BULLETIN OF THE CHEMICAL SOCIETY OF JAPAN VOL. 39 1—7 (1966)

The Preparation of Heavy Metal Hydride and Its Catalytic Activity. VIII.* Information on the Mechanism of Iron Hydride Formation**

By Yoshinobu TAKEGAMI, Toru UENO and Kiyoshi KAWAJIRI

Department of Fuel Chemistry, Faculty of Engineering, Kyoto University, Sakyo-ku, Kyoto

(Received March 26, 1965)

Some information on the mechanism of iron hydride formation in the reaction of iron(III) chloride with phenylmagnesium bromide under a hydrogen atmosphere has been presented. When the molar ratio ($C_6H_5MgBr/FeCl_3$) is larger than 5, 3—4 (mol./mol. $FeCl_3$) of hydrogen is absorbed during the synthesis of hydrides. The amounts of benzene, one of the by-products formed in the synthesis, have also been determined. The treatment of these hydrides with styrene under a nitrogen atmosphere has given ethylbenzene in amounts which correlate well with the amounts of hydrogen absorbed during the hydride synthesis. These observations can be taken as support for the formation of iron hydride. On the other hand, a mixture prepared by the reaction of iron(III) chloride with phenylmagnesium bromide under a nitrogen atmosphere evolved about 0.5 (mol./mol. $FeCl_3$) of hydrogen on hydrolysis. When the hydride prepared under a hydrogen atmosphere was hydrolyzed with dideuterosulfuric acid, D_2 as well as HD was evolved. These results seem to indicate that not only hydride sites but also metallic sites were formed during the iron hydride synthesis. On the basis of these observations, a possible mechanism for the formation of complex hydride containing iron and magnesium has been presented.

The formation of an iron hydride in the reaction of iron(III) chloride with phenylmagnesium bromide under a hydrogen atmosphere has been reported by several workers.[1-3] It was also demonstrated in our own earlier publications[4,5] that the iron hydride and several other transition metal hydrides were of interest for their high catalytic activities in the hydrogenation of olefins. Since the catalytic activity of the hydride is closely dependent on its composition (hydrogen content),[5] we investigated[6] the process of the iron hydride synthesis and found the following facts; 1) no hydrogen was absorbed so long as the ($C_6H_5MgBr/FeCl_3$) molar ratio was lower than 3; 2) a plot of the amounts of hydrogen absorbed during the hydride synthesis vs. the molar ratios was linear when the molar ratios were in the range from 3.5 to 7, and 3) about 4 mol. of hydrogen per mol. of iron(III) chloride was absorbed when the molar ratio was higher than 8. These observations suggested that the reaction scheme involved the following steps: 1) the formation of an intermediate; 2) the interaction of an excess of the Grignard reagent with the intermediate; 3) the replacement of phenyl groups with hydrogen atoms, and 4) the formation of a complex hydride.

$$FeCl_3 + 3C_6H_5MgBr \rightarrow Fe(C_6H_5)_3 + 3MgBrCl \quad (1)$$

$$Fe(C_6H_5)_3(C_6H_5MgBr)_{4/3} + H_2 \rightarrow FeH(C_6H_5)_2(C_6H_5MgBr)_{4/3} + C_6H_6 \quad (2)$$

$$FeH(C_6H_5)_2(C_6H_5MgBr)_{8/3} + H_2 \rightarrow FeH_2(C_6H_5)(C_6H_5MgBr)_{8/3} + C_6H_6 \quad (3)$$

$$FeH_2(C_6H_5)(C_6H_5MgBr)_4 + H_2 \rightarrow FeH_3(C_6H_5MgBr)_4 + C_6H_6 \quad (4)$$

$$FeH_3(C_6H_5MgBr)_{n>4} + C_6H_5MgBr + H_2 \rightarrow 1/2Mg(FeH_4)_2(C_6H_5MgBr)_{n>8} + 1/2MgBr_2 + C_6H_6 \quad (5)$$

However, in view of the instability of organo-iron compounds,[7] it appeared improbable that the $Fe(C_6H_5)_3$ could be an intermediate in the iron hydride synthesis. In this paper, several pieces of

* Part VII: Y. Takegami, T. Ueno and T. Fujii, This Bulletin, **38**, 1279 (1965).

** Part of this work was reported at the 17th Annual Meeting of the Chemical Society of Japan, Tokyo, April, 1964.

1) T. Weichselfelder, *Ann.*, **447**, 64 (1926).

2) B. Sarry, *Z. anorg. u. allgem. Chem.*, **288**, 48 (1956).

3) R. C. Ray and R. B. N. Sahai, *J. Indian Chem. Soc.*, **23**, 67 (1946).

4) Y. Takegami and T. Fujimaki, *J. Chem. Soc. Japan, Ind. Chem. Sect.* (*Kogyo Kagaku Zasshi*), **64**, 287 (1961).

5) Y. Takegami, T. Ueno and K. Kawajiri, *Catalyst* (*Shokubai*), **4**, 13 (1962).

6) Y. Takegami, T. Ueno and K. Kawajiri, *J. Chem. Soc. Japan, Ind. Chem. Sect.* (*Kogyo Kagaku Zasshi*), **66**, 1068 (1963).

7) F. A. Cotton, *Chem. Revs.*, **55**, 571 (1955).

information about the intermediate will be presented, and a probable mechanism based on them will be discussed.

Experimental

Materials.—Phenylmagnesium bromide was prepared under nitrogen by the reaction of freshly-distilled phenylbromide with a 10% excess of magnesium in dry tetrahydrofuran (THF) or diethyl ether. The Grignard reagent was filtered, and the concentration of the stock solution (0.6—0.9 mol./l.) was determined, prior to use, according to Gilman's method.[8] The solvent, tetrahydrofuran or diethyl ether, was dried over sodium and freshly distilled just before use.

The Preparation and Hydrolysis of Iron Hydride.—Since in all cases the hydrides were sensitive to air and moisture, all operations were carried out in a nitrogen or hydrogen atmosphere. The apparatus for the preparation of hydrides consisted of a four-necked flask equipped with a stirrer, a dropping funnel (60 ml.) and a thermometer; this was connected to a gas buret through a silica gel tube. Before the reaction, the apparatus was flushed with hydrogen. A solution of 70 ml. of tetrahydrofuran containing 0.005 mol. of iron(III) chloride was stirred at the reaction temperature for 40 min. To this solution a desired amount of the phenylmagnesium bromide solution (in THF) was then added through the dropping funnel. The solution immediately turned black, and a hydrogen absorption took place. The mixture was then stirred for 5 hr. or more, until the hydrogen absorption ceased. Then the hydride was hydrolyzed by the addition of 20 ml. of 15% aqueous hydrochloric acid, and the amount of hydrogen evolved was measured.

The Reaction of Iron Hydrides with Styrene under a Nitrogen Atomosphere.—The iron hydride was prepared at 0°C. The hydrogen gas in the system was exchanged with nitrogen, and then 5 ml. (0.0435 mol.) of styrene was added to the iron hydride solution. The mixture was stirred for 5 hr. at 0°C (styrene treatment). The mixture was hydrolyzed by the addition of aqueous hydrochloric acid, and the amount of hydrogen evolved was measured. The addition of ether produced two layers. The organic layer was separated, washed with water, concentrated by the evaporation of ether, and analyzed by gas chromatography.

The Determination of the Amounts of Benzene Produced during the Iron Hydride Synthesis.—Two variations of the determination procedure were used. In one method (procedure A), the iron hydride was prepared under hydrogen at 0°C, using ether as the solvent. At the end of the preparation, the stirrer was quickly replaced with a short distilling head, and the solvent, containing a small amount of benzene, was distilled under reduced pressure (10 mmHg) and at room temperature. The distillate collected in a dry ice trap was analyzed by gas chromatography, using cyclohexane as an internal reference. In order to check the validity of this method, another procedure (procedure B) was also employed. To the iron hydride prepared as above, 5 ml. of diethylketone was added, and the solution was stirred for 2 hr. at 0°C. The solution was then hydrolyzed and analyzed by gas chromatography, using cyclohexane as an internal reference. As a small amount of benzene was produced by the same treatment of Grignard reagent alone, it was necessary to correct the observed amount of benzene in gas chromatography in order to determine the true amount of benzene produced by the iron hydride synthesis.

The Hydrolysis of the Iron Hydride with Dideuterosulfuric Acid.—Dideuterosulfuric acid was prepared by the reaction of deuterium oxide with the sulfur trioxide which evolved from warm 30% fuming sulfuric acid. Several iron hydrides were hydrolyzed with dideuterosulfuric acid (30% D_2SO_4 in D_2O). The gas evolved during the hydrolysis was washed with concentrated sulfuric acid and analyzed by mass spectrography.

The Reaction of Iron(III) Chloride with 2, 4, 6-Trideuterophenylmagnesium Bromide.—2,4,6-Trideuterophenylmagnesium bromide was prepared by the reaction of 2,4,6-trideuterophenyl bromide with magnesium in THF. 2,4,6-Trideuterophenyl bromide was prepared by the reaction of phenyl bromide with dideuterosulfuric acid (50 mol.% D_2SO_4 in D_2O) according to Wilson's method.[9] The reaction of iron(III) chloride with the 2, 4, 6-trideuterophenylmagnesium bromide was carried out in THF at 25°C under a nitrogen atomosphere. The reaction mixture was then hydrolyzed by the addition of aqueous hydrochloric acid, and the gas evolved during the hydrolysis was analyzed by mass spectrography.

Results

The Synthesis of Iron Hydrides under a Hydrogen Atmosphere at Various Reaction Temperatures.—In order to elucidate the course of the iron hydride synthesis, reactions of iron(III) chloride with Grignard reagents were carried out at different molar ratios and at several reaction temperatures. The results are given in Tables I.

TABLE I. SYNTHESIS AND HYDROLYSIS OF IRON HYDRIDES*

$FeCl_3$ mmol.	Molar ratio $C_6H_5MgBr/FeCl_3$	H_2 absorbed	H_2 evolved on hydrolysis mol./mol.$FeCl_3$
		(at −20°C)	
5.55	2.99	0.09	0.37
4.95	3.96	1.04	—
5.23	4.88	2.27	2.46
4.80	5.72	2.70	—
4.95	6.10	2.50	2.74
5.28	8.04	1.63	1.80
5.18	8.20	1.35	1.52
5.14	12.2	1.88	2.06
		(at −40°C)	
5.73	3.59	(0.65)	0.83
6.71	4.90	(1.70)	—
		(at −70°C)	
5.39	6.06	0	0.20

* Solvent: THF, about 100 ml.

8) H. Gilman, E. A. Zoellner and J. B. Dickey, *J. Am. Chem. Soc.*, **51**, 1576 (1929).

9) A. P. Best and C. L. Wilson, *J. Chem. Soc.*, **1946**, 239.

Table II. Synthesis of iron hydrides at 0°C and their styrene treatment*

$FeCl_3$ mmol.	Molar ratio $C_6H_5MgBr/FeCl_3$	H_2 absorbed mol./mol.$FeCl_3$	H_2 evolved** mol./mol.$FeCl_3$	Ethylbenzene %	Ethylbenzene mol./mol.$FeCl_3$
5.31	3.77	0.96	0.81	4.6	0.38
5.56	3.96	1.14	0.79	6.7	0.52
5.32	4.46	1.89	0.59	17.0	1.39
5.16	5.36	2.79	0.52	27.6	2.33
5.12	6.96	3.61	0.63	37.6	3.19
4.82	8.49	3.79	0.61	37.7	3.40
3.89	11.42	3.90	0.58	29.6	3.31
5.31	15.10	3.72	0.49	42.1	3.45

* Styrene treatment: at 0°C for 5 ml. (43.5 mmol.) of styrene. Solvent: THF, about 100 ml.
** Amounts of hydrogen evolved on the hydrolysis subsequent to the styrene treatment.

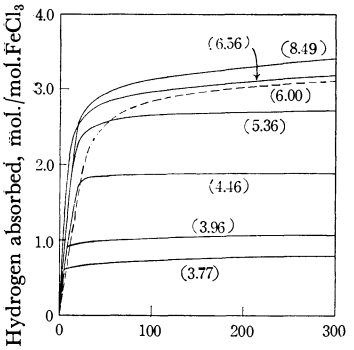

Fig. 1. Hydrogen absorption curves in the reactions carried out at 0°C.
Numerals in parentheses represent the molar ratios ($C_6H_5MgBr/FeCl_3$). Dotted line shows the results of the reaction of ($FeCl_3+1/4\ LiAlH_4$) with 6 C_6H_5MgBr.

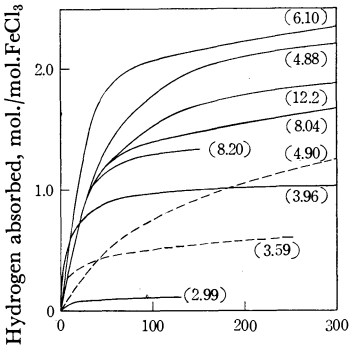

Fig. 2. Hydrogen absorption curves in the reactions carried out −20°C and −40°C.
Solid lines: at −20°C Dotted lines: at −40°C
Others are same in Fig. 1.

and II. The hydrogen absorption curves obatined from the reaction carried out at 0°C are shown in Fig. 1. At the relatively low molar ratios of 3 and 4, the total amount of hydrogen absorbed was small, though the initial rate of the hydrogen absorption was high. At relatively high molar ratios between 6 and 12, the hydrogen absorption proceeded rapidly up to about 3 (mol./mol. iron(III) chloride) but there followed a sluggish hydrogen absorption; the total amount of hydrogen absorbed reached about 4 (mol./mol. iron(III) chloride). This correlation between the hydrogen absorption curves and the molar ratios is almost the same as that observed in the reactions carried out at 35°C.[6]

The experiments performed at lower temperatures (Fig. 2) show that the rates of hydrogen absorption slowed down as the reaction temperature was lowered. At −40°C, the rate was very slow and, therefore, no end point of the hydrogen absorption was detected exactly. At −70°C, no hydrogen absorption was observed, and the reaction mixture did not turn black.

The amount of hydrogen absorbed during the hydride synthesis is closely dependent on the molar ratio. The amounts of hydrogen absorbed plotted

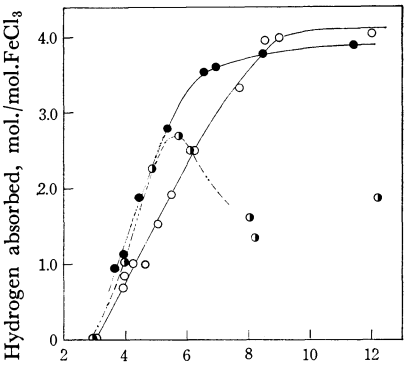

Fig. 3. Molar ratios vs. amounts of hydrogen absorbed.
-○-: At 35°C
-●-: At 0°C
-◑-: At −20°C

against the molar ratios (Fig. 3) show that the amounts of hydrogen absorbed at 0°C are more dependent on the molar ratio than those absorbed at 35°C. At −20°C, the amount of hydrogen absorbed reaches a maximum when the molar ratio is 6.10, decreasing with any further increase

in the molar ratio. Evidently, this dependence of the amount of absorbed hydrogen on the molar ratio is different from those observed at 0°C and 35°C. When the iron hydride was prepared at −20°C in the molar ratio of 6, and when phenylmagnesium bromide was added to the reaction mixture at the same temperature, no hydrogen evolution was observed, even though the molar ratio was as high as 12. It now seems impossible to find any probable interpretation for this decrease in the amount of hydrogen absorbed with the increase in the molar ratio.

On the hydrolysis of the hydrides prepared above, a hydrogen evolution was observed. The amounts of hydrogen evolved are given in the last column of Table I. They are somewhat larger than those absorbed during the hydride synthesis.

The Styrene Treatment of the Iron Hydrides.—Ethylbenzene was produced by the reaction of the iron hydride with styrene under a nitrogen atmosphere. The amounts of ethylbenzene produced are given in Table II. They are also shown graphically in Fig. 4 as a function of the amounts of hydrogen absorbed during the hydride synthesis. As may be seen in Fig. 4, a linear relationship is observed between the amounts of ethylbenzene produced during the styrene treatment and the amounts of hydrogen absorbed during the hydride synthesis.

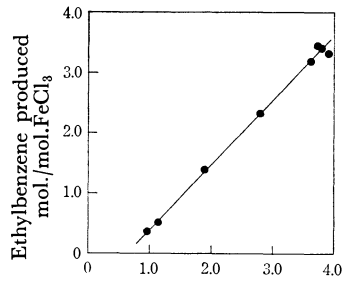

Fig. 4. Amounts of hydrogen absorbed during hydride synthesis vs. amounts of ethylbenzene produced during styrene treatment.

The Determination of the Amounts of Benzene Produced during the Iron Hydride Synthesis.—One mole of benzene should be produced per mole of hydrogen absorbed so long as the iron hydride formation proceeds according to Eqs. 1—5. Therefore, the amounts of benzene produced during the iron hydride synthesis were determined in order to check the scheme. As may be seen in Fig. 5, plots of the amounts of benzene produced against the amounts of hydrogen absorbed during the hydride synthesis gave a straight line, with a slope of 1.0. These results show that one mole of benzene is produced per mole of hydrogen absorbed. However, when the data are extrapolated to zero hydrogen absorbed, about 0.6

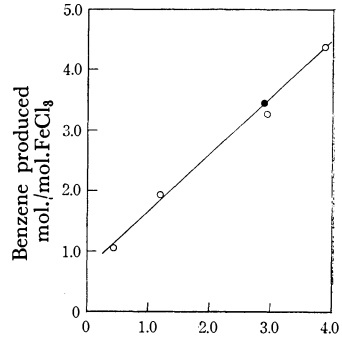

Fig. 5. Amounts of hydrogen absorbed during hydride synthesis vs. amounts of benzene produced.
○: Procedure A
●: Procedure B (See Experimental)

(mol./mol. iron(III) chloride) of benzene is to be produced.

The Reaction of Iron(III) Chloride with a Grignard Reagent under a Nitrogen Atmosphere,—Even when the reaction of iron(III) chloride with a Grignard reagent was carried out under a nitrogen atmosphere, a black solution was produced and about 0.5 mol. of hydrogen per mole of iron(III) cholride was evolved on the hydrolysis, as is shown in Table III. The amount of hydrogen evolved increased steadily as the molar ratio increased from 3 to 5, and then it reached a plateau. It was also observed that the amount of hydrogen evolved on the hydrolysis of the nickel (II) chloride - Grignard reagent system was somewhat larger than that evolved from the iron(III) chloride - Grignard reagent system.

Table III. Hydrolysis of reaction mixtures prepared under a nitrogen atmosphere*

MX_n mmol.	Molar ratio C_6H_5MgBr/MX_n	H_2 evolved on hydrolysis mol./mol.MX_n
	($FeCl_3$-Grignard reagent)	
5.53	1.99	0.11
5.42	2.93	0.36
4.93	4.03	0.51
5.18	5.12	0.55
5.38	6.45	0.49
5.02	7.98	0.46
	($NiCl_2$-Grignard reagent)	
5.37	2.94	0.62
5.23	5.88	0.77

* Metal halides was treated with phenylmagnesium bromide at 0°C for 2 hr. prior to the hydrolysis. Solvent: THF, about 100 ml.

Figure 6 shows that, in the styrene treatment of the reaction mixture prepared under a nitrogen atmosphere, the ethylbenzene produced and the hydrogen evolved on the hydrolysis subsequent to

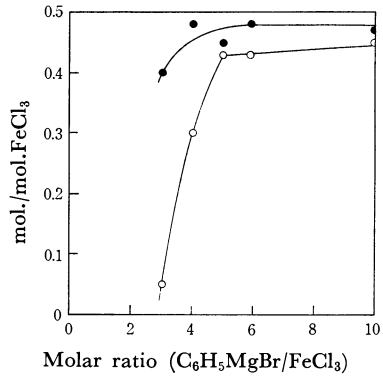

Fig. 6. Styrene treatment of reaction mixture prepared under a nitrogen atmosphere.
○: Amounts of ethylbenzene produced.
●: Amounts of hydrogen evolved on the hydrolysis subsequent to the styrene treatment.

the styrene treatment was about 0.5 (mol./mol. iron(III) chloride) when the molar ratio was higher than 5.

Hydrogen Absorption Subsequent to the Reaction Carried Out under a Nitrogen Atmosphere.—The reaction of iron(III) chloride with the Grignard reagent was carried out under a nitrogen atmosphere (the first step), and then under a hydrogen atmosphere (the second step).*1 The amount of hydrogen absorbed was measured in the course of the second step. The hydrogen absorption curves are shown in Fig. 7. A comparison between Fig. 1 and Fig. 7 shows that the hydrogen absorption rate and the amounts of hydrogen absorbed are quite the same as those in the one-step reactions. As is shown in Table IV, the amounts of hydrogen evolved during the hydrolysis subsequent to the hydrogen absorption are larger by 0.3—0.4 than the amounts of hydrogen absorbed in the second step as expressed by the mol. hydrogen/mol. iron(III) cholride ratio. In the cases of the nickel(II) chloride - Grignard reagent system, these increments in the amount of hydrogen evolved on the hydrolysis amounted to 0.6—1.0. The increase in the amount of hydrogen seemingly comes from the hydrogen which the reaction product of the first step evolves in the hydrolysis.

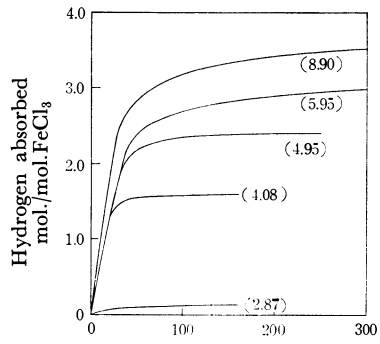

Fig. 7. Hydrogen absorption curves in the second-step reactions.
Numerals in parentheses represent the molar ratios ($C_6H_5MgBr/FeCl_3$).

TABLE IV. AMOUNT OF HYDROGEN ABSORBED IN THE SECOND STEP AND EVOLVED ON HYDROLYSIS OF THE PRODUCT FROM TWO-STEP REACTION*

MX_n mmol.	Molar ratio C_6H_5MgBr/MX_n	H_2 absorbed mol./mol.MX_n	H_2 evolved on hydrolysis mol./mol.MX_n
	($FeCl_3$-Grignard reagent)		
5.22	2.87	0.14	0.40
5.62	4.08	1.60	1.63
5.25	4.95	2.43	2.81
6.39	5.86	2.57**	2.91
5.04	5.95	3.32	3.63
5.52	8.90	4.00	3.96
	($NiCl_2$-Grignard reagent)		
5.49	1.91	0.29	0.91
5.82	3.04	0.83	1.66
5.86	4.12	1.23	2.22
5.08	7.19	1.63	2.41

* Metal halide was treated with phenylmagnesium bromide at 0°C for 2 hr. under a nitrogen atmosphere prior to the hydrogen absorption. Solvent: THF, about 100 ml.
** The first-step reaction was conducted under nitrogen atmosphere for 48 hr. and then the second-step reaction under hydrogen atmosphere.

The Hydrolysis of Iron Hydrides with Dideuterosulfuric Acid.—It has been assumed that the hydrogen evolved on the hydrolysis should be attributed to the hydride. However, there is still another possibility, that a metallic compound which evolves hydrogen on the hydrolysis may be included in the reaction system. Therefore, several reaction products of the reaction of iron(III) chloride with phenylmagnesium bromide were hydrolyzed with dideuterosulfuric acid, and the gas evolved, a mixture of D_2, HD and H_2, was analyzed by mass spectrography. Although the mechanism of the evolution of D_2, HD and H_2 has not yet been constructed, we assume that the amount of D_2 evolved can be an index of the amount of the free metal and/or the reaction product not containing hydrogen as a constituent, and that the amount of HD evolved can be an index of the amount of hydride. The results are listed in Table V. The D-purity of the dideuterosulfuric acid was about 92% as determined by the hydrolysis of iron metal (Run 1).

The agreement between the compositions of the

*1 The preparation of hydride which takes two steps (first and second steps) will be described as "two-step reaction," while the preparation carried out under a hydrogen atmosphere from the beginning of the reaction will be described as "one-step reaction" in the discussion below.

TABLE V. HYDROLYSIS OF IRON HYDRIDE WITH DIDEUTEROSULFURIC ACID

Run	Sample	Acid	Mass number, %		
			2	3	4
1	Fe-metal	D_2SO_4	2	13	85
2	PhMgBr-$FeCl_3$ in N_2	D_2SO_4	5	16	79
3	PhMgBr-$FeCl_3$, $N_2 \rightarrow H_2$*	D_2SO_4	26	45	29
4	PhMgBr-$FeCl_3$ in H_2**	D_2SO_4	20	43	37
5	$C_6H_2D_3MgBr$-$FeCl_3$ in N_2	HCl	>99	<1	—

* Prepared by the two-step reaction: the amount of hydrogen absorbed was 3.2 mol./mol.$FeCl_3$.

** Prepared by the one-step reaction: the amount of hydrogen absorbed was 3.2 mol./mol.$FeCl_3$.

gas evolved in Runs 1 and 2 demonstrates that the major product in the reaction of iron(III) chloride with phenylmagnesium bromide under a nitrogen atmosphere is indeed the free metal and/or the reaction product not containing hydrogen as a constituent. In the cases of the hydrides which absorbed hydrogen, the gas evolved was about 45% (1.6 mol./mol. iron(III) chloride) HD, which can be taken as further support for the presence of the iron hydride. On the other hand, there was about 30% (1.4 mol./mol. iron(III) chloride) D_2; this can not be explained by Eqs. 1—5. About 20% (1.0 mol./mol. iron(III) chloride) of H_2 was also evolved.*2

As may be seen in Run 5, no appreciable D-fraction was detected in the gas evolved during the hydrochloric acid hydrolysis of the product of the reaction of ferric chloride with 2, 4, 6-trideutero phenylmagnesium bromide.

Discussion

The linear relationship between the amounts of hydrogen absorbed during the hydride synthesis and the amounts of ethylbenzene produced during the styrene treatment of the hydrides (Fig. 4) indicates that the hydrogen absorbed during the synthesis was consumed in the formation of the hydride. The evolution of HD during the hydrolysis with dideuterosulfuric acid subsequent to the hydrogen absorption (Table V) is conceivably due to the presence of the hydride.

The facts that one mole of benzene was produced per mole of hydrogen absorbed during the iron hydride synthesis and that plots of the amounts of hydrogen absorbed against the molar ratios were linear in the reaction carried out at 0°C, as well as at 35°C, can be taken as further confirmations of the proposed scheme, Eqs. 1—5.

However, there are several facts that can not be explained by the proposed scheme. About 0.5 mol. of hydrogen per mole of iron(III) chloride was evolved during the hydrolysis of the reaction mixture produced under a nitrogen atmosphere (Table III). Since 0.5 mol. of ethylbenzene per mole iron(III) chloride was produced when this reaction mixture was treated with styrene under a nitrogen atmosphere (Fig. 6), it seems plausible that a small amount of hydride was formed under a nitrogen atmosphere by the elimination of FeH from the intermediate, $Fe(C_6H_5)_3$.*3 This view, however, is discarded by the fact that no appreciable deuterium fraction was detected in the gas evolved on the hydrolysis, with hydrochloric acid, of the reaction mixture prepared by the reaction of iron(III) chloride with 2, 4, 6-trideuterophenylmagnesium bromide under a nitrogen atmosphere. The mass spectral data also show that the reaction mixture produced by the reaction of iron(III) chloride with phenylmagnesium bromide under nitrogen does not contain hydrogen as a constituent. This compound absorbs hydrogen to give the nearly same amount of the hydride as that formed in the one-step reaction under a hydrogen atmosphere. A reasonable scheme must be proposed for the hydrogen absorption in the two-step reaction.

The $Fe(C_6H_5)_3$ intermediate has been considered to be formed in the reaction of iron(III) chloride with phenylmagnesium bromide. This intermediate, however, does not evolve hydrogen in the hydrolysis, and it is improbable that the intermediate is left intact for 2 hr. or more. Therefore, the intermediate in the two-step reaction is considered to be one of the decomposition products of $Fe(C_6H_5)_3$,*4 i. e., $Fe(C_6H_5)_2$, $Fe(C_6H_5)$ or Fe. If Fe is the intermediate, 1.0 mole. of hydrogen should be evolved on the hydrolysis, while no hydrogen evolution should be observed if $Fe(C_6H_5)_2$ is the intermediate. Thus, $Fe(C_6H_5)$

*2 Three points can be considered as the source of this H_2; 1) the H-fraction in the dideuterosulfuric acid used in the hydrolysis; 2) the hydrolysis of iron hydride which contains a relatively large amount of hydrogen (for example, $FeH_3 + 2D_2SO_4 \rightarrow FeSO_4 + 2HD + 1/2\ H_2$), and 3) hydrogen which is adsorbed on the metal surface. We now consider that 1) and 2) contribute greatly to the H_2-evolution.

*3 When cyclohexylmagnesium bromide is used instead of phenylmagnesium bromide, 1.4 mol. of hydrogen per mole of iron(III) chloride is evolved on the hydrolysis of the reaction mixture prepared under a nitrogen atmosphere, presumably indicating the formation of iron hydride through cyclohexene-elimination from the iron-cyclohexyl intermediate; Y. Takegami, T. Ueno, K. Shinoki and T. Sakata, *J. Chem. Soc. Japan, Ind. Chem. Sect.* (*Kogyo Kagaku Zasshi*), **67**, 316 (1964).

*4 Kharasch and his co-workers (*J. Am. Chem. Soc.*, **83**, 3229 (1961)) reported, in their study of the modification of the Grignard reaction in the presence of a small amount of iron(III) chloride serving as a catalyst, that phenylmagnesium bromide combines with iron(III) chloride to produce an unstable organo-iron compound, which then decomposes to give a biphenyl and a reduced iron salt in the following way: $2C_6H_5MgBr + FeCl_3 \rightarrow (C_6H_5)_2FeCl + 2MgBrCl$, $(C_6H_5)_2FeCl \rightarrow FeCl + C_6H_5\text{-}C_6H_5$. Our assumption of $Fe(C_6H_5)_3$ as an unstabe intermediate in place of $Fe(C_6H_6)Cl$ is based on the fact that hydrogen is absorbed only when the molar ratio is higher than 3 (Fig. 3), indicating that 3 mol. of Grignard reagent has been consumed before the hydrogen absorption takes place in the reaction.

appears to be the best choice as the intermediate which evolves 0.5 mol. of hydrogen in the hydrolysis.*5 The fact that the product in the reaction of iron(II) chloride, as well as iron(III) chloride, with the Grignard reagent under a nitrogen atmosphere evolved about 0.5 mol. of hydrogen per mole of iron(III) chloride is also in agreement with the prediction of such an intermediate as $Fe(C_6H_5)$.

As may be seen in Table III, 4—8 mol. of the Grignard reagent per mole of iron(III) chloride is necessary for the hydrogen absorption. The effect of the excess Grignard reagent appears quite similar to that considered in Eqs. 1—5. Therefore, the hydrogen absorption in the two-step reaction is assumed to be initiated by the interaction of the Grignard reagent with $Fe(C_6H_5)$ to form an iron subphenyl-Grignard reagent complex such as II, followed by the replacement of phenyl groups with hydrogen atoms by the attack of hydrogen molecule. Thus, a complex hydride such as III should be produced when 3 mol. of hydrogen per mole of iron(III) chloride is absorbed. On the hydrolysis of III, 3.5 mole. of hydrogen per mole of iron(III) chloride should be evolved. Since this corresponds to the results presented above, the shceme I→II→III can be assumed in the two-step reaction:

$$FeCl_3 + 3\,C_6H_5MgBr \rightarrow Fe(C_6H_5)_3 + 3\,MgBrCl$$

$$\underset{\mathbf{I}}{Fe(C_6H_5)_3} \rightarrow Fe(C_6H_5) + C_6H_5\text{–}C_6H_5{}^{*6} \quad (6)$$

$$Fe(C_6H_5) + 2\,C_6H_5MgBr \rightarrow \underset{\mathbf{II}}{\begin{matrix} & MgBr \\ & \vdots \\ & C_6H_5 \\ & \vdots \\ Fe & \text{–} C_6H_5 \\ & \vdots \\ & C_6H_5 \\ & \vdots \\ & MgBr \end{matrix}} \quad (7)$$

$$II + 3\,H_2 \rightarrow \underset{\mathbf{III}}{\begin{matrix} & MgBr \\ & \vdots \\ & H \\ & \vdots \\ Fe & \text{–} H \\ & \vdots \\ & H \\ & \vdots \\ & MgBr \end{matrix}} \quad (8)$$

Although this new scheme is proposed for the formation of the iron hydride in the two-step reaction, it seems almost certain that this scheme also contributes greatly to the iron hydride formation in the one-step reaction under hydrogen. If this is the case, the following experimental results in the one-step reaction, which can not be explained by the earlier scheme, can be explained: 1) the rate of the absorption and the amount of hydrogen absorbed are nearly the same in the one-tsep reaction as in the two-step reaction (Fig. 1 vs. Fig. 7); 2) the amounts of hydrogen evolved in the hydrolysis are somewhat larger than those absorbed during the hydride synthesis (Table II); 3) the composition of the gas evolved in the hydrolysis with dideuterosulfuric acid is nearly the same as that in the two-step reaction (Table V); 4) about 5 mol. of Grignard reagent per mole of iron(III) chloride is needed to absorb 3 mol. of hydrogen in the iron hydride synthesis (the reaction carried out at 0°C, in Fig. 3), and 5) almost the same results were obtained when iron(III) chloride was used instead of iron(III) chloride (Fig. 1).

It can be reasonably concluded, therefore, that the scheme I→II→III is also valid in the one-step reaction. A more detailed discussion of this hypothesis must, however, await the accumulation of additional data on the composition of the gas evolved by the hydrolysis of hydrides of various hydrogen contents with dideuterosulfuric acid, as well as on other reaction parameters. These data are now being gathered.

The authors wish to express their gratitude to Professor Yoshimasa Takezaki of the Chemical Research Institute, Kyoto University, for his kind mass spectrographic analysis. Thanks are also due to Mr. Takeki Sakata and Mr. Takao Fujii for their skillful assistance in the experiments.

*5 $Fe(C_6H_6) + 2\,HCl \rightarrow FeCl_2 + C_6H_6 + 1/2\,H_2$. This intermediate is being studied by means of electron-spin resonance.

*6 Like Kharasch, we assume a production of one mole of biphenyl. However, a small amount of phenyl radicals may also be produced, which then abstracts the hydrogen atom from the solvent to give benzene. This hypothesis may explain the production of about 0.6 mol. of benzene when the amount of hydrogen absorbed during the iron hydride synthesis is zero (Fig. 5).

BULLETIN OF THE CHEMICAL SOCIETY OF JAPAN VOL. 39 8—14 (1966)

Studies of Organic Catalytic Reactions. III.[1] The Hydration Mechanism of Nitriles to Amides with Nickel Catalysts

By Ken-ichi WATANABE and Koji SAKAI

Department of Chemistry, Faculty of Science, Tokyo Metropolitan University, Setagaya-ku, Tokyo

(Received March 26, 1965)

Benzonitrile, benzyl cyanide, acetonitrile and 2-cyanopyridine give the corresponding amides by the hydration with nickel catalysts and water. The effect of pyridine and thiophene on the hydration has been investigated. In general, the yield of amides increases upon the addition of a suitable amount of pyridine. On the contrary, the reaction is distinctly suppressed by the addition of thiophene. This fact is in striking contrast to the effect on the hydrogenation of nitriles. The correlation of the catalytic functions in hydration and the hydrogenation of nitriles has been studied, and the hydration mechanism with nickel catalysts has been discussed.

Nitriles are hydrated to the corresponding amides by refluxing them with metal catalysts (a nickel catalyst is the best) in water[1]. In this novel reaction, neither acid nor alkali is necessary, and the reaction is generally stopped at the amide stage, especially in the reaction of aromatic nitriles. However, the reaction of aliphatic nitriles is somewhat complicated because of the side reactions with accompany the hydration. The present paper will deal with the mechanism of this catalytic hydration reaction of nitriles from the points of view of organic reaction and catalytic function.

It has been reported that a nickel catalyst acts in two different ways, exhibiting both acidic and basic functions. In this paper, this conception will be developed further by some experiments and discussed. In the hydration of benzonitrile, benzyl cyanide, benzamide and acetonitrile, when pyridine was used as a basic substance, it accelerated the hydration. While thiophene, when used as an acidic substance, suppressed the hydration. In addition, pyridine also suppressed side reactions. As a result of many facts mentioned below, the hydration mechanism of nitriles to amides with nickel catalysts will be presented.

The Hydration of Benzyl Cyanide, Acetonitrile and 2-Cyanopyridine with Nickel Catalysts.—Though Raney nickel is effective enough for this reaction,[1] Urushibara nickel catalyst-B (U-Ni-B)[1,2] was used in these experiments. Some results of the hydration of three nitriles are shown in Table I and in Figs. 1 and 2. In the hydration of acetonitrile, hydrogen cyanide was generated as well as ammonia. The formation of propionic acid, hydrogen cyanide and formic acid suggests that catalytic cleavages of acetonitrile and

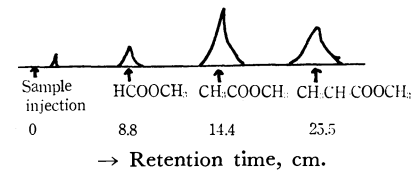

Fig. 1. Gas chromatographic chart of analysis of acids. (Acids were converted to methylesters respectively.)

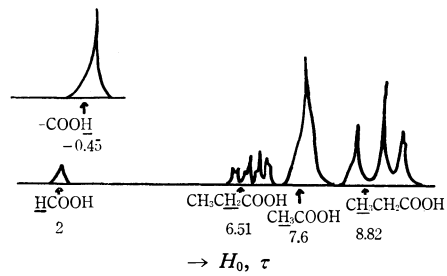

Fig. 2. NMR spectrum chart of acids.

new bond formations take place in addition to the hydration reaction. It is of great interest that such reactions occur in the liquid phase around at 100°C.*1 The effect of the electronegative character of the nitrogen atom in the pyridine nucleus was so predominant in the hydration of cyanopyridines that a remarkably good result was obtained in the case of 3-cyanopyridine (amide yield: 89%),[1] while a nickel complex was obtained in the case of 2-cyanopyridine.

1) Paper II: K. Watanabe, This Bulletin, **37**, 1325 (1964).
2) Y. Urushibara and S. Nishimura, This Bulletin, **28**, 466 (1955).

*1 The hydration of adiponitrile gave the corresponding amide in a poor yield (ca. 20%) and was accompanied by various kinds of side reactions. By the gas chromatographic analysis of the oily by-product, five components were detected. It seemed that an acidic substance was included in the oil. It can only be preumed that the reaction was much more complicated than that of acetonitrile.

TABLE I. THE HYDRATION OF NITRILES TO AMIDES WITH U-Ni-B IN WATER

Exp. No.	Nitrile g.	Catalyst g.	Water ml.	Reaction time hr.	Yield[1] of amide %	Recovered[2] nitrile	Other product	Remark
1	Benzyl cyanide 10	4	150	10	58	+	Phenylacetic acid, Phenethylamine, Benzaldehyde (?)	
2	Acetonitrile 7	4	100	5	28[3]	+	Acids,[4] Amine (+)	5)
3	Acetonitrile 7	4	100	7.5	47.2	+	Acids, Amine (+)	5)
4	Acetonitrile 7	8	100	5	49.6	+	Acids, Amine (+)	5)
5[6]	Acetonitrile 35	20	500	8	70	+	Acids, Amine (+)	5)
6	2-Cyanopyridine 7	4	100	10	ca. 40	—	Nickel complex	
7[7]	3-Cyanopyridine 7	4	100	10	89	—		

1) Yield of amide was calculated from the weight of amide obtained in pretty pure.
2) Recovered nitrile was analyzed by gas chromatography.
3) This is the highest yield of the reaction products by this condition.
4) Acids are propionic acid, acetic acid and a trace of formic acid.
5) Besides ammonia gas, hydrogen cyanide was detected.
6) The content was stirred with efficient stirrer during the refluxing.
7) Paper II.

TABLE II. THE HYDRATION OF BENZONITRILE TO BENZAMIDE WITH VARIOUS CATALYSTS

Exp. No.	Catalyst g.		Weight of sample g.	Solvent (water) ml.	Reaction time hr.	Yield[1] of benzamide %
1	U-Ni-B	4	5	80	8	78
2	Stabilized-Ni (F50)	25	5	80	8	78
3	ZnO	4	5	80	8	—
4	$Cu\text{-}CrO_2$	4	5	80	8	20

1) Yield of amides was calculated from the weight of amides obtained.

Studies of Catalysts for the Hydration.—The effect of the nature of many catalysts on this hydration has been examined.[1] It has been found that the usual catalysts for hydrogenation are generally effective in the hydration of nitriles.

For this paper, some other catalysts have also been tested in the hydration of benzonitrile. The catalysts used were U-Ni-B, Stabilized-Ni (F50),*2 zinc oxide, and copper chromium oxide. The results of representative experiments are shown in Table II. The highest yield of benzamide was given with U-Ni-B (Exp. No. 1), the other substances gave poor results as catalysts for the hydration.

The Effect of Ammonia Gas on the Hydration.—During the hydration of any nitrile, a small quantity of ammonia gas is gradually generated. The quantity of ammonia gas generated during the reaction with benzonitrile was examined every hour,*3 this was also tried in the case of the hydrolysis of benzamide with U-Ni-B in water. The

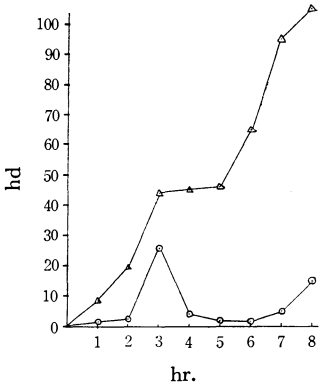

Fig. 3. The relative quantity of ammonia gas generated during the hydration with U-Ni-B.
—△— Benzonitrile —○— Benzamide

results of the measurements are shown in Fig. 3. It may easily be assumed that the ammonia gas generation was caused by the cleavage of the C–N bond of the nitrile groups. The quantitative analysis of all the ammonia gas generated from benzonitrile throughout the eight-hour reaction always gave constant results (ca. 20% yield), while benzamide was obtained in a 77 per cent yield. On the contrary, the hydrolysis of benzamide was much slower than that of benzonitrile, and no constant

*2 Obtained from the Nikko Scientiffic & Chemical Industry Co., Ltd., Tokyo, this was a kind of nickel catalyst on kieselguhr (50%) made from nickel formate, stabilized with inert gas.

*3 The reaction apparatus was connected to a gas samplemetric tube of the gas chromatography, and the ammonia gas generated was introduced to the tube for just three minutes and then analyzed by the usual method. Gas chromatography: column, 30% Carbo-wax 1500 on Celite ca. 30—40 mesh; length, 2 m.; temp., 75°C; flow rate, 6/10 ml./sec.; carrier gas, H_2.

TABLE III. THE EFFECT OF AMMONIA ON THE HYDRATION OF BENZONITRILE

Exp. No.	Weight of sample g.	Catalyst g.	Ammonia added	Solvent ml.		Reaction time hr.	Yield of amide %
1	5	—	NH_4OH conc. 2—3 drops (pH 8.8—9.2)	Water	80	8	4.3
2	5	—	NH_4OH conc. 80 ml.	NH_4OHaq.	80	8	4.3
3	5	—	Constant flow of ammonia gas	Water	80	8	22.0
4	5	U-Ni-B, 4	—	Water	80	5	1)
5	5	U-Ni-B, 4	NH_4OH conc. 2—3 drops (pH 8.8—9.2)	Water	80	5	2)

1) Benzonitrile unreacted after the reaction for five hours; 19%.
2) Benzonitrile unreacted after the reaction for five hours; 12%.

TABLE IV. THE EFFECTS OF PYRIDINE AND THIOPHENE ON THE HYDRATION OF NITRILES TO AMIDES IN WATER WITHOUT NICKEL CATALYST

Exp. No.	Nitrile	Weight of sample g.	Admixture ml.	Water ml.	Reaction time hr.	Yield of amide	Generated ammonia gas	Recovered nitrile g.
1	Benzyl cyanide	10	—	150	10	Trace	—	7.20
2	Benzyl cyanide	10	Pyridine, 1	150	10	Trace	—	8.30
3	Benzyl cyanide	10	Thiophene, 1	150	10	Trace	—	8.10
4	Benzonitrile	5	—	80	8	Trace	—	4.10
5	Benzonitrile	5	Pyridine, 1	80	8	Trace	—	4.00
6	Benzonitrile	5	Thiophene, 1	80	8	Trace	—	3.85

TABLE V. THE HYDRATION OF BENZYL CYANIDE TO PHENYLACETAMIDE WITH U-Ni-B IN WATER[1)]

Exp. No.	Admixture	Yield of amide %	Recovered nitrile %	Other product
1[2)]	—	58	6	Phenylacetic acid, Phenethylamine, Benzaldehyde (?)
2	Pyridine (1 ml.)	83	2.5	—
3	Pyridine (1.5 ml.)	51	7	—
4	Thiophene (1 ml.)	16	31	Amine
5[3)]	Pyridine (0.5 g.)	72	2.3	—
6	Pyridine (1 g.)	69	2.9	—
7	Pyridine (1.5 g.)	49	6.5	—

1) 10 g. of benzyl cyanide, 4 g. of catalyst and 150 ml. of water were refluxed for ten hours in each run.
2) The catalyst prepared at one time was divided into four parts of the same quantity and they were used respectively in each run of Exp. No. 1—4 at the same time.
3) Same way with 2).

results were observed with regard to the ammonia generation. A part of the ammonia generated during the reaction may form an ammonium salt of the acid that is produced by the hydrolysis of nitriles. On the basis of the results of experiments with benzonitrile, however, it may be assumed that the ammonium salts are too unstable under these reaction conditions and that they are likely to decompose and free the ammonia gas. In order to establish whether ammonia gas itself behaves as a catalyst for the hydration of nitriles, some experiments were carried out. Benzonitrile was refluxed with water containing a few drops of concentrated ammonium hydroxide without a nickel catalyst or was refluxed with concentrated ammonium hydroxide without a catalyst.*4 In one case, ammonia gas was introduced constantly throughout the reaction in the absence of a nickel catalyst. The results of the experiments are shown in Table III. It has been proved that ammonia gas itself generally effective to some extent as a catalyst for the hydration.

The Effect of Pyridine and Thiophene on the Hydration of Nitriles.—The effect of pyridine and thiophene on the hydration of some nitriles was studied in detail in the examination of this

*4 Krewson and Couch reported that concentrated ammonium hydroxide was only effective for the hydrolysis of nicotinonitrile in the sealed-tube (at 108°C for twelve hours). C. F. Krewson and J. F. Couch, *J. Am. Chem. Soc.*, **65**, 2256 (1943).

catalytic reaction mechanism. Blank tests with pyridine and thiophene showed that neither of them had any influence upon the hydration of benzonitrile and benzyl cyanide without catalysts (Table IV). In the hydration of benzyl cyanide, benzonitrile and acetonitrile, however, pyridine had favorable effects, while thiophene had unfavorable effects. This effect of pyridine was observed conspicuously in the reactions of benzyl cyanide. As is shown in Table V, the yield of phenylacetamide increased a great deal upon the addition of a suitable amount of pyridine (ca. 20% of a nickel catalyst). Further, it is noteworthy that no by-product could be obtained.

The results of the experiments with benzonitrile are shown in Figs. 4 and 5. Figure 4 shows the amount of the diminution of benzonitrile during the reaction with pyridine. The most desirable amount of pyridine added was ca. 1 g. (ca. 25% of a nickel catalyst). As is shown in Fig. 5,*5 it has been found that thiophene has a distinct effect in suppressing the reaction. The effect of pyridine on the hydration of acetonitrile was somewhat different from that of the other cases. Pyridine did not promote the hydration of acetonitrile, and the yield of acetamide was decreased. However, it was found that no propionic acid or formic acid was obtained, only acetic acid and acetamide were obtained by the addition of pyridine. Therefore, pyridine seemed to suppress the catalytic cleavages of acetonitrile. As for the effect of thiophene, it was as large as in the other cases. When acetamide was refluxed with a newly-prepared catalyst in water, the reaction hardly ever took place suprisingly. The reaction of acetonitrile may be assumed to be as shown in Fig. 6. Benzoic acid was obtained in a poor yield by the hydrolysis of benzamide,*6 a small quantity of ammonia gas was hardly ever generated. The effect of pyridine and thiophene was also observed by the generation of ammonia, a generation which was of the same type as the hydration of benzonitrile.

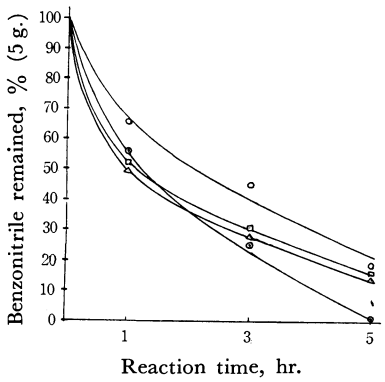

Fig. 4. Diminution of benzonitrile in the hydration with pyridine. (5 g. of benzonitrile and 4 g. of U-Ni-B were used in each run.)
Exp. No. 1 —○— Standard (without pyridine)
Exp. No. 2 —⊙— Addition of 1 g. of pyridine
Exp. No. 3 —△— Addition of 0.5 g. of pyridine
Exp. No. 4 —□— Addition of 2.5 g. of pyridine

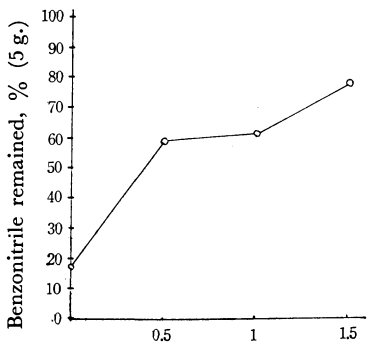

Fig. 5. Unreacted benzonitrile in the hydration with thiophene. (5 g. of benzonitrile and 4 g. of U-Ni-B were used in each run; reaction time, 5 hr.)

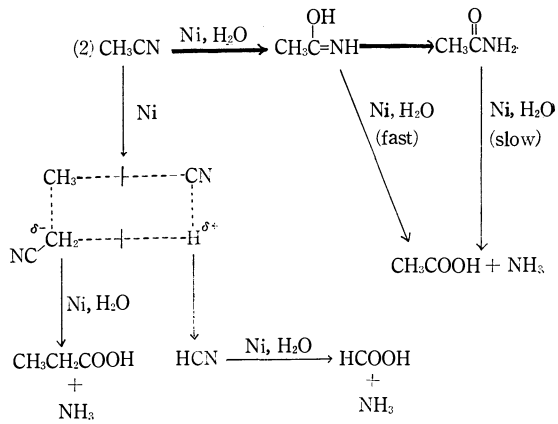

Fig. 6. Reactions of acetonitrile with nickel catalysts in water.

Discussion

As the result of many experiments, it is apparent, in the hydration of nitriles with nickel catalysts in water, that pyridine and organic bases have favorable effects on the reaction, while that thiophene and organic acids have unfavorable effects. It has previously been shown[1] that nitriles of a basic character afford the corresponding amides in good yields, and that those of an acidic character afford no hydration products. On the other hand, the effects of pyridine and thiophene on the hydrogenation of nitriles with nickel catalysts both

*5 The experimental method with thiophene was that 0.5 g., 1 g. or 1.5 g. of thiophene was added respectively in each run, after the reactions were over, the benzonitrile which remained was analyzed by gas chromatography (Fig. 5).

*6 The same reaction procedure with the hydration of benzonitrile.

in the liquid[3] and the vapor phases[4] have been studied in detail.[5] For instance, an organic base, ammonia or nitriles of a basic character effect an unfavorable hydrogenation. Thiophene does not. Consequently, it is significant that the effect of organic acids and bases on the hydration of nirtiles is in contrast to their effect on the hydrogenation of nitriles. It is of particular interest that *o*-aminobenzamide was obtained by the hydrogenation of *o*-nitrobenzonitrile with a nickel catalyst both in the liquid[6] and the vapor phase[5,7]. It is presumed that the hydrogenating activity of the nickel catalyst is greatly depressed by the nitro group, and also by the amino group produced by the reduction of the nitro group, and that the nitrile group is hydrated with the water produced by the hydrogenolysis of the nitro group. From these facts, it may be inferred that the hydrogenation of nitriles is due to the catalytic action of a kind of active center which may be expressed as acidic contact sites of the nickel catalysts. In this case, the electronegative nitrogen atom of the nitrile group may be first adsorbed on the acidic contact sites and then be activated to cause hydrogenation. So long as other atoms of a more electronegative character cover the acidic contact sites of the catalysts, the nitrogen atom of the nitrile group will hardly ever be adsorbed firmly on the sites, consequently, the hydrogenation of the nitrile group will be depressed. On the other hand, the hydration of the nitrile group with water may occur by means of the activation of the carbon atom of the nitrile group on the other kind of free active-contact sites of the catalysts in spite of the existence of hydrogen. Therefore, the hydration of nitriles is apt to take place instead of hydrogenation when the acidic contact sites of the catalysts are covered with bases or basic substances. From many experimental facts, it may be concluded that the active-contact sites serving to introduce the hydration of nitriles are endowed with a more electronegative character (they are, that is, the basic contact sites of the catalysts). This may be expressed as in Fig. 7 (A). On the contrary, acidic substances may cover the basic contact sites of the catalysts, and interfere with the strong adsorption of nitriles on the same sites, so suppressing the hydration. This may be expressed as in Fig. 7 (B).

The conception that the carbon atom of the nitrile group is adsorbed predominantly on the basic contact sites of the nickel catalysts has been proved

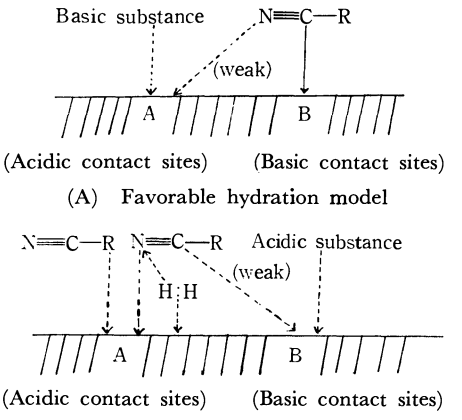

(A) Favorable hydration model

(B) Unfavorable hydration model

Fig. 7

by some other experiments. When benzonitrile was hydrogenated with a nickel catalyst in the vapor phase (250°C), toluene was obtained (87%) by the cleavage of the C–N bond. However, in the reaction at 350°C, about 35% of benzene was formed, and when amine was added to the benzonitrile, the yield of benzene increased to 47%.[5] The formation of benzene is apparently due to the cleavage of the C–CN bond, in this hydrogenolysis, the carbon atom of the nitrile group should be adsorbed on the other kind of active-contact sites of the catalysts (the basic contact sites). It was proved that the cleavage of the C–CN bond occurs before the hydrogenation of the nitrile group.[8] Amine worked on the acidic contact sites to accentuate the function of the basic contact sites of the catalysts. When *o*-nitrobenzonitrile was hydrogenated, 48 per cent of aniline was obtained at a reaction temprature of 300°C.[7] It was about the same with the reaction of *o*-aminobenzonitrile.[5] When benzonitrile mixed with about 35 per cent of water was hydrogenated at 250°C, the yield of toluene was decreased to 60 per cent and amines and unreacted nitrile were obtained.[5] On the other hand, *o*- and *p*-hydroxybenzonitrile afforded no phenols in reactions at 300°C, and only the *o*-compound afforded even 11 per cent of phenol at 350°C.[9] From these results, it can be concluded that the carbon atom of the nitrile group is likely to be adsorbed on the basic contact sites of the nickel catalysts and so cause the hydrogenolysis of the C–CN bond at elevated temperatures. Amine and water relate to the acidic contact sites of the catalysts. The hydroxyl group relates to the basic contact sites and suppreses the hydrogenolysis. As for the cleavage of the C–CN bond in water, it has obviously been shown that hydrogen cyanide, formic acid and propionic

3) T. Okazawa, M. Hayashi, K. Watanabe and K. Hata, *J. Chem. Soc. Japan, Pure Chem. Sect.* (*Nippon Kagaku Zasshi*), **82**, 254 (1961); *Chem. Abstr.*, **56** 1003 7h (1962).

4) K. Watanabe, ibid., **78**, 1478 (1957); *Chem. Abstr.*, **54**, 1370b (1960).

5) K. Hata and K. Watanabe, This Bulletin, **32**, 861 (1959); *Chem. Abstr.*, **54**, 1305 4h (1960).

6) H. Rupe, *Helv. Chim. Acta*, **8**, 832 (1925).

7) K. Watanabe, *J. Chem. Soc. Japan, Pure Chem. Sect.* (*Nippon Kagaku Zasshi*), **76**, 398 (1955); *Chem. Abstr.*, **51**, 17815 i (1957).

8) M. Tanaka, K. Watanabe and K. Hata, ibid., **76**, 1392 (1955); *Chem. Abstr.*, **51**, 17813 a (1957).

9) M. Tanaka, K. Watanabe and K. Hata, ibid., **77**, 980 (1956); *Chem. Abstr.*, **52** 9015 a (1958).

acid are formed in the hydrolysis of acetonitrile with a nickel catalyst. Thus, it may also be assumed that the cleavage of the C–CN bond takes place on the basic contact sites of the catalysts. As was shown in a previous paper,[1] it is of interest that no hydration product was obtained in the reaction of *p*-hydroxybenzonitrile with a nickel catalyst in water. This fact suggests a strong interaction between the hydrogen atom of the hydroxy group and the basic contact sites of the catalysts.

When benzonitrile is hydrogenated with a nickel catalyst in ethanol, amines are obtained as the main products (ordinary hydrogenation). However, it has now been observed that no reaction takes place when water is used as the solvent instead of ethanol at room temperature (the carbylamine test is negative), while, the hydration of the nitrile to benzamide occurs predominantly when the reaction mixture is refluxed with enough hydrogen gas (amide yield; 75%). To examine the effect of thiophene on the reactions mentioned above, 1 g. (25% of the nickel catalyst) and 0.2 g. (5% of the nickel catalyst) of thiophene were added to the catalysts. In the reactions, both at room temperature and at the refluxing temperature (ca. 100°C), even very small quantities of amines were hardly ever obtained. No favorable effect of thiophene on the hydrogenation was observed. On the other hand, the unfavorable effect of thiophene on the hydration of the nitrile was just the same as that shown in Fig. 5 when it was refluxed. Thus, it is evident that water suppresses the hydrogenation of nitriles, causing the hydration in some way. Apparently, the fact that water is the most suitable solvent for this hydration is important. That is, water has two functions, one is to react with nitriles, affording amides, while the other is to suppress other side reactions, especially the hydrogenation of nitriles. It may be assumed, consequently, that the free electron pair of the oxygen atom of the water molecule interacts with the acidic contact sites of the nickel catalysts and interferes with the strong adsorption of the nitrogen atom of the nitrile group on the same sites of the catalysts. The fact that the addition of basic substances to the catalysts does not have an unfavorable effect may mean that the interaction of water and catalysts is fairly strong. From a different point of view, however, if this nickel-catalyzed hydration is essentially due to the ionization or half-ionization of water on the catalysts, the hydrolysis of nitriles to acids should be the main reaction, as is observed in the hydrolysis with acid or base catalysts.

According to the conception of the acidic and basic functions of the nickel catalysts, the nitrile-catalysts-water interaction may be represented as in Fig. 8, while the course of the hydrolysis of nitriles to acids may be represented as in Fig. 9. However, it has not been proved that there are two kinds of active contact sites, A and B, really fixed

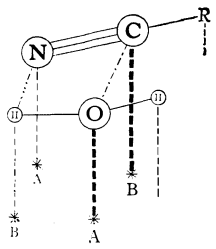

Fig. 8

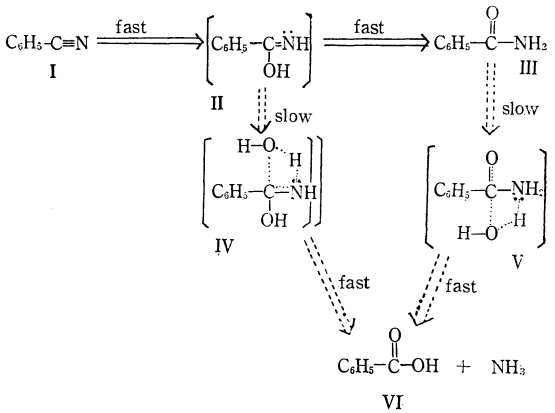

Fig. 9. The hydration of Benzonitrile

⇒ Main reaction

⇛ Hydrolysis

on the surface of the catalysts. This serves only to explain the phenomena and results of the nickel-catalyzed hydration and hydrogenation of nitriles. It is assumed that the hydrolysis of nitriles may arise also by the activation of the carbon atom of the amide group, and that it is less active than the hydration of nitriles. Attention should be focussed on the fact that the hydrolysis of benzamide and acetamide with a nickel catalyst is much more difficult than that of benzonitrile or acetonitrile. This is the reason why two courses, II–IV–VI and II–III–V–VI, have been postulated. The former is expected to be faster than the latter.

In the end, it is noteworthy that the nickel catalysts (U-Ni and Raney nickel) used in this hydration have been prepared somewhat differently from that used for hydrogenation. It does not matter if the catalyst is exposed to air and to common city water during the preparation.[1] This may lead to an assumption that oxygen in the air or in undistilled water attacks the acidic contact sites of the catalysts, but does not have the unfavorable effect on the basic contact sites of causing the hydration of nitriles.

Experimental

According to the common reaction procedure reported previously[1], were refluxed nitriles for eight hours in

water with U-Ni-B. After the reactions, the catalysts were separated by filtration, the filtrates were analyzed by gas chromatography, and the reaction products were obtained by the careful evaporation of the filtrates on a water bath. In general, rather pure amides were thus obtained.

The Hydration of Benzyl Cyanide.—Ten grams of benzyl cyanide and 150 ml. of water were refluxed vigorously with U-Ni-B (containing 4 g. of nickel) for ten hours. During the reaction a small quantity of ammonia was generated as was detected with litmus. After the reaction was over, the catalyst was separated by filtration while hot and washed with hot water. The filtrate, combined with the washings, was extracted with ether. When the aqueous solution (filtrate) was then evaported carefully on a water bath, phenylacetamide was obtained in a 58% yield as the main product, m. p. 153.5—154.2°C. A small quantity of an oily by-product was obtained from the ether extract and was analyzed successfully by gas chromatography.*7 The by-products seemed to be small quantities of phenylacetic acid, phenethylamine and benzaldehyde. However, the presence of benzaldehyde was somewhat doubtful, because the Tollens' test[10] for it varied between being positive and negative; moreover, the detection of benzaldehyde was not always successful by gas chromatography.

The Hydration of Acetonitrile.—Thirty-five grams of acetonitrile and the catalyst (containing 20 g. of nickel) in 500 ml. of water were placed in a 1000-ml., three-necked, round flask and stirred while being refluxed for eight hours. During the reaction, ammonia gas was detected; sometimes hydrogen cyanide was detected as well. The hydrogen cyanide was identified by the method used for picric acid.[11] After the reaction was over, the catalyst was separated by filtration. The filtrates were alkalized with sodium hydroxide and then evaporated to a solid mass on a water bath. When the dried mass was extracted with chloroform in a Soxhlet extractor, crude acetamide was obtained from the extract in rather pure form, m. p. 81.5—81.7°C. The yield was 30.05 g. (ca. 70%). The sodium salt which remained was put into a small quantity of water and acidified with concentrated hydrochloric acid. The free acids were extracted with ether. The total weight of the free acids thus obtained was 6 g. The mixture of the acids was analyzed by means of their NMR spectrum*8 (Fig. 2). On the other hand, they were esterified with diazomethane and the esters were analyzed by gas chromatography*9 (Fig. 1). The acids were propionic acid, acetic acid and a small amount of formic acid. They were identified by NMR and by gas chromatography with three pure acids. Amine was extracted by hydrochloric acid and was identified by carbylamine reaction.

The Hydration of 2-Cyanopyridine.—Seven grams of 2-cyanopyridine and 100 ml. of water were refluxed vigorously with U-Ni-B (containing 4 g. of nickel) for ten hours. During this reaction, the colorless contents turned violet and then blue and the pH value of the contents became 9.4—9.2 and then 8.4—8.2. A small quantity of ammonia gas was generated during the reaction, as could be detected with litmus. The product obtained by the same method as in the other cases was dissolved in ethanol and then separated by column chromatography with active alumina. Thus, pyridine-α-carboxylic acid amide was obtained in ca. 40% yield (m. p. 105°C), along with a blue nickel complex. The weight proportion of pyridine-α-carboxylic acid amide and the nickel complex was about 3 : 1. The nickel complex immediately absorbed moisture in air and had the property of a solid solution. The paramagnetic character was observed. When it was heated with hydrochloric acid, both pyridine-α-carboxylic acid and its amide were obtained. When it was treated with dimethylglyoxime, free pyridine-α-carboxylic acid amide was obtained. As a result of an infrared analysis, it seems that this complex might be formed by an interaction of the nickel and pyridine-α-carboxylic acid amide. By refluxing 2-cyanopyridine with Raney-Ni-W_7 in water, the contents (color and pH) were observed as well as when U–Ni–B was used. However, a small quantity of pyridine was obtained besides pyridine-α-carboxylic acid amide and the nickel complex.

The Hydration of Benzonitrile Accompanied with Hydrogen Gas.—1) Five grams of benzonitrile was refluxed in 80 ml. of water with U-Ni-B (4 g. of nickel) for eight hours. A constant flow of hydrogen gas was introduced into the reaction mixture throughout the refluxing. Benzamide was thus obtained in a 75% yield, along with a very small amount of amine (almost the same reaction and result as were obtained without hydrogen gas; cf. Exp. No 1, Table II).

2) Five grams of benzonitrile, together with U-Ni-B (4 g. of nickel) and 0.2 g. of thiophene (5% of nickel catalyst), was stirred for eight hours at room temperature. A constant flow of hydrogen gas was introduced into the reaction mixture throughout the reaction. Benzamide was thus obtained in a 7% yield, while 80% of the nitrile was recovered. Amine was extracted by hydrochloric acid and was analyzed by means of a study of its infrared spectrum. Benzylamine was obtained in a 2% yield.

3) Five grams of benzonitrile, together with U-Ni-B (4 g. of nickel) and 1 g. of thiophene (25% of nickel catalyst), was refluxed in 80 ml. of water for eight hours. A constant flow of hydrogen gas was introduced into the reaction mixture throughout the refluxing. Benzamide was thus obtained in a 36.5% yield as the main product, while 58% of the nitrile was recovered. A small quantity of amine was obtained as hydrogen chloride-salt, as was detected by carbylamine reaction (almost the same reaction as that with 1 g. of thiophene without hydrogen gas; cf. Fig. 5).

The authors wish to express their hearty thanks to Professor Kazuo Hata for his kind advice.

*7 Column, 30% Carbo-wax 1500 on Celite ca. 30—40 mesh; length, 2 m.; temp., 68°C; flow rate, 20/24 ml./sec.; carrier gas, H_2. Gas chromatograph: Yanagimoto GCG 220 Type, Yanagimoto Mfg. Co., Ltd, Kyoto, Japan.

10) R. L. Shriner, R. C. Fuson and D. Y. Curtin, "The Systematic Identification of Organic Compounds," Reprint, Maruzen, Tokyo (1956), p. 162.

11) H. Meyer, "Nachweiss und Bestimmung der organischen Verbindungen", Copyright by Julius Springer in Berlin (1933), p. 99.

*8 Solvent; CCl_4; filter bandwidth, 4 c.p.s.; r.f. field, 0.015 mG; sweep time, 500 sec.; sweep width, 500 c. p. s.; sweep offset, 200 c.p.s.

*9 Column; 30% Carbo-wax 1500 on Celite ca. 30—40 mesh; length, 2 m.; temp., 40°C; flow rate, 20/12 ml./sec.; carrier gas, H_2.

BULLETIN OF THE CHEMICAL SOCIETY OF JAPAN VOL. 39 15—19 (1966)

The Heats of Dilution of Atactic Polystyrene Solutions

By Akihiro KAGEMOTO, Sachio MURAKAMI and Ryoichi FUJISHIRO

Department of Chemistry, Faculty of Science, Osaka City University, Sumiyoshi-ku, Osaka

(Received March 29, 1965)

The heats of dilution of atactic polystyrene ($\bar{P}=244$) - various solvent systems have been measured by using a micro-twin-calorimeter at 25°C. Toluene, anisole, ethyl methyl ketone, dioxane and ethyl acetate were used as the solvents. For the analysis of the experimental data obtained by each dilution process, the simple Van Laar formula has been used, and the apparent enthalpy parameter between the polymer and the solvent has been derived. Since these interaction parameters seemed to depend on the concentration, we tried to analyze the experimental data with a modified Van Laar formula which contained interaction parameters depending on the concentration. The interaction parameters obtained by these analyses are considerably dependent on the concentration in good solvents, while those in poor solvents depend hardly at all on the concentration. This dependence of the interaction parameters on the concentration has been explained by using the dilute solution theory of polymer solutions proposed by Flory and Krigbaum (*J. Chem. phys.*, **18**, 1086 (1951)). The interaction parameters in the dilute region have been compared with those obtained by other methods, and the agreement between our values and those obtained by other methods has been found to be fairly good.

The direct measurement of the heats of dilution of polymer solutions is very important in investigating the interaction parameter between the polymer and the solvent molecules. In spite of the fact that such measurement is accompanied by considerable difficulties, several reports[1-5] have been published in this field. We have now constructed a twin-calorimeter and, by using this apparatus, have attempted thermal measurements in order to study the behavior of atactic polystyrene using such solvents as anisole, toluene, ethyl acetate, dioxane and ethyl methyl ketone.

Experimental

Apparatus and Procedure.—The twin calorimeter which is shown in Fig. 1 was designed to measure the heats of dilution. It consists of two copper cell holders (A), a mixing cell (B_1) and a reference cell (B_2). Around the outside surface of the holders, a thirty-junction copper-constantan thermocouple (C) is wound. The heating coil, with a resistance of about 40 ohm is fixed with araldite cement around the mixing cell (D). The mixing cell is made of glass and consists of an outer cell (E) and an inner cell (F), as is shown in Fig. 2. The outer cell (E) is filled with the polymer solution, and the inner cell (F) is charged with the solvent by using a hypodermic syringe; each cell is then sealed, at G and H, with mercury.

The polymer solution and solvent are mixed by pulling up the lid of the inner cell through the manipulation of the wire (I) from the outside of the calorimeter chamber.

The solution is mixed by being stirred by a synchronous (30 r. p. m.) motor (J). The reference cell (B_2), containing only the solvent, is the same type of cell as the mixing cell and acts as the reference bath for the thermocouple.

The electronic circuit for the measurement of the heat of dilution is the same as that described in a previous

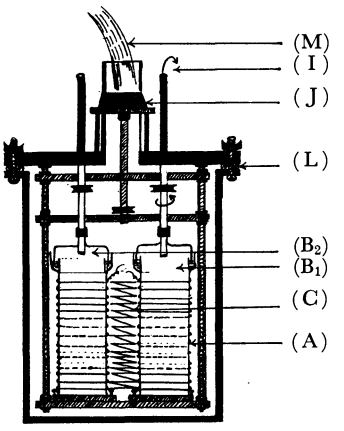

Fig. 1. Twin micro-calorimeter.
(A) Copper cell holder
(B_1) Mixing cell
(B_2) Reference cell
(C) Copper-constantan thermocouple
(L) Rubber ring
(J) 30 r. p. m. motor
(M) Lead wire
(I) Wire for pulling up the lid

1) H. Tompa, *J. Polymer Sci.*, **8**, 51 (1952).
2) G. H. Kabayama and H. Daoust, *Can. J. Chem.*, **36**, 556 (1958).
3) G. H. Schulz and H. Horbach, *Z. Physik Chem.*, **22**, 377 (1959).
4) M. Senez and H. Daoust, *Can. J. Chem.*, **40**, 734 (1962).
5) K. Amaya and R. Fujishiro, This Bulletin, **29**, 270 (1956).

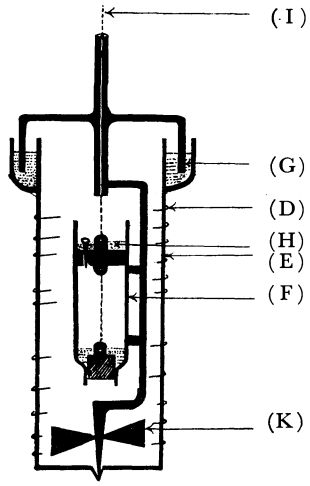

Fig. 2. Mixing cell.

(D)	Heating coil	(I)	Wire for pulling up the lid
(E)	Outer cell		
(F)	Inner cell	(K)	Stirrer
(G), (H)	Mercury seal		

paper[5]. The calorimeter was immersed in a water thermostat kept at 25.00±0.01°C.

Materials.—An atactic polystyrene sample (degree of polymerization: 244) was supplied by Dr. T. Matuo of the Chemical Institute of Kyoto University. This sample was purified by dissolving it in toluene, precipitated with methanol, and then dried under a pressure of 1 mmHg until the solvent has been completely removed. The solvents used were anisole, toluene, dioxane, ethyl acetate and ethyl methyl ketone. These solvents were purified by the ordinary methods described in the literature[6] and finally distilled.

Results and Discussion

The heats of the dilution of atactic polystyrene were measured over the concentration range from a 0.2 to a 0.015 volume fraction of the polymer by the successive addition of 5- or 20-ml. portions of the solvent to a solution of a known concentration. The results obtained are shown in Table I.

Three systems, the solutions of anisole, toluene and ethyl acetate, are exothermic, while the other two systems, those of dioxane and ethyl methyl ketone, are endothermic.

Assuming that the heat of mixing is expressed by the simple Van Laar equation and following the method of treatment by Tompa,[1] the heat of dilution, $\Delta\overline{H}_d$, from the volume fraction ϕ_2 to the volume fraction ϕ_2' can be represented by;

$$\Delta\overline{H}_d = \boldsymbol{R}T\chi_H\phi_2\phi_2'\Delta n_1 \qquad (1)$$

where Δn_1 is the number of moles of solvent added and χ_H is the interaction parameter between the polymer and the solvent. Instead of Eq. 1, we can also obtain the equivalent expression:

$$\Delta\overline{H}_d = \boldsymbol{R}Txn_2(\phi_2-\phi_2')\chi_H \qquad (1')$$

where n_2 is the number of moles of the structure unit and x the degree of the polymerization of the polymer.

By using the experimental data listed in Table I and Eq. 1 or 1', the interaciion parameter, χ_H, can be obtained for each stage of the dilution process of each system; these parameters are given in the last column of the same table.

For the polystyrene-toluene system, we previously measured the heats of dilution in the concentrated solution and so derived the values of the interaction parameter, χ_H, values which were in the vicinity of −0.2. The χ_H values in this experiment are about −0.2 in the concentrated range, which is in good agreement with those obtained in the previous experiment; there is also a decrease in the absolute value in the fairly diluted region. The tendency for the χ_H parameter to depend on the concentration seems to be observed not only in the toluene system but also in other systems. To test this behavior, we plotted the heat of dilution, $\Delta\overline{H}_d$, against $\phi_2\phi_2'\Delta n_1$ or $xn_2(\phi_2-\phi_2')$ in Fig. 3.

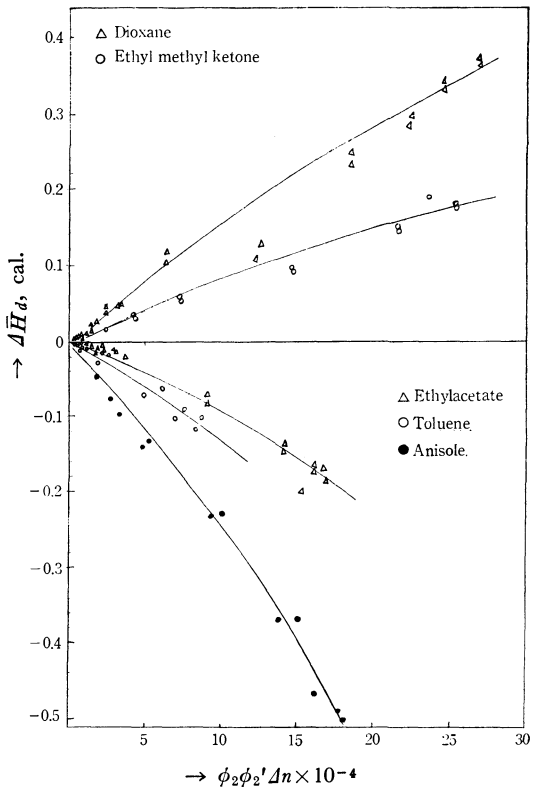

Fig. 3. The plot of the heat of dilution $\Delta\overline{H}_d$ against $\phi_2\phi_2'\Delta n_1$.

6) A. Weissberger and E. S. Proshauen, "Organic Solvent," Interscience Publishers, New York (1955).

TABLE I. HEATS OF DILUTION OF ATACTIC POLYSTYRENE SOLUTION AT 25°C

1. Polystyrene-Toluene

V, cc.	ϕ_2	V', cc.	ϕ_2'	$-\Delta\overline{H}_d$, cal.	χ_H
5	0.176	10	0.088	0.066	−0.15
10	0.088	15	0.058	0.029	−0.20
15	0.058	20	0.043	0.009	−0.14
5	0.166	10	0.083	0.074	−0.19
10	0.083	15	0.056	0.033	−0.25
15	0.056	20	0.042	0.014	−0.22
20	0.052	30	0.035	0.0134	−0.13
30	0.035	40	0.026	0.0044	−0.08
40	0.026	50	0.021	0.0016	−0.05
20	0.048	30	0.032	0.0087	−0.10
30	0.032	40	0.024	0.0035	−0.08
40	0.024	50	0.019	—	—
5	0.176	15	0.058	0.095	−0.16
5	0.176	20	0.043	0.104	−0.16
5	0.166	15	0.056	0.107	−0.20
5	0.166	20	0.042	0.121	−0.20
20	0.052	40	0.026	0.0178	−0.12
20	0.052	50	0.021	0.0194	−0.10
20	0.048	40	0.024	0.0123	−0.09

2. Polystyrene-Anisole

V, cc.	ϕ_2	V', cc.	ϕ_2'	$-\Delta\overline{H}_d$, cal.	χ_H
10	0.175	15	0.116	0.227	−0.42
15	0.116	20	0.087	0.153	−0.57
20	0.087	25	0.069	0.094	−0.59
25	0.069	30	0.058	0.036	−0.34
10	0.184	15	0.122	0.227	−0.38
15	0.122	20	0.091	0.148	−0.50
20	0.091	25	0.072	0.106	−0.61
10	0.175	20	0.087	0.380	−0.46
10	0.175	25	0.069	0.474	−0.49
10	0.175	30	0.058	0.510	−0.47
10	0.175	20	0.091	0.375	−0.42
10	0.184	25	0.072	0.481	−0.45

3. Polystyrene-Ethyl acetate

V, cc.	ϕ_2	V', cc.	ϕ_2'	$-\Delta\overline{H}_d$, cal.	χ_H
10	0.186	15	0.124	0.077	−0.11
15	0.124	20	0.093	0.066	−0.19
20	0.093	25	0.073	0.021	−0.10
25	0.073	30	0.060	0.013	−0.10
10	0.186	15	0.124	0.084	−0.12
15	0.124	20	0.093	0.063	−0.18
20	0.093	25	0.072	0.031	−0.15
25	0.072	30	0.060	0.014	−0.11
30	0.060	35	0.040	0.014	−0.20
20	0.050	40	0.025	0.0110	−0.073
40	0.025	50	0.020	0.0013	−0.046
50	0.020	60	0.016	0.0004	−0.023
60	0.016	70	0.014	—	—
20	0.059	40	0.029	0.0196	−0.095
40	0.029	50	0.024	0.0015	−0.039
10	0.186	20	0.093	0.141	−0.13
10	0.186	25	0.073	0.162	−0.13
10	0.186	30	0.060	0.175	−0.14
10	0.186	20	0.093	0.147	−0.14
10	0.186	25	0.072	0.178	−0.14
10	0.186	30	0.060	0.192	−0.15
10	0.186	35	0.040	0.206	−0.18
20	0.050	50	0.020	0.0123	−0.07
20	0.050	60	0.016	0.0127	−0.07
20	0.059	50	0.024	0.0212	−0.08

4. Polystyrene - Ethyl methyl ketone

V, cc.	ϕ_2	V', cc.	ϕ'_2	$\Delta\overline{H}_d$, cal.	χ_H
10	0.222	20	0.148	0.095	0.089
15	0.148	25	0.111	0.052	0.098
20	0.111	20	0.088	0.031	0.098
10	0.222	15	0.148	0.092	0.086
15	0.148	20	0.111	0.051	0.095
20	0.111	25	0.088	0.028	0.090
25	0.088	30	0.060	0.017	0.099
10	0.222	20	0.111	0.147	0.092
10	0.222	25	0.088	0.178	0.093
10	0.222	20	0.111	0.143	0.088
10	0.222	20	0.088	0.171	0.089
10	0.222	20	0.060	0.188	0.108

5. Polystyrene-Dioxane

V, cc.	ϕ_2	V', cc.	ϕ_2'	$\Delta\overline{H}_d$, cal.	χ_H
10	0.216	15	0.144	0.128	0.12
15	0.144	20	0.108	0.117	0.22
20	0.108	25	0.086	0.054	0.17
25	0.086	30	0.070	0.041	0.20
30	0.070	35	0.060	0.032	0.22
10	0.213	15	0.142	0.104	0.10
15	0.142	20	0.106	0.129	0.25
20	0.106	25	0.084	0.052	0.17
25	0.084	30	0.070	0.046	0.23
30	0.070	35	0.060	0.030	0.21
10.9	0.039	21.4	0.020	0.007	0.12
9.7	0.053	19.2	0.027	0.011	0.12
19.2	0.027	24.2	0.021	0.003	0.13
24.2	0.021	29.3	0.018	0.002	0.17
11.1	0.054	16.3	0.037	0.012	0.17
16.3	0.037	21.3	0.028	0.006	0.17
10	0.216	20	0.108	0.245	0.15
10	0.216	25	0.086	0.299	0.16
10	0.216	30	0.070	0.340	0.16
10	0.216	35	0.060	0.372	0.17
10	0.213	20	0.106	0.233	0.15
10	0.213	25	0.084	0.285	0.15
10	0.213	30	0.070	0.331	0.16
10	0.213	35	0.060	0.361	0.17
9.7	0.053	24.2	0.021	0.014	0.12
9.7	0.053	29.3	0.018	0.016	0.12

According to Eq. 1 a linear plot must be obtained, its slope giving the interaction parameter. However, as may be seen in Fig. 3, this plot is not linear, indicating that the interaction parameter depends on the concentration.

Assuming that the interaction parameter, χ_H, is expressed as:

$$\chi_H=\chi_1+\chi_2\phi_2$$

and making the same derivation as that of Eq. 1 or 1', we can obtain the following equation:

$$\Delta\overline{H}_d=\boldsymbol{R}T\phi_2\phi_2'\Delta n_1[\chi_1+\chi_2(\phi_2+\phi_2')/2] \quad (2)$$

or

$$\Delta\overline{H}_d=\boldsymbol{R}Txn_2(\phi_2-\phi_2')[\chi_1+\chi_2(\phi_2+\phi_2')/2] \quad (2')$$

where $\phi_2=xn_2/(n_1+xn_2)$

and $\phi_2'=xn_2/(n_1+\Delta n_1+xn_2)$.

In order to find χ_1 and χ_2, we tried to plot the $\Delta\overline{H}_d/\boldsymbol{R}T\phi_2\phi_2'\Delta n_1$ against $(\phi_2+\phi'_2)/2$ for each system of Fig. 4.

The experimental data, however, were too scattered for us to obtain accurate values. Therefore,

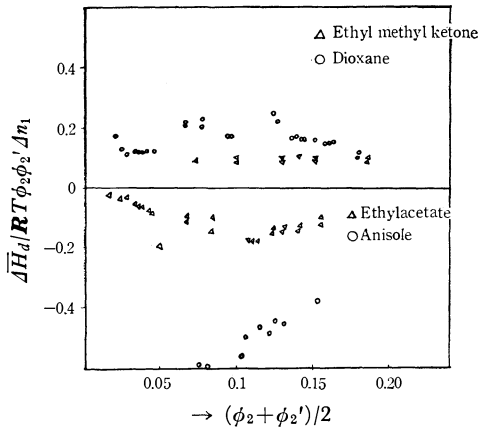

Fig. 4a. The variation of the apparent heat parameter with the average volume fraction of polystyrene-various solvents at 25°C.

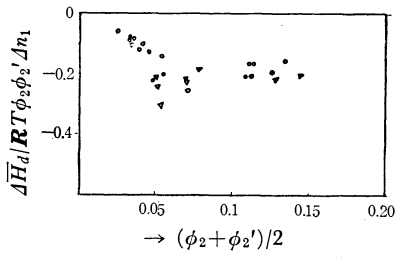

Fig. 4b. The variation of the apparent heat parameter with the average volume fraction of polystyrene-various solvents at 25°C.
Toluene, ○ $\overline{P}=244$, △ $\overline{P}=270$

Table II. Values of interaction parameter $\chi_H=\chi_1+\chi_2\phi_2$

Solvent	χ_1	χ_2
Toluene	−0.08	−0.94
Anisole	−0.60	−1.18
Ethyl acetate	−0.05	−0.66
Dioxane	0.16	−0.008
Ethyl methyl ketone	0.10	−0.08
Toluene[5]	−0.27	0.69

we carried out the least-squares treatment of the data according to Eq. 2; this gave the values for χ_1 and χ_2 shown in Table II.

By using the values of χ_1 and χ_2 listed in Table II, a $\Delta\overline{H}_d-\phi_2\phi_2'\Delta n_1$ curve has been calculated for each system; this curve, which is shown by the full line in Fig. 3, is in good agreement with the experimental data for each system.

As may be seen in Table II, the χ_H parameter in good solvents (exothermic systems) are considerable concentration-dependent, while those in poor solvents (endothermic systems) do not depend on the concentration. These tendencies indicate that the absolute values of the χ_H parameter in the dilute solution are considerably lower than those in the moderate concentration range in good solvents, while the values of the χ_H parameter in poor solvents hardly change.

According to the dilution theory of the polymer solution proposed by Flory,[7] the second virial coefficient, A_2, is expressed as:

$$A_2\propto(\psi_1-\kappa_1)F(X)$$

where: $X=2(\alpha^2-1)$,

$$F(X)=1-X/2!\cdot 2^{-3/2}+\cdots$$

An approximate treatment gives the interaction parameter as $\kappa_1F(X)$, which is an apparent interaction parameter in the dilute region. Now we may assume that Flory's formula also applies to the solution of good solvents, though this formula has hitherto been considered to be correct only in poor-solvent systems. Therefore, in good solvents α is greater than 1 and $F(X)$ is considerably less than 1. The apparent interaction parameter, $\kappa_1F(X)$, in the dilute region is, therefore, considerably smaller than that in the moderate concentration in terms of absolute value. On the other hand, in poor solvents the expansion factor α is nearly equal to 1, and $F(X)\simeq 1$, suggesting that the interaction parameter may be independent of the concentration.

The interaction parameter is usually studied by other methods, such as the temperature dependence of the osmotic pressure of the solution. The values for the interaction parameter obtained by various

7) P. J. Flory and W. R. Krigbaum, *J. Chem. Phys.*, **18**, 1086 (1950).

TABLE III. VALUES OF THE INTERACTION PARAMETER OBTAINED BY VARIOUS AUTHORS

Solvent	χ_1 (a)	χ_1 (b)	χ_1 (c)	χ_1 (d)	χ_1 (e)	χ_1 (f)	χ_1 (g)	χ_1 (h)
Toluene	−0.030	−0.101	0.06	0.06	−0.10 ∼−0.17	−0.008	−0.27	−0.08
Ethyl methyl ketone	−0.001		0.00	0.00		0.04		0.10
Ethyl acetate	0.019	0.025	0.02					−0.05
Dioxane			0.07					0.16

(a) See Ref. 8, osmotic pressure
(b) See Ref. 9, osmotic pressure
(c) See Ref. 10, viscosity
(d) See Ref. 11, viscosity
(e) See Ref. 1, *direct* measurement
(f) See Ref. 12, osmotic pressure
(g) See Ref. 5, direct measurement
(h) This paper, direct measurement

authors[1,5,8-12] using these methods are listed in Table III. Since these measurements have been carried out in a dilute solution, those of our values of the interaction parameter to be compared with those in Table III must also be in a dilute solution, that is, the χ_1 values, which are the concentration-independent terms in χ_H as determined by our experiment and shown in the last column in Table III.

The agreement between our parameters and those obtained by other methods may be fairly good in terms of absolute value, though there remain some questions concerning their signs.

Summary

We have constructed a twin calorimeter with a thirty-junction thermocouple in order to measure the slight temperature-change of a polymer solution. By using this apparatus, the heats of the dilution of atactic polystyrene ($\overline{P}$=244) have been measured, and from them the interaction parameters have been derived according to Van Laar's simple formula. Since the interaction parameters seemed to depend on the concentration, we tried to analyze the experimental data with a modified Van Laar formula which contained the interaction parameter depending on the concentration.

We found that the interaction parameters are considerably concentration-dependent in good solvents, while those in poor solvents do not depend on the concentration.

The authors wish to thank Dr. T. Matuo of the Chemical Institute of Kyoto University for supplying the sample to them.

8) G. H. Schulz and H. Hellfritz, *Z. Elektrochem.*, **57**, 835 (1953).
9) M. J. Schik, P. Doty and B. H. Zimm, *J. Am. Chem. Soc.*, **72**, 530 (1953).
10) L. H. Cragg and T. E. Dumitro, ibid., **74**, 1997 (1952).
11) T. G. Fox and P. J. Flory, ibid., **73**, 1915 (1952).
12) G. E. H. Bawn and M. A. Wajid, *J. Polymer Sci.*, **12**, 109 (1954).

BULLETIN OF THE CHEMICAL SOCIETY OF JAPAN VOL. 39 20—24 (1966)

The DTA of Polymer-Solvent Systems. The Solubility Curves of Isotactic Polypropylene-Decalin and Isotactic Polypropylene-Nitrobenzene Systems

By Katsutoshi TAMURA, Kunio NAKATSUKA and Ryoichi FUJISHIRO

Department of Chemistry, Faculty of Science, Osaka City University, Sumiyoshi-ku, Osaka

(Received April 5, 1965)

A DTA apparatus for a polymer solution has been constructed. The heating rate was adjusted to approximately 0.50 or 0.42°C/min., a favorable rate for a polymer solution. From the DTA curves obtained by the use of this apparatus, the temperatures of the end points of the melting or dissolution have been determined; their plots give the solubility curves. The solubility of the isotactic polypropylene in decalin system increases monotonously with the increase in the temperature, except for the abnormality in the region from 30 to 50 wt.% in polymer content. In the case of the isotactic polypropylene-nitrobenzene system, on the other hand, the melting curve has a horizontal part in the region with a polymer content of less than 50 wt.%; above this point lies the phase separation curve, which touches the melting curve at the point with a polymer content of approximately 50 wt.%. The double peaks which appear in the DTA curve of the melting of pure isotactic polypropylene, may be due to the paracrystalline smectic modification of isotactic polypropylene, as has been suggested by Natta (*Makromol. Chem.*, **35,** 93 (1960)). The heat of fusion for isotactic polypropylene has been estimated to be approximately 1000 cal./unit mol. by measuring the area under the melting peak of the DTA curve and the equation for the melting point depression.

It is known that differential thermal analysis (DTA) is very useful in investigating such a thermal change as the phase transition. The applications of the DTA method to polymeric materials, however, have been restricted mainly to the thermal change in a pure polymer or in one with only a small amount of diluents. In this paper we shall use this DTA method in studying the dissolution behavior of isotactic polypropylene-decahydronaphthalene (decalin) and isotactic polypropylene-nitrobenzene mixtures, over the whole concentration range. Decalin and nitrobenzene will be used as a typically good and a typically bad solvent respectively for isotactic polypropylene. Further, the analysis of DTA curves on pure isotactic polypropylene will also be carried out under some pretreatment conditions.

Experimental

Apparatus.—We constructed the DTA apparatus, equipped with a stirrer to secure the smooth dissolution of polymer during heating, illustrated in Fig. 1. A sample cell and a reference cell made of stainless steel were put into the cell holder and fitted with copper-constantan thermocouples at their bottoms.

The e. m. f. representing the temperature difference between the sample cell and the reference cell was amplified by the Okura AM101B amplifier, and the signals for the temperature difference were recorded on a time-base chart recorder (YEW ER1-30). The temperature was determined by measuring the potential difference between the reference substance and the ice point with the potentiometer.

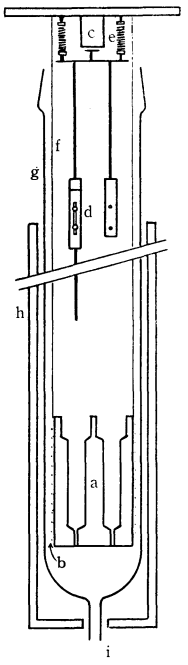

Fig. 1. The DTA apparatus.

(a) Cell holder
(b) Heater (nichrome wire)
(c) Magnetic vibrator for stirrers
(d) Joint of stirrer and vibrator
(e) Spring
(f) Wires for suspending the cell holder
(g) Glass mantle
(h) Heater mantle
(i) Outlet of thermocouples

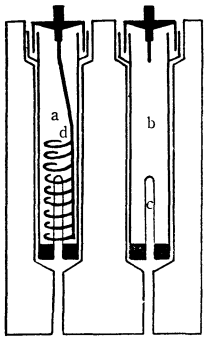

Fig. 2. The cell holder.

(a) Sample cell
(b) Reference cell
(c) Bored capillary for thermocouples
(d) Stirrer

The rate of heating was manually controlled.

Material.—Isotactic polypropylene, Avisun 101117-Q84, was reprecipitated through decalin-methanol, in which the antioxydant had been removed; the precipitate was then washed several times with methanol and dried in a vacuum. The mean molecular weight of the polymer was determined to be 3.7×10^5 by viscometric measurements in decalin.[1]

Decalin was purified by the ordinary method;[2] the ratio of *cis*- to *trans*-decalin was about 3 to 2, as determined by observing the density and the viscosity.

Nitrobenzene was distilled twice in a vacuum.

The urea to be used in calibrating the apparatus for calorimetry was reprecipitated from a methanol solution and dried in a vacuum.

The Pre-treatment of the Sample.—The sample was prepared by putting the weighed solvent and isotactic polypropylene into the sample cell; it was then melted so that the stirrer could be inserted. After the sample cell had been set at the apparatus, the sample was melted once more and then slowly cooled to room temperature at the rate of 0.3—0.5°C/min.; thus a definite condition was given to all samples.

Results and Discussion

The Effect of the Heating Rate.—A sample with an approximately 15% polymer content in a decalin solution was repeatedly run, at the heating rates of approximately 1.25, 0.83, 0.63, 0.50, 0.42 and 0.31°C/min., in order to check the effect of the heating rate on the peak temperature of the dissolution in a highly viscous solution.

We found that the heating rate is not very effective on the dissolution temperature at these rates, while the cooling rate in the pre-treatment is rather effective, as will be discussed later. Therefore, we took the heating rate of 0.50 or 0.42°C/min., in which the reproducibilities of DTA curves seem favorable.

The Isotactic Polypropylene-Decalin System.—The DTA curves obtained for the isotactic polypropylene-decalin system with various proportions of polymer are shown in Fig. 3. The dissolution of a polymer into a solvent is accompanied by each curve reaching a peak which represents the absorption of heat in this experiment. Each curve increases gradually in the low-temperature region,

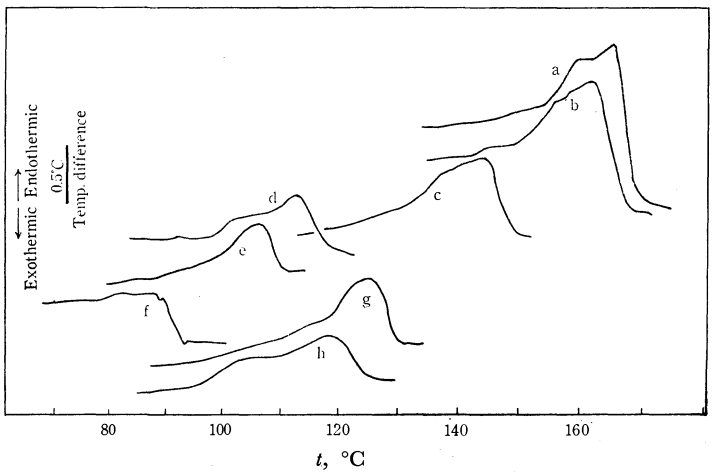

Fig. 3. The DTA curves of isotactic polypropylene-decalin system.

(a) 98% polymer content
(b) 95% polymer content
(c) 64.7% polymer content; stirred
(d) 24.9% polymer content; stirred
(e) 15% polymer content; stirred
(f) 1.05% polymer content; stirred
(g) 34.8% polymer content; annealed; stirre
(h) 34.8% polymer content; rapidly cooled; stirred

The heating rate is 0.5°C/min. except (d) and (f), that of (d) 0.43°C/min., and that of (f) 0.83°C/min.

1) F. Danusso and G. Moraglio, *Makromol. Chem.*, **28**' 250 (1958).

2) A. Weissberger and E. S. Proshauen, "Organic Solvent," Interscience Publisher Inc., New York (1955).

particularly for the mixture with a small polymer content, reaches the top of the peak, and then rapidly descends. The gradual increase in the low-temperature region suggests that the dissolution may begin at a fairly low temperature. Since the dissolution process is completed at the top of the peak, the corresponding temperature will be assigned to the end point of dissolution.

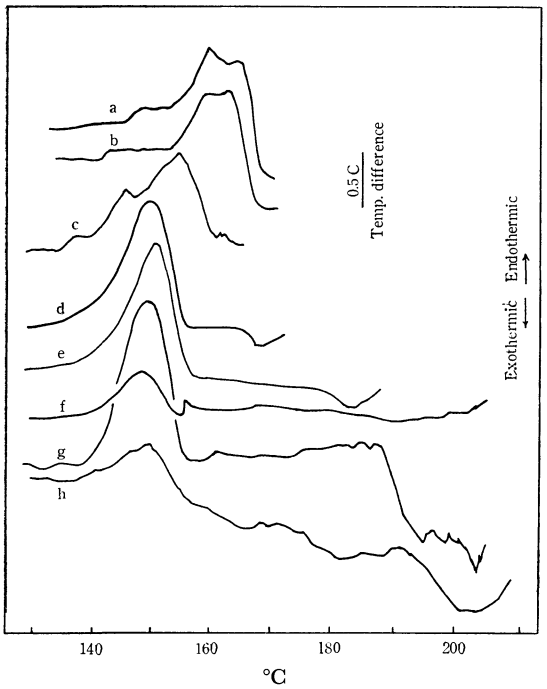

Fig. 4. The DTA curves of isotactic polypropylene-nitrobenzene system.

(a) 98% polymer content
(b) 95% polymer content
(c) 65% polymer content
(d) 41.4% polymer content
(e) 37.5% polymer content
(f) 21.5% polymer content
(g) 25.4% polymer content; stirred
(h) 15.0% polymer content; stirred
The heating rate is 0.5°C/min. for all samples.

By plotting the end points of the dissolution against the polymer content in the mixture, the solubility curve is obtained, as is shown in Fig. 6. Except for the region from 30 to 50% in polymer content, the curve increases smoothly with the polymer content, indicating that decalin is a good solvent for isotactic polypropylene. In the region of the polymer content of from 30 to 50%, the DTA curves are not so reproducible [see Fig. 3. (g) and (h)] and, hence, the end points determined from them are considerably scattered, suggesting that some anomalous states exist in this region. If we connect the curve of a lower polymer content with the other one of a higher content, we must

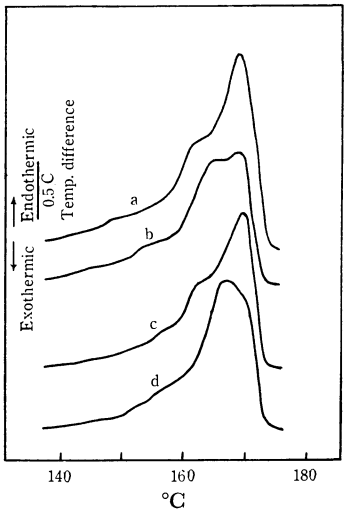

Fig. 5. The DTA curves of isotactic polypropylene.

(a) The sample crystallized by rapid cooling (3—5°C/min.) from the melt
(b) The sample crystallized by slow cooling (0.3—0.5°C/min.) from the melt
(c) The sample crystallized by rapid cooling from the melt with antioxidant
(d) The sample crystallized by slow cooling from the melt with antioxidant

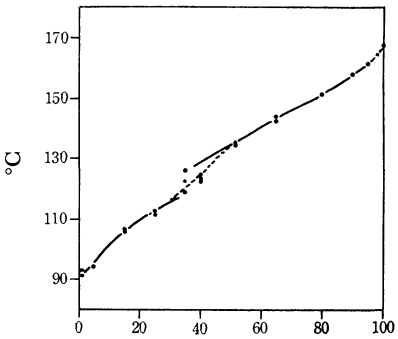

Fie. 6. The solubility curve of isotactic polypropylene-decalin system.

draw the discontinuous curve with a flection in this region shown by the dotted line in Fig. 6. We can not give a full explanation of this anomalous behavior, but it may be due to the existence of two crystal modifications, such as the usual one crystallized from the melt (or from the concentrated solution) and the other either the one from the dilute solution, as confirmed in polyethylene by Flory,[3] or the metastable paracrystalline smectic one.[4]

3) J. B. Jackson, P. J. Flory and R. Chiang, *Trans. Faraday Soc.*, **59**, 1906 (1963).
4) G. Natta, *Makromol. Chem.*, **35**, 93 (1960).

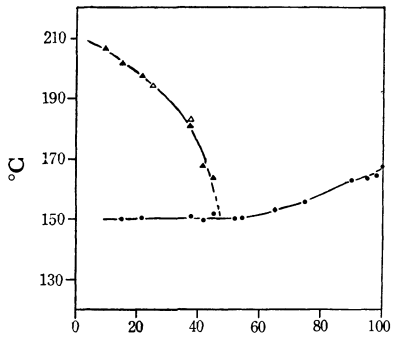

Fig. 7. The solubility curve of isotactic polypropylene-nitrobenzene system.
—●— dissolution point
—▲— phase separation point

The Isotactic Polypropylene-Nitrobenzene System.—The DTA curves obtained for the isotactic polypropylene-nitrobenzene system are shown in Fig. 4. These curves are divided into two types, one appearing in polymer-rich mixtures, and the other in polymer-poor mixtures. The former type contains a main peak the temperature of which decreases with the solvent content, indicating that these peaks may be due to the dissolution of the polymer into nitrobenzene, as in the cases of the decalin system. On the other hand, each curve of the latter type has a peak at almost the same temperature; then it gradually falls until it suddenly shows a small bend at the high-temperature region according to the solvent content, followed by another sharp, upward bend, a bend which is probably due to the beginning of the vaporization of the solvent. In the dilute solutions, the curve after the peak, as a whole, is curved in the endothermic direction as a result of the vaporization of the solvent. When the solution is stirred, as may be seen in Figs. 4. (g) and (h), the curve makes a sharp descent just before the first bend (the cause of this we can not find), and the curve, as a whole, becomes rugged.

By plotting the temperatures of the tops of the peaks and those of the first bends against the polymer contents in the mixtures, the solubility curve shown in Fig. 7 is obtained. "The first bend point-polymer content" curve closely resembles the phase separation curve in the polymer solution, suggesting that two liquid phases may coexist, because nitrobenzene is a bad solvent for isotactic polypropylene.

In order to ascertain if this curve is due to the phase separation, we tried to observe directly the temperature at which the mixture becomes homogeneous or at which the homogeneous solution separates into two phases; we attempted to do this by heating or cooling the polymer-solvent mixture in a test tube immersed in an oil bath. The temperatures obtained by this rough procedure are shown by open triangles in Fig. 7; they are close to the bend point curve, indicating that this curve may be the phase separation curve.

The peak temperature curve is very analogous to the melting curves of the polyethylene - *n*-butyl phthalate and polyethylene - *o*-nitrotoluene systems obtained by Mandelkern and his co-worker[5] with the dilatometric method. These curves show the characteristic feature that each curve contains a slope in the polymer-rich region and a horizontal line at a definite temperature in the polymer-poor region.

In Fig. 7, the extrapolation of the phase separation curve leads to an intersection with the peak temperature curve at an approximately 50% polymer content; this seems to correspond to the furthermost right end of the horizontal part of the peak temperature curve.

When a polymer-poor mixture with a polymer content of less than 50% is heated, the crystallites of the polymer may dissolve into nitrobenzene, forming two polymer solutions in equilibrium with each other at a definite temperature of 150°C, as is indicated by the horizontal line of the dissolution curve. This abrupt dissolution of the polymer shows as a sharp peak in the DTA curves.

The Melting of Pure Isotactic Polypropylene.—The DTA curves of pure isotactic polypropylene show a broad peak, accompanied by a small peak in the low temperature region, and have approximately a 9°C spread, as is illustrated in Fig. 5. The temperature of the top of the main peak, corresponding to the completion of melting, is in the range of 167.7±0.3°C for the samples pre-treated under various conditions.

As may be seen in Fig. 5, the cooling rate in the pre-treatment has a slight effect on the location of the small peak on the low-temperature side. The slower the cooling rate, the more the small peak seems to approach the main peak. The presence of an antioxidant may not produce any effect, showing that the existence of the earlier peak is not due to the thermal degradation and the oxidation of samples.

The double peaks of the melting of isotactic polypropylene have been reported by several authors.[6-8] Ke,[7] one of them, suggests that the double peaks are associated with structural differences, probably different stereospecificities (atactic or syndiotactic) in isotactic polypropylene. Atactic polypropylene has two transitions at 70

5) F. A. Quinn, Jr., and L. Mandelkern, *J. Am. Chem. Soc.*, **77**, 781 (1955).
6) I. M. Tolchinski, N. A. Nechitailo, and A. V. Topchiev, *Plasticheskie Massy*, **1960**, (No. 7) 3 (1960).
7) B. Ke, "Newer Methods of Polymer Characterization," Polymer Review, No. 6, Interscience Publisher Inc., New York (1964).
8) R. F. Schwenker, Jr., and R. K. Zuccarello, *J. Polymer Sci., Part C*, (No. 6) 1 (1964).

and 155°C,[9] but the heats of these transitions, 2.1 and 0.30 cal./g.[9] respectively, are too small in comparison with the heat of the fusion of isotactic polypropylene, 20 cal./g.,[9] to enable one to assign the earlier peak to the two transitions of atactic polypropylene. Syndiotactic polypropylene has been reported to melt at 183°C; this seems inadequate to explain the earlier peak.

Schwenker and his co-worker[8] have observed that the DTA curve of drawn polypropylene shows the double peaks at 158 and 174°C; they also observed that if the melt from the drawn fiber is cooled and rerun, the earlier peak disappears. They have concluded that the earlier peak may be ascribed to the disorientation of the crystallites, as has been confirmed in nylon 66 by White.[10] According to them, our samples crystallized by slow cooling and those crystallized by rapid cooling from the melt consist of disoriented and orientated crystallites respectively; this seems curious, though we can not deny the disorientation of crystallites because we have not carried out measurements of the drawn samples.

As may be seen in Figs. 3 (a), (b) and 4 (a), (b), the earlier peak seems to be enlarged by the addition of solvents; this may confirm that it is not due to disorientation, since, the addition of solvents makes it impossible for the disorientation of crystallites (perhaps perfectly at random in solvents) to occur.

On the other hand, on the bases of the X-ray and infrared spectra of samples rapidly cooled and annealed from the melted isotactic polypropylene, though there has been no information obtained by the thermal method, Natta[4] has reported that a rapid cooling of the melted isotactic polypropylene produces a metastable paracrystalline smectic modification in which right- and left-helices of polymers are placed at random in a psuedo-hexagonal cell, while in the usual samples, produced by slow cooling and annealing, they are regularly disposed facing one another, two by two. Though we can not give an explicit conclusion for the earlier peak, since we have not examined the sample by X-ray, it may be suggested that the earlier peak, produced by rapid cooling, is due to the melting of the metastable paracrystalline smectic modification, and that the location and magnitude of the earlier peak varies with the degree of randomness and with the amount of modification.

The Heat of the Fusion of Isotactic Polypropylene.—The heat of the fusion, ΔH_u, of isotactic polypropylene is easily found by the ratio of the area under the DTA peak of the fusion of isotactic polypropylene to that of a known heat change (e. g., the heat of the fusion of urea), or by Flory's equation of melting point depression:[11]

$$1/T_m - 1/T^\circ_m = (R/\Delta H_u)[(V_{2u}/V_1)v_1 - \chi v_1^2] \quad (1)$$

where T°_m is the melting temperature of a pure polymer; T_m, the melting temperature of a polymer with a diluent; ΔH_u, the heat of the fusion of the polymer per structural-unit mole; χ, the interaction parameter; V_{2u}, the unit molar volume of the polymer; V_1, the molar volume of the diluent, and v_1, the volume fraction of the diluent. The former method gives a value of 1070±100 cal./unit mol. for the heat of fusion, while the latter method gives values of 870±50 cal./unit mol. for a decalin system and 920±50 cal./unit mol. for a nitrobenzene system. These values are in good agreement with each other. The values of the interaction parameter, χ, are estimated to be 0.88 and 2.93 for decalin and nitrobenzene respectively by the above equation. These values may, however, be considered to be a little large.

TABLE I. THE VALUES OF THE HEAT OF FUSION OF ISOTACTIC POLYPROPYLENE

Method	Value of ΔH_u cal./unit mole	Reference
Area of DTA curve	1070±100	This work
Eq. 1		
in decalin	870±50	This work
in nitrobenzene	920±50	This work
Dilatometry	1700	12
Dilatometry	2500	13
Area of DTA curve	650	14
Specific heat	870 (1500)*	9
$dP/dT = \Delta H/T\Delta V$	630	15
$dP/dT = \Delta H/T\Delta V$	2370	16

* Calculated for 100% crystallized.

The above values of the heat of fusion are listed in Table I, together with the values[9,12-16] determined by other authors by using various methods; our values are reasonable, especially considering that Wilkinson and his co-worker,[9] by specific heat measurement, calculated the value to be 1500 cal./unit mol. for the heat of the fusion of the 100% crystallized isotactic polypropylene.

Summary

A DTA apparatus for a polymer solution has been constructed. By using this apparatus, we have investigated the solubility curves of isotactic polypropylene-decalin and isotactic polypropylene-nitrobenzene systems; we have then discussed the DTA curves obtained for these systems, and also

9) R. W. Wilkinson and M. Dole, *J. Polymer Sci.*, **58**, 1089 (1962).
10) T. R. White, *Nature*, **175**, 895 (1955).
11) P. J. Flory, *J. Chem. Phys.*, **17**, 223 (1949).
12) O. Ishizuka, *J. Chem. Soc. Japan, Ind. Chem. Sect.* (*Kogyo Kagaku Zasshi*), **65**, 244 (1962).
13) F. Danusso, G. Moraglio and E. Flores, *Atti accad. nazl. Lincei. Rend., classe sci. fis., mat. e nat.*, **25**, 420 (1958).
14) B. Ke., *J. Polymer Sci.*, **42**, 15 (1960).
15) G. Gee, *Proc. Chem. Soc.*, **1957**, 111.
16) J. R. Schaefgen, *J. Polymer Sci.*, **38**, 549 (1959).

the double peaks which appear in the melting of pure isotactic polypropylene, peaks which may be due to the paracrystalline smectic modification of isotactic polypropylene. The heat of the fusion of isotactic polypropylene has been estimated to be approximately 1000 cal./unit mol. by the methods of measuring the area under the melting peak and of the equation of the melting point depression.

The authors wish to express their deep sense of gratitude to the Mitsubishi Rayon Co., Ltd., for supplying the samples.

BULLETIN OF THE CHEMICAL SOCIETY OF JAPAN VOL. 39 25—30 (1966)

Kinetic Studies of the Solution Polymerization of Trioxane Catalyzed by $BF_3 \cdot O(C_2H_5)_2$. II. The Effect of Catalyst and Water Concentrations of the Molecular Weight of the Polymer

By Toshinobu HIGASHIMURA, Tetsuro MIKI and Seizo OKAMURA

Department of Polymer Chemistry, Kyoto University, Sakyo-ku, Kyoto

(Received April 5, 1965)

In the solution polymerization of trioxane catalyzed by $BF_3 \cdot O(C_2H_5)_2$, the dependence of the molecular weight of the polymer formed on the polymerization conditions has been studied. In general, the molecular weight of the polymer formed increases in the course of polymerization, keeps a constant value over a certain range of conversion, and then again incerases remarkably. The molecular weight of the polymers formed decrease with an increase in the catalyst and water concentrations. This phenomenon can be explained qualitatively on the assumptions that the rate of the propagation reaction is smaller than that of the initiation reaction and that the chain breaking occurs through the reaction with water, which is consumed as the polymerization proceeds. This is equal to the assumption that the chain carrier is an oxonium ion in the cationic polymerization of trioxane.

It is neccessary for a study of the characteristics of the polymerization of the cyclic compound to know the molecular weight of the produced polymer as well as the rate of polymerization. None of the papers on the solution polymerization of trioxane has, however, dealt with the relation between the polymerization conditions and the molecular weight of the produced polymer, This relation has been discussed only in connection with the polymerization of molten trioxane.[1,2]

The effect of the concentrations of $BF_3 \cdot O(C_2H_5)_2$ and of water on the rate of polymerization in various solvents was described in previous paper.[3] For the present paper, the molecular weight of the polymer obtained in the previous paper was measured, and its dependence on the concentrations of catalyst and water was studied. The exact relationship between the solution viscosity and the molecular weight for polyoxymethylene has not yet been obtained, so we used the viscosity number instead of the molecular weight of the produced polymer.

The peculiar phenomenon was found that the molecular weight of the produced polymer increased as the polymerization proceeded but decreased as the catalyst concentration increased; no such phenomenon has been found in the cationic polymerization of vinyl monomers.

Experimental

After the polymer obtained in the previous paper[3] had been throughly dried, viscosity number (η_{sp}/C; C=0.6 g./100 ml. solution) was measured in a *p*-chlorophenol solution including 2% α-pinene at 60°C. The polymer was dissoved in *p*-chlorophenol under nitrogen gas by heating it at 120°C for 2—4 min. Under such conditions, it was not clear whether the polymer was decomposed or not during dissolution. The decomposition of the polymer during dissolution was, however, inferred to be negligible since the reproducibility of the measurements of the same sample within 5 min. of heating was very good and since the value of η_{sp}/C varied regularly with the polymerization conditions.

Results

The Effect of the Catslyst Concentration and the Conversion.—The effects of both the

1) M. Kučera and E. Spousta, *Makromol. Chem.*, **76**, 183 (1964).
2) M, Kučera and E. Spousta, ibid., **76**, 190 (1964).
3) T. Higashimura, T. Miki and S. Okamura, This Bulletin, **38**. 2067 (1965).

catalyst concentration and the conversion on the molecular weight of the resulting polymer in various solvents were studied. The polymerization conditions were the same as those in the corresponding figures in the previous paper.[3]

The results for the polymers obtained in benzene and ethylene dichloride are shown in Figs. 1 and 2. The molecular weight of both polymers increased with the conversion. Moreover, the molecular weight is the smaller at larger catalyst concentrations.

Although the catalyst concentration did not affect the rate of polymerization at a high-monomer concentration (3.3 mol./l.) in nitrobenzene, the

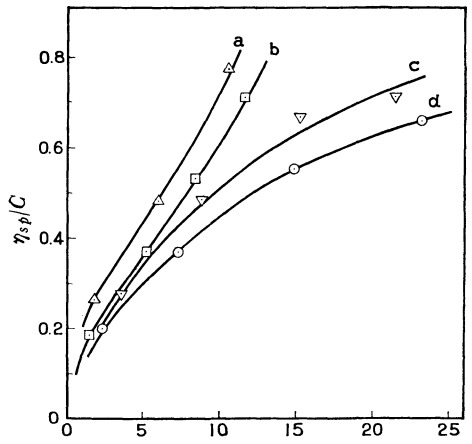

Fig. 1. Effect of catalyst concentration on the molecular weight of resultant polymers in benzene solution at 30°C.
$[M]_0$; 3.3 mol./l., $[H_2O]$; 2.5 mmol./l., $[BF_3 \cdot O(C_2H_5)_2]$; a(△): 5, b(□): 10, c(▽): 20 and d(○): 30 mmol./l.

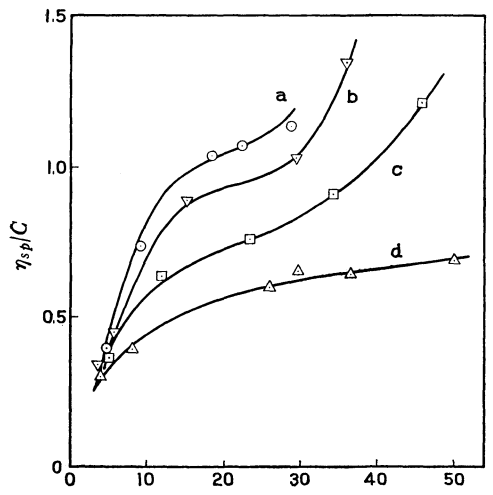

Fig. 2. Effect of catalyst concentration on the molecular weight of resultant polymers in ethylene chloride solution at 30°C.
$[M]_0$; 3.3 mol./l., $[H_2O]$; 2.9 mmol./l., $[BF_3 \cdot O(C_2H_5)_2]$; a(○): 2.5, b(▽); 5, c(□): 10 and d(△): 20 mmol./l.

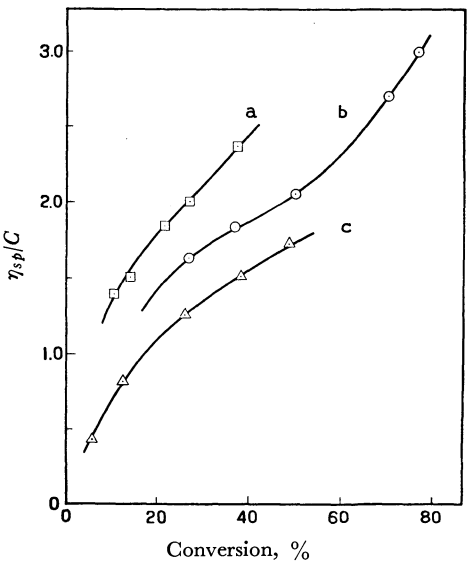

Fig. 3. Effect of catalyst concentration on the molecular weight of resultant polymers in nitrobenzene solution at 30°C.
$[M]_0$; 3.3 mol./l., $[H_2O]$; 1.8 mmol./l., $[BF_3 \cdot O(C_2H_5)_2]$; a(□): 0.5, b(○): 1.0 and c(△): 2.5 mmol./.

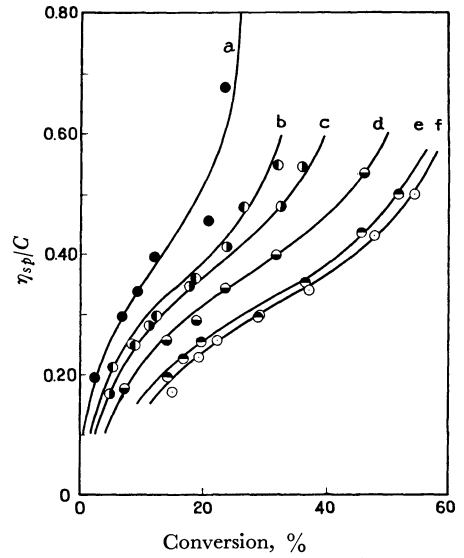

Fig. 4. Effect of water concentration on the molecular weight of resultant polymers in *n*-hexane at 30°C.
$[M]_0$; 0.37 mol./l., $[BF_3 \cdot O(C_2H_5)_2]$; 9.4 mmol./l., $[H_2O]$; a(●): 0.4, b(◐): 0.9, c(◑): 1.1, d(◒): 1.7, e(◓): 2.2 and f(○): 3.4 mmol./l.

molecular weight of the produced polymers decreased regularly with an increase in the catalyst concentration and increased remarkably with the conversion, as is shown in Fig. 3. A similar behavior was found in the nitroethane solvent.

The Effect of the Water Concentration— The addition of water also decreased the molecular weight of the produced polymer. The results in *n*-hexane and ethylene dichloride are shown in Figs. 4 and 5, respectively. A similar result was obtained in benzene. In these solvents a small amount of water accelerates the polymerization, but an excessive addition of water decreases the rate. In all these solvents, it may be noted that the molecular weight decreases monotonously with the increase of water, but not with the conversion. In ethylene dichloride, for examlpe, the rate of the increase in molecular weight is remarkably raised at certain conversions.

In nitrobenzene the relation between the molecular weight and the water concentration was also curious. As is shown in Fig 6, when the monomer concentration was equal to 3.3 mol./l., a small amount of water did not affect the molecular weight. However, when the monomer concentration was low, the molecular weight was decreased

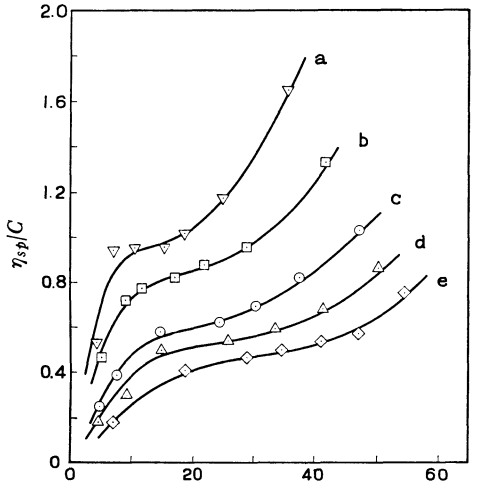

Fig. 5. Effect of water concentration on the molecular weight of resultant polymers in ethylene dichloride at 30°C.
$[M]_0$; 3.3 mol./l., $[BF_3 \cdot O(C_2H_5)_2]$; 10 mmol./l., $[H_2O]$; a(▽): 0.3, b(□): 1.6, c(○): 3.7, d(△): 5.9 and e(◇): 10.8 mmol./l.

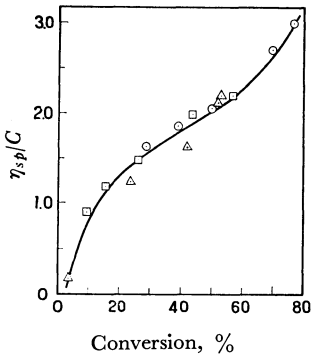

Fih. 6. Effect of water concentration on the molecular weight of resultant polymers in nitrobenzene at 30°C.
$[M]_0$; 3.3 mol./l., $[BF_3 \cdot O(C_2H_5)_2]$; 1.0 mmol./l., $[H_2O]$; ○: 1.8, △: 4.7 and □: 8.3 mmol./l.

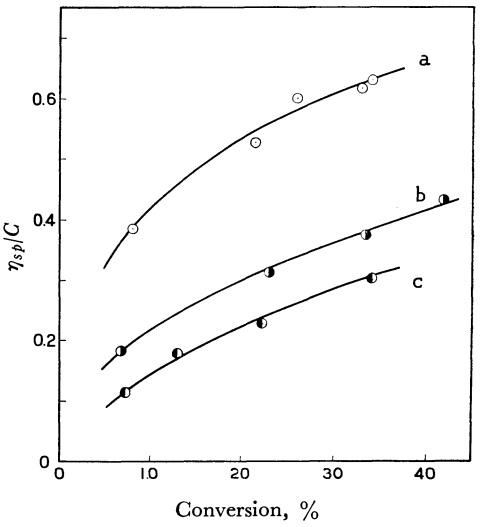

Fig. 7. Effect of methanol concentration on the molecular weight of resultant polymers in ethylene dichloride at 30°C.
$[M]_0$: 3.3 mol./l., $[BF_3 \cdot O(C_2H_5)_2]$; 20 mmol./l., $[H_2O]$; 2.7 mmol./l., $[CH_3OH]$; a(○): 0, b(◑): 10.0 and c(◐): 20.0 mmol./l.

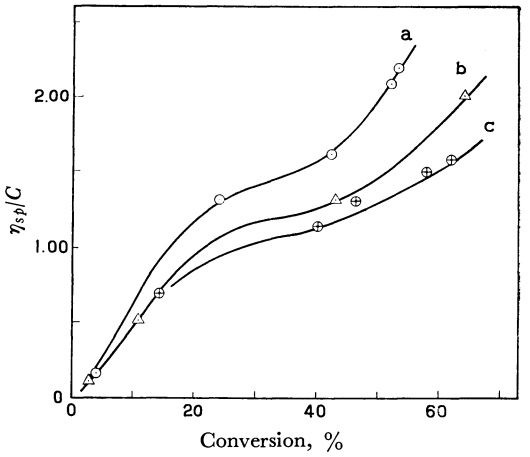

Fig. 8. Effect of methanol concentration on the molecular weight of resultant polymers in nitrobenzene at 30°C.
$[M]_0$; 3.3 mol./l., $[BF_3 \cdot O(C_2H_5)_2]$; 1.0 mmol./l., $[H_2O]$; 4.7 mmol./l., $[CH_3OH]$; a(○): 0, b(△): 2.5 and c(⊕): 5.0 mmol./l.

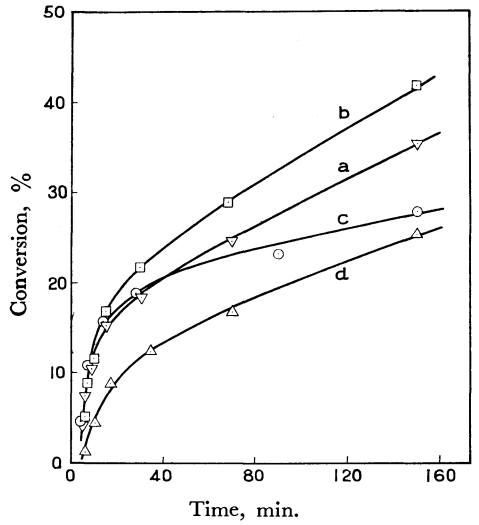

Fig. 9. Comparison between the rate of polymerization in ethylene dichloride and that in methylene chloride at 30°C.
$[M]_0$; 3.3 mol./l., $[BF_3 \cdot O(C_2H_5)_2]$; 10 mmol./l.,
a(▽); $(CH_2Cl)_2$ solvent, $[H_2O]$: 0.3 mmol./l.,
b(□); $(CH_2Cl)_2$ solvent, $[H_2O]$: 1.6 mmol./l.,
c(○); $(CH_2Cl)_2$ and CH_2Cl_2 mixed solvent (equal volume), $[H_2O]$: 0.9 mmol./l.,
d(△); CH_2Cl_2 solvent, $[H_2O]$: 0.9 mmol./l.

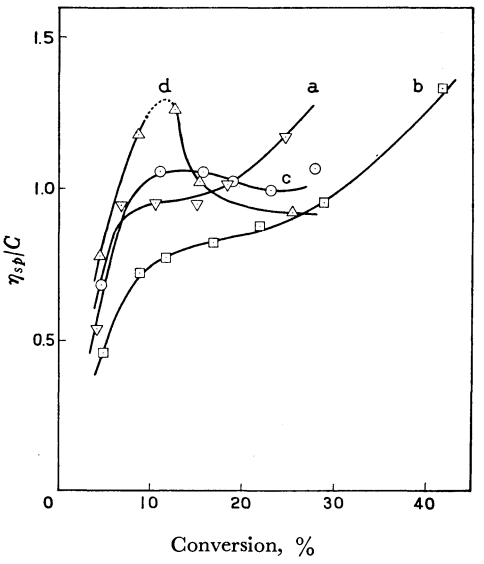

Fig. 10. Comparison between molecular weight of polymer obtained in ethylene chloride and that in methylene chloride at 30°C.
Polymerization condition and notes of courves are the same as in Fig. 9.

by an increase in the water concentration. As the relation between the conversion and the molecular weight at a low-monomer concentration was extraordinary, this matter will be discussed in the next paper.[4]

The Effect of the Addition of Methanol.—The effect of added methanol in ethylene dichloride and nitrobenzene was also studied. As is shown in Figs. 7 and 8, the molecular weight of the polymer decreased with an increase in the concentration of methanol. At a fixed conversion, the rate of the decrease in molecular weight by the addition of methanol in ethylene dichloride was larger than that in nitrobenzene.

Abnormality in Methylene Chloride.—It has been reported that, in the case of the polymerization of trioxane by iron(III) chloride in cyclohexane, the molecular weight of the produced polymer decreased with an increase in the conversion.[5] In our results on the solution polymerization of trioxane, however, the molecular weight of the polymer increased in the course of polymerization. Therefore, we have studied whether the molecular weight of the resultant polymers decreased or not with an increase in the conversion in a $BF_3 \cdot O(C_2H_5)_2$-methylene chloride which is considered to act as a transfer agent.

As is shown in Fig. 9, the rate of the polymerization of trioxane in methylene chloride was smaller than that in ethylene dichloride, but there was no essential difference in the behavior between two solvents. The molecular weight of the produced polymer in methylene chloride, however, was found to exhibit the characteristic behavior as is shown in Fig. 10. In methylene chloride the molecular weight of the polymer increased in the course of polymerization at the initial stage of polymerization, reached a maximum at a certain conversion, and then decreased.

Discussion

Generally in the cationic polymerization of vinyl monomers, the molecular weight of the produced polymers is independent of the catalyst concentration and the conversion. However, in the solution polymerization of trioxane catalyzed by $BF_3 \cdot O(C_2H_5)_2$, the molecular weight of the polymers formed increases in the course of polymerization but decreases with an increase in the catalyst and water concentrations.

The change in the molecular weight in the course of the polymerization of trioxane can be characterized as follows. The molecular weight increases monotonously up to 10—20% conversion; the rate of its increase decreases in the middle stage of the polymerization, and then again increases rapidly at a high conversion. As may be seen from Figs. 4 and 5, the range in which the molecular weight did not increase with the conversion was influenced by the quantity of water. In order

4) T. Higashimura, T. Miki and S. Okamura, ibid., **39**, 31 (1966).
5) V. Jaacks and W. Kern, *Makromol. Chem.*, **62**, 1 (1963).

to clarify the reaction mechanism, we shall first try to explain the relation between the change in molecular weight and the conversion.

Other instances where the moleculat weight of the polymers formed increases in the course of polymerization have been found in the cationic polymerization of such cyclic ethers as ethylene oxide and 1, 3-dioxolane,[6,7] and in the anionic polymerization of the cyclic monomers and vinyl monomers. These results have been summarized[8] and explained by the concept of "successive" polymerization[9] by Kagiya et al.

As for trioxane, this phenomenon was recognized in the cationic polymerization in the molten state.[1] It has been regarded as being caused by the polymerization's proceeding step by step through a living end and by the impurities which act as chain breakers being consumed in the course of polymerization. This suggestion involved the two points that the molecular weight of the polymers formed was independent of the catalyst concentration and that the molecular weight at 0% conversion was not equal to zero.

These proposals[1,8,9] could explain many things, but not the complicated behavior of the solution polymerization of trioxane found in this paper. To explain the observed change in molecular weight, then, the following three elementary reactions are assumed for the solution polymerization of trioxane:

$$\text{Initiation reaction} \quad M + C \xrightarrow{k_i} M_1^* \tag{1}$$

$$\text{Propagation reaction} \quad M_r^* + M \xrightarrow{k_p} M_{r+1}^* \tag{2}$$

$$\text{Transfer reaction} \quad M_r^* + X_{tr} \xrightarrow{k_{tr}} P_n + X'_{tr} \tag{3}$$

Where M, C, and X_{tr} denote a monomer, a catalyst and a chain-transfer reagent like water respectively. If X_{tr} is water, X'_{tr} implies a proton. Consequently, X_{tr} is consumed during the polymerization according to reaction 3. It may be inferred that, in the cationic polymerization of trioxane, the transfer reactions to monomer and solvents used in this paper scarcely ever occur.

According to Kagiya et al.[9] the phenomenon of the molecular weight of the polymers formed increasing in the course of polymerization is found only when the rate of the initiation reaction is larger than those of the propagation and the transfer reaction. In such a system the average degree of polymerization ($\bar{P}$) corresponding to the elementary reactions 1—3 is shown by Eq. 4[9]:

$$\bar{P} = \frac{[M]_0 - [M]}{\alpha[C]_0 + k_{tr}\int [M^*][X_{tr}]dt} \tag{4}$$

where α is a constant which denotes the mole concentration of active center produced per mole of catalyst and where the suffix 0 denotes the initial concentration. If X_{tr} is not consumed during the polymerization (e. g., if $[X_{tr}]$ is a constant), Eq. 5 is obtained by substituting Eq. 2 into Eq. 4:

$$\bar{P} = \frac{[M]_0 - [M]}{\alpha[C]_0 + (k_{tr}/k_p)[X_{tr}]_0 \ln([M]_0/[M])} \tag{5}$$

Equation 5, as derived by Kagiya et al., implies that the degree of polymerization increases with the conversion to the limited value and that after that it again decreases. This behavior is shown schematically in curve c in Fig. 11. This does not agree with our experimental results.

As is shown in Eq. 3, X_{tr} decreases in the course of polymerization. In such a case, the relation between $[X_{tr}]$ and [M] has already been indicated, as is shown in Eq. 6[1]:

$$[X_{tr}] = [X_{tr}]_0([M]/[M]_0)^{k_{tr}/k_p} \tag{6}$$

Equation 7 is obtained by putting Eqs. 2 and 6 into Eq. 4 and integrating;

$$\bar{P} = \frac{[M]_0 - [M]}{\alpha[C]_0 + [X_{tr}]_0\{1 - ([M]/[M]_0)^a\}} \tag{7}$$

$$= \frac{[M]_0 x}{\alpha[C]_0 + [X_{tr}]_0\{1 - (1-x)^a\}} \tag{7'}$$

where $a = k_{tr}/k_p$ and where x denotes the fractional conversion. This is equal to the equation obtained by Kucera[1] except for the first term of the denominator.

In our experiments, η_{sp}/C was measured, but not the molecular weight. There was also the added complexity that the polymer formed precipitated from the reaction system during the polymerization. Therefore, the experimental results will be compared qualitatively.

If the transfer reaction (Eq. 3) does not occur, the second term of the denominator in Eq. 7' may be omitted and $\bar{P}$ increases in proportion to the conversion. This is shown by line a in Fig. 11. If $\bar{P}$, as proposed by Kučera,[1] depends on only the transfer reaction, $\bar{P}$ is indicated by curve b in Fig. 11. If the transfer reagent (X_{tr}) is not consumed during the polymerization, $\bar{P}$ is indicated by Eq. 5 and its change will obey curve c in Fig. 11. These lines do not agree with our experimental results. When a in Eq. 7' is smaller than 1, $\bar{P}$ indicates curve d. However, the rapid increase in the molecular weight at a high conversion cannot be explained. On the other hand, when a is larger than 1, curve e is obtained and the shape of the curve agrees qualitatively with the experimental data. According to this result, it is recognized that, as the water is consumed during the initial

6) D. J. Worsfold and A. M. Eastham, *J. Am. Chem. Soc.*, **79**, 897 (1957).
7) T. Kagiya, M. Hatta, T. Shimizu and K. Fukui, *J. Chem. Soc. Japan, Ind. Chem. Sect.* (*Kogyo Kagaku Zasshi*), **66**, 1890 (1963).
8) T. Kagiya, M. Hatta and K. Fukui, *Chem. High Polymers Japan* (*Kobunshi Kagaku*), **20**, 737 (1963).
9) T. Kagiya, M. Hatta and K. Fukui, ibid., **20**, 730 (1963).

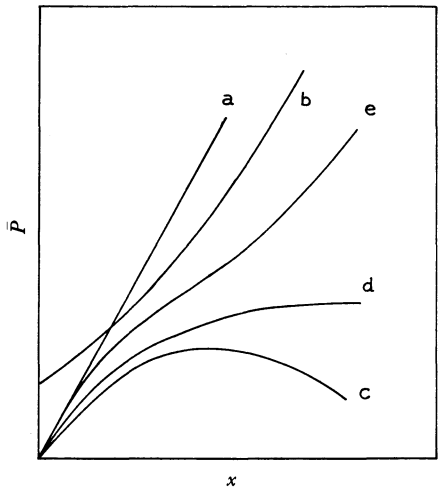

Fig. 11. Schematic diagram of the relationship between the degree of polymerization ($\bar{P}$) and the fractional conversion (x).

stages of polymerization, such a η_{sp}/C-conversion curve is observed. Also, the rate of the transfer reaction may be fairly fast, because k_{tr}/k_p is larger than unity. However, another reason can be given for this phenomenon. Polymer transfer reactions have been reported in the cationic polymerization of trioxane[10] and tetrahydrofuran[11]. Therefore, the transfer reaction of the growing chain to the dead polymer may be considered to exist in this system also.

If α in Eq. 7 is independent of the catalyst concentration,[9] it is recognized that the molecular weight of the polymers decreases with the increase in the catalyst concentration. It is also clear from this equation that an increase in the transfer reagent concentration decreases the molecular weight of the polymers.

In methylene chloride the molecular weight of the polymers decreased at a high conversion. It has also been found that, in the polymerization of trioxane in cyclohexane catalyzed by iron(III) chloride the molecular weight of the polymers decreases in the course of the polymerization.[5] It is considered that these phenomena are caused by the decomposition of the resultant polymers. It is not clear, however, why the decomposition of the polymers takes place only in methylene chloride and cyclohexane.

It has been considered that, in the cationic polymerization of vinyl monomers, the rate of the propagation reaction is larger than that of the other elementary reactions. However, as has been mentioned above, Eq. 7 was derived on the assumption that the rate of the initiation reaction is larger than that of the propagation reaction. This fact is understandable assuming that the growing chain is stable in the cationic polymerization of trioxane. If the active chain end produced from trioxane has the structure shown in Eq. 8, however, this chain end is more unstable than that of vinyl monomers, and the reactivity of the former should be larger than that of the latter;

$$\sim\!\sim CH_2\text{-}O\text{-}\overset{+}{C}H_2\cdots B^- \qquad (8)$$

Nevertheless, the rate of the propagation reaction was smaller than that of the other elementary reaction, according to our results. This may be because the chain carrier is stabilized in a shape of the oxonium ion shown in Eq. 9, as is considered to be the case in the cationic polymerization of many cyclic ethers.

$$\sim\!\sim CH_2\text{-}O\text{-}CH_2\text{-}\overset{+}{O}\begin{matrix}CH_2\text{-}O\\ \vdots\\ B^-\end{matrix}\!\!\diagdown\!\!\diagup\begin{matrix}CH_2\text{-}O\\ CH_2\end{matrix} \qquad (9)$$

Even if the polymerization reaction would proceed through the oxonium ion, there are many cases in which the molecular weight of the polymers formed does not increase in the course of polymerization.[12,13] However, in a system in which the molecular weight of the polymers increases rapidly with the conversion, it may be reasonable to consider the chain carrier to be a stable oxonium ion.

10) K. Weissermel, E. Fischer, K. Gutweiler and H. D. Hermann, *Kunststoffe*, **54**, 410 (1964).
11) A. Rosenberg, E. B. Lyudvig, A. R. Gantmakher and S. S. Medvedev, *Visokomol. Soed.*, **7**, 188 (1965).
12) J. B. Rose, *J. Chem. Soc.*, **1956**, 542.
13) I. Penczek and S. Penczek, *Makromol. Chem.*, **67**, 203 (1963).

BULLETIN OF THE CHEMICAL SOCIETY OF JAPAN VOL. 39 31—36 (1966)

Kinetic Studies of the Solution Polymerization of Trioxane Catalyzed by $BF_3 \cdot O(C_2H_5)_2$. III. The Effect of the Monomer Concentration

By Toshinobu HIGASHIMURA, Tetsuro MIKI and Seizo OKAMURA

Department of Polymer Chemistry, Kyoto University, Sakyo-ku, Kyoto

(Received April 5, 1965)

In the solution polymerization of trioxane catalyzed by $BF_3 \cdot O(C_2H_5)_2$, the dependence of the monomer concentration on the polymerization reaction has been studied. The kinetic order of the monomer concentration as determined from the course of polymerization is close to 2 (except in a non-polar solvent). The kinetic order of the initial monomer concentration is extraordinarily large in the polar solvent. On the other hand, the molecular weight of the polymers formed increases with an increase in the initial monomer concentration. In the polymerization of trioxane in a polar solvent such as nitrobenzene at a low monomer concentration, the molecular weight of the polymers does not increase in the course of polymerization, even at the initial stage of polymerization. The reason for this has been discussed in terms of the nature of the chain carrier.

It has been recognized that, in the cationic, solution polymerization of trioxane catalyzed by $BF_3 \cdot O(C_2H_5)_2$, the molecular weitht of the resultant polymers increases in the course of polymerization, not as in the cationic polymerization of vinyl monomers.[1] This has been explained in terms of the rate of the propagation reaction being smaller than that of the initiation reaction. It has been suggested as the cause of this that the chain carrier in the solution polymerization of trioxane is not a carbonium ion but a stable oxonium ion solvated by monomers. If a condition were selected so that a more reactive carbonium ion than the oxonium ion were easily produced or the reactivity of initiating species were decreased, it might be expected that the relation between the conversion and the molecular weight of polymers would be changed.

Since a decrease in the trioxane concentration corresponds to a decrease in the concentration of the monomeric ether group which solvates the active ends, the behavior of the cationic polymerization of trioxane at a low monomer concentration will be studied in this paper.

It should also be noted that the effect of the catalyst and water concentrations on the polymerization rate is complicated and that the kinetic order of these concentrations varies remarkably with the kind of solvent.[2] Because of this, as well as for the above-mentioned purpose, the effect of the monomer concentration on the polymerization rate has been studied.

As a result, we have found that the kinetic order of the initial monomer concentration to the initial rate is large and that the molecular weight of the polymers produced at a low monomer concentration in a solvent with a high dielectric constant is nearly constant at the initial state of polymerization.

Experimental

The procedures of the polymerization and purification of materials were the same as were used in the first paper.[2] The molecular weights of the polymers formed were compared by the viscosity numbers (η_{sp}/C), which were measured in a *p*-chlorophenol solution.[1]

Results

The Effect of the Monomer Concentration on the Rate of Polymerization.—As non-polar solvents, such as *n*-hexane, do not have a high solubility toward trioxane, ethylene dichloride was used as a polar solvent and nitrobenzene, as a highly-polar solvent.

The time-conversion curves at various monomer concentrations in ethylene dichloride at a fixed catalyst concentration are shown in Fig. 1. With an increase in the initial monomer concentration, the rate of polymerization increased and the induction period decreased. Figure 2 shows the logarithmic plot of the initial monomer concentration against that of the initial rate as determined graphically from Fig. 1. It may be seen that the kinetic order of the initial monomer concentration to the initial rate is approximately 3.

In Fig. 3 is similarly shown the time-conversion curves at various monomer concentrations in nitrobenzene. It may be seen that the effect of the initial monomer concentration on the initial rate was remarkably large. In fact, on plotting the initial rate against the initial monomer concen-

1) T. Higashimura, T. Miki and S. Okamura, This Bulletin, **39**, 25 (1966).
2) T. Higashimura, T. Miki and S. Okamura, ibid., **38**, 2067 (1965).

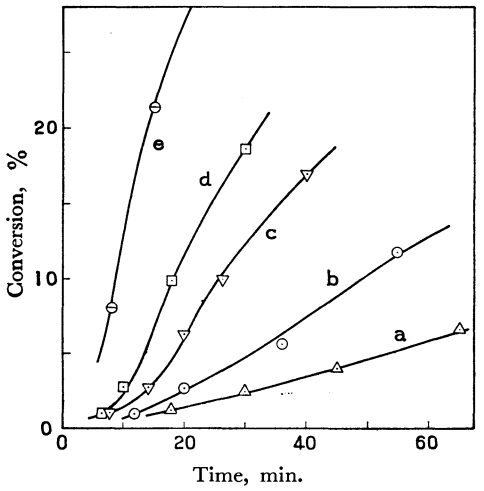

Fig. 1. Effect of the monomer concentration on the rate of polymerization in ethylene dichloride at 30°C.
$[BF_3 \cdot O(C_2H_5)_2]$; 20 mmol./l., $[H_2O]$; 2.7—3.0 mmol./l., $[M]_0$; a(△): 1.4, b(○): 1.7, c(▽): 2.2, d(□): 2.8 and e(⊖): 3.3 mol./l.

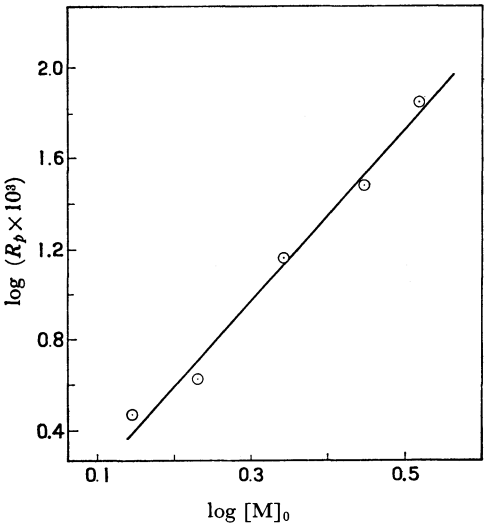

Fig. 2. Relationship between the initial rate and the initial concentration of monomer in ethylene dichloride at 30°C.
Calculated from Fig. 1.

tration, Fig. 4 was obtained; it was found that the initial polymerization rate was proportional to the sixth power of the initial monomer concentration. The induction period also decreased with an increase in the initial monomer concentration, but no simple stoichiometric relation has been found.

The Effect of the Monomer Concentration on the Molecular Weight of Polymers.— Figure 5 shows the relation between the conversion and the molecular weight of polymers obtained in ethylene dichloride at various initial monomer concentrations. The molecular weight of the

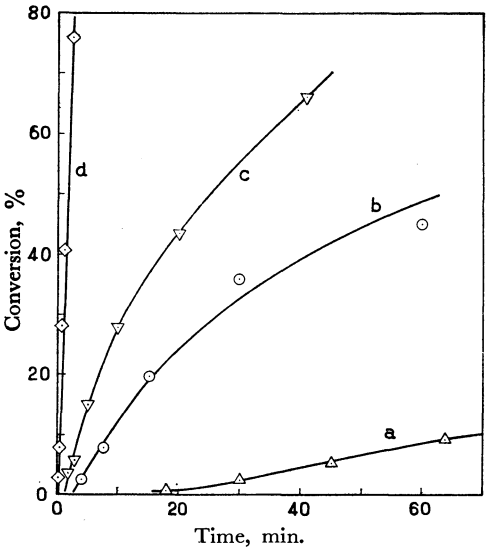

Fig. 3. Effect of the monomer concentration on the rate of polymerization in nitrobenzene at 30°C.
$[BF_3 \cdot O(C_2H_5)_2]$; 10 mmol./l., $[H_2O]$; 2.3—3.9 mmol./l., $[M]_0$; a(△): 0.83, b(○): 1.0, c(▽): 1.1 and d(◇): 2.2 mol./l.

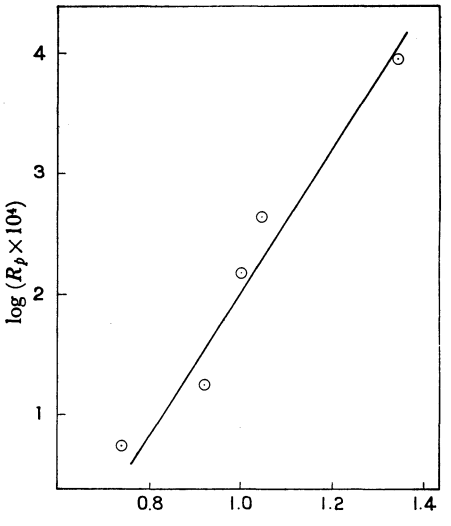

Fig. 4. Relationship between the initial rate and the initial concentration of monomer in nitrobenzene at 30°C.
Calculated from Fig. 3.

polymers increased in the course of the polymerization, even with a low initial concentration of monomer. The relation between the initial monomer concentration and the value of η_{sp}/C at the fixed conversion as determined graphically from Fig. 5 is shown in Fig. 6. The value of η_{sp}/C was proportional to the initial monomer concentration up to a 10% conversion.

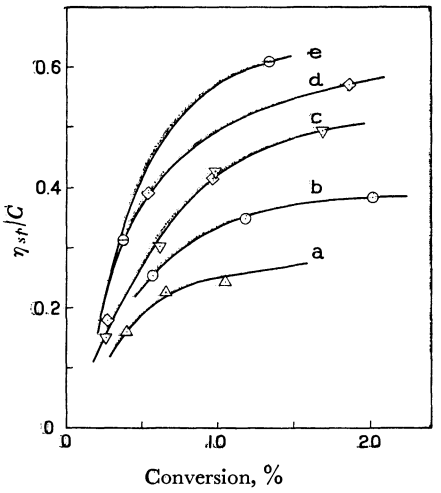

Fig. 5. Effect of the monomer concentration on the molecular weight of resultant polymers in ethylene dichloride at 30°C.
Polymerization conditions are the same as in Fig. 1. $[M]_0$; a(△): 1.4, b(○): 1.7, c(▽): 2.2, d(□): 2.8 and e(⊖): 3.3 mol./l.

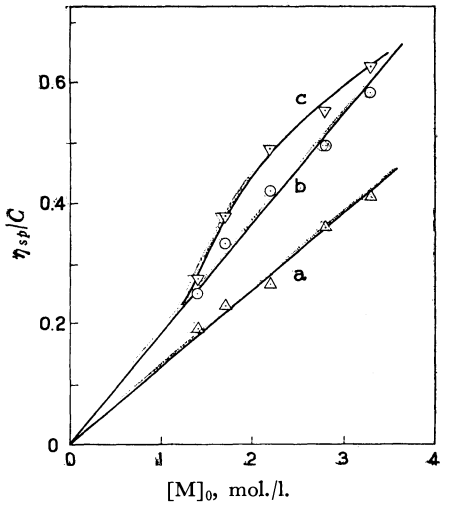

Fig. 6. Relationship between the molecular weight of polymers and the initial concentration of monomer at various conversion in ethylene dichloride at 30°C.
Calculated from Fig. 5. Conversion; a(△): 5.0, b(○): 10 and c(▽): 15%

The behavior in nitrobenzene was different. As is shown in Fig. 7, at a low initial concentration of the monomer no increase of the molecular weight with the conversion was seen in the initial state of polymerization. To clarify this unusual behavior at a low monomer concentration, a relation was obtained between the conversion and the molecular weight of polymers formed at various concentrations of catalyst and water when the initial concentration of the monomer was equal

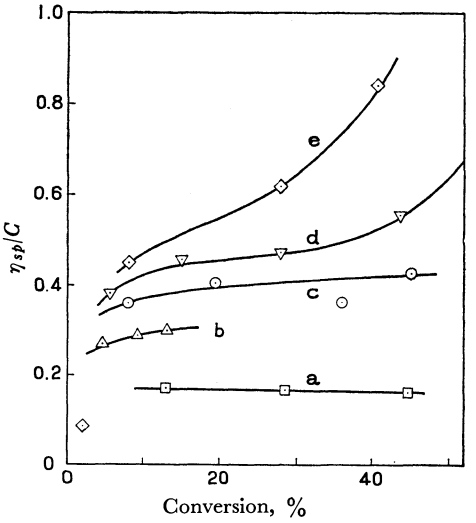

Fig. 7. Effect of the monomer concentration on the molecular weight of resultant polymers in nitrobenzene at 30°C.
Polymerization conditions are the same as in Fig. 3. $[M]_0$; a(□): 0.55, b(△): 0.83, c(○): 1.0, d(▽): 1.1 and e(◇): 2.2 mol./l.

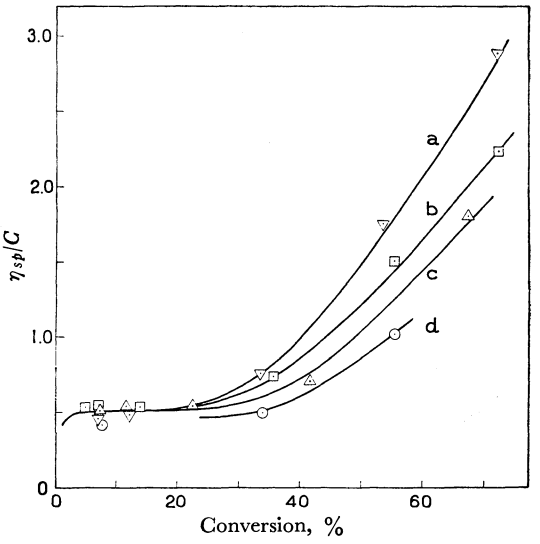

Fig. 8. Effect of the catalyst concentration on the molecular weight of resultant polymers at low monomer concentration in nitrobenzene at 30°C.
$[M]_0$; 1.1 mol./l., $[H_2O]$; 2.4 mmol./l., $[BF_3 \cdot O(C_2H_5)_2]$; a(▽): 2.5, b(□): 5.0, c(△): 10 and d(○): 20 mmol./l.

to 1.1 mol./l. The rate of polymerization with respect to this system has already been reported in a previous paper,[2] Figures 8 and 9 show the effects of the concentrations of the catalyst and of water respectively. In both cases the molecular weight was nearly constant, independent of the conversion, up to 30%. Figure 10 was

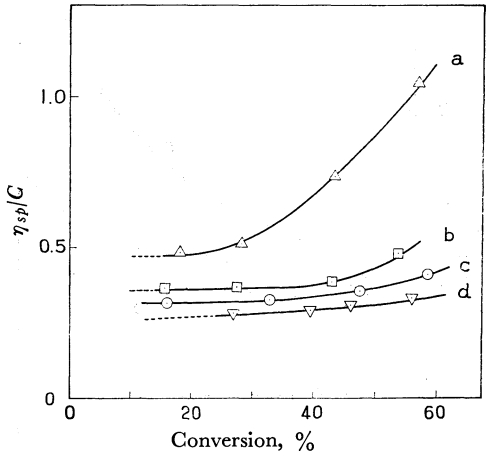

Fig. 9. Effect of the water concentration on the molecular weight of resultant polymers at low monomer concentration in nitrobenzene at 30°C. $[M]_0$; 1.1 mol./l., $[BF_3 \cdot O(C_2H_5)_2]$; 10 mmol./l., $[H_2O]$; a(△): 2.2, b(□): 4.0, c(○): 5.9 and d(▽): 7.8 mmol./l.

obtained upon plotting the initial monomer concentration against η_{sp}/C at a 10% conversion as determined graphically from Fig. 7. It may be suggested that the polymerization behavior at a monomer concentration below about 1 mol./l. differs from that at a monomer concentration larger than 1 mol./l.

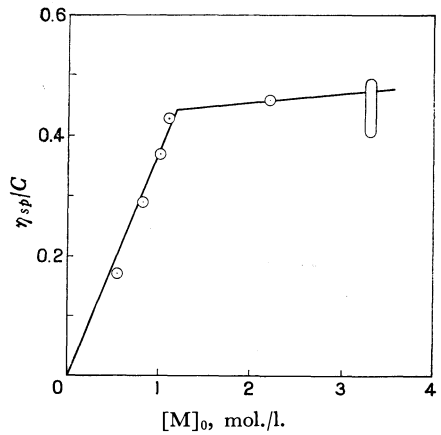

Fig. 10. Relationship between the molecular weight of polymers and the initial concentration of monomer at 10% conversion.
Calculated from Fig. 7.

The Kinetic Order of Monomer Concentration as Determined from the Course of Polymerization.—The kinetic order of the monomer concentration to the polymerization rate can be determined from the relation between the polymerization rate and the residual monomer concentration at a settled time in the time-conversion curve.

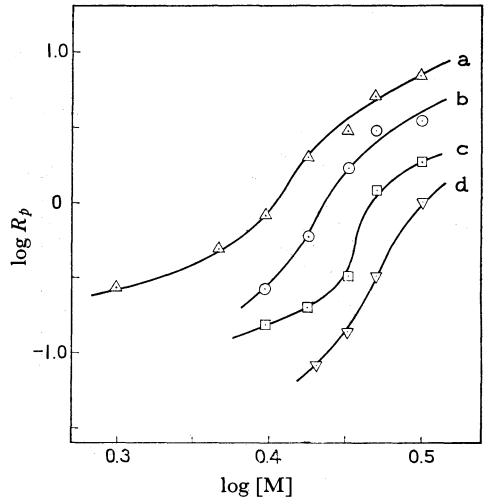

Fig. 11. Relationship between the rate of polymerization and the residual monomer concentration in the course of polymerization in ethylene dichloride at various temperatures.
$[M]_0$; 3.3 mol./l., $[BF_3 \cdot O(C_2H_5)_2]$; 5.0 mmol./l., Polymerization temp.; a(△): 46, b(○): 38.5, c(□): 30 and d(▽): 23°C

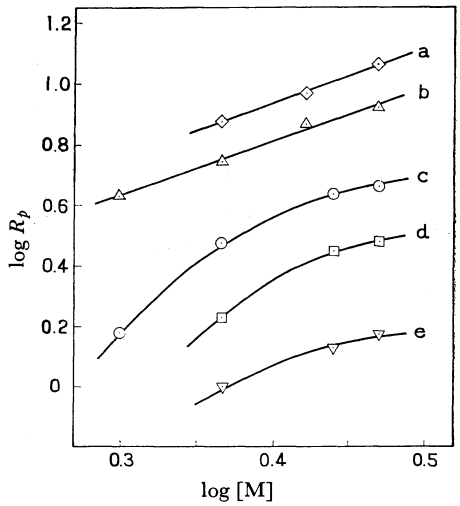

Fig. 12. Relationship between the rate of polymerization and the residual monomer concentration in the course of polymerization in nitroethane at various temperatures.
$[M]_0$; 3.3 mol./l., $[BF_3 \cdot O(C_2H_5)_2]$; 2.5 mmol./l., $[H_2O]$; 2.7 mmol./l., Polymerization temp.; a(◇): 50, b(△): 45, c(○): 38, d(□): 30 and e(▽): 23°C

The results of the analysis of the time-conversion curves of polymerization carried out in the various solvents are shown in Figs. 11, 12 and 13, where the concentrations of the monomer and of the catalyst were fixed and where only the reaction temperature was varied. (All the time-conversion curves will be shown in the fifth paper of this series.)

Excluding the complicated behavior in ethylene dichloride and that at a very low temperature, it may be concluded that the kinetic order of monomer concentration as determined from the course of polymerization is close to 2.

Although an abnormality was found in the relation between the conversion and the molecular weight in nitrobenzene at a low initial monomer concentration, the kinetic order of monomer concentration as determined from the course of polymerization was close to 2 in these systems, much as in systems with a high monomer concentration.

Discussion

The relation between the initial monomer concentration and the polymerization rate is very complicated, as is the relation between the catalyst or water concentration and the polymerization rate. Particularly, it was found that the initial polymerization rate is proportional to the sixth power of the initial monomer concentration in nitrobenzene

On the other hand, the kinetic order of the monomer as determined from the course of the time-conversion curve was close to 2 over a wide range of conversion in a polar solvent such as nitrobenzene, as is shown in Fig. 13. The constant kinetic order of the monomer over the wide range of conversion suggests that, in spite of the heterogeneous polymerization, a kinetic treatment is possible just as in an homogeneous polymerization. In the polymerization at a low temperature and in a less-polar solvent, however, the polymerization rate decreased remarkably in the course of the polymerization reaction. This may be due to the fact that the concentration of the active center was decreased remarkably by the precipitation of the resultant polymers, including catalysts. In a less-polar solvent it may be also considered that the rapid decrease in the polymerization rate in the course of the polymerization reaction is caused by the consumption of water as a co-catalyst.

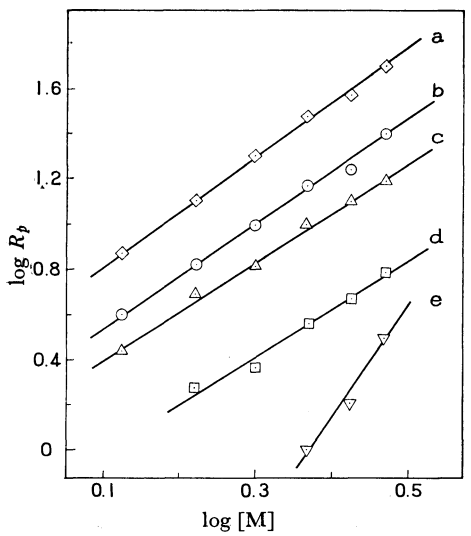

Fig. 13. Relationship between the rate of polymerization and the residual monomer concentration in the course of polymerization in nitrobenzene at various temperatures.
$[M]_0$; 3.3 mol./l., $[BF_3 \cdot O(C_2H_5)_2]$; 2.5 mmol./l., $[H_2O]$; 3.6 mmol./l., Polymerization temp.; a(◇): 30, b(△): 23, c(○): 15, d(□): 8.0 and e(▽): 3.0°C

While the kinetic order of the monomer as determined from the course of polymerization was close to 2, the kinetic order of the initial monomer concentration was extraordinarily large in the polar solvent. This suggests that the monomer or solvents participate in processes other than the propagation reaction. In a previous paper,[1] the relation between the polymerization conditions and the molecular weight of the polymers formed was explained on the assumption of the simple elementary reactions. The expression for the rate of polymerization derived from such simple elementary reactions, however, can not explain the kinetic order of the monomer. An explanation of this will be given in the next paper.[4]

Another remarkable result of the change in the monomer concentration was that, at a low monomer concentration, the molecular weight of the polymers formed was constant, independent of the conversion up to a 20—40% conversion in nitrobenzene.

In a previous paper[1] the increase in the molecular weight of the polymers formed with the conversion at the initial stage of polymerization was considered to be due mainly to the rate of the initiation reaction being larger than that of the propagation and other reactions[5] It has been supposed that, for this reason, in the cationic polymerization of trioxane the chain carrier is not a carbonium ion, but a oxonium ion which is stabilized by the solvation of the former with monomers. The formation of the oxonium ion in the polymerization of cyclic ethers is due to the instability of the corresponding carbonium ion and to the high concentration of ether groups in the reaction system.[3] Therefore, if the carbonium ion is stabilized and if the concentration of ether groups is small, it may be expected that a carbonium ion with a large reactivity exists and that the rate of the propagation reaction will increase. That is, in a solvent with great solvation ability, such as nitrobenzene, the carbonium ion is stabilized and, as the monomer concentration is small (i. e., if

3) E. g., A. M. Eastham, "The Chemistry of Cationic Polymerization," Ed. by P. H. Plesch, Pergamon Press, London (1963), p. 401.
4) T. Miki, T. Higashimura and S. Okamura, This Bulletin, **39**, 41 (1966).
5) T. Kagiya, M. Hatta and K. Fukui, *Chem. High Polymers Japan* (*Kobunshi Kagaku*), **20**, 737 (1963).

the concentration of the ether groups which solvate the carbonium ion is small), the active end will be able to exist in the form of the carbonium ion. Therefore, in the polymerization of trioxane in nitrobenzene at a low monomer concentration, the molecular weight of the polymers will not vary with the conversion as in the polymerization of vinyl monomers. The increase in the molecular weight in the course of polymerization at a high conversion may be due to the consumption of a chainbreaking or transfer reagent during the polymerization.

Of course, there is another possible explanation of this phenomenon. If the rate of the initiation reaction is decreased in the polymerization at a low monomer concentration in nitrobenzene, we will observe the more usual relationship, in which the molecular weight of the polymer is independent of the conversion.[5] This possibility will be discussed in the next paper.[4]

On the other hand, the cationic polymerization of 3, 3-bis(chloromethyl)oxethane (BCMO) is a typical example of how the reaction proceeds through the oxonium ion. In the polymerization of BCMO the molecular weight of the polymers formed was independent of the conversion.[6,7] From this point of view, it may be unreasonable to conclude that the chain carrier in the polymerization of trioxane in nitrobenzene at a low monomer concentration is not an oxonium ion. However, it could also be concluded that the rate of the initiation reaction is not so large as that of the propagation reaction. To clarify the nature of the chain carrier, a further investigation must be carried out.

6) J. B. Rose, *J. Chem. Soc.*, **1956**, 542.
7) I. Penczek and S. Penczec, *Makromol. Chem.*, **67**, 203 (1963).

BULLETIN OF THE CHEMICAL SOCIETY OF JAPAN VOL. 39 36—41 (1966)

Kinetic Studies of the Solution Polymerization of Trioxane Catalyzed by $BF_3 \cdot O(C_2H_5)_2$. IV. The Change in the Formaldehyde Concentration during Polymerization

By Tetsuro MIKI, Toshinobu HIGASHIMURA and Seizo OKAMURA

Department of Polymer Chemistry, Kyoto University, Sakyo-ku, Kyoto

(Received April 5, 1965)

In the solution polymerization of trioxane catalyzed by $BF_3 \cdot O(C_2H_5)_2$ and boron fluoride, the dependence of the yield of CH_2O produced in the induction period on the polymerization conditions has been studied at 30°C. In the case of the $BF_3 \cdot O(C_2H_5)_2$ catalyst, the formation of CH_2O has been recognized in *n*-hexane just after the addition of the catalyst while no induction period of the polymerization was seen. In polar solvents, both the formation of CH_2O and the polymerization were retarded as the water concentration increased. In these systems the concentration of the CH_2O formed changed with time, and no equilibrium or stationary concentration was recognized. In the case of the boron fluoride catalyst, an increase in the water concentration remarkably increased the induction period, also. For either catalyst the induction period was not decreased by the addition of CH_2O to the polymerization system in advance of the catalyst addition. Therefore, it has been deduced that, in the polymerization system catalyzed by $BF_3 \cdot O(C_2H_5)_2$, the polymerization and depolymerization reaction took place simultaneously and that the induction period was caused by water, which inhibits the formation of high polymers.

In the solution polymerization of trioxane by an acidic catalyst, an induction period and the formation of formaldehyde (CH_2O) have been recognized under certain conditions. Kern et al.[1] considered that, during the initial stage of polymerization, a certain concentration of CH_2O was obtained by the depolymerization of CH_2O from the active centers. Monomeric CH_2O must be present in an equilibrium concentration before the polymerization of trioxane can take place; they regarded the induction period as the time during which such a concentration of CH_2O was obtained. Thereafter, kinetic studies of the induction period of the polymerization were carried out by Kučera[2] and by Rakova.[3] While they have agreed that

1) W. Kern and V. Jaacks, *J. Polymer Sci.*, **48**, 399 (1960).

2) M. Kučera and E. Spousta, ibid., **A2**, 3443 (1964).

3) G. V. Rakova, L. M. Ramanov and N. S. Enikolopyan, *Vysokomol. Soed.*, **6**, 2178 (1964).

the free CH_2O produced at the initial stages of polymerization reacts rapidly with the catalyst to form the active centers, they differed on the relationship to the yield of CH_2O during polymerization. Moreover, since they worked under different polymerization conditions, it is impossible to apply their results to our system.

For the present paper, the yield of CH_2O produced during the polymerization of trioxane catalyzed by $BF_3 \cdot O(C_2H_5)_2$ was measured under the same conditions as in the previous papers. For comparison, the polymerization catalyzed by boron fluoride was also carried out. Considering the relation between the induction period and the yield of CH_2O, it may be deduced that the induction period is caused mainly by water in the reaction system.

Experimental

The procedures of the polymerization except for the stopping of the reaction, and of the purification of the materials were the same as in the previous paper.[4] Commercial boron fluoride (Matheson Co., Inc., boron fluride content: 99.5%) was used without purification. In the case of the addition of CH_2O to the polymerization system, the necessary quantity of the formaldehyde solution was prepared by the thermal decomposition of polyoxymethylene at 250—300°C under nitrogen.

The concentration of CH_2O was determined by the sodium sulfite method.[5]

For the measurement of the concentration of CH_2O produced in the polymerization system, the polymerization at a fixed time was stopped by adding a certain quantity of a 1 M sodium sulfite aqueous solution, in which the free sodium hydroxide had previously been neutralized, using thymolphthalein (0.1% alcohol soln.) as an indicator. When necessary, the polymers were separated and CH_2O was measured immediately after the polymerization was stopped. As this solution showed a blue color if CH_2O had been produced, it was quickly titrated by 1/20 N hydrogen chloride until its color disappeared. As the catalyst present in the polymerization system acts as an acid, sodium hydroxide corresponding to the initial catalyst concentration was added before the titration.

Results

The Formation of CH_2O in the Polymerization System Catalyzed by $BF_3 \cdot O(C_2H_5)_2$.—In the polymerization of trioxane catalyzed by $BF_3 \cdot O(C_2H_5)_2$ in various solvents, the relation between the reaction time and the yields of polymer and CH_2O was studied. Here "polymer" is defined as that polyoxymethylene which was insoluble in methanol, and the CH_2O formed means all those CH_2O units which could be measured by the method described in the Experimantal section.

In *n*-hexane, as Fig. 1 shows, the polymerization took place without any induction period. The formation of CH_2O could be detected immediately after the addition of the catalyst (within 6 sec.), and the concentration of CH_2O was almost constant up to a 10% conversion. These results did not change even if the concentrations of catalyst and water were changed.

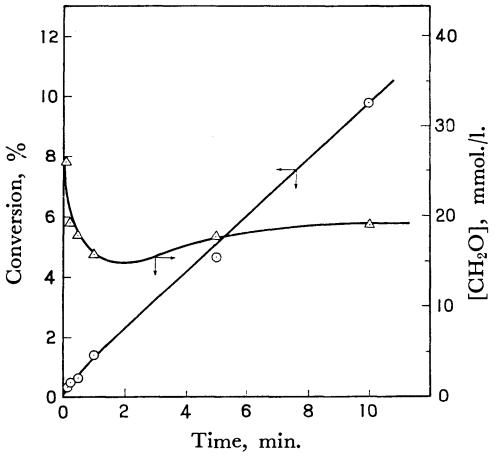

Fig. 1. Relationship between conversion and the concentration of produced CH_2O during polymerization in *n*-hexane catalyzed by $BF_3 \cdot O(C_2H_5)_2$ at 30°C.
$[M]_0$; 0.35 mol./l., [C]; 2.0 mmol./l., $[H_2O]$; 0.8 mmol./l.

In ethylene dichloride, as is shown in Fig. 2, an increase in the water concentration increased both the initial rate of polymerization and the induction period. At a low concentration

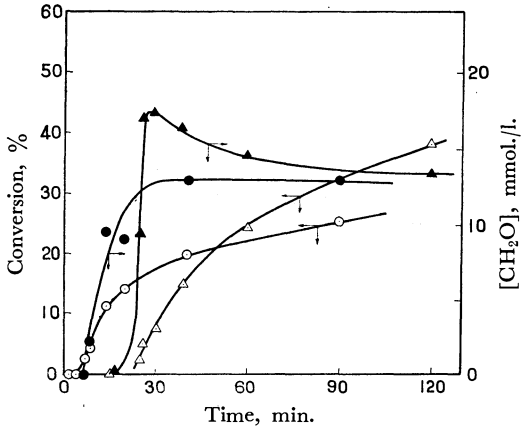

Fig. 2. Effect of water on the rate of polymerization and the concentration of produced CH_2O during polymerization in ethylene dichloride catalyzed by $BF_3 \cdot O(C_2H_5)_2$ at 30°C.
$[M]_0$; 3.3 mol./l., [C]; 10 mmol./l., $[H_2O]$; ○ and ●: 2.3, △ and ▲: 9.8 mmol./l.

4) T. Higashimura, T. Miki and S. Okamura, This Bulletin, **38**, 2067 (1965).
5) J. Frederic Walker, "Formaldehyde," Reinhold Publishing Corporation, New York (1953), Chap. 18.

of water the induction period for the formation of CH_2O was short (CH_2O was found just after the production of polymer), while at a high concentration of water the induction period for the formation of CH_2O was long; here the formation of CH_2O and the polymerization occurred simultaneously.

In nitrobenzene we studied two systems, in one of which the concentration of water was low and, in the other, extremely high. In the former system, as Fig. 3 shows, both the polymer and CH_2O were produced less than one minute after the addition of the catalyst. The maximum concentration of CH_2O was about 15 mmol./l., as in ethylene dichloride. The concentration of the CH_2O formed tended to decrease during the course of the polymerization. However, in a system containing much water, a large quantity of CH_2O was produced during the induction period, the concentration of the CH_2O decreased just before

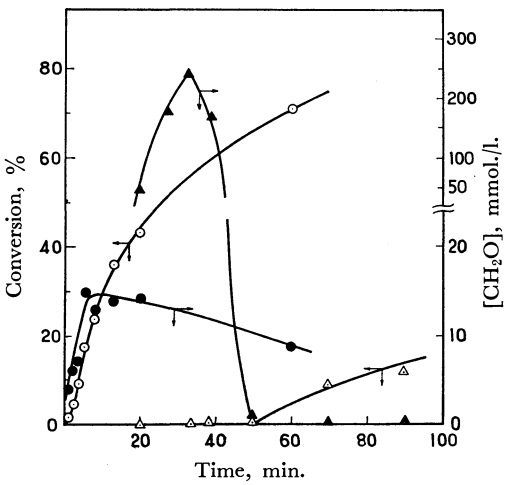

Fig. 3. Effect of water on the rate of polymerization and the concentration of produced CH_2O during polymerization in nitrobenzene catalyzed by $BF_3 \cdot O(C_2H_5)_2$ at 30°C.
$[M]_0$; 1.1 mol./l., [C]; 10 mmol./l., $[H_2O]$; ○ and ●: 2.2, △ and ▲: 18.6 mmol./l.

polymerization occurred, and no CH_2O was found in the system after the polymerization had taken place. So far as Fig. 3 is concerned, no equilibrium concentration of CH_2O was observed.

The Effect of CH_2O Added to the Polymerization System Catalyzed by $BF_3 \cdot O(C_2H_5)_2$.—The effect of the added CH_2O was studied in ethylene dichloride, using $BF_3 \cdot O(C_2H_5)_2$ as a catalyst. When CH_2O was present, the polymerization system became turbid immediately after the addition of the catalyst and the polymerization of trioxane seemed to occur. Nevertheless, the yield of polymers did not increase during a given period, and the true induction period was not changed by

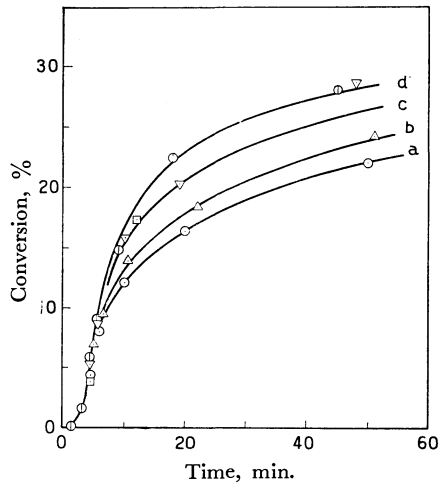

Fig. 4. Effect of addition of CH_2O on the rate of polymerization in ethylene dichloride catalyzed by $BF_3 \cdot O(C_2H_5)_2$ at 30°C. (The exact curve for *e* could not be determined.)
$[M]_0$; 3.3 mol./l., [C]; 10 mmol./l., $[H_2O]$; 1.7 mmol./l., $[CH_2O]$; a(○): 0, b(△): 14, c(▽): 28, d(◫): 58 and e(□): 93 mmol./l.

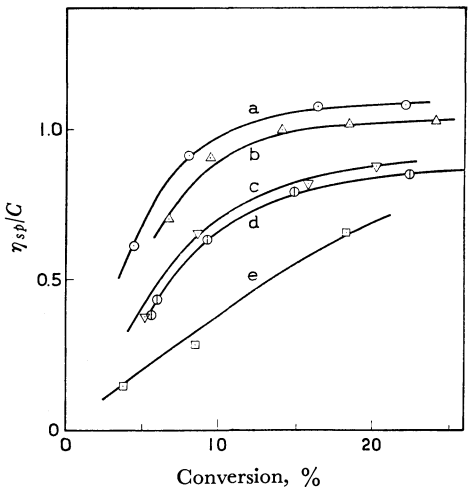

Fig. 5. Effect of addition of CH_2O on the molecular weight of resultant polymers in ethylene dichloride catalyzed by $BF_3 \cdot O(C_2H_5)_2$ at 30°C. Polymerization conditions are the same as in Fig. 4.

the addition of CH_2O, as Fig. 4 shows. These facts indicate that the added CH_2O was polymerized upon the addition of the catalyst, thus giving the observed turbidity. It apparently did not participate in the induction period of the polymerization of trioxane. Increasing the amount of CH_2O added did, however, increase the rate of the polymerization of trioxane and, as Fig. 5 shows, decrease the molecular weight of the resulting polymer. This same tendency was also caused by the increase

in the catalyst concentration.

The Formation of CH_2O in the Polymerization System Catalyzed by Boron Fluoride.— As the CH_2O formation in the polymerization system catalyzed by BF_3, which had been reported earlier,[1] differed from that of the $BF_3 \cdot O(C_2H_5)_2$ catalyst reported in this paper, we again studied the former polymerization system. The effect of the water concentration was studied in ethylene dichloride at a fixed catalyst concentration. As Fig. 6 shows, an increase in the water concentration increased the rate of polymerization and the induction period. When the water concentration was larger than that of the catalyst, the time-conversion curve assumed a typical S-shape, as in the results obtained by Kern et al.[1] in methylene chloride. The saturated yield of the polymer was found to be independent of the water concentration in the case of the BF_3 catalyst. Figure 7 shows that, although the molecular weight of the resulting polymers increased with the conversion (as in $BF_3 \cdot O(C_2H_5)_2$ catalysis), the water concentrations used did not affect the molecular weight of the polymers.

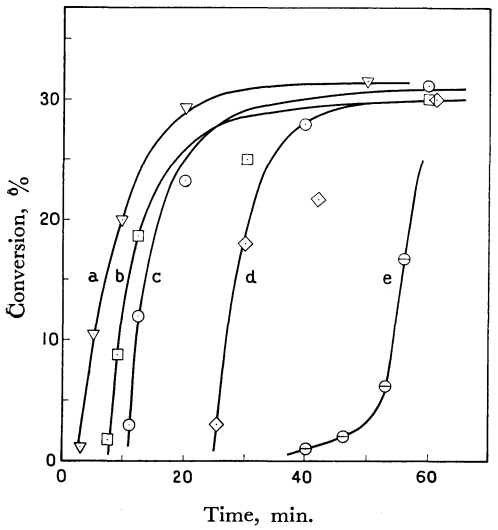

Fig. 6. Effect of water on the rate of polymerization in ethylene dichloride catalyzed by BF_3 at 30°C.
$[M]_0$; 4.4 mol./l., [C]; 3.8 mmol./l., $[H_2O]$; a(▽): 2.7, b(□): 3.6, c(○): 4.0, d(◇): 4.5 and e(⊖): 5.5 mmol./l.

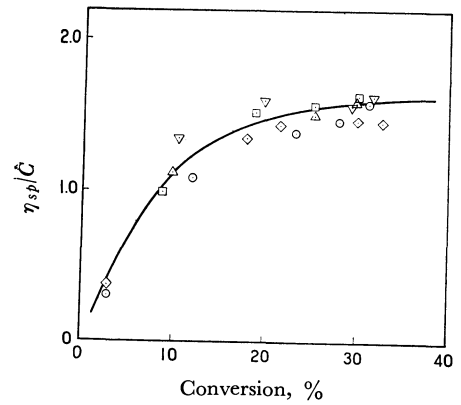

Fig. 7. Effect of water on the molecular weight of resultant polymers in ethylene dichloride catalyzed by BF_3 at 30°C.
$[M]_0$; 4.4 mol./l., [C]; 3.8 mmol./l., $[H_2O]$; ▽: 2.7, △: 3.4, □: 3.6, ○: 4.0 and ◇: 4.5 mmol./l.

In the same system the change in the concentration of CH_2O produced during the induction period of the polymerization was also measured. As Fig. 8 shows, CH_2O was produced during the induction period. When the concentration of CH_2O seemed to reach a maximum, the polymerization of trioxane took place. Thereafter, the concentration of CH_2O suddenly decreased. Here no equilibrium concentration of CH_2O was found, either. The change in the CH_2O concentration was so sudden both before and after the polymerization

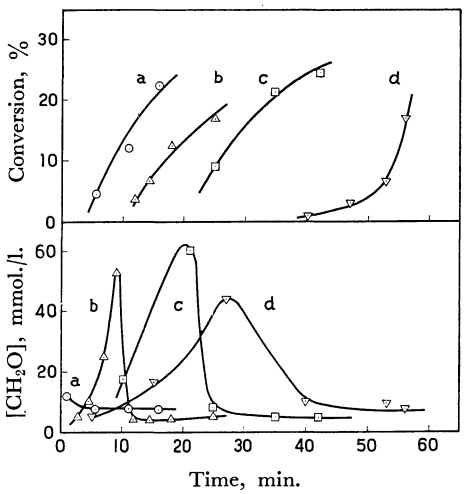

Fig. 8. Effect of water on the rate of polymerization and the concentration of produced CH_2O during polymerization in ethylene dichloride catalyzed by BF_3 at 30°C.
$[M]_0$; 4.4 mol./l., $[BF_3]$; a(○) and d(▽): 3.5 mmol./l., b(△) and c(□): 3.0 mmol./l., $[H_2O]$; a(○): 2.4, b(△): 2.2, c(□) 4.8 and d(▽): 5.5 mmol./l.

that the measurement of the maximum concentration of CH_2O was very difficult.

The Effect of the CH_2O Added to the Polymerization System Catalyzed by Boron Fluoride. — The effect of the added CH_2O on the polymerization reaction was studied in ethylene dichloride, as in the case of the $BF_3 \cdot O(C_2H_5)_2$ catalyst. Similarly to the case of the $BF_3 \cdot O(C_2H_5)_2$ catalyst, when CH_2O was present the reaction system became turbid just after the addition of

the catalyst, but the quantity of polymers was fairly small and did not increase during the settled period. As Fig. 9 shows, a small amount of the added CH_2O did not greatly affect the rate of polymerization and did not decrease the induction period. It was impossible to conclude that these results were caused only by the added CH_2O because of the possibilities that water came into the solvent during the preparation of the CH_2O solution by our method and that CH_2O reacted with water in the polymerization system.

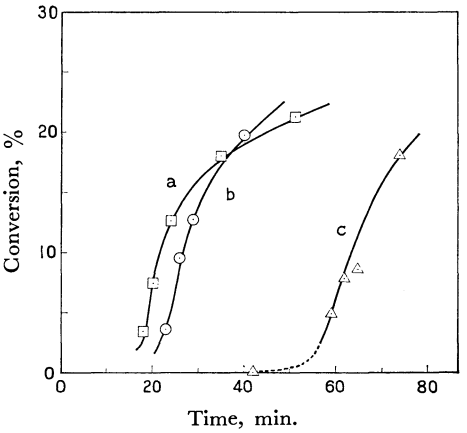

Fig. 9. Effect of addition of CH_2O on the rate of polymerization in ethylene dichloride catalyzed by BF_3 at 30°C.
$[M]_0$; 4.4 mol./l., $[BF_3]$; 2.5 mmol./l., $[H_2O]$; 2.0 mmol./l., $[CH_2O]$; a(□): 0, b(○): 25 and c(△): 71 mmol./l.

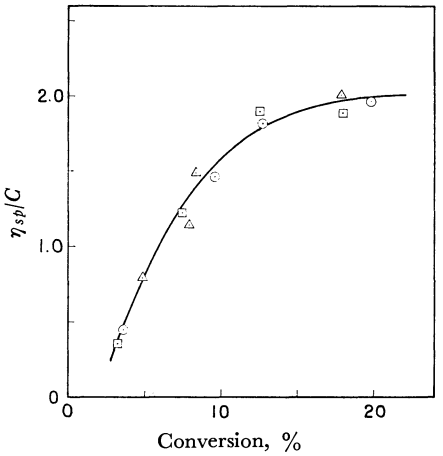

Fig. 10. Effect of addition of CH_2O on the molecular weight of resultant polymers in ethylene dichloride catalyzed by BF_3 at 30°C. (Polymerization conditions are the same as in Fig. 9.)

The molecular weight of the resulting polymers was not affected by the added CH_2O, as Fig. 10. shows. While in the case of the $BF_3{\cdot}O(C_2H_5)_2$ catalyst the addition of water and CH_2O decreased the molecular weight of the polymers, in the case of the BF_3 catalyst the addition of water and CH_2O did not affect the molecular weight of the polymers.

Discussion

In the cationic solution-polymerization of trioxane, the induction period of the polymerization and the formation of CH_2O during the polymerization have often been recognized. In Table I we have summarized our experimental results on the induction period. Here the relation between the induction period and the concentrations of the catalyst and of the monomer was too complicated to be explained quantitatively, as was the relation between the polymerization rate and the concentrations of the catalyst and of the monomer.

In *n*-hexane, no induction period of the polymerization was observed. This agrees with Rakova's result[3] in a non-polar solvent wherein the formation of CH_2O was recognized immediately after the addition of a catalyst. This is probably due to the facile depolymerization of the unsolvated growing-chain end.

On the other hand, our results in polar solvents showed that the factor which most greatly influences the induction period of the polymerization seemed to be the concentration of water. This relation was considered to hold not only in the case of the $BF_3{\cdot}O(C_2H_5)_2$ catalyst, but also in the case of the boron fluoride catalyst, as Fig. 6 shows. In the latter case, when the water concentration was about 1.5 times larger than that of the boron fluoride catalyst, a very long induction period was observed and the time-conversion curve assumed a typical S-shape. In earlier papers, this view has not been dealt with at all.

Kern et al.[1] have indicated that, in the polymerization of trioxane catalyzed by boron fluoride, the active chains were depolymerized, thus liberating free, monomeric CH_2O, whose concentration reached a certain value (i. e., the equilibrium concentration) before the polymerization reaction took place. This conception has been supported by

TABLE I. SUMMARY OF THE RELATIONSHIP BETWEEN INDUCTION PERIOD (t_i) AND REACTION CONDITIONS

Solvent	*n*-C_6H_{14}	C_6H_6	$(CH_2Cl)_2$	$C_2H_5NO_2$	$C_2H_5NO_2$
$[BF_3{\cdot}O(C_2H_5)_2]$	None	$t_i \propto 1/[C]^{0.6}$	$t_i \propto 1/[C]^{1.0}$	$t_i \propto 1/[C]^{1.7}$	$t_i \propto 1/[C]^{2.0}$
[Trioxane]	—	—	$t_i \propto 1/[M]^{1.3}$	—	$t_i \propto 1/[M]^{a*}$
$[H_2O]$	None	—	$[H_2O]\uparrow$ $t_i\uparrow$	—	$[H_2O]\uparrow$ $t_i\uparrow$

* *a* was a very large number, but the value could not be settled.

Kučera in the cationic polymerization of molten trioxane.[2]

In our results concerning the $BF_3 \cdot O(C_2H_5)_2$ catalyst, as long as the water content in the reaction system was not very large, the polymerization reaction and the formation of CH_2O took place simultaneously; we did not observe that the polymerization reaction occurred only when a certain concentration of CH_2O is present. As the change in the induction period was not observed when CH_2O had been added to the polymerization system, the conception of Kern et al.[1] can not be applied to the polymerization catalyzed by $BF_3 \cdot O(C_2H_5)_2$.

Rakova et al.[3] dealt quantitatively with the induction period in the solution-polymerization of trioxane. Considering that, in their results, the stationary concentration of CH_2O varied with the polymerization conditions, and also considering that in our results no stationary or equilibrium concentration was clearly recognized, it is doubtful whether the equilibrium concentration of CH_2O is present.

The behavior of a system containing a large amount of water should be considered, also. In general, an increase in the water concentration increased the induction period during which a high concentration of CH_2O was attained. We have defined "polymer" as the methanol-insoluble polyoxymethylene. Therefore, it seems that the polymerization does not occur if only the methanol-soluble oligomer is formed. Besides, it is well known[6] that, in water, this oligomer decomposes into CH_2O, the decomposition being facilitated by an acid or a base. As the determination of the CH_2O concentration was carried out by using a sodium sulfite aqueous solution, the free monomeric CH_2O could not be distinguished from the CH_2O unit which was decomposed from the oligomer. As water might act as a transfer agent or as an inhibitor and much more oligomer would be produced in the presence of much water, a large quantity of CH_2O might be measured experimentally during the induction period. The decrease in the concentration of CH_2O in the course of polymerization was probably due to the growth of these oligomers to high polymers. Without exact knowledge of the concentration of the free monomeric CH_2O in the polymerization system, however, it will be difficult to discuss the induction period in detail. At any rate, it is clear that the induction period is caused by water, which inhibits the formation of high polymers.

Such aspects of the polymerization catalyzed by $BF_3 \cdot O(C_2H_5)_2$ as the effect of water differed from those of the polymerization catalyzed by boron fluoride; it must be established by future studies whether a consistent mechanism can be applied to both systems.

6) J. Löbering, *Ber.*, **69**, 1884 (1936).

BULLETIN OF THE CHEMICAL SOCIETY OF JAPAN VOL. 39 41—46 (1966)

Kinetic Studies of the Solution Polymerization of Trioxane Catalyzed by $BF_3 \cdot O(C_2H_5)_2$. V. The Effect of the Solvent and of the Polymerization Temperature

By Tetsuro MIKI, Toshinobu HIGASHIMURA and Seizo OKAMURA

Department of Polymer Chemistry, Kyoto University, Sakyo-ku, Kyoto

(Received April 5, 1965)

The effect of the polarity of solvents in the solution polymerization of trioxane catalyzed by $BF_3 \cdot O(C_2H_5)_2$ has been studied. While the molecular weight of the resulting polymer is almost independent of the kind of solvent, the rate of polymerization in a polar solvent is large at a high initial monomer concentration. At a low monomer concentration, however, the rate of polymerization in a non-polar solvent is larger than that in a polar solvent. This fact can probably be explained by observing that, at the low monomer concentration, the initiation species produced from the catalyst is solvated by the solvent molecule rather than by trioxane because of the small basicity of trioxane. The activation energies of the over-all polymerization rate as determined in ethylene dichloride, nitroethane and nitrobenzene are all about 16 kcal./mol. The decrease in the molecular weight of the resulting polymers caused by raising the temperature is very small.

In the cationic polymerization of vinyl monomers, the dielectric constant of the reaction system remarkably affects the rate of polymerization and the molecular weight of the resultant polymers. It is well known that in the polymerization of styrene, the rate of polymerization increases with the dielectric constant.[1] However, the relation between the molecular weight of the polymers and the dielectric constant varies with the kind of solvent. While in the cationic polymerization of the styrene and its derivatives the molecular weight of the resultant polymers increases with the dielectric constant,[1,2] a reverse relation is shown in the polymerization of isobutene[3] and of vinyl ethers.[4] This may be ascribed mainly to the difference between the mechanisms of the monomer transfer reactions.

If, in the cationic polymerization of trioxane, an ionic active species is produced by the interaction between the neutral molecules, as in the cationic polymerization of vinyl monomers, it is to be expected that the increase in the dielectric constant of the reaction system will increases the rate of polymerization.

In the present paper we will try to clarify the effect of the polarity of solvents in the ring-opening polymerization. Therefore, the findings on solvent variation will be summarized from the previous papers in this series and then the temperature dependence in several solvents will be studied. It will be found that the effect of a sovlent in the cationic polymerization of trioxane is not always the same as in the polymerization of vinyl monomers.

Experimental

The procedures of the polymerization and of the purification of the materials were the same as in the previous papers.[5]

Results

The Effect of the Solvent.—As the kinetic orders of the monomer and catalyst to the polymerization rate are changed by the kind of solvent, it was impossible to compare the polymerization rates in various solvents exactly. Figure 1, therefore, compares the polymerization rates in various solvents on the condition that the concentrations of the reagents were selected to be as equal as possible. From this result it can be seen that, at a high monomer concentration (3.3 mol./l.), the polymerization rate increases with the dielectric constant. Nitrobenzene is also found to be a very useful solvent, one in which high polymers can be obtained at high yields.

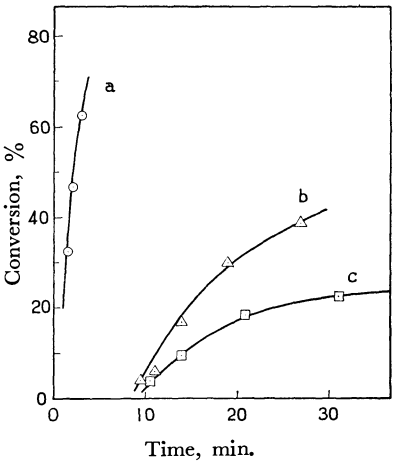

Fig. 1. Effect of a kind of solvents on the rate of polymerization at 30°C.
$[M]_0$; 3.3 mol./l., [C]; 2.5 mmol./l., Solvent; a(○); nitrobenzene ($[H_2O]$: 3.6 mmol./l.), b(△): nitroethane (2.7) and c(□): ethylene dichloride (2.9)

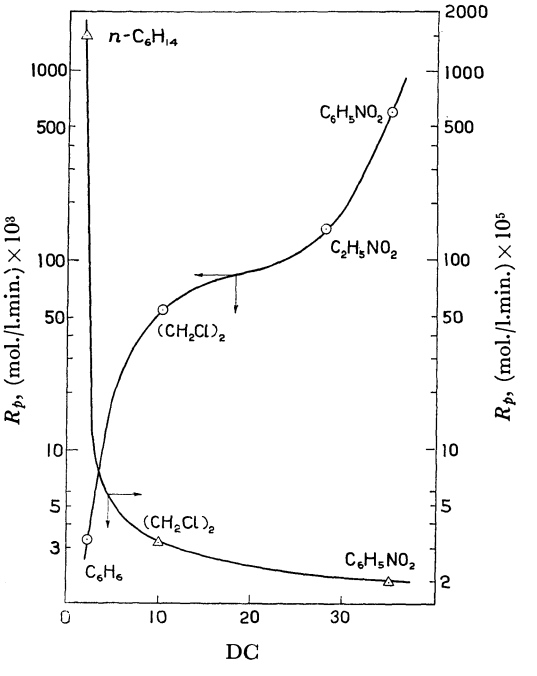

Fig. 2. Effect of a kind of solvents on the initial rate at low and high monomer concentrations at 30°C.
$[H_2O]$; 2–3 mmol./l., $[M]_0$; ○: 3.3 and △: 0.4 mol./l., $[C]_0$; ○: 2.5 and △: 10 mmol./l.

1) D. C. Pepper, *Trans. Faraday Soc.*, **45**, 397 (1949); J. George and H. Wechsler, *J. Polymer Sci.*, **6**, 725 (1951); T. Higashimura, and S. Okamura, *Chem. High Polymers Japan* (*Kobunshi Kagaku*), **13**, 338 (1956).
2) E. g., Y. Sakurada, T. Higashimura and S. Okamura, *J. Chem. Soc. Japan, Ind. Chem. Sect.* (*Kogyo Kagaku Zassi*), **61**, 1640 (1958); Y. Imanishi, S. Matsushita, T. Higashimura and S. Okamura, *Makromol. Chem.*, **70**, 68 (1964).
3) Y. Imanishi, T. Higashimura and S. Okamura, *Chem. High Polymers Japan* (*Kobunshi Kagaku*), **18**, 333 (1961).
4) Y. Imanishi, H. Nakayama, T. Higashimura and S. Okamura, ibid., **19**, 154, 565 (1962).
5) T. Higashimura, T. Miki and S. Okamura, This Bulletin, **38**, 2067 (1965); **39**, 25 (1966).

As *n*-h exane did not have a large solubility of trioxane, the rate of polymerization in *n*-hexane was compared with the rates in polar solvents at only a low monomer concentration. In this case, as the experimental data were not obtained at a very low monomer concentration in the polar solvents, the extrapolated values were used as the rates in the polar solvents. Figure 2 shows the resultant relation between the dielectric constant of the solvent and the rate of polymerization. At a high monomer concentration, as Fig. 1 shows, the rate of polymerization in a polar solvent was larger than that in a non-polar solvent, but the reverse tendency was found at the low monomer concentration. Although it may be difficult to compare these data quantitatively because some of them are extrapolated, this tendency seems to be correct qualitatively.

On the other hand, Fig. 3 shows the molecular weight of the polymers which should be produced under the conditions corresponding to those in Fig. 2. Here the molecular weight was compared at a low conversion (10%). It can be said that the molecular weight of the resultant polymers is independent of the kind of solvent if the other conditions are equal.

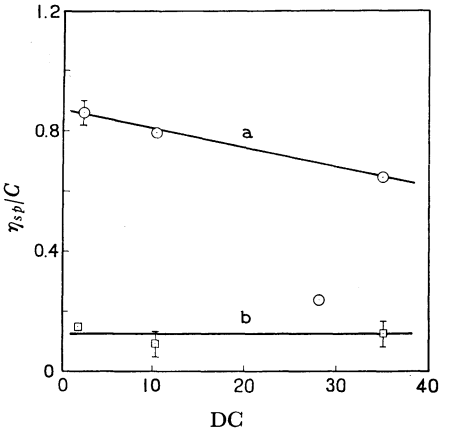

Fig. 3. Effect of a kind of solvents on the molecular weight of resultant polymers at conversion 10%.
Polymerization conditions are the same as in Fig. 2. $[M]_0$; a(○): 3.3 and b(□): 0.4 mol./l.

The Effect of the Polymerization Temperature.—In the polymerization of trioxane at a high monomer concentration, the increase in the polarity of the solvent remarkably increased the rate of polymerization. Therefore, the dependence of the polymerization reaction on the reaction temperature was studied in various solvents.

Figures 4, 5 and 6 show the time-conversion curves at various temperatures in ethylene dichloride, nitroethane and nitrobenzene respectively. The increaes in the reaction temperature increase the

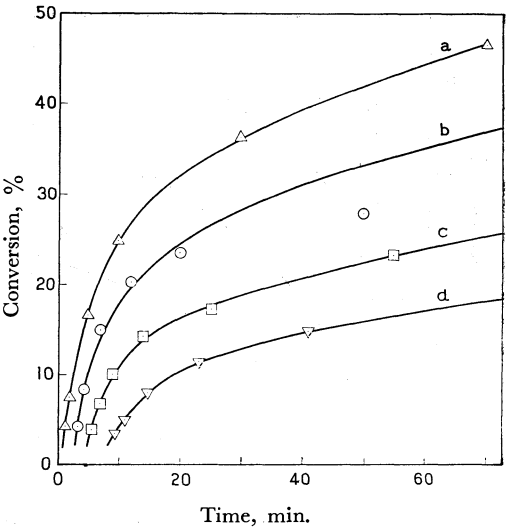

Fig. 4. Effect of temperature on the rate of polymerization in ethylene dichloride.
$[M]_0$; 3.3 mml./l., [C]; 5.0 mmol./l., $[H_2O]$; 2.5 mml./l., Polymerization temp.; a(△): 46.0, b(○): 38.5, c(□): 30.0 and d(▽): 23.0°C

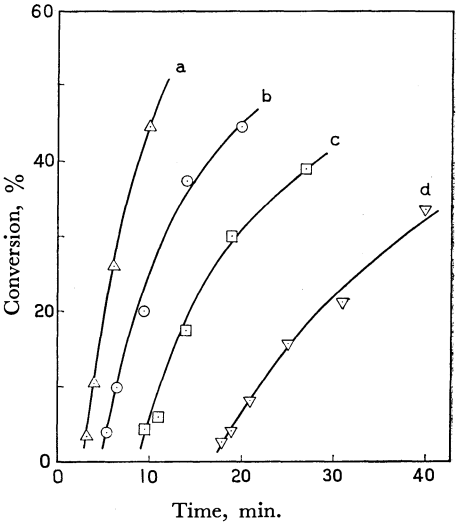

Fig. 5. Effect of temperature on the rate of polymerization in nitroethane.
$[M]_0$; 3.3 mol./l., [C], 2.5 mmol./l., $[H_2O]$; 2.7 mmol./l., Polymerization temp.; a(△): 45.0, b(○): 38.0, c(□): 30.0 and d(▽): 23.0°C

rate of polymerization and decreased the induction period of the polymerization. Except for the polymerization at a low temperature, the reaction order of the monomer as determined from the course of polymerization, as described in the previous paper,[6] was independent of the reaction temperature.

The activation energy determined from the initial

6) T. Higashimura, T. Miki and S. Okamura, ibid., **39**, 31 (1966).

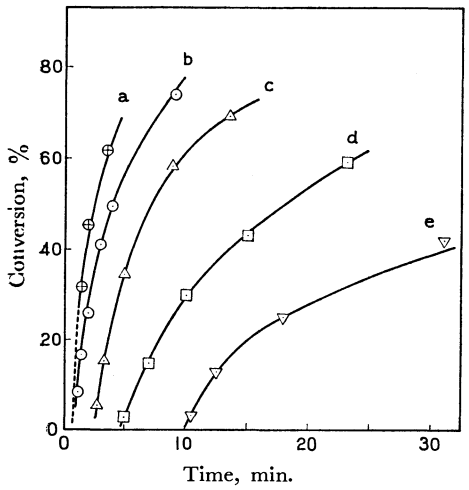

Fig. 6. Effect of temperature on the rate of polymerization in nitrobenzene.
$[M]_0$; 3.3 mol./l., [C]; 2.5 mmol./l., $[H_2O]$; 3.6 mmol./l., Polymerization temp.; a(⊕): 30.0, b(○): 23.0, c(△): 15.0, d(□): 8.0 and e(▽): 3.0°C

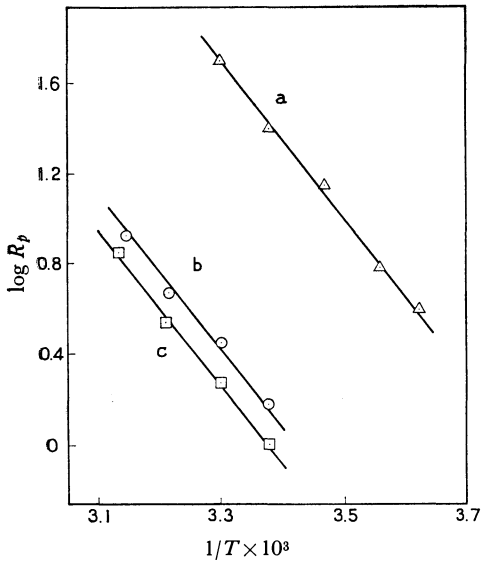

Fig. 7. Arrhenius plot of the initial rate in various solvents.
Calculated from Figs. 4—6. Solvent; a(△): nitrobenzene, b(○): nitroethane and c(□): ethylene dichloride

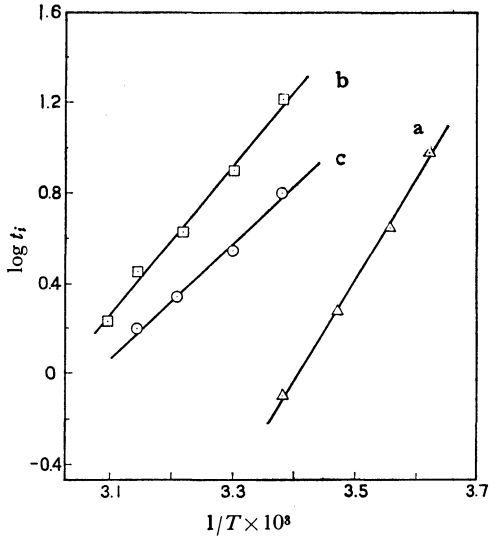

Fig. 8. Arrhenius plot of the induction period in various solvents.
Calculated from Figs. 4—6. Solvent; a(△): nitrobenzene, b(□): nitroethane and c(○): ethylene dichloride

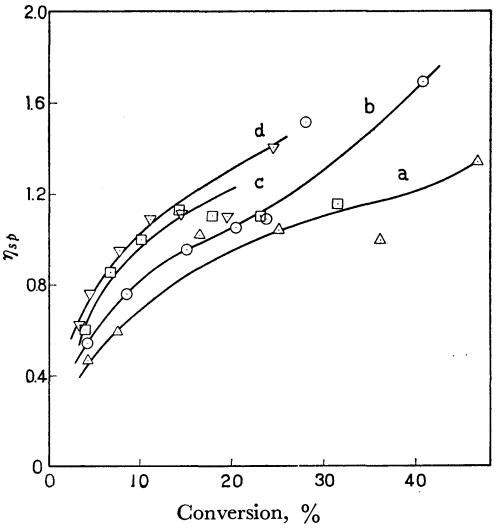

Fig. 9. Effect of temperature on the molecular weight of resultant polymers in ethylene dichloride.
Polymerization conditions are the same as in Fig. 4. Temp.; a(△): 46.0, b(○): 38.5, c(□): 30.0 and d(▽): 23.0°C

rate of these curves was about 16 kcal./mol., as is shown in Fig. 7, in each solvent,

By plotting the logarithms of the induction period against the reciprocal of temperature, the linear correlation was obtained in all the solvents, as Fig. 8 shows. The activation energy with respect to the induction period, as determined from the slope of each line in Fig. 8, was smaller the smaller the dielectric constant of the solvent.

The polymerization temperature also affected the molecular weight of the resultant polymers. Figures 9, 10 and 11 show the relations between the conversion and the molecular weights of the polymers obtained in Figs. 4, 5 and 6 respectively. An increase in the polymerization temperature decreased the molecular weight of the resultant

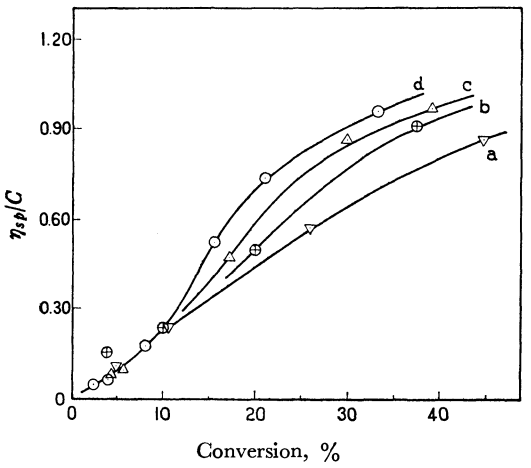

Fig. 10. Effect to temperature on the molecular weight of resultant polymers in nitroethane. Polymerization conditions are the same as in Fig. 5. Temp.; a(▽): 45.0, b(⊕): 38.0, c(△): 30.0 and d(○): 23.0°C

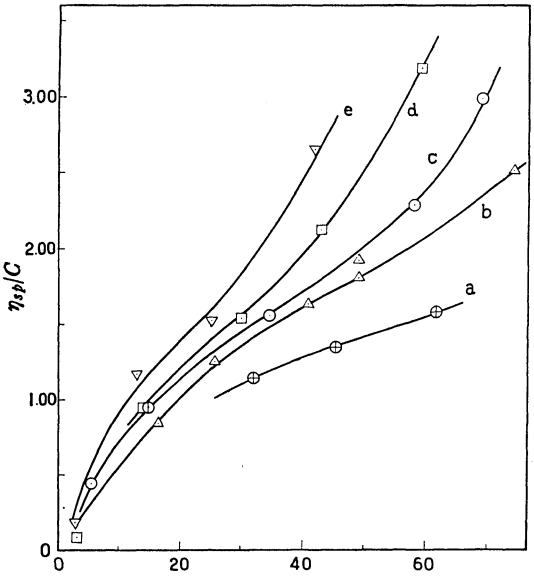

Fig. 11. Effect of temperature on the molecular weight of resultant polymers in nitrobenzene. Polymerization conditions are the same as in Fig. 6. Temp.; a(⊕): 30.0, b(△): 23.0, c(○): 15.0, d(□): 8.0 and e(▽): 3.0°C

polymers. This tendency has also been found in the polymerization of trioxane in toluene, a non-polar solvent.[7]

Discussion

One of the most remarkable characteristics of the solution polymerization of trioxane is the effect of the polarity of the solvent on the polymerization rate. At a high monomer concentration, an increase in the dielectric constant of the solvent increased the rate of polymerization, as in vinyl polymerization. On the other hand, at a low monomer concentration, an increase in the dielectric constant decreased the rate of polymerization. As the molecular weight of the polymers produced did not greatly depend on the dielectric constant of the solvent, the change in the polymerization rate with the kind of solvent is probably caused by the initiation reaction.

In general, an increase in the dielectric constant of a solvent ought to facilitate a reaction in which the neutral catalyst molecule itself dissociates to produce an ionic species. Therefore, the behavior observed at the high monomer concentration is probably normal. The unusual behavior observed at the low monomer concentration suggests that some reactions which decrease the polymerization rate are present. This postulate is also supported by the large kinetic order of the initial monomer concentration in a olar solvent.[6] It may be considered that the catalyst (AB) dissociates to the ion-pairs ($A^+—B^-$), and that they then are stabilized by solvation with monomer (M) or solvent molecules (S), as is shown in Eq. 1. The solvation of ion-pairs with a monomer implies the

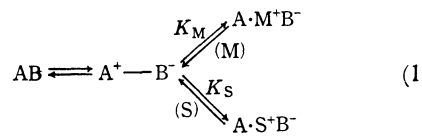

(1)

occurrence of the initiation reaction. As A^+ will be solvated mainly with monomers at a high monomer concentration, the rate-determining step in the initiation reaction is possibly the process in which AB dissociates. In this case, the dissociation constant, K_1, increases with the dielectric constant, and the active centers (AM^+) are rapidly formed as the dielectric constant of the system increases.

At a low monomer concentration the formation of the active centers is in competition with the reaction in which A^+ is solvated with solvent molecules. It has been reported that the trioxane molecule has no great complex-forming ability with the carbonium ion indicated in Eq. 2, i. e., the basicity of trioxane is not very large.[8] In

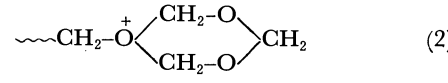

(2)

fact, in the copolymerization of 3, 3-bis(chloromethyl)oxethane (BCMO) with trioxane, the copolymer was not obtained, was obtained only the

7) T. Higashimura, M. Tomikawa and S. Okamura, *J. Chem. Soc. Japan, Ind. Chem. Sect.* (*Kogyo Kagaku Zasshi*), **65**, 712 (1962).
8) S. Iwatsuki, M. Okada, Y. Yamashita and Y. Ishii, ibid., **67**, 1236 (1964).

homopolymer of BCMO.[9] Therefore, it may be expected that, in a polar solvent, K_S will be larger than K_M and that the active center will be produced with difficulty at a low monomer concentration because A^+ will be solvated with the solvent and so become inert. It has been reported that nitro compounds act strongly as transfer agents in the cationic polymerization of styrene.[10] This is one instance in which a polar solvent may stabilize a carbonium ion. On the other hand, in a non-polar solvent such as *n*-hexane, A^+ is not stabilized by solvation with a solvent, but by solvation with a monomer. Such a consideration can explain qualitatively the dependence of the polymeriz ation rate onthe dielectric constant of the solvent.

If the relation indicated in Eq. 1 is valid, the large kinetic order of the initial monomer concentration in the polar solvent is understandable. That is, in the polar solvent, a decrease in the initial monomer concentration implies an increase in the solvent molecule (S), which so stabilizes A^+ that the active centers are not produced. Consequently, a decrease in the initial monomer concentration rapidly decreases the rate of polymerization.

Although the meaning of the induction period is not clear, it must be related to the time during which a certain amount of the active center is produced. It is also clear that the formation of the active centers is hindered by water. This may be explained by the idea which has been described above, the idea that the temperature coefficient is smaller, the smaller the dielectric constant of the solvent. That is, the destruction of the ionic active-center by a water molecule should be easier in a non-polar solvent than in a polar solvent.

The activation energy of the initial rate of polymerization in a polar solvent was independent of the kind of solvent. Although no detailed discussion can be carried out becuase of the obscurity of the elementary reactions in each solvent, it may be inferred that the reaction mechanisms in these halogenated and nitronized solvents is not graetly different. The activation energy in benzene, a non-polar solvent, was reported by Rakova et al.[11] to be 12 kcal./mol.; this value was estimated by a method different from ours.

The activation energy for the decomposition of polyoxymethylene catalyzed by acids has been reported to be about 19 kcal./mol.[12] Since the molecular weight of polymers decreased slightly as the reaction temperature was raised in our work, it is clear that the decomposition of the polymers during polymerization did not greatly affect the molecular weight.

9) T. Higashimura, Y. Kitagawa and S. Okamura, unpublished data.
10) D. H. Jenkinson and D. C. Pepper, *Proc. Roy. Soc.*, **A263** 82 (1961).
11) G. V. Rakova, L. M. Romanov and N. S. Enikolopyan, *Vysokomol. Soed.*, **6**, 2178 (1964).
12) J. Mejzlik, *Macromol. Chem.*, **59**, 184 (1963).

BULLETIN OF THE CHEMICAL SOCIETY OF JAPAN VOL. 39 46—52 (1966)

Silent Discharge Reactions in Aqueous Solutions. I. An Acidic Aqueous Solution of Ferrous Sulfate in Atmospheres of Helium and Argon*

By Akira YOKOHATA and Satoru TSUDA

Department of Chemistry, Faculty of Engineering, Hiroshima University, Senda-machi, Hiroshima

(Received April 6, 1965)

In an atmosphere of helium or argon, the silent discharge reactions of aqueous solutions have been investigated from the point of view of radiation chemistry. A discharge tube with two coaxial glass tubes was used. In a dilute oxygen-free aqueous solution of sulfuric acid, hydrogen peroxide appeared as a result of discharge. Also, the oxidation of ferrous ions to ferric ions has been found. It has been confirmed, first, that neither the effect of metastable excited states of helium and argon nor that of luminescence is serious, and, second, that the reaction may well be interpreted by taking into consideration the actions of slow electrons generated in the gas phase on the liquid water. The yield of hydrogen atoms plus hydroxyl radicals has been estimated from the yields of hydrogen peroxide and ferric ions. The ratios of the yield of hydrogen peroxide to that of radicals show that the silent discharge reaction corresponds to the reaction by ionizing radiation of high LET, the value of which apparently equals 3eV./Å in helium and 8 eV./Å in argon. The $G(Fe^{3+})$

* Presented in part at the 17th Annual Meeting of the Chemical Society of Japan, Tokyo, April, 1964.

value and the absorbed dose (E) estimated were, respectively, as follows: In helium: $G(Fe^{3+})=4.6$, $E=3.8\times10^6$ r./hr.; in argon: $G(Fe^{3+})=4.3$, $E=7.2\times10^6$ r./hr.

In the field of silent discharge reaction, the work has hitherto been chiefly confined to studies of the gas phase; the study of the solutions is, however, currently receiving increasing attention.[1,2] The discharge reactions in the gas phase have been investigated exhaustively,[3-5] and their reaction mechanisms have been elucidated from the point of view of the reactivity of active species. In the studies of liquids,[6-8] the reaction mechanisms have also been interpreted as the reactions of active species generated in an atmosphere to solutes or solvents; the actions on them of low-energy electrons generated in an atmosphere have been neglected or forgotten.

As far as we have been able to determine, few studies of the silent discharge reactions in aqueous solutions from the point of view of radiation chemistry by the low-energy electron generated in an atmosphere have been made. Moreover, their importance has not adequately been explored.

We began our studies with the purpose of rectifying these omissions and so explored the mechanism of the silent discharge reactions, comparing this mechanism with the findings of radiation chemistry. The method we have developed also makes it possible to determine the apparent energy absorbed in a solution by silent discharge if adequate chemical systems are selected.

In the present work the oxidation of ferrous ion in the dilute sulfuric acid solution, well known as a chemical dosimeter, has been studied, using helium or argon as an atmosphere[9]; as has already been pointed out by Davis,[1] the contributions of their metastable-excited states to chemical reactions, to, for example, the oxidation of ferrous ion to ferric ion, seem to be very small.

According to our experimental results, hydrogen peroxide is formed in the dilute sulfuric acid solution; ferrous ion is oxidized to ferric ion, and the yield of ferric ions is always larger than that which would be expected from the oxidation by the hydrogen peroxide formed. Now, assuming that the net effect by the slow electrons is similar to that of the usual ionizing radiation,[10] the yield of hydrogen atoms plus hydroxyl radicals can be estimated from the yields of hydrogen peroxide and ferric ions according to the well-established reaction mechanism. Moreover, the ratio of the yield of hydrogen peroxide to that of radicals shows clearly that the silent discharge reaction[11] in the aqueous solutions corresponds to the reactions by ionizing radiations of high LET. Also, the apparent dose rate in each case of helium and argon under our experimental conditions was estimated by considering carefully our findings on the relations of LET and $G(Fe^{3+})$.

Experimental

Apparatus.—Most of the previous studies of the discharge reaction have been made by means of glow discharge. It is impossible, however, to study the aqueous solution by this method. In this work, a discharge tube of the ozonizer type (Fig. 1) was used;

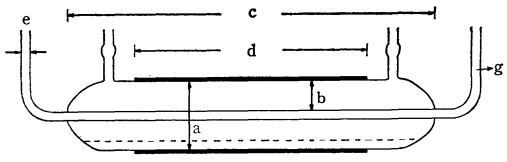

Fig. 1. Schematic diagram of discharge tube.

a	26 mm.	e	10 mm.ϕ
b	8 mm.		
c	300 mm.	---	surface of solution
d	230 mm.	—	tin foil

this makes the study of solutions possible. It is composed of two coaxial, hard-glass tubes; the part consisting of tin foil stuck on the outer tube was used for one electrode, and the part containing the dilute sulfuric acid in the inner tube (g) was used for the other electrode (high-tension side). After the sample solution had been poured into the discharge tube, the discharge was made by applying a high tension between those two electrodes, letting helium or argon flow through the gas space of the discharge tube.

All experiments were made at a constant volume of the solution, 10 ml. The surface of the solution was vibrated gently by the discharge. This may be useful for the renewal of the surface of the solution.

All experiments were made after the dissolved oxygen in the solution had been completely removed by bubbling helium or argon gas into the solution. Sometimes samples were degassed by four successive cycles of freezing, evacuation, and melting on a vacuum line.

1) T. W. Davis, S. Gordon and E. J. Hart, *J. Am. Chem. Soc.*, **80**, 4487 (1958).
2) G. Gzapski and G. Stein, *Nature*, **182**, 598 (1958); *J. Phys. Chem.*, **63**, 850 (1959); *Israel J. Chem.*, **2**, 15 (1964).
3) M. Suzuki, *Proc. Japan Acad.*, **26**, 20 (1950).
4) K. Sugino, E. Inoue, T. Wakabayashi and T. Matsuda, *J. Elect. Chem. Japan*, **25**, 70 (1957).
5) G. Glockler and S. C. Lind, "The Electrochemistry of Gases and Other Dielectrics," John Wiley & Sons, London (1939).
6) T. Okamoto and H. Kobayashi, *J. Soc. Org. Synth. Chem. Japan*, **7**, 10 (1949).
7) Y. Isomura, *J. Elect. Chem. Japan*, **17**, 9 (1949).
8) M. Gotoda, *Railway Technical Research Report (Tetsudo Gizitsu Kenkyu Hōkoku)*, No. 226, June (1961).
9) Even though the effects of such ions as Ar^+ and He^+ have been considered, the effect would probably be very small since their mobility is quite low compared with that of electrons.
10) It is generally accepted that the chemical change produced by a high-energy radiation, such as those of beta-, alpha- and gamma-rays, can be explained as the reaction by secondary electrons with a mean energy of about 100 eV.
11) Since the electron energy is very small, most of the energy might be dissipated by one event. Accordingly, the term "LET", as herein used, may not be adequate, the electron generated by silent discharge being very slow.

For the washing of the discharge tube, a mixed solution of alcohol and a saturated aqueous solution of sodium hydroxide was used, besides the usual cleaning solution. The discharge tube was dried by evacuation.

Sometimes, a quartz discharge tube of the same size was used to test the effect of the light arising from the discharge. In this case. the test was made after the sample had been poured into the inner tube, g in Fig. 1. If the effect were predominant, some contributions would be expected; however, this was not the case.

Another discharge tube (Fig. 2) was also used. This is a vertical one. Samples were tested in the position of A. This experiment makes it possible to estimate the contributions of active species with a long life, such as He^{m*} and Ar^{m*}, and also those of the oxidizing products, such as the trace of ozone formed in the gas phase.

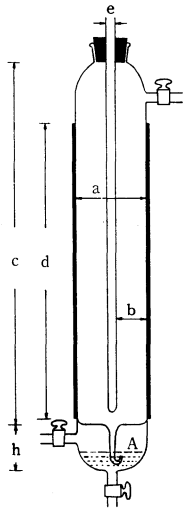

Fig. 2. Schematic diagram of discharge tube.

a	26 mm.	d	230 mm.
b	8 mm.	e	10 mm.ϕ
c	300 mm.	h	40 mm.

Electric Circuit.—An electric circuit (Fig. 3) was used for measuring the discharge current running through the discharge tube. In general the wave form shown in Fig. 4 is found, where V and I are the voltage and the current respectively. The phase difference was about 80 degrees.

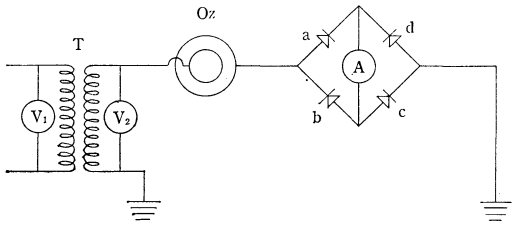

Fig. 3. Electric circuit.

V_1 Voltmeter	V_2 Static electric voltmeter
a, b, c, d, Cu_2O rectifier	A Direct ammeter
Oz, Discharge tube	T Transformer

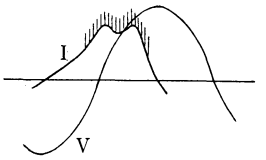

Fig. 4. General waveform of discharge current.
I Discharge current
V Voltage

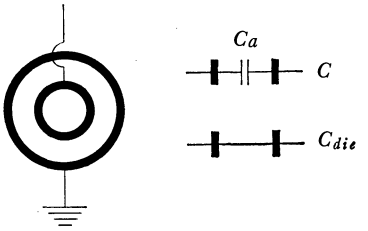

Fig. 5. Cut-away diagram of discharge tube.

The discharge tube is a sort of condenser, the capacitance of which is shown by C and which consists of two parts C_{die} and C_a; the former depends on the thickness of the outer and inner glass tubes, and the latter, on the gap distance of the discharge tube (Fig. 5). The capacitance during discharge may be approximately shown by C_{die}, because it has a short circuit because of the discharge.[12]

Materials.—The water used was purified by the multiple distillation described by Johnson and Allen.[13] Reagent-grade sulfuric acid and ferrous ammonium sulfate were used without further purification. Helium and argon (purity: >99.99%) were also used without further treatment.

Analysis.—The amount of hydrogen peroxide produced in the dilute sulfuric acid solution was determined by the method of Ghormley.[14] The ferric ions in ferrous sulfate solutions were determined by light absorption at 3040 Å.

Results

Figure 6 shows the relation between the applied voltage and the electric current when 10 ml. of solution is contained in the discharge tube, where B or B' shows the firing voltage (V_1) for helium and argon respectively. The AB or AB' part before discharge is expressed by the formula[10] $I=\omega CV$. For BC or B'C' during discharge, $I=\omega CV_1+\omega C_{die}(V-V_1)$: $\omega=2\pi f$; V_1: firing voltage; V: applied voltage; f: frequency. Most of the experiments were made at a constant discharge current, $I=$ 1 mamp. The electric current as measured by the method shown in Fig. 2 shows the low frequency component principally, not the high frequency component. For the latter another method, such as

12) T. Biyodo, *J. Japan Chem.* (*Kagaku-no-Ryoiki*), **3**, 172 (1950).
13) E. R. Johnson and A. O. Allen, *J. Am. Chem. Soc.*, **74**, 4147 (1952).
14) A. O. Allen, C. J. Hochanadel, J. A. Ghormley and T. W. Davis, *J. Phys. Chem.*, **56**, 575 (1952).

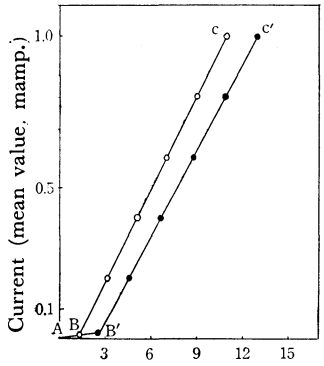

Fig. 6. Relation between applied voltage and electric current.
○ case of helium
● case of argon

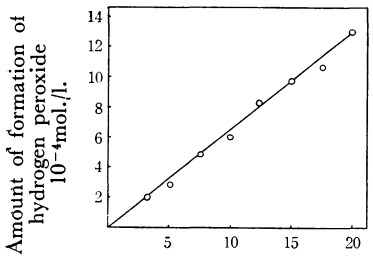

Fig. 7a.

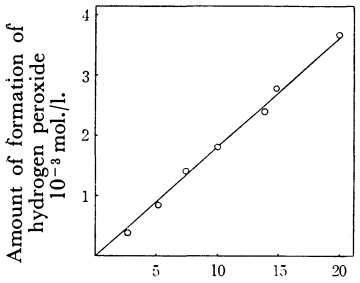

Fig. 7b.

Fig. 7. Relationship between amount of formation of hydrogen peroxide and duration time of discharge in 0.8 N sulfuric acid.
a case of helium b case of argon

one using a thermoammeter, seems to be needed. Recently we have made extensive studies of this point,[15] but we will not discuss them here.

The Formation of Hydrogen Peroxide from a Dilute Aqueous Solution of Sulfuric Acid.—In the oxygen-free aqueous solution of sulfuric acid, hydrogen peroxide appeared as a result of discharge in argon or helium. The concentration of sulfuric acid in the range from 2×10^{-2} N to 1.5 N had no effect on the yield of hydrogen peroxide within the range of experimental error (Figs. 7a and 7b). The yield of hydrogen peroxide also showed a good linear correlation with the duration of discharge. A larger amount of hydrogen peroxide was found in argon than in helium. Although the formation of hydrogen peroxide from the water vapor in the gas phase may be expected, it was negligibly small under our experimental conditions, in which the gas passed at a velocity of about 120 ml./min. and the duration time of the discharge (20 min.) was very short.

The formation of hydrogen peroxide, therefore, may be considered to be caused by the actions of low energy electrons generated by discharge on water molecules, just as in radiation chemistry.

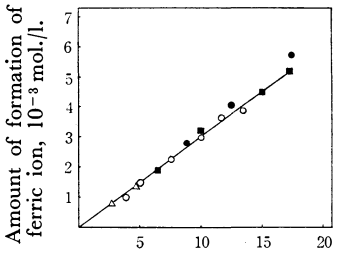

Fig. 8a.

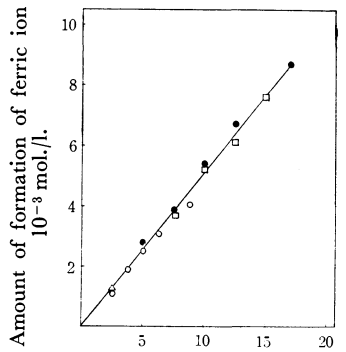

Fig. 8b.

Fig. 8. Relationship between amount of formation of ferric ion and duration time of discharge.
a case of helium b case of argon
● 4×10^{-1} mol./l. □ 4×10^{-2} mol./l.
■ 1×10^{-2} mol./l. ○ 5×10^{-3} mol./l.
△ 2×10^{-3} mol./l.

The Formation of Ferric Ions.—Ferric ions were found to be formed in an aqueous ferrous sulfate solution acidified with sulfuric acid. Figures 8a and 8b show the relationship between the amount of ferric ions formed and the duration of the discharge in a helium or an argon atmosphere respectively. The yield of ferric ions was independent of the concentration of ferrous ions in the

15) A. Yokohata and S. Tsuda, *J. Chem. Soc. Japan, Pure Chem. Sect.* (*Nippon Kagaku Zassi*), **86**, 682, 686, 689 (1965).

range from 2×10^{-3} M to 4×10^{-1} M, and of the concentration of sulfuric acid in the range from 2×10^{-2} N to 1.5 N; it also showed a good linear correlation with the duration of discharge. These results suggest that the mechanism of the silent discharge reaction may be interpreted as that of radiolysis by slow electrons.

Discussion

The silent discharge on aqueous solutions in an atmosphere of helium or argon will give many numbers of electrons; excited molecules such as He^{m*} and Ar^{m*}, and atoms or radicals like the H-atom and the OH-radical due to the interaction of the water molecule with an electron or an excited molecule such as He^{m*}; it is also accompanied by a weak luminescence. Accordingly, the effect of the silent discharge may naturally be considered to be the superposed effect caused by those electrons, active species, and luminescence.

It is, however, very important to clarify which of them plays the main role. This is our purpose in the present study.

The Effect of Active Species.—First, let us consider the effect of the excited molecule alone. It is very difficult to clear up this effect quantitatively, but it is possible to do so qualitatively. For this purpose, the discharge tube shown in Fig. 2 was used. 10 ml. samples were tested in the position of A. After the oxygen dissolved in a sample in the A section had been completely excluded by bubbling argon or helium in, a discharge was made. In order to pass the discharged gas rapidly into the sample solution, the gas was sent forth through the capillary tube. The experimental results showed only a very small amount of ferric ions under such these conditions: duration time of discharge =30 min.; flow velocity of gas =120 ml./min., and electric current=1 mamp. If the effect of the excited molecules is predominant, larger amounts of ferric ion may be expected.

Our results are consistent with the work by Davis et al.,[1] in which the oxidation of ferrous ions was checked by introducing argon treated by glow discharge into an aqueous solution. They found only a very slow oxidation. Therefore, the effect of the excited molecule itself may be concluded to be very small. However, when water vapor is present, the situation may be different.

In the study of the total ionization in gases by single alpha-particles, Jesse[16] showed that the number of ion pairs in pure helium or neon is greatly increased by the addition of a small amout of almost any impurity; he then suggested that the additional ionization arose from reactions of the following type:

$$He^* + X \rightarrow He + X^+ + e^- \qquad (1)$$

The metastable-excited states of helium have a sufficiently long life to encounter an impure atom or molecule and ionize it in a collision of the second kind (the Penning effect). With helium, most of the contaminants show this effect. As expected, other ionizing radiations (beta-rays, gamma-rays) show exactly the same effect.

Since the presence of water vapor should be considered in our case, the following reaction may occur in the gas phase:

$$He^* + H_2O \rightarrow He + H_2O^+ + e^- \qquad (2)$$

However, it can, alternatively, result in the "dissociation" of the molecule.[17]

$$He^* + H_2O \rightarrow He + H + OH \qquad (3)$$

One of the reaction products may be electronically excited. If the hydrogen exists in the excited state, reaction 4 may be expected:

$$H^* + H_2O \rightarrow H_2 + OH \qquad (4)$$

In argon also the circumstances are just the same, except that the excitation energy of the metastable state is smaller than that of helium. Since the excitation energy of argon is smaller than the ionization potential of the water vapor molecule, a reaction like 2 may not be expected.

As has already been pointed out,[1] the effect of water vapor cannot be neglected. In the present stage, it is very difficult to estimate separately the effects of H-atoms and OH-radicals arising from the water vapor and those arising from the interaction of liquid water with the slow electrons generated in the gas phase. However, we have already obtained the experimental result that the yield of hydrogen peroxide formed in the gas phase is negligibly small under the experimental conditions. This seems to show that the contribution of the hydroxyl radical from the water vapor is not very great. Also, hydrogen atoms will not naturally make an important contribution.

The Effect of Luminescence.—The silent discharge gives a luminescence, although the intensity is weak. Therefore, photochemical reactions[18] may be expected, although their contribution in this case is thought to be small.

In order to clear up this point, we made an experiment, where a quartz discharge tube was used; the aqueous ferrous sulfate solution to be tested was put in an inner tube (Fig. 1. g). Since quartz is transparent for light of wavelengths of $\lambda>2000$Å, it might be possible to learn the order of contributions due to photons of the wavelengths $\lambda>2000$Å by this experiment. Experimental results showed that this effect was negligibly small.

Evidence that the light below 2000Å is effective in the flash photolysis of aqueous ferrous sulfate

16) W. P. Jesse and J. Sadauskis, *Phys. Rev.*, **88**, 417 (1952); **100**, 1755 (1955).
17) R. L. Platzman, *Vortex*, **23**, 372 (1962).
18) T. Rigg and J. Weiss, *J. Chem. Phys.*, **20**, 1194 (1952).

has recently been given by Baxendale and Mansell.[19] They concluded that the observed $Fe^{2+} \rightarrow Fe^{3+}$ oxidation was an indirect effect, the primary one being the photolysis of water to give products which oxidize Fe^{2+}. Although the contribution of ultraviolet rays (<2000Å) may exist in our case, we have not yet performed any experiment to test such effects because of the great difficulty. However, judging from the fact that the effect of luminescence was clearly negligibly small in the case of nitrogen molecule which has $\lambda \fallingdotseq$ 2000Å (E=6.1 eV.) as a resonance line,[20] the resonance lines of helium and argon are also too weak to make contributions.[21]

The Effect of Electrons.—As has been mentioned above, the effects of the metastable-excited state of helium and argon and of the luminescence cannot be serious.

However, the contributions of hydrogen atoms and hydroxyl radicals from the water vapor cannot be neglected, although they might also not be very large. The yield of hydrogen peroxide from the water vapor was very small. On the other hand, our present work shows that the yield of hydrogen peroxide formed in the aqueous solutions is fairly great (Table I). Also, the yield of ferric ions was always larger than that which could be expected from the oxidation by the hydrogen peroxide formed. These phenomena may be interpreted by taking into consideration the actions of the slow electrons generated in the gas phase on the solvent.

About the energy distribution of electrons produced by such silent discharge under an atmospheric pressure, we do not yet have any exact information. The electrons, however, may be considered to have an energy distribution from just above zero to somewhat above the ionization potential for the gas in which the discharge occurs.[22,23] On the other hand, to produce a hydrogen atom and a hydroxyl radical through the excited state of a water molecule, it is well known that the energy 7.4 eV. is necessary.[24] Accordingly, in the silent discharge also, the formation of a hydrogen atom and a hydroxyl radical can be expected. In other words, the effect of electrons may be interpreted in the same way as in radiation chemistry:

$$H_2O \text{ -W-} \rightarrow H, OH, H_2, H_2O_2 \qquad (5)$$

Some part of the hydrogen atoms and the hydroxyl radicals may come from the water vapor. The overall reaction, however, proceeds irrespective of whether they are produced from the water vapor or the liquid water,

Therefore,[25] the following relation is obtained:

$$Y(Fe^{3+}) = 2Y(H_2O_2) + Y(OH) + Y(H) \qquad (6)$$

where Y shows the yield of each product under given conditions.

Table I shows each value of $Y(H_2O_2)$, $Y(Fe^{3+})$, $Y(H+OH)$ estimated by (6), and $Y(H_2O_2)/Y(H+OH)$ in the cases of helium and argon respectively.

Table I. Estimation of $Y(H_2O_2)/Y[(H)+(OH)]$

	$Y(H_2O_2)$ mol./l.	$Y(Fe^{3+})$ mol./l.	$Y[(H)+(OH)]$ mol./l.	$Y(H_2O_2)/Y[(H)+(OH)]$
He	6.5×10^{-4}	3.0×10^{-3}	1.7×10^{-3}	0.38
Ar	1.8×10^{-3}	5.1×10^{-3}	1.5×10^{-3}	1.2

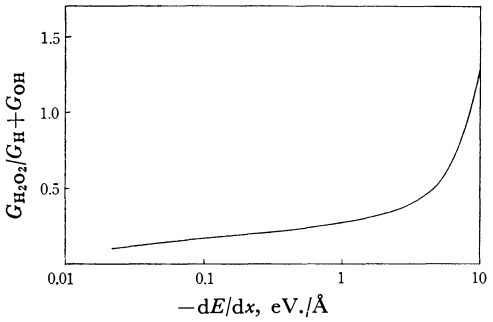

Fig. 9. Relation between $G_{H_2O_2}/G_H+G_{OH}$ and $-dE/dx$.

Figure 9 shows the relations between $G(H_2O_2)/G(H+OH)$ and LET, arranged using the data from Allen, Lefort and Barr.[26-28] The linear energy transfer (LET) in Fig. 9 is expressed by $-dE/dx$ (eV./Å), where ^{60}Co gamma rays: LET 0.02 eV./Å, 40 keV. electron: 0.08 eV./Å, 18 MeV. deuteron: 0.5 eV./Å and 5.5 MeV. alpha-rays: 9 eV./Å, as is already known,[29]

The radical yields decrease with an increase in the LET, and molecular yields increase until the radical yields approach zero at a sufficiently high LET.

By comparing the results in Table I with Fig. 9, the following interesting conclusions can be derived. In an atmosphere of helium, the chemical effect of the silent discharge apparently corresponds to that of the ionizing radiation with a LET of

19) J. H. Baxendale and A. L. Mansell, *Nature*, **190**, 622 (1961).
20) G. Herzberg, "Molecular Spectra and Molecular Structure (I. Spectra of Diatomic Molecules)," D. Van Nostrand Company, New York (1963), p. 448.
21) A long exposure time (for example, 1—4 hr.) was necessary to take spectrograms with a small "Riken" quartz spectrograph and with "Sakura S. G. 100" photographic plates.
22) L. B. Loeb, "Basic Processes of Gaseous Electronics," Univ. of California Press, Berkeley (1955), p. 269.
23) H. Kokado, Y. Mori and I. Tanaka, *J. Chem. Soc. Japan, Pure Chem. Sect.* (*Nippon Kagaku Zassi*), **78**, 151 (1957).
24) M. Burton, J. S. Kirby-Smith and J. L. Magee, "Comparative Effects of Radiation," John Wiley & Sons, New York (1960), p. 179.
25) $H_2O_2 + Fe^{2+} \rightarrow Fe^{3+} + OH^- + OH$
$OH + Fe^{2+} \rightarrow Fe^{3+} + OH^-$
$H + H^+ + Fe^{2+} \rightarrow Fe^{3+} + H_2$
26) A. O. Allen, *Radiation Res.*, **1**, 85 (1954).
27) M. Lefort, *J. Chem. Phys.*, **54**, 782 (1957).
28) N. F. Barr and R. H. Schuler, *Radiation Res.*, **7**, 302 (1957).
29) A. O. Allen, "Radiation Chemistry of Water and Aqueous Solutions," D. Van Nostrand Company, New York (1961), p. 10.

about 3 eV./Å, while in argon it corresponds to a radiation with a LET of about 8 eV./Å. In argon it seems to be very close to the effect of alpha rays. This is consistent with Hochanadel's finding that, for very low-energy electrons, the radicals are formed in high concentrations along the track in the same way as for alpha particles and low-energy protons.[30]

The slight difference between helium and argon is thought to be due to their different discharge characters; in the former the discharge is very gentle and the high frequency part of the discharge current is very small, while in the latter the discharge is quite vigorous and the high frequency part is relatively large.[15] Also, from the relation between $-dE/dx$ and $G(Fe^{3+})$[31] it becomes possible to estimate the apparent $G(Fe^{3+})$ in helium and in argon. The former is $G(Fe^{3+}) \fallingdotseq 4.6$, and the latter, $G(Fe^{3+}) \fallingdotseq 4.3$.

The Estimation of the Apparent Dose Absorbed.[32]—It is very important to ascertain the absorbed energy or the dose in the silent-discharge chemistry. As a method of measuring the total dissipated energy, the electrical method using a synchroscope has been proposed.[33] In our experience, however, this method was very difficult because the high-frequency component of the electric current fluctuates very vigorously. An approach by theoretical calculations has also been made. The following formula has been proposed for the energy dissipated per second by the silent discharge[34]:

$$A=\frac{f(C_{die}+C_a)(V_i+V_d)\{2E_m-(V_i+V_d)(1+C_a/C_{die})\}}{1+C_a/C_{die}} \qquad (7)$$

A : the energy dissipated per second by the silent discharge
f : the frequency of the electric source used
C_{die} : the total capacitance of the insulator
C_a : the capacitance due to the gap distance in the discharge tube
V_i : the voltage across the gap space at the firing voltage
V_d : the stopping voltage
E_m : the maximum value of the applied voltage

Of couse, this formula is an approximate one, in which the contributions of the high-frequency parts are neglected. Also, V_i means the voltage in the gas space and is correlated by the $V_i=V_1(C_{die}/(C_a+C_{die}))$ formula to the firing voltage, V_1. Now, let us suppose that discharge occurs when the voltage of the gap space attains V_i and stops at V_d. The relation between V_d and V_i is not well known, but the value of V_d/V_i is said to be approximately 0.4—0.2[35]

In our experimental conditions $C_{die}=180$ pF,[36] $C_a=36$ pF, $V_i=1.3$ kV. and $E_m=15.4$kV. in helium, and $V_i=2.4$kV. and $E_m=17.2$ kV. in argon. By putting these values into (7), the ratio of the energy dissipated by the silent discharge in helium and argon can be estimated.[37] Table II shows the results of the calculation for each case of $V_d/V_i=0.2$ and 0.4.

TABLE II. CALCULATION RESULTS OF DISSIPATED ENERGY IN HELIUM AND ARGON (NORMALIZED TO THE CASE OF HELIUM)

Kind of atmosphere	V_d/V_i	Dissipated energy
He	0.2	1
Ar		2.0
He	0.4	1
Ar		2.0

Next, let us estimate approximately in roentgen units the dose absorbed in helium and in argon. By combining $G(Fe^{3+})=4.6$ with $Y(Fe^{3+})=3.0\times10^{-3}$ M in helium and $G(Fe^{3+})=4.3$ with $Y(Fe^{3+})=5.1\times10^{-3}$ M in argon, it becomes possible to estimate them. In helium, the apparent dose rate equals about 3.8×10^6 r./hr. and in argon to 7.2×10^6 r./hr. These values, of course, vary with the value of the electric discharge current. This is the case of 1 mamp. The values also indicate the average integral dose absorbed by the aqueous solution in the apparatus used by the authors, where a solution with a volume of 10 ml. is used. The dose rate in argon is larger than that in helium and its ratio is about 1.9, which is almost consistent with the calculated result.

30) C. J. Hochanadel, *J. Phys. Chem.*, **56**, 587 (1952).
31) A. O. Allen, "Radiation Chemistry of Water and Aqueous Solutions," D. Van Nostrand Company, New York (1961), p. 54.
32) The absorbed dose cannot be measured directly by the instruments connected in the circuit, since a part of it has been changed to heat or light. The extent of the real chemical utilization can best be measured by chemical dosimetry.
33) M. Suzuki, "Ozonizer Handbook," Koronasha, Tokyo (1960), p. 232.
34) S. Fuji and N. Takimura, *Bulletin of the Electrotechnical Laboratory (Denki Shikensho Hokoku)*, **16**, 837 (1952).
35) M. Suzuki, *J. Electrochem. Soc. Japan (Denki Kagaku)*, **24**, 354 (1956).
36) This value was estimated approximately from a curve showing the relation between the applied voltage and the discharge current.
37) The value of A means the total energy dissipated per second by the silent discharge. The energy absorbed in a solution occupies only a small amount (x%) of A. Since it is impossible to estimate the value of x, the absolute value of A is not so important. The value of the A_{Ar}/A_{He} ratio, however, would be useful for us as a means to check the value of the absorbed dose as measured by the chemical dosimeter.

BULLETIN OF THE CHEMICAL SOCIETY OF JAPAN VOL. 39 53—55 (1966)

Silent Discharge Reactions in Aqueous Solutions. II. An Acidic Aqueous Solution of Ceric Sulfate in Atmospheres of Helium and Argon*

By Akira YOKOHATA and Satoru TSUDA

Department of Chemistry, Faculty of Engineering, Hiroshima University, Senda-machi, Hiroshima

(Received April 6, 1965)

In an atmosphere of helium or argon, the silent discharge reaction of an acidic aqueous solution of ceric sulfate has been investigated from the point of view of radiation chemistry. The results show the reduction of ceric ions to cerous ions. The situation is very similar to that in the case of radiation chemistry. From the known mechanism of the radiolysis of a ceric sulfate solution, the yield of "hydrogen atoms minus hydroxyl radicals" has been determined. Also, combining this yield with that of "hydrogen atoms plus hydroxyl radicals" previously obtained gave the respective yields of hydrogen atoms and hydroxyl radicals. Moreover, on the basis of the value of the dose rate previously determined, the G values of the hydrogen atom, the hydroxyl radical and the cerous ion were determined to be as follows: in helium: $G(H)=1.1$, $G(OH)=1.6$, $G(Ce^{3+})=1.6$; in argon: $G(H)=0.6$, $G(OH)=0.7$, $G(Ce^{3+})=2.9$. On the basis of these results, it may be concluded that the silent discharge reactions in an aqueous solution in inert gas can well be interpreted in terms of the radiolysis caused by the ionizing radiation of high LET.

In the previous report[1] it was pointed out, first, that in the atmospheres of helium and argon, the chemical reaction in an aqueous solution of ferrous sulfate by silent discharge may well be interpreted in terms of the actions of slow electrons generated in the gas phase on the solvent, and, then, that neither the effect of the metastable-excited states of helium and argon nor of the luminescence can be serious.

Using the methods described in that, the present work will deal with a silent discharge reaction, in the atmospheres of helium and argon, on an aqueous solution of ceric sulfate acidified with dilute sulfuric acid.

The reaction mechanism of this system has already been well established in the field of radiation chemistry,[2] in which ceric ions have been reduced to cerous ions.

The silent discharge also showed the reduction of ceric ions. As was established in the previous report, the net effect of slow electrons generated by the silent discharge may be considered to be similar to that of radiation chemistry introduced by alpha- or gamma-ray irradiation. Therefore, combining the yield of cerous ions with that of hydrogen peroxide should give the yield of "hydrogen atoms minus hydroxyl radicals" under given conditions. Accordingly, it may be expected that the yield of hydrogen atoms and hydroxyl radicals can be separately estimated by combining the yield of "hydrogen atoms plus hydroxyl radicals" (described in the previous report) with that of "hydrogen atoms minus hydroxyl radicals."

In this report, the G values of H, OH and Ce^{3+} in the silent discharge will be estimated. Also, it will be pointed out that, in atmospheres of helium and argon, the silent discharge reactions in the aqueous solutions can apparently be interpreted well in terms of the radiolysis caused by a particle of a high LET value.

Experimental

The discharge tube, the electric circuit, and the experimental conditions were the same as have previously been reported.

Merck guaranteed-reagent ceric sulfate was used without further purification. All the other materials were also of a reagent grade. The helium and argon (purity: >99.99%) were used without further treatment.

The ceric-ion concentration was measured directly by spectrophotometry, using the molar extinction coefficient of 5580 at 3200 Å (25°C).

Results

Figures 1a and 1b show the relationship between the amount of cerous ions formed and the duration time of the discharge in the cases of helium and argon respectively. The yield of cerous ions in a ceric sulfate solution acidified with 0.8 N sulfuric acid was independent of the concentration of ceric ions in the range from 1×10^{-3} M to 2×10^{-2}M. The effect of the solute concentration, however, was found at concentrations higher than 5×10^{-2} M (cf. Fig. 1b). The situation is very similar to the

* Presented in part at the 17th Annual Meeting of the Chemical Society of Japan, Tokyo, April, 1964.

1) Part I of this series: A. Yokohata and S. Tsuda, This Bulletin, **39**, 46 (1966).

2) A. O. Allen, *Radiation Res.*, **1**, 85 (1954).

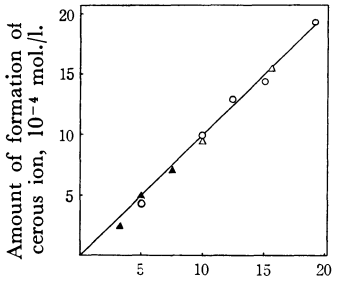

Duration time of discharge, min.

Fig. 1a

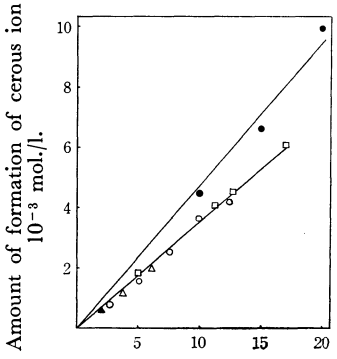

Duration time of discharge, min.

Fig. 1b

Fig. 1. Relationship between amount of formation of cerous ion and duration time of discharge.
a Helium b Argon
Initial concentrations of ceric ion
● 5×10^{-2} M, □ 2×10^{-2} M, ○ 5×10^{-3} M,
△ 3×10^{-3} M, ▲ 1×10^{-3} M

case in radiation chemistry. This point will be discussed later.

Discussion

Harlan and Hart,[3] using a concentrated solution, studied the upper limit of the usefulness of ceric dosimetry; they found that the relation between the change in the ceric-ion molarity and the dose absorbed was not linear. The initial slope corresponded to $G(Ce^{3+})=3.1$, and the final slope to $G=1.7$. Also, the effect of the solute concentration has been determined. For example, in the concentration range from 10^{-4} M to 10^{-3} M, $G(Ce^{3+})$ equals 2.50 and 2.9 at 0.1 M. In a 0.39 M ceric-sulfate solution, $G(Ce^{3+})$ increases to 3.1 because the $H+Ce^{4+}$ reaction now scavenges hydrogen atoms that normally combine to form hydrogen in dilute solutions,

3) J. T. Harlan and E. J. Hart, *Nucleonics*, **17** (No. 8), 102 (1959).

Taimuty et al.[4] irradiated the same system and obtained almost the same results. In the range from 1×10^{-3} M to 5×10^{-2} M, they got $G(Ce^{3+})=2.5$. Also, their results showed no dose-rate dependence; on the other hand a small effect of the temperature was found at temperatures higher than 27°C.

The present work will show that $Y(Ce^{3+})$ is independent of the ceric-ion concentration in the range from 1×10^{-3} M to 2×10^{-2} M within the range of experimental error, but that it is dependent on ceric ions in concentrations higher than 5×10^{-2} M. This point might well be interpreted by taking the $H+Ce^{4+}$ reaction into consideration in the same way as has been described by Harlan and Hart.

Now, in the same manner as was pointed out in the previous report, we may assume a radiolysis by the interaction of slow electrons with the water molecules.

Therefore, in the range of the linear correlation of each yield to the dose, the observed yield of cerous ion may be expressed by (1)[5,6]:

$$Y(Ce^{3+})=2Y(H_2O_2)+Y[(H)-(OH)] \qquad (1)$$

Table I shows $Y[(H)-(OH)]$ as estimated from (1) by combining the $Y(Ce^{3+})$ with the $Y(H_2O_2)$ previously obtained.[1] The cases of both helium and argon give a negative value: $Y(OH)>Y(H)$.

Hochanadel[7] has published the yields of the intermediate H, OH in the decomposition of a 0.4 M sulfuric acid solution as a function of the initial LET (linear energy transfer) value of the incident particle. In the LET range above 10 eV./Å, $G(OH)$ exceeds $G(H)$ and $G(H_2)$ exceeds $G(H_2O_2)$.

TABLE I. YIELD OF "HYDROGEN ATOM MINUS HYDROXYL RADICAL"

	$Y(H_2O_2)$ mol./l.	$Y(Ce^{3+})$ mol./l.	$Y[(H)-(OH)]$ mol./l.
He	6.5×10^{-4}	1.0×10^{-3}	-3×10^{-4}
Ar	1.8×10^{-3}	3.5×10^{-3}	-1×10^{-4}

Our results show that the silent discharge reactions apparently correspond to the reactions induced by particles with values of LET larger than about 10 (eV./Å). In the previous report we showed that the silent discharge reaction in helium

4) S. I. Taimuty, L. H. Towle and D. L. Peterson, ibid., **17** (No. 8), 103 (1959).

5) The following reaction scheme may be expected:

$$H_2O \rightsquigarrow H, OH, H_2O_2, H_2$$
$$H + Ce^{4+} \rightarrow Ce^{3+} + H^+$$
$$H_2O_2 + 2Ce^{4+} \rightarrow 2Ce^{3+} + 2H^+ + O_2$$
$$OH + Ce^{3+} \rightarrow Ce^{4+} + OH^-$$

Accordingly, $G(Ce^{3+}) = 2G(H_2O_2) + G(H) - G(OH)$

6) Y shows the yield of products under these given conditions: discharge current: 1 mamp., and duration time of discharge: 10 min.

7) M. Burton, J. S. Kirby-Smith and J. L. Magee, "Comparative Effects of Radiation," John Willy & Sons, New York (1960), p. 179.

and in argon under given conditions apparently corresponded to that by particles with the LET values of 3 and 8 (eV./Å) respectively. A small discrepancy can be seen in helium. In estimating the value of LET, however, it seems to be more reasonable to take into consideration the ratio of $Y(H_2O_2)$ to $Y[(H)+(OH)]$ than the ratio of $Y(OH)$ to $Y(H)$. Accordingly, the values of 3 (eV./Å) in helium and 8(eV./Å) in argon were used in this work.

Of couse, the yield of hydrogen atoms and hydroxyl radicals from the water vapor may also be present in the case of a silent discharge on an aqueous solution. Our interest, however, was in the net yield of H and OH.

We previously reported the yield of the "hydrogen atom plus the hydroxyl radical":

$$\left.\begin{array}{ll}\text{In helium:} & Y[(H)+(OH)]=1.7\times10^{-3}\ \text{M}\\ \text{In argon:} & Y[(H)+(OH)]=1.5\times10^{-3}\ \text{M}\end{array}\right\} \quad (2)$$

Combining (2) with the results shown in Table I gives these yields of H and OH:

$$\left.\begin{array}{ll}\text{In helum:} & Y(H)=0.7\times10^{-3}\ \text{M}\\ & Y(OH)=1.0\times10^{-3}\ \text{M}\\ \text{In argon:} & Y(H)=0.7\times10^{-3}\ \text{M}\\ & Y(OH)=0.8\times10^{-3}\ \text{M}\end{array}\right\} \quad (3)$$

These values will hereafter be checked further by means of studies of other chemical systems.

Table II shows the relation between G_{obs} and G_{est}. Each G_{obs} indicates a G value obtained by combining $Y(H)$, $Y(OH)$ and $Y(H_2O_2)$ with the dose previously determined. Each G_{est} means a G value estimated from the figure[7] showing the relations of $G(H)$, $G(OH)$ and $G(H_2O_2)$ to LET, using 3 (eV./Å) in helium and 8 (eV./Å) in argon as the LET values. The correspondence of G_{obs} to G_{est} is relatively good, except for $G(OH)$ in helium.

Table II. Relation between G_{est} and G_{obs}

	He		Ar	
	G_{est}	G_{obs}	G_{est}	G_{obs}
H	1.2	1.1	0.7	0.6
OH	1.0	1.6	0.7	0.7
H_2O_2	1.2	1.0	1.4	1.5

Also, the values of $G(Ce^{3+})=1.6$ in helium and $G(Ce^{3+})=2.9$ in argon were obtained. The differences in $G(Ce^{3+})$ in helium and in argon, and also between $G_{obs}(OH)$ and $G_{est}(OH)$ in helium, may be due to the different discharge characters, the locality of the discharge being higher in argon than in helium. Besides, the difference in the formation mode of the hydrogen atom and of the hydroxyl radical from the water vapor may be a reason (cf. part I). These points will be left as a future problem.

It is our conclusion that silent discharge reactions in an aqueous solution in atmospheres of helium and argon may apparently be well interpreted in terms of radiolysis caused by a particle with a high LET value.

BULLETIN OF THE CHEMICAL SOCIETY OF JAPAN VOL. 39 55—57 (1966)

The Color Reaction between Chromium(III) Ion and Potassium Ferrocyanide*

By Yoshio MATSUMOTO and Michiko SHIRAI

Department of Chemistry, Faculty of Hygienic Science, Kitasato University, Minato-ku, Tokyo

(Received April 8, 1965)

The observation of the orange-coloring reaction between potassium ferrocyanide and the chromium(III) ion on filter paper and its application in the paper chromatographical analysis of the chromium(III) ion has been reported on previously by the present authors. The color reaction has now been observed in an aqueous solution as well and studied in relation to the reaction temperature, the reaction time, the characteristic absorption, the species of chromium(III) salts, the chromium(III) ion concentration, the pH level, and the presence of an acetic acid buffer, by measuring the absorption spectra of the reaction solutions. The recommended conditions for getting a satisfactory color reaction and a suitable wavelength for the measurement of this color reaction have been presented.

In continuation of previous work[1] on the color reaction of potassium ferrocyanide with chromium(III) ions on filter paper, the present paper will report on the coloration which takes place in an aqueous solution.

When Cr^{3+} and $K_4[Fe(CN)_6]$ were mixed together in an aqueous solution, the color of the solution gradually changed to reddish orange and its intensity reached near the maximum within 1.5—3 hr. at room temperature; on the other hand, the reaction proceeded more quickly at a higher temperature, a satisfactory coloration being obtained in 15 min. at 50°C.

With regard to the reaction solution described above, the absorption spectra at various Cr^{3+} concentrations for visible light and the variation in the spectra during the reaction were measured. It was thus found that the maximum variation in color intensity was observed at a wavelength between 410 and 420 mμ. It was also found that, in the case of a reaction for 15 min. at 50°C, a strictly linear relationship held between the extinction at 415 mμ and the Cr^{3+} concentration.

The major part of the experiments in this work was done with chrome alum as the representative source salt of Cr^{3+}, and the chromium(III) ion will be referred as having a more general significance in the statement of the experimental results, because of the preliminary experimental proof of the agreement in extinction at 415 mμ of the reaction solutions derived from different chromium(III) salts, such as chromic chloride and chrome alum.

In the course of studying the relation between the pH value and the coloration, interference with the coloration by the acetic acid - sodium acetate buffer was found.

The coloration caused by the present reaction is thought to be due to the formation of a complex anion containing chromium; attempts to isolate such a complex in a crystalline form are now in progress.

Experimental

The Absorption Spectra of Reaction Solutions at Various Cr^{3+} Concentrations.—Solutions of chromium(III) ions from $KCr(SO_4)_2 \cdot 12H_2O$ and potassium ferrocyanide solutions were mixed together in the various ratios shown in Fig. 1, and the absorption spectrum of each solution was measured after 3-hr.'s reaction at room temperature (Fig. 1). The extinction was found to vary widely in accordance with the Cr^{3+} concentration in the wavelength range between 410 and 420 mμ.

The Relation between the Color Intensity and the Reaction Time.—With the Cr^{3+} and $K_4[Fe(CN)_6] \cdot 3H_2O$ used in the final concentrations of 40 μg./cc. and 10 mg./cc. respectively, the absorption spectra were measured after reaction at room temperature for the times of 0, 20, 40, 60, 100, 140 and 180 min. (Fig. 2). In this experiment, the color intensity almost attained its maximum within 100 min. after mixing.

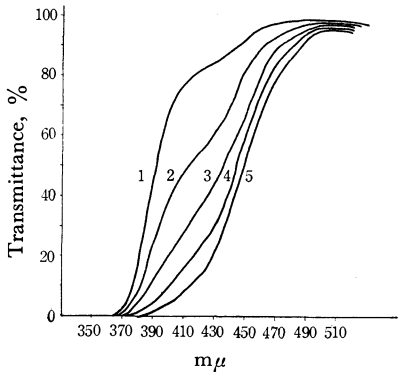

Fig. 1. Absorption curves of the reaction solutions at varying Cr^{3+} concentrations observed after 3-hr.'s reaction at room temperature.
Concentration of $K_4[Fe(CN)_6] \cdot 3H_2O$ after mixing is 10 mg./cc. in each case.

Curve No.	1	2	3	4	5
Cr^{3+} concn. after mixing, μg./cc.	0	10	20	30	40

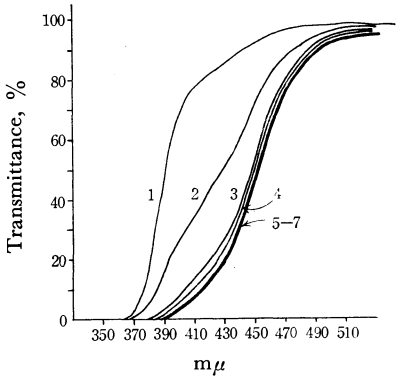

Fig. 2. Absorption curves at varying times after mixing.
Concentrations of Cr^{3+} and $K_4[Fe(CN)_6] \cdot 3H_2O$ after mixing are 40 μg./cc. and 10 mg./cc. respectively.

Curve No.	1	2	3	4	5	6	7
Period of time after mixing, min.	0	20	40	60	100	140	180

Experiments at 50°C.—The reaction time could be shortened with the elevation of the reaction temperature until the temperature attained 50°C, at which point a satisfactory coloration was obtained in only 15 min. A temperature above 50°C, however, was not desirable because the reaction solution became turbid.

The Relation between the Extinction at 415 mμ and the Cr^{3+} Concentration.—The solutions of chromium(III) ions and potassium ferrocyanide were mixed together in the various ratios shown in Fig. 3 and allowed to react together for 15 min. at 50°C;

* A part of this work was orally disclosed at the 11th Annual Meeting of the Japanese Society of Analytical Chemistry, Sapporo, July, 1962.

1) Y. Matsumoto and M. Shirai, *Japan Analyst* (*Bunsekikagaku*), **12**, 608 (1963).

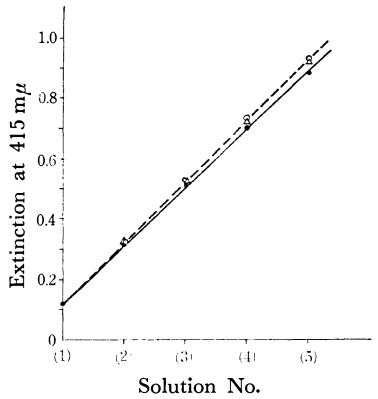

Fig. 3. Relation between color intensity and Cr^{3+} concentration after the reaction for 15 min. at 50°C.
(○) green, (△) blue } chromic chloride soln. (----)
(●) chrome alum soln. (——)
Concentration of $K_4[Fe(CN)_6]\cdot 3H_2O$ after mixing is 5 mg./cc. in each case.

Solution No.	(1)	(2)	(3)	(4)	(5)
Cr^{3+} concn. after mixing, μg./cc.	0	10	20	30	40

then the extinction of each reaction solution was measured at 415 mμ (Fig. 3). The results showed a strictly linear relationship between the color intensity and the Cr^{3+} concentration.

A Comparison of the Different Chromium(III) Salts.—A chromic chloride solution in a green color and one in a blue color, considered to contain chiefly the species $[Cr(H_2O)_4Cl_2]^+$ and $[Cr(H_2O)_5Cl]^{2+}$ respectively, were prepared; then the chromium(III) concentration in each solution was determined by the titration method using potassium permanganate and iron(II) sulfate solutions. These chromic chloride solutions were treated with a potassium ferrocyanide solution, and the extinction was measured under the conditions stated in Fig. 3, and compared with the chrome alum solution, which corresponds to $[Cr(H_2O)_6]^{3+}$. The extinctions of the both chromic chloride solutions agreed exactly with each other, and agreed fairly well with that of the chrome alum solution at the same chromium(III) concentrations.

Restriction in pH Value.—This color reaction was not satisfactory at low pH levels, especially below 2, and not an orange but a light blue color was caused at pH levels below 1.5 due to the decomposition of potassium ferrocyanide.

The Effects of Using an Acetic Acid - Sodium Acetate Buffer.—An acetic acid - sodium acetate buffer was found to interfere considerably with this coloration. One evidence responsible for the interference was that the acetic acid itself, reacting with potassium ferrocyanide, gave rise to some coloration during the requisite time for the purposed reaction, which is 1.5—3 hr. in the case of room temperature. At 50°C, however, the purposed reaction proceeded so quickly that the coloration by the reaction between acetic acid and potassium ferrocyanide was found to be negligible. The other interfering factor of acetic acid was its reaction with chromium, which resulted in a considerable decrease in the color intensity of the reaction solution. Thus the presence of acetic acid as a buffering agent is undesirable for this color reaction.

Summary

The color reaction of potassium ferrocyanide with chromium(III) ions in an aqueous solution has been observed. The absorption spectra of the reaction solutions for visible light were measured, and the coloration in relation to the reaction temperature, the reaction time, the characteristic absorption, the species of chromium(III) salts, the Cr^{3+} concentration, the pH level, and the presence of an acetic acid buffer has been studied.

For getting a satisfactory color reaction and for measuring it, a reaction for 15 min. at 50°C and an extinction measurement at 415 mμ were found to be best.

Between the extinction and the Cr^{3+} concentration in the solution of a given chromium(III) salt, a strictly linear relationship held. The same concentration of Cr^{3+} ions from different chromium(III) salts, such as chrome alum and chromic chloride, proved to give almost the same extinction.

This color reaction was not satisfactory at low pH levels. An acetic acid buffer interfered strongly with the coloration.

The authors are grateful to Dr. Konomu Matsumura and Dr. Akiji Fujita for their kind advice and their encouragement of this work, and Dr. Mamoru Mitomi for his kind cooperation in the absorption spectra measurements.

BULLETIN OF THE CHEMICAL SOCIETY OF JAPAN VOL. 39 58—64 (1966)

Copper(II) Halide Complexes with Substituted Pyridine *N*-Oxides

By Yoneichiro MUTO* and Hans B. JONASSEN

Department of Chemistry, Tulane University, New Orleans, Luisiana, U. S. A.

(Received April 14, 1965)

Pyridine *N*-oxide copper(II) chloride, the structure of which has recently been elucidated by X-ray analysis [J. C. Morrow and H. L. Schäfer, private communication], has a subnormal magnetic moment (0.85 B. M. [J. V. Quagliano, J. Fujita, G. Franz, D. J. Phillips, J. A. Walmsley and S. Y. Tyree (*J. Am. Chem. Soc.*, **83**, 3770 (1961)]). It consists of a binuclear molecule $[Cu(C_5H_5NO)Cl_2]_2$ in which copper atoms are bridged in pairs by two oxygen atoms. In this work, copper(II) complexes with the empirical formulae of CuX_2L, CuX_2L_2 and CuX_2LY (X=Cl, Br; L=pyridine *N*-oxide, 3-picoline *N*-oxide, 4-picoline *N*-oxide, 4-chloropyridine *N*-oxide, 2, 4-lutidine *N*-oxide, 2, 4, 6-collidine *N*-oxide, 4-nitroquinoline *N*-oxide; Y=*N*, *N'*-dimethylformamide, dimethylsulfoxide) have been prepared, and magnetic and spectral studies of these complexes have been made. The room-temperature magnetic susceptibilities of CuX_2L complexes have been found to be correlated with the pK_a (acid-dissociation constant) values of the attached *N*-oxides. The absorption band in the 735—900 mμ region (the so-called copper band) in the solid-state reflectance spectra of CuX_2L complexes has been found to shift towards a lower frequency as the ligand field strength decreases, and a good parallelism between the frequencies and the magnetic moments has been observed. The effect of the attached ligand on the magnetic interaction has been discussed in terms of the electronic effect of the substituent on the pyridine ring. The infrared spectral data on the N–O stretching frequency indicate the absence of Cu–O–Cu linkage in the CuX_2L_2 complexes with normal magnetic moments.

Quagliano et al.[1] prepared pyridine *N*-oxide copper(II) chloride with an abnormally low magnetic moment of 0.85 B. M. Kubo et al.[2] then suggested that this low magnetic moment is caused by the formation of binuclear oxygen-bridged molecules. Very recently this binuclear structure has been determined by a complete X-ray analysis[3] (Fig. 1.). Harris et al.[4] suggested, in a study of the temperature dependence of the magnetic susceptibility for this complex, that electron exchange demagnetization can occur between pairs of adjacent copper(II) ions via the oxygen atoms. In this case, the following two pathways for the migration of an electron may be set up:

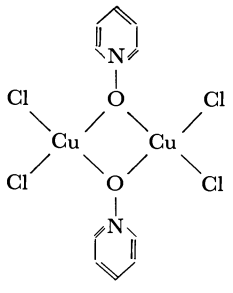

Fig. 1

σ-path: $3d_\sigma(Cu)-2sp_\sigma^2(O)-3d_\sigma(Cu)$

π-path: $3d_\pi(Cu)-2p_\pi(O)-3d_\pi(Cu)$

Either way, via the σ-path or via the π-path, the electron exchange interaction between Cu–O–Cu will become larger as the covalent bond between Cu–O becomes stronger.

The present work was undertaken in an attempt to elucidate the magnetic property in the dihalo copper(II) complexes with pyridine *N*-oxides. First, the complex of the empirical formula CuX_2L (1:1 complex) CuX_2L_2 (1:2 complex) and CuX_2L (1:1 complex) CuX_2L_2 (1:2 complex) and CuX_2LY (X=Cl, Br; L=pyridine *N*-oxide, 3-picoline *N*-oxide, 4-picoline *N*-oxide, 4-chloropyridine *N*-oxide, 2, 6-lutidine *N*-oxide, 2, 4, 6-collidine *N*-oxide, 4-nitroquinoline *N*-oxide; Y=*N*, *N'*-dimethylformamide, dimethylsulfoxide) were prepared. Secondly, the acid-dissociation constants (pK_a) of pyridine *N*-oxides and the magnetic susceptibilities of the copper(II) complexes at room temperature were determined in order to investigate the effect of the nature of the attached ligand on the magnetic interaction. Thirdly, the infrared and visible absorption spectra and the

* Presented address: Department of Chemistry, Saga University, Saga.

1) J. V. Quagliano, J. Fujita, G. Franz, D. J. Phillips, J. A. Walmsley and S. Y. Tyree, *J. Am. Chem. Soc.*, **83**, 3770 (1961).

2) M. Kubo, Y. Kuroda, M. Kishita and Y. Muto, *Australian J. Chem.*, **16**, 7 (1963).

3) J. C. Morrow and H. L. Schäfer, private communication.

4) C. M. Harris, E. Kokot, S. L. Lenzer and T. N. Lockyer, *Chem. & Ind.*, **1962**, 651.

Table I. Analytical date

Compound		Analysis, % C	H	N	Cu
$CuCl_2 \cdot 3\text{-}CH_3C_5H_4ON$	Found	29.65	2.98	5.61	26.11
	Calcd.	29.59	2.90	5.75	26.09
$CuBr_2 \cdot 3\text{-}CH_3C_5H_4ON$	Found	21.68	2.14	3.51	19.24
	Calcd.	21.68	2.12	4.21	19.11
$CuCl_2 \cdot 4\text{-}CH_3C_5H_4ON$	Found	29.73	3.03	5.81	26.06
	Calcd.	29.59	2.90	5.75	26.09
$CuBr_2 \cdot 4\text{-}CH_3C_5H_4ON$	Found	21.79	2.26	4.17	19.19
	Calcd.	21.68	2.12	4.21	19.11
$CuBr_2 \cdot (4\text{-}CH_3C_5H_4ON)_2$	Found	32.10	3.24	6.32	14.64
	Calcd.	32.64	3.20	6.34	14.39
$CuBr_2 \cdot (4\text{-}CH_3C_5H_4ON) \cdot (CH_3)_2SO$	Found	23.10	3.34	3.28	15.43
	Calcd.	23.40	3.19	3.41	15.47
$CuCl_2 \cdot 4\text{-}ClC_5H_4ON$	Found	23.09	1.71	4.79	23.95
	Calcd.	22.75	1.53	5.31	24.07
$CuCl_2 \cdot (4\text{-}ClC_5H_4ON)_2$	Found	30.33	2.19	6.75	16.34
	Calcd.	30.52	2.05	7.12	16.15
$CuBr_2 \cdot 4\text{-}ClC_5H_4ON$	Found	17.71	1.36	4.17	17.81
	Calcd.	17.02	1.14	3.97	18.00
$CuCl_2 \cdot 2,6\text{-}(CH_3)_2C_5H_3ON$	Found	32.82	3.52	5.37	24.79
	Calcd.	32.64	3.52	5.44	24.67
$CuBr_2 \cdot 2,6\text{-}(CH_3)_2C_5H_3ON$	Found	24.57	2.75	3.60	18.27
	Calcd.	24.26	2.62	4.06	18.34
$CuCl_2 \cdot 2,4,6\text{-}(CH_3)_3C_5H_2ON$	Found	35.42	4.13	4.87	23.20
	Calcd.	35.38	4.08	5.16	23.39
$CuCl_2 \cdot [2,4,6\text{-}(CH_3)_3C_5H_2ON]_2$	Found	46.98	5.53	6.91	15.66
	Calcd.	47.00	5.42	6.85	15.44
$CuBr_2 \cdot 2,4,6\text{-}(CH_3)_3C_5H_2ON$	Found	26.63	3.19	3.42	17.48
	Calcd.	26.65	3.06	3.89	17.62
$CuBr_2 \cdot [2,4,6\text{-}(CH_3)_3C_5H_2ON]_2$	Found	38.60	4.50	5.03	12.61
	Calcd.	38.61	4.46	5.63	12.77
$CuCl_2 \cdot 4\text{-}NO_2C_9H_6ON$	Found	33.22	1.80	8.08	19.55
	Calcd.	33.30	1.86	8.63	19.57
$CuCl_2 \cdot (4\text{-}NO_2C_9H_6ON)_2$	Found	42.16	2.26	10.77	12.32
	Calcd.	42.00	2.35	10.88	12.34

reflectance spectra were measured for the complexes in order to study the relation between the structure and the magnetic property.

Experimental

Materials.—Pyridine *N*-oxides were obtained commercially. The HCl salts of pyridine *N*-oxides for the pK_a determination were purified by recrystallization from ethanol.

The Preparation of the Copper(II) Complexes. —*1:1 Complexes.*—The complexes were prepared by mixing ethanol solutions of copper(II) halide and pyridine *N*-oxides in a 1:1 molar ratio. In the case of 2,4,6-collidine *N*-oxide, even though ethanol solutions of copper(II) halide and the *N*-oxide in a 1:1 molar ratio were mixed, the 1:2 complexes precipitated immediately. The 1:1 complexes were prepared by refluxing the 1:2 complexes and anhydrous copper(II) halide in a 1:1.5 molar ratio in ethanol for 1 to 2 hr. on a heater plate. However, the 1:1 complexes were rapidly converted to the 1:2 complexes in water, moist air, acetonitril, dioxane, dimethylformamide or dimethylsulfoxide.

1:2 Complexes.—The complexes were prepared by mixing ethanol solutions of copper(II) halide and

Table II. Magnetic susceptibility data (c. g. s., e. m. u.)

Ligand (L)	Complex	$10^6\chi_g$[b]	T °K	μ B. M.
4-Nitroquinoline *N*-oxide	$CuCl_2L$	4.72	297	1.99
	$CuCl_2L_2$	2.57	299	1.93
4-Chloropyridine *N*-oxide	$CuCl_2L$	−0.06	296	0.49
	$CuCl_2L_2$	2.79	284	1.71
	$CuBr_2L$	−0.14	294	0.45
3-Picoline *N*-oxide	$CuCl_2L$	0.05	297	0.55
	$CuBr_2L$	−0.10	291	0.48
4-Picoline *N*-oxide	$CuCl_2L$	0.00	298	0.52
	$CuBr_2L$	−0.12	291	0.47
	$CuBr_2L_2$	1.30	291	1.34
	$CuBr_2L \cdot DMS$[a]	0.77	291	1.07
2,6-Lutidine *N*-oxide	$CuCl_2L$	−0.39	297	0.22
	$CuCl_2L_2$	2.86	292	1.74
	$CuBr_2L$	−0.34	298	0.30
	$CuBr_2L_2$	2.48	289	1.80
2,4,6-Collidine *N*-oxide	$CuCl_2L$	−0.38	294	0.27
	$CuCl_2L_2$	4.44	298	2.20
	$CuBr_2L$	−0.22	289	0.42
	$CuBr_2L_2$	2.45	292	1.85

a) DMS is an abbreviation for dimethylsulfoxide.
b) χ_g is the gram susceptibility of the copper(II) complex.

TABLE III. CORRELATION BETWEEN pK_a VALUES OF THE LIGAND AND MAGNETIC MOMENTS OF THE COMPLEXES

Ligand (L)	pK_a (at 20±1°C)	Magnetic moment of complex, B. M.			
		$CuCl_2L$	$CuBr_2L$	$CuCl_2L_2$	$CuBr_2L_2$
4-Nitroquinoline *N*-oxide	−0.8	1.99		1.93	
4-Chloropyridine *N*-oxide	0.60	0.49	0.45	1.71	g)
		0.58[b]	0.23[b]	1.75[b]	
Pyridine *N*-oxide	0.79[a]	0.73[c]	0.53[c]	0.59[c]	1.46[c]
		0.77[d]	0.65[d]	0.63[e]	
		0.85[e]			
3-Picoline *N*-oxide	1.08[a]	0.55	0.48	g)	g)
4-Picoline *N*-oxide	1.29[a]	0.52	0.47	g)	1.34
		0.51[b]	0.26[b]		1.33[b]
2,6-Lutidine *N*-oxide	1.60	0.22	0.30	1.74	1.80
2,4,6-Collidine *N*-oxide	2.07	0.27	0.42[f]	2.20	1.85

a) These values were quoted from H. H. Jaffé and G. O. Dork, *J. Am. Chem. Soc.*, **77**, 4441 (1955).
b) Ref. 6.
c) M. Kishita, Y. Muto, M. Inoue and M. Kubo, presented at the 16th Annual Meeting of the Chemical Society of Japan, Tokyo, March—April, 1963.
d) Ref. 4.
e) Ref. 1.
f) The reason for the relatively high value seems to be that this sample is contaminated with a very small amount of the 1 : 2 complex; see the Experimental section.
g) These complexes have not been obtained.

pyridine *N*-oxides in a 1:2 molar ratio. Bis-2,4,6-collidine *N*-oxide copper(II) halide was purified by recrystallization from dimethylformamide, while the other complexes were purified by repeatedly washing them with cold ethanol. Except for the collidine *N*-oxide complexes, they all easily lost one mole of the ligand when heated in ethanol. Bis-4-picoline *N*-oxide copper(II) bromide, for instance, gradually lost one mole of 4-picoline *N*-oxide, even in cold ethanol.

The addition compounds of dimethylformamide or dimethylsulfoxide with 1:1 complexes were prepared by the recrystallization of the 1:1 complexes from the respective solvents.

The results of elementary analysis of the complexes are listed in Table I.

Magnetic Susceptibility Determinations.—These were made by the Gouy method at room temperature. The effective magnetic moment, μ, per copper atom was calculated from the expression $\mu=2.83\sqrt{\chi_M \cdot T}$ B. M. where χ_M is the molar susceptibility corrected using Pascal's constants[5] for the diamagnetism of the other atoms in the compounds. The experimental results are presented in detail in Table II, while the correlation between the pK_a values of the ligands and the magnetic moments of the complexes are listed in Table III.

pK_a Determination.—The pK_a values of the various bases were determined by ultraviolet absorption spectroscopy, which was used to measure the concentration of the free and protonated *N*-oxide bases in solutions with measured pH values. The pH measurements were made with a Beckman Zeromatic pH meter which had been calibrated with buffers; the pH values were determined at 20°C 1.07, 2.27, 3.33 and 7.00. The ultraviolet absorption spectra were obtained with a Beckman DB spectrophotometer.

5) G. Foëx, "Constantes Sélectionées Diamagnétisme et Paramagnétisme," Masson & Cie, Paris (1957), p. 222.

Infrared Spectra.—These were recorded on a Beckman IR-8 recording spectrophotometer. The

TABLE IV. ENERGIES OF THE N-O STRETCHING VIBRATION FOR THE PYRIDINE *N*-OXIDES AND COMPLEXES*

N-Oxide (L)	ν, cm^{-1}	Complex	ν, cm^{-1}
Pyridine *N*-oxide	1265[a]	$CuCl_2L$	1203[b]
		$CuCl_2L_2$	1223, 1206[b]
		$CuCl_2L$·DMF**	1203
		$CuCl_2L$·DMS	1203
		$CuBr_2L$	1200
		$CuBr_2L_2$	1211, 1201
		$CuBr_2L$·DMF	1202
3-Picoline *N*-oxide	1285[a]	$CuCl_2L$	1248
		$CuBr_2L$	1244
4-Chloropyridine *N*-oxide	1269[a]	$CuCl_2L$	1195
		$CuCl_2L_2$	1209, 1195
		$CuBr_2L$	1199
4-Picoline *N*-oxide	1260[a]	$CuCl_2L$	1200
		$CuBr_2L$	1203
		$CuBr_2L_2$	1240, 1209
		$CuBr_2L$·DMS	1211
2,6-Lutidine *N*-oxide	1255[a]	$CuCl_2L$	1199
		$CuCl_2L_2$	1208
		$CuBr_2L$	1195
		$CuBr_2L_2$	1203
2,4,6-Collidine *N*-oxide	1247[a]	$CuCl_2L$	1199
		$CuCl_2L_2$	1208
		$CuBr_2L$	1202
		$CuBr_2L_2$	1205

* The values with superscript a and b were quoted from Ref. 7 and Ref. 1, respectively.
** DMF is an abbreviation for *N*,*N'*-Dimethylformamide.

TABLE V. REFLECTANCE SPECTRA DATA: λ_{max} (mμ)

Ligand (L)	$CuCl_2L$		$CuBr_2L$		
	λ_1	λ_2	λ_1	λ_2	λ_{Br}
1. 2,4,6-Collidine *N*-oxide	750	410	735	425	530
2. 2,6-Lutidine *N*-oxide	760	425	745	440	530
3. 4-Chloropyridine *N*-oxide	800	430	800	*	525
4. 4-Picoline *N*-oxide	835	425	830	*	505
5. 3-Picoline *N*-oxide	850	420	840	455	520
6. Pyridine *N*-oxide	940	418	900	*	510
7. 4-Nitroquinoline *N*-oxide		400			

* The band with this mark is so broad that the exact band peak can not be determined.

TABLE VI. VISIBLE SPECTRA DATA IN A VARIETY OF SOLVENTS: λ_{max} (mμ)

Solvents: A, Methanol; B, Nitromethane; C, Dioxane; D, Acetone; E, Acetonitril; F, *N*,*N*'-Dimethylformamide; G, Dimethylsulfoxide.

1. 2,4,6-Collidine *N*-oxide $CuCl_2$*

	λ_1	λ_2
B	783	

2. 2,4,6-Collidine *N*-oxide $CuBr_2$*

	λ_1	λ_2	λ_{Br}
B	775		630

3. 2,6-Lutidine *N*-oxide $CuCl_2$

	λ_1	λ_2
A	802	
B	789	
C	795	
D	793	
E	790	445
F	794	436
G	802	—**

3. 2,6-Lutidine *N*-oxide $CuBr_2$

	λ_1	λ_2	λ_{Br}
A	800		
B	773		658
C	795		
D	795		
E		429	637
F		—	593
G	799	—	

5. 4-Chloropyridine *N*-oxide $CuCl_2$

	λ_1	λ_2
A	785	
B	786	
C	795	
D	780	480
E	781	458
F	786	435
G	781	—

6. 4-Chloropyridine *N*-oxide $CuBr_2$

	λ_1	λ_2	λ_{Br}
A	790		
B	772		623
C	795		
D			651
E		429	636
F		—	593
G	778	—	

7. 3-Picoline *N*-oxide $CuCl_2$

	λ_1	λ_2
A	778	
B	780	
C	785	
D	777	472
E	780	468
F	780	435
G	778	—

8. 3-Picoline *N*-oxide $CuBr_2$

	λ_1	λ_2	λ_{Br}
A	787		
B	775		618
C	800		
D		428	653
E		425	637
F		—	597
G	778	—	

9. 4-Picoline *N*-oxide $CuCl_2$

	λ_1	λ_2
A	785	
B	785	
C	793	
D	785	470
E	782	457
F	785	435
G	778	—

10. 4-Picoline *N*-oxide $CuBr_2$

	λ_1	λ_2	λ_{Br}
A	788		
B	780		622
C	780		
D		436	652
E		425	638
F		—	592
G	780	—	

11. Pyridine *N*-oxide $CuCl_2$

	λ_1	λ_2
A	791	
B	784	
C	790	
D	782	477
E	784	453
F	782	434
G	795	430

12. Pyridine *N*-oxide $CuBr_2$

	λ_1	λ_2	λ_{Br}
A	783		
B	784		632
C	787		
D		472	653
E		435	632
F		—	590
G	780	—	

13. 4-Nitroquinoline *N*-oxide $CuCl_2$

	λ_1	λ_2
A	778	
B	778	
C	778	
D	788	465
E	778	455
F	788	438
G	790	—

* Compound 1 and 2 converted to the 1 : 2 complex in each solvents employed except nitromethane.

** The band with this mark should be hidden in the absorption band of the ligand.

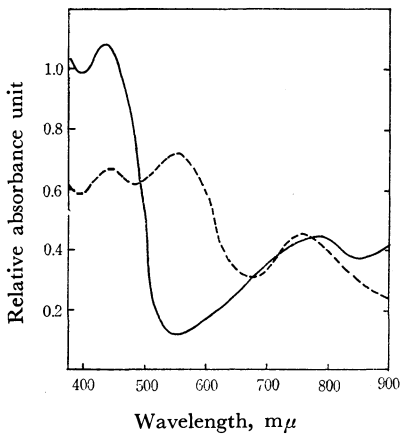

Fig. 2a. Reflectance spectra of 2,6-lutidine *N*-oxide Cu(II) halide.
—— Chloride complex ---- Bromide complex

spectra were taken in both Nujol mulls and KBr disks. The energy of the intense band near 1200 cm^{-1} for each of the complexes and the free ligand are given in Table IV.

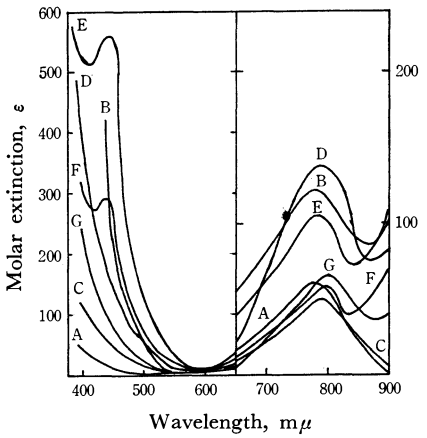

Fig. 2b. Absorption spectra of 2,6-lutidine *N*-oxide $CuCl_2$ in seven different solvents. The letters indicate the solvents noted in Table VI.

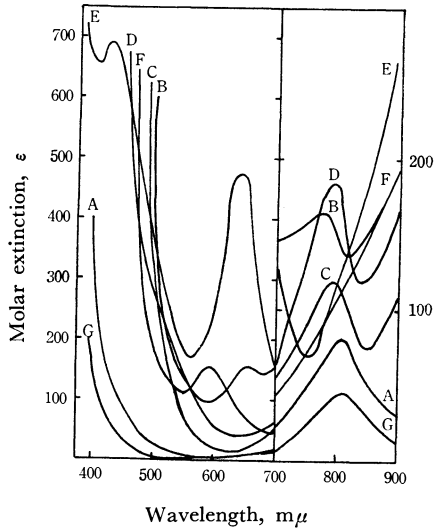

Fig. 2c. Absorption spectra of 2,6-lutidine *N*-oxide $CuBr_2$ in seven different solvents. The letters indicate the solvents noted in Table VI.

Diffuse Reflectance Spectra.—The diffuse reflectance spectra of the 1:1 complexes were measured in the 375—900 mμ region on a Beckman DU spectrophotometer with a reflectance attachment. The band maxima are recorded in Table V. Fig. 2a gives the reflectance spectra for 2,6-lutidine *N*-oxide complexes.

Visible Absorption Spectra.—The visible absorption spectra of the 1:1 complexes in a variety of solvents were determined on a Cary model 14 recording spectrophotometer in the 400—900 mμ region. The absorption maxima are recorded in Table VI, while the absorption curves for 2,6-lutidine *N*-oxide complexes are shown in Figs. 2b and 2c.

Results and Discussion

The pK_a Values of Ligands and Magnetic Moments of Complexes.—The 1:1 Complex (CuX_2L).—As is sown in Table II, there is a good correlation between the pK_a values of the *N*-oxides and the magnetic moments of the 1:1 complexes with the oxides, except with 4-chloropyridine *N*-oxide. These data demonstrate that the larger tendency of the *N*-oxide to coordinate with the copper(II) ion results in a larger magnetic interaction.

The introduction of the methyl group on the pyridine ring results in an increase in the pK_a value. Since the pK_a value of the *N*-oxides reflects the σ-electron density on the oxygen atom, such an increase in the value is considered to be caused by the inductive effect of the methyl group. The increase in the electron density on the oxygen atom results in an increase in the Cu-O σ-bond strength, leading to a greater magnetic interaction through the σ-path of the Cu–O–Cu bridge.

The introduction of a chlorine atom on the pyridine ring results in a decrease in the pK_a value as a result of the σ-electron-attracting effect of the chlorine atom. Although the magnetic moment of 4-chloropyridine *N*-oxide copper(II) halide is to be expected in view of the pK_a value of the ligand being smaller than that of the pyridine *N*-oxide complex, just the opposite was observed. However, it is a well-known fact that the chlorine atom conjugated to an aromatic ring has both σ-attracting and π-releasing effects. It seems reasonable, therefore, to conclude that the π-electron on the chlorine atom in the 4-position is conjugated with the π-electron system of pyridine *N*-oxide to increase the π-electron density on the oxygen atom. Consequently, the lowering of the magnetic moment may be interpreted as resulting from the superexchange interaction through the π-path, provided the π-path is more effective for the interaction than the σ-path. The magnetic data for 4-hydroxypyridine *N*-oxide copper(II) chloride (molar magnetic susceptibility: χ_M= 0 at 24.8°C)[6] also suggest the superexchange interaction through the π-path. It is, however, difficult to evaluate the effects of the σ- and π-paths separately at present. Further studies along this line are in progress.

The 1:2 Complex (CuX_2L_2).—No regular correlation between the pK_a value of the ligand and the magnetic interaction in the 1:2 complexes is observed. The observed magnetic moments seem to indicate that the further addition of a ligand to a 1:1 complex produces either a slight or a complete structural change, because the magnetic interaction must be affected by even a slight change in the bond angle in the Cu–O–Cu bridge. The structure shown in Fig. 3 is reasonable for 1:2 complexes with a normal magnetic moment. In the case of complexes with a subnormal magnetic moment, the easy removal of one ligand molecule

6) W. E. Hatfield, Y. Muto, H. B. Jonassen and J. S. Paschal, *Inorg. Chem.*, **4**, 97 (1965).

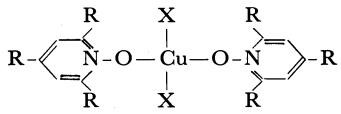

(R: H, CH_3; X: Cl, Br)

Fig. 3

seems to indicate that one molecule of ligand is weakly bonded to the copper(II) atom, whereas the other forms the Cu–O–Cu linkage with copper atoms. The infrared spectra studies of the N–O stretching frequency support the above conclusion for the 1:2 complexes also, as will be seen in the next section.

Infrared Spectra.—The strong absorption in the 1200—1300 cm^{-1} region in the infrared spectrum of pyridine *N*-oxide and its derivatives has been assigned to their characteristic N–O stretching vibration.[7,8] Kida et al.[9] reported that the coordination of pyridine *N*-oxide with metal ions results in a decrease in the contribution of the mesomeric structure B shown in Fig. 4 and, consequently, in a decrease of the NO double-bond character and in a lowering of the N–O stretching frequency.

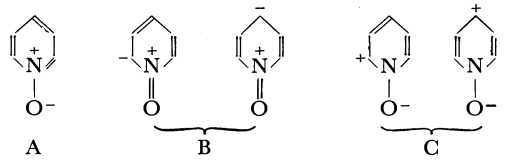

Fig. 4

The NO double-bond character in the 1:1 complexes is expected to be smaller than that in the 1:2 complexes with a normal magnetic moment. This is because a larger electron donation from NO groups is necessary to form the Cu–O–Cu linkage than to form the single coordination shown in Fig. 3 (see also Table IV). The absorption energies of the N–O stretching vibration of the 1:1 complexes were lower than the values for the 1:2 complexes with a normal magnetic moment. This observation is in agreement with our expectation. On the other hand, 1:2 complexes with a subnormal magnetic moment show two N–O stretching frequencies, suggestive of two kinds of NO bonds, for instance, 1223 and 1206 cm^{-1} in bis-pyridine *N*-oxide copper(II) chloride. The assignment of 1223 cm^{-1} to the NO frequency of weakly-bonded pyridine *N*-oxide and 1206 cm^{-1} to the NO frequency of bridged pyridine *N*-oxide are reasonable in view of the chemical property, the magnetic moment and the double-bond character.

Reflectance Spectra.—The spectra which are observed may be conveniently classified into three groups by region: λ_1, 735—940 mμ; λ_2, 400—435 mμ; λ_{Br}505—530 mμ.

λ_1: A band of a relatively low intensity is observed in this region for all the 1:1 complexes studied. From the frequency and the intensity, the band in this region can undoubtedly be attributed to the so-called copper band, a transition within the d shell. This shifts towards lower frequencies as the ligand field strength decreases (cf. Table V). A good parallelism is seen between the frequencies and the magnetic moments. In all the 1:1 complexes the copper atom is combined with two halogen atoms; hence, it may be presumed that the ligand field strength provided by the halogen atoms for the copper atom is almost the same in all the 1:1 complexes.

According to the molecular orbital theory, the splitting of metal d orbitals is essentially attributed to covalent bonding. The greater the overlap of metal d orbitals with the ligand orbitals, the higher in energy will be the antibonding orbital (σd*).[10] Therefore, the frequency of this band may be taken as a measure of the degree of covalency in the Cu–O linkage. The magnetic interaction will become greater as the orbital overlap between the copper and oxygen atoms becomes larger. It may thus be concluded, provided that the ligand-field strength reflects the σ-bond strength of Cu–O linkage, that the superexchange interaction occurs through the σ-path of the Cu–O–Cu bridge.

λ_2: A band of a relatively high intensity is observed in this region for all the 1:1 complexes studied. This corresponds to the band at 350—400 mμ for bivalent metal complexes with picolinic acid *N*-oxide which has been observed and tentatively assigned to a charge transfer, $d_\varepsilon \rightarrow \pi^*$, by Lever et al.[11] A similar band has been observed in solutions, as will be seen in the next section, though this appears at lower frequencies than the band in crystals.

λ_{Br}: In addition to λ_1 and λ_2, a band of a relatively high intensity is observed in this region for all the bromide complexes studied. It is missing, however from the spectra of all the chloride complexes studied. This band has been observed also in solutions of bromide complexes. This band seems to appear by cooperation of copper(II) ion, bromide ion and π-acceptor in a certain environment. However, more work is necessary before we can give it a definite assignment.[12]

7) H. Shindo, *Chem. Pharm. Bull.* (*Tokyo*), **4**, 460 (1956); **6**, 117 (1958); **7**, 191 (1959).
8) G. Costa and P. Blasina, *Z. Phys. Chem.* (*Frankfurt*), **4**, 24 (1955).
9) S. Kida, J. V. Quagliano, J. A. Walmsley and S. Y. Tyree, *Spectrochemica Acta*, **19**, 189 (1963).
10) See, for example, K. Ito and Y. Kuroda, *J. Chem. Soc. Japan, Pure Chem. Sect.* (*Nippon Kagaku Zassi*), **76**, 766, 934 (1955); B. Basolo and R. Johnson, "Coordination Chemistry," W. A. Benjamin, New York, N. Y. (1964), p. 56.
11) A. B. P. Lever, J. Lewis and R. S. Nyholm, *J. Chem. Soc.*, **1962**, 5262.
12) M. Kato, Y. Muto and H. B. Jonassen, unpublished.

Visible Absorption Spectra in a Variety of Solvents.—All the 1:1 complexes are very insoluble in solvents with practically no coordination tendency, such as benzene or chloroform, but they are soluble in organic solvents capable of coordination. The spectra in solutions are somewhat different from the reflectance spectra, as is shown in Table VI and in Figs. 2a, b, and c. This shows that solvation occurs even when the coordination power of the solvent is not high, such as in methanol or nitromethane.

Although the absorption bands for various 1:1 complexes in different solvents differ from one another, they may be classified into three groups just as those of crystals: λ_1, 770—800 mμ; λ_2, 420—460 mμ; λ_{Br}, 590—660 mμ.

λ_1: An absorption band of a low intensity ($\varepsilon \sim 100$) is observed in this region for all the chloride complexes in each solvent. In the case of bromide complexes, an absorption band in this region is observed in weak coordinating solvents, but not in relatively strong coordinating solvents. However, it seems from the shape of the absorption curves that the band peaks in strong coordinating solvents exist at lower frequencies, perhaps near 900 mμ, outside the range of the present measurements.

λ_2: An absorption band is observed in this region for all the complexes in relatively strong coordinating solvents, such as dimethylsulfoxide, *N, N'*-dimethylformamide, acetonitrile and acetone. It is absent, however, from the spectra of the complexes in weak coordinating solvents, such as methanol, nitromethane and dioxane. It has a considerable intensity (ε 300—700) and shifts towards higher frequencies with an increase in the coordination power of the solvents. Recently, a similar band in the near ultraviolet region has been observed for a number of copper(II) complexes; it has been variously ascribed to a d-d transition,[13] a ligand transition,[14] or a charge transfer.[11,15] However, more experimental and theoretical studies are necessary before this band can be assigned definitely.

λ_{Br}: A band in this region is observed for the bromide complexes but not for the chloride complexes, as in crystals. Furthermore, this band is observed in solvents which have a π-electron accepting ability, but not in solvents which do not have an appreciable π-character.

The financial support of the Office of Naval Reseach under Contract No. 47509 is gratefully acknowledged. Fruitful discussions with Dr. M. Kato of Aichi Women's College are also gratefully acknowledged.

13) D. P. Graddon, *J. Inorg. Nuclear Chem.*, **14**, 161 (1960).
14) T. S. Piper and R. L. Belford, *Mol. Phys.*, **5**, 169 (1962); R. L. Belford and T. S. Piper, ibid., **5**, 251 (1962); G. Basu, R. L. Belford and R. E. Dickerson, *Inorg. Chem.*, **1**, 438 (1962).
15) D. W. Barnum, *J. Inorg. Nuclear Chem.*, **21**, 221 (1961); R. L. Carlin, *J. Am. Chem. Soc.*, **83**, 3773 (1961).

BULLETIN OF THE CHEMICAL SOCIETY OF JAPAN VOL. 39 64—71 (1966)

Molecular Structure Determination by Gas Electron Diffraction at High Temperatures. I. Arsenic

By Yonezo MORINO,† Takeshi UKAJI††,* and Tetsuzo ITO†,**

†*Department of Chemistry, Faculty of Science, The University of Tokyo, Hongo, Tokyo*
††*Department of Chemistry, Ibaraki University, Mito*

(Received April 17, 1965)

A high-temperature nozzle assembly for gas-electron diffraction has been designed and constructed. The molecular structure of gaseous arsenic at 485°C has then been investigated by the use of this nozzle. The regular tetrahedral structure of the molecule has been confirmed from the observed index of resolution; the interatomic distance has been determined to be r_g(As-As)= 2.435±0.004Å, while the mean amplitude has been determined for the first time (l(As-As)= 0.085±0.006Å). The observed amplitude has led to the evaluation of the bond-stretching force constant, f_r(As-As)=1.5±0.3 mdyn./Å.

Recent technical and theoretical developments in the method of gas electron diffraction have made it possible to determine interatomic distances and the mean amplitudes of thermal vibrations in molecules with a precision of a few thousandths of an angstrom. These data are important for elucidating molecular structure. For instance,

* Present address: Ikutoku Kosen, Atsugi, Kanagawa.
** Present address: The Institute of Physical and Chemical Research, Komagome, Tokyo.

the observed interatomic distances reveal various effects of thermal vibrations, and the mean amplitudes afford information on intramolecular forces. However, almost all such high-precision data have been obtained at room temperature; experiments at higher temperatures are usually much more difficult.

About thirty years ago, Maxwell and his co-workers investigated the molecular structure of alkali halides[1] and other molecules[2] at temperatures up to about 1300°C by the visual method. Since then, several investigators have designed and used high temperature nozzles for determining the molecular structure of compounds with low vapor pressures. For example, Kimura and Aoki (1953)[3] investigated acetamide and *N*-methylacetamide at about 250°C by the visual method; Bauer and his co-workers (1960)[4] studied lithium chloride at about 820°C by the same method, and Akishin and his co-workers (1958–) studied alkali halides[5] and other molecules[6,7] in the temperature range up to about 1500°C by the sector-microphotometer method.[8] The uncertainties in the observed interatomic distances ranged from 0.02 to 0.04 Å, and the values of mean amplitudes were only tentative even when they were reported. More recently, Hedberg and Iwasaki (1962)[9] for the first time observed the temperature effects on the interatomic distances and mean amplitudes of phosphorus trichloride by taking diffraction photographs at 27 and 232°C and by applying a least-squares treatment to the molecular intensity curves.

For the present work, a high-temperature nozzle assembly for high-precision studies was designed, constructed, and used for the study of the molecular structure of arsenic in the vapor phase. When the structure of this molecule was studied by Maxwell and his co-workers (1935)[2] at about 500°C by the visual method of gas electron diffraction, they observed one interatomic distance, 2.44 ± 0.03 Å; with the aid of the vapor density data,[10] which indicate that the molecule is predominantly tetratomic below 800°C, they concluded that the molecule has a regular tetrahedral structure. No spectroscopic information has up until now been available on the force field of this molecule.

1) L. R. Maxwell, S. B. Hendricks and V. M. Moseley, *Phys. Rev.*, **52**, 968 (1937).
2) L. R. Maxwell, S. B. Hendricks and V. M. Moseley, *J. Chem. Phys.*, **3**, 699 (1935).
3) M. Kimura and M. Aoki, This Bulletin, **26**, 429 (1953).
4) S. H. Bauer, T. Ino and R. F. Porter, *J. Chem. Phys.*, **33**, 685 (1960).
5) P. A. Akishin and N. G. Rambidi, *Z. Phys. Chem.*, **213**, 111 (1960).
6) P. A. Akishin, V. A. Naumov and V. M. Tachevskiy, *Moscow University Report* (*U. S. S. R.*), **1**, 229 (1959).
7) V. P. Spiridonov, P. A. Akishin and V. I. Tsirelinikov, *J. Structural Chem.* (*U. S. S. R.*), **3**, 329 (1962).
8) P. A. Akishin, M. I. Vinogradov, K. D. Danilov, N. P. Levkin, E. N. Martinson, N. G. Rambidi and V. P. Spiridonov, *Instruments and Experimental Technique* (*U. S. S. R.*), **2**, 70 (1958).
9) K. Hedberg and M. Iwasaki, *J. Chem. Phys.*, **36**, 589 (1962).
10) J. W. Mellor, "A Comprehensive Treatise on Inorganic and Theoretical Chemistry," Vol. IX, Longmans, London (1929), p. 23.

Experimental

The Construction of the High-Temperature Nozzle Assembly.—After a series of preliminary tests on possible difficulties which were expected to arise in electron-diffraction experiments at high temperatures (the chemical and thermal instability of materials, difficulty in the control of the rate of gas effusion, the fogging of photographic plates due to radiation from the heated assembly, etc.), a nozzle assembly useful for high-precision studies in the temperature range up to 600°C was designed and constructed.

A diagram of the nozzle assembly is shown in Fig. 1. The sample is heated to a required temperature in the oven, 1; the stopcock valve, 2, is then opened, and the vapor is ejected through the capillary nozzle, 3, into the diffraction camera, where it scatters electron beams at about 0.4 mm. above the nozzle outlet. About 2 cm. above the nozzle, there is a brass cold trap cooled with liquid nitrogen designed to condense the ejected vapor. The distinctive features of this nozzle assembly are the material of the nozzle and the construction of the stopcock valve. The oven and the nozzle are made of quartz, which is suitable because of its chemical and thermal stability (the linear expansion coefficient: 4.8×10^{-7}/deg.; the softening temperature: 1300°C). The thermal stability of the nozzle is essential for the accurate determination of the camera length. The nozzle is equipped with a stopcock valve lubricated with a small amount of fine graphite powder in order that the gas can be introduced into the camera chamber for a desired length of time; it also enables a fine control of the rate of sample effusion. Diffraction photographs can be obtained at any fixed temperatures up to 600°C by the use of this valve. The valve is also useful for the study of a reaction system in the vapor phase because it prevents any one of the reactants from evaporating out of the oven through the outlet before the system attains the thermal equilibrium at the desired temperature.

The oven, the capillary nozzle and the cover-framework, 4, are all made of quartz. The oven, about 15 ml. in volume, contains enough sample gas for three successive 4-mmHgl. exposures. The length of the capillary nozzle is about 20 mm., while the inner diameter at the outlet is about 0.2 mm. The edge of the top of the nozzle is cut off lest it should interrupt the scattered electrons. The upper part of the nozzle is covered with gold foil grounded through a fine wire in order to avoid the charging-up of the nozzle, which might cause a drift of the electron beam.

The oven and the nozzle are individually heated with a 10—40 V. a. c. current supplied through coils of nichrome wires, which are supported by a number of small projections of quartz attached to the walls of the oven and the nozzle and which are covered with quartz-wool. The magnetic field produced by the electric current is minimized by a dual winding of nichrome wires in opposite directions. The fluctuation of the electron beam due to the magnetic field is found to be negligible under these working conditions (the electric current up to about 1 amp.). The temperatures of the oven and the nozzle are measured with two alumel-

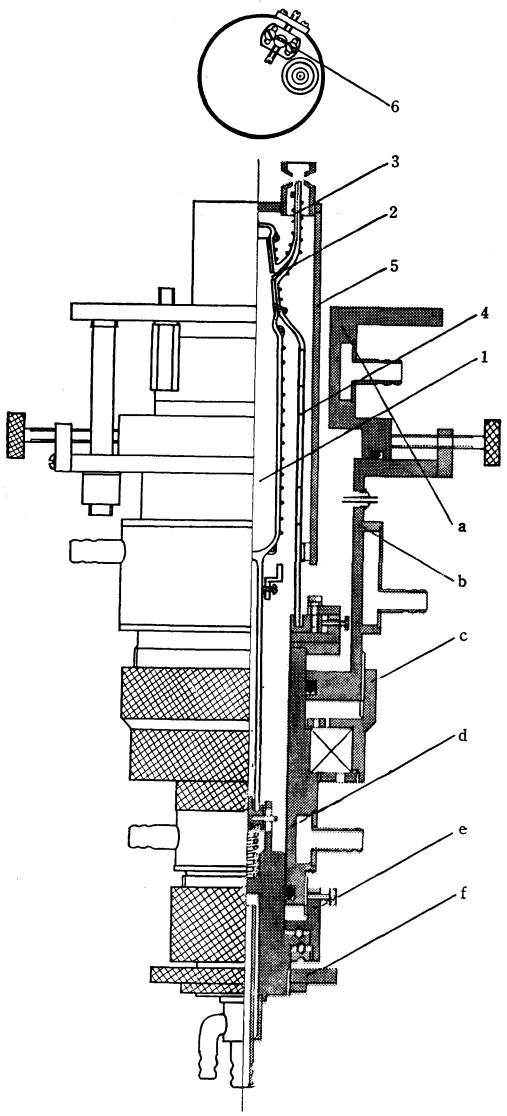

Fig. 1. High-temperature nozzle assembly.
1 Oven, 2 Stopcock, 3 Nozzle, 4 Framework, 5 Shield, 6 Gold-foil support, a—f Parts of the oven holder.

chromel thermocouples placed in contact with the walls. The difference between the temperature of the ejected gas and that of the nozzle, as measured by the thermocouple, is estimated to be less than 30°C.* The oven and the nozzle can be heated to 600°C in about 15 min. A little degassing from the nozzle assembly during heating does not affect the vacuum of the diffraction camera (ca. 2×10^{-5} mmHg). In the temperature range up to 600°C, the fogging of photographic plates due to radiation from the heated assembly is easily eliminated by means of a radiation shield, 5, which covers the oven and the nozzle. A support, 6, for mounting the gold foil necessary for the calibration of the electron wavelength and the camera distance is attached to the shield.

The oven and the cover-framework are supported by an oven-holder which consists of the following six parts, a to f. Part a is designed for fixing the whole assembly on to the diffraction camera; Part b, for adjusting the position of the nozzle in a plane parallel to the electron beam; Part c, for changing the height of the nozzle, and Part d, for rotating the assembly in such a way that the gold foil is placed in the beam, and also for supporting the cover-framework of the oven. (The framework is cemented to the support with the epoxy adhesive "Araldite.") The vacuum-tightness of the stopcock is assured by Part e, which pushes the oven against the cover-framework, while Part f supports the oven and transmits to the axis of the oven the rotation necessary for opening and shutting the stopcock. A steel spring is inserted between Part f and the axis in order to apply proper pressures on the stopcock and to make allowance for any possible mechanical eccentricity of the male part of the stopcock with respect to the female part. The sample can be easily loaded and unloaded by pulling down the oven, together with Part e and Part f. All parts are made of brass, and Parts a, b, d and f are water-cooled. Various parts of the assembly are made vacuum-tight with O-rings; they are operated independently by means of ball-bearing systems. The whole assembly was processed in the workshop of the Tokyo Shibaura Electric Co.

The Calibration of the Camera Length.—The nozzle assembly was attached to a diffraction camera equipped with an r^3-sector.[11] The cold trap which covered the nozzle was replaced by a glass-window, and the plate-to-gold foil distance, L_g, was adjusted so as to be equal to the camera length, L_c (the distance from the plate to the center of the nozzle outlet) using a comparator. Fine adjustments were made by means of a screw attached to the gold-foil support. The error in the agreement between L_g and L_c was kept to within 0.05 mm., a value which could introduce an error of only about 0.05% in the scale factor, since the camera length was 106 mm. Deviations in the camera length during the heating up to 600°C were also found to be within 0.05 mm.

During the diffraction experiments, however, the rotation of the nozzle assembly necessary for locating the center of the gold foil in the electron beam could not be adjusted using a comparator, since the cold trap obstructed the field of vision. The adjustment was thus made by observing, through a side-window, the images of the electron beam and of the gold-foil support on a fluorescent screen. Another sheet of gold foil was placed in front of the nozzle assembly in order to make the images during the adjustments. An uncertainty in the angle of rotation of the nozzle assembly could be another source of the error in the scale factor.

Figure 2 shows a schematic diagram of the top-view of the nozzle assembly, where R is the radius of the circumference on which the centers of the nozzle outlet

* The temperature measured by the thermocouple was calibrated at 270°C by the following procedure. A small crystal of anthraquinone was placed on top of the nozzle above the outlet while heated iodine gas was ejected through the capillary nozzle. The temperature, as measured by the thermocouple, was 270°C when the crystal began to melt. This temperature was in agreement with the observed melting point of the crystal within a range of experimental error of about ±5°C.

11) Y. Morino, K. Kuchitsu and E. Hirota, "Experimental Chemistry" (Jikken Kagaku Koza), Vol. 3, Maruzen Co., Tokyo (1957), p. 253.

and of the gold foil move, and O is the center of rotation. As is evident from the figure, an error in the angle of rotation, $\Delta\theta$, introduces an error in the camera distance:

$$\Delta Lc = R\Delta\theta\sin\theta$$

In order to assure a 0.1% accuracy in the scale factor, ΔLc must be less than 0.1 mm. If we take the radius of the gold foil, 1 mm., as approtimately the maximum of $R\Delta\theta$, it is necessary to adjust θ to be less than 6°. In the following experiments, care was taken to adjust the center of the rotation of the nozzle assembly to just below the electron beam, as well as to minimize errors in the angle or rotation.

By the use of this nozzle assembly, diffraction photographs of iodine vapor have recently been taken at 80°C, 300°C and 500°C by one of the present authors.[12] A preliminary analysis has shown that the observed interatomic distances r_g(I-I) at these temperatures are in agreement with the values calculated from the spectroscopic data[13,14] within 0.15%. This uncertainty can be regarded as a measure of the total error in the scale factor of this nozzle assembly.

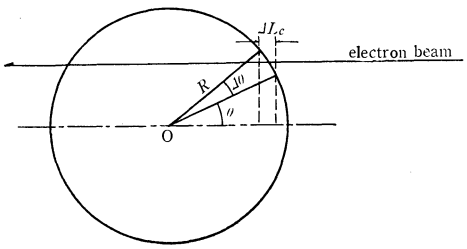

Fig. 2. Error in the camera distance ΔLc caused by the error in the angle of rotation $\Delta\theta$.

Diffraction Photographs of Arsenic. — Solid arsenic was kindly supplied by the Tokyo Shibaura Electric Co. The oxide which had covered the surface of the crystal was easily removed by heating it to about 300°C in a vacuum. The diffraction photographs were taken on Fuji Process-hard plates, with a camera distance of 106 mm., an accelerating voltage of the electron beam of about 43 kV., a beam current of about 0.005 μamp., and exposure times of from two to three minutes. The nozzle temperature was 485±30°C. The photographs were developed for five minutes in a FD-131 developer diluted twice at 20°C. The optical densities of the photographs ranged from 0.1 to 0.4, and the measured range of the scattering angle was from 20 to 100 in the q-scale.

Analytical Procedure

The interatomic distance and the root-mean-square amplitude of arsenic in the vapor phase were determined from the diffraction photographs by a procedure similar to that usually applied.[15] The final results were obtained by a least-squares analysis of the molecular intensity curves, $qM(q)$. All the calculations were carried out by using an electronic computer, PC-2.[16]

Molecular Intensity.—Four diffraction photographs were selected for the analysis; they were traced across the diameter of the diffraction pattern with a Rigaku-Denki MP-3 microphotometer while being rotated rapidly around the center of the pattern. In order to record fine details of the pattern, the transmittancy range corresponding to the undulations of the curve was magnified to about five times the original scale (full scale; 24 cm.) by the use of an electronic amplifier built into the photometer. The magnification ratio was later determined by a least-squares fit of the magnified curve to that of the original scale.

The photometer curves of the magnified and the original scales were measured at intervals of $\Delta q=1$; a value taken from one side of a curve was combined with the corresponding value from the other side, and an average was taken point by point. The distance, $x(q)$, on the abscissa of a photometer chart corresponding to the scattering angle, q, was calculated by using the value of $L_c\lambda$, which was obtained as $L_g\lambda$ from a transmission pattern of gold foil after L_g was corrected for the inclination of the photographic plate by the method of Iijima.[17],* A linear relation between the density and the intensity was assumed, since the densities of all the photographs used for the analysis were less than 0.4.[17]

After the intensity curve was corrected for the deficiency of the sector opening[18] (i. e., for the deviations from the defined opening of cr^3), it was divided by a levelling function, $f(q)$, in order to obtain a levelled intensity curve, $I_L(q)$, which facilitated the drawing of a background line, $I_B(q)$. The $f(q)$ function was derived by a least-squares fit of the intensity curve to a quadratic function. The most probable background line was obtained after two cycles of redrawing the line according to the non-negativity criterion with respect to the radial distribution curve, in which only one peak was observed. The artificial damping factor was so chosen as to reduce the molecular intensity to one-tenth of the original at $q=100$.

The experimental molecular intensity curve, $qM(q)$, was calculated as:

$$qM(q) = q\{I_L(q) - I_B(q)\}/I_B(q) \qquad (1)$$

while the theoretical expression for a tetratomic molecule, As_4, is given by the equation;[15]

12) Y. Morino and T. Ukaji, to be published.
13) G. Herzberg, "Molecular Spectra and Molecular Structure," D. Van Nostrand Company, New York (1950), p. 541; L. S. Bartell, *J. Chem. Phys.*, **23**, 1219 (1955).
14) K. Kuchitsu and L. S. Bartell, ibid., **35**, 1945 (1961).
15) Y. Morino, Y. Nakamura and T. Iijima, *J. Chem. Phys.*, **32**, 643 (1960).
16) Y. Murata, T. Ito and K. Kuchitsu, "Bussei," **2**, 39 (1964).
17) Y. Morino and T. Iijima, This Bulletin, **35**, 1661 (1962).
* The inclinations of the photographic plates placed in the three positions, A, B and and C, were re-examined because the setting of the disk on which the three plates were mounted had been changed during recent leak tests. The following correction factors, which were not very different from those reported by Iijima, were obtained:
A −0.23±0.02%, B 0.06±0.03%, C 0.01±0.03%.
18) Y. Morino and Y. Murata, ibid., **38**, 104 (1965).

$$qM(q) = k(120/\pi r_a)\{|F_{As}(q)|^2/I'_B(q)\} \cdot\exp(-\pi^2q^2l^2/200) \cdot\sin(\pi q/10)(r_a-\pi^2q^2\kappa/100) \quad (2)$$

where k is the index of resolution; κ is the anharmonicity parameter, and $I_{B'}(q)$ is the sum of the coherent and incoherent atomic scattering.

Least-Squares Analysis.—The experimental intensity curve, Eq. 1, was fitted to the theoretical expression, Eq. 2 (for the tetratomic model), by the least-squares treatment, with the following four variable parameters: the apparent interatomic distance, r_a(As–As); the mean amplitude, l(As–As); the anharmonicity parameter, κ(As–As), and the index of resolution, k. According to the principle of the least-squares method, the weight function, $p(q)$, of the molecular intensity curve should be so chosen as to be inversely proportional to $\sigma^2(q)$, the square of the standard deviation at q. The standard deviation, $\sigma(q)$, was estimated[17] from the standard deviation of the four experimental molecular intensity curves used for the analysis. By this procedure, a discontinuous weight function, $p_d(q)$, was obtained. The elastic scattering factor, $|F_{As}(q)|$, was taken from the table of Ibers and Hoerni,[19] while the inelastic scattering factor, $S_{As}(q)$, was taken from the table of Bewilogua.[20]

The apparent interatomic distance, r_a, determined by the least-squares treatment was converted to r_g by the relation[15]:

$$r_g = r_a + l^2/r_a \quad (3)$$

The distance r_g is the interatomic distance averaged over the anharmonic vibrations of the two end-atoms; it is expressed as[21]:

$$r_g = r_e + \langle\Delta z\rangle + (1/2r_e)(\langle x^2\rangle + \langle\Delta y^2\rangle) + \delta_r \quad (4)$$

where the second and the third terms represent the effects of anharmonic and perpendicular vibrations respectively, and δ_r represents the centrifugal distortion. It should be noted that all the terms except for r_e depend on the temperature.

The Estimation of Errors.—Random and systematic errors in the molecular parameters as determined by gas-electron diffraction have been critically discussed by Kuchitsu,[22] and by Morino, Kuchitsu and Murata.[23] In the present work, the errors were estimated essentially according to their schemes.

Random Errors.—The most probable value, x_m, of a certain molecular parameter, x, was obtained as the arithmetic mean of the most probable values, x_i, derived from N molecular intensity curves (N is the number of plates used for the analysis; it was four in the present case):

$$x_m = \sum x_i/N \quad (5)$$

The random error associated with the most probable value, x_m, was estimated in two different ways[22]: $\sigma_1(x_m)$ and $\sigma_2(x_m)$. They were calculated as:

$$\sigma_1(x_m) = \bar{\sigma}(x)/\sqrt{N} \quad (6)$$

and:

$$\sigma_2(x_m) = \sum\{(x_i - x_m)^2/N(N-1)\}^{1/2} \quad (7)$$

where $\bar{\sigma}(x)$ is the arithmetic mean of N standard deviations of the least-squares treatment. The statistical treatment, Eq. 6, is valid only when the values, x_i, agree with each other within the range of $\bar{\sigma}(x)$. Therefore, σ_2 gives another useful measure of the random error; the larger, σ_1 or σ_2, was taken as the random error.

Systematic Errors.—The following possible sources of important systematic errors were taken into consideration:

i) For the Interatomic Distance:

a) The drift of the wave length of the electron beam, 0.05%.

b) Uncertainty in the lattice constant of the gold foil, 0.05%.

c) Uncertainty in the camera distance, 0.1%. The plate-to-gold foil distance was adjusted to be equal to the camera distance within the range of 0.1% uncertainty.

d) Uncertainty in the corrections for the inclinations of the plates, 0.04%. The camera distance was corrected for the inclination of the photographic plate. The uncertainty in the correction factors, 2.5 σ, was taken as the limit of error.

e) Uncertainty in the anharmonicity parameter. The difference between the most probable value of r_a when κ was taken as a variable parameter and that when κ was fixed at zero was taken as the limit of error.

ii) For the Mean Amplitude:

a) The effect of the finite sample size. The delocalization of the silicon tetrachloride gas near the nozzle outlet was studied by Murata[24] for a needle-type nozzle; it was shown there to be about a half of that for an ordinary drum-type nozzle; the corrections in the mean amplitudes were shown to be about −1.5%. The delocalization was expected to be even smaller for the high-temperature nozzle used in the present work because the inner diameter of the nozzle, 0.2 mm., was less than that of the nozzle used for the silicon tetrachloride, 0.55 mm., while the distance from the outlet to the electron beam was almost the same (about 0.4 mm.). Therefore, no correction was made for the effect of the finite sample size on the mean amplitude; the possible order of magnitude of the correction, which was estimated assuming the same distribution of the sample gas

19) J. A. Ibers and J. A. Hoerni, *Acta Cryst.*, **7**, 405 (1954).
20) L. Bewilogua, *Physik. Z.*, **32**, 740 (1931).
21) Y. Morino, K. Kuchitsu and T. Oka, *J. Chem. Phys.*, **36**, 1108 (1962).
22) K. Kuchitsu, This Bulletin, **32**, 748 (1959).
23) Y. Morino, K. Kuchitsu and Y. Murata, *Acta Cryst.*, to be published.
24) Y. Morino and Y. Murata, This Bulletin, **38**, 114 (1965).

TABLE I. RESULTS OF THE LEAST SQUARES ANALYSIS OF $qM(q)$ OF As_4 AT 485°C

Plate	I	II	III	IV	$\bar{\sigma}$*
r_a(As-As)	2.4313	2.4306	2.4328	2.4315	0.0014 Å
l(As-As)	0.0897	0.0828	0.0834	0.0825	0.0013 Å
κ(As-As)	1.46	0.11	0.25	1.78	0.54 10^{-5}Å^3
Index	1.04	0.91	0.98	0.93	0.02

* The arithmetic mean of four standard deviations.

as that of silicon tetrachloride, was regarded as the limit of error.

b) Uncertainty in the weight function. The mean amplitude was found to be influenced slightly by the choice of the weight function. The effect was estimated by using the following smooth-weight function in place of the discontinuous one, and the difference in the most probable value of l was taken as the limit of error;

$$p_s(q)=1 \quad \text{for} \quad q\leq 65$$
$$p_s(q)=\exp\{-0.001(q-65)^2\} \quad \text{for} \quad 65\leq q \qquad (8)$$

c) Uncertainty in the theoretical atomic-scattering factor. The error caused by this uncertainty was estimated by using the values of the atomic-scattering factor taken from different sources in the literature;[25] the largest discrepancy in the most probable value was regarded as the limit of error.

d) The effect of the extraneous scattering. This effect was estimated from a comparison of the results derived from $qM(q)$ with those derived from the molecular intensity curves of a slightly different form, $qN(q)$[26] which were expected to be less influenced by the extraneous scattering; the difference in the most probable value was taken as the limit of error.

Limit of Error.—The limit of error corresponding to the 99 per cent confidence interval was estimated as:

$$\text{Limit of error} = \{(2.5\sigma_r)^2 + \sigma_s^2\}^{1/2} \qquad (9)$$

where σ_r was the random error (the larger of σ_1 and σ_2), and σ_s^2 was the sum of the squares of all the systematic errors discussed above.

Results and Discussion

Molecular Structure.—One of the radial distribution curves is shown in Fig. 3. The results of the least-squares analysis of the molecular intensity curves, $qM(q)$, are listed in Table I, where $\bar{\sigma}$ in the last column denotes the arithmetic mean of the four standard deviations, all of which were found to be nearly equal; for instance, the $\sigma(r_a)$ values of Plates I to IV were 0.0015, 0.0015, 0.0014 and 0.0012 Å respectively. In Fig. 4 one of the experimental molecular intensity curves, $qM(q)$, is compared with the theoretical curve calculated with the parameters obtained above. The correction from the apparent distance, r_a, to the average

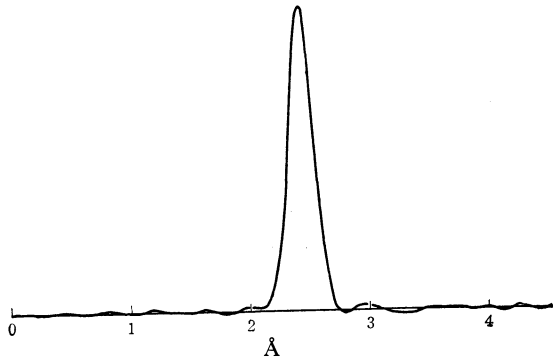

Fig. 3. Radial distribution curve of As_4 at 485°C.

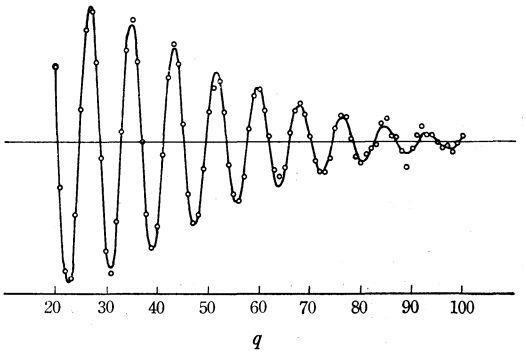

Fig. 4. Calculated and observed molecular intensity curves of As_4 at 485°C.
— Calcd.
○ Obs.

TABLE II. ERRORS IN THE INTERATOMIC DISTANCE

Source of error		r_g(As-As)
Random:		
$2.5\sigma_1$	0.0018 Å	
$2.5\sigma_2$	(0.0013)	
Systematic:		
scale factor total	0.13%	0.0032
a) drift of wavelength	0.05%	
b) lattice constant	0.05%	
c) camera distance	0.10%	
d) inclination of plate	0.04%	
e) effect of κ		0.0019
Limit of error:		0.0041

25) A. J. Freeman and R. E. Watson, "International Tables for X-Ray Crystallography," Vol. III, Kynoch press, Birmingham (1962), p. 206; M. Kimura, private communication.

26) Y. Morino, T. Ukaji and T. Ito, This Bulletin, **39**, 71 (1966).

Table III. Errors in the mean amplitude

Source of error	l(As-As)
Random:	
2.5 σ_1	(0.0016) Å
2.5 σ_2	0.0043
Systematic:	
a) sample size	0.0008
b) weight	0.0020
c) scattering factor	negligible
d) extraneous scattering	0.0037
Limit of error:	0.0061

Table IV. Final results of the molecular parameters of As_4 at 485°C

r_g(As-As)	l(As-As)	κ(As-As)
2.435±0.004 Å	0.085±0.006 Å	0.9±1.3×10^{-5}Å^3

distance, r_g, was +0.0030 Å. The estimates of the errors in the final values of r_g and l are summarized in Tables II and III respectively. The limit of error in the anharmonicity parameter, $\kappa \times 10^5$ Å^3, was estimated to be 1.3; this comprised the random error, 2.5 σ_2, of 1.05 and the systematic error, 0.74, arising from the choice of the weight function. The final results of the molecular parameters are listed in Table IV.

The index of resolution was found to be 0.96± 0.07. The limit of error was estimated from the random error, 2.5σ_2, of 0.07. Evidence for the tetratomic structure of at least the predominant part of the arsenic molecules at this temperature was given by the small deviation in the observed index from unity. This is evident from the following consideration. The molecular intensity, $qM(q)$, is proportional to the ratio of the number of the atom-pairs to the number of atoms in the molecule. Since the ratios for the diatomic, triatomic, and tetratomic structrues are 1/2, 3/3, and 6/4 respectively, analyses based on the tetratomic model must result in indices of about 0.33, 0.67, and 1, if the molecule has one of the above structures. The observed index of nearly unity clearly eliminates the possibilities of diatomic and triatomic structures.

Force Constants.—The mean amplitude and the anharmonicity parameter obtained above provide information on the intramolecular force field of the arsenic molecule, for which no spectroscopic studies of the vibrational frequencies have been made. The theory of correlating the mean amplitudes to the force constants has been developed by Morino and his co-workers[27] by using Wilson's ***GF*** matrix method, while an X_4 molecule (T_d symmetry) has been treated by Cyvin.[28]

The general quadratic potential function of the As_4 molecule (T_d symmetry) is given by:

$$2V = \sum f_r \Delta r_i^2 + 2\sum f_{rr} \Delta r_i \Delta r_j + 2\sum f_{rr'} \Delta r_i \Delta r_k \quad (10)$$

where Δr_i ($i=1,\cdots,6$) is the change in length of the ith bond, and the interaction constants, f_{rr} and $f_{rr'}$, correspond to the neighboring and the opposite bond pairs respectively. The mean-square amplitude of the As–As bond is given by[28]:

$$l^2 = (\mu/3)\ (2\Delta_1 + \Delta_2 + 3\Delta_3) \quad (11)$$

where μ is the reciprocal mass of the arsenic atom, and Δ_i is the mean square amplitude of the i th normal coordinate:

$$\Delta i = (\hbar/8\pi^2 c\nu_i)\coth(hc\nu_i/2kT) \quad (12)$$

It should be noted that the mean amplitude, l, is a function of the three force constants and of the temperature.

All of the three force constants can not be determined from a single observed value of the mean amplitude. The interaction constants, f_{rr} and $f_{rr'}$, therefore, tentatively assumed to be zero:

$$f_{rr} = f_{rr'} = 0 \quad (13)$$

The relation between the bond-stretching constant, f_r, and the amplitude, l, assuming Eq. 13 is shown in Fig. 5 for the three temperatures: 455°C (the lower limit), 485°C, and 515°C (the upper limit). As is shown in the figure, the observed value of l= 0.085 Å at 485°C corresponds to f_r=1.5 mdyn./Å, while the error caused by the uncertainties in the

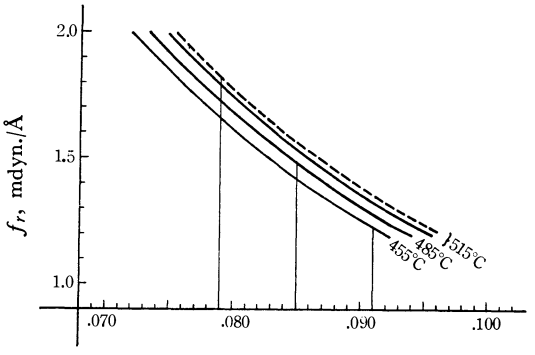

Fig. 5. Relation between the force constant f_r and the mean amplitude l(As-As) of As_4.
—— $f_{rr}=f_{rr'}=0$
---- f_r : f_{rr} : $f_{rr'}$ transferred from P_4

temperature and in the amplitude is ±0.28 mdyn./Å. The error in f_r introduced by the assumption of Eq. 13 was roughly estimated with reference to the P_4 molecule, which has the same T_d structure.[29] The force constants of P_4 have been determined by Pistorius[30] from the Raman spectra: f_r=2.065, f_{rr}=−0.122, and $f_{rr'}$=0.096 mdyn./Å.

27) Y. Morino, K. Kuchitsu and T. Shimanouchi, *J. Chem. Phys.*, **20**, 726 (1952).
28) S. J. Cyvin, *Spectrochim. Acta*, **17**, 1219 (1961).
29) H. J. Bernstein and J. Powling, *J. Chem. Phys.*, **18**, 1018 (1950).
30) C. W. F. T. Pistorius, ibid., **29**, 1421 (1958).

If the $f_r:f_{rr}:f_{rr'}$ ratios of the P_4 molecule are transferred to those of the As_4 molecule, the correlation curves in Fig. 5 are shifted by about 0.05 mdyn./Å, as is shown for the temperature of 515°C. Twice this shift, i. e., 0.1 mdyn./Å, was taken as a measure of the error due to the above assumption. Thus, the bond-stretching constant compatible with the observed mean amplitude was determined to be $f_r=1.5\pm0.3$ mdyn./Å, which is in agreement with the estimate, 1.5 mdyn./Å, from Badger's rule.[31] This shows the covalent nature of the As–As bond of this molecule. The corresponding estimates of the vibrational frequencies are $\nu_1(A_1)=350\pm30$, $\nu_2(E)=180\pm30$ and $\nu_3(F_2)=250\pm30$ cm^{-1}. However, no experimental observation has yet been made because of the difficulty of spectroscopic instrumentation.

The observed value of the anharmonicity parameter of $0.9\pm1.3\times10^{-5}$Å^3 may be compared with the values estimated from other sources. If a Morse-type potential function is assumed for the As–As bond, the anharmonicity parameter, κ, is approximately represented by[14]:

$$\kappa = (\alpha/6)l^4 \qquad (14)$$

where:

$$\alpha = (f_r/2D)^{1/2} \qquad (15)$$

is the asymmetry constant of the Morse function. When we insert the observed values of $l=0.085$Å and $f_r=1.5$ mdyn./Å, together with the binding energy, D, of 34 kcal./mol.,[32] into the above equations, κ is estimated to be 1.5×10^{-5}Å^3. Even though the observed and estimated values are both crude, the orders of magnitude are in essential agreement.

With the force constant obtained above, it is possible to estimate the apparent elongation of the As–As bond due to the perpendicular amplitudes and the elongation caused by the centrifugal force, represented by the third and the fourth terms of Eq. 4 respectively. The former is expressed as $\mu(\Delta_2+\Delta_3)/2r_e$ and is estimated to be 0.0022 Å at 485°C. The centrifugal elongation is estimated by the method of Iwasaki and Hedberg[33] as follows: $\delta_r(\text{As–As})=kT/2F_1r_e=0.0014$Å at 485°C, where $F_1=f_r+f_{rr}+f_{rr'}$. The distance parameter, which is obtained by subtracting the above two terms from r_g, is denoted as r_α[20]; thus, r_α(As–As) is estimated to be 2.431Å at 485°C.

The authors wish to express their sincere gratitude to the Tokyo Shibaura Electric Co. for the constructioh of the nozzle assembly and for the kind gift of the sample. They are also indebted to Mr. Masakatsu Kochi for his assistance.

31) R. M. Badger, ibid., **3**, 710 (1935).

32) E. H. E. Pietsch ed., "Gmelins Handbuch der Anorganischen Chemie," Vol. 17, Verlag Chemie, Weinheim (1952), p. 115.

33) M. Iwasaki and K. Hedberg, *J. Chem. Phys.*, **36**, 2961 (1962).

BULLETIN OF THE CHEMICAL SOCIETY OF JAPAN VOL. 39 71—78 (1966)

Molecular Structure Determination by Gas Electron Diffraction at High Temperatures. II. Arsenic Triiodide and Gallium Triiodide

By Yonezo MORINO,† Takeshi UKAJI††,* and Tetsuzo ITO†,**

† *Department of Chemistry, Faculty of Science, The University of Tokyo, Hongo, Tokyo*
†† *Department of Chemistry, Ibaraki University, Mito*

(Received April 17, 1965)

The precise molecular structures of arsenic triiodide and gallium triiodide in the vapor phase have been determined by the sector-microphotometer method of electron diffraction at the nozzle temperatures of 230°C and 255°C respectively. The results of gallium triiodide have confirmed the regular triangle structure of the molecule. The force constants of these molecules have been estimated from the observed mean amplitudes.

In the preceding paper (Part I),[1] a high-temperature nozzle assembly for electron diffraction was reported, together with the results of its application to the determination of the molecular structure of arsenic in the vapor phase. The purpose of the present work is to determine the precise molecular structures of arsenic triiodide and gallium triiodide in the vapor phase, and to obtain information on the force field of these molecules on the basis of the observed mean amplitudes.

* Present address: Ikutoku Kosen, Atsugi, Kanagawa.
** Present address: The Institute of Physical and Chemical Research, Komagome, Tokyo.

1) Y. Morino, T. Ukaji and T. Ito, This Bulletin, **39**, 64 (1966).

The molecular structure of arsenic triiodide has been studied by the visual method of electron diffraction by several investigators; the findings of Finbak and Hassel (1941) (r(As–I)=2.54Å and θ(IAsI)=98.5°) and the preliminary findings of Swingle (1949) (r(As–I)=2.55±0.03Å and θ(IAsI) =101±1.5°) are cited by Sutton.[2] The mean amplitudes have never been observed. The Raman frequencies of the molecule in the $CHBr_3$ and carbon disulfide solutions have been observed by Stammreich and his co-workers.[3] Akishin and his co-workers (1959)[4] investigated the molecular structure of gallium triiodide by the sector-microphotometer method of electron diffraction, with r(Ga–I)=2.44±0.03Å; they concluded that the molecule has a planar, regular triangle structure. They also estimated the mean amplitudes from the radial distribution curve. No spectroscopic data are, however, now available concerning the force field of the molecule.

Experimental

A sample of arsenic triiodide was synthesized by the $AsCl_3+3KI \rightarrow AsI_3+3KCl$ reaction.[5] The melting point of the sample was found to be 140°C, which was lower than the value of 149°C cited in the literature. This was probably due to the potassium chloride remaining in the sample. However, the sample was not further purified, since the melting point of potassium chloride, 776°C, was so much higher than the nozzle temperature that this impurity did not interfere with the present experiment. A sample of gallium triiodide was synthesized by a direct reaction of the gallium and iodine elements.[6] Stoichiometric quantities of gallium and iodine were heated in a vacuum to about 300°C; the resulting gallium triiodide was then purified by sublimation in a vacuum.

The conditions of the diffraction experiments were almost the same as those used in Part I for the arsenic except that the nozzle temperatures were 230±30°C and 255±30°C for the arsenic triiodide and the gallium triiodide respectively. During the exposures for the arsenic triiodide sample, a slight change in the direction of the electron beam was observed at the early stages of the experiments; this was found to be caused by the electronic charge piled up on the sample condensed onto the cold trap. The drift was eliminated by widening the space between the cold trap and the electron beam from the ordinary space of about 2 cm. to about 5 cm. Since the gallium triiodide sample was strongly hygroscopic, it was degassed in the oven of the nozzle assembly in a vacuum for more than an hour at room temperature, and then for a few minutes at about 100°C, immediately before making exposures. The optical densities of the diffraction photographs ranged from 0.15 to 0.5.

Analytical Procedure

The diffraction photographs of the arsenic triiodide and the gallium triiodide were analyzed by almost the same procedure as that described in Part I. The final results were obtained by the least-squares analysis of the molecular intensity curves, $qM(q)$. A least-squares analysis of the molecular intensity curves of a slightly different form, $qN(q)$, was also carried out in order to examine the effects of the extraneous fogging of the photographic plates on the final values of the molecular parameters.

The experimental molecular intensity curve,

$$qM(q)=q(I_L-I_B)/I_B \qquad (1)$$

was fitted by the least-squares method to its theoretical expression:

$$qM(q)=k(10/\pi)\sum\sum(|F_i||F_j|/I_B')\cos \Delta\eta \cdot\exp(-\pi^2q^2l^2/200)(1/r_a')\sin(\pi qr_a'/10) \qquad (2)$$

where r_a' stands for $r_a-\pi^2q^2\kappa/100$, and the subscripts are omitted from $\Delta\eta$, l and r_a' for the sake of simplicity. The parameters to be determined were the interatomic distances, r_a', the root-mean-square amplitudes, l, and the index of resolution, k. The anharmonicity parameters, κ, were fixed to zero because the outputs of the successive cycles did not converge when they were taken as variable parameters. This was because of a strong correlation between r_a and κ, and because the molecular intensity curves could not afford information sufficient to determine r_a and κ separately. The interatomic distances as determined by the leaset-squares procedure are, therefore, not r_a but r_a', i. e., $r_a-\pi^2q^2\kappa/100$ averaged over the observed range of the scattering angle (q=20—100). The values of the elastic scattering factors, $|F_i|$, and of the complex phases, η_i were taken from the tables of Ibers and Hoerni.[7]

When the fogging of the photographic plate is not negligible, as indicated by an appreciable decrease in the index of resolution of gallium triiodide from the ideal value of unity (k=0.8), the experimental molecular intensity, Eq. 1, can not be directly compared with the theoretical expression, Eq. 2, since the experimental background, I_B, in Eq. 1 contains an extraneous scattering which might affect the final values of the molecular parameters, particularly those of the mean amplitudes. As it is difficult to estimate the extraneous scattering, and as the molecular term, I_L-I_B, in Eq. 1 was probably little influenced by the extraneous scattering, an analysis of the molecular intensity curves, $qN(q)$, described below was carried out, and the results compared with those obtained

2) L. E. Sutton et al. ed., "Tables of Interatomic Distances and Configuration in Molecules and Ions," The Chemical Society, London (1958).

3) H. Stammreich, R. Forneris and Y. Tavares, *J. Chem. Phys.*, **25**, 580 (1956).

4) P. A. Akishin, V. A. Naumov and V. M. Tachevskiy, *Moscow University Report* (*U. S. S. R.*), **1**, 229 (1959).

5) H. S. Booth ed., "Inorganic Syntheses," Vol. 1, 103 (1939).

6) G. Brauer ed., "Handbüch der Präparativen Anorganischen Chemie," Ferdinand Enke Verlag, Stuttgart (1954), p. 637.

7) J. A. Ibers and J. A. Hoerni, *Acta Cryst.*, **7**, 405 (1954).

TABLE I. RESULTS OF THE LEAST SQUARES ANALYSIS OF $qM(q)$ OF AsI_3 AT 230°C

Plate	I	II	III	IV	$\bar{\sigma}$*
r_a'(As-I)	2.5503	2.5568	2.5531	2.5576	0.0017Å
r_a'(I-I)	3.9192	3.9080	3.9137	3.9201	0.0055Å
l(As-I)	0.0747	0.0788	0.0721	0.0711	0.0022Å
l(I-I)	0.1507	0.1495	0.1474	0.1424	0.0043Å
Index	1.02	1.07	0.89	0.79	0.03

* The arithmetic mean of four standard deviations.

from $qM(q)$. This type of molecular intensity curve has usually been used by the Norwegian group.[8] The experimental molecular intensity, $qN(q)$, was calculated as:

$$qN(q)=A(q)(I_L-I_B) \tag{3}$$

where $A(q)=f(q)q^2\{1-(\lambda q/40)^2\}^{-3/2}$. The multiplication of the $A(q)$* factor was necessary for a least-squares fit of the curve to the theoretical expression:

$$qN(q)=K\sum\sum|F_i||F_j|\cos\Delta\eta \cdot\exp(-\pi^2q^2l^2/200)(1/r_a')\sin(\pi qr_a'/10) \tag{4}$$

where K is an adjustable constant similar to the index of resolution, k, in Eq. 2 but with less physical importance, since it is difficult to know the absolute intensity of the scattered electrons either from experimental diffraction photographs or from theoretical calculations.

The apparent interatomic distances, r_a', were converted to the average distances, r_g', by the $r_g'=r_a'+l^2/r_a'$ relation, while the bond angles, θ_g'(IMI) (where M denotes arsenic or gallium), were calculated from the average distances by the relation:

$$\sin(\theta_g'/2)=r_g'(\text{I-I})/2r_g'(\text{M-I}) \tag{5}$$

The errors in the observed interatomic distances and the mean amplitudes were estimated by the procedure described in Part I. Although the most probable values of the interatomic distances are, in general, not influenced by the weight functions taken in the course of the least-squares treatment, the effect of the weight function was not negligible in the case of gallium triiodide. The errors were estimated by using the smooth weight function, Eq. 8 of Part I, in place of the discontinuous one. The mean amplitude of a pair of atoms with different atomic numbers is influenced by possible errors in the theoretical phases, η_i, since $\cos\Delta\eta$ has a q-dependence almost the same as that of the exponential damping factor of thermal vibrations. The cosine factor of the As–I ($\Delta Z=20$) or the Ga–I ($\Delta Z=22$) pair, when reduced to the amplitude scale, is about one-tenth of the amplitude. The uncertainties in the values of η_i given by Ibers and Hoerni have been discussed by Karle and Bonham[9] for argon ($Z=18$) and for uranium ($Z=92$); they showed them to be less than 10%. Although uncertainties in the differences, $\Delta\eta$, are expected to be even smaller, 10% was regarded as the limit of error.

The random error in the bond angles was estimated in two ways: as 2.5 σ_2—from the fluctuation among the values derived from the individual plates according to Eq. 7 of Part I, and as 2.5 σ_1—from the errors, σ_1, in the interatomic distances obtained by applying the law of the propagation of errors to Eq. 5:

$$\sigma(\theta)=(360/\pi)\tan(\theta/2)[\{\sigma(r_1)/r_1\}^2+\{\sigma(r_2)/r_2\}^2]^{1/2}$$

where r_1 and r_2 stand for r_g'(M–I) and r_g'(I–I) respectively. The systematic errors in the interatomic distances, other than that introduced by the uncertainty in the weight function, do not influence the bond angles.

Results and Discussion

Arsenic Triiodide.—*Molecular Structure.*—Four diffraction photographs were used for the analysis. One of the radial distribution curves is shown in Fig. 1. The results of the least-squares analysis of the molecular intensity curves, $qM(q)$, are listed in Table I. It should be noted that the mean amplitudes derived from the four plates are in fairly good agreement with one another in spite of the large deviations in the indices of resolution. A typical experimental molecular intensity curve is compared with the best-fit theoretical one in Fig. 2. The corrections from r_a' to r_g' were +0.0022Å and +0.0056Å for the As–I and I–I distances respectively. A deviation of +0.0066Å was observed in the most probable value of l(I–I) when the real atomic scattering factors[10] were used in place of the complex ones. Since there was no suitable way to compare the reliabilities of the scattering factors, the mean of the two values was taken as the final value. The estimates of the errors in the

8) O. Bastiansen, L. Hedberg and K. Hedberg, *J. Chem. Phys.*, **27**, 1311 (1957).

* $A(q)$ is proportional to $f(q)\{R(q)\}^2q^5/\alpha(q)\cos\theta$, where θ is the scattering angle; $f(q)$ is the levelling function; $R(q)$ is the distance from the nozzle to the point on the plate corresponding to the angle, θ, and $\alpha(q)$ is the sector function and is proportional to $\tan^3\theta$ for the r^3-sector. The cosine term in the denominator comes from the fact that the plate is perpendicular to the incident electron beam.

9) J. Karle and R. A. Bonham, ibid., **40**, 1396 (1964).

10) A. J. Freeman and R. E. Watson, "International Tables for X-Ray Crystallography," Vol. III, Kynoch Press, Birmingham (1962), pp. 204—206; H. L. Thomas and K. Umeda, *J. Chem. Phys.*, **26**, 293 (1957); M. Kimura, private communication.

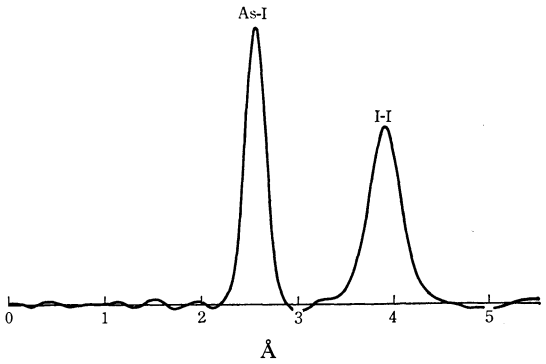

Fig. 1. Radial distribution curve of AsI_3 at 230°C.

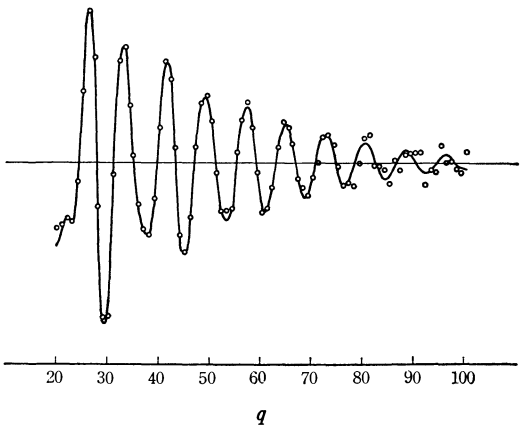

Fig. 2. Calculated and observed molecular intensity curves of AsI_3 at 230°C.
— Calcd. ○ Obs.

interatomic distances and the mean amplitudes are summarized in Tables II and III respectively. The index of resolution was found to be 0.94± 0.17. The limit of error, ±0.17, was estimated from the random error of 0.16 ($2.5\,\sigma_2$), plus the systematic error, 0.07, due to the uncertainties in the scattering factors. The final results of the molecular parameters are listed in Table IV. The results of the least-squares analysis of the molecular intensity curves, $qN(q)$, are listed in Table V. They were in good agreement with

TABLE II. ERRORS IN THE INTERATOMIC DISTANCES OF AsI_3

Source of error	r_g'(As-I)	r_g'(I-I)
Random:		
$2.5\,\sigma_1$	(0.0021)Å	(0.0069)Å
$2.5\,\sigma_2$	0.0043	0.0069
Systematic:		
scale factor 0.13%	0.0033	0.0051
weight	negligible	negligible
Limit of error:	0.0054	0.0085

TABLE III. ERRORS IN THE MEAN AMPLITUDES OF AsI_3

Source of error	l(As-I)	l(I-I)
Random:		
$2.5\,\sigma_1$	(0.0028)Å	(0.0053)Å
$2.5\,\sigma_2$	0.0043	0.0054
Systematic:		
a) sample size	0.0010	0.0012
b) weight	0.0029	0.0027
c) scattering factor	negligible	0.0066
d) extraneous scattering	0.0022	0.0017
e) $\Delta\eta$	0.0007	none
Limit of error:	0.0057	0.0092

TABLE IV. FINAL RESULTS OF THE MOLECULAR PARAMETERS OF AsI_3 AT 230°C

	r_g'	l	θ_g'(IAsI)
As-I	2.557±0.005Å	0.074±0.006Å	100.2°±0.4°
I-I	3.921±0.009	0.151±0.009	

TABLE V. RESULTS OF THE LEAST SQUARES ANALYSIS OF $qN(q)$ OF AsI_3 AT 230°C

	r_g'	l	θ_g'(IAsI)
As-I	2.557±0.005Å	0.076±0.006Å	100.2°±0.4°
I-I	3.920±0.011	0.149±0.007	

the results obtained from $qM(q)$.

Force Constants. — The relations between the mean amplitudes and the force constants of an XY_3 molecule (C_{3v} symmetry) have been discussed by Iwasaki and Hedberg[11] for phosphorus trichloride. The general quadratic potential function of arsenic triiodide is expressed by a set of six force constants, for example, by F_{11}, F_{12}, F_{22}, (A_1 species), F_{33}, F_{34}, and F_{44} (E species), in terms of the ordinary symmetry coordinates as defined in the reference. They are related to the force constants in terms of the internal coordinates:

$$\left.\begin{aligned} F_{11}&=f_r+2f_{rr}, \quad F_{12}=2f_{r\theta}+f_{r\theta'},\\ F_{22}&=f_\theta+2f_{\theta\theta}, \quad F_{33}=f_r-f_{rr},\\ F_{34}&=f_{r\theta}-f_{r\theta'}, \quad F_{44}=f_\theta-f_{\theta\theta} \end{aligned}\right\} \qquad (6)$$

where f_r and f_θ are the stretching and bending force constants respectively, and where f_{rr}, $f_{\theta\theta}$, $f_{r\theta}$ and $f_{r\theta'}$ are the interaction constants corresponding to the neighboring bonds, neighboring angles, neighboring bond and angle, and opposite bond and angle respectively.

The four Raman frequencies, combined with the two observed mean amplitudes, are sufficient for the determination of all the force constants. It should be noted that the values of the force constants are restricted by a set of relations imposed by the four frequencies. This is due to the requirement that force constants be real quantities; it will be shown below for the A_1 species. If the observed

11) M. Iwasaki and K. Hedberg, *J. Chem. Phys.*, **36**, 594 (1962).

frequencies, ν_1 and ν_2, are substituted into the secular equation, $|\boldsymbol{GF}-\lambda_i\boldsymbol{E}|=0$, the following two equations are obtained for the three force constants:

$$\left.\begin{aligned}\lambda_1+\lambda_2&=G_{11}F_{11}+2G_{12}F_{12}+G_{22}F_{22}\\ \lambda_1\lambda_2&=(G_{11}G_{22}-G_{12}^2)(F_{11}F_{22}-F_{12}^2)\end{aligned}\right\} \quad (7)$$

where $\lambda_i=(2\pi c\nu_i)^2$. By eliminating one of the force constants, say, F_{22}, from the above two equations, a quadratic equation for F_{11} and F_{12} is obtained. Then, from the requirement that F_{11} be real, F_{12} is limited to the $-0.03<F_{12}<1.17$ mdyn./Å range. Similarly, F_{34} is limited to the $-0.18<F_{34}<1.03$ mdyn./Å range.

Since the number of unknown force constants is six, a correlation curve (a biquadratic curve) is obtained on the (F_{12}, F_{34}) plane from the four frequencies and one mean amplitude. From the other set of the four frequencies and the remaining

Table VI. Fundamental frequencies of AsI_3[3]

$\nu_1(A_1)$	$\nu_2(A_1)$	$\nu_3(E)$	$\nu_4(E)$
216	94	221	70 cm^{-1}

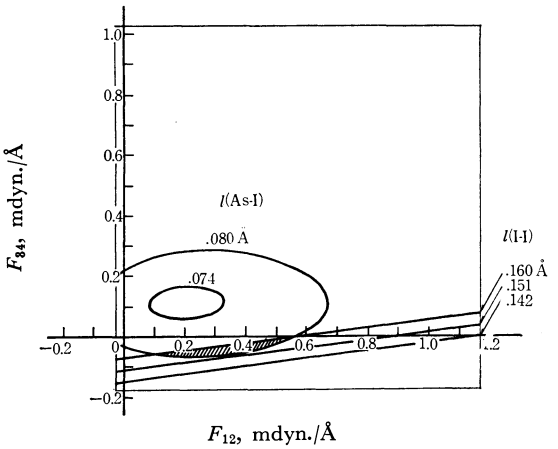

Fig. 3. Correlation curve of F_{34} and F_{12} of AsI_3 at 230°C.

mean amplitude, the other curve is obtained. Thus, the force constants can be determined as the crossing point or points of the two curves. The two correlation curves, as calculated from the Raman frequencies in Table VI and the mean amplitudes in Table IV at the temperature of 230°C, are shown in Fig. 3. The curves corresponding to the limits of error of the mean amplitudes are also shown in the figure. The curve corresponding to the lower limit of l(As–I) of 0.068Å does not exist on the real plane. Contrary to the above expectation, the crossing did not appear for the most probable values. The two curves crossed only for the upper limits of the amplitudes. Thus, the most probable values of the mean amplitudes were found to be hardly compatible with the Raman frequencies. This inconsistency may be ascribed

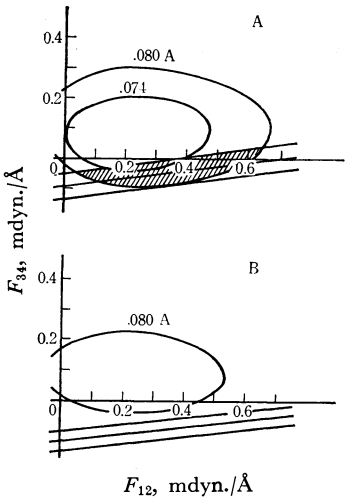

Fig. 4. Correlation curve of F_{34} and F_{12} of AsI_3 (cf. Fig. 3).
A: at 200°C, B: at 260°C

to errors in the Raman frequencies and in the measurement of the temperature in the present experiments. The Raman frequencies were obseved in the solution and not in the gas phase. For the time being, however, the frequencies were assumed to be correct, and the effects of the uncertainty of the temperature were examined. The correlation curves at 200°C and 260°C, corresponding to the lower and the upper limits of the temperature respectively, are shown in Fig. 4. At 200°C, the two curves corresponding to the most probable values of the mean amplitudes came closer, and the overlapped area increased, while at 260°C no crossing of the curves occurred at all.

The force constants, F_{12} and F_{34}, compatible with the observed Raman frequencies and the mean amplitudes were determined from the overlapped areas in Figs. 3 and 4 as follows: $F_{12}=0.3_5\pm0.3_0$ and $F_{34}=-0.0_3\pm0.0_7$ mdyn./Å The six force constants were determined accordingly; they are listed in Table VII, together with the force constants in terms of the internal coordinates. It must be mentioned that these force constants are subject to possible errors in the Raman frequencies used. The observed stretching constant of $1.4_7+0.2_2$ mdyn./Å is in agreement with the estimate, 1.3 mdyn./Å, derived from Badger's rule[12] of $f=1.24/(r_e-d_{ij})^3$, if we define the parameter, d_{ij}, so as to reproduce the force constant of the diatomic molecule, GaI,[13] i. e., if $d_{45}=1.57$Å. This parameter is also consistent with the observed stretching constant, f_r(Ga–I), of gallium triiodide. It should be noted that the interaction constant,

12) R. M. Badger, ibid., **3**, 710 (1935).
13) S. S. Mitra, ibid., **22**, 2097 (1954); A. H. Barret and M. Mandrel, *Phys. Rev.*, **109**, 1572 (1958).

$f_{r\theta}'$, is of the same order of magnitude as f_θ and $f_{r\theta}$, although the associated errors are large; in fact, the assumption of the Urey-Bradley force field, $f_{r\theta}=f_{r\theta}'=0$, is not compatible with the frequencies of Table VI.

TABLE VII. FORCE CONSTANTS OF AsI_3

For symmetry coordinates		For internal coordinates	
F_{11}	$2.2_4\pm0.6_0$ mdyn./Å	f_r	$1.4_7\pm0.2_2$ mdyn./Å
F_{12}	$0.3_5\pm0.3_0$	f_{rr}	$0.3_8\pm0.2_1$
F_{22}	$0.1_6\pm0.0_5$	$f_{r\theta}$	$0.1_1\pm0.1_0$
F_{33}	$1.0_9\pm0.1_5$	$f_{r\theta}'$	$0.1_4\pm0.1_1$
F_{34}	$-0.0_3\pm0.0_7$	f_θ	$0.1_3\pm0.0_2$
F_{44}	$0.1_1\pm0.0_2$	$f_{\theta\theta}$	$0.0_2\pm0.0_2$

Gallium Triiodide. — *Molecular Structure.*— Three diffraction photographs were selected for analysis. The radial distribution curve is shown in Fig. 5. The results of the least-squares analysis are listed in Table VIII. One of the experimental molecular intensity curves is compared in Fig. 6 with the theoretical curve calculated from the parameters as determined by the least-squares treatment. The most probable value of the interatomic distance, r_g'(I-I), was shifted by -0.014 Å (-0.33%) when the smooth weight function, Eq. 8 of Part I, was used in place of the discontinuous one obtained from the fluctuation of the three molecular intensity curves. The discontinuous weight function can not be considered to be more reliable than the smooth one, since it was estimated from only three observations. Therefore, the average of the two values was taken as the final value, and the discrepancy was included in the estimate of the error The estimates of the errors in the interatomic distances and in the mean amplitudes are summarized in Tables IX and X respectively. The corrections from r_a' to r_g' were $+0.0018$ Å and $+0.0060$ Å for the Ga-I and for the I-I distances respectively. As was the case for arsenic triiodide, the mean amplitude, l(I-I), was influenced by the choice of the atomic scattering factors and was corrected by $+0.0033$ Å. The final results of the molecular parameters are listed in Table XI.

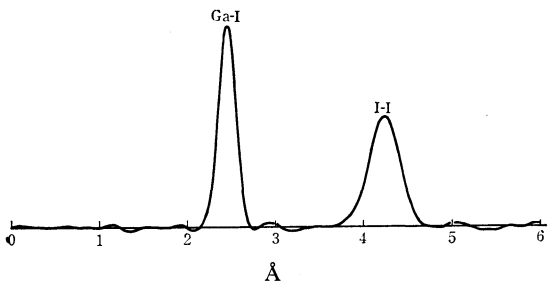

Fig. 5. Radial distribution curve of GaI_3 at 255°C.

TABLE VIII. RESULTS OF THE LEAST SQUARES ANALYSIS OF $qM(q)$ OF GaI_3 AT 255°C

Plate	I	II	III	$\bar{\sigma}$*
r_a'(Ga-I)	2.4559	2.4579	2.4535	0.0013Å
r_a'(I-I)	4.2536	4.2603	4.2563	0.0072Å
l(Ga-I)	0.0670	0.0662	0.0680	0.0018Å
l(I-I)	0.1600	0.1552	0.1641	0.0048Å
Index	0.82	0.78	0.79	0.02

* The arithmetic mean of three standard deviations.

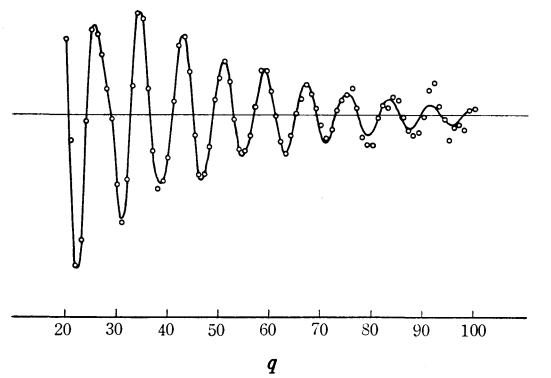

Fig. 6. Calculated and observed molecular intensity curves of GaI_3 at 255°C.
— Calcd. ○ Obs.

TABLE IX. ERRORS IN THE INTERATOMIC DISTANCES OF CaI_3

Source of error	r_g'(Ga-I)	r_g'(I-I)
Random:		
$2.5\,\sigma_1$	(0.0022)Å	0.0103Å
$2.5\,\sigma_2$	0.0031	(0.0082)
Systematic:		
scale factor 0.13%	0.0032	0.0055
weight	0.0013	0.0140
Limit of error:	0.0046	0.0182

TABLE X. ERRORS IN THE MEAN AMPLITUDES OF GaI_3

Source of error	l(Ga-I)	l(I-I)
Random:		
$2.5\,\sigma_1$	0.0028Å	0.0071Å
$2.5\,\sigma_2$	(0.0013)	(0.0064)
Systematic:		
a) sample size	0.0010	0.0013
b) weight	0.0012	0.0021
c) scattering factor	0.0017	0.0065
d) extraneous scattering	0.0014	0.0014
e) $\Delta\eta$	0.0009	none
Limit of error:	0.0040	0.0100

TABLE XI. FINAL RESULTS OF THE MOLECULAR PARAMETERS OF GaI_3 AT 255°C

	r_g'	l	θ_g'(IGaI)
Ga-I	2.458 ± 0.005Å	0.067 ± 0.004Å	$120.0°\pm0.7°$
I-I	4.256 ± 0.018	0.163 ± 0.010	

The observed bond angle of 120.0°±0.7° has confirmed the planar regular triangle structure of the molecule. It is also consistent with the results of the vapor-pressure measurement[14] and the mass-spectroscopic analysis[15], which indicate that the molecule is predominantly (about 97%[14]) monomeric at 255°C. The r_g'-structure determined above is different from the equilibrium structure (see Eq. 4 of Part I). Aside from the anharmonic contribution, the average distance, r_g', contains additional contributions due to the centrifugal distortion and the perpendicular amplitudes. The centrifugal distortion of the gallium triiodide molecule was estimated, using the force constant obtained from the observed mean amplitudes, to be $\delta_r = kT/(f_r+2f_{rr})r_e(\text{Ga-I}) = 0.0017$ Å for the Ga-I bond. The distortion does not change the bond angle of the molecule, since it is totally symmetric. The effects of the perpendicular amplitudes were estimated as follows: $(L^2_{22}\Delta_2+2L^2_{43}\Delta_3+2L^2_{44}\Delta_4)/18r_e(\text{Ga-I}) = 0.0074$ Å for the Ga-I bond, and $\{(\sqrt{3}L_{33}-L_{43})^2\Delta_3+(\sqrt{3}L_{34}-L_{44})^2\Delta_4\}/12r_e(\text{I-I}) = 0.0026$ Å for the I-I bond. (As for the notations, see the definitions following Eq. 9.) In the above estimate, ν_2 was assumed to be equal to ν_1. If the average distances, r_g', are corrected for the perpendicular amplitudes, the bond angle is 120.4°; this is different from the planar angle of 120°, but the discrepancy is within the range of experimental error.

The index of resolution was found to be 0.80± 0.06. The limit of error was estimated from the random error of 0.03 (2.5 σ_2) plus the systematic error, 0.05, due to the uncertainty in the scattering factors. Since the rather large deviation of the observed index from unity was considered to be due to extraneous scattering, $qN(q)$ was analyzed in order to examine the effect of the extraneous scattering on the molecular parameters. The results of the least-squares analysis of $qN(q)$ are listed in Table XII. In spite of the small index of resolution, the results were in fairly good agreement with those obtained from $qM(q)$. The discrepancies in the mean amplitudes were less than those due to the uncertainties in the theoretical scattering factors. In Fig. 7 the experimental background line, which was obtained as the average of the three lines, is compared with the two theoretical lines; the theoretical background lines, denoted as C and R, were calculated from the complex and from the real[10] atomic scattering factors respectively. The lines are normalized to unity at $q=48$. The experimental background line lies between the theoretical lines, C and R. Therefore, it can be concluded that the extraneous scattering raised the background uniformly, and hence decreased the index of resolution; fortunately, however, it did not seriously affect the values of the mean amplitudes.

Table XII. Results of the least squares analysis of $qN(q)$ of GaI_3 at 255°C

	r_g'	l	θ_g'(IGaI)
Ga-I	2.456±0.005Å	0.066±0.004Å	120.2°±0.8°
I-I	4.258±0.020	0.162±0.011	

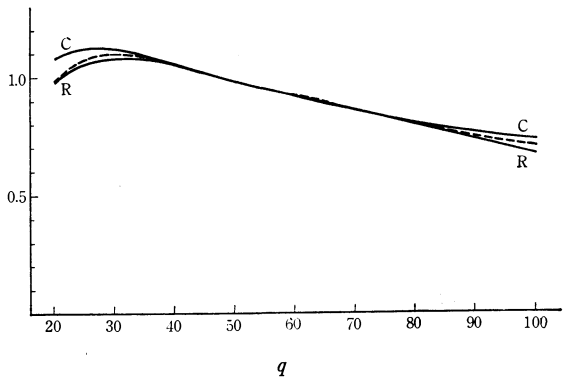

Fig. 7. Calculated and observed background lines of GaI_3.
Calc. { C: Complex scattering factors (by partial-waves), R: Real scattering factors (by the first Born approximation).
— Calcd. -- Obs.

Force Constants.—Since spectroscopic data regarding the force field of gallium triiodide are not available, we must resort to the approximation of the valence forces in order to estimate the stretching and bending force constants, f_r and f_θ, from the two observed mean amplitudes. The general quadratic potential function of a GaI_3 molecule (D_{3h} symmetry) in terms of the internal coordinates is given by:

$$\begin{aligned}2V = &\sum f_r \Delta r_i^2 + 2\sum f_{rr}\Delta r_i \Delta r_j + 2\sum f_{r\theta}\Delta r_i (R\Delta\theta_j) \\ &+ 2\sum f_{r\theta}'\Delta r_i (R\Delta\theta_i) + \sum f_\theta (R\Delta\theta_i)^2 \\ &+ 2\sum f_{\theta\theta}(R\Delta\theta_i)(R\Delta\theta_j) + f_\tau (R\Delta\gamma)^2 \end{aligned} \quad (8)$$

where Δr_i and $\Delta\theta_i$ are the changes in the ith bond and in the bond angle respectively; R is the Ga-I distance, and the $R\Delta\gamma$ coordinate is the distance of the central gallium atom from the plane of the three iodine atoms. The number of independent force constants is reduced from seven to five when the potential function is expressed in terms of symmetry coordinates. By an ordinary procedure,[16] the mean-square amplitudes, l^2(Ga-I) and l^2(I-I), are expressed as:

$$\begin{aligned} l^2(\text{Ga-I}) &= (1/3)L^2_{11}\Delta_1 + (2/3)(L^2_{33}\Delta_3 + L^2_{34}\Delta_4) \\ l^2(\text{I-I}) &= L^2_{11}\Delta_1 + (1/6)(\sqrt{3}L_{33}-L_{43})^2\Delta_3 \\ &\quad + (1/6)(\sqrt{3}L_{34}-L_{44})^2\Delta_4 \end{aligned} \quad (9)$$

14) W. Fischer and O. Jübermann, *Z. anorg. u. allgem. Chem.*, **227**, 227 (1936).
15) T. Tsuchiya, private communication.
16) Y. Morino, K. Kuchitsu and T. Shimanouchi, *J. Chem. Phys.*, **20**, 726 (1952).

where L_{ij} is the element of the $\boldsymbol{L}$ matrix connecting the symmetry coordinates to the normal coordinates, and Δ_i is the mean-square amplitudes of the ith normal coordinate. The subscripts 1, 3 and 4 specify the symmetric stretching (A_1') and the degenerate stretching and bending (E_1') vibrations respectively. It should be noted that the out-of-plane vibration (A_2') has no influence on either of the amplitudes in this order of approximation.

When the approximation of the valence force field is introduced, i. e., when all the cross terms are assumed to be zero, the number of the force constants is reduced to two besides f_r, and a correlation diagram similar to those used for arsenic triiodide is obtained on the (f_r, f_θ) plane by using the values of the mean amplitudes as parameters. Figure 8 shows a diagram for the gallium triiodide at the temperature of 255°C. The correlation curves for the observed mean amplitudes and those corresponding to the limits of error are also shown in the figure. From the shaded area of the figure, the force constants were estimated as follows: $f_r=1.7\pm0.2$ mdyn./Å, $f_\theta=0.06\pm0.02$ mdyn./Å. The corresponding estimates of the vibrational frequencies are $\nu_1(A'_1)=150\pm10$, $\nu_2(E')=300\pm20$ and $\nu_4(E')=65\pm10$ cm^{-1}. The uncertainty in the temperature (±30°C) was taken into consideration in the estimates of the errors, while the uncertainty due to the approximation of the valence force field was not included.

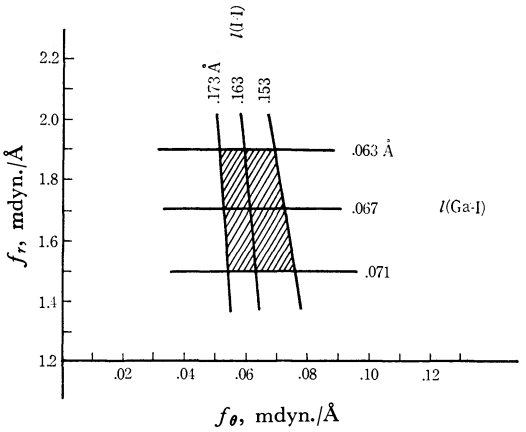

Fig. 8. Correlation curve of f_r and f_θ of GaI_3 at 255°C.

The authors wish to express their gratitude to the Tokyo Shibaura Electric Co. for the supply of gallium. They are also indebted to Dr. Toshikazu Tsuchiya of the Government Chemical Industrial Research Institute, Tokyo, for his mass-spectroscopic analysis of gallium triiodide.

BULLETIN OF THE CHEMICAL SOCIETY OF JAPAN VOL. 39 78—83 (1966)

The Formation Conditions and the Properties of Copper, Zinc, Ammonium Sulfites*

By Keiichi OMORI

Department of Mineralogy, Faculty of Science, Tokyo University

and

Akitsugu OKUWAKI, Takahiro SUZUKI, Hiroshi ITO and Taijiro OKABE

Department of Applied Chemistry, Faculty of Engineering, Tohoku University, Katahira-cho, Sendai

(Received April 19, 1965)

On the reaction of an ammonium sulfite solution with a mixed solution of cupric sulfate and zinc sulfate, ten or more complex sulfite salts have been identified by chemical analysis and X-ray diffraction, and their formation regions have been shown with equilateral triangle coordinates. Their crystallographic properties have been examined through optical observation and X-ray diffraction. Usually some of them are formed simultaneously, but sometimes only one of them is formed, depending on the reaction conditions. The newly-found compounds are as follows:

$Cu_2SO_3 \cdot 7(NH_4)_2SO_3 \cdot 9H_2O$	Tetragonal
$Cu_2SO_3 \cdot ZnSO_3 \cdot 6(NH_4)_2SO_3 \cdot 10H_2O$	Tetragonal
$Cu_2SO_3 \cdot 2ZnSO_3 \cdot 5(NH_4)_2SO_3 \cdot 12H_2O$	Monoclinic
$Cu_2SO_3 \cdot 4ZnSO_3 \cdot 3(NH_4)_2SO_3 \cdot 12H_2O$	Hexagonal

* Presented at the 17th Annual Meeting of the Chemical Society of Japan, Tokyo, April, 1964.

The authors have already proposed a new hydrometallurgical process for copper, a process includes the sulfatizing roasting of copper sulfide ores, the extraction of cupric sulfate, the reduction of cupric sulfate with ammonium sulfite, the separation of metallic copper, and the recovery of ammonium sulfate.[1] In the case of simple sulfide ores, there is no technical problem in the process, but in the case of complex sulfide ores containing zinc, lead and other heavy metals besides copper, the reduction of cupric sulfate proceeds unsatisfactorily. The reason for this trouble seems to be due to the formation of inactive complex copper-zinc-ammonium sulfites, which are easily produced with both metal sulfates and ammonium sulfite in an aqueous solution.

In the present paper, an effort will be made to determine the composition, the properties, and the formation conditions of the complex sulfites.

Experimental

Procedure.—A mixed solution of cupric sulfate and zinc sulfate, prepared by the dissolution of an E. P. reagnt, was placed in a 200-ml. Erlenmeyer flask; then a freshly-prepared ammonium sulfite solution was added drop by drop to the sulfate solution until the three component salts reach a desirable mole fractions. The mixture was vigorously shaken, sealed tightly and allowed to stand for 1—20 days. The crystals which formed were separated from the solution, washed with water and then with methyl alchohl, and dried for 30 min. in a vacuum.

Analysis.—The complex salts formed in the reaction were dissolved by treatment with bromine water. The solution was then boiled on a sand bath until the bromine was completely expelled. The copper and zinc contents were determined by iodometry and by chelatometry respectively. The ammonia content was determined by alkalimetry after distillation, and sulfurous acid, as barium sulfate by oxidation.

Results and Discussion

Complex Sulfite Salts and the Conditions of Their Formation.—When an ammonium sulfite solution is added to a mixed solution of the two metal sulfates, an amorphous, yellowish-brown precipitate is immediately formed, this then gradually changes into transparent crystals. When the mixture is vigorously stirred, the amorphous precipitate tends to coagulate into a plastic mass, one which seems very stretchable without any trace of recovery. If more than a 0.78 mol. fraction of the ammonium sulfite solution is added, the amorphous precipitate is dissolved again, and a wine-red solution is obtained.

The complex salts formed in the reaction are listed in Table I, among which the compounds from III to VI have not been previously reported in the literature; their analytical values are shown in Table II. Besides, the existence of other complex sulfites, XII, XIII, XIV and XV, were recognized by means of X-ray diffraction, but regrettably, these compounds could not be isolated or identified.

Table I. The complex salts formed in the reaction

Compd. No.	Chemical formula
I	$7Cu_2SO_3 \cdot 2CuSO_3 \cdot 3(NH_4)_2SO_3 \cdot 24H_2O$
II	$Cu_2SO_3 \cdot 7(NH_4)_2SO_3 \cdot 10H_2O$
III	$Cu_2SO_3 \cdot 7(NH_4)_2SO_3 \cdot 9H_2O$
IV	$Cu_2SO_3 \cdot ZnSO_3 \cdot 6(NH_4)_2SO_3 \cdot 10H_2O$
V	$Cu_2SO_3 \cdot 2ZnSO_3 \cdot 5(NH_4)_2SO_3 \cdot 12H_2O$
VI	$Cu_2SO_3 \cdot 4ZnSO_3 \cdot 3(NH_4)_2SO_3 \cdot 12H_2O$
VII	$ZnSO_3 \cdot (NH_4)_2SO_3$
VIII	$Cu_2SO_3 \cdot (NH_4)_2SO_3$
IX	$Cu_2SO_3 \cdot CuSO_3 \cdot 2H_2O$ (Chevreul's salt)
X	$ZnSO_4 \cdot (NH_4)_2SO_4 \cdot 6H_2O$ (Tutton's salt)
XI	$ZnSO_3 \cdot 2.5H_2O$
XII	Unknown (Cotton-like crystal)
XIII	Unknown (Calcite-like crystal)
XIV	$Cu_2SO_3 \cdot 5ZnSO_3 \cdot (NH_4)_2SO_3 \cdot 18H_2O$
XV	Unknown (Chevreul's salt-like crystal)
XVI	Non-recoverable plastic mass

The region where the complex salts are formed is shown in Figs. 1(a) and (b). The three component salts are placed at the vertexes of the coordinates, while the mole fractions of their salts in the original mixture are indicated on the internal points. The regions where the complex salts are formed are regularly distributed in the order of II, III, IV, V and VI, from the region rich in ammonium sulfite to the region of little ammonium sulfite.

Properties and Methods of Preparation.—Since some of the above salts contain copper as cuprous sulfite, they are easily oxidized with atmospheric oxygen.

Compound I: $7Cu_2SO_3 \cdot 2CuSO_3 \cdot 3(NH_4)_2SO_3 \cdot 24H_2O$.[2] — Colorless, transparent, square, thin plates, or an aggregate of spherical microcrystals observed as a yellowish-green powder by the naked eye. This salt is easily formed in a very wide region, together with other salts, and it is slowly converted into Chevreul's salt in a low-mole fraction of copper ion. That is, in the region where the mole fraction of cupric sulfate is less than 0.1, the formation of this salt takes place first with an extreme decrease in the quantity of copper ions; consequently, both ramentum-like crystals of compound XIII and Tutton's salt of zinc, $ZnSO_4 \cdot (NH_4)_2SO_4 \cdot 6H_2O$, appear. Besides, in the region where the mole fraction of ammonium sulfite is about 0.65, compound VI appears, as a result of the change in the

1) T. Okabe and H. Ito, *Tech. Repts, Tohoku University*, **29**, 157 (1964).

2) T. Okabe, A. Kanbe and S. Hori, *J. Chem. Soc. Japan, Ind. Chem. Sect.* (*Kogyo Kagaku Zasshi*), **64**, 2091 (1961).

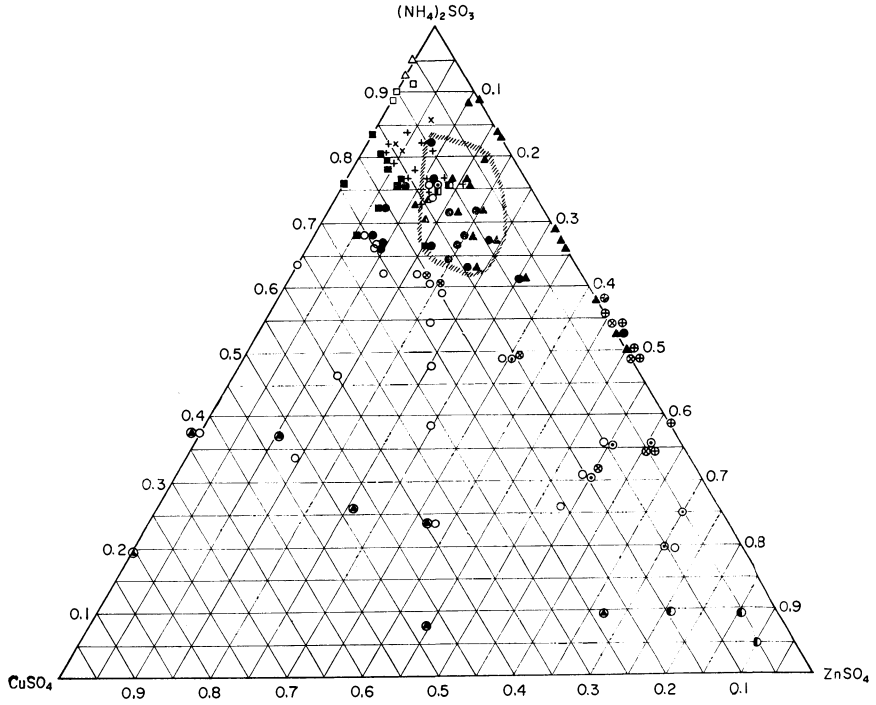

Fig. 1. (a). The formation region of copper, zinc, ammonium sulfites.

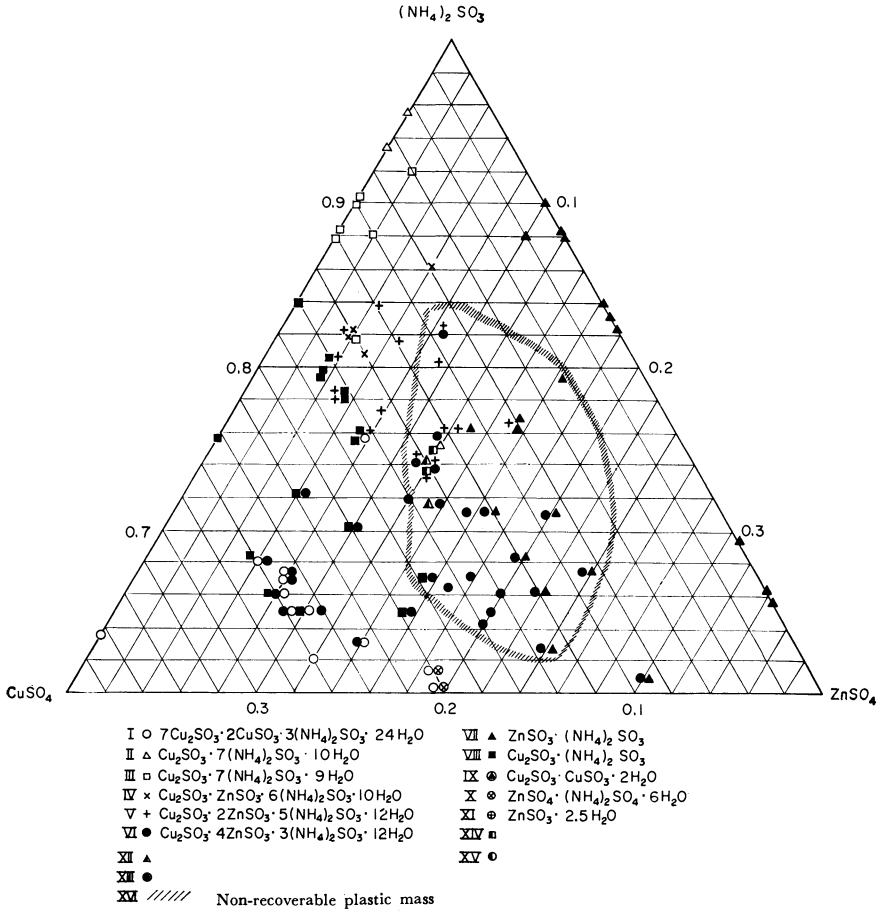

Fig. 1 (b). Developed formation region enriched with ammonium sulfite.

Table II. Analytical values of the new sulfites (%)

Compd. No.	Found					Calcd.				
	NH_4	Zn	Cu	SO_3	H_2O	NH_4	Zn	Cu	SO_3	H_2O
III	20.84	—	10.59	54.18	13.76	21.36	—	10.74	54.17	13.73
IV	16.68	5.30	9.93	52.85	15.24	17.60	5.32	10.33	52.10	14.65
V	13.93	10.10	9.81	49.46	16.70	13.40	9.97	9.85	50.20	16.58
VI	8.00	19.32	9.39	47.32	15.97	7.91	18.75	10.01	47.71	15.62

composition of the solution, in the zinc-rich region after the formation of the compound I.

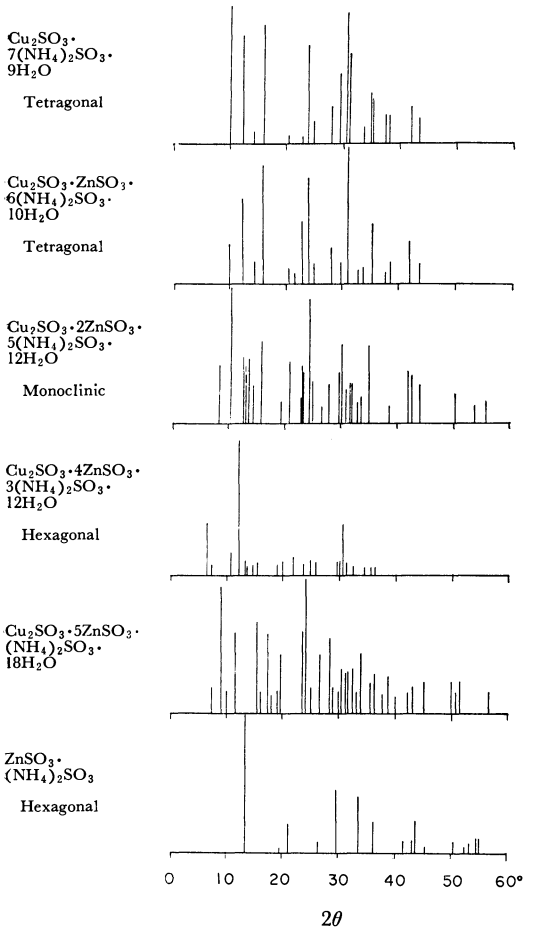

Fig. 2. The X-ray diffraction patterns of some complex sulfites.

Compound II: $Cu_2SO_3 \cdot 7(NH_4)_2SO_3 \cdot 10H_2O$.[2]—Transparent, colorless needles. Very soluble in water. This salt is prepared easily by the drop-by-drop addition of a cupric sulfate solution to a 3-mol./l. or a more concentrated solution of ammonium sulfite in the region where the mole fraction of cupric sulfate is less than 0.06.

Compound III: $Cu_2SO_3 \cdot 7(NH_4)_2SO_3 \cdot 9H_2O$.—Tetragonal (4/m 2/m 2/m). $c=0.3223$. Soluble in water. This salt is formed in a pale wine-red solution at about a 0.9 in mole fraction of ammonium sulfite. When zinc ions are absent in the solution, this salt is obtained as transparent, colorless plates as a result of the good development of the (110) face, and also occasionally as large crystals with a sandglass structure of a wine-red color, while in the presence of a few zinc ions in the solution, this salt is obtained as prisms, as is shown in Fig. 3. This salt bears a resemblance to the compound II and to the $Cu_2SO_3 \cdot 7(NH_4)_2SO_3 \cdot 14H_2O$ reported by Svensson[3] in composition; apparently, however, these salts are not the same, for their chemical properties, X-ray diffraction patterns and formation regions are different.

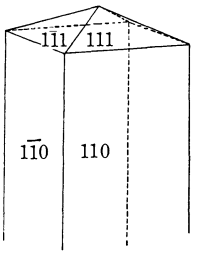

Fig. 3. Cuprous, ammonium sulfite, III.

Compound IV: $Cu_2SO_3 \cdot ZnSO_3 \cdot 6(NH_4)_2SO_3 \cdot 10H_2O$.—Tetragonal, transparent, colorless prisms. Soluble in water. When this salt is oxidized in moist air, it gradually turns yellow. The X-ray diffraction pattern is almost equal to that of the compound III except for the peak corresponding to d: 2.88 Å. This salt is obtained in the region where the amount of zinc ions is larger than that in the formation region of the compound III. This salt is obtained as transparent prisms, for example, in a mixed solution of metal sulfates to which 2—2.5 mol./l. ammonium sulfite solution is added until the mole fractions of cupric sulfate zinc sulfate and ammonium sulfite reach 0.08, 0.06 and 0.86 respectively, and which has stood for several days.

Compound V: $Cu_2SO_3 \cdot 2ZnSO_3 \cdot 5(NH_4)_2SO_3 \cdot 12H_2O$.—Monoclinic prisms, as are shown in Fig. 4 and in Photograph 1. $a : b : c=0.9325 : 1 : 0.4557$, $\beta=93°$ or 87°. Easily soluble in water. The solution of this salt is yellowish green. This salt is formed slowly as large crystals, together with the plastic mass in the region where the mole fraction of cupric sulfate is nearly equal

3) N. Svensson, *Ber.*, **4**, 713 (1871).

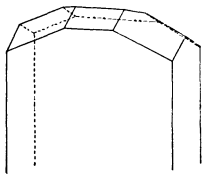

Fig. 4. Cuprous, zinc, ammonium sulfite, V.

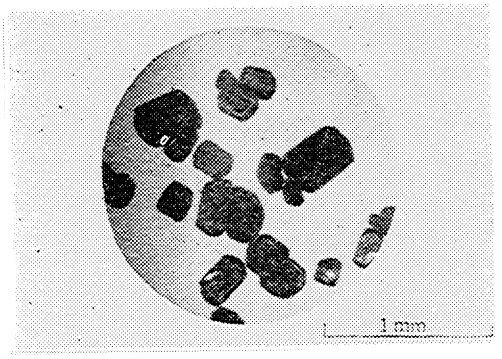

Photograph 1.

to that of zinc sulfate and where the mole fraction of ammonium sulfite is 0.75—0.83. When the number of zinc ions is large, the compound VII, $ZnSO_3 \cdot (NH_4)_2SO_3$, is formed, while when the number of copper ions is large, the compound VIII, $Cu_2SO_3 \cdot (NH_4)_2SO_3$, is formed.

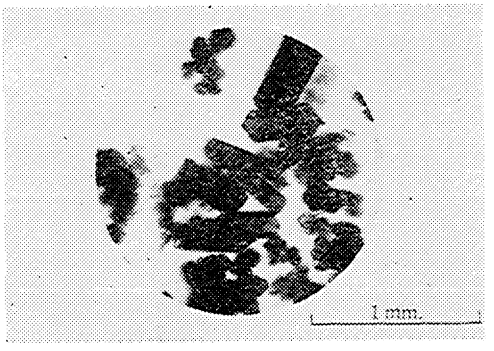

Photograph 2.

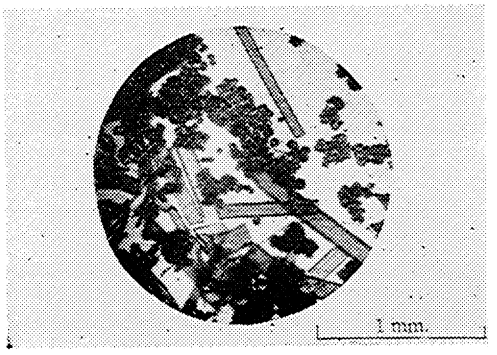

Photograph 3.

Compound VI: $Cu_2SO_3 \cdot 4ZnSO_3 \cdot 3(NH_4)_2SO_3 \cdot 12H_2O$. — Hexagonal crystals, as are shown in Photographs 2 and 3. Insoluble in water and stable in the air. This salt is formed as plates since the $(10\bar{1}0)$ face grows well in the region where the mole fraction of ammonium sulfite is 0.63—0.73. This salt is prepared by adding a 2 mol./l. ammonium sulfite solution to a mixed solution of metal sulfates until the mole fractions of cupric sulfate, zinc sulfate and ammonium sulfite become 0.15, 0.20 and 0.65 respectively. At this state, the mixture must be shaken sufficiently to dissolve the plastic mass and then allowed to stand for a few days, isolated from the atomsphere.

Compound VII: $ZnSO_3 \cdot (NH_4)_2SO_3$.[4]—Hexagonal, transparent and colorless crystals. Slightly soluble in water and relatively stable in the air. The X-ray diffraction pattern and the Miller indices of this salt resemble those of the monohydrate registered on the ASTM X-ray Card 7-0426, but the results of the chemical analysis are apparently different from that of the monohydrate. This salt is formed easily at a 0.25 molar ratio between zinc sulfate and ammonium sulfite. Hexagonal plates are formed in the presence of copper ions, and bipyramidal plates, in the absence of copper ions or at a low concentration of ammonium sulfite. The primary formation of this salt is usually followed by that of the compound V or VI. (Found: NH_4, 13.19; Zn, 25.19; SO_3, 61.55%).

Compound VIII: $Cu_2SO_3 \cdot (NH_4)_2SO_3$.[5]—Rhombohedral, $c=9.0139$. Insoluble in water and stable in the air. Bipyramidal crystals are formed in the presence of zinc ions, and hexagonal plates, in the absence of zinc ions. This salt is obtained over a wide region by adding cupric sulfate to an ammonium sulfite solution until the molar ratio of cupric sulfate to ammonium sulfite becomes nearly 0.25.

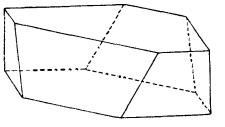

Fig. 5. Cuprous, ammonium sulfite, VIII.

Compound IX: $Cu_2SO_3 \cdot CuSO_3 \cdot 2H_2O$.[6]—Pseudo orthorhombic.

$a=8.34$ Å
$b=7.64$ Å
$c=5.56$ Å

Insoluble in water, but slightly soluble in sulfurous acid. This salt is always formed easily in a

4) F. L. Hahn, H. A. Meier and H. Siegert, *Z. anorg. Chem.*, **150**, 126 (1926).
5) A. Rosenheim and S. Steinhauser, ibid., **25**, 98 (1900).
6) G. Brauer and M. Eichner, *Z. anorg. u. allgem. Chem.*, **287**, 95 (1956).

small mole fraction of ammonium sulfite, or in a relatively large one through the conversion of the compound I.

Compound X: $ZnSO_4 \cdot (NH_4)_2SO_4 \cdot 6H_2O$.—This salt is formed slowly in the zinc-rich region as large crystals after the formation of zinc sulfite.

Compound XI: $ZnSO_3 \cdot 2.5H_2O$.[7]—This salt is formed when the mole fraction of ammonium sulfite is smaller than 0.55. Below a 0.4 mol. fraction of ammonium sulfite, only this salt is formed, but at about 0.45 it is accompanied by Tutton's salt.

The following compounds have also been obtained, but their properties have not been identified.

Unknown Compound XII.—This salt is obtained as a cotton-like aggregate of needles, together with a plastic mass, when a 3 mol./l. or more concentrated solution of ammonium sulfite is added to a mixed solution of the two metal sulfates. The X-ray diffraction pattern of this salt resembles that of the compound II, but the peak at d: 11.7 Å disappears and the intensity of the peak at d: 2.12 Å decreases compared with that of the compound II.

Unknown Compound XIII.—Transparent, colorless and calcite-like crystals. This salt is obtained in the same region as the compound XII is formed. However, the conditions under which only this salt is obtained could not be discovered.

Compound XIV: $Cu_2SO_3 \cdot 5ZnSO_3 \cdot (NH_4)_2SO_3 \cdot 18H_2O$.—This salt is formed as transparent and ink crystals in the clear solution after the dissolution of the plastic mass first formed. Besides, several salts with X-ray diffraction patterns similar to that of the compound II are formed in the region where the mole fraction of copper is below 0.1. (Found: NH_4, 2.56; Zn, 23.00; Cu, 8.96; SO_3, 42.18; H_2O, 23.30%).

Unknown Compound XV.—In the presence of zinc sulfate the color of the Chevreul salt formed in the reaction varies from a reddish brown through orange to yellow with the increase in the amount of zinc sulfate. The change in color may be due to the partial replacement of copper by zinc. The X-ray diffraction pattern varies with the color change until the formation of a certain pattern of this salt is established.

The Non-recoverable Plastic Mass. — Upon the drop-by-drop addition of an ammonium sulfite solution to a mixed solution of metal sulfates in the region where the molar ratio of zinc to copper is 1—2.5 and where the mole fraction of ammonium sulfite is 0.63—0.78, yellowish brown amorphous precipitates are rapidly formed at first; when stirred, these turn into a paste-like material which has no elasticity but which does have a good plasticity; this is named the "non-recoverable plastic mass."

The mass gradually hardens when the occluded water is released, and it is partly converted into the compounds I and VI within a few days or weeks.

Summary

In the reaction of an ammonium sulfite solution with a mixed solution of cupric sulfate and zinc sulfate, ten or more of the complex salts formed have been identified, and their formation regions and properties have been examined. Usually some of them are formed simultaneously, but sometimes only one is formed, depending on the reaction conditions. The newly-found compounds are as follows;

$Cu_2SO_3 \cdot 7(NH_4)_2SO_3 \cdot 9H_2O$
$Cu_2SO_3 \cdot ZnSO_3 \cdot 6(NH_4)_2SO_3 \cdot 10H_2O$
$Cu_2SO_3 \cdot 2ZnSO_3 \cdot 5(NH_4)_2SO_3 \cdot 12H_2O$
$Cu_2SO_3 \cdot 4ZnSO_3 \cdot 3(NH_4)_2SO_3 \cdot 12H_2O$

Among these salts, some may be represented by the general formula of $Cu_2SO_3 \cdot mZnSO_3 \cdot n(NH_4)_2SO_3 \cdot xH_2O$, in which $(m+n)=7$. Possibly, ammonium ions may be replaced by zinc ions to a certain extent.

7) T. Okabe, K. Kanzawa and S. Hori, *J. Chem. Soc. Japan, Pure Chem. Sect.* (*Nippon Kagaku Zasshi*), **81**, 531 (1960).

BULLETIN OF THE CHEMICAL SOCIETY OF JAPAN VOL. 39 84—88 (1966)

The Solvent Effect on the Equilibrium of a Chemical Reaction in a Non-electrolyte Solution: Application to the Keto-enol Tautomerism and Dimerization of Nitrogen Dioxide

By Satohiro TANAKA

Government Chemical Industrial Research Institute, Tokyo, Shibuya-ku, Tokyo

(Received April 27, 1965)

A simple lattice theory of a non-electrolyte solution in which the equilibrium of chemical reaction is reached has been presented and compared with the data of the enolization of ethyl acetoacetate in various solvents and with those of the dimerization of nitrogen dioxide in chloroform. Predicted linear relationships has been obtained for the data of the enolization in non-polar solvents, but they could not be obtained for the reaction in ethyl alcohol or for the dimerization of nitrogen oxide in chloroform. The van't Hoff-Dimroth relation has been derived by the present theory.

It is generally found that the equilibrium of a chemical reaction in a liquid solution is influenced by its medium; this is usually known as the solvent effect. The equilibria in electrolyte solutions has been discussed from the point of view of molecular theory, but those in non-electrolyte solutions have usually been treated only in terms of macroscopic thermodynamic quantities, such as activity and activity coefficient[1-3]; they have hardly been discussed at all from the standpoint of molecular theory.

Recently, the idea[4-6] of accounting for the behavior of associated solutions, in which hydrogen bonding and other weak bonding can occur between the molecules, by considering the system as an ideal mixture of the pure component and the associated complexes has been presented. In this case it is assumed that a chemical equilibrium between the monomers and the associated complexes occurs, and that the equilibrium ratio, as represented in terms of their mole fractions, is independent of the concentrations. However, this idea and its assumptions are very doubtful in the case of real mixtures.

Therefore, some further consideration of the non-electrolyte solution in which the equilibrium of the chemical reaction occurs is desirable in order to account for the medium effect. Such a consideration would contribute to a clearer interpretation of the behavior of associated solutions.

The A⇄B Type Reaction in a Solvent.— The system of a non-electrolyte solution in which a simple equilibrium of the chemical reaction, A⇄B, such as keto-enol tautomerism, occurs in an inert solvent, S, will be considered first. Then the lattice model may be applied to this system, the components of which are A, B and S. Although the lattice model does not describe the behavior of real liquid mixtures exactly,[7] it is convenient for calculating any thermodynamic quantity in the case of a multi-component system, and it can be used as one of approximations for real liquid mixtures.

In addition to the usual assumptions[8] of the lattice theory, these further assumptions were made:

1) All molecules are similar in size.

2) There is no long-range molecular interaction.

Then, using a simple zeroth approximation[9] for the sake of simplicity in calculation, one obtains the partition function (PF) of this system as:

$$(\mathrm{PF}) = \mathrm{e}^{-N_{\mathrm{B}}\varepsilon_0/kT} f_{\mathrm{A}}^{N_{\mathrm{A}}} f_{\mathrm{B}}^{N_{\mathrm{B}}} f_{\mathrm{S}}^{N_{\mathrm{S}}} \frac{N!}{N_{\mathrm{A}}!\, N_{\mathrm{B}}!\, N_{\mathrm{S}}!} \times \exp\left\{-\frac{z}{kT}\left(\frac{N_{\mathrm{A}}N_{\mathrm{B}}}{N} w_{\mathrm{AB}} + \frac{N_{\mathrm{B}}N_{\mathrm{S}}}{N} w_{\mathrm{BS}} + \frac{N_{\mathrm{S}}N_{\mathrm{A}}}{N} w_{\mathrm{SA}}\right)\right\} \quad (1)$$

where N_{A}, N_{B}, and N_{S} are the numbers of A, B, and C molecules respectively; N is the total number of molecules, $N_{\mathrm{A}}+N_{\mathrm{B}}+N_{\mathrm{S}}$; f_{A}, f_{B}, and f_{S} are the partition functions of A, B, and C

1) E. A. Moelwyn-Hughes, "The Kinetics of Reactions in Solution," 2nd Ed., Oxford University Press, London (1950), Chap. VI.

2) G. N. Lewis and M. Randall, "Thermodynamics," 2nd Ed., Rev. by K. S. Pitzer and L. Brewer, McGraw-Hill, N. Y. (1961), Chap. 20.

3) J. E. Leffler and E. Grundwald, "Rates and Equilibria of Organic Reactions," John Wiley & Sons, N. Y. (1963).

4) I. Prigogine and R. Defay, "Chemical Thermodynamics," translated and revised by D. H. Everett, Longmans, London (1954), Chap. XXVI.

5) I. Prigogine, A. Bellemans and V. Mathot, "The Molecular Theory of Solutions," North-Holland, Amsterdam (1957), Chap. XV.

6) A. G. Williamson, *Annual Rev. Phys. Chem.*, **15**, 63 (1964).

7) J. H. Hildebrand and R. L. Scott, "Regular Solution," Prentice-Hall, New Jersey (1962), Chap. 5.

8) E. A. Guggenheim, "Mixture," Oxford University Press, London (1952), p. 16.

9) E. A. Guggenheim, ibid., p. 30.

respectively: ε_0 is the energy change in the $A \rightleftarrows B$ reaction in the gaseous phase; and w_{AB}, w_{BS}, and w_{SA} are molecular interchange energies between the species identified in the subscript.

The Helmholtz free energy of the system is, then, given by:

$$\frac{F}{kT} = -\ln(PF) = \frac{N_B\varepsilon_0}{kT} - N_A \ln f_A - N_B \ln f_B - N_S \ln f_S + N_A \ln \frac{N_A}{N} + N_B \ln \frac{N_B}{N} + N_S \ln \frac{N_S}{N} + \frac{z}{kT}\left(\frac{N_A N_B}{N} w_{AB} + \frac{N_B N_S}{N} w_{BS} + \frac{N_S N_A}{N} w_{SA}\right) \quad (2)$$

Differentiating with respect to N_A and N_B, one obtains for the chemical potential μ_A and μ_B;

$$\frac{\mu_A}{kT} = -\ln f_A + \ln x_A + \frac{z}{kT}\{x_B(1-x_A)w_{AB} - x_B x_S w_{BS} + x_S(1-x_A)w_{SA}\} \quad (3)$$

$$\frac{\mu_B}{kT} = \frac{\varepsilon_0}{kT} - \ln f_B + \ln x_B + \{x_A(1-x_B)w_{AB} - x_S x_A w_{SA} + x_S(1-x_B)w_{BS}\}\frac{z}{kT} \quad (4)$$

where x_A, x_B, and x_S are the mole fractions of A, B, and S respectively.

$$x_A + x_B + x_S = 1 \quad (5)$$

As in the equilibrium,

$$\mu_A = \mu_B \quad (6)$$

the following expressions can be obtained:

$$\ln K = \ln \frac{x_B}{x_A} = -\frac{\varepsilon_0}{kT} + \ln \frac{f_B}{f_A} + \frac{z}{kT}\{(x_B - x_A)w_{AB} + x_S(w_{SA} - w_{BS})\} \quad (7)$$

$$K = \frac{x_B}{x_A} = e^{-\varepsilon_0/kT}\frac{f_B}{f_A}\exp\left[\frac{z}{kT}\{(x_B - x_A)w_{AB} + x_S(w_{SA} - w_{SB})\}\right] \quad (8)$$

From Eqs. 7 and 8, it may easily be seen that the equilibrium ratio, $K = x_B/x_A$, where x_A and x_B are the mole fractions of A and B, contains a factor which represents the solvent effect in terms of x_S, w_{SA}, w_{SB}. A similar formula was also obtained by Moelwyn-Hughes,[10] but he did not develop his formula further or apply it to any experimental data.

For the convenience of analyzing the experimental data, formula 7 is transformed as follows. By substituting $x_S = 1 - x_A - x_B$ into 7, one obtains:

$$\ln K = -\frac{\varepsilon_0}{kT} + \ln \frac{f_B}{f_A} + \frac{z}{kT}(w_{SA} - w_{SB}) + \frac{z}{kT}(w_{AB} - w_{SA} + w_{SB})x_B + \frac{z}{kT}(w_{SB} - w_{SA} - w_{AB})x_A \quad (9)$$

$$= \gamma + \beta x_B + \alpha x_A \quad (10)$$

with:

$$\alpha = \frac{z}{kT}(w_{SB} - w_{SA} - w_{AB})$$

$$\beta = \frac{z}{kT}(w_{AB} + w_{BS} - w_{SA})$$

$$\gamma = \frac{\varepsilon_0}{kT} + \ln \frac{f_B}{f_A} + \frac{z}{kT}(w_{SA} - w_{SB})$$

For $x_S = 0$, formula 10 becomes:

$$\ln K^0 = \gamma + \beta x_B^0 + \alpha x_A^0 \quad (11)$$

where K^0, x_A^0, and x_B^0 are the values of K, x_A, and x_B respectively in the absence of a solvent. When 11 is subtracted from 10, the following equation is obtained:

$$\frac{\ln K - \ln K^0}{x_A - x_A^0} = \alpha + \beta \frac{x_B - x_B^0}{x_A - x_A^0} \quad (12)$$

The $2A \rightleftarrows B$ Type Reaction in a Solvent.—This is also a non-electrolyte solution system containing three components, A, B, and S.

In equilibrium,

$$2\mu_A = \mu_B \quad (13)$$

Then, using a procedure similar to that previously used, the following formula can be obtained:

$$\ln K = \ln \frac{x_B}{x_A^2} = -\frac{\varepsilon^0}{kT} + \ln \frac{f_B}{f_A^2} + \{2x_B - x_A x_B - x_A)w_{AB} + x_S(2 - x_A)w_{SA} - x_S(1 + x_B)w_{SB}\}\frac{z}{kT} \quad (14)$$

This formula will be tested later on the dimerization reaction of nitrogen dioxide.

A Comparison with the Experimental Data of the Keto-enol Isomerization of Ethyl Acetoacetate.—Any adequate comparison of the present formula with the experimental data requires the experimental determination of the mole fractions of the reacting species in non-electrolyte solutions over a wide range of composition. Unfortunately, there are only a few reactions for which such measurements have been made.

As an example of older measurements, the keto-enol isomerizations of ethyl acetoacetate in *n*-hexane, carbon disulfide, benzene and ethyl alcohol were studied by Meyer and Kappelmeier[11] over the whole concentration range. Figure 1

10) E. A. Moelwyn-Hughes, "Physical Chemistry," 2nd Ed., Pergamon, Oxford (1961), p. 1031.

11) K. H. Meyer and P. Kappelmeier, *Ber.*, **44**, 2718 (1911).

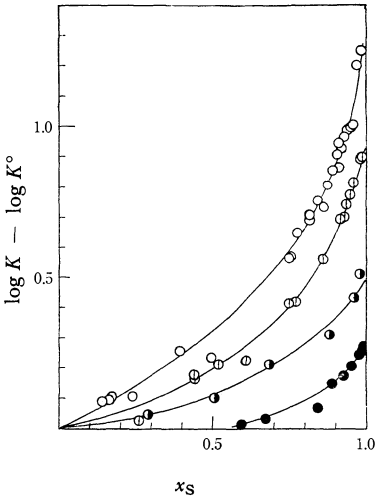

Fig. 1. Variation of equilibrium ratio K for keto-enol isomerization of ethyl acetoacetate with the concentration of the solvent *n*-hexane ○, carbon disulfide ⓘ, benzene ◑ and ethyl alcohol ● in their mole fractions. Recalculated from Meyer et al.'s[11] data.

shows the variations in the equilibrium ratio with the solvent concentration, which was recalculated from their data. These recalculated equilibrium ratios, $K=x_B/x_A$, where A and B represent keto and enol forms respectively, were used to test formula 12; the results are shown in Fig. 2. In these tests, the equilibrium ratio, K^0, for a pure reactant was chosen as the standard of comparison because the K^0 ratio was measured most accurately in their measurements. Despite scattering in the original data and a wide variation in

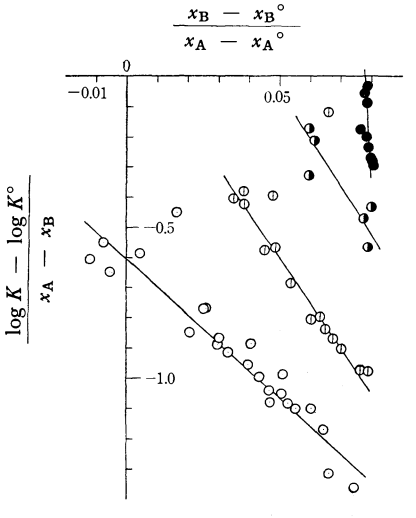

Fig. 2. A test of Eq. 12 for keto-enol isomerization of ethyl acetoacetate in *n*-hexane ○, carbon disulfide ⓘ, benzene ◑ and ethyl alcohol ●.

Table I. Interchange energy w_{AB} between keto and enol forms of ethyl acetoacetate in various solvents

Solvent	w_{AB}, kcal./mol.	
	$z=6$	$z=8$
n-Hexane	−0.9	−0.7
Carbon disulfide	−1.3	−0.9
Benzene	−0.8	−0.6
Ethyl alcohol	—	—

the solvent concentration, the plots describe a fairly satisfactory straight line, with a reasonable slope for each solvent except for ethyl alcohol. Alcohol is known as a polar-associated liquid, and the usual simple lattice theory cannot describe the equilibrium behavior of solution; therefore, a straight line perpendicular to the abscissa, which is not in accordance with the prediction of formula 12, might be obtained.

From Fig. 2 the values of α and β can be read. The value of w_{AB}, the molecular interchange energy between A and B, can also be calculated; they are given in Table I for all the solvents. The values of w_{AB} should be independent of the solvent, but the values for the carbon disulfide solvent differ from the values for *n*-hexane and benzene, and the differences exceed the range of experimental error. The difference may be due to the simplicity of the present model and approximation. However, the three values of w_{AB} are in fairly good accordance with each other in spite of the large difference in the influences of the solvents.

The Derivation of the van't Hoff-Dimroth Relation.—For the $A \rightleftarrows B$ reaction, the value of the equilibrium constant, K, given by the $K=C_B/C_A$ equation at a high dilution, varies from solvent to solvent if the concentrations, C_A and C_B respectively, of A and B are expressed either in moles per liter or in any other conventional unit. However, the constant, G (characteristic of the particular reaction), defined by the equation;

$$G = \frac{C_B/S_B}{C_A/S_A} \tag{15}$$

should be more or less independent of the solvent if the solubilities, S_A and S_B respectively, of A and B in the solvent of interest are not too great. This Eq. 15 is called the van't Hoff-Dimroth relation; it was derived by van't Hoff[12] from thermodynamic considerations and was tested by Dimroth[13] for the isomerism of 1-phenyl-5-aminotriazole carboxylic acid esters in various solvents. The relation has been shown to hold also for the equilibrium between tautomeric forms in various solvents in which the solubilities of the reactants are not too great.

It may easily be shown that the relation can be

12) J. H. van't Hoff, *Lectures on Theoret. Chem.*, **1**, 221 (1898).
13) O. Dimroth, *Ann.*, **377**, 127 (1910).

deduced from the present theory. Let us first obtain the solubility, x_A^*, of A in a solvent, S. In a saturated solution of A in S, we have:

$$\mu_A(s) = \mu_A(l) \tag{16}$$

where $\mu_A(s)$ and $\mu_A(l)$ are the chemical potentials of A in its solid and solution states respectively. By substituting 3 into 16, we obtain:

$$\ln x_A^* = \ln\frac{f_A^l}{f_A^s} - \frac{z}{kT}(1-x_A^*)^2 w_{AB} \tag{17}$$

where f_A^s and f_A^l are the partition functions of A in the solid and liquid states respectively. Similarly, the solubility, x_B^*, of B in S can be obtained:

$$\ln x_B^* = \ln\frac{f_B^l}{f_B^s} - \frac{z}{kT}(1-x_B^*)^2 w_{BS} \tag{18}$$

On the basis of, 17, and 18, the right-hand side of Eq. 15 can be expressed in this form:

$$\ln\frac{x_B/x_B^*}{x_A/x_A^*} = -\frac{\varepsilon_0}{kT} + \ln\frac{f_A^s}{f_B^s} + \frac{z}{kT}\{(w_{AB}+w_{BS}-w_{AS})(x_B-x_A) + w_{BS}(x_B^*-2)x_B^* - w_{AS}(x_A^*-2)x_A^*\} \tag{19}$$

The conditions under which the van't Hoff-Dimroth relation holds, when the equilibrium is at a high dilution and the solubilities of the reactants are not too great, are:

$$x_A,\ x_B,\ x_A^*,\ x_B^* \ll 1 \tag{20}$$

Therefore, x_A^{*2} and x_B^{*2} can be neglected compared with x_A^* and x_B^*, and 19 becomes:

$$\ln\frac{x_B/x_B^*}{x_A/x_A^*} \simeq -\frac{\varepsilon_0}{kT} + \ln\frac{f_B^s}{f_A^s} + \frac{z}{kT}\{(w_{AB}+w_{BS}-w_{AS})(x_B-x_A) - 2(w_{BS}x_B^* - w_{AS}x_A^*)\} \tag{21}$$

The third term on the right-hand side of 21, containing solvent parameters, is consisted of differences of small values if the conditions 20 are taken into consideration, and it may become appreciably small compared with the other terms. Therefore, the quantity on the left-hand side of 21 becomes hardly dependent at all on the solvent; it can thus easily be seen that 21 is equivalent to the van't Hoff-Dimroth relation 15.

A Comparison with the Experimental Data of the $2NO_2 \rightleftarrows N_2O_4$ Reaction in Chloroform.— Cundall[14] investigated the dimerization of nitrogen dioxide in chloroform at 0°C over the full range of concentration, and Lewis et al.[15] calculated the equilibrium ratio, $K=x_B/x_A^2$, at various values of x_S from Cundall's data; x_A, x_B, and x_S are the mole fractions of nitrogen dioxide, nitrogen tetraoxide and chloroform respectively.

14) J. T. Cundall, *J. Chem. Soc.*, **59**, 1076 (1895).
15) Reference 2, p. 273.

According to their results, the condition,

$$x_A \ll x_B,\ x_S$$

held over nearly the entire range of the concent ration. Therefore, formula 14 becomes:

$$\ln K \simeq -\frac{\varepsilon_0}{kT} + \ln\frac{f_B}{f_A^2} - \frac{2zw_{AB}}{kT}x_B + \frac{2z}{kT}(w_{SA}-w_{SB}-w_{AB})x_S + \frac{z}{kT}w_{BS}x_S^2 \tag{22}$$

In the absence of a solvent, i. e. when $x_S=0$, a similar condition,

$$x_A \ll x_B,$$

holds; then 14 becomes:

$$\ln K^0 = -\frac{\varepsilon_0}{kT} + \ln\frac{f_B}{f_A^2} - \frac{2zw_{AB}}{kT}x_B \simeq -\frac{\varepsilon_0}{kT} + \ln\frac{f_B}{f_A^2} - \frac{2zw_{AB}}{kT} \tag{23}$$

By subtracting 23 from 22, one obtains the following equation:

$$\frac{\ln K - \ln K^0}{x_S} = \frac{2z}{kT}(w_{SA}-w_{AB}-w_{SB}) + \frac{z}{kT}w_{BS}x_S \tag{24}$$

Again the ratio, K^0, for pure a reactant is chosen as a standard because it can be measured more accurately than at a high dilution.

The $(\ln K - \ln K^0)/x_S$ values obtained from Cundall's data are plotted in Fig. 3 against the

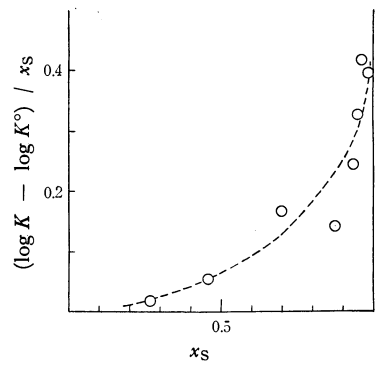

Fig. 3. A test of Eq. 23 for dimerization of nitrogen dioxide in chloroform.

x_S values, but the predicted linear plot cannot be obtained. This failure may be due to the simplicity of the present lattice model and the rough approximation, to the assumption that the dimers are the same size as the monomer; the long-range molecular interaction is neglected although a considerable change in dipole moment occurs in the dimerization in the polar solvent.

The author wishes to thank Dr. Kazuo Amaya for his interest and advice. He also wishes to thank Mrs. Kazuko Sasaki for her interest and encouragement.

BULLETIN OF THE CHEMICAL SOCIETY OF JAPAN VOL. 39 88—91 (1966)

The Flocculation of Kaolin and Precipitated Calcium Carbonate by Polymers

By Kahei SAKAGUCHI and Kunihiko NAGASE

Industrial Research Laboratories, Kao Soap Co., Ltd., Wakayama-shi

(Received May 7, 1965)

The subsidence rate of a suspension of kaolin or precipitated calcium carbonate flocculated by polyacrylamide increases with an increase in the intrinsic viscosity of the polymer, and it shows a marked acceleration above an intrinsic viscosity of 5—6. However, in the case of the flocculation of the precipitated calcium carbonate flocculated by sodium polyacrylate, the subsidence rate depends linearly upon the intrinsic viscosity of the polymer. The results have been discussed in terms of Verwey and Overbeek's theory. The real unperturbed dimension of polyacrylamide has been calculated from the equations proposed by Kurata, Stockmayer and Fixman. As a consequence, it has been suggested that the dimension of a polymer has a close relationship with its flocculation behavior.

It has been suggested by Michaels[1,2] and by other authors[3-5] that the flocculation of the suspension brought about by water-soluble high polymers is caused by the cross-linking of the solid particles with the adsorbed polymer molecules. In the case of the flocculation of a clay suspension by polyacrylamide, it has been reported by Toyoshima[5] that the subsidence rate depends linearly upon the molecular weight of the polymer. However, his observations were confined to the region where the intrinsic viscosity of the polymer solution was less than 6.

In the present work we have investigated the dependence of the molecular weight of polyacrylamide and sodium polyacrylate on the subsidence rate of kaolin or of precipitated calcium carbonate in suspensions. The results will be discussed in terms of Verwey and Overbeek's theory[6]; the conclusion that the flocculation is closely related to the dimension of a polymer will be obtained.

Experimental

Materials.—Both the polyacrylamides and the sodium polyacrylates used in this experiment were prepared by the aqueous polymerization of the corresponding monomers, using ammonium persulfate as an initiator. The viscosities of the resultant polymer solution were measured at 30°C with an Ubbelohde viscometer.

Kaolin was supplied by the Sanko Seiyaku Kogyo Co., Ltd.; its composition and particle-size distribution are shown in Table I and Fig. 1 respectively. The PH of a 5% suspension of this kaolin in water is 4.0.

The precipitated calcium carbonate was supplied by the Shiseido Seiyaku Co., Ltd.; its particle-size distribution is shown in Fig. 2. The PH of a 5% suspension of this carbonate is 9.5.

TABLE I

Componemt	Weight percentage
SiO_2	77.1
Al_2O_3	15.9
Fe_2O_3	0.1
CaO and MgO	trace
Ignition loss (800°C)	3.5

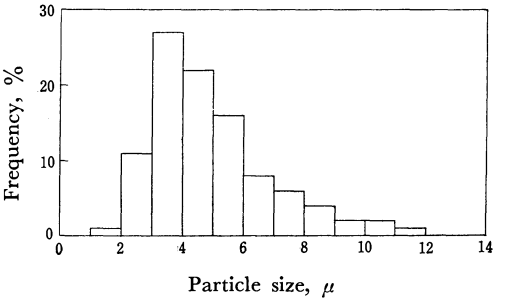

Fig. 1. Particle size distribution of kaolin.

1) A. S. Michaels, *Ind. Eng. Chem.*, **46**, 1485 (1954).
2) A. S. Michaels and O. Morelos, ibid., **47**, 1801 (1955).
3) V. K. LaMer et al., *J. Colloid Sci.*, **11**, 704, 710, 720 (1956); **12**, 230, 566 (1957); **13**, 589 (1958).
4) R. A. Ruhrwein and D. W. Ward, *Soil Sci.*, **73**, 485 (1952).
5) Y. Toyoshima, *J. Chem. Soc. Japan, Pure Chem. Sect.* (*Nippon Kagaku Zasshi*), **82**, 1295, 1297, 1301 (1961).
6) E. J. W. Verwey and J. Th. G. Overbeek, "Theory of the Stability of Lyophobic Colloids," Elesevier, Amsterdam, New York (1948).

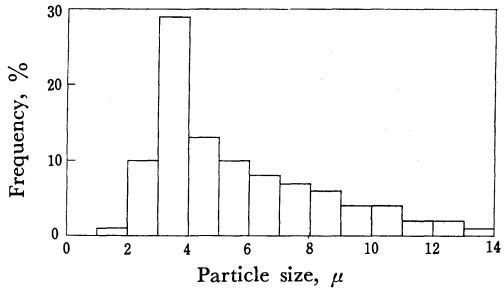

Fig. 2. Particle size distribution of precipitated calcium carbonate.

Methods.—The subsidence data were obtained at room temperature using 25-ml., graduated cylinders 1.2 cm. in inner diameter and 19.4 cm. long. After 1.25 g. of kaolin or calcium carbonate had been weighed into the cylinder, 20 ml. of water was added. The cylinder was then shaken vigorously in order to obtain a suspension. An aqueous solution of a polymer was added to make a total of 25 ml. The amount of the polymer was 0.01% of the solid. The content was mixed by inverting the cylinder 20 times a minute; then it was allowed to settle. The subsidence rates were determined by plotting the height of the solid-liquid boundary as a function of the time.

Results

Figure 3 shows the subsidence rate of a kaolin suspension flocculated by polyacrylamide as a function of the intrinsic viscosity of the polymer. Figure 4 shows the results of the flocculation of the precipitated calcium carbonate suspension by polyacrylamide. In each case, the subsidence rate increases with an increase in the intrinsic viscosity and shows a marked acceleration above an intrinsic viscosity of 5—6. Upon the sedimentation of precipitated calcium carbonate flocculated by sodium polyacrylate, as is shown in Fig. 5, the subsidence rate depends linearly upon the intrinsic viscosity of the polymer.

In the flocculation of a kaolin or precipitated calcium carbonate suspension by polyacrylamide, it appears that a polymer with an intrinsic viscosity

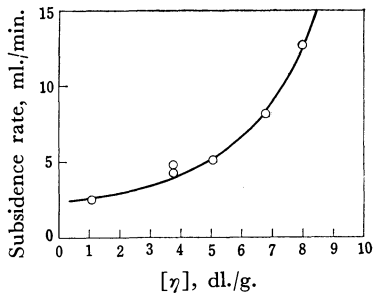

Fig. 3. The relation between the subsidence rate and the intrinsic viscosity of polyacrylamide in the flocculation of kaolin suspension.

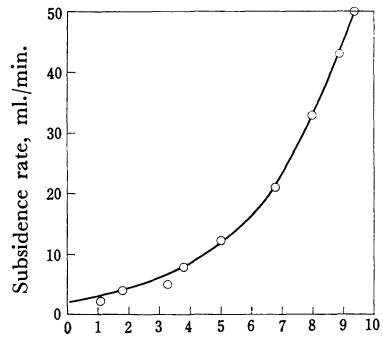

Fig. 4. The relation between the subsidence rate and the intrinsic viscosity of polyacrylamide at the flocculation of calcium carbonate suspension.

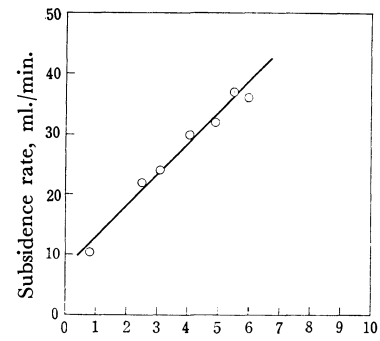

Fig. 5. The relation between the subsidence rate and the intrinsic viscosity (in 2 N NaOH aqueous solution) of sodium polyacrylate in the flocculation of precipitated calcium carbonate.

of 5 or more has a special property to facilitate the crosslinking of the suspended particles with each other. On the other hand, sodium polyacrylate, in contrast to polyacrylamide, shows a moderate flocculating power, even at a low intrinsic viscosity, and it shows a typical linear relationship between the subsidence rate and the intrinsic viscosity. Some of these results have been discussed in another paper.[7]

Discussion

These results seem to suggest that the dimensions of a polymer in an aqueous medium are closely related to the flocculating power. In a dilute aqueous solution of sodium polyacrylate, the configuration of the polymer chain may be greatly expanded by the electrostatic repulsion between carboxyl groups. The intrinsic viscosities of sodium polyacrylates were determined in 2 N sodium hydroxide. Consequently, the actual

7) K. Sakaguchi and K. Nagase, *J. Chem. Soc. Japan, Ind. Chem. Sect.* (*Kogyo Kagaku Zasshi*), to be published.

dimensions of the polymer chain in an aqueous solution may be much larger than that of polyacrylamide, even if the intrinsic viscosity is same. Polyacrylamide is essentially nonionic, and it is not believed that the configuration of the polymer chain is as expanded as in the case of a polyelectrolyte.

On the stability of lyophobic sols, Verwey and Overbeek[6] and Derjaguin and Landau[8-10] have proposed a theory that a flocculation occurs when the London - van der Waals' force exceeds the repulsion force. For coarser particles of polystyrene in dilute salt solutions, Schenkel and Kitchener[11] showed that flocculation takes place at the "secondary minimum" in the potential energy curves, at which the interparticle distance is 500—1000 Å. Hachisu and Furusawa[12] reported that, at low concentrations of sodium chloride, a loose flocculation of "tungustic acid sol" occurs at an interparticular distance of 800—1000 Å; this flocculation at the "secondary minimum" is explained as a balance between the London - van der Waals' force and the repulsion force. The bond combining the particles is easily broken by a mild shock, for the "secondary minimum" is in any case rather shallow. This state of flocculation is a "pseudo flocculation," in which flocculation-deflocculation is reversible.

In order to flocculate the suspension irreversibly, it is necessary to reduce the repulsion force (or the ζ-potential) between the particles by adding larger amounts of electrolytes. Then the interparticular distance becomes narrower than 100 Å, and the aggregate can not be destroyed easily by a mild shock.

The size of the kaolin or of the precipitated calcium carbonate used in the present study was rather coarse; its average diameter was 2—6μ. When these particles were suspended in water in the absence of a polyacrylamide flocculating agent, a loose flocculation of suspensions occurred spontaneously, and the suspensions were deflocculated easily by a mere mechanical shock. The interparticular distance under these conditions could be assumed to be around 1000 Å.

In order to obtain a stable aggregate, one in which the particles are combined stronlgy with each other, the dimensions of a polymer which is to be adsorbed onto the solid surface to facilitate the crosslinking of the particles should be at least larger than 1000 Å. As is demonstrated in Figs. 3 and 4, the polyacrylamides with intrinsic viscosities higher than 5—6 are very effective flocculants. Moreover, as the polyacrylamides used in this study were essentially nonionic, it can be assumed that the adsorption of this polymer causes little change in the repulsion force between particles. In this connection, it would be very interesting to calculate the dimensions of polyacrylamide molecules in water and to examine the relationship between these dimensions and its flocculating behavior.

Recent theoretical investigations by Stockmayer and Fixman[13-15] into the expansion factor of a coiled-chain molecule and its role in the viscosity give these simple intrinsic viscosity equations:

$$[\eta]=[\eta]_\theta \alpha_\eta{}^3 \tag{1}$$

$$[\eta]=KM^{1/2} \tag{2}$$

$$K=\Phi_0 A^3 \tag{3}$$

$$\alpha_\eta{}^3=1+1.55\,Z \tag{4}$$

where $[\eta]$ and $[\eta]_\theta$ represent the intrinsic viscosities in ordinary and theta solvents respectively. M is the molecular weight of the polymer; Φ_0 is an universal constant, 2.87×10^{23} (c. g. s.); α_η is the viscosity expansion factor, and A and Z are shown in Eqs. 5 and 6 respectively:

$$A^2=\langle R_0{}^2\rangle M^{-1} \tag{5}$$

$$Z=\left(\frac{3}{2\pi}\right)^{3/2} BA^{-3}M \tag{6}$$

where $\langle R_0{}^2\rangle$ is the mean-square dimension of the polymer chain and where B is a parameter measuring the polymer-solvent interactions. By combining these equations, we obtain:

$$[\eta]=KM^{1/2}+0.51\Phi_0 BM \tag{7}$$

Rewriting Eq. 7 gives:

$$[\eta]M^{-1/2}=K+0.51\Phi_0 BM^{1/2} \tag{8}$$

On plotting $[\eta]M^{-1/2}$ against $M^{1/2}$, the intercept is equal to K and the slope of the straight line is $0.51\Phi_0 B$. By substituting K in Eq. 3, $\langle R_0{}^2\rangle$ can be determined from Eq. 5. By then substituting B into Eq. 6, Z is determined. Then α_η can be calculated from Eq. 4. The relationship between the mean-square dimension of the polymer chain, $\langle R_0{}^2\rangle$, and the unperturbed mean-square radius of gyration, $\langle S_0{}^2\rangle$, is :

$$\langle S_0{}^2\rangle=(1/6)\langle R_0{}^2\rangle \tag{9}$$

The real unperturbed mean-square radius of gyration, $\langle S^2\rangle$, is :

$$\frac{\langle S^2\rangle}{\langle S_0{}^2\rangle}=\alpha_s \tag{10}$$

where

$$\alpha_s{}^3=\alpha_\eta{}^{2.43} \tag{11}$$

The relationship between the intrinsic viscosity

8) B. Derjaguin, *Trans. Faraday Soc.*, **36**, 203, 730 (1940).
9) B. Derjaguin and L. D. Landau, *Acta Physicochim. U. R. S. S.*, **14**, 633 (1941).
10) B. Derjaguin and L. D. Landau, *J. Exptl. Theoret. Phys.* U. S. S. R., **11**, 802 (1941).
11) J. H. Schenkel and J. A. Kitchener, *Trans. Faraday Soc.*, **56**, 161 (1960).
12) S. Hachisu and K. Furusawa, *Science of Light*, **12**, 1157 (1963).
13) M. Kurata and W. H. Stockmayer, *Fortschr. Hochpolym.-Forsch.*, **3**, 196 (1963).
14) M. Kurata and W. H. Stockmayer, *Rept. Prog. Polymer Phys. Japan*, **5**, 23 (1951).
15) W. H. Stockmayer and M. Fixman, *J. Polymer Sci.*, **C1**, 137 (1963).

and the molecular weight for polyacrylamide has been reported by Dainton et al.[16] to be:

$$[\eta]=6.8\times10^{-4}M^{0.66} \quad (12)$$

where $[\eta]$ is the intrinsic viscosity in an aqueous solution at 30°C, dl./g., and where M is the number-average molecular weight. By plotting $[\eta]M^{-1/2}$ against $M^{1/2}$, values which were calculated from Eq. 12, the curve shown in Fig. 6 was obtained.

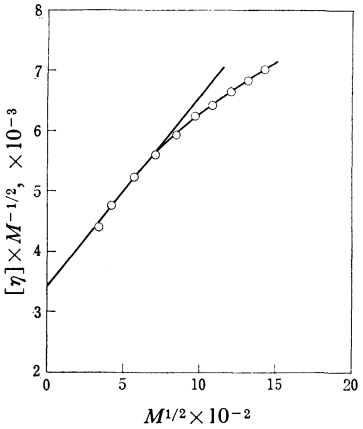

Fig. 6. Plots of $[\eta]M^{-1/2}$ versus $M^{1/2}$.

K and B were determined from the intercept and from the slope of a straight line in the lower molecular weight region respectively:

$$K=3.40\times10^{-3} \quad (13)$$

$$B=2.10\times10^{-27} \quad (14)$$

From Eq. 12, when $[\eta]$ is 6, M is 942000. Substituting K and M values into Eqs. 3 and 5 gives:

$$\langle R_0^2\rangle=1.047\times10^{-10} \quad (15)$$

$$\langle R_0^2\rangle^{1/2}=1.024\times10^{-5} \quad (15')$$

Consequently, the dimension of the polymer chain in a theta solvent is 1024 Å. Using a B value of 2.10×10^{-27}, the Z, α_η and α_s values were calculated successively:

$$Z=0.573 \quad (16)$$

$$\alpha_\eta=1.236 \quad (17)$$

$$\alpha_s=1.187 \quad (18)$$

Subsequently, $\langle S^2\rangle$, $\langle S^2\rangle^{1/2}$ and $\langle R^2\rangle^{1/2}$ were obtained:

$$\langle S^2\rangle=2.07\times10^{-9} \quad (19)$$

$$\langle S^2\rangle^{1/2}=4.55\times10^{-6} \quad (20)$$

$$\langle R^2\rangle^{1/2}=6^{1/2}\langle S^2\rangle^{1/2}=1.114\times10^{-5} \quad (21)$$

Thus, the "real dimension" (the root mean-square end-to-end distance of the chain, $\langle R^2\rangle^{1/2}$) of the polyacrylamide molecules with the intrinsic viscosity of 6 was calculated to be 1114 Å.

Figure 7 shows the relationship between $\langle R^2\rangle^{1/2}$ and the intrinsic viscosity of polyacrylamide. When $[\eta]$ is 5.3, $\langle R^2\rangle^{1/2}$ equals 1000 Å.

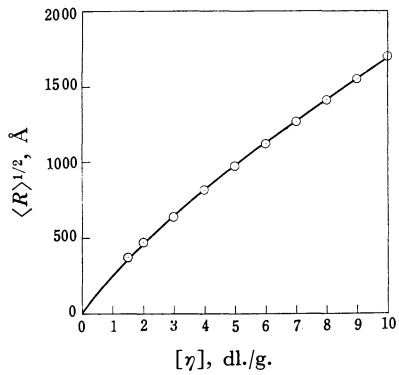

Fig. 7. Plots of $\langle R^2\rangle^{1/2}$ versus $[\eta]$.

This is in good accord with the value of 1000 Å which had been predicted.

Conclusion

At the "secondary minimum" in the potential curve of the Verwey and Overbeek theory, the particles can approach each other up to an inter-particular distance of 1000 Å. However, in this state, the flocculation is not complete. When a polymer with a dimension of 1000 Å or more is added to this suspension, the particles are bound together to give a stable aggregate. Thus, by the addition of polyacrylamide with a dimension larger than 1000 Å, which corresponds to the intrinsic viscosity of 5—6, the suspension is effectively flocculated. Sodium polyacrylate, on the other hand, because of its chain expansion in solution due to the repulsion between carboxyl groups, shows a moderate flocculating power even at a lower intrinsic viscosity. Thus, it gives a linear intrinsic viscosity - subsidence rate relation.

The authors wish to express their thanks to Dr. Eiichi Wada of the Institute of Physical and Chemical Research, Tokyo, for his valuable suggestions.

16) E. Collinson, F. S. Dainton and G. S. McNaughton, *Trans. Faraday Soc.*, **53**, 489 (1957).

BULLETIN OF THE CHEMICAL SOCIETY OF JAPAN VOL. 39 92—100 (1966)

The Crystal Structure of Tris(*l*-propylenediamine)cobalt(III) Bromide and the Absolute Configuration of the Complex Ion, [Co *l*-pn_3]$^{3+}$ *1

By Hitoshi IWASAKI and Yoshihiko SAITO

Institute for Solid State Physics, The University of Tokyo, Azabu, Tokyo

(Received May 13, 1965)

Crystals of L-[Co *l*-pn_3]Br_3 (pn: propylenediamine) were prepared and their crystal structure was completely determined by means of X-rays. They are hexagonal, with the space group $P6_3$; $a=11.08\pm0.03$, $c=8.59\pm0.02$Å and $Z=2$. The structure is essentially ionic, consisting of complex ions and bromide anions. A complex ion has a three-fold axis of symmetry through the central cobalt atom. Five-membered Co-pn rings are puckered, and the C–C bonds in these rings are nearly parallel to the threefold axis. The methyl carbon bonds are equatorial with respect to the plane of the ring. The absolute configuration of the complex ion has been determined by using the absorption-edge technique. The L*lll*-type complex ion has been found to be laevorotatory with respect to the NaD lines. By the introduction of an asymmetric carbon atom into the ligands, the absolute configuration of a series of tris(bidentate)-complexes could be successfully correlated to the configurational series in organic compounds.

In the study of the optical properties of complex compounds, tris(bidentate)-metal complexes are most frequently taken up since they have relatively simple structures and exhibit typical optical isomerism. When three bidentate ligands are coordinated to the central atom in an octahedral fashion, it is possible for two optically active isomers, D and L, to occur (Fig. 1). Niekerk et al. have shown that a [Cr ox_3]$^{3-}$ ion (ox=oxalate ion) essentially possesses the structure shown in Fig. 1.[1] When the chelating molecules are not planar, another kind of isomer appears. For example, when ethylenediamine molecules (usually denoted as "en") are chelated to a metal atom, they assume the "gauche" configuration, and the five-membered ring, consisting of metal and an ethylenediamine molecule, is puckered. If we denote the two possible and enantiomorphous conformations of ethylenediamine as *d* and *l*[*2]

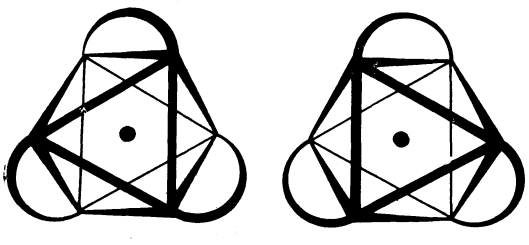

D L

Fig. 1. Two possible configurations of a tris-(bidentate)-complex ion.

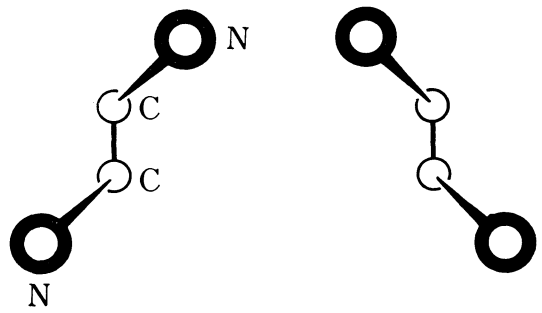

d *l*

Fig. 2. Two possible gauche forms of an ethylenediamine molecule.

(Fig. 2), there will be eight isomers of the [M en_3], such as D*ddd*, L*ddl*, etc.[3] Kuroya et al. found that the most stable form of the [Co en_3]$^{3+}$ ion has a three-fold symmetry and takes either the D*ddd* or the L*lll* form,[*3,3-5] forms which correspond to the "lel" type according to Corey and Bailar's notation.[2] The determination of the absolute configuration proved that the D-type complex is dextrorotatory with respect to the NaD lines.[4]

Now it is widely recognized that the optical rotatory dispersion (ORD) curve is diagnostic of the absolute configuration. In attempting to

*1 Part of this paper is taken from the Doctoral Thesis presented to the University of Tokyo by Hitoshi Iwasaki, 1965. Short Communication, This Bulletin, **36**, 1543 (1963).

*2 Corey and Bailar[2] called these two forms *k* and *k'*.

1) J. N. van Niekerk and F. R. L. Schoening, *Acta Cryst.*, **5**, 196, 475, 499 (1952).

2) E. J. Corey and J. C. Bailar, Jr., *J. Am. Chem. Soc.*, **81**, 2620 (1959).

3) K. Nakatsu, This Bulletin, **35**, 832 (1962).

*3 The notations refer to Figs. 1 and 2.

4) Y. Saito, K. Nakatsu, M. Shiro and H. Kuroya, *Acta Cryst.*, **8**, 729 (1955); This Bulletin, **30**, 158, 795 (1957).

5) K. Nakatsu, Y. Saito and H. Kuroya, ibid., **29**, 428 (1956).

verify this convention of correlating the configurations of various complex ions, the tris(l-propylenediamine)cobalt(III) ion, [Co l-pn$_3$]$^{3+}$, has been chosen and its absolute configuration determined by means of X-rays; the ORD curve of this ion bears a close resemblance to that of [Co en$_3$]$^{3+}$, whose absolute configuration had already been established. Moreover, by the introduction of the methyl groups in the ethylenediamine ring in [Co en$_3$]$^{3+}$ ion, the ligands themselves are optically activated, actually being the l-forms in the present case. The absolute configuration of the l-pn has been chemically correlated to that of D-alanine.[6,7] Accordingly, we may expect to find a correlation between the configurational series in organic chemistry and that of the complex compounds.

Experimental

Commercial racemic propylenediamine was resolved with d-tartaric acid according to the method described by O'Brien and Toole.[8] 5.5 g. of the l-pn was heated with 5.0 g. of chloropurpureo-salt, [CoCl(NH$_3$)$_5$]Cl$_2$. The reaction mixture was then dissolved in a small amount of water. When concentrated hydrobromic acid was added to the solution, crystals of the bromide of the aimed complex were precipitated. By recrystallization from an aqueous solution, single crystals of suitable sizes for X-ray works were obtained.

The crystals are reported to have two moles of water of crystallization.[9] However, no weight loss was observed after the specimen had been kept in an air bath at 123°C for 80 min. The results of the chemical analysis*4 also showed that the specimen was anhydrous. (Found: N, 16.18%; calcd. for [Co l-pn$_3$]Br$_3$: N, 16.15%; calcd. for [Co l-pn$_3$]Br$_3$·2H$_2$O: N, 14.61%). This was supported by the present X-ray structure analysis.

The crystals are deep orange-red in color and transparent. They are hexagonal prismatic, and stable in air at room temperature. An X-ray examination showed the prismatic axis of the crystal to be coincident with the c-axis of the hexagonal system, and the well-developed prismatic faces are indexed as $\{11\bar{2}0\}$. Since the crystals contain only the l-isomer of the propylenediamine, they are optically active. In fact, the crystal was found to be laevorotatory with respect to the NaD lines under a polarizing microscope.

Oscillation photographs were taken around the c-axis. When one uses the Cu$K\alpha$ radiation ($\lambda=1.542$ Å), the intensity distribution on the films was approximately of a mirror symmetry with respect to the equatorial line; i. e.,

$$I(hkl) \fallingdotseq I(hk\bar{l})$$

Detailed examination, however, revealed that this was not exactly true for many weak reflections, though the deviation from the strict mirror symmetry was generally quite small. The photographs taken with the Fe$K\alpha$ radiation ($\lambda=1.937$ Å), for which the effect of the anomalous scattering is expected to be smaller than in the case of Cu$K\alpha$, had a nearly perfect mirror symmetry with respect to the equatorial line. Therefore, it may safely be concluded that the deviation from the symmetry is attributable to the anomalous dispersion occurring in the acentric crystals. The equatorial and upper-level Weissenberg photographs showed the existence of a sixfold symmetry in each reciprocal plane perpendicular to the c-axis. Thus the Laue symmetry group to which the intensity distribution from this crystal belongs is 6 (C_6). The space group was uniquely determined from the systematic absences to be No. 173, $P6_3$ (C_6^6).

The lattice constants were determined from the Weissenberg photographs of crystals rotating about tha a and c axes. The following values were obtained:

$$a=11.08\pm0.03, \qquad c=8.59\pm0.02 \text{ Å}$$

A unit cell contains two formula units of [Co l-pn$_3$]Br$_3$ (Density: observed 1.91 g. cm^{-3}, calcd. 1.90 g. cm^{-3}).

The specimen used for the collection of the final intensity data was polished by emery paper into a cylindrical form with a diameter of 0.012 cm. Equi-inclination Weissenberg photographs were taken around the c-axis up to the seventh layer with the filtered Cu$K\alpha$ radiation. The $0kl$ reflections were also collected by the a-axis rotation. Intensities were estimated visually with a standard film strip. 541 independent reflections were observed. The usual Lorentz, polarization, spot-shape and absorption corrections were then applied. For the a-axis data it was found that the standard deviations of the intensities among the equivalent reflections were larger than those for the c-axis data, probably due to the irregular shape of the specimen. Therefore, these data were not used for the final refinement.

The Determination of the Crystal Structure

Since a unit cell contains only two cobalt atoms, they must be located at one of the two kinds of two-fold special positions: 2a and 2b. However, the former was decidedly ruled out on the basis of the packing consideration. The z-parameter of the cobalt atom was chosen to be zero without any loss of generality.

Thus the cobalt atoms are located on the threefold axis. Consequently, the complex ion [Co l-pn$_3$]$^{3+}$ must possess the symmetry 3 (C_3). The positions of the bromine atoms were easily deduced from the Patterson functions projected along the a- and c-axes. By making use of the results of the structure analyses of the related complex compounds,[3,10] a structural model of the complex ion [Co l-pn$_3$]$^{3+}$ could be easily set up. The positions of the cobalt and bromine atoms being already fixed, only the azimuthal orientation of the complex ion around the threefold axis was left to be determined. After several trials, an optimum

*4 The authors are indebted to Dr. Shohei Tamura for the chemical analysis of the sample.

6) H. Reihlen, E. Weinbrenner and G. v. Hessling, *Ann.*, **494**, 143 (1932).

7) S. Schnell and P. Karrer, *Helv. Chim. Acta*, **38**, 2036 (1955).

8) T. D. O'Brien and R. C. Toole, *J. Am. Chem. Soc.*, **76**, 6009 (1954).

9) A. P. Smirnoff, *Helv. Chim. Acta*, **3**, 177 (1920).

10) Y. Saito and H. Iwasaki, This Bulletin, **35**, 1131 (1962).

condition was obtained in which the discrepancy factor, $R=\sum||F_o|-|F_c||/\sum|F_o|$, became 0.26, where the summation was taken over all the observed $hk0$ data. Starting with this plausible position, the usual difference Fourier method was repeatedly applied to the (001) projection until the structure projected on this plane was completely established. An a-axis projection was also worked out at the same time. Using the results of the c-axis projection, together with the structural model quoted above, the R-factor for the $0kl$ reflections was only 0.25 for the first trial of the z-parametres, where the position of the bromine atoms was chosen so that it gave the N-Br contact of about 3.5 Å. Thus, these parameters were thought to be reasonable and essentially correct.

By the several Fourier refinements described below, the R factors were reduced to 0.12 for $hk0$ and 0.16 for $0kl$. The final refinement was performed on the full-matrix least-squares program, ORFLS, originally written by Busing, Martin and Levy, and slightly modified by Nakatsu and Sakurai to take the effect of the anomalous scattering into account. Anisotropic temperature factors were not used since the three-dimensional electron density map and the difference Fourier map did not indicate the existence of any large anisotropic thermal motions of the atoms. After three cycles of this refinement, the R value dropped and converged to 0.100. All the reflections were given the weight of 1. The extinction effect was corrected for the strongest 17 reflections. Atomic scattering curves were taken from the International Tables.[11]

In the calculations of the structure factors, the effect of the anomalous dispersion was strictly considered. The correction factors for the f-values were assumed as follows:[12]

$$\text{for Co, } \Delta f'=-2.2, \quad \Delta f''=3.9$$

and

$$\text{for Br, } \Delta f'=-0.9, \quad \Delta f''=1.5$$

In the final refinement alone was the angular dependence of these quantities[13] also taken into account.

In the calculations of the Fourier syntheses, the contributions from the anomalous scattering to the structure factors were directly subtracted from F_{obs}, whose phases were given those of F_c. The remainder was used as the Fourier coefficients; i. e.,

$$F(\text{coef.})=|F_o|\exp(i\alpha)-F_c''$$

Here α is the calculated phase factor, and F_c'' is the contribution of the correction terms of the atomic scattering factors to the structure factor. F_c'' contains only the contribution from the cobalt and bromine atoms whose positional parameters are easily fixed. At each step of the refinement, this quantity may take a different value, which is in line with the improvement of the temperature factors and also with a slight change in the position of the bromine atoms. Moreover, the scale factor of F_o may be slightly changed at each step. Therefore, these Fourier coefficients had to be re-calculated at each step of the Fourier refinement. This was made possible by successive approximation. Though such a procedure seems to be rather complicated, it takes the effect of the anomalous dispersion strictly into account, and probably it is one of the best ways to solve the problem when the correction of the anomalous scattering is necessary. A computer program was written for the entire course of calculating both the structure factors and the electron densities. The shifts of the atomic parameters were read from a Fourier map, and the results were used as the next input data for the calculation of the structure factors and electron densities.

In order to obtain the Fourier coefficients by such a procedure, it is necessary to fix the absolute sign of the z-parameters so as to calculate F_c''. Thus, the absolute structure of the crystal had also to be determined during the course of the Fourier refinement.

On oscillation photographs taken around the c-axis, the diffraction spots corresponding to hkl and $hk\bar{l}$, the latter being equivalent to $\overline{hkl}$ due to the symmetry of the space group, are recorded at the symmetrical positions on each side of the equatorial line. These two spots are not equal in intensity as a result of the breakdown of Friedel's law. If the proper indices are given to these spots, including the correct sign of l, inequality

Table I. Determination of the absolute configuration

h	k	l	Observed $\sqrt{I(hkl)/I(hk\bar{l})}$	Calculated $\lvert F(hkl)\rvert/\lvert F(hk\bar{l})\rvert$
8	1	1	0.77	0.88
9	1	1	0.72	0.86
10	1	1	0.71	0.83
8	2	1	0.91	0.88
9	2	1	0.75	0.84
1	3	1	1.31	1.50
3	4	1	0.91	0.78
4	4	1	1.10	1.07
1	5	1	1.21	1.70
3	5	1	0.60	0.43
5	5	1	1.39	1.10
1	6	1	0.73	0.59
4	6	1	0.82	0.75
6	7	1	0.80	0.88
1	9	1	0.54	0.61
2	9	1	0.86	0.75

11) "International Tables for X-ray Crystallography," Vol. III, Kynoch Press, Birmingham (1962), p. 164.
12) C. H. Dauben and D. H. Templeton, *Acta Cryst.*, 8, 841 (1955).
13) Reference 10, Vol. III, p. 214.

TABLE II. ATOMIC PARAMETERS

Atom	x	$\sigma(x)$	y	$\sigma(y)$	z	$\sigma(z)$	B (Å^2)
Co	0.6667	—	0.3333	—	0	—	1.912
Br	0.4526	0.0002	0.1189	0.0002	0.5103	0.0008	4.048
N(1)	0.4954	0.0014	0.2692	0.0014	−0.1295	0.0022	2.358
N(2)	0.5504	0.0014	0.1696	0.0014	0.1373	0.0021	2.768
C(1)	0.3863	0.0028	0.1243	0.0026	−0.0821	0.0037	4.194
C(2)	0.4011	0.0024	0.1182	0.0022	0.0998	0.0032	2.689
C(3)	0.2408	0.0018	0.0781	0.0018	−0.1389	0.0025	4.038

relations between $I(khl)$ and $I(hk\bar{l})$ will be established. The sense of the c^* direction could be easily determined with the help of a Weissenberg photograph. The differences between $I(hkl)$ and $I(hk\bar{l})$ were observed by several people independently at first, and later the intensities were estimated visually by the authors. Under the present conditions, the Lorentz, polarization and absorption factors take the same value for hkl and $hk\bar{l}$ reflections. Hence, the $\sqrt{I(hkl)/I(hk\bar{l})}$ ratio is equal to the ratio of the two structure factors, i. e., $|F(hkl)|/|F(hk\bar{l})|$. Some of the observed ratios, together with the calculated ratios, are listed in Table I. The latter are based on the parameters listed in Table II. Considering the general agreement in Table I, it may be concluded that these atomic parameters correspond to the absolute structure of the (−)-[Co *l*-pn$_3$]Br$_3$ crystal. A complex ion based on these parameters is illustrated in Fig. 3. Therefore, the complex ion shown in this figure must correspond to the (−)-[Co *l*-pn$_3$]$^{3+}$ ion.

The trial model with the reversed z-parameters was checked several times during the course of the Fourier refinement in order to justify the assumption of the absolute configuration of the complex ion. The calculations of the structure factor ratios were repeated at each cycle in these refinements. After the final refinement, the R values for all the hkl reflections became 0.100. If one takes a set of parameters in which the signs of the z-parameters of all the atoms are reversed, the R value becomes 0.123. Though the difference is small in terms of the values of the R-factors, a detailed examination of individual reflections clearly excludes the possibility of the reversal of the z-parameters.

The final set of the atomic parameters, together

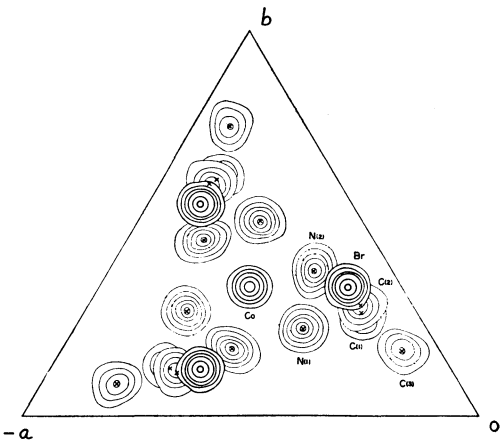

Fig. 4. Composite three dimensional Fourier diagram. Contours around the cobalt and bromine atoms are drawn at intervals of 10 e. Å^{-3}, and those for the light atoms, 2 e. Å^{-3}.

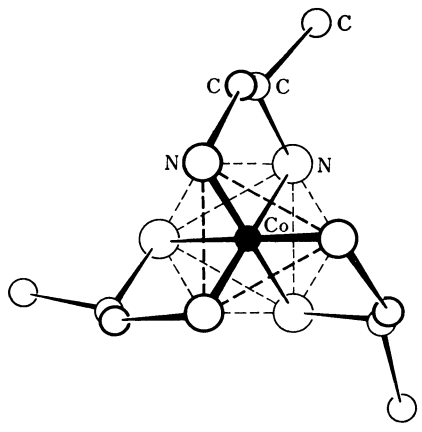

Fig. 3. The absolute configuration of a (−)-[Co *l*-pn$_3$]$^{3+}$ ion.

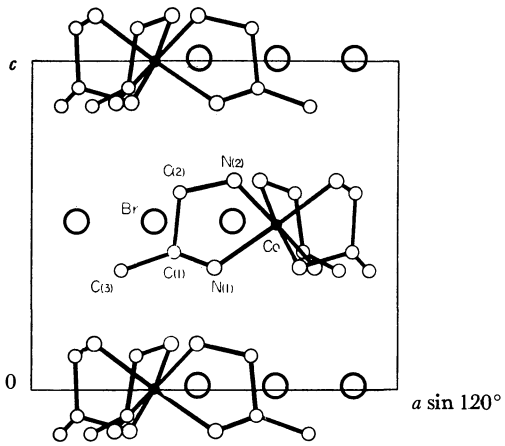

Fig. 5. Atomic arrangement projected along the a-axis.

TABLE III. THE OBSERVED AND CALCULATED STRUCTURE FACTORS

h	k	F_o	F_c	h	k	F_o	F_c	h	k	F_o	F_c	h	k	F_o	F_c
$l=0$				3	6	24.6	20.6	5	3	45.5	47.9	6	1	42.1	41.1
1	0	83.3*	87.6	4	6	33.3	28.7	6	3	17.5	10.1	7	1	6.8	3.7
2	0	26.2	24.6	6	6	4.8	4.4	7	3	34.0	38.9	8	1	12.2	9.9
3	0	10.3	6.9	7	6	9.8	11.0	9	3	5.5	6.5	9	1	14.5	17.9
4	0	65.5	66.4	2	7	19.3	18.0	1	4	37.5	28.3	10	1	15.0	14.9
5	0	66.3	67.8	3	7	26.5	25.9	2	4	68.2	66.4	11	1	10.7	12.2
6	0	29.1	30.5	4	7	8.2	8.5	3	4	20.8	18.0	1	2	80.2*	81.3
7	0	9.0	5.0	5	7	8.7	7.6	4	4	17.9	20.9	2	2	20.2	21.8
8	0	11.1	3.7	6	7	12.3	12.2	5	4	26.9	26.8	3	2	44.1	36.2
9	0	45.1	48.5	1	8	24.3	20.5	7	4	27.4	26.2	4	2	38.9	36.1
10	0	17.0	17.9	2	8	12.3	8.8	8	4	17.1	17.4	5	2	10.8	9.0
11	0	4.1	3.0	3	8	19.3	21.2	1	5	13.3	7.2	6	2	47.9	49.6
1	1	16.0	14.5	5	8	13.4	15.3	2	5	19.2	19.0	7	2	11.9	13.3
2	1	178.9*	171.3	1	9	23.5	21.9	3	5	16.7	11.7	8	2	6.6	7.5
3	1	39.9	43.0	2	9	12.7	6.3	4	5	24.7	23.8	9	2	14.0	11.2
4	1	97.1*	100.5	4	9	9.3	13.8	5	5	7.2	9.5	10	2	12.0	12.6
5	1	14.2	15.8	1	10	6.5	12.7	7	5	25.0	22.2	1	3	50.0	44.5
6	1	57.0	57.8	2	10	8.0	5.9	1	6	16.1	13.0	2	3	26.9	24.4
7	1	5.4	4.7	3	10	12.2	16.1	2	6	69.0	69.6	3	3	30.9	31.6
8	1	19.8	15.5	1	11	12.5	15.3	3	6	18.4	17.1	4	3	32.6	32.9
9	1	13.1	12.7					4	6	12.4	8.9	5	3	29.5	23.8
10	1	14.3	13.6	$l=-1$				5	6	6.8	11.1	6	3	20.5	17.6
11	1	11.6	12.5	1	0	26.5	13.6	6	6	23.9	25.5	7	3	15.7	17.0
1	2	100.1*	105.4	2	0	41.5	45.6	1	7	40.7	41.4	8	3	23.1	25.3
2	2	39.1	38.0	3	0	15.3	14.5	2	7	21.6	26.9	9	3	9.7	4.5
3	2	27.6	24.9	4	0	52.5	55.9	3	7	7.1	12.3	1	4	101.5*	101.8
4	2	47.9	50.1	5	0	64.1	65.6	4	7	20.5	18.6	2	4	40.6	42.5
5	2	33.5	29.8	6	0	14.8	13.3	5	7	13.7	13.0	3	4	40.9	38.4
6	2	34.1	36.8	7	0	40.5	38.2	6	7	18.3	22.4	4	4	39.8	42.3
7	2	12.4	15.3	10	0	16.6	14.9	2	8	21.2	18.5	5	4	28.2	31.0
9	2	12.7	8.1	11	0	13.5	11.6	3	8	33.4	38.6	6	4	12.1	7.6
10	2	13.3	12.6	1	1	56.3*	59.9	5	8	4.7	5.4	7	4	13.8	9.9
1	3	7.7	7.3	2	1	32.7	29.7	1	9	9.7	11.6	8	4	13.4	13.4
2	3	30.2	26.3	3	1	27.4	23.9	2	9	12.6	15.0	9	4	7.5	7.5
3	3	18.8	20.7	4	1	13.0	10.4	1	10	5.9	12.0	1	5	28.8	33.2
4	3	42.6	45.6	5	1	10.3	9.5	2	10	10.1	12.6	2	5	14.8	10.8
5	3	47.4	43.9	6	1	68.6	70.4	3	10	10.7	15.3	3	5	6.6	5.0
6	3	35.4	34.6	7	1	45.8	49.8	1	11	18.0	24.2	4	5	28.7	30.7
7	3	7.8	7.4	8	1	12.5	13.2					5	5	43.2	49.9
8	3	24.7	27.4	9	1	13.7	9.9	$l=-2$				6	5	11.4	10.0
1	4	95.2*	99.3	10	1	11.8	10.1	1	0	65.2*	64.0	7	5	6.0	8.0
2	4	31.1	35.5	11	1	8.7	8.3	2	0	29.5	26.6	8	5	9.5	15.4
3	4	28.5	28.1	1	2	158.9*	151.8	3	0	30.1	27.0	1	6	41.3	42.2
4	4	49.8	55.1	2	2	70.4	68.8	4	0	70.6	70.1	2	6	43.6	43.8
5	4	40.7	43.8	3	2	45.7	47.0	5	0	64.7	63.7	3	6	24.3	22.9
6	4	11.1	7.2	4	2	23.9	25.7	6	0	33.7	35.7	4	6	27.0	22.9
7	4	5.3	4.7	5	2	28.3	26.8	7	0	14.8	14.1	5	6	11.4	12.5
9	4	6.9	7.0	6	2	36.2	37.0	8	0	11.9	11.2	7	6	10.9	12.5
1	5	29.7	34.1	7	2	36.0	39.0	9	0	46.8	51.7	1	7	9.6	5.7
2	5	31.1	21.0	8	2	23.4	22.0	10	0	14.4	16.2	2	7	15.3	16.7
3	5	10.4	6.9	9	2	19.0	20.0	11	0	7.6	6.5	3	7	21.7	19.1
4	5	26.6	27.2	10	2	16.3	22.4	1	1	13.1	8.6	4	7	0.0	3.1
5	5	42.2	48.5	1	3	26.0	16.2	2	1	122.9*	122.6	5	7	10.7	10.0
8	5	10.0	14.2	2	3	39.6	38.9	3	1	55.5	54.8	6	7	12.6	13.2
1	6	47.1	48.5	3	3	80.7	89.0	4	1	88.1	87.6	1	8	26.5	22.4
2	6	39.4	39.7	4	3	74.5	81.3	5	1	16.9	14.0	2	8	9.8	8.5

Table III. (Continued)

h	k	F_o	F_c	h	k	F_o	F_c	h	k	F_o	F_c	h	k	F_o	F_c
3	8	18.1	19.8	4	4	7.1	8.6	7	2	11.7	9.5	3	1	35.4	35.1
5	8	11.2	13.6	5	4	27.9	25.8	8	2	10.6	10.2	4	1	18.8	16.1
1	9	22.1	20.0	7	4	13.9	14.2	9	2	11.7	9.3	5	1	16.2	10.1
2	9	11.4	8.1	8	4	16.2	17.9	10	2	6.3	8.0	6	1	41.6	42.1
3	9	5.5	5.6	1	5	17.7	17.7	1	3	17.9	13.0	7	1	22.4	22.7
4	9	6.2	11.0	2	5	19.1	19.3	2	3	20.6	19.2	8	1	10.2	7.8
1	10	10.5	12.7	3	5	17.3	15.0	3	3	24.7	21.9	9	1	13.3	9.4
2	10	11.5	11.1	4	5	28.3	27.9	4	3	24.6	21.2	10	1	7.1	7.9
3	10	7.5	9.8	6	5	9.5	8.1	5	3	14.1	6.0	1	2	82.3*	91.0
1	11	8.8	12.4	7	5	19.9	22.2	6	3	6.6	5.6	2	2	47.1	49.0
				8	5	4.2	4.7	7	3	23.2	23.6	3	2	46.9	49.5
$l=-3$				1	6	20.3	18.9	8	3	25.4	21.9	4	2	8.2	9.3
1	0	78.6*	63.3	2	6	59.3	65.9	9	3	7.5	6.3	5	2	19.1	14.9
2	0	71.8*	67.4	3	6	10.2	10.7	1	4	71.4	75.9	7	2	24.0	24.3
3	0	12.4	11.7	5	6	11.5	16.9	2	4	37.7	37.6	8	2	15.2	12.1
4	0	41.4	40.9	6	6	17.1	19.5	3	4	39.4	39.7	9	2	9.6	11.6
5	0	51.8	51.8	7	6	6.5	7.7	4	4	28.4	28.3	1	3	24.3	25.0
6	0	6.6	1.8	1	7	36.2	38.9	5	4	15.5	16.2	2	3	20.5	18.0
7	0	30.0	32.4	2	7	20.8	23.7	6	4	9.3	6.1	3	3	50.7	53.3
8	0	7.2	8.6	3	7	12.4	14.2	8	4	12.8	12.2	4	3	34.0	36.7
9	0	6.9	0.7	4	7	21.2	20.1	1	5	31.0	31.9	6	3	13.6	9.2
10	0	11.6	9.5	5	7	10.5	12.1	2	5	12.4	12.1	7	3	23.4	23.8
11	0	7.3	9.5	6	7	11.2	19.7	4	5	27.6	30.4	8	3	10.6	12.9
1	1	84.3*	78.2	2	8	13.5	16.0	5	5	41.6	45.2	1	4	16.9	17.5
2	1	39.3	34.6	3	8	28.3	35.0	7	5	4.5	6.0	2	4	37.5	36.9
3	1	50.2	49.1	5	8	6.2	2.3	1	6	34.0	34.3	3	4	22.8	22.1
4	1	10.0	8.2	2	9	6.3	8.6	2	6	33.5	34.2	4	4	9.0	8.9
5	1	23.5	17.9	1	11	10.3	17.1	3	6	16.3	17.0	5	4	22.3	19.5
6	1	57.1	54.7					4	6	19.2	14.9	7	4	7.0	7.6
7	1	30.9	29.7	$l=-4$				5	6	13.0	14.5	8	4	11.5	14.4
8	1	6.3	7.7	1	0	36.1	34.5	1	7	6.7	5.9	1	5	14.4	13.9
9	1	13.5	9.7	2	0	15.9	12.8	2	7	13.1	10.6	2	5	19.4	19.9
10	1	10.2	9.4	3	0	35.9	34.5	3	7	6.2	12.5	3	5	11.1	8.1
11	1	3.7	9.4	4	0	49.7	49.4	4	7	8.8	5.9	4	5	21.3	18.1
1	2	126.5*	119.2	5	0	48.4	47.0	1	8	19.6	17.3	5	5	5.8	5.3
2	2	68.7	70.4	6	0	35.1	37.7	2	8	8.8	5.9	6	5	7.2	8.4
3	2	57.0	57.6	8	0	15.4	17.2	3	8	17.6	18.3	7	5	12.7	14.2
4	2	11.8	9.8	9	0	38.7	47.3	4	8	6.9	7.6	1	6	18.9	16.7
5	2	24.6	19.9	10	0	12.8	14.6	1	9	18.0	14.8	2	6	40.7	45.4
6	2	10.1	6.8	11	0	3.9	3.7	2	9	7.9	4.7	3	6	10.6	7.4
7	2	30.1	31.0	1	1	18.6	14.0	3	9	7.5	6.2	4	6	7.8	9.2
8	2	17.3	15.4	2	1	55.6	59.3	1	10	7.0	10.0	5	6	10.2	11.4
9	2	15.1	19.4	3	1	46.0	51.7	2	10	9.7	12.6	6	6	13.0	16.5
10	2	13.4	21.4	4	1	67.1	70.9					1	7	28.9	27.4
1	3	17.3	15.5	5	1	15.3	13.5	$l=-5$				2	7	6.2	10.8
2	3	39.5	39.2	6	1	25.5	23.3	1	0	41.7	38.3	3	7	10.2	11.6
3	3	71.8	73.7	7	1	13.4	10.7	2	0	53.0	54.4	4	7	12.9	11.4
4	3	49.0	49.2	8	1	9.5	4.1	3	0	11.7	8.6	5	7	8.4	10.1
5	3	10.0	7.1	9	1	13.5	13.6	4	0	35.5	33.8	1	8	5.9	9.0
6	3	13.7	11.9	10	1	11.0	11.9	5	0	38.9	38.1	2	8	14.4	14.0
7	3	27.5	31.0	1	2	53.0	52.6	6	0	14.9	8.6	3	8	22.9	26.3
8	3	11.9	13.4	2	2	16.4	14.7	7	0	27.9	26.9	4	8	6.0	8.1
9	3	4.8	5.2	3	2	29.0	28.3	8	0	10.5	7.5	2	9	7.4	7.2
1	4	23.2	21.2	4	2	25.1	20.6	10	0	8.9	8.3				
2	4	51.6	50.2	5	2	23.0	26.3	1	1	57.2*	59.2	$l=-6$			
3	4	18.4	19.3	6	2	49.8	50.8	2	1	28.5	24.5	1	0	30.0	28.5

Table III. (Continued)

h	k	F_o	F_c	h	k	F_o	F_c	h	k	F_o	F_c	h	k	F_o	F_c
2	0	7.3	1.2	2	3	23.5	21.3	2	8	7.8	6.0	7	2	16.7	17.8
3	0	16.1	15.1	3	3	12.4	8.7	3	8	13.3	15.8	8	2	9.9	9.4
4	0	28.9	28.1	4	3	21.9	21.1	1	9	11.8	9.0	1	3	17.4	17.9
5	0	31.7	30.6	5	3	14.4	12.2					2	3	6.4	8.0
6	0	25.5	26.1	6	3	13.8	11.9	$l=-7$				3	3	32.7	34.3
7	0	8.0	4.6	7	3	15.0	13.8	1	0	15.0	13.5	4	3	30.0	32.7
8	0	13.7	12.1	8	3	14.1	17.0	2	0	28.8	29.9	5	3	14.5	17.8
9	0	26.1	29.8	1	4	36.7	36.4	3	0	10.3	5.4	6	3	10.0	4.8
10	0	8.3	12.3	2	4	25.7	27.2	4	0	27.0	27.6	7	3	15.2	17.3
1	1	19.7	18.8	3	4	24.9	24.4	5	0	27.4	26.9	1	4	6.5	3.9
2	1	35.8	37.4	4	4	24.0	26.0	6	0	9.4	4.7	2	4	24.3	24.8
3	1	29.6	30.3	5	4	14.9	15.5	7	0	20.0	18.1	3	4	19.9	16.9
4	1	47.6	54.9	6	4	8.7	6.8	8	0	5.8	5.8	5	4	13.2	11.4
5	1	14.0	11.4	1	5	23.0	24.5	1	1	30.5	32.1	6	4	6.5	4.5
6	1	22.2	20.8	2	5	9.7	8.2	2	1	12.4	13.8	1	5	6.4	7.7
7	1	10.9	10.6	3	5	6.0	6.8	3	1	18.7	14.0	2	5	14.2	13.0
8	1	5.3	5.8	4	5	21.2	22.9	4	1	11.2	9.5	3	5	6.9	5.0
9	1	8.8	9.5	5	5	28.8	30.6	5	1	11.2	8.1	4	5	14.3	10.3
1	2	34.6	37.4	1	6	29.3	29.4	6	1	29.1	30.7	1	6	11.2	9.4
2	2	14.8	15.7	2	6	20.0	18.0	7	1	17.2	18.2	2	6	24.5	24.5
3	2	10.7	8.0	3	6	9.1	9.0	8	1	5.1	4.1	3	6	8.1	5.4
4	2	14.1	12.8	4	6	15.3	11.8	1	2	47.6	56.0	1	7	18.5	15.2
5	2	11.2	10.3	5	6	6.9	9.3	2	2	28.2	26.6	2	7	5.6	6.0
6	2	28.7	28.3	1	7	7.7	9.4	3	2	28.2	28.5	3	7	7.6	6.7
7	2	9.6	8.8	2	7	15.6	18.7	4	2	11.2	12.9	1	8	5.1	7.9
8	2	6.2	8.1	3	7	13.4	13.3	5	2	11.5	10.2	2	8	8.4	8.6
1	3	15.7	13.9	1	8	11.5	8.9	6	2	11.3	14.1				

with their standard deviations, is shown in Table II. The standard deviations are calculated from the usual treatment of the errors, using the disagreement of the structure factors.[14] This corresponds to the standard errors of the positions of an average of about 0.007 Å for Br, 0.027 Å for N and 0.046 Å for C.

The observed and calculated structure factors are listed in Table III. In the table the asterisk * denotes those reflections which have already been corrected for the extinction effects.

A composite electron density diagram made from the sections of the three-dimensional Fourier synthesis is shown in Fig. 4. The structure projected along the a-axis is illustrated in Fig. 5.

The Description of the Structure and Discussion

The atomic arrangement in the crystal is shown in Figs. 4 and 5. The interatomic distances and bond angles are given in Table IV.

The structure is essentially ionic and consists of the positively-charged [Co l-pn_3]$^{3+}$ ions and Br^- ions. The Br–Br separation is 4.11$_2$ Å, corresponding to twice the ionic radius of Br^-. The cobalt and bromine atoms lie in approximately one

Table IV. Interatomic distances and bond angles (Å, degree)

Co-N(1)	1.998±0.030
Co-N(2)	2.001±0.030
N(1)-C(1)	1.50 ±0.07
N(2)-C(2)	1.49 ±0.06
C(1)-C(2)	1.58 ±0.07
C(1)-C(3)	1.51 ±0.07
Br-Br	4.112±0.011**
Br-N(1)	3.432±0.037*
Br-N(2)	3.339±0.037*
Br-C(1)	3.584±0.048*
Br-C(2)	3.573±0.040*
Br-C(3)	3.705±0.040**
Co-Br	4.985±0.007*
Co-Br	4.830±0.007*
Co-Br	4.499±0.007**
∠N Co N	86.5±1.5°
∠Co N(2)C(2)	108 ±3°
∠Co N(1)C(2)	110 ±4°
∠N(1)C(1)C(2)	106 ±5°
∠N(2)C(2)C(1)	108 ±5°
∠N(1)C(1)C(3)	115 ±6°
∠C(2)C(1)C(3)	115 ±6°

* Distances between layers.
** Distances within one layer.

14) D. W. J. Cruickshank, *Acta Cryst.*, **2**, 65 (1949).

layer, perpendicular to the *c*-axis. The whole structure can be obtained if exactly similar layers are placed on the first in such a way that they are all related by the operation of 6_3. A complex ion is surrounded by three Br^- ions within the same layer at a distance of 4.49_9 Å and by six anions at the apices of a trigonal prism. The Co atom lies approximately at the center of this prism, the Co–Br distances being 4.98_5 and 4.83_0 Å. The atomic group composed of three Br^- ions is surrounded by the complex ions in just the same way as the latter is surrounded by the anions.

There are some possibilities of the formation of weak hydrogen bonds between the Br^- and the nitrogen atoms in the propylenediamine rings. Two of the closest N–Br approaches occur at the distances of 3.36 and 3.43 Å. The directions of these close N–Br contacts are almost parallel to the *c*-axis. By these hydrogen bonds each layer seems to be held together. These distances are of the same order as those found in isoleucine hydrobromide[15] and 11-aminoundecanonic acid. $HBr \cdot 1/2H_2O$[16]. The existence of any water molecules is evidently excluded.

The complex ion has a three-fold symmetry because of the requirements of the space group. The three chelate rings must, therefore, be completely identical with each other. The CH–CH_2 bond in the chelate rings is nearly parallel to the three-fold axis of the complex ion, corresponding to the "lel" form. The shape and size of the five-membered ring, composed of Co and pn except for the methyl group, closely resembles that found in [Co en$_3$]$^{3+}$,[3-5] [$CoCl_2$en$_2$]$^+$[17] and [$CoBr_2$-en$_2$]$^+$[18]. The substituted methyl group does not disturb the overall features of the Co-en ring. The C–CH_3 bond lies in an approximately equatorial plane of the five-membered ring, in agreement with the prediction of Corey and Bailar that the equatorial orientation is of a lower energy than the axial one.[2] The shape and size of the Co-pn rings are essentially the same as those found in [$CoCl_2$ *l*-pn$_2$]$^+$.[10]

All the distances and angles within the chelate rings are normal. The Co–N separation is 2.00_0 Å, compared with 1.98—2.03 Å in [Co en$_3$]$^{3+}$ [3,5] and 1.94—2.02 Å in [$CoCl_2$*l*-pn$_2$]$^+$ [10]. Six nitrogen atoms form a slightly distorted octahedron around the central cobalt atom, the N–Co–N angle being 86.5°. The ligand molecule assumes a gauche configuration with an azimuthal angle of 51° between the planes determined by the C–C and C–N bonds.

The complex ion [Co *l*-pn$_3$]$^{3+}$ shown in Fig. 3 corresponds to the laevorotatory form with respect to the NaD lines. This form can be denoted as the L*lll* configuration.

If three methyl groups of L-(−)-[Co *l*-pn$_3$]$^{3+}$ are replaced by hydrogen atoms, the absolute configuration of the complex ion L-[Co en$_3$]$^{3+}$ is obtained. The latter is known also to be laevorotatory with respect to the NaD lines.[3,4] Smirnoff found that the ORD curves of (−)-[Co en$_3$]$^{3+}$ and (−)-[Co *l*-pn$_3$]$^{3+}$ correspond well to one another.[9] From this fact it has been deduced, without verification, that these two ions would possess the same absolute configuration; that is, the latter would also take the L-form. The present investigation has revealed that this is actually the case. Thus, the conventional method of correlating the absolute configurations with the ORD curves has been proved for the first time to be useful and reliable.

The absolute configuration of the propylenediamine, which has an asymmetric carbon atom in the molecule, could be determined at the same time. The result corresponds to the configuration correlated to D-alanine, which is in agreement with the previous conclusion about [$CoCl_2$ *l*-pn$_2$]$^+$ [10] and also with the chemical convention[6,7].

One of the most important conclusions of this study is that the absolute configuration of a series of tris(bidentate)-complexes can be successfully correlated to the configurational series in organic compounds. The complex ion [Co en$_3$]$^{3+}$, which is the simplest and the most familiar of the tris-(bidentate)-complexes, has been correlated to the *l*-pn and, consequently, to the whole system of the organic compounds through the intermediation of the absolute configuration of [Co *l*-pn$_3$]$^{3+}$. This was possible because the complex ion possesses a remarkable stereospecificity.[2] When three bidentates, en or pn, are co-ordinated to the cobalt atom, the central C–C bonds prefer the "lel" configuration to the oblique one. In the five-membered chelate rings, the C–CH_3 bond has a tendency to take the equatorial configuration rather than the axial one. Furthermore, the complex ion seems to favor the highest attainable symmetry, so that the three bidentates become identical with each other, as was pointed out by Jaeger et al.[19] If one accepts these three conditions, there is only one way in which three molecules of the *l*-pn can be co-ordinated to the cobalt atom. It may readily be seen that the resultant complex ion must assume the L-form shown in Fig. 1. These results are expected to be applied to the whole series of tris-(bidentate)-complexes. Investigations along these lines are now in progress for crystals of [Co cptn$_3$]$X_3 \cdot 4H_2O$ and [Co chxn$_3$]$X_3 \cdot 4H_2O$.

The calculations of the structure factors and electron densities were carried out on the PC 2

15) J. Trommel and J. M. Bijvoet, ibid., **7**, 703 (1954).
16) G. A. Sim, ibid., **8**, 833 (1955).
17) A. Nakahara, Y. Saito and H. Kuroya, This Bulletin, **25**, 331 (1952).
18) S. Ooi, Y. Komiyama, Y. Saito and H. Kuroya, ibid., **32**, 263 (1959).
19) F. M. Jaeger and L. Bijkerk, *Z. anorg. u. allgem. Chem.*, **233**, 97 (1937); earlier articles by Jaeger.

computer at this Institute and on the IBM 7090 computer at Mitsubishi Atomic Power Industries, Inc. The authors are indebted to Mrs. Hiroko Ota for her help in the early stages of this work.

Part of the cost of the present study was defrayed by a Scientific Research Grant of the Ministry of Education, to which the authors' thanks are due.

BULLETIN OF THE CHEMICAL SOCIETY OF JAPAN VOL. 39 100—105 (1966)

The Alkaline Sulfide Reduction of Aromatic Nitro Compounds. VII. The Induction Period of the Sodium Monosulfide Reduction of Sodium *m*-Nitrobenzene Sulfonate*

By Shizunobu HASHIMOTO and Junzo SUNAMOTO

Department of Applied Chemistry, Doshisha University, Karasuma-imadegawa, Kamikyo-ku, Kyoto

(Received May 15, 1965)

In the sodium monosulfide reduction of sodium *m*-nitrobenzene sulfonate, an induction period appears. The present investigation was undertaken in order to determine the causes of this induction period. The induction period is due not to the nitro compound, but to the reducing agent. The induction period is shortened by means of irradiation by ultraviolet light, the addition of potassium persulfate, ferric chloride, and α,α'-azobisisobutyronitrile, or under atmospheric conditions. On the other hand, the addition of phenol or alcohol lengthens the induction period. Further, on the basis of polarographic and spectroscopic studies of the induction period, it has been suggested that soduim disulfide is produced during this induction period. On the basis of these data, it seems reasonable to assume that, in the reduction of aromatic nitro compounds by sodium monosulfide, the reducing power of monosulfide is very small in itself, and that the nitro group is reduced by the disulfide produced by the radical oxidation of monosulfide. The formation of the sulfide ion radical and its dimerization appear to be responsible for the induction period of this reaction.

In an earlier presentation dealing with the kinetic studies of the alkaline sulfide reduction of sodium *m*-nitrobenzene sulfonate,[1] we reported that an induction period appeared in the sodium monosulfide reduction.

Although the alkaline sulfide reduction of aromatic nitro compounds is of much preparative significance, very little work has been carried out on it from the standpoint of reaction kinetics. One of the few available publications, with the exception of our own studies, is that of Goldschmidt and Larsen,[2] who measured the electric conductivity of the medium and followed the disappearance of sodium *m*-nitrobenzene sulfonate. However, they mistook the hydrosulfide for the monosulfide; when the aqueous monosulfide was prepared, gaseous hydrogen sulfide was introduced into the aqueous sodium hydroxide solution until the color of phenolphtalein disappeared. As sodium monosulfide undergoes hydrolysis, as is shown in Eq. 1, the sulfide which was prepared by Goldschmidt and Larsen is, then, hydrosulfide.

$$S^{2-} + H_2O \rightleftarrows SH^- + OH^- \qquad (1)$$

Another publication is that of Hojyo et al.,[3] who reported that the rate of the sodium monosulfide reduction of nitrobenzene in a 70 vol.% aqueous methanolic solution was too slow for the reaction to be followed kinetically. It may be supposed that they here observed the induction period which we later established.

The present investigation was undertaken in order to determine the causes of the appearance of the induction period in the sodium monosulfide reduction.

Experimental

Materials.—All the reactants and solvents were obtained commercially or by standard methods of preparation and were used after careful purification, either by distillation or by recrystallization. Sodium disulfide was freshly prepared by the method described in a previous paper.[4]

* Presented at the 18th Annual Meeting of the Chemical Society of Japan, Osaka, April, 1965.

1) S. Hashimoto, J. Sunamoto and K. Oshima, presented at the 16th Annual Meeting of the Chemical Society of Japan, Tokyo March, 1963.

2) H. Goldschmidt and H. Larsen, *Z. physik. Chem.*, **71**, 437 (1910).

3) M. Hojyo, Y. Takagi and Y. Ogata, *J. Am. Chem. Soc.*, **82**, 2459 (1960).

4) S. Hashimoto and J. Sunamoto, *J. Chem. Soc. Japan, Ind. Chem. Sect.* (*Kogyo Kagaku Zasshi*), **68**, 669 (1965).

Typical Procedure for Rate Measurements.—Appropriate amounts of a solvent, a nitro compound, and additives were placed in a 1000-ml. three-necked flask equipped with a reflux condenser, an outlet tube, and a nitrogen inlet tube with a trap containing the same solvent as the reaction flask. The flask was then immersed in a thermostat regulated and flushed by nitrogen at given temperatures for half an hour. The reaction was commenced by introducing a definite amount of an aqueous solution of sodium monosulfide which had previously been warmed to the reaction temperature. At appropriate time intervals aliquots (20 ml.) were withdrawn, poured into 20 ml. of a hydrochloric acid aqueous solution (1 : 2), and then warmed on a steam bath for half an hour.

Procedures for Irradiation.—In order to irradiate with ultraviolet light, a low-pressure mercury vapor lamp (2537 Å, 15 W.) was placed in the reaction flask; on the other hand, in order to irradiate with visible light, a National FCL-30D-SDL fluorescence lamp (4000—4500 Å, 20 W.) was set up at a distance of ca. 3 cm. from the reaction flask.

Analytical Procedures.—The above-mentioned acidic solutions were cooled below 10°C with ice, and the quantities of amine produced were determined by diazotizing titration according to the usual method.

Irradiation on an Aqueous Sodium Monosulfide Solution.—About 1000 ml. of a 1.33 mol./l. sodium monosulfide aqueous solution was placed in a flask equipped with a high-pressure mercury vapor lamp (3500—4000 Å, 100 W.), a reflux condenser, and an outlet tube. The flask was immersed in a thermostat regulated at 37—38°C, and then the internal atmosphere was substituted for nitrogen sufficiently. At appropriate time intervals samples were pressed out by nitrogen. The reaction was followed by the usual methods of acidimetry and iodometry and by polarography, as has previously been described.[4] The ultraviolet absorption spectra were run on a SHIMADZU Beckmann-type Model-DU spectrophotometer, while the visible absorption spectra were run on a SHIMADZU BAUSCH & LOMB Spectronic 20 photometer. Both absorption spectra were compared with that of an authentic solution of sodium disulfide. The coincidence was satisfactory.

Results and Discussion

The first investigation was undertaken in order to examine which species, the nitro compound or the reducing agent, exhibits an induction period in the reduction with sodium monosulfide. The results when the initial concentrations of the nitro compound and sodium monosulfide were changed with a varying molar ratio of the two reactants are shown in Figs. 1 and 2. The initial concentration of the reducing agent had an effect on both terms, the induction-period intervals and the rate of the main reaction. However, the initial concentration of the nitro compound had an effect only on the main reaction. It may, therefore, be concluded that the induction period is due not to the nitro compound, but to the reducing agent. Further, when nitrobenzene was used instead of sodium *m*-nitrobenzene sulfonate in the sodium monosulfide reduction, though the rate of the main reaction became slower, the induction period was certainly observed.

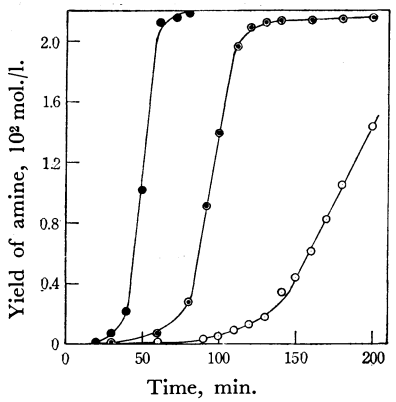

Fig. 1. Effect of initial concentration of reducing agent.
○ : Exp. No. 12 in Table I
⊙ : Exp. No. 17
● : Exp. No. 20

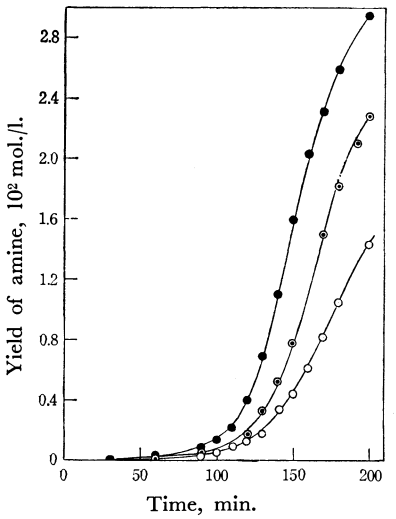

Fig. 2. Effect of initial concentration of nitro compound.
○ : Exp. No. 12 in Table I
⊙ : Exp. No. 25
● : Exp. No. 26

The rate of the main reaction is given by runs in which the initial concentrations of the nitro compound and sodium monosulfide were interchanged; it is certain that the rates can be expressed by Eq. 2:

$$d(Ar\text{–}NH_2)/dt = k_3(Ar\text{–}NO_2)(Na_2S)^2 \qquad (2)$$

This equation is the same as that given for the sodium hydrosulfide reduction in a previous presentation.[1]

Some complementary data on the induction-period intervals and the calculated apparent

TABLE I. THIRD-ORDER RATE CONSTANTS FOR REDUCTION OF SODIUM *m*-NITROBENZENE SULFONATE BY SODIUM MONOSULFIDE AQUEOUS SOLUTION

Exp. No.	(Ar-NO_2) 10^2 mol./l.	(Na_2S) 10^2 mol./l.	Additives 10^2 mol./l.	Temp. °C	Induction period min.	Rate constant k_3, $min^{-1} mol^{-2} l^{-2}$
1	1.563	5.625	None	35	121	2.790
2	1.563	5.625	None	35	42	3.416[a]
3	1.563	5.625	($FeCl_3$)=0.031	35	78	2.710
4	1.563	5.625	($FeCl_3$)=0.031, ($K_2S_2O_8$)=0.032	35	45	2.770
5	1.563	5.625	($NaHCO_3$)=5.625	35	126	2.123
6	1.563	5.625[b]	None	35	0	—
7	1.563	5.625[b]	($FeCl_3$)=0.031	35	0	—
8	1.563	9.631	None	35	45	2.331
9	1.563	9.631	None	35	120	0.844[c]
10	1.563	9.631	None	35	118	1.010[d]
11	1.563	9.631	None	35	118	0.067[e]
12	2.178	6.507	None	30	128	2.109
13	2.178	6.507	($K_2S_2O_8$)=0.533	30	20	3.741
14	2.178	6.507	(NaOH)=5.926	30	123	2.537
15	2.178	6.507	(ABIN)=0.136	30	116	2.066
16	2.178	6.507	(Phenol)=0.856	30	Very slow	Very small
17	2.178	11.73	None	30	74	1.725
18	2.178	11.73	None	30	60	1.715[f]
19	2.178	11.73	None	30	64	1.435[g]
20	2.178	19.49	None	30	40	1.281
21	2.682	5.126	None	30	138	0.917
22	2.682	5.126	None	30	138	5.676[h]
23	2.682	5.126	($Na_2S_2O_3$)=1.499	30	138	0.761
24	2.682	5.126	(Na_2S_2)=0.769	30	0	7.975
25	4.347	6.507	None	30	125	1.763
26	6.533	6.507	None	30	113	1.562

a) Inside irradiation of ultraviolet light, 2537 Å, 15 W.
b) Sodium disulfide
c) In 33.1 vol.% aqueous methanolic solution
d) In 33.1 vol.% aqueous isoproply alcohol solution
e) Nitrobenzene in 33.1 vol.% aqueous methanolic solution
f) Outside irradiation of visible light, 4000—4500 Å, 30 W.
g) Outside irradiation of visible light under atmospheric condition
h) Under atmospheric condition

third-order rate constants are shown in Table I.

The Effect of Light.—The effect of light on the induction period was also investigated. As is shown in Fig. 3, the induction periods were shortened by means of the inside irradiation of ultraviolet light and the outside irradiation of visible light, compared with the dark reaction. Of course, the effect was far better in the former, In neither case, however, was any effect on the main reaction observed.

On the basis of these data, it is reasonable to assume that the induction period contains a radical reaction, but the main reaction perhaps contains an ionic reaction.

Barret and his co-workers presented evidence that the sulfate ion radical was formed by the irradiation by ultraviolet light of an aqueous or methanolic sulfate solution.[5] It may be similarly

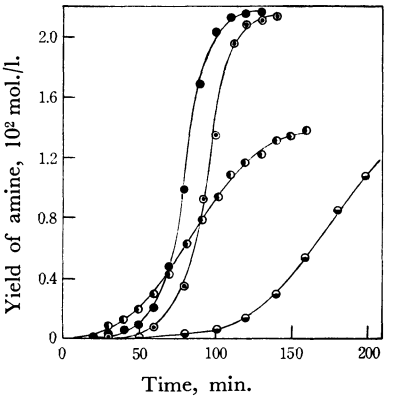

Fig. 3. Effect of light.
◒ : Exp. No. 1 in Table I
◐ : Exp. No. 2
⊙ : Exp. No. 17
● : Exp. No. 18

5) J. Barret, M. F. Fox and A. L. Mansell, *Nature*, **200**, 257 (1963).

reasonable to assume the following processes for the formation of the sulfide ion radical:

$$(S^{2-}H_2O) \xrightarrow{h\nu} (S\cdot^{-}H_2O^{-})^{*}$$
$$\rightarrow S\cdot^{-} + H\cdot + OH^{-} \quad (3)$$

The disulfide ion is immediately produced by the coupling of two sulfide ion radicals:

$$2S\cdot^{-} \rightarrow (S\text{-}S)^{2-} \quad (4)$$

Therefore, it was supposed that the reduction of the nitro group was proceeded by that of the disulfide ion produced.

The Effect of the Solvent.—Figure 4 shows that the induction-period intervals are longer in an aqueous alcoholic solution than in an aqueous solution. It can be considered that the sulfide ion radical was deactivated by the solvent.

$$S\cdot^{-} + \text{Solvent} \rightarrow \text{Deactivated species} \quad (5)$$

It is well known that the α-hydrogen of alcohol is more easily abstracted by the radical than is the hydrogen of water.[6] Also, the rate of the main reaction became a little solwer in an aqueous alcoholic solution than in an aqueous solution. This observation may be reasonable since the solubility of sodium *m*-nitrobenzene sulfonate is decreased, and the diminished solvent polarity may also be responsible.

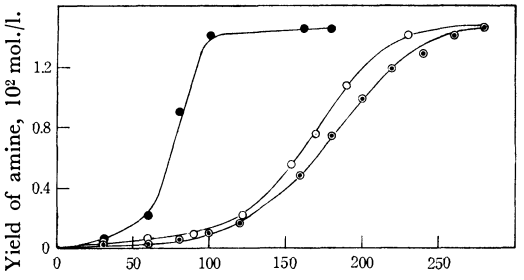

Fig. 4. Effect of solvent.
● : Exp. No. 8 in Table I
⊙ : Exp. No. 9
○ : Exp. No. 10

The Effect of Air.—Figure 5 shows that the induction period was only a little, though obvioulsy, shortened under the atmospheric conditions than a nitrogen atmosphere. It was earlier known that the oxidation of aqueous sodium sulfite is an auto-oxidation,[7] and that it is very sensitive to light and air in a chain oxidation process.[8] It may be reasonable to assume that the effect of air on the auto-oxidation of a sodium monosulfide solution is the same as on the auto-oxidation of a sodium sulfite solution; it may also be reasonable to suggest that the processes is as follows, for example:

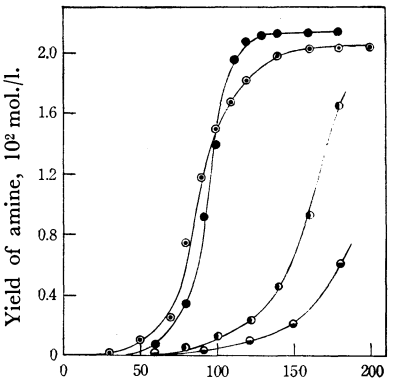

Fig. 5. Effect of air.
⊙ : Exp. No. 17 in Table I
● : Exp. No. 19
◒ : Exp. No. 21
◐ : Exp. No. 22

$$S\cdot^{-} + 3O \rightarrow SO_3\cdot^{-} \quad (6)$$

$$SO_3\cdot^{-} + S^{2-} \rightarrow SO_4^{2-} + S\cdot^{-} \quad (7)$$

In this case, however, it is necessary to reduce the rate of the main reaction with the air oxidation of the sodium disulfide produced.

The Effect of Sodium Disulfide and Sodium Thiosulfate.—The effects of the oxidation products of sodium monosulfide were also investigated. The addition of a catalytical amount of sodium disulfide made the induction period disappear. It may be reasonable to assume that the disulfide ion will make up for the sulfide ion radical, as in Eq. 8, and may be useful as an initiator:

$$(S\text{-}S)^{2-} \rightarrow S\cdot^{-} + S\cdot^{-} \quad (8)$$

However, the addition of sodium thiosulfate had scarcely any effect on the induction period or on the main reaction.

The Effect of ABIN and Phenol.—The addition of ABIN (α,α'-azobisisobutyronitrile) shortened the induction period, but it had scarcely any effect on the rate of the main reaction. On the other hand, the addition of phenol, which is often used as an inhibitor or a retarder for a radical reaction,[9] made the rate of the over-all reaction much slower.

The Effect of Potassium Persulfate and Ferric Chloride.—The salt of some metals of a variable valency is used as a radical source for a polymerization in an aqueous solution, such as a redox polymerization or an emulsion polymerization. If the induction period is due to the radical oxidation of sodium monosulfide to sodium disulfide,

6) C. F. Wells, *Trans. Faraday Soc.*, **57**, 1703 (1961).
7) N. N. Semenov, "Some Problems of Chemical Kinetics and Reactivity," translated by J. E. S. Bradley, Vol. I, Pergamon Press, New York (1958), p. 178.
8) H. L. J. Bäckström., *Z. physik. Chem.*, **B25**, 122 (1934).
9) P. G. Ashmore, "Catalysts and Inhibition of Chemical Reactions," Butterworth, London (1963), p. 266.

as was previously assumed, it may naturally be supposed that these salts have an effect on the induction period. In fact, the addition of a catalytical amount of potassium persulfate or ferric chloride shortened the induction period, as is shown in Fig. 6. When both salts were used together, it shortened it greatly.

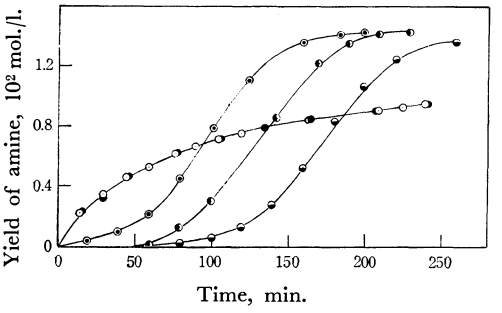

Fig. 6. Effect of ferric chloride.
◒ : Exp. No. 1 in Table I
◐ : Exp. No. 3
⊙ : Exp. No. 4
○ : Exp. No. 6
● : Exp. No. 7

At the present time, the sulfide ion radical is believed to be formed as follows:

$$Fe^{3+} + 2S^{2-} \rightarrow Fe^{2+} + 2S\cdot^{-} \quad (9)$$

$$S_2O_8^{2-} + S^{2-} \rightarrow SO_4^{2-} + SO_4\cdot^{-} + S\cdot^{-} \quad (10)$$

$$SO_4\cdot^{-} + S^{2-} \rightarrow SO_4^{2-} + S\cdot^{-} \quad (11)$$

In a system containing potassium persulfate and ferrous chloride, the formation of the ion radical is believed to start as follows[10]:

$$Fe^{2+} + S_2O_8^{2-} \rightarrow Fe^{3+} + SO_4^{2-} + SO_4\cdot^{-} \quad (12)$$

Ion radicals derived from the salts of these metals of a variable valency may exchange electrons with stable species and thereby form active-ion radicals in, e. g., the reaction of a sulfide with a salt of a trivalent iron. In this case an electron is transferred from the monosulfide ion to the ferric ion, producing the highly-active radical ion; this active-ion radical immediately dimerizes to disulfide, as in Eq. 4.

These reduction-oxidation systems, then, shortened the induction period due to the auto-oxidation of monosulfide to disulfide; the oxidation appeared to proceed even in the dark if traces of these salts were present.

On the other hand, in no case did the addition of these catalysts have any effect on the main reaction. The addition of ferric chloride in the sodium disulfide reduction, in fact, had no effect at all on its reduction rate.

When persulfate is used as a catalyst for a usual reaction, thiosulfate, as well as ferrous or ferric ion, is used as a promoter.[11] In the alkaline sulfide reduction of aromatic nitro compounds, thiosulfate, which is an oxidation product of sulfide, is certainly produced; therefore, it may be reasonable to assume that the reduction of persulfate by thiosulfate occurs. However, as disulfide or monosulfide has a far larger reducing power than thiosulfate,* there is no need to consider the effect of thiosulfate.

The Effect of pH.—In an aqueous solution the monosulfide undergoes hydrolysis, as Eq. 1 shows. Therefore, it may be considered that the pH will also have a large effect on the induction period. As is shown in Fig. 7, the addition of neither sodium hydroxide nor sodium hydrogen carbonate had, in fact, any effect on the induction period; rather, each had a large effect on the main reaction. Between the monosulfide ion and the hydrosulfide ion, we could not determine which species is more rapidly oxidized to the disulfide ion.

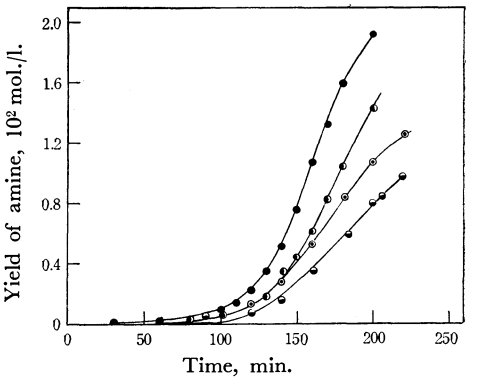

Fig. 7. Effect of pH.
⊙ : Exp. No. 1 in Table I
◒ : Exp. No. 5
◐ : Exp. No. 12
● : Exp. No. 14

Hojyo et al.,[3] stated that, in the reduction of nitrobenzene by sodium disulfide in a 70% aqueous methanolic solution, the rate of reaction shows a first-order dependence on the hydroxide ion concentration. They also stated that the reaction mechanism involved an attack by the disulfide ion, which is the kinetically effective species, on the positive nitrogen of the nitro group in conjunction with the hydrolytic equilibrium of the disulfide ion:

$$S_2^{2-} + H_2O \rightleftarrows S_2H^{-} + OH^{-} \quad (13)$$

10) J. W. L. Fordham and H. L. Williams, *J. Am. Chem. Soc.*, **73**, 4855 (1951).

11) D. Dunn, *Trans. Faraday Soc.*, **42**, 190 (1946).

* Their mercury anodic oxidation potentials clearly show this difference in reducing power.

The effect of the pH on the main reaction in our experiments may be similarly analyzed.

The Irradiation of an Aqueous Sodium Monosulfide Solution.—In order to examine the above hypothesis in detail, the irradiation of an aqueous sodium monosulfide solution was investigated. An aqueous solution of pure sodium monosulfide is colorless, but an aqueous disulfide solution is yellow.[12] When the monosulfide solution was irradiated, it turned yellow. Figure 8 shows that the absorption at 360 mμ, which is not observed before irradiation, appears upon irradiation and thereafter gradually increases in intensity. After a long irradiation its position and the intensity of the maximum absorption of irradiated monosulfide were essentialy identical with those of disulfide which had not been irradiated. The polarograms of the irradiated monosulfide solution support the discussion of the results of spectrophotometry.

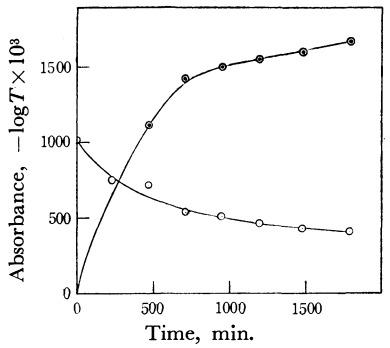

Fig. 8. Irradiation on aqueous sodium monosulfide solution; change of intensity of absorption in visible and ultraviolet region.
Initial concentration of sodium monosulfide aqueous solution: 1.33×10^{-2} mol./l.
Temp.: 37—38°C
⊙ : Intensity of absorption at 360 mμ
○ : Intensity of absorption at 230 mμ

12) For example, Gmelins Handbuch d. anorg. chem. syst. No. 21, (1928), pp. 481—494.

Conclusion

In view of the above facts, the most reasonable conclusion to be drawn from the available data is as follows. In the reduction of aromatic nitro compounds by sodium monosulfide, the reducing power of monosulfide is very small in itself, and the reduction of the nitro compound hardly proceeds at all. However, after the formation of disulfide by the radical oxidation of monosulfide, which involves the dimerization of the sulfide ion radical, the reduction of the nitro group is furthered by the disulfide produced. This step, containing of the formation of the sulfide ion radical and its dimerization, appears as the induction period in the sodium monosulfide reduction of aromatic nitro compounds.

Thanks are due to Mr. Takao Shima for his assistance in some of the experimental work. The authors are also indebted to the Daiwa Dyestuff Co., Ltd., for its gift of materials.

BULLETIN OF THE CHEMICAL SOCIETY OF JAPAN VOL. 39 105—112 (1966)

Studies on Long Chain Alkyl Amides of Water-soluble Poly-α-amino Acids. III. The Association of Poly-DL-alanine Dodecylamides in Aqueous Solution

By Shoichi IKEDA, Masakazu MAEKAWA* and Toshizo ISEMURA

Department of Biology, Faculty of Science, Osaka University, Toyonaka, Osaka

(Received May 15, 1965)

Poly-DL-alanine dodecylamide, prepared by the polymerization of *N*-carboxy-DL-alanine anhydride with dodecylamine initiation at different anhydride-to-initiator ratios, ([A]/[I]), is soluble in aqueous hydrochloric acid solutions to form micelles. Its micellar properties at pH 2.0 have been investigated by means of hydrodynamic methods. The material prepared at [A]/[I] 5 has a critical micelle concentration around 0.2—0.3 g. dl^{-1}, which can be detected by Archibald sedimentation measurements. The micelle has been determined by the Archibald method to consist of about 13 monomer molecules. The molecules in the micelle are hydrogen bonded intermolecularly to form a structure similar to the β-conformation. Hydrogen bonding

* Present address: Mitsubishi Paper Mills, Inc., Takasago, Hyogo.

between peptide groups is more important for the micelle formation than hydrophobic bonds between dodecyl groups. The materials prepared at [A]/[I] 15 and 20 associate into large micelles, consisting of about 320 and 240 monomers respectively, as deduced from the sedimentation and viscosity measurements. The micelles exhibit even a flow birefringence. The structure of micelles seems to be a disordered one composed of randomly coiled monomer molecules; intermolecular hydrogen bonding and hydrophobic bonding are cooperative in its stabilization.

A series of amphipathic polypeptides, poly-DL-alanine dodecylamide (PADA) with degrees of polymerization from 5 to 30, has been synthesized by the polymerization of *N*-carboxy-DL-alanine anhydride with dodecylamine initiation, and their physical chemical properties have been investigated in relation to the degree of polymerization.[1,2] PADA is soluble in aqueous hydrochloric acid solution of pH below 5.5, and the surface tension of its aqueous solution decreases considerably with the concentration. The surface activity of PADA decreases with increasing the degree of polymerization, but the lowest molecular weight PADA behaves like a typical amphipathic substance or a surface active agent. It is then expected that PADA molecules will be associated in aqueous solution to form micelles.

It has been accepted that intermolecular hydrophobic bonds, which should be strong between long chain alkyl groups, are important as a cohesive force for micelle formation. In the case of PADA, an additional cohesion, i. e., intermolecular hydrogen bonds between peptide groups, will also contribute to the stability of its micelle. Therefore, the effect of hydrogen bonding should be reflected in the associated states of PADA molecules such as the size of micelle. While PADA has a constitution somewhat similar to that of polyoxyethylene dodecyl ether, the latter being unable to form intermolecular hydrogen bond, it would be of interest to examine the micellar properties of PADA in comparison with those of polyoxyethylene dodecyl ether.

In the present work, the micellar properties of PADA in aqueous hydrochloric acid solutions have been investigated by means of measurements of viscosity, sedimentation and flow birefringence. It was found that the association of PADA is specifically dependent on its degree of polymerization. Since it has been confirmed[3] that poly-DL-alanine is molecularly dispersed in an aqueous solution, the hydrophobic force between dodecyl groups is operative and important in the association of PADA as in the other amphipathic substances; here evidence was also obtained that intermolecular hydrogen bonding between peptide groups also exerts a profound effect on the micellar association. The size and structure of the micelles were discussed in the light of the intermolecular forces and the molecular conformation.

Experimental

Materials.—PADA was synthesized by the polymerization of *N*-carboxy-DL-alanine anhydride by dodecylamine initiation in dioxane.[1] The anhydride-to-initiator molar ratio, [A]/[I], was varied from 5 to 20, to obtain PADA samples with different degrees of polymerization.

Titration of Terminal Amino Groups.—To obtain the number-average degree of polymerization of PADA, the anhydrous titration of terminal amino groups were carried out.[4] About 3 mg. of PADA were dissolved in 1 ml. of a formic acid - acetic acid (1 : 9 v/v) mixture, and the solution was titrated to a blue point of crystal violet with 0.05 N perchloric acid dissolved in acetic acid. The blank titer was then subtracted from the solution titer. The mixed solvent was used, because the indicator color was blue in formic acid even without any titer, and also because PADA was insoluble in acetic acid alone.

Preparation of Aqueous Solutions.—Almost all the experiments were made with PADA solutions in aqueous hydrochloric acid at pH 2.0. The pH's of the solutions were adjusted by the addition of hydrochloric acid a day after solutions were made. Solutions of different concentrations were prepared by diluting a ca. 1 g. dl^{-1} stock solution with water and by readjusting the pH's with hydrochloric acid. The pH values were measured by a Horiba Model H pH-meter. Each solution was filtered through a No. 4 glass filter before use.

Electric Conductivity.—The specific conductances were measured at 25°C with a Yanagimoto MT-7 Conductivity Bridge. The electrodes of a conductivity cell were made of white platinum, since platinized platinum electrodes blocked the electric current completely because of the adsorption of PADA on their surfaces. The cell constant was 0.450, as calibrated by 0.01 M potassium chloride.

Density.—The densities of the solutions were determined at 25°C by an Ostwald type pycnometer with a volume of 3 ml. The partial specific volume of PADA, $\bar{v}$ (ml. g^{-1}), was calculated from the equation

$$\rho = \rho_0 + (1 - \bar{v}\rho_0)c$$

where ρ (g. ml^{-1}) is the density of the solution at a given concentration, c (g. ml^{-1}), and ρ_0 (g. ml^{-1}) is the density of the solvent, i. e., of 0.01 N hydrochloric acid.

Viscosity.—An Ubbelohde type viscometer with a flow time 140 sec. for water was used for the viscosity measurements. The relative viscosities were referred to 0.01 N hydrochloric acid at 25°C.

1) T. Isemura, S. Ikeda, F. Tokiwa and J. Noguchi, This Bulletin, **34**, 1236 (1961).
2) S. Ikeda and T. Isemura, ibid., **35**, 1523 (1962).
3) S. Ikeda, unpublished.
4) M. Sela and A. Berger, *J. Am. Chem. Soc.*, **77**, 1893 (1955).

Sedimentation. — *The Archibald Method.* — The Archibald method[5-7] was adapted to the determination of the micellar molecular weight of PADA [A]/[I] 5. The measurements were performed in a Hitachi UCA-1 Analytical Ultracentrifuge using a schlieren optical system. A piece of stretched human hair was drawn in place of a schlieren diaphragm. The rotor speed read by an odometer was 41000 r. p. m., and the temperature measured by a radiation thermocouple was 30±1°C. The solutions were centrifuged in a standard cell, putting a thin layer of Dow-Corning Silicone 555 at the cell bottom.[8] Photographic films were enlarged tenfold on an Olympus Model CP-20 Precision Contour Projector and traced on graphic paper. For the calibration of the schlieren pattern to the concentration scale, a synthetic boundary cell of the Pickels type was utilized.

Sedimentation Velocity.—The sedimentation coefficients of PADA [A]/[I] 15 and 20 were determined in a Spinco Model E Analytical Ultracentrifuge using a schlieren optical system. The rotor speed was 44770 r.p.m. The sedimentation coefficients were reduced to those at 25°C by the correction of the solvent viscosity coefficients.

Flow Birefringence.—Both the extinction angles and the birefringences were measured in a Rao Flow Birefringence Instrument, Model 7-B. The birefringence was determined at 517 mμ of a zirconium lamp. The rotor speed was read by counting the speed of the driving motor with a tachometer.

Refractive Index Increment.—The refractive index increments at 547 mμ were measured in a Shimadzu Differential Refractometer of the Debye type against 0.01 M hydrochloric acid at 25°C.

Results

Characterization.—PADA is soluble in formic acid, dichloroacetic acid, phenol and *m*-cresol, in which it will be molecularly dispersed without association. The determination of the molecular weight of PADA in these solvents, however, involves numerous difficulties.* Therefore, the number of terminal amino groups was determined by the anhydrous titration to estimate an approximate number-average degree of polymerization. As is shown in Table I, the degree of polymerization, x_{NH_2}, derived from the number of amino groups is almost equal to the [A]/[I] value, indicating that the synthetic procedure can be well controlled in obtaining PADA of desired molecular weight. The number-average degree of polymerization, x_n, was thus assumed to be equal to the [A]/[I] value. The weight-average degree of polymerization, x_w, was estimated from the number-average one, assuming that the molecular weight distribution follows the Poisson distribution.[12] The results are summarized in Table I.

Table I. Degree of polymerization of PADA

Sample number	[A]/[I] $=x_n$	x_{NH_2}	x_w	M_n	M_w	$[\eta]$ at 25°C in 85% HCOOH
B4201	5	6.4	5.8	539	596	0.036
B4202	10	10.9	10.9	959	1023	0.043
B4203	15	17.5	15.9	1427	1493	0.053
B4204	20	22.8	21.0	1804	1872	0.063
A808	$NaOCH_3$	49				0.086

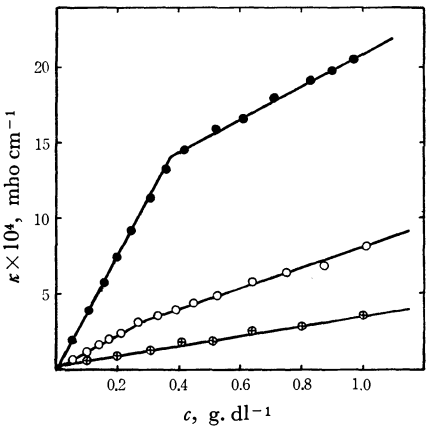

Fig. 1. Specific conductances of PADA solutions at pH 5.0.
○, [A]/[I] 5; ⊕, [A]/[I] 15; ●, dodecylammonium chloride in water

The specific conductances of PADA solutions at pH 5.0 are shown in Fig. 1, together with those of dodecylammonium chloride in water. The latter data are in accord with the published ones.[13] On the conductance curve of PADA [A]/[I] 5, a break similar to the critical micelle concentration (CMC) for dodecylammonium chloride appeared. The CMC of PADA [A]/[I] 5 was found to be 0.295 g. dl^{-1} or 5.4×10^{-3} M. A similar break was observed in the surface tension curve.[1] The CMC was somewhat lower as the pH was lowered.

The [A]/[I] 10 preparation was unstable in an aqueous solution. Its relative viscosity markedly increased with the time elapsed after the solution

5) W. J. Archibald, *J. Phys. Chem.*, **51**, 1204 (1947).
6) S. M. Klainer and G. Kegeles, ibid., **59**, 952 (1955).
7) H. K. Schachman "Ultracentrifugation in Biochemistry," Academic Press, New York (1959), p. 181.
8) A. Ginsburg, P. Appel and H. K. Schachman, *Arch. Biochem. Biophys.*, **65**, 545 (1956).
* The application of the Archibald method was limited by such factors as the negative value of the $1-\bar{v}\rho_0$ term in organic acids, as has been observed elsewhere,[9] the corrosive nature of these acids against the available cell materials and the high viscosity of *m*-cresol. The freezing point depression in formic acid or phenol was much larger than that to be expected from the [A]/[I] value and it was also strongly dependent on the concentration in a dilute region, probably because PADA is ionized at its terminal amino groups or at each peptide group, as has been noted in polyamides.[10,11]
9) M. Goodman, E. S. Schmitt and D. A. Yphantis, *J. Am. Chem. Soc.*, **84**, 1283 (1962).
10) J. R. Schaefgen and C. F. Trivisonno, ibid., **73**, 4580 (1951).
11) H. G. Fendler and H. A. Stuart, *Makromol. Chem.*, **25**, 159 (1957).
12) S. G. Waley and J. Waston, *Proc. Roy. Soc.*, **A199**, 499 (1949).
13) A. W. Ralston, C. W. Hoerr and F. J. Hoffman, *J. Am. Chem. Soc.*, **64**, 97 (1942).

was made up, and it did not settle within several days. The sedimentation pattern of the same solution consisted of many discrete peaks. Thus this preparation was not investigated further.

The reduced viscosities of PADA of solutions at pH 2.0 are shown in Fig. 2. The values of the intrinsic viscosities, $[\eta]$, are given in Table II together with those of the partial specific volumes. The latter was also calculated from the partial molar volumes of the constituent atoms.[14] Assuming the micelles to be unhydrated ellipsoids of revolution, the axial ratios of the PADA micelles were estimated from the intrinsic viscosities and partial specific volumes by means of the Simha's equation.[15]

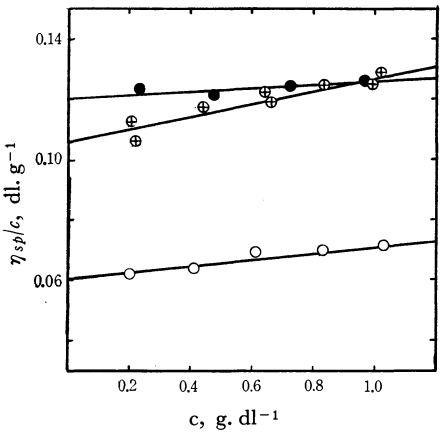

Fig. 2. Reduced viscosities of PADA solutions at pH 2.0.
○, [A]/[I] 5; ⊕, [A]/[I] 15; ●, [A]/[I] 20

TABLE II. INTRINSIC VISCOSITY AND PARTIAL SPECIFIC VOLUME OF PADA AT pH 2.0

Sample number	$[\eta]$ dl. g^{-1}	$\bar{v}$* ml. g^{-1}	Axial ratio, a/b	
			Prolate	Oblate
B4201	0.060	0.834 (0.861)	6.1	1/ 8.7
B4203	0.106	0.793 (0.811)	9.90	1/17.9
B4204	0.120	0.782 (0.770)	10.9	1/20.8
A808**	0.079	0.726 (0.735)		

* Values in parentheses were calculated from molar volumes of constituent atoms.[14]
** Data in distilled water.

The electrostatic effect of ionized terminal groups has not been taken into account in all cases, since it seems likely that a good amount of hydrochloric acid exists to suppress the effect, at least, at pH 2.0.

The Association of PADA [A]/[I] 5.—The Archibald method of sedimentation is based on the fact that the equation for sedimentation equilibrium is formally satisfied at both the meniscus and the bottom of a solution in a sedimentation cell, irrespective of the time of centrifugation. If a solution is centrifuged in a cell with an angular velocity, ω (sec^{-1}), and if the concentration at a distance, r (cm.), from the rotor axis is given by c (g. ml^{-1}) at time t, the apparent molecular weight at the meniscus or the bottom can be obtained by the equation[5-7,16,17]:

$$M_{app}(t)=\frac{\boldsymbol{R}T}{\omega^2(1-\bar{v}\rho)}\left(\frac{dc/dr}{rc}\right)_{m \text{ or } b}$$

where T is the temperature and $\boldsymbol{R}$ is the gas constant. The suffix m or b denotes the meniscus or the bottom. For a given initial concentration, c_0 (g. ml^{-1}), $M_{app}(t)$ can be evaluated from the schlieren pattern at any time, t, and then extrapolated to zero time to obtain $M_{app}(0)$ for c_0. The extrapolation is usually performed by postulating a linear relation of $M_{app}(t)$ with t. The apparent molecular weight, $M_{app}(0)$, obtained in this way should be equal at both the meniscus and the bottom; it can be related to the weight-average molecular weight, M_w, of the solute by

$$M_{app}{}^{-1}(0)=M_w{}^{-1}+2Bc_0+\cdots$$

where B is the second virial coefficient.

The determination of the micellar molecular weight of PADA [A]/[I] 5 is somewhat complicated, since it has the CMC. The validity of the Archibald method has been demonstrated even for association-dissociation systems, whether the conversion velocity is fast or slow.[18] However, as far as monomers and micelles coexist in a solution, the usual procedure of the Archibald method, as described above, can not be applied; an extrapolation must be made to the CMC rather than that to an infinite dilution. A similar procedure has been widely adopted in the case of light scattering in micellar solutions.[19-21] In the Archibald method the values of CMC and $\{(dc/dr)/r\}_{CMC}$ must be first determined from the plots such as those of $\{(dc/dr)/r\}_{m \text{ or } b}$ against c_m or c_b, in order to obtain the micellar molecular weight. However, these values could not be determined very accurately for the present system, probably because the rates of the mutual conversion between monomers and micelles were not sufficiently fast as compared with the sedimentation velocities, so that the values $M_{app}(t)$ were not independent of the initial concentration.

Consequently, the usual procedure was first adopted for the determination of the molecular weight. Nevertheless, it gave an approximate

14) E. Friedman, T. J. Gill, III, and P. Doty, ibid., **83**, 4050 (1961).
15) R. Simha, *J. Phys. Chem.*, **44**, 25 (1940).
16) G. Kegeles, S. M. Klainer and W. J. Salem, ibid., **61**, 1286 (1957).
17) H. Fujita, H. Inagaki, T. Kotaka and H. Utiyama, ibid., **66**, 4 (1962).
18) G. Kegeles and M. S. N. Rao, *J. Am. Chem. Soc.*, **80**, 5721 (1958).
19) P. Debye, *J. Phys. Colloid. Chem.*, **53**, 1 (1949).
20) P. Debye and E. W. Anacker, ibid., **55**, 644 (1951).
21) L. M. Kushner and W. D. Hubbard, *J. Phys. Chem.*, **58**, 1163 (1954).

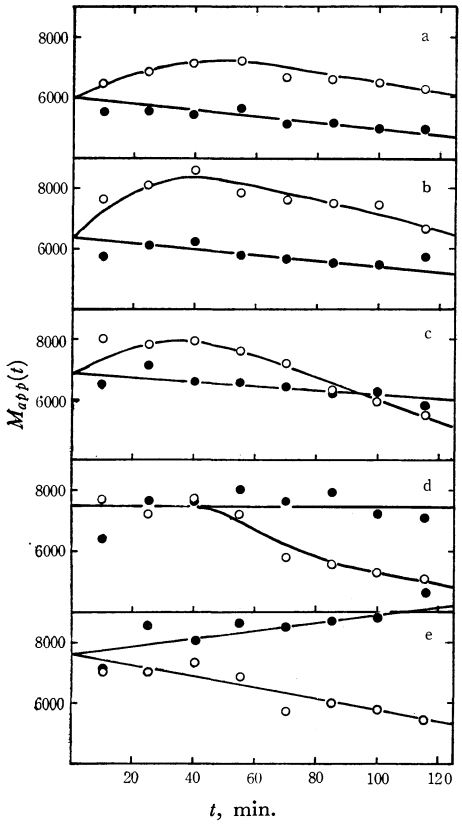

Fig. 3. The $M_{app}(t)$ versus t curves of PADA [A]/[I] 5 solutions at pH 2.0.
○, meniscus; ●, bottom
Rotor speed, 41000 r. p. m.; temp.; 30°C
Concn. (g. dl^{-1}): a, 1.02; b, 0.82; c, 0.61; d, 0.41; e, 0.20.

value for the CMC. The plots of $M_{app}(t)$ against t were drawn for different initial concentrations and the curves were extrapolated to zero time of centrifugation to obtain $M_{app}(0)$. They are shown in Fig. 3. Linear extrapolation was always possible at the cell bottoms, but the slopes of the straight lines varied from negative to positive as the inital concentrations were lowered. On the other hand, some of the plots at the menisci were not linear but upward convex: they initially rise up and then fall gradually with time. Then the intercept at zero time at the meniscus can be made coincident with that at the bottom, thus giving an identical value of $M_{app}(0)$ for a given initial concentration. Such anomalous behavior may be qualitatively explained in the following way.

In general, the fractionation effect of a polydisperse system under centrifugal field results in a decrease in $M_{app}(t)$ with time at the meniscus and in its increase at the bottom. On the contrary, the non-ideality of the system has an opposite effect on the change in $M_{app}(t)$ with time.[16,17] In the present system, however, the micelle formation at the bottom or the dissociation of micelles into monomers at the meniscus seems to be more important than the fractionation effect. At the bottoms for high initial concentrations, the decrease in $M_{app}(t)$ with time can be ascribed to the non-ideality of the micellar solutions. For the lowest initial concentration investigated, the concentration at the bottom increases with time, reaching and then exceeding the CMC after some time of centrifugation; micelles are formed and accumulate there to increase the $M_{app}(t)$ value with time. At the intermediate initial concentration, the micelle-forming effect compensates for the non-ideality of the micellar solution, and $M_{app}(t)$ becomes practically independent of the time.

The initial rise in $M_{app}(t)$ at the meniscus can also be attributed to the non-ideality of the micellar solution. The decrease in $M_{app}(t)$ after some time reflects the dissociation of micelle into monomers through the CMC region. At the lowest initial concentration, the curve monotonously decreases with time, suggesting the dissociation of micelle into monomers. Near the CMC or even above it, micelles leaves the meniscus faster than monomers, and the dilution at the meniscus brings about the dissociation of the remaining micelles; thus $M_{app}(t)$ decreases with time. These results indicate the presence of rather a broad concentration region for micelle formation.

After such a justification for the non-linear relation of $M_{app}(t)$ with t, the same intercept, $M_{app}(0)$, can be derived from both the meniscus and the bottom.* Then the intercept, $M_{app}(0)$, was plotted against c_0, as is shown in Fig. 4. The curve clearly indicates[22] that the CMC locates around 0.3 g. dl^{-1}. The linear part of the curve is extrapolated to the CMC The intercept gives

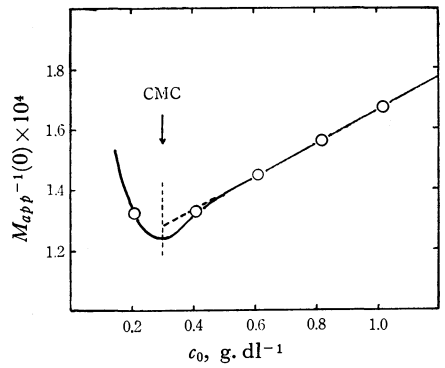

Fig. 4. The $M_{app}^{-1}(0)$ versus c_0 curve of PADA [A]/[I] 5 solutions at pH 2.0.

* There is no reason, however, to have an identical value for $M_{app}(0)$ at the meniscus and at the bottom, epecially for the present system. Solute molecules adsorbed at the meniscus, i. e., at the air-water interface, need not necessarily have an identical apparent molecular weight with that in solution or at the bottom, for they may have different conformations or different associated states.

22) E. Hutchinson, *J. Colloid Sci.*, **9**, 191 (1954).

TABLE III. MICELLAR PROPERTIES OF PADA [A]/[I] 5 (B4201)

CMC g. dl^{-1}	M_w	m (Number of association)	B mol. ml. g^{-1}
0.3	7700	13	2.5×10^{-3}

the weight-average molecular weight of the micelle, while the slope gives its second virial coefficient, omitting some contribution of the monomers present. The micellar molecular weight and the second virial coefficient of PADA [A]/[I] 5 obtained in this way are listed in Table III. The molecular weight, 7700, or the number of association, 13, is very small as compared with that of the corresponding derivatives of polyoxyethylene.[23-25]

A method similar to that described above was applied to a solution of 1.0 g. dl^{-1} at pH 5.0; it gave a value of $M_{app}(0)$ 3300. The micellar molecular weight would be lower than that at pH 2.0, even if the second virial coefficient is taken into account. Hence, lowering the pH serves merely to promote the association of PADA; free hydrochloric acid would act to suppress the electrostatic interaction.

The Association of PADA [A]/[I] 15 and 20. —The sedimentation velocities of PADA [A]/[I] 15 and 20 in solution were both sufficiently high, even at low rotor speeds. The sedimentation pattern of PADA [A]/[I] 15 consisted of two components, one amounting to about 95% and the other appearing as a faster shoulder. The shoulder is probably a remnant of discretely heterogeneous aggregates, as was observed in the [A]/[I] 10 preparation. PADA [A]/[I] 20 gave a symmetrical peak. The sedimentation coefficients of the main peaks are plotted against the concentration in Fig. 5. From the extrapolation to infinite dilution,

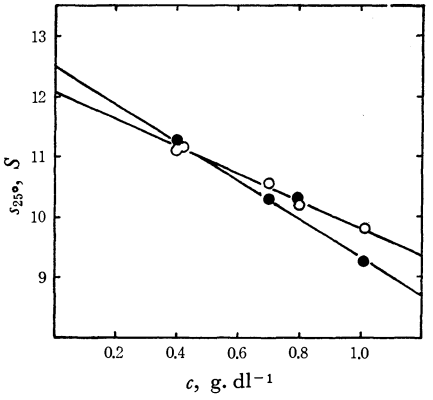

Fig. 5. Sedimentation coefficients of PADA solutions at pH 2.0.
●, [A]/[I] 15 (main component); ○, [A]/[I] 20

TABLE IV. MICELLAR PROPERTIES OF PADA [A]/[I] 15 AND 20

[A]/[I]	$s^0_{25°}$ / S	Simha-Perrin	M	m	Scheraga-Mandelkern M	Scheraga-Mandelkern m
15 (B4203)	12.5	Prolate	509000	340	477000	320
		Oblate	599000	400		
20 (B4204)	12.1	Prolate	468000	250	447000	240
		Oblate	576000	310		

the sedimentation constants, $s°$, were obtained; they are given in Table IV.

Assuming the micelles to be unhydrated ellipsoids of revolution, and omitting the contribution of minor components in the [A]/[I] 15 preparation, the micellar molecular weights were estimated by means of the Simha-Perrin tretament.[15,26,27] The values for both prolate and oblate ellipsoids are listed in Table IV. They may be limits of the micellar molecular weights. Alternatively, assuming the micelles to have a structure similar to random coils, the Scheraga-Mandelkern equation[28]

$$M^{2/3}=\frac{N s^0[\eta]^{1/3}\eta_0}{\beta(1-\bar{v}\rho_0)}$$

can give another estimate of the micellar molecular weights, as is also given in Table IV. Here η_0 is the viscosity coefficient of the solvent, N the Avogadro number and β is a shape factor having a value of 2.5×10^6 for random coils.

The micellar molecular weights obtained by the Scheraga-Mandelkern treatment are rather in better agreement with those obtained by the Simha-Perrin treatment for the prolate ellipsoidal model, although the latters are extreme cases without hydration. PADA might have the micellar molecular weights of 480000 and 450000 for [A]/[I] 15 and 20, respectively. Their numbers of association are 320 and 240, respectively. Therefore, the PADA micelles are much larger than those of the corresponding polyoxyethylene derivatives.[23-25] Since poly-DL-alanine does not associate in an aqueous solution,[3] it seems likely that the number of association of PADA micelle decreases with increasing the degree of polymerization, as far as the latter exceeds about ten.

At pH 5.0 the sedimentation experiments were performed on solutions of about 1 g. dl^{-1}. The sedimentation coefficients were 5.6 S and 5.4 S for [A]/[I] 15 and 20, respectively. They are lower than those at pH 2.0, This again indicates that the micelles at higher pH's consist of a smaller number of molecules than those at lower pH's, and that the excess hydrochloric acid merely suppresses the electrostatic effect.

23) J. Stauff and J. Rasper, *Kolloid-Z.*, **151**, 148 (1957).
24) T. Nakagawa, H. Inoue, K. Kuriyama and T. Oyama, *J. Chem. Soc. Japan, Pure Chem. Sect.* (*Nippon Kagaku Zassi*), **79**, 345 (1958).
25) F. Tokiwa and T. Isemura, This Bulletin, **35**, 1737 (1962).
26) F. Perrin, *J. phys. radium*, [7] 7, 1 (1936).
27) J. W. Mehl, J. L. Oncley and R. Simha, *Science*, **92**, 132 (1940).
28) H. A. Scheraga and L. Mandelkern, *J. Am. Chem. Soc.*, **75**, 179 (1953).

Discussion

It may be supposed that the instability of the solution of the [A]/[I] 10 preparation that there are two kinds of PADA micelles, depending on the degree of polymerization. In fact, the low molecular weight PADA forms a micelle consisting of only 13 monomer molecules, while the higher molecular weight PADA forms a micelle the number of association of which amounts to a few hundred for [A]/[I] 15 and 20.

Structure of the Small Micelle.—It has been shown from infrared spectral studies[1,2] that PADA [A]/[I] 5 assumes the β-conformation in the solid state. In the β-conformation the polypeptide chains are extended and arranged in an antiparallel way, and hydrogen bonds are formed between peptide groups of different chains. A similar structure may be expected to exist in the micelle. In solutions of acid pH's, however, the intermolecular hydrogen bonds would compete with the electric repulsion between ionized amino groups. If the solution is not dilute enough, ionized amino groups would be shielded electrically by other ionized molecules and the PADA molecules would associate into a micelle through the intermolecular hydrogen bonds: PADA has a structure similar to the β-conformation. If the solution is so dilute that the electric repulsion is not sufficiently suppressed, the intermolecular hydrogen bonds would be disrupted and the PADA molecules would assume a random coil conformation without associating with one another. Therefore, a sharp change in solution properties should occur at some intermediate concentration. The CMC would correspond to this concentration, where the association-dissociation of molecules and the coil-β transition of conformation take place simultaneously.

If the micelle has a structure similar to the β-conformation in the solid, dodecyl groups are directed outwards within the plane of polypeptide chains alternately. The micellar dimension can be roughly estimated for this model. This axial ratio of an oblate ellipsoid approximating this model was about 9, which is comparable with that derived from the intrinsic viscosity. Alternatively, by converting the model into an equivalent disk, the second virial coefficient may be evaluated by means of an excluded volume equation.[29] It was found to be $1—2\times10^{-3}$ c. g. s., which was of the same order of magnitude as the observed value, 2.5×10^{-3} c. g. s. The correction for polydispersity and intermolecular interaction may explain the discrepancy between the calculated and observed values.

From these considerations regarding the micellar size and shape in relation to the conformation of PADA in solid, it may be concluded that the micelle of PADA [A]/[I] 5 has a structure similar to the β-conformation.

Structure of the Large Micelles.—The micelles of high molecular weight PADA are different from the small micelle of the [A]/[I] 5 preparation. The micellar size decreases with the degree of polymerization, and poly-DL-alanine does not associate in an aqueous solution. Such a dependence of the micellar size on the monomer size is similar to that of polyoxyethylene derivatives.[25] Hydrophobic bonds between dodecyl groups are certainly an important factor in the cohesion of the micelles. However, intermolecular hydrogen bonding between peptide groups is also effective in the association, since the micellar size of PADA is much larger than that of polyoxyethylene derivatives. In connection with the conformation in the solid state and the hydrodynamic behavior of the micelles, it can be concluded that the large micelles of PADA [A]/[I] 15 and 20 have a structure similar to that of random coils; the conformation of each molecule is randomly coiled in these micelles.

It may be expected that the large PADA molecule can be oriented by shear flow to exhibit flow birefringence. Preliminary experiments on flow birefringence were made with the two preparations, [A]/[I] 15 and 20. The results concerning PADA [A]/[I] 20 are shown in Fig. 6. A slight dependence of the extinction angle, χ, and of the birefrigence increment, $\Delta n/c$ on the concentration was observed. Since the micellar structure and its rigidness are not known accurately, no definite conclusion on the micellar size and shape can be derived from these results. If the micellar shape is assumed to be a hydrodynamically

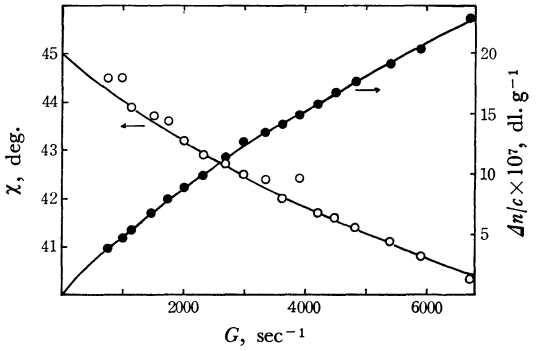

Fig. 6. Flow birefringence of PADA [A]/[I] 20 solution at pH 2.0.
Concn., 0.94 g. dl^{-1}; temp., 16°C
○, Extinction angle; ●, Birefringence increment

Table V. Optical properties of PADA micelles

[A]/[I]	Θ sec^{-1}	g_1-g_2 $\times10^{-3}$	dn/dc ml.g^{-1}	Ellipsoid	n_1	n_2
15 (B4203)	1000	0.6	0.185	Prolate	1.55	1.59
20 (B4204)	5000	1.0	0.187	Oblate	1.64	1.56

29) A. Isihara, *J. Chem. Phys.*, 18, 1446 (1950).

equivalent ellipsoid derived by the Simha treatment, the rotary diffusion coefficient, Θ, and the optical anisotropy factor, g_1-g_2, can be obtained by the use of the equations of Peterlin and Stuart.[30] These values are listed in Table V. The rotary diffusion coefficients, however, lead to too large micellar dimensions when they are compared with those derived from the sedimentation experiments. This may be due to the polydispersity of the micelles and to the concentration dependence of the extinction angle.

If the data on birefringence increment, $\Delta n/c$, and refractive index increment, dn/dc, are combined, the principal refractive indices, n_1 and n_2, for the ellipsoids of revolution can be obtained; these values are also given in Table V. It was found that the principal refractive indices of the micelles are equal to each other for the two preparations, [A]/[I] 15 and 20, whether a prolate or an oblate ellipsoid is postulated. This suggests that the micelles formed from these two preparations have similar structures.

30) A. Peterlin and H. A. Stuart, *Z. Physik*, **112**, 1 (1939).

BULLETIN OF THE CHEMICAL SOCIETY OF JAPAN VOL. 39 112—117 (1966)

The Vibrational Assignment and Rotational Isomerism of *n*-Propyl Mercaptan

By Michiro HAYASHI, Yuji SHIRO and Hiromu MURATA

Department of Chemistry, Faculty of Science, Hiroshima University, Higashisenda-machi, Hiroshima

(Received May 17, 1965)

The infrared and Raman spectra of *n*-propyl mercaptan have been measured and vibrational assignments made with relation to the rotational isomerism. The normal vibration calculation has been carried out in a modified Urey-Bradley force field. In the gaseous and liquid states, TT and GT molecular forms have been confirmed to exist. An appreciable energy difference in the isomers has been found even in the liquid state. The TT form has a lower energy than the GT form. The CH_2 hydrogen deformation frequencies of CH_2CH_2 groups in molecules similar to *n*-propyl mercatpan have been listed and discussed in relation to their molecular forms.

In a series of studies[1,2] we have studied the Raman and infrared spectra of molecules containing sulfur atoms in relation to the rotational isomerism. As a continuation of this reseach, we shall now report on the vibrational spectra of *n*-propyl mercaptan. This is the third of this series of papers.

For this substance, Scott et al.[3] pointed out the possibility of rotational isomers and gave a brief assignment of the observed spectra as a mixture of the trans and the gauche isomers around the C–C bond. This assignment, unfortunately, requires many improvements when a comparison is made with other members of the series of molecules we have studied.

In the previous papers, we pointed out a tendency toward hydrogen deformation frequencies in molecules containing sulfur atoms. In this paper, we will summarize the results of all the studies of this series of molecules.

1) M. Hayashi, Y. Shiro, T. Oshima and H. Murata, This Bulletin, **38**, 1734 (1965).
2) M. Hayashi, Y. Shiro, M. Murakami and H. Murata, ibid., **38**, 1740 (1965).
3) R. E. Pennington, D. W. Scott, H. L. Finke, J. P. McCullough, J. F. Messerly, I. A. Hossenlopp and G. Waddington, *J. Am. Chem. Soc.*, **78**, 3266 (1956).

Experimental

The sample used for the measurements was commercial *n*-propyl mercaptan which had been carefully redistilled. B. p. 67°C; n_D^{20} 1.4351.

The spectra were obtained by the same apparatus and under the same conditions as we have described in the previous papers. We attempted to measure the infrared spectra in the crystalline state for a sample cooled by liquid nitrogen at about −120°C. However, we could not make the sample in the crystalline state, though we could measure the spectra in a very viscous liquid state. The observed spectra in the liquid state were in a good agreement with those reported by Scott et al.

Rotational Isomerism

Though the spectra in the crystalline state are not available, the infrared spectra recorded at about −120°C have shown large changes in their relative absorption intensities.

Around 800 cm^{-1}, we have three bands, at 815, 793 and 779 cm^{-1}, of which the one at 779 cm^{-1} appears as a shoulder of the strongest band at 793 cm^{-1} at room temperature, while at a low temperature, the one at 815 cm^{-1} becomes the

TABLE I. OBSERVED SPECTRA OF *n*-PROPYL MERCAPTAN IN cm^{-1}

Infrared			Raman	Assignment[b]
Gas	Liquid (Room temp.)	Liquid[a] (Low temp.)	Liquid	
			233	Skeletal def. (G), C–SH torsion (T, G)
			290	CH_3 torsion (T)
			363	Skeletal def. (T)
			417	Skeletal def. (G)
655 s	655 s		651	CS str. (G)
710 s	706 m	706 vs	701	CS str. (T)
735 m	736 m	736 vs	736	CH_2 rock. (T)
780 w	779 sh	780 w	779	CH_2 rock. (G)
793 s	793 s	790 sh	805	CSH def. (G)
815 w	815 w	810 s		CSH def. (T)
880 sh	880 m	880 sh	880	CH_2 rock. (G)
890 s	892 s	891 vs	905	CH_2 rock. (T)
920 w	925 w	918 w		CH_3 rock. (G)
961 vw	961 m	960 w	964	CH_3 rock. (T)
1032 w	1032 w	1030 m	1032	CC str. (T, G)
1060 w	1060 sh	1062 m		CH_3 rock. (G)
1085 s	1088 s	1082 m		CH_3 rock. (T), CC str. (G)
1105 m	1105 s	1108 s	1103	CC str. (T)
1210 w	1208 sh		1205	CH_2 twist. (G)
1225 sh	1225 sh	1221 s		CH_2 twist. (T)
1240 s	1246 s	1249 s	1256	CH_2 wag. (T), CH_2 twist. (G)
1298 s	1298 s	1297 s	1294	CH_2 twist. (T), CH_2 wag. (G)
1340 w	1339 m	1340 m	1330	CH_2 wag. (T, G)
1380 s	1380 s	1380 m		CH_3 sym. def. (T, G)
1450 s	1440 s	1440 s	1440	CH_2 bend. (T, G)
	1458 s	1458 s		CH_3 deg. def. (T, G)
2565 s	2564 s	2560 s	—[c]	SH str. (T, G)
2950 br.	2950 br.	2950 br.	—[c]	CH str. (T, G)

a) Measured at about −120°C.
b) Molecular forms around the C–C bond are shown in parentheses.
c) Not measured.

strongest band, and the band at 793 cm^{-1} appears as a shoulder of a weak band at 779 cm^{-1}.

Around 900 cm^{-1}, three bands are seen at room temperature, at 925, 892 and 880 cm^{-1}, with weak, strong and medium intensities respectively, while at a low temperature, the band at 892 cm^{-1} becomes much more intense, that at 925 cm^{-1} shifts to 918 cm^{-1} and that at 880 cm^{-1} appears as a shoulder of 892 cm^{-1}. At 1225 cm^{-1}, we have a shoulder of a strong band at 1246 cm^{-1} at room temperature, while at a low temperature, this shoulder gains in intensity and appears as a doublet with that at 1246 cm^{-1}.

There are too many observed spectra for unique molecular form, and, as Scott et al. have pointed out, we may also conclude that for this substance rotational isomers exist which have different energies even in the liquid state. The skeletal deformation frequencies have been calculated as a four-body problem using the reported values[1,4] of the force constants in the Urey-Bradley force field. The calculations have been carried out for seven different isomers around the C–C bond. It has been found that a Raman line observed at 363 cm^{-1} belongs to the trans isomer, while the lines at 233 and 417 cm^{-1} belong to the gauche isomer around the C–C bond.

When the molecular form around the C–S bond is taken into consideration, we would expect five different isomers, TT, TG, GT, GG and GG′ in the notation described in the previous papers, where the first symbol refers to the molecular form around the C–C bond, and the second, to those around the C–S bond. In the second paper of this series, we mentioned that the molecular form of the CH_2CH_2SH part of the molecule affects strongly only the CSH deformation frequencies, while its influence is negligible for the other vibrational modes. For β-chloroethyl mercaptan, a refinement of the normal vibration calculation has shown that CSH deformation frequencies for five different isomers would be arrayed in the sequence

4) S. Mizushima, T. Shimanouchi, I. Nakagawa and A. Miyake, *J. Chem. Phys.*, **21**, 215 (1953).

of GG', TG, TT and GT ranging from the higher frequencies to the lower frequencies. The highest frequency for β-chloroethyl mercaptan is 928 cm^{-1}, whie the lowest is 860 cm^{-1}.

For *n*-propyl mercaptan CSH deformation mode would be expected at a frequency region lower than those of β-chloroethyl mercaptan for two reasons; (1) the lack of C–Cl stretching modes in the lower frequency region, and (2) the introduction of the CH_3 rocking modes at the frequency region higher than the region where the CSH deformations would be expected.

We have five infrared bands, at 925, 892, 880, 815 and 793 cm^{-1}, of which those at 925, 880 and 793 cm^{-1} may be attributed to the gauche bands around the C–C bond on the basis of intensity measurements at different temperatures. The bands at 925, 892 and 880 cm^{-1} are assigned to the CH_3 rocking modes on the basis of a comparison of the spectra with those of propane which Takahashi[5] reported. The bands at 815 and 793cm^{-1} might be the CSH deformation frequencies, of which that at 815 cm^{-1} arises from the trans isomer around the C–C bond. A refinement of the normal vibration calculation, which will be described below, indicates that these should be attributed to TT and GT molecular forms. As for the other three isomers (GG', GG and TG), since the CH_3 rocking modes might overlap in the region expected, we could not confirm their existence.

A Refinement of the Normal Vibration Calculation

In the previous papers we attempted to test the set of force constants in a modified Urey-Bradley force field, considering all the vibrational freedoms which we obtained from the observed frequencies of 1, 2-ethanedithiol in the first paper of this series. (The details of the modifications of the Urey-Bradley force field were described in that paper.) For *n*-propyl mercaptan, we have also attempted to find the transferability of the set of force constants. All the force constants are listed in Table II. To make the treatment simple, the C–H and S–H stretching modes were split out from the $\boldsymbol{G}$ and $\boldsymbol{F}$ matrices by the high-frequency splitting technique. Thirty force constants are required, of which twenty can be transferred from the set obtained from 1, 2-ethanedithiol, while ten can be transferred from propane, for which Takahashi reported the force constants.[5] The calculation has been carried out on the assumption that the molecular forms are TT and GT. The results are shown in Table III, with forty-one observed frequencies. The assignments have been found to be very satisfactory (average error, 1.9%). In the table we have also added brief descriptions of the potential energy distributions. For the other molecules of this series, we found that all the vibrational modes have relatively well-localized potential energy distributions. However, we found,

TABLE II. FORCE CONSTANTS

Force constants transferred from the set obtained from 1,2-ethanedithiol.

K(C-S)	md./Å	1.9	$\kappa(CH_2)$	md.·Å	0.058
K(C-C)	md./Å	2.2	$l(CH_2)$	md.·Å	0.057
K(C-H)	md./Å	4.33	$t(CH_2CH_2)$	md.·Å	0.136
K(S-H)	md./Å	3.46	$g(CH_2CH_2)$	md.·Å	−0.051
H(HCH)	md./Å	0.331	F(HCH)	md./Å	0.2
H(HCS)	md./Å	0.294	F(HCS)	md./Å	0.192
H(HCC)	md./Å	0.156	F(HCC)	md./Å	0.459
H(SCC)	md./Å	0.052	F(SCC)	md./Å	0.560
H(CSH)	md./Å	0.086	F(CSH)	md./Å	0.620
$Y(CH_2CH_2)$	md.·Å	0.15	$Y(CH_2SH)$	md.·Å	0.052

Force constants transferred from the set reported for propane by Takahashi.

H(HCH)	md./Å	0.37	F(HCH)	md./Å	0.2
H(HCC)	md./Å	0.186	F(HCC)	md./Å	0.54
H(CCC)	md./Å	0.275	F(CCC)	md./Å	0.335
$\kappa(CH_3)$	md.·Å	0.008	$Y(CH_3CH_2)$	md.·Å	0.15
$t(CH_3CH_2)$	md.·Å	0.118	$g(CH_3CH_2)$	md.·Å	0.0

$F' = -(1/10)F$

l; Interaction term within the CH_2 groups

t, g; Trans and gauche interaction terms for the CH_2CH_2 group and the CH_3CH_2 group

Y; Force constant for torsional vibration

5) H. Takahashi, *J. Chem. Soc. Japan, Pure Chem. Sect.* (*Nippon Kagaku Zasshi*), **83**, 978 (1962).

TABLE III. OBSERVED AND CALCULATED FREQUENCIES OF *n*-PROPYL MERCAPTAN IN cm^{-1} c)

Trans form (TT)a)			Gauche form (GT)a)		
Obs.	Calcd.	Interpretationb)	Obs.	Calcd.	Interpretationb)
1458	1457	CH_3 deg. def. (80)	1458	1453	CH_3 deg. def. (80)
1458	1449	CH_3 deg. def. (80)	1458	1445	CH_3 deg. def. (80)
1440	1437	CH_2 bend. (90)	1440	1423	CH_2 bend. (90)
1440	1421	CH_2 bend. (90)	1440	1421	CH_2 bend. (90)
1380	1371	CH_3 sym. def. (95)	1380	1373	CH_3 sym. def. (95)
1339	1334	CH_2 wag. (70)	1339	1333	CH_2 wag. (70)
1298	1277	CH_2 twist. (90)	1298	1279	CH_2 wag. (60), CH_2 twist. (20)
1246	1266	CH_2 wag. (70)	1246	1236	CH_2 twist. (50), CH_2 wag. (20)
1225	1232	CH_2 twist. (60), CH_3 rock. (30)	1208	1199	CH_2 twist. (70)
1105	1101	CC str. (40), CH_3 rock. (35)	1088	1062	CC str. (50), CH_2 rock. (30)
1088	1081	CH_3 rock. (60), CH_2 twist. (30)	1060	1051	CH_3 rock. (45), CH_2 wag. (45)
1032	1031	CC str. (90)	1032	1019	CC str. (60), CH_2 twist. (20)
961	947	CH_3 rock. (30), CC str. 20) CSH def. (30)	925	940	CH_3 rock. (30), CC str. (30) CSH def. (30)
892	860	CH_2 rock. (40), CH_3 rock. (50)	880	870	CH_2 rock. (40), CH_3 rock. (40)
815	829	CSH def. (50), CC str. (30)	793	821	CSH def. (50), CC str. (30)
736	715	CH_2 rock. (80)	779	750	CH_2 rock, (90)
706	694	CS str. (80)	655	644	CS str. (90)
363	358	CCS def. (60), CC str. (20)	417	435	CCS def. (80)
290	298	CH_3CH_2 torsion (90)	—	313	CH_3CH_2 torsion (70), CCC def. (20)
233	240	CH_2SH torsion (90)	233	243	CH_2SH torsion (80)
—	211	CCS def. (100)	233	222	CCC def. (60), CH_2CH_2 torsion (40)
—	130	CH_2CH_2 torsion (90)	—	123	CH_2CH_2 torsion (80), CCC def. (20)

a) Trans form (TT); the trans form around the C-C bond and the trans form around the C-S bond.
Gauche form (GT); the gauche form around the C-C bond and the trans form around the C-S bond.

b) Diagonal elements of the potential energy distributions for mainly contributing internal coordinates are added in parentheses in %, and the underlines indecate the assignments of the spectra.

c) CH and SH stretching modes were split out in the treatments. The averaged difference between the observed and the calculated frequencies is 1.9% and the maximum difference is 6.0%.

as special features of *n*-propyl mercaptan, that some of the vibrational modes are largely mixing and that their potential energy distributions are not localized in special internal coordinates.

The Energy Difference between the Isomers

We determined the change in the absorption intensities of the spectra at a lower temperature and used it as one of the most important data for the assignment of the observed spectra to different rotational isomers.

Since these changes were observed in the liquid state, the rotational isomers are shown to have different energies, even in the liquid state. For this molecule we would think the electrostatic interaction might not depend on the molecular forms so strongly. Therefore, it seems natural to expect that the energy difference is not large in either the liquid or the gaseous state, as in the works by Mizushima and his co-workers.[6] However, Scott et al. reported that, in the gaseous state, the trans isomer around the C–C bond has an energy about 400 cal./mol. lower than the gauche isomer. We also found that there is some energy difference in the liquid state, and that the trans has a lower energy than the gauche isomer. We have no idea at present how to explain this fact.

The Assignment of the Spectra

As we have mentioned above, a mixing of the vibrational modes sometimes makes the assignments of the observed spectra difficult. For example, the band at 880 cm^{-1} has almost equal contributions from the CH_3 and CH_2 rocking modes of the gauche isomer. However, we will call this band a CH_2 rocking mode, since we can find the bands at 1060 and 925 cm^{-1} for two CH_3 rocking modes, and since this band corresponds well to a CH_2 rocking mode for the other molecules of the

6) S. Mizushima "Structure of Molecules and Internal Rotation," Academic Press, New York (1964).

series which we previously reported on. In the table, the underlining indicates the names of vibrations given in this way.

Scott et al. did not report the spectra at a lower temperature, and they did not notice that the spectra show appreciable changes in their absorption intensities. Furthermore, they took *n*-propyl bromide as the sample for comparison, while we have taken 1, 2-ethanedithiol and β-halogenoethyl mercaptan, in assigning the observed spectra. When we compare the infrared spectra of these substances, we immediately find that the spectra of *n*-propyl mercaptan resemble those of 1, 2-ethanedithiol and β-halogenoethyl mercaptan, but that they are different from those of *n*-propyl bromide both in the shapes of the bands and in their frequency values. Therefore, our choice of the sample for comparison would be much better than theirs. Therefore, we believe that our assignments are better than theirs.

Actually, we have the sum rule of $\sum\nu^2(TT)=8.949\times10^7$ and $\sum\nu^2(GT)=8.925\times10^7$ (0.3% difference), in which the CH and SH stretching frequencies are excluded from the calculation, while they reported a 1.25% difference between the sums. The most appreciable difference in the assignments between ours and theris may be those of the CH_2 rocking frequencies, which would have a great influence on the assignments of the other spectra. They took 767 and 1105 cm^{-1} for the trans isomer and 793 and 1105 cm^{-1} for the gauche isomer. It seems to us, according to this assignment, that the frequency differences between the two CH_2 rockings are too large, and also that the frequency differences between different isomers are too small. As we will discuss again below, when we take the ratio of the frequencies of different isomers, we would expect that it would be around 0.65, while it is 0.89 according to their assignments. Therefore, we think their assignments are not acceptable.

CH_2 Hydrogen Deformation Frequencies in Relation to Molecular Forms

It is well known that the CH_2 hydrogen deformation frequencies for molecules with the $-CH_2CH_2-$ structures are strongly influenced by molecular forms around the C–C bond. Especially, the frequency difference between two CH_2 rocking frequencies for the trans isomer is found, in general, to be much larger than those for the gauche isomer. In Table IV we have listed the CH_2 rocking frequencies of the molecules with rotational isomers. In the tenth column of Table IV, we have added the ratio of the frequency differences for the trans and the gauche isomers in order to make the above tendencies clear. From the table, it can be seen that this ratio is less than unity; we always have a larger ratio for the molecules containing sulfur atoms than for the typical example, 1, 2-dichloroethane. Larger ratios are also obtained for molecules which do not contain sulfur atoms. For example, it is 0.62 for succinonitrile.[7] The averages

TABLE IV. CH_2 ROCKING FREQUENCIES OF THE MOLECULES (XCH_2CH_2Y) (cm^{-1})

Molecule[a]	Trans isomer[b]				Gauche isomer[b]				Ratio[e]	Ref.
	ν_1^T	ν_2^T	Av.[c]	Dif.[d]	ν_1^G	ν_2^G	Av.[c]	Dif.[d]		
(HS, SH)	1027	718	873	309	972	769	871	203	0.66	1
(HS, Cl)	1021	724	873	297	967	778	872	189	0.64	2
(HS, Br)	1022	710	866	311	962	764	863	198	0.64	2
(HS, SCH_3)	1019	728	873	291	963	778	871	185	0.64	8
(CH_3S, SCH_3)	1010	739	875	271	958	840	899	118	0.43	9
(CH_3S, Cl)	1005	746	876	259	957	845	901	112	0.43	8
(CH_3S, Br)	1015	738	878	278	958	838	898	120	0.43	8
(HS, CH_3)	892	736	814	156	880	779	830	101	0.65	This work
(Cl, Cl)	989	768	879	221	943	881	912	62	0.28	6
(Cl, Br)	955	761	858	194	921	861	891	60	0.31	6
(Cl, CH_3)	863	729	796	134	856	788	822	68	0.51	6
(Br, Br)	934	747	841	187	897	838	868	59	0.32	6
(Br, CH_3)	849	737	793	112	838	777	808	61	0.54	6
(CN, CN)	1005	762	884	243	963	813	888	150	0.62	7

a) The formulas of the molecules are abridged. For example, (HS, SH) means $HSCH_2CH_2SH$.
b) The trans and the gauche isomers around the C–C bonds.
c) The averaged frequency values of two CH_2 rocking frequencies.
d) The differences in two rocking frequencies.
e) The ratio of the frequency differences for the trans and the gauche isomers. That is, dif.(gauche)/dif. (trans).

7) T. Fujiyama, K. Tokumaru and T. Shimanouchi, *Spectrochim. Acta*, **20**, 415 (1964).
8) M. Hayashi, Y. Shiro, T. Kawakita and H. Murata, to be published.
9) M. Hayashi, Y. Shiro, T. Oshima and H. Murata, This Bulletin, **39**, 118 (1966).

of two CH_2 rocking frequencies for the trans isomers of molecules containing sulfur atoms are found to be nearly 872 $cm^{-1}\pm10$ cm^{-1}, except for *n*-propyl mercaptan, while for the other molecules the averages are far from the above range.

If we arrange the molecules in the sequence of X, which stands for SH, CH_3, SCH_3, Br and Cl, we find that the ratio is strongly influenced by the exchange of X, as is shown in Table V.

For $HSCH_2CH_2X$, the ratio decreases slightly as X changes. For four other series of molecules, that is, for the $CH_3CH_2CH_2X$, $CH_3SCH_2CH_2X$, $BrCH_2CH_2X$ and $ClCH_2CH_2X$ series, the ratio decreases appreciably. In general, this ratio is largest when X is SH, becomes smaller as X changes to CH_3, SCH_3 Br and Cl successively, and is smallest when X is Cl.

Table V. Ratio of frequency differences in two CH_2 rocking frequencies

Y=	SH	CH_3	SCH_3	Br	Cl
$HSCH_2CH_2Y$	0.66	0.65	0.64	0.64	0.64
$CH_3CH_2CH_2Y$	0.65	—	—	0.54	0.51
$CH_3SCH_2CH_2Y$	0.64	—	0.43	0.43	0.43
$BrCH_2CH_2Y$	0.64	0.54	0.43	0.32	0.31
$ClCH_2CH_2Y$	0.64	0.51	0.43	0.31	0.28

Table VI is a similar table given for the CH_2 wagging frequencies. The frequency differences in two wagging frequencies are, in general, much smaller than those of the CH_2 rocking frequencies. Therefore, a large uncertainty is introduced into the ratio of the frequency differences of isomers. However, when X and Y stand for one of the groups, SH, CH_3, Br or Cl, the ratio of the frequency diffrences for the XCH_2CH_2Y molecule always takes a value between those of the XCH_2CH_2X and YCH_2CH_2Y molecules.

We believe, then, that the above tendencies for the CH_2 rocking and wagging frequencies will be useful in the assignment of the observed spectra.

Table VI. CH_2 wagging frequencies of the molecules (XCH_2CH_2Y) (cm^{-1})

Molecule	Trans isomer			Gauche isomer			Ratio[a]	Ref.
	ν_1^T	ν_2^T	Dif.	ν_1^G	ν_2^G	Dif.		
(HS, SH)	1292	1220	72	1292	1273	19	0.26	1
(HS, Cl)	1298	1222	76	1306	1281	25	0.33	2
(HS, Br)	1291	1199	92	1291	1260	31	0.34	2
(HS, SCH_3)	1290	1215	75	1290	1271	19	0.25	8
(CH_3S, SCH_3)	1285	1209	76	1285	1267	19	0.25	9
(CH_3S, Cl)	1294	1217	77	1294	1272	22	0.29	8
(CH_3S, Br)	1295	1213	82	1295	1270	25	0.31	8
(HS, CH_3)	1339	1246	93	1339	1298	41	0.44	This work
(Cl, Cl)	1304	1230	74	1304	1264	40	0.54	6
(Cl, Br)	1300	1203	97	1295	1258	37	0.38	6
(Cl, CH_3)	1338	1258	80	1338	1304	34	0.43	6
(Br, Br)	1284	1190	94	1284	1252	32	0.34	6
(CN, CN)	1359	1272	87	1339	1322	17	0.20	7

a) The ratio of the frequency differences for the trans and the gauche isomers.

BULLETIN OF THE CHEMICAL SOCIETY OF JAPAN VOL. 39 118—121 (1966)

The Vibrational Assignment and Rotational Isomerism of 1, 2-Dithiamethyl Ethane

By Michiro HAYASHI, Yuji SHIRO, Toshiyuki OSHIMA and Hiromu MURATA

Department of Chemistry, Faculty of Science, Hiroshima University, Higashisenda-machi, Hiroshima

(Received May 17, 1965)

The infrared and Raman spectra of 1, 2-dithiamethyl ethane have been measured in gaseous, liquid and solid states. Vibrational assignments have been made in relation to the rotational isomerism. The normal vibration calculation has been carried out in a modified Urey-Bradley force field. In the gaseous and liquid states, GTG' and GGG molecular forms exist, while in the solid state the GTG' form alone persists. The energy difference between GTG' and GGG molecular forms has been found to be 1.1 kcal./mol. in the gaseous state and very small in the liquid state. The GTG' form is more stable than the GGG form, in both the gaseous and liquid states.

In previous papers, we have dealt with the vibrational spectra of 1, 2-ethanedithiol,[1] β-halogenoethyl mercaptan[2] and *n*-propyl mercaptan[3] in relation to the rotational isomerism. The present work, the fourth of a series of papers, will deal with the vibrational spectra of 1, 2-dithiamethyl ethane. For this substance Sweeny et al.[4] discussed the possibility of rotational isomers in relation to its metal complex. However, they did not mention details of the vibrational assignments of the observed spectra, and they also did not consider the molecular forms around two C–S bonds.

In the present work, we will attempt assignments of the spectra and will consider the molecular forms around two C–S bonds as well as the C–C bond. The energy differences between the isomers will also be measured.

Experimental

1, 2-Dithiamethyl ethane was prepared by the reaction of 1, 2-dichloroethane with sodium methyl mercaptide in absolute alcohol. B. p. 84°C/20 mmHg; n_D^{20} 1.5297.

The spectra were obtained by the same apparatus and under the same conditions as we have described in the previous papers.

The infrared spectra in the crystalline state were recorded for a sample cooled with liquid nitrogen at about −120°C.

Rotational Isomerism

From a comparison of the observed spectra in the gaseous and the liquid states with those in the crystalline state, and also from a comparison of the spectra with those of 1,2-ethanedithiol which we reported in a previous paper, the following evidence of rotational isomers has been obtained.

The CH_2 wagging frequencies found for 1, 2-ethanedithiol at 1220, 1273 and 1292 cm^{-1} are also seen at 1202, 1273 and 1292 cm^{-1}, of which only 1202 cm^{-1} persists in the crystalline state. One C–C stretching frequency is seen at 1008 cm^{-1}; it disappears in the crystalline state. These are similar to those found for 1, 2-ethanedithiol. As Sweeny et al. pointed out, we may conclude that the isomer persisting in the crystalline state has the center of symmetry, which is the trans form around the C–C bond, while the other, which disappears in the crystalline state, might be the gauche form around the C–C bond.

The assignments of the observed spectra are easy from a comparison with those of 1, 2-ethanedithiol and β-halogenoethyl mercaptan. The assignments of the spectra are shown in Table I. It is important to note that there are no unassigned spectra over the spectral region obtained.

When we take the molecular forms around the two C–S bonds into consideration, ten different isomers may be expected for this substance. Four of them have the trans form, and six have the gauche form, around the C–C bond. We will use the symbols G and T for the molecular forms around each internal-rotation axis, as we did in the previous papers.

The actual molecular form in the crystalline state should be either TTT or GTG' in this notation, because the observed spectra demonstrate the mutual exclusion rule between the infrared and the Raman spectra.

To get information on the detailed molecular form, the skeletal deformation frequencies have been calculated in the Urey-Bradley force field for

1) M. Hayashi, Y. Shiro, T. Oshima and H. Murata, This Bulletin, **38**, 1734 (1965).
2) M. Hayashi, Y. Shiro, M. Murakami and H. Murata, ibid., **38**, 1740 (1965).
3) M. Hayashi, Y. Shiro and H. Murata, ibid., **39**, 112 (1966).
4) D. M. Sweeny, S. Mizushima and J. V. Quagliano, *J. Am. Chem. Soc.*, **77**, 6521 (1955).

Table I. Observed frequencies of 1,2-dithiamethyl ethane (cm^{-1})

Infrared			Raman	Assignment[a]
Gas	Liquid	Solid	Liquid	
			143 w	(G)
			235 m	(T)
			257 m	(G)
			340 s	(T, G)
	418 w		420 w	(G)
			644 w	CS str. (G)
	655 w	656 w	651 m	CS str. (T, G)
687 m	688 s	683 m	690 s	CS str. (T)
		729 s	729 m	CH_2 rock. (T)
739 m	739 s	739 s	735 m	CS str. (T)
840 w	840 w	—		CH_2 rock. (G)
960 s	960 s	—	965 w	CH_2 rock. (G), CH_3 rock. (T, G)
	972 sh	969 s		CH_3 rock. (T, G)
1010 w	1020 w	—	1026 vw	CC str. (T, G), CH_2 rock. (T)
	1130 sh	—		CH_2 twist. (G)
1137 s	1140 s	1137 m		CH_2 twist. (T)
	1200 sh	—	1200 vw	CH_2 twist. (G)
1204 s	1209 s	1206 s		CH_2 wag. (T)
	1268 s	—		CH_2 wag. (G), CH_2 twist. (G)
1280 s	1285 sh	—		CH_2 wag. (T, G)
1324 m	1320 m	1317 m, 1322 sh	1325 vw	CH_3 sym. def. (T, G)
	1419 sh	1425 s		CH_2 bend. (T, G)
1435 s	1432 vs	1435 vs	1429 m	CH_3 deg. def. (T, G)
2900 s	2900 s	2900 s	2915 vs	CH str. (T, G)
2950 s	2950 s	2950 s	2951 m	CH str. (T, G)

skeletal def.

a) Molecular forms around the C-C bond have been given in parentheses.

six different molecular forms as a four-body problem, using the reported values[1,5] of the six necessary force constants; these values are $K(CH_2\text{-}S)=2.60$, $K(CH_2\text{-}CH_2)=3.70$, $H(CH_2CH_2S)=0.15$, $H(CH_2SCH_3)=0.157$, $F(CH_2CH_2S)=0.50$ and $F(CH_2SCH_3)=0.211$ md./Å.

The results are shown in Fig. 1, where we have also added the observed Raman lines below 500 cm^{-1}. There are five observed Raman lines below 500 cm^{-1}, where the skeletal deformation frequencies are expected, while four skeletal deformation frequencies are calculated for a unique molecular form. If the form has the center of symmetry, two of the four frequencies become inactive in the Raman effect.

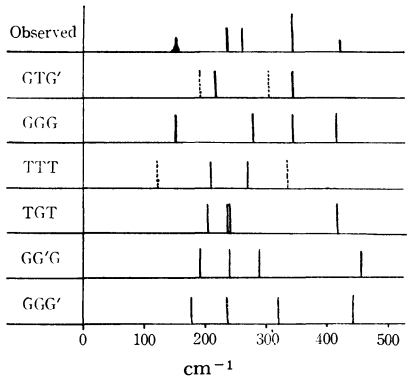

Fig. 1. Observed and calculated skeletal vibration frequencies below 500 cm^{-1}.
(·····Raman inactive)

The calculated frequencies of the skeletal deformation modes show a strong dependance on the molecular forms, as we expected. The results suggest that the gauche forms for two C–S bonds are more favorable than the trans form for predicting the observed lines. Especially, the strong Raman line at 340 cm^{-1} should only belong to the frequencies for either GTG' or GGG, while the weak Raman line at 143 cm^{-1} should also only belong to the frequency for GGG. It may be noted that GTG' has the center of symmetry; this could be the molecular form in the crystalline state.

In general, the above treatment of normal vibrations is relatively uncertain, and there is difficulty in measuring weak Raman lines. Therefore, we could not determine whether GTG' is a unique molecular form in the crystalline state, and whether the other form exists in the gaseous and the

5) M. Hayashi, *J. Chem. Soc. Japan, Pure Chem. Sect.* (*Nippon Kagaku Zassi*), **78**, 627 (1957).

liquid states in addition GTG' and GGG. However, we believe that GTG' and GGG are the main molecular forms for this substance.

The absorption intensity of the spectra were measured at ten different temperatures in the range from 50 to 140°C in the gaseous state, and at five different temperatures in the range from −20 to 50°C in the liquid state.

Three wagging frequencies around 1250 cm^{-1} were used in the measurements. From the observed optical densities, the energy difference of the isomers around the C–C bond has been computed to be 1.1 kcal./mol. in the gaseous state. In the liquid state, it has been found to be very small (<0.1 kcal./mol.).

A Refined Treatment of Normal Vibration Calculations

In the previous papers, we attempted to determine the force constants in a modified Urey-Bradley force field, considering all the vibrational freedoms. The purpose of this attempt was to determine a set of transferrable force constants which we could apply to every molecule with the $-SCH_2CH_2S-$ structure and, finally, to polyalkyl polysulfides.

In the first paper of this series, we determined a set from the observed spectra of 1, 2-ethanedithiol. In the second and the third papers, we tested it for the cases of β-halogenoethyl mercaptan and *n*-propyl mercaptan and found that the agreement between the observed and the calculated frequencies is quite satisfactory. In the present work, we have tried to apply the set to 1, 2-dithiamethyl ethane.

The force field adopted in the calculation is a modified Urey-Bradley force field, which has been described fully in the first paper of this series; it will also be described separately in a paper in which we will use dimethyl sulfide as an example.[6] All the force constants used are listed in Table II. To simplify the treatment, the C–H stretching modes were split from the $\boldsymbol{G}$ and $\boldsymbol{F}$ matrices by the high-frequency splitting technique.

Twenty-seven force constants are required, of which sixteen can be transferred from the set obtained from 1, 2-ethanedithiol, while eleven can be transferred from the set obtained from dimethyl sulfide. The calculations have been carried out on the assumption of two pairs of molecular forms. One of them is a pair (TTT and TGT) which have the trans form around two C–S bonds, while the other is a pair (GTG' and GGG) which have the gauche form around two C–S bonds. The results are shown in Table III for fifty-one observed frequencies.

From the table, it may be seen that the influence of the molecular forms around two C–S bonds makes no essential difference in the calculated frequencies except in the frequencies of skeletal deformation modes. This indicates that we will have no chance to confirm the molecular forms around the C–S bond unless we examine the skeletal deformation modes. Though the observed Raman lines for the skeletal deformation frequencies are all relatively weak, the five observed Raman lines assigned to skeletal deformation modes can be much better predicted on the assumption of one pair (GTG' and GGG) than on that of the other pair (TTT and TGT).

Therefore, we have concluded that GTG' and GGG are the actual molecular forms for this substance; of these, GTG' persists in the crystalline state.

The agreement between the calculated and the observed frequencies, assuming that the molecular forms are GTG' and GGG, is quite satisfactory; the transferability of the set of force constants has also been proved for this substance.

TABLE II. FORCE CONSTANTS

Force constants transferred from the set obtained from 1, 2-ethanedithiol

K(C-S)	md./Å	2.9	$t(CH_2CH_2)$	md·Å	0.136
K(C-C)	md./Å	2.0	$g(CH_2CH_2)$	md·Å	−0.051
K(C-H)	md./Å	4.33	$l(CH_2)$	md·Å	0.057
H(HCH)	md./Å	0.331	F(HCH)	md./Å	0.2
H(HCS)	md./Å	0.294	F(HCS)	md./Å	0.192
H(HCC)	md./Å	0.156	F(HCC)	md./Å	0.459
H(SCC)	md./Å	0.052	F(SCC)	md./Å	0.560
$\kappa(CH_2)$	md·Å	0.058	$Y(CH_2CH_2)$	md·Å	0.15

Force constants transferred from the set obtained from dimethyl sulfide

H(HCS)	md./Å	0.04	F(HCS)	md./Å	0.76
H(HCH)	md./Å	0.38	F(HCH)	md./Å	0.2
H(CSC)	md./Å	0.22	F(CSC)	md./Å	0.21
$t(CH_3SC)$	md·Å	0.07	$g(CH_3SC)$	md·Å	−0.07
$Y(CH_3S)$	md·Å	0.052	$\kappa(CH_3)$	md·Å	0.06
$n(CH_3)$	md·Å	0.03			

$F' = -(1/10)F$

l; Interaction term within the CH_2 group

t, g; Trans and gauche interaction terms for the CH_2CH_2 group and the CH_3SC group

Y; Force constants for torsional vibration

n; Interaction term within the CH_3 group

The Assignment of CH_2 Rocking Frequencies

As is shown in Table I, there are several differences in the assignments of the observed spectra between ours and those reported by Sweeny et al. They reported that 840 and 900 cm^{-1} were two CH_2 rocking vibrations for the gauche isomer. We found a very weak band at 890 cm^{-1} at first. However, this disappeared after careful distillation, while that at 840 cm^{-1} remained unchanged.

6) M. Hayashi, Y. Shiro and H. Murata, to be published.

TABLE III. OBSERVED AND CALCULATED FREQUENCIES OF 1, 2-DITHIAMETHYL ETHANE IN cm^{-1}

Trans form[a]			Gauche form[a]			
Obs.	Calcd.		Obs.	Calcd.		Assignment
	TTT	GTG'		TGT	GGG	
1432	1448	1448	1432	1447	1448	CH_3 deg. def.
1419	1426	1420	1419	1425	1428	CH_2 bend.
1321	1348	1348	1321	1347	1348	CH_3 sym. def.
1285	1296	1293	1268	1253	1254	CH_2 wag.
965	Ag 969	g 980	972	983	984	CH_3 rock.
1020	1020	1009	1020	997	1013	CC str.
735	726	713	651	654	647	CS str.
651	653	649	644	634	629	CS str.
340	281	344	143	A 245	A 138	CCS def.
235	208	214	340	204	340	CSC def.
1432	1447	1448	1432	1448	1448	CH_3 deg. def.
1140	1163	1159	1195	1180	1176	CH_2 twist.
959	961	964	972	981	980	CH_3 rock.
739	Au 717	u 724	960	960	959	CH_3 rock.
—	184	198	—	168	177	CH_3S torsion
—	110	77	—	84	110	CH_2CH_2 torsion
—	46	47	—	56	41	CH_2S torsion
1432	1450	1448	1432	1448	1448	CH_3 deg. def.
1419	1420	1420	1419	1423	1425	CH_3 deg. def.
1321	1347	1347	1321	1348	1348	CH_3 sym. def.
1209	1215	1211	1285	1298	1291	CH_2 wag.
972	Bu 986	u 985	972	983	980	CH_3 rock.
683	690	695	651	650	655	CS str.
655	646	660	644	648	642	CS str.
—	334	309	257	231	272	CSC def.
—	99	142	420	B 446	B 428	CCS def.
1432	1447	1448	1432	1448	1448	CH_3 deg. def.
1268	1282	1280	1130	1151	1151	CH_2 twist.
965	960	978	960	975	965	CH_3 rock.
1020	Bg 1023	g 1039	840	779	785	CH_2 rock.
—	176	169	—	176	170	CH_3S torsion
—	104	91	—	49	51	CH_2S torsion

a) Molecular form around the C-C bond.

Therefore, the band at 900 cm^{-1} may be caused by an impurity.

We regarded one of the CH_2 rocking modes as overlapping with a CH_3 rocking frequency at 960 cm^{-1}. For the trans isomer, since in the crystalline state the band at 739 cm^{-1} exists as a doublet, this band has two components, that is, one of the CH_2 rocking modes and one of the C–S stretching modes, as Sweeny et al. pointed out. The other CH_2 rocking modes for the trans isomer might be at 1020 cm^{-1}.

The frequency differences in the two CH_2 rocking modes are found to be 281 and 120 cm^{-1} for the trans and the gauche isomers respectively, while 221 and 62 cm^{-1} are found for 1, 2-dichloroethane, which Sweeny et al. chose as the standard. If the band at 900 cm^{-1} actually existed, the frequency differences for this substance could be close to those for 1, 2-dichloroethane. Since the band at 900 cm^{-1} does not exist, we have a large difference between these substances. However, when all the CH_2 rocking frequencies of the series of molecules which we studied are taken into consideration, the assignment of the two CH_2 rocking modes to 840 and 960 cm^{-1} for the gauche isomer is not only reasonable but inevitable.

The results of normal vibration calculations support the present assignment.

As we pointed out in the third paper of this series, we believe that this is a characteristic difference for the series of molecules containing sulfur atoms. It is worth noting that this improvement in the assignment does not have any influence on the discussions of the metal complex which Sweeny et al. reported on.

BULLETIN OF THE CHEMICAL SOCIETY OF JAPAN VOL. 39 122—127 (1966)

Influence of Metal Ions and of Metal Chelates on the Hydrolysis of α-D-Glucose 1-Phosphate*

By Yukito MURAKAMI and Michio TANAKA

Department of Organic Synthesis, Faculty of Engineering, Kyushu University, Hakozaki, Fukuoka

(Received May 18, 1965)

The hydrolysis reaction of α-D-glucose 1-phosphate has been studied in the presence of several metal ions and metal chelates at 40.0 and 60.0°C, in the pH range of 1.69—2.71, and at an ionic strength of 0.10 M (KNO_3). The reaction rate was followed by the colorimetric method using a combination of the amidol reagent and 8.3% molybdate solution. Among the metal ions employed in this work, dipositive ions, such as manganese(II), cobalt(II), nickel(II), copper(II), zinc(II) and uranyl ions, were observed to be nearly without effect on the rate of hydrolysis, while iron(III) and thorium(IV) ions demonstrated a negative catalytic effect. On the other hand, all the chelating agents employed tend to restore the reaction rate in reference to the corresponding metal-ion-effected reactions. With the 1:1 thorium(IV)-EDTA and the 1:1 iron(III)-EDTA chelate system, the rate was completely restored. Both iron(III)-kojate and thorium(IV)-Tiron chelate systems restored the reaction rate to a lesser extent. The roles of the chelating agents were discussed. The reaction mechanism in the presence of the catalyst species has been considered, and two possible mechanisms have been put forward for the present reactions.

The hydrolysis of organic orthophosphates are in general complicated by several factors[1] even in the absence of metal ions and of metal chelates. Firstly, an organic phosphate exists in various ionic forms in aqueous media, the composition of which depends on the nature of the medium, the structure of the alcohol substituent, and the acid dissociation constants of the phosphate. Secondly, each ionic species of the substrate undergoes either carbon-oxygen or phosphorus-oxygen bond fission, or both simultaneously in the course of hydrolysis. Thirdly, the reactivity of each ionic species is controlled by the structure and the physical properties of the alcohol substituent, and by the nature of the medium. The reactivity is also affected by a reaction process through which hydrolysis of a substrate proceeds.

Among the organic phosphates of biological interest, α-D-glucose 1-phosphate is known to form as an intermediate in biological system during the course of degradation of sugars. The hydrolysis of this phosphate has been extensively studied by Bunton and co-workers[2] and the neutral species was found to be the most reactive one among the neutral, monoionic and diionic species. A unimolecular mechanism was assigned to the hydrolysis of both the neutral and the monoionic species.

Present research has been carried out to investigate the participation of metal ions and metal chelates in the hydrolysis of α-D-glucose 1-phosphate. Since a series of studies on the hydrolysis of salicyl phosphate analogs have been carried out previously[3-5] to investigate the catalytic roles of metal ions and of metal chelates, this work may provide some additional information on the role of metals in such reactions.

Experimental

Reagents.—The dihydrate form of dipotassium α-D-glucose 1-phosphate was purchased from Sigma Chemical Company, St. Louis, Mo., U. S. A. The purity of this compound, which was established by phosphorus analysis and potentiometric titration, was sufficiently high, so that further purification was not necessary.

The disodium salt of ethylenediaminetetraacetic acid and Tiron (sodium pyrocatechol-3, 5-disulfonate) were the products of the Research Laboratories of Dojindo & Co., Ltd.; both were used without further purification. Kojic acid was purchased from Tokyo Kasei Kogyo Co., Ltd. and was purified by sublimation in vacuo.

The nitrates of divalent metals, $Co(NO_3)_2 \cdot 6H_2O$, $Ni(NO_3)_2 \cdot 6H_2O$, $Cu(NO_3)_2 \cdot 3H_2O$, and $Zn(NO_3)_2 \cdot 6H_2O$; and manganese sulfate, $MnSO_4 \cdot nH_2O$, of an analytical grade were purchased from Wako Pure Chemical Industries, Ltd. The nitrates of actinide metals, $UO_2(NO_3)_2 \cdot 6H_2O$ and $Th(NO_3)_4 \cdot 4H_2O$, of an analytical

* Contribution No. 82 from the Department of Organic Synthesis, Faculty of Engineering, Kyushu University.

1) See for general review: J. R. Cox, Jr., and O. B. Ramsey, *Chem. Revs.*, **64**, 317 (1964).

2) C. A. Bunton, D. R. Llewellyn, K. G. Oldham and C. A. Vernon, *J. Chem. Soc.*, **1958**, 3588.

3) R. Hofstetter, Y. Murakami, G. Mont and A. E. Martell, *J. Am. Chem. Soc.*, **84**, 3031 (1962).

4) Y. Murakami and A. E. Martell, *J. Phys. Chem.*, **67**, 582 (1963).

5) Y. Murakami and A. E. Martell, *J. Am. Chem. Soc.*, **86**, 2119 (1964).

grade are the products of the British Drug Houses Ltd. and Wako Pure Chemical Industries, Ltd. respectively. The ferric nitrate nonahydrate was a pure grade reagent of the latter company. Standardization of aqueous stock solutions of these metal salts was established by the usual method of chelatometric titration.

Potentiometric Measurements.—The apparatus and procedures for potentiometric titrations have been mentioned elsewhere.[6] Potentiometric titrations of α-D-glucose 1-phosphate were carried out at temperatures of 34.8, 39.8, 45.0 and 60.0°C, and at an ionic strength of 0.10 M with added potassium nitrate. In order to avoid any perturbation of the data which may be caused by hydrolysis of the phosphate during the course of titrations, the reliability of titration data was confirmed by repeated titration runs and by the detection of any liberated inorganic phosphate.

Kinetic Measurements.—The pH value of an experimental solution was maintained constant during each run without adding any base or acid, since each solution was sufficiently acidic that the chemical reactions occurring did not cause any significant change in its acidity. Nevertheless, the pH value of each experimental solution was checked from time to time with an HRL Model P pH meter of the Horiba Instruments Inc. fitted with extension glass and calomel electrodes. The ionic strength of the experimental solutions was maintained at 0.10 M with potassium nitrate. Two reaction temperatures were selected; 40.0±0.1 and 60.0±0.1°C. The rate of hydrolysis was determined by measuring the amount of phosphoric acid liberated in the course of hydrolysis.

The analytical method for the liberated inorganic orthophosphate, employed in this work, essentially followed the procedure established by Allen.[7] The two kinds of solutions were prepared: Amidol reagent was prepared by dissolving 2.5 g. of amidol (product of Naniwa Chemical Co., Ltd.) recrystallized from water-methanol and 50 g. of sodium bisulfite (Wako analytical grade) in mineral-free water, and diluting to 250 ml. This mixed solution was allowed to stand overnight in a refrigerator after a small amount of active charcoal being added, and then filtered to remove active charcoal and any other precipitates. The activity of this reagent was checked from time to time to assure the accurate analysis of orthophosphate. The second reagent is the 8.3% molybdate solution. To prepare this solution, 22.035 g. of ammonium molybdate $(NH_4)_6(Mo_7O_{24})\cdot 4H_2O$ (Wako analytical grade) was dissolved in 228 ml. of mineral-free water.

The following analytical procedure was employed in this study. A 2.0 ml. sample was pipetted from the experimental solution and was transferred to a 25 ml. volumetric flask containing 10 ml. of water, which had been cooled in an ice bath. The reaction stopped immediately because of low temperature. Two milliliters of 60% perchloric acid (Wako analytical grade), 2.0 ml. of the amidol reagent, and 1.0 ml. of the 8.3% molybdate solution were added in this order, and the mixture was diluted to 25 ml. with mineral-free water. The volumetric flask was then placed in a constant temperature bath at 15.0±0.5°C for 5 min. to develop the violet color. The absorbance was measured at 720 mμ with a Shimadzu-Bausch & Lomb Spectronic 20 Colorimeter immediately after the development of the color. The amount of inorganic phosphate was determined by reference to a calibration curve obtained with the use of a standard potassium dihydrogen phosphate (Wako analytical grade) solution.

Results

Determination of Acid Dissociation Constants.—The evaluated acid dissociation constants of α-D-glucose 1-phosphate are summarized in Table I. Some different values of pK_{HA} were reported by Ashby and co-workers,[8] and the discrepancy can be ascribed to the difference in experimental ionic strength among this work and theirs. Another set of pK values reported by Cori and co-workers[9] are in a rather close agreement with the present data.

Kinetics of Spontaneous Hydrolysis.—Hydrolysis of α-D-glucose 1-phosphate has been studied at 40 and 60°C in the lower pH region ranging from 1.72 to 3.38. This hydrolysis reaction was found to follow the apparent first order kinetics, rate constants obtained at various pH's being summarized in Table II. The reaction rate is seen to increase as the pH of the solution decreases.

Table I. Acid dissociation constants of α-D-glucose 1-phosphate

Temp., °C	μ	pK_{H_2A}	pK_{HA}	Ref.
34.8±0.1	0.10 (KNO_3)	1.44±0.04	—	This work
39.8±0.1	0.10 (KNO_3)	1.43±0.04	—	This work
45.0±0.1	0.10 (KNO_3)	1.42±0.04	—	This work
60.0±0.1	0.10 (KNO_3)	1.40±0.05	6.09±0.01	This work
35	—	—	6.519*	8
40	—	—	6.531*	8
45	—	—	6.545*	8
50	—	—	6.561*	8
30	—	1.10	6.13	9

* Thermodynamic constant

6) Y. Murakami, This Bulletin, **35**, 52 (1962).
7) R. J. L. Allen, *Biochem. J.*, **34**, 858 (1940).
8) J. H. Ashby, H. B. Clarke, E. M. Crook and S. P. Datta, ibid., **59**, 203 (1955).
9) C. J. Cori, S. P. Colowick and G. T. Cori, *J. Biol. Chem.*, **121**, 465 (1937).

Table II. First order rate constants of the hydrolysis of α-D-glucose 1-phosphate
$\mu=0.10$ M (KNO_3); $T_S=1.00\times10^{-3}$ M

	60.0±0.1°C							40.0±0.1°C
$-\log[H^+]$	1.72	1.91	2.04	2.07	2.25	2.71	3.38	1.72
$10^5 k$, sec^{-1}	6.83	4.19	3.08	2.83	1.94	0.617	0.139	0.385

T_S: Initial total concentration of the phosphate species

Table III. Hydrolysis rates of α-D-glucose 1-phosphate in the presence of metal ions
$\mu=0.10$ M (KNO_3); $T_M/T_S=1.0$; $T_S=1.00\times10^{-3}$ M

	$k\times10^6$, sec^{-1}			
	60.0±0.1°C			40.0±0.1°C
Metal ion	$-\log[H^+]=1.72$	$-\log[H^+]=2.04$	$-\log[H^+]=2.71$	$-\log[H^+]=1.72$
none	68.3	30.8	6.17	3.85
Mn(II)	67.2	29.7	4.49	3.13
Co(II)	68.6	31.8	—	3.43
Ni(II)	69.3	31.8	6.81	3.32
Cu(II)	67.9	32.5	6.17	3.20
Zn(II)	68.5	32.2	—	3.73
Fe(III)	32.0	13.9	5.28	1.69
UO_2(VI)	60.3	28.9	—	—
Th(IV)	10.9	—a)	—a)	—

T_M: Total concentration of the metal ion
T_S: Total concentration of the phosphate species
a) Not first order

Kinetics of Hydrolysis in the Presence of Metal Ions.—In order to investigate effects and roles of metal ions in the hydrolysis reaction of α-D-glucose 1-phosphate, several metal ions of the first transition series and of the actinide series have been employed in this study. The hydrolysis reaction has been studied at a 1:1 molar ratio of substrate to metal ion and the reaction was observed to proceed homogeneously in all cases. The experimental data obtained at 60.0 and 40.0°C indicate an apparent first order rate with respect to the total concentration of unreacted organic phosphate species in most instances. All the rate data obtained for the metal-ion-effected hydrolysis reactions are listed in Table III. In most cases where the hydrolysis reaction followed first order kinetics, the divalent metal ions and uranyl ion did not cause any significant change in reaction rate in reference to the spontaneous rate. As can be seen, those metal ions which caused a significant change in reaction rate acted as negative catalysts. Although the thorium ion provided a first order rate constant at $-\log[H^+]=1.72$ and 60°C, the hydrolysis did not follow first order kinetics under other experimental conditions with this metal ion present. Moreover, the apparent reaction rate increases as pH value is raised in the presence of the thorium ion, while the rate of spontaneous hydrolysis and of other metal ion-effected reactions decreases. The rate profiles at various pH's for the thorium-effected reaction are shown in Fig. 1 along with those for the spontaneous reaction.

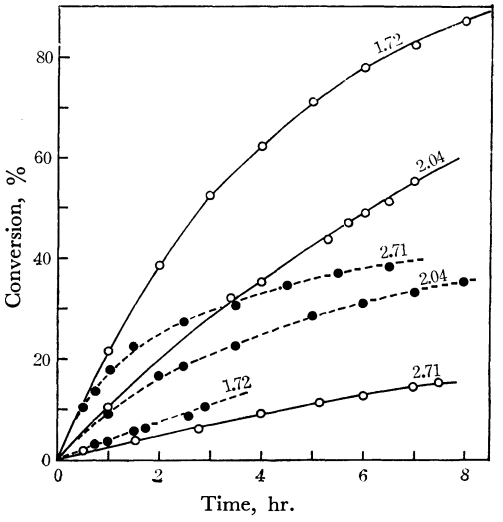

Fig. 1. Hydrolysis of α-D-glucose 1-phosphate at 60.0°C in 0.10 M KNO_3, with the total substrate concentration of 1.00×10^{-3} M; ○, spontaneous reaction; ●, thorium(IV)-ion-effected reaction ($T_S/T_M=1.0$). Numbers refer to the hydrogen ion concentration in $-\log[H^+]$. T_M=total concentration of the thorium ion; T_S=total concentration of the phosphate species.

Kinetics of Hydrolysis in the Presence of Metal Chelates.—Four different chelate systems have been employed in the present work to investigate the interaction of each chelate system with α-D-glucose 1-phosphate in the course of

hydrolysis reaction of the latter. These chelate systems are iron(III)-kojate, iron(III)-EDTA, thorium(IV)-Tiron, and thorium(IV)-EDTA. The hydrolysis reaction was studied at 60.0°C and was observed to follow first order kinetics in all instances; all the experimental solutions contained a 1:1:1 molar ratio of metal ion, ligand, and substrate. The specific rate constants determined experimentally are listed in Table IV.

Table IV. Hydrolysis rates of α-D-glucose 1-phosphate in the presence of metal chelates
60.0±0.1°C; μ=0.10 M (KNO_3); T_M/T_S=1.0; $T_S=1.00\times10^{-3}$ M; T_M/T_L=1.0

Metal chelate system		$k\times10^5$, sec^{-1}	
Metal ion	Ligand	$-\log[H^+]=1.69\pm0.02$	$-\log[H^+]=2.00\pm0.02$
none	none	6.83[a]	3.08[b]
Fe(III)	none	3.20[a]	1.39[b]
Fe(III)	kojate	4.87	2.35
Fe(III)	EDTA	7.47	3.78
Th(IV)	none	1.09[a]	—[c]
Th(IV)	Tiron	1.52	1.18
Th(IV)	EDTA	7.33	3.80

T_M: Total concentration of the metal species
T_S: Total concentration of the phosphate species
T_L: Total concentration of the ligand species
$-\log[H^+]$ values: a, 1.72; b, 2.04
c) Not first order.

As shown in Table IV, at both pH's the interaction of metal ion alone with the phosphate resulted in a much slower rate of hydrolysis than the spontaneous hydrolysis rate. The presence of a ligand capable of coordinating to metal ion, however, tends to restore the rate to the spontaneous one. With the two chelate systems, Fe(III)-EDTA and Th(IV)-EDTA, the rate is recovered completely. The concentration effect of the Fe(III)-kojate chelate system was studied at a selected hydrogen ion concentration ($-\log[H^+]=2.07$), and the rate-concentration profile is shown in Fig. 2. The reaction rate is seen to decrease with an increase of the chelate concentration.

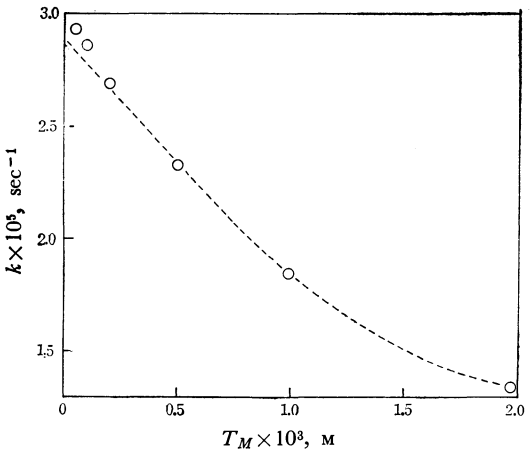

Fig. 2. Variation of the first order rate constant of the hydrolysis of α-D-glucose 1-phosphate with the concentration of Fe(III)-kojate chelate species at $-\log[H^+]=2.07$; μ=0.10 M (KNO_3); 60.0°C; T_M=total concentration of the Fe(III) species (free metal ion and chelate species).

Discussion

Spontaneous Hydrolysis.—The substrate, α-D-glucose 1-phosphate, is considered as a dibasic acid and exists in three different forms, I, II, and III, the composition of which is dependent on the pH value of a solution.

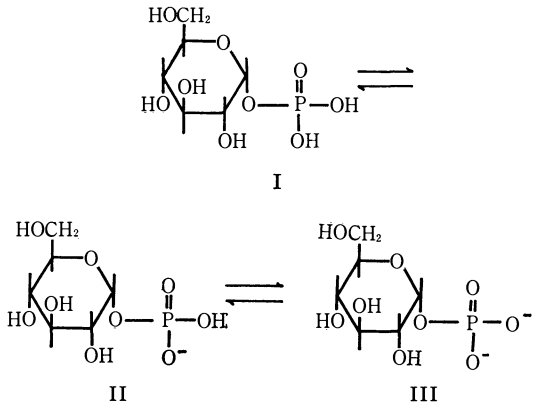

The mole fractions of these three substrate species at various hydrogen ion concentrations are shown in Table V together with the hydrolysis rate constant at each hydrogen ion concentration. A plot of

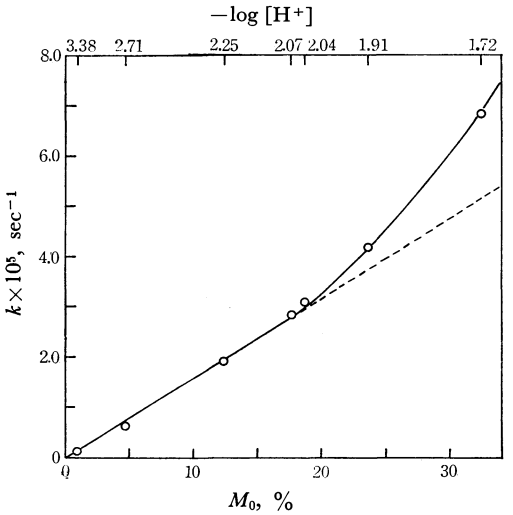

Fig. 3. Variation of the first order rate constant for the spontaneous hydrolysis of α-D-glucose 1-phosphate with the mole fraction of the neutral phosphate species at 60.0°C; μ=0.10 M (KNO_3). Dotted line indicates an extrapolated straight line.

Table V. Correlation of mole fractions of the substrate species with hydrolysis rates at various hydrogen ion concentrations

60.0±0.1°C; μ=0.10 M (KNO_3)

$-\log[H^+]$	$[H^+]$, M	M_0	M_I	M_{II}	$k\times10^5$, sec^{-1}
1.72	1.91×10^{-2}	3.24×10^{-1}	6.76×10^{-1}	2.89×10^{-5}	6.83
1.91	1.23×10^{-2}	2.36×10^{-1}	7.64×10^{-1}	5.05×10^{-5}	4.19
2.04	9.13×10^{-3}	1.87×10^{-1}	8.13×10^{-1}	7.25×10^{-5}	3.08
2.07	8.51×10^{-3}	1.76×10^{-1}	8.24×10^{-1}	7.87×10^{-5}	2.83
2.25	5.63×10^{-3}	1.24×10^{-1}	8.76×10^{-1}	1.26×10^{-4}	1.94
2.71	1.95×10^{-3}	4.67×10^{-2}	9.53×10^{-1}	3.97×10^{-4}	0.617
3.38	4.17×10^{-4}	1.04×10^{-2}	9.90×10^{-1}	1.76×10^{-3}	0.139

M_0: Mole fraction of the neutral species
M_I: Mole fraction of the monoionic species
M_{II}: Mole fraction of the diionic species

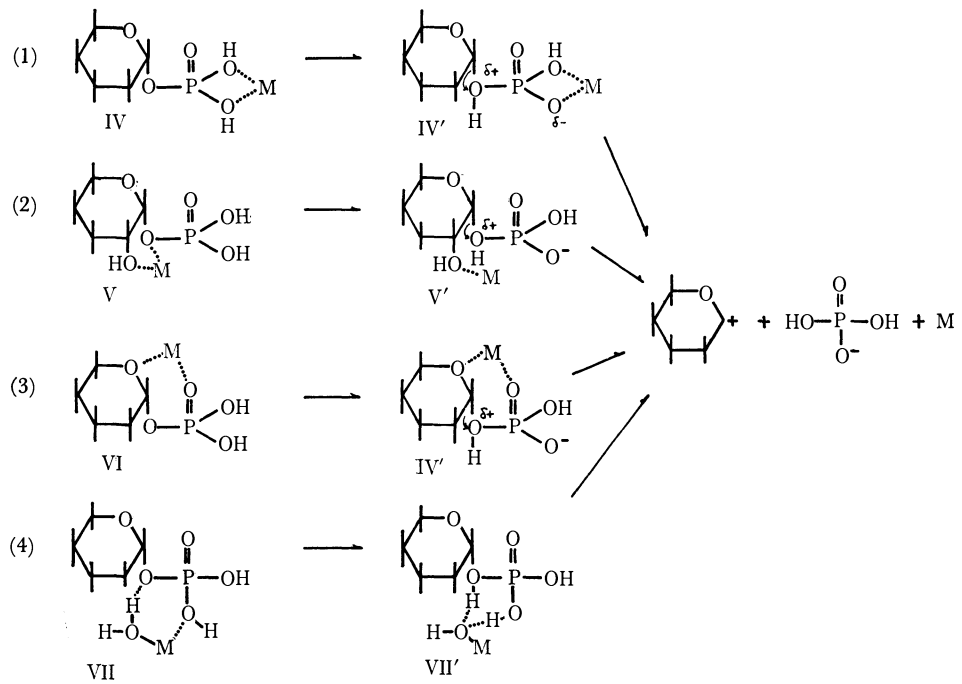

Chart 1. Probable mechanisms for the hydrolysis of α-D-glucose 1-phosphate in the presence of metal species.

a mole fraction of the neutral species against corresponding spontaneous rate constant resulted in a straight line in the region lying below a mole fraction 0.18, as is seen in Fig. 3.

Therefore, the main active species existing in this pH region may be assumed to be the neutral phosphate species. In the higher mole fraction range, the specific rate constant plot deviates from linearity. Thus, an acid catalyzed reaction is considered to be superimposed upon the spontaneous hydrolysis of the neutral species. These considerations are in agreement with and in support of the results obtained by Bunton et al.[2]

Effects of Metal Ions.—In this investigation the pH value of experimental solutions was maintained in the range, 1.72—2.71. Therefore, the acid catalyzed reaction may not be significant under present experimental conditions. The effect of metal ions on the hydrolysis reaction is obviously dependent on the positive charge that these metal ions possess, as illustrated in Table III. Thus, all the divalent metal ions and even the uranyl ion do not cause any significant change in reaction rate. As the mechanism in which metal ions can show any profound effect in the hydrolysis reaction, four cases illustrated in Chart 1 may be considered probable. The four mechanisms proposed are based upon two principal concepts: firstly, that a proton-transfer process plays a vital role in the transition state, and secondly, that the spontaneous hydrolysis mechanism, which results in the formation of a carbonium cation, is not disturbed to

a significant extent so that an S_N1 process still holds in the presence of metal ions. Mechanisms 1 and 4 would be favored if the reaction were accelerated in the presence of metal ions. A mechanism similar to the first one involving metal ion attack at the site of the phosphate group was given previously for the hydrolysis of salicyl phosphate and its derivatives.[3-5] In the activated complex of structure IV, the metal ion may act to accelerate the transfer of a phosphate proton to the ester oxygen. This proton-transfer results in the formation of structure IV', which undergoes degradation to yield the carbonium cation. On the other hand, a proton of a hydrated water in structure VII may be transferred to the ester oxygen by the help of the electron-withdrawing effect of the metal ion, with the C–O bond being subsequently cleaved to give the carbonium ion.

A different situation is expected for mechanisms 2 and 3. The proton-accepting capacity of the ester oxygen would be reduced by the presence of metal ion where the metal ion acts on the ester oxygen as shown in structure V. The coordination of the metal ion to the ether oxygen of the glycoside ring and to the phosphate oxygen, as illustrated in structure VI, acts to reduce the electron-donating power of the ether oxygen on one hand, and to diminish the proton accepting tendency of the ester oxygen on the other. The former effect would be unfavorable for the formation of the carbonium ion and the latter unfavorable for C–O bond cleavage. Therefore, from the above consideration, mechanisms 2 and 3 may be reasonable for the cases where a diminished rate of hydrolysis was observed.

Effects of Metal Chelates.—With the thorium-EDTA chelate system, the hydrolysis rate was found to be comparable with the spontaneous one. The predominant species present in the experimental solutions is the 1:1 chelate species even in the low pH region used in this investigation due to an extremely high stability of the chelate.[10] Since only two coordination sites are left on the nuclear metal of the Th(IV)-EDTA chelate[11] and the thorium ion is well-shielded with the ligand from the substrate species, the steric interaction of the substrate with this thorium chelate may prohibit the formation of the activated complexes mentioned above with the exception of IV. A similar explanation can be given for the effect of the Fe(III)-EDTA chelate system on the hydrolysis reaction. The presence of both Fe(III)-kojate and Th(IV)-Tiron chelate systems resulted in an increased rate of hydrolysis in comparison with the corresponding free metal ions. However, there still remains a negative catalytic effect with these chelates. Under these conditions of hydrogen ion concentration, the 1:1 Fe(III)-kojate[12] and Th(IV)-Tiron[13] chelate systems consist primarily of two components, free metal ion and the 1:1 chelate species. Therefore, these two chelating agents seem to demonstrate their roles in two aspects in the course of hydrolysis:

(1) the reduction of the concentration of the free metal ion, which is the most active negative catalyst;

(2) the reduction of the affinity of metal toward the substrate species through the chelation.

In conclusion, the catalytic hydrolysis reaction of organic phosphates may be explained in terms of the proton-transfer mechanism, whenever the substrate species involve any active protons. When metal ions and metal chelates showed any catalytic effect in this work, they acted to reduce the reaction rate in contrast to the hydrolysis of salicyl phosphate analogs.[3-5] Thus, whether the catalytic effect is positive or negative seems to be controlled by the three factors; ionic forms of a substrate, structure of an alcoholic residue, and hydrolytic reaction mechanism. Some further studies on the roles of metal ions and of metal chelates in the hydrolysis of organic phosphates are under progress in these laboratories.

10) G. Schwarzenbach, R. Gut and G. Anderegg, *Helv. Chim. Acta*, **37**, 937 (1954).

11) R. F. Bogucki and A. E. Martell, *J. Am. Chem. Soc.*, **80**, 4170 (1958).

12) Y. Murakami, *J. Inorg. Nucl. Chem.*, **24**, 679 (1962); W. A. E. McBryde and G. F. Atkinson, *Can. J. Chem.*, **39**, 510 (1959); L. Sommer and A. Losmanova, *Collection Czechoslov. Chem. Commun.*, **26**, 2781 (1961).

13) Y. Murakami and A. E. Martell, This Bulletin, in press.

BULLETIN OF THE CHEMICAL SOCIETY OF JAPAN VOL. 39 128—131 (1966)

The Direct Iodination of Polyalkylbenzenes Bearing Bulky Groups[1)]

By Hitomi SUZUKI,* Kiyomi NAKAMURA and Ryozo GOTO

Department of Chemistry, Faculty of Science, Kyoto University, Sakyo-ku, Kyoto

(Received May 20, 1965)

The following polyalkylbenzenes bearing bulky groups have been subjected to direct iodination using iodine and periodic acid, and the corresponding mono-iodinated products have been obtained in fairly high yields: 4-*t*-butyl-1, 2-dimethylbenzene, 5-*t*-butyl-1, 3-dimethylbenzene, 5-*t*-butyl-1, 2, 3-trimethylbenzene, 1, 2, 4, 5-tetraisopropylbenzene and *p*-di-*t*-butylbenzene. The polyiodination of polymethylbenzenes has also proceeded smoothly, giving polyiodo compounds in high yields. A comparison of various direct methods has proved the above reagent to be the best iodinating agent for a variety of polyalkylbenzenes.

Because of our interest in the disproportionation of aromatic iodo compounds in sulfuric acid, some attempts to prepare the iodo derivatives of some polyalkylbenzenes bearing bulky groups by ordinary direct methods have been made. Up to the present, however, little attempt has been made to introduce an iodine atom into the rings of such polyalkylbenzenes. As the polyalkylbenzenes are unreactive towards molecular iodine, it is necessary to use some oxidizing agents for a successful direct iodination. In order to determine the best oxidizing agent for the reaction, we carried out a series of preliminary tests, using 5-*t*-butyl-1, 3-dimethylbenzene as a common substrate. Seven reagents have been tested as oxidizing agents or iodinium cation sources: silver sulfate,[2)] silver perchlorate,[3)] mercuric oxide,[4)] potassium persulfate,[5)] iodic acid,[6)] periodic acid, and *o*-iodoanisole.[7)] The experimental procedures employed for the tests were nearly the same as those described in the original papers. The results are shown in Table I. As is apparent from the table, *iodine used with periodic acid* was found to be the best iodinating agent for polyalkylbenzenes possessing bulky groups.

The following five polyalkylbenzenes have been subjected to the direct iodination: 4-*t*-butyl-1, 2-dimethylbenzene, 5-*t*-butyl-1, 3-dimethylbenzene, 5-*t*-butyl-1, 2, 3-trimethylbenzene, 1, 2, 4, 5-tetraisopropylbenzene and *p*-di-*t*-butylbenzene. All five polyalkylbenzenes underwent the iodination and afforded new iodo derivatives. Even 1, 2, 4, 5-tetraisopropylbenzene, which was almost completely inert towards the other iodinating agents, gave the iodo product in an acceptable yield. It is interesting that 5-*t*-butyl-1, 2, 3-trimethylbenzene was, in spite of its apparently highly-crowded structure, readily iodinated to give 5-*t*-butyl-4-iodo-1, 2, 3-trimethylbenzene. This is probably because the steric aversion towards the entry of the bulky iodine atom is in part surmounted by the combined inductive effects of the four alkyl groups. In sharp contrast to the iodo derivatives of lightly-alkylated benzenes,[8)] these iodinated products were relatively stable towards sulfuric acid and did not liberate iodine until they were heated with sulfuric acid at a moderately high temperature. Nor did they undergo disproportionation under ordinary conditions of the Jacobsen reaction.

As an extension of this work, the polyiodination of some polymethylbenzenes was also carried out. Subjected to the reaction were *o*-xylene, *p*-xylene, durene and prehnitene. The reaction occurred fairly smoothly and afforded polyiodo products in high yields. The increased introduction of the iodine atoms into the ring usually diminishes the reactivity of the compound, so the tri- or tetra-iodination of xylenes was difficult to effect. For the purpose of synthesizing highly-iodinated compounds, therefore, the disproportionation of diiodo compounds by the action of sulfuric acid (Jacobsen reaction) is preferable.[9)]

Although no exhaustive investigation to find the optimum conditions was carried out, the excellent results in the present experiments showed the superiority of this reagent. The ready availability and convenience of the agent, the simple reaction conditions, the complete absence of

1) Part VIII. On the Reaction of Polysubstituted Aromatics. Part VII: This Bulletin, **38**, 1590 (1965).

* Present address: Bedford College, University of London, Regent's Park, London, N. W. 1.

2) I. R. L. Barker and W. A. Waters, *J. Chem. Soc.*, **1952**, 150.

3) L. Birckenbach and J. Goubeau, *Ber.*, **65**, 395 (1932).

4) A. Töhl, ibid., **25**, 1521 (1892).

5) K. Elbs and A. Jaroslawzew, *J. prakt. Chem.*, (2), **88**, 92 (1913).

6) H. O. Wirth, O. Königstein and W. Kern, *Ann.*, **634**, 84 (1960).

7) H. Suzuki, T. Sugiyama and R. Goto, This Bulletin, **37**, 1858 (1964).

8) H. Suzuki and R. Goto, *J. Chem. Soc. Japan, Pure Chem. Sect.* (*Nippon Kagaku Zasshi*), **84**, 284 (1963).

9) H. Suzuki and R. Goto, This Bulletin, **36**, 389 (1963).

Table I. Direct iodination of 5-*t*-butyl-1, 3-dimethylbenzene by various methods

Reagent, g.		Solvent, ml.		Hydrocarbon g.	Temp. °C	Time hr.	Yield %	Remark
Iodine	3.39	Acetic acid	17	5.40	60—65	4	91	All iodine disappeared within 4 hr. On cooling, the product separated out as white crystals. No by-product. The use of iodic acid gave similar result (86%), except that the reaction needed much longer time for completion.
Periodic acid dihydrate	1.54	Water Sulfuric acid	3 0.6					
Iodine	10.77	Cyclohexane	10	3.32	10—15	4	46	Removal of silver iodide from the product was troublesome. At elevated temperature (35—40°C), resinous materials and an oil with a camphor-like odor were formed.
Silver sulfate	4.13	Sulfuric acid Water	20 2					
Iodine	5.10	Chloroform	30	3.58	10—15	3	43	Resinous materials always accompanied the reaction. In one experiment, a violent explosion occurred.*
Silver perchlorate	4.14							
Iodine	8.50	Cyclohexane	30	5.40	40—43	3	26	Resinous materials were always formed.
Silver perchlorate	6.91							
Magnesium oxide	1.30						50**	
Iodine	10.86	Cyclohexane	20	3.25	45—50	35	55	Reactions were slow and incomplete. Mercuric oxide became pasty and greatly disturbed the smooth agitation.
Mercuric oxide	4.38							
Iodine	2.78	Acetic acid	20	3.62	60—65	6	62	Reactions proceeded slowly. Persulfate was in part consumed for the formation of iodic acid.
Potassium persulfate	2.64	Water	5					
o-Iodoanisole	4.68	Cyclohexane	10	3.25	25—30	4	83**	Small amounts of 2, 4-diiodoanisole tenaciously clinged to the product were difficult to remove.
		Sulfuric acid	10					

* The reaction had been being carried out at sunny window side, magnetically stirring with a plastic-covered stirrer, when the explosion suddenly occurred.

** Yields based on unrecovered hydrocarbon.

polymeric by-products in the final reaction mixtures, and the excellent yields of iodo derivatives recommend this method for a wide variety of polyalkylbenzenes.

Experimental

Materials.—Commercially-available *o*- and *p-xylene* were used. *Durene* and *prehnitene* were prepared according to the literature.[10,11] *4-t-Butyl-1, 2-dimethylbenzene* (I; b. p. 101—103°C/22—23 mmHg), *5-t-butyl-1, 3-dimethylbenzene* (II; b. p. 95—96°C/22—23 mmHg), and *p-di-t-butylbenzene* (III; m. p. 78—79°C) were prepared by the *t*-butylation of *o*-xylene, *m*-xylene and *t*-butylbenzene respectively.

1, 2, 4, 5-Tetraisopropylbenzene (VI) was prepared by the direct isopropylation of cumene using propylene and small amounts of 98% sulfuric acid as the catalyst. A white, oily, crystalline cake which formed in the flask was scraped out and filtered by suction until no more oil could be removed. Several recrystallizations from hot 2-propanol yielded large white needles; m. p. 118—119°C.[12]

5-t-Butyl-1, 2, 3-trimethylbenzene was prepared by the lithium hydride reduction[13] of 4-*t*-butyl-2, 6-dimethylbenzyl chloride, which had been prepared by the chloromethylation of 5-*t*-butyl-1, 3-dimethylbenzene.

4-t-Butyl-2, 6-dimethylbenzyl Chloride (V).—A mixture of II (160 g.), 37% formalin (180 g.) and concentrated hydrochloric acid (500 ml.) was stirred and heated to 65—70°C over a 7 hr. period, while a stream of hydrogen chloride was being bubbled through this mixture. After it had stood overnight, the upper organic phase was extracted with ether, washed with a saturated aqueous sodium bicarbonate solution, dried over calcium chloride, and fractionated. Colorless, rather thick oil distilled at 151—152°C/24 mmHg.[14,15] Yield, 171 g. (82%).

5-t-Butyl-1, 2, 3-trimethylbenzene (VI).—In a 500-ml. four-necked flask, fitted with a thermometer, a reflux

10) "Organic Syntheses," Coll. Vol. 2, 248 (1948).

11) "Organic Reactions," Vol. 1, John Wiley and Sons, Inc., New York, N. Y. (1942), p. 382; S. F. Birch, R. A. Dean, F. A. Fidler and R. A. Lowry, *J. Am. Chem. Soc.*, **71**, 1362 (1949); L. Horner and W. Spietschka, *Ann.*, **579**, 159 (1953).

12) A. Newton, *J. Am. Chm. Soc.*, **65**, 320 (1943).

13) J. E. Johnson, R. H. Blizzard and H. W. Carhart, ibid., **70**, 3664 (1948).

14) R. C. Fuson, J. J. Denton and J. W. Kneisley, ibid., **63**, 2652 (1941).

15) M. J. Schlatter, ibid., **76**, 4952 (1954).

condenser and a dropping funnel containing 125 g. of V dissolved in a small amount of tetrahydrofuran, lithium hydride (10 g.), lithium aluminum hydride (4 g.) and tetrahydrofuran (300 ml.) were placed and rapidly stirred with a mechanical stirrer. Then a solution of V was added drop by drop at such a rate that a gentle refluxing was maintained in the system. After the completion of dropping, the flask was immersed in a water bath and warmed at 50—60°C for several hours in order to complete the reaction. The reaction mixture was then carefully poured into large amounts of water, and the crystalline solid which precipitated was extracted with ether. Drying over calcium chloride, followed by fractional distillation, gave 96 g. (92%) of colorless oil, b. p. 115—116°C/19 mmHg, which readily solidifieds to large plates and which melted at 30—31°C.[14,15]

The use of magnesium ribbon or zinc dust as reducing agents leads to a remarkable formation of the coupling product, 4, 4'-di-*t*-butyl-2, 2', 6, 6'-tetramethyl-1, 2-diphenylethane, m. p. 215—217°C.[14]

Solvent.—The solvent used for the reaction was aqueous acetic acid, with small amounts of sulfuric acid added as a catalyst ($CH_3COOH : H_2O : H_2SO_4 = 100 : 20 : 3$).

Monoiodinated Products.—*4-t-Butyl-2, 6-dimethyliodobenzene.*—A mixture of II (5.40 g.), periodic acid dihydrate (1.54 g.), iodine (3.39 g.) and the solvent (20 ml.) was magnetically stirred and warmed at 60—65°C. After 4 hr., the elementary iodine had almost entirely disappeared and a heavy oil had precipitated. Upon cooling, the solidified product was collected by filtration and recrystallized from petroleum ether to give large plates, m. p. 59—60°C. The yield was 8.7 g. (90%). Because of its great tendency to avoid the hindered position, the iodine atom is supposed to be present at a position para to the *t*-butyl group.

Found: C, 49.73; H, 5.74. Calcd. for $C_{12}H_{17}I$: C, 50.00; H, 5.95%.

I was iodinated in a similar manner. This reaction, however, needed a little more time (6—7 hr.). The oil which precipitated was extracted with ether, and the ethereal solution was distilled after being washed with a dilute aqueous sodium bisulfite solution. There was obtained *5-t-butyl-2, 3-dimethyl-iodobenzene,* boiling at 146—147°C/14 mmHg, in a 81% yield. The unsymmetrical structure was confirmed by the aromatic substitution pattern of an infrared spectrum.

Found: C, 50.27; H, 6.07. Calcd. for $C_{12}H_{17}I$: C, 50.00; H, 5.95%.

6-t-Butyl-2, 3, 4-trimethyliodobenzene.—This was obtained, using a similar procedure, from VI (5.86 g.), periodic acid dihydrate (1.56 g.), iodine (3.39 g.) and the solvent (20 ml.). The crude product was chromatographed with an alumina column (1.7×35 cm.) using petroleum ether as an eluant; it was then recrystallized from hot ethanol to afford 8.9 g. of colorless plates melting at 74—75°C.

Found: C, 51.54; H, 6.41. Calcd. for $C_{13}H_{19}I$: C, 51.77, H, 6.35%.

2, 3, 5, 6-Tetraisopropyliodobenzene.—A mixture of IV (8.25 g.), periodic acid (1.54 g.), iodine (3.30 g.) and the solvent (35 ml.) was stirred and heated in such a manner that the temperature of the reaction mixture was held in the 75—80°C range. The iodine which sublimed on the upper part of the reaction vessel was scraped off by an occasional shaking. After 30 hr.'s heating, the hot mixture was poured into water, and the crystalline mass which precipitated was collected by filtration. Direct chromatography on an alumina column (1.7×65 cm.), using petroleum ether as an eluant, gave the unchanged hydrocarbon (7.0 g.), followed by the monoiodo product (1.9 g.). The latter compound was recrystallized several times from hot ethanol to obtain about 1.6 g. of white needles, m. p. 161—163°C.

Found: C, 58.35; H, 7.93. Calcd. for $C_{18}H_{29}I$: C, 58.07; H, 7.85%.

2, 5-Di-t-butyliodobenzene. — To a solution of III (6.38 g.) and iodine (3.38 g.) in the solvent (30 ml.), periodic acid dihydrate (1.60 g.) was added. The mixture was then agitated and heated at 75—80°C for about 30 hr. The reaction proceeded so slowly that the frequent shaking of the reaction vessel was necessary to scrape off the iodine which sublimed. After it had cooled, the solidified material was collected by filtration and washed with a dilute aqueous sodium bisulfite solution. As an attempted separation of the iodinated product from the unchanged hydrocarbon by alumina chromatography was found to be unsuccessful, the white crystalline cake was subjected to fractional distillation. There was obtained, after the removal of the low-boiling, unchanged hydrocarbon, 2.2 g. of a colorless oil boiling at 156—157°C/13—14 mmHg.

Found: C, 54.11; H, 6.96. Calcd. for $C_{14}H_{21}I$: C, 54.11, H, 6.70%.

Polyiodinated Products. — *4, 5-Diiodo-1, 2-dimethylbenzene.*—A mixture of *o*-xylene (3.54 g.), periodic acid dihydrate (3.04 g.), iodine (6.8 g.) and the solvent (20 ml.) was heated to 70°C and stirred until the purple color of the elementary iodine had almost disappeared (3—4 hr.). Then the mixture was poured into a dilute sodium bisulfite solution in order to remove the unreacted iodine. The tan solid which precipitated was then collected and chromatographed over a short alumina column (1.7×20 cm.). Recrystallization from ethanol gave 10.2 g. (85%) of colorless plates, m. p. 93—94°C. Raman and Varma reported a m. p. of 74—76°C.[16] Since they used nitric acid as an oxidizing agent, their product was necessarily contaminated with a small amount of nitro compounds. The symmetrical structure of the product was confirmed by the substitution pattern of an infrared spectrum.

Found: C, 26.69; H, 2.03. Calcd. for $C_8H_8I_2$: C, 26.84; H, 2.26%.

By a similar procedure, *2, 5-diiodo-1, 4-dimethylbenzene* was obtained from *p*-xylene. The product, recrystallized from benzene-ethanol, melted at 104—105°C. (Reported, m. p. 104°C).[16]

Found: C, 26.90; H, 2.31. Calcd. for $C_8H_8I_2$: C, 26.85; H, 2.26%.

The use of double the amounts of iodine and periodic acid has proved to have no effect. The reaction stopped at the stage of diiodination, and no tri- or tetra-iodo compounds were formed.

Diiodoprehnitene.—Prehnitene (4.47 g.) dissolved in the solvent (20 ml.) was iodinated with iodine (6.8 g.) and periodic acid (3.04 g.) in the manner described above. The reaction was completed within 1.5 hr,

16) P. S. Varma and K. S. V. Raman, *J. Indian Chem. Soc.*, **12**, 343 (1935).

and a pink-colored solid was precipitated. The product was collected and recrystallized from hot benzene. White needles; m. p. 190—191°C. Sparingly soluble in ethanol and petroleum ether. The yield was 10.8 g. (84%).

Found: C, 30.99; H, 3.38. Calcd. for $C_{10}H_{12}I_2$: C, 31.11; H, 3.13%.

Durene was converted by the same procedure to diiododurene, m. p. 140—141°C. Slightly soluble in hot ethanol and readily soluble in hot benzene, but nearly insoluble in petroleum ether.

Found: C, 31.00; H, 3.26. Calcd. for $C_{10}H_{12}I_2$: C, 31.11; H, 3.13%.

BULLETIN OF THE CHEMICAL SOCIETY OF JAPAN VOL. 39 131—137 (1966)

The Simultaneous First- and Second-Order Esterifications of *l*-Menthol by Acyl Chlorides: Autocatalyses by Menthol in Acetonitrile and in Liquid Sulfur Dioxide*

By Fuminori AKIYAMA and Niichiro TOKURA

Department of Applied Chemistry, Faculty of Engineering, Osaka University, Higashinoda, Osaka

(Received May 21, 1965)

The propionylation and *p*-methoxybenzoylation of *l*-menthol in various solvents have been studied. In chloroform, benzene, ethyl methyl ketone and carbon tetrachloride, the reaction follows the second-order rate law. However, in acetonitrile or in liquid sulfur dioxide, the rate follows the second-order rate law only at the initial stage of the reaction; thereafter it gradually deviates from the second-order type to the first-order one. Moreover, the first-order rate equations both in acetonitrile and liquid sulfur dioxide are dependent on the initial concentration of the alcohol; the over-all rates being expressed as:

$$\text{Rate} = k_1^{\circ}\,(\text{AcCl})\,(\text{ROH})_0 + k_2\,(\text{AcCl})\,(\text{ROH})$$

where $(\text{ROH})_0$, (ROH), (AcCl), k_1° and k_2 are the concentrations of the alcohol at time zero and t, that of the acyl chloride at time t, the first-order rate constant and the second-order rate constant respectively.

It has been reported in a preceding paper[1] that the initial rates of the esterifications between *l*-menthol and acetyl chloride in various solvents obey the second-order and the first-order rate laws with the alcohol and the acetyl chloride respectively and that the rates depend neither upon the dielectric constants nor upon the Z values[2] of the solvents. The rate constant in liquid sulfur dioxide is the largest, the reason for this has also been discussed.

However, the inspection of the conversion vs. time curve in liquid sulfur dioxide revealed that the order of the reaction varies gradually and that the reaction obeys the first-order rate law after the middle stage of the reaction has passed.

Since the reaction rate of acetyl chloride with menthol in liquid sulfur dioxide is so rapid, the rate constant has only been determined by an extrapolation method. In the present paper, a further investigation of the esterification has been undertaken on slower rate systems, the propionylation and *p*-methoxybenzoylation of *l*-menthol in various solvents, thus we hope to make an unambiguous scrutiny of the reaction mechanism.

The reaction processes in various solvents, from the initial stages through the completion of the reactions, have been examined and analyzed; we found that the first-and second-order esterifications take place simultaneously in some of the solvents used, such as acetonitrile, liquid sulfur dioxide and nitromethane. When nitromethane is used as the solvent, another phenomenon in addition to the simultaneous reactions has also been observed; this finding will be published elsewhere in the near future.

The simultaneous nucleophilic substitutions (S_N1 and S_N2), the so-called border-line cases, in liquid sulfur dioxide have already been reported by Ingold et al.[3], and the possibility of such a phenomenon has been discussed by Tokura and Kondo[4] in connection with the Menschutkin reaction in liquid sulfur dioxide. Moreover, the first-order reaction rates in acetonitrile and in liquid sulfur dioxide have been found to be enhanced by the initial concentration of the *l*-menthol

* Substitution in Liquid Sulfur Dioxide, Part V. Part IV: Ref. 1)

1) N. Tokura and F. Akiyama, This Bulletin, **37**, 1723 (1964).

2) E. M. Kosower, *J. Am. Chem. Soc.*, **80**, 3253 (1958).

3) M. L. Bird, E. D. Hughes and C. K. Ingold, *J. Chem. Soc.*, **1954**, 634.

4) N. Tokura and Y. Kondo, This Bulletin, **36**, 200 (1963).

employed. This means that the autocatalyses by the alcohol and/or the material produced from the alcohol are taking place in the esterification in these solvents.

Experimental

Solvents.—The following materials were purified by the methods described in the preceding paper[1] and were used as the solvents; liquid sulfur dioxide, chloroform, acetonitrile, benzene, ethyl methyl ketone, nitromethane and carbon tetrachloride.

Materials.—Commercial extra-pure-grade *l*-menthol was used without further purification; m. p. 41.5—43°C, $[\alpha]_D^{25}$ −47.6° (benzene). Preliminary examinations in liquid sulfur dioxide and in other solvents verified that the optical rotations of the solutions of *l*-menthol were stable over all the reaction times employed. Propionyl chloride was distilled, and the fraction boiling from 76.6 to 78.2°C was used. *p*-Methoxybenzoic acid and thionyl chloride (1 : 1.5 molar ratio) were heated together on a water bath for a half hour; the chloride produced was then distilled, the fraction with a b. p. of 132—133°C/11 mmHg being used.

The Identification of the Esters Obtained.—The reaction mixture after the esterification was concentrated in vacuo, and the residual oil was fractionated. The yield was almost quantitative. *l*-Menthyl propionate: b. p. 116°C/8 mmHg, $[\alpha]_D^{25}$ −82.18°, (benzene);

Found: C, 73.63; H, 11.64. Calcd. for $C_{13}H_{24}O_2$: C, 73.53; H, 11.39%.

l-Menthyl *p*-methoxybenzoate: b. p. 197°C/7 mmHg $[\alpha]_D^{25}=-80.0°$ (benzene);

Found: C, 74.87; H, 8.83. Calcd. for $C_{18}H_{26}O_3$: C, 74.44; H, 9.02%.

The specific rotations of *l*-menthyl propionate in various solvents are listed in the following table.

Table I. The specific rotations of *l*-menthyl propionate in solvents

Solvent	$-[\alpha]_D^{25}$ degree·dm^{-1}·g^{-1}·ml.
Liq.SO_2	79.04
Chloroform	84.19
Acetonitrile	77.25
Ethyl methyl ketone	78.86
Benzene	82.18
Nitromethane	80.44

The Kinetic Procedure.—The polarimetric procedure used for the kinetic followings was described earlier,[1] a graphic representation of the apparatus (a polarimeter equipped with a pressure-cell for use in the reaction in liquid sulfur dioxide) will also be found therein. *l*-Menthol dissolved in a solvent was placed in the cell. An acyl chloride in an ampoule was deposited in a cell situated in a polarimeter before a menthol solution was introduced. After the temperature equilibration of the apparatus containing the menthol solution in the thermostat had been attained, the ampoule in the cell was broken by a vigorous shaking and the solution was mixed. Then the kinetic following by means of polarimetry was began.

The Estimation of the Rate Constant.—The second-order rate constant, k_2, may be obtained from the slope of the linear plot:

$$\log\frac{(ROH)_0\{l([R]^\circ_E-[R]^\circ_A)(AcCl)_0-(\alpha-\alpha_0)\}}{(AcCl)_0(\alpha_\infty-\alpha)} \text{ vs. } t,$$

since

$$\frac{1}{(AcCl)-(ROH)_0}\times \ln\frac{(ROH)_0\{l([R]^\circ_E-[R]^\circ_A)(AcCl)_0-(\alpha-\alpha_0)\}}{(AcCl)_0(\alpha_\infty-\alpha)}=k_2\cdot t \quad (1)$$

where $(ROH)_0$ and $(AcCl)_0$ are the initial concentrations of the alcohol and the acyl chloride and $(R)^\circ_A$ and $(R)^\circ_E$ are the specific rotations of the alcohol and the ester in the solvents in degree·dm^{-1}·mol^{-1}·l. respectively. l, α, α_0 and α_∞ are the length of the cell, dm., and the rotations of the solution at time t, zero and infinity.

When equimolar concentrations of menthol and acyl chloride were used, the rate constant, k_2, was given by the slope of the linear plot of :

$$\frac{1}{\alpha_\infty-\alpha} \text{ vs. the time, } t,$$

since:

$$\frac{1}{\alpha_\infty-\alpha}-\frac{1}{\alpha_\infty-\alpha_0}=\frac{k_2\cdot t}{l[(R)^\circ_E-(R)^\circ_A]} \quad (2)$$

First-order Rate Constant.—The first-order rate constant, k_1, will be expressed as;

$$\ln\frac{\alpha_\infty-\alpha_0}{\alpha_\infty-\alpha}=k_1\cdot t \quad (3)$$

Therefore, the $-\log(\alpha_\infty-\alpha)$ vs. t plot will give a straight line, whose slope will be the value of k_1.

Typical Runs.—The second-order plots of the esterifications in chloroform, ethyl methyl ketone and benzene are visualized in Fig. 1. The second-order plots of the reactions in acetonitrile and in liquid sulfur dioxide are shown in Figs. 2 and 5, which show the deviations from linearity as the reactions proceed.

The first-order plots of the same esterifications are seen in Figs. 3 and 6, which again exhibit the deviations from linearity in the initial periods of the reactions.

Results

The Propionylation of *l*-Menthol.—In chloroform, ethyl methyl ketone, benzene and carbon tetrachloride, the esterification reactions strictly obey the second-order rate law throughout the reaction (Fig. 1). These results, together with the second-order rate constants in acetonitrile, in liquid sulfur dioxide and in nitromethane, are listed in Table II.

That the second-order rate law consists of the first order with both the alcohol and the acyl chloride has already been established[5]; evidence for this was also given in the previous paper.[1]

On the contrary, in acetonitrile, liquid sulfur dioxide or nitromethane, the apparent kinetic order of the reaction varies as the reaction proceeds.

5) J. F. Norris and A. A. Ashdown, *J. Am. Chem. Soc.*, **47**, 873 (1925).

TABLE II. THE SECOND-ORDER RATE CONSTANTS (k_2, $sec^{-1} \cdot mol^{-1} \cdot l.$) OF THE PROPIONYLATION OF *l*-MENTHOL IN VARIOUS SOLVENTS

Solvent	Reaction temp., °C				
	5	15	25	30	35
Liq.SO_2	2.11×10^{-2}	3.12×10^{-2}	4.70×10^{-2}		
Nitromethane			1.50×10^{-3}		
Chloroform		8.99×10^{-4}	1.35×10^{-3}		2.17×10^{-3}
Benzene		2.39×10^{-4}	4.40×10^{-4}	5.70×10^{-4}	
Carbon Tetrachloride			8.13×10^{-4}		
Acetonitrile		2.12×10^{-4}	3.33×10^{-4}		5.70×10^{-4}
Ethyl methyl ketone		4.21×10^{-5}	9.18×10^{-5}		2.29×10^{-4}

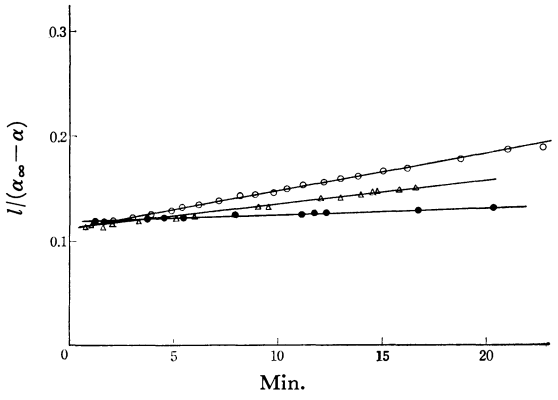

Fig. 1. Propionylation of *l*-menthol at 25°C.
-○- Chloroform
-△- Benzene
-●- Ethyl methyl ketone

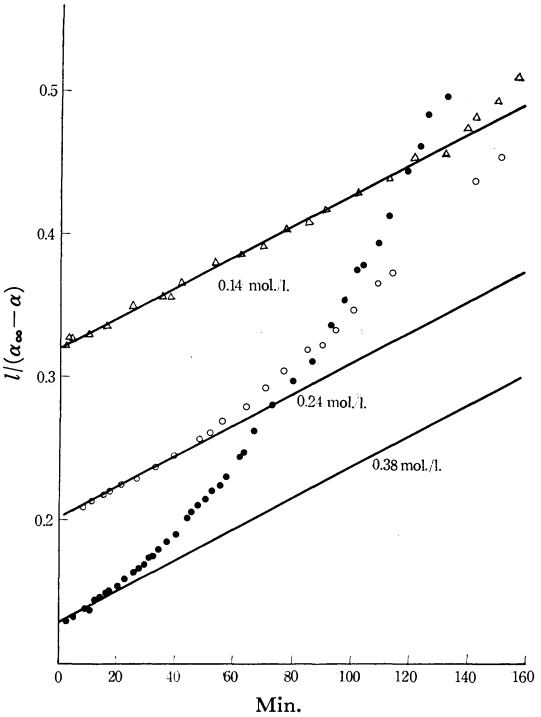

Fig. 2. Second-order plots in acetonitrile. 25°C

During the initial stage of the reaction, a second-order law was directive, this was followed by a gradual transition to an apparent first-order rate law, first order in acyl chloride and zero order in the alcohol. In the present paper, the findings and the discussion of the esterification in nitromethane are omitted, since another interesting feature has been found in nitromethane.

Propionylation in Acetonitrile.—As may be seen in Fig. 2, the second-order plot of the reaction deviates from linearity as the reaction proceeds. Figure 3 is the first-order plot of the esterification in the middle and the final periods of the reaction, following the first-order rate law.

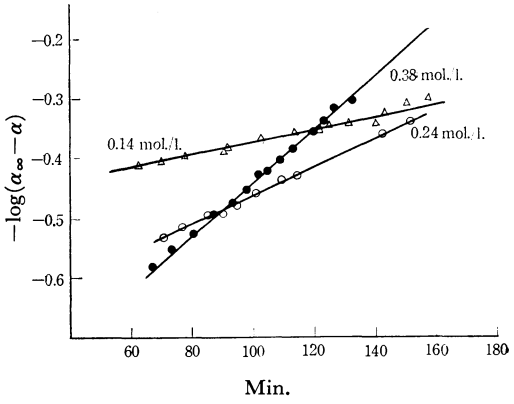

Fig. 3. First-order plots in acetonitrile. 25°C

The deviation from the second-order law is greatly affected by the initial concentration of the alcohol. Also, the rate constant of the first-order reaction is affected by the initial concentration of the alcohol, although the rate law is zero-th order in the alcohol concentration. The transition or the deviation points which are shown by the conversions from the second law, may be seen in Fig. 2 and are listed in Table III.

The larger the initial concentration, the earlier the transition point appears, as may be seen in Table III. The dependency of the rate constant, k_1 on the initial concentration is visualized in Fig. 4, which shows a linear correlation between k_1 and $(ROH)_0$.

Table III. First-order rate constants of the esterification in acetonitrile, 25°C
The dependence of thf rate constants on the initial concentrations

$(ROH)_0$ mol./l.	$(AcCl)_0$ mol./l.	k_1, sec^{-1}	Conversion at the transition point, %
0.14	0.14	3.85×10^{-5}	35
0.24	0.24	9.19×10^{-5}	18
0.36	0.24	1.43×10^{-4}	
0.38	0.38	1.63×10^{-4}	11
0.38	0.19	1.53×10^{-4}	
0.48	0.24	2.28×10^{-4}	
0.67	0.38	3.11×10^{-4}	

The rate expression, then, will be

$$\text{Rate} = k_1^\circ(\text{ROH})_0(\text{AcCl}) \quad (4)$$

since

$$k_1 = k_1^\circ(\text{ROH})_0 \quad (5)$$

while k_1° is estimated to be $k_1^\circ = 5.14 + 10^{-4}\ sec^{-1}\cdot mol^{-1}\cdot l.$ at 25°C.

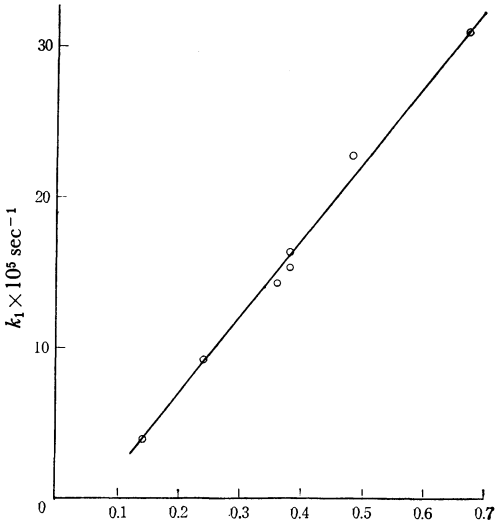

Fig. 4. Dependency of k_1 on $(ROH)_0$ in acetonitrile at 25°C.

Propionylation in Liquid Sulfur Dioxide.—The results resemble those in acetonitrile, but the transition to the first order occurs at a later period of the reaction, as may be seen in Fig. 5 and in Table IV. The first-order plots are also visualized in Fig. 6, which confirms a linear dependency on the initial concentration of menthol, as in the case of acetonitrile.

Table IV. The transition from the second-order law at 25°C in $Liq.SO_2$

Initial concn. mol./l.	Transition point conversion, %
0.27	76
0.13	78
0.11	81

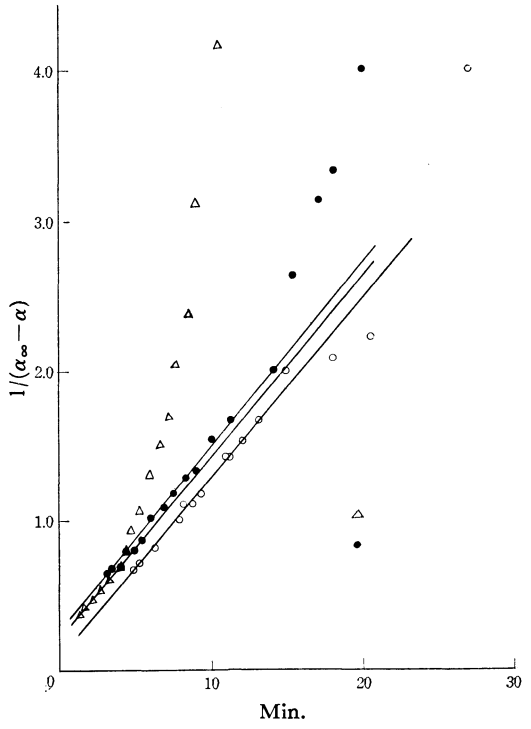

Fig. 5. Second-order plots in liquid sulfur dioxide. 25°C
△ 0.27 mol./l. ● 0.13 mol./l. ○ 0.11 mol./l.

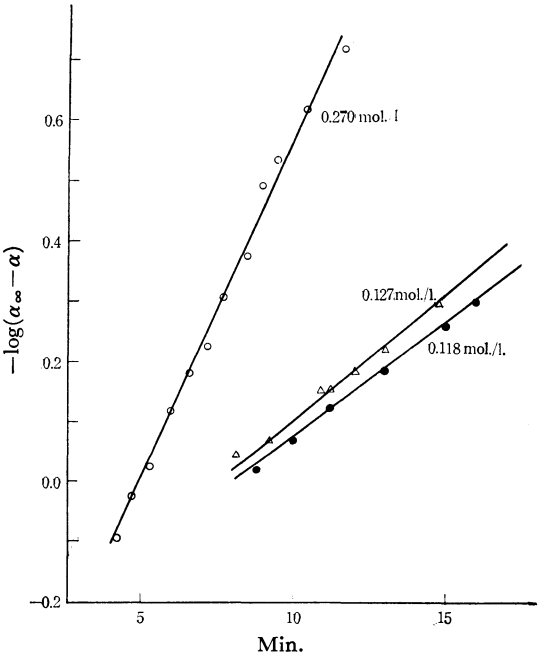

Fig. 6. First-order plots in liquid sulfur dioxide. 25°C

The higher the initial concentrations, the earlier

the deviations from the second-order rate law; however, in liquid sulfur dioxide the deviation occurs at a later stage, at over a 76% conversion, as is shown in Fig. 5.

Table V. First-order rate constants, k_1 in various initial concentrations of $(ROH)_0$ at 25°C

$(ROH)_0$, mol./l.	k_1, sec^{-1}
0.27	4.15×10^{-3}
0.133	1.72×10^{-3}
0.127	1.63×10^{-3}
0.120	1.46×10^{-3}

As is illustrated in Fig. 7 and Table V, the dependency of k_1 on $(ROH)_0$ in liquid sulfur dioxide is linear and the $k_1°$ value is given as;

$$\text{Rate}=k_1(\text{AcCl})$$
$$=k_1°(ROH)_0(\text{AcCl}) \quad (6)$$

since $$k_1=k_1°(ROH)_0 \quad (7)$$

$$k_1°=1.77\times10^{-2}\,sec^{-1}\cdot mol^{-1}\cdot l. \text{ at } 25°C$$

The Kinetic Parameter of the Second-order Reaction.— The activation parameters for the second-order reaction in various solvents as estimated from the

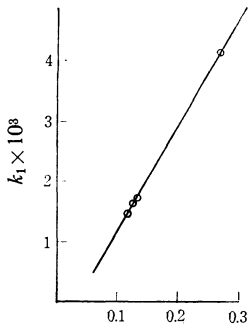

Fig. 7. Dependency of k_1 on $(ROH)_0$ in liquid sulfur dioxide at 25°C.

Table VI. The activation parameters of the esterification of *l*-menthol with propionly chloride in solvents

Solvent	$\Delta E^{\ddagger}$ kcal./mol.	$\Delta H^{\ddagger}$ kcal./mol.	$\Delta S^{\ddagger}$, e. u.
Liq. SO_2	6.57	5.98	−44.55
Chloroform	7.75	7.16	−47.6
Acetonitrile	8.53	7.94	−47.7
Benzene	11.40	10.81	−37.6
Ethyl methyl ketone	15.00	14.41	−28.52

Table VII. The activation parameters of the esterification of *l*-menthol with *p*-methoxybenzoyl chloride in Liq. SO_2 and $CHCl_3$

Solvent	$\Delta E^{\ddagger}$	$\Delta H^{\ddagger}$	$\Delta S^{\ddagger}$
liq. SO_2	10.07	9.48	−35.3
$CHCl_3$	17.96	17.37	−23.4

results in Table II are listed in Tables VI and VII.

Discussion

The results may be summarized as follows. The reactions, the propionylations and the *p*-methoxybenzoylations of *l*-menthol follow the second-order rate law in chloroform, benzene, ethyl methyl ketone and carbon tetrachloride at 25°C, as they do in the acetylations of *l*-menthol, which were reported on earlier.[1]

However, in acetonitrile or in liquid sulfur dioxide, the rate obeys the second-order rate law at the initial stage of the reaction, the second-order plot, deviates from linearity as the reaction proceeds, and gradually changes into a first-order rate reaction. The apparent transition or the deviation from the second-order rate law is prompted when the initial concentration of the alcohol is increased and acetonitrile is used as the solvent.

The inversion of the rate laws during an acylation in a solvent has not hitherto been reported, although the change in the rate orders in the acylation of an alcohol by solvents has been reported by Brown and Hudson.[6] The change in the reaction orders during a reaction course in a solvent, as is reported in the present paper, may be plausibly explained as the results of simultaneous reactions consisting of a first-order type and a second-order type reaction, such as have been frequently encountered and discussed in nucleophilic substitutions in various solvents[7] including liquid sulfur dioxide.[3] Thus, it may be shown by the following expression:

$$\text{Rate}=k_1(\text{AcCl})+k_2(\text{AcCl})(ROH) \quad (8)$$

or, for equimolar initial concentrations of the alcohol and the acyl chloride:

$$\text{Rate}=dx/dt=k_1(a-x)+k_2(a-x)^2 \quad (9)$$

where a and x are the concentrations of the alcohol initially added and of the ester formed respectively.

The integration of Eq. 9 gives this relation:

$$\log\frac{a-x}{a-x+k_1/k_2}=\frac{-k_1}{2.303}t+\log\frac{a}{a+k_1/k_2} \quad (10)$$

By substituting the values, k_1 and k_2, obtained experimentally into the left term of Eq. 10, the plots of $\log\frac{a-x}{a-x+k_1/k_2}$ vs. time t are linear, as is shown in Figs. 8 and 9, in both acetonitrile and liquid sulfur dioxide. The slopes of the respective plots are fairly coincident with the experimentally-attained values of k_1's in the range of experimental error.

6) D. A. Brown and R. F. Hudson, *J. Chem. Soc.*, **1953**, 883, 3352.

7) a) W. G. Young and L. J. Keefer, *J. Am. Chem. Soc.*, **66**, 421 (1944). b) V. Gold, ibid., **78**, 4633 (1956). c) Y. Pocker, *J. Chem. Soc.*, **1954**, 3939, 3943. d) P. Casapieri and R. E. Swart, ibid., **1961**, 4342.

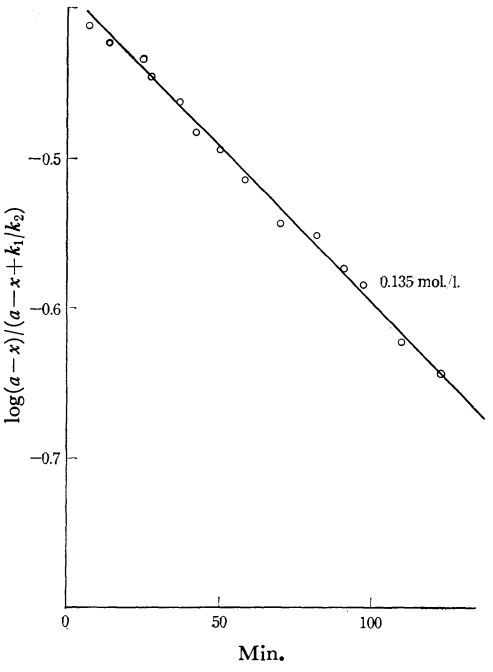

Fig. 8. Plots of the simultaneous reactions in acetonitrile at 35°C.

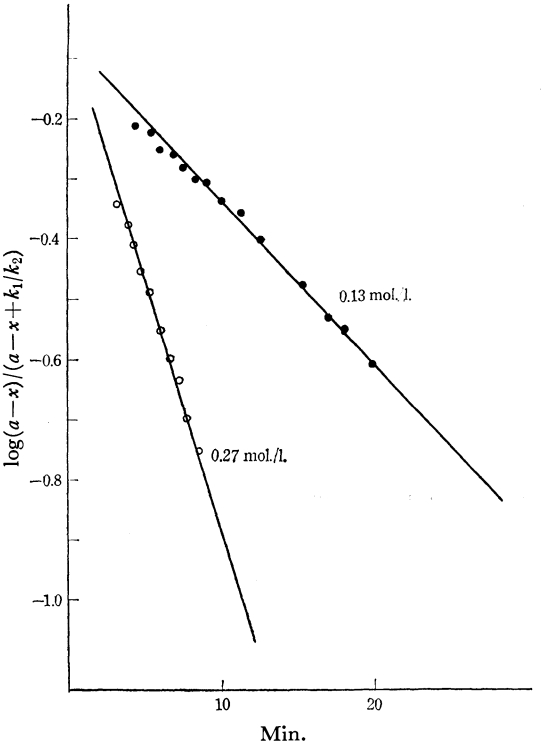

Fig. 9. Plots of the simultaneous reactions in liquid sulfur dioxide at 25°C.

These results satisfactorily confirm the assumption of the simultaneous nature of the reaction in two solvents.

Moreover, in both solvents the first-order rate constants, the k_1 values, are dependent upon the initial concentrations of the alcohol; the higher the initial concentration, the larger the first-order rate constant, as is shown in Figs. 4 and 7. This suggests that the alcohol and/or a compound produced from the alcohol (perhaps the ester or HCl) might be responsible for the apparent autocatalysis in the propionylation of the alcohol, and that the over-all kinetics of the reaction may be expressed as;

$$\text{Rate}=k_1^{\circ}(\text{AcCl})(\text{ROH})_0+k_2(\text{AcCl})(\text{ROH}) \quad (11)$$

	k_1°, $\text{sec}^{-1}\cdot\text{mol}^{-1}\cdot\text{l}.$	k_2, $\text{sec}^{-1}\cdot\text{mol}^{-1}\cdot\text{l}.$ at 25°C
Acetonitrile	5.14×10^{-4}	3.33×10^{-4}
Liq. SO_2	1.77×10^{-2}	4.70×10^{-2}

The multimolecularity of alcohol in the rate law of the esterification was first recognized by Ashdown[8] as early as in 1930 in his study of the ethanolysis of *p*-nitrobenzoyl chloride, where the reaction followed a third-order rate law, while it followed a second order in ethanol and a first order in the acyl chloride.

Ingold et al.[9] have also observed, in a nucleophilic substitution by ethanol in nitromethane, that the first-order rate constant is dependent on the initial concentration of the alcohol. The dependency of k_1 on the initial concentration of menthol $(\text{ROH})_0$ can be most adequately elucidated in terms of the solvation of the alcohol to enhance the rate-determining ionization of the acyl chloride.

The rate constants, both k_1 and k_2, are largest in liquid sulfur dioxide, as may be seen in Tables II, III and IV.

One might suspect that the expression 11 could be replaced by a simpler equation, such as;

$$\text{Rate} = k(\text{AcCl})(\text{ROH})_0 \quad (12)$$

since Eq. 12 is also consistent with the experimental fact that the reaction is second-order at the initial stage but soon changes to a first-order rate law. However, this rate equation is not adequate to explain the reaction in liquid sulfur dioxide where the second-order rate law predominates until a 80% conversion or so.

$(\text{ROH})_0$ can be explained in terms of the alcohol present in the reaction mixture and/or the compound produced as the result of the reaction of the alcohol in an equivalent molarity, such as that of the ester or of HCl.

An inspection of Table II will reveal that the second-order esterifications are more reactive in the electrophilic solvent than in the electrodonative solvent, suggesting that the rate-determining step is the formation of an ionic compound such as:

8) A. A. Ashdown, *J. Am. Chem. Soc.*, **52**, 269 (1930).
9) E. Gilles, E. D. Hughes and C. K. Ingold, *J. Chem. Soc.*, **1954**, 2918.

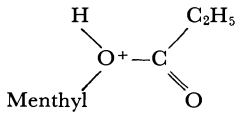

It is interesting to note that, in both acetonitrile and liquid sulfur dioxide, which are the two extreme solvents (viz., a Lewis base and a Lewis acid), the reactions are simultaneous. One explanation for this is that acylium ions (RCO^+) are formed in an appreciable amount in these dipolar aprotic solvents with large polarities:

$$RCOCl \rightleftarrows RC^+O+Cl^-$$

Summary

The propionylation and *p*-methoxybenzoylation of *l*-menthol in various solvents have been studied. In chloroform, benzene, ethyl methyl ketone and carbon tetrachloride, and at the initial stages of the reaction courses in acetonitrile and in liquid sulfur dioxide, the reactions follow the second-order rate law. However, in acetonitrile or liquid sulfur dioxide, the rate gradually varies from the second-order type to the first-order type apparently as the reaction proceeds.

The phenomena in both solvents have been elucidated as resulting from simultaneous unimolecular and bimolecular reactions. Moreover, the first-order rate constants in both acetonitrile and liquid sulfur dioxide, are dependent on the initial concentration of the alcohol.

The over-all rates in the two solvents are expressed as:

$$\text{Rate}=k_1^\circ(\text{AcCl})(\text{ROH})_0+k_2(\text{AcCl})(\text{ROH})$$

The rate constants in liquid sulfur dioxide, both k_1 and k_2, are the largest among those in the solvents used.

The authors are indebted to the Seitetsu Kagaku Co., Ltd., for its donation of liquid sulfur dioxide.

BULLETIN OF THE CHEMICAL SOCIETY OF JAPAN VOL. 39 137—140 (1966)

The Adsorption Equilibria of DL-Mandelic Acid on Starch in an Aqueous Phase

By Masaaki OHARA, Chau-Yang CHEN and Takao KWAN

Division of Physicochemical Technology, Faculty of Pharmaceutical Sciences, The University of Tokyo, Hongo, Tokyo

(Received May 25, 1965)

The selective adsorption of D- or L-mandelic acid on starch from an aqueous solution of racemate has been quantitatively investigated. L-Mandelic acid has been judged from the distinct negative value of the optical rotation in the solution to be adsorbed preferentially over the D-isomer. The separation factor for the adsorption of the two enantiomers was 1.06 ± 0.02 at 0°C. From the saturation value estimated by the Langmuir equation for adsorption, the ratio of the glucose residue to the DL-mandelic acid adsorbed has been calculated as 5, indicating that not all the glucose residues in the starch constitute adsorption sites for mandelic acid.

The asymmetric adsorption of racemate on optically active adsorbents has so far been studied by the batch adsorption or the chromatographic technique.[1] Despite the effort devoted to this subject, however, little progress has been made in the quantitative estimation of the stereospecific adsorption of optical antipodes. The lack of the observation of large rotation angles and the absence of a distinct difference in adsorption between enantiomers in the systems investigated have hampered any further clarification of this subject, although several reliable and somewhat systematic attempts using the batch method have been reported for such systems as wool - DL-mandelic acid,[2] and silica-gel - DL-*s*-butanol.[3]

It has been investigated by several authors,[4] and well established in this laboratory,[1] that starch, when used as an optically active column packing, takes up the L-(+)-isomer selectively

1) See, for example, M. Ohara, I. Fujita and T. Kwan, This Bulletin, **35**, 2049 (1962); M. Ohara, K. Ohta and T. Kwan, ibid., **37**, 76 (1964).

2) W. Bradley and G. C. Easty, *J. Chem. Soc.*, **1951**, 499; ibid., **1953**, 1519; W. Bradley and R. A. Brindley, ibid., **1956**, 1622; W. Bradley, R. A. Brindley and G. C. Easty, *Discussions Faraday Soc.*, **No. 16**, 152 (1954).

3) E. I. Klabunovskii, A. E. Agoronomov, L. M. Volkova and A. A. Balandin, *Izv., A. N. S. S. S. R. Otd. Chim. Nauk.*, **1963**, 228.

4) H. Krebs, J. Diewald and J. A. Wagner, *Chem. Ber.*, **89**, 1875 (1956); W. Lautsch and D. Heinicke, *Kolloid Z.*, **154**, 1 (1957); D. Braun, "Anomalien bei Ionenaustauschvorgängen," Ionenaustauscher in Einzeldarstellungen, Bd. 2, Vol. I, Akademie-Verlag, Berlin (1962), p. 393.

through the passage of DL-mandelic acid from an aqueous solution. The selective adsorption of this kind has now been further investigated by utilizing a batch technique. In this paper, we will report on the first quantitative investigation on the adsorption equilibria of DL-mandelic acid on starch, in which the separation factor of the isomers is evaluated as 1.06 ± 0.02 at the temperature of 0°C.

Experimental

Materials.—Commercial DL-mandelic acid of a high grade was used (m. p. 118°C). The elementary analysis showed:

Found: C, 63.28; H, 5.32; O, 31.40. Calcd. for $C_6H_8O_3$: C, 63.15; H, 5.30; O, 31.55%.

Potato starch of a reagent grade was used without special pretreatment. It contained 18 ± 0.1% moisture.

General Procedure.—Samples of starch, weighing 18 g., 13.5 g., 9 g. and 4.5 g., were immersed in a 50 ml. Erlenmeyer flask equipped with a stopper. The closed flask was then kept at 0°C for 48 hr. with occasional agitation until equilibrium was attained. After the starch had been allowed to settle, the supernatant liquid equilibrated was withdrawn; the optical rotation of the solution α_D^{15} was then determined in a 10 cm. tube in a Yanagimoto Model OR-20-type photomagnetic polarimeter within a ±0.002 accuracy. The concentration of the acid was determined by means of the optical absorption at 257 mμ.

Results

First, the adsorption of DL-mandelic acid on starch was studied by means of the optical rotatory dispersion. The results were compared with those of the two control experiments. Hence the systems studied were:

1) 10 w/v% DL-mandelic acid aqueous solution (30 ml.) - untreated starch (18 g.)
2) water (30 ml.) - starch (18 g.)
3) 14.3 w/v% glycolic acid aqueous solution* (30 ml.) - starch (18 g.).

The optical rotatory dispersion was determined in a 5 cm. tube on a Nippon Bunko Model ORD/UV-5-type recording spectrophotometer. In Fig. 1

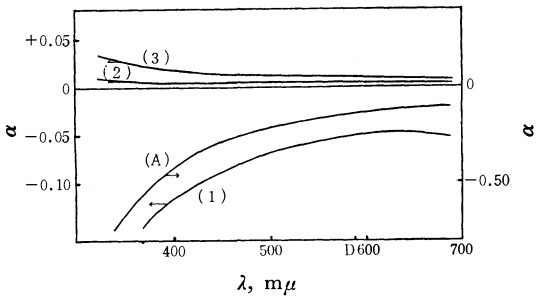

Fig. 1. The optical rotatory dispersion curves of DL-mandelic acid solution (1), water (2) and glycolic acid solution (3) in contact with starch as compared with that of D-(−)-mandelic acid (A).
Cell length: 5 cm.
Temp. : 12—14.5°C
D : Sodium D line

the observed curves are compared with that of authentic D-(−)-mandelic acid.

The curve 3 bends slightly to the (+) side, while the curve 2 indicates no definite rotation, suggesting that glycolic acid slightly decomposes or extracts the optically active starch component. On the other hand, the curve 1 bends on a large scale to the (−) side, as does that of the authentic sample. The difference between 1 and 3 gives a (−) sign of rotation; this may be ascribed to the net rotation value of mandelic acid in a solution. It is apparent, therefore, that L-(+)-mandelic acid is preferentially adsorbed from the racemate solution. This finding is consistent with those revealed by the column chromatography.[1]

Let us proceed to the principal subject. It was previously confirmed that the adsorption of DL-mandelic acid on starch reaches an equilibrium within 8 hr. at 0°C. However, the equilibrium data were recorded after the solution had been left standing over 2 days. By carying the amount of DL-mandelic acid, on the one hand, and the amount of starch on the other, the adsorption isotherm was determined as usual at the temperature of 0°C. Table I lists some of the adsorption data,

TABLE I. ADSORPTION EQUILIBRIUM DATA OF DL-MANDELIC ACID ON STARCH (T=0°C)

Sample No.	C_i	C_e	Amount adsorbed	Optical rotation of solution		$\Delta W/W$	f
	mg./ml.	mg./ml.	mg.	α_D^{15}	$[\alpha]_D^{15}$	%	
B1	25.05	21.8	137	−0.017	−0.78	2.2	1.05
B2	50.0	43.8	265	−0.036	−0.82	2.4	1.06
B3	74.5	66.5	360	−0.045	−0.68	2.2	1.05
B4	100.3	91.8	420	−0.060	−0.66	2.6	1.06
D1	25.05	19.7	232	−0.035	−1.8	2.5	1.07
D2	50.0	39.4	461	−0.061	−1.6	2.2	1.07
D3	74.5	61.4	614	−0.082	−1.3	2.2	1.06
D4	100.3	84.2	785	−0.103	−1.2	2.2	1.06

* Glycolic acid was chosen as the control sample, since (1) it is of almost the same acidity as mandelic acid; (2) it has a chemical structure similar to that of mandelic acid, and (3) it is an optically-inactive organic acid.

obtained along with parameters estimated therefrom.

In Table I, the signs B and D stand for the amount of starch used, 9 g. and 18 g. respectively, while C_i and C_e are the initial and equilibrium concentrations of the acid respectively. To determine the amount of mandelic acid adsorbed, W, the usual method would be to measure the change in the concentration of the solution after equilibrium. However, this method was thought to be inadequate for the present investigation, as the untreated starch, which contains 18% moisture, sorbs addition water, Consequently, W was estimated from the following revised equation:

$$W=30C_i-(30-Gw)C_e$$

where G is the amount of the untreated starch and w, the volume of the additionally sorbed water (ml.) per gram of the untreated starch. It was estimated at about 0.2 ml. from the difference between the amount of moisture in the untreated starch and that of water bound to potato starch suspended in an aqueous solution. The amount of bound water, about 33%, was based upon the data in the literature.[5] ΔW is the difference between enantiomers in the amount of mandelic acid adsorbed, and f is the separation factor, which will be defined later.

The net angle of rotation of mandelic acid in the solution is indicated in the 5 th column of Table I. These values were corrected for the rotation due to the optically active starch component produced by the interaction of the acid with starch. In Table II typical data are given on the interaction of an acid with starch.

Table II. α_D^{15} of the glycolic acid solution in contact with starch (T=0°C)

Concn. of glycolic acid mg./ml.	Weight of starch g.	Reaction time hr.	α_D^{15} of the solution after reaction
143	4.5	48	+0.001
143	9.0	48	+0.003
143	13.5	48	+0.006
143	18.0	48	+0.009

It was recognized that the α_D^{15} of the solution was little dependent on the concentration of the glycolic acid, but very dependent on the amount of starch used.

Using the data of Table I, the adsorption isotherm of DL-mandelic acid on starch is plotted in Fig. 2. The equilibrium concentration of the acid was in the range from 3.1 to 95 mg./ml.

The limited solubility of the acid did not permit the observation of the adsorption over the higher equilibrium concentrations. However, the Langmuir equation, $W=W_m bC_e/(1+bC_e)$, seemed to apply to the observed data. The Langmuir

5) F. Schierbaum and K. Täufel, *Die Stärke*, **15**, 161 (1963).

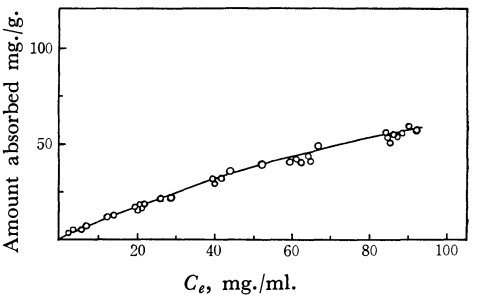

Fig. 2. Adsorption isotherm of DL-mandelic acid on starch at 0°C.

equation may be tested by arranging it in the form:

$$C_e/W=C_e/W_m+1/bW_m$$

In Fig. 3 plots of C_e vs. C_e/W are shown. They yield approximately a straight line. From the slope $1/W_m$, a reciprocal of the saturated amount of adsorption can be calculated. It was found to be W_m=188 mg.

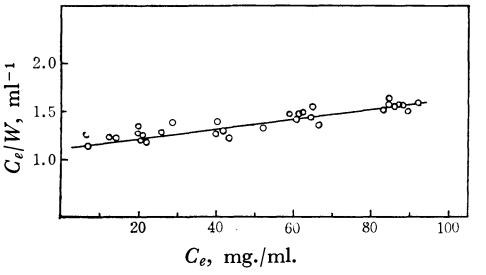

Fig. 3. Adsorption isotherm of DL-mandelic acid plotted according to the Langmuir equation.

The amounts of D- or L-isomers adsorbed on the surface of the starch were computed from the data of the specific rotation in the solution. The concentration of each isomer in the solution may be calculated by assuming that the additivity rule holds between $[\alpha]_D$ and the composition of each isomer, and that the $[\alpha]_{DP}$ of the acid is independent of the concentration. Here, $[\alpha]_{DP}$ is the specific rotation of optically pure mandelic acid. The difference between enantiomers in the amount adsorbed may be expressed as:

$$\Delta W=W_d-W_l=(30-Gw)C_e \mid [\alpha]_D/[\alpha]_{DP} \mid$$

where W_d and W_l are, respectively, the amount of the L- or D-isomer adsorbed. Consequently, $\Delta W/W$ may be obtained as:

$$\Delta W/W=(30-Gw) \mid [\alpha]_D/[\alpha]_{DP} \mid C_e/W$$

The substitution of 0.2 and $\pm$157 for w and $[\alpha]_{DP}$ respectively in the above equation yields a $\Delta W/W$ value for each G, values which range between 2.1% and 2.6%. These values are shown in the 7 th column of Table I.

Finally, the separation factor, f, as defined by the ratio of the adsorption equilibrium constants of the isomers, is expressed as:

$$f=\frac{W_d/C_{ed}}{W_l/C_{el}}=\frac{1+|[\alpha]_D/[\alpha]_{DP}|}{1-|[\alpha]_D/[\alpha]_{DP}|}\times\frac{1+\Delta W/W}{1-\Delta W/W}$$

where C_{ed} and C_{el} are the concentrations of L- and D-isomers respectively in the liquid phase at equilibrium.

On the basis of this equation, f may be estimated to be 1.06 ± 0.02. The values of f are presented in the last column of Table I.

Discussion

It is interesting to note that the adsorption of mandelic acid on starch obeys the Langmuir equation. This would mean that the surface of starch is rather homogeneous for the adsorption of mandelic acid, and that no interaction between the adsorbed molecules is present. The saturation value for the adsorption was found, according to the Langmuir equation, to be 188 mg./g. starch. This value corresponds to 7.4×10^{20} molecules. Since one gram of starch consists of about 3.7×10^{21} glucose residues, the following stoichiometric relation may hold at saturation:

Glucose residue: Mandelic acid $\approx$ 5 : 1

Let us discuss the problem in connection with bound water. In a series of investigations bearing the title of "The Hydration of Starch," Schierbaum and Täufel have definitely shown that bound water in the starch may be distinguished from free water. The literature[5] estimates the amount of bound water to be 32.5—33.8% for potato starch. This value corresponds to:

Glucose residue : Water molecule $\approx$ 1 : 4

The logical sites for the adsorption of mandelic acid or water seem to be the hydroxyl groups of the starch. If so, three available sites are found in each glucose residue. It may be suggested, therefore, that not all glucose residue are effective in the adsorption of mandelic acid, and that bound water occupies almost all the active sites.

The surface area of starch effective in the adsorption of mandelic acid may be evaluated from the saturation value.

Assuming that the molecular shape of mandelic acid is a sphere, the molecular area, σ_m, of acid is estimated to be:

$$\sigma_m=34 \text{ sq. Å}$$

Consequently, the surface area is given by $S=250$ m^2/g.

The surface area of potato starch was determined by Hellman and Melvin[6] by the BET method, using nitrogen as the adsorbate at -195°C. Accordingly, the area was 0.11 m^2/g. The same author found that the surface area of the same starch was about 300 m^2/g. when the adsorption of water vapor was applied to the BET plot at 25°C.

The amount of water adsorbed at the monolayer, according to these authors, corresponded to:

Glucose residue : Water molecule $\approx$ 1 : 1

Therefore, the amount of bound water is about four times as great as that of the monolayer.

The discrepancy between the BET area obtained by the nitrogen adsorption at -195°C and that due to the water adsorption at room temperature is well known in the surface area of organic high polymers, such as cellulosic fibers and proteins[7] and coal[8]. In Table III the surface areas of some organic polymers as determined by the nitrogen adsorption method and by the water (methanol) adsorption method are compared, using those of titanium dioxide (anatase) as a reference sample.

TABLE III. THE SURFACE AREA OF SOME ORGANIC HIGH POLYMERS AS DETERMINED BY DIFFERENT METHODS

Material	Area Determined by nitrogen at -195°C m^2/g.	Area Determined by water at 25°C m^2/g.	Lit.
Potato starch	0.11	296	6
Wool	0.96	206	7
Cotton	0.76	108	7
Nylon	0.31	45.0	7
Coal	0.1—10	20—200**	8
Titanium dioxide	7.90	7.0	7

Obviously, the nitrogen adsorption method at -195°C would be inadequate for the measurement of the surface area of organic polymers. On the other hand, the surface area of starch, estimated from the saturation of the mandelic acid adsorption, is not very different from that of water adsorption as determined by Hellman and Melvin. The adsorption of mandelic acid on starch is probably to be considered as a kind of inclusion of the adsorbate molecule on the internal surface of starch.

The difference in the adsorption of D- and L-mandelic acid, established in this paper, must be investigated further with regard to the structural correlation of the adsorbate molecule with starch.

The authors wish to express their gratitude to Professor Syun-ichi Yamada and Dr. Kazuo Achiwa of The University of Tokyo for letting them use both the ORD spectrophotometer and the polarimeter.

6) N. N. Hellman and E. H. Melvin, *J. Am. Chem. Soc.*, **72**, 5186 (1950).

7) J. W. Rowen and R. L. Blaine, *Ind. Eng. Chem.*, **39**, 1659 (1947).

8) D. W. Van Krevelen and J. Schuyer, "Coal Science," Elsevier Publishing Company, Amsterdam (1957), p. 129.

** Determined by methanol.

BULLETIN OF THE CHEMICAL SOCIETY OF JAPAN VOL. 39 141—145 (1966)

Organic Syntheses by Means of Noble Metal Compounds. XIV. The Carbonylation of Cyclooctadienes

By Jiro Tsuji, Shuntaro Hosaka, Jitsuo Kiji and Tosaku Susuki

Basic Research Laboratories, Toyo Rayon Company, Kamakura

(Received May 27, 1965)

The 1, 5-cyclooctadiene - palladium chloride complex and carbon monoxide react in ethanol to form ethyl 4-cyclooctenecarboxylate. The carbonylation of 1, 5-cyclooctadiene catalyzed by palladium chloride has given ethyl 4-cyclooctenecarboxylate and cyclooctanedicarboxylate. It has been found that the monoester can be obtained selectively under certain conditions; the further carbonylation of the monoester gives the diester. Under the same reaction conditions, 1, 3-cyclooctadiene gives ethyl 2-cyclooctenecarboxylate in a low yield. Metallic palladium has been found to be the true catalyst and the presence of hydrogen chloride has been found to be essential for the catalysis. It has also been found that the 1, 5-cyclooctadiene - palladium chloride complex can be formed from 1, 5-cyclooctadiene, metallic palladium and hydrogen chloride by heating them in an autoclave under nitrogen. It seems likely that the catalytic carbonylation of 1,5-cyclooctadiene proceeds through the formation of the 1,5-cyclooctadiene - palladium chloride complex.

Previous work in this series has shown that palladium chloride complexes of simple olefins,[1] allylic compounds,[2,3] and conjugated dienes[4] can be carbonylated easily to form saturated or unsaturated esters in an alcoholic solution, and acid chlorides in a benzene solution. In the present paper, we wish to report the carbonylation of the 1, 5-cyclooctadiene (1, 5-COD) - palladium chloride complex (I). It was of special interest to study the carbonylation of 1, 5-COD complex in view of the fact that the complex is unusually stable and has a monomeric structure which is different from halogen-bridged olefinic and π-allylic complexes of palladium chloride.[5] In addition, the direct carbonylation of 1, 5-COD to form a mono- or a di-ester in the presence of a catalytic amount of palladium chloride seemed to be worthy of study.

Experimental

The NMR spectra were determined with high-resolution spectrometer, models DP 60 and HR 100, using tetramethylsilane as an internal standard; the peak positions are expressed in terms of τ values. Gas chromatographic analyses were carried out on a Thermol-3 column, 2 m. long, at 220°C for higher-boiling products, or on a Silicone DC 550 columm, 2 m. long, at 180°C for lower-boiling products. All boiling points are uncorrected. The molecular weights were determined in benzene using a Mechrolab vapor-pressure osmometer, or by mass spectroscopy.

Materials. — Commercially available anhydrous palladium chloride was used without further purification. Carbon monoxide (99.5% pure) was purchased from the Matheson Co., U.S.A. 1, 5-COD was also a commercial product (99% pure). 1, 3-COD was prepared from 1, 5-COD by Devaprabhakara's method.[6]

3-Bromocyclooctene was prepared by refluxing a mixture of cyclooctene (80 g.), N-bromosuccinimide (110 g.), benzoyl peroxide (0.2 g.), and carbon tetrachloride (400 ml.) for 1 hr. The product (b. p. 73—75°C/ 7mmHg) was obtained in a 69% (96 g.) yield.

The Carbonylation of 1, 5-COD in Ethanol.— The reaction conditions are given in Table I. The general procedure is as follows. To avoid the effect of the metal surface of a stainless steel autoclave, the reaction was carried out in a glass vessel with a gas-inlet capillary. In the glass vessel, a mixture of ethanol (or an ethanolic solution of hydrogen chloride), 1, 5-COD, and palladium chloride (or metallic palladium, or palladium acetylacetonate) was placed; the vessel was then set in the autoclave. Then carbon monoxide was introduced (100 kg./cm^2), and the mixture was shaken at 100°C for a certain period of time. After the reaction, the reaction mixture was poured into five times its volume of water, and the solution was extracted several times with ether. The ethereal solution was dried over anhydrous magnesium sulfate. Distillation under reduced pressure gave COD (40°C/14 mmHg), the monoester (102°C/15 mmHg), and the diesters (143°C/4 mmHg). The recovered COD consisted of 1, 5- and 1, 3-isomers. Their relative amounts varied

1) J. Tsuji, M. Morikawa and J. Kiji, *Tetrahedron Letters*, **1963**, 1061; *J. Am. Chem. Soc.*, **86**, 4851 (1964).
2) J. Tsuji, J. Kiji, S. Imamura and M. Morikawa, *Tetrahedron Letters*, **1963**, 1811; *J. Am. Chem. Soc.*, **86**, 4350 (1964).
3) R. Long and G. H. Whitfield, *J. Chem. Soc.*, **1964**, 1852.
4) J. Tsuji, J. Kiji and S. Hosaka, *Tetrahedron Letters*, **1964**, 605.
5) For general reference, see E. O. Fischer and H. Werner, "Metall π-Komplexe mit di- und oligoolefinischen Liganden," Verlag Chemie, Weinheim (1963).
6) D. Devaprabhakara, C. G. Cardenas and P. D. Gardner, *J. Am. Chem. Soc.*, **85**, 1553 (1963).

with the reaction conditions. Ethyl 4-cyclooctenecarboxylate was converted into crystalline amide by heating it with excess concentrated ammonia in a sealed tube at 100° for 10 hr; m. p. 203°C[7] (from ethanol). When the ester was hydrogenated in ethanol in the presence of palladium on carbon, ethyl cyclooctanecarboxylate was obtained (b. p. 120°C/20 mmHg.). On hydrolysis with 15% alcoholic potassium hydroxide, cyclooctane-carboxylic acid was obtained (b. p. 110—120°C/1 mmHg). The acid was converted into acid chloride by treatment with oxalyl chloride in benzene. The crude acid chloride was converted into amide by treatment with ammonia; m. p. 194—196°C (from ethanol) reported m. p. 195.8°C),[8] hydrazide, m. p, 67—68°C.

The Carbonylation of Cyclooctene.—To a mixtrue of 30 ml. of ethanol, 3g. of palladium chloride, and 17 g. of cyclooctene in a glass vessel set in the autoclave, carbon monoxide was introduced (97 kg./cm^2); this mixture was then shaken at 100°C for 25 hr, After the usual work-up, 8.4 g. of cyclooctanecarboxylate was collected by distillation (108—115°C/14 mmHg). The ester was converted into crystalline amide in the manner described above.

The Carbonylation of 1, 3-COD.—A mixture of 1, 3-COD (16 g.), ethanol (30 ml.), and palladium chloride (5 g.) was allowed to react under 155 kg./cm^2 of carbon monoxide at 100°C for 23 hr. After the usual work-up, distillation gave 1, 3-COD (4.3 g., 50—75°C/46 mmHg) and crude ester (5.0 g., 75—145°C/46 mmHg). The purification of the crude ester by preparative gas chromatography gave ethyl 2-cyclooctenecarboxylate and a small amount of 3-ethoxycyclooctene. Analytical results of the monoester;

Found: C, 72.21; H, 9.89; mol. wt., 184. Calcd. for $C_{11}H_{18}O_2$; C, 72.49; H, 9.96%; mol. wt., 182.

NMR spectrum: 8.77 (triplet, 3 methyl protons), 8.44 (multiplet, ring methylenes), 7.92 (multiplet, 2 allylic protons), 6.70 (multiplet, 1 proton at the carbethoxy-bearing carbon), 5.95 (diffuse quartet, 2 protons $-O-CH_2-$), and 4.34 (multiplet, 2 vinyl protons). Ethyl 2-cyclooctenecarboxylate was converted into amide by treating it with ammonia in a sealed tube at 100°C for 10 hr; m. p. 185—186°C (from ethanol).

Found: C, 70.50; H, 9.87; N, 9.11. Calcd. for $C_9H_{15}O_1N$; C, 70.55; H, 9.87; N, 9.14%.

3-Ethoxycyclooctene was identified, by means of its NMR and infrared spectra, with an authentic sample prepared by refluxing 3-bromocyclooctene with sodium ethoxide in ethanol. Mol. wt., Found: 154 (mass spectroscopy). Calcd. for $C_{10}H_{18}O_1$: 154.

The ether had the following NMR peaks; 8.87 (triplet, 3 methyl protons), 8.51 (diffuse multiplet, ring methylenes), 7.87 (multiplet, 2 allylic protons), 6.65 (multiplet, 2 protons $-O-CH_2-$), 5.91 (multiplet, 1 proton $-CH-O-$), and 4.52 (multiplet, 2 vinyl protons). Two protons of the ethoxy (5.91) and carbethoxr groups (5.95) do not show a clear quartet, because of the effect of the neighboring asymmetric carbon (the carbethoxy- or ethoxy-bearing carbon). A similar observation has been reported with cortisone acetate.[9]

In addition, 1.5 g. of unidentified diester (mol. wt., 240) was obtained.

The Carbonylation of 3-Bromocyclooctene.—A mixture of 3-bromocyclooctene (8 g.) and palladium chloride (1.8 g.) in ethanol (60 ml.) was allowed to react under 92 kg./cm^2 of carbon monoxide at 100°C for 14 hr. The crude product then obtained by distillation (62—94°C/5 mmHg) was purified by preparative gas chromatography; 3-ethoxycyclooctene (yield based on 3-bromocyclooctene 16.9%) and ethyl 2-cyclooctenecarboxylate (yield 36.4%) were thus obtained.

The Carbonylation of the 1, 5-COD Complex.—The complex (15 g.) was suspended in 30 ml. of ethanol in a glass vessel. Carbon monoxide was then introduced (100 kg./cm^2), and the mixture was shaken for 24 hr. at 110°C. After the usual work-up, 2.4 g. of crude monoester (100—120°C/21 mmHg), together with a small amount of 1, 5-COD, was obtained. Further distillation gave 0.3 g. of the diesters (140°C/5 mmHg).

The Formation of the 1, 5-COD Complex from Metallic Palladium.—In a glass vessel, 20 ml. of a 15% alcoholic solution of hydrogen chloride, 0.2 g. of palladium black, and 8 ml. of 1, 5-COD were mixed. The mixture was then shaken in the autoclave at 110°C under a nitrogen atmosphere (40 kg./cm^2). After 18 hr., a yellow precipitate contaminated with palladium black was collected by filtration and recrystallized from acetic acid to give 0.12 g. of the 1, 5-COD palladium chloride complex. The complex was identified by a comparison of its infrared spectrum with that of an authentic sample.

Found: C, 33.76; H, 4.28; Cl, 24.62. Calcd. for $C_8H_{12}Pd_1Cl_2$: C, 33.62; H, 4.23; Cl, 24.80%.

The recovered COD consisted of a 1 : 2.3 muxture of 1, 5- and 1, 3-isomers.

The Carbonylation of Di-μ-chloro-bis(8-methoxycyclooct-4-enyl)-dipalladium.—This complex was prepared by the treatment of the 1, 5-COD complex with sodium carbonate in methanol following the method of Chatt et al.[10] To a suspension in the autoclave of the complex (5.5 g.) in 50 ml. of benzene, carbon monoxide was introduced (50 kg./cm^2). The mixture was then stirred at 60°C for 20 hr. After the reaction, the palladium which had precipitated was removed. An infrared spectrum of the crude solution showed an absorption band at 1735 cm^{-1} due to an ester. No absorption at 1800 cm^{-1} due to an acid chloride was observed. To ensure the conversion of an acid chloride, if present, into an ester, the solution was then refluxed with 10 ml. of methanol for 30 min. When the solvent was removed, 1.2 g. of an oily residue was obtained. Gas chromatographic analysis showed the presence of two main products, which were separated by preparative gas chromatography. The first fraction was identified as 1, 5-COD. The second fraction was determined to be methyl 8-methoxy-4-cyclooctenecarboxylate.

Found: C, 66.39; H, 9.03 mol. wt. 198. Calcd. for $C_{11}H_{18}O_3$: C, 66.64; H, 9.15%; mol. wt. 198.3.

The NMR spectrum had the following peaks; 4.43τ (multiplet, 2 vinyl protons), 6.43τ (singlet, methyl protons of the ester,), 6.79τ (singlet methoxy protons),

7) G. Stork and H. K. Landesman, *J. Am. Chem. Soc.*, **78**, 5129 (1956).

8) A. C. Cope, M. Grug and S. W. Fenton, ibid., **74**, 174 (1952); E. Muller and H. Hubner, *Chem. Ber.*, **96**, 670 (1963).

9) J. N. Shoolery and M. T. Rogers, *J. Am. Chem. Soc.*, **80**, 5121 (1958).

10) J. Chatt, L. M. Vallarino and L. M. Venanzi, *J. Chem. Soc.*, **1957**, 3413.

7.28τ (multiplet, proton at the carbomethoxy-bearing carbon), 6.5τ (multiplet, 1 proton at the methoxy-bearing carbon), broad multiplets centered at 7.8 (4 allylic protons), and 8.24 (4 ring methylene protons). Furthermore, a small amount of methyl 4-cyclooctene-carboxylate was detected.

The Conversion of Ethyl 4-Cyclooctenecarboxylate (II) into Ethyl 3-Carbethoxyl-2-oxocyclopentanepropionate.—Fourteen grams of II were oxidized by the drop-by-drop addition of 220 ml. of a sodium permanganate solution (12%) for 3 hr., with the occasional addition of small pieces of dry ice. After the oxidation, sulfur dioxide gas was passed through until the solution became clear. Then the product was extracted with ether. The ether was then evaporated, and the residue was esterified in a mixture of benzene and ethanol by the azeotropic method. The benzene and ethanol were then evaportaed; the distillation of the residue gave 9 g. of ethyl 1, 3, 6-hexanetricarboxylate (b. p. 145—152°C/2 mmHg. Found: mol. wt., 293, Calcd. for $C_{15}H_{26}O_6$: 302).

The triester (5 g.) in 50 ml. of benzene was refluxed overnight with 1.2 g. of sodium hydride. The reaction mixture was washed with aqueous acetic acid and then with water. Distillation gave 2.1 g. of ethyl 3-carbethoxy-2-oxocyclopentanepropionate (b. p. 130—140°C (bath temp.)/ 1 mmHg). The ester gave a positive test with ferric chloride.

The ester (2 g.) was dissolved in a mixture of concentrated hydrocholric acid (8 ml.) and acetic acid (8 ml.); the mixture was then refluxed for 5 hr. The reaction mixture was concentrated under reduced pressure, and the residue was treated with 2, 4-dinitrophenylhydrazine to give the hydrazone of 2-oxocyclopentanepropionic acid; m. p. 171—172°C (reported m. p. 170°C[11]).

Found: C, 49.57; H, 4.69; N, 16.60. Calcd. for $C_{14}H_{16}O_6N_8$: C, 50.00: H, 4.76; N, 16.66%. Furthermore, the residue was esterified in a mixture of benzene and ethanol by the azeotropic method. After the solvents had been evaporated, the residue was treated with 2, 4-dinitrophenylhydrazine. The hydrazone of ethyl 2-oxocyclopentanepropionate thus obtained was recrystallized from ethanol; m. p. 87.5—88.5°C.

Found: C, 52.61; H, 5.56; N, 15.08. Calcd. for $C_{16}H_{20}O_6N_4$: C, 52.74; H, 5.53; N, 15.38%.

The Synthesis of Ethyl 2-Oxocyclopentanepropionate.—An enamine (30 g.) was prepared from cyclopentanone (21 g.) and pyrrolidine (30 g.) by the usual azeotropic method.[12]

The enamine (7 g.) was dissolved in 30 ml. of ethanol. To the solution 7 g. of ethyl 3-bromopropionate was added; then the mixture was refluxed for 5 hr. The enamine was hydrolyzed by warming it with excess dilute hydrochloric acid. After most of the ethanol had been evaporated, the residue was dissolved in ether. The ethereal solution was washed successively with a sodium bicarbonate solution and with water. The distillation of the solution gave 2 g. of ethyl 2-oxocyclopentanepropionate (b. p. 114—115°C/5 mmHg). 2, 4-Dinitrophenylhydrazone was prepared; its melting point was undepressed on admixture with the 2, 4-dinitrophenylhydrazone obtained above. (Found: C, 52.87; H, 5.61; N, 15.50%).

11) M. Lamant and M. Delepine, *Compt. rend.*, **242**, 380 (1956).
12) G. Stork, A. Brizzolara, H. Landesman and J. Szmuszkovics, *J. Am. Chem. Soc.*, **84**, 1755 (1962).

Results and Discussion

The Carbonylation of the 1, 5-COD Complex.—It was found that, unlike the other olefinic complexes previously studied,[1,2] the 1, 5-COD complex did not react with carbon monoxide in benzene, even at 100°C, under a carbon monoxide pressure of 100 kg./cm^2; unchanged complex was recovered. The complex, however, reacted smoothly with carbon monoxide in ethanol at about 100°C; an unsaturated monoester was the main product, along with a small amount of saturated diesters. The infrared and NMR spectra, the gas chromatography and the crystalline amide of the monoester were identical with those of ethyl 4-cyclooctenecarboxylate (II) as synthesized by Stork's method.[7] II was converted into ethyl cyclooctanecarboxylate by hydrogenation and identified with the ester obtained by the carbonylation of cyclooctene catalyzed by palladium chloride. The diesters were considered to be a mixture of 1, 4- and 1, 5-cyclooctane dicarboxylates (III). Their separation was not possible, and they did not give sharp melting points after hydrolysis. The interesting reactions of the mixed esters will be described later in a separate paper.

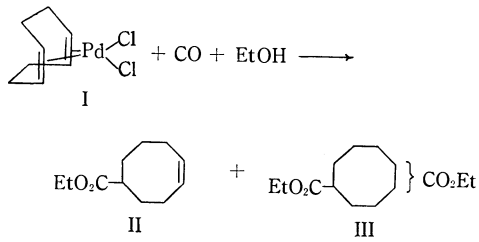

The Carbonylation of 1, 5-COD.—Considering that the complex can easily be formed from palladium chloride and 1, 5-COD, we attempted the direct carbonylation of 1, 5-COD without the prior formation of the complex. When 1, 5-COD in ethanol was smoothly carbonylated in the presence of palladium chloride, the monoester (II), accompanied by the mixed diesters (III), was obtained. As is shown in Table I, it was confirmed that only a catalytic amount of palladium chloride is necessary. Interestingly, it was found that a metallic palladium such as palladium on carbon or palladium black can be used as an active catalyst when the reaction is carried out in ethanol containing hydrogen chloride. Palladium acetylacetonate was found effective only when hydrogen chloride was added to the reaction medium. The concentration of hydrogen chloride has a marked effect on the reaction products. When the concentration was high, the yield of the diesters increased. When palladium iodide, instead of chloride, was used,

Table I. Reaction of 1, 5-COD with carbon monoxide[d]

Expt.	1, 5-COD ml.	Solvent	Catalyst, g.	Reaction Temp. °C	Reaction Time hr.	Yield, %[a] Monoester	Yield, %[a] Diester
1	20	EtOH 30	$PdCl_2$ 3	100	3	58.4	19.8
2	20	EtOH 30	$PdCl_2$ 0.5	100	24	16.8	trace
3	20	EtOH 30	$PdCl_2$ 3	200—250	4	58.0	0.8
4	8	EtOH 12	$PdBr_2$ 1.2	100	1.5	52.2	45.5
5	8	EtOH 12	PdI_2 1.2	100	3.5	5.0	95.0
6	20	10% HCl[c]/EtOH 30	$Pd(acac)_2$[b] 1	100	2	75.0	3.8
7	20	30% HCl/EtOH 30	$Pd(acac)_2$[b] 1	100	1	37.5	59.0
8	20	10% HCl/EtOH 30	Pd-black 0.5	100	24	18.6	trace
9	20	10% HCl/EtOH 30	10% Pd on charcoal 5	100	24	31.0	31.0

a) Yield based on 1, 5-COD
b) Palladium acetylacetonate
c) 10% hydrogen chloride in absolute ethanol
d) Carbon monoxide pressure was 100 kg./cm² in all cases.

an almost exclusive formation of the diesters was observed. The catalytic action of the hydrogen chloride - palladium system in the carbonylation of olefins,[13] allylic compounds[2] and acetylene[14] has already been reported.

It is known that 1, 5-COD can be easily isomerized to 1, 3-COD by the catalytic action of palladium chloride.[15] Therefore, we should consider the possibility of the double bond migration during the carbonylation reaction to give isomers of ethyl cyclooctenecarboxylate. The position of the double bond in the monoester II was determined in the following way. The oxidation of II with sodium permanganate gave 1, 3, 6-hexanetricarboxylic acid, which was then esterified. The Dieckmann condensation of the ester gave ethyl 3-carbethoxy-2-oxocyclopentanepropionate, which in turn gave a low melting 2, 4-dinitrophenylhydrazone. The ketoester was converted into 2-oxocyclopentanepropionic acid and then to ethyl 2-oxocyclopentanepropionate, both of which gave 2, 4-dinitrophenylhydrazones as crystalline substances with sharp melting points. An authentic sample of ethyl 2-oxocyclopentanepropionate was synthesized by the reaction of cyclopentanone with ethyl 3-bromopropionate by the enamine method. Its identity was confirmed by a mixed melting point determination. Thus, the reaction sequences described above give convincing evidence for the structure of ethyl 4-cyclooctenecarboxylate. It can be concluded that the double bond of the monocarbonylation product remained at the original position, at least in the major portion, though not necessarily all, even in the presence of palladium; this suggests that the rate of carbonylation is larger than that of the double bond migration.

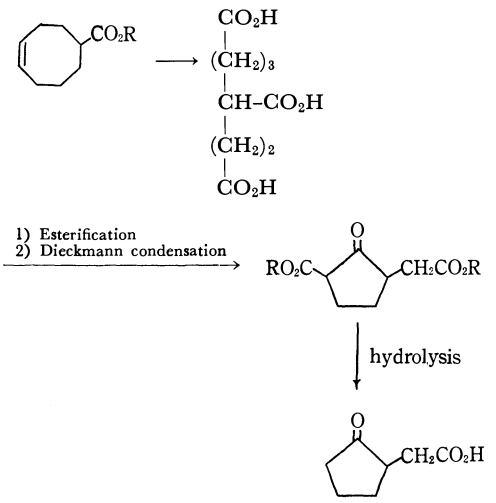

The first step in the carbonylation reaction of 1, 5-COD catalyzed by palladium - hydrogen chloride is evidently the formation of the 1, 5-COD complex. The complex is known to be formed by the direct contact of 1, 5-COD with palladium chloride or its complex.[10] Interestingly, we have confirmed that the complex can be prepared by the reaction of metallic palladium, not palladium chloride, with 1, 5-COD in ethanol containing hydrogen chloride (15%) at 100°C.

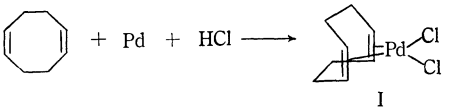

I

In connection with our observation, it should be mentioned that π-allylpalladium bromide can be prepared from metallic palladium and allyl bromide.[16]

13) J. Tsuji, M. Morikawa and J. Kiji, *Tetrahedron Letters*, **1964**, 1437.
14) G. Jacobsen and H. Spathe, German Pat. 1138760 (1962); *Chem. Abstr.*, **58**, 6699 (1963).
15) S. A. Rhone-Poulenc, French. Pat. 1337889 (1963); *Chem. Abstr.*, **60**, 2802 (1964).
16) E. O. Fischer and G. Burger, *Z. Naturforsch.*, **16b**, 702 (1961).

Table II. Comparative studies of carbonylation of dienes

CO pressure: 100 kg./cm²; reaction temp.: 100°C

Diene ml.	EtOH ml.	$PdCl_2$ g.	Time hr.	Yield of monoester %	By-product %
1,3-COD 20	30	3	23	2-Cyclooctene-carboxylate (IV) 9.5	3-Ethoxycyclooctene 1.3
1,5-COD 20	30	3	3	4-Cyclooctene-carboxylate (II) 58.4	1,4- and 1,5-Cyclo-octanedicarboxylate 19.8
1,3-Cyclohexa-diene 5	12	1.2	24	2-Cyclohexene-carboxylate 79.8	

The second step in the carbonylation is the coordination of carbon monoxide on the palladium of the complex. When the 1, 5-COD complex in ethanol was shaken under 100 kg./cm² of carbon monoxide at room temperature, the complex changed into another yellow complex, while absorbing carbon monoxide. The new complex was quite unstable and decomposed when exposed to the air. Although no further elucidation of the new complex has been undertaken because of its instability, it is reasonable to expect that the complex is an intermediate in the carbonylation.

The Carbonylation of 1, 3-COD.—As has been mentioned, the COD recovered from the carbonylation was a mixture of 1, 5- and 1, 3-isomers. Therefore, the carbonylation of pure 1, 3-COD was studied. Ethyl 2-cyclooctenecarboxylate (IV) was obtained in a low yield. As is shown in Table II, the carbonylation of 1, 3-COD is much slower than that of 1, 5-COD. Under comparable conditions, 1, 3-cyclohexadiene gave 2-cyclohexenecarboxylate in a higher yield. In general, conjugated dienes such as butadiene can be carbonylated easily to form β, γ-unsaturated esters,[4] the steric factors of 1, 3-COD seem to be responsible for this difference in reactivity. The same ester was obtained by the carbonylation of 3-bromocyclooctene. The formation of the β, γ-unsaturated ester by a carbonylation of the allylic halogen catalyzed by palladium is a general reaction.[2]

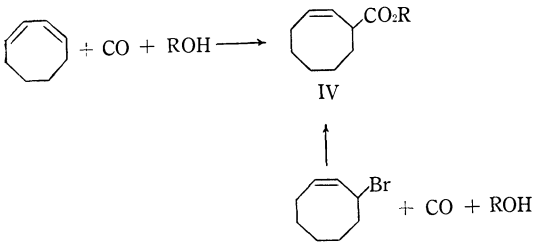

The Carbonylation of Di-μ-chloro-bis (8-methoxycyclooct-4-enyl)-dipalladium. — The 1, 5-COD complex can be converted into a halogen-bridged alkoxy-substituted complex (V) by means of the action of sodium carbonate on the complex in alcohol.[10] The complex involves σ-bonds, which may be expected to be carbonylated more easily than the original 1, 5-COD complex. Actually the complex was carbonylated in benzene at 60°C to form an alkoxycyclooctenecarboxylate. Although no identification with an authentic sample has been made, it is highly probable that the product is methyl 8-methoxy-4-cyclooctenecarboxylate (IV); this suggestion is based on its NMR spectrum. In addition, 1, 5-COD and its palladium chloride complex were detected in the reaction mixture.

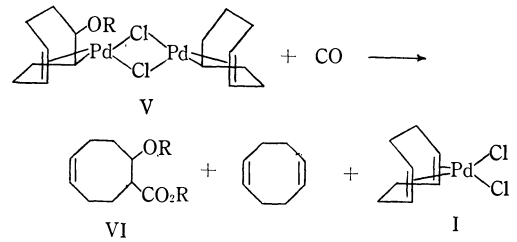

Although the reaction was carried out in a benzene solution, a methyl ester was obtained, instead of the expected acid chloride.[1] Undoubtedly the methoxy group is supplied by the decomposition of the methoxysubstituted complex.

Summary

1, 5-Cyclooctadiene - palladium chloride complex and carbon monoxide react in ethanol to form ethyl 4-cyclooctenecarboxylate. The carbonylation of the 1, 5-cyclooctadiene catalyzed by palladium chloride has given 4-cyclooctenecarboxylate and cyclooctanedicarboxylate. Under the same conditions, 1, 3-cyclooctadiene has given 2-cyclooctenecarboxylate in a low yield.

BULLETIN OF THE CHEMICAL SOCIETY OF JAPAN VOL. 39 146—149 (1966)

Organic Syntheses by Means of Noble Metal Compounds. XV. The Carbonylation of 1, 5, 9-Cyclododecatriene Catalyzed by Palladium

By Jiro Tsuji and Tatsuo Nogi

Basic Research Laboratories, Toyo Rayon Company, Kamakura

(Received May 27, 1965)

The carbonylation of 1, 5, 9-cyclododecatriene has been carried out in ethanol in the presence of palladium chloride; mono- and diesters have thus been obtained without ring contraction. It has been observed, by means of a study of the NMR and infrared spectra, that the first attack of carbon monoxide occurred at the trans double bond, giving ethyl cyclododecadienecarboxylate. The second attack of carbon monoxide occurred randomly, giving an isomeric mixture of ethyl cyclododecenedicarboxylate. No triester was obtained even under prolonged carbonylation. The true catalyst has been found to be metallic palladium, and the presence of hydrogen chloride has been found to be essential for the catalysis. The oxidation of ethyl cyclododecadienecarboxylate, followed by esterification, has given ethyl succinate and 1, 3, 6-hexanetricarboxylate. This result indicates that the double bonds of ethyl cyclododecadienecarboxylate remain at the original positions.

We have reported that pallaium chloride or metallic palladium, in the presence of hydrogen chloride, is an active catalyst for the carbonylation of olefins in alcohol, thus forming carboxylic esters.[1] The reaction proceeds quite smoothly under rather mild conditions. The palladium-catalyzed carbonylation reaction was then extended to various allylic compounds[2] and conjugated dienes[3] to form β, γ-unsaturated esters. Furthermore, it was found that 1, 5-cyclooctadiene (1, 5-COD) can be carbonylated smoothly to form mono- or diester, depending on the reaction conditions.[4] The above-mentioned olefinic compounds are known to form π- or π-allylic complexes with palladium chloride,[5] and certainly their carbonylations proceed through the formation of these complexes.

Like 1, 5-COD, 1, 5, 9-cyclododecatriene (1, 5, 9-CDT) can be easily prepared from butadiene by the catalytic action of several transition metal complexes. However, unlike 1, 5-COD, which is known to form a stable palladium chloride complex, 1, 5, 9-CDT does not easily form a complex with palladium chloride. Only recently it was reported that a complex can be prepared after the prolonged contact of 1, 5, 9-CDT with palladium chloride - benzonitrile complex, but its structure is not yet known.[6] It seems likely that the three double bonds of 1, 5, 9-CDT are not orientated in a way suitable for forming a stable complex with palladium chloride. From these considerations, it seemed worthwhile investigating the carbonylation of 1, 5, 9-CDT by the catalytic action of palladium. The carbonylation of 1, 5, 9-CDT has been reported by Rull,[7] who obtained methyl cyclododecanecarboxylate by the catalytic action of cobalt carbonyl in methanol. In this case, two double bonds were hydrogenated. In addition, the carbonylation of 1, 5, 9-CDT by the catalytic action of Lewis acids to give carboxylic acids is known, but in this case ring contractions due to transannular reaction have occurred, giving a variety of carboxylic acids.[8a,b] In contrast, the carbonylation reaction reported in this paper gives mono- and dicarbonylation products without ring contraction or the reduction of the double bonds.

Experimental

The gas chromatographic analyses were carried out on a Thermol-3 column, 2 m. long, at 220°C. All the boiling points are uncorrected. The molecular weights were determined in benzene by the ebullioscopic method, using a Mechrolab vapor pressure osmometer. The NMR spectra were recorded on a high resolution spectrometer, model DP 60, and the peak positions are expressed in τ values. The infrared spectra were recorded on a Hitachi infrared spectrometer, model EPI-S2.

1) J. Tsuji, M. Morikawa and J. Kiji, *Tetrahedron Letters*, **1963**, 1437.
2) J. Tsuji, J. Kiji, S. Imamura and M. Morikawa, *J. Am. Chem. Soc.*, **86**, 4350 (1964).
3) J. Tsuji, S. Hosaka and J. Kiji, *Tetrahedron Letters*, **1964**, 605.
4) J. Tsuji, S. Hosaka, J. Kiji and T. Susuki, This Bulletin, **39**, 141 (1966).
5) For general reference, see E. O. Fisher and H. Werner, "Metall π-Komplexe mit di- und oligoolefinischen Liganden," Verlag Chemie, Weinheim (1963).
6) E. Kuljian and H. Frye, *Z. Naturforsch.*, **19b**, 651 (1964).
7) T. Rull, *Bull. soc. chim. France*, **1964**, 2680.
8) a) K. E. Moller, *Brennstoff Chemie*, **45**, 129 (1964); *Angew. Chem.*, **75**, 1122 (1963). b) M. Genas and T. Rull, *Bull. soc. chim. France*, **1962**, 1837.

Materials. — Commercially - available palladium chloride was used without further purification. *cis, trans, trans*-1, 5, 9-CDT was prepared in the Central Research Laboratories, Toyo Rayon Company, and distilled before use.

The Carbonylation of 1, 5, 9-CDT—The reaction conditions and the amounts of the reactants used are shown in Table I. A typical example of the carbonylation is as follows. One gram of palladium chloride, 20 ml. of ethanol containing a certain amount of hydrogen chloride, and 10 g. of 1, 5, 9-CDT were introduced into a glass vessel with a gas-inlet capillary. The vessel was then set in a stainless steel autoclave (made by Sakashita Seisakusho), and carbon monoxide was introduced (100 kg./cm^2). After the autoclave had been set in an electrical furnace preheated to 100°C, the furnace was shaken. After a certain period of time, the autoclave was quenched in a water bath. The catalyst was removed by filtration, and the solution was distilled. The 1, 5, 9-CDT recovered was collected at 90—95°C/8 mmHg. Ethyl cyclododecadiencarboxylate (140—145°C/5 mmHg) and ethyl cyclododecenedicarboxylate (165—175°C/4 mmHg) were easily separated by fractional distillation.

The presence of four olefinic protons was confirmed by a study of the NMR spectrum of ethyl cyclododecadienecarboxylate (Fig. 1). Also, the monoester was hydrogenated in ethanol in the presence of an Adams platinum catalyst, with the absorption of 2 mol. of hydrogen; it gave ethyl cyclododecanecarboxylate.

Found: C, 74.57; H, 11.60; mol. wt., 240. Calcd. for $C_{15}H_{28}O_2$: C, 74.95; H, 11.74%; mol. wt., 240.

The hydrolysis of ethyl cyclododecanecarboxylate was carried out by refluxing it in a 10% alcoholic potassium hydroxide solution for 5 hr. After the usual work-up, cyclododecanecarboxylic acid was recrystallized from hexane, m. p. 97—98°C (reported m. p. 99.5°C[7]).

Found: C, 73.45; H, 11.39%. Calcd. for $C_{13}H_{24}O_2$: C, 73.53; H, 11.39%.

An NMR spectrum of ethyl cyclododecenedicarboxylate showed the presence of 2 olefinic protons (Fig. 2), and the hydrogenation of the diester consumed 1 mol. of hydrogen. The hydrolysis of the hydrogenated diester with 10% ethanolic potassium hydroxide gave the corresponding solid acid, which did not show a sharp melting point, even after chromatographic purfication.

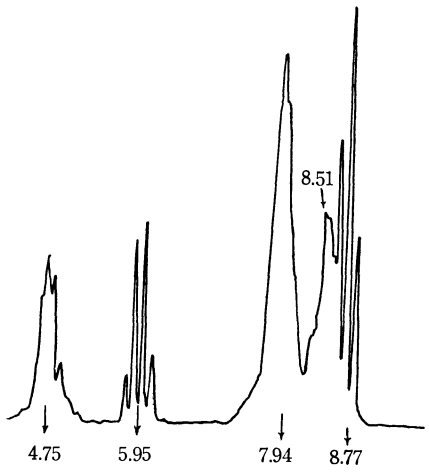

Fig. 1. NMR spectrum of ethyl cyclododecadienecarboxylate.

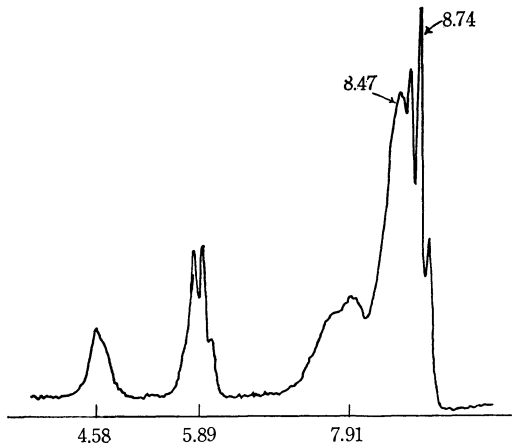

Fig. 2. NMR spectrum of ethyl cyclododecenedicarboxylate.

Found: C, 65.41; H, 9.41. Calcd. for $C_{14}H_{24}O_4$: C, 65.59; H, 9.44%.

The Carbonylation of Cyclododecene.—A mixture of 1 g. of palladium chloride, 20 ml. of ethanol containing hydrogen chloride (7.5%), and 6 g. of cyclododecene was placed in a glass vessel; the reaction was then carried out at 120°C for 20 hr. under a pressure of carbon monoxide (100 kg./cm^2). After the usual work-up, 8.0 g. (93%) of ethyl cyclododecanecarboxylate was obtained by distillation (148—150°C/10 mmHg). The ester was then hydrolyzed to crystalline cyclododecanecarboxylic acid.

The Oxidation of Ethyl Cyclododecadienecarboxylate.—The ester (10 g.) was mixed with 20 ml. of cyclohexane and 20 ml. of water in a 1-l. round-bottomed flask. To the mixture there was then vigorously stirred 250 ml. of a sodium permanganate solution (12.5%) over a 3-hr. period, with the occasional addition of small pieces of dry ice. The oxidation product was then esterified in a manner described before,[4] and distilled. A lower-boiling fraction was confirmed to be ethyl succinate by gas chromatography and infrared spectrum; then it was hydrolyzed to succinic acid, m. p. 186—188°C. A higher-boiling fraction (b. p. ca. 150°C/2 mmHg, mol. wt., 300; yield 4 g.) was identified by infrared and NMR spectra, with the ethyl 1, 3, 6-hexanetricarboxylate obtained from ethyl cyclooctenecarboxylate, and by converting it into ethyl 2-oxocyclopentanepropionate.

Results and Discussion

There are three isomers of 1, 5, 9-CDT, namely, cis-trans-trans, cis-cis-trans and trans-trans-trans. In this study, the most easily obtainable cis-trans-trans isomer was used. The carbonylation proceeded smoothly, and mono- and di-carbonylation were observed, giving ethyl cyclododecadienecarboxylate and ethyl cyclododecenedicarboxylate respectively. The presence of, respectively, two and one double bonds in these esters was confirmed clearly by the

Table I. Carbonylation of 1,5,9-CDT[a]

Cat.[b]	HCl/EtOH[c] wt.%	Reaction Temp. °C	Reaction Time hr.	CO kg./cm²	Yield, %[d] monoester	Yield, % diester
$PdCl_2$	0	100	24	100	20	0
$PdCl_2$	7.5	100	1	100	54	37
$PdCl_2$	15	100	1	100	50	41
$PdCl_2$	15	30	15	100	0	0
$PdCl_2$	7.5	100	1/3	100	30	0
$PdCl_2$	7.5	100	1/2	100	64	3
$PdCl_2$	7.5	100	10	100	trace	85
$PdCl_2$	7.5	100	5	50	33	45
$PdCl_2$	7.5	100	1	150	60	25
Pd-C	0	100	24	100	0	0
Pd-C	7.5	100	1	100	50	30

a) Amount of 1,5,9-CDT 10 g. b) Amount of $PdCl_2$ 1 g. Pd-C (10%) 3 g.
c) Volume of ethanol 20 ml. d) Yield based on 1,5,9-CDT (10 g.).

NMR spectra (Fig. 1 and 2) and hydrogenation, showing that no ring contraction occurs during the carbonylation reaction.

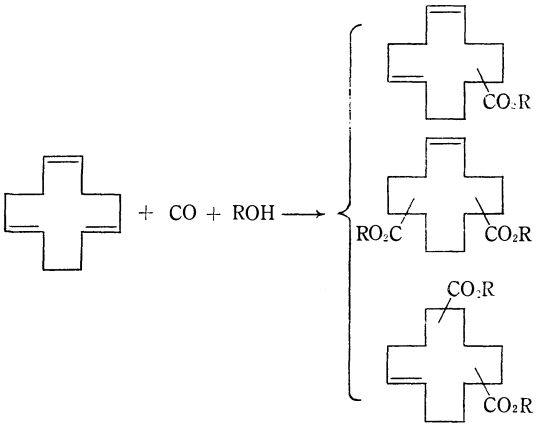

When 1, 5-COD was carbonylated, it was rather easy to control the reaction so that mono- and diester were selectively obtained,[4] because the double bonds of 1, 5-COD behave as a bidentate ligand, forming a stable complex with palladium. Although the trans double bond was attacked first, as will be described later, there was not much difference in the reaction rate between mono- and dicarbonylation, as is shown in Table I, and it seemed likely that the double bonds of 1, 5, 9-CDT behaved almost independently. The only way to obtain the monoester as a main product was to stop the reaction after a comparatively short period. A longer reaction time gave rise to the diester exclusively. The reaction stopped at the dicarbonylation stage and the further carbonylation of the remaining double bond to form a saturated triester was almost impossible. It is supposed that the two ester groups of cyclododecenedicarboxylate inhibit the access of palladium to the remaining double bond, thus making the carbonylation almost impossible. On the other hand, cyclododecene, which has no such steric hindrance, was carbonylated easily to give ethyl cyclododecanecarboxylate.

It is known that there is considerable diffrence in reactivity between the cis and trans double bonds of *cis, trans, trans*-1, 5, 9-CDT.[9] In general, one of the trans double bonds is attacked first. In this carbonylation reaction, as was expected, it was found, by comparing the changes of intensities of the infrared bands at 968 cm^{-1} (trans) and 707 cm^{-1} (cis), that the first attack of carbon monoxide occurred at the trans double bond. As is shown in Figs. 3, 4 and 5, the intensity ratio of the cis and trans bonds of 1, 5, 9-CDT is about 1 : 2, while those of the monoester and diester are nearly equal. Therefore, it is apparent that the second attsck is not selective and that both the cis and trans double bonds are randomly attacked.

By mono- and dicarbonylation, considerable numbers of isomers can be formed on the basis

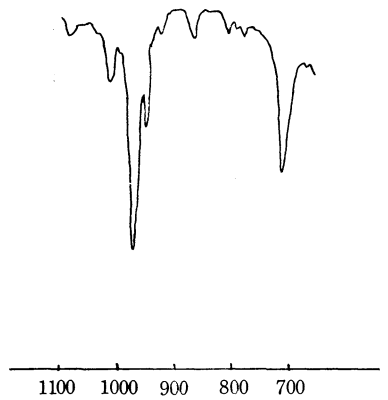

Fig. 3. Infrared spectrum of 1,5,9-cyclododecatriene (in CCl_4).

9) M. Ohno and S. Torimitsu, *Tetrahedron Letters*, **1964**, 2259.

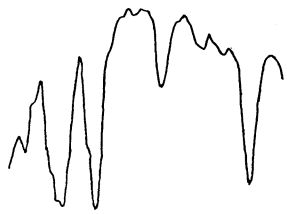

Fig. 4. Infrared spectrum of ethyl cyclododecadienecarboxylate (in CCl_4).

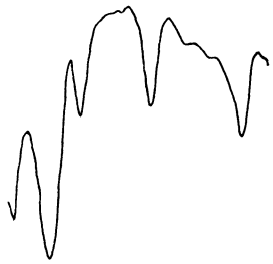

Fig. 5. Infrared spectrum of ethyl cyclododecenedicarboxylate (in CCl_4).

of the relative position of the carbethoxy groups. There are two possible sites of the carbethoxy group in ethyl cyclododecadienecarboxylate relative to the remaning cis and trans double bonds. Actually, two peaks were observed closely by gas chromatography, but it was impossible to separate them by any means. By hydrogenation, a single peak was observed; this was identified with the ethyl cyclododecanecarboxylate obtained by the carbonylation of cyclododecene catalyzed by palladium chloride. The hydrolysis of the hydrogenated ester gave cyclododecanecarboxylic acid as a crystal.

It is known that palladium chloride is an active catalyst for double bonds migration. For example, 1, 5-COD can be isomerized to 1, 3-COD by the action of palladium chloride.[10] In view of this the possibility of the double bond migration after the monocarbonylation was investigated by the oxidation of the monoester with sodium permanganate. When the oxidation product was esterified, the presence of ethyl succinate was detected by gas chromatography. The ester was isolated by distillation. Ethyl 1, 3, 6-hexanetricarboxylate was also isolated. This ester's identity with the ester isolated from the oxidation product of ethyl 4-cyclooctenecarboxylate was confirmed by means of a study of their infrared and NMR spectra. Furthermore, the structure of ethyl 1, 3, 6-hexanetricarboxylate was confirmed by its conversion into ethyl 2-oxocyclopentanepropionate, as has been described in the structural determination of ethyl 4-cyclooctenecarboxylate.[4] Thus, the oxidation studies have confirmed that the double bonds of ethyl cyclododecadienecarboxylate remain at the original positions, at least usually, even in the presence of palladium chloride.

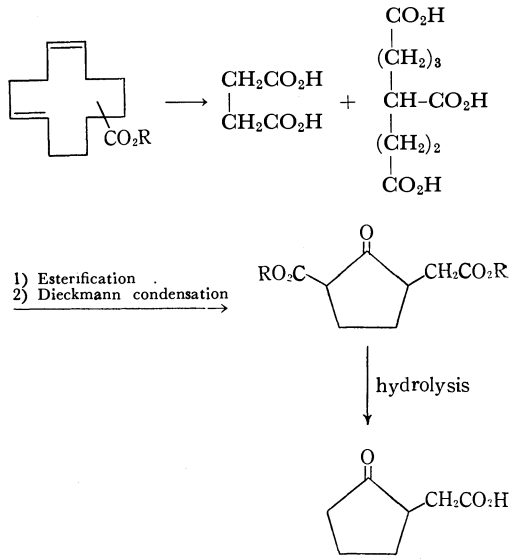

For ethyl cyclododecenedicarboxylate, there exist six possible isomers without considering optical isomerism, and their differentation and separation were impossible by any means. By hydrogenation, the number of the isomers decreased to three, and after hydrolysis the product did not give a sharp melting point, even after an attempted chromatographic separation.

In this carbonylation, as has been described before,[4] metallic palladium and hydrogen chloride are essential for the catalysis. Palladium on carbon alone was inactive. The concentration of hydrogen chloride in the reaction medium has a marked influence on the reaction rate, as can be seen in Table I.

10) Rhono-Poulene, French Pat. 1337889 (1963); *Chem. Abstr.*, **60**, 2802 (1964).

BULLETIN OF THE CHEMICAL SOCIETY OF JAPAN VOL. 39 150—155 (1966)

A Mass Spectrometric Study of Phosphorus Oxide

By Akio HASHIZUME, Nobuhide WASADA and Toshikazu TSUCHIYA

Government Chemical Industrial Research Institute, Tokyo, Shibuya-ku, Tokyo

(Received May 28, 1965)

Phosphorus pentoxide has been investigated with a mass spectrometer over the temperature range from 60°C to 650°C. A Knudsen cell has been installed in the source of the mass spectrometer. Two samples were used in the experiment. One was commercially-available phosphorus pentoxide, while the other had been purified from the commercial phosphorus pentoxide by Finch's method. The ionization efficiency curves near the appearance potential of $P_4O_9^+$ and $P_4O_{10}^+$, and the fractional yield of each ion versus the ionizing voltage have been investigated and interpreted as evidence for the presence of the P_4O_9 molecule. Three curves representing the intensity of the mass 284 ($P_4O_{10}^+$) peak as a function of the temperature have been obtained. Two of them, which set on at about 250°C and 450°C respectively, are related to the known vapor pressure curves of phosphorus pentoxide. The curve with the lowest onset temperature, about 100°C, may be interpreted as a vapor pressure of a new low temperature phase of phosphorus pentoxide.

The nature of phosphorus oxides has been investigated by various authors,[1-3] since the oxides have a great significance in the chemistry of fertilizer manufacture, and an accurate knowledge of their behavior in the pure state is a prequisite to a complete understanding of complex systems of a more practical importance. Especially, phosphorus pentoxide is known to be a component of several phase systems. This has not, however, been determined unequivocally, because the oxides cannot be handled conveniently, as they absorb moisture from air immediately and attack glass at elevated temperatures.

Some people believe that "phosphorus pentoxide" is not as a very favorable drying agent for a vacuum system, as lower oxides of phosphorus sublime.

Several works have been published studying the sublimation products from solid state compounds by mass spectrometry.[4,5] Manometric investigations based upon various principles have been reported and used; these studies have measured a quantity which is proportional, in some sense, to the total pressure of the gas under investigation, whereas mass spectrometry gives information about the partial pressure of each species of molecules contained in the gas phase. Such being the case, the present study was undertaken in order to investigate the properties of phosphorus oxides with a mass spectrometer.

Experimental

The phosphorus oxides used in this investigation were obtained from two sources. One was an extra pure phosphorus pentoxide available commercially (hereafter referred to as commercial phosphorus pentoxide) and obtained from Miyazaki Shōten, while the other was prepared from the commercial product by sublimation in a current of oxygen in an iron tube at about 800°C, according to the method of Finch and Frazer.[6] The iron tube was heated electrically instead of by gas. In this process the lower oxides of the phosphorus are reported to be oxidized completely. After sublimation, the oxidized product (hereafter referred to as purified phosphorus pentoxide) was handled carefully so as to prevent it from absorbing moisture.

Most of the work was carried out with a 60° Nier-type mass spectrometer of our own construction.[7] The median radius of the stainless-steel analyzer of this instrument was 20 cm., and the resolving power was about 150. The ion current was amplified by an Applied Physics Corporation, model 36, vibrating reed amplifier. The other electronic circuits and the construction of the ion source were much the same as those reported by Nier.[8] Figure 1 shows the mass spectrometer mounting, containing a Knudsen effusion cell similar to that of Porter, Schissel and Inghram.[4] The cell consisted of two crucibles, an outer stainless-steel crucible and an inner crucible made of aluminum oxide; the latter contained the phosphorus oxide to be

1) J. R. van Wazer, "Phosphorus and its Compounds," Vol. I, Interscience Publishers, New York (1958).
2) J. C. Southard and R. A. Nelson, *J. Am. Chem. Soc.*, **59**, 911 (1937).
3) W. L. Hill, G. T. Faust and S. B. Hendricks, ibid., **65**, 794 (1943).
4) R. F. Porter, P. Schissel and M. G. Inghram, *J. Chem. Phys.*, **23**, 339 (1955).
5) J. D. Louw and J. W. L. DeVilliers, *Rev. Sci. Instr.*, **25**, 1226 (1954); M. G. Inghham, W. A. Chupka and J. Berkowitz, *J. Chem. Phys.*, **27**, 569 (1957); M. G. Inghram, W. A. Chupka and J. Berkowitz, *Mem. soc. roy. sci. Liege*, **18**, 513 (1957); T. A. Milne, H. M. Klein and D. Cubicciotti, *J. Chem. Phys.*, **28**, 718 (1958); R. E. Powell, *J. Sci. Instr.*, **37**, 252 (1950); R. P. Burns, G. Demaria, J. Droward and M. G. Inghram, *J. Chem. Phys.*, **38**, 1035 (1963).
6) G. I. Finch and R. P. Fraser, *J. Chem. Soc.*, **129**, 117 (1926).
7) To be reported elsewhere.
8) A. O. Nier, *Rev. Sci. Instr.*, **18**, 398 (1947).

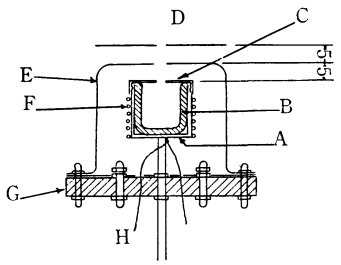

Fig. 1. Crucible for mass spectrometer.
(A) Stainless-steel crucible, (B) Alumina crucible, (C) Cap, (D) Position of ionization chamber, (E) Radiation shield (F) Filament (G) Steatite base, (H) Thermocouple

investigated. The stainless-steel cover of the outer crucible had an effusion hole (0.15 mm. in diameter). As the ratio of the total vaporizing area of the phosphorus oxide to the effusion area was approximately 1000, a true equilibrium partial pressure of each gaseous species with the charged oxide can exist inside the Knudsen cell. The stainless-steel crucible was heated directly by means of a surrounding tungsten filament coated with aluminum oxide or by electron bombardment from the filament. The Knudsen cell and the heating filament were enclosed by a stainless-steel radiation shielding, which had an effusion hole 2 mm. in diameter. The distance between the holes of the outer crucible and the radiation shielding was about 5 mm. The temperature was measured with a platinum-platinum-rhodium thermocouple attached to the bottom of the stainless-steel crucible. Gases effusing out of the Knudsen cell pass through the hole in the top of the radiation shielding and enter the ionization chamber of the ion source, where they are ionized.

As soon as the compound to be investigated was loaded in the inner crucible, the stainless-steel cover was placed on; then, in about 5 min., the ion source system, including the crucible, was mounted on the analyzer of the mass spectrometer and evacuated.

Since thr resolving power of the mass spectrometer described above was insufficient, a CEC 21-103C mass spectrometer was used to determine the mass numbers of those ions which have mass numbers higher than 150. In this case the material to be investigated was charged in an ampoule. The ampoule was then positioned at the necessary depth in a flask of liquid nitrogen just prior to the evacuation and during the sealing. The ampoule was attached directly to the

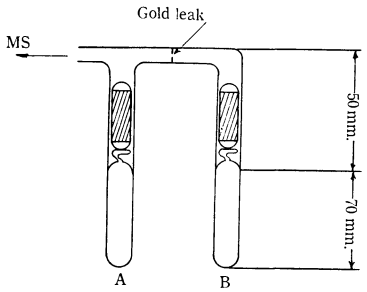

Fig. 2. Mounting of ampoules containing sample.
(A) Phosphorus pentoxide, (B) *n*-eicosane

sample manifold of the mass spectrometer, as is shown in Fig. 2. Such ampoules were fabricated from pyrex and in the approximate dimensions shown.

In order to determine the mass numbers of the ion peaks, *n*-eicosane was introduced simultaneously with phosphorus oxide as a reference. The location of the ampoule containing *n*-eicosane is shown in Fig. 2. The vapor of the sample was extracted from the ampoule by breaking the breakable seal and by then heating the ampoule to an appropriate temperature with an electric furnace. The vapor was introduced into the ion source of the mass spectrometer directly or through the gold leak. The mass numbers of the spectral peaks of phosphorus oxides were determined by comparing them with those of *n*-eicosane. In some cases, the intensity of the isotope peak contributed by ^{18}O was calculated[9] and used to indentify the mass number.

A Pirani-type manometer was constructed, and the vapor pressure of phosphorus pentoxide was checked through the temperature range from 90°C to 260°C. The manometer, which had a platinum filament 30 μ in diameter, was of an ordinary type and was calibrated with reference to a thermocouple gauge obtained from the Showa Rikagakukikai Co. At a constant wall temperature of the manometer, the calibration curve was a straight line, the tangent of which was a function of the temperature. A glass tube containing the phosphorus pentoxide was connected directly with the manometer. After the interior was pumped down to 10^{-4} mm Hg or lower, the glass tube with the manometer was closed off, with the vacuum still applied. Then it was immersed in a thermostat and the pressure was measured.

Results

Pattern Coefficient.—Table I shows the pattern coefficients of the mass spectra of the phosphorus oxides corresponding to *m/e* values greater than 47. No peak of an *m/e* value greater than

Table I. Pattern coefficients of phosphorus pentoxides

m/e	Purified phosphorus pentoxide*	Commercially available phosphorus pentoxide**	Constitution
286	2.1	2.1	$P_4O_9{}^{18}O$
284	100	100	P_4O_{10}
268	1.1	30.1	P_4O_9
205	26.0	34.0	P_3O_7
142	2.9	4.1	P_2O_5
63	22.3	54.8	PO_2
47	70.4	224.8	PO

Mass spectrometer: CEC 21-103C
Electron accelerating voltages: 70 V.
* Oxidized according to Finch and Frazer from the guaranteed reagent phosphorus pentoxide at Kanto Kagaku Co.
** Extra pure phosphorus pentoxide obtained from Miyazaki Shōten.

9) J. H. Beynon, "Mass Spectrometry and its Applications to Organic Chemistry," Elsevier Publ. Co., Amsterdam (1960), pp. 294—298.

that at 288, which is due to an isotope peak of $P_4O_{10}^+$, was observed. Under the present experimental conditions, the pattern coefficients corresponding to $P_4O_6^+$ or $P_2O_3^+$ were smaller than 1. The pattern coefficients of the commercial phosphorus pentoxide varied with the time. The variation in the pattern coefficients of the $P_4O_9^+$ is shown in Table II. The pattern coefficient of the *m/e* 47 ion was found to have a poor reproducibility, the reason for this was not studied.

TABLE II. VARIATION OF THE PATTERN COEFFICIENTS OF P_4O_9 WITH TIME

m/e	1	2	3	4
284	100	100	100	100
268	153.5	78.0	51.2	40.4

Measurement was made at about every 10 min.
Temperature of the crucible was at 100°C during the measurements.
Phosphorus pentoxide used in this measurement was extra pure.

The Intensity of the Peaks as a Function of the Electron Accelerating Voltage.—Figures 3 and 4 show the fractional yields (the percentage ratio of a peak height to the sum of all peaks in a mass spectrum of a substance) of several main peaks in the spectra of the commercial phosphorus pentoxide and in the purified phosphorus pentoxide respectively; the yields are shown as a function of the electron-accelerating voltage above the appearance potential. The voltage scale is not corrected for contact potentials or any other conditions.

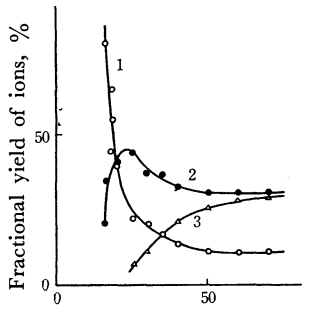

Fig. 3. Fractional yield of ions.
Commercial phosphorus pentoxide. Curve 1, *m/e* 268; Curve 2, *m/e* 284; Curve 3, *m/e* 47

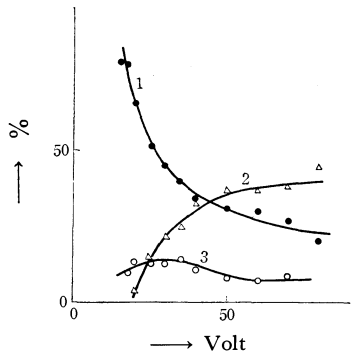

Fig. 4. Fractional yield of ions.
Purified phosphorus pentoxide. Curve 1, *m/e* 284; Curve 2, *m/e* 47; Curve 3, *m/e* 268

The ionization efficiency curves near the appearance potentials of the *m/e* 268 and *m/e* 284 ions from the commercial phosphorus pentoxide are shown in Fig. 5. Though the energy scale was not corrected and though the absolute values of the appearance potentials of the ions were not estimated, it is clear that the *m/e* 268 ion, $P_4O_9^+$, appears at an ionizing voltage about 0.5 eV. lower than that of the *m/e* 284 ion, $P_4O_{10}^+$.

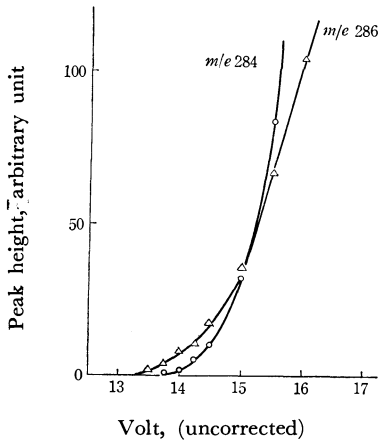

Fig. 5. Ionization efficiency curves. Commercial phosphorus pentoxide.

The Variation in *m/e* 284 Ion Intensity with the Temperature.—Figure 6 shows the relation between the *m/e* 284, $P_4O_{10}^+$, ion intensity and the temperature of phosphorus pentoxide. In the intermediate temperature ranges between curves 1, 2 and 3 of Figure 6, which had onset points at about 100°C, 250°C and 500°C respectively, the ion intensity was found to be zero. After the sample had been heated at about 200°C for a while, the intensity of the ion corresponding to curve 1 gradually dropped; after the temperature had been maintained for a few hours, the ion disappeared completely. Then when the temperature was raised, the ion began to appear again at about 250°C and curve 2 could be traced. A phosphorus pentoxide sample, previously heated to a temperature higher than 250°C in the crucible, gave almost no *m/e* 284 ions at about 200°C.

While vapor pressure curves which are very similar in shape and onset point to curves 2 and 3 have been reported by other authors[1,2,10,11] (curves

10) A. Smits, *Z. phys. Chem.*, **B46**, 43 (1940).
11) A. Smits and A. J. Rutgers, *J. Chem. Soc.*, **125**, 2573 (1924).

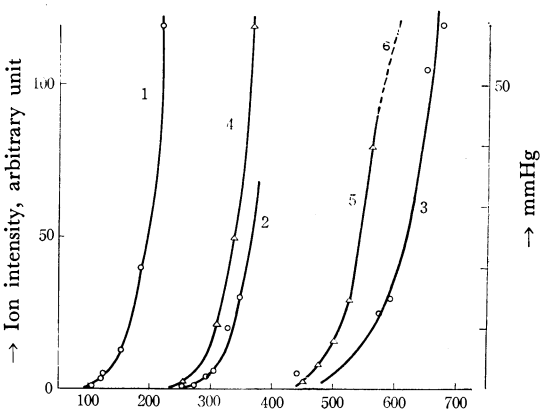

Fig. 6. Intensity of *m/e* 284 ion versus temperature of purified phosphorus pentoxide.
Curves 1, 2 and 3, ion intensity of *m/e* 284 ion; Curves 4, 5 and 6, vapor pressure obtained by A. Smits and A. J. Rutgers.[11]

4 and 5 in Fig. 6[2]), the one which sets on at about 100°C has not yet been reported. A Pirani gauge was used in order to check the vapor pressure in this temperature range by a means other than mass spectrometry. The determination of the absolute value of the pressure was not carried out, however, as the sample material may corrode the filament of the gauge during the measurement. However, as in the case of determination with the mass spectrometer, the pressure rise was observed to begin at about 100°C. The pressure was roughly estimated to be at least of an order of magnitude higher than the value estimated by the extrapolation of curve 4 in Fig. 6, which was obtained by Southard and Nelson.[2]

Discussion

Previous Works on Phosphorus Pentoxide.—The vapor pressures of phosphorus pentoxide have been investigated, either with a Jackson-type manometer or with a platinum bulb gauge, by many authors.[1-3,10,11] From these vapor pressure data, together with their microscopic observation of the crystalline form of the compound, Hill, Faust and Hendricks[3] have concluded that phosphorus pentoxide exists in three crystalline modifications. The low-temperautre polymorph belongs to the rhombohedral division of the hexagonal system (referred to as the H-form). A high-temperature form obtained by heating the hexagonal crystals below 420°C for an appropriate period belongs to the orthorhombic system (referred to as the O-form). When the aggregate of the O-form is heated at 450°C for twenty-four hours, it is converted into a stable crystalline modifications, which is thought to be tetragonal (designated as the T-form). The H-form is metastable with respect to the O-form. This change takes place very slowly at 70°C, but it is completed in one hour at 378°C. Alternatively, the O-form is metastable with respect to the T-form. The H-, the O- and the T-forms exist, respectively, in the three temperature ranges bounded by curve 4 and curve 5 in Fig. 5. While various papers have since been published discussing the higher temperature forms, the H- and the O-forms have been considered to be corroborated. Curve 6 has been reported by Southard and Nelson to be a vapor pressure curve on a liquid phase.

According to Southard and Nelson, the vapor pressure curves, 4, 5, and 6, are represented by the following equations respectively:
Low temperature form:

$$\log p = -(50000/T) + 9.792 \quad (1)$$

High temperature form:

$$\log p = -(7930/T) + 11.113 \quad (2)$$

Liquid:

$$\log p = -(4320/T) + 6.809 \quad (3)$$

They determined the heats of vaporization per gram of the molecule from Eqs. 1, 2 and 3 for the low-temperature form (the H-form according to Hill et al.), the high-temperature form (the O-form) and the liquid respectively. The data are listed in the last column of Table III.

Table III. Heats of vaporization
L (kcal./mol.) of P_4O_{10}

Curve	*L*	Crystalline form	*L**
1	19.2		
2	23.8	H	22.8
		O	36.3
3	20.6	liq.	19.7

* J. C. Southard and R. A. Nelson, *J. Am. Chem. Soc.*, **59**, 911 (1937).

The only available calorimetric work on the heat of vaporization is that of Frandsen[12] on the low-temperature form. He obtained the value of 8800+1300 cal. per gram formula weight of phosphorus pentoxide. On the basis of the assumption that the molecular formula P_4O_{10} is nearly correct, the heat of vaporization was calculated to be 17600 +2600 cal. par gram mole, which deviates considerably from the value of 22800 obtained by Southard and Nelson and from the 22600 calculated from the data of Hoeflake and Scheffer.[13]

Heats of Vaporization.—The curves 1, 2 and 3 obtained in the present experiment are represented by Eqs. 4, 5 and 6 respectively:

$$\log p = -(42 \times 10^2/T) + 13.06 \quad (4)$$

$$\log p = -(52 \times 10^2/T) + 11.06 \quad (5)$$

12) M. Frandsen, *Bur. Standards J. Res.*, **10**, 54 (1933).
13) J. M. A. Hoeflake and F. E. C. Scheffer, *Rec. trav. chim.*, **45**, 191 (1926).

$$\log p = -(45 \times 10^2/T) + 7.55 \quad (6)$$

The constants in Eqs. 1—6 are functions of the sensitivity of the manometer used and of the unit of pressure. The heats of vaporization calculated from Eqs. 4—6 are listed in column two, Table III. When we compare these values with those of Southard and Nelson given in column four, and when we take the temperautre range of each curve into account, we see that curve 2 and curve 3 of the intensity correspond to curve 4 and curve 6 of the vapor pressure respectively.

As has been shown in the present study, no polymer of P_4O_{10} was observed in the gas phase. This shows that Frandsen's assumption is correct. As may be seen in Table III, Frandsen's value, 17600±2600 cal. per gram mole, is in agreement with the one calculated from curve 1 within the tolerance of experimental error.

A New Modification of Phosphorus Pentoxide.—In mass spectrometry, a measured ion-peak height is proportional to the pressure, in the ionization chamber, of the parent compound of the ion, as long as an ion peak of a certain mass number is concerned. In the present instance, although the pressure coefficient of the peak height may be a function of the temperature of the parent molecules, the peak height was assumed to be approximately proportional to the pressure, since the temperature range was not very wide. From the arrangements of the Knudsen cell and the ionization chamber, the pressure in the chamber was properly assumed to be proportional to the P_4O_{10} vapor pressure, which is in equilibrium, at that temperature, with the charged phosphorus pentoxide in the cell.

While curves 2 and 3 of the intensity obtained in the present study are considered to correspond to curves 4 and 6 of the vapor pressure respectively, given by Southard and Nelson, no vapor pressure curve which corresponds to the curve 1 of the intensity obtained in the present study is yet known. One of the significant differences in the experimental conditions between those of Southard and Nelson and ours is the treatment of the sample materials. Whereas they distilled the sample directly into a measuring manifold, we exposed the sample to air for a short time in a room kept at a low humidity. This procedure has been mentioned previoulsy. Under these circumstances, the possible amount of water absorbed by the sample is estimated to be of the order of a 10^{-2} weight percentage of the sample.[13] Nothing is known about the pressure of P_4O_{10} vapor on a phosphorus pentoxide containing a minute quantity of water. The pressure of P_4O_{10} vapor on a phosphorus pentoxide containing a minute quantity of water cannot be considered to exceed that on a pure phosphorus pentoxide by an order of magnitude. As has been mentioned already, the evaporation of P_4O_{10} vapor near 200°C lasts for a few hours and the heat of evaporation coincides with the calorimetric value. Taking these circumstances into consideration, we infer that curve 1 in Fig. 6 is a vapor pressure curve attributable to a phase of pure phosphorus pentoxide, and that there exists a new phase (which we shall refer to as the α-form phosphorus pentoxide), which has not yet been reported on, corresponding to the curve. The behavior of the *m/e* 284 ion in the temperature range between 100°C and 250°C may be understood if we assume that the α-form substance changes readily into a higher temperature form, presumably into the H-form. One possible explanation of the fact that the α-form or curve 1 has not been reported by previous investigators may be that from the outset they investigated phosphorus pentoxide in a form other than the α-form. If the distilled phosphorus pentoxide condenses on a wall at a temperature higher than about 250°C, the prepared substance may be in a form other than the α-form.

P_4O_9—King and Long[14], in a study of the mass spectrum of some simple esters, showed that the curves representing the fractional yield of each ion versus the ionizing voltage fall into three distinct types. According to these authors, the first group of curves, designated by them as Type I, is for those ions whose fractional yields vary inversely with the electron energy. Type I curves are observed only for parent ions and for primary ions with a low activation energy. Type II curves are for those ions whose relative yields rise rapidly to a maximum at about 10 V. above the ionization potential, and then drop off slightly at higher voltages. This type of curve arises from primary products with a slightly higher energy; the slight drop in yield observed at the higher electron voltages probably arises from competition with primary processes with still higher activation energies or from a slight secondary decomposition. Type III curves are for those ions whose relative yields rise slowly and do not level off until at much higher voltages. Type III ions result from high energy processes; they are either primary ions with a high activation energy, or secondary or further fragmentation products which require a high energy for their formation.

Their conclusion is for a pure substance, but according to circumstances it may furnish useful information on a composite system. Curve 1 in Fig. 3 and curve 1 in Fig. 4; curve 2 in Fig. 3 and curve 3 in Fig. 4; and curve 3 in Fig. 3 and curve 2 in Fig. 4 of the present investigation assume forms typical of curves of types I, II and III respectively.

In the spectrum of commercial phosphorus pentoxide, the appearance potential of the $P_4O_9^+$ ion is lower than that of the $P_4O_{10}^+$ ion, as may be

14) A. B. King and F. A. Long, *J. Chem. Phys.*, **29**, 374 (1958).

seen in Fig. 5, and no ion peak of a mass greater than the *m/e* 284 ion, $P_4O_{10}^+$, is observed, as has been mentioned previously. Table II shows that the peak height of the $P_4O_9^+$ ion, at a constant temperature, decreased with time. These results suggest that some part of the $P_4O_9^+$ may not be produced by electron bombardment from the P_4O_{10} molecule by the loss of an oxygen atom and an electron, but that the P_4O_9 itself is a parent molecule. Curve 1 in Fig. 3, indeed, assumes a typical parent ion type, i. e., type I. In the oxidation process of commercial phosphorus pentoxide, lower oxides of phosphorus are reported to be oxidized completely. Curve 3 in Fig. 4, which represents the behavior of the *m/e* 268 ion, $P_4O_9^+$, of purified phosphorus pentoxide, shows that the ion current is far less intense at lower electron energies, where further fragmentations of the P_4O_9 are of minor importance, than that of commercial phosphorus pentoxide. The finding that curve 2 in Fig. 3, the $P_4O_{10}^+$ ion curve from commercial phosphorus pentoxide, is not of the parent ion type, i. e., type I of King and Long, can be accepted if we consider that the oxide contanis a P_4O_9 molecule, the appearance potential of its parent ion, $P_4O_9^+$, being lower than that of $P_4O_{10}^+$ from the P_4O_{10} molecule. In fact, curve 1 in Fig. 4, for $P_4O_{10}^+$ from purified phosphorus pentoxide which contains no P_4O_9 molecule at all, is of the typical parent ion type. A graph similar to Fig. 3 was also obtained from a commercial phosphorus pentoxide at 295°C.

From the standpoint of mass spectrometry, we may conclude that a vapor equilibrium with a commercial phosphorus pentoxide, which is oxidized incompletely, contains the P_4O_9 molecule as well as the P_4O_{10} molecule, and no stable polymers heavier than P_4O_{10}. The molecular structrues of P_4O_{10} and P_4O_6 have been well established by electron diffraction studies.[15] In P_4O_6 the four phosphorus atoms are at the corners of a tetrahedron, each bonded to three oxygen atoms along the tetrahedron edges. The P_4O_{10} molecule is very similar to the P_4O_6 molecule in structure, with the addition of an oxygen atom to each phosphorus atom completing the PO_4 tetrahedra. The structure of P_4O_9 might be much the same as the P_4O_{10} molecule, with the exception of the loss of an unshared oxygen atom from a phosphorus atom. This phosphorus will be trivalent, while the other three atoms are pentavalent. Recently, Thilo, Heinz and Host[16] and Heinz[17] have reported on a mixed crystal consisting of P_4O_9 and P_4O_8 molecules.

From the difference in pattern coefficients between purified phosphorus pentoxide and the commercially-available guaranteed reagent phosphorus pentoxide, the amount of P_4O_9 contained in the latter is estimated to be of an order of a percentage points.

Summary

Phosphorus oxides have been investigated by means of mass spectrometers. The mass spectrometers used were a Nier-type spectrometer equipped with a Knudsen cell and a CEC 21-103C type. From the ionization efficiency curves, P_4O_9 molecules have been found to be contained in vapor equilibrium with a commercially available phosphorus pentoxide. From the relation between the vapor pressure and the temperature of phosphorus pentoxide, the existence of a new low-temperature phase of the oxide has been inferred.

The authors wish to thank Dr. Kazuo Someno and Dr. Etsuro Kobayashi for their helpful discussions. We are also indebted to Miss Hiroko Hoshino for her cooperation in constructing the mass spectrometer, and to Mr. Toshio Nishikawa, Mr. Ichiro Kuga and Mr. Kazuo Maruyama for their help in the measurements. We are also indebted to Mr. Ryuzo Shiota for reading and discussing this manuscript prior to publication.

15) G. C. Hampson and A. J. Stosick, *J. Am. Chem. Soc.*, **60** 1814 (1938); L. R. Maxwell, S. B. Hendricks and L. S. Deming, *J. Chem. Phys.*, **5**, 626 (1937).

16) E. Thilo, D. Heinz and K.-H. Host, *Angew. Chem.* **76**, 229 (1964).

17) D. Heinz, *Z. anorg. u. allgem. Chem.*, **336**, 137 (1965).

BULLETIN OF THE CHEMICAL SOCIETY OF JAPAN VOL. 39 156—160 (1966)

Nitrous Oxide as an Electron Scavenger in the Radiolysis of Hydrocarbons

By Shin SATO, Rei YUGETA, Kyoji SHINSAKA and Terumi TERAO

Department of Applied Physics, Tokyo Institute of Technology, Ookayama, Meguro-ku, Tokyo

(Received June 4, 1965)

Nitrous oxide has been used as an electron scavenger in the radiolysis of hydrocarbons: cyclohexane, cyclohexene, benzene, and their mixtures. Considering that the energy for the formation of an ion pair is about 25 eV. in hydrocarbons, 0.4 mol.l^{-1} of nitrous oxide is not enough to capture all the electrons ejected from irradiated hydrocarbons. In the case of cyclohexane, 70% of the ejected electrons seem to be captured by 0.4 mol.l^{-1} of nitrous oxide. In the case of benzene, $G(N_2)$ is about a half of that for cyclohexane. This has been explained tentatively in terms of the ability of benzene to capture electrons. The $G(H_2)$'s in the cases of cyclohexene and benzene have not shown any noticeable dependence on the concentration of nitrous oxide. This shows that hydrogen does not result from the neutralization in these systems. In order to clarify them, the primary processes in the radiolysis of cyclohexane have been further considered using the data previously obtained.

In an attempt to investigate the charge separation in the radiolysis of liquid hydrocarbons, various electron scavengers, such as iodine, methyl iodide and tetrachloromethane, have been used as solutes.[1,2] However, these compounds are known to be reactive to the free radicals as well as to the electrons produced in the radiolysis, so they are not quite suitable for discriminating the reactions of free radicals and charged species, both of which are believed to participate in the radiolysis of hydrocarbons.

Recently it has become clear that nitrous oxide is highly reactive to electrons, but not to free radicals.[3] The compound has been used as an additive in the radiolysis of water[4,5] and its reaction with hydrated electrons has been interpreted in terms of the following dissociative mechanism:

$$e_{aq} + N_2O \rightarrow N_2 + O^-$$

In the radiolysis of hydrocarbons, it is possible that nitrous oxide are capable of capturing the electrons ejected from irradiated hydrocarbons if its concentration is high enough. In fact, Scholes and Simic suggested in a preliminary report that such a reaction occurs in the radiolysis of cyclohexane.[6]

The present paper will report the results of an independently-undertaken study of the applicability of this technique to the radiolysis of cyclohexane, cyclohexene, and benzene, and mixtures of these hydrocarbons.

Experimental

Guaranteed-grade cyclohexane, cyclohexene and benzene, supplied by the Tooa-gosei Co., have been purified by the conventional method described elsewhere.[7] The final step in the purification was to pass the liquids separately through 1-m. silica gel columns. Impurities of less than 0.1% were detected in the purified cyclohexene by gas chromatography; such small impurities are believed to have no appreciable effect on the radiolysis studied. In the case of cyclohexane, special precaution was taken to eliminate olefin contamination.[7] Nitrous oxide supplied by the Takachiho-shoji Co. was used as supplied; no impurities were detected by gas chromatography.

Samples consisting of 5 ml. of each liquid were irradiated with ^{60}Co-γ rays at room temperature, at a does rate of 1.60×10^{17} eV. ml^{-1} min^{-1}. In estimating the dose, $G(Fe^{3+})=15.6$ was used in the Fricke dosimetry.

The products not condensable at the temperature of liquid nitrogen were measured by a Toepler pump attached to a gas burette and a cuprous oxide furnace kept at 240°C. In this furnace, hydrogen is combusted into water, which is then trapped at the temperature of liquid nitrogen. In the cyclohexane radiolysis, a fair amount of water was detected as a product in some cases, although the amounts measured by gas chromatography were not quantitatively reliable.

Since the solubilities of nitrous oxide in cyclohexane and cyclohexene were not known, they were determined at room temperature using the technique reported by Loprest.[8] The Ostwald absorption coefficients obtained are shown in Table I. The value obtained for

1) L. J. Forrestal and W. H. Hamill, *J. Am. Chem. Soc.*, **83**, 1535 (1961).
2) J. A. Stone and P. J. Dyne, *Can. J. Chem.*, **42**, 669 (1964).
3) G. Czapski and J. Jortner, *Nature*, **188**, 50 (1960).
4) F. S. Dainton and D. B. Peterson, *Proc. Roy. Soc.*, **A267**, 443 (1962).
5) G. Scholes and M. Simic, *J. Phys. Chem.*, **68**, 1731 (1964).
6) G. Scholes and M. Simic, *Nature*, **202**, 895 (1964).
7) S. Sato and S. Shida, *J. Chem. Soc. Japan, Pure Chem. Sect.* (*Nippon Kagaku Zasshi*), **81**, 555 (1960).
8) F. J. Loprest, *J. Phys. Chem.*, **61**, 1128 (1957).

benzene is in good agreement with the value 3.668 at 20°C listed in the International Critical Tables.

Table I. Ostwald absorption coefficients of nitrous oxide (22.9°C)

Solvent	Benzene	Cyclohexane	Cyclohexene
Coefficient	3.45	2.62	3.10

Results

Figure 1 shows the dose dependence of products in the radiolysis of cyclohexane containing 0.05 mol.l^{-1} of nitrous oxide. Hydrogen and nitrogen increase linearly with the dose up to 3×10^{20} eV.ml^{-1}, while cyclohexene shows a non-linear dependence on the dose. The initial G-value of

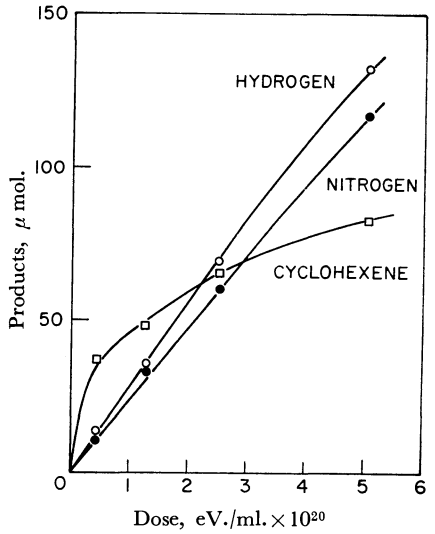

Fig. 1. Dose dependence of the products of the radiolysis of cyclohexane containing 0.05 mol.l^{-1} N_2O.

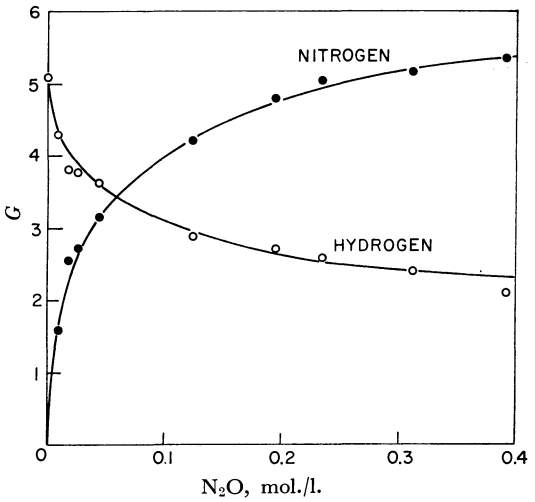

Fig. 2. G-Values of hydrogen and nitrogen from N_2O cyclohexane solution.

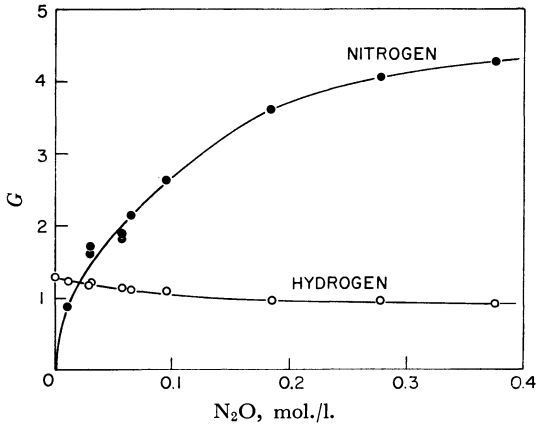

Fig. 3. G-Values of hydrogen and nitrogen from N_2O cyclohexene solution.

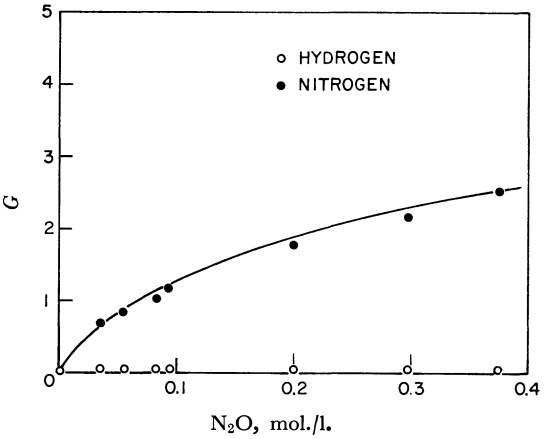

Fig. 4. G-Values of hydrogen and nitrogen from N_2O benzene solution.

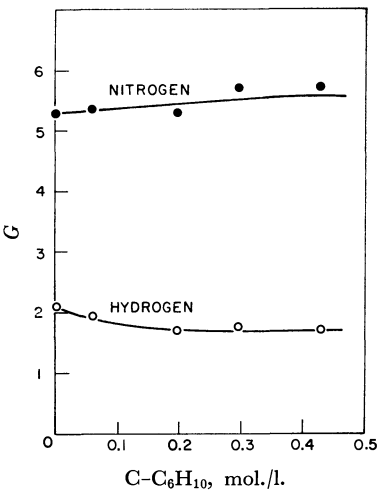

Fig. 5. The effect of cyclohexene on the radiolysis of cyclohexane containing 0.39 mol. l^{-1} N_2O.

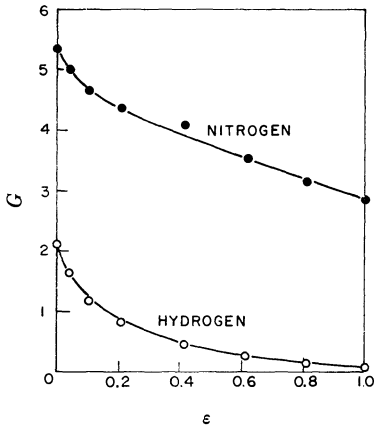

Fig. 6. The effect of N_2O on the radiolysis of mixtures of cyclohexane and benzene. ε is the electron fraction of benzene.

cyclohexene is about twice as large as that in pure cyclohexane.

When the concentration of nitrous oxide is increased, the nitrogen yield increases and the hydrogen yield decreases, though both tend to level-off at high N_2O concentrations, as is shown in Fig. 2. At any N_2O concentration in Fig. 2, the following relationship is found to hold exactly:

$$G(N_2) = 2\Delta G(H_2)$$

where $\Delta G(H_2)$ is the decrease in the G-value of hydrogen. Although quantitative measurements could not be made, the yields of water and cyclohexene were observed to increase with an increase in the concentration of nitrous oxide.

Similar experiments were carried out using cyclohexene and benzene as solvents; the results are shown in Figs. 3 and 4. In these cases water was not detected in the products.

Since olefins are known to act as radical scavengers in the radiolysis of cyclohexane, the effect of the presence of cyclohexene has also been investigated. The results are shown in Fig. 5, where the nitrous oxide concentration is 0.39 mol.l^{-1}. As can be seen from Fig. 2, this concentration is not high enough for $G(N_2)$ and $G(H_2)$ to reach their limiting values. However, in order to obtain a concentration higher than 0.39 mol.l^{-1}, the pressure of N_2O gas inside the cell would have to be in excess of 3 atm., which was the limiting value in the apparatus used.

Figure 6 shows the effect of nitrous oxide on the radiolysis of mixtures of cyclohexane and benzene. The dependence of the nitrogen and hydrogen yields on the electron fraction of benzene evidently indicates an interaction between the two solvents.

9) G. J. Schulz, *J. Chem. Phys.*, **34**, 1778 (1961).
10) S. C. Lind, "Radiation Chemistry of Gases," Reinhold Pub. Corp., New York (1961).

Discussion

Nitrous Oxide as an Electron Scavenger.— The initial processes in the radiolysis of cyclohexane may be represented as follows:

$$C_6H_{12} \rightsquigarrow C_6H_{12}^+ + e \quad (1)$$
$$C_6H_{12} \rightsquigarrow C_6H_{12}^* \quad (2)$$

Reaction 1 corresponds to the ionization, and reaction 2 to the excitation, while $C_6H_{12}^*$ does not necessarily mean an excited state of cyclohexane but a precursor of the decomposition into neutral fragments. The nitrous oxide is known to react with electrons as follows:[9]

$$N_2O + e \rightarrow N_2 + O^- \quad (3)$$

Therefore, if electrons ejected from irradiated cyclohexane are captured by nitrous oxide according to this reaction, the succeeding reactions may be represented as follows:

$$O^- + C_6H_{12}^+ \rightarrow C_6H_{11} + OH \quad (4)$$
$$OH + C_6H_{12} \rightarrow H_2O + C_6H_{11} \quad (5)$$

These reactions explain the formation of water and the increase in the G-value of cyclohexene in the radiolysis of a cyclohexane solution.

If reaction 3 is the only source of nitrogen, $G(N_2)$ should be equal to the G-value of the electrons captured by nitrous oxide. At the highest concentration of nitrous oxide used, $G(N_2)$ reaches 5.3, which means that the energy for the formation of an ion pair should be lower than 20 eV. in this system, while the value observed in the gas phase of many hydrocarbons ranges from 20 to 30 eV.,[10] although the value for cyclohexane has not been reported. Another possible source of nitrogen is the reaction of O^- with nitrous oxide; this has been suggested by Johnson and Warman[11] in the gas phase radiolysis of propane:

$$O^- + N_2O \rightarrow N_2 + O_2^- \quad (6)$$

According to Adams et al.,[12] the rate of the reaction of O^- with the oxygen molecule in an alkaline solution is 2.6×10^9 l. mol^{-1} sec^{-1}. If we take this value for the rate of reaction 6 and assume the rate of reaction of O^- with cyclohexane to be equal to that of a hydrogen atom with cyclohexane, which is lower than 10^7 l.mol^{-1} sec^{-1}, a concentration of 0.1 mol. l^{-1} of nitrous oxide is large enough for the reaction between O^- and cyclohexane to become negligible. However, it is not certain that even a concentration of 0.5 mol.l^{-1} of nitrous oxide is high enough to capture all the electrons ejected from the irradiated cyclohexane.

The highest value of $G(N_2)$ obtained in the radiolysis of cyclohexene solution is 4.3, which is

11) G. R. A. Johnson and J. M. Warman, *Nature*, **203**, 73 (1964).
12) G. E. Adams, J. W. Boag and B. D. Michael, ibid., **205**, 898 (1965).

lower than that for cyclohexane by 1.0. The difference may be explained by the higher reactivity of cyclohexene with O^- than that of cyclohexane.

As is shown in Fig. 5, $G(N_2)$ from a 0.39 mol. l^{-1} N_2O cyclohexane solution slightly increases upon the addition of cyclohexene. The addition of cyclohexene may be considered to assist nitrous oxide in scavenging electrons as follows:

$$e + C_6H_{10} \rightarrow C_6H_{10}^- \quad (7)$$

$$C_6H_{10}^- + N_2O \rightarrow C_6H_{10} + N_2 + O^- \quad (8)$$

where $C_6H_{10}^-$ does not necessarily represent a real ion. In other words, cyclohexene provides a shallow trap for electrons. However, this suggestion seems to contradict the observation that $G(N_2)$ from cyclohexene is lower than that from cyclohexane. Evidently, this matter requires further investigation.

Benzene as an Electron Scavenger.—It has recently been established, from studies of the absorption spectra, that aromatic compounds capture electrons to form negative ions; for example, negative naphthalene ions have been observed in the radiolysis at the temperature of liquid nitrogen[13] and diphenyl ions, in the pulsed radiolysis at room temperature.[14] Similarly, benzene may be expected to capture electrons in the radiolysis, although its ability to do so may be weaker. As is shown in Fig. 4, the $G(N_2)$ from a benzene solution of nitrous oxide is about a half of that from a cyclohexane solution at the same concentration of nitrous oxide. This difference may be explained in terms of the competition between nitrous oxide and benzene for electrons. The reactions of benzene may be represented as follows:

$$C_6H_6 + e \rightarrow C_6H_6^- \quad (9)$$

$$C_6H_6^- + C_6H_6^+ \rightarrow 2C_6H_6 \quad (10)$$

i. e., some of the electrons ejected from the molecules are captured by benzene to form negative ions, and these ions are then neutralized by their parent ions without decomposing. The ratio of the rates of the competitive reactions, 3 and 9, is estimated to be 20 to 1 from the plots of $G(N_2)$'s in Figs. 4 and 6. The reported value for this ratio is about 100 to 1.[6]

The dependence of $G(H_2)$ on the electron fraction of benzene in Fig. 6 may be tentatively explained by the following charge transfer reaction:

$$C_6H_{12}^+ + C_6H_6 \rightarrow C_6H_{12} + C_6H_6^+ \quad (11)$$

The possibility of this reaction has already been suggested.[7]

Initial Processes in the Radiolysis of Cyclohexane.—All the important initial steps which can be envisaged in the radiolysis of cyclohexane may be written as follows:

Initial ionization and excitation:

$$C_6H_{12} \begin{cases} \rightsquigarrow C_6H_{12}^+ + e \\ \rightsquigarrow C_6H_{12}^* \\ \rightsquigarrow C_6H_{12}^{*+} + e \end{cases}$$

Neutralization:

$$C_6H_{12}^+ + e \begin{cases} \rightarrow C_6H_{12} & (a) \\ \rightarrow H + C_6H_{11} & (b) \\ \rightarrow H_2 + C_6H_{10} & (c) \end{cases}$$

Neutral decomposition:

$$C_6H_{12}^* \begin{cases} \rightarrow C_6H_{12} & (d) \\ \rightarrow H + C_6H_{11} & (e) \\ \rightarrow H_2 + C_6H_{10} & (f) \end{cases}$$

The decomposition of the excited ion:

$$C_6H_{12}^{*+} \begin{cases} \rightarrow H + C_6H_{11}^+ & (g) \\ \rightarrow H_2 + C_6H_{10}^+ & (h) \end{cases}$$

where $C_6H_{12}^{*+}$ stands for a precursor ion decomposing before neutralization, if this ever occurs. Reaction h does not necessarily mean a unimolecular decomposition; it can stand for an ion-molecule reaction, such as:

$$C_6H_{12}^+ + C_6H_{12} \rightarrow H_2 + \text{residue} \quad (12)$$

If we now take the letters $a, b, \ldots$, etc. to represent the G-values for the respective reactions, we can obtain the following simultaneous equations (I to V):

For the case of the radiolysis of pure cyclohexane:

$$G(H_2) = b + c + e + f + g + h = 5.6 \quad (I)$$

because hydrogen atoms from reactions b, e and g react as follows:

$$H + C_6H_{12} \rightarrow H_2 + C_6H_{11} \quad (13)$$

and because the observed initial G-value of hydrogen is 5.6.[7]

In the gas phase, the energy needed for the formation of an ion pair of many hydrocarbons is observed to be around 25 eV.; i. e., the G-value of the electron may be assumed to be 4, even in the liquid phase. Therefore:

$$a + b + c + g + h = 4 \quad (II)$$

The relation observed above, $G(N_2) = 2\Delta G(H_2)$, gives:

$$e + f + g + h = 5.6 - G_e = 1.6 \quad (III)$$

When cyclohexene is present in sufficient amounts, the reactions involving hydrogen atoms may be omitted; i. e.,

$$G(H_2) = c + f + h = 2.8 \quad (IV)$$

This value has been estimated to be 2.8 in a previous paper.[7]

When both nitrous oxide and cyclohexene are

13) M. R. Ronayne, J. P. Guarino and W. H. Hamill, *J. Am. Chem. Soc.*, **84**, 4230 (1962).

14) S. Arai and L. M. Dorfman, *J. Chem. Phys.*, **41**, 2190 (1964).

present in sufficient concentrations, the G-value of hydrogen should be given by:

$$G(H_2)=f+h \qquad (V)$$

the observed value of which is 1.7, very close to the 1.6 in III. We will now adopt the latter value.

These simultaneous equations give the following solutions:

$$a=e=g=h=0,\ b=2.8,\ c=1.2 \text{ and } f=1.6$$

If this reasoning is correct, the main primary processes in the radiolysis of cyclohexane can be simply expressed as follows, with their approximate G-values as indicated:

$$C_6H_{12} \begin{cases} \rightsquigarrow C_6H_{12}^{+} + e \\ \rightsquigarrow C_6H_{12}^{*} \end{cases}$$

$$C_6H_{12}^{+}+e \begin{cases} \rightarrow H + C_6H_{11} & G \sim 2.8 \\ \rightarrow H_2 + C_6H_{10} & G \sim 1.2 \end{cases}$$

$$C_6H_{12}^{*} \rightarrow H_2 + C_6H_{10} \qquad G \sim 1.6$$

The last reaction does not necessarily represent only a unimolecular reaction; it may also include a bimolecular reaction. Deuterium labeling can discriminate between these two possibilities.

The authors wish to express their deep thanks to Professor Shoji Shida (Tokyo Institute of Technology) for his interest in and encouragement of the present work. They are also indebted to Dr. R. J. Cvetanovic (National Research Council, Canada) for reading the present manuscript.

BULLETIN OF THE CHEMICAL SOCIETY OF JAPAN VOL. 39 160—164 (1966)

Perchloro-(dimethylene-1, 2-cyclobutanedione) and Its Solvolytic Degradation*

By Akira FUJINO, Kousuke KUSUDA and Takeo SAKAN

Organic Chemistry Division, Research Institute for Atomic Energy, Osaka City University, Kita-ku, Osaka

(Received June 5, 1965)

Perchloro-(3, 4-dimethylenecyclobutene) has been converted to 1, 3', 3', 4', 4'-pentachloro-2-methoxy-3, 4-dimethylenecyclobutene; in some solutions exposed to the air, this then gradually decomposed to perchloro-(dimethylene-1, 2-cyclobutanedione). The further spontaneous degradation of the last compound in an aqueous ethanol solution has also been investigated in order to elucidate the structures of an unstable intermediate (an adduct of ethanol to the carbonyl) and the end product (the hemi-ketal lactone ester). The physical and chemical properties of these compounds have been given and discussed. A possible bicyclic intermediate caused by the interaction between the hydroxyl group and the diagonally-positioned dichloromethylene group in above unstable ethanol adduct has been suggested in the process from the latter compound to the end product.

In a preceding paper,[1] which reported on some chemical properties of perchloro-(3, 4-dimethylenecyclobutene) (I), it was demonstrated that the double bond at the C_{1-2} position of this chlorocarbon is readily cleaved by the attack of various oxidizing agents. Although the extremely high reactivity of the corresponding hydrocarbon,[2,3] which rapidly polymerizes upon being exposed to the air, placed it beyond direct comparison, the expectation of valuable information about the hitherto little mentioned complicated triene system in chlorocarbon led us to initiate this study of the chemical behavior of I. Perchloro-substitution positively effects a retardation of the polymerization tendency of the triene, as in the case of open-chain compounds.[4] Another reason for examining the chemical properties of I as well as of the related compounds is that the reactivity would be closely connected with both the electronic and the steric characters of the chlorine substituents in the molecule. This paper will deal with the action of some bases on I, the subsequent air oxidation of the product to a four-membered α-diketone, and the ethanolysis of the latter, which involves unique type of ring cleavage, to a lactone ester.

* Perchlorocompounds II.

1) A. Fujino, Y. Nagata and T. Sakan, This Bulletin, **38**, 295 (1965).

2) A. T. Blomquist and F. M. Maitlis, *Proc. Chem. Soc.*, **1961**, 332.

3) W. D. Huntsman and H. J. Wristers, *J. Am. Chem. Soc.*, **85**, 3308 (1963).

4) A. Roedig, G. Voss and E. Kuchinke, *Ann.*, **580**, 24 (1953).

Results and Discussion

Compound II (m. p. 124°C), in which one of the chlorine atoms in I is replaced by a methoxy-group, was obtained almost quantitatively when I was treated for a short period with a methanolic sodium or potassium hydroxide solution containing a total of 2.5 equivalents base to I. Similar results were observed with the use of a sodium methoxide solution. Both the infrared spectrum ($\nu_{C=C}$ 1705 s and 1605 vs cm^{-1}, and 935 cm^{-1} assigned to the $-\underset{|}{C}=CCl_2$ group[5]) and the ultraviolet absorption (in Fig. 1, along with that of I) of II indicate that no remarkable change either in its skelton or in the double system has occurred in the transformation of I.

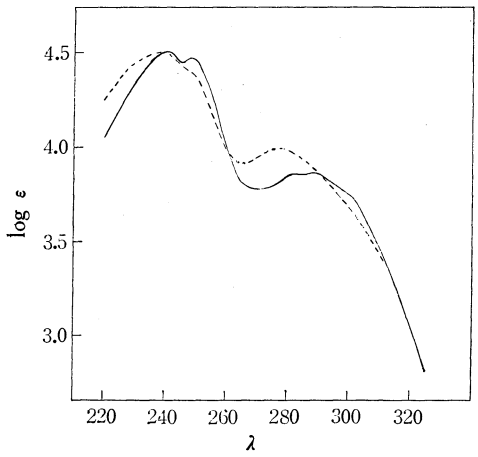

Fig. 1.
---- Perchloro-(3, 4-dimethylenecyclobutene) (I)
—— 1, 3', 3', 4', 4'-Pentachloro-2-methoxy-3, 4-dimethylenecyclobutene (II)

The 1605 cm^{-1} band is the most intense one over the whole absorption range; it is approximately twice as strong as the 1705 cm^{-1} band. This suggests that two bands with the same wave number coincide in the former. In addition, the data are also in accord with the reported observation that the replacement of a chlorine substituent by a methoxy-group in some polychloro-cyclopentadiene[6] and cyclobutene[7] derivatives has caused a shift of their $\nu_{C=C}$ frequencies to a higher region. The oxidation of II with hydrogen peroxide in ether gave perchloro-(dimethylenesuccinic acid).[1] (III) (m. p. 215°C (decomp.)), revealing that the location of the methoxy-group is on the ring carbon. The structural proof for III has been established by the catalytic reduction of III to a chlorine-free dicarboxylic acid (m. p. 211°C), an acid which is identical with the *meso*-dimethylsuccinic acid synthesized from 2-bromopropionic acid. Therefore, the structure shown in Chart I may, without doubt, be given to II.

II was gradually decomposed in benzene or in carbon tetrachloride, while hydrogen chloride was evolved, when the solution was exposed to the air for a long period. The product was a red oil from which scarlet crystals of $C_6Cl_4O_2$ (IV) (m. p. 167°C) were obtained. The structural evidence for its giving the four-membered α-diketone may be enumerated as follows: 1) infrared absorption: $\nu_{C=O}$ 1805 m, 1755 s; $\nu_{C=C}$ 1595 s, 1515 m cm^{-1}; 935cm^{-1} ($-\underset{|}{C}=CCl_2$).[5] 2) IV was oxidized with 30% hydrogen peroxide to the anhydride (V)[1] (m. p. 119—120°C) of III. A similar type of oxidation has been reported by several authors[8-11] for members of the substituted cyclobutadienoquinone series, sometimes as a diagnostic method for α-diketone. 3) IV was normally condensed with *o*-phenylenediamine in acetic acid to give a quinoxaline derivative (IV) (m. p. 197.5—198°C), the ultraviolet spectrum of which is shown, along with that of IV, in Fig. 2. No ring opening as in the reaction of mono-[11] or diphenylcyclobutadienoquinone[12] with the diamine has been observed in this case.

IV may be sublimed under a vacuum and recrystallized from ether. Most interestingly, however, IV was spontaneously decomposed in a solution

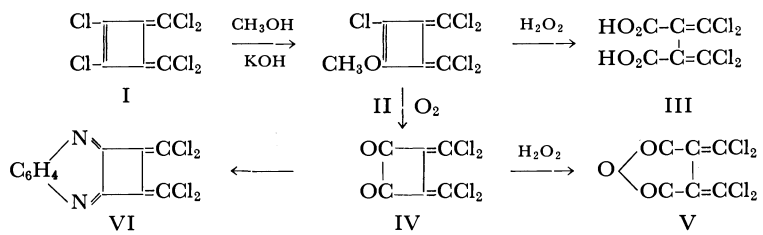

Chart 1

5) See Ref. 1, footnote 11.
6) E. T. McBee, D. L. Crain, R. D. Crain, L. R. Belohlav and H. P. Braendlin, *J. Am. Chem. Soc.*, **84**, 3557 (1962).
7) J. D. Park, J. R. Dick and J. H. Adams, *J. Org. Chem.*, **30**, 400 (1965).
8) A. T. Blomquist and R. A. Vierling, *Tetrahedron Letters*, **1961**, 655.
9) A. T. Blomquist and E. A. LaLancette, *J. Am. Chem. Soc.*, **83**, 1387 (1961).
10) A. Roedig and R. Kohlhaupt, *Tetrahedron Letters*, **1964**, 1107.
11) E. J. Smunty, M. C. Caserio and J. D. Roberts, *J. Am. Chem. Soc.*, **82**, 1793 (1960).
12) A. T. Blomquist and E. A. LaLancette, ibid., **84**, 220 (1962).

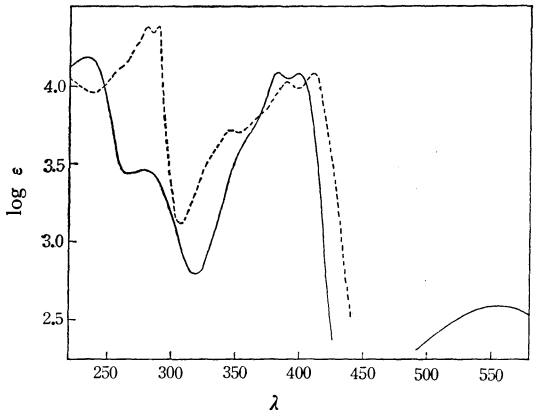

Fig. 2.
—— Perchloro-(dimethylene-1, 2-cyclobutanedione) (IV)
---- Quinoxaline derivative (VI) from IV

in the presence of ethanol and water. It has been observed that, when a small amount of 99% ethanol was added to the system, the peak heights at 234, 280, 383 and 400 (mμ) in the ultraviolet absorption of IV in cyclohexane began to lower at a markedly rapid rate, and then went on to produce, less rapidly, a new absorption peak at 335 mμ. This new peak also started to decay, after reaching a certain height, and finally became a complete transparency. In ethanol alone the original spectral features of IV disappeared too quickly for it to be precisely followed. A more detailed plot of the slower decay at 335 mμ against the time with a highly-diluted, freshly-prepared ethanol solution revealed its half life period to be ca. 30 min. This observation suggests that some unstable reaction intermediate is formed from IV and ethanol, and that the intermediate collapses a little more slowly than IV itself. The isolation of this intermediate has not been successful; the attempted procedures have resulted only in the regeneration of IV as a sublimate. It is highly probable that ethanol has first been added to one of the carbonyls, thus establishing an equilibrium between the adduct (VIIa) and the components, as has been suggested by Mallory and Roberts[13] in the thermal methanolysis of phenylcyclobutadienoquinone. Blomquist and LaLancette[9] reported a smooth ethanolysis of diphenylcyclobutadienoquinone at 25°C; it then proceeds to diethyl α, α'-diphenylsuccinate, probably via bisphenylketene. In the case of IV, however, there can be no transformation like this, for the bis-ketene formation is structurally disallowed. Uhler, Shechter and Tiers[14] also observed the instability of 3, 4-bis(diphenylmethylene)-1, 2-cyclobutanedione in ethanol near room temperature, but they provided no other information on its degradation process. The speculation about the mono-hemiketal intermediate VIIa is further supported by the observation that perchloro-(2, 3-dimethylenecyclobutanone)[15] (VIIb) absorbs the ultraviolet light at 344 mμ in cyclohexane.

IV was refluxed with 99% ethanol in order to examine the decomposition product. The reaction mixture soon turned strongly acidic, and the evolution of hydrogen chloride was observed. The chromatographically-fractionated neutral product was an oily material, $C_{10}Cl_2H_{12}O_5$ (b. p. 170°C (bath temp.)/3.5 mmHg), in a 70% yield. The hemi-ketal lactone ester formula VIIIa is the only one which rigorously accounts for its infrared ($\nu_{C=O}$ 1780m and 1730 s cm^{-1}, $\nu_{C=C}$ 1580 m cm^{-1} and 920 s cm^{-1} for $-C=CCl_2$ group[5]), ultraviolet (λ_{max}^{EtOH} 260 mμ, ε 4500) and NMR (5.64, 5.86, 8.60 and 8.73 τ for the protons in the ethoxy-group and 6.41 τ for the two protons in the $-CH_2CO-$ group) spectral properties. The chain structure (IX), the most possible alternative, may be ruled out in view of the observed high value of the first $\nu_{C=O}$ frequency. The ultraviolet absorption was drastically changed by the addition of alkali;

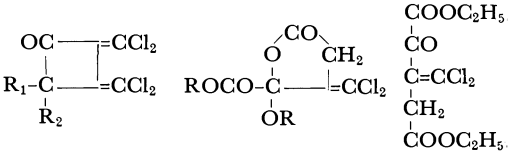

VII a: R_1=OH, R_2=OC_2H_5 b: R_1=R_2=Cl
VIII a: R=C_2H_5 b: R=H
IX

it did not reproduce the original curve on acidification. Further, the 2, 4-dinitrophenylhydrazine test proved the existence of a ketonic group in VIIIa. Both the Tollens' reagent and phosphomolybdic acid in aqueous ammonia normally reacted with VIIIa, whereas the fuchsin-sulfurous acid did not bring about a parallel result. This irregularity in the aldehyde test can well be interpreted as what may reasonably be expected if it is assumed that the dichloromethylene group in VIIIa is a potential aldehyde which, in effect, functions only in the alkaline medium. The alkaline hydrolysis converted VIIIa to a carboxylic acid, $C_6Cl_2H_4O_5$ (VIIIb) (m. p. 131°C). The evidence for the structure included: 1) neutralization equivalent: 114; 2) pK_a value: 1.65 and 4.08; 3) ultraviolet (λ_{max}^{EtOH} 254.5, ε 2100), infrared (ν_{OH} 3200, $\nu_{C=O}$ 1770, 1730; $\nu_{C=C}$ 1670 cm^{-1}) and NMR (5. 79 τ in D_2O) spectra; 4) an indication of a potential aldehyde in the test similar to those for VIIIa. An additional confirmation of the structure has been achieved by the hydrogenation of the dichloromethylene group to a methyl group, followed by an alkaline

13) E. B. Mallory and J. D. Roberts, *J. Am. Chem. Soc.*, **83**, 393 (1961).
14) R. O. Uhler, H. Shechter and G. V. D. Tiers, ibid., **84**, 3397 (1962).
15) This compound will be reported in detail in the succeeding paper.

hydrolysis, presumably to β-methyl α-ketoglutaric acid (X) (the 2, 4-dinitrophenylhydrazone of its monoethyl ester: m. p. 171°C).

In the process VIIa→VIIIa, the initial hydrolysis of the dichloromethylene group β-positioned to the residual carbonyl in VIIa appears to have occurred by way of an acid chloride or its analog. It should be noted here, however, that there is is an another possibility, that the initial participation of the hydroxyl group in VIIa to the diagonally-positioned dichloromethylene moiety is more important in this degradation. Because of the enhanced puckering of the four-membered ring in VIIa due to the two severely-interacting chlorine atoms on each exocyclic methylene carbon, the hydroxyl group is made so closely accessable to the diagonal dichloromethylene or chloroethoxymethylene group as to cause the subsequent formation of a potential lactone, such as XIa or XIb. At the present stage it seems fairly difficult to conclude which one is the true transformation process. However, one piece of evidence which favors the speculation that the ring puckering makes the vinylogical chlorine substituent less reactive toward hydrolysis has been experimentally observed; the fading rate of the red color of IV in dioxan-water (9 : 1 by vol.) was much slower than in an alcoholic system. Even when the solution was heated at 100°C, the hydrolytic degradation took place very gradually. This suggests that the chlorine-substituent hydrolysis of either one or of both, in VIIa will also be slow and will not precede the formation of XI.

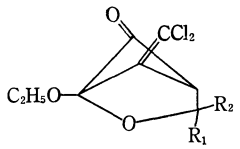

XI a: $R_1=R_2=Cl$
b: $R_1=Cl$, $R_2=OC_2H_5$

An inspection of the model also supports this speculation about the stereospecific approach. Perhaps, as the following step, the hydrolysis of the geminated dichloromethylene or chloro-hemiketal group and the alcoholytic cleavage of the ketone would take place almost concertedly because of its highly-strained bicyclic structure.

Other alcohols, such as methanol (1), propanol (2), isopropyl alcohol (3), *n*-butanol (4), *t*-butanol (5), *n*-hexanol (6), cyclohexanol (7) and benzyl alcohol (8), were preliminarily examined in terms of the ketone degradation. It was found that, except for 3, 5 and 8, they react with IV much like ethanol. IV was decomposed very slowly in the isopropyl alcohol solution, while no noticeable change was observed in *t*-butanol and benzyl alcohol. These definite differences in the reactivity of alcohols may be well interpreted by assuming a difference in the ease of their initial addition to the carbonyl group in IV.

Experimental[16]

1,3',3',4',4'-Pentachloro-2-methoxy-3, 4-dimethylenecyclobutene (II). — A mixture of perchloro-(3, 4-dimethylenecyclobutene) (I) (10 g.) dissolved in benzene (80 ml.) and methanolic potassium hydroxide (4.8 g. of potassum hydroxide in 50 ml. of anhydrous methanol) was stirred at room temperature for 3 hr. The solution was then repeatedly washed with water, and the neutral fraction was separated. The crystalline product was collected after the evaporation of the solvent as white needles, which were recrystallized from methanol to give a material with a melting point of 118—120°C. 5.3 g. (55%). The pure sample for analysis melted at 124°C.

Found: C, 30.11; H, 1.48; Cl, 63.25. Calcd, for $C_7Cl_5H_3O$: C, 29.98; H, 1.08; Cl, 63.23%. UV: λ_{max}^{EtOH} 238(30200), 277(10000); λ_{sh} 233(28200); λ_{min} 264—267(9100), mμ(ε).

The Oxidation of II with Hydrogen Peroxide. —A reagent solution was first prepared by shaking an aqueous hydrogen peroxide solution (30%, 30 ml.) twice with ether (each 25 ml.). II (327 mg.) was dissolved in the ether containing the peroxide, after which the entire solution was allowed to stand at room temperature for 17 days. A part of the acidic fraction (37 mg.) crystallized to give a material which is, in a comparison of their infrared charts, identical with the perchloro-(dimethylenesuccinic acid) (III) previously reported.[1]

The Reduction of III to *meso*-Dimethylsuccinic Acid.—III (266 mg.) dissolved in ethanol (5 ml.) was hydrogenated with 5% palladium chloride on charcoal (200 mg.). After the absorption of the calculated amount of hydrogen, the separated acidic fraction was vacuum-sublimed (120—130°C (bath temp.)/5 mmHg) to give 34 mg. of the material with a melting point of 211°C.

Found: C, 49.44; H, 6.91. Calcd. for $C_6H_{10}O_4$: C, 49.31; H, 6.90%.

meso-Dimethylsuccinic acid was synthesized by heating a mixture of 5 g. each of 2-bromopropionic acid and of silver powder at 150—160°C in a sealed tube for 3 hr. The crystalline product was then collected from a viscous acidic oil after the solution had been kept in a refrigerator. The crystals were purified by sublimation, after being pressed between a folded filter paper, a to material with a melting point of 204—208°C. The infrared absorption of this acid was identical with that of that obtained above by the reduction of III.

Perchloro-(dimethylene-1, 2-cyclobutanedione) (IV).—The benzene (10 ml.) solution of II (2.77 g.) was shaken with oxygen gas at room temperature. A little more than one equimolar amount of oxygen was absorbed in 3 hr. While it was being kept in the open air, the solution gradually turned red and there was a slow evolution of hydrogen chloride, and the solid material crystallized out as red leaflets. The filtered crystals, after being washed with a small amount of carbon tetrachloride, weighed 1.02 g. (42%). Recrystallization from ether afforded a pure sample of diketone IV (m. p. 167°C). The yield of IV was lower when the run was carried out in carbon tetrachloride.

16) All meltng points given are uncorrected.

Found: C, 29.52; H, 0.44; Cl, 57.31. Calcd. for $C_6Cl_4O_2$: C, 29.31; H, 0.00; Cl, 57.68%. UV: $\lambda_{max}^{cyclohexane}$ 233—234(14700), 280(2900), 383(11500), 402—403(11500), 550—560(400); λ_{min} 270(2800), 320(600), 395(10700), mμ(ε).

The Oxidation of IV to Perchloro-(dimethylenesuccinic) Anhydride.—A mixture of a chloroform (4 ml.) solution of IV (100 mg.) and 30% aqueous hydrogen peroxide (1 ml.) was efficiently shaken and allowed to stand at room temperature for 48 hr. The neutral solid mass was then collected and recrystallized from petroleum ether to give a sample of V with a melting point of 119—120°C. 14 mg. The infrared absorption is identical with that previously reported.[15]

1, 2 - Bis (dichloromethylene) cyclobuta [b] quinoxaline (VI).—A mixture of IV (105 mg.) and *o*-phenylenediamine (46 mg.) was heated in acetic acid at 100°C for one hour. After it had been cooled, the solid product was filtered under reduced pressure and recrystallized from ethanol as long yellow needles (m. p. 197.5—198°C). 79 mg.

Found: C, 45.56; H, 1.57; N, 8.75. Calcd. for $C_{12}Cl_4H_4N_2$: C, 45.32, H, 1.27; N, 8.81%. UV: λ_{max}^{EtOH} 270—271(23700), 279(23300), 335—337(5400), 378(10500), 400—402(12200), mμ(ε). IR: $\nu_{C=C}^{Nujol}$ 1665 s, 1640 m, 1610 s, 1583 m cm.$^{-1}$

The Ethyanolytic Degradation of IV to the Hemiketal Lactone Ester (VIIIa).—IV (4.79 g.) was, after the addition of ethanol (40 ml.), heated on a water bath for 10 min. The neutral fraction was then separated and chromatographed on silica gel (10 g.) with benzene. The light yellow main fraction (4.64 g.) was vacuum-distilled at 170°C (bath temp.)/3.5 mmHg to give a colorless oil of VIIIa.

Found: C, 42.35; H, 4.49. Calcd. for $C_{10}Cl_2H_{12}O_5$: C, 42.42; H, 4.27%.

The Hydrolysis of VIIIa to the Hydroxylactone Acid (VIIIb).—To VIIIa (381 mg.) an aqueous sodium hydroxide solution (N, 2.8 ml.) was added; the mixture was then shaken for 10 min. at room temperature. The acidic fraction, when separated in the usual manner, furnished a viscous oil (207 mg.) which gradually solidified to give colorless fine crystals, (m. p. 128—131°C). Repeated recrystallization from chloroform afforded a sample of VIIIb with a melting point of 131—133°C.

Found: C, 31.88; H, 2.04. Calcd. for $C_6Cl_2H_4O_5$: C, 31.74; H, 1.78%.

The Hydrogenation of VIIIb and the Subsequent Hydrolysis to β-Methyl-α-ketoglutaric Acid (X).—The ethanol (5 ml.) solution of VIIIb (1.72 g.) was shaken with hydrogen under atmospheric pressure in the presence of 5% palladium chloride on charcoal. After the calculated amount of hydrogen had been absorbed, the catalyst was filtered off and the filtrate was passed through a column packed with aluminum oxide (5 g.). After the solvent had been removed, the residual oil was vacuum-distilled at 100—120°C (bath temp.)/5 mmHg.

Found: C, 54.96; H, 7.58. Calcd. for $C_{10}H_{16}O_5$: C, 55.54; H, 7.46%. IR: $\nu_{C=C}$ 1800, 1725 cm.$^{-1}$

The distillate above (230 mg.) was heated with an aqueous sodium hydroxide solution (0.1 N, 20 ml.) for 10 min. on a water bath; the acidic product was then continuously extracted with ether. After the ether had been removed After the solution had been dried, the hygroscopic residue remained oily and its infrared spectrum showed a very intense and broad ν_{OH} band.[17] This material (70 mg.) was heated with 2, 4-dinitrophenylhydrazine (60 mg.) in ethanol, the quantity of which was enough to dissolve both of them. A small amount of water (2 ml.) was added, and the whole solution was then strongly heated under refluxing for one hour. The acidic fraction was separated and chromatographed on silica gel, with a developing solvent of benzene - methanol - acetic acid (25: 8 : 4 by vol.), to acid crystals with a melting point of 167—171°C.

Found: C, 45.67; H, 4.33; N, 15.23. Calcd. for $C_{14}H_{16}N_4O_8$: C, 45.65; H, 4.38; N, 15.21%.

We wish to express our thanks to Mr. Junichi Goda and Miss Hiromi Tokuda of Osaka City University for his elemental analyses and her infrared spectra measurement, and also to Dr. Kazuo Tori of Shionogi Research Laboratory for NMR spectra data.

17) Although G. Cauquil reported the melting point of 167°C for X (*Compt. rend.*, **208**, 1156 (1939)), it is doubtful whether the precursory compound (m. p. 186°C), obtained by the oxidation of pulegon with selenium oxide, really has a triketone structure. Our infrared datum indicated the presence of alcoholic group in this compound.

BULLETIN OF THE CHEMICAL SOCIETY OF JAPAN VOL. 39 165—169 (1966)

The Solvent Extraction of Europium Ions with Benzoyltrifluoroacetone. The Synergistic Effect of Oxygen- and Nitrogen-containing Solvents

By Tsunenobu SHIGEMATSU, Masayuki TABUSHI, Masakazu MATSUI and Takaharu HONJYO

Institute for Chemical Research, Kyoto University, Sakyo-ku, Kyoto

(Received June 7, 1965)

The synergistic effect of many kinds of oxygen- and nitrogen-containing solvents on the extraction of europium ions with benzoyltrifluoroacetone in *n*-hexane has been studied. The addition of alcohols, esters, ketones, amines and heterocyclic compounds enhances the extraction, and in general, the solvents with longer carbon chain, especially alcohols and amines, have the larger synergistic effects. At a constant benzoyltrifluoroacetone concentration, the logarithm of the distribution coefficient is linear with pH. The slope of the log D vs. pH plot is about 1.5 in the extraction with 0.05 M benzoyltrifluoroacetone in *n*-hexane, but it is 2 in the presence of 0.04 M oxygen-containing compound and 3 in the presence of 0.04 M nitrogen-containing compound. It may be considered that europium benzoyltrifluoroacetonate forms some adducts with these oxygen- or nitrogen-containing Lewis bases, and that the coordination of nitrogen-containing Lewis bases to the chelates is stronger than that of oxygen-containing ones. Since the solvent extraction of neodymium and lutetium ions with β-diketones is performed as well as that of europium ions, it seems to be a favorable procedure for the extraction of rare earth ions with β-diketones to utilize the adduct formation between β-diketonates and active oxygen- or nitrogen-containing Lewis bases.

The nature of the organic solvent is important in the extraction of metal ions with a suitable chelating reagent.[1] Here the neutral chelate compounds may be extracted into the organic phase, there forming addition compounds with some molecules of water, a solvent and/or an uncoordinated chelating reagent.

In the case of the extraction with such an inert solvent as benzene, chloroform, carbon tetrachloride, *n*-hexane and cyclohexane, the addition of an active oxygen- or nitrogen-containing solvent to the extraction system often increases the extraction. This phenomenon, the synergistic effect of the solvent, may be attributed to the formation of adducts or solvates between the metal chelates and the polar oxygen- or nitrogen-containing solvents. This synergistic effect of the solvent has been observed in the solvent extractions of thorium TTA chelates in the presence of tri-*n*-octylamine[2] and acetic acid[3]; in the solvent extractions of copper(II) and zinc(II) TTA or β-isopropyltropolone chelates in the presence of TBP or hexone,[4] and in the solvent extraction of alkali earth oxinates in the presence of *n*-butyl amine.[5] The synergistic effect has also appeared in the thorium TTA and phosphate ester systems,[2,6] the uranyl DBP-TBP system,[7] and the actinide TTA, TBP and TBPO systems.[8] The chelating reagent also reacts as a donor molecule in the case of a UO_2R_2HR-type complex with uranium(VI) and TTA.[9-11]

On the other hand, there have been severa-investigations of the adduct or solvate formation by the crystallization of chelates, such as the halomethane solvates of tervalent metal acetylacetonates[12]; the solvates of the rare earth acetylacetonates with water and methanol[12,13]; the adducts of copper(II) β-diketonates with heterocyclic bases[14]; the adducts between UO_2 β-diketonates and amine, ammonia, water, ketones or alcohols,[15-17] and europium(III) dibenzoylmethide

1) I. P. Alimarin and Yu. A. Zolotov, *Talanta*, **9**, 891 (1962).
2) L. Newman and P. Klotz, *J. Phys. Chem.*, **67**, 204 (1963).
3) G. Goldstein, O. Menis and D. L. Manning, *Anal. Chem.*, **32**, 400 (1960).
4) T. Sekine and D. Dyrssen, *J. Inorg. Nucl. Chem.*, **26**, 1727 (1964).
5) F. Umland, W. Hoffmann and K. U. Meckenstock, *Z. anal. Chem.*, **173**, 211 (1960).
6) T. V. Healy, *J. Inorg. Nucl. Chem.*, **19**, 314 (1961).
7) D. Dyrssen and L. Kuča, *Acta Chem. Scand.*, **14**, 1945 (1960).
8) H. Irving and D. N. Edgington, *J. Inorg. Nucl. Chem.*, **15**, 158 (1960); **20**, 314, 321 (1961).
9) A. M. Poskazer and B. M. Foreman, Jr., ibid., **16**, 323 (1961).
10) S. Peterson, ibid., **14**, 126 (1960).
11) M. Ishibashi, T. Shigematsu and M. Tabushi, *J. Chem. Soc. Japan, Pure Chem. Sect.* (*Nippon Kagaku Zasshi*), **80**, 1018 (1959).
12) F. R. Clarke, J. F. Steinbach and W. F. Wagner, *J. Inorg. Nucl. Chem.*, **26**, 1311 (1964).
13) G. W. Pope, J. F. Steinbach and W. F. Wagner, ibid., **20**, 304 (1961).
14) D. P. Graddon and E. C. Watton, ibid., **21**, 49 (1961).
15) A. E. Comyns, B. M. Gatehouse and E. Wait, *J. Chem. Soc.*, **1958**, 4655.
16) W. W. Wendlandt, J. L. Bear and G. R. Horton, *J. Phys. Chem.*, **64**, 1289 (1960).
17) L. Sacconi, G. Caroti and P. Paoletti, *J. Chem. Soc.*, **1958**, 4257.

adducts with a number of oxygen- and nitrogen-containing Lewis bases.[18]

During the course of the authors investigations of the extraction of many metal ions with β-diketones,[11,19-23] it has been found that rare earth and uranyl β-diketonates are extracted better with a polar oxygen-containing solvent, such as butyl acetate, than with chloroform or benzene. It may be inferred that rare earth β-diketonates form adducts with the active solvents as well as uranyl chelates do.

In this paper, the synergistic effect of a number of oxygen- and nitrogen-containing solvents on the extraction of europium ions with a fluorinated β-diketone, benzoyltrifluoroacetone in *n*-hexane, will be studied, and the usefulness of this effect in the extraction of rare earth(III) ions with β-diketones will be discussed.

Experimental

Apparatus.—Radioactivity countings were made with a Kobe Kogyo NaI(Tl) (4.45 cm.×5.08 cm.) well-type scintillation counter, model PS-300, connected to a transistorized scaler, model SA-230. A Hitach-Horiba glass electrode pH meter, model M-3, was used for the pH measurements.

Materials.—The radioisotopes of neodyminum-147, europium-152, 154 and lutetium-177 were supplied from ORNL, U. S. A. or from The Radiochemical Center, Amersham, England.

The benzoyltrifluoroacetone was obtained from the Dojindo Co., Ltd., Research Laboratories.

The chloroform was purified by washing it with a diluted sodium hydroxide solution, water, a diluted hydrochloric acid solution and three portions of water, followed by distillation. The butyl acetate was washed with water and distilled. The ethers were shaken with an aqueous ferrous sulphate solution. The furan was refluxed with cuprous chloride and then distilled. All the other reagents were reagent-grade materials and were used without further purification.

Procedure.—The extractions are made by shaking 10 ml. of the aqueous sample solution with 10 ml. of the organic solvent. The aqueous sample solution, adjusted to a desired pH, contains europium ions in the concentration of about 1 p. p. m. (^{152,154}Eu 2—3×10^4 c. p. m.), sodium chloride and acetic acid in each 0.1 molar concentration respectively. When the effect of the nitrogen-containing solvent is investigated, the material is added to the aqueous solution to make a 0.04 M solution. The organic solvent phase is composed of 0.05 M benzoyltrifluoroacetone and a 0.04 M oxygen-containing compound in the studies of the effect of an oxygen-containing solvent.

The aqueous and the organic phase are taken into a 50 ml. separating funnel and then shaken for 15 to 30 min. Two milliliters of each of the two phases are then pipetted into test tubes (14 mm. in diameter); the gamma activities are measured with the NaI scintillation counter, and the pH values of the aqueous phase after the extraction are obtained with the pH meter.

Results

The distribution ratio, D, and the per cent of extraction, $\%E$, were calculated by the following equations;

$$D=\frac{\gamma\text{-count rate per 2 ml. of the org. phase}}{\gamma\text{-count rate per 2 ml. of the aq. phase}}$$

$$\%E=(D/(1+D))\cdot 100$$

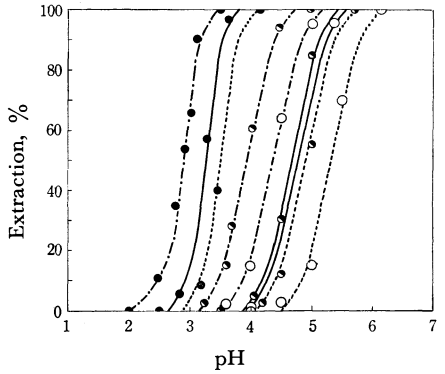

Fig. 1. Extration of rare earth(III) benzoyltrifluoroacetonate.
Rare earth: ····· neodymium, —— europium, —·— lutetium
Solvent: —●— butyl acetate, —◔— benzene, —○— chloroform

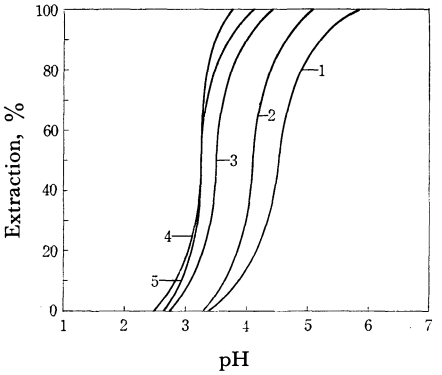

Fig. 2. Extraction of europium benzoyltrifluoroacetonate.
Solvent: *n*-hexane, BTFA: 5×10^{-2} M,
Concentration of added butyl acetate
1 None
2 6.0×10^{-2} M
3 7.6×10^{-1} M
4 3.0 M
5 Pure butyl acetate

18) R. G. Charles and R. C. Ohlmann, *J. Inorg. Nucl. Chem.*, **27**, 119 (1965).
19) T. Shigematsu, M. Tabushi and M. Matsui, This Bulletin, **37**, 1333 (1964).
20) T. Shigematsu, M. Tabushi, M. Matsui, Y. Nishikawa and S. Goda, *J. Chem. Soc. Japan, Pure. Chem. Sect.* (*Nippon Kagaku Zasshi*), **84**, 263 (1963).
21) M. Tabushi, *Bull. Inst. Chem. Res., Kyoto Univ.*, **37**, 252, 226, 237 (1959).
22) T. Shigematsu and M. Tabushi, *J. Chem. Soc. Japan, Pure Chem. Sect.* (*Nippon Kagaku Zasshi*), **81**, 265 (1960).
23) T. Shigematsu, Y. Takenobu and H. Tsujita, unpublished.

The extraction curves for neodymium-, europium- and lutetium-benzoyltrifluoroacetonates with butyl acetate, chloroform and benzene are shown in Fig. 1. From the figure, it may be seen that the extraction of rare earth benzoyltrifluoroacetonates is performed better with butyl acetate than with chloroform or benzene. Figure 2 represents the extraction behavior of the europium chelate in mixed solvents which are prepared by changing the concentration of butyl acetate using *n*-hexane as the diluent. The extraction is much enhanced, even at a low concentration of butyl acetate such as 0.06 M.

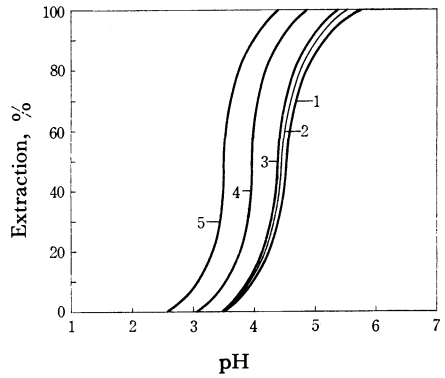

Fig. 3. Extraction of europium benzoyltrifluoroacetonate.
Solvent: *n*-hexane BTFA: 5×10^{-2} M
Molarity of added alcohol: 4×10^{-2} M
1 None or ethyl alcohol
2 *t*-Butyl alcohol
3 *n*-Butyl alcohol, *s*-butyl alcohol, isobutyl alcohol or benzyl alcohol
4 *n*-Amyl alcohol or isoamyl alcohol
5 *n*-Hexyl alcohol, *n*-octyl alcohol, *n*-decyl alcohol or dodecyl alcohol

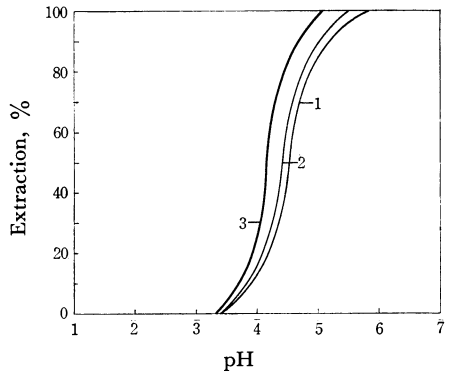

Fig. 4. Extraction of europium benzoyltrifluoroacetonate.
Solvent: *n*-hexane BTFA: 5×10^{-2} M
Molarity of added ester: 4×10^{-2} M
1 None
2 Methyl acetate
3 Ethyl acetate, butyl acetate, amyl acetate or hexyl acetate

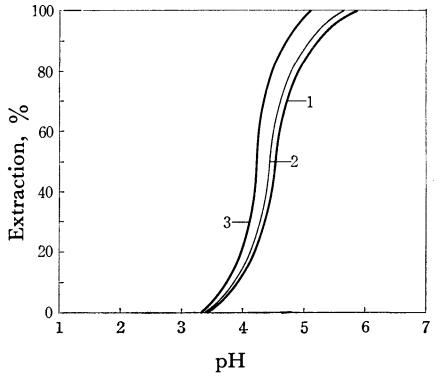

Fig. 5. Extraction of europium benzoyltrifluoroacetonate.
Solvent: *n*-hexane BTFA: 5×10^{-2} M
Molarity of added ketone: 4×10^{-2} M
1 None or acetone
2 Diethyl ketone
3 Methyl isobutyl ketone, methyl *n*-amyl ketone methyl *n*-hexyl ketone or heptyl methyl ketone

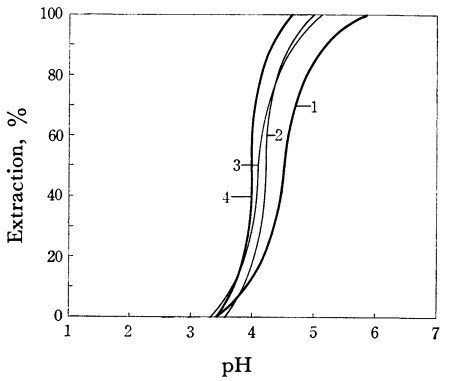

Fig. 6. Extraction of europium benzoyltrifluoroacetonate.
Solvent: *n*-hexane BTFA: 5×10^{-2} M
Molarity of added heterocyclic compound: 4×10^{-2} M
1 None, furan or pyrrole
2 Pyrrolidine
3 Tetrahydrofuran
4 Pyridine or piperidine

The effects of alcohols, esters, ketones and ethers have also been investigated according to the above-described procedure; the extraction curves obtained in the presence of 0.04 M oxygen-containing compounds are shown in Fig. 3 (alcohols), Fig. 4 (esters) and Fig. 5 (ketones). Figure 3 indicates that the higher alcohols have the larger solvent effects. Esters and ketones show effects similar to those of alcohols, although the effect of the latter is much greater than that of the former. Ethers do not have such an influence. The effect of heterocyclic bases has also been studied; the results are shown in Fig. 6. Furan and pyrrole do not exert any effects,

whereas tetrahydrofuran, pyrrolidine, pyridine and piperidine increase the extraction. As is shown in Fig. 7, amines have the same effect as alcohols, and the presence of amines and other nitrogen-containing Lewis bases causes a steeper rise in the extraction curves than does that of oxygen-containing compounds.

This fact becomes more evident from the results in Fig. 8, which presents the slope of the log-D vs. pH plot obtained at 0.05 M benzoyltrifluoroacetone. When the extraction is carried out using n-hexane as the extracting solvent, the slope of the log D vs. pH plot is about 1.5. This slope is 2 in the extraction using n-hexane containing 0.04 M oxygen-containing compounds as the extracting solvents, and 3 in the presence of 0.04 M nitrogen-containing Lewis bases.

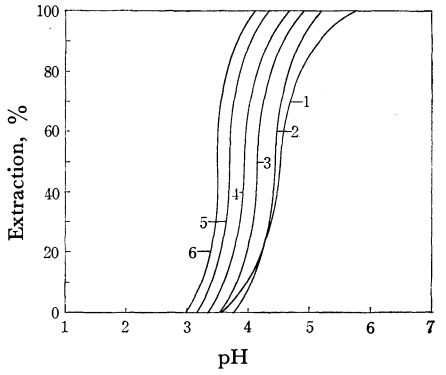

Fig. 7. Extraction of europium benzoyltrifluoroacetonate.
Solvent: n-hexane BTFA: 5×10^{-2} M
Molarity of added amine: 4×10^{-2} M
1 None
2 Ethyl amine
3 t-Butyl amine
4 n-Butyl amine
5 n-Hexyl amine
6 Octyl amine

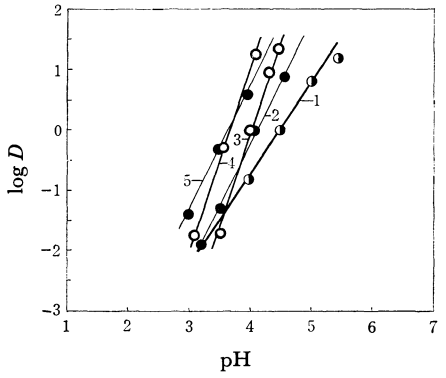

Fig. 8. Variation of the distribution ratio, D as a function of pH.
Solvent: n-hexane BTFA: 5×10^{-2} M
Molarity of added Lewis base: 4×10^{-2}
Slope: 1 None (1.5)
2 Tetrahydrofuran (2.0)
3 Pyridine (3.0)
4 n-Hexyl amine (3.0)
5 n-Hexyl alcohol (2.0)

Discussion

The extraction of rare earth benzoyltrifluoroacetonates improves in the order of lutetium, europium, and neodymium, as is shown in Fig. 1. Generally, the stability of rare earth β-diketonates increases with the decrease in the ionic size, that is, with the decrease in basicity,[24-26] while their extraction is enhanced with the decreasing basicity of the central metal ions.[27] The results in Fig. 1 are in agreement with these facts.

Table I shows the shifts of the $pH_{1/2}$s of the extraction caused by the addition of several sorts of oxygen- or nitrogen-containing compounds (Lewis base). In general, the $pH_{1/2}$ shifts seem to enlarge with the increase in the length of the carbon chain of the base. These effects of the carbon cahin length could be ascribed to the decreasing solubility of the higher base in water.

The role of these Lewis bases in the extraction behavior of the chelate can be explained as follows. If a neutral metal chelate extracted reacts with a Lewis base to form the adduct compound, the concentration of the chelate in the organic phase decreases. Then the overall extraction equilibrium of the metal chelate shifts in the direction that favors the rise of the distribution ratio (organic/aqueous) of the metal.

Table I suggests an attractive technique for the solvent extraction of rare earth ions. By utilizing the adduct formation between rare earth benzoyltrifluoroacetone chelate and Lewis bases, the extraction can be undertaken at a lower pH region.

The differences found among the solvent effects of alcohols, esters, ketones and ethers are probably due to the basicity of the oxygen atoms in the solvent molecules. Figure 6 suggests that lone-pair electrons of furan and pyrrole participate in the resonance stabilization of the molecule, whereas lone-pair electrons of tetrahydrofuran, pyrrolidine, pyridine and piperidine are utilized in the adduct formation.

The difference observed between the solvent effect of oxygen- and nitrogen-containing Lewis bases may be attributed to the differences in the donating power of the active oxygen and nitrogen atoms in the molecules, indicating that the bonding of the former to the metal chelates is weaker than that of the latter.

24) N. K. Dutt and P. Bandyopadhyay, *J. Inorg. Nucl. Chem.*, **26**, 729 (1964).
25) R. M. Izatt et al., *J. Phys. Chem.*, **59**, 80, 170 (1955).
26) I. Grenthe and W. C. Fernelius, *J. Am. Chem. Soc.*, **82**, 6258 (1960).
27) W. B. Brown, J. F. Steinbach and W. F. Wagner, *J. Inorg. Nucl. Chem.*, **13**, 119 (1960).

Table I. Shift of $pH_{1/2}$ of the extraction curve obtained by the addition of 4×10^{-2} M oxygen- and nitrogen-containig solvent or Lewis base to water - *n*-hexane extraction system

Organic solvent of Lewis base	$-\Delta pH_{1/2}$	Organic solvent or Lewis base	$-\Delta pH_{1/2}$
n-Hexane	—	Diethyl ketone	0.16
Ethyl alcohol	0	Methyl isobutyl ketone	0.39
n-Butyl alcohol	0.19	Methyl *n*-amyl ketone	0.42
s-Butyl alcohol	0.16	Methyl *n*-hexyl ketone	0.43
t-Butyl alcohol	0.09	Heptyl methyl ketone	0.45
Isobutyl alcohol	0.18	Ethyl ether	0
n-Amyl alcohol	0.64	Isopropyl ether	0
Isoamyl alcohol	0.63	Furan	0
n-Hexyl alcohol	1.10	Tetrahydrofuran	0.41
n-Octyl alcohol	1.11	Pyrrole	0
n-Decyl alcohol	1.12	Pyrrolidine	0.25
Dodecyl alcohol	1.12	Pyridine	0.50
Benzyl alcohol	0.16	Piperidine	0.50
Methyl acetate	0.17	Ethyl amine	0.05
Ethyl acetate	0.44	*t*-Butyl amine	0.35
n-Butyl acetate	0.49	*n*-Butyl amine	0.53
n-Amyl acetate	0.54	*n*-Hexyl amine	0.80
Hexyl acetate	0.55	Octyl amine	1.03
Acetone	0		

The bondings of the donor molecules (including water molecules) to the metal chelates have been widely studied by various methods; they have generally been classified into two groups; (1) donor molecules bond to the coordinated chelating reagents by dipole-dipole interaction or hydrogen bonding,[12] and (2) donor molecules coordinate directly to the central metal ions.[17,18] Both monomers and dimers of the chelates also exist in a non-aqueous solution.[13,28,29] There are several pieces of evidence that rare earth β-diketonates have coordination numbers greater than six,[30] and the coordination number of seven may be expected from the fact that one water molecule is always tightly held on the crystal of rare earth β-diketonates.[12,13,31] From the results in Fig. 6 and Fig. 7, it might be considered that nitrogen-containing Lewis bases substitute with the water molecule directly coordinated to central metal ions, although more detailed experiments must be undertaken before a definite conclusion can be reached.

At any rate, it is evident that the adduct formation with Lewis bases is favorable for the solvent extraction of rare earths as the benzoyltrifluoroacetone chelates; it is also probable that a similar advantage can be expected in some other cases of the extraction of metal β-diketonates, which show a poor extractability in the absence of adduct-forming materials.

28) S. Freed, S. I. Weissman and F. E. Fortess, *J. Am. Chem. Soc.*, **63**, 1079 (1941).
29) T. Moeller and W. F. Ulrich, *J. Inorg. Nucl. Chem.*, **2**, 164 (1956).
30) L. C. Thompson and J. A. Lorass, *Inorg. Chem.*, **2**, 89 (1963).
31) R. G. Charles and A. Perrotto, *J. Inorg. Nucl. Chem.*, **26**, 373 (1964).

BULLETIN OF THE CHEMICAL SOCIETY OF JAPAN VOL. 39 170—178 (1966)

Aminocyclitols. VIII. A Synthesis of Inosamines and Inosadiamines*

By Tetsuo SUAMI,† Frieder W. LICHTENTHALER†† and Seiichiro OGAWA†

† *Department of Applied Chemistry, Faculty of Engineering, Keio University, Koganei-shi, Tokyo*
†† *Institut für Organische Chemie, Technische Hochschule, 61 Darmstadt, Germany*

(Received June 8, 1965; in revised form July 23, 1965)

muco-Inosamine-1, *scyllo*-inosamine, *muco*-inosadiamine-1, 5 and *myo*-inosadiamine-1, 2 have been synthesized from *myo*-inositol. Their structures have also been established by a study of the NMR spectra of their acetyl derivatives. When 1, 4, 5, 6-tetra-*O*-acetyl-3-*O*-mesyl-*myo*-inositol is treated with sodium azide in boiling aqueous 2-methoxyethanol, an azido derivative is obtained. The azido compound is hydrogenated in the presence of a catalyst and subsequently acetylated to give muco-inosamine-1. The stereochemical course of the reaction has been proposed to be an anchimeric reaction. When the analogous reaction is carried out with 2, 3-di-*O*-mesyl-*myo*-inositol tetraacetate, *myo*-inosadiamine-1, 2 or *muco*-inosadiamine-1, 5 is obtained as the main product, depending on the solvent applied.

In connection with a previous communication,[1] a new synthesis of *muco*-inosamine-1,[4] *scyllo*-inosamine,[8] *muco*-inosadiamine-1, 5 and *myo*-inosadiamine-1, 2, and their structures as established by means of the NMR spectra, will be described in the present paper.

scyllo- and *muco*-1-Inosamine

1, 4, 5, 6-Tetra-*O*-acetyl-*myo*-inositol (I)[2] has been used as the starting material. By treating I with one mole of methanesulfonyl chloride in pyridine, 1, 4, 5, 6-tetra-*O*-acetyl-3-*O*-mesyl-*myo*-inositol (II) is obtained in a fairly good yield. Then the acetylation of II gives 3-*O*-mesyl-*myo*-inositol pentaacetate (III).[3] The sturctures of II and III have been established by means of the NMR spectra, along with chemical evidence.[1] The spectrum of III in chloroform (Fig. 1) reveals a sharp signal at 7.00 τ, which is assigned to the protons of an equatorial mesyloxy group.[3] The signal at 7.78 τ corresponds to an axial acetoxy group, and the

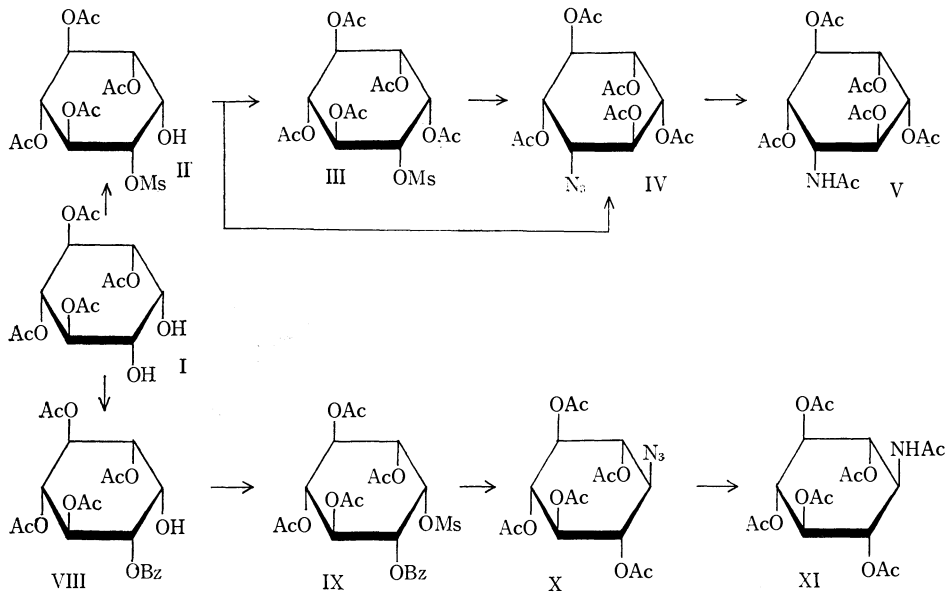

* A part of this research has been presented at the 18th Annual Meeting of the Chemical Society of Japan, Osaka, April, 1965.

1) T. Suami and S. Ogawa, This Bulletin, **37**, 1238 (1964).

2) S. J. Angyal, P. T. Gilham and C. G. Macdonald, *J. Chem. Soc.*, **1957**, 1417.

3) T. Suami, F. W. Lichtenthaler and S. Ogawa, This Bulletin, **38**, 754 (1965).

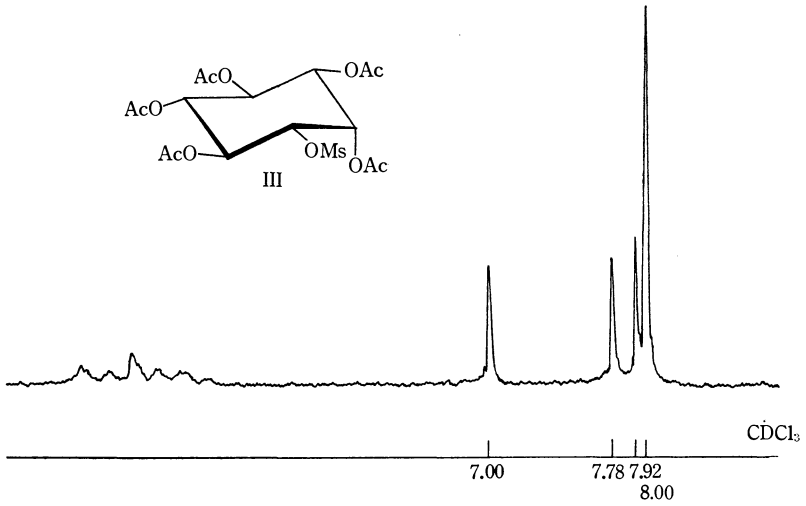

Fig. 1

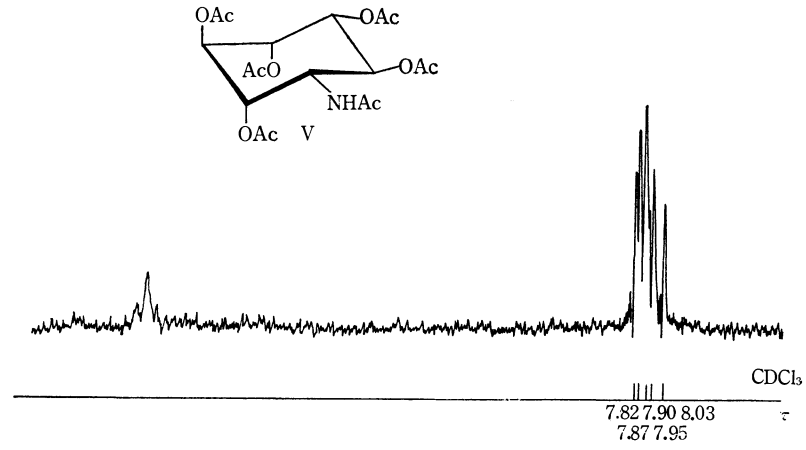

Fig. 2

signals at 7.92 and 8.00 τ with a 1 : 3-intensity are expected from four equatorial acetoxy groups.

When III is treated with sodium azide in boiling aqueous 2-methoxyethanol and subsequently acetylated, an azido acetate (IV) is obtained. Upon the catalytic reduction of IV, followed by acetylation, hexaacetyl-*muco*-inosamine-1 (V) is obtained in 32% yield; it has been identified by a mixed melting point determination.[4] V can also be prepared from II by an analogous reaction sequence.

Considering the configuration of the product obtained, the demesylation of III seems to proceed through an intermediate formation of a dioxolane-ring by participation of the vicinal, trans-orientated acetoxy group, which is then cleaved by a nucleophilic attack of the azide ion in the manner of a diaxial opening.[3]

V can also be prepared in 40% yield from II by treatment with ammonia in methanol under pressure and by subsequent acetylation. Since the first step of this reaction is a de-*O*-acetylation, the formation of V must proceed via an oxirane ring between C-3 and C-4, a ring which is diaxially opened.[5]

The stereochemical courses of these reactions are analogous to an attack of the acetate ion on

4) M. Nakajima, A. Hasegawa and N. Kurihara, *Chem. Ber.*, **95**, 2708 (1962): The melting point determination has kindly been carried out by Professor Minoru Nakajima of Kyoto University.

5) E. W. Bodycote, W. N. Haworth and E. L. Hirst, *J. Chem. Soc.* **1934**, 151; R. W. Jeanloz and A. M. C. Rapin, *J. Org. Chem.*, **28**, 2978 (1963); R. S. Tipson, "Advances in Carbohydrate Chemistry," Vol. 8, Academic Press, New York (1953), pp. 176—177.

the anchimeric intermediate acetoxonium ion[6] and to an opening of a highly-strained oxirane ring by a nucleophile.[7]

NMR-spectroscopical data support the muco-configuration: the hexaacetate V shows sharp signals at 8.03 τ, as is to be expected from an equatorial acetamido group, and at 7.82, 7.87, 7.90 and 7.95 τ (1 : 1 : 1 : 2), arising from three axial and two equatorial acetoxy groups.

The NMR spectrum of *N*-acetyl-*muco*-inosamine-1 (VI), prepared by the de-*O*-acetylation of V, in D_2O (Fig. 3) reveals one sharp signal at 7.98 τ due to the acetamido group in an equatorial orientation.

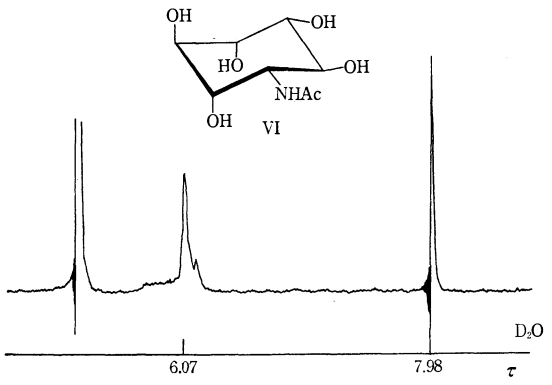

p. p. m., $H \rightarrow$

Fig. 3

When the demesylation of III with sodium azide is carried out in dimethylformamide instead of in 2-methoxyethanol, an as-yet-unidentified hexaacetyl-inosamine (VII) is obtained besides V, and this substance shows a remarkable depression in a mixed melting point determination with hexaacetyl-*rac*-inosamine-2.[8]

In analogy to the monomesylation of tetraacetyl-*myo*-inositol (I→II), a selective monobenzoylation to the 3-*O*-benzoyl derivative should also be possible by treating I with benzoyl chloride under appropriate conditions. When one mole of benzoyl chloride is added to I in pyridine at 5°C, a tetra-*O*-acetyl-3-*O*-benzoyl derivative (VIII) is obtained in a good yield. It can easily be mesylated with methanesulfonyl chloride to 3-*O*-benzoyl-2-*O*-mesyl-*myo*-inositol tetraacetate (IX). This product IX is quite different in its physical properties from the 2-*O*-benzoyl-3-*O*-mesyl-*myo*-inositol tetraacetate (XIX) prepared by the benzoylation of II. Also, their NMR spectra are distinctly different (cf. Figs. 4 and 5 respectively). The spectrum of IX reveals a sharp signal at 6.94 τ corresponding to an axial mesyloxy group, while in the case of XIX the signal of the mesyl protons is shifted to a higher field (6.98 τ), as is to be expected from an equatorial mesyloxy group. Therefore, it is reasonable to conclude that IX is 3-*O*-benzoyl-2-*O*-mesyl-*myo*-inositol tetraacetate. It must be noticed that benzoyl chloride attacks an equatorial hydroxyl group rather than an axial one, as does *p*-toluenesulfonyl chloride[9] or methanesulfonyl chloride[1].

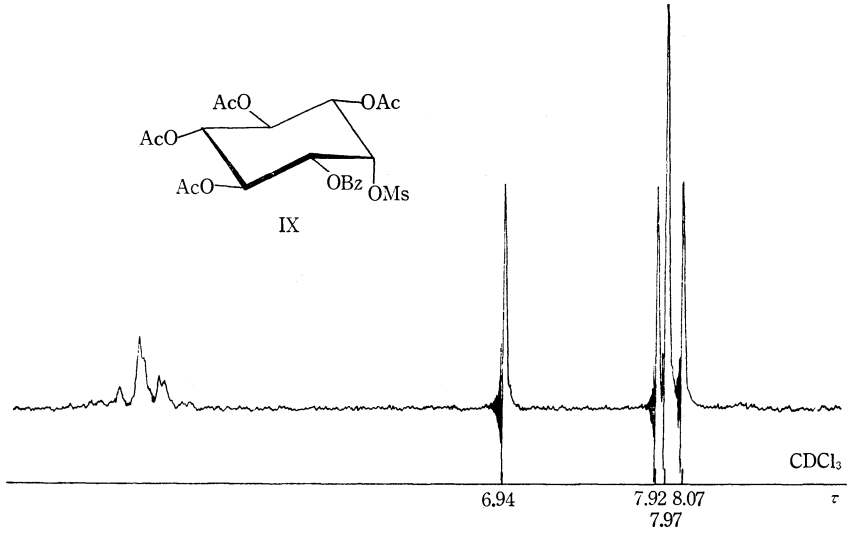

p. p. m., $H \rightarrow$

Fig. 4

6) E. S. Gould, "Mechanism and Structure in Organic Chemistry," Rinehart & Winston, New York (1959), pp. 565—566.

7) E. Eliel, in M. S. Newman, "Steric Effects in Organic Chemistry," J. Wiley & Sons, New York (1956), pp. 130—134; M. Nakajima, A. Hasegawa and F. W. Lichtenthaler, *Ann. Chem.*, **669**, 75 (1963).

8) M. Nakajima, N. Kurihara and A. Hasegawa, *Chem. Ber.*, **95**, 141 (1962); an authentic sample of hexaacetyl-*rac*-inosamine-2 has been presented by Professor Minoru Nakajima of Kyoto University.

9) S. J. Angyal and L. Anderson, "Advances in Carbohydrate Chemistry," Vol. XIV, Academic Press, New York (1959), p. 167.

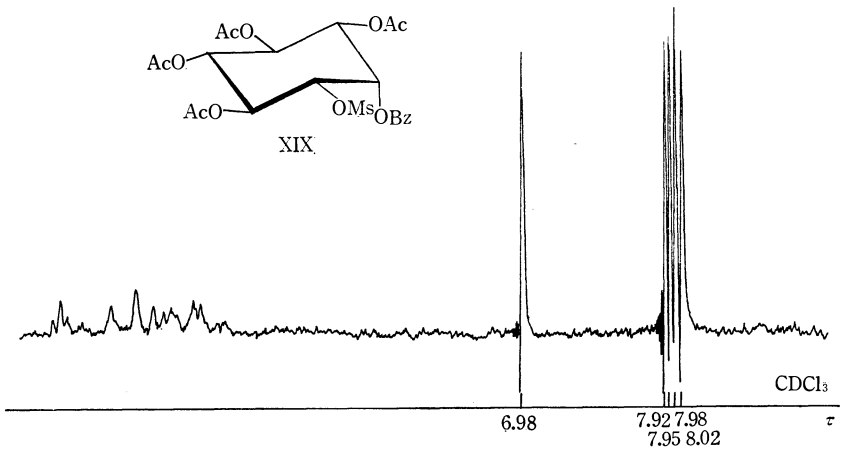

p. p. m., $H \rightarrow$

Fig. 5

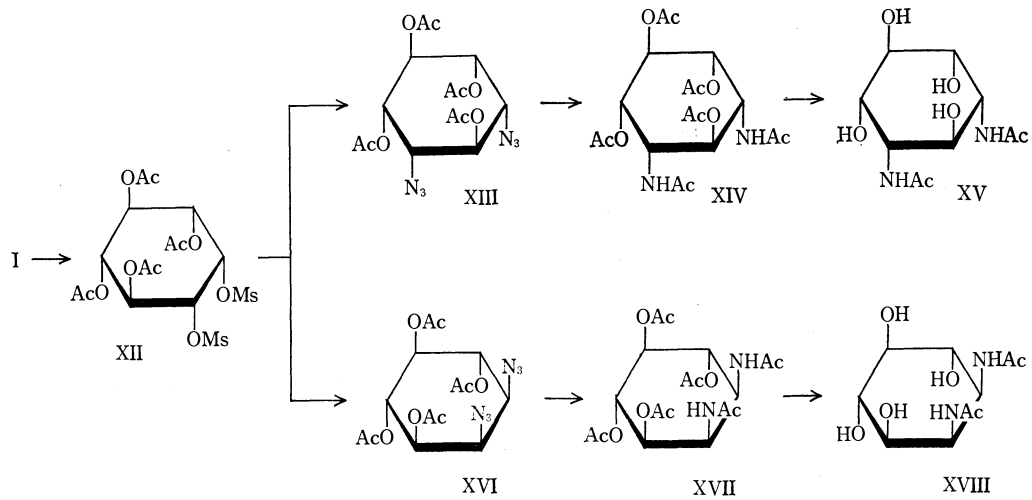

When IX is treated with sodium azide in boiling aqueous 2-methoxyethanol, an azido compound (X) is obtained; upon hydrogenation and subsequent acetylation, this compound yields hexaacetyl-*scyllo*-inosamine (XI).[10]

In the case of compound IX, the two vicinal acyloxy groups are located in an anchimerically-unassisted cis configuration to the mesyloxy group. Thus a neighboring group participation is improbable, and a direct S_N2 mechanism[11] must be proposed for the demesylation of IX with sodium azide.

myo-1, 2 and *muco*-1, 5-Inosadiamine

Upon the treatment of tetraacetyl-*myo*-inositol (I) with two moles of methanesulfonyl chloride in pyridine, 2,3-di-*O*-mesyl-*myo*-inositol tetraacetate (XII) is obtained in a good yield. Its NMR spectrum (Fig. 6) reveals two sharp signals at 6.80 and 6.89 τ, corresponding to an axial and an equatorial mesyloxy group respectively.

By treating XII with sodium azide in aqueous 2-methoxyethanol, a diazido derivative (XIII) is obtained; this is converted to hexaacetyl-*muco*-inosadiamine-1, 5 (XIV) by hydrogenation and by subsequent acetylation.

The structure of XIV as a *m*-inosadiamine and its *muco*-1, 5-configuration is established on the basis of the following data: 1) The hexaacetate XIV is easily de-*O*-acetylated with methanolic ammonia to its di-*N*-acetate (XV), which, upon periodation, consumes 2.2 mol. of periodate in 43 hr. Thus the two acetamido groups must be located in a 1, 3-position. 2) Since the hexaacetate XIV is insoluble in chloroform, the NMR spectrum was measured in pyridine and in d_6-dimethylsulfoxide (DMSO). In pyridine, signals

10) H. E. Carter, R. K. Clark, Jr., B. Lytle and G. E. McCasland, *J. Biol. Chem.*, **175**, 683 (1948).

11) B. R. Baker and A. H. Haines, *J. Org. Chem.*, **28**, 442 (1963).

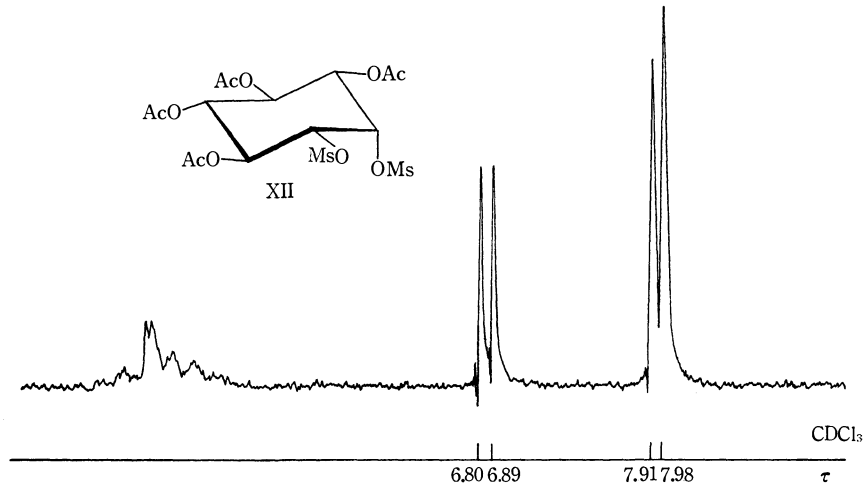

p. p. m., $H \rightarrow$

Fig. 6

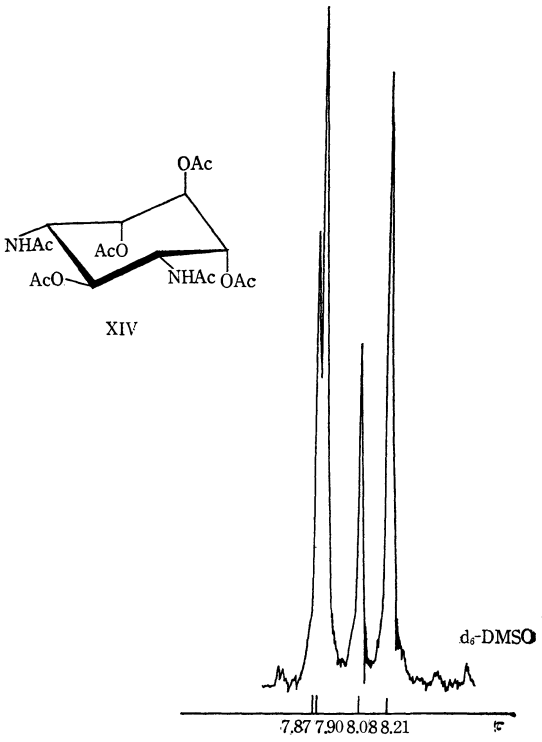

p. p. m., $H \rightarrow$

Fig. 7

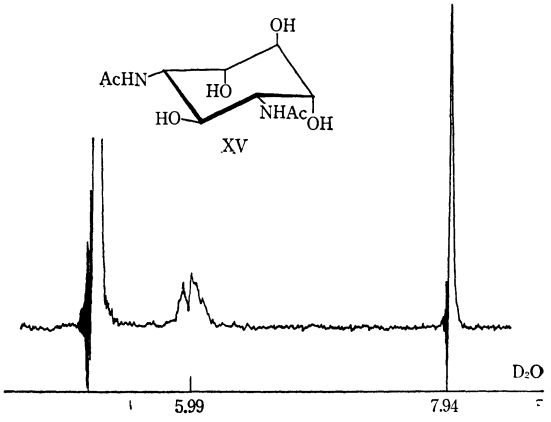

p. p. m., $H \rightarrow$

Fig. 8

were obtained in the 8 τ-region; however, when compared with the signals in similar compounds, these signals showed no apparent correlation with the configuration. In d_6-DMSO however, nicely-resolved signals for the acetyl groups were obtained in the 8 τ-region (Fig. 7): a four signal pattern with a 1 : 2 : 1 : 2-intensity. Since the absorption ranges obtained for axial and equatorial acetoxy or acetamido-groups in chloroform solution[12] cannot be applied for other solvents, a series of compounds have been measured in d_6-DMSO; on the basis of these measurements the following ranges could be established: a) acetoxy-groups, axial 7.86—7.91 τ; equatorial 8.05—8.11 τ; b) equatorial acetamido-groups 8.19—8.30 τ.[13] Subsequently, the NMR-signals of XIV in d_6-DMSO can be convincingly assigned to three axial acetoxy groups, 7.87 τ (1) and 7.90 τ (2), one equatorial acetoxy group (8.08 τ), and two equatorial acetamido groups (8.21 τ), thus establishing the *muco*-1, 5-configuration for XIV.

The di-*N*-acetate (XV) has, in its NMR-spectrum in D_2O (Fig. 8), one sharp signal at 7.94 τ, showing the presence of two sterically-equivalent

12) F. W. Lichtenthaler, *Chem. Ber.*, **96**, 2047 (1963).
13) F. W. Lichtenthaler, H. Leinert and H. P. Albrecht, *Tetrahedron Letters*, in press.

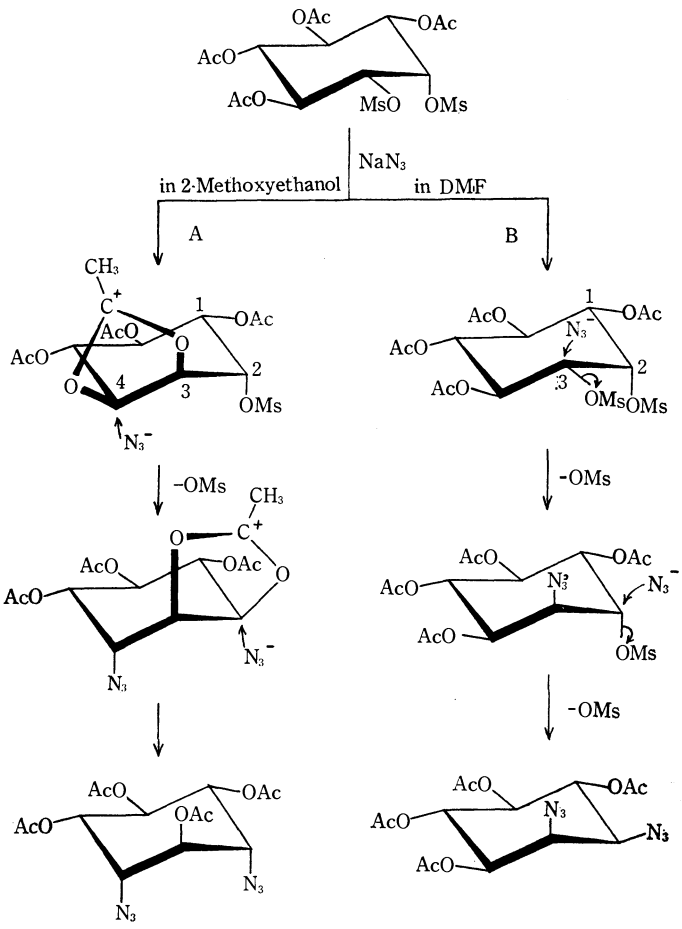

(equatorial) acetamido-groups, thus supporting the *muco*-1, 5-configuration.

The course of the reaction can be explained by assuming the formation of an acetoxonium ion in an anchimeric mechanism with the displacement of the mesyloxy group on C-3. Then an nucleophilic attack by an azide ion can occur in the manner of a trans-diaxial opening of a dioxolane ring.[6] Now again, a mesyloxy group and an acetoxy group are in a trans orientation, resulting in the formation of another acetoxonium ion and subsequent clevage by the azide ion. This reaction sequence is shown in the following chart (course A).

When XII is treated with ammonia under pressure, the same *muco*-inosadiamine-1, 5 is obtained. In this reaction, de-*O*-acetylation takes place at first and an oxirane ring may be formed;[5] this ring is then cleaved by the nucleophilic attack of ammonia in the manner described above.

When XII is reacted with sodium azide in aqueous dimethylformamide instead of 2-methoxyethanol and subsequently treated in a manner analogous to that in which XIV is obtained, hexaacetyl-*myo*-inosadiamine-1, 2 (XVII) is obtained.

The structural and configurational proof was obtained from the following data; the NMR spectrum of XVII in d_6-DMSO (Fig. 9) gives two sharp signals, with an equal intensity, at 8.14 and 8.23 τ; these signals are to be assigned to an axial and an equatorial acetamido group respectively. The four equatorial acetoxy groups give two signals with a 1 : 3-intensity at 8.05 and 8.08 τ. The NMR spectrum of the di-*N*-acetate (XVIII), obtained by the de-*O*-acetylation of XVII with methanolic ammonia is shown in Fig. 10: two sharp signals, with an intensity of 1 : 1, at 7.96 and 8.07 τ, corresponding to an axial and an equatorial acetamido group respectively. Furthermore, it shows a triplet at 5.47 τ (J= 3.5 c. p. s.), as i expected[14] for the C-2-hydrogen in XVIII. Also, XVIII consumes 3.3 mol. of periodate in 43 hr., showing that the two acetamido groups are in a vicinal position, thus establishing unequivocally the *myo*-1, 2-configuration. Considering the structure and configuration of the product obtained, a quite different mechanism must operate in the course of this reaction; the

14) G. Slomp and F. A. MacKellar, ibid., **12** 521 (1962).

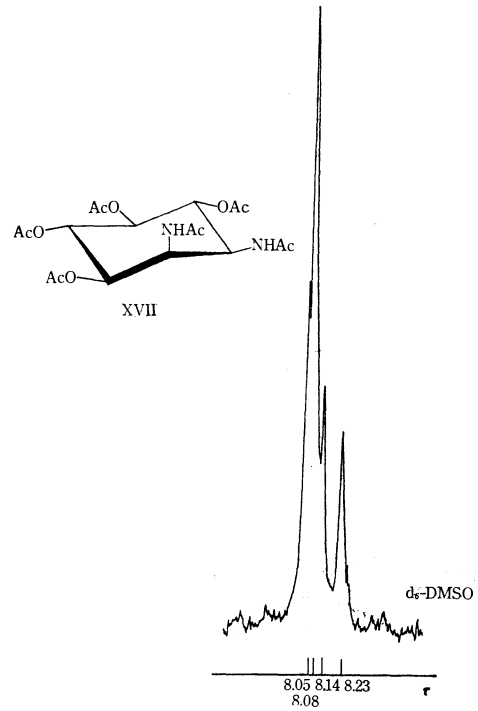

p. p. m., $H \rightarrow$

Fig. 9

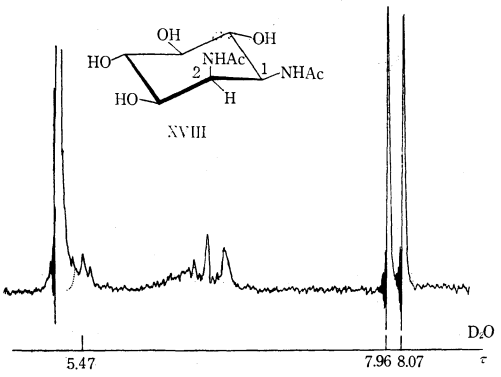

p. p. m., $H \rightarrow$

Fig. 10

replacement of the mesyloxy groups on C-2 and C-3 must proceed predominantly through a direct S_N2 mechanism and, hence, Walden inversions must occur on C-2 and C-3 (course B).

The different reaction mechanisms caused by a change in solvent in the displacement of a mesyloxy group have been reported in previous communications;[3,15] this is another valid example of a solvent effect on a stereochemical course of the reaction. That is, in 2-methoxyethanol an anchimeric reaction is predominant, while a direct S_N2 reaction is dominant in dimethylformamide.

15) B. R. Baker and H. S. Sachdev, *J. Org. Chem.*, **28**, 2132 (1963).

Experimental

The melting points reported were determined on a Mitamura Riken micro hot stage. The melting points marked with asterisks were measured in a liquid bath and are uncorrected. The infrared spectra were determined by pressed potassium bromide disks. The NMR spectra of the samples were determined at a frequency of 60 Mc. p. s. in deuteriochloroform, deuterium oxide or deuteriodimethylsulfoxide with tetramethylsilane, sodium trimethylsilylpropanesulfonate or tetramethylsilane respectively as an internal standard. The peak positions are given in τ-values.

1, 4, 5, 6-Tetra-*O*-acetyl-3-*O*-mesyl-*myo*-inositol (II).—To a stirred solution of 3.45 g. of 1, 4, 5, 6-tetra-*O*-acetyl-*myo*-inositol (I) in 40 ml. of pyridine, 1.5 g. of methanesulfonyl chloride was added at 5°C. The mixture was kept at room temperature overnight and then poured into ice and water, after which the solution was evaporated under reduced pressure to dryness. The residue was digested with cold water, and the product was collected by filtration. The crude product (3.9 g.) was recrystallized from methanol to give 2.7 g. (72%) of colorless crystals at *210—213°C. Further recrystallization afforded an analytical sample of II, m. p. *210.5—212°C.

Found: C, 41.86; H, 5.31; S, 7.83. Calcd. for $C_{15}H_{22}O_{12}S$: C, 42.25; H, 5.20; S, 7.52%.

3-*O*-Mesyl-*myo*-inositol Pentaacetate (III).—A 200 mg. portion of II was treated with 3 ml. of acetic anhydride in pyridine at 90°C. The mixture was then evaporated under reduced pressure to dryness, and the residue was crystallized from a mixtrue of methanol and petroleum ether to give 220 mg, of white crystals melting at 158—160°C. Recrystallization from ethanol furnished 193 mg. (87.7%) of colorless needles, m. p. 159—161°C.

Found: C, 43.42; H, 5.34; S, 6.58. Calcd. for $C_{17}H_{24}O_{13}S$: C, 43.59; H, 5.17; S, 6.85%.

2-*O*-Mesyl-*myo*-inositol Pentaacetate.—To a stirred mixture of 37 mg. of 1, 3, 4, 5, 6-penta-*O*-acetyl-*myo*-inositol[16] and 0.5 ml. of pyridine, 0.1 g. of methanesulfonyl chloride was added. After it had stood overnight at room temperature, the mixture was poured into 1 ml. of cold water. The solution was then evaporated to dryness, and the residue was crystallized from ethanol to give 15 mg. of colorless needles melting at 190—192°C.

Found: C, 43.45; H, 5.35. Calcd. for $C_{17}H_{24}O_{13}S$: C, 43.59; H, 5.17%.

Hexaacetyl-*muco*-inosamine-1 (V).—a) A mixture of III (0.907 g.), sodium azide (0.255 g.) and 90% aqueous 2-methoxyethanol was refluxed for 16 hr. A brown mixture was evaporated under reduced pressure to dryness. The residue was dissolved in 10 ml. of ethanol, and an insoluble material was removed by filtration. The filtrate was then evaporated to give a brown oil, which showed an infrared absorption characteristic of an azide group at 2100 cm^{-1}. Then the oil was acetylated with acetic anhydride in pyridine to give an oily product (IV).

IV was hydrogenated in 20 ml. of ethanol over Raney nickel T4[17] under 50 p.s.i.g. of initial hydrogen pressure for 6 hr. After the catalyst had been removed,

16) E. L. May, ibid., **17**, 286 (1952).
17) S. Nishimura, This Bulletin, **32**, 61 (1959).

the filtrate was evaporated and the residue was acetylated with acetic anhydride in pyridine to yield 0.273 g. (32.3%) of crystals melting at 204°C after sintering at 190°C. Recrystallizations from methanol gave rhombic crystals of V melting at 205—205.5°C.

Found: C, 50.08; H, 5.97; N, 3.30. Calcd. for $C_{18}H_{25}NO_{11}$: C, 50.11; H, 5.84; N, 3.23%.

b) A mixture of II (1.02 g.), sodium azide (0.32 g.) and 90% aqueous 2-methoxyethanol was heated under reflux for 15 hr. The reaction mixture was then treated in the manner described above, giving 0.409 g. (39.2%) of crystals melting at 204—205°C after sintering at 197°C. Recrystallization from ethanol afforded crystals melting at 205—205.5°C.

c) A mixture of II (1.00 g.), sodium azide (1.00 g.) and 90% aqueous dimethylformamide was heated under reflux for 40 hr. The mixture was treated in the manner described above to give 0.26 g. (25%) of crude hexaacetyl-inosamine, m. p. 170—190°C. Fractional recrystallizations from a mixture of ethanol and ether gave 0.10 g. (9.6%) of V, m. p. 197—199°C. and 0.03 g. of an unidentified product (VII), m. p. *175—178°C.

When VII was mixed with an authentic sample of hexaacetyl-*rac*-inosamine-2, a remarkable depression of the melting point was observed.

IR: 3260, 1685, 1655, 1550 (amide), 1750 cm^{-1} (OAc).

Found: C, 49.95; H, 6.59; N, 3.43%.

After hydrolysis with 6 N hydrochloric acid, VII gave a single spot of R_f 0.26 in ascending paper chromatography in an ethyl acetate - pyridine - acetic acid - water (5 : 5 : 1 : 3) system[18] at 20°C (R_f of D-glucosamine hydrochloride: 0.35).

d) A mixture of III (7.08 g.) and 350ml. of methanol. saturated with ammonia was heated at 110°C for 24 hr. in an autoclave. After it had then been cooled, the mixture was evaporated in vacuo and the residue was acetylated with acetic anhydride (10 ml.) and sodium acetate (0.5 g.) at 100°C for 2 hr. to give a crude product. The product was recrystallized from ethanol to yield colorless crystals of V (2.52 g., 40.5%), m. p. 204.5—205°C. From the mother liquor, an unidentified product (0.22 g.), m. p. 192—218°C, was obtained.

N-Acetyl-*muco*-inosamine-1 (VI).—A 297 mg. portion of V was added to 25 ml. of methanol saturated with ammonia. The mixture was kept at room temperature overnight and evaporated under reduced pressure; a colorless oil was thus obtained. The product was washed with 5 ml. of ethyl acetate and crystallized from 90% ethanol to yield 118 mg. (77.7%) of colorless plate melting at 222—224°C. The second crop, m. p. 221.5—224°C (14 mg., 86.5%), was recovered from the mother liquor. Recrystallization from ethanol gave fine plates melting at 223—225°C.

Found: C, 43.55; H, 6.96; N, 6.37. Calcd. for $C_8H_{15}O_6N$: C, 43.43; H, 6.84; N, 6.33%.

1, 4, 5, 6-Tetra-*O*-acetyl-3-*O*-benzoyl-*myo*-inositol (VIII).—To a solution of 9.4 g. of I in 60 ml. of pyridine there was added, portion by portion, 3.5 ml. of benzoyl chloride at 5°C. The mixture was kept at room temperature for 20 hr. and then poured into 100 ml. of ice and water. The solution was extracted four times with chloroform (50 ml.), and the extracts were washed with water. After it had been dried over anhydrous sodium sulfate, the chloroform was evaporated in vacuo to give a crystalline residue. The crystals were washed with ethanol. The crude product (8.9 g., 73%) melted at *201.5—203°C. A second crop (1.3 g., 84%) was obtained from the washings. Recrystallization from ethanol afforded fine needles which melted at *202—203°C.

Found: C, 55.81; H, 5.26; Calcd. for $C_{21}H_{24}O_{11}$: C, 55.76; H, 5.35%.

1, 4, 5, 6-Tetra-*O*-acetyl-2-*O*-mesyl-3-*O*-benzoyl-*myo*-inositol (IX).—To a solution of 8.0 g. of VIII in 80 ml. of pyridine, 3.5 g. of methanesulfonyl chloride was added. The mixture was kept at room temperature for 2 days, and then poured into 300 ml. of ice and water. The precipitate was collected and washed with ethanol. The crude product weighed 8.0 g. (85%). Recrystallization from 2-methoxyethanol gave colorless rhombics (6.34 g., 67%) which melted at 240.5—242°C.

Found: C, 50.08; H, 5.07; S, 5.78. Calcd. for $C_{22}H_{26}O_{13}S$: C, 49.80; H, 4.94; S, 6.04%.

1-Azido-1-deoxy-*scyllo*-inositol Pentaacetate (X).—A mixture of 5.0 g. of IX, 2.0 g. of sodium azide and 170 ml. of 90% aqueous 2-methoxyethanol was refluxed for 20 hr. The brown mixture was evaporated under reduced pressure, and the residue was acetylated by heating it with acetic anhydride and pyridine at 100°C for 1 hr. After the solution had cooled, the insoluble material was removed and the filtrate was evaporated under reduced pressure to give a partly-crystallized residue. The residue was triturated with ethanol and filtered to yield 3.02 g. (77%) of crystals melting at *200—203°C. Recrystallization from ethanol gave colorless needles (2.04 g.) melting at *205—205.5°C.

Found: C, 46.57; H, 5.05; N, 9.78. Calcd. for $C_{16}H_{21}N_3O_{10}$: C, 46.26; H, 5.10; N, 10.12%.

Hexaacetyl-*scyllo*-inosamine (XI).—X (0.547 g.) was dissolved in glacial acetic acid (30 ml.) and hydrogenated at room temperature in a Parr shaker type apparatus at an initial pressure of 50 p.s.i.g. of hydrogen over Adams platinum oxide (33 mg.) for 13 hr. The catalyst was then removed, and the filtrate was evaporated in vacuo. The residual oil was treated with 10 ml. of pyridine - acetic anhydride (1 : 1) to give crude hexaacetyl-*scyllo*-inosamine (0.518 g., 91.3%) melting at *269—272°C with decomposition after sintering at 230°C. Recrystallization from 2-methoxyethanol gave colorless needles (0.397 g.) melting at *271—272°C with decomposition after coloring at 240°C. (Lit.[8,10] m. p. 275—276 and 288°C)

Found: C, 50.56; H, 5.79; N, 3.22. Calcd. for $C_{18}H_{22}NO_{11}$: C, 50.11; H, 5.84; N, 3.23%.

The NMR spectrum was superimposable upon that of an authentic sample.

N-Acetyl-*scyllo*-inosamine, m. p. *285—286°C (decomp), was prepared by an ordinary method of selective deacetylation [Lit.[10] m. p. 289—301°C (decomp.)].

1, 4, 5, 6-Tetra-*O*-acetyl-2, 3-di-*O*-benzoyl-*myo*-inositol.—A mixture of I (1 g.), benzoyl chloride (1 ml.) and pyridine (5 ml.) was heated on a boiling-water bath for 30 min. After it had been cooled, the mixture was diluted with cold water and the precipitate was collected and washed with water. The crude

18) F. G. Fischer and H. Dorfel, *Hoppe-Seyler's Z. physiol. Chem.*, **301**, 224 (1955).

product weighed 1.46 g. (91%) and melted at 157—163°C. The analytical sample was obtained by recrystallizations from methanol; it melted at 180.5—182°C.

Found: C, 60.31; H, 4.89. Calcd. for $C_{28}H_{28}O_{12}$: C, 60.43; H, 5.07%.

1, 4, 5, 6-Tetra-*O*-acetyl-2-*O*-benzoyl-3-*O*-mesyl-*myo*-inositol.—A mixture of II (0.408 g.), benzoyl chloride (0.5 ml.) and pyridine (5 ml.) was treated similarly to give 0.285 g. (56%) of crystals melting at 150—153°C. The analytical sample was obtained by recrystallization from ethanol m. p. *152—154.5°C, 154—155.5°C.

Found: C, 49.66; H, 5.00; S, 6.17. Calcd. for $C_{22}H_{26}O_{13}S$: C, 49.80; H, 4.94; S, 6.04%.

2, 3-Di-*O*-mesyl-*myo*-inositol Tetraacetate (XII).—To a solution of 1.0 g. of I in 10 ml. of pyridine, 1.3 g. of methanesulfonyl chloride was added under ice cooling. The mixture was treated in the manner described for II to give 1.25 g. (87.5%) of the product, m. p. *205.5—209°C. Recrystallizations from ethanol afforded 1.12 g. (78.5%) of needles, m. p. *211—213°C.

Found: C, 38.34; H, 4.98; S, 12.48. Calcd. for $C_{16}H_{24}O_{14}S_2$: C, 38.10; H, 4.80; S, 12.72%.

A mixed melting point determination with II showed a remarkable depression.

Hexaacetyl-*muco*-inosadiamine-1, 5 (XIV). — a) A mixture of XII (2.06 g.), sodium azide (1.05 g.) and 95% aqeous 2-methoxyethanol (75 ml.) was refluxed for 19 hr. The mixture was then treated in the manner described for V a) to give 193 mg. of the crude product, m. p. *282—283°C (decomp.). Recrystallizations from ethanol afforded 134 mg. (7.6%) of the crystals, m. p. *305—306°C.

Found: C, 50.14; H, 6.22; N, 6.50. Calcd. for $C_{18}H_{26}N_2O_{10}$: C, 50.23; H, 6.09; N, 6.51%.

No other crystalline isomer could be obtained from the mother liquor.

b) A mixture of XII (3.0 g.) and methanol (180 ml.) which had previously been saturated with ammonia was heated in an autoclave at 110°C for 20 hr. Then the reaction mixture was treated in the manner described for V c) to give 646 mg. (25.0%) of the crude XIV, m. p. *292.5—294.5°C (decomp.). Recrystallizations from ethanol gave 438 mg. (16.9%) of colorless needles, which melted at *306.5—307°C.

Di-*N*-acetyl-*muco*-inosadiamine-1, 5 (XV).—XIV (100 mg.) was selectively deacetylated by the ordinary method described for VI to give 66 mg. of the crude product of XV, m. p. 235—237°C. Recrystallization from aqueous alcohol gave 43 mg. (71%) of colorless plates, m. p. 238.5—239°C.

Found: C, 45.25; H, 7.09; N, 10.38. Calcd. for $C_{10}H_{18}N_2O_6$: C, 45.79; H, 6.92; N, 10.68%.

Periodate Oxidation.—A 21.9 mg. portion of XV was treated with 25 ml. of a 0.0301 M sodium metaperiodate solution at 15°C. Iodometric titrations with sodium arsenite[19] showed that 2.18 mol. of periodate was consumed per mole of XV in 43 hr.

***muco*-Inosadiamine-1, 5 Dihydrochloride.**—XIV (300 mg.) was heated in 6 N hydrochloric acid on a boiling water bath for 1.5 hr. The solution was then evaporated under reduced pressure to give a crystalline residue. The residue was recrystallized from a mixture of methanol and ethanol to give 175 mg. (60.6%) of crystals melting at *300°C (decomp.) after coloring at 260°C.

Found: C, 29.24; H, 6.28; N, 10.74; Cl, 27.83. Calcd. for $C_6H_{14}N_2O_4 \cdot 2HCl$: C, 28.70; H, 6.42; N, 11.15; Cl, 28.24%.

Hexaacetyl-*myo*-inosadiamine-1, 2 (XVII). — A mixture of XII (5.0 g.), sodium azide (3.0 g.) and 80% aqueous dimethylformamide (120 ml.) was refluxed for 18 hr. The reaction mixture was then evaporated under reduced pressure and extracted with ethanol (30 ml. × 3). The extracts were evaporated in vacuo to dryness, pyridine - acetic anhydride (1 : 1) (50 ml.) was added, and the mitture was kept at room temperature overnight. The insoluble material was removed, and the solution was evaporated under reduced pressure to give an oil. This oil was dissolved in ethanol (20 ml.) and kept in a refrigerator overnight. The precipitate (the starting material) was filtered off and treated again with toluene (20 ml.) in a similar manner. The filtrate was evaporated, and the residual oil was dissolved in ethanol (20 ml.) containing Adams platinum oxide (100 mg.). The mixture was hydrogenated at room temperature in a Parr shaker-type apparatus at an initial pressure of 50 p.s.i.g. of hydrogen for 20 hr. The catalyst was filtered off, and the filtrate was evaporated. The residual oil was treated again with pyridine-acetic anhydride (1 : 1) (10 ml.) and crystallized from ethanol/ether to give the crude product (152 mg.), which melted at *270—274°C with decomposition after sintering at 260°C. The second crop was obtained from the mother liquor, 123 mg., melting at *250—262°C with decomposition after sintering at 245°C. The total yield was 6.4%. The crude product was recrystallized from ethanol with carbon to give colorless needles (151 mg.) which melted at *275—277°C with decomposition after sintering at 267°C.

Found: C, 50.14; H, 6.18; N 6.67. Calcd. for $C_{18}H_{26}N_2O_{10}$: C. 50.23; H, 60.9; N, 6.51%.

Di-*N*-acetyl-*myo*-inosadiamine-1, 2 (XVIII). — XVII (150 mg.) was treated in the manner described for XV to give 85.9 mg. (94.1%) of crystals, m. p. 262—264°C The analytical sample was obtained, by recrystallization from a mixture of ethanol, ether and water, as plates melting at 270—271°C.

Found: C, 45 62; H, 6.85; N, 10.47. Calcd. for $C_{10}H_{18}N_2O_6$: C, 45.79; H, 6.92; N, 10.68%.

Periodate Oxidation. — A 25.1 mg. portion of XVIII was dissolved in 50 ml. of a 0.0301 M sodium metaperiodate solution at 15°C. Iodometric titrations with sodium arsenite[17] showed that 3.30 mol. of periodate was consumed per mole of XVIII in 43 hr.

The authors are grateful to Professor Sumio Umezawa for his helpful advice and to Mr. Saburo Nakada for his elementary analyses. The authors are also indebted to Mr. Hiroyasu Suzuki for his assistance in the measurements, and to the Japan Electron Optics Co., Ltd., for the NMR spectra. This research has been financially supported in part by a grant of the Ministry of Education and by the Deutsche Forschungsgemeinschaft, to which the authors' thanks are due.

19) J. M. Bobbitt, "Advances in Carbohydrate Chemistry," Vol. XI, Academic Press, New York (1956), pp. 1—41.

BULLETIN OF THE CHEMICAL SOCIETY OF JAPAN VOL. 39 179—185 (1966)

The Interaction between a Polysoap and a Monosoap

By Fumikatsu TOKIWA

Kao-Atlas Laboratory, Kao Soap Co., Ltd., Minato-Yakushubata, Wakayama

(Received June 10, 1965)

The way in which a cationic polysoap, prepared by quaternizing the nitrogen of poly-2-vinylpyridine with *n*-dodecyl bromide, interacts with additives, such as a cationic monosoap (*n*-dodecyl-α-picolinium bromide), a non-ionic surfactant (polyoxyethylene dodecyl ether) and potassium bromide, has been studied in aqueous solutions in terms of the viscosity and solubilizing power for oil-soluble dyes of the mixed solutions of the polysoap and the additives. An experiment on the effects of these additives on the behavior of a polyelectrolyte (poly-2-vinyl-*N*-ethylpyridinium bromide), prepared from the same parent polymer as the polysoap, has also been included for the purpose of comparison. The hydrophobic hydrocarbon chains in the polysoap and additive molecules play an important role in the interaction of the polysoap with the additives. Co-micellization or mixed micellization occurs between the polysoap and the monosoap or the non-ionic surfactant in aqueous solutions.

In previous papers[1,2] the solubilization behavior of cationic polysoap and monosoap was compared in terms of the spectra of some oil-soluble dyes solubilized by both soaps,[1] as well as in terms of the solubilizing power, the viscosity and the electrical conductivity of the soap solutions.[2] In general, a polysoap molecule has been regarded as a model of a micelle of ordinary soaps in the sense that the molecule acts as a prefabricated soap micelle.[3] However, this is not necessarily true. It has, for instance, been pointed out by the present author that the polysoap, *n*-dodecyl bromide addition compound of poly-2-vinylpyridine, differs considerably in its behavior, such as in the solubilization of oil-soluble dyes, from the monosoap, *n*-dodecyl-α-picolinium bromide, which is considered to be very similar in its chemical structure to the polymeric unit of the polysoap.[1,2] It will also be of interest to study the properties of mixed solutions of the polysoap, which is a long flexible chain of a macroion with a great number of hydrocarbon side chains, with the monosoap.

With respect to the properties of aqueous solutions of the mixtures of a cationic polysoap and a monosoap, Narasaki and Ito[4,5] have reported that whether the addition of the monosoap to the polysoap solutions leads to a synergistic or to an antigistic effect on some physicochemical property varies from case to case.

The present paper is a study of mixed solutions of a polysoap and a monosoap in terms of viscosity and solubilization; this study leads to an understanding of the way in which the polysoap and the monosoap interact in aqueous solutions. The effects of a simple electrolyte and a non-ionic surfactant upon the behavior of the polysoap are also included. An experiment in which the polysoap was replaced by the polyelectrolyte prepared from the same parent polymer as the polysoap is also included for purposes of comparison.

Experimental

Materials.—The polysoap, *n*-dodecyl bromide addition compound of poly-2-vinylpyridine, was prepared and purified by a method previously described.[1] The molecular weight of the parent polymer, poly-2-vinylpyridine, was 1.16×10^5, as estimated from its intrinsic viscosity in 92% ethanol by weight[6]; this value corresponds to a degree of polymerization of 1.10×10^3. The analysis of the polysoap revealed that 32.5% of the nitrogen was quaternized with *n*-dodecyl bromide, while 9.6% carried hydrogen bromide.

The monosoap, *n*-dodecyl-α-picolinium bromide, was prepared by the quaternization of α-picoline with *n*-dodecyl bromide according to the ordinary method. The soap was then purified by repeated recrystallizations from acetone.

The polyelectrolyte, poly-2-vinyl-*N*-ethylpyridinium bromide, was prepared from ethyl bromide and the poly-2-vinylpyridine described above. The method of Strauss et al.[7] was employed from preparing poly-4-vinyl-*N*-ethylpyridinium bromide. Analysis gave nitrogen 7.57% bromine 32.3%.

The non-ionic surfactant, polyoxyethylene dodecyl ether (abbreviated hereafter as PODE), was the same sample as that used in a previous investigation[8]. The

1) F. Tokiwa, This Bulletin, **36**, 1585 (1963).
2) F. Tokiwa, ibid., **36**, 1589 (1963).
3) L. H. Layton and U. P. Strauss, *J. Colloid. Sci.*, **9**, 149 (1954).
4) H. Narasaki and N. Ito, *J. Chem. Soc. Japan, Ind. Chem. Sect.* (*Kogyo Kagaku Zasshi*), **64**, 1790 (1961).
5) H. Narasaki, ibid., **64**, 1955 (1961).
6) A. G. Boyes and U. P. Strauss, *J. Polymer Sci.*, **22**, 463 (1956).
7) U. P. Strauss and N. L. Gershfeld, *J. Phys. Chem.*, **58**, 747 (1954).
8) F. Tokiwa, This Bulletin, **36**, 222 (1963).

average degrees of the polymerization of polyoxyethylene chain, p, of the two samples used were 7.6 and 15.8, the number written after PODE representing the value of p.

The potassium bromide was a special-grade product obtained from the Wako Pure Chemicals Co. Solubilizates, the 1-benzeneazo-2-naphthol and 1-*p*-nitrobenzeneazo-2-naphthol (abbreviated hereafter as BAN and *p*-nitro-BAN respectively) were the same samples as those described in a previous paper.[1] The details of these samples were reported in that paper

Procedure.—The solubilizations were run in a water bath at 30±0.1°C for 40 hr. in order to attain equilibrium, the method described in a previous paper[8] being employed. The amount of solubilized dyes was determined by optical density measurements using a spectrophotometer, Shimadzu Model B60.

The viscosities were measured in a water bath at 30±0.01°C with Ostwald-type viscometers, the flow times for pure water at 30°C being 102.8 and 128.3 sec.

Results

The viscometric behavior of the polysoap in pure water and in aqueous solutions of additives, i. e., monosoap, potassium bromide and PODE, is shown in Figs. 1 and 2, where the reduced viscosity, η_{sp}/c of the polysoap is plotted against the concentration, c. In this paper the aqueous solution with the same concentration of one of the above additives was taken to be the solvent for the polysoap.

Figure 1 shows the η_{sp}/c - c curves of the polysoap at a constant concentration of the additives. The

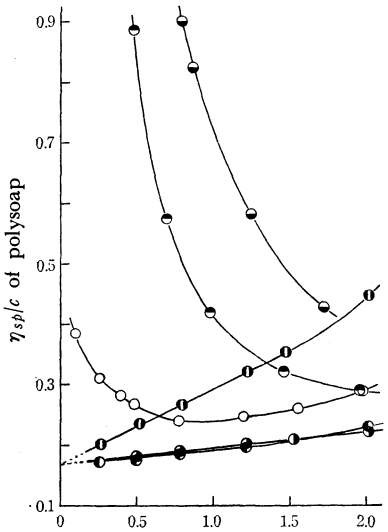

Fig. 1. The reduced viscosity vs. concentration of polysoap curves at a constant concentration of 0.77×10^{-2} M monosoap (◐), 2.26×10^{-2} M monosoap (◑), 2.05×10^{-2} M PODE-7.6 (◓), 2.11×10^{-2} M PODE-15.8 (◒) or 2.03×10^{-2} M KBr (◐); polysoap alone (○) at 30°C.

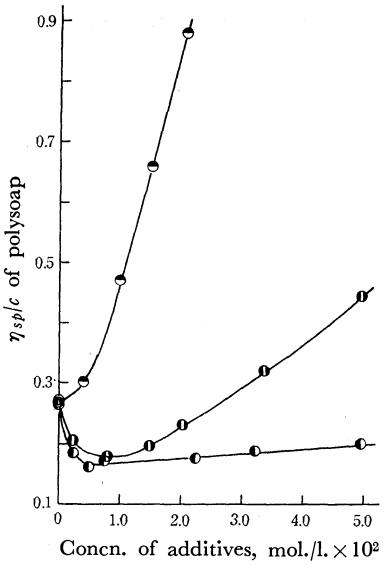

Fig. 2. The effect of additive concentrations on the reduced viscosity of polysoap of a constant concentration at 30°C: ◐, monosoap (polysoap concn. 0.407 g./100 ml.); ◓, PODE-7.6 (polysoap concn. 0.498 g./100 ml.); ◐, KBr (polysoap concn. 0.497 g./100 ml.).

η_{sp}/c of the polysoap in the monosoap solution is lower than that in water, and the η_{sp}/c - c curve runs linearly with c, giving an intrinsic viscosity, $[\eta]$, of 0.17. The curve in the potassium bromide solution is also linear and $[\eta]=0.17$. On the other hand, the η_{sp}/c in the PODE solution becomes abnormally higher as the concentration of the polysoap decreases. Figure 2 illustrates the effect of the concentration of the additives on the η_{sp}/c of the polysoap. Each additive influences the polysoap viscosity in a different way. The viscosity in the PODE solution increases abruptly with the increase in the PODE concentration. The viscosity rise of the polysoap in the PODE solution became more striking with the increase in the polyoxyethylene chain-length of PODE.

The results of the solubilzation of BAN by the mixed solutions of the polysoap with the monosoap, potassium bromide or PODE are shown in Figs. 3 and 4. Figure 3 shows the amounts of BAN solubilized by that mixed solution in which the concentration of the polysoap is varied while that of the additive remains constant. Since the monosoap and PODE have a solubilizing power above their critical micelle concentration (CMC), the amount of BAN solubilized by the mixed solutions is greater than that solubilized by the polysoap solution alone. However, the effect of the monosoap on the solubilization differs from that of PODE. Figure 4 illustrates the effect of the additive concentrations on the solubilizing power of that mixed solution in which the concentration

of the polysoap remains constant while that of the additive is varied. For comparison, the solubilizing power of the solution of the monosoap or PODE without the polysoap is also given in Fig. 4. The presence of potassium bromide slightly lowers the solubilizing power of the polysoap.

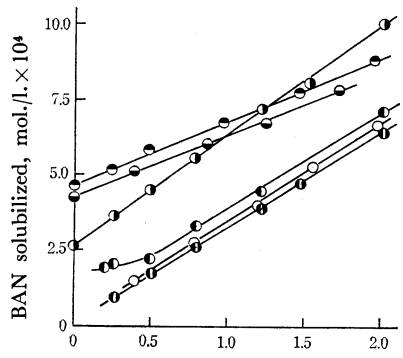

Fig. 3. The solubilization of BAN vs. concentration of polysoap curves at a constant concentration of 0.77×10^{-2} M monosoap (◐), 2.26×10^{-2} M monosoap (◑), 2.05×10^{-2} M PODE-7.6 (◓), 2.11×10^{-2} M PODE-15.8 (◒) or 2.03×10^{-2} M KBr (◐); polysoap alone (○) at 30°C.

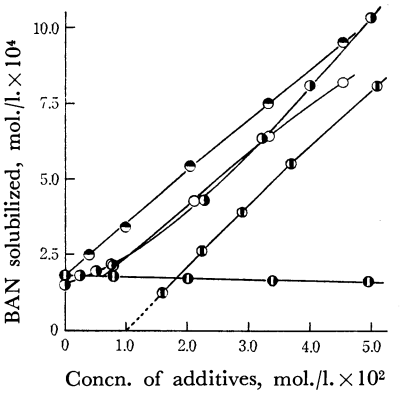

Fig. 4. The effect of additive concentrations on the solubilization of BAN by the mixed solutions of polysoap and additive at 30°C: ◑, monosoap (polysoap concn. 0.407 g./100 ml.); ◓, PODE-7.6 (polysoap concn. 0.498 g./100 ml.); ◐, KBr (polysoap concn. 0.497 g./100 ml.); ◑, monosoap alone; ○, PODE-7.6 alone.

The results of the solubilization of *p*-nitro-BAN by the same solutions are shown in Fig. 5. *p*-Nitro-BAN showed a more characteristic solubilization behavior than the two other nitro substituents studied in a previous experiment.[2] The amount of *p*-nitro-BAN solubilized by the mixed solution of the polysoap with the monosoap or PODE is considerably smaller than that solubilized by the polyaoap solution alone, in spite of the presence of the monosoap or PODE with solubilizing power.

For comparison, the viscosities of the polyelectrolyte with no dodecyl side chain, in the absence of and in the presence of the additives, are shown in Fig. 6. The η_{sp}/c - c curve of the polyelectrolyte

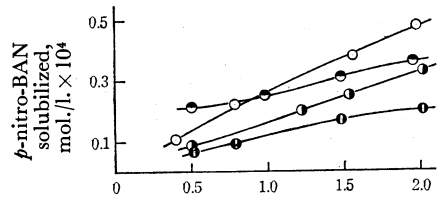

Fig. 5. The solubilization of *p*-nitro-BAN vs. concentration of polysoap curves at a constant concentration of 2.26×10^{-2} M monosoap (◑), 2.05×10^{-2} M PODE-7.6 (◓) or 2.03×10^{-2} M KBr (◐); polysoap alone (○) at 30°C.

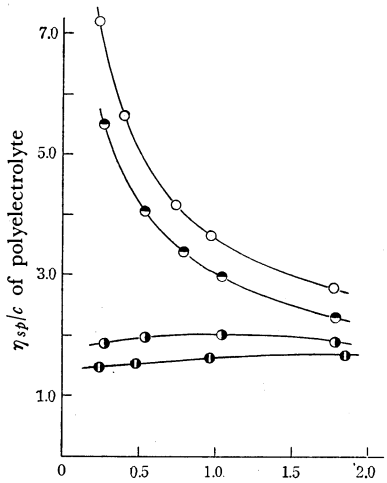

Fig. 6. The reduced viscosity vs. concentration of polyelectrolyte curves at a contant concentration of 2.03×10^{-2} M monosoap (◑), 2.06×10^{-2} M PODE-7.6 (◓) or 2.00×10^{-2} M KBr (◐); polyelectrolyte alone (○) at 30°C.

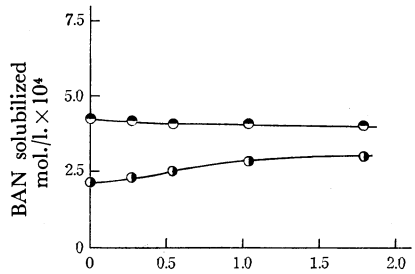

Fig. 7. The effect of poly electrolyte concentration on the solubilization of BAN by 2.03×10^{-2} M monosoap (◑) or 2.06×10^{-2} M PODE-7.6 (◓) at 30°C; the polyelectrolyte alone has no solubilizing power.

in water shows a familiar pattern. In the monosoap or potassium bromide solution, the reduced viscosity depression at the lower concentrations is remarkable. However, the polyelectrolyte molecule in a PODE solution behaves similarly to that in water.

Figure 7 shows the effect of polyelectrolyte concentrations on the solubilizing power of the monosoap and PODE for BAN. The polyelectrolyte makes the solubilizing power of the monosoap slightly higher, while it leaves that of PODE almost unchanged.

Discussion

Interaction between the Polysoap and the Monosoap.—The effect of potassium bromide on the viscosity of the polysoap has already been investigated by Strauss et al.[9] While at first the reduced viscosity of the polysoap decreases with an increase in the potassium bromide concentration, in time it reaches a minimum and then rises sharply, as may be seen in Fig. 2. They ascribed the initial viscosity decrease to the contraction of the polysoap molecule, and the viscosity rise with the added potassium bromide to interaction between the molecules. It the monosoap, which is a kind of electrolyte although it has a long hydrocarbon chain, would act on the polysoap only like potassium bromide, it might be expected to show a viscosity behavior similar to that in a potassium bromide solution. However, the results obtained in the monosoap solution are different from those obtained in the potassium bromide solution, as is shown in Figs. 1 and 2. This difference in viscosity behavior can be considered to arise from the long hydrocarbon chain in the monosoap molecule.

It is known that such polar materials with long hydrocarbon chain as higher alcohols are solubilized, with their polar groups located in the polar region near the polymer backbone and with their hydrocarbon chains penetrating into the hydrocarbon region of the polysoap molecule, in a way similar to their penetration into micelle. The solubilized hydrocarbon which supplies additional van der Waals' force to the hydrocarbon atomsphere inside the polysoap molecule causes the molecule to contract further.[3,7]

If the hydrocarbon chains of the monosoap cations penetrate into the interior of the polysoap molecule in the similar manner described above, this penetration will cause a contraction of the polysoap molecule. At the same time the surface of the polysoap molecule will be covered for the most part with hydrophilic ionized groups of the monosoap cations. An increase in the electrical charge on the surface leads to an enhancement of the electrostatic repulsion between different polysoap molecules, which will simultanously diminish the interaction between them. Although this will cause a swelling of the polysoap molecule, the van der Waals' attraction between hydrocarbon chains compensates for the ionic repulsion, so the resulting polysoap molecule is more compact than the initial molecule. This interaction between the polysoap and the monosoap may be regarded as a type of "co-micellization" or" mixed micellization." If the above argument is reasonable, the interaction may not be involved in the micelle formation of the monosoap. In fact, an insignificant change in viscosity could be found below and above the CMC of the monosoap (1.02×10^{-2} mol./l.), as may be seen in Fig. 1. After the penetration of the monosoap reaches the saturation point, the free monosoaps, which do not contribute directly to the co-micellization with the polysoap, will act on the polysoap in a way similar to potassium bromide.

On the other hand, in the case of the polyelectrolyte, there is no significant difference between the monosoap and potassium bromide in their effects on the reduced viscosity, as Fig. 6 shows. The hydrocarbon chain of the monosoap cation, which plays an important role in the interaction with the polysoap, can not act effectively with regard to the interaction with the polyelectrolyte having no long hydrocarbon side chains. In this case the monosoap cation seems to act on the polyelectrolyte as an electrolyte. This indicates the importance of the hydrocarbon chains of the polysoap, and supports the mechanism described above. However, the action of the monosoap cations on the polyelectrolyte is not completely negligible. The monosoap cations seem to interact slightly with the polyelectrolyte between the hydrocarbon chain of the cation and the hydrophobic portion in the backbone of the polyelectrolyte. The slight increase in the solubilizing power of the monosoap in a polyelectrolyte solution to be seen in Fig. 7 may be attributed to this interaction.

It is instructive to consider the intrinsic viscosity of the polysoap in the monosoap solution in the light of the general principle developed by Flory et al.[10] The Θ-solvent intrinsic viscosity, $[\eta]_\theta$, of poly-4-vinylpyridine[7] is:

$$[\eta]_\theta = 8.1 \times 10^{-4} M^{1/2}$$

Assuming that the $[\eta]_\theta$ of poly-2-vinylpyridine is equal to that of poly-4-vinylpyridine, the $[\eta]_\theta$ of the parent polymer used in this experiment, whose molecular wieght is 1.16×10^5, equals 0.276. From this value, according to Strauss' assumption,[7] one can calculate the expected value for the $[\eta]_\theta$ of the quaternization product, i. e., the polysoap, by the relation:

9) U. P. Strauss, N. L. Gershfeld and E. H. Crook, *J. Phys. Chem.*, **60**, 577 (1956).

10) P. J. Flory, "Principles of Polymer Chemistry," Cornell University Press, Ithaca, N. Y. (1953), Chap. 12—14.

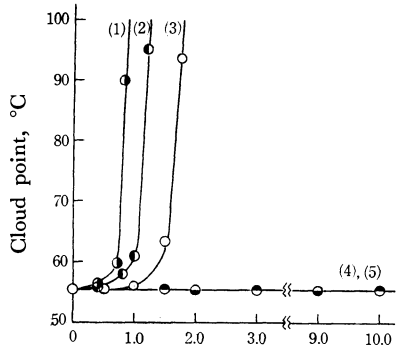

Fig. 8. The effect of polysoap and polyelectrolyte on the cloud point of PODE-7.6 solution of 10 ml.; PODE concn. (1) 0.82, (2) 1.13, (3) 1.63, (4) 0.80, (5) 1.60 g./100 ml. (1), (2) and (3) refer to the polysoap, and (4) and (5) refer to the polyelectrolyte.

$$[\eta]_{\theta,Q} = [\eta]_{\theta,P} (M_P/M_Q)$$

where the subscripts P and Q refer to the parent polymer and the quaternization product respectively. The resulting estimate of $[\eta]_{\theta,Q}$ is 0.15, slightly lower than the observed intrinsic viscosity of 0.17 shown in Fig. 1. It has been reported[9] that polysoaps can dissolve in aqueous media without phase separation, even when the intrinsic viscosity, $[\eta]$, is lower than the value of $[\eta]_\theta$. Further, the Einstein figure for a compact sphere is 0.025. Thus there is considerable room left inside the polysoap molecule for the solubilization for oil-soluble materials, even when the polysoap molecule is contracted by the penetration of monosoap cations.

The oil-soluble dye, BAN, would be mainly solubilized in an interior of a micelle, i. e., a dense hydrocarbon region of a micelle.[2] Therefore, it may be expected that an increase in the hydrocarbon region in the interior of the polysoap molecule, as a result of its co-micellization with monosoap molecules, will enhance the solubilizing power of the polysoap similarly to the effect of alcohols with a long hydrocarbon chain on the solubilizing power of ordinary soaps.[11] As may be seen in Figs. 3 and 4, the amount of BAN solubilized by the mixed solution of the polysoap and the monosoap is greater than the total amount solubilized by the respective solution of the corresponding concentration. This is an indication of the synergistic effect of the mixed micelle of the polysoap and the monosoap. It is noteworthy that an increase in solubilizing power is appreciable in the mixed solution in which the concentration of the monosoap is lower than the CMC. On the other hand, the addition of potassium bromide slightly lowers the solubilizing power of the polysoap, because potassium bromide acts as only a simple electrolyte.

The results of the solubilization of *p*-nitro-BAN are very interesting in contrast with that of BAN. The amount of *p*-nitro-BAN solubilized by the mixed solution of the polysoap and the monosoap is considerably smaller than that solubilized by the polysoap solution alone. Essentially, *p*-nitro-BAN is not so solubilized by soaps as is BAN.[2] The present author has previously pointed out that the loci of the solubilization of oil-soluble dyes in the polysoap molecule are not only in the dense hydrocarbon region in the interior but also in the polar region near the polymer backbone. In the case of the solubilization of *p*-nitro-BAN especially, the polar region of the polysoap molecule acts as a strong solubilizing locus.[1,2] With this picture in mind, the electrical charge on the surface of the polysoap molecule appears to be more correlated with the solubilization of *p*-nitro-BAN than the interior of the polysoap molecule. The addition of the monosoap or potassium bromide may change the electrical charge on the surface and at the same time change the atomosphere of the polar region. These changes, which may be disadvantageous for the solubilization of *p*-nitro-BAN, will lead to a lowering of the solubilizing power of the polysoap.

The Effect of a Non-ionic surfactant on the Behavior of the Polysoap.—Since PODE has no ionized group in its molecule, at first it may be expected to be able to show only the hydrocarbon effect on the polysoap. However, unexpected results for the viscosity were obtained. That is, the polysoap exhibited an extraordinary viscosity rise in the presence of PODE. In Figs. 1 and 2 we can see that the viscosity rise of the polysoap becomes higher with an increase in the ratio of PODE to the polysoap. A similar result was obtained by Narasaki when non-ionic surfactants, such as polyoxyethylene compounds, were added to the aqueous solution of the cationic polysoap prepared by quaternizing the nitrogen of poly-α-vinyl-β-ethylpyridine with *n*-dodecyl bromide and ethyl bromide.[5] The steep rise in the viscosity curves may be an indication of either an anomalous extension of the polysoap molecules or of an anomalous interaction between different polysoap molecules. The effect of the length of the polyoxyethylene tail on the viscosity of the polysoap —the longer the tail, the higher the viscosity— suggests that the polyoxyehtylene tail is responsible for the viscosity rise. Furthermore, the fact that the viscosity of the polyelectrolyte with no long hydrocarbon chain is almost not affected at all by PODE, as may be seen in Fig. 6, suggests the importance of the interaction by van der Waals'

11) M. E. L. McBain and E. Hutchinson, "Solubilization and Related Phenomena," Academic Press, New York (1955), pp. 45, 147.

force between the hydrocarbon chain of the polysoap and that of PODE. The two following mechanisms seem possible ways by which the polysoap interacts with PODE:

1) The PODE molecules penetrate into the hydrocarbon-water interface of the polysoap molecule in such a way that the polyoxyethylene tails are in the water, while the hydrocarbon chains are anchored in the hydrocharbon region of the polysoap molecule. The polyoxyethylene tails thus exposed on the surface of the polysoap molecule will interact with similarly-exposed polyoxyethylene tails belonging to other polysoap molecules, with the result that the viscosity of the poysoap will tend to increase. This interaction between polyoxyethylene tails may occur through the hydrogen bonding between the tails, probably by the medium of the water.

2) It is well-known that ordinary soap micelles swell as a result of hydrocarbon solubilization,[11] and that sometimes polysoap molecules also swell under certain conditions of solubilization.[9] The swelling of the polysoap molecules may be another type of mechanism to explain the reduced viscosity increase. When the PODE molecules penetrate into the polysoap molecule, the bulky polyoxyethylene tails may reduce the van der Waals' force between different parts of the same polysoap molecule as a result of a steric effect. As a result, the polysoap molecules will swell and extend beyond their original size, resulting in the viscosity rise.

Of course, it is difficult, on the basis of only the present experiment, to say which type of the mechanism is the more probable. The clear resolution of this problem will have to await further study. At any rate, however, the importance of polyoxyethylene tails in this interaction may easily be understood from the effect of the tail length.

In contrast to the synergistic effect of the solubilization exhibited by the polysoap and the monosoap, the amount of BAN solubilized by the mixed solution consisting of the polysoap and PODE is smaller than the total amount solubilized by the respective solution of the corresponding concentration. Namely, the PODE exerts an antigistic effect with regard to the solubilization of BAN. A similar effect has been observed when ethyl alcohol is added to some soaps.[11] Whether the presence of additives leads to a greater or a lesser solubilizing power varies from case to case; no valid generalization is possible at this stage.

Evidence for the existence of the interaction between the polysoap and PODE is also provided by the disappearance of the "clouding phenomenon" which is observed in the aqueous PODE-7.6 solution. As Fig. 8 shows, the addition of a very small amount of the polysoap to the PODE solution raises the "cloud point." A further addition makes the cloud point disappear. This may be an indication of the formation of the co-micelle or mixed micelle of the polysoap and PODE.[12] The amount of the polysoap required to make the clouding disppear increases in proportional to the concentration of PODE, the value being 5.4×10^{-2} g. polysoap/1 g. PODE. The clouding phenomenon is generally considered to be a phase separation resulting from the breaking of the hydrogen-bonding between the polyoxyehtylene portion of PODE and the water at a high temperature.[13] Therefore, the disappearance of the clouding means that the polysoap makes the PODE, which is insoluble in water at an elevated temperature, soluble in water in terms of interaction or co-micellization.[12]

On the other hand, the polyelectrolyte has no influence upon the cloud point of the PODE-7.6 solution, even when a fairly large amount of the polyelectrolyte is added to the solution, as may be seen in Fig. 8. This indicates that no interaction occurs between the polyelectrolyte and PODE.[14] The absence of interaction must be due to the lack of long hydrophobic side chains in the polyelectrolyte molecule, for it is only in this respect that the two types of polymers, i. e., the polysoap and the polyelectrolyte, are chemically distinct. The interaction between the polysoap and PODE is, therefore, characterized by the presence of the dodecyl side chains in the polysoap molecules.

Summary

The viscosity and solubilizing power of a polysoap (the *n*-dodecyl bromide addition compound of poly-2-vinylpyridine) in aqueous solutions of a monosoap (*n*-dodecyl-α-picolinium bromide), a non-ionic surfactant (polyoxyethylene dodecyl ether, PODE) or potassium bromide have been measured. A similar experiment with a polyelectrolyte (poly-2-vinyl-*N*-ethylpyridinium bromide) has also been carried out for purposes of comparison. The effect of the polysoap on the cloud point of PODE has also been included.

The presence of the monosoap in the polysoap solution lowers the reduced viscosity, η_{sp}/c, of the polysoap. Potassium bromide has a similar effect at lower concentrations, while it causes the η_{sp}/c of the polysoap to rise at higher concentrations. The η_{sp}/c in the PODE solution is markedly high, and it becomes even higher as the PODE/polysoap-ratio increases. In the case of the polyelectrolyte, on the other hand, the monosoap and potassium bromide show a similar effect on the η_{sp}/c of the

12) W. N. Macley, *J. Colloid Sci.*, **11**, 272 (1956).
13) A. M. Schwartz, J. W. Perry and J. Berch, "Surface Active Agents and Detergents," Vol. II, Interscience Publishers, New York (1957), p. 120.
14) I. Murata, *J. Chem. Soc. Japan, Pure Chem. Sect.* (*Nippon Kagaku Zasshi*), **83**, 861 (1962).

polyelectrolyte, and the PODE deos not affect the η_{sp}/c significantly. The addition of the monosoap to the polysoap solution promotes the solubilization for 1-benzeneazo-2-naphthol, while that of PODE lowers the solubilization. 1-*p*-Nitrobenzeneazo-2-naphthol exhibits an interesting behavior with regard to solubilization, and it is less solubilized by the mixed solution of the polysoap with the monosoap or PODE than by the polysoap solution alone. The cloud point of the aqueous PODE solution disappears when a very small amount of the polysoap is added.

From these results, the way in which the polysoap interacts with the monosoap or the non-ionic surfactant has been discussed. The interaction can be explained by the co-micellization or the mixed micellization of the polysoap and the nonosoap or the non-ionic surfactant.

The author wishes to express his hearty thanks to Professor Toshizo Isemura of Osaka University for his helpful discussion. He also wishes to express his appreciation to Kao Soap Co., Ltd. for permission to publish this paper.

BULLETIN OF THE CHEMICAL SOCIETY OF JAPAN VOL. 39 185—190 (1966)

Studies on Amino-hexoses. IX. The *N*-Deacetylation of Methyl *N*-Acetyl-β-D-glucosaminide, Methyl *N*-Acetyl-3-*O*-methyl-α- and β-D-glucosaminide, and Methyl *N*-Acetyl-4, 6-*O*-ethylidene-α-D-glcosaminide

By Mamoru FUJINAGA and Yoshio MATSUSHIMA

Department of Chemistry, College of Science, Osaka University, Nakanoshima, Osaka

(Received June 11, 1965)

The efficiency of hydrazine as a mild *N*-deacetylating reagent has been studied in the reaction of hydrazine with four *N*-acetylaminosugars. This reagent has been shown to be of great use in the *N*-deacetylation of methyl *N*-acetyl-β-D-glucosaminide and methyl *N*-acetyl-4, 6-*O*-ethylidene-α-D-glucosaminide. It may be noted that the 3-*O*-substitution of the sugars makes the deacetylation reaction reluctant. The synthesis of methyl *N*-acetyl-4, 6-*O*-ethylidene-α-D-glucosaminide and the isolation of crystalline methyl β-D-glucosaminide and methyl 4, 6-*O*-ethylidene-α-D-glucosaminide in the free-base form have been described.

The hydrazine treatment of methyl *N*-acetyl-α D-glucosaminide (Ia) was described in a previous paper of this series.[1] The *N*-acetyl group in Ia was there shown to be well removed by the hydrazine treatment, and methyl α-D-glucosaminide (IVa) was isolated in a fairly good yield as the deacetylated product. It was also shown that both anhydrous and hydrated hydrazine had a minimal influence on the glycosidic linkage of Ia.

The present paper will describe the hydrazine treatment of four glucosamine derivatives: methyl *N*-acetyl-β-D-glucosaminide (Ib), methyl *N*-acetyl-3-*O*-methyl-α-D-glucosaminide (IIa), methyl *N*-acetyl-3-*O*-methyl-β-D-glucosaminide (IIb) and methyl *N*-acetyl-4, 6-*O*-ethylidene-α-D-glucosaminide (III). Anomerically-pure Ib was obtained, together with pure Ia by the chromatography on Dowex 1×3 (OH^- form), as has been described by Matsushima, Miyazaki and Park.[3] A pure 3-*O*-methyl α-compound (IIa) was prepared from Ia according to the method of Neuberger.[3] The β-anomer (IIb) was prepared from Ib by the known methods.[2-5] In the preparation of IIb, the physical data of the intermediate compounds were in good agreement with those described by Roth and Pigman,[5] whose data were different from those of Masamune, Okuyama and Sinohara.[4] The ethylidene compound (III) was newly synthesized by a slight modification of the method of Helferich and Appel.[6] The structure of III was verified by leading it to methyl *N*-carbobenzyloxy-4, 6-*O*-ethylidene-α-D-glucosaminide (VII), which had been prepared by Akiya and Osawa,[7] and by the periodate oxidation of the *N*-deacetylated product of III, methyl 4, 6-*O*-ethylidene-α-D-glucosaminide (VI). The deacetylation yield was assayed by the Van Slyke method in the case of Ib and by the micro

1) M. Fujinaga and Y. Matsushima, This Bulletin, **37**, 468 (1964).

2) Y. Matsushima, T. Miyazaki and J. T. Park, *J. Biochem.*, **54**, 109 (1963).

3) A. Neuberger, *J. Chem. Soc.*, **1941**, 50.

4) H. Masamune, T. Okuyama and H. Shinohara, *Tohoku J. Exp. Med.*, **68**, 181 (1958).

5) W. Roth and W. Pigman, *J. Am. Chem. Soc.*, **82**, 4608 (1960).

6) B. Helferich and H. Appel, *Ber.*, **64**, 1841 (1931).

7) S. Akiya and T. Osawa, *Yakugaku Zasshi*, **76**, 1276 (1956).

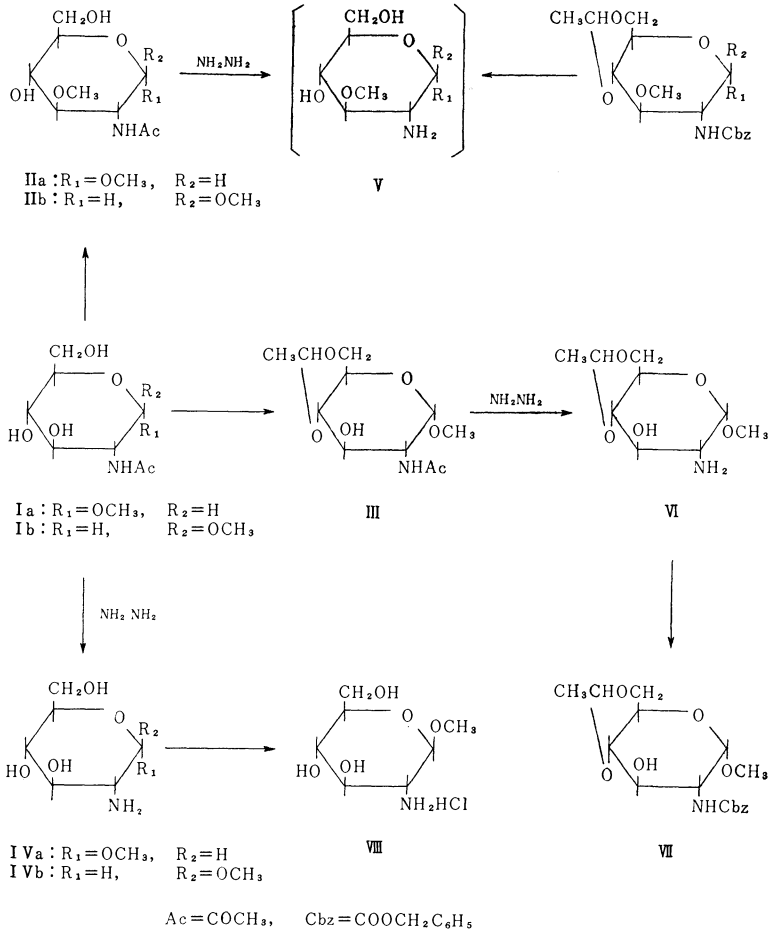

Chart 1.

Kjeldahl method in the case of IIa, IIb and III. A Hitachi amino acid autoanalyzer was also used to determine the deacetylation yield in the case of III. The starting compound which remained was assayed by isolation in every case. The results are shown in Tables I-IV. Methyl N-acetyl-β-D-glucosaminide (Ib) was well deacetylated, as in the case of the α-anomer (Ia);[1] the ethylidene compound (III) was also well deacetylated by the treatment with hydrated hydrazine, while the 3-*O*-methyl compounds (IIa and IIb) were both deacetylated in an unexpectedly low yield. These findings may give some suggestions about the reaction mechanism.

The reaction courses followed in this investigation are shown in Chart 1.

Experimental

Methyl β-D-Glucosaminide (IVb).—The starting methyl *N*-acetyl-β-D-glucosaminide (Ib)[2] (Chart 2) had a m. p. of 202—203°C and $[\alpha]_D^{29}$ −39.7° (*c* 2.890, water). A mixture of Ib (1 g.) and hydrazine (3 ml.) was kept in a sealed tube at 100°C for 20 hr.; it was then treated in a manner similar to that described in a previous paper.[1] The colorless crystals obtained from ethanol had a m. p. of 132—133°C and $[\alpha]_D^{14}$ −41.2° (*c* 1.608, water). Yield, 0.45 g. (55%).

Found: C, 43.56; H, 7.93, N, 7.26. Calcd. for $C_7H_{15}O_5N$: C, 43.52; H, 7.83; N, 7.25%.

The infrared spectrum of IVb is shown in Chart 2.

Methyl β-D-Glucosaminide Hydrochloride (VIII).—The treatment of IVb with 1 N hydrochloric acid gave a hydrochloride which ahd a m. p. of 187—188°C and $[\alpha]_D^{14}$ −23.6° (*c* 1.824, water) after recrystallization from ethanol.

Found: C, 35.81; H, 7.00; N, 6.04; Cl, 15.49. Calcd. for $C_7H_{16}O_5NCl$: C, 36.61; H, 7.02; N, 6.10; Cl, 15.44%.

Methyl *N*-Acetyl-4, 6-*O*-Benzylidene-β-D-glucosaminide.—A mixture of Ib, benzaldehyde and zinc chloride was shaken for 16 hr. The resulting benzylidene compound was then isolated by the usual method. Recrystallization from methanol gave the pure substance. Yield, 80%. M. p. 270—274°C. $[\alpha]_D^{18}$ −17.4° (*c* 0.432, dimethylsulfoxide).

Found: C, 59.39; H, 6.54; N, 4.28. Calcd. for $C_{16}H_{21}O_6N$: C, 59.43; H, 6.55; N, 4.33%.

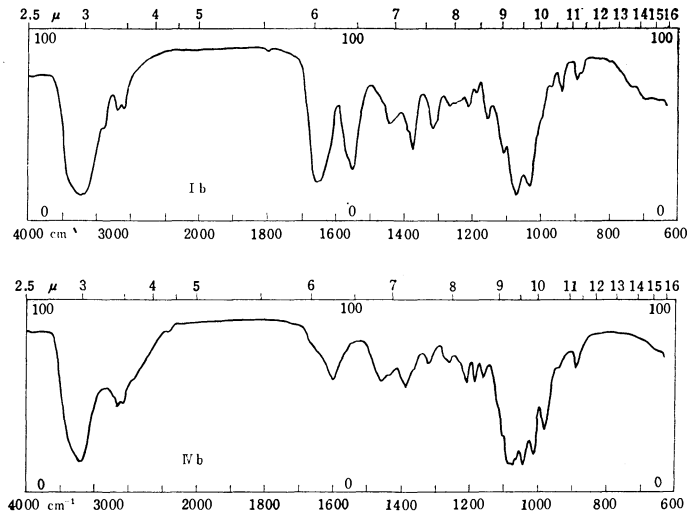

Chart 2. Infrared spectra of methyl *N*-acetyl-β-D-glucosaminide (Ib) and methyl β-D-glucosaminide (IVb).

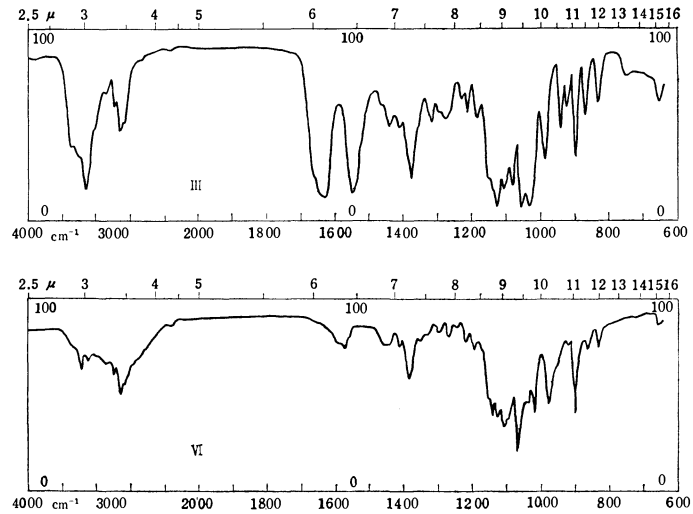

Chart 3. Infrared spectra of methyl *N*-acetyl-4,6-*O*-ethylidene-α-D-glucosaminide (III) and methyl 4,6-*O*-ethylidene-α-D-glucosaminide (VI).

Methyl *N*-Acetyl-4, 6-*O*-benzylidene-3-*O*-methyl-β-D-glucosami-nide.—Methyl *N*-acetyl-4, 6-*O*-benzylidene-β-D-glucosaminide was treated with dimethylsulfate and 30% sodium hydroxide in a large amount of dioxane. The reaction mixture was then poured into water, and the precipitates were collected and recrystallized from methanol. Yield, 57%. M. p. 276—280°C; $[\alpha]_D^{18}$ −64.8 (*c* 0.432, dimethylsulfoxide).

Found: C, 60.45; H, 6.70; N, 4.13. Calcd. for $C_{17}H_{23}O_6N$: C, 60.52; H, 6.87; N, 4.15%.

Methyl *N*-Acetyl-3-*O*-Methyl-β-D-Glucosaminide (IIb).—Methyl *N*-acetyl-4, 6-*O*-benzylidene-3-*O*-methyl-β-D-glucosaminide was heated with 60% acetic acid for 15 min. The clear solution was then evaporated in vacuo, and the residue was recrystallized from ethanol. Yield, 55%. M. p. 220—22°C; $[\alpha]_D^{14}$ −50.1 (*c* 2.176, water).

Found: C, 48.40; H, 7.71; N, 5.65. Calcd. for $C_{10}H_{19}O_6N$: C, 48.18; H, 7.68; N, 5.62%.

Methyl *N*-Acetyl-4, 6-*O*-ethylidene-α-D-glucosaminide (III).—Into a cooled suspension of Ia (4g.) in freshly-distilled paraldehyde (80 ml.), two drops of concentrated sulfuric acid were mechanically stirred. After the mixtrue had then been warmed at 60°C for 4 hr., a large amount of chloroform was added. The insoluble materials were then filtered off, and the filtrate was treated with solid potassium carbonate and then evaporated in vacuo. The crystalline residue was recrystallized twice from ethyl acetate. Yield, 3.6 g. (80%). M. p. 237—238°C; $[\alpha]_D^{12}$ +118.9° (*c* 1.968, ethanol).

Found: C, 50.31; H, 7.33; N, 5.34. Calcd. for $C_{11}H_{19}O_6N$: C. 50.56; H, 7.33; N, 5.36%.

The infrared spectrum of III is shown in Chart 3.

TABLE I. HYDRAZINOLYSIS OF METHYL *N*-ACETYL-β-D-GLUCOSAMINIDE (Ib)

Reagent	Starting compound mg.	Yield of the deacetylated product, %	Recovery of the starting compound			Total recovery %
			mg.	%	m. p.,* °C	
Hydrazine hydrate (90%)	500.4	99.1	5.2	1.0	148—150	100.1
Anhydrous hydrazine	500.2	74.1	135.5	27.1	163—164	101.2

* Before recrystallization

TABLE II. HYDRAZINOLYSIS OF METHYL *N*-ACETYL-3-*O*-METHYL-α-D-GLUCOSAMINIDE (IIa)

Reagent	Starting compound mg.	Yield of the deacetylation product, %	Recovery of the starting compound			Total recovery %
			mg.	%	m. p.,* °C	
Hydrazine hydrate (90%)	1001.2	27.0	716.6	71.6	205—207	98.6
Anhydrous hydrazine	1000.4	10.4	869.7	86.6	210—211	97.0

* Before recrystallization

Methyl 4, 6-*O*-Ethylidene-α-D-glucosaminide (VI).—A mixture of III (1.0 g.) and hydrazine hydrate (6 ml.) was kept, with occasional shaking, in a sealed tube at 100°C for 20 hr. The crystalline residue obtained by the evaporation of the reaction mixture was dissolved in hot cyclohexane, and then the solution was cooled gradually. The soft colorless needles thus obtained had a m. p. of 134—135°C ($[\alpha]_D^{18}$ +110.8° (*c* 2.048, water)) and 6.49% nitrogen. Yield, 0.7 g. (83%). Recrystallization from cyclohexane gave a pure VI, m. p. 135—136°C, $[\alpha]_D^{18}$ +111.1° (*c* 1.980, water).

Found: C, 49.13; H, 7.69; N, 6.34. Calcd. for $C_9H_{17}O_5N$: C, 49.30; H, 7.82; N, 6.39%.

The infrared spectrum of VI is given in Chart 3.

Methyl *N*-Carbobenzyloxy-4, 6-*O*-ethylidene-α-D-glucosaminide (VII).—Sodium bicarbonate (0.5 g.) and carbobenzyloxychloride (1 ml.) were stirred into an aqueous solution of VI (0.5 g.) at room temperature. After the stirring had been continued for an hour, the precipitates were filtered and washed with water. Recrystallization from ethanol gave fine needles; m. p. 176—177°C, $[\alpha]_D^{18}$ +67.5° (*c* 2.058, chloroform). Yield, 0.42 g. (52%).

Found: C, 57.69; H, 6.39; N, 3.96. Calcd. for $C_{17}H_{23}O_7N$: C, 57.78; H, 6.56; N, 3.96%.

No depression of the melting point was observed when VII was mixed with an authentic specimen which has been prepared according to the method of Akiya and Osawa,[7] and it had a m. p. of 176—177°C; $[\alpha]_D^{17}$ +67.4° (*c* 1.720, chloroform).

The Hydrazine Treatment of Methyl *N*-Acetyl-β-D-glucosaminide (Ib).—An about 500 mg. portion of Ib was treated with hydrazine (1.5 ml.) at 100°C for 20 hr. in a sealed tube, and then it was treated in a manner similar to that described in the previous paper.[1] The recovered substance obtained by passing the reaction mixture through a column of Dowex 50×4 (H^+ form) was characterized as the starting compound, Ib, by chromatographic examination and by a study of the infrared spectra, though a slight difference in melting point was observed. The results are shown in Table I.

The Hydrazine Treatment of Methyl *N*-Acetyl-3-*O*-methyl-α-D-glucosaminide (IIa).—The starting methyl *N*-acetyl-3-*O*-methyl-α-D-glucosaminide (IIa)[8] had a m. p. of 212—213°C; $[\alpha]_D^{12}$ +113.6° (*c* 1.690, water). In a sealed tube, IIa (1 g.) and hydrazine (3 ml.) were kept at 100°C for 20 hr. After it had then cooled, the reaction mixture was dissolved in absolute ethanol and concentrated in vacuo on a boiling water bath. An aqueous solution of the crystalline residue was passed through a column of Dowex 50×4 (2×18 cm., H^+ form), and then washed with water (300 ml.). The effluent and washings were combined and concentrated in vacuo to dryness, and the final crystalline residue was weighed. The compound thus recovered was identified as the starting compound, IIa, by a melting point determination, a study of its infrared spectra, and thin-layer chromatography.

The column of Dowex 50×4 was eluted with 0.5 N hydrochloric acid. The effluent solution was collected in about 6 ml. fractions, which were then checked with ninhydrin and *p*-dimethylaminobenzaldehyde - hydrochloric acid reagents. Hydrazine and hydrazide react with the latter reagent to form an intensely-yellow to orange-colored substance and a yellow fluorescent product respectively.[8,9] The fractions which were positive with the ninhydrin and negative with the *p*-dimethylaminobenzaldehyde reagent were collected, passed through a column of Dowex 1×4 (2.2×25 cm., OH^- form), and then washed with water. The effluent, combined with washings, was concentrated in vacuo to a syrup, which was then dissolvend in an appropriate amount of water. The aqueous solution thus obtained was subjected to micro Kjeldahl nitrogen determination, from which the yield of the deacetylated product was calculated. The results are shown in Table II.

The Hydrazine Treatment of Methyl *N*-Acetyl-3-*O*-methyl-β-D-glucosaminide (IIb).—One gram of IIb was treated with hydrazine as in the case of IIa. The results are shown in Table III.

The Hydrazine Treatment of Methyl *N*-Acetyl-4, 6-*O*-ethylidene-α-D-glucosaminide (III).—A two-hundred-mg. portion of III was treated with hydrazine (1.2 ml.) and then treated in a manner similar to that

8) F. Feigle, "Spot Tests in Organic Analysis," Elsevier Publishing Co., Amsterdam (1960), p. 313.

9) S. Seifter, P. M. Gallop, S. Michaels and E. Meuman, *J. Biol. Chem.*, **235**, 2613 (1960).

Table III. Hydrazinolysis of methyl *N*-acetyl-3-*O*-methyl-β-D-glucosaminide (IIb)

Reagent	Starting compound mg.	Yield of the deacetylation product, %	Recovery of the starting compound			Total recovery %
			mg.	%	m. p.,* °C	
Hydrazine hydrate (90%)	1001.7	8.2	911.5	91.0	186—187	99.2
Anhydrous hydrazine	1000.2	2.5	963.9	96.4	196—198	98.9

* Before recrystallization

Tablf IV. Hydrazinolysis of methyl *N*-acetyl-4,6-*O*-ethylidene-α-D-glucosaminide (III)

Reagent	Starting compound mg.	Yield of the deacetylated product, %	Recovery of the starting compound			Total recovery %
			mg.	%	m. p.,* °C	
Hydrazine hydrate (90%)	204.3	99.8 (97.5)**	6.7	3.3	206—210	103.1
Anhydrous hydrazine	203.2	58.7 (60.3)**	85.8	42.2	220—222	100.9

* Before recrystallization
** Determined by an amino acid autoanalyzer

used in the case of IIa, except that a column of Dowex 50×4 cooled with ice-water was used to avoid the splitting of the ethylidene group. The Hitachi amino acid autoanalyzedr was used to determine the yield of the deacetylated product. An aqueous solution (1 ml.) containing about 0.5 μmol. of the deacetylated product, from which hydrazine and hydrazide had been removed as thoroughly as possible by repeated evaporation, was introduced into an amino acid analyzer (0.9×7 cm. column, pH 5.28, 0.2 N citrate buffer). A small peak due to acthydrazide, a low broad peak due to hydrazine, and a main peak of methyl 4, 6-*O*-ethylidene-α-D-glucosaminide (VI) were observed. The results are shown in Table IV.

The Periodate Oxidation of Methyl 4, 6-*O*-Ethylidene-α-D-Glucosaminide (VI). — One milliliter of a 0.05 M potassium periodate solution was added to 9 ml. of a 10^{-3} M aqueous solution of VI at 25°C in a dark place, and the optical density at 290 mμ was read at several intervals against the reagent blank.[10] The decrease in the optical density at this wave lengh: after 72 hr. was 0.194, which corresponded to the consumption of one mole of periodate per mole of VI.

Discussion

Methyl β-D-glucosaminide (IVb) has also been obtained, by a different method, by Matsushima and Miyazaki,[11] who gave a m. p. of 130—132°C, $[\alpha]_D^{18}$ −40.7°. As has been described above, the compound isolated from the reaction mixture gave identical physical constants. The hydrochloride of IVb had melting point and optical rotation values consistent with those described by Foster, Horton and Stacey,[12] who prepared the compound via methyl *N*-carbobenzyloxy-β-D-glucosaminide and gave a m. p. of 189—190°C, $[\alpha]_D^{20}$ −24°. The infrared spectrum of IVb (Chart 2) shows the existence of the free amino group. Thin-layer chromatography using a moving phase of buthanol: acetic acid: water=4 : 1 : 5 (upper layer) revealed that the reaction mixture contained only two components, Ib and IVb. These findings together with the data in Table I, show that Ib was well deacetylated by the hydrazine treatment and gave IVb as the sole deacetylated product. The glycosidic linkage in Ib was stable under the hydrazine treatment.

While methyl 3-*O*-methyl-D-glucosaminides (V) have not been reported yet, their 4, 6-*O*-ethylidene and 4, 6-*O*-benzylidene compounds have been prepared by Akiya and Osawa.[7] By the method of these authors, 4, 6-*O*-ethylidene compounds of IIa and IIb were prepared and the ethylidene group was split with 60% acetic acid. The resultant amorphous substances (both of which we tried to crystallize, but all in vain), were used as the standard methyl 3-*O*-methyl-D-glucosaminides in the chromatographic examinations. The hydrazinolyzed products of IIa and IIb were thus characterized without isolating them.

Tables II and III show that the greater part of the starting compounds, IIa and IIb, were recovered, the *N*-deacetylation occurring in an unexpectedly low yield.

As has been mentioned above, the hydrazinolyzed product of III was characterized as a *N*-carbobenzyloxy derivative, one with a melting point and optical rotation data consistent with those of an authentic specimen prepared by the method of Akiya and Osawa.[7] A thin-layer chromatogram and its infrared spectra showed that VII was identical with the authentic specimen.[7] The infrared spectrum (Chart 3) and the elemental analyses support the structure of VI. These results and the

10) T. Ikenaka, *J. Biochem.*, **54**, 328 (1963).
11) Y. Matsushima and T. Miyazaki, This Bulletin, **38**, 1325 (1965).
12) A. B. Foster, D. Horton and M. Stacey, *J. Chem. Soc.*, **1957**, 81.

periodate oxidation of VI show definitely that an ethylidene group in III or VI is in the 4, 6-position.

Hydrazine hydrate seems to have a greater power to deacetylate than does anhydrous hydrazine (Tables I—IV). Another trait observed is that the compounds with a free hydroxyl group vicinal to the *N*-acetyl group undergo deacetylation more easily. The results obtained in the case of IIa and IIb are consistent with the fact that the hydrazine treatment of *N*-acetylaminopolysaccharides with a substituent of C-3, such as chondroitin sulfate,[13-15] hyaluronic acid[15] and the cell wall mucopolysaccharide of Micrococcus lysodeikticus,[16] resulted in low yields.

The total recovery (Table I—IV) and the chromatographic examinations show that hydrazine treatment caused little cleavage of glycosidic likages. These findings are consistent with the reported fact that the hydrazine treatment of a simple polysaccharide such as soluble starch and glycogen[17] does not cause any extensive cleavage of glycosidic linkages. As regards the hydrazinolysis of mucopolysaccharides,[13-15] which ended in a considerable degradation of the molecule, some specific interpretations will be required.

13) Y. Matsushima and N. Fujii, This Bulletin, **30**, 48 (1957).
14) M. L. Wolfrom and B. O. Juliano, *J. Am. Chem. Soc.*, **82**, 2588 (1960).
15) Z. Yosizawa and T. Sato, *J. Biochem.*, **51**, 155 (1962).
16) S. Hara Y. Matsushima, in preparation.
17) Z. Yosizawa and T. Sato, *Tohoku J. Exp. Med.*, **76**, 100 (1962).

Summary

Methyl *N*-acetyl-β-D-glucosaminide, methyl *N*-acetyl-3-*O*-methyl-α- and β-D-glucosaminide and methyl *N*-acetyl-4, 6-*O*-ethylidene-α-D-glucosaminide have been deacetylated using anhydrous and hydrated hydrazine. It has been found that the 3-*O*-substitution slowed the deacetylation reaction considerably.

Crystalline methyl β-D-glucosaminide (IVb) and methyl 4, 6-*O*-ethylidene-α-D-glucosaminide (VI) have been newly obtained in the free base form from the corresponding *N*-acetyl compounds.

This investigation was supported by U. S. Public Health Service Grant No. AI-04586-03.

NOTE

An Electron Diffraction Investigation of the Molecular Species in the Vapor Phase of the GaAs-I_2 System

By Yonezo MORINO,† Takeshi UKAJI††,* and Tetsuzo ITO†,**

† *Department of Chemistry, Faculty of Science, The University of Tokyo, Hongo, Tokyo*

†† *Department of Chemistry, Ibaragi University, Mito*

(Received April 17, 1965)

The growth of single crystals from a vapor phase has become an important technique in the preparation of single crystals of such semiconducting compounds as GaAs. It has recently been discovered[1] that, when a small quantity of iodine is added as a carrier to polycrystals of GaAs, the starting material, the growth takes place at relatively low temperatures of about 700°C, although GaAs itself has only a negligible vapor pressure at such temperatures. It is, therefore, important to identify the reacting species in the vapor phase in order to understand the mechanism of the crystal growth. After we had started the high-temperature diffraction work for this purpose, Silvestri and Lyons[2] published their work on this system by vapor-pressure measurements; they showed that the vapor phase of this system consists mainly of GaI_3 and As_4 and established the $2GaAs(s)+GaI_3(v)\leftrightarrow 3GaI(v)+(1/2)As_4(v)$ reaction in the 560—850°C temperature range.

In the present work, in pursuit of a possible change in the species present in the mixture at different temperatures, a vapor-phase equilibrium of the GaAs-I_2 system at a lower temperature of 440°C has been studied by the sector-microphotometer method of electron diffraction. The above temperature was also selected because the operation of the present high-temperature nozzle was easier below 500°C.

Experimental

Polycrystals of GaAs of a high purity were kindly supplied by the Tokyo Shibaura Electric Co. The sample of iodine was purified by sublimation. About 0.1 g. of the iodine and an excess amount (about 1 g.) of the crystals were placed in the oven of the nozzle at the same time. After the mixture had been degassed for about ten minutes in a vacuum, it was slowly heated to 440°C in about 30 min. The diffraction photographs were taken under conditions almost the same as those described in a preceding paper.[3]

Results and Discussion

One diffraction photograph of the GaAs-I_2 reaction system was analyzed. The molecular intensity curve, $qM(q)$, which was obtained by the drawing of a smooth background line across the experimental total intensity curve was found to be similar to those of the GaI_3 described in a preceding paper.[4] The molecular intensity curve thus obtained is compared with the theoretical curve of the GaI_3 in Fig. 1.

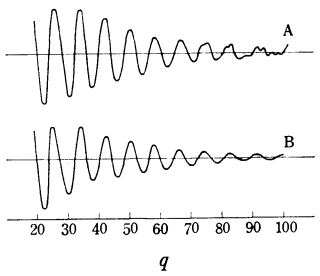

Fig. 1. Molecular intensity curve of GaAs-I_2 at 440°C.
A: Observed $qM(q)$ of GaAs-I_2
B: Calculated $qMq(q)$ for the GaI_3 model

Since the intensity of a small-angle region is sensitive to the specimen, it seemed desirable to examine the $q<20$ region in order to confirm that the system was indeed GaI_3. The photograph taken by the usual procedure was not suitable for this study, since the beam trap of the sector interfered with the observation of the diffraction pattern in this region. Moreover, the nozzle

* Present address: Ikutoku Kosen, Atsugi, Kanagawa.
** Present address: The Institute for Physical and Chemical Research, Komagome, Tokyo.

1) G. Antell and D. Effer, *J. Electrochem. Soc.*, **106**, 509 (1959).
2) V. J. Silvestri and V. J. Lyons, ibid., **109**, 963 (1962).
3) Y. Morino, T. Ukaji and T. Ito, This Bulletin, **39**, 64 (1965).
4) Y. Morino, T. Ukaji and T. Ito, ibid., **39**, 71 (1965).

assembly was not designed for use at a longer camera distance. The features of the diffraction pattern in that range of the scattering angles were, therefore, examined qualitatively by the following procedure. The sector was removed, and the photographs were taken with two different exposure times: about one second, and one and a half seconds. The photographs were then traced with a microphotometer across the diameter of the pattern, and the two intensity curves corresponding to the above exposure times were joined together at the q of about 13, and the curve thus obtained was converted to the molecular intensity curve, $qM(q)$. In Fig. 2 this curve is compared with the theoretical molecular intensity curve calculated with the molecular parameters of the GaI_3 (r_a'(Ga-I)=2.456, r_a'(I-I)=4.250 Å. The mean amplitudes were corrected for the change in temperature as follows: l(Ga-I)=0.076 and l(I-I)=0.185 Å).

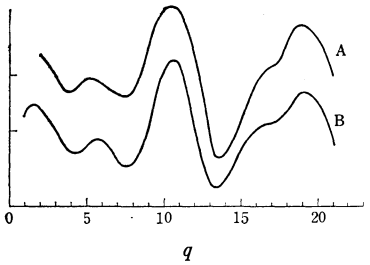

Fig. 2. Small-angle intensity curve of $GaAs\text{-}I_2$ at 440°C.
A: Observed $qM(q)$ of $GaAs\text{-}I_2$
B: Calculated $qM(q)$ for the GaI_3 model

The features of the experimental intensity curve are in qualitative agreement with the theoretical curve. The radial distribution curve was, therefore, obtained from the experimental molecular intensity curve spliced in the range of the scattering angles q less than 20 by a theoretical curve calculated with the molecular parameters of the GaI_3. The curve is shown in Fig. 3A; it is essentially similar to that of the GaI_3. It should be mentioned, however, that in this curve two fairly large negative areas between the two main peaks are observed, as is an appreciable distortion from the Gaussian form for the I-I peak.

Synthetic radial distribution curve for the GaI_3 model mentioned above was then calculated and subtracted from the experimental curve of Fig. 3A. The curve obtained as the difference between the two curves is shown in Fig. 3B. Three peaks are observed in this curve. Although the peak at about 2.5 Å might correspond to the As—As distance of As_4 (r_a=2.432Å)[3] and the As—I distance of AsI_3 (r_a'=2.554 Å)[4], and the peak at about 3.9 Å, to the I—I distance of AsI_3 (r_a'=3.915 Å), no quantitative discussions can be made, since the heights of these peaks are of the same orders of magnitude as those of ghosts (the negative peaks). The peak at about 3.1 Å has not been assigned to any, possible interatomic distance; it may be a ghost.

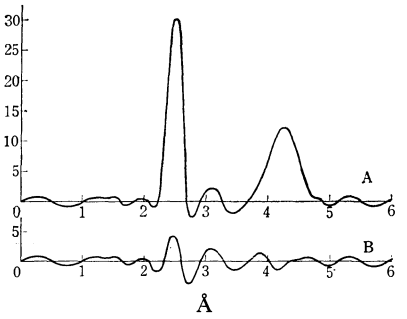

Fig. 3.
A: Radial distribution curve of $GaAs\text{-}I_2$ at 440°C
B: Difference between the RD curve of $GaAs\text{-}I_2$ and that of the GaI_3 model

In conclusion, the present study has shown that the predominant species in the vapor phase of the $GaAs\text{-}I_2$ reaction system at 440°C is GaI_3. It may, therefore, be inferred that a reaction similar to that reported by Silvestri and Lyons takes place at this temperature. The vapor pressure of the GaI_3 is about 700 mmHg (estimated from the amount of the starting iodine), while the arsenic which results from the reaction is expected to remain mainly in the solid phase (the vapor pressure of arsenic is about 10 mmHg at 440°C); it has, therefore, only a little influence on the diffraction photograph.

The authors wish to express their deep gratitude to the Tokyo Shibaura Electric Co. for kindly supplying the sample of GaAs.

SHORT COMMUNICATIONS

A New Spectrophotometric Method for the Determination of Tungsten with Stilbazogall I

By Hajime ISHII and Hisahiko EINAGA

Central Research Laboratory, Onoda Cement Co., Ltd., Koto-ku, Tokyo

(Received October 20, 1965)

A new spectrophotometric method for the determination of a trace of tungsten has been developed. It is based upon the formation of a red tungsten(VI) complex of Stilbazogall I, stilbene-4, 4' - bis [(1-azo)-2, 3, 4-trihydroxybenzene] - 2, 2'-disulfonic acid (I), which was synthesized by Cherkesov et al.[1] and which has recently been reported to be a reagent for the determination of zirconium.

The absorption spectra of the complex at various pH values are shown in Fig. 1, from which it may be seen that tungsten(VI) froms more than one type of complex. In detailed experiments, two types of complexes were found. One of them was a 1 : 1 metal-to-reagent complex formed at about pH 2, while the other was a 1 : 2 complex

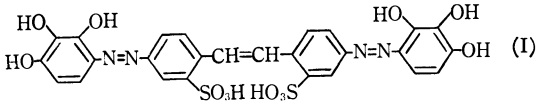

(I)

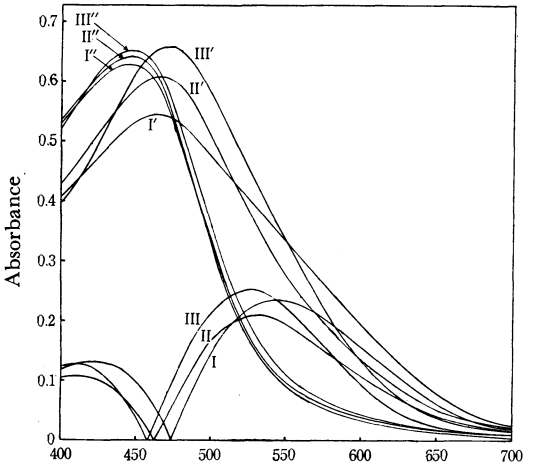

Fig. 1. Absorption spectra of W(VI) - Stilbazogall I complex.
W(VI): 1×10^{-5}; Stilbazogall I: 2×10^{-5} mol./l.
pH: I, I', II'', 2.2; II, II', II'', 3.5; III, III' III'', 4.8.
Reference: I, II, III, reagent blank
I', II', III', I'', II'', III'', water
I'', II'', III'' stilbarogall I alone

1) A. I. Cherkesov and Yu. V. Pushinov, *Zhur. Anal. Khim.*, **20**, 665 (1965).

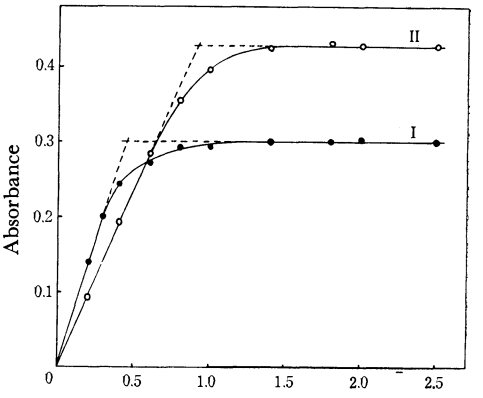

Fig. 2. Determination of mole ratio of W(VI) - Stilbazogall I complex by the mole ratio method.
Stillazogall I: 2×10^{-5} mol./l.
I: pH 4.9, 520 mμ II: pH 2.2, 550 mμ

formed at about pH 5. The composition of the complex was found to change continuously from 1 : 1 to 1 : 2 with an increase in the pH value. Figure 2 shows the results obtained by the mole ratio method as an example. A linear relationship was found between the concentration of tungsten(VI) and the absorbance. The molar extinction coefficients of 1 : 1 and 1 : 2 complexes were about 2.1×10^4 and 3.7×10^4, and the sensitivities were 8.7×10^{-3} and 4.9×10^{-3} μg.W/cm^2 respectively, corresponding to log $(I_0/I)=0.001$. The proposed procedure for the determination is as follows. To a sample solution containing tungsten(VI) in a 25-ml. volumetric flask, 5.0 ml. of a Stilbazogall I solution (10^{-4} mol./l.) and 5 ml. of a sodium acetate - acetic acid buffer solution (pH=4.9) are added. The solution is then diluted to the mark with distilled water. The absorbance of the solution is measured at 520 mμ against a reagent blank solution between 5 and 15 min. after the addition of the reagent solution. Some metals, such as aluminum(III) copper(II), molybdenum(VI), titanium(IV), and zirconium(IV), interfere under the conditions proposed.

The details of this study will be reported elsewhere.

A New Colorimetric Method for the Determination of Beryllium with Sodium *p*-Chlorophenol-azo-1, 8-dihydroxynaphthalene-3, 6-disulfonate

By Katsuya UESUGI and Yukiteru KATSUBE

Himeji Institute of Technology, Idei 600, Himeji

(Received October, 21, 1965)

A new colorimetric method for the determination of traces of beryllium has been developed. It is based upon the stable blue beryllium complex of sodium *p*-chlorophenol-azo-1, 8-dihydroxynaphthalene-3,6-disulfonate in an aqueous solution. This compound has been used for the colorimetric determinations of calcium and magnesium in serum,[1] urin[2] and cast iron[3].

The absorption spectra of the beryllium complex are shown in Fig. 1. At pH 6.5, the maximum absorbance is found at 610 mμ. The complex is formed by adding a small amount of beryllium to the mixture of 10 ml. of a sodium acetate - acetic acid buffer solution and 2.0 ml. of a 0.1% reagent solution in a 25 ml. volumetric flask. The solution is diluted to the mark with distilled water and thoroughly mixed. The beryllium complex has a maximum absorbance in the pH range from 6.2 to 6.8. The color under these conditions develops completely within 10 min. and is stable for at least 30 min. There is no variation in the absorbance of the color over the temperature range of 10 to 30°C. When the color is measured spectrophotometrically at its absorption peak, 610 mμ, the beryllium complex obeys Beer's law within the range from 0.02 to 0.3 p.p.m. of beryllium (Fig. 2).

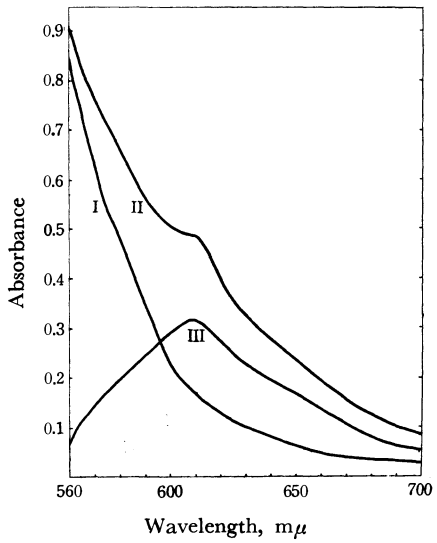

Fig. 1. Absorption spectra. pH 6.5

I. Reagent (40 p.p.m.), against water
II. Reagent (40 p.p.m.) + Be (0.28 p.p.m.), against water
III. Reagent (40 p.p.m.) + Be (0.28 p.p.m.), against reagent blank

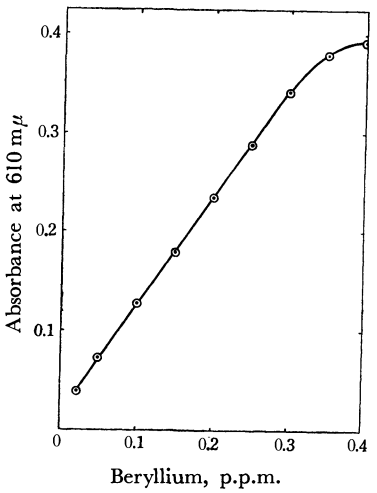

Fig. 2. Beer's law curve. pH 6.5

At 610 mμ, the molar extinction coefficient is about 11000, the sensitivity being 0.0008 μg. Be/cm^2, corresponding to log I_0/I=0.001.

5 μg. of beryllium can be determined satisfactorily in the presence of 50 μg. of iron (II, III), manganese(II), calcium and magnesium. Copper-(II), aluminum, zinc, cobalt and nickel interfere.

Further, detailed studies are now in progress.

1) F. Yanagisawa, *J. Biochem.*, **42**, 3 (1955).
2) G. R. Kingsley, *Anal. Chem.*, **29**, 615 (1957).
3) K. Ota, *J. Japan Inst. Metals, Sendai*, **24**, 46 (1960).

A Novel Direct Synthesis of the *N*-Oxides of Quinoline Derivatives

By Yusuf AHMAD and Shamim Ahmad SHAMSI

Chemical Research Division, Central Laboratories, Pakistan Council of Scientific and Industrial Research Karachi, West Pakistan

(Received October 27, 1965)

The *N*-oxides of quinoline compounds are usually obtained by the oxidation of corresponding quinoline derivatives. No synthesis resulting in the direct formation of the *N*-oxide of quinoline derivatives seems to have been recorded so far. Perhaps the only exception is the report of Loudon et al.[1] regarding the syntheses of some 1, 4-dihydro-1-hydroxy-4-oxoquinolines, which in their tautomeric form can be regarded as 4-hydroxyquinoline *N*-oxide derivatives.

We record below a novel quinoline synthesis, in which the nitro group of a benzene derivative interacts with the side chain in the ortho position, in the presence of a base, and results in the direct formation of the *N*-oxide of a quinoline derivative.

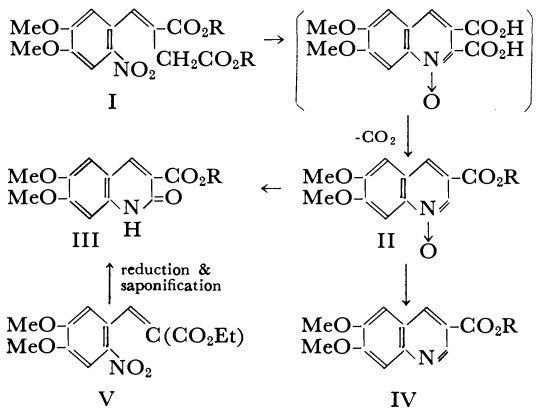

a) R=H, b) R=Et, c) R=Me

Veratraldehyde was condensed with ethyl succinate to obtain veratrylidenesuccinic acid,[2] m. p. 174—175°C, which on nitration gave *o*-nitroveratrylidenesuccinic acid[3] (Ia) as yellow needles, m. p. 214—415°C. Ia, on being warmed with 20% aqueous potassium hydroxide, gave an acid (m. p. 282—283°C decomp.) which was then purified by precipitation with acid from its sodium bicarbonate solution. The constitution of this acid was confirmed to be 6,7-dimethoxyquinoline-1-oxide-3-carboxylic acid (IIa), as it underwent the known rearrangement[4] of the *N*-oxides of quinoline to carbostyrils on being heated with acetic anhydride, and gave 2-hydroxy-6, 7-dimethoxyquinoline-3-carboxylic acid (IIIa) as yellow needles (m. p. 310°C decomp.), an acid which was identical (delete infrared spectrum and mixed melting point) with an authentic sample[5], synthesised through a previously-reported unambiguous route, involving the reduction of the intermediate (V) and its simultaneous cyclisation, followed by the saponification of the resulting ester. IIIa obtained by either of the routes, on sublimation in vacuo, decarboxylated to the same 6, 7-dimethoxycarbostyril (III, H for CO_2R) (m. p. 232—234°C); the two samples had identical infrared spectra, and their melting point and mixed melting point were the same. On esterification, 6, 7-dimethoxyquinoline-1-oxide-3-carboxylic acid (IIa) gave the ethyl ester (IIb), as white needles (m. p. 214—215°C) and the methyl ester (IIc), as white needles (m. p. 211—212°C). The ethyl ester, on deoxygenation[6] with PCl_3, gave ethyl 6, 7-dimethoxyquinoline-3-carboxylate (IVb) as white needles, m. p. 140—141°C; on saponification this gave 6, 7-dimethoxyquinoline-3-carboxylic acid (IVa), as white micro-needles (m. p. 267—268°C). All the compounds reported above gave satisfactory C, H and N analyses.

Similar work in an analogous series has been completed; it will be described in detail in a subsequent publication.

1) J. D. Loudon and I. Wellings, *J. Chem. Soc.*, **1960**, 3462, 3470; J. D. Loudon and G. Tennant, ibid., **1960**, 3466.
2) J. W. Cornforth, G. K. Hughes and F. Lions, *J. Proc. Roy. Soc. N. S. Wales.*, **72**, 228 (1939).
3) N. J. Cartwright and R. D. Haworth, *J. Chem. Soc.*, **1944**, 535.
4) E. Ochiai and T. Okamoto, *J. Pharm. Soc. Japan*, **68**, 88 (1948); E. Ochiai, *J. Org. Chem.*, **18**, 534 (1953); cf. S. Oae and S. Kozuka, *Tetrahedron*, **20**, 2691 (1964).
5) S. Somasekhara and R. Phadke, *J. Indian Inst. Sci.*, **37**, 120 (1955).
6) S. Takahashi and H. Kano, *Chem. Pharm. Bull.* (*Tokyo*), **12**, 783 (1964); M. Hamana, *Yakugaku Zasshi*, **71**, 263 (1951).

The Electron Spin Resonance of Sodium Polyphosphate Glass Irradiated with γ-Rays

By Masaji MIURA and Akinori HASEGAWA

Department of Chemistry, Faculty of Science, Hiroshima University, Hiroshima

(Received October 29, 1965)

Phosphate glass is easily colored upon irradiation with γ-rays. Krapetyan and Yudin have reported that the red color of phosphate glass induced by the irradiation of γ-rays is to be attributed to the electron trapped by phosphorus atoms.[1] By taking the g values and the coupling constant into account, however, it has recently been concluded that the color is caused by the hole trapped by the oxygen atom rather than by the electron trapped by the phosphorus atom.[2]

These authors have used phosphate glasses, but the degrees of polymerization were not determined. No relationship between the effect of γ-rays on the glass and its degree of polymerization, $\bar{n}$, has yet been established. The purpose of the present work is to investigate this relationship by using sodium polyphosphate, which is so-called Graham's salt. Samples of sodium polyphosphate glass with various values of $\bar{n}$ were prepared and irradiated with γ-rays from a ^{60}Co source at room temperature. The ESR and optical-absorption measurements were then carried out on these glasses.

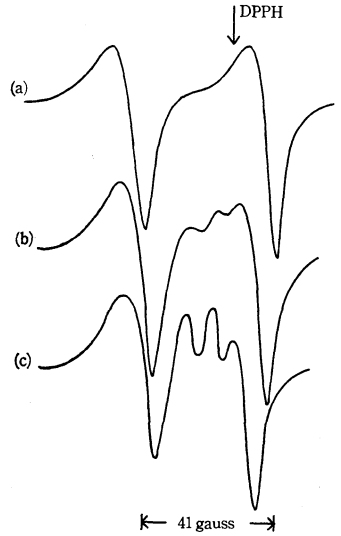

Fig. 1. The ESR spectra of γ-irradiated sodium polyphosphate glasses with (a) $\bar{n}=86$, (b) $\bar{n}=11$ and (c) $\bar{n}=4.8$.

The glass with a higher value of $\bar{n}$, as is shown in Fig. 1a, gave two asymmetric ESR absorptions which are hyperfine structures originating from the interaction between the ^{31}P nucleus and the hole trapped in the non-bonding orbital of the oxygen atom. The coupling constant between these two absorptions became smaller and, at the same time, a new doublet appeared more definitely with a decrease in the $\bar{n}$ value (Figs. 1b and 1c). The latter doublet may be attributed to the hole trapped in the oxygen ion of the end group, PO_4^{2-}, because it has a much smaller coupling constant than that of the former doublet and becomes more evident with an increase in the content of the end groups.

After the irradiation of 5×10^5 r., the ESR measurement on each glass was carried out at room temperature. The intensity of the larger doublet decreases rapidly as the value of $\bar{n}$ decreases.

Each transparent sheet of these glasses showed an intrinsic absorption band in the ultraviolet region. After the irradiation with γ-rays, however, each gave two additional bands, one in the visible, and the other in the ultraviolet region. The wavelengths of the maximum absorption of these bands depend upon the value of $\bar{n}$. The visible absorption band may be due to the electronic transition between the excited level of the non-bonding orbital, where the trapped hole is mainly localized, and the lower levels of the bonding orbital. On the other hand, the ultraviolet absorption may be caused by the charge transfer of the trapped electron to the neighbors.

Thus, from the ESR spectra of γ-irradiated sodium polyphosphate glasses, two doublets were found; the larger doublet is due to the hole trapped by the main chain of polyphosphate, while the smaller doublet is due to the hole trapped by the end group. The ESR of the larger doublet and the optical absorption of the glass may be modified by the change in the distortion of the P-O-P bond caused by the variation in the degree of polymerization.

1) G. O. Krapetyan and D. M. Yudin, *Fiz. Tverd. Tela*, **3**, 2827 (1961).
2) Y. Nakai, This Bulletin, **38**, 1308 (1965).

Stable *trans*-Isomers of Bis(acetato)-triethylenetetramine-cobalt(III) and Bis(propionato)-triethylenetetramine-cobalt(III) Complexes

By Kashiro KURODA and Motoko GOTO

Department of Chemistry, Kyoto-Gakugei University, Fushimi-ku, Kyoto

(Received November 4, 1965)

Although a diacido-triethylenetetramine-cobalt-(III) complex may exist in three stereoisomeric forms, two *cis*- and one *trans*-isomers, all of the complexes prepared so far have been *cis*-isomers except for *trans*-[$CoBr_2$trien]X.[1] Concerning the complex, however, the absorption spectrum has not been measured because of its instability in solution. In our previous studies of [Co(halac)$_2$-$(NH_3)_4$]X and [Co(halac)$_2$(en)$_2$]X,[2] where halac= acetato and halogenoacetato ligands, we have noticed that *trans*-isomers occur when the reaction mixture of a carbonato-complex and a halogeno-acetic acid is evaporated at a high temperature and that they are apt to arise in the cases of halac ligands with low halogen contents. In the light of this knowledge, two compounds, [Co$(CH_3CO_2)_2$-trien]ClO_4·$HClO_4$ and [Co$(C_2H_5CO_2)_2$]trienClO_4·$HClO_4$, have been obtained which must be *trans*-isomers judging from their preparation procedures[3] and absorption spectra.

Figure 1 and Table I show the absorption spectra of the complexes prepared, together with those of some related complexes. It has been well-established that, in a [Coa_4b_2]-type complex, the first band of the *trans*-isomer splits much more significantly than that of the *cis*-isomer.[4,5] As may be seen in Fig. 1, the absorption curves of the prepared complexes obviously exhibit the features of a *trans*-isomer. In addition, the absorption maxima are in good correspondence with those of *trans*-[Co$(CH_3CO_2)_2$-$(en)_2$]ClO_4. The identification is also reasonable in view of the preparation procedures. Much as in the procedures for some *trans*-[Co(halac)$_2$$(en)_2$]-$ClO_4$,[2] the reaction mixture of [$CoCO_3$trien]ClO_4 and CH_3CO_2H (or $C_2H_5CO_2H$) was boiled for a few minutes at the final period of the evaporation. Moreover, just as *trans*-[Co(halac)$_2$$(en)_2$]$^+$ precipitate as acidic salts upon the addition of perchloric acid,[2] so do the present complexes.

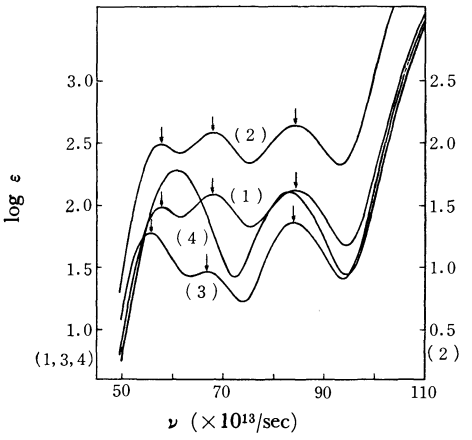

Fig. 1. Absorption spectra of *trans*-[Co$(CH_3CO_2)_2$-trien]ClO_4 and some related complexes.
1 : *trans*-[Co$(CH_3CO_2)_2$ trien]ClO_4
2 : *trans*-[Co$(C_2H_5CO_2)_2$ trien]ClO_4
3 : *trans*-[Co$(CH_3CO_2)_2$ $(en)_2$]ClO_4
4 : *cis*-[Co$(CHCl_2CO_2)_2$ trien]ClO_4

The intensity is the most significant difference between the spectra of *trans*-[Co$(CH_3CO_2)_2(en)_2$]$^+$ and of *trans*-[Co$(CH_3CO_2)_2$ trien]$^+$. The high intensity of the latter is probably due to the low symmetry of the complex. Because the trien molecule is constrained by the square planar coordination and because there is no chelation at one side of the square, the square is necessalily distorted to some extent. That is, the symmetry of the complex is much lower than those of the $(NH_3)_4$- and $(en)_2$- analogues. This may effect the increase in the transition moment and, hence, the high extinction coefficients.

TABLE I. ABSORPTION SPECTRA OF *trans*-[Co$(CH_3CO_2)_2$ trien]ClO_4

	ν_{1a} (10^{13}/sec.)	log ε_{1a}	ν_{1b} (10^{13}/sec.)	log ε_{1b}	ν_2 (10^{13}/sec.)	log ε_2
trans-[Co$(CH_3CO_2)_2$trien]$^+$	57.7	1.981	67.8	2.083	84.3	2.122
trans-[Co$(C_2H_5CO_2)_2$trien]$^+$	57.7	1.989	67.8	2.082	84.2	2.139
trans-[Co$(CH_3CO_2)_2(en)_2$]$^+$	55.8	1.778	66.7	1.462	84.0	1.863

1) J. Selbin and J. C. Bailar, *J. Am. Chem. Soc.*, **82**, 1524 (1960).
2) K. Kuroda and P. S. Gentile, This Bulletin, **38**, 1362, 1368 (1965).
3) To be published in detail shortly.
4) M. Linhard and M. Weigel, *Z. anorg. Chem.*, **264**, 321 (1951).
5) Y. Shimura, This Bulletin, **25**, 49 (1952).

Photooxidation with Cupric Ions. A Novel Dimethoxylation and Diacetoxylation of Styrene

By Shinji MURAI and Shigeru TSUTSUMI

Department of Chemical Technology, Faculty of Engineering, Osaka University, Miyakojima-ku, Osaka

(Received November 4, 1965)

Previous investigations of photooxidation with transition metal ions have dealt almost exclusively with aqeuous solutions.[1] The hydroxylation of benzene[2] and benzoic acid[3,4] to the corresponding phenols by irradiation with ultraviolet light in an aqeuous ferric ion solution have been reported. Recently Kochi has reported the photochemical chlorination of organic compounds in organic media.[5]

We wish now to report some novel photooxidations in nonaqeuous solutions: the photochemical reactions of styrene with methanol or with acetic acid in the presence of cupric ions. The over-all reactions are shown below:

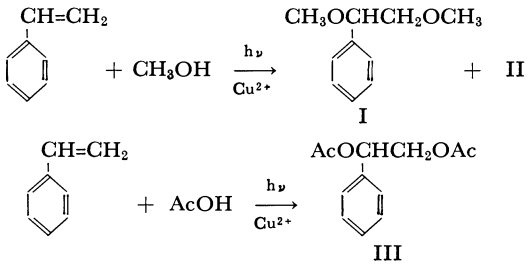

A homogeneous solution of styrene (0.1 mol.) and cupric perchlorate hexahydrate (0.1 mol.) in methanol (200 mol.) was irradiated by 2537Å light for 24 hr. The reaction mixture was then diluted with water and extracted with ether.[6] The ether extract was dried and distilled to give 2.4 g. of styrene glycol dimethyl ether (I), b. p. 90—95°C/11 mmHg, and 1.7 g. of an almost colorless oil, b. p. 110—120°C/0.5 mmHg, which was partially crystallized on standing and which was separated by filtration into 0.2 g. of crystalline *meso*-1, 4-dimethoxy-2, 3-diphenylbutane (II) and an oil. This oil, obtained also in the absence of cupric perchlorate, was presumably a mixture of styrene dimers (infrared). When compound I was purified by preparative gas chromatography, it showed an infrared spectrum identical with that of an authentic sample.[7] Found: C, 72.29; H, 8.77. Calcd. for $C_{10}H_{14}O_2$: C, 72.26; H, 8.49%. II was recrystallyzed from methanol, m. p. 129—130°C, underpessed on admixture with an authentic sample.[7] When the reaction of styrene with methanol was carried out, under irradiation, using cupric sulfate pentahydrate in place of cupric perchlorate, I (0.3 g.) and II (0.2 g.) were also obtained.

In the same manner, a homogeneous solution of styrene (0.1 mol.) and cupric perchlorate hexahydrate (0.1 mo.l) in acetic acid (400 ml.) was irradiated by 2537Å light for 24 hr. No gas evolution was observed during the reaction. On working up as has been described above, 1.5 g. of styrene diacetate (III), b. p. 102—105°C/0.3 mmHg was obtained. III was identified by gas chromatography on a polyester-DA column at 185°C. III also showed an infrared spectrum identical with that of an authentic sample.[8] III gave styrene glycol upon hydrolysis, m. p. and m. m. p. 65—66°C (ligroin).

Upon irradiation in the absence of styrene, a solution of cupric perchlorate in methanol gave formaldehyde, while in acetic acid the products were mainly CH_4 and CO_2, with small amounts of H_2 and C_2H_6. Therefore, in these reactions the methoxy radical or the acetoxy radical are probably formed initially by the photooxidation of methanol or acetic acid with cupric ions. Then addition of these radicals to styrene probably takes place, thus yielding intermediate radicals such as IV.

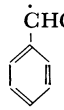

IV R=CH_3, Ac

Finally, IV gives I or III by the usual cupric ion oxidation of free radicals.[9] Small amounts of fine precipitates of metallic copper were obtained throughout these reactions. Cupric ions might be reduced to cuprous ions, which might then disproportionate to cupric ions and metallic copper. However, the possibility of the initial formation of the styrene cation radical by a photochemical one-electron oxidation of styrene with cupric ions and the trapping of the cation radical by solvents, thus yielding IV, has not been eliminated.

1) N. Uri, *Chem. Revs.*, **50**, 375 (1952).
2) J. H. Baxendale and J. Magee, *Trans. Faraday Soc.*, **51**, 205 (1955).
3) H. G. C. Bates and N. Uri, *J. Am. Chem. Soc.*, **75**, 2754 (1953).
4) J. Saldick and A. O. Allen, ibid., **77**, 1388 (1955).
5) J. K. Kochi, ibid., **84**, 2121 (1962).
6) *Caution;* Avoid concentrating the reaction mixture or serious explosion would take place.
7) T. Inoue and S. Tsutsumi, This Bulletein, **38**, 661 (1965).
8) W. L. Evans and L. H. Morgan, *J. Am. Chem. Soc.*, **35**, 54 (1913).
9) J. K. Kochi, *Tetrahedron*, **18**, 483 (1962).

The Determination of Singlet-Triplet Separation from the Anomalous Hyperfine Structure Observed with a Radical Pair

By Hisaharu HAYASHI, Koichi ITOH and Saburo NAGAKURA

The Institute for Solid State Physics, The University of Tokyo, Azabu, Tokyo

(Received November 12, 1965)

It has recently been found by ESR studies that radical pairs are stably trapped in the single crystals of several oximes X-irradiated at 77°K.[1-3] In particular, the radical pair, "K", of dimethylglyoxime shows an anomalous hyperfine structure; i. e., the observed central three lines among the nine hyperfine lines corresponding to the $\Delta m=\pm 1$ transitions of the radical pair are not equally spaced.[1] This can not be explained by a first-order treatment which considers only the nonequivalence of the hyperfine tensors of two interacting radicals.[1] We have attempted to interpret the anomaly by considering the mixing between the singlet and triplet states through the hyperfine interaction and the electronic Zeeman term.

The Hamiltonian for the system under consideration consists of the electronic Coulomb, electronic Zeeman, electron spin-spin interaction, hyperfine interaction and nuclear Zeeman terms. The effective energy difference due to the first term between the singlet and triplet states is expressed by the exchange term, $-2J\mathbf{s}_1\mathbf{s}_2$, where J is the exchange integral. On the assumptions that the second term is much larger than the third and fourth terms, and that the fourth term is much larger than the fifth term, the energy level, $E(m, M^a, M^b)$, of the triplet state can easily be evaluated by the aid of the second-order perturbation. In this case, the interacting nucleus is only one nitrogen ($I=1$) for each radical.[1,4] The two radical sites are designated as a and b, and m and M^p are the z-components of the electron spin of the triplet state and of the nitrogen nuclear spin on the p site respectively. Only the allowed transitions of $\Delta m=\pm 1$ and $\Delta M^a=\Delta M^b=0$ are considered.

Since the anomaly is noticeable for the hyperfine lines due to $M^a+M^b=0$, the deviation, $\delta_\pm$, defined below should be considered,

$$\delta_\pm=\{\Delta E_\pm(1,\ -1)-\Delta E_\pm(-1,\ 1)\}/2-\Delta E_\pm(0,\ 0) \qquad (1)$$

where the transition energies, $\Delta E_+(M^a, M^b)$ and $\Delta E_-(M^a,M^b)$, are represented by $E(1, M^a, M^b)-E(0, M^a, M^b)$ and $E(0, M^a, M^b)-E(-1, M^a, M^b)$ respectively. When the perturbation is applied to the second order, $\delta_\pm$ is given as follows:

$$\delta_\pm=\pm A/(2J\mp g\beta H-d/6)\pm B/(2J+d/3)-C_\pm \qquad (2)$$

where:

$$A=\{A^a{}_{xx}{}^2+2A^a{}_{xy}{}^2+A^a{}_{yy}{}^2+A^b{}_{xx}{}^2+2A^b{}_{xy}{}^2+A^b{}_{yy}{}^2-2(A^a{}_{xz}+A^b{}_{xz})^2-2(A^a{}_{yz}+A^b{}_{yz})^2\}/16 \qquad (3)$$

$$B=\{2(A^a{}_{zz}+A^b{}_{zz})^2-A^a{}_{zx}{}^2-A^a{}_{zy}{}^2-A^b{}_{zx}{}^2-A^b{}_{zy}{}^2\}/8 \qquad (4)$$

$$C_\pm=(A+A^a{}_{xz}A^b{}_{zx}/2+A^a{}_{yz}A^b{}_{yz}/2)\times\{2/(g\beta H\pm d/2)-1/(g\beta H\mp d/2)\} \qquad (5)$$

The laboratory coordinates are taken as x, y and z, and the external magnetic field is parallel to the z-axis. $A^p{}_{ij}$ is the ij-element of the hyperfine tensor for the p site, g is equal to $(g^a{}_{zz}+g^b{}_{zz})/2$, and d is represented by $D(3\cos^2\Theta-1)/3$, where Θ is the angle between the axis of symmetry and the external magnetic field. D may be of the negative sign, since the odd electron is localized on the =N–O· group of the oxime[1,4] and the distance between the groups of the interactng radicals is very large (5.6 Å).[1] E is negligibly small in this case[1]. The first and second terms of Eq. 2 arise from the mixing of the singlet state with the $m=\pm 1$ and $m=0$ states of the triplet state respectively. On the other hand, the third term is brought about by the mixing within the triplet state.

From the $\delta_\pm$ values measured with four crystal orientations at the X-band, J was evaluated as $-(1.24\pm 0.12)\times 10^{-5}$ eV. In this case the second term of Eq. 2 was found to be predominant. Thus, the system is proved to be a ground-state singlet.

It may be emphasized that magnitudes and signs of J as small as 10^{-5} eV. can be determined by the present method. Details will be published elsewhere.

1) Y. Kurita, *J. Chem. Phys.*, **42**, 3926 (1964); *J. Chem. Soc. Japan, Pure Chem. Sect.* (*Nippon Kagaku Zasshi*), **85**, 833 (1964). $D_\parallel$ and $D_\perp$ in these papers are to be negative and positive, respectively.

2) H. Hayashi, K. Itoh and S. Nagakura, to be published.

3) Y. Kurita, private communication.

4) I. Miyagawa and W. Gordy, *J. Chem. Phys.* **30**, 1590).

The Base-catalyzed Oxidation of Friedelin with Molecular Oxygen

By Tadaaki NISHIHAMA and Takeyoshi TAKAHASHI

Department of Chemistry, Faculty of Science, The University of Tokyo, Hongo, Tokyo

(Received December 2, 1965)

The autoxidation of 3-ketotriterpenes and 3-keto-4,4-dimethylsteroids in the presence of potassium *t*-butoxide has been reported by Hanna and Ourisson, who also recorded the isolation of the corresponding 2,3-dione (I) together with lactol (II).[1)]

We now wish to report the oxidation of friedelin (III) under the same conditions, this oxidation leads to a product of a different type. Oxygen was passed into a solution of friedelin in *t*-butyl alcohol in the presence of a ten-molar excess of potassium *t*-butoxide at room temperature for 40 hr. The residue obtained, when methylated with diazomethane, gave, after separation by chromatography, an unsaturated ester (IV, R=CH_3), m. p. 214.5—215°C, λ_{max}^{EtOH} 253 mμ (ε, 8900), IR: $\nu_{C=O}$ 1720 (ester), $\nu_{C=C}$ 1640 cm^{-1}, NMR: τ 7.92 (doublet, J=2 c. p. s., 1 H, C=CH-CH), τ 6.21 (singlet, 3 H, $COOCH_3$), τ 6.08 (quartet, J=7 c. p. s., 1 H, -O-CH-CH_3) and τ 3.99 (doublet, J=2 c. p. s., 1 H, C=CH-CH), $C_{31}H_{50}O_3$ (Found: C, 78.70; H, 10.79. Calcd.: C, 79.10; H, 10.71%), whose mass spectrum shows a peak at *m/e* 470 (M^+), together with other peaks due to skeletal fragmentations.

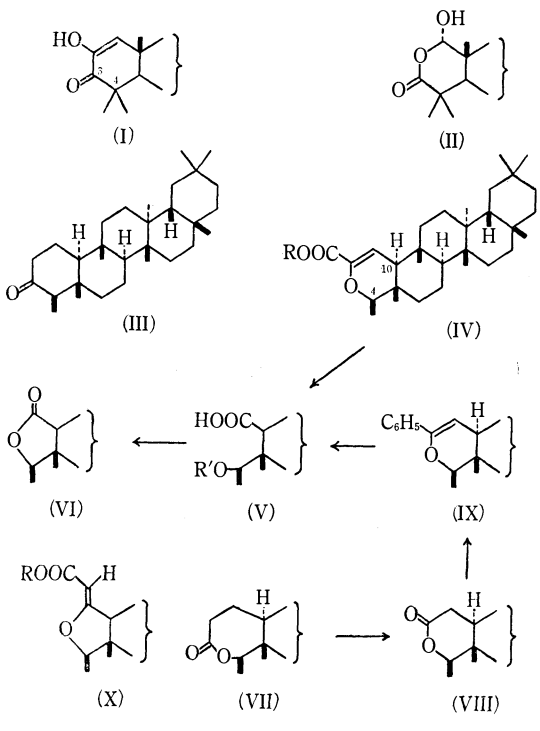

The oxidation of IV (R=CH_3) with ozone and hydrogen peroxide gave V (not isolated); on partial reduction with lithium aluminum hydride, followed by treatment with hydrochloric acid, this afforded a lactone (VI), m. p. 269°C, $\nu_{C=O}$ 1765 cm^{-1}. The same γ-lactone was also obtained by an alternative route. 3-Keto-3a-oxa-A-homo-friedelane (VII) was, by the Barbier-Wieland procedure, converted into 2-keto-3-oxa-friedelane (VIII), m. p. 263—266°C, $\nu_{C=O}$ 1735 cm^{-1}. VIII was, then, submitted to a Grignard reaction using phenylmagnesium bromide; it yielded 2-phenyl-3-oxa-1-friedelene (IX), m. p. 223—225°C, $\nu_{C=C}$ 1640 cm^{-1}, NMR: τ 7.88 (doublet, J=2 c. p. s., 1 H, C=CH-CH), τ 6.03 (quartet, J=7 c. p. s., 1 H, -O-CH-CH_3) and τ 4.79 (doublet, J=2 c. p. s., 1 H, C=CH-CH), $C_{35}H_{52}O$ (Found: C, 86.22; H, 10.71. Calcd.: C, 86.00; H, 10.72%). The oxidation of IX with chromium trioxide afforded V (R'=COC_6H_5); on partial reduction with lithium aluminum hydride and subsequent treatment with dilute hydrochloric acid, this gave a lactone, m. p. 273—273.5°C, $\nu_{C=O}$ 1765 cm^{-1}, $C_{28}H_{46}O_2$ (Found: C, 81.40; H, 11.17. Calcd.: C, 81.10; H, 11.18%), identical (IR, m. p. and mixed m. p.) with γ-lactone (VI).

The γ-lactone (VI) obtained by either procedure described above gave one spot on a thin-layer chromatogram, while an alkaline saponification of V (R'=COC_6H_5), followed by acidification, afforded γ-lactone which showed one more spot on the same chromatogram. This indicates that the configuration at C_{10} in VI is the same as that of friedelin, and that a partial isomerization at C_{10} has taken place under alkaline conditions. On the other hand, in a conversion of VII into VI, the configuration at C_4 is untouched. Along with the information obtained from the NMR data, these results established the constitution and stereochemistry of the unsaturated ester (IV, R=CH_3). As no γ-lactone was isolated on the normal ozonolysis of the unsaturated ester, the alternative structure (X, R=CH_3) for this unsaturated ester could be eliminated. Thus the structure of IV (R=H) for the unsaturated acid initially formed was established.

1) R. Hanna and G. Ourisson, *Bull. Soc. Chim. France*, **1961** 1945.

BULLETIN OF THE CHEMICAL SOCIETY OF JAPAN VOL. 39 201—207 (1966)

Vibrational Analysis of Substituted and Perturbed Molecules. III. Green's Function Determination of Force Constants for XY_3 Planar Molecules

By Thomas WOLFRAM, C. D. BASS, Roger E. DEWAMES and L. LYNDS

North American Aviation Science Center, Thousand Oaks, California, U. S. A.

(Received Junary 26, 1965)

Using the Green's function formulae for isotopic frequencies of the XY_3 molecule together with the spectral theorem, explicit formulae for the molecular force constants directly in terms of the vibrational frequencies have been obtained. The relationship between the Wilson force constants and the cartesian force constants is discussed and leads to the above formulae. The procedure is applied to the BCl_3 and BBr_3 molecules and force constants are obtained. A simple procedure for calculating the variations in the force constants with variations in vibrational frequencies is suggested.

In previous papers[1,2] (hereafter referred to as VAI and VAII), it was shown that the vibrational frequencies of isotopically substituted molecules can be calculated using a Green's function procedure, thereby avoiding the construction of a force constant model. It was pointed out in VAI that a unique set of force constants for the molecule can be generated directly from the vibrational frequencies once the mixing parameters were known. This procedure leads to explicit expressions for the force constants in terms of the vibrational frequencies. These formulae are the inverted relationships between the force constants and frequencies. One customarily obtains by the FG procedure explicit expressions for the frequencies involving non-linear combinations of the force constants. For example, the procedure employed recently by Ladd, Orville-Thomas, and Cox[3] in the treatment of the boron trihalides involves the solution of two simultaneous non-linear equations with the three unknown force constants (for the two doubly degenerate frequencies). By assuming value for one force constant, the corresponding values of the other two are calculated. When the sets of values of the three are plotted graphically, the resulting figure is an ellipse. The isotopic frequencies yield another, intersecting ellipse. One of the intersection points corresponds to a physically acceptable set of force constants. In this paper we illustrate a quite different approach which makes use of the spectral theorem together with the Green's function isotopic formulae and leads to exact, explicit formulae for the force constants. The procedure is easily applied to the BX_3 molecules, however it is clear that the solution of the isotopic Green's function equations can become a sizable task for larger molecules with lower symmetry. Determination of the mixing parameters may approach in more complex cases the difficulty associated with a standard force constant analysis. On the other hand, once the mixing parameters are known the Green's function procedure is extremely convenient for the analysis of related or perturbed molecular systems as discussed in previous papers[1,2] and in the companion paper.

In section I the relationships between the cartesian coordinate force constants and the Wilson internal coordinate force constants are reviewed. The spectral theorem for the force constants in the Wilson FG representation is derived. Explicit formulae for force constants of XY_3 planar molecules are derived in terms of the vibrational frequencies and the mixing parameter. The discussion in section I is given in some detail because it serves as the theoretical foundation for the development of the Green's function procedure in the internal coordinate system which is presented in the companion paper. In section II the explicit formulae developed in I are used to calculate the force constants for $^{10}BCl_3$, $^{11}BCl_3$, $^{10}BBr_3$, and $^{11}BBr_3$. The mixing parameters necessary for these calculations were obtained by application of the Green's function isotopic formulae discussed in VAII. The results of the calculations are presented in section III. A simple procedure of calculating the variation of the force constants with variations in the input data (frequencies) is discussed.

I. Valence and Cartesian Molecular Force Constants

A. General Formalism.—Consider a molecule with n atoms numbered 1 through n and label

1) R. E. DeWames and T. Wolfram, *J. Chem. Phys.*, **40**, 853 (1964).
2) C. D. Bass, L. Lynds, T. Wolfram and R. E. DeWames, ibid., **40**, 3611 (1964).
3) J. A. Ladd, W. J. Orville-Thomas and B. C. Cox, *Spectrochem. Acta*, **19**, 1911 (1963).

the cartesian coordinates x_i $(i=1,2,...,3n)$ so that, for example, the three cartesian coordinates of atom 1 are x_1, x_2, x_3, and those of atom 2 are x_4, x_5, and x_6. The internal coordinates are designated by α_i $[i=1,2,...,(3n-6+r)]$ where r is the number of redundant coordinates. An arbitrary motion of the entire molecule may be represented by a supervector, $\boldsymbol{X}$ in the cartesian system

$$\boldsymbol{X}=\begin{pmatrix} x_1 \\ x_2 \\ \vdots \\ x_{3n} \end{pmatrix} \tag{1}$$

The internal symmetry coordinates do not span the entire vector space, but excluding translation and rotation, a vibratory motion of the molecule can be represented by a supervector, $\boldsymbol{\alpha}$, in the internal coordinate system

$$\boldsymbol{\alpha}=\begin{pmatrix} \alpha_1 \\ \alpha_2 \\ \vdots \\ \alpha_{3n-6+r} \end{pmatrix} \tag{2}$$

Because the cartesian coordinates span a larger vector space than the internal coordinates it is not possible to define transformation from the external to the internal coordinate system. In order to relate the two systems we must eliminate the redundant coordinates from the internal system and rotations and translations from the external system. This task is conveniently accomplished by transforming to symmetry coordinates. Let $\boldsymbol{X}_t$ $[t=(\Gamma, \nu_i)]$ be a supervector in the cartesian coordinate representation which transforms according to the νth row of the Γth irreducible representation of the group of the molecule.[4] (The subscript i on ν indexes different coordinates with identical transformation properties.) A new set of orthogonal symmetry coordinates, $\boldsymbol{S}_t$, may be constructed from the $\boldsymbol{X}_t$ as follows: The $\boldsymbol{X}_t$ corresponding to translations and rotations (about the center of mass) are mass weighted. The mass weighted vibrational type motions with identical transformation properties are then orthogonalized to the translation and rotation vectors and to each other. The symmetry coordinates, $\boldsymbol{S}_t$, then consist of orthogonalized mass weighted, translations, rotations and vibrational type motions which tranform according to the irreducible representations of the group of the molecule. The set of internal symmetry coordinates, $\boldsymbol{\sigma}_r$, which define the representation for the Wilson reduced $\boldsymbol{F}^W$ matrix do not contain translations or rotation and are not mass weighted. The $\boldsymbol{\sigma}_r$ coordinates are simply those linear combinations of the internal coordinates α_i which transform irreducibly according to the molecular group. The internal symmetry coordinates can be expressed uniquely in terms of the external coordinates (although the converse is not true) by the usual procedure[4] so that a rectangular matrix, $\boldsymbol{T}$ $(3n-6\times 3n)$, may be constructed which transforms the $\boldsymbol{\sigma}_r$ into the cartesian representation. Let us define the matrix $\boldsymbol{\sigma}$ to be a $(3n-6+r\times 3n-6)$ matrix whose columns are the non-redundant $\boldsymbol{\sigma}_r$ and let $\boldsymbol{f}$ be the matrix of (valence) force constants $(3n-6+r\times 3n-6+r)$ in the internal coordinate system, then the Wilson reduced force constant matrix, $\boldsymbol{F}^W$, $(3n-6\times 3n-6)$ in the internal symmetry coordinate system is given by

$$\boldsymbol{F}^W=\tilde{\boldsymbol{\sigma}}\boldsymbol{f}\boldsymbol{\sigma} \tag{3}$$

where $\tilde{\boldsymbol{\sigma}}$ $(3n-6\times 3n-6+r)$ is the transpose of the matrix $\boldsymbol{\sigma}$.

The cartesian coordinate matrix of force constants $\boldsymbol{F}^c$ $(3n\times 3n)$ is then given by

$$\tilde{\boldsymbol{F}}^c=\tilde{\boldsymbol{T}}\boldsymbol{F}^W\boldsymbol{T} \tag{4}$$

We may now transform the mass transformed interaction matrix[1] or dynamical matrix $\boldsymbol{D}=\boldsymbol{M}^{-1/2}\boldsymbol{F}^c\boldsymbol{M}^{-1/2}$ to the external symmetry coordinate system defined by the symmetry vectors $\boldsymbol{S}_t$ with result that

$$\boldsymbol{D}^s=\boldsymbol{S}^+\boldsymbol{D}\boldsymbol{S}=\boldsymbol{S}^+\boldsymbol{M}^{-1/2}\tilde{\boldsymbol{T}}\boldsymbol{F}^W\boldsymbol{T}\boldsymbol{M}^{-1/2}\boldsymbol{S} \tag{5}$$

where $\boldsymbol{S}^+$ is the Hermetian conjugate of $\boldsymbol{S}$, and $\boldsymbol{D}^s$ is the dynamical matrix in the cartesian or external symmetry coordinate system. $\boldsymbol{S}$, the unitary transformation from cartesian to cartesian symmetry coordinates and $\boldsymbol{M}$ the diagonal mass matrix, are discussed in Refs. 1 and 2.

A few properties of $\boldsymbol{D}^s$ should be noted; first, $\boldsymbol{D}^s$ is block diagonal in the different irreducible representations of the molecule. Furthermore, since the vibrational symmetry coordinates of $\boldsymbol{S}$ are orthogonalized to the rotation and translation eigenvectors there are no matrix elements joining the vectors to the remaining symmetry coordinates. Thus the rows and columns corresponding to rotations and translations have zero matrix elements. The matrix $\boldsymbol{D}^s$ is Hermitian and its eigenvalues are the frequencies squared. If we arrange the rotations and translations to correspond to the last 6 columns of $\boldsymbol{S}$ then a square matrix $\boldsymbol{B}$ can be defined[5]

$$\boldsymbol{B}=\{\boldsymbol{T}\boldsymbol{M}^{-1/2}\boldsymbol{S}\}_{\text{truncated}} \tag{6}$$

by removing the last 6 columns of $\boldsymbol{T}\boldsymbol{M}^{-1/2}\boldsymbol{S}$. Whereas the matrix $\boldsymbol{T}\boldsymbol{M}^{-1/2}\boldsymbol{S}$ is singular, the $\boldsymbol{B}$ matrix is non-singular, block diagonal, and its inverse can be constructed so that the Wilson $\boldsymbol{F}^W$ matrix elements can be given in terms of the symmetrized dynamical matrix.

4) See for example, Wilson, Decius and Cross, "Molecular Vibrations," McGraw-Hill, New York (1955). The connection between internal and cartesian coordinates has been discusssed previously by D. E. Mann (*J. Chem. Phys.*, **22**, 764 (1954)) and also by T. Shimanouchi and M. Tsuboi (*J. Chem. Phys.*, **35**, 1597 (1961)).

5) E. B. Wilson, J. C. Decius and P. C. Cross, *J. Mol. Spectroscopy*, ibid., **12**, 61, 74 (1964).

$$\boldsymbol{F}^W=\tilde{\boldsymbol{B}}^{-1}\boldsymbol{D}^s\boldsymbol{B}^{-1} \tag{7}$$

From Eq. 7 it follows that $\boldsymbol{B}\tilde{\boldsymbol{B}}$ is the Wilson $\boldsymbol{G}$ matrix for the molecule. The Wilson force constants can now of course be related directly to the cartesian force constants since $\boldsymbol{D}^s=\boldsymbol{S}^+\boldsymbol{D}\boldsymbol{S}=\boldsymbol{S}^+\boldsymbol{M}^{-1/2}\boldsymbol{F}^c\boldsymbol{M}^{-1/2}\boldsymbol{S}$. The relation between the internal force constants and the external cartesian force constants is given by

$$\boldsymbol{f}=\bar{\boldsymbol{\sigma}}\tilde{\boldsymbol{B}}^{-1}\boldsymbol{S}^+\boldsymbol{M}^{-1/2}\boldsymbol{F}^c\boldsymbol{M}^{-1/2}\boldsymbol{S}\boldsymbol{B}^{-1}\bar{\boldsymbol{\sigma}}^+ \tag{8}$$

where $\bar{\boldsymbol{\sigma}}$ is the $(3n-6+r\times 3n-6+r)$ matrix of all the $\boldsymbol{\sigma}_r$ including the redundant symmetry coordinates and r rows and columns of zero have been added to $\boldsymbol{F}^W$ to match the dimensionality of $\bar{\boldsymbol{\sigma}}$. (It is important to note that this corresponds to an arbitrary *definition* of f since as pointed out by Crawford and Overend[6] there is a true indeterminacy in the matrix elements associated with the redundant or null coordinates. This difinition is the same as that used in almost all force constant calculations and in particular for previous calculations for BX_3 force constants and allows us to make direct comparison with these other results. Other difinitions are, however, possible.) The matrix elements of $\boldsymbol{F}^W$ can be given directly in terms of the vibrational frequencies by making use of the spectral theorem. The matrix $\boldsymbol{D}^s$ is block diagonal and may be diagonalized by a unitary matrix $\boldsymbol{A}$ (the matrix of mixing parameters) which has non-zero matrix element only between rows and columns which correspond to the same row of the same irreducible representation, and thus $\boldsymbol{A}$ is also block diagonal. We have that

$$\boldsymbol{A}^+\boldsymbol{D}^s\boldsymbol{A}=\boldsymbol{\Lambda}$$

where

$$\boldsymbol{\Lambda}=\begin{bmatrix}\lambda_1 & & & & \\ & \lambda_2 & & & \\ & & \lambda_3 & & \\ & & & \ddots & \\ & & & & \lambda_{3N}\end{bmatrix} \tag{9}$$

is the diagonal matrix of eigenvalues. It should be noted that a knowledge of the mixing parameter matrix, $\boldsymbol{A}$, is equivalent to a knowledge of the $\boldsymbol{L}$ matrix discussed by Wilson, Decius, and Cross.[5] From Eq. 9 we can write

$$\boldsymbol{D}^s=\boldsymbol{A}\boldsymbol{\Lambda}\boldsymbol{A}^+ \tag{10}$$

so that

$$\boldsymbol{F}^W=\tilde{\boldsymbol{B}}^{-1}\boldsymbol{A}\boldsymbol{\Lambda}\boldsymbol{A}^+\boldsymbol{B}^{-1} \tag{11}$$

Since both $\boldsymbol{B}$ and $\boldsymbol{A}$ are block diagonal we can write an equation for the force constants corresponding to a particular symmetry type Γ_ν (the ν row of the Γth irreducible representation) involving only the mixing parameters for that block:

$$\{\boldsymbol{F}^W\}^{\Gamma_\nu}=\{\tilde{\boldsymbol{B}}^{-1}\}^{\Gamma_\nu}\{\boldsymbol{A}\}^{\Gamma_\nu}\{\boldsymbol{\Lambda}\}^{\Gamma_\nu}\{\boldsymbol{A}^+\}^{\Gamma_\nu}\{\boldsymbol{B}^{-1}\}^{\Gamma_\nu} \tag{12}$$

where $\{\ \}^{\Gamma_\nu}$ means the block whose rows and columns correspond to the νth row of the Γth irreducible representation. The dimensionality of the matrix Eq. 12 is equal to the number of vibrational symmetry coordinates which transform according to Γ_ν.

In VAI and VAII formulae for obtaining the mixing parameters using the Green's function approach were given. The mixing parameters, of course, allow the construction of the matrix A and thus the calculation of $\boldsymbol{F}^W$ from Eq. 11 or 12.

B. Application to the XY_3 Planar Molecule. —In this section we apply the preceding formalism to the XY_3 molecule and obtain the relations between the external and internal force constants. In anticipation of a following paper which deals with the XY_2Z planar molecule we have generalized the diagrams and force constants to the case of the XY_2Z molecule. The internal and external coordinate systems for the XY_3 and XY_2Z molecule are shown in Fig. 1.

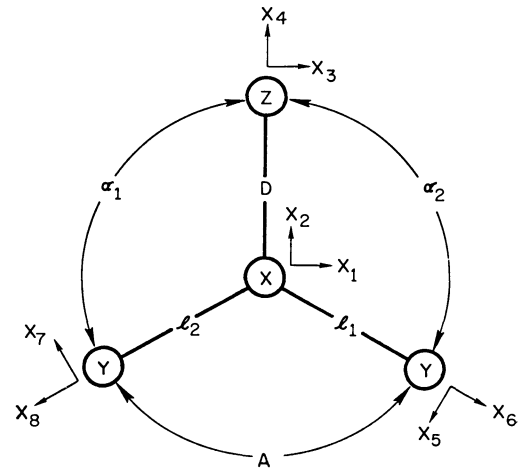

Fig. 1. Showing the internal and cartesian coordinate systems for the XY_2Z planer molecule.

In this section we shall be concerned with XY_3 molecules for which the bond lengths D, l_1 and l_2 are all of length l and the angles A, α_1 and α_2 are 120°, although no such restrictions need apply to the XY_2Z molecule. The external mass weighted symmetry coordinates for the XY_3 planar molecule given in VAII may be orthonormalized to give the unitary $\boldsymbol{S}$ matrix (13).

where $r^2=m_y/m_x$, $d_1{}^2=3r^2+1$, and $d_2{}^2=3r^2+2$. The first column of S corresponds to the A_1 symmetric stretch; the second column is a mass weighted E′ bending symmetry coordinate, and the third column is an E′ stretching symmetry coordinate which has been orthogonalized to column two. These three coordinates transform according to

6) B. Crawford and J. Overend, ibid., **12**, 307 (1964).

$$\boldsymbol{S}=\begin{pmatrix}
0 & 0 & 0 & \frac{\sqrt{3}r}{d_2} & \frac{-\sqrt{3}r}{d_1 d_2} & 0 & \frac{1}{d_1} & 0 \\
0 & \frac{\sqrt{3}r}{d_2} & \frac{-\sqrt{3}r}{d_1 d_2} & 0 & 0 & 0 & 0 & \frac{1}{d_1} \\
0 & 0 & 0 & \frac{-2}{\sqrt{3}d_2} & \frac{-\sqrt{3}r^2}{d_1 d_2} & \frac{1}{\sqrt{3}} & \frac{r}{d_1} & 0 \\
\frac{1}{\sqrt{3}} & 0 & \frac{d_2}{\sqrt{3}d_1} & 0 & 0 & 0 & 0 & \frac{r}{d_1} \\
0 & \frac{1}{d_2} & \frac{3r^2}{2d_1 d_2} & \frac{1}{\sqrt{3}d_2} & \frac{\sqrt{3}r^2}{2d_1 d_2} & \frac{1}{\sqrt{3}} & \frac{-r}{2d_1} & \frac{-\sqrt{3}r}{2d_1} \\
\frac{1}{\sqrt{3}} & 0 & \frac{-d_2}{2\sqrt{3}d_1} & 0 & \frac{d_2}{2d_1} & 0 & \frac{\sqrt{3}r}{2d_1} & \frac{-r}{2d_1} \\
0 & \frac{-1}{d_2} & \frac{-3r^2}{2d_1 d_2} & \frac{1}{\sqrt{3}d_2} & \frac{\sqrt{3}r^2}{2d_1 d_2} & \frac{1}{\sqrt{3}} & \frac{-r}{2d_1} & \frac{\sqrt{3}r}{2d_1} \\
\frac{1}{\sqrt{3}} & 0 & \frac{-d_2}{2\sqrt{3}d_1} & 0 & \frac{-d_2}{2d_1} & 0 & \frac{-\sqrt{3}r}{2d_1} & \frac{-r}{2d_1}
\end{pmatrix} \tag{13}$$

the A_1 irreducible representation for the group of the XY_2Z molecule. The fourth and fifth columns are E' bending and stretching coordinates which correspond to B_1 type coordinates for the XY_2Z molecule. The remaining columns are the in-plane rotation and translation normal modes. The internal coordinates are taken to be ΔD, Δl_1, Δl_2, $l\Delta A$, $l\Delta\alpha_1$, and $l\Delta\alpha_2$. The internal symmetry coordinates for the XY_3 molecule define the $\bar{\boldsymbol{\sigma}}$ matrix given below:

$$\bar{\boldsymbol{\sigma}}=\begin{pmatrix}
\frac{1}{\sqrt{3}} & \frac{2}{\sqrt{6}} & 0 & 0 & 0 & 0 \\
\frac{1}{\sqrt{3}} & \frac{-1}{\sqrt{6}} & 0 & \frac{1}{\sqrt{2}} & 0 & 0 \\
\frac{1}{\sqrt{3}} & \frac{-1}{\sqrt{6}} & 0 & \frac{-1}{\sqrt{2}} & 0 & 0 \\
0 & 0 & \frac{2}{\sqrt{6}} & 0 & 0 & \frac{1}{\sqrt{3}} \\
0 & 0 & \frac{-1}{\sqrt{6}} & 0 & \frac{-1}{\sqrt{2}} & \frac{1}{\sqrt{3}} \\
0 & 0 & \frac{-1}{\sqrt{6}} & 0 & \frac{1}{\sqrt{2}} & \frac{1}{\sqrt{3}}
\end{pmatrix} \tag{14}$$

The first of $\bar{\boldsymbol{\sigma}}$ is the A_1 symmetric stretch, the second is the E' stretching coordinate and the third is the E' bending. These three coordinates transform like A_1 modes for the XY_2Z symmetry. The fourth and fifth columns are E' stretching and bending coordinates which transform like B_1 modes for the XY_2Z molecule. The remaining column is the redundant symmetry coordinate and corresponds to a null vector in the cartesian coordinate system. The rectangular σ matrix is obtained from $\bar{\boldsymbol{\sigma}}$ by omitting the last column. The $\tilde{\boldsymbol{B}}$ and $\tilde{\boldsymbol{B}}^{-1}$ matrices for the XY_3 molecule are

$$\tilde{\boldsymbol{B}}=(m_y)^{-1/2}\begin{pmatrix}
1 & 0 & 0 & 0 & 0 \\
0 & \frac{-3r^2}{\sqrt{2}d_2} & \frac{-3d_2}{\sqrt{6}} & 0 & 0 \\
0 & \frac{\sqrt{2}d_1}{d_2} & 0 & 0 & 0 \\
0 & 0 & 0 & \frac{-3r^2}{\sqrt{2}d_2} & \frac{-3d_2}{\sqrt{6}} \\
0 & 0 & 0 & \frac{\sqrt{2}d_1}{d_2} & 0
\end{pmatrix} \tag{15}$$

and

$$\tilde{\boldsymbol{B}}^{-1}=(m_y)^{1/2}\begin{pmatrix}
1 & 0 & 0 & 0 & 0 \\
0 & 0 & \frac{d_2}{\sqrt{2}d_1} & 0 & 0 \\
0 & \frac{-\sqrt{6}}{3d_2} & \frac{-3r^2}{\sqrt{6}d_1 d_2} & 0 & 0 \\
0 & 0 & 0 & 0 & \frac{d_2}{\sqrt{2}d_1} \\
0 & 0 & 0 & \frac{-\sqrt{6}}{3d_2} & \frac{-3r^2}{\sqrt{6}d_1 d_2}
\end{pmatrix} \tag{16}$$

The internal force constant matrix $\boldsymbol{f}$ is

$$\boldsymbol{f}=\begin{pmatrix}
f_D & f_{Dd} & f_{Dd} & f_{DA} & f_{D\alpha} & f_{D\alpha} \\
f_{Dd} & f_d & f_{dd} & f_{dA} & f_{d\alpha} & f'_{d\alpha} \\
f_{Dd} & f_{dd} & f_d & f_{dA} & f'_{d\alpha} & f_{d\alpha} \\
f_{DA} & f_{dA} & f_{dA} & f_A & f_{A\alpha} & f_{A\alpha} \\
f_{D\alpha} & f'_{d\alpha} & f'_{d\alpha} & f_{A\alpha} & f_\alpha & f_{\alpha\alpha} \\
f_{D\alpha} & f_{d\alpha} & f_{d\alpha} & f_{A\alpha} & f_{\alpha\alpha} & f_\alpha
\end{pmatrix} \tag{17}$$

in the case of the XY_3 planar molecule $f_D=f_d\equiv f_r$, $f_A=f_\alpha\equiv f_\alpha$, $f_{dA}=f_{d\alpha}\equiv f_{r\alpha}$, $f_{DA}=f'_{d\alpha}\equiv f'_{r\alpha}$, $f_{dd}=f_{Dd}\equiv f_{rr}$, and $f_{A\alpha}=f_{\alpha\alpha}\equiv f_{\alpha\alpha}$.

where, following Lindeman and Wilson,[7] we have distinguished the adjacent angle-bond force constant, $f_{d\alpha}$, from the opposite angle-bond interaction, $f'_{d\alpha}$.

The redundancy conditions reduce the number of independent internal force constants to 9 in the case of the XY_2Z molecule with the relations

$$\left.\begin{aligned} f_{D\alpha} &= -\frac{1}{2}f_{DA} \\ f'_{d\alpha} &= -(f_{dA}+f_{d\alpha}) \\ f_{A\alpha} &= -\frac{1}{2}f_{A} \\ f_{\alpha\alpha} &= \frac{1}{2}f_{A}-f_{\alpha} \end{aligned}\right\} \quad (18)$$

For XY_3 molecules, $f_D=f_d$, $f_{Dd}=f_{dd}$, $f_A=f_\alpha$, $f_{DA}=f'_{d\alpha}$, and $f_{dA}=f_{d\alpha}$, which leaves four independent force constants. The Wilson reduced $\boldsymbol{F}^W$ matrix in the internal symmetry coordinates for the XY_2Z molcecule is

$$\boldsymbol{F}^W=\tilde{\boldsymbol{\sigma}}\boldsymbol{f}\boldsymbol{\sigma}=\left\{\begin{pmatrix} F_{11} & F_{12} & F_{13} \\ F_{12} & F_{22} & F_{23} \\ F_{13} & F_{23} & F_{33} \end{pmatrix}\begin{pmatrix} 0 & 0 \\ 0 & 0 \\ 0 & 0 \end{pmatrix}\right\} \quad (19)$$
$$\left\{\begin{pmatrix} 0 & 0 & 0 \\ 0 & 0 & 0 \end{pmatrix}\begin{pmatrix} F_{44} & F_{45} \\ F_{54} & F_{55} \end{pmatrix}\right\}$$

The F_{ij} have been given in terms of the f_{ij} by Lindeman and Wilson; however, because of a number of typographical errors in their paper the corrected relations are listed here.[7]

$$\left.\begin{aligned} F_{11} &= \frac{1}{3}(f_D+2f_d+4f_{Dd}+2f_{dd}) \\ F_{12} &= \frac{1}{3\sqrt{2}}(2f_D-2f_d+2f_{Dd}-2f_{dd}) \\ F_{13} &= \frac{1}{3\sqrt{2}}(2f_{DA}-2f'_{d\alpha}+4f_{dA} \\ &\quad -2f_{d\alpha}-2f_{d\alpha}) \\ &= \frac{1}{\sqrt{2}}(f_{DA}+2f_{dA}) \\ F_{22} &= \frac{1}{6}(4f_D+2f_d-8f_{Dd}+2f_{dd}) \\ F_{23} &= \frac{1}{6}(4f_{DA}+2f'_{d\alpha}-4f_{dA}-4f_{D\alpha} \\ &\quad +2f_{d\alpha}) = f_{DA}-f_{dA} \\ F_{33} &= \frac{1}{6}(4f_A+2f_\alpha-8f_{A\alpha}+2f_{\alpha\alpha}) \\ &= \frac{3}{2}f_A \\ F_{44} &= f_d-f_{dd} \\ F_{45} &= f'_{d\alpha}-f_{d\alpha} = -(2f_{d\alpha}+f_{dA}) \\ F_{55} &= f_\alpha-f_{\alpha\alpha} = -\frac{1}{2}f_A+2f_\alpha \end{aligned}\right\} \quad (20)$$

In the case of the XY_3 molecule, $F_{12}=F_{13}=0$, $F_{22}=F_{44}$, $F_{33}=F_{55}$, and $F_{23}=F_{45}$. Using Eq. 7 one obtains the relations between the external symmetrized (mass weighted) force constants D_{ij}^s and the Wilson $\boldsymbol{F}^W$ force constants for the XY_3 molecule:

$$\left.\begin{aligned} F_{11} &= m_y D_{11}^s \\ F_{22} &= F_{44} = \frac{m_y d_2^2}{2d_1^2}D_{33}^s \\ F_{33} &= F_{55} = m_y\frac{2}{3d_2^2}D_{22}^s+\frac{2m_y r^2}{d_1 d_2^2}D_{23}^s \\ &\quad +\frac{3}{2}m_y\frac{r^4}{d_1^2 d_2^2}D_{33}^s \\ F_{23} &= -m_y\frac{1}{3d_1^2}\left\{d_1 D_{23}^s+\frac{3}{2}r^2 D_{33}^s\right\} \end{aligned}\right\} \quad (21)$$

Equation 7 may be inverted to give

$$\left.\begin{aligned} D_{11}^s &= F_{11}/m_y \\ D_{12}^s &= D_{13}^s = 0 \\ D_{22}^s &= \frac{9}{2m_y}\left(\frac{r^4}{d_2^2}F_{22}+\frac{2r^2}{\sqrt{3}}F_{23}\right. \\ &\quad \left.+\frac{d_2^2}{3}F_{33}\right) \\ D_{23}^s &= \frac{-3d_1}{m_y}\left(\frac{r^2}{d_2^2}F_{22}+\frac{1}{\sqrt{3}}F_{23}\right) \\ D_{33}^s &= \frac{2}{m_y}\frac{d_1^2}{d_2^2}F_{22} \\ D_{44}^s &= D_{22}^s \\ D_{45}^s &= D_{23}^s \\ D_{55}^s &= D_{33}^s \end{aligned}\right\} \quad (22)$$

The mixing parameter matrix for the XY_3 molecule is (see VAII)

$$\boldsymbol{A}=\begin{pmatrix} 1 & & & & & \\ & \frac{1}{A_0}\begin{pmatrix} a & 1 \\ 1 & -a \end{pmatrix} & & & & \\ & & \frac{1}{A_0}\begin{pmatrix} a & 1 \\ 1 & -a \end{pmatrix} & & & \\ & & & 1 & & \\ & & & & 1 & \\ & & & & & 1 \end{pmatrix} \quad (23)$$

where $A_0=(a^2+1)^{1/2}$.

Using Eq. 11 one obtains the Wilson force constants directly in terms of the frequencies of vibration and the mixing parameter a:

7) L. P. Lindeman and M. K. Wilson, *J. Chem. Phys.*, **24**, 242 (1956).

TABLE I. FREQUENCY DATA (cm^{-1}) AND MOLECULAR PARAMETERS FOR BORON TRIHALIDES

Molecule		ν_1	ν_2	ν_3	Ref.	m_B	$m_{halogen}$
$^{10}BF_3$		888	1481.9	485.46	8	10.01	19.00
$^{11}BF_3$		888	1428.8	483.74	8		
$^{10}BCl_3$		471	993.7	243	9	10.01	35.456
$^{11}BCl_3$		471	954.2	243	9		
$^{10}BBr_3$	Set 1	278	856	150	10	10.01	79.916
$^{11}BBr_3$	Set 1	278	820	150	10		
$^{10}BBr_3$	Set 2	282.5	856	155	8	10.01	79.916
$^{11}BBr_3$	Set 2	282.5	819	155	8		

TABLE II. FORCE CONSTANTS (mdyn./Å)

Molecule	Calculation	f_r	f_{rr}	f_α	$f_{\alpha\alpha}$	$f'_{r\alpha}$	$f_{r\alpha}$	$\omega_2^2+\omega_3^2$ (obs.) ($cm^{-2}\times 10^{-6}$)	$\omega_2^2+\omega_3^2$ (calcd.) ($cm^{-2}\times 10^{-6}$)
$^{10}BF_3$[a]	This work	7.14787	0.83787	0.35177	−0.17588	−0.21288	0.10644	14.321	14.324
$^{10}BF_3$	Ref. 1	7.14810	0.83819	0.35184	−0.17593	−0.21267	0.10633	14.321	14.326
$^{10}BCl_3$[b]	This work	3.78813	0.41925	0.15233	−0.07617	−0.13548	0.06774	6.1632	6.1638
$^{10}BCl_3$	Ref. 1	3.64622	0.49279	0.15818	−0.07909	−0.09206	0.04603	6.1632	6.1652
$^{10}BBr_3$[c] Set. 1	This work	3.5788	0.029105	0.12662	−0.06331	−0.30715	0.15357		
$^{10}BBr_3$[d]	This work	3.0669	0.34457	0.13587	−0.06794	−0.12279	0.06140	4.4569	4.4566
$^{10}BBr_3$	Ref. 1	2.95092	0.40233	0.14123	−0.07061	−0.09133	0.04566	4.4569	4.4586

a) Mixing parameter $a=-1.2765$
b) Mixing parameter $a=-1.7040$
c) Mixing parameter $a=-2.1889$
d) Mixing parameter $a=-2.6693$

$$\left.\begin{aligned}
F_{11}&=m_y\lambda_1\\
F_{22}=F_{44}&=\frac{m_y d_2{}^2(\lambda_2+a^2\lambda_3)}{2A_0{}^2 d_1{}^2}\\
F_{33}=F_{55}&=\frac{m_y}{2}\left\{\left(\frac{2ad_1+3r^2}{\sqrt{3}A_0 d_1 d_2}\right)^2\lambda_2\right.\\
&\quad\left.+\left(\frac{2d_1-3ar^2}{\sqrt{3}A_0 d_1 d_2}\right)^2\lambda_3\right\}\\
F_{23}=F_{45}&=m_y\left\{\frac{-(2ad_1+3r^2)}{2\sqrt{3}A_0{}^2 d_1{}^2}\lambda_2\right.\\
&\quad\left.+\frac{a(2d_1-3ar^2)}{2\sqrt{3}A_0{}^2 d_1{}^2}\lambda_3\right\}
\end{aligned}\right\}\quad(24)$$

where in Eq. 24 we have used the fact that $\lambda_2=\lambda_4$ and $\lambda_3=\lambda_5$. $\boldsymbol{F}^W$ can also be given directly in terms of $\boldsymbol{F}^c$ with the result that for the XY_3 molecule

$$\left.\begin{aligned}
F_{11}&=F_{44}{}^c+2F_{46}{}^c\\
F_{33}&=\frac{1}{2}F_{33}{}^c\\
F_{23}&=F_{36}{}^c\\
F_{22}&=F_{44}{}^c-F_{46}{}^c
\end{aligned}\right\}\quad(25)$$

II. Force Constants For BCl_3 and BBr_3

In this section we apply the equations given by 24 and calculate the Wilson force constants. In order to accomplish this we must first determine the mixing parameter a. The quadratic equation which determines a is (see VAII)

$$\begin{aligned}
a^2\left\{\frac{\lambda_2+\lambda_3}{(1+\varepsilon)d_1{}^2}(d_1{}^2+\varepsilon)+\frac{3r^2\varepsilon}{(1+\varepsilon)d_1{}^2 d_2{}^2}(d_1{}^2\lambda_3+\lambda_2)\right.\\
\left.-(\lambda_2{}^{(i)}+\lambda_3{}^{(i)})^2\right\}+a\left(\frac{6r^2\varepsilon}{(1+\varepsilon)d_1 d_2}(\lambda_2-\lambda_3)\right)\\
+\left\{\frac{\lambda_2+\lambda_3}{(1+\varepsilon)d_1{}^2}(d_1{}^2+\varepsilon)+\frac{3r^2\varepsilon}{(1+\varepsilon)d_1{}^2 d_2{}^2}\right.\\
\left.\times(d_1{}^2\lambda_2+\lambda_3)-(\lambda_2{}^{(i)}+\lambda_3{}^{(i)})\right\}=0\qquad(26)
\end{aligned}$$

where $\varepsilon=(m^{(i)}-m)/m$, λ_1 is the symmetric stretching frequency, λ_2 is the degenerate asymmetric stretching frequency, and λ_3 is the degenerate bending frequency. $\lambda_2{}^{(i)}$ and $\lambda_3{}^{(i)}$ are the corresponding frequencies for the isotopic molecule. If m is in atomic mass units, and $\lambda_i=5.8894\times 10^{-2}\ \nu_i{}^2$ (ν_i is the observed frequency in cm^{-1}) then the F's are in units of dynes/cm. The λ's should be the zero order frequencies, and if these are available, then the equations constitute an exact determination of the molecular force constants.

The valence force constants are given by

$$\left.\begin{aligned}
f_r&=\frac{1}{3}(F_{11}+2F_{44}),\quad f'_{r\alpha}-f_{r\alpha}=F_{23}\\
f_{rr}&=\frac{1}{3}(F_{11}-F_{44}),\quad f_\alpha-f_{\alpha\alpha}=F_{55}
\end{aligned}\right\}\quad(27)$$

A number of sets of force constants available in the literature have recently been tabulated by Duncan[8] and consequently no summary of these calculations will be given in this paper. Various sets of observed frequencies are also available.[7,9,10] The frequencies used to compute the mixing parameters and force constants are listed in Table I. These sets were selected on the basis of reproducing results of other experiments on "perturbed systems" derived from the BX_3 molecules.[11] Selection of the mixing parameters from the two solutions of Eq. 26 was also made on this basis. Results for two sets of frequencies for the same molecule, BBr_3, are included to illustrate the effect of small changes in frequencies on the values of the force constants.

The results are shown in Table II. Calculations were made for $^{10}BY_3$ as the unperturbed molecule. Starting with the ^{11}B-species leads to slightly different values, due to anharmonicities. The force constants are quoted to five places only for comparison with those calculated in Ref. 3 for identical frequencies, which are also listed in Table I. The differences between our values and those of Ladd, Orville-Thomas, and Cox[3] are rather large. Small changes in F_{22} and F_{33} require a large change in F_{23}. This illustrates the inherent numeralogical difficulty of dealing with the non-linear equations. Inspection of the results for two different sets of input frequencies for BBr_3 emphasizes this point even more strongly. Thus, while it is possible, using the Green's function, to obtain a high degree of internal consistency, the force constants should in reality be considered known to, at most, two significant figures. The reason for the large variation in force constants with a small change in frequencies becomes apparent on inspection of Eq. 26: the mixing parameter is critically dependent on a small number, which is the difference between two large numbers.

8) J. L. Duncan, *J. Mol. Spectroscopy*, **13**, 338 (1964).
9) C. W. F. T. Pistorius, *J. Chem. Phys.*, **29**, 1174 (1958).
10) K. Nakamoto, "Infrared Spectra of Inorganic and Coordination Compounds," Wiley, New York (1963), p. 90.
11) See VAII for results on BCl_3-$HBCl_2$. Also, we have carried out calculations on a series of mixed boron halides, and on $HBBr_2$ and HBF_2 which have subsequently been prepared and observed (L. Lynds). The results of these experiments and calculations will be reported at a later date.

Conclusions

Using the Green's function approach to analyze the dynamics of molecular systems, we have obtained explicit expressions for the force constants of XY_3 planar molecules. Application of these formulae is quite simple and extremely convenient. It is important to point out that the variation in the force constants with the frequencies can be studied quite simply from Eqs. 24 and 26. For example, if a range of values is specified for the XY_3 and $XY_3{}^{(i)}$ vibrational frequencies then the corresponding range in the mixing parameter can be determined from Eq. 26. This range in the mixing parameter then determines the range of values for the force constants by use of Eq. 24.

BULLETIN OF THE CHEMICAL SOCIETY OF JAPAN VOL. 39 207—214 (1966)

Internal Coordinate Green's Function Analysis of Molecular Vibrations with Application to XY_2Z Planar Molecules

By Thomas WOLFRAM and Roger E. DEWAMES

North American Aviation Science Center, Thousand Oaks, California, U. S. A.

(Received January 26, 1965)

The Green's function formalism for the analysis of molecular vibrations has been formulated for the internal or valence coordinate system. A general procedure for calculating isotopic frequencies and changes in force constants associated with the characterization of a perturbed molecule in terms of the unperturbed molecule is developed. It is shown that the internal molecular Green's function can be constructed from the vibrational frequencies of the unperturbed molecule. Application is made to the XY_2Z planar molecule. Exact formulae for the $XY_2Y^{(i)}$ molecule are obtained. The shifts in the frequencies of an XY_2Z planar molecule due to mass and bond length changes are obtained. It is shown that the A_1 modes are unaffected by a change in the X–Z bond length while the B_1 modes move to higher frequencies as the bond distance decreases. An explicit expression for the change in the valence bond bending force constant, f_α, is obtained as an example of how force constant changes can be studied by means of the Green's function procedure. Qualitative results for $HBCl_2$ and $HBBr_2$ are obtained which indicate that f_α decreases in going from $BCl_3 \rightarrow HBCl_2$.

The purpose of this paper is to develop a well defined and exact procedure for relating the vibrational properties of similar molecules. The use of the Green's function procedure to obtain frequencies of isotopic molecules and approximate frequencies for $HBCl_2$ has been described in previous papers;[1-3] (hereafter referred to as VAI–III).

In these previous papers the Green's function procedure was developed for use in the cartesian coordinate system. The cartesian coordinate representation is reasonably convenient for treating the isotope problem but completely unsuited for introducing geometry changes. The Wilson FG representation appears to be the most convenient representation for formulating the general problem of relating the dynamics of similar molecules. For example, since the $\boldsymbol{G}$ matrix contains the geometry and masses of the molecule, changes in these parameters are conveniently handled by introducing a change in the $\boldsymbol{G}$ matrix, $\Delta\boldsymbol{G}$. It is also desirable to be able to separate the effects of force constant changes from these other effects. The essential idea of the approach may be illustrated as follows. Consider the problem of determining the force field of $HBCl_2$. One has at one's disposal the observed fundamental frequencies of $HBCl_2$ as well as those of BCl_3 and its isotopes. Using the Green's function formulae for isotopic substitution $XY_3 \rightarrow X^{(i)}Y_3$ one can determine the Green's function for BCl_3 as was demonstrated in a previous paper.[2] The first step in the analysis of $HBCl_2$ is to treat this molecule as if it possessed the same force field as BCl_3 and differed from BCl_3 only in that the hydrogen mass has replaced the chlorine mass and that the B–H bond length may be different from the B–Cl bond. The frequencies of this fictitious molecule, the mass-geometry shifted frequenceis, may be easily calculated using the Green's function procedure. These fictitious frequencies may be compared with the actual observed frequencies and the differences attributed entirely to changes in the Wilson $\boldsymbol{F}$ matrix. The point here is that two different molecules with identical $\boldsymbol{F}$ matrices will have different vibrational frequencies because of mass and geometry differences. The fictitious frequencies are corrected for these effects and comparison of these frequencies with the observed frequencies gives immediately a qualitative measure of the changes in the force constants. The last step in the analysis is to obtain by use of the Green's function method the change in force constants directly from the observed frequencies. This step-by-step analysis allows one to make maximum use of the similarity between the two systems. It should be pointed out here that the idea of using knowledge about one molecule to calculate the properties of another is not new. Previous techniques[4] which have been suggested, however, are perturbation schemes and depend upon the smallness of the off diagonal matrix elements. The Green's function procedure, on the other hand, is formally exact and imposes no such restrictions. A similar procedure has also been developed by the Uppsala Quantum Chemistry Group[5] for the study of molecular wave functions. In this paper we develop the Green's function approach for the internal or valence coordinate system. One advantage of this system is, of course, that one avoids the necessity of constructing the rotation and translation eigenvectors. Furthermore, correlation of molecules with different geometries appears to be most conveniently treated in the internal coordinate system because the geometry is contained explicitly in the Wilson $\boldsymbol{G}$ matrix.

In section I, the Green's function formalism is developed in the internal coordinate system for both the GF and FG representation. The analysis is oriented towards either calculating the frequencies of isotopic molecules or the force constants changes which characterize a new species.

By making extensive use of the spectral theorem for the dynamical matrix, and the transformation between internal and cartesian coordinates, it is shown in section II that the Green's function for the internal coordinates can be constructed directly from the "unperturbed" vibrational frequencies without a knowledge of the molecular force constants.

In section III the procedure is applied to the XY_2Z planar molecule. The frequencies of this molecule differ from those of the XY_3 molecule because of changes in mass, geometry and force constants. Explicit formulas for the mass and geometry corrected frequencies of an XY_2Z molecule whose X–Z bond length differs from the X–Y bond length of the XY_3 molecule are obtained. It is shown that this bond length change affects only the B_1 type vibrational modes and that the resulting frequency shifts can be quite large when the mass of the Z atom is much less than that of the Y atom. An explicit expression for studying the change in the valence bond-bending force constants, f_α, which includes the effects of changes in mass and X–Y bond length is derived. Using an X–Z bond length of 1.20 Å for $HBCl_2$ one arrives at the qualitative result that the bond bending force constant, f_α, is decreased on the order of 20% on going from BCl_3 to $HBCl_2$.

1) R. E. DeWames and T. Wolfram, *J. Chem. Phys.*, **40**, 853 (1964).
2) C. D. Bass, L. Lynds, T. Wolfram and R. E. DeWames, ibid., **40**, 3611 (1964).
3) T. Wolfram, C. D. Bass, R. E. DeWames and L. Lynds, This Bulletin, **39**, 201 (1966).
4) W. H. Edgell and T. R. Riethof, *J. Phys. Chem.*, **56**, 326 (1952).
5) See for example, J. E. Harriman, Scientific Report No. 19. Quantum Chemistry Group, University of Uppsala, Uppsala Sweden. Also see, P. O. Löwdin, *J. Math. Phys.*, **3**, 969 (1961).

I. Internal Coordinate Green's Functions

In this section the Green's function formalism is developed in the internal or valence coordinate system from which the vibrational frequencies of a "perturbed" molecule can be obtained exactly in terms of the vibrational frequencies of the "unperturbed" molecule. The "perturbed" and "unperturbed" molecules are any two molecules whose internal coordinates can be set in a one to one correspondence. The utility of the approach is greatly enhanced when the two molecules whose vibrational properties are to be correlated are, in addition, physically similar. For example, if $^{10}B^{35}Cl_3$ is considered to be the "unperturbed" molecule, then the isotopes $^{11}B^{35}Cl_3$ and $^{10}B^{35}Cl_2{}^{37}Cl$ or the new species $H^{10}B^{35}Cl_2$ and $D^{10}B^{35}Cl_2$ may be selected as "perturbed" molecules.

The unperturbed molecule's vibrational frequencies are (in the internal symmetry coordinate system) determined, according to the Wilson procedure, by the secular matrix equation

$$(\boldsymbol{G}_0\boldsymbol{F}_0-\lambda)\boldsymbol{R}=0 \tag{1}$$

or

$$(\boldsymbol{F}_0\boldsymbol{G}_0-\lambda)\boldsymbol{G}_0{}^{-1}\boldsymbol{R}=0 \tag{2}$$

where $\boldsymbol{G}_0$ and $\boldsymbol{F}_0$ are the reduced Wilson $\boldsymbol{G}$ and $\boldsymbol{F}$ matrices for the unperturbed molecule. (The redundant coordinates are omitted) λ is the square of the angular frequency, $\boldsymbol{\omega}$ and $\boldsymbol{R}$ symbolize the internal symmetry coordinate vectors. Equation 2, of course, can be obtained from Eq. 1 by a similarity transformation with the matrix $\boldsymbol{G}_0$. The secular equation for the perturbed molecule is

$$\{(\boldsymbol{G}_0+\Delta\boldsymbol{G})(\boldsymbol{F}_0+\Delta\boldsymbol{F})-\lambda\}\boldsymbol{R}=0 \tag{3}$$

or

$$\{(\boldsymbol{F}_0+\Delta\boldsymbol{F})(\boldsymbol{G}_0+\Delta\boldsymbol{G})-\lambda\}\boldsymbol{G}_0{}^{-1}\boldsymbol{R}=0 \tag{4}$$

where $\boldsymbol{G}_p=\boldsymbol{G}_0+\Delta\boldsymbol{G}$ is the $\boldsymbol{G}$ matrix for the perturbed molecule. The $\Delta\boldsymbol{G}$ matrix accounts for changes in mass and geometry in going from the unperturbed to the perturbed system and $\Delta\boldsymbol{F}$ accounts for the force constant differences.

1. Isotope Case, $\Delta\boldsymbol{F}=0$.—When the perturbed molecule is an isotope of the initial molecule so that $\Delta\boldsymbol{F}=0$ we have for Eqs. 3 and 4

$$(\boldsymbol{G}_0\boldsymbol{F}_0-\lambda+\Delta\boldsymbol{G}\boldsymbol{F}_0)\boldsymbol{R}=0 \tag{5}$$

or

$$(\boldsymbol{F}_0\boldsymbol{G}_0-\lambda+\boldsymbol{F}_0\Delta\boldsymbol{G})\boldsymbol{G}_p{}^{-1}\boldsymbol{R}=0 \tag{6}$$

The eigenvalues are obtained by requiring the determinant to vanish. By factoring out $(\lambda-\boldsymbol{G}_0\boldsymbol{F}_0)$ from Eq. 5 we obtain the secular equations

$$|\boldsymbol{I}-\boldsymbol{J}_0(\lambda)\Delta\boldsymbol{G}\boldsymbol{F}_0|=0 \tag{7}$$

and

$$|\boldsymbol{J}_0{}^{-1}(\lambda)|=0 \tag{8}$$

where

$$\boldsymbol{J}_0(\lambda)=(\lambda-\boldsymbol{G}_0\boldsymbol{F}_0)^{-1}$$

is the Green's function for the unperturbed molecule and $\boldsymbol{I}$ is a unit matrix. Equation 8 gives the frequencies for the unperturbed molecule and Eq. 7 determines the isotopically shifted frequencies. Similarly we obtain from Eq. 6 the secular determinants

$$|\boldsymbol{I}-\boldsymbol{L}_0(\lambda)\boldsymbol{F}_0\Delta\boldsymbol{G}|=0 \tag{9}$$

$$|\boldsymbol{L}_0(\lambda)^{-1}|=0 \tag{10}$$

where

$$\boldsymbol{L}_0(\lambda)=(\lambda-\boldsymbol{F}_0\boldsymbol{G}_0)^{-1}=\boldsymbol{G}_0{}^{-1}\boldsymbol{J}_0(\lambda)\boldsymbol{G}_0 \tag{11}$$

Equation 9 is preferred to Eq. 7 when the $\Delta\boldsymbol{G}$ matrix is dimensionally smaller than $\boldsymbol{F}_0$ since Eq. 9 is truncated to the size of $\Delta\boldsymbol{G}$. Both Eqs. 7 and 9 can also be applied to the case in which geometry changes are considered. The utility of these equations obviously depends upon the elimination of the matrix $\boldsymbol{F}_0$. We shall show in the next section that the $\boldsymbol{F}_0$ matrix can, by making use of the spectral theorem, be replaced by a matrix involving the unperturbed vibrational frequencies.

All of the matrices involved are block diagonal according to the irreducible representation of the unperturbed molecule except for $\Delta\boldsymbol{G}$ which is block diagonalized according to the perturbed symmetry. Consequently, Eqs. 7 and 9 hold for each perturbed symmetry type, Γ,

$$|\boldsymbol{I}-\boldsymbol{J}_0{}^{\Gamma}(\lambda)\Delta\boldsymbol{G}^{\Gamma}\boldsymbol{F}_0{}^{\Gamma}|=0 \tag{7a}$$

or

$$|\boldsymbol{I}-\boldsymbol{L}_0{}^{\Gamma}(\lambda)\boldsymbol{F}_0{}^{\Gamma}\Delta\boldsymbol{G}^{\Gamma}|=0 \tag{9a}$$

where the superscript Γ refers to the Γ-type block of the matrices. $\boldsymbol{F}_0{}^{\Gamma}$, for example, contains those symmetry blocks of $\boldsymbol{F}_0$ which are coupled by $\Delta\boldsymbol{G}^{\Gamma}$ and gives rise to the Γ block of the perturbed symmetry. In subsequent equations it is to be assumed that an equivalent equation holds for each perturbed symmetry type.

2. General Case.—In the most general case both $\Delta\boldsymbol{F}$ and $\Delta\boldsymbol{G}$ are non-vanishing. One then obtains the determinantal equations

$$|\boldsymbol{I}-\boldsymbol{J}_p(\lambda)\boldsymbol{G}_p\Delta\boldsymbol{F}|=0 \tag{12}$$

$$|\boldsymbol{J}_p{}^{-1}(\lambda)|=0 \tag{13}$$

where

$$\boldsymbol{J}_p(\lambda)=(\lambda-\boldsymbol{G}_p\boldsymbol{F}_0)^{-1} \tag{14}$$

The matrix $\boldsymbol{J}_p(\lambda)$ is evidently the Green's function for a fictitious molecule having the geometry and mass of the perturbed molecule and the force constants of the unperturbed molecule. The eigenvalues of Eq. 12 are the vibrational frequencies of the perturbed molecule which are affected by $\Delta\boldsymbol{F}$ as well as $\Delta\boldsymbol{G}$. In the circumstance that a frequency is unaffected by $\Delta\boldsymbol{F}$ but shifted by $\Delta\boldsymbol{G}$ then this eigenvalue will be determined by Eq. 13.

(In section II we show that $\boldsymbol{J}_p(\lambda)$ can be obtained from $\boldsymbol{J}_0(\lambda)$. We can also obtain from Eq. 2

$$\boldsymbol{K}_p(\lambda)^{-1}[\boldsymbol{I}-\boldsymbol{K}_p(\lambda)(\boldsymbol{F}_0+\Delta\boldsymbol{F})\Delta\boldsymbol{G}]=0 \quad (15)$$

where

$$\boldsymbol{K}_p(\lambda)=[\lambda-(\boldsymbol{F}_0+\Delta\boldsymbol{F})\boldsymbol{G}_0]^{-1} \quad (16)$$

which leads to the determinants

$$|\boldsymbol{I}-\boldsymbol{K}_p(\lambda)(\boldsymbol{F}_0+\Delta\boldsymbol{F})\Delta\boldsymbol{G}|=0 \quad (17)$$

and

$$|\boldsymbol{K}_p(\lambda)^{-1}|=0 \quad (18)$$

Equation 18 gives the eigenvalues of a fictitious molecule with the perturbed molecule force constants and the geometry and mass of the unperturbed molecule, and Eq. 17 gives the perturbed molecular frequencies. This form of the secular equation is convenient when $\Delta\boldsymbol{G}$ truncates the matrix to a small dimension, or in the case that one makes a power series expansion of $\boldsymbol{K}_p(\lambda)$ for small $\Delta\boldsymbol{F}$.

A calculation of the force constant changes, $\Delta\boldsymbol{F}$, associated with the characterization of the new species XY_2Z may be made by using either Eq. 12 or 17. The matrix elements of $\Delta\boldsymbol{F}$ appear as parameters in the equations and if the perturbed frequencies are known then $\Delta\boldsymbol{F}$ may be determined. The frequencies of any isotope of the perturbed XY_2Z molecule can be utilized to give additiona equations for the $\Delta\boldsymbol{F}$ matrix elements. In Eq. 17 one simply substitutes $\Delta\boldsymbol{G}+\Delta\boldsymbol{G}_p(\text{isotope})$ for $\Delta\boldsymbol{G}$ where

$$\Delta\boldsymbol{G}_p(\text{isotope})=\boldsymbol{G}_p(\text{isotope})-\boldsymbol{G}_p \quad (19)$$

In Eq. 12 one must use the new Green's function

$$\begin{aligned}\boldsymbol{J}_p(\lambda)(\text{isotope})&=(\lambda-\boldsymbol{G}_p(\text{isotope})\boldsymbol{F}_0)^{-1}\\&=(\boldsymbol{I}-\boldsymbol{J}_p(\lambda)\Delta\boldsymbol{G}_p(\text{isotope})\boldsymbol{F}_0)^{-1}\boldsymbol{J}_p(\lambda)\end{aligned} \quad (20)$$

II. Construction of Green's Functions

In this section we show how the Green's functions $\boldsymbol{J}_0(\lambda)$, $\boldsymbol{J}_p(\lambda)$, $\boldsymbol{L}_0(\lambda)$, and $\boldsymbol{K}_p(\lambda)$ can be constructed starting from the spectral representation. It was shown in VAIII[3] that the vibrational part of the dynamical matrix in the cartesian symmetry representation, $\boldsymbol{D}^s$, was related to the Wilson reduced force constant matrix $\boldsymbol{F}$ by the congruent transformation

$$\tilde{\boldsymbol{B}}\boldsymbol{F}\boldsymbol{B}=\boldsymbol{D}^s \quad (21)$$

and that

$$\boldsymbol{B}\tilde{\boldsymbol{B}}=\boldsymbol{G} \quad (22)$$

where

$$\boldsymbol{B}=\boldsymbol{T}\boldsymbol{M}^{-1/2}\boldsymbol{S} \quad (23)$$

and $\tilde{\boldsymbol{B}}$ is the transpose of $\boldsymbol{B}$. $\boldsymbol{T}$ is the transformation from the internal symmetry coordinates to the cartesian coordinates, $\boldsymbol{M}$ is the diagonal mass matrix and $\boldsymbol{S}$ is the transformation from the cartesian coordinates to the orthonormal mass weighted cartesian vibrational symmetry coordinates.

The matrix $\boldsymbol{D}^s$ has the square of the angular vibrational frequencies, λ_i, for its eigenvalues and is diagonalized by the unitary matrix $\boldsymbol{A}$

$$\boldsymbol{A}^+\boldsymbol{D}^s\boldsymbol{A}=\boldsymbol{\Lambda} \quad (24)$$

$$\Lambda_{ij}=0 \quad i\neq j \quad (25)$$

$$\Lambda_{ii}=\lambda_i \quad (26)$$

where $\boldsymbol{A}^+$ is the Hermetian conjugate of $\boldsymbol{A}$. The matrix $\boldsymbol{A}$ is the matrix of mixing parameters discussed in previous papers,[1-3] where it was shown that $\boldsymbol{A}$ can be determined directly from isotope data on the XY_3 molecule. Making use of the above equations one finds that

$$\boldsymbol{F}_0=\tilde{\boldsymbol{H}}^{-1}\boldsymbol{\Lambda}\boldsymbol{H}^{-1} \quad (27)$$

$$\boldsymbol{G}_0\boldsymbol{F}_0=\boldsymbol{H}\boldsymbol{\Lambda}\boldsymbol{H}^{-1} \quad (28)$$

and

$$\boldsymbol{F}_0\boldsymbol{G}_0=\tilde{\boldsymbol{H}}^{-1}\boldsymbol{\Lambda}\tilde{\boldsymbol{H}} \quad (29)$$

where

$$\boldsymbol{H}=\boldsymbol{B}\boldsymbol{A} \quad (30)$$

Thus,

$$\boldsymbol{J}_0(\lambda)=\boldsymbol{H}(\lambda-\boldsymbol{\Lambda})^{-1}\boldsymbol{H}^{-1} \quad (31)$$

and

$$\boldsymbol{L}_0(\lambda)=\tilde{\boldsymbol{H}}^{-1}(\lambda-\boldsymbol{\Lambda})^{-1}\tilde{\boldsymbol{H}}=\tilde{\boldsymbol{J}}_0(\lambda) \quad (32)$$

Thus we see that $\boldsymbol{J}_0$ and $\boldsymbol{L}_0$ can be constructed from the unperturbed vibrational frequencies and the mixing parameters. The mixing parameters can be obtained from isotope data as discussed in VAI[1] and II[2] or from Coriolis and centrifugal distortion constants.[6] From Fq. 31 it is clear that $\boldsymbol{J}_0(\lambda)$ is just the internal coordinate representation of the vibrational part of the cartesian symmetry coordinate Green's function $\boldsymbol{D}^s$ discussed in VAIII.[3]

It should be pointed out again that all of the above equations hold for each of the symmetry types, Γ.

The matrix $\boldsymbol{J}_p(\lambda)$ can be constructed directly with the result that

$$\boldsymbol{J}_p(\lambda)=\boldsymbol{H}(\lambda-(\boldsymbol{I}+\Delta\boldsymbol{G}_t)\boldsymbol{\Lambda})^{-1}\boldsymbol{H}^{-1} \quad (33)$$

where $\Delta\boldsymbol{G}_t$ is the transformed $\Delta\boldsymbol{G}$ matrix

$$\Delta\boldsymbol{G}_t=\boldsymbol{H}^{-1}\Delta\boldsymbol{G}\tilde{\boldsymbol{H}}^{-1} \quad (34)$$

We may also construct $\boldsymbol{J}_p(\lambda)$ from $\boldsymbol{J}_0(\lambda)$ since

$$\boldsymbol{J}_p(\lambda)=[\boldsymbol{I}-\boldsymbol{J}_0(\lambda)\Delta\boldsymbol{G}\tilde{\boldsymbol{H}}^{-1}\boldsymbol{\Lambda}\boldsymbol{H}^{-1}]^{-1}\boldsymbol{J}_0(\lambda) \quad (35)$$

Similarly for $\boldsymbol{K}_p(\lambda)$ we obtain,

$$\boldsymbol{K}_p(\lambda)=\tilde{\boldsymbol{H}}^{-1}(\lambda-\boldsymbol{\Lambda}-\Delta\boldsymbol{F}_t)^{-1}\tilde{\boldsymbol{H}} \quad (36)$$

where $\Delta\boldsymbol{F}_t$ is the transformed $\Delta\boldsymbol{F}$ matrix

$$\Delta\boldsymbol{F}_t=\tilde{\boldsymbol{H}}\Delta\boldsymbol{F}\boldsymbol{H} \quad (37)$$

6) J. S. Margolis and C. D. Bass, *J. Chem. Phys.*, **40**, 1590 (1964).

$\boldsymbol{K}_p$ may also be written in terms of $\boldsymbol{L}_0$,

$$\boldsymbol{K}_p(\lambda)=[\boldsymbol{I}-\boldsymbol{L}_0(\lambda)\Delta\boldsymbol{F}\boldsymbol{G}_0]^{-1}\boldsymbol{L}_0(\lambda) \tag{38}$$

It is important to realize that in all cases the $\boldsymbol{H}$ matrix refers to the unperturbed molecule and one never needs the $\boldsymbol{H}$ matrix for the perturbed molecule.

III. Application to XY_2Z Planar Molecules

In this section, as an example, we apply the Green's function formalism developed in the preceding sections to the problem of the in-plane vibrational frequencies of the XY_2Z planar molecule. In determining the force constant changes, $\Delta\boldsymbol{F}$, associated with the characterization of the XY_3Z molecule in terms of the corresponding XY_3 molecule it is important to first calculate the frequency shifts due to changes in mass and geometry. These mass-geometry corrected frequencies can then be compared with the observed XY_2Z frequencies and the differences attributed to pure force constant changes. We consider in this section the problem of obtaining the mass-geometry corrected frequencies of XY_2Z planar molecules whose X–Z bond length differs from the X–Y bond length of the unperturbed XY_3 molecule. This situation arises in connection with the analysis of the dihaloboranes in terms of the parent boron trihalide. For example, $HBCl_2$ has the same 120° bond angles as BCl_3 but the H–B bond length is believed to be smaller than the B–Cl bond length.[7] The same circumstance obtains in the case of $HBBr_2$.

The internal coordinates and $\boldsymbol{G}$ matrix for an XY_2Z planar molecule with 120° bond angles has been discussed by Lindeman and Wilson.[8] The internal coordinates used in VAIII[3] are the same as those discussed by Lindeman and Wilson except that the angular coordinates are multiplied by the X–Y bond distance. Following this convention the $\Delta\boldsymbol{G}$ matrix elements associated with the characterization of the XY_2Z planar molecule are given by

$$\Delta G_{11}=\frac{1}{3}\Delta\mu$$

$$\Delta G_{12}=\frac{\sqrt{2}}{3}\Delta\mu$$

$$\Delta G_{22}=\frac{2}{3}\Delta\mu$$

$$\Delta G_{45}=\sqrt{3}\,\Delta l\mu_x$$

$$\Delta G_{55}=2\Delta\mu+2\Delta l[\mu_z(\Delta l+2)+\mu_x(\Delta l+3)]$$

$$\Delta\mu=\mu_z-\mu_y$$

$$\Delta l=(l-l')/l'$$

where μ_α is the reciprocal of the αth atom's mass, l is the X–Y bond length and l' is the Z–X bond length. All other $\Delta\boldsymbol{G}$ matrix elements vanish. It is evident that the A_1 modes are independent of the geometry change since the A_1 part of $\Delta\boldsymbol{G}$ (the upper 3×3) involves only mass changes. The ΔG_{45} matrix elements involve only pure geometry effects while ΔG_{55} contains both mass and geometry effects.

1. A_1 Modes.—In order to calculate the A_1 vibrational frequencies we solve the secular determinant given by Eq. 9

$$|\boldsymbol{I}-\boldsymbol{Z}|=0 \tag{40}$$

where

$$\boldsymbol{Z}=[\boldsymbol{L}_0(\lambda)\boldsymbol{F}_0\Delta\boldsymbol{G}]_{A_1} \tag{41}$$

The subscript refers to the A_1 block; the upper 3×3 matrix. It is convenient to transform Eq. 40 to a representation in which ΔG is diagonal

$$|\boldsymbol{I}-\boldsymbol{U}^+\boldsymbol{Z}\boldsymbol{U}|=0 \tag{40a}$$

where

$$\boldsymbol{U}=\frac{1}{\sqrt{3}}\begin{pmatrix}1 & \sqrt{2} & 0\\ \sqrt{2} & -1 & 0\\ 0 & 0 & \sqrt{3}\end{pmatrix} \tag{42}$$

In this representation $\Delta\boldsymbol{G}$ assumes the simple form

$$\boldsymbol{U}^+\Delta\boldsymbol{G}\boldsymbol{U}=\begin{pmatrix}\Delta\mu & 0 & 0\\ 0 & 0 & 0\\ 0 & 0 & 0\end{pmatrix} \tag{43}$$

so that Eq. 40a reduces to a 1×1 transcendental determinant

$$1-\{\boldsymbol{U}^+\boldsymbol{L}_0(\lambda)\boldsymbol{F}_0\boldsymbol{U}\}_{11}\Delta\mu=0 \tag{44}$$

where $\{\ \}_{11}$ is the $1-1$ matrix element. Thus we need only a single matrix element to determine the A_1 isotope frequencies. Using Eqs. 27 and 32 we find that

$$\begin{aligned}\{\boldsymbol{U}^+\boldsymbol{L}_0(\lambda)\boldsymbol{F}_0\boldsymbol{U}\}_{11}&=\{\boldsymbol{U}^+\tilde{\boldsymbol{H}}^{-1}[\Lambda(\lambda-\Lambda)^{-1}]\boldsymbol{H}^{-1}\boldsymbol{U}\}_{11}\\&=\{\boldsymbol{U}^+{}_1,\tilde{\boldsymbol{H}}^{-1}[\Lambda(\lambda-\Lambda)^{-1}]\boldsymbol{H}^{-1}\boldsymbol{U}_1\}\end{aligned} \tag{45}$$

One need only calculate the inner product given by Eq. 45 where $\boldsymbol{U}_1$ is the first column of $\boldsymbol{U}$ and $\boldsymbol{U}^+{}_1$ is the first row of $\boldsymbol{U}^+$. The matrices $\boldsymbol{A}$ and $\boldsymbol{B}$ are given in VAIII[3] and their product, $\boldsymbol{H}$, is

$$\boldsymbol{H}=\boldsymbol{B}\boldsymbol{A}=\begin{pmatrix}(BA)_{A_1} & 0\\ 0 & (BA)_{B_1}\end{pmatrix} \tag{46}$$

where

$$(BA)_{B_1}=\frac{\mu_y{}^{1/2}}{\sqrt{2}\,A_0d_2}\begin{pmatrix}(2d_1-3r^2a) & -(3r^2+2ad_1)\\ -\sqrt{3}\,d_2{}^2a & -\sqrt{3}\,d_2{}^2\end{pmatrix} \tag{47}$$

and

$$(BA)_{A_1}=\begin{pmatrix}\mu_y{}^{+1/2} & 0\\ 0 & (BA)_{B_1}\end{pmatrix} \tag{48}$$

7) L. Lynds and C. D. Bass, ibid., **40**, 1590 (1964).
8) P. Lindeman and M. K. Wilson, ibid., **24**, 242 (1956).

where

$$\left.\begin{aligned} d_1^2&=1+3r^2\\ d_2^2&=2+3r^2\\ r^2&=m_y/m_x\\ A_0^2&=1+a^2 \end{aligned}\right\} \qquad (49)$$

a=mixing parameter

Equation 45 leads to the following equations for mass shifted A_1 frequencies of the XY_2Z molecule,

$$\lambda_1^p\lambda_2^p\lambda_3^p=\lambda_1\lambda_2\lambda_3\left\{1+\frac{\Delta\mu}{3\mu}\left(1+\frac{d_2^2}{d_1^2}\right)\right\}, \qquad (50)$$

$$\lambda_1^p\lambda_2^p+\lambda_1^p\lambda_3^p+\lambda_2^p\lambda_3^p=\lambda_1\lambda_2+\lambda_1\lambda_3+\lambda_2\lambda_3 +\frac{\Delta\mu}{3\mu_y}\left\{\lambda_1(\lambda_2+\lambda_3)+\frac{d_2^2\lambda_1}{d_1^2A_0^2}(\lambda_2+a^2\lambda_3) +\frac{d_2^2}{d_1^2}\lambda_2\lambda_3\right\} \qquad (51)$$

$$\lambda_1^p+\lambda_2^p+\lambda_3^p=\lambda_1+\lambda_2+\lambda_3 +\frac{\Delta\mu}{3\mu_y}\left\{\lambda_1+\frac{d_2^2}{d_1^2A_0^2}(\lambda_2+a^2\lambda_3)\right\} \qquad (52)$$

where the λ^p are the square of the XY_2Z A_1 angular frequencies. λ_1 refers to the A_1 totally symmetric mode of the XY_3 molecule and λ_2 and λ_3 refer to the E′ modes of the XY_3 molecule. Equations 50—52 were derived in VAII[2] using the cartesian coordinate Green's function and are exact for the isotopic case $Z \rightarrow Y^{(i)}$.

2. B_1 Modes.—The mass and geometry corrected B_1 modes may be easily calculated from Eq. 7 which takes the form

$$|\boldsymbol{I}-\boldsymbol{Z}|=0 \qquad (53)$$

$$\boldsymbol{Z}=[\boldsymbol{J}_0(\lambda)\Delta\boldsymbol{G}\boldsymbol{F}_0]_{B1} \qquad (54)$$

It is convenient to proceed from the relation (for a 2×2 matrix)

$$|\boldsymbol{I}-\boldsymbol{Z}|=1+|\boldsymbol{Z}|-\mathrm{Tr}\boldsymbol{Z} \qquad (55)$$

since the determinant of Z can be written down by inspection,

$$|\boldsymbol{Z}|=\frac{|\boldsymbol{J}_0(\lambda)||\boldsymbol{G}_0\boldsymbol{F}_0||\Delta\boldsymbol{G}|}{|\boldsymbol{G}_0|} =\left[\frac{1}{(\lambda-\lambda_4)(\lambda-\lambda_5)}\right]\frac{(\lambda_4\lambda_5)(-3\Delta l\mu_x^2)}{3\mu_y(\mu_y+3\mu_x)} \qquad (56)$$

The trace of Z is given by

$$\mathrm{Tr}\boldsymbol{Z}=\mathrm{Tr}(\boldsymbol{J}_0(\lambda)\Delta\boldsymbol{G}\boldsymbol{F}_0)=\mathrm{Tr}(\boldsymbol{F}_0\boldsymbol{J}_0(\lambda)\Delta\boldsymbol{G}) =\frac{\lambda_4}{\lambda-\lambda_4}(\Delta\boldsymbol{G}_t)_{44}+\frac{\lambda_5}{\lambda-\lambda_5}(\Delta\boldsymbol{G}_t)_{55} \qquad (57)$$

where $\Delta\boldsymbol{G}_t$ is given by Eq. 34.

Equation 55 gives rise to the following set of equations for the mass-geometry corrected B_1 frequencies of the XY_2Z molecule,

$$\lambda_4^p\lambda_5^p=\lambda_4\lambda_5\left\{1-\frac{3\Delta l\mu_x}{\mu_y d_1^2}\left(\frac{\Delta l\mu_x}{3\mu_y}+r^2\right) +\frac{(\beta+2\Delta\mu)}{6\mu_y d_1^2}d_2^2\right\} \qquad (58)$$

$$\lambda_4^p+\lambda_5^p=(\lambda_4+\lambda_5) +\frac{\lambda_4}{\mu_y A_0^2}\left[\frac{-\sqrt{2}\,\alpha d_2}{d_1}+(\beta+2\Delta\mu) \times\left(\frac{\sqrt{6}\,a}{3d_2}+\frac{3r^2}{\sqrt{6}\,d_1d_2}\right)\right]\left[\frac{\sqrt{6}\,a}{3d_2}+\frac{3r^2}{\sqrt{6}\,d_1d_2}\right] +\frac{\lambda_5}{\mu_y A_0^2}\left[-\frac{\sqrt{2}\,\alpha d_2}{d_1}+(\beta+2\Delta\mu) \times\left(\frac{-\sqrt{6}}{3d_2}+\frac{3r^2a}{\sqrt{6}\,d_1d_2}\right)\right]\left[\frac{-\sqrt{6}}{3d_2}+\frac{3r^2a}{\sqrt{6}\,d_1d_2}\right] \qquad (59)$$

where

$$\alpha=\sqrt{3}\,\Delta l\mu_x \qquad (60)$$

and

$$\beta=2\Delta l[\mu_z(\Delta l+2)+\mu_x(\Delta l+3)] \qquad (61)$$

In the above equations λ_4^p and λ_5^p are the mass-geometry corrected B_1 eigenvalues of the XY_2Z molecule while λ_4 and λ_5 ($\lambda_4=\lambda_2$, $\lambda_5=\lambda_3$) are the E′ eigenvalues of the XY_3 molecule.

When $\Delta l=0$ Eqs. 58 and 59 reduce to the exact isotopic equations given in VAII[2] for $XY_2Y^{(i)}$. Positive (negative) Δl has an effect similar to decreasing (increasing) the molecular mass so that the geometry shift is towards higher (lower) frequencies. Furthermore, if μ_z is much larger than either μ_x or μ_y then the term with β will dominate the geometry dependent terms. In the case of the dihaloboranes this effect is comparable to the pure isotope or mass shift and explicit results will be published in a subsequent paper.

3. Example of Force Constant, Mass and Geometry Change.—As an example of how the force constant changes can be studied by means of the Green's function procedure let us consider the XY_2Z planar molecule treated in the preceding section in which the valence force constant f_α differs from that of the XY_3 unperturbed molecule. Knowing the XY_3 and XY_2Z vibrational frequencies we wish to calculate *directly* the change in f_α. We use Eq. 12 for this calculation. The bond bending constant f_α affects only the B_1 modes and ΔF is given by

$$\left.\begin{aligned} (\Delta F)_{44}&=0\\ (\Delta F)_{45}&=0\\ (\Delta F)_{55}&=2\Delta f_\alpha \end{aligned}\right\} \qquad (62)$$

and Eq. 12 can be rewritten in the simple form

$$\Delta f_\alpha=\frac{1}{2\{\boldsymbol{J}_p(\lambda)\boldsymbol{G}\}_{55}} \qquad (63)$$

The quantity $\{\boldsymbol{J}_p(\lambda)\boldsymbol{G}_p\}_{55}$ is the 5-5 matrix element of the matrix product of the B_1 block. A little manipulation shows that

$$\{\boldsymbol{J}_p(\lambda)\boldsymbol{G}_p\}_{55}=|\boldsymbol{J}_p(\lambda)|\{\lambda(\boldsymbol{G}_p)_{55}-|\boldsymbol{G}_p|F_{44}\} \qquad (64)$$

where F_{44} is the 4—4 element of the force constant matrix for the XY_3 unperturbed molecule and may be expressed directly in terms of the vibrational frequencies by application of Eq. 27 which (see VAIII) gives

$$F_{44}=\frac{m_y {d_2}^2(\lambda_2+a^2\lambda_3)}{2{A_0}^2{d_1}^2} \tag{65}$$

Next we make use of the fact that

$$|\boldsymbol{J}_p(\lambda)|=\frac{1}{(\lambda-\lambda^*_4)(\lambda-\lambda^*_5)}=\frac{1}{\mu(\lambda-\lambda^*)} \tag{66}$$

where $\lambda^*_{4,5}$ are the mass-geometry corrected frequencies calculated in section I.2. Thus we obtain the final result that

$$\Delta f_\alpha=\frac{\pi(\lambda-\lambda^*)}{2\{\lambda(\boldsymbol{G}_p)_{55}-|\boldsymbol{G}_p|F_{44}\}} \tag{67}$$

In this example Δf_α is overdetermined. Evaluating Eq. 67 by substitution of an XY_2Z B_1 frequency $\lambda_4{}^p$ or $\lambda_5{}^p$ for λ yields two values of Δf_α. If the fundamental (anharmonically corrected) frequencies were available and if only changes in f_α were involved the two values of Δf_α would coincide.

4. $HBCl_2$ Force Field.—The infrared spectrum of $HBCl_2$ was discussed in VAII. In this work an assignment of the vibrational bands was made on the basis of an "isotope" calculation in which $HBCl_2$ was treated as if the hydrogen was an isotope of chlorine. The observed in-plane frequencies for $H^{11}BCl_2$ were $\nu_1=740(729)$, $\nu_2=2617(2607)$, $\nu_4=1089(1000)$ and $\nu_5=892(851)$ cm^{-1}. (The isotopically calculated frequencies are in parenthesis.) ν_3 was calculated to be at 287 cm^{-1} and was outside the range of the instrument. The A_1 frequencies (ν_1, ν_2, and ν_3) are so close to the calculated values that corrections for force constant changes would be meaningless. Anharmonic corrections can be greater than these differences.

The apparent agreement of the calculated B_1 frequencies with the observed values is somewhat fortuitous. In the above calculation no correction was made for the change in bond length. When Eqs. 58 and 59 are used to obtain the mass-geometry corrected frequencies one gets the results $\nu_4=1363$ and $\nu_5=912$ for a B–H bond length of 1.20Å. The A_1 modes are not affected by the bond length change. If we assume that the force constants involved in the A_1 modes are essentially unchanged as suggested by the fact that the calculated frequencies are so close, then we must have changes in the force field which affect only the B_1 modes. There are two such constants, f_α and $f_{d\alpha}$ (see VAIII). Application of Eq. 67 (the frequencies and mixing parameter are given in VAII) using $\lambda_4{}^p(\lambda_4{}^p=\nu_4{}^2/4\pi^2)$ gives a value of $\Delta f_\alpha=-0.038$ mdynes/Å or 25% decrease in f_α in going from BCl_3 $\rightarrow HBCl_2$. With this single force constant change the calculated frequencies are $\nu_5=1089$, $\nu_5=912$. ν_5 is about 20 wave numbers higher than the value estimated from the band center in VAII indicating that some other small force constant changes may be involved. A similar calculation for $DBCl_2$ indicates about a 15% decrease in f_α and predicts frequencies $\nu_4=1005$ and $\nu_5=793$. ν_4 agrees exactly with the observed $DBCl_2$ frequency but ν_5 was not observed. The change in f_α is therefore qualitatively the same for both $HBCl_2$ and $DBCl_2$. This calculation is of course not intended to constitute an accurate determination of the force field. In fact, it is not possible to obtain accurate force constants without having the anharmonically corrected frequencies. For example, in VAIII one finds that two sets of BBr_3 data which differ by less than 5 wave numbers gives values of f_α which differ by 10%. Nevertheless, the preceding analysis gives a fairly quantitative picture of the $HBCl_2$ force field; it is nearly identical to the BCl_3 force field with a 15 to 25% decrease in the bending force constant f_α. A calculation for the molecules $HBBr_2$ and $DBBr_2$ in terms of BBr_3 yields almost identical results. A more detailed account of these results along with the infrared spectra will be published at a later date.

A more accurate determination of the force constants does not seem to be meaningful until the anharmonic corrections are known. It should also be noted that the change in f_α becomes smaller as one increases the B–H bond length and in fact goes to zero at about 1.56Å.

Discussion and Conclusions

In the preceding sections we have developed the Green's function procedure for molecular analysis in the internal coordinate system.

By making use of the spectral representation of the cartesian dynamical matrix and the transformation between internal and cartesian symmetry coordinates we have shown how to construct the internal molecular Green's function directly from observed vibrational frequencies of the unperturbed molecule. It was shown that the changes in force constants associated with the characterization of a perturbed molecule can be calculated without reference to the unperturbed force constants. This procedure circumvents to a large degree the difficulties encountered in a direct procedure in which the unperturbed molecular force constants vary wildly with small changes in the unperturbed molecular frequencies. It was shown that all of the internal Green's functions can be constructed from a knowledge of the transformation matrix $\boldsymbol{B}$ and the mixing parameters.

In section III we obtained explicit formulae for the mass and geometry frequency shifts in going from an XY_3 to an XY_2Z planar molecule with a different bond length. It was shown that the A_1 modes are unaffected by the change in bond length and that the B_1 modes were shifted to higher

(lower) frequencies whenever $\Delta l > 0$ ($\Delta l < 0$).

As an example of force constant changes, an explicit formula was obtained for the change in f_α directly in terms of the perturbed and unperturbed frequencies.

The Green's function formalism in the internal coordinate system appears to be a particularly simple and appealing procedure for correlating the vibrational properties of families of related molecular species.

A qualitative analysis of the $HBCl_2$ and $DBCl_2$ was given which shows that these molecules have a force field almost identical with the BCl_3 force field except that the bending force constant f_α is decreased by about 20%.

The authors wish to express their appreciation to G. W. Lehman and L. Lynds for valuable suggestions concerning the topics in this paper.

BULLETIN OF THE CHEMICAL SOCIETY OF JAPAN VOL. 39. 214—219 (1966)

The Reactions of *N*-Phenyl Ethanolamine with Imido Phosphites, Amido Phosphites and Amino Phosphines

By Oyo MITSUNOBU,* Takashi OHASHI, Motokazu KIKUCHI and Teruaki MUKAIYAMA*

Technical Research Department, Bridgestone Tire Co., Ltd., Kodaira, Tokyo

(Received March 2, 1965)

Various symmetrical and unsymmetrical triesters of phosphorous acid have been obtained by the reactions of phosphazo compounds with alcohols or phenols. When a phosphazo compound, amido phosphites or amino phosphine is treated with 2 mol. of *N*-substituted ethanolamine, the corresponding bis(β-aminoethyl) phosphites or phosphonite is obtained. On the other hand, when the same reaction is carried out with 1 mol. of the ethanolamine, cyclic phosphorous compounds are obtained in fairly good yields. Further, it has been found that the treatment of bis(β-anilinoethyl)phenyl phosphonite with phenyl isocyanate gives 2-phenylimino-3-phenyl-1, 3-oxazolidine.

The reaction of ethyl *N*-phenylimino phosphite (ethoxyphosphazobenzene) with benzaldehyde and ethanol has recently been reported to afford diethyl phosphite and benzilideneaniline.[1] In the present study, addition reactions of phosphazo compounds with active hydrogen compounds, such as amines, alcohols, phenols and aminoalcohols, were attempted. When *N*-phenylamino *N'*-phenylimino phosphine (I) was treated with an equimolar amount of aniline in boiling toluene, trisanilino phosphine (II), an addition compound, could not be obtained; rather, 53.8% of the starting material (I) was recovered, along with an unidentified product (Eq. 1):

$$\underset{\text{I}}{C_6H_5\text{-}N{=}P\text{-}NHC_6H_5} + C_6H_5NH_2 \xrightarrow{\times} \underset{\text{II}}{P(NHC_6H_5)_3} \quad (1)$$

Ethyl dianilino phosphite (III), the expected addition compound, could not be obtained when I was treated with an equimolar amount of ethanol in boiling toluene, but triethyl phosphite and aniline were produced in 23.3 and 33.3% yields, and 21% of I was also recovered (Eq. 2):

$$\text{I} + \text{EtOH} \begin{cases} \xrightarrow{\times} \underset{\text{III}}{(C_6H_5NH)_2P\text{-}OEt} \\ \longrightarrow (EtO)_3P + 2C_6H_5NH_2 \end{cases} \quad (2)$$

On the other hand, the yield of triethyl phosphite was increased to 46% when 3 mol. of ethanol were used in the above reaction. In a similar manner, various trialkyl or triaryl phosphites were prepared by the reactions of 1 mol. of I with 3 mol. of alcohols or phenols (see Table I).

Similarly, unsymmetrical ethyl dialkyl or ethyl diphenyl phosphite was produced by the reaction of 1 mol. of ethyl *N*-phenylimino phosphite (IV) with 2 mol. of alcohols or phenol (Eq. 3). The results are summarized in Table II.

$$\underset{\text{IV}}{C_6H_5\text{-}N{=}P\text{-}OEt} + 2ROH \longrightarrow (RO)_2P\text{-}OEt + C_6H_5NH_2 \quad (3)$$

R=alkyl or phenyl

* Laboratory of Organic Chemistry, Tokyo Institute of Technology, Ookayama, Meguro-ku, Tokyo

1) O. Mitsunobu and T. Mukaiyama, *J. Org. Chem.*, **29**, 3005 (1964).

Table I. The reaction of *N*-phenylamino *N'*-phenylimino phosphine with alcohols and phenols

Material	Product: Phosphite	Yield, %	B. p., °C/mmHg	Aniline, Yield, %
EtOH	$(EtO)_3P$	45.8	52—63/26	94.7
n-BuOH	$(n\text{-}BuO)_3P$	77.6	90—91/1	64.6
C_6H_5OH	$(C_6H_5O)_3P$	81.5	117—136/0.05	86.0
p-Cl-C_6H_4OH	$(p\text{-}Cl\text{-}C_6H_4O)_3P$	78.2	119—146/0.08	78.6

Table II. The reaction of ethyl *N*-phenylimino phosphite with alcohols and phenol

Material	Product: Phosphite	Yield, %	B. p., °C/mmHg	Aniline, Yield, %
EtOH	$(EtO)_3P$	72.6	75—78/40	98.5
n-PrOH	$(n\text{-}PrO)_2POEt$	50.0	79—81/15	170*
n-BuOH	$(n\text{-}BuO)_2POEt$	80.8	82—84/18	96.5
C_6H_5OH	$(C_6H_5O)_2POEt$	78.3	73—96/0.02	88.9

* In this case, the aniline fraction was contaminated with the phosphite.

Table III. The synthesis of bis(β-aminoethyl)-phosphorous compounds

$$R\text{-}P\left(OCH_2CH_2N\begin{matrix}R'\\H\end{matrix}\right)_2$$

Starting material: Phosphorous compound	Ethanolamine	Reaction condition: Solvent	Time hr.	Temp. °C	Product: R	R'	Yield %	B. p. °C/mmHg	Analysis N, %
$EtO\text{-}P(NEt_2)_2$	$CH_3NHCH_2CH_2OH$	Toluene	4	110	EtO-	CH_3-	60.3	54—57/2	Found 12.50 Calcd. 12.50
$EtO\text{-}P(NEt_2)_2$	$C_2H_5NHCH_2CH_2OH$	Toluene	7	110	EtO-	C_2H_5-	50.7	71—73/0.1	Found 11.35 Calcd. 11.11
EtO-P=N-Ph	$C_6H_5NHCH_2CH_2OH$	—	5	120	EtO-	C_6H_5-	32.6	99—101/0.005	Found 7.99 Calcd. 8.05
$C_6H_5\text{-}P(NEt_2)_2$	$C_6H_5NHCH_2CH_2OH$	—	4	120	C_6H_5-	C_6H_5-	69.4	105—107/0.001	Found 7.45 Calcd. 7.37
$C_6H_5\text{-}P(O\text{-}CH_2\text{-}N(C_6H_5)\text{-}CH_2)$	$C_6H_5NHCH_2CH_2OH$	Xylene	4	140	C_6H_5-	C_6H_5-	31.4	124—126/0.03	Found 7.35 Calcd. 7.37

Table IV. The synthesis of 1, 3, 2-oxazaphospholidines

$$R\text{-}P\begin{matrix}O\text{-}CH_2\\|\\N\text{-}CH_2\\|\\R'\end{matrix}$$

Starting material: Phosphorous compound	Ethanolamine	Reaction condition: Solvent	Time hr.	Temp. °C	Product: R	R'	Yield %	B. p. °C/mmHg	Analysis N, %
$C_6H_5\text{-}P(NEt_2)_2$	$C_6H_5NHCH_2CH_2OH$	Xylene	2.5	140	C_6H_5-	C_6H_5-	85	130—132/0.03	Found 5.88 Calcd. 5.76
$EtO\text{-}P(NEt_2)_2$	$C_6H_5NHCH_2CH_2OH$	—	3	120	EtO-	C_6H_5-	84.3	88—91/0.02	Found 6.79 Calcd. 6.64
$C_6H_5\text{-}P(NEt_2)_2$	$CH_3NHCH_2CH_2OH$	—	2.5	120	C_6H_5-	CH_3-	24.6	64—66/0.03	Found 7.83 Calcd. 7.74
$EtO\text{-}P{=}NC_6H_5$	$C_6H_5NHCH_2CH_2OH$	Toluene	5	110	EtO-	C_6H_5-	54.6	91—92/0.02	Found 6.70 Calcd. 6.64

It has recently been reported by Burgade[2] and Petrov et al.[3] that alcohols or phenols react with amido phosphites and amino phosphines to give the corresponding phosphites or phosphonites, with the elimination of the original amino groups.

In view of the finding that imido phosphites, amido phosphites or amino phosphines react with alcohols much more readily than amines, such phosphorous compounds may be expected to react with amino alcohols to form ω-aminoalkyl phosphites or phosphonites primarily. For instance, when 2-diethylamino-4-methyl-1, 3, 2-dioxaphospholane (V) is treated with an equimolar amount of *N*-phenyl ethanolamine in boiling toluene for 3 hr., β-anilinoethyl propylene phosphite (VI) is obtained in a 86% yield (Eq. 4):

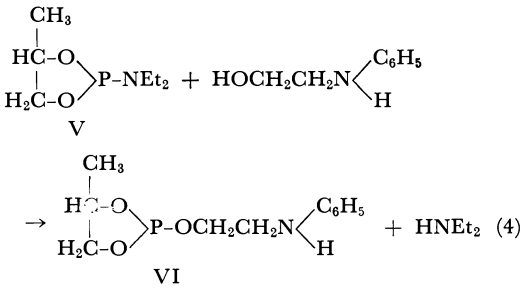

The structure of VI was confirmed by means of elemental analysis and a study of its infrared spectrum. The VI reacts with phenyl isocyanate to give a viscous oily product, the infrared spectrum of which shows the absorption at 1660 cm^{-1} due to the urea linkage. The liquid is readily hydrolyzed to give *N*-(β-hydroxyethyl)-*N*, *N'*-diphenyl urea (VII) in a good yield (Eq. 5):

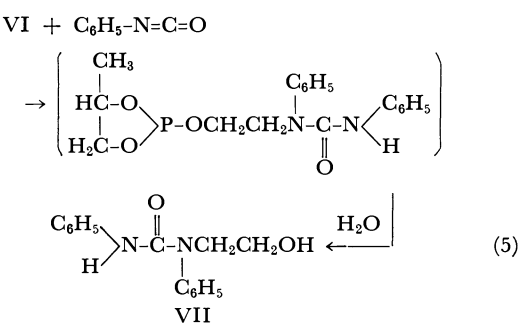

This fact shows that the nitrogen of the trivalent phosphorus-nitrogen bond is selectively replaced with the oxygen of the ethanolamine.

Further, when IV was treated with 2 mol. of *N*-phenyl ethanolamine while being refluxed in toluene for 5 hr., ethyl bis(β-anilinoethyl) phosphite (IXb) (b. p. 114—116°C/0.009 mmHg) was obtained in a 27% yield (Eq. 6):

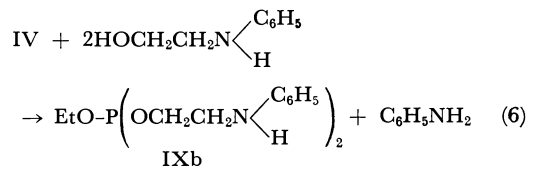

Similarly, when phenyl bis(diethylamino) phosphine (VIIIa) or ethyl bis(diethylamido) phosphite (VIIIb) was treated with 2 mol. of *N*-phenyl ethanolamine at 130°C for 4 hr., bis(β-anilinoethyl)phenyl phosphonite (IXa) or ethyl bis(β-anilinoethyl) phosphite (IXb) was obtained in a 69% or a 20% yield respectively (Eq. 7):

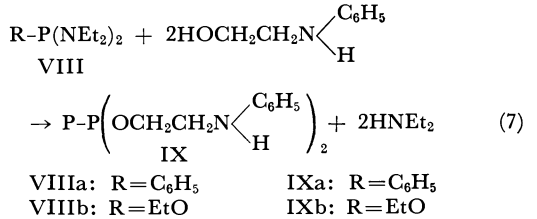

The resulting ethyl bis(β-anilinoethyl) phosphite or bis(β-anilinoethyl)phenyl phosphonite is rather unstable and is partly decomposed into *N*, *N'*-diphenyl piperazine (X) during distillation (Eq. 8):

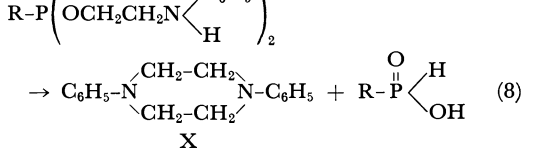

The solvents, yields, and physical properties of the bis(β-aminoethyl) phosphites and phosphonite as well as the results of elementary analyses of these substances, are listed in Table III.

On the other hand, when VIIIa or VIIIb was reacted with an equimolar amount of amino alcohol, 2, 3-diphenyl-1, 3, 2-oxazaphospholidine (XI) or 2-ethoxy-3-phenyl-1, 3, 2-oxazaphospholidine (XII) was obtained in a fairly good yield. In the case of the reaction of 1 mol. of ethyl *N*-phenylimino phosphite with 1 mol. of *N*-phenyl ethanolamine, 2-ethoxy-3-phenyl-1, 3, 2-oxazaphospholidine and ethyl bis(β-anilinoethyl) phosphite were obtained in 55 and 21% yields respectively, along with a small amount of *N*,*N'*-diphenyl piperazine (Eq. 9): The results are summarized in Table IV.

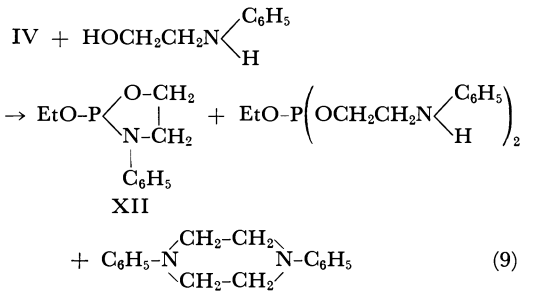

2) R. Burgada, a) *Ann. Chim.* (*France*), 347 (1963); b) *Bull. soc. chim. France*, **1963**, 2335.

3) K. A. Petrov, E. E. Nifantev, T. N. Lysenko and V. P. Evdakov, *Zh. Obshch. Khim.*, **31**, 2377 (1961).

The resulting cyclic phosphorous compounds may be expected to yield bis(β-aminoethyl) phosphite or phosphonite by the ring-opening addition of the other amino alcohol, as is shown in the following equation (10):

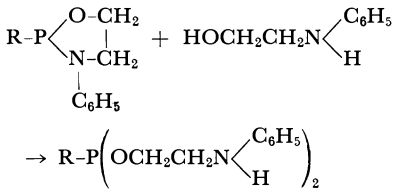

(10)

When 2, 3 - diphenyl-1, 3, 2-oxazaphospholidine was treated with an equimolar amount of *N*-phenyl ethanolamine in xylene, bis(β-anilinoethyl)phenyl phosphonite was obtained in a 31% yield; 15% of the cyclic phosphorous compound was also recovered.

Next, in order to prepare the corresponding urea derivatives of bis(β-aminoethyl) phosphorous compounds, the reaction of bis(β-anilinoethyl)phenyl phosphonite with 2 mol. of phenyl isocyanate was attempted. Contrary to our expectation, the urea could not be isolated, although 2-phenylimino-3-phenyl-1, 3-oxazolidine was obtained in a 58.5% yield. The unexpected oxazolidine formation may result in the subsequent decomposition of the initially-formed ureas. Futher study of this new synthesis of oxazolidine derivatives is now in progress.

Experimental

Materials.—Aminoalcohols and phenyl isocyanate were obtained commercially and purified by distillation. *N*-Phenylamino *N'*-phenylimino phosphine[4] (m. p. 246—248°C), ethyl phosphorodichloridite[5] (b. p. 48—50°C/80 mmHg), ethyl *N*-phenylimino phosphite[1] (b. p. 153—155°C/0.09 mmHg), phenyl phosphonous dichloride[6] (b. p. 59—61°C/2 mmHg) and 2-chloro-4-methyl-1, 3, 2-dioxaphospholane[7] (b. p. 75—76°C/50 mmHg) were prepared according to the methods in the literature.

The Preparation of Phenyl Bis(diethylamino) Phosphine.—A solution of phenyl phosphonous dichloride (179 g., 1.0 mol.) in 800 ml. of dry benzene was stirred, drop by drop over a period of 1.5 hr., into a solution of diethylamine (146 g., 2.0 mol.) and triethylamine (202 g., 2.0 mol.) in 300 ml. of dry benzene which had been cooled in an ice-water bath. The mixture was then stirred for another hour and subsequently heated to reflux. Triethylamine hydrochloride was removed by filtration. After the solvent had been removed under reduced pressure from the filtrate, the residue was distilled to give 217 g. (86.3%) of phenyl bis(diethylamino) phosphine (b. p. 123—125°C/0.2 mmHg).

Found: N, 11.08. Calcd. for $C_{14}H_{25}N_2P$: N, 11.10%.

By the same procedure, ethyl bis(diethylamido) phosphite was prepared in a 71.3% yield; b. p. 81—83°C/9 mmHg.

Found: N, 12.62. Calcd. for $C_{10}H_{25}N_2PO$: N, 12.73%.

The Preparation of 2-Diethylamino-4-methyl-1, 3, 2-dioxaphospholane.—A solution of diethylamine (75 g., 1.03 mol.) in 100 ml. of ligroin was vigorously stirred, drop by drop, into a solution of 2-chloro-4-methyl-1, 3, 2-dioxaphospholane (70 g., 0.5 mol.) in 300 ml. of ligroin which had been cooled in an ice-water bath. The mixture was then stirred for an additional 2 hr. at room temperature. Diethylamine hydrochloride was removed by filtration. After the solvent had been removed from the filtrate under reduced pressure, the residue was distilled to give 2-diethylamino-4-methyl-1, 3, 2-dioxaphospholane, (52 g., 59.1%; b. p. 67—68°C/6.5 mmHg).

Found: N, 7.85. Calcd. for $C_7H_{16}NPO_2$: N, 7.91%.

The Reaction of *N*-Phenylamino *N'*-Phenylimino Phosphine (I) (1 mol.) with Aniline (1 mol.).—A solution of aniline (1.86 g., 0.02 mol.) in 10 ml. of dry toluene was added to a solution of I (4.28 g., 0.02 mol.) in 10 ml. of dry toluene at room temperature. The mixture was then refluxed for 5 hr. After the solution had been cooled, the starting material was recovered as precipitates (2.30 g., 53.8%). The filtrate was concentrated under reduced pressure to give unidentified solids (2.09 g.; m. p. 139—169°C) which could not be purified further.

The Reaction of *N*-Phenylamino *N'*-Phenylimino Phosphine (I) (1 mol.) with Ethanol (1 mol.).—A solution of ethanol (0.46 g., 0.01 mol.) in 5 ml. of dry toluene was added to a solution of I (2.14 g., 0.01 mol.) in 15 ml. of dry toluene at room temperature. The reaction mixture was then refluxed for 5 hr., after which time the reaction mixture was concentrated and the separated I (0.45 g., 21%; m. p. 234—241°C) was removed by filtration. The filtrate was fractionated in vacuo to give curde triethyl phosphite (0.39 g., 23.3%; b. p. 54—58°C/16 mmHg) and aniline (0.21 g., 33.3%; b. p. 34—39°C/3 mmHg). The infrared spectrum of triethyl phosphite was identical with that of an authentic sample.

The Reaction of *N*-Phenylamino *N'*-Phenylimino Phosphine (I) (1 mol.) with Ethanol (3 mol.).—In the same manner 3 mol. of ethanol (1.38 g., 0.03 mol.) was allowed to react with I (2.14 g., 0.01 mol.) thus producing triethyl phosphite (0.76 g., 45.8%; b. p. 52—63°C/26 mmHg) and aniline (1.76 g., 94.7%; b. p. 74—86°C/27 mmHg).

By a similar procedure, several trialkyl and triaryl phosphites were obtained, as Table I shows.

The Reaction of Ethyl *N*-Phenylimino Phosphite (IV) (1 mol.) with Ethanol (2 mol.).—A solution of ethanol (0.92 g., 0.02 mol.) in 10 ml. of dry benzene was added to a solution of IV(1.67 g., 0.01 mol.) in 10 ml. of dry beznene at room temperature. The reaction mixture was refluxed for 3 hr. After the solvent had been removed, triethyl phosphite (1.21 g., 72.6%; b. p. 75—78°C/40 mmHg) and aniline (0.91 g.,

4) H. W. Grimmel, A. Guenther and J. F. Morgan, *J. Am. Chem. Soc.*, **68**, 539 (1946).
5) R. W. Young, K. H. Wood, R. J. Joyce and G. W. Anderson, ibid., **78**, 2126 (1956).
6) B. Buchner and L. B. Lockhart, Jr., "Organic Syntheses," **31**, 88 (1951).
7) H. J. Lucas, F. W. Mitchell, Jr., and C. N. Scully, *J. Am. Chem. Soc.*, **72**, 5491 (1950).

98.5%; b. p. 94—97°C/40 mmHg) were obtained by fractionation.

Similarly, some unsymmetrical phosphites were obtained, as is shown in Table II. In each case, a small amount of a mixture of various phosphites was formed by transesterification.

The Reaction of 2-Diethylamino-4-methyl-1, 3, 2-dioxaphospholane (V) (1 mol.) with *N*-Phenyl Ethanolamine (1 mol.).—A solution of V (10.62 g., 0.06 mol.) and *N*-phenyl ethanolamine (8.22 g., 0.06 mol.) in 20 ml. of dry toluene was refluxed for 3 hr. After the solvent and the evolved diethylamine had been removed under reduced pressure, the residure was distilled in vacuo, giving β-anilinoethyl propylene phosphite (12.5 g., 86.3%; b. p. 107—109°C/0.1 mmHg). Redistillation gave the pure phosphite (b. p. 107—109°C/0.1 mmHg).

Found: N, 5.89. Calcd. for $C_{11}H_{16}NPO_3$: N, 5.81%.

The Reaction of β-Anilinoethyl Propylene Phosphite (VI) (1 mol.) with Phenyl Isocyanate (1 mol.).—A solution of phenyl isocyanate (1.19 g., 0.01 mol.) in 10 ml. of dry toluene was added, drop by drop, to a solution (2.41 g., 0.01 mol.) of VI in 10 ml. of dry toluene. After an initial exothermic reaction had ceased, the reaction mixture was refluxed for 3 hr. After the solvent had then been removed under reduced pressure, an oily substance was obtained. The oily substance was solidified, with a slight heat liberation, by treatment with 5 ml. of water. The solid was filtered to give 2.46 g. (68.4%) of *N*-(β-hydroxyethyl)-*N*, *N'*-diphenyl urea (m. p. 80—83°C; recrystallized from ethyl acetate, m. p. 82—83°C).

Found: C, 69.92; H, 6.42; N, 11.23. Calcd. for $C_{15}H_{16}N_2O_2$: C, 70.29; H, 6.29; N, 10.94%.

The Reaction of Ethyl *N*-Phenylimino Phosphite (IV) (1 mol.) with *N*-Phenyl Ethanolamine (2 mol.).—A solution of IV (1.67 g., 0.01 mol.) and *N*-phenyl ethanolamine (2.74 g., 0.02 mol.) in 20 ml. of dry toluene was refluxed for 5 hr. After the solvent had been removed under reduced pressure, the residue was distilled, in vacuo giving aniline (0.19 g., 22%; b. p. 34—35°C/2 mmHg) and ethyl bis(β-anilinoethyl) phosphite (0.94 g., 27%; b.p. 114—116°C/0.009 mmHg); a tarry residue also remained. From this residue, *N*, *N'*-diphenyl piperazine (0.12 g.; m. p. 163—165°C) was extracted with boiling toluene; the residual substance gave an unidentified gray colored solid (m. p. 235°C).

The Reaction of Phenyl Bis(diethylamino) Phosphine (VIIIa) (1 mol.) with *N*-Phenyl Ethanolamine (2 mol.)—A mixture of VIIIa (5.04 g., 0.02 mol.) and *N*-phenyl ethanolamine (5.48 g., 0.04 mol.) was heated at 125—135°C (oil bath temperature) for 4 hr. After the diethylamine had been removed under reduced pressure, the residue was distilled in vacuo to give bis(β-anilinoethyl)phenyl phosphonite (5.27 g., 69.4%; b. p. 105—107°C/0.001 mmHg). Its infrared spectra showed absorption bands at 3350 (m), 1430 (m), 1175 (m), 1050(s), and 925(s) cm^{-1}.

Found: N, 7.45. Cacld. for $C_{22}H_{25}N_2PO_2$: N, 7.37%.

In a similar way, ethyl bis(β-anilinoethyl) phosphite, ethyl bis(β-ethylaminoethyl) phosphite and ethyl bis-(β-methylaminoethyl) phophite were prepared by the reactions of the corresponding ethanolamines with ethyl bis(diethylamido) phosphite (Table III).

The Reaction of Ethyl Bis(diethylamido) Phosphite (VIIIb) (1 mol.) with *N*-Phenyl Ethanolamine (1 mol.).—A mixture of VIIIb (22 g., 0.1 mol.) and *N*-phenyl ethanolamine (13.7 g., 0.1 mol.) was heated at 120—130°C (oil bath temperature) for 3 hr. The diethylamine was then collected in a trap cooled in an ice-water bath. The reaction mixture was distilled under reduced pressure to give 2-ethoxy-3-phenyl-1, 3, 2-oxazaphospholidine (17.79 g., 84.3%; b. p. 88—91°C/0.02 mmHg). Its infrared spectra displayed absorption bands at 1304(s), 1150(w), 1030(s), and 920(s) cm^{-1}.

Found: N, 6.79; mol. wt. (Ebulliometric) 218. Calcd. for $C_{10}H_{14}NPO_2$: N, 6.64%; mol. wt. 211.

In a similar way, 2, 3-diphenyl-1, 3, 2-oxazaphospholidine and 2-phenyl-3-methyl-1, 3, 2-oxazaphospholidine were prepared from phenyl bis(diethylamino) phosphine and the corresponding ethanolamines, as is shown in Table IV.

The Reaction of Ethyl *N*-Phenylimino Phosphite (IV) (1 mol.) with *N*-Phenyl Ethanolamine (1 mol.).—A solution of IV (16.7 g., 0.1 mol.) and *N*-phenyl ethanolamine (13.7 g., 0.1 mol.) in 200 ml. of dry toluene was refluxed for 5 hr. After the solvent had been removed, the residue was fractionated into four major fractions. Fraction 1: aniline (5.77 g., 62.2%; b. p. 58—64°C/6 mmHg). Fraction 2: 2-ethoxy-3-phenyl-1, 3, 2-oxazaphospholidine (11.48 g., 54.6%; b. p. 91—92°C/0.02 mmHg). (This fraction shows an infrared spectrum identical with that of the 2-ethoxy-3-phenyl-1, 3, 2-oxazaphospholidine obtained in the above experiment). Fraction 3: ethyl bis(β-anilinoethyl) phosphite (3.59 g., 20.6%; b. p. 117—119°C/0.03 mmHg). (Its infrared spectra shows absorption bands at 3350(m), 1270(s), 1150(m), 1020(s), 900(s) cm^{-1}. Fraction 4: 6.58 g., b. p. 131—151°C/0.006 mmHg. This fraction was partly solidified. The fraction was extracted with boiling toluene. After the extract had been cooled, *N*, *N'*-diphenyl piperazine (0.89 g., m. p. 163—165°C) was obtained. Recrystallization from toluene raised the melting point to 166—167°C, and the melting point was undepressed on admixture with an authentic sample.

Found: C, 79.63; H, 8.09; N, 11.96. Calcd. for $C_{16}H_{18}N_2$: C, 80.67; H, 7.57; N, 11.77%.

The Reaction of 2, 3-Diphenyl-1, 3, 2-Oxazaphospholidine (XII) (1 mol.) with *N*-Phenyl Ethanolamine (1 mol.)—A solution of XII (2.84 g., 0.01 mol.) and *N*-phenyl ethanolamine (1.53 g., 0.01 mol.) in 7 ml. of dry xylene was refluxed for 4 hr. After the solvent had been removed, the residue was fractionated into two fractions. Fraction 1: 0.65 g. (42.2%); b. p. 82—84°C/0.005 mmHg. (The infrared spectrum of the product was identical with that of *N*-phenyl ethanolamine). Fraction 2: 3.07 g., b. p. 104—110°C/0.008 mmHg. After this substance had stood in a refrigerator, 0.43 g. (15%) of XII (m. p. 75—77°C) was recovered. After the XII had been removed by filtration, the residue was distilled to give 1.39 g. (31%) of bis(β-anilinoethyl)phenyl phosphonite (b. p. 124—126°C/0.03 mmHg).

The Reaction of Bis(β-anilinoethyl) Phenyl Phosphonite (IXa) with Phenyl Isocyanate.—A solution of phenyl isocyanate (2.38 g., 0.02 mol.) in 10 ml. of dry toluene was stirred, drop by drop, into a solution of IXa (3.80 g., 0.01 mol.) in 10 ml. of dry

toluene at room temperature. After an initial exothermic reaction had ceased, the reaction mixture was refluxed for 3 hr. The solvent was removed under reduced pressure, and an oily substance was obtained. After the oily substance had been stored for several days at room temperature, a small amount of a white crystalline compound was precipitated. When 5 ml. of 99.5% ethanol was added to the mixture, a white crystalline compound (1.44 g., 58.5%; m. p. 115—116°C) was again obtained. This crystalline compound was purified by recrystallization from ethanol (m. p. 117—118°C). The compound was identical in its infrared spectrum with that of an authentic 2-phenylimino-3-phenyl-1, 3-oxazolidine[8] and with the results of the elemental analysis.

Found: C, 75.60; H, 6.11; N, 11.83. Calcd. for $C_{15}H_{14}N_2O$: C, 75.63; H, 5.83; N, 11.76%.

The authors wish to thank the Bridgestone Tire Co., Ltd., especially, its General Director, Mr. Kunio Yasutake, for permission to publish this work; they wish also to acknowledge the helpful advice given by Mr. Yoshitake Kubota and the late Mr. Koshiro Fujiwara.

8) H. Nohira, Y. Nishikawa and T. Mukaiyama, This Bulletin, **37**, 797 (1964).

BULLETIN OF THE CHEMICAL SOCIETY OF JAPAN VOL. 39 219—222 (1966)

The Fluorination of Ethylene and Ethane*

By Shunji NAGASE,† Kiyoshi TANAKA,†† Hajime BABA† and Takashi ABE†

† *Government Industrial Research Institute, Nagoya, Kita-ku, Nagoya*

†† *Research Laboratories, Central Glass Co., Ltd., Ohte-machi, Chiyoda-ku, Tokyo*

(Received March 15, 1965)

Ethylene and ethane were electrochemically fluorinated in an electrolytic fluorination cell equipped with a bubbler. Several fluorinated ethanes were obtained from these samples in reasonable total-yields with reasonable current efficiencies. The influence of operating conditions on the reaction was investigated. A probable mechanism was described for the formation of the characteristic procucts obtained in the fluorination reaction.

There have been a number of papers dealing with the fluorination of substituted ethylenes by various methods. However, no successful report has yet described the fluorination of ethylene itself by an electrochemical process.[1] The present work was carried out in order to examine the possibility of the electrochemical fluorination of ethylene which may undergo polymerization, fragmentation, or simple fluorination. It has been found that ethylene can be fluorinated without difficulty by using an electrolytic fluorination cell equipped with a bubbling arrangement[2]; fluorinated ethanes are thus produced in a reasonable yield and at a reasonable current efficiency. The electrochemical fluorination of ethane, which has already been reported briefly by Sartori,[3] was also carried out in order to compare the results with those of ethylene.

A representative mechanism will be described to account for the formation of the characteristic products obtained in the present electrochemical fluorination.

Experimental

Materials. — The ethylene, obtained from the Ohio Chemical & Surgical Equipment Co., was more than 99.5% pure. The ethane (99.7% pure) was obtained from the Takachiho Chemical Industrial Co. The hydrogen fluoride (more than 99% pure) was supplied by the Daikin Industries Co. The diluent employed was Airco helium gas.

Apparatus and Procedure.—The apparatus used for this fluorination was essentially the same as that used for the fluorination of methane.[2] The characteristic part of the fluorination cell was the bubbler. Many minute bubbles of the sample gas were produced in hydrogen fluoride by the use of this bubbler.

The experimental procedure was as follows. Hydrogen fluoride (1 l.) was placed in the cell, and before the introduction of the sample, electrolysis was carried out in a nitrogen atmosphere in order to remove a trace of an impurity; the electrolysis was carried out at an anodic current density of 2.7 amp./dm^2 and at 5—6°C until the cell voltage rose to 6.0 V. Then sodium fluoride was added, and the metered sample was introduced from the bottom of the cell, through the bubbler, into hydrogen fluoride maintained at 6—7°C,

* "Electrochemical Fluorination of Gases" Part II.

1) After this work had been completed, the authors read a review article (M. Schemisser and P. Sartori, *Chemie-Ing.-Techn.*, **36**, 9 (1964)) stating that the electrochemical fluorination of ethylene was not accomplished due to the polymerization of ethylene.

2) S. Nagase, K. Tanaka and H. Baba, This Bulletin, **38**, 834 (1965).

3) P. Sartori, *Angew. Chem.*, **75**, 417 (1963).

using a calibrated flow meter connected to a sample cylinder. In a few experiments, helium was admitted simultaneously with the sample into the bubbler. The sample was fluorinated at the anodic current density of 2.2 amp./dm^2. When the cell voltage became almost steady at 6—6.5 V. (after about 1 hr.), traps were immersed in ice and liquid nitrogen respectively, and electrolysis was carried out for the designated amp.-hr. period. Since the bubbler was found to be very effective in the fluorination of methane, all the present reactions were carried out using the bubbler.

The fluorinated gas evolved from the cell was passed through a condenser kept at −15°C and over sodium fluoride pellets in order to remove the hydrogen fluoride; then it was bubbled through a sodim sulfite solution containing a small amount of potassium iodide in order to eliminate a trace amount of explosive oxygen difluoride. The gas was subsequently passed through a trap in ice, and finally condensed in two traps placed in series in liquid nitrogen. Fluorination took place smoothly in all the experiments.

The product thus obtained was rectified in a low-temperature rectification unit and weighed in a glass ampule. The molecular weight of each fraction was measured by means of gas density balance. The mixture was then further separated by gas chromatography, using an activated charcoal column (2 m.) maintained at 120°C, using helium as the carrier.

The Fluorination of Ethylene.—The reaction conditions of six representative runs, and a typical example of the results of low-temperature rectification and chromatographic separation are given in Tables I and II respectively. As in the case of the fluorination of methane, the quantitative analysis by means of a gas chromatograph of the separated component was made on the assumption that the ratio of the peak areas of chromatogram is a direct measure of the percentage weight of the components.[4] However, in the case of fraction 1, which consisted of tetrafluoromethane, ethylene, and hexafluoroethane, the latter two components were not separated from each other chromatographically under the conditions applied; therefore this fraction was analyzed quantitatively by the use of the baseline method for the infrared spectrum.

Fraction 2 corresponded to hexafluoroethane but was contaminated by a negligible amount of trifluoromethane. Rather unexpectedly, ethane was also contained in this fraction, obtained from runs 2 and 5, in the amounts of 3 and 5 mol.% of the total fractions. (The amount of ethane was determined by means of the baseline method for the infrared spectrum).

Fraction 3 consisted of 1, 1, 1-trifluoroethane and pentafluoroethane. The azeotropic mixture of these two compounds is known to boil at −45°C.[5] Fraction 4 consisted of a mixture of isomers of 1, 1, 1, 2-tetrafluoroethane and 1, 1, 2, 2-tetrafluoroethane with the observed molecular weight of 102 to 103. The boiling point of the azeotropic mixture of these two compounds is known to be −29°C.[5]

Fraction 5 consisted mainly of a mixture of 1, 1-difluoroethane and 1, 1, 2, 2-tetrafluoroethane, plus a

4) M. J. Root, "Gas Chromatography," Ed. by V. J. Coates, H. J. Noebels and I. S. Fagerson, Academic Press, New York (1958), p. 99.

5) J. A. Cuculo and L. A. Bigelow, *J. Am. Chem. Soc.*, **74**, 710 (1952).

TABLE I. CONDITIONS FOR FLUORINATION OF ETHYLENE[a]

Run No.	Total amount of C_2H_4 fed mol.	NaF used g.	He used ml./min	Temp. °C	Note
1	0.274	10	0	7—8	Effect of feed rate
2	0.446	10	0	6—7	
3	0.218	50	0	6—7	Effect of NaF
4	0.283	10	104[b]	6—7	Effect of diluent
5	0.563	10	150[c]	6—7	
6	0.309	10	0	16—17	Effect of temp.

a) Electrolysis was carried out for 76 amp.hr. in all the experiments.
b) Dilution ratio (C_2H_4: He) was 1: 4 by volume.
c) Dilution ratio (C_2H_4: He) was 1: 3 by volume.

TABLE II. RECTIFICATION OF FLUORINATED ETHYLENE[a]

Fract. No.	B. p., °C	Wt., g.	Component[b]
1	−105——100	8.7	CF_4(trace),[c] CH_2=CH_2, CF_3CF_3[c]
2	−90——77	5.9	CF_3CF_3, CHF_3 (trace),[c] CH_3CH_3
3	−49——45	9.3	CF_3CH_3,[d] CF_3CHF_2[c]
4	−29——23	5.0	CF_3CH_2F, CHF_2CHF_2
5	Hold up	3.9	CHF_2CH_3,[d] CHF_2CHF_2, X

a) This example was taken from the result of low-temperature rectification and chromatographic separation of the products obtained in run 2.
b) The components of each fraction in this table and in Table IV were arranged in the order of the peak appearance of gas chromatogram.
c,d) The infrared spectra of these compounds respectively agree with those listed in Weiblen's "Fluorine Cehmistry," Vol. II, Ed. by J. H. Simons, Academic Press Inc., New York (1954), p. 469, and "Infrared Spectral Data," American Petroleum Institute, Research Project 44, Carnegie Institute Technology, 1959, Serial number 977 and 979.

TABLE III. CONDITIONS FOR FLUORINATION OF ETHANE[a]

Run No.	Total amount of C_2H_6 fed mol.	NaF used g.	He used ml./min.	Temp. °C	Note
1	0.517	10	0	6—7	Effect of feed rate
2	0.607	10	0	6—7	
3	0.481	50	0	6—7	Effect of NaF
4	0.506	10	107[b]	6—7	Effect of diluent
5	0.573	10	0	16—17	Effect of temp.

a) Electrolysis was carried out for 108 amp.hr. in all the experiments.
b) Dilution ratio (C_2H_6: He) was 1 : 3 by volume.

Table IV. Rectification of fluorinated ethane[a]

Fract. No.	B. p., °C	Wt. g.	Component
1	−95——92	25.8	CF_4(trace), CF_3CF_3, CH_3CH_3
2	−91——89	2.4	CH_3CH_3
3	−50——46	6.5	CF_3CH_3, CF_3CHF_2
4	−29——22	3.2	CF_3CH_2F, CHF_2CHF_2
5	Hold up	2.8	CF_3CH_2F, CHF_2CHF_2

a) This example was taken from run 2.

small amount of a compound, X, which could not be identified chemically or spectroscopically.

A small amount (0.2—0.4 g.) of a tarry polymeric material whose infrared spectrum showed the presence of a C-F bond and a C-H bond was found in the residue in the electrolytic cell after the distillation of hydrogen fluoride from the cell.

The Fluorination of Ethane.—The fluorination of ethane was carried out under the reaction conditions shown in Table III. Table IV shows a typical example of the results of low-temperature rectification and chromatographic separation. The products were analyzed quantitatively by a method similar to that used for ethylene. Fraction 1 consisted of an azeotropic mixture of hexafluoroethane and ethane, along with an insignificant amount of tetrafluoromethane. The elements of this azeotropic mixture, reported to boil at −92°C,[6] could not be separated from each other by gas chromatography under the conditions used. In a few runs, a negligible amount of trifluoromethane was detected in this fraction.

Fraction 2 corresponded to ehtane, but it was often contaminated with hexafluoroethane. Fractions 3 and 4 were essentially the same as those of fractions 3 and 4 in Table II. The components of fraction 5 were the same as those of fraction 4. In the other runs, however, an unidentified compound whose infrared spectrum was identical with that of the compound X obtained from ethylene was present.

It was interesting that monofluoroethane* was obtained in a considerable amount under the mild reaction conditions of run 4.

Results and Discussion

The results obtained from the fluorination of ethylene and ethane are summarized in Tables V and VI respectively; these results show that the milder and controllable fluorination reaction can be carried out by the use of an electrolytic cell equipped with a bubbler.

Table V. Collected results in the fluorination of ethylene

Run No.	Total yield mol.%	Total current eff., %[a]	Product comp., mol.%							
			CF_3CF_3	CF_3CHF_2	CF_3CH_2F	CHF_2CHF_2	CF_3CH_3	CHF_2CH_3	CF_4	X[b]
1	78.0	60.8	46.2	17.1	9.3	14.4	6.2	4.3	2.5	0
2	50.3	56.1	23.6	9.6	18.0	7.9	32.3	8.6	trace	1.2
3	73.5	42.9	36.5	14.6	13.7	20.7	7.3	5.9	1.3	2.2
4	79.9	59.3	36.8	12.6	10.5	19.7	6.7	11.4	2.3	0
5	44.5	59.6	18.2	16.8	22.1	16.0	19.2	4.8	2.9	2.0
6	73.2	57.7	28.2	16.6	16.1	20.3	12.0	6.0	0.8	0

a) The calculation of current efficiency was based on the amount of current assumed to be necessary for forming fluorine with a discharging fluoride ion which would react with the sample according to the following equations. Total current efficiency shown is the sum total of the current efficiency for each component.

$C_2H_4 + 10F = CF_3CF_3 + 4HF$ (1)
$C_2H_4 + 8F = CF_3CHF_2 + 3HF$ (2)
$C_2H_4 + 6F = CF_3CH_2F + 2HF$ (3)
$C_2H_4 + 6F = CHF_2CHF_2 + 2HF$ (4)
$C_2H_4 + 5F + H = CF_3CH_3 + 2HF$ (5)
$C_2H_4 + 3F + H = CH_3CHF_2 + HF$ (6)
$C_2H_4 + 12F = 2CF_4 + 4HF$ (7)

b) The amounts of X were given in unit of grams in this table and in Table VI.

Table VI. Collected results in the fluorination of ethane

Run No.	Total yield mol.%	Total current eff., %[a]	Product comp., mol.%						
			CF_3CF_3	CF_3CHF_2	CF_3CH_2F	CHF_2CHF_2	CF_3CH_3	CH_2FCH_3	X
1	48.5	65.0	56.2	14.2	12.1	10.3	7.2	0	0.9
2	40.7	62.2	51.2	14.8	13.4	10.4	10.2	0	0
3	40.4	49.6	49.5	20.6	10.3	13.9	5.7	0	1.6
4	48.1	52.7	44.8	8.6	10.7	9.4	7.5	19.0	1.8
5	54.1	79.6	53.0	13.0	12.1	17.9	4.0	0	1.9

a) The calculation of the current efficiency shown was made on the similar assumption to that in the case of ethylene, for instance, $C_2H_6 + 12F = C_2F_6 + 6HF$

6) J. D. Calfee, N. Fukuhara and L. A. Bigelow, ibid., **61**, 3552 (1939).

* The reference infrared spectrum obtained from the American Petroleum Institute, serial number 1302, was identical with this product.

With regard to the partial fluorination of these samples, the results obtained were not as striking as for methane.[1] The sample feed rate had a large effect, especially on the partial fluorination of ethylene. A higher feed rate made the reaction milder and gave less hexafluoroethane in the products. The amount of sodium fluoride and the electrolysis temperature also affected the results in the present experiments. Above all, the dilution of the feed with helium appeared to make the reaction milder and to give a large amount of less-fluorinated ethane from ethylene and a considerable amount of monofluoroethane from ethane.

Except for a kinetic study of fluorine addition to ethylene,[7] no information has been available on the fluorination of ethylene with elementary fluorine, but the kind and the ratio of the reaction products reported here appeared to be very close to what might be expected from the very mild fluorination of ethylene with elementary fluorine. Furthermore, the characteristics associated with the results obtained from the fluorination of ethane were comparable in many respects to those obtained from the vapor-phase fluorination of ethane with elementary fluorine,[6,8,9] which is known to proceed via a free-radical mechanism.

The fluorinating agent and the reaction mechanism in electrochemical fluorination are much in dispute.[10] However, the basic reaction which takes place during the present fluorination appears very likely to be a free-radical reaction on the anode surface. The effective dispersion of the reaction heat, the good agitation, the sparing solubility of the sample and fluorinated products, and the reaction in the very inert solvent, hydrogen fluoride, to fluorinating agent may account for the mildness of this fluorination reaction.

The important products from ethylene were 1, 1-difluoroethane and 1, 1, 1-trifluoroethane, which was isolated in a considerable amount. The formation of these may perhaps be represented simply as follows:

$$CH_2{=}CH_2 \xrightarrow{[F]} \underset{(I)}{CH_2F\text{-}CH_2F} \xrightarrow{-HF} \underset{(II)}{CHF{=}CH_2}$$

$$\xrightarrow{HF} \underset{(III)}{CHF_2\text{-}CH_3} \xrightarrow{[F]} \underset{(IV)}{CF_3CH_3}$$

The initial product I, which is well known to be unstable, may undergo dehydrofluorination to give II under these reaction conditions. The addition of hydrogen fluoride to II, which is known to proceed readily in accordance with Markownikoff's rule,[11] could yield III, which could be further fluorinated to give IV. The increasing stability of compounds with fluorine atoms attached to the same carbon atom[12] may suggest a possible pathway, although the reaction could and probably did follow different routes simultaneously.

In the case of ethane, which did not afford 1, 1-difluoroethane in a detectable amount, such isomerization could have occurred to a certain extent, but the lower concentration of the initial product I compared with that from ethylene can account for the observed fact. Ethylene may always give I in the initial step of the reaction.

A quite unexpected and interesting by-product from ethylene was ethane. It is believed that this was formed by the cathodic reduction of ethylene. Only one report has described the cathodic reduction, and that not in a typical electrochemical fluorination.[13]

The formation of a detectable amount of any other compound with a double bond or more carbon atoms than the parent compounds could not be confirmed through the experiments.

Summary

The electrochemical fluorination of ethylene and ethane has been carried out using a cell equipped with a bubbling arrangement. It appeared that the fluorination reaction could be controlled, especially for ethylene, in order to obtain either perfluoroethane or partially-fluorinated ethanes preferentially, in a reasonable yield and with reasonable current efficiency.

From ethylene, without any significant polymerisation or fragmentation, hexafluoroethane, pentafluoroethane, 1, 1, 1, 2-tetrafluoroethane, 1, 1, 2, 2-tetrafluoroethane, 1, 1, 1-trifluoroethane, 1, 1-difluoroethane, tetrafluoromethane, and a reduced product, ethane, and an unidentified minor product were formed. Ethane afforded similar fluorinated ethanes, together with monofluoroethane and a trace of tetrafluoromethane, but not 1,1-difluoroethane.

The influence of the operating conditions on these fluorination reactions and the mechanism involved have been discussed.

The authors wish to express their deep thanks to the Daikin Industries Co. for supplying some of the materials, and to Dr. Kan Inukai of this Institute for his interest in this work.

7) G. A. Kapralova, L. Yu. Rusin, A. M. Chaikin and A. E. Shilov, *Dokl. Akad. Nauk, SSSR*, **150**, 1282 (1963).
8) D. S. Young, N. Fukuhara and L. A. Bigelow, *J. Am. Chem. Soc.*, **62**, 1171 (1940).
9) E. A. Tyczkowski and L. A. Bigelow, ibid., **77**, 3007 (1955).
10) For example, see J. Burdon and J. C. Tatlow, "Advances in Fluorine Chemistry," Vol. I, Ed. by M. Stacey, J. C. Tatlow and A. G. Sharpe, Butterworths Scientific Publications, London (1959), p. 160.
11) A. M. Lovelace, D. A. Rausch and W. Postelnek, "Aliphatic Fluorine Compounds," Reinhold Publishing Co., New York (1958), p. 14.
12) J. Hine, *J. Am. Chem. Soc.*, **85**, 3239 (1963).
13) H. Schmidt and H. D. Schmidt, *J. pr. Chem.*, **2**, 105 (1955).

BULLETIN OF THE CHEMICAL SOCIETY OF JAPAN VOL. 39 223—227 (1966)

A Spectrophotometric Study of the Complex Formation between Iron(III) and Sulfosalicylic Acid

By Kin'ya OGAWA and Nobuko TOBE

Hitachi Research Laboratory, Hitachi, Ltd., Hitachi, Ibaraki

(Received April 8, 1965)

A spectrophotometric study of the complex formation between iron(III) and sulfosalicylic acid was carried out over the pH range up to 8; further, an attempt was made to test the applicability of sulfosalicylic acid as a reagent for the spectrophotometric determination of iron(III) in the presence of iron(II). The absorption maxima are found at 510 mμ independently of the pH between 1 to 2.5, while they shift in the direction of shorter wavelength as the pH rises. It was concluded that three complex species, Fe(Su), $Fe(Su)_2^{3-}$, and $Fe(Su)_3^{6-}$, are formed successively in acid solutions; their stability constants were determined to be:

$$\frac{[Fe(Su)]}{[Fe^{3+}][Su^{3-}]}=1.13\times10^{14} \qquad \frac{[Fe(Su)_2^{3-}]}{[Fe^{3+}][Su^{3-}]^2}=2.14\times10^{24} \qquad \frac{[Fe(Su)_3^{6-}]}{[Fe^{3+}][Su^{3-}]^3}=1.25\times10^{33}$$

where Su^{3-} denotes the sulfosalicylate anion, $C_6H_3(O^-)(COO^-)(SO_3^-)$. If the pH of the solution is adjusted from 3 to 4.5 and if the absorbancy measurements are made at 480 to 490 mμ, sulfosalicylic acid can be used as a reagent for determining iron(III) in the presence of iron(II). The optimum concentration of iron(III) is 2 to 10 p. p. m.; iron(II) does not interfere, even at a concentration of 100 p. p. m.

Sulfosalicylic acid, because it gives characteristic colors with iron(III), has been known as a reagent[1] for the colorimetric determination of iron(III). However, though several investigators have studied this complex-forming reaction, there have been some discrepancies between their results. For instance, Foley and Anderson[2,3] studied this reaction spectrophotometrically; they concluded that a 1 to 1 complex was formed in the pH range up to 8. On the other hand, Banks and Patterson[4] reported in their polarographic investigation that the molar ratio of sulfosalicylic acid to iron(III) in a complex formed in a solution of pH 9 was 3 to 1. Afterwards, Ågren[5] and Vareille[6] demonstrated the formation of more than one complex in their potentiometric and photometric studies.

The present study was undertaken in order to make possible a choice between the above alternative explanations and to test the applicability of sulfosalicylic acid as a reagent for determining spectrophotometrically iron(III) in the presence of iron(II).

1) E. B. Sandell, "Colorimetric Determination of Traces of Metal," 3rd. Ed., Interscience Publishers, New York (1959), p. 544.
2) R. T. Foley and R. C. Anderson, *J. Am. Chem. Soc.*, **70**, 1195 (1948).
3) R. T. Foley and R. C. Anderson, ibid., **72**, 5609 (1950).
4) C. V. Banks and J. H. Patterson, ibid., **73**, 3062 (1951).
5) A. Ågren, *Acta Chem. Scand.*, **8**, 266 (1954); *Chem. Abstr.*, **48**, 11970 (1954).
6) L. Vareille *Bull. Soc. Chim. France*, **1955**, 870; *Chem. Abstr.*, **49**, 12173 (1955).

Experimental

Reagents.—A standard solution of iron(III) was prepared by dissolving ammonium iron(III) sulfate, $Fe_2(SO_4)_3(NH_4)_2SO_4\cdot24H_2O$, in sulfuric acid. A standard solution of iron(II) was prepared by dissolving ammonium iron(II) sulfate, $FeSO_4(NH_4)_2SO_4\cdot6H_2O$, in sulfuric acid. The final concentration of acid in these solutions was adjusted to about 0.05 N. A solution of sulfosalicylic acid was prepared by dissolving a commercial product, $C_6H_3(OH)(COOH)(SO_3H)\cdot2H_2O$, in distilled water. For the adjustment of the pH, 1 N hydrochloric acid (pH<2), a 0.5 M monochloroacetic acid - sodium hydroxide solution (pH 2—3), a 1 M acetic acid - sodium acetate solution (pH 3—6.5), and a 1 M ammonium chloride - ammonium hydroxide solution (pH>7.5) were used. All the chemicals used were of the reagent grade.

Apparatus.—The absorption curves were recorded by using a Hitachi EPS-2-type Automatic Pen Recording Spectrophotometer, while a Hitachi EPU-2A-type Spectrophotometer was used for the absorbancy measurements. These spectrophotometers were equipped with absorption cells 10 mm. thick. The pH values were measured with a Horiba M-3-type pH meter equipped with a glass electrode.

Procedures.—An aliquot of a standard solution of iron(III) was taken, and the pH was adjusted to the required value by adding a buffer solution. After an aliquot of a solution of sulfosalicylic acid had been added, the solution was diluted to 100 ml. with distilled water. An absorbancy measurement was made on a part of the resulting solution within 3 hr. after the solution had been prepared, and, if necessary, an absorption curve

covering the range from 400 to 600 mμ was recorded and the pH was measured for the other part.

Preliminary experiments showed that solutions containing both 1.83×10^{-4} M of iron(III) and 7.3×10^{-3} M of sulfosalicylic acid gave the same absorption curves after 3 hr. of standing at room temperature for each pH value: 3.4, 4.5 and 5.2.

Results and Discussion

The Effects of the pH Values on the Absorption Curves.—Figure 1 shows the absorption curves for the solutions which contain 1.83×10^{-4} M of iron(III) and 8×10^{-3} M of sulfosalicylic acid at different pH values. The absorption maxima are found at 510 mμ independently of the pH between 1 to 2.5, while they shift to shorter wavelength as the pH rises. These color variations, from violet through deep red or rose in acid solutions to yellow in alkaline, suggest that more than one complex may be formed in aqueous solutions.

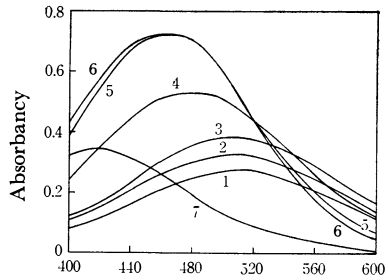

Fig. 1. Absorption curves. Solutions were 1.83×10^{-4} M in iron(III) and 8×10^{-3} M in sulfosalicylic acid.
Curve 1, at pH 1.38 in 0.05 M hydrochloric acid: 2, at pH 2.00; 3, at pH 2.49 in 0.05 M of total monochloroacetate: 4, at pH 3.08; 5, at pH 4.40; 6, at pH 5.34 in 0.05 M of total acetate: 7, at pH 7.88 in 0.05 M of total ammonium

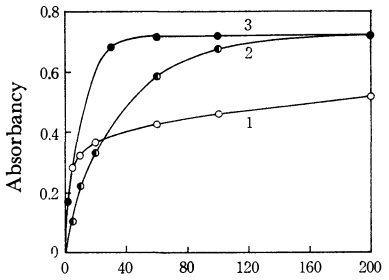

Fig. 2. Relation between absorbancy and C_{Su}/C_{Fe}, keeping C_{Fe} at 1.83×10^{-4} and varying C_{Su} up to 3.66×10^{-2} M in 0.05 M of total acetate.
Curve 1, at pH 3.39 for 480 mμ; 2 at pH 4.46 for 470 mμ; 3, pH 5.20 for 470 mμ

The Effects of the Molar Ratio of Sulfosalicylic Acid to Iron(III).—The relations between the absorbancies and the molar ratios of sulfosalicylic acid to iron(III) in solutions were obtained at different pH values; the results are shown in Fig. 2. In a solution of pH 5.20, a constant absorbancy is obtained with increasing molar ratios of over sixty parts of sufosalicylic acid to one of iron(III), while solutions in the lower pH region do not level off to a constant absorbancy in spite of the presence of more than a hundred moles of sulfosalicylic acid to one mole of iron(III). Judging from this, higher complexes seem to be produced successively with an increasing concentration of sulfosalicylic acid.

The Composition of the Complex.—The compositions of the complexes were determined by applying the continuous variation method.[7] Figure 3 shows the results obtained at different pH values by plotting Y, the difference between the observed absorbancy and that calculated assuming no complex formation, against the ratio of the total concentration of sulfosalicylic acid, C_{Su}, to the sum of the total concentration of iron(III) and that of sulfosalicylic acid, $C_{Fe}+C_{Su}$. The maximum value of Y in curve 1 occurs at a ratio of 0.5, indicating that a 1 to 1 complex is formed here. In curve 2 the maximum value of Y is found at a ratio of 0.6, and in curve 3, at a ratio of 0.75; this suggests that complex species in which the molar ratios of sulfosalicylic acid to iron(III) are 2 to 1 and/or 3 to 1 are formed in addition to the 1 to 1 complex at higher pH values.

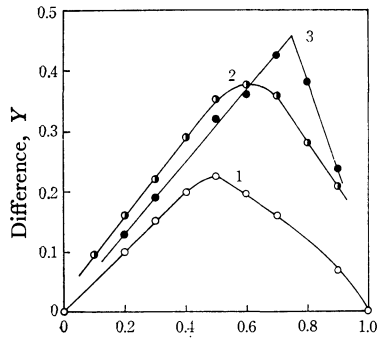

Fig. 3. Relation between Y and $C_{Su}/(C_{Fe}+C_{Su})$ in the application of the continuous variation method. Solutions were 4.57×10^{-4} M in $C_{Fe}+C_{Su}$, and 0.05 M in total monochloroacetate (curve 1) or 0.05 M in total acetate (curves 2 and 3).
Curve 1, at pH 2.20 for 500 mμ; 2, at pH 3.40 for 480 mμ; 3, at pH 4.46 for 470 mμ

7) A. E. Martell and M. Calvin, "Chemistry of the Metal Chelate Compounds," Prentice-Hall, New York (1952), p. 28.

The Stability Constant of the Complex.— From the aforementioned results, the complex-forming reaction between iron(III) and sulfosalicylic acid in an acid solution may be assumed to be represented in general as three successive steps:

$$Fe^{3+} + Su^{3-} \rightleftarrows Fe(Su) \quad (1)$$

$$Fe(Su) + Su^{3-} \rightleftarrows Fe(Su)_2^{3-} \quad (2)$$

$$Fe(Su)_2^{3-} + Su^{3-} \rightleftarrows Fe(Su)_3^{6-} \quad (3)$$

The corresponding equilibrium constants are, then:

$$K_1 = \frac{[Fe(Su)]}{[Fe^{3+}][Su^{3-}]} \quad (4)$$

$$K_2 = \frac{[Fe(Su)_2^{3-}]}{[Fe(Su)][Su^{3-}]} \quad (5)$$

$$K_3 = \frac{[Fe(Su)_3^{6-}]}{[Fe(Su)_2^{3-}][Su^{3-}]} \quad (6)$$

where Su^{3-} denotes the sulfosalicylate anion, $C_6H_3(O^-)(COO^-)(SO_3^-)$. The absorptions of both iron(III) and sulfosalicylic acid in the solution are so weak that they are negligible compared with the absorption of complexes over the range from 450 to 600 mμ. Therefore, the observed absorbancy, As, is expressed in general as:

$$As = \varepsilon_1[Fe(Su)] + \varepsilon_2[Fe(Su)_2^{3-}] + \varepsilon_3[Fe(Su)_3^{6-}] \quad (7)$$

where ε_1, ε_2 and ε_3 are the molar absorbancy indices of $Fe(Su)$, $Fe(Su)_2^{3-}$ and $Fe(Su)_3^{6-}$ respectively.

If a condition is now selected where only a 1 to 1 complex is formed, $[Fe(Su)_2^{3-}]$ and $[Fe(Su)_3^{6-}]$ become zero and K_1 is expressed as:

$$K_1 = \frac{[Fe(Su)]\Phi}{\{C_{Fe} - [Fe(Su)]\}\{C_{Su} - [Fe(Su)]\}} \quad (8)$$

$$= \frac{\varepsilon_1 As\Phi}{(\varepsilon_1 C_{Fe} - As)(\varepsilon_1 C_{Su} - As)} \quad (9)$$

where:

$$\Phi = 1 + \frac{[H^+]}{k_3} + \frac{[H^+]^2}{k_2 k_3} \quad (10)$$

where k_2 and k_3 are the second and the third acid dissociation constants of sulfosalicylic acid; these values, which were described in the literature,[8] will be used in subsequent calculations. The data at pH 2.20 were applied to Eq. 9, and K_1 and ε_1 were determined by the successive approximation method. As a first approximation, ε_1 for 480 mμ was assumed to be equal to 1.78×10^3 M^{-1} cm^{-1}, and the first approximations to K_1 were calculated from Eq. 9. Using the mean of these K_1 values, the second approximations to ε_1 were calculated from the absorbancy. Again using the mean of these values of ε_1, new values of K_1 were obtained from Eq. 9. This procedure was repeated four times. The results of these calculations are summarized in Table I.

Next, K_2 and K_3 can be determined when sulfosalicylic acid is present in a large excess over iron(III). Under these conditions, the concentration of the sulfosalicylic acid combining with iron(III) is negligible in comparison with its total concentration, so C_{Su} is nearly equal to $[Su^{3-}]\Phi$.

If a condition can be found where the reaction for the complex formation is represented as the two successive steps of reactions 1 and 2, $[Fe(Su)_3^{6-}]$ becomes zero, and from Eqs. 4, 5 and 7 the following relationship is derived;

$$\frac{C_{Fe}}{As} = \frac{1}{\varepsilon_1} + \frac{F_2}{\varepsilon_2\beta_2} \quad (11)$$

where:

$$F_2 = \frac{\Phi^2}{C_{Su}^2}\left\{1 + \frac{K_1}{\Phi}C_{Su} - \frac{\varepsilon_1 K_1 C_{Fe} C_{Su}}{As\Phi}\right\} \quad (12)$$

and where β is the overall stability constant of the complex, which is expressed in general as $\beta_n = \Pi K_n$. The plot of C_{Fe}/As against F_2 in Eq. 11 was applied to the data at pH 3.39, which gave a straight line, as is shown in Fig. 4. From the slope

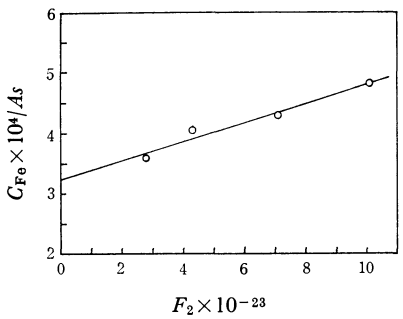

Fig. 4. Plot of C_{Fe}/As vs. F_2 at pH 3.39 for 480 mμ, keeping C_{Fe} at 1.83×10^{-4} M and varying C_{Su} from 3.6×10^{-3} to 3.66×10^{-2} M in 0.05 M of total acetate.

and the intercept at $F_2=0$, ε_2 and β_2 were then calculated: the results are included in Table II.

If, finally, a condition is selected where three complex species are formed, from Eqs. 4, 5, 6 and 7 the following equation is derived:

$$\frac{C_{Fe}}{As} = \frac{1}{\varepsilon_3} + \frac{F_3}{\varepsilon_3\beta_3} \quad (13)$$

where:

$$F_3 = \frac{\Phi}{C_{Su}^3}\left\{1 + \frac{K_1}{\Phi}C_{Su} + \frac{\beta_2}{\Phi^2}C^2{}_{Su}\right\} - \frac{C_{Fe}C_{Su}\left(\varepsilon_1\frac{K_1}{\Phi} + \varepsilon_2\frac{\beta_2 C_{Su}}{\Phi^2}\right)}{As} \quad (14)$$

The application of Eq. 13 to the data at pH 5.20

8) J. Bierrum, G. Schwarzenbach and L. G. Sillen, "Stability Constants, Part I: Organic Ligands," The Chemical Society, London (1956), p. 56.

TABLE I. DETERMINATION OF ε_1 AND K_1 BY SUCCESSIVE APPROXIMATIONS*

Approximation							Mean
	$C_{Fe}\times10^4$ (M)	1.37	1.83	2.28	2.74	3.20	
	$C_{Su}\times10^4$ (M)	3.20	2.74	2.28	1.83	1.37	
	As (at 480 mμ)	0.158	0.195	0.225	0.195	0.150	
1	$\varepsilon_1\times10^{-3}$	—	—	—	—	—	1.78
	$K_1\times10^{-14}$	1.07	1.24	1.68	1.24	0.93	1.23
2	$\varepsilon_1\times10^{-3}$	1.93	1.77	1.96	1.77	1.83	1.87
	$K_1\times10^{-14}$	0.84	1.07	1.43	1.07	0.81	1.04
3	$\varepsilon_1\times10^{-3}$	1.68	1.89	2.08	1.89	1.60	1.83
	$K_1\times10^{-14}$	1.00	1.14	1.53	1.14	0.85	1.13
4	$\varepsilon_1\times10^{-3}$	1.75	1.84	2.03	1.84	1.67	1.83
	$K_1\times10^{-14}$	1.00	1.14	1.53	1.14	0.85	1.13

* Measurements were made at pH 2.20. Solutions were 0.05 M in total monochloroacetate. $\Phi=1.37\times10^{10}$.

TABLE II. CALCULATION OF K_2 AND K_3

Calculation of K_2 from Fig. 4

pH	Φ $\times10^{-8}$	Intercept $\times10^4$	Slope $\times10^{26}$	ε_2 $\times10^{-3}$	β_2 $\times10^{-24}$	K_2 $\times10^{-10}$
3.39	2.67	3.24	1.53	3.08	2.12	1.88

Calculation of K_3 from Fig. 5

pH	Φ $\times10^{-6}$	Intercept $\times10^4$	Slope $\times10^{34}$	ε_3 $\times10^{-3}$	β_3 $\times10^{-33}$	K_3 $\times10^{-8}$
5.20	3.48	2.73	2.19	3.66	1.25	5.90

TABLE III. THE OVERALL STABILITY CONSTANTS

Method*1	Medium	Temp., °C	log K_1	log β_2	log β_3	Reference
sp.	0.05 M monochloroacetate or acetate	Room temp. (25—28)	14.05	24.33	33.10	Present
pot.	3 M $NaClO_4$	25	14.42	25.18	32.24	Ågren[8]
sp.	*2	18	14.64	25.18	32.12	Vareille[8]

*1 The two abbreviations, "sp." and "pot." mean "spectrophotometric" and "potentiometric" respectively.

*2 Ionic strengths is 0.25 M.

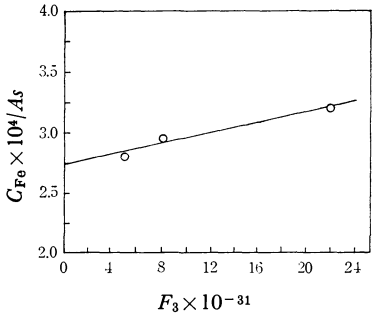

Fig. 5. Plots of C_{Fe}/As vs. for 480 mμ at pH 5.20 keeping C_{Fe} at 1.83×10^{-4} M and varying C_{Su} from 5.5×10^{-3} to 2.95×10^{-2} M in 0.05 M of total acetate.

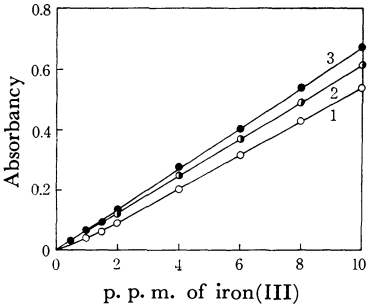

Fig. 6. Calibration curves. Solutions were 0.016 M in sulfosalicylic acid and 0.5 M in total acetate. Curve 1, at pH 3.40 for 480 mμ; 2, at pH 4.50 for 470 mμ; 3, at pH 5.20 for 470 mμ

gave a straight line plot, as is shown in Fig. 5. The results of the calculation of ε_3 and β_3 from the slope and the intercept at $F_3=0$ are included in Table II.

The logarithmic values of the stability constants calculated above are given in Table III, where they are also compared with those determined by Ågren[3] and by Vareille[6]. There are differences in ionic strength, temperature and buffer components between the findings of these investigations. Nevertheless, it may be concluded that the results obtained in these investigations are in

reasonable agreement.

The Spectrophotometric Determination of Iron(III) in the Presence of Iron(II).—*Calibration Curves.*—The calibration curves prepared for different pH values with a series of solutions containing up to 10 p.p.m. of iron(III) are shown in Fig. 6. A linear or nearly linear relation has been found between the absorbancy and the concentration of iron(III).

The Effect of Iron(II).—As is shown in Table IV, the determination of iron(III) at pH 3.40 and 4.50 is not interfered with or is given a negative error of only a few percentage points because of the presence of iron(II). At pH 5.20, the sensitivity is greater, but even small quantities of iron(II) produce a large positive error.

Table IV. Spectrophotometric determination of iron(III) with sulfosalicylic acid in the presence of iron(II)*

pH	Fe(II) present p. p. m.	Absorbancy	Fe(III) found p. p. m.	Error %
3.40	10	0.409(480 mμ)	7.8	−3
	50	0.408(480 mμ)	7.7	−4
	100	0.408(480 mμ)	7.7	−4
4.50	10	0.499(470 mμ)	8.1	+1
	50	0.490(470 mμ)	8.0	0
	100	0.490(470 mμ)	8.0	0
5.20	10	0.552(470 mμ)	8.2	+3
	50	0.577(470 mμ)	8.6	+8
	100	0.784(470 mμ)	11.7	+46

* The amount of Fe(III) taken in each case was 8 p. p. m. Solutions were 0.016 M in sulfosalicylic acid and 0.5 M in total acetate.

Summary

A spectrophotometric study of the complex formation between iron(III) and sulfosalicylic acid has been carried out over the pH range up to 8. Three complex species, Fe(Su), $Fe(Su)_2^{3-}$, and $Fe(Su)_3^{6-}$, have been concluded to be formed in acid solutions, and their stability constants have been determined to be:

$$\frac{[Fe(Su)]}{[Fe^{3+}][Su^{3-}]} = 1.13 \times 10^{13}$$

$$\frac{[Fe(Su)_2^{3-}]}{[Fe^{3+}][Su^{3-}]^2} = 2.12 \times 10^{24}$$

$$\frac{[Fe(Su)_3^{6-}]}{[Fe^{3+}][Su^{3-}]^3} = 1.25 \times 10^{33}$$

Also, it has been ascertained that sulfosalicylic acid can be used as a reagent for determining iron(III) in the presence of iron(II) if the spectrophotometric measurements are made in the pH range from 3 to 4.5.

The authors wish to express their deep gratitude to Professor Sôichirô Musha of the University of Osaka Prefecture for his interest, as well as to Assistant Professor Makoto Munemori for his helpful discussions, and to Dr. Takeshi Nakatogawa and Dr. Natsuki Kawashima of the Hitachi Research Laboratory, Hitachi, Ltd., for their guidance and encouragement throughout this work.

BULLETIN OF THE CHEMICAL SOCIETY OF JAPAN VOL. 39 227—232 (1966)

A Spectrophotometric Study of the Complex Formation between Iron(III) and Salicylic Acid

By Kin'ya OGAWA and Nobuko TOBE

Hitachi Research Laboratory, Hitachi, Ltd., Hitachi, Ibaraki

(Received April 8, 1965)

A spectrophotometric study of the complex formation between iron(III) and salicylic acid was carried out over the pH range up to 6; further, an attempt was made to test the applicability of salicylic acid as a reagent for the spectrophotometric determination of iron(III) in the presence of iron(II). The absorption maxima of the mixture of iron(III) and salicylic acid are found at 530 mμ independently of the pH between 0.7 to 2.5, while they shift to shorter wavelength when the pH rises above 3. The isosbestic point occurs at 550 mμ between pH values from 3 to 6. It was concluded that three complex species, $Fe(Sa)^{+}$, $Fe(Sa)_2^{-}$, and $Fe(Sa)_3^{3-}$, are formed successively in acid solutions; their stability constants were determined to be:

$$\frac{[Fe(Sa)^{+}]}{[Fe^{3+}][Sa^{2-}]}=2.25\times10^{15} \qquad \frac{[Fe(Sa)_2^{-}]}{[Fe^{3+}][Sa^{2-}]^2}=1.57\times10^{27} \qquad \frac{[Fe(Sa)_3^{3-}]}{[Fe^{3+}][Sa^{2-}]^3}=1.86\times10^{36}$$

where Sa^{2-} denotes the salicylate anion, $C_6H_4(O^-)(COO^-)$. If the pH of the solution is adjusted from 2 to 3 and if absorbancy measurements are made at 515 to 500 mμ, salicylic acid can be used as a reagent for determining iron(III) in the presence of iron(II). The optimum concentration of iron(III) is 2 to 12 p. p. m.; iron(II) does not interfere, even at a concentration of 100 p. p. m.

Salicylic acid has been known as a reagent[1] for determining iron(III), since it gives characteristic colors with iron(III). The initial investigation of the nature of the complex formation between iron(III) and salicylic acid was undertaken by Babko,[2,3] who demonstrated the formation of more than one complex in an aqueous solution. Afterward, Ågren[4] determined the equilibrium constants for the complex-forming reaction.

The present authors were interested in the color variations, from violet through red to yellow with a rise on the pH values, which had been noted in earlier analytical studies.[5,6] For the present paper, therefore, the color-forming reaction between iron(III) and salicylic acid was studied spectrophotometrically, and, further, an attempt was made to test the applicability of salicylic acid as a reagent for the spectrophotometric determination of iron(III) in the presence of iron(II).

Experimental

Reagents.—The iron(III), iron(II) and buffer solutions were prepared in manners described previously.[7] A solution of salicylic acid was prepared by dissolving a commercial product, $C_6H_4(OH)(COOH)$, in ethanol.

Apparatus.—The two spectrophotometers and the pH meter used in the present work were the same as those described previously.[7]

Procedure.—The volume of the iron(III) solution was calculated and the pH was adjusted to the required value by adding a buffer solution. After the calculated volume of the salicylic acid solution had been added, the whole was diluted to the proper volume and allowed to stand for two hours. The absorbancy was observed in a part of the resulting solution, and/or, if necessary, the absorption curve over the range from 400 to 600 mμ was recorded, while the pH was measured for the other part. Preliminary experiments showed that the solutions reached an equilibrium within two hours and showed no measurable variation thereafter for periods of less than twenty-four hours.

Results and Discussion

The Effects of pH on the Absorption Curve.—Figure 1 shows the absorption curves for the mixture of iron(III) and salicylic acid at different pH values. The absorption maxima are found at 530 mμ, independently of the pH values when those values are between 0.7 to 2.5, while they shift to a shorter wavelength when the pH rises above 3. The isosbestic point occurs at 550 mμ at pH values between 3 and 6. This behavior suggests that only one complex is formed in a strongly acid solution between pH 0.7 and 2.5, but that the formation of more than one complex may be involved in a weakly acid solution between pH 3 and 6.

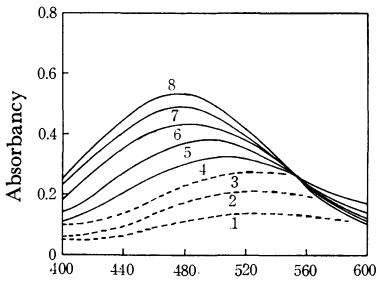

Fig. 1. Absorption curves. Solutions were 1.83×10^{-4} M in iron(III) and 7.3×10^{-3} M (for dotted line) or 1.45×10^{-2} M (for full line) in salicylic acid.
Curve 1, at pH 0.74; 2, at pH 1.71; 3, at pH 2.45; 4, at pH 3.20; 5, at pH 3.63; 6, at pH 4.04; 7, at pH 4.60; 8, at pH 5.30

The Effects of the Molar Ratio of Salicylic Acid to Iron(III).—The relations between the absorbancy and the molar ratio of salicylic acid

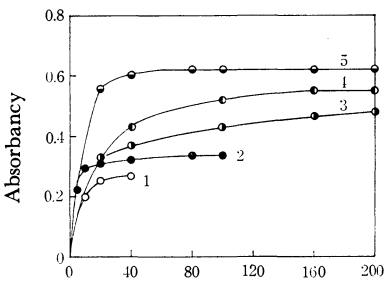

Fig. 2. Relations between absorbancy and C_{Sa}/C_{Fe}. Solutions were 1.83×10^{-4} M in iron(III) and 0.05 M in total monochloroacetate (curves 1 and 2) or 0.05 M in total acetate (curves 3, 4 and 5).
Curve, 1, at pH 2.04 for 530 mμ; 2, at pH 2.81 for 515 mμ; 3, at pH 3.51 for 490 mμ; 4, at pH 4.58 for 480 mμ; 5, at pH 5.96 for 475 mμ

1) F. J. Welcher, "Organic Analytical Reagents Vol. II," D. van Nostrand Co., New York (1947), p. 118.
2) A. K. Babko, *J. Gen. Chem.* (*U.S.S.R.*), **15**, 745 (1945); *Chem. Abstr.*, **40**, 7041 (1946).
3) A. K. Babko, *J. Gen. Chem.* (*U.S.S.R.*), **15**, 758 (1945); *Chem. Abstr.*, **40**, 7042 (1946).
4) A. Ågren, *Acta Chem. Scand.*, **8**, 1059 (1954); *Chem. Abstr.*, **49**, 2929 (1955).
5) J. P. Mehlig, *Ind. Eng. Chem. Anal. Ed.*, **10**, 136 (1938).
6) R. O. Scott, *Analyst*, **66**, 142 (1941).
7) K. Ogawa and N. Tobe, This Bulletin, **39**, 223 (1966).

to iron(III) in their mixture were obtained at different pH values. The results are shown in Fig. 2. There is neither a sharp break nor a leveling-off to a constant absorbancy at any pH value for ratios up to as high as ten moles of salicylic acid to one mole of iron(III); this shows that the colored complexes are appreciably dissociated and that, hence, a large excess of salicylic acid over iron(III) is required to bring the reaction to completion.

The Composition of the Complex.—The compositions of the complexes were determined by applying the continuous variation method.[8] Figure 3 shows the results obtained at different pH values by plotting Y, the difference between the observed absorbancy and that which would be obtained if no reaction had taken place, against the ratio of the total concentration of salicylic acid, C_{Sa}, to the sum of the total concentration of iron(III) and that of salicylic acid, $C_{Fe}+C_{Sa}$. The maximum value of Y in curve 1 occurs at a ratio of 0.5, indicating that salicylic acid combines with iron(III) in a molar ratio of 1 to 1. In each of the curves from 2 to 5 the maximum of Y is found in the neighborhood of a ratio of 0.7, while in curve 6 it is found at a ratio of about 0.75. This indicates that complex species in which salicylic acid combines with iron(III) in molar ratios of two to one and/or three to one are formed in addition to the 1 to 1 complex, and that the molar ratio of salicylic acid to iron(III) in the complex increases with the rising pH values. This behavior is interpreted as taking place because iron(III) competes with hydrogen ions in taking away salicylate anions.

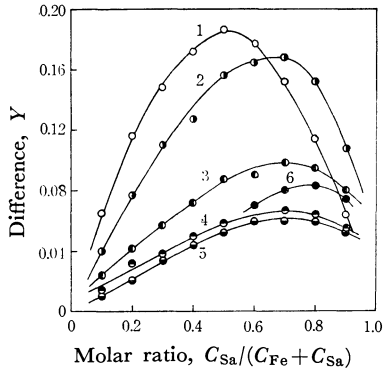

Fig. 3. Relations between Y and $C_{Sa}/(C_{Fe}+C_{Sa})$ in the application of continuous variation method. Solutions were 4.57×10^{-4} M (curves 1 to 5) or 9.13×10^{-1} M (curves 6) in $C_{Fe}+C_{Sa}$ and 0.05 M in total monochloroacetate (curve 1) or 0.05 M in total acetate (curves 2 to 6).
Curve 1, at pH 2.70 for 520 mμ; 2, at pH 3.33 for 505 mμ; 3, at pH 3.80 for 500 mμ; 4, at pH 4.02 for 485 mμ; 5, at pH 4.80 for 480 mμ; 6, at pH 5.94 for 475 mμ

The Stability Constant of the Complex.—The method described by McConell and Davidson[9] was used for determining the stability constants of the complexes. Since there are three complex species in the acid solution, the reaction for the complex formation may be written in general in terms of the following successive steps:

$$Fe^{3+}+Sa^{2-} \rightleftarrows Fe(Sa)^{+} \quad (1)$$

$$Fe(Sa)^{+}+Sa^{2-} \rightleftarrows Fe(Sa)_2^{-} \quad (2)$$

$$Fe(Sa)_2^{-}+Sa^{2-} \rightleftarrows Fe(Sa)_3^{3-} \quad (3)$$

where Sa^{2-} denotes the salicylate anion, $C_6H_4(O^-)(COO^-)$. The corresponding equilibrium constants are, then;

$$K_1=\frac{[Fe(Sa)^{+}]}{[Fe^{3+}][Sa^{2-}]} \quad (4)$$

$$K_2=\frac{[Fe(Sa)_2^{-}]}{[Fe(Sa)^{+}][Sa^{2-}]} \quad (5)$$

$$K_3=\frac{[Fe(Sa)_3^{3-}]}{[Fe(Sa)_2^{-}][Sa^{2-}]} \quad (6)$$

When salicylic acid is present in a large excess over iron(III), the concentration of the salicylic acid combining with iron(III) is negligible compared with its total concentration. Therefore, Eqs. 4, 5, and 6 are converted into the following:

$$K_1=\frac{[Fe(Sa)^{+}]\Phi}{\{C_{Fe}-([Fe(Sa)^{+}]+[Fe(Sa)_2^{-}]+[Fe(Sa)_3^{3-}])\}C_{Sa}} \quad (7)$$

$$K_2=\frac{[Fe(Sa)_2^{-}]\Phi}{[Fe(Sa)^{+}]C_{Sa}} \quad (8)$$

$$K_3=\frac{[Fe(Sa)_3^{3-}]\Phi}{[Fe(Sa)_2^{-}]C_{Sa}} \quad (9)$$

where C_{Fe} and C_{Sa} represent the total concentrations of iron(III) and of salicylic acid respectively, and

$$\Phi = 1+\frac{[H^+]}{k_2}+\frac{[H^+]^2}{k_1k_2} \quad (10)$$

where k_1 and k_2 are the first and the second acid dissociation constants of salicylic acid. The absorptions of both iron(III) and salicylic acid in the solution are so weak that they are negligible compared with the absorption of the complexes over the range from 450 to 600 mμ. Therefore, the observed absorbancy, As, may be expressed as:

$$A_S=\varepsilon_1[Fe(Sa)^{+}]+\varepsilon_2[Fe(Sa)_2^{-}]+\varepsilon_3[Fe(Sa)_3^{3-}] \quad (11)$$

where ε_1, ε_2, and ε_3 represent the molar absorbancy

8) A. E. Martell and M. Calvin, "Chemistry of the Metal Chelate Compounds," Prentice-Hall, New York (1952), p. 28.

9) H. McConell and N. Davidson, *J. Am. Chem. Soc.*, **72**, 3164 (1950).

indexes of $Fe(Sa)^+$, $Fe(Sa)_2^-$, and $Fe(Sa)_3^{3-}$ respectively.

From Eqs. 7, 8, 9, and 11 the following equation is derived:

$$\frac{C_{Fe}}{As}=\frac{1}{\varepsilon_3}+\frac{F_3}{\varepsilon_3\beta_3} \tag{12}$$

where:

$$F_3=\frac{\Phi^3}{C_{Sa}{}^3}\left\{1+\frac{K_1}{\Phi}C_{Sa}+\frac{\beta_2}{\Phi^2}C_{Sa}{}^2-\frac{C_{Fe}C_{Sa}\left(\varepsilon_1\frac{K_1}{\Phi}+\varepsilon_2\frac{\beta_3 C_{Sa}}{\Phi^2}\right)}{As}\right\} \tag{13}$$

and where β is the overall stability constant of the complex, which is expressed in general as $\beta_n=\Pi K_n$. In Eqs. 12 and 13, C_{Fe} and C_{Sa} have known values; As is an observed quantity, and ε_1, ε_2, K_1 and β_2 can be obtained from subsequent equations. If a suitable condition is chosen, the plotting of C_{Fe}/As against F_3 gives a straight line, the slope of which is $1/\varepsilon_3\beta_3$. The molar absorbancy index, ε_3, can be estimated from the intercept at $F_3=0$, which is obtained by extrapolation. In all subsequent equations, as in this, C_{Fe}/As is plotted against F terms, and the desired constants are obtained from the slopes and the intercepts of the straight lines.

If a condition is now selected where the reaction for the complex formation is represented as the two successive steps of reactions 1 and 2, $[Fe(Sa)_3^{3-}]$ becomes zero, and, from Eqs. 7, 8 and 11, it follows that:

$$\frac{C_{Fe}}{As}=\frac{1}{\varepsilon_2}+\frac{F_2}{\varepsilon_2\beta_2} \tag{14}$$

where:

$$F_2=\frac{\Phi^2}{C_{Sa}{}^2}\left\{1+\frac{K_1}{\Phi}C_{Sa}-\frac{\varepsilon_1 K_1 C_{Fe}C_{Sa}}{As\Phi}\right\} \tag{15}$$

Equations 14 and 15 permit the determination of both ε_2 and β_2, which are necessary for Eq. 13.

If a condition can be found where only a 1 to 1 complex is formed, both $[Fe(Sa)_2^-]$ and $[Fe(Sa)_3^{3-}]$ become zero, and, from Eqs. 7 and 11, there comes the following equation:

$$\frac{C_{Fe}}{As}=\frac{1}{\varepsilon_1}+\frac{F_1}{\varepsilon_1 K_1} \tag{16}$$

where $F_1=\Phi/C_{Sa}$, which permits the determination of both ε_1 and K_1, necessary for Eq. 14.

First, in order to determine the K_1 value, plots of Eq. 16 were applied to the data at pH 2.04 and 2.81; the results are shown in Fig. 4. Next, plots of Eq. 14 were applied to the data at pH 3.51 in order to determine β_2; the results are given in Fig. 5. Finally, β_3 was determined from the results of the application of Eq. 12 to the data at pH 5.96, as is shown in Fig. 6.

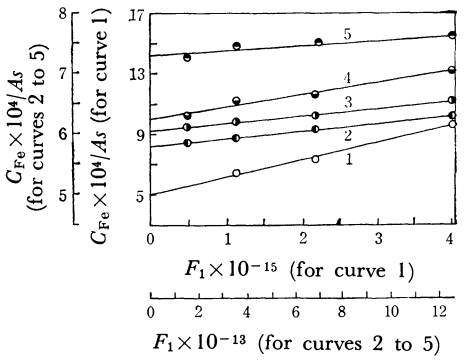

Fig. 4. Plots of C_{Fe}/As vs. F_1, keeping C_{Fe} at 1.83×10^{-4} M and varying C_{Sa} from 2.0×10^{-3} to 1.45×10^{-2} M in 0.05 M of total monochloroacetate.
Curve 1, at pH 2.04 for 530 mμ; 2, at pH 2.81 for 530 mμ; 3, at pH 2.81 for 550 mμ; 4, at pH 2.81 for 480 mμ; 5, at pH 2.81 for 460 mμ.

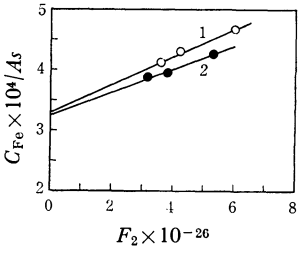

Fig. 5. Plots of C_{Fe}/As vs. F_2 at pH 3.51, keeping C_{Fe} at 1.83×10^{-4} M and varying C_{Sa} from 7.3×10^{-3} to 3.62×10^{-2} M in 0.05 M of total acetate.
Curve 1, for 460 mμ; 2, for 480 mμ.

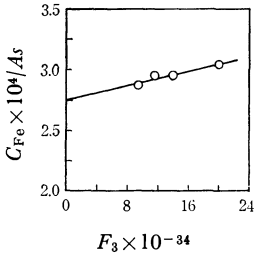

Fig. 6. Plots of C_{Fe}/As vs. F_3 at pH 5.96 for 480 mμ, keeping C_{Fe} at 1.83×10^{-4} M and varying C_{Sa} from 3.6×10^{-3} to 2.90×10^{-2} M in 0.05 M of total acetate.

In Table I are tabulated the results of the calculation of the desired constants from Figs. 4, 5 and 6. The values of the first and the second acid dissociation constants of salicylic acid used in these calculations were those described in the literature.[10] The logarithmic values of the stability constants calculated above are given in Table II, where they are also compared with those determined by

Table I. Calculation of stability constants

Calculation of K_1 from Fig. 4

pH	Φ $\times 10^{-12}$	Wavelength $m\mu$	Intercept $\times 10^{4}$	Slope $\times 10^{19}$	ε_1 $\times 10^{-3}$	K_1 $\times 10^{-15}$
2.04	8.07	530	5.00	1.14	2.00	4.39
2.81	0.249	460	7.30	2.58	1.37	2.83
2.81	0.249	480	6.25	6.33	1.60	0.99
2.81	0.249	530	5.80	3.95	1.72	1.47
2.81	0.249	550	6.05	3.95	1.65	1.53
					Mean	2.24

Calculation of β_2 from Fig. 5

pH	Φ $\times 10^{-10}$	Wavelength $m\mu$	Intercept $\times 10^{4}$	Slope $\times 10^{31}$	ε_2 $\times 10^{-3}$	β_2 $\times 10^{-27}$
3.51	1.32	460	3.30	2.30	3.03	1.43
3.51	1.32	480	3.25	1.90	3.07	1.71
					Mean	1.57

Calculation of β_3 from Fig. 6

pH	Φ $\times 10^{-7}$	Wavelength $m\mu$	Intercept $\times 10^{4}$	Slope $\times 10^{40}$	ε_3 $\times 10^{-3}$	β_3 $\times 10^{-36}$
5.96	1.47	480	2.75	1.48	3.64	1.86

Table II. Logarithmic values of overall stability constants

Method*	Medium	Temp., °C	log K_1	log β_2	log β_3	Reference
sp.	0.05 M monochloroacetate or acetate	20—25	15.35	27.20	36.27	Present
pol.	3 M $NaClO_4$	25	15.82	27.49	35.31	Ågren[4,10]

* The two abbreviations, "sp." and "pol." mean "spectrophotometric" and "polarographic" respectively.

Ågren.[4,10] The present values of log K_1 and log β_2 agree reasonable well those obtained by Ågren, while there are considerable discrepancies between them in the two values of log β_3. These discrepancies may be due to the difference in ionic strength and temperature, and also to some unknown factor such as the influence of buffer components in the equilibria.

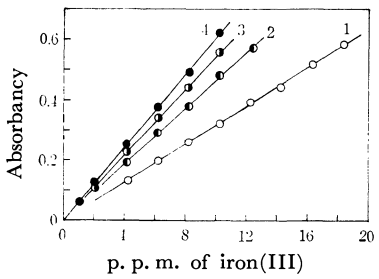

Fig. 7. Calibration curves. Solutions were 0.036 M in salicylic acid and 0.5 M in total monochloroacetate (curve 1) or 0.5 M in total acetate (curves 2 to 4).
Curve 1, at pH 2.80 for 515 $m\mu$; 2, at pH 3.50 for 490 $m\mu$; 3, at pH 4.50 for 480 $m\mu$; 4, at pH 6.00 for 475 $m\mu$

10) J. Bjerrum, G. Schwarzenbach and L. G. Sillen, "Stability Constants, Part I: Organic Ligands," The Chemical Society, London (1956), p. 53.

The Spectrophotometric Determination of Iron(III) in the Presence of Iron(II).—*Calibration Curves*—The calibration curves prepared for different pH values with a series of solutions containing up to 10 p. p. m. of iron(III) are shown in Fig. 7. A linear or nearly linear relation is found between the absorbancy and the concentration of iron(III) at each pH value.

The Effects of Iron(II).—As is shown in Table III, the determination of iron(III) at pH 2.80

Table III. Spectrophotometric determinations of iron(III) by salicylic acid in the presence of iron(II)*

pH	Fe(II) present p. p. m.	Absorbancy	Fr(III) found p. p. m.	Error %
2.80	10.2	0.262(515 $m\mu$)	8.30	+ 2
	51.0	0.264(515 $m\mu$)	8.30	+ 2
	102	0.267(515 $m\mu$)	8.35	+ 2
3.50	10.2	0.372(490 $m\mu$)	8.05	− 1
	51.0	0.389(490 $m\mu$)	8.40	+ 3
	102	0.402(490 $m\mu$)	8.55	+ 5
4.50	10.2	0.535(480 $m\mu$)	9.80	+20
	51.0	0.659(480 $m\mu$)	122	+50
	102	0.799(480 $m\mu$)	150	+84

* The amount of iron(III) taken in each case was 8.16 p. p. m. Solutions were 0.036 M in salicylic acid and 0.5 M in total monochloroacetate or total acetate.

and 3.70 has a positive error of a few percentage points because of the presence of iron(II). At pH 4.50, the sensitivity is greater, but even small quantities of iron(II) produce a large positive error.

Summary

A spectrophotometric study of the complex formation between iron(III) and salicylic acid has been carried out over the pH range up to 6. Three complex species, $Fe(Sa)^+$, $Fe(Sa)_2^-$, and $Fe(Sa)_3^{3-}$, have been concluded to be formed in acid solutions, and their stability constants have been determined to be:

$$\frac{[Fe(Sa)^+]}{[Fe^{3+}][Sa^{2-}]}=2.24\times10^{15}$$

$$\frac{[Fe(Sa)_2^-]}{[Fe^{3+}][Sa^{2-}]^2}=1.57\times10^{27}$$

$$\frac{[Fe(Sa)_3^{3-}]}{[Fe^{3+}][Sa^{2-}]^3}=1.86\times10^{36}$$

Also, it has been ascertained that salicylic acid can be used as a reagent for determining iron(III) in the presence of iron(II) if the spectrophotometric measurements are made in the pH range from 2 to 3.

The authors wish to express their deep gratitude to Professor Sôichirô Musha of the University of Osaka Prefecture for his interest, as well as to Assistant Professor Makoto Munemori for his helpful discussions. Thanks are due also to Dr. Takeshi Nakatogawa and Dr. Natsuki Kawashima of the Hitachi Research Laboratory, Hitachi, Ltd., for their guidance and encouragement throughout this work.

BULLETIN OF THE CHEMICAL SOCIETY OF JAPAN VOL. 39 232—239 (1966)

Intermediates in the Photoreduction of Eosine as Revealed by a Flash-Photolysis Study

By Takeshi OHNO, Shunji KATO and Masao KOIZUMI

Department of Chemistry, Facultry of Science, Tohoku University, Katahira-cho, Sendai

(Received April 15, 1965)

Besides the triplet state, semi-reduced eosine (Rd) and semi-oxidized eosine (Ox) were observed as transient intermediates in an aqueous solution; the former has a peak at 408 mμ, and the latter, one at 456 mμ. These two species are produced by the reaction $D^T + D \rightarrow Rd + Ox$ or $D^T + D^T \rightarrow Rd + Ox$. The sum of the rate constants for the reactions $D^T + D \rightarrow Ox + Rd$ and $D^T + D \rightarrow 2D$ is about 8.0×10^8 M^{-1} sec^{-1}, approximately equal to the sum of the rate constants for $D^T + D^T \rightarrow 2D$ and $D^T + D^T \rightarrow Ox + Rd$. Triplet eosine, by reacting with ATU or EDTA, produces two kinds of half-reduced eosine, Rd' and Rd'', which have absorption spectra similar to those of Rd but with different life-times. These are perhaps loose compounds of half-reduced dye and a half-oxidized reductant. The rate constants for $D^T + ATU \rightarrow Rd'$ and $D^T + EDTA \rightarrow Rd''$ are 3.4×10^5 M^{-1} sec^{-1} and 5×10^5 M^{-1} sec^{-1} respectively. Rd disappears bimolecularly by means of the $Rd + Ox \rightarrow 2D$ reaction with the rate constant of 8.8×10^7 M^{-1} sec^{-1}. Ox, by reacting with EDTA or ATU, regenerates the original dye with the rate constants of 1×10^6 and 8×10^5 M^{-1} sec^{-1} respectively. The results enable us to conclude that the D-D mechanism occurs under suitable conditions.

It has been proposed by two of the present authors[1] (Koizumi and Ohno) that, in the continuous-light photoreduction of eosine by allylthiourea (ATU), the reaction proceeds by one of two alternative paths, depending on the experimental conditions. Thus, in the case of higher ATU concentrations, the primary step is the reaction between the triplet dye (D^T) and a reducing agent (the D-R mechanism), while at lower concentrations of ATU the primary step is the electron transfer between D^T and D (the D-D mechanism). The rate constants of some elementary processes have also been evaluated.

The first evidence for the electron transfer between two D^T molecules or between D^T and D was presented by Lindqvist in his extensive study of the transient intermediates of fluorescein by means of a flash technique[2]; further evidence was presented by Kato et al. in the case of methylene blue.[3]

1) T. Ohno, Y. Usui and M. Koizumi, This Bulletin, **38**, *1022 (1965)*.

2) L. Lindqvist, *Arkiv för Kemi*, **16**, 79 (1960).

3) S. Kato, M. Morita and M. Koizumi, This Bulletin, **37**, *117 (1964)*.

Meanwhile, Grossweiner and Zwicker reported,[4] in their paper dealing with a flash-photolytic investigation of the eosine-phenol system, that there is no evidence for the production of semi-reduced and semi-oxidized eosine in an evacuated aqueous eosine solution. These quite different aspects of the behavior of fluorescein and eosine seemed to us rather odd, although Grossweiner himself attributed them to their different electronic configurations.

In view of our findings in steady-illumination experiments and the above disagreement between the two groups of investigators, we made flash-photolytic studies of aqueous solutions of eosine in connection with our steady-light studies.

The purpose of the present paper is to report that half-reduced and half-oxidized eosine does come into existence in the flash-illuminated aqueous eosine solution.

In addition, we have investigated the behavior of these intermediates as well as that of the triplet dye.

Experimental

Apparatus.—The flash apparatus reported on in a previous paper[3] was used to record the transient spectra.

Another apparatus, with a shorter duration of the photolysis flash, was used to trace the change in the transient absorption. It was assembled from a grating monochrometer (Narumi RM-23), a synchroscope (Iwasaki SS-5151) and a 150W. xenon short arc lamp (Ushio UXL-150). Two quartz flash lamps filled with xenon were set parallel and were connected, in series, with an air gap for triggering and a carbon rod (15 cm. long and 4.5 mm. in diameter) for electric damping. The lamps were powered by a 1 μF condenser and operated at 10 kV. The half-height duration of the flash was 4.5 μsec.

The relative light doses of flashes with and without the carbon rod were compared by the use of a ferrioxalate actinometer; it was found that the rod reduced the light dose to 55 per cent of the value without it. Thus, the flash energies recorded in this paper are 55 per cent of the input electrical energies.

The green plastic plates, always used as filters were transparent from 420 to 600 mμ and had a maximum transmittance of 60 per cent at 520 mμ. To change the light intensity, darkened photographic plates with a known transmittance were employed as neutral filters, instead of changing the electrical conditions. Accordingly, the profile of the incident flash light was always of the same shape.

Materials.—Eosine (Merck) was recrystallized three times from an ethanol solution. ATU, β-sulfonylanthraquinone, disodium hydrogen phosphate, potassium dihydrogen phosphate and $NaClO_3$, all of a G. R. grade, were recrystallized three times from aqueous solutions. Benzoquinone was recrystallized two times from ethanol and then washed with water. The other substances, all of a G. R. grade, were used without further purification.

All the sample solutions were prepared in a 0.1 M phosphate buffer solution, pH=7.2. The samples were degassed by cycles of freezing, pumping and thawing.

Results

General Features of the Reaction and the Assignment of the Transient Absorption Spectra.—It was established that the permanent bleaching of dye by a single flash (19J) is less than 1%. The transient spectra at 65, 360 and 1410 μ sec. after the excitation flash are shown in Fig. 1. Four maxima are apparent, at 580, 456, 408 and 325 mμ, of which the first one and the last one

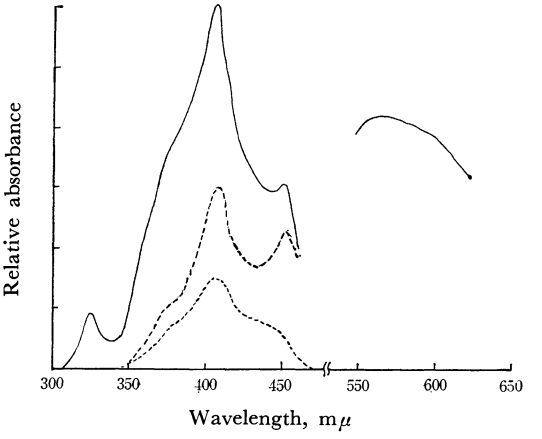

Fig. 1. Absorption spectra of transient species in the phosphate buffer solution (pH 7.2). Eosine concentration is 13 μM.
—— 65 μ sec. after flashing (input-energy 19J)
---- 360 μ sec. (upper curve) and 1410 μ sec. (lower curve) after flashing (input-energy 19J)

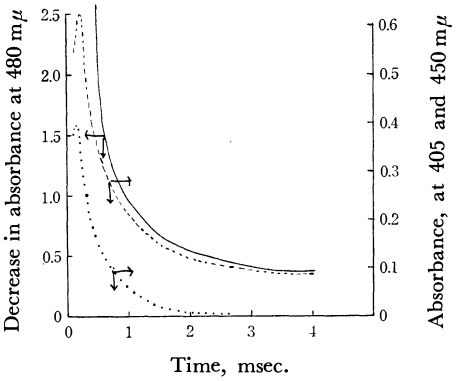

Fig. 2. Change in the absorbance of transient species and eosine. Eosine concentration is 10 μM.
—— 480 mμ (eosine) ---- 405 mμ
····· 450 mμ

4) E. F. Zwicker and L. I. Grossweiner, *J. Phys. Chem.*, **67**, 549 (1963).

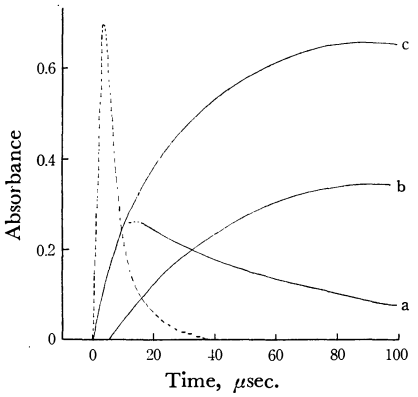

Fig. 3. Rise and fall of transient species during and after flash irradiation. Eosine concentration is 10 μM.
Dotted line; flash (55J), a, 610 mμ; b, 450 mμ; c, 405 mμ

completely disappear at 360 μsec., of the two remaining peaks, 408 mμ has the longer life. This is clear from Fig. 2, in which the decay at 405 and at 450 mμ in a later stage is shown. The recovery of the main absorption band of the original dye (480 mμ) is also included in this figure.

The rise and fall of each absorption maximum in an early stage are shown in Fig. 3. There is no doubt from these three figures that 325 mμ and 508 mμ, which appear to be produced only during illumination and which decay at the same rate, belong to a primary intermediate. These two bands may most plausibly be assigned to the triplet state of the dye. The peaks at 405 and 450 mμ, which grow with the decline of 325 and 580 mμ, can be attributed to the second-step intermediates.

When ATU, EDTA, $NaClO_3$, $NaHAsO_4$ or oxygen was added, a more or less permanent bleaching of the dye resulted from a single flash. The extent of bleaching is particularly large in the cases of EDTA and ATU.

In the cases of β-sulfonylanthraquinone and *p*-benzoquinone, there is scarcely any permanent bleaching observed. The triplet absorption spectra were not observable when an ample quantity of any of the above-mentioned substances, except $NaClO_3$ and $NaHAsO_4$, were added.

The transient spectra from the system containing ATU or EDTA have only a 408 mμ peak, as is shown in Fig. 4, whereas the only observable peak in the case of the system to which β-sulfonylanthraquinone or oxygen has been added is the one at 456 mμ. $NaClO_3$ and $NaHAsO_4$ scarcely affect the transient spectra at all.

The spectra for the system containing *p*-benzoquinone are complicated, as can be seen in Fig. 5. Besides the 450—460 mμ band, four peaks are apparent, at 430, 410, 380 and 355 mμ; these may most plausibly be attributed to the half-reduced forms of benzoquinone, in ionic and neutral forms.

To sum up the effect of the added substances, there is scarcely any doubt that the peaks at 408 and 456 mμ can be assigned to semiquinone (Rd) and half-oxidized eosine (Ox) respectively, because

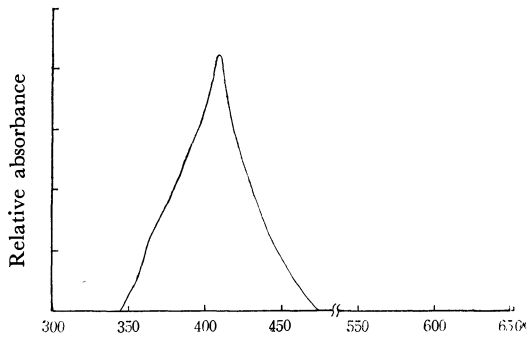

Fig. 4. Absorption spectra of transient species in the presence of 3×10^{-2} M allylthiourea at 65 μsec. after flashing. Eosine: 13 μM

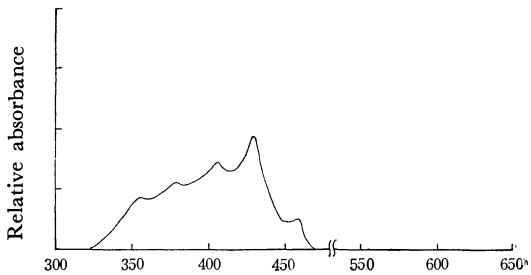

Fig. 5. Absorption spectra of transcient species in the presence of 10^{-3} M *p*-benzoquinone at 360 μ sec. after flashing. Eosine: 13 μM

the addition of oxidants removes the 405 mμ peak, while reductants eliminate the 456 mμ absorption. This conclusion will be further substantiated below.

Some Observations Concerning the Behavior of Transient Intermediates.—The relation between the absorbances at 450 and 408 mμ, due, respectively, to the existence of Ox and Rd at 80 μsec. after flashing, is shown in Fig. 6; the concentrations of these intermediates were varied by changing the intensity of the light flash. It is certain from this figure that the two intermediates are always produced in the same ratio, irrespective of the experimental conditions. In order to determine this ratio, one must know the molar extinction coefficients of Rd and Ox. These were derived in the following way.

As is evident from Fig. 2, only Rd survives at a later stage. If one assumes that both Rd and Ox return completely to the ground-state dye under any circumstances, the molar extinction coefficient

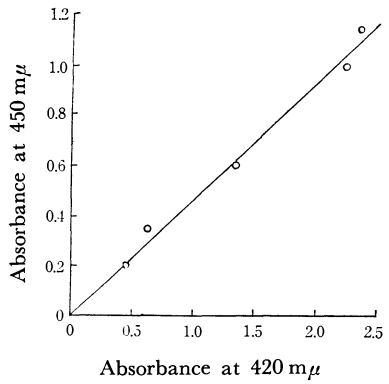

Fig. 6. Relation between the formation of Ox and Rd at 80 μsec. after flashing. Eosine concentration is 13 μM.

of Rd can easily be calculated, since its concentration in the later stage can be equated to that of the ground-state dye recovered after the corresponding time point. This, although not conclusive, appears to be justified if one recalls that the fluorescein semiquinone produced from the interaction of leuco- and oxidized-forms returns completely to the ground-state dye, probably by losing molecular hydrogen.[5] The molar extinction coefficient of Rd at 408 mμ thus obtained is 2.5×10^4. The molar extinction coefficient of Ox can, then, be obtained from the absorbance at 458 mμ in the stage where there is no triplet absorption remaining, by using the concentration data of the ground-state eosine and of Rd, both of whose coefficients are known. The coefficient of Ox thus obtained at 458 mμ is 1.2×10^4.

By the use of the above ε-values, the ratio of Rd to Ox was found to be about unity. This implies that Rd and Ox are produced by the reaction:

$$D^T + D \rightarrow Rd + Ox \qquad (1)$$

or

$$D^T + D^T \rightarrow Rd + Ox \qquad (2)$$

Although the procedure used above is somewhat ambiguous, the coefficients so obtained are used tentatively in the present paper. Grossweiner's value[4] for ε_{408} is $3.8\times10^4\pm0.4$, which is not very different from ours.

The relation between the yield of Rd and the dye concentration was examined using a flash light of such an intensity that most of the dye was converted to the triplet state, while the production of the triplet state was considered to be roughly proportional to the dye concentration.

In Fig. 7 the absorbances at 408 mμ measured 80 μ sec. after flashing are plotted against the dye concentration. The shape of the curve favors the view that the predominant reaction is $D^T+D^T \rightarrow Rd+Ox$, but it does not obviate the possible participation of the process $D^T+D \rightarrow Rd+Ox$.

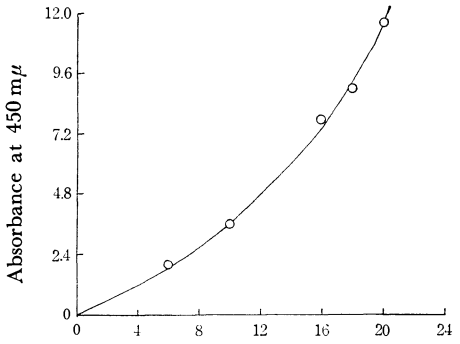

Fig. 7. Formation of Ox at various eosine concentrations at 80 μsec. after flashing. (55J, 77.5J)

To investigate further which reaction, 1 or 2, is the more efficient, the dependence of the yield of Rd on the triplet dye concentration was examined. Since the decay of the triplet state is exponential with the rate constant, independent of the light intensity (see below), the quantities of the triplet state produced by single flashes of various intensities are proportional to the absorbance density at 610 mμ at a fixed time point after flashing. Figure 8 gives the plot of the absorbance at 610 mμ, A_{610}, against the relative light intensity.

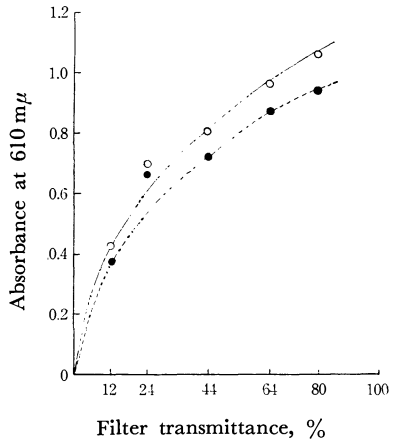

Fig. 8. Formation of triplet state by various light energies observed at various time interval.
—○— 30 μsec. after flashing
—●— 40 μsec. after flashing

Then, at various light intensities, the maximum values of A_{408} after flashing were compared with the values of A_{610}. As is shown in Fig. 9, A_{408} is approximately proportional to A^2_{610}. Although exact analysis is difficult, the results strongly suggest

5) Y. Momose, K. Uchida and M. Koizumi, This Bulletin, 38, 1601 (1965).

the predominance of the reaction 2 under the present experimental conditions.

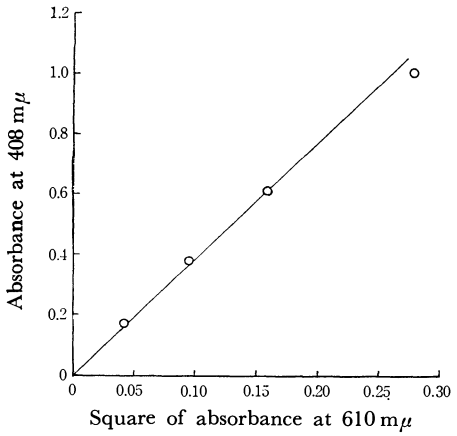

Fig. 9. Relation between the formation of Rd and triplet state.

When ATU or EDTA is added, the yield of Ox decreases with the increase in the reductant concentration. The yield of Rd, on the other hand, is not affected to any large extent. However, the decay of Rd, which will be treated quantitatively later, shows a sharp breaking point, after which the rate becomes very slow; yet the shape of the absorption spectrum remains the same. The phenomenon is similar in both reductants. It is reasonable to explain this break by assuming two somewhat different species, species which have the same absorption spectra but which differ in life time. The one with the shorter life time and that with a longer life time will conventionally be denoted as Rd and Rd' respectively in the case of ATU, and as Rd and Rd'' respectively in the case of EDTA. Both Rd' and Rd'' increase with the concentration of reductants. Tables I and II give some of the results; one example is shown in Fig. 10.

TABLE I

[ATU] $\times 10^2$	Rd+Rd' (Op. dens.)	Rd (Op. dens.)	Rd' (Op. dens.)	Ox
0	0.670	0.670	0	0.360
2	0.609	0.385	0.244	0.12
4	0.560	0.243	0.316	0
5	0.652	0.286	0.366	0

TABLE II

[EDTA] $\times 10^2$	Rd+Rd''	Rd	Rd''	Ox
0	0.670	0.67	0	0.360
1	0.49	0.26	0.24	0.24
2	0.95	0.56	0.39	0
3	0.97			0
5	1.14	0.76	0.38	0

At first sight there appear to be two ways in which the nature of Rd' and Rd'' can be explained. One is to consider, as has been mentioned above, that they are slightly different species from Rd and are produced by a direct reaction between D^T and the reductants; the other interpretation is to consider that they are the same species as Rd but that, since the reductants eliminate Ox, the remaining Rd, with no Ox to react, behaves in quite a different way. The data in the above table show that quite a large quantity of Rd still exists after the Ox has been exhausted; hence, the first interpretation is more plausible. The problem will be discussed later, after the studies of the decay of the transient intermediates have been described.

The quantity of Rd' is proportional to the quantity of the permanent bleaching of the dye; if one assumes that the extinction coefficients of Rd' and Rd'' are same as that of Rd, then the quantity of Rd' is exactly the same as the permanent bleaching. Thus Rd' is completely converted to leuco eosine. Rd'' is also proportional to the quantity of permanent bleaching, but the ratio of the former to the latter is 1 : 2.3 in this case. (Fig. 11)

When 10^{-3} M of *p*-benzoquinone is added, the absorption spectra of the triplet dye do not appear

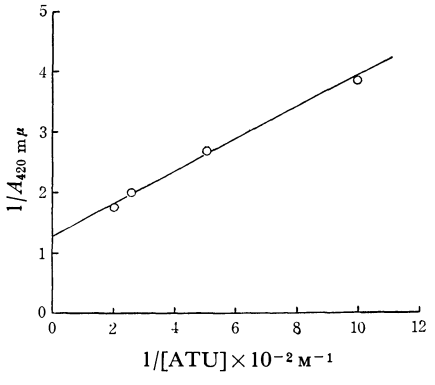

Fig. 10. Formation of Rd' for various allylthiourea concentration.

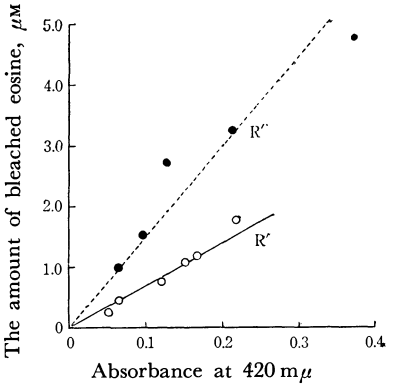

Fig. 11. Relation between the formation of Rd' or Rd'' and permanent bleaching of eosine.

at all, and the quantity of Ox reaches its maximum value immediately after the flashing. The quantity of Ox is exactly proportional to the absorbance at 430 mμ which is due to benzosemiquinone. This is shown in Fig. 12. Hence, one may say that the reaction between benzoquinone and D^T yields Ox and the half-reduced form of *p*-benzoquinone very efficiently.

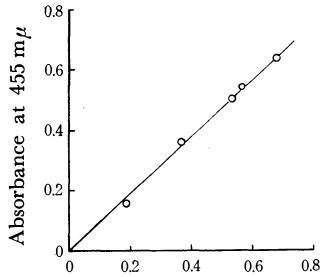

Fig. 12. Relation between the formation of Ox and that of benzosemiquinone ion.

The Decay of the Intermediates.—The decay of the triplet state was measured at 580 mμ.

As Fig. 13 shows, the decay rate is scarcely influenced at all by a variation in the intensity of the exciting light. This suggests that the decay is not affected by the concentration of D^T. The decay is well expressed as a first-order process, seemingly suggesting the absence of any bimolecular processes. However, this is not the case, because the first order decay constant increases with the concentration of dye, as is shown in Fig. 14. Hence, the rate formula for the decay should be written as follows:

$$\frac{-d[D^T]}{dt}=\{k_{sp}+k[D]_0\}[D^T] \qquad (3)$$

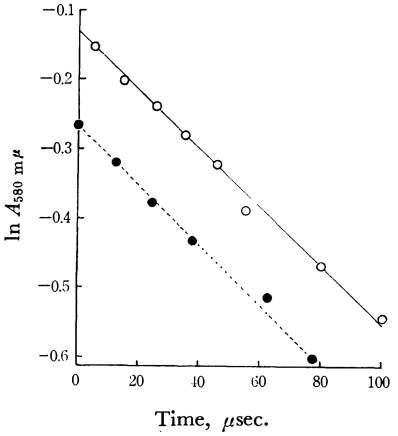

Fig. 13. Decay of triplet state for various light energies. Eosine concentration is 25 μM.
—○— Input-energy 55J
—●— Input-energy 2.5J

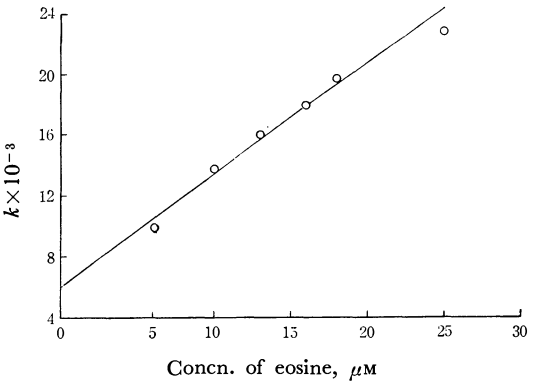

Fig. 14. Decay constant of triplet state for various eosine concentrations.

where k_{sp} is a unimolecular rate constant and $[D]_0$ is the concentration of the dye. From the intercept, $k_{sp}\approx6\times10^3\ sec^{-1}$, and from the slope, $k=8.0\times10^8\ M^{-1}\ sec^{-1}$.

The above results imply that, along with the reaction between two triplet molecules, deactivation by the ground-state dye takes place at about the same efficiency, for at an initial stage, where no appreciable quantities of Rd and Ox exist, the sum of $[D^T]$ and [D] is equal to $[D]_0$.

In a later stage of the decay curves in Fig. 14, quite a large quantity of Rd and Ox may be expected to exist, so there is a great possibility that these species are equally efficient quenchers of D^T. From the above results, one may approximately put $k_{T-T}=k_{T-S}=8.0\times10^8\ M^{-1}\ sec^{-1}$, where k_{T-T} and k_{T-S} are the second-order rate constants for, respectively reaction $D^T+D^T\rightarrow$ and the $D^T+D\rightarrow$reaction.

The decay of Rd was measured at 405 mμ. As Fig. 15 shows, the decay is a second-order process with regard to Rd, but deviation becomes apparent at a later stage. A second-order rate constant is 8.8—$10^7\ M^{-1}\ sec^{-1}$.

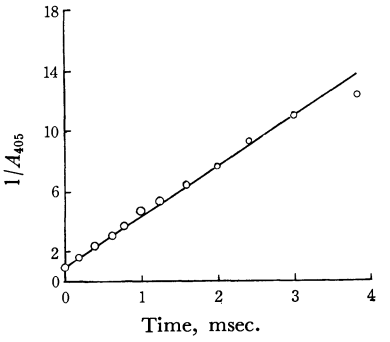

Fig. 15. Decay of Rd at 20 μM eosine.

The decay of Ox was measured at 450 mμ. The decay is complicated and cannot be expressed by a simple rate formula. It seems that first-order

and second-order processes are superimposed. At higher concentrations of Ox, the participation of the second-order process seems to increase.

If one puts

$$-\frac{dC}{dt}=k_1C+k_2C^2$$

then one can estimate the values of k_1 and k_2 by analysing the experimental data. They are $k_2=8.7\times10^8$ M^{-1} sec^{-1} and $k_1=9\times10^2$ sec^{-1}. The value of k_2, although not so reliable, agrees with the value of the decay constant for Rd, supporting the occurrence of the process Rx+Od→2D.

The nature of the superimposing first-order process is unknown.

As for the decay of the triplet state of the dye, it is accelerated more or less by the addition of oxygen, β-sulfonylanthraquinone, *p*-benzoquinone, ATU and EDTA. The air-saturated solution (10^{-4} M) and the solution containing 10^{-3} M *p*-benzoquinone do not give any appreciable triplet absorption spectra.

Figure 16 shows the relation between the first-order decay constant and the concentrations of EDTA and ATU.

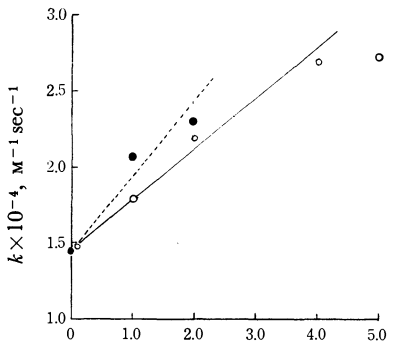

Fig. 16. Decay constant of triplet state for various reductant concentrations. Eosine: 10 μM
—○— Allylthiourea
--●-- EDTA

From the plots, one obtains, as the second-order rate constant for D^T+ATU→ and D^T+EDTA→ respectively, 3.4×10^5 M^{-1} sec^{-1} and 5×10^5 M^{-1} sec^{-1}.

The addition of ATU or EDTA promotes the decay of Ox. The decay curve is expressed by a simple first-order rate formula, as is shown in Fig. 17. From the plots, the rate constants for Ox+EDTA→D+EDTA$^+$ and Ox+ATU→D+ATU$^+$ are found to be respectively, 8×10^5 M^{-1} sec^{-1} and 1.0×10^6 M^{-1} sec^{-1}.

In the air-saturated solution, the absorption spectra near 450 mμ appear slightly only with quite a large input of energy. The addition of

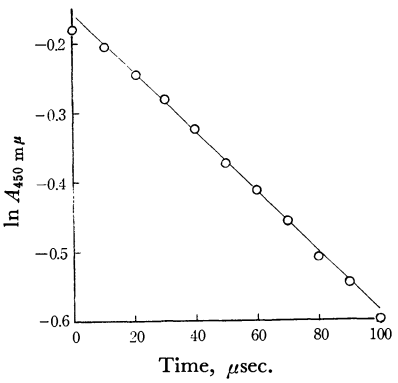

Fig. 17

$NaClO_3$ or $NaHAsO_4$ slightly lengthens the life of Ox. In the system containing *p*-benzoquinone, the life of Ox is only about 20 μsec., and the decay cannot be analyzed.

In the system containing $NaClO_3$ or $NaHAsO_4$, the decay of Rd at an earlier stage is a second-order process, while in a later stage it is a first-order process. The latter process may be attributed to the reaction between Rd and oxidants. Its rate constant is below 10^4 M^{-1} sec^{-1}.

In the case of ATU and EDTA, the decay consists of two parts, as has already been described. The decay for Rd'' (in the case of EDTA) is a first-order process, as Fig. 18 shows.

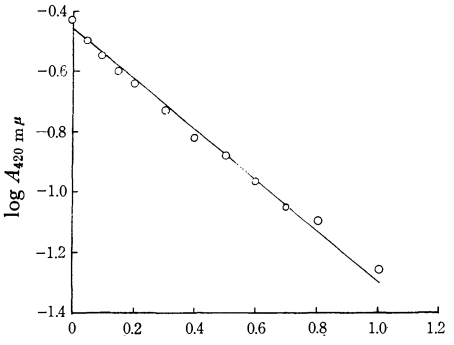

Fig. 18

The first-order rate constants is 1.0 sec^{-1}, independent of the concentration of EDTA. For ATU we did not succeed in getting a reliable value because of the bad reproducibility of the experiment.

Summary and Discussion

The elementary reactions established in the present paper may be summarized as follows:

D^T

$D^T \rightarrow D$ $\quad k \approx 6\times10^3\ sec^{-1}$

$D^T + D \rightarrow Ox + Rd$ (1a)
$D^T + D \rightarrow 2D$ (1b)
} For the sum of the two $k = 8.0\times10^8\ l.mol^{-1}\ sec^{-1}$

$D^T + D^T \rightarrow Ox + Rd$ (2a)
$D^T + D^T \rightarrow 2D$ (2b)
} For the sum of the two $k = 8.0\times10^8\ l.mol^{-1}\ sec^{-1}$

$D^T + ATU \rightarrow Rd'$ (3) $\quad k = 3.4\times10^5\ l.mol^{-1}\ sec^{-1}$

$D^T + EDTA \rightarrow Rd''$ (3') $\quad k = 5\times10^5\ l.mol^{-1}\ sec^{-1}$

The rate constants for 3 and 3', which had been obtained from the steady-light experiments,[1] are, respectively, $k = 3.1\times10^5$ and 4.1×10^5; these values are in excellent agreement with the above values.

The rate of reaction 2a is probably larger than that of 2b, but no comparison can be made between la and 1b.

Rd. Rd produced by la or 2a disappears by a second-order process, at least in the initial stage;

$$k = 8.8\times10^7\ l.mol^{-1}\ sec^{-1} \quad (4)$$

$Rd' \rightarrow$ leuco eosine
$Rd'' \rightarrow$ leuco eosine
} (not certain)

O x The reaction of Ox is rather complicated; it seems to be a superimposition of a first-order and a second-order reaction. The rate constants are, respectively:

$$k_5 = 9\times10^{-2}\ sec^{-1} \quad (5)$$

$$k_6 = 8.7\times10^8\ M^{-1}\ sec^{-1} \quad (6)$$

These data are not very reliable.

$$Ox + EDTA \rightarrow D + (EDTA)^+$$
$$k = 1\times10^6\ M^{-1}\ sec^{-1} \quad (7)$$

$$Ox + ATU \rightarrow D + (ATU)^+$$
$$k = 8\times10^5\ M^{-1}\ sec^{-1} \quad (7)$$

From the above rate constants, one can say definitely that the D–D mechanism (in the present case, the reaction between two D^T molecules) occurs under certain experimental conditions. Thus, from the rate constants for reactions 1, 2 and 3, the rate for the reaction between two dye molecules (the D–D-mechanism) is of the same order as that for the reaction between eosine and a reductant (ATU or EDTA) when the concentration of [D] is $\sim10^{-5}$ M and that of the reductant is $\sim10^{-2}$ M. If the reductant concentration is lower, the reaction due to the D-D mechanism will predominate.

The Ox thus produced will then react with the reductant or disappear according to 5 or 6. From the rate constant for 6, $8\times10^5\ M^{-1}\ sec^{-1}$, and for 7, $1\times10^6\ M^{-1}\ sec^{-1}$, the reaction 7 will predominate if $[Ox]=[Rd]\leqq10^{-8}$ M and if EDTA $\approx10^{-2}$ M. Hence, in such situations Rd will survive and will turn into leuco dye. This is just what may be expected via a D–D mechanism. Thus, the discussion so far, we believe, thoroughly confirms a D–D mechanism.

Most of the other results obtained in the present paper can be understood in terms of this scheme. Thus, the finding that $[Rd]\propto[D^T]^2$ can be interpreted on the assumption that the rate of the reaction is proportional to $D^T\times D^T$. No comment is needed for the fact that the yield ratio of Rd and Ox is 1 : 1.

However, the extent to which the back reaction, $Rd + Ox \rightarrow 2D$, occurs, is not yet clear enough, since some of Rd and some of Ox react independently of each other. The answers to such questions must await further study.

As to the nature of Rd' and Rd'', they are probably loose compounds of a half-reduced dye and a half-oxidized reductant. This conclusion depends on the following reasons: Firstly, from the rate constant of la on the one hand and that of 3 and 3' on the other, one can say that D–D and D–R mechanisms occur as competing processes under the experimental conditions in which Rd' and Rd'' are produced (see Tables I and II). Secondly, the fact that Rd'' obeys the first-order decay with the same rate constant, irrespective of the concentration of EDTA, can be interpeted by the above model, but perhaps not so well by other models.

It is very interesting that such a compound has a life as long as l sec., and that its absorption spectra are quite similar to those of free semiquinone. There is no assurance, however, that its molar absorbance is the same as that of the latter. Hence, the statement given regarding the ratio of Rd' or Rd'' to leuco dye is not decisive.

BULLETIN OF THE CHEMICAL SOCIETY OF JAPAN VOL. 39 240—243 (1966)

Studies of Scandium in Various Solutions. I. An Ion-Exchange Study of Scandium(III) Chloride and Nitrate Complexes

By Tatsuya SEKINE and Yuko HASEGAWA

Department of Chemistry, Tokyo College of Science, Kagurazaka, Shinjuku-ku, Tokyo

(Received April 30, 1965)

The complex formation of scandium(III) with chloride and nitrate ions has been investigated at 25°C. Scandium-46 was employed in conjunction with a cation-exchange resin (Dowex 50W X-12, 100—200 mesh) in the H^+-form and the ionic strength was maintained at 4.0 M with perchloric acid. The stability constants have been obtained graphically by a curve-fitting method and the following results were obtained.

	$\beta_n=[ScL_n^{3-n}]/[Sc^{3+}][L^-]^n$		
	$\log \beta_1$	$\log \beta_2$	$\log \beta_3$
Chloride	−0.12	−0.84	−1.40
Nitrate	0.28	−0.28	—

The chemical properties of trivalent scandium are known to be somewhat similar to those of trivalent lanthanides and yttrium. Scandium(III) is often included among the rare earth elements. However, its smaller ionic size and its higher electronegativity sometimes make this ion different from the other rare earth ions. Actually, the scandium ion in solutions is believed to be a better acceptor of various complex-forming ligands than the other rare earth ions.

This series will report on our studies of the chemical behavior of scandium in various solutions. Paper I will report on a study of scandium(III) complexes with chloride or nitrate ions.

The complex formation of scandium(III) in concentrated hydrochloric acid and nitric acid may easily be supposed from the ion-exchange adsorption or the solvent extraction of this ion from these acid media.[1-3] However, because of the low stability of these complexes, no quantitative data on the stabilities have been presented until quite recently.

The stability constants of scandium(III) chloride complexes were first studied by Paul[4] by potentiometry in perchlorate solutions at 0.5 M. The stability constants were also determined by Reed, Sutton and Morris[5] from an ion-exchange study in perchloric acid media at 0.691 M. However, no report on the stability constants of scandium(III) nitrate complexes seems to have been presented.

In the present work, the cation-exchange equilibria of scandium(III) at a tracer concentration were determined radiometrically at 25°C between an ion-exchange resin and 4.0 M H(Cl, ClO_4) or 4.0 M H(NO_3, ClO_4). These ionic media were chosen in order to make it possible to compare the results with those on trivalent lanthanide and americium complexes obtained in other work.[6]

The stability constants were determined graphically by a curve-fitting method[7] from the decrease in the ion-exchange adsorption with the increase in the ligand concentration in the aqueous phase.

Statistical Treatment

The distribution ratio of scandium(III) in equilibrium between a cation-exchange resin phase and an aqueous phase is defined as:

$$D=\frac{[Sc(III)]_R}{[Sc(III)]}=\frac{\text{Sc(III) per g. resin}}{\text{Sc(III) per ml. solution}} \quad (1)$$

where the subscript "R" denotes a species in the resin phase.

This can be calculated by radioactivity measurements as:

$$D=(T-vA)/(G\times A) \quad (2)$$

where T is the total radioactivity in the whole

1) K. A. Kraus and F. Nelson, "Proceedings International Conference on Peaceful Uses of Atomic Energy Geneva, 1955, Vol. VII," United Nations Publication, New York (1956), p. 837.
2) D. F. Peppard, G. W. Mason and J. L. Maier, *J. Inorg. Nucl. Chem.* **3**, 215 (1956).
3) T. Ishimori and E. Nakamura, "Data of Inorganic Solvent Extraction (1)." JAERI 1047, Japan Atomic Research Institute (1963).
4) A. D. Paul, *J. Phys. Chem.*, **66**, 1248 (1962).
5) G. L. Reed, K. J. Sutton and D. F. C. Morris, *J. Inorg. Nucl. Chem.*, **26**, 1463 (1964).
6) T. Sekine, *J. Inorg. Nucl. Chem.*, **26**, 1463 (1964); *Acta Chem. Scand.*, **19**, 1435 (1965).
7) F. J. C. Rossotti and H. Rossotti, "The Determination of Stability Constants in Solution," McGraw-Hill Book Co., Inc., New York (1961).

system; A is the radioactivity per ml. of the aqueous phase in equilibrium with the resin; v is the volume of the aqueous phase (ml.), and G is the weight of the resin (g.).

When no complex-forming ligand exists in the system, the distribution constant, K_{d_0}, can be written as:

$$K_{d_0}=[Sc^{3+}]_R/[Sc^{3+}] \quad (3)$$

where the subscript "0" denotes the absence of the ligand.

When the metal ion forms complexes with a mono-negative ligand, L^-, the net distribution ratio of the metal ion between the resin and the aqueous phase can be written as:

$$D=\frac{[Sc^{3+}]_R+[ScL^{2+}]_R+[ScL_2^{+}]_R}{[Sc^{3+}]+[ScL^{2+}]+[ScL_2^{+}]+[ScL_3]+\cdots} \quad (4)$$

The ion-exchange equilibrium constant for the "nth" complex may be defined as:

$$K_{d_n}=[ScL_n^{3-n}]_R/[ScL_n^{3-n}] \quad (5)$$

The formation and the over-all stability constant, β_n, of the "nth" complex can be described as:

$$Sc^{3+}+nL^- \rightleftarrows ScL_n^{3-n} \quad (6)$$

$$\beta_n=[Sc_n^{3-n}]/[Sc^{3+}][L^-]^n \quad (7)$$

By introducing Eqs. 3, 5 and 7 into Eq. 4, the following equation is obtained:

$$\frac{D}{K_{d_0}}=\frac{1+(K_{d_1}/K_{d_0})\beta_1[L^-]+(K_{d_2}/K_{d_0})\beta_2[L^-]^2}{1+\beta_1[L^-]+\beta_2[L^-]^2+\beta_3[L^-]^3+\cdots} \quad (8)$$

The constants in Eq. 8 can be determined by a curve-fitting method.[7]

In order to obtain a simpler function, a variable, a, and two parameters, R and B, are introduced into Eq. 8. Here a, R and B are $\beta_2^{1/2}$ $[L^-]$, $\beta_1\beta_2^{-1/2}$ and K_{d_1}/K_{d_0} respectively. Then:

$$\frac{D}{K_{d_0}}=\frac{1+BRa+(K_{d_2}/K_{d_0})a^2}{1+Ra+a^2+\beta_3\beta_2^{-3/2}a^3+\cdots} \quad (9)$$

It may be possible to discuss the problem more generally, but here the following assumptions are made as the first approximation:

(i) K_{d_2} is negligible compared to K_{d_1}.

(ii) Only the first and the second complexes exist in the solution.

On the basis of these assumptions, Eq. 9 can be written as:

$$y=(1+BRa)/(1+Ra+a^2) \quad (10)$$

By introducing various sets of values into R and B in Eq. 10, families of standard curves represented by the following equations are obtained:

$$\left.\begin{aligned} Y=\log y&=-\log(1+Ra+a^2)+\log(1+BRa)\\ X&=\log a\end{aligned}\right\} \quad (11)$$

One of these curves will be found to fit the plot of the experimental data, $\log(D/K_{d_0})$ vs. $\log[L^-]$.

The equilibrium constants can be determined from the parameters of this particular standard curve as follows:

From the definition,

$$\log a=\frac{1}{2}\log\beta_2+\log[L^-]$$

The value of $1/2\log\beta_2$ can be determined graphically from the difference between the value on the abscissa of the standard curve ($X=\log a$) and the value on the abscissa of the experimental data ($X=\log[L^-]$).

For example, one may compare the abscissa of the experimental data (plotted as $\log D/K_{d_0}$ vs. $\log[L^-]$) with that of the best-fitted curve (plotted as $\log y$ vs. $\log a$ (Eq. 11)). Then one can read the $\log[L^-]_0$ value on the abscissa of the experimental plot which coincides with the point, $\log a=0$, on the abscissa of the standard curve; this $\log[L^-]_0$ value should give the $\log a$—$\log[L^-]$ value.

From this $\log[L^-]_0$, $\log\beta_2$ can be determined as:

$$\log\beta_2=-2\log[L^-]_0$$

The $\log\beta_1$ value can then be determined as:

$$\log\beta_1=\log R+\frac{1}{2}\log\beta_2$$

and K_{d_1} can be determined as:

$$K_{d_1}=BK_{d_0}$$

If the assumptions i and ii cannot be adopted, the terms K_{d_2}/K_{d_0} and/or $\beta_3\beta_2^{-3/2}a^3$, etc., should be introduced into Eq. 11. Then the followings are obtained:

$$\log y=-\log(1+Ra+a^2+\beta_3\beta_2^{-3/2}a^3)+\log(1+BRa) \quad (12)$$

$$\log y=-\log(1+Ra+a^2)+\log\{1+BRa+(K_{d_2}/K_{d_0})a^2\} \quad (12')$$

$$\log y=-\log(1+Ra+a^2+\beta_3\beta_2^{-3/2}a^3)+\log\{1+BRa+(K_{d_2}/K_{d_0})a^2\} \quad (12'')$$

.....

and the curve-fitting can be continued as above.

More details of this method may be found in other articles (for instance, Ref. 7).

Experimental

Reagents.—The perchloric acid, the hydrochloric acid and the nitric acid used were of a reagent grade. The concentration of the acids was determined by titrations using potassium acid carbonate as the standard substance.

Radioactive Tracer.—Scandium-46 was used as the tracer. It was obtained from the Radiochemical Center, Amersham, England, as a hydrochloric acid solution. This tracer was purified by a solvent extraction method and diluted with 4.00 M hydrochloric

acid, nitric acid or perchloric acid. These solutions were then used as the stock solutions.

Cation-exchange Regin.—A Dowex 50 W X-12, 100—200 mesh, was used. The resin was conditioned alternately with 4 M hydrochloric acid and 4 M sodium chloride solution several times. The resin was finally made into a H^+-form and dried in an air-bath at 60°C overnight. Then it was equilibrated in the open air for several days and stored in a closed bottle. The exchange capacities of this resin were 3.62 meq./g. for Na^+ and 3.60 meq./g. for H^+.

Procedures.—All of the procedures were carried out in a thermostatted room at 25±0.5°C. About 100 mg. of resin was placed in glass-stoppered tubes (volume, 20 ml.) and weighed. The tracer solution and various amounts of hydrochloric acid or nitric acid were placed in the tubes, and then perchloric acid was added to make the aqueous phase 5.0 ml. and the ionic strength 4.0 M. The tubes with the contents were agitated by a mechanical rotator for about four hours in order to ensure an equilibrium. It was found in the preliminary experiments that the ion-exchange equilibrium was reached within two hours by the rotation. After the rotation was finished, the substances were centrifuged at 2000 r.p.m. for about three minutes. A two-milliliter aliquot of the solution was then pipetted out and transferred into a small test tube, and the γ-radioactivity of the aqueous phase was measured with a well-type (NaI) scintillation counter.

Results

The distribution ratios of scandium(III) between the resin and the aqueous perchlorate solutions with various amounts of chloride ions or nitrate ions are given in Table I. The plots of log (D/K_{d_0}) against log $[Cl^-]$ and log $[NO_3^-]$ are shown in Fig. 1.

The stability constants of the complexes were determined by the curve-fitting as follows. The plots in Fig. 1 were first compared with the families of the standard curves defined by Eq. 11. The plot of the data in the nitrate system was found to be well fitted by a standard curve which was obtained with the parameters $R=2.5$ and $B=0$. The stability constants were therefore determined from these values and $\log[L^-]_0=-0.14$. However, it was not possible to find a standard curve for the chloride system among the curves defined by Eq. 11, which fits the plot over all the ligand concentration region. The standard curve obtained by introducing $R=2$ and $B=0$ into Eq. 11 fits the plot in the lower concentration region when $\log[L^-]_0$ was 0.42, but it deviated from the plot upward as the ligand concentration increased. This seemed to indicate the formation of the third complex, $ScCl_3$. After many trials, a curve given by Eq. 12 was found to fits best when $R=2$, $B=0$ and $\beta_3\beta_2^{-3/2}=0.6$ were introduced into the equation. The log $[L^-]_0$ value was found to be 0.42 even after the introduction of the third term. The equilibrium constants were calculated from these values.

TABLE I. THE DISTRIBUTION RATIO OF Sc(III) AT 25°C
Ion-exchange resin: Dowex 50 W X-12

(A) 4.0 M H(Cl, ClO_4)

$[Cl^-]$	D	$[Cl^-]$	D
4.00	3.90×10	1.44	1.31×10^2
4.00	3.86×10	1.36	1.33×10^2
3.84	4.09×10	1.36	1.39×10^2
3.68	3.90×10	1.28	1.40×10^2
3.52	4.56×10	1.20	1.47×10^2
3.36	4.98×10	1.12	1.48×10^2
3.20	5.30×10	1.04	1.56×10^2
3.20	5.63×10	0.96	1.57×10^2
3.04	5.81×10	0.88	1.74×10^2
2.88	6.21×10	0.80	1.60×10^2
2.72	6.89×10	0.72	1.86×10^2
2.56	6.80×10	0.64	1.94×10^2
2.40	7.75×10	0.56	2.00×10^2
2.40	7.91×10	0.48	2.08×10^2
2.08	9.26×10	0.48	2.13×10^2
2.00	9.76×10	0.40	2.32×10^2
1.92	1.08×10^2	0.32	2.31×10^2
1.76	1.11×10^2	0.28	2.50×10^2
1.76	1.11×10^2	0.24	2.51×10^2
1.68	1.11×10^2	0.20	2.43×10^2
1.60	1.12×10^2	0.16	2.72×10^2
1.60	1.18×10^2	0.12	2.69×10^2
1.52	1.27×10^2	0.08	2.84×10^2
1.44	1.19×10^2	0.04	2.85×10^2

(B) 4.0 M H(NO_3, ClO_4)

$[NO_3^-]$	D	$[NO_3^-]$	D
4.00	1.83×10	1.20	7.63×10
3.84	1.94×10	1.12	7.50×10
3.68	1.99×10	1.04	8.05×10
3.52	1.98×10	0.96	8.64×10
3.20	2.37×10	0.80	1.03×10^2
3.04	2.43×10	0.68	1.16×10^2
2.88	2.70×10	0.56	1.30×10^2
2.72	2.79×10	0.52	1.43×10^2
2.56	3.19×10	0.48	1.38×10^2
2.40	3.40×10	0.40	1.59×10^2
2.24	3.46×10	0.32	1.72×10^2
2.08	3.81×10	0.28	1.86×10^2
2.00	4.51×10	0.24	1.96×10^2
1.92	4.59×10	0.22	2.14×10^2
1.84	4.82×10	0.20	2.23×10^2
1.68	5.41×10	0.20	2.21×10^2
1.60	5.74×10	0.12	2.54×10^2
1.52	5.92×10	0.08	2.55×10^2
1.44	6.15×10	0.04	2.65×10^2
1.28	6.66×10		

From these results, the constants were determined to be as shown in Table II.

Conclusion

From the results, the following conclusions may be drawn:

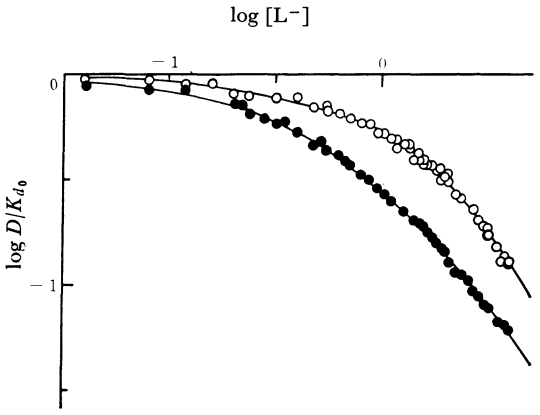

Fig. 1. The plot $\log D/K_{d_0}$ vs. $\log [L^-]$ of scandium(III) in nitrate and chloride media.
Ion-exchange resin: Dowex 50 W X-12 100—200 mesh
Aqueous phase: 4.0 M H(Cl, ClO_4) -○-
4.0 M H(NO_3, ClO_4) -●-
The curves drawn for the plots are
$\log D/299 = -\log (1+1.9[NO_3^-]+0.53[NO_3^-]^2)$
$\log D/299 = -\log (1+0.76[Cl^-]+0.14[Cl^-]^2 +0.04[Cl^-]^3)$

(1) The adsorption of scandium(III) from 4 M H(Cl, ClO_4) or 4 M H(NO_3, ClO_4) to Dowex 50W X-12 decrease with the increase in the ligand concentration. When the ligand concentration is the same, the decrease is always larger in the nitrate system.

(2) The change in the distribution ratio is explained by Eq. 4, together with the equilibrium constants in Table II.

(3) The constants in Table II seem to indicate that:

(a) The ScL^{2+} and ScL_2^+ species are formed both in the nitrate and in the chloride system.

(b) The ScL_3 species is negligible in the nitrate system, but it is formed in the chloride system.

(c) The adsorption of the ScL^{2+} or ScL_2^+ complexes to the ion-exchange resin is negligible.

Table II. Equilibrium constants for the ion-exchange adsorption and the stability constants for the chloride and the nitrate complexes of scandium(III) in 4.0 M H(Cl, ClO_4) and 4.0 M H(NO_3, ClO_4) at 25°C
Ion-exchange resin: Dowex 50 W X-12
$K_{d_0}=[Sc^{3+}]_R/[Sc^{3+}]$, $K_{d_1}=[ScL^{2+}]_R/[ScL^{2+}]$
$\beta_n=[ScL_n^{3-n}]/[Sc^{3+}][L^-]^n$

	Chloride	Nitrate
K_{d_0}	299	
K_{d_1}	0	0
$\log \beta_1$	−0.12	0.28
$\log \beta_2$	−0.84	−0.28
$\log \beta_3$	−1.40	—

In the present study, the above conclusions were reached by assuming the constancy of the activity coefficients of the chemical species. More precise argument will be possible when many more thermodynamical data are available.

The stability constants reported by Paul[4] and by Reed et al.[5] are summarized in Table III. The present results may not, however, be compared directly with those results because those experiments were carried out in aqueous solutions of a lower ionic concentration.

Table IV summarizes the stability constants of chloride complexes of lanthanum(III), europium(III), lutetium(III) and americium(III) in 4 M Na(Cl, ClO_4).[6]

From Tables II and IV, it may be concluded that the stability constants for the complexes MCl^{2+} and MCl_2^+ of these five metal ions are in the same order, but that only scandium(III) forms a MCl_3 complex under these experimental conditions.

Some part of the work was carried out at the Laboratory of Nuclear Chemistry, Institute o Physical and Chemical Research, Tokyo. The authors are so grateful to Professor Nobufusa Saito, the head of the laboratory.

Table III. Summary of stability constants of scandium(III) chloride complexes in previous work

Temp. °C	Ionic medium	β_1	β_2	K_1	K_2	Ref.
25°C	I=0.50	(11.7)	(128)	11.7±0.5	10.9±1.0	4
20°C	I=0.691	1.1±0.1	0.75±0.1	(1.1)	(0.7)	5

$K_n=\beta_n/\beta_{n-1}$

Table IV. Summary of the stability constants of chloride complexes of some lanthanides and americium in Ref. 6

Ionic medium 4 M Na(Cl, ClO_4)
Temp., 25°C

	La(III)	Eu(III)	Lu(III)	Am(III)
$\log \beta_1$	−0.22±0.11	−0.15±0.10	−0.35±0.07	−0.15±0.07
$\log \beta_2$	−0.64±0.11	−0.72±0.17	−0.57±0.05	−0.69±0.10

BULLETIN OF THE CHEMICAL SOCIETY OF JAPAN VOL. 39 244—246 (1966)

Studies of Scandium in Various Solutions. II. The Extraction of Scandium(III) with Tributyl Phosphate from Perchlorate-Chloride and Perchlorate-Nitrate Media

By Tatsuya SEKINE, Takeshi HAMADA and Mitsuo SAKAIRI

Department of Chemistry, Tokyo College of Science, Kagurazaka, Shinjuku-ku, Tokyo

(Received June 12, 1965)

The distribution of scandium(III) between organic tributyl phosphate solutions and aqueous perchlorate, nitrate, chloride solutions or mixed solutions of perchlorate-nitrate, perchlorate-chloride has been determined.

The distribution of scandium between 50% tributyl phosphate - chloroform and 4 M H(Cl, ClO_4) or 4 M H(NO_3, ClO_4) in some chloride or nitrate concentration region was higher than any of that distribution between the organic phase and 4 M perchloric acid, 4 M hydrochloric acid or 4 M nitric acid. It seems that the enhancement of the distribution ratios can be attributed to the extraction of mixed ligand complexes, but no simple relationship has been established between the distribution ratios and the proportion of the complex species in the aqueous phase as calculated from the previous data.

The extraction of scandium(III) in hydrochloric or nitric acid solutions with tributyl phosphate (TBP) was studied by Peppard, Mason and Maier.[1] They reported that the extraction of the metal ion increases very sharply with the increase in the acid concentration.

The complex formation of scandium(III) with chloride ions or nitrate ions in 4 M perchloric acid media was studied by Sekine and Hasegawa[2] by an ion-exchange method, and the stability constants for the complex species, $ScCl^{2+}$, $ScCl_2^+$, $ScCl_3$, $ScNO_3^{2+}$ and $Sc(NO_3)_2^+$, were determined.

For the present work, the authors determined the distribution of scandium(III) between organic solutions containing TBP and aqueous solutions of 4 M H(Cl, ClO_4) or 4 M H(NO_3, ClO_4) in order to study the variation in the metal distribution with the formation of scandium complexes in the aqueous phase.

Experimental

Tracers and Reagents.—^{46}Sc, ^{140}La, $^{152+154}Eu$, ^{177}Lu and ^{241}Am were used as the radioactive tracers. All the reagents used were of analytical grade. The preparation and the purification of the tracers and the reagents were carried out in ways which have been described previously.[2-5]

Procedures.—All the procedures were carried out in a thermostatted room at 25±0.5°C. The concentration of the sodium perchlorate solutions was determined by weighing the residue left after a certain amount of the solution had been evaporated in an air-bath at 120°C. The concentration of the acids was determined by titrations using potassium hydrogen carbonate as the standard. The organic phases were pre-equilibrated with the corresponding aqueous phase just before the experiments. In the experiments with sodium perchlorate, the aqueous phase was buffered with a small amount of acetate at pH 4 to 5. The organic and aqueous phases were agitated in glass tubes with a stopper by a mechanical shaker and then centrifuged. Two-milliliter aliquots were pipetted from both phases, and the γ-radioactivity was determined. The distribution ratios of the metal ions were calculated as:

$$D=\frac{\gamma\text{-count-rate per ml. of org. phase}}{\gamma\text{-count-rate per ml. of aq. phase}}$$

Results and Discussion

The results are given in Figs. 1 to 4. The organic phase was 10% TBP (by volume) in hexane for the experiments in Fig. 1, and 50% TBP (by volume) in chloroform for the other experiments.

The results in the figures may be summarized as follows:

i) Scandium(III) is extracted from perchlorate media into the organic phase better than trivalent lanthanides or americium. The results for the other four ions showed nearly the same tendency as had been reported previously.[6,7] (Fig. 1)

ii) The distribution of scandium(III) from 4 M (H, Na)ClO_4 is independent of the change in

1) D. F. Peppard, G. W. Mason and J. L. Maier, *J. Inorg. Nucl. Chem.*, **3**, 215 (1956).
2) T. Sekine and Y. Hasegawa, This Bulletin, **39**, 240 (1966).
3) T. Sekine, *J. Inorg. Nucl. Chem.*, **26**, 1463 (1964); *Acta. Chem. Scand.* **19**, 1435 (1965).
4) T. Sekine, This Bulletin, **38**, 1972 (1965).
5) T. Sekine and M. Ono, ibid., **38**, 2087 (1965).
6) S. Siekierski, *Polish Academy of Science, Institute of Nuclear Research*, 130/v (1960); *J. Inorg. Nucl. Chem.*, **12**, 129 (1959).
7) H. Yoshida, ibid., **26**, 619 (1964).

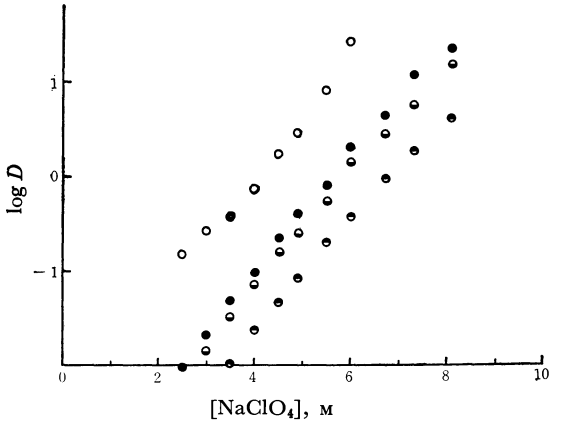

Fig. 1. Variation of the distribution ratios of Sc(III) (○), La(III) (●), Lu(III) (◒) and Am(III) (◓) between 10% TBP in hexane and sodium perchlorate solutions at various concentrations (pH 4—5). The results of Eu(III) are nearly the same as La(III).

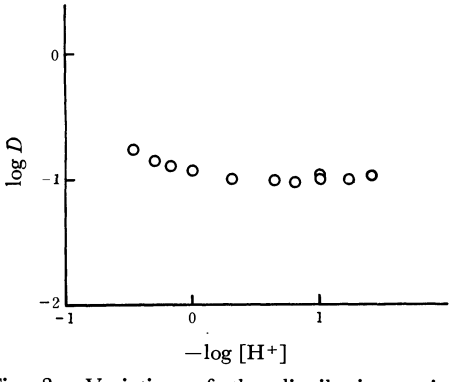

Fig. 2. Variation of the distribution ratio of Sc(III) between 50% TBP in chloroform and 4 M (H, Na)ClO_4 with the hydrogen ion concentration.

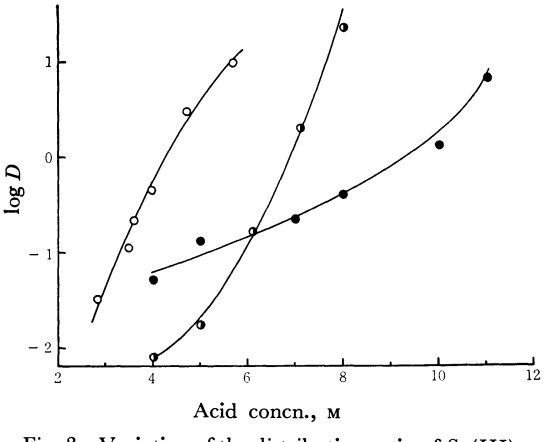

Fig. 3. Variation of the distribution ratio of Sc(III) between 50% TBP in chloroform and perchloric acid (○), hydrochloric acid (◑) or nitric acid (●) with the acid concentration.

the hydrogen ion concentration. However, it is slightly increased when the hydrogen ion concentration is above 1 M. (Fig. 2)

iii) The distribution of scandium from the perchloric acid solutions into the organic phase is much higher than that from hydrochloric or nitric acid solutions. Below 6 M, the distribution of scandium(III) from nitric acid is higher than that from hydrochloric acid, but the distribution ratios show an inverse order above 6 M. (Fig. 3)

iv) The distribution of scandium(III) from 4 M perchloric acid is enhanced by a replacement of the acid with 4 M hydrochloric or nitric acid. The enhancement is made larger by replacements with nitric acid than by those with hydrochloric acid. When the nitric acid content in the aqueous phase is about 0.6 M, the distribution ratio is four times that from pure perchloric acid, but the distribution ratio becomes lower than that from pure perchloric acid when more than half of the

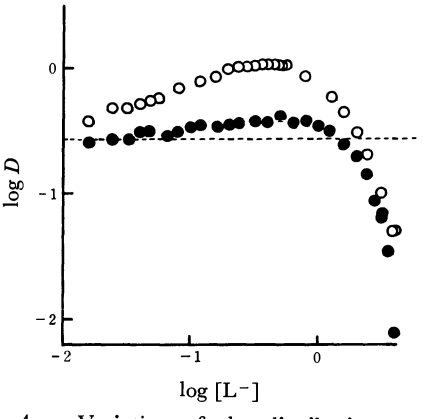

Fig. 4-a. Variation of the distribution ratio of Sc(III) between 50% TBP in chloroform and 4 M H(Cl, ClO_4) (●) or 4 M H(NO_3, ClO_4) (○) as functions of the chloride or nitrate concentration.

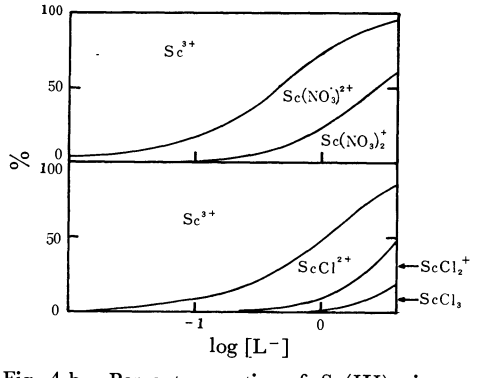

Fig. 4-b. Percentage ratios of Sc(III) nitrate or chloride complex species in 4 M perchloric acid as a function of the ligand concentration calculated from the stability constants given in Ref. 2.

acid is replaced with nitric or hydrochloric acid. (Fig. 4-a)

When L denotes nitrate or chloride ions, the scandium species in the organic phase distributed from the mixed acid media may generally be described as;

$$Sc(ClO_4)_aL_bH_{a+b-3}(TBP)_c$$

From the results in Fig. 4-a, one may conclude that the distribution of the mixed complex species is higher than that of the species containing only one kind of anion.

However, it seems difficult to establish any simple relationship between the variation in the distribution ratios and the compositions of the complex species in the corresponding aqueous phase, which are given in Fig. 4-b.

Part of the work was carried out at the Laboratory of Nuclear Chemistry, Institute of Physical and Chemical Research, Tokyo. The authors are very grateful to Professor Nobufusa Saito, the head of the laboratory. The authors are also grateful to Miss Yuko Hasegawa and Mr. Ichiro Kobayashi of the present laboratory for their experimental aid and valuable discussions.

BULLETIN OF THE CHEMICAL SOCIETY OF JAPAN VOL. 39 246—249 (1966)

The Spectra and the Conductances of Alizarine Saphirol SE in Water-Ethanol Mixtures

By Masaru MITSUISHI and Gensaku AIDA

Faculty of Fiber Science and Technology, Shinshu University, Ueda, Nagano

(Received April 30, 1965)

In order to explore the behavior of Alizarine Saphirol SE in water-ethanol mixtures, the absorption spectrum and the conductance of the dye solution were obtained. A characteristic spectrum of the dye aggregate in water is found to change gradually into a monomer spectrum with an increase in the proportion of an added ethanol. Moreover, the dye is found to show marked McBain effect in water, while showing a conductance curve typical of a weak electrolyte in 58.7% (v/v) ethanol.

A characteristic spectrum for an aggregate has been found in some solutions of such aromatic compounds as dyes.[1-4] In the spectrum of the solution of such compounds, with an increase in the proportion of an added organic solvent, the monomer peak is found to be intensified at the expense of the dimer and the higher multimers. This reduction of the aggregation has generally been ascribed to the reduced polarity of the medium.

Further, the so-called McBain effect has been found in equivalent conductances of such compounds in aqueous solutions, in which ionic micells are formed.[5-7] The McBain effect is, however, supposed to diminish as a result of the reduction of the aggregation of such compound in water-ethanol mixtures.

Some of these compounds, which behave as strong electrolytes in water, are supposed to behave as weak electrolytes in water - organic solvent mixtures with low dielectric constants as a result of the increase in the Coulombic attraction between ions of opposite charges.

Very little comparative investigation of the spectrum and the above-described conductance has been made. Alizarine Saphirol SE (sodium salt of 1, 5-dihydroxy-4, 8-diamino anthraquinone-2-sulfonic acid) may be considered, judging from its structure, to aggregate strongly in an aqueous solution. Therefore, it seemed valuable to explore the behavior of the dye in water-ethanol mixtures.

Experimental

Materials.—Alizarine Saphirol SE (C. I. Acid Blue 43, sodium salt of 1, 5-dihydroxy-4, 8-diaminoanthraquinone-2-sulfonic acid) was supplied by the Mitsui Chemical Industries Co., Ltd., and was purified as follows. The benzene-soluble impurities in the dye were removed by extraction with purified benzene. After the salting-out with sodium chloride from an aqueous solution had been repeated, sodium ions and chloride ions were removed completely through cation exchange

1) E. Rabinowitch and L. F. Epstein, *J. Am. Chem. Soc.*, **63**, 69 (1941).
2) L. Michaelis and S. Granick, ibid., **67**, 1212 (1944).
3) D. R. Lemin and T. Vickerstaff, *Trans. Faraday Soc.*, **43**, 491 (1947).
4) P. Mukerjee and A. K. Ghosh, *J. Phys. Chem.*, **67**, 193 (1963).
5) C. Robinson, *Trans. Faraday Soc.*, **31**, 245 (1935).
6) C. Robinson and H. E. Garret, ibid., **35**, 771 (1935).
7) N. Ando, *J. Chem. Soc., Japan (Nippon Kwagaku Kwaisi)*, **64**, 1305, 1431 (1943).

resin (Amberlite IR-120) and also anion exchange resin (Amberlite IRA-410). Finally, the solution was neutralized with sodium hydroxide, concentrated under reduced pressure, and dried at 105°C.

Ethanol and urea of a guaranteed reagent grade were used.

Spectrophotometric Measurements.—The spectrophotometric measurements were carried out in a Shimadzu Spectrophotometer, QV50, using a 10 mm. cell.

Conductance Measurements.—The circuit of the conductance bridge is shown in Fig. 1, in which R is a General Radio variable resistance (10 kΩ—0.1 Ω)

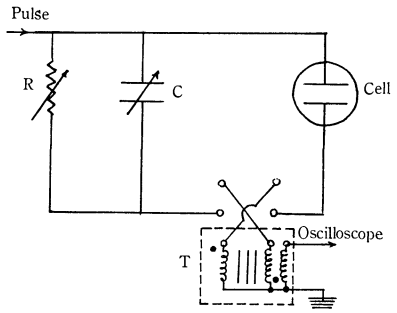

Fig. 1. Circuit of bridge.

with an error of 0.05%, C is an air-variable condenser, and T is a pulse-transformer. An oscilloscope was used as an indicator of the bridge balance. Conductances were measured at 25±0.1°C in a Komatsu-Yamato Coolnics CTR-1 thermostat. The specific conductances of the solvents were always less than 1.0×10^{-6} mhos. Two conductance cells with different cell constants, 0.05336 and 0.26706, were used.

Results and Discussion

The absorption spectra of Alizarine Saphirol in water are shown in Fig. 2, in which the spectrum is characterized by a prominent peak at about 590 mμ, or an α band, and a small shoulder at about 620 mμ, or a β band. With an increase in the concentration of the dye, Beer's law does not hold; the extinction coefficients at about 590 mμ and 620 mμ diminish, and also the shoulder falls progressively. This may be ascribed to the formation of aggregates of the dye in water.

The absorption spectra of Alizarine Saphirol in water-ethanol mixtures are shown in Fig. 3, in which both the α and β band are intensified and shift slightly towards longer wavelengths, with an increase in the proportion of an added ethanol, and in which the β band is more intensified than the α band in 30%, 40% (v/v) and richer ethanol solvents. This effect of ethanol on the spectrum of the dye is supposed to be the reduction of the aggregation due to the reduced polarity of the medium. A similar effect of ethanol was found by Rabinowitch and Epstein on Methylene Blue.[1]

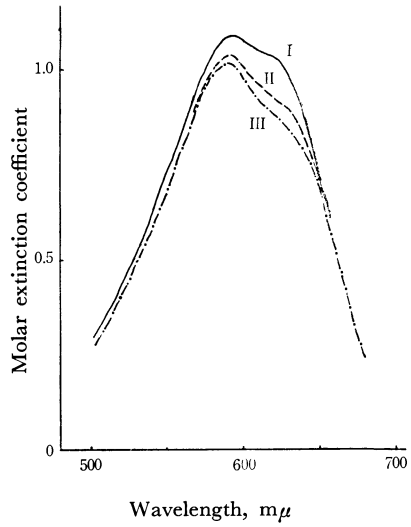

Fig. 2. Spectrum of Alizarine Saphirol SE in water at room temperature.
Concentration of the dye:
Curve I, 1.274×10^{-5} M; II, 6.370×10^{-5} M; III, 12.74×10^{-5} M

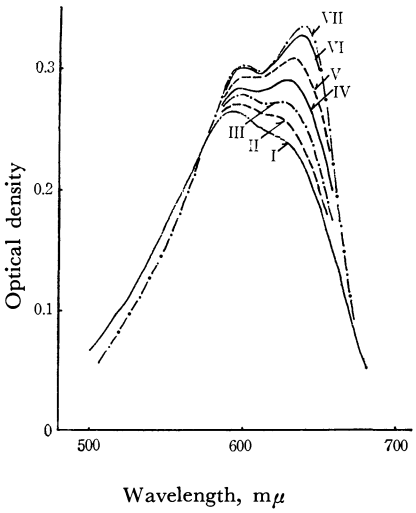

Fig. 3. Spectrum of Alizarine Saphirol SE in water-ethanol mixtures at room temperature.
Optical densities determined in 10 mm. cells.
Concentration of ethanol by volume: curve I, 0%; II, 10%; III, 20%; IV, 30%; V, 40%; VI, 60%; VII, 90%(v/v)

In order to compare the effect of ethanol with that of urea on the spectrum of the dye, the spectrum of Alizarine Saphirol in the presence of urea is shown in Fig. 4, in which, with an increase in the proportion of an added urea, both the α and the β band shift towards longer wavelengths. The optical density of the β band is larger than that of the α band in 7.2 M urea aqueous solution. The effect of the addition of urea is very similar

qualitatively to that of ethanol, as is shown in Fig. 3. Thus urea is considered to reduce the aggregation of the dye in water.

The effects of the temperature on the spectra of Alizarine Saphirol in water-ethanol mixtures are shown in Fig. 5. In Fig. 5, both the α and β bands of the dye in water and 30% (v/v) ethanol are intensified with raising the temperature, although β band appears to be intensified more than the α band. The rise in the temperature seems to reduce the aggregation due to the change in structural properties of water. No marked temperature effect on the spectrum of Alizarine Saphirol is, however, found in either 60 or 90% (v/v) ethanol. From these findings in the spectra, it may be considered that the shift of the spectra with an increase in the concentration of Alizarine Saphirol in an aqueous solution in Fig. 2 is due to the increase in number of aggregates, while the shift of the spectra with an increase in the proportion of an added ethanol (in Fig. 3) or urea (in Fig. 4) is due to the inhibition of the aggregation. These findings in the spectra, however, give no suggestion whether ethanol and urea prevent aggregation by interacting with water molecules related with the aggregation mechanism, or by interacting with Alizarine Saphirol directly.

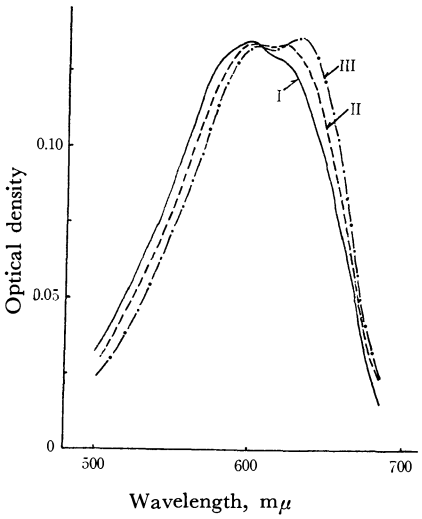

Fig. 4. Effect of urea on the spectrum of Alizarine Saphirol SE in aqueous solution. Optical densities determined in 10 mm. cells. Concentration of urea: curve I, 0 M; II, 1.6 M; III, 7.2 M

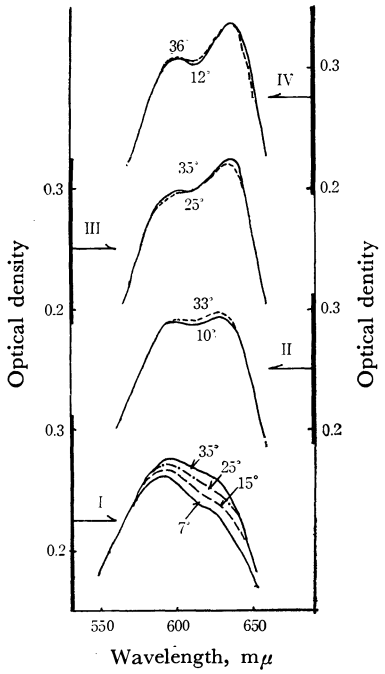

Fig. 5. Effect of temperature on the spectrum of Alizarine Saphirol SE in water-ethanol mixtures. Optical densities determined in 10 mm. cells. Concentration of ethanol by volume: curve I, 0%; II, 30%; III, 60%; IV, 90%

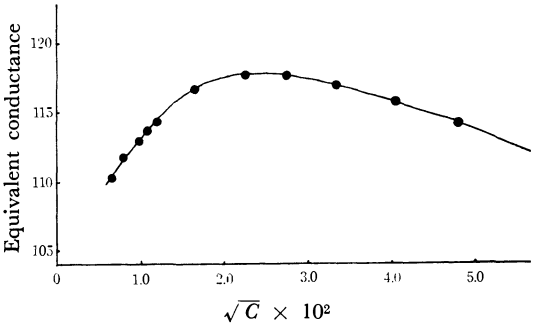

Fig. 6. Equivalent conductance of Alizarine Saphirol SE in water at 25±0.1°C.

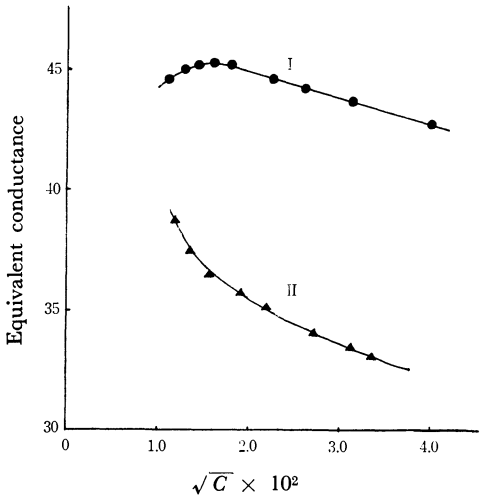

Fig. 7. Equivalent conductance of Alizarine Saphirol SE in water-ethanol mixtures at 25± 0.1°C.
Concentration of ethanol by weight: curve I, 34.9%, II, 58.7%.

The equivalent conductances (Λ) of Alizarine Saphirol in water are plotted against the square root of the molar concentration, $\sqrt{C}$, in Fig. 6. The Λ-$\sqrt{C}$ curve reaches a maximum, and the so-called McBain effect is found in the curve which suggests the presence of ionic micells. The curves I and II in Fig. 7 show the equivalent conductances in 34.9 and 58.7% (v/v) ethanol respectively. Also the McBain effect is found in 34.9% ethanol (curve I), the conductances decrease gradually with an increase in the concentration of the dye in 58.7% ethanol (curve II). This conductance behavior of curve II is similar to that of a weak electrolyte. Thus, in 58.7% ethanol, Alizarine Saphirol is supposed not to form aggregates, but to exist as a monomer. These conductance findings are in agreement with the considerations made from the spectrophotometric evidence.

Since Alizarine Saphirol is the sodium salt of a sulfonic acid, it will behave as a strong electrolyte in an aqueous solution. However, it is natural for Alizarine Saphirol to behave as a weak electrolyte in water-ethanol mixtures of a low dielectric constant due to the increase in Coulombic attraction between ions of opposite charges.

Summary

The absorption spectra and the conductances of Alizarine Saphirol SE (sodium salt of 1, 5-dihydroxy-4, 8-diaminoanthraquinone-2-sulfonic acid) in water-ethanol mixtures have been obtained, and the dispersed states of the dye have been examined qualitatively.

1) A characteristic spectrum of the dye aggregate in water has been obtained; a prominent peak at about 590 mμ and a small shoulder at about 620 mμ were found in the spectrum, and Beer's law did not hold. Alizarine Saphirol showed a marked McBain effect in an equivalent conductance in water.

2) The small shoulder of the spectrum at about 620 mμ changed to a prominent peak with an increase in the proportion of ethanol added, and the absorptions at both about 590 and about 620 mμ shifted towards longer wavelengths. The dye did not show any McBain effect, and the typical conductance curve of a weak electrolyte was obtained in 58.7% (v/v) ethanol.

The authors wish to thank Professor Masatoki Yokoi for his helpful discussions.

BULLETIN OF THE CHEMICAL SOCIETY OF JAPAN VOL. 39 249—253 (1966)

The Chlorine Quadrupole Resonances of Ethane Derivatives

By Seiichi KONDO

Laboratory of Physical Chemistry, Osaka University of Liberal Arts and Education, Tennoji-ku, Osaka

(Received May 1, 1965)

The temperature broadening of the chlorine quadrupole resonance line-width was studied in three ethane derivatives (1, 1, 1-trichloroethane, hexachloroethane and 1, 1, 1, 2-tetrachloro-2, 2-dimethylethane) below the plastic crystalline phases. Most of the resonance frequencies observed at the temperature of liquid nitrogen were equal to those reported in the literature. The energies of activation (2.2, 2.6 and 4 kcal./mol. respectively for the three compounds mentioned above) were obtained from the line-width versus temperature curves in the low temperature phases. It was suggested, considering the smallness of the energies of activation, that the vibrational rotation of the molecule as a whole rather than the internal axial rotation may exist in those phases.

Gutowsky and McCall[1] and Tatsuzaki and Yokogawa[2] reported a temperature shift of the chlorine quadrupole resonance frequencies in chlorine-substituted hydrocarbons. Many of these compounds possess plastic crystal phases just below the melting points, and the molecules are in rotational or disordered states in such phases. These authors showed, from an analysis of the temperature shift of the resonance frequencies, that the resonance signals of these compounds fades out at certain temperatures below the plastic crystal phases; they interpreted this phenomenon as resulting from the increase in the degree of molecular rotation. The purpose of the present investigation is to study this phenomenon in further detail with respect to the temperature effect of the line-width and of the

1) H. S. Gutowsky and D. W. McCall, *J. Chem. Phys.*, **32**, 548 (1960).
2) I. Tatsuzaki and Y. Yokogawa, *J. Phys. Soc. Japan*, **12**, 802 (1957).

TABLE I. SUMMARY OF RESULTS OF THE PRESENT EXPERIMENTAL STUDIES

	CH_3CCl_3	C_2Cl_6	$CCl_3CCl(CH_3)_2$
Melting point, °K	240	—	452
Transition point, °K	224 205	344 318	234
Resonance frequency at 77°K, kc.	38216(a) 38036(b) 37820(c)	40752(a) 40710(b) 40678(c) 40539(d)	39159(a) 39092(b) 35192(c)
Fade-out temperature, °K	150	250	230
Activation energy, kcal./mol.	2.2	2.6	4.0

signal-to-noise ratio of chlorine quadrupole resonance signals for 1, 1, 1-trichloroethane, hexachloroethane and 1, 1, 1, 2-tetrachloro-2, 2-dimethylethane at atmospheric pressure.

Experiments

Materials.—Hexachloroethane and 1, 1, 1-trichloroethane of a commericial reagent grade were vacuum-sublimed into glass ampoules for the resonance measurement. The observed melting and transition points are summerized in Table I; they are in satisfactory agreement with those reported in the literature. 1, 1, 1, 2-Tetrachloro-2, 2-dimethylethane was synthesized from chloretone and phosphorus pentachloride by the method reported by McElvin and Stevens.[3] The raw material thus obtained was recrystallized several times from an ethanol solution and sublimed under vacuum into glass ampoules for the measurement. The same material was used for the dielectric measurement. The observed melting and transition points are listed in Table I. The chlorine content of the material purified in this way was analyzed to be 71.74%, almost equal to the calculated values of 72.4%. The electric capacity versus the temperature curve changed quite sharply at the transition point, as is shown in Fig. 1, indicating that the material was quite pure. The plastic crystal phase of this material was observed to be isotropic by optical measurements, and the X-ray diffraction lines of a powder sample of this phase were interpreted satisfactorily as having a body-centered cubic structure.

Chlorine Quadrupole Resonance Measurements.—A self-quenching super-regenerative detector described by Dean[4] was used for the detection of the resonance signals. When the signal was strong, the resonance frequency was measured by an oscilloscope with a heterodyne-frequency meter calibrated by JJY, with an accuracy of ±1 k c. p. s. In order to determine the resonance characteristics, the resonance signal was frequency-modulated with the modulation frequency of 80 c. p. s. amplified with a narrow-band amplifier of the feed-back type, with a band-width of 2 c. p. s. and 80 db. amplification, and then recorded through a phase-sensitive detector. In this case, the accuracy of the frequency measurement was about ±2 k c. p. s.

Measurements at Low Temperatures.—The samples were kept in a petroleum ether bath cooled with liquid nitrogen from outside of the container bath. Below the solidifying temperature of petroleum ether, approximately 120°K, powder of the sodium chloride was mixed with petroleum ether in order to increase the thermal conductivity of solid ether; the temperature was kept very nearly constant, within ±0.1°C/min., during the measurements. Since these substances have marked phase transitions, they have to be cooled very slowly through the transition point in order to make the resonance characteristics reproducible under thermal equilibrium conditions. In the present case, about three hours were required to cool the sample from room temperature to stable and reproducible resonance conditons at the temperature of liquid nitrogen.

Dielectric Measurements.—The dielectric measurements of 1, 1, 1, 2-tetrachloro-2, 2-dimethylethane were carried out using a low-frequency bridge described elsewhere.[5] Since this material decomposes quite easily near the melting point, the measurement was undertaken only below room tempareture with a powder sample kept in a vacuum-sealed glass cell and with a platinum electrode installed inside the cell. By this apparatus, the absolute value of the dielectric constant could not be obtained, but a relative change in the electric capacity of the sample cell with the variation in temperature was measured, as shown in Fig. 1.

Experimental Results and Discussion

1, 1, 1-Trichloroethane.—Three resonance lines a, b and c were observed at the temperature of liquid nitrogen, as Table I shows, in an intensity ratio of roughly 2 : 3 : 1. The a and b lines were identified with those already reported by Gutowsky and McCall.[1] The curves of the temperature versus frequency, the half-value width and the signal-to-noise ratio for the b line are illustrated in Figs. 2, 3 and 4 respectively. The a and c lines have characteristics similar to those of the b line. The contribution of the intramolecular or overall rotational motions of the molecule to the line-width, $\Delta\nu$, of the signal becomes important as the temperature approaches the rotational phase transition point, as is shown by the broken line in Fig. 3 (from 110°K to 170°K). As has been discussed by Das and Hahn,[6] the activation energy, E, for

3) S. M. McElvin and C. Stevens, *J. Am. Chem. Soc.*, **69**, 2667 (1947).
4) C. Dean, *Phys. Rev.*, **96**, 1053 (1954).
5) S. Kondo and T. Oda, This Bulletine, **27**, 567 (1954).
6) T. P. Das and E. L. Hahn, "Nuclear Quadrupole Resonance Spectroscopy," Academic Press, New York (1958) PP. 64—70.

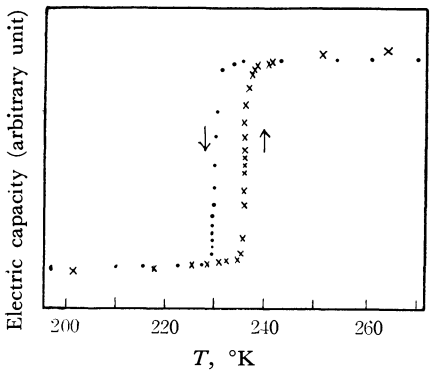

Fig. 1. Electric capacity versus temperature curve of $Cl_3CCl(CH_3)_2$.

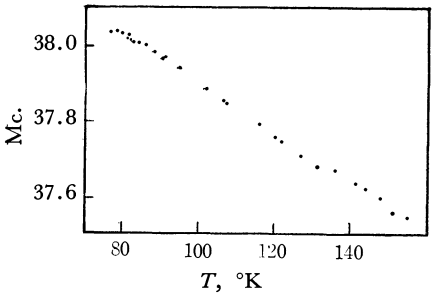

Fig. 2. Frequency versus temperature curve of the b line of Cl_3CCH_3.

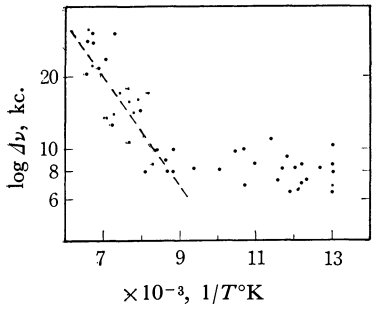

Fig. 3. Half-value width versus temperature curve of the b line of Cl_3CCH_3.

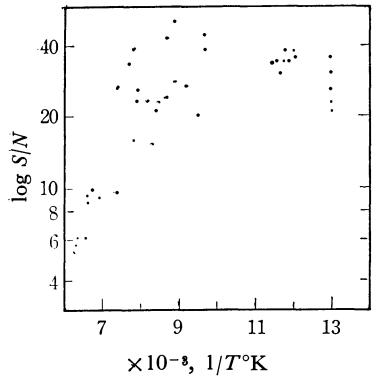

Fig. 4. Signal-to-noise ratio versus temperature curve of the b line of Cl_3CCH_3.

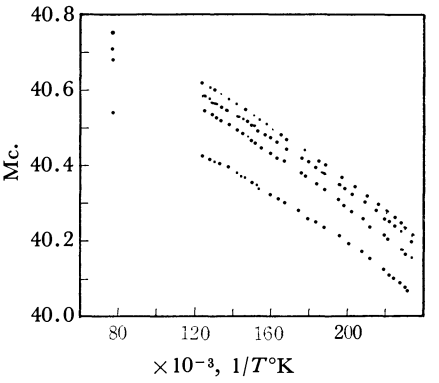

Fig. 5. Frequency versus temperature curves of four lines of C_2Cl_6.

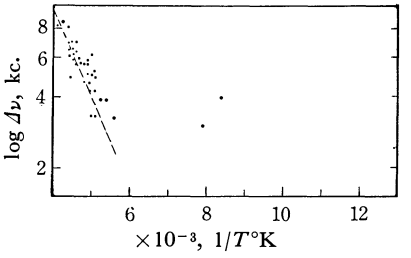

Fig. 6. Half-value width versus temperature curve of the a line of C_2Cl_6.

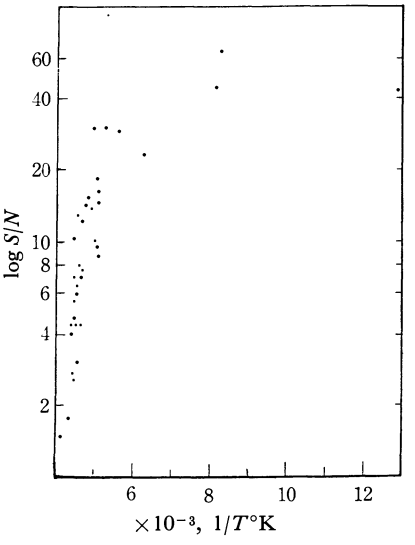

Fig. 7. Signal-to-noise ratio versus temperature curve of the a line of C_2Cl_6.

the molecular rotation can be obtained from the slope of the curve shown in Fig. 3. For example, Buyl-Bodin[7] described this curve by the following expression;

7) M. Buyl-Bodin, *Ann. Phys.*, (12) **10**, 533 (1955).

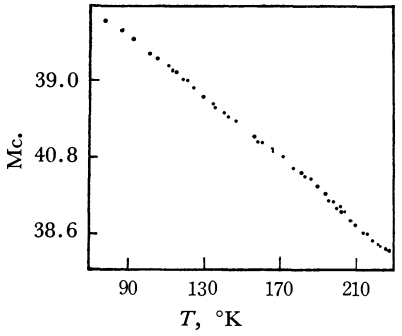

Fig. 8. Frequency versus temperature curve of the a line of $CCl_3CCl(CH_3)_2$.

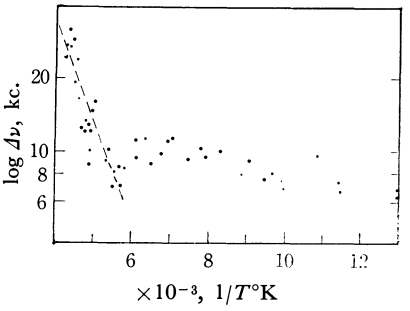

Fig. 9. Half-value width versus temperature curve of the a line of $CCl_3CCl(CH_3)_2$.

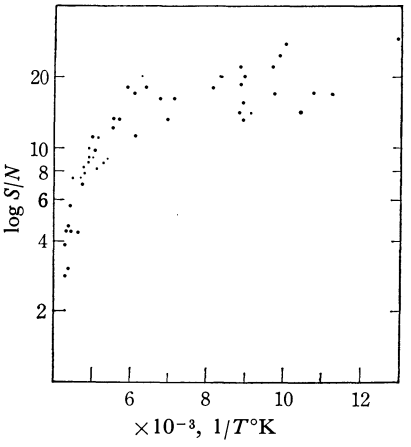

Fig. 10. Signal-to-noise ratio versus temperature curve of the a line of $CCl_3CCl(CH_3)_2$.

$$\frac{1}{\Delta\nu}\frac{d\Delta\nu}{dT}=\frac{E}{RT^2}$$

where T is the absolute temperature and R is the gas constant. From this equation, the value of E is calculated to be 2.2 kcal./mol. in the temperature range from 110°K to 170°K. Since the methyl groups of this molecule start rotating at about −180°C, according to the study of nuclear magnetic resonance by Powles and Gutowsky,[8] it seems that the internal rotation of the constituent groups and

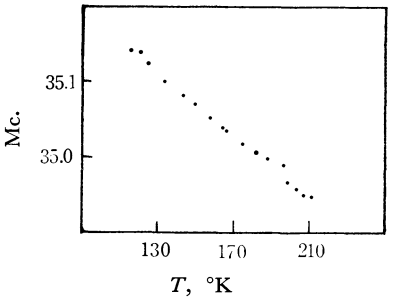

Fig. 11. Frequency versus temperature curve of the c line of $CCl_3CCl(CH_3)_2$.

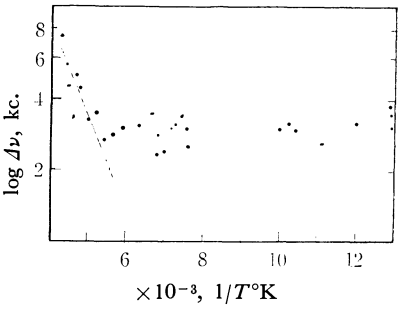

Fig. 12. Half-value width versus temperature curve of the c line of $CCl_3CCl(CH_3)_2$.

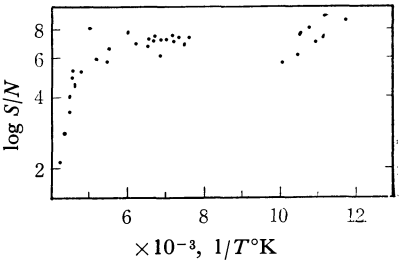

Fig. 13. Signal-to-noise ratio versus temperature curve of the c line of $CCl_3CCl(CH_3)_2$.

the rotatation of the molecule as a whole occur simultaneously near the fade-out temperature.

Hexachloroethane.—The four resonance lines, a, b, c and d, observed at 77°K, can clearly be identified with those reported by Gutowsky and McCall[1] and by Tatsuzaki and Yokogawa[2]. The curves of the frequency, the line-width and the signal-to-noise ratio versus the temperature for the a line are shown in Figs. 5, 6 and 7 respectively. The corresponding curves of the other lines are similar to those of the a line. The activation energy for rotation, obtained in the same way as in the case of 1, 1, 1-trichloroethane from Fig. 6, (in the temperature range from 160°K to 250°K), is about 2.6 kcal./mol. This value seems to correspond

8) J. P. Powles and H. S. Gutowsky, *J. Chem. Phys.*, **21**, 1695 (1953).
9) R. Livingston, *J. Phys. Chem.*, **57**, 496 (1957).

to the activation energy of the rotation of the molecule as a whole, since the value is much smaller than the activation energy of the internal rotation of this molecule (about 10 kcal./mol.) obtained by Morino and Iwasaki.[10]

1, 1, 1, 2-Tetrachloro-2, 2-dimethylethane.— Three resonance lines a, b and c were observed as shown in Table I. The a and b lines have frequencies higher than that of the c line. As has been discussed by Hooper and Bray,[11] the a and b lines can be assigned to the three chlorine atoms bonded (more covalently) to the same carbon atom at the position 1 while the c line can be assigned to the single carbon atom bonded (less covalently) to carbon 2.

The curves of the frequency, the line-width and the signal-to-noise ratio versus the temperature for the a and c lines are shown in Figs. 8 through 13. These three lines fade out at about 230°K; this is just below the phase transition temperature (234°K) obtained by the dielectric measurements illustrated in Fig. 1. The activation energies obtained from the line-width versus the temperature curves of the lines a and c shown in Figs. 9 and 12 are about 4 kcal./mol. Figures 9, 10, 12 and 13 indicate that the activation energy and the temperature dependence of the line-width and the signal-to-noise ratio are quite similar in the lines a and c; this may imply that the motions of the chlorine atoms at the positions 1 and 2 are nearly alike as far as the present measurements are concerned. This result may provide further indirect support for the assumption that the molecule as a whole rotates in this temperature range.

The author wishes to express his thanks to Professor Shizuo Fujiwara for his help in the course of the present study, and also to Miss Michiko Motoi, and Messrs. Sumitoshi Kumimoto, Masaji Ura, Tatsuyoshi Matsu-ura for their experimental assistance.

10) Y. Morino and M. Iwasaki, *J. Chem. Phys.*, **17**, 216 (1949).
11) H. O. Hooper and P. J. Bray, ibid., **33**, 334 (1960).

BULLETIN OF THE CHEMICAL SOCIETY OF JAPAN VOL. 39 253—256 (1966)

Pyrazolotropolones and Their Derivatives[1)]

By Shô Itô, Kahei Takase, Norio Kawabe and Hiroshi Sugiyama

Department of Chemistry, Faculty of Science, Tohoku University, Katahira-cho, Sendai

(Received May 4, 1965)

Two new methods have been developed to synthesize pyrazolotropone derivatives. 2-Methoxy-3, 5, 7-tribromotropone reacts with diazomethane to yield 4, 6-dibromo-7-methoxy-1-methyl-8(1*H*)-cyclohepta[c]pyrazolone, whereas the alkaline treatment of 4-acetyltropolone tosylhydrazone provides 3′-methylpyrazolo[3, 4-c]tropolone and 3′-methylpyrazolo[4, 3-d]tropolone. The structure of these products has been elucidated.

The reaction of diazomethane with troponoids, apart from the normal methylation of the tropolone hydroxyl, has been studied by Nozoe et al.,[2)] who found that the reagent attacked 2-halotropones and 4-methoxytropone to form pyrazolotropone derivatives, although the exact location of the pyrazole ring on the tropone nucleus was not established. We now wish to report on the structure of the products from a similar reaction of halomethoxytropones, as well as a new method to synthesize pyrazolotropolones.

3, 5, 7-Tribromotropolone[3)] (I), when treated in methanol with an excess of ethereal diazomethane at room temperature, first formed 2-methoxy-3, 5, 7-tribromotropone (II); this soon dissolved to an orange-red solution. The evaporation of the solvent, which served to liberate the hydrogen bromide, followed by alumina chromatography, yielded pale yellow, silky needles of III (m. p. 158°C) in a 30% yield. The same compound was also prepared in a 54% yield by the action of diazomethane on II.

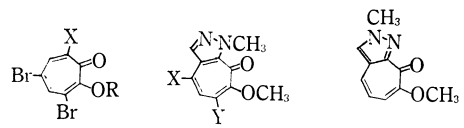

I R=H, X=Br
II R=CH_3, X=Br
XII R=X=H

III X=Y=Br
IV X=Cl, Y=Br or X=Br, Y=Cl
Va X=Y=H

Vb

1) Presented in part at the Tohoku Local Meeting of the Chemical Society of Japan, Yonezawa, June, 1963.
2) T. Nozoe, T. Mukai and T. Asao, to be published.
3) T. Nozoe, S. Seto, K. Kitahara, M. Kunori and Y. Nakayama, *Proc. Japan Acad.*, **26**, (7), 38 (1950).

Table I. NMR data*1

Compd No.	C-CH_3	O-CH_3	N-CH_3	CH_3CO	Aromatic protons on 7-membered ring	Aromatic protons on 5-membered ring
III		3.97*2	4.47		7.63	8.08
IV		3.96	4.47		7.40	8.11
V		3.88	4.46		6.4—6.9(m)*3	7.84
					7.0—7.3(q)*3	
IX	2.49			2.36	7.16(d, J=13)	
				3.61	7.40	
					8.88(d, J=13)	
XI	2.51	3.94	4.47		6.5—6.9(m)*3	
					7.0—7.3(q)*3	
XIII		3.93	4.15		7.80	8.46

*1 Spectra are refered to for deuteriochloroform solution. Chemical shift (δ) is expressed in p. p. m. from internal tetramethylsilane, coupling constants (J) being in c. p. s.
*2 Singlet unless shape of signal is stated by d for doublet, q for quartet and m for multiplet.
*3 ABX type of pattern, representing two and one proton respectively.

The ultraviolet spectrum indicates the presence of a tropone nucleus in III, while its NMR spectrum (cf. Table I) shows the presence of O-CH_3 (3.97 p. p. m.),[4] N-CH_3 (4.47 p. p. m.), and two isolated nuclear protons at 7.63 p. p. m. and 8.08 p. p. m. These spectroscopic observations, together with the analytical data and the fact that hydrogen bromide was liberated during the reaction, indicate that III is a dibromomethoxy-*N*-methylpyrazolotropone.

The permanganate oxidation of III gave, after thermal decarboxylation, 1-methylpyrazole-4-carboxylic acid, the structure of which was confirmed by the NMR spectrum of its methyl ester. This reaction establishes the presence of a pyrazole ring in III. The functional groups in the compound III are very inactive, and the only reaction registered was the acid-catalyzed exchange of one of the bromine atoms for a chlorine, thus yielding the corresponding bromochloro compound, IV (NMR Table I), although the position of the chlorine atom was not established. The catalytic reduction of III resulted in the absorption of two moles of hydrogen, and yielded V as yellow granules; the analysis and the ultraviolet spectrum of these granules suggest that the product is the corresponding methoxy-*N*-methylpyrazolotropone. Its NMR spectrum (cf. Table I) showed a singlet at 7.84 p. p. m. due to a proton on the pyrazole ring, and a complex multiplet, representing 3 protons, probably of the ABX type, between 6.4 and 7.3 p. p. m., besides signals due to a O-CH_3 (3.88 p.p.m.) and a N-CH_3 (4.46 p.p.m.). Compound V must, therefore, have one of the alternative structures, Va and Vb, deduced from the above evidence and from a consideration of the mode of action of diazomethane on α, β-unsaturated ketones. However, the appearance of the *N*-methyl signal at such a low field in the NMR spectrum of V and no substantial deviation between those signals in IV and V can more easily be explained on the basis of the structure Va; the low field shift is apparently due to the paramagnetic anisotropy of the carbonyl group at the peri-position.[5]

During the investigation of the various reactions of 4-acetyltropolone, we have also found an effective, simple method for the synthesis of pyrazolotropolone. The *p*-tosylhydrazone VI of 4-acetyltropolone[6] was treated with potassium hydroxide in ethanol. The product was a mixture of VII (pale yellow needles; 40% yield) and VIII (orange prisms; 22% yield), both of which showed a positive ferric chloride coloration and exhibited ultraviolet spectra

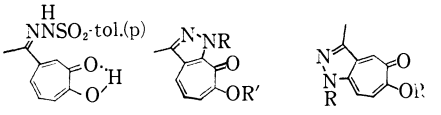

VI VII R=R'=H VIII R=H
X R=H, R'=$COCH_3$ IX R=$COCH_3$
XI R=R'=CH_3

suggestive of the presence of a tropolone ring. That both VII and VIII contain a pyrazole ring fused with the tropolone nucleus was established by their permanganate oxidation, which yielded 5-methylpyrazole-3, 4-dicarboxylic acid. Although the acetylation of VIII gave the colorless *O*, *N*-diacetate (IX), the same reagent under similar conditions converted VII to only a pale yellow *O*-acetate (X), which gave a negative ferric chloride test. The methylation of VII, under the conditions described above for tribromotropolone, gave the corresponding *O*, *N*-dimethyl compound (XI), the NMR spectrum of which (Table I) could almost be imposed on that of V, except for the appearance of a

4) The assignment followed many precedences in bromotropolone methyl ethers; the methyl signal invariably appears in the region from 3.90 to 4.00 p. p. m. (J. Tsunetsugu and S. Itô, unpublished observation).

5) Similar situations can be found in the Varian NMR spectra catalog, Vol. I and II, Varian Associate, Palo Alto.

6) T. Nozoe, K. Takase and M. Ogata, *Chem. & Ind.*, **1957**, 1070.

singlet due to a C–CH_3 at 2.51 p.p.m. and the disappearance of the singlet at 7.84 p.p.m. due to the pyrazole proton. Once again, the appearance of the N–CH_3 signal at such a low field suggests the position of the methyl group. On the other hand, the NMR spectrum of IX showed an AB-type quartet and a singlet (Table I) in the aromatic region, thus disclosing the structures.

The reaction of diazomethane on tribromotropolone was extended to other bromotropolones, but it gave no definite product besides their methyl ether with the exception of 3, 5-dibromotropolone (XII). In the reaction, XII gave, together with 3, 5-dibromo-2-methoxytropone and 3, 5-dibromo-7-methoxytropone, colorless needles (XIII) with a m. p. of 235—236°C(decomp.), and with a molecular formula of $C_{10}H_8O_2N_2Br_2$. XIII exhibits an

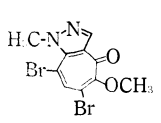

XIIIa

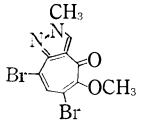

XIIIb

ultraviolet spectra completely different from that of III, although it still retain a tropone nucleus. NMR spectrum (Table I) of XIII discloses the presence of O–CH_3, N–CH_3 and two isolated aromatic protons. The N–CH_3 signal appears at a much higher field than those in III, IV, V and XI, showing that they are free from the paramagnetic anisotropy of a carbonyl group, and that, therefore, they are remote from the carbonyl groups. On the other hand, the pyrazole proton at 8.46 p. p. m. is in an extremely low field compared with its counterparts in III, IV and V; this indicates that the pyrazole protons suffer from the anisotropy of the carbonyl group. With this information, the two alternative structures, XIIIa and XIIIb, were derived. However, study was discontinued because of the limited amount of material available.

Experimental[7]

4, 6-Dibromo-7-methoxy-1-methyl-8(1*H*)-cycloheptapyrazolone (III).[8]— *a) From 3, 5, 7-Tribromotropolone (I).*—An excess of diazomethane (an ethereal solution) was added to the warm suspension of I (10 g.) in methanol (150 ml.). After all the solid had disappeared, leaving an orange red solution, the reaction mixture was left in the dark for two days at room temperature with further addition of diazomethane. The colorless needles (m. p. 155—156°C) which crystallized out were collected (2.77 g.) by filtration; the filtrate was evaporated to leave a dark tarry material (the liberation of hydrogen bromide was detected), which was then chromatographed on alumina, eluted with ether to give a further 0.70 g. of the material. Total yield; 2.97 g. (30.6%). Recrystallization from methanol-chloroform gave colorless silky needles (m. p. 158°C).

Found: C, 34.58; H, 2.47; N, 7.62. Calcd. for $C_{10}H_8O_2N_2Br_2$: C, 34.51; H, 2.32; N, 8.05%.

UV λ_{max}^{MeOH} mμ (log ε): 245 (sh. 4.27), 264(4.34), 324(3.74), 335(sh. 3.70), 370(3.78).

IR: 1608, 1572, 1420, 1220, 986, 895, 861 cm^{-1}.

b) From 2-Methoxy-3, 5, 7-tribromotropone (II).—An ethereal diazomethane was added to a solution of 2.181 g. of II in 150 ml. of methanol; the solution thus obtained was left in the dark at room temperature for 2 days. After crystals had formed (943 mg., m. p. 148—151°C), the solution was treated exactly in the manner described above. The total yield of the crystals was 1.087 g. (53.5%). The compound was identified as III by a mixed melting point determination and by a comparison of the ultraviolet, infrared and NMR spectra.

7-Methoxy-1-methyl-8(1*H*)-cycloheptapyrazolone (V).—III (1.247 g.) was hydrogenated in a mixture of acetic acid (6 ml.) and ethyl acetate (60 ml.) in the presence of sodium acetate (990 mg.) and 5% palladium on charcoal (93 mg.). After a 2-molar uptake of hydrogen and the removal of the catalyst, the solvent was removed by distillation, leaving a brown residue; this residue was sublimed in vacuo to give yellow prisms (361 mg., 53%). Recrystallization from ethyl acetate yielded pale yellow prisms (m. p. 135—136°C).

Found: C, 63.06; H, 4.79; N, 14.48. Calcd. for $C_{10}H_{10}O_2N_2$: C, 63.15; H, 5.30; N, 14.73%.

UV λ_{max}^{MeOH} mμ (log ε): 230(4.56), 255(4.41), 306 (4.06), 321(4.10), 380(3.91).

IR: 1600, 1553, 1429, 1215, 1052, 896, 854, 794, 780 cm^{-1}.

4(or 6)-Bromo-6(or 4)-chloro-7-methoxy-8-(1*H*)-cycloheptapyrazolone (IV).—III (93 mg.) was heated under reflux for 3 hrs. with 6 N hydrochloric acid (9 ml.) in methanol (20 ml.), and then left overnight at room temperature. The colorless crystals which were thus formed were taken up (64 mg., 79%). Recrystallization from methanol yielded colorless plates (m. p. 143.5—144.5°C).

Found: C, 39.59; H, 2.82; N, 8.55. Calcd. for $C_{10}H_8O_2N_2BrCl$: C, 39.57; H, 2.66; N, 9.23%.

1-Methylpyrazole-4-carboxylic Acid.—An aqueous solution (100 ml.) of potassium permanganate (4.5 g.) was added, at 65—75°C, to III (679 mg.) dissolved in acetone (150 ml.). After the temperature had been kept constant for 6 hr., the reaction mixture was left overnight. The removal of the MnO_2 which had been precipitated and the evaporation of the solvent from a yellow filtrate left a colorless solid. The extraction of the residue by dry acetone and the concentration of the solvent gave colorless crystals (m. p. 175—177°C; 126 mg.; 38% yield). The sublimation of the crystal at 160°C yielded 65 mg. of colorless crystals (m. p. 169°C).

Found: C, 47.88; H, 4.72; N, 21.31, mol. wt. 124 (titration). Calcd. for $C_5H_6O_2N_2$: C, 47.62; H,

7) All melting points are uncorrected. The infrared spectra are referred to Nujol mull unless otherwise stated.

8) This nomenclature is based on the name, 1, 8-dihydrocycloheptapyrazole, of the hypothetic compound XV (numbering shown).

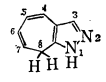

XV

4.82; N, 21.22%; mol. wt. 126.11.

UV λ_{max}^{MeOH} mμ (log ε); 227(3.91).

IR: 1715, 1560, 1258, 1000, 931, 887 cm^{-1}.

Methyl Ester.—Prepared by the action of diazomethane and purified by alumina chromatography. Colorless leaflets; m. p. 62—62.5°C.

Found: C, 51.38; H, 5.82; N, 20.06. Calcd. for $C_9H_8O_2N_2$: C, 51.42; H, 5.75; N, 19.99%.

IR (KBr): 3145, 1706, 1553, 1458, 1431, 1232, 1008, 763 cm^{-1}.

NMR δ^{CDCl_3}: 3.81(3H, S), 3.92(3H, S), 7.98(1H, S), 8.00 p. p. m. (1H, S).

p-Toluenesulfonylhydrazone (VI) of 4-Acetyltropolone.—A mixture of 4-acetyltropolone (5.00 g.), *p*-toluenesulfonylhydrazine (6.00 g.) and ethanol (30 ml.) was heated. The mixture changed into a solution at once, and soon the *p*-toluenesulfonylhydrazone (VI) was crystallized out as pale yellow prisms (m. p. 220°C (decomp.)) (10.52 g.).

Found: C, 57.57; H, 4.52; N, 8.22. Calcd. for $C_{16}H_{16}O_4SN_2$: C, 57.83; H, 4.85; N, 8.43%.

UV λ_{max}^{MeOH} mμ (log ε); 228 (4.36), 292(4.19), 384 (3.68).

3'-Methylpyrazolo[3, 4-c]tropolone (VII) and 3'-Methylpyrazolo[4, 3-d]tropolone (VIII).—To a solution of potassium hydroxide (3.0 g.) in ethanol (60 ml.), VI (5.10 g.) was added; the mixture was then refluxed for 7 hr. After the addition of water (40 ml.) and acidification with 6 N hydrochloric acid, the solution was allowed to stand overnight. The crystals thereby formed were colledted by filtration and recrystallized from dimethylformamide to give 3'-methylpyrazolo-[3, 4-c]tropolone (VII) as pale yellow needles (m. p. 211—212°C) (1.09 g.).

Found: C, 58.15; H, 4.38; N, 15.11. Calcd. for $C_9H_8O_2N_2 \cdot 1/2H_2O$: C, 58.73; H, 4.90; N, 15.13%.

UV λ_{max}^{MeOH} mμ (log ε): 226(4.28), 255(4.38), 305(3.80), 318(3.87), 379(sh. 3.88), 390(3.93).

Acetate X: m. p. 216—218°C, pale yellow needles (from ethanol).

Found: C, 60.51; H, 4.30; N, 12.83. Calcd. for $C_{11}H_{10}O_3N_2$: C, 60.54; H, 4.62; N, 12.84%.

UV λ_{max}^{MeOH} mμ (log ε): 233(4.30), 294(3.82), 307(3.79), 365(3.79), 380 (sh. 3.73).

The removal of ethanol from the mother liquor gave an oily material, which was solidified by allowing it to stand. This was warmed with methanol, and the sparingly-soluble part (m. p. 215—222°C) (1.00 g.) was recrystallized from dimethylformamide to give 3'-methylpyrazolo[4, 3-d]tropolone (VIII) as orange prisms (m. p. 225—226°C) (0.60 g.).

Found: C, 60.83; H, 4.34; N, 15.72. Calcd. for $C_9H_8O_2N_2$: C, 61.36; H, 4.58; N, 15.90%.

UV λ_{max}^{MeOH} mμ (log ε): 228(4.27), 280(sh. 4.27), 287(4.31), 296(sh. 4.28), 398(3.61), 435(3.55).

Acetate IX: m. p. 169—170°C; colorless micro-needles (from acetic acid).

Found: C, 60.16; H, 4.26; N, 10.51. Calcd. for $C_{13}H_{12}O_2N_2$: C, 59.99; H, 4.65; N, 10.77%.

UV λ_{max}^{MeOH} mμ (log ε): 282(4.46), 315(sh. 4.02).

From the methanol-soluble part, *p*-tolyl *p*-toluenethiolsulfonate (0.60 g.), was obtained as colorless needles (m. p. 75—76°C (reported 76°C[9])) after recrystallization from methanol.

1, 3-Dimethyl-7-methoxy-8-(1*H*)-cycloheptapyrazolone (XI).—VII (603 mg.) was methylated with diazomethane under the conditions described for the compound III. After the reaction mixture had been left overnight, the solvent was distilled off, and the residue was chromatographed on alumina. Elution with benzene gave yellow crystals (587 mg., 84.5%). Recrystallization from benzene - petroleum ether (b. p. 60—80°C) gave yellow prisms (m. p. 81.5—82°C).

Found: C, 64.96; H, 5.55; N. 13.50. Calcd. for $C_{11}H_{12}O_2N_2$: C, 64.69; H, 5.90; N, 13.70%.

UV λ_{max}^{MeOH} mμ (log ε): 230(4.37), 250(4.37), 302(3.98), 316(4.03), 370(3.94).

IR: 1623, 1603, 1553, 1425, 1214, 1028, 793, 768 cm^{-1}.

The Permanganate Oxidation of Pyrazolotropolones VII and VIII.—Into a solution of VII (0.53 g.) in a 0.4 N potassium hydroxide solution (25 ml.), finely-powdered potassium permanganate was stirred in small portions at room temperature; 2.65 g. of permanganate was thus smoothly consumed. After the mixture had been allowed to stand overnight, the excess permanganate was decomposed on the addition of methanol and the manganese dioxide was filtered off. The filtrate was slightly acidified with 6 N hydrochloric acid and concentrated under reduced pressure until crystals had begun to separate out. Acetone was then added, and the inorganic salts thereby separated were filtered off. After the mother liquor had been treated repeatedly in the same way, the acetone solution was evaporated to dryness; the subsequent addition of a small amount of water gave oxalic acid. From the water-soluble part, 5-methylpyrazole-3, 4-dicarboxylic acid (0.11 g.) was obtained as colorless microcrystals; this acid was identified with an authentic specimen[10] by a comparison of the infrared spectra.

Found: C, 38.60; H, 4.30; N, 14.77. Calcd. for $C_6H_6N_2 \cdot H_2O$: C, 38.30; H, 4.29; N, 14.89%.

The same oxidation of VIII (0.30 g.) with potassium permanganate also gave 5-methylpyrazole-3, 4-dicarboxylic acid (0.05 g.).

The Reaction of Diazomethane with 3, 5-dibromotropolone (XII).—The reaction was carried out with 100 mg. of XII in exactly the same way as was described in the above section. The product obtained by the evaporation of the solvent from the reaction mixture in vacuo was chromatographed on alumina. Elution with benzene gave colorless cytstals (30 mg.), which were recrystallized from chloroform to give colorless silky needles (XIII) (m. p. 235—236°C(decomp.)).

Found: C, 34.61; H, 2.30; N, 7.54. Calcd. for $C_{10}H_8O_2N_2Br_2$: C, 34.51; H, 2.32; N. 8.02%.

UV λ_{max}^{MeOH} mμ (log ε): 240(sh. 4.70), 253(4.77), 260 (sh. 4.69), 347(4.24).

IR: 3125, 1616, 1587, 1221, 1012, 903, 865, 785, 765 cm^{-1}.

The authors wish to express their gratitude to Professor Tetsuo Nozoe, Tohoku University, for his interest, and to Professor W. A. Ayer, University of Alberta, Canada, for some of the NMR spectra included in this paper.

9) J. L. Kice and K. W. Bowers, *J. Am. Chem. Soc.*, **84**, 605 (1962).

10) K. V. Auwers and E. Cauer, *Ann.*, **470**, 304 (1929).

BULLETIN OF THE CHEMICAL SOCIETY OF JAPAN VOL. 39 257—263 (1966)

Studies of the Chemiluminescence of Several Xanthene Dyes. I. Kinetic Studies of Uranine and Eosine Chemiluminescence

By Isao KAMIYA

Department of General Education, Nagoya University, Chikusa-ku, Nagoya

and Ryojirô IWAKI

Aichi Gakugei University, Chemical Laboratories, Okazaki, Aichi

(Received May 12, 1965)

A kinetic study of the chemiluminescence in alkaline solutions of several xanthene dyes with hydrogen peroxide was carried out in the hope of gaining some insight into the mechanism of the luminescent reaction. When the concentrations of sodium hydroxide and hydrogen peroxide were kept constant, the decay curve of the luminescence was represented by $I_t = A \exp(-at)$, where I_t is the light intensity at time t ; a is equal to the rate constant of the decomposition of the dye (first order with respect to the dye concentration) and A is a parameter proportional to the initial dye concentration. The lifetime of the luminescent reaction was prolonged by the addition of such organic solvents as alcohol and dioxane; the a value decreased, while the A value remained unchanged. Both the a value and the A value increased with the elevation of the reaction temperature.

In 1924, Keaney[1] observed a glow when ozonized oxygen was passed through a solution of aesculin in water, methyl alcohol, ethyl alcohol or propyl alcohol. A short time later, Biswas and Dhar[2] investigated a similar glow, using fifty different fluorescent and non-fluorescent dyes; they concluded that the luminescent intensity was roughly proportional to the fluorescence efficiency of the dyes. Moreover, they found that the same glow was obtained when the dyes were oxidized by hydrogen peroxide, using ferrous sulfate as a catalyst. Strehlar and Shoup[3] have discovered the chemiluminescence of riboflavin and showed that the spectral energy distribution of the luminescence is very similar to that of the fluorescence emission of riboflavin.

Thus, it is very probable that the light emitted in the chemiluminescence of a fluorescent dye is the fluorescence emission of the dye, although little is known as to how the dye can be excited to emit fluorescence in the chemiluminescent reaction. It was with this in mind that the present authors[4] began to study the chemiluminescence of several xanthene dyes.

It has been established that, when the dyes are oxidized by hydrogen peroxide, hydroxyl ion, iodide ion, hypochlorite ion or lead acetate acts as a catalyst for the light production, as does ferrous sulfate. Moreover, when a hydrogen peroxide solution is added to alkaline solutions of the dyes, the emission is very much enhanced and is quite reproducible.

For the present paper, kinetic studies of uranine and eosine chemiluminescence were carried out in order to establish the mechanism for light production.

Experimental

The Preparation of the Luminescent System.—Two milliliters of a sodium hydroxide solution was added to 6 ml. of a uranine or eosine solution; the mixed solution was then kept at a definite temperature. After 1 ml. of a hydrogen peroxide solution has been added to the mixed solution, a portion of the reacting solution (4—5 ml.) was transferred quickly into a cell (2.8 cm. high, 2.0 cm. wide and 1.0 cm. thick); then the cell was placed in a thermostat, with water circulating at a constant temperature.

Uranine and eosine were recrystallized from a 60—70% ethanol solution. One gram of each dye was dissolved into 100 ml. of water or a water - organic solvent mixture in order to prepare the original solution; when necessary, this was further diluted to 1/2, 1/4, 1/8, and so on. The sodium hydroxide, the hydrogen peroxide solution (30 %) and organic solvents of an analytical grade were used without further purification.

Measurements of the Light Intensity versus the Time.—The light-measuring apparatus is shown diagramatically in Fig. 1. It was composed of a small thermostat and a photomultiplier-tube box, both of which were covered with a large dark box. The reaction cell in the thermostat was clamped on so as to face a glass window, through which the emitted light was

1) M. Kearney, *Phil. Mag.*, **47**, 648 (1924).
2) N. N. Biswas and N. R. Dhar, *Z. anorg. u. allgem. Chem.*, **173**, 125 (1928); **186**, 154 (1930); **144**, 400 (1931).
3) B. L. Strehler and C. S. Shoup, *Arch. Biochem. Biophys.*, **47**, 8 (1953).
4) R. Iwaki and I. Kamiya, *J. Chem. Soc. Japan, Pure Chem. Sect.* (*Nipppn Kagaku Zassi*), **79**, 251, 255 (1958).

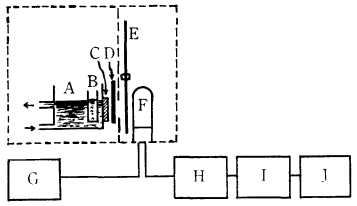

Fig. Diagram of measuring system.

A, Small thermostat. B, Reaction cell. C, Glass window. D, Shutter. E, Sector. F, Photomultiplier. G, High-voltage supply. H, Cathode follower. I, Linear amplifier. J, Self-recording micro-ammeter.

detected with a photomutiplier-tube (Matzuda MS9SY). The tube was coupled with a linear amplifier, and the output current was lead to a self-recording micro-ammeter, so that the curve of the light intensity versus the time could be recorded automatically.

Measurements of the Decomposition Rate of the Dyes.—The dyes were decomposed during the luminescent reaction; no emission was observed when the dye was not decomposed. In order to determine the decomposition rate of the dye, 1 ml. of the reacting solution was withdrawn at a definete interval in order to mix it with 250 ml. of water (the reaction was stopped upon dilution); the concentration of unoxidized dye was determined spectro-photometrically with a Shimadzu QR-50-type electro-spectrophotometer, at the wavelength of 492 mμ for uranine and of 517 mμ for eosine.

Experimental Results

In general, the curve of the emission intensity versus the time (the *I-t* curve) rises to reach a maximum at the initial stage and then decays slowly. The *I-t* curve was reproducible except in the initial stage. (The initial curve was not quite reproducible because hydrogen peroxide decomposed after a short induction period.)

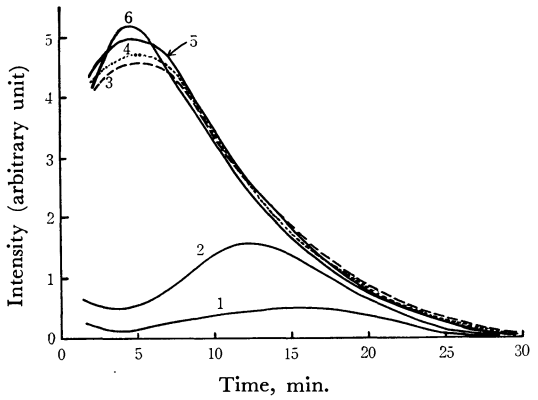

Fig. 2. Effect of hydrogen peroxide concentration on *I-t* curve for uranine chemiluminescence.
(Original solution, 2.5 N NaHOaq., 30°C)
(1) 5%, (2) 10%, (3) 15%, (4) 20%, (5) 25%, (6) 30%

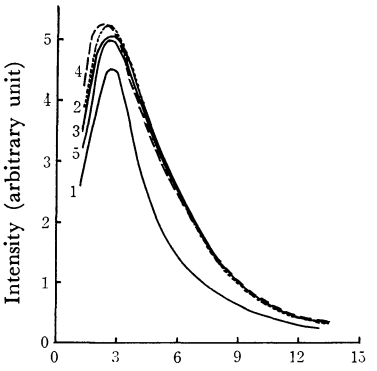

Fig. 3. Effect of hydrogen peroxide concentration on *I-t* curve for eosine chemiluminescence.
(Original solution, 0.5 N NaOHaq., 41°C)
(1) 10%, (2) 15%, (3) 20%, (4) 25%, (5) 30%

The Effect of the Hydrogen Peroxide Concentration on the *I-t* Curve—The results are shown in Figs. 2 and 3. It is there demonstrated that the decay curve is little affected by the change in the concentration of the added hydrogen peroxide solution when its concentration is comparatively high (20—30%). When the concentration is low, however, the *I-t* curve becomes lower and is greatly affected by a change in the concentration of the added hydrogen peroxide solution. The optimum concentration of the added hydrogen peroxide solution for the kinetic studies is found to be 20—30%.

The Effect of the Sodium Hyroxide Concentration on the *I-t* Curve.—The correlation between the *I-t* curve and the added sodium

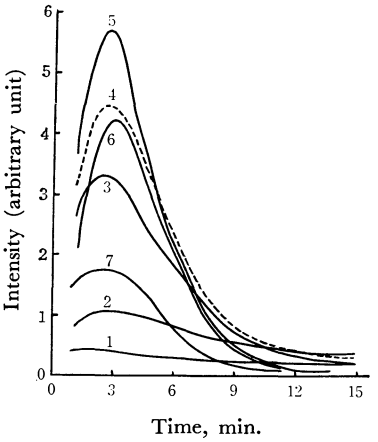

Fig. 4. Effect of sodium hydroxide concentration on *I-t* curve for uranine chemiluminescence.
(1/4 conc. to original solution, 15% H_2O_2aq., 45°C)
(1) 0.5 N, (2) 1.0 N, (3) 1.5 N, (4) 2.0 N, (5) 2.5 N, (6) 3.0 N, (7) 4.0 N

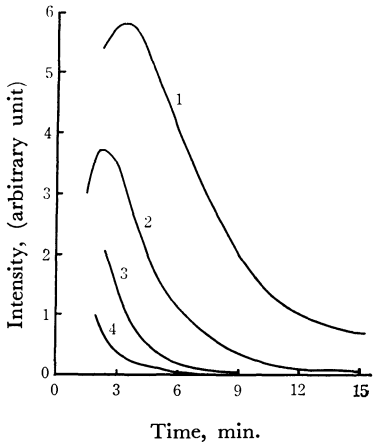

Fig. 5. Effect of sodium hydroxide concentration on *I-t* curve for eosine chemiluminescence.
(1/2 conc. to original solution, 30% H_2O_2aq., 41°C)
(1) 0.5 N, (2) 1.0 N, (3) 2.0 N, (4) 3.0 N

hydroxide concentration is not so simple, because the aspects of the *I-t* curve differ according to the concentration of hydrogen peroxide as well as according to the dye concentration. The effect is probably due to the fact that the alkali concentration controls both the rate of the decomposition of hydrogen peroxide and the luminescent reactivity of the dye. Typical examples are shown in Fig. 4 for uranine and in Fig. 5 for eosine. These figures show that the optimum concentration of the added sodium hydroxide solution should be 2—3 N for uranine and 0.5 N for eosine.

The Effect of the Dye Concentration on the *I-t* Curve.—*I-t* curves measured at 16°C in uranine chemiluminescent systems of different

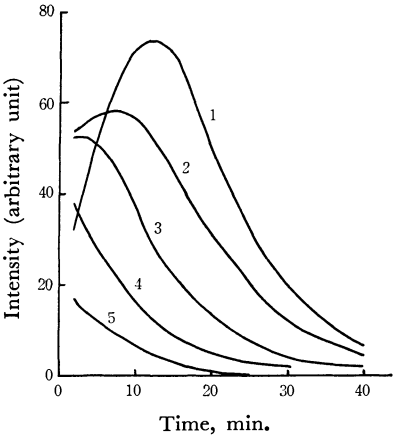

Fig. 6. Effect of uranine concentration on *I-t* curve for uranine chemiluminescence.
(3.0 N NaOHaq., 20% H_2O_2aq., 16°C)
(1) Original solution, (2) 1/2 conc. to original solution, (3) 1/4 conc. to original solution, (4) 1/8 conc. to original solution, (5) 1/16 conc. to original solution.

Table I. The effect of varying uranine concentration on the intensity-time relation
(3 N NaOHaq., 20% H_2O_2aq., 16°C)

Dye concn.	Original soln.		1/2 concn. to original soln.		1/4 concn. to original soln.		1/8 concn. to original soln.		1/16 concn. to original soln.	
Time min.	Eq. 1a		Eq. 1b		Eq. 1c		Eq. 1d		Eq. 1e	
	Calcd.	Obs.	Calcd.	Obs.	Calcd.	Obs.	Calcd.	Obs.	Calcd.	Obs.
2	32.3	32.0	42.0	53.0	51.6	54.0	39.3	35.5	17.6	16.8
4	42.7	44.0	49.4	57.0	50.3	51.0	32.3	30.0	15.2	14.5
6	53.6	54.5	54.9	59.0	46.1	47.0	26.3	25.0	11.3	10.5
8	65.9	64.2	58.7	60.0	41.5	41.5	21.5	20.0	9.1	8.5
10	75.0	71.0	57.5	57.5	34.7	35.0	17.7	16.5	7.3	7.0
12	77.2	74.2	52.5	52.5	29.2	29.5	14.4	13.5	6.5	5.5
14	76.1	71.0	48.6	48.0	24.7	24.0	11.8	10.5	4.8	4.5
16	67.9	65.2	43.8	43.0	20.2	19.5	9.7	9.0	3.7	3.0
18	59.5	59.5	37.9	37.0	16.5	16.0	7.0	7.0	2.5	2.2
20	50.5	52.0	32.0	32.0	13.5	13.5	6.5	6.0	2.2	2.0
22	43.3	43.3	28.0	28.0	11.5	11.5	5.3	5.0	0.9	1.5
24	36.3	36.5	23.0	23.5	8.2	6.9	4.4	4.5	0.7	0.5
26	29.6	33.2	18.0	18.5	6.1	6.0	3.9	3.5	—	—
28	24.3	30.0	16.0	15.0	5.1	5.0	2.9	2.8	—	—
30	20.0	24.0	13.4	12.5	4.1	4.0	2.4	2.4	—	—
32	16.3	16.8	11.2	11.5	3.3	3.0	—	—	—	—
34	13.4	13.5	9.4	9.8	2.7	2.5	—	—	—	—
36	10.9	10.5	7.6	7.5	—	—	—	—	—	—
38	8.9	8.5	6.4	6.5	—	—	—	—	—	—
40	7.3	8.0	5.4	4.5	—	—	—	—	—	—

dye concentrations are shown in Fig. 6, where the concentrations of the added sodium hydroxide and hydrogen peroxide solutions are 3.0 N and 20% respectively (optimum concentration). From numerical analysis, every curve can be represented by the following general equation (1):

$$I_t = A\exp(-at)/\{1+B\exp(-bt)\} \qquad (1)$$

where I_t is the emission intensity at time t; a is the decay costant, and A, B and b are parameters which differ according to the experimental conditions. The curves shown in Fig. 6 can be represented by the following equation:

Uranine concn. (ratio to the original soln.)	Equation
1	$I_t=400\exp(-0.10t)/\{1+16\exp(-0.28t)\}$
1/2	$I_t=200\exp(-0.09t)/\{1+5\exp(-0.25t)\}$
1/4	$I_t=100\exp(-0.10t)/\{1+\exp(-0.28t)\}$
1/8	$I_t=48\exp(-0.10t)$
1/16	$I_t=22\exp(-0.10t)$

Table I shows both the calculated values and the observed values. The calculated values are in fairly good agreement with the observed values except for a slight deviation at the initial stage. From the results, the following important conclusions are obtained:

i) Since the second term of the denominator in Eq. 1, $B\exp(-bt)$, can be disregarded except in the initial stage, the decay part of the I-t curve is represented by:

$$I_t = A\exp(-at) \qquad (2)$$

ii) The decay constant, a, is not affected by the dye concentration.

iii) The value of A is proportional to the initial dye concentration. This fact indicates that the luminescent decay is of the first order with respect to the dye concentration.

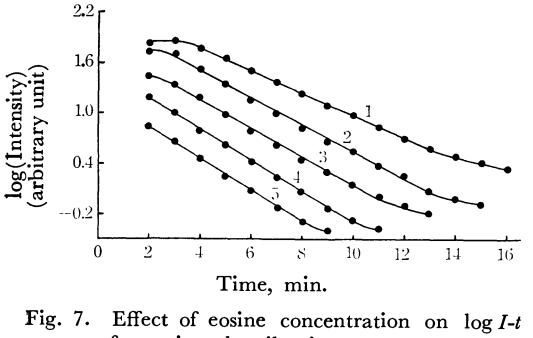

Fig. 7. Effect of eosine concentration on log I-t curve for eosine chemiluminescence.
(0.5 N NaOHaq., 30% H_2O_2aq., 41°C)
(1) Original solution, (2) 1/2 conc. to original solution, (3) 1/4 conc. to original solution, (4) 1/8 conc. to original solution, (5) 1/16 conc. to original solution

The intensities of emission measured at 41°C in eosine chemiluminescent systems of different dye concentrations are shown in Fig. 7, where the logarithm of I_t is plotted against the time. These plots are almost on straight lines except in the initial and final stages. Therefore, the decay curves may also be represented as follows:

Eosine concn. (ratio to the original soln.)	Equation
1	$I_t=180\exp(-0.28t)$
1/2	$I_t=150\exp(-0.41t)$
1/4	$I_t=78\exp(-0.41t)$
1/8	$I_t=39\exp(-0.41t)$
1/16	$I_t=20\exp(-0.41t)$

It is shown that, when the concentration of eosine is comparatively high, the values of A and a are smaller than the expected values. Moreover, the curves deviate from Eq. 2 at the final stages in both uranine and eosine chemiluminescence.

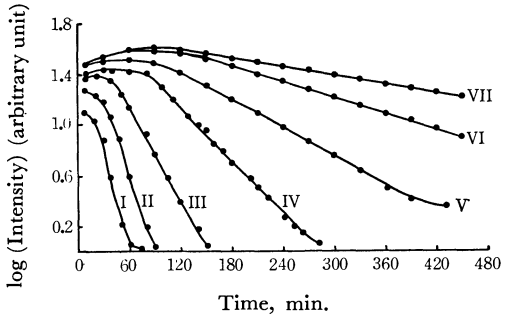

Fig. 8. Effect of methanol concentration on log I-t curve for uranine chemiluminescence.
(Original solution, 2.5N NaOHaq., 20% H_2O_2aq., 20°C)
I 0%, II 15%, III 25%, IV 35%, V 45%, VI 55%, VII 65%

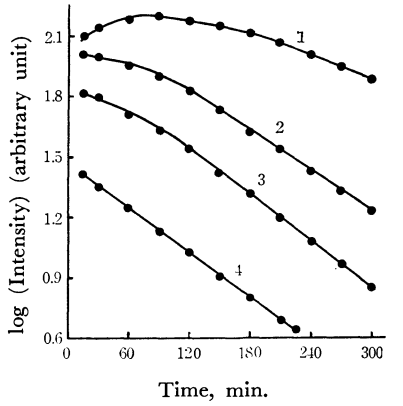

Fig. 9. Effect of uranine concentration on log I-t curve in 65% methanol system at 26°C.
(1) Original solution, (2) 1/2 conc. to original solution, (3) 1/4 conc. to original solution, (4) 1/8 conc. to original solution

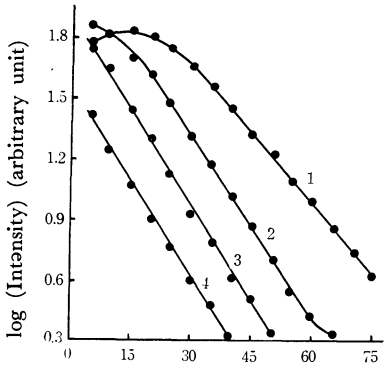

Fig. 10. Effect of uranine concentration on log *I-t* curve in 25% methanol system at 28°C. (1) Original solution, (2) 1/2 conc. to original solution, (3) 1/4 conc. to original solution, (4) 1/8 conc. to original solution

This deviation will be discussed in a succeeding paper.

The Effect of an Added Organic Solvent on the *I-t* Curve.—In general, the emission intensity was enhanced when such organic solvents as alcohol, dioxane and glycerol were added to the system. The *I-t* curves obtained from uranine chemiluminescence in water-methanol systems of different methanol concentrations at 20°C, with the uranine concentration kept constant, are shown in Fig. 8. The curves obtained from the systems with different uranine concentrations and with a constant methanol concentration are shown in Figs. 9 and 10. These curves were also represented as:

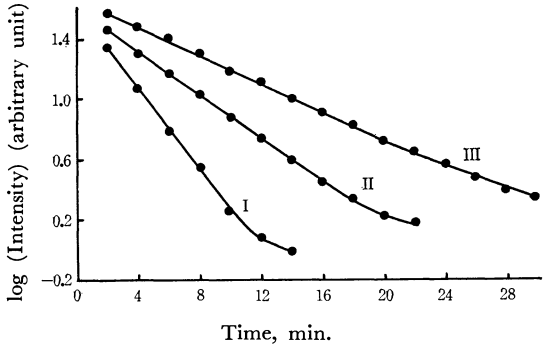

Fig. 11a. Effect of methanol concentration on log *I-t* curve for eosine chemiluminescence. (1/8 conc. to original solution, 0.5 N NaOHaq., 30% H_2O_2aq., 41°C)
I 10%, II 30%, III 50%

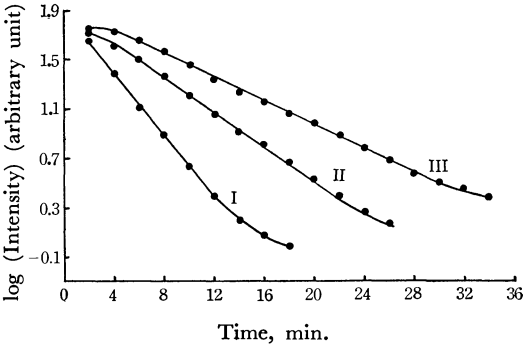

Fig. 11b. Effect of methanol concentration on log *I-t* curve for eosine chemiluminescence. (1/4 conc. to original solution, 0.5 N NaOHaq., 30% H_2O_2aq., 41°C)
I 10%, II 30%, III 50%

Table II. Effect of the concentration of added organic solvent on the values of *A* and *a* in uranine and eosine chemiluminescence

Solvent	%	Dye	Concn.	NaOHaq., N	Temp., °C	*A*	*a*
Ethanol	20	Uranine	1/2	2.5	20	105	0.030
Ethanol	40	Uranine	1/2	2.5	20	105	0.015
Ethanol	60	Uranine	1/2	2.5	20	91	0.005
Isopropanol	20	Uranine	1/2	2.5	20	102	0.027
Isopropanol	20	Eosine	1/2	0.5	30	127	0.071
Isopropanol	40	Uranine	1/2	2.5	20	98	0.008
Isopropanol	40	Eosine	1/2	0.5	30	126	0.022
Isopropanol	60	Eosine	1/2	0.5	30	126	0.009
n-Propanol	20	Uranine	1/2	2.5	20	99	0.019
n-Propanol	40	Uranine	1/2	2.5	20	99	0.006
n-Propanol	60	Uranine	1/2	2.5	20	80	0.004
Dioxane	20	Uranine	1/2	2.5	20	109	0.030
Dioxane	20	Eosine	1/2	0.5	30	120	0.098
Dioxane	40	Uranine	1/2	2.5	20	104	0.016
Dioxane	40	Eosine	1/2	0.5	30	118	0.050
Dioxane	60	Eosine	1/2	0.5	30	107	0.021
Glycerol	20	Uranine	1/2	2.5	20	104	0.031
Glycerol	40	Uranine	1/2	2.5	20	105	0.021

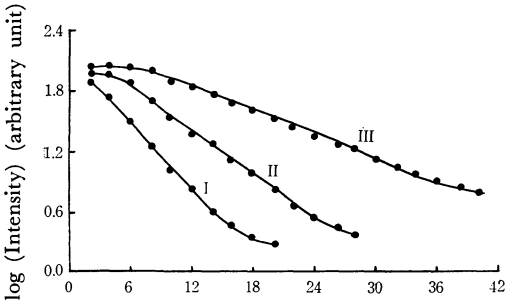

Fig. 11c. Effect of methanol concentration on log *I-t* curve for eosine chemiluminescence.
(1/2 conc. to original solution, 0.5 N NaOHaq., 30% H_2O_2aq., 41°C)
I 10%, II 30%, III 50%

Curves in Fig. 8 (original uranine soln.)

Methanol concn. (% in volume)	Equation
0	$I_t=100\exp(-0.078t)/\{1+7.4\exp(-0.11t)\}$
15	$I_t=100\exp(-0.051t)/\{1+6.0\exp(-0.10t)\}$
25	$I_t=100\exp(-0.030t)/\{1+3.9\exp(-0.067t)\}$
35	$I_t=100\exp(-0.016t)/\{1+3.2\exp(-0.050t)\}$
45	$I_t=91\exp(-0.0091t)/\{1+2.6\exp(-0.029t)\}$
55	$I_t=73\exp(-0.0047t)/\{1+2.0\exp(-0.024t)\}$
65	$I_t=68\exp(-0.0043t)/\{1+1.7\exp(-0.022t)\}$

Curves in Fig. 9 (65% methanol soln.)

Dye concn. (ratio to the original soln.)	Equation
1	$I_t=290\exp(-0.0045t)/\{1+1.4\exp(-0.019t)\}$
1/2	$I_t=210\exp(-0.0085t)/\{1+1.1\exp(-0.016t)\}$
1/4	$I_t=94\exp(-0.0085t)/\{1+0.35\exp(-0.021t)\}$
1/8	$I_t=30\exp(-0.0085t)$

Curves in Fig. 10 (25% methanol soln.)

Dye concn. (ratio to the original soln.)	Equation
1	$I_t=347\exp(-0.067t)/\{1+4.9\exp(-0.10t)\}$
1/2	$I_t=172\exp(-0.067t)/\{1+\exp(-0.10t)\}$
1/4	$I_t=84\exp(-0.074t)$
1/8	$I_t=37\exp(-0.074t)$

I-t curves obtained from eosine chemiluminescence in water-methanol systems of different eosine and methanol concentrations at 41°C are shown in Fig. 11 (a—c); the corresponding equations are shown below.

Dye concn. (ratio to the original soln.)	Methanol concn. (% in volume)	Equation
1/2	10	$I_t=171\exp(-0.30t)$
1/2	30	$I_t=171\exp(-0.16t)$
1/2	50	$I_t=170\exp(-0.08t)$
1/4	10	$I_t=78\exp(-0.30t)$

TABLE III. EFFECT OF TEMPERATURE ON THE VALUES OF *A* AND *a* UNDER SEVERAL EXPERIMENTAL CONDITIONS

1. Uranine chemiluminescence in aqueous solution
(1/4 concn. to original solution, 20% H_2O_2aq.)

NaOHaq., N	Temp., °C	*A*	*a*
3.0	21	155	0.13
3.0	31	800	0.35
3.0	41	3100	0.47
3.0	50	7700	1.02
3.0	59	17400	1.63
2.0	21	105	0.072
2.0	31	580	0.20
2.0	41	2640	0.40
2.0	50	6660	0.70
2.0	59	14000	1.05

2. Eosine chemiluminescence in aqueous solution
(1/4 concn. to original solution, 0.5 N NaOHaq., 30% H_2O_2aq.)

Temp., °C	*A*	*a*
21	11	0.11
32	35	0.27
41	80	0.41
51	180	0.77
59	390	1.38

3. Uranine chemiluminescence in water-methanol system (25%).
(Original solution, 2.5 N NaOHaq., 20% H_2O_2aq.)

Temp., °C	*A*	*a*
22	147	0.031
30	412	0.060
39	1540	0.10
51	4980	0.28
57	13800	0.47

4. Eosine chemiluminescence in water-isopropanol system (40%)
(1/2 concn. to original solution, 0.5 N NaOHaq., 30% H_2O_2aq.)

Temp., °C	*A*	*a*
23	83.5	0.017
30	126	0.022
37	221	0.038
45	394	0.063
52	1338	0.14

1/4	30	$I_t = 72\exp(-0.14t)$
1/4	50	$I_t = 78\exp(-0.08t)$
1/8	10	$I_t = 40\exp(-0.31t)$
1/8	30	$I_t = 38\exp(-0.15t)$
1/8	50	$I_t = 38\exp(-0.08t)$

From these results, it can be seen that the decay constant, a, which is independent of the dye concentration, decreases with an increase in the concentration of added methanol, while A, which is proportional to the initial dye concentration, is little affected by the addition of methanol. It may, therefore, be concluded that the stimulation of luminescence by the addition of methanol is due to the prolongation of the luminescent lifetime. In other water - organic solvent systems, the same correlation is obtained between the values of A and a and the concentration of the added organic solvent. These results are shown in Table II.

The Effect of the Temperature on the *I-t* Curve.—*I-t* curves were also investigated at several different temperatures. Every curve can be represented by Eq. 2. The values of A and a obtained either in an aqueous system or in a water - organic solvent system are listed in Table III. It may be seen that in all of the systems both A and a increase with the increase in the temperature.

The Decomposition Rate of Dye in the Luminescent Reaction.—Typical decomposition curves obtained from uranine and eosine chemiluminescence are shown in Figs. 12 snd 13 respectively, where the logarithm of the dye concentration (in arbitrary units) is poltted against the reaction time. An almost straight line is obtained in each

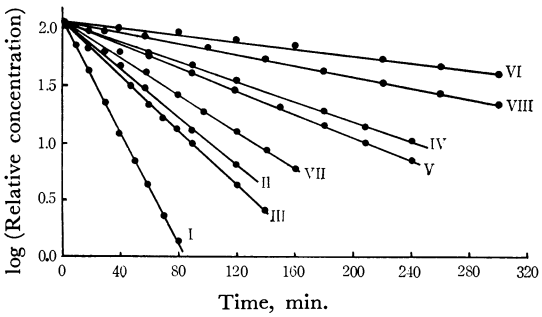

Fig. 12. Rate of uranine decomposition in water-organic solvent systems.
(Original solution, 2.5 N NaOHaq., 20% H_2O_2-aq., 20°C)

I	20% Methanol	V	20% *n*-Propanol
II	40% Methanol	VI	40% *n*-Propanol
III	20% Ethanol	VII	20% Isopropanol
IV	40% Ethanol	VIII	40% Isopropanol

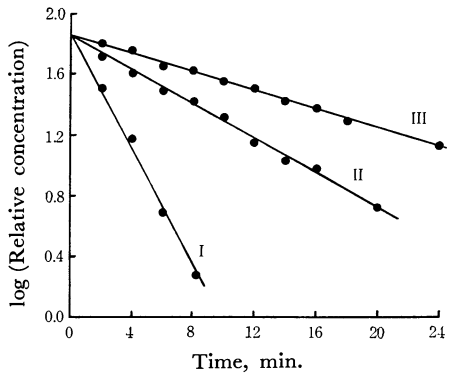

Fig. 13. Rate of eosine decomposition in water-methanol systems.
(1/8 conc. to original solution, 0.5 N NaOHaq., 30% H_2O_2aq., 41°C)
I 10%, II 30%, III 50%

Table IV. Rate constants of uranine decomposition and of eosine decomposition under several experimental conditions

Solvent	%	Dye	Conc.*	NaOHaq. N	H_2O_2aq. %	Temp. °C	Rate const.	a
Water	—	Uranine	1	3	20	16	0.07	0.10
Water	—	Uranine	1/2	3	20	16	0.07	0.09
Water	—	Uranine	1/4	3	20	16	0.07	0.10
Water	—	Uranine	1/8	3	20	16	0.08	0.10
Water	—	Uranine	1/16	3	20	16	0.08	0.10
Methanol	20	Uranine	1	2.5	20	20	0.05	0.050
Methanol	40	Uranine	1	2.5	20	20	0.02	0.025
Ethanol	20	Uranine	1	2.5	20	20	0.03	0.030
Ethanol	40	Uranine	1	2.5	20	20	0.01	0.015
n-Propanol	20	Uranine	1	2.5	20	20	0.01	0.019
n-Propanol	40	Uranine	1	2.5	20	20	0.004	0.006
Isopropanol	20	Uranine	1	2.5	20	20	0.02	0.027
Isopropanol	40	Uranine	1	2.5	20	20	0.005	0.008
Methanol	10	Eosine	1/8	0.5	30	41	0.4	0.31
Methanol	30	Eosine	1/8	0.5	30	41	0.2	0.15
Methanol	50	Eosine	1/8	0.5	30	41	0.08	0.08

* Ratio to the original solution.

case. These results indicate that the decomposition is first order with respect to the dye concentration. The decomposition rate constants under several different expermental conditions are tabulated in Table IV. The values of a (the decay constant) obtained under the same experimental conditions are also given in the last column. It is interesting to note that the decomposition rate constant is almost equal to the corresponding a value in every system.

Studies of several different aspects of chemiluminescence will be presented in a succeeding paper; the combined results, including those of the present experiment, will be discussed thereafter.

BULLETIN OF THE CHEMICAL SOCIETY OF JAPAN VOL. 39 264—269 (1966)

Studies of the Chemiluminescence of Several Xanthene Dyes. II. The Chemiluminescence Emission Spectra of Uranine and Eosine

By Isao KAMIYA

Department of General Education, Nagoya University, Chikusa-ku, Nagoya

and Ryojirô IWAKI

Aichi Gakugei University, Chemical Laboratories, Okazaki, Aichi

(Received May 12, 1965)

The emission spectra of uranine and esoine chemiluminescence with hydrogen peroxide were measured photoelectrically and were compared with the fluorescence spectra of the dyes. The apparent spectra did not give the true energy distribution of the emitted light, because self-absorption took place. When the dyes were oxidized with ozonized air, the apparent emission spectra were very similar to those obtained when the dyes were oxidized with hydrogen peroxide. This would indicate that the emitting species are the same in the two reaction systems. The emission from the dye-ozone reaction was intense, and the spectrum could be compared with the fluorescence spectrum by employing a system with a low dye concentration. The coincidence of the two spectra was clearly demonstrated. The chemiluminescence spectrum of uranine at a high dye concentration in the presence of hydrogen peroxide was compared to the "chemi-fluorescence" spectrum of the luminol-dye system. The two systems gave almost the same spectrum. It may be concluded that the emissions from uranine and eosine chemiluminescence are the fluorescence emissions of the dyes and that the emitting species are the excited singlet states of uranine and eosine.

Since organic compounds which emit chemiluminescent light often fluoresce, the chemiluminescence emission spectra can conveniently be compared with the fluorescence emission spectra. The chemiluminescence spectrum is not always the same as the fluorescence spectrum; in luminol chemiluminescence, it has been found[1] that the emitting species is the excited aminophthalic acid ion produced by the reaction. Light emittted by lophin chemiluminescence has also been found[2] not to correspond to the fluorescence of the compound.

On the other hand, the chemiluminescence emission spectra of lucigenin[3] and riboflavin[4] were found to be very similar to their fluorescence emission spectra. The chemiluminescence emission observed when hydrogen peroxide was added to an alkaline solution of uranine or eosine seemed to correspond to the fluorescence of the dye. However, no comparison of the two spectra has yet been made except for a rough observation with the naked eye.[5]

There is a severe restriction in the measurement of the emission spectra; the apparent chemiluminescence spectra of the dyes do not give the true energy distribution, because the dye solutions absorb the emitted light. In a dilute dye solution where the self-absorption is not apreciable, the intensity

1) E. H. White and M. M. Bursey, *J. Am. Chem. Soc.*, **86**, 941 (1964).
2) K. Maeda, H. Ojima and T. Hayashi, This Bulletin, **38**, 76 (1965); E. H. White and M. C. Harding, *J. Am. Chem. Soc.*, **86**, 5686 (1964).
3) A. V. Karyakin, *Optica i. Spektroskopia*, **7**, 122 (1959).
4) B. L. Strehler and C. S. Shoup, *Arch. Biochem. Biophys.*, **47**, 8 (1953).
5) N. N. Biswas and N. R. Dhar, *Z. anorg. u. allegem. Chem.*, **173**, 125 (1928).

of the chemiluminescence is too weak for reliable measurements. Therefore, other, supplementary methods for estimating the emission spectra should be employed together with direct measurements.

Experimental

Measurements of Emission Spectra in Uranine and Eosine Chemiluminescence with Hydrogen Peroxide.—The luminescent system was prepared in the method described previously.[6] The emission spectra were measured photo-electrically with the apparatus shown diagramatically in Fig. 1. A was a hard-glass reaction tube about 20 mm. in diameter; it was placed in a cylindrical copper thermostat, B. Water circulated between the cylinder, B, and a large thermostat through pipes, D, so the reaction tube could be kept at a constant temperature. C was a dark box. Light emitted from the reaction tube was conducted through a convex lens, E, into a electro-spectrophotometer, F. By dialing a wavelength adjuster with a motor, a spectral curve was recorded on G. It took about 2 min. to scan the whole curve. As a result of the decay of the emission intensity during the recording, the recorded spectral curve was corrected by the decay curve which had been measured under the same experimental conditions. In the present work, where the chemiluminescence emission spectra are compared with the fluorescence spectra, no correction was made for the characteristic sensitivity of the photomultiplier, because the fluorescence was measured with the same photomultiplier.

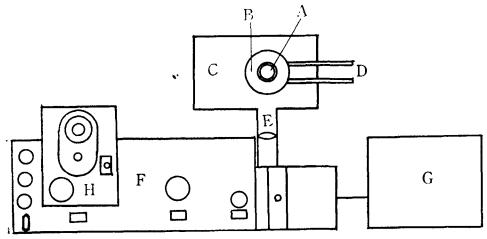

Fig. 1. Diagram of measuring apparatus for the emission spectra of dye chemiluminescence with hydrogen peroxide.

A: Reaction tube B: Thermostat
C: Dark box D: Pipes
E: Convex lens F: Spectrophotometer
G: Selfrecording micro-ammeter
H: Dialing wavelength adjuster

The Measurement of Emission Spectra in Uranine and Eosine Chemiluminescence with Ozone.—When ozonized air was passed through ethanol solutions of uranine and eosine, light was also produced and the apparent emission spectra were similar to those observed when the dyes were oxidized with hydrogen peroxide. The intensity of the emission in this system was more pronounced, although the reproducibility was somewhat poor; hence, the emission spectra could be measured in a solution of such a low dye concentration that self-absorption was not appreciable.

6) I. Kamiya and R. Iwaki, This Bulletin, **39**, 257 (1966).

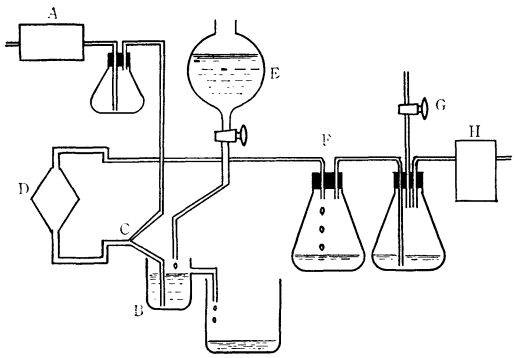

Fig. 2. Diagram of measuring apparatus for the emission spectra of dye chemiluminescence with ozone.

A: Ozonizer B: Beaker
C: Nozzle D: Reaction vessel
E: Sample-solution flask
F: Waste-solution flask
G: Cock H: Pump

The measurement of the emission spectra in the system was carried out with the apparatus shown diagramatically in Fig. 2. Four hundred milliliters of an ethanol solution of uranine or eosine in a flask, E, was dropped into a beaker, B. By pumping out the entire vessel via H, the ozonized air produced in an ozonizer, A, was introduced from a nozzle, C, and reacted with the dye solution. The reacting solution was carried to F through a vessel, D. D is a lozenge-shaped vessel (3.7 cm. wide, 5.4 cm. high) consisting of two parallel glass plates 2 mm. apart, the back of one glass plate being coated with silver. The spectra were measured by inserting D into the A of Fig. 1. As the intensity of emission was practically constant for about 10 min., no correction was needed for the variation with the reaction time. All the measurements were carried out at room temperature because the temperature dependence of the intensity was not appreciable.

Experimental Results

The apparent emission spectra observed in uranine and eosine chemiluminescence with hydrogen peroxide are shown in Figs. 3 and 4. The conentrations of uranine and eosine were 1 g. per 100 ml. and 0.5 g. per 100 ml. respectively. The measurements were carried out in a 60% methanol solution at 60°C. Figures 5 and 6 show the same spectral curves in other solvents, such as ethanol, *n*-propanol, isopropanol and glycerol. It is sohwn that every (apparent) spectrum has the same maximum, at 560 mμ for uranine and at 580 mμ for eosine. These apparent spectra, however, do not give the true energy distribution of the emitted light, because the dye solutions absorb the light. (The absorption spectra of uranine and eosine have maxima at 492 mμ and 517 mμ respectively.) Therefore, no direct comparison of the spectra with fluorescence spectra could be made.

The apparent chemiluminescence spectra observed when ozonized air was passed through ethanol solutions of different uranine concentrations are shown in Fig. 7. The spectra for eosine solutions are shown in Fig. 8. The apparent spectra in a concentrated dye solution are similar to those obtained with hydrogen peroxide. This would indicate that the emitting species is the same in the two reactions. It is very interesting to see that the peak shifts towared a shorter wavelength with a decrease in the dye concentration. In dilute dye solutions, the spectra have maxima at 530 mμ for uranine and at 560 mμ for eosine.

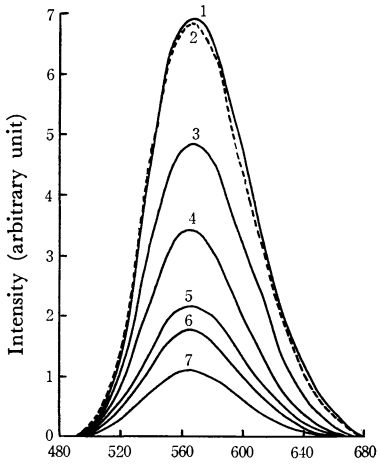

Fig. 3. The emission spectra of uranine chemiluminescence in methanol with hydrogen peroxide at 63°C.

7 ml. of uranine solution (1 g. of uranine in 100 ml. of 60% methanol) + 2 ml. of 2.5 N NaOHaq. + 1 ml. of 20% H_2O_2aq.

1: After 80 sec. 2: After 170 sec.
3: After 241 sec. 4: After 309 sec.
5: After 400 sec. 6: After 470 sec.
7: After 580 sec.

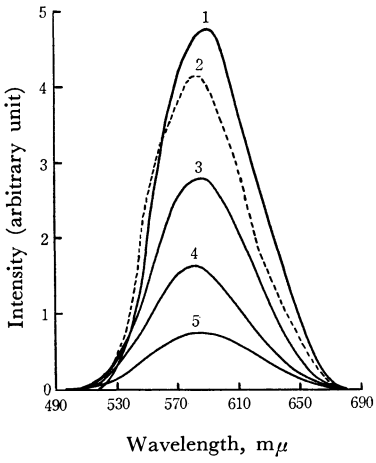

Fig. 4. The emission spectra of eosine chemiluminescence in methanol with hydrogen peroxide at 60°C.

7 ml. of eosin solution (0.5 g. of eosine in 100 ml. of 60% methanol) + 2 ml. of 0.5 N NaOHaq. + 1 ml. of 30% H_2O_2aq.

1: After 43 sec. 2: After 112 sec.
3: After 175 sec. 4: After 236 sec.
5: After 293 sec.

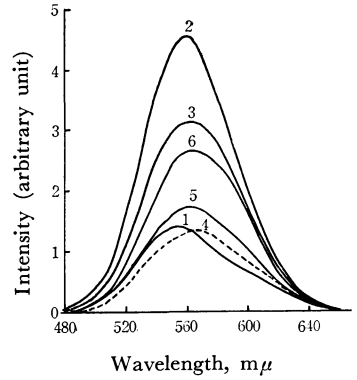

Fig. 5. The emission spectra of uranine chemiluminescence in various solvents with hydrogen peroxide at 57°C.

7 ml. of uranine solution (1 g. of uranine in 100 ml. of solvent) + 2 ml. of 2.5 N NaOHaq. + 1 ml. of 20% H_2O_2aq.

1: Water 2: 60% methanol
3: 60% ethanol 4: 60% *n*-propanol
5: 60% isopropanol 6: 60% glycerine

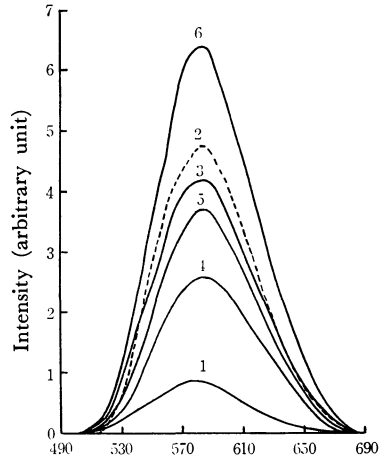

Fig. 6. The emission spectra of eosine chemiluminescence in various solvents with hydrogen peroxide at 60°C.

7 ml. of eosine solution (0.5 g. of eosine in 100 ml. of solvent) + 2 ml. of 0.5 N NaOHaq. + 1 ml. of 30% H_2O_2aq.

1: Water 2: 60% methanol
3: 60% ethanol 4: 60% *n*-propanol
5: 60% isopropanol 6: 60% glycerine

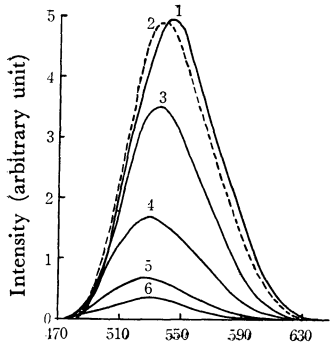

Fig. 7. The emission spectra of uranine chemiluminescence in ethanol with ozone at 12°C.
Concentration of uranine solution in ethanol:
1: 1.33×10^{-2} mol./l. 2: 6.64×10^{-3} mol./l.
3: 3.32×10^{-3} mol./l. 4: 1.66×10^{-3} mol./l.
5: 8.31×10^{-4} mol./l. 6: 4.10×10^{-4} mol./l.

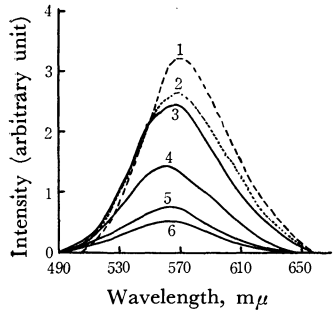

Fig. 8. The emission spectra of eosine chemiluminescene in ethanol with ozone at 12°C.
Concentration of eosine solution in ethanol:
1: 1.44×10^{-2} mol./l. 2: 7.22×10^{-3} mol./l.
3: 3.61×10^{-3} mol./l. 4: 1.81×10^{-3} mol./l.
5: 9.03×10^{-4} mol./l. 6: 4.52×10^{-4} mol./l.

As will be shown later, these maxima correspond to the peaks of the fluorescence of the dyes.

Chemi-fluorescence Emission Spectra in Luminol-Uranine and Luminol-Eosine Systems.—When a dilute hydrogen peroxide solution was added to an aqueous alkaline solution of luminol and a fluorescent dye such as uranine or eosine, a green fluorescence of the dye appeared at the expense of the blue luminescence of luminol. (In such a reaction system, the added dye is almost unoxidized as a result of the low concentration of hydrogen peroxide.) This phenomenon was discovered by Plotnikov[7] and called "Chemi-fluorescence" or "Induced Chemiluminescence." Tamamushi[8] investigated it further and found that both blue light and green light were observed when less than 0.02% of fluoresceine was added to 0.0025% of a luminol solution, and that the blue

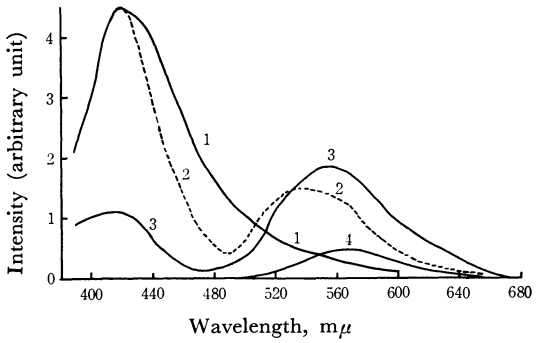

Fig. 9. The emission spectra of luminol and uranine-luminol chemiluminescence at 31°C.
6 ml. of alkaline luminol solution (0.25 g. of luminol and 2 g. of sodium hydroxide in 100 ml. of water) + 21 ml. of uranine aqueous solution of various concentrations + 3 ml. of 10% H_2O_2aq.
Concentration of uranine aqueous solution:
1: 0 g./l. 2: 0.01 g./l.
3: 0.1 g./l. 4: 0.625 g./l.

light changed completely to green light when the dye was more than 0.02%. The light was gradually enfeebled by the further addition of the dye.

With the aid of this phenomenon, the variation in the shape of apparent emission spectra with the dye concentration could be investigated. To initiate the luminol reaction, 3 ml. of 10% of a hydrogen peroxide solution was added to mixtures of 6 ml. of an alkaline luminol solution (0.25 g. of luminol and 2 g. of sodium hydroxide were dissolved in 100 ml. of water) and 21-ml. portions of uranine solutions of various concentrations. The chemi-fluorescence spectra were measured with the apparatus shown in Fig. 1. The reaction was carried out at 31°C; the results are illustrated in Fig. 9. It is shown that the spectrum in a dilute dye solution has two maxima, at 420 mμ and 530 mμ, due to luminol chemiluminescence and uranine chemi-fluorescence respectively. The second peak shifts to longer wavelengths with an increase in the dye concentration, which is very similar to the red shift observed in the apparent chemiluminescence emission spectrum of the uranine-ozone system. This similarity would indicate that the chemiluminescence is the fluorescence of the dye.

Fluorescence Spectra of Uranine and Eosine.—In order to compare the chemiluminescence emission spectra with the fluorescence spectra, the apparent fluorescence spectra were investigated in methanol solutions of uranine and eosine of various concentrations. The spectra were measured with a fluoro-meter attached to the electro-spectro-photometer of Fig. 1 (Fig. 10). The results are shown in Figs. 11 and 12. It is there shown that the peaks of the apparent fluorescence spectra also shift towards longer wavelengths with an increase in the dye concentration.

The chemiluminescence emission spectra o

7) I. Plotnikov, *Umchau*, **42**, 981 (1938).
8) B. Tamamushi, *Naturwiss.*, **28**, 722 (1940).

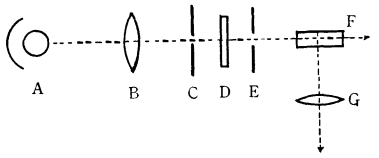

Fig. 10. Diagram of measuring apparatus for fluorescence emission spectra.
A: Mercury lamp B, G: Condencer
C: Iris D: Filter
E: Slit F: Quartz cuvett

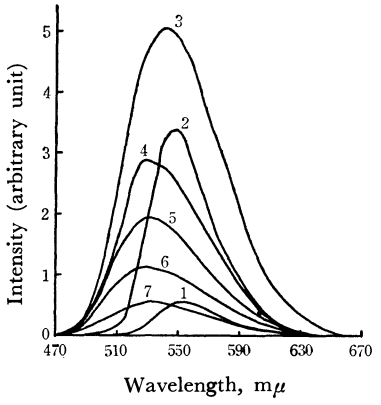

Fig. 11. Fluorescence emission spectra of uranine solutions in ethanol at 28°C.
1: 1.66×10^{-3} mol./l. 2: 4.10×10^{-4} mol./l.
3: 1.03×10^{-4} mol./l. 4: 2.56×10^{-5} mol./l.
5: 1.28×10^{-5} mol./l. 6: 6.41×10^{-6} mol./l.
7: 3.21×10^{-6} mol./l.

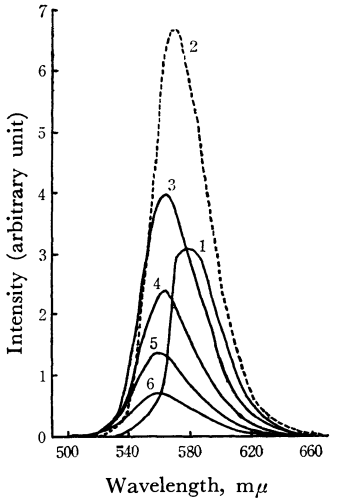

Fig. 12. Fluorescence emission spectra of eosine solutions in ethanol at 12°C.
1: 4.52×10^{-4} mol./l. 2: 1.13×10^{-4} mol./l.
3: 2.32×10^{-5} mol./l. 4: 1.16×10^{-5} mol./l.
5: 5.81×10^{-6} mol./l. 6: 2.90×10^{-6} mol./l.

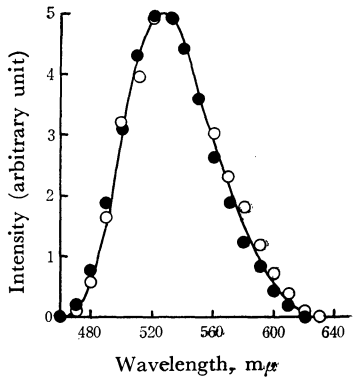

Fig. 13. Fluorescence and chemiluminescence emission spectra of uranine solution in ethanol.
—●— Chemiluminescence (curve 6 in Fig. 7)
—○— Fluorescence (curve 7 in Fig. 11)

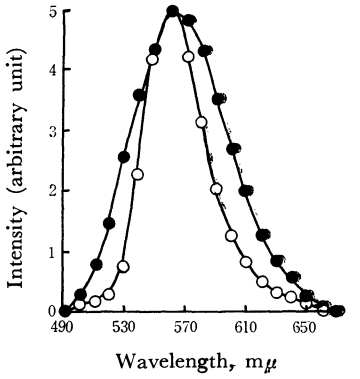

Fig. 14. Fluorescence and chemiluminescence emission spectra of eosine solution in ethanol.
—●— Chemiluminescence (curve 6 in Fig. 8)
—○— Fluorescence (curve 6 in Fig. 12)

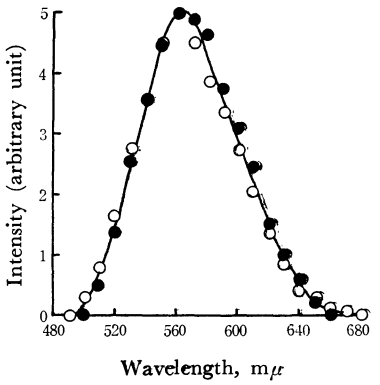

Fig. 15. Chemiluminescence emission spectrum of uranine and compared with the chemi-fluorescence spectrum of uranine-luminol system.
—○— Uranine system (curve 1 in Fig. 3)
—●— Uranine-luminol system (curve 4 in Fig. 9)

Figs. 7 and 8 are compared with the fluorescence spectra of Figs. 11 and 12 in Figs. 13 for uranine and in Fig. 14 for eosine. A correspondence between the two spectral curves is clearly demonstrated, although a slight deviation is found in the eosine system. The same comparison was made between the spectrum of uranine chemiluminescence in the presence of hydrogen peroxide and that of chemi-fluorescence in the luminol-uranine system. This is shown in Fig. 15. The coincidence is apparent.

On the basis of this experimental evidence, it may be concluded that the emissions from the uranine and eosine chemiluminescence are fluorescence emissions of the dyes and that the emitting species are the excited singlet states of uranine and eosine.

Further evidence in support of the present conclusion will be given in a succeeding paper.

BULLETIN OF THE CHEMICAL SOCIETY OF JAPAN VOL. 39 269—276 (1966)

Studies of the Chemiluminescence of Several Xanthene Dyes. III. The Effect of Added Foreign Dyes on Light Production

By Isao KAMIYA

Department of General Education, Nagoya University, Chikusa-ku, Nagoya

and Ryojirô IWAKI

Aichi Gakugei University, Chemical Laboratories, Okazaki, Aichi

(Received May 12, 1965)

The intensity of uranine chemiluminescence decreased when trypaflavine was added to the system. The enfeebling action seemed to be due to external quenching. On the contrary, the intensity of eosine chemiluminescence was enhanced by the presense of uranine. The values of Δ and σ are defined by the following equations:

$$\Delta=\int_0^T (I_{UE}-I_U-I_E)dt \qquad \sigma=\Delta\Big/\int_0^T I_E dt$$

where I_{UE}, I_U and I_E are the intensities measured in uranine-eosine, uranine and eosine systems respectively, and where T is the duration of eosine chemiluminescence. Δ increased with the increase in either the concentration of uranine or that of eosine, while σ increased only when the ratio of the uranine concentration to the eosine concentration increased. Δ increased with the increase in the temperature, while σ was little affected by the temperature. Δ increased upon the addition of organic solvents, while σ was little affected by the addition of the organic solvents. The enhancing action is due neither to the production of a stable compound which emits strongly nor to the increase in the rate of the decomposition of the dye. One possible mechanism of the enhancing action is that energy is transferred from an energy-rich intermediate produced by the reaction to an unoxidized uranine or eosine.

The intensity of chemiluminescence is affected more or less by the addition of foreign substances. Biswas and Dhar[1] have studied the subject extensively with a number of foreign substances and have found that all of them were inhibitors of the luminescent reaction. Bersis,[2] however, has succeeded in showing that the intensity of the chemiluminescence of polyphenol is remarkably enhanced by the presence of rhodamine B. In the present paper, the chemiluminescence of uranine and eosine will be investigated in the presence o foreign dyes, in the hope that a full examination of the effect of foreign substances will give some insight into the mechanism of the luminescent reaction. The results may be summarized as follows:

1) The intensity of uranine chemiluminescence decreases in the presence of trypaflavine (an enfeebling action). This has also been found to be true in uranine-erythrosine and in eosine-erythrosine systems.

2) The intensity of eosine chemiluminescence

1) N. N. Biswas and N. R. Dhar, *Z. anorg. u. allgem. Chem.*, **173**, 125 (1928).

2) D. S. Bersis, *Z. phys. Chem.* (*Neue Folge*), **26**, 359 (1960).

increases in the presence of uranine, and (an enhancing action).

Experimental

The luminescent systems were prepared, and both the luminescence intensities and the rates of the decomposition of the dyes were measured in the ways described in a preceding paper.[3]

Results and Discussion

I) Enfeebling Action.

Figure 1 shows the effect of added trypaflavine on the intensity of uranine chemiluminescence; curves I, II, III and IV represent, respectively, the results obtained from the uranine-trypaflavine sample solutions of I, II, III and IV listed in Table I. Each luminescent reaction was started by the addition of 1 ml. of a 20% hydrogen peroxide solution to a mixture of 7 ml. of the sample solution and 2 ml. of a 2.5 N sodium hydroxide solution at 40°C. We can see an "enfeebling action" of the added trypaflavine. The higher the concentration of added trypaflavine, the stronger becomes the enfeebling action. By numerical analysis, the curves can be represented as:

$$I_t = A\exp(-at)/\{B + Q\exp(-qt) + C\exp(-ct)\} \quad (1)$$

where I_t is the intensity of the emission at time t and A, a, B, Q, q, C and c are all parameters which differ according to the experimental conditions. Curves I, II, III and IV of Fig. 1 can be represented as the following equations:

Curve

$$\text{I:}\quad I_t = 500\exp(-0.46t)/\{1 + 6.0\exp(-0.80t)\} \quad (1a)$$

$$\text{II:}\quad I_t = 460\exp(-0.46t)/\{1.14 + 5.5\exp(-0.80t) + 6.3\exp(-0.53t)\} \quad (1b)$$

$$\text{III:}\quad I_t = 430\exp(-0.46t)/\{1.29 + 5.2\exp(-0.80t) + 16.2\exp(-0.51t)\} \quad (1c)$$

$$\text{IV:}\quad I_t = 357\exp(-0.46t)/\{1.53 + 4.5\exp(-0.80t) + 26.4\exp(-0.47t)\} \quad (1d)$$

Both the calculated values and the observed values are tabulated in Table II. The calculated values are in fairly good agreement with the observed values except for a slight deviation at the initial stage.

In the reaction system of uranine-trypaflavine, no emission was observed as resulting from the decomposition of trypaflavine. It is difficult to determine the decomposition rate of trypaflavine in the uranine-trypaflavine system by measuring the absorbancy of the dye at 452 mμ, because uranine absorbed light appreciably at that wavelength. However, as the rate of the decomposition of trypaflavine was found to be almost independent of the amount of uranine, its rate in the system could be estimated from a separate experiment in an isolated trypaflavine system. The rate of the decomposition of trypaflavine was measured in a system composed of 7 ml. of a trypaflavine solution, 2 ml. of a 2.5 N sodium hydroxide solution, and 1 ml. of a 20% hydrogen peroxide solution. The results are shown in Fig. 2, where the concentrations of trypaflavine in II', III' and IV' are equal to those in II, III and IV of Fig. 1 respectively. These decomposition curves can be represented as:

$$[D]_t = \alpha + \beta(-k_t t) \quad (2)$$

where $[D]_t$ is the concentration of trypaflavine at time t, both α and β are parameters which differ according to the experimental conditions, and k_t is the rate constant. The curves of Fig. 2 can be expressed as:

$$\text{Curve II'}\quad [D]_t = 0.036 + 1.74\exp(-0.53t) \quad (2a)$$

$$\text{Curve III'}\quad [D]_t = 0.076 + 4.27\exp(-0.53t) \quad (2b)$$

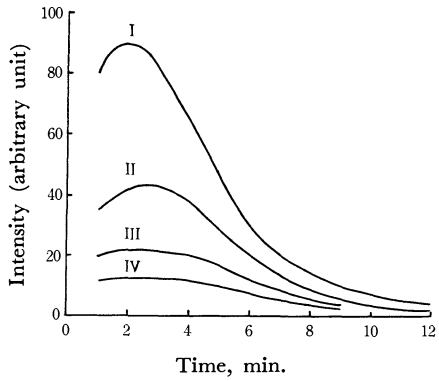

Fig. 1. *I-t* curves in uranine and uranine-trypaflavine systems.
(2.5 N NaOHaq., 20% H_2O_2 aq., 40°C)

TABLE I. THE RATIOS OF URANINE, TRYPAFLAVINE AND WATER IN VOLUME

Sample No.	Uranine solution (10 g./l.)	Trypaflavine solution (10 g./l.)	Water
I	3.5	0.0	3.5
II	3.5	0.5	3.0
III	3.5	1.0	2.5
IV	3.5	1.5	2.0

3) I. Kamiya and R. Iwaki, This Bulletin, **39**, 257 (1966).

TABLE II. QUENCHING REACTION BY TRYPAFLAVINE ON THE CHEMILUMINESCENCE OF URANINE AT 40°C

Time min.	Sample No. I Eq. 1a Calcd.	I Eq. 1a Obs.	II Eq. 1b Calcd.	II Eq. 1b Obs.	III Eq. 1c Calcd.	III Eq. 1c Obs.	IV Eq. 1d Calcd.	IV Eq. 1d Obs.
1.0	85.4	79.2	39.0	36.0	20.3	19.5	11.8	12.9
1.5	89.9	86.8	40.9	39.0	20.8	21.2	11.9	12.7
2.0	90.0	90.0	41.5	41.6	22.2	21.8	11.9	12.6
2.5	87.6	88.0	41.1	42.8	20.9	20.9	11.8	11.9
3.0	81.7	81.7	39.7	42.2	20.6	20.4	11.3	11.5
3.5	73.0	73.0	37.6	40.0	19.9	19.6	10.9	11.2
4.0	63.7	63.0	34.5	36.8	18.9	18.2	10.3	10.8
4.5	54.2	53.2	31.0	32.3	17.8	17.0	9.8	10.0
5.0	45.0	45.0	27.0	28.0	16.2	16.0	9.1	9.2
5.5	37.4	36.0	23.8	24.0	14.7	13.2	8.4	8.4
6.0	29.9	29.0	20.0	19.0	12.6	11.3	7.5	7.3
7.0	19.6	19.0	14.0	12.6	9.8	8.0	5.9	5.2
8.0	12.8	12.2	9.7	8.4	7.2	5.2	4.3	3.6
9.0	8.0	8.0	6.2	6.4	4.7	4.3	3.1	2.6
10.0	5.1	5.0	3.8	4.0	—	—	—	—
11.0	3.2	3.0	2.5	2.4	—	—	—	—
12.0	2.0	2.0	1.6	1.6	—	—	—	—

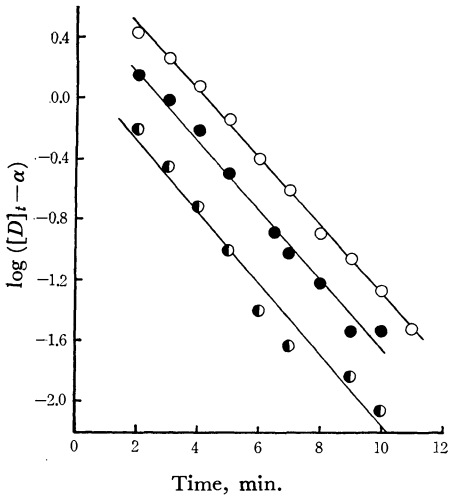

Fig. 2. Decomposition of trypaflavine at 40°C.
◐ II′ ● III′ ○ IV′

Curve IV′ $[D]_t = 0.141 + 6.92\exp(-0.53t)$ (2c)

The results indicate that the decomposition of trypaflavine is first order with respect to its concentration.

We shall first discuss the physical meaning of the parameters, a, A, etc.

Parameter a.—It was shown in a previous paper[3] that all the curves of the intensity versus the time measured in uranine chemiluminescence could be represented by a single equation in the form of Eq. 1a, in which a was found to correspond to the rate of the decomposition of uranine. Perhaps this may also be the case with Eqs. 1b—1d. We may also assume that parameter a is the rate of the decomposition of uranine, which is not affected by the addition of trypaflavine.

Parameter A.—From the same argument, A should be a value proportional to the initial concentration of uranine. Since an equal amount of uranine was added to each solution, the values A should be equal to one another. However, the values of A in the equations of 1b—1d are not constant. This deviation can be accounted for by the following consideration.

When a large amount of trypaflavine was added to a uranine solution, a small amount of a white precipitate was produced. Assuming that the amount of the precipitate is proportional to the product of the initial concentrations of uranine $[U]_0$ and trypaflavine $[T]_0$, the final concentration of uranine is given as $[U]=[U]_0(1-p[T]_0)$, where p is a proportionality constant. In the present case, [U] is given by the following equations, since the ratio of $[T]_0$ is 0 : 1 : 2 : 3.

Sample	Equation
I	$[U]=[U]_0$
II	$[U]=[U]_0(1-p')$
III	$[U]=[U]_0(1-2p')$
IV	$[U]=[U]_0(1-3p')$

where p' is a new constant. If $[U]_0$ and p' are put equal to 500 and 0.08 respectively in arbitrary units, the [U] values in the four specimens are

calculated to be 500, 460, 420 and 380 respectively. These values agree with the corresponding A value in Eqs. 1b—1d. Therefore, it may be concluded that A is a value proportional to the initial concentration of uranine.

Parameters c and C.—The third term of the denominator in Eq. 1, $C\exp(-ct)$, is found only in Eqs. 1b, 1c and 1d, not in Eq. 1a. This would indicate that the term corresponds to the effect of the addition of trypaflavine. If we assume the values of c in Eqs. 1b, 1c and 1d (0.53, 0.51 and 0.47 min^{-1}) to be approximately equal to one another, c is very likely to be the rate constant of the decomposition of trypaflavine (0.53 min^{-1} under the same experimental conditions). Moreover, the values of C in Eqs. 1b, 1c and 1d are almost proportional to the values of β in Eqs. 2a, 2b and 2c. Hence, it may be concluded that C is a value proportional to the initial concentration of trypaflavine. The actual concentration of trypaflavine may decrease upon the addition of uranine, but it is still proportional to the initial concentration (Table I).

Parameter B.—The mutual ratio of (B-1) values (0.14 : 0.29 : 0.53) is approximately equal to the ratio of α values in Eqs. 2a, 2b and 2c. The value of (B-1), therefore, is proportional to the initial concentration of trypaflavine.

From the same argument, parameters q and Q seem to correspond, respectively, to the decomposition rate constant and the initial concentration of a substance inhibiting light production.

On the basis of this discussion, Eq. 1 can be rewritten as:

$$I_t = A'[\mathrm{U}]_0 \exp(-k_\mathrm{U}t)/[1 + Q\exp(-qt) + [\mathrm{T}]_0 \times \{1 + B' \exp(-k_\mathrm{T}t)\}] \quad (3)$$

where A' and B' new constants, $[\mathrm{U}]_0$ and $[\mathrm{T}]_0$ are the initial concentrations of uranine and of trypaflavine respectively, and K_U and K_T are the rate constants of the decomposition of uranine and trypaflavine respectively.

At the initial stage of the reaction, Eq. 3 becomes:

$$I_t = A'[\mathrm{U}]_0/\{1 + Q + (1 + B)[\mathrm{T}]_0\} \quad (4)$$

This equation is similar to the Stern-Volmer equation for the quenching of fluorescence, if Q and $[\mathrm{T}]_0$ are the concentrations of the quenching substances. According to Wilhelmann, Lumry and Eyring,[4] the fraction of excited molecules which emit light in the chemiluminescence is given by:

$$\phi = k_1/(k_1 + k_2 + \sum_i k_i q_i)$$

where k_1, k_2 and k_i are the rates of the emission process, the internal quenching and the external quenching respectively, and q_i is the concentration of the ith quencher. The equation is very similar to Eq. 4.

From the above considerations, it may be concluded that the enfeebling action of trypaflavine is probably the external quenching.

II) Enhancing Action.

Figure 3 shows the curves of the intensity versus the time measured in a reaction system composed of 1 ml. of a 20% hydrogen peroxide solution, 2 ml. of a 3 N sodium hydroxide solution and 6 ml. of a uranine, eosine or uranine-eosine mixed solution, where the notation I_UE (3-1-2), for example, refers to a system composed of 3 ml. of a uranine

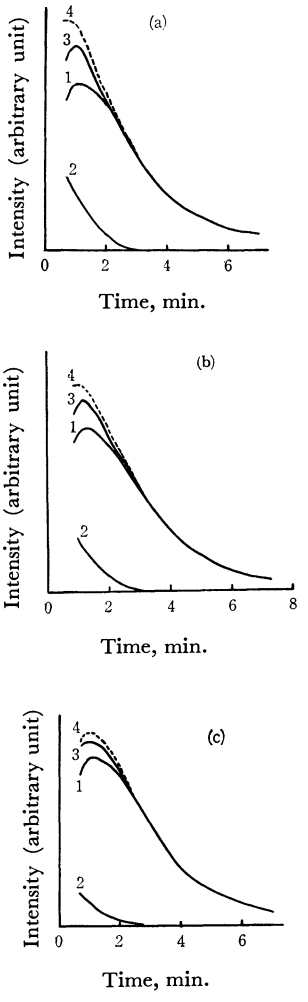

Fig. 3. I-t curves in uranine-eosine systems. (3 N NaOHaq., 20% H_2O_2aq., 45°C)

(a) 1: I_U (3-0-3); 2: I_E (0-3-3); 3: I_UE (3-3-0); 4: $I_\mathrm{U}+I_\mathrm{E}$

(b) 1: I_U (3-0-3); 2: I_E (0-2-4); 3: I_UE (3-1-2); 4: $I_\mathrm{U}+I_\mathrm{E}$

(c) 1: I_U (3-0-3); 2: I_E (0-1-5); 3: I_UE (3-1-2); 4: $I_\mathrm{U}+I_\mathrm{E}$

4) P. C. Wilhelmann, R. Lumry and H. Eyring, "The Luminescence of Biological Systems," John Wiley & Sons, New York, N. Y. (1955), p. 75.

solution (0.5 g./100 ml.), 1 ml. of an eosine solution (0.5 g./100 ml.) and 2 ml. of water. Similarly, I_U (3-0-3) and I_E(0-3-3), for example, refer respectively to the systems of (3 ml. of a uranine solution)+(3 ml. of water) and (3 ml. of an eosine solution)+(3 ml. of water). In every case, the I_{UE}-curve is lower than the corresponding (I_U+I_E) curve (shown by a dotted line); that is, an enfeebling action was found under these experimental conditions. Figure 4 involves similar intensity-time curves, which have been measured with the systems except that the 3 N sodium hydroxide solution is replaced by a 1.5 N solution. In this case, the I_{UE}-curve is slightly higher than the (I_U+I_E)-curve; that is, the enhancing action is exhibited under the conditions employed. This enhancing

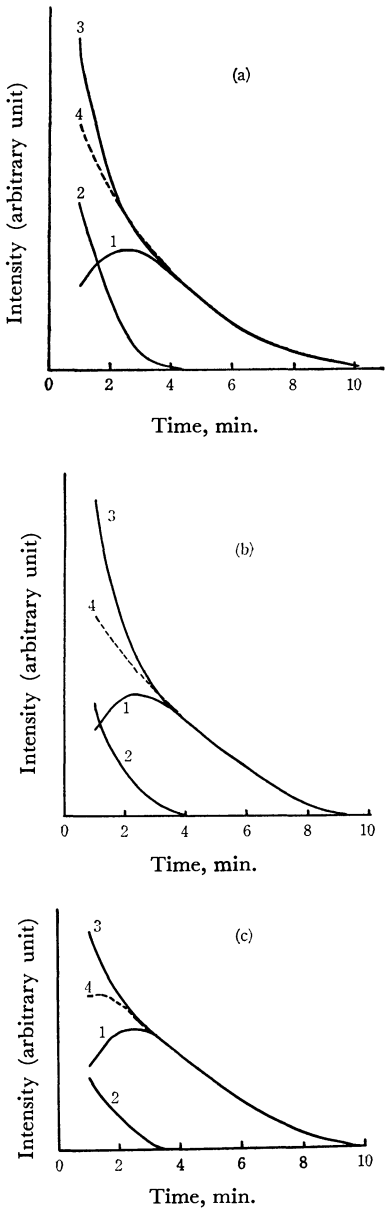

Fig. 4. *I-t* curves in uranine-eosine systems. (1.5 N NaOHaq., 20% H_2O_2aq., 45°C)

(a) { 1: I_U (3-0-3); 2: I_E (0-3-3); 3: I_{UE} (3-3-0); 4: I_U+I_E }

(b) { 1: I_U (3-0-3); 2: I_E (0-2-4); 3: I_{UE} (3-2-1); 4: I_U+I_E }

(c) { 1: I_U (3-0-3); 2: I_E (0-1-5); 3: I_{UE} (3-1-2); 4: I_U+I_E }

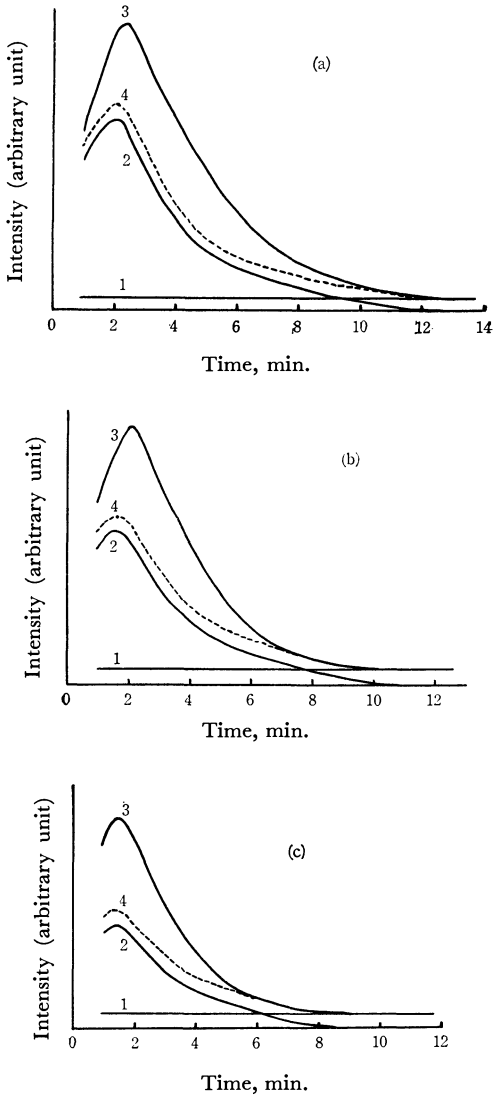

Fig. 5. *I-t* curves in uranine-eosine systems. (0.5 N NaOHaq., 20% H_2O_2aq., 45°C)

(a) { 1: I_U (3-0-3); 2: I_E (0-3-3); 3: I_{UE} (3-3-0); 4: I_U+I_E }

(b) { 1: I_U (3-0-3); 2: I_E (0-2-4); 3: I_{UE} (3-2-1); 4: I_U+I_E }

(c) { 1: I_U (3-0-3); 2: I_E (0-1-5); 3: I_{UE} (3-1-2); 4: I_U+I_E }

TABLE III. THE VALUES OF Δ AND σ AS A FUNCTION OF DYE CONCENTRATION AT 40°C
(0.3 N NaOHaq., 20% H_2O_2aq.)

Dye concentration (Ratio to original solution)						
Uranine	Eosine	$\int I_U dt$	$\int I_E dt$	$\int I_{UE} dt$	Δ	σ
1/2	1/2	1.5	35.5	80.0	43.0	1.3
1/2	1/4	1.5	17.5	50.0	31.0	1.8
1/2	1/8	1.5	9.1	33.0	22.4	2.5
1/2	1/16	1.5	3.5	16.3	11.3	3.2
1/2	1/32	1.5	1.5	9.8	6.8	4.5
1/2	1/64	1.5	0.6	6.0	3.9	6.5
1/2	1/2	1.5	35.5	80.0	43.0	1.3
1/4	1/2	0.8	35.5	66.0	29.7	0.83
1/8	1/2	0.4	35.5	52.0	16.1	0.44
1/16	1/2	0.2	35.5	46.0	10.3	0.30
1/32	1/2	0.0	35.5	41.8	6.3	0.17
1/64	1/2	0.0	35.5	39.0	3.5	0.078

TABLE IV. EFFECT OF TEMPERATURE ON THE VALUES OF Δ AND σ IN AQUEOUS SYSTEM WITH $[U]_0/[E]_0=1$
(0.5 N NaOHaq., 20% H_2O_2aq.)

Temp., °C	$\int I_U dt$	$\int I_E dt$	$\int I_{UE} dt$	Δ	σ
37	0.0	8.0	17.5	9.5	1.2
29	0.0	5.2	11.4	6.2	1.2
20	0.0	3.5	7.75	4.25	1.2
9	0.0	1.6	3.47	1.87	1.1

TABLE V. THE EFFECT OF THE CONCENTRATION OF ADDED ORGANIC SOLVENTS ON THE VALUES OF Δ AND σ
($[U]_0/[E]_0=5$, 0.5 N NaOHaq., 20% H_2O_2aq., 45°C)

Solvent	% (In volume)	$\int I_U dt$	$\int I_E dt$	$\int I_{UE} dt$	Δ	σ
Water	—	192.4	43.1	324.3	88.8	2.0
Methanol	20	220.8	80.3	461.2	160.1	2.0
	30	398.4	124.2	768.3	245.7	2.0
	40	405.8	153.8	839.8	280.2	1.8
	60	632.8	207.7	1244.3	403.8	1.9
Ethanol	20	408.0	135.1	812.5	269.4	2.0
	30	547.8	169.0	1059.2	342.4	2.0
	40	796.8	223.6	1488.0	467.6	2.1
	60	1223.2	259.6	1999.6	516.8	2.0
n-Propanol	20	474.5	122.4	839.7	242.8	2.0
	30	481.4	131.8	882.2	269.0	2.0
	60	921.4	198.1	1495.0	375.5	1.9
Isopropanol	20	559.3	128.6	953.0	265.1	2.1
	30	654.0	131.1	1066.7	281.6	2.1
	40	880.0	165.2	1404.0	358.8	2.1
Glycerol	20	174.0	73.0	409.4	162.4	2.2
	30	184.1	96.2	491.6	211.3	2.2
	40	193.9	122.2	571.8	255.7	2.1
	50	250.4	168.3	739.3	320.6	1.9
Dioxane	20	472.7	156.6	898.0	268.7	1.7
	30	723.2	217.0	1314.2	374.0	1.7
	40	910.8	245.0	1560.6	404.8	1.7
	50	1626.6	258.6	2294.0	408.8	1.6

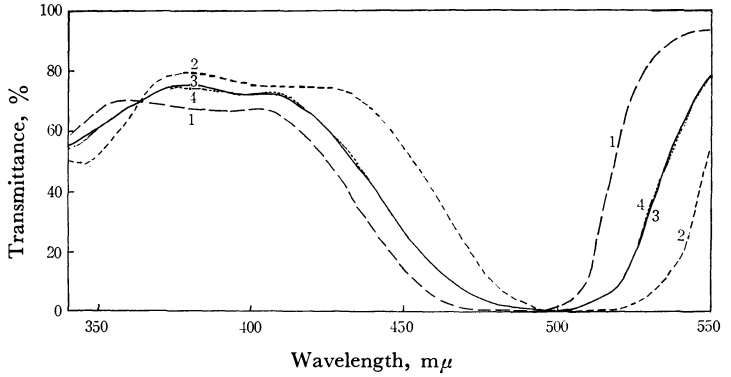

Fig. 6. Absorption spectra of uranine, eosine and uranine-eosine systems. (1/2 conc. to original solution, 0.5 N NaOHaq.)
1: T_U; 2: T_E; 3: T_{UE}; 4: $\sqrt{T_U \times T_E}$

action becomes stronger when 2 ml. of a 0.5 N sodium hydroxide solution is used instead. Hence, it may be concluded that the enhancing action arises only in a system of low alkali concentration.

It is worth noting that every I_{UE}-curve in Fig. 5 approaches the I_U-curve when the I_E-curve falls to zero. This allows the "increment of the total light emission" to be defined as:

$$\Delta = \int_0^T (I_{UE} - I_U - I_E)dt \qquad (5)$$

where I_{UE}, I_U and I_E are the intensities of the emission measured in uranine-eosine, uranine and eosine systems respectively, and T is the duration of eosine chemiluminescence. Furthermore, the results indicate that the enhancing action can be seen only when eosine chemiluminescence takes place; in other words, the processes of eosine chemiluminescence seem to be necessary for the enhancing action. In a system of such a low alkali concentration, uranine decomposes so slowly that the intensity of its chemiluminescence is practically zero, so the ratio of Δ to the total light emission of eosine chemiluminescence can be taken as the value of the "relative increment," σ:

$$\sigma = \Delta \Big/ \int_0^T I_E dt \qquad (6)$$

The values of Δ and σ were investigated under various experimental conditions. In order to obtain the pertinent values for I_{UE}, I_U and I_E, the I-t cruves were integrated graphically.

The Dependence of Δ and σ on the Concentration of the Dye.—The values of Δ and σ measured in systems with different uranine concentrations but with a constant eosine concentration are shown in Table III. The Δ and σ values in the systems with different eosine concentrations but with a constant uranine concentration are also shown in Table III. These results indicate that Δ increases with an increase in the initial concentration of either uranine ($[U]_0$) or eosine ($[E]_0$), while σ increases only when the ratio of $[U]_0/[E]_0$ increases. As will be discussed in a succeeding paper, Δ and σ are given by:

$$\Delta = M[U]_0 \log \{1 + N([E]_0/[U]_0)\}$$

$$\sigma = M'([U]_0/[E]_0) \log \{1 + N([E]_0/[U]_0)\}$$

where M, M' and N are the parameters.

The Temperature Dependence of Δ and σ.—Table IV illustrates the values of Δ and σ as measured in systems of (3-3-0), (3-0-3) and (0-3-3) at several different temperatures. It is there shown that Δ increases with an increase in the temperature, while σ is almost completely insensitive to the temperature.

The Dependence of Δ and σ on the Concentration of Added Organic Solvent.—It has been found that the total amount of emission is enhanced when organic solvents, such as alcohol, acetone, dioxane and glycerol, are added to the luminescent system. Therefore, Δ and σ have been determined in several water-organic solvent systems (Table V). We see that Δ increases as the concentration of the organic solvent increases, while σ remains constant. The results will be discussed in a succeeding paper.

The Absorption Spectrum of the Uranine-Eosine System.—The enhancing action arises from an interaction between uranine and eosine. To decide what kind of the interraction this is, the absorption spectrum of the uranine-eosine system was measured. The results are shown in Fig. 6, where T_U and T_E are the absorption curves of the solutions of uranine (0.5 g./100 ml.) and eosine (0.5 g./100 ml.), and T_{UE} is that of a uranine-eosine mixed solution (0.5 g. uranine and 0.5 g. eosine per 100 ml.). It can be seen that the I_{UE}-curve is very close to the $\sqrt{T_U \times T_E}$-curve (shown by a dotted line). This fact indicates that no stable substance is produced when the two dyes are mixed.

The Rates of the Decomposition of Uranine and Eosine in the Uranine-Eosine System.—

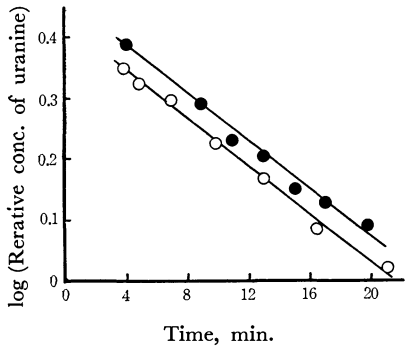

Fig. 7. Rates of uranine decomposition in uranine eosine system and in isolated uranine system. (0.5 N NaOHaq., 20% H_2O_2aq., 41°C)
-●- Isolated uranine system
-○- Uranine-eosine system

The rate of the decomposition of uranine in the system of uranine-eosine can easily be determined by spectrophotometry at 490 mμ, bceause practically no eosine absorbed that light. The measurements were carried out in a system composed of 12 ml. of a (6-6-0) sample solution, 4 ml. of a 0.5 N sodium hydroxide solution and 2 ml. of a 20% hydrogen peroxide solution. The results are shown in Fig. 7. It shows that the decomposition of uranine in the uranine-eosine system is first order with respect to the uranine concentration. The rate constant is 0.048 min^{-1}, which is almost identical with the decay constant of uranine chemiluminescence in an isolated uranine system under the same experimental conditions. Hence, it may be concluded that the rate of uranine decomposition is not affected by the addition of eosine.

As has been shown before, the I_{UE}-curve approaches the I_U-curve when the I_E-curve falls to zero. This fact would mean that the duration of eosine chemiluminescence in mixed system is the same as that in an isolated system, because the enhancing action is found only when the chemiluminescent reaction of eosine takes place. Hence, it seems that the rate decomposition of eosine is little affected by the addition of uranine.

It follows from the above considerations that the enhancing action is due neither to the production of a stable substance which emits strongly nor to the increase in the rate of the decomposition of uranine or eosine.

One possible mechanism for the enhancing action would be that eosine is oxidized to an energy-rich intermediate at the first stage of the reaction; then the energy is transferred from the intermediate to an oxidized dye, thereby exciting both eosine and uranine to emit fluorescence. The same mechanism for the light production was proposed by Kautsky,[5] who studied the luminescent reaction of siloxen ($Si_6O_3H_6$) in the presence of rhodamine. He found that the spectral distribution of the luminescence was similar to that of the fluorescence of rhodamine, although the dye was not oxidized; he concluded that energy was transferred from siloxene to the dye by some sort of collision. Similar results have been reported by Schales,[6] Tamamushi[7] and Vassil'ev[8].

Spruit van der Burg[9] has reported that the emission of lucigenin chemiluminescence is blue in a hot, dilute solution and that it may arise from the energy-rich product, methyl acridone, while the emission is green in a cold, concentrated solution. This fact is suggestive of the same energy-transfer mechanism as that of the emission in the uranine-eosine system.

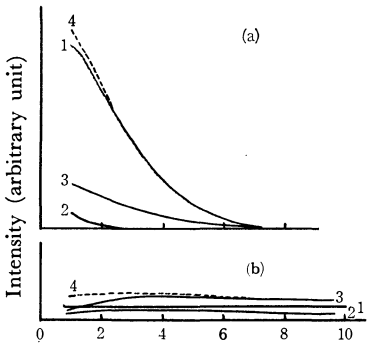

Fig. 8. *I-t* curves in uranine-erythrosine systems.
(a) 3 N NaOHaq., 20% H_2O_2aq., 45°C
(b) 0.5 N NaOHaq., 20% H_2O_2aq., 45°C
1: I_U (3-0-3) 2: I_{Er} (0-3-3)
3: I_{UEr} (3-3-0) 4: I_U+I_{Er}

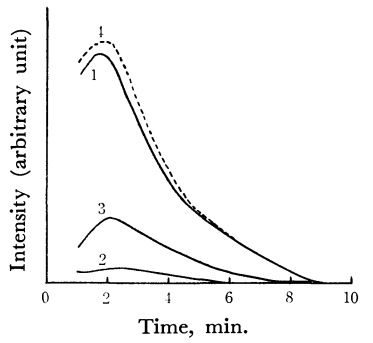

Fig. 9. *I-t* curves in eosine-erythrosine system. (0.5 N NaOHaq., 20% H_2O_2aq., 45°C)
1: I_E (3-0-3) 2: I_{Er} (0-3-3)
3: I_{EEr} (3-3-0) 4: I_E+I_{Er}

Chemiluminescence in such other systems as uranine-erythrosine and eosine-erythrosine has also been investigated; the results are illustrated in Figs. 8 and 9. They exhibit no enhancing action.

5) H. Kautsky and H. Zocher, *Z. Phys.*, **9**, 267 (1922).
6) O. Schales, *Ber.*, **172**, 1155 (1939).
7) B. Tamamushi, *Naturwiss.*, **28**, 722 (1940).
8) R. F. Vassil'ev, *Nature*, **196**, 668 (1962).
9) A. Spruit van der Burg, *Rec. Trav. Chim.*, **69**, 1526 (1950).

BULLETIN OF THE CHEMICAL SOCIETY OF JAPAN VOL. 39 277—281 (1966)

Studies of the Chemiluminescence of Several Xanthene Dyes. IV. Theoretical Considerations

By Isao KAMIYA

Department of General Education, Nagoya University Chikusa-ku, Nagoya

and Ryojirô IWAKI

Aichi Gakugei University, Chemical Laboratories, Okazaki, Aichi

(Received May 12, 1965)

On the basis of the results shown in the previous papers, the following reaction scheme was proposed for the chemiluminescent reaction. Hydrogen peroxide decomposes spontaneously to the radical (R·). A portion of the radical then reacts with the dye molecule (E) to produce an energy-rich intermediate (M_E*): $E+R\cdot \rightarrow M_E^*$ The energy-transfer takes place from M_E* to an unoxidized dye, so the dye is excited electronically: $M_E^*+E \rightarrow E^*+\cdots$ However, most of the M_E* is decomposed by non-radiative processes. E* is deactivated by fluorescence emission processes ($E^* \rightarrow E+h\nu$) or quenching processes ($E^*+E \rightarrow E+E$). According to this reaction scheme, most of the experimental results can be explained reasonably. It is expected that further experimental evidence, such as the detection of an intermediate, will verify the theory.

The present authors have investigated the chemiluminescence of several xanthene dyes and obtained the following results:[1]

1) The intensity of the emission versus the time at the decay stage was represented by:

$$I_t = A \exp(-a t) \quad (1)$$

where I_t is the intensity of the emission at time t, a (the decay constant) is equal to the rate constant of the decomposition of the dye, and A is a parameter which is proportional to the initial concentration of the dye. This indicates that the decay of the luminescence is first order with respect to the concentration of the dye. The curve was much affected by the concentration of the added sodium hydroxide solution, while it was not affected by the concentration of added hydrogen peroxide when its concentration was high.

2) The energy distribution of the chemiluminescence emission was very similar to that of the fluorescence emission. This indicates that the emitting species are probably excited singlet states of the dye molecule.

3) The luminescent light was enfeebled by the addition of some kind of foreign dye. The enfeebling action seemed to be due to external quenching; it was found in all of the uranine-trypaflavine, uranine-erythrosine and eosine-erythrosine systems.

On the contrary, the intensity of the emission was enhanced when uranine was added to the eosine chemiluminescent system. However, the enhancing action was found only when the concentration of alkali was too low to cause the decomposition of uranine. The enhancing action was due neither to the production of a stable compound which emitted light strongly nor to the increase in the rate of decomposition of the dyes. A possible mechanism may be proposed, in which eosine is oxidized to an energy-rich intermediate and the energy is transferred from the intermediate to unoxidized eosine and uranine, thereby exciting both dyes to emit fluorescence.

Concideration

Reaction Scheme.—On the basis of the results summarized above, the following mechanism seems plausible for the luminescent reaction.

In an alkaline solution, hydrogen peroxide decomposes spontaneously to radicals, R·, such as OH· and O_2H·. Some of the radicals react with the dye to produce an energy-rich intermediate. In a uranine-eosine system with a low alkali concentration, the radical reacts only with eosine, E, to produce an energy-rich intermediate, M^*_E:

$$E + R\cdot \rightarrow M^*_E \quad [I] \text{ reaction rate: } k_1$$

Recently, Hayashi and Maeda[2] have shown that the intermediate in lophin chemiluminescence is a radical. Steele[3] has reported, in his studies of the photo-induced chemiluminescence of riboflavin in water containing hydrogen peroxide, that the emission is mediated by an excited metastable triplet state of riboflavin. White and

1) I. Kamiya and R. Iwaki, This Bulletin, **39**, 257, 264, 269 (1966).

2) T. Hayashi and K. Maeda, ibid., **35**, 2057 (1962).

3) R. H. Steele, *Biochem.*, **2**, 529 (1963).

Bursey[4] proposed that an excited triplet state of the aminophthalic acid ion was an intermediate in luminol chemiluminescence. However, no information as to M^*_E has yet been obtained.

An energy-transfer takes place from M^*_E to unoxidized eosine and uranine, so the dyes are excited electronically.

$$M^*_E + E \rightarrow E^* + \cdots \qquad [II]: k_2$$
$$M^*_E + U \rightarrow U^* + \cdots \qquad [III]: k_3$$

Since the efficiency of the emission of the luminescent reaction is low, most of M^*_E would be decomposed or deactivated by non-radiative processes. E* and U* are deactivated either by fluorescence emission processes or by quenching processes:

$$M^*_E \rightarrow \cdots \qquad [IV]: k_4$$

E* and U* are deactivated either by fluorescence emission processes or by quenching processes:

$$E^* \rightarrow E + h\nu \qquad [V]: k_5$$
$$U^* \rightarrow U + h\nu \qquad [VI]: k_6$$
$$E^* + E \rightarrow E + E \qquad [VII]: k_7$$
$$E^* + U \rightarrow E + U \qquad [VIII]: k_8$$
$$U^* + E \rightarrow U + E \qquad [IX]: k_9$$
$$U^* + U \rightarrow U + U \qquad [X]: k_{10}$$

Although further quenching may take place at the initial stage, as has been shown in a previous paper, our discussion will be limited to the decay stage, where the intensity versus time is represented by Eq. 1.

The Curve of the Intensity versus the Time ((I-t Curve) in a Uranine-Eosine System with Low Alkali Concentration.—According to the mechanism proposed above, the intensity of chemiluminescence in a uranine-eosine system, I_{UE}, is given by:

$$I_{UE} = \phi_E[E^*] + \phi_U[U^*] = k_2[M^*_E][E]\phi_E + k_3[M^*_E][U]\phi_U \qquad (2)$$

where ϕ_E and ϕ_U are the fluorescence efficiencies of eosine and uranine respectively and are given by:

$$\phi_E = k_5/\{k_5+k_7[E]+k_8[U]\}$$
$$\text{and} \quad \phi_U = k_6/\{k_6+k_9[E]+k_{10}[U]\}$$

In luminescent reaction systems, the apparent fluorescence is so weak that

$$\left.\begin{aligned} k_5 &\ll k_7[E] + k_8[U] \\ \text{and} \\ k_6 &\ll k_9[E] + k_{10}[U] \end{aligned}\right\} \qquad (3)$$

are obeyed approximately.

From Eq. 3 and the assumption that $k_7=k_9$ and $k_8=k_{10}$, I_{UE} is reduced to:

$$I_{UE} = [\{k_2k_5[E]+k_3k_6[U]\}/\{k_7[E]+k_8[U]\}][M^*_E] \qquad (4)$$

$d[M^*_E]/dt$ is then given by:

$$d[M^*_E]/dt = k_1[R\cdot][E]-k_2[M^*_E][E]-k_3[M^*_E][U]-k_4[M^*_E] \qquad (5)$$
$$= k_1[R\cdot][E]-k_4[M^*_E]$$

because $k_4 \gg k_2 + k_3$.

It has been found that the decay curve is not affected by the concentration of hydrogen peroxide when its concentration is high and that the intensity of emission is increased by the addition of a dye solution at the final stage of the reaction. These facts indicate that the concentration of R· does not vary during the luminescent reaction, provided the concentration of the added hydrogen peroxide is high (in excess). Furthermore, the experimental results show that the concentrations of eosine and uranine are given by:

$$[E]=[E]_0\exp(-K_Et), \quad [U]=[U]_0$$

where $[E]_0$ and $[U]_0$ are the initial concentrations of eosine and uranine respectively, and where K_E is the rate constant of the decomposition of eosine. (The decomposition of uranine can be disregarded.) Therefore, Eq. 5 can be rewritten approximately as:

$$d[M^*_E]/dt = k_1[R\cdot][E]_0\exp(-K_Et) - k_4[M^*_E] \qquad (6)$$

Since [R·] is independent of the time, Eq. 6 can easily be resolved to:

$$[M^*_E] = \{k_1[R\cdot][E]_0/(k_4-K_E)\} \times \{\exp(-K_Et)-\exp(-k_4t)\}$$

It seems likely that $k_4 \gg K_E$, so:

$$[M^*_E] = \{k_1[R\cdot][E]_0/k_4\}\exp(-K_Et) \qquad (7)^{**}$$

From Eqs. 4 and 7, I_{UE} is finally given by:

$$I_{UE} = k_1[R\cdot](k_2k_5[E]^2+k_3k_6[E][U]_0)/k_4(k_7[E]+k_8[U]_0) \qquad (8)$$

The I-t Curve for Eosine and Uranine Systems.—By taking into account reactions I, II, IV and VII, the intensity of the emission of eosine chemiluminescence, I_E, at time t can similarly be derived as:

$$I_E = k_1k_2k_5[R\cdot][E]/k_4k_7 = (k_1k_2k_5[R\cdot][E]_0/k_4k_7)\exp(-K_Et) \qquad (9)$$

Similarly, the intensity of the emission of uranine chemiluminescence, I_U, in a solution with a high alkali concentration is given by:

$$I_U = k_1'k_2'k_5'[R\cdot][U]/k_4'k_7' = (k_1'k_2'k_5'[R\cdot][U]_0/k_4'k_7')\exp(-K_Ut) \qquad (10)$$

4) E. H. White and M. M. Bursey, *J. Am. Chem. Soc.*, **86**, 941 (1964).

** Equation 7 can also be obtained by the "Steady-State Method," $d[M^*_E]dt=0$.

The experimental results in a previous paper have shown that I_E and I_U can be represented by Eq. 1. This seems to give support to the present equations of 9 and 10. However, when the concentration of hydrogen peroxide is low, Eqs. 9 and 10 are no more obeyed, because [R·] is no longer constant during the reaction. Moreover, k_5 is not ignorable compared to k_7[E] in the final stage, because the concentration of the dye becomes low.

The Value of Δ in a Uranine-Eosine System with a Low Alkali Concentration.—The value of Δ (the increment of the total emission) observed in a uranine-eosine chemiluminescent system with a low alkali concentration was defined as:

$$\Delta=\int_0^T (I_{UE}-I_U-I_E)\mathrm{d}t \tag{11}$$

where T is the duration of the chemiluminescence of eosine. Using Eqs. 8 and 9, and recalling that $I_U=0$, Eq. 11 becomes:

$$\Delta=(k_1[\mathrm{R}\cdot]/k_4)\int_0^T \{(k_2k_5[\mathrm{E}]^2+k_3k_6[\mathrm{E}][\mathrm{U}]_0)/(k_7[E]+k_8[\mathrm{U}]_0)-(k_2k_5/k_7)[\mathrm{E}]\}\mathrm{d}t$$

or

$$\Delta=(k_1[\mathrm{R}\cdot][\mathrm{U}]_0/k_4)(k_3k_6-k_2k_5k_8/k_7)\times\int_0^T \{[\mathrm{E}]/(k_7[\mathrm{E}]+k_8[\mathrm{U}]_0)\}\mathrm{d}t \tag{12}$$

On substituting the relation $[\mathrm{E}]=[\mathrm{E}]_0\exp(-K_Et)$ and $[\mathrm{E}]_0\exp(-K_ET)=0$, Eq. 12 is integrated to:

$$\left.\begin{aligned}\Delta&=(k_1[\mathrm{R}\cdot]/k_4K_Ek_7)(k_3k_6-k_2k_5k_8/k_7)[\mathrm{U}]_0\times\ln(1+k_7[\mathrm{E}]_0/k_8[\mathrm{U}]_0)\\ \text{or}\\ \Delta&=2.30P[\mathrm{U}]_0\log(1+Q[\mathrm{E}]_0/[\mathrm{U}]_0)\end{aligned}\right\} \tag{13}$$

where

$$P=(k_1[\mathrm{R}\cdot]/k_4K_Ek_7)(k_3k_6-k_2k_5k_8/k_7)$$
$$Q=k_7/k_8$$

Table I. Observed and calculated Δ-values in uranine-eosine system
(0.3N NaOHaq., 20% H_2O_2aq., 40°C)

$[\mathrm{U}]_0$ (mu)	$[\mathrm{E}]_0$ (ne)	$\int I_E\mathrm{d}t$	$\int I_U\mathrm{d}t$	$\int I_{UE}\mathrm{d}t$	Δcalcd.*	Δobs.
		(in arbitrary unit)				
32	32	35.5	1.5	80.0	44.8	43.0
16	32	35.5	0.8	66.0	29.3	29.7
8	32	35.5	0.4	52.0	18.3	16.1
4	32	35.5	0.2	46.0	11.0	10.3
2	32	35.5	0.0	41.8	6.5	6.3
1	32	35.5	0.0	39.0	3.7	3.5
32	16	17.5	1.5	50.0	32.2	31.0
32	8	9.1	1.5	33.0	25.1	22.4
32	4	3.5	1.5	16.3	13.3	11.3
32	2	1.5	1.5	9.8	7.5	6.8
32	1	0.6	1.5	6.0	4.1	3.9

* Δcalcd.$=1.6m\log(1+6.5n/m)$

Table II. Observed and calculated Δ-values in uranine-eosine system
(0.5N NaOHaq., 20% H_2O_2aq., 42°C)

$[\mathrm{U}]_0$ (mu')	$[\mathrm{E}]_0$ (ne')	$\int I_E\mathrm{d}t$	$\int I_U\mathrm{d}t$	$\int I_{UE}\mathrm{d}t$	Δcalcd.*	Δobs.
		(in arbitrary unite)				
37	59	28.2	10.0	63.4	25.4	25.2
37	37	19.1	10.0	50.2	22.1	21.1
37	22	16.2	10.0	40.8	16.1	16.2
37	15	13.7	10.0	33.8	13.4	13.7
37	11	11.9	10.0	28.2	11.3	11.9

$u'=37u/16$, $e'=37e/16$;
* Δcalcd.$=6.5m\log(1+6.5n/m)$

In a system composed of 3 ml. of an eosine solution (1 g./100 ml.), 3 ml. of a uranine solution (1 g./100 ml.), 2 ml. of a 0.3 N sodium hydroxide solution and 1 ml. of a 20% hydrogen peroxide solution, $[\mathrm{U}]_0$ and $[\mathrm{E}]_0$ are put, for illustrative convenience, as $32u$ and $32e$ respectively, so u and e are equal to 1.4×10^{-4} and 7.5×10^{-5} mol./l. respectively. The concentration of uranine or eosine is successively reduced by half ($16u$, $8u$, etc.) and the values of Δ are calculated with Eq. 13, where $2.3\times(Pu)$ is taken to be 1.6 and (Qe/u), 6.5:

$\Delta=1.6\,m\log(1+6.5n/m)$ (m and n are integers). They are shown in Table I, together with the observed values. Table II tabulates the Δ-values observed when the concentration of the added sodium hydroxide solution is slightly higher (0.5 N), so that I_U can no longer be ignored. It also includes values calculated by the following equation:

$$\Delta=6.5m\log(1+6.5n/m) \tag{14}$$

In both cases, the calculated values are in fairly good agreement with the observed values. It is worth noting that, whether I_U is smaller or not, the values of Δ can be expressed by the same equation. This means that the uranine chemiluminescence is not enhanced by the presence of eosine.

The Values of σ.—The relative increment, σ, was defined as:

$$\sigma = \Delta\Big/\int_0^T I_E\mathrm{d}t \tag{15}$$

From Eqs. 9 and 15, we obtain:

$$\int_0^T I_E\mathrm{d}t = k_1[\mathrm{R}\cdot]k_2k_5[\mathrm{E}]_0/k_4K_Ek_7 \tag{16}$$

since $[\mathrm{E}]_0\exp(-K_ET)=0$.

On substituting Eqs. 13 and 16 into Eq. 15, we obtain:

$$\sigma=\{(k_3k_6/k_2k_5)-k_8/k_7\}([\mathrm{U}]_0/[\mathrm{E}]_0)\times\ln(1+k_7[\mathrm{E}]_0/k_8[\mathrm{U}]_0) \tag{17}$$

Equation 17 indicates that σ is constant when the ratio of $[\mathrm{U}]_0$ to $[\mathrm{E}]_0$ remains constant (at a constant temperature). The experimental values

of σ obtained at several different concentrations of uranine and eosine but at a constant ratio of $[U]_0/[E]_0$ are shown in Table III. As is to be expected, the values of σ are almost constant except in the systems with low dye concentrations. The value of σ probably decreases in a system with a low dye concentration because the energy-transfer from M^*_E to U can no longer take place.

TABLE III. OBSERVED VALUES OF σ IN URANINE-EOSINE SYSTEMS WITH THE CONSTANT RATIO OF $[U]_0$ TO $[E]_0$
(0.5N NaOHaq., 20% H_2O_2aq., 40°C)

$[U]_0$	$32u$	$16u$	$10.7u$	$8u$	$5.3u$	$4u$	$2.7u$
$[E]_0$	$32e$	$16e$	$10.7e$	$8e$	$5.3e$	$4e$	$2.7e$
σ	1.24	1.22	1.20	1.23	0.59	0.43	0.22

The Effect of the Temperature on the Luminescent Reaction.—It is reasonable to assume that there are two processes with a heat of activation in the reaction; one is the process of reaction I, reaction between R· and the dye, the other is that of II (III); an energy-transfer from an energy-rich intermediate to an unoxidized dye. Thus, the rate constants of k_1 and k_2 (and k_3) are much more affected by the temperature than any other rate constants in the reaction scheme. On this arguments, we can derive the conclusion that the values of A and a in Eq. 1 and the value of Δ increase with an increase in the temperature, while σ is not affected by the temperature from the consideration that A is second order; a and Δ are first order, and σ is zero-th order with respect to the rate constants of k_1 and k_2 (k_3) since K_E seems to be k_1.

The activation energy of reaction I can be estimated from the plot of log a (log K_E) against the reciprocal of the absolute temperature. Figure 1 is the plot obtained from the system composed of 6 ml. of a uranine solution, 2 ml. of a sodium hydroxide solution, and 1 ml. of 20% hydrogen peroxide. Figure 2 is a similar plot in eosine chemiluminescence (6 ml. of an eosine solution, 2 ml. of a 0.5 N sodium hydroxide solution, and 1 ml. of 30% hydrogen peroxide). The activation energies of uranine and eosine chemiluminescent reactions are found to be 13 and 11 kcal./mol. respectively. We can see that the activation energy for the reaction in an aqueous system is equal to that in a water-organic solvent system, although the light intensity in the former is lower than that in the later. Moreover, the energy is practically the same, irrespective of the concentration of the added sodium hydroxide solution.

The Effect of the Added Organic Solvent on the Intensity of Emission.—In Table IV, the products of Δ and K_E in methanol-water and ethanol-water systems of different alcohol concentrations are shown. It may be seen that the product is almost constant in each system.

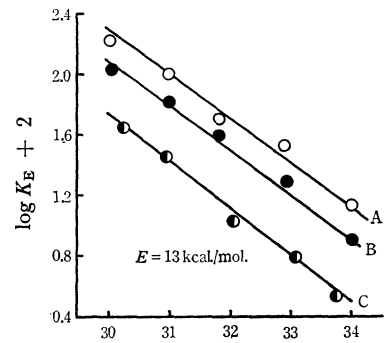

Fig. 1. Log K_E - 1/T plots in uranine chemiluminescence.
A: 3N NaOHaq., 20% H_2O_2, 1/4 conc. to original solution ($[U]_0=8u$): aq. solution
B: 2N NaOHaq., 20% H_2O_2, original solution ($[U]_0=32u$): aq. solution
C: 2.5N NaOHaq., 20% H_2O_2, original solution ($[U]_0=32u$): 25% water-methanol solution

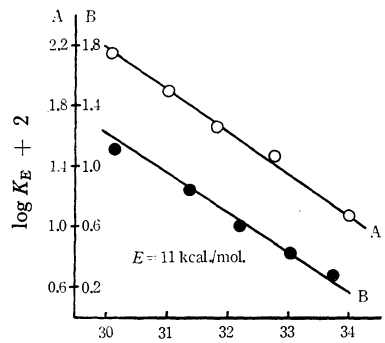

Fig. 2. Log K_E - 1/T plots in eosine chemiluminescence.
A: 0.5N NaOHaq., 30% H_2O_2, 1/4 conc. to original solution ($[E]_0=8e$): aq. solution
B: 0.5N NaOHaq., 30% H_2O_2, 1/2 conc. to original solution ($[E]_0=16e$): 30% water-isopropanol solution

TABLE IV. RELATIONSHIP BETWEEN Δ-VALUE AND K_E (EOSINE)

(1) Ethanol-water systems (at 25°C)

Ethanol concentration (% in volume)	10	20	30	40	60
K_E (min^{-1})	0.32	0.11	0.083	0.062	0.046
Δ (relative unit)	8.9	26.9	34.2	46.8	51.7
$K_E\Delta$ (×10)	28.5	29.6	28.4	29.1	23.8

(2) Methanol-water systems (at 45°C)

Methanol concentration (% in volume)	10	20	40	60
K_E (min^{-1})	0.30	0.20	0.16	0.09
Δ (relative unit)	16.0	24.6	28.0	40.4
$K_E\Delta$	4.8	4.9	4.5	3.6

From Eqs. 13 and 17, $K_E \times \Delta/\sigma$ is given by the following equation:

$$K_E \times \Delta/\sigma = k_1 k_2 k_5 [R\cdot][E]_0/k_4 k_7 = A[E]_0 \quad (18)$$

σ, as has been shown in a previous paper, does not change in the systems; hence, A ($E_E \times \Delta/\sigma$) should remain constant. This invariability of A is consistent with the experimental finding that the value of A remains constant upon the addition of organic solvent.

Conclusion

By the reaction scheme proposed in the present paper, most of the experimental results reported in preceding papers can be explained reasonably. This would indicate that the present theory is plausible. It is expected that further experimental evidence, such as the detection of an intermediate or end product, will verify the theory.

BULLETIN OF THE CHEMICAL SOCIETY OF JAPAN VOL. 39 281—285 (1966)

The Reaction of Aminotropones with Diketene. II. The Structure of the By-product in the Reaction of 5-Aminotropolone with Diketene

By Shuichi SETO, Hiroko SASAKI and Kyozo OGURA

The Chemical Research Institute of Non-Aqueous Solutions, Tohoku University, Katahira-cho, Sendai

(Received May 19, 1965)

The reaction of 5-aminotropolone with diketene gave a minor product and 5-aceto acetamidotropolone, which had previously been described (K. Ogura et al., This Bulletin, **38**, 306 (1965)). This unknown compound was obtained as a main product when 5-acetoacetamidotropolone was treated with diketene in the presence of triethylamine. From its oxidative degradation and its NMR spectrum, this compound was proved to be 3-acetyl-4-hydroxy-6-methyl-1-(tropolon-5'-yl)pyridone-2. Furthermore, for the sake of the structural determination, 3-acetyl-4-hydroxy-6-methylpyridone-2 and its deacetylated product were prepared.

In the previous paper of this series, it was reported that the reaction products of aminotropones with diketene were useful for the synthesis of 3-acetyl derivatives of 1-azaazulan-2-one and their related compounds. For example, the reaction of 5-aminotropolone (I) with diketene gave 5-acetoacetamidotropolone (II), which could then be converted into 3-acetyl-2-hydroxycyclohepta-[b]pyrrol(1*H*)-5-one (III).[1]

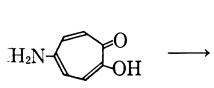

I

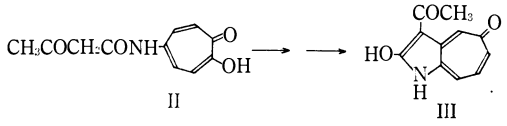

II III

The present authors have since examined the reaction of I with diketene in more detail, and found that another product, IV, was a by-product in this reaction. This paper will concern the structure of the compound IV.

The mixture of the reaction products obtained by the treatment of I with a large excess of diketene was separated by recrystallization into II and IV, the yields of which were 65 and 10% respectively. The compound IV was considered to be a *N*, *N*-disubstituted derivative of I from the fact that its ultraviolet absorption spectrum is of the *N*-acyl-aminotropolone type and from its infrared absorption spectrum. It shows a broad band at 3200 cm^{-1} due to the hydroxyl group and two bands at 1660 and 1625 cm^{-1} for the carbonyl groups in the chloroform solution. The NMR spectrum of IV in deuterochloroform exhibits signals for a methyl group attached to the double bond (2.04), an acetyl group (2.61), aromatic protons of the tropolone ring (near 7.2), and two signals for hydroxyl groups at 9.00 and 16.10 p.p.m. (with tetramethylsilane as a standard). The signal at the lower field (16.10) can be attributed to the enolic hydroxyl group, which is strongly chelated with the carbonyl group, while the higher one (9.00 p.p.m.) corresponds to the hydroxyl group of tropolone.

The treatment of IV with diazomethane gave a monomethyl ether (V). In the NMR spectrum of V, a new signal, at 3.97 p.p.m., for the methoxyl

1) K. Ogura, H. Sasaki and S. Seto, This Bulletin, **38**, 306 (1965).

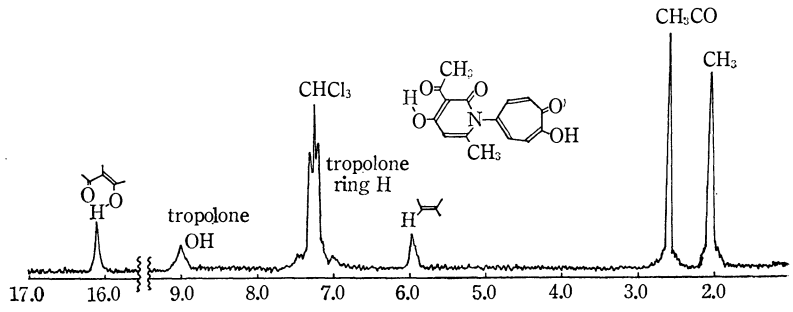

Fig. 1. NMR spectrum of IV in $CDCl_3$.

group appears instead of the hydroxyl group of tropolone in IV, while the signal for the enolic hydroxyl group is still observed at 15.90 p. p. m., indicating that V is the 2-methoxytropone derivative.

These facts and the elemental analysis of IV corresponding to $C_{15}H_{13}O_5N$ suggest that IV has a pyridone moiety formed by the addition of II to another molar equivalent of diketene, followed by dehydration. Two kinds of pyridone derivatives, the 4-hydroxy type (IVa) and the 6-hydroxy type (IVb), can be expected, according to the manner of addition. Garatt and Shemin reported that the reaction of glycine with diketene in the alkaline solution gave no *N*-acetoacetylglycine, but it did give 3-acetyl-1-carboxymethyl-4-hydroxy-6-methyl-pyridone-2 (VI).[2] Kato also obtained the corresponding pyridone derivative from 4-amino-pyridine.[3]

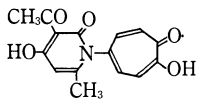

IVa

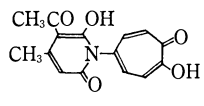

IVb

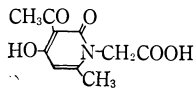

VI

Our spectral data for compound IV mentioned above correspond well with those for VI obtained by Garatt; IV seems to be 3-acetyl-4-hydroxy-6-methyl-1-(tropolon-5'-yl)pyridone-2 (IVa) by analogy. These data alone, however, can not exclude another structure (IVb), so the following experiments were carried out in order to determine the structure precisely.

The oxidation of IV with potassium permanganate gave colorless needles (VII). The fact that VII has an absorption maximum at 326 mμ indicates that VII is no longer a tropolone derivative, but a pyridone derivative which is probably a key compound for the structural determination of IV. The same compound VII could be obtained by the reaction of acetoacetamide with diketene in the presence of triethylamine. The infrared spectrum exhibits complicated bands in the region

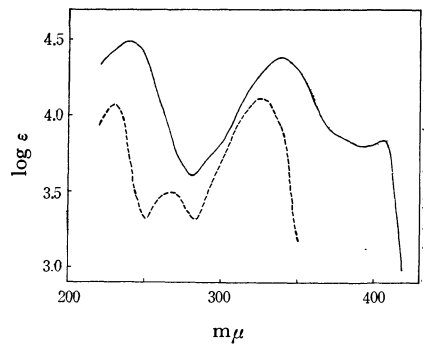

Fig. 2. Ultraviolet spectra of IV (——) and VII (----) in methanol.

3200—2500 cm^{-1} and ν_{CO} bands at 1670 and 1625 cm^{-1}. The NMR spectrum of VII in deuterodimethylsulfoxide indicates the existence of an enolic hydroxyl group (15.65) which chelates strongly with the acetyl group (2.50 p.p.m.).

The ultraviolet spectrum and the chemical behavior of both 4-hydroxy- and 6-hydroxypyridone-2 are known through the literature,[4,5] but no data on their acyl derivatives have yet been reported. It is also known that the treatment of dehydroacetic acid (VIII) with ammonia gives 4-lutidone (IX) and that 4-hydroxy-6-methyl-pyrone-2 (X) obtained from VIII, on treatment with ammonia, is converted into the corresponding pyridone derivative XI.[6,7] The present authors examined these reactions and obtained compound XI, whose structure was confirmed by

2) S. Garatt and D. Shemin, *J. Org. Chem.*, **28**, 1372 (1963).
3) T. Kato, H. Yamanaka, T. Niitsuma, K. Wagatsuma and M. Oizumi, *Chem. Pharm. Bull.*, **12**, 910 (1964).
4) H. J. den Hertog and D. J. Buuman, *Rec. Trav. Chim.*, **75**, 257 (1956).
5) L. Gattermann and A. Skita, *Ber.*, **49**, 495 (1916).
6) R. C. Elderfield, "Heterocyclic Compounds," John Wiley & Sons, New York and London (1959), p. 528.
7) M. A. Butt and J. A. Elvidge, *J. Chem. Soc.*, **1963**, 4483.

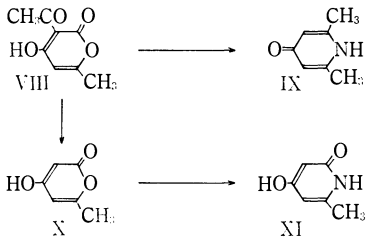

a study of its ultraviolet, infrared and NMR spectra. Thus, the removal of the acetyl group from the compound VII was desirable for the elucidation of the structure.

The deacetylation of VII was successful in affording colorless crystals, crystals which a comparison of the ultraviolet and infrared absorption spectra showed to be quite identical with IX. The compound XI shows an absorption maximum at 283 mμ in methanol and at 265 mμ in the acidic solution.

The NMR spectrum of XI in deuterodimethylsulfoxide exhibits a doublet (J, 2.5 c.p.s.) at 5.34 p.p.m. for the proton in the 3-position and a multiplet at 5.58 p.p.m. for the proton in the 5-position.

This identification undoubtedly indicates that the by-product IV is 3-acetyl-4-hydroxy-6-methyl-1-(tropolon-5'-yl)pyridone-2 (IVa). Furthermore,

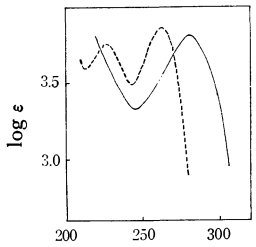

Fig. 3. Ultraviolet absorption spectra of XI in methanol (——), and in 0.1 N HCl - methanol (----).

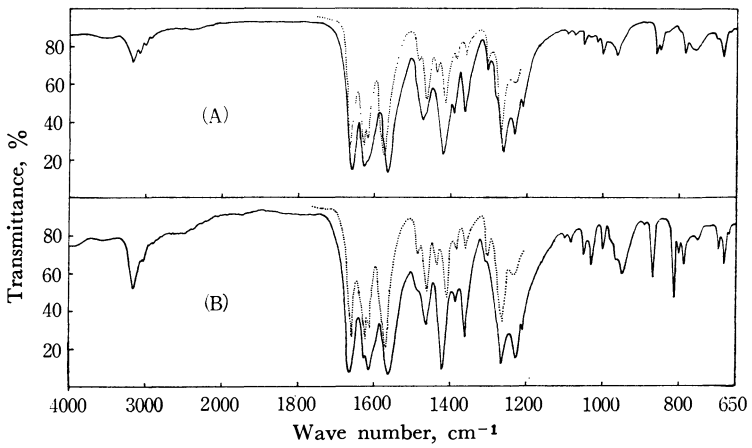

Fig. 4. Infrared absorption spectra of IV (crystals A and B) in KBr disk (——) and in chloroform solution (----).

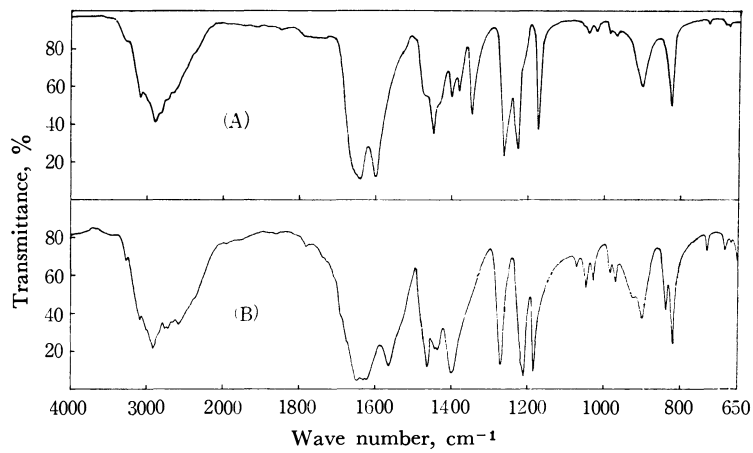

Fig. 5. Infrared absorption spectra of XI (crystals A and B) in KBr disk.

it was found that the treatment of IV with sulfuric acid gave the deacetylated compound XII, from which XI was also obtained, though in such a low yield that identification was possible only by a means of comparison of the ultraviolet absorption spectrum in both methanolic and acidic solutions.

The treatment of II with an equivalent amount of diketene in benzene resulted only in the recovery of II. However, IV could be obtained in a good yield when a small amount of triethylamine was added to the above reaction mixture. The reaction of I with diketene in the presence of triethylamine gave IV directly and exclusively. These facts suggest that, in the reaction of I and diketene in the absence of triethylamine, 5-aminotropolone (I) itself acts as a catalyzer to give a small amount of IV.

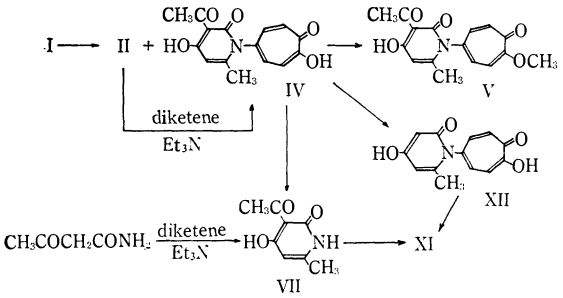

The compound IV has two crystalline forms (A and B), which are convertible into one other. These two forms exhibit slightly different infrared absorption spectra in the solid state, as is shown in Fig. 4, but their spectra in the solution, as well as their ultraviolet and NMR spectra, are quite identical. Analogous phenomena are observed also in the case of the compound XI. The infrared spectra of the two forms (A and B) of XI are shown in Fig. 5.

Experimental*

3-Acetyl-4-hydroxy-6-methyl-1-(tropolon-5'-yl)-pyridone-2 (IV).—a) A solution of I (4 g.) in diketene (20 ml.) was heated at 80°C for 1 hr. The yellow crystalline mixture that separated out on cooling was then collected. The recrystallization of this mixture from methanol-chloroform gave a major product, II (4.2 g.), which had been already reported in our previous paper,[1] and pale yellow crystals (IV). Yield, 850 mg. The repeated recrystallization of IV from methanol-chloroform gave two forms of crystals, A (globules) and B (prisms). Both A and B decomposed at 250 °C, and no depression of the mixed melting point was observed. The crystals A, when recrystallized from their methanol-chloroform solution by adding tiny crystals of B as seed, were converted into crystals B. The crystals B, however, were easily changed again to A by the acidification of the alkaline solution of B.

b) A suspension of I (500 mg.) in dry benzene (10 ml.), with a catalytic amount of triethylamine added, was stirred at 80°C, while a solution of diketene (680 mg.) in dry benzene (5 ml.) was being dropped into the suspension over a 30 min. The mixture was then kept at the same temperature while being stirred for 1 hr. During this reaction the crystals of I gradually dissolved, and orange crystals newly appeared. The crystals were collected and recrystallized from methanol-chloroform to give IV. Yield, 300 mg.

c) A suspension of II (550 mg.) in dry benzene (10 ml.), with one drop of triethylamine added, was heated at 80°C and stirred, while a solution of diketene (450 mg.) in dry benzene (5 ml.) was being added, drop by drop, to the suspension over a 1 hr. Then the mixture was stirred at 80°C for 2 hr. The crystals that separated out on cooling were collected and recrystallized from methanol-chloroform to give IV. Yield, 500 mg. λ_{max}^{MeOH} mμ (log ε): 240(4.49), 340(4.39), 405(3.85).

Found: C, 62.55; H, 4.78; N, 4.11. Calcd. for $C_{15}H_{13}O_5N$: C, 62.71; H, 4.65; N, 4.56%.

3-Acetyl-4-hydroxy-6-methylpyridone-2 (VII).—a) To a mixture of IV (100 mg.) and a potassium hydroxide solution (potassium hydroxide, 70 mg.; water, 1 ml.), a potassium permanganate solution (potassium permanganate, 580 mg.; water, 15 ml.) was added slowly. After the addition of potassium permanganate solution had been completed, the manganese dioxide was removed by filtration. This filtrate was acidified with hydrochloric acid, adjusted to pH 3. After the water had been completely removed under reduced pressure, the residue was extracted with acetone. The evaporation of the acetone afforded colorless crystals, which were then collected and recrystallized from acetone to give colorless needles, m. p. 256°C (decomp.).

b) A suspension of acetoacetamide (1 g.) in dry benzene (20 ml.), with a catalytic amount of triethylamine added, was heated at 80°C while being stirred. After a solution of diketene (1.3 g.) in dry benzene (10 ml.) had been slowly added, the mixture was stirred at 80—85°C for an additional 1.5 hr. The precipitate that separated out on cooling was collected and recrystallized from acetone-methanol to give colorless needles (m. p. 256°C (decomp.)). Yield, 500 mg. λ_{max}^{MeOH} mμ (log ε): 260(4.07), 263(3.49), 326(4.11).

Found: C, 57.68; H, 5.30; N, 8.38. Calcd. for $C_8H_9O_3N$: C, 57.48; H, 5.43; N, 8.38%.

The Methylation of IV.—After ethereal diazomethane had been added to a suspension of IV (100 mg.) in methanol (10 ml.) until portions of the solution were no longer colored with ferric chloride, the mixture was allowed to stand at room temperature for 2 hr. The pale yellow crystals that separated out were collected and recrystallized from methanol to give V (225°C (decomp.)). Yield, 45 mg. λ_{max}^{MeOH} mμ (log ε): 230(4.52), 330(4.30).

Found: C, 63.51; H, 4.31; N, 4.91. Calcd. for $C_{16}H_{15}O_8N$: C, 63.78; H, 5.02; N, 4.65%.

The Deacetylation of IV.—A mixture of IV (500

* All melting points are uncorrected. The microanalyses were carried out by Misses Yoko Endo and Noriko Matsukawa of this Institute, to whom the authors are indebted. The measurements of the ultraviolet and infrared absorption spectra were made with a Cary recording spectrophotometer model 14 and with a Hitachi EPI-S2 spectrophotometer respectively. The NMR spectra were measured in a deuterochloroform or deuterodimethylsulfoxide solution, using tetramethylsilane as an internal standard, on a Varian A-60 spectrometer.

mg.) and sulfuric acid (2 ml.) was heated at 200°C for 30 min.; then the mixture was poured into ice water. The colorless precipitate thereby obtained was recrystallized from methanol to give colorless crystals, m. p. 284—285°C (decomp.). Yield, 270 mg. λ_{max}^{MeOH} $m\mu$ (log ε): 206(4.55), 240(4.49), 290(3.81), 340(4.09).

Found: C, 63.75; H, 4.49; N, 4.93. Calcd. for $C_{13}H_{11}O_4N$: C, 63.67; H, 4.52; N, 5.71%.

4-Hydroxy-6-methylpyridone-2 (XI).—a) After a mixture of VIII (2.0 g.) and 93% sulfuric acid (6 g.) had been allowed to stand at room temperature for 1 hr., the mixture was heated at 130°C for 7 min. When cracked ice was added into the reaction mixture, a pale yellow precipitate was immediately deposited. The recrystallization of this precipitate gave pale yellow crystals of X (1.9 g.), m. p. 183—184°C. A solution of X (350 mg.) in a 28% ammonium hydroxide solution (4 ml.) was heated on a water bath. The removal of an excess of ammonium hydroxide gave colorless crystals, which were then recrystallized from water to afford colorless needles, m. p. 320°C (decomp.). Yield, 50 mg.

b) A mixture of VII (200 mg.) and concentrated sulfuric acid (0.4 ml.) was heated at 180°C for 7 min. After it had been cooled, the mixture was poured into ice water and neutralized with a barium hydroxide solution. The barium sulfate that separated out was removed by filtration. When the filtrate was concentrated under reduced pressure, colorless needles of XI were obtained.

c) To a solution of XII (120 mg.) in a potassium hydroxide solution (potassium hydroxide, 90 mg.; water, 2 ml.), a potassium permanganate solution (potassium permanganate, 790 mg.; water, 20 ml.) was added slowly. After this addition had been completed, the manganese dioxide that precipitated out was removed by filtration and the filtrate was acidified with hydrochloric acid, adjusted to pH 3. After the water from the filtrate had been completely removed under reduced pressure, the residue was extracted with acetone. The evaporation of the acetone gave colorless crystals in a very poor yield. λ_{max}^{MeOH} $m\mu$ (log ε): 280(3.82). $\lambda_{max}^{MeOH-HCl}$ $m\mu$ (log ε): 225(3.75), 263(3.86).

Found: C, 57.40; H, 5.42; N, 11.34. Calcd. for $C_6H_7O_2N$: C, 57.59; H. 5.64; N, 11.20%.

The authors wish to express their thanks to the Sankyo Co., Ltd., which defrayed a part of the expenses of the present research.

BULLETIN OF THE CHEMICAL SOCIETY OF JAPAN VOL. 39 285—287 (1966)

Mineral Acids as Photoinitiators of Vinyl Polymerization in Aqueous Media

By Mihir K. SAHA*

Indian Association for the Cultivation of Science, Jadavpur, Calcutta-32, India

(Received May 26, 1965)

A few mineral acids, namely hydrochloric, hydrobromic and sulfuric acid, have been used as photoinitiators for the polymerization of methyl methacrylate in aqueous media in the presence of ultraviolet light. The endgroups incorporated in the resulting polymers have been determined by the application of the sensitive "Dye Techniques" lately developed in our laboratory. On the basis of the endgroup results, attempts have then been made to explain the mechanism of such polymerization, and also the nature of the initiating species involved.

Mineral acids have been used as the initiators of vinyl polymerization to a very limited extent; a few of the instances quoted in the literature[1,2] are supposed to proceed through an ionic mechanism. The present communication will describe the use of some mineral acids, viz., hydrochloric, hydrobromic and sulfuric acids, as photoinitiators for the aqueous polymerization of methyl methacrylate. The endgroups incorporated in the resulting polymers have been determined by the application of the "Dye Techniques"[3] lately developed in our laboratory in order to get an idea of the nature of the initiating species involved in such processes.

Experimental

Purified methyl methacrylate (MMA) was used as the monomer. The acids employed as initiators were of an analytical grade and were free of traces of iron.

* Present address: Department of Chemistry, University of Notre Dame, Notre Dame, Indiana, U. S. A.

1) M. J. Hayes and D. C. Pepper, a) *Trans. Faraday Soc.*, **57**, 432 (1961); b) *Proc. Roy. Soc.*, **A263**, 63 (1961); c) *Proc. Chem. Soc.*, **1961**, 228.

2) D. C. Pepper and P. J. Reilly, *J. Polymer Sci.*, **58**, 639 (1962).

3) S. R. Palit, a) *Chem. & Ind.*, **1960**, 1531; *Makromol. Chem.*, **36**, 89 (1959); **38**, 96 (1960).

Polymerization experiments were carried out in clean pyrex conical flasks in a nitrogen atmosphere in the presence of ultraviolet light, without any filter, and at a temperature of 30°C, the concentration of the monomer being kept at 0.094 mol./l. in all the experiments. The induction period for the polymerization varied from about half an hour to about 3 hr., depending on the nature and concentration of the acids empolyed as initiators. Polymers were obtained as a coarse precipitate after the polymerization was over. The polymers were then washed free of acid, dried in an air oven at 45°C, and purified by repeated reprecipitations from a benzene solution by a mixture of alcohol and petroleum ether.

The purified polymers were then subjected to the "Dye Tests" in order to determine the endgroups incorporated in them. The halogen endgroups were determined by the application of the "Dye partition test" using a Disulfine blue reagent after the quaternisation of the polymers with pyridine.[4] The sulfate endgroup was estimated by the "Dye partition test" employing a methylene blue reagent.[5]

Results and Discussion

The usual features of these polymerization, e. g., the initiation of polymerization only in the presence of light, a fairly long induction period, the polymerization over a considerable period of time (about 2—5 hr.), and the complete inhibition of the polymerization in the presence of oxygen, are suggestive of a typical radical polymerization process.

Initiation by Halo Acids.—Both hydrochloric and hydrobromic acid could initiate the polymerization of MMA in the presence of ultraviolet light, while hydroiodic acid failed to do so under identical conditions, probably because of the strong inhibitive action of the iodine liberated. The polymers obtained with both hydrochloric and hydrobromic acid were found to bear halogen endgroups to a varying extent (about 0.3 to 0.8 per chain) (Table I). This definitely indicates that some of the polymer chains are initiated by halogen atoms generated in the systems by the photolysis of the halo acids or, more precisely, by that of the halide ions in question; thereby they appear as polymer endgroups. The generation of halogen atoms probably takes place by the following mechanism:

$$HX \rightleftarrows H^+ + X^-$$

$$X^- + HOH \xrightarrow{h\nu} X\cdot + H\cdot + OH^- \quad [X=Cl \text{ or } Br]$$

It appears, therefore, that both the radicals, X· (Cl· in the case of hydrogen chloride and Br· in the case of hydrogen bromide) and the hydrogen atom (H·), may bring about the initiation of polymerization. (It has been indicated by Dainton[6] that the hydrogen atom (H) produced by irradiation with X-ray or γ-ray can initiate the polymerization of acrylonitrile in aqueous media.)

Table I. Endgroup analysis of polymethyl methacrylate obtained by the aqueous photoinitiation with mineral acids

Initiator concn. (normality)	$[\eta]$[a] of the polymer	Average halogen or sulfate endgroup/chain
[HCl]		[Cl]
0.012	2.85	0.80
0.024	2.65	0.50
0.036	2.53	0.50
0.048	2.40	0.27
0.096	2.10	trace
0.120	1.80	trace
0.240	Polymer is almost insoluble in benzene and chloroform.	
[HBr]		[Br]
0.012	3.60	—
0.030	2.68	0.31
0.060	1.70	0.38
0.120	1.60	0.34
0.180	1.50	0.29
0.360	1.00	0.23
0.600	0.91	0.40
[H_2SO_4]		[Sulfate]
0.036	1.00	0.11
0.072	0.90	0.18
0.180	0.84	0.12
0.360	0.80	0.15
0.720	Polymer is almost insoluble in benzene and chloroform.	

a) Number average molecular weight ($\overline{M}_n$) of the polymers was obtained viscometrically by the application of the following equation[9]:

$$\overline{M}_n = 2.81 \times 10^5 \times [\eta]^{1.32}$$

(for P. MMA in benzene)

The hydroxyl endgroups in these polymers could not be determined by the application of "dye techniques" due to the extensive hydrolysis of the ester units to a carboxyl group, a process which rendered the polymer increasingly insoluble in benzene and chloroform. The determination of the halogen endgroup in the polymer by the above spectrophotometric method is based on the process of quaternisation, which is extremely slow and sluggish at the end of the reaction,[7] especially when the quantity of halogen is extremely low, as in the case of the polymer endgroup. This leads to some uncertainty as to the quantitative values obtained herein; hence, there is hardly any order in the endgroup values obtained. However, allowing for these uncertainties, it can be easily demonstrated that the polymers obtained by using

4) M. K. Saha, P. Ghosh and S. R. Palit, *J. Polymer Sci.*, **A2**, 1365 (1964).
5) P. Ghosh, S. C. Chadha, A. R. Mukherjee and S. R. Palit, ibid., **A2**, 4433 (1964).
6) F. S. Dainton, *Nature*, **160**, 268 (1947).
7) a) R. M. Fuoss and U. P. Strauss, *J. Polymer Sci.*, **3**, 246 (1948); b) R. M. Fuoss, M. Watanabe and B. D. Coleman, ibid., **48**, 5 (1960).

hydrogen chloride and hydrogen bromide as photoinitiators incorporate halogen endgroups at least in part.

Initiation by Sulfuric Acid.—The polymers obtained with sulfuric acid as a photoinitiator have been found to incorporate sulfate endgroups to an average extent of about only 0.1 to 0.2 per chain (Table I); this is indicative of initiation by sulfate ion radicals, at least in part. The generation of sulfate ion radicals may take place in the following way:

$$H_2SO_4 \rightleftarrows 2H^+ + SO_4^{2-}$$

$$SO_4^{2-} + HOH \xrightarrow{h\nu} S\overline{O}_4\cdot + H\cdot + OH^-$$

Both $S\overline{O}_4\cdot$ and $H\cdot$ may initiate the polymer chain and may, thereby, appear as polymer endgroups. The ability of $S\overline{O}_4\cdot$ to initiate the vinyl polymerization has been widely studied.[5,8] It is also probable that, due to the acidity of the medium, sulfate ion radicals react readily with water to generate hydroxyl radicals, e. g.;

$$S\overline{O}_4\cdot + \begin{matrix} H \\ \diagdown \\ \overset{+}{O}—H \\ \diagup \\ H \end{matrix} \rightarrow H_2SO_4 + OH\cdot$$

This reaction probably occurs more readily at higher concentrations of acids.[5] However, the hydroxyl endgroups in these polymers could not be examined because of a difficulty similar to that indicated in the case of halo acids.

Thanks are due to Professer Santi R. Palit for his encouragement and helpful discussions. Thanks are also due to Dr. P. Ghosh for discussion. Thanks are also due to the C. S. I. R. (Govt. of India) for financial support.

8) I. M. Kolthoff, A. I. Medalia and H. P. Raaen, *J. Am. Chem. Soc.*, **73**, 1733 (1951).
9) J. H. Baxendale, S. Bywater and M. G. Evans, *J. Polymer Sci.*, **1**, 237 (1946).

BULLETIN OF THE CHEMICAL SOCIETY OF JAPAN VOL. 39 287—295 (1966)

Fractures in Thin-sectioned Corundum Crystals

By Goro YAMAGUCHI, Yasushi KUBO and Hiroshi OGAWA

Department of Industrial Chemistry, Faculty of Engineering, The University of Tokyo, Hongo, Tokyo

(Received May 26, 1965)

The fracture properties of corundum crystals have been examined on various artificial corundums, such as electrically-fused corundum, Verneuil-flame-fused corundum and hydrothermally-synthetised corundum. The specimens were ground to a tihckness of less than 5/100 mm. The microcracks generated in the grinding process were observed by means of a polarizing microscope. The orientation of the c-axis (C) and the crack normal to the section normal (T) was measured using a universal stage. The direction of the crack has a close relation to the crystal orientation of the thin section. Frequent irregular cracks intercrossing one another occur in crystals ground with T$\wedge$C angles from 0° to 50°. Cleavage cracks along the $\{10\bar{1}1\}$ plane take place prominently in the range of T$\wedge$C angles from 50° to 80°. Rare irregular cracks streaming in one direction take place in the range of T$\wedge$C angles from 80° to 90°. The heat treatment in air of titania-containing corundum decreases the number of cracks in the crystal. The results have been interpreted on the basis of the cohesion strength theory of M. D. Shappel (*Am. Mineralogist,* **21**, 75 (1936)). In order to explain the limited range of the ocurrence of cleavage cracks, a model has been proposed in which the shearing along the cleavage plane takes place prior to the crack nucleation in the corundum crystal.

The fracture properties of corundum are of practical importance as well as of theoretical interest. Its abrasive properties are inferred to depend on the relation between the hardness and the toughness of the corundum.

According to the literature, fabricators of jewel bearings know by experience a certain technique for avoiding breakage loss. The fracture mechanisms in such materials as metals and ductile minerals have been discussed on the basis of the dislocation theory, but discussion of such brittle minerals of a high hardness and strength as corundum has not progressed.

Information has, however, been provided on the fracture properties of artificial corundums observed in thin sections. In a microscopic observation of electric-furnace-fused alumina abrasives, attention was called to the fact that many microcracks, regular or irregular, were generated in corundum crystals lying in various crystallographic

orientations in thin sections. These carcks were found to develop when the crystal was ground to a thickness of below about 5/100 mm. Careful observation of these cracks by quantitative determination revealed a certain law of fracture in thin-sectioned corundum. Various artificial specimens from electrically-fused corundum, Verneuil-flame-fused corundum and hydrothermally-synthesized corundum were observed.

The results will, in this paper, be compared with a model based on the cohesion strength theory of the crystal plane. A mechanism will be proposed which gives an adequate explanation of the discrepancy in the minimum cohesion strength model and which agrees splendidly with the observations.

Experimental

Specimens.—*Regular and White Alumina.*—Most of the specimens employed were commercial 16-mesh grains of electric-furnace-fused alumina abrasives produced by the Carborundum Company, abrasives which contain from 95 to 97% alumina and the impurities shown in Table I. Corundum is the predominating crystalline phase, and impurities are present for the most part as impure minerals, except that only titania is present in corundum in a solid solution, as is shown in the fifth and sixth rows in Table I.

TABLE I. THE IMPURITY COMPOSITION OF THE SPECIMENS

Specimen	SiO_2	Fe_2O_3	TiO_2	
C32	0.51	0.12	2.46	
R41	0.49	0.15	2.49	
C37	0.26	0.04	tr.	
Japanese commercial abrasive	0.86	0.21	2.34	#24 as-received
	0.10	0.10	1.50	#220 treated with Na_2CO_3-K_2CO_3-H_3BO_3 flux

These grains are made up of from one to twenty corundum crystals, euhedral or anhedral, 2 mm. to 1/10 mm. in size. Small amounts of impure minerals are contained in corundum or form the matrix. Titania-containing corundums in the specimens designated as C32 and R41 range in color from brown to pink. The C37 specimen is the one made from Bayer-process white alumina, with few impurities, though it contains some beta alumina.

Heat-treated Titania-containing Abrasive Grains.—Corundum containing titania in a solid solution is known to change color from pink or brown to bluish, and then to opaline, upon the segregation of titania along a certain crystal plane by heat treatment in air. In titania-containing abrasive aluminas, this change in color is accompanied by a marked improvement in the toughness of the grains.

Fracture properties in thin section were observed to change in this process when Japanese commercial 24-mesh grains were used as received and heat-treated in air at 1250°C for 1 hr.; the latter turns bluish with 3.1% weight increase upon oxidation. The impurity compositions of these grains are shown in the fifth and sixth rows in Table I.

Verneuil and Hydrothermally-synthesized Corundum.—The effect of the crystal-growth technique on fracture properties in thin sections was examined using Verneuil corundum and hydrothermally-synthesized corundum which had been grown on the seed of Verneuil corundum.

The Observation of Microcracks in Thin Sections.—Specimens were ground with a 600-mesh SiC abrasive on a motor-driven disk to a thickness of about 5/100 mm., and then refined with boron carbide finer than 600-mesh by manual grinding to about 2/100 mm. Microcracks were generated in this grinding process, as Fig. 1 shows, when the specimens were thinner than 5/100 mm.

The orientation of the c-axis and of the crack normal relative to the section normal was determined by the microscopic method using a universal stage and subsidiarily by the X-ray Laue back-reflection method.

Results

Characteristics of Fractures Related to the Crystallographic Orientation of the Ground Surface.—Figures 1(a), 1(b), 2(a) and 2(b) show thin sections of grains composed of a number of corundum crystals with various crystallographic orientations relative to the section normal. One can see fractures of various kinds exhibited in each of the crystals, depending on their orientations.

The disposition of the c-axis (C) measured on each of crystals with respect to the section normal (T) and the aspect of fracturing are expressed on stereographic projections of Fig. 1(c) and Fig. 2(c).

One can see a definite tendency, in the range of the $T \wedge C$ angle from 0° to 60°, for fracturing to be prominent; from 60° to 80°, it is prominent or medium, while from 80° to 90° there is little fracturing. Smooth crystals with no fractures, such as 2, 3 and 15 in Fig. 1 and 8, 15 and 16 in Fig. 2, have, almost without exception, the c-axis lying in the section plane.

Irregular Cracks.—Two sorts of fractures can be discriminated in Fig. 1(a) and Fig. 2(a); one consists of linear cracks occurring parallel to one another, while the other consists of curved irregular cracks occurring in random directions. The latter is the cleavage crack taking place parallel to a particular crystal plane. In Fig. 1(a) the irregular crack is prominent, while in Fig. 2(a) the cleavage crack is prominent.

Irregular cracks show a definite dependency on the inclination of the c-axis with respect to the section normal. Characteristic irregular cracks intercrossing in three directions, as is shown in Fig. 3, take place in the crystal with the c-axis perpendicular to the section plane ($T \wedge C = 0$). Inclining from this disposition up to the $T \wedge C$ angle of about 60° gives rise to irregular cracks with a tendency to intercross with one another, as Fig.

Fig. 1 (a) Fig. 1 (b) Fig. 1 (c)

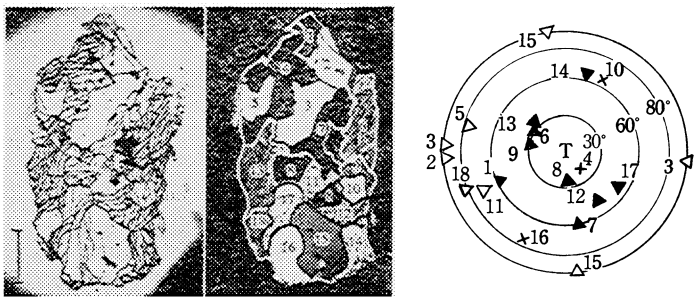

Fig. 1. Aspect of fractures in corundum crystals with various orientations in thin section. Disposition of the c-axis is expressed in (c) by stereographic projection on the section plane where all projections are of the upper intersection, with solid triangles for prominently fractured crystals, open triangles for fractured ones and crosses for medium ones, respectively. Figures affixed to crystals in (b) correspond to ones in (c). ((a) Parallel nicols, (b) Crossed nicols, Specimen R41)

Fig. 2 (a) Fig. 2 (b) Fig. 2 (c)

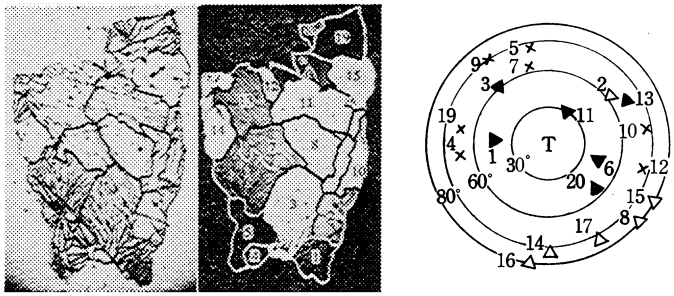

Fig. 2. Aspect of fractures in corundum crystals with various orientations in thin section. Expression is the same as Fig. 1. ((a) Parallel nicols, (b) Crossed nicols, Specimen C32)

Fig. 3 (a) Fig. 3 (b) Fig. 3 (c)

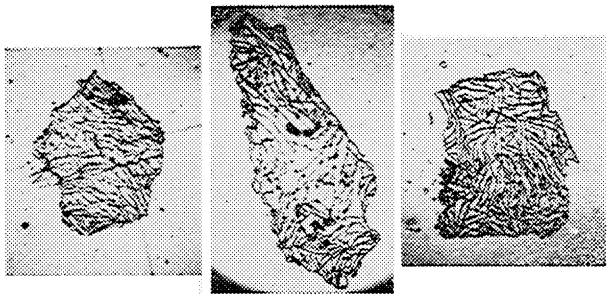

Fig. 3. Fractures in crystals ground perpendicular to the c-axis. (a) Specimen C32, (b) Specimen R41 and (c) Specimen C37

4 shows. The irregular cracks occurring in the region of the T∧C angle between 80° to 90° have a tendency to stream in one direction, as is shown in Fig. 5. In the T∧C range from 50° to 80°, cleavage cracks are the predominating fractures, as will be mentioned in the following section, while at the T∧C angle of 90° no fractures occur.

The dependency on the azimuthal orientation can not be treated separately because of experimental difficulties.

The Cleavage Crack.—The orientation of the c-axis (C) and the cleavage crack normals (P_1, P_2 and P_3, in the order of predominance) with respect to the section normal (T) were determined for crystals in which cleavage cracks take place in different directions in two or three sets. The results for various cases are shown by

Fig. 4. Fig. 5

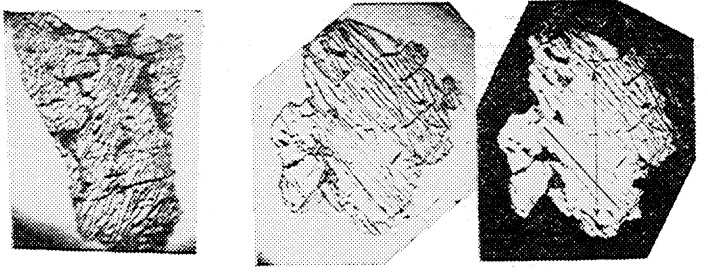

Fig. 4. Fractures in the crystal ground with the angle T∧C less than 60°.
Fig. 5. Fractures in the crystal ground near parallel to the c-axis. (Left; Parallel nicols, Right; Crossed nicols, Specimen C37)

Fig. 6 (a) Fig. 6 (b) Fig. 6 (c)

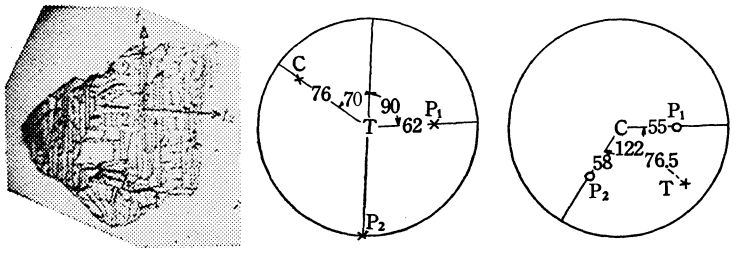

Fig. 6. Orientation of the crystal and the cleavage cracks in thin section of (a) determined by an universal stage and expressed by the stereographic projection (b) on the section plane and (c) on the basal plane. C and T represent the c-axis and the section normal, respectively. P_1, P_2,..... represent the cleavage crack planes less prominent in this order. (Specimen C37)

Fig. 7 (a) Fig. 7 (b) Fig. 7 (c)

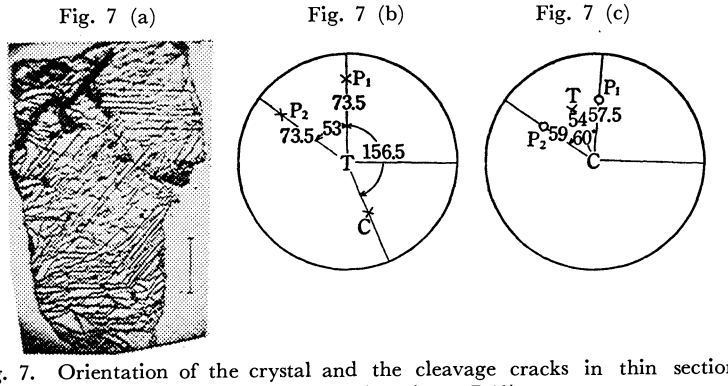

Fig. 7. Orientation of the crystal and the cleavage cracks in thin section. Expression is the same as in Fig. 6. (Specimen R41)

Fig. 8 (a) Fig. 8 (b) Fig. 6 (c)

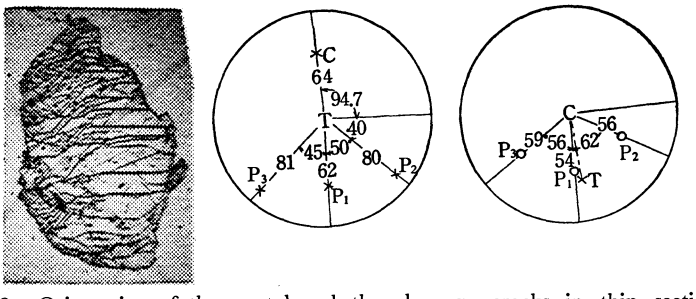

Fig. 8. Orientation of the crystal and the cleavage cracks in thin section. Expression is the same as in Fig. 6. (Specimen C32)

Fig. 9 (a) Fig. 9 (b) Fig. 9 (c)

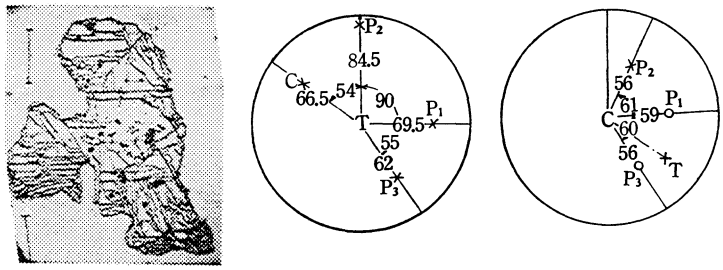

Fig. 9. Orientation of the crystal and the cleavage cracks in thin section. Expression is the same as in Fig. 6. (Specimen R41)

the stereographic projection on the section plane in Fig. 6(b)—9(b), where the orientation corresponds to that of Fig. 6(a)—9(a). These were converted into the stereographic projection on the basal (0001) plane in Fig. 6(c)—9(c) to show the symmetry and the polar angle with respect to the c-axis. The plots by the cross and the open circle represent, as usual, the projection of the upper intersection and the lower intersection respectively. The value of the polar angle measured on a number of crystals is in the 57.5°±5° range, corresponding to that of the rhombohedral $\{10\bar{1}1\}$ plane. The symmetry of the cleavage crack patterns, however, can be interpreted as trigonal or hexagonal for Fig. 6(c), but only as hexagonal for Fig. 7(c)—9(c). This incompatibility may be considered to be due to the formation of basal twinning in electric-furnace-fused corundum.

The conditions for the generation of the cleavage crack were examined, on all of the crystals exhibiting the cleavage crack in a section containing about

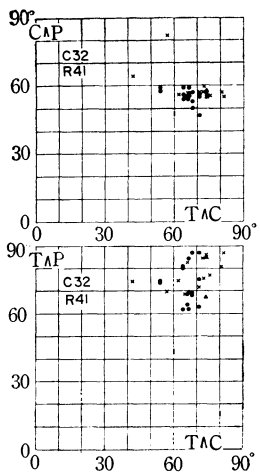

Fig. 10. Condition for generation of the cleavage crack expressed by the angles T∧C, T∧P and C∧P. solid circles represent cleavage cracks with hexagonal arrangement due to basal twinning, solid triangles ones with trigonal and crosses ones with single, respectively. (Specimen C32, R41)

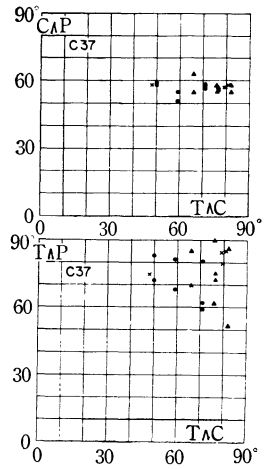

Fig. 11. Condition for generation of the cleavage crack. Expression is the same as in Fig. 10. (Specimen C37)

eighty grains, for the C32, R41(titania-containing) and C37(white alumina) specimens by measuring the T∧C, T∧P and C∧P angles. The results are plotted in Figs. 10 and 11, with solid circles for the hexagonal cleavage, solid triangles for the apparent trigonal cleavage, and crosses for the single cleavage.

It is clear that almost all of the cleavage cracks occur when the crystal is ground with a T∧C angle between 50° and 80° and with a T∧P angle between 60° and 90°.

The Effect of the Heat Treatment on the Fracture Properties of Titania-containing Corundum.—Fig. 12(a) shows the thin sections of corundum crystals as received, containing titania in a solid solution and colored a pale brown. Figure 12(b) shows that of crystals treated in air at 1250°C for 1 hr.; they turned bluish.

A remarkable change in fracture properties is observed when specimens are heat-treated. In the heat-treated specimen, the cleavage crack comes not to take place, but large cracks dividing the crystal into relatively small numbers of blocks appear characteristically.

Fig. 12 (a)

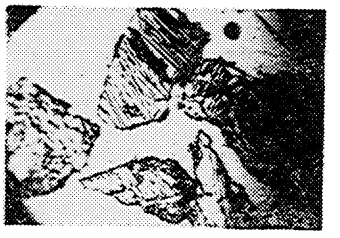

Fig. 12 (b)

Fig. 12. Change of fracture property of titania-containing corundums by heat treatment, (a) as-received and (b) heat treated in air at 1250°C for 1hr to bluish.

Fractures in Verneuil Corundum and Hydrothermal Corundum.—Figure 13 shows a microphotograph with crossed nicols of a thin section of Verneuil corundum on the left of the dividing line, and one of hydrothermal corundum on the right, which has been grown on the seed of the Verneuil corundum with the same crystallographic orientation. Basal fractures are striking in the hydrothermal corundum: they occur in the contact region along the stripes with a high birefringence, but they are interrupted at some distance from the boundary. This region of high birefringence has been shown by an electron probe microanalyzer to be twice as rich in iron content introduced from an autoclave as other regions of the hydrothermal corundum. Outside the contact region of the hydrothermal corundum and in the Verneuil corundum, the cleavage cracks along $r\{10\bar{1}1\}$ take place as usual. The crystal has an orientation with a T∧C angle of 81° and a T∧P angle of 77°.

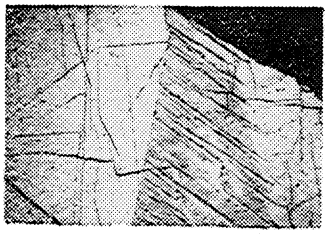

Fig. 13. Fractures in Verneuil corundum and in hydrothermal corundum. Hydrothermal corundum on the right was grown on the seed of Verneuil corundum on the left with the same crystallographic orientation. Stripes in hydrothermal corundum are regions with high birefringence. The crystal was ground with the angle T∧C of 81° and T∧P of 77°. The trace of $r\{10\bar{1}1\}$ and $c\{0001\}$ is shown in the figure. (Crossed nicols)

Discussion

Regarding fracture properties, corundim is known[1] to show no cleavages but two possible partings, one parallel to the basal {0001} plane, and the other parallel to the rhombohedral $\{10\bar{1}1\}$ plane, which is often characterized by the appearance of twin laminations along the same plane. This description is based on a study by Judd[2] which demonstrated that the supposed cleavages in corundum are due to alteration along definite planes of the crystal. When alteration does not exist, the natural corundum is quite destitute of any trace of cleavage, but is usually breaking with an irregular or conchoidal fracture as in quartz; however, a tendency to break up along certain planes, such as $c\{0001\}$, $r\{10\bar{1}1\}$ and $m\{10\bar{1}0\}$, is the result of the incipient alteration, which gives rise to corroded cavities along these planes.

This is obviously incorrect in the case of artificial corundum, such as the electrically-fused, the flame-fused or the hydrothermally-synthesized corundum, which exhibits well-defined cleavages along $r\{10\bar{1}1\}$ in thin sections, as has been shown above.

The fracture properties of materials are usually determined on a relatively large rod, as in loading tests. In such tests corundum exhibits rather conchoidal fractures which bear no clear relation to its crystal structure or to the inherent structural weakness. In thin sections, however, where the bulk strength is extremely reduced, fractures characterized by the structure become predominant. This means that the type of fracture depends on the way it is produced. Therefore, such discussion of corundum as concerns cleavage, parting and conchoidal fracture is meaningless unless the testing method is clearly described.

The cohesion strength of the crystal plane in thin sections has been estimated on corundum and compared with the results obtained above. Using Shappel's cleavability,[3] $V_{|hkl|}$ is defined as:

$$V_{|hkl|} = \frac{A_{|hkl|}}{\sum_i n_i f_i \cos\theta_i}$$

where f_i is the bond strength between a pair of the ions with the cleavage face interpose between them; θ_i, the angle between the bond and the normal of the crystal plane; n_i, the number of such bonds for the ith ion, and $A_{|hkl|}$, the area element

1) J. D. Dana and E. S. Dana, "The System of Mineralogy," 7th ed., Vol. 1, John Wiley & Sons, Inc., New York (1944), p. 520.
2) J. W. Judd, *Min. Mag.*, **11**, 49 (1895).
3) M. D. Shappel, *Am. Mineralogist*, **21**, 75 (1936).

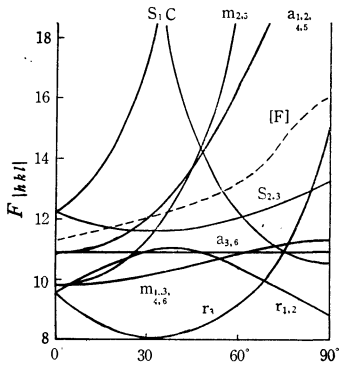

$\Phi=-30°$ T∧C

Fig. 14 (a)

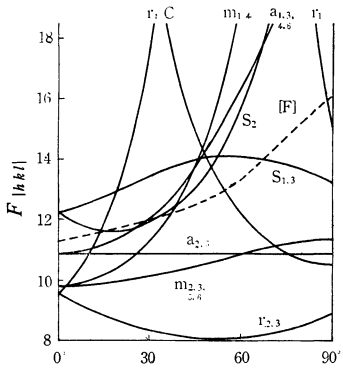

$\Phi=30°$ T∧C

Fig. 14 (b)

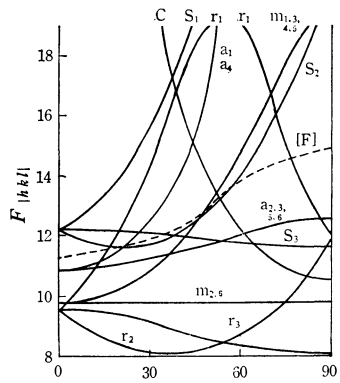

$\Phi=0°$, (60°) T∧C

Fig. 14 (c)

Fig. 14. Dependence of the cohesion strength of crystal plane in thin scetion, $F_{|hkl|}$, on the polar grinding direction on main zones, T∧C.

of the crystal plane. The estimated cohesion strength, $F_{|hkl|}$, of the crystal plane in thin sections is derived as:

$$F_{|hkl|} = \frac{\text{cosec}(\text{T}\wedge\text{P})}{V_{|hkl|}}$$

where T∧P is the angle between the section normal and the normal of the crystal plane and where cosec(T∧P) represents the cross area of the crystal plane in thin sections. The value of the cleavability, $V_{|hkl|}$, of corundum was calculated by Shappel to be as given in the seventh column of Table II, where the bond strength, f_i, is estimated from the coordination theory of ionic structures.

The value of the cohesion strength, $F_{|hkl|}$, at different T∧C angles along main zones has been calculated for each of the crystal planes, as is given in Fig. 14. The crystallographic data on main crystal planes of corundum are shown in Table II and Fig. 15.

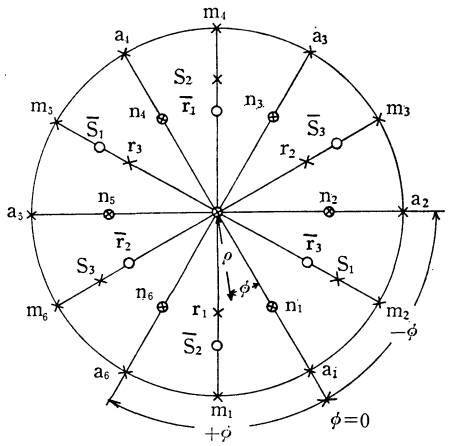

Fig. 15. Stereographic projection showing main crystal planes of corundum and designation in this paper.

In the range of T∧C angles larger than about 20°, the cohesion strength of $r\{10\bar{1}1\}$ becomes conspicuously lower than in other ranges. The basal (0001) plane can not be a cleavage plane; this conclusion, based on the cohesion strength calculation, is in conformity with the fact that the basal fracture in hydrothermally-synthesized corundum, in the contact region with the seed, may be referred to as the parting which is produced by the zonal segregation of the impurity iron along the same plane.

For the crack in the thin section with the T∧C angle of 0°, a possible interpretation is that the main direction of the irregular cracks are parallel to the $m\{10\bar{1}0\}$; the crack faces are nearly perpendicular to the section plane, and the small differences in cohesion strength among the crystal planes in this orientation cause an irregular deviation in the crack direction.

In order to estimate the strength of corundum at various crystallographic orientations of the ground surface, we will define the strength factor, [F], as:

TABLE II. CRYSTALLOGRAPHIC DATA ON MAIN CRYSTAL PLANES OF CORUNDUM

Form	Index: Morphological rhombohedral	Index: Hexagonal (adopted in this paper)	Index: Structural hexagonal	σ in Fig. 15	Φ in Fig. 15	Shappel's cleavability
c	111	0001	0001	0°00′	—	9.5
m	$2\bar{1}\bar{1}$	$10\bar{1}0$	$01\bar{1}0$	90°00′	30°00′	10.2
a	$10\bar{1}$	$11\bar{2}0$	$11\bar{2}0$	90°00′	0°00′	9.2
r	100	$10\bar{1}1$	$01\bar{1}2$	57°35′	30°00′	12.4
s	$11\bar{1}$	$02\bar{2}1$	$10\bar{1}1$	72°23′	−30°00′	8.6
n	$31\bar{1}$	$22\bar{4}3$	$11\bar{2}3$	61°11½′	0°00′	

$$\frac{1}{[F]} = \frac{1}{n}\sum_{i=1}^{n}\left(\frac{1}{F_i}\right)$$

where F_i corresponds to $F_{|hkl|}$ and where $[F]$ is shown approximately as follows:

$$\frac{1}{[F]} = \frac{1}{13}\left(\frac{1}{F_{a_1}}+\frac{1}{F_{a_2}}+\frac{1}{F_{a_3}}+\frac{1}{F_{s_1}}+\frac{1}{F_{s_2}}+\frac{1}{F_{s_3}}+\frac{1}{F_{m_1}}+\frac{1}{F_{m_2}}+\frac{1}{F_{m_3}}+\frac{1}{F_c}+\frac{1}{F_{r_1}}+\frac{1}{F_{r_2}}+\frac{1}{F_{r_3}}\right)$$

We may expect qualitatively that the increase of $[F]$ will correspond to the decrease in fracturing. The calculated values in each azimuthal direction (ϕ) are shown by dotted lines in Fig. 14. From this we can see that $[F]$ increase as the T∧C angle increases from 0° to 90°, regardless of the azimuthal direction; this finding coincides with the observation that fracturing decreases as the T∧C angle increases from 0° to 90°.

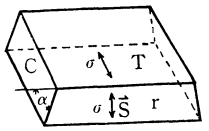

Fig. 16. Schematic representation of each planes, T the surface plane, c the basal plane and r the cleavage plane. Cleavage cracks take place only in the range of the angle T∧C from 50° to 80°. α represents the angle T∧C.

The limited range of the occurrence of cleavage cracks might have the significance explained below, in view of the crystal structure of corundum. Figure 17 illustrates the packing of ions parallel to the $\{10\bar{1}1\}$ plane. On the cleavage surface, there exist the directions shown by the arrows designated $\vec{S}$, with the angle of 18° from the trace of the basal (0001) plane and with the T∧C angle of 75°, which corresponds to the direction leading to a saddle point, and the other direction shown by the arrows $\vec{R}$ with the angle of 29° from the trace of the basal (0001) plane and with the T∧C angle

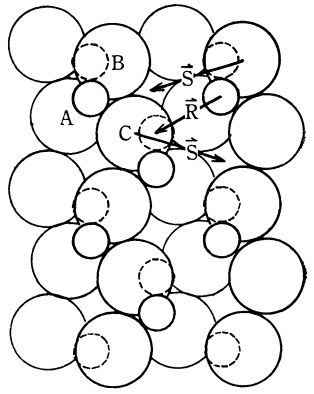

Fig. 17 (a)

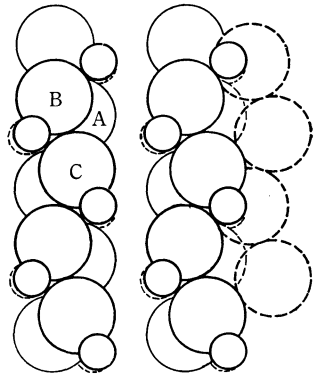

Fig. 17 (b)

Fig. 17. Packing of ions normal to $\{10\bar{1}1\}$. Two layers of ions on both sides of cleavage surface are shown in (a), and arrangement after the shear $\vec{R}$ is shown in (b).

of 66°, which corresponds to the direction in which the Al ions on the upper layer may be transported to just above the Al ions on the lower layer. Most of the plots fall in the T∧C regions between 66° and 75°. If a shear is applied between these two layers, a great resistance may be anticipated in directions other than the adjacent region of the $\vec{S}$ direction. When the shear shown by the $\vec{R}$ vector is applied, it gives rise to the arrangement of ions on both sides of the cleavage surface shown

in Fig. 17, where no bonding exists between the two crystal faces, and where only repulsions work between anions and between cations. Therefore, the experimental results have been interpreted as suggesting a fracture mechanism in which a shear along the cleavage face is required prior to the cleavage-crack nucleation.

The change in fracture properties upon heat treatment on titania-containing corundum may be interpreted on the assumption of this mechanism that the exsolution of the titania[4] nuclei in the corundum makes the shear quite difficult by nailing up the crystal plane.

Conclusion

1) When corundum crystals are ground in thin sections below the thickness of about 5/100 mm., fractures characterized by the inherent structure occur in the grinding process. The previous descriptions of the fracture properties of corundum are not sufficient in that they neglect the dependence of the type of fracture on the testing method.

2) These microcracks have a close relation to the section direction with respect to the crystal orientation. Irregular cracks with a tendency to intercross with one another occur frequently in crystals ground with T∧C angles from 0° to 50°. Cleavage cracks along the $r\{10\bar{1}1\}$ plane take place prominently in the range of the T∧C angles from 50° to 80°. Irregular cracks with a tendency to stream in one direction occur rarely in the range from 80° to 90°.

3) The results have been interpreted in terms of the cohesion strength of the crystal plane calculated on the basis of the ionic-bonding-strength theory. In order to explain the limited range of the occurrence of cleavage cracks, a model based on the shearing along the cleavage face prior to the crack nucleation has been proposed.

4) Heat treatment in air on titania-containing corundum has a conspicuous effect on the fracture properties.

5) Verneuil corundum and hydrothermal corundum exhibit no conspicuous differences in fracture properties, and the basal parting in the contact region of hydrothermal corundum on a seed is due to the zonal segregation of the iron impurity.

4) T. Horibe and S. Kuwabara, *J. Chem. Soc. Japan, Ind. Chem. Sect.* (*Kogyo Kagaku Zasshi*), **67**, 2033 (1964).

BULLETIN OF THE CHEMICAL SOCIETY OF JAPAN VOL. 39 295—299 (1966)

Twinning in Electric Furnace-fused Corundum

By Goro YAMAGUCHI, Yasushi KUBO and Hiroshi OGAWA

Department of Industrial Chemistry, Faculty of Engineering, The University of Tokyo, Hongo, Tokyo

(Received July 20, 1965)

In an investigation into the fracture properties of thin-sectioned corundum crystals, it was noticed that microcracks in electrically-fused corundum obey a hexagonal symmetry in spite of the rhombohedral symmetry of the corundum structure. This fact suggests that the corundum crystals consist of several twins, which have the same optical direction and which cannot be distinguished microscopically. The X-ray Laue back-reflection and etching techniques were applied to commercial 16-mesh grains of electric furnace-fused alumina abrasives. Corundum crystals grown over the crystal size of hundreds of μ to 1 mm. in electric-furnace fusions were found to be generally composed of several penetration twins with a twinning plane (0001). The twins are considered to be growth twins arising in the cooling process. The impurity composition and heat treatment have no marked effect on twinning. The twin junction is highly stable both mechanically and chemically. Cleavage cracks generated in individual crystals are stopped at the twin boundary.

Recently many studies have been made of the imperfection structures of corundum as background for such applications as alumina ceramics, jewel instruments, lasers and masers.

In one investigation into the effect of imperfection sturctures on the abrasive properties of corundum, it was noticed that corundum crystals from electric-furnace-fused ingot consist of several twins ranging in size from hundreds of μ to 1 mm.; these twins have the same optic direction and can not be distinguished microscopically. This fact was initially noticed in examining microcracks generated in thin-sectioned corundum crystals,[1]

1) G. Yamaguchi, Y. Kubo and H. Ogawa, This Bulletin, **39**, 287 (1966).

which obey a hexagonal symmetry in spite of the rhombohedral symmetry of the corundum structure.[2] X-Ray Laue back-reflection and etching techniques were applied, thus revealing the characteristic features of this fine basal twinning with the penetration twin boundary. The cause of twinning and the effect on the abrasive properties will be discussed.

Experimental

Specimens.—Most of the specimens examined were commercial 16-mesh grains of electric-furnace-fused alumina abrasives obtained from Carborundum Company, with the impurity contents given in Table I. These specimens were obtained from large ingots of electric-furnace-fusions and were composed predominantly of corundum with crystal sizes of from 2 mm. to 1/10 mm. and of impure minerals forming a matrix or included in corundum crystals. Of these impurities, only titania was present in a conceivable amount in corundum in a solid solution. The texture varies depending on the raw materials and on the processing. A detailed description of the texture of these products may be found in the article by Baumann.[3]

TABLE I. IMPURITY COMPOSITION OF THE SPECIMENS

Specimen	SiO_2	Fe_2O_3	TiO_2	
C32	0.51	0.12	2.46	
R41	0.49	0.15	2.49	
C37	0.26	0.04	tr.	
Japanese commercial abrasives	0.86	0.21	2.43	# 24 as received
	0.10	0.10	1.50	# 220 treated by Na_2CO_3-K_2CO_3-H_3BO_3 flux

The specimens, designated G52, C32, R41 and C37, are so-called high or low-titania fused aluminas widely used for abrasives. C36 is an electric-furnace made white alumina made from Bayer-process raw material; it contains beta alumina as impurity. R71 is a special alumina containing a considerable amount of ZrO_2; in it corundum crystals grow as dendrite or fine euhedral crystalites in a matrix of impurities. Commercial Verneuil corundum and hydrothermally-synthesized corundum were also studied for the sake of comparison.

The effect of heat treatment on twinning was examined using as received Japanese commercial 24-mesh abrasive alumina containing titania in a solid solution; it has been heat-treated in air at 1250°C for 1 hr.

The Observation of Cleavage Cracks in Thin Sections.—When corundum crystals were ground in thin sections, numerous microcracks, regular or irregular, appeared in various places. These microcracks were not observed until the section was ground to a thickness of less than 5/100 mm.; they were closely related to the crystallographic orientation of the ground section.

When the ground section made an angle of from 50° to 80° with the basal (0001) plane and one of from 60° to 90° with the rhombohedral $\{10\bar{1}1\}$ plane, cleavage cracks parallel to the $\{10\bar{1}1\}$ plane took place predominantly.

The orientation of the c-axis and the cleavage crack normals with respect to the section normal was determined on thin-sectioned corundum crystals approximately 2/100 mm. thick using a universal stage and expressed in terms of stereographic projection. The symmetry exhibited by the cleavage cracks was then examined.

X-Ray Laue Back-reflection Photographs.—By the Laue back-reflection method, the orientation of the crystal in thin sections was examined and compared with the data determined by the measurement of cleavage cracks. Crystals with the c-axis nearly perpendicular to the section plane were selected in thin sections. Laue back-reflection photographs of them were then taken, and the symmetry of the reflection patterns was examined. The Laue pattern obtained from the single corundum crystal should be of a trigonal symmetry, so the hexagonal crystal gives evidence of basal twinning.

Etching on the Basal (0001) Surface.—In order to examine the twin junction and the size of twin individuals, the basal (0001) surface was etched. Etching techniques developed by Scheuplein and Gipps[4] using phosphoric acid and by Stephens and Alford[5] using potassium bisulfate were applied.

Results

The Arrangement of Cleavage Cracks in Thin Sections.—The orientations of the section normal (T), the c-axis (C) and the cleavage crack normals (P_1, P_2 and P_3) as determined on a thin-sectioned corundum crystal of Fig. 1(a), which exhibits three sets of cleavage cracks, are shown in Figs. 1(b) and 1(c) by stereographic projection to show the symmetry of the cleavage cracks.

These cleavage cracks correspond to the rhombohedral $(10\bar{1}1)$ plane, with an angle of 57°35′ with relation to the basal plane. The arrangement of cracks, however, can only be interpreted as of a hexagonal symmetry. By careful observation of Fig. 1(a) it can be seen that the sets of cleavage cracks never intercross with each other and that they separates a crystal into regions, in each of which one of the sets predominates. Almost all of the crystals exhibiting more than two sets of cleavage cracks were found to possess hexagonal crack patterns.

A Laue Back-reflection Photograph.—One of the Laue back-reflection photographs taken along the c-axis of nearly basal sections of electric-furnace-fused corundum is given in Fig. 2(a); the corundum is seen to be made up, by basal twinning, of the superposition of the usal trigonal pattern of a single corundum crystal and its 180° rotated or mirror-reflected pattern.

2) J. D. Dana & E. S. Dana, "The System of Mineralogy," 7th ed., Vol. 1, John Wiley & Sons, Inc., New York (1944), p. 520.
3) H. N. Baumann, Jr., *Am. Ceram. Soc. Bull.* **37**, 179 (1958).
4) R. Sheuplein, *J. Am. Ceram. Soc.*, **43**, 458 (1960).
5) W. J. Alford, ibid., **46**, 193 (1963).

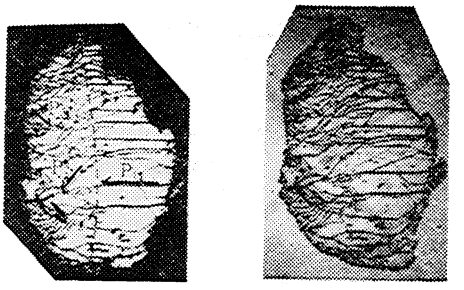

Fig. 1(a). A crystal made up of two twin individuals, one of which includes cleavage crack P_1, another includes P_2 and P_3. Each arrow is drawn parallel to the trace of cleavage crack on thin section. The twin boundary presumed from the distribution of cleavage cracks is shown by dotted line.

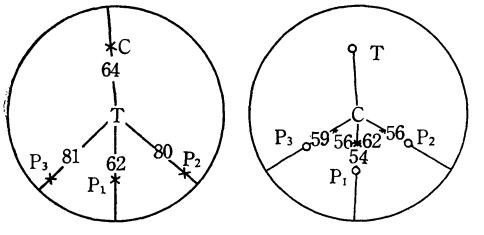

1(b) 1(c)

Fig. 1(b). Stereographic projection of cleavage cracks on the section plane.

1(c). Stereographic projection of cleavage cracks on the basal plane.

The Twin Structure Revealed by Etching on the Basal (0001) Plane.—Etch pits on the (0001) surface showed the region of twin individuals by means of the reversal of the triangular etch pits. Twin junctions were not affected at all or were only obscurely etched, as is shown in Fig. 3 and Fig. 4; this differs from Alford's observation of the basal twin of flux crystals, where the trace of the composition plane $(10\bar{1}0)$ on the basal plane was marked by a row of rectangular or diamond-shaped etch pits.[5]

The twin boundaries drawn from the distribution of etch pits are shown in Fig. 5. The size of the individual crystal is determined to vary from hundreds of μ to 1 mm. in diameter, and the twin boundary is not planar but interpenetrating.

The Effect of Impurities, Texture, and Heat Treatment on Twinning.—The presence of twinning was examined on each of the specimens, which differ in impurity composition and in texture. The results are shown in Fig. 6, where measured grains are marked at positions on the abscissa expressing the crystal size in mm.; the single crystal is marked by a one-sided arrow head, and twin composed of more than two individuals, by a two-sided arrow head.

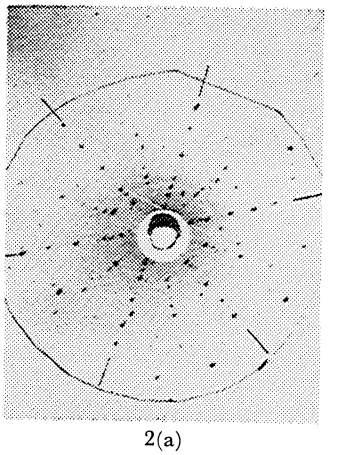

2(a)

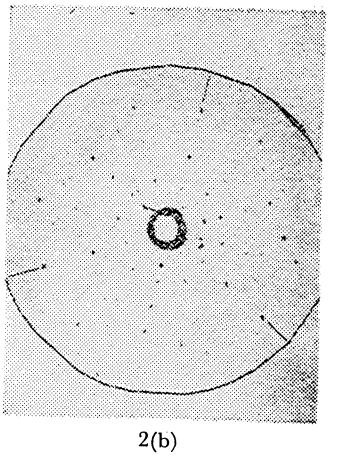

2(b)

Fig. 2(a). Laue photograph taken along the c-axis of electrically-fused corundum crystal. An X-ray beam with about 1 mm. in diameter is applied. The hexagonal distribution of the spots confirms the twinning of the crystal.

2(b). Laue photograph taken along the c-axis of Verneuil corundum crystal. An X-ray beam with about 1 mm. in diameter is applied. The trigonal distribution of the spots is that of single crystal's.

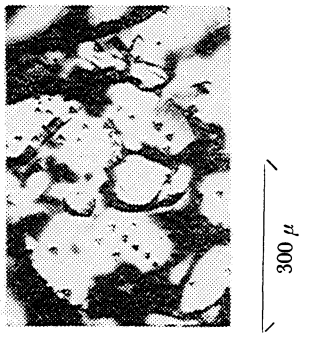

Fig. 3. Twin structure revealed by etching on the basal plane. Twin junction was not affected at all.

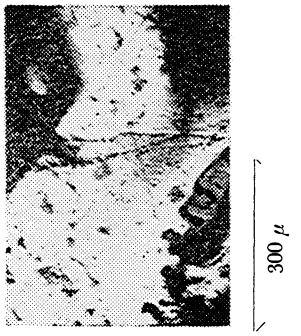

Fig. 4. Same as Fig. 3. Twin junction was obscurely etched.

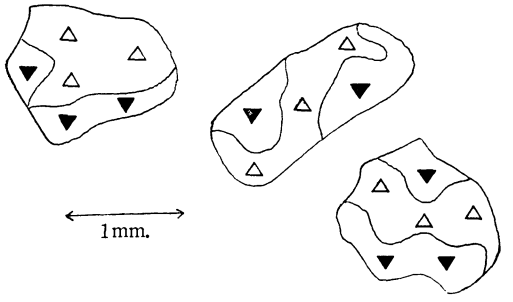

Fig. 5. Twin boundaries drawn from the distribution of etch pits.

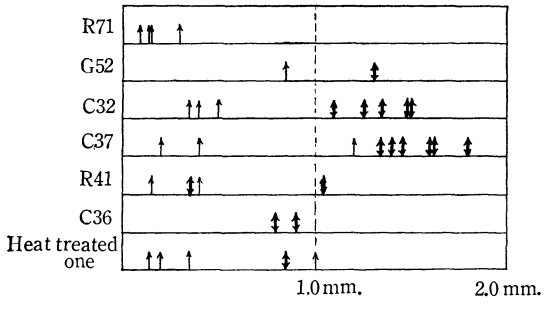

Fig. 6. Relations between crystal size and twin formation.
Crystal size is expressed by $(a+b)/2$ in mm.
a: The longest diameter
b: The diameter perpendicular to the direction of a
↕ Twin composed of more than two individuals
↑ Single crystal

Except for the R71 sample, which has a singular composition and texture, no striking difference was observed between the specimens with regard to twin formation. In any specimen corundum crystals grown over the crystal size of hundreds of μ are composed of interpenetrating basal twins. Heat treatment in air at 1300°C on titania-containing crystals caused no change in the twin structure.

Discussion

The twinning of corundum has been described in the literature as follows; commonly with a twinning plane $(10\bar{1}1)$ and less commonly with (0001), the latter being usually lamellar and producing a lamellar structure and striae on $c(0001)$ and $r(01\bar{1}1)$, and even less commonly, penetration twins or, rarely, arrowhead twins with tabular crystals parallel to $(11\bar{2}0)$.[2]

Recently, Stephans and Alford[6] reported that a basal twinning with a $(10\bar{1}0)$ composition plane and a (0001) twin axis, which was observed by Mekczer as a rare form on natural corundum, is generally present on flux crystals grown from PbO-PbF_2 flux systems at temperatures up to 1250°C. Pressure twinning produced on $(10\bar{1}1)$ and on (0001) under pressures of from 13000 to 18000 atmospheres was studied in detail by Veit[7] and interpreted on the basis of dislocation mechanisms by Kronberg.[8] This study has shown another form of twinning in electric-furnace fused corundum crystals.

Skeletal crystals (so designated by Baumann), which grow on the surface of shrinkage pipes in cooled ingots, were also found to be basal twins coupled on a longitudinal twin boundary, on each side of which rhombohedral corundum crystals pile up along the c-axis, thus forming a skeletal needle, on which no comment was made by Baumann.

The cause and process of twin formation can only be inferred qualitatively. The observed twins are considered to be growth twins arising from the strain peculiar to the cooling of large ingots of electric-furnace fusions. The cohesion of a twin junction is as strong as the internal cohesion of a single crystal; the etch pits usually observed in other cases on the traces of a twin boundary are not revealed, and the cleavage cracks generated in the region of single crystals are stopped at the twin boundary, not propagating beyond it, as is shown in Fig. 1(a).

The fracture properties of electrically-fused corundum are supposed to be affected by twinning. Whether twinning increases the toughness of corundum or not remains to be established, however.

Conclusion

1) Corundum crystals grown over the crystal size of from hundreds of μ to 1 mm. in electric-furnace fusions have been found generally to be composed of several penetration twins with a twinning plane (0001).

6) W. J. Alford, *J. Am. Ceram. Soc.*, **47**, 81 (1964).
7) K. Veit, *Jb. Min. Beil.*, **45**, 121 (1921).
8) M. L. Kronberg, *Acta. Met.*, **5**, 507 (1957).

2) These twins have been considered to be growth twins arising in the cooling process. The impure content and heat treatment have no marked effect on the twinning.

3) The twin junction is highly stable, both mechanically and chemically. Cleavage cracks generated in individual single crystal are stopped at the twin boundary. By chemical etching on the basal plane, the trace of the twin boundary is not affected at all or, in some cases, is only obscurely etched.

4) The fracture properties of corundum may be supposed to be affected by twinning, but the relation between the toughness of abrasives and the twinning remains to be established.

BULLETIN OF THE CHEMICAL SOCIETY OF JAPAN VOL. 39 299—306 (1966)

Kinetic Studies of Solvolysis. XI.* The Steric Course of the Phenolyses of Optically Active α-Phenylethyl Chloride in Mixtures of Various Phenols and Organic Solvents—A Mechanism for the S_N1 Reaction with a Net Retention of Configuration

By Kunio Okamoto, Hiroto Yamada, Issei Nitta and Haruo Shingu

Department of Fuel Chemistry, Faculty of Engineering, Kyoto University, Sakyo-ku, Kyoto

(Received May 27, 1965)

The S_N1 phenolyses of optically active α-phenylethyl chloride in binary mixtures of organic solvents and certain substituted phenols (i. e., phenol, *p*-cresol, *p*-chloro- and *p*-nitro-phenol) proceed in the presence of aniline and of triethylamine to give the corresponding α-phenylethyl substituted-phenyl ethers with a predominantly-retained configuration. In binary mixtures of benzene and various phenols, the extents of retention for the ethers are slightly reduced at the higher base concentrations. However, in binary solvents of acetonitrile and certain phenols, the optical purities of the ethers with retained configurations decrease continuously with the base concentrations, while at the higher concentrations (~0.4 M) the steric courses change to the inverted course. The *C*-alkylated (α-phenylethylated) derivatives of these phenols, isolated along with the phenyl ethers, have inverted configurations, irrespective of the configurations of the corresponding phenyl ethers. These results are all consistent with a mechanism in which a molecule of the phenol reacts with the S_N1 ion-pair intermediate of the phenolysis to give a phenyl ether with a retained configuration, probably by S_Ni-like four-center substitution, whereas the reaction of a phenoxide anion with the S_N1 intermediate proceeds predominantly by the Walden inversion mechanism yielding a phenyl ether and α-phenylethylated phenols with inverted configurations.

It has been demonstrated in the literature that the S_N1 solvolyses of optically active α-phenylethyl chloride ordinarily proceed with a net inversion of the configuration in methanol,[1] ethanol,[1] aqueous acetone[1] and acetic acid[2]. The results[3] in our laboratories have also revealed that a net inversion is standard for the α-phenylethyl system in S_N1 solvolyses in such solvents as cyclohexanol, formic acid, trifluoroacetic acid and pivalic acid.

In contrast to these facts, however, we found[4] that the S_N1 phenolysis of optically-active α-phenylethyl chloride in a phenol-benzene mixture gave α-phenylethyl phenyl ether with a net retention of the configuration in the presence of a base such as aniline. In this earlier investigation, it was not clear whether the retention of the configuration was a result typical of all phenolyses in the substituted phenols, nor was it clear which nucleophile (a phenoxide anion or a phenol molecule) was responsible for this unordinary steric course.

In this paper we wish to report on the results of studies undertaken in order to answer the above questions. It will be shown that the S_N1 phenolyses of optically active α-phenylethyl chloride in various

* Presented at the 15th Organic Reaction Mechanism Symposium of the Chemical Society of Japan, Nagoya, October, 1964. Part X of this series: K. Okamoto, Y. Matsui and H. Shingu, This Bulletin, **38**, 1844 (1965).

1) E. D. Hughes, C. K. Ingold and A. D. Scott, *J. Chem. Soc.*, **1937**, 1201.

2) J. Steigman and L. P. Hammett, *J. Am. Chem. Soc.*, **59**, 2536 (1937).

3) K. Okamoto and Y. Matsui, unpublished data.

4) K. Okamoto, K. Takeuchi and H. Shingu, This Bulletin, **35**, 525 (1962).

Table I. Effect of nature of organic solvent in phenol-organic solvent mixtures on steric course of phenolysis of optically active α-phenylethyl chloride in the presence of aniline at 40.0°C

Run. No.	Org. solvent	Phenol[a] M	Aniline M	RCl M	RCl[b] α_D	ROC_6H_5[c] α_D	Net steric course[d]	k_t min^{-1}
25	Cyclohexane	4.71[e]	0.256	0.088	−47.8°	+3.67°	20.6% ret.	7.45×10^{-2}
20	Anisole	6.11[f]	0.200	0.096	−48.1°	+5.45°	30.4% ret.	4.11×10^{-2}
83	Benzene	4.71	0.243	0.076	+41.02°	−5.36°	35.0% ret.	3.13×10^{-2}
85	Acetonitrile	4.71	0.248	0.076	+41.02°	−6.46°	42.2% ret.	2.42×10^{-3}
84	Acetone	4.71	0.246	0.076	+41.02°	−7.84°	51.2% ret.	4.13×10^{-4}

a) Calculated from composition (by weight) and density (at 40.0°C) of the mixture.
b) Rotations of starting α-phenylethyl chloride, taken neat, $l=1$ dm.
c) Rotations of α-phenylethyl phenyl ether, taken neat, $l=1$ dm.
d) Calculated taking into account lack of optical purity of starting chloride; the rotations of the optically pure materials are taken to be 125° (H. M. R. Hoffmann and E. D. Hughes, *J. Chem. Soc.*, **1964**, 1244) for α-phenylethyl chloride and 46.6° for α-phenylethyl phenyl ether; reported value, 41.1°,[11] for the ether was recalculated on the basis of the new value for the maximum rotation for the chloride (H. and H., loc. cit.).
e) Phenol-cyclohexane mixture (1 : 1 by weight).
f) Phenol-anisole mixture (1 : 1 by weight).

substituted phenols, i. e., *p*-cresol, *p*-chlorophenol, and *p*-nitrophenol, yielded the corresponding α-phenylethyl substituted-phenyl ether with a predominantly retained configuration, and that this retention of configuration is caused by the attack, probably of the four-center type, of the undissociated molecules of the phenols on the S_Ni ion-pair intermediate, whereas the ambident phenoxide anions react with the S_Ni intermediate by the Walden-inversion mechanism to yield the corresponding ethers and α-phenylethylphenols with an inverted configuration.

Part I. The Steric Course of Phenyl Ether Formation in the S_Ni Phenolyses of Optically Active α-Phenylethyl Chloride

The Effect of the Nature of the Organic Solvent on the Steric Course of the Formation of α-Phenylethyl Phenyl Ether from Optically Active α-Phenylethyl Chloride. — Optically active α-phenylethyl chloride was subjected to phenolysis in phenol-organic solvent mixtures (about 1 : 1 by weight). The reactions were carried out in the presence of aniline as a base at 40.0°C for ten half-lives. The half-life for each reaction was estimated from the results of the kinetic runs carried out at 40.0°C under conditions similar to those used in the product studies. α-Phenylethyl phenyl ether was isolated by chromatography on silica gel or basic alumina.

Table I compares the effect of the organic solvent variation on the stereochemical outcome of phenolysis. In all runs, α-phenylethyl phenyl ether had a retained configuration, accompanied by 50 to 80% racemization.

It has been postulated that the retained steric course in the decomposition of secondary aliphatic chlorosulfites is due to the back-side participation of the solvents, such as ethers or alkyl halides, in a positive center of the ion-pair intermediate of this reaction.[5] An examination of the data in Table I, however, reveals that there can be hardly any specific relationship between the nucleophilic coordination power of these organic solvents and the extent of the net retention of the configuration. Therefore, the organic solvent molecule seems to play no primary rôle in the retention of the configuration; rather, the presence of the compound "phenol," i. e., a phenol molecule, a phenoxide anion, or an ion-pair of the phenoxide ion, seems to control the net steric course.

Furthermore, in those runs carried out in similar phenol concentrations there is a clear trend toward a larger racemization of the product ether with higher phenolysis rates (Table I). This trend may be explained if one assumes that the higher rates are responsible for the looser ion-pair intermediates, which in turn result in a larger racemization of the ether so formed.

The Effect of the Composition of Phenol-Organic Solvent Mixtures on the Steric Course of the Formation of α-Phenylethyl Phenyl Ether from Optically Active α-Phenylethyl Chloride.—In order to obtain further evidence for the essential rôle of phenol in the retention of the configuration, phenolyses of α-phenylethyl chloride were carried out in phenol-benzene and the phenol-acetonitrile mixtures with various phenol concentrations. As is shown by the degree of the retention of the configuration of α-phenylethyl phenyl ether (Table II), the higher concentration of phenol is not a necessary condition for the retention of the steric course. In fact, in a phenol-acetonitrile mixture with such a small concentration as 0.55 M of phenol in the

5) E. S. Lewis and C. E. Boozer, *J. Am. Chem. Soc.*, **74**, 308 (1952); C. E. Boozer and E. S. Lewis, ibid., **75**, 3182 (1953).

Table II. Effect of the composition of phenol-organic solvent mixtures on the steric course of phenolysis of optically active α-phenylethyl chloride at 40.0°C

Run. No.	Phenol[a] M	Base M	RCl M	RCl[b] α_D	ROC_6H_5[c] α_D	Net steric course[d]	k_t min^{-1}
			Organic solvent, benzene; Base, aniline				
92	11.2[e]	0.248	0.076	−43.49°	+6.34°	39.1% ret.	—
83	4.71	0.243	0.076	+41.02°	−5.36°	35.1% ret.	3.18×10^{-2}
91	2.26	0.245	0.078	−43.49°	+5.64°	34.8% ret.	4.29×10^{-2}
			Organic solvent, acetonitrile; Base, triethylamine				
90	11.2[e]	0.176	0.076	+42.89°	−5.36°	33.5% ret.	—
	4.73	0.175	0.070			30.5% ret.[f]	1.42×10^{-3}[g]
67[h]	1.61	0.175	0.075	+54.13°	−4.95°	24.5% ret.	4.20×10^{-2}
88[i]	0.55	0.165	0.084	+41.13°	−3.71°	24.1% ret.	2.97×10^{-3}

a), b), c) and d) See foot notes a), b), c) and d), Table I.
e) 100% Phenol.
f) Interpolated from data cited in Table III.
g) Initial concentration of triethylamine was 0.424 M.
h) Carried out at 90.5°C.
i) Carried out at 111°C.

presence of 0.165 M triethylamine, the extent of retention for α-phenylethyl phenyl ether still amounts to 24.1%, in spite of the fact that the reaction was carried out at a rather higher temperature because of the low rate in the solvent ranges with such low phenol concentrations. This is another support for the conclusion in the preceding section, i. e., the primary rôle of the compound "phenol" in the steric course with a net retention of the configuration.

The Effect of the Base Concentration on the Steric Course of the Formation of α-Phenylethyl Phenyl Ether from α-Phenylethyl Chloride in *p*-Substituted Phenol-Organic Solvent Mixtures.—In order to differentiate the rôles of a phenol molecule and a phenoxide anion (or ion-pair) on the steric course of the phenyl ether formation, the effect of the base concentration on the extent of the retention of the configuration of α-phenylethyl *p*-substituted-phenyl ether was examined in mixtures of various *p*-substituted phenols and benzene (or acetonitrile). The results are illustrated in Fig. 1 and in Table IV (see Experimental Section).

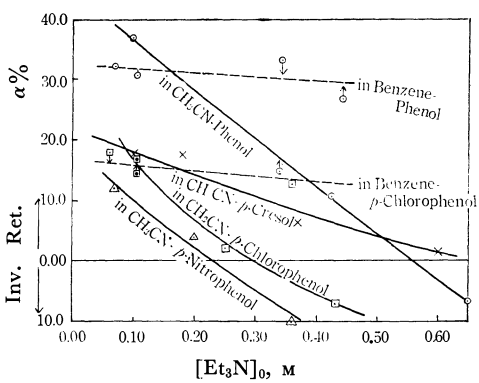

Fig. 1. Effect of base concentration on the steric course for the formation of α-phenylethyl *p*-substituted-phenyl ethers optically active α-phenylethyl chloride in *p*-substituted phenol-organic solvent mixtures (1 : 1 by weight).

In a benzene-phenol mixture (1 : 1 by weight) the extent of retention of α-phenylethyl phenyl ether shows a slight trend towards lower optical purities at higher triethylamine concentrations; this trend becomes more pronounced in an acetonitrile - phenol mixture (1 : 1 by weight). Finally, the run carried out in the presence of 0.65 M triethylamine afforded α-phenylethyl phenyl ether with an "inverted" configuration.

Similarly, in a *p*-chlorophenol - acetonitrile mixture (1 : 1 by weight), the net steric course of *p*-chlorophenolysis changes from a 37% retention to a 6.5% inversion as the concentration of triethylamine is increased from 0.1 to 0.6 M ,whereas in a benzene - *p*-chlorophenol mixture (1 : 1 by weight) the extent of retention of α-phenylethyl *p*-chlorophenyl ether does not show such a large decrease in optical purities as in the mixtures of acetonitrile - *p*-chlorophenol.

Similar trends are also observed in *p*-cresolysis and in *p*-nitrophenolysis in mixtures of these phenols and acetonitrile (1 : 1 by weight).

These results suggest that the reactions of the phenoxide anions of various phenols (or the triethylammonium salt of these phenols) with the S_Ni intermediate proceed predominantly with an inversion of the configuration. Accordingly, it may be concluded that the reaction of these undissociated phenol molecules with the intermediate is responsible for the retention of the configuration.

The most probable course for the retention of the configuration caused by the reaction of a phenol molecule and the S_Ni ion-pair intermediate would be a four-center reaction, such as the one depicted below:

Table III. Steric course of *C*-alkylation in phenolysis of α-phenylethyl chloride in *p*-substituted phenol-organic solvent mixtures (1 : 1 by weight) at 40.0°C

Run No.	*p*-Substituted phenol	Et_3N M	RCl M	RCl[a] α_D	*p*-Substituted-*o*-α-phenylethylphenol[b] $[\alpha]_D$ (temp., °C; *c*)	Yield %	Net steric course[c] Alkylation on carbon	oxygen[d]
				Organic solvent, benzene				
97	Phenol	0.408	0.175	+54.66°	ortho-isomer −4.65° (16.6; neat)	14.8	38.1% inv.	31.0% ret.
					para-isomer +1.845°(21.5; 30.4)	13.3	41.2% inv.	
70	*p*-Chlorophenol	0.106	0.084	−54.3°	+4.94° (30.3; 1.82)	16.5	25.4% inv.	14.7% ret.
				Organic solvent, acetonitrile				
53	Phenol	0.340	0.071	+29.5°	−5.38° (19.0; 39.4)[e]	19.4[e]	86.7%[f] inv.	14.9% ret.
52	Phenol	0.650	0.130	+29.5°	−3.16° (19.0; 76.4)[g]	21.4[g]	57.9%[f] inv.	6.5% inv.
59	*p*-Cresol	0.182	0.075	−50.2°	−4.43° (21.2; 31.3)	23.3	64.5% inv.	17.7% ret.
56	*p*-Cresol	0.370	0.075	+16.4°	+1.43° (20.2; 31.4)	24.9	64.0% inv.	6.9% ret.
57	*p*-Chlorophenol	0.249	0.074	−52.0°	−6.28° (25.3; 11.0)	6.4	33.8% inv.	2.1% ret.
58	*p*-Chlorophenol	0.429	0.073	−52.0°	−11.8° (26.3; 14.8)	11.5	63.4% inv.	7.3% inv.

a) Rotations of starting α-phenylethyl chloride, taken neat, calcd. for $l=1$ dm.
b) Specific rotations of *p*-substituted-*o*-α-phenylethylphenol, taken in benzene.
c) See foot note d), Table I; rotations (neat, $l=1$ dm.) for optically pure materials are taken to be 27.85° for *o*-α-phenylethylphenol (see text), 10.26° for *p*-α-phenylethylphenol (see text), 17.1° for *o*-α-phenylethyl-*p*-cresol,[7] and 44.7° for *o*-α-phenylethyl-*p*-chlorophenol (calculated from the results[13] of the S_N2 reaction between optically active α-phenylethyl chloride and potassium *p*-chlorophenoxide in acetone, assuming the same optical purities for the *O*-alkylated and the *C*-alkylated product.
d) See the 7th column, Table III, except the runs 97 and 70.
e) For the mixture of ortho-isomer (90%) and para-isomer (10%).
f) Calculated for the mixture, assuming the same optical purities for the ortho and the para isomer.
g) For the mixture of ortho-isomer (79%) and para-isomer (21%).

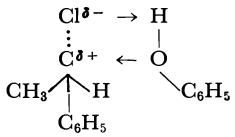

Considering that in relatively non-polar benzene-phenol mixtures the base concentration has not so much effect on the optical purities of the ethers as in polar acetonitrile-phenol mixtures, we may suggest that the more effective reaction species in the inversion of configuration would not be triethylammonium phenoxide (an ion-pair) but, rather, a phenoxide anion (a dissociated anion).

The Determination of the Configurations and Maximum Rotations of α-Phenylethyl *p*-Chlorophenyl Ether and α-Phenylethyl *p*-Nitrophenyl Ether.—In order to establish the configuration and the maximum rotation of α-phenylethyl *p*-chlorophenyl ether, a dioxan solution of α-phenylethyl chloride, ($[\alpha]_D^{16}$ −35.4° (benzene)) and sodium *p*-chlorophenoxide was refluxed for 6.5 hr.; this gave α-phenylethyl *p*-chlorophenyl ether ($[\alpha]_D^{15}$ −5.80° (benzene)) and unchanged α-phenylethyl chloride ($[\alpha]_D^{15}$ −35.7° benzene)). From these results of the S_N2 reaction, the maximum rotation, $[\alpha]_D$ in benzene, for R-α-phenylethyl *p*-chlorophenyl ether was estimated to be −22.40° (see Experimental Section).

In order to determine the configuration and the maximum rotation of α-phenylethyl *p*-nitrophenyl ether, a dimethyl sulfoxide solution of *p*-nitrobromobenzene and potassium α-phenylethoxide, which afforded α-phenylethyl alcohol (α_D^{24} +15.6° ($l=1$ dm., neat)) after hydrolysis, was maintained at 40.0°C for 17 hr. After the usual treatment, the reaction mixture afforded α-phenylethyl *p*-nitrophenyl ether ($[\alpha]_D^{26}$ +15.3° (benzene)) and unchanged potassium α-phenylethoxide, recovered as α-phenylethyl alcohol with α_D^{26} +13.4° ($l=1$ dm., neat). Assuming that the optical activity of potassium α-phenylethoxide decreases linearly during the reaction, we took the arithmetic mean of the rotations before and after the reaction as the rotation of the α-phenylethoxide in the course of the reaction. The estimated maximum rotation of R-α-phenylethyl *p*-nitrophenyl ether amounted to +46.6° (see Experimental Section).

Part II. The Steric Course of α-Phenylethylphenol Formation in the S_N1 Phenolyses of Optically Active α-Phenylethyl Chloride

The Steric Course of Various α-Phenylethylphenol Formations in *p*-Substituted Phenol - Organic Solvent Mixtures (1 : 1 by Weight).—The phenoxide anion, as an ambident

TABLE IV. EFFECT OF BASE CONCENTRATION ON PHENOLYSES OF OPTICALLY ACTIVE α-PHENYLETHYL CHLORIDE IN *p*-SUBSTITUTED PHENOL-ORGANIC SOLVENT MIXTURES (1 : 1 BY WEIGHT)

Run No.	*p*-Substituted phenol	Et_3N M	RCl M	RCl[a] α_D	ROR'[b] α_D or $[\alpha]_D$ (temp., °C; *c*)	Net steric course[c]	k_t min^{-1}
			Organic solvent, benzene; temp. 25.0°C				
45	Phenol	0.071	0.072	−32.4°	+3.90°	32.2% ret.	—
69	Phenol	0.107	0.075	−54.3°	+6.22°	30.8% ret.	1.68×10^{-2}
49	Phenol	0.293	0.073	+27.1°	−3.38°	33.4% ret.	—
48	Phenol	0.446	0.090	+42.1°	−4.30°	27.4% ret.	1.44×10^{-2}
43	*p*-Chlorophenol	0.061	0.066	−44.9°	+1.47° (15.6; 22.1)	18.3% ret.	—
70	*p*-Chlorophenol	0.106	0.084	−54.3°	+1.43° (30.3; 32.5)	14.7% ret.	3.38×10^{-2}
41	*p*-Chlorophenol	0.361	0.123	−44.9°	+1.03° (14.7; 11.9)	12.8% ret.	2.81×10^{-2}
			Organic solvent, acetonitrile; temp. 40.0°C				
50	Phenol	0.100	0.073	+27.1°	−3.74°	37.0% ret.	—
53	Phenol	0.340	0.071	+29.5°	−1.64°	14.9% ret.	—
51	Phenol	0.424	0.143	+27.1°	−1.10°	10.9% ret.	1.42×10^{-3}
52	Phenol	0.650	0.130	+29.5°	+0.71°	6.5% inv.	1.06×10^{-3}
55	*p*-Cresol	0.103	0.075	+16.4°	−0.47° (21.5; 46.8)	17.5% ret.	8.18×10^{-4}
59	*p*-Cresol	0.182	0.075	−50.2°	+1.45° (22.0; 46.2)	17.6% ret.	—
56	*p*-Cresol	0.370	0.075	+16.9°	−0.18° (21.5; 37.9)	6.5% ret.	—
60	*p*-Cresol	0.595	0.076	+24.6°	−0.065°(22.3; 46.2)	1.6% ret.	6.76×10^{-4}
54	*p*-Chlorophenol	0.105	0.076	+16.5°	−0.50° (27.5; 49.4)	16.9% ret.	—
57	*p*-Chlorophenol	0.249	0.074	−52.0°	+0.20° (22.0; 41.1)	2.1% ret.	7.06×10^{-4}
58	*p*-Chlorophenol	0.429	0.073	−52.0°	−0.68° (23.5; 44.0)	7.3% inv.	6.53×10^{-4}
40	*p*-Nitrophenol	0.071	0.061	+43.8°	+1.97° (23.6; 27.9)	12.1% ret.	6.58×10^{-2}
38	*p*-Nitrophenol	0.198	0.100	+43.8°	+0.63° (15.2; 3.2)	3.9% ret.	—
46	*p*-Nitrophenol	0.358	0.143	+42.1°	−1.55° (17.2; 6.3)	9.9% inv.	6.47×10^{-2}

a) Rotations of starting α-phenylethyl chloride, taken neat, calculated for $l=1$ dm.
b) Rotations of *p*-subsituted-phenyl α-phenylethyl ether, taken neat (calcd. for $l=1$ dm.) or in benzene.
c) See foot note d) Table I; the specific rotations (in benzene) of optically pure materials are taken to be −22.40° for R-α-phenylethyl *p*-chlorophenyl ether (see text), 46.6° for R-α-phenylethyl *p*-nitrophenyl ether (see text), 20.4° for S-α-phenylethyl *p*-cresyl ether. Reported value for the *p*-cresyl ether, 18°,[11] was recalculated on the basis of the new value for the maximum rotation of the chloride (see Table I, foot note d)).

ion,[6] reacts bimolecularly in acetone with α-phenylethyl chloride to afford not only α-phenylethyl phenyl ether but also *o*- or *p*-phenylethylphenol (*C*-alkylation products).[7] Accordingly, the S_N1 intermediate formed from α-phenylethyl chloride should also react with the phenoxide anion to give *C*-alkylation products as well as *O*-alkylation products (α-phenylethyl phenyl ethers). In this case, it may be anticipated that *C*- and *O*-alkylation will both have the same steric outcome, because both reactions proceed by the anion transfer mechanism. Regarding the steric course of such *O*-alkylation of the phenoxide anion, we concluded in the preceding part that the reaction proceeds with an inversion of the configuration with respect to α-phenylethyl chloride. Therefore, we can expect to obtain inverted α-phenylethylphenols also in the *C*-alkylation of the phenoxide anion by the S_N1 reaction.

The possibility of the concomitant *C*-alkylation of the phenol molecule by the S_N1 intermediate can be eliminated because its rate is slower[4] than the rate for the phenoxide anion.

Thus, we isolated the *C*-alkylated phenols in several runs carried out in the presence of a base. The yields and net steric courses of the *C*-alkylation are summarized in Table III. For purposes of comparison, the net steric courses of the *O*-alkylations are also illustrated in that table.

As expected, in all runs carried out for ten half-lives, the *C*-alkylated phenols, i. e. α-phenylethylphenol (the ortho and the para isomer), *o*-α-phenylethyl-*p*-cresol and *o*-α-phenylethyl-*p*-chlorophenol, had rotations which demonstrated that the *C*-alkylation process involved a predominant inversion of the configuration.

The Determination of the Configuration and the Maximum Rotation for *p*-α-Phenylethylphenol.—In order to determine the configuration and the maximum specific rotation for *p*-α-phenylethylphenol, the permanganate oxidation[7] of optically active *p*-α-phenylethylphenol ($[\alpha]_D^{21.5}$ +1.845° (benzene)) was conducted in acetone.

6) N. Kornblum, R. A. Smiley, R. K. Blackwood and D. C. Iffland, ibid., 77, 6269 (1955).
7) H. Hart and H. S. Eleuterio, ibid., 76, 516 (1954).

From the specific rotation of the α-phenylpropionic acid so obtained ($[\alpha]_D^{23.1}$ +14.57°), the maximum rotation of *p*-s-α-phenylethylphenol was estimated to be +10.26° (benzene). Using this value for the optically-pure para isomer and the value, −24.8°, estimated for the mixture of optically pure *o*- and *p*-s-α-phenylethylphenol (92 : 8),[7] the specific rotation for the pure ortho isomer was evaluated as −27.85° (s-configuration).

Experimental[8]

Materials.—The preparations of racemic and optically active α-phenylethyl chloride followed previous practice.[9] All the reagents employed were of a reagent-grade quality, and all were purified by fractional distillation except *p*-nitrophenol (commercial material, m. p. 111—114°C); acetone, b. p. 55.0—56.0°C; acetonitrile, b. p. 82.0—83.0°C; anisole, b. p. 152.0°C; benzene, b. p. 79.5—80.0°C; *p*-chlorophenol, b. p. 110—116°C/32 mmHg, m. p. 42.5—43.5°C; *p*-cresol, 99.5—102.0°C/24 mmHg; phenol, b. p. 180—181°C; aniline, b. p. 182—183°C; triethylamine, b. p. 89.3°C.

Kinetic Measurements.—The previous procedure[10] was followed. For the runs measured at 25.0±0.05°C, 1-cc. aliquots were removed at intervals from 20 cc. of the reaction mixture placed in a glass-stoppered flask. For the runs at 40.0±0.05°C, the usual sealed-ampoule (1 cc.) technique was employed. The diminution of base concentrations was followed by titration with standard perchloric acid in acetic acid, using crystal violet as an indicator. The phenol concentrations at the reaction temperature were calculated from the weight compositions and the densities of the phenol-organic solvent mixtures. All the rate data were treated graphically by a plot of log $a/(a-x)$ against the time. In each case the reaction was followed to at least 80% conversion and a smooth linear relationship was obtained. Infinity titers were determined after at least ten half-lives and gave reproducible results. These results are summarized in Tables I, II and IV.

The Isolation of the Reaction Products (General Procedure).—In a 100-cc. ampoule or a 100-cc. glass-stoppered round-bottomed flask, there were placed ca. 100 cc. of a mixture of a phenol, an organic solvent and the calculated amount of base (triethylamine or aniline). The concentration of the base was determined by titration of a 1-cc. aliquot (see Kinetic Measurement section). Finally, 1-cc. (0.00757 mol.) of optically active α-phenylethyl chloride was added. The sealed tube or the flask was then placed in a constant-temperature bath for at least ten half-lives. To the reaction mixture, 100 cc. of benzene was added; then the benzene solution was washed with three 70 cc.-portions of 10% aqueous sodium chloride, three 100 cc.-portions of 10% aqueous sodium hydroxide, and several 70 cc.-portions of 10% aqueous sodium chloride. After being dried with magnesium sulfate, the benzene solution was distilled and the residual oil was chromatographed over 25 g. of basic alumina. The *n*-hexane fractions afforded α-phenylethyl phenyl ether, whereas various α-phenylethyl substituted-phenyl ethers were obtained from the *n*-hexane - benzene (1 : 1 by volume) eluent. In the run in which aniline was used as the base, an excess of aniline was recovered from the benzene fractions. Various α-phenylethylphenols were obtained from the ethanol fractions. The phenyl ethers so obtained were used for the measurement of the rotation after structural verification by means of a comparison of the infrared spectrum with that of an authentic sample. Some of the ethers were sent for microanalysis. The *C*-alkylation products were distilled under reduced pressure, and the rotations of the distillates were taken in a benzene solution. These phenols were identified by infrared spectra and by microanalyses. The ortho and para compositions of α-phenylethylphenol were estimated by using the infrared spectrum of the mixture. Some of the mixtures were separated by chromatography on silica gel. The results are summarized in Tables I—IV. The details of the experimental procedure for representative runs are cited below.

The Phenolysis of Optically Active α-Phenylethyl Chloride in a Phenol-Acetonitrile (1 : 1 by Weight) Mixture (Run 53).—In a 100-cc. ampoule, 100 cc. of a mixture of phenol-acetonitrile (1 : 1 by weight), 5.00 cc. of triethylamine (0.340 mol./l.), and 1.00 cc. (0.00757 mol.) of α-phenylethyl chloride (b. p. 45—46°C/1mmHg, $\alpha_D^{15.5}$ +14.75±0.01°, 0.5 dm., neat) were placed. The ampoule was then sealed and maintained at 40.0°C for 46 hr. After the treatment mentioned above, 1.26 g. of an oily material was chromatographed over 25.0 g. of basic alumina. *n*-Hexane - benzene (1 : 1 by volume) eluent left 0.900 g. (60.1% yield, based on the starting chloride) of α-phenylethyl phenyl ether. M. p. 34.0—35.3°C (Lit. m. p. 38—39°C[11]) (Found: C, 85.09; H, 7.32. Calcd. for $C_{14}H_{14}O$: C, 84.81; H, 7.12%); λ_{max}^{neat} 8.07 μ; $\alpha_D^{15.5}$ −0.82±0.01°, 0.5 dm., neat. The ethanol (99%) fractions afforded 0.291 g. of a pale yellow oil, which was then distilled under reduced pressure to give 0.85 g. (5.67% yield) of a mixture of *o*- and *p*-α-phenylethylphenol; b. p. 110—115°C (bath, 0.3 mmHg) (Found: C, 83.17; H, 7.30. Calcd. for $C_{14}H_{14}O$: C, 84.81; H, 7.12%); $[\alpha]_D^{25.5}$ −5.38±0.33°, benzene, *c* 39.4. The ratio between the *o*- and the *p*-α-phenylethylphenol in the mixture was estimated to be 90 : 10 by infrared analysis. The characteristic bands used for the analysis were 6.62 and 6.72 μ.

The *p*-Cresolysis of Optically Active α-Phenylethyl Chloride in a Mixture of *p*-Cresol and Acetonitrile (1 : 1 by Weight) (Run 59).—Into a 100-cc. ampoule, 100 cc. of a mixture of *p*-cresol and acetonitrile (1 : 1 by weight), 2.60 cc. of triethylamine (0.182 M), and 1.00 cc. (0.00757 mol.) of α-phenylethyl chloride (b. p. 45—46°C/1 mmHg, $\alpha_D^{25.5}$ −25.11±0.015°, 0.5 dm., neat) were placed; the ampoule was sealed. After the mixture had been maintained for 65.7 hr. 40.8°C and subsequent usual treatment, 1.312 g. of an oily material was chromatographed over 25.0 g. of basic alumina. The *n*-hexane - benzene (1 : 1 by volume) eluent left 0.905 g. (56.4% of the starting chloride) of α-phenylethyl *p*-cresyl ether; m. p. 54.0—56.0°C.

8) All melting points are uncorrected. The microanalyses were performed by the Microanalytical Center, Kyoto University, Kyoto. The infrared spectra were obtained from a Shimadzu model IR-27 spectrometer. Optical rotations were measured with a Zeiss-Winkel "Kreispolarimeter 0.01°."

9) K. Okamoto, K. Takeuchi and H. Shingu, This Bulletin, **34**, 1137 (1961).

10) K. Okamoto and H. Shingu, ibid., **34**, 1131 (1961).

11) H. Hart and H. S. Eleuterio, *J. Am. Chem. Soc.*, **76**, 519 (1954).

54.0—56.0°C (Lit. m. p. 49—50°C[11]); (Found; C, 85.02; H, 7.84. Calcd. for $C_{15}H_{16}O$: C, 84.87; H, 7.60%); $\lambda_{max}^{CCl_4}$ 8.07 μ; $[\alpha]_D^{22.0}$ +1.45±0.11° (benzene, *c* 46.16). A pale yellow oily material (0.905 g.), obtained from ethanol fractions, was distilled in vacuo giving 0.295 g. (18.4% yield) of *o*-α-phenylethyl-*p*-cresol; b. p. 125°C (bath, 0.2 mmHg.) (Lit. b. p. 175—177°C/13 mmHg[12]); (Found: C, 84.09; H, 7.90. Calcd. for $C_{15}H_{16}O$: C, 84.87 H, 7.60%); $[\alpha]_D^{21.2}$ −4.43±0.39° (benzene, *c* 31.34); λ_{max}^{neat} 2.82 and 2.96 μ.

The *p*-Chlorophenolysis of Optically-Active α-Phenylethyl Chloride in a Mixture of *p*-Chlorophenol and Acetonitrile (1 : 1) by Weight (Run 57). —A reaction mixture was prepared from 100 cc. of a mixture of *p*-chlorophenol and acetonitrile (1 : 1 by weight), 3.75 cc. of triethylamine (0.249 M; determined by titration), and 1.00 cc. (0.00757 mol.) of α-phenylethyl chloride (b. p. 45—46°C/1 mmHg, α_D^{18} −26.01±0.015°, 0.5 dm., neat.). A part (10 cc.) of the mixture was pipetted out for the rate measurement. The remaining part was sealed into a 100-cc. ampoule and kept at 40.0°C for 90.8 hr. After the usual treatment, 1.086 g. of white crystals was chromatographed over 25.0 g. of basic alumina. The *n*-hexane - benzene (1 : 1 by volume) fractions gave 0.879 g. (56.5% of the starting chloride) of α-phenylethyl *p*-chlorophenyl ether; m. p. 65—67.6°C (Lit. m. p. 66.4—67.0°C[13]); (Found: C, 72.01; H, 5.52. Calcd. for $C_{14}H_{13}OCl$: C. 72.26; H, 5.63%); $\lambda_{max}^{CCl_4}$ 8.07 μ; $[\alpha]_D^{22}$ +0.195±0.15° (benzene, *c* 41.08). An oily material (0.112 g.), obtained from ethanol fractions, was distilled in vacuo to give 0.0805 g. (a 5.7% yield) of *o*-(α-phenylethyl)-*p*-chlorophenol, b. p. 120°C (bath temp., 0.1 mmHg) (Lit. b. p. 155°C/2 mmHg[13]); (Found: C, 72.30; H, 6.38. Calcd. for $C_{14}H_{13}OCl$: C, 72.26; H, 5.63%); $[\alpha]_D^{25.8}$ −6.28±0.46° (benzene, *c* 10.98); λ_{max}^{neat} 2.85 and 2.96 μ.

The *p*-Nitrophenolysis of Optically Active α-Phenylethyl Chloride in a Mixture of *p*-Nitrophenol and Acetonitrile (1 : 1 by Weight) (Run 46).—A mixture of 49.97 g. of *p*-nitrophenol, 49.89 g. of acetonitrile, and 3.75 g. of triethylamine (0.358 M, as determined by titration) was prepared. To 100 cc. of the mixture there was added 2.00 cc. (0.0150 mol.) of α-phenylethyl chloride (b. p. 43—47°C/2 mmHg; $\alpha_D^{17.0}$ +21.07°, 0.5 dm., neat). From the reaction mixture so prepared, 8 cc. of an aliquot was removed for the rate measurement; the remaining mixture was sealed into an 100-cc. ampoule and kept at 40.0°C for 54 hr. To the reaction mixture were added 150 cc. of benzene and 150 cc. of 10% aqueous sodium hydroxide. The crystals of sodium *p*-nitrophenoxide, which precipitated in an aqueous layer, were filtered off; then the benzene solution was treated in the usual manner described above. Benzene was distilled off from the dried benzene solution, and the residue was distilled in vacuo to give 1.35 g. (37% yield, based on the chloride) of α-phenylethyl *p*-nitrophenyl ether; b. p. 122—124°C/0.1 mmHg; $[\alpha]_D^{17.2}$ −1.55±0.04° (benzene, *c* 6.29); (Found: C, 69.92; H, 5.47. Calcd. for $C_{14}H_{13}O_3N$: C, 69.12; H, 5.39%). For the authentic sample, see below.

12) Ng. Ph. Buu-Hoi, H. Le Bihan and F. Binon, *J. Org. Chem.*, **17**, 246 (1952).
13) H. Hart, W. L. Spliethoff and H. S. Eleuterio, *J. Am. Chem. Soc.*, **76**, 4547 (1954).

Optically Active α-Phenylethyl *p*-Nitrophenyl Ether from Optically Active Potassium α-Phenylethoxide and *p*-Bromonitrobenzene.—Potassium α-phenylethoxide was prepared in 50 cc. of *t*-butanol (b. p. 81.8°C) from 5.10 g. (0.042 mol.) of α-phenylethyl alcohol (b. p. 68.5°C/5 mmHg, $\alpha_D^{22.3}$ +9.995°, 0.5 dm., neat) and potassium *t*-butoxide, which had been prepared by the addition of 1.41 g. (0.036 g.-atom) of potassium to *t*-butanol. After the distillation of the *t*-butanol, the excess α-phenylethyl alcohol was evaporated in vacuo, leaving 5.95 g. (0.036 mol.) of crude potassium α-phenylethoxide.

The optical purity of the potassium α-phenylethoxide was determined by the measurement of that of the recovered α-phenylethyl alcohol after the hydrolysis. A part (1.53 g.) of the potassium α-phenylethoxide was hydrolysed by the addition of 10 cc. of water; the alcohol was extracted with ether, and the oily material obtained after the evaporation of the ether was chromatographed over 25 g. of basic alumina. Ether fractions afforded 0.226 g. of acetophenone (identity established by a study of the infrared spectrum), and the ethanol fractions gave 0.574 g. of a yellow oil, which was distilled in vacuo to yield 0.4373 g. of α-phenylethyl alcohol, b. p. 75°C/6 mmHg, $\alpha_D^{24.4}$ +7.78±0.02° (0.5 dm., neat), identified by a study of the infrared spectrum.

To the solution of the optically active potassium α-phenylethoxide (1.60 g.) in dimethyl sulfoxide (50 cc., b. p. 81.0°C/2 mmHg.), 1.80 g. (0.00892 mol.) of *p*-bromonitrobenzene (m. p. 117—120°C) was added. After 17 hr. at 40.0°C under a nitrogen atmosphere, 40 cc. of ether was added to the black reaction mixture; the mixture was then washed with 50 cc. of 10% aqueous sodium chloride. The ether solution was dried with magnesium sulfate and evaporated under reduced pressure to give a black viscous mass, which was then extracted with *n*-hexane. The aqueous layer was extracted with *n*-hexane, and the combined *n*-hexane extracts were dried with magnesium sulfate and evaporated in vacuo to yield 1.4023 g. of an oil containing yellow crystals. The mixture was chromatographed over 25 g. of basic alumina. The first half of the *n*-hexane - benzene fractions gave 0.5108 g. of *p*-bromonitrobenzene (m. p. 111—119°C), while the second half afforded 0.1475 g. of α-phenylethyl *p*-nitrophenyl ether, m. p. 65.5—67.0°C; $[\alpha]_D^{25.9}$ +15.28 ±0.43° (benzene, *c* 14.22); $\lambda_{max}^{CCl_4}$ 7.97 μ.

Found: C, 68.70; H, 5.41. Calcd. for $C_{14}H_{13}O_3N$: C, 69.12; H, 5.39%.

The ether fractions afforded 0.013 g. of an oil, while the ether-ethanol (1 : 1 by volume) fractions gave 0.2527 g. of an oil. The combined oily materials were distilled under reduced pressure to give 0.1369 g. of α-phenylethyl alcohol, b. p. 58.0°C/2 mmHg, $\alpha_D^{25.6}$ +6.70±0.104° (0.5 dm., neat). From these results, the maximum specific rotation of α-phenylethyl *p*-nitrophenyl ether has been estimated to be as follows: 15.28×44.2/(7.78×6.70)=46.6° (benzene) (see text).

Optically Active α-Phenylethyl *p*-Chlorophenyl Ether from Sodium *p*-Chlorophenoxide and Optically Active α-Phenylethyl Chloride. — To ethanolic sodium ethoxide, prepared from 0.33 g. (0.0147 g.-atom) of metallic sodium and 25 cc. of 99% ethanol, there was added 1.92 g. (0.0149 mol.) of *p*-chlorophenol; the solution was then evaporated in

vacuo to give white crystalls of sodium *p*-chlorophenoxide. A solution of sodium *p*-chlorophenoxide was prepared by refluxing a mixture of the chlorophenoxide crystals so prepared and 88 cc. of dioxan (b. p. 101.0—102.0°C). α-Phenylethyl chloride (1.00 cc., 0.00760 mol., b. p. 45—46°C/1 mmHg), $\alpha_D^{16.6}$ −16.20° (0.5 dm., neat), $[\alpha]_D^{16.0}$ −35.43° (benzene, *c* 6.833) was then added to the solution, and the mixture was refluxed for 6.3 hr. The reaction mixture was concentrated, and, after the addition of 80 cc. of benzene, the solution was washed with 120 cc. of 10% aqueous sodium chloride, two 50-cc. portions of aqueous sodium hydroxide, and seven 50-cc. portions of 10% aqueous sodium chloride. The benzene layer was dried with magnesium sulfate and evaporated under reduced pressure to give an oily material, which was distilled in vacuo to afford 0.40 g., of α-phenylethyl chloride (b. p. 35—37°C/0.5—0.8 mmHg, $[\alpha]_D^{15.2}$ −35.7°, benzene, *c* 13.78) and 0.30 g. of an oil (b. p. 105—120°C/0.7—1.0 mmHg.). The redistillation of the oil afforded 0.20 g. of *p*-chlorophenyl α-phenylethyl ether, b. p. 130—140°C (bath temp., 0.5 mmHg); $[\alpha]_D^{15.2}$ −5.80±0.06°, benzene, *c* 17.23; m. p. 64.0—65.5°C (99% ethanol) (lit. m. p. 66.4—67.0°C[13]); (Found: C, 72.01; H, 5.52. Calcd. for $C_{14}H_{13}OCl$: C, 72.25; H, 5.63%); $\lambda_{max}^{CCl_4}$ 48.07 μ. The maximum specific rotation of α-phenylethyl *p*-chlorophenyl ether was estimated to be as follows: (5.80×125)/(16.20×2)=22.40° (benzene) (see text).

The Phenolysis of Optically Active α-Phenylethyl Chloride in a Phenol Benzene Mixture (1 : 1 by Weight) (Run 97).—A triethylamine solution (0.408 M) in a phenol-benzene mixture was prepared from 11.4 cc. of triethylamine and 190 cc. of a mixture of benzene and phenol (1 : 1 by weight). After the solution had been kept in a 200-cc. round-bottomed flask at 40.0°C for 0.5 hr., 5.06 g. of α-phenylethyl chloride ($\alpha_D^{17.8}$ +27.33°, 0.5 dm., neat) was added to the solution. After a 3 hr. reaction and the subsequent addition of 200 cc. of benzene, the benzene solution was washed with two 50-cc. portions of 10% aqueous sodium hydroxide, and ten 100-cc. portions of 10% aqueous sodium hydroxide, and ten 100-cc. portions of 10% aqueous sodium chloride, and then dried with magnesium sulfate. After the concentration of the solution, 7.4 g. of a yellow-brown oil was chromatrographed over 70 g. of silica-gel (Nakarai, No. F 1, 100—200 mesh). The column was eluted with *n*-hexane - benzene (1 : 1 by volume) and then with benzene, 45-cc. portions being taken. Fractions 1—6, using *n*-hexane - benzene, gave 4.204 g. of α-phenylethyl ether, m. p. 30.0—31.5°C, $\alpha_D^{16.6}$ −2.325° (0.5 dm., neat); λ_{max}^{neat} 8.07 μ, while fractions 8—15, using benzene, gave 0.980 g. of *o*-(α-phenylethyl)-phenol, b. p. 130—131°C/2 mmHg (Lit. b. p. 127—127.5°C/0.9 mmHg[14]); n_D^{30} 1.5850 (Lit.[14] n_D^{20} 1.5923); $\alpha_D^{16.6}$ −2.325° (0.5 dm. neat); λ_{max}^{neat} 2.34 μ; (Found: C, 84.26; H, 7.14. Calcd. for $C_{14}H_{14}O$: C, 84.81; H, 7.12%) and fractions 19—52, using benzene, afforded 0.914 g. of *p*-(α-phenylethyl)-phenol, m. p. 49.0-51.0°C (Lit. m. p. 56.0—56.3°C[14]); $[\alpha]_D^{21.5}$ +1.845±0.07° (benzene, C 30.37); $\lambda_{max}^{CCl_4}$ 2.73 and 2.99μ; (Found: C, 84.84; H, 6.88. Calcd. for $C_{14}H_{14}O$: C, 84.81; H, 7.12%). An intermediate fraction, 7, using benzene, 10.6 mg. of a mixture of α-phenylethyl phenyl ether and *o*-(α-phenylethyl)-phenol, and the other intermediate fractions, 16—18, afforded 39.6 mg. of a mixture of *o*- and *p*-(α-phenylethyl)-phenol. On the basis of the infrared spectra, the intermediate fractions were estimated to be 1 : 1 mixtures of the relevant two components. The total analysis was 4.209 g. (62.5% of the chloride) of α-phenylethyl phenyl ether; 1.054 g. (14.8% yield) of *o*-(α-phenylethyl)-phenol, and 0.934 g. (13.3% yield) of *p*-(α-phenylethyl)-phenol.

The Oxidation of Optically Active *p*-(α-Phenylethyl) - Phenol to α-Phenylpropionic Acid. — Optically active *p*-(α-phenylethyl)-phenol was oxidized according to the procedure of Hart and Eleuterio.[7] To a solution of 0.6722 g. (0.00339 mol.) of *p*-(α-phenylethyl)-phenol, obtained in the run 97 ($[\alpha]_D^{21.5}$ +1.845°, benzene, *c* 30.37), in 200 cc. of acetone, there was added 4.1 g. of potassium permanganate in 200 cc. of water at 13—15.5°C for 25 min. The mixture was then stirred for 1.8 hr. and acidified with 6 N sulfuric acid, and the precipitated manganese dioxide was destroyed with sodium bisulfite. The mixture was extracted with 10% sodium bicarbonate (four 50-cc. portions), and the extracts were acidified with 90-cc. of 6 N hydrochloric acid and extracted with four 50-cc. portions of benzene. The benzene solution was dried with magnesium sulfate, after the solvent had been removed, it was distilled in vacuo to give 96.8 mg. (19.0% yield) of α-phenyl-propionic acid, b. p. 120°C (bath temp., 0.2 mmHg) (Lit. b. p. 145—148°C/15 mmHg[7]); n_D^{20} 1.5239; neut. equiv. 151.4 (Calcd. 150); $[\alpha]_D^{23.1}$ +14.57° (ethanol, *c* 14.46). Since this reaction does not involve the asymmetric carbon atom, the configurations of α-phenylpropionic acid and *p*-(α-phenylethyl)-phenol should be identical. Thus, the specific rotation of optically pure *p*-(s-α-phenylethyl)-phenol may be estimated to be +10.26° (in benzene) (Lit. $[\alpha]_D$ +7.78°, benzene[15]) on the basis of the value for optically pure s-α-phenylpropionic acid, +81.1° (in ethanol).[7]

14) H. Hart, *Anal. Chem.*, **24**, 1500 (1952).

15) R. H. Pickard and W. O. Littlebury, *J. Chem. Soc.*, **89**, 467 (1906).

BULLETIN OF THE CHEMICAL SOCIETY OF JAPAN VOL. 39 307—311 (1966)

Kinetic Studies of Solvolysis. XII.* The Question of a Single Mechanism for the "Borderline" S_N Reactions — The Solvolysis of Optically Active α-Phenylethyl Chloride in Aqueous Ethanol

By Kunio OKAMOTO, Nobuko UCHIDA, Seiki SAITÔ and Haruo SHINGU

Department of Fuel Chemistry, Faculty of Engineering, Kyoto University, Sakyo-ku, Kyoto

(Received July 14, 1965)

Competitive solvolysis has been conducted in binary solvents of water and ethanol on optically active α-phenylethyl chloride at 40.0°C. The extents of inversion (α%) for solvolysis products, i. e., α-phenylethyl alcohol and α-phenylethyl ethyl ether, have been calculated from the optical rotations of these products isolated after ten half-lives, and the values of α% have been plotted vs. the volume percentage of water. In the region of 90% aqueous ethanol, the two α% lines for the alcohol and the ether intersect with each other. This intersection of the two lines conflicts with any single mechanism for the borderline S_N reactions, whereas the dual mechanism can explain this phenomenon without any difficulty. In the region of a 100% water-solvent (a typical medium for the S_N1 solvolysis), the two lines do not converge to the same α% value. On the basis of these findings, a general mechanism of racemization for the S_N1 solvolysis has also been discussed.

The single and the dual mechanisms for the "borderline" S_N reactions have been a long-standing question, and there have been several arguments in support of both sides.[1-6]

On the basis of reaction kinetics, which describes the homogeneous reaction in a solution or in the gas phase as a combination of elementary reactions (Urreaktionen[7]) with "integral" molecularity, the view[4,6] that a borderline reaction must be expressible as a sum of concurrent elementary reactions, i. e., the unimolecular (S_N1) and the bimolecular (S_N2) process, seems to be only the self-evident representation of the borderline cases; there have been in the literature several examples of borderline cases which cauld be explained on the basis of the dual mechanism.[8]

On the other hand, if one ignored the significance of the reaction-kinetical mechanism mentioned above, the view[1-3] that a single mechanism of an intermediate character operates in borderline S_N reactions might be superficially tempting inasmuch as there have been presented no definitive experimental results which are inexplicable by this single mechanism.

Thus, the question as to which picture is more reasonable has been currently described as "difficult"[9] or "to some extent a question of definition."[10]

However, Weiner and Sneen[5] recently presented data which they interpreted to mean that two distinct paths, i. e., the S_N1 and the S_N2 processes, were followed in a borderline case. Namely, when the hydrolysis of optically active 2-octyl brosylate was conducted in the presence of large amounts of sodium azide, the resulting inverted 2-octanol, formed in competition with 2-octyl azide, proved to be 100% optically pure. If one recognized that sodium azide (a strong nucleophile) would react preferentially with the S_N1 intermediate to form alkyl azide, thus preventing its conversion to alcohol, and that a nucleophilic S_N2 displacement by water would furnish inverted alcohol, the data mentioned above would consequently mean the presence of two distinct paths for the hydrolysis of 2-octyl brosylate.

In this paper we will report on a new phenomenon observed in the competitive hydrolysis and ethanolysis of optically active α-phenylethyl chloride, a phenomenon which also seems to favor the dual mechanism.

* Part XI of this series: K. Okamoto, H. Yamada, I. Nitta and H. Shingu, This Bulletin, **39**, 299 (1966).

1) S. Winstein, E. Grunwald and H. W. Jones, *J. Am. Chem. Soc.*, **73**, 2700 (1951).

2) M. L. Bird, E. D. Hughes and C. K. Ingold, *J. Chem. Soc.*, **1954**, 634.

3) C. G. Swain, *J. Am. Chem. Soc.*, **70**, 1119 (1948).

4) V. Gold, *J. Chem. Soc.*, **1956**, 4633.

5) H. Weiner and R. A. Sneen, *J. Am. Chem. Soc.*, **84**, 3599 (1962).

6) H. Shingu and K. Okamoto, "Theoretical Significance of Differentiation of the S_N1 and S_N2 Mechanism," presented at Organic Reaction Mechanism Symposium of the Chemical Society of Japan, Osaka, October, 1952.

7) A. Skrabal, "Homogenkinetik," T. Steinkopf, Dresden (1941), p. 39.

8) E. g. a) H. Shingu and K. Okamoto, *J. Chem. Soc. Japan, Pure Chem. Sect.* (*Nippon Kagaku Zassi*), **78**, 547 (1957); b) Y. Pocker, *J. Chem. Soc.*, **1959**, 3944, 3939; c) P. Casapieri and E. R. Swart, ibid., **1963**, 1254.

9) E. S. Gould, "Mechanism and Structure in Organic Chemistry," Henry Holt and Co., New York (1959), p. 258.

10) J. Hine, "Physical Organic Chemistry," 2nd ed., McGraw-Hill Book Co., New York (1962), p. 138.

The Extent of Inversion for the Products of the Competitive Solvolyses of Optically Active α-Phenylethyl Chloride in Aqueous Ethanol. —Solvolysis was conducted in mixtures of water with ethanol at 40.0°C on optically active α-phenylethyl chloride. After ten half-lives, as calculated from the rate constants interpolated from the data[11] at other temperatures, α-phenylethyl alcohol and α-phenylethyl ethyl ether with an inverted configuration, accompanied by racemization, were isolated by elution chromatography over basic alumina. The styrene were found to amount at most to 3% of the chloride in the solvent range from 50 to a 95% aqueous ethanol (see Table II). The extent of inversion for the alcohol and that for the ether were calculated from the optical rotations of these reaction products. The results are shown in Fig. 1 in the form of a plot of α% (the degree of inversion) vs. the volume percentage of water in aqueous ethanol solvents.

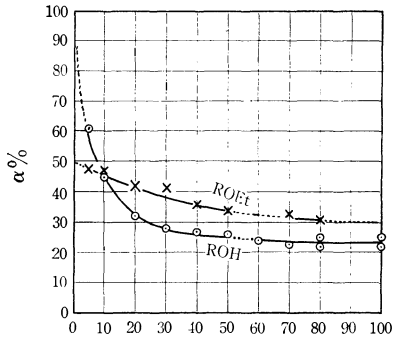

Fig. 1. Extent of inversion (α%) of solvolysis products of α-phenylethyl chloride in aqueous ethanol at 40.0°C.

For the solvent ranges of 60 to 100% water, the solvolyses were conducted under heterogeneous conditions; the reaction was continued until at least 98% of the chloride has been converted to hydrogen chloride. Despite the difference in stirring conditions, the extents of inversion for duplicate runs carried out in 100% water and in 80% water were similar to each other (see Fig. 1). Therefore, these results in heterogeneous regions seem actually to be caused by homogeneous reactions with rather low concentrations of the chloride.

As is illustrated by the α% line in Fig. 1, the degree of inversion for the α-phenylethyl alcohol so formed decreases from 61 to 25% as the water content of these binary solvents is increased from 5 to 50%; then at higher water contents it remains relatively constant at a level of from 22 to 25%.

The extent of inversion for α-phenylethyl ethyl ether also diminishes from 47 to 34% upon an increase in water content from 5 to 50%, while at higher water contents it remains at a level of about 30%.

The possible racemization of α-phenylethyl alcohol in the presence of hydrogen chloride under the reaction conditions has been ruled out, since it was found that in 90 and 70% aqueous ethanol and in water optically active α-phenylethyl alcohol was not appreciably racemized (less than 3%) in the presence of 0.1 to 0.5 N hydrogen chloride at 40.0°C for the reaction time for which each solvolysis was conducted (Table III).

An Interpretation of the Results in Solvent Ranges Close to 100% Water.—In 100% water or in the solvent ranges close to it, the solvolysis of α-phenylethyl chloride proceeds by a typical S_N1 mechanism; this may be understood as follows.

The solvolysis rate of this compound is known to be 10^5[12] as high in water as in 100% ethanol; this rate ratio is enormously high compared with the ratio (10-10^2[13]) to be expected in "S_N2" solvolyses in water and in 100% ethanol. Therefore, the possibility of inversion due to the S_N2 hydrolysis may be ruled out in these solvent ranges and the observed extent of inversion may be derived exactly from the stereochemical characteristics of the "S_N1" solvolysis.

If one assumes for the S_N1 solvolyses that an optically active S_N1 intermediate reacts with all molecules of the nucleophile on its back-side as a result of the presence of the anionic-leaving group on the front-side, and that the racemization of the product is caused only by the intramolecular inversion of the intermediate to its antipode,[14] the extents of the inversions of the products of two kinds, formed by the competitive back-side attack of nucleophiles of two kinds, should be the same as one another. Actually, however, this is not the case. The α% line for α-phenylethyl ethyl ether runs at a higher level than that for α-phenylethyl alcohol, as is illustrated in Fig. 1.

This gap in the α% lines can be explained by the following general mechanism for the racemization, a mechanism which contains a third path to the product, i. e., the front-side attack of a nucleophile on the intermediate, in addition to the above mentinoed two paths to the products (an intramolecular inversion of the intermediate and a back-side attack of a nucleophile on the intermediate). This may be schematically illustrated as follows.

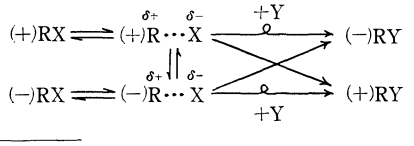

11) A. H. Fainberg and S. Winstein, *J. Am. Chem. Soc.*, **79**, 1597 (1957).

12) At 50°C, Ref. 11.

13) e. g., for the S_N2 solvolyses of methyl bromide k_{H_2O}: k_{EtOH} ratio is estimated to be 26.8 at 50°C.[1]

14) See a) K. Okamoto, K. Takeuchi and H. Shingu, This Bulletin, **35**, 525 (1962); b) H. Weiner and R. A. Sneen, *J. Am. Chem. Soc.*, **87**, 292 (1965).

According to this general mechanism for racemization, the extent of the inversion of the product is controlled not only by the intramolecular inversion of the optically active intermediates, but also by the competition of the front- and back-side attack of a nucleophile. As a result of this competition, the extents of inversion (or retention) should vary significantly with the nature of the nucleophile. In our experiments, as may be expected from this mechanism, the extents of inversion for α-phenylethyl alcohol and α-phenylethyl ethyl ether are not the same; this is reflected by the different natures of the two attacking nucleophiles, water and ethanol.

An Interpretation of the Results in Solvent Ranges Close to 100% Ethanol.—In 95% aqueous ethanol, both α-phenylethyl alcohol and α-phenylethyl ethyl ether show rather high optical purities, 61 and 47% respectively. In addition, as is illustrated in Fig. 1, the α% line of α-phenylethyl alcohol for the solvent ranges close to 100% ethanol can be extrapolated to 100% from the values for 95 and 90% aqueous ethanol solvents, whereas the α% line for α-phenylethyl ethyl ether points to a value of about 50% for a 100% ethanol solvent.

According to the dual mechanism, this would indicate that in the solvent ranges from 95 to 100% ethanol most of the water molecules react with α-phenylethyl chloride by means of S_N2 mechanism, whereas in the same solvent ranges ethanol molecules react by means of both S_N1 and S_N2 mechanisms and a significant part (at least 50%) of the ethanol molecules still react by means of the S_N1 mechanism.

The facts observed in these solvent ranges might also be explicable by the single mechanism. According to the single mechanisms,[1-3] which postulate only one transition state for a single borderline case, one could assume transition states of two kinds corresponding to the competitive hydrolysis and ethanolysis in 95% aqueous ethanol. Thus, if one uses the representation for the transition state of the single mechanism proposed by Winstein et al.,[1] the greater extent of inversion for α-phenylethyl alcohol as compared with that for α-phenylethyl ethyl ether would be explained by the greater contribution of the sturcture II[1] (see below) for the transition state containing more nucleophilic water molecules as compared with that for the transition state composed of less-nucleophilic ethanol molecules.

$$\underset{\text{I}}{Z:\ R\text{–}X} \longleftrightarrow \underset{\text{II}}{Z\text{–}R:\ X} \longleftrightarrow \underset{\text{III}}{Z:\ R:\ X}$$

(RX, α-phenylethyl chloride; Z, water or ethanol)

Furthermore, if one uses the terms[15] derived from the conception of a "concerted" displacement reaction, i. e., a single mechanism proposed by Swain,[3,15] this fact would be explicable as due to the greater "bond-making" extent at the transition state of hydrolysis as compared to that of the ethanolysis, since the extents of "bond-breaking" in ethanolysis and hydrolysis would be identical in this binary solvent.

However, as will be illustrated in the following section, the intersection of two α% lines for α-phenylethyl alcohol and for α-phenylethyl ethyl ether seems difficult to explain by any single mechanism.

The Inadequacies of the Single Mechanism in Interpreting the Intersection of Two α% Lines.—According to the single mechanism, the greater extent of inversion for α-phenylethyl alcohol than that for α-phenylethyl ethyl ether may be anticipated not only for a 95% aqueous ethanol solvent but also for the solvent ranges with a much greater water content in this binary solvent, because the contribution of the structure II or the extent of "bond-making" for the transition state composed of the water molecule with the greater nucleophilic reactivity should become greater as the content of water is increased in aqueous ethanol solvents, whereas the extent of "bond-breaking" or the contribution of the structure III in the transition state would be of the same magnitude for both hydrolysis and ethanolysis in this binary solvolytic medium.

As is illustrated in Fig. 1, however, the two α% lines intersect with each other in the region of 90% aqueous ethanol, and in the solvent ranges with a higher water content the α% line for α-phenylethyl alcohol runs at a lower level than that for α-phenylethyl ethyl ether. This is in conflict with the above-mentioned anticipation of the single mechanism, which expected the α% line for the alcohol to run at a higher level than that for the ether over the entire range of this binary solvent.

On the other hand, the intersection of two α% lines does not conflict with the dual mechanism; it may be interpreted as an incidental result of the superposition of two α% lines corresponding to the concurrency of two independent reaction, i. e., hydrolysis and ethanolysis, each of which is composed of S_N1- and S_N2-type reactions.

Experimental[16]

Materials.—The preparation of optically active and racemic α-phenylethyl chloride followed previous practice.[17] The solvolysis infinity values indicated a purity of from 98 to 99% for the chloride. Ethanol

15) C. G. Swain and W. P. Langsforf, *J. Am. Chem. Soc.*, **73**, 2813 (1951).

16) Optical rotations were measured with a Zeiss-Winkel "Kreis-Polarimeter 0.01°." The infrared spectra were obtained on a Shimadzu model IR-27. The ultraviolet spectra were obtained with an Shimadzu model UV-50M. The gas-liquid chromatograms were obtained with an Ohkura model 2100 equipped with a flame ionization detector.

17) K. Okamoto, K. Takeuchi and H. Shingu, This Bulletin, **34**, 1142 (1961).

Table I. The extents of inversion (α%) of products in solvolyses of optically active α-phenylethyl chloride in aqueous ethanol at 40.0±0.05°C

Run No.	Solvent vol. %[a] EtOH	RCl[b] M	Reaction time hr.	α_D (neat, 0.5 dm.)[c] RCl	ROH	ROEt	α%[d] ROH	ROEt
	100							(27.8)[e]
10	95	0.149	524	+9.975°	−2.15°	−3.585°	61.0	47.4
1	90	0.149	118	−21.44°	+3.44°	+7.59°	45.4	46.7
11	80	0.151	30.2	−13.240°	+1.475°	+4.20°	31.5	41.9
3	70	0.148	15.4	+12.225°	−1.190°	−3.815°	27.5	41.1
7	60	0.044	4.0	+5.755°	−0.540°	−1.580°	26.5	36.2
15	50	0.0226	1.8	−7.635°	+0.690°	+1.985°	25.6	34.4
21	40	0.0770[f]	0.8	+15.645°	−1.335°	—	24.2	—
3′	30	0.363[f]	3.9	+14.120°	−1.160°	−3.565°	23.3	33.3
20	20	0.0746[f]	0.9	+15.815°	−1.405°	—	25.1	—
4′	20	0.333[f]	1.5	−13.650°	+1.070°	+3.210°	22.2	31.0
6	H_2O	0.0750[f]	1.1	+6.060°	−0.540°	—	25.2	—
4	H_2O	0.127[f]	1.1	+6.155°	−0.488°	—	22.4	—

a) See Experimental.
b) Initial concentration of optically active α-phenylethyl chloride.
c) Taken at 24—30°C.
d) Rotations for optically pure substances were taken to be 125° for α-phenylethyl chloride (H. M. R. Hoffmann and E. D. Hughes, *J. Chem. Soc.*, **1964**, 1244.), 44.2° for α-phenylethyl alcohol (D. J. Cram, K. R. Kopecky, F. Hauck and A. Langemann, *J. Am. Chem. Soc.*, **81**, 5754 (1959)), and 94.8° for α-phenylethyl ethyl ether (K. Mislow, *J. Am. Chem. Soc.*, **73**, 4043 (1951)).
e) At 70.0°C, calculated from the data by Hughes et al. (E. D. Hughes, C. K. Ingold and A. D. Scott, *J. Chem. Soc.*, **1937**, 1201).
f) Heterogeneous conditions, mol. of RCl/1 l. of the solvent.

Table II. Composition of solvolysis products of α-phenylethyl chloride in aqueous ethanol at 40.0±0.05°C

Run No.	Solvent vol. %[a] EtOH	RCl[b] M	Reaction time hr.	Product compositon ROH[d] %	ROEt[d] %	Styrene[e] %	10^5 k_1 (sec^{-1})[c]
101	95	0.100	524	30	67	3	—
102	90	0.100	118	38	60	2	1.26
103	80	0.100	30	49	50	1	5.75
105	70	0.140	17	58	41	1	19.5
104	60	0.100	4.0	68	31.5	0.5	63.1
106	50	0.0226	2.0	78.5	21	0.5	174

a) and b) See foot notes a) and b) Table I.
c) Interpolated from the data at other temperatures.[11]
d) Analyses by gas-liquid chromatography, ROH%=ROH% (estimated by g. l. c.) - Styrene%, See Experimental.
e) Analyses by ultraviolet spectroscopy.

Table III. Racemization of α-phenylethyl alcohol in the presence of hydrogen chloride in aqueous ethanol at 40.0°C

Run No.	Solvent vol. %[a] EtOH	ROH M	HCl N	Reaction time hr.	α_D (neat, 0.5 dm.)[a] of ROH Initial	After the reaction	Racemization %
1	90	0.150	0.150	120	+5.965°	+5.965°	0.0
2	70	0.140	0.120	16	+5.985°	+6.010°	(0.0)
3	H_2O	0.120	0.100	1.3	+5.980°	+5.785°	3.3

a) Taken at 25—28°C.

was purified by the process of Lund and Bjerrum.[18] Aqueous ethanol solvents (x vol.%) were prepared by mixing x volumes of ethanol and $100-x$ volumes of water, each with temperatures of from 20 to 25°C before mixing. Racemic α-phenylethyl ethyl ether for an authentic sample was prepared by refluxing α-phenylethyl chloride (6.7 g.) in 99% ethanol (175 cc.) for 10 hr. After the usual treatment, 5.19 g. (71.2% yield) of racemic α-phenylethyl ethyl ether, b. p. 54.0°C/5 mmHg; $n_D^{30.0}$ 1.4821, was obtained. Racemic α-phenylethyl alcohol, the commercial material, was distilled in vacuo b. p. 85—86°C/7 mmHg.

Results.—The details of the results for solvolyses in aqueous ethanols are tabulated in Table I. The results of composition analyses of the solvolysis products are illustrated in Table II. α-Phenylethyl alcohol and α-phenylethyl ethyl ether were estimated by the gas-liquid chromatography of the reaction mixtures. The column was made from 4.0 mm. i. d. × 4 m. annealed copper tubing. The packing was prepared from Diasolid (60—80 mesh) using PEG 6000 as a liquid; the packing was 5% liquid phase by weight. The retention times for α-phenylethyl alcohol and α-phenylethyl ethyl ether were, respectively, 7.5—8.5 and 17.5—18.0 min.; these times were determined at 160°C using nitrogen as the carrier gas (flow rate 50—60 cc./min.). Because of the failure to separate the styrene peak and the α-phenylethyl alcohol peak under the operation conditions of this chromatography, the concentration of styrene in the reaction mixtures was estimated by ultraviolet spectroscopy, using 244 mμ as a characteristic band for styrene. The cell length was 1 cm.; one volume of the reaction mixture was diluted with 99 volumes of distilled water. Absorbances caused by the benzenoid absorption of α-phenylethyl alcohol and α-phenylethyl ether were subtracted from the observed styrene absorbance of the sample. The precentage of α-phenylethyl alcohol as estimated by gas-liquid chromatography was corrected by the subtraction of the styrene percentage.

The results of racemization experiments for α-phenylethyl alcohol in the presence of hydrogen chloride are illustrated in Table III. The details of procedures for the isolation of the solvolysis products and for the racemization experiments of α-phenylethyl alcohol are illustrated in the descriptions of some representative runs which follow.

The Solvolysis of Optically Active α-Phenylethyl Chloride in 80 vol.% Aqueous Ethanol at 40.0°C.—To 100 cc. of 80 vol.% aqueous ethanol in a 200-cc. round-bottomed flask maintained at 40.0°C, 2.16 g. (0.0154 mol.) of α-phenylethyl chloride, $\alpha_D^{24.9}$ −13.240° (0.5 dm., neat); b. p. 56.0°C/3 mmHg. was added. After it has been maintained for 30.2 hr. at 40.0±0.05°C, the reaction mixture was neutralized with 0.65 g. of sodium hydroxide pellets and then fractionally distilled to give 80 cc. of ethanol, b. p. 77—80°C. To the residue 7.0 g. of sodium chloride was added, and the organic layer was extracted with three 15-cc. portions of ether. The concentration of the combined ether solutions, dried with magnesium sulfate, afforded an oily material which was distilled in vacuo to give 1.01 g. of the mixture of α-phenylethyl alcohol and α-phenylethyl ethyl ether, b. p. 55—60°C/5—4 mmHg. The mixture was then chromatographed over 25 g. of basic alumina. The fractions (No. 1—5, for each 25 cc.) eluted with n-hexane consisted of α-phenylethyl ethyl ether, (0.29 g., b. p. 37°C/2 mmHg; $\alpha_D^{24.2}$ +4.20° (0.5 dm., neat) n_D^{30} 1.4840). α-Phenylethyl alcohol (0.309 g.; b. p. 64°C/3 mmHg; $\alpha_D^{25.2}$ +1.475° (0.5 dm., neat) n_D^{30} 1.5231) was eluted with 99% ethanol fractions (Nos. 8 and 9, for each 15 cc.). The alcohol and the ether showed infrared spectra identical with those of the authentic samples.

The Heterogeneous Solvolysis of Optically Active α-Phenylethyl Chloride in Water.—To 110 cc. of water, maintained at 40.0°C, in a 100-cc. four-necked flask equipped with a reflux condenser, a stirrer and a thermometer, there was added 2.00 g. (0.0142 mol.) of α-phenylethyl chloride, $\alpha_D^{24.1}$ +6.155° (0.5 dm., neat); b. p. 54.0°C/5 mmHg, in one portion. After a 0.7 hr. stirring, the reaction mixture was extracted with five 20-cc. portions of ether. The concentration of the combined ether solutions, dried with magnesium sulfate, afforded 1.76 g. of an oily material which was then distilled in vacuo to give 1.47 g. of α-phenylethyl alcohol, $\alpha_D^{24.4}$ −0.488° (0.5 dm., neat); n_D^{30} 1.5239; b. p. 66°C/5 mmHg; identical infrared spectrum with an authentic sample.

An Examination of the Racemization of Optically Active α-Phenylethyl Alcohol in 90% Aqueous Ethanol in the Presence of 0.15 N Hydrogen Chloride.—To 54 cc. of 0.15 N hydrogen chloride in 90% aqueous ethanol, prepared by mixing 7.00 cc. of concentrated hydrogen chloride and 63 cc. of 100% ethanol in a 100-cc. round-bottomed flask, 1.00 g. (0.00821 mol.) of α-phenylethyl alcohol ($\alpha_D^{22.9}$ +5.965° (0.5 dm., neat)) was added. After it had stood for 120 hr. at 40.0°C, the mixture was neutralized with 0.30 g. of sodium hydroxide pellets (silightly basic to litmus) and then fractionally distilled to give 36 cc. of ethanol. To the residue 10 g. of sodium chloride was added; it was then extracted with five 15-cc. portions of ether. The combined ether extracts were concentrated and distilled in vacuo to give 0.80 g. of α-phenylethyl alcohol, b. p. 84°C/6 mmHg, $\alpha_D^{24.9}$ +5.965° (0.5 dm., neat.)

The authors wish to thank Mr. Yoshihisa Matsui for his assistance in the analyses of styrene.

18) L. F. Fieser, "Experiments in Organic Chemistry," 3rd ed., D. C. Heath and Co., Boston (1955), p. 286.

BULLETIN OF THE CHEMICAL SOCIETY OF JAPAN VOL. 39 312—315 (1966)

The Volatile Constituents of Some Plants of the Compositae Family

By Naoko TSUBAKI, Kiichi NISHIMURA and Yoshio HIROSE

The Institute of Food Chemistry, Kita-ku, Osaka

(Received May 27, 1965)

Full analyses of the essential oils obtained from Yomena (*Aster indicus* L.), Yomogi (*Artemisia princepts* Pamp.) and Hog weed (*Ambrosia elatior* L.) were carried out. Each essential oil was separated by fractional distillation under reduced pressure, and the fractions thus obtained were identified.

The so-called Yomena and Yomogi (the *Aster indicus* L. and *Artemisia princepts* Pamp. respectively) are the most common plants of the Compositae family which grow wild all over in Japan. Hog weed (*Ambrosia elatior* L.), which was derived from North America at the beginning of the Meiji era, has been naturalized and is widely distributed in this country now.

Some studies have been reported on the essential oils obtained from these plants. Uchida[1], for instance, analyzed the oil derived from all ground parts of the Yomena obtained in the northeastern district of China and found dipentene, bornyl formate, bornyl acetate, a monoterpene alcohol with a myrtenol-like odor, a sesquiterpene hydrocarbon, and a monocyclic tertiary sesquiterpene alcohol. Nakao and Shibue[2] isolated cineol and α-thujone from the volatile oil derived from Japanese Yomogi grass, and Sörensen[3] identified a polyacetylene compound called dehydromatricaria ester in the same plant of foreign origin.

This paper will present full analyses of the essential oils obtained from these three plants of the Compositae family, Yomena, Yomogi, and hog weed.

Method

The analyses of these oils were carried out as follows. Each essential oil was subjected to fractional distillation under reduced pressure with a Podbielniaks 13 mm. Heli-Grid column, and the fractions thus obtained were analyzed by gas chromatography (GLC) and infrared spectroscopy (IR). Further fractionations by means of column chromatography on silicic acid were applied to the fractions which seemed to be complicated. Moreover, for the final estimation these methods were supplemented with ultraviolet spectroscopy, nuclear magnetic resonance spectroscopy and mass spectrometry (MS).

Gas Chromatography.—Gas chromatography was carried out using a Shimadzu GC-2C-type gas chromatograph with polyethylene glycol (30%) on celite and a Hitachi F-6 gas chromatograph with a capillary column (HB-2000). In both of these cases, nitrogen was adopted as the carrier gas.

Liquid Chromatography. — Mallinchrodt's silicic acid was used as the adsorbent, and a hexane solution of ether (3%, 5%, 10%, 30%), as the elute solvent.

Mass Spectrometry.—The mass spectrometry was measured by means of a Hitachi mass spectrometer, RMU 6-type, under the following conditions: ionization voltage, 80 V.; ion source temperature, 250°C, ion accelerative voltage, 2 kV.; inlet vapor temperature, 150°C.

Experimental and Results

Yomena Oil.—Eighty-seven kilograms of the leaves and above-ground parts of the grass gathered at the beginning of October was steam-distilled; 34 cc. of the essential oil was thus obtained. This oil was subjected to fractional distillation and divided into seven fractions. The distillation residue was then steam-distilled to recover the higher boiling components.

The results are summarized in Table I.

TABLE I. FRACTIONS OF THE YOMENA OIL

Fraction No.	Volume ml.	Calcd. b. p. °C/760 mmHg
1	2	170—223
2	2	223—247
3	2	247—251
4	2	251—266
5	2	266—267
6	2	267—268
7	3.5	268—271
Steam-distd. fraction	2.5	—
Residue	15.0	—

1) S. Uchida, *J. Soc. Chem. Ind., Japan* (*Kôgyo Kwagaku Zasshi*), **29**, 124 (1926).
2) M. Nakao and C. Shibue, *J. Pharm. Soc. Japan* (*Yakugaku Zasshi*), **1924**, 639.
3) K. Stavholt and N. A. Sörensen, *Acta Chem. Scand.*, **4**, 1567 (1950).

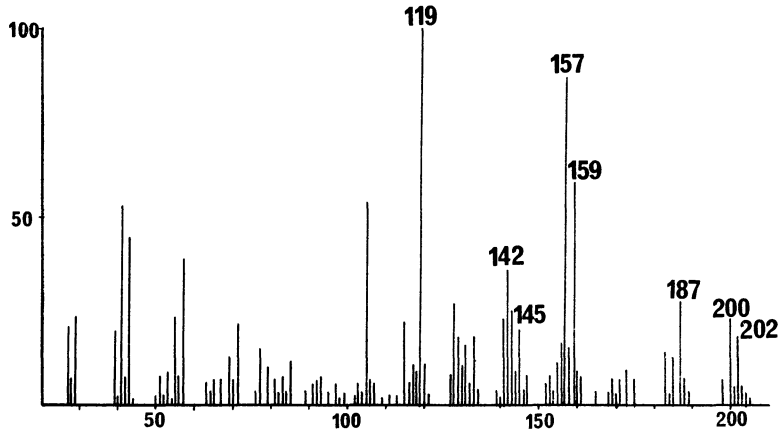

Fig. 1. The mass spectrum of calamenene fraction.

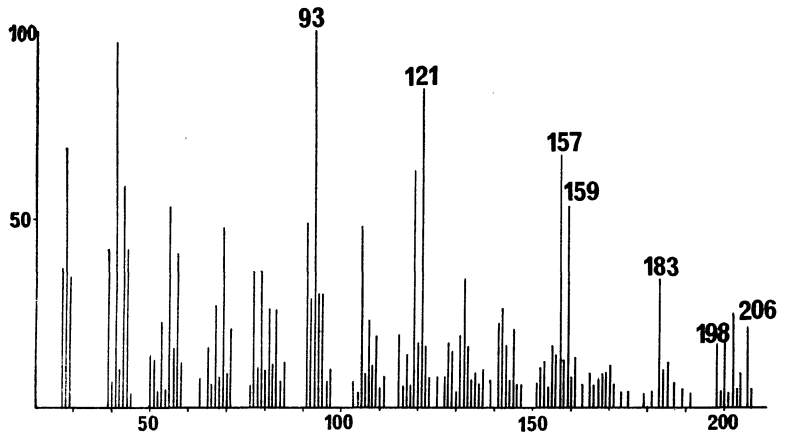

Fig. 2. The mass spectrum of calamenene and calacorene fraction.

Fraction 1 contained *p*-cymene, limonene, bornyl acetate, citronellyl acetate, phenylethyl acetate, borneol and terpineol. A hydrocarbon which was very similar to myrcene in its IR spectrum but not in its GLC was isolated from this fraction. Its spectroscopic character (IR: 6.1, 6.2, 9.02, 10.1, 11.2, 13.2 μ. UV: $\lambda_{max}^{Ethanol}$ 234.9 mμ) indicates the presence of conjugated dienes, at least one of which has an end methylenic feature. This is further supported by the fact that the hydrocarbon suffers oxidation and polymerization rather soon after being exposed to the atmosphere. These characteristics suggest that the hydrocarbon is likely to be ocimene.

Fractions 2 to 4 were found to contain β-elemene as the main constituent, together with small amounts of bornyl acetate, benzyl alcohol, camphor, borneol and phenylethyl alcohol.

Fractions 5 to 7 and the volatile part recovered from the distillation residue were composed solely of sesquiterpene hydrocarbons. From these fractions, β-elemene, caryophyllene, humulene, α-curcumene, calamenene, δ-cadinene and γ-cadinene were identified by means of IR and GLC measurements. In addition to these compounds, a hydrocarbon corresponding to β-selinene in GLC was isolated. Its MS spectrum was also very similar to that of β-selinene. However, the IR and MS spectra of β-selinene has no remarkable characteristics to distinguish them from others, and further attempts to identify it definitely were discontinued because of the limited amount of material available.

The volatiles recovered from the distillation residue contained humulene, caryophyllene, γ- and δ-cadinene, calamenene and a sesquiterpene hydrocarbon whose IR spectrum was very similar to β-cadinene. The calamenene separated by the chromatography of this fraction was shown to include calacorene by IR, GLC and MS spectrum studies. The MS spectrum of calamenene fraction is shown in Fig. 1.

The peaks at *m/e* 187, 159, 145 and 202 are derived by the fragmentation of calamenene (MW. 202), while the peaks at *m/e* 200, 185, 157 and 142 are derived by the fragmentation of calacorene (MW.

200). These fragments can be illustrated as follows:

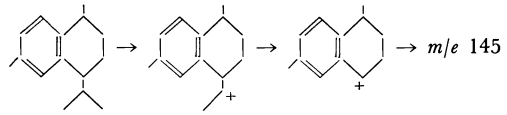

Calamenene

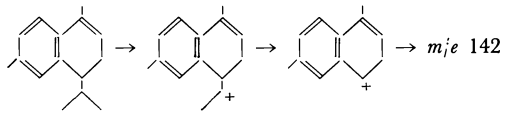

Calacorene

The compounds identified from Yomena oil are listed in Table II.

Table II. Compounds identified from Yomena oil

Compound	Content, %
p-Cymene	0.4
Ocimene ?	0.9
Limonene	0.3
Aromatic hydrocarbon	0.3
Borneol	0.3
Camphor	0.3
Bornyl acetate	6.1
Citronellyl acetate	+
Terpinyl acetate	+
Phenylethyl acetate	+
Terpineol	+
Phenylethyl alcohol	+
Benzyl alcohol	0.3
β-Elemene	22.8
Caryophyllene	2.9
Humulene	4.9
γ-Cadinene	3.4
δ-Cadinene	0.7
β-Cadinene	+
α-Curcumene	1.3
Calamenene	4.2
Calacorene	2.8

Yomogi Oil.—Yomogi oil (160 cc.) obtained by the steam distillation of 58 kg. of the grass dried in the shade was submitted to fractional distillation under diminished pressure and then divided into 16 fractions. A mixture of borneol and camphor (15 g.) was removed from the pot material by filtration in the course of distillation, because the crystallization of those compounds at the take-off arm of the distillation column obstructs further operation; the distillation was then carried on again. The distillation residue was steam-distilled to recover the volatiles (Fraction 17).

The results are summarized in Table III.

Fractions 1 to 3 consisted of α-pinene, camphene, myrcene, *p*-cymene and cineol, which was the principal constituent of these fractions.

Table III. Fraction of the Yomogi oil

Fraction No.	Volume ml.	Calcd. b. p. °C/760 mmHg
1	5	165—184
2	5	184
3	5	184
4	10	184—208
5	10	208—211
6	1	211—213
7	5	213—235
8	5	235—268
9	5	268—269
10	6	269
11	4	269—276
12	2	276—281
13	2	281—285
14	4	285—287
15	2	287—288
16	4	288—290
17	4	—
Residue	71	—

γ-Terpinene, cineol, artemisia ketone, matsutakeol and α-thujone were separated from Fraction 4 by column chromatography. Artemisia ketone was identified by comparing its IR, MS spectra and GLC results with those of an authentic sample*1 obtained from the volatile oil of *Artemisia annua* L.

Fractions 5 to 7 contained bornyl acetate, camphor, piperitone and borneol. A sesquiterpene hydrocarbon which was separated by the chromatography of Fraction 7 displayed major absorption peaks in the IR spectrum at 11.1 and 14.3 μ and gave predominant peaks in its MS spectrum at *m/e* 189, 175, 161 and 119 (base peak) indicating that it might be a patchoulene-type compound.

Fraction 8 contained ylangene, caryophyllene, β-elemene, creosol, borneol and an aromatic acid. Fractions 9 and 10 consisted mainly of caryophyllene. As Fractions 8 to 10 were shown to contain some carbonyl compounds by a study of their IR spectra, a mixture of these fractions was treated by a Girard T reagent in the usual manner; the small amounts of carbonyl compounds were separated which were shown by GLC to contain at least three compounds. One of them was identified as α-ionone by means of IR, MS spectra and GLC.

Fractions 11 to 16 contained β-elemene, caryophyllene, humulene, curcumene, γ-cadinene, δ-cadinene and a sesquiterpene keotne, which gave a 2, 4-dinitrophenyl hydrazone (m. p. 167—173°C). The chromatographic fraction containing calamenene and calacorene separated from Fraction 17 was shown by its MS spectrum to include two additional hydrocarbons.

*1 The authors wish to thank Professor Tsunematsu Takemoto for providing us with an authentic sample of artemisia ketone.

The two series of peaks at *m/e* 202 and 159 and at *m/e* 200 and 157 are derived by the fragmentation of calamenene and calacorene respectively. The peaks at *m/e* 206, 121 and 93 show the existence and the fragmentation of a perhydro-sesquiterpene hydrocarbon whose molecular weight is 206. The peaks at *m/e* 198 and 183 are derived from a dehydrogenated sesquiterpene hydrocarbon, which is likely to be a naphthalene compound, such as cadalene or eudalene, with a molecular weight of 198.

The results of the analysis of Yomogi oil are shown in Table IV.

Table IV. The constituents of Yomogi oil

Compound	Content, %
α-Pinene	0.6
Camphene	1.6
Myrcene	1.5
p-Cymene	0.2
γ-Terpinene	2.2
Cineol	3.2
Artemisia ketone	2.5
Matsutakeol	2.7
α-Thujone	1.0
Bornyl acetate	2.5
Camphor	10.5
Piperitone	0.5
Borneol	15.4
α-Ionone	+
Creosol	0.2
Ylangene	1.0
Caryophyllene	2.9
β-Elemene	+
Humulene	4.1
γ, δ-Cadinene	2.6
β-Cadinene	0.5
α-Curcumene	5.2
Calamenene	1.6
Calacorene	0.5
β-Selinene ?	0.1
Hydrocarbon (MW 206)	+
Hydrocarbon (MW 198)	+
Sesquiterpene hydrocarbon	0.1
Sesquiterpene ketone	0.9

Hog Weed Oil.—Upon the steam distillation of the hog weed grass (60 kg.) collected in the middle of October, 19 cc. of volatile oil was obtained. The oil was subjected to fractional distillation and was divided into four fractions (Table V). Each fraction was treated in the way described above.

Table V. Fraction of hog weed grass oil

Fraction No.	Volume ml.	Calcd. b. p. °C/760 mmHg
1	2.9	155—190
2	2	190—252
3	2	252—273
4	0.7	273—300

Fraction 1 consisted solely of monoterpene hydrocarbons; the gas chromatogram of this fraction showed that these hydrocarbons were α-pinene, camphene, β-pinene, myrcene and limonene.

Fractions 2 to 4 consisted of rather complicated sesquiterpene hydrocarbons and contained at least nine compounds. The chromatographic analyses of those fractions showed the presence of ylangene, δ-cadinene, γ-cadinene and curcumene. As to the other compounds, however, no further characterization could be attained owing to the small quantities of them available and difficulties in separating them from each other.

The composition of hog weed oil is shown in Table VI.

Table VI. Composition of the volatile fraction of hog weed grass

Compound	Content, %
α-Pinene	4.7
Camphene	0.1
β-Pinene	0.5
Myrcene	0.5
Limonene	9.8
Ylangene	0.5
δ-Cadinene	2.5
γ-Cadinene	2.0
α-Curcumene	5.0
Unidentified five hydrocarbons	24.3

Summary

Volatile oils obtained from three kinds of plants of the Compositae family have been analyzed.

Yomena oil contained *p*-cymene, ocimene, limonene, borneol, camphor, bornyl acetate, citronellyl acetate, terpinyl acetate, phenylethyl acetate, terpineol, phenylethyl alcohol, benzyl alcohol, β-elemene, caryophyllene, humulene, γ-cadinene, δ-cadinene, β-cadinene, α-curcumene, calamenene, calacorene, and an aromatic hydrocarbon.

Yomogi oil contained α-pinene, camphene, myrcene, *p*-cymene, γ-terpinene, cineol, artemisia ketone, matsutakeol, α-thujone, bornyl acetate, camphor, piperitone, borneol, α-ionone, creosol, ylangene, caryophyllene, β-elemene, humulene, γ-cadinene, δ-cadinene, β-cadinene, α-curcumene, calamenene, calacorene, β-selinene, three kinds of sesquiterpene hydrocarbon, and a sesquiterpene ketone.

Hog weed oil contained α-pinene, camphene, β-pinene, myrcene, limonene, ylangene, δ-cadinene, γ-cadinene, α-curcumene and five unidentified hydrocarbons.

BULLETIN OF THE CHEMICAL SOCIETY OF JAPAN VOL. 39 316—320 (1966)

The Reactions of *cis, trans, trans*-1, 5, 9-Cyclododecatriene. IV.[1] Selective Reactions with *cis*-Addition Reagents

By Masaji OHNO, Masaru OKAMOTO and Seiichi TORIMITSU

Basic Research Laboratories, Toyo Rayon Company Ltd., Tebiro, Kamakura

(Received June 1, 1965)

The addition reactions of *cis, trans, trans*-1, 5, 9-cyclododecatriene with *cis*-addition reagents, such as osmium tetroxide, potassium permanganate, diimide, and nitrosyl chloride, have been investigated. It has been shown that the first attack of each reagent preferentially takes place at one of the *trans* double bonds. The reactions with osmium tetroxide and potassium permanganate at room temperature afforded *cis*-5, *trans*-9-cyclododecadiene-*trans*-1, 2-diol in 89 and 59% yields respectively. The glycol was then further oxidized with osmium tetroxide into *cis*-9-cyclododecene-1, 2, 5, 6-tetrol in a 60% yield. The reduction of the cyclotriene with diimide, generated in situ by the oxidation of hydrazine, afforded *cis*-cyclododecene in 60—82% yields. The addition of nitrosyl chloride in the presence of hydrochloric acid afforded 2-chlorocyclododecadienone oxime in a quantitative yield; this was then reduced into cyclododecanone oxime, obtained in a quantitative yield, by catalytic reduction with palladium-charcoal.

The discovery of an elegant synthesis of *cis, trans, trans*-1, 5, 9-cyclododecatriene (I) by means of the cyclotrimerization of butadiene with Ziegler catalysts[2,3] has prompted investigations into the reactions of this cyclotriene; the results of these investigations are summarized in Table I. On the basis of our own findings and these previous results, we would like to point out that the competitive reactivities between the *cis* and *trans* double bonds are closely connected with the mode of the addition of reagents.

The oxidation of *cis, trans, trans*-1, 5, 9-cyclododecatriene with osmium tetroxide or potassium permanganate showed a high selectivity and afforded *cis*-5, *trans*-9-cyclododecadiene-*trans*-1, 2-diol; the results are shown in the following scheme:

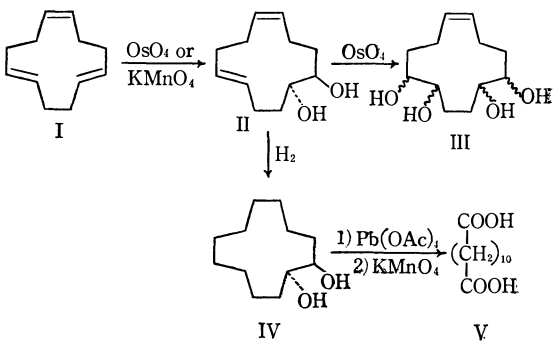

TABLE I. REACTIONS WITH VARIOUS REAGENTS

Reagent	Mole	Product	Addition mechanism	Double bond preferentially attacked	Yield, %	Ref.
Br_2	1	1-Bromocyclododecatriene Tetrabromocyclododecene	*trans*	no selectivity	61 20—30	7
Br_2	2	Tetrabromocyclododecene	*trans*	*cis* and *trans*	20—40	5, 7
Cl_2	1	Dichlorocyclododecadiene	*trans*	no selectivity	70	7
$PhCO_3H$	1	Monoepoxide	*cis*	*trans*	80—90	4, 5a
$PhCO_3H$	2	Diepoxide	*cis*	*trans* and *cis*	80	4, 5a
H_2O_2-HCO_2H	1	Monoepoxide	*cis*	*trans*	76	5b
Et_2BH	3	$(C_{12}H_{21})(BEt_2)_3$	*cis*	*	80	6
$HCl/FeCl_3$	Excess	Mono- and dichlorides	*trans*	no selectivity	20—40	8
$AcOH/BF_3$	Excess	Monoacetate	*trans*	no selectivity	50	8

* It was observed that the *trans* double bond reacted faster than the *cis* one.

1) Part III of this series: M. Ohno, M. Okamoto and N. Naruse, *Tetrahedron Letters*, in press (1965). Presented at the 15th Symposium on Organic Reaction Mechanisms of the Chemical Society of Japan, Nagoya, October, 1964.

2) G. Wilke, *Angew. Chem.*, **69**, 97 (1957).

3) G. Wilke, ibid., **75**, 10 (1963).

4) G. Wilke, *J. Polymer Sci.*, **38**, 45 (1959).

5) a) L. I. Zakharkin and V. V. Korneva, *Dokl. Akad. Nauk S. S. S. R.*, **132**, 1078 (1960); b) H. Takahashi and M. Yamaguchi, This Bulletin, **36**, 1390 (1963).

6) R. Köster and G. Griaznov, *Angew. Chem.*, **73**, 171 (1961).

7) H. Takahashi and M. Yamaguchi, *J. Chem. Soc. Japan, Pure Chem. Sect.* (*Nippon Kagaku Zasshi*), **83**, 1042 (1962).

8) L. I. Zakharkin, V. V. Korneva and A. V. Iogansen, *Dokl. Akad. Nauk S. S. S. R.*, **138**, 378 (1961).

cis, trans, trans-1, 5, 9-Cyclododecatriene in aqueous acetone was treated with a one-mole equivalent of potassium permanganate with stirring while being kept at 20°C. A colorless crystalline material, m. p. 168—169°C, was batined in a 59% yield and was proved to be *cis*-5, *trans*-9-cyclododecadiene-*trans*-1, 2-diol (II) by an elemental analysis of it and a study of its infrared spectrum. The infrared spectrum showed that the absorption intensity characteristic of the *trans* double bond at 980 cm^{-1} decreased, while that of the *cis* double bond at 707 cm^{-1} remained unchanged, showing that only one of the *trans* double bonds was subjected to the oxidation. The glycol was quantitatively converted into known cyclododecane-*trans*-1, 2-diol[9] (IV), m. p. 102—103°C, by catalytic hydrogenation; in turn this was converted into known dodecanedioic acid[10] (V) oxidation with lead tetraacetate and then with potassium permanganate. The same *cis*-5, *trans*-9-cyclododecadiene-*trans*-1, 2-diol was also obtained in a 89% yield from a reaction with a one-mole equivalent of osmium tetroxide at room temperature.

The further oxidation of *cis*-5, *trans*-9-cyclododecadiene-1, 2-diol with osmium tetroxide gave *cis*-9-cyclododecane-1, 2, 5, 6-tetrol (III), m. p. 212—214°C, in a 60% yield. The infrared spectrum showed only an absorption characteristic of the *cis* double bond at 707 cm^{-1}; the catalytic hydrogenation of the unsaturated tetrol yielded cyclododecane-1, 2, 5, 6-tetrol, showing no infrared absorption at 707 cm^{-1}.

Clearly, the first attack by such reagents takes place at one of the *trans* double bonds, and there is difference enough in reactivity between the *cis* and *trans* double bonds to control the product.

The above oxidation provides a simple method of preparing cyclododecane-*trans*-1, 2-diol, which has previously been obtained by a reaction of *trans*-cyclododecene with osmium tetroxide.[9]

Next, the reduction of *cis, trans, trans*-1, 5, 9-cyclododecatriene with diimide has been investigated in order to clarify which double bond of I is more easily reduced with diimide. As for other olefins, Hünig[11] showed that fumaric acid is more rapidly reduced than maleic acid with diimide, although Aylward[12] showed that elaidic acid is more slowly reduced than oleic acid.

cis, trans, trans-1, 5, 9-Cyclododecatriene dissolved in ethanol was treated with a large excess of hydrazine hydrate in the presence of a catalytic amount of cupric sulfate with a vigorous bubbling-in of air and with vigorous stirring for 24—48 hr. The reaction was found to be highly exothermic. Aliquots of the reaction mixture were subjected to spectroscopic and vapor-phase chromatographic analyses at intervals.

Their infrared spectra showed that only the absorption intensity at 980 cm^{-1} for the *trans* double bond decreased; that at 707 cm^{-1} for the *cis* double bond remained unchanged during the reaction.

Vapor-phase chromatography showed the presence of three components. On the basis of their retention times, two of them were confirmed to be the starting material and *cis*-cyclododecene (VII); another fraction was attributed to *cis, trans*-1, 5-cyclododecadiene (VI). No detectable amount of *trans*-cyclododecene was identified. The reaction was continued until the absorption band at 980 cm^{-1} essentially disappeared, affording a colorless liquid, b. p. 64—65°C/1.0 mmHg, in 60—82% yields from the reaction product. Vapor-phase chromatography using PEG 6000 showed that the liquid was 90—95% *cis*-cyclododecene (VII) and 5—10% cyclododecane. Pure *cis*-cyclododecene was esaily obtained by preparative gas chromatography; its infrared spectrum is completely identical with that of an authentic sample.[9] The above reactions are shown in the following scheme:

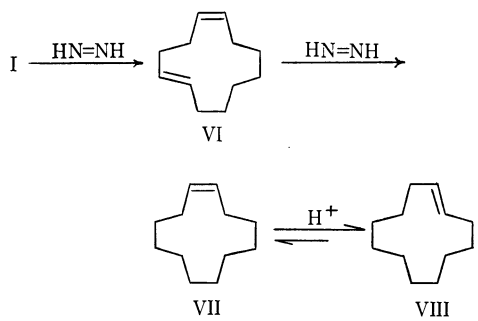

On the other hand, when the cyclododecene was subjected to equlibration by Cope's method,[13] it afforded a mixture of *trans*-cyclododecene (VIII) and *cis*-cyclododecene (VII) in a ratio of about 2 to 1.

Therefore, the attack by diimide takes palce more easily at the *trans* double bonds, and the reduction presents a simple and valuable method of synthesizing *cis*-cyclododecene, which has previously been prepared by a tedious method.[9]

Finally, the reaction of the cyclododecatriene with nitrosyl chloride was studied. The addition of one mole equivalent of nitrosyl chloride in the presence of hydrochloric acid to *cis, trans, trans*-1, 5, 9-cyclododecatriene (I), in either methylene chloride at −10°C or trichloroethylene at 10°C, was found to be exothermic and to provide 2-chlorocyclododecadienone oxime in nearly quantitative yields. It melted at 110—115°C, even after several recrystallizations from ligroin, and it was easily

9) V. Prelog and M. Speck, *Helv. Chim. Acta*, **38**, 1786 (1955).
10) J. Walker, *J. Chem. Soc.*, **1940**, 1304.
11) S. Hünig and H. R. Müller, *Angew. Chem.*, **74**, 215 (1962).
12) F. Aylward and M. Sawistowska, *Chem. & Ind.*, **1962**, 484.
13) A. C. Cope, P. T. Moore and W. R. Moore, *J. Am. Chem. Soc.*, **82**, 1744 (1960).

Table II. Reactions with *cis*-addition reagents

Reagent	Mole	Product	Double bond preferentially attacked	Yield, %
OsO_4	1	*cis*-5, *trans*-9-Cyclododecadiene-*trans*-1, 2-diol (II)	*trans*	89
OsO_4	2	*cis*-9-Cyclododecene-1, 2, 5, 6-tetrol (III)	*trans*	60
$KMnO_4$	1	*cis*-5, *trans*-9-Cyclododecadiene-*trans*-1, 2-diol (II)	*trans*	59
HN=NH	Excess	*cis*-Cyclododecene (VII)	*trans*	60—82
NOCl/HCl	1	2-Chlorocyclododecadienone oxime (IXa and IXb)	*trans*	95

hydrogenated to a known cyclododecanone oxime (X) by catalytic reduction. Its infrared spectra showed only that the absorption intensity at 980 cm^{-1} characteristic of the *trans* double bond decreased and that the one at 707 cm^{-1} characteristic of the *cis* double bond remained unchanged. Therefore, the product is probably a mixture of 2-chloro-*cis*-5, *trans*-9-cyclododecadienone oxime (IXa) and 2-chloro-*trans*-5, *cis*-9-cyclododecadienone oxime (IXb).

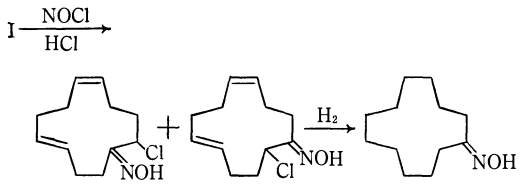

XIa XIb X

All the results obtained above are summarized in Table II.

Discussion

The results obtained by the present investigation have shown clearly that the first attack by *cis*-addition reagents, such as osmium tetroxide,[14] potassium permanganate, diimide,[15] and nitrosyl chloride,[16-18] takes place at one of the *trans* double bonds of *cis*, *trans*, *trans*-1, 5, 9-cyclododecatriene, and that, as far as *cis* addition reagents are concerned, there is difference enough in reactivity between the *cis* and *trans* double bonds to control the product.

Obviously, the selectivity of the reactions of *cis*, *trans*, *trans*-1, 5, 9-cyclododecatriene depends on the addition mechanism of the reagents, as is shown in Tables I and II.

A survey of *cis*, *trans*, *trans*-1, 5, 9-cyclododecatriene using the Dreiding model shows that there is no considerable difference in steric approach control toward the *cis* and *trans* double bonds, and that the cyclic system is so flexible that no rigid conformation can be considered.

cis, *trans*, *trans*-1, 5, 9-Cyclododecatriene is very stable to usual Lewis acids and bases[3]; this suggests that there is no marked difference in the thermodynamic stability of the *cis* and *trans* double bonds.

The reactions of mixture of *cis*- and *trans*-cyclododecene with osmium tetroxide[19] and nitrosyl chloride[3] also show a high selectivity, high enough to control the product; thus, only *trans*-cyclododecene can be converted into addition products. Therefore, it may be reasonable to assume that the reactivity of the *cis* and *trans* double bonds of *cis*, *trans*, *trans*-1, 5, 9-cyclododecatriene is very similar to that of a mixture of *cis*- and *trans*-cyclododecene.

On the other hand, Cope[20] has shown that there is a slight predominance of the *trans* isomer at equilibrium for cyclododecene (ΔF=0.49 kcal./mol.).

More strained acyclic olefins or *cis* olefins react much faster than *trans* olefins with *cis*-addition reagents, as has been demonstrated by Brown[21] in the case of the hydroboration of olefins.

However, the present investigation has disclosed that the more stable *trans* double bond of the 12-membered ring reacts preferentially with *cis*-addition reagents; no satisfactory explanation of this can be obtained from a discussion of the thermodynamic stability of the normal state of the starting material.

Such competitive reactivities might be explained in terms of the conformational stability at four-, five- and six-center transition states or intermediates in the *cis*-addition reactions. The transition states or intermediates for the *trans* double bonds seem to be more stable than those for the *cis* double bond because of the difference in eclipsing effect.[22]

Experimental

All melting points are uncorrected.

The Reaction of *cis*, *trans*, *trans*-1, 5, 9-Cyclododecatriene (I) with Potassium Permanganate.—

14) E. L. Eliel, "Stereochemistry of Carbon Compounds," McGraw-Hill Book Company, Inc., New York (1962), p. 358.
15) E. J. Corey, D. J. Pasto and W. L. Mock, *J. Am. Chem. Soc.*, **83**, 2957 (1961).
16) J. Meinwald, Y. C. Meinwald and T. N. Baker, III, ibid., **86**, 4074 (1964).
17) W. J. Serfontein, J. H. Jordaan and J. White, *Tetrahedron Letters*, **1964**, 1909.
18) R. U. Lemieux, T. L. Nagabhushan and I. K. Oneill, ibid., **1964**, 1909.
19) M. Ohno, unpublished results. The *trans*-olefin reacts much faster than the *cis* one.
20) A. C. Cope, P. T. Moore and W. R. Moore, *J. Am. Chem. Soc.*, **81**, 3153 (1959).
21) H. C. Brown and A. W. Moerikofer, ibid., **83**, 3417 (1961).
22) D. Y. Curtin and D. B. Kellom, ibid., **75**, 6011 (1953).

The cyclotriene[23] (I, 10 g.), dissolved in 200 ml. of acetone, and 40 ml. of water were placed in a 500-ml. three-necked flask equipped with a stirrer, a thermometer, and a reflux condenser. Potassium permanganate (7 g.) was added into the solution in small portions, and then the mixture was cooled at 20°C for one hour. After the reaction mixture had been stirred for 2 more hr. at room temperature, a solid fraction was removed by filtration and washed with 50 ml. of acetone. After the acetone had been removed under reduced pressure from the filtrate, a colorless solid material (7.6 g., 59%) was separated from the residue by filtration. It melted at 168—169°C after recrystallization from benzene; its infrared spectrum showed absorptions at 980 cm^{-1} for the *trans* double bond and at 707 cm^{-1} for the *cis* double bond. Therefore, the *cis*-5, *trans*-9-cyclododecadiene-*trans*-1, 2-diol (II) structure was assigned.

Found: C, 73.51; H, 10.47. Calcd. for $C_{12}H_{20}C_2$: C, 73.43; H, 10.27%.

The Reaction of *cis, trans, trans*-1, 5, 9-Cyclododecatriene (I) with Osmium Tetroxide.—The cyclotriene (I, 1.27 g.), dissolved in 50 ml. of ether, and pyridine (0.8 g.) were placed in a 100-ml. three-necked flask equipped with a stirrer, a thermometer, and a separatory funnel. An ethereal solution of osmium tetroxide (2.0 g.) was then added into the solution, the reaction temperature was kept at 0°C for over 2 hr. After the reaction mixture had been allowed to stand for 12 hr. at room temperature, it was treated with sodium bisulfite and extracted with chloroform, according to Baran's method.[24] The chloroform solution was dried over sodium sulfate; the removal of the solvent afforded 1.37 g. (89%) of a colorless material. This material melted at 168—169°C after recrystallization from benzene and was proved by a mixed melting point determination and by a study of its infrared spectrum to be identical with the product of permanganate oxidation.

The Hydrogenation of *cis*-5, *trans*-9-Cyclododecadiene-1, 2-diol (II).—The diol (II, 7 g.) dissolved in a mixed solvent of ethanol (50 ml.) and cyclohexane (50 ml.) was hydrogenated with 1 g. of 5% palladium charcoal under atomospheric pressure at room temperature.

It took 12 hr. to absorb 2 mol. equivalents of hydrogen. When, after the reaction, the solvents were removed under reduced pressure, a colorless solid (7 g.) was obtained. It melted at 103—104°C after recrystallization from ether, and its infrared spectrum was identical with that of cyclododecane-*trans*-1, 2-diol.[9]

Found: C, 71.73; H, 11.91. Calcd. for $C_{12}H_{24}O_2$: C, 71.95; H, 12.08%.

The Oxidative Cleavage of Cyclododecane-*trans*-1, 2-diol (IV).—Lead tetraacetate (6.4 g.) was added to a benzene solution of the saturated diol (IV, 3 g.). The reaction mixture was then heated for 40 min. over a steam bath. After the precipitate had been removed by filtration, the benzene solution was washed with water and dried over sodium sulfate. The removal of the solvent left 3.0 g. of a colorless solid. Its infrared spectrum showed the absorptions at 1725 cm^{-1} and 2800 cm^{-1} characteristic of an aldehyde; it was therefore considered to be dodecanedial. It was dissolved in 10% aqueous acetone (100 ml.) and further oxidized with potassium permanganate (6 g.). After the usual treatment, 2.5 g. of a colorless solid was obtained. This solid melted at 125—126°C after recrystallization from aqueous methanol and was proved to be dodecanedioic acid (V) by a study of its infrared spectrum.

Found: C, 62.79; H, 9.63. Calcd. for $C_{12}H_{24}O_4$: C, 62.58; H, 9.63%.

The Reaction of *cis*-5, *trans*-9-Cyclododecadiene-*trans*-1, 2-diol (II) with Osmium Tetroxide.—According to a procedure similar to that described above, the treatment of the unsaturated diol (II, 2.3 g.) with osmium tetroxide (3 g.) afforded 1.7 g. of a colorless solid. It was recrystallized from ether and melted at 212—214°C. Its infrared spectrum showed no absorption 980 cm^{-1} for the *trans* double bond, only an absorption at 707 cm^{-1} for the *cis* double bond; it was therefore considered to be *cis*-9-cyclododecene-1, 2, 5, 6-tetrol (III).

Found: C, 62.45; H, 9.63. Calcd. for $C_{12}H_{22}O_4$: C, 62.58; H, 9.63%.

When the unsaturated tetrol (III) was hydrogenated with palladium-charcoal, a saturated tetrol, m. p. 169—170°C, was obtained in a quantitative yield. Its infrared spectrum showed no absorption at 707 cm^{-1}.

Found: C, 61.83; H, 10.49. Calcd. for $C_{12}H_{24}O_4$: C, 62.04; H, 10.41%.

The Reduction of *cis, trans, trans*-1, 5, 9-Cyclododecatriene (I) with Diimide.—The cyclotriene (I, 60 g.), hydrazine hydrate (300 g.) and cupric sulfate (3 g.) were placed in a one-liter three-necked round-bottom flask equipped with a stirrer, a condenser, and an inlet air tube. Ethanol (200 ml.) was added to the above mixture until the reaction mixture became homogeneous. Air was bubbled into the solution with vigorous stirring. The reaction generated a considerable amount of heat, and the reaction temperature easily rose as high as 50—60°C. It was kept below 50°C by cooling it with ice-water. The reaction mixture gradually turned brown, and the blue color of the cupric ion was deposited on the wall of the reaction vessel in 30—40 hr. It took about 45 hr. for the generation of heat to become negligible. Then the reaction mixture was filtered to remove the catalyst and extracted with ether. The ethereal solution was washed with 2 N hydrochloric acid to remove the excess hydrazine; then it was washed with water and dried over sodium sulfate. The ether was removed under reduced pressure, the residue was distilled in a vacuum. A fraction (42 g.), b. p. 64—65°C/1.0 mmHg, was the main component of the reaction product, which was proved by gas chromatography (PEG 6000) to consist of 91% *cis*-cyclododecene (VII) and 9% cyclododecane. Pure *cis*-cyclododecene was obtained by a preparative gas chromatography, and the compound showed an infrared spectrum identical with that of an authentic sample.[9]

Found: C, 86.48; H, 13.32. Calcd. for $C_{12}H_{22}$: C, 86.66; H, 13.34%.

On the other hand, aliquots of the reaction mixture were subjected to infrared and vapor phase chromatographic analyses at intervals during the reaction. Their infrared spectra showed that only the absorption intensity at 980 cm^{-1} for the *trans* double bond diminished,

23) Supplied by Hüls Co., Ltd., and the sample contained 98% of *cis, trans, trans*-1, 5, 9-cyclodedecatriene and 1.8% of *trans, trans, trans*-1, 5, 9-cyclododecatriene.

24) J. S. Baran, *J. Org. Chem.*, **25**, 257 (1960).

while that at 707 cm^{-1} for the *cis* double bond remained unchanged during the reaction. Vapor phase chromatography showed the presence of three components. Two of them were confirmed by their retention times to be the starting material and *cis*-cyclododecene (VII), while the other fraction was attributed to *cis, trans*-1, 5-cyclododecadiene (VI). No detectable amount of *trans*-cyclododecene was identified.

At the end of the reaction, a small amount of cyclododecane was observed by vapor phase chromatography, and the ratio of *cis*-cyclododecene to cyclododecane was seen to depend upon the reaction time. Prolonged treatment with diimide caused an increase in the amount of cyclododecane, showing that *cis*-cyclododecene was slowly hydrogenated.

In order to confirm the structure further, the cyclododecene obtained by means of diimide was converted into cyclododecane-*cis*-1, 2-diol in the following way. The cyclododecene (1.32 g.) was dissolved in ether (40 ml.) and treated with pyridine (2 ml.) and osmium tetroxide (2 g.) for 3 days. After the adduct had been decomposed with Baran's reagent,[23] a crude glycol (1.42 g.) was obtained. It melted at 157—158°C after recrystallization from a mixed solvent of benzene and ligroin and was proved by a study of its infrared spectrum to be identical with an authentic sample prepared by Prelog.[9]

Found: C, 72.04; H, 12.05. Calcd. for $C_{12}H_{24}O_2$: C, 71.95; H, 12.08%.

The Reaction of *cis, trans, trans*-1, 5, 9-Cyclododecatriene (I) with Nitrosyl Chloride in the Presence of Hydrochloric Acid.—The cyclododecatriene (I, 200 g.) dissolved in 1 l. of trichloroethylene was placed in two-liter three-necked flask equipped with a stirrer, a condenser, and an inlet tube for nitrosyl chloride. Nitrosyl chloride (81 g.) and hydrogen chloride gas were bubbled into the solution over 3 hr. while the reaction temperature was kept below 12°C. After the addition of nitrosyl chloride, hydrogen chloride was further passed into the solution for 1 hr. After the reaction, the solvent was removed under reduced pressure and a pale yellow crude product (287 g.) was obtained. When this was recrystallized from ligroin, it showed a m. p. of 110—115°C; when it was further recrystallized from aqueous ethanol, it showed a m. p. of 127—129°C.

Found: C, 63.15; H, 7.85; N, 5.85; Cl, 15.99. Calcd. for $C_{12}H_{18}NOCl$: C, 63.3; H, 7.92; N, 6.16; Cl, 15.6%.

Its infrared spectrum showed an absorption at 980 cm^{-1} characteristic of the *trans* double bond and one at 707 cm^{-1} characteristic of the *cis* double bond, showing that one of the *trans* double bond was preferentially attacked by nitrosyl chloride. Besides the above absorptions, a N–OH absorption was observed at 3210 cm^{-1}. No skeletal change or transannular reaction was observed, since its hydrogenation with palladium charcoal afforded cyclododecanone oxime in a quantitative yield. Therefore, the product must be 2-chlorocyclododecadienone oxime (IXa and IXb).

Similar reactions using methylene chloride, chloroform, and carbon tetrachloride showed that there was no essential change in the product; 2-chlorocyclododecadienone oxime was thus afforded in yields of 60—90%.

Summary

Addition reactions of *cis, trans, trans*-1, 5, 9-cyclododecatriene (I) with *cis* addition reagents, such as osmium tetroxide, potassium permanganate, diimide, and nitrosyl chloride, have been investigated. It has been shown that the first attack of each reagent preferentially takes place at one of the *trans* double bonds. From a synthetic point of view, simple methods for preparing cyclododecane-*trans*-1, 2-diol (IV), *cis*-cyclododecene (VII), and cyclododecanone oxime (X) have been presented. An account of such selective reactions has been given in terms of conformational stabilities of the transition states or intermediates in the *cis* manner addition reactions.

The authors wish to express their thanks to Messrs. Keizo Ono, Sei Ogura and Isamu Usui for their help with these experiments.

BULLETIN OF THE CHEMICAL SOCIETY OF JAPAN VOL. 39 321—326 (1966)

Studies of the Chemical Reactions of Uranium Iodide with Oxygen and Iodine at High Temperatures

By Muneo HANDA

Division of Fuel Research and Development, Japan Atomic Energy Research Institute, Tokai-mura, Naka-gun, Ibaraki

(Received June 4, 1965)

Uranium tetraiodide is oxidized to triuranium octoxide through three intermediates, which are deposited on silica powder heated to temperatures of about 400, 300 and 200°C respectively. The intermediates are produced by the action of oxygen contained in small amounts in a helium stream (1/100—1/10000 atm.) on uranium tetraiodide. The intermediates are considered to be compounds consisting of uranium, iodine and oxygen. Chemical analysis, the measurement of the melting point and X-ray analysis show that the compound deposited at the temperature of 400°C is uranium triiodide, while the compounds deposited at 300 and 200°C are both uranium tetraiodides. Three hypotheses have been formulated to interpret the above phenomenon, in which the reaction of uranium iodides with iodine has been studied.

In the author's previous studies of the chemical behavior of fission products captured in graphite powder, it was found that fission iodine diffusing out of the uranium dioxide and graphite is not an elementary iodine but a chemical form of uranium tetraiodide.[1-2] Uranium tetraiodide attracts moisture and is oxidized in air to triuranium octoxide and iodine; therefore, it should be handled in a dry, inert atmosphere. The graphite and beryllia used as moderators for a high-temperature gas-cooled reactor have many gaseous impurities, such as hydrogen, oxygen, and water vapor, adsorbed on the surface.[3] These gaseous impurities are released gradually as the reactor operates. In order to ascertain the chemical behavior of fission iodine in a reactor fuel, the reactions between uranium tetraiodide and these gaseous impurities must be studied carefully.

As has already been reported in a previous paper,[4] the reactions between uranium tetraiodide and oxygen were studied by using a thermochromatograph. It was found that uranium tetraiodide was oxidized to triuranium octoxide through three intermediates, which deposited on silica powder heated to temperatures of about 400, 300 and 200°C.

These intermediates were produced by the action of oxygen contained in small amounts in a helium stream (1/100—1/10000 atm.) on uranium tetraiodide. The intermediates were considered to be compounds consisting of uranium, iodine and oxygen, although the existence of these compounds in their solid state has not been reported in the literature.

The present work was undertaken in order to estimate the chemical form of these intermediates. Chemical analysis, melting-point measurements and X-ray analysis were carried out for these intermediates. The results of these experiments showed that these intermediates were not compounds consisting of uranium, iodine and oxygen; the compound deposited at the temperature of 400°C was uranium triiodide, while the compounds deposited at 300°C and at 200°C both consisted of uranium tetraiodide. These results indicate that uranium triiodide and tetraiodide moved to positions in the thermochromato-tube at which the temperatures were much lower than the melting points. Three hypotheses were made in order to interpret the above phenomenon; by means of these hypotheses, the reaction of uranium iodides with iodine was studied.

As a result, the following mechanism was found to account for the above phenomenon. First, the oxygen reacts with uranium tetraiodide and produces an elementary iodine. Then this iodine reacts with adjacent uranium tetraiodide, producing a compound of uranium tetraiodide to which iodine has been added. This addition compound has a low melting point, and so moves to a lower temperature in the thermochromato-tube and is decomposed to uranium triiodide, tetraiodide and iodine.

Experimental and Results

Sample Preparation. — *Uranium Tetraiodide Packed in Silica Breakable.*—Uranium tetraiodide

1) S. Yajima, K. Shiba and M. Handa, This Bulletin, **36**, 253 (1963).
2) S. Yajima, K. Shiba and M. Handa, ibid., **36**, 258 (1963).
3) J. P. Redmond and P. L. Walker, Jr., *Nature*, **186**, 73 (1960).
4) S. Yajima, K. Shiba and M. Handa, This Bulletin, **38**, 278 (1965).

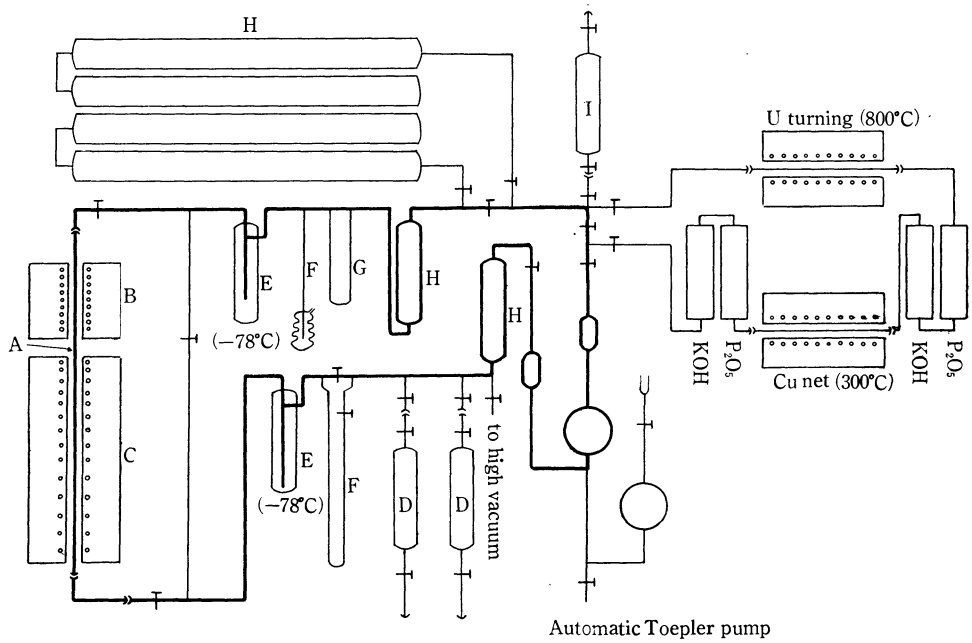

Fig. 1. Flow system of thermochromatograph.

A: Thermochromato-tube
B: Sample heating furnace (600°C)
C: Thermochromato-furnace (600°C to room-temperature)
D: Carrier gas vessel
E: Mercury trap
F: Mano-meter
G: Flow-meter
H: Buffer tank
I: Vessel for trapping carrier gas

was prepared by the direct combination of uranium and iodine, as has been described in the literature.[5] From 0.2 to 10 g. of the uranium tetraiodide was packed in a silica breakable with a ball joint, which was in turn placed in a glove box filled with purified helium gas. Then a cock was attached to the breakable with a ball-joint holder, and the entire assembly was taken out of the glove box. The helium gas in the breakable was evacuated, and the part of the breakable containing the sample was sealed off by an oxy-hydrogen flame.[4]

Apparatus.—The apparatus used is shown schematically in Fig. 1. The apparatus had an automatic Toepler pump, making possible experiments with oxygen of various concentrations as the carrier gas. Buffer tanks were installed at the entrance and exit of the automatic Toepler pump, in order to stabilize the flow rate of the carrier gas; the volumes of these buffer tanks were 0.5 and 25.0 l. respectively. These large-volume buffer tanks can be used to keep the concentration of oxygen constant when some of it is consumed in the oxidation of the sample material.

The experimental apparatus also had a bypass gas purification system which made possible experiments with purified helium carrier gas. The thermochromato-tube, made of transparent silica, was 1.2 cm. in inner diameter and 100 cm. long. An empty silica tube was used as the thermochromato-tube, and so the sample packed in the silica breakable was held by silica wool packed in the tube. The tube was heated by the thermochromato-furnace so as to produce a linear temperature gradient of 600°C to room-temperature along its axis.

Procedure.—The entire apparatus was evacuated with a rotary pump, and then arbitrary volumes of helium and oxygen were introduced into the apparatus to a one-tenth atmosphere. The gases were completely mixed together by circulating them for 5 hr. through the apparatus with the automatic Toepler pump.

However, when the experiment was carried out in an inert atmosphere, only helium was introduced; the gas was purified by circulation for 5 hr. through the gas purification system with the automatic Toepler pump. After the apparatus had been filled with the carrier gas, the breakable containing the sample was broken, with an iron bar sealed in the silica tube, from outside the thermochromato-tube. Then the thermochromato-furnace was started in order to heat the tube. After the temperature of the furnace had reached 600°C, the circulation of the carrier gas was continued for a further 5 to 10 hr. The thermochromato-tube was then cooled, and the top and bottom of the tube were sealed by an oxy-hydrogen flame. The sealed tube was transferred to a glove box

5) N. W. Gregory, UCRL, RL-4, 6, 272 (1944).

filled with purified helium, and the compounds deposited on the wall of the silica tube, which had been heated at 400, 300 and 200°C, were taken out of the tube by cutting it with a baby grinder. These compounds were weighed and packed in silica breakables for chemical analysis and for measurement of the melting point; they were also packed in capillary tubes for X-ray analysis.

The Determination of the Uranium and Iodine in the Compounds Deposited on Silica Tubes Heated at 400, 300 and 200°C.—The breakable containing a sample was broken above a beaker of water and rapidly immersed. The three samples were completely dissolved in water. A reddish-purple solution was obtained from the compound deposited at 400°C, while a green solution was obtained from the compounds deposited at 300 and 200°C. The reddish-purple solution immediately turned green. Each solution was placed in a 100-ml. measuring flask and was diluted with water to 100 ml. A few milliliters of the solution were then put in a separating funnel and nitric acid was added. The iodine was extracted by carbon tetrachloride. The iodine in the carbon tetrachloride, which turned reddish-purple, was directly determined by colorimetry at the wavelength of 575 mμ. Sulfuric acid was added to the residue solution, from which the iodine had been extracted, and the solution was heated almost to dryness. After the nitric acid had been expelled by repeating the above procedure three times, the pH of the solution was adjusted with ammonium hydroxide (not containing the carbonate radical) and the uranium was extracted by an oxine-chloroform solution. The uranium content of the chloroform was determined by colorimetry at 380 mμ. The analytical results are shown in Table III.

The Determination of Oxygen in the Compounds Deposited at 400 and 300°C.—The method of determining oxygen by subtracting the weights of uranium and iodine from the total weight of the sample is inferior to the method of determining oxygen directly. Therefore, the oxygen was determined directly. The compounds of uranium, iodine and oxygen were oxidized to triuranium octoxide and iodine when heated in the air at 600°C. From the determinations of the uranium and iodine in these compounds, it was shown that the iodine/uranium ratio was 3.0 for the compound deposited at 400°C and 4.0 for the compounds deposited at 300 and 200°C. If oxygen is present in these compounds, the amount consumed in their oxidation should decrease in proportion to that which they already contain. This is because these compounds, like the oxidation products, must consist of stoichiometric compositions of uranium, iodine or oxygen. The calculated volumes of oxygen consumed in the oxidation of 1 g. of various compounds are shown in Table I.

Table I. Oxygen volumes consumed to oxidize 1 g. of compound ($U_xI_yO_z$) to uranium oxide and iodine

Compound	Oxygen volumes consumed for reaction ml. at S.T.P.	Chemical equation
U	130.0	$3U+4O_2=U_3O_8$
UI_2	69.9	$3UI_2+4O_2=U_3O_8+3I_2$
UI_3	48.3	$6UI_3+8O_2=2U_3O_8+9I_2$
UI_4	40.2	$3UI_4+4O_2=U_3O_8+6I_2$
UOI_3	29.9	$6UOI_3+5O_2=2U_3O_8+9I_2$
UOI_4	24.5	$6UOI_4+5O_2=2U_3O_8+12I_2$
UO_2I_3	11.4	$6UO_2I_3+2O_2=2U_3O_8+9I_2$
UO_2I_4	9.7	$3UO_2I_4+O_2=U_3O_8+6I_2$

The oxygen consumed for the reactions was measured by means of a B. E. T. apparatus.[6] The B. E. T. apparatus can measure amounts of oxygen as small as 0.02 ml. at S. T. P. The results obtained are shown in Table II.

Table II. Determination of oxygen in the compounds deposited at the temperatures of 400 and 300°C

Compound	Sample weight g.	Oxygen consumed ml. at S.T.P.	Oxygen consumed to oxidize 1 g. of sample ml. at S.T.P.	Ref.
Compound deposited at 400°C	0.356	16.6	46.5	
	0.692	31.5	45.5	UI_3(1 g.)
	1.117	56.1	47.9	48.3 ml.
	0.319	14.7	46.2	
Compound deposited at 300°C	0.643	25.3	39.4	UI_4(1 g.)
	0.377	15.5	41.1	40.2 ml.

The Measurement of the Melting Point.—The melting point was measured in an inert gas atmosphere, using a fused salt bath (lithium chloride - potassium chloride eutectic mixture). The apparatus for measuring the melting point is shown in Fig. 2. The melting point of the compound deposited at 400°C was found to be 788±10°C, while that for the compound at 300°C, was 506±10°C.

Discussion

Before the experiment, it was thought that the compounds depositing at 400, 300 and 200°C would all consist of uranium, iodine and oxygen. However, the results of their chemical analyses, which are given in Table III, show that the deposit at 400°C was uranium triiodide, while the deposits at 300 and 200°C were uranium tetraiodide.

6) S. Brunauer, P. H. Emmett and E. Teller, *J. Am. Chem. Soc.*, **60**, 309 (1938).

TABLE III. CHEMICAL FROM OF THE COMPOUNDS DEPOSITED AT 400, 300 AND 200°C

Compound	Sample No.	Iodine g. atom	Uranium g. atom	Oxygen g. atom	Ratio of I/U	Result
Compound deposited at 400°C	1	2.86×10^{-3}	9.86×10^{-4}	0	2.90	UI_3
	2	2.69×10^{-3}	9.19×10^{-4}	0	2.93	
	3	4.33×10^{-3}	1.44×10^{-3}	0	2.90	
	4	1.73×10^{-3}	5.76×10^{-4}	0	2.95	
Compound deposited at 300°C	1	3.48×10^{-3}	8.64×10^{-4}	0	4.03	UI_4
	2	2.00×10^{-3}	5.19×10^{-4}	0	3.85	
Compound deposited at 200°C	1	8.66×10^{-5}	2.09×10^{-5}	—*	4.14	UI_4
	2	8.27×10^{-5}	2.17×10^{-5}	—*	3.81	
	3	9.29×10^{-5}	2.30×10^{-5}	—*	4.04	

* The oxygen was not analyzed since only a small amount of sample could be obtained.

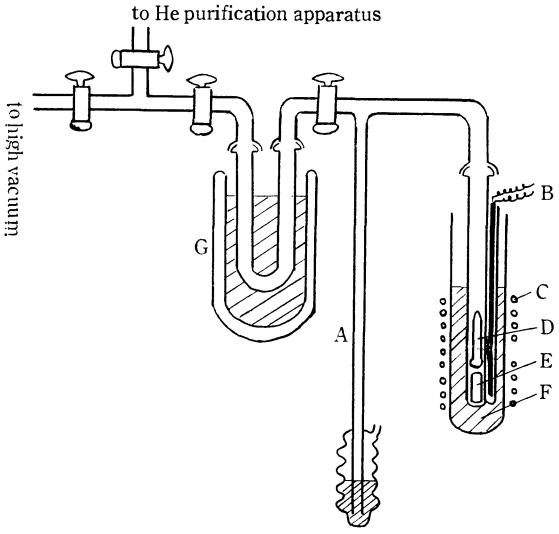

Fig. 2. Apparatus for measuring the melting point.
A: Mercury bubbler
B: Pt-PtRh thermocouple
C: Nichrome heater
D: Sample
E: Sample breaker
F: Mixed fused bath (KCl-LiCl eutectic)
G: Iodine trap (cooled with liquid nitrogen)

Further, the melting points of the compounds deposited at 400 and 300°C were 788 and 506°C, nearly equal to those of uranium triiodide (780°C) and uranium tetraiodide (508°C), as reported by other workers.[7-8] The X-ray patterns (powder method) obtained for the compounds deposited at 400 and 300°C also agreed with those for the uranium triiodide and tetraiodide prepared in the laboratory. When the compound deposited at 400°C was dissolved in water, the reddish-purple color characteristic of the uranium ion (III) appeared. The compounds deposited at 300 and 200°C, on the other hand, exhibited a green color characteristic of the uranium ion (IV).

On the basis of these data, it may be reasonable to conclude that the compound deposited at 400°C is uranium triiodide and that the compound deposited at 300 and 200°C is uranium tetraiodide.

Using a thermochromatograph, the deposition temperature was determined for many metal iodides in an inert gas atmosphere using an experimental time of 2 hr. It was found that many metal iodides deposited at temperatures near their melting points.[9]

When purified helium was used as the carrier gas, uranium tetraiodide deposited on the wall of a silica tube heated at 550°C. When the carrier gas contained a small amount of oxygen (1/10000 to 1/10 atm.), uranium triiodide and uranium tetraiodide deposited at 400, 300 and 200°C.

The above observations indicate that there must be a metastable compound present with a low melting point. The discussions below will deal with mechanisms for the movement of uranium tetraiodide and triiodide toward temperatures lower than the melting points.

Three possible mechanisms may be considered in accounting for the above phenomenon:

1) A metastable compound, consisting of uranium, iodine and oxygen, is produced by the action of oxygen on uranium tetraiodide. The compound moves toward lower temperatures, being carried by the helium gas, and decomposes to uranium triiodide, uranium tetraiodide, iodine and oxygen. The chemical equation postulated is as follows:

$$aUI_4+bO_2 \rightarrow cU_xI_yO_z \begin{cases} \nearrow dUI_4+eI_2+fO_2 \\ \searrow gUI_3+hI_2+iI_2 \end{cases} \quad (1)$$

2) A metastable compound, produced similarly, disproportionates to uranium triiodide, uranium tetraiodide, uranium oxide and iodine:

$$aUI_4+bO_2 \rightarrow cU_xI_yO_z \begin{cases} \nearrow dUI_4+eU_3O_8+fI_2 \\ \searrow gUI_3+hU_3O_8+iI_2 \end{cases} \quad (2)$$

7) J. J. Katz and E. Rabinowitch, "The Chemistry of Uranium: The Element, Its Binary and Related Compounds," Dover Publications, New York (1951).
8) M. M. Popov and M. D. Senin, *Zh. Neorgan. Khim.*, **2**, 1479 (1957).
9) S. Yajima, K. Shiba and M. Handa, unpublished work.

3) In the first step of a third mechanism, oxygen reacts with uranium tetraiodide, producing elementary iodine and uranium oxide. Then this iodine reacts with uranium tetraiodide, present nearby, and the addition compound which is produced moves toward lower temperatures, decomposing to uranium triiodide, uranium tetraiodide and iodine:

$$3UI_4+4O_2 \rightarrow U_3O_8+6I_2 \quad (3)$$

$$aUI_4+bI_2 \rightarrow cUI_{4+x} \begin{cases} \nearrow dUI_4+eI_2 \\ \searrow fUI_3+gI_2 \end{cases} \quad (4)$$

The first mechanism appears unreasonable in explaining the phenomenon because of the reported heats of formation for uranium iodides and uranium oxides:[7]

$$U(\text{solid})+3/2I_2(\text{gas})=UI_3(\text{solid}) \quad (5)$$

$\Delta H_{298°K}=-136.9\pm0.6$ kcal. per mol.

$$U(\text{solid})+2I_2(\text{gas})=UI_4(\text{solid}) \quad (6)$$

$\Delta H_{298°K}=-156.6\pm0.6$ kcal. per mol.

$$U(\text{solid})+O_2(\text{gas})=UO_2(\text{solid}) \quad (7)$$

$\Delta H_{298°K}=-256.6$ kcal. per g. of U

$$U(\text{solid})+4/3O_2(\text{gas})=1/3U_3O_8(\text{solid}) \quad (8)$$

$\Delta H_{298°K}=-281.7$ kcal. per g. of U

The heats of formation for uranium oxides are much greater than those for uranium iodides. In other words, the binding energy of uranium with oxygen is much greater than that with iodine. Therefore, the postulated metastable compound, $U_xI_yO_z$, which decomposes to uranium iodides, iodine and oxygen, cannot be considered seriously.

In view of the heats of formation mentioned above, it seems that the disproportionation reaction of the metastable compound is probable, as has been suggested in the second mechanism. The binding energy of uranium with oxygen is much greater than that with iodine. Uranium oxide is isolated first, from the metastable compound; the chemical bond between uranium and iodine is left as it is, and the excess iodine is released as elementary iodine. Since the uranium oxide is isolated as a compound with a high melting point, it cannot move in the thermochromato-tube once it separates from the metastable compound. Consequently, uranium oxide must deposit near the uranium iodide if the intermediate is present and moves toward lower temperatures. However, uranium oxide could not be found at any positions of the thermochromato-tube except where the sample had been packed. Therefore, it is not reasonable to assume this mechanism for the phenomenon mentioned above.

Two kinds of experiments were carried out in attempting to confirm the third mechanism. In one experiment, an amount of elementary iodine equal to that produced when a sample is completely oxidized was sealed in a silica breakable in a similar manner. The silica breakable containing this elementary iodine was placed on a sample in the thermochromato-tube, the temperature there being about 60°C. The helium carrier gas was purified and the thermochromato-furnace was heated to produce a linear temperature gradient from 600°C to room-temperature. Both of the silica breakables were broken, and then the sample heating furnace was started. The temperature was maintained for 2 hr. after it reached 600°C. The iodine sublimate passed through the sample, flowing down the tube. Iodine from the tube was trapped in a liquid nitrogen-cooled trap. Then the reactions of iodine with uranium tetraiodide and triiodide were examined. The results obtained for the reactions were the same as those obtained for the oxygen-helium mixed carrier gas; that is, uranium triiodide deposited at 400°C and uranium tetraiodide at 300 and 200°C. The amount of uranium tetraiodide deposited at 200°C was very small. From these facts, it may be considered that the uranium tetraiodide deposited at 200°C is formed by the action of iodine on the uranium iodides already deposited at 400 and 300°C, through the mechanism by which uranium iodides move and deposit at 400 and 300°C.

In the second experiment, stoichiometric amounts of iodine, required to produce uranium hexaiodide (UI_6) and uranium decaiodide (UI_{10}), were mixed with uranium tetraiodide in a helium gas atmosphere; these mixtures were sealed in silica vessels after the helium gas had been evacuated. Then the silica vessels were heated for 10 hr. at 600 to 700°C. After the vessels, had been cooled, the substances obtained were taken out, weighed, and placed in silica breakables. These materials were unstable compounds, releasing iodine vapor even when they were taken out in a helium gas atmosphere.

The experimental results obtained for both the samples with a purified helium carrier were the same as those obtained when iodine was placed on the uranium tetraiodide.

The results in the first experiment indicate that there exists a compound, UI_{4+x}, with a much lower melting point than that of uranium tetraiodide. In the second experiment, because the materials release iodine in the helium gas atmosphere, they exist only under a certain iodine vapor pressure. The results obtained for the uranium hexaiodide and uranium decaiodide show that these compounds decompose to uranium triiodide, uranium tetraiodide and iodine in an inert gas atmosphere.

From the foregoing experiments and discussions, it seems reasonable to conclude that the phenomenon in which uranium triiodide and uranium tetraiodide move toward temperatures

lower than their melting points and deposit there takes place via the formation of an iodine addition compound of uranium tetraiodide.

Foster and Tvrzicky have reported that, when uranium tetraiodide is left in air, uranyl iodide (UO_2I_2) and uranous oxyiodide (UOI_2) are produced.[6] However, the results of the present studies on the oxidation of uranium tetraiodide have shown that such compounds are too unstable to be produced by the direct oxidation of uranium tetraiodide.

The author wishes to thank Professor Seishi Yajima and Mr. Koreyuki Shiba for valuable discussions and suggestions, and Professor Takanobu Shiokawa for his continuing interest in and encouragement of this work. He is also indebted to Dr. Thomas Olsen for his kindness in making corrections of the grammatical errors in English.

BULLETIN OF THE CHEMICAL SOCIETY OF JAPAN VOL. 39 326—329 (1966)

Oxidation of Alcohols with *t*-Butyl Chromate. IV. The Course of the Formation of the Ester*

By Takayuki SUGA and Tamon MATSUURA

Department of Chemistry, Faculty of Science, Hiroshima University

(Received June 7, 1965)

The results obtained in the preceding papers (Parts I—III) of this series showed that, on oxidation with *t*-butyl chromate, the primary alcohol without a π-electron system on the carbon α to the hydroxymethyl group yields the corresponding ester in a comparable yield, together with the aldehyde and the acid, and also that the cyclic α-glycol with two secondary hydroxyl groups affords the corresponding cyclic ester, along with the glycol fission product. Chemical examination and infrared spectroscopic study have now proved that the course of the formation of these esters does not follow the direct esterification of the alcohol with the acid formed from it by oxidation, but rather involves the formation of a hemiacetal intermediate between the original alcohol and the aldehyde produced from the alcohol, and the subsequent oxidation of the hemiacetal. The oxidation of alcohols with *t*-butyl chromate has also been discussed generally on the basis of the results of our previous papers and of the present work.

Our previous papers[1-3] showed that, on oxidation with *t*-butyl chromate, saturated primary alcohols, such as aliphatic and β-phenylethyl alcohols and cyclohexylcarbinol, yielded mixtures of the corresponding aldehyde, acid and ester in comparable yields, while unsaturated primary alcohols, such as *trans*-cinnamyl and benzyl alcohols, geraniol and myrtenol, did not produce the ester, but yielded only the corresponding aldehyde and acid.

The ester might be formed in one of the following two courses: the direct esterification of the alcohol with the acid formed from it by oxidation,[4,5] or the hemiacetal formation between the original alcohol and the aldehyde produced from it by oxidation, and the subsequent oxidation to the ester.[6,7] We have now tried to clarify the course of the formation of the ester, together with the reason for the oxidation mode being different depending on the type of alcohol. In addition, generalizations as to the *t*-butyl chromate oxidation of alcohols have been given.

In the *t*-butyl chromate oxidation of *n*-butyl alcohol, *n*-butyric acid produced was removed by extracting the benzene solution with alkali before the solvent was removed (Exp. 1). The amount of *n*-butyl *n*-butyrate thus obtained was identical with that of the ester (Exp. 5 in Ref. 1) obtained without this treatment. A similar result (Exp. 2) was also observed in the oxidation of cyclohexane-*trans*-1, 2-diol, which yielded *trans*-1, 2-adipoxycyclohexane (II) as an ester (Exp. 5 in Ref. 3). Besides, *n*-butyl alcohol was not esterified (Exp. 3) by *n*-butyric acid during the agitation

* Partly presented at the Local Meeting of the Chûgoku-Shikoku district of the Chemical Society of Japan, Hiroshima, November, 1960, and at the 15th Annual Meeting of the Chemical Society of Japan, Kyoto, April, 1962.

1) T. Suga, K. Kihara and T. Matsuura, This Bulletin, **38**, 893 (1965).

2) T. Suga, K. Kihara and T. Matsuura, ibid., **38**, 1141 (1965).

3) T. Suga and T. Matsuura, ibid., **38**, 1503 (1965).

4) L. Bouveaut, *Bull. Soc. Chim. France*, **1904**, 1306.

5) G. R. Robertson, "Organic Syntheses," Coll. Vol. I, 138 (1941).

6) W. A. Mosher and D. M. Preiss, *J. Am. Chem. Soc.*, **75**, 5605 (1953).

7) J. C. Craig and E. G. Horning, *J. Org. Chem.*, **25**, 2098 (1960).

of a mixture of the alcohol and the acid in benzene under conditions similar to those in the oxidation. Moreover, if the ester were formed by direct esterification, *n*-hexyl acetate would be produced together with *n*-hexyl *n*-caproate when *n*-hexyl alcohol is oxidized in the presence of acetic acid. However, this oxidation (Exp. 4) did not give any *n*-hexyl acetate; it afforded only *n*-hexyl *n*-caparoate.

If another aldehyde (R''-CHO) is added to a mixture of an alcohol (R'-CH_2OH) and an aldehyde (R'-CHO) produced from it, two kinds of hemiacetals (R'-CH(OH)·O·CH_2-R' and R'-CH(OH)·O·CH_2-R'') should be formed and then oxidized to two esters (R'-CO·O·CH_2-R' and R'-CO·O·CH_2-R'' respectively). The oxidation of an equimolar mixture of *n*-hexyl alcohol and *n*-butyraldehyde (Exp. 5) showed the formation of *n*-hexyl *n*-butyrate and *n*-hexyl *n*-caproate; this was in agreement with the expectation. These results suggest that the course to the ester involves the hemiacetal oxidation.

The infrared spectra of mixtures of an aldehyde and an alcohol were examined in order to establish the formation of a hemiacetal as an intermediate. Two absorption cells, one filled with an aldehyde and the other with an alcohol, were placed in series so that the recorded spectrum was the sum of the spectra of two samples. On the other hand, an equimolar mixture of an aldehyde and an alcohol was placed in one cell and the spectrum was again recorded. A comparison was then made between the "separate" and "mixed" spectra. The spectra of the pair, *n*-butyraldehyde and *n*-hexyl alcohol (Fig. 1), showed considerable

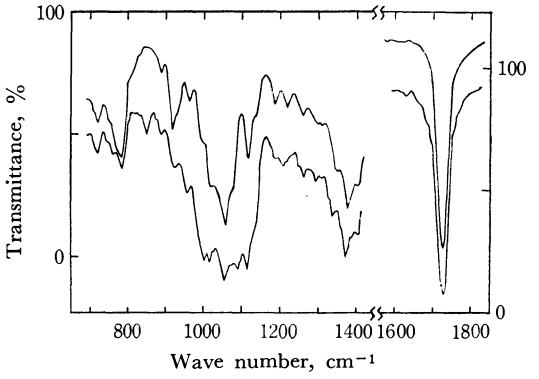

Fig. 1. The "separate" (upper line) and "mixed" (lower line) infrared spectra of *n*-butyraldehyde and *n*-hexyl alcohol in a carbon disulfide solution.

differences between the "separate" and "mixed" spectra. In the "mixed" spectrum the strong new bands were found at about 850, 1000—1015, 1090, 1115, and 1140 cm^{-1} and were assignable to an ether-linkage of a hemiacetal.[8,9] The same phenomena as above were also observed in the spectra of the other pairs, *n*-butyraldehyde and *n*-butyl alcohol, and β-phenylacetaldehyde and β-phenylethyl alcohol. The formation of the ester has been observed in the oxidation of these alcohols and is in harmony with the appearance of new bands which can be ascribed to the formation of an intermediate hemiacetal in the spectra of mixtures of the alcohols and the corresponding aldehydes. In contrast, a complete agreement was observed between the "separate" and "mixed" spectra of the two pairs, benzaldehyde and benzyl alcohol, and *trans*-cinnamaldehyde and *trans*-cinnamyl alcohol. This is coincident with the finding of our previous work[2] that the *t*-butyl chromate oxidation of these alcohols does not produce the ester; this can be ascribed to the failure of these pairs to form a hemiacetal.

The agreement observed between the "separate" and "mixed" spectra of the two pairs, benzaldehyde and *n*-hexyl alcohol, and *trans*-cinnamaldehyde and *n*-butyl alcohol, also indicated no formation of a hemiacetal between these pairs, while the formation of a hemiacetal was shown by the differences observed between the spectra of two other pairs, caproaldehyde and benzyl alcohol, and *n*-butyraldehyde and *trans*-cinnamyl alcohol. Accordingly, it was found that the hemiacetal formation does not depend on the structure of the alcohol, but on that of the aldehyde, namely, on the substitution system on the carbon α to the carbonyl group.

A previous paper[3] of this series showed that the *t*-butyl chromate oxidation of *trans*-cyclohexane-1, 2-diol produces *trans*-1, 2-adipoxycyclohexane (II), the formation of which has not yet been reported in the oxidation of this diol. Recently, Head[10] has observed the reaction of *trans*-cyclohexane-1, 2-diol with glyoxal at room temperature to give a crystalline bishemiacetal, *trans*-hexahydro-2, 3-dihydroxy-1, 4-benzodioxane. The formation of II can, therefore, be explained by the process by which the hemiacetal (I) shown in the following equation is first formed by the

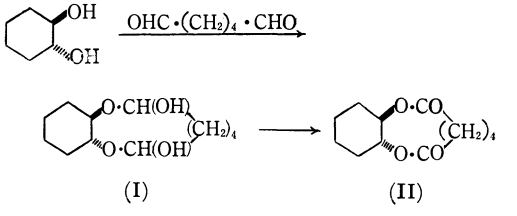

(I) (II)

interaction of *trans*-cyclohexane-1, 2-diol and adipaldehyde probably produced by the glycol-fission of the 1, 2-diol, and is subsequently oxidized.

In conclusion, our previous findings[1-3] and the present work on the *t*-butyl chromate oxidation of alcohols permit us to generalize the oxidation

8) A. Ashdown and T. A. Kletz, *J. Chem. Soc.*, **1948**, 1454.
9) E. D. Bergmann and S. Pinchas, *Rec. Trav. Chim.*, **71**, 161 (1952).
10) F. S. H. Head, *J. Chem. Soc.*, **1960**, 1778.

as follows. The oxidation of the primary alcohol without a π-electron system on the carbon α to the carbinol carbon, such as the alcohol which contains the group shown below:

$$R\text{-}CH_2\cdot CH_2OH \quad (R=H, \text{Alkyl, or Phenyl})$$

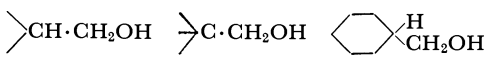

yields a mixture of the corresponding aldehyde, acid and ester in a comparable yield. On the other hand, the oxidation of the primary alcohol with a π-electron system on the carbon α to the hydroxymethyl group, such as the following system:

$$-CR{=}CR\cdot CH_2OH \quad (R=H \text{ or Alkyl})$$

$$C_6H_5\cdot CH_2OH$$

produces not the ester, but the corresponding aldehyde in a high yield and acid in a low yield. A secondary alicyclic alcohol and a cyclic α-glycol with a secondary and a tertiary hydroxyl groups are selectively oxidized to the corresponding ketone and α-hydroxyketone respectively, while the oxidation of a cyclic α-glycol with two secondary hydroxyl groups does not give the corresponding α-diketone, but the glycol fission product and the cyclic ester.

Moreover, there was evidence that the course of the formation of the ester did not involve direct esterification, but hemiacetal oxidation.

Experimental

Samples.—The alcohols were the same ones as were used in the previous papers[1-3] of this series; the aldehydes were obtained from a commercial source. All the samples were purified repeatedly by distillation or recrystallization just before use.

Oxidation or Reaction.—A benzene solution of *t*-butyl chromate was prepared in the manner used in a preceding paper.[1] The quantity of each component in this solution is shown in Table I, which also lists the quantity of the sample and its solvent. After the oxidation or the reaction was carried out at 1—2°C for 6 hr. (except in Exp. 2, which had a reaction time of 3 hr. at 35°C), the reaction mixture was treated with oxalic acid and water, as has been shown in Ref. 1. The separated benzene solution was subjected to the described examinations in each experiment. Each of the constituents of the reaction product was identified by a comparison of its infrared spectrum with that of the authentic sample and by a mixed melting point determination; the yield of the constituents is shown below.

The Oxidation of *n*-Butyl Alcohol (Exp. 1).—After the oxidation, the reaction mixture was treated with oxalic acid and water, and then the separated benzene solution was repeatedly extracted with a sufficient amount of a 5% sodium carbonate solution; this alkaline solution gave *n*-butyric acid (31.5% yield based on the alcohol; b. p. 99—100°C/79 mmHg, n_D^{25} 1.3957, d_4^{25} 0.9614) on acidification. The removal of the solvent from the neutral benzene solution afforded *n*-butyl *n*-butyrate (34.3%; b. p. 94—95°C/77 mmHg, n_D^{25} 1.4059, d_4^{25} 0.8663; $\nu_{ester}^{liq.}$ 1741, 1187 cm^{-1}).

The Oxidation of Cyclohexane-*trans*-1, 2-diol (Exp. 2).—The reaction mixture was treated in the manner described in Exp. 1. The neutral product obtained was subjected to examinations similar to those used in Exp. 5 in Ref. 3; *trans*-1,2-adipoxycyclohexane (m.p. and mixed m.p. 103—104°C; ν_{ester}^{KBr} 1733, 1270, 1154 cm^{-1}) was thus obtained in a 7% yield.

The Agitation of a Mixture of *n*-Butyl Alcohol and *n*-Butyric Acid in Benzene (Exp. 3).—After a mixture of *n*-butyl alcohol and *n*-butyric acid in benzene had been stirred under the conditions shown above, the solvent was removed from the solution under an atmospheric pressure without previous treatment by an alkaline solution. The remaining liquid was analyzed by gas chromatography (column: silicone DC-550 on Celite, 130°C, 50 ml. helium/min.) and infrared spectroscopy. Not even a trace of *n*-butyl *n*-butyrate was detected; the liquid consisted of only the original samples.

The Oxidation of *n*-Hexyl Alcohol in the Presence of Acetic Acid (Exp. 4).—After the oxidation had been carried out in benzene containing acetic acid corresponding to about a 5% concentration in the whole reaction mixture, the reaction mixture was treated as in Exp. 1. The sodium carbonate extracts afforded *n*-caproic acid (26.0%; b. p. 195—200°C, n_D^{25} 1.4129, d_4^{25} 0.9284) on acidification, while the removal of the solvent from the neutral benzene solution gave a neutral product; this was then fractionated by distillation and subjected to gas chromatographic analysis (column: silicone DC-550 on Celite, 140°C, 60 ml. helium/min.). The reaction product did not contain even a trace of *n*-hexyl acetate; it consisted of capraldehyde (12.3%; b. p. 128—135°C, n_D^{25} 1.4070, d_4^{25}

Table I. The weights of the sample used and each component in the oxidant

Exp.	Sample			Oxidant		
	Material		C_6H_6	CrO_3	*t*-BuOH	C_6H_6
		g.	g.	g.	g.	g.
1	*n*-Butyl alcohol	20.0	60	27.0	54.0	100
2	Cyclohexane-*trans*-1,2-diol	30.0	26	77.4	143.4	774
3	*n*-Butyl alcohol *n*-Butyric acid	20.0 10.0	140	—	—	—
4[a]	*n*-Hexyl alcohol	40.0	87	39.1	66.6	159
5	*n*-Hexyl alcohol *n*-Butyraldehyde	51.1 36.1	111	50.0	100.0	195

a) To the benzene solution of *t*-butyl chromate, 20 g. of glacial acetic acid was added.

0.8238; $\nu_{CHO}^{liq.}$ 1724, 2723 cm^{-1}), *n*-hexyl *n*-caproate (46.5%; b. p. 110—113°C/8 mmHg; n_D^{25} 1.4226, d_4^{25} 0.8573; $\nu_{e\ ter}^{liq.}$ 1738, 1168 cm^{-1}) and unchanged alcohol (3.3%; b. p. 93—100°C/49 mmHg).

The Oxidation of a Mixture of *n*-Hexyl Alcohol and *n*-Butyraldehyde (Exp. 5).—As soon as a benzene solution of an equimolar mixture of *n*-hexyl alcohol and *n*-butyraldehyde had been prepared under ice-cooling, the oxidation was conducted under the conditions shown above; then the reaction mixture was worked up as has been described above. The distillation of the acidic product gave *n*-butyric acid (10.5%; b. p. 83.5—84°C/40 mmHg, n_D^{25} 1.3958, d_4^{25} 0.9535) and *n*-caproic acid (8.4%; b. p. 121°C/40 mmHg, n_D^{25} 1.4136, d_4^{25} 0.9236). On the other hand, a combination of fractional distillation, gas chromatography and infrared spectroscopy indicated that the neutral product consisted of caproaldehyde (6.5%; b. p. 125—132°C, n_D^{25} 1.4041, d_4^{25} 0.8290), *n*-hexyl *n*-butyrate (18.6%; b.p. 97—98°C/19 mmHg, n_D^{25} 1.4142, d_4^{25} 0.8612; $\nu_{ester}^{liq.}$ 1734, 1184 cm^{-1}; ester number 331), *n*-hexyl *n*-caproate (5.4%; b. p. 127°C/19 mmHg, n_D^{25} 1.4224, d_4^{25} 0.8601; $\nu_{ester}^{liq.}$ 1741, 1170 cm^{-1}; ester number 280), unchanged alcohol (9.2%), and unchanged aldehyde (14.7%). The hydrolysis of the esters gave the corresponding alcohol and acid respectively.

The Measurement of the "Separate" and "Mixed" Infrared Spectra of the Aldehydes and the Alcohols.—The spectrometer used was a Hilger H-800 double-beam spectrophotometer fitted with a sodium chloride prism. Each of the cells used for the "separate" spectra measurements was 0.1 mm. thick, and the aldehyde and the alcohol were each a carbon disulfide solution of 1 molar concentration. In the "mixed" spectra measurements, the cell was 0.2 mm. long, and a carbon disulfide solution of an equimolar mixture of an aldehyde and an alcohol was prepared in a 1-molar concentration of each sample.

Summary

1) The formation of the ester which is produced when the alcohol without a π-electron system on the carbon α to the carbinol carbon and the cyclic α-glycol with two secondary hydroxyl groups are oxidized with *t*-butyl chromate, has been found to follow the course of the formation of an intermediate hemiacetal between the original alcohol and the aldehyde produced from it by oxidation, and subsequent oxidation.

2) The oxidation of alcohols with *t*-butyl chromate has been generally described on the basis of results obtained in our previous papers (Parts I—III) and in the present work.

The authors are indebted to Messrs. Keiichi Kihara and Tadahisa Yanagihara for their help in this research. This work was partly supported by a grant-in-aid of the Ministry of Education.

BULLETIN OF THE CHEMICAL SOCIETY OF JAPAN VOL. 39 329—333 (1966)

The Hydroxide-Blacks of Ruthenium and Rhodium as Catalysts for the Hydrogenation of Organic Compounds. II.[1] The Effects of Solvents and Added Alkalis in the Hydrogenation of Aniline

By Shigeo NISHIMURA, Tetsuo SHU and Tomoyoshi HARA

Department of Industrial Chemistry, Tokyo University of Agriculture and Technology, Koganei, Tokyo

and Yuzuru TAKAGI

The Institute of Physical and Chemical Research, Bunkyo-ku, Tokyo

(Received June 8, 1965)

The hydrogenation of aniline with the hydroxide-black catalysts of ruthenium and rhodium was investigated, using various alcohols as solvents. The formation of dicyclohexylamine increased in the following order with respect to the solvents: *t*-butyl alcohol≅isopropyl alcohol≪ethyl alcohol<methyl alcohol. It was shown that the addition of a small amount of alkali greatly hinders the formation of dicyclohexylamine. The effects of added ammonia and dicyclohexylamine were also investigated. The addition of ammonia retarded the rhodium-catalyzed hydrogenation much more seriously than the hydrogenation with ruthenium, but it was found that in the presence of alkali the hydrogenation with rhodium was not inhibited by the addition of ammonia.

In the preceding paper,[1] it was reported that the hydroxide-blacks of ruthenium and rhodium are catalysts excellent in activity and selectivity in the hydrogenation of aromatic compounds. The method of the preparation of the hydroxides is very simple; ruthenium hydroxide is much more

1) Part I: Y. Takagi, T. Naito and S. Nishimura, This Bulletin, **38**, 2119 (1965).

active than the ruthenium dioxide prepared by the method of Pichler and Buffleb,[2] and rhodium hydroxide is nearly as active as the rhodium oxide of the Adams type.[3] It was further suggested that the hydroxides, though they were precipitated with a strong alkali, contained much less alkali than the oxides mentioned above. This paper will deal with the hydrogenation of aniline and the effects of solvents and added alkalis on the reactions using the hydroxide-black catalysts of ruthenium and rhodium.

Usually the hydrogenation of aniline to cyclohexylamine is accompanied by the formation of dicyclohexylamine, and it has been known that the addition of metal oxides of a basic character, such as the oxides of calcium and magnesium, is effective in depressing the formation of the secondary amine in the hydrogenations with cobalt and nickel catalysts.[4-7] It has recently been accepted that ruthenium is the most effective of the platinum metals for the hydrogenation of aromatic amines to alicyclic amines.[8-14] Ruthenium dioxide has often been used for this hydrogenation.[8-10,12,13] More recently, rhodium and rhodium-platinum catalysts have been used successfully for the hydrogenation of aniline.[14-16] However, no detailed study of the effects of added alkalis and solvents seems to have been done in the hydrogenation of aniline, especially with ruthenium and rhodium catalysts. Only the effects of added ammonia and dicyclohexylamine have recently been studied with reference to ruthenium and rhodium catalysts supported on carbon.[14]

Experimental

Catalysts.—The hydroxides of ruthenium and rhodium were prepared in a method described previously.[1] Ruthenium dioxide was prepared by the method of Pichler and Buffleb.[2] Rhodium oxide was prepared by a modification of Adams' method described in a previous paper.[3]

Hydrogenation.—A 200 ml. autoclave of an electromagnetically-stirring type was charged with 0.1 g. of the catalyst, 0.1 mol. of aniline, and 50 ml. of the solvent at an initial hydrogen pressure of 80 kg./cm^2. The temperature was raised to 80°C under stirring and maintained constant during the hydrogenation. After the completion of the hydrogenation, the hydrogen pressure dropped to 45 kg./cm^2 at 80°C. For the addition of ammonia, ammonia gas was led into the solvent through a soda-lime tube; the amount of ammonia dissolved was determined by the titration method. Probably some loss of the ammonia occurred during loading and purging operations. Sodium hydroxide and lithium hydroxide were added as a 10% aqueous solution. The products were analyzed directly by means of gas chromatography using a column containing PEG-6000.

Results and Discussion

The Effects of Solvents.—An acidic medium is often used with platinum catalysts to avoid poisoning by nitrogen bases, but it has been shown that the use of acetic acid increases the formation of dicyclohexylamine in hydrogenation with a (7 : 3) rhodium-platinum catalyst, although the rate is the greatest in the acid.[16] In this study, the effects of various alcohols on the selectivity of the hydrogenation of aniline were investigated, using ruthenium hydroxide as the catalyst. From the results shown in Table I, it may be seen that the formation of dicyclohexylamine increases in the following order with respect to the solvents: *t*-butyl alcohol$\cong$isopropyl alcohol$\ll$ethyl alcohol $<$methyl alcohol. The formation of dicyclohexylamine was observed to be very little in *t*-butyl and isopropyl alcohols, whereas it was much larger in ethyl and methyl alcohols. This order of selectivity indicates that the more basic the alcohol used as the solvent, the more unfavorable it is for the formation of dicyclohexylamine;[17] this is in line with the previous observation that acetic acid increases the formation of dicyclohexylamine.

When the hydrogenation was carried out using alcohols as the solvents, the hydrogenation with ruthenium hydroxide proceeded rather rapidly to completion, whereas the hydrogenation with rhodium hydroxide was almost completely inhibited after about 80 to 90% of aniline had been hydrogenated. These results suggest that the rhodium catalyst is much more easily poisoned by nitrogen bases than is the ruthenium catalyst.

The Effects of Added Alkalis.—The addition of ammonia has been shown to suppress the formation of secondary amines in the hydrogenation of nitriles[18] and aniline[4]. However, the presence

2) H. Pichler and H. Buffleb, *Brennstoff-Chem.*, **21**, 257 (1940).
3) S. Nishimura, This Bulletin, **34**, 1544 (1961).
4) C. F. Winans, *Ind. Eng. Chem.*, **32**, 1215 (1940).
5) A. I. Naumov, Z. G. Lapteva and M. M. Shumilina, U. S. S. R. Pat. 114260 (1958) [*Chem. Abstr.*, **53**, 14026 (1959)].
6) P. Richter, J. Pasek, V. Ruzicka and L. Jarkovsky, Czech. Pat. 98263 (1959) [*Chem. Abstr.*, **56**, 12771 (1962)].
7) H. Hagihara and E. Echigoya, *Catalyst (Shokubai)*, **6**, 345 (1964); This Bulletin, **38**, 2094 (1965).
8) L. C. Behr, J. E. Kirby, R. N. MacDonald and C. W. Todd, *J. Am. Chem. Soc.*, **68**, 1296 (1946).
9) G. M. Whitman, U. S. Pat. 2606925 (1952) [*Chem. Abstr.*, **47**, 3874 (1953)].
10) A. E. Barkdoll, D. C. England, H. W. Gray, W. Kirk, Jr., and G. M. Whitman, *J. Am. Chem. Soc.*, **75**, 1156 (1953).
11) G. M. Illich, Jr., and R. M. Robinson, German Pat. 1106319 (1958) [*Chem. Abstr.*, **56**, 2351 (1962)].
12) M. Freifelder and G. R. Stone, *J. Am. Chem. Soc.*, **80**, 5270 (1958).
13) M. Freifelder and G. R. Stone, *J. Org. Chem.*, **27**, 4568 (1962).
14) H. Greenfield, ibid., **29**, 3082 (1964).
15) Abbott Laboratories, Brit Pat. 881512 (1961) [*Chem. Abstr.*, **56**, 11465 (1962)].
16) S. Nishimura and H. Taguchi, This Bulletin, **36**, 873 (1963).
17) It is of interest that similar effects of solvent alcohols were reported on the selectivity of the hydrogenation of benzyl alcohol using a platinum oxide catalyst (Y. Ichinohe and H. Ito, This Bulletin, **37**, 887 (1964)).
18) E. J. Schwoegler and H. Adkins, *J. Am. Chem. Soc.*, **61**, 3499 (1939).

Table I. Hydrogenation of aniline with ruthenium and rhodium catalysts in various alcohols[a]

Catalyst	Solvent	Time for hydrogenation hr.	Yield of product,[b] %			
			Cyclohexylamine	Dicyclohexylamine	Cyclohexanol	Aniline unreacted
Ru hydroxide	MeOH	3.0	87.5	11.9	0.6	0.0
Ru hydroxide	EtOH	3.2	91.4	6.9	1.7	0.0
Ru hydroxide	*i*-PrOH	1.0	100.0	trace	0.0	0.0
Ru hydroxide	*t*-BuOH	1.5	99.7	0.3	0.0	0.0
Rh hydroxide	*i*-PrOH	1.5[c]	79.1	3.5	0.0	17.4
Rh hydroxide	*t*-BuOH	1.5[c]	90.0	2.0	trace	8.0

a) Aniline (0.1 mol.) was hydrogenated with 0.1 g. of the hydroxide in 50 ml. of the solvent at 80°C and 80 kg./cm^2 of initial hydrogen pressure.
b) Yields are given in weight per cent of the products.
c) Hydrogenation was strongly inhibited in the course of the reaction and not completed.

Table II. Effects of added alkalis on the hydrogenation with ruthenium and rhodium catalysts[a]

Catalyst	Solvent	Additive mg.	Time for hydrogenation hr.	Yield of product,[b] %			
				Cyclohexylamine	Dicyclohexylamine	Cyclohexanol	Aniline unreacted
Ru hydroxide	EtOH[c]	NaOH, 4	1.6	97.7	1.7	0.6	0.0
Ru hydroxide	*i*-PrOH	NaOH, 4	0.6	100.0	0.0	0.0	trace
Ru hydroxide	*t*-BuOH	LiOH, 5	2.0	99.6	0.2	0.0	0.2
Ru hydroxide	*t*-BuOH	LiOH, 20	1.8	100.0	trace	0.0	0.0
Ru hydroxide	*t*-BuOH	NaOH, 4	1.3	100.0	0.0	0.0	0.0
Ru hydroxide	*t*-BuOH	NaOH, 7	2.0	98.6	0.0	0.0	1.4
Ru dioxide	*t*-BuOH	—	6.5	99.3	0.0	trace	0.7
5% Ru-C	*t*-BuOH	—	4.5	83.7	12.6	3.7	0.0
5% Ru-C	*t*-BuOH	NaOH, 7	5.0	84.8	10.2	5.0	0.0
Rh hydroxide	*t*-BuOH	LiOH, 20	0.7	99.8	0.2	trace	0.0
Rh hydroxide	*t*-BuOH	NaOH, 4	0.8	99.7	0.3	trace	0.0
Rh hydroxide	*t*-BuOH	NaOH, 7	0.7[d]	61.6	0.2	0.0	38.2
Rh oxide	*t*-BuOH	—	0.6	100.0	0.0	trace	0.0
5% Rh-C	*t*-BuOH	—	0.8	64.0	34.6	1.4	0.0

a) Aniline (0.1 mol.) was hydrogenated with 0.1 g. of unsupported catalysts or 1 g. of supported catalysts in 50 ml. of the solvent at 80°C and 80 kg./cm^2 of initial hydrogen pressure.
b) Yields are given in weight per cent of the products.
c) The use of carefully purified ethanol was necessary for rapid hydrogenation, otherwise the rate decreased markedly with the coloration of the solvent.
d) Hydrogenation was strongly inhibited in the course of the reaction and not completed.

of ammonia strongly retards the hydrogenation of aniline,[4] especially with rhodium and ruthenium catalysts.[14] Probably the most effective and simplest way to suppress the formation of secondary amines is to add a small amount of strong alkali to the reaction mixture.[19,20] Thus, it was found that the addition of only 4 mg. of sodium hydroxide or 20 mg. of lithium hydroxide per 100 mg. of the hydroxide catalyst extremely depresses the formation of dicyclohexylamine with ruthenium hydroxide and almost completely inhibits it with rhodium hydroxide (see Table II). It is noteworthy that, in the presence of the added alkali, the rhodium-catalyzed hydrogenation proceeded rapidly to completion, although the hydrogenation in the absence of alkali was strongly poisoned in the course of the hydrogenation. The addition of an excess amount of alkali (7 mg. of sodium hydroxide) prevented the hydrogenation with rhodium hydroxide from being completed, but not that with ruthenium hydroxide. Neither the ruthenium dioxide prepared by Pichler's method nor the rhodium oxide of the Adams type gave any dicyclohexylamine, even in the absence of added alkali.

19) M. Fluchaire and F. Chambret, *Bull. Soc. Chim. France*, **11**, 22 (1944).
20) M. Taniyama, N. Sawa, T. Nagaoka and T. Takeda, Japanese Pat. 21353 (1963) [*Chem. Abstr.*, **60**, 2756 (1964)].

It is obvious that these oxide catalysts in themselves contain alkaline substances which were contaminated during preparation.[21] Commercial 5% ruthenium- and rhodium-on-carbon catalysts* gave considerable yields of dicyclohexylamine, even in *t*-butyl alcohol, and the addition of a small amount of alkali was of little effect in supressing the formation of the secondary amine (see Table II). Presumably the added alkali was adsorbed on carbon rather than on the catalyst metal.

From the fact that, without the addition of alkali, the hydrogenation with rhodium hydroxide was strongly inhibited before it could be completed, it was supposed that the ammonia and/or dicyclohexylamine produced during the hydrogenation may have poisoned the catalyst. Therefore, the effects of the addition of ammonia and of dicyclohexylamine were studied in isopropyl alcohol using rhodium hydroxide as the catalyst. As may be seen in Fig. 1, the addition of 0.06 mol. of dry ammonia inhibited the hydrogenation almost completely, whereas the addition of 0.05 mol. of dicyclohexylamine retarded the hydrogenation only to a little extent.[22] Thus it is obvious that it was ammonia rather than dicyclohexylamine which inhibited the hydrogenation seriously. The hydrogenation with ruthenium hydroxide was also retarded by the addition of ammonia, though to a much lesser extent. The decrease in the rate observed at the later stages of the hydrogenations in ethyl alcohol and in methyl alcohol, when compared with those in isopropyl and *t*-butyl alcohols, may be attributed to the action of the ammonia formed along with dicyclohexylamine in the course of the hydrogenation (see Fig. 2 and Table I). However, it has been found that, in the presence of a slight amount of added alkali, the hydrogenation with rhodium hydroxide proceeded rapidly to completion, even when 0.077 mol. of ammonia was added (Fig. 1)[23] It is probable that the added alkali eliminated the poisoning action of ammonia by preventing or weakening its adsorption on the catalyst. In connection with these findings, it is of interest to note that, in the synthesis of ammonia, the role of potassium oxide in the doubly-promoted iron catalysts may be explained by assuming that the alkali metal oxide eliminates the poisoning by adsorbed NH-NH_2- and NH_3-species, thus promoting the synthesis of ammonia.[24,25]

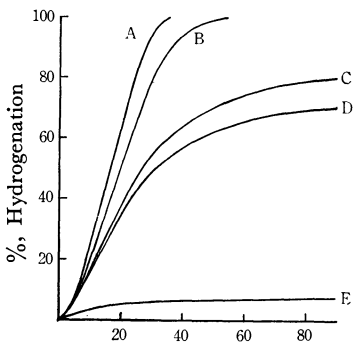

Fig. 1. Hydrogenation of aniline with rhodium hydroxide catalyst in isopropyl alcohol with addition of the following substances.

A LiOH, 10 mg.
B NH_3, 0.077 mol. + LiOH, 10 mg.
C None
D Dicyclohexylamine, 0.05 mol.
E NH_3, 0.063 mol.

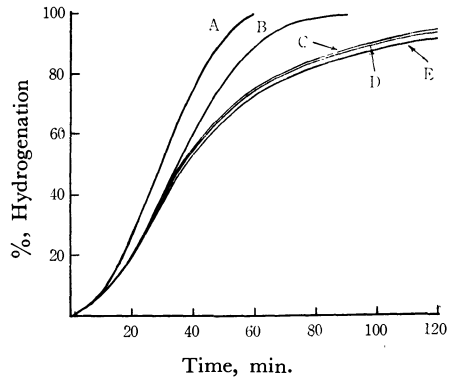

Fig. 2. Hydrogenation of aniline with ruthenium hydroxide catalyst in various solvents and the effect of added ammonia.

A *i*-PrOH B *t*-BuOH
C MeOH D *i*-PrOH + 0.06 mol. NH_3
E EtOH

The mechanism of the formation of dicyclohexylamine is probably the same as that proposed for the production of secondary amines in the hydrogenation of nitriles.[26] Dicyclohexylamine is probably formed by the following reaction sequence via enamine and imine intermediates.[14] However, it is not obvious which step of the reaction leading

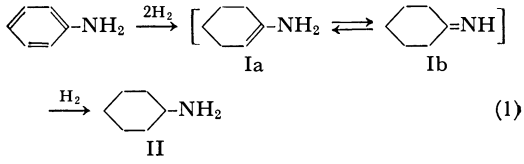

(1)

21) Cf. Ref. 1 and C. W. Keenan, B. W. Giesemann and H. A. Smith, *J. Am. Chem. Soc.*, **76**, 229 (1954).
* Obtained from Engelhard Industries, Inc., Newark, New Jersey, U. S. A.
22) Similar results have been reported with supported ruthenium and rhodium catalysts (Ref. 14).
23) The hydrogenations of aniline with added cyclohexylamine and dicyclohexylamine were similarly rapidly completed in the presence of alkali.
24) W. G. Frankenburg, "Catalysis," Vol. III, Reinhold Publishing Corp., New York (1955), p. 171.
25) R. Krabetz and C. Peters, *Angew. Chem.*, **77**, 333 (1965).
26) J. von Braun, G. Blessing and F. Zobel, *Ber.*, **56B**, 1988 (1923).

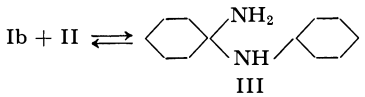

(2)

III

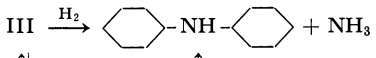

(3)

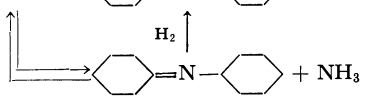

(4)

IV

to the formation of dicyclohexylamine is retarded by alkali. It is probable that the elimination of ammonia by reaction 3 or by reaction 4 is depressed by the presence of alkali, but the present results also suggest another possibility, that the alkali prevents a longer stay of cyclohexylamine on the catalyst surface and thus depresses the addition of it to the Ib imine by reaction 2. In some cases, a small amount of cyclohexanol was obtained (see Tables I and II), the formation of which probably results from the hydrolysis of imine intermediates (Ib and IV). The formation of dicyclohexylamine from two moles of cyclohexylamine was not observed at all under the conditions used in this study, though the condensation is known to occur at higher temperatures.

The authors are indebted to the Mitsubishi Chemical Industries Co., Ltd., for the financial support. Ruthenium-carbon and rhodium-carbon catalysts were kindly supplied by the Nippon Engelhard Co., Ltd.

BULLETIN OF THE CHEMICAL SOCIETY OF JAPAN VOL. 39 333—343 (1966)

An Analysis of the Proton Magnetic Resonance Spectra of Acrylic Acid in Solution: A Comparative Discussion of the Methods of the Analysis of ABC Spin Systems

By Takeo YAMAMOTO and Shizuo FUJIWARA

Department of Chemistry, Faculty of Science, The University of Tokyo, Hongo, Tokyo

(Received June 14, 1965)

In an attempt to examine various existing methods for the analysis of high-resolution NMR spectra, the statistical theory has been applied to the least-squares iteration method presented by Arata, Shimizu and Fujiwara. The standard errors of chemical shifts and spin-spin coupling constants, and the singularity in the normal equation, have been discussed. Two sets of parameters which are placed close together have a possibility of producing a singularity in the normal equation. A way of eliminating the singularity has been presented. The method thus presented has then been applied to an analysis of the vinyl proton spectra of acrylic acid in carbon tetrachloride and in aqueous solutions of various pH values. It has been found that the spin-spin coupling constants do not change beyond the range of experimental errors under the conditions of the present study. The change in chemical shifts has been discussed in terms of the possible conformations of the molecules.

The theory of the analysis of high-resolution NMR spectra seems to be fairly complete. When a set of chemical shifts and coupling constants (molecular constants) is given, ordinary methods[1] of perturbation or exact diagonalization, as well as the direct method of Banwell and Primas,[2] can be used to calculate the spectrum. When a series of measurements is given in an attempt to estimate the most probable molecular constants, the experimental spectrum must first be assigned to the transitions among the energy levels. This is usually done by the trial-and-error method, supplemented by intensity and frequency sum rules.[3,4] Because of the non-uniqueness of the assignments and because of the inevitable experimental errors, however, the procedure is often difficult, and ^{13}C–H satellite line data[5] and double-quantum line data[6] have been used to confirm

1) J. A. Pople, W. G. Schneider and H. J. Bernstein, "High-resolution Nuclear Magnetic Resonance," McGraw-Hill, New York (1959).

2) C. N. Banwell and H. Primas, *J. Mol. Phys.*, **6**, 225 (1963).

3) S. Castellano and J. S. Waugh, *J. Chem. Phys.*, **34**, 295 (1961).

4) J. D. Swalen and C. A. Reilly, ibid., **37**, 21 (1962).

5) R. T. Hobgood, Jr., R. E. Mayo and J. H. Goldstein, ibid., **39**, 2501 (1963).

6) W. A. Anderson, R. Freeman and C. A. Reilly, ibid., **39**, 1518 (1963).

the assignment.

For an ABC spin system, however, Castellano and Waugh[3] have shown that all the possible assignments (energy diagrams) can be obtained from a precise knowledge of all the 15 absorption line positions (the CW method for assignment). When an assignment is obtained, there are two ways to use the observed data for the calculation of the molecular constants. One is to use the data directly for a least-squares adjustment of the molecular constants; the other is to use the absorption line-position data to obtain a set of energy levels, and subsequently to deduce the molecular constants from the energy levels. The former method (the ASF method) was developed by Arata, Shimizu and Fujiwara[7]. Swalen and Reilly[4] (the SR method) obtained the molecular constants by adjusting the calculated energy levels to the "observed" constants by least-squares iterations. Castellano and Waugh[3] (the CW method for calculating molecular constants) used the "observed" energy levels to find, by explicit algebraic calculations, all the sets of molecular constants that regenerate the energy-level diagram.

The ASF method has the advantage over other methods that a suitable choice of the Jacobian matrix enables us to use not only the line positions and intensities, but also the other physical quantities, as input data.[8] The more fundamental advantage of the method is that it provides direct and unambiguous relations between the variance in the observed values and that in the calculated results. These points, which were not fully examined in the previous paper,[7] will be discussed later.[9] The above-mentioned relations are expressed rather indirectly in the SR method, and no such relation has been given for CW method. There are, however, some limitations in the practice of the ASF method, most of which limitations are shared by all least-squares iteration calculations. It will be shown that one of the most serious limitations, i. e., the problem of finding suitable starting constants for all the possible solutions, can be solved by a reduction in the order of the normal equation and by a complementary use of the CW method. Another limitation, the singularity of the normal equation and its eventual omission, will also be discussed.

The analysis was applied to acrylic acid in carbon tetrachloride and in aqueous alkaline media. The chemical shifts and coupling constants obtained will be discussed in connection with possible states of acrylic acid in the above media. The changes in chemical shifts are internal and do not suffer from the large and ambiguous variations caused by macroscopic susceptibility and by other interactions affecting the entire solute molecule.

Method of Analysis

The Calculation of the Spectra.—A spin Hamiltonian for a ABC-type nuclear spin system can be written as follows:

$$\mathscr{H} = -\nu_A I_{AZ} - \nu_B I_{BZ} - \nu_C I_{CZ} + J_{AB}\vec{I_A}\cdot\vec{I_B} + J_{BC}\vec{I_B}\cdot\vec{I_C} + J_{CA}\vec{I_C}\cdot\vec{I_A} \quad (1)$$

Here notations are used in the usual way. In the present work, the vinyl protons cis, geminal and trans to the carboxylic group in an acrylic acid molecule were assigned to A, B and C respectively. When the ν_A, ν_B, ν_C, J_{AB}, J_{BC}, and J_{CA} molecular constants (hereafter called collectively $\{q_i\}$ or $\{q\}$) are known, one can calculate the positions of the absorption lines $\{\omega_j\}$ and the corresponding relative intensities $\{I_j\}$. On the basis of the zeroth order eigenfunctions $\{\varphi_m{}^0\}$ $(m=1,\ldots,8)$ for a three spin $(I=1/2)$ system, the Hamiltonian (1) is represented in a matrix form:

$$(\mathscr{H}_{mn}) = \begin{pmatrix} A & & & & & & & \\ & B & R & Q & & & & \\ & R & C & P & & 0 & & \\ & Q & P & D & & & & \\ & & & & E & R & Q & \\ & 0 & & & R & F & P & \\ & & & & Q & P & G & \\ & & & & & & & H \end{pmatrix} \quad (2)$$

Matrix 2 can be diagonalized by some orthogonal matrices, T, without violating the ordering among the partial matrices in 2:

$$\tilde{T}(\mathscr{H}_{mn})T = \begin{pmatrix} E_1 & & & & & & & \\ & E_2 & & & & & & \\ & & E_3 & & 0 & & & \\ & & & E_4 & & & & \\ & & & & E_5 & & & \\ & & 0 & & & E_6 & & \\ & & & & & & E_7 & \\ & & & & & & & E_8 \end{pmatrix} \quad (3)$$

Since the matrix consists of two 1×1 and two 3×3 matrices, there are $(1!)^2\cdot(3!)^2=36$ T transformations of 2 into Form 4. The eigenfunctions, $\{\varphi_m\}$ $(m=1,\ldots,8)$, are calculated as:

$$T\begin{pmatrix} \varphi_1{}^0 \\ \vdots \\ \varphi_8{}^0 \end{pmatrix} = \begin{pmatrix} \varphi_1 \\ \vdots \\ \varphi_8 \end{pmatrix}$$

The positions of the absorption lines $\{\omega_j\}$ and the relative intensities $\{I_j\}$ are obtained as:

$$\omega_j = \omega_{m\leftarrow n} = E_m - E_n$$

$$I_j = I_{m\leftarrow n} = a|\langle\varphi_m|I_x|\varphi_n\rangle|^2$$

7) Y. Arata, H. Shimizu and S. Fujiwara, ibid., **36**, 1951 (1962).

8) J. Aldous and I. M. Mills, *Spectrochimica Acta*, **18**, 1073 (1962).

9) Recently, Castellano and Bothner-By[10] published their method of analysis based on the Hoffman's method.[11] They expressed same interest with us on the general features of the problem of analysis. Our results shown in this paper will present more concrete an example of the problem.

10) S. Castellano and A. A. Bothner-By, *J. Chem. Phys.*, **41**, 3865 (1963).

11) R. A. Hoffman, ibid., **33**, 1256 (1960).

The normalization coefficient, a, is taken to be $\sum_j I_j = 100$ in the present work.

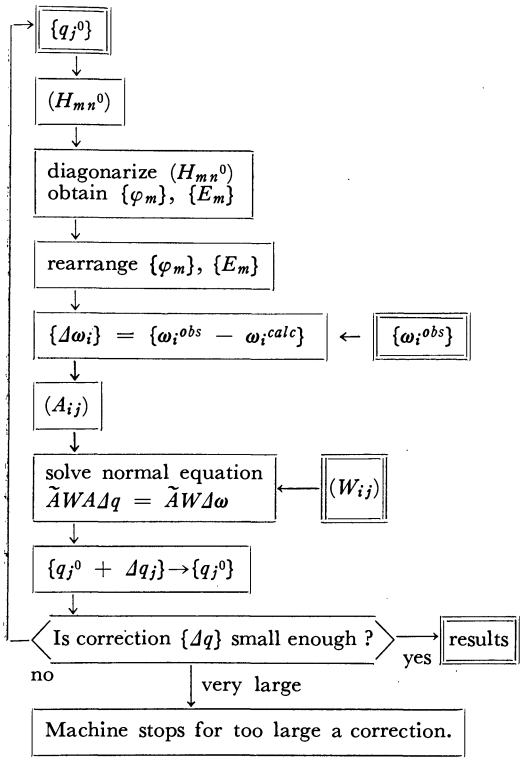

Fig. 1. Flow chart for the ASF method.

Double frames stand for the input and the output data.

The ASF Method.—The flow-chart for the ASF method is reproduced in Fig. 1, where W is the weight matrix for the observed quantities and A is the Jacobian matrix, which contains the differential of the observed quantities with respect to the parameters to be determined. The figure refers to a special case where the weighted squares of the residuals of line positions at a certain resonance frequency are minimized. The method is, however, applicable to any physical quantities expressed as functions of q_i, such as the intensities and the resonant positions at several radiofrequencies.

The estimated variance of the most probable q_i value (the solution of the analysis), $\sigma^2[q_i]$, may be expressed by the variance of an observation of unit weight, σ^2, and by the ii-component of the inverse matrix of the coefficient matrix $\tilde{A}WA$, of the normal equation, $(\tilde{A}WA)^{-1}{}_{ii}$:

$$\sigma^2[q_i] = (\tilde{A}WA)^{-1}{}_{ii} \cdot \sigma^2 \tag{4}$$

The correlation factor between two most probable values of the parameters, q_i and q_j, is given by:

$$\rho[q_i, q_j] = (\tilde{A}WA)^{-1}{}_{ij} \cdot \frac{\sigma^2}{\sigma[q_i] \cdot \sigma[q_j]} = \frac{(\tilde{A}WA)^{-1}{}_{ij}}{\{(\tilde{A}WA)^{-1}{}_{ii} \cdot (\tilde{A}WA)^{-1}{}_{jj}\}^{1/2}} \tag{5}$$

The σ^2 quantity in Eq. 4 can be evaluated in two ways.[12] One way consists of estimating it from the differences (residual vector) between the "observed" and the "calculated" values:

$$\sigma_1{}^2 = \frac{\Delta\tilde{\omega}W\Delta\omega}{N - M} \tag{6}$$

where N is the number of observed quantities (here, the number of absorption lines) and M is the dimension of the normal equation. It must be noted that the "observed" value is obtained by averaging several measurements. The "calculated" value is obtained from the converged parameters $\{q_i\}$.

The other way consists of estimating σ^2 from the variance of the values in individual observations around their mean values, that is, the "observed values" for the analysis:

$$\sigma_2{}^2 = \frac{\sum_{j=1}^{n} (x_j - x)^2}{n(n-1)} \tag{7}$$

where x is the average line position of unit weight; x_j is the jth observed value for that position, and n is the number of runs in the observation. The $\sigma_2{}^2$'s thus obtained are different for all the lines; their average can be used to estimate σ^2. In each analysis, σ_1 and σ_2 must be normally of the same order of magnitude. When $\sigma_1 \gg \sigma_2$ or $\sigma_1 \ll \sigma_2$, the σ in Eq. 4 must be estimated from the larger value, σ_1 or σ_2.

When the analysis is confined to the line positions obtained at a single frequency, the Jacobian matrix (A_{ij}) can be calculated[7]:

$$\begin{aligned}\tilde{A}_{ij} = A_{ji} &= \left(\frac{\partial E_m}{\partial q_i}\right)_{q^0} - \left(\frac{\partial E_n}{\partial q_i}\right)_{q^0} \\ &\simeq 1/\Delta q_i \{\langle\varphi_m|\mathscr{H}(q_i{}^0 + \Delta q_i)|\varphi_m\rangle \\ &\quad - \langle\varphi_m|\mathscr{H}(q_i{}^0)|\varphi_m\rangle - \langle\varphi_n|\mathscr{H}(q_i{}^0 \\ &\quad + \Delta q_i)|\varphi_n{}^0\rangle + \langle\varphi_n{}^0|\mathscr{H}(q_i{}^0)|\varphi_n\rangle\}\end{aligned} \tag{8}$$

where $q_i{}^0$ is the assumed value of the parameter, q_i, and, where Δq_i is the coreection for it.

A Discussion of the ASF Method

The Order in Energy Levels.—In the present work, the Hamiltonian matrix 2 was diagonalized into Form 3 by the Jacobi method. In this method, the choice of the transformation, T, from the 36 possible transformations cannot be controlled, and sometimes a sudden jump in the ordering of the calculated spectrum is observed. The iteration is impossible, in such a case.

12) Y. Murata and Y. Morino, This Bulletin, **38**, 104 (1965).

In order to avoid this inconvenience, the transformation, T, which gives a definite inequality in energy levels (i. e., $E_2 \geq E_3 \geq E_4$ and $E_5 \geq E_6 \geq E_7$) was chosen for the subsequent analysis.

This, however, introduces another difficulty, one which will be discussed in the next section.

The Validity of Approximation for the Jacobian Matrix.—Two conditions are required for the first-order approximation (8) for the Jacobian matrix: (1) the non-degeneracy of energy levels (E_2, E_3, E_4) and (E_5, E_6, E_7) and (2) the closeness of the starting constants, $\{q^0\}$, to the final value, $\{q\}$.

Condition 1 is not always warranted; i. e., there can be "cross-over" among the energy levels, in each 3×3 partial matrix in Eq. 3, as the parameters, $\{q\}$, are varied. In the case of cross-over, second-order or higher-order perturbation methods might be applied. However, another difficulty would occur in that case. Figure 2-1 and 2-2 illustrate this kind of situation. In Fig. 2-1, the values of a parameter q_i are plotted against the remaining parameters, $\{q'\}$. A point on the plane represents a point in the multidimensional space, $\{q\}$, that is, a set of values of the parameters. When a set of observed line positions, $\{\omega_j^{obs}\}$, and the weight matrix, W, are given, the weighted sum of residuals for the data, $\Delta\tilde{\omega}W\Delta\omega$, can be calculated for each $\{q\}$ point. The contour lines in the figure build hypersurfaces, on which the values of $\Delta\tilde{\omega}W\Delta\omega$ are invariant. Figure 2-2 shows a sectional diagram of Fig. 2-1 cut along the straight line X–Y. Point O gives a minimum in $\Delta\tilde{\omega}W\Delta\omega$. On the PQR curve (hypersurface), a cross-over occurs in the energy levels. When the $\{q\}$ parameters are varied on XY from O to Q, the displacement in the calculated line positions makes $\Delta\tilde{\omega}W\Delta\omega$ increase. The differential function is discontinuous at Q. Then, $\Delta\tilde{\omega}W\Delta\omega$ decreases as $\{q\}$ values are varied from Q to Y. This phenomenon has nothing to do with the fact that the estimation of the Jacobian matrix was not carried on above the first-order of approximation. At any rate, the least-square calculation cannot converge into the true minimum, O, when the starting set of constants, $\{q^0\}$, is on the right-hand side of the PQR curve in Fig. 2-1. This means that, when the true solution is near the "cross-over region," a spectrum is hard to analyze unless the starting constants are known with a sufficiently good approximation, as is stated in Condition 2.

When the set of starting constants, $\{q^0\}$, is not beyond the cross-over, the violence of Condition 2 may lead to three faults: a halt of the iteration, a falling into a trap on a hillside, and a jumping over the cross-over line. When Condition 2 is violated, the value of the correction, $\{\Delta q\}$, obtained from $\{q^0\}$ may be such that the Jacobian matrix for the

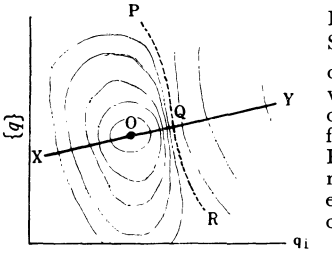

Fig. 2-1. Schematic behavior of $\Delta\tilde{\omega}W\Delta\omega$, the weighted square sum of residuals, as function of $\{q\}$. PQR represents a ridge way where energy levels cross over each other.

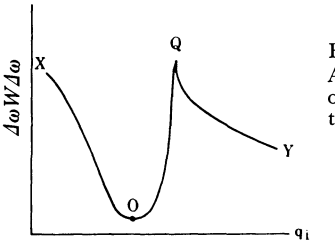

Fig. 2-2. A sectional diagram of Fig. 2-1 cut along the line X–Y.

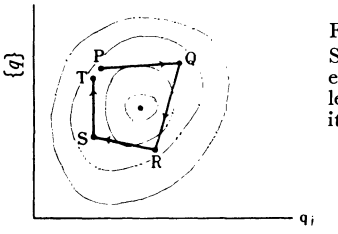

Fig. 2-3. Schematic representation of a halted least-squares iteration.

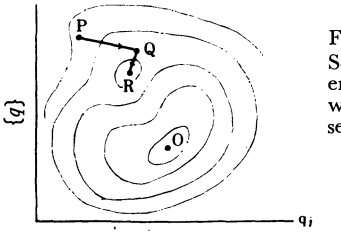

Fig. 2-4. Schematic representation of a case where the iteration settles in a trap.

next cycle of iteration (A_{ij}^1) is significantly different from the original one (A_{ij}^0). Then (A_{ij}^2) may also differ significantly from (A_{ij}^1), in which case an oscillation or circulation of the iteration sets in. This is shown in Fig. 2-3, where the coordinates and the contour lines have the same meaning as in Fig. 2-1. The iteration procedure gives the P, Q, R, S and T points in turn. If there is a trap on the way, the iteration may converge into the trap. This is shown in Fig. 2-4. Starting from P, a false set of constants R is obtained. Near the "cross-over" line, the large correction, $\{\Delta q\}$, may cause the next set of constant, $\{q\}$, to jump over the line. This is the third case.

The Singularity of the Normal Equation.—In the present work, 10 to 14 data of line positions were used to obtain 6 parameters in the least-squares analysis. The symmetry of the molecule

is sufficiently low for there to be no identity among the molecular constants. It might be supposed that there would be little possibility for the normal equation to be singular. It was, however, found that the normal equation could sometimes be almost singular.

Table I shows a set of observed line positions and five weight matrices. Table II lists the results obtained for the five weight matrices by the standard ASF least-squares method. These tables show that small changes in input data sometimes result in considerable variations in the converged constants. In Cases I and II, the same line positions and only one change of weight, from 1 to 0, resulted in a difference of 0.3 c.p.s., or of 15%, in the J_{AC} value. When the starting constants or the line positions were varied by small amounts, the least-squares iterations sometimes showed a slow convergence, and in some cases oscillation resulted.

In the above cases, the inverse matrix of the coefficient matrix of the left-hand side of the normal equation $(\tilde{A}WA)^{-1}$ had abnormally large elements. Table III shows the matrix $(\tilde{A}WA)^{-1}$ for the converged value of Case II in Table II. Accordingly, the estimated normal deviations for the resultant values of parameters, $\sigma[q_i]$, were large. This may be seen, for example, in the values in Table III, Column 1, obtained for the 1 data in Table I. In this case, the accuracy for the observed values and that for the result, $\{q\}$, are not, as has often been assumed, of the same order of magnitude.

TABLE I. ABSORPTION LINE POSITION DATA FOR PURE ACRYLIC ACID

The same set of line position data ω_j was used with five sets of weight matrices W_{jj}. Line positions ω_j were obtained by averaging 30 charts, measured at 60 Mc., at room temperature, from an arbitrary zero-point, by c.p.s. Intensities I_j and standard deviations σ_2 were used in the subsequent analysis.

Line No.	ω_j	W_{jj} I	II	III	IV	V	σ_2	I_j
1	36.104	1	0	0	1	1	0.22	0.2
2	31.155	1	1	1	1	1	0.06	2.4
3	26.122	1	1	1	1	1	0.06	3.0
4	16.525	1	1	1	1	1	0.04	8.3
5	11.527	1	1	1	1	1	0.05	14.8
6	8.685	1	1	1	1	1	0.04	9.0
7	6.914	1	1	1	1	1	0.05	5.5
8	−0.897	1	1	1	1	1	0.07	17.6
9	−6.014	1	1	0	1	1	0.07	0.5
10	−10.648	1	1	1	1	1	0.04	13.7
11	−15.604	1	1	1	1	0	0.05	20.4
12		1	1	1	0	0		
13	−20.232	1	1	1	1	1	0.06	4.3
14	−25.250	1	1	1	1	1	0.10	0.5
15	—	0	0	0	0	0	—	0.0

The correlation matrix for the six parameters, $(R_{ij})=(\rho[q_i, q_j])$, was calculated, as is shown in Table IV, from the inverse matrix in Table III. It has large off-diagonal elements near unity, indicating strong correlations among the parameters.

The above-mentioned features indicate that the normal equation is nearly singular in these cases. The iteration calculations were, therefore, carried out with one parameter fixed. First, the J_{AB}

TABLE II. MOLECULAR CONSTANTS OBTAINED FROM A SET OF LINE POSITION DATA WITH VARIOUS WEIGHT MATRICES

Molecular constants q_i and residuals for line positions (in c.p.s.) were calculated for the five weight matrices I—V in Table I.

Weight matrix data No.	I	II	III	IV	V
q_i					
ν_{AC}	33.456	33.527	33.528	33.371	33.245
ν_{BC}	12.276	12.310	12.308	12.229	12.151
J_{AB}	17.052	16.851	16.841	17.140	17.322
J_{BC}	10.439	10.350	10.359	10.463	10.503
J_{CA}	1.767	2.058	2.059	1.613	1.385
Line No.	Residuals for line positions, $\Delta\omega$				
1	0.18	—	—	0.17	0.15
2	−0.07	−0.02	−0.01	−0.06	−0.07
3	−0.10	−0.05	−0.04	−0.09	−0.07
4	−0.04	0.01	0.01	−0.05	−0.07
5	−0.03	0.02	0.01	−0.05	−0.03
6	−0.02	0.02	0.01	−0.01	0.01
7	0.06	0.03	0.04	0.07	0.09
8	0.00	0.04	0.04	−0.01	−0.02
9	−0.06	−0.02	—	−0.07	−0.05
10	0.01	−0.02	−0.03	0.02	0.04
11	−0.05	−0.01	−0.02	−0.08	—
12	0.06	0.02	0.02	—	—
13	0.03	−0.01	−0.00	0.02	0.01
14	0.01	−0.02	−0.02	0.00	0.02
15	—	—	—	—	—

TABLE III. INVERSE MATRIX FOR THE COEFFICIENTS OF THE NORMAL EQUATION, $(\tilde{A}WA)^{-1}$, FOR A "NEARLY SINGULAR" CASE

Values of molecular constants for this cycle of the iteration are; $\nu_A=21.217728$ c.p.s., $\nu_B=0$ c.p.s., $\nu_C=-12.310128$ c.p.s., $J_{AB}=16.851388$ c.p.s., $J_{BC}=10.350362$ c.p.s., $J_{CA}=2.058250$ c.p.s., representing the converged set of molecular constants for weight matrix No. II, Table I. The matrix is symmetric.

j \ i	ν_A	ν_B	ν_C	J_{BC}	J_{CA}	J_{AB}
ν_A	4.22					
ν_B	1.16	0.84				
ν_C	−5.39	−1.80	7.77			
J_{BC}	−3.52	−1.28	4.84	3.59		
J_{CA}	15.23	4.78	−20.91	−13.36	59.50	
J_{AB}	−11.65	−3.50	15.80	10.16	−44.27	33.78

TABLE IV. A CORRELATION MATRIX (R_{ij}) AMONG THE SIX PARAMETERS FOR A "NEARLY SINGULAR" CASE

Molecular constants used are the same as in Table III. The matrix is symmetric.

j \ i	ν_A	ν_B	ν_C	J_{BC}	J_{CA}	J_{AB}
ν_A	1					
ν_B	0.61	1				
ν_C	0.94	0.71	1			
J_{BC}	0.90	0.74	0.92	1		
J_{CA}	0.96	0.68	0.97	0.91	1	
J_{AB}	0.98	0.66	0.98	0.92	0.99	1

parameter was fixed. Then, the remaining five parameters, $\{q'\}$, were no more correlated. As may be seen from Table V and Table VI, the inverse matrix has no diagonal element much larger than unity, and the off-diagonal elements in the correlation matrix are much smaller than unity.

The result obtained when J_{AB} is fixed at J_0, $\{q'; J_0\}$, is a point on the $J_{AB}=J_0$ hypersurface, where the square sum of weighted residuals, $\Delta\tilde{\omega}W\Delta\omega$, reaches a minimum. When J_0 is varied by small increments and $\{q'; J_0\}$ is obtained for each J_0 value, the sum, $\Delta\tilde{\omega}W\Delta\omega$, is a function of J_0 and can be minimized at $J_0=J_0{}^{min}$. Then, the point $\{q'; J_0{}^{min}\}$ gives a minimum point of the sum in the $\{q\}$ space. Although this procedure gives the same result as that obtained by directly solving the original 6×6 normal equation, it enables us to start from more crude trial constants, $\{q^0\}$. Sometimes, as in the analysis of the pH-5.03 aqueous solution of acrylic acid in Table X, the 6×6 method failed to converge from all the starting constants tried; the 5×5 method was the only means to obtain a solution.

TABLE V. A 5×5 INVERSE MATRIX $(\tilde{A}WA)^{-1}{}_{ij}$ OBTAINED BY FIXING J_{AB}

Molecular constants are the same as in Table III.

j \ i	ν_A	ν_B	ν_C	J_{BC}	J_{CA}
ν_A	0.20				
ν_B	−0.04	0.48			
ν_C	0.05	−0.17	0.38		
J_{BC}	−0.02	−0.25	0.10	0.55	
J_{CA}	−0.05	0.22	−0.22	−0.08	1.54

TABLE VI. A CORRELATION MATRIX (R_{ij}) AMONG THE REMAINING FIVE PARAMETERS WHEN A PARAMETER J_{AB} IS FIXED

Molecular constants used are the same as in Table III.

j \ i	ν_A	ν_B	ν_C	J_{BC}	J_{CA}
ν_A	1				
ν_B	0.13	1			
ν_C	0.21	0.39	1		
J_{BC}	0.05	0.49	0.22	1	
J_{CA}	0.08	0.26	0.28	0.09	1

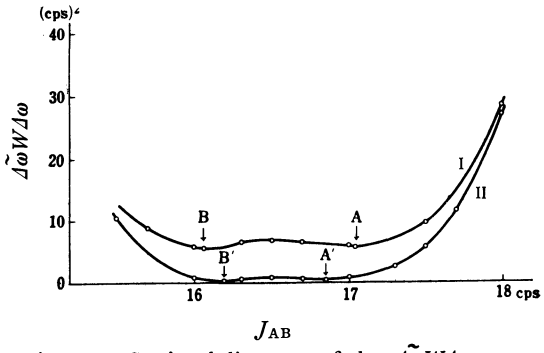

Fig. 3-1. Sectional diagrams of the $\Delta\tilde{\omega}W\Delta\omega$ surface, as obtained by fixing J_{AB}. Curves I and II correspond to data I and II of Table II. Singularity is produced when the saddle point between A and B is low.

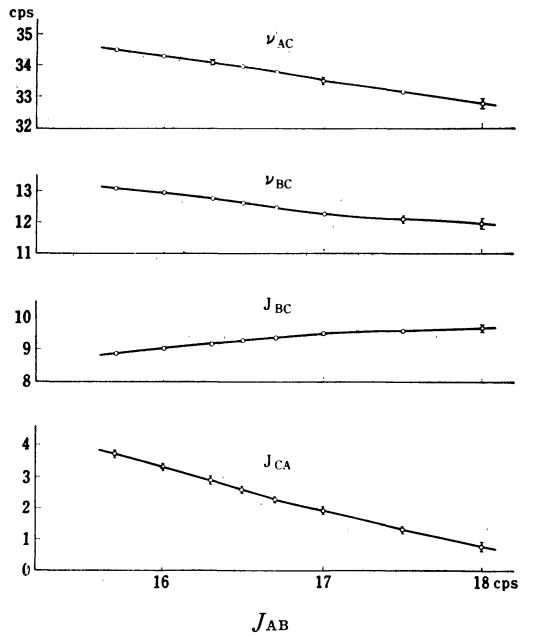

Fig. 3-2. The remaining constants $\{q'\}$ obtained by fixing J_{AB}.

Furthermore, the 5×5 method may be used to study the detailed shape of $\Delta\tilde{\omega}W\Delta\omega$ as a function of $\{q\}$. The values of $\Delta\tilde{\omega}W\Delta\omega$ and the corresponding $\{q'; J_0\}$ are plotted against J_0 in Figs. 3-1 and 3-2. The two curves in Fig. 3-1 are sectional sideviews similar to the curve in Fig. 2-2. The straight line, X–Y, in Fig. 2-2 is now replaced by a curve tracing the bottom of the valley. The abscissa is J_{AB}. Curves I and II correspond to data I and II in Table I respectively.

TABLE VII. CALCULATED SPECTRA CORRESPONDING TO SEVERAL SETS OF MOLECULAR CONSTANTS, $\{q'\ ;\ J_0\}$

ν_{AC}		34.506	34.294	33.903	33.499	33.108	32.741
ν_{BC}		13.075	12.918	12.604	12.304	12.076	11.923
$J_0 = J_{AB}$		15.700	16.000	16.500	17.000	17.500	18.000
J_{BC}		9.858	10.010	10.247	10.425	10.531	10.589
J_{CA}		3.647	3.243	2.523	1.836	1.232	0.123
Line positions	1	35.94	35.93	35.92	35.92	35.96	36.01
	2	31.22	31.22	31.21	31.22	31.27	31.36
	3	26.15	26.21	26.25	26.22	26.18	26.13
	4	16.65	16.57	16.54	16.56	16.61	16.68
	5	11.56	11.56	11.57	11.56	11.52	11.45
	6	8.65	8.69	8.72	8.72	8.67	8.64
	7	6.84	6.85	6.87	6.86	6.83	6.80
	8	−0.90	−0.90	−0.91	−0.90	−0.85	−0.75
	9	−5.94	−5.96	−5.96	−5.96	−5.98	−6.04
	10	−10.66	−10.66	−10.66	−10.66	−10.67	−10.67
	11	−15.49	−15.55	−15.59	−15.56	−15.50	−15.44
	12	−15.74	−15.68	−15.62	−15.66	−15.76	−15.92
	13	−20.21	−20.25	−20.29	−20.27	−20.20	−20.09
	14	−25.28	−25.27	−25.26	−25.26	−25.28	−25.32
	15	−42.78	−42.78	−42.78	−42.78	−42.79	−42.81
Intensities	1	0.12	0.16	0.24	0.32	0.40	0.48
	2	2.91	2.84	2.73	2.61	2.49	2.37
	3	3.82	3.73	3.57	3.40	3.22	3.03
	4	9.81	9.57	9.05	8.45	7.85	7.29
	5	14.89	14.84	14.73	14.62	14.55	14.51
	6	7.49	7.62	7.85	8.10	8.38	8.66
	7	1.75	2.16	2.99	3.90	4.79	5.63
	8	18.97	18.96	18.93	18.88	18.82	18.77
	9	0.00	0.00	0.11	0.35	0.65	0.99
	10	14.59	14.53	14.41	14.27	14.12	13.96
	11	8.48	8.73	9.18	9.57	9.85	10.04
	12	11.23	11.17	10.94	10.59	10.16	9.70
	13	4.25	4.21	4.13	4.07	4.05	4.06
	14	1.61	1.41	1.08	0.80	0.59	0.43
	15	0.00	0.00	0.00	0.00	0.00	0.00

In Fig. 3-2, the remaining constants, $\{q'\}$, for the data I are plotted. The short perpendicular bars are the standard deviations estimated from Formulas 4 and 6.

A remarkable feature of the curves in Fig. 3-1 is that each of them has two minima with a low saddle point. The two minima in the curve gave the same line positions and very similar absorption intensities. $\{q'\ ;\ J_0\}$ points between and near the minima also gave very similar spectra. Table VII shows the calculated spectra for several points, $\{q'\ ;\ J_0\}$, on Curve I, Fig. 3-1. It may be seen that a large (and correlated) variation in the constants causes little variation in the line positions. For example, the variation in J_{AC} from 3.65 c.p.s. to 0.12 c.p.s. causes line 11 to displace only 0.30 c.p.s, and this is the most prominent of all the line position displacements. The calculated intensities for the two minima for the data are presented in Table VIII. The intensities are not very different.

The above-mentioned results show that, when there are two closely-placed minima in the $\Delta\tilde{\omega}W\Delta\omega$ vs. $\{q\}$ curve, there may be an incomplete singularity in the original least-squares method and a large inaccuracy in the results obtained. Therefore, it is not appropriate to ask whether or not two results of analysis, $\{q^1\}$ and $\{q^2\}$, represent the same solution without considering their normal deviations. A set of data may give $\{q^1\}$, while another set, a little different from the former, or even the same data when processed on another computor, may give $\{q^2\}$, which seems to be substantially different from $\{q^1\}$.

The same situation may be encountered[13] in dealing with the CW method for calculating molecular constants. In the above-mentioned cases of two minima, the solutions from the CW method were also strongly affected by minute changes in the adjusted (observed) line positions and rounding

13) J. R. Cavanaugh, *J. Chem. Phys.*, **40**, 248 (1964).

TABLE VIII. ALL THE POSSIBLE SETS OF MOLECULAR CONSTANTS FOR THE LINE POSITION DATA OF PURE ACRYLIC ACID AT 60 Mc.

The four sets were obtained by analyzing the data set I, Table I. All the four sets of molecular constants give the same calculated line positions. Sets I and II are presented with the estimated normal deviations of the constants.

	Set			
q_i	I	II	III	IV
ν_{AC}	33.46±0.26	34.24±0.20	29.63	27.91
ν_{BC}	12.28±0.20	12.87±0.18	9.09	7.45
J_{AB}	17.05±0.39	16.07±0.34	18.11	21.51
J_{BC}	10.44±0.11	10.05±0.20	7.75	8.55
J_{CA}	1.77±0.50	3.14±0.52	12.82	8.62

Line No.	Line positions		Intensities				
	Calcd.	Obs.	Calcd. I	II	III	IV	Obs.
1	35.93	36.10	0.33	0.17	0.05	0.79	0.2
2	31.22	31.16	2.60	2.82	2.23	1.91	2.4
3	26.22	26.12	3.38	3.71	2.77	1.75	3.0
4	16.56	16.53	8.39	9.51	9.06	4.97	8.3
5	11.56	11.53	14.61	14.83	19.10	18.68	14.8
6	8.70	8.69	8.13	7.65	3.78	4.68	9.0
7	6.86	6.91	4.00	2.27	0.15	5.24	5.5
8	−0.90	−0.90	18.87	18.96	24.48	24.18	17.6
9	−5.96	−6.01	0.37	0.01	1.49	2.61	0.5
10	−10.66	−10.65	14.26	14.52	18.98	18.39	13.7
11	−15.56	−15.60	9.60	8.80	3.60	6.26	20.4
12	−15.66		10.55	11.14	9.00	7.60	
13	−20.26	−20.23	4.07	4.19	2.88	2.80	4.3
14	−25.26	−25.25	0.77	1.36	2.29	0.04	0.5
15	−42.78	—	0.00	0.00	0.06	0.02	0.0

errors in the calculations.

In conclusion, two closely-placed minima cause a poor convergence in the calculation and large estimated normal deviations in the result. The convergence may be improved by the reduction of the parameter, but the only way to eliminate uncertainty in the result is to introduce independent information, such as a change in the medium, data at another radiofrequency, or the parameters of related compounds.

The Starting Constants.—In an analysis of an unknown ABC spin system with the ASF method, the first one or two sets of solutions are usually easy to obtain. A few trial-and-error assumptions of starting constants based on a first-order analysis, chemical or structural considerations or explicit analysis can give the desired result. When the iteration does not converge, it may be improved by reducing a parameter.[14]

However, it is sometimes difficult to obtain all the possible solutions by the trial-and-error method.[15] The CW method for calculating molecular constants is suitable for this purpose. The calculated spectrum of the first solution can be used for the "adjusted absorption frequencies data." When the biquadratic equation described in Ref. 3 yields complex solutions with small imaginary components, the real part may be used to obtain an approximate set of molecular constants. The refinement by the ASF method then removes the uncertainty about the line-adjustment[13] and the reliability of the result.

14) In order to reduce the parameters, the choice of the new set of parameters is important. In principle, it may be selected by solving a secular equation for the $\{q\}\sim\Delta\omega W\Delta\omega$ solid. A set of linear combinations of the original parameters is obtained. The most efficient way to eliminate the singularity is to fix one of the linear combinations and to take the others for the new set of parameters. In the present work, in order to simplify matters, the new set chosen was similar to the original one except for the fixed parameter. The parameter, J_{AB}, was fixed because the correlation matrix had comparatively large elements in the corresponding column. The choice proved to be effective, as has been discussed in the text. We also tried to fix all the parameters in turn and to make the calculation self-consistent; that is, one parameter was fixed in a cycle and the solution was used for the input data of the next cycle, where another parameter was fixed. This method failed to improve the convergence, however.

15) Swalen and Reilly[4] say that there is no problem of uniqueness about their iteration method. However, energy levels are not uniquely determined from a set of observed line positions. Even when the levels are determined from double quantum lines or by other techniques, other sets of solutions are still possible. Their "transformation vector," which diagonalizes the approximate Hamiltonian, is not a constant vector when the correction, $\{\Delta q\}$, is large. It follows that if they start from different sets of approximate constants, different solutions will be obtained. The situation is the same between the SR method and the ASF method as far as the uniqueness is concerned.

TABLE IX. TWO SETS OF MOLECULAR CONSTANTS FOR THE LINE POSITION DATA OF 11% BY WEIGHT ACRYLIC ACID IN CCl_4

q_i	Set I	Set II
ν_{AC}	34.08±0.15	35.61±0.11
ν_{BC}	10.88±0.13	12.19±0.11
J_{AB}	17.36±0.22	15.29±0.20
J_{BC}	10.42±0.06	9.76±0.12
J_{CA}	1.42±0.25	4.14±0.29

Line No.	Line positions		Intensities		
	Calcd.	Obs.	Calcd. I	II	Obs.
1	36.22	36.17	0.52	0.13	0.5
2	31.93	31.95	2.88	3.28	3.1
3	26.59	26.55	3.45	4.20	3.7
4	17.67	17.71	7.52	9.70	8.0
5	12.34	12.35	14.21	14.60	13.1
6	8.05	—	4.79	1.46	
7	7.91	7.94	7.72	6.80	14.6
8	−1.70	−1.67	18.74	18.90	15.4
9	−6.35	−6.39	0.70	0.03	0.7
10	−10.64	−10.66	14.39	14.91	12.5
11	−15.96	−15.94	10.43	8.92	23.9
12	−15.97		10.50	11.58	
13	−20.25	−20.29	3.80	4.02	4.1
14	−25.58	−25.58	0.35	1.47	0.2
15	−44.26	—	0.00	0.00	0.0

TABLE X. TWO SETS OF MOLECULAR CONSTANTS OBTAINED FOR ALKALINE SOLUTIONS OF ACRYLIC ACID

	q_i	pH: Aq. soln.	3.70	3.96	4.37	5.03	5.40	13
Set I	ν_{AC}	24.86±0.10	24.21±0.10	23.88±0.11	23.09±0.18	22.4±10.5	22.30±0.65	22.01±0.10
	ν_{BC}	10.38±0.10	15.31±0.14	17.10±0.12	21.85±0.20	26.2±13.3	27.37±0.83	28.60±0.12
	J_{AB}	17.29±0.10	17.42±0.10	17.29±0.07	17.36±0.06	17.3± 5.0	17.52±0.41	17.52±0.08
	J_{BC}	10.56±0.09	10.60±0.12	10.36±0.08	10.47±0.10	10.6± 6.3	10.54±0.55	10.45±0.10
	J_{CA}	1.27±0.10	1.14±0.16	1.28±0.12	1.42±0.16	1.4±11.2	1.36±0.76	1.54±0.12
Set II	ν_{AC}	27.98	26.94	23.88	23.09	22.84	23.32	23.72
	ν_{BC}	12.37	16.05	17.39	25.98	25.16	24.90	24.20
	J_{AB}	13.41	15.10	15.47	16.33	17.62	18.33	19.05
	J_{BC}	8.39	7.55	6.92	8.63	10.99	11.43	11.90
	J_{CA}	7.32	6.50	6.55	4.27	0.70	−0.34	−1.44

Experimental

The acrylic acid and carbon tetrachloride were purified by distillation from commercial products. The pH measurements were made to a precision of ±0.1 pH units with glass electrodes calibrated with standard buffer solutions. The concentrations were determined by weight.

The NMR measurements were made with a standard 60 Mc. apparatus without NMR control, at room temperature. The sideband frequencies were calibrated by a frequency counter to a precision of ±0.1 c.p.s. The absorption line positions were measured from a line in the spectrum which served as a zero point. One sample was measured for 5—40 sweeps. These charts were then averaged to obtain one set of observed data.

A digital computor, PC-2, was used for the statistical processing of the charts, the CW method for calculating molecular constants, and the ASF least-squares calculations. The ASF method with or without the J_{AB} parameter fixed, and the CW method were used for analyses.

In the ASF method, the weight matrices were taken to be diagonal.[16] Except for the data listed in Table I, the diagonal elements were taken to be 1 or 0, depending on whether or not the corresponding line was observed. The lines which were not observed clearly because of weakness or line overlapping were given weights of 0.5 or 0.

16) In the above case, the line-position data from a chart sheet are not mutually-independent measurements, and the weight matrix may have some off-diagonal elements.[12] This point was, however, not studied in the present work. When the diagonal elements were varied, there were no significant changes in the results provided the normal deviation was taken into account.

Results and Discussion

Acrylic Acid in Carbon Tetrachloride.— Four sets of molecular constants, $\{q\}$, were obtained as the results of the analysis of pure acrylic acid. They are shown in Table IX. In view of the intensity data, Sets III and IV are obviously not suitable, whereas Sets I and II almost equally fit to the observed spectrum. Though the intensities of Lines No. 9 and No. 14 seem to be favorable to Set I, the choice is not clear. The estimated standard deviations are large in both cases.

In order to determine which of the two sets is the more suitable, the spectrum of a carbon tetrachloride solution of acrylic acid, 11% by weight, was analyzed. Two sets of molecular constants were obtained near Sets I and II of the pure substance, as is shown in Table IX. One of them, Set I, has very similar coupling constants to those of Set I in the pure substance. Though the observed spectra of the two systems are rather similar, the other sets of molecular constants, the II sets, were considerably different. The saddle-point between the two minima was found to increase in height, and the calculated absorption intensity for the two sets I and II was also appreciably different, in the 11% solution. In this case, therefore, there was little ambiguity in choosing Set I as the better set.

The spectra in 63% and 2% solutions were also analyzed. Again there was a series of sets of constants with small variations in coupling constants and with good agreement in intensities. From those facts we have concluded that the sets corresponding to the Set I in pure substance are the correct sets of the molecular constants of the systems. These results are shown in Fig. 4, together with other results.

Acrylic Acid in Aqueous Alkaline Media.— The variation in $\{q\}$ was studied for a 10%-in-wt. aqueous solution of acrylic acid at various pH values. The pH was adjusted by the addition of sodium hydroxide. In these systems, the fact that we again obtained the Set II of molecular constants caused some difficulty. The variation in these two sets of solutions with the pH of the system is shown in Table X. This table shows that, in Set I, J_{AB} and J_{AC} are not changed by more than ± 0.2 c.p.s. by the cange in pH, while in Set II they vary over a wide range. The pH dependence of the shifts is smooth in Set I, while in Set II it is irregular. These facts suggest that Set I is the more suitable solution. Moreover, a comparison of the intensities shows that in the two extreme cases, i. e., in the aqueous solution and in the pH-13 solution, Set I gives the correct intensity while Set II does not. Hence, Set I may be said to represent the true molecular constants over the entire pH range.

In the intermediate range of pH, where the two sets approach and cross each other, the estimated normal deviations of $\{q\}$ became broad and convergence was difficult to obtain, as has been discussed in the previous section. At pH 5.03, the least-squares analysis was made by the 5×5 method because convergence was not reached by the 6×6 method. The corresponding reliability range, shown in Table XIII, is very large. When, however, the calculation is made by assuming the J_{AB} constant to be in the same reliability range as it is at the other pH's, i. e., at 17.4 ± 0.2 c.p.s, the corresponding range of the other parameters becomes much narrower, as is shown by the perpendicular bars in Fig. 4.

Figure 4 also shows that the coupling constants do not vary appreciably with the pH. The following assumptions were made to explain the pH dependence of the chemical shifts:

(a) The only solute species in a 10% aqueous solution and in a pH $\sim$13 alkaline solution are an acid monomer molecule, HA, and a monoanion, A^-, respectively.

(b) In a solution with an intermediate pH

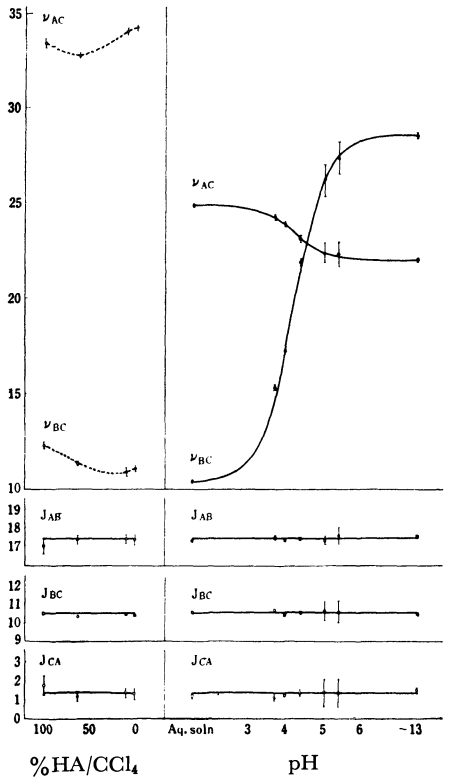

Fig. 4. Variation of the molecular constants. The left half of the figure shows the molecular constants of acrylic acid in CCl_4, and the right one those in 10% aqueous solutions of various pH. Perpendicular bars are the estimated normal deviations (see text). Solid curves for ν_{AC} and ν_{BC} represent theoretical lines for a pK_a of 4.20.

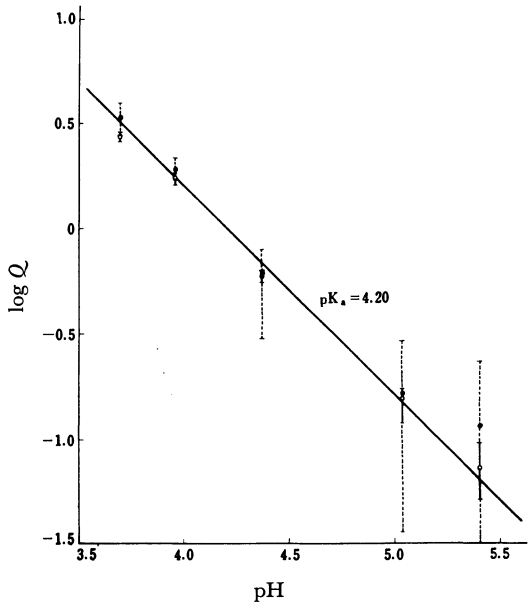

Fig. 5. The relation between log Q and pH. White circles refer to log Q's obtained by ν_{AC} and black circles to those by ν_{BC}. Solid or broken bars attached to each circle represents the variation in each value.

value, HA and A^- exist in a chemical equilibrium:

$$[H^+]\cdot[A^-] = [HA]\cdot 10^{-pK_a} \quad (9)$$

and the exchange between them is sufficiently fast. The activity expressed in Eq. 9 by a square bracket can be approximated by the analytical concentration.

Therefore,

$$pK_a - pH = \log Q$$

where

$$Q = \frac{q_A - q_{HA}}{q - q_{HA}} - 1$$

Figure 5 shows the log Q vs. pH plot for $q=\nu_{AC}$ and for $q=\nu_{BC}$. The perpendicular bars are estimated widths, corresponding to the standard deviations of q, q_{A^-} and q_{HA}. The points agree with the solid straight line with a gradient of -1. From the intercept of the straight line with the line for log $Q=1$, $pK_a=4.20\pm0.10$ was deduced. This value agrees fairly well with the value of 4.25 reported in the literature, which was determined potentiometrically.

The results given above suggest that the molecular constants for a 10% aqueous solution and a pH ~13 aqueous solution of acrylic acid represent those of a monomer acid molecule and a monoanion respectively. The chemical shifts can be explained in terms of bond-anisotropy. It was assumed that an acid monomer molecule has a *s-cis* structure; that the C=O bond susceptibility tensor is axially symmetric with an anisotropy of $\Delta\chi$ and with the axis perpendicular to the molecular plane, and that the induced dipole is at the center of the bond. The monoanion COO^- group was assumed to have a similar group anisotropy, $\Delta\chi'$, and the induced dipole was assumed to be at the center of gravity of two C–O bonds. The reported values of anisotropy in C=O[17,18] and CO_3^{2-} [19] groups leads to $\Delta\chi$ and $\Delta\chi'$ values of -5——10×10^{-6} e.m.u. If we take $\Delta\chi=\Delta\chi'=-8\times10^{-6}$ e.m.u., $\nu_{AC}=22.6$ c.p.s. and $\nu_{BC}=13.9$ c.p.s. in an acid monomer, and $\nu_{AC}=12.1$ c.p.s. and $\nu_{BC}=22.3$ c.p.s. in a monoanion. These values are in fairly good agreeement, in order of magnitude and in sense of variation, with the observed values. The difference of about 10 c.p.s. in ν_{AC} value between the 10% aqueous solution and carbon tetrachloride solutions seems to reflect the change from the acid monomer structure interacting with the solvent water molecules to the acid dimer or polymer structure interacting with the other solute molecules. A simple explanation in terms of bond-anisotropy was not sufficient for a more quantitative discussion. Solutions in carbon tetrachloride showed only a small change in chemical shifts with the concentration, suggesting that dilution with the nonpolar solvent carbon tetrachloride down to 2 wt.% or 5 mol.% affects the solute-solute interactions little.

According to the concept of electronegativity, a –COOH group must be considerably different from a $-COO^-$ group, and the relationship between coupling constants and electronegativity in vinyl compounds predicts corresponding changes in coupling constants. Such changes were not observed, however. The coupling constants and, particularly, their sums are quite invariable in spite of the great change in molecular states and in chemical shifts.

The authors wish to thank Drs. Yuzuru Fujiwara, Masaharu Toyama and Yoji Arata for valuable discussions. We are also much indebted to Dr. Osamu Yamamoto of the Government Chemical Research Institute, Tokyo, and Dr. Ichiro Yamaguchi of Japan Atomic Energy Research Institute for their aid in NMR measurements.

17) P. T. Narashimhan and M. T. Rogers, *J. Phys. Chem.*, **63**, 1388 (1959).
18) J. A. Pople, *J. Chem. Phys.* **37**, 60 (1962).
19) J. A. Pople, ibid., **38**, 1276 (1963).

BULLETIN OF THE CHEMICAL SOCIETY OF JAPAN VOL. 39 344—347 (1966)

The Effect of the pH Value on the Crystallization of Strontium Sulfate in the Presence of Triphosphate

By Masaji MIURA, Hiromitu NAONO and Mitunori HARA

Department of Chemistry, Faculty of Science, Hiroshima University, Higashisenda-machi, Hiroshima

(Received June 16, 1965)

The crystallization of strontium sulfate has been conductometrically investigated in the presence of triphosphate under various pH values of the solution. The amount of triphosphate adsorbed on the crystal surface of strontium sulfate has been estimated as a function of the pH of the solution. The action of triphosphate in stabilizing the supersaturated solution of strontium sulfate and the amount of triphosphate adsorbed on the crystal surface depend remarkably on the pH of the solution; further, the two are closely correlated with each other. It has been concluded from these facts that the adsorption of triphosphate plays an important role in the stabilization of the supersaturated solution of strontium sulfate.

Several investigators have studied the characteristic phenomena caused by the action of condensed phosphates on the crystallization of sparingly-soluble inorganic salts from their supersaturated solution.[1-5] As has been reported previously,[2-4] the crystallization of strontium sulfate is extremely retarded and its supersaturated solution is stabilized by the coexistence of a minute amount of triphosphate. Recently, it has been clarified that the main function of triphosphate is the suppression of nuclei formation from the supersaturated solution of strontium sulfate.[6] On the other hand, such a stabilizing action is closely correlated to the adsorption of triphosphate on the crystal surface of strontium sulfate.[2-4]

The works mentioned above have treated the stabilizing action and the adsorptive behavior of triphosphate in a neutral solution.[2-4] It has been found, however, that when the pH of the solution is varied, remarkable differences arise in the stabilizing action, and also in the adsorptive behavior, of triphosphate. Accordingly, it seems of great interest to investigate these problems at various pH values.

Experimental

Materials.—Strontium chloride and potassium sulfate were purified by recrystallizing the special-grade reagents three times from their aqueous solutions. Pure sodium triphosphate labeled with ^{32}P was prepared by a procedure which has been described previously.[5] Strontium sulfate crystals used as an adsorbent were prepared by a procedure similar to that described in a previous paper,[3] except that the experiment was carried out in a nitrogen atmosphere in order to avoid the formation of strontium carbonate.

Crystallization.—The crystallization of strontium sulfate was traced by measuring the conductivity decrease in the supersaturated solution, which was prepared by mixing equal volumes of 0.02 M solutions of strontium chloride and potassium sulfate, the latter containing various amounts of triphosphate.

Adsorption.—The experiment of adsorption was carried out by a radiotracer method with the aid of triphosphate labeled with ^{32}P.[2]

The pH of the solution was adjusted by adding hydrochloric acid or sodium hydroxide. Crystallization and adsorption experiments were carried out at 25°C in a nitrogen atmosphere in order to restrain the pH change during the procedures.

Results and Discussion

As has been reported in the previous papers,[3,4] such a minute amount of triphosphate as 5×10^{-6} M practically inhibits the crystallization from a 0.01 M strontium sulfate solution when the solution is neutral. With its concentration kept at 5×10^{-6} M, the action of triphosphate on the crystallization of strontium sulfate was examined conductometrically at various pH values. As may be seen in Fig. 1, the stabilizing action of triphosphate becomes weak as the pH of the solution is lowered. In Fig. 3, the decrease in specific conductivity after 100 min, is plotted as a function of the pH of the solution. It must be emphasized that the stabilizing action changes abruptly within a certain pH range and practically disappears below pH 5. Figure 2 shows the pH dependence of the stabilizing

1) L. Rosenstein, U. S. Pat. 2038316 (1936); G. B. Hatch and O. Rice, *Ind. Eng. Chem.*, **31**, 51 (1939); R. F. Reitemeier and T. B. Buehrer, *J. Phys. Chem.*, **44**, 535, 552 (1940); R. F. Reitemeier and A. D. Ayers, *J. Am. Chem. Soc.*, **69**, 2759 (1947); B. Raistrick, *Discussions Faraday Soc.*, **5**, 234 (1949); E. J. Burcik, *Producers Monthly*, **19**, No. 1, 42 (1954).

2) S. Otani, This Bulletin, **33**, 1544, 1549 (1960).

3) M. Miura, S. Otani, M. Kodama and K. Shinagawa, *J. Phys. Chem.*, **66**, 252 (1962).

4) M. Miura, S. Otani, Y. Abe and C. Fukumura, This Bulletin, **36**, 1091 (1963).

5) M. Miura, H. Naono and S. Otani, *J. Chem. Soc. Japan, Ind. Chem. Sect.* (*Kogyo Kagaku Zasshi*), **66**, 597 (1963).

6) H. Naono and M. Miura, This Bulletin, **38**, 80 (1965).

action of triphosphate, its concentration being 3×10^{-5} M. An abrupt change in the stabilizing action is also observed, but it occurs in a somewhat lower pH region than in the above case, as may be seen in Fig. 3.

Next, the crystallization of strontium sulfate was studied at various pH values in the absence of triphosphate. Figure 4 shows that the crystallizations are somewhat different at different pH values. The lower the pH of the solution, the more rapidly the crystallization begins, but the effect of pH on the crystallization is small compared with that in the presence of triphosphate mentioned above. Consequently, it is clear that the remarkable change in the stabilizing action with the pH value in the presence of triphosphate is mainly due to the change in the action of triphosphate with the pH.

It has been considered so far that the stabilization of the supersaturated solution of strontium sulfate by triphosphate is to be attributed to the adsorption of triphosphate. It may, therefore, be expected that a remarkable difference will also appear in the adsorptive behavior of triphosphate on the surfaces of strontium sulfate crystals.

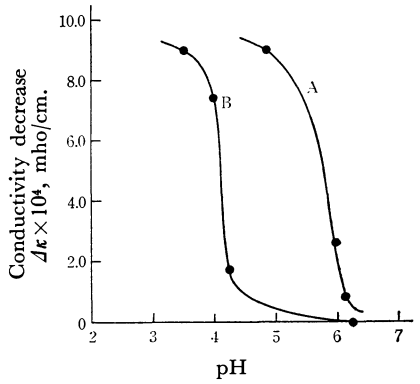

Fig. 3. Conductivity decrease after 100 min.
Concentration of triphosphate:
A 5.0×10^{-6} M, B 3.0×10^{-5} M

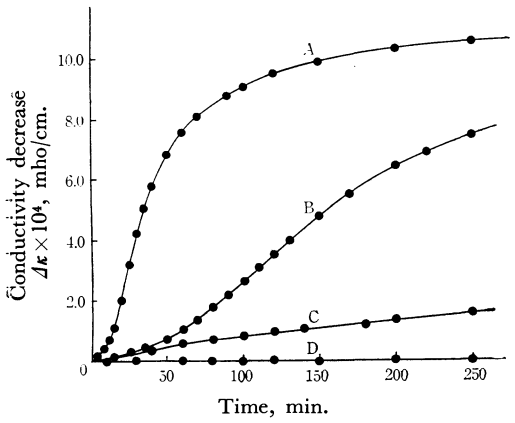

Fig. 1. Effect of pH on the crystallization of strontium sulfate from 0.01 M solution in the presence of 5.0×10^{-6} M triphosphate.
A pH=4.85, B pH=5.98, C pH=6.12, D pH=9.97

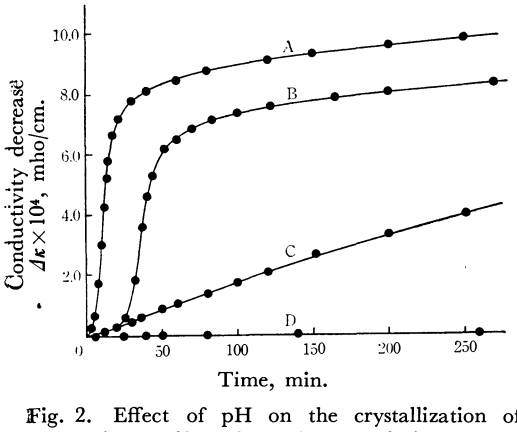

Fig. 2. Effect of pH on the crystallization of strontium sulfate from 0.01 M solution in the presence of 3.0×10^{-5} M triphosphate.
A pH=3.45, B pH=3.98, C pH=4.08, D pH=6.20

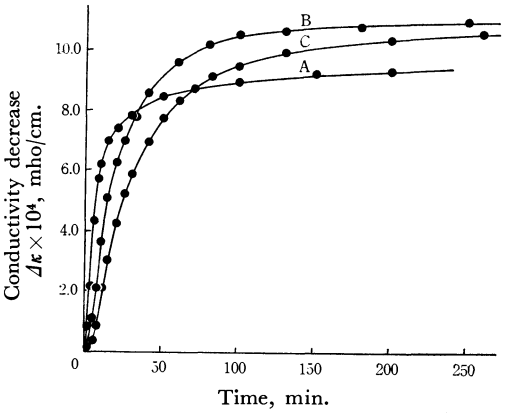

Fig. 4. Effect of pH on the crystallization of strontium sulfate from 0.01 M solution.
A pH=3.32, B pH=6.50, C pH=9.95

It has been reported previously that triphosphate adsorbed from a neutral solution forms a monomolecular layer on the surfaces of strontium sulfate crystals.[3] It is, therefore, apparent from the

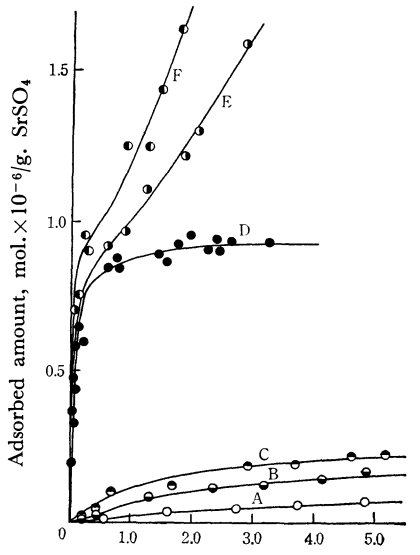

Fig. 5. Adsorption isotherms of triphosphate at various pH.
A pH=2.5, B pH=3.2, C pH=3.5,
D pH=6.8, E pH=10.9, F pH=11.3

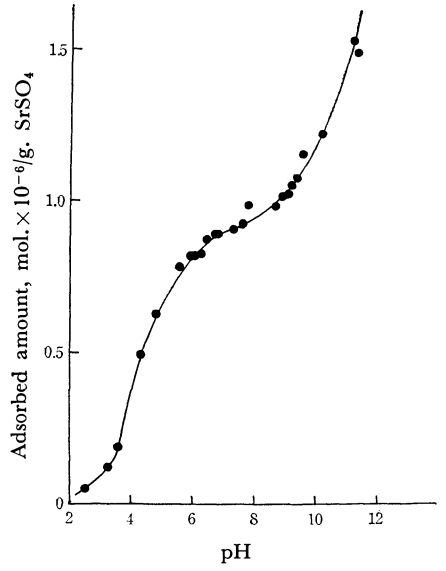

Fig. 6. Relation between adsorbed amount and pH of solution at the equilibrium concentration of 3×10^{-5} M triphosphate.

isotherms in the acid region that the adsorbed triphosphate covers merely a small fraction of the adsorbent surface. On the other hand, on the alkaline side the amount adsorbed far exceeds that corresponding to the monomolecular layer.

Now, let us discuss the pH dependence of the stabilizing action of triphosphate in connection with that of the amount adsorbed at the concentration of triphosphate, 3×10^{-5} M. It is obvious from Figs. 2 and 6 that both the stabilizing action and the adsorbed amount change remarkably in the vicinity of pH 4; that is, the stabilizing action increases rapidly with the abrupt change in the adsorbed amount. This fact indicates that the adsorption plays an important role in the stabilizing action, as has been considered previously. In the present work, no large difference in the stabilizing action was observed on the alkaline side, though the amount adsorbed was far larger than that in the neutral region.

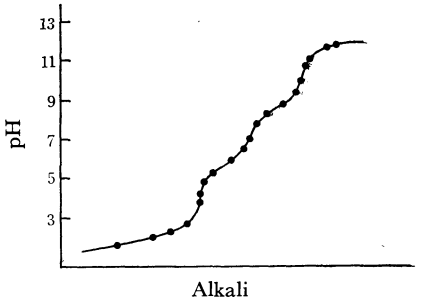

Fig. 7. Titration curve of triphosphoric acid with tetramethyl ammonium hydroxide. After J. I. Watter et al.[7]

When triphosphoric acid is titrated with alkali, three inflection points can be obtained, corresponding to three different ionic species, namely, $H_2P_3O_{10}^{3-}$, $HP_3O_{10}^{4-}$ and $P_3O_{10}^{5-}$, as may be seen in Fig. 7.[7] A comparison between the titration (Fig. 7) and the adsorption (Fig. 6) curves shows that the ionic species, $HP_3O_{10}^{4-}$ and $P_3O_{10}^{5-}$, have a much greater ability to be adsorbed on the crystal surface than does $H_2P_3O_{10}^{3-}$. On the other hand, the stability of the complex between strontium and triphosphate ions increases with an increase in the pH of the solution.[8] Therefore, triphosphate ions of a higher valency may be adsorbed on the strontium sulfate crystal, forming a surface complex with strontium ions and thus playing an important role in stabilizing the supersaturated solution of sutrontium sulfate.

Summary

The pH of the solution exerts a profound influence on the action of triphosphate in stabilizing the supersaturated solution of strontium sulfate, and also on the amount of triphosphate adsorbed on its crystal surface. Both of these functions of triphosphate show a remarkable change in the vicinity of pH 4 when the concentration of triphosphate is 3×10^{-5} M. Above pH 4, the stabilizing action and the amount of triphosphate adsorbed

7) J. I. Watters, S. M. Lambert and E. D. Loughran, *J. Am. Chem. Soc.*, **79**, 3651 (1957).
8) A. Roppongi and T. Kato, This Bulletin, **35**, 1086 (1962).

increase remarkably. On the other hand, it has been reported that the stability of the strontium complex with triphosphate increases with the increase in the pH. These facts have led us to the conclustion that the stabilizing action in the higher pH range is mainly due to the strong interaction between triphosphate ions of a higher valency and the surfaces of strontium sulfate crystals.

BULLETIN OF THE CHEMICAL SOCIETY OF JAPAN VOL. 39 347—352 (1966)

The Effects of Polyamines on the Melting of Polyriboinosinic Acid Plus Polyribocytidylic Acid Complex in Solution

By Kimiko MATSUO and Masamichi TSUBOI

Faculty of Pharmaceutical Sciences, The University of Tokyo, Hongo Tokyo

(Received June 21, 1965)

The thermal transition profile (melting profile) of the double-helical complex of polyriboinosinic acid plus polyribocytidylic acid, poly(I+C), into random coils in solution has been examined by the observation of the ultraviolet absorbance at 248 mμ of the solution. The effects of Na^+, Mg^{2+}, NH_4^+, $CH_3NH_3^+$, $NH_3^+(CH_2)_nNH_3^+$ (where $n=2$, 3, 4, 5, 6, and 8), spermidine, spermine, actinomycin D, and poly-L-lysine upon the melting profile have been observed. Among the diamines examined, that with $n=3$ has been found to have the maximum effect. Poly-L-lysine has been found to form a complex with poly(I+C) in the solution with a stoichiometric mole ratio of $NH_2 : P = 0.5 : 1$.

The interactions of polyamines with nucleic acids seem to play important roles in some stages of many biological processes. Spermine NH_3^+-$(CH_2)_3NH_2^+(CH_2)_4NH_2^+(CH_2)_3NH_3^+$, for example, which is widely distributed in biological materials,[1] is known to affect the deoxyribonucleic acid (DNA) multiplication in some bacterial systems. In the chromosomes of higher organisms, DNA is found as a complex with histon, which is a lysine- and arginine-rich basic protein. In view of such biological importance, we have attempted to obtain fundamental knowledge about the interactions of polyamines with nucleic acids.

Polyriboinosinic acid (poly I) and polyribocytidylic acid (poly C) are synthetic polymers which have the same ribosephosphate backbone as natural ribonucleic acid (RNA).[2] A 1 : 1 mixture of poly I and poly C is known to form a double-stranded helical complex, poly(I+C), in solution.[3] Its structure[4] is considered to be similar to that of natural double-stranded DNA.[5] Some general discussions of the "melting" of such a double-helical nucleic acid were given in a previous paper.[6] Along this line we have been observing the effects of polyamines on the "melting" profile of poly-(I+C) in solution. Quite recently, however, a similar work with poly(I+C), which was done independently of our work, has been reported by Mehrotra and Mahler,[7] as have been a few similar examinations made previously with DNA.[8-10] Some of our results, which differ from those reported in other papers, will be presented in this paper and Discussed.

Experimental

The polyriboinosinic acid (poly I) and polyribocytidylic acid (poly C) used in this work were prepared by the use of the polynucleotide phosphorylase obtained from *Azotobacter vinelandii*. Both polynucleotides showed a sedimentation coefficient of 4s—8s in ultracentrifugal examination. The polynucleotide concentration in each standard solution was determined by measuring the phosphorus content.[11,12] Ethylenediamine dihydrochloride $NH_3^+(CH_2)_2NH_3^+ \cdot 2Cl^-$, 1, 4-diaminobutane

1) H. Tabor, C. W. Tabor and S. M. Rosenthal, *Ann. Rev. Biochem.*, **30**, 579 (1961).
2) M. Grunberg-Manago, P. J. Ortiz and S. Ochoa, *Science*, **122**, 907 (1955).
3) D. R. Davies and A. Rich, *J. Am. Chem. Soc.*, **80**, 1003 (1958).
4) D. R. Davies, *Nature*, **186**, 1030 (1960).
5) R. Langridge, W. E. Seeds, H. R. Wilson, C. W. Hooper, M. H. F. Wilkins and L. D. Hamilton, *J. Biophys. Biochem Cytol.*, **3**, 767 (1957).
6) M. Tsuboi, This Bulletin, **37**, 1514 (1964).
7) B. D. Mehrotra and H. R. Mahler, *Biochim. Biophys. Acta*, **91**, 78 (1964).
8) H. R. Mahler, B. D. Mehrotra and C. W. Sharp, *Biochem. Biophys. Res. Comm.*, **4**, 79 (1961).
9) M. Mandel, *J. Mol. Biol.*, **5**, 435 (1962).
10) H. Tabor, *Biochemistry*, **1**, 496 (1962).
11) P. S. Chen, T. Y. Toubarer and H. Warner, *Anal. Chem.*, **28**, 1756 (1956).
12) B. N. Ames and D. T. Dubin, *J. Biol. Chem.*, **235**, 769 (1960).

dihydrochloride $NH_3^+(CH_2)_4NH_3^+\cdot 2Cl^-$, 1, 5-diaminopentane dihydrochloride $NH_3^+(CH_2)_5NH_3^+\cdot 2Cl^-$, 1, 6-diaminohexane dihydrochloride $NH_3^+(CH_2)_6NH_3^+\cdot 2Cl^-$ and 1, 8-diaminooctane dihydrochloride $NH_3^+(CH_2)_8NH_3^+\cdot 2Cl^-$ were obtained from the Tokyo Kasei Co. 1, 3-Diaminopropane dihydrochloride was obtained by introducing hydrogen chloride into 1, 3-diaminopropane (purchased from the Tokyo Kasei Co.) dissolved in ethanol. Spermidine trihydrochloride $NH_3^+(CH_2)_3NH_2^+(CH_2)_4NH_3^+\cdot 3Cl^-$ was obtained from the Nutritional Biochemicals Corporation, and spermine tetrahydrochloride $NH_3^+(CH_2)_3NH_2^+(CH_2)_4NH_2^+(CH_2)_3NH_3^+\cdot 4Cl^-$ from the Sigma Chemical Co. Poly-L-lysine hydrobromide with average molecular weight of 60000 was purchased from Pilot Chemicals, Inc. The poly-L-lysine concentration in our standard solution was determined by hydrolyzing it with 6 N hydrochloric acid and by then measuring the lysine content by the use of 2, 4-dinitrofluorobenzene.[13]

The ultraviolet absorption measurements were made by the use of an Ito Spectrophotometer, model QU-3. The temperature of the sample chamber was controlled by circulating ethylene glycol from a Haake Thermostat, model F. The sample chamber was thermally insulated from the other parts of the spectrophotometer by using two insulating plates and by having cooling water flow between the two plates. The temperature of the sample solution was measured with a cupper-Constantan thermocouple.

Results and Discussion

The Melting of Poly(I+C) Observed by Tracing the Absorbance at 248 mμ.—First, a few preliminary examinations were made of the ultraviolet absorption spectra of our samples of polyribonucleotides and their mixtures. It was found that our poly I and poly C in a citrate buffer (pH 7.0) give exactly the same spectra as those reported by Davies and Rich[3] in the 220—300 mμ region. The spectrum of a 1 : 1 mixture of these polymers indicates that a strong interaction takes place in 0.01 M sodium chloride plus 0.01 M sodium citrate buffer (pH 7.0), while no interaction takes place in a 0.001 M sodium-citrate buffer (pH 7.0) without sodium chloride. In the 0.05 M sodium chloride plus 0.01 M sodium-citrate buffer (pH 7.0), the absorbance was measured at 233 mμ for several mixtures containing varying proportions of poly I and poly C, while the total nucleotide concentration was kept constant. The resulting mixing curve is similar to what Davies and Rich[3] observed at 235 mμ in a cacodylate buffer (pH 6.7). It is composed of two straight lines which intersect sharply at a 1 : 1 mole ratio, demonstrating the formation of a 1 : 1 complex, poly(I+C). This complex is considered to have a double-helical conformation.[3,4] When solution of this complex is heated, there is a general increase in absorbance in the 230—270 mμ region. This increase is considered to correspond to the "melting" of the double-helical poly(I+C) into single-stranded random coils, poly I and poly C. The increase in absorbance is greatest at 248 mμ. Therefore, the melting process of poly(I+C) was followed by observing the absorbance at 248 mμ throughout the rest of the present work. The melting temperature, T_m, is defined as the midpoint of the increase in absorbance just mentioned.

The Effect of Na^+.—The melting process of poly(I+C) is influenced by the Na^+ concentration in the solvent in two ways. When the Na^+ concentration is lowered, the melting temperature, T_m, of poly(I+C) is lowered, and at the same time the melting process loses its reversibility. As may be seen in Fig. 1, the T_m of poly(I+C) is 65°C in the medium with 0.1 M Na^+ while it is 49.5°C with 0.01 M Na^+. In the former solution the reformation of the complex takes place rapidly (within 9 min.), while in the latter it takes a very long time (about 24 hr.). This lower reaction rate may be attributed to a high activation energy. Without shielding by a cation atmosphere, two negatively-charged polymers (poly I and poly C) cannot easily approach to each other. In Fig. 2, T_m is plotted against the logarithm of the Na^+ concentration [s]. As was expected in a previous paper,[6] the curve gives an S shape. On the basis of what was described in Section 3 in a previous paper,[6] $K'=1/[s]$ at the inflection point. Here, K' is the equilibrium constant at T_m of each of the reactions:

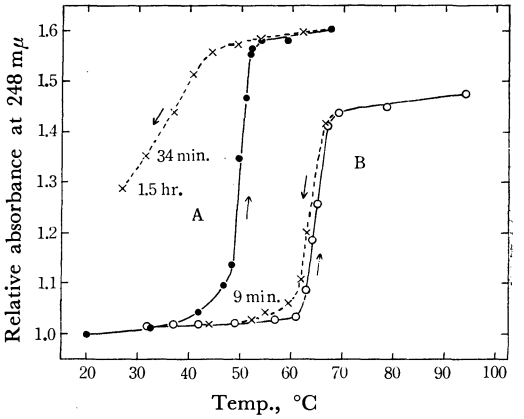

Fig. 1. The variation of the absorbance of poly-(I+C) solutions at 248 mμ with temperature. Full line: heating curve, broken line: cooling curve.
A Poly I 2.5×10^{-5} M plus poly C 2.5×10^{-5} M in 0.01 M NaCl plus 0.01 M Li-citrate buffer, pH 7.0.
B poly I 2.5×10^{-5} M plus poly C 2.5×10^{-5} M in 0.1 M NaCl plus 0.01 M Li-citrate buffer, pH 7.0.
Each of the figures given on the cooling curves indicates the time taken by cooling the solution from the highest temerature given to the temperature in question.

13) D. T. Dubin, *J. Biol. Chem.*, **235**, 783 (1960).

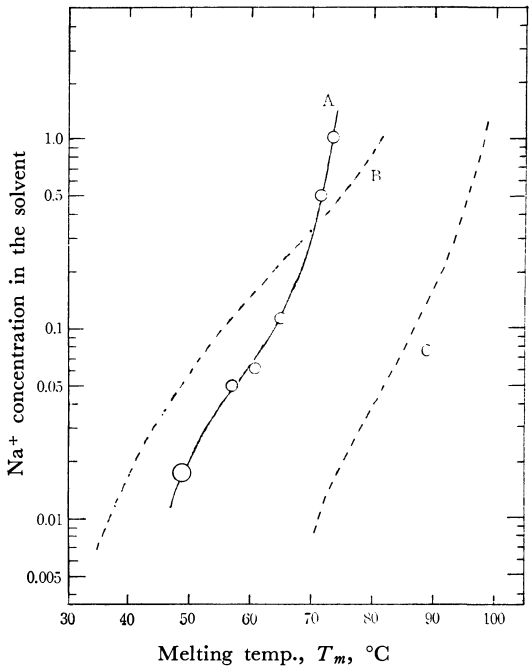

Fig. 2. The dependence of T_m on Na^+ concentration.
A Equimolar mixture of poly I and poly C.
B Equimolar mixture of poly A and poly U (Details will be given in our next paper.)
C DNA (the dependence of T_m on K^+ concentration, J. Marmur and P. Doty, *J. Mol. Biol.*, **5**, 109 (1961).)

$$\text{Poly(I + C)} + Na^+ = \text{poly(I + C)}Na^+$$

$$\text{poly(I + C)}Na^+ + Na^+ = \text{poly(I + C)}{Na^+}_2$$

.....

and

$$\text{poly(I+C)}{Na^+}_{N-1} + Na^+ = \text{poly(I+C)}{Na^+}_N$$

From an inspection of Fig. 2, $K'=15$—$20\ M^{-1}$. An inspection of Fig. 2 also shows that the T_m change in the variation of $[s]$ is smaller than that for poly(A+U) and that for DNA. Very probably this means that the α value is smaller for poly(I+C) than for poly(A+U) or for DNA.[6] Here α is the increase in the enthalpy of the melting of poly(I+C) caused by the adsorption of one cation.[6]

The Effects of a Few Other Cations.—As may be seen in Fig. 3, the effect of the ammonium ion on the T_m of poly(I+C) is almost the same as that of Na^+. The effect of the methylammonium ion is somewhat smaller, while the effect of Mg^{2+} is markedly greater than the effect of the ammonium ion.

The Effects of Diamines.—When a NH_3^+-$(CH_2)_n NH_3^+$-type diamine is added to the poly(I+C) solution, an appreciable elevation of T_m is again observed (Fig. 4). The amount of elevation ΔT_m, is found to depend upon the value of

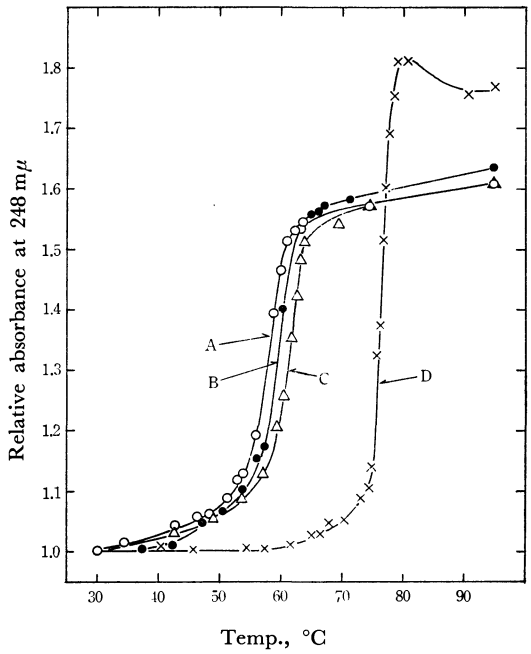

Fig. 3. The variation of the absorbance of poly(I+C) solutions at 248 mμ with temperature.
A Poly I 2.5×10^{-5} M plus poly C 2.5×10^{-5} M in 0.05 M NaCl plus 0.001 Na-citrate buffer, pH 7.0
B Solution A plus 0.02 M $CH_3NH_3^+Cl^-$
C Solution A plus 0.02 M NH_4Cl
D Solution A plus 0.01 M $MgCl_2$

n, the number of the methylene groups placed between the two amino groups of the diamine. When the concentration of the diamines is kept constant (0.01 M), the greatest ΔT_m value of poly(I+C) is found at $n=3$. $NH_3^+(CH_2)_3NH_3^+$ has an effect on the T_m of poly(I+C) greater not only than $NH_3^+(CH_2)_2NH_3^+$ but also than Mg^{2+}. This fact suggests that the $n=3$ cation functions not only as a shielder of the PO_2^- charges of the poly I and poly C chains, but also as a clamp which tends to keep the two polynucleotide chains together and gives an additional stability to the intertwined double-helical structure. If so, the $NH_3^+\cdots NH_3^+$ distance in this cation should reflect the distance from an oxygen atom of a PO_2^- group belonging to a poly I chain to that belonging to the poly C chain which is intertwined with the poly I chain.

The Effects of Spermidine and Spermine.—The effect of spermidine, $NH_3^+(CH_2)_3NH_2^+$-$(CH_2)_4NH_3^+$ (see Fig. 5, B), is much greater than that of the 1, 3-diaminopropane described above (Fig. 4, C). Thus, the addition of the former in only half the amount (0.005 M) of the latter causes a greater change in the T_m value (from 57°C to 84°C, i. e., $\Delta T_m=27$°C). The effect of spermine, $NH_3^+(CH_2)_3NH_2^+(CH_2)_4NH_2^+(CH_2)_3NH_3^+$, is even more dramatic (Fig. 5, C). Only 0.0005 M

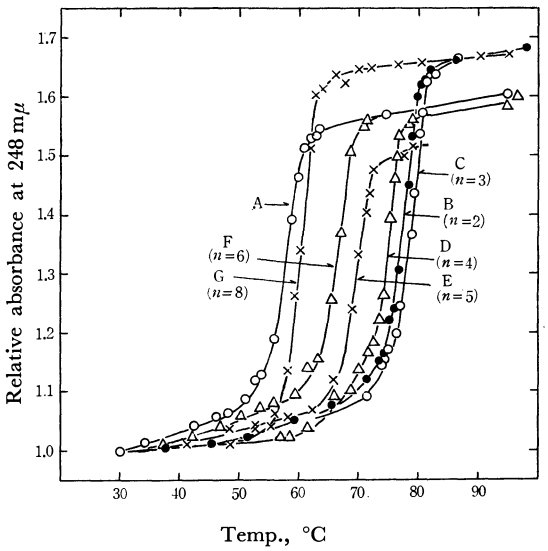

Fig. 4. The variation of the absorbance of poly-(I+C) plus diamine ($NH_3^+(CH_2)_nNH_3^+$) solutions at 248 mμ with temperature.

A Poly I 2.5×10^{-5} M plus poly C 2.5×10^{-5} M in 0.05 M NaCl plus 0.001 M Na-citrate buffer, pH 7.0
B Solution A plus 0.01 M $NH_3^+CH_2CH_2NH_3^+$
C Solution A plus 0.01 M $NH_3^+(CH_2)_3NH_3^+$
D Solution A plus 0.01 M $NH_3^+(CH_2)_4NH_3^+$
E Solution A plus 0.01 M $NH_3^+(CH_2)_5NH_3^+$
F Solution A plus 0.01 M $NH_3^+(CH_2)_6NH_3^+$
G Solution A plus 0.01 M $NH_3^+(CH_2)_8NH_3^+$

of it causes an elevation of T_m from 57°C to 91°C. This suggests that the equilibrium constant, K', of the binding reaction of spermine to poly(I+C) is to the order of 10^4 or more. Mandel[9] examined the interaction of spermine with DNA, and found that the extent of the increase in T_m is proportional to the adenine-thymine content of the DNA sample. On the basis of what he found, one might suggest that there is no effect of spermine upon a double-helical polynucleotide structure without an adenine-thymine pair. What we have observed here, however, shows that this is not necessarily the case. There is certainly a marked effect of spermine upon poly(I+C), a double-helical polynucleotide without an adenine-thymine or an adenine-uracil pair. As may be seen in Fig. 5, D, the dialysis of the poly(I+C) plus spermine solution against the buffer for 40 hr. results in a great lowering of T_m, from 91°C to 66°C. Its T_m, however, is still appreciably higher than that of poly(I+C) alone in the same buffer. This fact indicates that the poly(I+C)-spermine binding is a very strong one; however, there seems to be no chemical reaction between them.

The Effect of Actinomycin D.—In a previous work,[14] 31.8 μg./ml. of actinomycin D was found

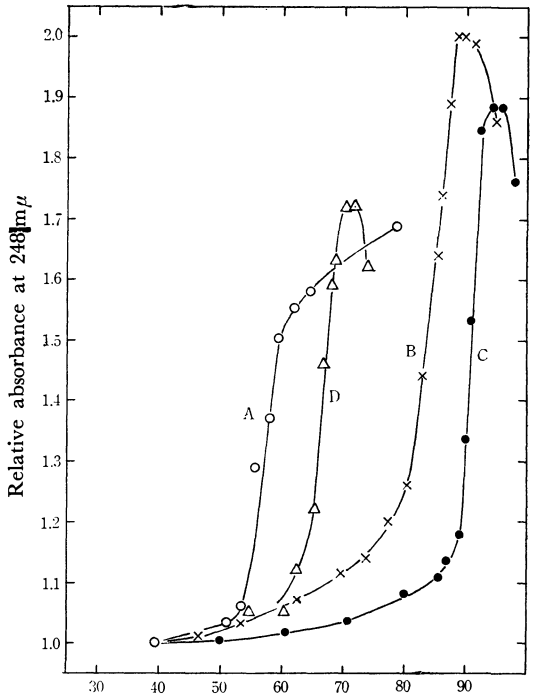

Fig. 5. The variation of the absorbance of poly-(I+C) plus polyamines at 248 mμ with temperature.

A Poly I 2.5×10^{-5} M plus poly C 2.5×10^{-5} M in 0.05 M NaCl plus 0.001 M Na-citrate buffer, pH 7.0
B Solution A puls 0.005 M spermidine trihydrochloride
C Solution A plus 0.0005 M spermine tetrachloride
D A solution obtained by a dialysis of the solution C against 0.05 M NaCl plus 0.001 M Na-citrate buffer, pH 7.0, for 40 hr.

to cause an elevation of the T_m of DNA from 72°C to 87°C in a 0.01 M tris buffer. The same amount of actinomycin D, however, has now been found to have almost no effect on the melting profile of poly(I+C) in 0.05 M sodium chloride plus a 0.01 M sodium citrate buffer.

The Effect of Poly-L-lysine.—When poly-L-lysine is added to $0.8_3\times10^{-5}$ M to a solution of 2.5×10^{-5} M poly(I+C) ($NH_2:P=0.16_6:1$), two-step melting is observed instead of one-step melting (Fig. 6, A). Roughly two-thirds of the total increase in absorbance at 248 mμ takes place at 57°C, and the rest at 89°C. When the concentration of poly-L-lysine is increased to $1.6_6\times10^{-5}$ M (now $NH_2:P=0.33:1$), only 1/3 of the total increase in absorbance takes place at the first-step melting; the rest takes place at the second step. However, the melting temperatures remain at 57°C and 89°C (Fig. 6, B). The melting temperature of the first step (57°C) is the same as

14) M. Tsuboi, S. Higuchi, Y. Kyogoku, K. Matsuo and A. Wada, *Chem. Pharm. Bull.*, **12**, 501 (1964).

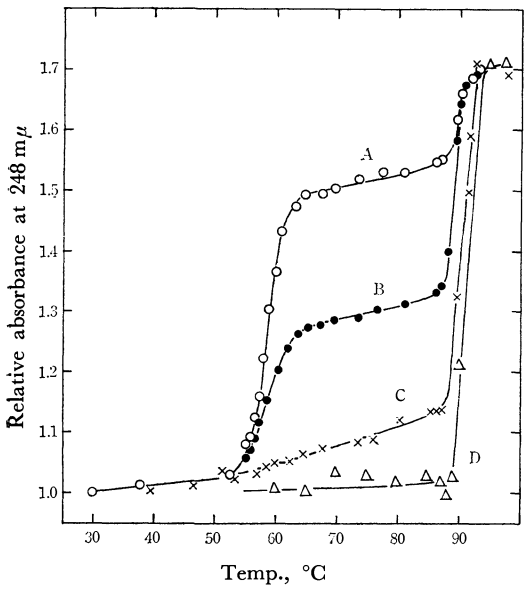

Fig. 6. The variation of the absorbance of poly-(I+C) plus poly-L-lysine solutions with temperature. Solvent: 0.05 M NaCl in 0.001 M Na-citrate buffer, pH 7.0.

A Poly I 2.5×10^{-5} M plus poly C 2.5×10^{-5} M plus poly-L-lysine $0.8_3\times10^{-5}$ M (NH_2 : P= 0.16_6 : 1).

B Poly I 2.5×10^{-5} M plus poly C 2.5×10^{-5} M plus poly-L-lysine $1.6_6\times10^{-5}$ M (NH_2 : P= 0.33 : 1).

C Poly I 2.5×10^{-5} M plus poly C 2.5×10^{-5} M plus poly-L-lysine 2.5×10^{-5} M (NH_2 : P= 0.5 : 1).

D Poly I 2.5×10^{-5} M plus poly C 2.5×10^{-5} M plus poly-L-lysine $3.7_5\times10^{-5}$ M (NH_2 : P= 0.75 : 1).

the T_m value of poly(I+C) alone in the solvent in question (0.05 M sodium chloride plus 0.001 M sodium citrate buffer, pH 7.0). When the concentration of poly-L-lysine is increased to 2.5×10^{-5} M (now NH_2 : P=0.5 : 1), the first-step melting at 57°C almost disappears, and only the melting at 89°C takes place (Fig. 6, C).

These experimental results indicate that there is a complex of poly-L-lysine and poly(I+C) with a definite mole ratio and with a T_m of 89°C in the solution. It has recently been shown[15] that, in poly-L-lysine plus DNA system, all the poly-L-lysine molecules added are bound by the DNA molecules and no poly-L-lysine molecules remain free, if the amount added is less than the amount sufficient to saturate the DNA molecules with poly-L-lysine. This is probably the case also for the poly-L-lysine plus poly(I+C) system. If so, the composition of the poly-L-lysine+poly-(I+C) complex in question can easily be determined. The NH_2: P ratio in the complex should be 0.5 : 1, since the melting of poly(I+C) free from poly-L-lysine (at 57°C) disappears at this mole ratio. This knowledge of the composition of the complex enables us to conjecture to some extent about its structure. It may be concluded, for example, that a molecular model similar to that of deoxyribonucleoprotamine, as proposed by Wilkins et al.[16,17] is not acceptable for the poly-L-lysine+poly(I+C) complex. In this model, an almost fully-extended polypeptide chain winds helically around the doubly-stranded polynucleotide chains. The pitch of the polypeptide helix is the same as that of polynucleotide helices. This model requires one amino acid residue per nucleotide residue, i. e., NH_2 : P=1 : 1, while in the poly-L-lysine+poly(I+C) complex in question, NH_2: P=0.5 : 1. In a fully-extended polypeptide chain, one amino acid residue corresponds to a translation of 3.4 Å along the chain axis. In the A-form of poly(I+C), the translation along the helix axis per nucleotide pair is 3.0 Å.[4] Therefore, such a chain axis of poly-L-lysine should be inclined about

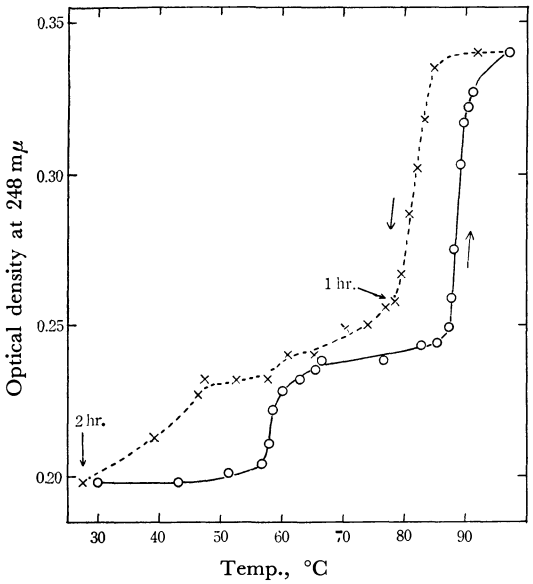

Fig. 7. The variation of the absorbance of a poly(I+C) plus poly-L-lysine solution on heating (full line) and on cooling (broken line). Poly I 2.5×10^{-5} M plus poly C 2.5×10^{-5} M plus poly-L-lysine $1.6_6\times10^{-5}$ M (NH_2 : P=0.33: 1) in 0.05 M NaCl plus 0.001 M Na-citrate buffer, pH 7.0. Each of the figures given on the cooling curve indicates the time taken by cooling the solution from 97°C to the temperature in question.

15) M. Tsuboi, K. Matsuo and P. O. P. Ts'o, *J. Mol. Biol.*, in press.

16) M. Feughelman, R. Langidger, W. E. Seeds, A. R. Stokes, H. R. Wilson, C. W. Hooper, M. H. F. Wilkins, R. K. Barclay and L. D. Hamilton, *Nature*, **175**, 834 (1955).

17) M. H. F. Wilkins, *Cold Spring Har. Quant. Biol.*, **21**, 75 (1956).

arc cos (3.0/3.4)=28° to the helix axis of the poly-(I+C) in the complex in question. Thus a possible model of the complex may be suggested in which the fully-extended poly-L-lysine chain winds around the double helices of poly(I+C) core along a helix with a long pitch.

The poly-L-lysine concentration was further increased from that corresponding to $NH_2 : P=0.5 : 1$. As may be seen in Figs. 6, C and D, the poly-L-lysine plus poly(I+C) solution with $NH_2 : P=0.75 : 1$ gives a heating curve similar to that of the solution with $NH_2 : P=0.5 : 1$. There is, however, a slight difference between them. In the latter there is a gradual increase in absorbance from 50°C to 88°C before a steep increase in absorbance takes place, whereas in the former no such gradual increase is observed; the curve is practically horizontal up to 89°. This fact may be taken as indicating that the excess poly-L-lysine molecules in the solution with $NH_2 : P=0.75 : 1$ serve to keep the complex rigid throughout the emperature range from 50°C to 89°C, and that without such excess poly-L-lysine molecules the poly-L-lysine+poly(I+C) complex is somewhat flexible.

Figure 7 shows the results of an examination of the reversibility of the two-step meltings now in question. As may be seen here, an almost complete reformation of the poly-L-lysine+poly(I+C) complex takes place in the solvent in question when the solution is kept at about 80°C for an hour after the melting.

The authors wish to express their deep thanks to Professor Fujio Egami, Professor Tyunosin Ukita, Professor Den-ich Mizuno, and their collaborators, and to the members of the Research Laboratories of the Meiji Seika Kaisha, Ltd., for their kind help in our preparation of poly I and poly C. This work was supported by a grant from the United States Public Health Service (No. GM 10024-02) and a grant from the Ministry of Education of Japan.

BULLETIN OF THE CHEMICAL SOCIETY OF JAPAN VOL. 39 352—356 (1966)

The Determination of Micro Amounts of Polythionates. III.* A Photometric Method for the Determination of Tetrathionate by Means of Its Cyanolysis[1]

By Tomozo KOH and Iwaji IWASAKI

Laboratory of Analytical Chemistry and Geochemistry, Tokyo Institute of Technology, Ookayama, Tokyo

(Received June 22, 1965)

A photometric method capable of determining tetrathionate by exactly the same procedure as that used for pentathionate and hexathionate has been established. The optimum pH ranges for the reactions of tetrathionate, pentathionate and hexathionate with cyanide are 8.3—12.1, 8.0—8.8, and 7.8—8.9 respectively for the recommended procedure. From a consideration of the above experimental facts, it has been concluded that tetrathionate can be determined accurately by exactly the same procedure as that used for pentathionate and hexathionate when the pH value is within the range from 8.3 to 8.8. To the standard tetrathionate solution first the buffer solution and then a solution of sodium cyanide are added in order that the pH value of the mixture solution after the addition of the cyanide solution may be within the 8.3—8.8 range. The mixed solution is kept in the thermostat at 40°C for 30 min.; the tetrathionate is thereby converted into thiocyanate quantitatively. After the addition of a ferric nitrate - perchloric acid solution, the absorbancy of the solution of ferric-thiocyanate complex formed is measured at the wavelength of 460 mμ.

Nietzel and DeSesa[2] have presented a spectrophotometric method for the determination of low concentrations of tetrathionate, a method which is based on the formation of thiocyanate from tetrathionate by reaction with cyanide in an alkaline medium, and on the subsequent formation of a ferric-thiocyanate complex with ferric iron. At the same time, they have pointed out that their method can also be used for pentathionate and

* Part II: This Bulletin, **38**, 2135 (1965).

1) Presented at the Scientific Meeting on Chemistry, Tokyo, November, 1964.

2) O. A. Nietzel and M. A. DeSesa, *Anal. Chem.*, **27**, 1839 (1955).

hexathionate, because the higher polythionates react more easily with cyanide to form thiocyanate.

On the other hand, Urban[3] has modified the Nietzel-DeSesa method and applied it to the evaluation of n, the mean number of sulfur atoms in the formula, $S_nO_6^{2-}$, for polythionates above trithionate, on the assumption that pentathionate and hexathionate would react with cyanide to be quantitatively converted into thiocyanate under the same conditions as those used for the estimation of tetrathionate.

However, the higher polythionates, as has been reported in the first paper of this series,[4] undergo a partial alkaline decomposition under the conditions of the Nietzel-DeSesa and the Urban methods,[2,3] because of the higher pH value arising from the addition of a sodium cyanide solution. Therefore, their methods are not suitable for the higher polythionates.

The present authors[5] have previoulsy reported a method for the determination of a small amount of hexathionate, a method based on the reaction of hexathionate with cyanide, with the subsequent formation of thiocyanate from hexathionate, and on the photometric determination of the thiocyanate with ferric iron. In the above investigation, it has been found that the hexathionate can be determined sufficiently rapidly, precisely, and accurately by the very same procedure as is used for pentathionate.[4]

The present authors have now investigated, in greater detail, a method for the determination of tetrathionate using the reaction:

$$S_4O_6^{2-}+3CN^-+H_2O = S_2O_3^{2-}+SO_4^{2-}+2HCN+SCN^-$$

followed by the photometric determination of the thiocyanate thus formed with ferric iron; they have thus established an excellent method for determining a small amount of tetrathionate by the very same procedure as is used for pentathionate[4] and hexathionate[5]; they have found the conditions under which tetrathionate is also quantitatively converted into thiocyanate under the same conditions as are used for pentathionate and hexathionate, by varying the cyanide amount, the pH, the reaction time, and the temperature.

The present investigation was undertaken to see if the method for the determination of pentathionate[4] and hexathionate[5] could be used for tetrathionate also; the authors have their ultimate object analyzing the polythionates when they are mixed with one another.

Experimental

Apparatus and Materials.—Unless otherwise stated, the apparatus and materials used in this study were the same as those described in the first paper of this series.[4]

Potassium Tetrathionate.—This salt was prepared according to the directions of Stamm and Goehring.[6] The raw tetrathionate obtained was recrystallized with redistilled water at a temperature below 60°C and dried at room temperature for 4 days. The water content physically adsorbed in the tetrathionate was estimated to be 0.6% by the Karl Fischer method.

The purity of this salt was estimated by determining the total potassium and sulfur as follows. The potassium tetrathionate was decomposed into potassium sulfate by heating it at about 800°C; $K_2S_4O_6 \rightarrow K_2SO_4$. The potassium was determined by weighing[7] the potassium sulfate thus formed.

As for the sulfur, the tetrathionate was oxidized[4,5,7] by bromine in an alkaline medium upon heating; the sulfate ions formed were determined by the usual gravimetric method.

Table I. Determination of K for the potassium tetrathionate* used in the present study

Sample taken mg.	As $K_2S_4O_6$ mg.	Found as K_2SO_4 mg.	K found for $K_2S_4O_6$ %	K calcd. for $K_2S_4O_6$ %
261.6	260.0	149.8	25.86	25.86
198.7	197.5	113.7	25.83	

Table II. Determination of S for the potassium tetrathionate* used in the present study

Sample taken mg.	As $K_2S_4O_6$ mg.	Found as $BaSO_4$ mg.	S found for $K_2S_4O_6$ %	K calcd. for $K_2S_4O_6$ %
273.2	271.6	832.2	42.09	42.40
233.2	231.8	710.5	42.10	

* Water content was estimated to be 0.6%.

Tables I and II show that this potassium tetrathionate is pure enough for the purposes of this investigation.

The Standard Tetrathionate Solution.—The standard solution, a 1.0×10^{-3} M stock solution of tetrathionate, was prepared by dissolving 152.1 mg. of the potassium tetrathionate (water content: 0.6%) in redistilled water, and then diluting it to 500 ml. This stock solution proved to be stable; even after six months, no measurable change was found by the present method when it was kept at 5±2°C in a refrigerator. The working standard solutions were prepared by diluting the stock solution properly.

Buffer Solution.—Phosphate buffer (0.2 M) and sodium hydroxide (0.01 to 1 N) solutions were employed to adjust the pH to the values required.

Procedure.—A sample solution of 10.0 ml. is placed in a 25 ml. volumetric flask. To this solution there are added, first 4.0 ml. of the phosphate buffer solution of pH 7.4, and then 2.6 ml. of 0.05 M sodium cyanide; the pH of the solution is thereby brought to 8.6.

The volumetric flask is kept in the thermostat at 40±1°C for 30 min.; the tetrathionate is thereby converted into thiocyanate quantitatively. Then 3.0 ml. of a .1.5 M ferric nitrate - perchloric acid solution is

3) P. J. Urban, *Z. anal. Chem.*, **180**, 110 (1961).
4) T. Koh, This Bulletin, **38**, 1510 (1965).
5) T. Koh and I. Iwasaki, ibid., **38**, 2135 (1965).
6) H. Stamm and M. Goehring, *Z. anorg. u. allgem. Chem.*, **250**, 226 (1942).
7) F. Martin and L. Metz, ibid., **127**, 83 (1923).

added. After the flask has been filled with redistilled water to the mark, the contents are mixed well. The absorbancy of the solution of the ferric-thiocyanate complex thus formed is measured at the wavelength of 460 mμ, using distilled water as a reference.

Results and Discussion

Calibration Curves.—The calibration curves shown in Fig. 1 were obtained by the procedure described above, using standard tetrathionate and thiocyanate solutions.

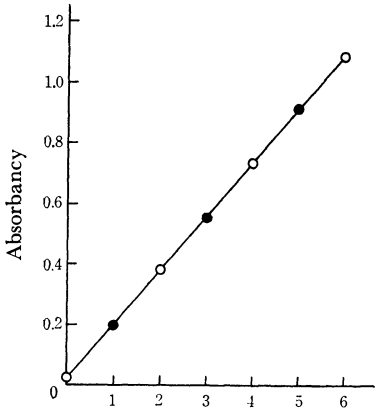

Fig. 1. Calibration curves.
○ Tetrathionate ● Thiocyanate

The absorbancy and the concentration were in a good linear relationaship, as can be seen in Fig. 1. When one ion of tetrathionate undergoes cyanolysis, one ion of thiocyanate is formed. Therefore, if the tetrathionate is pure enough and if it is, moreover, converted into thiocyanate stoichiometrically and quantitatively, the calibration curve of tetrathionate should be in full accord wtih that of thiocyanate when plotted by the mole concentration for tetrathionate and thiocyanate. In fact, Fig. 1 shows that the calibration curve for tetrathionate is in exact accordance with that for thiocyanate, demonstrating that the reaction of tetrathionate with cyanide goes well to completion and that it is stoichiometric.

The Effect of the Amount of Sodium Cyanide.—As will be disclosed below, it was confirmed that the optimum pH value for the reaction of tetrathionate with cyanide ranges from 8.3 to 12.1 under the conditions of the procedure mentioned above. 0.5 ml. of a 0.025 M sodium cyanide solution and from 0.5 to 4.0 ml. of a 0.05 M sodium cyanide solution were employed, in all cases the final solution being buffered to the optimum pH value. The resulting effect of the amount of sodium cyanide upon the cyanolysis is shown in Fig. 2.

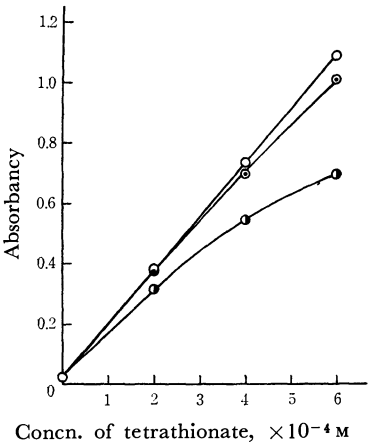

Fig. 2. The effect of the amount of sodium cyanide.
The pH was adjusted to 8.4—12.1 in all cases.
Cyanolysis time: 30 min. at 40°C
◑ 0.025 M NaCN 0.5 ml. (I)
⊙ 0.05 M NaCN 0.5 ml. (II)
○ 0.05 M NaCN 1.0, 2.0, 2.6, and 4.0 ml. (III)

The calibration curves with 0.5 ml. portions of 0.025 and 0.05 M sodium cyanide solutions do not form straight lines (see I and II), indicating that tetrathionate is not completely converted into thiocyanate because of insufficient amounts of cyanide. It can be concluded from Fig. 2 that 1.0 ml. of a 0.05 M sodium cyanide solution is sufficient for the complete conversion of tetrathionate into thiocyanate, and that the amount of sodium cyanide does not have any effect on this method as long as it is sufficient and the pH is adjusted to an optimum value.

The Effect of the pH.—The reaction should be carried out below a pH value of 12.1, because tetrathionate undergoes alkaline decomposition in addition to cyanolysis at higher pH levels.

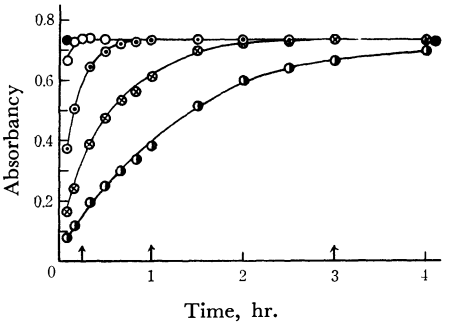

Fig. 3. Effect of pH on the rate of cyanolysis at 25°C.
● 4.0×10^{-4} M SCN^-
○ pH 10.3 and 11.8 (I)
⊙ pH 8.7 (II)
⊗ pH 8.0 (III)
◑ pH 7.5 (IV)
} 4.0×10^{-4} M $S_4O_6^{2-}$

Figure 3 shows the dependence of the rate of cyanolysis on the pH of the solution at 25°C.

The maximum absorbancy, which corresponds to the complete and stoichiometric reaction of tetrathionate with cyanide, is attained in 15 min. at pH 10.3 and 11.8, and thereafter remains constant (see I), while the reactions at pH 8.7 and 8.0 go to completion in 1 hr. and 3 hr. respectively (see II and III). However, the reaction at pH 7.5 does not reach completion even within 4 hr. (see IV).

As can also be seen from Fig. 3, the higher the pH of the solution, the more rapid the rate of cyanolysis; therefore, it is desirable that the procedure is carried out at a higher pH level as long as it is below 12.1. However, pentathionate and hexathionate, as has been reported in previous papers,[4,5] undergo a partial alkaline decomposition at pH levels higher than pH 9.0. Consequently, we made our study at pH values below 8.7. In order to accelerate the rate of cyanolysis, the reaction temperature was raised from 25°C to 40°C. Figure 4 shows how the pH of the solution affects the rate of cyanolysis at 40°C.

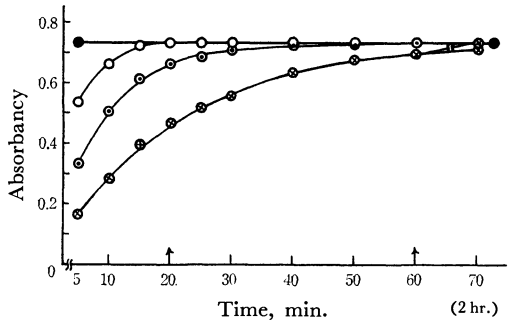

Fig. 4. Effect of pH on the rate of cyanolysis at 40°C.

● 4.0×10^{-4} M SCN^-
○ pH 8.7 (I)
⊙ pH 8.0 (II) } 4.0×10^{-4} M $S_4O_6^{2-}$
⊗ pH 7.5 (III)

The reactions at pH 8.7 and 8.0 go well to completion, and are stoichiometric, in 20 min. and 1 hr. respectively (see I and II in Fig. 4). On the other hand, the reaction at pH 7.5 goes stoichiometrically to completion in 2 hr. (see III).

It was observed that tetrathionate also undergoes thermal decomposition as well as cyanolysis at 70°C, as do pentathionate and hexathionate.

The reaction of tetrathionate with cyanide at various pH values was carried out both at 25°C for 70 min. and at 40°C for 30 min. The results are shown in Fig. 5, where the complete and stoichiometric reaction occurs over the pH range from 8.5 to 12.1 at 25°C for 70 min. (see I) and over the pH range from 8.3 to 12.1 at 40°C for 30 min. (see II).

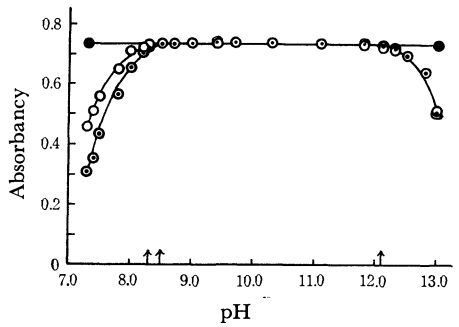

Fig. 5. Effect of pH.

● 4.0×10^{-4} M SCN^-
○ 30 min. at 40°C (II) } 4.0×10^{-4} M $S_4O_6^{2-}$
⊙ 70 min. at 25°C (I) }

The decrease in absorbancy above the pH value of 12.2 may be due to the alkaline decomposition of tetrathionate. The optimum pH range for the reaction of tetrathionate with cyanide can be extended from either 8.3 or 8.5 to a lower pH by making the cyanolysis time longer, because the rate of cyanolysis decreases with a lowering of the pH value.

Figure 6 shows how the pH affects the cyanolysis of tetrathionate, pentathionate, and hexathionate under the conditions of the procedure described above.

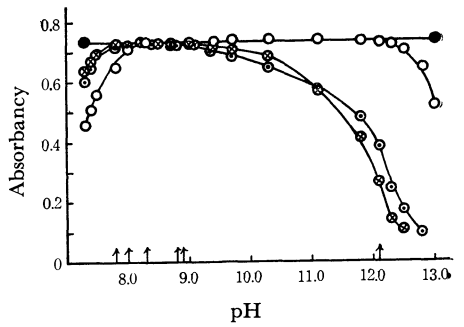

Fig. 6. Effect of pH.
Cyanolysis time: 30 min. at 40°C

● 4.0×10^{-4} M SCN^-
○ 4.0×10^{-4} M $S_4O_6^{2-}$
⊙ 2.0×10^{-4} M $S_5O_6^{2-}$
⊗ 1.33×10^{-4} M $S_6O_6^{2-}$

As can be seen in Fig. 6, the optimum pH ranges for tetrathionate, pentathionate, and hexathionate are between 8.3 and 12.1, 8.0 and 8.8, and 7.8 and 8.9 respectively. In view of the experimental results shown in Fig. 6, it may be concluded that tetrathionate can be determined accurately by the very same procedure as that used for pentathionate and hexathionate, where the pH value is 8.6.

Calibration Curves of Tetrathionate, Pentathionate, and Hexathionate.—Solutions

containing various amounts of thiocyanate, tetrathionate, pentathionate, and hexathionate were treated by the preceding procedure; the results are shown in Figs. 7 and 8. When one ion of tetrathionate, pentathionate, and hexathionate undergoes cyanolysis, one, two, and three ions of thiocyanate are, respectively, formed.

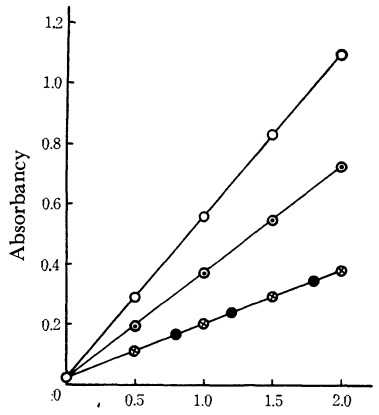

Fig. 7. Calibration curves
● Thiocyanate ⊗ Tetrathionate
⊙ Pentathionate ○ Hexathionate

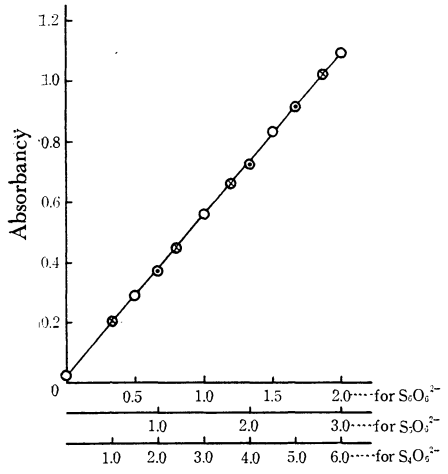

Fig. 8. Calibration curves.
⊗ Tetrathionate ⊙ Pentathionate
○ Hexathionate

In fact, Fig. 7 shows that the calibration curves of tetrathionate, pentathionate, and hexathionate are once, twice, and three times, respectively, as sensitive as that of thiocyanate. As can also be seen in Fig. 8, their calibration curves exactly coincide with one another when the scales of the concentration of tetrathionate and pentathionate are made one-third and two-thirds of the hexathionate concentration, indicating that all three of these polythionates can be easily determined by the same procedure.

A similar method, one suitable for the determination and for the evaluation of the composition of the polythionates mixed with each other, will be reported on in another paper.

Summary

The photometric method for the determination of a small amount of tetrathionate has been developed; it is based on the formation of thiocyanate equivalent to the tetrathionate, and on the determination of the thiocyanate with an excess of ferric iron. The conditions capable of determining a small quantity of tetrathionate by the very same procedure as that used for pentathionate and hexathionate have been established by varying the cyanide amount, the pH, the reaction time and the temperature.

The authors wish to thank Dr. Satori Utsumi of Nihon University, and Mr. Takejiro Ozawa and Dr. Minoru Yoshida of the Tokyo Institute of Technology for their many valuable discussions and suggestions during this study. Thanks are also given to Dr. Kaname Muroi, the Central Research Laboratory of Mitsubishi Chemical Industries, Ltd., for the estimation of the water content in the tetrathionate by the Karl Fischer method.

BULLETIN OF THE CHEMICAL SOCIETY OF JAPAN VOL. 39 357—361 (1966)

The Polarographic Behavior of Tris(1, 10-phenanthroline)cobalt Complexes and the Univalent Phenanthroline-Cobalt Complex.*1

By Kenichi MORINAGA, Kunio NAKANO, Shigeru SAITO*2 and Keizo NAKAMURA*3

Department of Chemistry, College of Science, St. Paul's University (Rikkyo Daigaku), Toshima-ku, Tokyo

(Received June 22, 1965)

The oxidation-reduction behavior of tris(1, 10-phenanthroline)cobalt complexes at a dropping mercury electrode has been studied by the d. c. and a. c. polarographic methods. The trivalent cobalt-phenanthroline complex ion is reduced in two steps in 1 M sodium sulfate in a quite similar way as the trivalent cobalt-dipyridyl complex ion. Both electrode processes, cobalt(III)→cobalt(II) and cobalt(II)→cobalt(I), are considered to be reversible. The univalent cobalt-phenphenanthroline complex has been obtained as a black powder by the reduction of the divalent cobalt complex with sodium borohydride; the atomic ratio of nitrogen to cobalt has been found to be close to six. The ethanolic solution is brown-black, in remarkable contrast with that of the corresponding dipyridyl complex, deep blue.

It is well known that the lower valency states of transition metals can be stabilized by coordinating ligands, such as carbonyl, cyanide, and dipyridyl which are likely to form bonds of a partly double-bond character between a central metal ion and the ligands.[1] A polarographic method has been proved to be very useful for detecting such abnormal valency states in many metal complex compounds.[2-9] From polarographic studies of cobalt-dipyridyl complexes, it has been shown that the tris(2, 2'-dipyridyl)cobalt(III) complex ion is reduced in two steps, from cobalt(III) to cobalt(II) and from cobalt(II) to cobalt(I). The isolation of the univalent cobalt complex has also been reported.[4,6] The cobalt complexes of phenanthroline, however, in spite of its strong resemblance to dipyridyl as a ligand, have never been studied in detail by the polarographic method. Therefore, the present authors have investigated the polarographic behavior of the tris(1, 10-phenanthroline)cobalt(III or II) ion in a 1 M sodium sulfate medium and found a great similarity between the d. c. polarogram of the tris(1, 10-phenanthroline)cobalt ion and that of the tris-(2, 2'-dipyridyl)cobalt ion, which has been reported on in a previous short communication.[10] They have also attempted to isolate the univalent cobalt complex and define its formula. The results will be presented in the present paper.

Experimental

Direct-current (d. c.) and alternating-current (a. c.) polarograms were recorded with a Yanagimoto model PS-52 photorecording polarograph and a Yanagimoto model PA-101 pen-recording polarograph respectively. A Yanagimoto controlled-potential electrolyzer was also used in an attempt to prepare and to identify the univalent cobalt complex in a solution. The absorption spectra were measured using a Hitachi EPU 2 spectrophotometer. The cell equipment used for the polarographic measurements was the same as has been reported on previously except that the saturated calomel electrode was replaced by the saturated mercurous sulfate electrode.[11] The dropping mercury electrode employed had an m value of 0.855_9 mg./sec. and a drop-time of 8.52 sec. when measured in distilled water at a 58.2 cm. height of the mercury reservoir with an open circuit. The cell temperature was maintained at 25 ± 0.1°C by means of a water thermostat. The oxygen dissolved in the electrolytic solution was removed by bubbling pure nitrogen gas through the solution. $[Co(phen)_3](ClO_4)_2$ and $[Co(phen)_3](ClO_4)_3 \cdot 2H_2O$ (phen=1, 10-phenanthroline) were prepared according to the procedures described in the literature.[12] A 1 M sodium sulfate solution was used as a supporting electrolyte, while no maximum suppressor was added. Solutions

*1 Presented at the 9th Symposium on Polarography, Kyoto, October, 1962, and at the 13th Symposium on Coordination Chemistry, Nagoya, October, 1963.

*2 Present address: Hosei University, Chiyoda-ku, Tokyo.

*3 Present address: Toyo Soda Kogyo Co., Ltd., Nanyo-cho, Yamaguchi.

1) L. E. Orgel, "An Introduction to Transition-Metal Chemistry," Methuen & Co., London (1961), p. 133.

2) D. N. Hume and I. M. Kolthoff, *J. Am. Chem. Soc.*, **71**, 867 (1949).

3) A. A. Vlček, *Nature*, **177**, 1043 (1956).

4) A. A. Vlček, ibid., **180**, 753 (1957); *Z. phys. Chem.*, Sonderheft, 143 (1958).

5) A. A. Vlček, *Z. Elektrochem.*, **61**, 1014 (1957).

6) G. M. Waind, B. Martin, *J. Inorg. & Nuclear Chem.*, **8**, 551 (1958).

7) N. Maki, J. Fujita and R. Tsuchida, *Nature*, **183**, 458 (1959); N. Maki, ibid., **185**, 682 (1960).

8) N. Maki and R. Tsuchida, This Bulletin, **34**, 891 (1961).

9) N. Maki and K. Okawa, ibid., **37**, 1233 (1964).

10) K. Morinaga, K. Nakano and K. Nakamura, *J. Chem. Soc. Japan, Pure Chem. Sect.* (*Nippon Kagaku Zasshi*), **84**, 198 (1963).

11) K. Morinaga, This Bulletin, **29**, 793 (1956).

12) P. Pfeiffer and Br. Werdelmann, *Z. anorg. u. allgem. Chem.*, **261**, 197 (1950); ibid., **263**, 31 (1950).

Table I. Dependence of limiting currents on a mercury column height for 0.2_9 mM $[Co(phen)_3]^{3+}$ in 1 M Na_2SO_4

H_{corr} cm.	i_{l_1}* μamp.	$i_{l_1}/\sqrt{H_{corr}}$	i_a* μamp.	$i_a/\sqrt{H_{corr}}$	i_{l_2}* μamp.	$i_{l_2}/\sqrt{H_{corr}}$
64.1	0.425	0.053	0.074	0.009_2	0.425	0.053
56.1	0.387	0.051	0.060	0.008_0	0.385	0.051
48.1	0.369	0.053	0.051	0.007_1	0.360	0.052
41.1	0.332	0.051	0.042	0.006_0	0.323	0.050

* i_{l_1}, i_a and i_{l_2} represent the limiting current for the first wave, the prewave and the total limiting current for the second wave including the prewave, respectively.

Table II. Characteristics of d. c. waves for $[Co(phen)_3]^{3+}$ in 1 M Na_2SO_4

Concentration of depolarizer	1st reduction wave		2nd reduction wave			
	i_d	$E_{1/2}$	i_d*	i_a**	$E_{1/2}$**	E_d***
mM	μamp.	V. vs. SCE	μamp.	μamp.	V. vs. SCE	V. vs. SCE
1.27	1.61	$+0.08_6$	1.59	0.04_6	−0.83	−0.98
0.86	1.05	$+0.09_8$	1.03	0.05_9	−0.84	−1.00
0.63	0.83_1	$+0.10_1$	0.82_1	0.06_5	−0.84	−1.03
0.32	0.44_3	$+0.10_4$	0.42_4	0.06_5	−0.83	−1.08
0.12	0.17_5	$+0.08_5$	0.13_5	0.05_8	−0.83	−1.13

* The total diffusion current including the prewave
** The values for the prewave
*** The decomposition potential for the main second wave

containing the divalent cobalt complex were carefully prepared in order to prevent it from oxidation. All the chemicals used were of guaranteed reagent grade.

Results and Discussion

On the D. C. and A. C. Polarograms.—$[Co(phen)_3]^{3+}$ ions are reduced in two steps in 1 M sodium sulfate, as has been shown in Fig. 1 of a previous paper.[10] The first wave appears around +0.10 V. vs. SCE, and the second one accompanying a small prewave appears around −1.0 V. vs. SCE. A small minimum was observed on the plateau of the first wave. $[Co(phen)_3]^{2+}$ ions show an oxidation wave and a reduction wave at the respective potentials corresponding to the first and the second waves of $[Co(phen)_3]^{3+}$ ions. Since the solubility of $[Co\ phen_3]\ (ClO_4)_2$ was very low, the reduction waves of the $[Co(phen)_3]^{3+}$ ion were studied under varied conditions. The dependence of the limiting current on the mercury column height is given in Table I. The characteristics of the d. c. polarograms at various concentrations of the depolarizer are given in Table II.

A typical example of the logarithmic plot for the first reduction wave with 0.6_3 mmol./l. $[Co(phen)_3]^{3+}$ is shown in Fig. 1. The reciprocal slope in the upper part decreases with the increase in the depolarizer concentration up to 1.5 mmol./l. Beyond that point, the d. c. polarogram is distorted to a greater extent with an increase in the concentration. The main second wave has a discontinuity at its beginning, and the decomposition potential shifts to a more positive potential with an incerase

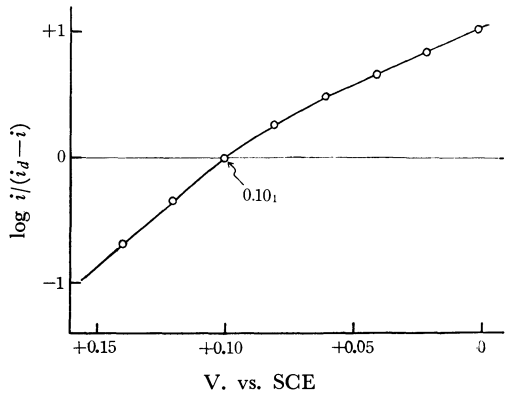

Fig. 1. Logarithmic plot for the reduction wave of 0.6_3 mM $[Co(phen)_3](ClO_4)_3$ in 1 M Na_2SO_4.

in the depolarizer concentration. The first and the second (including the prewave) waves are concentration-dependent and are evidently diffusion-controlled. The prewave has the characteristic of an adsorption wave in that its height is independent of the depolarizer concentration.[13] Since adsorption phenomena seem to play an important role over a wide potential range, the drop time was measured at different potentials. The results are shown in Fig. 2. The irregularity of the electrocapillary curve is exactly reflected in the d. c. and a. c. polarograms. The a. c. polarograms at various concentrations of the depolarizer are shown in Fig. 3, together with the a. c. polarograms obtained in the presence of gelatine.

13) R. Brdička, *Z. Elektrochem.*, **48**, 278 (1942).

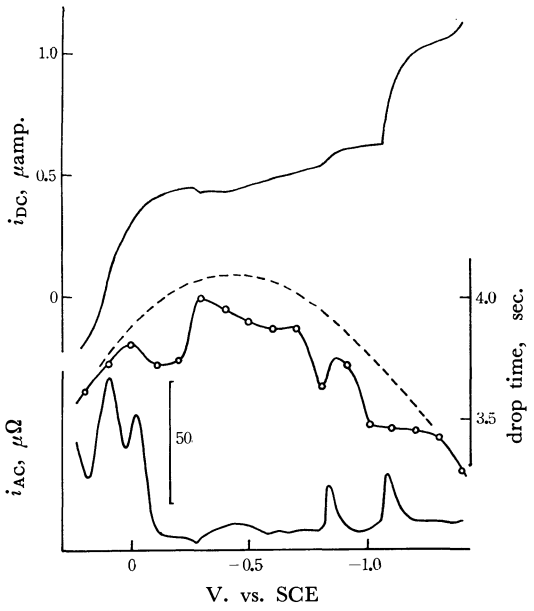

Fig. 2. Electrocapillary curve and d.c. and a.c. polarograms of 0.3 mM $[Co(phen)_3](ClO_4)_3$ in 1 M Na_2SO_4.

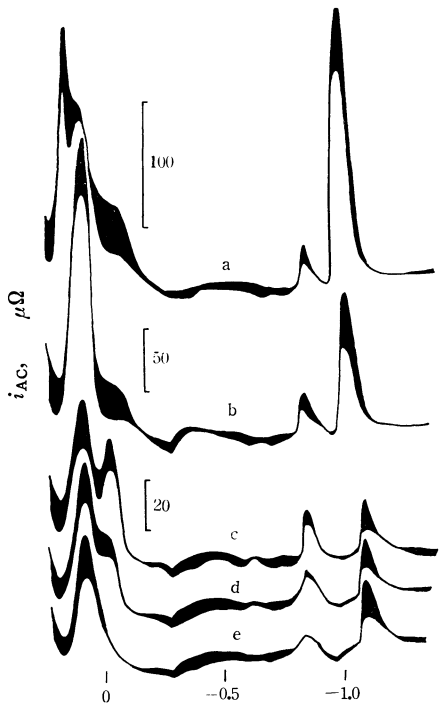

Fig. 3. A. c. polarograms of $[Co(phen)_3](ClO_4)_3$ in 1 M Na_2SO_4. The concentration of $[Co(phen)_3](ClO_4)_3$: a) 1.5 mM, b) 0.9 mM, c) 0.3 mM, d) 0.3 mM (+0.01% gelatine) and e) 0.3 mM (+0.03% gelatine).

It should be noted that the a. c. peak height corresponding to the first d. c. wave is not proportionate to the concentration of the depolarizer, and that the two a. c. peaks are observed at the potential for the first d. c. wave with 0.3 mmol./l. $[Co(phen)_3]^{3+}$.

On the Reduction Mechanism.—From the diffusion current constants for the first and the second waves, the first wave can be attributed to the reduction of cobalt from a trivalent to a divalent state and the second, to the reduction of divalent to univalent cobalt. A similar reduction process has been already proposed for several cobalt complexes.[4-7] In the case of the tris(dipyridyl) complex, Waind and Martin[6] concluded that the first reduction wave is reversible, while Vlček[4] pointed out that the second reduction wave is reversible.

The inflection of the logarithmic plot at the upper part for the first step and the appearance of a minimum on the d. c. polarogram may be explained qualitatively by assuming the following electrode reaction:

$$[Co(phen)_3]^{3+} + e^- \rightarrow [Co(phen)_3]^{2+}$$
$$\downarrow\uparrow$$
$$\text{Hg-phen complex} + e^- \leftarrow Hg + phen + [Co(phen)_2]^{2+}$$

The $[Co(phen)_3]^{2+}$ ion produced at the electrode surface, because of its lower stability, dissociates partly to the lower complex, liberating phenanthroline; the phenanthroline is very likely to be adsorbed onto the electrode surface, where it will interfere with the passage of the current and cause a minimum. At a certain potential dependent on the depolarizer concentration, the free phenanthroline adsorbed on the surface accelerates the dissolution of mercury through the formation of a mercury-phenanthroline complex; this oxidation process will compensate for a part of the reduction current, thus causing an inflection of the logarithmic plot and also a distinct deformation of the d. c. polarograms with an increase in the depolarizer concentration. These reduction and oxidation processes give the two peaks around +0.1 V. on an a. c. polarogram.

The peak at a negative potential is confirmed to correspond to the oxidation process since its peak height increases when a small amount of excess free phenanthroline is added. At higher concentrations of the depolarizer, the two opposite processes take place at almost the same potential, resulting in an apparent lowering of the a. c. peak height. If a more strongly adsorbable substance than phenanthroline covers the electrode surface, the dissolution of mercury will be hindered. This expectation can be fully realized by adding 0.03% gelatine to the electrolytic solution, as has been shown in Fig. 3. In spite of the addition of gelatine, however, the polarographic reversibility is very high, as is shown in Table III. The polarographic

TABLE III. VALUES OF $i_p/(ni_d\sqrt{\tau})$

Electrolyte	Electrode reaction	$i_p/(ni_d\sqrt{\tau})$ kΩ amp^{-1}sec$^{-1/2}$
0.3 mM$[Co(phen)_3]^{3+}$+1 M Na_2SO_4 +0.03% gelatine	Co(III) ⟷ Co(II)	0.052_0
	Co(II) ⟷ Co(I)	0.03*
0.3 mM Tl^++1 M Na_2SO_4	Tl(I) ⟷ Tl(Hg)	0.054_0
0.3 mM Cd^{2+}+1 M Na_2SO_4	Cd(II) ⟷ Cd(Hg)	0.052_5
0.3 mM Zn^{2+}+1 M NaCl +0.001% gelatine	Zn(II) ⟷ Zn(Hg)	0.020_1
0.3 mM$[Co(NH_3)_6]^{3+}$+1 M Na_2SO_4	Co(III) ⟷ Co(II)	0.007_0

* 0.05 with 0.8 mM$[Co(phen)_3]^{3+}$

reversibility is defined as $i_p/(ni_d\sqrt{\tau})$, where i_p, i_d and τ represent an a. c. peak height, a limiting diffusion current of the d. c. polarogram and a drop time respectively.[14] Also, from the approximate coincidence of the half-wave potential values for the oxidation of cobalt(II) (aver. +0.093 V.) and the reduction of cobalt(III) (aver. +0.095 V.), it can be concluded that the electrode process for the reduction of cobalt(III) to cobalt(II) is highly reversible in the phenanthroline system.

The prewave of the second wave can be attributed to the adsorption of the cobalt(I)-complex produced through the following electrode reaction:

$$[Co(phen)_{2-3}]^{2+} + e^- \rightarrow [Co(phen)_{2-3}]^+$$

The uncommon univalent cobalt complex ion can be produced in solution by the controlled-potential electrolysis method. The existence of the cobalt(I)-complex can be shown by the oxidation curve, as is shown in Fig. 4. From the polarographic reversibility and the constancy of the half-wave potential for the redox waves, the reduction of cobalt(II) to cobalt(I) is also considered

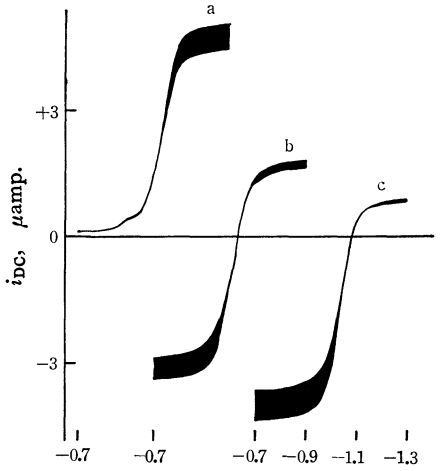

Fig. 4. D. c. polarograms obtained with a 1 : 3 mixture of cobalt(II) and phenanthroline in 0.5 M LiCl ethanolic solution: (a) 0, (b) 0.5 and (c) more than 3 hr. after controlled-potential electrolysis was started.

to be reversible in the present system.

From the above results, it can definitely be concluded that the polarographic behavior of the tris-(1,10-phenanthroline)cobalt complex is quite similar to that of the tris(dipyridyl) complex as regards both the mechanism and the reversibility of the electrode reaction.

On the Composition of the Univalent Cobalt Complex.—In the case of the dipyridyl complex, two formulas, $[Co(dipy)_3]ClO_4$ and $[Co(dipy)_2]ClO_4$, have been proposed for the univalent cobalt complex by different authors.[4,6] Therefore, the present authors attempted to isolate the univalent cobalt phenanthroline complex in a pure state and to determine its chemical composition. Since the controlled-potential electrolysis method proved unsuccessful in its isolation, a reduction method similar to that employed in the preparation of the dipyridyl complex was used; $[Co(phen)_3](ClO_4)_2$ suspended in an ice-cold methanol (20%)-water mixture was reduced by slowly adding a cold aqueous solution of sodium borohydride in an atmosphere of nitrogen. The black solid which had precipitated was filtered, washed with cold water, and dried in a vacuum desiccator. It is highly sensitive to oxidation and turns brown-black on exposure to the air. Chemical analysis gave the atomic ratio of Co : N : Cl = 1 : 5.75 : 0.90. (Found: Co, 8.2; N, 11.20; ClO_4, 12.4%). Preliminary measurements revealed that the magnetic moment is much less than the value to be expected for a complex of octahedral symmetry, with its central metal ion having a d^8-electron configuration. From these results and from the fact that the prolonged electrolysis did not completely diminish the reduction wave of divalent cobalt, it may be supposed that the univalent cobalt complex obtained by the above method is not in a pure state. The color of the solid and the solution also suggests the possibility that the product is either entirely or partly a polynuclear complex. This situation leads to the conclusion that the authors are unable to decide definitely whether the univalent cobalt complex is $[Co(phen)_3]^+$ or $[Co(phen)_2]^+$,

14) M. Senda, M. Senda and I. Tachi, *J. Electrochem. Soc. Japan (Denki Kagaku)*, **27**, 83 (1959).

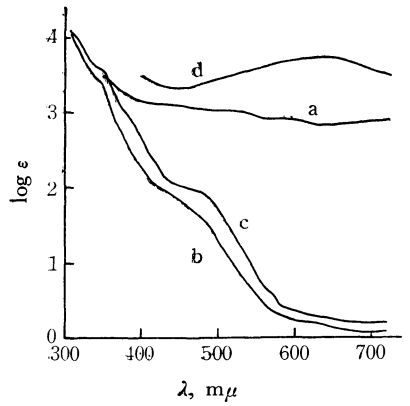

Fig. 5. Absorption spectra.
(a) $[Co(phen)_{2-8}]^{+}$, (b) $[Co(phen)_3]^{2+}$, (c) $[Co(phen)_3]^{3+}$, (d) $[Co(dipy)_3]^{+}$ plotted from the data obtained by Waind and Martin.[6]

although the atomic ratio of nitrogen to cobalt is close to six.*

The brown-black solution obtained by electrolyzing the 1 : 3 mixture of cobalt(II) and phenanthroline in a 0.5 M lithium chloride ethanolic solution (50% by volume) was used to measure the absorption spectrum. No definite absorption maxima are observed on the absorption curve, as is shown in Fig. 5. The color of the solution is in remarkable contrast with that of the dipyridyl complex, which has been shown to be a deep blue, its λ_{max} being 640 mμ.[6] Although the color of the solution and that of the solid are quite similar, there still remains some uncertainty with regard to the identity of the primary electrode reaction product and the solid obtained above. More detailed studies are needed.

* Independent of the present work, it has been reported that the phenanthroline cobalt(I) perchlorate is the hexacoordinated complex, $[Co(phen)_3]ClO_4$. N. Maki, M. Yamagami and H. Itatani, *J. Am. Chem. Soc.*, **86**, 514 (1964).

Summary

Tris(1, 10-phenanthroline)cobalt(III) complex ions are reduced in two steps in 1 M sodium sulfate. The first wave, which appears around +0.10 V. vs. SCE, corresponds to the reduction of cobalt from a trivalent state to a divalent, while the second, which appears around −1.0 V. vs. SCE, corresponds to the reduction of divalent to univalent cobalt. Tris(1, 10-phenanthroline)cobalt(II) ions show an oxidation wave and a reduction wave at the respective potentials corresponding to the first and the second waves of trivalent cobalt complex ions. A small minimum is observed on the plateau of the first wave, and a small prewave is accompanied by the second wave. Both electrode processes are considered to be reversible.

The univalent cobalt-phenanthroline complex has been prepared by the reduction of the divalent cobalt complex with sodium borohydride. It is a black powder, and the atomic ratio of nitrogen to cobalt is found to be nearly six, though not exactly six.

This work was supported in part by Scientific Research Grant of the Ministry of Education, to which the authors are grateful.

BULLETIN OF THE CHEMICAL SOCIETY OF JAPAN VOL. 39 361—364 (1966)

Asymmetric Hydrogenation with Modified Raney Nickel. VI

By Yoshiharu IZUMI, Susumu TATSUMI, Masami IMAIDA
Yoshio FUKUDA and Shiro AKABORI

Division of Organic Chemistry, Institute for Protein Research, Osaka University, Kita-ku, Osaka

(Received June 26, 1965)

The asymmetric hydrogenation catalyst has been prepared by the modification of Raney nickel with solutions of (−)-2-methyltartaric acid (A), (+)-2-methyltartaric acid (B) and (+)-2, 3-dimethyltartaric acid, and its asymmetric hydrogenation activity has been measured by the hydrogenation of methyl acetoacetate to optically active methyl 3-hydroxybutyrate. The asymmetric activity of the catalyst is much influenced by the pH and the temperature of the modifying solution. Generally, (+)-2-methyltartaric acid (B) and (+)-2, 3-dimethyltartaric acid have a high asymmetric activity in reaction to Raney nickel. The highest asymmetric activity has been obtained by modification with (+)-2-methyltartaric acid (B) and with it the specific rotation of the hydrogenation product has been found to be $[\alpha]_D^{20}$ +11.72° (without a solvent) under the optimum conditions. This value means that the product is 78% composed

of the dextro- and 22% of the levorotatory form. On the other hand, the asymmetric activity of the catalyst modified with (−)-2-methyltartaric acid (A) is very low and quite different from that of the catalyst modified with (+)-2-methyltartaric acid (B). It has been supposed that this difference depends on the stereoisomerism of the threo-erythro form of the 2-methyltartaric acid molecule.

The previous papers of this series[1-5] reported the asymmetric hydrogenation of methyl acetoacetate to methyl 3-hydroxybutyrate using Raney nickel catalysts modified with optically active 2-amino and 2-hydroxy carboxylic acids. It was found that the asymmetric activity of the catalysts is much influenced by the pH and temperature of the modifying solution. An especially high asymmetic activity was obtained when the catalyst was modified at 100°C with a D-tartaric acid solution, the pH of which had been adjusted to 5.1—5.2.[2]

In the present work, optically active 2-methyltartaric and 2, 3-dimethyltartaric acid will be tested as modifying reagents in an attempt to study the role of substituents on asymmetric carbon atoms of tartaric acid in the modification of the Raney nickel catalyst.

Materials

Modifying Reagents.*—2-Methyltartaric acid has two racemic forms, the melting points of which are 146°C and 161°C. Both racemic substances were synthesized from ethyl acetoacetate and resolved with brucine by the fractional crystallization of the diastereomers in water. The optical rotation values of the four isomers were as follows;

(A) From the racemic form with the lower melting point (2-methyltartaric acid A):

(+)-isomer $[\alpha]_D^{20}$ +8.90° (*c* 3.7, water) (I)

(−)-isomer $[\alpha]_D^{20}$ −8.94° (*c* 3.7, water) (II)

(B) From the racemic form with the higher melting point (2-methyltartaric acid B);

(+)-isomer $[\alpha]_D^{20}$ +5.88° (*c* 3.2, water) (III)

(−)-isomer $[\alpha]_D^{20}$ −5.60° (*c* 3.2, water) (IV)

2, 3-Dimethyltartaric acid has two optically inactive modifications; the one is the racemic (m. p. 187°C), and the other is the meso form (m. p. 180°C). Both substances were prepared from diacetyl, while the optical resolution of the racemic form was performed with brucine. The optical rotation values of the two optical isomers of this hydroxy carboxylic acid were as follows:

(+)-isomer $[\alpha]_D^{20}$ +13.4° (*c* 4.0, water) (V)

(−)-isomer $[\alpha]_D^{20}$ −13.4° (*c* 4.0, water) (VI)

In the present asymmetric hydrogenation experiments, optically active (−)-2-methyltartaric acid (A) (II), derived from the racemate with the lower melting point; (+)-2-methyltartaric acid (B) (III), derived from the racemate with the higher melting point, and (+)-2, 3-dimethyltartaric acid (V) were used as the modifying reagents.

Results and Discussion

The Effect of the pH of the Modifying Solution.—Measurements were made of the asymmetric activities of catalysts modified at 0°C with aqueous solutions of substances II, III and V, the pH of which had been adjusted to specified values with a 1 N (*f*=0.893) sodium hydroxide solution according to the titration curve shown in Fig. 1. The results are shown in Fig. 2.

The catalysts modified at 0°C with these hydroxy carboxylic acids hydrogenated methyl acetoacetate predominantly to dextrorotatory methyl 3-hydroxybutyrate. Higher asymmetric activities were observed on modification with III and V, when the catalysts were less influenced by the pH of the modifying solutions. In the case of modification

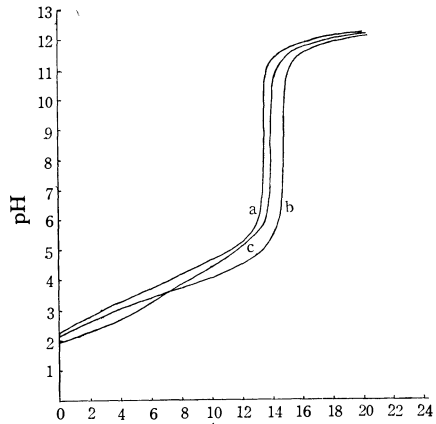

Fig. 1. Titration curve of 1% hydroxy carboxylic acid solution with N NaOH.
a (−)-2-Methyltartaric acid (A)
b (+)-2-Methyltartaric acid (B)
c (+)-2, 3-Dimethyltartaric acid

1) Y. Izumi, M. Imaida, H. Fukawa and S. Akabori, This Bulletin, **36**, 21 (1963).
2) Y. Izumi, M. Imaida, H. Fukawa and S. Akabori, ibid., **36**, 155 (1963).
3) S. Tatsumi, M. Imaida, Y. Fukuda, Y. Izumi and S. Akabori, ibid., **37**, 846 (1964).
4) Y. Izumi, S. Akabori, H. Fukawa, S. Tatsumi, M. Imaida, Y. Fukuda and S. Komatsu, *Proceedings of the 3rd International Congress on Catalysis*, **2**, 1364 (1964).
5) Y. Izumi, S. Tatsumi, M. Imaida, Y. Fukuda and S. Akabori, This Bulletin, **38**, 1206 (1965).
* The preparation of optically active 2-methyltartaric acids and 2, 3-dimethyltartaric acid will be published by the present authors in this Bulletin in the near future.

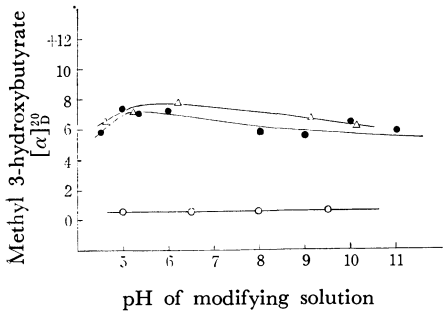

Fig. 2. Effect of pH of modifying solution at 0°C.
—○— (−)-2-Methyltartaric acid (A)
—●— (+)-2-Methyltartaric acid (B)
—△— (+)-2, 3-Dimethyltartaric acid

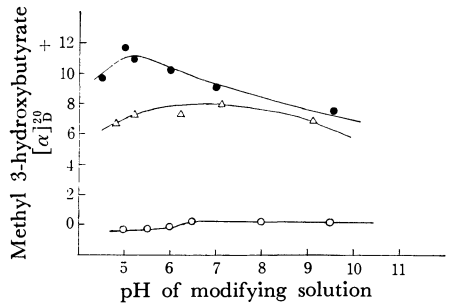

Fig. 3. Effect of pH of modifying solution at 100°C.
—○— (−)-2-Methyltartaric acid (A)
—●— (+)-2-Methyltartaric acid (B)
—△— (+)-2, 3-Dimethyltartaric acid

with II, however, the asymmetric activity was very low and was not at all influenced by the pH of the modifying solution.

The effect of the pH value of the modifying solution at 100°C on the asymmetric activities of the modified catalysts is shown in Fig. 3.

As is shown in Fig. 3, upon modification with III the asymmetric activity was greater and was much influenced by the pH of the modifying solution. The greatest asymmetric activity was obtained at pH 5.0 when the specific rotation value of the hydrogenation product was $[\alpha]_D^{20}$ +11.72° (without a solvent). There was a considerable decrease in activity at both lower and higher pH values. Under acidic conditions below pH 4.5, the catalytic activity of the modified catalyst was too low to permit any hydrogenation experiments. On modification with V, although a high asymmetric activity was obtained, it was lower than with III; and the asymmetric activity curve showed a tendency similar to that shown on modification at 0°C. In the case of modification with II, however, the asymmetric activity was very low and the levorotatory product was obtained at pH values below the pH jump of the titration curve of this acid shown in Fig. 1.

The Effect of the Modifying Temperature. —The effect of the temperature of the modifying solution was studied at pH 5.0—5.2; the results are shown in Fig. 4.

As is shown in Fig. 4, the asymmetric activity of the catalyst modified with III was greater than

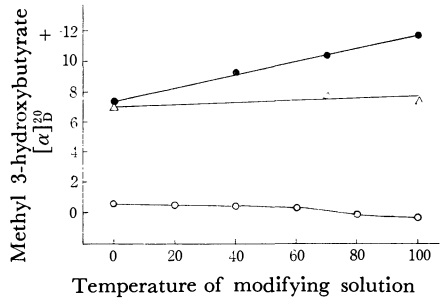

Fig. 4. Effect of temperature of modifying solution.
—○— (−)-2-Methyltartaric acid (A) (pH 5.0)
—●— (+)-2-Methyltartaric acid (B) (pH 5.0)
—△— (+)-2, 3-Dimethyltartaric acid (pH 5.1—5.2)

that of the catalyst modified with V, and it clearly increased with elevation of the modifying temperature. On modification with V, however, the activity was hardly influenced at all by the temperature. In the case of modification with II, the asymmetric activity was very low and the hydrogenation product was dextrorotatory below 70°C, although it showed the opposite optical rotation above this temperature.

As is shown in Figs. 2, 3 and 4, on modification with (+)-2-methyltartaric acid (B) (III), the catalyst had a higher asymmetric activity than tartaric acid[2] and gave the dextrorotatory product. Under optimum conditions the specific rotation value of the product was $[\alpha]_D^{20}$ +11.72°; this means that the product was 78% composed of the dextro- and 22% of the levorotatory form. On the other hand, (−)-2-methyltartaric acid (A) (II) has only a small asymmetric effect upon Raney nickel.

2-Methyltartaric acid has a structure in which a methyl group is introduced into one of the asymmetric carbons of tartaric acid in place of a hydrogen atom. Thus it is characterized by the existence of two types, the threo and erythro form, which are 2-methyltartaric acid (A) and (B). Although it is unknown at the present time which steric isomer is threo and which is erythro, it is conceivable that the difference in the asymmetric effects of (−)-2-methyltartaric acid (A) and (+)-2-methyltartaric acid (B) depends on their threo-erythro isomerism. On modification with (+)-2, 3-dimethyltartaric acid, however, the asymmetric activity shows a tendency similar to that shown on modification with tartaric acid, except for the difference in the asymmetric direction.

The relationship between the asymmetric activity of the catalyst and the stereoisomerism of the modifying reagent will be discussed after the steric configurations of (−)-2-methyltartaric acid (A), (+)-2-methyltartaric acid (B) and (+)-2, 3-dimethyltartaric acid have been confirmed.

Experimental

The preparation and modification of the Raney nickel catalyst, the hydrogenation of methyl acetoacetate, and the measurement of the asymmetric activity of the catalyst were performed as described in a previous paper.[3]

Summary

1) The asymmetric activities of Raney nickel catalysts modified with (−)-2-methyltartaric acid (A), (+)-2-methyltartaric acid (B) and (+)-2, 3-dimethyltartaric acid have been measured by the hydrogenation of methyl acetoacetate.

2) The highest asymmetric acitivity has been obtained by modification with (+)-2-methyltartaric acid; with it the specific rotation of the hydrogenation product was $[\alpha]_D^{20}$ +11.72° under optimum conditions.

3) The asymmetric activity of the catalyst modified with (−)-2-methyltartaric acid (A) was very low and quite different from that of the catalyst modified with (+)-2-methyltartaric acid (B). This difference depends on the stereoisomerism of the threo-erythro form. On modification with (+)-2, 3-dimethyltartaric acid, the asymmetric activity showed a tendency similar to that shown on modification with D-tartaric acid, except for the difference in the asymmetric direction.

This research was made possible through support from the Kawaken Fine Chemicals Co., Ltd., Tokyo, and the Ajinomoto Co., Inc., Tokyo.

BULLETIN OF THE CHEMICAL SOCIETY OF JAPAN VOL. 39 364—366 (1966)

The Synthesis of Sulfoxides by the Oxidation of Sulfide with the Bromine Complex of 1, 4-Diazabicyclo(2, 2, 2)octane[1,2]

By Shigeru OAE, Yutaka OHNISHI, Seizi KOZUKA and Waichiro TAGAKI

Department of Applied Chemistry, Faculty of Engineering, Osaka City University, Sumiyoshi-ku, Osaka

(Received July 5, 1965)

1, 4-Diazabicyclo(2, 2, 2)octane readily forms an addition complex with two moles of bromine. This complex has been found to be an excellent oxidizing agent for the selective oxidation of various sulfides to the corresponding sulfoxides when the reaction is performed in an aqueous medium. The bromine-addition complexes of pyridine and quinoline have also been found to be useful for the same purpose. The reaction has been shown to be a superb way of incorporating ^{18}O into sulfoxides.

A number of methods for the oxidation of sulfides to sulfoxides are known.[3] Among these, the oxidation by halogenating agents, such as molecular halogens or hypohalites, is one of the least-studied procedures. Molecular halogens have been known to add to sulfides to form addition compounds which are then readily hydrolyzed to give sulfoxides; on the other hand, hypohalites have been shown to oxidize higher dialkyl sulfides to the corresponding sulfoxides,[3] while lower sulfides are likely to be oxidized by the reagents directly to their sulfones.[3] However, the use of such halogenating agents for the oxidation of sulfides has been limited to only a certain type of sulfides, since many sulfides are known to undergo different reactions to give undesirable side products.

Recently we have found that some sulfides are successfully oxidized to the corresponding sulfoxides in high yields when the sulfides are treated with *N*-bromosuccinimide (NBS) in aqueous media.[4] Meanwhile, *p*-substituted phenyl methyl sulfides have been found to form, with bromine, the corresponding bromine addition complexes which, upon hydrolyses, are found to afford the corresponding sulfoxides.[5] The same sulfides, however, gave only the C–S bond cleavage products when treated with NBS. These observations seem to

1) This work was supported by the Petroleum Research Fund, administered by the American Chemical Society.

2) Paper X on Sulfoxides.

3) H. H. Szmant, Chapter 16, in "Organic Sulfur Compounds," Pergamon Press, London (1961).

4) W. Tagaki, K. Kikukawa, K. Ando and S. Oae, *Chem. & Ind.*, **1964**, 1924.

5) a) Th. Zincke and W. Frohnberg, *Ber.*, **43**, 837 (1909); b) S. Oae, W. Tagaki and K. Kikukawa, unpublished work.

Table I. The oxidation of sulfides with the bromine complexes of tertiary amines in 70% aqueous acetic acid

Sulfide	Product	Yield, %			
		NBS[a]	$C_6H_{12}N_2nBr_2$[b]	$C_5H_5NBr_2$[c]	$C_9H_7NBr_2$[d]
$(n\text{-}C_4H_9)_2S$	$(n\text{-}C_4H_9)_2SO$	C–S cleavage	85	—	—
$p\text{-}CH_3C_6H_4SCH_3$	$p\text{-}CH_3C_6H_5SOCH_3$	C–S cleavage	85	—	—
$C_6H_5CH_2SC_2H_5$	$C_6H_5CH_2SOC_2H_5$	C–S cleavage	70	—	—
$C_6H_5CH_2SC_6H_5$	$C_6H_5CH_2SOC_2H_5$	85	95	65	90
$C_6H_5SC_6H_5$	$C_6H_5SOC_6H_5$	75	95	—	—
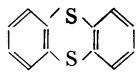	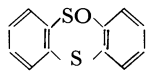	60	95	—	—
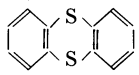	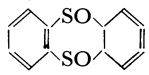	30	95	—	—

a) Previous results, Ref. 4. b) The bromine complex of 1, 4-diazabicyclo(2, 2, 2)octane. c) The bromine complex of pyridine. d) The bromine complex of quinoline.

suggest that the mode of oxidation varies with the type of halogenating agent.

In the present investigation, we have examined the possibility of the oxidation of sulfides by the bromine complexes of a few stable tertiary amines; we have found that the bromine complex of 1, 4-diazabicyclo(2, 2, 2)octane can oxidize a variety of sulfides to sulfoxides without the formation of sulfones. Some of the sulfides which could not be oxidized to the corresponding sulfoxides either by NBS or molecular bromine were readily oxidized to the sulfoxides by this reagent.

Tertiary amines, such as pyridine and quinoline, are known to form bromine-addition complexes when treated with bromine in an inert solvent,[6-12] and these complexes can be used in situ as brominatting agents.[8,9] These complexes are usually very sensitive to light, heat and moisture, and hence have to be used immediately after they are prepared. Unlike the bromine complexes of other amines, however, that of 1, 4-diazabicyclo-(2, 2, 2)octane is very stable,[13] although its structure and the reason for its stability are not well understood yet.

The six different sulfides subjected to this oxidation were dialkyl, aryl-alkyl, benzyl-alkyl, benzyl-aryl, diaryl sulfides and thianthrene. The first three sulfides undergo C–S bond cleavage by NBS, but they were found to be readily oxidized selectively by the new method to the corresponding sulfoxides. All these sulfides were oxidized with the above three complexes in 70% aqueous acetic acid. The reactions were very rapid, like the similar oxidation by NBS. When the reaction proceeded nicely, the initial heterogeneous reaction mixture usually turned to a homogeneous solution within a few minutes, with or without heating. Therefore, one could use the rapid change of the state of solution for the diagnosis of the successful oxidation. The results are shown in Table I, where they may be compared with the results obtained by the oxidation with NBS.

In all cases, the bromine complex of 1, 4-diazabicyclo(2, 2, 2)octane gave the corresponding sulfoxides in satisfactory yields. Neither the cleavage of the aliphatic C–S bond, which was observed in the oxidation of aliphatic sulfides by NBS, nor the bromination of the aromatic ring, which takes place in the oxidation by molecular bromine, was observed. Here again the sulfoxides thus obtained were found to be completely free from the sulfones. When ^{18}O-enriched water was used in the reaction of diphenyl sulfide, a ^{18}O-labeled sulfoxide was obtained in which the sulfoxide oxygen was found to be incorporated with almost the same ^{18}O-enrichment as that of the original water, as is shown in Table II. This implies that the ^{18}O scrambling between acetic acid and water is not important in this rapid reaction. The present oxidation is therefore, a more convenient and a better method for labeling sulfoxide oxygen with ^{18}O than our previous methods, that by the oxygen-exchange reaction of sulfoxide in concentrated sulfuric acid[14,15] or

Table II. ^{18}O-labeling with the bromine complex of 1, 4-diazabicyclo(2, 2, 2)octane

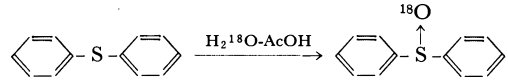

	^{18}O Content (atom%)
$H_2{}^{18}O$ used	1.65
Sulfoxide	1.45

6) D. M. Williams, *J. Chem. Soc.*, **1931**, 2783.
7) S. M. McElvain and M. A. Goese, *J. Am. Chem. Soc.*, **65**, 2227 (1943).
8) S. M. McElvain and L. R. Morris, ibid., **73**, 206 (1951).
9) N. A. Domnin and V. A. Cherkasova, *Zhur. Obshchei Khim.*, **23**, 1731 (1953).
10) J. Eisch, *Chem. & Ind.*, **1959**, 1449.
11) J. Eisch, *J. Org. Chem.*, **27**, 1318 (1962).
12) J. Eisch and B. Jaselskis, ibid., **28**, 2865 (1963).
13) E. C. Herich, U. S. Pat. 29654529 (1962).
14) S. Oae, T. Kitao and Y. Kitaoka, *Chem. & Ind.*, **1961**, 291.
15) S. Oae, T. Kitao, Y. Kitaoka and S. Kawamura, This Bulletin, **38**, 546 (1965).

that by the oxidation of sulfide with NBS in ^{18}O-enriched water.[4]

Experimental

Oxidation with Bromine Complexes of Pyridine and Quinoline.—The quinoline-bromine complex was prepared by slowly mixing equimolecular amounts of quinoline and bromine in carbon tetrachloride.[11] The pyridine-bromine complex was prepared similarly.

To a solution of benzyl phenyl sulfied (0.68 g., 0.0034 mol.) in 70% aqueous acetic acid, the freshly-prepared quinoline-bromine complex (0.99 g., 0.0034 mol.) was added; the whole mixture was then stirred at room temperature until it became homogeneous (within a few minutes). The resulting solution was poured into an excess of water, and the benzyl phenyl sulfoxides which separated were collected and recrystallized; yield, 0.65 g. (89%). If necessary, the quenched reaction mixture was made alkaline with potassium carbonate, and the sulfoxide was extracted with ether. The oxidation by the pyridine-bromine complex was carried out similarly. The results are shown in Table I.

The Bromine Complex of 1, 4-diazabicyclo-(2, 2, 2)octane.—The diamine was supplied by the Houdry Corp. and was recrystallized from *n*-hexane before use. Into the diamine solution of an inert solvent, such as carbon tetrachloride or benzene, equimolar amounts of bromine in the same solvent were slowly stirred at room temperature in the case of benzene and warmed up to 50°C in the case of carbon tetrachloride. The pale yellow precipitates which formed immediately were collected, washed with a fresh solvent, and dried (m. p. 150—160°C with decomposition). The same precipitates (m. p. 150—160°C with decomposition) were also obtained by adding two moles of bromine. The complexes can be used for the reaction in a similar manner.

Calcd. for $C_6H_{12}N_2Br_2$: Br, 74.07; found Br, 70.80 (obtained from the treatment of 1-to-1 mol. of bromine) and 73.30% (obtained from the treatment of 2 mol. of bromine).

Oxidation with the Bromine Complex of 1, 4-diazabicyclo(2, 2, 2)octane. — Half-molar amounts of the complex which had been prepared by treatment with 2 mol. of bromine were used, and a small excess was employed for the complex which had been prepared by treatment with 1 mol. of bromine. Diamine could be recovered from the reaction mixture as a hydrobromide salt. The procedure for the oxidation of various sulfides with the diamine-bromine complex was similarly applied to those of pyridine- or quinoline-dibromide.

The Identification of the Sulfoxides.—*Di-n-butyl Sulfoxide,* $(n\text{-}C_4H_9)_2SO$.—B. p. 105°C/3 mmHg; very hygroscopic.

p-Tolyl Methyl Sulfoxide, $p\text{-}CH_3C_6H_4SOCH_3$—B. p. 107°C/3 mmHg; m. p. 38.5°C (from benzene-hexane).

Found: C, 62.69, H, 6.75. Calcd. for $C_8H_{10}SO$: C, 62.33, H, 6.49%.

Benzyl Ethyl Sulfoxide, $C_6H_5CH_2SOC_2H_5$.—B. p. 141°C/3 mmHg; m. p. 51—52°C (from benzene-hexane).

Found: C, 64.52, H. 7.22. Calcd. for $C_9H_{12}SO$: C, 64.28, H, 7.14%.

Benzyl Phenyl Sulfoxide, $C_6H_5CH_2SOC_6H_5$.—M. p. and mixed m. p. 122—123°C (with an authentic sample).

Thianthrene Monoxide, 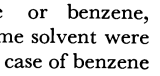 —M. p. and mixed m. p. 143°C (with an authentic sample).

Thianthrene dioxide, 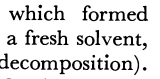 .—M. p. and mixed m. p. >200°C (sublimation).

Diphenyl sulfoxide, $C_6H_5SOC_6H_5$.—M. p. and mixed m. p. 69—71°C (with an authentic sample).

All these sulfoxides showed the infrared bands at 1040—1050 cm^{-1} characteristic of sulfoxides.

BULLETIN OF THE CHEMICAL SOCIETY OF JAPAN VOL. 39 366—369 (1966)

Ion-pair Formation of Some Substitution-inert Complexes and Sulfate Ions. Determination of Association Constants Using Polarographic Diffusion Current

By Nobuyuki TANAKA, Kazuko OGINO (née EBATA) and Gen SATÔ*

Department of Chemistry, Faculty of Science, Tohoku University, Katahira-cho, Sendai

(Received July 6, 1965)

The polarographic diffusion current of some tervalent substitution-inert complex cations decreases by the addition of sulfate. From the change in diffusion current the association constants of substitution-inert complex and sulfate ions are obtained at ionic strength 0.1 ($NaClO_4$) and 25°C. The values are 69 ± 8, 58 ± 8 and 4×10 for $[Co(NH_3)_6]^{3+}$–SO_4^{2-}, $[Cr(NH_3)_6]^{3+}$–SO_4^{2-} and $[Cr(H_2O)_6]^{3+}$–SO_4^{2-} respectively. The formation of $[Co(NH_3)_6]^{3+}$–HSO_4^- is negligibly small compared with that of $[Co(NH_3)_6]^{3+}$–SO_4^{2-}.

* Present address: Department of Chemistry, Sophia University, Chiyoda-ku, Tokyo.

It has been reported that the polarographic reduction waves of tervalent complex cations such as $[Co(NH_3)_6]^{3+}$ and $[Cr(NH_3)_6]^{3+}$ are affected by the presence of sulfate[1-5]; the half-wave potential shifts to more negative potentials and the diffusion current decreases upon the addition of sulfate. These were attributed mainly to the effect of ion-pair formation of the tervalent complex cations and sulfate ions. The shift in the half-wave potential was used for the determination of the association constants both in the case of a reversible electrode process[2,5] and in that of an irreversible electrode process[4]. However, the change of the structure of the electrical double layer caused by the addition of sulfate ions affects the rate of the electrochemical step, and hence the half-wave potential when the electrode process is irreversible. In such cases, it seems not appropriate to determine the association constant from the change of the half-wave potential.

In this paper, a method for the determination of the association constant using the polarographic diffusion current is presented and is applied to the ion-pairs $[Co(NH_3)_6]^{3+}$–SO_4^{2-}, $[Cr(NH_3)_6]^{3+}$–SO_4^{2-} and $[Cr(H_2O)_6]^{3+}$–SO_4^{2-}.

Experimental

Hexamminecobalt(III) perchlorate and hexamminechromium(III) perchlorate were obtained by the precipitation from aqueous solutions of the corresponding chlorides by the addition of perchloric acid, the chlorides of the ammine complexes being prepared with procedures given in literatures.[6,7] The solution of hexaquochromium(III) in perchloric acid was obtained by the reduction of sodium dichromate with hydrogen peroxide.[8]

Measurements were carried out at 25°C in solutions of ionic strength 0.1 ($NaClO_4$) containing 0.005% gelatin and an appropriate amount of perchloric acid. The diffusion current was recorded with a Yanagimoto PB-4 pen-recording polarograph.

Treatment of the Data

Consider the electrode reaction

$$M^{m+} + X^{x-} \rightleftarrows MX^{(m-x)+} \quad (1)$$

$$M^{m+} \text{ or } MX^{(m-x)+} + ne \rightarrow \text{Reduction product} \quad (2)$$

where M^{m+} corresponds to a complex cation, X^{x-} a counter ion and $MX^{(m-x)+}$ an ion-pair. The magnitude of the polarographic diffusion current for this system depends on the ion-pair formation: When reaction 1 is in equilibrium, the apparent diffusion coefficient, D, is given by[9,10]

$$D=\frac{D_M+KD_{MX}C_X}{1+KC_X} \quad (3)$$

where C_X is the concentration of X^{x-}, D_M and D_{MX}, the diffusion coefficients of M^{m+} and $MX^{(m-x)+}$ respectively and K the association constant of M^{m+} and X^{x-}:

$$K=C_{MX}/(C_MC_X) \quad (4)$$

where C_M and C_{MX} denote concentrations of M^{m+} and $MX^{(m-x)+}$ respectively. When values of D_M and D at various C_X are available, several methods,[11] i. e., elimination methods, linear plots methods and curve fitting methods, can be used for the calculation of the association constant. Among them, one of the linear plots methods is most appropriate in the present case. Eq. 3 is transformed to

$$\frac{C_X}{D_M-D}=\frac{1+KC_X}{K(D_M-D_{MX})} \quad (5)$$

where the left-hand side can be obtained experimentally. Equation 5 shows that when its left-hand side is plotted against C_X, a straight line is obtained and from the ratio of its slope and intercept, the association constant is obtained.

The advantage of this method is that it can be applied both to reversible and to irreversible electrode processes, irrespective of the relative electroactivity of M^{m+} and $MX^{(m-x)+}$.

Results

Since a part of sulfate ion combines with hydrogen ion to form hydrogensulfate ion in solutions of pH<3, the effect of hydrogensulfate ion on the equilibrium of the ion association was examined with hexamminecobalt(III) which shows a well-difined one-electron reduction wave both in neutral and in acid media. A series of measurements was carried out in solutions with 0.08 M hydrogen ion and in neutral solutions. The changes in current at −0.7 V. vs. SCE (saturated calomel electrode) with the increase of sodium sulfate concentration are shown in Figs. 1 and 2. In Fig. 1, where the abscissa is the total concentration of sulfate (the sum of sulfate ion and hydrogensulfate ion), the change of the current in acid media is less pronounced than that in neutral media. The sulfate ion concentration, which was calculated

1) H. A. Laitinen, A. J. Frank and P. Kivalo, *J. Am. Chem. Soc.*, **75**, 2865 (1953).
2) H. A. Laitinen and M. W. Grieb, ibid., **77**, 5201 (1955).
3) N. Tanaka, K. Ebata and G. Satô, This Bulletin, **36**, 912 (1963).
4) A. A. Vlček, "Progress in Inorganic Chemistry," Ed. by F. A. Cotton, Interscience Publishers, New York (1963), p. 211.
5) D. Konrád and A. A. Vlček, *Collection Czech. Chem. Commun.*, **26**, 595 (1963).
6) J. Bjerrum and J. P. McReynolds, "Inorganic Syntheses," Vol. II, McGraw-Hill, New York (1946), p. 216.
7) M. Mori, *J. Chem. Soc. Japan, Pure Chem. Sect.* (*Nippon Kagaku Zassi*), **74**, 253 (1953).
8) K. M. Sancier and J. S. Mills, *J. Phys. Chem.*, **67**, 1438 (1963).
9) J. Koutecký, *Collection Czech. Chem. Commun.*, **19**, 857 (1954).
10) H. Matsuda and Y. Ayabe, *Z. Elektrochem.*, **66**, 469 (1962).
11) F. J. C. Rossoti and H. Rossoti, "The Determination of Stability Constants," McGraw-Hill, New York (1961), p. 83.

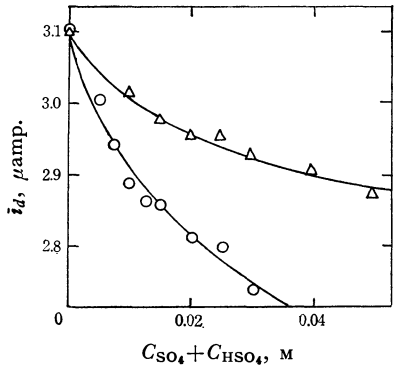

Fig. 1. Variation of the mean diffusion current ($\bar{i}_d$) of the reduction wave of $[Co(NH_3)_6]^{3+}$ with the change of the total sulfate concentration in neutral solutions (○) and in solutions containing 0.08 M hydrogen ion (△).

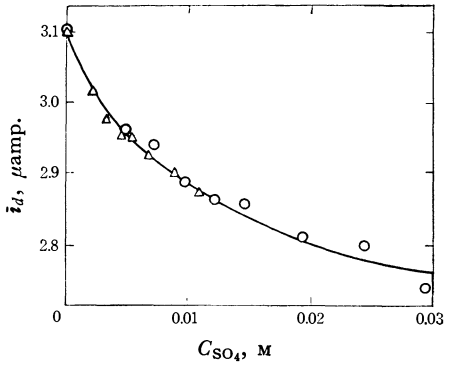

Fig. 2. Variation of the mean diffusion current ($\bar{i}_d$) of the reduction wave of $[Co(NH_3)_6]^{3+}$ with the change of the concentration of sulfate ion in neutral solutions (○) and in solutions containing 0.08 M hydrogen ion (△).

from the total sulfate and the hydrogen ion concentrations and the second dissociation constant of sulfuric acid,* is taken as the abscissa in Fig. 2, where the two sets of plots lie almost on a single curve. It may be concluded from these plots that the association of hydrogensulfate ion is negligible compared with that of sulfate ion.

The measurements for the determination of association constants were carried out in 0.003 N perchloric acid solutions because it was reported that the reduction wave of hexamminechromium(III) is not well-defined in neutral media, but well-defined in acid solutions,[3,12] and that hexaquochromium(III) ions polymerize and hydrolyze in pH ranges higher than 3 and lower than 0.[8] In plotting the left-hand side of Eq. 5, the sulfate

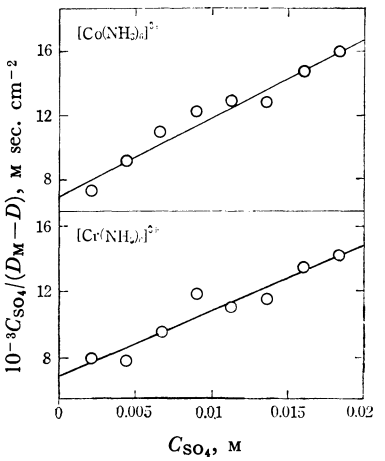

Fig. 3. Relation between the value of the left-hand side of Eq. 5 and sulfate concentration.

concentration, C_{SO_4}, was obtained by subtracting the concentrations of the ion-pair and the hydrogensulfate from the total sulfate concentration. The diffusion coefficient was calculated by the Ilkovič equation from the mean diffusion currents at −0.8 V. in the case of hexamminecobalt(III) and those at −1.1 V. in the cases of hexamminechromium(III) and hexaquochromium(III). The values of D_M were obtained from the diffusion current observed in the absence of sodium sulfate. The plots of of Eq. 5 are shown in Fig. 3. The slopes and the intercepts of the straight lines were calculated by the method of least square, and the association constants were obtained as given in Table I.

TABLE I. ASSOCIATION CONSTANTS OF ION-PAIRS
μ=0.1, 25°C

Ion-pair	K
$[Co(NH_3)_6]^{3+}$-SO_4^{2-}	69±8
$[Cr(NH_3)_6]^{3+}$-SO_4^{2-}	58±8
$[Cr(H_2O)_6]^{3+}$-SO_4^{2-}	4×10

Discussion

The association constant of hexamminecobalt(III) with sulfate ion has been reported by several researchers[13]; the logarithmic constant at infinite dilution ranges between 2.89 and 3.60. Corrected for the effect of activity coefficient,[14] the logarithmic association constant at infinite dilution obtained from our result becomes 3.21, which is in agreement with the values in the literature, and with that expected from Bjerrum's theory[15] of ion as-

* The pK_a of the second dissociation step of sulfuric acid at ionic strength 0.1 was taken as 1.6, which was obtained from the value at infinite dilution (L. G. Sillén and A. E. Martell, "Stability Constants of Metal-Ion Complexes," Chemical Society, London (1964), p. 232.) by correcting for the effect of activity coefficient.

12) N. Tanaka and G. Satô, *Nature*, **197**, 176 (1963).

13) L. G. Sillén and A. E. Martell, "Stability Constants of Metal-Ion Complexes," Chemical Society, London (1964), p. 241.

14) I. Kielland, *J. Am. Chem. Soc.*, **59**, 1675 (1937).

15) H. S. Harned and B. B. Owen, "The Physical Chemistry of Electrolyte Solutions," Reinhold Publishing, New York (1950), p. 42.

sociation due to coulombic interaction between tervalent and bivalent ions of opposite charge at the distance of closest approach 5 Å.

The association constant of $[Cr(NH_3)]_6^{3+}-SO_4^{2-}$ has not been reported. Though detailed comparison of the constant with that of $[Co(NH_3)_6]^{3+}-SO_4^{2-}$ is limited because of the rather large error, it may be said that $[Cr(NH_3)_6]^{3+}-SO_4^{2-}$ is slightly less stable than $[Co(NH_3)_6]^{3+}-SO_4^{2-}$.

In the case of hexaquochromium(III), only a rough estimate of the association constant is obtained because of the rather small change in diffusion coefficient accompanying association. But it may be concluded that the value of K for $[Cr(H_2O)_6]^{3+}-SO_4^{2-}$ is about the same with or less than those for [hexammine complexes]$^{3+}-SO_4^{2-}$, contrary to the result by Tsuchiya and Umayahara[16] who reported that the association constant of $[Cr(H_2O)_6]^{3+}-SO_4^{2-}$ was about twenty times larger than that of $[Co(NH_3)_6]^{3+}-SO_4^{2-}$.

In deriving Eq. 5, only the association of one cation and one anion was taken into consideration. With the precision of the present experiment it is difficult to determine the extent of the ion association involving more than one sulfate ion. The formation of such species is negligibly small compared with the formation of the species such as $[Co(NH_3)_6]^{3+}-SO_4^{2-}$, as far as the association is assumed to depend mainly on the coulombic interaction between ions.

The authors wish to thank the Ministry of Education for the financial support granted for this research.

16) R. Tsuchiya and A. Umayahara, This Bulletin, **36**, 554 (1963).

BULLETIN OF THE CHEMICAL SOCIETY OF JAPAN VOL. 39 369—375 (1966)

The Electron Spin Resonance and Electronic Spectra of 4-Substituted Pyridinyl Radicals

By Michiya ITOH* and Saburo NAGAKURA

The Institute for Solid State Physics, The University of Tokyo, Azabu, Tokyo

(Received July 7, 1965)

The ESR and electronic absorption spectra have been measured with the 1-methyl-4-carbomethoxy-, 1-methyl-4-carbamido-, 1-methyl-4-acetyl- and 1-methyl-4-cyanopyridinyl radicals. From the analysis of their ESR spectra by the aid of a spectrum accumulator, we have been able to determine the nitrogen and hydrogen hyperfine splitting constants of these pyridinyl radicals, from which the spin distributions have then been evaluated. These radicals except for the 1-methyl-4-carbamidopyridinyl radical, have been found to show three absorption bands, at 300—350 mμ, at about 400 mμ and at about 600 mμ. From the results of the ESR and electronic absorption spectra, the electronic structures of these pyridinyl radicals have been concluded to be similar to those of the 4-substituted pyridine anion radicals. The preparation of 1, 2, 6- and 1, 3, 5-trimethyl-4-substituted pyridinyl radicals has been attempted. The latter radicals, except for the 1, 3, 5-trimethyl-4-cyanopyridinyl radical, were not detected by the ESR and electronic absorption spectra, because the steric hindrance of the methyl groups at the 3 and 5 positions prevents them from achieving the resonance stabilization due to the 4-substituent.

Schwarz et al.[1] have reported that the electrochemical reduction of the pyridinium ion in acetonitrile produces a dilute solution of the pyridinyl radical in the presence of tetra-*n*-butylammonium perchlorate as an electrolyte. Kosower et al.[2] have reported that a stable free radical can be prepared by bringing 1-ethyl-4-carbomethoxypyridinium iodide into contact with zinc dust in acetonitrile, and that the radical can be isolated in a pure form by distillation under a high vacuum. They proposed that this free radical is the 1-ethyl-4-carbomethoxypyridinyl radical.

The present authors[3] have studied the electronic structures of 3- and 4-nitropyridine anion radicals by combining the experimental results of the ESR and electronic spectra with the theoretical studies based on the molecular orbital method.

* Present address: The Faculty of Pharmaceutical Sciences, The University of Tokyo, Hongo, Tokyo.

1) W. M. Schwarz, E. M. Kosower and I. Shain, *J. Am. Chem. Soc.*, **83**, 2013 (1961).

2) E. M. Kosower and E. J. Poziomek, ibid., **85**, 2035 (1963); **86**, 5516 (1964).

3) M. Itoh, T. Okamoto and S. Nagakura, This Bulletin, **36**, 1665 (1963); M. Itoh and S. Nagakura, ibid., **38**, 825 (1965).

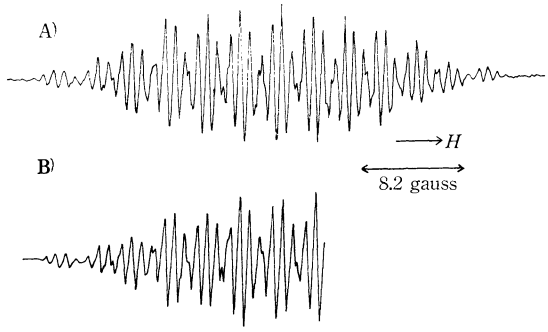

Fig. 1a. A) The ESR spectrum (first derivative) of the acetonitrile solution of 1-methyl-4-carbomethoxypyridinyl radical. B) The theoretically simulated spectrum based on the splitting constants by the aid of the spectrum accumulator. The line width was estimated to be 0.4 gauss and the line shape was considered to be a Lorentzian line.

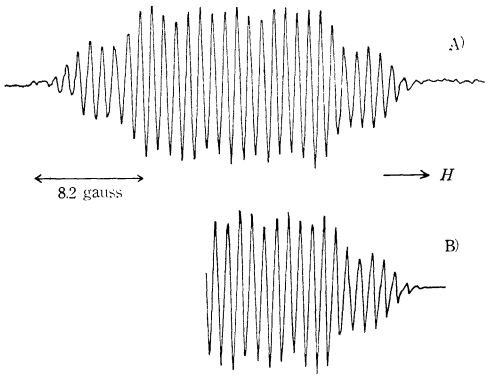

Fig. 1b. A) The ESR spectrum of the acetonitrile solution of the 1-deuteromethyl-4-carbomethoxypyridinyl radical. B) The simulated spectrum based on the splitting constants. The line witdth was estimated to be 0.4 gauss.

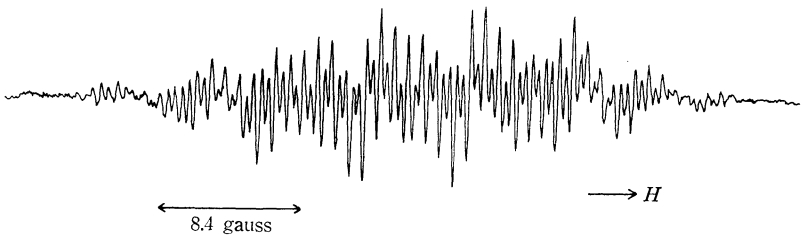

Fig. 1c. The ESR spectrum of the dioxane solution of the 1-methyl-4-carbomethoxypyridinyl radical.

In the course of their investigations, the present authors have attempted to prepare various substituted pyridinyl radicals and to measure their ESR electronic spectra. The present investigation includes the 1-methyl-4-carbomethoxy-, 1-methyl-4-carbamido-, 1-methyl-4-acetyl-, and 1-methyl-4-cyanopyridinyl radicals. The spin distributions and electronic structures of the pyridinyl radicals will be discussed on the basis of the ESR hyperfine splitting constants and the electronic spectra, special attention being paid to a comparison of these results with those concerning the substituted pyridine anion radicals which were reported in previous papers.[3]

Experimental

Materials. — 1-Methyl-4-carbomethoxypyridinium iodide, m. p. 190—191°C,[4] 1-methyl-4-cyanopyridinium iodide, m. p. 197°C,[4] 1-methyl-4-acetylpyridinium iodide, m. p. 172—173°C,[5] and 1-methyl-4-carbamidopyridinium iodide, m. p. 255°C[6], were prepared from the respective 4-substituted pyridines and methyl iodide. Ion exchange resin IRA-410 was used to prepare the 1-methyl-4-carbomethoxypyridinium chloride, m. p. 265—270°C (decomp.). The melting points of these compounds were in good agreement with those reported in the literature.

1-Deuteromethyl-4-carbomethoxy pyridinium bromide was obtained by the treatment of the corresponding substituted pyridines with deuteromethyl bromide (Merck; molecular weight 97.96). 1-Deuteromethyl-4-carbomethoxypyridinium bromide, m. p. 165°C.

Found: C, 40.97, H, (D), 6.04; N, 5.97. Calcd. for $C_8H_7D_3NO_2Br$: C, 40.85; H (D), 5.53; N, 5.95%.

1, 3, 5-Trimethyl- and 1, 2, 6-trimethyl-4-carbomethoxypyridinium iodides, m. p. 218—219°C and m. p. 198°C (decomp.), 1, 3, 5-trimethyl- and 1, 2, 6-trimethyl-4-cyanopyridinium iodides, m. p. 217°C and m. p. 225°C (decomp.), and 1, 3, 5-trimethyl- and 1, 2, 6-trimethyl-4-carbamidopyridinium iodides, m. p. 258°C and m. p. 215°C (decomp.) were prepared from the 2, 6-dimethyl- and 3, 5-dimethyl-4-substituted pyridines which had been obtained from the corresponding dimethyl-4-cyanopyridines.[7,8] The 2, 6-dimethyl-4-cyanopyridine was prepared by the reaction of the 1-methoxy-2, 6-dimethylpyridinium iodide with potassium

4) E. M. Kosower, *J. Am. Chem. Soc.*, **80**, 3253 (1958).
5) A. R. Katritzky, *J. Chem. Soc.*, **1955**, 2586.
6) E. M. Kosower and S. W. Bauer, *J. Am. Chem. Soc.*, 82, 2191 (1960).
7) T. Okamoto, M. Hirobe and A. Ohsawa, to be published in *Chem. Pharm. Bull.*
8) T. Okamoto and H. Tani, ibid., **7**, 925 (1959).

cyanide.[8] The 3, 5-dimethyl-4-cyanopyridine was obtained from 1-amino-3, 5-dimethylpyridinium iodide and potassium cyanide.[9] The melting points of these pyridinium iodides are in good agreement with those reported in the literature.

Solvents.—Acetonitrile was purified by repeated distillation from phosphorus pentoxide. Dimethoxyethane (DME) and dioxane were treated with potassium metal and distilled from lithium aluminum hydride.

The Preparation of Pyridinyl Radicals and Measurements.—The substituted pyridinyl radicals were prepared at room temperature by bringing the corresponding pyridinium salts into contact with zinc mirror in acetonitrile. In DME or doixane, the pyridinyl radicals were prepared by bringing them into contact with sublimated potassium metal. All the solvents were purified and degassed before use. The zinc and potassium metals were purified by repeated sublimation in vacuo. The preparation of the pyridinyl radicals and the measurements of ESR and electronic spectra were performed in vacuo by the method described in previous papers.[8] The ESR and electronic spectra were measured with a Hitachi ESR spectrometer, model MPU-2B (X-band 100 kc. modulation) and with a Cary recording spectrophotometer, model 14 M, respectively.

Experimental Results

The 1-Methyl-4-carbomethoxypyridinyl Radical. — The acetonitrile solutions of 1-methyl-4-carbomethoxypyridinium chloride and 1-deuteromethyl-4-carbomethoxypyridinium bromide (10^{-3} -10^{-4} mol./l.) were colored a yellowish green by coming into contact with pure sublimated zinc metal in vacuo. The observed ESR spectra of these solutions are shown in Figs. 1a and 1b.

The DME or dioxane solution of the 1-methyl-4-carbomethoxypyridinium chloride became slightly yellow upon coming into contact with sublimated potassium mirror in vacuo. As is shown in Fig. 1c, the ESR spectrum of the dioxane solution showed an intense hyperfine structure. The ESR spectra of the DME or dioxane solution of the 1-deuteromethyl-4-carbomethoxypyridinyl radical were also measured. Furthermore, 1-methyl-4-carbomethoxypyridinyl radical was prepared by zinc metal in dioxane. The ESR spectrum of the radical prepared by zinc metal in dioxane was exactly the same as that of the radical prepared by potassium metal in the same solvent. Therefore, it may be said that the metal cation does not exert any observable effect upon the hyperfine structure of the ESR spectrum.

The electronic absorption spectrum of the acetonitrile solution of the 1-methyl-4-carbomethoxypyridinyl radical was measured parallel with the ESR spectrum. The results are shown in Fig. 2. The spectrum consists of three absorption bands, at 307, 396 and 650 mμ. The electronic spectra

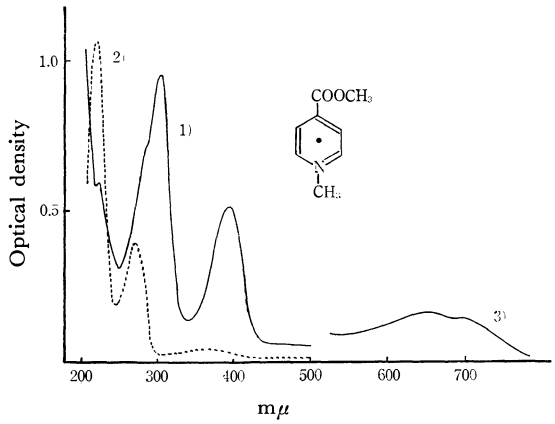

Fig. 2. The electronic absorption spectrum of the 1-methyl-4-carbomethoxypyridinyl radical. (The vertical axis is arbitrary scale.)
1) The acetonitrile solution of the radical.
2) The radical solution exposed to air.
3) The solution about ten times as concentrated as solution 1).

of this pyridinyl radical in the other solvents are similar to those obtained with the acetonitrile solution. The three absorption bands of the radical solution disappeared when the solutions were exposed to air.

The 1-Methyl-4-acetylpyridinyl Radical.—The acetonitrile solution of the 1-methyl-4-acetylpyridinium iodide turned reddish yellow when it came into contact with sublimated zinc metal in vacuo.* The ESR and electronic absorption spectra of this solution were measured, with the results given in Figs. 3 and 4 respectively.

The 1-Methyl-4-carbamidopyridinyl Radical.—The 1-methyl-4-carbamidopyridinyl radical was prepared by bringing it into contact with zinc mirror in acetonitrile or DME.* The ESR and electronic spectra of this radical are shown in Figs. 5 and 6 respectively. This radical is rather unstable and, therefore, shows an ESR spectrum with a less resolved hyperfine structure.

The 1-Methyl-4-cyanopyridinyl Radical.—The DME solution of 1-methyl-4-cyanopyridinium iodide became an orange yellow when brought into contact with sublimated potassium metal. The observed ESR spectrum of this radical is shown in Fig. 7. The electronic spectrum was also measured with the DME solution of the radical. As is shown in Fig. 8, the spectrum consists of three absorption bands, at 342, 410 and ca. 600 mμ. These bands disappeared when the solution was exposed to air.

The acetonitrile solution of 1-methyl-4-cyanopyridinium iodide became an intense blue-black when brought into contact with zinc metal. The ESR and electronic spectra of the acetonitrile

9) T. Okamoto, M. Hirobe, C. Mizushima and A. Ohsawa, ibid., **11**, 780 (1963).

* The radicals were prepared by the reaction with potassium metal in DME.

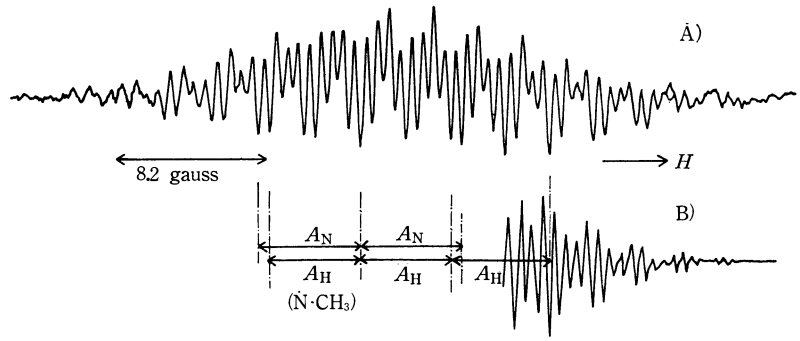

Fig. 3. The ESR spectrum of the acetonitrile solution of 1-methyl-4-acetylpyridinyl radical and a part of the reconstruction based on the splitting constants.

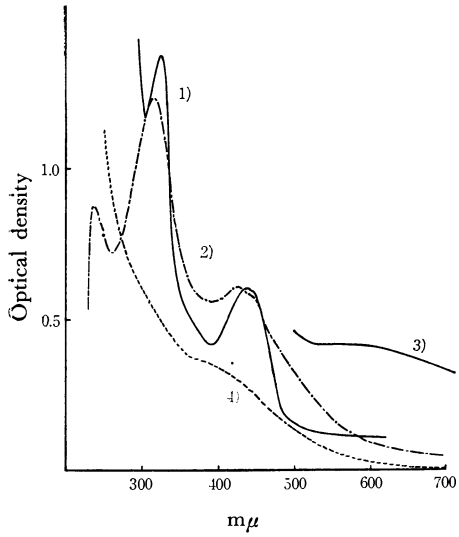

Fig. 4. The electronic spectrum of 1-methyl-4-acetylpyridinyl radical.
1) The acetonitrile solution of the radical.
2) The solution about ten times as concentrated as solution 1).
3) The DME solution of the radical.
4) The acetonitrile solution of the radical exposed to air.

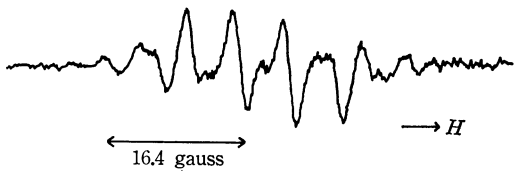

Fig. 5. The ESR spectrum of the acetonitrile solution of the 1-methyl-4-carbamidopyridinyl radical.

solution were measured. The observed ESR and electronic spectra were exactly identical with those of the methylviologen cation radical recently reported by Kosower et al.[10] It may be inferred from the present experimental results that the 1-methyl-4-cyanopyridinyl radical easily dimerizes to form the methylviologen cation radical in polar solvents such as acetonitrile, although it is considerably stable in such less polar solvents as DME.

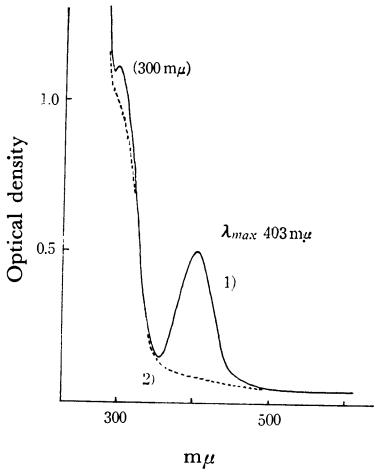

Fig. 6. The electronic absorption spectrum of the 1-methyl-4-carbamidopyridinyl radical. (The vertical axis is arbitrary scale.)
1) The acetonitrile solution of the radical.
2) The radical solution exposed to air.

The Determination of the Hyperfine Splitting Constants and Simulated Spectra. — The hyperfine splitting constants associated with the nitrogen and hydrogen (deuterium) atoms of the above-mentioned pyridinyl radicals were determined from the ESR spectra. All the results are summarized in Table I. The theoretical spectra were simulated from the estimated splitting constants by the aid of a spectrum accumulator, JNM-RA-1, of the Japan Electron Optics Laboratory. The simulated spectra match well with the observed spectra, as is shown in Figs. 1, 3 and 7.

The Preparation of the Other Methyl Substituted Pyridinyl Radicals and Their

10) E. M. Kosower and J. L. Cotter, *J. Am. Chem. Soc.*, **86**, 5524 (1964).

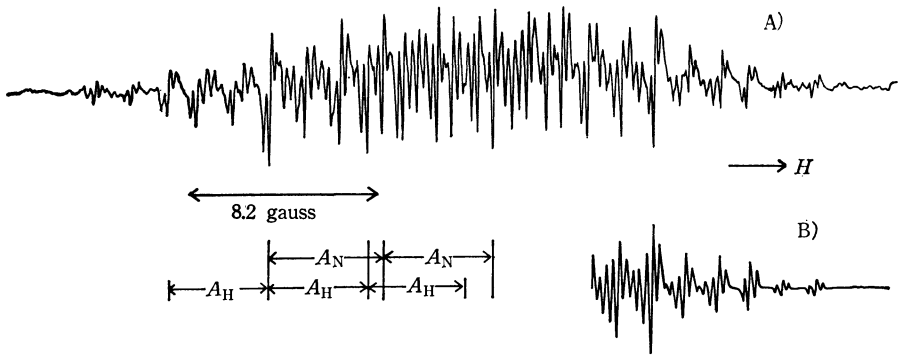

Fig. 7. A) The ESR spectrum of the DME solution of the 1-methyl-4-cyanopyridinyl radical. B) A part of the theoretically simulated spectrum based on the splitting constants. The line width was estimated to be 0.22 gauss. The line shape is considered to be a Lorentzian line.

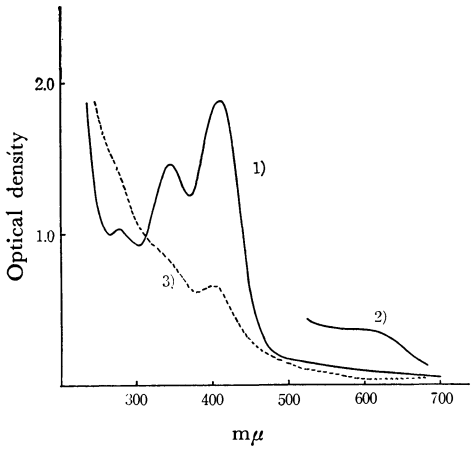

Fig. 8. The electronic absorption spectrum of the 1-methyl-4-cyanopyridinyl radical. (The vertical axis is arbitrary scale.)
1) The DME solution of the radical.
2) The solution about ten times as concentrated as solution 1).
3) The DME solution exposed to air.

Stability.—We also attempted to prepare 1, 2, 6-trimethyl-and, 1, 3, 5-trimethyl-4-substituted (substituents: $-COOCH_3$, $-CONH_2$, and $-CN$) pyridinyl radicals. The three 1, 2, 6-trimethyl-4-substituted pyridinyl radicals and the 1, 3, 5-trimethyl-4-cyanopyridinyl radical could be obtained from the respective pyridinium iodides. However, the 1, 3, 5-trimethyl-4-carbomethoxy and 1, 3, 5-trimethyl-4-carbamidopyridinyl radicals could not be obtained despite careful and repeated experiments. The stability of these substituted pyridinyl radicals in acetonitrile is summarized in Table II. It seems that the results given in Table II can be explained by considering the steric hindrance of the methyl groups at the 3 and 5 positions. This point will be discussed in a later part of the present paper.

Discussion

The Spin Distribution of Pyridinyl Radicals.—The hyperfine splitting constant associated with the nitrogen atom of the aromatic ring has been

Table I. Hyperfine splitting constants due to nitrogen and hydrogen atoms of substituted pyridinyls radicals (gauss unit)

	4-$COOCH_3$	4-CN*	4-$COCH_3$
A_N (ring)	6.26	6.4±0.2	6.5±0.3
A_H (N-CH_3)	5.56 (0.84)**	5.6±0.2	5.16±0.2
A_H (2,6-)	3.56	3.8±0.1	3.2±0.1
A_H (3,5-)	0.84	0.35±0.1	0.6±0.1
	A_H (OCH_3) 0.84	A_N (CN) 1.9±0.1	A_H (CH_3) 2.63±0.2

* The result of DME solution.
** The result of the 1-deuteromethyl-4-carbomethoxypyridinyl radical.

Table II. Stability of substituted pyridinyl radicals at room temerature*

Alkyl substituents	4-$COOCH_3$	4-$CONH_2$	4-CN
None	2—3 days	1—2 hrs.	2—3 days**
3,5-Dimethyl	No radical	No radical	ca. 2 days
2,6-Dimethyl	10—20 min.	ca. 10 min.	1—2 hr.

* Time, until the ESR hyperfine structures disappeared.
** The result of the DME solution.

Table III. The spin densities of the nitrogen and carbon atoms of the pyridinyl radicals evaluated from the ESR splitting constants

	Pyridinyl			Anion radical			
	4-$COOCH_3$	4-CN	4-$COCH_3$	4-NO_2[c]	4-$NO_2N\rightarrow O$[c]	4-CN[d]	4-$COCH_3$[e]
Ring N	0.195	0.200	0.203	0.124	0.181	—	0.171
2,6-C	0.158	0.168	0.142	0.052	0.159	0.059	0.021 (0.008)
3,6-C	0.037	0.015	0.026	0.033	0.068	0.110	0.124 (0.143)
N (CN)[a]	—	0.101	—	—	—	0.124	—
C (CO)[b]	—	—	0.095	—	—	—	0.205

a) The spin density on the nitrile-nitrogen, using $Q_N=18.8$ gauss.[13]
b) The spin density on the carbonyl-carbon atom calculated from methyl proton splitting, using $Q^H_{CCH_3}=27.2$ gauss.[15]
c) The results of the 4-nitropyridine and its 1-oxide anion radicals.[3]
d) The result of the 4-cyanopyridine anion radical obtained by Fraenkel et al.[13]
e) The result of the 4-acetylpyridine anion radical obtained by Fraenkel et al.[15]

considered to depend not only on the spin density of the nitrogen atom, but also, via indirect polarization, on the spin densities of the adjacent atoms. Carrington et al.,[11] however, proposed the following equation for the relationship between the nitrogen splitting constant, A_N, and the spin density on the nitrogen atom concerned, ρ_N, by disregarding the indirect polarization;

$$A_N=Q_N\rho_N \quad (1)$$

They estimated Q_N to be 25.3 gauss for the anion radicals.

Bolton et al.[12] suggested that the hyperfine splitting constant associated with the protonated nitrogen atom in the nitrogen semiquinone cation radical could be represented similarly by Eq. 1. By combining the observed nitrogen splitting constants with the spin densities on the 4,4'-dipyridyl semiquinone cation and the pyrazine semiquinone cation radicals as calculated by the Hückel molecular orbital method, they determined the value of Q_N to be 32—36 gauss[12] for the cation radicals. Rieger and Fraenkel[13] studied the spin density distribution in a number of nitrile anion radicals. They reported that the nitrile-nitrogen splitting, A_N, should be approximately proportional to the spin density, ρ_N, on the nitrogen atom: $A_N=K\rho_N$. Furthermore, they showed that when the least-squares method is applied to the observed nitrile-nitrogen splitting constants, it gives $K=18.8\pm0.7$ gauss for the Hückel spin densities.

In the present paper, the electronic state of the nitrogen atom in the pyridinyl radicals was assumed to be the same as that of the protonated nitrogen atom in the nitrogen semiquinone cation radicals. In other words, the value of Q_N in Eq. 1 was taken to be 32 gauss for the pyridinyl radical. By combining the observed hyperfine splitting constants with the above-mentioned relations for nitrogen splittings and the well-known relation for the proton hyperfine splittings ($A_H=-22.5\rho_C$), we have evaluated the spin densities on the nitrogen and carbon atoms of the substituted pyridinyl radicals. The results are summarized in Table III. The hydrogen splitting constant of the *N*-methyl group is considered to be proportional to the spin density of the nitrogen atom concerned, as in the case of the hydrogen splitting of the methyl group attached to the aromatic carbon atom[14]:

$$A'_H=Q'_H\rho_N \quad (2)$$

According to the present results, the Q'_H value is 28.4 gauss on the basis of the nitrogen spin densities of the pyridinyl radicals and the methyl hydrogen splitting constants shown in Table I.

From the spin densities summarized in Table III, it may be inferred that an odd electron is not localized on the ring nitrogen atom which has a positive formal charge in the pyridinium cation, but is distributed over the pyridinyl radical. This shows that the neutral pyridinyl radicals are of the π-type, as is usual for aromatic anion radicals.

The present authors[3] have reported elsewhere their studies of the ESR and electronic structures of the 4-nitropyridine and its 1-oxide anion radicals. Fraenkel et al.[13,15] have reported on the spin distribution of the electrochemically-generated 4-cyano- and 4-acetylpyridine anion radicals. The spin densities of these anion radicals are also shown in Table III. The results summarized in Table III show that the spin densities on the ring nitrogen and carbon atoms are remarkably larger in the substituted pyridinyl radicals than in the substituted pyridine anions. Furthermore, by comparing the spin densities of the 1-methyl-4-cyano- and 1-methyl-4-acetylpyridinyl radicals with those of the

11) A. Carrington and J. dos Santos-Veiga, *Mol. Phys.*, **5**, 21 (1962).
12) J. R. Bolton, A. Carrington, A. Forman and L. F. Orgel, ibid., **5**, 466 (1962).
13) H. Rieger and G. K. Fraenkel, *J. Chem. Phys.*, **37**, 2795 (1962).
14) J. R. Bolton, A. Carrington and A. D. McLachlan, *Mol. Phys.*, **5**, 31 (1962).
15) P. H. Rieger and G. K. Fraenkel, *J. Chem. Phys.*, **37**, 2811 (1962).

pyridine anion radicals with the same substituent groups at the 4-position, we can conclude that the spin densities on the nitrile-nitrogen or carbonyl-carbon atoms of the neutral radicals are smaller than those of the anion radicals. This is because the pyridinium ring is more electronegative than the pyridine ring; therefore, the spin density of the pyridinyl ring of these neutral radicals is larger than that of the pyridine ring in the corresponding pyridine anion.

The Electronic Spectra of Pyridinyl Radicals.—As is clearly seen from Figs. 2, 4, 6 and 8, all these pyridinyl radicals in acetonitrile, except for the 1-methyl-4-carbamidopyridinyl radical, show three absorption bands in the visible and ultraviolet regions. The observed maximum wavelengths summarized in Table IV show that the shortest wavelength absorption bands of these neutral radicals shift to longer wavelengths with the increase in the electron-attracting ability of the 4-substituents. The order is as follows: $-CONH_2 < -COOCH_3 < -COCH_3 < -CN$.

Table IV. The electronic absorption band of substituted pyridinyl radicals

Pyridinyl radical	λ_{max} mμ		
4-$CONH_2$	300	403	—
4-$COOCH_3$	307	396	650*
4-$COCH_3$	326	432	ca. 600*
4-CN**	342	410	ca. 610*

* Very weak band.
** The result of the DME solution.

The present authors[3] have also demonstrated elsewhere that the electronic spectrum of the 4-nitropyridine anion showed three absorption bands, at 313, 440 and 640 mμ. The molecular orbital calculation allows us to regard the 440 mμ and 313 mμ bands as the intramolecular charge-transfer band and as the blue-shifted band of the band pertinent to the pyridine anion respectively. The electronic structures of the pyridinyl radicals with the electron-attracting groups, like the carbomethoxy, nitrile or acetyl groups, may be essentially similar to that of the 4-nitropyridine anion, although the valence state ionization potential of the nitrogen atom is considerably greater in the *N*-methyl pyridinyl radical than in the pyridine anion. On this assumption, the 300—350 mμ bands and the 390—440 mμ bands of the pyridinyl radicals may be thought to correspond to the 313 mμ band and the 440 mμ band of the 4-nitropyridine anion radical respectively.

The Effect of the Steric Hindrance of Methyl Groups upon the Stability of the Radicals.—The 1, 3, 5-trimethyl-4-carbomethoxy- and 1, 3, 5-trimethyl-4-carbamidopyridinyl radicals could not be obtained. It seems that this fact can be explained by considering the steric hindrance of the methyl groups at 3- and 5-positions. The $-COOCH_3$ and $-CONH_2$ groups at the 4-position can probably be prohibited by the steric hindrance from coplanarity with the pyridinium ring. This noncoplanarity decreases the resonance stabilization due to the $COOCH_3$ and $CONH_2$ groups.[16] This seems to be a reason why the 1, 3, 5-trimethyl-4-carbomethoxy- and 1, 3, 5-trimethyl-4-carbamidopyridinyl radicals could not be obtained. The above explanation is also supported by the fact that the 1, 3, 5-trimethyl-4-cyanopyridinyl radical can be prepared stably. In this case, the cyano group may reasonably be thought not to be susceptible to the steric hindrance of the methyl groups.

The Metal Cation Effect upon the Hyperfine Splitting Constants.—One electron transfer from zinc or alkali metal into the substituted pyridinium cation results in the formation of the neutral pyridinyl radicals and the metal cations. The alkali metal effect upon the nitrogen and hydrogen hyperfine splittings has been observed for the substituted nitrobenzene or substituted benzophenone anion radical reduced by alkali metal in THF or DME[17,18] This metal effect has been attributed to the electronic interaction between the anion radical and the metal cation.[19] As for the 1-methyl-4-carbomethoxypyridinyl radical, no metal effect upon the ESR hyperfine splitting was observed. This seems to show that the neutral pyridinyl radicals are different from the usual ion radicals in their interaction with the metal cations.

The authors wish to thank Mr. Masaaki Hirobe and Mr. Akio Ohsawa of the Faculty of Pharmaceutical Sciences, the University of Tokyo, for supplying some of the materials. The kind help given by Mr. Eiji Tsurumachi and Mr. Kohji Yanagi of the Japan Optics Lab. Co., Ltd., in obtaining the simulated ESR spectra is also gratefully acknowledged.

16) S. Nagakura, M. Kojima and Y. Maruyama, *J. Mol. Spectroscopy*, **13**, 174 (1964).
17) K. Umemoto, Y. Deguchi and H. Takaki, This Bulletin, **35**, 260 (1962); P. Ludwig, T. Layloff and R. N. Adams, *J. Am. Chem. Soc.*, **86**, (1964).
18) N. Hirota, *J. Chem. Phys.*, **37**, 1884 (1962).
19) N. Hirota and S. I. Weissman, *J. Am. Chem. Soc.*, **86**, 2538 (1964).

BULLETIN OF THE CHEMICAL SOCIETY OF JAPAN VOL. 39 376—379 (1966)

The Reaction of Thiols with Propylene Oxide in the Presence of Free Radical Sources[1]

By Matsuji TAKEBAYASHI, Tadao SHINGAKI and Takakimi MIHARA

Department of Chemistry, College of General Education, Osaka University, Toyonaka, Osaka

(Received July 19, 1965)

The effect of free radical sources on the reaction of thiols with propylene oxide has been studied. In the presence of free radical sources, such as benzoyl peroxide, tetraphenylhydrazine and tetramethylthiuram disulfide, the reaction gives a single addition product, 1-aryl(or aralkyl)thio-2-propanol, in the same manner as when alkaline catalysts are employed. When *l*(+)-propylene oxide is used, an optically-active 1-thio-2-propanol is obtained. However, azobisisobutyronitrile manifests no catalytic influence on the reaction. Mercury-vapor light also has no effect on the interaction of thiols and propylene oxide, while the light leads to the decomposition of thiols. The mechanism of the reaction has been discussed in terms of a thiyl anion intermediate.

It has been reported that the reactions of thiols with cyclic ethers to give hydroxysulfides are promoted by alkaline catalysts.[2] Searles,[3] investigating the reaction of thiophenol with trimethylene oxide, obtained a good yield of 3-phenylthio-1-propanol with an alkaline catalyst, but a very poor yield of the product with an acid catalyst. The observation of Schuetz[4] has shown that the interaction of thiophenol and propylene oxide in the presence of an alkaline catalyst gives a single product, 1-phenylthio-2-propanol, in an excellent yield, while in the presence of an acid catalyst a mixture of the two possible isomers, 1-phenylthio-2-propanol and 2-phenylthio-1-propanol, is obtained in a poor yield. In these reactions, thiophenol reacts ionically on cyclic ethers, and the position of the ring opening of the cyclic ethers depends on the nature of the catalysts employed and also on the polarity or the steric effect of substituents on the carbon atom of the oxide ring.[5]

On the other hand, it has been recognized that benzoyl peroxide[6] and azobisisobutyronitrile[7] are effective catalysts in the homolytic addition of thiophenol to unsaturated compounds, and that tetraphenylhydrazine, triphenylmethyl peroxide and hexaphenylethane also accelerate the radical decomposition of aromatic azides in thiols.[8] In the light of such experimients, we investigated the reaction of thiols with propylene oxide in the presence of such free radical sources as benzoyl peroxide, tetraphenylhydrazine, tetramethylthiuram disulfide and azobisisobutyronitrile.

Results and Discussion

The reaction of thiols (0.3 mol.) with propylene oxide (0.2 mol.) has been carried out with a small amount (0.01 mol.) of free radical sources at 80°C in an atmosphere of nitrogen. The results are shown in Table I.

Two kinds of reaction products, I and II, may be expected.

$$CH_3CH-CH_2 + RSH \quad (\text{O bridge}) \rightarrow \begin{cases} CH_3CH(OH)-CH_2SR & (I) \\ CH_3CH(SR)-CH_2OH & (II) \end{cases} \qquad (1)$$

However, the reaction gave a single product (I) in the same manner as when alkaline catalysts were employed. No reaction took place in the absence of free radical sources.

Among the free radical sources employed, tetraphenylhydrazine and tatramethylthiuram disulfide act as the most effective catalysts on the reaction. Benzoyl peroxide promotes the reaction to some extent, though without any conspicuous evolution of carbon dioxide. On the other hand, azobisisobutyronitrile manifests practically no catalytic influence on the reaction.

1) Presented in part at the Symposium of Organic Reaction Mechanism, Fukuoka, October, 1963.
2) R. E. Parker and N. S. Isaacs, *Chem. Revs.*, **59**, 737 (1959).
3) S. Searles, *J. Am. Chem. Soc.*, **73**, 4515 (1951).
4) R. D. Schuetz, ibid., **73**, 1881 (1951).
5) E. L. Eliel, "Substitution at Saturated Carbon Atoms," in "Steric Effects in Organic Chemistry," Ed. by M. S. Newman (1956), p. 106.
6) M. S. Kharasch, A. T. Read and F. R. Mayo, *Chem. & Ind.*, **57**, 752 (1938).
7) Cf., for instance, T. Hoshino et al., *J. Chem. Soc. Japan, Pure Chem. Sect.* (*Nippon Kagaku Zassi*), **74**, 510 (1953); ibid., **75**, 1086 (1954); This Bulletin, **29**, 447 (1956).
8) M. Takebayashi and T. Shingaki, *J. Chem. Soc. Japan, Ind. Chem. Sect.* (*Kogyo Kagaku Zasshi*), **64**, 469 (1961); M. Takebayashi, T. Shingaki and T. Mitsuyama, *Science Reports, Osaka Univ.*, **10**, 35 (1961).

TABLE I. REACTION OF THIOLS WITH PROPYLENE OXIDE AT 80° C FOR SIX HOURS
Propylene oxide 0.2 mol., Thiol 0.3 mol., Free radical source 0.01 mol.

Thiol (RSH)	Free Radical Source (R'-R')	Yields of Products $CH_3-CH(OH)-CH_2SR$ % [a]	RS-SR % [b]	R'H % [b]
C_6H_5SH	None	0	0	0
	$(C_6H_5)_2N-N(C_6H_5)_2$	92	96	93
	$C_6H_5CO-OC-C_6H_5$ (O, O)	9.3	96	93
	$(CH_3)_2NCS-SCN(CH_3)_2$ (S, S)	75	90	
	$(CH_3)_2CN=NC(CH_3)_2$ (CN, CN)	0	99	
$C_6H_5CH_2SH$	None	0	0	0
	$(C_6H_5)_2N-N(C_6H_5)_2$	99	98	98
	$C_6H_5CO-OCC_6H_5$ (O, O)	18	66	c)
	$(CH_3)_2NCS-SCN(CH_3)_2$ (S, S)	85	99	
	$(CH_3)_2CN=NC(CH_3)_2$ (CN, CN)	0	90	

a) Mole % based on the amount of propylene oxide.
b) Mole % based on the amount of free radical source added.
c) Syrupy oil (2.36 g.) containing sulfur atom.

In these experiments, the disulfides corresponding to the thiols used were obtained nearly quantitatively; diphenylamine and benzoic acid were also produced in good yields during the reactions with tetraphenylhydrazine and benzoyl peroxide respectively.

Another experiment investigated the reaction using L(+)-propylene oxide. The L(+)-propylene oxide shows practically no change in its optical activity ($[\alpha]_D^{15}$: +16.51° in ether) during the course of being heated with benzylmercaptan at 80°C for six hours in an atmosphere of nitrogen. Therefore, the reaction of L(+)-propylene oxide with benzylmercaptan has been carried out in the presence of tetramethylthiuram disulfide under the conditions described above. (−)-Benzylthio-2-propanol ($[\alpha]_D^{15}$: −17.73° in ether) was obtained in a good yield (78%). This suggests that no bonds at the asymmetric carbon atom of propylene oxide are made or broken during the reaction.

When quinone or hydroquinone was added as a free radical scavenger in the reaction mixture, the reaction was slightly suppressed. Therefore, a mixture of propylene oxide (0.30 mol.) and thiophenol (0.45 mol.) was exposed to a mercury-vapor light of 2537 and 3500 Å at 10°C for 24 hr. in an atmosphere of nitrogen. Diphenyl disulfide, hydrogen sulfide and hydrogen were thus obtained, without any reaction product corresponding to I or II; most of the propylene oxide was also recovered.

Thiophenol has strong absorption bands in the regions of 2350 Å (ε_{max} 8500) and 2690 Å (ε_{max} 720),[9] and the ArS–H and Ar–SH bond dissociation energies of thiophenol are close to 86 and 74 kcal./mol. respectively. The absorption of light of 2537 Å in one mole of a substance corresponds to that of an energy ($E=N_A h\nu$) of 112 kcal. per mol. Therefore, thiophenol may be dissociated in two ways by the absorption of the light:

$$C_6H_5SH \xrightarrow{h\nu} \cdot C_6H_5 + \cdot SH \qquad (2)[10]$$

$$C_6H_5SH \xrightarrow{h\nu} C_6H_5S\cdot + H\cdot \qquad (3)[11]$$

The free radicals, $\cdot C_6H_5$, $\cdot SH$ and H, produced by the reactions 2 and 3 react on thiophenol to give the thiyl radical, $C_6H_5S\cdot$:

$$C_6H_5SH + \cdot C_6H_5 \rightarrow C_6H_5S\cdot + C_6H_6 \qquad (4)$$

$$C_6H_5SH + \cdot SH \rightarrow C_6H_5S\cdot + H_2S \qquad (5)$$

$$C_6H_5SH + H\cdot \rightarrow C_6H_5S\cdot + H_2 \qquad (6)$$

If the thiyl radical attacks propylene oxide, the reaction products, I and/or II, should be produced. However, the thiyl radical dimerized to give disulfide without any reaction toward propylene oxide.

9) K. Browden, E. A. Braude and E. R. H. Jones, *J. Chem. Soc.*, **1946**, 948.
10) W. M. Malisoff and E. M. Marks, *Ind. Eng. Chem.*, **23**, 1114 (1931).
11) C. Walling and R. Rabinowitz, *J. Am. Chem. Soc.*, **81**, 1137 (1954).

$$2\ C_6H_5S \rightarrow C_6H_5S\text{-}SC_6H_5 \quad (7)$$

The results presented above suggest that the reaction is not initiated by thiyl radicals derived from the reactions of thiols with free radical sources. The reaction may, then, reasonably explained as follows.

In the first place, the thermal decomposition of free radical sources occurs, giving rise to the corresponding free radicals:

$$\left.\begin{array}{l} (C_6H_5)_2N\text{-}N(C_6H_5)_2 \rightarrow 2\ (C_6H_5)_2N\cdot \\ C_6H_5CO\text{-}OCC_6H_5 \rightarrow 2\ C_6H_5CO\cdot \\ \quad\ \ O\quad\ \ O\qquad\qquad\quad\ \ O \\ (CH_3)_2NCS\text{-}SCN(CH_3)_2 \rightarrow \\ \quad\ \ S\quad\ \ S \\ \qquad\qquad 2\ CS_2 + 2(CH_3)_3N\cdot \end{array}\right\} \quad (8)$$

These free radicals have lone-pair electrons on their free radical atoms. Therefore, a proton-transfer reaction 9 to give thiyl anion must take place in addition to the abstraction of hydrogen (10). For instance:

$$(C_6H_5)_2N\cdot + RSH \rightarrow (C_6H_5)_2\overset{+}{N}H + RS^- \quad (9)$$

$$(C_6H_5)_2N\cdot + RSH \rightarrow (C_6H_5)_2NH + RS\cdot \quad (10)$$

The thiyl anion attacks the primary carbon atom of propylene oxide as a result of the inductive effect of the methyl group, and the reactions 11 and 12 will proceed in a chain mechanism:

$$CH_3\text{-}\underset{\diagdown O \diagup}{CH} - CH_2 + RS^- \rightarrow CH_3\text{-}\underset{O^-}{CH}\text{-}CH_2SR \quad (11)$$

$$CH_3\text{-}\underset{O^-}{CH}\text{-}CH_2SR + RSH \rightarrow CH_3\text{-}\underset{OH}{CH}\text{-}CH_2SR + RS^- \quad (12)$$

The reaction chain my be terminated by the reactions 13 and 14:

$$(C_6H_5)_2\overset{+}{N}H + RS^- \rightarrow (C_6H_5)_2NH + RS\cdot \quad (13)$$

$$2\ RS\cdot \rightarrow RS\text{-}SR \quad (14)$$

Experimental

Materials.—*Propylene Oxide (racemic).*—Commercial propylene oxide was refluxed for 2 hr. over pellet potassium hydroxide and fractionated, the fraction boiling at 34.5—35°C being used.[12]

L(+)-*Propylene Oxide.*—Levene's synthesis was employed.[12] α-Bromoacetone was converted to acetol by treating it with ethyl formate in methanolic potassium hydroxide; the acetol was then reduced to L-propylene glycol by the reductase of yeast. The propylene glycol was converted to L-propylenebromohydrin with dry hydrogen bromide, and the bromohydrin was then cyclized to L(+)-propylene oxide with concentrated aqueous potassium hydroxide. The crude material was purified by refluxing it over potassium hydroxide pellets; b. p. 34.5—35°C, $[\alpha]_D^{15}$: +16.51° (in ether).

Thiophenol.—Benzenesulfonyl chloride was reduced by zinc and sulfuric acid to thiophenol.[13] The crude distillate was fractionated; b. p. 61°C/15 mmHg.

Benzylmercaptan.—A mixture of benzyl alcohol and hydrobromic acid (48%) was refluxed for 12 hr.; the reaction product was then hydrolyzed by an alkaline solution.[14] The benzyl mercaptan produced was purified by fractionation; b. p. 65°C.

Tetraphenylhydrazine.—A solution of diphenylamine in acetone was oxidized by potassium permanganate.[15] The crude material was recrystallized in benzene; m. p. 144°C

Tetramethylthiuram Disulfide.—To a hot solution of commercial material in chloroform, ethanol was added; then the mixture was cooled. The precipitate was dissolved again in hot benzene and cooled after ether had been added.[16] The treatment was repeated twice; the disulfide melting at 146°C was used.

Benzoyl Peroxide was purified by treating it with chloroform and methanol;[17] m. p. 107—107.5°C.

Azobisisobutyronitrile was recrystallized in 95%-alcohol;[18] m. p. 102—103°C.

The Reaction of Thiols with Propylene Oxide in the Presence of Free Radical Sources.—Propylene oxide (0.2 mol., 11.6 g.), thiol (0.3 mol.) and a free radical source (0.01 mol.) were placed in a hard glass reaction tube, which had been cooled in an ice-salt bath, avoiding the entrance of moisture. After it had been flushed with dry nitrogen, the tube was sealed immediately. The sealed tube was then agitated and placed in a constant temperature bath (at 80—0.5°C) for an appropriate time. After the required reaction time, the tube was cooled in ice water and opened. After the unreacted propylene oxide had then been evaporated at room temperature under diminished pressure, the unreacted thiophenol and benzylmercaptan were distilled off at 61—62°C/15 mmHg and 64—65°C/3 mmHg, respectively, and the reaction products were separated by fractionation and column chromatography.

(A) In the reaction of thiophenol with propylene oxide, a fraction boiling at 103—110°C/1 mmHg was collected and redistilled. Nearly all of the fraction was distilled at 103—105°C/1 mmHg, and the liquid product was confirmed to be 1-phenylthio-2-propanol (Found: C, 64.16; H, 7.21; S, 18.90%).[19] The ultraviolet absorption curve (λ_{max} 254 mμ, ε_{max} 8.70×10^3) of this product accorded completely with that of the 1-phenylthio-2-propanol, which had been prepared according

12) C. C. Price and M. Osgan, *J. Am. Chem. Soc.*, **78**, 4787 (1956).

13) H. Gilman, "Organic Syntheses," Coll, Vol. I. John Wiley & Sons, New York (1941), p. 490.

14) R. L. Frank and P. V. Smith, *J. Am. Chem. Soc.*, **68** 2103 (1946).

15) L. Gattermann, "Die Praxis des Organischen Chemikers," 36 Aufl., Walter de Gruyler and Co., Berlin (1954), p. 308.

16) T. E. Ferington and A. V. Tobolsky, *J. Am. Chem. Soc.*, **73**, 1881 (1951); **77**, 4510 (1955).

17) K. Nozaki and P. D. Bartlett, ibid., **68**, 1686 (1946).

18) C. G. Overberger, ibid., **71**, 2661 (1949).

19) The isomer, 2-phenylthio-1-propanol: b. p. 125—126°C/1 mmHg; UV absorption band, λ_{max} 256 mμ, ε_{max} 5.97×10^3.

to the directions of Schuetz,[20] and the 3, 5-dinitrophthalate of this product showed no melting-point depression when mixed with an authentic sample (m. p. 112°C). The residue, a crystalline mass, was treated as follows.

When tetraphenylhydrazine was used as a free radical source, the residue was dissolved in a small amount of alcohol, dried on a water bath after concentrated hydrochloric acid had been added, and treated with benzene. Diphenyl disulfide (2.09 g.) was obtained from the benzene solution, and diphenylamine hydrochloride (3.82 g.) from the residue.

When benzoyl peroxide was used, the residue was dissolved in ether and treated with a 10%-aqueous solution of sodium hydroxide. Diphenyl disulfide (2.18 g.) was obtained from the ether layer, and benzoic acid (2.27 g.) from the aqueous layer, after acidification.

When tetramethylthiuram disulfide was used, the residue was recrystallized from a small amount of alchohol. Diphenyl disufide (2.72 g.) was thus separated from the solution. The solution was then evaporated, and the residue was treated by column chromatography using 50 g. of active alumina. Diphenyl disulfide (1.20 g.) was isolated again by elution with petroleum ether (b. p. 30—40°C); a small amount of a syrupy substance was also obtained by elution with methanol.

When azobisisobutyronitrile was used, no principal product, phenylthiopropanol, was detected in spite of the evolution of nitrogen, while diphenyl disulfide was obtained in a good yield (3.91 g.).

(B) In the reaction of benzyl mercaptan with propylene oxide, the reaction products were treated in the way described above. The fraction boiling at 115—116°C/1 mmHg was identified as 1-benzylthio-2-propanol (Found: C, 65.82; H, 7.80; S, 17.52%).[21] The ultraviolet absorption curve of this product accorded completely with that of 1-benzylthio-2-propanol (λ_{max} 260.3 mμ, ε_{max} 3.40×10^3 and λ_{max} 267.0 mμ, ε_{max} 2.03×10^3).

Dibenzyl disulfide was also obtained nearly quantitatively except when benzoyl peroxide was used as a free radical source. In the latter case, the residue of fractionation was treated by column chromatography using active alumina. Dibenzyl disulfide (1.60 g.) was isolated by elution with petroleum ether, while syrupy products, boiling at 120—123°C/0.5 mmHg (1.0 g.) and 134—145°C/0.5 mmHg (1.36 g.), were obtained by elution with benzene and methanol respectively. The syrupy products gave positive results in tests to detect sulfur.

20) R. D. Schuetz, *J. Am. Chem. Soc.*, **73**, 1881 (1951).

21) The isomer, 2-benzylthio-1-propanol: b. p. 124—125°C/1 mmHg.

Summary

The reaction of thiols with propylene oxide leads to the formation of 1-aryl(or aralkyl)-thio-2-propanol in the presence of such free radical sources as tetraphenylhydrazine, tetramethylthiuram disulfide and benzoyl peroxide. In the presence of azobisisobutyronitrile, however, no principal product is obtained.

The reaction of benzylmercaptan with L(+)-propylene oxide in the presence of tetramethylthiuram disulfide gives (−)-benzylthio-2-propanol. When a mixture of thiol and propylene oxide is exposed to a mercury-vapor light, no principal procuct is detected.

It has been suggested that the reaction proceeds not by means of thiyl radicals but by means of thiyl anions in a chain mechanism.

The authors wish to express their hearty thanks to Professor Naoki Inamoto and to Dr. Katsumi Tokumaru for their kind discussions.

BULLETIN OF THE CHEMICAL SOCIETY OF JAPAN VOL. 39 380—386 (1966)

Color Reactions of Dinitrobenzyl Pyridine and Related Compounds

By Hiroyuki HIRAOKA* and Russell E. HARDWICK

Department of Chemistry, University of California, Los Angeles 24, California, U. S. A.

(Received July 19, 1965)

Upon treatment with certain reagents, the photochromes, α- and γ-(2, 4-dinitrobenzyl)pyridine and 2, 4, 2', 4'-tetranitrodiphenylmethane form stable, blue-colored compounds which probably have chromophoric structures similar to those of the photochromic modifications of the original compounds (two examples of the permanently colored compounds are the N-methyl bases and the products from reactions with epoxy compounds). Kinetic and spectrophotometric studies of these colored compounds and of the anions of the original photochromes are reported. These results are compared with data on the photochromic tautomers.

It is well known,[1] that α-(2, 4-dinitrobenzyl)-pyridine (α-DNBP) develops a deep blue color upon irradiation with ultraviolet light (4000 to 3000 Å) either in the crystalline state or in solutions. In the crystals, the blue color fades quite slowly in the dark but in solutions disappears rapidly (within a few milliseconds to a few seconds at room temperatures depending upon the solvent and the acidity). The γ isomer of DNBP shows the same behavior in solution, but the crystals are not phototropic.** The blue colored substances may also be generated chemically, but transiently, upon neutralization of the anions of the photochromic compounds.

In the present investigation, we continue our study of the photochromic reaction and its products, primarily through comparison with the ordinary chemistry of DNBP. This report covers the following:

A. Formation and properties of stable, conjugated molecular modifications of DNBP.
B. Spectral properties of these conjugated species.
C. Kinetic studies, including
   1. Formation of the DNBP anion in base solutions.
   2. Kinetics of the reaction of DNBP with epoxides.
   3. Comparison of the fading rates of the conjugated form of α- and γ-DNBP as produced chemically and phototropically.

Experimental

The γ-DNBP was prepared by the method[1b] already described. Carbon disulfide, benzene, and isooctane were of spectro grade, Matheson, Coleman and Bell, and carbon tetrachloride of spectro grade, Merck. All other chemicals were Eastman CP and were used without further purification.

To prepare the epoxy addition compounds, DNBP was dissolved in an excess of epichlorohydrin; this solution was used directly for some measurements. To prepare the solid for extinction measurements, the solution was allowed to reach equilibrium, i. e., the optical density reached a constant value, then the solvent was evaporated away under high vacuum. The resulting platelets were ground with KBr and pressed into pellets for the infrared spectra. Other samples of the platelets were dissolved in various solvents for taking spectral and reaction data.

The spectra were taken with a Cary 14 spectrophotometer, and the rate measurements were made by a "stop-flow method" with a detection system having a DuMont 6292 photomultiplier, a simple monochromater and a Speedomax recorder type C. The scanning beam was passed through a Corning glass filter 3-69 and a heat filter before entering a reaction tube. The schematic diagram of the reaction tube is shown in Fig. 1.

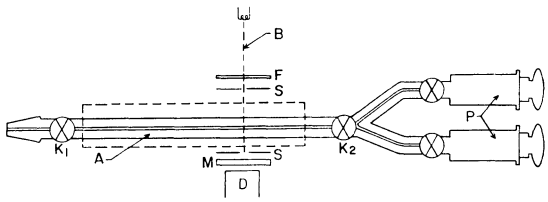

Fig. 1. Schematic diagram of stop-flow apparatus.

The reaction takes place in the 3 mm. capillary cell A, into which liquid is driven by the pressurized pistons P. Sequentially, the cell is evacuated through stopcock K_1, which is then closed; K_2 is opened and solutions flow from the separate cylinders, mixing at the tube junction. As the front of the rapidly moving

* The Central Research Institute, Teijin Company, Hino-shi, Tokyo, Japan.

1) a) A. E. Chichibabin, B. Kundshi and S. V. Benwalenskaja, *Ber. deut. Chem. Ges.*, **58**, 1580 (1925); b) R. Hardwick, H. S. Mosher ane P. Passailaigue, *Trans. Faraday Soc.*, **56**, 44 (1960); c) H. S. Mosher, C. Souers and R. Hardwick, *J. Chem. Phys.*, **32**, 1888 (1960); d) H. S. Mosher, R. Hardwick and D. Ben Hur, ibid., **37**, 904 (1962).

** We have found that liquid γ-DNBP is pale blue at its melting point[5] and that crystals immersed in H_2O or D_2O show blue color at even lower temperatures than the melting point. The α-isomer does not display these characteristics.

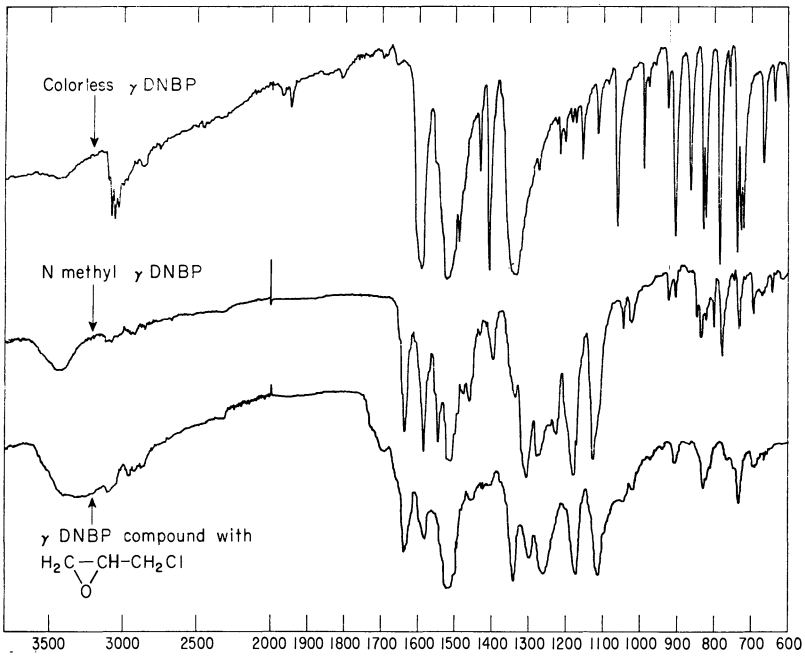

Fig. 2. Infrared spectra.

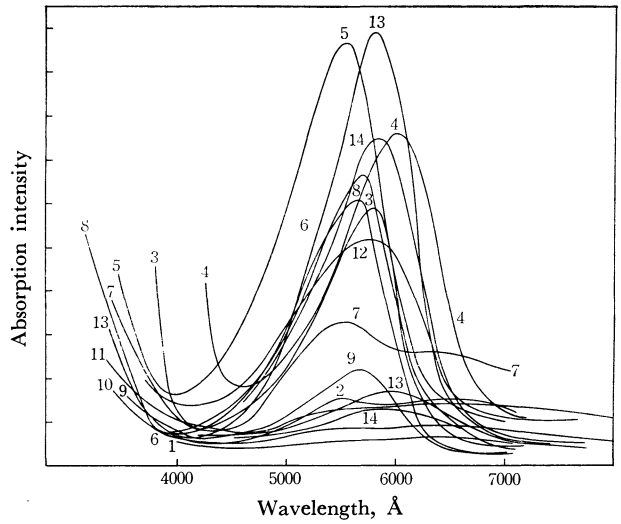

Fig. 3. Shift of visible spectra with solvent.

1	Isooctane	2	Cyclohexane	3	Carbon disulfide
4	Nitrobenzene	5	Carbon tetrachloride	6	C_6H_6
7	Freon 113	8	Mesitylene	9	*p*-Oxane
10	Isooctane	11	Heptane	12	Tetrahydrofuran
13	Acetone	14	Chloroform		

liquid passes the scanning beam, B, it triggers an oscilloscope monitoring device. M represents a monochromator while S indicates slits and F a filter.

Results and Discussion

A. Stable Conjugated Compounds with Photochromic Absorption Spectra.—We have found that when dissolved in epoxy compounds such as epichlorohydrin, epoxy benzene, etc., such photochromic compounds as α-DNBP, γ-DNBP, and 2, 4, 2′ 4′-tetranitrodiphenylmethane acquire absorption spectra which are the same as those typical of their photochromic reactions. The blue colors formed by the photochromic substances and epoxy compounds are stable in the dark,

unlike those arising from photochromic reactions, although the former colors fade upon irradiation by near ultraviolet light. It is noticed that α-DNBP, and especially 2, 4, 2', 4'-tetranitrodiphenylmethane, do not form the blue substance in as great an amount as that characteristic of γ-DNBP.

The nature of this visible absorption is probably the allowed transition, discussed below, which is also very likely the source of the photochromic colors. The blue color disappears upon the addition of H^+ and appears again upon the addition of OH^-.* The color appears more rapidly upon the addition of the epoxy compounds to the anions of the photochromic substances than to the neutral photochrome. In a solution originally neutral, the amount of H^+ necessary to destroy the blue color is just equivalent to the number of the moles of the photochromic substances contained.

One possibility for the reaction between γ-DNBP +epichlorohydrin is the following:

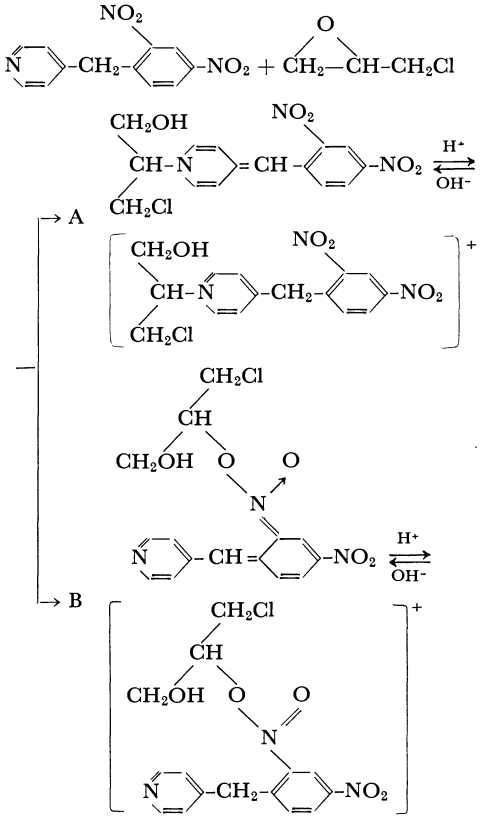

The fact that 2, 4, 2', 4'-tetranitrodiphenylmethane also forms a blue substance in epoxy compounds, albeit with low intensity, indicates that B can not be neglected. However, the infrared spectrum of the blue substances, Fig. 2, clearly shows the $\equiv C-\overset{+}{N}\diagdown$ frequency at 1635 cm^{-1}, which is also found with similar intensity in

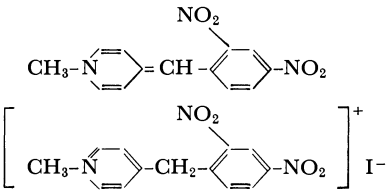

where ordinary DNBP does not have any absorption at this frequeccy. Although a C–O–N structure might possibly exhibit absorption at this energy, this more usually occurs at smaller frequencies, i. e., lower than 1600 cm^{-1}. We have prepared *N*-methyl γ-DNBP from γ-DNBP+CH_3I, followed by the addition of aqueous sodium hydroxide solutions; m. p. 161°C. The hydrogen bond frequency (3450 cm^{-1}) is displayed by crystals of the blue substance prepared from the solutions of γ-DNBP and epoxy compounds as well as in *N*-methyl γ-DNBP. The most characteristic feature in the infrared spectrum common to all the permanent blue modifications, (the epoxy complex and the *N*-alkylated compounds) is the near disappearance of the C–H stretching frequency peaks around 3000 cm^{-1}. The light induced and thermo-chromic blue mixtures show no detectable change at 3000 cm^{-1} presumably because only a very small proportion of the compound is changed.

B. Visible Absorption Spectra of the Conjugated Compounds.—In the process of taking extinction coefficients of the product of γ-DNBP and epichlorohydrin, we made Beer Law plots by successively diluting solutions which were prepared by dissolving crystals of the product in isopropyl alcohol. These gave curves which were linear within our experimental error of about 1%. From these measurements, the calculated decadic extinction coefficient was 2.40×10^4 l./mol.-cm. at the absorption peak at 5880 Å, taken on the basis of 100% conversion.*

As we have seen, the two rings of γ-DNBP may also be coupled through methylation of the ring nitrogen, giving a deep blue solution. As with the epoxide complex, this blue product shows a peak at 5800 Å; its decadic extinction coefficient is 2.4×10^4 l./mol.-cm. for the γ-isomer and 1.97×10^4 l./mol.-cm. for the α-isomer.

So far, we do not know the extinction coefficient

* The appearance of blue color is immediate when base is added to an acidified solution of DNBP-epoxy compound, even though the original reaction between DNBP and epoxy is usually very slow. For this reason, we feel that the DNBP-epoxy compound is not decomposed by acid and reconstituted by base, but that it merely assumes a colorless, cationic form in the presence of acid.

* We believe that the equilibrium between γ-DNBP and epichlorohydrin favors almost complete formation of the complex. The reasons for this conclusion are that the extinction coefficient of the complex (calculated on 100% conversion) is the same as that of the *N*-methyl base (see below), which has a similar absorbing structure. Moreover, when the complex is isolated by pumping off the solvent, no trace of the original γ-DNBP remains.

The fact that Beer's Law is followed to extreme dilution by both alcohol and epichlorohydrin solutions of the blue compound argues that the equilibrium constant of the reaction of γ-DNBP+ epichlorohydrin must be extremely high.

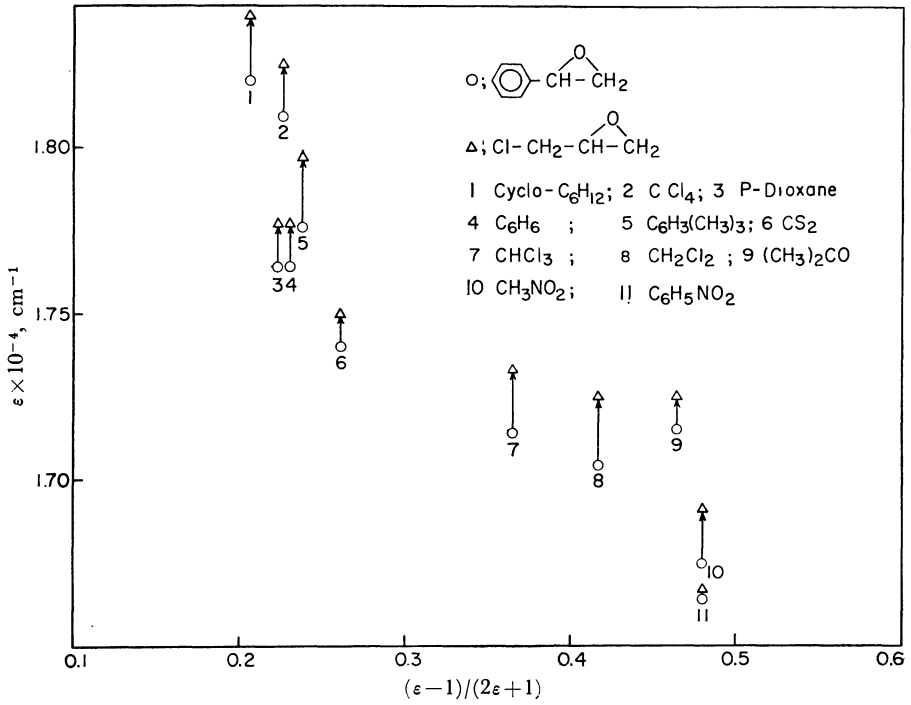

Fig. 4. Relation between frequency shift and dielectric constant.

of the blue photochromic product of γ-DNBP, but it is reasonable to believe that it might very well be approximately the same as that of the conjugated structure produced by either of the permanent chemical reactions discussed above. If we take this assumption, however, we find that the amount of photochromic conversion in solutions of γ-DNBP (or for that matter in either the crystalline form or the solutions of α-DNBP) can be only a few percent. As proposed in an earlier paper of this series, this effect may arise from a photoequilibrium which is established through the destruction of the blue tautomer by radiation in the ultraviolet region (all the photochromic products are stable to irradiation at 5800 Å). We are continuing to investigate this possibility.

The maximum color density developed by either α-DNBP or 2, 4, 2', 4'-tetranitrodiphenylmethane in epichlorohydrin never even remotely reaches that shown by the gamma isomer, the "apparent" decadic extinction coefficients being only 53 l. mol^{-1} cm^{-1} and 9.3 l. mol^{-1} cm^{-1} respectively at 36°C. Since we know of no obvious reason why the conjugated forms of these two substances should not have approximately the same absorption efficiency, we believe that the effect must be caused in the former compounds by incomplete dissociation of the bridge hydrogen or by the existence of an equilibrium which is not favorable to the product formed with epichlorohydrin.

We have found that the color formed by γ-DNBP and various epoxy compounds shifts from blue to pink as the original product is diluted with solvents of decreasing dielectric constant. Figure 3 shows several spectra of solutions made up by mixing 10 ml. of various solvents with 0.1 ml. of a solution consisting of 10^{-3} mol. of γ-DNBP in 1 ml. of epichlorohydrin;* it may be seen that the absorption curve moves to longer wavelengths with increasing dielectric constant of the medium. This red shift would be expected if the excited state of the absorbing molecule were to be of a more polar nature than the ground state, i. e., increasing interaction with the solvent would lower the energy of the excited state. One transition which would fulfill this requirement is that to the antibonding π^* state.

According to theory,[2] the relative frequency shift of the absorption, $\Delta\nu/\nu$, of a vibrating dipole in a spherical cavity of radius a, surrounded by a continuum of dielectric constant ε, is proportional to $(\varepsilon-1)/(2\varepsilon+1)\cdot(1/a^3)$. In Fig. 4, the

* Similar results are found for the product of the reaction between γ-DNBP and 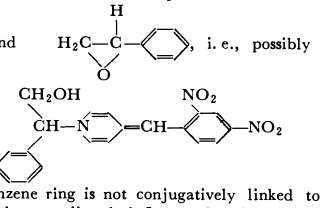 , i. e., possibly

Since the added benzene ring is not conjugatively linked to the DNBP structure, it does not directly influence the $\pi^*\leftarrow\pi$ transition.

2) H. H. Jaffe and M. Orchin, "Theory and Application of Ultraviolet Spectroscopy," John Wiley & Sons, Inc., New York (1962), pp. 190, 222.

maximum absorption frequency of the γ-DNBP epoxy compound is shown as a function of $(\varepsilon-1)/(2\varepsilon+1)$ of the solvent. The approximate linear relationship suggests that the absorption may be the $\pi^*\leftarrow\pi$ transition of the conjugated system.

If the solutions are made using solvents with very weak intermolecular forces: e. g., isooctane ($\delta=6.9$), freon 113 ($\delta=7.3$) and cyclohexane ($\delta=8.2$), there appear two maximum absorption peaks, which are not found in the solvents with solubility parameter[3] higher than carbon tetrachloride ($\delta=8.6$). In these bifurcated spectra, the absorption peak of shorter wavelength, ~5400 Å or less may correspond to the absorption found in the other solvents; however, the long wavelength peak, 6000 to 7000 Å, is probably different in nature, because even in the highly polar solvents no absorption has been found in this region. The latter transition may arise from dimers or higher aggregates which could not be dispersed to monomer form owing to the weaker intermolecular forces of the solvents.

The absorption wavelength arising from the transiton of a π-electron to its first excited state is given by the free electron model[2] as:

$$\lambda=\frac{8ma^2C}{(2k+1)\boldsymbol{h}}$$

where a is the length of the potential well, k the number of orbitals occupied by the π-electrons in the conjugated systems, m the electron mass, C the light velocity, and $\boldsymbol{h}$ Planck's constant. In applying the free electron theory to our systems there are very serious problems of hetero atoms with different electronegativity; however as a zeroth order approximation, we neglect this difference. Taking an average C–C bond distance of 1.4 Å and those of C–N and of N–O as 1.2 Å we obtain the following results for the neutral conjugated systems and for the anion (in the latter, we use k_N+1 to account for the extra electron), Table I.

Table I. Calculated and experimental absorption wavelengths

Species	Absorption wavelength mμ: Neutral molecule Calcd.	Neutral molecule Obs.	Anion Calcd.	Anion Obs.
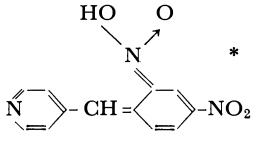 *	585	575	585 500	640 480
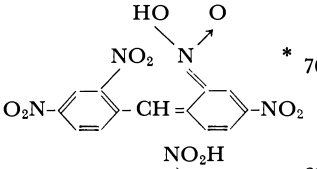 *	700	712	700 610	700 —
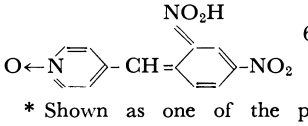	690	650	690 527	650 527

* Shown as one of the possible photochromic modifications.

In the anion, calculations are made for transition of the extra electron ($n=6$ to $n=7$) and again for the optical electron as in the neutral molecule ($n=5$ to $n=6$); this action is supported by the double peak found in the anion spectrum. It may be seen that, at least in the neutral molecule, the free electron theory makes a fairly good prediction of the wavelength which is observed, thus lending support to the proposed structures and to the assignment of $\pi^*\leftarrow\pi$ for the transition. In the 585 mμ band for γ-DNBP it is noticed that, although the agreement between calculation and experiment is good for the neutral molecule, in the anion the discrepancy runs to ~65 mμ. This misbehavior of the ion may be due to large solvation effects arising out of the fact that the anion has a charge. The agreement of the calculated wavelengths and the observed ones is excellent when we consider the approximation used. Probably this is largely fortuitous, yet the evidence does support the conclusion that the absorption is due to the $\pi^*\leftarrow\pi$ transition.

When the anions of γ-DNBP are diluted with certain polar solvents such as nitromethane or *p*-dioxane, the characteristic green color disappears, and the typical blue-violet color of the neutral conjugated systems appears transiently. This may possibly be caused by transfer of the excess charge from the anion to the solvent. In acetone, however, a stable pink color gradually appears, Figure 5, possibly arising from complex formation.

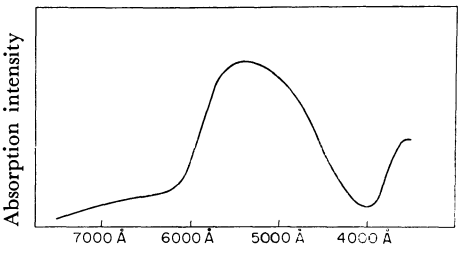

Fig. 5. Spectrum of pink solution of DNBP anion in acetone. (Concn. 2.08×10^{-7} mol./l.)

C. Kinetic Studies. — *1) Anion Formation Reaction.*—The rates of formation of the anions of DNBP have been measured with the "stop-flow method." Typically, α-DNBP solution of 1.07×10^{-4} mol. dissolved in 25 ml. of isopropanol was mixed in the reaction tube with an aqueous solution of 0.098 molar sodium carbonate. The relative proportions of DNBP solution to base solution varied from 1.0 to 2.0; however, the rate

3) J. H. Hildebrand and R. L. Scott, "Regular Solutions," Prentice-Hall Inc., New Jersey (1962).

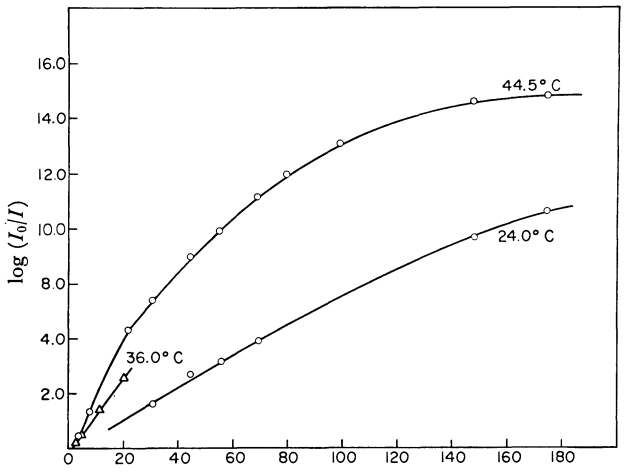

Fig. 6. Reaction rate of γ-DNBP+Cl·CH_2·CH·CH_2·O.

constants measured did not change in this range of concentration. The final pH of the one-to-one solution was 12.8. The rate of formation of the anion was found to follow first order kinetics under our conditions of a large excess of base. Sample rates of anion formation in solutions of α-DNBP mixed with sodium hydroxide are shown in Table II. With OH^- in excess, our observed rate constant is given by:

for α-DNBP

$$k_{\text{anion}}=1.29\times10^{6}\exp\left(-\frac{10.5\times10^{3}}{RT}\right)\text{sec}^{-1}$$

Table II. The rate of formation of anions from α-DNBP+aq. NaOH

Concn. of α-DNBP in isopropanol; 3.8×10^{-6} mol./ml.,
pH of aq. NaOH=12.0

Temp. °C	Vol. of α-DNBP / Vol. of aq. NaOH	$\tau_{1/2}$ sec.	k sec^{-1}
27.5	0.50/0.50	24.8	2.80×10^{-2}
27.0	0.45/0.50	23.6	2.94×10^{-2}
27.0	0.40/0.60	23.6	2.94×10^{-2}
27.0	—	23.6	2.94×10^{-2}
26.5	0.45/0.55	24.0	2.89×10^{-2}
36.0	0.40/0.65	16.5	4.20×10^{-2}
37.0	0.35/0.60	13.8	5.03×10^{-2}
37.0	0.65/0.55	14.1	4.92×10^{-2}
43.0	0.45/0.55	9.2	7.55×10^{-2}
43.0	0.45/0.50	8.2	8.46×10^{-2}
43.0	0.50/0.60	11.0	6.30×10^{-2}
43.0	0.45/0.60	10.0	6.94×10^{-2}
15.5	0.35/0.50	38.0	1.825×10^{-2}
14.5	0.30/0.50	42.2	1.644×10^{-2}
16.0	0.40/0.60	37.4	1.735×10^{-2}
16.0	0.40/0.50	32.0	2.165×10^{-2}

and for γ-DNBP

$$k_{\text{anion}}=2.82\times10^{7}\exp\left(-\frac{11.2\times10^{3}}{RT}\right)\text{sec}^{-1}$$

2) Reaction of DNBP+Epoxy Compounds.— α-DNBP and γ-DNBP were dissolved in pure Cl·CH_2·CH·CH_2O and the rates of formation of the blue conjugated compounds were measured by following the absorption intensity at the wavelength of the maximum absorption. It was found that the rate followed 1st order kinetics. The results are given by the following:

for α-DNBP

$$k=5.4\times10^{4}\exp\left(-\frac{13.6\times10^{3}}{RT}\right)\text{sec}^{-1}$$

for γ-DNBP

$$k=1.06\times10^{3}\exp\left(-\frac{12.6\times10^{3}}{RT}\right)\text{sec}^{-1}$$

It is seen that the reaction, α-DNBP+$ClCH_2$·CHCH$_2$O requires a slightly higher activation energy than that of γ-DNBP+$ClCH_2$·CHCH$_2$O, but the former has the higher frequency factor, probably due to the proximity of nitrogen atom in pyridine ring to $-CH_2-$ bridge. As mentioned earlier, the equilibrium is far more favorable to the formation of the conjugated system in γ-DNBP than in α-DNBP.

3) Study of the Conjugated Form of γ-DNBP as Produced Chemically and Phototropically. — Other work in this laboratory[4] has shown that when the brown-green anion of γ-DNBP is neutralized, the blue color, characteristic of the phototropic modification, appears fleetingly before the solution becomes colorless. We feel that it

is reasonable to assume that the species which gives the blue color upon neutralization may very well be the same as that which arises photochemically, thus we are attempting to compare the two in as many ways as possible. The previous report has discussed the low temperature decay rates and spectra of the two systems of γ-DNBP, the discussion below gives rates at higher temperatures and compares activation energies for the fading of the systems as produced chemically and phototropically.

This experiment was made by mixing solutions of γ-DNBP anion with HCl solutions, the concentrations being adjusted such that the pH of the final mixtures came very near to pH=7. In order to increase the solubility of γ-DNBP, isopropanol was added, the concentration of which was 25% of the final solution upon neutralization, With these conditions we have found the following results, Table III.

Table III. Fading-rate of the blue, conjugated form as chemically produced

Temp., °C	k, sec^{-1}
11.0	0.56±0.09
2.1	0.14±0.02

It has been reported previously[4] that the rate of the disappearance of the blue, colored form of γ-DNBP chemically produced was about 2×10^{-3} sec^{-1} at 173°K. By combination with this result, we may calculate the activation energy to be 5.0×10^{3} cal./mol. for the fading rate. This value may be compared to that of 4.5×10^{3} cal. reported earlier[5] for the fading of the phototropic blue γ-DNBP in tetrahydrofuran solutions. The comparison is only approximate because of the differences in solvent and the sensitivity of the stop-flow measurements to small errors in pH adjustment, but taken with other reported similarities, this agreement again supports the argument that the chemically and phototropically produced species are identical.

This research was supported by the Atomic Energy Commission under Contract No. AT(11-1)-34, Project 88. We also gratefully acknowledge many conversation, suggestions and other valuable contributions made by Professor Harry S. Mosher.

4) R. Hardwick and H. S. Mosher, *J. Chem. Phsy.*, **36**, 1402 (1962).
5) H. Hiraoka and R. Hardwick, ibid., **41**, 2568 (1964).

BULLETIN OF THE CHEMICAL SOCIETY OF JAPAN VOL. 39 386—390 (1966)

Electrical Conduction of Organic Semiconductors under High Pressure

By Ichimin SHIROTANI, Hiroo INOKUCHI and Shigeru MINOMURA

The Institute for Solid State Physics, The University of Tokyo, Azabu, Tokyo

(Received July 27, 1965)

The electrical conductivity and the temperature dependency of the organic semiconductors, five simple polycyclic aromatic compounds, two charge transfer complexes and a free radical, have been observed up to 1.6×10^5 kg./cm^2. The conductivity thus increases to 10^5-10^7 times that at atmospheric pressure, while the band gaps decrease to about one fifth of the ordinary values. These abrupt changes may be caused by the overlapping of π-electron clouds of adjacent aromatic molecules.

In 1955, we studied the effect of pressure on the resistance of an organic semiconductor, iso-violanthrone, by means of a simple instrument and found that the resistance at 8×10^3 kg./cm^2 was decreased to five-hundredths that at atmospheric pressure.[1] Recently, Drickamer and his collaborators have found that the electrical conductivity of polycyclic aromatics rises very rapidly until the pressure reaches the 10^5 kg./cm^2 region.[2] No quantitative treatment for these abrupt changes has, however, yet been reported.

It is reasonable to assume that the increase in the electrical conductivity is caused by the overlapping of π-electron clouds of adjacent aromatic molecules. In this report, we will present some findings on the electrical conductivity and on the temperature dependency of polycyclic aromatic compounds and will discuss the contraction of the band gaps of the organic semiconductors.

Experimental Procedures

Materials.—The materials applied were purified by several methods, as will be described in the following

1) H. Inokuchi, This Bulletin, **28**, 570 (1955).
2) G. A. Samara and H. G. Drickamer, *J. Chem. Phys.* **37**, 474 (1962).

paragraphs.

Polycyclic Aromatic Compounds.—1) Coronene ($C_{24}H_{12}$). This compounds was provided by the Badish Anilin Soda Fabrik A. G., of Germany. By repeated recrystallizations from 1, 2, 4-trichlorobenzene, plate-like crystallites of the hydrocarbon were obtained. When this material was then chromatographed under argon, it yielded pale yellow needles; these were twice sublimed at 200°C under a vacuum of 10^{-5} mmHg.[3]

2) Quaterrylene ($C_{40}H_{20}$). This stable aromatic hydrocarbon was purified by a method of vacuum sublimation, because it is virtually insoluble in all solvents at room temperature. Before applying the sublimation techique, an extraction of the impurities included in the matrix with trichlorobenzene was effective. After a vacuum sublimation was repeated at about 450°C, the compound was composed of dark green microcrystals. The details of the purification of this compound have already been reported.[4]

3) Pentacene ($C_{22}H_{14}$). This dark-blue five-ringed aromatic hydrocarbon was provided by the Rütgerswerk A. G., of Germany. In order to purify the material, pentacene was sublimed in vacuo at about 250°C. Because of its instability against ultraviolet light, the hydrocarbon had to be kept in a dark room.

4) Tetrathiotetracene ($C_{18}H_8S_4$). The compound was provided by Matsunaga.[5] This sulphur compound was purified by recrystallizations from trichlorobenzene and also by fractional sublimation. The electronic properties of the material will be reported elsewhere.[6]

5) α, α' - Diphenyl - β - picrylhydrazyl (DPPH). DPPH was prepared by the reaction of α, α'-diphenylhydrazine with picrylchloride in chloroform.[7] To prevent a complex formation with an applied solvent, a recrystallization of the free radical from a carbon disulphide solution was carried out.

6) Violanthrone (Violanthrone A; $C_{34}H_{16}O_2$). This dyestuff was synthesized from purified benzanthrone by a carefully-controlled alkali-fusion. An unstable by-product, denoted as violanthrone B, was removed by a vatting method.[8] The synthesized violanthrone was washed with chlorobenzene or with a sodium hydroxide solution and then recrystallized from concentrated sulphuric acid. Further, the material was repeatedly sublimed under a vacuum, it thus yielded dark-blue needle crystallites.

The Charge Transfer Complexes.—1) Violanthrene-iodine Complex ($C_{34}H_{18}$-$2I_2$). The complex was provided by Uchida. The complex formation between purified violanthrene and pure iodine was carried out by Clar's method.[9,10]

2) Perylene-iodine Complex ($C_{20}H_{12}$-$3I_2$). This complex was also prepared by Clar's method from perylene, which was purified through repeated chromatographical purification, and pure iodine.

Both of the complexes had to be kept in sealed glass vessels to avoid decomposition.

Resistance Cell.—The materials described above were compressed between two steel plates under a few kbars* pressure to make a thin sheet, the thickness of which was about 0.1 mm. These samples were then fitted into a high pressure resistance cell. The cell applied in the experiment was similar to those used by Balchan and Drickamer.[11] Figure 1 shows a schematic diagram of the cell.

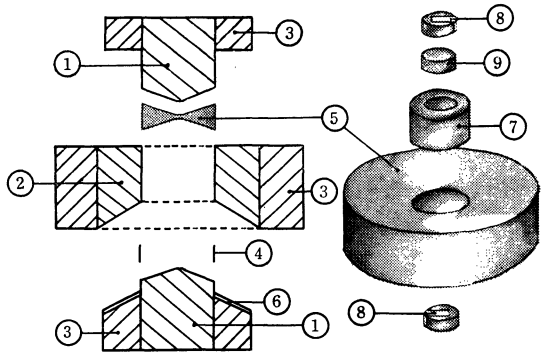

Fig. 1. Resistance cell.
1 Carboloy piston, 2 Carboloy insert, 3 steel jackets, 4 0.02 mm. mica ring, 5 pyrophyllete pellet, 6 Bakelite insulating ring, 7 pyrophyllete ring, 8 electrodes and 9 specimen

The Carboloy insert (2) was ground to a tight slip fit on the Carboloy pistons (1), and then pressed into the steel outer jacket (3). One end of each insert was ground in the truncated cone shape, with an 18° taper and 2.4 mm. diameter flat. One of the pistons was reduced in outside diameter by 0.02 mm. to permit an electrical insulation from the chamber wall with a thin strip of mica (4). A pellet of pyrophyllite (5), 0.33 mm. thick at the centre, was applied as the supporting medium for the taper. Bofore use, the pellet was dried in an electric oven for a few hours to remove a small amount of adsorbed water. The details of the arrangement of the electrodes in the resistance cell are illustrated in the same figure. The electrical resistances of the samples were measured by the potential drop method. To increase the electrical insulation of the cell, a boron nitride pellet (5) and ring (7) were used instead of pyrophyllite ones. As a result of this imporvement, the bulk resistance of the cell reached around 10^8 Ω.

Pressure Calibrations**—A sharp change in the electrical resistance of bisumth at 2.54×10^4 kg./cm^2 and 8.8×10^4 kg./cm^2 was used in the calibration of the pressure of the resistance cell, Further, the phase transition point of lead at 1.61×10^5 kg./cm^2 was used.

3) H. Inokuchi, Y. Harada and T. Kondow, *J. Opt. Soc. Am.*, **54**, 842 (1962).
4) Y. Maruyama, Y. Harada and H. Inokuchi, This Bulletin, **36**, 1193 (1963).
5) Y. Matsunaga, *J. Chem. Phys.*, **42**, 2248 (1965).
6) M. Kochi, H. Inokuchi and Y. Harada, Private Communication.
7) S. Goldschmit and K. Renn, *Ber.*, **55**, 628 (1922); H. Inokuchi, Y. Harada and Y. Maruyama, This Bulletin, **35**, 1559 (1962).
8) J. Aoki, ibid., **34**, 1817, 1820 (1961).
9) T. Uchida and H. Akamatu, ibid., **35**, 981 (1962).
10) K. Brass and E. Clar, *Ber.*, **65**, 1660 (1932).

* 1 kbar=10^3 kg./cm^2
11) A. S. Balchan and H. G. Drickamer, *Rev. Sci. Inst.*, **32**, 308 (1961).
** Usually, there is a discrepancy between an applied pressure and a real compression on a specimen. The cause of this discrepancy is that friction and pressure in the gasket zones adsorb some of the thrust force on the piston elements.

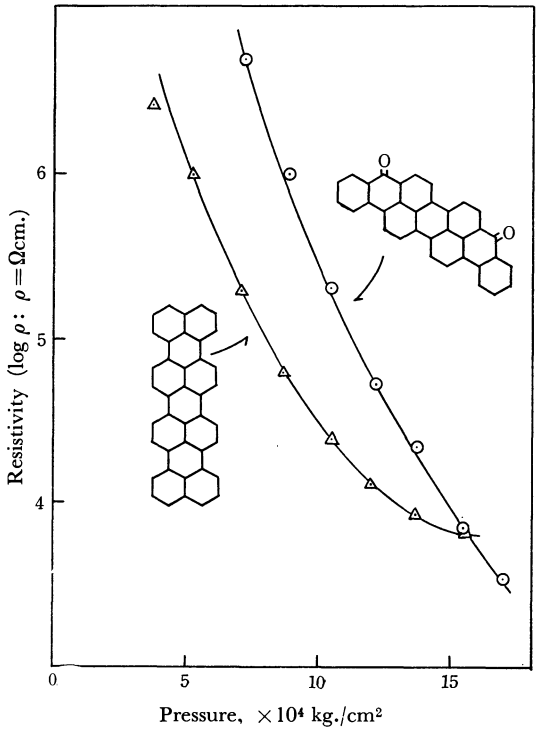

Fig. 2-(a)

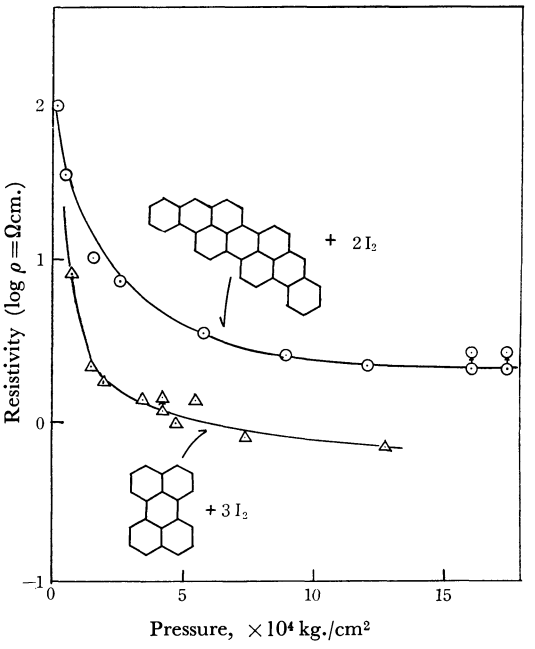

Fig. 2-(b)-2

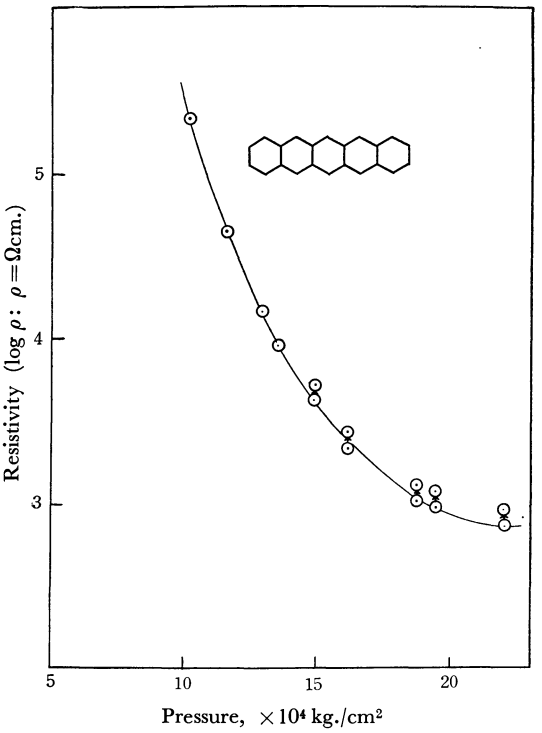

Fig. 2-(b)-1

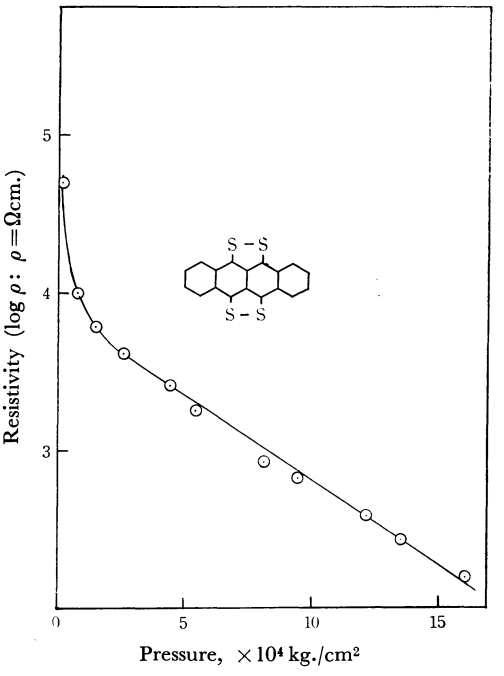

Fig. 2-(c)

Fig. 2. The electrical resistivity of organic semiconductors as a function of hydrostatic pressure (a) quaterrylene and violanthrone, (b) pentacene and two charge transfer complexes and (c) tetrathiotetracene.

Experimental Results

As has been mentioned previously,[12] the abrupt change in the electrical resistance of the purified organic semiconductors was found at a lower pressure range, 10^4 kg./cm^2. At a higher pressure region, three different curves between the applied pressure and the resistivity were found. Figure 2-(a) shows the pressure-resistivity curve for the first group, which displayed a leveling-off behaviour. Quaterrylene and violanthrone belonged to this group.

Table I. The electrical resistivity of organic semiconductors under high pressure
($\rho=\rho_0 \exp(\Delta\varepsilon/2kT)$)

Compound	At atmospheric pressure		at 1.61×10^5 kg./cm^2	
	ρ_{15}(Ωcm.)	$\Delta\varepsilon$	ρ_{15}(Ωcm.)	$\Delta\varepsilon$
Quaterrylene	10^8	0.60	7×10^3	0.16
Violanthrone A	2.3×10^{10}	0.78	3.7×10^3	0.20
Coronene	1.7×10^{17}	1.7	$>10^6$	—
DPPH	10^{13}	1.7	1.1×10^4*	0.21*
Pentacene	10^{14}	1.5	2.3×10^3	0.14
Violanthrene-iodine	96**	0.15	2.3***	0.17
Peryleneiodine	10	0.06	0.6	—
Tetrathiotetracene	4×10^4**	0.4—0.5	1.6×10^2	0.34

* Under a pressure of 1.27×10^5 kg./cm^2
** Under a pressure of 10^3 kg./cm^2
*** At 1.20×10^5 kg./cm^2 compression

In the second group, the behaviour of the pressure-resistivity relation was almost identical with that of the first group. However, the resistivity was increased gradually under a constant pressure of around 10^5 kg./cm^2 (Fig. 2-(b)). Two charge transfer complexes, pentacene and DPPH, belonged to this group. In the second one, the resistivity of tetrathiotetracene decreased monotonously, even at a higher pressure range (Fig. 2-(c)). All of the materials examined in this experiment exhibited a sharp decrease in the band gap, as was observed from the temperature dependency of the resistivity, which is listed in Table I.

Discussion

In a previous work,[12] we assumed that the increment in electrical conductivity under the high pressure is contributed by electroncloud overlappings between molecules in the molecular lattice. The compressibility of a few of the organic molecular crystals has been observed as a function of the applied pressure.[2] Recently, Danno and Kajiwara have measured the Young modulus of a series of polycyclic aromatic compounds by means of a vibrating-reed method under atmospheric pressure; the value for triphenylene was 1.19×10^{10} dyne/cm^2; for 1, 2, 3, 4-dibenzanthracene, 2.81×10^{10} dyne/cm^2; for coronene, 1.10×10^{10} dyne/cm^2, and for the acridine-I_2 complex, 1.67×10^{11} dyne/cm^2.[13] From their results, we found that the average compressibility of these molecular crystals is one hundred times those of ordinary metals. The volume contraction of organic crystals by compression was expected to be anomalously large: the volumes at 1.6×10^5 kg./cm^2 for these molecular crystals were estimated to be 69% of those at atmospheric pressure.[2]

The decrease in the volume upon compression is caused by the contraction of the lattice distances of adjacent molecules. The contraction, however, is not isotropic, because almost all of the crystals examined in this experiment have monoclinic or triclinic crystal structures. It is not difficult to assume that the direction perpendicular to the molecular plane, the distances of which are listed in Table II, is more compressible than the other directions. Therefore, a great increase in the electron flow in that direction of the crystal may be expected under compression.

To simplify the theoretical treatment of the charge flow in the compressed crystal, we assumed that the contraction of the crystal was isotropic. When we applied these contractions to the treatment of the tight-binding approximation, and also assumed that the carrier-scattering can be described by the constant mean free time, $\tau(k)=\tau_0$, the mobility components were given by:

$$\mu_{ij}=e\tau_0\langle v_i v_j\rangle/kT$$

where v_i is the ith component of the carrier velocity, v, which is described by $v=(1/\hbar)\ \partial E(k)/\partial k$.[14] The $\langle v_i v_j\rangle$ quantity is a statistical average over the band. The average value of μ_{ij} in the three directions of the crystal was estimated to be 10^1—10^2 times larger than those at atmospheric pressure.[14],*

Therefore, the remarkable increase in electrical conductivity upon compression, $10^5\sim10^7$ times, must result from the increase in the number of charge carriers, n in $\sigma=ne\mu$; this increment is produced from an unexpected decrease in the band gap. A similar order of decrease in the band gap was also found for some inorganic semiconductors, as is mentioned in Table III.

12) H. Inokuchi, I. Shirotani and S. Minomura, This Bulletin, **37**, 1234 (1964).

13) T. Danno and T. Kajiwara, Private Communication.

14) Y. Harada, Y. Maruyama, I. Shirotani and H. Inokuchi, This Bulletin, **37**, 1378 (1964).

* The anisotropic compression of some simple organic molecular crystals has been observed by Kabalkina (S. S. Kabalkina, *Fizika Tverdogo Tela.*, **4**, 3124 (1962)). When we applied this finding to the tight-binding approximation roughly, the increase of mobility was estimated to be around $5\times10^1-10^2$ times value for isotropic compression, $1\times10^1-10^2$ times.

TABLE II. THE INTERMOLECULAR DISTANCE (d) OF POLYCYCLIC AROMATIC COMPOUNDS

Compound	Crystal structure	d, Å
Benzene	Orthorhombic	3.6
Anthracene	Monoclinic	3.8
Tetracene	Triclinic	3.68
Pyrene	Monoclinic	3.53
Coronene	Monoclinic	3.4
Quaterrylene	Monoclinic	3.47
Graphite	Hexagonal	3.345

TABLE III. THE DECREASE IN THE ENERGY GAP FOR ORGANIC AND INORGANIC SEMICONDUCTORS

Compound	$(d\Delta\varepsilon/dp)_T$ (in 10^{-6} eV./bar)
Quaterrylene	2.75
Violanthrone A	3.6
Pentacene	8.5
Silicon	2.0[a]
AlSb	1.6[a]

a) W. Paul and D. M. Warschauer, in "Solids under Pressure," McGraw-Hill Co., New York (1963), p. 177.

TABLE IV. THE RED-SHIFT OF THE OPTICAL ABSORPTION PEAK FOR VARIOUS POLYCYCLIC AROMATIC COMPOUNDS

Compound	Absorption peak	Applied pressure	Shift per unit of pressure
	cm^{-1}	$\times 10^3$ kg./cm^2	$\times 10^{-6}$ eV./bar
Anthracene	25300	100	4.7
Tetracene	19200*	90	6.8
	19235*	5.2	13.4
	19810	5.2	9.4
Pentacene	15000	55	9.3
Coronene	26810	4.5	13
Perylene	21368	5.2	12.5
Cu-phthalocyanine	16420	55	0.75

* 19200 cm^{-1}, observed by Drickamer, is corresponded to 19235 cm^{-1} band found by the present authors.

On the other hand, we have already determined several characteristic points in the behaviour of the optical properties of aromatic compounds under high pressure; a remarkable increase in Davydov splitting in a tetracene crystal with an increase in the pressure,[15] a strong red-shift of the energy transfer luminescence spectra of the anthracene-tetracene mixed crystal, and a red-shift of the absorption spectra.[16] Table IV shows the red-shift of the absorption peak of aromatic compounds. Generally speaking, the value of the shift is comparable to the contractions of the band gaps; that is to say, both the anomalous changes, electrical and optical, may happen for same reasons.

In the case of a remarkable increase in Davydov splitting, the increase can be explained qualitatively by the following contribution: a decrease in lattice distances and also a rotation of molecules in the lattice points.[15] Under hydrostatic pressure, the crystal lattice may be diminished anisotropically; this is in contrast to the assumption adopted above. Furthermore, the contribution to the intermolecular force from dipole-quadrapole interaction and also quadrapole-quadrapole interaction between adjacent molecules must be considered.

In addition to these theoretical treatments, the accurate experimental values of compressibility in all crystal directions, and also those of electronic mobility under high pressure, which are now being examined, may be introduced as a reasonable explanation for the anomalous change in the electrical and optical properties of aromatic compounds.

The relation between pressure and resistivity above 1×10^5—2×10^5 kg./cm^2 for almost all samples was a leveling off; this parallels the leveling off of the compressibility of organic materials in the pressure range. The curve for tetrathiotetracene is an exceptional one, as is illustrated in Fig. 2-(c). Above 1×10^5 kg./cm^2, the electrical resistance still decreases monotonously.

In the second group, the resistance, after it has been leveling off, gradually increases with time. The change is assumed to be introduced by a chemical reaction between two components of the complexes or by a decomposition of the material itself. After compression, the decomposition of pentacene was confirmed by a detection of the electron spin resonance absorption signal. To the contrary of Drickamer's work, we could not find any "metallic" character of pentacene with a positive temperature coefficient.

The authors wish to thank Dr. Hiroshi Nagasaki for his kind assistance throughout this work.

15) H. Ohigashi, I. Shirotani, H. Inokuchi and S. Minomura, *J. Chem. Phys.*, **43**, 314 (1965).

16) H. Ohigashi, I. Shirotani, H. Inokuchi and S. Minomura, *J. Phys. Soc. Japan*, **19**, 1996 (1964).

BULLETIN OF THE CHEMICAL SOCIETY OF JAPAN VOL. 39 391—395 (1966)

The Synthesis of Some Peptides Related to the Active Site of Enzymes[1]

By Tadao HAYAKAWA,[2] Kaoru HARADA and Sidney W. FOX

Institute of Molecular Evolution, University of Miami, Coral Gables, Florida, U. S. A.; Institute for Space Biosciences and Chemistry Department, The Florida State University, Tallahassee, Florida, U. S. A.

(Received May 10, 1965)

The sequences, α-aspartyl-L-serylglycine and α-glutamyl-L-serylglycine, appear in the "active site" of many esteratic enzymes. The free tripeptides were synthesized in this study. In order to avoid difficulties encountered in more conventional synthetic routes, *N*-carbobenzoxy-L-aspartyl (β-benzyl ester)-*O*-benzyl-L-serylglycine dibenzyl ester and *N*-carbobenzoxy-L-glutamyl (γ-benzyl ester)-*O*-benzyl-L-serylglycine dibenzyl ester were synthesized. These protected peptides were converted to the free tripeptides upon hydrogenolysis, which removed all of the four protecting groups simultaneously. Several derivatives of these tripeptides were also synthesized.

The α-aspartyl-L-serylglycine sequence has been found in many esteratic enzymes in the so-called "active site."[3] The synthesis of this free tripeptide[4] is accordingly of interest for the preparation of derivatives including other peptides of defined constitution, as a standard reference substance in tests of catalytic activity with derivatives, and for investigation as a co-monomer in copolymerizations. For the latter objective, in particular, combination with histidine residues in the same macromolecule would be of interest.

The difficulties of preparation of the free tripeptide posed special requirements. One of these was protection of the unstable seryl residue during the syntheses. Another problem was avoidance of saponification of the ester of β-benzyl *N*-carbobenzoxy-L-aspartate, an intermediate in some projected syntheses. Bernhard et al.[5] found that the saponification of β-benzyl *N*-carbobenzoxy-L-aspartyl residues involved the formation of an imide intermediate. The most rapid reaction, both in the formation of the imide intermediate and its subsequent hydrolysis, was observed with *N*-carbobenzoxyaspartyl (β-benzyl ester)-serinamide. The hydroxyl group of the serine residue was found to be required for the most rapid hydrolysis of this benzyl ester. Bernhard et al. also isolated the intermediate imide compound. These findings suggested that alkaline conditions should be avoided during the synthesis and that protection of the hydroxyl group of the serine residue is desirable.

Attempts in this laboratory to saponify selectively the ethyl ester of *N*-carbobenzoxy-L-aspartyl (β-benzylester)-*O*-benzyl-L-serylglycine were unsuccessful. Hydrogenolysis of the saponified product resulted in hygroscopic peptides composed of aspartic acid, serine, and glycine. These were presumably mixtures of α- and β-aspartyl peptides which could result from saponification of an intermediate imide.

The ethyl esters of glycyl-α-L-aspartyl-L-serylglycine[7] and of L-aspartyl-*O*-acetyl-L-serylglycine[7] have been reported. However, saponification of the ethyl esters and of the *O*-acetate also is difficult to control.

In order to avoid all of the difficulties mentioned, *N*-carbobenzoxy-L-aspartyl-*O*-benzyl-L-serylglycine dibenzyl ester was synthesized because the four protecting groups would presumably be removable by hydrogenolysis, and alkaline treatments during synthetic steps would thus be avoided. A test of this hypothesis showed that the free tripeptide could indeed be prepared in this way. The α-L-glutamyl-L-serylglycine was then similarly prepared. This sequence has also been found in the active site of esteratic enzymes.[3]

Recently, the synthesis of an octapeptide corresponding to a sequence containing the active site of chymotrypsin has been reported.[8]

Experimental

β-Benzyl L-Aspartate.—β-Benzyl L-aspartate was prepared by the sulfuric acid method.[9] m. p. 221°C,

1) Aided by Grant no. NsG-173-62 of the National Aeronautics and Space Administration, U. S. A. Contribution no. 051 of the Institute for Space Biosciences. Presented at the 145th Meeting of the American Chemical Society, New York, September, 1963.

2) Presented adress: Hokkaido University, Sapporo, Japan.

3) J. A. Cohen, B. A. Osterbaan, H. S. Jansz and F. Berends, *J. Cell. Comp. Physiol.*, **54**, Suppl. 1, 231 (1959).

4) S. W. Fox, T. Hayakawa and K. Harada, This Bulletin, **36**, 1050 (1963).

5) S. A. Bernhard, A. Berger, J. H. Carter, E. Katchalski, M. Sela and Y. Shalitin, *J. Am. Chem. Soc.*, **84**, 2421 (1962).

6) A. Van de Linde, H. Kienhuis, A. Verweij and J. P. J. Van der Holst, *Rec. trav. chim.*, **80**, 1305 (1961).

7) L. Benoiton and H. N. Rydon, *J. Chem. Soc.*, **1960**, 3328.

8) H. T. Cheung, T. S. Murthy and E. R. Blout, *J. Am. Chem. Soc.*, **86**, 4200 (1964).

9) T. Hayakawa, H. Nishi, J. Noguchi, K. Ikeda, T. Yamashita and T. Isemura, *J. Chem. Soc. Japan, Pure Chem. Sect.*, (*Nippon Kagaku Zasshi*), **82**, 601 (1961).

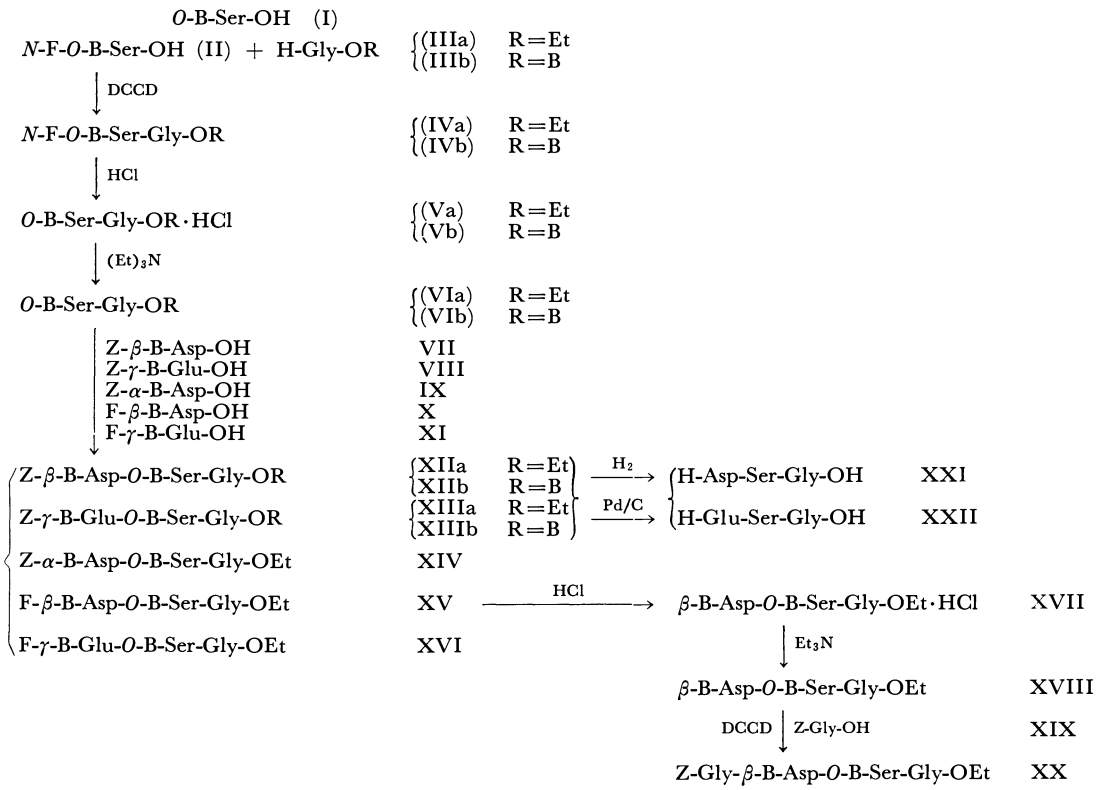

B: Benzyl F: Formyl Z: Carbobenzoxy Et: Ethyl

$[\alpha]_D^{26}$ +24.2° (*c* 1.18, 1 N HCl).

γ-Benzyl L-Glutamate.—γ-Benzyl L-glutamate was also prepared by the sulfuric acid method.[9] m. p. 174°C, $[\alpha]_D^{26}$ +21.8° (*c* 1.87, AcOH).

***O*-Benzyl-L-serine.**—*O*-Benzyl-L-serine was prepared from methyl acrylate by Okawa's method,[10] The *O*-benzyl-DL-serine was acetylated and the resulting *N*-acetyl *O*-benzyl-DL-serine was resolved by Takaacylase, m. p. 219—221°C (decomp.), $[\alpha]_D^{26}$ +5.0° (*c* 1.00, 3 N HCl).

β-Benzyl *N*-Carbobenzoxy-L-aspartate (VII).—β-Benzyl *N*-carbobenzoxy-L-aspartate was prepared by the usual Schotten-Bauman reaction.[11] m. p. 105—106°C, $[\alpha]_D^{27}$ +12.0° (*c* 1.50, AcOH).

γ-Benzyl *N*-Carbobenzoxy-L-glutamate (VIII).—γ-Benzyl *N*-carbobenzoxy-L-glutamate was prepared as described by Hanby et al.[12] m. p. 75—76°C, $[\alpha]_D^{27}$ −22.7° (*c* 1.41, N $KHCO_3$).

β-Benzyl *N*-Formyl-L-aspartate (X).—β-Benzyl L-aspartate, 31.3 g. (0.13 mol.), was dissolved in 200 ml. of 98% formic acid. To this was added dropwise 78 ml. of acetic anhydride at 5—10°C under agitation during a period of 1 hr. After addition was complete, the mixture was stirred for 2 hr. at room temperature. The solution was evaporated to dryness under reduced pressure at 50°C in a water bath. The residue was dried in a vacuum desiccator overnight over sodium hydroxide. The dried residue was dissolved in 150 ml. of acetone and filtered to remove the insoluble material (1.05 g., m. p. 155—160°C). Petroleum ether was added to the acetone solution to crystallize the β-benzyl *N*-formyl-L-aspartate, 28.2 g. (81%), m. p. 122—125°C. This product was recrystallized from acetone and petroleum ether, m. p. 123—125°C, $[\alpha]_D^{25}$ +28.6° (*c* 1.75, ethanol).

Found: N, 5.61. Calcd. for $C_{12}H_{13}O_5N$: N, 5.58%. COOH titration,[13] Found: M=248, Calcd: M=251.2.

γ-Benzyl *N*-Formyl-L-glutamate (XI).—γ-Benzyl *N*-formyl-L-glutamate was synthesized in a way similar to that described above. m. p. 130—131°C, $[\alpha]_D^{25}$ +17.9° (*c* 1.98, ethanol).

Found: N, 5.32. Calcd. for $C_{13}H_{15}O_5N$: N, 5.28%. COOH titration: Found, M=264; Calcd. M=265.3.

***N*-Formyl-*O*-benzyl-L-serine (II).** — *N*-Formyl-*O*-benzyl-L-serine was prepared from *O*-benzyl-L-serine by use of a method similar to that described above. Yield, 78%, m. p. 123—128°C. This was recrystallized from ethyl acetate and petroleum ether, m. p. 129—130°C, $[\alpha]_D^{25}$ +54.8 (*c* 2.75, ethanol).

Found: N, 6.23. Calcd. for $C_{11}H_{13}O_4N$: N, 6.28%. COOH titration, Found: M=223; Calcd. M=223.2.

***N*-Formyl-*O*-benzyl-L-serylglycine Ethyl Ester (IVa).**—*N*-Formyl-*O*-benzyl-L-serine, 6.00 g., was dissolved in 60 ml. of tetrahydrofuran. To this was

10) K. Okawa, This Bulletin, **29**, 486 (1956).
11) A. Berger and E. Katchalski, *J. Am. Chem. Soct.* **73**, 4084 (1951).
12) W. E. Hanby, S. G. Waley and J. Watson, *J. Chem. Soc.*, **1950**, 3239.
13) The carboxyl group was titrated with methanolic sodium methoxide in dimethylformamide or in dioxane by use of thymol blue as the indicator. Elemental Analyses were carried out by Micro-Tech Laboratories, INC., Skokie, Illinois, U. S. A.

added 2.77 g. of freshly distilled glycine ethyl ester (IIIa). To this solution, 5.90 g. of dicyclohexylcarbodiimide (DCCD) in 15 ml. of tetrahydrofuran was added dropwise under cooling with ice water. After 30 min. of cooling, the mixture was allowed to attain room temperature. Precipitated dicyclohexylurea was filtered after 24 hr. of standing, and the filtrate was evaporated under reduced pressure at 40°C. The residue was dissolved in ethyl acetate and filtered to remove dicyclohexylurea. The solvent was evaporated to 25 ml. and petroleum ether was added slowly to precipitate *N*-formyl-*O*-benzyl-L-serylglycine ethyl ester. The mixture was kept in the ice box for 3 hr., then filtered to collect the *N*-acyldipeptide ester, 6.2 g. (75%). This was recrystallized from 10 ml. of ethyl acetate, 15 ml. of ether and 35 ml. of petroleum ether, 5.0 g., m. p. 63—64°C, $[\alpha]_D^{25}$ +4.1° (*c* 2.48, ethanol).

Found: C, 58.44; H, 6.60; N, 9.03. Calcd. for $C_{13}H_{20}O_5N$: C, 58.44; H, 6.55; N, 9.09%.

O-Benzyl-L-serylglycine Ethyl Ester Hydrochloride (Va).—*N*-Formyl-*O*-benzyl-L-serylglycine ethyl ester (IVa), 4.62 g., was dissolved in 18.8 ml. of methanol. To this was added 16.5 ml. of 1 N hydrochloric acid in methanol under cooling (2 ml. of concentrated hydrochloric acid was diluted to 24 ml. with methanol). The solution was allowed to stand at room temperature for 48 hr. The solvent was evaporated under reduced pressure, and the residual syrup was dissolved in 20 ml. of water. The insoluble material was filtered and the filtrate was twice extracted with ether. The aqueous solution was then lyophilized. A slightly yellowish vitreous dipeptide ester hydrochloride was obtained; 4.68 g. (98%). This peptide ester hydrochloride was used for subsequent syntheses without further purification.

N-Carbobenzoxy-L-aspartyl (β-benzyl ester)-O-benzyl-L-serylglycine Ethyl Ester (XIIa).—*O*-Benzyl-L-serylglycine ethyl ester hydrochloride (Va), 14.05 g., was dissolved in 150 ml. of dry dioxane. To this solution, 4.80 g. of triethylamine was added under cooling. The resultant triethylamine hydrochloride was filtered. In this filtrate, 15.85 g. of β-benzyl *N*-carbobenzoxy-L-aspartate was dissolved. To the mixture, a solution of 9.17 g. of DCCD in 50 ml. of dioxane was added slowly under cooling. After 5 min., dicyclohexylurea began to precipitate. The reaction mixture was allowed to stand overnight. Precipitated urea was filtered out and the filtrate was evaporated at 40—45°C under diminished pressure. The residual syrup was dissolved in 180 ml. of ethyl acetate at 45°C and filtered. The filtrate was washed twice with each of the following: 0.3 N hydrochloric acid, 5% sodium hydrogen carbonate, and water. The washed solution was dried over anhydrous sodium sulfate. The ethyl acetate was evaporated to about 80 ml. and then petroleum ether was added solwly to precipitate the protected tripeptide ester. The mixture was kept in the refrigerator overnight. The crystals were filtered and washed with ether and dried; 19.80 g., m. p. 117—120°C. From the mother liquor an additional 1.50 g. of crystals was obtained; yield 78%. This was recrystallized from ethyl acetate, acetone, and petroleum ether; m. p. 121—124°C, $[\alpha]_D^{25}$ −5.6° (*c* 1.51, ethanol).

Found: C, 64.05; H, 6.10; N, 6.79. Calcd. for $C_{37}H_{37}O_9N$: C, 63.96; H, 6.02; N, 6.78%.

N-Carbobenzoxy-L-glutamyl (γ-benzyl ester)-O-benzyl-L-serylglycine Ethyl Ester (XIIIa).—The protected tripeptide ester (XIIIa) was prepared in a way similar to that described above. After washing the ethyl acetate solution with 0.3 N hydrochloric acid, a yield of 10.1 g. (74%) of XIIIa was obtained. This was recrystallized by dissolving in acetone - ethyl acetate mixture and by precipitating with petroleum ether. By this recrystallization procedure, two fractions of different melting points were isolated. One (A), (0.21 g.), has a m. p. 133—134°C and the other (B), (5.10 g.), melted at 147—148°C. The compound A melted at 133—134°C, then solidified, and the solid remelted at 146—147°C. Accordingly, compound A is probably converted to compound B by heating. Elemental analyses of compound A and B each agree with the theoretical value.

Compound A, Found: C, 64.59; H, 6.27; N, 6.81.
Compound B, Found: C, 64.83; H, 6.06; N, 6.68.
Calcd. for $C_{34}H_{39}O_9N_3$: C, 64.54; H, 6.31; N, 6.63%.

N-Formyl-L-aspartyl (β-benzyl ester)-O-benzyl-L-serylglycine Ethyl Ester (XV).—A solution of 23 g. of *O*-benzyl-L-serylglycine ethyl ester hydrochloride (Va) in 200 ml. of dioxane was treated with 11.0 ml. of triethylamine. The free dipeptide ester (VIa) was condensed with 19.1 g. of β-benzyl *N*-formyl-L-aspartate (X) by use of 16.6 g. of DCCD. A yield of 33.0 g. (89%) of protected tripeptide ester (XV) was obtained, m. p. 83—86°C. This was recrystallized from ethyl acetate; m. p. 91—93°C, $[\alpha]_D^{25}$ −5.8° (*c* 1.67, AcOH).

Found: C, 61.52; H, 6.48; N, 7.90. Calcd. for $C_{27}H_{33}O_8N_3$: C, 61.47; H, 6.30; N, 7.97%.

L-Aspartyl (β-benzyl ester)-O-benzyl-L-serylglycine Ethyl Ester Hydrochloride (XVII).—β-Benzyl ester of *N*-formyl-L-aspartyl-L-serylglycine ethyl ester (XV), 16.0 g., was dissolved in 60 ml. of absolute ethanol. To this solution, 40 ml. of 1 N ethanolic hydrogen chloride was added. The mixture was allowed to stand at room temperature for three days. The solvent was evaporated under reduced pressure and the residue was dissolved in 30 ml. of water. The insoluble material was filtered off and the filtrate was extracted with ethyl acetate to remove the unreacted *N*-formyl derivative. The aqueous solution was lyophilized; yield, 3.60 g. (22%).

N-Carbobenzoxy-glycyl-L-aspartyl (β-benzyl ester)-O-benzyl-L-serylglycine Ethyl Ester (XX).—A solution of 2.1 g. of carbobenzoxyglycine (XIX) in 15 ml. of dioxane was added to 50 ml. of acetonitrile solution of L-aspartyl (β-benzyl ester)-*O*-benzyl-L-serylglycine ethyl ester (XVIII) which was prepared from 5.3 g. of L-aspartyl (β-benzyl ester)-*O*-benzyl-L-serylglycine ethyl ester hydrochloride (XVII) and an equimolar amount of triethylamine. The two compounds were condensed by 2.1 g. of DCCD under stirring and cooling. After standing overnight the reaction mixture was treated in the same way as described above. The protected tetrapeptide, 4.0g. (60%), was obtained from ethyl acetate solution by addition of ether, m. p. 68—73°C. This was recrystallized twice from ethyl acetate and ether, m. p. 85—89°C, $[\alpha]_D^{25}$ −13.0° (*c* 2.17, dioxane).

Found: C, 61.55; H, 6.11; N, 8.35. Calcd. for $C_{35}H_{40}O_4N_4$: C, 62.12; H, 5.96; N, 8.28%.

α-Benzyl N-Carbobenzoxy-L-aspartate (IX).—

This compound was prepared by the method of Bergmann et al.[14] The crude product (m. p. 71—78°C) was recrystallized repeatedly from ethyl acetate by petroleum ether. The material which melted at 82—85°C was used for further synthesis, $[\alpha]_D^{25}$ −15.3° (*c* 1.60, ethanol).

Found: N, 3.95. Calcd. for $C_{19}H_{19}O_6N$: N, 3.93%. COOH titration, Found: M=358; Calcd.: M=357.5.

***N*-Carbobenzoxy-L-aspartyl (*α*-benzyl ester)-*O*-benzyl-L-serylglycine Ethyl Ester (XIV).**—Compound Va, 4.00 g., in 30 ml. of tetrahydrofuran, was treated with 1.28 g. of triethylamine. The precipitated amine salt was removed by filtration. To the filtrate, 4.50 g. of *α*-benzyl *N*-carbobenzoxy-L-aspartate (IX) was dissolved. DCCD (2.88 g.), in 10 ml. of tetrahydrofuran, was added slowly to the above mixture while stirring and cooling. The reaction mixture was treated in the same way as described earlier. The product obtained weighed 6.0 g. (77%). This was recrystallized from ethyl acetate (45 ml.) and petroleum ether (40 ml.). Yield, 4.1 g., m. p. 134—136°C (sintering at 128°C).

Found: C, 64.05; H, 6.10; N, 6.76. Calcd. for $C_{33}H_{37}O_9N_3$: C, 63.96; H, 6.02; N, 6.78%.

Glycine Benzyl Ester (IIIb).—The *p*-toluensulfonate of glycine ester was prepared by the method of Zervas, et al.[15] Yield, 80—90%, m. p. 130—132°C. Free glycine benzyl ester was prepared by treating with an excess of anhydrous potassium carbonate and ether while cooling and stirring. The resulting free ester was used for further synthesis without purification.

***N*-Formyl-*O*-benzyl-L-serylglycine Benzyl Ester (IVb).**—To the mixture consisting of 11.2 g. of *N*-formyl-*O*-benzyl-L-serine, 9.1 g. of glycine benzyl ester in 50 ml. of dioxane, 11.0 g. of DCCD in 20 ml. of dioxane was added under cooling. The mixture was allowed to stand overnight. The reaction mixture was treated in the same way as was described earlier. The resultant dipeptide benzyl ester was dissolved in ethyl acetate and precipitated with ether, yield, 15.0 g. (81%), m. p. 89—90°C. The precipitate was further purified by treating it twice with ethyl acetate and ether, 13.0 g., m. p. 91—92°C, $[\alpha]_D^{25}$ +2.2° (*c* 2.43, AcOH), $[\alpha]_D^{25}$ +0.26° (*c* 3.0, ethanol).

Found: C, 65.02; H, 5.92; N, 7.53. Calcd. for $C_{20}H_{22}O_5N_2$: C, 64.85; H, 5.97; N, 7.56%.

***O*-Benyzl-L-serylglycine Benzyl Ester Hydrochloride (Vb).** — *N*-Formyl-*O*-benzyl-L-serylglycine benzyl ester (IVb), 2.0 g., was dissolved in 6.4 ml. of dioxane and 6 ml. of 1 N ethanolic hydrochloric acid. This solution was allowed to stand at room temperature for 3 days. The reaction mixture was evaporated under reduced pressure at 40°C. The resudue was dissolved in water and the insoluble material was filtered off; the filtrate was extracted with ethyl acetate. The aqueous solution was lyophilized. Yield, 1.40 g. (69%). $[\alpha]_D^{27}$ +8.3° (*c* 6.3, water).

***N*-Carbobenzoxy-L-aspartyl-*O*-benzyl-L-serylglycine Dibenzyl Ester (XIIb).**—*β*-Benzyl *N*-carbobenzoxy-L-aspartate (VII), 6.0 g., was mixed with *O*-benzyl-L-serylglycine benzyl ester (VIb) in 60 ml. of dioxane which was prepared from 7.3 g. of its hydrochloride (Vb) and 2.7 ml. of triethylamine. To this mixture, 4.0 g. of DCCD in 10 ml. of dioxane was added under cooling and stirring. The mixture was allowed to stand overnight at room temperature. The reaction mixture was processed in the usual manner. The protected tripeptide ester was crystallized from ethyl acetate and ether. The crystals were washed with petroleum ether and dried, yield, 5.3 g., (41%), m. p. 119—125°C. This was recrystallized from ethyl acetate and ether, m. p. 129—131°C, $[\alpha]_D^{25}$ −4.7° (*c* 1.43, dioxane).

Found: C, 67.41; H, 5.99; N, 6.25. Calcd. for $C_{38}H_{39}O_9N_3$: C, 66.95; H, 5.77; N, 6.16%.

***α*-Aspartyl-L-serylglycine (XXI).** — *N*-Carbobenzoxy-*α*-L-aspartyl-*O*-benzyl-L-serylglycine dibenzyl ester (XIIb), 1.36 g., was dissolved in 60 ml. of methanol and 5 ml. of 0.4 N hydrochloric acid. This solution was mixed with 3.5 g. of 5% palladium on charcoal. Hydrogenolysis of the mixture was carried out at room temperature for 5 hr. After the reaction was completed, the catalyst was filtered and the filtrate was concentrated to dryness under reduced pressure. The residue was dissolved in a small amount of water and filtered. The filtrate was lyophilized. A yield of 550 mg. of material was obtained. The tripeptide hydrochloride was dissolved in absolute alcohol and the insoluble part was filtered off. To the filtrate was added 0.03 ml. of pyridine and the solution was kept in the refrigerator overnight. The precipitated free tripeptide was collected by centrifugation and washed with absolute alcohol and ether and dried. This was recrystallized by dissolving in water and precipitating with absolute ethanol; yield, 250 mg. (45%). The crystals are not hygroscopic. m. p. 174—176°C (decomp.), $[\alpha]_D^{25}$ −7.3° (*c* 1.54, water).

Found: C, 38.93; H, 5.45; N, 15.16. Calcd. for $C_9H_{15}O_7N_3$: C, 38.99; H, 5.45; N, 15.16%.

By paper chromatography in 80% phenol, the peptide showed an R_f=0.17. Amino acid composition analyzed by the Phoenix K 5000 amino acid analyzer showed 97 aspartic acid: 98 serine: 100 glycine.

***N*-Carbobenzoxy-L-glutamyl-*O*-benzyl-L-serylglycine Dibenzyl Ester (XIIIb).**—*O*-Benzyl-L-serylglycine benzyl ester hydrochloride (Vb), 2.36 g. in 20 ml. of dioxane, was treated with 0.66 g. of triethylamine. Precipitated amine hydrochloride was removed by filtration. To the filtrate, 2.50 g. of *γ*-benzyl *N*-carbobenzoxy-L-glutamate (VIII) and 1.45 g. of DCCD in 5 ml. of dioxane were added. The reaction mixture was kept at room temperature overnight. This was treated in the way described earlier. The protected tripeptide ester was crystallized from ethyl acetate and ether, 2.45 g., m. p. 108—111°C. This solid was recrystallized from ethyl acetate, m. p. 109—112°C, $[\alpha]_D^{25}$ −1.83° (*c* 1.81, dioxane).

Found: C, 67.31; H, 5.97; Calcd. for $C_{39}H_{41}O_9N_3$: C, 67.32; H, 5.94%.

***α*-L-Glutamyl-L-seryl-glycine (XXII).**—*N*-Carbobenzoxy-L-glutamyl-*O*-benzyl-L-serylglycine dibenzyl ester (XIIIb), 1.35 g., was dissolved in a mixture of 60 ml. of methanol, 30 ml. of ethanol, 2.15 ml. of 1 N hydrochloric acid, and 3 ml. of water. To this mixture, 3.0 g. of 5% palladium on charcoal was added. Hydrogenolysis was carried out at room temperature for 10 hr. After the reaction was completed, the catalyst

14) M. Bergmann, L. Zervas and L. Salzmann, *Ber.*, **66**, 1288 (1933).
15) L. Zervas, M. Winitz and J. P. Greenstein, *J. Org. Chem.*, **22**, 1515 (1957).

was removed by filtration and the filtrate was evaporated to dryness under reduced pressure at 40°C. The residue was dissolved in a small amount of water. The insoluble material was filtered and the filtrate was lyophilized. The dried residue (tripeptide hydrochloride) was dissolved in 15 ml. of ethanol and 1.4 millimole of pyridine was added slowly. The tripeptide crystallized at once. The crystals were collected by centrifugation, and were washed with ether and dried, yield, 0.25 g. (44%). This solid was recrystallized by dissolving in 2.5 ml. of water and precipitating by 15 ml. of absolute ethanol. Tripeptide, 202 mg., was obtained, m. p. 191—192°C (decomp.), $[\alpha]_D^{27}$ +8.62° (*c* 1.24, water).

Found: C, 41.23; H, 5.93; N, 14.18. Calcd. for $C_{10}H_{17}N_3O_7$: C, 41.23; H, 5.88; N, 14.43%.

The tripeptide is not hygroscopic. By paper chromatography in 80% phenol, the peptide showed an R_f=0.35. The amino acid composition analyzed showed 100 glutamic acid: 98 serine: 99 glycine.

Summary

Syntheses of the free tripeptides found in the active site of various enzymes,[3] α-L-aspartyl-L-serylglycine and α-L-glutamyl-L-serylglycine, are described. Difficulties in the synthesis included the rapid saponification of β-benzyl *N*-carbobenzoxy-L-aspartyl residues.[5] Also, although many protected tri- and tetra-peptide esters were synthesized, attempts to obtain pure products by saponification were unsuccessful.

The synthesis was accomplished by using intermediates protected only with groups that could be simultaneously removed by hydrogenolysis. The intermediates thus employed were the *N*-carbobenzoxy-α-L-aspartyl-*O*-benzyl-L-serylglycine dibenzyl ester (XIIb) and the α-L-glutamyl analog (XIIIb). The syntheses of these two intermediates are also described.

NOTES

Complexing Behavior of Kojic Acid with Metal Ions. III. Infrared Studies of Bivalent Metal-Kojate Chelates*

By Yukito MURAKAMI and Katsumi MERA

Department of Organic Synthesis, Faculty of Engineering, Kyushu University, Hakozaki, Fukuoka

(Received April 19, 1965)

In previous studies, the interaction of bivalent magnesium, manganese and tervalent iron ions with kojic acid in aqueous media has been investigated and the corresponding stability constants evaluated.[1,2] However, the majority of the bivalent first-transition metals do not yield the corresponding soluble kojate chelates in aqueous solutions. Therefore, most of the potentiometric studies aiming to obtain chelate stability constants have been carried out in dioxane-water media.[3,4] The stability of these kojate chelates with respect to the bivalent metals has been found to follow the sequence:

$$Cu(II) > Zn(II) > Ni(II) \sim Mn(II) \sim Co(II)$$

It is interesting to note that a zinc ion forms a much more stable chelate than do nickel, cobalt and manganese ions in the kojate chelate system. In addition, the comparable stability of the manganese chelates with the corresponding nickel and cobalt chelates is rather unexpected.

In order to investigate the structural change in the ligand molecule brought about through its coordination to the metal ions and the correlation of the structural change with the stability sequence, infrared spectral measurements of the kojate chelates of copper(II), zinc(II), nickel(II) and cobalt(II) have been performed in the present study. The absorption peaks of interest for these metal chelates are listed in Table I for the sake of comparison. The absorption spectra obtained for the zinc, nickel and cobalt chelates were almost identical with each other, and slightly different from that for the copper chelate. The most significant difference among these two types of metal chelates (zinc, nickel, cobalt; copper) is the OH-stretching vibration appeared in the region ranging 3200—2400 cm^{-1}. Another difference is observed in the range between 905 and 850 cm^{-1}, where the copper chelate gives three

TABLE I. SIGNIFICANT PEAKS IN THE INFRARED SPECTRA OF SOME METAL-KOJATE CHELATES

Kojic acid	Cu(II)-kojate	Zn(II)-kojate	Ni(II)-kojate	Co(II)-kojate	Assignment
3290 m	3175 m, b				O-H str. (CH_2OH)
	3090 m	3085 m	3085 m	3090 m	
3215 m, b					O-H str. (phenol)
	2680 w	2760 w	2755 w	2760 w	OH str. (H-bonded)
		2610 w, b	2590 w, b	2590 w, b	
		2440 w	2440 w	2450 w	
1710 w					C=O str.
1668 s	1635 s	1634 s	1634 s	1635 s	
1640 s					C=C str.
1621 s	1580 s	1572 s	1570 s	1570 s	
1591 s	1535 s	1540 s	1540 s	1550 s	
865 s	895 m	905 m	905 m	905 m	
	876 w				
	867 m				

s: strong; m: medium; w: weak; b: broad

* Contribution No. 81 from the Department of Organic Synthesis, Faculty of Engineering, Kyushu University.

1) Y. Murakami, This Bulletin, **35**, 52 (1962).

2) Y. Murakami, *J. Inorg. Nucl. Chem.*, **24**, 679 (1962).

3) B. E. Bryant and W. C. Fernelius, *J. Am. Chem. Soc.*, **76**, 5351 (1962).

4) H. Kido, W. C. Fernelius and C. G. Haas, Jr., *Anal. Chim. Acta*, **23**, 116 (1960).

absorption peaks while the other chelates give only one significant peak. In view of the spectral shift of the OH vibrations for the metal chelates from that of the ligand alone, it seems that the stronger hydrogen bonding is secured through metal coordination. In addition, the zinc, nickel and cobalt chelates seem to contain some sorts of hydrogen bonding stronger than that in the corresponding copper chelate, since the former chelate species demonstrated several absorption peaks in the range between 2800 and 2400 cm^{-1}, where the latter chelate does not show any significant peak. Moreover, the nearly-identical spectral behavior among the zinc, nickel and cobalt chelates seems to suggest that these chelates possess coordinate bonds of nearly identical characters.

The following four resonance structures (I—IV) may be drawn for kojic acid:

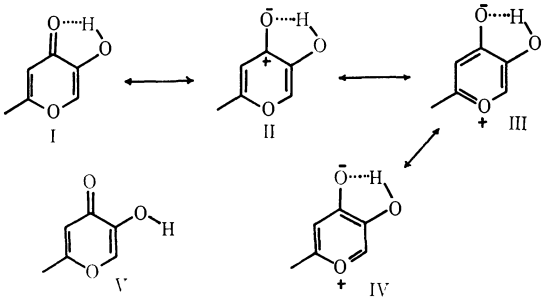

The absorption bands which appear at 1710 and 1668 cm^{-1} are most likely due to the non-hydrogen-bonded (cf. structure V) and to the hydrogen-bonded carbonyl vibrational modes (cf. structures I—IV) respectively. When kojic acid

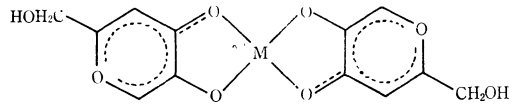

VI

forms a complex with a metal ion (as is illustrated by structure VI), the former mode disappears and the latter shifts to lower frequencies. The other significant bands, appearing at 1640, 1621 and 1591 cm^{-1} in the free kojic acid, are assigned to the C=C stretching modes. These bands also were observed to shift to lower frequencies through the formation of metal coordinate bonds. These shifts of C=O and C=C bands to lower frequencies seem to indicate that the contribution of resonance structures of the II, III and IV types, in which a hydrogen atom is replaced by a metal ion, becomes greater as metal coordinate bonds are formed. The resonance interaction involving structures II, III and IV tends to delocalize olefinic and carbonyl π-electrons over both γ-pyron and chelate rings, thus decreasing the double-bond character of olefinic and carbonyl bonds.

The infrared spectral data do not provide any significant correlation with the stability sequence among these bivalent metal kojate chelates. Thus, some further studies are needed to clarify the problems of the stability order.

Experimental

The kojic acid used was a product of the Nutritional Biochemical Corporation, U. S. A., and was purified by sublimation in vacuo: m. p. 156—156.6°C. All the kojate complexes used in this work were prepared by standard methods described in the literature. The analyses are listed in Table II.

Table II. Analyses of metal-kojate chelates

Chelate	Carbon,* %	Hydrogen,* %
$Cu(C_6H_5O_4)_2$	41.19 (41.68)	3.23 (2.92)
$Zn(C_6H_5O_4)_2$	41.04 (41.46)	3.20 (2.90)
$Ni(C_6H_5O_4)_2$	41.08 (42.28)	3.23 (2.96)
$Co(C_6H_5O_4)_2$	41.89 (42.25)	3.03 (2.95)

* Calculated values for the specified formula are given in parentheses.

The infrared spectra of the kojate chelates were measured by the Nujol mull method with a Koken Model DS-301 Spectrophotometer equipped with sodium chloride optics.

A Modified Method of Preparing of ω, p-Dihydroxyacetophenone

By J. S. CHADHA* and G. K. SHARMA**

Department of Chemistry, Delhi University, Delhi-7, India

(Received May 31, 1965)

The earlier method for the preparation of ω, p-dihydroxyacetophenone (IV)[1,2] needed an improvement because of difficulties encountered in the isolation of the key intermediate, ω-chloro-p-hydroxyacetophenone,[1,3] which in its crude form is extremely lachrymatory. In the present investigation, a modified procedure has been employed to eliminate the use of ω-chloro-p-hydroxyacetophenone.

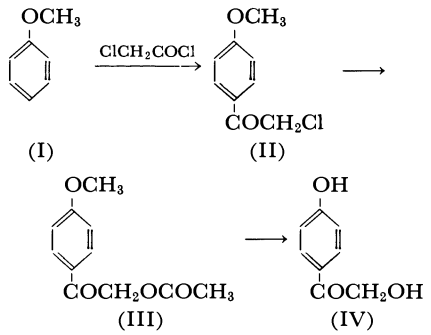

Chloroacetyl chloride and anisole (I) are condensed in cold in the presence of aluminium chloride[4] to give ω-chloro-p-methoxyacetophenone (II). This compound II, on treatment with anhydrous potassium acetate in absolute ethanol, yields ω-acetoxy-p-methoxyacetophenone[5] (III). This III is then demethylated with aluminium chloride. In the last reaction, deacetylation takes place simultaneously, and thus the final product, ω, p-dihydroxyacetophenone (IV), is directly obtained.

Experimental

ω, p-Dihydroxyacetophenone (IV, obtained by the demethylation and deacetylation of III): ω-Acetoxy-p-methoxyacetophenone (1.30 g.) was dissolved in dry benzene (30 ml.), and anhydrous aluminium chloride (4.0 g.) was added to the solution. The reaction mixture was refluxed for 3 hr., and the solvent removed under reduced pressure. The residual mass was hydrolysed with ice and hydrochloric acid to give a solid, which was extracted with ethyl acetate. The ethyl acetate solution was evaporated and the residual mass crystallised from hot water to yield colourless prisms of the final product, ω, p-dihydroxyacetophenone (0.76 g., 80%); m. p. 177—178°C (sinters at 170°C). (Found: C, 63.2; H, 5.2. Calcd. for $C_8H_8O_3$: C, 63.2; H, 5.2%).

The authors are thankful to Dr. Miss Krishna K. Vashistha, Department of Chemistry, Delhi University, Delhi-7, India, for her valuable help and constant encouragement during this work.

* Present address: Unilever Research Laboratory, The Frythe, Welwyn, Herts., England.

** Present address: Glaxo Laboratories Ltd., Ulverston (Lancs), England.

1) A. Robertson and R. Robinson, *J. Chem. Soc.*, **1928**, 1464.

2) A. Leon, A. Robertson, R. Robinson and T. R. Seshadri, ibid., **1931**, 2672.

3) F. Tutin, F. W. Caton and A. C. O. Hann, ibid., **95**, 2113 (1909).

4) F. Tutin, ibid., **97**, 2503 (1910).

5) M. Tiffeneau, *Compt. rend.*, **150**, 1181 (1910).

A Study of the Hydration of Calcium Orthoplumbate. IV. The Behavior of Dehydration

By Masumi KOISHI and Kenjiro MEGURO

Department of Applied Chemistry, Faculty of Science, Tokyo College of Science, Kagurazaka, Shinjuku-ku, Tokyo

(Received June 15, 1965)

In the previous papers[1] it was demonstrated that Kissinger's method[2] of differential thermal analysis could be used to analyze the reaction kinetics of the dehydration of calcium orthoplumbate hydrates. That is, the reaction order and the activation energy of dehydration were determined, and the information thus obtained was used to analyze the behavior of the dehydration.

In the present paper, the authors will attempt to confirm the previous conclusion by thermogravimetric analysis. The reaction order and the activation energy of the dehydration will also be examined by Freeman's method[3] of thermogravimetric analysis.

The results of present experiments will support the conclusions of the previous papers.

Experimental Procedure

Material.—*Calcium Orthoplumbate Hydrate-Calcium Hydroxide Mixtures.*—The mixture used in this experiment was prepared by hydrating calcium orthoplumbate. The process of hydration was carried out with the apparatus and procedure previously described.[1] Hydrated mixtures were identified by X-ray diffraction patterns, differential thermal and thermogravimetric curves, and chemical analysis.

Calcium Orthoplumbate Hydrate.—Franke's method[4] was used to remove calcium hydroxide from hydrated mixtures, as has been described before.[1]

The samples employed for thermal analysis are the same as those used in the previous work.

Apparatus and Procedure.—The DTA-TGA unit (Automatic Differential Thermobalance, made by the Rigaku Denki Company, Tokyo), designed for simultaneous differential thermal and thermogravimetric analyses, was used in this work. Specimen holders made of platinum and beryllium oxide were employed. A platinum-rhodium thermocouple was used. The reference material was α-alumina. Each of the eight samples was run in analysis at the rate of 2.5 and 10°C per min. in order to determine the activation energy and the reaction order. The samples were ground enongh to pass them through a 250-mesh sieve. Specimen holders were filled loosely with 400—600 mg. of the sample. The differential temperature variation and the weight change as a function of the time and the temperature were recorded continuously.

Results and Discussion

The continuous tracings of the weight change accompanying the heat treatment of calcium orthoplumbate hydrate and calcium orthoplumbate hydrate - calcium hydroxide mixtures are given in Figs. 1 and 2 respectively. A typical comparison of simultaneously-recorded curves of thermogravimetric and differential thermal analyses is then given in Fig. 3.

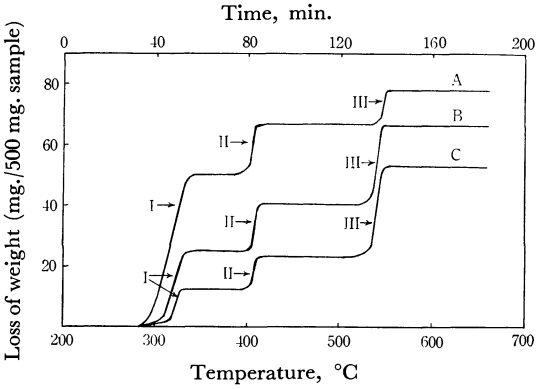

Fig. 1. Thermogravimetric analysis curves for calcium orthoplumbate hydrate - calcium hydroxide mixtures.

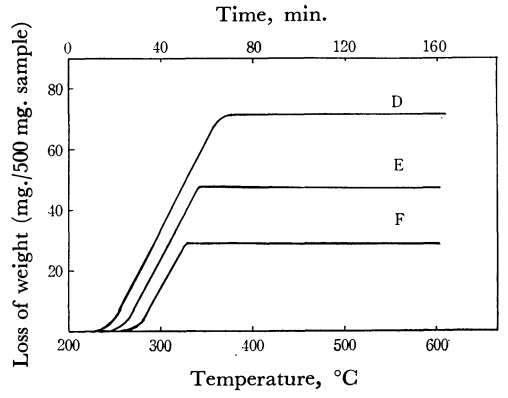

Fig. 2. Thermogravimetric analysis curves for calcium orthoplumbate hydrate.

1) M. Koishi and K. Meguro, *J. Chem. Soc. Japan, Ind. Chem. Sect.* (*Kogyo Kagaku Zasshi*), **67**, 2001, 2005 (1964); M. Koishi, This Bulletin, **37**, 1570 (1964).

2) H. E. Kissinger, *J. Research Natl. Bur. Standard*, **57**, 217 (1956); *Anal. Chem.*, **29**, 1702 (1957).

3) E. D. Freeman and B. Carroll, *J. Phys. Chem.*, **62**, 394 (1958).

4) E. E. Pressler, S. Brunauer and D. L. Kantro, *Anal. Chem.*, **28**, 897 (1956).

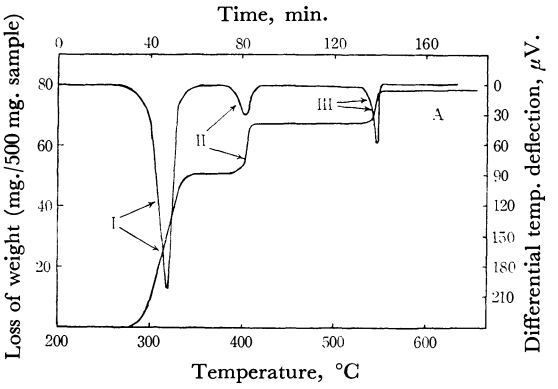

Fig. 3. Comparison of simultaneously recorded thermogravimetric and differential thermal curves.

It is apparent from Figs. 1 and 2 that the dehydration of samples D, E and F proceeds in one stage, while that of samples A, B and C, proceeds in three stages. Stages I and II in Fig. 1 show the first and second stage of the dehydration respectively; Stage III shows the decomposition of calcium hydroxide.

When the thermogravimetric analysis data of Figs. 1 and 2 were plotted according to Freeman's method, straight lines were obtained for each cases, thus enabling us to calculate the activation energy. The results of the thermogravimetric studies in the present work are compared with the values obtained by Kissinger's method based on differential thermal analysis, in Table I.

The value of the reaction order of magnesium hydroxide (1.00) reported in this paper (Table I) differs from those reported by Kissinger and by Gregg and Razouk[2] (0.67), but the agreement with the differential thermal analysis value (0.99) is good. The activation energy (25.0 kcal. per mol.) differs slightly from their values (27.2—31.4 kcal. per mol.) in order of magnitude. This discrepancy may be attributed to the difference in the particle size and in the mineral origin of the samples.

The values of the reaction order derived from the thermogravimetric analysis are nearly equal to unity in the cases of samples A, B and C. While the activation energies of the first dehydration were found to be 20.1, 21.0 and 20.1 kcal. per mol., those of the second dehydration were from 41.0 to 45.7 kcal. per mol. The activation energies for samples D, E and F were found to 11.8, 12.6 and 12.6 kcal. per mol. while their reaction orders were nearly equal to unity.

Table I. Comparison of results with thermogravimetric and differential thermal analysis methods

Material		x TGA	x DTA	E, kcal./mol. TGA	E, kcal./mol. DTA
A	I*1	1.10	1.08	20.1	18.2
	II*2	0.90	—	41.0	—
	III*3	0.70	0.66	32.8	33.0
B	I	1.10	1.10	21.0	18.0
	II	0.90	0.92	43.8	41.0
	III	0.70	0.66	32.8	33.0
C	III	1.00	1.09	20.1	18.0
	II	1.01	0.92	45.7	43.0
	III	0.70	0.66	32.8	33.0
D		0.90	0.88	11.8	11.5
E		1.00	0.96	12.6	11.5
F		1.00	1.05	12.6	12.1
G		0.70	0.66	30.1	30.7
H		1.00	0.99	25.0	25.0
I	a)	0.55 to	0.44	31.4	
	b)	0.69		27.2	

*1 First dehydration step.
*2 Second dehydration step.
*3 Dehydration of liberated calcium hydroxide.
a) Kissinger's data[2] by DTA method for Brucite.
b) Kissinger's data[2] by isothermal weight-loss measurements for Brucite.

As was concluded in the previous paper, the difference in activation energy between the first and second dehydration processes indicates that the dehydration is influenced by the inhibitive action of the calcium hydroxide liberated; that is, the elevation of the activation energy of the second dehydration seems to result from the fact that small particles of calcium hydroxide liberated in hydrate mixtures are firmly bonded to the hydrate.

The results of the thermogravimetric studies by Freeman's method in the present work agree well with the values obtained by Kissinger's method which based on the differential thermal analysis. It may be concluded from the results of this kinetic investigation that the method of thermogravimetric analysis can be used to obtain information about the kinetics of simple dehydration reactions.

However, several factors which may influence the patterns have not examined, such as pressure, atmosphere and particle size.

The Syntheses of Substituted 4-Indanyl Phenyl Ketones and Aceanthrenes

By Tosio MORIWAKE

Department of Industrial Chemistry, School of Engineering, Okayama University, Tsushima, Okayama

(Received June 19, 1965)

According to Cook,[1] it appears that the carcinogenic potency of methylcholanthrene cannot be attributed to its special pentacyclic structure. Fieser and Hershberg[2] have suggested that methylcholanthrene owes its high activity to the presence of the 1, 2-benzanthracene ring system with a simple substituent at the 10-position. These facts have prompted the present author to synthesize the derivatives of aceanthrene, which has a structural analogy to cholanthrene but which possesses no carcinogenic activity by itself.

The Elbs reaction[3] has been extensively used for the preparation of polycyclic aromatic hydrocarbons. The syntheses of 1, 2-cyclopentenoaceanthrene and 1, 2-dimethylaceanthrene by this reaction have been reported by Fieser and Hershberg.[2] There are also several other methods[4] for preparing aceanthrene derivatives, but the method using the pyrolysis of substituted 4-indanyl phenyl ketone seems to be the most convenient. This paper will deal with the synthesis and the pyrolysis of some substituted 4-indanyl phenyl ketones.

The condensation of benzonitrile with 4-indanyllithium, which had been prepared by the reaction of 4-bromoindane with lithium in ether, gave 4-indanyl phenyl ketone in a 78% yield, whereas the reaction of benzoyl chloride or benzonitrile with 4-indanylmagnesium bromide, which had been prepared from 4-bromoindane and magnesium in ether, gave 4-indanyl phenyl ketone in yields of 40 and 27% respectively. The author then prepared other 4-indanyl phenyl ketones, which are summarized in Table I, by the condensation of benzonitrile with 4-indanyllithium.

The pyrolysis of 4-indanyl phenyl ketone at 350—355°C for 5 hr. gave a product, which was identified as aceanthrene by a study of its melting point, picrate and spectra, in a 27.2% yield. The pyrolysis of 4-indanyl *p*-tolyl ketone gave 9-methylaceanthrene in a 25.0% yield.

On the other hand, the pyrolysis of 4-indanyl *o*-tolyl ketone gave a viscous material, from which small amount of picrate was then obtained. The analytical data of the picrate agreed well with the values calculated for $C_{17}H_{14}\cdot C_6H_3O_7N_3$. In view of the structure of the ketone, 1, 2-cyclopentenoanthracene or 7-methylaceanthrene might be the pyrolytic product. However, the attempted isolation of hydrocarbon from the picrate failed. The pyrolysis of other ketones failed to give pure substances.

Experimental[5]

4-Indanyl Phenyl Ketone: Method A (from Benzonitrile and 4-Indanyllithium).—A solution of 9.8 g. of 4-bromoindane[6] in 30 ml. of ether was added

TABLE I. 4-INDANYL PHENYL KETONES

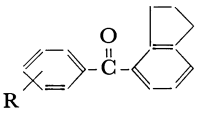

Substituent R	M. p. or b. p. °C/mmHg	Yield %	C, % Found	C, % Calcd.	H, % Found	H, % Calcd.
H	153—152/2[a]	72	86.37	86.45	6.78	6.35
o-CH_3-	158—160/3[b]	65	86.63	86.40	7.17	6.83
p-CH_3-	159—161/2[c]	57	86.08	86.40	7.13	6.83
o-CH_3O-	72—73	56	81.43	80.92	6.55	6.39
p-CH_3O-	55—56	63	81.24	80.92	6.42	6.39
p-CH_3S-	61—62	52	76.06	76.10	6.07	6.01

a) n^{15} 1.6080 b) n^{25} 1.5943 c) n^{15} 1.6030

1) J. W. Cook, *Ber.*, **69A**, 38 (1936).
2) L. F. Fieser and E. B. Hershberg, *J. Am. Chem. Soc.*, **59**, 394 (1937).
3) L. F. Fieser, "Organic Reactions," Vol. I, Ed. by R. Adams, John Wiley & Sons, New York, N. Y. (1942), p. 129.
4) a) L. F. Fieser and M. A. Peters, *J. Am. Chem. Soc.*, **54**, 4373 (1932); b) E. D. Bergman and R. Ikan, *J. Org. Chem.*, **23**, 907 (1958); c) C. R. Clemo and N. G. Chatge, *J. Chem. Soc.*, **1956**, 1067; d) L. F. Fieser and E. Berliner, *J. Am. Chem. Soc.*, **74**, 536 (1952).
5) The boiling and melting points are uncorrected.
6) L. F. Fieser and A. M. Seligman, *J. Am. Chem. Soc.*, **57**, 942 (1935).

to a suspension of 0.8 g. of lithium in 30 ml. of ether at such a rate that moderate refluxing was continued; this refluxing was continued for a further 5 hr. To the resulting solution there was added, with ice-cooling, 5.2 g. of benzonitrile dissolved in a mixture of 20 ml. of ether and 20 ml. of benzene over a 30-min. period. After the mixture had been refluxed for 2 hr., it was decomposed by the addition of 50 ml. of 10% hydrochloric acid. After the organic solvent had been distilled off, 10 ml. of water, 10 ml. of concentrated hydrochloric acid and 5 ml. of acetic acid were added; the mixture was then refluxed for 2 hr. to complete the decomposition of the resulting ketimine. The product was extracted with a mixture of ether and benzene, and the extract was washed with a saturated sodium bicarbonate solution, and with water, dried, concentrated, and distilled to give 8.0 g. (72%) of 4-indanyl phenyl ketone (b. p. 153—155°C/2 mmHg; n^{15} 1.6080). Attempts to prepare the oxime and semicarbazone of the ketone failed.

Found: C, 86.37; H, 6.78. Calcd. for $C_{16}H_{14}O$: C, 86.45; H, 6.35%.

The other indanyl phenyl ketones summarized in Table I were prepared by this method.

Method B (from Benzoyl Chloride and 4-Indanylmagnesium Bromide).—A solution of 9.8 g. of 4-bromoindane in 30 ml. of ether was added under refluxing to 1.2 g. of magnesium covered with 30 ml. of ether over a 10-min. period. Refluxing was then continued for an additional 1.5 hr. to complete the reaction. The mixture was cooled with an ice bath; a solution of 7.0 g. of benzoyl chloride in 30 ml. of ether was then added over a 15-min. period, and the mixture was refluxed for 1 hr. The cooled reaction mixture was decomposed by the addition of 60 ml. of 10% hydrochloric acid, extracted with ether, and treated as usual. Distillation gave 4-indanyl phenyl ketone in a 40% yield.

Method C (from Benzonitrile and 4-Indanylmagnesium Bromide).—To an ethereal solution of 4-indanylmagnesium bromide (prepared from 3.3 g. of 4-bromoindane and 0.4 g. of magnesium in ether) there was added a solution of 2.0 g. of benzonitrile in 20 ml. of ether over a 10-min. period. The resulting mixture was treated with in the same manner as has been described in method A. 4-Indanyl phenyl ketone was obtained in a yield of 27%.

Aceanthrene (The Pyrolysis of 4-Indanyl Phenyl Ketone).—When 2.0 g. of 4-indanyl phenyl ketone was heated at 350—355°C for 5 hr. in a metal-bath and distilled at 2 mmHg, a viscous distillate was obtained, which crystallized on standing. The recrystallization of the resulting yellow crystalline from ethanol gave 0.5 g. (27.2%) of aceanthrene; m. p. 114.5—115.5°C (lit.[3] 113°C); λ_{max}^{EtOH} 254 mμ (ε 13800), 258(115000), 356(3100), 375(6300) and 396(3600); (Found: C, 93.91; H, 5.98%.

The picrate (from ethanol) melted at 120—120.5°C (lit.[3] m. p. 120°C).

9-Methylaceanthrene (The Pyrolysis of 4-Indanyl *p*-Tolyl Ketone).—2.2 g. of 4-indanyl *p*-tolyl ketone was heated at 360—370°C for 4 hr. and distilled at 3 mmHg to give 500 mg. (25.0%) of yellow crystals, m. p. 115—118°C. The recrystallization of this material from ethanol gave an analytically pure sample; m. p. 118—118.5°C; λ_{max}^{EtOH} 259 mμ (ε 113000), 355(3000), 373(6200) and 394(3500).

Found: C, 93.36; H, 6.41. Calcd. for $C_{17}H_{14}$: C, 93.53; H, 6.47%.

The picrate, as fine, dark-red needles, melted at 121—122°C after recrystallization from ethanol.

Found: C, 61.64; H, 3.94. Calcd. for $C_{23}H_{17}O_7N_3$: C, 61.74; H, 3.83%.

The Pyrolysis of 4-Indanyl *o*-Tolyl Ketone.—When 2.0 g. of 4-indanyl *o*-tolyl ketone was heated at 350—360°C for 5 hr. and distilled at 5 mmHg, a reddish oil was obtained. To this distillate there was added a saturated ethanolic solution of picric acid, and the dark-red fine needles which separated were collected. Recrystallizations from ethanol gave a pure picrate, m. p. 123.5—124°C.

Found: C, 61.94; H, 4.04. Calcd. for $C_{23}H_{17}O_7N_3$: C, 61.74; H, 3.83%.

The analytical data agreed well with the values calculated for $C_{17}H_{14}\cdot C_6H_3O_7N_3$, the picrate of 7-methylaceanthrene or 1, 2-cyclopentenoanthracene, but the attempt to isolate the corresponding hydrocarbon from the picrate failed.

The Separation of Selenium(IV) and Selenium(VI) by Solvent Extraction

By Mariko INARIDA

The Institute of Physical and Chemical Research, Komagome, Bunkyo-ku, Tokyo

(Received June 24, 1965)

As a method for the mutual separation of selenium(IV) and selenium(VI), precipitation with sulfur dioxide gas[1] has been used. The present author has now tried to separate them by extraction with TBP (tributyl phosphate) and Na(DDTC) (sodium diethyldithio carbamate). As a result, a more rapid and simple method will be elaborated.

Selenium(IV) forms a yellow compound in hydrochloric acid media with DDTC, this chelate can be extracted by TBP from a 0.05 N—0.1 N hydrochloric acid solution quantitatively, while selenium(VI) does not form DDTC complexes under these conditions. The author has devised the following separation prosedure based on the above properties.

Experimental and Results

The Preparation of the Radioactive Selenium(IV) Solution and the Radioactive Selenium(VI) Solution.—^{75}Se was added to a nitric acid solution (1 : 1) of standard selenium(IV) solution. The solution was then evaporated, dried up, and dissolved with a 0.1 N hydrochloric acid solution. One milliliter of this solution contained 100 μg. of Se*(IV). The radioactive selenium(VI) solution was prepared using radioactive selenium-(IV) by the method of Dennis and Koller.[2]

The Determination of the Distribution Ratios.—The distribution ratios of selenium(IV) and selenium(VI) in the DDTC-HCl-TBP system were studied. The radioactive selenium(IV) solution (or the radioactive selenium(VI) solution) and 0.1 M Na(DDTC) were mixed with 5 ml. of hydrochloric acid in various concentrations and then shaken with an equal volume of TBP(pre-equilibrated with each hydrochloric acid solution). The equilibrium was established within 1 min. The two phases were then separated by centrifuging, and a 1 ml. portion was taken from each phase. The γ-radioactivity was measured with a well-type scintillation counter. The data obtained are shown in Fig. 1, where D is the distribution ratio. It is clear from this figure that the mutual separation of selenium(IV) and selenium(VI) is possible at the acidity of a hydrochloric acid solution of 0.05—0.1 N.

The effects of the ratio of DDTC to selenium were next investigated. The smallest DDTC-to-selenium ratio, giving the highest extraction, was between 4 and 5 to 1 on a molar basis.

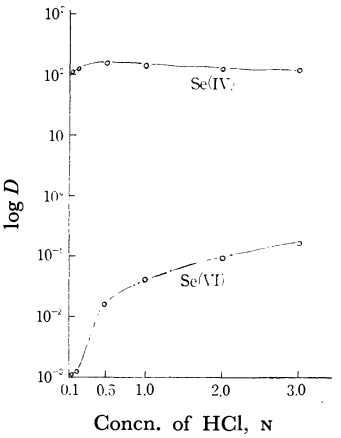

Fig. 1. Distribution of selenium in DDTC-HCl-TBP system.

The Back-Extraction of Selenium(IV).—Selenium(IV) in the TBP phase is back-extracted by shaking for one minute with 20 ml. of a 10% perchloric acid solution and 1 ml. of a hydrogen peroxide solution. More than 99% of the selenium-(IV) was recovered in the aqueous phase by two back extractions.

The Mutual Separation of Selenium(IV) and Selenium(V).—A radioactive (or inactive) selenium(IV) solution and an inactive (or radioactive) selenium(VI) solution were mixed (selenium-(IV): 10 mg., selenium(VI): 10 mg.). The solution was then adjusted to the acidity of a 0.05—0.1 N hydrochloric acid solution. The total volume was 20 ml. After the addition of 2 ml. of a 10% Na(DDTC) solution, the solution was shaken with 5 ml. of TBP in a separating funnel for one minute. The extraction was then repeated two times. After the selenium(IV) has been extracted with TBP, leaving selenium(VI) in the aqueous phase, the selenium(IV) was back-extracted twice as above. Then the aqueous phase was separated. The γ-activity of the aqueous and organic phases was measured with a well-type scintillation counter. By this simple procedure, these ions can be separated quantitatively.

The author is grateful to Dr. Nobufusa Saito, Chief of the Laboratory of Nuclear Chemistry, for his helpful discussions.

1) H. Bode and H. D. Stemmer, *Z. Anal. Chem.*, **155**, 96 (1957).
2) L. M. Dennis and J. P. Koller, *J. Am. Chem. Soc.*, **41**, 949 (1919).

SHORT COMMUNICATIONS

The Catalytic Activity of Bis-cyclopentadienyltransitionmetal Compounds for Ethylene Polymerization

By Yoshio TAZIMA and Sadao YUGUCHI

Central Research Laboratory, Toyo Rayon Co., Ltd., Otsu, Shiga

(Received June 24, 1965)

The catalytic activity of the binary sytsem of the biscyclopentadienyltransitionmetal compound and of the organoaluminum compound has been investigated. The transition metal π-complexes used as components of the binary system were biscyclopentadienyltransitionmetal halide, -chromate, -dichromate, -phosphate, -thiocyanate, -tetrathiocyanatodiamminechromate (VI), etc., while the center elements of the π-complexes tried were titanium, vanadium and zirconium.

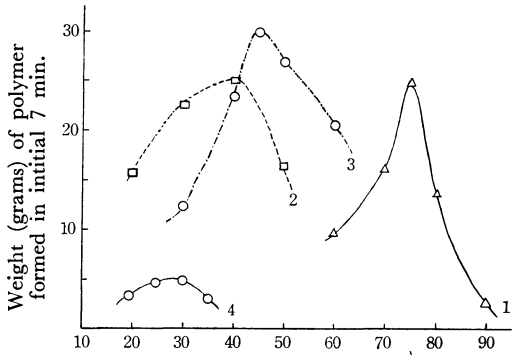

Fig. 1. Catalytic activity of the binary system for echylene polymerization at various temperature.
1. $Cp_2TiCr_2O_7$ - $AlEt_2Cl$
2. $Cp_2TiCr_2O_4$ - $AlEt_2Cl$
3. $Cp_2Ti[C_6H_2(NO_2)_3O]_2$ - $AlEt_2Cl$
4. $Cp_2Ti[(NH_3)_2Cr(SCN)_4]_2$ - $AlEt_2Cl$

Figure 1 shows the relations of the polymerization temperature and the weight of the polymer formed during the initial seven minutes by the binary catalyst systems of 0.1 g. of biscyclopentadienyltitanium compounds and 1 cc. of $AlEt_2Cl$, using 50 cc. of toluene as a solvent under 40 kg./cm^2 of ethylene pressure. The temperature at which the catalyst system showed a maximum activity was 75°C in the $Cp_2TiCr_2O_7$ - $AlEt_2Cl$ system, 50°C in the Cp_2TiCrO_4 - $AlEt_2Cl$ system, and 45°C in the $Cp_2Ti[C_6H_2(NO_2)_3]_2$ - $AlEt_2Cl$ system.

When vanadium or zirconium was the center element instead of titanium, the same tendency was observed.

The results are summarized in Table I and Table II. In Table I the temperature of the maxiumm catalytic acitivity of the system is shown for each center element of titanium, vanadium, zirconium. In Table II the maxium catalytic activity of each binary system (the transitional π-complex - $AlEt_2Cl$) is shown. The catalytic activity is expressed as grams of polymer formed in an hour per gram of transition metal complex under the experimental conditions.

TABLE I. THE TEMPERATURE (°C) OF THE MAXIMUM CATALYTIC ACTIVITY OF THE (Cp_2MX_2 - $AlEt_2Cl$) SYSTEM

M: Ti, V, Zr.

Center element / Anion species	Ti	V	Zr
Cl^- (Br^-)*	25	25	30
$Cr_2O_7^{2-}$	75	75	80
CrO_4^{2-}	40	40	50
$C_6H_2(NO_2)_3O^-$	45	45	50
$[(NH_3)_2Cr(SCN)_4]^-$	30	30	40
PO_4^{3-}	30	30	40

* Cp_2ZrBr_2

TABLE II. THE MAXIMUM CATALYTIC ACTIVITY OF THE SYSTEM

Center element / Anion species	Tt	V	Zr
Cl^- (Br^-)*	31740	130	15
$Cr_2O_7^{2-}$	2180	100	2.2
CrO_4^{2-}	2100	75	4.4
$C_6H_2(NO_2)_3O^-$	2580	8200	2.4
$(NH_3)_2Cr(SCN)_4^-$	330	50	7.2
PO_4^{3-}	40	20	0.9

* Cp_2ZrBr_2

Therefore, the following points were concluded.

1) The activity of the catalyst system depends principally on the nature of the center element of the π-complex, and the order of catalytic activity is conspicious;

$$(Ti \gg V \gg Zr)$$

2) The temperature of the maximum catalytic activity of the binary system depends on the anion species of the π-complex, and it is independent of the center element.

3) Exceptionally, the system of biscyclopentadienylvanadiumpicrate $\simeq$ aluminumdiethylchloride is extraordinarily active at 45°C.

4) As an organoaluminum compound, $AlEt_2Cl$ is better than $AlEt_3$, $AlEtCl_2$, $Al(i\text{-}Bu)_3$, etc.

The Reaction Between Benzylsulfonyl Halide and Phenyllithium

By Yasuhiko SHIROTA, Toshikazu NAGAI and Niichiro TOKURA

Department of Applied Chemistry, Faculty of Engineering, Osaka University, Higashinoda, Miyakojima-ku, Osaka

(Received November 6, 1965)

When benzylsulfonyl chloride (Ia) was treated with phenyllithium at 20—25°C, lithium benzylsulfinate (I), α-chlorobenzyl phenyl sulfone (II), m. p. 179—180°C, chlorobenzene (III), *trans*-stilbene (IV), m. p. 123°C, α, α-dichlorobenzyl phenyl sulfone (V), m. p. 151—152°C, *trans*-1, 2-diphenyl vinyl phenyl sulfone (VI), m. p. 182.5—183°C, benzyl phenyl sulfone (VII), m. p. 146°C, α-benzylsulfonyl-α'-benzenesulfonyl dibenzyl sulfone (VIII), m. p. 199—201°C and α-benzylsulfonyl-α-benzenesulfonyl toluene (IX), m. p. 237—242°C (decomp.) were obtained and identified.

(I), $C_6H_5CH_2SO_2Li$, was verified by converting it to benzyl methyl sulfone,[1] m. p. 126°C and to Ia. I was the major product; it was obtained in an overwhelming yield. II, IV and VII were identified by means of mixed melting point methods and by the coincidences of the infrared spectra with those of the respective authentic specimens.[2-4] The ields were 9.1, 3.6 and 0.4% respectively. III was identified by the coincidences of the boiling point, the infrared spectrum and the retention time obtained by V. P. C. with those of the standard sample, the yield being 16%.

V, VI and VIII were identified on the basis of elemental analyses, mol. wt. determinations,[5] and infrared, NMR or ultraviolet spectra. The yields were 0.7, 6.0 and 1.6% respectively. (V), $C_6H_5C(Cl_2)SO_2C_6H_5$, IR: ν_{max}^{Nujol} 1330 and 1050 cm^{-1} (SO_2), NMR: τ 2.35 (phenyl protons). Found: C, 51.54; H, 3.06; Cl, 23.75: Calcd. for $C_{13}H_{10}Cl_2O_2S$: C, 51.84: H, 3.34; Cl, 23.54%. (VI), $C_6H_5CH{=}C(C_6H_5)SO_2C_6H_5$, IR: ν_{max}^{Nujol} 1300, 1140 (SO_2), 1620(C=C) and 820 cm^{-1} (tri-substituted ethylene), UV: λ_{max}^{EtOH} 216 mμ (ε 21600) and 275 mμ (ε 18900), NMR: τ 2 (vinyl proton, singlet, 1H) and τ 2.65 (phenyl protons, 15 H). Found: C, 74.64; H, 5.05; S, 10.09; mol. wt., 316, Calcd. for $C_{20}H_{16}O_2S$: C, 74.97; H, 5.03; S, 10.00%; mol. wt., 320.

(VIII), $C_6H_5{-}SO_2{-}CH_D(C_5H_6){-}SO_2{-}CH_C(C_5H_6){-}SO_2{-}C(H_A)(C_5H_6){-}H_B$,
IR: 1340, 1330, 1320, 1150 and 1120 cm^{-1} (SO_2), NMR: τ 5.63 (H_A snd H_B, quartet with J_{AB}= 13.5 c.p.s.), τ 3.3 (H_C singlet), τ 3.08 (H_D, singlet) and τ 2.6 (phenyl protons). The relative areas were 2 : 1 : 1 : 20. Found: C, 60.01; H, 4.54; S, 17.49; mol. wt., 543, Calcd. for $C_{27}H_{24}O_6S_3$: C, 59.98; H, 4.47; S, 17.78%; mol. wt., 541. (IX), IR; ν_{max}^{Nujol} 1320, 1310, 1150 and 1135 cm^{-1} (SO_2), NMR (in DMSO at 100°C): τ 2.6 (phenyl protons), τ 3.5 ($SO_2{-}CH(C_6H_5){-}SO_2$) and τ 5.2 (methylene protons), the relative areas being around 15 : 1 : 1.8. Found: C, 61.99; H, 4.69; S, 16.33; mol. wt., 374. Calcd. for $C_{20}H_{18}O_4S_2$: C, 62.15; H, 4.70; S, 16.59%; mol. wt., 386. Yield: 3.7%.

$C_6H_5CH_2SO_2Cl + C_6H_5Li \rightarrow$

$C_6H_5CH_2SO_2Li$ (I) main product

$C_6H_5CH_2SO_2F + C_6H_5Li \rightarrow$

$C_6H_5{-}SO_2{-}CH(C_6H_5){-}SO_2{-}CH_2(C_6H_5)$ (IX) main product

On the other hand, the similar treatment of benzylsulfonyl fluoride (Ib) with phenyllithium gave the disulfone (IX) with a m. p. of 248—250°C (decomp.) exclusively (60% yield), together with 3.9% of IV, 1.8% of VII, 4.0% of VIII and 3.0% of I. The corresponding fluorocompounds of II, V and VI, however, were not formed.

The results above described indicate that, in the reaction of Ia with phenyllithium, Li–Cl interconversion is the predominant reaction course; it contains both the direct Li–Cl interconversion between Ia and C_6H_5Li and the Li–Cl interconversion after the metalation at the α-position to the sulfone group, whereas the reaction of Ib with phenyllithium takes a different course. The formation of IV and VI suggests the possibility of the intermediacy of a phenylsulfene[6] resulting from α-lithium benzylsulfonyl halide, followed by the β-elimination of LiX. The details, including the the formation of a polysulfone, $(C_6H_5CHSO_2)_n$,[7] at a low temperature (−80°C), will be reported in the near future.

1) E. Fromm and J. de S. Palma, *Ber.*, **39**, 3308 (1906).
2) R. Otto, *J. Prakt. Chem.*, (2), **40**, 516 (1889).
3) L. F. Fieser, "Experiments in Org. Chem.," Heath and Maruzen, Japan (1956), p. 178.
4) R. Otto and W. Otto, *Ber.*, **21**, 1696 (1885).
5) The molecular weight was determined with a Mecrolab Vapor Pressure Osmometer.
6) J. E. King and T. Durst, *Tetrahedron Letters* **1963**, 585.
7) It has a higher molecular weight than VIII.

Long Range Interaction between Hydrated Electrons

By Hideo TSUJIKAWA, Kenji FUEKI and Zenichiro KURI

Department of Synthetic Chemistry, Faculty of Engineering, Nagoya University, Chikusa-ku, Nagoya

(Received November 26, 1965)

The pulse radiolysis technique has made it possible to observe directly the formation and reactivity of the hydrated electron in liquid water. The bimolecular reaction of the hydrated electron has been found to be a fast reaction[1] and a subject for discussion, since it is the reaction of two negative species in which only a repulsive interaction would be expected from a simple classical consideration.

In order to understand this reaction, it is necessary to consider the interaction between hydrated electrons on a theoretical basis. We have, therefore, made a calculation, using the polaron model, of the long range interaction between hydrated electrons.

The interaction energies between two hydrated electrons in the electronic ground state are expressed as follows:

$$E\left\{\begin{matrix}{}^1\Sigma_g^+\\ {}^3\Sigma_u^+\end{matrix}\right\}=\frac{1}{1\pm S^2}\left[-2\beta e^2\left\{\frac{1}{r_0}\int_{r_{b1}\leq r_0}\phi_a^2(1)\mathrm{d}v_1+\int_{r_{b1}\geq r_0}\frac{\phi_a^2(1)}{r_{b1}}\mathrm{d}v_1\pm S\left(\frac{1}{r_0}\int_{r_{b1}\leq r_0}\phi_a(1)\phi_b(1)\mathrm{d}v_1+\int_{r_{b1}\geq r_0}\frac{\phi_a(1)\phi_b(1)}{r_{b1}}\mathrm{d}v_1\right)\right\}+\frac{e^2}{D}\left\{\int\frac{\phi_a^2(1)\phi_b^2(2)}{r_{12}}\mathrm{d}v_1\mathrm{d}v_2\pm\int\frac{\phi_a(1)\phi_b(2)\phi_a(2)\phi_b(1)}{r_{12}}\mathrm{d}v_1\mathrm{d}v_2\right\}\right]$$

where the upper and lower signs on the right-hand side correspond to the ${}^1\Sigma_g^+$ and ${}^3\Sigma_u^+$ states respectively; a and b represent the cavities which are formed by each electron; r_0 is the cavity radius; ϕ_a and ϕ_b are the wave function of the hydrated electron in the cavities a and b respectively; r_{b1} is the distance between the center of the b cavity and the 1 electron; r_{12} is the distance between the electrons; S is the overlap integral between ϕ_a and ϕ_b, and $\beta=(1/D_{op})-(1/D_s)$, D_{op} and D_s being the optical and static dielectric constants of water respectively.

The wave function of the hydrated electron is obtained by the SCF dielectric treatment,[2] while the effective dielectric constant, D, has been estimated in the following way:

$D=D_s$ for $R\geq 12$Å

$D=f(R)$ for $12\text{Å}\geq R\geq 6\text{Å}$

$D=D_{op}$[3] for $6\text{Å}\geq R$

where $f(R)$ is a cubic function with srepect to the distance, R, between the cavities and is connected smoothly with D_{op} at $R=6$Å and with D_s at $R=12$ Å.

Figure 1 shows the interaction energy, E, calculated as a function of R for the different cavity radii, $r_0=0$ and 1.8 Å. The interaction potentials for both the ${}^1\Sigma_g^+$ and ${}^3\Sigma_u^+$ states are attractive rather than repulsive except at short distances. The potential curve for the ground state (${}^1\Sigma_g^+$) has a minimum at 7.5 Å. The increase in the cavity radius lowers the ${}^1\Sigma_g^+$ state slightly and raises the ${}^3\Sigma_u^+$ state to the same extent.

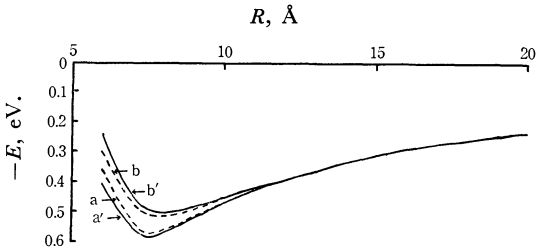

Fig. 1. The interaction energy between hydrated electrons.
a: ${}^1\Sigma_g^+$, $r_0=0$; a′: ${}^1\Sigma_g^+$, $r_0=1.8$Å
b: ${}^3\Sigma_u^+$, $r_0=0$; b′: ${}^3\Sigma_u^+$, $r_0=1.8$Å

The present results suggest that the activation energy for the bimolecular reaction of the hydrated electron arises from a short range interaction when the activation energy for diffusion is properly taken into account, and that it is not justifiable to use a simple electrostatic interaction between hydrated electrons in applying the Debye equation to the second-order rate constant.

1) S. Gordon, E. J. Hart, M. S. Matheson and J. Rabani, *Discusions Faraday Soc.*, No. **36**, 193 (1963).

2) J. Jortner, *Radiation Res., Suppl.* **4**, 24 (1964).

3) The high frequency limiting value of the dielectric constant, 5.5, has been used for D_{op}. J. B. Hasted, D. M. Ritson and C. H. Collie, *J. Chem. Phys.*, **16**, 1 (1948).

Four Isomers of Monobromo-2-stilbazole

By Takumi KATSUMOTO and Akiko HONDA

Faculty of Science, Kwansei Gakuin University, Nishinomiya, Hyogo

(Received November 30, 1965)

Monobromo-2-stilbazole, Ph-(CH=CBr)-Py-2, is expected to have four isomers: *cis*- and *trans*-2-(α-bromostyryl)-pyridine, Ph-CBr=CH-Py-2 and *cis*- and *trans*-2-(β-bromostyryl)-pyridine, Ph-CH=CBr-Py-2. However, only one species (m. p. 74—75°C) has been obtained by the dehydrobromination of 2-stilbazole dibromide,[1-3] its structure had not yet been established. The three other possible but unknown isomers have now been prepared in our laboratory, after which the structures and configurations of all the isomers have been established:

cis-2-(α-bromostyryl)-pyridine,
Ph-CBr=CH-Py-2 (I)

trans-2-(α-bromostyryl)-pyridine,
Ph-CBr=CH-Py-2 (II)

cis-2-(β-bromostyryl)-pyridine,
Ph-CH=CBr-Py-2 (III)

trans-2-(β-bromostyryl)-pyridine,
Ph-CH=CBr-Py-2 (IV)

I was prepared by the dehydrobromination of *threo*-2-stilbazole dibromide. Colorless prisms, m. p. 146.5—147.2°C (Found: Br, 31.08. Calcd. for $C_{13}H_{10}NBr$: Br, 30.73%). UV in heptane: 242 mμ (log ε, 3.90), 290 mμ (3.57). II was prepared either by the action of phosphorus pentabromide upon 2-phenacylpyridine, Ph-CO-CH_2-Py-2, or by hydrogen bromide addition to 2-tolazole, Ph-C≡C-Py-2. Liquid, b. p. 123°C/3 mmHg, n_D^{25} 1.6638. (Found: C, 59.93; H, 3.94; N, 5,50; Br, 30.55. Calcd. for $C_{13}H_{10}NBr$: C, 60.02; H, 3.87; N, 5.38; Br, 30.73%). UV: 220 mμ (4.05), 292 mμ(4.31). III was prepared by the dehydrobromination of *erythro*-2-stilbazole dibromide. Colorless prisms, m. p. 72.7—74.5°C. (Found: C, 60.06; H, 3.98; N, 5.57; Br, 30.69%). UV: 230 mμ (4.12), 286 mμ(3.89). IV was prepared by the action of phosphorus pentabromide upon 2-Pyridyl benzyl ketone, Ph-CH_2-CO-Py-2. Liquid, b. p. 127°C/3 mmHg, n_D^{25} 1.6710. (Found: C, 59.99, H, 4.06; N, 5.34; Br, 30.96%). UV: 223 mμ (4.17), 303 mμ(4.38).

The above-described structures of these isomers were established by the following experiments. (a) The process of preparing II and IV using pentabromide on the -CO-CH_2-group suggests that the bromine atom is combined with α-carbon in II and with β-carbon in IV respectively, and that they are both trans isomers. (b) III is the main product of the dehydrobromination of *erythro*-dibromide in an alcoholic potassium hydroxide solution and is supposed to be cis form as the result of trans elimination. (c) I and III are converted into II and IV respectively when heated at 200°C, while the reverse reactions from II and IV do not occur under the same conditions. (d) All isomers are converted into 2-tolazole by further dehydrobromination. The reactions of I and III are by far slower than those of II and IV. (e) By the reduction of bromine with zinc, II and IV are converted into *trans*-2-stilibazole, Ph-CH=CH-Py-2, almost quantitatively, while I and III are converted into *cis* 2-stilbazole. (f) The bathochromic shifts and remarkable increases in the absorption intensity occur as usual on passing from the cis isomers to the trans isomers.

A cis isomer usually melts at a much lower temperature than a trans isomer does, but in this case the cis isomers are crystal and the trans isomers are liquid. It is also interesting to note that the cis isomer I was the main product obtained from *threo*-dibromide, because the trans elimination of *threo*-dibromide generally gives the trans isomer.

1) J. W. Blood and B. D. Shaw, *J. Chem. Soc.*, **1930**, 504.
2) T. Katsumoto and A. Honda, *J. Chem. Soc. Japan, Pure Chem. Sect.* (*Nippon Kagaku Zasshi*), **84**, 527 (1963).
3) T. Nakajima, *J. Pharm. Soc. Japan* (*Nippon Yakugaku Zasshi*), **77**, 1298 (1957).

The S_N1 Hydrolysis of α-Phenylethyl Chloride Proceeding with the Retention of the Configuration in Binary Mixtures of Phenol and Water

By Kunio OKAMOTO, Masayuki HAYASHI and Haruo SHINGU

Department of Fuel Chemistry, Faculty of Engineering, Kyoto University, Sakyo-ku, Kyoto

(Received December 2, 1965)

In recent publications, Goering and his collaborators[1] have reported that the S_N1 hydrolysis (alkyl-oxygen cleavage) of *p*-chlorobenzhydryl *p*-nitrobenzoate proceeds with an excess retention of the configuration in 80—90% aqueous acetone. Despite extensive investigations of the steric course of S_N1 hydrolysis, no other examples which follow the retained steric course are known for such a system without a configuration-retaining group adjacent to the reaction center. The present report is of significance both because it will present another example of hydrolysis with the retention of configuration for a simple secondary carbon system, and because it can throw light on the hitherto elusive nature of the retention mechanism for this system in general.

Solvolyses of optically active α-phenylethyl chloride (0.106 M) were conducted in 75, 80, and 90 wt.% aqueous phenols in the presence of triethylamine (0.114—0.118 M) for ten half-lives at 30.0°C. The products of the competitive phenolysis and hydrolysis were chromatographed over basic alumina and purified by distillation in vacuo. From the rotations of α-phenylethyl alcohol (α_D, $-1.58°$, $-1.64°$ and $+1.16°$ (neat, 0.5 dm.) for the respective solvolyses) and α-phenylethyl phenyl ether (α_D, $+0.62°$, $+0.76°$ and $-1.97°$, neat, 0.5 dm.) thus obtained, it was found that the configurations of the chlorides (α_D, $-27.39°$, $-26.30°$ and $+27.06°$, neat, 0.5 dm.) were retained for both hydrolysis and phenolysis over the entire solvent range examined. The extents of retention[2] were calculated on the basis of the rotaions of the starting chloride to be 16.3, 17.6 and 12.1% for α-phenylethyl alcohol and 6.08, 7.76 and 19.5% for α-phenylethyl phenyl ether for the respective solvolyses. In previous papers,[3] with regard to phenolyses in various mixtures of phenol and organic solvents (e. g.,benzene, cyclohexane, and acetonitrile), we reported that the formation of α-phenylethyl phenyl ether from α-phenylethyl chloride proceeded with a net retention of configuration, and suggested a mechanism involving a S_Ni-like four-center reaction between a molecule of phenol and the ion-pair intermediate.

For the retention of the steric course of the hydrolysis, we have considered two possible explanations. The shielding by a phenol molecule might be operative from the back-side of the S_N1 intermediate; this concept has been used in explaining the decrease in inversion in the hydroxylic solvents of a higher content of such co-solvents as ether, dioxane, nitrobenzene and acetone.[4] However, this possibility is unlikely since the extent of retention for the α-phenylethyl alcohol shows a decreasing tendency, passing through a maximum value in the solvents with the higher phenol contents. It appears that some intermolecular complexes between water and phenol molecules of different degrees of association favor the front-side attack, as is depicted in the case of the 1 : 2 complex as follows:

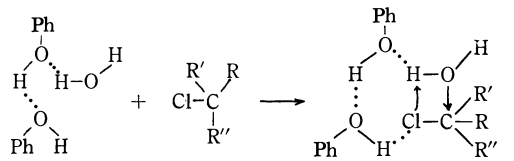

This may be regarded as a detailed expression of the "polymolecular"[5] attack of hydroxylic molecules on the halogen atom in the S_N1 solvolysis.

The details of this work and descriptions of some further extention experiments with methanolic phenol solvents will be published in the near future.

1) a) H. L. Goering, R. G. Briody and J. F. Levy, *J. Am. Chem. Soc.*, **85**, 3059 (1963); b) H. L. Goering and and J. F. Levy, ibid., **86**, 120 (1964).

2) The maximum rotation of the chloride was taken to be 125° (neat, 1 dm.; H. M. R. Hoffman and E. D. Hughes, *J. Chem. Soc.*,**1964**, 1244), and those of α-phenylethyl alcohol and α-phenylethyl ether, as 44.2° (D. J. Cram, K. R. Kopecky, F. Hauck and A. Langemann, *J. Am. Chem. Soc.*, **81**, 5754 (1959)) and 46.6°, Ref. 3b.

3) a) K. Okamoto, K. Takeuchi and H. Shingu, This Bulletin, **35**, 525 (1962); b) K. Okamoto, H. Yamada, I. Nitta and H. Shingu, This Bulletin, **39**, 299 (1966).

4) a) W. v. E. Doering and A. Streitwieser, Jr. Cf. A. Streitwieser, Jr., *Chem. Revs.*, **56**, 571 (1956); b) A. Streitwieser, Jr., and W. D. Schaeffer, *J. Am. Chem. Soc.*, **79**, 6233 (1957); c) A. Streitwieser, Jr., and S. Andreades, ibid., **80**, 6553 (1958); d) H. Weiner and R. A. Sneen, ibid., **87**, 287, 292 (1965).

5) a) L. P. Hammett, "Physical Organic Chemistry," McGraw-Hill Book Co., New York (1940), p. 169; b) K. Okamoto and H. Shingu, This Bulletin, **34**, 1131 (1961).

The Absolute and Relative Stereochemical Correlation of Isoflavanone, Sophorol and Naturally-occurring Isoflavan Derivatives

By Hiroshi SUGINOME

Department of Chemistry, Faculty of Science, Hokkaido University, Sapporo

(Received December 10, 1965)

The absolute and relative stereochemical correlations between corresponding asymmetric centers of optically acitve isoflavanone, sophorol[1] and various chromanocoumarans, including (−) homopterocarpin[2a] (I) X=H, Y=OMe, Z=Me, (−) maackiain[2b] (I) X and Y=methylenedioxy, Z=H and (−) trifolirhizin[11,2c] (I) X and Y=methylenedioxy, Z=-D-glucose, have not yet been defined.

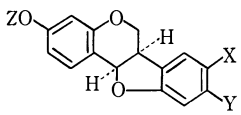

(I)

The optical rotatory-dispersion curves of sophorol, the oxidation product of *O*-methyldihydropterocarpin[3] and *O*-dimethylsophorol, exhibit virtually identical plain positive dispersion curves throughout the spectral range under examination. This result can be taken as conclusive evidence of an identical absolute configuration at C^3 in sophorol and the corresponding asymmetric center[4] of maackiain and the related compounds; it thus confirms previous assumptions.[5] The rotatory-dispersion curves of homopterocarpin, pterocarpin and maackiain all exhibit negative cotton effect curves. In these cases C^3 asymmetric carbon in the chromanocoumaran molecule makes a very weak negative contribution,[6] as is shown in the dispersion curve of dihydro-*O*-methylmaackiain *O*-methylether. Therefore, the relatively strong negative rotation accompanying by the cotton effects in these compounds is probably produced by the C^4 asymmetric center.

Lyle[7] reported that the compounds of the II, III, IV, (I) ephedrine and (−)-ϕ-ephedrine types showed negative cotton effects of a similar shape, and he identified the absolute configuration of (−) halostachine (II) as R on the basis of an unequivocal chemical correlation.[7]

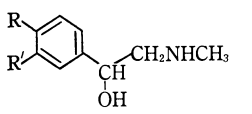

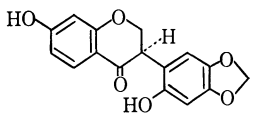

(II) R=R′=H
(III) R=H, R′=OH
(IV) R=R′=OH

(V)

Attention must be drawn to the structural similarity between the asymmetric center of halostachine (II) and the environment of the corresponding asymmetric center of pterocarpin. Although, in the series of compounds in the present case, the aromatic ring is not free to rotate, and the enhancement of the optical activity can be observed,[8] the negative cotton effects by the asymmetric center of the R configuration in halostachine (II) and the C^4 environment of pterocarpin are strong evidence for assuming that the asymmetric centers of these compounds have the same absolute configuration R.

Since the B/C ring junction in pterocarpin is cis,[9] pterocarpin is represented as the C^4R, C^3R, configuration (I). Consequently, all the other chromanocoumarans which have been reported to exhibit negative rotation can be identified as having the C^4R, C^3R, configuration. Since it is apparent from the O. R. D. curve that C^3 in the isoflavan equol[10] and the corresponding asymmetric center of dihydro *O*-methylmaackiain-*O*-methylether have the same absolute configuration, the C^3 center of equol is assigned the R configuration. Therefore, sophojaponicin[11] must have the C^4S, C^3S configuration.

Furthermore, it follows that the absolute configuration of C^3 of sophorol is R (V). The present assignment of the absolute configuration should, however, be examined by an unequivocal chemical correlation.*

1) a) H. Suginome, *J. Org. Chem.*, **24**, 1655 (1959); *Tetrahedron Letters*, **1960** 16.
2) a) E. Späth and J. Schläger, *Ber.*, **73**, 1 (1940). b) H. Suginome, *Experientia*, **18**, 161 (1962). c) J. B. Bredenberg and P. K. Hietala, *Acta. Chem. Scand.*, **936**, 15 (1961); Y. Fujise, T. Toda and S. Ito, *Chem. Pharm. Bull. Japan*, **11**, 167 (1963).
3) A. McGookin, A. Robertson and W. B. Whalley, *J. Chem. Soc.*, **1940** 787.
4) The numbering system of chromanocoumaran was chosen arbitrarily since it is an isoflavone derivative.
5) W. B. Whally, "The Chemistry of Flavonoid Compounds," T. A. Geissman ed., Pergamon Press London (1962), p. 441.
6) The formation of ring compounds from open chains is accompanied by an increase in the optical rotation.[8]
7) G. G. Lyle, *J. Org. Chem.*, **25**, 1779 (1960).
8) W. J. Kauzmann, J. E. Walter and H. Eyring, *Chem. Revs.*, **26**, 339 (1940).
9) H. Suginome and T. Iwadare, *Experientia*, **18**, 163 (1962).
10) G. F. Marrian and D. Beall, *Biochem. J.*, **29**, 1586 (1935).
11) S. Shibata and Y. Nishikawa, *Chem. & Pharm. Bull.*, **11**, 167 (1963).

* After this paper was prepared, Professor S. Ito informed us that he and his colleagues had assigned C^4R, C^3R as the absolute configuration of trifolirhizin on the basis of the chemical correlation.

Isopyrrolnitrin: A Metabolite from Pseudomonas

By Masashi HASHIMOTO and Kiyoshi HATTORI

Research Laboratories, Fujisawa Pharmaceutical Co. Ltd., Higashi-yodogawa, Osaka

(Received December, 13, 1965)

Pyrrolnitrin (I) was isolated as a metabolite of Pseudomonas and its structure established by Arima and others.[1] During our investigation of metabolites of Pseudomonas, an isomer of pyrrolnitrin was found in the acetone extracts of the bacterial cells. First the existence of isopyrrolnitrin has been recognized by silica-gel thin-layer chromatography: R_f-values, 0.50 for pyrrolnitrin and 0.67 for isopyrrolnitrin, as determined by chloroform developing.

Isopyrrolnitrin has been isolated as yellowish crystals; m. p. 105—108°C, mol. wt. 257 by mass spectrometry.

Found: C, 46.82; H, 2.12; N, 11.27. Calcd. for $C_{10}H_6N_2O_2Cl_2$: C, 46.71; H, 2.35; N, 10.90%.

The infrared spectrum shows the presence of a –NH-group (3460 cm^{-1}) and characteristic absorption bands of the nitro group (1515 and 1349 cm^{-1}); the whole pattern of the spectrum is very similar to that of pyrrolnitrin. A color reaction by the Ehrlich reagent is positive (blue-violet). These data have suggested that isopyrrolnitrin has a structure similar to that of pyrrolnitrin. Conclusive information has been obtained from the NMR spectrum; the α-proton of the pyrrole ring appears at 6.76 p.p.m. as a doublet signal (coupling with the NH-proton of pyrrole), a proton adjacent to the nitro group in the benzen ring appears at 7.90 p.p.m. as a quartet signal, the multiplet signals from three protons appear at 7.3—7.7 p.p.m. of the aromatic proton region, and the proton of the NH-group appears at 8.4 p.p.m. as a broad signal (measured in $CDCl_3$ at 60 M c.p.s.). It follows from these data that the structure of isopyrrolnitrin is *o*-nitrophenyl-dichloropyrrole. The infrared absorption band at 743 cm^{-1} also shows that the compound is of a *o*-nitrophenyl substitution type, and the bands appearing in the region of 700—900 cm^{-1} are of a characteristic absorption which is common in the spectra of 2-substituted derivatives of pyrrolnitrin.

As a result of these studies, it may be supposed that the structure of isopyrrolnitrin is 2, 3-dichloro-4-(2'-nitrophenyl)-pyrrole (II). The correctness of this deduction has been proved by the synthesis.

The details will be published later.

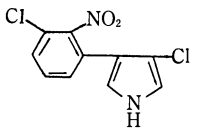

(I)

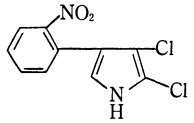

(II)

1) K. Arima, H. Imanaka, M. Kousaka, A. Fukuta and G. Tamura, *Agr. Biol. Chem.*, **28**, 575 (1964).

A New Method for the Synthesis of Alkyl Aryl Sulfides

By Hiroshi YOSHIDA, Saburo INOKAWA and Tsuyoshi OGATA

Department of Synthetic Chemistry, Faculty of Technology, Shizuoka University, Oiwake, Hamamatsu

(Received December 15, 1965)

Alkyl aryl sulfides are generally produced by the condensation of alkyl halides with thiophenolates.[1,2] In previous papers,[3,4] the authors have reported that methyl xanthates, $MeOCS_2R$ (R= Me, Et, *n*-Pr), reacted with triethylamine to form the ammonium salts, $Et_3\overset{\oplus}{N}(Me)\overset{\ominus}{S}COSR$, at room temperature and to form dithiolcarbonates at an elevated temperature. In a similar reaction of *S*-phenyl xanthates with triethylamine, alkyl aryl sulfides were obtained in a good yield, this reaction will be described in this communication.

Upon mixing *S*-phenyl methyl xanthate (I, b. p. 100—102°C/2 mmHg, n_D^{14} 1.6304. Found: S, 34.2%. Calcd. for $C_8H_8OS_2$: S, 34.6%) and triethylamine at room temperature, immediate exotherms were observed with the evolution of carbonyl sulfide gas. After several minutes, methyl phenyl sulfide (b. p. 74.5—75°C/15 mmHg, n_D^{13} 1.5918) was produced in a 93% yield, while the amine remained almost unchanged. The equimolar mixture of I and triethylamine gave, at −20°C after 12 hr. in the form of pale yellow hygroscopic crystals needles (m. p. 57—59.5°C) in only a 3% yield by weight. These crystals were decomposed with aqueous hydrochloric acid to thiophenol, carbonyl sulfide and methyltriethylammonium chloride. Thus the structure of these crystals was concluded to be II (R=Et), similar to that of the salts[3] produced from $MeOCS_2R$ (R=Me, Et, *n*-Pr) and triethylamine. I and trimethylamine in benzene gave, at room temperature after 12 hr., white crystals (m. p. 130—134°C); these crystals showed reactions similar to those of II (R=Et) with aqueous hydrochloric acid. II (R=Me, Et) gave methyl or ethyl phenyl sulfide with methyl or ethyl iodide.

Methyl phenyl sulfide was also produced in a good yield by treating I with II (R=Et) at room temperature or with II (R=Me) at 70°C. These reactions may be summarized as follows:

$$MeOCS_2Ph \xrightarrow[(R=Me,\ Et)]{R_3N} \underset{(I)}{} MeSPh + \underset{(II)}{R_3\overset{\oplus}{N}(Me)\overset{\ominus}{S}COSPh} + COS$$

$$MeOCS_2Ph \xrightarrow{II} MeSPh + COS$$

$$R_3\overset{\oplus}{N}(Me)\overset{\ominus}{S}COSPh \xrightarrow[(R'=Me,\ Et)]{R'I} R'SPh + COS + R_3\overset{\oplus}{N}(Me)\overset{\ominus}{I}$$

Similarly, ethyl phenyl sulfide[5] (b. p. 80—81°C/13.5 mmHg, n_D^{13} 1.5669) was obtained by the catalytic decomposition of *S*-phenyl ethyl xanthate[1] (b. p. 95—97°C/1.5 mmHg, $n_D^{17.5}$ 1.6100) with triethylamine at 80°C with only a small amount of oily ammonium salt.

1) R. Leuckart, *J. prakt. Chem.*, **1890** (ii), **41**, 179.
2) C. M. Suter and H. L. Hansen, *J. Am. Chem. Soc.*, **54**, 4101 (1932).
3) H. Yoshida and S. Inokawa, *J. Chem. Soc. Japan, Pure Chem. Sect.* (*Nippon Kagaku Zasshi*) **86**, 950 (1965).
4) H. Yoshida, S. Inokawa and T. Ogata, ibid., **86**, 1179 (1965).
5) A. I. Vogel, *J. Chem. Soc.*, **1948**, 1820.

The Sulfuryl Chloride Chlorination of Alkyl Silanes. The Electronic Effect of Some Silyl Groups

By Yoichiro NAGAI, Noboru MACHIDA and Toshihiko MIGITA

Department of Chemistry, Gunma University, Kiryu, Gunma

(Received December, 24, 1965)

The free radical halogenation of alkylsilanes is one of the most convenient methods of introducing functional groups into the organic substituents attached to silicon. While much of the work in this field has been expended for synthetic purposes,[1] relatively little is known about the effect of changes in the structure of the silanes on the reactivities of each position of the alkyl groups.[2]

In order to obtain quantitative data on the effect of silyl groups in directing substitution, the sulfuryl chloride chlorination of ethyltrichloro-, ethylmethyldichloro-, ethyldimethylchloro-, *n*-propyltrichloro- and *n*-butyltrichloro-silane has been studied competitively in the presence of toluene.

Table I lists the relative reactivities per hydrogen atom at each carbon atom of those silanes, the aliphatic hydrogen atom in toluene being taken as unity.

Table I.[a] The relative reactivities of C–H bonds in the sulfuryl chloride chlorination of silanes

CH_3–CH_2SiCl_3		CH_3–$CH_2SiMeCl_2$		CH_3[b]–CH_2SiMe_2Cl
0.17	0.15	0.35	0.41	— 0.82

CH_3–CH_2–CH_2SiCl_3			CH_3–CH_2–CH_2–CH_2SiCl_3			
0.27	0.57	0.19	0.25	1.1	0.49	0.09

a) All the experiments were carried out in carbon tetrachloride at the reflux temperature. Product analyses were made by means of vapor-phase chromatography (QF-1, Silicone Grease).

b) The β-chloroethyl compound has not yet been positively characterized.

It may be seen from the table that the values for the methyl groups of *n*-propyltrichlorosilane and *n*-butyltrichlorosilane are very similar, indicating that the trichlorosilyl group exerts only the slightest influence, if any, on the γ- and δ-carbon atoms. Therefore, it follows that the β-position of ethyltrichlorosilane is less reactive, and that of ethylmethyldichlorosilane is more reactive, than ordinary primary hydrogens. From the electrophilic character of chlorination,[2] it is, then, obvious that the trichlorosilyl group is electron-withdrawing and that the methyldichlorosilyl group is electron-releasing. This seems to be the first comment to have been made concerning the electronic effects of those groups.

Another notable feature of the table is the marked decrease in the reactivity of hydrogens on carbons alpha to silicon. In fact, the reactivity ratio of α-methylene to an ordinary methylene is 0.14 (0.15/1.1), 0.37 (0.47/1.1) and 0.75 (0.82/1.1) for ethyltrichlorosilane, ethylmethyldichlorosilane and ethyldimethylchlorosilane respectively. It should be noted, however, that these methylene groups on silicon have only three adjacent C–H bonds capable of stabilizing the incipient α-radicals by hyperconjugation.

There are indications in the literature that radical formation at the alpha position of alkylsilanes is quite difficult relative to that at the beta position. For example, the chlorination of 1, 1-dichlorosilacyclopentane under radical conditions produces more beta than alpha.[3] Similarly, the sulfuryl chloride chlorination of ethylmethyldichlorosilane yields the chloroethyl compounds only, no substitution occurring at the methyl group alpha to silicon.[4]

The reduced possibilities of alpha radicals for hyperconjugation are apparently responsible for these observations.

1) C. Eaborn, "Organosilicon Compounds," Butterworths Scientific Publications, London (1960), p. 379.

2) C. Walling, "Free Radicals in Solution," John Wiley & Sons, New York (1957), p. 369.

3) R. A. Benkeser, Y. Nagai, J. L. Noe, R. F. Cunico and P. H. Gund, *J. Am. Chem. Soc.*, **86**, 2446 (1964).

4) D. T. Hurd, ibid., **67**, 1813 (1945).

BULLETIN OF THE CHEMICAL SOCIETY OF JAPAN VOL. 39 413—417 (1966)

Some Reactions of the Glycidyl Esters of Sulfonic Acids

By Nobuo NAKABAYASHI, Eiichi MASUHARA and Yoshio IWAKURA

Research Institute of Dental Materials, Tokyo Medical and Dental University, Yushima, Bunkyo-ku, Tokyo; Department of Synthetic Chemistry, The Faculty of Engineering, The University of Tokyo, Hongo, Tokyo

(Received March 4, 1965)

1-Chloro-2-hydroxypropyl sulfonates are obtained by the reaction of glycidyl sulfonates with hydrochloric acid at room temperature. They are converted into 1, 3-dichloro-2-propanol by the action of hydrochloric acid at 100°C, or into epichlorohydrin by that of bases. The reaction of glycidyl sulfonates and sodium carboxylates affords glycidyl carboxylates. In the preparation of glycidyl carboxylates, glycidyl sulfonates act as a direct alkylation agent for sodium carboxylates. The addition of amines to the epoxide is carried out at first in the reaction of glycidyl sulfonates and amines. The adducts are converted into glycidyl amines by the action of sodium hydroxide, or into *N*-[β-hydroxypropylene(α, γ)]-ammonium sulfonates by the isomerization, by heating them or letting them stand for a long time. The latter is an intermediate used in preparing 1, 4-dioxane derivatives in the presence of sodium hydroxide.

Glycidyl vinylsulfonate, glycidyl allylsulfonate, and glycidyl β-styrenesulfonate have been prepared and copolymerized with acrylonitrile, styrene and methyl methacrylate to obtain reactive polymers containing a glycidyl sulfonate group.[1-3] During our recent study of the reaction of the copolymers with amines, it has been demonstrated that a ring-opening addition of epoxide competes with a carbon-oxygen bond scission of sulfonate. The latter reaction is unfavorable for the purpose of polymer reaction because of the elimination of the reaction site from the polymers.

The present work was undertaken in order to investigate in more detail the reactions of glycidyl sulfonates with hydrochloric acid, sodium carboxylates and amines.

Results and Discussion

The Preparation of Glycidyl Sulfonates and Their Reaction with Hydrochloric Acid.— Glycidyl esters of methane-, allyl-, 2-propane-, butane-, and *p*-toluenesulfonic acid were prepared from glycidol and the corresponding sulfonyl chlorides. The results are shown in Table I.

$$RSO_2Cl + HOCH_2CH(\diagdown O \diagup)CH_2 \rightarrow RSO_2OCH_2CH(\diagdown O \diagup)CH_2$$

Glycidyl sulfonates reacted with hydrochloric acid to give 3-chloro-2-hydroxypropyl sulfonates in a good yield at room temperature. The results are shown in Table II.

$$RSO_2OCH_2CH(\diagdown O \diagup)CH_2 + HCl \rightarrow RSO_2OCH_2CH(OH)CH_2Cl$$

3-Chloro-2-hydroxypropyl sulfonates afforded 1, 3-dichloro-2-propanol in the reaction with hydrochloric acid at 100°C, whereas they formed epichlorohydrin in the presence of sodium hydroxide or triethylamine. This indicates that the scission of the carbon-oxygen bond of sulfonic ester

Table I. Preparations of glycidyl sulfonates

R	Yield %	B. p. °C/mmHg	Anal. $C_{Calcd.}$	$H_{Calcd.}$	C_{Found}	H_{Found}	n_D^{25}
CH_3	74.5	109—110/1 (lit.[4] 115—116/2)					1.4497
$(CH_3)_2CH$	69.2	113—115/2	40.00	6.71	40.00	6.54	1.4493
n-C_4H_9	70.9	122—123/1	43.29	7.27	43.19	7.24	1.4522
p-$CH_3C_6H_4$	45.0	167—172/2 (lit.[4] 162/1)					1.5243

1) Y. Iwakura and N. Nakabayashi, *Makromol. Chem.*, **66**, 142 (1963).
2) Y. Iwakura, N. Nakabayashi and M. H. Lee, Unpublished results.
3) Y. Iwakura, K. Uno, N. Nakabayashi, T. Tani and W. Y. Chiang, *J. Chem. Soc. Japan, Ind. Chem. Sect.* (*Kogyo Kagaku Zasshi*), **68**, 1222 (1965).
4) K. Ichikawa, *Yûki Gôsei Kagaku Kyôkai Shi*, **22**, 553 (1964).

Table II. Addition of hydrochloric acid to glycidyl sulfonates

R	Yield %	B. p. °C/mmHg	Anal. $C_{Calcd.}$	$H_{Calcd.}$	C_{Found}	H_{Found}	n_D^{25}
CH_3	67	140—141/1	25.47	4.81	25.00	5.10	1.4711
$(CH_3)_2CH$	91	148—150/1.5	33.26	6.05	33.22	6.09	1.4680
$CH_2=CHCH_2$	86	154—156/1	33.57	5.17	33.25	5.35	1.4667
n-C_4H_9	95	150—152/1	36.44	6.55	36.09	6.50	1.4680

Table III. Preparations of glycidyl acetate (Nos. 1—12) and glycidyl methacrylate (No. 13)

No.	R in $RSO_2OCH_2CH(O)CH_2$	g.	Time hr.	Yield g. (%)	The recovered glycidyl sulfonate g. (%)
1	CH_3	3.0	0.5	1.2 (50)	0.8 (27)
2[1]	CH_3	3.0	0.5	—	2.8 (93)
3[2]	CH_3	15.2	0.5	0.6 (26)	12.5
4[3]	CH_3	3.0	11.5	0.3 (13)	2.0 (67)
5	$(CH_3)_2CH$	3.6	0.5	0.4 (17)	2.1 (57)
6	$CH_2=CHCH_2$	3.6	0.5	0.3 (13)	2.5 (69)
7	n-C_4H_9	3.9	0.5	0.3 (13)	2.5 (64)
8	p-$CH_3C_6H_4$	4.6	0.5	0.2 (8.6)	3.2 (70)
9	p-$CH_3C_6H_4$	4.6	0.5	0.2 (8.6)	3.6 (78)
10	p-$CH_3C_6H_4$	4.6	4	0.3 (13)	2.5 (54)
11[1]	p-$CH_3C_6H_4$	4.6	0.5	—	3.6 (78)
12	ECH[4]	1.9	4	<0.1	—
13	CH_3	3.0	0.5	1.2 (42)	0.8 (37)

1) Triethylbenzylammonium chloride was not used.
2) Excess GMS was used as a reagent and solvent.
3) The solvent was water and the catalyst was not used.
4) ECH indicates epichlorohydrin. It was used in place of glycidyl sulfonates.

predominates over that of the carbon-chlorine bond.

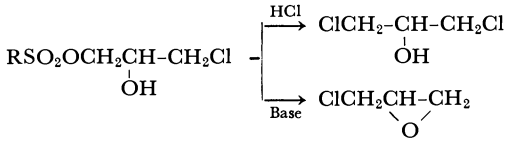

The Reaction of Glycidyl Sulfonates with Sodium Carboxylates.—Next, the preparations of glycidyl carboxylates by the reactions of sodium acetate or sodium methacrylate and glycidyl sulfonates in the presence of a catalytic amount of triethylbenzylammonium chloride[5,6] were studied (Table III).

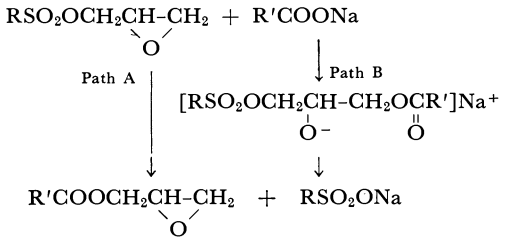

As is shown in the above scheme, there can be considered to be two alternative pathways for the formation of glycidyl carboxylates; namely, the direct displacement of sulfonate by carboxylate (Path A), or the attack of the carboxylate ion on the terminal carbon of the epoxide, thus giving rise to an intermediate alkoxide ion, which subsequently reforms the epoxide by the displacement of sulfonate (Path B), similar as in the case of the reaction of epichlorohydrin with sodium carboxylate.[6] It was found that the reaction of n-propyl methanesulfonate with sodium acetate gave n-propyl acetate in the same yield as in the case of glycidyl acetate. In view of this finding, it may be said that the reaction proceeds through Path A.

5) Y. Iwakura, T. Kurosaki and N. Nakabayashi, *Makromol. Chem.*, **44/46**, 570 (1961).
6) O. Maerker, J. F. Carmichael and W. S. Port, *J. Org. Chem.*, **26**, 2681 (1961).

The Reaction of Glycidyl Sulfonates with Amines.—When glycidyl methanesulfonate (GMS) was allowed to stand with morpholine at 25°C for an hour, the formation of 2-hydroxy-3-(4-morpholinyl)-propyl methanesulfonate (I) was observed by means of a study of the infrared spectrum. The treatment of the reaction mixture (hereafter we will call it the "first stage reaction mixture," which might be composed mainly of I) with sodium hydroxide at 25°C for an hour gave 4-(2, 3-epoxypropyl)-morpholine (III) in a 70% yield. III was also obtained by the reaction of GMS with morpholine in the presence of sodium hydroxide at −5°C for 30 min.

The isomerization of I to 4-[β-hydroxypropylene-(α, γ)]-morpholinium methanesulfonate (II)[4] was observed by the change in the infrared spectrum when the first stage reaction mixture was allowed

Table IV. Reactions of glycidyl sulfonates and amines[1]

No.	R	Amine[2]	H_2O g.	Condition of treatments[3] 1st. °C	1st. hr.	NaOH	2nd °C	2nd hr.	Product,[4]	Yield %
1	CH_3	Mo	trace	25	1	B	25	1	III	70
2	CH_3	Mo	5	−5	1/2	A			III	53
3[5]	CH_3	Mo	5	0	1	A			III	39, IV 25
4	CH_3	Mo	5	80	1/3	A			III	17, IV 35
5	CH_3	Mo	5	25	45	B	75	1/3	IV	45
6	CH_3	Mo	5	80	1/3	B	80	1/3	IV	56
7	CH_3	Mo	5	80	1/3	B	25	1		—[6]
8	$(CH_3)_2CH$	Mo	5	80	1/3	B	90	1/3	IV	53
9	*p*-$CH_3C_6H_4$	Mo	5	80	1/2	B	90	1/4	IV	53
10	CH_3	Py	5	90	1/2	B	90	1/2	V	32
11	CH_3	Pi	5	90	1/2	B	90	1/2	VI	39
12	CH_3	Et	5	25	1	B	25	1	VII	27
13	CH_3	Py	5	0	1/3	B	25	1	VIII	20

1) The reaction was carried out in 0.02 mol. scale.
2) Mo indicates morpholine, Py: pyrrolidine, Pi: piperidine, and Et: diethylamine
3) 1st: First treatment of an aqueous mixture of glycidyl sulfonates and amines.
NaOH: A or B shows that addition of sodium hydroxide to the mixture of glycidyl sulfonates and amines was performed together with 1st or 2nd treatment.
After 1st treatment, 2nd treatment was carried out.
4) III is 1-(2,3-epoxypropyl)-morpholine, IV: 2,5-bis-(4-morpholinylmethyl)-1,4-dioxane, V: 2,5-bis-(1-pyrrolidinylmethyl)-1,4-dioxane, VI: 2,5-bis-(1-piperidinylmethyl)-1,4-dioxane, VII: *N*-(2,3-epoxypropyl)-*N*,*N*-diethylamine, and VIII: 1-(2,3-epoxypropyl)-pyrrolidine.
5) The reaction temperature was raised by the heat of reaction for an instant.
6) A resinous product was obtained.

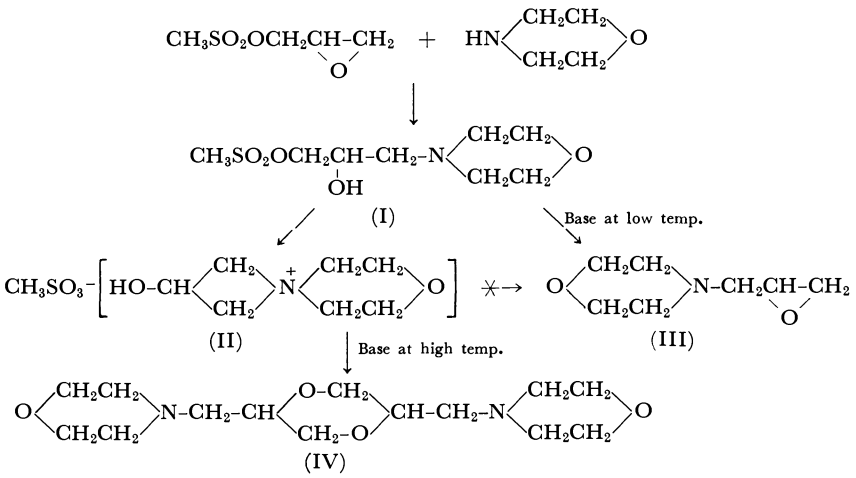

Fig. 1. The process of the reaction of GMS with morpholine.

to stand at 25°C for 45 hr. or at 80°C for 20 min. (we will call the reaction mixture at this stage the "second stage reaction mixture," which might be composed mainly of II). By treating the second stage reaction mixture with sodium hydroxide at 80°C for 20 min., 2, 5-bis-(4-morpholinylmethyl)-1, 4-dioxane (IV) was obtained in a 56% yield. On the other hand, the treatment of the above mixture with sodium hydroxide at 25°C resulted in the formation of a resinous product. The reaction of GMS with morpholine in the presence of sodium hydroxide at 80°C gave a mixture of III (17%) and IV (35%) after 20 min.

Both glycidyl 2-propanesulfonate or glycidyl *p*-toluenesulfonate and morpholine gave IV in a 53% yield when the reaction mixture (after standing at 80°C for 20—30 min.) was treated with sodium hydroxide at 90°C for 15—20 min.

The reaction of piperidine or pyrrolidine with GMS and sodium hydroxide also afforded 2, 5-bis-(1-piperidinylmethyl)-1, 4-dioxane or 1-(2, 3-epoxypropyl)-pyrrolidine and 2, 5-bis-(1-pyrrolidinylmethyl)-1, 4-dioxane, just as in the reaction of piperidine or pyrrolidine with epichlorohydrin.[7,8] By the treatment of GMS with diethylamine and sodium hydroxide, *N*-(2, 3-epoxypropyl)-*N*, *N*-diethylamine was obtained, but no dioxane derivative was detected as was in the reaction of epichlorohydrin with diethylamine and sodium hydroxide.[8,9] The above results are summarized in Table IV.

The process of the reaction of GMS with morpholine may be depicted as Fig. 1.

As the reaction of GMS with morpholine in the presence of sodium hydroxide to give III proceeded faster than that of *n*-propyl methanesulfonate with morpholine to give 4-(*n*-propyl)-morpholine under the same reaction conditions, it seems rational to consider the former reaction to proceed via an intermediate such as I rather than via the direct replacement of the ester group by an amino group. The isomerization of I to II, which was favored in the absence of sodium hydroxide, and the formation of III from I may be considered to be competitive reactions on the basis of the following facts. (1) When the mixture of GMS and morpholine was allowed to stand without sodium hydroxide to afford the second stage reaction mixture, only IV was obtained upon subsequent treatment with sodium hydroxide. (2) On the other hand, when sodium hydroxide was added earlier to the reaction mixture (first stage), III was obtained in a 70% yield. (3) The reaction of GMS with morpholine, carried out in the presence of sodium hydroxide from the beginning at 80°C, gave a mixture of III and IV.

TABLE V. M. P. (B. P.) AND YIELD OF V—VIII

Compound	M. p. (b. p.) °C (°C/mmHg) Found	lit.[8]	Yield %
V	106—108	107.5—109.5	32
VI	102—104	101 —104	39
VII	(58—58.5/19)	(58—60/20)	27
VIII	(61—63/11)	(63—64/12)	20

Experimental

Raw Materials.—Methanesulfonyl chloride, 2-propyl bromide, *n*-butyl bromide, sodium sulfite, phosphorus pentachloride, glycidol and *p*-toluenesulfonyl chloride were commercially available. Sodium 2-propanesulfonate,[10] sodium butanesulfonate, 2-propanesulfonyl chloride (b.p. 83°C/25 mm.; lit.[11] 74.5°C/15 mm.), *n*-butanesulfonyl chloride (b. p. 96°C/16 mm.; lit.[12] 93.5°C/15 mmHg), glycidyl methanesulfonate[4] (GMS) and glycidyl *p*-toluenesulfonate[4] (GTS) were prepared by methods reported previously.

Glycidyl 2-Propanesulfonate (GPS).—To a solution of 22.3 g. (0.301 mol.) of glycidol and 30.3 g. (0.300 mol.) of triethylamine in 200 ml. of dry toluene, there was added, drop by drop, a mixture of 40.7 g. (0.286 mol.) of 2-propanesulfonyl chloride and 20 ml. of dry toluene under cooling in an ice-salt bath. The reaction mixture was then stirred for 3 hr. at room temperature. The triethylamine hydrochloride formed was removed by filtration, and the toluene was distilled off in vacuo. The residue was distilled under reduced pressure to give 35.8 g. of GPS boiling at 114—115°C/1 mmHg. The yield was 69.2%.

2-Hydroxy-3-chloropropyl 2-Propanesulfonate.—A mixture of 7.8 g. of GPS and 20 ml. of concentrated hydrochloric acid was occasionally stirred over a 2 hr. period while being kept at room temperature. The fractionation of the residue after the water had been removed gave 8.5 g. (91%) of 2-hydroxy-3-chloropropyl 2-propanesulfonate boiling at 148—150°C/1.5 mmHg.

Glycidyl Acetate from GMS. — a) A mixture of 3.0 g. (0.02 mol.) of GMS, 1.6 g. (0.02 mol.) of sodium acetate, 0.2 g. of triethylbenzylammonium chloride and 20 ml. of dry toluene was refluxed for 0.5 hr. After the precipitate had been removed by filtration and the toluene had been removed by distillation in vacuo, the fractional distillation of the residue afforded 1.2 g. (50%) of glycidyl acetate (b. p. 71°C/17 mmHg) and 0.8 g. (27%) of GMS.

b) A suspension of 15.2 g. (0.10 mol.) of GMS and 1.6 g. (0.02 mol.) of sodium acetate and 0.2 g. of triethylbenzylammonium chloride was stirred for 0.5 hr. at 110°C. After the precipitate had been removed, the residue was fractionated to give 0.6 g. (26% yield based on the sodium acetate charged) of glycidyl acetate and 12.5 g. of GMS.

c) A suspension of 3.0 g. of GMS and 1.6 g. of sodium acetate in 5.0 g. of water was stirred for 11.5 hr. at

7) R. Rothstein and K. Binovic, *Compt. rend.*, **236**, 1050 (1953).
8) D. L. Heywood and B. Phillips, *J. Am. Chem. Soc.*, **80**, 1257 (1958).
9) J. H. Ross, D. Baker and A. T. Coscia, *J. Org. Chem.*, **29**, 824 (1964).
10) S. Zuffanti, *J. Am. Chem. Soc.*, **62**, 1044 (1940).
11) F. Asinger, W. Schmidt and F. Ebeneder, *Ber.*, **75**, 34 (1942).
12) F. Asinger, F. Ebeneder and E. Bock, ibid., **75**, 42 (1942).

room temperature. The reaction mixture was then extracted with ether. After the ether had been removed, the distillation of the residue gave 0.3 g. (13%) of glycidyl acetate boiling at 57—59°C/11 mmHg and 2.0 g. (67%) of GMS.

Glycidyl Methacrylate from GMS.—Glycidyl methacrylate was prepared exactly as was glycidyl acetate, except that sodium methacrylate was treated with GMS in place of sodium acetate. From 2.2 g. of sodium methacrylate and 3.0 g. of GMS, 1.2 g. (42%) of glycidyl methacrylate (b. p. 84—85°C/15 mmHg) (lit.[5] 85°C/15 mmHg) was obtained and 0.8 g. (37%) of GMS was recovered.

4-(2, 3-Epoxypropyl)-morpholine (III).—a) Under occasional cooling with a dry-ice methanol bath in order to maintain the reaction temperature below 30°C, there were mixed 3.0 g. (0.02 mol.) of GMS and 1.7 g. (0.02 mol.) of morpholine. After the initial exothermic reaction had subsided, the reaction mixture was allowed to stand for an hour at room temperature. The infrared spectrum of the mixture showed a hydroxyl band at 3390 cm.$^{-1}$ and sulfonic ester bands at 1350 and 1170 cm.$^{-1}$, but no epoxide bands. The mixture was then treated, with occasional stirring, with a solution of 0.9 g. (0.023 mol.) of sodium hydroxide in 2 ml. of water for 1 hr. at room temperature. The solution was extracted with ether continuously. After the ether had been removed, the fractionation of the residue afforded 2.0 g. (70%) of III boiling at 93—97°C/12 mmHg (lit.[8] 93—95°C/12 mmHg).

b) Into 3.0 g. (0.02 mol.) of GMS in an ice-salt bath there was stirred a solution of 1.7 g. (0.02 mol.) of morpholine and 1.0 g. (0.025 mol.) of sodium hydroxide in 5.0 ml. of water at −5°C. The reaction mixture was then allowed to stand for 0.5 hr. at this temperature. The other treatment was same as that described above. The yield of III was 1.5 g. (53%).

2, 5-Bis-(4-morpholinylmethyl)-1, 4-dixoane (IV).—a) GMS (3.0 g., 0.02 mol.) was mixed with a solution of 1.7 g. (0.02 mol.) of morpholine in 5 ml. of water under moderate cooling in order to maintain the temperature below 30°C. The mixture was allowed to stand for 20 min. at 80°C. The infrared spectrum of the mixture obtained showed sulfonate ion bands at 1200 and 1030 cm^{-1} and a hydroxyl band at 3220 cm^{-1}; it was essentially identical with that reported by Ichikawa.[4] The above mixture was then treated with 0.9 g. (0.023 mol.) of sodium hydroxide at 80°C for 20 min. and extracted continuously with ether. After the ether had been removed, 1.6 g. (56%) of IV was obtained as a crystalline product. It was recrystallized from ether. The melting point of IV was 107—108°C (lit.[8] 108—110°C).

b) IV was also prepared by the reaction of GPS or GTS with morpholine in a manner similar to that used with GMS (see above). The yield was 53% in both cases.

2, 5-Bis-(1-pyrrolidinylmethyl)-1, 4-dioxane (V), 2, 5-Bis-(1-piperidinylmethyl)-1, 4-dioxane (VI), *N*-(2, 3-Epoxypropyl)-*N*,*N*-diethylamine (VII) and 1-(2, 3-Epoxypropyl)-pyrrolidine (VIII).—The reaction of GMS with the secondary amines was carried out in a manner similar to that used for GMS with morpholine (III and IV).

BULLETIN OF THE CHEMICAL SOCIETY OF JAPAN VOL. 39 417—422 (1966)

Thermal and Radiation Oxidations of Benzene to Phenol in Aqueous Solutions Containing Metal Ions at Elevated Temperatures. VII. The Mechanisms of Phenol Formation as Studied by Stable Isotopes*

By Hiroshi HOTTA, Nobutake SUZUKI and Toshihiko ABE

Takasaki Radiation Chemistry Research Establishment, Japan Atomic Energy Research Institute, Takasaki, Gunma

(Received April 21, 1965)

When benzene was oxidized to phenol in an oxygen-18 enriched aqueous solution of iron and copper sulfates, the oxygen-18 was much concentrated to phenol. The oxygen-18 content depended on the kind of metal ion and on the temperature. This suggests that the oxygen in the phenol produced is donated not only by the molecular oxygen, but also by the water. Therefore, it is assumed for the termination process that phenol is formed by the ionic reactions. Furthermore, when an equimolar mixture of benzene and benzene-d_6 was oxidized, the isotope effect of hydrogen, k_H/k_D, as estimated from the isotopic composition of the phenol produced, was about 1.2. This value seems to be small for the hydrogen abstraction reaction of radicals. Therefore, when we compare these results with the other facts reported previously, the main reaction of the propagation process may be supposed to be the abstraction reaction of hydrogen by phenyl peroxide. In this experiment, it was also found that phenol exchanges hydrogen with water. The rate constant of the exchange reaction was estimated by Bateman's equation. The rate constant is the highest in the ferric sulfate solution.

* Partly Presented at the 15th Symposium on Organic Reaction Mechanisms, Nagoya, October, 1964.

The effects of metal ions on the autoxidation of benzene to phenol in aqueous solutions of iron and copper sulfates have previously been studied in our laboratory.[1-6] The present paper will describe the results of the studies which were carried out by using stable isotopes, i. e., oxygen-18 enriched water, benzene-d_6 and deuterium oxide, in order to confirm the reaction scheme hitherto assumed. The reactions in the oxygen-18 enriched water solution other than phenol formation will be discussed in the following paper, also in this Bulletin.

Experimental

Oxidation Procedure.—Benzene was oxidized in oxygen-18 enriched aqueous solutions of ferrous, ferric and cupric sulfates by the following procedure, described in a previous paper.[2] These sulfate solutions were prepared by dissolving 0.01 M of metal ion.[1] Oxygen-18 enriched water (1.63 oxygen-18 atom %) was obtained from the Weizman Institute of Science, Israel.

One cubic centimeter of benzene was put on 15 cc. of the aqueous phase in a hard-glass tube in a 50 cc. stainless-steel reactor under an oxygen pressure of 30 atm. This system was then heated by a controlled procedure and kept 30 min. at a given temperature. When it was irradiated, a dose of about 13000 r. of cobalt-60 gamma rays was given for 25 min. Some related experiments were also carried out under other conditions for the sake of reference.

The Analysis of Oxygen-18 in Phenol.—Phenol was separated into 30 cc. of water after ether extraction from the above aqueous phase. It was precipitated as tribromophenol by adding 50 cc. of a 0.1 N bromide solution, a solution of potassium bromate and potassium bromide, and 10 cc. of 12 N hydrogen chloride. The precipitate was purified by sublimation at 100°C using the suction of an aspirator. The oxygen-18 content was analyzed using a mass spectrometer according to the method of Rittenburg and Ponticorvo.[7]

The Experiment on Benzene-d_6.—In order to study the isotope effect of hydrogen at the above oxidation, benzene-d_6 (Merck Sharp & Dohme of Canada, Ltd.) was mixed with benzene in the ratio, $C_6H_6 : C_6D_6 : C_6HD_5 : C_6H_2D_4 : C_6H_3D_3 : C_6H_4D_2 : C_6H_5D = 100 : 93.7 : 4.1 : 0.4 : 0.4 : 0.1 : 0.1 : 0.0$, according to mass spectrometry.[8] This benzene mixture was then oxidized in the solutions of natural water by the above oxidation procedure. This ratio did not change for the unreacted benzene within the range of experimental error after oxidation in the present degree of conversion.

After the phenol produced, which was extracted into ether by the previous method,[2] had been separated by gas chromatographic fractionation using the column of PEG 6000 at 170°C, the abundance ratio between various deuterated phenols in the product (cf. Table III) was determined from the mass spectrum on the following assumption. That is, the ion abundance ratio between $C_6H_5O^+$, $C_6H_5OH^+$ and $^{12}C_5{}^{13}CH_5OH^+$ for the mass spectrum of phenol is 2.06 : 100 : 6.69. Since the formation of these ions is independent of hydrogens of the benzene ring, the ratio between $i-1$., i and $i+1$'th peaks ($i=m/e$ of parent peak) is assumed to be the same for the mass spectrum of various deuterated phenols.

Benzene was also oxidized in the solution of deuterium oxide (99.75%, Showa Denko Co., Tokyo) by the same procedure.

Results

Oxygen-18 in Phenol.—Since the previous papers[1-6] have shown that the yield of phenol in

Table I. Atom-% of oxygen-18 in phenol produced at benzene oxidation

No.	Additive	Temp., °C	Atom-% of ^{18}O	Oxygen of phenol from water, F_w, %[d]	Ref.
1	$FeSO_4$	150	0.48	19	2
2	$FeSO_4$	180	0.99	55	2
3[a]	$FeSO_4$	180	0.90	49	2
4[b]	$FeSO_4$	180	0.90	49	4
5	$FeSO_4$	200	0.88	46	2
6	$Fe_2(SO_4)_3$	180	0.93	51	2
7[a]	$Fe_2(SO_4)_3$	180	1.06	60	2
8	$CuSO_4$	200	0.62	30	3
9[a]	$CuSO_4$	200	0.61	29	3
10[b]	$CuSO_4$	200	0.76	39	4
11[b]	$CuSO_4$+Cu-pieces	200	0.53	23	3
12[b]	Cu-pieces	200	0.48	19	3
13[c]	$CuSO_4$	200	0.44	15	4

a) Irradiated run b) Using purified benzene c) The 0.001 M $CuSO_4$ solution
d) Estimated from Eq. i

1) H. Hotta and N. Suzuki, This Bulletin, **36**, 717 (1963).
2) H. Hotta, A. Terakawa, K. Shimada and N. Suzuki, ibid., **36**, 721 (1963).
3) H. Hotta, N. Suzuki and A. Terakawa, ibid., **36**, 1255 (1963).
4) N. Suzuki and H. Hotta, ibid., **37**, 244 (1964).
5) K. Shimada, N. Suzuki, N. Itatani and H. Hotta, ibid., **37**, 1143 (1964).
6) H. Hotta, N. Suzuki, N. Itatani, K. Shimada, ibid., **37**, 1147 (1964).
7) D. Rittenburg and L. Ponticorvo, *J. Appl. Rad. Isotopes*, **1**, 208 (1956).
8) API Mass Spectral Data, Series No. 609, Carnegie Inst. Techn., Pittsburgh (1956).

the oxidation of benzene depends on the kind of metal ions, the impurities in the benzene, irradiation with gamma rays, and so on, the atom percentage of oxygen-18 in the phenol produced was examined in oxygen-18 enriched aqueous solutions at the various conditions listed in Table I. Experiments 3, 7 and 9 were carried out with gamma-ray irradiation. The purified benzene was used for experiments 4, 10, 11 and 12. The purity of the benzene used for the other experiments was the same as was shown in Table I of Part VI.[6] Two grams of copper pieces were added for experiments 11 and 12. Experiment 13 was carried out in an aqueous solution of 0.001 M cupric sulfate. The significance of these conditions is described in the previous paper referred to the last columm of Table I.

For reference, the aqueous solutions of phenol (0.021 M) were also treated by the same procedure as was used in the benzene oxidation under the pressure of either oxygen or nitrogen (30 atm. at 20°C). The results, shown in Table II, show that the content of oxygen-18 in phenol is not changed by the present procedure.

Therefore, the increase in oxygen-18 in Table I is not due to the exchange reaction of oxygen between water and the phenol produced, but to some reaction in the oxidation process of benzene.

Table II. Atom-% of oxygen-18 in treated phenol

No.	Additive	Temp. °C	Atmosphere[a]	Atom-% of ^{18}O
14	None	180	Oxygen	0.21
15	$FeSO_4$	180	Nitrogen	0.21
16	$Fe_2(SO_4)_3$	180	Nitrogen	0.20
17	$Fe_2(SO_4)_3$	180	Oxygen	0.21

a) 30 atm. at 25°C.

This means that some part of the oxygen in the phenol produced does not come from gaseous oxygen but from water during the phenol formation. The percentage of such oxygen given from water, F_w, is estimated by the equation:

$$F_w=\frac{(x-0.20)}{(1.63-0.20)}\times 100 \qquad \text{(i)}$$

as is shown in Table I, where x is the observed value of the atom percentage of oxygen-18 in phenol.

When the results are compared, it may be concluded that 52±3% of oxygen are transferred from water to phenol at 180°C in an aqueous solution of iron sulfates, regardless of ferrous or ferric sulfate, purification of benzene, and irradiation, and that the corresponding percentage is 33±5% at 200°C in an aqueous solution of cupric sulfate.

Table III. Deuterium distribution in phenol

No.	20	21	22	23	24	25
Reactant	$C_6H_6+C_6D_6$	$C_6H_6+C_6D_6$	$C_6H_6+C_6D_6$	C_6H_6	C_6H_6	C_6H_6
Additive	$FeSO_4$	$FeSO_4$	$CuSO_4$	$FeSO_4$	$FeSO_4$	$Fe_2(SO_4)_3$
Medium	H_2O	H_2O	H_2O	D_2O	D_2O	D_2O
Temp., °C	150	180	200	150	180	200
Ratio of products						
C_6H_5OH	100	100	100	100	100	100
C_6H_4DOH	3.9	2.3	2.4	15.8	77.1	66.8
$C_6H_3D_2OH$	1.4	4.0	0.8	2.7	61.4	108.1
$C_6H_2D_3OH$	2.1	15.0	2.8	0.4	25.2	408.5
C_6HD_4HOH	13.2	26.8	16.3	0.0	2.0	40.8
C_6D_5OH	62.5	29.3	62.9	0.0	0.2	2.7
Total of d-phenols	83.1	77.4	85.2	18.9	165.9	626.9
k_H/k_D	1.19	1.28	1.16	—	—	—

No.	26	27	28	28	30
Reactant	C_6H_6	C_6H_5OH	C_6H_5OH	C_6H_5OH	C_6H_5OH
Additive	$CuSO_4$	$FeSO_4$	$FeSO_4$	$Fe_2(SO_4)_3$	$CuSO_4$
Medium	D_2O	D_2O	D_2O	D_2O	D_2O
Temp., °C	200	150	180	200	200
Ratio of products					
C_6H_5OH	100	100	100	100	100
C_6H_4DOH	38.7	4.0	51.0	401.7	46.2
$C_6H_3D_2OH$	12.5	0.6	13.4	724.3	11.6
$C_6H_2D_3OH$	3.3	0.5	1.8	457.9	2.0
C_6HD_4OH	0.3	0.4	0.1	38.0	0.1
C_6D_5OH	0.1	0.0	0.1	2.7	0.0
Total of d-phenols	54.9	5.5	66.4	1624.6	59.9
k_H/k_D	—	—	—	—	—

When experiments 1 and 13 are compared with others, it may be seen that the value of F_w increases with the temperature and with the concentration of metal ions.

Deuterium Distribution in Phenol.—Under the conditions shown in Table III, the benzene mixed with deuterated benzene was oxidized in natural water (experiments 20—32), while benzene without deuterated benzene was oxidized in deuterium oxide (experiments 23—26). For reference, the solution of phenol in deuterium oxide was also treated by the same procedure as was used for the benzene oxidation.

After experimentation, the abundance ratios between various deuterated phenol were determined as to be shown in Table III by the procedure mentioned above. The ratios in experiments 20—22 are quite different from the original benzene mixture. Such deuterium transfer appears to be independent of the oxidation process of benzene, for it also occurs to a considerable extent in the solution of phenol, as is shown for experiments 27—30. The hydroxyl group of phenol formed in deuterium oxide was changed to OH-group during separation of phenol from the aqueous solution, even if it was OD-group (experiments 23—30).

Discussion

Oxygen of the Hydroxyl Group.—It has been assumed that the present autoxidation of benzene is propagated by the abstraction of the hydrogen atom from benzene (reaction 3) as follows:

$$RO_2 + PhH = RO_2H + Ph\cdot \quad (1)$$

$$Ph\cdot + O_2 = PhO_2 \quad (2)$$

$$PhO_2 + PhH = PhO_2H + Ph\cdot \quad (3)$$

$$PhO_2H + M^+ = PhO\cdot + OH^- + M^{2+} \quad (4)$$

$$PhO_2H + M^{2+} = PhO_2 + H^+ + M^+ \quad (5)$$

$$2PhO_2 = 2PhO\cdot + O_2 \quad (6)$$

where M^+ represents a ferrous or cuprous ion, and M^{2+}, a ferric or cupric ion. The initiation process of the peroxide formation (RO_2) is omitted in the present paper.[4]

However, it is not explained in the above reaction scheme how to form phenol from the phenoxy radicals accumulated. The process for it can be interpreted on the basis of the present finding in Table I, by taking the ionic reaction scheme as follows[9,10]:

$$PhO\cdot + M^+ = PhO^{-}\cdot + M^{2+} \quad (7)$$

$$PhO^{-}\cdot + H^+ = PhOH \quad (8)$$

and

$$PhO_2 + M^{2+} = Ph^{+}\cdot + O_2 + M^+ \quad (9)$$

$$Ph^{+}\cdot + O^*H^- = PhO^*H \quad (10)$$

where O* is the oxygen atom from water. The values of F_w in Table I obtained from Eq. i can be interpreted as the result of the competition between reactions 4 and 7 and reactions 5 and 9.

Benzene is not oxidized to phenol in the cupric sulfate solution, even with irradiation at temperatures lower than 180°C, because cuprous ions are immediately oxidized by oxygen if produced by reaction 5.[3,4] The fact suggests that, in the above reaction scheme, the rate of reaction 9 is extremely slow at the lower temperature, because phenol is not formed by the aid of cupric ions, and because reaction 7, another path of phenol formation, can not occur due to the lack of cuprous ions. On the other hand, a considerable amount of phenol is produced at 200°C.[3,4] Therefore, it may be supposed that the rate of reaction 5 is so fast at 200°C that a larger amount of cuprous ions is produced than is consumed by their oxidation. The low value of F_w in Table I suggests that the rate of reaction 9 becomes significant at 200°C, but that it is not so fast as for iron ion to be discussed below.

Since ferrous ions are not oxidized as quickly as cuprous ions,[1] phenol is produced by reaction 7 in the iron sulfate solutions.[2,4] Since the values of F_w in Table I increase between 150°C and 180°C, the rate of reaction 9 is sure to increase in this temtemperature range. This is consistent with the above assumption that the rate of reaction 9 for cupric ions is very dependent on temperature in the same range. Almost all the iron species are ferrous in solutions after the oxidation of benzene.[2] This accumulation of ferrous species is due to the fast rate of reaction 5 and the slow oxidation of ferrous ions rather than to the fast rate of reaction 9. Phenyl peroxides, accumulated by reactions 3 and 5, might be converted to phenoxy radicals by reaction 6, and then to phenol by reaction 7. Therefore, it may be concluded that phenol is mainly produced by reaction 4—7, not by reaction 9, at least at lower temperatures.

The oxygen-18 content in the phenol produced in Table I, is larger in iron sulfate solutions than in a 0.01 M cupric sulfate solution as well as in a 0.001 M cupric sulfate solution. The concentration of iron species in iron sulfate solutions at 180°C (experiments 2, 3, 4, 6 and 7) is about 0.0002 M due to the precipitation of ferric oxides.[1,2] This means that iron ions are much more reactive than copper ions in the present process, and that the rate of reaction 9 for ferric ions is quite different from that for cupric ions.

Recently, Vysotskaya reported that the phenol which was produced by hydrogen peroxide in the presence of ferrous or ferric ions in oxygen-18 enriched water contained some of oxygen-18.[11] Although this is of much interest in relation to the

9) A. V. Tobolosky and R. S. Mesrobian, "Organic Peroxides," Interscience Publ., New York (1954), p. 103.
10) K. U. Ingold, *Chem. Revs.*, **61**, 563 (1961).
11) N. A. Vysotskaya, *Zh. Fis. Khim.*, **38**, 1688 (1964).

present study, it must be noted that phenol is produced through the non-chain process at room temperature, not through the chain process as in the present study.

The Isotope Effect of Hydrogen on Benzene Oxidation.—The isotope effect of hydrogen on the oxidation of deuterated benzene might prove the abstraction reaction of the hydrogen atom from benzene by a free radical (reaction 3), because the reactions above-mentioned scheme are independent of the dueterium atom except reaction 3. For this purpose, since the conversion of benzene is very low in the present study, the rate-constant ratio, k_H/k_D, is estimated for experiments 20—22 in Table III by the equation:

$$\frac{k_H}{k_D}=\frac{(C_6H_5OH)}{(C_6H_6)}\times\frac{\sum_{i=1}^{5}(C_6H_iD_{6-i})}{\sum_{i=1}^{4}(C_6H_iD_{5-i}OH)} \qquad \text{(ii)}$$

Although the isotope effect or the rate-constant ratio, k_H/k_D, is usually larger than the values in Table III, i. e., about 1.2, for the hydrogen abstraction reaction by free radicals, the reactions with the smaller activation energy have the smaller isotope effect.[12] The rate of the autoxidations is mainly controlled by the rate of the abstraction reaction by peroxides, as in reaction 3. However, it is very difficult in the present system to obtain an activation energy which is physically meaningful, due to the complexity of the pre-equilibration between reactants related to the reaction in question. At any rate, the temperature-dependent coefficient apparently corresponds to about 10 kcal./mol. between 150°C and 180°C for the oxidation of purified benzene in the aqueous solution of ferrous sulfate, judging from the result reported previously.[4] The value obtained by Terakawa et al. is 6 kcal./mol.[13] Both values are smaller than the value for the autoxidation of parrafins, 15 kcal./mol.[14]

It is confirmed that the formation of phenol in the aqueous solution of benzene at room temperature, by radiation and the Fenton's reagent, is to be attributed to the addition reaction of the hydroxyl radical.[15,16] On the other hand, the present chain autoxidation of benzene at elevated temperatures cannot be understood by the same mechanisms due to the following facts. a) No ferric ions are reduced in the mechanisms of the Fenton's reagent, but almost all the iron species are ferrous after the present experimentation.[2] Especially, in the presence of oxygen, it is very difficult to see how ferric ions are reduced. b) The yield of phenol increases abruptly above 170°C.[4] This fact cannot be interpreted without assumption of reactions 1 and 3, because the yield of the hydroxyl radical cannot increase like the yield of phenol. c) The effect of the impurities in benzene indicates that the initiation of the present process is not the direct reaction between benzene and hydroxyl radical.[4] Therefore, reaction 1 must be assumed at first for the oxidation of benzene.

The Exchange Reaction of Hydrogen.—As has already been shown in the section on "Results," the isotopic composition of the phenol produced in Table III is quite different from that of the original benzene mixture. This is due to the exchange reaction of hydrogen between phenol and water, which is independent of the oxidation process of benzene.

Phenol makes phenolate with ferric ions, not with ferrous or cupric ions, so phenol is usually analyzed qualitatively as ferric phenolate. It has been reported that phenol in deuterium oxide exchanges the hydrogen atom of *o*- and *p*-positions only and hydroxyl group with water.[17] On the other hand, in Table III, the exchange of the hydrogen atom is extremely high in the ferric sulfate solution (experiments 28—30), and the phenol having more than three deuterium atoms is very little. Therefore, it may be concluded that the formation of a Ph-O-M bond (M=metal ion) induces the hydrogen exchange of the *o*- and *p*-positions electronically.

Since the exchange reaction of hydrogen is consecutive, as in:

$$\underset{(N_1)}{C_6H_5OH}\xrightarrow[k_1]{}\underset{(N_2)}{C_6H_4DOH}\xrightarrow[k_2]{}\underset{(N_3)}{C_6H_3D_2OH}\xrightarrow[k_3]{}\underset{(N_4)}{C_6H_2D_3OH}\xrightarrow[k_4]{} \qquad (11)$$

the rate constant of the exchange reaction for the i'th deuterium atom, k_i, can be estimated by Bateman's equation[18]:

$$N_1=N_{01}e^{-k_1t} \qquad \text{(iii)}$$

$$\frac{N_i}{N_{01}}=\frac{k_1k_2k_3\cdots k_{i-1}}{(k_2-k_1)(k_3-k_1)(k_4-k_1)\cdots(k_i-k_1)}e^{-k_1t}+\frac{k_1k_2k_3\cdots k_{i-1}}{(k_1-k_2)(k_3-k_2)\cdots(k_i-k_2)}e^{-k_2t}+\cdots+\frac{k_1k_2k_3\cdots k_{i-1}}{(k_1-k_i)(k_2-k_i)\cdots(k_{i-1}-k_i)}e^{-k_it} \qquad \text{(iv)}$$

where N_i is the number of phenol molecules attacked by the i'th deuterium atom at time $t=t$, which is N_{01} at $t=0$.

The rate constants shown in Table IV are

12) K. B. Wiberg, *Chem. Revs.*, **55**, 713 (1955).
13) A. Terakawa, Y. Hosaki, M. Nitto and T. Hirayama, *J. Chem. Soc. Japan, Ind. Chem. Sect.* (*Kogyo Kagaku Zasshi*), **66**, 80 (1963).
14) G. H. Twigg, *Chem. Eng. Sci.*, **1954**, 3 Spec. Suppl., 5.
15) L. M. Dorfman, I. A. Taub and R. E. Bühler *J. Chem. Phys.*, **36**, 3051 (1962).
16) J. R. L. Smith and R. O. C. Norman, *J. Chem. Soc.*, **1963**, 2897.
17) A. Murry and D. L. Williams, "Organic Syntheses with Isotopes," Part II, Interscience Publ., New York (1958), p. 1652.
18) H. Bateman, *Proc. Cambridge Phil. Soc.*, **15**, 423 (1910).

estimated for experiments 27—30 by the above equations from the observed values listed in Table III on the assumption that the reaction time, t, is 1800 sec. Since the true time should be longer than this time because of some contribution of the reaction during heating and cooling,[1,2] the corrected rate constants would be faster than the present values. This increase would be ten percent at most. Furthermore, since the sulfate solutions containing benzene or phenol become a ferrous and ferric mixture at elevated temperatures, regardless of whether they are ferrous or ferric originally,[2,5] the true rate should be faster for ferric ions and slower for ferrous ions than the present values. For the cupric sulfate solution, the contribution of cuprous ions can be ignored because of their fast autoxidation.[3]

In comparing the rate constants in Table IV, it can be seen that the first rate constants, k_1, are not very different from the second rate constants, k_2, but are larger than the third rate constants, k_3. However, the accuracy of the third rate constants is the lowest.

Table IV. Rate constants of exchange reaction of hydrogen in sec^{-1}

No.	27	28	29	30
k_1	2.97×10^{-5}	2.83×10^{-4}	1.58×10^{-3}	2.57×10^{-4}
k_2	3.00×10^{-5}	2.60×10^{-4}	1.20×10^{-3}	2.58×10^{-4}
k_3	1.70×10^{-5}	1.35×10^{-4}	0.65×10^{-3}	2.49×10^{-4}

The authors wish to express their appreciation to Miss Reiko Kiritani of the Radiation Center of Osaka Prefecture, Sakai, for her kind guidance and co-operation in oxygen-18 analysis, and to Mrs. Nobue Itatani of JAERI for her preliminary experiments on oxygen-18.

BULLETIN OF THE CHEMICAL SOCIETY OF JAPAN VOL. 39 422—425 (1966)

The Transfer of the Oxygen Atom of Water in an Aqueous Solution of Iron and Copper Sulfates*

By Nobutake SUZUKI, Hiroshi HOTTA and Hitoshi HASHIMOTO

Takasaki Radiation Chemistry Research Establishment, Japan Atomic Energy Research Institute, Takasaki, Gunma

(Received April 21, 1965)

When an oxygen-18 enriched aqueous solution of ferrous, ferric and cupric sulfates was heated between 130 and 200°C, the oxygen-18 content decreased in the order of $Fe^{II} > Fe^{III} > Cu^{II}$ in water; and it increased in the sulfate group and in the molecular oxygen of the gaseous phase. A transfer of oxygen from water to the sulfate group was also observed, even in a nitrogen atmosphere. The oxygen transfer was promoted in all the cases in the presence of molecular oxygen, and it increased further in the presence of benzene. Since the exchange reaction of oxygen does not occur between water and sulfate ions, the above facts may be attributed to the reactions between water and the thermal decomposition products of the sulfate group, and between water and the hydrogen peroxide produced. The peroxy species, produced by the oxidation of the decomposition products, are more reactive in such a transfer of oxygen, since the reaction is promoted in the presence of oxygen. The peroxides in the autoxidation of benzene seem also to be reactive in it.

The oxidation reaction of benzene to phenol in aqueous solutions of ferrous, ferric and cupric sulfates has previously been studied in our laboratory.[1-3] We showed that some of the oxygen atoms of the phenol produced originated in the water, using oxygen-18 enriched water.[4] In connection with this, the phenomena of the oxygen transfer in the oxygen-18 enriched aqueous solutions of these sulfates, which were studied with and without benzene, will be described in the present paper. Some properies of these solutions, studied without benzene under the same conditions as in the benzene oxidation, had already been reported in a previous paper.[5]

Experimental

Procedure.—The solutions of ferrous, ferric and cupric sulfates were prepared by dissolving 0.01 M of

* Thermal and Radiation Oxidations of Benzene to Phenol in Aqueous Solutions Containing Metal Ions at Elevated Temperatures. VIII.

1) H. Hotta, A. Terakawa, K. Shimada and N. Suzuki, This Bulletin, **36**, 721 (1963).

2) H. Hotta, N. Suzuki and A Terakawa, ibid., **36**, 1255 (1963).

3) N. Suzuki and H. Hotta, ibid., **37**, 244 (1964).

4) H. Hotta, N. Suzuki and T. Abe, ibid., **39**, 417 (1966).

5) H. Hotta and N. Suzuki, ibid., **36**, 717 (1963).

metal ion in oxygen-18 enriched water (1.63 oxygen-18 atom%) obtained from the Weizman Institute of Science, Israel. These solutions were treated by the same procedure as was used in a previous paper.[5] That is, 15 cc. was put in a hard-glass tube in a 50 cc. stainless-steel reactor at an oxygen pressure of 30 atm. This system was then heated by a controlled heater and kept for 30 min. at a given temperature. Some of the experiments were performed under other conditions (see Table I). For example, experiments 44—47 were carried out at a nitrogen pressure of 30 atm., while 1 cc. of benzene was added for experiments 48—50. The experiments for the cupric sulfate solution were carried out only at 200°C under various conditions; experiment 40 was carried out under the standard condition described above; for experiment 40 the 0.001 M solution was used instead of the 0.01 M solution; experiment 42 was carried out in the presence of copper metal pieces alone[2]; and a 0.1 N sulfuric acid solution of 0.01 M cupric sulfate was used for experiment 43.

Although oxygen-18 7.56-atom-% enriched water was used to measure the change in the oxygen-18 content in the gaseous phase, the value in Table I is corrected as measured in 1.63-atom-% enriched water.

Analytical.—The oxygen-18 content in the water was determined as the atom percentage of oxygen-18 by the mass spectrum of carbon dioxide after equilibration with it by shaking it at 30°C for four hours.[6]

The oxygen-18 content in the sulfate group was also determined by the mass spectrum of carbon dioxide according to the method of Rittenburg and Ponticorvo after it was precipitated as barium sulfate and dried in vacumm for 48 hr.[7,8]

Although the observed values for the original enriched water as the standard fluctuated within ± 0.02 atom %, the decrements after experimentation were in good agreement within ± 0.001 atom% between the different runs. Therefore, the decrements or the differences between the values after and before experimentation are shown in the present paper.

Since the decomposition of the sulfate group must be expected at higher temperatures,[5] its concentration in the solutions after the above procedure was determined roughly as the residual ratio of the sulfate group:

$$R = \frac{(BaSO_4)_{treated}}{(BaSO_4)_{untreated}} \times 100 \qquad (i)$$

where $(BaSO_4)_{untreated}$ and $(BaSO_4)_{treated}$ represent the weights of dry barium sulfate precipitated from 50 cc. of the original and treated solutions respectively.

Results

The Decrements of the Oxygen-18 Atom Percentage in Water.—The results are shown in Table I. The decrements in the ferrous sulfate solution mount with increasing temperature (experiments 31—35). The decrements in the ferric sulfate solution are somewhat smaller than in the ferrous solution. When the solution was irradiated by 13000 r. of cobalt-60 gamma rays,[5] the decrements were nearly the same or a little larger than in the unirradiated solutions (experiments 37 and 39). The decrement in the cupric sulfate solution is smaller than in the iron sulfate solutions.

The results in 0.1 N sulfuric acid solutions are not very different from those in aqueous solutions (experiments 34 and 43); the effect of sulfuric acid is considerable in a nitrogen atmosphere (experiment 47).

The results in Table Ib) show that the decrement is appreciable even in a nitrogen atmosphere, although it is smaller than in an oxygen atmosphere. The results in Table Ic) will be discussed later.

Oxygen-18 in the Sulfate Group.—The increments of the oxygen-18 atom percentage in the sulfate group, less by 0.20 than the observed value, are shown in Table I. They are larger in an oxygen atmosphere than in a nitrogen atmosphere, except in the cupric sulfate solution (experiment 46). The value in the presence of benzene is the largest among experiments 40, 46 and 50.

Iron sulfates are precipitated as ferric oxides at temperatures higher than 150°C in aqueous solutions[5] while few precipitates are found in an aqueous solution of cupric sulfate, even at 200°C. However, the concentration of the sulfate group in the iron sulfate solutions does not decrease so much as iron ions are precipitated, as is shown by the residual ratio of Eq. i in Table I.

Discussion

The results in Table Ib) show that there is some exchange reaction of oxygen between water and the sulfate group, independent of the presence of molecular oxygen. Brodsky and Vysotskaya have suggested the following scheme:

$$-X{=}O + H_2O^* \rightarrow -X\begin{matrix}O^*H\\OH\end{matrix} \rightarrow -X{=}O^* + H_2O \qquad (1)$$

for a similar reaction.[9] Since the exchange of the oxygen atom does not occur between water and sulfate ions,[10] the transfer of oxygen may be supposed to be due to the reaction not with the sulfate ion but with the sulfur trioxide produced by the thermal decomposition of the sulfate group; that is, the reaction may be similarly assumed to be:

$$MSO_4 \rightarrow MO + SO_3 \qquad (2)$$

$$\begin{matrix}O\\O\end{matrix}\!\!>\!S{=}O + H_2O^* \rightarrow \begin{matrix}O\\O\end{matrix}\!\!>\!S\!<\!\begin{matrix}O^*H\\OH\end{matrix} \qquad (3)$$

6) M. Cohn and H. C. Urey, *J. Am. Chem. Soc.*, **60**, 679 (1938).
7) D. Rittenburg and L. Ponticorvo, *J. Appl. Rad. Isotopes*, **1**, 208 (1956).
8) I. Maass, *Kernenergie*, **5**, 402 (1962).
9) A. E. Brodsky and N. A. Vysotskaya, *Zh. Fis. Khim.*, **32**, 1521 (1958).
10) T. C. Hoering and J. M. Kennedy, *J. Am. Chem. Soc.*, **79**, 56 (1957).

Table I. Change of oxygen-18 atom percentage and residual ratio of sulfate

No.	Sulfate	Temp °C	Decrement in water	Increment in SO_4	Residual ratio of SO_4, R, %	Increment in gas phase	Remark
	a) Aqueous solutions under oxygen pressure						
31	$FeSO_4$	130	0.006	—	—	—	—
32	$FeSO_4$	150	0.010	—	—	—	—
33	$FeSO_4$	180	0.015	0.78	85	0.0012	—
34	$FeSO_4$	180	0.014	—	—	—	0.1 N H_2SO_4 soln.
35	$FeSO_4$	200	0.014	—	—	—	—
36	$Fe_2(SO_4)_3$	150	0.006	—	—	—	—
37	$Fe_2(SO_4)_3$	150	0.007	—	—	—	Irradiated
38	$Fe_2(SO_4)_3$	180	0.013	1.07	85	—	—
39	$Fe_2(SO_4)_3$	180	0.014	—	—	—	Irradiated
40	$CuSO_4$	200	0.011	0.53	94	0.0018	—
41	$CuSO_4$	200	0.002	—	—	—	0.001 M $CuSO_4$
42	Cu-metal pieces	200	0.001	—	—	—	No sulfate
43	$CuSO_4$	200	0.009	1.09	97	—	0.1 N H_2SO_4 soln.
	b) Aqueous solutions under nitrogen pressure						
44	$FeSO_4$	180	0.009	0.12	89	—	—
45	$Fe_2(SO_4)_3$	180	0.006	0.94	83	—	—
46	$CuSO_4$	200	0.004	0.68	91	—	—
47	$CuSO_4$	200	0.007	0.96	96	—	0.1 N H_2SO_4 soln.
	c) Aqueous solutions with benzene under oxygen pressure						
48	$FeSO_4$	180	0.022	—	—	—	—
49	$Fe_2(SO_4)_3$	180	0.020	—	—	—	—
50	$CuSO_4$	200	0.015	0.97	98	0.0018	—

In fact, the increment of the oxygen-18 content in the sulfate group is larger in experiment 45 than in experiment 46 (in the order of the unstability of sulfates) and larger in experiment 47 than in experiment 46 (in the order of the concentration of the sulfate group). It is also explained by reactions 2 and 3 why the concentration of the sulfate group does not decrease in spite of the precipitation of ferric oxides, as is shown by the residual ratio of Eq. i. However, the result of experiment 44 is still obscure.

When the results in the oxygen and nitrogen atmospheres are compared, it may be seen that the transfer of the oxygen atom from water is promoted in the oxygen atmosphere, although the oxygen atom is not necessarily transferred from water to the sulfate group. Although the thermal decomposition of iron sulfates is independent of the presence of the molecular oxygen,[5] the decomposition products from the sulfate group are oxidized to peroxy acids, which are capable of exchanging oxygen with water, in the presence of oxygen.[11-13]

It has been assumed so far that hydrogen peroxide is formed in the oxygenated solution of iron and copper sulfates, as a result of the reaction:[1,14]

$$O_2 + M^+ = O_2^- + M^{2+} \quad (4)$$

Furthermore, it is known that the oxygen exchange reaction between hydrogen peroxide and water is induced in the presence of iron and copper ions (which are represented by M^+):

$$HOOH + M^+ = MOOH + H^+ \quad (5)$$

$$MOOH + H_2O^* = HOO^*H + MOH \quad (6)$$

and that reaction 6 is also induced by sulfur trioxide.[15,16] The oxygen exchange reaction might also occur between water and sulfur peroxides resulting from the oxidation of the decomposition products, in a manner similar to reaction 6.[10,13] These products, labeled by oxygen-18 as the result of these exchange reactions, namely, the labeled hydrogen peroxide and sulfur peroxides, provide not only the labeled sulfate and molecular oxygen, but also various products containing oxygen-18 which were not detected in the present study. In fact, even in experiment 46, the amount of oxygen-18 transferred from water (0.6 mg.) is fairly large in comparison with that transferred to the sulfate group (0.1 mg.); the amount transferred into gaseous oxygen, in experiment 40, is 0.1 mg. at most.

In summarizing the above discussion, the oxygen transfer reactions from water may be classified

11) J. M. Monger and O. Redlich, *J. Phys. Chem.*, **60**, 797 (1956).
12) M. Tsao and W. K. Wilmarth, ibid., **63**, 346 (1959).
13) C. R. Giuliano, N. Schwarz and W. K. Wilmarth, ibid., **63**, 353 (1959).
14) G. Czapski and M. Dorfman, ibid., **68**, 1169 (1964).
15) M. Anbar, *J. Am. Chem. Soc.*, **83**, 2031 (1961).
16) M. Anbar and S. Guttmann, ibid., **83**, 2035 (1961).

into 1) reaction 3 through the thermal decomposition products of the sulfate group, independent of the presence of molecular oxygen; 2) some reactions through peroxy products from the above decomposition products in the presence of oxygen; and 3) reaction 6 through the formation of hydrogen peroxide.

As was pointed out in the foregoing paper,[4] the concentration of iron species in the solution is about 0.0001 M at 180°C and 200°C as a result of the precipitation of ferric oxides.[5] Although this is much smaller than in experiment 41 (0.001 M $CuSO_4$), the observed value of the decrement of the oxygen-18 content in water is much larger in experiments 33 and 38 than in experiment 41. The efficiency for the decrement is in the order of $Fe^{II} > Fe^{III} > Cu^{II}$. This suggests that the oxidation of metal ion, as well as the decomposition of sulfate, plays an important role in the transfer of the oxygen atom from water.

The Effect of Benzene Oxidation.—The results in Table I c) show that the decrement of the oxygen-18 content in water increases in the presence of benzene by 0.007 atom% at 180°C in either ferrous or ferric sulfate, and by 0.004 atom% at 200°C in cupric sulfate, in addition to the decrement when there is no benzene (Table I a), (experiments 33, 38 and 40), and that the increment of the oxygen-18 content in the sulfate group also increases considerably (experiments 40 and 50).

Since phenyl peroxide and its hydroperoxide are accumulated in the chain process of the benzene oxidation,[4] the above effect may be attributed to some reaction with them. For example, phenyl peroxide and its hydroperoxide might exchange oxygen with water in a manner similar to reaction 6:

$$PhOOM + H_2O^* = PhOO^*H + MOH \qquad (7)$$

When M is sulfur trioxide, it may give the labeled sulfate group or its precursor.

When the results in Table I a) are compared with those in the previous papers,[1-3] it may be seen that a large amount of benzene is oxidized to phenol when the decrement of the oxygen-18 content in water is greater than 0.010 atom% in Table I, independent of the other conditions. This suggests that the initiation process of the benzene oxidation is related to one of the oxygen-transfer process discussed above. Especially, the oxidation of benzene above 180°C in the unirradiated ferric and cupric sulfate solutions is considered to be initiated by the decomposition products of the sulfate group and their peroxides, since such decomposition is confirmed by the present study using oxygen-18. It has been reported that various aromatics, as well as benzene, are oxidized by sulfuric acid[17] and aqueous sulfate[18], which are decomposed to oxidizing reagents.

17) M. Kilpatrick, M. W. Meyer and M. L. Kilpatrick, *J. Phys. Chem.*, **64**, 1433 (1960).
18) W. G. Toland, *J. Am. Chem. Soc.*, **82**, 1911 (1960).

BULLETIN OF THE CHEMICAL SOCIETY OF JAPAN VOL. 39 425—428 (1966)

The Spectrophotometric Determination of Iron(III) with Methylthymol Blue

By Kôichi TONOSAKI

Department of Chemistry, Faculty of Literature and Science, Hirosaki University, Hirosaki, Aomori

(Received May 13, 1965)

The reaction between iron(III) and methylthymol blue has been studied spectrophotometrically in an attempt to establish the optimum conditions for determining small amounts of iron. Depending on the acidities of a solution, iron(III) reacts with methylthymol blue to form one of two complexes. The 1-to-1 complex, which has its maximum absorbance in the acidity range from 0.07 to 1.00 M with respect to perchloric acid, has an absorption maximum at about 580 mμ against a reagent blank. The 1-to-2 (metal-reagent ratio) complex, which has its maximum absorbance in the pH range from 4.5 to 5.5, has an absorption maximum at about 520 mμ against a reagent blank. With either complex, Beer's law is obeyed over the range from 5 to 50 μg. of iron(III) in 25 ml. of complex. The apparent molar extinction coefficients of the two complexes at their absorption maxima were calculated to be 15000 and 14000 respectively (the former, at 0.08 M HClO; the latter, at pH 5). According to Sandell's notation, the sensitivities of the reactions are 0.004 μg. of iron(III) per cm^2 at 580 mμ and 0.005 μg. of iron(III) per cm^2 at 520 mμ respectively. The effect of diverse ions was examined with a solution containing iron(III) and 25 cations.

* This work was presented at the 12th Annual Meeting of the Japan Society for Analytical Chemistry, Kanazawa, October, 1963.

Methylthymol blue was first prepared by Körbl et al.[1] It has since been widely used as a universal metallochromic indicator in complexometric titrations. The color reaction between this reagent and such metal cations as zirconium(IV),[2,3] yttrium(III),[4] lanthanum(III),[4] mercury(II),[5] thorium(IV),[6,7] and gallium(III)[8] has been studied spectrophotometrically in determining these cations.

It has been found that, depending on the acidity of a solution, iron(III) reacts with methylthymol blue to form two complexes, with metal-ligand ratios of 1 to 1 and 1 to 2, and that these reactions are applicable to the spectrophotometric determination of iron. The proposed metho dis very sensitive; it is comparable in sensitivity with the method using xylenol orange,[9] ferron,[10] hydrazinophthalazine,[11] or salicylaldoxime.[12]

Experimental

Reagents.—*The Standard Ferric Perchlorate Solution.*—This was prepared by dissolving the freshly-precipitated ferric hydroxide in hot 4.5 M perchloric acid and then diluting it with water to make the solution about 0.01 M with respect to iron. The solution was standardized by the complexometric titration[13] using α-pyridyl-β-azonaphthol as an indicator. Working solutions of iron were then prepared by diluting the standard solution with distilled water.

Methylthymol Blue Solution.—A 1×10^{-3} M methylthymol blue solution was prepared by dissolving the Dotite MTB reagent (disodium salt), which was used without further purification, in distilled water.

An acetate buffer solution and nitric acid were used for the adjustment of the pH values. Solutions of diverse ions were prepared by dissolving the respective compounds (all reagent-grade chemicals) in distilled water in appropriate concentrations.

Apparatus.—A Hitachi spectrophotometer, model EPV-2, was employed, with 1 cm. cells for all the absorbance measurements. A Hitachi glass-electrode pH meter, model EHP-1, was employed for all the pH determinations.

Results and Discussion

Absorption Curves.—The absorption curves of the solutions containing iron(III) and methylthymol blue at different acidities are shown in Figs. 1 and 2. These curves were obtained by measuring the absorbance of the colored solutions against a reagent blank which contained the same amount of methylthymol blue.

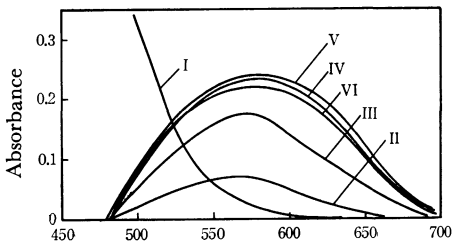

Fig. 1. Absorption curves of methylthymol blue and its iron complex at various acidities.
Iron: 26.8 μg.; MTB: 1.96×10^{-4} M
I: MTB vs. water at pH 0-6; II: Iron complex vs. a reagent blank
$HClO_4$ concn.: II 0.30 M; III 0.20 M; IV 0.15 M; V 0.08 M; VI 0.05 M

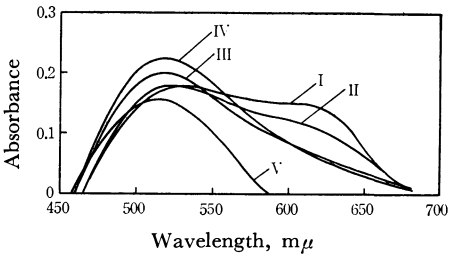

Fig. 2. Absorption curves of the iron-methylthymol blue mixture at various acidities.
Iron: 26.8 μg., Reference: a reagent blank
pH value: I 2.5; II 3.0; III 4.0; IV 4.5—5.5; V 6.5

When the concentration of perchloric acid is 0.05 to 0.20 M, the solutions give essentially identical absorption curves, with an absorption maximum at about 580 mμ. Above pH 2, the position of the maximum absorption shifts toward shorter wavelengths with the increase in the pH value. The curves obtained at pH 2.5 and 3.0 have a shoulder at about 610 mμ. Between pH 3.5 and 6.5, however, the solutions give absorption curves with an absorption maximum at about 520 mμ. Therefore, it may be concluded that, in the presence of an excess of methylthymol blue, two complexes are formed between iron(III) and the reagent.

The Effect of the Acidity.—The effect of the acidity on the absorbance of the solution was examined by measuring, at two wavelengths, 580 and 520 mμ, the absorbance of a solution containing 26.8 μg. of iron and a 5- to 10-fold excess of methylthymol blue. From the curves shown

1) J. Körbl and R. Pribil, *Collection Czech. Chem. Commun.*, **23**, 873 (1958).
2) V. F. Lukyanov and E. M. Knyazeva, *Zavodsk. Lab.*, **26**, 263 (1960).
3) A. K. Babko and V. D. Vasilenko, *Ukrain. Khim. Zhur.*, **26**, 514 (1960).
4) H. Okada, K. Kaneko and S. Goseki, *Japan Analyst*, **12**, 822 (1963).
5) N. Iritani and T. Miyahara, ibid., **12**, 1182 (1963).
6) M. Otomo, ibid., **14**, 229 (1965).
7) V. D. Vasilenko and M. V. Shanya, *Zh. Analit. Khim.*, **20**, 636 (1965).
8) K. Tonosaki and K. Sakai, *Japan Analyst*, **14**, 495 (1965).
9) M. Otomo, This Bulletin, **38**, 624 (1965).
10) F. D. Snell and C. T. Snell, "Colorimetric Methods of Analysis," 3rd Ed., Van Nostrand Co., New York (1953), p. 324.
11) R. Raggieri, *Anal. Chim. Acta*, **16**, 242 (1957).
12) D. E. Howe and M. G. Mellon, *Ind. Eng. Chem., Anal. Ed.*, **12**, 448 (1940).
13) K. Ueno, "Kireto Tekitei (Chelatometric Titration)" (in Japanese), Nankodo, Tokyo (1960), p. 257.

in Fig. 3, it may be seen that the maximum absorbance is obtained in the acidity range from 0.07 to 0.1 M with respect to perchloric acid when measured at 580 mμ, and in the pH range from 4.5 to 5.5 when measured at 520 mμ.

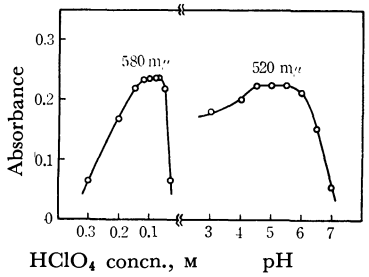

Fig. 3. Effect of acidity.
Iron: 26.8 μg.; MTB: 1.96×10^{-4} M
Reference: a reagent blank

The Stability of the Color.—The color development between iron(III) and the reagent occurs instantaneously at room temperature. The color intensity of the solution remained almost constant for at least 4 hr. after preparation, either at the acidity of 0.08 M or at pH 5.0.

Calibration Curves.—From the foregoing results, two optimum conditions for determining iron were found. The procedure for preparing the calibration curves for iron was as follows: An aliquot of the standard iron(III) solution was pipetted into a 25-ml. volumetric flask. The acidity of the solution was then adjusted to 0.08 M in the final concentration with perchloric acid or to pH 5.0 with an acetate buffer. To the solution, 2.5 to 3.5 ml. of a 1×10^{-3} M methylthymol blue solution was added, and the resulting solution was diluted with water to the mark. After about 30 min., the absorbance of the solution was measured at 580 or 520 mμ against the reagent blank.

The results shown in Fig. 4 indicate that Beer's law is followed by solutions containing up to at least 50 μg. of iron. The sensitivities of the methods

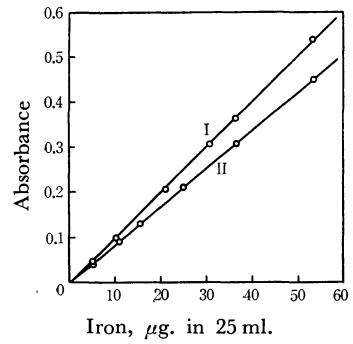

Fig. 4. Calibration curves.
I: MTB 1.15×10^{-4} M; $HClO_4$ 0.08 M; 580 mμ
II: MTB 1.37×10^{-4} M; pH 5.0; 520 mμ

are 0.004 μg. of iron per cm^2 at 580 mμ and 0.005 μg. of iron per cm^2 at 520 mμ.

The Effect of Diverse Ions.—The effect of diverse ions was examined with a solution containing 26.8 μg. of iron and diverse ions. The acid concentration of the solution was adjusted to 0.08 M with perchloric acid. Of the 25 cations tested, such ter- or quadrivalent cations as bismuth, gallium, indium, thallium, thorium, uranium, vanadium, and zirconium gave a positive error, while common divalent cations and some rare earth elements did not interfere. The following anions did not interfere under the conditions described: chloride, nitrate and sulfate up to at least 100 μmol., fluoride up to 5 μmol., tartrate and citrate up to 50 μmol. and phosphate up to 30 μmol. Oxalate, nitrilotriacetate and ethylenediaminetetraacetate, however, inhibit the formation of the complex, even when only trace amounts are present.

The Composition of the Complexes.—*The Complex with an Absorption Maximum at* 580 mμ. —The method described by Frank and Oswalt[14] was applied. This method is effective in the identification of a 1-to-1 complex with a formation constant of less than about 10^4.

An attempt was made with solutions with a given molar concentration of iron at a given perchloric acid concentration, but with varying methylthymol blue concentrations. If only a 1-to-1 complex is formed under the conditions, and if the absorbance of the solution, A, is measured against the reagent blank, the following relationship may be derived:

$$ab/A = (a+b)/(\varepsilon_C - (\varepsilon_O)_H) + 1/(K_1')_H(\varepsilon_C - (\varepsilon_O)_H) \quad (1)$$

where a and b represent the total molar concentration of iron and that of the reagent respectively; ε_C is the molar extinction coefficient of the complex, and $(\varepsilon_O)_H$ is the apparent molar extinction coefficient of the reagent at a given acidity. $(K_1')_H$ is defined as:

$$(K_1')_H = x/(a-x)(b-x) \quad (2)$$

where x represents the equilibrium molar concentration of the complex at a given acidity.

In Fig. 5 ab/A is plotted against $(a+b)$ at 580 mμ. In these solutions, the concentration of iron was 1.92×10^{-5} M, while that of methylthymol blue varied from 1.0×10^{-4} to 1.2×10^{-3} M; the acidity was held constant at 0.02 M with respect to perchloric acid. The good linearity of the plots supports the assumption inherent in Eq. 1, indicating that only a 1-to-1 complex is found under the conditions investigated. The molar extinction coefficient was calculated to be 15000 at 580 mμ, and the value of $(K_1')_H$, to be 8.4×10^3.

14) H. S. Frank and R. L. Oswalt, *J. Am. Chem. Soc.*, **69**, 1321 (1947).

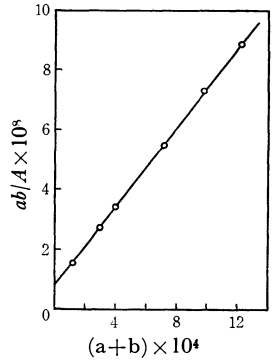

Fig. 5. Plot of ab/A vs. $(a+b)$ at 580 mμ.
a: 1.92×10^{-5} M; b: 1.0×10^{-4}—1.2×10^{-3} M
$HClO_4$: 0.20 M

The Complex with an Absorption Maximum at 520mμ. —The mole ratio of iron to the reagent was confirmed by the mole ratio method at pH 5.5. In this work, each solution was 1.02×10^{-4} M in the total concentration of methylthymol blue. The results are shown in Fig. 6, which indicates that probably a 1-to-2 complex is formed between iron and the reagent. The wavelengths, 540 and 550 mμ, were chosen because the reagent itself has too high an absorbance at 520 mμ. The molar extinction coefficient of this complex was calculated to be about 14000 at 520 mμ.

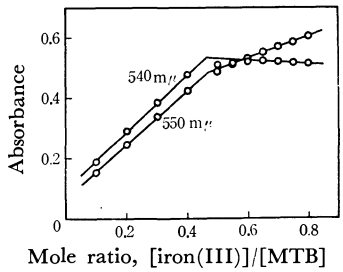

Fig. 6. Mole ratio method.
MTB: 1.02×10^{-4} M, pH: 5.5

The author wishes to thank Mr. Makoto Otomo for his discussion and Mr. Fujio Maeda for his assistance. This investigation was partly supported by a grant from the Ministry of Education.

BULLETIN OF THE CHEMICAL SOCIETY OF JAPAN VOL. 39 428—434 (1966)

Studies of Poly-2-vinylpyridine. I. Suspension Polymerization and Molecular Weight Distribution

By Shizuo ARICHI, Seiji MITSUTA, Noriyuki SAKAMOTO and Hiromu MURATA

Department of Chemistry, Faculty of Science, Hiroshima University, Higashisenda-machi, Hiroshima

(Received May 19, 1965)

2-Vinylpyridine has been polymerized by the suspension method. A stable suspension has been obtained using a mixture of sodium butylnaphthalene sulfonate and gelatine as a stabilizer in the concentration ranges of 0.025—0.75 per cent (for the former) and 0.75—1.0 per cent (for the latter) in water. The molecular weight of polymers thus obtained from this stable suspension system could be controlled by varying the concentration of azo-bis-isobutyronitrile and the temperature. The M_w/M_n ratios of the polymers obtained by the above method are relatively large; from 3.5 to 5. Precipitation fractionation has been carried out for a polymer obtained using ethyl methyl ketone as a solvent and ligroin as a precipitant at a constant temperature. Three kinds of molecular weight distribution curves have been obtained by applying the data of fractionation to (1) Tung's method, (2) exponential-type and (3) logarithmic normal-type molecular weight distribution functions. By comparing the average molecular weights, M_w and M_n calculated from each curve with the experimental values, it was found that the molecular weight distribution of the fraction can be well represented by the function 2 or 3.

Various copolymers[1-4] of 2-vinylpyridine have been extensively studied because of their practical importance. The derivatives of poly-2-vinylpyridine have also fully been investigated from the point of view of polyelectrolytes[5-8] and

1) W. W. Rinne and J. E. Rose, *Ind. Eng. Chem.*, **40**, 1437 (1948).
2) S. Yuguchi and M. Watanabe, *Kobunshi Kagaku*, **17**, 465 (1960).
3) K. Mizutani and S. Suzuki, *J. Chem. Soc. Japan, Ind. Chem. Sect.* (*Kogyo Kagaku Zasshi*), **64**, 577 (1961).
4) T. Ida, S. Kishi, S. Takahashi and I. Utsumi, *J. Pharm. Sci.*, **51**, 1061 (1962).
5) W. N. Maclay and R. M. Fuoss, *J. Polymer Sci.*, **6**, 511 (1951).
6) H. L. Wagner and F. A. Long, *J. Phys. & Colloid Chem.*, **55**, 1512 (1951).
7) A. Katchalsky and I. R. Miller, *J. Polymer Sci.*, **13**, 57 (1954).
8) I. R. Miller, *J. Colloid Sci.*, **9**, 579 (1954).

polysoaps[9-13] by Fuoss, Strauss and others. One of the present authors has studied this polymer as an emulsifying agent[14] in the polymerization of acrylonitrile in an acidic medium; he has also studied some properties of the aqueous solution of a polysoap[15] derived from poly-2-vinylpyridine. As for poly-2-vinylpyridine itself, however, relatively few investigations have been reported.

It is considered that studies of the polymerization, the fractionation, the relation between the intrinsic viscosity and molecular weight, etc., are important for the practical use of this polymer. In addition, by investigating the solution properties of the polymer, it may be possible to obtain some information about the effect of the polarity of pyridine nitrogen on its solubility and conformation in a solution. Recently, the effect of the tacticity of a polymer on solution behavior has become an interesting subject; data in this field have been collected for many polymers. Isotactic crystalline poly-2-vinylpyridine was first polymerized by Natta and others[16] in 1960 using Grignard's reagent as a catalyst. As both isotactic and atactic poly-2-vinylpyridine are soluble in various solvents at ordinary temperatures, they are considered to be suitable samples for the investigation into the effect of tacticity on the solution properties.

In the present work, the suspension polymerization of 2-vinylpyridine was studied with regard to the effect of the concentrations of the stabilizer and the initiator and to that of the temperature. The results of the study of the molecular weight distribution of the polymer will also be reported here.

Experimental

Materials. — 2-Vinylpyridine monomer (Tokyo Yukigoseikogyo Inc.) was distilled immediately before use under a vacuum with a 100-cm. jacketed column containing Podvielniak single-turn helix packing. A middle portion (b. p. 71°C/32 mmHg) was used for polymerization. All the solvents were purified by the usual procedure. Sodium butylnaphthalene sulfonate (Pelex-NBK, Kao Sekken Inc.) was purified by recrystallization.

Polymerization.—2-Vinylpyridine was polymerized in a sealed glass ampoule under a nitrogen atmosphere by the suspension method. Gelatine and Pelex-NBK were used as stabilizers, and azo-bis-isobutyronitrile (AIBN), as an initiator. An aqueous solution of gelatine and Pelex-NBK and a monomer in which AIBN had been dissolved under cooling were introduced in an ampoule successively. The ampoule was then cooled with a mixture of dry ice and acetone, and the air was replaced by a nitrogen atomsphere. After the ampoule had been sealed, polymerization was performed in a water bath with stirring by the revolution of the ampoule. After the required time, the polymerization was stopped by pouring the suspension into a large amount of water. The supernatant liquid was decanted off after most of polymer particles had precipitated. The particles were washed at least four times with hot water on a No. 2 sintered glass filter.

Intrinsic Viscosity.—A modified Ubbelohde-type viscometer was used for the measurement of the viscosity. The flow time for 92.01 weight per cent ethanol varied from 120 to 300 sec. according to the viscometer used. All the solutions were filtered through a No. 3 sintered glass filter immediately before measurement and were successively diluted in the viscometer. The initial concentration was determined by a weighing method. The intrinsic viscosity $[\eta]$, was obtained according to Eq. 1:

$$\eta_{sp}/c = [\eta] + k'[\eta]^2 c \qquad (1)$$

where η_{sp} is the specific viscosity; c, the concentration of the polymer in g./100 ml., and k', Huggins' constant.

Osmotic Pressure.—The osmotic pressure was measured statically with a Zimm-Myerson-type osmometer (Shibayama Rikagaku Kikai Seizosho) at 25± 0.003°C. Gel cellophane No. 300 (Tokyo Serohanshi Inc.) was used as the membrane after the usual treatment. The leakage of low-molecular-weight polymer through the membrane could not be prevented because all the samples were unfractionated polymers. Thus, the pressure decreased slowly and linearly after the attainment of an apparent equilibrium. Consequently, the measurement was carried on for 5 or 6 days, employing the method of extrapolation to zero time. The number-average molecular weight, M_n, was obtained according to Eq. 2:

$$\pi/c = \boldsymbol{R}T(1/M_n + A_2 c) \qquad (2)$$

where π is the osmotic pressure; $\boldsymbol{R}$, the gas constant; T, the absolute temperature, and A_2, the second virial coefficient.

Light Scattering.—Light scattering was measured with a Brice-type microphotometer (Shimadzu Seisakusho Inc.) with unpolarized and monochromatized incident light (436 mμ) and using the dissymmetry method. The refractive index increment was measured with a Debye-type instrument (Shimadzu Seisakusho Inc.). Data were arranged according to Eq. 3:

$$Kc/R_\theta = 1/\{M_w P(\theta)\} + 2A_2 c \qquad (3)$$

where $K = 2\pi^2 n_0^2 (\mathrm{d}n/\mathrm{d}c)^2/(\lambda^4 \boldsymbol{N})$

and where n_0 is the refractive index of solvent: $\mathrm{d}n/\mathrm{d}c$, the refractive index increment; λ, the wavelength of incident light; $\boldsymbol{N}$, the Avogadro number; R_θ, the reduced intensity of scattered light at an angle of θ, and $1/P(\theta)$, the dissymmetry correction. $[Kc/R_\theta]_0$ was obtained by the extrapolation of the linear line obtained by plotting Kc/R_θ versus c, while $1/P(90)$ was obtained from the dissymmetry, $z=[Kc/R_{135}]_0/[Kc/R_{45}]_0$, using the table

9) U. P. Strauss and E. G. Jackson, *J. Polymer Sci.*, **6**, 649 (1951).
10) L. H. Layton, E. G. Jackson and U. P. Strauss, ibid., **9**, 295 (1952).
11) L. H. Layton and U. P. Strauss, *J. Colloid Sci.*, **9**, 149 (1954).
12) U. P. Strauss and S. S. Slowata, *J. Phys. Chem.*, **61**, 411 (1957).
13) H. E. Jorgensen and U. P. Strauss, ibid., **65**, 1873 (1961).
14) S. Arichi, *J. Sci. Hiroshima Univ. Ser. A-II*, **25**, 419 (1962).
15) M. Miura, S. Arichi and T. Morita, *J. Chem. Soc. Japan, Pure Chem. Sect.* (*Nippon Kagaku Zasshi*), **83**, 32 (1962).
16) G. Natta, G. Mazzanti, G. Dall'Asta and P. Longi, *Makromol. Chem.*, **37**, 160 (1960).

TABLE I. THE EXPERIMENTAL RESULTS OF POLYMERIZATION[a]

Sample No.	Temp. °C	Concn. of AIBN[b]	Time hr.	Conv. %	$[\eta]$[c] dl./g.	$M_w \times 10^{-4}$	$M_n \times 10^{-4}$	M_w/M_n
9	85	1.5	6	84.2	0.41	8.12		
10	85	1.0	6	80.8	0.49	9.10		
11	85	0.5	6	87.8	0.59			
12	85	0.1	6	74.8	0.94	21.10	5.57	3.8
1	65	2.5	12	91.8	0.56	14.27	4.15	3.4
2	65	1.5	12	82.4	0.64		4.91	
3	65	0.5	12	79.7	0.86	19.74		
4	65	0.2	12	45.0	0.90			
5	45	1.0	96	92.1	1.17	27.23	6.66	4.1
6	45	0.5	96	67.7	1.29	32.40	7.73	4.2
7	45	0.1	137	37.5	1.69			
8	45	0.05	137	34.9	1.48	39.10	8.00	4.9
13	40	0.2	288	58.7	—[d]			
14	40	0.1	288	49.2	—[d]			

a) Weight ratio of water to monomer was 2 : 1, the concentrations of gelatine and Pelex-NBK were 0.75 and 0.025 per cent with respect to water.
b) Weight per cent with respect to monomer.
c) In 92.01 weight per cent ethanol at 25±0.01°C.
d) The polymer did not dissolve in hot solvent within a month.

of Doty and Steiner[17] for the unfractionated polymers. The instrument was calibrated with benzene which had been purified by three recrystallizations and distillations, using $R_{90}=48.5\times10^{-6}$ (436 mμ).[18]

Fractionation.—The fractional precipitation method was used. Ethyl methyl ketone and ligroin were used as a pair, as a solvent and a precipitant. The polymer solution (of 1 or 2 weight per cent) was poured into a heart-type flask, and then ligroin was added slowly while the solution was stirred vigorously at 30°C. After the appearance of a proper turbidity, stirring was still continued for 1 or 2 more hours; then the system was allowed to stand overnight. The gel thus obtained was separated from the supernatant liquid by decantation. A solid polymer was obtained by pouring excessive petroleum ether into the gel. The product was washed with petroleum ether and dried in a vacuum dryer.

Results and Discussion

The Effect of Concentrations of Gelatine and Pelex-NBK on the Stability of the Suspension.—The effect of concentrations of gelatine and Pelex-NBK on the stability of the suspension was investigated with a 20 ml. ampoule scale. The polymerization conditions were as follows: water, 10 g.; monomer, 5 g.; AIBN, 0.1 g.; temperature, 45°C and revolution velocity of ampoule, 40 r. p. m. while the concentrations of gelatine and Pelex-NBK varied. After 5 hours' polymerization, the states of suspension were observed and the diameter of particles was measured with a microscope.

Neither gelatine and Pelex-NBK, when used separately, had any dispersion power up to the concentrations of 2.0 and 0.5 weight per cent respectively in water. Even when they were used as a mixture, the stability of the suspension was poor, regardless of the concentration of gelatine, until the concentration of Pelex-NBK was 0.02 per cent. When the concentrations of gelatine and Pelex-NBK exceeded 0.75 and 0.025 per cent respectively, however, the suspension became very stable; the stability showed no remarkable change with the concentrations of gelatine and Pelex-NBK until they were 1 and 0.75 per cent respectively. However, the size of the particle became smaller and the polydispersity decreased wtih the increase in the concentration of gelatine at a constant concentration of Pelex-NBK.

The diameter of most particles was smaller than ca. 0.2 mm. There was also a small amount of very fine particles.

The Effect of the Concentration of AIBN and of the Temperature on the Conversion and the Intrinsic Viscosity of the Polymer.—The polymerization for the preparation of samples was performed in a 400 ml. ampoule. The conditions were as follows; the weight ratio of water to the monomer was 2 : 1; the concentrations of gelatine and Pelex-NBK were 0.75 and 0.025 weight per cent in water respectively; the revolution velocity of ampoule was 40 r.p.m., and the concentrations of AIBN and the temperature varied. The intrinsic viscosity of the polymer solutions in 92.01 weight per cent ethanol was measured at 25±0.01°C.

The results of polymerization are shown in Table I. As may be seen in this table, the conversion is sufficiently high in most cases. When we denote the concentration of AIBN as p (weight per cent with respect to the monomer), the relation between $p^{-1/2}$ and $[\eta]$ at each temperature is

17) P. Doty and R. F. Steiner, *J. Chem. Phys.*, **18**, 1211 (1950).
18) C. I. Carr and B. H. Zimm, ibid., **18**, 1616 (1950).

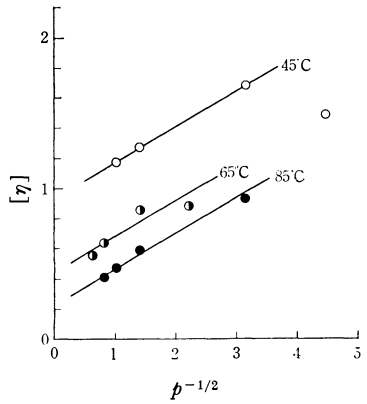

Fig. 1. Effect of AIBN concentration, p (weight per cent with respect to monomer), on the intrinsic viscosity of poly-2-vinylpyridine at constant temperature indicated.

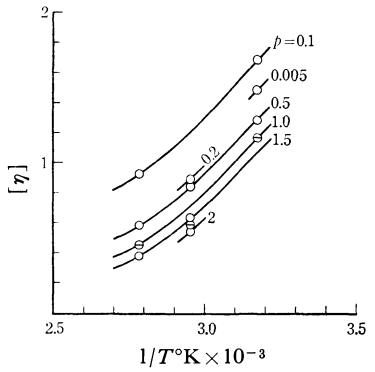

Fig. 2. Effect of temperature on the intrinsic viscosity of poly-2-vinylpyridine at constant concentration of AIBN indicated.

linear except at a very low concentration of catalyst, as may be seen in Fig. 1.

The relation between $1/T°K$ and $[\eta]$ at a constant concentration of AIBN is shown in Fig. 2. The temperature dependence of $[\eta]$ seems to be nearly the same for all the concentrations of AIBN studied. It is apparent that, in the present method of suspension polymerization, it is possible to control the molecular weight of the polymer by varying the concentration of AIBN and the temperature.

The Weight-average and Number-average Molecular Weight of the Polymer.—The M_w and M_n values of several samples were determined by measuring the light scattering of the polymer in methanol and the osmotic pressure of the polymer solution in ethyl methyl ketone respectively. The results are shown in Figs. 3 and 4 and are summarized in Table I. The values of M_w/M_n given in column 9 of the table show that the width of the molecular weight distribution of the polymers is quite large, but the values do not vary very much with polymerization conditions.

In Fig. 5 the intrinsic viscosity in 92.01 weight per cent ethanol is plotted against the M_w and M_n values in double logarithmic scales. Sufficiently exact information has been obtained on the relation between the intrinsic viscosity and the molecular weight of the polymer obtained under the experimental conditions described. The results on the fractionated polymers will be reported in Part III.[19]

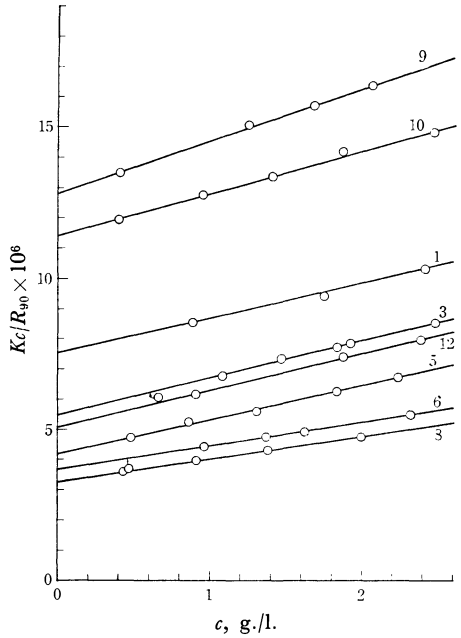

Fig. 3. Plots of reciprocal reduced scattering intensity vs. concentration of poly-2-vinylpyridine in methanol at 25°C.

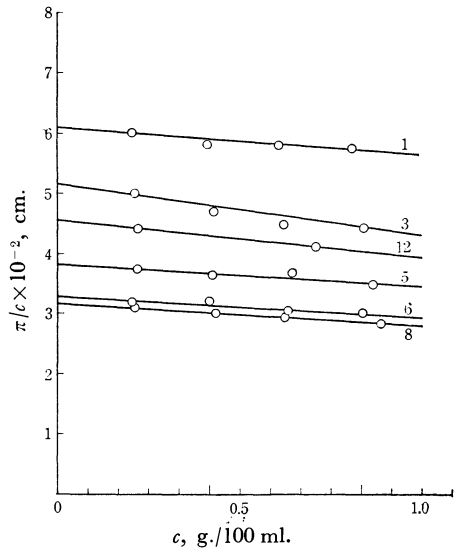

Fig. 4. Plots of reduced osmotic pressure vs. concentration of poly-2-vinylpyridine in ethyl methyl ketone at 25°C.

19) S. Arichi, This Bulletin, **39**, 439 (1966).

TABLE II. RESULTS OF FRACTIONATION

Primary fractionation

	Sample No.	W_i g.	$[\eta]$ dl./g.
Input	6	61.6	1.29
Output	6A	17.1	2.23
	6B	12.9	1.66
	6C	13.6	1.19
	6D	18.9	0.68
	6E	1.1	0.16

Secondary fractionation

	Sample No.	W_i g.	$[\eta]_i$ dl./g.	$W_i/\sum W_i$ %
Input	6A	16.6	2.23	—
Output	6A-1	2.48	3.01	4.51
	6A-2	1.98	2.57	3.60
	6A-3	1.62	2.51	2.94
	6A-4	1.53	2.34	2.78
	6A-5	1.42	2.23	2.58
	6A-6	1.42	2.27	2.56
	6A-7	1.68	1.61	3.05
	6A-8	1.04.	1.36	1.89
	6A-9	1.73	0.89	3.14
Input	6B	12.2	1.66	—
Output	6B-1	2.38	2.09	4.32
	6B-2	2.07	2.03	3.76
	6B-3	0.80	1.83	1.45
	6B-4	1.00	1.45	1.82
	6B-5	1.00	1.45	1.82
	6B-6	0.74	1.50	1.34
	6B-7	0.71	1.36	1.29
	6B-8	0.96	1.26	1.74
	6B-9	0.57	1.09	1.04
	6B-10	0.50	0.54	0.91
Input	6C	13.1	1.19	—
Output	6C-1	1.20	1.55	2.18
	6C-2	1.40	1.69	2.54
	6C-3	0.99	1.51	1.80
	6C-4	1.61	1.48	2.93
	6C-5	1.38	0.86	2.51
	6C-6	1.37	0.90	2.49
	6C-7	1.97	0.52	3.58
	6C-8	1.70	0.66	3.09
Input	6D	17.8	0.68	—
Output	6D-1	1.91	1.09	3.47
	6D-2	1.38	0.83	2.51
	6D-3	1.54	0.71	2.80
	6D-4	1.51	0.58	2.87
	6D-5	1.41	0.51	2.56
	6D-6	1.71	0.84	3.11
	6D-7	2.46	0.58	4.47
	6D-8	2.00	0.41	3.63
	6D-9	2.71	0.23	4.92

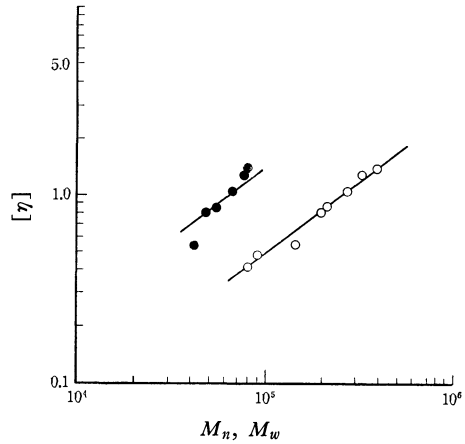

Fig. 5. Log-log plots of $[\eta]$ vs. M_n (-●-) and of $[\eta]$ vs. M_w (-○-) in 92.01 weight per cent ethanol at 25°C for unfractionated poly-2-vinylpyridine.

Results of Fractionation.—Unfractionated poly-2-vinylpyridine (No. 6 listed in Table I) was chosen as the sample for the measurement of the molecular weight distribution. Using the method described previously, 61.6 g. of this polymer was fractionated into five fractions; each of the first four fractions was refractionated into eight or ten subfractions, and the intrinsic viscosity was measured in 92.01 weight per cent ethanol at 25±0.01°C. The results of fractionation are shown in Table II.

The Molecular Weight Distribution (MWD) Curve.—Three kinds of MWD curves were obtained by applying the data in Table II to (1) Tung's method,[20] which is a modification of Schulz',[21] (2) exponential-type[22] and (3) logarithmic normal-type MWD functions[23] respectively.

Schulz-Tung's Method.—According to Tung,[20] the S-shape integral distribution, $I(M)$, was assumed to be given by:

$$I(M) = 1-\exp(-aM^b) \quad (4)$$

If $\log[1/\{1-I(M)\}]$ is plotted against M on a double logarithmic paper, the plots will fall on a straight line with a slope of b and an intercept of $\log(a\log e)$. The differential weight distribution function, $w(M)$, can be obtained from Eq. 4 as follows:

$$w(M) = \mathrm{d}I(M)/\mathrm{d}M = ab\exp(-aM^b)M^{b-1} \quad (5)$$

When the molecular weight, M, is replaced by the intrinsic viscosity, the constants a and b are

20) L. H. Tung, *J. Polymer Sci.*, **20**, 495 (1956).
21) G. V. Schulz and A. Dinglinger, *Z. physik. Chem.*, **B43**, 47 (1939).
22) G. V. Schulz, ibid., **B30**, 379 (1935); B. H. Zimm, *J. Chem. Phys.*, **16**, 1099 (1948).
23) R. Koningsveld and C. A. F. Tuijnman, *J. Polymer Sci.*, **39**, 445 (1959).

replaced by a' and b'; the relations among them are given[24] by:

$$a' = aK'^{-b/\nu}, \quad b' = b/\nu$$

where K' and ν are the constants in the Mark-Houwink equation, $[\eta]=K'M^{\nu}$.

The Tung plot is shown in Fig. 6. The values of a' and b' obtained from this figure are 0.532 and 1.60 respectively. As will be shown in Part III,[19] the Mark-Houwink equation with fractionated poly-2-vinylpyridine in 92.01 weight per cent ethanol at 25±0.01°C is expressed by $[\eta]=1.22\times10^{-4}M_w^{0.73}$. Using this equation and the values of a' and b' obtained above, the values of a and b are calculated to be 2.95×10^{-7} and 1.17 respectively. The calculated $w(M)$ value is shown in Fig. 7 by curve I.

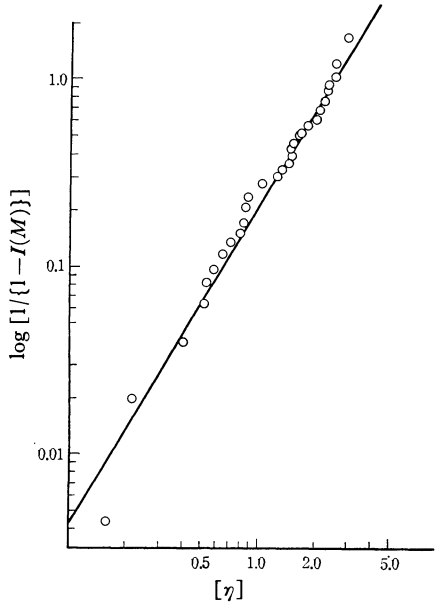

Fig. 6. Fractionation data for poly-2-vinylpyridine (sample, No. 6) arranged by Tung's method.

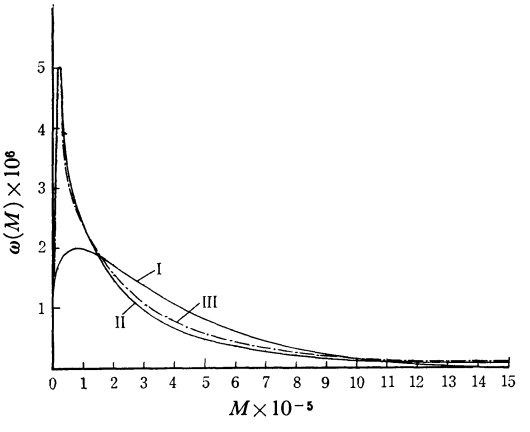

Fig. 7. Differential weight distribution curves of poly-2-vinylpyridine (sample, No. 6).
I Tung's method, II Exponential type, III Logarithmic normal type

The Exponential-type MWD Curve.—The MWD function proposed by Schulz and Zimm[22] and treated by the statistical method of Booth and Beason[25] is expressed by Eqs. 6 and 7:

$$w_i(M)=\{Y_i^{h_i+1}/\Gamma(h_i+1)\}M^{h_i}\exp(-Y_iM) \quad (6)$$

$$w(M)=\sum w_i(M) \quad (7)$$

where $w_i(M)$ and $w(M)$ are differential MWD functions of the ith fraction and the original polymer respectively. Parameters Y_i and h_i are related by Eq. 8 to the molecular weights, M_{wi} and M_{ni} of the ith fraction:

$$Y_i = h_i/M_{ni} = (h_i+1)/M_{wi} \quad (8)$$

In this work, these parameters for each fraction were calculated from the values of M_{wi} and M_{ni} which had been obtained from the Mark-Houwink equation for M_w described above and that for M_n[19]; $[\eta]=2.13\times10^{-4}M_n^{0.73}$. The result for MWD is shown by the curve II in Fig. 7.

The Logarithmic Normal-type MWD Curve.—The logarithmic normal distribution function proposed by Koningsveld and Tuijinman[23] is expressed by Eq. 9:

$$w_i(M) = MA_i\exp\{-p_i^2(\ln M/M_{oi})^2\} \quad (9)$$

where $w_i(M)$ is the differential weight distribution function of the ith fraction and A_i, a parameter normalizing the function to a desired total number of weight; p_i, a parameter related to the width of the distribution; and M_{oi}, the molecular weight at which the function reaches its maximum value. The values of A_i, p_i and M_{oi} can be calculated by the following equations, using the average molecular weights, M_{wi} and M_{ni}, of the ith fraction:

$$A_i = (W_i/M_{wi}M_{ni})\exp(-1/p_i^2)(\pi^{1/2}/p_i) \quad (10)$$

$$M_{wi}/Mn_i = \exp(1/2p_i^2) \quad (11)$$

$$M_{oi} = M_{wi}/\exp(5/4p_i^2) \quad (12)$$

In this work these parameters were again obtained from the values of M_{wi} and M_{ni} which were calculated from the intrinsic viscosity of each fraction. The value of $w(M)$ for the original sample can be calculated by Eq. 13:

$$w(M) = \sum w_i(M) \quad (13)$$

The MWD curve thus obtained is shown by the curve III in Fig. 7.

An Examination of the MWD Curves.—As may be seen in Fig. 7, the MWD curves, II and III, closely resemble each other. Each of them has a maximum at a very low molecular weight and a characteristic long tail in the higher

24) J. H. Green, *Chem. & Ind.*, **1959**, 924.

25) C. Booth and L. R. Beason, *J. Polymer Sci.*, **42**, 81 (1960).

TABLE III. COMPARISON OF $[\eta]$, M_w AND M_n OF UNFRACTIONATED POLY-2-VINYLPYRIDINE (SAMPLE NO. 6)

	Obs.	Calcd. From data of each fraction	Calcd. From MWD curve I	Calcd. From MWD curve II	Calcd. From MWD curve III
$[\eta]$	1.29	$\frac{\sum W_i[\eta]_i}{\sum W_i}=1.33$	1.33	—	—
$M_w\times10^{-4}$	32.40	$\frac{\sum W_iM_{wi}}{\sum W_i}=34.8$	36.9	29.7	31.3
$M_n\times10^{-4}$	7.73	$\frac{\sum W_i}{\sum(W_i/W_{ni})}=6.7$	11.1	7.6	8.1
M_w/M_n	4.2	5.2	3.3	3.9	3.9

molecular weight range. In contrast to these, the curve I has a lower maximum of $w(M)$ at a higher molecular weight.

To examine the validity of these MWD curves, the M_w, M_n and $[\eta]$ values of the original polymer were calculated from these curves and compared with the experimental values. In the case of Tung's treatment, the values of M_w and $[\eta]$ were calculated by Eqs. 14 and 15[24]:

$$[\eta] = a'^{-1/b'}\Gamma(1+1/b') \tag{14}$$

$$M_w = a^{-1/b}\Gamma(1+1/b) \tag{15}$$

The results are shown in Table III. The values cited in column 3 of this table were calculated by means of the equations in the same column, using the weight, W_i; the intrinsic viscosity, $[\eta]_i$, and the molecular weights, M_{wi} and M_{ni}, which were obtained from $[\eta]_i$. From these values the Mark-Houwink equations described above have been proved to be applicable to the fractions in this study.

In Table III it is noticeable that the values of M_w and M_n from the exponential-type MWD curve, II, and those from the logarithmic normal-type one, III, are in good agreement with the experimental values. On the other hand, those from Tung's method, I, are considerably larger than the experimental values. These results show that the MWD of each fraction is well represented by the above two functions; they also show that the overlapping of various molecular weights in each fraction can not be neglected in reality. These results resemble closely those for isotactic polypropyrene reported by Kotera and others.[26]

26) A. Kotera, K. Takamizawa, T. Kamata, H. Kawaguchi, M. Nireki, M. Kuwabara and K. Yamashita, presented at the 10th Symposium on High Polymers, Tokyo, November, 1961.

BULLETIN OF THE CHEMICAL SOCIETY OF JAPAN VOL. 39 434—439 (1966)

Studies of Poly-2-vinylpyridine. II. Solubilities in Various Solvents

By Shizuo ARICHI, Hiroatsu MATSUURA, Yoshio TANIMOTO and Hiromu MURATA

Department of Chemistry, Faculty of Science, Hiroshima University, Higashisenda-machi, Hiroshima

(Received May 19, 1965)

The viscosity and osmotic pressure of a fraction of poly-2-vinylpyridine have been measured in various solvents, and the parameters concerning the solubility of this polymer, that is, the osmotic second virial coefficient, A_2, the polymer-solvent interaction parameter, μ, and the solubility parameter, δ_2, have been obtained. From the values of these parameters, the following conclusions have been obtained: poly-2-vinylpyridine has a solubility parameter of ca. 10.4 $(\text{cal./cc.})^{1/2}$ and acts as an electron donor. As a result of the specific interaction between a solvent and the pyridine nitrogen of this polymer, the solvent power is greater in an acidic solvent and smaller in a basic than would be expected from the solubility parameter alone. An especially strong interaction between poly-2-vinylpyridine and aliphatic alcohols, chloroform and nitroethane has been observed and its nature has been discussed.

The interaction between a polymer and a solvent is the very important factor which influences the behavior of the polymer in solution.[1,2] The nitrogen atom which is situated at the α-position of pyridine ring of poly-2-vinylpyridine has a lone

1) T. Alfrey, Jr., A. I. Goldberg and J. A. Price, *J. Colloid Sci.*, **5**, 251 (1950).
2) H. Daoust and M. Rinfret, ibid., **7**, 11 (1952).

electron-pair and, consequently, shows a fairly strong basic character. The solubilities of this polymer in various solvents are much influenced by the basicity and the structural position of nitrogen. In the present study, the viscosity and osmotic pressure of a fraction of poly-2-vinylpyridine was measured in various solvents, and the nature of the polymer-solvent interaction will be discussed using the various solubility parameters obtained by these measurements.

Experimental

Polymer.—A fraction of poly-2-vinylpyridine, our sample number H-2, was used for this investigation. The procedure of the polymerization of this polymer has been described in Part I,[3] while that of the fractionation will be given in Part III.[4]

Solvents.—The solvents used were treated by the usual procedure and distilled before use.

The Viscosity and the Osmotic Pressure.—All parts of the apparatus and all procedures for the measurement of the viscosity and the osmotic pressure were the same as in Part I.[3] In order to measure the intrinsic viscosity of one fraction in various solvents, many viscometers with capillaries of different diameters were used; the correction of kinetic energy could be neglected. The osmotic pressure was measured by the static method with a gel cellophane membrane No. 300.

Results and Discussion

Huggins' Polymer-Solvent Interaction Parameter.—According to Huggins,[5] the partial molar free energy of dilution, ΔF_1, is given by the expression:

$$\Delta F_1 = \boldsymbol{R}T\{\ln(1-v_2) + (1-1/x)v^2 + \mu v_2^2\} \quad (1)$$

where v_2 is the volume fraction of the polymer; x, the ratio of the molar volume of polymer to that of solvent, and μ, a polymer-solvent interaction parameter which is independent of the molecular weight and the concentration of the polymer. The μ value is related to the osmotic second virial coefficient, A_2, by the following equation[6]:

$$A_2 = \bar{v}_2^2/\boldsymbol{N}V_1'(1/2-\mu) \quad (2)$$

where $\bar{v}_2$ is the specific volume of the polymer; $\boldsymbol{N}$, the Avogadro number, and V_1', the molecular volume of the solvent.

The results of osmotic pressure measurements of the H-2 fraction in ethanol, methanol, isopropanol, benzene and ethyl methyl ketone at 25±0.003°C are shown in Fig. 1. The relation between the π/c and c values in each solvent is shown by a linear line, from the slope of which the values of A_2 and μ were calculated by using

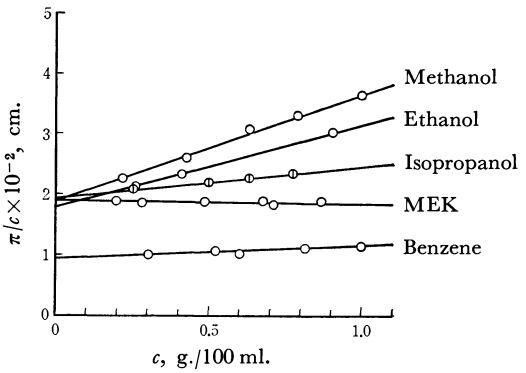

Fig. 1. Plots of reduced osmotic pressure vs. concentration of poly-2-vinylpyridine (fraction H-2) in various solvents at 25°C.

Eq. 2. As for the value of $\bar{v}_2$, the observed value of 0.856 ml./g. was used. The value of π/c in a benzene solution is small over the whole range of concentration. From the observed value of the intrinsic viscosity in benzene, this abnormality of π/c is considered to be caused by the leak of solute molecules through the membrane, and not by such an abnormality of the molecular dispersion state as association[7] in solution. The leak of solute molecules, however, may not influence the value of A_2 very much.[8] The values of A_2 and μ are shown in columns 4 and 5 of Table I.

The value of μ can also be evaluated from the data of the intrinsic viscosity.[9] From the theory of Flory and Fox,[10,11] the relation between the intrinsic viscosity $[\eta]$ in a solvent and the $[\eta]_\theta$ value in a θ-solvent is expressed by Eq. 3 for a homogeneous fraction of the polymer:

$$[\eta] = [\eta]_\theta \alpha^3 \quad (3)$$

where α is the viscosity expansion factor, which can be expressed by Eq. 4:

$$\alpha^5 - \alpha^3 = 2C_m(1/2-\mu)M^{1/2} \quad (4)$$

where C_m is a constant which depends on the specific volume of the polymer, $\bar{v}_2$, and on the molar volume of solvent, V_1; it can be expressed by: $C_m = (27/2^{5/2}\pi^{3/2})(\bar{v}_2^2/\boldsymbol{N}V_1)(\langle L^2\rangle_0/M)^{-3/2}$, where $\langle L^2\rangle_0$ is the mean-square displacement length of the chain in a θ-solvent. By rearranging Eqs. 3 and 4, the following equation can be obtained:

$$(1/2-\mu) = (V_1/2C_m'\Phi_0 M)([\eta]^{5/3}/[\eta]_\theta^{2/3} - [\eta]) \quad (5)$$

where C_m' is a constant expressed by $(27/2^{5/2}\pi^{3/2})(\bar{v}_2^2/\boldsymbol{N})$ and Φ_0, a universal constant.

3) S. Arichi, S. Mitsuta, N. Sakamoto and H. Murata, This Bulletin, **39**, 428 (1966).
4) S. Arichi, ibid., **39**, 439 (1966).
5) M. L. Huggins, *Ann. New York Acad.*, **43**, 9 (1942).
6) P. J. Flory and W. R. Krigbaum, *J. Chem. Phys.*, **18**, 1086 (1950).
7) P. Doty, H. Wagner and S. Singer, *J. Phys. & Colloid Chem.*, **51**, 32 (1947).
8) H. Tompa, "Polymer Solutions," Butterworths Scientific Publications, London (1956).
9) G. M. Bristow and W. F. Watson, *Trans. Faraday Soc.*, **54**, 1742 (1958).
10) P. J. Flory and T. G. Fox, Jr., *J. Am. Chem. Soc.*, **73**, 1904 (1951).
11) P. J. Flory, *J. Chem. Phys.*, **17**, 303 (1949).

TABLE I. SOLUBILITY DATA FOR POLY-2-VINYLPYRIDINE[a]

No.	Name	$[\eta]$ dl./g.	A_2 cm.^{3} mol./2 $\times 10^4$	μ[b]	μ[c]	δ_1[d] (cal./cc.)$^{1/2}$	k'	k_s
1	Nitroethane					11.1		
2	92.01 wt. % Ethanol	1.30					0.20	0.16
3	Chloroform	1.23			0.443	9.3	0.23	0.13
4	*n*-Heptanol	1.22			0.400	10.6	0.28	0.11
5	*i*-Butanol	1.17			0.441	9.8	0.23	0.09
6	*n*-Pentanol	1.16			0.402	10.9	0.27	0.11
7	Methanol	1.16	6.29	0.45	0.474	13.4	0.29	0.12
8	*n*-Butanol	1.15			0.445	10.1	0.37	0.14
9	*n*-Propanol	1.09			0.460	11.9	0.32	0.13
10	Ethanol	1.03	5.52	0.45	0.473	11.6	0.29	0.11
11	Pyridine	0.867			0.476	11.5	0.25	0.10
12	Nitrobenzene	0.853			0.471	10.0	0.36	0.14
13	Dimethylformamide	0.701			0.467	11.8	0.36	0.15
14	Tetramethyleneoxide	0.673			0.489	9.3	0.53	0.17
15	Isopropanol	0.670	2.18	0.47	0.490	10.2	0.33	0.13
16	Chlorobenzene	0.670			0.486	9.5	0.42	0.17
17	Benzene	0.530	0.96	0.49	0.495	9.2	0.31	0.13
18	Dioxane	0.470			0.498	10.0	0.60	0.19
19	Ethyl methyl ketone	0.385	−0.25	0.50	0.500	9.3	0.61	0.22

a) Our sample number, H-2.
b) The values from measurement of osmotic pressure, Eq. 2.
c) The values from measurement of viscosity, Eq. 5.
d) The values of δ_1 are taken from Hildebrand and Scott[14] for most of the solvents and are calculated with the aid of Hildebrand's rule[14] for the rest.

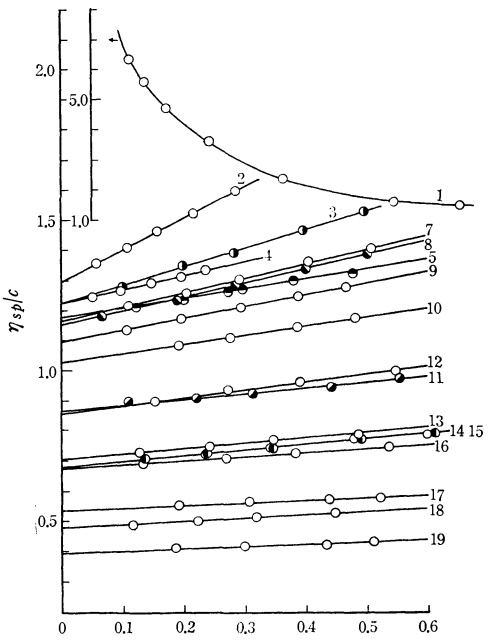

Fig. 2. Plots of reduced viscosity vs. concentration of poly-2-vinylpyridine (fraction H-2) in various solvents at 25°C. The number on each line corresponds to that of solvent cited in Table I.

The value of μ was evaluated by Eq. 5. The results of the viscosity measurements of the H-2 fraction in various solvents at 25±0.01°C are shown in Fig. 2 and are listed in Table I. The value of $[\eta]_\theta$ was evaluated by the following equation of Krigbaum[12]:

$$[\eta] = [\eta]_\theta + 5.0 \times 10^{-3} A_2 M \qquad (6)$$

The values of A_2 and $[\eta]$ are plotted in Fig. 3,

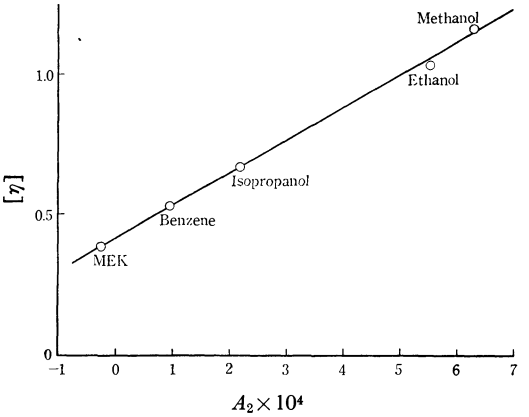

Fig. 3. Plots of intrinsic viscosity vs. osmotic second virial coefficient of poly-2-vinylpyridine (fraction H-2) in various solvents at 25°C.

12) W. R. Krigbaum, *J. Polymer Sci.*, **28**, 213 (1958).

from which the value of $[\eta]_\theta$ can be found to be 0.415. The measurement of the molecular weight, $M_w(30.08\times10^4)$, of this polymer will be described in Part III.[4] The values of μ in various solvents, which were calculated by inserting these data in Eq. 5, are shown in column 6 of Table I.

The values of the intrinsic viscosities, the osmotic second virial coefficients and the interaction parameters cited in Table I show that Lewis bases such as ethyl methyl ketone and dioxane and neutral solvents such as benzene are poor solvents, while Lewis acids such as nitroethane, chloroform and aliphatic alcohols are good solvents.

The Cohesive Energy Density of Poly-2-vinylpyridine.—According to the theory of Huggins,[13] μ can be divided into the term of entropy, μ_s, and that of the heat of mixing, μ_h:

$$\mu = \mu_s + \mu_h \tag{7}$$

When the contribution of μ_h is endothermic, it is related to the solubility parameters of the solvent, δ_1, and to that of the polymer, δ_2, as follows[14]:

$$\mu_h = V_1/\boldsymbol{R}T(\delta_1-\delta_2)^2 \tag{8}$$

where δ_1 and δ_2 are the square roots of the cohesive energy densities of the solvent and the polymer respectively. Equation 8 shows that the closer the value of δ_2 gets to δ_1, the stronger the solvent power becomes. Therefore, δ_2 is a useful key in selecting the solvent for the polymer.[15]

The method for evaluating the δ_2 value for the linear polymer has also been proposed by Bristow and Watson,[16] who obtained the following equation by combining Eqs. 7 and 8:

$$\delta_1^2/\boldsymbol{R}T = \mu/V_1$$
$$= 2(\delta_2/\boldsymbol{R}T)\delta_1 - (\delta_2^2/\boldsymbol{R}T+\mu_s/V_1) \tag{9}$$

$(\delta_1^2/\boldsymbol{R}T-\mu/V_1)$ was plotted against δ_1 in Fig. 4 using the values of μ and δ_1 cited in columns 6 and 7 of Table I. The value of δ_2 evaluated from the slope of the line and that evaluated from the intercept at the ordinate, neglecting the term of μ_s/V_1 are 10.4 and 10.5 $(\text{cal./cc.})^{1/2}$ respectively.

In principle Eq. 8 should be applied to the system in which the heat of mixing, μ_h, is only endothermic. If this is the case for poly-2-vinylpyridine-solvents systems, the solvent which has a value of δ_1 closer to 10.4 $(\text{cal./cc.})^{1/2}$ should have a stronger solvent power. Consequently, the intrinsic viscosities in such solvents must be large.

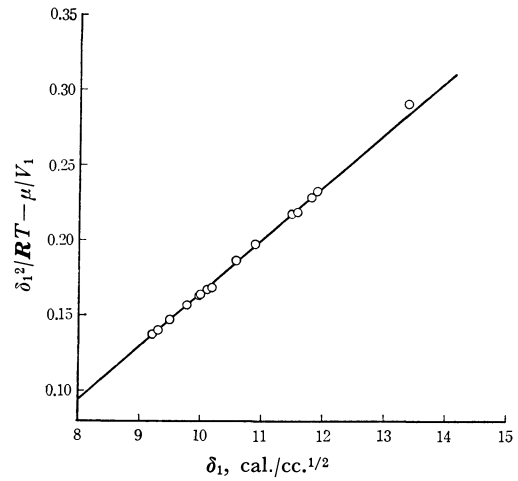

Fig. 4. Plots of $(\delta_1^2/\boldsymbol{R}T-\mu/V_1)$ vs. solubility paremeter of solvents for poly-2-vinylpyridine (fraction H-2).

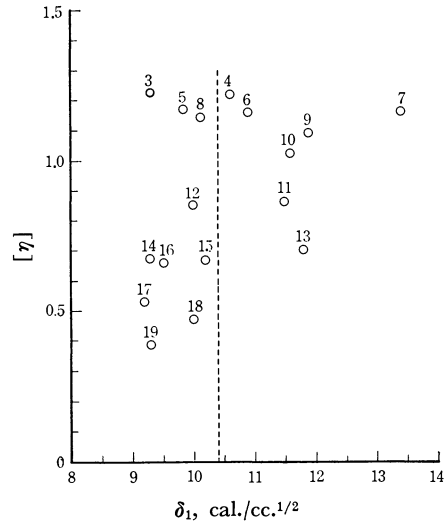

Fig. 5. Plots of intrinsic viscosity vs. solubility parameter of solvents for poly-2-vinylpyridine (fraction H-2). The number on each point corresponds to that of solvent cited in Table I.

In Fig. 5 the intrinsic viscosities in Table I are plotted against the δ_1 values of the corresponding solvents. From this figure no clear correlation can be seen between $[\eta]$ and δ_1. Thus, it may be considered that there exists some exothermic interaction between poly-2-vinylpyridine and some solvents.

Interaction between Poly-2-vinylpyridine and Solvents.—The nature of the specific interaction between poly-2-vinylpyridine and solvents described above was investigated from the viewpoint of Spurlin.[17] The nitrogen atom at the α-position of the pyridine ring has a lone electron-pair and acts as an electron donor, and so poly-2-vinylpyridine is quite a strong base. When a solvent is a Lewis acid or can act as an electron acceptor, its solvent power with regard to the

13) M. L. Huggins, ibid, **16**, 209 (1955).
14) J. H. Hildebrand and R. L. Scott, "The Solubility of Nonelectrolytes," Reinhold, New York (1950).
15) R. Johannsen, *Deut. Farben-Z.*, **17**, 264 (1963).
16) G. M. Bristow and W. F. Watson, *Trans. Faraday Soc.*, **54**, 1731 (1958).
17) H. M. Spurlin, *J. Polymer Sci.*, **3**, 714 (1948).

polymer may be increased because of solvation.

A typical example of such solvents is alcohols. As may be seen in Table I, it is remarkable that all the intrinsic viscosities of the polymer in various aliphatic alcohols are quite high except that in isopropanol. The intrinsic viscosities in methanol, ethanol and *n*-propanol are much higher than those which would be predicted on the basis of their solubility parameters alone. It is known that the lower aliphatic alcohol can act as a Lewis acid.[18,19] Alcohols, as a result, may be solvated to pyridine nitrogen, probably through the hydrogen bond.

The intrinsic viscosity of the H-2 fraction in chloroform, which has an acidic hydrogen atom, is also much higher than that which would be predicted on the basis of its solubility parameter alone. In contrast to this, carbon tetrachloride, which has no hydrogen atom, is nonsolvent of poly-2-vinylpyridine. These facts may be explained by the solvation of chloroform through hydrogen bonding to the polymer. A similar effect of solvated chloroform on the intrinsic viscosity was reported for polymethyl methacrylate.[20]

The existence of the hydrogen bond between the pyridine nitrogen in the polymer and alcohol or chloroform was supported by the following experiments. When the precipitant, *n*-hexane, was added to a poly-2-vinylpyridine solution in isopropanol or chloroform, and also when water was added to the solution in methanol, the lower the temperature, the larger the volume of the precipitant required for the first appearance of turbidity, as may be seen in Table II. Furthermore, the turbid solution thus produced became clear when it was cooled while this clear solution again became cloudy when heated. Obviously the temperature coefficient of the solubility of this polymer in these mixed solvents is negative; this may lead us to the conclusion that the polymer forms a hydrogen bond with the alcohol and chloroform.

Table II. Precipitation measurement of poly-2-vinylpyridine solution[a]

Solvent	Isopropanol		Methanol		Chloroform	
Precipitant	*n*-Hexane		Water		*n*-Hexane	
	Temp. °C	φ[b]	Temp. °C	φ[b]	Temp. °C	φ[b]
	20	40.26	10	53.98	10	55.75
	30	40.19	25	52.47	25	55.04
	40	39.02	40	51.10	35	54.02
	50	37.88			50	52.58

a) Our sample No. 5. Concentration was 1.0 g./100 ml.

b) Volume per cent of precipitant at the time of the first appearance of turbidity.

In the process of hydrogen bonding, it is probable that there is a steric hindrance for the orientation of solvent molecules. The fact that the H-2 fraction is practically insoluble in *t*-butanol is considered to be due to the steric hindrance. Such a steric hindrance may be small in the case of poly-4-vinylpyridine, in which the nitrogen atom is located at the γ-position of the pyridine ring. In fact, poly-4-vinylpyridine dissolves even *t*-butanol, and Strauss[21] has recognized the existence of hydrogen bonding in the poly-4-vinylpyridine-*t*-butanol system because of the negative temperature coefficient of the solubility of this polymer in a *t*-butanol - benzene mixture.

An extreme case of the specific interaction between poly-2-vinylpyridine and an acidic solvent is seen in the results of the viscosity measurement of the H-2 fraction in nitroethane. As may be seen in Fig. 2, the relation between the reduced viscosity and the concentration is similar to that of typical polyelectrolyte.[22] A similar result has been obtained by Cashin[23] in the case of poly-2-vinylpyridine in nitromethane. Nitroalkyl is tautomerized into nitro and acid forms, the latter of which behaves as an acid.[24] Nitroalkyl in the acid form may, therefore, quaternize the pyridine nitrogen. Thus, poly-2-vinylpyridine in nitroalkyl behaves as a polyelectrolyte.

The oxygen of the carbonyl group in ethyl methyl ketone has two lone electron-pairs, and so this solvent can act as a typical Lewis base.[18] Dioxane and nitrobenzene also act as bases to Lewis acid.[18] As may be seen in Fig. 5 the intrinsic viscosities in these solvents are lower than would be predicted on the basis of their solublity parameters alone. These results may also be explained as resulting from the interaction between pyridine

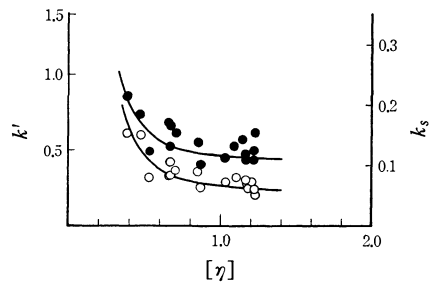

Fig. 6. Plots of Huggins' constant (○) and Spurlin's constant (●) vs. intrinsic viscosity of poly-2-vinylpyridine (fraction H-2) in various solvents.

18) S. G. Cohen, "Progress in Physical Organic Chemistry," Vol. 1, Interscience, New York-London (1964).
19) R. P. Bell, "Acids and Bases," Methuen, London, John Wiley and Sons, New York (1952).
20) W. R. Moore and R. J. Fort, *J. Polymer Sci.*, Part **A1**, 929 (1963).
21) A. G. Boyes and U. P. Strauss, ibid., **22**, 463 (1956).
22) R. M. Fuoss and U. P. Strauss, ibid., **3**, 246 (1948); R. M. Fuoss, ibid., **3**, 603 (1948).
23) W. M. Cashin, *J. Colloid Sci.*, **6**, 271 (1951).
24) D. Turnbull and S. H. Maron, *J. Am. Chem. Soc.*, **65**, 212 (1943).

nitrogen and solvents.

The intrinsic viscosity of the H-2 fraction in isopropanol is relatively low in spite of the value of δ_1 being closer to 10.4 (cal./cc.)$^{1/2}$ and in spite of its acidity. This is considered to be due to the steric hindrance to hydrogen-bond formation described previously.

Benzene is a typical neutral solvent, and the viscosity behavior of the polymer in this solvent coincides with that which is to be expected from its solubility parameter.

Huggins' Constant and Spurlin's Constant. —It has generally been recognized that Huggins' constant, k', defined by Eq. 1 in Part I[3] and Spurlin's constant, k_s, the ratio of the slope in the plots of $\log(\eta_{sp}/c)$ against c to the intrinsic viscosity, decrease with solvent power.[20,25] The values of k' and k_s obtained from the measurement of viscosity for the H-2 fraction in various solvents are cited in columns 8 and 9 of Table I and are plotted against the corresponding intrinsic viscosity in Fig. 6, which shows that the general rule described above is applicable to the present results.

25) L. H. Cragg and R. J. Sones, *J. Polymer Sci.*, **9**, 585 (1952).

BULLETIN OF THE CHEMICAL SOCIETY OF JAPAN VOL. 39 439—446 (1966)

Studies of Poly-2-vinylpyridine. III. Intrinsic Viscosity and Molecular Weight

By Shizuo ARICHI

Department of Chemistry, Faculty of Science, Hiroshima University, Higashisenda-machi, Hiroshima

(Received May 19, 1965)

The viscosity, osmotic pressure and light-scattering of a series of 14 fractions of poly-2-vinylpyridine in various solvents have been measured. The following results have been obtained: The constants, K_w' and ν, in the Mark-Houwink equation have been determined for the solutions of: (a) 92.01 weight per cent ethanol, (b) methanol, (c) dimethylformamide, (d) benzene and (e) dioxane as follows:

(a) $[\eta] = 1.22\times10^{-4} M_w^{0.73}$ (d) $[\eta] = 1.70\times10^{-4} M_w^{0.64}$
(b) $[\eta] = 1.13\times10^{-4} M_w^{0.73}$ (e) $[\eta] = 3.09\times10^{-4} M_w^{0.58}$
(c) $[\eta] = 1.47\times10^{-4} M_w^{0.67}$

The molecular weight of the polymers ranged from 3.4×10^4 to 93×10^4, while the viscosity was measured at 25±0.01°C. The constant, K', in the Mark-Houwink equation in the case of a homogeneous molecular weight has been calculated assuming the exponential- and logarithmic normal-type molecular weight distribution functions for each fraction. The Flory constant, K, defined as $[\eta]_\theta = KM^{1/2}$ has been found by the method of Fixman and Krigbaum to be: $(8.7\pm1.0)\times10^{-4}$ at 25°C. The K value has also been found to be $(9.1\pm1.1)\times10^{-4}$ by measuring the intrinsic viscosity in benzene at the θ-point, 16.2°C. The short range interactions of this polymer have also been discussed.

The Mark-Houwink viscosity equation and the unperturbed chain dimension of poly-2-vinylpyridine have not been reported in spite of their importance in the investigation of the polymer solution. The Mark-Houwink equation for poly-4-vinylpyridine, which, in chemical structure, closely resembles poly-2-vinylpyridine, has been reported by Strauss[1] and Fuoss[2], and the data concerning to the unperturbed chain dimension of poly-4-vinylpyridine, together with those of many other polymers, have recently been summarized by Kurata and Stockmayer.[3] The Mark-Houwink equation for poly-2-vinylpyridine may not be so much different from that of poly-4-vinylpyridine. However, the solubility characters of these two polymers in certain solvents differ from each other, as has been shown in Part II[4]; so it is considered important to obtain the equation for poly-2-vinylpyridine. In addition, by comparing the unperturbed chain dimension of poly-2-vinylpyridine with those of poly-4-vinylpyridine and polystyrene, it may be possible to obtain information about the effect of the polarity and the structural position of pyridine nitrogen on the conformation of the polymers in solution.

As most polymer samples have a distribution

1) A. G. Boyes and U. P. Strauss, *J. Polymer Sci.*, **22**, 463 (1956).
2) J. B. Berkowitz, M. Yamin and R. M. Fuoss, ibid., **28**, 69 (1958).
3) M. Kurata and W. H. Stockmayer, *Fortschr. Hochpolym.-Forsh.*, **3**, 196 (1963).
4) S. Arichi, H. Matsuura, Y. Tanimoto and H. Murata, This Bulletin, **39**, 434 (1966).

of molecular weight, corrections for the distribution must be applied to the experimentally obtained parameters, such as the constants, K' in the Mark-Houwink equation and K in the Flory equation. These corrections can be made by means of the proper equation based on a molecular weight distribution function; in this case the M_w/M_n ratio of the sample is always an important factor. In this study, both M_w and M_n were measured for 14 fractions of poly-2-vinylpyridine, and corrected values of the constants in the Mark-Houwink equation in five solvents and the unperturbed dimensions of the polymer were obtained.

Experimental

Polymers.—The polymer samples used in this investigation were prepared by the fractionation of the original polymers, which were described in Part I.[5] The composition of the solvent-precipitant and the technique of the fractionation were similar to those reported previously.[5] Each of the ten original polymers was first divided into 3 or 5 fractions; the fractions whose intrinsic viscosities were close to one another were put together. Thus, 13 fractions were obtained, they were named A, B, C, etc. Each of these fractions was then refractionated into three fractions, which were denoted A-1, A-2, A-3, B-1, etc.; of these, the middle fractions (A-2, B-2, C-2, etc.) were mainly used in this investigation.

In order to obtain the fractions whose molecular weights are higher than those obtained by the above method, the polymerization was performed by the method of Pritchard and others,[6] using potassium persulfate-sodium bisulfite as a redox initiator in an aqueous solution of the monomer acidified with hydrochloric acid at 45°C. The polymer was then fractionated as has been described above. Two of the resultant fractions N-3 and N-4, were used in this study.

Solvents.—The solvents used were guaranteed or first class reagents and were distilled before use, as has been described in Part I.[5]

The Phase Separation Temperature.—The polymer-solvent phase separation temperature was measured using a heart-type flask, to which a reflux condenser, a drying column containing phosphorous pentoxide and a glass stirrer were attached.

Viscosity, Osmotic Pressure and Light-scattering.—All apparatus for the measurement of viscosity, osmotic pressure, light-scattering and the refractive index increment were described in Part I.[5] The viscosities of a series of fractions were mesaured in various solvents at 25±0.01°C by the method of dilution in a viscometer. The correction for kinetic energy was neglected. The osmotic pressure was measured by a static method at 25±0.003°C, using a gel cellophane membrane (No. 300). No leakage of the solute molecule through the membrane was observed except for the sample with the lowest molecular weight (A-2, $M_w = 3.40\times10^4$); within 6 to 12 hr. the pressure reached an equilibrium which showed no change even after 24 hr. The reproducibility was checked by the reduced osmotic pressures, $(\pi/c)_0$, measured three times with the E-2 fraction in methanol, which were 3.41 3.43, and 3.30 ($\times10^2$ cm.).

Light-scattering was measured by a dissymmetry method with unpolarized incident light (436 mμ) at 25±1°C. The instrument was calibrated by using benzene[7] and also by means of a standard scattering plate.[8] The instrumental constants obtained by these two methods agreed with each other within the range of experimental error. The values of the molecular weight of the standard polystyrene, MS-1,[9] determined by using this instrumental constant were 23.7×10^4 and 23.6×10^4; these values were in good agreement with the mean value reported.[9] The solution and solvent were filtered through a cellafilter, "fein" or "mittel" (Membran Geselschaft, Göttingen, Germany). The concentration of the solution was determined by a weighing method. The dissymmetry was determined by the $[Kc/R_{135}]_0/[Kc/R_{45}]_0$ ratio, which was corrected for the back reflection of the incident light.

Results and Discussion

The Intrinsic Viscosity.—The results of the viscosity measurement of a series of fractions in methanol at 25±0.01°C are shown in Fig. 1. The measurements were also carried out for the same fractions in 92.01 weight per cent ethanol, dimethylformamide, benzene and dioxane.

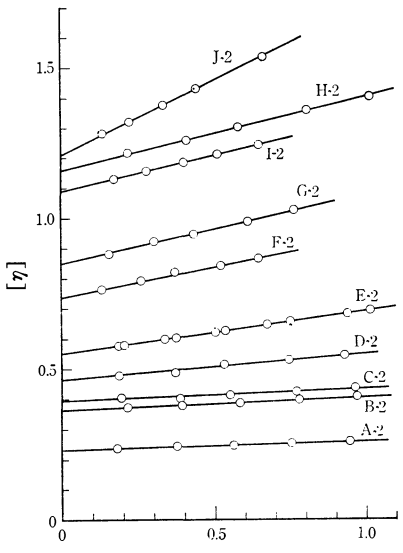

Fig. 1. Plots of reduced viscosity vs. concentration of poly-2-vinylpyridine fractions in methanol at 25°C.

5) S. Arichi, S. Mitsuta, N. Sakamoto and H. Murata, ibid., **39**, 428 (1966).

6) J. E. Pritchard, M. H. Opheim and P. H. Moyer, *Ind. Eng. Chem.*, **47**, 863 (1955).

7) C. I. Carr and B. H. Zimm, *J. Chem. Phys.*, **18**, 1616 (1950).

8) B. A. Brice, M. Halwer and R. Speiser, *J. Opt. Soc. Am.*, **40**, 768 (1950).

9) The Committee on Molecular Weight and Molecular Weight Distribution, *Rept. Progr. Polymer Phys. Japan*, **4**, 141 (1960).

The Osmotic Pressure.—The results of the measurement of the osmotic pressure of a series of fractions in methanol at 25±0.003°C are shown in Fig. 3. The results for the H-2 fraction in ethanol, methanol, isopropanol, benzene and ethyl methyl ketone were presented earlier, in Part II.[4]

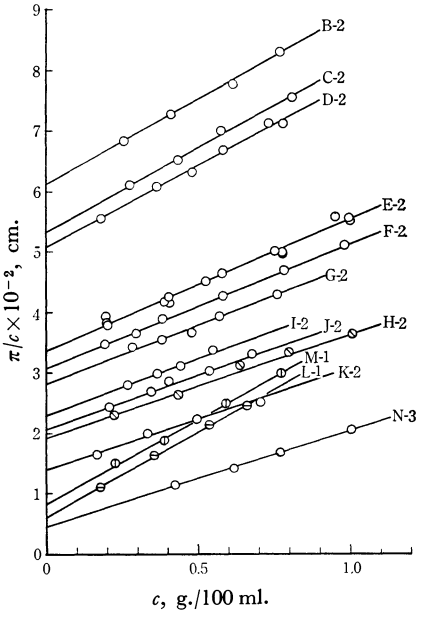

Fig. 2. Plots of reduced osmotic pressure vs. concentration of poly-2-vinylpyridine fractions in methanol at 25°C.

The Light-scattering.—The light-scattering of several of the fractions was measured in methanol, ethanol, isopropanol, ethyl methyl ketone, dioxane and benzene. In spite of the normal behavior shown in R_{90}, the angular distribution of scattered light showed a noticeable abnormality in all solvents; an extremely small dissymmetry (sometimes less than unity) was observed over the whole range of concentrations measured. A typical example is shown in Fig. 3 by the Zimm plot. The same behavior was observed irrespective of whether the incident light was polarized or unpolarized.

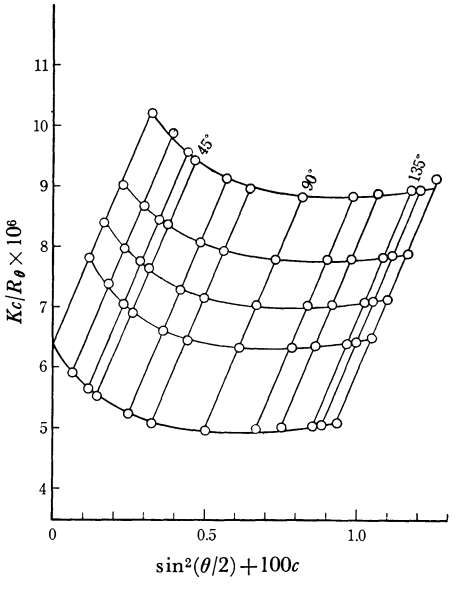

Fig. 3. The Zimm plots of faction G-2 in methanol at 25°C.

An abnormalilty in the angular distribution has also been reported by Miura and others[10] for poly-2-methyl-5-vinylpyridine in methanol. Fuoss and others[2] measured the light scattering of poly-4-vinylpyridine in absolute ethanol containing 0.02 mol. of dry ammonia per 1000 cc. "in order to suppress any possible ionization of pyridine nitrogen." In fact, an abnormal behavior in dissymmetry, which resembles that of a polyelectrolyte in a solution of a low ionic strength, has also been found for poly-2-vinylpyridine in absolute ethanol[11] and in nitromethane.[12]

On the other hand, no abnormality has been reported for poly-4-vinylpyridine in 92.01 weight per cent ethanol[1] or for poly-2-vinylpyridine in methanol[13] or in dioxane[12]. Since the abnormality described above was not observed in the

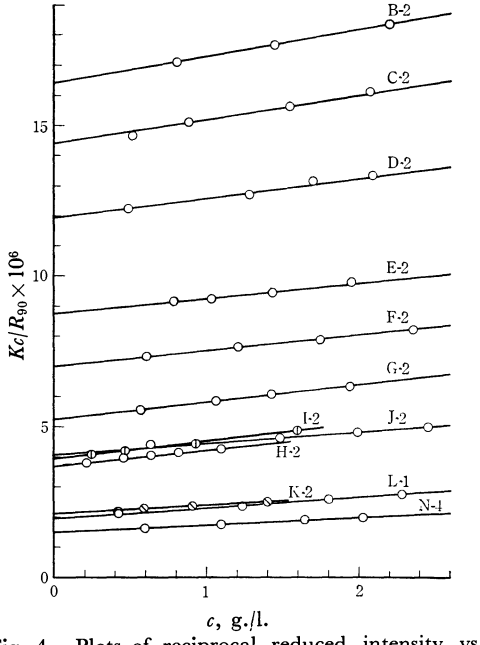

Fig. 4. Plots of reciprocal reduced intensity vs. concetration of poly-2-vinylpyridine fractions in methanol contained 0.02 mol. of dry ammonia per 1000 cc. at 25°C.

10) M. Miura, Y. Kubota and T. Masuzukawa, This Bulletin, **38**, 316 (1965).
11) A. J. Hyde and R. B. Taylor, *Makromol. Chem.*, **62**, 204 (1963).
12) W. M. Cashin, *J. Colloid Sci.*, **6**, 271 (1951).
13) H. Inoue, *Kolloid-Z. u. Z. Polymere*, **195**, 102 (1964).

TABLE I. THE RESULTS OF LIGHT SCATTERING, OSMOTIC PRESSURE AND VISCOSITY MEASUREMENT FOR A SERIES OF FRACTIONS OF POLY-2-VINYLPYRIDINE

P2VP No.	M_w $\times 10^{-4}$	M_n $\times 10^{-4}$	M_w/M_n	$(A_2)_{LS}$ $\times 10^4$	$(A_2)_{OP}$ $\times 10^4$	z	$\langle L^2\rangle^{1/2}$ Å	$[\eta]$ (dl./g.) in 92.01 wt. % Ethanol	Methanol	DMF	Benzene	Dioxane
A-2	3.04	—	—	8.10	—	1.04	250	0.255	0.230	0.160	0.140	0.134
B-2	6.28	4.15	1.51	8.24	11.4	1.06	315	0.399	0.361	0.250	0.201	0.200
C-2	7.27	4.77	1.52	7.75	11.1	1.07	342	0.420	0.394	0.280	0.220	0.214
D-2	9.30	5.00	1.86	5.67	10.7	1.07	342	0.498	0.462	0.308	0.259	0.231
E-2	12.01	7.42	1.62	5.30	8.3	1.08	368	0.636	0.550	0.360	0.305	0.275
F-2	16.05	8.16	1.97	6.62	8.0	1.18	559	0.838	0.735	0.471	0.374	0.340
G-2	21.95	8.84	2.48	5.75	7.5	1.20	585	0.942	0.847	0.530	0.420	0.371
H-2	30.08	12.97	2.32	6.20	6.3	1.16	532	1.30	1.16	0.700	0.530	0.460
I-2	31.10	10.95	2.84	6.00	7.3	1.25	651	1.20	1.09	0.640	0.502	0.441
J-2	30.75	12.10	2.54	4.56	6.9	1.29	693	1.30	1.21	0.640	0.537	0.433
K-2	52.06	18.07	2.88	4.75	6.2	1.29	693	1.78	1.69	1.02	0.790	0.610
L-1	84.97	39.51	2.15	3.98	(9.7)	1.77	1130	2.47	2.41	1.44	1.13	0.870
M-1	81.29	31.60	2.57	4.23	(10.8)	1.70	1078	2.40	2.39	1.39	1.09	0.863
N-4	93.10	—	—	3.50	—	1.90	1229	2.95	2.55	1.54	1.15	0.943
N-3	—	50.58	—	—	6.1	—	—	3.50	3.15	2.42	1.63	1.34

case of unfractionated poly-2-vinylpyridine[5] it may be possible to explain this phenomenon in terms of the contamination of polymers by some electrolytes in the course of fractionation, but the dissymmetrical behavior in benzene, dioxane and ethyl methyl ketone can not be explained in the same way. This phenomenon may also arise from the optical anisotropy of segments.[14,15]

Although the origin of the abnormality has not yet been clarified, it disappeared when methanol containing 0.02 mol. of dry ammonia per 1000 cc. was used as the solvent.[2] This solvent, therefore, was used in this study for the measurement of light-scattering of a series of poly-2-vinylpyridine fractions. The results are shown in Fig. 4.

The results of the measurements of the viscosity, the osmotic pressure, and the light-scattering are summarized in Table I, where M_n and $(A_2)_{OP}$ are the number average molecular weight and the second-virial coefficient in osmometry, and where M_w, z, $\langle L^2\rangle^{1/2}$ and $(A_2)_{LS}$ are the weight average moleclar weight, the intrinsic dissymmetry, the root mean square displacement length and the second-virial coefficient in turbidimetry respectively.

Relations among A_2, M_w and $\langle L^2\rangle^{1/2}$.—The plots of A_2 versus M_w and of $\langle L^2\rangle^{1/2}$ versus M_w are shown in Figs. 5 and 6 respectively. The expressions obtained from these plots are given in Table II. The relation between A_2 and M_w is almost the same as those obtained with other linear polymer-solvent systems, such as the polystyrene-toluene system.[16]

The exponent in the relation between $\langle L^2\rangle^{1/2}$

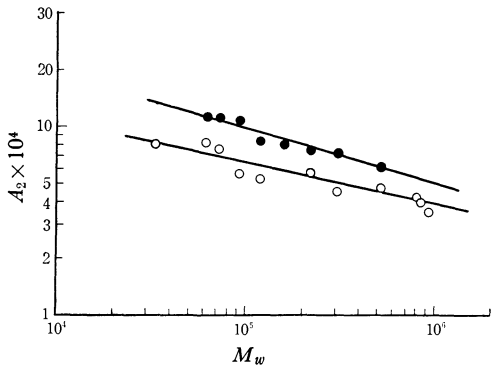

Fig. 5. Log-log plots of osmotic second virial coefficient vs. M_w in methanol (-●-) and of light scattering second virial coefficient vs. M_w in methanol contained 0.02 mol. of dry ammonia per 1000 cc. (-○-) at 25°C.

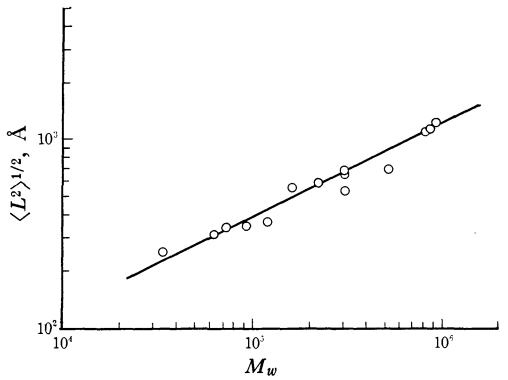

Fig. 6. Log-log plots of $\langle L^2\rangle^{1/2}$ vs. M_w for poly-2-vinylpyridine fractions in methanol contained 0.02 mol. of dry ammonia per 1000 cc. at 25°C.

14) M. Nakagaki, This Bulletin, **34**, 834 (1961).
15) H. Utiyama and M. Kurata, *Bull. Inst. Chem. Research, Kyoto Univ.*, **42**, 128 (1964).
16) E. F. Casassa and H. Markovitz, *J. Chem. Phys.*, **29**, 493 (1958).

Table II. Relations among A_2, M_w and $\langle L^2\rangle^{1/2}$

Solvent	Temp., °C	Formula
Methanol-NH_3	25±1	$(A_2)_{LS} \propto M_w^{-0.22}$
Methanol	25±0.003	$(A_2)_{OP} \propto M_w^{-0.29}$
Methanol-NH_3	25±1	$\langle L^2\rangle^{1/2} \propto M_w^{0.5}$

and M_w seems to be smaller than that which might be expected from the following facts: the relations between M_w and the intrinsic viscosities in pure methanol and methanol containing 0.02 mol. of dry ammonia per 1000 cc. are almost the same for all the fractions measured; moreover, methanol is an extremely good solvent for this polymer.[4]

Relations among M_w, M_n and $[\eta]$.—For polymer samples which are homogeneous with respect to the molecular weight, the relation between the intrinsic viscosity and the molecular weight can be expressed by the Mark-Houwink equation:

$$[\eta] = K_i' M^{\nu} \tag{1}$$

where K_i' and ν are constants independent of the molecular weight. However, it is well known that the empirically determined values of K' in the form of Eq. 1 for heterogeneous samples vary with the kind of average, and also with the width of the distribution of the molecular weight.[17-19]

In such cases, if the molecular weight distribution of the sample is known, a quantitative relation between K' and the degree of homogeneity can be obtained.[20,21] For example, when the molecular weight distribution of each fraction can be represented by the exponential-type function[22]:

$$w(M) = \{Y^{h+1}/\Gamma(h+1)\} M^h \exp(-YM) \tag{2}$$

the following relations are given:

$$[\eta] = K_w' M_w^{\nu} = K_i' \{\Gamma(\nu+h+1)/ \Gamma(h+1)(h+1)^{\nu}\} M_w^{\nu} \tag{3}$$

$$[\eta] = K_n' M_n^{\nu} = K_i' \{\Gamma(\nu+h+1)/ \Gamma(h+1)h^{\nu}\} M_n^{\nu} \tag{4}$$

The parameters in Eq. 2 have the same meaning as in Eq. 6 in Part I,[5] while the constants, K_w' and K_n' in Eqs. 3 and 4 refer to weight and number average respectively.

On the other hand, if we take the logarithmic normal-type distribution function[23]:

$$w(M) = MA \exp\{-p^2(\ln M/M_0)^2\} \tag{5}$$

the relations are given by:

$$[\eta] = K_w' M_w^{\nu} = K_i' (M_w/M_n)^{\nu(\nu-1)/2} M_w^{\nu} \tag{6}$$

$$[\eta] = K_n' M_n^{\nu} = K_i' (M_w/M_n)^{\nu(\nu+1)/2} M_n^{\nu} \tag{7}$$

The parameters in Eq. 5 are the same as in Eq. 9 in Part I.[5]

As the variation in the K_w' value in Eq. 3 or 6 with the change in M_w/M_n is comparatively small, the value of ν can be assumed to be nearly the same as the slope of the linear line in the double logarithmic plots of $[\eta]$ versus M_w for fractionated samples. Thus, the value of K_i' can be calculated by means of the above equations.

The intrinsic viscosities of fourteen fractions in five kinds of solvents and those in methanol are plotted against M_w and M_n respectively in Fig. 7. The plots of $[\eta]$ versus M_n can be expressed by linear lines, whereas the plots of $[\eta]$ versus M_n scatter considerably. This is considered to be due to the heterogeneity of the samples, as is shown by the M_w/M_n values cited in Table I.

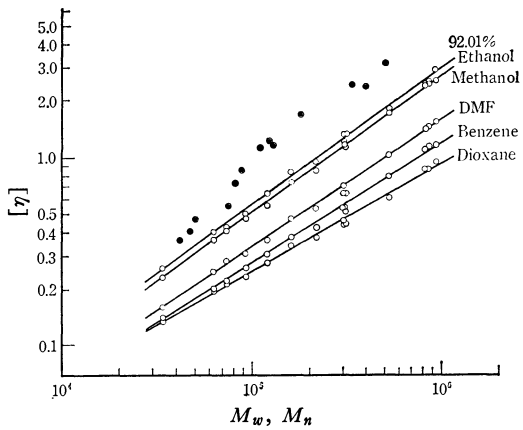

Fig. 7. Log-log plots of $[\eta]$ vs. M_n in methanol (-⊙-) and of $[\eta]$ vs. M_w in various solvents indicated (-○-) for poly-2-vinylpyridine fractions at 25°C.

The constants, ν and K_w', evaluated from the linear lines in Fig. 7 are shown in columns 2 and 3 respectively in Table III. The values of K_n' in column 4 of the table are the mean values of K_n' for all fractions; these values were calculated

Table III. The constants in the Mark-Houwink equation at 25°±0.01°C

Solvent	ν	$K_w' \times 10^4$	$K_n' \times 10^4$	$K_i' \times 10^4$ Eqs. 3 and 4	$K_i' \times 10^4$ Eqs. 6 and 7
92.01 wt.% Ethanol	0.73	1.22	2.13	1.28	1.31
Methanol	0.73	1.13	1.99	1.19	1.21
Dimethyl formamide	0.67	1.47	2.45	1.58	1.60
Benzene	0.64	1.70	2.71	1.80	1.85
Dioxane	0.58	3.09	4.78	3.30	3.38

17) H. P. Frank and J. W. Breitenbach, *J. Polymer Sci.*, **6**, 609 (1951).
18) H. P. Frank, ibid., **7**, 567 (1951).
19) H. P. Frank and G. B. Levy, ibid., **10**, 371 (1953).
20) R. Koningsveld and C. A. F. Tuijnman, *Makromol. Chem.*, **38**, 39 (1960).
21) A. Kotera, K. Takamizawa, T. Kamata, H. Kawaguchi, M. Nireki, M. Kuwabara and K. Yamashita, presented at the 10th Symposium on High Polymers, Tokyo, November, 1961.
22) G. V. Schulz, *Z. physik. Chem.*, **B30**, 379 (1935); B. H. Zimm, *J. Chem. Phys.*, **16**, 1099 (1948).
23) R. Koningsveld and C. A. F. Tuijnman, *J. Polymer Sci.*, **39**, 445 (1959).

from the equation, $[\eta]=K_n'M_n^{\nu}$, the values of ν being assumed to be the same as those for the relation between $[\eta]$ and M_w.

Assuming that the molecular weight distribution of each fraction can be represented by Eqs. 2 and 5, the values of K_i' were evaluated by inserting the values of ν, K_w' and K_n' cited in Table III into Eqs. 3 and 4 and Eqs. 6 and 7. The results are shown in columns 5 and 6 of Table III.

The values of K_i' calculated by assuming the two functions given above are in good agreement with each other. The validity of the values of K_i' and ν is shown with the methanol solution,

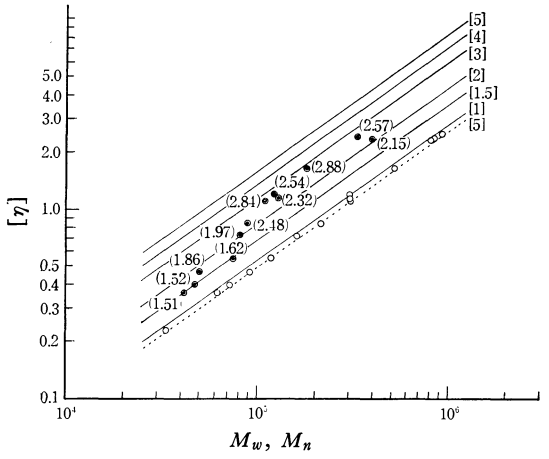

Fig. 8. Log-log plots of $[\eta]$ vs. M_w (---, Eq. 3) and $[\eta]$ vs. M_n (——, Eq. 4) for different M_w/M_n ratios indicated in [ ] assuming $K_i'=1.19\times10^{-4}$ and $\nu=0.73$ in methanol at 25°C. Points show plots of $[\eta]$ vs. M_w (-○-) and $[\eta]$ vs. M_n (-⊙-) for observed values of M_w/M_n indicated in ( ).

as an example, in Fig. 8. The figure in the parenthesis at each point in Fig. 8 shows the observed value of M_w/M_n. The straight lines correspond to the values of K_w' and K_n' which are obtained from Eqs. 3 and 4 by inserting the values of K_i' (1.19×10^{-4}) and ν (0.73) and the voluntarily selected values of M_w/M_n which are shown in the brackets. Almost the same results were obtained from Eqs. 6 and 7.

These results show that the values of K_i' and ν thus obtained are quite reasonable. The relation between the molecular weight and the $[\eta]$ value for sufficiently fractionated samples can be expressed by the Mark-Houwink equation containing the constants, K_i' and ν, cited in Table III.

The direction of the variation in the values of ν with the solvent is the same as the solvent power described in Part II.[4] The constants, K_w' and ν, for poly-2-vinylpyridine in 92.01 weight per cent ethanol at 25°C cited in Table III are almost the same as those for poly-4-vinylpyridine in the same solvent and temperature[1]:

$$[\eta]=1.20\times10^{-4}M_w^{0.73}$$

The Unperturbed Chain Dimension of Poly-2-vinylpyridine.—The intrinsic viscosities of a flexible linear polymer in theta and nontheta solvents are expressed by Eqs. 8 and 9 respectively[24]:

$$[\eta]_\theta = KM^{1/2} \tag{8}$$

$$[\eta] = KM^{1/2}\alpha^3 \tag{9}$$

Here K is a constant for a given polymer independent of the solvent and the molecular weight; it is related to the mean square displacement length of the chain, $\langle L^2\rangle_0^{1/2}$, in an ideal solvent as follows:

$$K=\Phi_0A^3, \qquad A^2=\langle L^2\rangle_0/M \tag{10}$$

where Φ_0 (0.87×10^{21}) is the universal viscosity constant for chain polymers in a theta solvent, while α in Eq. 9 is the viscosity expansion factor. According to a recent perturbation theory,[24-27] α is a function of z, which is defined by:

$$z = (3/2\pi)^{3/2}BA^{-3}M^{1/2} \tag{11}$$

where A is a parameter concerned with the short range interaction of segments defined by Eq. 10, and B, a parameter on the long range interaction of segments which is related to the excluded volume effect. The relation between α and z obtained by Stockmayer and Fixman[24] is:

$$\alpha^3 = 1 + 1.55z \tag{12}$$

From these equations they derived the following expression:

$$[\eta]/M^{1/2} = K + 0.51\Phi_0BM^{1/2} \tag{13}$$

The values of $[\eta]$ and M_w cited in Table I are plotted according to this equation in Fig. 9.

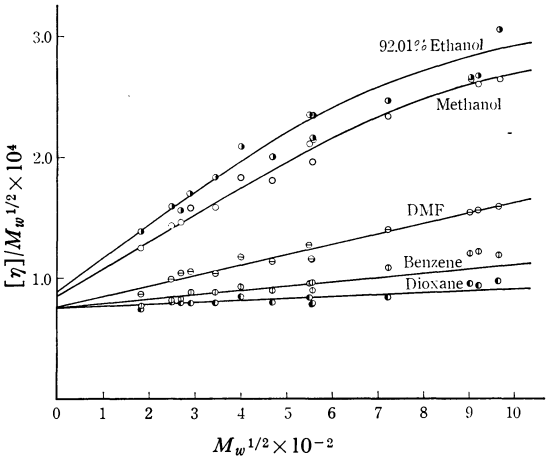

Fig. 9. Plots of $[\eta]/M_w^{1/2}$ vs. $M_w^{1/2}$ for poly-2-vinylpyridine fractions at 25°C.

24) W. H. Stockmayer and M. Fixman, ibid., **C1**, 137 (1963).
25) M. Kurata, W. H. Stockmayer and A. Roig, *J. Chem. Phys.*, **33**, 151 (1960).
26) M. Fixman, ibid., **36**, 3123 (1962).
27) O. B. Ptitsyn and Y. Y. Eisner, *Vysokomolekulyarye Soedineniya*, **1**, 1200 (1959).

The lines for the viscosities in the relatively poor solvents, dimethylformamide, benzene and dioxane, pass through the same intercept and are linear, as was to be expected from Eq. 13, whereas the lines for the good solvents, 92.01 weight per cent ethanol and methanol, have an upward curvature and the intercepts are larger than other one. Consequently, the K_w values obtained from these intercepts lie between 7.5×10^{-4} and 8.9×10^{-4}. A similar solvent dependence of the intercept has been reported for polymethyl methacrylate.[3,28,29] In Part II,[4] the existence of the solvation of alcohol molecules to pyridine nitrogen was suggested; therefore, it is of interest to investigate the solvent effect[30] on the unperturbed dimension of the chain. However, the present data seem insufficient for discussing this problem.

The value of K can also be obtained by the following semi-empirical equation of Krigbaum[31]:

$$[\eta] = [\eta]_\theta + 5.0\times10^{-3}A_2M \qquad (14)$$

As has been described in Part II,[4] the relation between $[\eta]$ and A_2 for the H-2 fraction in various solvents at 25°C can be expressed by Eq. 15:

$$[\eta] = 0.415 + 1.10\times10^3A_2 \qquad (15)$$

When the value of M_w, 30.08×10^4, for the H-2 fraction is inserted into Eq. 14, the following equation can be obtained:

$$[\eta] = [\eta]_\theta + 1.50\times10^3A_2 \qquad (16)$$

The difference between the coefficient of A_2 in Eq. 15 and that in Eq. 16 may be due to the molecular weight inhomogeneity and to experimental errors in M_w and A_2. The agreement, however, is satisfactory, and so it is reasonable to take the value of 0.415 for $[\eta]_\theta$. By inserting the values of $[\eta]_\theta$ and M_w for the H-2 fraction in Eq. 8, the value of K_w is found to be 7.6×10^{-4}. The probable error of K_w is $\pm(0.5\times10^{-4})$.

The value of K can be obtained by the more direct method, namely, by measuring the $[\eta]$ value of a fraction of poly-2-vinylpyridine in a θ-solvent. Flory and Shultz[32] have derived the following relation between the critical temperature, $T_c(°K)$, in a binary polymer-solvent system and the number of segments, x or M_w:

$$1/T_c = (1/\theta)\{1 + (1/\psi_1)(1/x^{1/2} + 1/2x)\}$$
$$\cong (1/\theta)(1 + b/M_w^{1/2}) \qquad (17)$$

where θ is the theta-temperature and ψ_1, an entropy parameter.

Benzene was used as the solvent in this experiment, and the critical temperature was determined by the method of Flory[32] for the E-2, J-2, K-2 and N-3 fractions. The results are plotted in Fig. 10 according to Eq. 17. The value of θ obtained from the intercept of the linear line in Fig. 10 is 16.2°C. The intrinsic viscosity of the H-2 fraction in benzene at 16.2°C was found to be 0.465; this, by definition, is the $[\eta]_\theta$ of this fraction. Thus, the value of K_w is calculated by means of Eq. 8 as 8.5×10^{-4} at 16.2°C. The probable error of K_w is $\pm(1.0\times10^{-4})$ in this case.

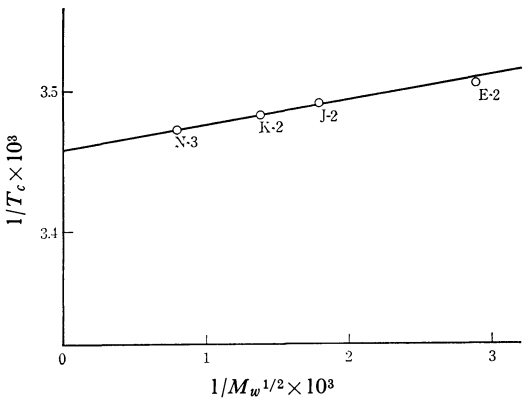

Fig. 10. Plots of reciprocal critical temperature in benzene vs. $1/M_w^{1/2}$ for poly-2-vinylpyridine fractions.

As the values of K_w obtained above were based on the data for samples which are not numerous enough to discuss them as a molecular homogeneous polymer, the correction for the molecular weight distribution was applied to them. Assuming again the exponential function[22] for the distribution of the molecular weight, the K_w values were corrected by the following equations[3]:

$$[\eta]_\theta/M_w^{1/2} = K_w = q_wK \qquad (18)$$

$$q_w = \Gamma(h+1.5)/(h+1)^{1/2}\Gamma(h+1) \qquad (19)$$

As may be seen in Table I, the M_w/M_n ratio for a series of fractions is ca. 2 as a mean value, while the ratio for the H-2 fraction is 2.32. Thus, q_w was calculated by using $h = 1$ for the value of K_w obtained by the Fixman plot and $h = 0.758$ for the values of K_w obtained by the latter two methods. The corrected K values are shown in Table IV.

Table IV. Corrected values of the Flory constant, K

Method	Temp. °C	$K_w\times10^4$	q_w	$K\times10^4$
Fixman (Eq. 13)	25.0	8.2±0.7	0.94	8.7±0.8
Krigbaum (Eq. 14)	25.0	7.6±0.5	0.93	8.2±0.6
Flory (Eq. 17)	16.2	8.5±1.0	0.93	9.1±1.1

The K values obtained by the methods of Fixman and Krigbaum are, as may be seen in Table IV, in good agreement with each other. This implies

28) W. Burchard, *Makromol. Chem.*, **50**, 20 (1961).
29) W. R. Moore and R. J. Fort, *J. Polymer Sci.*, **A1**, 929 (1963).
30) S. Lifson and I. Oppenheim, *J. Chem. Phys.*, **33**, 109 (1960).
31) W. R. Krigbaum, *J. Polymer Sci.*, **28**, 213 (1958).
32) A. R. Shultz and P. J. Flory, *J. Am. Chem. Soc.*, **74**, 4760 (1952).

TABLE V. UNPERTURBED CHAIN DIMENSION CALCULATED FROM K VALUES

Polymer	Temp. °C	$K\times10^4$	$\left[\frac{\langle L^2\rangle_0}{M}\right]^{1/2}\times10^{11}$	$\left[\frac{\langle L^2\rangle_{0f}}{M}\right]^{1/2}\times10^{11}$	σ	V_x
Polyethylene[3]	ca. 100	23.0±3.0	950±40	582	1.63±0.08	8
Polystyrene[3]	ca. 30	8.2±0.5	670±15	302	2.22±0.05	89
Poly-4-vinylpyridine[3]	25	9.4±1.0	710±30	300	2.37±0.10	81
Poly-2-vinylpyridine	25	8.7±1.0	673±30	300	2.24±0.10	81

that these two methods are closely correlated with each other. In fact, an extremely close resemblance between Fixman's equation (Eq. 13) and a deformation of Krigbaum's equation:

$$[\eta]/M^{1/2} = K + 0.63\Phi_0 Bh(z)M^{1/2} \qquad (20)$$

has been discussed by Stockmayer and Fixman.[24]

Considering that the hindrance to internal rotation about the C–C bond generally decreases with a rise in the temperature,[33] the value of K at 16.2°C is reasonable.

Using the values of $K = (8.7\pm1.0)\times10^{-4}$ and $\Phi_0 = 2.87\times10^{21}$, the value of $[\langle L^2\rangle_0/M]^{1/2}$ for poly-2-vinylpyridine was calculated by means of Eq. 10 as $(673\pm30)\times10^{-11}$ at 25°C.

By denoting the unperturbed root mean square displacement length of the polymer chain in the case of free rotation about C–C bond as $\langle L^2\rangle_{0f}^{1/2}$, and by assuming the C–C bond length and tetrahedral angle to be 1.54 Å and 109.5° respectively, the value of $[\langle L^2\rangle_{0f}/M^{1/2}]$ was found to be 300×10^{-11}.

As a measure of the hindrance to internal rotation, the following factor, σ, was calculated for the polymer using the values of $\langle L^2\rangle_0/M$ and $\langle L^2\rangle_{0f}/M$ described above:

$$\sigma^2 = \langle L^2\rangle_0/\langle L^2\rangle_{0f} \qquad (21)$$

The results are shown in Table V, together with those[3] for polyethylene, polystyrene and poly-4-vinylpyridine. The molar volumes, V_x, of side groups of these polymers, hydrogen, the benzene ring and the pyridine ring, are shown in column 7 of Table V.

When we compare the values of σ for these four polymers, we can find relatively large σ values for the latter three polymers; these are considered to be due to the steric hindrance caused by large groups of atoms in the side chain.[3,33] Further, as the V_x value of pyridine is smaller than that of benzene, the steric hindrance to internal rotation is considered to be somewhat smaller in polyvinylpyridines than in polystyrene. In spite of this difference in the values of V_x, the values of σ for the polyvinylpyridines are, on the other hand, a little larger than that for polystyrene, as may be seen in Table V. This may be interpreted as being due to electrostatic interaction between pyridine rings.

The small difference between the σ values for poly-2-vinylpyridine and poly-4-vinylpyridine may be due to the difference in the degree of short range interactions, for example, the interaction between the nitrogen and the hydrogen in the neighboring pyridine rings or in the main chain.

However, further systematic investigation will be required to clarify this problem, together with the solvent effect on the value of K described previously.

The author wishes to express deep appreciation to Professor Hiromu Murata for making this study possible and for his kind advice, and to Professor Masaji Miura for his encouragement and many valuable discussions throughout this work.

33) P. J. Flory, "Principles of Polymer Chemistry," Cornell Univ. Press, Ithaca, New York (1953).

BULLETIN OF THE CHEMICAL SOCIETY OF JAPAN VOL. 39 447—452 (1966)

The Rheological Study of Aqueous Solutions of Polyvinyl Alcohol at Ultrasonic Frequencies

By Kiyoshi ARAKAWA and Nobuo TAKENAKA

Research Institute of Applied Electricity, Hokkaido University, Sapporo

(Received June 3, 1965)

The ultrasonic velocity and the absorption have been measured over the 5—45 Mc./sec. frequency range for aqueous solutions of polyvinyl alcohol by means of an ultrasonic pulse technique which was similar in principle to that used by Pinkerton (*Proc. Phys. Soc.* **B62,** 286 (1949)). The temperature varied over the 3—70°C range. The velocity-versus-temperature curves have been found to be convex upwards, like that of pure water, but the peak shifts upwards and to the lower-temperature side with an increase in the concentration. The ultrasonic absorptions of aqueous solutions of partly-saponified polyvinyl alcohol have been found to be larger than those of perfectly-saponified alcohol at the same concentrations. Two relaxation mechanisms have been found for each sample. For the solutions of the perfectly-saponified sample, the first relaxation frequency, f_1, is 35 Mc./sec. at 12°C, while the second relaxation frequency f_2 is 40 Mc./sec. at 60°C, for example. On the other hand, these values have been found to be nearly equal for the solutions of the partly-saponified sample. The activation energy, ΔH_2, obtained from the temperature dependence of f_2 is about 4 kcal./mol., irrespective of the quantity of resuidal acetate groups, and the ΔH_1 value for f_1 is of the order of 10 kcal./mol.

In a previous paper[1] some results of rheological investigations of concentrated aqueous solutions of polyvinyl alcohol using an ultrasonic pulse technique have been reported; the adiabatic compressibility of polymer molecules in solutions have been discussed elsewhere.[2] However, the previous data concern one ultrasonic frequency in the mega cycle region; therefore, we have attempted in the present experiment to obtain ultrasonic data on the solutions of polyvinyl alcohol over a wider range of frequencies using a newly-constructed apparatus for the measurement of the ultrasonic velocity and the absorption by the pulse method.[1,3]

The oscillational displacement, ξ, in a longitudinal wave through the solution at a distance, x, from a source of sound is:

$$\xi = \xi_0 \exp(-\alpha x) \exp\{i\omega(t - x/c)\} \quad (1)$$

where c is the sound velocity; ω, the angular frequency; ξ_0, the amplitude of oscillation; α, the absorption coefficient, and t, the time. We will here obtain c and α values for various frequencies and temperatures.

Experimental

Apparatus and Procedure.—The apparatus used in this experiment is similar to that reported in the previous paper,[1] but this apparatus can be used for a wider range of frequencies. A block diagram of it is shown in Fig. 1.

A pulse generator supplies an electric pulse of about 5—10 μ sec. duration, and with a repetition rate of 2—5 kc./sec., into a high-frequency oscillator, which operates as an oscillator only during the loading period of the pulse. The oscillator is constructed from three independent parts, each of which is used for each available frequency range between 1—50Mc./sec.; for the measurement in the range of 50—100 Mc./sec., a frequency doubler unit[4] is inserted in a position series to the oscillator. The pulse-modulated high-frequency voltage from the oscillator is led to a transmitter quartz in a cell which contains a sample solution; there it is transduced into an ultrasonic pulse. The pulse which has been propagated through the solution is again transduced into an electric pulse by a receiver quartz and then led to an attenuator. The pulse from the attenuator is amplified and supplied into a vertical axis of a synchroscope.

The velocity of sound, c, is measured according to the procedure described in the previous paper.[1] The amount of attenuation is determined by the compensation method, using the attenuator. That is, the difference in the attenuator reading gives the amount of attenuation for the given path length between the two positions of the movable receiver quartz when attenuator is adjusted so that the pulse pattern in the synchroscope screen has the same height for the two positions of the receiver quartz. The absorption coefficient, α, is determined from the tangent of a linear plot of the amount of attenuation against the length of the ultrasonic path.

* Presented in part at the 18th Annual Meeting of the Chemical Society of Japan and at the 14th Annual Meeting of the Society of Polymer Science, Japan.

1) K. Arakawa, N. Takenaka, M. Watase and K. Kubota, This Bulletin, **37**, 559 (1964).

2) Y. Miyahara and Y. Masuda, *Science* (*Kagaku*), **30**, 588 (1960); Y. Masuda, T. Hasegawa and Y. Miyahara, *J. Chem. Soc. Japan, Pure Chem. Sect.* (*Nippon Kagaku Zasshi*), **82**, 1131 (1961); H. Shiio and H. Yoshihashi, *J. Phys. Chem.*, **60**, 1049 (1956).

3) J. M. Pinkerton, *Proc. Phys. Soc.*, **B62**, 86 (1949); L. Melchor and A. A. Petrauskas, *Ind. Eng. Chem.*, **44**, 716 (1952); D. G. Ivey, B. A. Mrowca and E. Guth, *J. Appl. Phys.*, **20**, 486 (1949); J. H. Andreas and P. L. Joyce, *Brit. J. Appl. Phys.*, **13**, 462 (1962).

4) H. J. McSkimin, *J. Acoust. Soc. Am.*, **34**, 404 (1962).

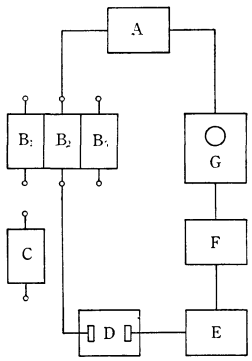

Fig. 1. Block diagram of the apparatus.
A: Pulse generator
B_1, B_2, B_3,: Oscillator
B_1, 1—15 Mc./sec.
B_2, 15—30 Mc./sec.
B_3, 30—50 Mc./sec.
C: Doubler, 60—100 Mc./sec.
D: Cell
E: Attenuator
F: Amplifier
G: Synchroscope

Samples.—The two samples, A and B, used were the same as those reported in the preceding paper.[1] The average molecular weight was 8.0×10^4 for the perfectly-saponified P.V.A. sample A and about 9×10^4 for the sample B, which is the partly saponified P. V. A. and which has 12.2 mole % of the residual acetate groups. The preparation procedure of the aqueous solution is similar to that reported previously.[1]

Measurement.—In this experiment the sound velocity and absorption were measured for 5 and 10 wt. % solutions of the two samples. The temperature was varied within the range of 3—70°C. The frequency range used was 5—45 Mc./sec.

Results and Discussion

The Effect of Aging on Ultrasonic Absorption.

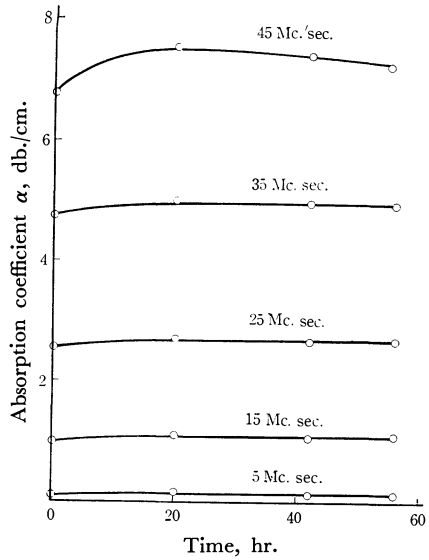

Fig. 2. Aging curve for the 10 wt.% solution of sample A.

—Concentrated polymer solutions are often found to exhibit an aging behavior. In Fig. 2 the absorption coefficient, α, which was measured for the 10 wt.% solution of sample A is plotted against the standing time after the thermal equilibration of the solution has been reached at room temperature. As may clearly be seen in Fig. 2, the

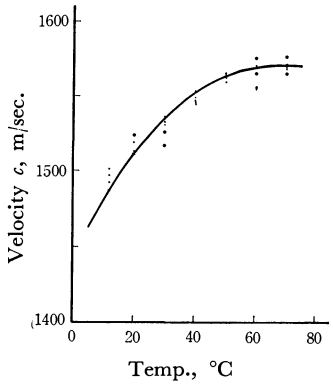

Fig. 3(a). Sound velocity, sample A, 5%.
Horizontal shift Δh: −5°C
Vertical shift Δv: +15 m/sec.

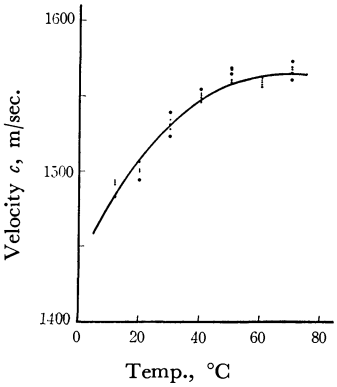

Eig. 3(b). Sound velocity, sample B, 5%.
Δh: −5°C, Δv: +10 m/sec.

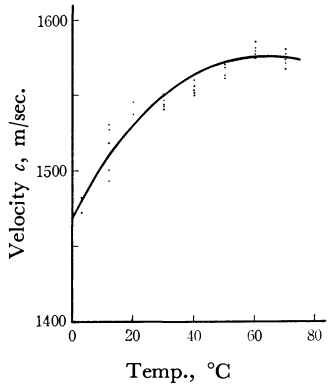

Fig. 3(c). Sound velocity, sample A, 10%.
Δh: −10°C, Δv: +20 m/sec.

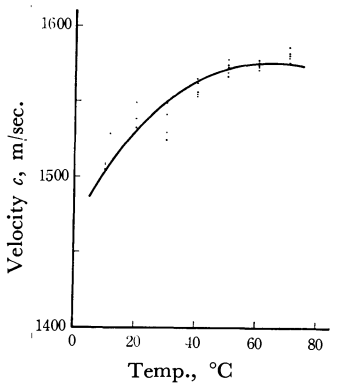

Fig. 3(d). Sound velocity, sample B, 10%.
Δh: −10°C, Δv: +20 m/sec.

effect of aging is not very large, but it has a tendency to increase with the frequency; the primary effect of aging is confined within 20 hr., while after more than 20 hr. the absorption coefficient is found to reach a constant value. Therefore, in the present experiment the measurements were made after the prepared solution had been allowed to stand at room temperature for more than 20 hr. after its preparation.

Data of Ultrasonic Velocity.—In Figs. 3(a), (b), (c), and (d) the sound velocities obtained for solutions of samples A and B are plotted against the temperature for each concentration; here the frequency dependence is not very clear. All the data for the 5—45 Mc./sec. frequency range are also plotted together against the temperature. Each solid line is one which is obtained by the parallel shift of the velocity vs. the temperature curve for pure water[5] (the amount of the shift is given in each figure). The sound velocity in pure water is found to have a maximum value, 1555.5 m/sec., at 74°C.[5] It may be seen in Fig. 3 that the peak in the velocity vs. the temperature curve shifts toward a temperature lower than that for pure water; it may also be seen that the amount of shift increases with the increase in the concentration.

Data of Sound Absorption.—In Figs. 4(a), (b), (c), and (d) the absorption coefficient, α, is plotted against the temperature; the frequency is varied within the 5—45 Mc./sec. range. It is found that the absorption of aqueous solutions of sample B is larger than that of sample A at the same concentration. It may be seen especially in Figs. 4(c) and (d) that absorption curves have two characters, that is, a peak or shoulder at about the 0—20°C range and a shoulder at about the 30—40°C range; it may also be seen that the two peaks or shoulders shift to a higher temperature region with the increase in frequency.

5) M. Greenspan and C. E. Sschiegg, *J. Res. Natl. Bur. Std.*, **58**, 249 (1957); *J. Acoust. Soc. Am.*, **31**, 75 (1959).

It is well known that the ultrasonic absorption of pure water decreases monotonously with the increase in temperature in this frequency range. Therefore, from these two characteristics we may

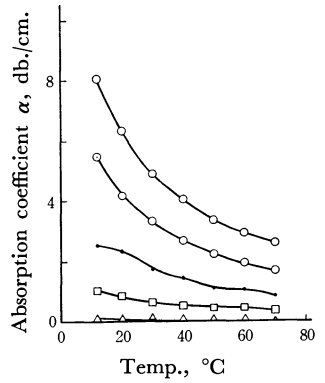

Fig. 4(a). Absorption coefficient, sample A, 5% solution.
○ 45 Mc. ⊙ 35 Mc. • 25 Mc. □ 15 Mc. △ 5 Mc.

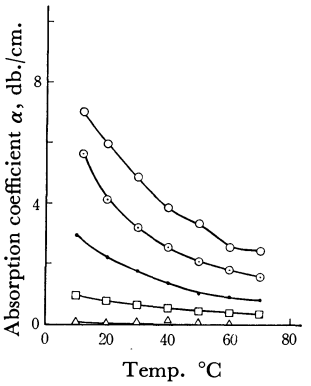

Fig. 4(b). Absorption coefficient, sample B, 5% solution.

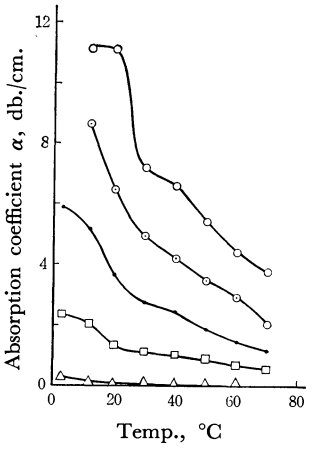

Fig. 4(c). Absorption coefficient, sample A, 10% solution.

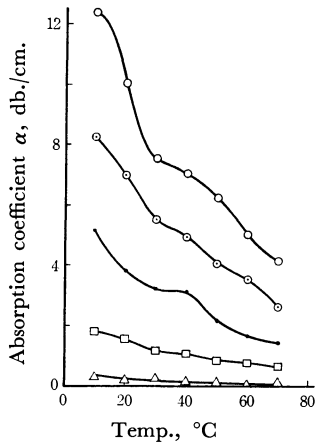

Fig. 4(d). Absorption coefficient, sample B, 10% solution.

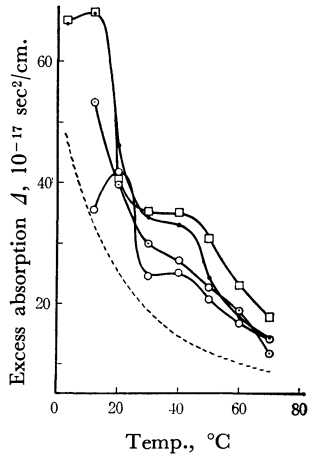

Fig. 5(a). Excess absorption, sample A, 10%.
○ 45 Mc ⊙ 35 Mc • 25 Mc □ 15 Mc.

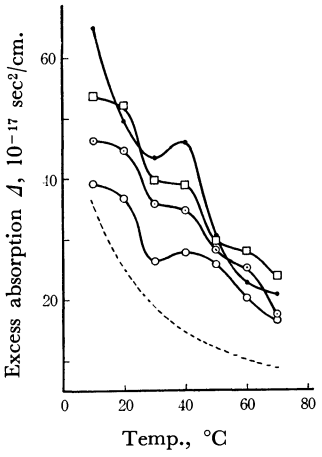

Fig. 5(b). Excess absorption, Sample B, 10%.

say that in this range of temperature and frequency the ultrasonic absorption of aqueous solutions of polyvinyl alcohol is approximately composed of three parts. The first one is, of course, to be attributed to free water, which is the greater part by weight in these solutions. The contribution from this part to the total absorption is, however, not necessarily the greater part of the total absorption. In the case of a 10% solution it is about one-third of the total absorption. The second and the third parts are to be attributed to polymer molecules, including the contribution from hydrated bound water. The second corresponds to the peak or shoulder at about the 0—20°C range, and the third, to the shoulder at about 30—40°C, as has been described above.

In Figs. 5(a) and (b), the excess absorption, Δ, for the 10 wt.% solution;

$$\Delta=\left(\frac{\alpha}{f^2}\right)_{\text{solution}}-0.9\left(\frac{\alpha}{f^2}\right)_{\text{water}} \qquad (2)$$

is plotted against the temperature. The dashed lines are the values (α/f^2) for pure water,[6] which may be, so to speak, regarded as back ground curves in the total absorption. The amount of Δ is the part of the absorption attributed to polymer molecules in solutions, including the excess contribution of hydrated water molecules, that is, the difference between the amount of the absorption of hydrated water molecules and the amount of the absorption of the water molecules when they are allowed to be free. The presence of the two absorption mechanisms may clearly be seen in Figs. 5(a) and (b). Therefore, it may safely be said that the ultrasonic absorption of a polyvinyl alcohol solution in this temperature range is approximately given by the summation of three parts, as is shown in Fig. 6, for example, where, however, the proportion of the absolute amount of each component is, of course, somewhat arbitrary.

Frequency Dependence of Ultrasonic Absorption.—In order to obtain the frequency dependence of the ultrasonic absorption we have given here, in Figs. 7(a) and (b), the α/f^2 vs. f curve, and also the $\alpha\lambda$ vs. f curve in Figs. 8(a) and (b), where λ is the wavelength, obtained from the data shown in Figs. 4(c) and (d).

As has been stated before on the basis of a consideration of the temperature dependence of the absorption, the presence of two relaxation mechanisms may be concluded. They are characterized by two relaxation frequencies, f_1 and f_2, each, which are numbered in order from the low temperature side in the α vs. T curve. For example, in the case of the 10 wt.% solution of the sample A, the value of f_1 and f_2 is determined from the

6) J. M. M. Pinkerton, *Proc. Phys. Soc.*, **B62**, 129, 286 (1949); *Nature*, **160**, 68 (1947); M. Pancholy, *J. Acoust. Soc. Am.*, **25**, 1003 (1953); T. Kishimoto and O. Nomoto, *J. Phys. Soc. Japan*, **9**, 1021 (1954).

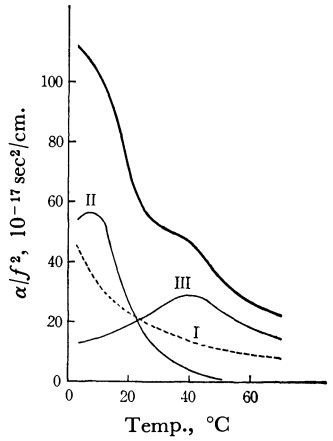

Fig. 6. Three parts of the absorption curve for the 10% solution of sample A at 25 Mc./sec.
I: 1st part (free water), II: 2nd part
III: 3rd part

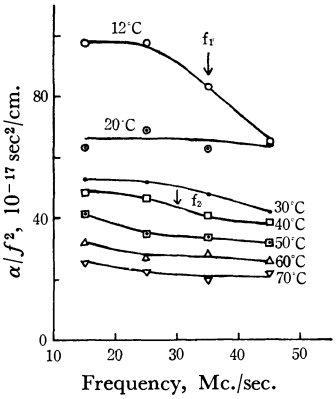

Fig. 7(a). Frequency dependence of the absorption, 10% solution of sample A.

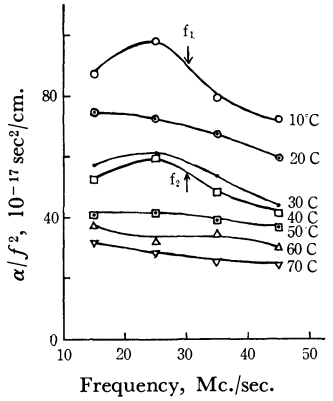

Fig. 7(b). Frequency dependence of the absorption, 10% solution of sample B.

curves in Fig. 7(a) and Fig. 8(a). In Fig. 8(a) the large peak in the curve at 12°C, which is characterized by the relaxation frequency f_1, is

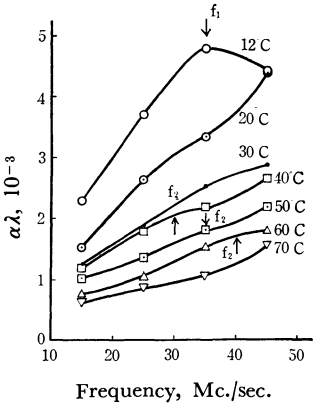

Fig. 8(a). $\alpha\lambda$ vs. f curve for the 10% solution of sample A.

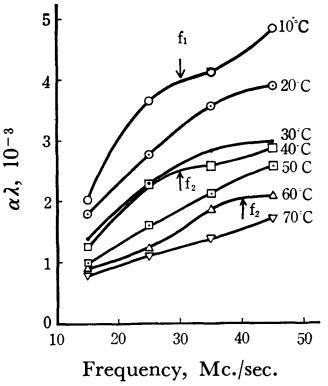

Fig. 8(b). $\alpha\lambda$ vs. f curve for the 10% solution of sample B.

found to correspond to the peak at 0—20°C in Fig. 5(a), while this peak is found to be shifted at the high frequency end at 20°C in Fig. 8(a). The shoulder[7] found at 30 Mc./sec. in the 40°C curve in Fig. 8(a), which corresponds to the shoulder near 40°C in Fig. 5(a), seems to shift gradually to the high frequency side with the increase in temperature; this shoulder is thought to be characterized by the relaxation frequency f_2. A similar consideration holds for the 10 wt.% solution of the sample B.

The value of the activation energy, ΔH_2, may be determined to be 4.2 kcal./mol. for both samples, A and B, from the temperature dependence of f_2. The value of ΔH_1 for f_1 can not be determined, but it may be estimated to be larger than 10 kcal./mol. from the curves in Figs. 8(a) and (b).

In Fig. 7(b) it may be seen that the values of α/f_2 decrease with the decrease in frequency at low temperatures. This may be attributed to the presence of Rayleigh scattering because of the co-existence of some larger colloidal particles;

7) M. Pancholy and S. P. Singal, ibid., **18**, 582 (1963).

this scattering follows the f^4 law. The fact that the decrease in α/f^2 with the decrease in frequency occurs at low temperatures only may be said to support this consideration.* Though the reason why this tendency is stronger for the sample B than for the sample A is not clear at present, it seems that it is to be attributed to the presence of residual acetate groups in the sample B which amount to about 1/8 in the mole fraction.

Longitudinal Wave Modulus.—From the values of the ultrasonic velocity and the absorption coefficient, the real part and imaginary part of the longitudinal wave modulus, M_1 and M_2, are obtained.

$$M_1=\rho c^2\frac{1-(\alpha c/\omega)^2}{\{1+(\alpha c/\omega)^2\}^2} \tag{3}$$

$$M_2=\rho c^2\frac{2(\alpha c/\omega)}{\{1+(\alpha c/\omega)^2\}^2} \tag{4}$$

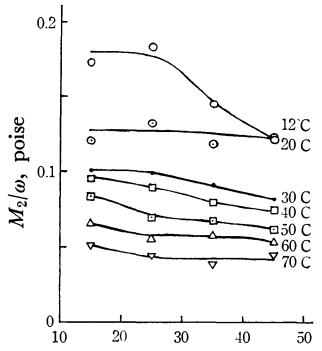

Fig. 9. Values of M_2/ω for the 10% solution of sample A.

* In Fig. 7(b) it may be seen that the curve at 20°C only is flat at low frequencies, in contrast to the above-described behavior of other curves at 10—40°C. This is because, if the Rayleigh dispersion is absent, the 20°C curve may be expected to go down rapidly with an increase in the frequency, while the 10, 30, and 40°C curves are more flat or slowly decrease on this low frequency side with an increase in the frequency.

From the values obtained in this work, the $(\alpha c/\omega)$ value is found to be very small compared with unity; therefore, the following relation is derived:

$$\frac{M_2}{\omega}=2\rho c^3\left(\frac{\alpha}{\omega^2}\right) \tag{5}$$

The M_2/ω quantity has the dimension of viscosity. In the preceding paper[1] it was found that the values of M_2/ω amount to 2—3 poises for the 10 wt.% solutions at 1.4 Mc./sec. From the present data we can determine the M_2/ω values to be of the order of 0.1 poises; these values are given in Fig. 9.

Summary and Conclusions

Data concerning ultrasonic velocity and absorption have been obtained by means of an ultrasonic pulse technique for aqueous solutions of polyvinyl alcohol.

1) The ultrasonic velocity and absorption have been measured over the temperature range of 3—70°C and the frequency range of 5—45 Mc./sec.

2) The ultrasonic absorption of aqueous solutions of partly-saponified polyvinyl alcohol is larger than that of perfectly-saponified polyvinyl alcohol at the same concentration.

3) Two relaxation mechanisms are present; one, which has been obtained from the temperature dependence of the relaxation frequency, is characterized by the activation energy of about 4 kcal./mol., and the other, by the activation energy of the order of 10 kcal./mol.

4) The value of the longitudinal wave modulus, M_2/ω, has been found to be of the order of 0.1 poises.

The authors wish to thank Miss Mitsuko Kobayashi for her cooperation in performing this study.

BULLETIN OF THE CHEMICAL SOCIETY OF JAPAN VOL. 39 453—456 (1966)

The Heterogeneous Adsorption of Carbon Dioxide on the Nickel Surface as Studied by the Isotopic Desorption Method

By Yasushi KOBAYASHI and Kozo HIROTA

Department of Chemistry, Faculty of Science, Osaka University, Toyonaka, Osaka

(Received June 11, 1965)

Further evidence on the adsorptive heterogeneity of the nickel surface has been presented by the use of the technique described in our previous paper. The results support the conclusion already proposed that more than 20—30% of the surface can adsorb carbon dioxide strongly over the temperature range between −78° and 300°C.

The heterogeneity of the adsorptive power of the nickel surface has often been reported by using various physical techniques, e. g., infrared spectroscopy,[1] measurements of the electric resistance[2] and of the surface potential,[3] and electron microscopy.[4] Nevertheless, the question why the heterogeneous adsorptivity can be observed at all has not yet been answered satisfactorily. Besides, the fractions of the individual nickel surfaces, which differ in their activity, to the total surface have rarely been determined without ambiguity, though their determination is important to an understanding of the occurrence of heterogeneity in the study of adsorption and catalysis.

Several years ago, the present authors[5] applied the isotopic desorption method (or the differential isotopic method) of Roginsky[6] to the present problem; they then found that about 20—30% of the BET area of the nickel surface can adsorb carbon dioxide more strongly over the temperature range from −78°C to 300°C than the other fraction of the surface. Since carbon dioxide is soluble into the nickel bulk with much difficulty, the result is free from any ambiguity of absorption, the disturbing effect of which was confirmed in the application of this method by Takeuchi and Asano, when tritium was used as the tracer.[7] The heterogeneity observed, therefore, may be suggested as being due to the co-existence of various crystal planes rather than to such peculiar sites as lattice defects on the surface. Selwood et al.[8] reported the same conclusion for nickelkieselguhr on the basis of the method of magnetization-volume isotherms; they concluded the coverage of the stronger adsorption to be one-sixteenth. Quinn and Robert[9] and Suhrmann et al.[10] also found heterogeneity in the adsorption of carbon dioxide and carbon monoxide respectively on nickel films. Moreover, recently one of the present authors could explain the poisoning effect of carbon dioxide on the self-hydrogenation of ethylene[11] in terms of the above findings.

Such being the situation, it will be significant to report here some supplementary data obtained since the report mentioned above,[5] which will be denoted hereafter as "Paper I." The object of the investigation is to obtain some knowledge on the physical equilibration of the adsorbed carbon dioxide and also to clarify the adsorbed state, because both points seem to involve some questions, when the previous results are discussed. In the present paper, therefore, two kinds of experiments will be reported, with the desorption time changed on one hand, and with $^{13}CO_2$ and $CO^{18}O$ used as the adsorbate gases on the other.

Experimental

The apparatus and procedure were the same as those adopted in Paper I, except for minor differences to be mentioned below. The reduced nickel powders used as the adsorbent were a different lot from the same source. The weight was 19.8 g., and the BET area, 0.178 cc./g. These powders will be denoted as "Cat. B," if necessary, so as to discriminate them from the "Cat. A" used in Paper I. Heavy carbon dioxide $^{13}CO_2$ (19.7 atom%) was prepared by oxydizing $^{13}CH_4$ which had been given to the authors by Professor S. Horibe.[12] It was enriched

1) R. P. Eischens and W. A. Plinskin, *Advan. Catalysis*, **10**, 1 (1958).
2) W. M. H. Sachtler and G. J. H. Dorgelo, *J. Chem. Phys.*, **54**, 27 (1957).
3) R. Suhrmann, Y. Mizushima, A. Hermann and G. Wedler, *Z. physik. Chem., N. F.*, **20**, 332 (1959).
4) W. M. H. Sachtler and G. J. H. Dorgelo, "Proc. 4th Intern. Conf. on Electron Microscopy," Berlin (1960), p. 802.
5) K. Hirota, Y. Kobayashi and J. Kiji, This Bulletin, **34**, 1213 (1961); "Preprint of the Catalysis Symposium of Japan (Osaka)" (1959), p. 1.
6) N. Keier and S. Roginsky, *DAN USSR*, **57**, 157 (1947).
7) T. Takeuchi and T. Asano, *Z. physik. Chem., N.F.*, **36**, 118 (1963).
8) I. E. Den Besten, P. G. Fox and P. W. Selwood, *J. Phys. Chem.*, **66**, 450 (1962); P. W. Selwood, "Adsorption and Collective Paramagnetism," Academic Press, New York (1962), p. 162.
9) C. M. Quinn and M. W. Roberts, *Trans. Faraday Soc.*, **58**, 569 (1962).
10) R. Suhrmann, H. J. Heyne and G. Wedler, *J. Catalysis*, **1**, 208 (1962).
11) K. Hirota and S. Teratani, *Sci. Pep. Inst. Phys. Chem. Research (Tokyo)*, **57**, 206 (1963).
12) S. Horibe, *J. Chem. Soc. Japan, Pure Chem. Sect. (Nippon Kagakaku Zasshi)* **80**, 1206 (1959).

TABLE I. EXPERIMENT TO INVESTIGATE THE EQUILIBRATION OF ADSORBED CARBON DIOXIDE

Catalyst B. Carbon dioxide: $CO^{18}O$ 29.1 atom % in No. 7 and 29.7 atom % in Nos. 8, 9, and 10

Run No.	Adsorption procedure: Temp. °C	Introduced order	Introduced amount cc.	Desorption procedure: Temp. °C	Desorption time min.	Desorbed gas amount cc.	Isotopic concn. of the gas %	Residual amount V_r cc.
7	−78	I	V_1 =4.22	−78	30	(6.74)	1.5	1.61
			V_1'=1.50		780	0.20	—	1.41
		II	V_2 =6.85	17—20	180	0.07	19.2	1.34
				100	180	0.07	19.4	1.27
				300	900	0.78	16.8	0.49
8	−78	I	V_1 =4.36	−78	120	(5.36)	1.7	1.43
			V_1'=1.43	0	90	0.08	17.0	1.35
		II	V_2 =5.36	100	90	0.12	19.3	1.23
				300	70	0.59	17.5	0.64
9	−78	I	V_1 =4.73	−78	60	(4.87)	1.9	1.54
			V_1'=1.44	0	60	0.15	18.1	1.39
		II	V_2 =4.97	100	60	0.12	19.3	1.27
				300	70	0.71	19.1	0.56
10	0	I	V_1 =4.12	0	120	(4.00)	2.9	1.63
			V_1'=1.55	100	120	0.41	16.3	1.22
		II	V_2 =4.08	300	120	0.74	20.2	0.48

N.B. Runs of Nos. 1—6 are shown in Paper I.
Numbers in paentheses denote the desorbed gas after the introduction of the second gas.

TABE II. EXPERIMENT, USING $^{13}CO_2$ AS ADSORBATE

Carbon dioxide $^{13}CO_2$=19.7 atom% Contact of the second gas is always 120 min.

Run No.	Adsorption procedure: Temp. °C	Introduced order	Introduced amount cc.	Desorption procedure: Temp. °C	Desorption time min.	Desorbed amount cc.	Isotopic concn., % ^{13}C	Isotopic concn., % ^{18}O	Residual amount V_r, cc.
11	0	I	V_1 =2.94	0	120	(4.16)	1.5	14.0	1.64
		($^{13}CO_2$)	V_1'=1.64	100	120	0.30	17.5	3.3	1.32
		II	V_2 =4.16	300	120	0.73	18.2	2.9	0.59
		($C^{18}O$, 14.8 atom%)							
12	−78	I	V_1 =3.89	−78	120	(3.70)	2.0	—	1.41
		($^{13}CO_2$)	V_1'=1.41	0	120	0.11	12.8	—	1.30
		II	V_2 =3.70	100	120	0.09	15.1	—	1.21
		(CO_2)		300	120	0.61	19.1	—	0.60

by the thermal diffusion column set at the Titani Laboratory of Tokyo Metropolitan University. $CO^{18}O$ was prepared by the present laboratory; its ^{18}O concentration was high enough to fulfill the object of the present research (ca. 29 or 15 atom%). The mass spectrometer used for isotopic analysis was a Hitachi (model RMB).

It might be mentioned that the desorption of carbon dioxide was always carried out by condensing it at the temperature of liquid nitrogen (−195°C), as was done in Paper I; i. e., desorption was continued until the vapor pressure of the adsorbed carbon dioxide decreased to 10^{-5} mmHg.[13] Special care was always taken in materials and manipulation so that no poison appeared on the nickel surface.

Results and Discussion

Table I summarizes the runs (Nos. 7—10) which were carried out to study the effect of the desorption time after introduction of the second gas. In Table II are shown the runs (Nos. 11 and 12) in which $^{13}CO_2$ was used as the first introduced gas, the desorption time being 120 min. In the tables, V_1 denotes the amount of the first gas introduced; V_1', that of the first gas which remained

13) Landolt-Börnstein, "physik. u. Chem. Tabellen," II band, 2 Teil (1960), p. 54.

after the desorption; V_2, that of the second gas introduced in the adsorption vessel (A), and V_r, the gas remaining after the second desorption at the same temperature. According to the data of Paper I, all the V_1+V_2 values in these runs are enough to form a monolayer of carbon dioxide on the surface.

No. 7 shows that the desorption time after the introduction of the second gas will not affect the result very much because the change in the residual amount on the surface was small, as is shown in Table II. The first residual gases of No. 7, 8, and 9 agree well with that of Paper I; i. e., 0.72 cc./g. was given for No. 8, while 0.67 cc./g. was given for the mean of Nos. 1 and 4, the desorption time of which was the same (120 min.) as that of No. 8. Thus, the desorption time of the second introduced gas, 110 or 120 min., is enough to make possible the conclusion drawn in Paper I. In other words, the present result means that the second portion of the introduced gas reached a physical equilibration after two hours, but that the isotopic equilibration with the first introduced gas was nevertheless not realized in the present system.

Table II shows that the amount of gas strongly adsorbed was practically unchanged at the same temperature, even if carbon dioxide was labelled by carbon instead of oxygen. (Compare Nos. 12 and 11 with Nos. 8 and 10 respectively.) The second point to be mentioned is the production of $^{13}CO^{18}O$ in the first desorbed gas. However, it could not be identified in the portions of the gas desorbed thereafter, for their quantities were too small. This finding tells us that the following exchange reaction (A) proceeds during the adsorption:

$$^{13}CO_2 + CO^{18}O \rightarrow {}^{13}CO^{18}O + CO_2 \qquad (A)$$

In other words, a kind of dissociative adsorption of carbon dioxide occurs. However, the dissociation may mean the formation of CO (ads)+O(ads), but not of C (ads)+2O(ats), considering the findings of Suhrmann et al.[10] as well as the energetic reason.

As Table II shows, it is now evident that the numerical value of the "strong" area, one-third, becomes more reliable and that carbon dioxide strongly adsorbed may exist as a dissociative state, as has been proposed.[5,9] However, there still exists a possibility of exchange without dissociation, similarly to that proposed by Webb and Eischens[14] in the case of exchange reaction (B):

$$^{13}CO + C^{18}O \rightarrow {}^{13}C^{18}O + CO \qquad (B)$$

The possibility of such a reaction without dissociation will be taken up again in the next section.

General Discussion

As has been mentioned above, there are at least two kinds of adsorption sites on the nickel surface. It is possible, however, that the above conclusion is of an apparent nature, considering that the "induced heterogeneity" may be produced as a result of mutual interactions between adsorbed molecules or between them and catalyst atoms. This possibility, which would be useful in explaining the gradual change in the adsorption heat, cannot be applied to the present findings, however, because since the desorption was carried out after the formation of a monolayer of carbon dioxide, it must occur at random if the surface is homogeneous.*

However, it must be admitted that there was gradual change in the adsorptive power of the strong sites now observed, because the fraction of the strongly-adsorbed carbon dioxide, reaching ca. 38% over the temperature range from −78°C—100°C, decreased to ca. 10% at 300°C. The above tendency can be explained in run No. 7 as follows. The residual amount of 1.4 cc. at −78°C decreased only by 9% at 100°C, but by 65% at 300°C, the isotopic concentration of the gas desorbed being that of the first gas. Moreover, the desorption at 300°C for 15 hr. could not make the decrease in the amount of adsorbed gas less than 0.49 cc. Now that the presence of stronger adsorption sites seems very plausible, let us discuss its nature.

As has been suggested in Paper I, the difference in the adsorptive power of each crystal plane may be its cause, judging from the magnitude of the ratio of the strong to the weak sites. The word "heterogeneity" must, however, be understood by a conventional standard, because the "strong" adsorption in this research means that the thermodynamical activity of strongly-adsorbed carbon dioxide is less than that of a carbon dioxide trapped at −195°C. Therefore, the strong adsorption sites could be classified in more detail if the relation between the residual amount of $C^{18}O_2$ (last column in Table I) and the desorption temperature could be analyzed more precisely. Thus, the discrepancy in the magnitude of stronger sites between the value of Selwood[8] and that of the present authors may be explained. However, the problem can not be answered quantitatively by the present method of investigation, because there remains a possibility that the decrease in residual $C^{18}O_2$ can be realized to some degree by the slow isotopic exchange (A) without dissociation between the adsorbed carbon dioxide on strong and weak sites. This possibility, if it does occur, may be small, however, considering

14) A. N. Webb and R. P. Eischens, *J. Am. Chem. Soc.*, **77**, 4710 (1955).

* This argument owes much to the kind suggestion of Professor Tomiyuki Toya, Hokkaido University.

15) Cf. G. Ehrlich, *Advan. Catalysis*, **14**, 255—427 (1963).

that the numerical value of the "strong" area determined by the present research coincides well that obtained by the adsorption measurement.[9]

Besides, the difference in adsorptive power between several crystal planes may also be supported by the adsorption measurements obtained on hydrogen by electron microscopy[4] or by field emission microscopy.[15] The possibility of relating the adsorptive to the catalytic heterogeneity has already been mentioned by one of the present authors[11]; it will be discussed elsewhere* in connection with the self-hydrogenation of ethylene on nickel.

Summary

The so-called adsorptive heterogeneity of the nickel surface has been studied at −78°C and 0°C by the isotopic desorption method, using labeled carbon dioxides ($CO_2{}^{18}$ and $^{13}CO_2$). The following results have been obtained:

(i) The fraction of the nickel surface which can adsorb carbon dioxide "strongly" at −78—300°C has been found to be about 20—30% of the total area, a proportion which is unchanged even when the desorption time is varied after the introduction of the second gas; (ii) When $^{13}CO_2$ and $C^{18}O_2$ are used as the first and second gas respectively, $^{13}CO^{18}O$ can be produced, indicating a dissociation of carbon dioxide on the strong stites of the surface.

These findings seem to offer some new evidence of the surface-heterogeneity which may be brought about by different crystal planes of the nickel surface, judging from the percentage of the area of the strong sites.

* K. Hirota and S. Teratani, *Z. physik. Chem. N.F.*, in press (1966). (Literature added in proof.)

BULLETIN OF THE CHEMICAL SOCIETY OF JAPAN VOL. 39 456—459 (1966)

The Photolysis of *cis*-2-Butene and Its Implications for Radiation Chemistry

By Yoshihiko HATANO and Shoji SHIDA

Laboratory of Physical Chemistry, Tokyo Institute of Technology, Ookayama, Tokyo

(Received June 14, 1965)

The direct photolysis at 1849 Å and the mercury-photosensitized reaction at 2537 Å of *cis*-2-butene have been studied in the gas phase at room temperature. It may be considered that the excited singlet state of *cis*-2-butene is formed in the former, and that the excited triplet state of *cis*-2-butene is formed in the latter. *trans*-2-Butene is predominantly produced in the latter, while the decomposition products (e. g., hydrogen, methane, ethane, ethylene, propylene, etc.) predominate in the former. The rates of the formation of all the products are pressure-independent in the former, while in the latter those of all products except *trans*-2-butene decrease rapidly with an increase in the initial pressure. The rate of *trans*-2-butene formation in the latter, however, increases gradually with an increase in the initial pressure until it becomes constant above 100 mmHg. By comparing the pressure-dependence and the product-distribution of these two reactions with the results of the radiolysis of liquid *cis*-2-butene, one may conclude that the excited triplet state of *cis*-2-butene contributes chiefly to the formation of *trans*-2-butene in the radiolysis, while the excited singlet state of *cis*-2-butene contributes chiefly to the decomposition products.

There are two ways in which excited molecules can be formed by ionizing radiation. One is from the neutralization of a positive ion by an electron or by a negative ion; the other is the direct excitation by the high-energy radiation itself. It is generally considered that these excited states consist of high levels of the different state manifolds. However, little attention has been paid to the nature of these states.

In a previous paper[1] on the radiolysis of liquid *cis*-2-butene, it was considered that *trans*-2-butene, which may be produced for the most part through the molecular mechanism, is formed not through the excited singlet state but through the excited triplet state. Moreover, on the basis of this inference, the effects of added aromatic hydrocarbons[1] and nitrous oxide[2],* on the radiolysis could be explained consistently.

The present investigation was undertaken in

1) Y. Hatano, S. Shida and S. Sato, This Bulletin, **37**, 1854 (1964).

2) Y. Hatano and S. Shida, The 18th Annual Meeting of the Chemical Society of Japan, Osaka, 1965.

* Nitrous oxide has been considered as an effective electron scavenger: $N_2O + e \rightarrow N_2 + O^-$. The addition of nitrous oxide to liquid *cis*-2-butene has the same effect on the formation of *trans*-2-butene as in the case of benzene as an additive.[1]

an attempt to confirm the above inference experimentally. The excited singlet and triplet states of gaseous *cis*-2-butene were formed photochemically. The former was formed by the direct photoexcitation at 1849 Å, while the latter was formed by the mercury-photosensitization at 2537 Å.

Gary and Pickett[3] investigated the ultraviolet absorption of *cis*-2-butene and reported that *cis*-2-butene has a maximum absorption in the region near 1849 Å. The energy level of the first excited singlet state of *cis*-2-butene has been estimated[4,5] to be a little lower than that of $Hg6^1P_1$, 6.7 eV., corresponding to 1849 Å. Therefore, the excited singlet state of *cis*-2-butene may be formed by the direct photo-excitation at 1849 Å. There has been, to the authors' knowledge, no report dealing with the direct photolysis of *cis*-2-butene.

On the other hand, many works have been done on the mercury-photosensitized reaction of olefins.[6] It is generally considered that olefins are excited by the collision between olefin molecules and excited mercury atoms, $Hg6^3P_1$, formed by the irradiation of light at 2537 Å. These excited olefin molecules return to the ground states through decomposition or collisional deactivation. On the basis of the results of the benzene-photosensitized reaction of *cis*-2-butene[7-9] and other evidence,[4,5] the energy level of the first excited triplet state of *cis*-2-butene is estimated to be about 4 eV. which is lower than that of $Hg6^3P_1$, 4.8 eV. Therefore, the excited triplet state of *cis*-2-butene may be formed by the mercury-photosensitization at 2537 Å. The mercury-photosensitized reaction of 2-butenes, especially the cis-trans isomerization, has been reported by Cundall et al.[10] According to them, the overall reaction can be explained in terms of the formation of the vibrationally-excited triplet state of 2-butene.

In this paper, experiments on the direct photolysis and the mercury-photosensitized reaction of *cis*-2-butene were undertaken in order to get some information about the role of lower excited singlet and triplet states in the radiolysis of *cis*-2-butene.

Experimental

Materials.—Matheson research-grade *cis*-2-butene was used after the usual degassing and bulb-to-bulb distillations. It was found by gas chromatography to contain less than 0.4% *trans*-2-butene.

In the experiments on the direct photolysis of gaseous *cis*-2-butene, it was prepared using the mercury-free vacuum line and was purified using gold foil in a cold trap.

Irradiation.—In the experiments on the direct photolysis at 1849 Å, an ordinary mercury resonance lamp was used as the light source. A cylindrical quartz cell, 50 mm. in diameter and 20 mm. thick, was connected to a mercury-free vacuum line. Moreover, the absence of mercury in the system was confirmed by making sure that the reaction did not take place at all when *cis*-2-butene was irradiated for 30 min. with the light source of 2537 Å.

In the experiments on the mercury-photosensitized reaction at 2537 Å, the light source and the reaction cell were the same as those used in the experiments on the direct photolysis. A droplet of mercury in the reaction cell provided a constant pressure of mercury vapor. The light shorter than 2100 Å was cut off with a filter.

All runs were made statically at room temperature, 25±3°C.

Analysis.—The analytical procedures were almost the same as in the radiolysis.[1]

After irradiation the gases noncondensable at −196°C (hydrogen and methane) were collected and measured by an analysis device composed of a Toepler pump, a McLeod gauge, and a copper oxide furnace. Products condensable at −196°C were analyzed by a home-made reduced-pressure-type gas chromatograph. A benzyl ether column was used mainly at room temperature, for the separation of C_1—C_4 hydrocarbons.

Results and Discussion

Table I shows the amounts of the major products of the direct photolysis of gaseous *cis*-2-butene at 1849 Å, the mercury-photosensitized decomposition of gaseous *cis*-2-butene at 2537 Å, and the γ-radiolysis[1] of liquid *cis*-2-butene. A marked difference between the relative rates of formation for

Table I. Products from the direct photolysis of gaseous *cis*-2-butene at 1849 Å and the mercury-photosensitized reaction of gaseous *cis*-2-butene at 2537 Å and the γ-radiolysis of liquid *cis*-2-butene

	Direct photolysis[a]	Mercury-photosensitized reaction[b]	γ-Radiolysis[c]
	10^{-7} mol./min.	10^{-7} mol./min.	molec./100 eV.
H_2	1.73	0.00	1.02
CH_4	0.97	0.00	0.21
$C_2H_6+C_2H_4$	1.03	0.00	0.11
C_2H_2	0.33	0.00	0.11
C_3H_6	1.03	0.02	0.13
n-C_4H_{10}	0.40	0.10	0.83
1-C_4H_8	1.47	0.06	0.40
trans-2-C_4H_8	0.50	10.8	2.29

a) The irradiation time: 3 min.
The initial pressure of *cis*-2-butene: 120 mmHg.
b) The irradiation time: 5 min.
The initial pressure of *cis*-2-butene: 100 mmHg.
c) The dose rate: 2.21×10^{19} eV./g. hr.
The total dose: $(0.30—3.59)\times10^{21}$ eV./g.

3) J. T. Gary and L. W. Pickett, *J. Chem. Phys.*, **22**, 599 (1954).
4) D. F. Evans, *J. Chem. Soc.*, **1960**, 1735.
5) J. R. Platt, *J. Chem. Phys.*, **18**, 1168, (1950).
6) E. W. R. Steacie, "Atomic and Free Radical Reactions," Reinhold Pub. Co., New York (1954).
7) S. Sato, K. Kikuchi and M. Tanaka, *J. Chem. Phys.*, **39** 239 (1963).
8) R. B. Cundall, F. J. Fletcher and D. G. Milne, *Trans. Faraday Soc.*, **60**, 1146 (1964).
9) P. Siegel, *J. Chem. Phys.*, **42**, 1953 (1965).
10) R. B. Cundall and T. F. Pamler, *Trans. Faraday. Soc.*, **56**, 1211 (1960).

these reactions may be noted. In the mercury-photosensitized decomposition, *trans*-2-butene is a major product, but not in the direct photolysis. To compare these reactions more precisely, the dependence of the rates of formation on the irradiation time and the pressure was examined.

The amount of the major products were measured at various irradiation times in the direct photolysis. The initial pressure of *cis*-2-butene was 40 mmHg. Until 3 min. of irradiation every product increased linearly with the time, showing no measurable secondary reaction of the product at this stage of reaction, although it decreased with time after 3 min. Figure 1 shows the rates of the formation of major products at various initial pressures for the irradiation time of 3 min. It may clearly be seen that the rates of the formation of all products are practically constant at pressures between 20 and 120 mmHg. These features agree with the results of the direct photolysis of propylene,[11] 1-butene[12] and cyclopentene[13] at 1849 Å.

The amounts of the major products were also measured at various irradiation times in the mercury-photosensitized reaction. The initial pressure of *cis*-2-butene was again 40 mmHg. Until 5 min. of irradiation every product increased linearly with the time; then it decreased with time after 5 min. Figure 2 shows the rates of the formation of major products at various initial pressures for the irradiation time of 5 min. It may clearly be seen that the rates of the formation of all products except *trans*-2-butene are strongly pressure-dependent. This is remarkably different from the results of the direct photolysis. The rates of the formation of all products except *trans*-2-butene rapidly decrease with an increase in the initial pressure. The rate of *trans*-2-butene formation,

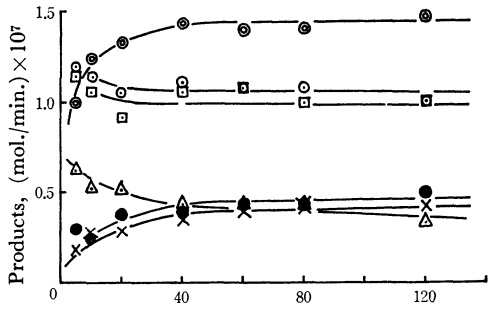

Fig. 1. Pressure-dependence of the formation of major products in the direct photolysis of *cis*-2-butene at 1849 Å

—◎— 1-C_4H_8 —⊙— $C_2H_4+C_2H_6$
—⊡— C_3H_6 —●— *trans*-2-C_4H_8
—×— *n*-C_4H_{10} —△— C_2H_2

11) T. Nishikawa, S. Arai and S. Shida, to be published.
12) N. Harumiya and S. Shida, This Bulettin, **38**, 142 (1965).
13) N. Sakai and S. Shida, to be published.

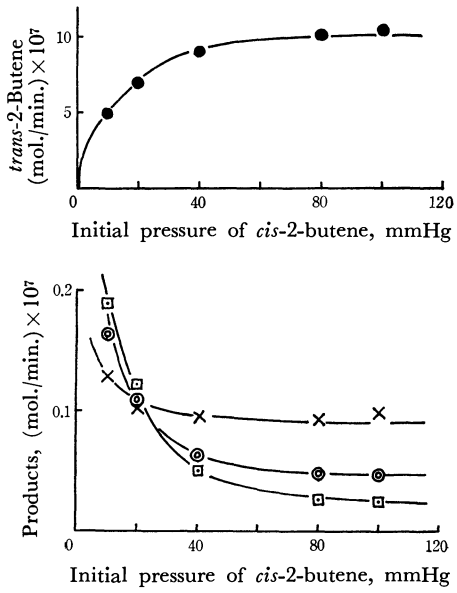

Fig. 2. Pressure-dependence of the formation of *trans*-2-butene and other products in the mercury-photosensitized reaction of *cis*-2-butene at 2537 Å.

—×— *n*-C_4H_{10} —◎— 1-C_4H_8
—⊡— C_3H_6 —●— *trans*-2-C_4H_8

however, increases gradually with an increase in the initial pressure until it becomes constant above 100 mmHg.

On the basis of these data, it seems reasonable to assume that the excited triplet state of *cis*-2-butene is more readily deactivated than the excited singlet state of *cis*-2-butene. In other words, the life-time of the latter is shorter than that of the former, and the latter decomposes with a larger probability before the collisional deactivation. The ratio of the cis-trans isomerization to the decomposition is 60 at the pressure of 100 mmHg in the mercury-photosensitized reaction, while it is 0.07 at the pressure of 120 mmHg in the direct photolysis. Thus, the excited triplet state may contribute much more effectively to the formation of *trans*-2-butene than does the excited singlet state.

These results may reasonably be explained by the following mechanisms.

In the direct photolysis of gaseous *cis*-2-butene at 1849 Å, the excited singlet state of *cis*-2-butene is formed, giving chiefly such decomposition products as C_1, C_2 and C_3 hydrocarbons:

$$\text{Cis} + h\nu \rightarrow \text{Cis}^* \text{ (singlet)} \quad (1)$$

$$\text{Cis}^* \text{ (singlet)} \rightarrow \text{Decomp. products} \quad (2)$$

where Cis and Cis*(singlet) indicate the ground state and the first excited singlet state of *cis*-2-butene respectively.

In the mercury-photosensitized reaction, on the other hand, the overall reaction is explained by

the formation of a vibrationally-excited triplet state of *cis*-2-butene in a fashion similar to that described by Cundall:[10]

$$Hg^1S_0 + h\nu \rightarrow Hg^3P_1 \quad (3)$$

$$Hg^3P_1 \rightarrow Hg^1S_0 + h\nu \quad (4)$$

$$Hg^3P_1 + Cis \rightarrow Cis^{**}\ (triplet) + Hg^1S_0 \quad (5)$$

$$Cis^{**}\ (triplet) + Cis \rightarrow Cis^{*}\ (triplet) + Cis \quad (6)$$

$$Cis^{*}\ (triplet) \rightarrow Trans \quad (7)$$

$$\searrow\ Cis \quad (8)$$

$$Cis^{**}\ (triplet) \rightarrow Decomp.\ products \quad (9)$$

where Cis*(triplet) and Cis**(triplet) indicate the first excited triplet state and the vibrationally-excited triplet state of *cis*-2-butene respectively. The steady-state treatment leads to Eqs. I and II:

$$R_t \simeq \frac{k_7 I}{k_7+k_8} \quad \text{at a higher pressure} \quad (I)$$

$$R_d = \frac{k_5 k_9 IP}{(k_4+k_5P)(k_9+k_6P)} \quad (II)$$

(P=the initial pressure of *cis*-2-butene)

where R_t and R_d indicate the rate of the formation of *trans*-2-butene and that of the decomposition products respectively. From Eq. I, it seems that the rate of the formation of *trans*-2-butene should be pressure-independent at a higher pressure. From Eq. II, it seems that the rate of the formation of decomposition products should become zero at higher pressures.

In view of the fact that the radiolysis of *cis*-2-butene mentioned above[1] is the reaction in the liquid phase, the most reasonable conclusion to be drawn from the above discussion is that the excited triplet state of *cis*-2-butene may contribute chiefly to the formation of *trans*-2-butene in the radiolysis, while the excited singlet state of *cis*-2-butene may contribute chiefly to the decomposition products. Comparing the patterns of the distribution of decomposition products in the three reactions, one may find that the pattern of the distribution in the radiolysis is similar to that in the direct photolysis. Thus, the following mechanism may be proposed for the radiolysis of liquid *cis*-2-butene:

$$\begin{array}{l} \quad\quad\quad\

BULLETIN OF THE CHEMICAL SOCIETY OF JAPAN VOL. 39 460—465 (1966)

The Infrared Spectra of Artificial Coal made from Submerged Wood at Uozu, Toyama Prefecture, Japan

By Hiroshi TSUKASHIMA

Department of Industrial Chemistry, Faculty of Engineering, Toyama University, Takaoka

(Received June 15, 1965)

The infrared spectra of artificial coal prepared from Submerged Wood were observed and compared with those of lignin and cellulose. The artificial coalification seems to proceed in three stages, characterized by the corresponding infrared spectra, i. e., a cellulose-like spectrum, a lignin-like spectrum, and a spectrum resembling that of natural coal. The infrared spectrum of artificial coal is generally similar to that of natural coal with a little higher carbon content, suggesting that the degree of coalification is more advanced in artificial coal than in natural coal. The background absorption in the infrared spectra of artificial coal of a low coalification is weak, while that in the infrared spectra of artificial coal of a high coalification is strong.

The infrared spectra of coal have frequently been used to investigate its structure.[1] The present report will deal with the mechanism of artificial coalification by observing the infrared spectra of the artificial coal prepared from Submerged Wood at Uozu, Toyama Prefecture, Japan, and by comparing these spectra with those of lignin and cellulose.

Experimental

One series of samples of artificial coal was prepared as follows. Fifty grams of the powdered sample (40—100 mesh) of the Submerged Wood was placed in a stainless steel autoclave of the shaking type (capacity; 1 l.) with 500 ml. of water. This was then heated at 150, 170, 200, 250, 260, 270, 280, 300, 325 and 350°C for 8, 24, 40 and 72 hr. under gas-steam pressure at 4, 13, 25, 50, 58, 65, 80, 105, 154 and 210 atom. (gauge pressure). The artificial coal (AC) thus obtained from the Submerged Wood was separated by filtration, washed with water, and air-dried.

Another series of samples of the artificial coal was prepared as follows. After 50 g. of the powdered sample of the Submerged Wood had been placed in a stainless steel autoclave of the rotating type (capacity; 5 l.) with 700 ml. of water, the air in the autoclave was replaced with nitrogen. Then the powdered sample in the autoclave was heated at 375 and 400°C for 8 and 40 hr. under gas-steam pressure at 210 and 270 atm. (gauge pressure). The artificial coal (AC) thus obtained was separated by filtration, then washed with water and air-dried. The conditions of artificial coalification are shown in Table I, while the elementary analysis and the yield of the artificial coal are given in Table II.

The infrared (IR) spectra of AC free from bitumen, lignins and cellulose were also measured. Powdered filter paper (No. 2) of the Toyoroshi Co., Ltd., was used as a sample of cellulose in measuring the IR spectra.

The lignin samples were prepared as follows. About 20 g. of powdered saw dust (60—100 mesh) from needle-leaved trees (Japanese red pin trees) was treated with a mixed solvent of ethyl alcohol and benzene (1 : 1) in order to extract the resinous matter and then treated with 400 ml. of concentrated hydrochloric acid (42%) and left to stand at room temperature for 24 hr., during which time it was occasionally shaken. Then the mixture was diluted with 3.6 l. of water and heated to boiling. The lignin thus obtained was filtered and thoroughly washed with hot water until the washings were free from chlorine ions. The yield was 13—16 g. of the so-called hydrochloric acid lignin, a light brownish powder.

About 100 ml. of concentrated hydrochloric acid was added to 400 ml. of waste liquor (specific gravity; 1.097 at 14°C) of sodium sulfate pulp made from pine trees and some broad-leaved trees (1 : 3), and then heated on a water bath for 1 hr. The thioalkali lignin thus precipitated was washed with hot water on a Buchner funnel until no chlorine ions were detected in the washings, and then dried at room temperature. The thioalkali lignin (30—40 g.) was thus obtained. The analytical data are listed in Table III.[2]

The IR spectra of the AC, lignins and cellulose were measured on potassium bromide disks in the following way. Five milligrams of the above sample in a small glass tube was dried in a vacuum desiccator with phosphorus pentoxide at 110°C for 6 hr., and then the tube was sealed. At a constant temperature (20°C) and at a constant humidity (35%) the sealed glass tube

1) S. Fujii, *J. Fuel Soc. Japan*, **37**, 643 (1958); **38**, 422 (1959); *Fuel*, **42**, 17, 341 (1963); The 1st Meeting of Coal Science, Tokyo, November, 1964. H. A. van Vucht, R. J. Rietveld and D. W. van Krevelen, *Fuel*, **34**, 50 (1955). D. W. van Krevelen, "Coal," pp. 363—372 (1961). J. K. Brown, *J. Chem. Soc.*, **1955**, 744. G. Bergman, G. Huck, J. Karweil and H. Luther, *Brenn. Chem.*, **38**, 193 (1957). M. M. Roy, *Fuel*, **36**, 249 (1957). W. A. Kirkby, J. R. A. Lakey and R. J. Sarjant, *Fuel*, **33**, 480 (1954). C. G. Cannon, *Nature*, **171**, 308 (1953). H. S. Rao, P. L. Gupta, F. Kaiser and A. Lahiri, *Fuel*, **41**, 417 (1962).

2) H. Tsukashima, *Bull. Fac. Eng. Toyama Univ.*, **5**, 54 (1954); **7**, 39 (1956); **8**, 22 (1957); **9**, 34 (1958); **11**, 41 (1960); **12**, 33 (1961); **13**, 41 (1962); *J. Chem. Soc. Japan, Ind. Chem. Sect.* (*Kogyo Kagaku Zassi*), **57**, 69 (1954); The 7 th, 9 th, 10 th, 11 th, 12 th, 13 th, 15 th Annual Meeting of the Chemical Society of Japan, Tokyo or Kyoto, April, 1954, 1956, 1957, 1958, 1959, 1960, 1962; Coal Utilization Technical Congress of Japan, Tokyo, November, 1959.

Table I. Artificial coalification condition

Sample	Coalification temp., °C	Coalification index	Beginning temp. of coalification, °C	Coalification time, hr.	Color
150, 8	150	1.16	14.0	8	Faint brown
150,72	150	8.31	14.0	72	Brown
170, 8	170	1.29	22.0	8	Brown
170,72	170	9.33	18.0	72	Umber
200, 8	200	1.73	18.0	8	Umber
200,32	200	5.72	12.2	32	Umber
200,40	200	6.69	12.5	40	Brownish black
200,72	200	11.30	16.0	72	Deep brownish black
250, 8	250	2.50	2.5	8	Violet black
250,72	250	15.50	3.5	72	Black
260, 8	260	2.44	17.5	8	Violet black
260,72	260	15.44	14.0	72	Black
270, 8	270	2.61	14.0	8	Black
270,72	270	16.00	15.5	72	Black
280, 8	280	2.78	13.0	8	Black
280,72	280	16.83	13.2	72	Black
300, 8	300	3.18	6.0	8	Black
325,72	325	19.93	12.0	72	Black
350,72	350	22.13	5.0	72	Black
375,40	375	13.34	24.0	40	Black
400,36	400	13.31	20.5	36	Black

Coalification velocity index 55°

Table II. Elementary analysis of AC (%, dry ash free)

Sample	C	H	O*	N	Yield
Untreated wood	52.74	6.30	40.85	0.11	
150, 8	53.63	6.03	40.32	0.02	89.37
150,72	55.56	5.85	38.55	0.04	84.33
170, 8	54.95	5.83	39.19	0.03	83.39
170,72	59.09	5.89	34.98	0.04	82.81
200, 8	59.80	6.17	33.92	0.11	79.47
200,32	65.26	5.86	28.76	0.12	71.93
200,40	66.88	5.99	26.99	0.14	69.57
200,72	70.79	5.73	23.36	0.12	66.22
250, 8	73.63	5.57	20.62	0.18	55.48
250,72	76.34	5.71	17.81	0.13	55.84
260, 8	74.90	5.77	19.16	0.17	55.99
260,72	77.54	5.64	16.65	0.17	53.36
270, 8	75.51	5.44	18.93	0.12	55.47
270,72	77.13	5.29	17.55	0.13	50.73
280, 8	74.90	5.10	19.90	0.10	53.04
280,72	77.72	4.78	17.31	0.12	46.61
300, 8	79.93	5.44	14.63		44.93
325,72	82.68	4.83	12.49		39.86
350,72	84.39	4.52	11.09		31.10
375,40	88.43	4.20	7.37		35,96
400,36	89.56	4.20	6.21		35.66

* By difference

mentioned above was broken and the sample was mixed with 500 mg. of potassium bromide which had been prepared by heating special-grade potassium bromide commercially obtained in a platinum crucible in an electric furnace at 260°C for 6 hr. and by then cooling it in a vacuum desiccator with phosphorus pentoxide; the sample was then pulverized in an agate mortar for about 20 min. Five hundred milligrams of this mixture was weighed and pressed under a 10-ton pressure for 7 min. in a vacuum. The disk obtained was 20 mm. in diameter and 0.6 mm. thick. Double-beam IR spectrophotometers (OYOKOKEN 310

Table III. Analyses of lignins
(%, dry ash free)

Lignin	C	H	S	O*
Hydrochloric acid lignin	65.13	5.28	—	29.59
Thioalkali lignin	65.54	5.02	4.74	25.70

* By difference

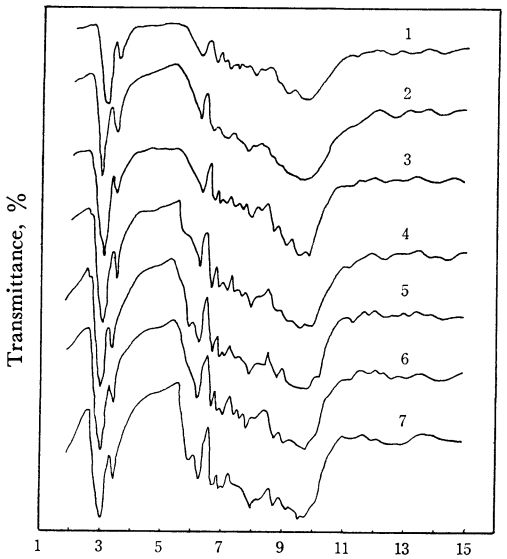

Fig. 1. IR spectra of AC.
1. Submerged wood 2. 150°C, 8 hr.
3. 150°C, 72 hr. 4. 170°C, 8 hr.
5. 170°C, 72 hr. 6. 200°C, 8 hr.
7. 200°C, 32 hr.

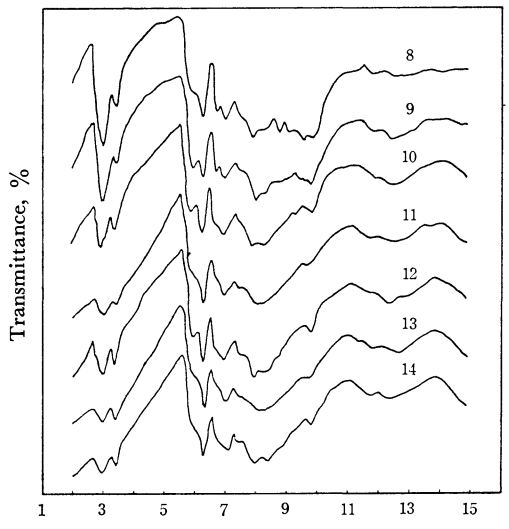

Fig. 1. (continued) IR spectra of AC.
8. 200°C, 40 hr. 9. 200°C, 72 hr.
10. 250°C, 8 hr. 11. 250°C, 72 hr.
12. 260°C, 8 hr. 13. 260°C, 72 hr.
14. 270°C, 8 hr.

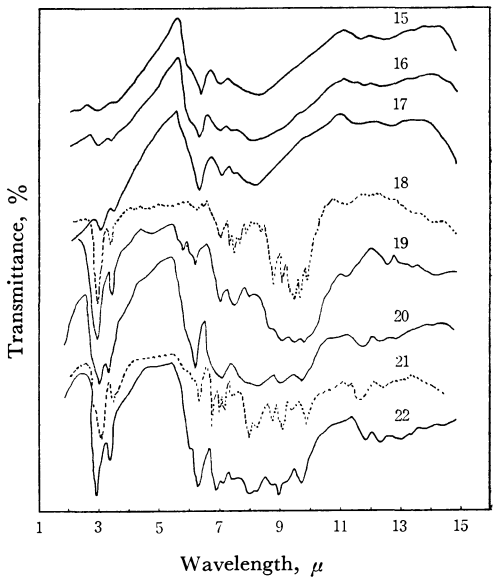

Fig. 1. (continued) IR spectra of AC.
15. 270°C, 72 hr. 16. 280°C, 8 hr.
17. 280°C, 72 hr. 18. Cell.[3] 19. Cell.
20. HCl lig. 21. Red pine lig.[7]
22. Thio lig.

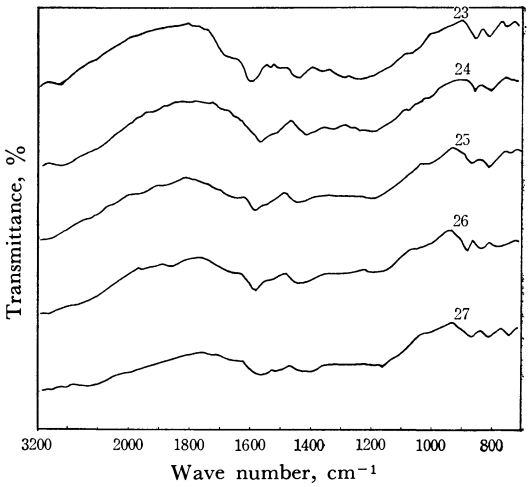

Fig. 1. (continued) IR spectra of AC.
23. 300°C, 8 hr. 24. 300°C, 72 hr.
25. 350°C, 72 hr. 26. 375°C, 40 hr.
27. 400°C, 40 hr.

type and HITACHI EPI-2 type), equipped with rock-salt prisms, were used.

Results

The IR spectra of the Submerged Wood, AC, lignins and cellulose were measured. The results are shown in Fig. 1. The IR spectra of lignin and cellulose reported by previous authors are also shown, for the purpose of comparison, in Fig. 1.

Discussion

1) There have been two explanations for the strong background absorption of the IR spectra of coal.[1] One is that it is caused by the size of the particle of the sample. The other is that it is caused by the growth of graphite crystallites as the condensation of the aromatic cluster proceeds. When there is a low degree of the coalification of AC, the background absorption is weak, but it is very strong with a high degree of coalification, especially in the region from 4 μ to 6 μ, possibly because of the growth of graphite crystallites and the abundantly distributed particles of a comparatively large size. The background absorption is stronger in the spectra of AC than in that of natural coal of a similar carbon content. This might be caused by the greater refractivity of AC.

2) The IR spectrum of AC is generally similar to that of natural coal with a little higher carbon content, suggesting that the degree of coalification is more advanced in AC than in natural coal.

3) 3.03 μ (3300 cm^{-1}). The H-bonded OH group. The absorption of the H-bonded OH group increases with an advance in coalification under 200°C and decreases with an advance in coalification above 200°C. Similar results have been reported both in other kinds of AC and in natural coal.[1]

4) 3.25 μ (3000—3100 cm^{-1}). The aromatic CH group. There was no absorption of the aromatic CH group in the AC spectra, but it appears in the spectra of natural coal in which the carbon content is above 80 per cent.[1]

5) 3.43 μ (2800—3000 cm^{-1}). The aliphatic CH (CH_2, CH_3) group. The absorption of the aliphatic CH group appears at a medium intensity and then gradually decreases above 200°C because the aliphatic CH group in AC is broken up.

6) 5.85 μ (1700 cm^{-1}) The carbonyl and carboxyl CO group. There is no absorption of the CO group in the spectra of Submerged Wood and the AC obtained at 150°C; it appears in the spectra of the AC obtained at 200°C and increases in those of the AC obtained at 200—250°C, while it diminishes in the AC obtained above 250°C. The cellulose that contains no CO group vanishes at about 200°C. The remaining lignin that contains a CO group causes the absorption band of the CO group to appear; this gradually increases up to 250°C, possibly because of the oxidations of the lignin,[4] and then decreases above 250°C, possibly because of the conversion of lignin into a coaly matter by dehydration and deoxidation.

7) 6.25 μ (1600 cm^{-1}). Aromatic C–C bond and oxygen-containing groups (H-bonded carbonyl groups). This absorption is mainly due to the C–C double bond in the aromatic structure of coal. On the other hand, it has been reported[1] that the absorption intensity of this C–C vibration is enhanced by oxygen-containing groups and that the H-bonded carbonyl group is responsible for this absorption. It appears at a considerable intensity in the AC spectra and increases with an advance in the coalification of AC. In the spectra of the AC obtained above 280°C, it is weak, possibly because the background absorption has increased.[1]

8) 6.64 μ (1500 cm^{-1}) The aromatic C–C bond. The absorption of the aromatic C–C bond is very strong in the spectra of lignins.[1,5] In the spectra of the AC of a low coalification (obtained under 200°C), the absorption of the aromatic C–C bond at 6.64 μ is stronger than those of the aromatic C–C bond and oxygen-containing groups at 6.25 μ, but in the spectra of the AC of a high coalification (obtained at 200—250°C), the former is weaker than the latter. This shows that the oxidation of lignin in AC occurs at 200—250°C (cf. 6)).

9) 6.85, 7.00, 7.33 μ (1460, 1430, 1360 cm^{-1}). Aliphatic CH_2, CH_3, and cyclic CH_2 groups. The absorption intensities of aliphatic CH and cyclic CH groups decrease with an advance in the coalification.

10) 7.92, 8.30 μ (1260, 1200 cm^{-1}). The aromatic C–O (phenolic OH, aryl ether and methoxyl benzene) bond. The absorption of the aromatic C–O bond increases up to 250—260°C with an advance in the coalification and then decreases above 260°C.

11) 8.66—9.70 μ (1150—1030 cm^{-1}). The carboxyl CO group, the aliphatic ether C–O–C bond and the alcohol OH group. The absorptions of

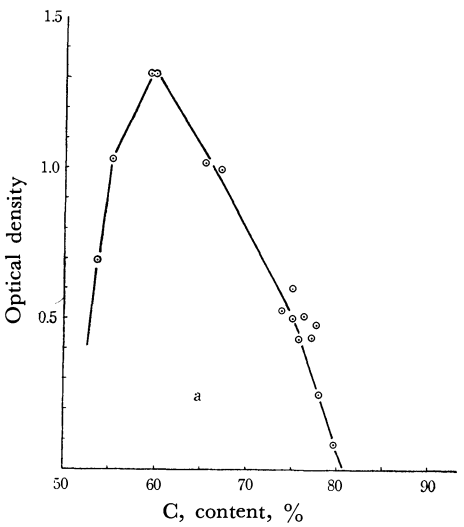

Fig. 2. Relation between carbon content and functional group optical density.
a. 3.03 μ

3) Infrared Data Committee of Japan, "IRDC Card" (1960).
4) S. Fujii and F. Yokoyama, *J. Fuel Soc. Japan*, **38**, 98 (1959).
5) S. Fujii, ibid., **38**, 267 (1959).

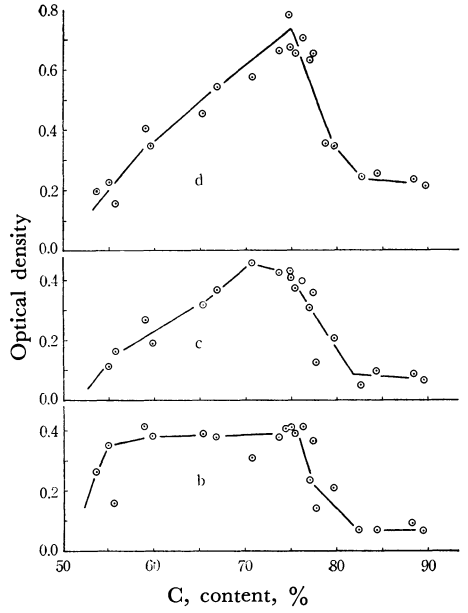

Fig. 2. (continued) Relation between carbon content and functional group optical density.
b. 3.43 μ c. 5.85 μ d. 6.25 μ

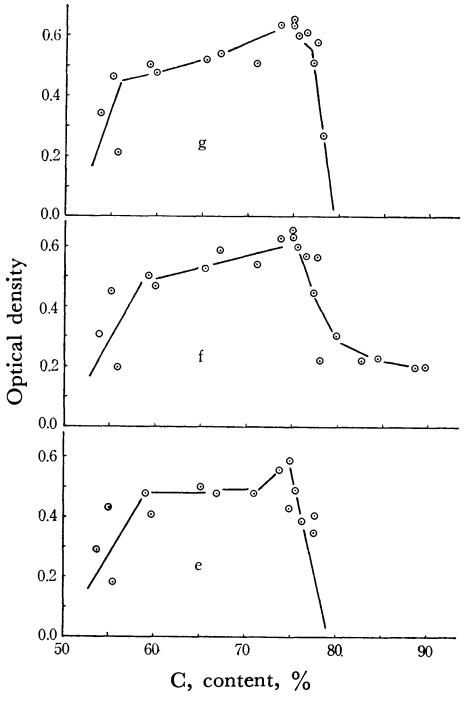

Fig. 2. (continued) Relation between carbon content and function functional group optical density.
e. 6.64 μ f. 6.85 μ g. 7.00 μ

the carboxyl CO group, the aliphatic ether C–O–C group and the alcohol OH group are very strong in the spectra of the AC obtained at 150—200°C, but they decrease in intensity in the spectra of the

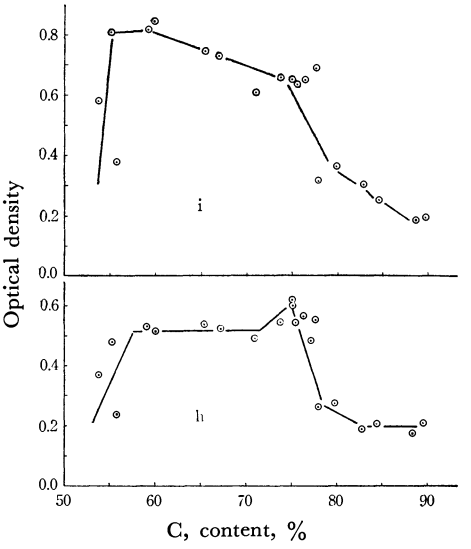

Fig. 2. (continued) Relation between carbon content and functional group optical density.
h. 7.33 μ i. 8.66 μ

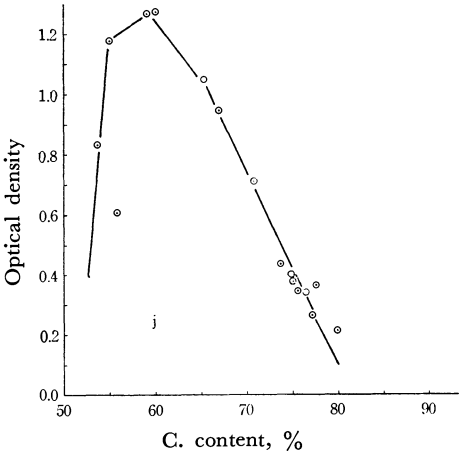

Fig. 2. (continued) Relation between carbon content and functional group optical density.
j. 9.75 μ

AC obtained above 200°C.

12) The absorption bands of the aromatic CH groups at 11—14.5 μ (690—900 cm^{-1}) do not appear clearly in the AC spectra.

13) The functional group absorptions in the IR spectrum of material of a complicated structure with a great molecular weight are difficult to discriminate because of the interference of each group with the others. In such a case, a comparison of the figures of the IR spectra of the materials is useful. For instance, the IR spectra of the AC obtained at 150—200°C are similar to that of cellulose between 5.00—6.00 μ, 7.00—7.33 μ and 9.00—9.70 μ. The IR spectra of the AC obtained at 250—260°C are similar to those of lignins between

5.00—6.00 μ, 6.25—7.92 μ and 9.00—9.70 μ. The IR srectra of the AC obtained at 270—280°C are different from those of lignins, and their absorption bands between 9.00—9.70 μ are weak.

14) The remarkable change in the IR spectra and in the results of the rational analyses of AC obtained at 200—250°C shows that a very important change in its chemical structure has occurred in this temperature range.

15) The relation between the carbon content of AC and the optical density of the bands of the functional groups is illustrated in Fig. 2.[6] The percentage transmission near 5.26 μ (1900 cm^{-1}) was chosen for the base line in calculating the optical density. In Fig. 2 there are two clearly discernible turning points at carbon percentages, about 60 and 75. Thus artificial coalification seems to proceed in three stages. In the first stage, at carbon percentages of 60 and less (coalification temperature; 150—200°C), the IR spectra of the AC are similar to that of cellulose. In the second stage, at carbon percentages from 60 to 75 (coalification temperature; 200—250°C), they are similar to those of lignins. In the third stage, at carbon percentages of 75 and more (coalification temperature; above 250°C), they are rather similar to those of natural coal. These results agree with those mentioned above (6, 13 and 14) and with those presented in a previous report by the present author.[2]

6) W. Funasaka and C. Yokokawa, "Coal Chemistry," Kyoritsu Shuppan, Tokyo (1960), p. 111.

7) H. Sobue and S. Fukuhara, *J. Chem. Soc. Japan, Ind. Chem. Sect.* (*Kogyo Kagaku Zassi*), **61**, 1070 (1958).

BULLETIN OF THE CHEMICAL SOCIETY OF JAPAN VOL. 39 465—469 (1966)

The Liquid-Liquid Extraction of Alkali Metals as Their Poly-Iodides

By Ikuko AKAZA

Department of Chemistry, Faculty of Science, Kanazawa University, Kanazawa

(Received June 16, 1965)

It has been known that alkali metal ions can be extracted into nitrobenzene as their poly-iodides, but the extraction has not been attempted for various salts of alkali metals except in the case of their iodides. In this research ammonium iodide and elemental iodine were preferentially added to the extraction system in order to convert various alkali metal salts into poly-iodides. Ammonium iodide should be larger than the equivalent amount to an alkali metal present in an aqueous solution. The ratio of free iodine to ammonium iodide is an important factor; when the ratio is more than three, a higher distribution ratio is obtained. The ratio of iodine to iodide in the organic phase after the extraction is estimated to be six; therefore, the extracted species seems to be heptaiodide. The extractability of alkali metals increases in the order: Li–Na–K–Rb–Cs, and the distribution ratio decreases with the increase in the amount of metal ions taken in. Back extraction is achieved by shaking the organic phase with 10 M nitric acid. The separation factor between the metals is too low for them to be separated from one another.

Dawson et al. demonstrated at the turn of the century that alkali metal ions could be extracted into nitrobenzene and other solvents with the poly-iodide anion.[1-3] Later Bock and Hoppe[4] investigated the distribution of alkali poly-iodides between aqueous solutions and various organic solvents, and obtained much valuable information on the liquid-liquid extraction of alkali metal ions and their separability from one another. However, in their experiments, metal iodides and iodine were added to the extraction system, and other alkali salts, such as chloride and sulfate, were left outside their scope. Many problems pertinent to the practical application of the method have remained unsolved, e. g., how to convert the chloride or sulfate into iodide easily in an aqueous solution, what distribution ratio is to be established in the presence of diverse ions, and what are the optimum conditions to be kept during the extraction process. The present author has studied the above subjects using nitrobenzene as an extracting solvent. This paper will describe a device for the conversion of other salts of alkali metals into iodides; ammonium iodide is preferred as the reagent for the conversion. Also described will be the relation of the distribution ratio to the concentrations of various alkali salts in the aqueous phase and of the elemental iodine added to the system. It can be concluded that the metals may be divided into two groups: the first, which has lower distribution ratios in

1) H. M. Dawson and R. Gawler, *J. Chem. Soc.*, **81**, 524 (1902).
2) H. M. Dawson, ibid., **85**, 467 (1904); **93**, 1308 (1908).
3) H. M. Dawson and M. S. Leslie, ibid., **99**, 1601 (1911).
4) R. Bock and T. Hoppe, *Anal. Chim. Acta*, **16**, 406 (1957).

the nitrobenzene, includes sodium and lithium, while the second, which has higher distribution ratios, consists of potassium, rubidium and cesium. The separation of the metals within each group, even by multiple extraction in the batch system, seems to be difficult because of their low separation factor. The present author aims to accomplish a satisfactory separation of these metals by reversed-phase partition chromatography based on liquid-liquid extraction. The techniques employed and the separability obtained will be described in a following paper.

Experimental

Into a 50-ml. separatory funnel there was put 10 ml. of an aqueous solution containing a known amount of alkali salt and a varying amount of ammonium iodide; then 10 ml. of nitrobenzene was added. After solid iodine in varying amounts had been put into the funnel, the vessel was tightly stoppered and shaken for five minutes with an Iwaki-V-S shaking machine, operating at 230 double strokes per minute. After the phases became disengaged, the lower organic phase was drained into an Erlenmyer flask, from which 5 ml. of the organic phase was then pipetted into a porcelain crucible. The nitrobenzene and free iodine were driven off by heating them with an infrared lamp. When the residue became white, 1 ml. of 5 M sulfuric acid was dropped onto it and heating was continued under the infrared lamp until the white fumes of sulfuric acid ceased to evolve. The crucible was then put in an electric furnace and heated to 750°C in the cases of potassium and sodium and to 600°C in the cases of lithium, rubidium and cesium. The weight of alkali sulfate was determined in order to calculate the distribution ratio as well as the recovery of the metal. However, in the presence of free iodine, the volumes of the aqueous and organic phases after the equilibration both remarkably differed from that taken initially of the aqueous solution and the nitrobenzene; therefore, the distribution ratio of the metal was computed with the volumes which resulted. The composition of the organic phase was estimated as follows: a part of the phase was taken out and the amount of free iodine was titrated with a standard sodium thiosulfate solution using starch as the indicator. The total iodine content was estimated by titration in hydrochloric acid with a standard potassium iodate solution, as has been described in a general text-book.[5]

Results and Discussion

The Formation and Extraction of Poly-iodides.—If alkali chlorides or sulfates only are present in the sample solution, they cannot be extracted with nitrobenzene. Therefore, a method should first be established to convert them into polyiodides. For this purpose a mixture of hydriodic acid and iodine, another of ammonium iodide, sulfuric acid and iodine, and a third of ammonium iodide and iodine were tried separately for the solution containing alkali metal salts. From the results obtained after the extraction in the presence of each mixture, the last one was found to be the best for the conversion of alkali metals into poly-iodides in an aqueous solution, with respect to the stability of the reagents and the ease of maintaining the optimum conditions.

Definite amounts of a potassium sulfate solution and a solution of ammonium iodide, varying in amount from one to five equivalents to the potassium ion, were put into a separatory funnel; the total volume was made 10 ml. Ten milliliters of nitrobenzene were then added, 1.00 to 2.00 g. of solid iodine was thrown into the funnel, and the extraction was attempted according to the standard procedure. As is shown in Table I, the maximum recovery was obtained at the NH_4I : K ratio close to two at a fixed amount of iodine. The recovery of potassium increased with the amount of iodine added and with the ratio of iodine to iodide; when 2 g. of iodine was used the recovery was as high as 93%, while when the iodine was absent scarcely any extraction was accomplished. Thus the extraction seemed to depend upon the amounts of both ammonium iodide and iodine in the system. In other words two variable factors, the NH_4I : K and the I_2 : NH_4I ratios, may be considered to affect the extraction of potassium. Next, the extraction process was carried further, keeping the NH_4I : K ratio at two and varying the I_2 : I^- ratio from unity to five in the reaction system.

TABLE I. EXTRACTION OF POTASSIUM AS POLY-IODIDE WITH NITROBENZENE IN THE PRESENCE OF VARIOUS AMOUNTS OF AMMONIUM IODIDE AND IODINE

Ammonium iodide taken, mg.	NH_4I : K	Iodine taken g.	Distribution ratio (D)	Recovery %
174.6	1	1.0	5.85	85.4
349.2	2	1.0	9.85	90.8
523.8	3	1.0	2.28	69.6
698.4	4	1.0	2.28	69.6
873.2	5	1.0	3.47	77.6
174.6	1	1.5	2.49	71.3
349.2	2	1.5	4.41	81.5
523.8	3	1.5	4.39	81.5
698.4	4	1.5	1.91	65.6
873.2	5	1.5	3.01	75.1
174.6	1	2.0	4.03	80.1
349.2	2	2.0	14.0	93.3
523.8	3	2.0	5.83	85.4
698.4	4	2.0	2.96	74.7
873.2	5	2.0	2.16	68.3
174.6	1	0.0	0.015	1.5

In each case 47.1 mg. of potassium was taken as 105.0 mg. of potassium sulfate in 10 ml. of an aqueous phase, and 10 ml. of nitrobenzene was used as an extractant.

5) I. M. Kolthoff and R. Belcher, "Volumetric Analysis," Vol. 3, Interscience Publ., New York (1957), p. 447.

The larger the amount of iodine added, the larger was the recovery of potassium in the organic phase, as is shown in Table II, and it was also found that as large a recovery as 97% was obtained when the $I_2 : I^-$ ratio was 5.0.

Table II. Dependence of recovery on the ratio of free iodine to iodide in the extraction system

$I_2 : I^-$ initially added to system	Recovery of potassium in organic phase %	*D*	$I : I^-$ in org. phase after extn.	Recovery of NH_4^+ in organic phase %	*D*
1.0	64.1	1.73	3.9	9.1	0.09
2.0	86.6	6.16	4.7	32.5	0.45
3.0	96.5	25.60	6.0	48.1	0.87
4.0	96.0	21.67	6.6	57.6	1.23
5.0	97.4	33.33	6.4	58.8	1.28

In each case 47.1 mg. of potassium as 105.0 mg. of sulfate and 400 mg. of ammonium iodide were taken in 10 ml. of an aqueous phase. Free iodine was added to nitrobenzene to make the ratio $I_2 : I^-$ in the system as shown in the first column.

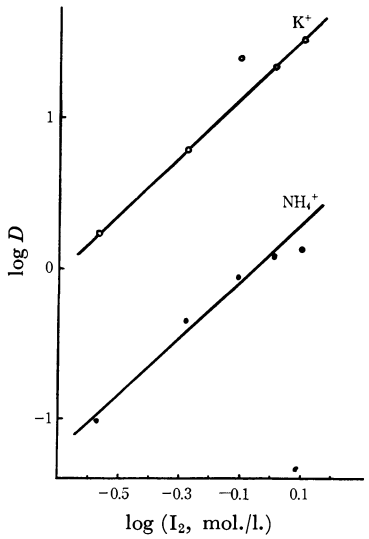

Fig. 1. Relation between distribution ratio and the concentration of iodine added in the system.

In order to examine the composition of the organic phase after the extraction, a part of it was taken out and the amounts of free iodine and iodide were determined volumetrically. From the results shown in the fourth column of Table II, it can be seen that the ratio of iodine to iodide in the organic phase in which the largest recovery of potassium was accomplished was approximately six; therefore, the extracted compound of potassium seemed to be the heptaiodide KI_7, the formation of which has been described by Dawson.[2] In this process the ammonium ion was also extracted into nitrobenzene as its poly-iodide, as is shown in the last column of Table II. Generally, it may be concluded that when the molar ratio of iodine to ammonium iodide exceeds three, a nearly constant distribution ratio is maintained, and the extracted species is the hepta- or a higher poly-iodide of the metal.

In the extraction the relation between the distribution ratio of the metal and the amount of free iodine added to the system may give information as to the composition of the compound extracted as well as the extraction mechanism in the process. In Fig. 1, the relation is shown in a graph of log *D* vs. log (I_2); this relation is a straight line with a slope of 2. Taking the results in Table II and Fig. 1 into account, it can be assumed that potassium and ammonium ions form their triiodides readily in the aqueous phase and that two molecules of free iodine subsequently combine with the triiodide to form the heptaiodide.

In Table III are shown the results of the extraction in which the $I_2 : I^-$ ratio was kept constant while the amount of ammonium iodide was varied. From the results it is clear that if the $I_2 : I^-$ ratio is kept constant at 3.2, the recovery of potassium in the organic phase is also held constant, so the ratio is an important factor, while the amount of ammonium iodide is not. Aqueous solutions containing various amounts of potassium were submitted to extraction by nitrobenzene, as has been described above, at the nearly constant ratio $I_2 : I^-$. The results are shown in Table IV, from which it may be seen that the larger the amount of potassium taken, the lower is the recovery of its poly-iodide; however, the distribution ratio remains constant for a given amount of potassium, even when 20 ml. of the solvent is used. The relation of the distribution ratio to the amount of potassium taken is clearly shown in Fig. 2, in which a straight line with a slope of -1 may be drawn between the distribution ratio and the amount of potassium, both in the logarithmic scale. In these experiments the composition of the organic phase was also examined in the manner shown previously; the extracted species could be identified as potassium heptaiodide, regardless of

Table III. Extraction of potassium as poly-iodide with nitrobenzene at constant ratio of $I_2 : I^-$ in the extraction system

Ammonium iodide added mg.	Free iodine added g.	$I_2 : I^-$	Recovery of potassium in org. phase %
349.2	2.0	3.2	96.5
523.8	3.0	3.2	98.3
698.4	4.0	3.2	99.8
873.2	5.0	3.2	96.9

In each case 47.1 mg. of potassium as sulfate was taken in 10 ml. of the aqueous phase, and 10 ml. of nitrobenzene was used.

TABLE IV. EXTRACTION OF POTASSIUM OF VARIOUS AMOUNTS

Potassium taken mg.	Potassium recovered %	Distribution ratio D	$I : I^-$ in org. phase	Condition of extraction
17.9	98.8	74.0		(1) and (3)
26.9	98.1	48.5		
44.8	96.0	22.2		
62.8	94.6	16.2		
71.7	92.4	11.1		
89.7	89.9	8.2		
0.0	—	—	6.4	(2) and (3)
50.0	95.4	14.4		
75.0	95.1	13.3	6.2	
100.0	92.7	8.8		
125.0	90.1	6.3	5.9	
150.0	90.7	6.7		
175.0	86.4	4.4	6.0	
25.0	100.0	infin.		(2) and (4)
75.0	96.2	17.3		
100.0	94.2	6.7		
125.0	93.5	5.7		
150.0	92.6	4.6		
175.0	93.5	5.6		
200.0	92.4	4.4		

Extractions were carried out with potassium taken as sulfate and under the following conditions.

(1) 0.40 g. NH_4I and 2.80 g. I_2 were put into the system.
(2) 1.48 g. NH_4I and 9.08 g. I_2 were put into the system.
(3) 10 ml. of nitrobenzene was used as an extractant.
(4) 20 ml. of nitrobenzene was used as an extractant.

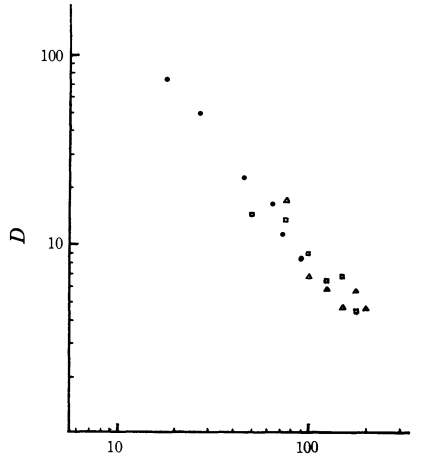

Fig. 2. Dependence of distribution ratio on the amount of potassium taken in the system. Condition of extraction (1), (2), (3) and (4) are shown in Table IV.
• (1) and (3), □ (2) and (3), △ (2) and (4)

the amount of potassium in the original solution.

The extraction procedure was also applied to an aqueous solution containing various kinds of potassium salt, as is shown in Table V; satisfactory recoveries were obtained, even when their amount present was large. Therefore, this procedure must be applicable to solutions containing neutral potassium salts. Other alkali metal ions, lithium, sodium, rubidium and cesium, were subjected to extraction under the same conditions as for potassium, but the detailed results will be

TABLE V. EXTRACTION OF POTASSIUM FROM AQUEOUS SOLUTION CONTAINING VARIOUS KINDS OF POTASSIUM SALT

Potassium salt kind	Potassium salt taken mg.	Potassium taken mg.	Distribution ratio (D)	Recovery of K^+ %
KNO_3	323.0	125.0	6.58	86.8
KSCN	311.0	125.0	7.62	88.4
K_2CO_3	221.0	125.0	8.69	89.7
KH_2PO_4	435.0	125.0	6.62	86.9
KBr	381.0	125.0	6.76	87.1
KCl	238.0	125.0	7.39	88.1
KI	531.0	125.0	10.40	91.2
K_2SO_4	279.0	125.0	7.50	88.1

In the above experiment 1.48 g. of NH_4I and 9.08 g. of iodine were added to each extraction system.

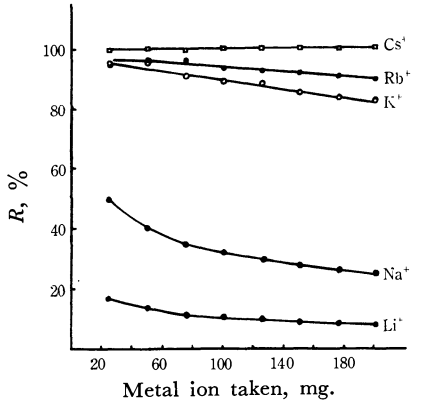

Fig. 3. Recovery of extraction of various metal chlorides as poly-iodides in nitrobenzene. In each case 1.483 g. of NH_4I, 10 ml. of nitrobenzene and 9.09 g. of free iodine were present in the system.

omitted here, since these ions behaved exactly like potassium. The summarization in Fig. 3 shows the behavior of individual metal ions when extracted with nitrobenzene from an aqueous solution containing the corresponding chloride. The same results were obtained for their sulfates. Cesium was the most easily extractable in both cases, followed by rubidium, potassium, sodium, and lithium in that order. Because the distribution ratios of cesium, rubidium and potassium are

approximately equal, these metals may be included in one group, while sodium and lithium may be put in another for the same reason. Because of the marked difference in distribution ratio between potassium and sodium, these ions may be separated from each other by the method of continuous extraction.

The Effect of Acids on the Extraction.—If a free acid is present in the aqueous solution, it may affect the extraction of alkali poly-iodides. As an example, the data found in the case of perchloric acid are given in Table VI. It may be concluded that the stronger the acid, the less satisfactory the extraction.

Table VI. Effect of acids on the extraction

a) Perchloric acid:

$HClO_4$ in aq. phase M	Extraction of Na		Extraction of K	
	D	Recovery %	D	Recovery %
0.00	0.471	32.0	8.90	89.0
0.02	0.429	30.0	11.00	91.7
0.06	0.410	29.1	9.75	90.7
0.10	0.404	28.8	9.53	90.5
0.20	0.412	29.2	9.64	90.6
0.40	0.377	27.4	6.69	78.3
0.50	0.357	26.3	2.01	66.8
1.00	0.280	22.4	0.48	32.8

b) Organic acids:

Acid, 100 mg. equivalent	pH of aqueous phase before extraction	Extraction of Na	
		D	Recovery %
Citric acid	1.95	0.464	31.7
Oxalic acid	0.90	0.477	32.3
Succinic acid	2.32	0.456	31.3
Tartaric acid	1.61	0.473	32.1
Without org. acid	6.18	0.471	32.0

In the above experiment 1.48 g. of ammonium iodide and 9.08 g. of iodine were put into the system, and 100 mg. of sodium or potassium ion was taken in each case.

The Back-extraction of the Metals from the Organic Phase.—The organic phase can be readily stripped, by the following method, of the metal it has taken up. The organic phase separated with a separating funnel was mixed with an equal volume of 10 M nitric acid; the free iodine separating out as a solid by the oxidative action of the acid was then filtered off with a sintered-glass-filter and washed well with water. In the filtrate and washings, two layers of liquid were seen; one of them was nitrobenzene, and the other, a solution of the nitrate of the metal. The organic layer was rejected, and the aqueous phase was evaporated to dryness under an infrared lamp. Thus the alkali metal in the nitrobenzene layer was isolated as its nitrate. The residual iodine on the filter was found to have adsorbed a small quantity of the metal. The yield in the stripping process reached 97.0%.

Summary

The author has described how alkali metal ions in an aqueous solution can be extracted as their hepta- or higher poly-iodides into nitrobenzene in the presence of ammonium iodide in an aqueous solution and in the presence of free iodine in an organic solvent. The extractability of the metals increased in the order; Li–Na–K–Rb–Cs. The equivalence ratio of free iodine to ammonium iodide was an important factor in the satisfactory extraction of the metallic poly-iodide; the ratio had to be kept above three. Acids in the aqueous phase inhibited the extraction, and the removal of metals from the nitrobenzene could be achieved by shaking it with 10 M nitric acid.

The author wishes to express her hearty thanks to Professor Toshiyasu Kiba for his advice and encouragement.

BULLETIN OF THE CHEMICAL SOCIETY OF JAPAN VOL. 39 470—476 (1966)

Intramolecular Interaction between Hydroxyl Group and π-Electrons. XIX.[1] Steric Effects on the Interaction in *o*-(1-Alkenyl)phenols

By Michinori Ōki and Hiizu Iwamura

Department of Chemistry, Faculty of Science, The University of Tokyo, Hongo, Tokyo

(Received June 17, 1965)

Nine *o*-(1-alkenyl)phenols, *o*-$HOC_6H_4CR^1{=}CR^2R^3$, have been prepared and their ultraviolet absorptions and the O–H stretching bands (ν_{O-H}) in the infrared absorption measured in an effort to explore the effect of the substituents, R^1—R^3, on the strength of the intramolecular interaction between the OH group and the π-electron system. The K-band of the styrene chromophore at 240—250 mμ is lost in the samples involving R^1, which is bulkier than methyl. As the size of R^1 increases from H, by way of Me, Et, and *i*-Pr, to *t*-Bu, the angle of the twist between the planes made by the benzene ring and the ethylenic group must increase; this trend is nearly parallel with the amount of the interacting ν_{O-H} in the infrared spectrum. The phenomenon is interpreted mainly by means of the favorable overlap between the O–H group and π-orbitals. *o*-Isobutenylphenol shows a ν_{O-H} triplet at 3610, 3576 and 3539 cm^{-1}. The latter two bands are assigned to the hydroxyl group interacting with π-electrons on the vinyl group intramolecularly. A tentative explanation has been developed which attributes the two interacting bands to the presence of two interacting conformations. The solvent effect on the ultraviolet absorptions is in accord with this explanation.

o-Vinylphenol shows a doublet O–H stretching vibration (ν_{O-H}) at 3611 and 3557 cm^{-1} in the infrared absorption spectra[2]; the latter band has been assigned to the hydroxyl group taking part in the intramolecular interaction with the π-electrons on the vinyl group. Although the interaction does not involve the lone pair of electrons as a proton acceptor, it has been found to be analogous to the ordinary hydrogen bonding in that the polarizable π-electrons play the role of the electron donor. Thus, in *o*-(*trans*-1-propenyl)-phenol, the electron-releasing methyl substituent on the vinyl group enhances the strength of the interaction, as is visualized by a greater shift of the ν_{O-H} to the lower frequency,[3,4] while in 2-hydroxy-*trans*-stilbene[2] and 2-hydroxy-ω-nitrostyrene,[5] the electron-attracting phenyl and nitro groups diminish and extinguish the interaction[6] respectively. These electronic effects have been fully discussed in a series of 2-hydroxybiphenyls,[7] which are aromatic analogs of *o*-vinylphenols.

Since the strength of the interaction must be sharply dependent on the overlap between the π-orbitals in the electron donor and the electron-accepting O–H orbital, the steric hindrance in the neighborhood of the interacting group may be expected to alter the interaction to a great extent. In the present paper, it will be shown that the substituents in the alkenyl group of *o*-(1-alkenyl)phenols (I—VIII) exert a conspicuous steric effect on the interaction in addition to the expected electronic effect. The steric environment of the phenols will be evaluated as a steric inhibition of the resonance between the benzene ring and the alkenyl group through the ultraviolet absorption spectra.

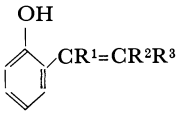

	R^1	R^2	R^3
I	H	H	H
II	Me	H	H
III	*t*-Bu	H	H
IV	H	Me	Me
IV′	H	Me	Et
V	Me	Me	Me
VI	*i*-Pr	Me	Me
VII	H	Me	H
VIII	Et	Me	H

Experimental

The Measurement of the Absorption Spectra.— The infrared measurements were carried out with a Perkin-Elmer 112 G grating infrared spectrometer, the spectral slit width under the 3 μ region being adjusted to 0.8 cm^{-1}. Samples were dissolved in carbon tetrachloride (redistilled over phosphorus pentoxide) with a

1) Part XVIII: M. Ōki and H. Iwamura, This Bulletin, **36**, 1 (1963).
2) M. Ōki and H. Iwamura, ibid., **33**, 681 (1960).
3) M. Ōki, H. Hosoya and and H. Iwamura, ibid., **34** 1391 (1961).
4) A. W. Baker and A. T. Shulgin, *Spectrochimica Acta*, **20**, 153 (1964).
5) The phenol shows a single symmetric band at 3597.5 cm^{-1} which, though shifted to a lower frequency, can be assigned to the free ν_{O-H}.
6) Undoubtedly the planarity of the molecule is unfavorable to the interaction in these compounds, as will be discussed later. However, the presence of the interaction in 2-hydroxy-*trans*-stilbene is an indication of a non-planar conformation, at least to a small extent, in comparison with the absence of the interaction in 1-naphthol.
7) M. Ōki and H. Iwamura, This Bulletin, **34**, 1395 (1961).

Table I. Physical constants and analytical data of the *o*-(1-alkenyl)phenols

	Obs.		Lit.		Anal., %	
	B. p., °C/mmHg	n_D (°C)	B. p., °C/mmHg	n_D (°C)	Found	Calcd.
I	112/17	1.5775 (27)	93—94/12	1.577 (35.7)[9]		
II	92—93/16	1.5463 (20.5)	204/760[10]			
III	105—107/16	1.5171 (20.5)			C: 81.84 H: 9.25	31.77 9.15
IV	100—101/16	1.5606 (19.5)			C: 80.74 H: 8.32	81.04 8.16
IV'	84/4	1.5475 (24.2)			C: 81.41 H: 8.99	81.44 8.70
V	99—100/15.5	1.5390 (23.2)			C: 81.26 H: 8.99	81.44 8.70
VI	116—117/16	1.5170 (21)			C: 82.03 H: 9.35	82.06 9.54
VII	M. p., 36°C		M. p., 36.5—37°C[11]			
VIII	98—99/14	1.5320 (21.5)	112—113/19	1.53234 (17)[12]		

Table II. Physical constants and analytical data of the *o*-(1-alkenyl)anisoles (o-MeO·C_6H_4·CR^1=CR^2R^3)

	Obs.		Lit.		Anal., %	
	B. p., °C/mmHg	n_D (°C)	B. p., °C/mmHg	n_D (°C)	Found	Calcd.
I	89—90/15	1.5552 (24)	73—75/10	1.5530 (20)[13]		
II	91—92/16	1.5304 (28)	56.5—57/2	1.5340 (20)[14]		
III	112/22	1.5111 (28)			C: 82.12 H: 9.52	82.06 9.53
IV	115/22	1.5460 (27)			C: 81.62 H: 8.79	81.44 8.70
IV'	102/15	1.5400 (26.8)			C: 81.70 H: 9.29	81.77 9.15
V	107/18	1.5183 (29)			C: 81.65 H: 9.02	81.77 9.15
VI	117—118/17	1.5178 (24.5)			C: 82.23 H: 9.64	82.30 9.87
VII	101/22	1.5562 (22)	104—105/13	1.5600 (30)[15]		
VIII	112—113/17	1.5188 (21)	113—115/19	1.52013 (17)[12]		

concentration of around 0.001 mol./l., unless otherwise stated. Quartz cells 2.0 and 5.0 cm. in optical length were employed in order to obtain the desired absorption intensity. The apparent absorptions were assumed to be expressed by means of the Lorentz curves and separated into the individual absorptions when they are overlapped. Each integrated intensity (A) was computed from the equation[8]:

$$A = K\frac{\pi}{2cl} \times \ln\left(\frac{I_0}{I}\right)_{max} \Delta\nu^a{}_{1/2}$$

where K was put at unity, $\Delta\nu^a{}_{1/2}$ being the apparent half band width.

The ultraviolet absorptions were measured with a Beckman DU spectrophotometer. The concentration of the samples in 95% aqueous ethanol or in *n*-heptane of a spectro-grade was nearly 10^{-5} mol./l. throughout.

The Preparation of the Samples.—*3, 3-Dimethyl-2-(2-hydroxyphenyl)-2-butanol.*—To a Grignard solution prepared from 41 g. (0.5 mol.) of *t*-butyl chloride, 12 g. (0.5 atom) of magnesium and 300 mol. of ether, was added 20.5 g. (0.15 mol.) of *o*-hydroxyacetophenone in 50 ml. of ether with efficient stirring and cooling. The mixture was heated under reflux for 2 hr., and then 600 ml. of anhydrous benzene added. The solvent was removed by distillation until the boiling point was attained (75°C). The remainder was heated for a further 6 hr. and, after cooling, decomposed with 500 ml. of 15% aqueous acetic acid. Stirring was continued throughout the process. The organic layer was separated, and the aqueous layer extracted with benzene. The combined benzene solution was washed with aqueous sodium bicarbonate, dried, and fractionally distilled to give 7.0 g. of recovered *o*-hydroxyacetophenone and 5.0 g. (17%) of the desired product as a highly viscous colorless oil, b. p. 118—120°C/4 mmHg. The oil later solidified and was recrystallized from petroleum ether to give colorless prisms, m. p. 75—77°C.

8) D. A. Ramsay, *J. Am. Chem. Soc.*, **74**, 72 (1952).

9) K. Fries and G. Fickewirth, *Ber.*, **41**, 367 (1908).

10) K. Fries, W. Gross-Selbeck and O. Wicke, *Ann.*, **402**, 305 (1914).

11) D. S. Tarbell, "Organic Reactions," Vol. II, John-Wiley & Sons, Inc., New York (1944), p. 27.

12) A. Mounié, *Bull. Soc. Chim. France*, [3] **29**, 350 (1903).

13) C. S. Marvell and D. W. Hein, *J. Am. Chem. Soc.*, **70**, 1895 (1948).

14) Y. Okamoto and H. C. Brown, ibid., **79**, 1912 (1957).

15) T. R. Govindachari and B. R. Pai, *J. Org. Chem.*, **18**, 1256 (1953).

Found: C, 74.20; H, 9.45. Calcd for $C_{12}H_{18}O_2$: C, 74.19; H, 9.34%.

2, 4-Dimethyl-3-(2-hydroxyphenyl)-3-pentanol.—This was similarly prepared from methyl salicylate and isopropylmagnesium bromide; it was obtained as needles, m. p. 114—116°C, in a 40% yield.

Found: C, 75.36; H, 9.73. Calcd for $C_{13}H_{20}O_2$: C, 74.96; H, 9.68%.

o-(1-t-Butylvinyl)phenol.—3, 3-Dimethyl-2-(2-hydroxyphenyl)-2-butanol (5 g.) and 10 mg. of iodine were heated in vacuo. The dehydration took place at ca. 100°C, and the product distilled at about 150°C (bath temperature). The distillate was taken up in ether, washed with aqueous sodium thiosulfate, and dried. Distillation gave 3 g. (60%) of a colorless oil.

Other *o*-(1-alkenyl)phenols were prepared similarly. The physical constants and the analytical data are collected in Table I.

The methyl ethers of the phenols were prepared by the methylation of the corresponding phenols with sodium hydroxide and dimethyl sulfate, or by the dehydration of dialkyl-*o*-methoxyphenylcarbinol. The physical constants and the analytical data are listed in Table II.

2, 4-Dimethyl-3-(2-methoxyphenyl)-3-pentanol.—This was an unknown compound and was prepared from methyl 2-methoxybenzoate and isopropylmagnesium bromide. It was a colorless oil boiling at 124—126°C/4 mmHg and was obtained in a 72% yield.

Found: C, 75.36; H, 9.73%. Calcd. for $C_{14}H_{22}O_2$: C, 75.63; H, 9.98%.

Results and Discussion

The apparent ν_{O-H} absorption curves at around 3600 cm^{-1} are shown in Figs. 1, 2 and 3. In Table III are listed the ν_{O-H} maxima, the apparent half band widths ($\Delta\nu^a_{1/2}$), the integrated intensities, the shifts ($\Delta\nu_{max}$) of the interacting ν_{O-H} (ν_i) from the corresponding free ν_{O-H} (ν_f) and the ratios of A_i to A_f.

Although the phenols vary widely, there always appears an absorption of a certain intensity at about 3610 cm^{-1} in each phenol examined. Since phenol itself absorbs in this region in its monomeric state, it is reasonable to assign the absorption which appears here to the free ν_{O-H} band of the phenols.

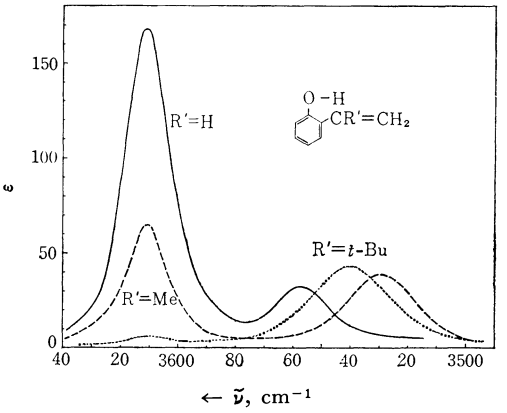

Fig. 1. ν_{O-H} absorptions of I, II and III.

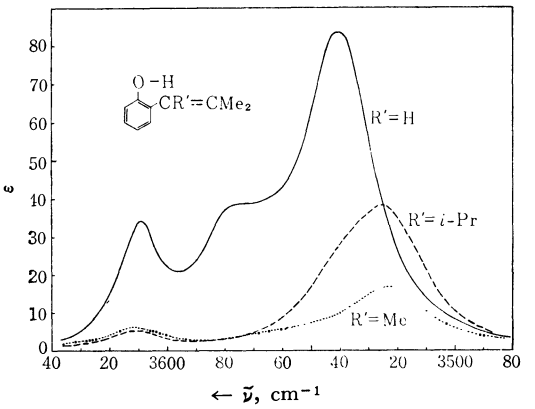

Fig. 2. ν_{O-H} absorptions of IV, V and VI.

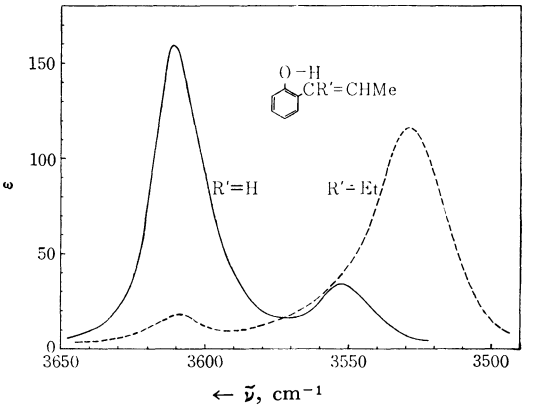

Fig. 3. ν_{O-H} absorptions of VII and VIII.

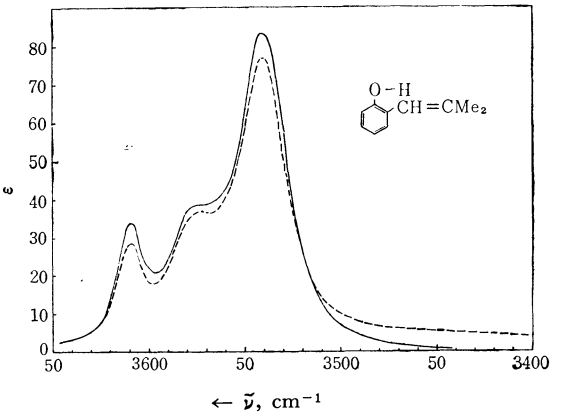

Fig. 4. Variation in ν_{O-H} absorption of *o*-isobutenylphenol (IV) with concentration.
—— 0.00154 mol./l. - - - 0.113 mol./l.

Some of the ν_{O-H} curves are very unusual in shape; this complexity can be interpreted only when the curves are assumed to be overlaps of at least three symmetric curves, each expressed

in terms of the Lorentz function.[8] It has first been confirmed through dilution study that all these ν_{O-H} bands belong to the monomeric molecules of the phenols. Over a wide range of concentration, ν_{O-H} curves hardly change at all in any spectral properties, as is shown in Fig. 4. Secondly, the possibility of the incidental occurrence of the overtone or the combination bands in the midst of the ν_{O-H} region was discarded as a result of a deuterium-substitution experiment in the hydroxyl group. As is shown in Fig. 5, with the example of *o*-(2-methyl-1-propenyl)-phenol-*O*-d, the ν_{O-D} curve appears in the expected region of the lower frequency, with almost the same band shape as the original ν_{O-H} curve. Three absorptions in this case have the same ν_{O-H} to ν_{O-D} ratio of 1.35. It is quite natural that the anharmonicity of ν_{O-H} would not vary significantly after the O–H···π interaction, since it is suggested that ν_{O-H} is of normal anharmonicity or is possibly slightly more harmonic after the hydrogen bond formation.[16] Therefore, the lower ν_{O-H} bands appearing below 3600 cm^{-1} were all thought to result from the hydroxyl group interacting somehow with π-electrons in the vinyl group intramolecularly.

Table III. ν_{O-H} Absorptions of *o*-(1-alkenyl)-phenols

No.	ν_{max} cm^{-1}	$\Delta\nu^a_{1/2}$ cm^{-1}	$A\times10^{-4}$ mol^{-1} l. cm^{-2}	$\Delta\nu_{max}$ cm^{-1}	A_i/A_f
I	3611.0	17.8	1.08	53.9	0.26
	3556.8	24.4	0.28		
II	3610.7	17.6	0.41	81.4	0.95
	3529.3	28.3	0.39		
III	3610.5	19.0	0.028	70.6	18.6
	3539.9	32.8	0.52		
IV	3609.8	14.6	0.12	33.7	10.1
	3576.1	37.0	0.40	70.5	
	3539.3	26.8	0.81		
IV′	3609.2	14.8	0.12	32.8	10.5
	3576.4	38.4	0.36	71.4	
	3537.8	29.6	0.90		
V	3612.2	27.2	0.051	52.9	4.6
	3559.3	39.0	0.043	87.8	
	3524.4	33.4	0.19		
VI	3611.1	20.2	0.026	69.6	18.8
	3541.5	23.4	0.086	86.4	
	3524.7	32.0	0.40		
VII	3611.1	16.8	0.84	9.9	0.67
	3601.2	19.2	0.29	58.9	
	3552.2	24.0	0.27		
VIII	3609.4	21.0	0.14	52.4	9.4
	3557.0	32.0	0.084	80.6	
	3528.8	29.6	1.23		

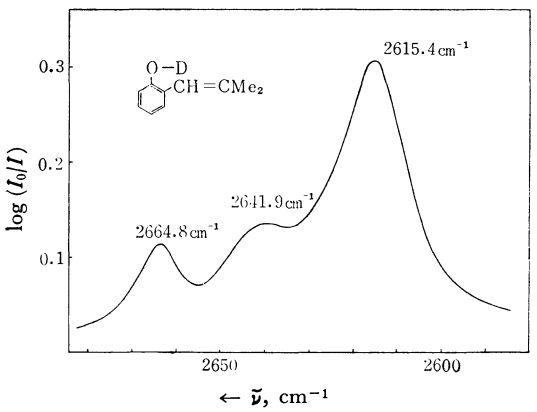

Fig. 5. ν_{O-D} absorption curve of *o*-isobutenyl-phenol-*O*-d.

By assigning in these ways, the remarkable effects of the substituents on the apparent absorption curves can be summarized as follows.

a) It is obvious from Figs. 1, 2 and 3, and also from the last column of Table III, that the degree of the interaction increases as the α-substituent on the vinyl group varies from methyl to ethyl, isopropyl and to *t*-butyl, because the intensity of the free ν_{O-H} band decreases, while the relative intensity of the interacting ν_{O-H} to the free one increases, in this descending order of substituents.

b) The phenols with a sterically-crowded alkenyl group show a rather less total intensity of the ν_{O-H} band.

c) In some instances, two or more kinds of ν_{O-H} bands appear interacting with π-electrons. This suggests the possible presence of more than one kind of interacting forms of a comparable stabilization.

d) The ν_{O-H} shifts following the interaction, which may be reagrded as corresponding to the

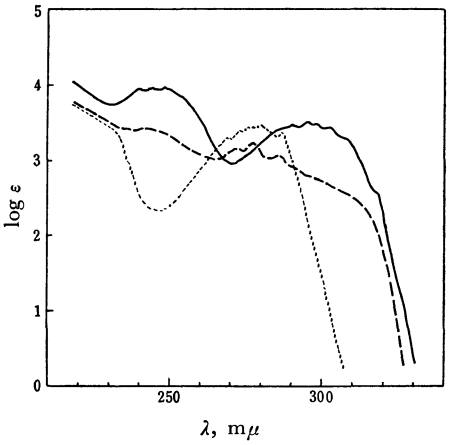

Fig. 6. The ultraviolet absorptions of I, II and III in *n*-heptane.

16) C. C. Pimentel and A. L. McClellan, "The Hydrogen Bond," W. H. Freeman and Co., San Francisco and London (1960), p. 114.

energy of the interaction, are not always in the order of the degree of the interaction, A_t/A_f.

Before ascribing these effects mainly to the steric factors and discussing them further, it would be more instructive to inspect here the configuration of the molecules with reference to the ultraviolet absorption spectra, together with the corresponding anisoles which lack the O–H···π interaction. Figure 6 illustrates the ultraviolet absorption curves of the selected examples in the region from 215 to 350 mμ, the numerical data of these, together with other phenols, being tabulated in Tables IV and V.

The absorption bands may be classified into two groups. The first, appearing in the 240—250 mμ region with a greater intensity, can only include the samples without a rather bulky group in the α-position of the vinyl group; the K-band of styrene chromophore[17] is characteristic. Styrene has been shown to be planar and, according to the thermochemical data,[18] to be stabilized through conjugation between the benzene ring and the vinyl group by 1.5 kcal./mol. Though no direct data is available for *o*-vinylphenol, it is not unreasonable to regard the molecule as planar, since the K-band is actually observed and there is no benefit in the non-planar structure with a loss of the resonance energy. The α-methyl substituent is not enough to make this conjugation band vanish and so retains it as a shoulder. The second bands appear in the 270—300 mμ region, with the maximum molar absorptivity in the neighborhood of $2-3\times10^3$. This is assigned to the B-band of the benzene derivatives with an oxygen function, such as phenol and anisole.[19]

Those homologs with a rather bulky α-substituent have only the latter absorption; it is, in addition, very akin to that of phenol itself in its shape and in the location of the absorption peak. There is no conjugation between the vinyl group and the benzene ring in these cases. It is most probable that the loss of the conjugation is due to the non-bonded repulsion between the group(s) on the vinyl group on the one hand and the hydroxyl group (the methoxyl group, in the case of anisoles) and the hydrogen atom of the benzene ring ortho to the alkenyl group on the other, and that it arises from the rotation of the alkenyl group around the bond through which it is connected to the benzene ring and from the consequent non-coplanarity between the two planar systems concerned. As the angle between them increases by way of a change in the α-substituents from methyl to ethyl, isopropyl, and to *t*-butyl, the non-bonded repulsive energy is relieved at the expense of the resonance energy. The compromise is attained at a certain angle of twist; thus, the conformation of the *o*-(1-alkenyl)phenols is determined. Since their

Table IV. The ultraviolet absorptions of *o*-(1-alkenyl)phenols in *n*-heptane (H) and 95% aqueous ethanol (A)

No.	Solv.	K-band		B-band	
		λ_{max}	log ε_{max}	λ_{max}	log ε_{max}
I	H	245.5	3.96	296.5	3.49
				310.0	3.21
	A	246.5	4.04	302.5	3.63
II	H	243.0	3.41	271.5	3.15
				278.0	3.22
				283.5	3.09
	A	245.0	3.46	277.5	3.21
III	H			280.0	3.47
				286.0	3.34
	A			278.0	3.44
IV	H	235.0	3.79	282.0	3.41
	A	242.0	3.96	287.5	3.57
IV′	H	235.0	3.75	281.5	3.47
	A	242.0	3.98	287.0	3.56
V	H			281.5	3.48
				288.5	3.42
	A			278.0	3.45
				280.5	3.48
VI	H			281.0	3.48
				288.5	3.36
	A			280.0	3.47
VII	H	243.0	3.94	291.0	3.57
		247.0	3.97	300.0	3.55
		251.5	3.97	312.5	3.21
	A	245.0	3.99	298.0	3.67
		254.5	4.04	305.0	3.68
VIII	H			274.5	3.33
				279.5	3.37
	A			279.0	3.39

Table V. The ultraviolet absorptions of *o*-(1-alkenyl)anisoles (*o*-MeO·C_6H_4·CR^1=CR^2R^3) in *n*-heptane

No.	K-band		B-band	
	λ_{max}	log ε_{max}	λ_{max}	log ε_{max}
I	247.0	4.03	301.0	3.58
			312.5	3.32
II	237.0	3.84	273.5	3.30
			279.5	3.36
III			280.0	3.49
			287.0	3.36
IV	245.0	4.05	286.0	3.58
IV′	247.5	4.03	285.0	3.57
V			274.5	3.36
			280.0	3.38
VI			281.0	3.52
			289.0	3.45
VII	248.0	4.05	293.0	3.60
	253.0	4.06	300.0	3.61
VIII			275.0	3.37
			280.0	3.38

17) R. Y. Mixer, R. F. Hech, S. Winstein and W. G. Young, *J. Am. Chem. Soc.*, **75**, 4094 (1953).
18) H. Grasshof, *Chem. Ber.*, **84**, 916 (1951).
19) R. A. Friedel and M. Orchin, "Ultraviolet Spectra of Aromatic Compounds," John Wiley & Sons, New York (1951).

ultraviolet absorptions are, with one exception to be discussed later, very similar to the corresponding anisoles, it may be concluded that a third effect, that of the intramolecular interaction between the hydroxyl group and π-electrons on the conformation of the molecule, is a minor one and that the interaction takes place in a steric environment determined mainly by the resonance and the steric hindrance of the alkenyl group.

The trend mentioned in a) can now be explained. As the angle between the planes made by the benzene ring and the vinyl group increases, the localization of the π-electrons on the vinyl group commences to reduce their ionization potential, and so the strength as the electron donor of the π-electron system increases. This tendency is in the same direction as the inductive electron-donating ability of the alkyl groups, and it must be a factor in the observed substituent effect. In addition, the increased rotation of the plane of the vinyl group from that of the benzene ring is sure to produce a more favorable overlap between the π- and O–H orbitals, because the directional O–H anti-bonding orbital can approach the highest-occupied π-orbital in the vinyl group from the upper side of the electron cloud. Thus, the following order of the $\Delta\nu_{max}$ values is reasonable: II>I; III>I; V>IV; VIII>VII. It must be a reflection of the electronic effect that V and VII have greater $\Delta\nu_{max}$ than II and I, respectively. Nevertheless, the orders, II>III and V>VI, which are obtained by assuming that the $\Delta\nu_{max}$ values are direct measures of the strength of the interaction, can not be explained satisfactorily by the above interpretation. An inspection of the molecular models suggests that, when the α-substituents are greater than the methyl group, the dihedral angle made by the planes of the vinyl group and the benzene ring becomes great enough to make the hydroxyl and the vinyl groups overlap in the desired direction, but that the distance between the two groups increases a little, thus resulting in a reduction of their overlap. Thus, if the energy of the interaction is expressed by $\Delta\nu_{max}$, then methyl group as an α-substituent seems to afford the optimum among the two opposing steric effects, in addition to the favorable electronic effect.

The steric effect may be an attractive means of interpreting of the decrease in the total intensity of the phenols with a rather sterically-crowded alkenyl group, since the bulky alkenyl group may dislocate the hydrogen atom of the hydroxyl group out of the benzene ring, thus giving a lower absorption intensity, from the analogy of comparison of the intensities of phenols and alcohols. However, this is not the case for sterically-hindered phenols. Ingold and Taylor[20] have reported that, among the homologous series of alkyl- or alkenyl-substituted phenols, the molar absorptivity did not change significantly. The present authors are tentatively inclined to attribute this phenomenon to the electronic effect of the substituent. That is, the vinyl group withdraws the electron, thus increasing the molar absorptivity of the ν_{O-H}, unless the steric effect is operating. When the steric effect forces the vinyl group to rotate out of the plane of the benzene ring, the vinyl group which is carrying some alkyl groups now acts as an electron-releasing group to lessen the molar absorptivity. We have to await further investigations to confirm this hypothesis, but the authors are postulating this on the basis that the compound V gives the least total intensity, whereas the second least is that of the compound VI, and the third least, that of the compound III.

As has been discussed above, the ultraviolet spectra indicate that I and VII are planar. If the molecule is perfectly planar, however, even the conformation IX cannot show the O–H···π interaction, because the hydroxyl group is pointing to the node of the π-orbitals on the vinyl group. A slight rotation around the bond which connects the vinyl group with the benzene ring will not lose the resonance energy materially, while the overlap between the O–H and π-orbitals may become possible; this must be the case in I.

The free ν_{O-H} in I is practically symmetric under the resolution of the present spectrometer. In VII, on the contrary, the band at the higher frequency is asymmetric. The tailing on the lower frequency side is reminiscent of the second absorption at 3601 cm^{-1}. Since it is shifted only 10 cm^{-1} from the free ν_{O-H}, the band is in its nature free. In this latter case, the basicity of the

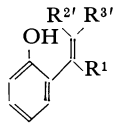

IX

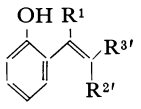

X

π-electron system as the proton acceptor is enriched by the β-alkyl substitution, and the hydroxyl group in the conformation X may be perturbed a little. Since the energy gained by the O–H···π interaction is not enough to compensate for the loss in the resonance energy in X, X cannot be a form which has a strongly interacting ν_{O-H}; it shows only a perturbed free ν_{O-H}.

When $R^{2'}$ is methyl, the vinyl group must be buttressed out of the plane of the benzene ring by the hydrogen at the 3-position with respect to the hydroxyl group, and some overlap between the hydroxyl group and the π-orbital becomes possible in X, giving an interacting ν_{O-H} curve different from that in IX. This must be the reason for the doublet interacting ν_{O-H} bands

20) K. U. Ingold and D. R. Taylor, *Can. J. Chem.*, **39**, 471 (1961).

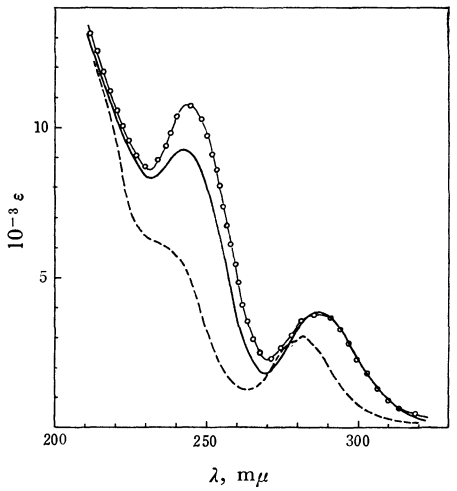

Fig. 7. The effect of solvents on the ultraviolet absorptions of *o*-isobutenylphenol (IV) and its methyl ether.

——— IV in 95% ethanol (A)
----- IV in *n*-heptane (H)
—○— IV methyl ether in A and H

in IV and IV'. This explanation has already been adopted by Baker and Shulgin[4] for the ν_{O-H} curves of IV and *o*-(*cis*-1-propenyl)phenol.

In this connection, it should be mentioned that the solvents and *O*-methylation have marked effects on the ultraviolet spectra of IV. Figure 7 shows the ultraviolet absorptions of IV in 95% aqueous ethanol and in *n*-heptane. The corresponding methyl ether has, in both solvents, the same absorption pattern as that of IV in ethanol, the data of which can be seen in Tables IV and V. Since the ether exhibits the K-band characteristic of the styrene chromophore, the molecule can be assumed to have a fairly planar structure. This must hold true in IV in ethanol. It is only in IV in *n*-heptane that the intramolecular interaction between the hydroxyl group and the π-electrons of the vinyl group takes place in this system. From the fact that it is only under these conditions that the K-band is weakened, it may be concluded that, when the interaction is possible, the angle made by the planes of the isobutenyl group and the benzene ring increases, thus producing better overlap of the orbitals of the hydroxyl group and the π-cloud on the isobutenyl group. This is the first observation of the effect of the intramolecular O–H$\cdots\pi$ interaction on the ultraviolet absorption spectra.

As regards the remaining assignment, concerning which of the two bands, at 3576 and 3539 cm^{-1}, should correspond to the conformations represented by IX and X, it is effective to compare the $\Delta\nu_{max}$ value of IV with those of I and VII. Since the $\Delta\nu_{max}$ values of 53.9 and 58.9 cm^{-1} of I and VII respectively, can be regarded as originating from the conformation IX, this form of IV must have a greater $\Delta\nu_{max}$ value because the basicity of the π-electrons is increased by one more methyl substitution. It is the band at 3539 cm^{-1} which conforms to this requirement; therefore, it may rather safely be concluded that the bands at 3576 and 3539 cm^{-1} should be assigned to the interacting hydroxyl groups in X and IX respectively.

A confirmative support of this assignment is now being investigated; it will be presented in a forthcoming paper.

The authors are indebted to the Ministry of Education for a grant-in-aid for Fundamental Scientific Research.

BULLETIN OF THE CHEMICAL SOCIETY OF JAPAN VOL. 39 476—480 (1966)

The Absorption Spectra of Dyes. X.[1] Note on the Configuration of the Component Molecules in the Complex State*

By Toshihiko Hoshi and Yoshié Tanizaki

Department of Chemistry, Tokyo Institute of Technology, Ookayama, Tokyo

(Received June 22, 1965)

The configuration of the component molecules in the complexes formed between Chrysophenine G (G) and the direct dyes (P), such as Chlorazol Sky Blue FF, has been discussed qualitatively with respect to the relation between the steric structure of the individual P molecules and the enthalpy or the entropy changes in the complex formations. The electrons to be transferred from

1) Part IX of this series: T. Hoshi, Y. Tanizaki and N. Ando, This Bulletin, 38, 725 (1965).

* Presented at the 7th Discussions on Dyeing Chemistry (May, 1965) held by the Chemical Society of Japan and the Society of Fiber Sience and Technology, Japan.

the partner (P) to the G molecule are the π electrons of the functional (hydroxy) groups and are those of the inner-side groups when the respective coupling components of the dye have more than one functional group. The larger the charge density of such an effective functional group becomes, the more the enthalpy change ($-\Delta H$) is increased. It may be said with certainty that there must exist a certain configuration of the component molecules peculiar to the complex formation. Such a configuration may be seen for the combination of G and ND (NW-acid←dianisidine→NW-acid). For other combinations of which the partner of G is more deformed in free than ND state, the shifts of equilibrium to the configuration for the complex state are almost due to an entropy change ($-\Delta S$) which increases in proportion to the magnitude of the deformation.

Hitherto in this series, the complex formation between the disazo direct dyes and Chrysophenine G has been studied.[1-4] According to the conclusion reached on the complex state, the component molecules are arranged side by side when the charge transfer from the partner (to be abbreviated as P) to the G molecule (Chrysophenine G) occurs[1,3]; that is, the π electron on the functional group of the P molecule transfers to the lowest vacant MO (π_G^*) of G.[1] Since the charge transfer, as is well known, plays an important role in the intermolecular force, the enthalpy change ($-\Delta H$) for the complex formation should be directly affected by the π electron density of the functional group. Moreover, as the π electron possesses the directional property, there may exist a certain configuration of P and G suitable for a charge transfer. The shifts to such a peculiar configuration of the component molecules must be reflected in the entropy change ($-\Delta S$).

The purpose of the present study is therefore to consider the thermodynamic quantities qualitatively and in connection with the configuration. At the same time, a supplement to the previous discussion will be given, on the basis of the experimental results accumulated so far, regarding the configuration of the complexes formed.

Experimental

The experimental procedure and the treatment of the data obtained were the same as have been described before.[4]

The dyes used here were the symmetric disazo dyes prepared in the usual way from the following diazo and the coupling components, which will hereforth be called by the notations indicated in parentheses; benzidine (B), tolidine (T), dianisidine (D) and 3, 3'-dichlorobenzidine (Cl), and NW-acid (N), J-acid (J), SS-acid (S), H-acid (H) and chromotropic acid (C). A dye, for example, NW-acid←benzidine→NW-acid, will be represented by NB. CT and CCl were excluded because they could not be obtained in a pure enough form to indicate only one spot on the paper chromatograph. The other dyes, when combined with G, showed the spectral change corresponding to the 1 : 1 and 1 : 2 complex formations. However, there were some combinations for which the equilibrium constants for the complex formations could not be estimated for several reasons; some dyes with the first absorption peaks at 530 mμ or at shorter wavelengths were affected by the absorption tail of G at its higher concentrations; others when combined with G did not indicate large enough spectral changes at the isosbestic points for reliable equilibrium constants to be calculated, and so on. The estimated thermodynamic quantities are shown in Table I, in which 1 : 1 means the complex

Table I. ΔH kcal./mol. and ΔS e.u. for the 1:1 (P+G→PG) and the 1:2 complex formations (PG+G→GPG)

		B		T		D*		Cl	
		1:1	1:2	1:1	1:2	1:1	1:2	1:1	1:2
N	ΔH	a)		c)		−7.4	−6.7	c)	
	ΔS					1	0		
J	ΔH	a)		c)		−13	−11	a)	
	ΔS					−19	−20		
S	ΔH	b)		g)		−24	−20	f)	−23
	ΔS					−44	−45		−50
H	ΔH	−18	e)	−19	e)	−25	−19	−26	−19
	ΔS	−37		−36		−57	−47	−57	−46
C	ΔH	−15	−11	d)		−27	−19	d)	
	ΔS	−29	−22			−60	−40		

* Taken from Ref. 4.

a) The isosbestic points due to the influence of the tail of G did not appear because the first absorption peaks of P's were at too short wavelengths (530 mμ).

b) The equilibrium constants could not be calculated because the spectral change corresponding to the 1 : 2 complex formation did not retain well-defined isosbestic points.

c) In spite of the indication of the well-defined isosbestic points due to the complex formations, the spectral changes corresponding to the 1 : 1 and the 1 : 2 complex formations at the 1 : 2 and the 1 : 1 isosbestic points respectively were too small for the equilibrium constants to be calculated.

d) The sample could not be purified so as to provide only one spot on the paper chromatograph as the other samples could.

e) The spectral change due to the 1 : 2 complex formation at the 1 : 1 isosbestic point was too small for K_2 to be calculated.

f) The spectral change due to the 1 : 1 complex formation at the 1 : 2 isosbestic point was too small for K_1 to be calculated.

g) The values obtained were extensively dispersed; for example, the $-\Delta H$ values were dispersed from −18 to −23.

2) T. Kobayashi, Y. Tanizaki and N. Ando, This Bulletin, **33**, 661 (1960).
3) T. Kobayashi, K. Saito, Y. Tanizaki and N. Ando, ibid., **35**, 935 (1962).
4) Y. Tanizaki, T. Hoshi and N. Ando, ibid., **38**, 264 (1965).

formation of the P+G→PG type, and 1 : 2, that of the PG+G→GPG type.

Results and Discussion

The thermodynamic quantities for the complex formations of 1 : 1 (P+G→PG) and 1 : 2 (P+2G →GPG) are summarized in Tables II and III for the D and the H series respectively. There can be discussed by means of the data in Table II the effect of the structural differences for the coupling components, and, by means of the data in Table III, that for the diazo components.

Table II. The enthalpy and entropy changes for the D series; ΔH_1, ΔS_1 for P+G→PG, and ΔH_2, ΔS_2 for P+2G→GPG.

P	ND	JD	SD	HD	CD
ΔH_1, kcal./mol.	−7.4	−13	−24	−25	−27
ΔH_2, kcal./mol.	−14	−24	−44	−44	−46
ΔS_1, e. u.	1	−19	−44	−57	−60
ΔS_2, e. u.	1	−39	−89	−104	−100

Table III. The enthalpy and entropy changes for the H series; ΔH_1, ΔS_1 for P+G→PG, and ΔH_2, ΔS_2 for P+2G→GPG.

P	HB	HT	HD	HCl
ΔH_1, kcal./mol.	−18	−19	−25	−26
ΔH_2, kcal./mol.	—	—	−44	−45
ΔS_1, e. u.	−37	−36	−57	−57
ΔS_2, e. u.	—	—	−104	−103

The Enthalpy Change.—It has been clarified that the lone pair electrons on the amino group of SS-acid (S) cannot conjugate to the naphthalene link due to the intramolecular hydrogen bond formation of the N···H–O type, as is shown in Fig. 1.[5] The π electrons of the hydroxyl groups must, therefore, be alone responsible for the SD→G charge transfer, provided the SD molecule allows of the above-mentioned situation for S. On the other hand, all the amino and/or the hydroxyl groups of H and C have π type lone pair electrons, because of the hydrogen bond formation in the N–H···O or O–H···O form respectively (Fig. 1).[5] That is, the HD and the CD molecule have twice as many functional groups with π type lone pair electrons as the SD molecule. According to Table II, however, the ΔH's of SD, HS and CD are nearly in the same order. This suggests strongly that only the π electrons of the internal functional groups (the hydroxyl groups) of P are responsible for the charge transfer. The reason why the π electrons on the end functional groups attached to the outside ring of naphthalene are ineffective could not be found. At any rate, the internal hydroxyl groups will be discussed with the above facts in mind.

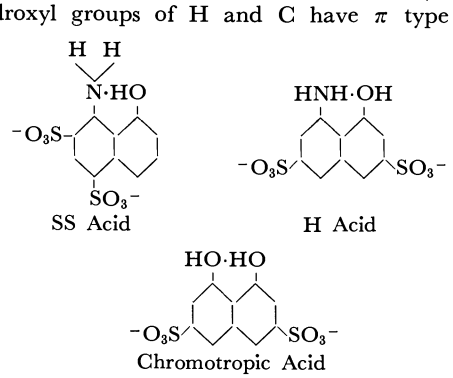

Fig. 1. The type of the hydrogen bonding of SS acid, H acid and chromotropic acid.

The effective functional groups of the P dyes used here are, therefore, just the hydroxyl groups. According to the findings described above, it ought to be possible to explain the relative magnitude of $-\Delta H$ in connection with the π electron densities of such hydroxyl groups. The relative π electron density will be comparable with that of the total charge density in the usual sense. It can be said that the larger the charge density of the hydroxyl group, the more the difficulty of the proton dissociation of the group. The order of the starting pH value for the dissociation of the hydroxyl groups has been found to be C(4.2)<J(5.6)<N(6.2)<S(8.0)≒H(8.4), where the figures in parentheses indicate the approximate pH values.[5] As the solvent water used here had a pH value of 6, nearly a half of C and also a small amount of J could be dissociated in the solution. Accordingly, the plausible order of the charge density is N<J≒S<H<C in the solution. If it is assumed that the condition of the hydroxyl groups is preserved because of the same coupling positions of the components,* the charge densities of the hydroxyl groups of the P dyes in the D series may plausibly be arranged in the same order as that of the coupling components, i. e., (ND)<JD<SD≒HD≒CD. Indeed, the order just mentioned corresponds well—including ND—with that of the magnitude of the $-\Delta H$'s in Table II.

In the H series, the coupling component, H-acid, is the common ingredient; therefore, the kinds of substituents at the 3,3′ positions of the biphenyl skeleton must be correlated with the charge density on the hydroxyl groups. The resonance effect of the substituent will hinder the electron of the hydroxyl group from migrating to the inner conjugate system. If this is the case, the π electron density of the hydroxyl group

5) Y. Tanizaki, H. Inoué and N. Ando, This Bulletin, **38**, 1419 (1965).

* This assumption is adequate except in the case of ND, because, as will be shown in the following section, all of the dyes in the D series but ND are affected by some steric effects and, consequently, the relative situation of the charge densities of the hydroxyl groups could not be altered. At present, however, no reason can be found for arranging ND on the left side as above.

will be larger in the case of HD and HCl than in that of HB and HT. Consequently, the transition probability of P→G in the former case will become larger than in the latter. In fact, the order of the magnitude of $-\Delta H$'s in Table III comes up to this expectation.

The above consideration can equally be applied to both the PG (1 : 1) and the GPG (1 : 2) complexes.

In the 1 : 2 complex state, the two G molecules have been considered to be equivalent to one another.[1,2] This is not inconsistent with the magnitude of the ΔH values obtained here, because, for all cases, the $-2\Delta H_1 > -\Delta H_2$ relation is always maintained.

Entropy Change.—First of all, concerning the ΔS value, it is interesting to notice the following relations which appear in Table II;

for the ND–G system: $\Delta S_1 \fallingdotseq \Delta S_2 \fallingdotseq 0$ (1)

for the JD–G and SD–G systems:

$$2\Delta S_1 \fallingdotseq \Delta S_2 \quad (2)$$

for the HD–G and CD–G systems:

$$-2\Delta S_1 < -\Delta S_2 \quad (3)$$

and for both ΔS_1 and ΔS_2 :

$$0 \fallingdotseq -\Delta S(\mathrm{ND}) < -\Delta S(\mathrm{JD}) < -\Delta S(\mathrm{SD}) < -\Delta S(\mathrm{HD}) \fallingdotseq -\Delta S(\mathrm{CD}) \quad (4)$$

Relation 1 implies that ND and G have not been suffered from any structural restriction by the complex formation; Relation 2, that the amount of deformation is equally distributed to the first (P+G →PG) and the second process (PG+G→GPG), and Relation 3, that the deformation is larger in the first process than in the second.

In order to enable the charge transfer to take place, the π_P orbital of the hydroxyl groups of P and the π_G^* orbital of G must overlap with each other. Besides, the π_P orbital originally has a directional property, as has been described above. For that reason, both of the component molecules are required to change the configuration into that suitable for the above conditions.

Though all of the P dyes take similar chemical structures, some differences may be seen in the three-dimensional structures between them, i. e., the differences in the torsional angles about the bonds shown in Fig. 2, as R_0, R_1 and R_2 are dependent on the sort of coupling components, though R_0 and R_1 may be almost independent. In the case of ND (see Fig. 2), the hydrogen bond formation is possible ($R_2=0°$), while in HD the electrostatic repulsion between the negative charge on the sulfonic group and the lone-pair electrons of the azo group exceeds the sum of the hydrogen bonding force and the resonance force of the C–N bond, $R_2=50$—$60°$.[6] That to is say, the $R_2(\mathrm{ND}) \ll R_2(\mathrm{HD})$ relation can

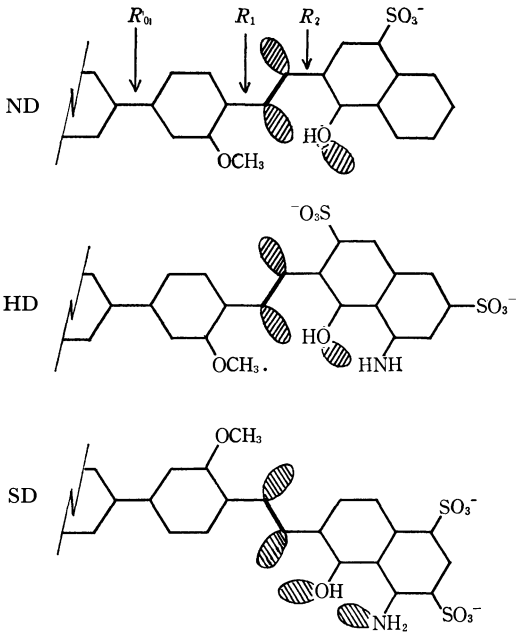

Fig. 2. Steric structures of ND, HD and SD; shadings indicate the σ type lone pair electrons.

well be correlated to the $-\Delta S(\mathrm{ND}) \ll -\Delta S(\mathrm{HD})$ relation. Therefore, it may be expected that a parallelism exists between the order of the tortional angle, R_2, in the free state and that of the entropy change.

Let us assume here that the ND molecule keeps the ideal conformation for the complex formation, because it can form the complexes without any entropy change. According to this assumption, the other P dyes have to become somewhat deformed in order to approach such an ideal conformation.

JD and CD have previously been considered to have nearly the same order of R_2 as HD.[6] However, JD has amino groups at the end β positions of the naphthalene links, while HD has these at the end α positions. The resonance effect of the amino group of J slightly increases the charge density at the opposite β position to be coupled with the diazo component, while that of the amino group of H cannot do that.[7] In the case of JD, therefore, the amino group could increase the resonance force of the C–N bond (R_2) and could also increase the charge density of the azo-nitrogen atom adjacent to biphenyl. For that reason, the R_2 angle of JD may become smaller than that of HD. The order of the torsion angles is considered to be as follows (R_2(SD) will not be considered here):

$$0° \fallingdotseq R_2(\mathrm{ND}) < R_2(\mathrm{JD}) < R_2(\mathrm{HD}) \fallingdotseq R_2(\mathrm{CD}) \quad (5)$$

Relation 5 coincides with Relation 4 except for

6) T. Kobayashi, Y. Tanizaki and N. Ando, ibid., **33**, 913 (1960).

7) H. Baba and S. Suzuki, ibid., **34**, 82 (1961).

SD. If Relations 4 and 5 are parallel, it must be said that R_2(SD) can be positioned between R_2(JD) and R_2(HD), indicating that the R_2 of SD is also fairly large. This, together with the drawing of SD in Fig. 2, implies the existence of some repulsive force acting between the σ type lone-pair electrons of the hydroxyl group and those of the azo-nitrogen atom. The fact of the steric structure of SD just mentioned must be emphasized, because the conventional image of the SD molecule has been one in which an intramolecular hydrogen bond is formed like the ND molecule shown in Fig. 2, that, i. e., the R_2 angle of SD is zero.[6]

In the H series, since R_0 and R_2 can be assumed to be invariant because of the common coupling components, the difference in the entropy change of Table III may be attributed to the difference in R_1 values. As may be seen from the drawing of HD in Fig. 2, the torsion of R_1 is mainly due to the electrostatic repulsion or the steric hindrance of the methoxy group in relation to the σ type lone-pair electrons of the azo-nitrogen atom. Also, in the case of HCl, a similar situation involving the chlorine atom can be taken into consideration. Such substituent effects may be larger for HD and HCl than for HB and perhaps for HT as well. The corresponding torsion angles R_1 for the former class will, therefore, become larger than those for the latter. Thus, the entropy change difference appearing in the two classes, (HB, HT) and (HD, HCl), can reasonably be explained.

One of the present authors (T. H.) wishes to express his hearty thanks to Dr. Harutada Negoro, Sankyo Co., Ltd., for his encouragement and advice.

BULLETIN OF THE CHEMICAL SOCIETY OF JAPAN VOL. 39 480—484 (1966)

The Synthesis of α, ω-Disubstituted Higher Alkanes from $\alpha, \alpha, \alpha, \omega$-Tetrachloroalkanes

By Kazuo SAOTOME, Hiroshi KOMOTO and Toshiaki YAMAZAKI

Technical Research Laboratory, Asahi Chemical Industry Co., Itabashi-ku, Tokyo

(Received June 22, 1965)

Higher ω-chloroalkanoic acids than ω-chlorooctanoic acid were prepared in good yields (over 90%) by improved methods of the hydrolysis of $\alpha, \alpha, \alpha, \omega$-tetrachloroalkanes. The reactions were carried out in fuming nitric acid, with the addition of nitrogen dioxide during the reaction or in the presence of a small amount of phosphoric anhydride. α, ω-Dichloroalkanes were derived from the ω-chloroalkanoic acids by the Kolbe electrolytic synthesis. Various other novel α, ω-disubstituted alkanes with very long methylene chains, such as glycols, dinitriles, dicarboxylic acids, and diamines, were also prepared starting from the tetrachloroalkanes.

Many kinds of bifunctional derivatives have been prepared by several Russian authors[1] from $\alpha, \alpha, \alpha, \omega$-tetrachloroalkanes which had been obtained by the telomerization of ethylene with carbon tetrachloride. Some of the lone-chained derivatives have also been synthesized. For example, α, ω-dodecanedioic and α,ω-hexadecanedioic acids were obtained through the dimeric compounds produced by the catalytic hydrogenation of these tetrachloroalkanes:[2]

$$Cl(CH_2)_nCCl_3 \rightarrow [Cl(CH_2)_nCCl_2\text{-}]_2 \rightarrow$$
$$Cl(CH_2)_{2n+2}Cl \rightarrow HOOC(CH_2)_{2n+2}COOH$$

In the present work, α, ω-disubstituted derivatives with a long methylene chain have been prepared by the Kolbe electrolytic synthesis of the ω-substituted alkanoic acids derived from $\alpha, \alpha, \alpha, \omega$-tetrachloroalkanes.

The preparation of lower ω-chloroalkanoic acids from the tetrachloroalkanes with sulfuric acid was also well investigated by the previously-mentioned authors. Freidlina et al.[3] obtained higher ω-chloroalkanoic acids (C_9—C_{13}) in yields of 60—70% by treating the tetrachloroalkanes with fuming nitric acid. A careful hydrolysis of these higher tetrachloroalkanes in concentrated sulfuric acid also gave the acids in nearly the same yields.[4]

We have found that the yield of these higher ω-chloroalkanoic acids (C_9–C_{15}) is remarkably affected by the density of fuming nitric acid, and that the

1) A. N. Nesmeyanov, R. Kh. Freidlina and L. I. Zakharkin, *Quart. Rev.*, **10**, 330 (1956).
2) A. N. Nesmeyanov, L. I. Zakharkin and T. A. Kost, *Izv. Acad. Nauk S. S. S. R., Otd. Khim. Nauk*, **1955**, 657.
3) R. Kh. Freidlina and Ye. I. Vasil'eva, *Doklady Akad. Nauk S. S. S. R.*, **100**, 85 (1955).
4) Sh. A. Karapetyan and N. A. Semenov, *Zh. Prikl. Khim.*, **37**, 2003 (1964).

Table I. The preparation of higher ω-chloroalkanoic acids

$Cl(CH_2)_nCCl_3$		HNO_3	$Cl(CH_2)_nCCl_3$		$Cl(CH_2)_nCOOH$	
			Recovered	Conversion		
n	g.	g.	g.	%	g.	Yield, %*
8	130	350	6.0	95.5	87.0	96.0
10	120	400	19.0	84.0	74.0	97.5
12	120	450	31.0	74.0	66.5	96.5
14	100	450	30.0	70.0	51.0	92.0

* The yield was calculated by taking the recovered tetrachloroalkane into account.

yield is much improved to over 90% by adding nitrogen dioxide to the reaction mixture during the course of the reaction. The yield has also been found to increase when the reaction is carried out in a fuming nitric acid solution containing a small amount of phosphoric anhydride. ω-Chloroalkanoic and ω-hydroxyalkanoic acids derived from the tetrachloroalkanes were subjected to the Kolbe electrolysis to afford α, ω-disubstituted long alkanes according to the following scheme;

$$\begin{array}{l} Cl(CH_2)_nCCl_3 \\ \downarrow \\ Cl(CH_2)_nCOOH \rightarrow HO(CH_2)_nCOOH \\ \downarrow \quad \text{Kolbe electrolysis} \quad \downarrow \\ Cl(CH_2)_{2n}Cl \qquad HO(CH_2)_{2n}OH \\ \downarrow \\ CN(CH_2)_{2n}CN \rightarrow H_2N(CH_2)_{2n+2}NH_2 \\ \downarrow \\ HOOC(CH_2)_{2n}COOH \end{array}$$

The Kolbe electrolytic syntheses of some ω-chloroalkanoic[5] and ω-hydroxyalkanoic[6] acids have been reported.[7] In this work, however, very long α, ω-dichloroalkanes (up to α, ω-dichlorotetracosane) were prepared. Dinitriles, dicarboxylic acids, and diamines were also derived from these long α, ω-dichloroalkanes.

Experimental and Results

δ-Chlorovaleric, ω-chloroenanthic and ω-chloropelargonic acids were prepared by hydrolyzing the corresponding tetrachloroalkanes in sulfuric acid according to the method in the literatures.[8]

The Preparation of Higher ω-Chloroalkanoic Acids in Fuming Nitric Acid with Nitrogen Dioxide Added.—A mixture of $\alpha, \alpha, \alpha, \omega$-tetrachloroalkane and fuming nitric acid (d=1.52) was stirred in a water bath. The reaction started at about 40°C with the generation of gas. When the initial generation of gas stopped (at 45—50°C, after 2—2.5 hr.), a stream of an excess of nitrogen dioxide was passed through the solution. Then the temperature was gradually raised to 70°C until the gas genaration practically ceased. 2—2.5 hr. were needed to complete the reaction under the flow of nitrogen dioxide. The reaction was carried out for about 5 hr. in all. A crystalline product was precipitated by adding ice-water to the reaction mixture. The precipitate was then filtered and washed several times with water. White crystals were obtained after recrystallization from ether - petroleum ether. From the mother liquor, the unreacted tetrachloroalkane was recovered by distillation under reduced pressure. The repeated recrystallization of the crystals from the same solvents afforded the following specimens: ω-chloropelargonic acid (a fraction of b. p. 140—143°C/2 mmHg was recrystallized), m. p. 30°C (lit. 30°C); ω-chloroundecanoic acid, m. p. 42°C (lit. 42°C); ω-chlorotridecanoic acid, m. p. 53°C (lit. 52°C); and ω-chloropentadecanoic acid, m. p. 62°C (lit. 62°C).

The details of the reaction are shown in Table I.

The Preparation of Higher ω-Chloroalkanoic Acids in Fuming Nitric Acid Containing Phosphoric Anhydride.—1) A mixture consisting of 55 g. of 1, 1, 1, 9-tetrachlorononane, 150 g. of fuming nitric acid (d=1.52) and 6 g. of phosphoric anhydride was stirred. The reaction started at 40°C with the generation of gas. The temperature was then gradually raised to 70°C as the reaction proceeded. After a 3 hr. reaction, the mixture was treated as above. Distillation under reduced pressure afforded a crystalline product without the unreacted tetrachloroalkane. Yield, 38.5 g. (96.5%).

2) A mixture consisting of 60 g. of 1,1,1,11-tetrachloroundecane, 180 g. of fuming nitric acid and 4 g. of phosphoric anhydride was treated as above. The reaction was carried out at temperatures between 40—60°C for 5 hr. Recrystallization from ether - petroleum ether gave white crystals. From the mother liquor, 3.5 g. of the unreacted tetrachloroalkane was recovered; conversion, 94%. Yield, 37.5 g. (89%).

The Preparation of ω-Hydroxyalkanoic Acids.—A mixture of ω-chloroalkanoic acid and its two moles of sodium hydroxide (a 5% aqueous solution) was refluxed for 6 hr. The solution was

5) F. L. M. Pattison, J. B. Stothers and R. G. Woolford, *J. Am. Chem., Soc.*, **78**, 2255 (1956).
6) G. E. Svadkovskaya, S. A. Voitkevich, Y. K. Smol'yaninova and V. N. Belov, *Zh. Obsch. Khim.*, **27**, 2146 (1957).
7) B. C. L. Weedon, "Advances in Organic Chemistry (Methods and Results), I," Interscience Publisher, New York (1960), p. 1.
8) R. M. Joyce, W. E. Hanford and J. Harmon, *J. Am. Chem. Soc.*, **70**, 2529 (1948).

Table II. The kolbe electrolysis of ω-substituted alkanoic acids

$X(CH_2)_nCOOH$			MeOH	Na	$X(CH_2)_{2n}X$	
X,	n,	g.	ml.	g.	g.	Yield, %*
Cl	4	137	500	2.3	51.5	56.0 (51.5)**
Cl	5	150	500	1.1	68.0	65.0 (55.0)
Cl	6	165	500	1.1	66.0	55.0
Cl	8	190	500	1.1	76.5	52.5
Cl	10	220	500	1.2	75.5	43.0
Cl	12	120	400	0.8	48.0	49.0
OH	8	170	500	1.1	34.5	27.5
OH	10	100	400	0.8	9.3	12.0

* A large part of the by-products was found to be the methyl ester of the initial carboxylic acid.
** Yields in ( ) are cited from the literature.[5]

Table III. Characteristics and analytical results of α,ω-disubstituted alkanes

Formula	B. p. (lit.) °C/mmHg	n_D^{25} or M. p. (lit.) °C	Elementary Analysis, % Found C	Found H	Found Cl	Calcd. C	Calcd. H	Calcd. Cl
$Cl(CH_2)_8Cl$	75—76/2 (115—116/10)	1.4568 (1.4570)						
$Cl(CH_2)_{10}Cl$	101—102/1 (140—142/11)	1.4580 (1.4585)						
$Cl(CH_2)_{12}Cl$	170—172/10	27—28	60.20	9.86	29.57	60.25	10.11	29.65
$Cl(CH_2)_{16}Cl$		52—53	64.98	10.59	24.32	65.07	10.92	24.01
$Cl(CH_2)_{20}Cl$		60—61	68.17	11.49	20.46	68.35	11.47	20.18
$Cl(CH_2)_{24}Cl$		69—70	70.53	11.92	17.18	70.73	11.87	17.40
$HO(CH_2)_{16}OH$		89—90 (90.5)						
$HO(CH_2)_{20}OH$		102—103	76.32	13.38		76.37	13.46	

then acidified with sulfuric acid while being cooled with ice-water in order to separate the product. The precipitate was filtered, washed with water, and dissolved in ether - petroleum ether. The crystals which were separated after the evaporation of a large part of the solvents were again recrystallized from ethyl acetate. The following ω-hydroxyalkanoic acids were thus obtained: ω-hydroxypelargonic acid, m. p. 51°C (lit. 51.5°C); yield 86%; ω-hydroxyundecanoic acid, m. p. 69°C (lit. 70°C); yield 89%; ω-hydroxyundecanoic acid, m. p. 69°C (lit. 70°C); yield 89%; ω-hydroxytridecanoic acid, m. p. 79°C (lit. 79°C); yield 83%; and ω-hydroxypentadecanoic acid, m. p. 82°C (lit. 82°C); yield 78%.

The Kolbe Electrolysis of ω-Substituted Alkanoic Acids.—The apparatus used for the electrolysis was as follows. In a glass cell ($10\times10\times1$ cm^3), electrodes of titanium plates plated with platinum ($8\times8\times0.3$ cm^3) were settled 2 mm. apart. The cell was then placed in a cooling bath, and a sample solution was vigorously circulated through it. Commercial absolute methanol was used as the solvent, and small amounts of metallic sodium were added. The current density was maintained between 0.10 and 0.12 amp./sq. cm. throughout the reaction. The temperature in the cell was controlled below 50°C (30—40°C), while the solution outside the cell was cooled with ice-water in order to deposit crystalline products. A glass filter was placed between the outer section and the cell in order to protect the circulation pump from the solid precipitate. The reaction was continued until the solution was just alkaline to litmus; the time needed for this to occur was usually 100—150% longer than that calculated. The product, after being acidified with hydrochloric acid, was condensed almost to dryness, then the residue was extracted with ether. The ether extract was washed with a dilute solution of sodium carbonate in order to remove the unreacted acid, and then dried. The product which was obtained after the evaporation of the ether was recrystallized from ethanol. In the cases of α, ω-dichloroalkanes, in which carbon atoms in a molecule are less than 16, however, the products were purified by distillation under reduced pressure.

The details of the reaction and the characteristics of the products are shown in Tables II and III.

The Preparation of Dinitriles from α, ω-Dichloroalkanes.—α, ω-Dicyanoalkanes were prepared by treating these dichloroalkanes with potassium cyanide in the solvent of dimethylformamide (DMF). The reaction products were filtered to remove precipitated potassium chloride, and the filtrates were condensed by heating under reduced

Table IV. The cyanation of α,ω-dichloroalkanes

$Cl(CH_2)_nCl$		DMF	KCN	Reaction		$CN(CH_2)_nCN$	
				Temp.	Time		
n	g.	ml.	g.	°C	hr.	g.	Yield, %
8	60	200	50	120—130	8	44.0	82.0
10	60	200	45	110—115	8	40.5	74.5
12	65	250	40	130—140	10	43.5	73.0
16	85	300	40	140—150	12	55.0	70.0
20	35	100	15	140—150	15	17.2	55.0

Table V. Characteristics and analytical results of α,ω-dicyanoalkanes

Formula	B. p. (lit.) °C/mmHg	n_D or M. p. (lit.) °C	Elementary analysis N%	
			Found	Calcd.
$CN(CH_2)_8CN$	153—155/2 (199—200/15)	n_D^{16} 1.4528 (n_D^{20} 1.4474)		
$CN(CH_2)_{10}CN$	145—146/2	n_D^{16} 1.4550	14.60	14.57
$CN(CH_2)_{12}CN$	164—166/1.5	n_D^{16} 1.4578	12.75	12.71
$CN(CH_2)_{16}CN$		45—46	10.20	10.13
$CN(CH_2)_{20}CN$		56—57	8.25	8.42

pressure in order to evaporate the solvent. The lower dinitriles were separated and purified by distillation under reduced pressure, while the higher ones were obtained as white crystals after repeated recrystallizations from ethanol. The yields in Table IV are the values after the first distillation or recrystallization. The characteristics and the analytical results are shown in Table V.

The Preparation of α,ω-Alkanedioic Acids.—1) The oxidation of ω-hydroxyalkanoic acids. ω-Hydroxyundecanoic, ω-hydroxytridecanoic and ω-hydroxypentadecanoic acids were oxidized with nitric acid. For example, a mixture of 11 g. of ω-hydroxytridecanoic acid and 150 g. of nitric acid (98%) was stirred at room temperature for 1.5 hr. Then the temperature was gradually raised to 60°C over a 1-hr. period and then maintained between 60 and 70°C for 5 more hours. The mixture was diluted with water, and a crystalline product was filtered, washed with water and recrystallized from ethyl acetate. The pure crystals were obtained after repeated recrystallization from benzene.

2) The oxidation of glycols. Hexadecamethylene and eicosamethylene glycols were oxidized with potassium permanganate in acetone-water. For example, 5 g. of hexadecamethylene glycol was added to a solution of acetone (200 ml.) and water (20 ml.) containing 10 g. of potassium permanganate. The mixture was then heated at 70°C for 8 hr. while being stirred. After being allowed to stand overnight, the mixture was acidified with hydrochloric acid; then an aqueous solution of sodium hydrogen sulfite was added in order to dissolve precipitated manganese dioxide. The separation and the purification of a crystalline product were carried out as above.

3) The hydrolysis of dinitriles. Into a mixture consisting of 25 ml. of sulfuric acid (96%), 20 ml. of water and to 80 ml. of acetic anhydride, 25 g. of the dinitrile shown in Table V was added and the mixture was then refluxed for 15 hr. The reaction mixture was cooled and diluted with water to afford a crystalline precipitate, which was then separated and purified much above.

The yields and the melting points of these dicarboxylic acids are shown in Table VI.

The Preparation of Diamines.—The dinitriles shown in Table V were hydrogenated in the presence of the Raney cobalt or nickel (recipe W-7) under hydrogen pressures of 110—130 atm. The reaction was carried out for 2 hr. in 200 ml. of methanol containing 20 g. of ammonia. The absorption of hydrogen generally reached the theoretical amount after 1 hr. From the reaction mixture, the catalyst was filtered off, and the filtrate

Table VI. The preparation of α,ω-alkanedioic acids

$HOOC(CH_2)_n$-COOH	Process	Yield %	M. p., °C	
n			Found	Lit.
8	3	96	134—134.5	134.5
9	1	94	111—111.5	111
10	3	87	127—127.5	128
11	1	86	113—113.5	113.5
12	3	79	125—126	127
13	1	83	114—115	114.5
14	2	78	123—124	124
16	3	82	124—125	125
18	2	72	121—122	123
20	3	78	124—125	124

Table VII. The preparation of α,ω-diaminoalkanes

$CN(CH_2)_nCN$		Catalyst		Temp.	$H_2N(CH_2)_{n+2}NH_2$					
					Yield		B. p.	M. p.	N% (HCl salt)	
n	g.		g.	°C	g.	%	°C/mmHg	°C	Found	Calcd.
8	25	Co	10	100—105	17.5	72.0	128—130/2	59—59.5 (60—61)*		
10	20	Ni	8	100—110	13.8	70.5	145—148/2	65.5—66 (66—67)		
12	20	Ni	10	130—140	13.5	66.0	154—156/2	70.5—71	9.30	9.30
16	15	Ni	8	140—150	9.5	64.0	193—195/2	85—85.5	7.62	7.84

* The values in ( ) show the melting points of the literature.

was condensed by evaporating the solvent and ammonia. A fraction with a higher boiling point was again distilled under reduced pressure to give a product with a constant boiling point.

The details of the reaction and the products are summarized in Table VII.

Discussion

In the hydrolysis of the higher tetrachloroalkanes in fuming nitric acid, the yields of ω-chloroalkanoic acids were much improved by the addition of either nitrogen dioxide or phosphoric anhydride. The hydrolysis of the trichloromethyl group is denoted by:

$$RCl_3 + 2H_2O \rightarrow RCOOH + 3HCl$$

The hydrogen chloride produced is immediately oxidized by an attack of nitric acid to give 3 mol. of water:

$$3HCl + 3HNO_3 \rightarrow 3NO_2 + 3/2Cl_2 + 3H_2O$$

As a matter of fact, the gas generated from the reaction mixture is a mixture of nitrogen dioxide and chlorine. The actual reactions taking place in the nitric acid solution may be summarized as:

$$RCCl_3 + 3HNO_3 = RCOOH + 3NO_2 + 3/2Cl_2 + H_2O$$

According to the above equation, one mole of water is produced to dilute the nitric acid when one mole of the tetrachloroalkane is converted. The facts that the yield is greatly affected by the density of the fuming nitric acid and that relatively poor yields are obtained in a simple treatment with fuming nitric acid, reveal the prohibiting effect of dilution by the produced water. Moreover, the reaction is actually interrupted by the small addition of water into the system. It is obvious that the nitrogen dioxide and the phosphoric anhydride in the reaction mixture catch the water, thus maintaining the system free from the dilution. The characteristic feature of these acidic media with regard to the progress of the reaction is much affected by the dilution with water. The remarkable improvements in the yields of the higher ω-chloroalkanoic acids in these experiments may be explained by the above explanation.

On the other hand, the hydrolysis of the lower tetrachloroalkanes ($<C_9$) in fuming nitric acid proceeds smoothly enough to give a high conversion even without the addition of these dehydrating agents. The products, however, are somewhat yellow, and this color could not be removed even by repeated distillations. The infrared spectra of the colored products denote the presence of some nitro-compounds as impurities.

BULLETIN OF THE CHEMICAL SOCIETY OF JAPAN VOL. 39 485—489 (1966)

The Synthesis of Novel α, ω-Oxaalkanedioic Acids with Long Methylene Chain Units

By Kazuo SAOTOME and Kenichiro SATO

Technical Research Laboratory, Asahi Chemical Industry Co., Nakadai, Itabashi-ku, Tokyo

(Recieved June 22, 1965)

α, ω-Oxaalkanedioic acids with the general formula $HOOC(CH_2)_mO(CH_2)_nCOOH$ (m, n= 3—10, but in unsymmetric structures m=3 or 4) were synthesized. The symmetric acids were prepared by the catalytic dehydration of ω-hydroxyalkanoic acids or by the condensation of ω-chloroalkanoic acids in the presence of alkali hydroxide. The unsymmetric acids (m=3 or 4) were prepared by the reaction of γ-butyrolactone or δ-valerolactone with alkali alcoholates of ω-hydroxyalkanoic acids. The reaction mechanisms were also discussed. In the plots of the melting points of the two unsymmetric series (m=3, 4 in m/n) against the carbon atoms in a molecule, the minimum melting points are found at 3/5 and 4/5 respectively.

The synthesis of some α, ω-oxaalkanedioic acids with a formula $O[(CH_2)_nCOOH]_2$ (n= 2—5) has been reported hitherto.

Alexander and Schniepp[1] prepared 6-oxaundecanedioic acid from bis(4-chlorobutyl)ether through its biscyano derivative. 7-Oxatridecanedioic acid was also derived from bis(4-bromobutyl)-ether by malonic ester synthesis.[2] Reppe et al.[3] prepared 5-oxaazelaic acid by treating γ-butyrolactone with alkali hydroxide at temperatures above 200°C.[4-6] The conversion of β-propiolactone to 4-oxapimelic acid proceeds easily in the presence of water at about 100°C.[7,8]

In the present work, the authors will report on the synthesis of α, ω-oxaalkanedioic acids with the general formula of $HOOC(CH_2)_mO(CH_2)_n$ COOH, in which m and n are integers from 3 to 10 respectively, although m is 3 or 4 in unsymmetric structures. In the synthesis of the above α, ω-oxaalkanedioic acids, the ω-carboxyalkyl groups of C_4 and C_5 are derived from γ-butyrolactone and δ-valerolactone as raw materials in each case. The reaction between γ-butyrolactone and alkali alcoholates to form γ-carboxypropyl derivatives was precisely investigated by Reppe et al.[3] The reaction is considered to proceed through alkyl-fission in the γ-butyrolactone ring. On the other hand, the reactivities of δ-valerolactone have been little studied.

The synthesis and the polymerization of δ-valerolactone were reported on in previous papers.[9,10] During the course of the investigation of the reactivities of δ-valerolactone in comparison with those of γ-butyrolactone, it was found that δ-valerolactone reacts with alkali alcoholates in the same manner as γ-butyrolactone to afford δ-carboxybutyl derivatives.

For example, a mixture of sodium phenolate and δ-valerolactone gives δ-phenoxyvaleric acid in a good yield.[11] The preparation of 6-oxaundecanedioic acid from δ-valerolactone was carried out by three different methods, in which the formation of the ether linkage was effected through the following processes: 1) the dehydration of alkali δ-hydroxyvalerate in the presence of alumina as the catalyst, 2) the reaction between δ-valerolactone and the alkali alcoholate of sodium δ-hydroxyvalerate, and 3) the reaction of δ-valerolactone with sodium carbonate. By the second type of reaction, unsymmetric 5-oxasebacic acid was also found to be produced by the reaction between γ-butyrolactone and the sodium alcoholate of sodium δ-hydroxyvalerate, which had been prepared by heating a mixture of δ-valerolactone and two times as many moles of sodium hydroxide under reduced pressure. The reactions of the first two types were investigated using various lactones, ω-hydroxyalkanoic and ω-chloroalkanoic acids; novel α, ω-oxaalkanedioic acids with both symmetric and unsymmetric structures were thus obtained. It was found that δ-valerolactone reacted with alkali alcoholates of ω-hydroxyalkanoic salts in the same manner as γ-butyrolactone to give both symmetric and unsymmetric α, ω-oxaalkanedioic acids. ε-Caprolactone, however, did not react with the

1) K. Alexander and L. E. Schniepp, *J. Am. Chem. Soc.*, **70**, 1839 (1948).
2) V. Prelog, M. Fausy EL-Neweihy and O. Häfliger, *Helv. Chim. Acta*, **33**, 1937 (1950).
3) W. Reppe et al., *Ann.*, **596**, 194 (1955).
4) I. Nishigori, B. Tatsuya and S. Murahashi, *Chem. High Polymer (Japan)*, **8**, 249 (1951).
5) K. Heintz, German Pat. 836936 (1952); *Chem. Abstr.*, **51**, 15557 (1957).
6) H. Haussman and G. Gräfinger, German Pat. 919167 (1954); *Chem. Abstr.*, **49**, 11690 (1955).
7) H. J. Hagemeyer, Jr., U. S. Pat. 2466419 (1949); *Chem. Abstr.*, **43**, 5037 (1949).
8) K. Nagakubo, Y. Iwakura and T. Fujii, *J. Chem. Soc. Japan, Ind. Chem. Sect. (Kogyo Kagaku Zassi)*, **62**, 817 (1959).
9) K. Saotomo, This Bulletin, **37**, 956 (1964).
10) K. Saotome and Y. Kodaira, *Makromol. Chem.*, **82**, 41 (1965).
11) A. N. Nesmeyanov and L. L. Zakharkin, *Izv. Akad. Nauk S. S. S. R., Otd. Khim. Nauk*, **1955**, 224.

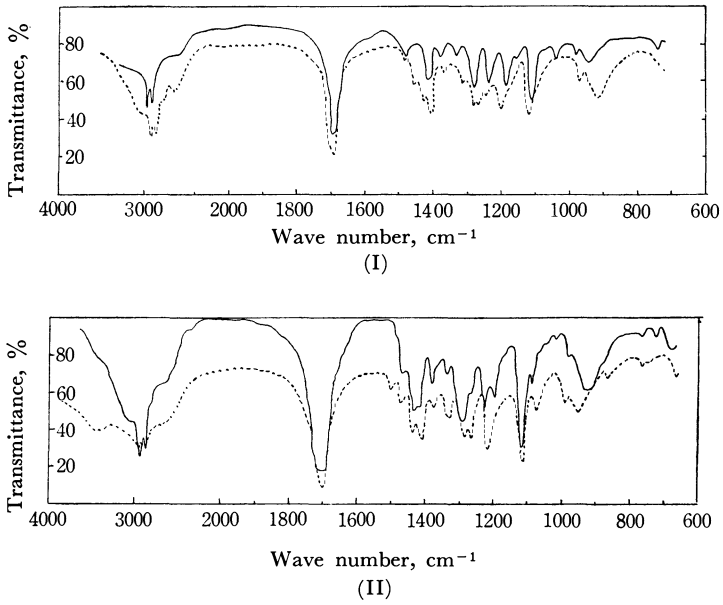

Fig. 1. Infrared spectra of α, ω-oxaalkanedioic acids.

(I) —— $HOOC(CH_2)_6O(CH_2)_6COOH$, ····· $HOOC(CH_2)_4O(CH_2)_6COOH$
(II) —— $HOOC(CH_2)_3O(CH_2)_8COOH$, ····· $HOOC(CH_2)_3O(CH_2)_4COOH$

alcoholates as above; rather, a resinous product was obtained under severe conditions. The symmetric α, ω-oxaalkanedioic acids with longer methylene chain units than C_4 were prepared either by the condensation of ω-hydroxyalkanoic salts in the presence of the dehydration catalyst or by the treatment of ω-chloroalkanoic acids with potassium hydroxide. We tried to obtain unsymmetric α, ω-oxaalkanedioic acids of which had methylene chain units longer than C_4, by the reaction between ω-chloroalkanoic acids and the alkali alcoholates of ω-hydroxyalkanoic salts with carbon numbers different from those of the chloro-acids. However, the reaction products seemed to be mixtures of symmetric and unsymmetric α, ω-oxaalaknedioic acids, each with the ω-carboxy-alkyl group of the starting compounds. It was difficult to separate the individual α, ω-oxa-alkanedioic acids from the reaction mixtures.

The mechanisms of these condensation reactions will be discussed.

Experimental

Materials.—δ-Valerolactone was prepared according to the method described in a previous paper.[9] ω-Chloroalkanoic and ω-hydroxyalkanoic acids were also prepared from the telomers of ethylene with carbon tetrachloride. The characteristics of these intermediates agreed with those in the literature.[12]

6-Oxaundecanedioic Acid.—1) A mixture of 50 g. of δ-valerolactone and 20 g. of sodium hydroxide was heated at about 200°C in order to make a homogeneous solution. Then, 10 g. of activated alumina (grains) was added to the solution, and the temperature was gradually raised to 260—265°C over a 3 hr. period. During this period, a vigorous foaming due to the dehydration reaction was observed. After the reaction mixture had been kept at that temperature for a further 6 hr., the product was cooled and dissolved in 500 ml. of water. The aqueous solution was acidified by adding sulfuric acid a little over the neutral point of methyl orange. The precipitate and the solution were extracted with ether. After the evaporation of the ether, the residue was distilled under reduced pressure. The recrystallization of a fraction (b. p. 200—230°C/1 mmHg) from ethyl acetate afforded white crystals; m. p. 89.5—90°C (lit.[1] 88.5—89°C). Yield, 29 g. (53%).

A mixture of 25 g. of δ-valerolactone and 14 g. of potassium hydroxide was treated as above, but the reaction was carried out at temperatures of 255—260°C for 4 hr. White crystals of the same melting point were obtained. Yield, 19 g. (70%).

Found: C, 55.13; H, 8.29; mol. wt. (titration), 219. Calcd. for $C_{10}H_{18}O_5$: C, 55.03; H, 8.31%; mol. wt., 218.3.

2) A solution of 42 g. of sodium hydroxide dissolved in 50 ml. of water was gradually added to 50 g. of δ-valerolactone under cooling. After the evaporation of water with an aspirator, the mixture was heated to 220°C under the reduced pressure of 1 mmHg for 3 hr. until the water in the system was completely removed. Then, 60 g. of δ-valerolactone was added, and the mixture was refluxed under the atmosphere of nitrogen. When the mixture became homogeneous after several minutes, the temperature was raised to 255—260°C and kept there for a further 8 hr. When the product was treated as above, 88 g. (74%)

12) A. N. Nesmeyanov, R. Kh. Freidlina and L. I. Zakharkin, *Quart. Rev.*, **10**, 330 (1956).

of 6-oxaundecanedioic acid was obtained.

3) A mixture of 25 g. of δ-valerolactone and 14 g. of sodium carbonate was refluxed. The temperature was gradually raised to 260°C over a 1.5 hr. period and then maintained at that point for 3 hr. During this period, the generation of 2.5 l. of carbon dioxide (nearly theoretical) was observed. When the reaction product was treated as above, 14 g. (51%) of 6-oxaundecanedioic acid was obtained.

5-Oxaazelaic Acid.—The preparation of this acid from γ-butyrolactone has already been reported in the cited articles. In these experiments, however, the reaction was carried out under somewhat different conditions; γ-butyrolactone was treated with potassium hydroxide and sodium carbonate under conditions similar to those in the cases of δ-valerolactone described above. No large difference in the yields between the two lactones was observed in either case, and the melting point of the obtained crystals agreed with that of the literature (81°C).

5-Oxasebacic Acid.—From a mixture of 50 g. of δ-valerolactone and 42 g. of sodium hydroxide in 60 ml. of water, the water was completely removed by heating it to 250°C for 3 hr. under the reduced pressure of 1 mmHg. Then 60 g. of γ-butyrolactone was added, and the mixture was heated at 250—260°C for 8 hr. under nitrogen. Just before the end of the reaction, the unreacted lactone was recovered by distillation under reduced pressure. The treatment of the product was carried out much as in the case of 6-oxaundecanedioic acid. From the ether extract, a fraction with a b. p. of 180—210°C/2 mmHg was separated by distillation. Recrystallization from ether-petroleum ether afforded white crystals; m. p. 67°C. Yield based on δ-valerolactone, 72 g. (71%).

Found: C, 53.00; H, 8.06; mol. wt. (titration), 206. Calcd. for $C_9H_{16}O_5$: C, 52.93; H, 7.90%; mol. wt., 204.2.

A mixture of 43 g. of γ-butyrolactone and 42 g. of sodium hydroxide was treated as above. Then 60 g. of δ-valerolactone was added, and the mixture was heated similarly. Crystals identical with the above product were separated. Yield based on γ-butyrolactone, 62 g. (61%). The infrared spectrum is shown in Fig. 1.

5-Oxaundecanedioic Acid.—A mixture of 28 g. of ε-caprolactone and 32 g. of potassium hydroxide in 50 ml. of water was treated as in the case of 6-oxaundecanedioic acid (2). Then 25 g. of γ-butyrolactone was added, and the mixture was treated similarly. A fraction with a b. p. of 200—215°C/1 mmHg was distilled from the ether extract. Recrystallization from ether - petroleum ether gave white crystals; m. p. 34—35°C. Yield based on ε-caprolactone, 38 g. (71%).

Found: C, 54.96; H, 8.07; mol. wt. (titration), 220. Calcd. for $C_{10}H_{18}O_5$: C, 55.03; H, 8.31%; mol. wt., 218.3.

5-Oxadodecanedioic Acid.—A mixture of 55 g. of ω-chloroenanthic acid and 64 g. of potassium hydroxide in 150 ml. of water was refluxed for 4 hr. After the complete evaporation of the water from the mixture according to the above procedure, 35 g. of γ-butyrolactone was added; and the mixture was then treated similarly. The recrystallization of a fraction with a b. p. of 200—220°C/1 mmHg with ether - petroleum ether afforded white crystals; m. p. 57.5—58°C. Yield based on ω-chloroenanthic acid, 45 g. (58%).

Found: C, 56.72; H, 8.52; mol. wt. (titration), 229. Calcd. for $C_{11}H_{20}O_5$: C, 56.88; H, 8.68%; mol. wt., 232.3.

5-Oxatetradecanedioic Acid.—Into a solution of 9.2 g. of metallic sodium dissolved in 100 ml. of dry methanol, 35 g. of crystalline ω-hydroxypelargonic acid was added. The methanol was completely removed from the mixture by heating it to 220°C over a 3 hr. period under the reduced pressure of 1 mmHg. To the residue 20 g. of γ-butyrolactone was then added, and the mixture was refluxed for 2 hr. Then the excess γ-butyrolactone was recovered by distillation under reduced pressure. The reaction was continued for a further 6 hr. at temperatures of 250—260°C. The product was treated as above. The recrystallization of a fraction with a b. p. of 220—250°C/0.4—0.8 mmHg with ether - petroleum ether afforded white crystals; m. p. 64.5—65°C. Yield based on ω-hydroxypelargonic acid, 31 g. (59%).

Found: C, 59.82; H, 9.35; mol. wt. (titration), 264. Calcd. for $C_{13}H_{24}O_5$: C, 59.98; H, 9.29%; mol. wt., 260.3.

The infrared spectrum is shown in Fig. 1.

5-Oxahexadecanedioic Acid.—The reaction was carried out under conditions similar to those above. Thus 35 g. of ω-hydroxyundecanoic acid was treated with 8.0 g. of metallic sodium and 20 g. of γ-butyrolactone. A crystalline product was obtained after the evaporation of ether from the extract. Recrystallization from an ether - petroleum ether solution afforded white crystals; m. p. 74—74.5°C. Yield based on ω-hydroxyundecanoic acid, 26 g. (52%).

Found: C, 62.39; H, 9.67; mol. wt. (titration), 286. Calcd. for $C_{15}H_{28}O_5$: C, 62.47; H, 9.79%; mol. wt., 288.4.

6-Oxadodecanedioic Acid.—The reaction was carried out under conditions similar to those in the case of 5-oxaundecanedioic acid. The intermediate product from 28 g. of ε-caprolactone and 32 g. of potassium hydroxide was treated with 29 g. of δ-valerolactone. The recrystallization of a fraction with a b.p. of 200—220°C/1mmHg from an ether - petroleum ether solution afforded white crystals; m. p. 52.5—53°C. Yield based on ε-caprolactone, 37 g. (65%).

Found: C, 56.91; H, 8.58; mol wt. (titration), 234. Calcd. for $C_{11}H_{20}O_5$: C, 56.88; H, 8.68%; mol. wt., 232.3.

6-Oxatridecanedioic Acid.—The reaction was carried out under conditions similar to those in the case of 5-oxadodecanedioic acid. The intermediate product from 55 g. of ω-chloroenanthic acid and 64 g. of potassium hydroxide was treated with 41 g. of δ-valerolactone. The recrystallization of a fraction with a b. p. of 200—225°C/1 mmHg with ether-petroleum ether afforded white crystals; m. p. 57.5—58°C. Yield based on ω-chloroenanthic acid, 56 g. (68%).

Found: C, 58.17; H, 8.94; mol. wt., (titration), 249. Calcd. for $C_{12}H_{22}O_5$: C, 58.51; H, 9.00%; mol. wt., 246.3.

The infrared spectrum is shown in Fig. 1.

6-Oxapentadecanedioic Acid.—The reaction was carried out under conditions similar to those in the case of 5-oxatetradecanedioic acid. The intermediate product from 35 g. of ω-hydroxypelargonic acid and

9.2 g. of metallic sodium was treated with 24 g. of δ-valerolactone. The recrystallization of a fraction with a b. p. of 210—240°C/0.5—1 mmHg from ether-petroleum ether afforded white crystals; m. p. 64.5—65°C. Yield based on ω-hydroxypelargonic acid, 34 g. (62%).

Found: C, 62.89; H, 9.10; mol. wt. (titration), 277. Calcd. for $C_{14}H_{26}O_5$: C, 62.91; H, 9.15%; mol. wt., 274.3.

6-Oxaheptadecanedioic Acid.—The reaction was carried out under conditions similar to those in the case of 5-oxahexadecanedioic acid. The intermediate product from 35 g. of ω-hydroxyundecanoic acid and 8.0 g. of metallic sodium was treated with 24 g. of δ-valerolactone. A crystalline product was obtained after the evaporation of ether from the extract. Recrystallization from ether-petroleum ether afforded white crystals; m. p. 84.5—85°C. Yield based on ω-hydroxyundecanoic acid, 33 g. (63%).

Found: C, 63.36; H, 9.70; mol. wt. (titration), 304. Calcd. for $C_{16}H_{30}O_5$: C, 63.54; H, 10.00%; mol. wt., 302.4.

7-Oxatridecanedioic Acid.—A mixture of 28 g. of ε-caprolactone and 15 g. of potassium hydroxide in 20 ml. of water was treated much as in the case of 6-oxaundecanedioic acid (1). The recrystallization of a fraction with a b. p. of 210—250°C/1 mmHg from water-ethanol afforded white crystals; m. p. 90—91°C, (lit. 91°C). Yield, 16 g. (53%).

Found: C, 58.49; H, 8.90; mol. wt. (titration), 245. Calcd. for $C_{12}H_{22}O_5$: C, 58.51; H, 9.00%; mol. wt., 246.3.

8-Oxapentadecanedioic Acid.—From a mixture of 55 g. of ω-chloroenanthic acid and 39 g. of potassium hydroxide in 40 ml. of water, the water was rapidly removed (within 20 min.) by heating the mixture to 240°C under reduced pressure. After the evaporation of the water, the mixture was kept at temperatures of 250—260°C for 8 hr. under the reduced pressure of 1 mmHg. The product was then treated as above. The recrystallization of a fraction with a b. p. of 210—250°C/0.5—1 mmHg from water-ethanol afforded white crystals; m. p. 95.5—96°C. Yield, 28 g. (61%).

Found: C, 61.19; H, 9.50; mol. wt. (titration), 271. Calcd. for $C_{14}H_{26}O_5$: C, 61.29; H, 9.55%; mol. wt., 274.3.

10-Oxanonadecanedioic Acid.—A mixture of 48 g. of ω-chloropelargonic acid and 29 g. of potassium hydroxide was treated much as above. A crystalline product was obtained after the evaporation of ether from the extract. Recrystallization from toluene afforded white crystals; m. p. 99—99.5°C. Yield, 21 g. (51%).

Found: C, 65.56; H, 10.08; mol. wt. (titration), 327. Calcd. for $C_{18}H_{34}O_5$: C, 65.45; H, 10.30%; mol. wt., 330.4.

The infrared spectra of some of these novel α, ω-oxaalkanedioic acids are shown in Fig. 1. The characteristic band at 1110—1125 cm^{-1} due to the ether linkages of these α, ω-oxaalkanedioic acids is observed in every chart.

The melting points of these dicarboxylic acids are plotted against the carbon numbers of the oxaalkylene groups in Fig. 2.

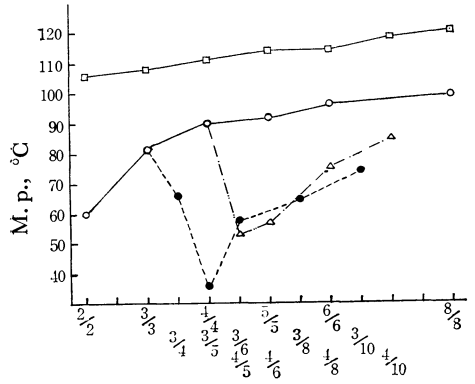

Carbon number; $^{m}/_{n}$,
$HOOC(CH_2)_mO(CH_2)_nCOOH$

Fig. 2. M. p. of α, ω-oxaalkanedioic acids.
—□— $HOOC(CH_2)_pCOOH$, p, odd
—○— $HOOC(CH_2)_nO(CH_2)_nCOOH$
···●··· $HOOC(CH_2)_3O(CH_2)_nCOOH$
–··△··– $HOOC(CH_2)_4O(CH_2)_nCOOH$

Discussion

The synthetic processes for the preparation of these α, ω-oxaalkanedioic acids may be classified into the following four types. During every course of the reaction, the carboxyl groups are protected as alkali salts.

1) The catalytic dehydration of ω-hydroxyalkanoic acids:

$$2HO(CH_2)_nCOOM \xrightarrow[-H_2O]{} MOOC(CH_2)_nO(CH_2)_nCOOM$$

where M denotes sodium or potassium.

2) The addition of γ-butyrolactone or δ-valerolactone to the alkali alcoholates of ω-hydroxyalkanoic acids:

$$\left[O(CH_2)_mCO\ (m=3 \text{ or } 4)\right] + MO(CH_2)_nCOOM \rightarrow MOOC(CH_2)_mO(CH_2)_nCOOM$$

3) The reaction of γ-butyrolactone or δ-valerolactone with sodium carbonate:

$$2\left[O(CH_2)_mCO\right] + Na_2CO_3 \rightarrow NaOOC(CH_2)_mO(CH_2)_mCOONa + CO_2$$

4) The condensation of ω-chloroalkanoic acids with alkali hydroxide:

$$2\,Cl(CH_2)_nCOOH + 4MOH \xrightarrow[-3\,H_2O]{} MOOC(CH_2)_nO(CH_2)_nCOOM + 2MCl$$

The unsymmetric α, ω-oxaalkanedioic acids, in which one of the methylene chain units interrupted by an ether linkage consists of 3 or 4 methylene units, can be prepared through the Type 2 process. In the synthesis of 5-oxasebacic acid, it is interesting that no symmetric dicarboxylic acid (neither 5-oxaazelaic nor 6-oxaundecanedioic acid) was found in the product. Moreover, the same product was obtained in similar yields whichever of the two lactones had been treated with sodium hydroxide first. These facts indicate that no interchange reaction between these lactones

and the alcoholates occurs. The mechanisms of the addition of γ-butyrolactone and δ-valerolactone to the alkali alcoholates of ω-hydroxyalkanoic salts may thus be presented as follows:

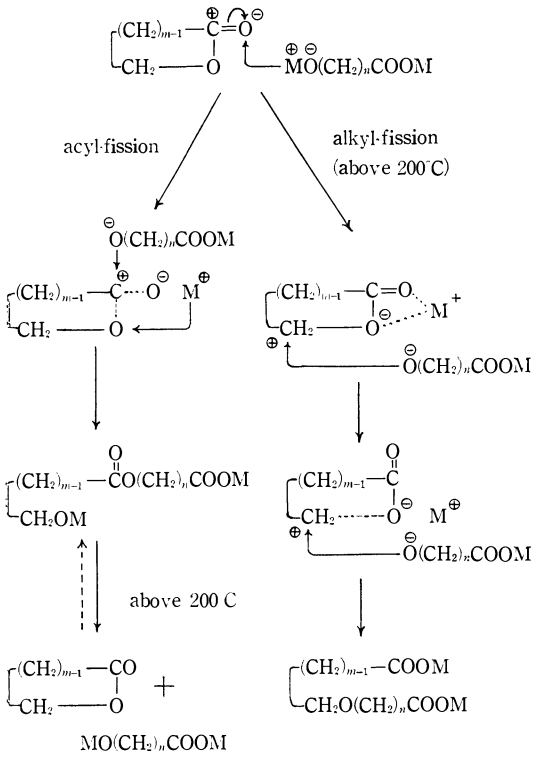

The acyl-fission is considered to occur more smoothly than the alkyl-fission in the ring opening of these lactones under these experimental conditions. In the polymerization of δ-valerolactone initiated with sodium alcoholate, the acyl-fission mechanism is supported by the presence of the end hydroxyl groups in a polyvalerolactone molecule.[10] The ester intermediate of δ-valerolactone formed by the acyl-fission is unstable at elevated temperatures, and δ-valerolactone is recovered almost quantitatively by distillation under reduced pressure. In the case of γ-butyrolactone, which can not usually be polymerized, the ester intermediate is supposed to be far more unstable and to be dissociated into the monomeric lactone immediately. Therefore, the acyl-fission can be disregarded for these reaction mechanisms. In the case of ε-caprolactone, however, the ester intermediate is stable enough, and the lactone can not be recovered, even at elevated temperatures. No large difference is observed in the tendencies toward the acyl-fission between γ-butyrolactone and δ-valerolactone, because the yields of the corresponding α, ω-oxaalkanedioic acids are much alike under similar conditions.

In the Type 4 process, the chlorine atom may be considered to be eliminated, thus forming ω-hydroxyalkanoic salts at the initial stage of the reaction. However, large differences between the Type 1 and Type 4 reactions are observed. When ω-hydroxyenanthic and ω-hydroxypelargonic acids were treated according to the directions for the Type 1 process, only poor yields of the corresponding dicarboxylic acids were obtained, even in the presence of relatively large amounts of alumina. Therefore, the reaction mechanism in the Type 4 process is considered to be differed from that of Type 1. The eminent depression of yields was actually observed when the water was evaporated slowly (for one hour or more) in the preparation of 8-oxapentadecanedioic and 10-oxanonadecanedioic acids. Moreover, when ω-chloroalkanoic acids of which carbon atoms in a molecule are less than 6 were subjected to this process, only poor yields of the dicarboxylic acids were obtained. Perhaps the rapid hydrolysis of the chloride due to the formation of lactonic rings prevented the progress of the reaction of this type. In an experiment in which an equimolar mixture of ω-chloroenanthic and ω-hydroxypelargonic acids was treated with potassium hydroxide according to the procedure for the preparation of 8-oxapentadecanedioic acid, a crystalline product was separated from a water-ethanol solution. From the molecular weight and the elementary analysis, this product was estimated to be a mixture consisting of three α, ω-oxaalkanedioic acids: 8-oxaheptadecanedioic, 8-oxapentadecanedioic, and a small amount of 10-oxanonadecanedioic acids.

From these experimental results, the reaction of the following mechanism is considered to take place dominantly for the formation of the ether linkage:

$$Cl(CH_2)_nCOOM + MO(CH_2)_nCOOM \rightarrow MOOC(CH_2)_nO(CH_2)_nCOOM + MCl$$

In the relations between the melting points of the dicarboxylic acids of two types—$HOOC(CH_2)_3O(CH_2)_nCOOH$ and $HOOC(CH_2)_4O(CH_2)_nCOOH$—and their carbon atoms in a molecule, shown in Fig. 2, the minimum melting points are observed at 3/5 and 4/5 respectively. The remarkable depression of melting point around these minimum points may be attributed to the decrease in the symmetry in the configuration, in other words, the increase in the entropy of fusion (ΔS_m).

Polyamides from these α, ω-oxaalkanedioic acids have also been prepared. They will be reported in detail in the near future.

BULLETIN OF THE CHEMICAL SOCIETY OF JAPAN VOL. 39 490—497 (1966)

The Chemistry of Protactinium. I. The Preparation of Protactinium-233 and the Purification of Protactinium-231

By Shin SUZUKI and Yasushi INOUE

The Research Institute for Iron, Steel and Other Metals, Tohoku University, Katahira-cho, Sendai

(Received June 22, 1965)

Many methods, such as the co-precipitation method, the solvent extraction method and the ion exchange method, had previously been proposed for the separation and the purification of protactinium. However, these methods have some defects for the separation of Pa-233 produced by the thermal neutron irradiation of thorium dioxide and the purification of commercial Pa-231, when an attempt is made to study the chemistry of protactinium. From the above point of view, a combined method of solvent extraction and anion exchange was investigated. In the present paper, the detailed conditions for the TBP extraction of protactinium from a hydrochloric acid solution and the method for its final purification by anion exchange were described. The present method is comparatively simple and rapid, and chemically- and radiochemically-pure protactinium can thus be obtained.

Although protactinium has been known for a long time, its chemical properties are still far from having been thoroughly investigated; this is because of its comparative natural scarcity, its lack of usefulness, and the difficulties involved in its separation due to the remarkable similarity of its chemical properties to such Vb elements as niobium and tantalum, which usually accompany protactinium. This backwardness in the investigation is also attributable to its unstability in an aqueous solution; that is, it has a strong tendency to hydrolyze and to precipitate, even in a relatively strong acid solution. Recently, however, the chemistry of protactinium has become of interest in nuclear reactor technology because one of its isotopes, ^{233}Pa, is an intermediate in the thorium-uranium breeding cycle, being the parent of the fissionable isotope ^{233}U. Some investigations have therefore been carried out on the chemistry of protactinium.[1-3] However, the results are not always acceptable because the unstability in aqueous solution has resulted in some confusion in published works. Therefore, we have attempted to study its chemistry exhaustively, using the various methods available.

In this paper simple and relatively rapid methods will be described for the preparation of ^{233}Pa and for the purification of commerical ^{231}Pa.

Protactinium-233 can be produced by the ^{232}Th(n, γ) ^{233}Th $\xrightarrow[\beta^-]{}$ ^{233}Pa reaction. Many methods for the separation of protactinium from neutron-irradiated thorium have been proposed, but they are not satisfactory because of the necessity for the special reagents or because of the complexity of the procedures. Among these, the ion exchange method is excellent in this respect, but it is generally most useful in the treatment of a microamount of materials, so that its direct application to the complete separation of a large amount of materials will make for a cumbersome procedure. Therefore, it is desirable to use a preliminary separation method before ion exchange. For this purpose, McCormack and his co-workers[4] used diisopropylcarbinol extraction from a nitric acid solution, but this reagent is not easily available. Will[5] used diisopropyl ketone after the ion exchange separation and finally purified ^{233}Pa by the use of another small anion exchange column. His procedure, however, is complicated.

In this experiment, tri-*n*-butyl phosphate was chosen for its easy availability, its ease of handling and its powerful extractability. This reagent was used for the separation of thorium, protactinium and uranium by the countercurrent extraction method from a hydrochloric acid solution;[6] its behavior toward the accompanying fission products will not be given. In this paper the conditions for the TBP extraction of ^{233}Pa from a hydrochloric acid solution and the method for its final purification by anion exchange will be described in detail.

For the purification of commercial ^{231}Pa, this anion exchange method was modified on the basis of its chemical and radiochemical purity.

Experiments

Reagents.—*Radioactive Isotopes.*—The kinds of radioactive isotopes, their suppliers, the commercial forms

1) H. W. Kirby, "The Radiochemistry of Protactinium," NAS-NS 3016, U. S. A. E. C., Washington D. C. (1959).

2) M. Haissinsky and G. Bouissières, "Protactinium," Nouveau Traité de Chimie Minérale, XII, Ed. by P. Pascal, Masson et Cie., Paris (1958), p. 617.

3) R. E. Elson, "The Chemistry of Protactinium," The Actinide Elements, Ed. by G. T. Seaborg and J. J. Katz, McGraw-Hill Book Co., New York (1954), p. 103.

4) J. J. McCormack, F. H. Cripps and W. A. Wiblin, *Anal. Chim. Acta*, **22**, 408 (1960).

5) M. W. Will, U. S. A. E. C., UCRL-8423 (1958).

6) D. F. Peppard, G. W. Mason and M. V. Gergel, *J. Inorg. Nucl. Chem.*, **3**, 370 (1957).

Table I. Radioactive isotopes used in this work

Nuclide	Supplier	Commercial form	Pre-treatment
^{106}Ru	Radiochemical Center, England	Trichloride	
^{95}Zr-^{95}Nb	Oak Ridge National Laboratory, U. S. A.	Oxalate	If necessary, each nuclide is separated by means of TTA extraction; Converted to HCl form
^{137}Cs	Oak Ridge National Laboratory, U. S. A.	Chloride	
^{144}Ce	Radiochemical Center, England	Trichloride	
^{90}Sr-^{90}Y	N. V. Philips-Roxane Pharmaceutisch-Chemische Industrie "Duphar", Holland	Chloride	
^{231}Pa	Radiochemical Center, England	Pentoxide	
^{233}Pa	Prepared by this method		

and the methods of pretreatment are shown in Table I. Their radiochemical purities were certified by γ-ray and α-ray spectrometries, or by analyses of their β-ray absorption curves, before use.

Ion Exchanger.—A strong basic anion exchange resin, Dowex-1, 100—200 mesh, was used. It was conditioned in the usual manner and converted to the chloride form before use.

Solvent.—Highest purity-grade TBP was washed with a diluted sodium hydroxide solution and then with distilled water in order to remove any hydrolysis product. Immediately before use, it was then equilibrated with the aqueous solution to be used.

The other chemicals, such as thorium dioxide, hydrochloric acid and hydrofluoric acid, were of highest purity grade.

Apparatus.—The β- and γ-rays were measured by a Hitachi G. M. counter and a Hitachi well-type scintillation counter respectively. A Kobe-Kogyo Model PS-400 well-type scintillation probe and a Osaka-Dempa Model 4 gridded ionization chamber, both of them connected to a TMC-400 channel pulse height analyzer, Model 406-6, were used for the measurements of the γ- and α-ray spectra respectively. For the solvent extraction procedures, a Iwaki universal mechanical shaker, Model V-S, was used. The ion exchange column, the separatory funnel and the centrifuge cone were made of polyethylene in order to minimize the adsorption of protactinium on the wall.

Procedures.—The experimental procedure was as follows unless otherwise stated.

Solvent Extraction.—Ten-milliliter portions of the aqueous phase which had been adjusted to the desired condition and of the organic phase were mixed for 10 min. with a mechanical shaker. After the two phases had been completely separated, an aliquot of each phase was taken for the measurement of its gamma radioactivity by the use of a scintillation counter. Each value given is the average of the results of at least two determinations. Care was taken to check the material balance in each case.

Ion Exchange.—The column was prepared as follows. Ten milliliters of an exchanger immersed in distilled water was poured into a polyethylene column, 9 mm. in internal diameter, using finely-cut polyethylene cloth as a column support. The column thus prepared had a height of about 150 mm. After that, the column was treated passing through 30 ml. of the solution to be used at the flow rate of 0.2—0.3 ml./min. When the level of the solution reached the top of the exchanger bed, the sample solution was introduced and ion exchange separation was started. The flow rate of the influent was kept nearly constant, 0.2—0.3 ml./min., throughout this experiment.

For making elution curves, effluents were received in polyethylene test tubes for every suitable aliquot; their radioactivities were measured with the well-type scintillation counter.

The Preparation of the Sample for the Measurement of the α-Ray Spectra.—The method recommended by Kirby[7] was used: An aliquot of a diluted acidic sample solution was transferred to a stainless-steel disk coated with a thin collodion film. The solution was then evaporated to dryness under an infrared lamp, with the plate tilted as necessary to retain the solution in the center of the plate. The plate was then cooled, and the residue was covered with one milliliter of 0.1 N nitric acid. One drop of concentrated ammonium hydroxide solution was added, and the solution was again evaporated to dryness. The position of the lamp was lowered sufficiently to drive off all the ammonium nitrate, and then the plate was ignited over a flame until the organic coating had burned off. This was used for the measurement of the α-ray spectrum.

The Determination of Thorium and Uranium.—The thorium and uranium were determined by the neothorone[8] and the peroxide methods[9] respectively.

Results

I. The Preparation of Protactinium-233.—The Irradiation and Dissolution of the Target.—Two-tenths grams of thorium dioxide, sealed in a quartz ampoule under reduced pressure, was irradiated with thermal neutrons for 20 min. in the

7) p. 33 of Ref. 1.
8) M. Ishibashi and S. Higashi, *Japan Analyst* (*Bunsekikagaku*). **4**, 14 (1955).
9) Y. Inoue, S. Suzuki and H. Gotô, This Bulletin, **37**, 1547 (1964).

pneumatic tube of the JRR-2 atomic pile (total flux; 6.4×10^{13}) of the Japan Atomic Energy Research Institute, or, if circumstances did not permit, this 2 g. of thorium dioxide, sealed in a polyethylene bag, was irradiated with thermal neutrons for 2 hr. in the pneumatic tube of the JRR-1 atomic pile (total flux; 3×10^{11}). The sample was allowed to decay for one day for the complete conversion of ^{233}Th into ^{233}Pa, and then dissolved by heating it with a concentrated hydrochloric acid solution containing several drops of diluted hydrofluoric acid (1 : 30) as a catalyst. Care must be taken not to add excess hydrofluoric acid solution, because too much fluoride ions prevent the complete dissolution of the target.

Conditions for the TBP Extraction.—*The Effect of the Shaking Time.*—The effect of the shaking time on the extraction of protactinium from a 6 N hydrochloric acid solution was investigated. It was found that 10 min. shaking is sufficient, therefore, extraction will hereafter be performed by shaking for 10 min.

The Effect of the Hydrochloric Acid Concentration.—The effect of the hydrochloric acid concentration on the extraction of protactinium was also investigated. It is apparent from Fig. 1 that the extraction is almost complete at hydrochloric acid concentration above 5 N.

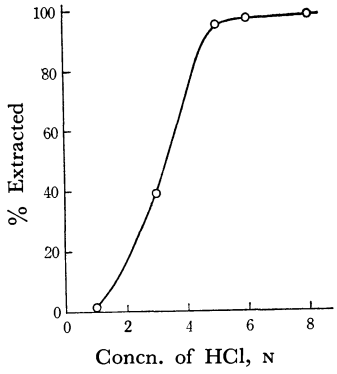

Fig. 1. The effect of hydrochloric acid concentration on the extraction of protactinium.
Shaking time: 10 min.

The Effect of the Hydrofluoric Acid Concentration.—The effect of the hydrofluoric acid concentration on the stripping of protactinium was investigated at a hydrochloric acid concentration of 6 N. The results presented in Fig. 2 show that the extraction percentage is constant over a hydrofluoric acid concentration of 0.4 N, so a 6 N HCl - 0.5 N HF solution is sufficient for the stripping of ^{233}Pa.

The Effect of the Thorium Concentration.—The effect of thorium on the extraction of protactinium was investigated at a hydrochloric acid concentration of 6 N, as is shown in Table II. With the

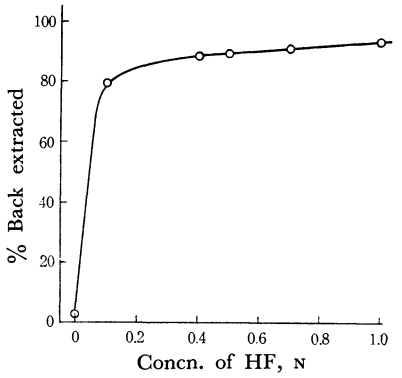

Fig. 2. The effect of hydrofluoric acid concentration on the stripping of protactinium.
Shaking time: 10 min., Acidity: 6 N HCl

TABLE II. THE EFFECTS OF THORIUM ON THE EXTRACTION OF ^{233}Pa

Amount of Th added as ThO_2, mg.	Per cent extracted of ^{233}Pa
None	97.1
400	95.4
800	94.4

increase in the concentration of thorium, the extraction of protactinium was somewhat decreased, but the effect was not very great.

The Masking of Fluoride Ions by Means of Aluminium Chloride.—If re-extraction is needed, it is essential to mask the fluoride ions added for the back extraction of protactinium. Aluminum chloride and boric acid are efficient for this purpose. In this experiment aluminum chloride was chosen, and the effect of its concentration was examined. The experiments were performed by the addition of a 3 M aluminium chloride solution to 10 ml.

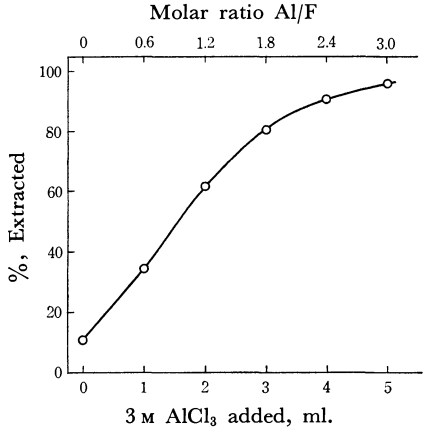

Fig. 3. The masking of fluoride ion with aluminum chloride.
Shaking time: 10 min.
Acidity: 6 N HCl - 0.5 N HF

of an aqueous solution which had the same composition as the stripping solution, 6 N HCl - 0.5 N HF. As is clearly shown in Fig. 3, the addition of 5 ml. or more of the aluminum chloride solution was needed for the complete extraction of protactinium from the stripping solution. This corresponds to the aluminum to fluoride molar ratio of 3.0.

The Extraction of Ions to Co-exist.—The main impurities in the irradiated thorium dioxide are considered to be ^{233}U and long-lived fission products; ^{95}Zr-^{95}Nb, ^{137}Cs, ^{106}Ru, ^{90}Sr-^{90}Y and rare earths (mainly ^{144}Ce). The separation of them from protactinium by the TBP extraction was examined, with the results shown in Table III. It is clear from the table that ^{137}Cs, ^{90}Sr-^{90}Y and ^{144}Ce can be separated from protactinium in the forward extraction, and uranium, in the backward one. The separation of ^{95}Zr-^{95}Nb and ^{106}Ru, was, however, incomplete. For their decontaminations, it is necessary to use other separation techniques.

Table IIIa. Extraction of long-lived fission products

Nuclide	Condition	Per cent extracted
^{95}Zr-^{95}Nb	6 N HCl	68.2
^{137}Cs	6 N HCl	1.40
^{106}Ru	6 N HCl	70.8
^{90}Sr-^{90}Y	6 N HCl	0.91
^{144}Ce	6 N HCl	0.73
^{95}Zr-^{95}Nb	6 N HCl - 0.5 N HF	56.0
^{137}Cs	6 N HCl - 0.5 N HF	0.87
^{106}Ru	6 N HCl - 0.5 N HF	67.2
^{90}Sr-^{90}Y	6 N HCl - 0.5 N HF	0.21
^{144}Ce	6 N HCl - 0.5 N HF	0.10

Table IIIb. Extraction of thorium and uranium

Element	Added mg.	Condition	Per cent extracted
Th	400	6 N HCl	0.0
Th	800	6 N HCl	7.8
Th	1.6	6 N HCl	0.0
Th	1.6	6 N HCl-0.5 N HF	91.9
U	2.38	6 N HCl	98.7
U	2.38	6 N HCl-0.5 N HF	98.7

Anion Exchange Separation.—Referring to Moore's method[10] the anion exchange method was investigated. After protactinium was adsorbed on the resin bed, elution was performed with a 9 N HCl-0.004 N HF solution and then a 9 N HCl - 0.2 N HF solutions. At the same time, the behaviour of ^{95}Zr-^{95}Nb and of ^{106}Ru was investigated under the same conditions as for protactinium. These results are presented in Fig. 4. ^{95}Zr-^{95}Nb could be separated quantitatively, but the separation of ruthenium was not complete. The removal of ruthenium, however, can be more easily and completely attained by the distillation from a perchloric acid solution[11] than by ion exchange, so no further experiments were conducted. It may be assumed from the investigation by Kraus[12] that the ions, which are almost all removed by solvent extraction, will not be adsorbed on the exchanger bed from a 10 N hydrochloric acid solution except uranium. Uranium, however, cannot be eluted by the eluant at all. Therefore, these elements may be separated again by this procedure, and so the decontamination factor may be extremely high. As is shown in Fig. 4a the elution curve of protactinium shows some tailing and a large volume of eluant is necessary for the complete recovery of protactinium. When the yield of fission products is considered to be extremely low, as in this case,[2] the use of an eluant with a higher fluoride concentration, such as 9 N HCl - 1 N HF, is convenient, because it hardly affects the behavior of any of the ions except zirconium and niobium, while the elution curve of protactinium becomes sharp, with a resultant decrease in the volume of eluant necessary for protactinium.

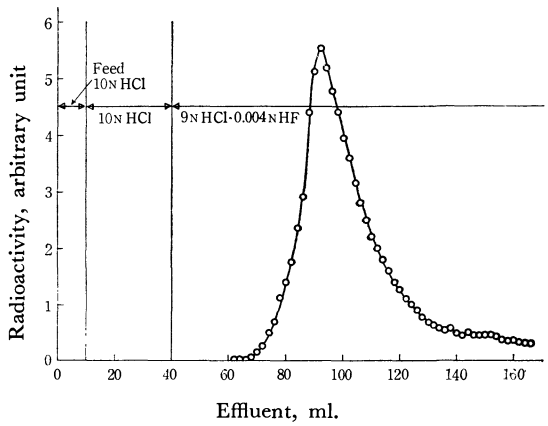

Fig. 4a. Elution of protactinium.

Recommended Procedure for the Separation of ^{233}Pa from Neutron-irradiated Thorium.—By putting the above results together, the best conditions for the separation of protactinium from thorium dioxide were decided upon. The irradiated thorium dioxide was dissolved by heating it in a platinum dish with concentrated hydrochloric acid containing several drops of a diluted hydrofluoric acid solution (1 : 30) to serve as a catalyst. This solution was initially evaporated almost to dryness, on a hot plate and then on a water bath. The residue was dissolved in possibly a small amount of a concentrated hydrochloric acid solution and

10) K. A. Kraus and G. E. Moore, *J. Am. Chem. Soc.*, **73**, 2900 (1951).

11) Y. Inoue, This Bulletin, **36**, 1316 (1963)

12) K. A. Kraus and F. Nelson, 1st International Conferences on the Peaceful Uses of Atomic Energy, Geneva, p. 837 (1955).

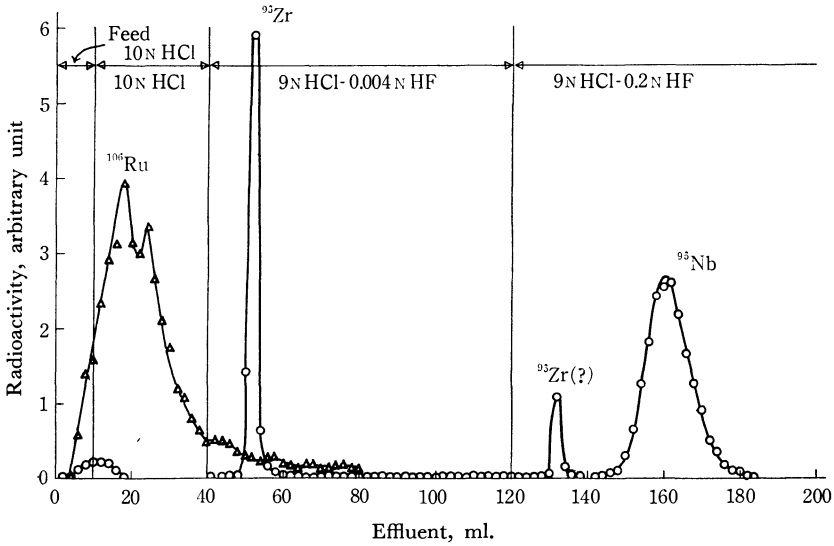

Fig. 4b. Elution of ^{95}Zr, ^{95}Nb and ^{106}Ru.
○: ^{95}Zr-^{95}Nb △: ^{106}Ru

again evaporated to dryness in the same manner. This was repeated a few times in order to eliminate the hydrofluoric acid completely. Then the residue was dissolved in 10 ml. of 6 N hydrochloric acid, and the solution was transferred to a separatory funnel. Ten milliliters of TBP was added, and the funnel was shaken mechanically for 10 min. After the two phases had separated, the aqueous layer (the lower) was run off and discarded. The TBP layer was then scrubbed with 10 ml. of a 6 N hydrochloric acid solution and its aqueous layer discarded. Then 10 ml. of a 6 N HCl - 0.5 N HF solution was added to the TBP extract, and the mixture was shaken mechanically for 10 min. The aqueous layer was run into another separatory funnel and scrubbed with fresh TBP. The aqueous layer was then transferred into another separatory funnel and washed with 10 ml. of distilled benzene in order to remove the remaining TBP. The aqueous layer was then placed in a platinum dish and heated almost to dryness, initially on a hot plate and finally on a water bath. After it had been cooled, 10 ml. of 10 N hydrochloric acid was added; the solution was heated in order to dissolve the residue and then poured into an ion exchanger bed; when the level of the solution reached the top of the exchanger bed, 50 ml. of a 10 N hydrochloric acid solution and 30 ml. of a 10 N HCl - 1.0 N HF solution were passed through the column successively. The protactinium-233 obtained in a 10 N HCl - 1.0 N HF solution was not only free from any thorium but also free from any solid materials. To make sure of its radiochemical purity, the γ-ray spectrum was measured. As is shown in Fig. 5, the spectrum completely coincided with the published data.[1]

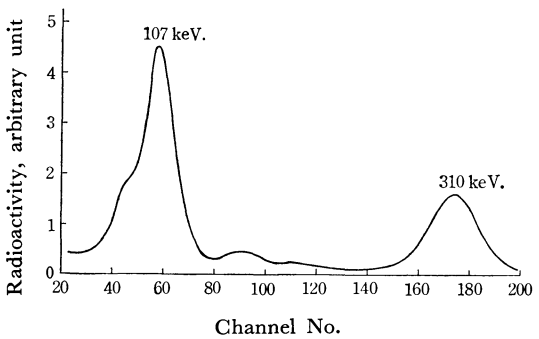

Fig. 5. γ-Ray spectrum of ^{233}Pa.

II. The Purification of Protactinium-231. —Basic considerations and Preliminary Experiments.—As is shown in Table I, ^{231}Pa was purchased in the form of protactinium pentoxide from the Radiochemical Center, Amersham, England. To check its chemical purity, emission spectrographic analysis was performed; a little niobium was detected in some cases. Although it was difficult to detect rare earths, they, as well as niobium, should be considered as chemical impurities. As to radiochemical impurities, it is assumed that ^{227}Ac, ^{227}Th and ^{233}Ra, the daughters of ^{231}Pa, are important enough to take consideration of their half lives. All the impurities listed above except niobium were considered not to be adsorbed on the anion exchange column from the concentrated hydrochloric acid solution, so the separation of niobium and protactinium was the main problem. The separation seems to be possible by means of the above-mentioned anion exchange procedures, but in the treatment of macro-amounts of protactinium, the hydrofluoric acid concentration of 0.004 N is so small that tailing may

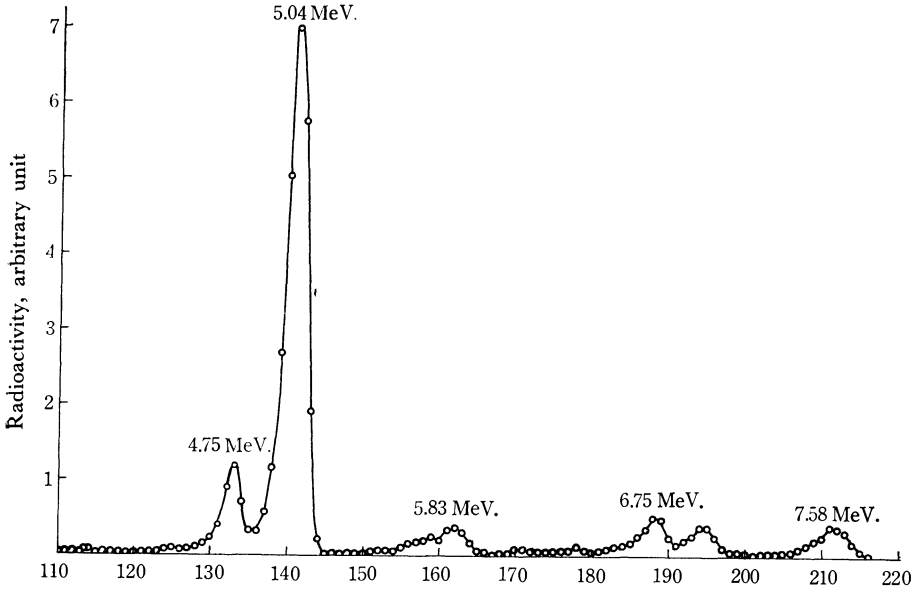

Fig. 6a. α-Ray spectrum of commercial ^{231}Pa.

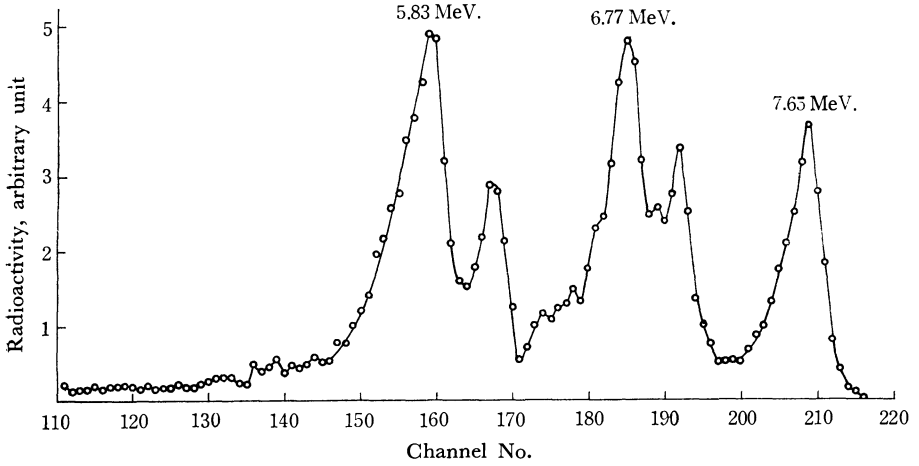

Fig. 6b. α-Ray spectrum of HCl washings.

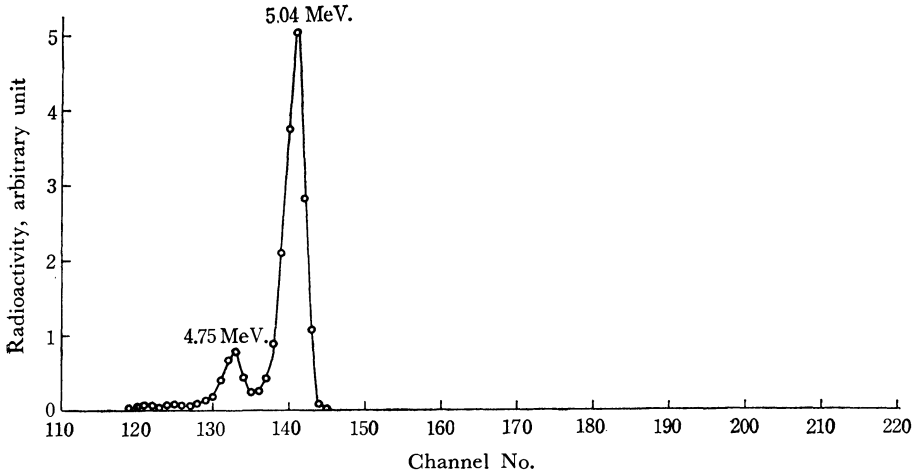

Fig. 6c. α-Ray spectrum of purified ^{231}Pa.

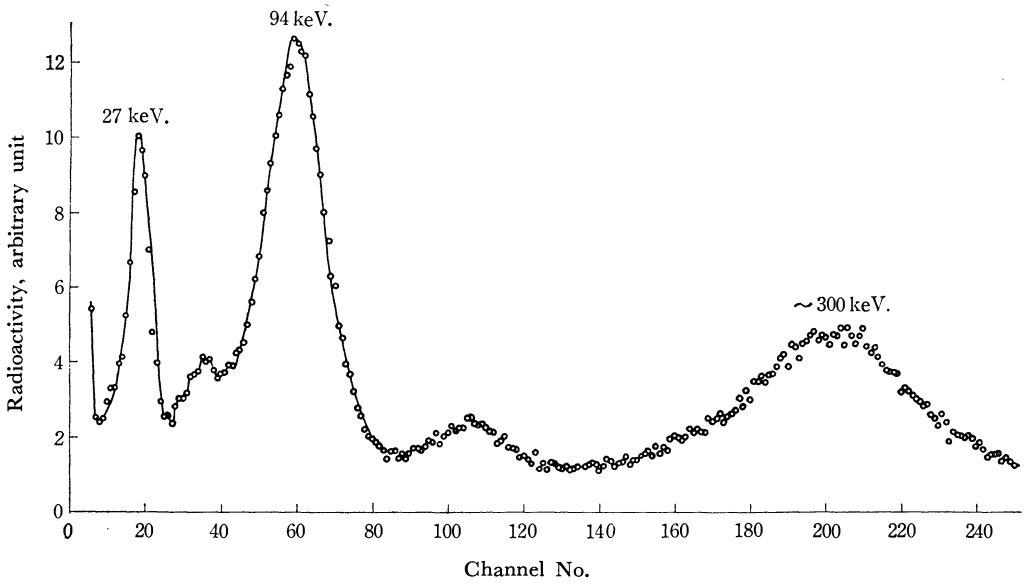

Fig. 7a. γ-Ray spectrum of commercial ^{231}Pa.

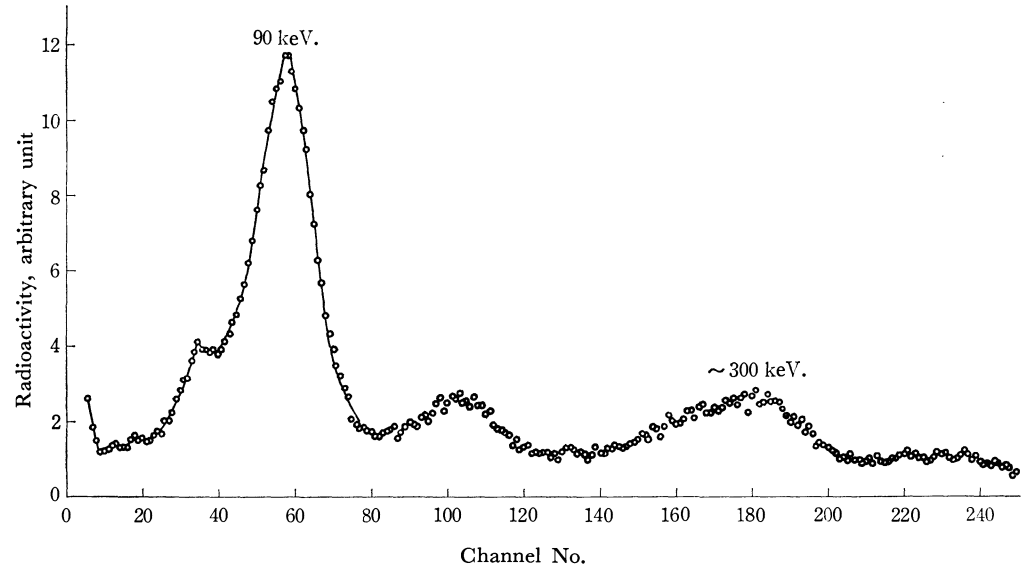

Fig. 7b. γ-Ray spectrum of HCl washings.

increase markedly. Furthermore, the ion exchange capacity should be large because a good separation is desired. Therefore, a high concentration of hydrofluoric acid and a large column are necessary for this purpose. Bearing this in mind, the preliminary separation of ^{95}Nb and ^{233}Pa was performed using 20 ml. of anion exchange resin and a 9 N HCl - 0.1 N HF solution as an eluant. In this case, niobium began to elute after 40 ml. of eluant had passed through. The elution of protactinium was complete before 30 ml. of eluant had passed through, so the complete mutual separation of these elements seemed possible.

Recommended Procedure for the Purification of Commercial Protactinium-231. — Putting the above results together, the recommended procedure for the purification of commercial protactinium was decided upon.

Protactinium pentoxide was dissolved in concentrated hydrochloric acid, containing possibly a small amount of hydrofluoric acid, in a platinum dish, the solution was then evaporated almost to dryness. This process was repeated until the hydrofluoric acid was completely expelled. The residue was dissolved in concentrated hydrochloric acid and diluted to 9 N with distilled water. This

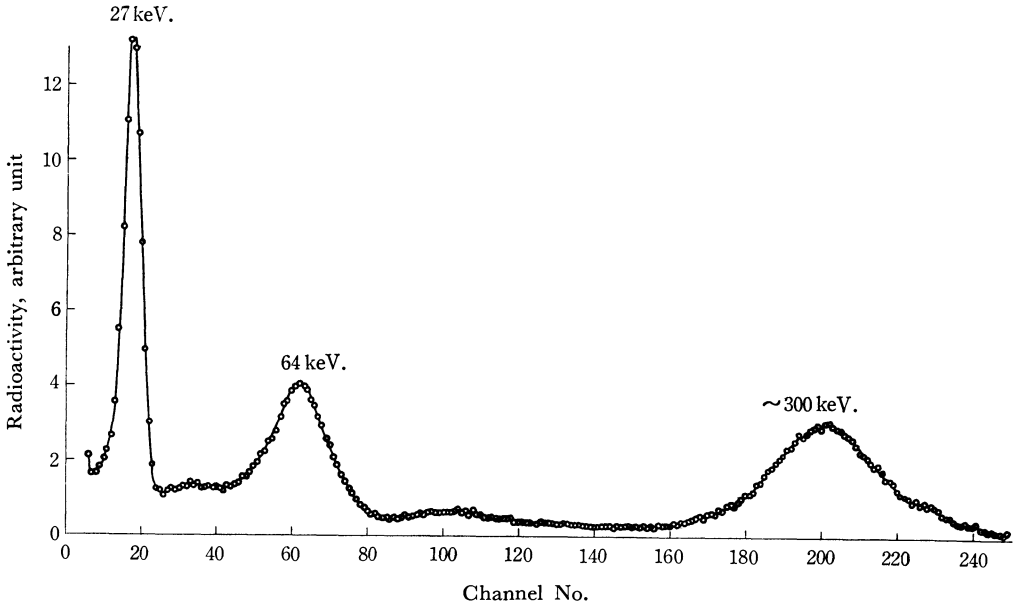

Fig. 7c. γ-Ray spectrum of purified ^{231}Pa.

sclution was percolated into the ion exchange column; when the level of the solution reached the top of the exchanger bed, 20 ml. of a 9 N hydrochloric acid solution was introduced in order to remove any radiochemical impurities. Then protactinium was eluted with 30 ml. of a 9 N HCl - 0.1 N HF solution. Care must be taken to check the characteristic γ-ray of 27 keV. throughout the ion exchange process in order to prevent any accidental loss due to the incomplete elimination of fluoride ions from the sample solution. The protactinium solution thus prepared was then evaporated almost to dryness and diluted with distilled water, and enough ammonium hydroxide solution was added to precipitate protactinium hydroxide. This precipitate was filtered, washed thoroughly, and ignited in a platinum crucible in the usual manner. For example, 29.8 mg. of pure protactinium pentoxide was obtained from 35.0 mg. of the crude sample. To check its radiochemical purity and to see the course of purification, the α- and γ-ray spectra of the original sample, the hydrochloric acid washings and the purified sample were measured, as is shown in Figs. 6 and 7. In Fig. 6 α-ray peaks more energetic than 5 MeV. are observed in the original sample. They have their origin in the decay products of ^{231}Pa. The α-ray spectrum of the hydrochloric acid washings shows no peaks of protactinium except those of daughters. On the contrary, the purified sample shows no peaks above 5 MeV., so it can be considered to be completely pure. In the γ-ray spectra, the circumstances are not as clear as in the α-ray spectra because of the complex overlapping of peaks, but the characteristic peak of ^{231}Pa (27 keV.) is not observed in the spectrum of hydrochloric acid washings, and that of the purified sample shows good agreement with the standard one.[1] Moreover, no niobium was detected in the purified sample by emission spectrographic analysis.

Summary

The methods for the separation of the ^{233}Pa produced by the thermal-neutron irradiation of thorium dioxide and the purification of commercial ^{231}Pa have been investigated. The separation of ^{233}Pa has been achieved by the combination of TBP extraction from a hydrochloric acid solution and anion exchange separation by a hydrochloric acid - hydrofluoric acid eluant. ^{231}Pa has been purified by a modification of the above anion exchange. Both processes can be conducted comparatively simply and rapidly, with the result that both isotopes are chemically and radiochemically pure enough for research work.

A part of the expense has been defrayed by a grant-in-aid by the Ministry of Education.

BULLETIN OF THE CHEMICAL SOCIETY OF JAPAN VOL. 39 498—503 (1966)

An MO-Theoretical Illumination for the Principle of Stereoselection

By Kenichi FUKUI

Faculty of Engineering, Kyoto University, Sakyo-ku, Kyoto

(Received June 23, 1965)

The principle of the stereoselection in organic chemistry has been discussed from the point of view of the molecular orbital theory. The stereoselectivity in the stereospecific ring-closure of conjugated polyenes and the stereospecific ring-cleavage of unsaturated carbon cycles, *trans*-1,2-noncycloadditions, *cis*-1,2-additions and *cis*-1,3-dipolar additions have been accounted for with a qualitative generalization. In many cases the symmetry relationship of certain particular molecular orbitals ("frontier orbitals") plays a conspicuously significant role in the steric control of stereochemical processes. This may be put in contrast with the role of the frontier electron density in the orientation process in organic reactions.

The purpose of the present paper is to make an attempt to furnish organic stereochemistry with a theoretical strategy. In view of the multifariousness noticed in the accumulation of recent stereochemical studies, it is hoped that a guiding principle to unravel the entanglements involved will appear. In order to be of practical applicability, such a guiding principle must first of all possess generality and simplicity. Therefore, the molecular orbital (MO) theory seems suitable.

The recent experimental information on the stereoselectivity in several cyclic reactions of unsaturated compounds[1] has been an incentive to start an MO-theoretical attack.[2-4] All these papers pointed out the importance of the symmetry of particular MO's in discussing the problem in question. These particular MO's were the highest-occupied MO (HO) and the lowest vacant MO (LV) of the ground state molecule. Oosterhoff[2] has suggested that the difference in stereochemical behavior between thermal and photo-induced reactions may be attributed to the symmetry characteristics of HO and LV. The important role of HO and LV (the frontier orbitals) in the course of the chemical interaction of organic compounds was early well established in the frontier electron theory,[5,6] and the symmetry of the frontier orbitals was also duly employed for the elucidation of Diels-Alder reactivity.[7]

However, it should be noted that the discrimination of the frontier orbitals from the other MO's should be based upon a proper comprehension of the theoretical grounds. Woodward and Hoffmann[3] discussed, in their elegant generalization of the problem of stereoselectivity, the ring-closure of conjugated olefins, and suggested that the steric course should be determined by the symmetry of HO only. However, this is evidently an "over-discrimination" of HO, since the overlap stabilization between two π atomic orbitals in a single conjugated system should be evaluated as the sum of the contributions from all occupied MO's.[4] The mere coincidence of the results does not justify such improper or less authentic neglect of the other MO's.

The basic idea, used throughout the present paper, for discussing the steric course in a consistent manner is to determine, from the MO perturbation calculation of the energy change of interaction, the direction of the overlap stabilization between interacting atomic orbitals; this will lead to the most likely correct steric course. The details will be illustrated by examples.

The Ring-Closure of Conjugated Polyenes. —Consider a linear conjugated polyene with k π electrons. So-called Hückel MO's of the simplest type are given by[8]:

$$\phi_j = \sum_{r=1}^{k} C_r^j \phi_r = \left(\frac{2}{k+1}\right)^{1/2} \sum_{r=1}^{k} \phi_r \sin\frac{jr\pi}{k+1} \qquad (j=1,\ 2,\cdots k)$$

where ϕ_r is rth carbon $2p\pi$ atomic orbital (AO), and C_r^j is the coefficient of ϕ_r in jth MO. These MO's are obtained by solving the usual secular equations, which yield the secular determinant:

1) a) E. Havinga, R. J. de Kock and M. P. Rappoldt, *Tetrahedron*, **11**, 276 (1960); b) E. Havinga and J. L. M. A. Schlatmann, ibid., **16**, 146 (1961); c) G. J. Fonken, *Tetrahedron Letters*, **1962**, 549; d) R. E. K. Winter, ibid., No. 17, 1207 (1965).

2) L. J. Oosterhoff, private suggestion to the authors of the paper cited in Ref. 1(b), a suggestion quoted on p. 151 of that paper.

3) R. B. Woodward and R. Hoffmann, *J. Am. Chem. Soc.*, **87**, 395 (1965).

4) K. Fukui, *Tetrahedron Letters*, No. 24, 2009 (1965).

5) a) K. Fukui, T. Yonezawa and H. Shingu, *J. Chem. Phys.*, **20**, 722 (1952); b) K. Fukui, T. Yonezawa, C. Nagata and H. Shingu, ibid., **22**, 1433 (1954).

6) a) K. Fukui, H. Kato and T. Yonezawa, This Bulletin, **33**, 1201 (1960); b) K. Fukui, H. Kato and T. Yonezawa, ibid., **34**, 442 (1961); c) K. Fukui, H. Kato and T. Yonezawz, ibid., **34**, 1111 (1961).

7) K. Fukui, "Molecular Orbitals in Chemistry, Physics, and Biology," Ed. by P.-O. Löwdin and B. Pullman, Academic Press, New York (1964), p. 513.

$$\Delta(\varepsilon)=\begin{vmatrix} -\varepsilon & \beta & \cdots & 0 & 0 \\ \beta & -\varepsilon & \cdots & 0 & 0 \\ \cdots & \cdots & \cdots & \cdots & \cdots \\ 0 & 0 & \cdots & -\varepsilon & \beta \\ 0 & 0 & \cdots & \beta & -\varepsilon \end{vmatrix} = \beta^k \frac{\sin(k+1)\theta}{\sin\theta} \quad (1)$$

$(\varepsilon=-2\beta\cos\theta)$

(k rows and k columns)

where the zero point of the energy, ε, is taken as equal to the Coulomb integral of carbon $2p\pi$ AO, β being the resonance integral between two adjacent $2p\pi$ AO's.

The change in the π-electronic energy in the case of the overlapping of the first and kth AO's is clearly approximated by:

$$\Delta E = 2\sum_{j=1}^{k} \nu_j C_1^j C_k^j \gamma = 2P_{1k}\gamma \quad (2)$$

by the first-order perturbation calculation, where ν_j is the number of π electrons occupying the jth MO, while γ is the resonance integral between ϕ_1 and ϕ_k in the case of the σ-like overlapping of these two orbitals in the distorted π electron system. The sign of γ is obvious, as is indicated by the scheme of Fig. 1.

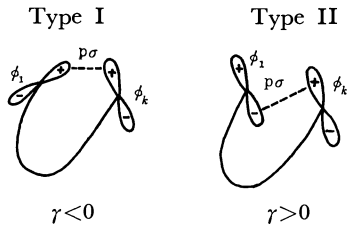

Fig. 1. Two types of overlap stabilization.

The quantity, P_{1k}, has the same form as that defined as the well-known "bond order," but in the present case it serves to determine the stability due to the overlapping of two π orbitals; it may thus appropriately be tentatively named the "overlap stabilization." If this quantity is positive, the overlapping of Type I is preferred, while if it is negative, Type II is more preferable, in the case of cyclization.

For the ground state of linear conjugated polyenes, P_{1k} is known to be easily expressed in an integral representation[9] as:

$$P_{1k} = \frac{\beta^{k-1}}{\pi}\int_{-\infty}^{+\infty}\frac{dy}{\Delta(iy)} = 4(-1)^{k/2+1}\frac{1}{\pi} \times \int_0^{\infty}\frac{\cosh^2\varphi d\varphi}{\cosh(k+1)\varphi} \quad (3)$$

$(y=-2\beta\sinh\varphi)$

which is immediately convertible into the form:

$$P_{1k} = \frac{(-1)^{k/2+1}}{k+1}\left(1+\frac{1}{\cos(\pi/(k+1))}\right) \quad (4)$$

Therefore, it follows clearly that, when $k=4m+2$, P_{1k} is positive, so that the cyclization of Type I occurs, while when $k=4m$, P_{1k} is negative, so that a Type II cyclization results; this is consistent with experimental facts in the case of $k=6$.[1]

This relationship is not limited to the cyclization due to the bonding between two termini. It is likewise very easy to prove mathematically that P_{rs} is positive in the cyclization forming a $(4m+2)$-membered ring, leading to a Type I course, whereas the cyclization forming a $4m$-membered ring would follow a Type II course. The discussion of this sort has already been made by numerical calculations more comprehensively and also more elaborately in connection with the theory of aromaticity by Fukui et al.[10]

A reverse relation holds in the first excited state, in which we assume the jumping of one π electron of HO into LV. In the present simple treatment, both the triplet and the singlet states will be discussed in terms of the same theoretical quantity. The overlap stabilization, which is in this case denoted by P_{1k}^*, is easily represented by:

$$P_{1k}^* = \frac{(-1)^{k/2}}{k+1}\frac{\cos(\pi/(k+1))+1}{\cos(\pi/(k+1))} \times\left(2\cos\frac{\pi}{k+1}-1\right) \quad (5)$$

Therefore, it is positive when $k=4m$, and negative when $k=4m+2$, provided $k\geqq 4$. Photo-induced cyclizations are known experimentally to take place by the Type II course when $k=6$.[1]

The steroselection in polyene cyclization, whether Type I or Type II, may thus be understood to be governed by the following rule:

	Thermal reaction	Photo-induced reaction
$k=4m$	Type II	Type I
$k=4m+2$	Type I	Type II

The steric courses, Type I and Type II, were named by Woodward and Hoffmann[3] "disrotatory" and "conrotatory" processes respectively, in their first generalization of this interesting cyclic conversion.

The Ring-Opening of Cyclic Olefins.— The reverse process to the above-mentioned cyclization have also been studied and found to follow the same stereoselection rule;[1] these reactions in two opposite directions were explained *en bloc* by Woodward and Hoffmann by emphasizing the symmetry of HO and LV.[3] This sort of ring-opening reaction is, however, supposed to

8) See, for instance, A. Streitwieser, Jr., "Molecular Orbital Theory for Organic Chemists," John Wiley & Sons, New York (1961), p. 50.

9) C. A. Coulson and H. C. Longuet-Higgins, *Proc. Roy. Soc.*, **A191**, 39 (1947); **A192**, 16 (1947).

10) K. Fukui, A. Imamura, T. Yonezawa and C. Nagata, This Bulletin, **33**, 1591 (1960).

be governed essentially by a sigma-pi interaction between a part of the π-electron system and the σ bond to be broken. A more plausible, separate explanation must be given on the basis of the direction of stabilization in this sigma-pi interaction.

The electrons to be taken into account are two σ-bonding electrons in the a—b bond to be broken and $(k\text{-}2)$ π electrons in the conjugated part of the ring, r-t-s in Fig. 2.

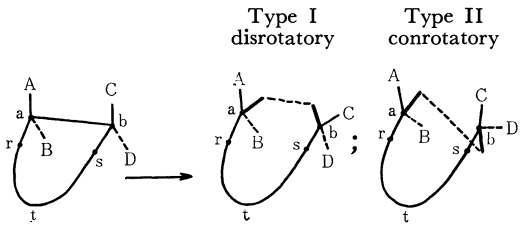

Fig. 2. Two types of interaction in the ring-cleavage.

The open-chain polyene to be produced has k π electrons. At the initial stage, the sigma and pi parts evidently have no appreciable interconjugation. As soon as the ring-cleavage begins to proceed, however, a π-like conjugation will take place between each of the two "incipient" orbitals appearing at the carbon atoms, a and b, and each end of the conjugated part, r-t-s.

The components of the two incipient orbitals perpendicular to the plane of the conjugated part are parallel and antiparallel to each other in the interactions of Type I and Type II respectively.[11]

The change in the energy of the system, ΔE, may be evaluated most simply by a perturbation treatment as a second-order term, if we regard the above-mentioned π-like conjugation as a small perturbation. The result is[12]:

$$\Delta E = \text{const.} + \left\{\sum_j \nu_j \frac{(C_r^j C_a'\gamma_a + C_s^j C_b'\gamma_b)^2}{\varepsilon_j - \varepsilon_0'} - \sum_j (2-\nu_j)\frac{C_r^j C_a\gamma_a + C_s^j C_b\gamma_b)^2}{\varepsilon_j - \varepsilon_0}\right\} + 0(\gamma^4) \quad (6)$$

where (1) ε_0 and ε_0' are the energies of a—b bonding and antibonding orbitals, which are denoted by $\chi = C_a\varphi_a + C_b\varphi_b$ and $\chi = C_a'\varphi_a + C_b'\varphi_b$ respectively, in which φ_a and φ_b are the initially-existing, carbon sp^3 hybridized orbitals of the a—b bond: (2) ε_j is the energy of the jth MO of the $(k-2)$ π electron system, which is written as $\varphi_j = \sum_t C_t^j \phi_t$, where ϕ_t is tth atomic orbital; (3) ν_j is the number of electrons occupying the jth MO; (4) γ_a and γ_b are the "resonance" integrals (although this terminology may be inadequate for their positive value) between each of the two incipient orbitals appearing at the carbon atoms, a and b, with the adjacent $2p\pi$ orbital at the carbon atoms, r or s; and (5) the term const. signifies the term which is involved almost always in both Type I and Type II interactions.

As may clearly be understood from the illustration, the sign, γ_a and γ_b which favors the minimization of ΔE will control the direction of the steric course. The same sign of γ_a and γ_b means the interaction of Type I, whereas Type II corresponds to γ_a and γ_b with opposite signs.

In the light of our knowledge about the parameters used in the MO treatment of σ electron systems developed by Fukui et al.,[13] the chief contributing terms on the right side of Eq. 6 are demonstrated to be those associated with HO and LV. Figure 3 indicates an example for the case of $k=6$. The charge transfer interaction of an HO electron with the a—b antibonding orbital will drive the σ bond into cleavage so as to cause a narrowing of the separation of ε_0' and ε_0, resulting in a stronger and stronger interaction.

If we take into account, for the sake of simplicity, only the most dominant term in each summation of the right side, Eq. 6 may be reduced to the following form:

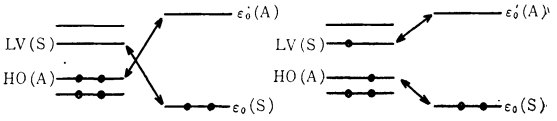

(S: symmetric; A: antisymmetric)

Fig. 3. Relation of energy levels occupied by interacting electrons in the ring-cleavage ($k=6$).

(a) For the case of the ground-state π electron system:

$$\Delta E \sim \text{const.} - 2\left\{\frac{(C_r^{HO}C_a'\gamma_a + C_s^{HO}C_b'\gamma_b)^2}{\varepsilon_0' - \varepsilon_{HO}} + \frac{(C_r^{LV}C_a\gamma_a + C_s^{LV}C_b\gamma_b)^2}{\varepsilon_{LV} - \varepsilon_0}\right\} \quad (7)$$

(b) For the case of the first-excited-state π electron system:

$$\Delta E \sim \text{const.} - \left\{\frac{(C_r^{LV}C_a'\gamma_a + C_s^{LV}C_b'\gamma_b)^2}{\varepsilon_0' - \varepsilon_{LV}} + \frac{(C_r^{HO}C_a\gamma_a + C_s^{HO}C_b\gamma_b)^2}{\varepsilon_{HO} - \varepsilon_0}\right\} \quad (8)$$

where the super- and subscript HO's and LV's signify the highest occupied and the lowest vacant MO's in the ground state.

11) The description of line 9, page 3 of Ref. 4 should be reversed with regard to "conrotatory" and "disrotatory" processes.

12) K. Fukui, C. Nagata, T. Yonezawa, H. Kato and K. Morokuma, *J. Chem. Phys.*, **31**, 287 (1959); also see Ref. 7.

13) K. Fukui, H. Kato and T. Yonezawa, This Bulletin, **33**, 1198 (1960); also see Ref. 6a).

The orbital symmetry[14] of HO is antisymmetric (A) when $k-2=4m$, and symmetric (S) when $k-2=4m-2$, while LV is S when $k-2=4m$ and A when $k-2=4m-2$. The symmetry of the ε_0 level is, of course, S, and ε_0' is A. Therefore, in order for ΔE to be minimized,

(a) For the ground state: γ_a and γ_b should have opposite signs when $k=4m$, and the same sign when $k=4m+2$;

(b) For the first excited state: γ_a and γ_b should have the same sign when $k=4m$, and opposite signs when $k=4m+2$.

Hence we are led to the following stereoselection rule, which has already been pointed out by Woodward and Hoffmann,[3] in accordance with the experimental results[1,3]:

	Thermal reaction	Photo-induced reaction
$k=4m$	Type II, conrotatory	Type I, disrotatory
$k=4m+2$	Type I, disrotatory	Type II, conrotatory

It should be noted that the orbital symmetry of HO and LV plays an essential role in determining the steric course. The discrimination of the "frontier orbitals" is thus justified in this case. This may be put in contrast with the fact that the "frontier electron density" plays an important role in determining the intramolecular orientation.

The *trans*-1, 2-Noncycloadditions. — The predominance of noncyclic *trans*-1, 2-additions in olefins has been well established in many experimental results in both ionic and radical additions.[15] It therefore appears appropriate to discuss the problem by dividing it into two items:

i) In the case in which the attacking reagent, XY, is used in highly dissociative conditions, the *trans*-selectivity may be attributed to the well-discussed symmetrical adduct of X to the ethylenic bond, which is supposed to be formed in the first stage.[16] No further, new way of explanation seems to be necessary in such a case, except a consideration of the orbital symmetry relation of X and the ethylenic bond which creates the possibility of forming such a symmetrical adduct. This point will be discussed in detail in the next section, on *cis*-1, 2-additions.

ii) For the case of almost simultaneous noncyclic additions, however, there seems to be a more plausible explanation than the existing ones if we consider the relationship of the orbital symmetry[14] between the reagent and the olefin. The direction of the approach of the reagent is supposed to be perpendicular to the plane of the ethylenic molecule.[17] The characteristic feature of the noncyclic addition of XY may be specified as the unfavorable square-form interaction of XY with the C-C double bond in the course of approach. For instance, a non-dissociated Br_2 molecule does not have any MO with a symmetry suitable for entering into square-form conjugation with ethylenic π orbitals. Its lowest vacant MO is antisymmetric, so that the interaction with ethylenic π electrons could be facilitated only by orbital overlapping in opposite directions at two terminals, as is illustrated in Fig. 4.[18] The formulation of this relation is in essence identical to the treatment of Eqs. 1—4 (Fig. 4(a)); it is also possible to apply Eq. 7 for the same purpose (Fig. 4(b)). The electron transfer from the π bond to the X-Y antibonding MO will give rise to the dissociation of XY, leading to the stage

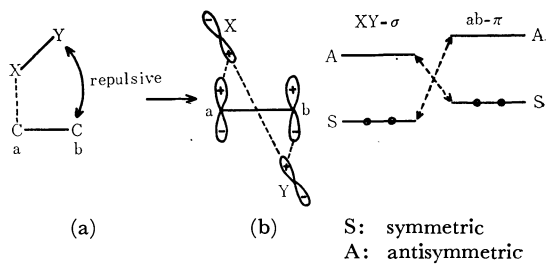

Fig. 4. The mode of initial interaction of the attacking reagent with an ethylenic bond.

indicated by (b) in Fig. 4. The explanation mentioned above may lead to a presumption of 1, 2-*cis*-noncycloaddition in the photo-excited state under suitable conditions.

No experimental results seem to be available for the stereoselectivity in noncyclic additions more distant than to 1, 2-positions of conjugated

14) More generally, it is, of course, not required to be exactly symmetric or antisymmetric. Only the relation between the signs of the coefficients in Eq. 7 is essential.

15) See, for instance, a) E. S. Gould, "Mechanism and Structure in Organic Chemistry," Henry Holt & Co., New York (1959), p. 514, 733 ff.; b) B. A. Bohm and P. I. Abell, *Chem. Revs.*, **62**, 599 (1962).

16) Evidence has been given early for the two-step additions (A. W. Francis, *J. Am. Chem. Soc.*, **47**, 2340 (1925)).

17) The opinion of Bader et al. (A. R. Bader, R. P. Buckley, F. Leavitt and M. Szwarc, *J. Am. Chem. Soc.*, **79**, 5621 (1957)) that the approach of the methyl radical in the additions to olefins was along the double bond axis was later corrected (M. Matsuoka and H. Szwarc, ibid., **83**, (1961)).

18) The author does not intend to reject the assumption of a bridged intermediate like the cyclic bromonium ion. Depending on conditions, we might have to take into account the interaction of X and C_b in addition to that of X and C_a. The essential point of the present discussion lies in pointing out the possibility of a mechanism with which we need no further, too-far-fetched views.

19) It should be noted that the terms "1, 4-" or "1, 6-addition" are used here in a purely mechanistic sense. They do not include a reaction composed of a series of successive processes. Hence, it is desirable that the starting conjugated polyene have a specific favorable structure: i. e., the *cis*-butadiene form for 1, 4-addition and the *cis-cis*-hexatriene form for 1, 6-addition. Also, we have to avoid confusion due to the term "*trans*-1, 4-addition," by which e. g., the following reaction is meant:

Butadiene + Cl_2 → *trans*-1, 2-Bischloromethyl ethylene

The term "*cis*-1, 4-addition" employed above signifies an addition of XY by the attack of X and Y from the same side of the molecular plane of conjugation.

olefins. Discussions similar to those for 1, 2-additions are possible if we make a consideration analogous to that of Fig. 4. The conclusion is that 1, 4-noncycloaddition should be *cis*, 1, 6-, *trans*, and so forth.[19]

The *cis*-1,2-Additions.—The *cis*-1,2-addition to an ethylenic bond can take place when the reagent has a vacant MO (of course, preferably LV, for the reason understood through Eq. 6), of a symmetry that is advantageous for interaction with the occupied MO of the ethylenic π bond. For this reason the reagents which have the LV orbital symmetrical with respect to the middle of their two reaction centers are qualified as having a possibility of *cis*-addition. The formation of the intermediates considered in the two-step mechanism of stereospecific *trans*-additions, such as the bridged cation of protonated ethylene, may clearly be understood by the fact that the reagent ion has a symmetrical LV orbital. The other reagents which can satisfy this symmetry requirement are the phenyl cation in the phenonium ion,[20] the oxygen atom in epoxidation, carbenes in their singlet-state adducts to olefins,[21] the permanganate ion,[22] osmium tetroxide,[23] dienes in the Diels-Alder addition, and so on. Among these the symmetry of LV in various dienes has already been investigated by numerical calculations.[7] With respect to the other species, it is also easy to show by an appropriate MO treatment that their LV satisfies the symmetry conditions mentioned above.

The *cis*-1, 2-addition in hydroboration is well known. The result of an extended Hückel calculation by Kato et al. for boron compounds[24] may be useful in comprehending how borane can add to the *cis* positions. The LV of the BH_3 molecule is completely localized at the central boron $2p\pi$ AO, so that a strong charge-transfer interaction is possible with bonding π electrons of the C-C double bond (Fig. 5). As the $p\sigma$-overlapping proceeds, the bond populations of B-H sigma as well as of C_a-C_b pi are seriously reduced, so as to repel the hydrogen atom and force it to combine with the C_b carbon. Thus, a square-form interaction[25] is performed to give rise to *cis*-addition. From this explanation it is easy to realize that the hydroboration is a reaction of an electrophilic nature.

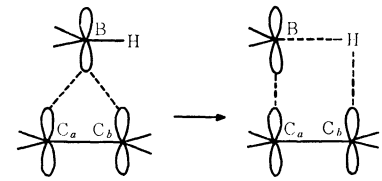

Fig. 5. The square-form interaction of BH_3 with C-C double bond.

Under these circumstances it is interesting that the easiness of the photo-induced cyclodimerization of olefins[26] in comparison with thermal reactions is also intimately connected with the symmetry relationship of HO and LV orbitals. In such cases, the *cis*-addition is geometrically desirable in order for the cyclodimerization to take place. Consequently, the orbital symmetry must be favorable for the square form interaction. As may easily be understood from the illustration in Fig. 6, in which acenaphthylene is chosen as an example, Eqs. 7 and 8 show that the square form interaction is thus facilitated in *excited-state* reactions.[27] The relation of the opposite symmetries of HO and LV in the ground state also holds as a general rule in alternant hydrocarbons, such as anthracene and pentacene, whose photodimerization has been well studied.

We have to remember that these circumstances must be similar in the case of the strong charge-transfer interaction in which one electron jumps from the olefin into the reagent orbital. The orbital symmetry requirement for a square-form

20) S. Winstein, E. Grunwald and L. L. Ingraham, *J. Am. Chem. Soc.*, **70**, 821 (1948); D. J. Cram, ibid., **71**, 3863 (1949); as regards the MO-theory, see Ref. 8, p. 382; the LV orbital of the phenyl cation is localized at the sp^2-like sigma orbital on the attached carbon atom (K. Fukui, H. Kato and T. Yonezawa, This Bulletin, **35**, 1475 (1962); K. Morokuma, S. Ohnishi, T. Masuda and K. Fukui, ibid., **36**, 1228 (1963)), which is, therefore, symmetrical with respect to the bisecting plane of the C-C double bond in the phenonium cation.

21) P. S. Skell and A. Y. Garner, *J. Am. Chem. Soc.*, **78**, 3409, 5430 (1956).

22) J. Boeseken, *Rec. Trav. Chim.*, **40**, 553 (1921); **47**, 683 (1928); K. B. Wiberg and K. A. Saegebarth, *J. Am. Chem. Soc.*, **79**, 2822 (1957); concerning the MnO_4^{2-} cis-addition, see J. S. F. Pode and W. A. Waters, *J. Chem. Soc.*, **1956**, 717.

23) R. Criegee, B. Marchand and H. Wannowius, *Ann.*, **522**, 75 (1936); **550**, 99 (1938).

24) H. Kato, T. Yonezawa and K. Fukui, Summary, 18th Annual Meeting of the Chemical Society of Japan (1965) (in Japanese), p. 440; H. Kato, K. Yamaguchi, T. Yonezawa and K. Fukui, This Bulletin, (in press).

25) Some alkyl borane compounds are known to react as a dimeric form. In such cases, the mode of interaction would resemble that of the S_N2 reaction of the halogen anion with alkyl halide.

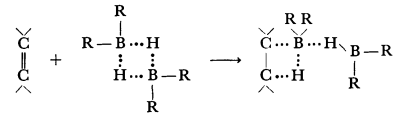

Thus, the structure near the transition state may be more or less similar to the square form.

26) E. L. Bowen and J. D. F. Marsh, *J. Chem. Soc.*, **1947**, 109; as regards the MO theory, see K. Fukui, K. Morokuma and T. Yonezawa, This Bulletin, **34**, 1178 (1960); A Schönberg and A. Mustafa, *J. Chem. Soc.*, **1948**, 2126; A. Mustafa, *Chem. Revs.*, **51**, 1 (1952); O_2 *cis*-addition is also described in G. O. Schenck and K. Ziegler, *Naturwissenschaften*, **32**, 157 (1944).

27) The perturbation theory is modified in case b where the second-order term in Eq. 8 should be replaced by the first-order term,

$$\{|C_r^{LV}C_{r'}^{LV}\gamma_a+C_s^{LV}C_{s'}^{LV}\gamma_b|^2 + |C_r^{HO}C_{r'}^{HO}\gamma_a+C_s^{HO}C_{s'}^{HO}\gamma_b|^2\}^{1/2}$$

where rs and $r's'$ are the two pairs of the reaction centers of the M and M′ molecules respectively.

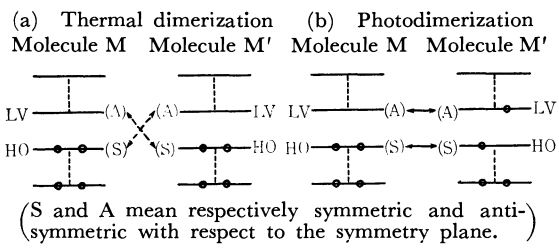

Fig. 6. The symmetry relationship of OH and LV of acenaphthylene in connection with dimerization reactivity.

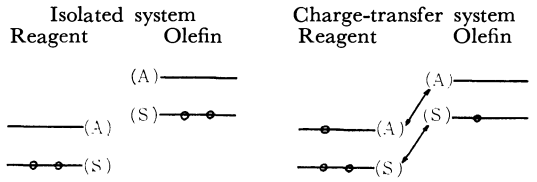

Fig. 7. The relation of orbital symmetry with charge-transfer interaction.

interaction, which the isolated systems are unable to fulfil, will then be satisfied. An instance for such a case is indicated in Fig. 7.

Here we should make reference to the recent finding in the field of polymerization chemistry that several stereospecific ionic polymerizations are thought to occur through successive *cis*-openings of the monomer double bond.[28] An interpretation of this fact has been given from a purely sterical point of view.[29] However, in view of the reasons above set forth it seems likely that the orbital symmetry of the system, including the growing chain end and the counter ion or catalyst part, should be examined after reliable information on the catalyst structure has been obtained. Also, whether or not circumstances like those in Fig. 7 might be realized in these cases is a matter of deep interest. We hope to re-examine the working mechanism of stereomodifiers in stereospecific vinyl polymerizations from the point of view of orbital symmetry. In addition, we may have to consider the participation of the neighboring group in the activated complex influencing the orbital symmetry when the monomer has any conspicuously influential group in the molecule. On this point, we shall present a report in the near future.

The 1, 3-Dipolar Additions.—The addition of 1, 3-dipoles to olefins occurs at positions *cis* with respect to both reactants.[30] Although various species of 1, 3-dipoles are known, the essential structure under reactive conditions may be characterized by the conjugated system which is indicated in Fig. 8.

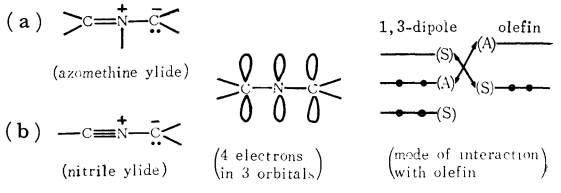

Fig. 8. The schematic representation of 1, 3-dipoles.

The LV orbital of 1, 3-dipoles is symmetric with respect to the two side AO's, so *cis*-interaction with olefin may be made favorable.

Other interesting problems, like the *trans*-1, 2-additions and the *endo*- and *exo*-additions in Diels-Alder reactions, as well as the stable conformations of organic molecular skeletons and the problem of *trans*-β-elimination, are left untouched in the present paper; they will be considered in several separate papers later.

28) G. Natta, M. Farina, M. Peraldo, P. Corradini, G. Bressan and P. Ganis, *Rend. Accad. naz. Lincei* (8), **28**, 442 (1960); G. Natta, M. Peraldo, M. Farina and G. Bressan, *Makromolekulare Chem.*, **55**, 139 (1962); M. Peraldo and M. Farina, *Chem. e Ind. (Milano)*, **42**, 1349 (1960); T. Miyazawa and Y. Ideguchi, *Polymer Letters*, **1**, 389 (1963); H. Tadokoro, M. Ukita, M. Kobayashi and S. Murahashi, ibid., **1**, 405 (1963); M. Tasumi, T. Shimanouchi, H. Tanaka and S. Ikeda, *J. Polymer Sci.*, **A2**, 1607 (1964); G. Natta, G. Dall'Asta and G. Mazzanti, *Angew. Chem.*, **76**, 765 (1964).

29) G. Dall'Asta and G. Mazzanti, *Makromolekulare Chem.*, **61**, 178 (1963).

30) R. Huisgen, *Proc. Chem. Soc.*, **1961**, 357.

BULLETIN OF THE CHEMICAL SOCIETY OF JAPAN VOL. 39 504—506 (1966)

The Infrared Absorption Spectra of the Condensation Products of Formaldehyde with Hydrazine

By Mitsuo MASHIMA

Department of Literature and Science, Saga University, Saga

(Received June 24, 1965)

The infrared absorption spectra of tetraformaltrisazine and formalazine have been obtained in the solid state. From a tentative assignment of the bands observed, it has been shown that a molecule of tetraformaltrisazine has the bicyclic structure proposed by Hofmann and Storm, while formalazine is a polymer with a four-membered heterocyclic ring.

Pulvermacher[1] first obtained a condensation product of formaldehyde with hydrazine hydrate. This compound, which is completely insoluble in water, has been designated as formalazine. Another water-soluble formaldehyde derivative of hydrazine, tetraformaltrisazine, was obtained by Hofmann and Storm.[2] On the basis of the results of molecular weight measurements and elemental analyses, they have proposed a bicyclic structure for this product.

In the present studies, the condensation products of formaldehyde with hydrazine were reexamined spectroscopically.

Experimental

Tetraformaltrisazine.—This compound was prepared by the gradual addition of 0.8 mol. of formaldehyde (ca. 37% solution) to one mole of hydrazine hydrate (ca. a 80% solution) under cooling.[2] The solution obtained was evaporated on a water bath, and then a great quantity of ethanol was added to the concentrated solution; the precipitate thus obtained was collected by suction filtration. When the precipitate was repeatedly dissolved in water and separated with ethanol, fine crystals were obtained. When heated, this compound begins to decompose partly over 200°C and then decomposes rapidly at 218°C (lit.[2] 225°C). The infrared spectra of this compound and its *N*-deuterated derivative were studied from 650 to 4000 cm^{-1} in the solid state.

Found: C, 33.09; H, 8.51; N, 58.11. Calcd. for $C_4N_6H_{12}$: C, 33.32; H, 8.39; N, 58.29%.

Formalazine.—This compound was prepared the by drop by drop addition of hydrazine hydrate (1 mol.) to formaldehyde (2 mol.) in a 37% solution. The precipitate obtained was washed with a large quantity of water and then dried; a white amorphous compound was obtained. This compound begins to decompose and turn brown at 265°C. The infrared spectra of this compound was studied in the solid state.

Found: C, 40.46; H, 7.51; N, 46.59. Calcd, for $C_{10}N_{10}H_{22}O$: C, 40.26; H, 7.38; N, 46.97%.

Measurements of the Infrared Spectra.—The infrared spectra were measured by using a double-beam Hitachi infrared spectrophotometer, type EPI-2, equipped with rock salt prisms. Potassium bromide disks were used to obtain the solid spectra.

Results and Discussion

Tetraformaltrisazine.—Hofmann and Storm[2] have proposed the molecular structure for this compound shown in Fig. 1. The spectroscopic

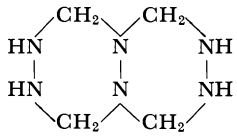

Fig. 1.

observations were also in agreement with this structure. The infrared spectra obtained are shown in Fig. 2: a solid curve shows the spectrum of this compound, and a dotted curve, the spectrum of its *N*-deuterated derivative.

The CH_2 group gives rise to bands corresponding to the C–H stretching vibrations and the CH_2 deformation vibrations. As may be seen from Fig. 2, the four bands at 2980, 2935, 2885, and 2830 cm^{-1} are scarcely changed in frequency on *N*-deuteration; they may be safely assigned to the CH_2 stretching vibrations. The CH_2 bending vibration gives rise to a band around 1465 cm^{-1} in *n*-paraffins. In cycloalkanes, there is a decrease in the CH_2 bending frequency; e. g., cyclopentane shows the corresponding band at 1455 cm^{-1}. Tetraformaltrisazine has two bands, at 1452 and 1437 cm^{-1}, which are little changed in frequency on *N*-deuteration. Consequently, they may be ascribed to the CH_2 bending vibration. The CH_2 twisting and wagging vibrations occur in the 1300—1200 cm^{-1} region. In *n*-paraffins a band near 1305 cm^{-1} has been assigned to the CH_2 wagging vibration. The present compound shows weak or moderately strong bands at 1379, 1349, 1303, and 1279 cm^{-1}; its *N*-deuterated derivative has bands corresponding to them at 1378, 1349, 1306, and 1275 cm^{-1}. These bands may be ascribed to

1) G. Pulvermacher, *Ber.*, **26**, 2360 (1893).
2) K. A. Hofmann and D. Storm, ibid., **45**, 1725 (1912).

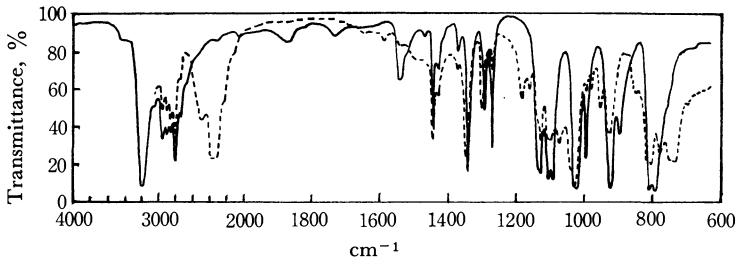

Fig. 2. Infrared spectra of tetraformaltrisazine (solid curve) and its *N*-deuterated derivative (dashed curve) in KBr disks.

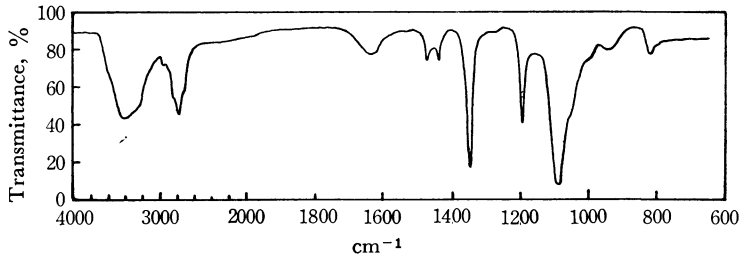

Fig. 3. Infrared spectrum of formalazine in KBr disks.

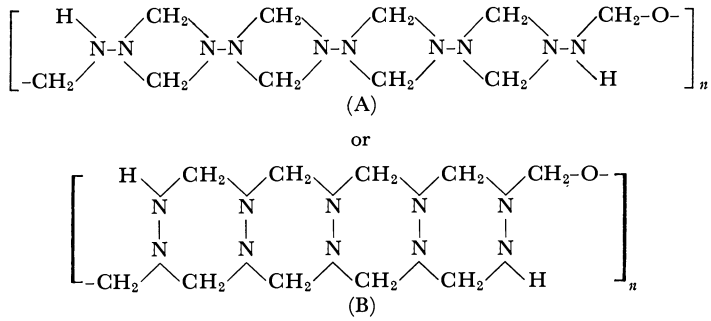

Fig. 4.

the CH_2 wagging and twisting vibrations. The CH_2 rocking vibration occurs near 720 cm^{-1} in *n*-paraffins, but this band is seen only when the number of the methylene group is more than two.[3] Tetraformaltrisazine has four CH_2 groups, which are isolated from each other; this compound shows no band in the 720 cm^{-1} region. Thus, the identification of the CH_2 rocking vibration is not easy.

Tetraformaltrisazine shows a strong band at 3220 cm^{-1}; it is displaced by a band at 2360 cm^{-1} on *N*-deuteration. Therefore, this band may safely be ascribed to the NH stretching vibration. In secondary amines, the NH deformation absorption usually occurs in the 1650—1550 cm^{-1} region. Tetraformaltrisazine shows a weak band at 1552 cm^{-1}, which falls in the range indicated above. This band is displaced by bands at 1186 and 1166 cm^{-1} on *N*-deuteration. Consequently, the 1552 cm^{-1} band may be ascribed to the NH deformation vibration.

In the 1150—800 cm^{-1} region, tetraformaltrisazine shows several strong or moderately strong bands; they are considered to be due to the C–N and N–N stretching vibrations. *N*-Deuterated tetraformaltrisazine shows new bands at 783 and 745 cm^{-1}. Therefore, it may surely be considered that the NH deformation vibration contributes to absorptions in this region. However, a detailed assignment of the above-indicated bands is not easy. The observed frequencies and some tentative assignments of them are summarized in Table I.

Formalazine.—The results of elemental analyses are in agreement with the structure shown in Fig. 4, but the results are inconsistent with the formula $(CH_2{=}N{-}N{=}CH_2)_x$ proposed by Pulvermacher.[1] The infrared absorption spectrum is shown in Fig. 3. As may be seen from Fig. 3, the number of absorption bands observed is not large. Consequently, it may be expected that at least the structural unit of molecules is relatively

3) C. N. R. Rao, "The Chemical Applications of Infrared Spectroscopy," Academic Press, New York and London (1963).

TABLE I. OBSERVED FREQUENCIES OF TETRAFORMALTRISAZINE (in cm^{-1})

Assignment	Tetraformaltrisazine	*N*-Deuterated tetraformaltrisazine
ν(NH)	3220 (vs)	
		2980 (m)
	2980 (m)	
$\nu(CH_2)$	2935 (m)	2935 (m)
	2885 (m)	2890 (m)
	2830 (s)	2830 (s)
	2765 (w)	
	2710 (w)	
ν(ND)		2360 (vs)
	2340 (vw)	
	2090 (vw)	
	1878 (vw)	
	1745 (vw)	
δ(NH)	1552 (m)	
	1480 (vw)	
$\beta(CH_2)$	1452 (m)	1449 (m)
	1437 (m)	1436 (m)
$\omega(CH_2)$, $\tau(CH_2)$	1379 (w)	1378 (w)
	1349 (s)	1349 (s)
	1303 (m)	1306 (m)
	1279 (s)	1275 (w)
δ(ND)		1186 (m)
		1166 (m)
	1144, 1138 (s)	1132 (m)
	1115 (s)	1107 (m)
Ring vibration,	1100 (s)	1077 (m)
π(NH), $\gamma(CH_2)$	1038, 1030 (vs)	1028 (vs)
	1005 (m)	1000 (w)
		984 (w)
		957 (m)
	933 (vs)	927 (s)
	905 (m)	854 (w)
	820 (s)	819 (s)
	800 (vs)	807 (s)
π(ND)		783 (s)
		745 (s)

ν, stretching; δ, in-plane deformation; β, bending; ω, wagging; τ, twisting; γ, rocking; π, out-of-plane deformation

simple. Since this compound is almost completely insoluble in water, we could not examine the effect of *N*-deuteration on the absorption spectrum. The observed frequencies were tentatively assigned by a comparison of the spectrum of this compound with that of tetraformaltrisazine (Fig. 2).

In the CH-stretching frequency range, this compound shows moderately strong or weak bands at 2960, 2860, and 2780 cm^{-1}. These bands may be assigned to the CH stretching vibration. The three bands at 1477, 1442, and 1349 cm^{-1} correspond in frequency to the 1452, 1437, and 1349 cm^{-1} bands of tetraformaltrisazine. Therefore, the 1477 and 1442 cm^{-1} bands were assigned to the CH_2 bending vibration, while the 1349 cm^{-1} band was assigned to the CH_2 wagging vibration. A sharp, moderately strong band at 1196 cm^{-1} may be considered to be due to the CH_2 twisting vibration. From these assignments of the observed bands, it may be concluded that a molecule of this compound contains the methylene group.

If this compound contains ether linkages, as is shown in Fig. 4, the intense absorption band will be shown in the 1150—1060 cm^{-1} range. For the identification of ether linkages in aliphatic ethers we have to depend upon the presence of intense bands within the range indicated above. Formalazine shows an intense band at 1088 cm^{-1}; this band has no partner band in the spectrum of tetraformaltrisazine. Therefore, the 1088 cm^{-1} band may be acribed to the CH_2–O–CH_2 stretching vibration.

In tetraformaltrisazine, which contains a ten-membered heterocyclic ring, several strong bands were observed in the 1150—800 cm^{-1} region. On the other hand, in formalazine no band corresponding to them was found. Therefore, out of the two structures indicated in Fig. 4, the former A is considered to be prefereable to B.

The broad band with its peak near 3400 cm^{-1} is considered to be due to the NH strecthing vibration.

The author is grateful to Professor Yoshiya Kanda of Kyushu University for letting him use the spectrophotometer. Thanks are also due to Mr. Michio Sido and Miss Takeko Tahara of the Centre of Elementary Analyses, Kyushu University, for their analyses of the C, H, and N contents.

BULLETIN OF THE CHEMICAL SOCIETY OF JAPAN VOL. 39 507—511 (1966)

A New Synthesis of Polyhydroxydihydroflavonols*

By Taichiro OYAMADA and Hajime BABA

Department of Applied Chemistry, Faculty of Engineering, Yamagata University, Yonezawa, Yamagata

(Received June 25, 1965)

An alkaline hydrogen peroxide oxidation of chalcones with methoxymethoxyl groups in the 2'-position and in other positions gave the corresponding poly(methoxymethoxy)chalcone oxides; these were then, in turn, easily converted into polyhydroxydihydroflavonols, with a simultaneous splitting of all the *O*-methoxymethyl groups, by warming with acid. The general applicability of the new method was illustrated by the synthesis of the following hydroxydihydroflavonols: 3, 7-dihydroxy- (m. p. 170—171°C), 3, 4'-dihydroxy- (m. p. 214—216°C), 3, 4'-dihydroxy-3'-methoxy- (m. p. 217—218°C), 3, 4', 7-trihydroxy- (m. p. 214—215°C), and 3, 3', 4', 7-tetrahydroxyflavanone (*dl*-fustin, m. p. 217—218°C). The first four new compounds were identified by converting them into known methyl ethers, while the last one was identified by comparing it with natural *dl*-fustin. Their structures were also confirmed by infrared and ultraviolet spectra.

The action of alkaline hydrogen peroxide on 2'-hydroxychalcones results in the formation of flavonols (3-hydroxyflavones)[1] or dihydroflavonols (3-hydroxyflavanones)[2], depending on the conditions employed. The course and mechanism of these reactions have been postulated by Geissman et al.[3] to involve an intermediary formation of the corresponding epoxides, which are immediately transformed into dihydroflavonols or aurones by the nucleophilic attack of the hydroxide or phenolate ions. The dihydroflavonols thus formed are readily oxidized in alkaline media into flavonols (the so-called Algar-Flynn-Oyamada reaction[4]); hence, the isolation of the former may be accomplished only under the appropriate conditions. Particularly polyhydroxychalcones, which carry one or more hydroxyl groups besides the 2'-hydroxyl group, often fail to give hydroxydihydroflavonols because of a further oxidation. Thus, only a few examples of the formation have been reported.[5]

The present authors have found that, from polyhydroxychalcones bearing one or more hydroxyl groups besides the 2'-hydroxyl one, the corresponding expoxides can be prepared by protecting all the hydroxyl groups by methoxymethylation during the course of the alkaline peroxide oxidation, and that the resulting poly(methoxymethoxy)chalcone oxides, when warmed with acid, readily cyclize to polyhydroxydihydroflavonols, with the simultaneous splitting of all *O*-methoxymethyl groups.

The general applicability of the new method will be illustrated by demonstrating the syntheses of the following hydroxydihydroflavonols: 3,3',4',7-tetrahydroxyflavanone (Va), 3,4',7-trihydroxyflavanone (Vb), 3,4'-dihydroxy-3'-methoxyflavanone (Vc), 3,7'-dihydroxyflavanone(Vd), and 3,4'-dihydroxyflavanone (Ve).

The synthetic scheme of Va (*dl*-fustin), for example, is:

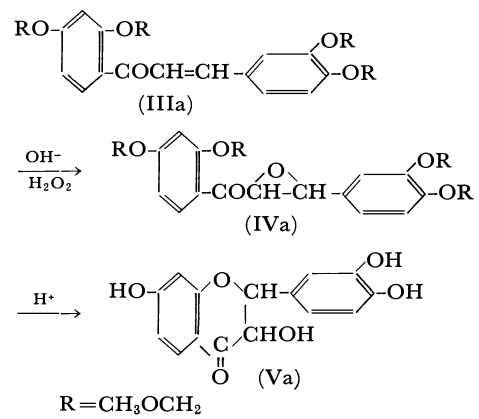

Of the above-mentioned compounds, the first one was identified by comparing it with the natural *dl*-fustin[6] obtained from the wood of *Rhus succedanea L.*, while the remaining four new compounds were identified by converting them into the known methyl ethers.[7-9] Their structures were also confirmed by infrared and ultraviolet spectra. Furthermore, these compounds gave a color reaction

* This was presented in part at the 18th Annual Meeting of the Chemical Society of Japan, Osaka, April, 1965, and published as a letter to the editor in *J. Chem. Soc. Japan, Pure Chem. Sect.* (*Nippon Kagaku Zasshi*), **86**, 750 (1965).

1) T. Oyamada, *J. Chem. Soc. Japan* (*Nippon Kwagaku Kwaishi*), **55**, 1256 (1934); This Bulletin, **10**, 182 (1935); J. Algar and J. P. Flynn, *Proc. Roy. Irish Imp. Acad.*, **B4**, 8 (1934).

2) M. Murakami and D. K. Irie, *Proc. Imp. Acad.* (*Tokyo*), **11**, 229 (1935).

3) T. A. Geissman and D. K. Fukushima, *J. Am. Chem. Soc.*, **70**, 1686 (1948).

4) J. E. Gowan and T. S. Wheeler, "Name Index of Organic Reactions," Longmans, London (1962), p. 3.

5) J. M. Guider, T. H. Simpson and D. E. Thomas, *J. Chem. Soc.*, **1955**, 170; H. Pacheoco, *Compt. rend.*, **251**, 1077 (1960); L. Reichel and J. Steudel, *Ann.*, **553**, 83 (1942).

6) T. Oyamada, *J. Chem. Soc. Japan* (*Nippon Kwagaku Kwaishi*), **55**, 755 (1934); T. Oyamada, *Ann.*, **538**, 44 (1939).

7) T. Oyamada, *J. Chem. Soc. Japan* (*Nippon Kwagaku Kwaishi*). **64**, 334 (1943).

8) T. Oyamada, ibid., **64**, 336 (1943).

9) T. Oyamada, ibid., **64**, 372 (1943).

TABLE I. INFRARED AND ULTRAVIOLET SPECTRAL DATA FOR DIHYDROFLAVONOLS AND FLAVANONES

	3-Hydroxyflavanone		Flavanone	
	IR(KBr) CO cm^{-1}	UV λ_{max}^{EtOH} mμ (log ε)	IR(KBr) CO cm^{-1}	UV λ_{max}^{EtOH} mμ (log ε)
3′,4′,7-Trihydroxy-	1674	235 (4.19) 279 (4.17) 310 (3.84)	1662	234 (4.11) 277 (4.12) 308 (3.71)
4′,7-Dihydroxy-	1660	232 (4.19) 275 (4.13) 310 (3.83)	1649	229[a] (3.99) 279 (3.90) 312 (3.64)
4′-Hydroxy-3′-methoxy-	1677	232[a] (4.06) 250 (3.95) 281 (3.58) 315 (3.51)	1676	232[a] (4.03) 250 (3.97) 281 (3.57) 318 (3.56)
7-Hydroxy	1677	234[a] (3.92) 277 (4.07) 308 (3.88)	1650	234 (4.01) 278 (4.08) 312 (3.87)
4′-Hydroxy-	1688	230[a] (4.21) 253 (4.10) 317 (3.65)	1669	230[a] (4.06) 252 (4.02) 317 (3.57)

a Inflection

characteristic of flavonoid compounds when they were reduced with magnesium or zinc and hydrochloric acid, and they were readily oxidized, by air in the presence of alkali or acid, into the corresponding flavonols. This facile dehydrogenation is a common feature of dihydroflavonols with trans-configurations. The stereochemistry of these dihydroflavonols and the steric course of this reaction will be discussed elsewhere.

In Table I are collected the infrared spectral data of the carbonyl group in the hydroxydihydroflavonols and the corresponding flavanones bearing no 3-hydroxyl groups, along with their ultraviolet absorption maxima. An examination of the infrared spectra will indicate that the introduction of a 3-hydroxyl group in the flavanones results in a rise in the carbonyl frequency, due probably to an inductive effect of the hydroxyl group. On the other hand, as might be expected, the ultraviolet absorption maxima of the dihydroflavonols and the corresponding flavanones are essentially identical.

Experimental

All melting points are uncorrected.

2′-(Methoxymethoxy)acetophenone (Ia).—A mixture of sodium salt of 2′-hydroxyacetophenone (30.0 g.), monochlorodimethyl ether (15.3 g.), calcium oxide (10.5 g.), and dioxane (240 cc.) was heated while being stirred at 40—45°C for 3 hr. The mixture was then filtered, and the filtrate was poured into water. The ether extract of the oily product was washed with 2% aqueous sodium hydroxide, dried over anhydrous sodium sulfate, and evaporated to yield 35.0 g. (89%) of a colorless liquid (Ia); b. p. 114—116°C/8 mmHg (lit. b. p. 139—140°C/12.5 mmHg[10]); n_D^{24} 1.5144. IR liquid film): 2990(sh), 2950, 2910(sh), 2830, 2780, 1082, 923 (CH_3OCH_2O); 1676 (CO); 1362 cm^{-1} (CH_3CO). (Found: C, 66.64; H, 6.91. Calcd. for $C_{10}H_{12}O_3$: C, 66.65; H, 6.71%).

2′,4′-Bis(methoxymethoxy)acetophenone (Ib).—To a solution of resacetophenone (37.5 g.) in absolute ethanol (150 cc.) containing sodium ethoxide (metallic sodium: 12.0 g.) there was added, drop by drop, monochlorodimethyl ether (40.0 g.) under cooling; the mixture was then stirred at room temperature (20°C) for 20 min. After the solvent had been removed, the residue was poured into water. The ether extract of the oily product was washed with 2% aqueous sodium hydroxide, dried over anhydrous sodium sulfate, and evaporated to yield 20.0 g. (33%) of a colorless liquid (Ib); b. p. 184°C/12 mmHg (lit. b. p. 140—150°C/0.2 mmHg[11]); n_D^{15} 1.5274. IR (liquid film): 2990(sh), 2960, 2900, 2835, 2775(sh), 1084, 924 (CH_3OCH_2O); 1669 (CO); 1363 cm^{-1} (CH_3CO). (Found: C, 59.89; H, 6.74. Calcd. for $C_{12}H_{16}O_5$: C, 59.99; H, 6.71%).

4-(Methoxymethoxy)benzaldehyde (IIa).—To a stirred suspension of a finely-divided sodium (3.4 g.) in toluene (90 cc.), a solution of 4-hydroxybenzaldehyde (18.0 g.) in absolute ethanol (20 cc.) was added; the mixture was then refluxed with stirring in order to complete the salt-formation. After the alcohol had been removed by fractional distillation the suspension of the sodium salt in toluene was treated with monochlorodimethyl ether (120.0 g.) under cooling the precipitate disappeared. The resulting solution was washed with 2% aqueous sodium hydroxide, dried over anhydrous sodium sulfate, and evaporated to yield 12.5 g. (86%) of a colorless liquid (IIa); b. p. 147—149°C/22 mmHg

10) C. Eneback, *Soc. Sci. Fennica, Commentations Phys.-Math.*, **28** (10), 95 (1963); *Chem. Abstr.*, **60**, 7972 (1964).
11) A. Bellini and P. Venturella, *Ann. chim. (Rome)*, **48**, 111-24 (1948); *Chem. Abstr.*, **52**, 1641 (1958).

(lit. b. p. 152—153°C/21 mmHg[12]): n_D^{15} 1.5434. IR (liquid film): 2960, 2910, 2840, 2740, 1082, 923 (CH_3OCH_2O); 2840, 2740, 1962 cm^{-1} (CHO). (Found: C, 65.04; H, 6.10. Calcd. for $C_9H_{10}O_3$: C, 65.05; H, 6.07%).

3, 4-Bis(methoxymethoxy)benzaldehyde (IIb).—This product was obtained from protocatechualdehyde by the procedure used for Ib; yield, 46%; m. p. 59—60°C (lit. m. p. 60°C[12]). IR (KBr): 2980(sh), 2940, 2840, 2740, 1083, 918 (CH_3OCH_2O); 2840, 2740, 1676 cm^{-1} (CHO). (Found: C, 58.66; H, 6.41. Calcd. for $C_{11}H_{14}O_5$: C, 58.40; H, 6.24%).

3-Methoxy-4-(methoxymethoxy)benzaldehyde (IIc).—To a solution of the sodium salt of vanillin (15.3 g.) in dioxane (76 cc.), chlorodimethyl ether (5.6 g.) was added, drop by drop, under ice-cooling; the mixture was then heated at 70—80°C for 1.5 hr. and poured into water. The toluene extract of the product was washed with 2% aqueous sodium hydroxide, dried over anhydrous sodium sulfate, and evaporated to yield an oily residue which crystallized on standing. Recrystallization from ether gave 10.0 g. (49%) of colorless plates (IIc); m. p. 39.5—41.5°C (lit m. p. 39—40°C[13]). IR (liquid film): 2990(sh), 2950, 2900, 2830, 2740, 1083, 924 (CH_3OCH_2O): 2830, 2740, 1685 cm^{-1} (CHO).

2', 3, 4, 4'-Tetrakis(methoxymethoxy)chalcone (IIIa).—To a solution of Ib (3.2 g.) and IIb (3.0 g.) in methanol (40 cc.) 50% aqueous sodium hydroxide (25.0 g.) was added; the mixture was then allowed to stand at room temperature overnight. The reaction mixture was poured into water, and the precipitate formed was collected and recrystallized from ligroin to give 3.0 g. (50%) of pale yellow needles (IIIa); m. p. 69—70°C. IR(KBr): 2990(sh), 2930(sh), 2900, 2830, 2800(sh), 1072, 918 (CH_3OCH_2O); 1640 cm^{-1} (CO).

Found: C, 61.98; H, 6.51. Calcd. for $C_{23}H_{28}O_9$: C, 61.59; H, 9.30%.

The Hydrolysis of IIIa with Hydrochloric Acid.—To a solution of IIIa (1.0 g.) in ethanol (20 cc.), 12 N hydrochloric acid (10 cc.) was added; the solution was then left at room temperature for 40 min. The reaction mixture was poured into water and the precipitate was collected and recrystallized from ethanol to give 0.15 g. of yellow crystals, m. p. 215—216°C. No depression of the melting point was observed on admixture with an authentic sample of butin.

2', 4, 4'-Tris(methoxymethoxy)chalcone (IIIb).—IIIb was obtained from Ib and IIa by the procedure described above. Yield, 90%; pale yellow needles; m. p. 47—48°C (*n*-hexane-carbon tetrachloride). IR (KBr): 2990, 2960, 2900, 2830, 2795(sh), 1077, 928 (CH_3OCH_2O); 1650 cm^{-1} (CO).

Found: C, 64.69; H, 6.38. Calcd. for $C_{21}H_{24}O_7$; C, 64.93: H, 6.24%.

2', 4-Bis(methoxymethoxy)-3-methoxychalcone (IIIc).—IIIc was obtained from Ia and IIc by the procedure described above. Yield, 67%; colorless needles; m. p. 64—64.5°C. IR(KBr): 2965, 2910, 2825, 2790(sh), 1080, 917 (CH_3OCH_2O); 1648 cm^{-1} (CO).

Found: C, 67.03; H, 6.34. Calcd. for $C_{20}H_{22}O_6$: C, 67.02; H, 6.20%.

2', 4'-Bis(methoxymethoxy)chalcone (IIId).—IIId was obtained from Ib and benzaldehyde by the procedure described above, except that the oily product was extracted with ether. The removal of the ether gave a pale yellow oil (IIId), which was used in the subsequent epoxidation without further purification. Yield, 80%; pale yellow liquid: n_D^{18} 1.5978. IR (liquid film): 3005, 2950, 2900, 2830, 2780(sh), 1080, 926 (CH_3OCH_2O); 1662 cm^{-1} (CO).

2', 4-Bis(methoxymethoxy)chalcone (IIIe).—IIIe was obtained from Ia and IIa by the procedure used for making IIId. Yield, 95%; pale yellow liquid; n_D^{13} 1.6067. This was used without further purification. IR (liquid film): 2990, 2940, 2900, 2835, 2780(sh), 1082, 924 (CH_3OCH_2O); 1660—1640 cm^{-1} (doublet) (CO).

2', 3, 4, 4'-Tetrakis(methoxymethoxy)chalcone Oxide (IVa).—To a solution of IIIa (3.0 g.) in methanol (160 cc.) there were adedd 15% aqueous hydrogen peroxide (9 cc.) and then 16% aqueous sodium hydroxide (15.0 g.) under cooling. The mixture was then allowed to stand in a refrigerator over night. The colorless precipitate formed was collected by filtration and recrystallized from carbon tetrachloride to give 1.5 g. (48%) of colorless needles (IVa), m. p. 77—79°C. A further amount (about 1.1 g.) of this compound was recovered from the filtrate by diluting it with water. IR (KBr): 2970, 2945, 2920, 2830, 2805, 1071, 924 (CH_3OCH_2O); 1678 (CO); 896 cm^{-1} (C(O)C—O).

Found: C, 59,74; H, 6.19; Calcd. for $C_{23}H_{28}O_{10}$: C, 59.47; H, 6.09%.

2', 4, 4'-Tris(methoxymethoxy)chalcone Oxide (IVb), 2', 4-Bis(methoxymethoxy)-3-methoxychalcone Oxide (IVc), 2', 4'-Bis(methoxymethoxy)-chalcone Oxide (IVd), and 2', 4-Bis(methoxymethoxy)chalcone Oxide (IVe).—IVb, IVc, IVd, and IVe were obtained from IIIb, IIIc, IIId, and IIIe respectively by the procedure described above for IVa.

IVb.—Yield, 76%; colorless needles; m. p. 95—96°C (carbon tetrachloride). IR (KBr): 3000, 2960, 2930(sh), 2830, 2800(sh), 1076, 910 (CH_3OCH_2O); 1681 (CO); 889 cm^{-1} (C(O)C—C).

Found: C, 62.67; H, 5.65. Calcd. for $C_{21}H_{24}O_8$: C, 62.36; H, 5.99%.

IVc.—Yield, 67%; liquid, n_D^{15} 1.6633. Attempts to crystallize the oily product (IVc) were unsuccessful. Thus, its elementary analysis gave no satisfactory results, although the infrared spectrum exhibited the expected bands as follows: IR (liquid film): 2990(sh), 2960, 2900(sh), 2820, 2780(sh), 1084, 924 (CH_3OCH_2O); 1679 (CO); 898 cm^{-1} (C(O)C—C).

IVd.—Yield, 68%; colorless needles; m.p. 61.5—62°C (carbon tetrachloride). IR(KBr): 2960, 2900, 2830, 2780(sh), 1086, 926 (CH_3OCH_2O); 1675 (CO); 898 cm^{-1} (C(O)C—C).

Found: C, 66.01; H, 5.93. Calcd, for $C_{19}H_{20}O_6$: C, 66.26; H, 5.86%.

IVe.—Yield, 79%; colorless prisms; m. p. 59—60°C (carbon tetrachloride). IR(KBr): 2991, 2970(sh), 2825(sh), 2785, 1084, 927 (CH_3OCH_2O); 1686 (CO); 890 cm^{-1} (C(O)C—C).

Found: C, 66.24; H, 6.29. Calcd. for $C_{19}H_{20}O_6$: C, 66.26; H, 5.86%.

3, 3', 4', 7-Tetrahydroxyflavanone (Va, *dl*-fustin).—A mixture of IVa (1.0 g.), methanol (10 cc.) and 12 N

12) H. Baum, D. R. Pat. 209608 (1909).
13) K. Freudenberg and H. G. Müller, *Ann.*, **584**, 40 (1953).

hydrochloric acid (3 cc.) was refluxed for 5 min. The reaction mixture was then diluted with water (about 20 cc.), and the methanol was removed at a temperature below 40°C in vacuo. The precipitate which had separated on cooling was collected and recrystallized from water to give 0.5 g. (80%) of colorless plates (Va), m. p. 217—218°C; this substance showed no melting point depression on admixture with an authentic sample of *dl*-fustin.[6] The infrared and ultraviolet spectra of Va were identical with those of the natural substance

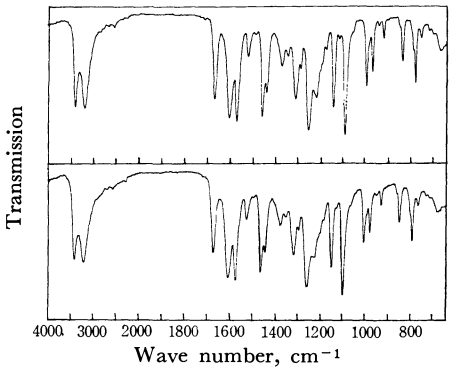

Fig. 1. The infrared spectra of natural (upper) and synthetic fustin (Va) (lower).

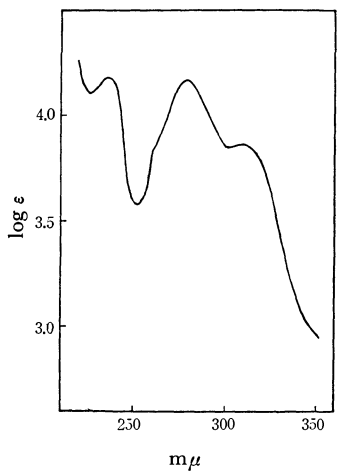

Fig. 2. The ultraviolet spectrum of synthetic fustin (Va) in ethanol.

(Figs. 1 and 2). Color reactions: magnesium - hydrochloric acid, orange red; zinc — hydrochloric acid, orange red; ferric chloride, green. IR(KBr): 3400, 3200, 1018 (OH); 1674 cm^{-1} (CO). UV λ_{max}^{EtOH} mμ (log ε): 235 (4.19), 279 (4.17), 310 (3.84). (Found: C, 62.61; H, 4.38. Calcd. for $C_{15}H_{12}O_6$: C, 62.50; H, 4.16%).

Tetraacetate: m. p. 148—149°C (lit. m. p. 150—151°C[6]). IR (KBr): 1752 (acetate CO); 1707 cm^{-1} (CO).

3', 4', 7-Trimethyl Ether: m. p. 140—140.5°C (lit. m. p. 143—144°C[6]). IR(KBr): 3450, 998 (OH); 3000—2900 (triplet), 2835 (CH_3O); 1679 cm^{-1} (CO).

3, 4', 7-Trihydroxyflavanone (Vb), 3, 4'-Dihydroxy-3'-methoxyflavanone (Vc), 3, 7-Dihydroxyflavanone (Vd), and 3, 4'-Dihydroxyflavanone (Ve). —Vb, Vc, Vd, and Ve were prepared from IVb, IVc, IVd, and IVe respectively by a slight modification of the procedure described above. The precipitate which had separated on the addition of water was collected and recrystallized from the appropriate solvents.

Vb.—Yield, 63%; colorless fine crystals; m. p. 214—215°C (ethanol). Color reactions: magnesium - hydrochloric acid, reddish violet; zinc - hydrochloric acid, reddish violet; phloroglucinol - hydrochloric acid, reddish violet; ferric chloride, none. IR (KBr): 3250 (broad), 1005 (OH); 1660 cm^{-1} (CO). UV λ_{max}^{EtOH} mμ (log ε): 232 (4.19), 275 (4.13), 310 (3.83).

Found: C, 66.17; H, 4.78. Calcd. for $C_{15}H_{12}O_5$: C, 66.17; H, 4.44%.

Triacetate: m. p. 149—150.5°C. IR (KBr): 1750 (acetate CO); 1707 cm^{-1} (CO).

Found: C, 63.19; H, 4.75. Calcd. for $C_{21}H_{18}O_8$: C, 63.31; H, 4.56%.

4', 7-Dimethyl Ether: m. p. 130—131°C (lit. m. p. 124—126°C[8]). IR (KBr): 3450, 1007 (OH); 3000—2900 (triplet), 2840 (CH_3O); 1683 cm^{-1} (CO).

The Oxidation of Vb to 3, 4', 7-Trihydroxyflavone (VIb). —A mixture of Vb (0.1 g.), 16% aqueous sodium hydroxide (4 cc.), and methanol (3 cc.) was warmed on a water bath for 10 min. The reaction mixture was then poured into water, and the precipitate formed was collected and recrystallized from ethanol to give VIb as yellow crystals, m. p. 296—297°C (lit. m. p. 302°C[14]).

Vc.—Yield, 45%; colorless needles; m. p. 217—218°C (ethyl acetate). Color reactions: magnesium - hydrochloric acid, reddish orange; zinc - hydrochloric acid, reddish orange; phloroglucinol - hydrochloric acid, violet; ferric chloride, none. IR(KBr): 3460, 1009 (OH); 1677 cm^{-1} (CO). UV λ_{max}^{EtOH} mμ (log ε): 232[a](4.06), 250(3.95), 281(3.58), 315(3.51).

Found: C, 67.10; H, 4.99. Calcd. for $C_{16}H_{14}O_5$: C, 67.12; H, 4.94%.

Diacetate: m. p. 144—145°C. IR (KBr): 1750 (acetate CO): 1699 cm^{-1} (CO).

Found: C, 65.07; H, 5.19. Calcd. for $C_{20}H_{18}O_7$: C, 64.85; H, 4.91%.

3', 4'-Dimethyl Ether: m. p. 155—157°C (lit. m. p. 155—157°C[8]). IR (KBr): 3450, 1005 (OH); 3000—2900 (triplet), 2840 (CH_3O); 1692 cm^{-1} (CO).

Vd.—Yield, 75%; colorless needles; m. p. 170—171°C (ethanol). Color reactions: magnesium - hydrochloric acid, reddish orange; zinc - hydrochloric acid, red; phloroglucinol - hydrochloric acid, orange; ferric chloride, none. IR(KBr): 3395, 3165, 1010 (OH); 1677 cm^{-1} (CO). UV λ_{max}^{EtOH} mμ (log ε): 234[a](3.92), 277-(4.07), 308(3.88).

Found: C, 69.66; H, 5.06. Calcd. for $C_{15}H_{12}O_4$: C, 70.30; H, 4.73%.

Diacetate: m. p. 129.5—130°C. IR (KBr): 1752 (acetate CO); 1700 cm^{-1} (CO).

Found: C, 66.95; H, 4.99. Calcd. for $C_{19}H_{16}O_6$: C, 67.04; H, 4.75%.

7-Methyl Ether: m. p. 148—149°C (lit. m. p. 146—147°C,[9] 149—150°C[10]). IR(KBr): 3450, 1012 (OH); 3000—2900 (triplet), 2840 (CH_3O); 1682 cm^{-1} (CO).

The Oxidation of Vd to 3, 7-Dihydroxyflavone (VId).—A

14) S. Yamaguchi, *J. Chem. Soc. Japan, Pure Chem. Sec.* (*Nippon Kagaku Zasshi*), **84**, 148 (1963).

mixture of Vd (0.05 g.), 2 N sulfuric acid (5 cc.), and methanol (2 cc.) was heated on a water bath for 15 hr. under reflux, while a gentle stream of air was passed into the flask. The work-up of the reaction product gave VId as pale yellow crystals, m. p. 251—252°C, which was identical with the sample prepared from 2', 4'-dihydroxychalcone by the Algar-Flynn-Oyamada method.

Ve.—Yield, 45%; colorless needles; m. p. 214—216°C (methanol). Color reactions: magnesium - hydrochloric acid, red; zinc - hydrochloric acid, reddish orange; phloroglucinol - hydrochloric acid, red; ferric chloride, none. IR(KBr): 3390, 1006 (OH); 1688 cm^{-1} (CO). UV λ_{max}^{EtOH} mμ (log ε): 230[a](4.21), 253(4.10), 317(3.65).

Found: C, 70.03; H, 5.03. Calcd. for $C_{15}H_{12}O_4$: C, 70.30; H, 4.73%.

Diacetate: m. p. 164.5—165.5°C. IR(KBr): 1742 (acetate CO); 1694 cm^{-1} (CO).

Found: C, 67.29; H, 4.99. Calcd. for $C_{19}H_{16}O_6$: C, 67.04; H, 4.75%.

4'-Methyl Ether: m. p. 171—172°C (lit. m. p. 172—174°C[7]). IR(KBr): 3450, 1003 (OH); 3000—2900 (triplet), 2840 (CH_3O); 1690 cm^{-1} (CO).

The Oxidation of Ve to 3, 4'-Dihydroxyflavone (VIe).—This oxidation was effected essentially by the method described above for Va. VIe was obtained as yellow needles, m. p. 266—268°C; it was identical with the sample prepared from 2', 4-dihydroxychalcone by the Algar-Flynn-Oyamada method.

As has been described above, except for *dl*-fustin, the hydroxydihydroflavonols obtained here, which contain a free 4'-, 7-hydroxyl, or 4', 7-dihydroxyl grouping, gave no color reaction with ferric chloride (carried out by the addition of aqueous ferric chloride to aqueous alcohol solutions of these compounds). This is not too surprising, for this observation is in agreement with that made by Briggs and Locker[15] in hydroxyflavones containing a similar hydroxyl grouping.

All of the above acetates were prepared by treating them with acetic anhydride and pyridine; all of the above methyl ethers were prepared by refluxing them with dimethyl sulfate and anhydrous potassium carbonate in an acetone solution.

The authors are indebted to Mr. Toru Sato, Mr. Yusuke Inoguchi, Mr. Masaki Kikuchi, and Mr. Kazuyuki Mori for their technical assistance, and to Miss Toshiko Koyama and Miss Yoshi Yamawaki for the ultraviolet and infrared spectral measurements.

15) L. H. Briggs and R. H. Locker, *J. Chem. Soc.*, **1951**, 3136.

BULLETIN OF THE CHEMICAL SOCIETY OF JAPAN VOL. 39 511—516 (1966)

A Geochemical Study of the Fumarolic Bismuthinite from Showashinzan

By Yoshihiko MIZUTANI

The Institute of Earth Sciences, Faculty of Science, Nagoya University, Chikusa-ku, Nagoya

(Received June 30, 1965)

In an active fumarole on the dome of the Showashinzan volcano, Hokkaido, Japan, a crystalline sublimate was found. It is lead grey, with a metallic luster, and forms loose clusters of acicular crystals. X-Ray diffraction, spectrographic and micro-chemical analyses have been made of the sublimate. The results indicate that the sublimate consists of bismuthinite Bi_2S_3, with traces of lead, zinc, aluminum, copper, iron and titanium. A colorimetric determination has also been made of the bismuth in the fumarolic gases from Showashinzan. The variation in the bismuth content of the gases with the gas temperature suggests that, when the temperature falls to about 500°C, bismuth compounds lose their volatility in the gases and are precipitated to form a sublimate. On the assumption that the chemical equilibrium is established in the gases, the stability of bismuth minerals and a possible reaction for the formation of bismuthinite in the gases have been discussed, and it has been suggested that the bismuthinite is formed by the $2BiCl_3 + 3H_2S = Bi_2S_3 + 6HCl$ reaction in the gases.

Showashinzan, Hokkaido, Japan, is an active volcano formed during the period from 1943 to 1945. It is composed of a platform-shaped mountain with a dome on it. The dome consists of new lava, hyperthene dacite. Fumarolic activity still persists on and around the dome, with the emission of large amounts of high-temperature volcanic gases.

Recently, Mizutani[1] has made chemical and mineralogical investigations of volcanic sublimates from Showashinzan. His results show that many primary volcanic sublimates, such as crystobalite, hematite, thenardite, glaserite, sal ammoniac, and sassolite, are deposited in the fumaroles of

1) Y. Mizutani, *J. Earth Sciences, Nagoya Univ.*, **10**, 149 (1962).

Showashinzan.

In the present research, a volcanic sublimate from fumarole B-1b (Mizutani's notation[2]) of Showashinzan was subjected to X-ray diffraction, spectrographic and micro-chemical analyses in order to clarify its mineralogical composition. An attempt was also made to explain the formation of the volcanic sublimate through a gas phase reaction.

Occurrence

The sublimate was found at fumarole B-1b (Fig. 1), about 10 cm. inside the opening of the fumarole. It had been developed on the inner wall of the fissure vent and had formed loose clusters of acicular crystals. The crystals are lead-grey

TABLE I. FUMAROLIC GASES FROM FUMAROLE B-1b

Date		1960	1961
Temp.	°C	260	227
H_2O,	l./1000 l.	986.2	991.7
CO_2,	l./1000 l.	12.2	7.06
H_2,	l./1000 l.	0.67	0.37
N_2,	l./1000 l.	0.70	0.64
HCl,	l./1000 l.	0.13	0.16
HF,	l./1000 l.	0.033	0.025
H_2S,	ml./1000 l.	100	74
SO_2,	ml./1000 l.	3	5
Ar,	ml./1000 l.	7.0	2.0
CH_4,	ml./1000 l.	16	11.2
CO,	ml./1000 l.	0.33	0.08
O_2,	ml./1000 l.	0.000	0.000

TABLE II. POWDER X-RAY DATA

Sample		Bismuthinite*1		Bismuthinite*2		Galenobismutite*3		Cannizzarite*4	
d, Å	I.	*d*, Å	I.	*d*, Å	I.	*d*, Å	I.	*d*, Å	I.
5.665	20	5.56	20	5.55	1.0	—	—	7.38	1
5.048	20	5.04	19	4.95	1.0	4.55	10	5.13	2
3.97	35	3.97	38	3.92	2.0	3.93	5	—	—
—	—	3.75	20	—	—	—	—	3.82	10
3.575	100	3.56	94	—	—	3.65	30	3.49	3
3.543	35	3.53	60	3.50	9.0	3.45	100	3.38	3
3.258	5	3.256	18	3.22	1.0	3.36	5	3.29	1
3.120	35	3.118	100	3.08	6.0	3.27	5	3.01	6
2.813	15	2.811	63	2.79	4.0	3.03	40	2.87	5
2.722	7	2.716	34	2.69	1.0	2.76	30	2.76	2
2.647	7	2.641	24	2.61	1.0	2.65	20	2.68	6
2.522	50	2.52	35	—	—	—	—	2.54	2
2.502	7	2.499	13	2.495	3.0	—	—	—	—
2.461	5	2.456	15	2.425	1.0	—	—	—	—
2.305	7	2.304	24	2.28	1.0	2.46	40	2.39	0.5
2.259	10	2.256	36	2.34	3.0	2.39	20	2.22	5
2.120	5	2.129	9	—	—	2.24	10	—	—
—	—	2.118	15	—	—	2.20	10	—	—
2.098	15	2.096	11	—	—	—	—	—	—
2.077	6	2.074	10	2.06	0.5	2.05	40	2.03	5
1.986	7	1.99	33	1.98	1.0	2.01	5	—	—
1.955	15	1.953	55	—	—	—	—	—	—
1.933	15	1.935	20	1.935	5.0	1.961	50	—	—
1.921	15	1.919	20	—	—	—	—	1.910	4
1.886	20	1.884	14	1.870	1.0	1.881	20	—	—
1.858	8	1.854	17	1.840	1.0	1.848	5	—	—
—	—	1.779	13	—	—	1.784	5	1.791	3
—	—	1.765	5	—	—	1.762	30	—	—
1.739	8	1.737	7	—	—	—	—	—	—
—	—	1.734	35	1.725	5.0	1.734	10	1.734	1
1.702	7	1.702	10	1.690	1.0	1.704	5	—	—

*1 ASTM X-ray powder card (6-0333)
*2 ibid. (11-138)
*3 Ref. 4
*4 Ref. 5

2) Y. Mizutani, *J. Earth Sciences, Nagoya Univ.*, **10**, 135 (1962).

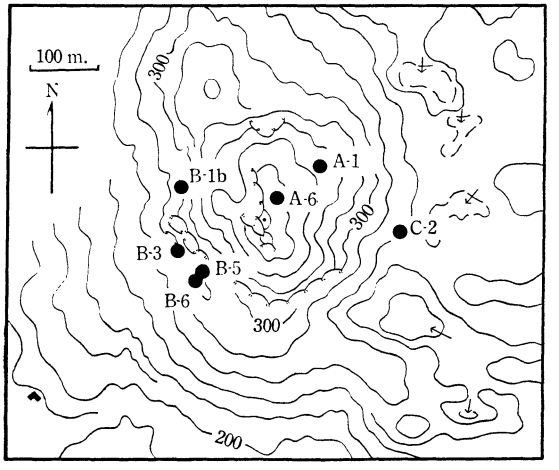

Fig. 1. Location of sampling.

with a metallic luster. Individual crystals reach a length of about 5 mm., but they are extremely thin. About 40 mg. of the sublimate was collected in 1960, and about 10 mg. in 1961, from the same place in the fumarole.

The vent of fumarole B-1b was 1—5 cm. wide and several meters long, running upwards on the slope of the dome. The surface of the inner wall of the fumarole was partly coated with a very thin film of a brown material, possibly hematite, but the inside of the wall rock, brecciated new lava, showed little evidence of having been attacked by fumarolic gases. From the fissure vent, gases with a temperature higher than 200°C were emitted at a rather low pressure, perhaps close to 1 atm. The temperature and chemical composition of the gases, determined at the same time as the sublimate was collected, are given in Table I.

Experimental

Identification.—A carefully-selected sample of the sublimate was subjected to qualitative spectrographic analysis and micro-chemical tests in order to get a provisional idea of its composition. The results showed that the sublimate consisted of bismuth sulfide, with trace amounts of lead, zinc, aluminum, copper, iron and titanium.

An X-ray powder pattern was prepared with a Norelco X-ray diffractometer using nickel-filtered copper radiation. The results obtained are given in Table II, together with the X-ray powder data of some bismuth minerals reported by ASTM,[3] Harcourt[4] and Graham et al.[5] The X-ray powder pattern of the sample is very similar to that of bismuthinite given by ASTM. Although they are identical in *d*-value, however, they are different in the intensities of some lines. The X-ray pattern of the bismuthinite given by Harcourt is also similar to that of the sample, though they differ slightly in the intensities and *d*-values of some lines. On the other hand, the X-ray patterns of the galenobismutite and cannizzarite given by ASTM and Graham et al. respectively are distinctly different from that of the sample.

The present identification is incomplete in the absence of quantitative chemical data, but it is thought to be sufficiently significant to prove that the sublimate examined consists of bismuthinite (Bi_2S_3).

The Determination of the Bismuth Content of Fumarolic Gases.—In order to discuss the formation of fumarolic bismuthinite throuhg a gas phase reaction, the bismuth content of the gases of Showashinzan was determined as follows.

Fumarolic gases were drawn into a cold trap containing a small amount of concentrated nitric acid by using a syringe through a silica tube inserted into the fumarole. By this process, the water vapor in the gases was condensed in the trap and bismuth compounds in the gases were completely dissolved in the condensed water. The nitric acid prevents the precipitation of bismuth as sulfide. The condensed water was then subjected to the following chemical analysis.

Two hundred and fifty milliliters of the condensed water was placed in a dish and concentrated to about 20 ml. Bismuth was separated from the solution as bismuth dithizonate in chloroform by Sandell's dithizone extraction method.[6] After the chloroform solution of bismuth dithizonate had been shaken with sulfuric acid (1 : 300), the aqueous phase was transferred to a small beaker and boiled gently until the odor of chloroform disappeared. Then the solution was subjected to Goto's colorimetric method.[7] The results obtained are given in Table III, together with the observed temperatures of the gases.

Table III. Bismuth content of fumarolic gases from Showashinzan

Sample*	Temp., °C	Bi, mg./kg. H_2O
A-1 (1960)	772	0.024
A-6 (1960)	695	0.026
C-2 (1960)	605	0.015
C-2 (1961)	560	0.046
B-5 (1960)	446	0.003
B-3 (1961)	375	0.003
B-6 (1960)	347	0.002
B-1b(1960)	260	0.002
B-1b (1961)	227	0.005
B-6 (1961)	211	0.003

*Sampling sites are shown in Fig. 1.

Discussion

The Behavior of the Bismuth in the Fumarolic Gases.—As may be seen from Table III, there is a notable decrease in the bismuth content at a temperature of about 500°C. This implies that, when the temperature falls to about 500°C, bismuth compounds lose their volatility in the gases

3) "X-Ray Powder Data File," American Society for Testing Materials.
4) G. A. Harcourt, *Am. Mineral*, **27**, 63 (1942).
5) A. R. Graham, R. M. Thompson and L. G. Berry, ibid., **38**, 536 (1953).
6) E. B. Sandell, "Colorimetric Determination of Traces of Metals," Interscience Publishers Inc., New York (1950).
7) H. Goto and S. Suzuki, *J. Chem. Soc. Japan, Pure Chem. Sect.* (*Nippon Kagaku Zassi*), **74**, 142 (1953).

and are precipitated to form volcanic sublimate. Therefore, it is suggested that the occurrence of the bismuth mineral may be common in low-temperature fumaroles of Showashinzan. The difficulty of finding fumarolic bismuth minerals may be attributable to the fact that the rate of the accumulation of the minerals in a fumarole is very small, as may be expected from the observed bismuth contents of the gases.

Stable Bismuth Minerals under Fumarolic Conditions.—Three minerals are considered: the metal itself, the sulfide and the oxide. Stability relationships among these minerals may be expressed as a function of the temperature and the chemical compositon of the gaseous phase in equilibrium with the minerals.

The reactions considered are:

$$2/3\,Bi + H_2O = 1/3\,Bi_2O_3 + H_2 \quad (1)$$

and

$$1/3\,Bi_2S_3 + H_2 = 2/3\,Bi + H_2S \quad (2)$$

The values of the free energy change, ΔG, for these reactions were obtained from the thermodynamic data given by Kubaschewski and Evans[8] and by Rossini et al.,[9] and the equilibrium constant of the reaction, K, was calculated from the $\Delta G = -RT\ln K$ relation, where R is the gas-law constant and T is the absolute temperature of the system. The equations of K thus obtained are: for Reaction 1,

($T<271$°C)

$$\log K_1 = -8.961 + 2.323\log T - 2.98\times10^{-4}T - 2320T^{-1} \quad (3)$$

($T>271$°C)

$$\log K_1 = -7.950 + 1.650\log T + 0.963\times10^{-4}T - 1973T^{-1} \quad (4)$$

$$K_1 = \frac{P_{H_2}}{P_{H_2O}}$$

and for Reaction 2:

($T<271$°C)

$$\log K = 8.36 - 2.02\log T - 1790\,T^{-1} \quad (5)$$

($T>271$°C)

$$\log K_2 = 7.35 - 1.35\log T - 0.394\times10^{-3}T - 2120\,T^{-1} \quad (6)$$

$$K_2 = \frac{P_{H_2S}}{P_{H_2}}$$

The stability relationships obtained from these equations are shown in Figs. 2 and 3. The observed values of P_{H_2}/P_{H_2O} and P_{H_2S}/P_{H_2} in fumarolic gases of Showashinzan[2,10] are also plotted in Figs. 2 and 3 respectively.

It may be seen from these figures that the equilibrium ratio, P_{H_2}/P_{H_2O}, is far below the ratios observed in the fumarolic gases, so the metal is more stable in the gases than is the oxide (Fig. 2), and similarly, that the sulfide is stable at temperatures below about 230°C with repect to the

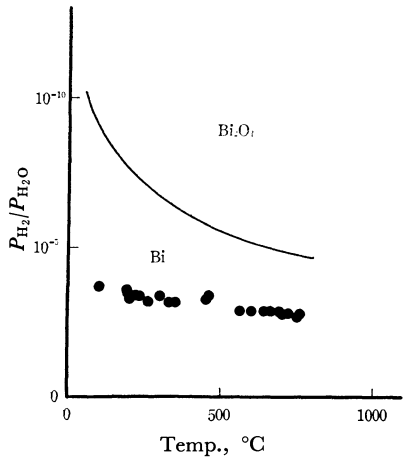

Fig. 2. Stability relationship between Bi_2O_3 and Bi as a function of temperature and P_{H_2}/P_{H_2O} ratio of the gas phase in equilibrium with the minerals.
—— : Bi_2O_3-Bi boundary
● : observed P_{H_2}/P_{H_2O} ratio of fumarolic gases of Showashinzan.

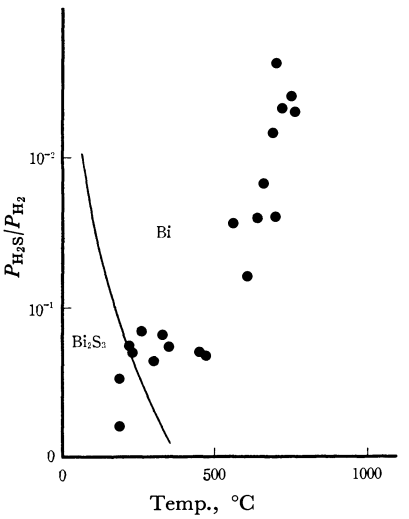

Fig. 3. Stability relationship between Bi and Bi_2S_3 as a function of temperature and P_{H_2S}/P_{H_2} ratio of the gas phase in equilibrium with the minerals.
—— : Bi - Bi_2S_3 boundary
● : observed P_{H_2S}/P_{H_2} ratio of fumarolic gases of Showashinzan

8) O. Kubaschewski and E. L. Evans, "Metallurgical Thermochemistry," John Wiley, New York (1956).
9) F. D. Rossini, D. D. Wagman, W. H. Evans, S. Levine and I. Jaffe, "Selected Values of Chemical Thermodynamic Properties," Natl. Bur. Standards, Circ. 500 (1952).
10) S. Oana and his co-workers, unpublished.

metal, but unstable at temperatures above 230°C (Fig. 3). Thus, in fumarolic gases of Showashinzan, bismuth, if present in an amount sufficient to form a solid, must exist as the sulfide or native metal.

A Possible Reaction to Form Bi_2S_3. — Theoretical evidence for the transportation of bismuth in magmatic vapor as chloride was adduced in Krauskopf's thermodynamic calculations[11] of the heavy metal content of magmatic vapor. His calculations suggest that high temperature magmatic vapor containing an appreciable amount of hydrogen chloride may transport bismuth in the form of bismuth chloride. On the basis of this theory, the following reaction may be offerred to account for the formation of bismuthinite under fumarolic conditions:

$$2\,BiCl_3 + 3\,H_2S = Bi_2S_3 + 6HCl \qquad (7)$$

This reaction may also be expressed as:

$$K_3 = \frac{X^6_{HCl} \cdot P}{X^2_{BiCl_3} \cdot X^3_{H_2S}} \qquad (8)$$

where K is the equilibrium constant, X is the molar fraction of the gaseous components in the system, and P is the total pressure on the system.

On the assumption that chemical equilibrium is attained in fumarolic gases of Showashinzan, the bismuth content of the gases may be estimated from the above relation if the equilibrium constant of the reaction, the chemical composition and pressure of the gases are given. The equilibrium constant for the reaction may be calculated in the way described above. The equation of the equilibrium constant thus obtained is:

$$\log K_3 = -17.23 + 5.34 \log T + 1.18 \times 10^{-3}\, T + 5190\, T^{-1} \qquad (9)$$

With respect to the chemical composition of the gases, Mizutani[2] showed that the variation in the hydrogen chloride and hydrogen sulfide contants of the fumarolic gases of Showashinzan could be approximately expressed as a function of the temperature. Thus the following relations, which are obtained from the analytical data of the fumarolic gases[2,12] by using the method of least squares, may be used for the estimation of the equilibrium bismuth chloride content of the gases:

$$C_{HCl} = 0.77 \times 10^{-3}\, T - 0.25 \qquad (10)$$

$$C_{H_2S} = -0.19 \times 10^{-3}\, T + 0.21 \qquad (11)$$

where C is the content of the chemical components in fumarolic gases in l./1000 l. and T is the temperature of fumarolic gases in °K. For the pressure it is assumed that the static pressure of fumarolic gases near the outlet is 1 atm. The result obtained is illustrated graphically in Fig. 4,

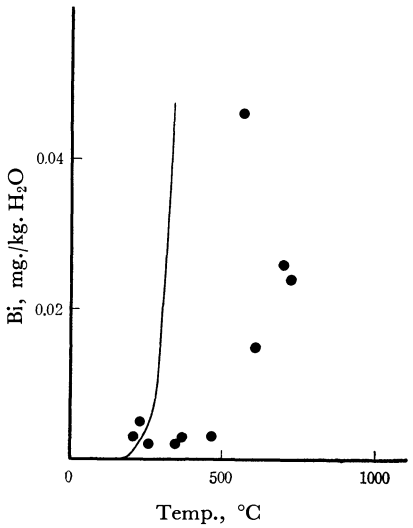

Fig. 4. Theoretical bismuth content in fumarolic gases of Showashinzan in equilibrium with Bi_2S_3 as a function of temperature at a total pressure of 1 atm., solid line.

● : observed bismuth content of fumarolic gases of Showashinzan
(0.01 mg. Bi/kg. $H_2O = 8.6 \times 10^{-4}$ ml. $BiCl_3$/1000 l. water vapor)

together with the observed bismuth contents of fumarolic gases.

Figure 4 indicates that the fumarolic gases are capable of forming bismuth sulfide when the temperature falls to about 250°C. This temperature of the formation of bismuth sulfide is in good agreement with that obtained by the field observations. This agreement suggests that the major part of the bismuth that is volatilized out of Showashinzan magma is transported as bismuth chloride and that the bismuthinite is formed by Reaction 7 in the fumarolic gases as the temperature falls. A problem, however, arises about the decrease in the actual bismuth content observed at a temperature of about 500°C. As is shown in Fig. 4, the theoretical curve deviates significantly from the observed bismuth contents at temperatures above 250°. This discrepancy may be due to uncertainties in the thermodynamic estimation or to the formation of bismuth minerals other than bismuthinite which are more stable in the fumarolic gases with temperatures between 250 and 500°C than is bismuthinite. This problem, however, remains unsolved, because available data are not enough to make discussion significant. Thus, it is necessary to find other bismuth minerals in fumaroles with gas temperatures between 250 and 500°C and to have more thermodynamic data on various bismuth compounds in order to be able to extend the discussions concerning the formation of fumarolic bismuth minerals.

11) K. B. Krauskopf, *Econ. Geol.*, **52**, 786 (1957).
12) S. Matsuo, *J. Earth Sciences, Nagoya Univ.*, **9**, 80 (1960).

Summary

A volcanic sublimate from fumarole B-1b of Showashinzan has been subjected to X-ray diffraction spectrographic and micro-chemical analyses. These analyses indicate that the sublimate consists of bismuthinite with trace amounts of lead, zinc, aluminum, copper and other substances. A possible reaction for the formation of bismuthinite in fumaroles of Showashinzan has been discussed by using the results of the analyses of fumarolic gases. It has been suggested that the bismuthinite is formed by the 2 $BiCl_3 + 3H_2S = Bi_2S_3 + 6HCl$ reaction in the fumarole.

The author wishes to express his deep appreciation to Professor Shinya Oana for his encouragement throughout this study. He is also indebted to Dr. Yoshiro Tsuzuki for his help in carrying out the preparation of the X-ray powder pattern, to Dr. Chuzo Iida for his spectrographic analysis, and to Mr. Tsutomu Sugiura for his help in the collection of samples.

BULLETIN OF THE CHEMICAL SOCIETY OF JAPAN VOL. 39 516—521 (1966)

Free Radical Reactions in Organic Electrode Processes. II. The Anodic Aroyloxylation of Anisole*

By Kikuhiko KOYAMA, Kunihisa YOSHIDA and Shigeru TSUTSUMI

Department of Chemical Technology, Faculty of Engineering, Osaka University, Miyakojima-ku, Osaka

(Received July 1, 1965)

Electrolyses of an acetonitrile solution of benzoic acid containing triethylamine have been carried out in the presence of anisole by the use of a platinum anode in an undivided cylindrical glass cell under various conditions. The electrolysis with benzoic acid at 15—23°C gave *o*- and *p*-methoxyphenyl benzoates (60%) as the main products, but the *m*-isomer could not be detected. The ratio of the isomers was 2 (*ortho*) : 1 (*para*). The other products identified in this experiment were carbon dioxide and biphenyl. The yield of the benzoates decreased when the electrolysis temperature was raised. The peaks of carbon dioxide and biphenyl on the vapor phase chromatograms in the experiment at 84°C, on the contrary, were relatively large compared with that observed in the low temperature electrolysis. Analogous products were obtained from the electrolysis of both *p*-toluic and *p*-anisic acids. These results have been compared with those obtained from the thermal decomposition of diaroyl peroxide in anisole. The mechanism of this anodic aroyloxylation of anisole has also been discussed.

It has been widely accepted that the anodic oxidation of carboxylate anions, generally known as the Kolbe electrolysis, proceeds via the direct formation of free radicals by the discharge of the carboxylate anions:[1,2]

$$RCOO^- \rightarrow RCOO\cdot + e \quad (1)$$

$$RCOO\cdot \rightarrow R\cdot + CO_2 \quad (2)$$

$$2R\cdot \rightarrow R\text{-}R \quad (3)$$

As a characteristic reaction of free radicals, the above sequence involves only the radical decomposition (Eq. 2) and the coupling reaction (Eq. 3). One might, however, expect that, when suitable conditions are employed, these intermediate radicals would react through the more varied processes observed in the other free radica reactions.[3] Indeed, this expectation has been partially realized in some studies.

It has already been suggested that the formation of some non-dimeric hydrocarbons could arise from either disproportionation or hydrogen abstraction from a solvent.[4] Evidence that the electrolysis of some carboxylates affords products which might be formed through a rearrangement of intermediate radicals has been provided by several groups of workers.[5,6]

Recently, Corey and his co-workers[7] have shown that electrolytically-generated aliphatic radicals readily undergo further oxidation to carbonium

* Presented at the 16th Annual Meeting of the Chemical Society of Japan, Tokyo, April, 1963.

1) M. J. Allen, "Organic Electrode Processes," Reinhold Publishing Corporation, New York (1958), p. 97.

2) B. C. L. Weedon, "Advances in Organic Chemistry," Vol. 1, Interscience Publishers, Inc., New York (1960), p. 3.

3) C. Walling, "Free Radicals in Solution," John Wiley & Sons, Inc., New York (1957), p. 31.

4) Ref. 3, p. 581.

5) Breederveld and Kooyman, *Rec. Trav. chim.*, **76**, 297 (1957).

6) P. J. Bunyan and D. H. Hey, *J. Chem. Soc.*, **1962**, 324.

7) E. J. Corey and R. R. Sauers, *J. Am. Chem. Soc.*, **81**, 1743 (1959); E. J. Corey, N. L. Bauld, R. T. La Londe, J. Casanova, Jr. and E. T. Kaiser, ibid., **82**, 2645 (1960).

TABLE I. ELECTROLYSES OF *p*-SUBSTITUTED BENZOIC ACIDS (0.075 mol.) IN THE PRESENCE OF ANISOLE (0.46 mol.)

Solvent: Acetonitrile (30 ml.)[a]
Electrodes: Pt-Foils (3×2 cm.; gap, about 5 mm.)

Substituent at *p*-position	Electrolysis-conditions				Acid not recovered mol.	Products					
	Temp. °C	Current amp.	Voltage V.	Time hr.		Methoxyphenyl esters		Biphenyls	Polymeric residue g.	Gases	
						Yield %	Ratio *o*-/*p*-			H_2	CO_2
H	15—23	0.33—0.05	83—100	41.5	0.072	60	2/1	T**	13.2	M*	T
H	84	0.3—0.08	55—98	59	0.049	42	2/1	T		M	T
CH_3	12	0.1—0.03	90—100	245	0.07	52	3/2		12.7	M	T
CH_3	10	0.1	50—99	66	0.055	34.7	3/2			M	T
CH_3O	8—12	0.1	40—95	100	0.054	13.5	3/2			M	T

a) Triethylamine (1.5 ml.) was added into the solvent, except for the experiment with *p*-anisic acid. In the case of *p*-anisic acid, 4 ml. of triethylamine was used.
* M: major ** T: trace

ions, which then attack the solvent.

In addition to the findings described above, the free radicals produced in the Kolbe electrolysis are capable of attacking organic substrates, giving rise to either an addition to double bonds or a substitution on aromatic nuclei. Interesting attempts to use the Kolbe electrolysis as a source of free radicals for the additive dimerization of dienes and for the polymerization of vinyl monomers have been made by many investigators.[8-11] The anodic acetoxylation and methylation of aromatic compounds, which takes place when acetate anions are subjected to electrolysis in the presence of the aromatic compounds, have previously been reported,[12-14] even though further attention has not yet been devoted to these substitutions.

On the other hand, analogous aromatic substitutions occur during the course of the decomposition of diacyl peroxides in aromatic solvents, the thermal decomposition of some lead tetracarboxylates in aromatic compounds, and the reaction of the complexes formed from a dry silver salt of a carboxylic acid and a halogen, with aromatic compounds, and it is well recognized that these compounds could readily undergo breakdown into acyloxy and hydrocarbon radicals, which then participate in aromatic substitutions.[15]

It thus becomes desirable to compare the products of the Kolbe electrolysis, which was carried out in the presence of an aromatic compound, with those of the decomposition of the corresponding diacyl peroxides in the aromatic solvent; we can thus extend our knowledge of the characteristics of the electrochemically-generated free radicals.

The present investigation will deal with the electrolysis of a salt of some aromatic acids in the presence of anisole, not merely because of the high availability of data on the decomposition of dibenzoyl peroxide in anisole, but also because of the paucity of information on the electrochemical behavior of aromatic acids.

Results and Discussion

The electrolyses which will now be reported on were carried out under various conditions in a mixture of anisole and acetonitrile containing triethylamine. Two platinum foil electrodes were used; a detailed description of the apparatus was given in a previous paper.[13]

In all cases, the mixtures became brownish, and a sticky non-conducting polymer was frequently deposited on the anode. The current, therefore, was gradually decreased until the end of the electrolysis.

The gaseous products evolved during these electrolyses were analyzed by vapor-phase chromatography, while the liquid products were generally treated as will be described below. After the electrolyzed mixtures were worked up to remove the solvents and recover the acids, the oils remaining were distilled under reduced pressure, and the distillates were chromatographed on alumina and/or treated with alcoholic potassium hydroxide. Qualitative and quantitative determinations of phenolic isomers and neutral fractions obtained from the hydrolysis products were carried out by vapor-phase chromatography, and the acidic fractions were characterized by mixed-melting-point measurements. The crystals isolated by column chromatography were identified as the esters

8) R. V. Lindsey, Jr., and M. L. Peterson, ibid., **78**, 2073 (1956).
9) W. Smith and H. G. Gilde, ibid., **81**, 5325 (1959).
10) W. Smith and H. G. Gilde, ibid., **82**, 659 (1960).
11) S. Goldschmidt and E. Stöckl, *Chem. Ber.*, **85**, 630 (1952).
12) C. L. Wilson and T. Hayashi, Abstracts of papers presented at the 126th Meeting of the American Chemical Society, New York, N. Y., 1954, p. 78—O.
13) K. Koyama, Y. Odaira and S. Tsutsumi, *Technol. Repts. Osaka Univ.*, **12**, 463 (1962).
14) L. F. Fieser, R. C. Clapp and W. H. Daudt, *J. Am. Chem. Soc.*, **64**, 2052 (1942).
15) G. H. Williams, "Homolytic Aromatic Substitution," Pergamon Press, Oxford (1960), pp. 41—42.

themselves by the usual methods.

The results obtained with benzoic, *p*-toluic and *p*-anisic acids are summarized in Table I. Percentage yields, based on the amount of the acid not recovered at the end of the electrolysis, are given for those products which were isolated quantitatively.

As has been indicated above (Table I), the major products in each experiment were *o*- and *p*-methoxyphenol esters of the corresponding aromatic acids; no *m*-isomers could be detected. The proportions of the isomers were nearly 2(*ortho*) to 1(*para*) with benzoic acid, and 3(*ortho*) to 2(*para*) with *p*-toluic and *p*-anisic acids.

From the results of the experiment with benzoic acid, it is evident that the extent of such anodic benzoyloxylation decreases when the temperature is raised to 84°C even though the value for the isomer distribution still remains constant. It might be expected that benzene, biphenyl, methoxybiphenyls and/or phenyl benzoate would be formed, either by the attack of phenyl radicals on the anisole or by the radical-recombination reaction. There was, however, no evidence for the presence of these products, except for the biphenyl, in our present studies with benzoic acid. In addition to the above observations, the formation of 1, 2-diphenoxyethane and phenoxymethylanisoles could not be observed in these electrolyses.

The gases evolved from these electrolyses consisted of hydrogen, accompanied by a trace of carbon dioxide.

The peak of carbon dioxide on the vapor phase chromatogram in the experiment with benzoic acid at 84°C, was relatively large compared with that observed in low temperature electrolysis.

The results thus obtained indicate that the high temperature electrolysis led to the decomposition of benzoyloxy radicals into carbon dioxide and phenyl radicals, which subsequently dimerized to give biphenyl as a normal Kolbe product.

In all cases, a considerable amount of polymeric residues was obtained. Although further treatment of the residues was unsuccessful because of their low solubility in usual organic solvents, their infrared spectra indicated the presence of both methoxyl and phenyl groups.

Results similar to those with benzoic acid were obtained in the experiments with *p*-toluic and *p*-anisic acids, except that both the yield of the esters and the value for the isomer distribution slightly varied. However, the differences in the isomer distribution are insignificant since the figures based on the peak area on the vapor-phase chromatograms admit some allowances in their calculations.

The results described herein exhibit a striking contrast to those obtained from the decomposition of dibenzoyl peroxide in anisole.[16-19] It may be suggested, in principle, that the radicals from dibenzoyl peroxide, both benzoyloxy and phenyl radicals, attack the aromatic substrates, giving rise to either the benzoyloxylation or the phenylation of aromatic nuclei. Both reactions, as a matter of course, have been observed in the homolytic aromatic substitutions. However, the extent of benzoyloxylation is generally small, especially with simple and monosubstituted aromatic compounds, since benzoyloxy radicals appear to be considerably less reactive entities than phenyl radicals in aromatic substitution.

Recently, Lynch and Moore[19] have found that the homolytic benzoyloxylation of anisole with dibenzoyl peroxide, which had been neglected in previous works, occurred to an appreciable extent at 80°C, even though phenylation still proceeded as the main reaction.

The predominance of benzoyloxylation over the phenylation in our experiment clearly indicates the characteristics of the anodically-generated benzoyloxy radical. An explanation for such an anomalous stability of benzoyloxy radicals is provided by the facts that this radical is generated at the anode, at a comparatively low temperature, and that biphenyl is only product which was formed with phenyl radicals by their coupling reaction. These facts imply that the anodically-produced benzoyloxy radicals are stabilized and suppressed to undergo their rapid decarboxylation by adsorption on the electrode surface, and that their subsequent reactions take place only on the electrode surface.

If free benzoyloxy radicals existed in a bulk solution during these electrolyses, a considerable amount of methoxybiphenyls would be produced through the spontaneous decomposition of the benzoyloxy radicals.

Furthermore, it may be assumed that the formation of biphenyl arose from the coupling of the phenyl radicals which were adsorbed on the electrode or which existed in the original solvent cage, since it seems that biphenyl and phenyl benzoate are formed by the "cage" recombination reaction of the radicals generated by the decomposition of dibenzoyl peroxides.[20]

The question may be raised, then, of how such stabilized benzoyloxy radicals react with anisole to afford methoxyphenyl benzoates. The recent work by Zweig et al.[21] has indicated that anisole can also be polarographically oxidized, with the

16) T. Suehiro, *J. Chem. Soc. Japan, Pure Chem. Sect.*, (*Nippon Kagaku Zassi*), **72**, 301 (1951).
17) C. S. Rondestvedt and H. S. Blanchard, *J. Org. Chem.*, **21**, 229 (1956).
18) D. R. Augood and G. H. Williams, *Chem. Revs.*, **57**, 123 (1957).
19) B. M. Lynch and R. B. Moore, *Canadian J. Chem.*, **40**, 1461 (1962).
20) C. G. Swain, L. J. Schaad and A. J. Kresge, *J. Am. Chem. Soc.*, **80**, 5313 (1958).
21) A. Zweig, W. G. Hodgson and W. H. Jura, ibid., **86**. 4124 (1964).

values of +1.76 V. (vs. SCE) and 19.4 μamp./mmole for the half-wave potential and the diffusion current respectively, to produce its cation radical in acetonitrile. Their finding will help provide an explanation of this question. It may suggest that the occurrence of the simultaneous oxidation of anisole molecules with benzoate anions would result in the facile attack of adsorbed benzoyloxy radicals on anisole cation radicals, which are produced by the loss of an electron from anisole at the anode, leading to the predominant formation of methoxyphenyl benzoates.

There is, as yet, an unsolved problem concerning the isomer distribution. The observed isomer distribution in this reaction is analogous to those in the anodic acetoxylation of anisole[12] and the benzoyloxylation with dibenzoyl peroxide,[19] in which no *m*-isomer could be detected and *ortho-para* orientation has been observed to be preferred. The predominance of *o*- and *p*- positions in this anodic substitution appears to be partly due to the polar character of the benzoyloxy radicals. The benzoyloxy radical, that is, seems to be an electrophilic species, it may thus be expected to attack preferentially the points of high electron density in the anisole.

However, a more satisfactory explanation for the orientation in this substitution will be given by the assumption that the coupling reaction of a benzoyloxy radical with an anisole cation radical will occur at the positions of high spin density in the cation radical. Lynch and Moore have already proposed the analogous coupling for the ortho benzoyloxylation of anisole with dibenzoyl peroxide[19]; i. e.:

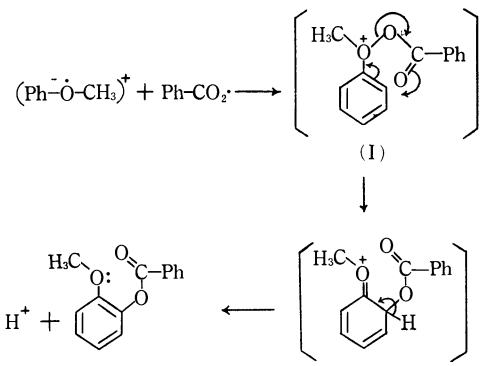

Furthermore, Zweig's calculation[21] of the spin densities for the ring and oxygen positions of the anisole cation radical affords abundant evidence in support of our assumption. The values of the spin density for each position are shown in Fig. 1.

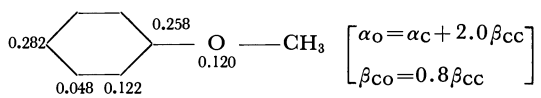

Fig. 1. The spin densities of the anisole cation radical.[21]

Although a high spin density on the substituted carbon atom in the benzene ring appears in their calculation, the possibility of the coupling at this position is very small because of the unfavorable steric requirement of this coupling or because of the low stability of a σ-complex (II) if one is formed in the transition state for this reaction.

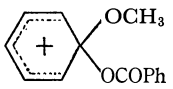

(II)

Accordingly, *o*- and *p*-methoxyphenyl benzoates would be formed by either process, a direct attack of benzoate radicals on *o*- and *p*-positions of the cation radical or a cyclic rearrangement of the indirect coupling intermediate (I), as has been suggested by Lynch et al.

On the basis of the argument described above, the most probable scheme for this anodic aromatic substitution may be shown thus:

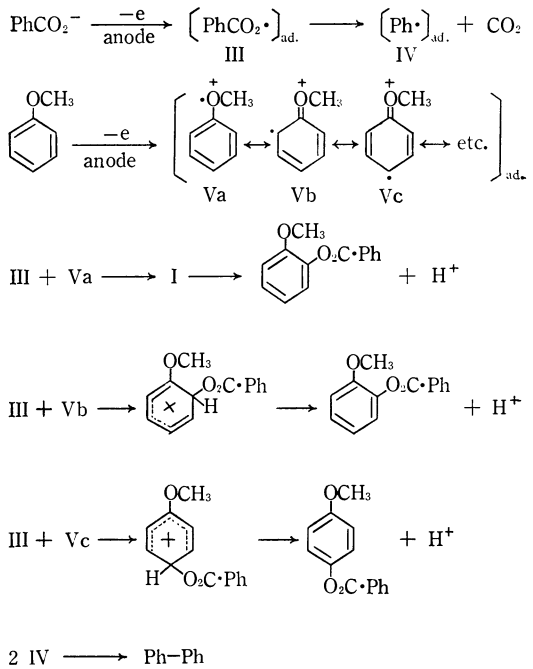

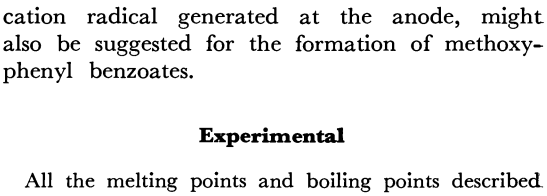

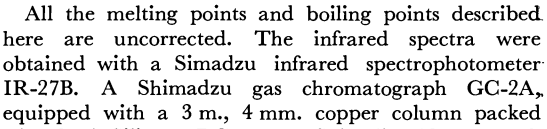

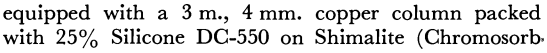

However, another mechanism, one involving the reaction of a benzoate anion with an anisole cation radical generated at the anode, might also be suggested for the formation of methoxyphenyl benzoates.

Experimental

All the melting points and boiling points described here are uncorrected. The infrared spectra were obtained with a Simadzu infrared spectrophotometer IR-27B. A Shimadzu gas chromatograph GC-2A, equipped with a 3 m., 4 mm. copper column packed with 25% Silicone DC-550 on Shimalite (Chromosorb P) was employed for the analysis of the phenolic and

neutral fractions; it was operated at 180°C, using hydrogen as a carrier gas. A vapor-phase chromatogram of the gaseous products was also obtained on the same instrument equipped with a 0.5 m., 4 mm. silica gel column, which was operated at 13°C. The carrier gas was nitrogen.

Electrolyses were carried out in a cylindrical cell fitted with a condenser; two platinum foil electrodes (3×2 cm.; gap about 5 mm.) were also used. During the electrolyses, the cell was cooled in a bath of cold water containing ice to control the temperature, and the contents were stirred magnetically.

Materials.—Commercially-available aetonitrile was dried over anhydrous magnesium sulfate and distilled (b. p. 81°C). Triethylamine was dried over potassium hydroxide and distilled. Anisole was washed with a 10% aqueous sodium hydroxide soultion and then with water, dried over calcium chloride, and distilled before use (b. p. 155°C). Benzoic, *p*-toluic and *p*-anisic acids were obtained commercially and used without further purification.

The Electrolysis of the Ammonium Salt of Benzoic Acid in the Presence of Anisole.—A solution of benzoic acid (9.2 g., 0.075 mol.) and anisole (50 ml., 0.46 mol.) in acetonitrile (30 ml.) containing triethylamine (1.5 ml.) was electrolyzed at 15—23°C, with an applied potential of 83—100V. for 41.5 hr. at a current of 0.33—0.05 amp.; the solution thus became slightly alkaline. The current was gradually decreased from 0.33 to 0.05 amp.; 0.47 faraday had been passed through the solution by the end of the electrolysis.

The acetonitrile was removed from the electrolyzed solution under reduced pressure, and the residue was dissolved in ether. The ethereal solution was then extracted with a saturated aqueous sodium hydrogen carbonate solution, washed with 10% hydrochloric acid and then with water, dried over anhydrous magnesium sulfate, filtered, and evaporated to yield 54.3 g. of a brownish residual oil.

When the aqueous solution was acidified with 10% hydrochloric acid, 0.3 g. of the unchanged benzoic acid was recovered. The residual oil, distilled under reduced pressure, gave the following fractions:

Fraction I: b. p. 58°C/15 mmHg, 30.8 g.

Fraction II: b. p. 148—154°C/2.5 mmHg, 10.3 g.

Residue: 10.2 g.

Fraction I consisted of anisole, which was identified by vapor-phase chromatography.

The infrared spectrum of Fraction II indicated the presence of benzoates. Thus, a portion (5 g.) of Fraction II was heated under reflux with 5% potassium hydroxide in ethanol for 16 hr. After the ethanol had been removed, the residue was acidified and extracted twice with ether. The combined extracts were worked up in the usual manner in order to separate them into acidic, phenolic and neutral fractions.

From the acidic fraction, 2.3 g. of the crude benzoic acid was obtained and recrystallized from benzene. The acid melted at 119.5—121°C (lit.[22] m. p. 122.4°C); the melting point was undepressed on admixture with an authentic sample. Moreover, the infrared spectrum of the acid (KBr disk) was essentially identical with that of authentic benzoic acid.

The phenolic fraction (2.4 g.) displayed two peaks with the same retention times as those of authentic *o*- and *p*-methoxyphenols on a vapor phase chromatogram; the ratio of the isomers was determined by an internal standard method to be 2 (*ortho*): 1(*para*). Moreover, the infrared spectrum of this fraction (liquid film) exhibited absorption bands at 733, 745, 825, 1022, 1037, 1105, 1150, 1175, 1220, 1260, 1300, 1380, 1440, 1450, 1510, 1600 and 3400 cm^{-1}. These absorption bands can easily be assigned to the *o*- and *p*-methoxyphenols respectively. If the phenolic fraction contained the *m*-isomer, it should show the additional absorption bands at 690, 770, 1160, 1200, 1290, 1500 and 1600 cm^{-1} in its infrared spectrum.

The neutral fraction (0.2 g.) obtained from the hydrolysis product of Fraction II displayed three peaks on a vapor-phase chromatogram. One of them had the same retention time as biphenyl, but this peak was relatively small compared to the other ones. No further attempts were made to determine the products which correspond to the other peaks. It is, however, evident that 1, 2-diphenoxyethane, phenoxymethylanisoles and methoxybiphenyls were not major constituents of this fraction. The fraction, however, displayed major absorption peaks in the infrared spectrum at 700, 755, 1025, 1228, 1450, 1600, 2860 and 3200 cm^{-1} (liquid film).

The remaining portion (5.3 g.) of Fraction II was chromatographed on alumina and eluted with benzene to afford two crude solids after the solvent had been removed. The solid rapidly eluted was recrystallized from ethanol and gave a white crystal (2.3 g.; m. p. 57—58°C, undepressed by admixture with *o*-methoxyphenyl benzoate prepared by an entirely different method). The infrared specturm (KBr disk) was essentially identical with that of an authentic sample.

Found: C, 73.63; H, 5.14. Calcd. for $C_{14}H_{12}O_3$: C, 73.67; H, 5.30%.

The recrystallization of the slowly-eluted solid from ethanol gave a white crystal (1.5 g.), m. p. 87.5—88.1°C; the melting point of this crystal was not depressed on admixture with *p*-methoxyphenyl benzoate. The infrared spectrum (KBr disk) was identical with that of an authentic sample.

Found: C, 73.62; H, 5.64. Calcd. for $C_{14}H_{12}O_3$: C, 73.67; H, 5.30%.

The brownish polymeric residue was insoluble in ether and ethanol, but slightly soluble in acetone and benzene. The infrared spectrum exhibited characteristic absorption bands which could be assigned to the methoxyl group and to the aromatic ring.

A vapor-phase chromatographic analysis indicated that the gaseous product consisted mainly of hydrogen, plus a trace of carbon dioxide.

The Electrolysis of the Benzoate Anion in the Presence of Anisole at a High Temperature.—The electrolysis was carried out at 84°C, with an applied potential of 55—98 V., at a current of 0.1—0.3 amp., for 59 hr. The results obtained from this electrolysis are summarized in Table I.

The peaks of carbon dioxide and biphenyl on the vapor-phase chromatograms were relatively large compared with those observed in a low-temperature electrolysis.

The Electrolysis of the Triethylammonium Salt of *p*-Toluic Acid in the Presence of Anisole.—A solution of *p*-toluic acid (10.2 g., 0.075 mol.) and

22) "The Merck Index" (seventh edition), Merck & Co., Inc., New Jersey (1960), p. 133.

anisole (50 ml., 0.46 mol.) in acetonitrile (30 ml.) containing triethylamine (1.5 ml.) was electrolyzed at 10°C, for 66 hr. A current of 0.1 amp. was maintained, while the voltage was varied from 50 to 99 V. By the end of electrolysis, about 0.25 faraday had been passed through the solution.

The procedure used for the isolation and the identification of the product was identical with that described in the experiment with benzoic acid.

After the work-up of the electrolyzed mixture, 2.6 g. of *p*-toluic acid was recovered. The distillation of the remaining oil under reduced pressure gave unreacted anisole (ca. 24.3 g.), a fraction (4.7 g.), b. p. 160—166°C/2.7 mmHg, and a residue.

The hydrolysis of 3.5 g. of the high-boiling fraction with 5% potassium hydroxide in ethanol for 20 hr. afforded an acid (1.7 g.), phenols (1.6 g.) and neutral substances (0.3 g.). The acid was characterized as *p*-toluic acid, m. p. 179—180.5°C, undepressed on admixture with an authentic sample. The infrared spectrum of the acid was identical with that of the authentic sample. The phenols were shown to be *o*- and *p*-methoxyphenols by vapor-phase chromatography; the ratio of these isomers was found to be 3 (*ortho*): 2 (*para*).

In addition, two crystals were isolated by chromatography; they were identified as *o*- and *p*-methoxyphenyl *p*-toluates.

The melting point of *o*-methoxyphenyl *p*-toluate was 75—76°C; infrared spectrum (KBr disk): 750, 835, 1020—1035 (2 bands), 1065, 1100, 1160, 1265, 1450, 1490, 1600 and 1710 cm^{-1}.

Found: C, 74.03; H, 5.91. Calcd. for $C_{15}H_{14}O_3$: C, 74.36; H, 5.83%.

The infrared spectrum of *p*-methoxyphenyl *p*-toluate, m. p. 95.5—96.5°C, exhibited characteristic bands at 835, 1025, 1035, 1065, 1100, 1165, 1200, 1265, 1450, 1500, 1600 and 1715 cm^{-1} (KBr disk).

Found: C, 74.27; H, 6.08. Calcd. for $C_{15}H_{14}O_3$: C, 74.36; H, 5.83%.

The Electrolysis of the Triethylammonium Salt of *p*-Anisic Acid in the Presence of Anisole. —A solution of *p*-anisic acid (11.4 g., 0.075 mol.) and anisole (50 ml., 0.46 mol.) in acetonitrile (30 ml.) containing triethylamine (4 ml.) was electrolyzed at 8—12°C, for 100 hr. The current was maintained at 0.1 amp., while the voltage was increased from 40 to 95 V.

After the electrolysis, unchanged anisic acid (3.1 g.) was recovered. The residual oil was distilled under reduced pressure to give the following fractions:

Fraction I: b. p. 46°C/11 mmHg, 23.4 g.

Fraction II: b. p. 92—181°C/3 mmHg, 2.1 g.

Residue: 9.4 g.

Fraction I was shown by vapor-phase chromatography to consist of anisole. A portion (0.8 g.) of Fraction II was submitted to hydrolysis. An acidic fraction obtained from the hydrolysis product consisted of *p*-anisic acid (0.4 g.), m. p. and m. m. p. 184°C. The infrared spectrum was identical with that of an authentic sample.

The phenolic fraction (0.4 g.) was found to be a mixture of *o*- and *p*-methoxyphenols (3 : 2 ratio).

Seven peaks were indicated on the vapor-phase chromatogram of the neutral fraction (0.1 g.) separated from the hydrolysis product, but this fraction could not be further identifed.

The Preparation of Authentic Samples. — Methoxybiphenyls were prepared by Gomberg's method,[23] and *o*- and *p*-methoxyphenyl benzoates were prepared by the reaction of benzoyl chloride with the corresponding methoxyphenols. 1, 2-Diphenoxyethane was prepared according to the directions of Drahowzal et al.[24] The syntheses of authentic phenoxymethylanisoles were carried out by the method of Claisen.[25]

23) W. E. Bachmann and R. A. Hoffman, "Organic Reactions," Vol. 2, John Wiley & Sons, New York (1944), p. 224.

24) F. Drahowzal and D. Klanann, *Chem. Abstr.*, **46**, 8036 (1952).

25) L. Claisen, *Annal.*, **442**, 244 (1925).

BULLETIN OF THE CHEMICAL SOCIETY OF JAPAN VOL. 29 521—524 (1966)

The Temperature Dependence of the Radio-Frequency Polarographic Wave Height

By Tomihito KAMBARA and Shogo WATARAI

Department of Chemistry, Faculty of Science, Hokkaido University, Sapporo

(Received July 1, 1965)

When the radio-frequency polarographic current, i_{RF}, is regarded approximately as the difference between the Fournier current and the ordinary DC polarographic current, i_{DC}, one can elucidate the temperature dependence of i_{RF}. It may be theoretically predicted that the relative temperature coefficient of i_{RF} for the completely-reversible system is less by 0.66% than that of i_{DC}. The plot of log $(i_{RF} \cdot T^2)$ against $1/T$, where T is the absolute temperature, gives two straight lines which join each other at a knick, coresponding to the transition from a completly reversible process to a less reversible one. Experiments with thallium(I) and zinc(II) ions in various supporting electrolytes reveal the essential validity of the present theory.

It was reported in our previous study[1] that the AC polarographic peak heights of the zinc ion in various supporting electrolytes, therefore with varying reversibilities, show different temperature dependencies. In the present study the effect of the temperature on the radio-frequency (R-F) polarographic wave heights observed with various redox systems will be investigated.

Theoretical

The R-F polarographic method developed by Barker[2,3] and the theoretical treatment of the Faradaic rectification developed by several authors[4-9] offer many complicated problems. Because of the mathematically-complicated expression for the R-F polarographic process, we will here employ the simplified concept suggested by Yasumori[10] that, during the half-period of R-F modulation, the electrolytic current observed is the Fournier current,[11] while the signal recorded in R-F polarography is the Fournier current minus the ordinary DC polarographic current, i_{DC}, as is illustrated in Fig. 1.

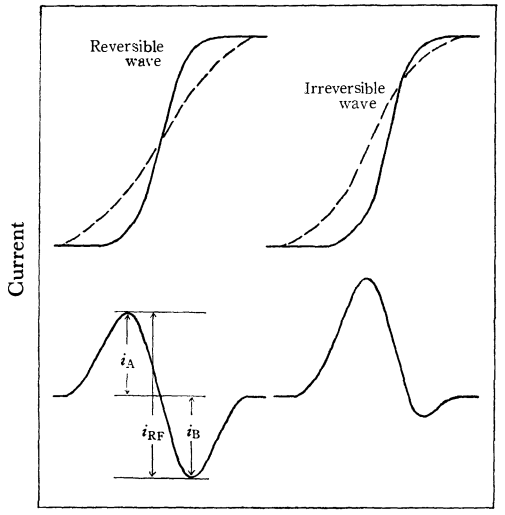

Fig. 1. Relation between the ordinary DC polarographic wave (full line), the Fournier polarogram (dashed line) and the R-F polarogram. (The construction method for evaluating the R-F wave heights, i.e. i_A, i_B and i_{RF}, are also schematically illustrated.)

Applying the Senda-Tachi[12] theory for the Fournier polarogram, one can derive the following expressions for a reversible system:

$$i_{DC} = j_0 i_d = \frac{i_d}{2}(1-\tanh x) \tag{1}$$

$$x = \frac{nF(E-E_{1/2})}{2RT} \tag{2}$$

$$i_F = i_{DC} + \frac{i_d}{4}\left(\frac{nF}{2RT}\right)^2 \frac{d^2 j_0}{dx^2} \Delta E^2 \tag{3}$$

$$i_{RF} = i_F - i_{DC} = \frac{i_d}{4}\left(\frac{nF}{2RT}\right)^2 \frac{d^2 j_0}{dx^2} \Delta E^2$$

$$= \frac{i_d}{4}\left(\frac{nF}{2RT}\right)^2 \Delta E^2 \frac{\sinh x}{\cosh^3 x} \tag{4}$$

In these equations, i_d is the DC diffusion current and ΔE the amplitude of the R-F voltage; the other symbols have their usual meanings.

The maximum and minimum in the R-F polarogram are obtained by solving $di_{RF}/dE = 0$ at:

$$x = \pm\frac{1}{2}\ln(2+\sqrt{3}) = \pm 0.6584 \tag{5}$$

Thus, it is found that:

$$i_{RF} = k \cdot i_d \cdot T^{-2} \cdot \Delta E^2 \tag{6}$$

where k is the proportionality factor. On the other hand, one has:

$$i_d \propto D^{1/2} \tag{7}$$

$$D = D_0 \cdot \exp\frac{-\Delta H_D}{RT} \tag{8}$$

where ΔH_D is the activation heat of diffusion.

Hence, it may be seen that:

$$\frac{1}{i_{RF}} \cdot \frac{di_{RF}}{dT} = \frac{1}{i_d} \cdot \frac{di_d}{dT} + \frac{2}{T} \tag{9}$$

It is thus expected that, for the completely reversible electrode process the R-F wave height would have a relative temperature coefficient less by 0.66% than that of the ordinary DC step height. Further, the plot of $\log(i_{RF}T^2)$ vs. $1/T$ would give a straight line in the reversible region.

Experimental

A Yanagimoto polarograph, type PF-500, was used; the radio frequency was 455 kC, and the square-wave frequency was 200 c. p. s.

1) T. Kambara and K. Kunimatsu, *Rev. Polarog. (Kyoto)*, **13**, 14 (1965).
2) G. C. Barker, *Anal. Chim. Acta*, **18**, 118 (1958).
3) G. C. Barker, "Transactions of the Symposium on Electrode Processes, Philadelphia, 1959," Ed. by E. Yeager, Wiley, New York (1961), pp. 325—365.
4) P. Delahay, M. Senda and C. H. Weis, *J. Am. Chem. Soc.*, **83**, 312 (1961).
5) M. Senda and P. Delahay, ibid., **83**, 3763 (1961).
6) P. Delahay, "Advance in Electrochemistry and Electrochemical Engineering," Vol. I, Interscience-Wiley, New York (1961), pp. 279—300.
7) H. Imai, *Rev. Polarog. (Kyoto)*, **10**, 209 (1962).
8) H. Schmidt and M. von Stackelberg, "Neuartige polarographische Methoden—ihr Prinzip und ihre Möglichkeiten," Verlag Chemie, Weinheim (1962); "Modern Polarographic Methods," English translation by R. E. W. Maddison, Academic Press, New York (1963).
9) B. Breyer and H. H. Bauer, "Alternating Current Polarography and Tensammetry," Interscience, New York (1963).
10) Y. Yasumori, M. Kurosaki and T. Nishimura, *Yakushinsuru Kiki (Yanagimoto Instr. Rev.)*, **6**, No. 3, 14 (1961).
11) M. Fournier, *Compt. rend.*, **232**, 1673 (1951).
12) M. Senda and I. Tachi, This Bulletin, **28**, 632 (1955).

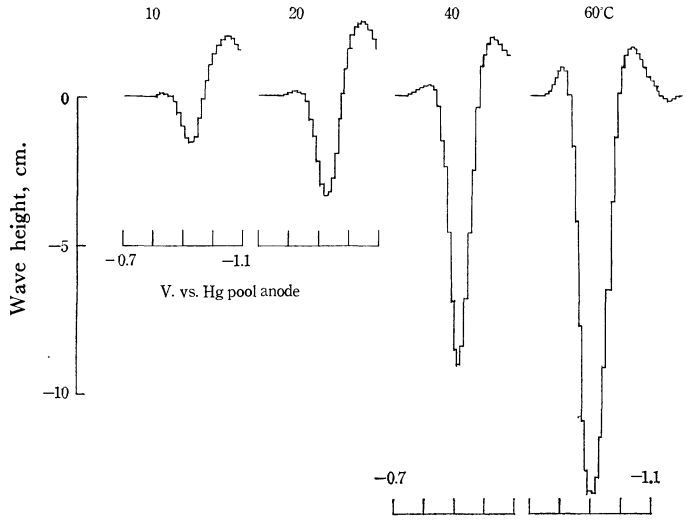

Fig. 2. R-F polarograms of 10^{-4} M Zn^{2+} in 1 M KCl at various temperatures.

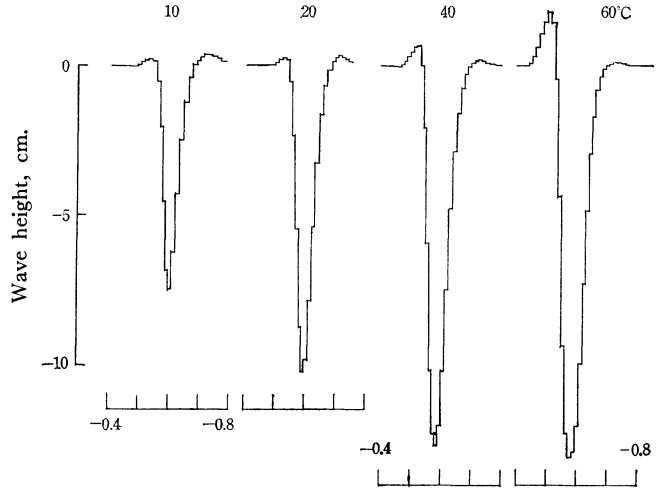

Fig. 3. R-F polarograms of 5×10^{-5} M Zn^{2+} in 1 M KI at various temperatures.

Table I. Relative temperature coefficient of the R-F polarographic wave height in percent

Absolute temp. T°K	10^{-4} M Zn^{2+} in 1 M KCl	10^{-4} M Zn^{2+} in 1 M KBr	5×10^{-5} M Zn^{2+} in 1 M KI	10^{-4} M Tl^{+} in 1 M KCl
283	7.6	6.5	3.9	4.3
293	6.4	5.9	2.1	2.6
303	5.0	4.1	1.2	1.8
313	4.2	1.7	0.6	1.1
323	1.7	0.6	0.5	0.6
333	1.0	0.3	0.3	0.4

The drop time was controlled to about 4 sec. at a constant mercury level, and the low frequency current was gated to a time interval from 2 to 3 sec. for each drop. The R-F voltage was 5 V., and the amplifier and recorder sensitivities were kept to 0.1.

Results

Figures 2 and 3 show some examples of the R-F polarograms recorded. The wave hieghts are plotted against the temperature in Fig. 4; the temperature coefficient is summarized in Table I. In Fig. 5 $\log(i_{RF}T^2)$ is plotted against the reciprocal of the absolute temperature.

Discussion

The temperature corresponding to the knick in the plot of $\log(i_{RF}T^2)$ vs. $1/T$ would indicate the transition of the rate-determining step from diffusion to electron-transfer. The transition temperature, as evaluated with AC peak heights

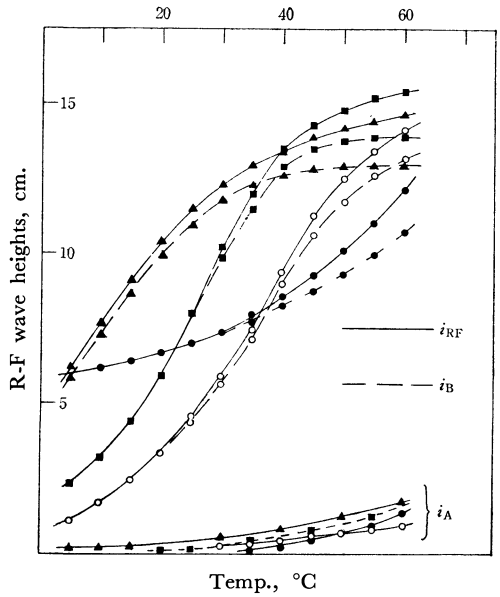

Fig. 4. R-F wave heights plotted against the temperature.

○ Zn^{2+} in KCl; ■ Zn^{2+} in KBr; ▲ Zn^{2+} in KI; ● Tl^{+} in KCl (Cf. Fig. 1 and Table I)

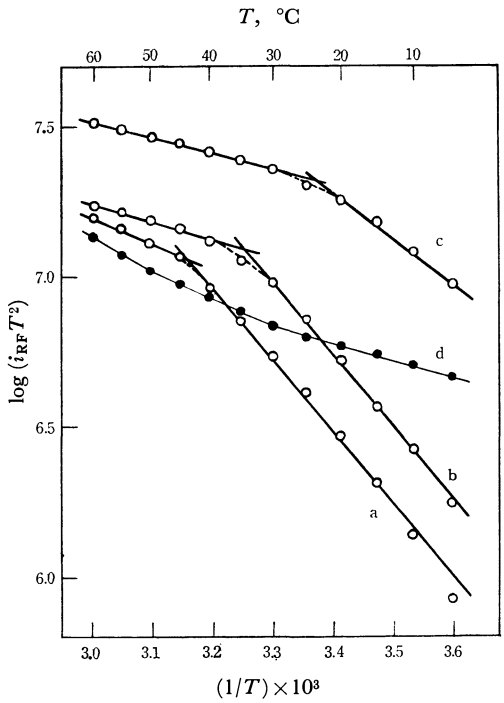

Fig. 5. log ($i_{RF}T^2$) vs. $1/T$.

a Zn^{2+} in KCl; b Zn^{2+} in KBr; c Zn^{2+} in KI; d Tl^{+} in KCl. In curve c i_{RF} was doubled for purposes of comparison.

in our previous study,[1] coincides well with that obtained by the present R-F method.

As for the R-F wave height of thallium(I), it may be safe to say that, in the temperature region higher than 35°C, another mechanism plays a role and that the temperature coefficient increases more rapidly than expected with an assumption of complete reversibility.

Summary

On the simplified model that the R-F polarographic current is the difference between the Fournier current and the ordinary DC polarographic current, one can clear up the temperature dependence of the R-F wave height. It has been concluded that, in the reversible case, the temperature coefficient of the R-F wave height is less by 0.66% than that of the DC step height. Further, a new method, in which the logarithm of the product of the R-F wave height and the square of the absolute temperature is plotted against the reciprocal of the absolute temperature, has been introduced and examined. In the reversible region the above plot gives a straight line, the slope of which corresponds to that of log i_{DC} plotted against $1/T$. At lower temperatures the reversibility decreases and the above plot shows a break, indicating the transition from a reversible electrode process to an irreversible one.

BULLETIN OF THE CHEMICAL SOCIETY OF JAPAN VOL. 39 525—530 (1966)

Further Study of Syntheses of *dl*-2, 3-Dicarboxycyclopentylacetic Acids

By Kazu KUROSAWA

Department of Chemistry, Faculty of Science, Tohoku University, Katahira-cho, Sendai

and Heitaro OBARA

Department of Applied Chemistry, Faculty of Engineering, Yamagata University, Yonezawa

(Received July 2, 1965)

The assignment of the configuration of racemic *trans-trans* and *cis-cis*-2, 3-dicarboxycyclopentylacetic acid previously proposed has been confirmed by the syntheses of these compounds through other unambiguous reaction sequences. The *trans-cis*-isomer has been prepared by the epimerization of the 3-carboxyl group of the *cis-cis*-isomer, but the attempt to synthesize the fourth isomer (*cis-trans*) has been unsuccessful.

It has been reported that the chromic acid oxidation of tetrahydroanhydrodesoxyaucubigenin (I) gives the optically active *cis-cis*-2, 3-dicarboxycyclopentylacetic acid (IIa) as the key compound for determining the carbon framework of aucubin; from this the *trans-trans* (IIb) and *trans-cis** isomer (IIc) can be derived by the epimerization of either one of two carboxyl groups attached to the cyclopentane ring. Moreover, the stereochemistry of each isomer has been established, along with the chemical properties and the course of formation.[1]

The synthesis of *dl-trans-trans*-tricarboxylic acid (IIb), on the other hand, has been accomplished by one of the present authors[2] starting from the Michael condensation of dimethyl Δ^2-cyclopentene-1, 2-dicarboxylate (III) with diethyl malonate.[3] IIb was transformed to the isomer, the configuration of which has been presumed to be a *cis-cis* relation (IIa) because of its identity with the natural IIa (see below).

The present paper will describe the syntheses of IIa and IIb according to alternative reaction sequences[4] and the isomerization of IIa to IIc.

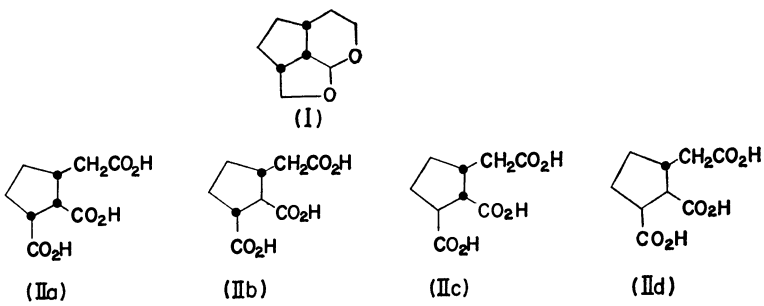

Fig. 1

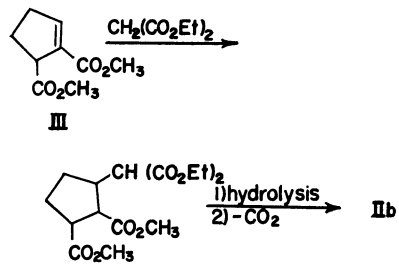

Fig. 2

* In this and other designations in this paper the relationship between two carboxyl groups attached to the cyclopentane ring is given first, and that between the carboxymethyl group and the adjacent carboxyl group, second.

1) a) S. Fujise, H. Obara and H. Uda, *Chem. & Ind.*, **1960**, 289; *J. Chem. Soc. Japan, Pure Chem. Sect.* (*Nippon Kagaku Zasshi*), **81**, 677 (1960). b) H. Uda, ibid., **81**, 1865 (1960).

2) H. Obara, ibid., **81**, 1871 (1960).

3) J. Grimshaw and H. R. Juneja (*Chem. & Ind.*, **1960**, 656) stated, without any evidence, that the migration of the double bond in III took place, giving the Δ^1-isomer, before the addition of diethyl malonate, and that, therefore, the final product was apparently 1, 2-dicarboxycyclopentylacetic acid (IV), not IIb. This possibility, however had already been excluded by the synthesis of IV through an unambiguous route,[2] and unlike III, the Δ^1-isomer undergoes the Michael addition accompanied by a migration of the double bond to the Δ^2-position, giving the same adduct as from III.[2]

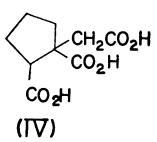

Fig. 3

4) An attempt to prepare IIa by the Dieckmann cyclization of diethyl 3-ethoxycarbonylmethyladipate was unsuccessful. S. Fujise, H. Obara and K. Kurosawa, *J. Chem. Soc. Japan, Pure Chem. Sect.* (*Nippon Kagaku Zasshi*), **82**, 370 (1961).

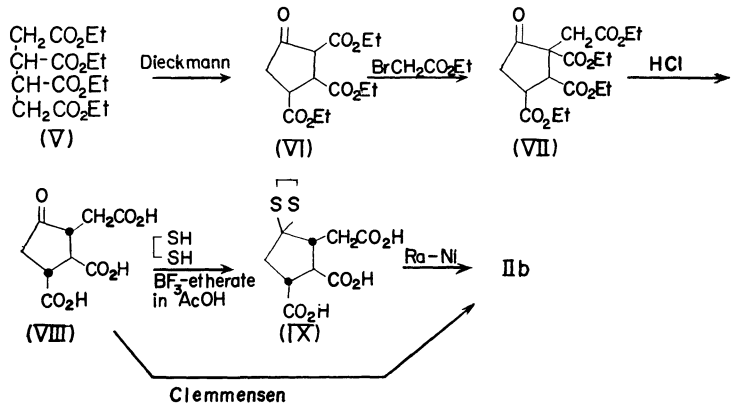

Fig. 4

2, 3, 4 - Triethoxycarbonylcyclopentanone (VI), which appeared to be the most satisfactory precursor for the synthesis of IIb, was prepared from tetraethyl butane-1, 2, 3, 4-tetracarboxylate (V) by the Dieckmann cyclization in a good yield. The condensation of the sodio derivative of VI with ethyl bromoacetate afforded a keto tetraester (VII), b. p. 195—210°C/2 mmHg; then VII was hydrolyzed and decarboxylated to yield 2, 3-dicarboxy-5-oxo-cyclopentylacetic acid (VIII), m.p. 215—216°C, by refluxing it with 6 N hydrochloric acid. The conversion of VIII into IIb was achieved by transforming it into a thioketal (IX) and then subjecting the IX to desulfurization with Raney nickel or directly by the Clemmensen reduction. The IIb thus obtained, m. p. 160°C, was identical with a sample of IIb which had been prepared from III, as has been mentioned above; this was determined by a comparison of the infrared spectra and by a mixed melting point determination. Since three substituents of VIII or of the Michael addition product of III will be preferentially oriented towards sterically less hindered (in another words, thermodynamically more stable) directions in such a strongly basic reaction condition, IIb must have the expected *trans-trans* arrangement.

In a series of experiments on the naturally-derived compounds, the *trans-trans* isomer (IIb), prepared by the epimerization of the triester of the *cis-cis*-tricarboxylic acid (IIa), produced the same dimeric trianhydride (X) as that obtained from IIa, involving the anomalous isomerization of one carboxyl group towards the sterically

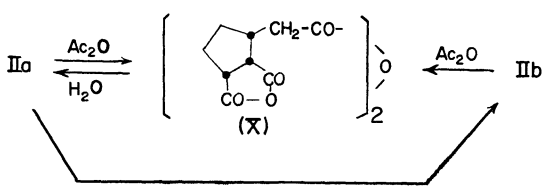

Fig. 5

unfavorable side, upon being treated with boiling acetic anhydride; X returned to IIa on hydrolysis.[1b] This process has been applied to the racemic IIb, giving an isomer.[2] However, there has been no definite evidence about the stereochemistry of this isomer; the assignment of *cis-cis* relationship as in the natural IIa has been tentatively made only on the basis of the course of formation and its identity with the natural IIa. In order to clarify this point, an alternative synthesis of IIa was carried out. The catalytic hydrogenation of the unsaturated lactone ester (XI) afforded the corresponding saturated compound, *cis-cis*-2-(2'-hydroxyethyl)-5-carboxycyclopentylcarboxylic acid δ-lactone (XII), resulting from the *cis* attack of hydrogen on the double bond from the side opposite an allylic substituent.[5] The chromic acid oxidation of XII gave the desired *cis-cis* isomer (IIa), m. p. 176—177°C,[5,6] which was identical with a sample of IIa derived from IIb via the dimeric trianhydride (X) as shown by a study of the infrared spectra and by a mixed melting point determination. These results provide convincing evidence for the correctness of the assumed reaction course from IIb to IIa via X and for the stereochemistry of IIa.

The procedure which was employed in the conversion of the natural IIa to another isomer, IIc,[1b] appeared to be most suitable for the synthesis of the third isomer, *trans-cis*-tricarboxylic acid (IIc). Upon being heated over its melting point, IIa was converted into an anhydride carboxylic acid (XIII) with a loss of water; it was then esterified with diazomethane to yield an anhydride ester (XIV). The methanolysis of XIV, followed by the epimerization of the resulting diester carboxylic acid (XV, R=CH_3), without purification, with sodium methoxide in boiling methanol,

5) For a preliminary communication, see K. Kurosawa and S. Fujise, *Chem. & Ind.*, **1963**, 1688; for a full publication, see K. Kurosawa, H. Obara and H. Uda, This Bulletin, **39**, 530 (1966).

6) The reported melting point of IIa is 161—162°C.[2] A further purified sample melts at 173—174°C.

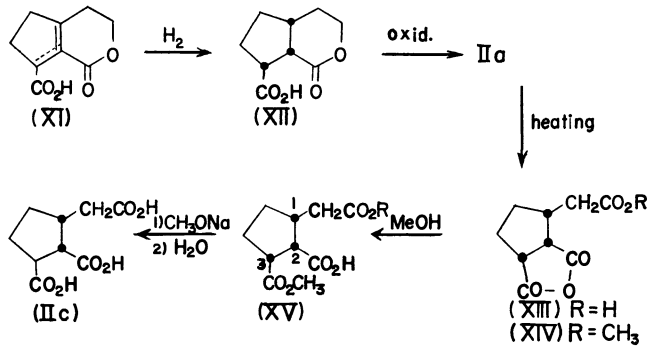

Fig. 6

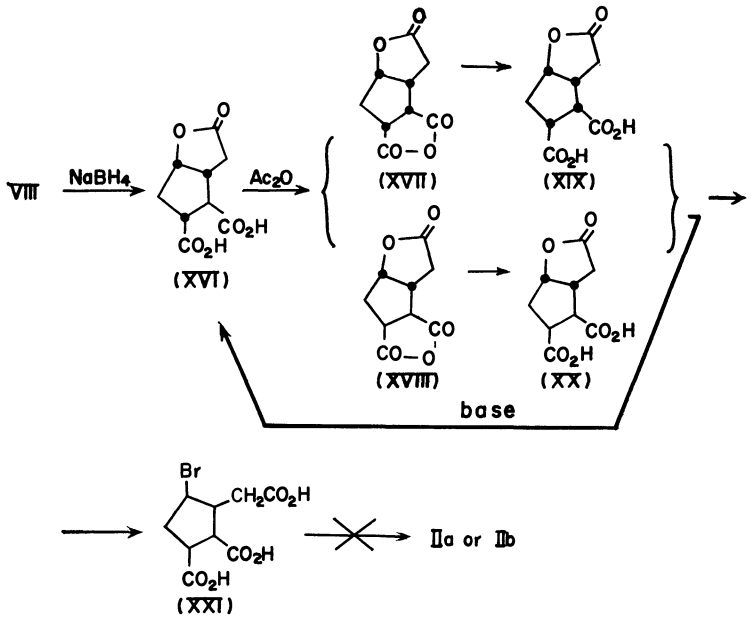

Fig. 7

and then the hydrolysis by addition of water produced the desired isomer (IIc) m. p. 156—157°C.[7] The method of synthesis and the chemical behavior[8] indicate that IIc must have a *trans-cis* configuration.

The following is an approach to the synthesis of the remaining *cis-trans* enantiomer (IId). The reduction of the keto tricarboxylic acid (VIII) with sodium borohydride afforded predominantly a lactone dicarboxylic acid (XVI), m. p. 192—193°C. The treatment of XVI with boiling acetic anhydride produced a single lactone anhydride, m. p. 164—165°C, accompanied by the rearrangement of one carboxyl group, the infrared spectrum of which manifested both succinic-type anhydride and γ-lactone carbonyl absorption (1850 and 1769 cm^{-1} [9] respectively). This compound is represented as the formula XVII or XVIII, according to the isomerization of either one of the two carboxyl groups. Thus, a lactone dicarboxylic acid, m. p. 198—199°C, isomeric with XVI and obtained by hydrolysis, possesses the structure XIX or XX respectively; this isomeric lactone carboxylic acid could be isomerized back to the starting material (XVI) on treatment with

7) The facts that the XV (R=H) naturally derived from XIII could undergo intramolecular anhydride (glutaric-type) formation, without isomerization, with hot acetic anhydride and that, after epimerization, the yield of the *trans-trans* isomer (IIb), evidently produced through the esterification of the C-2 carboxyl group,[1b] was very low prove the preferential ester-formation of the C-3 carboxyl group of the anhydride group in XIV on methanolysis and also indicate that the exclusive epimerization of the ester group takes place.

8) In addition to the glutaric-type anhydride formation in XV (R=H),[7] the thermostability of the natural IIc (no change upon heating) confirms the relative configuration of the three substituents of IIc to be *trans-cis*, since, if the configuration of the C-2 and C-3 carboxyl groups is *cis*, they must easily produce a succinic-type anhydride like IIa → XIII.[1b]

9) A succinic-type anhydride usually shows two carbonyl absorption bands, near 1855 and 1775 cm^{-1}. The latter hand in this compound presumably overlap with the lactone absorption.

base. Supposing that the epimerization of a carboxyl group takes place in the same mode as in the case of IIb→X during anhydride formation, the isomeric lactone dicarboxylic acid must be XIX with a *cis-syn-cis* configuration, whereas the epimerization of the other carboxyl group gives the alternative *cis-anti-cis* isomer (XX). The latter possibility seems to be sterically more favorable and has not, therefore, been eliminated. If this compound is actually XX, the expected *cis-trans* isomer (IId) would be obtained by the displacement of the hydroxyl group with hydrogen. The reaction of the compound (XIX or XX) with hydrogen bromide in anhydrous ethanol yielded a non-crystalline substance, which was supposed to be a bromotricarboxylic acid (XXI) because of the disappearance of lactone carbonyl absorption in its infrared spectrum. Successive attempts to reduce XXI to IIa or IId by means of zinc - hydrochloric acid or by means of catalytic hydrogenation under various conditions were all unsuccessful. Consequently, the preparation of IId or even the confirmation of the stereochemistry of the isomerized lactone dicarboxylic acid (XIX or XX) have not yet been accomplished.

Finally, a few remarks regarding the characterization of the Δ^1- and Δ^2-cyclopentene-1, 2-dicarboxylic acids, XXII and XXIII, used for the synthetic work[2] would be appropriate. The Δ^2- compound (XXIII), m. p. 144—145°C, has been obtained

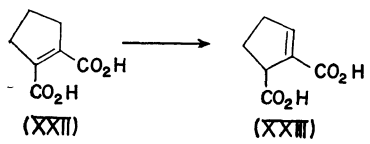

Fig. 8

from the Δ^1-isomer (XXII), m. p. 177—178°C, by treatment with boiling concentrated aqueous potassium hydroxide, involving a double-bond migration.[2,10] The further purification of this isomerized substance, m. p. 144—145°C, indicated that it was still a mixture of Δ^1- (XXII) and Δ^2-isomers (XXIII), which could be separated in the pure state. The structures of XXII and XXIII were verified beyond doubt by infrared and nuclear magnetic resonance spectroscopy. The former (XXII): 179—180°C, ν^{KBr}: 1685, 1620, 1585 and 1550 cm^{-1}, δ[11] = 2.97 (triplet, 4H, $-CH_2-C=$) and 1.67 (quintet, 2H, $-CH_2-$), pK_a : 3.36 and 7.18. The latter (XXIII): m. p. 178—179°C, ν^{KBr}: 1700, 1672 and 1636 cm^{-1}, δ = 4.12 (diffused singlet, 1H, $-CH=$) and 2.48 (multiplet, 5H, $-CH_2-$ and $-CH-$), pK_a: 4.03 and 5.92 respectively.

10) A. Hassell and C. K. Ingold, *J. Chem. Soc.*, **1962**, 1465; B. L. Nandi, *J. Indian Chem. Soc.*, **11**, 213 (1934).

11) Measured in a pyridine solution at 60 Mc. Chemical shifts are given in p.p.m. units, using tetramethylsilane as an internal standard.

Experimental

Tetraethyl Butane-1, 2, 3, 4-tetracarboxylate (V). —Commercial *cis*-Δ^4-cyclohexene-1, 2-dicarboxylic acid anhydride (100 g.) was dissolved into a solution of 75 g. of sodium carbonate, 2 kg. of cracked ice and 3 l. of water. To this solution 500 g. of well pulverized potassium permanganate was added portion by portion with efficient stirring; then the reaction mixture was stirred for 10 hr. with the temperature kept below 50°C. The precipitated manganese dioxide was filtered off, and the light brown filtrate was acidified (Congo red) with concentrated hydrochloric acid and evaporated to dryness. The residual solid was dried in vacuo over sulfuric acid and then extracted with boiling acetone three times; the acetone extracts were concentrated to a small volume, giving 55 g. of crude crystals. The second crop (21 g.) was obtained from the mother liquor. Recrystallization from acetone yielded 60 g. (39%) of pure butanetetracarboxylic acid, m. p. 188—189°C.

A solution of 380 g. of the above tetracarboxylic acid in 1.5 l. of ethanol containing 1 ml. of concentrated sulfuric acid was refluxed for 15 hr. The ethanol was removed by distillation, and the residue was again esterified with fresh ethanol by refluxing for an additional 15 hr. The ethanol was distilled off, and the residual oil was allowed to distill in vacuo. Tetraester (V), b. p. 178—183°C/1.0 mmHg; 395 g., 70%, was thus obtained.

2, 3, 4-Triethoxycarbonylcyclopentanone (VI).— To a suspension of 2.5 g. (0.11 g.atom) of finely-granulated sodium metal in 150 ml. of hot toluene there was carefully added 38 g. (0.11 mol.) of the tetraester (V) with vigorous stirring, so as to maintain a gentle refluxing and continuous evolution of hydrogen; after the addition of sodium, the stirring was continued for 2 hr. under refluxing. Then the cooled reaction mixture was poured into ice water containing an almost equimolar amount of acetic acid or hydrochloric acid with vigorous stirring. The water layer was separated and extracted with toluene two times. The combined toluene extracts were washed with water, dried over anhydrous sodium sulfate, and freed from toluene. The residual liquid was distilled in vacuo to give 25.5 g. of triethoxycarbonylcyclopentanone (VI), b. p. 175—182°C/2—3 mmHg (a slight decomposition was observed).

2, 3, 4-Triethoxycarbonyl-2-ethoxycarbonylmethylcyclopentanone (VII). — The sodio-derivative of VI was prepared from 85 g. (0.29 mol.) of VI and 7 g. (0.30 g.atom) of well-granulated metallic sodium in 400 ml. of anhydrous toluene in the usual manner. To this solution there was added dropwise 62 g. of ethyl bromoacetate with stirring and water-cooling, and the reaction mixture was heated under reflux for 6 hr. Then the mixture was poured into ice water, and the water layer was extracted with the same solvent three times. The combined toluene extracts were washed with dilute sodium bicarbonate solution and water, and then dried over anhydrous sodium sulfate and freed from toluene to give viscous liquid. Distillation in vacuo afforded 84 g. (76%) of 2, 3, 4,-triethoxycarbonyl- 2 -ethoxycarbonylmethylcyclopentanone (VII), b. p. 195—210°C/2.0 mmHg, ν^{neat} 1760 and 1733 cm^{-1}. The additional absorption bands at

1685 and 1638 cm^{-1} can be attributed to an *O*-alkylated by-product.

2, 3 - Dicarboxy - 5 - oxo-cyclopentylacetic Acid (VIII).—The mixture of VII and *O*-alkylated by-product from the preceding experiment (5 g.) was refluxed with 50 ml. of 6 N hydrochloric acid for 6 hr.; then the solvent was removed under reduced pressure. The residual viscous material crystallized when treated with ethyl acetate, and recrystallization from ethyl acetate gave 1.8 g. (47%) of a pure keto tricarboxylic acid (VIII), m. p. 215—216°C, ν^{KBr} 1747 (cyclopentanone) and 1700 cm^{-1} (carboxyl).

Found: C, 47.21; H, 4.45. Calcd. for $C_9H_{10}O_7$: C, 46.96; H, 4.38%. pK_{a_1} 3.32, pK_{a_2} 4.76, pK_{a_3} 5.92.

***trans - trans* - 2, 3 - Dicarboxycyclopentylacetic Acid (IIb).**—Keto tricarboxylic acid (VIII) (1.0 g.) was treated with 1.5 ml. of ethane dithiol and 1.5 ml. of boron trifluoride etherate, and then the mixture was allowed to stand at room temperature for 24 hr. The separated amorphous solid was collected by filtration, yielding 1 g., m. p. 190°C (decomp.) (no ketonic band in infrared); this was then subjected to desulfurization without purification. The above thioketal was refluxed with Raney nickel, prepared from 30 g. of alloy, in 100 ml. of 70% aqueous ethanol for 4 hr. Removal of the catalyst, followed by acidification and then evaporation of the solvent, gave crude crystals. Pure *trans-trans*-2,3-dicarboxycyclopentylacetic acid (IIb), 0.1 g., m. p. 160°C, was obtained by recrystallization from ethyl acetate, and showed an infrared spectrum completely identical with that of a sample prepared by the previously-reported procedure, starting from the Michael addition of dimethyl Δ^2-cyclopentene-1, 2-dicarboxylate (III) and diethyl malonate,[2] and there was no depression in a mixed melting point determination.

***cis-cis*-2,3-Dicarboxycyclopentylacetic Acid (IIa).**—A solution of *cis-cis*-2-(2'-hydroxyethyl)-5-carboxycyclopentylcarboxylic acid δ-lactone (XII)[5] (1.5 g.) in 250 ml. of glacial acetic acid was treated with a solution of 2.0 g. of chromium trioxide and 3.5 ml. of concentrated sulfuric acid in 7 ml. of water; the oxidation was then allowed to proceed at room temperature for three days. The excess oxidant was decomposed by addition of methanol, almost all of the acetic aicd was removed by distillation under reduced pressure with the aid of water, and then the solution was neutralized with a minimum amount of solid sodium bicarbonate, keeping the Congo red acidity. The resulting solution was saturated with sodium chloride and extracted continuously with ether for 65 hr. Evaporation of the ether extract gave 0.9 g. (51%) of *cis-cis*-2, 3-dicarboxycyclopentylacetic acid (IIa). The pure sample recrystallized from ethyl acetate had a melting point of 176—177°C.

Found: C, 50.00; H, 5.63. Calcd. for $C_9H_{12}O_6$: C, 50.00; H, 5.60%.

The infrared spectrum of this substance was completely indistinguishable from that of the sample obtained from IIb by isomerization via dimeric trianhydride (X),[2] and the mixed melting point of these samples was not depressed.

***trans-cis*-2, 3-Dicarboxycyclopentylacetic Acid (IIc)**—The *cis-cis* isomer (IIa) was heated over its melting point in a sublimation apparatus for half an hour and then distilled under diminished pressure. The resulting anhydride carboxylic acid (XIII) was treated with excess ethereal diazomethane. The anhydride methyl ester (XIV) (0.4 g.) thus obtained was refluxed in 4 ml. of anhydrous methanol for 1 hr., and, after removal of the methanol, a methanolic solution of sodium methoxide freshly prepared from 0.2 g. of metallic sodium and 10 ml. of anhydrous methanol was added and refluxing was continued for 2 hr. After water (3 ml.) had then been added, the reaction mixture was again refluxed for 30 min. to complete hydrolysis. The hydrolysate was worked up in the usual manner, i. e., evaporation of the methanol, dilution with water, acidification with mineral acid, and finally extraction with ethyl acetate, to give 0.25 g. of a crude product, m. p. 127—144°C. Recrystallization from ethyl acetate yielded pure *trans-cis*-2, 3-dicarboxycyclopentylacetic acid (IIc), m. p. 156—157°C, which revealed a different infrared spectrum from that of either IIa or IIb.

Found: C, 49.66; H, 5.56. Calcd. for $C_9H_{12}O_6$: C, 50.00; H, 5.60%.

2, 3-Dicarboxy-5-hydroxycyclopentylacetic Acid γ-Lactone (XVI).—To a solution of 0.2 g. of VIII in 5 ml. of water containing 0.15 g. of sodium hydroxide, there was added 0.1 g. of sodium borohydride; the reaction mixtrure was then stirred at 80°C for 2 hr. After acidification with concentrated hydrochloric acid, the solution was evaporated to dryness. The residual solid was treated with ethyl acetate, and then, after removal of the insoluble inorganic material by filtration, the filtrate was passed through a column of silica gel. Evaporation of the ethyl acetate gave 0.04 g. of a lactone dicarboxylic acid (XVI), m. p. 192—193°C, ν^{KBr} 1769 and 1685 cm^{-1}, pK_{a_1} 3.34, pK_{a_2} 5.51.

Found: C, 50.18: H, 4.82. Calcd. for $C_9H_{10}O_6$: C, 50.47; H, 4.71%.

2, 3-Dicarboxy-5-hydroxycyclopentylacetic Acid Anhydride γ-Lactone (XVII or XVIII).—A solution of 0.17 g. of XVI in 20 ml. of acetic anhydride was refluxed for 2 hr. After removal of the acetic anhydride under reduced pressure, the residual viscous liquid was distilled in vacuo using a sublimation apparatus and then treated with ethyl acetate to give a crystalline product. Recrystallization from ethyl acetate yielded 0.02 g. of pure anhydride lactone (XVII or XVIII), m. p. 164—165°C, ν^{KBr} 1850 and 1769 cm^{-1}.

Found: C, 55.25; H, 4.20. Calcd. for $C_9H_8O_5$: C, 55.10; H, 4.11%.

Isomeric 2, 3 - Dicarboxy-5-hydroxycyclopentylacetic Acid γ-Lactone (XIX or XX).—The anhydride lactone from the preceding experiment (0.17 g.) was treated with 5 ml. of water at 100°C for 30 min. and then dried up and recrystallized from ethyl acetate to give 0.13 g. (68%) of the isomeric lactone dicarboxylic acid (XIX or XX), m. p. 198—199°C, ν^{KBr} 1730 and 1692 cm^{-1}, pK_{a_1} 3.91, pK_{a_2} 5.92.

Found: C, 50.86; H, 4.69. Calcd. for $C_9H_{10}O_6$: C, 50.47; H, 4.71%.

Ethyl Diethoxycarbonyl - 5 - bromocyclopentylacetate (XXI).—The isomeric lactone dicarboxylic acid was treated overnight with anhydrous ethanol saturated with hydrogen bromide at room temperature. The hydrogen bromide and ethanol were then removed under reduced pressure to give a bromoester (XXI) (the lactone absorption disappeared) which,

without further purification or characterization, was then subjected to reduction. However, the reduction of XXI with zinc - hydrochloric acid or with hydrogen catalytically under various conditions failed to produce any crystalline product.

The authors wish to express their deep gratitude for the help of the late Professor Emeritus Shin-ichiro Fujise and of Professor Koji Nakanishi; they are also grateful to Mr. Hiroshi Honda for his technical assistance.

BULLETIN OF THE CHEMICAL SOCIETY OF JAPAN VOL. 39 530—535 (1966)

Syntheses of *dl*-Tetrahydroanhydrodesoxyaucubigenin and Related Compounds

By Kazu KUROSAWA,† Heitaro OBARA†† and Hisashi UDA†

† *Department of Chemistry, Faculty of Science, Tohoku University, Katahira-cho, Sendai*

†† *Department of Applied Chemistry, Faculty of Engineering, Yamagata University, Yonezawa*

(Received July 2, 1965)

The racemic tetrahydroanhydrodesoxyaucubigenin, one of the derivatives from a glycoside, aucubin, has been synthesized using *cis-cis*-2-(2'-hydroxyethyl)-5-methoxycarbonylcyclopentanecarboxylic acid δ-lactone as an intermediate. 6, 7-Dimethoxycarbonyl-2-oxa-bicyclo[3.3.0]-octane has also been synthesized, and the mechanism of the base-catalyzed rearrangement of the naturally-derived tetrahydroanhydroaucubigenin *p*-toluenesulfonate has been elucidated.

The recent achievement of the synthesis of a number of cyclic acetals fused to a five- or six-membered ring, for example, 1-ethoxyoctahydrocyclopenta[c]pyran,[1] has prompted the present authors to attempt the synthesis of tetrahydroanhydrodesoxyaucubigenin (II),[2] one of the most important derivatives from a glycoside, aucubin (I),[2a,3] and one with a unique tricyclic acetal-ring system.

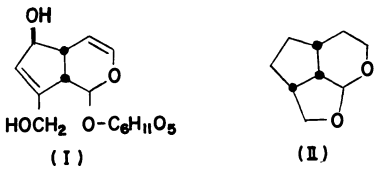

Fig. 1

In view of the previous findings,[1] an unsaturated lactone ester (X) appeared to be one of the most satisfactory intermediates for the synthesis of II, since the steric requirement (*cis-cis*) with respect to the three substituents on the cyclopentane ring in the precursor (XI) of II would be settled beyond difficulty by means of the catalytic hydrogenation of X; undoubtedly hydrogens add *cis* to the double bond from the side opposite to an allylic substituent, producing a *cis-cis* orientation. The most important and difficult problem, however, arises in the final step; that is, the lithium aluminum hydride reduction of XI must proceed selectively so as to reduce the ester group exhaustively to a primary alcohol, while reducing the lactone partially to an acetal. A controlled operation of this reduction has now been accomplished, resulting in the synthesis of racemic tetrahydroanhydrodesoxyaucubigenin (II), although in a low yield.[4] This paper will describe these results in detail, and also the syntheses of the related compounds.

The reaction of the sodio-derivative of 2-ethoxycarbonylcyclopentanone (III) with 2-iodoethyl methyl ether afforded a mixture (b. p. 130—135°C/5 mmHg) of the desired *C*-alkylated product (IV) and an undesired *O*-alkylated one (V) in a ratio of 3 : 1 (by v. p. c. analysis); the infrared spectrum showed absorption bands at 1748 and 1722 cm^{-1} due to IV and one at 1548 cm^{-1} due to V. Upon the treatment of the mixture with a boiling 0.1 molar-equivalent solution of sodium ethoxide in ethanol, the β-keto ester, a *C*-alkylated product (IV), underwent "acid-cleavage" to give diethyl 2-(2'-methoxyethyl)-adipate (VI), whereas V did not change; VI,

1) a) H. Obara, *J. Chem. Soc. Japan, Pure Chem. Sect.* (*Nippon Kagaku Zasshi*), **82**, 60, 62, 65 (1961); K. Kurosawa and S. Fujise, ibid., **83**, 327, (1962). b) K. Kurosawa and S. Fujise, ibid., **83**, 329 (1962).

2) a) S. Fujise, H. Obara and H. Uda, *Chem. & Ind.*, **1960**, 289; *J. Chem. Soc. Japan, Pure Chem. Sect.* (*Nippon Kagaku Zasshi*), **81**, 677 (1960); H. Uda, ibid., **81**, 1865 (1960). b) H. Uda, ibid., **81**, 1723 (1960).

3) a) J. Grimshaw and H. R. Juneja, *Chem. & Ind.*, **1960**, 656; A. J. Birch, J. Grimshaw and H. R. Juneja, *J. Chem. Soc.*, **1961**, 5194; M. W. Wendt, W. Haegele, E. Simonitsch and H. Schmid, *Helv. Chim. Acta*, **43**, 1440 (1960); W. Haegele, K. Kaplan and H. Schmid, *Tetrahedron Letters*, **1961**, 110. b) H. Uda, M. Maruyama, K. Kabuki and S. Fujise, *J. Chem. Soc. Japan, Pure Chem. Sect.* (*Nippon Kagaku Zasshi*), **85**, 279 (1964).

4) For a preliminary communication, see K. Kurosawa and S. Fujise, *Chem. & Ind.*, **1963**, 1688.

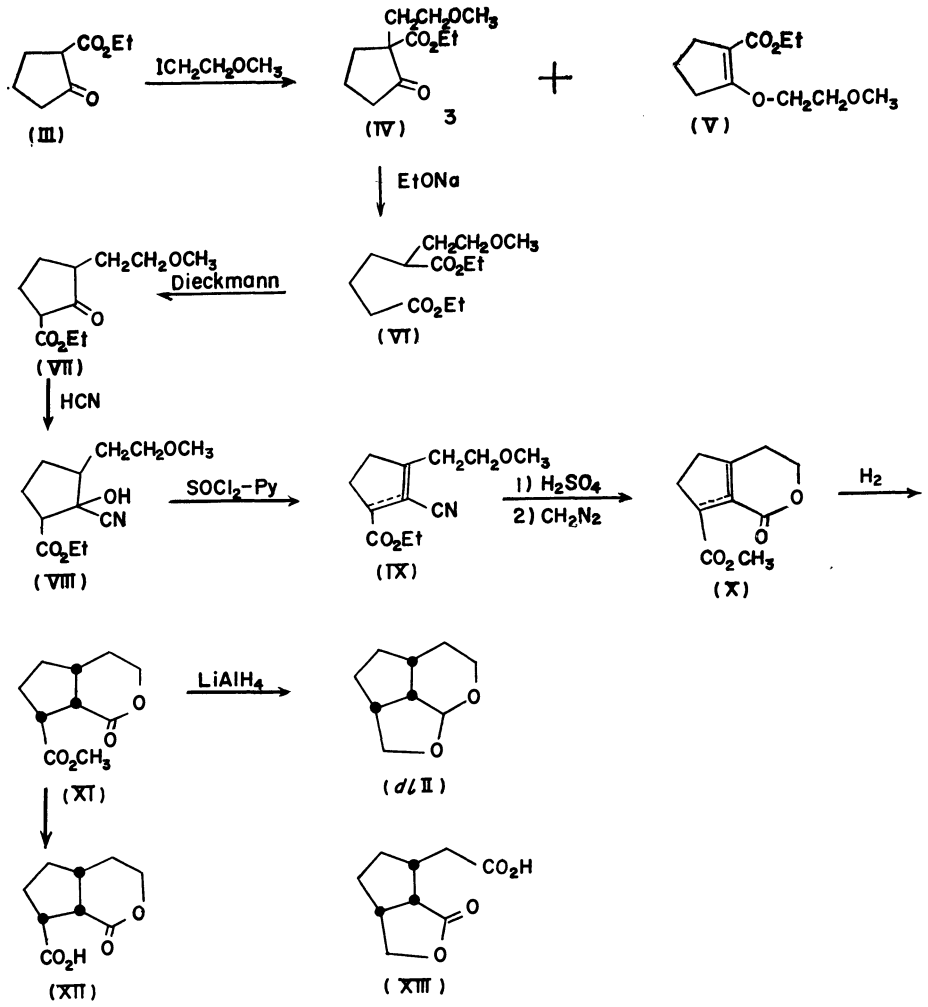

Fig. 2

b. p. 136—139°C/1 mmHg, was separated from V (distilled as a forerun) by fractional distillation through a 1 m. helix-packed column.[5] The Dieckmann cyclization of VI gave predominantly 5-ethoxycarbonyl - 2 - (2′ - methoxyethyl)cyclopentanone (VII), b. p. 155—162°C/3 mmHg, as expected, this was characterized by typical enol absorption bands at 1658 and 1625 cm^{-1} and a positive color test with ferric chloride. This was transformed readily into a cyanohydrin (VIII), b. p. 139—140°C/4.5 mmHg, by reaction with liquid hydrogen cyanide in the presence of a small amount of 50% potassium hydroxide; then the dehydration of VIII with thionyl chloride - pyridine gave an unsaturated nitrile ester (IX), b. p. 130—140°C/4.5 mmHg. The conversion to the desired intermediate, 2-(2′-hydroxyethyl)-5-methoxycarbonyl-Δ^1-(or Δ^5-)cyclopentenecarboxylic acid δ-lactone (X), was achieved by the hydrolysis of IX with boiling sulfuric acid - acetic acid - water, followed by the esterification of the resulting unsaturated lactone carboxylic acid with diazomethane. The pure X, obtained in a 29% yield,[6] b. p. 164—168°C/5 mmHg, ν^{neat} 1730 cm^{-1} (δ-lactone

5) 2-(2′-Acetoxyethyl) - 2 - ethoxycarbonylcyclopentanone (i)[1b] was also subjected to "acid-cleavage" reaction as one of the preliminary experiments on the introduction of the 2′-hydroxyethyl function; the product, however, was not the expected adipic acid derivative (iii), but rather an α-substituted butyrolactone derivative (ii, R = C_2H_5), b. p. 146—154°C/1.2 mmHg, ν(neat) 1768 and 1728 cm^{-1}, and the free acid (ii, R = H), m. p. 84—85°C, ν(KBr) 1760 and 1700 cm^{-1}.

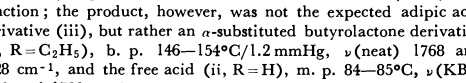

Fig. 3

6) A considerable amount of a by-product (as a low boiling fraction; b. p. 143—153°C/5 mmHg) was also isolated; it had the molecular formula of $C_{11}H_{18}O_5$ and neither a double bond nor a hydroxyl group, as was shown by infrared spectroscopy. The hydrolysis of this material gave a free carboxylic acid, $C_9H_{12}O_5$, m. p. 160—161°C. The analytical and spectral data of these compounds show the former to be the dimethyl ester of the latter, dicarboxylic acid, which possesses an oxygen-containing heterocyclic ring, but their structures have not been investigated further.

and ester) and 1648 cm^{-1} (double bond), was hydrogenated to the corresponding saturated lactone ester (XI), m. p. 72—73°C, using a platinum oxide catalyst in acetic acid, in which the stereochemistry of the three substituents on the cyclopentane ring must be *cis-cis*, as has been mentioned above.

In the final step, it is necessary to control the reduction of XI so as to discriminate each functional group to a reducing agent, lithium aluminum hydride; the ester group must be reduced exhaustively to a primary alcohol, and the lactone, partially to an acetal, in order to achieve the synthesis of II. Considering the environment of both functional groups in XI, it is obvious that the lactone would be more slowly reduced than the ester because of the steric obstruction of the ester and the hydroxyethyl moiety of the lactone ring; the ester is open to the approach of the reagent. In order to enhance this selectivity on reduction, a modified procedure was employed in which there was quite a slow reverse addition of a theoretical amount (0.75 mol.) of lithium aluminum hydride at a low temperature. Thus a mobile liquid, b. p. 112—120°C/20 mmHg, was obtained in a 10% yield; this synthetic material was identical with a sample of natural tetrahydroanhydrodesoxyaucubigenin (II) as determined by a comparison of their infrared spectra and their vapor-phase chromatographic behavior.

In addition to the above results, a few remarks regarding a comparison of synthetic lactone carboxylic acid (XII), m. p. 123—124°C, with a naturally-derived lactone carboxylic acid are appropriate. A δ-lactone structure, as XII, has been assigned on the basis of the lactone absorption band at 1755 cm^{-1} to the lactone carboxylic acid derived from the natural II by potassium permanganate oxidation in an acidic medium.[2a] The infrared spectra of the synthetic lactone carboxylic acid (XII) and its methyl ester (XI) are, however, completely different from those of the naturally-derived compounds, including the lactone carbonyl absorption which is at 1715 in XII and at 1725 cm^{-1} in XI, whereas it is at 1755 and 1766 cm^{-1} in the natural lactone carboxylic acid and methyl ester respectively. Consequently, the structure of the natural lactone carboxylic acid should be revised to the formula XIII with γ-lactone.[7]

7) The nuclear magnetic resonance spectrum of the natural lactone carboxylic acid also supports the structure XIII. Private communication of Dr. W. H. Tallent, G. D. Searle and Co. Two protons, H_A and H_B, attached to the carbon atom bearing lactone hydroxyl show a AB-type quartet at ca. $\delta = 4.2$ p.p.m., each peak of which is further split into a doublet by coupling with an adjacent proton, H_C ($J_{AB}=10$, $J_{AC}=9$—10, and $J_{BC}=3$—4 c.p.s.).

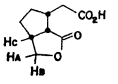

Fig. 4

Finally, as a part of the synthetic work on the aucubin derivative, the synthesis of 6, 7-dimethoxycarbonyl-2-oxa-bicyclo[3.3.0]octane (XXIII) should be mentioned.

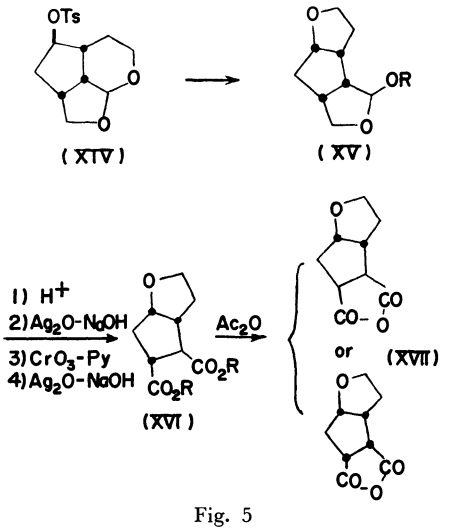

Fig. 5

It has been also reported that tetrahydroanhydroaucubigenin *p*-toluenesulfonate (XIV), when treated with alcoholic potassium hydroxide or sodium ethoxide, underwent acetal ring opening and a new oxygen-containing ring formation to give a compound XV, the structure of which was assumed to be that of a 2-oxa-bicyclo[3.3.0]octane derivative according to the successive transformation of XV into a succinic-type anhydride[8] (XVII), as is shown in Fig. 5; this unusual rearrangement has been explained in terms of the back-side attack of the ring-oxygen atom in the six-membered ring of XIV on the *p*-toluenesulfonyloxy group, facilitated by the attack of the hydroxy or ethoxy anion on the acetal carbon atom.[3b,9] It appeared, however, that the previous results were not sufficient to lead to a definite conclusion concerning the mechanism of rearrangement and the structure of product; hence, the final confirmation should be made by the synthesis of either compound from XV to XVII.

8) For the same type of epimerization involving one carboxyl group in the *trans*-cyclopentane-1, 2-dicarboxylic acid derivative during anhydride formation, see R. B. Bates, E. J. Eisenbraun and S. M. McElvain, *J. Am. Chem. Soc.*, **80**, 3413 (1958), and Refs. 2a and 10.

9) The alternative mechanism, in which another oxygen atom (in the five-membered ring) participates in this reaction, giving a bridged compound (iv), has been excluded because a dicarboxylic acid corresponding to XVI (R=H) would have to form a glutaric-type anhydride (v).

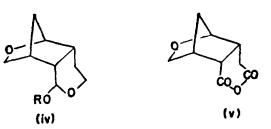

Fig. 6

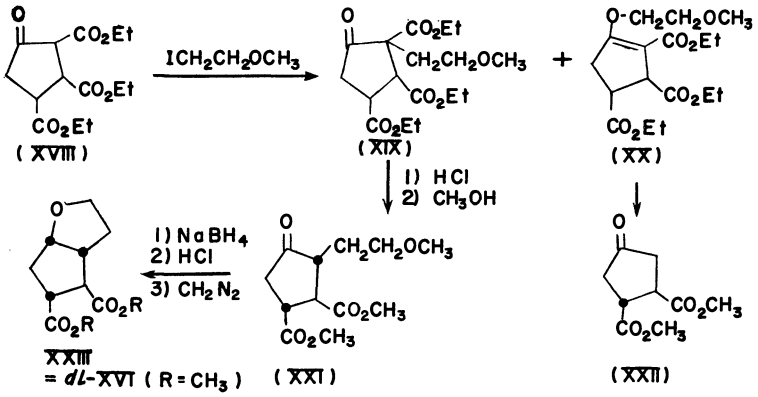

Fig. 7

The condensation of the sodio-derivative of 2, 3, 4-triethoxycarbonylcyclopentanone (XVIII)[10] with 2-iodoethyl methyl ether afforded a mixture of a *C*-alkylated (XIX) and an *O*-alkylated product (XX), in roughly equal amounts (as determined by v. p. c. analysis). The hydrolysis of them with boiling 6 N hydrochloric acid, followed by the esterification of the resulting carboxylic acid using methanol, gave a mixture of the desired compound (XXI) and a keto diester (XXII); these were readily separated by fractional distillation. XXI, b. p. 145—155°C/1.5 mmHg, was characterized by the formation of 2, 4-dinitrophenylhydrazone, $C_{18}H_{22}O_9N_4$, m. p. 123—124°C, and the relative configuration of three substituents must be a thermodynamically more stable or sterically more favorable *trans-trans* arrangement.

The reduction of XXI with sodium borohydride proceeded stereospecifically to produce a single hydroxy diester with *cis* hydroxyl to the adjacent methoxyethyl side chain, which was then transformed into a dicarboxylic acid (XXIII, R=H), accompanied by a simultaneous ring closure, by being refluxed in concentrated hydrochloric acid; subsequent esterification with diazomethane furnished 6, 7-dimethoxycarbonyl-2-oxa-bicyclo[3.3.0]-octane (XXIII, R=CH_3). The synthetic material (XXIII, R=CH_3) was identical with a sample of natural diester (XVI, R=CH_3) as was shown by vapor-phase chromatography and infrared spectroscopy. These results provide convincing evidence of the correctness of the proposed mechanism of transformation from XIV to XV, and also of the assigned structure for XVI; XVI must have a *trans-anti-cis*[11] configuration, and the epimerization of the acetal substituent in XV must take place during the oxidation sequence to XVI.

10) K. Kurosawa and H. Obara, This Bulletin, **39**, 525 (1966).
11) In this designation the relationship of the two carboxyl groups attached to the cyclopentane ring is given first.

Experimental

2-Chloroethyl Methyl Ether.—To a mixture of 500 g. (6.6 mol.) of ethylene glycol monomethyl ether and 500 ml. of pyridine, there was added 1 kg. (8.4 mol.) of thionyl chloride dropwise with stirring and ice cooling; after the mixture had been allowed to stand at room temperature for 48 hr., 500 ml. of water was added. The resulting mixture was extracted with ether three times, and the combined extracts were washed with 10% aqueous sodium hydroxide, dried over calcium chloride, and freed from ether. The residual liquid was distilled through a short fractional column to give 498 g. (80%) of 2-chloroethyl methyl ether, b. p. 89—90°C.

2-Iodoethyl Methyl Ether.—A solution of 438 g. of 2-chloroethyl methyl ether and 1 kg. of sodium iodide in 1 l. of dry acetone was refluxed for 50 hr.; the reaction mixture was then poured into ice water and extracted with ether. The extract was successively washed with aqueous sodium thiosulfate, water, and saturated sodium chloride solution, dried over calcium chloride, and freed from ether. Distillation of the residual liquid gave 782 g. (90%) of 2-iodoethyl methyl ether, b. p. 103—105°C.

Condensation of 2-Ethoxycarbonylcyclopentanone (III) with 2-Iodoethyl Methyl Ether.—To a suspension of 29 g. of finely-granulated sodium metal in 1 l. of anhydrous toluene was added 190 g. of 2-ethoxycarbonylcyclopentanone (III) dropwise with vigorous stirring; the mixture was then heated on an oil bath, while being continuously stirred, until all of the sodium was consumed, after about 5 hr. Then 323 g. of 2-iodoethyl methyl ether was added to the above jelly-like solution of the sodio-derivative of III, and the reaction mixture was refluxed for 10 hr. After cooling, the mixture was worked up by dilution with water, acidification with hydrochloric acid, and extraction in the usual manner to give a crude condensation product. Distillation in vacuo gave 218 g. (84%) of a mixture of two products, b. p. 130—135°C/5 mmHg. The mixture consisted of a *C*-alkylated (IV) and an *O*-alkylated product (V) in the ratio of about 3 : 1, as was determined by v. p. c. on a 3 m. silicone DC 550 column, there were two peaks at retention times of 25 min. (major) and 46 min. (minor) (200°C;

hydrogen flow 80 ml./min.). The major product (IV) gave 2, 4-dinitrophenylhydroazone, m. p. 69.5—70.5°C (from dilute ethanol), according to the usual procedure.

Found: C, 51.54; H, 5.62; N, 13.69. Calcd. for $C_{17}H_{22}O_7N_4$: C, 51.77; H, 5.62; N, 14.21%.

Diethyl 2-(2'-Methoxyethyl)adipate (VI).—The mixture of IV and V from the preceding experiment (624 g.) was treated with a sodium ethoxide solution prepared from 6.7 g. of metallic sodium and 1 l. of anhydrous ethanol; the resulting mixture was refluxed for 6 hr. The mixture was then neutralized with ethanolic hydrogen chloride and heated again for an additional 2 hr. The ethanol was removed by distillation, and the residual oil was poured into ice water and extracted with ether three times. The combined ether extracts were washed with water, dried over anhydrous sodium sulfate, and freed from ether to give 467 g. of the crude material. Fractional distillation in vacuo through a 1 m. helix-packed column gave, after a forerun of ca. 40 g., 425 g. (57%) of pure diethyl 2-(2'-methoxyethyl)-adipate (VI), b. p. 136—139°C/1 mmHg, n_D^{20} 1.4471, d_4^{20} 1.024, M. R. Obs.: 67.95; Calcd.: 67.19.

Found: C, 60.15; H, 9.55. Calcd. for $C_{13}H_{24}O_5$: C, 59.95; H, 9.29%.

5-Ethoxycarbonyl-2-(2'-methoxyethyl)cyclopentanone (VII).—To a suspension of 39 g. of finely-granulated sodium metal in 1 l. of dry benzene was added 425 g. of VI dropwise with efficient stirring; the reaction mixture was then warmed at 80°C for 2 hr., poured into cold 10% aqueous acetic acid, and extracted with benzene. The organic layer was thoroughly washed with saturated brine, dried over anhydrous sodium sulfate, and freed from benzene. The residual liquid was distilled in vacuo to give 227 g. (62%) of β-keto ester (VII), b. p. 155—162°C/3 mmHg, n_D^{18} 1.4600, d_4^{18} 1.073, M. R. Obs.: 54.58; Calcd.: 54.11, which gave a purple color with ferric chloride.

Found: C, 61.11; H, 8.55. Calcd for $C_{11}H_{18}O_4$: C, 61.66; H, 8.47%.

VII (5 g.) was hydrolyzed and decarboxylated by refluxing with 10% sulfuric acid; it thus gave 2.2 g. (67%) of 2-(2'-methoxyethyl)cyclopentanone, b. p. 104—108°C/24 mmHg, ν^{neat} 1755 cm^{-1}, n_D^{31} 1.4964, d_4^{31} 0.9799, M. R. Obs.: 38.37; Calcd.: 38.59, which in turn gave 2, 4-dinitrophenylhydrazone, m. p. 123—124°C.

Found: C, 52.31; H, 5.82; N, 17.37. Calcd. for $C_{14}H_{18}O_5N_4$: C, 52.17; H, 5.63; N, 17.38%.

This 2-(2'-methoxyethyl)cyclopentanone was also obtained from IV by hydrolysis and decarboxylation.

2-(2'-Methoxyethyl)-5-ethoxycarbonylcyclopentenylnitrile (IX).—Freshly-prepared liquid hydrogen cyanide (25 ml.) and a few drops of a 50% potassium hydroxide solution were added to 20 g. of the β-keto ester (VII) with ice cooling and vigorous stirring, and the reaction mixture was stored at 0°C for 20 hr. and carefully acidified with 80% phosphoric acid. The excess hydrogen cyanide was expelled under reduced pressure. Distillation of the residual liquid gave 18 g. of 5-ethoxycarbonyl-2-(2'-methoxyethyl)cyclopentanone cyanohydrin (VIII), b. p. 139—140°C/4.5 mmHg.

The above cyanohydrin (VIII) (18 g.) was dissolved in 20 ml. portions of anhydrous pyridine and benzene and treated with 18.5 g. (11 ml.) of thionyl chloride at 0°C. The reaction mixture was then allowed to stand at the same temperature for 20 hr., poured into ice water, and extracted with benzene. The benzene extracts were washed successively with dilute hydrochloric acid, sodium bicarbonate solution, and water, dried over anhydrous sodium sulfate, and freed from benzene to give a crude product. Distillation in vacuo gave 13.2 g. (79%) of an unsaturated nitrile ester (IX), b. p. 130—140°C/4.5 mmHg, n_D^{18} 1.4799, d_4^{18} 1.075, M. R. Obs.: 58.32. Calcd.: 58.06.

Found: C, 63.71 (low); H, 7.51; N, 6.47. Calcd. for $C_{12}H_{17}O_3N$: C, 64.55; H, 7.68; N, 6.27%.

2-(2'-Hydroxyethyl)-5-methoxycarbonylcyclopentenylcarboxylic Acid Lactone (X).—The unsaturated nitrile ester (IX) (13.2 g.) was dissolved in a solution of 23 ml. of concentrated sulfuric acid, 70 ml. of acetic acid, and 35 ml. of water, and the reaction mixture was refluxed for 15 hr. After cooling, the reaction mixture was diluted with ca. 130 ml. of water and extracted with ether. The ether extract was evaporated to dryness under reduced pressure; then the residual oil was dissolved in a dilute sodium hydroxide solution prepared from 20 g. of sodium hydroxide and 160 ml. of water. This solution was refluxed for 3 hr., acidified with concentrated hydrochloric acid, evaporated to dryness, and finally extracted with ethyl acetate. The ethyl acetate extract was treated with excess diazomethane in ether. The solvent was removed by distillation, and the residual liquid was fractionally distilled in vacuo through a short fractional column. After a forerun of 7 g. (b. p. 143—153°C/5 mmHg), the fraction (5.5 g.) was collected at b. p. 164—168°C/5 mmHg. This fraction consisted mainly of the desired unsaturated lactone ester (X). n_D^9 1.5042.

Found: C, 60.30 (low); H, 6.22. Calcd. for $C_{10}H_{12}O_4$: C, 61.21; H, 6.17%.

The forerun showed the following physical properties: n_D^{13} 1.4775, d_4^{13} 1.290, M. R. Obs.: 54.29; Calcd.: 53.55.

Found: C, 57.51; H, 7.29. Calcd. for $C_{11}H_{16}O_5$: C, 57.88; H, 7.01%.

The hydrolysis of this material with boiling dilute hydrochloric acid gave a crystalline substance, which was then recrystallized from chloroform. M. p. 160—161°C. There was neither hydroxy nor double bond absorption in the infrared spectrum.

Found: C, 53.61; H, 6.07. Calcd. for $C_9H_{12}O_5$: C, 53.99; H, 6.04%.

2-(2'-Hydroxyethyl)-5-methoxycarbonylcyclopentylcarboxylic Acid Lactone (XI).—The unsaturated lactone ester (X) (3.8 g.) in 25 ml. of acetic acid was hydrogenated using a platinum oxide catalyst at atomospheric pressure. A total of 375 ml. (70% of the theoretical amount) of hydrogen was absorbed. Filtration of the catalyst, followed by evaporation of the acetic acid to dryness, afforded a viscous liquid which was then distilled in vacuo to give 2.5 g. (65%) of a saturated lactone ester (XI), b. p. 163—167°C/3.5 mmHg, n_D^{13} 1.4886, d_4^{13} 1.220, M. R. Obs.: 46.87. Calcd.: 47.29. This distilled material gradually crystallized upon standing; it was recrystallized from ethyl acetate-petroleum ether to give pure XI, m. p. 72—73°C.

Found: C, 60.49; H, 7.48. Calcd. for $C_{10}H_{14}O_4$: C, 60.59; H, 7.12%.

***dl*-Tetrahydroanhydrodesoxyaucubigenin (II).**—A solution of 0.303 g. (7.95 mmol.) of lithium aluminum hydride in 20 ml. of anhydrous ether was added dropwise at −15 to −18°C to a stirred solution of 2.1 g. (10.6 mmol.) of the crystalline saturated lactone ester (XI) in 20 ml. of anhydrous ether; the reaction mixture was

then stored at 0°C overnight. Dilute sulfuric acid (10%) was slowly added to the reaction mixture with cooling and stirring until the solution became slightly acidic (Congo red); the organic layer was separated, and the water layer was extracted with ether three times. The combined ether extracts were then washed with water, dried over anhydrous sodium sulfate, and freed from ether. Distillation of the residual liquid in vacuo gave 0.15 g. (10%) of colorless *dl*-tetrahydroanhydrodesoxyaucubigenin (II), b. p. 112—120°C/15 mmHg, n_D^{19} 1.4987, d_4^{19} 1.124 (the reported values for the natural II: n_D^{20} 1.4961, d_4^{20} 1.1249),[2b] M. R. Obs.: 40.30. Calcd.: 40.43. Analysis by v. p. c. using a silicone DC 550 column indicated that this product was essentially pure; its behavior on this column (at 150°C) exactly matched that of pure natural tetrahydroanhydrodesoxyaucubigenin. The infrared spectrum of a sample of the synthetic product was completely indistinguishable from that of the authentic natural product II.

Found: C, 70.66; H, 9.59. Calcd. for $C_9H_{14}O_2$: C, 70.10; H, 9.15%.

2-(2′-Hydroxyethyl)-5-carboxycyclopentylcarboxylic Acid (XII).—The saturated lactone ester (XI) (4 g.) was hydrolyzed by refluxing with 30 ml. of 1.2 N hydrochloric acid for 3 hr.; the solution was then evaporated. The separated crystalline solid was collected and recrystallized from ethyl acetate-petroleum ether to give 1.5 g. (40%) of a lactone carboxylic acid (XII), m. p. 123—124°C.

Found: C, 59.03; H, 6.64. Calcd. for $C_9H_{12}O_4$: C, 58.69; H, 6.54%.

The infrared spectrum of this material was completely different from that of the lactone carboxylic acid derived from the natural II.

2-(3′-Ethoxycarbonylpropyl)butyrolactone (ii, R=C_2H_5) and the Free Acid (ii, R=H).—A solution of 24 g. of 2-(2′-acetoxyethyl)-2-ethoxycarbonylcyclopentanone (i)[1b] in 30 ml. of anhydrous ethanol containing 1.5 g. of sodium ethoxide was refluxed for 2 hr. The ethanol was then removed by distillation, and the residue was poured into ice water and extracted with ether. The ether extract was then washed with water, dried over anhydrous sodium sulfate, and freed from ether. Distillation of the residual liquid in vacuo gave 16 g. of a butyrolactone derivative (ii, R=C_2H_5), b. p. 146—154°C/1.2 mmHg, n_D^{12} 1.4574, d_4^{12} 1.087, M. R. Obs.: 49.25. Calcd.: 49.49.

Found: C, 59.88; H, 8.04. Calcd. for $C_{10}H_{16}O_4$: C, 59.98; H, 8.04%.

Hydrolysis of 2 g. of this material by refluxing with 30 ml. of 4 N hydrochloric acid, followed by recrystallization of the resulting semi-solid product from benzene, afforded 1.1 g. (64%) of 2-(2′-hydroxyethyl)adipic acid γ-lactone (ii, R=H), m. p. 84—85°C.

Found: C, 55.24; H, 6.92. Calcd. for $C_8H_{12}O_4$: C, 55.80; H, 7.03%.

Condensation of 2, 3, 4-Triethoxycarbonylcyclopentanone (XVIII) with 2-Iodoethyl Methyl Ether.—The sodio-derivative of XVIII was prepared from 21.5 g. of keto triester (XVIII)[10] and 3.5 g. of finely-granulated sodium metal in 150 ml. of dry xylene according to the usual procedure. To this solution there was added dropwise 30 g. of 2-iodoethyl methyl ether with stirring; the reaction mixture was then refluxed for 10 hr., and worked up in the usual manner, using benzene for extraction of the product to give 20 g. of a mixture of a *C*-alkylated and an *O*-alkylated product (XIX and XX) in roughly equal amount (as determined by v. p. c. analysis on a silicone DC 550 column), b. p. 160—195°C/2.0 mmHg.

3, 4-Dimethoxycarbonyl-2-(2′-methoxyethyl)cyclopentanone (XXI).—The mixture of XIX and XX obtained from the preceding experiment (20 g.) was hydrolyzed by boiling it in 150 ml. of 6 N hydrochloric acid for 4 hr. After removal of the hydrochloric acid and almost all of the water under reduced pressure, the oily residue was dissolved in anhydrous methanol containing a small amount of hydrogen chloride; the resulting solution was then refluxed for 36 hr. The methanol was removed by distillation, and the residual liquid was distilled in vacuo. After a forerun of 6 g. (major fraction, b. p. 122—129°C/1.5 mmHg), which consisted mainly of 3, 4-dimethoxycarbonylcyclopentanone (XXII), the minor fraction (2.5 g.) was collected at a boiling point of 145—155°C/1.5 mmHg. This fraction was the essentially-pure desired compound, 3, 4-dimethoxycarbonyl-2-(2′-methoxyethyl)cyclopentanone (XXI), as was shown by v. p. c. on a silicone DC 550 column. The 2, 4-dinitrophenylhydrazone of this material was prepared in the usual manner in a good yield. It had a melting point of 123—124°C.

Found: C, 49.83; H, 5.04; N, 12.59. Calcd. for $C_{18}H_{22}O_9N_4$: C, 49.31; H, 5.06; N, 12.78%.

***trans-anti-cis*[11]-6, 7-Dimethoxycarbonyl-2-oxabicyclo[3. 3. 0]octane (XXIII, R=CH_3) (*dl*-XVI, R=CH_3).**—A solution of 1.0 g. of XXI in a small amount of methanol was added to a solution of 0.55 g. of sodium borohydride in 4 ml. of methanol containing a trace of sodium hydroxide; the mixture was then refluxed for 4 hr. After the methanol had been removed, the residual solid was warmed with 5 ml. of concentrated hydrochloric acid on a steam bath for 2 hr., and then dried up to give a paste-like dicarboxylic acid (XXIII, R=H). This material, without further purification, was dissolved in a small amount of ethyl acetate and treated with excess ethereal diazomethane. The solvents were removed by distillation, and the residual liquid was distilled in vacuo to give 0.25 g. (30%) of the diester (XIII, R=CH_3), b. p. 123—125°C/1.0 mmHg. The infrared spectrum of a sample of the product collected by v. p. c. using a silicone DC 550 column was completely identical with that of a specimen of the naturally-derived diester (XVI, R=CH_3), and the v. p. c. behaviors of the two samples were also identical. An analytical sample was prepared by v. p. c.

Found: C, 57.56; H, 7.21. Calcd. for $C_{11}H_{16}O_5$: C, 57.88; H, 7.07%.

The authors are greatly indebted to the late Professor Emeritus Shin-ichiro Fujise and Professor Koji Nakanishi, Tohoku University, for their valuable discussions.

BULLETIN OF THE CHEMICAL SOCIETY OF JAPAN VOL. 39 536—537 (1966)

Vinylpolymerisation. CXXIX. Pfropfung von Methylmethacrylat auf Naturkautschuk in Abwesenheit von Initiatoren*

Von Mitsuru KONDO,† Kuniyoshi YAMADA,†† Kiichi TAKEMOTO und Minoru IMOTO

Abteilung der Angewandten Chemie, Technische Fakultät der Städtischen Universität Osaka, Sumiyoshi-ku, Osaka

(Eingegangen am 2. Juli, 1965)

The graft polymerization of methyl methacrylate on natural rubber was studied in an aqueous suspension at 90°C, in the absence of initiators. It was found that methyl methacrylate could be grafted fairly smoothly on uncured natural rubber crepe and latex, both of which had previously been extracted with acetone.

Die Pfropfung von Methylmethacrylat (abgekürzt MMA) auf Naturkautschuk in Anwesenheit von Initiatoren wurde bereits ausführlich untersucht,[1,2] und das Pfropfpolymerisat ist unter dem Handelsnamen Heveaplus MG bekannt. Neuerdings haben Imoto und seine Mitarbeiter gefunden, dass MMA in wässriger Emulsion ohne Hilfe von Initiatoren leicht auf Stärke, Dialdehydstärke und Maltose,[3] und ferner auf verschiedene Natur- und Kunstfasern, vor allem beträchtlich auf Seide und Cellulosefasern[4] gepfropft werden kann.

Im Zusammenhang mit einer Reihe von unseren Untersuchungen erschien es interessant, die Pfropfung von MMA auch auf Naturkautschuk unter analogen Bedingungen zu studieren. Es ist uns nun gelungen, MMA in Abwesenheit von Initiatoren auch auf nichtvulkanisierten Naturkautschuk mit höherem Umsatz zu pfropfen. Im folgenden sollen die Resultate der Versuche beschrieben werden.

Experimentelle Ergebnisse und Diskussion

Da die Pfropfung von Vinylmonomeren auf Stärke und einige Fasern am besten mit MMA gelingt, wurde auch in diesen Versuchen MMA als das zu pfropfende Monomere gewählt. Die Ergebnisse einer Reihe von Versuchen sind in Tabelle I zusammengestellt.

Wie aus dieser Tabelle ersichtlich, entsteht in Abwesenheit von Kautschuken (Vers. B) nur wenig Polymerisat. Während die Gewichtszunahme der Kautschuke in Anwesenheit vom Kunstkautschuk (Vers. K) und von vulkanisiertem Kautschuk (Vers. v. K.) nicht bemerkbar ist, verläuft die Polymerisation von Methylmethacrylat in Anwesenheit von nichtvulkanisierten Naturkautschuken glatt (Vers. C-2, 3, 4 und L-2, 3, 4). Bei den Versuchen, bei denen das gebildete Polymerisat nicht mit Aceton, sondern mit Methyläthylketon (abgekürzt MÄK)/Methanol-gemisch (10 : 1) extrahiert wurde (C-1 und L-1), beträgt die Gewichtszunahme wesentlich weniger; das beruht möglicherweise darauf, dass bei diesen Fällen sogar auch das Pfropfpolymerisat durch MÄK extrahiert worden ist. Im Unterschied zu den Versuchen in Anwesenheit von vorher nicht gereinigten Kautschuksproben ist zu beachten, dass MMA mit höherer Ausbeute auf die vorher mit Aceton extrahierte Kautschuksproben gepfropft werden kann (Vers. C-3, 4 und L-3, 4), während aber die Pfropfpolymerisation kaum an deproteiniertem Kautschuk eintritt (Vers. L-5). Aus der Beobachtung, dass die Pfropfpolymerisation beim Kunstkautschuk nicht eintritt, wird nahegelegt, dass die Pfropfpolymerisation durch die eigentlich im Naturkautschuk befindliche Proteine verursacht werken kann.

Hinzuzufügen ist, dass Luft den Pfropfungsumsatz fast gar nicht beeinflusst.

Zusammenfassend kann festgestellt werden, dass MMA unter den beschriebenen Bedingungen ähnlich wie auf Stärke und einige Fasern auch leicht auf nichtvulkanisierten Naturkautschuk gepfropft werden kann.

Experimenteller Teil

Reagenzien.—Der handelsübliche Krepp wurde 16 Stunden mit Aceton extrahiert. Der konz. Naturkautschukslatex wurde zuerst bei 70°C getrocknet, bis er durchsichtig wurde und ein konstantes Gewicht erreichte, und dann 16 Stunden mit Aceton extrahiert. Beide Proben wurden weiter im Vakuum bei Raumtemperatur getrocknet; die von den mit Aceton extrahierte Fraktionen betrugen 2.2% bzw. 2.4%. Der protein-

* CXXVIII Mitt.: A. Shimizu, T. Otsu und M. Imoto, *J. Polymer Sci.*, **B3**, 1031 (1965).

† Gegenwärtige Adresse: Matsutani Chem. Ind. AG.; Kitamura, Itami, Hyogo.

†† Gegenwärtige Adresse: Bando Kautschuk AG.; Hyogo-ku, Kobe.

1) F. M. Merrett und R. I. Wood, *Trans. IRI.*, **27**, 27 (1956).

2) Y. Mori, K. Sato und Y. Minoura, *J. Chem. Soc. Japan, Ind. Chem. Sect.* (*Kogyo Kagaku Zasshi*), **61**, 462 (1958).

3) S. Kimura, T. Takitani und M. Imoto, Diese Bulletin, **35**, 2012 (1962).

4) M. Imoto, M. Kondo und K. Takemoto, *Makromol. Chem.*, **89**, 165 (1965); *J. Chem. Soc. Japan, Ind. Chem. Sect.* (*Kogyo Kagaku Zasshi*), **68**, 1302 (1965).

Tabelle I. Pfropfpolymerisation von MMA auf Naturkautschuk
(MMA 1.68 g, H_2O 60 ml, Emulgator 0.15 g, 90°C, 2 Stunden)

Vers. Nr.	Polymerisationsbedingungen: Art des Kautschuks	Kautschuk g	Atmosphäre	Polymere: Gesamtausbeute %	Polym.-Umsatz %	Ausbeute d. Homopolymere, g	Gew. d. gepfropft. Kautschuks g	Gew.-Zunahme d. Kautschuks, %	Pfropf.-Umsatz %	Pfropf.-Wirkungsgrad %
B	—	—	unter Luft	0.3287	7.0	—	—	—	—	—
V-1	v. K.[e]	0.5153	unter Luft	0.5883	1.6	0.0730	0.5153	0	0	0
C-1	Krepp	0.5223	unter Luft	0.9742	9.7	0.4661	0.5081[c]	0	0	0
L-1	Latex	1.3632[b]	unter Luft	2.0050	13.7	0.5544	1.4506[c]	6.4	1.9	13.6
C-2	Krepp	0.5007	unter Luft	1.4909	21.2	0.7943	0.6966	39.1	4.2	19.8
L-2	Latex	0.5837[b]	unter Luft	1.4938	19.4	0.6402	0.8536	46.2	5.8	29.7
C-3	Krepp[a]	0.4940	unter Luft	2.5313	43.5	0.8070	1.7243	249.0	26.3	60.4
L-3	Latex[a]	0.4975	unter Luft	2.6204	45.4	1.0056	1.6148	224.6	23.9	52.6
C-4	Krepp[a]	0.4865	unter N_2	1.9918	32.2	0.6726	1.3192	171.2	17.8	55.3
L-4	Latex[a]	0.5062	unter N_2	1.6701	24.9	0.6109	1.0592	109.2	11.8	47.5
L-5	Latex[d]	0.5063	unter N_2	1.1826	14.4	0.5717	0.6109	20.7	2.2	15.5
K	KK.[f]	0.5143	unter N_2	0.5580	1.3	0.0591	0.4989	0	0	0

a) Die Kautschuke wurden vorher mit Aceton extrahiert.
b) Das Gewicht des Festkörperteils wurde als 62.7% (gemessener Wert) genommen.
c) Die gewonnenen Pfropfpolymerisate wurden mit MÄK/Methanol-gemisch (10 : 1) extrahiert. (Die anderen wurden alle mit Aceton extrahiert.)
d) Der Latex wurde durch Alkalibehandelung proteinfrei gemacht.
e) Vulkanisierter Kautschuk.
f) Kunstkautschuk (Polyisopren IR-305; Shell Chem. AG.)

freie Latex wurde nach der Methode von Pummerer[5] durch Alkalibehandlung des Latexkautschuks gewonnen. Als vulkanisierter Naturkautschuk wurde die handelsübliche Platte von ca. 2 mm Dicke gebraucht. Alle Kautschukproben wurden schliesslich im Vakuum bei Raumtemperatur über Calciumchlorid getrocknet. MMA wurde mit wassriger Natriumbisulfitlösung, 5% iger Natronlauge und dann mit 20% iger Natriumchloridlösung je dreimal gewaschen, über Natriumsulfat getrocknet, und anschliessend durch dreimalige Destillation im Vakuum unter Leitung von Stickstoffstrom gereinigt: Kp. 43°C (90 mmHg). Als Emulgator diente Emulgen 106 (Polyäthylenoxydderivat der Firma Kaô Sekken).

Pfropfpolymerisation.—4.68 g frisch destilliertes MMA wurden mit 0.15 g. Emulgator in 60 ml. Wasser suspendiert und die angegebene Menge von Kautschuk in kleinen Stückchen zugegeben. Das Reaktionsgemisch wurde unter ständigem Rühren 2 Stunden bei 90°C gehalten. Nach Abkühlen auf Raumtemperatur wurde das Reaktionsgemisch in überschüssiges Methanol eingegossen. Um das Homopolymere abzutrennen, wurde das Produkt nach dem Trocknen im Soxhlet-Apparat mit Aceton oder MÄK/Methanol-gemisch (10 : 1) extrahiert. Nach 18 bis 24 stündiger Extraktion war der Rückstand homopolymerfrei; er wird als Pfropfpolymerisat betrachtet. Pfropfungsumsatz, Pfropfungswirkungsgrad usw. ergeben sich aus folgenden Gleichungen:

$$\text{Gewichtszunahme des Kautschuks} = \frac{\text{Gew. des gepfropften Kautschuks} - \text{Gew. des Kautschuks}}{\text{Gew. des Kautschuks}} \cdot 100(\%)$$

$$\text{Polymerisationsumsatz} = \frac{\text{Gesamtausbeute} - \text{Gew. des Kautschuks}}{\text{Gew. des eingesetzten Monomeren}} \cdot 100(\%)$$

$$\text{Pfropfungsumsatz} = \frac{\text{Gew. des gepfropften Kautschuks} - \text{Gew. des Kautschuks}}{\text{Gew. des eingesetzten Monomeren}} \cdot 100(\%)$$

$$\text{Pfropfungswirkungsgrad} = \frac{\text{Gew. des gepfropften Kautschuks} - \text{Gew. des Kautschuks}}{\text{Gesamtausbeute} - \text{Gew. des Kautschuks}} \cdot 100(\%)$$

5) R. Pummerer und H. Pahl, *Ber.*, **60**, 2153 (1927).

Zusammenfassung

Die Pfropfpolymerisation von Methylmethacrylat auf Naturkautschuk wurde in wässriger Suspension in Abwesenheit von Initiatoren bei 90°C untersucht. Es ergab sich, dass Methylmethacrylat ziemlich glatt auf die nichtvulkanisierten, vorher mit Aceton extrahierten Naturkautschukskrepp und -latex gepfropft werden kann.

Herrn Dr. A. Kogure von Japan Synthetic Rubber Co., Ltd. danken wir verbindlich für die Lieferung der Kunstkautschuksproben.

BULLETIN OF THE CHEMICAL SOCIETY OF JAPAN VOL. 39 538—543 (1966)

The Mass Spectra of Chalcones, Flavones and Isoflavones*

By Yasuhiro ITAGAKI, Tadashi KUROKAWA and Shin-ichi SASAKI

Department of Chemistry, Tohoku University, Sendai

and

Chin-Te CHANG and Fa-Ching CHEN

Department of Chemistry, National Taiwan University, Taipei, Republic of China

(Received July 2, 1965)

The fragmentation of flavonoid compounds by electron impact has been studied and the following results described: 1) Chalcones gave the usual fragmentation pattern; however, 2'-hydroxy chalcones showed complex spectra according to the isomerization of chalcone to flavanone. 2) The fragmentation pathways of flavones were decided by comparison with many kinds of halogen-substituted flavones. 3) Isoflavone gave the M-1 ion as the base peak, and no loss of CO was observed.

A few reports on the mass spectral investigation of flavonoids have been published.[1] However, the fragmentation pathways of these compounds on electron impact have not always been established. The mass spectra of flavone and halogen-substituted flavones have been recorded; the natural isotopic abundance of halogen made the structures of most fragment ions clear. 2'-Hydroxychalcone and 2'-hydroxyhalochalcones give complex spectra because of the isomerization of chalcone to flavanone in the spectrometer. Furthermore, the mass spectra of isoflavones have been determined; in them M-1 ions are always characteristic base peaks and no loss of CO is observed, unlike as in flavones.

Experimental

All the mass spectra were obtained with an Hitachi RMU-6D Mass Spectrometer. Mass spectra were recorded with 70 V. electron energy and an 80 μamp. ionizing current. The temperature of the ion source was 250°C. All the samples were synthesized according to the known procedure.[2]

Results and Discussion

Chalcones.—The mass spectra of 4'-methoxychalcone (I) and 4-methoxychalcone (II) have been determined (Fig. 1). Both I and II give the molecular ion (a, a') (*m/e* 238), the M-1 ion (b, b') (*m/e* 237) and the M-CH_3 ion (c, c') (*m/e* 223) as common fragments. The peaks at *m/e* 103 (e) and *m/e* 131 (f) in I are shifted to *m/e* 133 (e') and *m/e* 161 (f') in II respectively; moreover, the peaks at *m/e* 105 (d') and *m/e* 77 (g') in II are shifted to *m/e* 135 (d) and *m/e* 107 (g) in I respectively. The difference between the two compounds is the location of the methoxyl group, that is, 30 mass units.

The spectra of the two compounds are very similar, but the process of cleavage is not fully identical; for instance, the phenyl cation (g') (*m/e* 77) in II is due to the loss of CO from the benzoyl cation (d') which was formed by the fragmentation of the methyl radical from the molecular ion (a') followed by the cleavage of the c' cation. However, an abnormally abundant phenyl cation (h) in I arises from the methoxyphenyl cation (g) and the styryl cation (e). All these pathways are ascertained by means of the presence of metastable ions (Table I). Furthermore, the supposition that the (h) ion deos not arise by the simple

TABLE I. METASTABLE IONS OF METHOXYCHALCONES

4'-Methoxychalcone Reaction	Metastable
$238^+ \rightarrow 223^+ + 15$	209
$238^+ \rightarrow 135^+ + 103$	76.5
$238^+ \rightarrow 103^+ + 135$	46.2
$223^+ \rightarrow 131^+ + 92$	77
$135^+ \rightarrow 28^+ + 107$	58
$103^+ \rightarrow 77^+ + 26$	56.5
4-Methoxychalcone Reaction	**Metastable**
$238^+ \rightarrow 223^+ + 15$	209
$238^+ \rightarrow 161^+ + 77$	109
$223^+ \rightarrow 105^+ + 118$	49.5
$161^+ \rightarrow 133^+ + 28$	109.5
$105^+ \rightarrow 77^+ + 28$	56.5

* Presented at the 18th Annual Meeting of the Chemical Society of Japan, Osaka, April, 1965.

1) a) J. H. Beynon, "Mass Spectrometry and its Application to Organic Chemistry," Elsevier Publishing Company, Amsterdam (1960), p. 270.
b) R. I. Reed and J. M. Wilson, *J. Chem. Soc.*, **1963**, 5949.
c) C. S. Barnes and J. L. Occolowitz, *Austral. J. Chem.*, **17**, 975 (1964).
d) H. Budzikiewicz, C. Djerassi and D. H. Williams, "Structure Elucidation of Natural Products by Mass Spectrometry," Vol. II Holden Day, Inc., Sanfrancisco (1964), p. 262.

2) F. C. Chen and T. H. Tsai, *J. Taiwan Pharm. Association*, **4**, 42 (1952) [*Chem. Abstr.*, **49**, 5374 (1955)]; F. C. Chen, C. T. Chang, T. T. Shi and T. Lin, *J. Chinese Chem. Soc.*, Ser. **II**, **1**, 159 (1954) [*Chem. Abstr.*, **50**, 2476 (1956)].

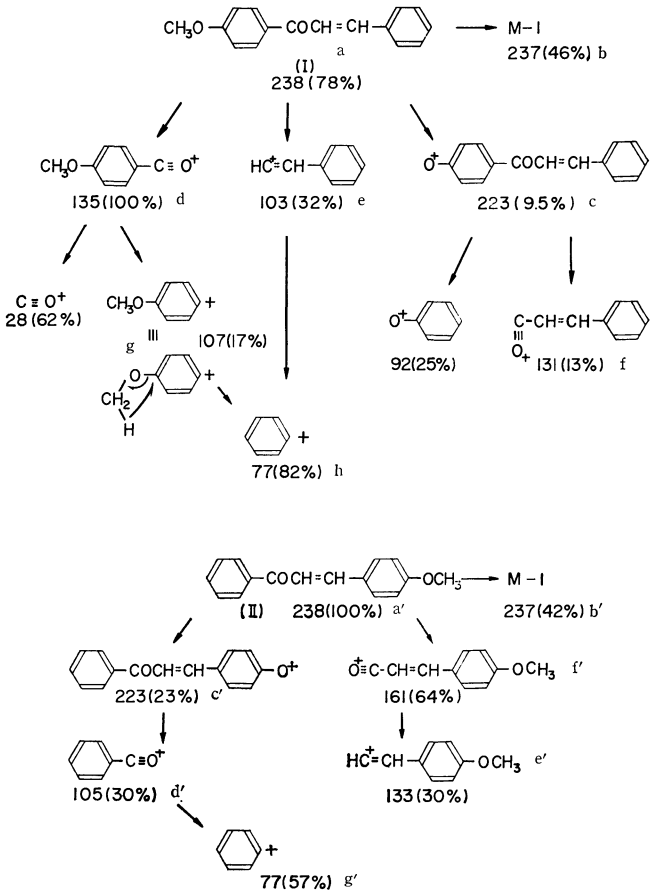

Fig. 1. Fragmentation of 4'-methoxy-(I) and 4-methoxychalcone (II).

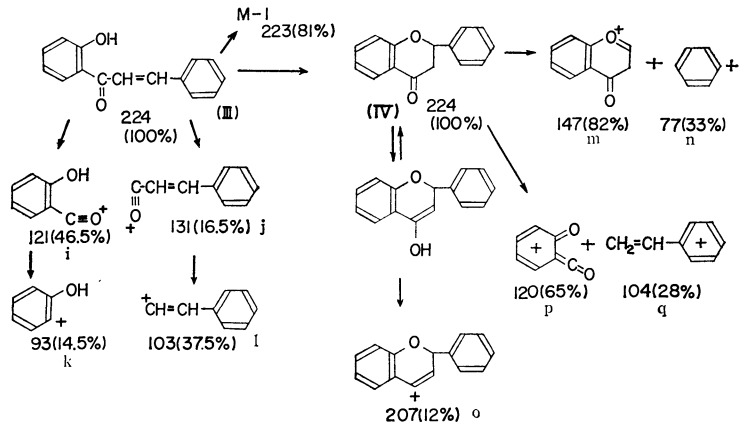

Fig. 2. Fragmentation of 2'-hydroxychalcone (III).

cleavage of the molecular ion (a) is supported by the fact that no CH_3O- -$COCH{=}CH^+$ ion appears in the spectrum of I.

The spectrum of 2'-hydroxychalcone (III) is interpreted in the same way as in the case of either I or II (Fig 2. Table II). The peaks at *m/e* 121 (i), *m/e* 131 (j), *m/e* 93 (k) and *m/e* 103 (l) must arise from 2'-hydroxychalcone itself. However, that the chalcone gives rise to the M–C_6H_5 ion (m) and the M–OH ion (o) is not conceivable; these cations, m and o, most probably arise from the loss of the phenyl radical and the hydroxyl radical respectively from the heat-isomerization product of the chalcone,

TABLE II. MASS SPECTRA OF 2'-HYDROXYCHALCONE AND 2'-HYDROXYHALOCHALCONES

				Fragments from chalcone				Fragments from flavanone				
	M	M-1	M-X	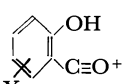	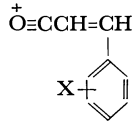	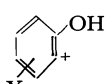	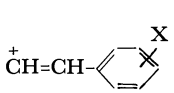	M-OH	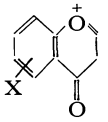	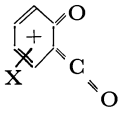	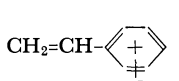	
				X=H	X=H	X=H	X=H		X=H	X=H	X=H	X=H
2'-Hydroxy-	224	223		121	131	93	103	207	147	120	104	77
chalcone (III)	(100)	(81)		(47)	(16)	(14)	(37)	(12)	(82)	(65)	(28)	(33)
				X=H	X=Cl	X=H	X=Cl		X=H	X=H	X=Cl	X=Cl
2'-Hydroxy-	258	257	223	121	165	93	137	241	147	120	138	111
3-chloro-	(100)	(74)	(12.5)	(60)	(56)	(16)	(11)	(12)	(95)	(69)	(7)	(7)
chalcone	260	259			167		139	243			140	113
(V)	(41)	(42)			(5)		(5)	(4)			(5)	(3)
				X=H	X=Cl	X=H	X=Cl		X=H	X=H	X=Cl	X=Cl
2'-Hydroxy-	258	257	223	121	165	93	137	241	147	120	138	111
4-chloro-	(100)	(72)	(12.5)	(33)	(18)	(16)	(16)	(15)	(40)	(38)	(29)	(8)
chalcone	260	259			167		139	243			140	113
(VI)	(34)	(36)			(6)		(9)	(5)			(12)	(3)
				X=H	X=Br	X=H	X=Br		X=H	X=H	X=Br	X=Br
2'-Hydroxy-	302	301	223	121	209	93	181	285	147	120	182	155
3-bromo-	(100)	(56)	(15)	(52)	(6)	(18)	(5)	(9.5)	(52)	(62)	(8)	(1)
chalcone	304	303			211		183	287			184	157
(VII)	(78)	(67)			(5.5)		(5)	(9)			(7.5)	(1)
				X=Br	X=H	X=Br	X=H		X=Br	X=Br	X=H	X=H
2'-Hydroxy-	302	301	223	199	131	171	103	285	225	198	104	77
4'-bromo-	(100)	(78)	(23)	(31)	(26)	(6)	(50)	(13)	(75)	(24)	(87)	(46.5)
chalcone	304	303		201		173		287	227	200		
(VIII)	(97)	(91)		(32)		(6)		(12)	(72)	(24)		
				X=Br	X=H	X=Br	X=H		X=Br	X=Br	X=H	X=H
2'-Hydroxy-	302	301	223	199	131	171	103	285	225	198	104	77
5'-bromo-	(100)	(78)	(12.5)	(20)	(21)	(5)	(56)	(7.5)	(48)	(96)	(83)	(42.5)
chalcone	304	303		201		173		287	227	200		
(IX)	(97)	(91)		(19)		(4.5)		(6.5)	(47)	(95)		
				X=Cl	X=H	X=Cl	X=H		X=Cl	X=Cl	X=H	X=H
2'-Hydroxy-	258	257	223	155	131	127	103	241	181	154	104	77
5'-chloro-	(100)	(67)	(9)	(31)	(16)	(9)	(45)	(9.5)	(63)	(76)	(58)	(58)
chalcone	260	259		157		129		243	183	156		
(X)	(44)	(42)		(9)		(7)		(3)	(22)	(50)		

TABLE III. MASS SPECTRA OF FLAVONE AND HALOFLAVONES

	M	M-1	M-CO 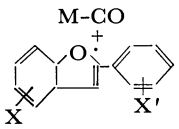	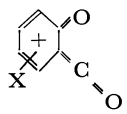	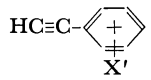	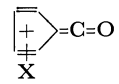
			X=X'=H	X=H	X'=H	X=H
Flavone (I)	222	221	194	120	102	92
	(100)	(33)	(52)	(80)	(12)	(43)
			X=Cl, X'=H	X=Cl	X'=H	X=Cl
6-Chloroflavone (II)	256	255	288	154	102	126
	(100)	(16)	(14)	(95)	(19)	(27)
	258	257	230	156		128
	(36)	(22)	(4)	(31)		(10)
			X=Cl, X'=H	X=Cl	X'=H	X=Cl
7-Chloroflavone (III)	256	255	228	154	102	126
	(100)	(23)	(48)	(50)	(37)	(35)
	258	257	230	156		128
	(31)	(21)	(14)	(15)		(11)
			X=Cl, X'=H	X=Cl	X'=H	X=Cl
8-Chloroflavone (IV)	256	255	228	154	102	126
	(90)	(12)	(15)	(100)	(15)	(20)
	258	257	230	156		128
	(25)	(15)	(7)	(44)		(7)
			X=H, X'=Cl	X=H	X'=Cl	X=H
4'-Chloroflavone (V)	256	255	228	120	136	92
	(92)	(13)	(32)	(100)	(12)	(70)
	258	257	230		138	
	(31)	(20)	(9)		(4)	
			X=Br, X'=H	X=Br	X'=H	X=Br
6-Bromoflavone (VI)	300	299	272	198	102	170
	(100)	(12)	(13)	(89)	(36)	(29)
	302	301	274	200		172
	(96)	(29)	(12.5)	(83)		(28.5)
			X=Br, X'=H	X=Br	X'=H	X=Br
7-Bromoflavone	300	299	272	198	102	170
(VII)	(100)	(20)	(45)	(50)	(60)	(30)
	302	301	274	200		172
	(98)	(37)	(44)	(49)		(29)
			X=Br, X'=H	X=Br	X'=H	X=Br
8-Bromoflavone	300	299	272	198	102	170
(VIII)	(100)	(13)	(15)	(87)	(22)	(13)
	302	301	274	200		172
	(96)	(28)	(15)	(84)		(12.5)
			X=I, X'=H	X=I	X'=H	X=I
6-Iodoflavone (IX)	348	347	320	246	102	218
	(100)	(7)	(8)	(52)	(14)	(20)
			X=I, X'=H	X=I	X'=H	X=I
7-Iodoflavone (X)	348	347	320	246	102	218
	(100)	(13)	(27)	(30)	(20)	(15)
			X=H, X'=I	X=H	X'=I	X=H
4'-Iodoflavone (XI)	348	347	320	120	228	92
	(100)	(5)	(14)	(75)	(9)	(41)

TABLE IV. MASS SPECTRA OF ISOFLAVONES

	M	M-1	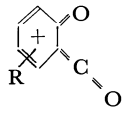	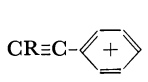	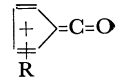
			R=H	R=H	R=H
Isoflavone (II)	222	221	120	102	92
	(91.5)	(100)	(40)	(11)	(34)
			$R=OCH_3$	R=H	$R=OCH_3$
7-Methoxy-isoflavone (III)	252	251	150	102	122
	(95)	(100)	(50)	(10)	(30)
	M	M-42	M-42-1	R=OH	$R=CH_3$
2-Methyl-7-acetoxy-isoflavone (IV)	294	252	251	136	116
	(13)	(81)	(100)	(2)	(8)

that is, flavanone (IV). Other peaks at *m/e* 120 (p) and *m/e* 104 (q) which are never observed in the spectrum of chalcone without a hydroxyl group at C-2', are also well-explained through the isomerization of III to IV.

The spectra of the following 2'-hydroxyhalochalcones have been determined (Table II): 2'-hydroxy-3-chloro-(V), 2'-hydroxy-4-chloro-(VI), 2'-hydroxy-3-bromo - (VII), 2'-hydroxy-4'-bromo-(VIII), 2'-hydroxy-5'-bromo-(IX) and 2'-hydroxy-5'-chlorochalcone (X). In all cases these hydroxyhalochalcones give molecular ions as the base peaks and M-X ions as the characteristic peaks. They also show both fragments from hydroxyhalochalcones (V-X) and the corresponding flavanones, as in the case of 2'-hydroxychalcone itself.

Flavones.—Barnes et al. reported that flavone (I) itself gives the molecular ion (*m/e* 222) as the base peak and shows the substantial loss of one hydrogen, thus giving an ion (*m/e* 221); one oxygen is readily eliminated as CO, but more readily by the retro-Diels-Alder fission of the heterocyclic ring, thus giving two ions, one with a quinonoid (*m/e* 120) (b), and the other a phenylacetylene

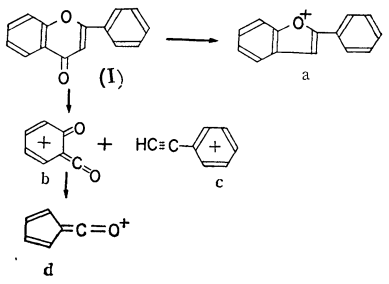

Fig. 3. Fragmentation of flavone.

(*m/e* 102) (c) structure. The d ion (*m/e* 92) arises from the loss of CO from the b ion (Fig. 3).

The spectra of 6-chloro- (II), 7-chloro- (III), 8-chloro- (IV), 4'-chloro- (V), 6-bromo- (VI), 7-bromo- (VII), 8-bromo- (VIII), 6-iodo- (IX), 7-iodo- (X) and 4'-iodoflavone (XI) have also been determined. All the characteristic peaks arise from the haloflavones correspond to the peaks of the molecular ion, the M-1 ion, and to the a, b, c and d of flavone itself. Therefore, the breakdown process of flavone proposed by Barnes may be regarded as quite reasonable (Table III).

Isoflavones.—It has been reported[1a] that the spectrum of daidzein dimethyl ether (I) shows a peak at *m/e* 282 (molecular ion) as the base peak, other peaks at *m/e* 150 (a) and *m/e* 132 (b), and no M-CO ion (Fig. 4).

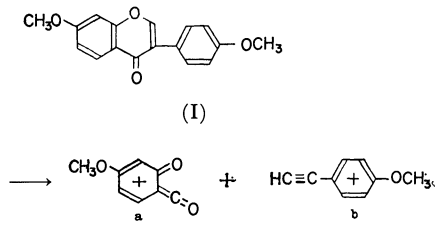

Fig. 4. Fragmentation of daidzein dimethyl ether.

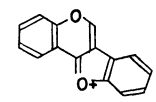

However, according to our determination of isoflavone (II) and 7-methoxyisoflavone (III), M-1 ions appear as the base peaks. In the case of 2-methyl-7-acetoxyisoflavone (IV), the ion loses a ketene molecule from the molecular ion; then it loses one hydrogen radical, which appears as the base peak. The structure of the M-1 ion is probably an oxonium ion (c) results from the

fragmentation of a hydrogen radical at C-2′ of the molecular ion. Because of the stability of the ion, no further fragmentation or loss of CO occurs, unlike as in flavones (Table IV).

Summary

The mass spectra of chalcones, flavones and isoflavones have been studied. From the metastable peaks or from a comparison with halogen-substituted compounds, the main fragmentation paths of chalcones and flavones on electron impact have been elucidated. The fragmentation of isoflavones, which give characteristic M-1 ions as base peaks has also been studied.

The authors wish to express their hearty thanks to Professor Koji Nakanishi for his encouragement throughout the course of this work.

BULLETIN OF THE CHEMICAL SOCIETY OF JAPAN VOL. 39 543—547 (1966)

The Interaction of Cumulene Systems with Organometallic π-Complexes. IV.[1] Novel π-Allyl Complexes Obtained from the Reactions of Allene with Iron and Cobalt Carbonyls

By Akira NAKAMURA*1

The Institute of Scientific and Industrial Research, Osaka University, Sakai, Osaka

(Received July 2, 1965)

2, 2'-Bi-π-allylene(hexacarbonyl)di-iron, $[(OC)_3Fe]\cdot\begin{matrix}CH_2\\CH_2\end{matrix}\!\!>\!C\!-\!C\!<\!\!\begin{matrix}CH_2\\CH_2\end{matrix}\cdot[Fe(CO)_3]$, was found to be a product of the reaction of allene with $Fe_3(CO)_{12}$. A study of the NMR spectrum, however, showed that a rapid valence tautomerisation takes place, even at −10°C between the 2, 2'-bi-π-allylene structure and the related butadiene-type structure. In the presence of an excess of $Co_2(CO)_8$, allene yielded the $[(C_3H_4)Co(CO)_3]_2$ complex. The structure of this complex in which a $\begin{matrix}CH_2\\CH_2\end{matrix}\!\!>\!C\!-\!C\!<\!\!\begin{matrix}O\\\end{matrix}$ skeleton was bound to two $Co(CO)_2$ groups via π-allyl and acyl groups, was suggested.

In a previous paper,[2] we have described the interaction of cumulene systems with organometallic π-complexes such as iron carbonyls to give a variety of stable π-complexes. As the first member of the cumulene system, allenic systems were examined for their ability to form π-complexes. Tetraphenylallene gave a stable iron tricarbonyl complex, $(Ph_4C_3)Fe(CO)_3$ and a cobalt complex, $(C_5H_5)Co(CO)(Ph_4C_3)$. Unsubstituted allene gave complexes of the compositions $[(C_3H_4)Fe(CO)_3]_2$ (I) and $[(C_3H_4)_2Fe(CO)_3]_{1-2}$. The structure of these complexes was not, however, clear. In this report, an investigation of the structure of the complex I will be described. A novel complex obtained from the reaction of allene with dicobalt octacarbonyl will also be reported.

Results and Discussion

The reaction of unsubstituted allene with tri-iron dodecacarbonyl at 120°C under pressure has been described in the previous paper.[2] The same reaction at atmospheric pressure in *n*-hexane, using an excess of tri-iron dodecacarbonyl gave a similar product, except that in this case the amount of the complex I increased and a new red compound was isolated in a small amount. When iron pentacarbonyl was used under the pressure of carbon monoxide at 140°C, no reaction was observed. In order to get a clue about the skeletal structure of the complexed organic part of complex I, the bromination of complex I was studied.*2 It gave colorless crystals upon bromination at room temperature. The crystal exhibited a reaction typical of allylic bromide, but it did not add another molecule of bromine. The presence of a double bond was shown by the permanganate test. The infrared spectrum of the crystals was found to be superimposable upon that of the authentic 2, 3-bis(bromomethyl)-1, 4-dibromobutene-2 prepared by the literature method.[3] If no coupling

1) For the previous paper of this series, cf. A. Nakamura, This Bulletin, **38**, 1868 (1965).

*1 Present address: Faculty of Engineering Science, Osaka University, Toyonaka, Osaka.

2) A. Nakamura, P.-J. Kim and N. Hagihara, *J. Organometal. Chem.*, **3**, 7 (1965).

*2 The preliminary results of the study have already been reported; cf. A. Nakamura and N. Hagihara, *J. Organometal. Chem.*, **3**, 480 (1965).

3) A. C. Cope and F. Kagan, *J. Am. Chem. Soc.*, **80**, 5499 (1958).

of the C_3H_4 moiety occurs during the bromination, the structure of the bromination product suggests that the skeletal structure of the organic part is $\begin{matrix} C \\ C \end{matrix}\!\!>\!C\!-\!C\!<\!\!\begin{matrix} C \\ C \end{matrix}$. Therefore, the 2, 2-bi-π-allylene structure may be present in I.*3 The infrared spectrum of I had strong maxima at 2068, 2030, 2003 and 1990 cm^{-1}, indicating the presence of terminal metal carbonyl groups. The infrared spectrum as a whole supported the π-allyl type structure. Recently, Emmerson et al.[4] reported the preparation of cyclic bi-π-allylene type iron carbonyl complexes such as are shown below.

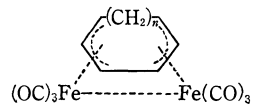

$n=1, 2$

These complexes can be regarded as derivatives of unknown 1, 1'-bi-π-allylene(hexacarbonyl)diiron. 2, 2'-Bis-π-allylenemetal complexes also have been unknown. If one assumes the 2, 2'-bi-π-allylene structure for I, the NMR spectrum would have two singlets, with a separation of ca. 1. p.p.m., corresponding to the syn and anti protons of the π-allylic group. The actual NMR spectrum in carbon tetrachloride at 35°C had two peaks, separated by only 0.07 p.p.m. and centered at 8.34 τ. The separation became smaller when the temperature was lowered, until finally the two peaks condensed into a sharp singlet at −10°C. This NMR behavior can be understood on the assumption that the following valence tautomerism occurs rapidly, even at −10°C in the solution. This rapid tautomerism averages out all the protons, and the NMR spectrum will have a single peak. The τ-value can be calculated approximately as follows on the assumption of this tautomerism. The calculation, which involves averaging out all the τ-values[5] of the terminal protons of butadiene(tricarbonyl)iron and the hypothetical τ-values for π-allyl(tricarbonyl)iron, results in a value of 8.35 τ. π-Allyl(tricarbonyl)iron is reported to be paramagnetic in a solution, and the NMR spectrum can not be obtained.[6] The hypothetical τ-value was calculated by averaging the known τ-values of the terminal protons in π-allyl(tetracarbonyl)-manganese and in π-allyl(tricarbonyl)cobalt.[7]

At much lower temperature, e. g., at −55°C in chloroform, the compound I showed three broad signals centered at about 8.3 τ; these may correspond to the tautomers slowly exchanging at the temperature. At higher temperatures, such as at 65°C, two peaks are observed. However, the oxidative degradation of the compounds I was occurring during the measurement by the solvent, carbon tetrachloride, and no satisfactorily accurate result could be obtained. These two NMR peaks at higher temperatures appeared to us to arise from

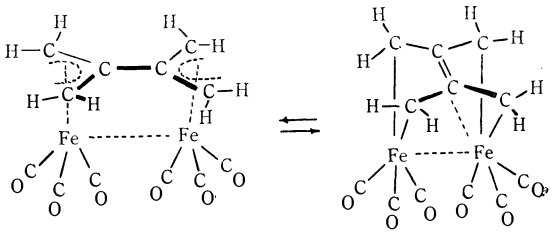

Fig. 1

the π-allylic tautomer (A). This fact suggests that the π-allylic form might be predominant at higher temperatures. The possible intervention of the π-allylic complex at higher temperatures has already been suggested in the deuterium exchange study[8] of polymethylcyclopentanes using such metal catalysts as palladium. Therefore, the predominance of the π-allylic form at higher temperatures is not unreasonable.

Rapid valence tautomerism has been postulated in the interpretation of the NMR spectra of some cyclic polyene-metal carbonyl complexes. For example, cyclooctatetraene(tricarbonyl)iron has only one sharp NMR signal.[9] This NMR behavior was once taken as evidence for the planar structure and aromaticity of the cyclooctatetraene ring on π-complex formation.[9a] X-ray structure analysis[10] of the compound, however, has shown that the ring is not planar in the crystalline state. The appearance of only one NMR signal has been understood as due to rapid valence tautomerism in the solution. More recently, two other similar examples[11] have been added to this type of tautomerism. It is of interest to regard compound I as the first example of rapid tautomerism occurring in the chain structure. Valence tautomerism now

*3 The author at first called this system "2, 2'-bis-π-allyl" to indicate two π-allyl systems connected at the center carbon atoms. However, it was later recommended that the system be called "2, 2'-bi-π-allylene" because of its bifunctional character. A confusion may indeed arise because allylene is a common name for 1-propyne. The author nevertheless prefers to use the latter nomenclature for the system, as he used it in the preliminary note.

4) G. F. Emmerson, J. E. Mahler, R. Pettit and R. Collins, ibid., **86**, 3590 (1964).

5) M. L. H. Green, L. Pratt and G. Wilkinson, *J. Chem. Soc.*, **1959**, 3753.

6) H. D. Murdoch and E. A. C. Lucken, *Helv. Chim. Acta*, **47**, 1517 (1964).

7) W. R. McClellan, H. H. Hoehn, H. N. Cripps, E. L. Muetterties and B. W. Howk, *J. Am. Chem. Soc.*, **83**, 1601 (1961).

8) J. J. Rooney and G. Webb. *J. Catalysis*, **3**, 488 (1964) and references therein.

9) a) T. A. Manuel and F. G. A. Stone, *Proc. Chem. Soc.*, **1959**, 90 (1959); b) M. D. Rausch and G. N. Schrauzer, *Chem. & Ind.*, **1959**, 957; c) A. Nakamura and N. Hagihara, This Bulletin, **32**, 880 (1959).

10) W. N. Lipscomb and B. Dickens, *J. Am. Chem. Soc.*, **83**, 4862 (1961).

11) a) R. B. King, *Inorg. Chem.*, **3**, 785 (1964); b) R. Pettit, J. E. Mahler and D. A. K. Jones, *J. Am. Chem. Soc.*, **86**, 3589 (1964).

seems to be possible not only in the cyclic polyene ligand, but also in the chain structure.

Our investigation suggests that a comparison of the thermodynamic stability between the π-allylic form (A) and the π-complexed butadiene form (B) is possible by means of the measurement of the NMR spectrum.

The 2, 2'-bi-π-allylene structure may yield compounds with many other transition metals, and other interesting properties may be found. We therefore intend to explore the chemistry of 2, 2'-bi-π-allylene complexes and related compounds further.

The Allene Complex of Cobalt Carbonyl.— The polymerization of allenic compounds by dicobalt octacarbonyl at room temperature was first reported by Greenfield et al.[12] The presence of metal carbonyl stretching bands in the infrared spectrum of the polymer attracted our interest. So far, only the formation of rather unstable diene-cobalt carbonyl complexes has been reported. However, the considerable stability of the metal carbonyl species in the allene polymer prepared by means of the cobalt carbonyl catalyst suggests the possibility of the formation of a stable allene complex of cobalt carbonyl. Thus, allene was slowly bubbled into a solution of dicobalt octacarbonyl in benzene at room temperature. A slight change in color to reddish brown and an evolution of heat was observed.

The sublimation of the reaction mixture gave air-sensitive yellow and black crystals. The black crystals were identified as tetracoblat dodecacarbonyl by means of their infrared spectrum. The yellow crystals were further purified and found to have the composition: $[(C_3H_4)Co(CO)_3]_2$ (II). A well-crystallized pure sample was stable in air for a few days, but the solution in organic solvents was unstable. Decomposition usually begins after the solution has stood in air at room temperature for about 10 min. The infrared spectrum showed two very strong bands at 2050 and 2010 cm^{-1}, indicating the presence of terminal metal carbonyl groups. The presence of a strong band at 1620 cm^{-1} suggests the presence of a keto carbonyl with an unusually low stretching frequency. This keto carbonyl may be of the acyl cobalt type. The NMR spectrum in carbon tetrachloride showed two singlets, at 6.39 and 7.72 τ, of equal intensity. The position of the peaks may be well accounted for by assuming the presence of a π-allyl group with an electro-negative group at the 2-position. For example, π-allyl cobalt tricarbonyl shows its NMR peak at 6.93 and 7.85 τ.[7] The peak at 6.93 τ has been assigned to the syn proton and the one at 7.85 τ, to the anti protons. The chemical shifts of the syn and anti protons in the known π-allyl cobalt tricarbonyl are, therefore, similar to those observed for the complex, except for the presence of a shift towards a lower field, which is probably due to an electron-withdrawing substituent at the 2-position.

The structure of the complex was investigated by bromination. The action of bromine at room temperature in carbon tetrachloride evolved 4 mol. of carbon monoxide. The composition of the complex indicates that six carbon monoxide groups are incorporated into the structure. Therefore, two carbon monoxide groups are bound to the organic part, and four such groups are present as terminal metal carbonyl groups. The bromination product was a complicated one. It contained an acid bromide of an unknown structure and other materials. The bromination in methanol at about 15°C gave a colorless crystals in a good yield. The elemental analysis and the molecular weight measurement, together with the infrared evidence, favor a diketone structure: $(BrCH_2)_2$-C–CO–CO–C$(BrCH_2)_2$. The bromination in methanol at higher temperatures resulted in a reduced yield of the diketone and in a mixture of bromoesters. The bromination product suggests that the skeletal structure of the organic part is $\begin{matrix}C\\C\end{matrix}\!>\!C\text{–}C\!<\!^{O}$. In addition, the presence of an acyl cobalt linkage is indicated by the isolation of an acid bromide, and also by the infrared band of II at 1620 cm^{-1}. The accumulated evidence suggests the following π-allyl-acyl cobalt carbonyl structure for the complex.

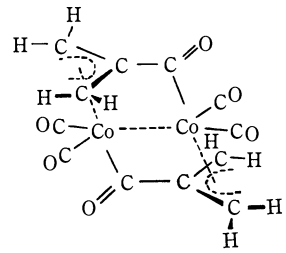

(II)

Fig. 2

A dimeric structure with a Co–Co bond, as indicated by its molecular weight, is necessary in explaining the diamagnetism of the compound. An alternative structure, in which one cobalt atom is bound to the π-allyl and the acyl groups simultaneously, is possible. However, this structure might allow dissociation in the solution, as in the case of the π-allyl-(tricarbonyl)iron dimer.[6] The considerable stability of the complex in solution and its diamagnetism in carbon tetrachloride makes the latter structural possibility less probable.

The reaction of II with triphenylphosphine occurred readily when the solution of the reactants was warmed in benzene; orange air-stable crystals

12) a) H. Greenfield and I. Wender and J. H. Wotiz, *J. Org. Chem.*, **21**, 875 (1956); b) I. W. Stolz, G. R. Dobson and R. K. Sheline, *Inorg. Chem.*, **2**, 1264 (1963).

were thus obtained. The crystals have strong infrared bands at 2002 cm^{-1} and at 1964 cm^{-1} and its NMR peaks mainly in the phenyl proton range. The composition was nearly $(C_3H_4)_2$-$Co_2(CO)_2(Ph_3P)_3$. The structure of the phosphine derivative is not clear at present.

The isolation of the iron and cobalt compounds is closely connected with the known polymerization[13] and carbonylation[14] of allene by organometallic catalysts. The π-allylic iron carbonyl compound (I) can be regarded as the stabilized form of the initiation step of the allene polymerization. The importance of π-allyl complexes of nickel and cobalt in the polymerization of butadiene and allene has already been shown.[13] In the reaction with allene, iron(0) in the iron carbonyl group ($Fe(CO)_3$) forms a stable complex, as has been described above, whereas nickel(0) does not. Possibly for this reason, nickel(0) complexes polymerize allene to a 1, 2-polymer with a very regular structure at room temperature.[13] The isolation of a stable complex of cobalt carbonyl with the $\overset{C}{C}\!>\!C\!-\!C\!<\!\overset{}{O}$ skeletal structure shows that this form might be the stabilized initial step of the carbonylation of allene. The catalytic carbonylation[14] of allene has been reported using a ruthenium(II) or a platinous chloride-stannic chloride system. In all cases, carbon monoxide adds to the central carbon atom of the allene system. The close similarity of the structure shows that the carbonylation of allene may be possible by means of a cobalt carbonyl catalyst.

The Interaction of Allene with Other Metal π-Complexes.—The interaction of allene with molybdenum hexacarbonyl with ultraviolet irradiation formed an orange solution under nitrogen. The attempt to isolate the allene complex failed, however, because of its instability. The orange complex may be stable only in the solution. We regard it as similar to the unstable olefin and acetylene complexes reported by Sheline et al.[12] No reaction of allene was observed in the thermal reaction with molybdenum hexacarbonyl at 70°C at atmospheric pressure or with dimanganese decacarbonyl at 150—160°C under pressure. No stable π-complexes have been isolated from the photochemical reaction of allene with cyclopentadienyl vanadium tetracarbonyl or with cyclopentadienyl manganese tricarbonyl. The polymerization of allene was observed, in the thermal reaction with nickelocene at 150—200°C to give a polymer with an irregular structure, together with a small amount of an unstable red compound. Tetraphenylallene was recovered unchanged in the reaction with nickelocene at 140°C.

Experimental

All melting points are uncorrected and were measured by a micro-melting point apparatus Yanagimoto Model MP-S2. The melting points and decomposition points in nitrogen were measured in a sealed capillary filled with nitrogen. The infrared spectra were obtained by a Hitachi Model EPI-2 and a Jasco Model DS-402G grating spectrometer. The NMR spectra were recorded by a Varian Model A-60 instrument and a Jeol JNM 4H-100 instrument using tetramethylsilane as an internal standard. The elemental analysis for carbon and hydrogen was performed by Mr. Shibano of this Institute. The molecular weights were measured in a bezene solution using a Mechrolab Vapor Pressure Osmometer, Model 301A.

Materials.—Allene was prepared by the debromination of 2, 3-dibromo-propene-1 with zinc dust. Tri-iron dodecacarbonyl and dicobalt octacarbonyl were prepared by the literature method.[15]

The Preparation of I.—a) The preparation of I in an autoclave under an autogeneous pressure of allene has been described in a previous paper.

b) In a 100 ml. round-bottomed flask, tri-iron dodecacarbonyl (1.5 g.) and a *n*-hexane solution of allene (1 ml. in 30 ml.) were placed. The mixture was then refluxed by stirring it for 3 hr. under nitrogen, using a condenser cooled with dry ice - acetone. At all times there was an excess of iron carbonyl. When the reaction mixture was treated in a way similar to that described previously, about 70 mg. of I was obtained. In addition to this I, a small amount of orange oil and red crystals were obtained.

The Bromination of I.—In a carbon tetrachloride solution of I (0.1 g. in 5 ml.), an excess of bromine (1 ml.) in carbon tetrachloride was slowly added at room temperature in air. An instant reaction occurred, with the evolution of a gas. The ferric bromide formed was removed by an addition of water, and the product was obtained after the evaporation of the solution. The crude product was purified by sublimation at 70°C/3 mmHg, followed by washing with *n*-hexane, to give 0.1 g. of colorless crystals. M. p. 174°C (in sealed tube).

The Preparation of II.—Into a solution of di-cobalt octacarbonyl (3.0 g.) in benzene (50 ml.), 1 ml. of liquid allene was slowly introduced in the gaseous state with stirring at 40°C during a 30 min. period under nitrogen. The evolution of a gas and slight heat was observed. After the reaction mixture had stood for 2 hr., then the solvent was evaporated under reduced pressure. A dark brown solid containing a yellow solid was thus obtained. The crude product was obtained by slow sublimation at 80°C/3 mmHg under nitrogen. The sublimate was a mixture of dark brown and yellow crystals. The dark brown sublimate consisted of di-cobalt octacarbonyl and teracobalt dodecacarbonyl and was sensitive towards air. The sublimate was stored under nitrogen for several days. During this period, the di-cobalt octacarbonyl decomposed. The product was then extracted with benzene.

13) a) S. Otsuka, M. Mori and F. Imaizumi, ibid., **87**, in press and references therein; b) R. E. Benson and R. V. Lindsey, Jr., ibid., **81**, 4247, 4250 (1959).

14) a) T. J. Kealy and R. E. Benson, *J. Org. Chem.*, **26**, 3126 (1961); b) E. L. Jenner and R. V. Lindsey, Jr., U. S. Pat. 2876254 (1959).

15) a) R. B. King and F. G. A. Stone, "Inorganic Syntheses," Vol. 7, McGraw Hill, New York (1963), p. 193; b) I. Wender, ibid., Vol. 5, McGraw Hill, New York (1959), p. 190.

The evaporation of the solvent under nitrogen, followed by sublimation, gave pure II as yellow crystals. The purified crystals were stable in air for a few days, and a slight decomposition was observed when it was stored in air for a longer period. The solution of II in benzene or in carbon tetrachloride began to decompose in air in 10—20 min.

The preparation of II can be performed under the pressure of carbon monoxide. A cooled *n*-hexane solution (20 ml.) of allene in an ampoule and dicobalt octacarbonyl in benzene (20 ml.) were placed in an autoclave at about 10°C. The carbon monoxide pressure was raised to 50 atm., and then the contents of the ampoule and the cobalt carbonyl solution were mixed. The autoclave was heated with rocking to 50—60°C for 1 hr. The product (0.7 g.) was isolated in this case by the evaporation of the solvent, followed by extraction with *n*-hexane and recrystallization. The purification of the product could be achieved by alumina chromatography under nitrogen.

Found: C, 39.76; H, 2.29. Calcd. for $[C_6H_4CoO_3]_2$: C, 39.37; H, 2.20%. mol. wt. 322: calcd. 366.

The Bromination of II.—a) In methanol: A suspension of II in methanol was mixed slowly with a solution of bromine in carbon tetrachloride at 10—15°C until the bromine was in excess. Water was then added to separate the cobaltous bromide formed, and the carbon tetrachloride layer was extracted with benzene. The evaporation of the solvent gave crude colorless crystals, which were further purified by recrystallization; m. p. 130—132°C in a sealed capillary.

Found: C, 15.6; H, 2.1. Calcd. for $C_4H_4Br_3O$: C, 15.60; H, 1.3%. mol. wt. 556. calcd. 615. infrared max., 1720cm^{-1} (strong, –CO–CO–).

The vicinal bromide structure was shown by the reaction with potassium iodide in acetone to give iodine.

b) In carbon tetrachloride: A solution of II in carbon tetrachloride was mixed with a solution of bromine at room temperature. The reaction occurred immediately. The product was isolated by distillation on a small scale and gave a colorless liquid. The characteristic smell and acidity of the liquid suggested the presence of an acid bromide. The presence of strong infrared band at 1780 cm^{-1} showed this compound to be acid bromide. The product hydrolyzed in air, and analysis was impossible. Another bromination, in a mixture of ethanol and carbon tetrachloride, gave a mixture of bromoesters (b. p. 100°C/3 mmHg), as evidenced by the presence of 1735 cm^{-1} band in the infrared spectrum.

Summary

The product with the $[C_3H_4Fe(CO)_3]_2$ composition obtained from the reaction of allene with tri-iron dodecacarbonyl has been found to be the first metal complex with a 2, 2'-bi-π-allylene structure. A study of the NMR spectrum has, however, shown an extensive valence tautomerism occurring, even at -10°C between the bi-π-allylene structure and the related butadiene-type structure. The reaction of allene with an excess of dicobalt octacarbonyl gave yellow crystals with the $[(C_3H)_4$-$Co(CO)_3]_2$ composition. A structure has been proposed in which a $\begin{matrix}CH_2\\CH_2\end{matrix}\!\!>\!C\text{–}C\!\!\begin{matrix}\diagup\!\!\!\!\diagup O\\\diagdown\end{matrix}$ skeleton is bound to cobalt atoms via π-allyl and acyl groups. The relation between the structures of these complexes and the catalytic reaction of allene have been discussed.

The author is grateful to Professor Nobue Hagihara for his invaluable discussions and encouragement during this study. He also wishes to express his appreciation of the advice and cooperation of Professor Sei Otsuka in the preparation of this report.

BULLETIN OF THE CHEMICAL SOCIETY OF JAPAN VOL. 39 547—551 (1966)

The Crystal Structure of the Pyrene-Tetracyanoethylene Complex

By Haruo KURODA, Isao IKEMOTO and Hideo AKAMATU

Department of Chemistry, Faculty of Science, The University of Tokyo, Hongo, Tokyo

(Received July 3, 1965)

The crystal structure of the pyrene-tetracyanoethylene (TCNE) complex has been determined by the two-dimensional Fourier method. The monoclinic unit cell dimensions are: $a=14.58$, $b=7.34$, $c=8.09$ Å and $\beta=92.4°$. The space group is $P2_1/a$. Two pyrene and two TCNE molecules are contained in a unit cell. Pyrene and TCNE molecules are stacked alternately along the c-axis direction, making their molecular planes parallel to each other. The center of a TCNE molecule is not directly above that of the neighboring pyrene molecule, but is displaced considerably along the long axis of pyrene. The mean separation of the molecular plane is 3.32 Å.

The crystal of the charge-transfer complex involving pyrene as the electron donor and tetracyanoethylene (TCNE) as the electron acceptor is an organic semiconductor, the resistivity of

which is about $10^{12}\Omega$·cm. at room temperature with an energy gap of 1.6 eV.[1] Interestingly, this complex exhibits a relatively high photoconductivity, which enables us to determine the drift mobilities of charge carriers.[2] Further investigation is going on in our laboratory in order to elucidate the nature of the electronic conduction. The determination of the crystal structure was undertaken, in the first place, in connection with these studies. There is, however, another point of interest in its crystal structure. The pyrene and the TCNE molecules are nonpolar and planar molecules, similar in shape and size to each other. In this case, the intermolecular forces other than the charge-transfer one do not seem to depend strongly on the relative orientation of the symmetry axes of the pyrene molecule to those of TCNE in so far as they are stacked face-to-face. One may, therefore, presume that the relative orientation is mainly determined by the charge-transfer interaction. It would be interesting to see if the orientation of the molecules in the crystal is the one expected from the charge-transfer theory.

Experimental

The dark purple crystals of a lath shape elongated in the c-axis direction, or of a square, thin plate with a (100) face, were obtained by slowly evaporating the solvent from the chloroform solution containing equimolar amounts of pyrene and TCNE. The mole ratio of pyrene and TCNE in the crystal was determined to be 1 : 1 by chemical analysis. The crystal is stable if it is kept in an atmosphere saturated with vapors of pyrene and TCNE, but it decomposes gradually in air. Thus, the crystal was sealed in a glass capillary with a very thin wall during the X-ray experiments.

The crystal data are as follows:

Pyrene-TCNE complex: $C_{16}H_{10}\cdot C_6N_4$

Monoclinic

$a=14.58\pm0.05$ Å

$b=7.34\pm0.03$ Å

$c=8.09\pm0.03$ Å

$\beta=92.4°$

Volume of the unit cell: 864.4 Å^3

Absent spectra: $h0l$ when h is odd, $0k0$ when k is odd.

Space group: $P2_1/a$ (C_{2h}^5)

Assuming that two molecules of pyrene and two molecules of TCNE are in a unit cell, the density is calculated to be 1.28 g.cm^{-3} (the density observed by the floatation method is 1.3 ± 0.02 g.cm^{-3}).

The intensities of $h0l$ and $hk0$ reflexions were measured visually from multiple-film Weissenberg photographs with Cu$K\alpha$ radiation. The number of the measured reflexions is 80 for $h0l$ and 92 for $hk0$. No correction was made for the absorption, while the corrections for the Lorentz and polarization factors were made in the usual way.

The Determination of the Crystal Structure

The crystal shows a marked dichroism.[3] It is known that the strong band at 830 mμ in the absorption spectrum of the crystal is the charge-transfer band, which is distinctly polarized in the c-axis direction. This fact indicates that the donor and the acceptor molecules are stacked alternately along the c-axis making their molecular planes parallel to each other, so as to give a large overlap between their molecular orbitals. From the consideration of the symmetry of the molecules and the space group of the crystal structure, one can fix the positions of the centers of two pyrene and two TCNE molecules in the unit cell as follows:

Pyrene: 0, 0, 0; 1/2, 1/2, 0

TCNE: 0, 0, 1/2; 1/2, 1/2, 1/2

Assuming the known bond distances from the crystal structures of pyrene[4] and TCNE[5] respectively, several trial structures were deduced; then the structure factors were calculated on each trial structure. The one that gives the best agreement between the calculated and the observed structure factors was chosen and refined by means of two-dimensional Fourier syntheses on ($h0l$) and ($hk0$). The calculation of the structure factors and the Fourier syntheses were repeated several times, and then the (F_o-F_c) syntheses were applied to correct the atomic coordinates. The temperature factors were assumed to be the same for all atoms, the values being 4.00 for ($h0l$) and 4.79 for ($hk0$).

The electron density projection along the b-axis and that along the c-axis are shown in Fig. 1 and Fig. 2 respectively. The atomic coordinates of the final structure are given in Table I, for

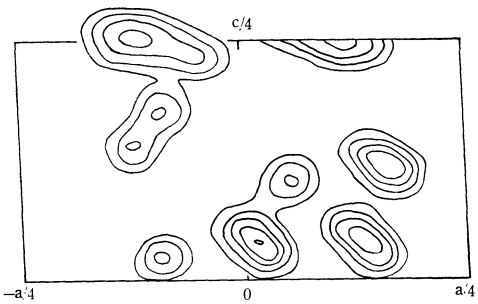

Fig. 1. Electron-density projection along [010]. Contours at intervals of 1.5 e.Å^{-2}, with the lowest solid contour of 4 e.Å^{-2}.

1) H. Kuroda, M. Kobayashi, M. Kinoshita and S. Takemoto, *J. Chem. Phys.*, **36**, 457 (1962).

2) H. Kuroda, K. Yoshihara and H. Akamatu, This Bulletin, **36**, 1365 (1963).

3) H. Kuroda and H. Akamatu, *J. Chem. Phys.*, **40**, 3748 (1964).

4) J. M. Robertson and J. G. White, *J. Chem. Soc.*, **1947**, 358.

5) D. A. Bekoe and K. N. Trueblood, *Zeit. Krist.*, **113**, 1 (1960).

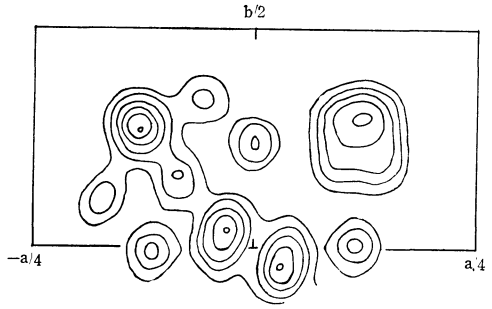

Fig. 2. Electron-density projection along [001]. Contours at intervals of 1.5 e.Å^{-2}, with the lowest solid contour of 4 e.Å^{-2}.

which the discrepancy index, $R=\sum||F_o|-|F_c||/\sum|F_o|$, is 19% for both ($hk0$) and ($h0l$). The observed and the calculated structure factors are given in Table II.

Table I. Atomic coordinates of pyrene-TCNE complex

Pyrene		X	Y	Z
C	1	0.146	−0.285	0.266
	2	0.176	−0.103	0.213
	3	0.119	0.007	0.106
	4	0.029	−0.057	0.053
	5	−0.002	−0.238	0.106
	6	0.055	−0.349	0.213
	7	0.149	0.189	0.053
	8	0.094	0.298	−0.053
TCNE				
C	9	0.042	0.009	0.530
	10	0.086	−0.133	0.630
	11	0.097	0.173	0.507
N	1	0.121	−0.247	0.710
	2	0.139	0.301	0.489

Description and Discussion of the Structure

The arrangement of molecules in the crystal is shown in Fig. 3. The donor and the acceptor molecules are stacked alternately along the c-axis. The molecules can be considered planar. The equations of the mean planes of pyrene and TCNE are:

$$-1.3361x+0.6639y+1.4371z=0$$

and

$$-1.6990x+0.8630y+2.0000z=1$$

respectively.

The departures of the atoms from the mean planes are less than 0.02 Å. The molecular planes of pyrene and TCNE are almost parallel to each other, the deviation from parallelism being about 2°. The average separation between the planes is 3.32 Å, which is smaller than the usual van der

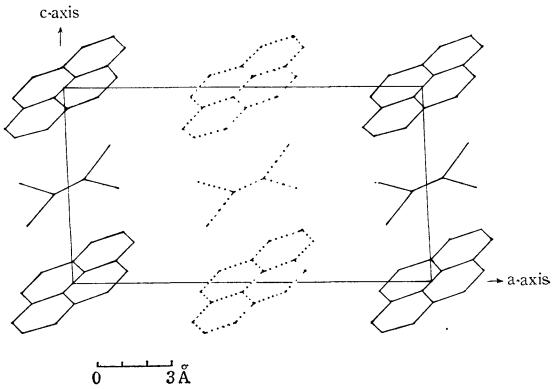

Fig. 3. Projection of the molecular arrangement on the (010) plane.

Waals separation. The distances between the atoms of the nearest neighbor pyrene and TCNE molecules are shown in Fig. 4, where the shortest one is 3.30 Å. Such close contact between the donor and the acceptor molecules suggests the presence of a strong intermolecular interaction between them.

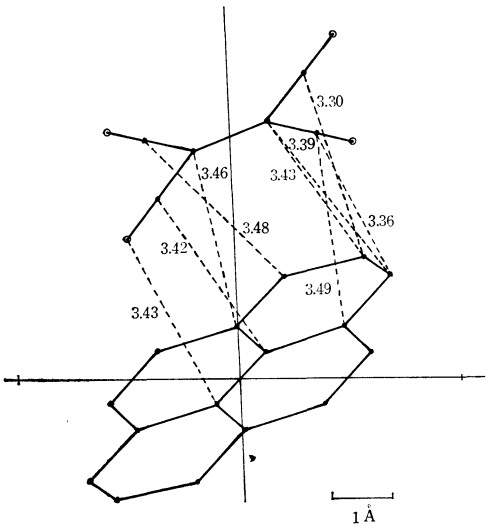

Fig. 4. Distances between atoms of the nearest neighbor pyrene and TCNE.

It is known that TCNE behaves as a very strong electron acceptor. There is reason to believe that nearly half of the binding energy between pyrene and TCNE is associated with the charge-transfer interaction in the case of the 1 : 1 complex formed in the solution. According to the charge-transfer theory, the donor molecule is supposed to take an orientation relative to the acceptor molecule, so as to give the largest overlap between the highest occupied orbital of the donor and the lowest vacant orbital of the acceptor, provided that the former is the donating orbital and the latter is the accepting one. This rule, known as

TABLE II. THE OBSERVED AND CALCULATED STRUCTURE FACTORS

h k l	F_o	F_c	h k l	F_o	F_c	h k l	F_o	F_c	h k l	F_o	F_c
0 0 1	22.36	14.08	−10 0 5	6.26	− 5.38	16 0 0	2.25	− 1.82	1 4 0	9.54	6.62
2	31.88	37.96	8	4.78	4.97	1 1 0	53.36	65.96	2	11.15	10.70
3	24.33	−23.01	−12 0 1	3.52	− 4.23	4	5.10	4.58	3	3.78	2.45
4	40.25	33.22	3	3.60	4.29	5	4.44	1.50	4	4.87	− 5.12
5	34.51	−26.49	4	5.51	− 9.21	6	21.07	17.21	5	4.69	2.65
6	11.32	− 6.34	−14 0 2	2.05	− 3.71	7	5.47	2.96	6	7.00	9.96
7	24.95	−21.54	−16 0 2	8.46	− 9.44	8	10.53	5.99	7	9.35	12.22
8	2.89	2.67	2 0 1	17.90	−15.17	9	0.94	1.71	8	22.26	20.13
9	3.54	− 4.50	2	20.42	−20.42	10	1.01	0.90	9	3.90	4.80
−2 0 0	48.68	76.89	5	21.91	−20.27	11	1.07	1.75	12	7.70	− 5.26
1	35.66	36.60	6	9.11	− 5.95	13	5.30	− 5.81	13	1.07	2.76
2	64.34	88.15	8	2.86	4.42	14	5.12	− 6.25	2 5 0	3.79	7.34
3	19.09	−16.55	9	3.85	3.32	15	5.78	− 5.30	3	7.14	9.10
4	14.43	−12.50	4 0 1	43.92	46.05	16	0.99	− 3.35	4	5.57	− 2.92
6	3.85	2.55	2	17.38	−17.70	0 2 0	65.94	−62.32	5	2.15	1.51
7	15.66	−11.07	3	8.30	6.10	1	13.17	10.31	6	5.96	− 6.64
8	4.57	− 2.58	4	21.45	−18.21	2	3.96	2.96	7	2.77	1.50
−4 0 0	59.50	−84.42	5	24.14	20.55	4	48.10	44.76	8	4.88	3.31
1	6.64	− 2.13	7	6.60	7.33	5	5.21	− 2.78	9	3.65	3.03
2	14.27	14.76	8	9.03	− 3.71	6	5.07	− 6.14	10	6.69	7.01
3	17.97	−15.50	9	11.73	11.42	7	0.85	1.82	11	4.16	− 1.63
4	26.96	−21.95	6 0 1	6.56	11.11	8	18.82	−21.42	12	1.05	3.11
5	7.31	5.94	2	5.50	− 5.96	9	3.71	− 3.50	13	0.96	− 1.21
−6 0 0	10.82	10.32	3	9.31	9.64	10	3.17	− 5.17	14	0.84	0.87
1	33.62	35.93	5	5.48	− 4.30	11	1.11	3.78	0 6 0	5.60	3.74
2	5.00	− 7.03	6	22.67	−20.38	12	11.48	− 8.87	1	1.94	− 1.91
3	26.28	−22.88	8	7.17	− 3.75	13	8.01	5.57	2	3.19	− 0.03
4	11.17	9.40	8 0 1	14.29	−16.88	14	12.61	−10.67	4	6.38	− 8.60
6	6.46	6.23	4	19.53	−17.89	1 3 0	26.67	24.89	5	4.00	4.92
7	7.21	5.54	5	29.61	−33.88	2	15.22	14.72	6	9.75	− 9.10
−8 0 0	22.64	20.58	6	24.23	−17.64	3	7.60	6.80	7	1.63	− 0.09
1	36.34	35.21	10 0 1	5.82	7.53	4	5.25	5.92	8	4.54	− 4.23
2	16.60	18.57	3	14.65	−12.13	5	5.60	− 2.77	9	1.10	2.39
3	6.96	9.48	4	25.00	−22.81	6	17.46	13.42	10	4.35	− 3.62
4	10.96	9.48	12 0 1	6.47	11.18	7	0.94	3.53	11	1.70	3.30
5	9.23	− 9.58	14 0 3	5.53	4.22	8	2.24	4.68	12	1.77	− 1.44
6	12.00	11.00	16 0 2	4.48	− 5.98	9	1.06	− 3.25	1 7 0	2.30	2.32
7	12.15	8.56	3	4.64	− 6.02	10	5.65	− 5.17	2	7.79	−12.73
8	7.75	6.32	2 0 0	73.96	77.64	11	15.40	−12.86	3	7.04	− 7.50
−10 0 0	2.56	− 3.96	4	83.05	−82.56	12	6.94	3.09	4	3.20	1.40
1	2.57	2.21	6	15.14	9.85	13	11.62	− 6.84	5	8.92	− 8.92
2	9.37	7.92	8	27.27	23.28	14	7.35	6.29	6	7.15	8.07
3	20.11	19.84	10	3.48	− 0.53	0 4 0	28.75	23.42			

the orientation and overlap principle, leads to the following structural model for the 1 : 1 complex of pyrene and TCNE: pyrene and TCNE molecules are stacked face-to-face, so that their molecular centers are directly over each other and the central double bond of TCNE is parallel to the short axis of pyrene. The relative orientation of pyrene to TCNE found in the crystal is, however, considerably different from the model described above, as is shown in Fig. 5. Naturally there can be several factors affecting the relative orientation of molecules in the crystal other than the charge-transfer interaction between the donor and the acceptor which are the nearest neighbors. Therefore, it is possible that the orientation in the crystal is not identical with the stable orientation for the 1 : 1 complex. It seems worthwhile, however, to examine the theoretical bases of the model for the 1 : 1 complex described previously.

According to the charge-transfer theory, the ground state of the complex is expressed by the resonance hybrid between the no-bond structure and the dative structure, or the charge-transfer state. Usually it is regarded enough for the first approximation to take as the dative structure merely the lowest charge-transfer state where

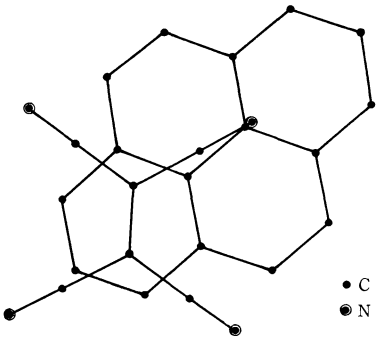

Fig. 5. Relative orientation of pyrene to TCNE found in the crystal.

an electron has been transferred from the highest occupied orbital of the donor to the acceptor. We have found, however, that the pyrene-TCNE complex shows two charge-transfer bands in the crystalline state as well as in the solution. The charge-transfer bands of the crystal are at 830 mμ and 510 mμ, and both of them are polarized in the c-axis direction. The first band is associated with the charge-transfer from the highest occupied orbital of pyrene to the lowest vacant orbital of TCNE, while the second one is associated with the charge transfer from the second highest occupied orbital of pyrene. The intensities of the two charge-transfer bands are comparable to each other. This can not be explained unless the charge-transfer state associated with the second band is as important a resonance structure as that of the lowest charge-transfer state. These facts suggest that the approximation neglecting the interactions of the charge-transfer states other than the lowest one is not satisfactory for the pyrene-TCNE complex. If such is the case, the orientation deduced from this approximation may not be the most stable structure, even for the 1 : 1 complex, since the overlap between the second highest occupied orbital of pyrene and the lowest vacant orbital of TCNE is largest when the central double bond of TCNE is parallel to the long axis, not the short axis, of pyrene. It is likely that the interactions of other charge-transfer states also make significant contributions to the binding energy. Further theoretical investigation seems to be necessary in this respect. Presumably the stable orientation for the 1 : 1 complex in solution will be similar, if not identical, to the one found in the crystal. Since there is a strong intermolecular interaction between pyrene and TCNE, we could expect deformations in the molecular structures. The bond distances determined at the present stage are, however, not accurate enough for us to determine conclusively if the molecules have been deformed by the complex formation or not. In order to solve this problem, refinements of the atomic coordinates as well as of the temperature factors are now in progress by means of three-dimensional analysis.

The authors wish to express their thanks to Professor Yōichi Iitaka, who has kindly allowed us to use the computer programs for the two-dimensional Fourier analysis.

BULLETIN OF THE CHEMICAL SOCIETY OF JAPAN VOL. 39 551—555 (1966)

Vulcanized Aniline Black. Its Electrical Conductivity and Catalysis upon the Decomposition of Hydrogen Peroxide*1,*2

By Hiroo INOUE, Yasuji KIDA and Eiji IMOTO

Department of Applied Chemistry, College of Engineering, The University of Osaka Prefecture, Sakai, Osaka

(Received July 5, 1965)

New semiconductive polymers have been prepared by the vulcanization of the oxidative condensation products of aniline. The polymers vulcanized are infusible black or black-violet powders insoluble in any organic solvent. The spin concentrations of the polymer vulcanized are about 1.5—2.5 $\times 10^{19}$ spins/g., about ten as much as those of the oxidative condensation products of aniline. The electrical conductivity increases with the increase in the sulfur content; the electrical resistivity at 20°C is 10^6—10^9 ohm-cm., and the activation energy is 0.68—1.18 eV. The polymers vulcanized have catalytic effects on the decomposition of hydrogen peroxide at 30°C. The catalytic effects of phenothiazine and the oxidative condensation products of aniline are, however, extremely slight. The catalytic ability depends not only on the structure of the polymer vulcanized, but also to some extent on its electrical conductivity.

*1 Part II of a series of studies of organic catalysts. The previous paper, also presented in This Bulletin (37, 326 (1964)), will be referred to as Part I of this series.

*2 Presented at the 18th Annual Meeting of the Chemical Society of Japan, Osaka, April, 1965.

The catalytic action of organic semiconductors on chemical reactions has received little attention. In a previous paper,[1] however, we have shown that some organic dyes catalyze the photo-oxidation of isopropyl alcohol in the liquid phase, and that the dyes classified as *p*-type organic semiconductors are more effective in catalytic activity than those classified as *n*-type organic semiconductors. Dawans, Gallard, Jeyssie and Traynard[2] have recently reported that the semiconductive polymers containing free radicals have catalytic activities on the decomposition of nitrous oxide, the dehydration of cyclohexanol and the isomerization of 1-butene.

In this paper we will describe how a new semiconductive polymer (shown as PAS in Fig. 1) synthesized by the vulcanization of the oxidative condensation product of aniline (shown as PA in Fig. 1) catalyses the decomposition of hydrogen peroxide at room temperature; the correlation between the catalytic activities of the polymer and their semiconductive properties will also be discussed.

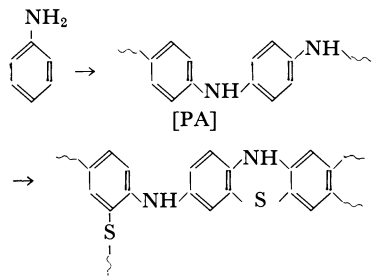

Fig. 1

Experimental

The Preparation of the Semiconductive Polymers.—*a) The Oxidative Condensation Product of Aniline (PA).*—A mixture of 50 ml. of 7.5% hydrogen peroxide and 0.25 g. of ferrous sulfate was gradually added to 5 g. of aniline at 60°C; the mixture was then allowed to stand overnight. The black precipitate obtained by filtration was poured into 100 ml. of 2 N sulfuric acid at 50°C. After the mixture had been filtered, the precipitate was washed with a boiling aqueous solution of ammonium hydroxide and then with water. When the washed precipitate was dried over calcium chloride at room temperature under the reduced pressure of 1 mmHg for a day, about 1.3 g. of black powder was obtained, m. p. 115—137°C.

Found: N, 13.68%.

b) The Oxidative Condensation Product of Aniline Hydrochloride (PA-Cl).—A mixture of 13.5 g. of concentrated hydrochloric acid, 38 ml. of 5% hydrogen peroxide and 0.9 g. of ferrous sulfate was gradually added to 4.66 g. of aniline dispersed in 200 ml. of water at 0°C; the mixture was stirred at 0°C for an hour, and then at room temperature for 44 hr. To this mixture 20 ml. of ammonium hydroxide was added, and the precipitate obtained was washed thoroughly with water and then dried over calcium chloride in the same way as has been described in the case of a). The yield of the product was 2.5 g.

c) The Vulcanized Product (PAS).—The vulcanization of PA or PA-Cl was carried out under the various conditions shown in Table I. Here the synthetic procedure of PAS, in which the molar ratio of sulfur to aniline unit was 2.1, will be described in detail as an example. A mixture of 0.56 g. of PA, 1.18 g. of sulfur and 0.08 g. of iodine was heated at 200—210°C for about 10 hr. under a nitrogen stream. During the course of the reaction, the evolution of hydrogen sulfide was observed. The solidified product was pulverized, and then extracted with carbon disulfide using a Soxhlet apparatus for a day in order to remove excess sulfur and low-molecular-weight compounds. With this extraction process, 0.91 g. of a mixture of sulfur and the black powder consisting of low-molecular-weight compounds was obtained. The traces of sulfur and iodine which remained in the extracted residue were removed by sublimation at about 120°C under the reduced pressure of 1—2 mmHg for 8 hr. About 0.78 g. of the infusible black powders was obtained. The results of the elementary analysis of nitrogen or sulfur for the black powders are shown in Table I.

Table I. The contents of nitrogen and sulfur in PAS

Starting material	S/-NHC_6H_4-*	PAS		
		N%	S%	r_s
PA	0	15.56	0	0
PA	1/2	11.16	16.61	0.65
PA	2	10.08	29.05	1.46
PA	6	7.81	37.05	2.08
PA	6**	5.44	46.72	3.74
PA	8	8.35	35.05	1.84
PA	20	6.90	37.74	2.39
PA-Cl	0	—	—	—
PA-Cl	6	—	32.98	—

* S/-NHC_6H_4- is the molar ratio of sulfur to aniline unit for the starting material.
** PA was vulcanized at 300°C.

Electrical Conductivities.—The d. c. resistivities of the polymers obtained were measured under a pressure of 1.0×10^3 kg./cm^2 at an applied electric field of 100—200 V./cm. according to the methods described in the preceding papers.[3] The current-voltage relationship was shown to be ohmic up to 10^4—10^5 V./cm. The electrical resistivity (ρ) at an ascending temperature was identical with that at a descending temperature, and a linear relationship between log ρ and $1/T$ was observed. The resistivity of all the polymers obtained fit the following equation, as does a typical organic semiconductor:

$$\rho = \rho_0 \exp(\Delta\varepsilon/2\boldsymbol{k}T)$$

1) H. Inoue, S. Hayashi and E. Imoto, This Bulletin, **37**, 326 (1964).
2) F. Dawans, J. Gallard, PH. Jeyssie and PH. Traynard, *J. Polymer Sci.*, **Part c**, 1385 (1964).
3) H. Inoue, S. Hayashi and E. Imoto, This Bulletin, **37**, 336 (1964).

Table II. Rate constants for the decomposition of hydrogen peroxide, and the values of spin concentrations, resistivity at 20°C (ρ_{20}) and $\Delta\varepsilon$

Compound	r_s	g-Value	Half width gauss	Spin concn. spins/g.	ρ_{20}, Ω·cm.	$\Delta\varepsilon$, eV.	k, min^{-1}
PA	0	2.0034	18.9	2.2×10^{18}	$>10^{13}$	—	very small
PAS	0.65	2.0045	15.7	2.1×10^{19}	2.7×10^{9}	1.05	1.2×10^{-3}
PAS	1.46	2.0047	15.0	1.7×10^{19}	2.4×10^{8}	0.95	2.5×10^{-3}
PAS	2.08	2.0045	16.4	2.4×10^{19}	2.3×10^{8}	0.97	5.5×10^{-3}
PAS	3.74	2.0049	15.0	1.5×10^{19}	3.8×10^{6}	0.68	1.2×10^{-4}
PAS	1.84	2.0043	13.2	2.0×10^{19}	2.2×10^{9}	1.18	6.1×10^{-3}
PAS	2.39	2.0054	17.7	2.2×10^{19}	3.5×10^{8}	0.98	5.5×10^{-3}
PA-Cl	—	—	—	—	2.8×10^{9}	1.28	very small
PAS-Cl	—	—	—	—	1.7×10^{5}	0.5	3.3×10^{-4}

The Decomposition of Hydrogen Peroxide.—The rate of the decomposition of 7.3% hydrogen peroxide was determined by measuring the amounts of oxygen generated. A weighed amount of a catalyst was dispersed in 5 ml. of distilled water in a reaction vessel placed in a thermostat. After the thermal equilibrium had been reached, 5 ml. of 7.3% hydrogen peroxide was added to the dispersed solution. The amounts of oxygen generated were measured at appropriate time intervals by a gas burette connected with the reaction vessel. In order to stop the reaction after a certain time, 2 N sulfuric acid was added to the above dispersed solution. The rest of the hydrogen peroxide was titrated with potassium permanganate. The amount of oxygen generated coincided with that of hydrogen peroxide calculated by the following equation:

$$2\,H_2O_2 = 2H_2O + O_2$$

Results and Discussion

The Properties of the Semiconductive Polymers.—PA was a black-brown powder and was partially soluble in dimethylformamide. However, when the powders were placed in a solution of concentrated sulfuric acid, the solution showed a red-brown color. The infrared spectra of PA showed the absorptions of the –NH– band at 3200—3300 cm^{-1} and the out-of-plane deformation band of two adjacent free hydrogen atoms at 825—840 cm^{-1}. The ESR spectrum of PA showed the existence of unpaired electrons, and the spin concentration was about 2.2×10^{18} spins/g. PA-Cl was infusible black powders and was insoluble in any organic solvent; it showed a blue-green color in concentrated sulfuric acid. The PAS obtained by the cross-linking of PA or PA-Cl with various amounts of sulfur was an infusible black powder, most of which was insoluble even in concentrated sulfuric acid. The molar ratio of sulfur to aniline unit in PAS (r_s) was calculated by the following equation:

$$\text{Molar ratio } (r_s) = \frac{S\% \times 14}{N\% \times 32}$$

As is shown in Table I, several polymers with different sulfur contents were obtained.

The infrared spectrum of PAS was similar to that of PA. The absorption bands of PAS at 825—840 cm^{-1} and 1450—1500 cm^{-1} were shifted toward a lower-wave-number side by 10—15 cm^{-1} as compared with those of PA.

The spin concentration of PAS calculated from the ESR spectra was about $1.5—2.5\times10^{19}$ spins/g., about ten times as much as that of PA. No remarkable difference in the spin concentration was, however, observed among the different sorts of PAS polymers. The g-value for PAS was close to that of a free electron, i. e., $g\simeq2.0023$. The half width of both PA and PAS was about 13.2—19.2 gauss, as narrow as that of the lattice polymer reported in preceding papers.[4]

Electrical Conductivities.—As can be seen in Table II, the ρ_{20} value of PA-Cl was low in comparison with that of PA ($>10^{13}$ ohm-cm.). The ρ_{20} value of PAS or PAS-Cl decreased with the increase in the sulfur contents; that is, the electrical conductivity increased with the increase in the degree of the vulcanization. This would imply that the degree of the conjugation of π

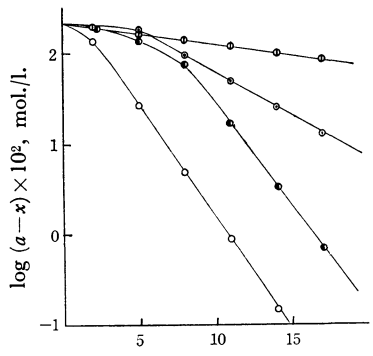

Fig. 2. Catalytic action of PAS on the decomposition of hydrogen peroxide: PAS of r_s, 1.84; a, 1.055 mol./l. and temp. 30°C.
○ PAS (r_s, 1.84), ◐ PAS (r_s, 2.39), ⊙ PAS (r_s, 1.49), ⓘ PAS-Cl

4) H. Inoue, T. Takiuchi and E. Imoto, *J. Chem. Soc. Japan, Ind. Chem. Sect.* (*Kogyo Kagaku Zasshi*), **65**, 1291 (1962); H. Inoue and E. Imoto, *J. Chem. Soc. Japan, Pure Chem. Sect.* (*Nippon Kagaku Zasshi*), **83**, 1052 (1962).

electrons in PAS increases.

The Effects of the Semiconductive Polymers on the Decomposition of Hydrogen Peroxide. —As can be seen in Fig. 2, phenothiazine showed no catalytic action on the decomposition of hydrogen peroxide, but PA, PA-Cl or PAS-Cl showed a slight catalytic action. On the other hand, PAS accelerated the decomposition of hydrogen peroxide to oxygen and water, and the catalytic activity of PAS depended on the sort of PAS. The logarithmic value of the concentration of hydrogen peroxide, log $(a-x)$. decreased linearly with the reaction time after a certain induction period. The first order rate constant, k, was calculated from the straight line in Fig. 2 by the following equation:

$$k = \frac{1}{t} \log \frac{a}{a - x}$$

where a and x are the initial and the decomposed concentrations of hydrogen peroxide respectively, and where t is the reaction time. The results calculated are shown in Table II. The relationships between the spin concentration, $\Delta\varepsilon$, log σ_0, or log k and r_s are shown in Fig. 3. No parallel relationship between the catalytic activity of PAS and the spin concentration or $\Delta\varepsilon$ was observed.

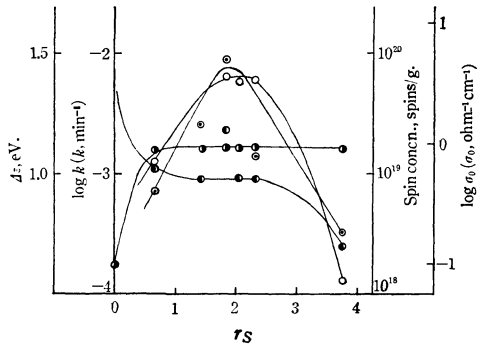

Fig. 3. Relationships between the spin concentration, $\Delta\varepsilon$, log σ_0, or log k and r_s.
◑ Spin concn., ◐ $\Delta\varepsilon$, ⊙ log σ_0, ○ log k

However, it is interesting to note that the spin concentration of PAS, which showed a catalytic activity was ten times larger than that of PA, which showed only a slight catalytic activity. The $\Delta\varepsilon$ value of PAS which shows the best catalytic activity was about 1 eV. Surprisingly, a parallel relationship was found between the variations in log σ_0 and log k for r_s. This seems to show that the catalytic activity is affected by the arrangement of the molecule, because log σ_0 is related more or less to the molecular arrangement.

The Effect of pH on the Catalytic Action.— Dokukina et al.[5] have reported that the nitrogen atoms contained in a catalyst acted as the active center on the decomposition of formic acid. In this connection, the fact that the catalytic activity of PAS decreases when $\Delta\varepsilon$ becomes smaller than 1 eV. may be caused by the decrease in the relative density of nitrogen atoms on the surface of a PAS solid. Therefore, we investigated the problem of whether the catalytic activity of PAS is affected by the variation of the pH in the solution of hydrogen peroxide. Here, the PAS with a r_s value of 1.8 was used as the catalyst, and the reaction was carried out at pH 3, 4, 5.2, 7.5, 9.8 and 11.2 respectively, in which Sörensen's buffer solutions for the 3—8 pH range, and Britton-Robinson's buffer solutions for the range of more than pH 9, were used. To 0.05 g. of PAS dispersed in 5 ml. of the buffer solution there was added 5 ml. of 7.3% hydrogen peroxide; then the amount of oxygen generated was measured at appropriate time intervals. In the solution of more than pH 9, oxygen was generated even with no addition of PAS, and so this amount was subtracted from the total amount of oxygen generated. As can be seen in Fig. 4, the catalytic effect in the acidic solution with pH values less than 4 was extremely slight. However, the PAS in neutral or alkaline solutions showed catalytic activity. This seems to show that the basicity of PAS plays an important role in the catalytic ability.

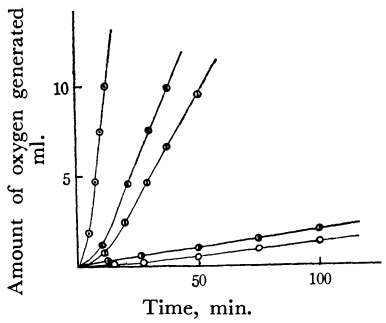

Fig. 4. Effect of pH on the catalytic action: PAS; r_s, 1.84.
○ pH 3, ◑ pH 4, ① pH 5.2, ◐ pH 9.8, ⊙ pH 11.2

The Effect of the Acceptor on the Catalytic Action.—The catalytic ability of PAS is considered also to be related to its nature as an electron donor. If so, the catalytic activity of PAS treated with an electron acceptor, for instance, iodine, 1, 3, 5 - trinitrobenzene or 7, 7, 8, 8 - tetracyanoquinodimethane, must decrease as compared with that of the untreated PAS. The treatment of PAS with the electron acceptor was carried out by dispersing PAS for 12 hr. in a solution of the electron acceptor in benzene or ethanol. As is shown in Fig. 5, the catalytic activity of the treated PAS was lower than that of the untreated PAS. Therefore, the nature of PAS as an electron donor

5) E. S. Dokukina, S. Z. Roginskii, M. M. Sakkarov, A. V. Topchiev, M. A. Geiderikh, B. E. Davydov and B. A. Krentsel, *Doklady Akad. Nauk. S. S. S. R.*, **137**, 893 (1961).

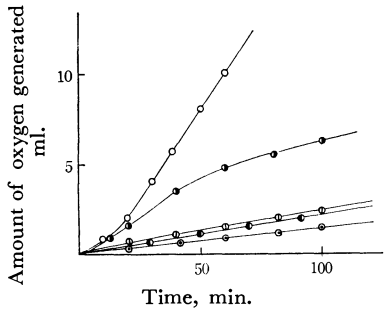

Fig. 5. Effect of the acceptor on the catalytic action: PAS; r_s, 1.84.
◑ Iodine, ⓘ 1, 3, 5-trinitrobenzene, ◐ sulfuric acid, ⊙ 7, 7, 8, 8-tetracyanoquinodimethane, ○ untreated PAS

seems to be important in the catalytic ability.

An Assumed Mechanism for the Catalytic Action of PAS.—As has been described above, it was assumed that the catalytic effect of the semiconductive polymers on the decomposition of hydrogen peroxide depends not only on the $\Delta\varepsilon$ value and their natures as electron donors, but also on the arrangement of the molecules and on the relative density of the nitrogen atom on the surface of the polymer solid. Though the details of the mechanism of the decomposition of hydrogen peroxide are not clear, it seems that hydrogen peroxide trapped on the nitrogen atoms on the catalyst is reduced by the conductive electron, decomposing to H_2O and O^-, and that O^- gives an electron to the hole on the catalyst, thus converting it to O_2, for example, by the following processes:

$$PAS + H_2O_2 \rightarrow PAS\cdots H_2O_2$$
$$\rightarrow PAS^+ + H_2O + O^-$$
$$PAS^+ + O^- \rightarrow PAS + O\cdot \rightarrow O_2 + PAS$$

Here, the catalytic ability must depend on the density and the arrangement of the active center such as the nitrogen atoms.

BULLETIN OF THE CHEMICAL SOCIETY OF JAPAN VOL. 39 555—558 (1966)

Phenazine Complexes. Their Preparation and Their Electrical Conductivity*

By Hiroo INOUE, Kentaro TAMAKI, Yoshihiro KIDA and Eiji IMOTO

Department of Applied Chemistry, College of Engineering, The University of Osaka Prefecture, Sakai, Osaka

(Received July 5, 1965)

The photo-reduction of phenazine was carried out in isopropyl alcohol in the presence of ferric chloride or stannic chloride. In the course of the photo-reduction, a metal chelate precipitated. The metal chelate was composed of unstable black needle crystals; it was presumed, from the results of the elementary analysis, the visible and the infrared absorption spectra and the ESR spectra, to be Fe^{2+}- or Sn^{2+}-chelate of *N*-monohydrophenazyl. On the other hand, the reduction of phenazine with stannous chloride and hydrochloric acid gave a phenazhydrin - stannic chloride-complex, which was more stable than the photo-reduction products. Their resistivities at 20°C had low values of from 10^5 to 10^8 ohm-cm.

The reduction of phenazine with stannous chloride and hydrochloric acid produces a complex containing stannic chloride; the structure of this complex is not yet known, however. When this complex is treated with an aqueous solution of sodium hydroxide, it loses stannic chloride and produces free phenazhydrin.[1] The irradiation of phenazine in isopropyl alcohol by ultraviolet light also produces phenazhydrin, together with acetone.[2] The intermediates of the photo-reduction to phenazhydrin from phenazine are not certain, but one of them is supposed to be the *N*-monohydrophenazyl radical. If the *N*-monohydrophenazyl radical is produced in this process and if an electron acceptor is also present in the system, the *N*-monohydrophenazyl radical may react with the electron acceptor to produce a complex. In order to verify this assumption, the photo-reduction of phenazine was carried out in isopropyl alcohol in the presence of ferric chloride or stannic chloride. As was expected, the complex of *N*-monohydrophenazyl with ferric chloride or stannic chloride was obtained as crystals of a plate form. These complexes have an electrical conductivity as organic semiconductors. In the

* Presented at the 17th Annual Meeting of the Chemical Society of Japan, Tokyo, April, 1964.

1) G. R. Clemo and H. McIlwain, *J. Chem. Soc.*, **1934**, 1991.

2) C. Dufraisse, A. Etienne and E. Toromanoff, *Bull. Soc. Chim. France*, **1953**, 140; G. A. Swan and D. G. I. Felton, "Phenazines," Interscience Publishers, New York (1957), p. 48.

TABLE I. THE VALUE OF SPIN CONCENTRATIONS, ρ_{20} AND $\Delta\varepsilon$ OF METAL CHELATES

Compound	g-Value	Half width gauss	Spin concn. spins/mol.	ρ_{20} ohm-cm.	$\Delta\varepsilon$ eV.
ph-phH_2	2.0033	7.1	3.8×10^{21}	3.7×10^{10}	1.32
(ph-phH_2)$_2$ $SnCl_4$	2.0033	6.2	3.1×10^{23}	1.6×10^{5}	0.75
phH·$SnCl_2$	2.0033	1.0	3.9×10^{23}	6.0×10^{8}	1.19
phH·$FeCl_2$	2.032	440	2.0×10^{22}	6.4×10^{7}	1.06

present paper we will report on the syntheses of these complexes and on their properties as organic semiconductors. In addition, the properties of the phenazhydrin - stannic chloride-complex will be investigated.

Experimental

Materials.—Phenazine was prepared according to the methods described in the literature[3]; it was purified by repeated recrystallizations from ethanol.

The Preparation of Metal Chelates.—*Reduction with Stannous Chloride and Hydrochloric Acid.*—To a solution of 0.54 g. of phenazine in 20 ml. of ethanol there was added at room temperature a solution of 0.56 g. of anhydrous stannous chloride in 10 ml. of ethanol. No crystals precipitated from the greenish reaction mixture. However, the acidification of the reaction mixture with 1—2 ml. of concentrated hydrochloric acid immediately gave black-green needle crystals. After the above acidified mixture had been further refluxed for five minutes, the hot mixture was filtered and left to cool. After the cooled filtrate had then been filtered out, 0.56 g. of the metal chelate was obtained as black-green needle crystals; this was then recrystallized from ethanol.

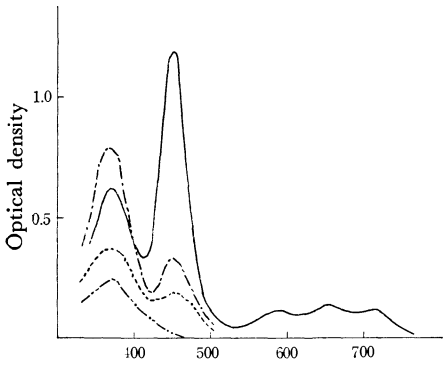

Fig. 1. The visible absorption spectra of a solution of phenazine, stannous chloride and hydrochloric acid (solvent: ethanol).
——: 1.01×10^{-4} mol./l. phenazine, 0.92×10^{-3} mol./l. $SnCl_2$
—·—: 7.23×10^{-5} mol./l. phenazine, 1.81×10^{-5} mol./l. $SnCl_2$
—··—: 2.02×10^{-5} mol./l. phenazine, 22.7×10^{-5} mol./l. $SnCl_2$
----: 4.04×10^{-5} mol./l. phenazine, 4.52×10^{-5} mol./l. $SnCl_2$

3) A. Wohl and W. Aue, *Ber.*, **34**, 2442 (1901).

Found: N, 11.40; Cl, 14.33. Calcd. for $C_{48}H_{36}N_8$-$SnCl_4$: N, 11.42; Cl, 14.46%.

The metal chelate decomposed to phenazine and stannic chloride when dissolved in ethanol. Therefore, the phenazine content in the metal chelate could be estimated from the optical densities of the ultraviolet and visible absorption spectra of phenazine at 250 mμ and 370 mμ in ethanol. The results showed the molar ratio of phenazine to stannic chloride to be 4 : 1.

The Photo-reduction of Phenazine with Isopropyl Alcohol.—*In the Presence of Stannic Chloride.*—A solution of 0.41 g. of phenazine and 0.69 g. of stannic chloride in 40 ml. of isopropyl alcohol was placed in a test tube of a vycol (30 mm. in inner diameter, 0.5 mm. in wall thickness) and irradiated under an atmosphere of nitrogen at room temperature for 30 hr. with a 100W. mercury lamp placed 5 cm. from the vessel. About 0.32 g. of black prism crystals were precipitated. The crystals collected by filtration were dried over phosphorus pentoxide under the reduced pressure of 2—5 mmHg.

Found: N, 7.43; Cl, 19.40. Calcd. for $C_{12}H_9N_2$-$SnCl_2$: N, 7.57; Cl, 19.20%.

From the results of the visible absorption spectra, the molar ratio of phenazine to stannous chloride in the product was estimated to be 1 : 1.

In the Presence of Anhydrous Ferric Chloride.—A solution of 0.12 g. of phenazine and 0.17 g. of anhydrous ferric chloride in 25 ml. of isopropyl alcohol was irradiated for 7 hr. in a manner similar to that described above. About 0.1 g. of black needle crystals were thus precipitated. The crystals were dried over phosphorus pentoxide under the reduced pressure of 2—5 mmHg in an atmosphere of nitrogen.

Found: N, 9.22; Cl, 23.38. Calcd. for $C_{12}H_9N_2$-$FeCl_2$: N, 9.20; Cl, 23.13%.

The molar ratio of phenazine to ferrous chloride in the product was estimated from its visible absorption spectra to be 1 : 1.

Results and Discussion

The Properites of Metal Chelates.—*The Reduction Product with Stannous Chloride and Hydrochloric Acid* (abbreviated as (ph-phH_2)$_2SnCl_4$).—The reduction product, infusible black-green needle crystals, was completely decomposed to phenazine and stannic chloride when it was dissolved in ethanol, although it was very stable in the crystalline form. The molar ratio of phenazine to stannic chloride in the product was 4 : 1.

The visible absorption spectra of a solution of phenazine, stannous chloride and hydrochloric acid dissolved in ethanol were measured at various

concentrations of the three components, phenazine, stannous chloride and hydrochloric acid. The results are shown in Fig. 1. As can be seen there, a new band appeared at 470 mμ, and the optical density of the new band increased with the increase in the molar ratio of phenazine to stannous chloride. This band seemed to be an absorption of the Sn^{2+}- or Sn^{4+}-chelate. When the concentration of each component in three components was increased, a new band appeared at about 650 mμ. This band must be a charge transfer absorption for phenazhydrin, ph-phH$_2$. On the other hand, the visible absorption spectrum as measured by the KBr disk showed two bands, at about 378 mμ and 470 mμ, while no band was observed at about 650 mμ.

The infrared absorption spectrum of the reduction product was similar to that of phenazhydrin, ph-phH$_2$, and showed the absorptions of the –N–H band at 3360 cm^{-1}, the –$\overset{+}{N}$= band at 2770 cm^{-1} and the out-of-plane deformation band at 735 cm^{-1}.

From the results described above, the following structural formula may be assigned to the structure of the metal chelate:

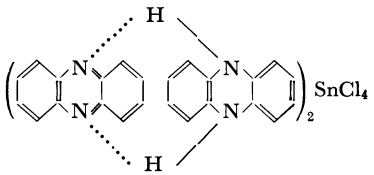

The spin concentration, the *g*-value and the half-width of the reduction product as calculated from the ESR spectra are shown in Table I. The ESR spectra consisted of a single narrow band; no fine structures were observed.

The Photo-reduction Product with Isopropyl Alcohol.— The photo-reduction of phenazine with isopropyl alcohol in the presence of ferric chloride gave the Fe^{2+}-chelate as black needle crystals (abbreviated as phH·FeCl$_2$). When the crystals were allowed to stand at room temperature in an atmosphere of air for a long time, their color gradually changed from black to yellow. Thus, the photo-reduction product seems to be unstable to oxygen.

The ultraviolet absorption spectrum of an ethanolic solution of the photo-reduction product, phH·FeCl$_2$, was found to be identical with that of phenazine because it was oxidized to decompose to phenazine and ferric chloride in the aerated ethanol. Therefore, the photo-reduction was carried out in a closed cell, and the variation in the visible absorption spectra during the course of the photo-reduction was measured. That is, a solution of phenazine and ferric chloride dissolved in isopropyl alcohol was sealed in the closed cell in an atmosphere of nitrogen and irradiated at room temperature for 95 hr. with a 100 W. mercury lamp; then the variation in its visible absorption spectrum with the reduction time was traced. As can be seen in Fig. 2, the absorption of phenazine at about 370 mμ decreased, while a new absorption appeared at about 500 mμ. The new band seems to be that of *N*-monohydrophenazyl, phH·

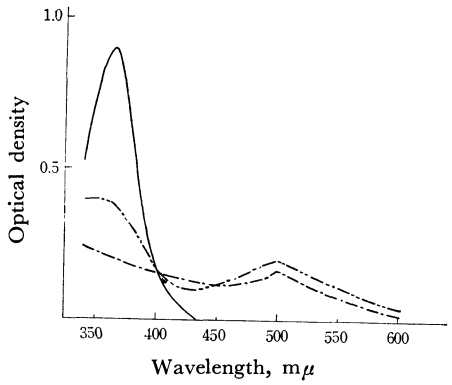

Fig. 2. The visible absorption spectra of the irradiated solution of phenazine in the presence of $FeCl_3$ or $SnCl_4$: Irradiated time; 95 hr. for $FeCl_3$ and 71 hr. for $SnCl_4$, Concentration; $FeCl_3$, 5.3×10^{-5} mol./l., $SnCl_4$, 6.09×10^{-5} mol./l. and phenazine, 6×10^{-5} mol./l.
—— Before irradiation, ---- $FeCl_3$,
-·-· $SnCl_4$

Its infrared absorption spectrum was similar to that of (ph-phH$_2$)$_2$SnCl$_4$. However, the out-of-plane deformation band showed the doublet at 740 cm^{-1} and 750 cm^{-1}, such as that of phenazine or dihydrophenazine.

The ESR spectrum was broad, although the features of the spectrum were similar to those of (ph-phH$_2$)$_2$SnCl$_4$. The *g*-value was large in comparison with that of the free electron, as is shown in Table I.

On the other hand, the ultraviolet and infrared spectral properties of the photo-reduction product obtained in the presence of stannic chloride (abbreviated as phH·SnCl$_2$) were similar to those of phH·FeCl$_2$, but the ESR spectrum was different, as is shown in Table I and Fig. 2.

As has been described above, the Fe^{2+}- and Sn^{2+}-chelates obtained by the photo-reduction both have free spins, and its visible spectrum shows an absorption at about 500 mμ. Also, the infrared spectrum shows an absorption of the –$\overset{+}{N}$= band; the molar ratio of the phenazine ring to ferrous chloride or stannous chloride is 1 : 1. Hence, the structural formula of the metal chelate might be formulated as follows:

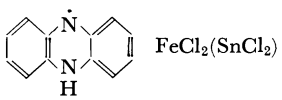

Namely, the intermediate photo-reduction product of phenazine would form the metal chelate with the Fe^{2+} or Sn^{2+} ion obtained by the photo-reduction of the Fe^{3+} or Sn^{4+} ion.

Electrical Conductivities.—The d. c. resistivity was measured under the pressure of 10^3 kg./cm^2 in vacuo according to the methods described in a previous paper.[4] In the case of phH·$FeCl_2$ or $SnCl_2$, the d. c. measurement was carried out with especial caution because it is unstable to oxygen. The dark-currents of all the metal chelates were ohmic up to 10^3 V./cm. The relationships between the d. c. resistivity and the temperature are shown in Fig. 3. The resistivity at an ascending temperature coincided with that at a descending temperature, and a linear relationship between $\log \rho$ and $1/T$ was observed. The value of $\Delta\varepsilon$ was calculated by the following equation:

$$\rho = \rho_0 \exp(\Delta\varepsilon/2\boldsymbol{k}T)$$

where $\Delta\varepsilon$ is the apparent energy gap; $\boldsymbol{k}$ is the Boltzman constant, and ρ is a specific electrical resistivity. The values of ρ_{20} and $\Delta\varepsilon$ are shown in Table I, which the values of ph-phH_2 are those reported in our previous paper.[4] The ρ_{20} values of all metal chelates were lower by about 10^2—10^5 than that of ph-phH_2. The ρ_{20} of (ph-phH_2)$_2$$SnCl_4$ was the lowest among those of all the metal chelates. The reason for this may be that the molecular arrangement of ph-phH_2 is more regular than that of the other chelates.

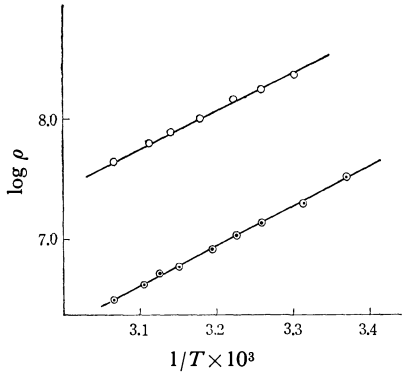

Fig. 3. The relationship between $\log \rho$ and $1/T$.
-○- phH·$SnCl_2$ -⊙- phH·$FeCl_2$

4) H. Inoue, S. Hayashi and E. Imoto, This Bulletin, **37**, 336 (1964).

BULLETIN OF THE CHEMICAL SOCIETY OF JAPAN VOL. 39 558—562 (1966)

The Absorption Spectra of Dyes. XI.[1] A Note on the Color Change in Some Azobenzene Dyes with Variation in the Acidity*

By Yoshié TANIZAKI, Tadashi KOBAYASHI and Toshihiko HOSHI

Department of Chemistry, Tokyo Institute of Technology, Ookayama, Tokyo

(Received July 8, 1965)

The absorption spectra of azobenzene and its para hydroxy, amino or dimethylamino derivative, and their sodium salts have been determined above 220 mμ in mixed solutions of water and ethanol (7 : 3 in volume) at various acidities. All the samples show characteristic changes in spectra with increase in the acidity, and the respective spectral changes keep well-defined isosbestic points, indicating a binary system spectrally. The wavelengths of the color band peaks and the corresponding spectral species have been determined. Consequently, the following order of the substitution effect has been obtained;

$$\left.\begin{matrix}-NH_3^+\\ -NHMe_2^+\end{matrix}\right)<-H<-OH<-NH_2<-O^-<-NMe_2$$

The color change in azobenzene derivatives with a variation in the pH value has been very often studied.[2] The conclusions on the proton addition, however, have not always coincided with one another. Klotz et al.,[3] for instance, have concluded that a first proton goes to the amino group and that a second proton goes to the azo group with an increase in the hydrogen ion concentration:

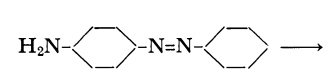

1) Part X of this series: T. Hoshi and Y. Tanizaki, This Bulletin, **39**, 476 (1966).

* Presented partly at the Nagoya Meeting of the Chemical Society of Japan, November, 1964.

2) G. Cilento, E. C. Miller and J. A. Miller, *J. Am. Chem. Soc.*, **78**, 1718 (1956); E. Sawicki and F. E. Ray, *J. Org. Chem.*, **19**, 1686 (1954); E. Sawicki and D. Gerber, ibid., **21**, 410 (1956); E. Sawicki, ibid., **21**, 605 (1956); **22**, 621, 743, 915, 1048 (1957); F. Gerson, E. Heilblonner, A. Van Veen and B. M. Wepster, *Helv. Chim. Acta*, **43**, 1899 (1960); A. Zenhäusern and H. Zollinger, ibid., **45**, 1882, 1890 (1962).

3) I. M. Klotz, H. A. Fiess, J. Y. Chen Ho and M. Mellody, *J. Am. Chem. Soc.*, **76**, 5136 (1954).

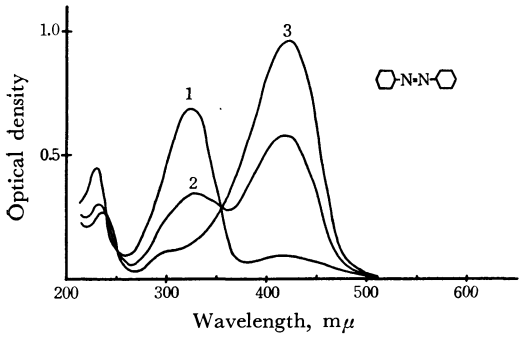

Fig. 1. Absorption spectra of AB.
Concentration of AB = 4.00×10^{-5} mol./l.
1. conc. H_2SO_4 20 ml. + 30% aqueous ethanol in 100 ml.
2. conc. H_2SO_4 40 ml.
3. conc. H_2SO_4 50 ml.

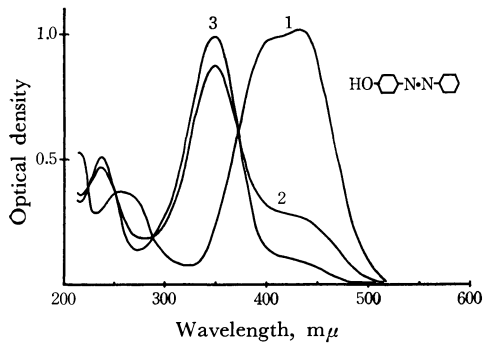

Fig. 2. Absorption spectra of HAB.
Concentration of HAB = 5.15×10^{-5} mol./l.
1. 30% aqueous ethanol
2. 1% HCl 1 ml. + 30% aqueous ethanol in 100 ml.
3. conc. HCl 1 ml.

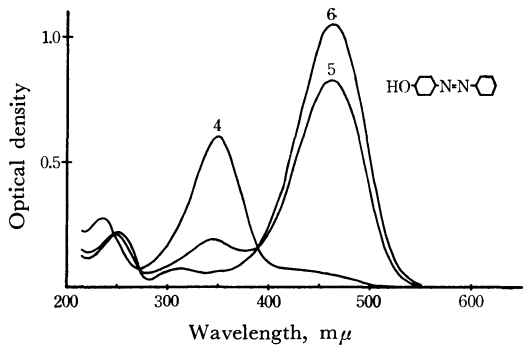

Fig. 3. Absorption spectra of HAB.
Concentration of HAB = 2.75×10^{-5} mol./l.
4. conc. H_2SO_4 5 ml. + 30% aqueous ethanol in 100 ml.
5. conc. H_2SO_4 20 ml.
6. conc. H_2SO_4 40 ml.

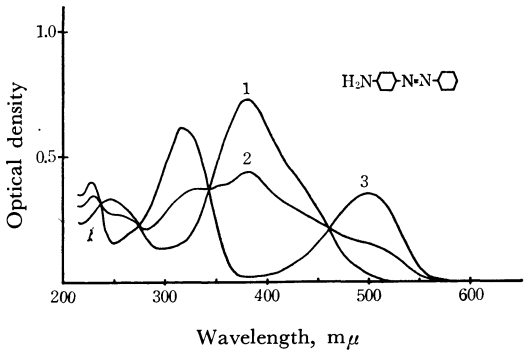

Fig. 4. Absorption spectra of AAB.
Concentration of AAB = 3.42×10^{-5} mol./l.
1. 30% aqueous ethanol
2. 25% H_2SO_4 0.03 ml. + 30% aqueous ethanol in 100 ml.
3. conc. H_2SO_4 1 ml.

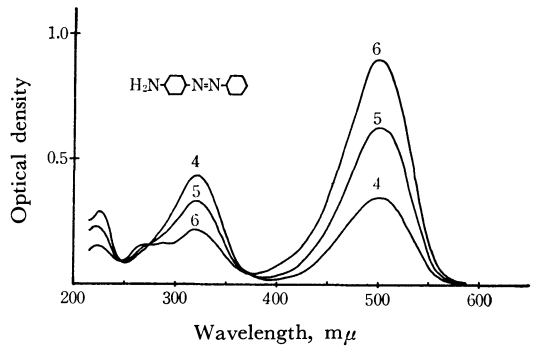

Fig. 5. Absorption spectra of AAB.
Concentration of AAB = 2.61×10^{-5} mol./l.
4. conc. H_2SO_4 8 ml. + 30% aqueous ethanol in 100 ml.
5. conc. H_2SO_4 20 ml.
6. conc. H_2SO_4 30 ml.

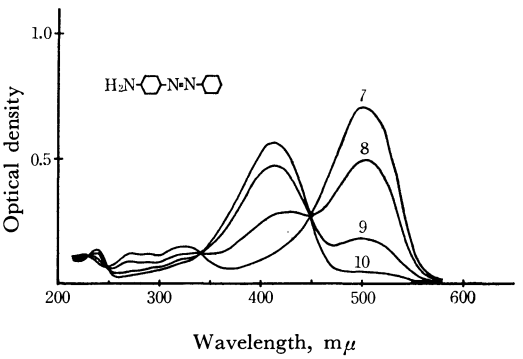

Fig. 6. Absorption spectra of AAB.
Concentration of AAB = 3.90×10^{-5} mol./l.
7. conc. H_2SO_4 35 ml. + 30% aqueous ethanol in 100 ml.
8. conc. H_2SO_4 40 ml.
9. conc. H_2SO_4 45 ml.
10. conc. H_2SO_4 50 ml.

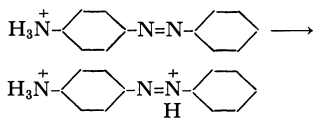

If this is true, the first proton addition must shift the color band to a shorter wavelength, because the electronic theory insists that the protonated amino group cannot conjugate with the ring system because of the loss of the π-type electrons. Therefore, this scheme cannot correspond to the red shift of the color band resulting from the first proton addition. On the other hand, Sawicki[4] has considered the tautomer concept of the proton addition, which is as follows;

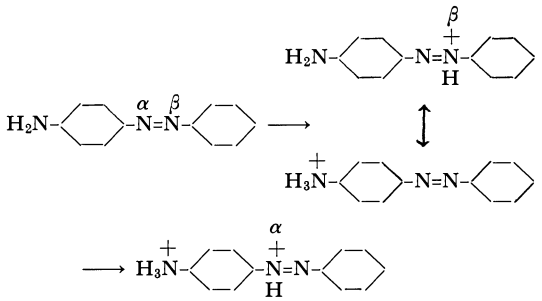

According to his scheme, either the first or the second protonation process could involve three spectral species. However, as will be shown later, a careful re-examination will make it evident that, in the course of an increase in the acidity, three kinds of spectral changes appear in turn, when a dicationic species is produced, and that each spectral change has well-defined isosbestic points, thus indicating a binary system spectrally.

In the present paper, a systematic interpretation will be given of the color band peaks with relation to the proton addition to some azobenzene derivatives. At the same time, the order of the substitution effect on neutral azobenzene and azobenzenium ions will be determined.

Experimental

The azo compounds used here were azobenzene (abbreviated to AB), *p*-hydroxyazobenzene (HAB), *p*-aminoazobenzene (AAB) and *N*, *N*-dimethylaminoazobenzene (DAB) prepared from the special-grade commercial materials by recrystallizations, repeated more than ten times, from the ethanol solution. The melting points of all the applied compounds were in agreement within ± 1 °C with those in the literature. The other compounds used here were the sodium salts of DAB - *m'*-sulfonic acid, HAB - *m'*-sulfonic acid and HAB - *p'*-sulfonic acid; they were synthesized in accordance with the usual steps and were purified by repeated recrystallizations in the same way as above.

The measurement of the absorption spectra was carried out over the 220—550 mμ region using a Shimadzu QR-50 manual spectrophotometer and a Hitachi EPS-2U recording spectrophotometer.

A mixed solution of water and ethanol (7 : 3 in volume) was used as the solvent.

The samples were carefully dealt with in order to avoid converting them to the cis isomer by light.

Results

The spectral change in various acid concentrations of AB, which is the prototype of the derivatives used here, is illustrated in Fig. 1. The first absorption peak moves from 320 mμ to the long wavelength at 425 mμ with an increase in the acid concentration.

The absorption spectra of HAB are shown in Fig. 2. The spectrum with a peak at 430 mμ in a neutral solution (curve 1) changes into another one with a 350 mμ band in an acid solution (curve 3) through the isosbestic points kept by the spectra in the intermediate solutions. With a further increase in the acid concentration, HAB reveals a new band at 460 mμ and a diminution of the 350 mμ band (Fig. 3).

The spectral changes of AAB are illustrated in Figs. 4, 5 and 6. Figure 4 shows that the intense band at 380 mμ in alkaline or neutral solutions (curve 1) is made to disappear by the addition of dilute sulfuric acid, while instead two new bands appear at 317 mμ and 500 mμ (curve 3). With a further increase in the acidity, absorption curve 3 (Fig. 4) varies as follows, keeping the isosbestic points (Fig. 5): the 317 mμ band decreases, and at the same time the 500 mμ band increases in intensity without a shifting of the peaks. After the almost total disappearance of the 317 mμ band (curve 7 in Fig. 6), the intensified 500 mμ band is moved to the shorter side at 415 mμ by a further-concentrated sulfuric acid, as is shown in Fig. 6.

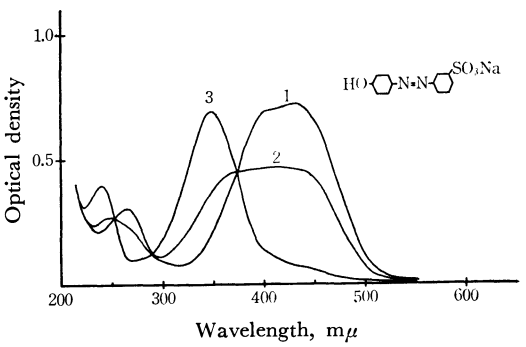

Fig. 7. Absorption spectra of HAB - *m'*-sulfonic acid sodium salt.
Concentration of HAB - *m'*-sulfonic acid sodium salt = 3.25×10^{-5} mol./l.
1. pH 9.70 (solvent water)
2. pH 9.05
3. pH 1.90

4) E. Sawicki, *J. Org. Chem.*, **22**, 365 (1957).

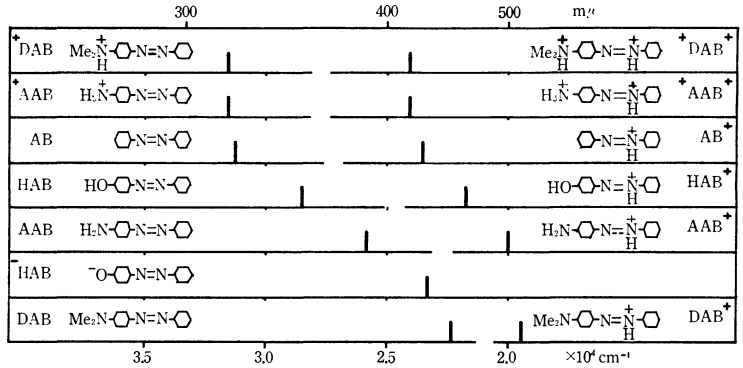

Fig. 8. Absorption maximum of the first band of azobenzene and its derivatives.

DAB behaved like AAB, though the spectral change corresponding to Fig. 5 was not so remarkable as in AAB.

The sulfonic sodium salts of HAB and AAB showed spectral changes quite similar to those of HAB and AAB, indicating essentially no effect of the sulfonic group. The spectral change of HAB - *m'*-sulfonic acid sodium salt is shown as an example in Fig. 7; it can be compared with HAB, which is shown in Fig. 2.

Discussion

The spectral change for the solvent variation in the sodium sulfonate of the azo compound is essentially identical with that of the parent azo compound. Accordingly, the discussion of the mechanism of the color change can be limited to the azo compounds, excluding the sulfonic groups, and the conclusion thus derived is also applicable to the corresponding compounds, including the sulfonic groups.

The proton addition to AB makes the 320 mμ band change to the 415 mμ band by attaching a proton to the electron pairs of one of the azo nitrogen atoms.[5] Let us describe this formally by:

$$AB(320\ m\mu) \rightarrow AB^{+}(425\ m\mu) \qquad (1)$$

As it is well known that the phenolic hydroxyl group can easily be dissociated, HAB in alkaline or neutral solutions has to be ionized; the 430 mμ band must be due to the $^{-}$HAB species. A first proton will go to the oxy-anion part of the $^{-}$HAB species, and a second one, this time preferentially, to the nonbonding σ electrons of β azo-nitrogen.[4,6] The spectral change of HAB may, therefore, be described as follows:

$$^{-}HAB(430\ m\mu) \rightarrow HAB(350\ m\mu) \rightarrow HAB^{+}(460\ m\mu) \qquad (2)$$

Now let us consider the case of AAB. According to Fig. 5, the 317 mμ and the 500 mμ band should be due to spectrally different species, while Fig. 4 indicates that the two bands behave as if they are only one species. This implies that, under such experimental conditions as are indicated in Fig. 4, there is no appreciable change in the amount-ratio of the two species. Since a first proton can be attached to either the amino-group or the β azo-nitrogen atom, representing the respective protonated species as $^{+}$AAB or AAB^{+}, the 317 mμ and the 500 mμ band may be assigned to the $^{+}$AAB and the AAB^{+} species respectively. Therefore, the spectral changes shown in Figs. 4, 5 and 6 can reasonably be explained by the following mechanism. At first, while the AAB species is usable, the amount-ratio of $^{+}$AAB and AAB^{+} is unchanged (Fig. 4); in the second step, the spectral change after using up the AAB species continues as a result of the increasing acidity until $^{+}$AAB is completely converted into AAB^{+} (Fig. 5); finally, AAB^{+} is protonated again by the further increase in acidity, thus producing the dicationic $^{+}$AAB^{+} species (Fig. 6). Thus, the following scheme is obtained for the protonation processes and the absorption peaks:

$$AAB(380\ m\mu) \rightarrow \begin{matrix} {}^{+}AAB(317\ m\mu) \\ AAB^{+}(500\ m\mu) \end{matrix} \rightarrow AAB^{+}(500\ m\mu) \rightarrow {}^{+}AAB^{+}(415\ m\mu) \qquad (3)$$

Similarly, scheme 4 may be considered to hold for the case of DAB:

$$DAB(460\ m\mu) \rightarrow \begin{matrix} {}^{+}DAB(317\ m\mu) \\ DAB^{+}(516\ m\mu) \end{matrix} \rightarrow DAB^{+}(516\ m\mu) \rightarrow {}^{+}DAB^{+}(420\ m\mu) \qquad (4)$$

where the [$^{+}$DAB]/[DAB^{+}] amount-ratio seems to be smaller than [$^{+}$AAB]/[AAB^{+}].

Correlations among the first band positions of the spectral species appearing in schemes 1—4 are summarized as a pattern in Fig. 8, which reveals quite clearly the order of the substitution effect.

5) H. H. Jaffé, *J. Chem. Phys.*, **21**, 415 (1953).
6) Cf. M. B. Robin and W. T. Simpson, ibid., **36**, 580 (1962).

The band positions of the left-side and the right-side series in Fig. 8 can be considered in relation to the substitution effect of the *p*-group to azobenzene and azobenzenium ions respectively, and they are understandable in terms of the electronic theory.

Thus we may conclude that the order of the substitution effect at the para position of both neutral and cationic azobenzene is:

$$\left.\begin{matrix}-NH_3^+ \\ -NHMe_2^+\end{matrix}\right) < -H < -OH < -NH_2 < -O^- < -NMe_2.$$

The authors are indebted to Dr. Harutada Negoro, Sankyo Co., Ltd., for permission to use that company's Hitachi EPS-2U recording spectrophotometer.

BULLETIN OF THE CHEMICAL SOCIETY OF JAPAN VOL. 39 562—565 (1966)

The Ring-opening Polymerization of Ethylene-methylphosphite

By Takeo SHIMIDZU, Tomio HAKOZAKI, Tsutomu KAGIYA and Kenichi FUKUI

Faculty of Engineering, Kyoto University, Sakyo-ku, Kyoto

(Received July 8, 1965)

Several Lewis acids have been found to be effective catalysts for the polymerization of ethylene-methylphosphite, giving a solid polymer with a poly(ethylene-methylphosphonate) structure. The use of $Al(C_2H_5)_3$ gave a wax-like polymer with the structure of poly(ethylene-methoxy-phosphinate), while Na and Li in liquid NH_3 at $-78°C$ produced a jelly-like polymer partly composed of poly(ethylene-methylphosphite).

Recently, there have been several studies of the ring-opening polymerization of species of phosphorus containing cyclic molecules, e. g., cyclic phosphonites,[1] cyclic phosphites,[2,3] cyclic phosphonates,[4] and cyclic phosphates.[5]

It can be seen in the patent descriptions that the ring-opening polymerization of cyclic phosphites has been investigated with several kinds of catalyst systems,[2] but no information on the structure of polymers has been given. The present authors have reported that the ring-opening polymerization of ethylene-alkylphosphites at higher temperatures gave a polymer with the structure of poly(ethylene-alkylphosphonate).[3] It is known that a tautomeric pair of trivalent and pentavalent structures exists in phosphorus compounds like enol- and keto-forms of carbonyl compounds, and that the former is less stable than the latter. In addition, Mukaiyama et al. reported that the polymerization products of cyclic phosphonites have the structure of poly-(ethylene-alkylphosphinate), and suggested an intermediate of an open-chain carbonium-cation type with a phosphoryl group.[4]

The present paper concerns a study of the catalyst and the polymerization products. It was found that the polymerization products were composed of the three types of polymers represented by the following formulae:

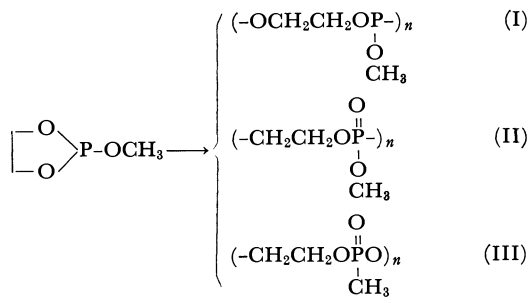

These structures were confirmed by means of infrared absorption spectra and their hydrolyzed products.

Experimental

Ethylene Methylphosphite.—This compound was prepared from ethylene phosphochloridite, methanol and dimethylaniline according to the method of Arbuzov and Zoroastrova[6]; b. p. 40—41°C/12 mmHg, n_D^{20} 1.4484. The infrared spectrum of this compound is shown in Fig. 1. The ethylene phosphochloridite employed was prepared by the following method: Into 1 mol. of ethylene glycol there was stirred drop by drop, 1.5 mol. of phosphorus trichloride at room temperature. Then the reaction mixture was refluxed

1) T. Mukaiyama, T. Fujisawa, Y. Tamura and Y. Yokota, *J. Org. Chem.*, **29**, 2572 (1964).
2) U. S. Pat. 2893961 (1959).
3) T. Shimidzu, T. Hakozaki, T. Kagiya and K. Fukui, *J. Polymer Sci.*, **B3**, 871 (1965).
4) V. V. Korshak, I. A. Gribova and M. A. Andreeva, *Izv. Akad. Nauk S. S. S. R., Otdel. Khim. Nauk*, **1957**, 631.
5) K. A. Petrov, E. E. Nifant'ev and L. V. Fedorchuk, *Vysokomolekulyarnye Soedineniya*, **2**, 417 (1960).
6) A. Y. Arbuzov and V. M. Zoroastrova, *Izv. Akad. Nauk U. S. S. R., Otdel. Khim. Nauk*, **1950**, 770.

TABLE I. SUMMARY OF THE RING-OPENING POLYMERIZATION OF ETHYLENE-METHYLPHOSPHITE

Run	Catalyst	Temp. °C	Time hr.	Yield g.	Appearance	[η]	Infrared (cm^{-1}) 1300	1255	1225	1175
1	—	180	9	0.92	White jelly	0.38	+	+	+	−
2-1	$AlCl_3$	100	6	0.88	Colorless jelly	0.40	±	+	+	+
2-2	$AlCl_3$	180	6	0.95	Colorless hard solid	1.24	+	+	+	−
3-1	$TiCl_3$	30	240	—	Not changed					
3-2	$TiCl_3$	100	7	0.80	Violet vis. liquid	0.12	+	+	+	−
4	BF_3 etherate	180	6	0.91	Brown tacky solid	1.01	+	+	+	−
5-1	P_2O_5	30	240	—	Not changed					
5-2	P_2O_5	180	7	0.81	Colorless liquid	0.08	+	+	+	−
6	96% H_2SO_4	160	5	0.56	Yellow vis. liquid	0.29	+	+	+	−
7	36% HCl	160	5	0.44	White vis. liquid	0.31	+	+	+	−
8	CH_3COOH	160	5	0.01	Colorless liquid	0.08	+	+	+	−
9	H_3PO_4	160	5	0.01	Colorless liquid	0.08	+	+	+	−
10	Na	0	—		Exothermal decomp.					
11	$NaOCH_3$	50	120	0.59	Colorless jelly	0.51	+	+	+	−
12	Na in NH_3	−78	480	0.05	Colorless jelly	0.55	−	+	+	+
13	Li in NH_3	−78	480	0.08	Colorless jelly	0.44	−	+	+	+
			Chloroform extract 0.03				(−	−	−	+)
14	$NaNH_2$ in THF	−78	480	0.05	Colorless jelly	0.39	−	+	+	+
15-1	$Al(C_2H_5)_3$	30	240	0.70	White vis. liquid	0.12	−	+	+	+
15-2	$Al(C_2H_5)_3$	180	7	0.95	White wax	1.34	+	+	+	+
16	$Al(C_2H_5)_3$ etherate	180	6	0.90	White wax	1.44	+	+	+	+
17	AIBN	180	7		Not changed					

(Monomer, 1.0 g. Catalyst, 0.04 g. The ratio of cat. and solvent = 1/20, when solv. is used.)

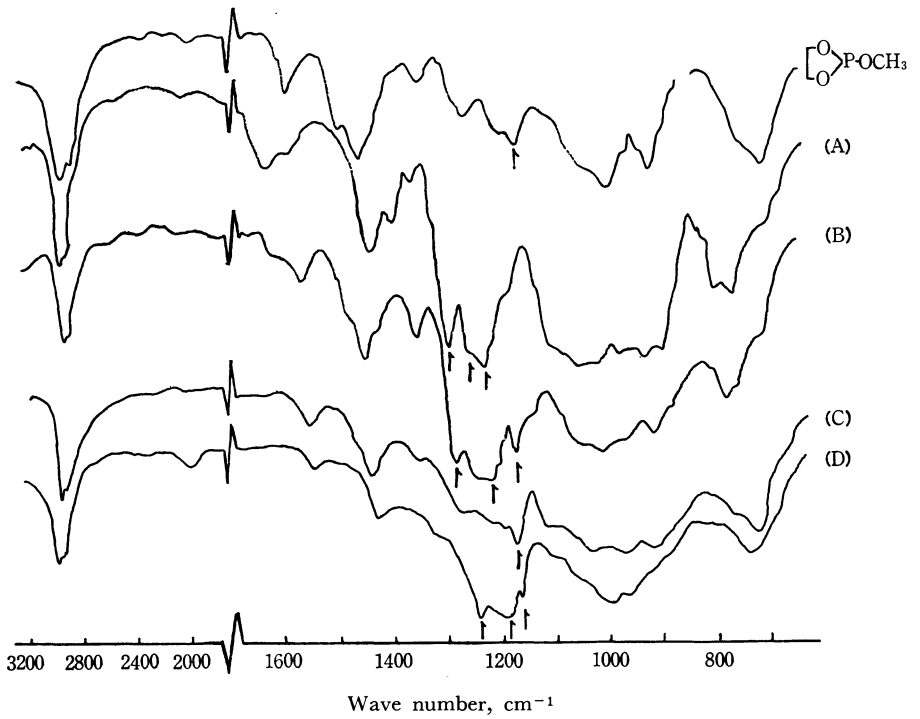

Fig. 1. Infrared spectra of the monomer and typical polymerized products.

TABLE II. THE RESULTS OF THE HYDROLYSIS OF THE POLYMERS

Polymer	Curve in Fig. 1	Product: Yield of hydrolysis	Product: Calcd.	Product: Found
Run 1	A	49%	$CH_3O_3PNa_2$: C, 8.58; H, 2.16	C, 8.41; H, 2.01
Run 15-2	B	41%	$C_2H_5O_4PNa_2$: C, 14.13; H, 2.97	C, 13.81; H, 3.08
Chloroform extract of run 13	C	ca. 54%	O_4PNa_3: C, 0; H, 0	C, 0.02; H, 0.04

for 5 hr. Ethylene phosphochloridite was distilled under reduced pressure: b. p. 64—69°C/45—50 mmHg, n_D^{20} 1.4953.

Catalyst.—Materials of a commercial grade were employed.

Polymerization was carried out in a sealed glass tube under a nitrogen atmosphere. The resultant polymer was washed by dry methanol, and the remaining monomer, as well as a volatile material, were removed under reduced pressure at a temperature below 50°C. The intrinsic viscosity was measured in a solution of dimethylformamide at 9°C.

The infrared absorption spectra were obtained from a KBr disk of the polymer.

The hydrolytic degradation of the polymer was carried out by refluxing it for three hours in 5 ml. of an aqueous 0.10 N sodium hydroxide solution with 30 ml. of dioxane under a nitrogen stream. After the contents had been kept standing overnight at room temperature, the precipitate was crystallized from ethanol. The identification of the polymer structure was aided by a study of its infrared spectrum and by its elementary analysis.

Results and Discussion

The results of the polymerization of ethylene-methylphosphite with various catalysts are summarized in Table I.

Ethylene-methylphosphite can be polymerized without a catalyst at high temperatures. Still, aluminum chloride and boron fluoride etherates are effective catalysts for the polymerization. They give solid polymer with the structure of poly(ethylene-methylphosphonate), $(-CH_2CH_2-\underset{\underset{CH_3}{|}}{\overset{\overset{O}{\|}}{O}}P-O-)_n$, as was reported in a preceding paper.[3] Sodium methylate also gives a jelly-like polymer at relatively low temperatures. Triethylaluminum is an effective catalyst, giving a brittle wax-like polymer the infrared spectrum of which differs a little from that of the above-mentioned polymers. This polymer has the structure of poly(ethylene-methoxyphosphinate), $(-CH_2CH_2\underset{\underset{OCH_3}{|}}{\overset{\overset{O}{\|}}{O}}P-)_n$, as is confirmed by the infrared spectrum indicated in Fig. 1 (curve B) and also by the hydrolyzed product, sodium β-hydroxyethylphosphonate.

Lithium and sodium in liquid ammonia can hardly be effective catalysts for the polymerization, but they give polymers with infrared spectra different from those of the polymers which are obtained by means of the other catalysts. Radical initiators such as 2, 2'-azobisisobutyronitrile do not polymerize ethylene-methylphosphite.

Figure 1 shows typical infrared spectra of the polymers. Curve A is that of run 1, while curve B is that of run 2-1. On the basis of these data, the absorptions at 1300 cm^{-1} (P-CH_3), 1255 and 1225 cm^{-1} (P=O) and 1175 cm^{-1} (P-OCH_3) were adopted as the key bands. These absorptions in each polymer are tabulated in Table I. Table II shows the results of the hydrolysis of the polymers.

The polymers which were obtained at the higher temperatures have absorptions at about 1300, 1255, and 1255 cm^{-1}, and their hydrolyzed products are mainly sodium salts of methyl-phosphonic acid. Conversely, the polymers which are obtained by triethylaluminum and at relatively lower temperatures (run 15 and run 2-1) have an absorption at 1175 cm^{-1} and their hydrolyzed products are mainly sodium β-hydroxyethylphosphonate. Besides, the polymers obtained by lithium and sodium in liquid ammonia at lower temperatures have a broad absorption spectrum in the range from 1170 to 1240 cm^{-1}. This suggests that the polymers have P=O and P-OCH_3 groups. To obtain those absorptions more evidently the polymer (run 13) was extracted in chloroform under nitrogen at room temperature. The results are shown in Tables II and III.

TABLE III. THE SEPARATION OF THE POLYMERS OF RUN 13 AND THEIR INFRARED ABSORPTIONS

	Absorptions at 1175	1225	1255	1300 cm^{-1}
Chloroform extr.	+	—	—	—
Residue	+	+	±	±

Extracted for 5 hr. under a nitrogen stream at 60°C.

The chloroform-extract of the polymer was readily oxidized when it was kept standing in the air; its infrared spectrum is shown in Fig. 1 (curve D). It has absorptions at about 1175, 1225, and 1255 cm^{-1}, but it has no characteristic absorption of the P-N bond and $-NH_2$ groups. On the basis of those data, we confirmed the

structure of the chloroform-extract to be poly(ethylene-methylphosphite), $(-CH_2CH_2OPO-)_n$ with OCH_3. No other chloroform extract with an infrared absorption spectrum of the type of curve D was found.

Thus the type of polymers produced by the ring-opening polymerization of ethylene-methylphosphite can be written as in the scheme presented at the beginning of the page. In Fig. 1, curves A, B, and C are obviously those of the polymers III, II, and I respectively.

It is interesting that the polymer of the type III is given, although it is not yet clear as to whether the polymer results from the methyl migration of an open-chain intermediate or from the ethylene-methylphosphonate which was primarily produced by a rearrangement of ethylene-methylphosphite. The latter scheme seems to be more plausible in view of the stability of the phosphoryl-type structure in phosphites.

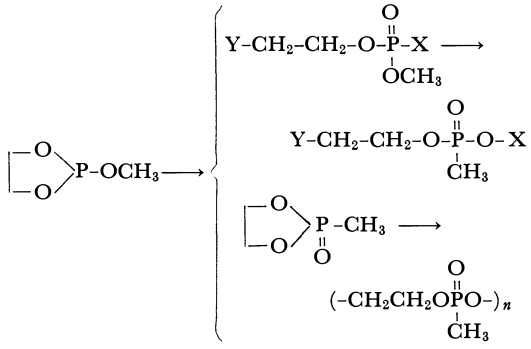

At any rate, ethylene-methylphosphite is not so stable at higher temperature or in the presence of sodium methylate. Korshak et al.[4] have reported that cyclic phosphonates can polymerize at 140°C with water or sodium. In the reaction mixtures of both runs 1 and 11, a little methyl ethylenephosphonate, which was confirmed by its boiling point and its molecular refraction, was recovered.

Recently Denny and Giacin have reported that trialkyl phosphite and *p*-toluene sulfonic acid methyl ester yield dialkyl methyl-phosphonate.[7] It should be noted that the preparation of ethylene-methylphosphite from ethylene-phosphochloridite and sodium methoxide is not easy since they are much more liable to methyl-phosphonate. The polymer of the type II may be produced through the so-called Arbuzov rearrangement. The polymer of the type I is a very particular one. The catalyst system, sodium in ammonia, gave the polymer of the type I while sodium amide did not yield this type of polymer. It goes without saying that sodium amide must exist in liquid ammonia. If it were not for an interaction of ammonia with trivalent *P* atom in ethylene-methylphosphite in the course of polymerization, it is hard to understand how such an enol-form could be stable.

Summary

The ring-opening polymerization of ethylene-methylphosphite has been carried out using several catalyst systems. By using an acidic catalyst, such as aluminum chloride, titanium(III) chloride, boron fluoride, etc., and by working at higher temperatures, we have produced a solid polymer with the structure of poly(ethylene-methylphosphonate), the intrinsic viscosity of which in DMF is ca. 1. When triethylaluminum was used, and when we worked at relatively lower temperatures, we obtained a wax-like polymer with the structure of poly(ethylene-methoxyphosphinate), the intrinsic viscosity of which in DMF is over 1. Sodium and lithium in liquid ammonia at −78°C, although they were not very effective catalysts for the polymerization, gave a jelly-like polymer with part of the structure of poly(ethylene-methylphosphite).

These structures have been confirmed by a study of their infrared spectra and their hydrolyzed products.

7) D. B. Denny and J. Giacin, *Tetrahedron Letters*, **1964**, 1747.

BULLETIN OF THE CHEMICAL SOCIETY OF JAPAN VOL. 39 566—568 (1966)

Phosphorylation via the Oxidation of Phosphite. II. The Preparation of the Diesters of Phosphorous Acid by the Reaction of Alcohols with Ethyl *N*-Phenylimino Phosphite and Acids*[1]

By Teruaki MUKAIYAMA and Kazutoshi OSAKA*[2]

Laboratory of Organic Chemistry, Tokyo Institute of Technology, Ookayama, Tokyo

(Received July 12, 1965)

The diesters of phosphorous acid were prepared in good yields by the reaction of primary or secondary alcohols, such as methanol, ethanol, and *s*-butanol, or of phenols, such as phenol, *p*-chlorophenol and *p*-cresol, with ethyl *N*-phenylimino phosphite and *p*-toluenesulfonic acid monohydrate. Similarly, when carboxylic acids, such as acetic acid, benzoic acid, *p*-chlorobenzoic acid and trichloroacetic acid, were used in place of the acid monohydrate in the above experiment, the diesters of phosphorous acid were also obtained. Ethyl *N*-*n*-propylimino or ethyl *N*-isopropylimino phosphite could be successfully used in place of ethyl *N*-phenylimino phosphite in the above experiments. Further, various derivatives of methylphosphinic acid, such as ethyl dicyanomethyl-, ethyl cyanocarboethoxymethyl- and ethyl dicarboethoxymethylphosphinate, were obtained by the reaction of ethyl *N*-phenylimino phosphite, *p*-toluenesulfonic acid monohydrate and active methylene compounds, such as malononitrile, ethyl cyanoacetate and diethyl malonate.

Recently, it has been found that diesters of phosphorous acid are successfully oxidized under mild conditions to give dialkyl hydrogen phosphates in high yields by means of monobromocyanoacetamide and benzyl alcohol. Therefore, a new useful method for the synthesis of diesters of phosphoric acid can be expected to be offered by the phosphonylation of alcohols and the subsequent oxidation of the phosphites. In this connection, the preparation of diesters of phosphorous acid by the reaction of alcohols with ethyl *N*-phenylimino phosphite and benzaldehyde was reported in the preceding paper.[1]

In the present study, the preparation of diesters of phosphorous acid from alcohols and metaphosphite, formed by the reaction of ethyl *N*-phenylimino phosphite and either carboxylic acid or *p*-toluenesulfonic acid, was attempted. The possible formation of metaphosphite from the reaction of ethyl *N*-phenylimino phosphite and carboxylic acids (Eq. 1) was suggested by the fact that the reaction of phenyl isocyanate with acetic acid resulted in the formation of acetanilide and carbon dioxide by way of a mixed anhydride of phenylcarbamic acid and acetic acid.[2]

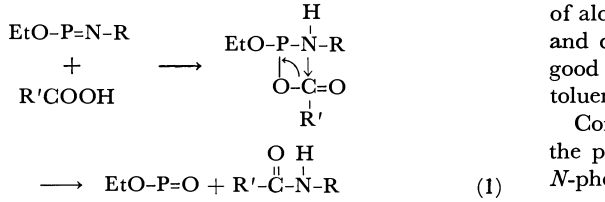

(1)

Indeed, when acetic acid and ethyl *N*-phenylimino phosphite were refluxed in anhydrous benzene for an hour, acetanilide was obtained in a 59% yield, but the expected metaphosphite could not be detected and an orange-colored resinous product was formed.

The presence of the intermediate, i. e., metaphosphite, is demonstrated by the formation of the corresponding diesters of phosphorous acid, diethyl phosphite or ethyl butyl phosphite, along with acetanilide, when acetic acid reacts with ethyl *N*-phenylimino phosphite in the presence of such alcohols as ethyl alcohol or butyl alcohol. Similarly, dialkyl phosphites were obtained, along with the corresponding anilides, when benzoic acid, *p*-chlorobenzoic acid or trichloroacetic acid was used in place of acetic acid in the above experiment. In these cases, ethyl alkyl phosphite was contaminated with small amounts of triethyl phosphite, a compound containing a carbonyl group and aniline, the presences of which were confirmed by the infrared spectra.

On the other hand, when ethyl *N*-phenylimino phosphite was treated with a strong acid such as *p*-toluenesulfonic acid monohydrate in the presence of alcohols, an exothermic reaction soon took place and diesters of phosphorous acid were obtained in good yields, along with the anilinium salt of *p*-toluenesulfonic acid (see Table I).

Contrary to the results obtained in the case of the phosphonylation of alcohols by means of ethyl *N*-phenylimino phosphite and benzaldehyde, both

*1 This paper was presented at the 17th Annual Meeting of the Chemical Society of Japan, Tokyo, April, 1964.

*2 Present address: Technical Research Laboratory, Asahi Chemical Co., Ltd., Nakadai, Itabashi-ku, Tokyo.

1) O. Mitsunobu and T. Mukaiyama, *J. Org. Chem.*, **29**, 3005 (1964).

2) T. Hoshino, T. Mukaiyama and H. Hoshino, *J. Am. Chem. Soc.*, **74**, 3097 (1952).

Table I. Reactions of alcohols with ethyl *N*-phenylimino phosphite and *p*-toluenesulfonic acid monohydrate

Alcohol	Reaction condition			Ethyl alkyl phosphite			Anilinium salt
	Solvent	Time hr.	Temp. °C	Yield %	b. p. °C/mmHg	$n_D^{°C}$	%
Methyl-	Benzene	2.0	65—78	61	59—61/14	?	93
Ethyl-	Benzene	2.0	80	59	70/14	n^{16} 1.4081	93
n-Propyl-	Benzene	2.0	80	54	52—53/4	n^{14} 1.4150	89
Isopropyl-	Benzene	2.1/3	80	63	38—39/3	n^{12} 1.4101	90
n-Butyl-	Benzene	2.0	80	64	55—72/3	n^{17} 1.4192	93
Isobutyl-	Benzene	1.2/3	80	61	52—62/3	n^{19} 1.4150	?
t-Butyl-	Benzene	2.0	80	—	—	—	95
Benzyl-	Benzene	2.0	80	54	113/3	n^{20} 1.4893	90

primary and secondary alcohols were similarly phosphonylated in good yields by the present method. However, in the case of the phosphonylation of such tertiary alcohols as *t*-butyl alcohol, the yield of phosphite decreased markedly.

Further, it was established, that phenols, such as phenol, *p*-chlorophenol and *p*-cresol, reacted with ethyl *N*-phenylimino phosphite and *p*-toluenesulfonic acid to give the corresponding ethyl aryl phosphites. Unfortunately, these phosphites could not be purified by distillation; a small amount of phenols always contaminated the phosphites.

In a similar way, it was also found that ethyl *N*-isopropylimino phosphite or ethyl *N*-*n*-propylimino phosphite gave the corresponding dialkyl phosphite by reaction with ethyl alcohol and *p*-toluenesulfonic acid.

The reaction may proceed through the initial formation of an intermediate, formed by the addition of the water of crystallization of *p*-toluenesulfonic acid to ethyl *N*-phenylimino phosphite, which in trun decomposes to metaphosphite and the anilinium salt of *p*-toluenesulfonic acid, as is shown in the following scheme (Eq. 2). Alcohols then join with the metaphosphite to form diesters of phosphorous acid.

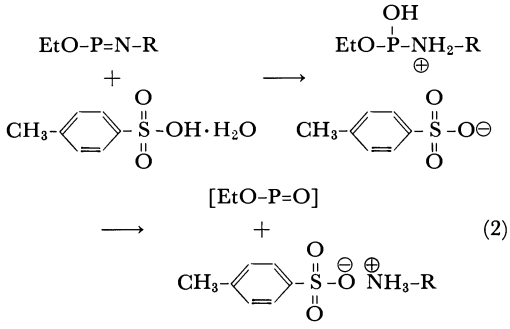

(2)

These results suggest that various derivatives of methylphosphinic acid can be prepared by the reaction of ethyl *N*-phenylimino phosphite, *p*-toluenesulfonic acid monohydrate and active methylene compounds. Indeed, when malononitrile, ethyl cyanoacetate or diethyl malonate was refluxed in benzene with ethyl *N*-phenylimino phosphite and *p*-toluenesulfonic acid monohydrate, the corresponding methylphosphinic acid derivatives, such as ethyl dicyanomethylphosphinate, were obtained (Eq. 3).

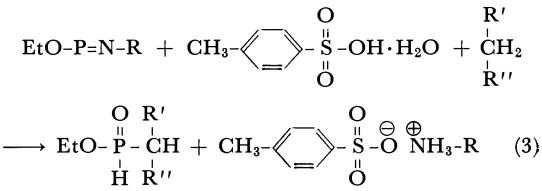

(3)

Experimental

All melting points and boiling points are uncorrected.

Solvents and Reagents.—The solvents and alcohols were dried and purified by ordinary procedures. Ethyl *N*-phenylimino phosphite was prepared from ethyl dichlorophosphite and aniline according to a method previously reported.[1]

Ethyl *N*-*n*-propylimino phosphite, b. p. 80—110°C/0.5 mmHg, 41%, and ethyl isopropylimino phosphite, b. p. 72—85°C/0.5 mmHg, 29%, were prepared by a method analogous to that used for ethyl *N*-phenylimino phosphite. These compounds were also obtained when ethyl dichlorophosphite was treated with an equimolar amount of isopropylamine or *n*-propylamine in the presence of triethylamine.

The Reaction of Ethyl *N*-Phenylimino Phosphite with Carboxylic Acids.—When a solution of acetic acid (1.20 g., 0.02 mol.) and ethyl *N*-phenylimino phosphite (1.67 g., 0.01 mol.) in 40 ml. of benzene was refluxed for an hour, acetanilide (0.80 g., 59%) was obtained, along with a colorless oily product. Similarly, benzanilide (88%) and trichloroacetanilide (96%) were obtained when benzoic acid and trichloroacetic acid respectively were used in place of acetic acid in the above experiment.

The Reaction of Ethyl Alcohol with Ethyl *N*-Phenylimino Phosphite and Acetic Acid.—Into a solution of ethyl *N*-phenylimino phosphite (1.67 g., 0.01 mol.) in 10 ml. of benzene there were stirred, at room temperature and in one portion, both a solution of acetic acid (0.60 g., 0.01 mol.) in 5 ml. of benzene and a solution of ethyl alcohol (0.46 g., 0.01 mol.) in 5 ml. of benzene. After the solvent had been removed under reduced pressure, acetanilide was separated by

TABLE II. THE REACTIONS OF ETHYL ALCOHOL WITH ETHYL *N*-PHENYLIMINO PHOSPHITE AND CARBOXYLIC ACIDS

Carboxylic acid	Reaction condition*1		Yield of anilide, %	Yield of*2 diethyl phosphite, %
Acetic	Reflux	7.5 hr.	59	72
Benzoic	Reflux	5.0 hr.	33	86
p-Chlorobenzoic	Reflux	6.0 hr.	*3	14
Trichloroacetic	Reflux	1.0 hr.	26	33

*1 Each reaction was carried out in dry benzene on the scale of 0.01 mol.
*2 In each case, the phosphites were contaminated with small amounts of aniline, triethyl phosphite and a substance containing a carbonyl group.
*3 0.76 g. (46%) of *p*-chlorobenzoic acid was recovered.

the addition of petroleum ether to the residue. The acetanilide was then removed by filtration; 0.30 g. (22%); m. p. 113—114°C. The filtrate was fractionally distilled to give 1.00 g. (72%) of crude diethyl phosphite (b. p. 38—45°C/5 mmHg, n_D^{22} 1.4184), and the residue was solidified to give 0.50 g. (37%) of acetanilide.

Similarly, crude ethyl *n*-butyl phosphite (0.87 g., 52%; b. p. 45—77°C/4 mmHg, n_D^{19} 1.4320) was obtained by the reaction of *n*-butyl alcohol (0.74 g., 0.01 mol.) with ethyl *N*-phenylimino phosphite (1.67 g., 0.01 mol.) and acetic acid (0.60 g., 0.01 mol.). The reactions of ethyl alcohol with ethyl *N*-phenylimino phosphite and benzoic acid, *p*-chlorobenzoic acid or trichloroacetic acid gave the corresponding anilides and crude diethyl phosphite (see Table II).

The Reaction of Ethyl *N*-Phenylimino Phosphite with *p*-Toluenesulfonic Acid Monohydrate.—When ethyl *N*-phenylimino phosphite (0.42 g., 0.025 mol.) and *p*-toluenesulfonic acid monohydrate (0.43 g., 0.026 mol.) were mixed in one portion by stirring them at room temperature, white needles were soon separated. The crystalline compound, 0.50 g. (80%), m. p. 229—232°C, was filtered off and identified by a comparison of its infrared spectrum with an authentic anilinium salt of *p*-toluenesulfonic acid.

The Reaction of Ethyl Alcohol with Ethyl *N*-Phenylimino Phosphite and *p*-Toluenesulfonic Acid Monohydrate.—To a solution of ethyl *N*-phenylimino phosphite (1.67 g., 0.01 mol.) in 20 ml. of benzene there was added a mixture of *p*-toluenesulfonic acid monohydrate (1.90 g., 0.01 mol.) and ethyl alcohol (0.46 g., 0.01 mol.) in 40 ml. of benzene. After the reaction mixture had been stirred for two hours at 80°C, a separated anilinium salt of *p*-toluenesulfonic acid (2.45 g.; 93%), was filtered off; the filtrate was then concentrated under reduced pressure. The fractionation of the residual oil gave diethyl phosphite, 0.82 g. (60%); b. p. 70°C/14 mmHg, n_D^{16} 1.4081, which was identified by a comparison with both its retention time of the gas chromatography and the infrared spectrum with these of an authentic sample (see Table I).

Similarly, when 1.41 g. (0.015 mol.) of phenol was treated with 3.34 g. (0.020 mol.) of ethyl *N*-phenylimino phosphite and 3.80 g. (0.02 mol.) of *p*-toluenesulfonic acid monohydrate, crude ethyl phenyl phosphite, 1.52 g. (82%); b. p. 110—117°C/5 mmHg, was obtained. Redistillation gave 0.48 g. (26%) of pure ethyl phenyl phosphite, b. p. 105°C/5 mmHg.

Infrared spectrum: 2420 (P–H), 1270 (P=O), 1595, 1495, 760 and 690 cm^{-1} (mono-substituted benzene).

Found: C, 52.09; H, 5.86. Calcd. for $C_8H_{11}O_3P$: C, 51.69; H, 5.96%.

The Reaction of Ethyl Alcohol with Ethyl *N*-Isopropylimino Phosphite and *p*-Toluenesulfonic Acid Monohydrate.—A solution of ethyl alcohol (0.51 g., 0.011 mol.) and *p*-toluenesulfonic acid monohydrate (2.09 g., 0.011 mol.) in 5 ml. of benzene was added, drop by drop, to a solution of ethyl *N*-isopropylimino phosphite (1.44 g., 0.011 mol.) in 20 ml. of benzene. The solution was refluxed for an hour. A separated isopropylammonium salt of *p*-toluenesulfonic acid 2.47 g. (97%); m. p. 137—139°C, was filtered off. After the solvent had been removed, diethyl phosphite, 1.21 g. (80%); b. p. 45—50°C/3 mmHg, n_D^{19} 1.4070, was obtained by distillation. Similarly, ethyl *N*-*n*-propylimino phosphite gave diethyl phosphite (50%).

The Reaction of Malononitrile with Ethyl *N*-Phenylimino Phosphite and *p*-Toluenesulfonic Acid Monohydrate.—A solution of 0.66 g. (0.01 mol.) of malononitrile and 1.90 g. (0.01 mol.) of *p*-toluenesulfonic acid monohydrate in 40 ml. of benzene was added to a solution of 1.67 g. (0.01 mol.) of ethyl *N*-phenylimono phosphite in 20 ml. of benzene. After the reaction mixture had been stirred for 2.1/4 hr. under refluxing, the anilinium salt of *p*-toluenesulfonic acid, 2.40 g.; (91%), was obtained by filtration. The filtrate was fractionated to give crude ethyl dicyanomethylphosphinate, 0.92 g, (58%); b. p. 60—63°C/4 mmHg, n_D^{13} 1.4138. Redistillation gave an analytical sample, b. p. 60—64°C/4 mmHg, n_D^{15} 1.4091.

Infrared spectrum; 2440 (P–H), 2260 (CN), 1250 cm^{-1} (P=O).

Found: N, 17.93. Calcd. for $C_5H_7O_2N_2P$: N, 17.72%.

Summary

Diesters of phosphorous acid have been prepared by the reaction of alcohols or phenols with ethyl *N*-phenylimino phosphite and acids, such as acetic acid, benzoic acid and *p*-toluenesulfonic acid monohydrate. Further, methylphosphonic acid derivatives have been obtained using active methylene compounds in place of alcohols in the above reaction.

The authers wish to express their hearty thanks to Dr. Tuziaki Hata and Mr. Oyo Mitsunobu for their kind advice given during the course of this experiment. They also wish to thank Miss Toshiko Aoyagi for her microanalyses.

BULLETIN OF THE CHEMICAL SOCIETY OF JAPAN VOL. 39 569—576 (1966)

Semi-empirical Treatments of the Nonlinearity of Free Energy Correlations in Aromatic Side-chain Reactions. The Multiplicity of Substituent Constants

By Takayuki FUENO, Tadashi OKUYAMA and Junji FURUKAWA

Department of Synthetic Chemistry, Kyoto University, Sakyo-ku, Kyoto

(Received July 15, 1965)

The nonlinearity of free energy correlations of the substituent effects in aromatic side-chain reactions has been treated by the simple LCAO MO method. The ionization equilibria of substituted phenylacetic acids, leading to the definition of "normal" substituent constants, σ^0, were taken as the basis for theoretical tests of the correlations. Thus, the integral parameters for various substituents were determined in such a way that the calculated π-electron charge densities for meta and para carbons in benzenes were proportional to the corresponding σ^0-constants. Several other typical side-chain reactions of substituted benzenes were simulated by the corresponding standard processes, and the effects of substituents on these reactions were examined by the perturbation calculations of the π-electron energy changes accompanying the reactions. It has been found that the substituent constants, σ, σ^+ and σ^-, are linearly related to the calculated energy changes. It is suggested that the treatment may be extended to other reactions to account for the sliding-scale variation in substituent constants from reaction to reaction.

It has been customary to utilize Hammett's $\rho\sigma$ equation[1] for correlating observations concerning the effects of ring substituents on the rate or equilibrium data for the reactions of benzene derivatives. The Hammett equation in its original form presumes that the standard free energy changes in certain types of reactions of substituted benzene derivatives are in a linear relation with those in the corresponding benzoic acid ionizations. This linear free energy relationship has been borne out well in many cases; indeed, there exists a voluminous literature that indicates the applicability of the Hammett equation.[2]

Several authors[3-9] have looked into the physical basis of the Hammett equation, particularly into the nature of the substituent constants, in terms of the simple molecular orbital method. These studies have been briefly reviewed in a recent article by Ehrenson.[9] Among others, Jaffé's attempts[3] to correlate the Hammett σ-constants with π-electron charge densities on the ring carbons bearing reaction sites seem to have illuminated, though with limited success, the role of mobile π-electrons in governing the relative magnitudes of σ-constants.

It is known, however, that the original Hammett relation suffers some limitations depending on the type of reaction and on the solvent conditions; thus, a number of modified sets of σ-values have been proposed by many authors.[2,10-13] The current belief that para substituents are more or less subject to multiplicity in σ-value is a conceptual outgrowth of these situations. This nonlinearity of free energy correlations, i. e., the "sliding-scale" character of sigma values, is believed to arise from the different extents of direct conjugation between substituents and reaction centers in different reactant structures and reaction types.[12,14] A molecular orbital consideration of such a multiplicity of substituent constants was first undertaken by Jaffé,[4] who was able to reproduce approximately the enhanced sigma values required for strongly electron-attracting para substituents in the ionizations of aniline and phenol.[1] The exalted electron-releasing character of some methylene anion-type para substituents in electrophilic substitutions was also accounted for by us from an examination of the effects of these substituents on the ring carbon localization energies.[7] Similar effects of this last group of substituents on the extracyclic reaction

1) L. P. Hammett, "Physical Organic Chemistry," McGraw-Hill, New York, N. Y. (1940), Chapter 7.
2) H. H. Jaffé, *Chem. Revs.*, **53**, 191 (1953).
3) H. H. Jaffé, *J. Chem. Phys.*, **20**, 279, 285, 1554 (1952); **21**, 415 (1953).
4) H. H. Jaffé, *J. Am. Chem. Soc.*, **76**, 5843 (1954).
5) F L. J. Sixma, *Rec. trav. chim.*, **72**, 273, 538, 543, 673 (1953); **73**, 235, 243 (1954); *J. Chem. Phys.*, **19**, 1209 (1951).
6) D. Peters, *J. Chem. Soc.*, **1957**, 2654.
7) T. Tsuruta, T. Fueno and J. Furukawa, *Bull. Inst. Chem. Res., Kyoto Univ.*, **34**, 214 (1956).
8) M. J. S. Dewar and P. J. Grisdale, *J. Am. Chem. Soc.*, **84**, 3539, 3548 (1962).
9) S. Ehrenson, "Progress in Physical Organic Chemistry," Vol. 2, Ed. by S. Cohen, A. Streitwieser, Jr., and R. W. Taft, Interscience, New York (1964), p. 195.
10) H. C. Brown and Y. Okamoto, *J. Am. Chem. Soc.*, **80**, 4979 (1958).
11) R. W. Taft, Jr., *J. Phys. Chem.*, **64**, 1805 (1960).
12) Y. Yukawa and Y. Tsuno, This Bulletin, **32**, 965, 971 (1959).
13) C. D. Ritchie and W. F. Sager, "Progress in Physical Organic Chemistry," Vol. 2, Ed. by S. Cohen, A. Streitwieser, Jr., and R. W. Taft, Interscience, New York (1964), p. 323.
14) H. van Bekkum, P. E. Verkade and B. M. Wepster, *Rec. trav. chim.*, **78**, 815 (1959).

sites have recently been discussed by Ehrenson.[9]

The purpose of the present paper is to analyze the relative magnitudes of various sets of substituent constants from a unified theoretical standpoint, and thereby clarify the cause of the above-mentioned nonlinearity of free energy correlations. To this end we will conduct second-order perturbation calculations of the energy changes of systems comprising substituted benzenes and reactive side-chains. In principle, this is a computational elaboration of the afore-mentioned treatment of Ehrenson.[9] As the basis for comparisons among different sets of substituent constants, the ionization equilibria of substituted phenylacetic acids, which lead to σ^0-values,[11] have been selected. This is because, in these compounds, the reaction site is insulated from the aromatic π-conjugation, which otherwise may blur the standard with which one may test the departure from the linear free energy relationships. The effects of substituents on other types of benzene side-chain reactions, leading to σ, σ^+ and σ^- constants,[1,10] will be examined by calculating the π-electronic energy changes accompanying the reactions. It will be shown that these calculated energy changes are closely related to the various substituent constants. It appears that extensions of the present treatment may provide a promising route to account for the sliding-scale variations of substituent constants from reaction to reaction.

The Method of Calculation

All the calculations were carried out by the simple LCAO MO method (overlap neglected). First, the π-electronic MO energies, $E_i=\alpha+m_i\beta$, and the corresponding MO coefficients, C_{it}, were calculated for various monosubstituted benzenes, XC_6H_5 (as the common unperturbed substrates). α and β have their usual meanings. Second, analogous calculations were made for isolated (unperturbed) extracyclic reaction centers, Y, whose energies and coefficients are $F_j=\alpha+n_j\beta$ and C_{ju} respectively. Third, the delocalization energies, DE, due to the linking of XC_6H_5 and Y to form disubstituted benzenes, XC_6H_4Y, were calculated from the following familiar expression,[15] which has been derived by the second-order perturbation method:

$$DE=2\left\{\sum_{i}^{\text{occ}}\sum_{j}^{\text{unocc}}-\sum_{j}^{\text{occ}}\sum_{i}^{\text{unocc}}\right\}\frac{(C_{ir})^2(C_{js})^2}{m_i-n_j}\left(-\frac{\gamma^2}{\beta}\right) \tag{1}$$

where the subscripts r and s denote the carbon atoms at which the components are bonded; γ is the resonance integral for such bonds. Equation 1 was used also for the system XC_6H_4Y' formed after the occurrence of the side-chain reactions. Finally, the total energy of the product, XC_6H_4Y', relative to that of the reactant, XC_6H_4Y, was obtained from

$$\Delta E_\pi=c-\Delta E \tag{2}$$

where

$$\Delta E=DE'-DE \tag{3}$$

and

$$c=2\sum_{j}^{\text{occ}}(F_j'-F_j) \tag{4}$$

The prime appearing in Eqs. 3 and 4 indicates that the quantities correspond to the product systems. Since c is independent of the substituents, X, the relative stabilities of the product systems may be expected to increase as the delocalization energy difference, ΔE, increases.

The integral parameters of heteroatoms and their bonds necessary for the calculation of the energies and coefficients of monosubstituted benzenes were determined by imposing the condition[16] that the charge densities on the para and meta ring carbons so obtained be proportional to the corresponding Taft σ^0-constants. The inductive effects of the substituents were roughly taken into account by assigning Coulomb integral increments to ring carbons.[3] Specifically, the ring carbon linked with a substituent atom, X, of the Coulomb integral parameter, k_X, was assumed to have a Coulomb integral increment, $\delta_{CX}k_X$; the inductive parameter, δ_{CX}, was taken to be 0.3 unless otherwise noted. The increments for the next-nearest ring carbons were assumed to be $\varepsilon\delta_{CX}$, with $\varepsilon=1/3$, but they were truncated for other carbon atoms.

For fixing the proportionality constant between charge densities and σ^0-values, only σ^0 meta and

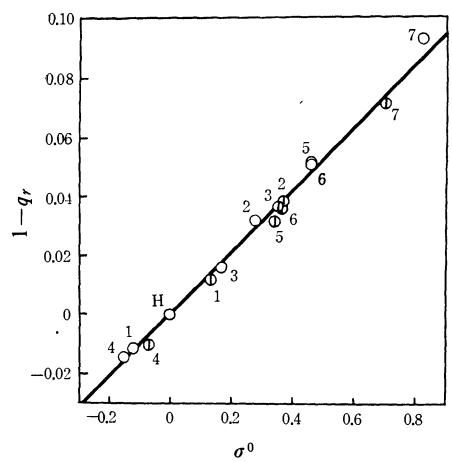

Fig. 1. The charge densities in substituted benzenes against σ^0-constants.
○, para; ⓘ, meta
Numbers correspond to the substituents given in Table I. The symbol H indicates hydrogen.

15) M. J. S. Dewar, *J. Am. Chem. Soc.*, **74**, 3341 (1952).

16) That is, $\sigma_r^0=\varepsilon(1-q_r)$, where q_r is the π-electron density calculated for a meta or para carbon, and where ε is a proportionality constant ($\varepsilon=9.68$).

Table I. Substituents and integral parameters

No.	Substituent	Integral parameters[a]		
1	CH_3O	$k_O=0.6$	$h_{C-O}=0.5$	$\delta_{CO}=0.3$
2	Cl	$k_{Cl}=0.9$	$h_{C-Cl}=0.45$	$\delta_{CCl}=0.6$
3	F	$k_F=1.0$	$h_{C-F}=0.6$	$\delta_{CF}=0.5$
4	CH_3	$k=-0.15$[b]		
5	$COCH_3$	$k_O=1.3$	$h_{C=O}=1.2$	
		$k_C=1.3$	$h_{C-C}=0.4$	$\delta_{CC}=0.3$
6	COOR	$k_O=1.3$	$h_{C=O}=1.2$	
		$k_{OR}=0.6$	$h_{C-OR}=0.5$	
		$k_C=1.3$	$h_{C-C}=0.4$	$\delta_{CC}=0.3$
7	NO_2	$k_N=3.0$	$h_{N=O}=1.0$	
		$k_O=1.3$	$h_{C-N}=0.3$	$\delta_{CN}=0.3$
	$COOH$[c]	$k_O=1.2$	$h_{C=O}=1.2$	
		$k_{OH}=0.6$	$h_{C-OH}=0.5$	
		$k_C=0.57$		
	COO^-[c]	$k_O=0.5$	$h_{C=O}=1.0$	
		$k_C=0.3$		

a) k, Coulomb integral parameter; h, resonance integral parameter; δ, inductive parameter for the ring carbon carrying substituents.
b) Inductive effect model. Ortho carbons are assigned a Coulomb integral increment 0.3 k.
c) Used for the calculations of ionization energies of benzoic acids.

para values of the methyl group will suffice in principle, provided that the group is assumed to be a non-conjugating (inductive) substituent. In practice, however, the σ^0-values for meta and para methoxy groups were also used for the above purpose. Three unknown parameters (two Coulomb integrals, $\alpha+k\beta$, for the methoxy and methyl groups and one resonance integral, $h\beta$, for the ring carbon-methoxy bond) were so adjusted as to give the best straight-line fit of the calculated charge densities when plotted against the four σ^0-values. The slope was thus fixed. The parameters for other substituents were chosen so that the corresponding plots would fall on this straight line. The parameter values finally adopted for the various substituents investigated are listed in Table I. The proportionality of the calculated charge densities to σ^0-values is shown in Fig. 1.

Results

σ^0-Constants.—As has already been mentioned, Jaffé[3] attempted to correlate π-electron densities on meta and para carbons of substituted benzenes with the corresponding Hammett σ-constants. However, such attempts are unjustifiable, since benzoic acids, and also their conjugate bases, more or less involve resonance interactions between substituents and reaction centers.

In contrast, in the case of phenylacetic acids, the reaction site is insulated from the aromatic conjugation, so that the interactions between the ring and its substituents in these acids will remain essentially the same as in substituted benzenes. From the ionization constants of substituted phenylacetic acids, Taft[11] defined the "normal" substituent constants, σ^0. It seems, then, more reasonable to correlate the π-electron distributions in substituted benzenes with Taft's σ^0-constants than with Hammett's σ-constants.

It may be shown that the π-electron distributions in substituted benzenes are related to the dissociation energies of the corresponding phenylacetic acids. The replacement of a benzene hydrogen atom by a CH_2COOH group will introduce a perturbation to the Coulomb integral of the ring carbon, r, at which such a replacement occurs. It is to be expected that the reaction:

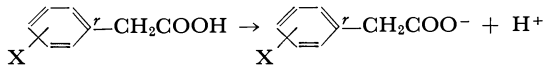

(5)

will accompany the change in this perturbation. Let us denote by $\delta\alpha_r$ and $\delta\alpha_r'$ these perturbations of the Coulomb integral before and after the reaction respectively. According to the simple LCAO MO theory, then, the total π-electronic energy change, ΔE^0, of the benzene part due to the above change in perturbation is given, to a first approximation, by

$$\Delta E^0 = q_r(\delta\alpha_r'-\delta\alpha_r) \qquad (6)$$

where q_r is the π-electron density on the ring carbon, r. Since the COO^- group is less electronegative than the COOH group, it is very likely that $\delta\alpha_r'-\delta\alpha_r>0$. Hence, the dissociation energy of phenylacetic acids will linearly increase with an increase in the q_r value.

Hammett's σ-Constants.—In the ionization of benzoic acids, the ΔE, defined by Eq. 3, is the difference in delocalization energy between benzoic acids and benzoate anions.

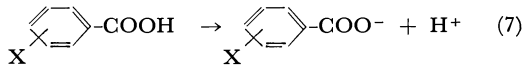

The integral parameters used for an isolated carboxyl group and the carboxylate anion are given in Table I. The parameter values assumed for COOH were the same as those used for COOR, except that the carbon atom in the former was assigned a smaller k value than in the latter. This assignment of a smaller k value was made in order to minimize the inductive effect of the COOH group on the ring in calculating the delocalization energies. Errors arising from such a minimization will be largely canceled by a similar disregard of the COO^- inductive effects in benzoate anions.

The values of ΔE calculated for various substituents are given in Table II. In every case the delocalization stabilization of the acid form was greater than that of the corresponding anion, i. e., $\Delta E<0$. This would mean that the smaller the ΔE in magnitude, the easier the ionization.

TABLE II. CHARGE DENSITIES IN SUBSTITUTED BENZENES AND ENERGY CHANGES FOR THE BENZOIC ACID IONIZATIONS

Substituent	$\sigma^{0a)}$	$1-q_r$	$\sigma^{b)}$	$-\Delta E(-\gamma^2/\beta)$
p-CH_3	−0.15	−0.0145	−0.170	0.0922
p-CH_3O	−0.12	−0.0119	−0.268	0.0975
m-CH_3	−0.07	−0.0103	−0.069	0.0896
H	0	0	0	0.0860
m-CH_3O	0.13	0.0152	0.115	0.0808
p-F	0.17	0.0158	0.062	0.0841
p-Cl	0.27	0.0317	0.227	0.0771
m-$COCH_3$	0.34	0.0309	0.376	0.0755
m-F	0.35	0.0363	0.337	0.0741
m-COOR	0.36	0.0353	0.37	0.0744
m-Cl	0.37	0.0383	0.373	0.0733
p-$COCH_3$	0.46	0.0521	0.502	0.0689
p-COOR	0.46	0.0508	0.45	0.0687
m-NO_2	0.70	0.0707	0.710	0.0633
p-NO_2	0.82	0.0930	0.778	0.0569

a) Ref. 11.
b) Ref. 1.

In Fig. 2 the calculated ΔE values relative to the value for unsubstituted benzoic acid are plotted against the σ-values. It may be seen there that the relative delocalization energy difference, $\delta\Delta E$, is proportional to σ, the symbol δ indicating the energy difference with respect to the substituents. It should be noted that the points for p-CH_3O and p-F groups, whose σ-values show relatively large deviations from σ^0-values, are well fitted to the straight line.

σ^+-Constants. — In electrophilic reactions, certain para-substituted compounds exhibit greater reactivities than would be expected from Hammett's σ-values of the substituents. From the data on the S_N1 solvolysis rates of substituted phenyldimethylcarbinyl chlorides (or, briefly, t-cumyl chlorides), Brown and Okamoto[10] defined the σ^+-values as a new set of electrophilic substituent constants.

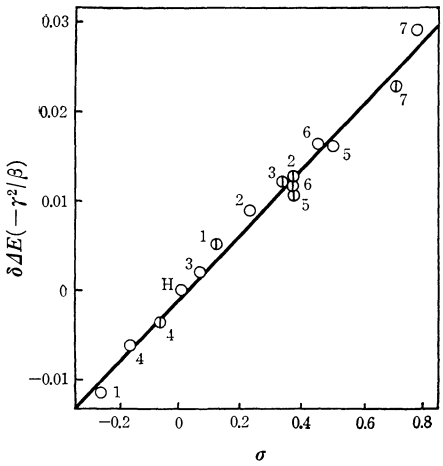

Fig. 2. The π-electronic energy changes in the ionization of substituted benzoic acids against σ-values.
○, para; ⓘ, meta
Numbers correspond to the substituents given in Table I.

In the present calculations, we have taken the following ionic cleavage of t-cumyl chlorides as a standard reaction:

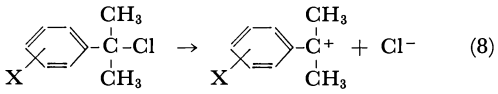

The total π-electronic energies of the chlorides may be assumed to be equal to those of the corresponding substituted benzenes. In the resulting carbonium ions, however, the side-chain, $-\overset{+}{C}(CH_3)_2$, is incorporated in the π-conjugation. Thus, the total π-electronic energies of the cations differ substantially from those of substituted benzenes. Since the carbonium ions are recognized to be very close to the transition state of the S_N1 reactions, the above energy increment, i. e., the delocalization energy which t-cumyl chlorides would acquire upon ionic cleavage, may be regarded as a measure of the relative ease of the reaction δ.[17,18]

The delocalization energies of t-cumyl chlorides may be calculated from Eq. 1, by assuming that the $-\overset{+}{C}(CH_3)_2$ group is a single heteroatom ion with a vacant π-type atomic orbital the Coulomb integral of which is $\alpha+k\beta$. These energies obtained

17) N. C. Deno, "Progress in Physical Organic Chemistry," Vol. 2, Ed. by S. Cohen, A. Streitwieser, Jr., and R. W. Taft, Interscience, New York (1964), p. 129.
18) A. Streitwieser, Jr., "Molecular Orbital Theory for Organic Chemists," John Wiley and Sons, New York, N. Y. (1961), Chapter 12.

TABLE III. THE DELOCALIZATION ENERGIES OF RING-SUBSTITUTED PHENYLDIMETHYLCARBINYL CHLORIDES

Substituent	σ^+ a)	$\Delta E_P^+(-\gamma^2/\beta)$			ΔE_V^+ $(-\beta)$
		kc)$=0$	$k=0.2$	$k=0.3$	
p-CH_3	−0.311	0.8730	1.0790	1.2270	0.7427
p-CH_3O	−0.778	0.9397	1.2655	1.6072	0.7769
m-CH_3	−0.066	0.8561	1.0521	1.1912	0.7335
H	0	0.8333	1.0185	1.1485	0.7206
m-CH_3O	0.047	0.8021	0.9986	1.1075	0.7023
p-F	−0.073	0.8323	1.0375	1.1931	0.7216
p-Cl	0.114	0.7857	0.9635	1.0934	0.6944
m-$COCH_3$	(0.376)b)	0.7683	0.9255	1.0325	0.6819
m-F	0.352	0.7605	0.9179	1.0267	0.6772
m-COOR	0.368	0.7633	0.9185	1.0241	0.6767
m-Cl	0.399	0.7553	0.9092	1.0147	0.6739
p-$COCH_3$	(0.502)b)	0.7296	0.8713	0.9661	0.6592
p-COOR	0.489	0.7301	0.8724	0.9681	0.6582
m-NO_2	0.674	0.6944	0.8237	0.9091	0.6343
p-NO_2	0.790	0.6552	0.7698	0.8440	0.6094

a) Ref. 10.
b) Hammett's σ-values.
c) k is the Coulomb integral parameter for the side-chain carbon cation.

by the perturbation method will be denoted by ΔE_P^+. The magnitudes of ΔE_P^+ were calculated for various substituents, using varying k values ($k = 0$, 0.2 and 0.3). The results are given in Table III, together with the corresponding σ^+-constants.

An inspection of the data listed in Table III will indicate that for each k value the ΔE_P^+ values are larger for those substituents which have smaller σ^+-constants. This trend is compatible with the qualitative expectation that carbonium ions will be more stabilized as the charge-center carbons of the ions become less electron-deficient.[19] Also noticeable in Table III is the tendency that, in each substituent examined, the ΔE_P^+ value increases with an increase in the k value that is, with an increasing affinity of the exocyclic carbons toward π-electrons. However, this in itself should by no means be related to observations on the relative stabilities of benzyl-type carbonium ions bearing different alkyl groups (or hydrogen atoms) on the exocyclic carbons.[20]

A rather more important feature to be noted in the $\Delta E_P^+ - \sigma^+$ relationship is that the Coulomb parameter, k, exerts a particularly large influence on the ΔE_P^+ values of some para-substituted compounds (p-methoxy and p-fluoro derivatives). The situations are illustrated in Fig. 3, where the relative delocalization energies, $\delta\Delta E_P^+$, taking the nonsubstituted t-cumyl chloride as the standard, are plotted against the σ^+-values for each assumed value of k. In each case, a straight line is seen to fit the plots for meta substituents. In order for the para points to show the best fits to the meta line, a value of $k=0.2$ would have to be assumed for the side chain.[21] If the side-chain carbon has an electronegativity different from that specified by $k=0.2$, the effects of some para substituents on reactions of the type 8 will deviate from those to be expected from their σ^+-values. The occurrence of such deviations may be taken as an indication that the relative importance of the resonance interaction between substituents and reaction sites varies according to the structure of the reactants. This view of the sliding-scale variation of substituent constants is compatible with the physical picture underlying the Yukawa-Tsuno four-parameter equation:[12]

$$\log k/k_H = \rho\{\sigma + r(\sigma^+ - \sigma)\} \qquad (9)$$

in which r is a reaction parameter which takes account of the degree of possible resonance interactions between substituents and reaction sites in the transition states. Thus, r would increase with an increase in the k value.

19) E. Berliner and N. Shien, *J. Am. Chem. Soc.*, **79**, 3849 (1957).

20) In addition to the π-electron delocalization, several other factors, such as the inductive and hyperconjugative effects of alkyl groups and the strain relief on ionization, need to be considered with regard to the carbonium ion stability. Nevertheless we feel that the ΔE_P^+ value may be useful in comparing the relative effects of ring substituents on the stabilities of different types of carbonium ions.

21) That the positively-charged side-chain carbon is more electronegative than the ring carbons may be confirmed by a self-consistent field treatment of the ion. The simplest test of this point may be achieved by the use of the conventional ω-technique.[22] In the case of the benzyl cation the charge density calculated for the exocyclic methylene carbon by this method is roughly 0.41.[18] The Coulomb integral parameter for the exocyclic carbon orbital of the t-cumyl cation in its ultimate self-consistency will be 0.41 times $\omega(=1.4)$ plus twice the inductive parameter (-0.15) of a methyl group. Thus, $k=0.41(1.4)+2(-0.15)=0.27$, a value which is of the correct order of magnitude.

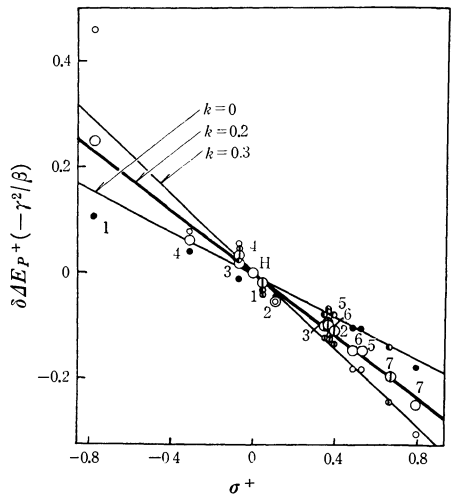

Fig. 3. The π-electronic energy changes in the dissociation of substituted *t*-cumyl chlorides against σ^+-values.
○, para; ⓘ, meta for $k=0.3$
○, para; ⓘ, meta for $k=0.2$
●, para; ◐, meta for $k=0$
Numbers correspond to the substituents given in Table I.

Another significant point in Fig. 3 is its indication that the k value also affects the slope of meta lines; the slope becomes steeper as the k value increases. If this is true, the reaction constant, ρ, should increase in magnitude with the increase in the resonance parameter, r, for reactions of the type 8. This expectation is borne out by the recent experimental results gained by Yukawa and Tsuno[23] who compared the substituent effects on the S_N1 solvolysis rates of *t*-cumyl and α-phenylethyl chlorides under the same conditions. They found that α-phenylethyl chlorides gave the values $r=1.16$ and $\rho=-4.95$ while *t*-cumyl derivatives had $r=1.00$ and $\rho=-4.54$. The variation in these values observed in going from *t*-cumyl to α-phenylethyl chlorides agrees at least qualitatively with our theoretical expectation.[24]

The delocalization energies were also calculated by the variation method for the case of $k=0$. The values obtained are included in Table III. The relative energies, $\delta\Delta E_V{}^+$, are found to be proportional to the corresponding $\delta\Delta E_P{}^+$ values, as is illustrated in Fig. 4. This remarkably good linear relationship confirms the validity of our present perturbation calculations.

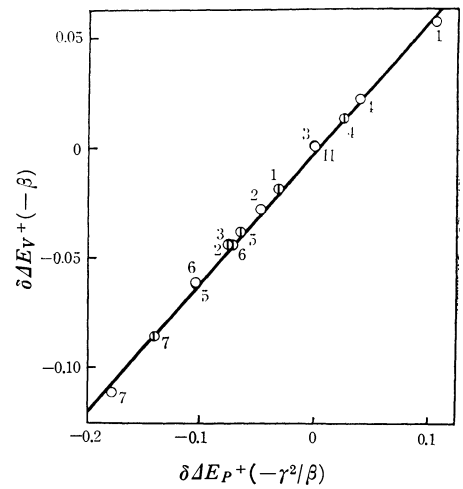

Fig. 4. Linear relationship between the π-electronic energy changes calculated by the perturbation and variation methods for the dissociation of substituted *t*-cumyl chlorides.
○, para; ⓘ, meta
Numbers correspond to the substituents given in Table I.

σ^--Constants.—Hammett first noted that, in the reactions of the derivatives of phenol and aniline, enhanced σ-values were required for such substituents as para-nitro and -cyano groups.[1] Just as the reactions whose transition states involve the electron-deficient side chains linked to an aromatic ring respond sensibly to electron-releasing para substituents, so the reactions which involve conjugating lone-pair electrons respond sensibly to electron-attracting para substituents. The special substituent constants for these substituents are designated by σ^-.

We calculated by the perturbation method the energy change, ΔE^-, accompanying the reaction:

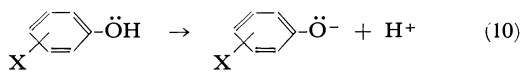

(10)

Here the Coulomb integral parameters of the OH and O^- atomic orbitals are assumed to be $k=1$ and 0.8 respectively, and the energy change, ΔE^-, is the difference between the benzene delocalization energies, as defined by Eq. 3. The calculated energy changes are given in Table IV, together with the available data for σ^-.

In Fig. 5 the values of ΔE^- relative to the unsubstituted phenol, $\delta\Delta E^-$, are plotted against σ- or σ^--values, whichever are appropriate.

22) A. Streitwieser, Jr., and P. M. Nair, *Tetrahedron*, **5**, 149 (1959); A. Streitwieser, Jr., *J. Am. Chem. Soc.*, **82**, 4123 (1960).
23) Y. Yukawa and Y. Tsuno, *J. Chem. Soc. Japan, Pure Chem. Sect.* (*Nippon Kagaku Zasshi*), **86**, 873 (1965). In applying Eq. 9 to these reactions, they replaced σ by σ^0.
24) Taking one step further, one may make a more quantitative comparison between theory and experiment. From the experimental r-values, we estimated the values of k which permitted the best linear correlationships between $\Delta E_P{}^+$ and $\sigma+r(\sigma^+-\sigma)$. The k-values thus estimated were 0.20 and 0.23 for the side chains $-\overset{+}{C}(CH_3)_2$ and $-\overset{+}{C}HCH_3$ respectively. The relative slopes of the theoretical lines corresponding to these k-values were found to be 1 and 1.07. The ratio 1 : 1.07 is in reasonable agreement with the experimental ρ ratio, 1 : 1.09, found between *t*-cumyl and α-phenylethyl chlorides.

Table IV. Energy changes for the phenol ionizations and anilinium ion dissociations

Substituent	σ^-	$\Delta E^-(-\gamma^2/\beta)$	$DE(-\gamma^2/\beta)$
p-CH_3		0.0430	0.4326
p-CH_3O	−0.13[a]	0.0443	0.4381
m-CH_3		0.0437	0.4366
H		0.0450	0.4444
m-CH_3O		0.0466	0.4553
p-F	0.005[a]	0.0491	0.4622
p-Cl		0.0505	0.4755
m-$COCH_3$		0.0487	0.4677
m-F		0.0496	0.4717
m-COOR		0.0492	0.4711
m-Cl		0.0499	0.4735
p-$COCH_3$	0.874[b]	0.0604	0.5028
p-COOR	0.678[b]	0.0573	0.4974
m-NO_2		0.0547	0.4999
p-NO_2	1.27[b]	0.0765	0.5480

a) A. I. Biggs and R. A. Robinson, *J. Chem. Soc.*, **1961**, 388.
b) Ref. 2.

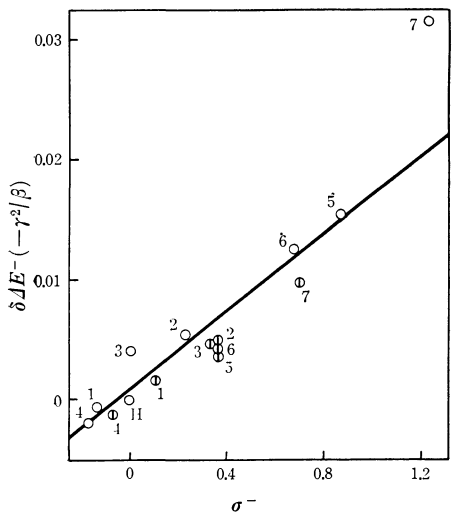

Fig. 5. The π-electronic energy changes calculated for the ionization of phenols against σ^--constants.
○, para; ⓘ, meta
Numbers correspond to the substituents given in Table I.

Although the points are somewhat scattered in comparison with those in Figs. 1 to 3, it does appear that a single straight line fits the plots here also. Different choices of Coulomb parameters for the OH and O^- orbitals neither improve nor worsen the situation materially.

As an alternative to the above theoretical quantity, $\delta\Delta E^-$, the benzene delocalization energy itself could be used as a measure of the σ^--constants. This would be particularly valid when the ionizations of anilinium salts are to be considered. The delocalization energies calculated for the case of $k=1$ are listed in Table IV and are plotted against σ- and σ^--values in Fig. 6. It may be seen in Fig. 6 that the plots corresponding to the σ^--values fall on the meta line, in agreement with Jaffé's previous conclusion reached by the use of a different set of integral parameters.[4]

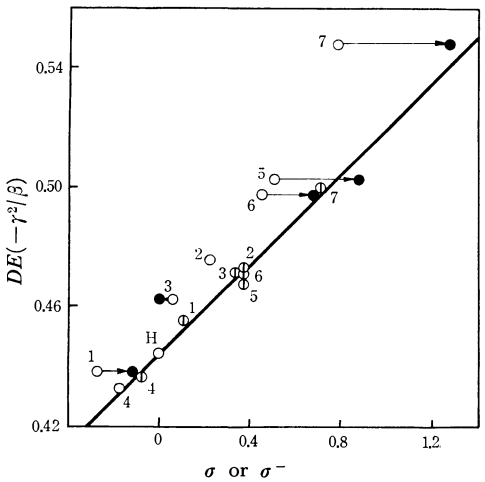

Fig. 6. Delocalization energies calculated for the acid dissociations of anilinium ions against σ and σ^-.
○, σ para; ⓘ, σ meta; ●, σ^-
Numbers correspond to the substituents given in Table I.

Discussion

Although it is definite that π-electrons make dominant contributions to the properties of conjugated compounds, any attempt to establish correlations between the distribution of such electrons and their role in controlling molecular reactivities must be judged with due caution. So far as the substituent effects on aromatic side-chain reactions are concerned, only those reactions which are governed by the normal substituent constants, σ^0, will respond directly to the electronic charge distributions effected by substituents. In other reactions, these two modes of substituent effects (on reactions and charge distributions) are more or less biased to the extent that they may permit discrimination. This is the basis of our present treatment of the nonlinearity of free energy correlations in aromatic side-chain reactions.

Our treatment is based on the assumption that the potential energy changes in the transition states caused by substituents would parallel the relative free energy changes for reactions. Although this assumption is a usual and irreplaceable starting point for the present sort of treatment, it is not always fulfilled in given reaction series.[13,25]

25) J. E. Leffler and E. Grunwald, "Rates and Equilibria of Organic Reactions," John Wiley & Sons, New York, N. Y. (1963), Chapter 9.

Nevertheless, we feel that imperfections arising from such difficulties will be minimized in the present treatment, inasmuch as our primary interest has been in the free energy correlations among different types of side-chain reactions. The integral parameters, which are used so as to mediate between substituent effects on different types of reactions, may partly absorb the uncertainties concerning the role of kinetic energy and entropy terms.

One major question which might be raised with regard to our treatment concerns the disregarding of the effects of factors other than π-conjugation. For instance, we have not considered explicitly the role of σ-inductive effects, which are definitely operative in reactions. Further, Dewar and Grisdale[8] have suggested that direct-field effects of substituents are even more important than σ-inductive effects and that the Hammett σ-constants may be related primarily to such effects and mesomeric effects. However, since there exists no justified way of separating σ-inductive (or, perhaps, direct-field) effects from mesomeric effects, we have avoided attempting to estimate these two contributions separately. Rather, in the interests of methodological simplicity, we have implicitly assumed that the inductive and field effects may at least be partly embodied in Hückel-type treatments by assigning relatively large inductive parameters to the ring carbons neighboring substituents.[26]

Finally, a word should be said about the inductive parameters, δ_{CX}, assumed for the C–Cl and C–F bonds. The adherence to the assignment $\delta_{CX}=0.3$ for these bonds has always resulted in anomalously large deviations of the *p*-chloro and *p*-fluoro points from the straight lines shown in Figs. 2, 3, 5 and 6. Since it turned out, from the calculations, that the choice of the values of 0.6 and 0.5 for the C–Cl and C–F bonds respectively greatly improved the corresponding plots in the ΔE-σ relationships, these values were used for testing the correlations of σ^0 with other substituent constants. It is conceivable that the parameters δ_{CX} are not constant over different bonds.

The authors wish to thank Professor Yasuhide Yukawa and Dr. Yuho Tsuno of Osaka University for their valuable suggestions and discussions.

26) It is agreed that relatively large inductive parameters are required in order to predict the reasonable magnitudes for meta electron densities.[3] Peters[6] has demonstrated that even equal π-electron densities can be predicted for para and meta carbons when the inductive parameters are assumed to propagate gradually along the bonds, diminishing by as large a constant factor as $\varepsilon=0.53$. Thus, the disregard of the π-inductive and field effects is largely counterbalanced by the choice of the parameters $\delta_{CX}=0.3$ and $\varepsilon=1/3$.

BULLETIN OF THE CHEMICAL SOCIETY OF JAPAN VOL. 39 576—580 (1966)

The Determination of Micro Amounts of Polythionates. IV.* A Photometric Method for the Determination of Tetrathionate by Decomposition with Sodium Sulfite[1)]

By Iwaji IWASAKI and Shigeru SUZUKI

Laboratory of Analytical Chemistry and Geochemistry, Tokyo Institute of Technology, Ookayama, Tokyo

(Received July 16, 1965)

A new photometric method for the determination of tetrathionate by means of its decomposition with sulfite has been developed. It is based on the formation of thiosulfate equivalent to the tetrathionate, and on the photometric determination of thiosulfate by measuring its decoloration of an iodine solution. 5×10^{-6}—1×10^{-3} M (1 mg./l.—0.2 g./l.) of tetrathionate can be determined easily and rapidly within a range of error of $\pm2\times10^{-6}$—2×10^{-5} M (0.4 mg./l.—4 mg./l.) by using 20 ml. of a sample. The tetrathionate solution is decomposed with sodium sulfite in a slightly alkaline medium. After the completion of the decomposition reaction, a formaldehyde solution is added to mask the interference of the excess sulfite remaining and this solution is acidified with acetic acid. Then the standard iodine solution is added. The absorbancy of the solution is measured at the wavelength of 372 or 440 mμ 20 min. after the addition of an iodine solution. By this method tetrathionate can be determined, even when it is coexistent with thiosulfate and sulfite in up to similar amounts. Many substances, such as aluminum, calcium, cadmium, magnesium, zinc, silicate, nitrate, sulfate, phosphate, chloride and fluoride, do not interfere, but iron(II, III), manganese(II), copper(II) and sulfide do interfere.

* T. Koh and I. Iwasaki, This Bulletin, **39**, 352 (1966).

1) Presented at the Scientific Meeting on Chemistry, Tokyo, November, 1961.

There have been no suitable procedures for the determination of the polythionates in such micro amounts as are present in hot springs, although a more rapid and accurate method for determining polythionates of low concentrations is desirable for the studies of the hydrolysis and oxidation products of sulfur and sulfide.

The reactions of polythionates with sulfite, cyanide and sulfide have been reported by Kurtenacker and Goldbach.[2] Goehring, Feldmann and Helbing[3] have then applied these reactions to the determination of polythionates, depending on the iodometric titration of the thiosulfate obtained. Nietzel and DeSesa[4] determined colorimetrically the thiocyanate obtained from the reactions between tetrathionates and cyanide. In our own series of studies[5-7] of determination of micro amounts of polythionates, many fundamental processes in the reaction of polythionates with cyanide have been studied in detail.

In the present investigation, it will be confirmed that micro amounts of tetrathionate from 5×10^{-6} to 10^{-3} M can be determined photometrically by measuring the degree of the decoloration of iodine, which depends on the amounts of thiosulfate formed from the reaction of tetrathionate with sulfite. Polythionates react with sulfite in an alkaline medium to form thiosulfate as follows[2,3]:

$$S_nO_6^{2-} + (n-3)SO_3^{2-} = (n-3)S_2O_3^{2-} + S_3O_6^{2-} \quad (1)$$
$$(n=4,\ 5,\ \text{and}\ 6)$$

In this reaction 1 mol. of thiosulfate is formed from 1 mol. of tetrathionate. The thiosulfate thus formed reacts quantitatively with iodine in an acid medium. Therefore, the degree of the decoloration of iodine indicates the amount of tetrathionate in the original solution.

This paper will be concerned with the presentation of the results of this investigation and with the determination of small amounts of tetrathionate in the presence of sulfite and thiosulfate by means of its decomposition with sodium sulfite.

Experimental

Apparatus and Reagents.—A Hirama electrophotocolorimeter model II, with 10.0 mm. cells and filters of 372 and 440 mμ (maximum transmission at 372 and 440 mμ respectively), was used to measure the absorbancy.

The Standard Potassium Tetrathionate Solution.—30.25 g. of potassium tetrathionate ($K_2S_4O_6$) was dissolved in water, the mixture was then diluted to 1 l. (M/10). This stock solution was standardized by iodometric titration after decomposing it with sulfite or cyanide,[2,3] and then diluted to an adequate concentration. Potassium tetrathionate was prepared by the reaction of potassium thiosulfate with iodine; it was recrystallized with aqueous alcohol and dried in a desiccator containing sulfuric acid.[8]

The Standard Iodine Solution.—A standardized N/10 iodine solution was diluted to a desirable concentration; in all cases the concentration of potassium iodide was N/5.

The Standard Sodium Thiosulfate Solution.—24.82 g. of guaranteed reagent sodium thiosulfate pentahydrate ($Na_2S_2O_3\cdot5H_2O$) was dissolved in water and diluted to 1 l. (N/10). This solution was standardized with potassium iodate and then diluted to a concentration required.

Procedure.—20.0 ml. of a sample solution is placed in a 50 ml. volumetric flask. Then 1.0 ml. of a 0.5 M sodium sulfite solution is added and mixed in well. When this solution does not show a pink color with a phenolphthalein indicator, a 1 N sodium or potassium hydroxide solution is added drop by drop until the pink color appears. After this mixture has stood for 5 min. or longer, 1.0 ml. of a 20% formaldehyde solution[2,9] is added; this solution is then acidified with 10 ml. of a 20% acetic acid solution. 5.00 ml. of N/2000 or N/200 standard iodine solution is then added. After the flask has been filled with water to the mark, the absorbancy of the solution is measured at the wavelength of 372 or 440 mμ 20 min. after the addition of an iodine solution.

Thiosulfate and sulfite can also be determined when both are present in the sample solution. Three 20.0-ml. aliquots of the sample solution are placed in three 50-ml. volumetric flasks. The first 20.0-ml. aliquot is treated by the procedure described above. To the second, 10 ml. of a 20% acetic acid solution and 5.00 ml. of the standard iodine solution are added. To the third, after the addition of 1.0 ml. of a 20% formaldehyde solution, a 1 N alkali hydroxide solution is added drop by drop until the solution becomes alkaline to a phenolphthalein indicator. Then the solution is acidified with 10 ml. of 20% acetic acid and 5.00 ml. of the standard iodine solution is added.

The degree of the decoloration of iodine observed in the first aliquot corresponds to the sum of the amount of tetrathionate and that of thiosulfate in the solution; that observed in the second, to the sum of the amount of thiosulfate and twice the amount to sulfite in the solution, and that observed in the third, to only the amount of thiosulfate in the solution.

Results and Discussion

Working Curves.—As the final purpose of this series of investigations is to determine the polythionates to such micro amounts as are present in hot springs, the working curves were prepared with the standard sodium thiosulfate solution

2) A. Kurtenacker and E. Goldbach, *Z. anorg. u. allgem. Chem.*, **166**, 177 (1927). A. Kurtenacker, "Analytische Chemie der Sauerstoffsauren des Schwefels," Stuttgart (1938).
3) M. Goehring, U. Feldmann and W. Helbing *Z. anal. Chem.*, **129**, 346 (1949).
4) O. A. Nietzel and M. A. DeSesa, *Anal. Chem.*, **27**, 1839 (1955).
5) T. Koh, This Bulletin, **38**, 1510 (1965).
6) T. Koh and I. Iwasaki, ibid., **38**, 2135 (1965).
7) T. Koh and I. Iwasaki, ibid., **39**, 352 (1966).
8) G. Bauer, "Handbuch der Preparativen Anorganischen Chemie," (1954), p. 311.
9) A. Kurtenacker, *Z. anal. Chem.*, **64**, 56 (1924).

instead of the standard potassium tetrathionate solution. Examples of the working curves are shown in Figs. 1 and 2.

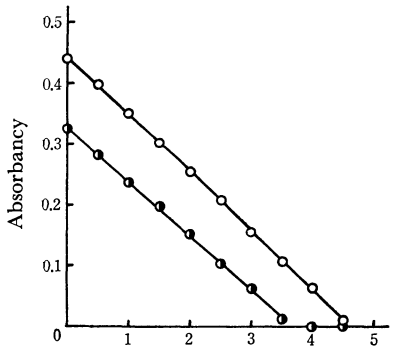

ml. of a 5.0×10^{-4} N standard thiosulfate solution

Fig. 1. Working curves.
Use is made of 5.0 ml. of a 5.0×10^{-4} N iodine standard solution. Absorbancy was measured at 372 mμ 20 and 90 min. respectively after the addition of a standard iodine solution.
—○— 20 min., —◑— 90 min.

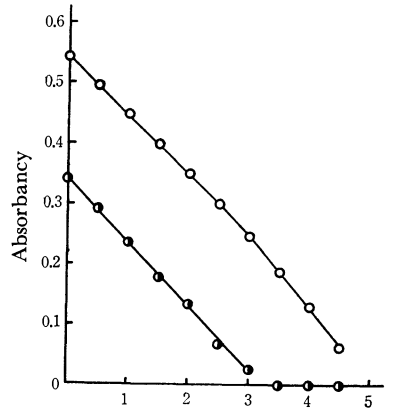

ml. of a 5.0×10^{-3} N standard thiosulfate solution

Fig. 2. Working curves.
Use is made of 5.0 ml. of a 5.0×10^{-3} N iodine standard solution. Absorbancy was measured at 440 mμ 20 min. and 22 hr. respectively after the addition of a standard iodine solution.
—○— 20 min., —◑— 22 hr.

The Effect of the Concentration of Iodide on the Absorbancy.—The absorbancies of iodine solutions become higher with an increase in the concentration of iodide at the wavelengths of both 372 and 440 mμ. Therefore, it is necessary to keep the concentration of iodide constant in the final solutions. However, no significant difference could be found between iodide concentrations of N/5 and N/50. In this study, N/50 of iodide was used as the final iodide concentration.

Time of Reaction.—The concentration of sodium sulfite seriously affects the velocity of the

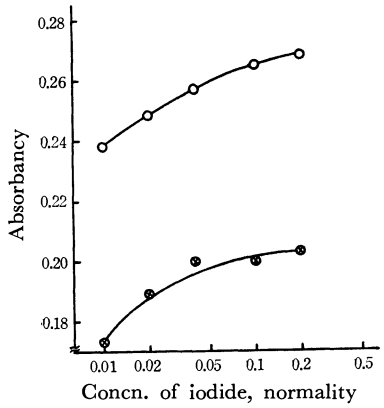

Fig. 3. Effect of the concentration of iodide on the absorbancy.
—○— 2.0×10^{-4} N iodine, at 440 mμ
—⊗— 2.0×10^{-5} N iodine, at 372 mμ

decomposition reaction of tetrathionate (Eq. 1), as is shown in Fig. 4. When 0.2 ml. of a 0.5 M sodium sulfite solution is used, it takes about 20 min. for the complete reaction, but it takes only 2 or 3 min. when 1.0 ml. of it is used. The absorbancies of the solutions obtained show the nearly constant value which is to be expected from Eq. 1. From these results it may be concluded that tetrathionate can be decomposed completely and that thiosulfate equivalent to the tetrathionate is formed quantitatively under these experimental conditions. Consequently, 1.0 ml. of a 0.5 M sodium sulfite solution was used in this study. However, when the pH value of the solution rises locally, there other

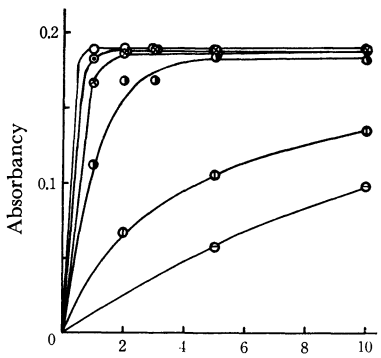

Fig. 4. Effect of the amount of sodium sulfite on the velocity of decomposition reaction.
2.0 ml. of a 5.0×10^{-3} M tetrathionate, 5.0 ml. of 20% formaldehyde, 10 ml. of 20% acetic acid, and 5.0 ml. of 5.0×10^{-3} N iodine were used. The absorbancy was measured at 440 mμ. Concn. of sodium sulfite: 0.5 M

⊖ 0.1 ml. ◐ 0.2 ml.
◑ 0.5 ml. ⊗ 1.0 ml.
⊙ 1.5 ml. ○ 2.0 ml.

decomposition reactions[2,3] occur; this may be a cause of error.

The Effect of Formaldehyde.—Since sulfite, as well as thiosulfate, reacts with iodine in an acid medium, it must be masked with formaldehyde, as has been proposed by Kurtenacker.[9] Figure 5 shows the decoloration of iodine solutions with formaldehyde on standing after the standard iodine solution has been added to sulfite solutions when thiosulfate and tetrathionate are absent. As may be seen in Fig. 5, the differences among the effects of 0.2 ml., 1.0 ml. and 5.0 ml. of a 20% formaldehyde solution are negligible. However, both when no formaldehyde was added and when it was added in an acidified medium, the iodine was completely consumed by the reaction with the excess sulfite remaining in the solution. Therefore, formaldehyde must be added to the solution in order to mask the action of the excessive sulfite before the solution is acidified with acetic acid.

On the other hand, the decoloration of the iodine solution proceeds when it stands after the addition of iodine, especially in its lower concentrations. From the results obtained in this study, 1.0 ml. of a 20% formaldehyde solution was used, and the absorbancies of the iodine solutions obtained were measured 20 min. after the addition of an iodine solution.

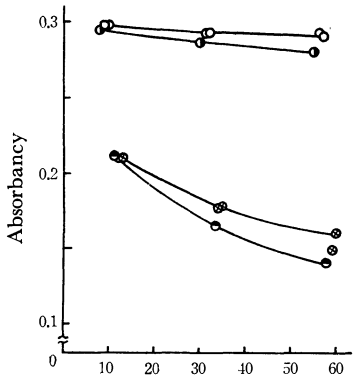

Fig. 5. Effect of formaldehyde on stability of color.
1.0 ml. of 0.5 M sodium sulfite and 10 ml. of acetic acid were used.
Concn. of formaldehyde: 20%
○ 1.0 and 5.0 ml.} 5.0×10^{-3} N I_2 2.5 ml.,
◑ 0.2 ml. } at 440 mμ
⊗ 1.0 and 5.0 ml.} 5.0×10^{-4} N I_2 2.5 ml.,
◓ 0.2 ml. } at 372 mμ

The Amounts of Acetic Acid.—It is necessary to acidify the solution for the reaction of thiosulfate with iodine. Figure 6 shows the absorbancies of the solutions against the amounts of acetic acid when 2.50 ml. of a N/2000 standard sodium thiosulfate solution and 5.00 ml. of a N/2000 standard iodine solution were used.

As will be seen in Fig. 6, when more than 5 ml. of 20% acetic acid were employed the absorbancies of the solutions reached a constant value; 10 ml. of 20% acetic acid was used in this study.

The Results of the Analyses of the Synthetic Solutions.—From the experimental results, the analytical procedures described above have been established. The working curves shown in Figs. 1 and 2 were obtained by these procedures.

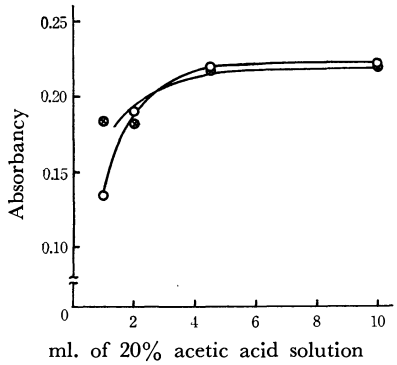

Fig. 6. Effect of the amount of acetic acid.
1.0 ml. of a 0.5 M sodium sulfite was used.
Absorbancy was measured 20 min. after the addition of iodine solution at 372 mμ.
○ 20% formaldehyde 1.0 ml.
⊗ 20% formaldehyde 5.0 ml.

Table I. Determination of tetrathionate in the synthetic solutions*

	Present ($\times10^{-4}$ M)			Found ($\times10^{-4}$ M)		
No.	$S_4O_6^{2-}$	$S_2O_3^{2-}$	SO_3^{2-}	$S_4O_6^{2-}$	$S_2O_3^{2-}$	SO_3^{2-}
1	0.09	—	—	0.10	—	—
2	0.34	—	—	0.34	—	—
3	0.80	—	—	0.79	—	—
4	1.08	—	—	1.07	—	—
5	0.05	1.00	—	0.03	0.99	—
6	0.05	0.50	—	0.03	0.51	—
7	0.10	0.90	—	0.07	0.90	—
8	0.10	0.80	—	0.05	0.82	—
9	0.10	0.45	—	0.10	0.46	—
10	0.25	0.45	—	0.24	0.45	—
11	0.50	0.15	—	0.48	0.17	—
12	0.90	0.05	—	0.88	0.06	—
13	0.10	0.05	0.50	0.10	0.06	0.50
14	0.20	0.50	0.20	0.22	0.49	0.20
15	0.50	0.05	0.50	0.48	0.07	0.50
16	0.50	0.10	0.10	0.49	0.12	0.10
17	0.50	0.50	0.05	0.50	0.51	0.05
18	0.60	0.10	0.40	0.59	0.12	0.40
19	0.50	—	10	0.51	0.00	—
20	0.50	—	100	0.52	0.02	—
21	0.10	0.80	10	0.04	0.79	—
22	0.10	0.80	100	0.06	0.80	—
23	0.80	0.10	10	0.75	0.11	—
24	0.80	0.10	100	0.81	0.12	—

* : 5×10^{-6} to 10^{-4} M at 372 mμ
— : Absent or not determined

Table II. Determination of tetrathionate in the synthetic solutions*

No.	Present ($\times 10^{-3}$ M) $S_4O_6^{2-}$	$S_2O_3^{2-}$	SO_3^{2-}	Found ($\times 10^{-3}$ M) $S_4O_6^{2-}$	$S_2O_3^{2-}$	SO_3^{2-}
1	0.20	—	—	0.20	—	—
2	0.58	—	—	0.59	—	—
3	0.73	—	—	0.74	—	—
4	0.95	—	—	0.96	—	—
5	0.10	0.90	—	0.10	0.89	—
6	0.20	0.50	—	0.21	0.48	—
7	0.50	0.25	—	0.51	0.24	—
8	0.80	0.10	—	0.79	0.11	—
9	0.10	0.10	0.10	0.10	0.11	0.10
10	0.10	0.10	0.50	0.12	0.10	0.50
11	0.20	0.20	0.20	0.19	0.21	0.19
12	0.30	0.30	0.10	0.29	0.31	0.10
13	0.30	0.50	0.20	0.28	0.50	0.20
14	0.50	0.10	0.30	0.48	0.12	0.29
15	0.50	—	1.0	0.54	0.00	—
16	0.50	—	10	0.50	0.00	—
17	0.25	0.80	1.0	0.24	0.80	—
18	0.25	0.80	10	0.24	0.80	—
19	0.80	0.25	1.0	0.79	0.25	—
20	0.80	0.25	10	0.77	0.26	—

* : 5×10^{-5} to 10^{-3} M at 440 mμ
— : Absent or not determined

The results of the analyses by the present method of the samples containing tetrathionate only, tetrathionate and thiosulfate, or tetrathionate, thiosulfate and sulfite are listed in Tables I and II. Very good agreements are seen, even in the lower concentrations of these chemical species.

The Influence of Diverse Ions.—The other polythionates would interfere,[2,3] but these, as well as thiosulfate and sulfite, might be individually determined by solving the simultaneous equations derived from Eq. 1 and the following reactions[2,3]:

$$S_nO_6^{2-}+(n-1)CN^-+H_2O=S_2O_3^{2-}+SO_4^{2-}+2HCN+(n-3)SCN^- \quad (n=4,\ 5,\ \text{and}\ 6) \qquad (2)$$

Table III. Effect of diverse ions

No.	Ionic species	Concn., w/v %	Form of salt	Absorbancy 372 mμ	440 mμ
0	—	—	—	0.309[a]	0.320[b]
1	Fe^{2+}	0.05	$FeSO_4\cdot7H_2O$	—[c]	0.457
2	Fe^{3+}	0.05	$Fe(NO_3)_3\cdot H_2O$	—[c]	0.502
3	Al^{3+}	0.05	$AlCl_3\cdot6H_2O$	0.312	0.320
4	Ca^{2+}	0.10	$CaCO_3$(HCl)	0.309	0.320
5	Mg^{2+}	0.06	MgO(HCl)	0.318	0.320
6	Mn^{2+}	0.01	$MnSO_4\cdot nH_2O$	—[c]	0.540
7	Zn^{2+}	0.5	$ZnSO_4\cdot7H_2O$	0.314	0.320
8	Cu^{2+}	0.013	$CuSO_4\cdot5H_2O$	0.364	0.338
9	Cd^{2+}	6.3[e]	$8CdSO_4\cdot3H_2O$	0.312	0.320
10	SiO_3^{2-}	0.02	$Na_2SiO_3\cdot nH_2O$	0.321	0.318
11	Cl^-	1.2	NaCl	0.301	0.317
12	SO_4^{2-}	1.0	Na_2SO_4	0.317	0.321
13	NO_3^-	0.9	KNO_3	0.306	0.321
14	S^{2-}	0.8	Na_2S	0.04[d]	0.01[d]
15	PO_4^{3-}	0.4	$Na_2HPO_4\cdot12H_2O$	0.310	0.319
16	F^-	0.005	NaF	0.310	0.320

a) 3×10^{-5} M concentration of tetrathionate.
b) 5×10^{-4} M concentration of tetrathionate.
c) Higher than 2.0 of absorbancy.
d) Slightly turbid.
e) Preliminary test for removal of sulfide.

$$S_nO_6^{2-}+S^{2-}=2S_2O_3^{2-}+(n-3)S \quad (n=3,\ 4,\ 5,\ \text{and}\ 6) \qquad (3)$$

$$2S_nO_6^{2-}+6OH^-=(2n-5)S_2O_3^{2-}+(10-2n)SO_3^{2-}+3H_2O \quad (n=3,\ 4,\ \text{and}\ 5) \qquad (4)$$

$$2S_6O_6^{2-}+6OH^-=5S_2O_3^{2-}+2S+3H_2O \qquad (4')$$

The influence on this method of the other ions commonly present in hot springs are given in Table III. Sulfide liberates colloidal sulfur. Iron(II) and manganese(II) are oxidized in an alkaline solution, and the iron(III) and manganese(IV) thus formed oxidize the iodide to produce iodine. The elimination of the interfering matter must be studied before we can apply this procedure to the various samples in their natural state.

BULLETIN OF THE CHEMICAL SOCIETY OF JAPAN VOL. 39 581—585 (1966)

The Coprecipitation Behavior of Strontium with Calcium Oxalate by Precipitation from a Homogeneous System

By Masakazu MATSUI

Institute for Chemical Research, Kyoto University, Sakyo-ku, Kyoto

(Received July 19, 1965)

The coprecipitation of strontium with calcium oxalate was studied using dimethyloxalate to precipitate calcium from a homogeneous solution. The several effects of the coprecipitation conditions on the distribution coefficients were investigated in the fractional precipitation process of calcium-strontium oxalate mixtures. Regardless of the pH value, the concentration of acetic acid and other factors, the coprecipitation curves of strontium showed similar shapes in almost all cases, although the curves well shifted up and dawn to some extent. It appears to be an anomalous system, because an increase in the fraction of the calcium precipitated tends to decrease the distribution coefficients. It is considered that two coprecipitation mechanisms are involved in the coprecipitation system; one is the surface adsorption on fine crystals, while the other is a normal systematic type. When the adsorption part was removed, it was found that the modified system obeyed the Doerner and Hoskins logarithmic distribution law and that the coefficient gave nearly a constant, 0.1.

The coprecipitation with calcium oxalate is generally used to separate strontium ions from other metals in dilute solutions.

When a strontium ion is coprecipitated with a calcium oxalate, there are two systematic ways in which strontium is distributed in crystals. One type of distribution is expressed by the homogeneous distribution law proposed by Chlopin[1] and Henderson and Kracek,[2] in which the strontium-calcium ratio in the precipitated crystals is proportional to the strontium-calcium ratio in the final solution:

$$\left(\frac{\mathrm{Sr}}{\mathrm{Ca}}\right)_{\mathrm{cryst.}} = D\left(\frac{\mathrm{Sr}}{\mathrm{Ca}}\right)_{\mathrm{soln.}} \quad (1)$$

where D is defined as the homogeneous distribution coefficient. This distribution law represents a state of true thermodynamic equilibrium, one in which the solid phase has been thoroughly digested in order to remove all the concentration gradients inside a crystal.

The other type is expressed by the logarithmic distribution law proposed by Doerner and Hoskins[3] and expressed as follows:

$$\log\frac{\text{Initial Sr}}{\text{Sr left in soln.}} = \lambda \log\frac{\text{Initial Ca}}{\text{Ca left in soln.}} \quad (2)$$

where λ is the logarithmic distribution coefficient; this law is obeyed when a replacement equilibrium is achieved on each layer of the crystal during the precipitation process. When λ is smaller than unity, the tracer component is enriched in the solution, and vice versa.

Ishibashi et al.[4] carried out an experiment in which oxalates were homogeneously precipitated, with a rise in pH value due to ammonium ions uniformly generated by the hydrolysis of urea. They found that strontium was distributed in calcium oxalate in accordance with the logarithmic distribution law, and that the extrapolation of the logarithmic distribution coefficients to 0% of calcium precipitated would give a constant value of about 0.30.

The coprecipitation behavior of scandium,[5] yttrium[6] and lanthanide[7] ions with calcium oxalate was studied by Shigematsu et al. and by the present author. Their results demonstrate that the most predominant factors affecting the coefficient are the pH value of the solution and the concentration of the organic acid used as a buffering agent, because the ionic concentrations of divalent macro and tervalent micro components vary with the coprecipitation conditions; the ionic radius also plays an important role in the coprecipitation process.

According to these papers, it may be deduced that the distribution coefficient in the case of a calcium-strontium system will not be very much affected by the precipitation condition, such as the pH value and the concentration of an organic acid, because the ratio of the complexing ability of macro and micro components with an organic acid is hardly affected at all by the above-mentioned

1) W. Chlopin, *Z. anorg. u. allgem. Chem.*, **143**, 97 (1925).
2) L. M. Henderson and F. C. Kracek, *J. Am. Chem. Soc.*, **49**, 738 (1927).
3) H. A. Doerner and W. M. Hoskins, ibid., **47**, 662 (1925).
4) M. Ishibashi, T. Shigematsu and T. Ishida, *Annual Rep. Research Committee on the Application of Artificial Radio-isotopes*, **3**, 6 (1953/4).
5) T. Shigematsu, M. Tabushi and M. Matsui, *Bull. Inst. Chem. Res., Kyoto Univ.*, **40**, 381 (1962).
6) T. Shigematsu, M. Tabushi and M. Matsui, This Bulletin, **37**, 1610 (1964).
7) M. Matsui, This Bulletin, in press.

factors.

This paper will deal with the variable influences of the coprecipitation conditions on the distribution coefficient in the fractional precipitation process of calcium-strontium oxalate mixtures.

Experimental

Apparatus and Reagents. — The radioactivity counting was performed with a Phillips halogen-quenched G-M tube connected to a Metro dekatron scaler, Model D-5. A Hitachi-Horiba pH meter, Model M-3, was used for the pH measurements.

Strontium-89 was supplied as chloride in hydrochloric acid by the Oak Ridge National Laboratory, Oak Ridge, Tennessee, U. S. A., and was diluted to make a solution of ~1 μc./ml. Reagent-grade dimethyloxalate was purified by recrystallizing it from anhydrous methanol; it was then stored in a dry atmosphere in a desiccator. The calcium solution was prepared by dissolving dry calcium carbonate with hydrochloric acid. The strontium solution was prepared by dissolving reagent-grade strontium chloride with water, after which it was standardized with a standard EDTA solution. The EDTA solution (0.00330 M), containing a magnesium EDTA complex, was standardized by means of a calcium standard solution; it was used for the determination of the calcium ions of the sample solutions.

The other chemicals were chemically-pure or reagent-grade materials.

Procedure.—The procedure of the coprecipitation and the determination of the macro and micro components were essentially the same as those described in previous papers.[6,7] The calcium was titrated with a EDTA solution containing its magnesium chelate.

The strontium activity would be contaminated very slightly by yttrium-90 existing as a radioactive daughter of strontium-90 impurity. The yttrium activity was estimated by the coprecipitation method with ferric hydroxide, while the strontium activity in the solution phase was corrected by means of the distribution values of yttrium.[6] The homogeneous and logarithmic distribution coefficients, D and λ, will be calculated from Eqs. 1 and 2.

Results

The Effect of the pH Value.—The percentages of coprecipitated strontium in the fraction of the calcium oxalate precipitate at different pH values are plotted in Fig. 1. The experimental conditions were as follows: The concentrations of calcium, strontium and dimethyloxalate were 2.50×10^{-1} M, 10^{-6} M and 0.1 M respectively. The total volume of the reacting solution was 200 ml.; this solution was buffered with 1 M acetate or formate, and the temperature was kept at 75.0°C. As is shown in Fig. 1, the strontium ion content was enriched in the solution phase, and unlike as in the case of the calcium - rare earth system, the coprecipitation behavior was the same regardless of the pH value and the species of organic acid.

The distribution coefficients, D and λ, were calculated from these experimental data; a few examples are presented in Table I. The results show that the increase in the amounts of precipitated calcium tends to decrease the coefficients.

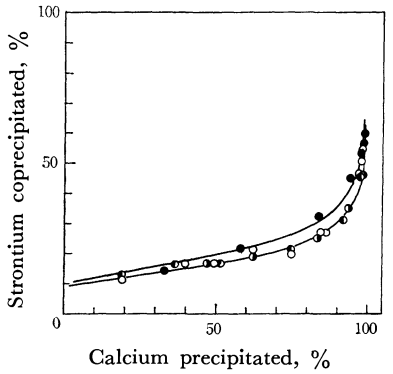

Fig. 1. The coprecipitation of strontium with calcium oxalate at different pH values.
Ca: 0.025 M, Sr: 10^{-6} M, dimethyloxalate: 0.1 M, acetate or formate: 1 M. Temp.: 75°C,
pH: ●; 2.88, ○; 3.62, ◐; 4.00, ◑; 4.79

The Effect of the Strontium Concentration.—While keeping the other variables constant, the calcium oxalate was precipitated at pH 4.00 in solutions containing 10^{-5} M, 10^{-6} M and 10^{-7} M of strontium respectively. The effect is indicated in Fig. 2; no significant change in the coprecipitation behavior was observed.

The Effect of the Acetate and Sodium Chloride Concentrations.—The effect of the acetate concentration was examined at pH 4.00 with regard to sample solutions of 0.5 M, 1.0 M and 2.0 M acetate, while the other variables were kept constant; the effect was found to be almost not noticeable in the range investigated, as is shown in Fig. 3. In order to study the effect

TABLE I. DEPENDENCE OF DISTRIBUTION COEFFICIENT ON THE PRECIPITATED FRACTION OF CALCIUM

Ca: 0.025 M, Sr: 10^{-6} M, dimethyloxalate: 0.1 M
Temp.: 75°C

Reacting time min.	Ca ppted. %	Sr coppted. %	D	λ
(A) pH: 4.80, acetate: 1 M				
120	28.31	11.52	0.330	0.368
240	46.96	16.74	0.227	0.289
300	62.17	18.81	0.141	0.214
450	83.47	25.29	0.0670	0.162
600	93.85	35.00	0.0353	0.155
700	98.35	46.34	0.0145	0.152
(B) pH: 2.88, formate: 1 M				
75	33.11	14.33	0.338	0.385
100	57.88	21.89	0.209	0.286
135	83.79	32.52	0.0932	0.216
180	94.53	45.03	0.0494	0.206
240	97.81	53.18	0.0254	0.199

of the ionic concentration in a reaction solution, an effect which is concerned with the adsorption in coprecipitation, final concentrations with nil, 1.0 M and 2.0 M of sodium chloride respectively were used. Figure 4 shows that the coprecipitation of strontium behaves in a similar manner, although it is appreciably influenced at the beginning of precipitation.

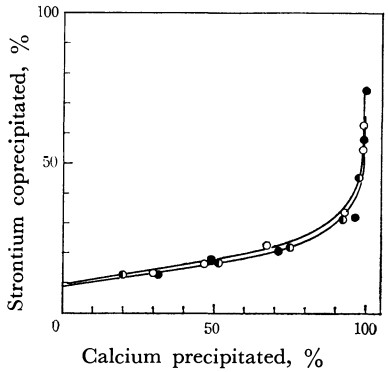

Fig. 2. The effect of the concentration of strontium.
Ca: 0.025 M, dimethyloxalate: 0.1 M, acetate: 1 M
Temp.: 75°C pH: 4.00
Sr: ○; 10^{-4} M, ●; 10^{-5} M, ◐; 10^{-6} M

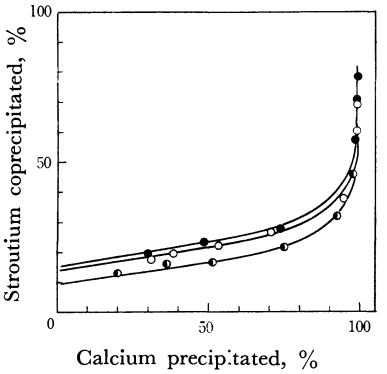

Fig. 3. The effect of acetate ion.
Ca: 0.025 M, Sr: 10^{-6} M,
Acetate: ○; 2.0 M, ◐; 1.0 M, ●; 0.5 M
Others are same to in Fig. 2.

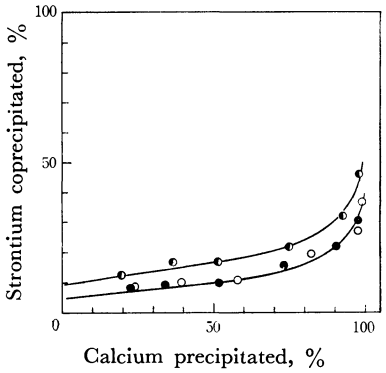

Fig. 4. The effect of sodium chloride concentration.
Ca: 0.025 M, Sr: 10^{-6} M,
NaCl: ◐; 0, ○; 1.0 M, ●; 2.0 M
Others are same to in Fig. 2.

The Effect of the Rate of Precipitation.— The effect of the ester was studied in order to examine the effect of the rate of precipitation. Figure 5 shows that the coprecipitation behavior almost does not change at all, except in the rapid precipitation, when the concentration of the ester changes from 0.0375 M to 0.25 M, corresponding to 1.5 and 10 times the stoichiometric quantity of calcium ions. The time required for the 90% precipitation of calcium is about 75, 580, 1350 and 2100 min. when the ratio of the ester to calcium is 10, 4, 2 and 1.5 respectively.

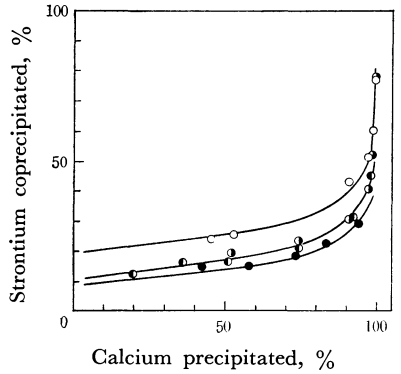

Fig. 5. The effect of the rate of precipitation.
dimethyloxalate: ◑; 0.0375 M, ●; 0.05 M,
◐; 0.10 M, ○; 0.25 M
others are same to in Fig. 2.

Discussion

As is shown in Figs. 1 to 5, the coprecipitation behavior of strontium was very similar in all cases, though the percentages of coprecipitation changed appreciably in the initial stage of the precipitation process.

The coprecipitation percentage of strontium increased very slowly to about 70 per cent, and then rapidly to the end of calcium precipitation.

An increase, in the fraction of precipitated calcium tends to decrease the distribution coefficient in all experiments, as is shown in Table I. If the decrease in λ-value is attributed to the aging of precipitate, as has been described in previous papers,[4,8] the coprecipitation behavior should be influenced by the rate of precipitation. However, the conprecipitation curves resemble each other except in the case of a very rapid precipitation.

8) M. L. Salutsky, J. G. Stites, Jr., and A. W. Martin, *Anal. Chem.*, **25**, 1677 (1953).

The coprecipitation behavior in the calcium-strontium oxalate system was postulated to be as follows: When a strontium ion is coprecipitated with calcium salt, two different mechanisms are involved. One type is the surface adsorption, with very fine crystals precipitating from a supersaturated solution. The other is a normal systematic type obeying the distribution law. When the curves are extrapolated to a zero percentage of the precipitated calcium, the adsorption part of the coprecipitation can be estimated. When the effect of the latter part is corrected, the logarithmic distribution law is followed and the coefficient can be calculated. These results are shown in Tables II to VI, in which the coefficients in the range of 40 to 95 per cent of calcium precipitated are adopted in order to make the error as small as possible, because there is a risk of producing a considerable error in the determination of the precipitated calcium or coprecipitated strontium beyond the above range.

The consistency of the λ values obtained in Table II to VI can not be explained by assuming random error. The mean values of the coefficient nearly gave a constant, about 0.1 of λ in almost all cases. Strontium, as well as other elements,

TABLE II. THE EFFECT OF pH ON λ AFTER CORRECTION OF ADSORPTION

	Ca ppted. %	Sr coppted. %	λ
(A) pH 4.80	46.96	6.74	0.110
(−10.00%)*	62.17	8.81	0.096
	83.47	15.29	0.092
	93.85	25.00	0.102
		Average	0.100
(B) pH 4.00	51.20	7.33	0.107
(−9.00%)*	74.83	12.33	0.097
	92.10	22.15	0.099
		Average	0.101
(C) pH 3.62	49.41	6.89	0.105
(−10.00%)*	62.47	10.96	0.118
	85.69	17.06	0.096
		Average	0.106
(D) pH 2.88	57.88	11.89	0.146
(−10.00%)*	83.79	22.52	0.140
	94.53	35.03	0.148
		Average	0.145

* The correction of adsorption for Sr.

TABLE III. THE EFFECT OF THE STRONTIUM CONCENTRATION AFTER CORRECTION OF ADSORPTION

	Ca ppted. %	Sr coppted. %	λ
(A) Sr: 10^{-4} M	46.77	6.23	0.102
(−10.20%)*	66.69	12.00	0.116
	92.41	23.52	0.104
		Average	0.107
(B) Sr: 10^{-5} M	49.24	6.68	0.102
(−9.00%)*	70.84	11.48	0.099
		Average	0.101

(C) Sr: 10^{-6} M see A) in Table II.

* The correction of adsorption for Sr.

TABLE IV. THE EFFECT OF THE ACETATE ION

	Ca ppted. %	Sr coppted. %	λ
(A) Acetate: 0.5 M	48.36	7.05	0.110
(−16.00%)*	73.62	11.91	0.095
		Average	0.103
(B) Acetate: 1.0 M	see A) in Table III		
(C) Acetate: 2.0 M	38.27	5.27	0.112
(−14.10%)*	53.06	7.99	0.110
	70.60	12.96	0.113
	94.20	23.73	0.090
		Average	0.106

* The correction of adsorption for Sr.

TABLE V. THE EFFECT OF SODIUM CHLORIDE CONCENTRATION

	Ca ppted. %	Sr coppted. %	λ
(A) NaCl: none added	see A) in Table II		
(B) NaCl: 1.0 M	57.47	7.89	0.096
(−2.60%)*	81.90	16.81	0.108
		Average	0.102
(C) NaCl: 2.0 M	51.37	7.79	0.113
(−2.00%)*	73.73	13.20	0.106
	90.33	19.15	0.091
	(96.99)	(28.91)	(0.097)
		Average	0.103

* The correction of adsorption for Sr.

TABLE VI. THF EFFECT OF THE RATE OF PRECIPITATION

	Ca ppted. %	Sr coppted. %	λ
(A) Dimethyloxalate:	52.58	9.11	0.113
0.25 M	90.96	26.27	0.130
(−17.00%)*	(96.77)	(34.02)	(0.121)
	(98.13)	(35.67)	(0.111)
		Average	0.122
(B) Dimethyloxalate: 0.1 M	see A) in Table II		
(C) Dimethyloxalate:	57.38	9.20	0.113
0.05 M	73.53	12.62	0.101
(−5.70%)*	83.12	17.04	0.105
	93.92	23.88	0.097
		Average	0.104

* The correction of adsorption for Sr.

such as scandium, yttrium and lanthanide, were also coprecipitated by calcium oxalate obeying along the logarithmic distribution law proposed by Doerner and Hoskins.[3]

Tables II and III show that, in the calcium-strontium oxalate system, λ is not influenced by the pH value and the acetate concentration, unlike as in the calcium - tervalent element system.

According to Chlopin's description,[9] the homogeneous distribution coefficient, D, will practically not change if the ratio of the ionic concentration of the micro component to that of the macro component does not vary even when the composition of the solution phase varies, while the value of D will increase if the ionic concentration of the macro component decreases more rapidly than that of the micro component, and vice versa. This explanation was applied in the calcium - tervalent metal ion system, which obeyed the logarithmic distribution law.[7] This rule can be applied to the present research, because the ratio of the ionic concentration of strontium to that of calcium scarcely does change, even if the precipitation conditions vary. The coefficient, λ, is nearly 0.1, meaning that strontium is enriched in the solution phase. The homogeneous distribution coefficient, D, of course decreased as the precipitation of calcium proceeded under all coprecipitation conditions.

When a strontium ion is brought together with the calcium oxalate carrier from the sample solutions, it may, in view of the above results, be concluded that: As the concentration of calcium left in solution phase becomes lower, the percentage of the coprecipitated strontium becomes higher. It is desirable to react with high pH values (if not influenced by the carbonate ion) and with an excess of oxalic acid in order to concentrate the strontium ions in the precipitate.

The author wishes to express his thanks to Professor Tsunenobu Shigematsu and Dr. Masayuki Tabushi for their valuable advice.

9) I. E. Starik, "Hoshakagaku no Kiso" (Fundamental Radiochemistry), translated from Russian by F. Ichikawa, H. Okashita and R. Ishiwatari, Nankodo, Tokyo (1962), p. 174.

BULLETIN OF THE CHEMICAL SOCIETY OF JAPAN VOL. 39 585—596 (1966)

The Separation of Alkali Metals as Poly-Iodides by Reversed-Phase Partition Chromatography

By Ikuko AKAZA

Department of Chemistry, Faculty of Science, Kanazawa University, Kanazawa

(Received July 22, 1965)

The liquid-liquid extraction of alkali metal ions as their poly-iodides had previously been investigated by the present author. In order to attain a good separation of each metal, this extraction system has now been extended to a reversed-phase partition chromatography in which Kel-F powder was used to support the organic phase of nitrobenzene-iodine-iodide. Column chromatographic separation was carried out in the presence of relatively large amounts of the metals by elution with water and 1 N or 6 N hydrochloric acid - eluting solutions. Chromatographic behavior of each metal ion was investigated and the elution from the column was found to be in the order of Li-Na-K-Rb-Cs. The distribution ratio of the metal ions varied with the quantity of the ions loaded on the column; the smaller the quantity of the ions used, the larger was the distribution ratio obtained. The actual separation of individual metal ions from the mixture was successfully achieved; a minute amount of cesium could be particularly isolated from large amounts of other alkali metals, even in a large volume of the sample solution. Elution curves of various amounts of metal were obtained as an aid to a discussion of the partition on the column. A comparison of the distribution ratio in the liquid-liquid extraction with that in the column chromatography showed that the extraction of the same mechanism proceeded in both cases.

Previously the author studied the liquid-liquid extraction of alkali metal ions as poly-iodides; the method presented consisted of the conversion of various kinds of alkali salts into iodides by double decomposition with ammonium iodide in an aqueous solution and the batch extraction of the iodide with nitrobenzene containing free iodine. The details of the investigation were described in a preceding paper.[1] It was found to be very difficult to separate alkali metals from one another by a batch extraction because the distribution ratios of the poly-iodides were too

1) I. Akaza, This Bulletin, **39**, 465 (1966).

close together in this extraction system. The low separation factor between each pair of metals of the alkali group led the author to seek other convenient methods which would be more efficient. Reversed-phase partition chromatography is closely related to liquid-liquid extraction, except that the water-insoluble extractant is immobilized on some stationary, inert support. In a column extraction of this type an aqueous solution containing the solute under consideration is always in contact with the fresh organic solvent on the column, and a multistage batch extraction can be carried on through the process; therefore, effective separation can be achieved even between substances with a low separation factor. Moreover, a larger quantity of material can be treated by this method.

A summary of the investigations of this method up to the end of 1964 has already been given by the present author,[2] so further description will be omitted here.

The author tested the qualifications of many substances which had been recommended for use as inert solid supporting materials to see if they were suitable for the poly-iodide extraction. Some of them could not retain nitrobenzene containing poly-iodide, while others were affected by the solvent system. However, the Kel-F (polytrifluorochloroethylene) moulding powder recommended by Hamlin et al.[3] was found to be very suitable because of its large absorptivity and capacity for the solvent and its strong resistivity against chemical agents. Therefore, this substance was finally chosen for this investigation.

Reversed-phase chromatography has never been applied in the separation of alkali metals, excepting the work of O'Laughlin and Banks[4] who separated sodium from lithium using bis(di-*n*-hexyl-phosphinyl)methane. Recently, however, Cerrai and his co-workers[5] attempted the paper chromatographic method with di-(2-ethylhexyl) orthophosphoric acid, HDEHP; the R_f value for each metal showed a good prospect of separation.

This paper will describe a column method of the reversed-phase chromatographic separation of alkali metals, using iodine - ammonium iodide - nitrobenzene as the stationary phase supported on Kel-F. The results of the investigation of the liquid-liquid extraction of poly-iodides of alkali metals described in a preceding paper[1] will be fully utilized. The elution of individual ions and their separation from their mixtures were both successfully achieved by the column method; the correlation between this chromatographic separation and the liquid-liquid extraction indicated by the detailed data obtained will be discussed.

Experimental

Apparatus. — *Column.*—A glass chromatographic column, 0.98 cm. in diameter and 23 cm. in length, and with a coase frit at the bottom, was used during this study; in order to keep the temperature constant, a water jacket was fitted so as surround the column tube, and water from the tap or a water-tank of a constant temperature was made to flow through it. A separating funnel as a reservoir of the eluting solution was fitted to the top of the column tube, a polyvinyl chloride tube 1 cm. in diameter was coiled around the funnel, and the constant-temperature water was allowed to flow through it before entering the water-jacket.

Fraction Collector.—A fraction collector (Model SF 200A of the Tōyō Roshi Co.) holding 200 tubes was employed.

Flame Photometer.—A spectrophotometer, Hitachi EPU-2, provided with a flame spectrophotometry accessory, H-2, was employed, hydrogen being used as the fuel.

Scintillation Counter.—A counting set made by the Kōbe Kōgyo Co. (Model EA-14, NaI(Tl) crystal and Model SA-250 scaler) was employed.

Pulse-height Analyzer.—A 100-channel pulse-height analyzer, model AN-100, of the Kōbe Kōgyo Co. was employed.

Reagents and Materials.—*Kel-F.*—Kel-F (polytrifluorochloroethylene), a trade name low-density 300 moulding powder, was imported from the Minnesota Mining and Manufacturing Co., U. S. A. When the material was ground with a mixing grinder and sieved through screens, particles between 42 to 80 mesh were collected for use.

Chemical Reagents.—The ammonium iodide, iodine, hydrochloric acid, nitrobenzene and alkali metal chlorides and sulfates were all of analytical reagent grade. Radio isotopes, ^{86}Rb as chloride and ^{137}Cs as nitrate, were purchased from the Radiochemical Center, Amersham, England. No diluted stock solutions were prepared; the original solutions were used as they were.

Organic Solvent as the Stationary Phase in the Column.—6.1 g. of iodine, 1 g. of ammonium iodide and 40 ml. of nitrobenzene were placed in a separatory funnel. Then there was added 40 ml. of an aqueous solution which had been selected from among distilled water, 6 N hydrochloric acid and 1 N hydrochloric acid, according to the kind of eluting solution to be used in the eluting process. After thirty minutes' shaking, the two phases were separated. The organic solvent thus treated contained iodine and iodide in the molar ratio of about 3 : 1; this ratio had been found in a preceding paper[1] to be the optimum for the extraction of alkali metal ions. The composition of the aqueous phase after the shaking should hold also in the eluting solution. Therefore, the amounts of iodine and iodide in the aqueous solution were determined and the same composition was adopted in the preparation of each eluting solution.

Eluting Solution.—*1) Aqueous Eluting Solution.*—Nitrobenzene was put in water in a separatory funnel

2) T. Kiba and I. Akaza, *Kagaku* (Chemistry), **19**, 984 (1964).
3) A. G. Hamlin, B. J. Roberts, W. Laughlin and S. G. Walker, *Anal. Chem.*, **33**, 1547 (1961).
4) J. W. O'Laughlin and C. V. Banks, *U. S. A. E. C. Rep.*, IS-737, 145 (1963).
5) E. Cerrai and G. Ghersini, *J. Chromatog.*, **13**, 211 (1964).

and shaken to produce a saturated solution, and the excess nitrobenzene was rejected through the stem of the funnel. The water thus treated was called nitrobenzene-saturated water in this investigation. On the other hand, 1.4 g. of iodine and 1.5 g. of ammonium iodide were dissolved in a small volume of the nitrobenzene-saturated water, and then the solution was diluted to 1 l. with the water.

2) 1 N Hydrochloric Acid Eluting Solution.—Nitrobenzene was dissolved to saturation in 1 N hydrochloric acid in the manner described in the case of nitrobenzene-saturated water; this solution was called nitrobenzene-saturated acid. In a small volume of the acid 0.78 g. of iodine and 0.61 g. of ammonium iodide were dissolved, and the solution was made up to 1 l. with the acid.

3) 6 N Hydrochloric Acid Eluting Solution.—Nitrobenzene-saturated 6 N hydrochloric acid was prepared in the way described above. In the 6 N acid 1.51 g. of iodine and 0.04 g. of ammonium iodide were dissolved, and the solution was made up to 1 l. with the same acid. It happened occasionally that iodine and ammonium iodide did not readily dissolve in the acid; shaking in a separatory funnel was resorted to in order to overcome this trouble. It is essential to keep the temperature constant both in the preparation of an organic solvent for the stationary phase and of eluting solutions for the mobile phase, and in carrying out the chromatographic separation.

Sample Solution.—It is often desirable, though not in all cases, that the sample solution has a composition alike to that of the eluting solution; for example, the correct amount of alkali metal salt was dissolved in a definite volume of the eluting solution mentioned above in order to make a sample solution to be tested. Three milliliters of the solution was usually employed for the chromatographic separation in the column method, but as much as 50 ml. of the solution was employed in the separation of trace amounts of ^{137}Cs from the mixture of sodium, potassium, rubidium and cesium salts.

Experimental Procedure.—*The Preparation of the Stationary Phase.*—Place in an Erlenmyer flask 6 g. of the Kel-F powder which had been dried at 80°C and stored in a calcium chloride desiccator, and then pour on it 4.5 ml. of the organic solvent solution prepared above. After stoppering the flask tigthly, shake it by hand until the content appears homogeneous and then let it stand over three hours. Add a small volume of a suitable eluting solution, stir gently to get rid of air bubbles, and pour the slurry little by little into the chromatographic column tube, taking care so as not to include any air bubbles. It is desirable to keep the temperature constant during the preparation by passing water of a constant temperature through the jacket fitted to the glass tube. Every time a portion of slurry is added, gently press the column bed with a glass rod in order to make it about 17.5 cm. in depth; meanwhile about 50 ml. of the eluting solution is passed through the column in order to remove any contaminant such as sodium that may be present in the column bed. The upper surface of the column should be below the surface of the eluting solution contained in the glass tube lest it becomes dry.

The Elution, Separation and Determination of Metals.—Pour 3 ml. of the sample solution on the upper surface of the column and allow it to percolate through the column at the rate of about 0.25 ml. per minute; then wash the inside of the glass tube above the top of the column bed twice with small portions of the eluting solution, letting them flow down at the same rate.

On the top of the glass tube, set a separatory funnel from which an eluting solution of a definite composition is supplied into the glass tube; then carry out the elution at the rate of 0.5 ml./min. During the preparation of the column and the elution of the material, the temperature should be kept constant— in this experiment 18°C was preferred. If the volume of the sample solution is large, the separatory funnel may be employed for the loading of the sample. Collect the effluent from the bottom of the column in suitable fractions with a fraction collector, and determine the content of alkali metal ions in each fraction by flame spectrophotometry. When a radioisotope was used, the activity in each fraction was counted by a scintillation counter and the nuclides separated were identified by γ-ray spectrometry.

Results and Discussion

The Characteristic Behavior of the Column.—*1) The Choice of Column Material.*—The application of the reversed-phase partition chromatography technique depends on the availability of a suitable supporting material. Several examples which had been reported were reviewed and discussed by the present author.[2] In the present work the organic phase consisted of nitrobenzene and poly-iodide; therefore, a more resistant material was sought.

The first choice was Kel-F moulding powder, previous experience having shown that the particular grade used had a large capacity for stationary phase and resistance against chemical agents.[3] A number of tests were made to find out whether other polymers or inorganic materials were equally suitable. Inorganic materials, such as alumina and silica gel, were found to be useless, as they failed to retain any nitrobenzene even after being treated with dimethyldichlorosilane. On the other hand, organic polymers such as cellulose powder, porous polyethylene chloride, and the polymer of tetrafluoroethylene (Teflon) had the disadvantages of reacting with iodine and of requiring difficult techniques in order to release the organic phase from them. The outstanding behavior of Kel-F moulding powder is presumably due to the large surface area of the aggregate and the resistance of the substance to chemical agents, but this has not been explained by organic chemists.

2) The Amounts of Nitrobenzene Adsorbed by Kel-F.—In an Erlenmyer flask fitted with a glass stopper, 45 ml. of nitrobenzene and 10 g. of Kel-F powder were left together overnight; the nitrobenzene unadsorbed was then drained through a small glass filter into a measuring cylinder placed in a slightly-evacuated vessel. The flask was washed with one milliliter of nitrobenzene, which was then poured

on the Kel-F powder, all of the excessive solvent being drained through the filter. The difference between the volume of nitrobenzene initially taken and that measured in the cylinder showed the volume of the solvent adsorbed by Kel-F; this was found to be 7.4 ml. per 10 g. of Kel-F powder.

3) The Volume of the Mobile Phase in the Column.—A column was packed with Kel-F loaded with nitrobenzene; a solution of sodium chloride saturated with nitrobenzene was poured onto the column and allowed to flow down to the bottom until the effluent became of the same concentration as the solution originally poured. After having been washed with water the inside of the glass tube below the fritted glass filter, the sodium chloride solution retained in the column was completely washed down by passing through water from the top of the column. The amount of sodium chloride contained in the washings was estimated argentimetrically. From this amount the volume of the sodium chloride solution in the column was computed as is usually done in chromatographic investigations. It was found that the volume of the mobile phase in the column was 4.68 ml. per 6 g. of Kel-F. The amount of nitrobenzene originally adsorbed on the Kel-F column was 4.5 ml., corresponding to the ratio of 7.4 ml./10 g. obtained in the experiment in 2); hence the volume ratio of the stationary phase to the mobile phase was 1 : 1 in this case. This indicates that the elution process consists of multiple extraction between equal volumes of the organic and the aqueous phases. The author's method of preparing the stationary phase and the eluting solution was built up consciously in order to maintain the above relation between the two phases during the elution.

4) Blank Test for the Column.—If alkali metal ions could be retained on the column of Kel-F without poly-iodide ions, separation by this method would not be satisfactory because of the complication caused by the adsorption on the stationary phase. To test the above phenomenon, a radioactive cesium tracer was passed through the column (cesium poly-iodide had been found by a preliminary experiment to be the most easily retained species). Six grams of Kel-F powder containing 4.5 ml. of nitrobenzene which had been pre-equilibrated with water was used for the column, while a trace of cesium-137 nitrate in 3 ml. of water pre-equilibrated with nitrobenzene was charged on the column. Elution was carried on by nitrobenzene-saturated water, and the effluent was collected in 10 ml. fractions. Strong radioactivity was found as early as in the first fraction, and the maximum appeared in the second. This showed that if poly-iodide ion was absent in the organic phase on Kel-F, no alkali metal ion will be retained on the column; there will be only a distribution caused by the poly-iodide ion in the chromatographic process.

5) Column Life and Stability.—After loading the column with 0.5 mg. of potassium, elution with an aqueous eluting solution was carried out; the usual elution curve was obtained. This experiment was repeated five times through the same column during a month's period; the band width and position of the peak were also examined. At the end of the five runs, the total volume of the eluting solution, including the preliminary washing with 1000 ml., was as large as 3070 ml. Table I shows the results. We can see that the column can stand the repeated uses, though a slight delay was observed at the front of the band and at the peak of the curve. As the nitrobenzene and poly-iodide of which the stationary phase consisted are tolerably soluble in an aqueous solution, the eluting solution and sample solution should have the same composition, as equilibrated with the organic solvent of the stationary phase, in order to prevent the degradation of the column during the continuous use.

TABLE I. VARIATION OF BAND WIDTH AND PEAK OF ELUTION CURVE DURING REPEATED USES OF THE COLUMN

Number of time	Band width shown as volume of effluent ml.	Peak of the curve shown as volume of effluent, ml.
1	243.8—413.4	300
2	249.1—408.1	300
3	265.0—402.8	307
4	254.4—413.4	315
5	242.5—388.0	291

6) The Recovery of Kel-F Powder.—The Kel-F powder could be recovered by the following method from a column degraded by long service; take out the Kel-F supporter from the column tube into a beaker, wash it with plenty of water, and filter it through a glass filter under suction. Put it back in the beaker, and pour a 30% ethanol-water mixture on it to remove roughly the nitrobenzene and poly-iodide remaining on the powder. Repeat this treatment if necessary, and finally wash it with water in order to drive off the ethanol. Stir 10 M nitric acid into the powder in order to separate the solid iodine from the poly-iodide, as in the case of the back extraction of alkali metal ions described in the preceding paper.[1] Filter the mixture of Kel-F powder and solid iodine under suction, and wash the residue with water in order to wash off the nitric acid. Transfer the residue into a beaker, and wash again with a 30% ethanol-water mixture to dissolve the iodine. Filter off the iodine solution. After preliminary washing with water, treat this Kel-F again with nitric acid and follow the serial procedure indicated, repeating the process three times. Wash the powder thus obtained by stirring it well with warm absolute alcohol in the beaker. Filter the powder under suction, and repeat the washing until the color of iodine disappears. Dry the white powder at 80°C before storing.

7) The Capacity of the Column.—The capacity of the column used was estimated by loading it with potassium salt and then examining its break through, shown in Fig. 1, in which the sharp rise of the curve indicates that the transfer rate of potassium ions is very high at the surface of and within the stationary phase. The capacity was estimated to be $17._1$ mg. of potassium when a solution containing 0.2 mg. of potassium per ml. was used as the feed solution, and $30._6$ mg. when a solution containing 5.0 mg. of potassium per ml. was used. As a matter of fact, the capacity in this case is distinctly different from that in the case of ion-exchange chromatography; the former merely depends on the partition of the substance between two phases, and its value varies remarkably with the concentration of the feed solution.

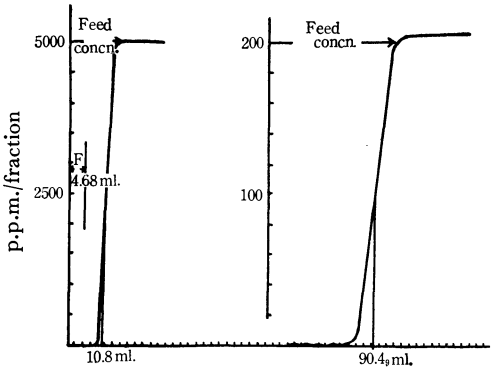

Fig. 1. Break-through curve of potassium.
Feed: 5 mg. potassium per ml. and 0.2 mg. potassium per ml. in aqueous eluting solution.
Flow rate: 0.2 ml. per minute.
F: Interstitial volume of the column.

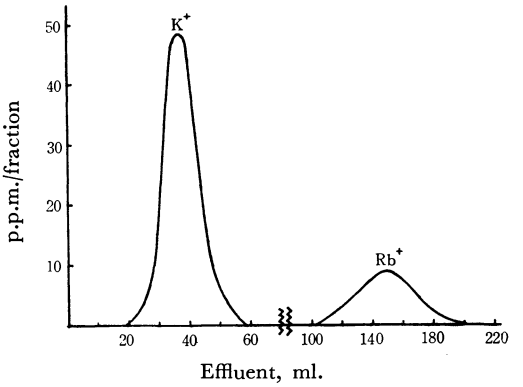

Fig. 3. Elution curves of potassium and rubidium. (Experiments with K and Rb conducted separately)
Loaded: 0.5 mg. of the element
Eluting solution: 1 N hydrochloric acid eluting solution

The Chromatographic Behavior of Alkali Metal Ions.—The chromatographic behavior of alkali metal ions is to be expected from the results obtained in the liquid-liquid extraction of alkali poly-iodides described in the preceding paper.[1] Their distribution ratios were found to depend on the ratio of free iodine to iodide ion in the system, on the acidity of the solution, and on the amounts of metal to be treated. Moreover, the temperature was also found to affect the distribution ratios. Because a marked effect will appear in the chromatographic process unless the temperature is kept constant, all the author's experiments were carried out at 18°C, except for the data shown in Figs. 2, 4, and 12, and in Table I. Since the distribution

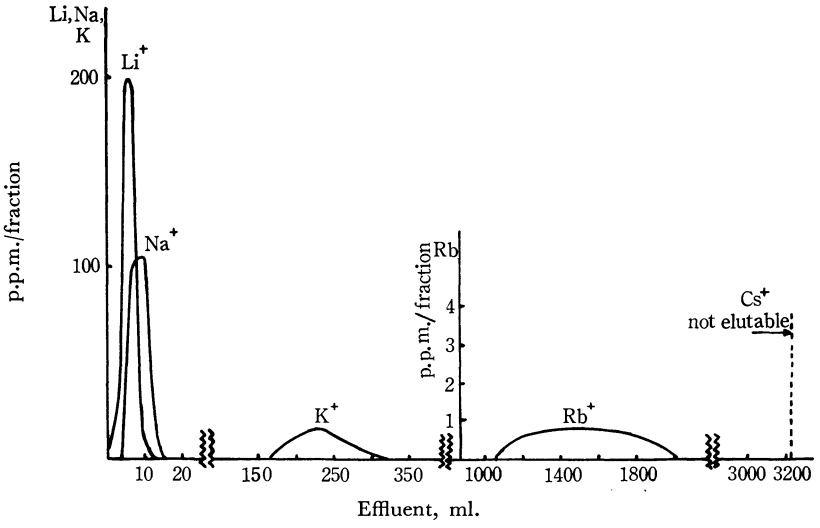

Fig. 2. Elution curves of individual ions.
Loaded: 0.5 mg. of the ion in each case Eluting solution: Aqueous

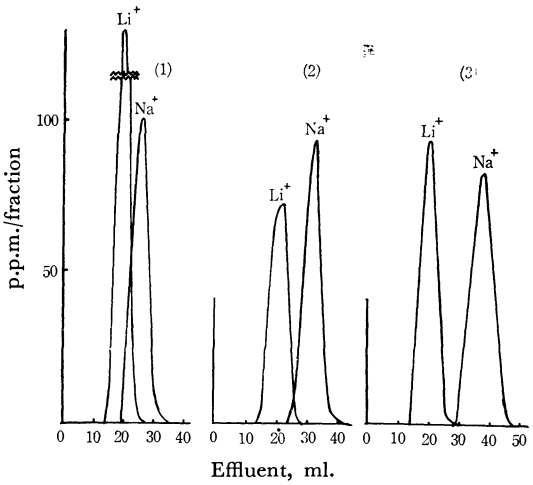

Fig. 4. Elution curves of lithium and sodium.
Stationary phase: 42—80 mesh Kel-F, 17 g. and 13 ml. of the organic solvent of nitrobenzene-iodine-iodide.
Column height: 49 cm.
Loaded: 0.5 mg. of the element.
(1) Composition of the organic solvent: Same as discribed in procedure.
Eluting solution: Aqueous.
(2) Organic solvent: 18.3 g. of iodine, 3 g. of ammonium iodide and 40 ml. of nitrobenzene shaken with 40 ml. of water.
Eluting solution: Aqueous eluting solution prepared by dissolving 2.54 g. of iodine and 2.91 g. of ammonium iodide in 1 l. of water saturated with nitrobenzene.
(3) Composition of organic solvent: A mixture of 24.4 g. of iodine, 4 g. of ammonium iodide and 40 ml. of nitrobenzene was used after shaking with 40 ml. of water.
Eluting solution: 3.4 g. of iodine and 4.0 g. of ammonium iodide dissolved in 1 l. of nitrobenzene-saturated water.

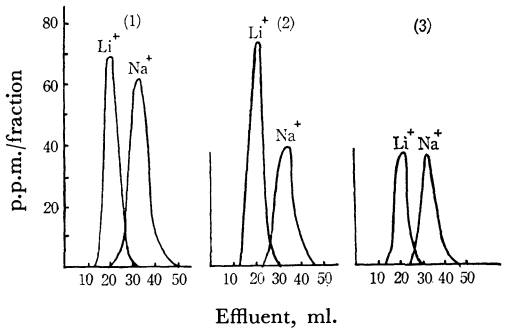

Fig. 5. Separation of lithium from sodium.
Loaded: (1) Li: 0.25 mg., Na: 0.25 mg.
(2) Li: 0.25 mg., Na: 0.1 mg.
(3) Li: 0.1 mg., Na: 0.1 mg.
Eluting solution: Aqueous

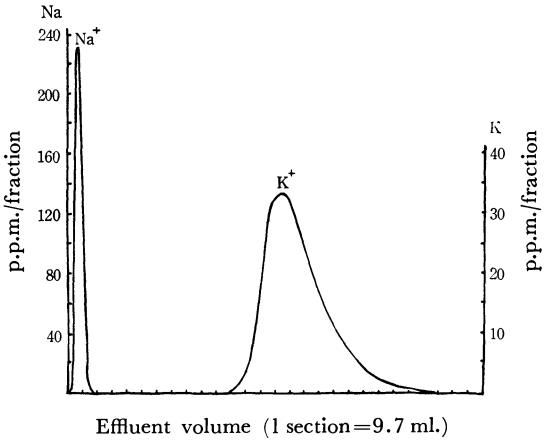

Fig. 6. Separation of sodium from potassium.
Loaded: Na: 1 mg., K: 1 mg.
Eluting solution: Aqueous

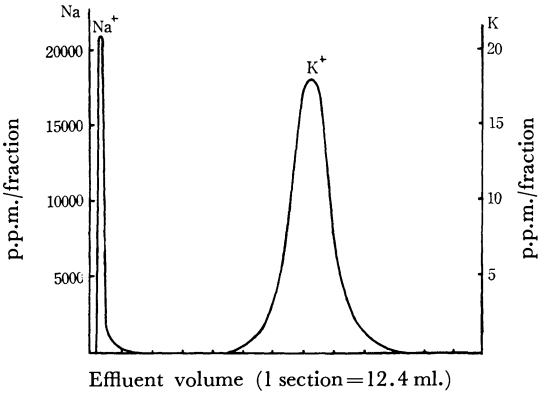

Fig. 7. Separation of potassium from sodium.
Loaded: Na: 100 mg., K: 0.5 mg.
Eluting solution: Aqueous

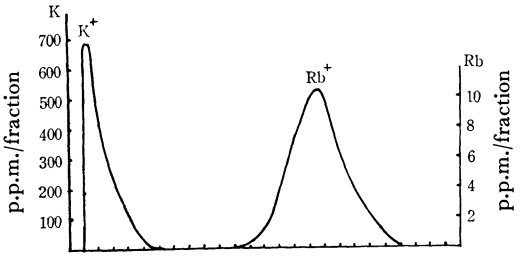

Fig. 8. Separation of potassium from rubidium.
Loaded: K: 12 mg., Rb: 0.5 mg.
Eluting solution: 1 N-hydrochloric acid eluting solution

ratio of individual alkali poly-iodide between nitrobenzene and an aqueous solution increased in the order of Li-Na-K-Rb-Cs, the elution from the column of Kel-F/nitrobenzene-iodine-iodide will show the expected resolution of alkali metals in

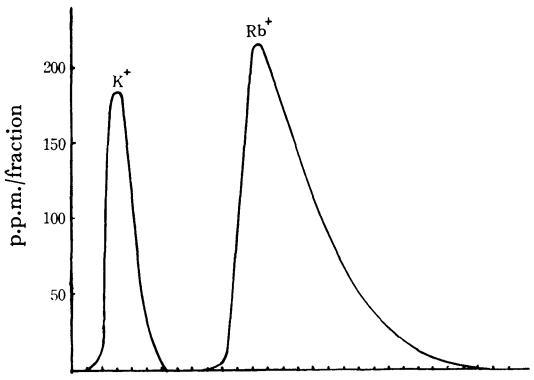

Fig. 9. Separation of potassium from rubidium.
Loaded: K: 0.5 mg., Rb: 10 mg.
Eluting solution: 1 N hydrochloric acid eluting solution.

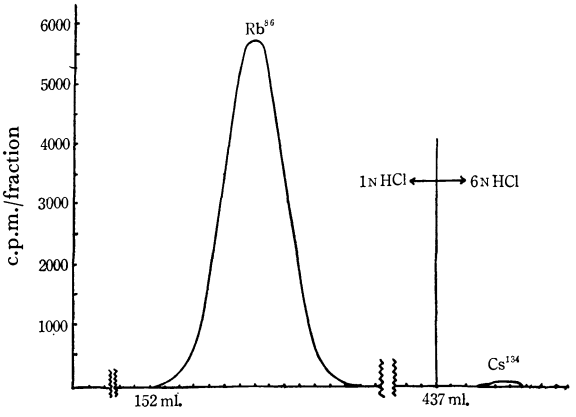

Fig. 11. Separation of cesium-134 from contaminated rubidium-86.
Loaded: A trace amount of rubidium-86.
Eluting solution: 1 N hydrochloric acid eluting solution followed by 6 N hydrochloric acid eluting solution.

the effluent, the lighter species appearing first and the heavier later.

1) The Elution Curve of Individual Ions.—In order to examine quantitatively the retention of individual ions on the column, a column prepared as described above was charged with 0.5 mg. of each ion; it was then eluted by a continuous stream of the aqueous eluting solution described above at a flow rate of 0.5 ml./min. The effluent was collected in 1.93-ml. fractions in the case of lithium and sodium, and in 9.86-ml. fractions in the case of heavier metals. The results are summarized in Fig. 2, in which it may be seen that lithium and sodium can easily be separated as a group from potassium, rubidium and cesium by this procedure. However, the later appearence of potassium and rubidium in the effluent, the plateau in their elution curves, and the failure of cesium to appear up to 3200 ml. of the effluent made it desirable to elute them faster in order to get a sharp peak on the curve. The acid eluting solution may serve for this purpose, because of the lower distribution ratio in an acid medium.

The other elution curves shown in Fig. 3 are those of potassium and rubidium eluted with a 1 N acid eluting solution; each has a relatively sharp peak. Therefore, this eluting solution is useful for the separation of potassium, rubidium and cesium from one another. On the other hand, the separation

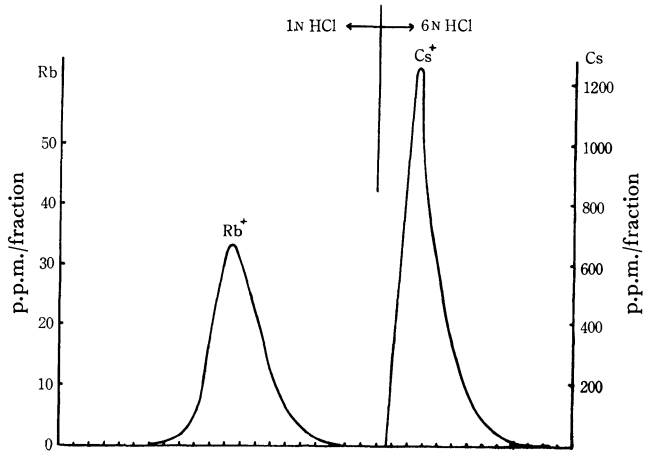

Fig. 10. Separation of rubidium from cesium.
Loaded: Rb: 0.5 mg, Cs: 25 mg.
Eluting solution: 1 N hydrochloric acid eluting solution followed by 6 N hydrochloric acid eluting solution.

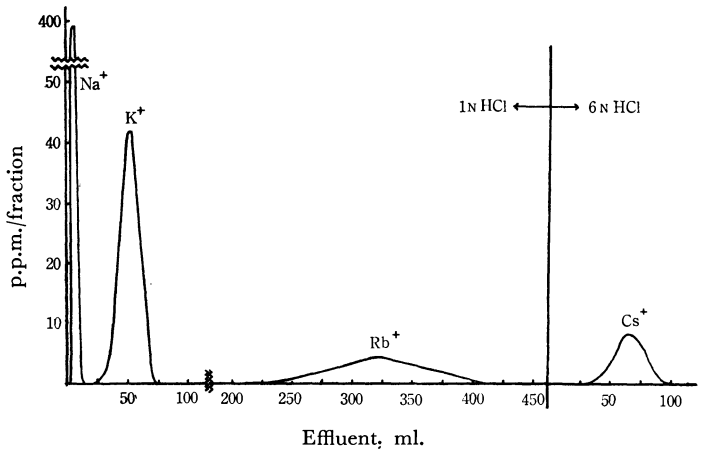

Fig. 12. Separation of Na-K-Rb-Cs.
Loaded: 0.5 mg. of each metal ion.
Eluting solution: 1 N hydrochloric acid eluting solution followed by 6 N hydrochloric acid eluting solution.

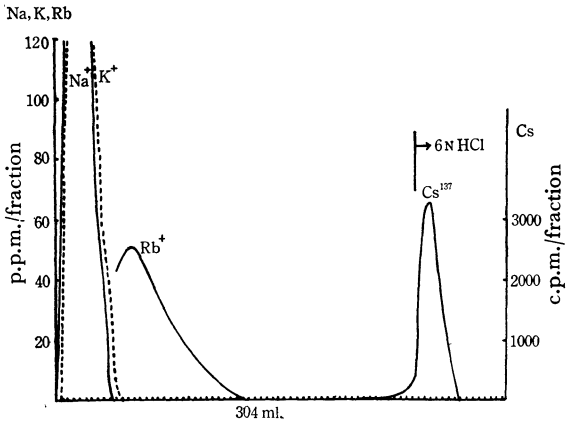

Fig. 13. Isolation of radioactive cesium from large amounts of sodium, potassium and rubidium.
Feed solution: 100 mg. each of Na, K, Rb and a trace amount of Cs-137 in 50 ml. of 1 N hydrochloric acid eluting solution.
Loaded: 50 ml. of the solution.
Eluting solution: 1 N hydrochloric acid eluting solution followed by 6 N hydrochloric acid eluting solution.

factor between lithium and sodium is so small that the separation of the two metals was found to be extremely difficult, as may be expected from the results of their liquid-liquid extraction. An attempt to increase the separability of these two metal ions was made by the elongation of the column bed in order to increase the plate number of the extraction. However, the experiment with a long column bed failed to give a good separation, as is shown in Fig. 4, in which (1) shows the results with a long column bed, and (2) and (3), with a stationary phase containing concentrated poly-iodide.

2) The Actual Separation of Metal Ions.—a) The Separation of Li-Na.—As has been described above, the separation of lithium from sodium seemed to be difficult, but the elution was performed for mixtures of various amounts of metal chlorides, with the results shown in Fig. 5. In these experiments the same stationary phase as in Fig. 4 (3) was employed, and the peaks of elution curves were easily distinguishable from each other, even though complete separation could not be achieved.

b) The Separation of Na-K.—The column prepared as described in the general procedure was loaded with 3 ml. of an aqueous solution containing 1 ml. each of sodium and potassium as chlorides, and elution was carried out with the aqueous eluting solution. Good separation was achieved as is shown in Fig. 6. Elution for a sample solution containing 100 mg. of sodium and 0.5 mg. of potassium was attempted in the same way with the results shown in Fig. 7.

c) The Separation of K-Rb.—Three milliliters of a 1 N hydrochloric acid eluting solution containing 12 mg. of potassium and 0.5 mg. of rubidium, and another 3 ml. of the solution containing 0.5 mg. of potassium and 10 mg. of rubidium were separately fed through the column, and then eluted with a 1 N hydrochloric acid eluting solution. The results are shown in Figs. 8 and 9.

d) The Separation of Rb-Cs.—Three milliliters of a 1 N hydrochloric acid eluting solution containing 0.5 mg. of rubidium and 25 mg. of cesium was fed through the column, and eluted first with a 1 N hydrochloric acid eluting solution and then with a 6 N hydrochloric acid eluting solution. The results are shown in Fig. 10.

e) The Separation of Cesium-134 from Contaminated Rubidium-86.—Radioactive rubidium-86 chloride

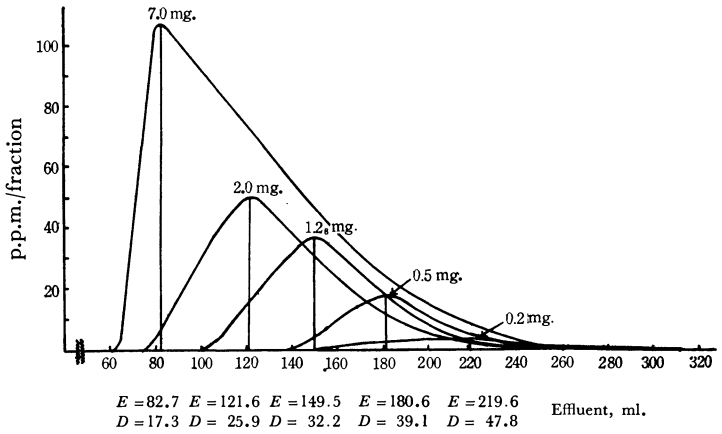

Fig. 14. Elution curve of various amounts of potassium loaded.
Potassium loaded: Given in mg. above each peak.
E, and D calculated from Eq. 1 are noted below each peak.

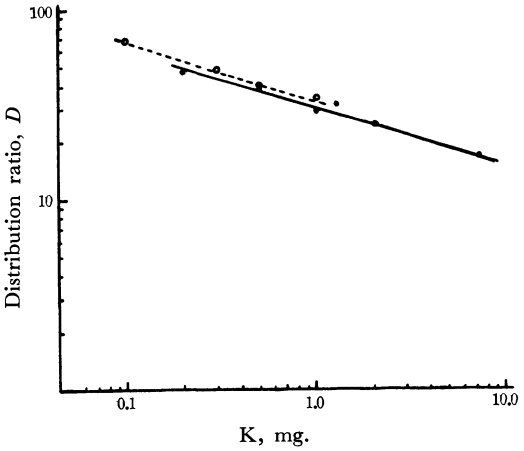

Fig. 15. Relation of potassium loaded to distribution ratio.
○----Refference data from liquid-liquid extraction under the same condition.

is sometimes contaminated with radioactive cesium derived from impurities in the target material. By eluting trace amounts of rubidium-86 chloride through the column, according to the standard procedure, with a 1 N hydrochloric acid eluting solution, the following fact was revealed. As is shown in Fig. 11, the proper elution curve was drawn up to 437 ml. of the effluent, and none of the activity seemed to remain in the column. Nevertheless, when a 6 N hydrochloric acid eluting solution was subsequently fed through the column, a minute amount of radioactivity was detected in the effluent after about 30 ml. of the new eluent had been spent. The radioactivity was shown by a γ-ray spectrometer to be the γ-activity of cesium-134. In the γ-ray spectrum no activity from rubidium was found; therefore, it was also revealed that the complete elution of rubidium had been accomplished with the 1 N hydrochloric acid eluting solution. Thus, this elution technique is useful for removing the

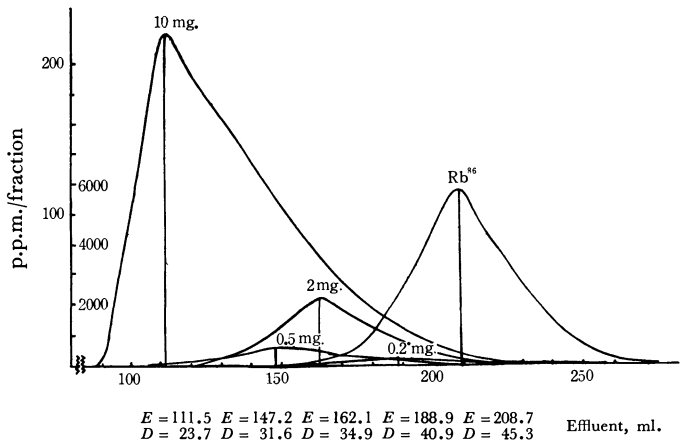

Fig. 16. Elution curve of various amounts of rubidium loaded.
Rubidium loaded: Noted in mg. above each peak.
E, and D calculated from Eq. 1 are noted below peak.

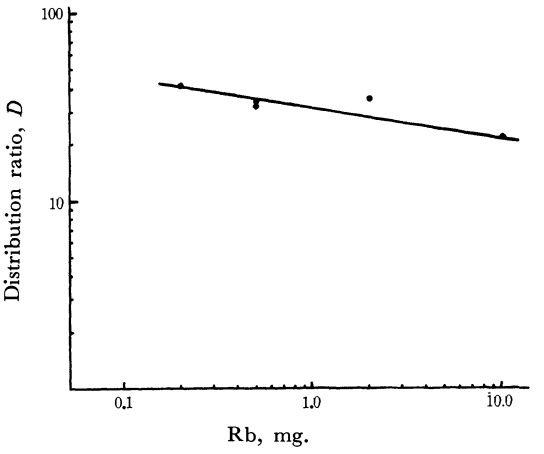

Fig. 17. Relation of potassium loaded to distribution ratio.

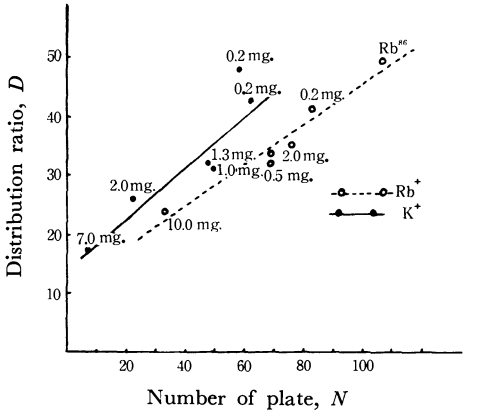

Fig. 18. Relation of distribution ratio to number of theoretical equivalent plates.

radioactive contaminants from rubidium-86, as well as for the determination of the amount of the contaminant.

f) The Separation of Na-K-Rb-Cs.—Three milliliters of a 1 N hydrochloric acid eluting solution containing 0.5 mg. each of the alkali metal ions together was fed to the column and eluted with a 1 N hydrochloric acid eluting solution up to 460 ml. of effluent and then further eluted with a 6 N hydrochloric acid eluting solution. The separation of the metal ions was achieved as shown in Fig. 12.

g) The Isolation of Radioactive Cesium from Large Amounts of Sodium, Potassium and Rubibium.—A mixed solution containing 100 mg. each of sodium, potassium, and rubidium, as well as a trace amount of radioactive cesium, was prepared with the 1 N hydrochloric acid eluting solution so as to bring the whole volume up to 50 ml. The entire amount was then fed to the column and eluted with the same eluting solution and then with a 6 N hydrochloric acid eluting solution. The results are shown in Fig. 13, in which it may be seen that a minute amount of cesium can be isolated from large amounts of other alkali metals, even in as large a volume of the solution as 50 ml.

h) The Separation and Recovery of Individual Ions from the Na-K-Rb-Cs Mixture.—The preceding experiments indicate that the extraction rate and the selectivity of the Kel-F/nitrobenzene-iodine-iodide column is adequate for the separation of an individual ion from other alkali metal ions. To demonstrate the practical usefulness of the method and to devise a convenient method, a typical simple separation was carried out without a fraction collector. In a few milliliters of the aqueous eluting solution, 847.28 mg. sodium chloride, 317.57 mg. potassium chloride, 9.42 mg. rubidium chloride and 9.07 mg. cesium sulfate were dissolved. Some of the nitrobenzene separated out from the solution because of the salting-out effect of the above added salts. To redissolve it, some water was added, little by little, to the above solution in a 100-ml. volumetric flask; finally, the aqueous eluting solution was added to bring it up to the mark. Three milliliters of this solution, containing 10 mg. of sodium, 5 mg. of potassium, 0.2 mg. of rubidium and 0.2 mg. of cesium, was placed in the column and eluted with the eluting solutions. Five fractions of the effluent were collected, without the help of a fraction collector, in five measuring flasks of the proper capacities. The first and second fractions, 50 ml. and 250 ml. respectively, were collected using the aqueous eluting solution; the third and fourth, 50 ml. and 250 ml. respectively, using 1 N acid eluting solution as the eluent, and the fifth, 100 ml., when the 6 N acid eluting solution was used. Each of the first three fractions was shaken well and submitted to flame photometry, at 589 mμ for sodium in the first fraction, and 768 mμ for potassium in the second. The fourth and fifth fractions were found too dilute for the determination of the amounts of rubidium and cesium, and so each fraction was evaporated to dryness under an infrared lamp and the residue was re-dissolved in 25 ml. of water. The solution thus obtained were submitted to flame photometry at 780 mμ for rubidium and at 852 mμ for cesium.

A known amount of each metal ion was dissolved in the same eluting solution as was used in the sample, and the solution was treated as above with the exception of the column process. The flame photometric value of the solution was compared with the value obtained from each fraction. Table II gives the results obtained in this separation process; each alkali metal ion was quantitatively recovered in each proper fraction without contamination.

The metal separated in each fraction could be recovered by evaporating the solution to dryness under an infrared lamp and in an electric furnace and by then treating the residue with a suitable

Table II. Recovery of alkali metal ions from their mixed solution by reversed-phase partition chromatography

Fraction of effluent No.	Eluting solution	Effluent volume ml.	Metal ion recovered mg.	Metal ion taken mg.
1	water	50	Na 10.03	Na 10.11
2	water	250	K 5.06	K 5.03
3	1 N HCl	50	—	—
4	1 N HCl	250	Rb 0.26	Rb 0.26
5	6 N HCl	100	Cs 0.20	Cs 0.20

The values in the last column were obtained from a reference solution of the identical composition.

acid to make its alkali salt, while the nitrobenzene and iodine contained in the effluent were all driven off by the heating with the strong acid.

The Relation to the Liquid-Liquid Extraction.—The reversed-phase partition chromatography is related to the liquid-liquid extraction of alkali poly-iodide into nitrobenzene described in the preceding paper.[1] The partition on the column, based on the theory of Martin and Synge,[6] seems to be equivalent to a counter current system consisting of a series of plates.

1) Distribution Ratio.—As has been described, the distribution ratio of alkali metal ions between the nitrobenzene-iodine-iodide solvent and an aqueous phase decreases with the increase in the number of metal ions; therefore, the effect of the amount of metal ions on the column upon the elution curve was also critically examined, especially in the case of potassium ions. The results shown in Fig. 14 reveal that the position of the peak of the elution curve (E in ml.) proceeds forward on the abscissa with the increase in the amount of metal ions loaded; this phenomenon seems to be caused by the decrease in the distribution ratio, which was calculated, from the data obtained by column chromatography, by the following equation[6,7];

$$D = A/RA_S - A_L/A_S = (E-F)/B \qquad (1)$$

where D is the distribution ratio; E, the volume of the effluent before the emergence of the solute in a maximal concentration; B, the volume of the stationary phase; F, the volume of the mobile phase, with empty space in the column; A, the cross-sectional area of the column; A_S, the cross-sectional area of the non-mobile phase (B/column length); A_L, the cross-sectional area of the mobile phase (F/column length), and R, the ratio of (the movement of the position of the maximum concentration of the solute) to (the simultaneous movement of the surface of the developing fluid in the empty part of the above column) (column length/E/A).

The values of D calculated from Eq. 1 by putting, for E, the volume of eluent at the peak of each elution curve are given under the respective peaks in Fig. 14. The logarithmic value of D calculated above is plotted against the logarithm of the mg. of the metal loaded on the column in Fig. 15, in which the relation is shown as a nearly straight line; if the line is elongated upward, the value of D at any point may show the value of D at any lower concentration of metal ions loaded. On the other hand, all of the tail ends of the elution curves are situated so close together on the abscissa in Fig. 14 that they seem to coincide with one another in the range of permissible error in all the procedure. Moreover, the E shifts rightward on the abscissa with the decrease in the amount of metal ions loaded on the column; the position of E when a trace amount of metal is treated may be assumed to be close to the tail end of the elution curve at last. The distribution ratio can usually be calculated from the value of E, so the position of the tail end can be used to calculate the distribution ratio at a very low concentration of the metal ions that probably may be focused on a constant value. The volume of the effluent at the tail end is 316.6 ml. in the author's experiment, while the value of D calculated from this volume is 69.3. This value of D is situated on the elongated part of the straight line in Fig. 15.

When the straight line is extended downward, it will show the relation of D to various larger amounts of potassium loaded. When potassium ions are converted into their poly-iodide, the amount of iodide present in the system may decide the maximum amount of poly-iodide to be formed; in this case, 4.5 ml. of the organic solvent held on the Kel-F supporter corresponds to 28.5 mg. of potassium ions, as calculated from the amount of iodide present in the system. On the other hand, the amount of potassium retained on the column had been estimated, from the value of one of its break-through curves in Fig. 1, as being equivalent to 30 mg. of potassium. These two values, one from the calculated and the other from the break-through, agree well with each other, though incidentally. This value seems to be the maximum amount of potassium loadable on the column; this amount is also the upper limit of the concentration of potassium on the straight line shown in Fig. 15.

As the straight solid line in Fig. 15 shows the relation of D to the amount of potassium loaded on the column, if the amount of potassium loaded on the column is known, the value of D can be estimated from the figure. Putting this value of D into Eq. 1, we get E, the location of the peak of the elution curve on the axis of the effluent volume.

Further liquid-liquid extraction experiments

6) A. J. P. Martin and R. L. M. Synge, *Biochem. J.*, **35**, 1358 (1941).
7) H. B. F. Dixon, *J. Chromatog.*, **7**, 467 (1962).

were carried out between 4.5 ml. of the same solvent as the stationary phase held on Kel-F and 4.5 ml. of the eluting solution containing exactly the same amounts of potassium ion as in the column. The volume of the phase was 4.5 ml.; this amount is equal to the organic solvent held on the column. The distribution ratios obtained in these experiments are also shown in Fig. 15 as ○ marks. This relation fairly agrees well with the relation between the amounts of metal ions and D obtained in the column extraction.

Moreover, similar results were obtained in the case of rubidium, as is shown in Figs. 16 and 17. In Fig. 16, the value of E when a minute amount of the metal is treated is situated close to the tail end, as in the case of potassium, Therefore, the author calculated D at a very low concentration of the metal ions, using 233 ml. as the mean of the effluent volumes of the tail ends of many elution curves; he estimated the value to be 50.7. On the other hand, the D value calculated from the E of the elution curve of Rb-86 tracer was 45.3. The above two values seem almost to agree with each other when the difference in sensitivity between flame photometry and radioactivity measurement is taken into account. These values are also nearly equal to the value obtained by extraporating upward the straight line in Fig. 17.

The distribution was also measured by batch extraction between a Kel-F/nitrobenzene-iodine-iodide mixture and an aqueous phase of the eluting solution containing potassium ions as follows. In a glass-stoppered Erlenmyer flask 6.0 g. of Kel-F powder containing 4.5 ml. of a nitrobenzene-iodine-iodide mixture and 13.5 ml. of a water-eluting solution were placed together; the vessel was then shaken for a while. The contents of the flask were then poured onto a No. 3 glass filter, and the aqueous solution was allowed to drain into a vessel before it was submitted to flame photometry for potassium, The distribution ratio thus estimated coincided with the value obtained in the case of batch extraction with the organic solvent and the aqueous solution in the same volume ratio. From this it may be concluded that Kel-F did not participate in this reversed-phase partition chromatography at all.

2) Column Efficiency.—Column efficiency is usually presented as the number of plates of equivalent extraction carried out on the column. The author tried to calculate the number of plates, N, in this reversed-phase partition chromatography, even though the partition process was far from ideal, in which the partition coefficient remains constant. The author's tentative calculations, based on the elution curve of potassium in Fig. 14 and that of rubidium in Fig. 16, are summarized in Fig. 18, which reveals that the smaller the amount of sample loaded, the larger the plate number, N, for the distribution ratio increases with the decrease in the number of ions treated; the relation between N and D may be assumed to be roughly proportional.

Summary

Partition chromatography and liquid-liquid extraction are closely related to each other with regard to the distribution of solute between two phases. The previous investigation by the present author has clarified that an alkali metal ion can be extracted from an aqueous phase into nitrobenzene containing iodine and ammonium iodide, but the metals are so similar in distribution behavior into the organic phase that they cannot be separated from one another, even by repeated batch extraction. The author has attempted to extend this extraction method to a reversed-phase partition chromatography in which Kel-F powder was used to support the organic phase of nitrobenzene-iodine-iodide; column chromatography has been carried out by eluting with three kinds of eluting solutions. Such characteristics of the column as the volume of the stationary phase held on Kel-F, the volume of the mobile phase in the column, the column life and the capacity of the column have been investigated. The elution of alkali metals has also been carried out with each individual ion. Actual separations, between lithum and sodium, potassium and sodium, potassium and rubidium, rubidium and cesium have been successfully achieved, in addition to the separation of radioactive cesium from rubidium and from large amounts of other alkali metals and the recovery of individual metals from their mixture. The capacity of the column can be estimated as the amount of solute that the column can retain, but the amount largely depends upon the distribution of the solute in the organic phase. Elution curves of various amounts of metal have been obtained for use in discussing the partition of the metal on the column. A comparison of the distribution ratio obtained in the liquid-liquid extraction with that obtained in the column chromatography has shown that same mechanism holds in both cases. The column efficiency has also been calculated, employing the band width of the elution curves and by using the equation commonly adopted. The distribution ratio varies with the amount of solute placed in the column; the larger the distribution, the smaller the amount. In this experiment, however, the number of the plates of equivalent extraction and the distribution ratio have been found to have a linear relationship; this shows that only the partition phenomenon is predominant in this chromatographic process.

The author is deeply indebted to Professor Toshiyasu Kiba for his kind help and advice.

BULLETIN OF THE CHEMICAL SOCIETY OF JAPAN VOL. 39 597—602 (1966)

An Application of the Quasi Chemical Approximation to the NMR Dilution Shift in Some Binary Mixtures

By Iwao SATAKE, Masujiro ARITA, Hideo KIMIZUKA and Ryohei MATUURA

Department of Chemistry, Faculty of Science, Kyushu University, Hakozaki, Fukuoka

(Received July 23, 1965)

The theoretical NMR dilution curves for the ethanol - carbon tetrachloride, water-acetone and water-dioxane systems have been derived without the assumption of any particular type of H-bonded complexes in the solution. The expressions so derived contain the interchange energies as variable parameters. The use of the appropriate values of interchange energies (a few kilocalories) gives reasonable quantitative fits of the experimental dilution curves over the entire concentration range of the solutions. These values suggest that the strength of hydrogen bonding in the present systems is in the order of: water-water > water-acetone > water-dioxane > ethanol-ethanol.

A number of papers have reported on the concentration dependence of the proton resonance lines in a variety of binary mixtures, and some quantitative treatments have been made for them. Huggins et al.[1] assumed the simple monomer-dimer equilibrium in order to elucidate the dilution curves of several phenol derivatives in the extremely low concentration range and obtained the association constants by using infrared data. Mavel[2] derived the theoretical dilution curves for various kinds of complex formations over the whole concentration range and compared them with the experimental results.

In most of the papers,[3-9] including those of the above authors, the treatments are based on the assumption that there exists an association equilibrium among the particular hydrogen bonded complexes in a given concentration range of the solution. It is, however, unreasonable to assume only the particular types of H-bonded complexes, since no conclusive evidence has yet been obtained for even the existence of such complexes.

From another point of view, the so-called "hydrogen bond" should be regarded as only a kind of intermolecular interaction which has a comparatively large interaction energy—a few kilocalories. In this connection, it is important to examine whether or not the concentration dependence of the proton chemical shifts in the H-bonded systems can be interpreted in terms of the statistical mechanics without the assumption of any particular H-bonded complex in the solution.

The purpose of this paper is to apply the quasi chemical approximation, developed by Guggenheim,[10] to the ethanol - carbon tetrachloride, water-acetone and water-dioxane systems, and to evaluate the dilution curves by means of information on the number of contacts which can be enumerated by Barker's method.[11] Although several reports[4,5,8,12-14] have already been published on these systems, we have chosen them as model systems for the present discussion.

Theoretical

In general, it can be said that the molecules and their functional groups give rise to molecular contacts with appropriate orientations in conformity with their thermodynamic probability. Thus, the protons of the type i, e. g., the hydroxyl proton of water in the water - organic solvent mixture, can be present as various kinds of pairs or of contacts, such as the proton-proton acceptor group of orgainc molecule, the proton-methylene group contact, and so on. The number of these pairs may then be denoted by N_{ij} ($j=1, 2, \cdots$), where j indicates the contact points of the molecule.

In H-bonded systems a single sharp line is usually

1) C. M. Huggins, G. C. Pimentel and J. N. Shoolery, *J. Phys. Chem.*, **60**, 1311 (1956).
2) G. Mavel, *J. Phys. et Radium*, **21**, 37 (1960).
3) C. M. Huggins, G. C. Pimentel and J. N. Shoolery, *J. Chem. Phys.*, **23**, 1244 (1955).
4) J. C. Davis, Jr., K. S. Pitzer and C. N. R. Rao, *J. Phys. Chem.*, **64**, 1744 (1960).
5) J. R. Holmes, D. Kivelson and W. C. Drinkard, *J. Am. Chem. Soc.*, **84**, 4677 (1962).
6) B. B. Haward, C. F. Jumper and M. T. Emerson, *J. Molec. Spec.*, **10**, 117 (1963).
7) R. Kaiser, *Can. J. Chem.*, **41**, 430 (1963).
8) A. Fratiello and D. C. Douglass, *J. Molec. Spec.*, **11**, 465 (1963).
9) A. L. McClellan, S. W. Nicksic and J. C. Guffy, ibid., **11**, 340 (1963).
10) E. A. Guggenheim, "Mixtures," Oxford Univ. Press, Oxford (1952).
11) J. A. Barker, *J. Chem. Phys.*, **20**, 1526 (1952).
12) A. Fratiello and J. P. Luongo, *J. Am. Chem. Soc.*, **85**, 3072 (1963).
13) W. Drinkard and D. Kivelson, *J. Phys. Chem.*, **62**, 1494 (1958).
14) E. D. Becker, U. Liddel and J. N. Shoolery, *J. Molec. Spec.*, **2**, 1 (1958).

observed for the protons under consideration because of a rapid exchange among the various types of protons present in the solution. In this case the chemical shift, δ_i, for the protons of the type i is known to be given by the weighted average of each contribution;

$$\delta_i = \sum_j N_{ij}\cdot\delta_{ij}/\sum_j N_{ij} \tag{1}$$

where δ_{ij} denotes the chemical shift for the protons of the type i in the i-j pairs. As may be seen in Eq. 1, the chemical shifts, as well as the proton fraction for each state, must be known in order to obtain the theoretical dilution curve for the H-bonded system.

Consider the mixture consisting of molecules of the types A, B,$\cdots$ arranged on a Z-coordinated lattice. For the numbers of N_{ij}^{AB} pairs, which are formed by the contacts between the i-th class of contact points of the A molecule $\binom{A}{i}$ and the j-th one of the B molecule $\binom{B}{j}$, we have:

$$2N_{ii}^{AA} + \sum_{B,j} N_{ij}^{AB} = Q_i^A\cdot N_A \tag{2}$$

and the quasi chemical equation:

$$(N_{ij}^{AB})^2 = 4\cdot N_{ii}^{AA}\cdot N_{jj}^{BB}\cdot\exp(-U_{ij}^{AB}/\boldsymbol{k}T) \tag{3}$$

where Q_i^A denotes the number of the contact points in the i-th class of the A molecule; N_A, the number of the A molecule, and U_{ij}^{AB}, the interchange energy per pair for the i-j contact.

By introducing the parameters[11]:

$$\eta_{ij}^{AB} = \exp(-U_{ij}^{AB}/\boldsymbol{k}T) = \eta_{ji}^{BA} = \eta_{ij} \tag{4}$$

and:

$$X_i^A = (N_{ii}^{AA}/N)^{1/2} \tag{5a}$$

$$X_j^B = (N_{jj}^{BB}/N)^{1/2} \tag{5b}$$

where N denotes the total number of molecules in the system, we have:

$$N_{ij}^{AB} = 2\cdot X_i^A\cdot X_j^B\eta_{ij}\cdot N \quad \text{for } \binom{A}{i} \neq \binom{B}{j} \tag{6a}$$

$$= (X_i^A)^2\cdot N \quad \text{for } \binom{A}{i} = \binom{B}{j} \tag{6b}$$

and;

$$X_i^A\sum_{B,j}\eta_{ij}X_j^B = Q_i^A x_A/2 \tag{7a}$$

$$X_j^B\sum_{A,i}\eta_{ij}X_i^A = Q_j^B x_B/2 \tag{7b}$$

where x_A and x_B denote the mole fraction of the A molecule and that of the B molecule respectively. Assuming appropriate models with reasonable values of Q_i^A's, the values of N_{ij}^{AB} can be estimated according to Eqs. 6a, 6b, 7a and 7b, provided that the values of the η_{ij}'s are known. Then the theoretical dilution curve can be obtained according to Eq. 1, provided that the δ_{ij}'s are known.

1) The Ethanol - Carbon Tetrachloride System.—We will start with the assumptions for the lattice model and molecular geometries; 1) From the approximate ratio of the molecular volume of ethanol to carbon tetrachloride, it is most reasonable to regard the ethanol molecule as a trimer and the carbon tetrachloride molecule as a pentamer. 2) We assume that each lattice point has four nearest neighbors; that is, $Z=4$. Then the number of contact points of ethanol is 8, and that of carbon tetrachloride is 12.

$$C_2H_5OH \quad r_e = 3, \quad Q_H^e = 1, \quad Q_O^e = 2, \quad Q_I^e = 5$$

$$CCl_4 \quad r_s = 5, \quad Q_s = 12$$

where the subscripts e and s refer to ethanol and carbon tetrachloride molecules respectively. Q_H^e, Q_O^e and Q_I^e denote the number of contact points of the hydroxyl hydrogen, hydroxyl oxygen and hydrocarbon parts of the ethanol molecule respectively. Further, it is necessary to assign the energy of interaction for each possible contact. The interchange energies among the equivalent contact points are zero by definition. The values of U_{OS}, U_{IS} and U_{HS} are considered to be so small, as compared with U_{HO}, that we may take them to be zero without serious error. The value of U_{HO} was determined so as to give the best fit of the NMR data.

On this simplification, Eqs. 7a and 7b may be written as:

$$\left.\begin{aligned} X_H(X_H+\eta X_O+X_I+X_S) &= x_e/2 \\ X_O(\eta X_H+X_O+X_I+X_S) &= x_e \\ X_I(X_H+X_O+X_I+X_S) &= 5x_e/2 \\ X_S(X_H+X_O+X_I+X_S) &= 6x_s = 6(1-x_e) \end{aligned}\right\} \tag{8}$$

where x_e is the mole fraction of ethanol and where $\eta = \exp(-U_{HO}/\boldsymbol{k}T)$.

The solutions of Eq. 8 can now be obtained by the convenient method described by Barker.[11] By the substitutions of the variables:

$$X_H = CY_1, \quad X_O = CY_2, \quad X_I = CY_3, \quad X_S = CY_4,$$
$$Y_1 = 1, \quad Y_2 = \alpha$$

Eq. 8 may be rewritten as:

$$\left.\begin{aligned} C^2(1+\alpha\eta+Y_3+Y_4) &= x_e/2 \\ C^2\alpha(\eta+\alpha+Y_3+Y_4) &= x_e \\ C^2Y_3(1+\alpha+Y_3+Y_4) &= 5x_e/2 \\ C^2Y_4(1+\alpha+Y_3+Y_4) &= 6x_s \end{aligned}\right\} \tag{9}$$

The solutions of Eq. 9 are given as:

$$\left.\begin{aligned} &Y_1 = 1, \quad Y_2 = \alpha, \quad Y_3 = 5(\alpha-1), \\ &Y_4 = [(2+\alpha\eta-\alpha^2)/(\alpha-2)] - Y_3 \end{aligned}\right\} \tag{10}$$

and:

$$C^2 = 6/[Y_4(1+\alpha+Y_3+Y_4) + 12(1+\alpha\eta+Y_3+Y_4)] \tag{11}$$

Any solution of Eq. 9 then serves to determine the mole fraction, x_e, as the function of α and η.

$$x_e = 12(\alpha-1)(\alpha-2)/[6\alpha^2+\alpha(\eta-21)+16] \quad (12)$$

The variable range of α is $2<\alpha<t$, where:

$$t = [(\eta+15)+\{(\eta+15)^2-192\}^{1/2}]/12 \quad (13)$$

By using Eqs. from 10 to 13, the numerical value of each number of possible contacts occurring in the ethanol - carbon tetrachloride mixture may be easily determined as a function of the concentration, provided the appropriate value of η is taken.

The hydroxyl protons participating in the rapid exchange among ethanol molecules may be classified into two groups from the electronic environmental point of view. To the first group are assigned the protons which participate in the (H-H), (H-I) and (H-S) contacts, and to the second, the H-bonded protons which participate in the (H-O) contacts. The chemical shifts of hydroxyl protons assigned to the first group are different from each other. However, we assign the same value of chemical shift, δ_F, to the protons for the (H-H), (H-I) and (H-S) contacts, since the differences among them may be considered to be fairly small.

The total number of hydroxyl protons in the mixture is $2(X_H^2+X_HX_I+\eta X_HX_O+X_HX_S)$. The number of protons assigned to the first group is $2(X_H^2+X_HX_I+X_HX_S)$, while the number assigned to the second is $2\eta X_HX_O$. If we denote the chemical shift of H-bonded protons as δ_B, the chemical shift of the –OH proton at a given concentration may be written as:

$$\begin{aligned}\delta &= [(X_H^2+X_HX_I+X_HX_S)\delta_F + \eta X_HX_O\delta_B]/\\ &\quad (X_H^2+X_HX_I+\eta X_HX_O+X_HX_S)\\ &= \delta_F + \alpha\eta(\delta_B-\delta_F)/(1+\alpha\eta+Y_3+Y_4) \quad (14)\end{aligned}$$

The substitution of Eq. 10 into Eq. 14 gives the simplified expression for δ; that is;

$$\delta = \delta_F + (\alpha-2)(\delta_B-\delta_F)\eta/(\alpha-1)(\eta-1) \quad (15)$$

Equation 15 gives the chemical shift, δ, of the –OH proton as the function of the parameter α, which is combined with the analytical mole fraction, x_e, through Eq. 12, and the unknown parameters, δ_F, δ_B and η. However, the parameters δ_F and δ_B can be eliminated from Eq. 15 by the use of boundary condition; i. e.,

$$\begin{aligned}&x_e \to 0 \qquad \alpha \to 2 \qquad \delta \to \delta_0\\ &x_e \to 1 \qquad \alpha \to t \qquad \delta \to \delta_1\end{aligned}$$

Here δ_0 is the limiting value of δ which corresponds to the chemical shift of the –OH proton extrapolated to infinite dilution, while δ_1 is the chemical shift of pure ethanol. It follows from Eq. 15 that:

$$\delta_F = \delta_0 \quad (16)$$

and that:

$$\delta_B = \delta_0 + (t-1)(\eta-1)(\delta_1-\delta_0)/\eta(t-2) \quad (17)$$

By the substitution of Eqs. 16 and 17 into Eq. 15, the final expression of the dilution curve is obtained:

$$\delta = \delta_0 + (\alpha-2)(t-1)(\delta_1-\delta_0)/(\alpha-1)(t-2) \quad (18)$$

In Eq. 18, the unknown parameter used to evaluate the value of t is η. The value of η must be determined so as to give the best fit of the observed chemical shifts.

2) The Water-Acetone System.—The elucidation of the dilution curve for water-acetone system is rather complicated, since there are two types of hydrogen bonds in solution. The molecular parameters assumed for this system are:

$$\begin{aligned}&H_2O \qquad r_w = 1 \qquad Q_H^W = 2 \qquad Q_O^W = 2\\ &(CH_3)_2CO \qquad r_a = 3 \qquad Q_H^A = 6 \qquad Q_O^A = 2\end{aligned}$$

and $Z=4$. Further, it is assumed that all of the interchange energies except U_{OH}^{WW} and U_{HO}^{WA} may be ignored. On the basis of these simplifications, two parameters,

$$\eta_1 = \exp(-U_{OH}^{WW}/\boldsymbol{k}T)$$

and

$$\eta_2 = \exp(-U_{HO}^{WA}/\boldsymbol{k}T)$$

are left to be determined. Taking the abbreviations $X_H^W=X_1$, $X_O^W=X_2$, $X_H^A=X_3$ and $X_O^A=X_4$, Eqs. 7a and 7b can be written in this form:

$$\left.\begin{aligned}&X_1(X_1+\eta_1X_2+X_3+\eta_2X_4) = x_w\\ &X_2(\eta_1X_1+X_2+X_3+X_4) = x_w\\ &X_3(X_1+X_2+X_3+X_4) = 3x_a = 3(1-x_w)\\ &X_4(\eta_2X_1+X_2+X_3+X_4) = x_a\end{aligned}\right\} \quad (19)$$

By substitutions of variables similar to those made in Sec. 1, the solutions of Eq. 19 may be easily obtained as follows:

$$\begin{aligned}&Y_1=1, \quad Y_2=\alpha, \quad Y_3=3(\alpha-1)(\eta_2+1)/(\eta_2-4\alpha+3)\\ &Y_4=2(\alpha-1)(2\alpha-1)/(\eta_2-4\alpha+3)\\ &C^2=1/[Y_4(\eta_2+\alpha+Y_3+Y_4)+(1+\alpha\eta_1+Y_3+\eta_2Y_4)]\end{aligned}$$

where the variable range of α is $1<\alpha<(\eta_2+3)/4$. The mole fraction of water, x_w, can be obtained by any one of the equations in Eq. 19.

Now, the states of the water protons in the solution may be classified into three groups. To the first are assigned the protons which come in contact with the hydroxyl proton of water or the methyl proton of acetone molecules. Their chemical shift is denoted by δ_F. To the second are assigned the protons which participate in the H-bond between the H and O atoms of water molecules. Their chemical shift is δ_W. To the third are assigned the protons which participate in the H-bond between the H atom of water and the O atom of acetone. Their chemical shift is δ_C. The chemical shift of the water proton at a given concentration is given as:

$$\delta = [(1+Y_3)\delta_F+\eta_2 Y_4\delta_C+\alpha\eta_1\delta_W]/(1+\alpha\eta_1+Y_3+\eta_2 Y_4) \quad (20)$$

By the use of boundary conditions, the unknown parameters, δ_W and δ_C, in Eq. 20 may be represented in terms of the chemical shift of pure water, δ_1, and that extrapolated to $x_w=0$, δ_0, i. e.:

$$x_w \to 1 \qquad \alpha \to 1 \qquad \delta \to \delta_1$$
$$x_w \to 0 \qquad \alpha \to (\eta_2+3)/4 \qquad \delta \to \delta_0$$

It follows, therefore, from Eq. 20 that:

$$\eta_1\delta_W = (1+\eta_1)\delta_1 - \delta_F \quad (21)$$

and that:

$$\eta_2\delta_C = (\eta_2+3)\delta_0 - 3\delta_F \quad (22)$$

The substitution of Eqs. 21 and 22 into Eq. 20 gives the final expression of δ for the water-acetone system:

$$\delta = [(1+Y_3-\alpha-3Y_4)\delta_F + \alpha(1+\eta_1)\delta_1 + Y_4(\eta_2+3)\delta_0]/(1+\alpha\eta_1+Y_3+\eta_2 Y_4) \quad (23)$$

Equation 23 contains three unknown parameters, δ_F, η_1 and η_2; the latter two must be estimated so as to give the best fit of the NMR data. If the protons in the first group can be assumed to be equivalent to the gaseous state, the chemical shift of the water vapor may be used in place of δ_F.

3) The Water-Dioxane System.—The molecular parameters assumed for the water-dioxane system are:

Water $\quad Q_H^W = 2 \quad Q_O^W = 2$

Dioxane $\quad Q_H^D = 10 \quad Q_O^D = 4$

and $Z=4$. We also assume that all of the interchange energies except U_{HO}^{WW} and U_{HO}^{WD} are negligibly The parameters to be determined are, then:

$$\eta_1 = \exp(-U_{HO}^{WW}/kT)$$

and:

$$\eta_2 = \exp(-U_{HO}^{WD}/kT)$$

By the same mathematical treatment as in Sec. 2, the theoretical dilution curve for the water-dioxane system may be derived as:

$$\delta = [(1+Y_3-\alpha-5Y_4/2)\delta_F + \alpha(1+\eta_1)\delta_1 + Y_4(\eta_2+5/2)\delta_0]/(1+\alpha\eta_1+Y_3+\eta_2 Y_4) \quad (24)$$

where:

$$Y_3 = 5(\alpha-1)(\eta_2+1)/(2\eta_2-7\alpha+5)$$
$$Y_4 = (7\alpha-3)(\alpha-1)/(2\eta_2-7\alpha+5)$$
$$1<\alpha<(2\eta_2+5)/7$$

Experimental

In the present experiment, the chemical shifts of the water proton in the water-acetone and water - 1, 4-dioxane mixtures were measured as a function of the composition (the concentration in mole fraction) of the mixture. The mixtures were prepared gravimetrically from the purified materials. Acetone was distilled twice with calcium sulfate, and 1, 4-dioxane, with metallic sodium, in order to remove traces of water. Water was distilled twice from the alkaline potassium permanganate solution.

The NMR shifts were obtained by using a Japan Electron Optics High Resolution NMR Spectrometer, JNM-3, operating at 40 Mc. The line separations were measured by the side-band technique, using cyclohexane as an external reference. The shifts were measured to an accuracy of ± 0.4 c. p. s., and each shift was corrected for the difference in the bulk diamagnetic susceptibilities of the reference and the solution.

Results and Discussion

In the present study, we applied Eq. 18 to the dilution curve of ethanol in carbon tetrachloride reported by Becker et al.[14] In Fig. 1, the chemical shift of the OH proton in the ethanol - carbon tetrachloride system determined by them is replotted against the concentration of ethanol. The

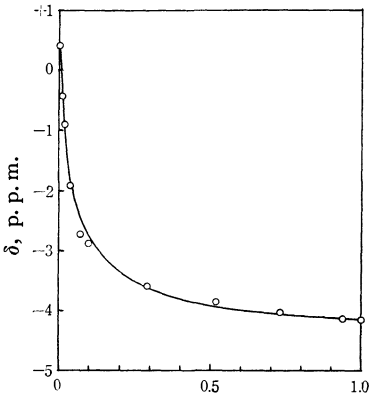

Fig. 1. The dilution curve of OH proton signal in C_2H_5OH—CCl_4 system at 27°C. The chemical shifts are referred to the central peak of the CH_3 triplet in ethanol.
○ Observed[14]
— Calculated from Eq. 18 with $\eta=180$.

most reliable value of η was found to be 180, corresponding to the interchange energy, U_{HO}, of about -3090 cal./mol. bonds at 27°C. The results calculated over the entire concentration range of ethanol is illustrated by the solid line in Fig. 1. Although slight deviations from the experimental values could not be eliminated, the agreement between the calculated and experimental curves is almost entirely satisfactory. Liddel and Becker[15] obtained 3.6 ± 0.8 kcal./mol. for the H-bond energy of this system on the basis of their infrared spectroscopic measurements.

15) U. Liddel and E. D. Becker, *Spectrochim. Acta*, **10**, 70 (1957).

The chemical shifts of water protons in water-acetone and water-dioxane mixtures, with reference to cyclohexane, at various concentrations x_w (mole fraction of water), are summarized in Table I.

Table I. Chemical shifts of water in the water-acetone mixture at 25°C and in the water-dioxane mixture at 35°C

Water-Acetone		Water-Dioxane	
x_w	$-\delta$, p.p.m.	x_w	$-\delta$, p.p.m.
0.020	1.415	0.068	1.168
0.050	1.521	0.102	1.314
0.100	1.668	0.145	1.459
0.149	1.823	0.190	1.607
0.197	1.961	0.237	1.747
0.249	2.100	0.295	1.929
0.296	2.198	0.342	2.026
0.315	2.270	0.393	2.129
0.391	2.384	0.493	2.332
0.486	2.607	0.595	2.531
0.605	2.765	0.693	2.729
0.703	2.910	0.795	2.934
0.805	3.090	0.898	3.154
0.904	3.258	1.000	3.360
1.000	3.391		

The concentration dependences of the water signals are also represented in Figs. 2 and 3. On applying Eqs. 23 and 24 to the water-acetone and water-dioxane systems respectively, we have used the value of +0.603 p.p.m. for δ_F, which has been determined by Schneider et al.[16] We have used the values, of −1.31 p. p. m. for δ_0 in Eq. 23 and −0.76 p. p. m. for that in Eq. 24, which have been determined by the extrapolation of the experimental dilution curves. The value of δ_0 for the water-acetone system agrees well with that (−1.308 p. p. m.) determined by Holmes et al.[5] The theoretical dilution curve calculated from Eq. 23 is given by the solid line in Fig. 2, and that calculated from Eq. 24, in Fig. 3. For the water-acetone system, the most reliable set of η_1 and η_2 vaules are found to be 1200 for η_1 and 500 for η_2; these values correspond to the interchange energies of −4200 and −3680 cal./mol. bonds respectively at 25°C. For the water-dioxane system, we find that $\eta_1=1300$ and $\eta_2=200$, corresponding to the interchange energies of −4400 and −3200 cal./mol. bonds respectively at 35°C.

Although the present treatment is an approximate one in nature, the agreement between calculated and experimental dilution curves seems almost entirely satisfactory over nearly all the concentration range. The slight deviations observed may be ascribed to the assumptions included in these treatments. The thermodynamic properties of hydrogen bonds have been determined by a number of authors, and the results have been summarized by Pimentel and McClellan.[17] However, the

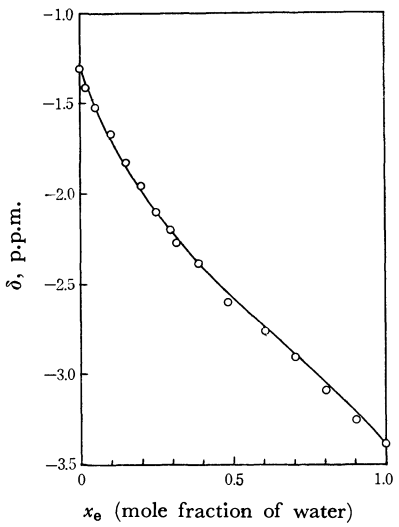

Fig. 2. The dilution curve of H_2O proton signal in H_2O—$(CH_3)_2CO$ system at 25°C. The chemical shifts are referred to the cyclohexane.
○ Observed
— Calculated from Eq. 23 with a set of $\eta_1=1200$ and $\eta_2=500$.

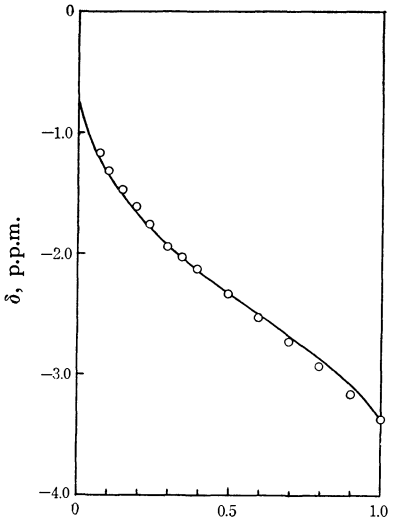

Fig. 3. The dilution curve of H_2O proton signal in H_2O-$C_4H_8O_2$ system at 35°C. The chemical shifts are referred to the cyclohexane.
○ Observed
— Calculated from Eq. 24 with a set of $\eta_1=1300$ and $\eta_2=200$.

16) W. G. Schneider, H. J. Bernstein and J. A. Pople, *J. Chem. Phys.*, **28**, 601 (1958).

17) G. C. Pimentel and A. L. McClellan, "The Hydrogen Bond," W. H. Freeman and Company, San Francisco and London (1960).

interchange energies obtained above are not directly comparable with them because of the considerable scattering of ΔH values. The values of the interchange energies obtained from the present discussion are in the order of H_2O-H_2O > H_2O-$(CH_3)_2CO$ > H_2O-$C_4H_8O_2$ > C_2H_5OH-C_2H_5OH, indicating that the strength of hydrogen bonding is in this order.

Summary

The generalized quasi-chemical approximation has been applied to the ethanol - carbon tetrachloride, water-acetone and water-dioxane systems for the elucidation of NMR dilution curves. The theoretical dilution curves can be derived as the function of the interchange energies and the proton fraction by assuming appropriate molecular models. The values of the interchange energies were determined so as to give the best fit of NMR data. The most reliable set of interchange energies so determined were −3090 cal./mol. bonds at 27°C for the ethanol - carbon tetrachloride system, −4200 and −3680 cal./mol. bonds at 25°C for the water-acetone system and −4400 and −3200 cal./mol. bonds at 35°C for the water-dioxane system. The agreements between the calculated and experimental dilution curves were almost entirely satisfactory over the entire concentration range. On the basis of the values of the interchange energies obtained in the present study, the strength of hydrogen bonding was found to be in the order of water-water > water-acetone > water-dioxane > ethanol-ethanol.

BULLETIN OF THE CHEMICAL SOCIETY OF JAPAN VOL. 39 602—604 (1966)

Studies of *C*-Substituted Tartaric Acid. I. The Preparation of Optically Active 2-Methyltartaric and 2, 3-Dimethyltartaric Acid

By Susumu TATSUMI, Yoshiharu IZUMI, Masami IMAIDA, Yoshio FUKUDA and Shiro AKABORI

Division of Organic Chemistry, Institute for Protein Research, Osaka University, Kita-ku, Osaka

(Received July 26, 1965)

Two racemic forms of 2-methyltartaric acid were prepared, and their optical resolutions were performed. Four optically active isomers were obtained. 2, 3-Dimethyltartaric acid was also prepared and separated into two isomeric optically inactive forms. The isomer with the higher melting point could be resolved into two optically active isomers, but the other, with the lower melting point, could not. The former was, therefore, assigned to the racemic configuration, and the latter, to the meso configuration.

Optically active 2-methyltartaric and 2, 3-dimethyltartaric acid are interesting substances to study from the stereochemical point of view in their relation to tartaric acid. Moreover, in a previous publication[1] from our laboratory, it was reported that a Raney nickel catalyst treated with aqueous solutions of these optically active hydroxy carboxylic acids has an asymmetric hydrogenation activity in the hydrogenation of methyl acetoacetate to methyl 3-hydroxybutyrate, and that an especially high asymmetric activity is obtained with optically active 2-methyltartaric acid (B) under optimum conditions. However, preparations of optically active 2-methyltartaric and 2, 3-dimethyltartaric acid have never been described.

In the present work, optically active 2-methyltartaric and 2, 3-dimethyltartaric acid will be prepared.

The two racemic forms of 2-methyltartaric acid (I), the melting points of which are 146°C (Ia) and 161°C (Ib), were prepared from ethyl α-acetoxyacetoacetate by a modification of Schmidt's procedure,[2] and their optical resolutions were performed with brucine by the method of the differential solubility of the diastereomers in water. The optical rotation values of the four isomers were as follows:

(A) From the racemic form with the lower melting point (2-methyltartaric acid A)···(Ia):

(+) isomer $[\alpha]_D^{20}$ +8.90° (*c* 3.7, water)

(−) isomer $[\alpha]_D^{20}$ −8.94° (*c* 3.7, water)

(B) From the racemic form with the higher melting point (2-methyltartaric acid B)···(Ib):

(+) isomer $[\alpha]_D^{20}$ +5.88° (*c* 3.2, water)

(−) isomer $[\alpha]_D^{20}$ −5.60° (*c* 3.2, water)

1) Y. Izumi, S. Tatsumi, M. Imaida, Y. Fukuda and S. Akabori, This Bulletin, in press.

2) O. T. Schmidt and W. Perkow, *Chem. Ber.*, **83**, 484 (1950).

2, 3-Dimethyltartaric acid (II) has two optically inactive modifications, the meso (IIa) and the racemic forms (IIb). This acid was synthesized from diacetyl and hydrogen cyanide, and the separation into two components, the meso and racemic form, was performed by means of the differential solubility of their barium salts in water. The melting points of the free meso and racemic acid are 180 and 187°C respectively. The optical resolution of the racemic form was performed in an aqueous solution with brucine, and the optical rotation values of the two isomers were as follows:

(+) isomer $[\alpha]_D^{20}$ +13.4° (*c* 4.0, water)

(−) isomer $[\alpha]_D^{20}$ −13.4° (*c* 4.0, water)

Experimental*

The Preparation of 2-Methyltartaric Acid (I) and Separation into Two Racemic Forms (Ia and Ib).—A mixture of 28.2 g. of ethyl α-acetoxyacetoacetate in 100 ml. of ethanol and 13 g. of potassium cyanide in 50 ml. of water was cooled to 0—5°C in an ice water bath; 200 ml. of N hydrochloric acid was then vigorously stirred, drop by drop, into the mixture. The flask was tightly stoppered, and the mixture was warmed in a water bath at 50—60°C for 4 hr. and then left to stand overnight at room temperature. After the reaction mixture had been cooled in an ice water bath, it was poured into 400 ml. of concentrated hydrochloric acid; the mixture was then allowed to stand for two days. The acidic solution was refluxed for an hour and concentrated in vacuo. During the concentration inorganic salts were removed by filtration. The residue was dissolved in a small amount of water and concentrated again in vacuo.

In order to remove the free hydrochloric acid, the above operation was then repeated. The residual syrup was taken up in 150 ml. of water and decolorized with charcoal; when it was neutralized with a 3% barium hydroxide solution, a great deal of the barium salt of Ia was precipitated. After it had been stored overnight in a refrigerator, the salt was collected by filtration, washed several times with hot water, and dried in air at 80°C. Yield, 15 g. The salt was dissolved in 50 ml. of N hydrochloric acid, and the resulting solution was then evaporated to dryness in vacuo. The residue was extracted with four 20-ml. portions of acetone. The acetone extracts were combined and evaporated to a syrup. The syrupy product was cooled and crystallized by the addition of a small amount of petroleum ether. Recrystallization from dry ethyl acetate gave pure, white, crystalline Ia. Yield, 5.5 g. M. p. 146°C.

Found: C, 36.73; H, 4.89. Calcd. for $C_5H_8O_6$: C, 36.59; H, 4.91%.

The mother liquor of the barium salt of Ia was concentrated to half its volume and then left to stand for 2 hr. in an ice box. A small amount of crystalline precipitate was filtered off, and the filtrate was treated with 10 ml. of 6 N hydrochloric acid and then evaporated to dryness. The residue was extracted with acetone and then treated as above.

In this way, four grams of white crystalline Ib were obtained. M. p. 161°C.

Found: C, 36.53; H, 4.93. Calcd. for $C_5H_8O_6$: C, 36.59; H, 4.91%.

The Optical Resolution of Ia.—Forty-nine grams of Ia and 118 g. of brucine were dissolved in 1000 ml. of boiling water; the resulting solution was allowed to stand overnight in a refrigerator. The needle-like crystals of the brucine salt which precipitated were collected by filtration; six recrystallizations of this salt from ten parts of boiling water gave 61 g. of the pure brucine salt of Ia. M. p. 236—237°C, $[\alpha]_D^{20}$ −21.9° (*c* 0.4, in water). This salt was then suspended in 100 ml. of cold water and decomposed with 225 ml. of a N sodium hydroxide solution. The precipitated brucine was removed by filtration, and the alkaline filtrate was washed twice with 50 ml. of chlorofoum, neutralized with 20 ml. of concentrated hydrochloric acid, and then evaporated to a syrup. To the residual syrup a small amount of water was added, and the resulting solution was decolorized with charcoal and evaporated to dryness in order to remove the free hydrochloric acid. The residue was extracted several times with 20 ml. of acetone. These acetone extracts were then combined and evaporated to a syrup. The syrupy product was dried over sulfuric acid in a vacuum desiccator. In this way, white, hygroscopic crystals of (−)-Ia were obtained. Recrystallization from dry ethyl acetate gave 14.9 g. of optically pure (−)-Ia. M. p. 115—116°C, $[\alpha]_D^{20}$ −8.94° (*c* 3.7, water).

Found: C, 36.53; H, 5.02. Calcd. for $C_5H_8O_6$: C, 36.59; H, 4.91%.

The mother liquor of the brucine salt of (−)-Ia was concentrated to a paste. After it had been stood for a week in a refrigerator, the brucine salt of (+)-Ia was collected. Optically pure (+)-Ia was obtained from this salt by the procedure described above. Yield, 8.0 g. M. p. 115°C, $[\alpha]_D^{20}$ +8.90° (*c* 3.7, water).

Found: C, 36.57; H, 4.94. Calcd. for $C_5H_8O_6$: C, 36.59; H, 4.91%.

The Optical Resolution of Ib.—Thirty-eight grams of Ib and 91.5 g. of brucine were dissolved in 1000 ml. of boiling water, and the resulting solution was treated as in the resolution of Ia. Forty grams of the pure brucine salt of (+)-Ib were, thus obtained. M. p. 234—235°C, $[\alpha]_D^{20}$ −16.5° (*c* 0.4, water). When the brucine salt was decomposed with alkali, 8.2 g. of optically pure (+)-Ib were obtained. M. p. 130—131°C, $[\alpha]_D^{20}$ +5.88° (*c* 3.2, water).

Found: C, 36.53; H, 4.88. Calcd. for $C_5H_8O_6$: C, 36.59; H, 4.91%.

From the mother liquor of the brucine salt of (+)-Ib, 5.1 g. of optically acitive (−)-Ib were obtained by the procedures described above. M. p. 129°C, $[\alpha]_D^{20}$ −5.60° (*c* 3.2, water).

Found: C, 36.63; H, 4.79. Calcd. for $C_5H_8O_6$: C, 36.59; H, 4.91%.

The Preparation of 2, 3-Dimethyltartaric Acid (II) and Its Separation into Meso (IIa) and Racemic Forms (IIb).—Into a solution of 520 g. of sodium cyanide in 1000 ml. of water, 800 ml. of concentrated hydrochloric acid was stirred vigorously, drop by drop, below 15°C in a hood. After the addition of hydrochloric acid, 74 ml. of a 20% aqueous potassium carbonate solution was added slowly. Then 344 ml. of diacetyl was stirred in drop by drop under sufficient

* All melting points are uncorrected.

cooling, and the reaction mixture was maintained at 15—20°C for 2 hr. Then 2.4 l. of concentrated hydrochloric acid were added cautiously (the temperature of the solution rose up to 40°C with foaming). After the reaction mixture had been kept at room temperature overnight, it was refluxed for 7 hr. Inorganic salt and tar were removed by suction from the cooled hydrolyzed solution, and the filtrate was concentrated to about 800 ml. in vacuo. On the addition of 300 ml. of acetone, inorganic salt was precipitated; this was filtered off, and the solution was concentrated again. The above treatment was repeated several times in order to remove the inorganic salts, and the residual syrup was dissolved in 1.5 l. of ethanol and was esterified with blowing dry hydrogen chloride gas into the solution. The alcohol was distilled off in vacuo, and the diethyl ester of II was collected at 110—115°C (4 mmHg). Yield, 240 g.

Two hundred and forty grams of diethyl ester were refluxed with 1000 ml. of 10% hydrochloric acid for 5 hr. The hydrolyzate was decolorized with charcoal and then concentrated to a syrup. The syrupy residue was taken up in 200 ml. of water and concentrated again. The above treatment was repeated in order to remove the free hydrochloric acid, and then the residue was dissolved in 2 l. of water and neutralized slowly to pH 5.0 with a barium hydroxide solution. A great deal of the barium salt of IIa was immediately precipitated. The barium salt was collected by suction, washed with a large quantity of hot water, and dried in air at 80°C. Yield, 160 g. When the mother liquor of the barium salt of IIa was adjusted to pH 8.0, a small amount of an additional salt appeared; this was removed by filtration. The filtrate was concentrated in vacuo, and the barium salt of IIb precipitating from the solution was collected successively by suction. It was washed with a small amount of water and dried in air at 80°C. Yield, 120 g.

IIa and IIb from their barium salts were prepared essentially as described in the preceding paragraph.

From 160 g. of the barium salt of IIa, 70 g. of IIa were obtained. M. p. 180°C.

Found: C, 40.31; H, 5.64. Calcd. for $C_6H_{10}O_6$: C, 40.45; H, 5.66%.

Similarly from 120 g. of the barium salt of IIb, 53 g. of IIb were obtained. M. p. 187°C.

Found: C, 41.00; H, 5.60. Calcd. for $C_6H_{10}O_6$: C, 40.45; H, 5.66%.

The Optical Resolution of IIb.—Sixty grams of IIb and 145 g. of brucine dihydrate were dissolved in 1300 ml. of boiling water. The resulting solution was treated by the method described for the resolution of Ia; 15.5 g. of optically pure (+)-IIb were thus obtained. M. p. 158°C, $[\alpha]_D^{20}$ +13.4° (*c* 4.0, water).

Found: C, 40.72; H, 5.60. Calcd. for $C_6H_{10}O_6$: C, 40.45; H, 5.66%.

From the mother liquor of the brucine salt of (+)-IIb, 13 g. of optically pure (−)-IIb were obtained. M. p. 160°C, $[\alpha]_D^{20}$ −13.4° (*c* 4.0, water).

Found: C, 40.38: H, 5.43. Calcd. for $C_6H_{10}O_6$: C, 40.45; H, 5.66%.

Summary

1) The optical resolutions of the two racemic forms of 2-methyltartaric acid, the melting points of which are 146 and 161°C, were performed using brucine as a resolving reagent; four optically active isomers were obtained.

2) 2, 3-Dimethyltartaric acid was prepared from diacetyl and hydrogen cyanide and was separated into meso (m. p. 180°C) and racemic forms (m. p. 187°C); the racemic form was then resolved into two optically active isomers.

The authors wish to express their thanks to Miss Kikue Koike and Miss Masako Kawakita of this Institute for performing the elemental analyses. This research was made possible by support from the Kawaken Fine Chemicals Co., Ltd., Tokyo, and the Ajinomoto Co., Inc., Tokyo.

BULLETIN OF THE CHEMICAL SOCIETY OF JAPAN VOL. 39 604—608 (1966)

Metal Complexes of Amino Acids. II.[1] The Absorption Spectra of Geometrical Isomers of Copper(II) Complexes

By Takaji YASUI and Yoichi SHIMURA

Department of Chemistry, Faculty of Science, Osaka University, Toyonaka, Osaka

(Received July 28, 1965)

The geometrical structures of bis(α-amino-acidato)copper(II) complexes have been determined from the data of diffuse reflectance spectra (α-amino-acid = glycine, L- and DL-α-alanine, L- and DL-valine, L- and DL-threonine, L- and DL-isoleucine and α-aminoisobutyric acid). It has been shown that pairs of cis(N) and trans(N) isomers exist in glycinato and valinato complexes. It has been clarified that the other amino-acidato complexes studied exist either only in the cis(N) form or only in the trans(N) form; that is, the needle and the scaly complexes of DL-alanine, the complexes of DL- and L-threonine, and the complex of α-aminoisobutyric acid exist only in the trans(N) form, while the complexes of L- and DL-isoleucine exist only in the cis(N) form.

1) Part I of this series: T. Yasui, This Bulletin, 38, 1746 (1965).

The well-known bright-blue crystal of copper(II) glycinate has been shown through X-ray analyses[2] to consist of the bis(glycinato)copper(II) complex, which has a cis(N) configuration involving the two nitrogen atoms of the two coplanar glycinate ligands. The other bluish-violet isomer of bis-(glycinato)copper(II) had been discovered by Mauthner and Suida[3]; it has been assumed to be the trans(N) isomer from a comparison of its infrared absorption spectrum with those of the corresponding trans isomers of bis(glycinato)platinum-(II) and -palladium(II).[4]

For other amino acids, however, no pair of the cis and trans isomers of a copper(II) complex has been known. All copper(II) amino-acid complexes the structures of which were determined by X-ray analysis, had the trans configuration except for the above-mentioned cis glycinato complex. Recently Hooper et al.[5] suggested, from their infrared study, that bis(DL-isoleucinato)copper(II) monohydrate has the cis structure. One of the purposes of the present investigation is to explore other pairs of the cis-trans isomers of copper(II) complexes.

We have shown already by a circular dichroism study[1,6] that a broad visible d→d absorption band of the bis(amino-acidato)copper(II) complex consists of four split components. The difference in symmetry between the cis and the trans isomers will be reflected in the behavior of the d→d absorption bands. In the present paper, the diffuse reflectance spectra of the powdered copper(II) complexes in the region from the near infrared to visible will be reported on, and the geometrical configurations of the complexes will be discussed.

Experimental

Measurement.—The measurements of diffuse reflectance spectra were made by a Hitachi EPU-2A spectrophotometer with a diffuse reflectance attachment. The samples were prepared by grinding the complexes as finely as possible in a porcelain mortar and then in an agatic one until no change appeared in the intensity of the spectra. Magnesium oxide was employed as the reference.

Materials.—The copper(II) complexes with amino acids and with amino acid derivatives were prepared from copper(II) hydroxide by a method similar to that of Abderhalden and Schnitzler.[7]

The *cis*-bis(glycinato)copper(II) complex and the bis(amino-acidato)copper(II) complexes of DL- and L-alanine, DL- and L-valine, DL- and L-threonine, DL-α-amino-*n*-butyric acid, and α-aminoisobutyric acid were recrystallized from aqueous alcohol. The bluish-violet glycine complex was obtained by the method of Mauthner and Suida,[3] and the scaly crystals of the DL-alanine complex by following the directions of Gol'braikh.[8]

Table I. Chemical analyses of the complexes

Complex*	C, %		H, %		N, %		H_2O, %	
	Found	Calcd.	Found	Calcd.	Found	Calcd.	Found	Calcd.
cis-[Cu gly_2]·H_2O	23.04	22.70	3.78	3.80	13.37	13.24	7.58	7.84
[Cu gly_2]·H_2O (scaly)	22.91	22.70	3.85	3.80	13.39	13.24	7.94	7.84
[Cu(DL-$ala)_2$]·H_2O (needle)	30.06	30.06	4.88	5.05	11.45	11.69	7.20	7.00
[Cu(DL-$ala)_2$] (scaly)	30.32	30.06	5.02	5.05	11.44	11.69	—	—
[Cu(DL-$val)_2$]	40.84	40.60	6.81	6.81	9.53	9.47	—	—
[Cu(DL-$thr)_2$]	32.25	32.05	5.37	5.38	9.32	9.35	—	—
[Cu(L-$isoleu)_2$]·H_2O	44.08	44.22	7.31	7.44	8.60	8.60	5.38	5.27
[Cu(DL-$isoleu)_2$]·H_2O	44.51	44.22	7.27	7.44	8.64	8.60	5.28	5.27
[Cu(DL-$Etgly)_2$]	36.05	35.88	5.99	6.03	10.50	10.46	—	—
[Cu($Me_2gly)_2$]	35.98	35.88	6.03	6.03	10.30	10.46	—	—
[Cu(ph_2edda)]·H_2O	55.28	55.44	4.67	4.66	7.23	7.19	4.46	4.42
[Cu(ph_2edpa)]·H_2O	57.68	57.47	5.36	5.32	6.96	6.70	4.41	4.13
[Cu(ediba)]·$3H_2O$	40.52	40.88	6.12	6.18	9.54	9.54	15.16	15.54
Cu(en)SO_4·$2H_2O$	9.26	9.39	4.64	4.74	10.20	10.95	—	—

* gly=glycinate, ala=α-alaninate, val=valinate, thr=threoninate, isoleu=isoleucinate, Etgly=α-amino-*n*-butyrate, Me_2gly=α-aminoisobutyrate, ph_2edda=ethylene-bis(α-iminophenylacetate), ph_2edpa=ethylene-bis(α-iminophenylpropionate), ediba=ethylene-bis(α-iminoisobutyrate), en=ethylenediamine.

2) H. C. Freeman, M. R. Snow, I. Nitta and K. Tomita, *Acta Cryst.*, **17**, 1463 (1964); K. Tomita and I. Nitta, This Bulletin, **34**, 286 (1961).
3) J. Mauthner and W. Suida, *Monatsh.*, **11**, 373 (1890).
4) T. J. Lane, J. A. Durkin and R. J. Hooper, *Spectrochim. Acta*, **20**, 1013 (1964).
5) R. J. Hooper, T. J. Lane and J. L. Walter, *Inorg. Chem.*, **3**, 1568 (1964).
6) T. Yasui, J. Hidaka and Y. Shimura, *J. Am. Chem. Soc.*, **87**, 2762 (1965).
7) E. Abderhalden and E. Schnitzler, *Z. physiol. Chem.*, **163**, 94 (1927).
8) Z. E. Gol'braikh, *Zhur. Neorg. Khim.*, **1**, 1739 (1956).

The copper(II) complexes of DL- and L-isoleucine, ethylene-bis(α-iminophenylacetic acid)[9a] and ethylene-bis(α-iminophenylpropionic acid)[9a] were recrystallized from hot water, and that of ethylene-bis(α-iminoisobutyric acid),[9b] from aqueous acetone. An ethylenediamine compound, $Cu(en)SO_4 \cdot 2H_2O$, was obtained by the method of Pfeiffer and Glaser[10] and recrystallized from aqueous alcohol.

The results of the chemical analyses are listed in Table I for all of the complexes obtained.

The preparations of the remaining complexes have already been reported in a previous report of this series.[1]

Results and Discussion

The spectral curves obtained by the diffuse reflectance measurements are shown in Figs. 1—5. The absorption spectrum of the glycine complex in an aqueous solution shows only one broad band and gives little information about the geometrical structures. Moreover, the cis and the trans isomers give identical spectra in an aqueous solution, probably reaching a cis-trans equilibrium mixture by the rapid rearrangement of the ligands.

The spectral difference between the bright blue *cis*-[Cu gly_2]$\cdot H_2O$ and the bluish-violet [Cu gly_2]$\cdot H_2O$, which can not be observed in an aqueous solution, definitely appears in the solid states, as may be seen in Fig. 1. The spectrum of the bluish violet [Cu gly_2]$\cdot H_2O$ is similar to that in an aqueous solution, but the *cis*-[Cu gly_2]$\cdot H_2O$ in the solid state has the peak at a longer wavelength than that of the bluish-violet form and an accompanying shoulder on the longer wavelength side. This fact indicates that the structure of *cis*-[Cu gly_2]$\cdot H_2O$ in the crystal is considerably different from that in an aqueous solution, and that the symmetry of the complex molecule is rather lowered. This agrees very well with the results of the X-ray study of the *cis*-[Cu gly_2]$\cdot H_2O$.[2] The spectra of the ethylene-bridged copper(II) complexes with cis structures are similar to that of the *cis*-[Cu gly_2]$\cdot H_2O$ (Fig. 2). The spectrum of the bluish-violet [Cu gly_2]$\cdot H_2O$ coincides exactly with that of *trans*-[Cu(DL-Etgly)$_2$], the structure of which has been determined by X-ray analysis.[11] It may be concluded, therefore, that the bluish-violet [Cu gly_2]$\cdot H_2O$ is the trans form. This conclusion is also consistent with the studies of infrared spectra.[4,12]

Another difference between the spectrum of *cis*-[Cu gly_2]$\cdot H_2O$ and that of bluish-violet [Cu gly_2]$\cdot H_2O$ lies in their intensities. The maximum absorption of the former is more intense than that of the latter, although not quite definitely so, since the intensities of diffuse reflectance spectra

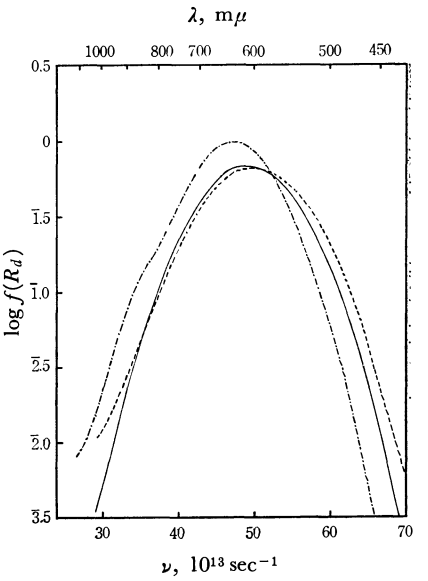

Fig. 1. The diffuse reflectance curves of *cis*-[Cu gly_2]$\cdot H_2O$ (-·-·-), bluish violet [Cu gly_2]$\cdot H_2O$ (——) and *trans*-[Cu(DL-Etgly)$_2$] (- - -).

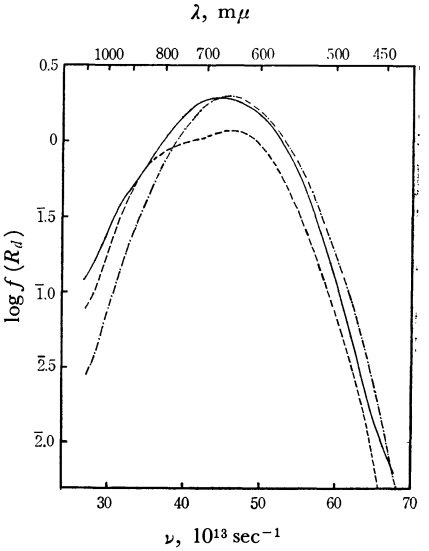

Fig. 2. The diffuse reflectance curves of [Cu(ph_2edda)]$\cdot H_2O$ (——), [Cu(ph_2edpa)]$\cdot H_2O$ (-·-·-), and $Cu(en)SO_4 \cdot 2H_2O$ (- - -).

depend on the particle size of the samples. According to Belford and Yeranos,[13] the intensities of the d→d absorption of copper(II) complexes are enhanced by the cis-structure or the strong interaction of the solvent to the fifth and/or sixth coordination positions.

In Fig. 3 the curves of [Cu(DL-ala)$_2$]$\cdot H_2O$ (needle) and of [Cu(DL-ala)$_2$] (scaly) almost coincide with that of the *trans*-[Cu(L-ala)$_2$], in which the

9) a) N. Schlesinger, *Ber.*, **45**, 1486 (1912); b) ibid., **44**, 1135 (1911).
10) P. Pfeiffer and H. Glaser, *J. prak. Chem.*, **151**, 134 (1938).
11) A. J. Stosick, *J. Am. Chem. Soc.*, **67**, 362 (1945).
12) K. Tomita, This Bulletin, **34**, 280 (1961).
13) R. L. Belford and W. A. Yeranos, *Mol. Phys.*, **6**, 121 (1963).

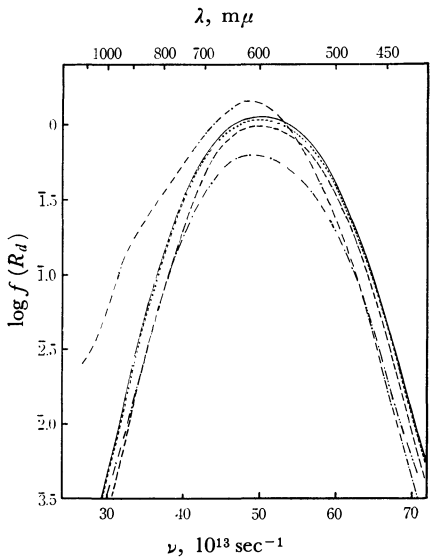

Fig. 3. The diffuse reflectance curves of [Cu(DL-ala)$_2$]·H_2O (——), [Cu(DL-ala)$_2$] (·····), [Cu(L-ala)$_2$] (- - -), [Cu(L-val)$_2$]·H_2O (-·-·) and [Cu-(DL-val)$_2$] (-·-·-·).

ligand L-alanine is coordinated to copper(II) in a trans planar configuration.[14] Therefore, it may be suggested that both the DL-alanine complexes take the trans structure, although their crystal forms and colors are different. In the valine complexes an interesting fact has been found; the spectrum of [Cu(L-val)$_2$]·H_2O corresponds to that of *cis*-[Cu gly$_2$]·H_2O, and the spectrum of [Cu-(DL-val)$_2$], to that of bluish-violet [Cu gly$_2$]·H_2O or *trans*-[Cu(DL-Etgly)$_2$] (Fig. 3). Moreover the band of [Cu(L-val)$_2$]·H_2O is more intense than that of [Cu(DL-val)$_2$]. From these facts, it may be concluded that the complex with L-valine is the cis form, and that with DL-valine is the trans form. Because of their different geometrical structures, it is possible that the interaction between the terminal isopropyl groups of the coordinated valines is smaller in the trans than in the cis complex of DL-valine, but it is smaller in the cis than in the trans complex of L-valine.

Similarly, it may be concluded from Fig. 4 that the complexes of isoleucine have the cis configuration, and that those of threonine have the trans configuration. The band of [Cu(DL-isoleu)$_2$]·H_2O has a higher intensity than that of [Cu(L-isoleu)$_2$]·H_2O; this may be interpreted as partly due to the aquo-ligand coordinated strongly to the copper atom and partly due to the cis structure.[13] The conclusion that [Cu(DL-isoleu)$_2$]·H_2O is the cis form also agrees with the conclusion which has been suggested from the infrared spectra.[5] The spectral behaviors of [Cu(DL-thr)$_2$] and [Cu(L-thr)$_2$]·

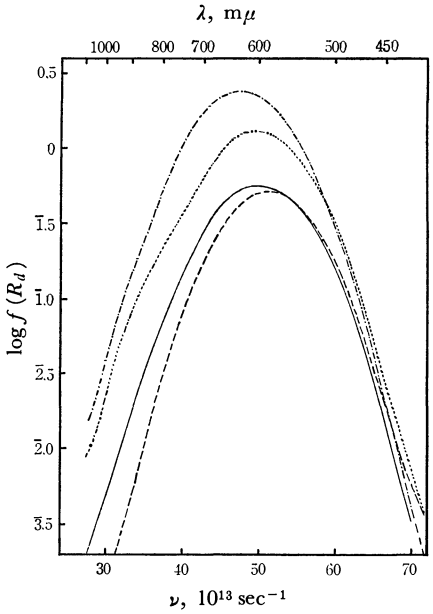

Fig. 4. The diffuse reflectance curves of [Cu(DL-(thr)$_2$] (——), [Cu(L-thr)$_2$]·H_2O (- - -), [Cu-(DL-isoleu)$_2$]·H_2O (-·-·) and [Cu(L-isoleu)$_2$]·H_2O (·····).

H_2O are almost identical with those of *trans*-[Cu(DL-Etgly)$_2$] and [Cu(DL-val)$_2$]; they show that they have the trans configuration.

The spectra of [Cu(Me$_2$gly)$_2$] and of the complex of isobutyric derivative, [Cu(ediba)]·3H_2O, show a different trend from those of the complexes with familiar amino acids mentioned above; that is, they show a shoulder on the shorter wavelength

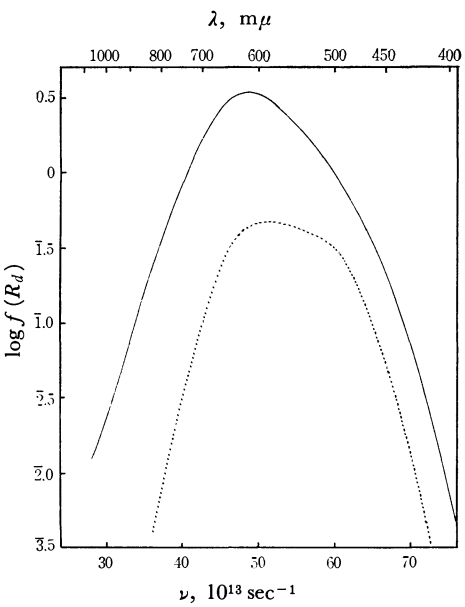

Fig. 5. The diffuse reflectance curves of [Cu-(ediba)]·3H_2O (——) and [Cu(Me$_2$gly)$_2$] (·····).

14) C. G. Vonk et al., quoted by C. Dijkgraaf, *Spectrochim. Acta*, **20**, 1227 (1964).

Table II. Colors and geometrical structures of the complexes

Complex	Color	Geometrical structure
$[Cu\,gly_2]\cdot H_2O$ (scaly)	Bluish violet	trans
$[Cu(DL\text{-}ala)_2]\cdot H_2O$ (needle)	Blue	trans
$[Cu(DL\text{-}ala)_2]$ (scaly)	Bluish violet	trans
$[Cu(L\text{-}val)_2]\cdot H_2O$	Blue	cis
$[Cu(DL\text{-}val)_2]$	Bluish violet	trans
$[Cu(L\text{-}thr)_2]\cdot H_2O$	Blue	trans
$[Cu(DL\text{-}thr)_2]$	Bluish violet	trans
$[Cu(L\text{-}isoleu)_2]\cdot H_2O$	Bluish violet	cis
$[Cu(DL\text{-}isoleu)_2]\cdot H_2O$	Bright blue	cis
$[Cu(Me_2gly)_2]$	Violet	trans

side (Fig. 5). Graddon and Munday[15] suggested, from the shoulder of $[Cu(Me_2gly)_2]$ on the shorter wavelength side, that the complex molecule has a purely tetragonal planar structure. The lower intensity of the band of this complex may be due to its trans-structure.

The geometrical structures of the bis(amino-acidato)copper(II) complexes which have been determined from the data of diffuse reflectance spectra are summarized in Table II.

15) D. P. Graddon and L. Munday, *J. Inorg. Nucl. Chem.*, **23**, 231 (1961).

BULLETIN OF THE CHEMICAL SOCIETY OF JAPAN VOL. 39 608—610 (1966)

The Dipole Moments of the Oligether of Ethylene Glycol

By Ko KIMURA and Ryoichi FUJISHIRO

Department of Chemistry, Faculty of Science, Osaka City University, Sumiyoshi-ku, Osaka

(Received July 31, 1965)

The dipole moments of ethylene glycol dimethyl ether ($N=1$), diethylene glycol dimethyl ether ($N=2$), triethylene glycol dimethyl ether ($N=3$), and tetraethylene glycol dimethyl ether ($N=4$), were measured in *n*-hexane or benzene at 25°C and 45°C. The observed dipole moments of $N=1$, $N=2$, $N=3$, and $N=4$ are 1.59 D, 1.92 D, 2.16 D, and 2.44 D, respectively, in *n*-hexane at 25°C, 1.71 D, 1.97 D, 2.22 D, and 2.45 D, respectively, in benzene at 25°C, and 1.72 D, 1.98 D, 2.27 D, and 2.50 D, respectively, in benzene at 45°C. The dipole moments were theoretically calculated on the assumptions that: (i) the dipole moments of these chain molecules are given by the vector sum of the polar groups of ether whose group moment is 1.20 D, and (ii) all the internal rotations of a chain molecule are free. The calculated values of $N=1$, $N=2$, $N=3$, and $N=4$ are 1.67 D, 2.03 D, 2.33 D, and 2.60 D, respectively. The agreement between the observed and the calculated values is satisfactory. The solvent effect and the temperature dependence of the observed dipole moments have also been discussed in terms of chain flexibility.

The study of the electric dipole moments of the oligomer of ethylene glycol in solutions from the point of view of thermodynamic behavior is important as well as from that of the molecular structure. The molecular structure of the oligomer of ethylene glycol in dioxane had been discussed,[1] but there is some difficulty in analyzing the experimental results because of the intra- and intermolecular hydrogen-bonding between hydroxyl groups of the solutes and the solvent. The hydrogen-bonding of the end groups may determine the configuration of chain molecules when their chain lengths are as short as those in oligomers. This paper, therefore, will present a study of the dipole moments of the dimethyl ether of monomer (ethylene glycol), dimer, trimer, or tetramer in solvents such as benzene and *n*-hexane, and will describe their correlation with their molecular configurations.

Experimental

Dimethyl ethers of the oligomer (products of the Tokyo Kasei Chemicals Co., Ltd.) were dried over calcium chloride and distilled under nitrogen several times. Benzene was purified by shaking it with concentrated

1) T. Uchida, Y. Kurita, N. Koizumi and M. Kubo, *J. Polymer Sci.*, **21**, 313 (1956); J. Marchal and H. Benoit., ibid., **23**, 223 (1957).

Table I. Observed values of ε and v expressed by linear equations of w

	H* 25°C	B* 25°C	B 45°C
Monomer ($N=1$)	$\varepsilon=1.8929+1.98w$	$\varepsilon=2.2725+3.21w$	$\varepsilon=2.2331+2.95w$
	$v=1.49776-0.272w$	$v=1.14508+0.050w$	$v=1.17444+0.014w$
Dimer ($N=2$)	$\varepsilon=1.8867+2.01w$	$\varepsilon=2.2725+3.00w$	$\varepsilon=2.2331+2.95w$
	$v=1.50969-0.427w$	$v=1.14465-0.084w$	$v=1.17458-0.098w$
Trimer (N=3)	$\varepsilon=1.8912+1.98w$	$\varepsilon=2.2725+2.91w$	$\varepsilon=2.2331+2.73w$
	$v=1.50126-0.483w$	$v=1.14475-0.115w$	$v=1.17442-0.134w$
Tetramer ($N=4$)	$\varepsilon=1.8877+2.01w$	$\varepsilon=2.2725+2.87w$	$\varepsilon=2.2331+2.69w$
	$v=1.50946-0.499w$	$v=1.14481-0.147w$	$v=1.17451-0.161w$

* B and H are abbreviations of benzene and hexane, respectively. Values of w's used in these measurements are from zero to about 0.03.

sulfuric acid and by fractional distillation through a 100 cm. column packed with stainless-steel helices. Hexane was purified by letting it stand with fuming sulfuric acid for a few months and by fractional distillation.

The measurements of the dielectric constants, ε, and the specific volumes, v, were carried out with an apparatus devised by Le Fevre and his collaborators.[2]

Results

The observed values of ε and v are expressed by linear equations of the solute concentrations, w (the weight fraction of solutes); they are summarized in Table I. Measurements were carried out at 25°C and 45°C. The calculation of the molecular polarizations, P, from these experimental data was performed according to the standard method.[3] Molecular refractions, R_D, for the sodium D line were calculated on the assumption of the additivity of bond refractions, and the distortion polarizations were assumed to be equal to $1.1\times R_D$.[1] The observed dipole moments, μ, are tabulated in Table II, together with the polarization values.

Table II. Observed dipole moments

		H 25° C	B 25° C	B 45°C
$N=1$	p_∞	0.8682 cc.	0.9600	0.9262
	P	78.25 cc.	86.52	83.48
	$1.1\times R_D$	26.64 cc.		
	μ	1.59 D	1.71	1.72
$N=2$	p_∞	0.8496	0.8802	0.8485
	P	114.0	118.1	113.8
	$1.1\times R_D$	38.83		
	μ	1.92	1.97	1.98
$N=3$	p_∞	0.8222	0.8540	0.8398
	P	146.5	152.1	149.6
	$1.1\times R_D$	51.0		
	μ	2.16	2.22	2.27
$N=4$	p_∞	0.8329	0.8371	0.8242
	P	185.1	186.1	183.2
	$1.1\times R_D$	63.2		
	μ	2.44	2.45	2.50

* p_∞ stands for the specific polarization.

Table III. Comparison between the calculated dipole moments and the observed ones

		$\mu_{obs.}$		
N	$\mu_{calc.}$	H 25°C	B 25°C	B 45°C
1	1.67D	1.59	1.71	1.72
2	2.03	1.92	1.97	1.98
3	2.33	2.16	2.22	2.27
4	2.60	2.44	2.45	2.50

Discussion

The dipole moment of a chain molecule consisting of n polar units is equal to:

$$\vec{\mu} = \sum_{i=1}^{n} \vec{\mu}_i \qquad (1)$$

where $\vec{\mu}_i$ is the dipole moment of each unit. In the present case, it is a group moment of ether, which is directed along the bisectrix of the C–O–C valence angle with the positive center at the side of carbon atoms. Its value, μ_0, is assumed to be 1.20 D. As a monomer consists of two units, n is equal to $N+1$. The scalar product of $\vec{\mu}$ gives:

$$\overline{\mu^2} = \sum_{i=1}^{n} \mu_i^2 + 2\sum_{i=1,\ i<j}^{n} \overline{(\vec{\mu}_i \cdot \vec{\mu}_j)} \qquad (2)$$

where $\overline{\mu^2}$ is the average μ^2 value over the angles of all internal rotations. The second term on the right hand side of (2) can be easily calculated if all the internal rotations are free.[4] The calculated results of (2) are as follows:

$$\overline{\mu^2} = (2-2\lambda^2\eta^2)\mu_0^2 \qquad \text{for } N=1$$

$$\overline{\mu^2}/2 = (3/2-2\lambda^2\eta^2-\lambda^5\eta^2)\mu_0^2 \qquad \text{for } N=2$$

2) R. J. W. Le Fevre, I. G. Ross and B. M. Smythe, *J. Chem. Soc.*, **1950**, 276.

3) I. F. Halverstadt and W. D. Kumler, *J. Am. Chem. Soc.*, **64**, 2988 (1942).

4) S. Oka, *Proc. Phys. Math. Soc. Japan*, **24**, 657 (1942); M. V. Volkenstein, "Configurational Statistics of Polymeric Chains," Interscience Publishers, New York (1963), p. 301; J. Marchal and H. Benoit, *J. Chim. Phys.*, **52**, 818 (1955).

TABLE IV. DISTANCES BETWEEN TWO METHYL GROUPS IN THE CASE OF $N=1$, WHEN A MOLECULE IS FIXED AT THE GAUCHE CONFIGURATION ABOUT THE CENTRAL BOND

GG	GT	GG'	TG	TT	TG'	G'G	G'T	G'G'
(1.32Å)	(3.06)	(3.36)	(3.06)	4.67	3.97	(1.83)	3.97	(3.20)

$$\overline{\mu^2}/3 = (4/3-2\lambda^2\eta^2-4/3\cdot\lambda^5\eta^2-2/3\cdot\lambda^8\eta^2)\mu_0^2 \quad \text{for } N=3$$

$$\overline{\mu^2}/4 = (5/4-2\lambda^2\eta^2-3/2\cdot\lambda^5\eta^2-\lambda^8\eta^2 -1/2\cdot\lambda^{11}\eta^2)\mu_0^2 \quad \text{for } N=4$$

$$\overline{\mu^2}/N = [1+1/N-2\lambda^2\eta^2\{1/(1-\lambda^3) -\lambda^3(1-\lambda^{3N})/N(1-\lambda^3)^2\}]\mu_0^2 \quad \text{for } N$$

$$= \{(1-2\lambda^2\eta^2/(1-\lambda^3))\}\mu_0^2 = 12/13\cdot\mu_0^2 \quad \text{for } N\to\infty$$

where λ and η are $\cos\omega$ and $\sin\omega/2$, respectively. For the sake of simplicity, the valence angle $(\pi\text{-}\omega)$ is assumed to be tetrahedral about the oxygen atoms as well as about the carbon atoms of ether. The calculated dipole moments are tabulated in Table III, together with the observed moments. From a comparison of the calculated dipole moments with the observed ones, we can see that the former agrees satisfactorily with the latter. It may, therefore, be suggested that the oligether of ethylene glycol in non-polar solvents is in a random coil state. For $N=1$, the solvent effect makes a considerable contribution to the dipole moment compared with the temperature effect, but for $N=4$, two effects are reversed, as is shown in Table III. This result may be expected if the steric effect of the rotational isomers is taken into consideration. The distances between two methyl groups for $N=1$ are estimated for nine configurations in Table IV, when the *gauche* configuration is kept about the central bond. Only three rotational isomers among the nine are possible as a result of the overlapping of two methyl groups. This means that chain flexibility is not expected for $N=1$. Therefore, no temperature dependence of its dipole moments was observed. On the contrary, the observed dipole moments at 25°C are constant for $N=4$ within the range of experimental errors, irrespective of the solvents used, but their temperature dependence was observed. The observed moments at 45°C approach the calculated moments more closely than those at 25°C. It may, therefore, be expected that the temperature effect rather than the solvent effect will become important as a result of the increase in chain flexibility when the chain length is lengthened.

Raman spectra at low frequencies (250 cm^{-1} to 600 cm^{-1}) corresponding to the skeletal deformation show the feature already described, although measurements of Raman spectra[5] were carried out for pure liquids. Only four sharp lines are observed for $N=1$. However, as N increases, broader bands are observed at these frequencies.

Summary

The dipole moments of the oligether of ethylene glycol have been measured in *n*-hexane and benzene at 25°C and 45°C. The observed values have been compared with the calculated values derived on the assumption that all internal rotations are free. The agreement between them is satisfactory. The solvent effect and the temperature dependence of the observed dipole moments have also been discussed.

5) K. Kimura and R. Fujishiro, unpublished work.

BULLETIN OF THE CHEMICAL SOCIETY OF JAPAN VOL. 39 611—614 (1966)

The Formation of Phenolic Ethers by the Acid-catalyzed Condensation of Phenols and Alcohols[1,2]

By Shigeru Oae

Department of Applied Chemistry, Faculty of Engineering, Osaka City University, Sumiyoshi-ku, Osaka

and Reiko Kiritani

Department of Chemistry, Radiation Center of Osaka Prefecture, Sakai, Osaka

(Received August 2, 1965)

The reaction of phenol with ethyl alcohol in strong acidic media at a somewhat high temperature gave phenyl ethyl ether in a 61% yield. The product isolated from a similar reaction between phenol and *n*-propyl alcohol was practically pure phenyl *n*-propyl ether, and no isopropyl isomer was detected. When ^{18}O-labeled phenol was treated with unlabeled ethyl alcohol, the phenetole isolated was found not to contain any excess ^{18}O. The reaction of phenol with ethyl alcohol in the presence of hydrogen chloride gave no isolable amount of phenetole. The mechanism for these reactions was then discussed.

Previously, we have reported that phenols undergo a facile oxygen-isotopic exchange with solvent water in strong acidic media at a high temperature.[3] It was suggested that, in a strong acidic media, phenol readily accepts a proton at either the ortho- or para-position to form a quasi-stable quinoid-type intermediate, whereby a nucleophilic attack of water at carbon-1 leads to the exchange of the oxygen, as is shown below.[3,4]

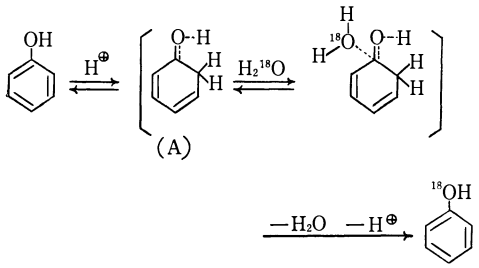

Fig. 1.

As an extension of this remarkable ^{18}O exchange reaction, it was expected that the phenolic hydroxy group would be replaced by more nucleophilic reagents, such as alcohols and mercaptans. Indeed, such reactions have been found to take place, and the details of the acid-catalyzed condensation of phenols with mercaptans have been reported in a previous paper of this series[5]. This paper will describe a more detailed investigation into the nature of the acid-catalyzed condensation of phenols and alcohols.

Results and Discussion

The acid-catalyzed formation of aryl ethers from aromatic phenols and alcohols[6] is not an entirely new reaction. Wiberg and Saegebarth[7] have reported recently that β-naphthyl methyl ether was obtained in a 70% yield when β-naphthol was heated at 100°C with methanol for 40 hr. in the presence of anhydrous *p*-toluenesulfonic acid in a sealed tube. It was suggested, on the basis of the ^{18}O tracer experiments using ^{18}O-labeled methanol, that this reaction proceeds in the following manner, similar to what was suggested by us for the oxygen-exchange reaction of phenols:

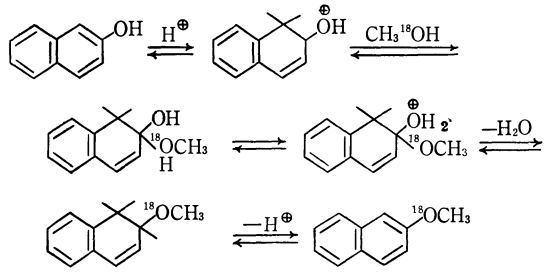

Fig. 2.

Resorcinol, which is known to have a carbonyl character, was also found to undergo a condensation reaction with methanol. However, phenol, catechol and hydroquinone were found not to undergo any condensation under the same reaction conditions.

Under the somewhat more drastic conditions under

1) Paper VII: Reactions of Phenols and Phenolic Esters.
2) For preliminary account of this paper, see S. Oae and R. Kiritani, This Bulletin, **36**, 346 (1963); **37**, 770 (1964); **38**, 765, 1381, 1543 (1965).
3) S. Oae, T. Fukumoto and R. Kiritani, ibid., **36**, 346 (1963).
4) S. Oae and R. Kiritani, ibid., **37**, 770 (1964).
5) S. Oae and R. Kiritani, ibid., **38**, 1381 (1965).
6) L. Gattermann, *Ann.*, **244**, 72 (1888).
7) K. B. Wiberg and K. A. Saegebarth, *J. Org. Chem.*, **25**, 832 (1960).

which the ^{18}O exchange takes place, phenol undergoes a condensation with alcohol, as is shown in Table I.

Table I. The reactions of phenols with alcohols

Reactants		Reaction condition			Yield %
Phenol	Alcohol	Mole ratio	Time hr.	Temp. °C	
Phenol	EtOH	1 : 5	48	180	58.4
Phenol	EtOH[a)]	1 : 5	48	180	61.0
Phenol	EtOH[b)]	1 : 5	48	180	none
Phenol	EtOH[c)]	1 : 5	48	180	none
Phenol	EtOH[c)]	1 : 5	48	110	none
Phenol	*n*-PrOH	1 : 5	48	180	55.1
β-Naphthol	EtOH	1 : 1	48	180	52.3
p-Cresol	EtOH	1 : 5	48	180	33.3
p-Nitrophenol	EtOH	1 : 5	48	180	trace

a) no H_2O; *p*-toluenesulfonic acid catalyst
b) no H_2O; no catalyst
c) no H_2O; hydrogen chloride catalyst

Although the reaction is considered to proceed through the following pathway, similar to that proposed by Wiberg for the formation of β-naphthyl methyl ether:

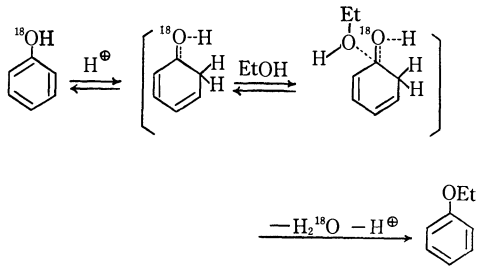

Fig. 3.

other possibilities have also to be scrutinized, because, after all, the conditions used here are so drastic that the formation of alkyl chloride or of the alkyl carbonium ion intermediate is quite conceivable during this reaction.

However, the mechanism involving the incipient formation of the alkyl carbonium ion or of alkyl chloride was excluded on the basis of the following observations:

a) When ^{18}O-labeled phenol (1.3 atom.% ^{18}O) was treated with unlabeled ethyl alcohol in an ^{18}O-enriched water (1.3 atom.% ^{18}O) solution of 12 N hydrochloric acid, the phenetole obtained was found to possess a natural abundance of oxygen (0.20 atom.% ^{18}O).

b) The product isolated in a 55.1% yield from the similar reaction between phenol and *n*-propyl alcohol was practically pure phenyl *n*-propyl ether; no isopropyl isomer was detected in the product within the range of experimental error. The carbonium ion formed from *n*-propyl alcohol must be the isopropyl cation. Hence, the reaction involving the alkyl carbonium ion should definitely give phenyl isopropyl ether as the product.

c) The reaction was found to proceed quite well with a small amount of anhydrous toluenesulfonic acid as the acid catalyst under anhydrous conditions. However, when water was excluded in the hydrochloric acid-catalyzed reaction between phenol and ethanol, no isolable amount of phenetole was obtained. The evolution of gas, presumably ethyl chloride, was noticed when the sealed tubes were opened. Probably, under anhydrous conditions, hydrochloric acid was consumed in the formation of ethyl chloride in the following equilibrium:

$$EtOH + HCl \rightleftharpoons EtCl + H_2O$$

On the other hand, the equilibrium of the reaction between ethanol and toluenesulfonic acid is undoubtedly shifted toward the left-hand side.

$$EtOH + TsOH \rightleftharpoons EtOTs + H_2O$$

It is also difficult to accept the direct aromatic nucleophilic substitution, shown below, in view of the results of previous work on the oxygen exchange reaction[8)] as well as in view of the sulfide-

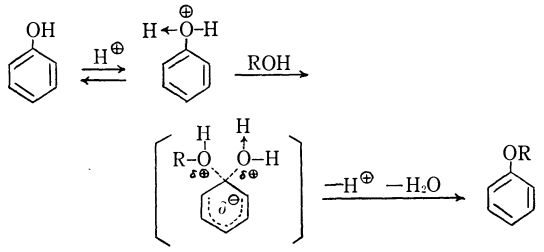

Fig. 4.

forming reaction.[5)] According to this reaction scheme, the substitution of an electron-withdrawing group at the *o*- or *p*-position will accelerate the reaction; however, the nitro group at the para position was found to retard the reaction substantially.

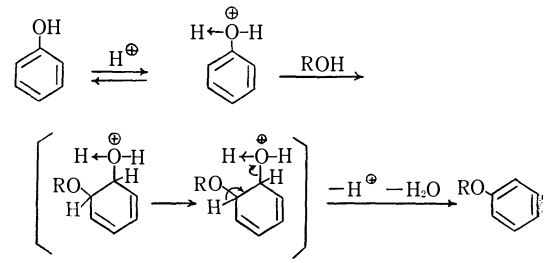

Fig. 5.

8) S. Oae and R. Kiritani, This Bulletin, to be submitted.

The other possible pathway (shown below), involving the nucleophilic attack of alcohol at the ortho or para-position of phenol and the subsequent elimination of water, can also be excluded.

There was no formation of any detectable amount of the rearranged ether from the reaction with *p*-cresol and β-naphthol.

Therefore, the only plausible pathway that can explain all these observations is the one involving the nucleophilic attack of alcohol on the incipient carbonium ion (A) formed during the reaction.

Recently, Gold and Satchell[9] have also postulated a similar ortho- or para-protonated σ-complex formation in a strong acid solution of phenolic compounds, while Kresge et al.[10] have obtained rather conclusive evidence for the protonated σ-complex through proton NMR spectroscopic measurements and through a study of the ultraviolet spectra in the case of phloroglucinol.

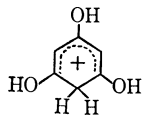

Fig. 6.

On the other hand, the formation of the σ-complex intermediate has never been successfully observed in the case of monohydroxylic phenol. However, in view of the very facile hydrogen isotopic exchange in strong acid solutions of phenol, the steady concentration of the incipient carbonium ion (A) or of the σ-complex will probably increase substantially, or the nucleophilic attack of alcohol on the carbonium ion (A) will take place more readily, or more probably the combination of the two reactions will become more facile, when the reaction temperature is elevated.

In order to shed further light on the nature of this and related reactions, condensation reactions with other nucleophilic reagents are now underway in these laboratories.

Experimental

β-Naphthyl Ethyl Ether.—β-Naphthol (1 g.) was added to 5 ml. of 10 N hydrochloric acid containing ^{18}O-enriched water (0.74 atom.% ^{18}O). The mixture was then heated in a sealed tube at 180°C for 24 hr. The recovered β-naphthol was subjected to ^{18}O analysis (0.53 atom.% ^{18}O). A mixture of 4.8 g. (0.033 mol.) of the labeled β-naphthol and 1 ml. of 12 N hydrochloric acid in 1.6 g. (0.033 mol.) of ethyl alcohol was sealed in a tube and heated at 180°C for 48 hr. Then the sealed tube was broken and, after the excess alcohol had been removed in vacuo, the whole content was extracted with ether. The ether layer was sufficiently washed with aqueous sodium carbonate and water to remove unreacted β-naphthol, and then dried over calcium chloride. When the ether extract was distilled under reduced pressure, 3 g. of a fragrant white precipitate was obtained (yield 52.3%). The product, β-naphthyl ethyl ether, was identified by means of its infrared spectrum and subjected to ^{18}O analysis (0.20 atom.% ^{18}O). M. p. 37—38°C; b. p. 124°C/5 mmHg; n_D^{20} 1.5932. Found: C, 83.78; H, 7.11%.

Phenetole.—A mixture of 2 g. (0.021 mol.) of phenol and 1 ml. of 12 N hydrochloric acid in 5 g. (0.109 mol.) of ethyl alcohol was sealed in a tube and kept at 180°C for 48 hr. After it had cooled the sealed tube was treated as has been described above. The distillate gave 1.5 g. of phenetole (yield 58.4%). The infrared spectrum was identical with that of an authentic sample. In a separate experiment, a mixture of 2 g. (0.021 mol.) of phenol and 0.2 g. (0.0012 mol.) of *p*-toluenesulfonic acid in 5 g. (0.109 mol.) of absolute ethyl alcohol was sealed in a tube and heated at 180°C for 48 hr. The sealed tube was then treated as has been described above. The ether layer was washed with aqueous sodium carbonate to remove unreacted phenol and *p*-toluenesulfonic acid, and then distilled under reduced pressure; thereby 1.6 g. of phenetole was obtained (yield 61%). B. p. 171—173°C; n_D^{20} 1.5129. Found: C, 78.68; H, 8.20%.

When the other sealed tube, which contained the same reactants, was kept at 110°C for 48 hr., no detectable amount of the product was obtained, while all of the reactants were recovered.

A solution of phenol 2 g. (0.021 mol.) in 5 g. (0.109 mol.) of ethyl alcohol in the absence of an acid catalyst was sealed in a tube. An alcohol solution of 1.3 N acid was then prepared by absorbing hydrogen chloride dried over sulfuric acid into absolute ethyl alcohol. A solution of phenol 2 g. (0.021 mol.) in 6 g. of the acidic ethyl alcohol was sealed in another tube. Both sealed tubes were heated at 180°C for 48 hr. and treated as described above; however, no phenetole was obtained.

^{18}O labeled phenol was prepared by the acid-catalyzed oxygen exchange reaction.[6] Using the ^{18}O enriched phenol (1.3 atom.% ^{18}O) thus prepared and unlabeled ethyl alcohol, the condensation reactions were carried out in the presence of an unlabeled or ^{18}O enriched (1.3 atom.% ^{18}O) water solution of hydrochloric acid in sealed tubes at 180°C for 48 hr. The products obtained in both reactions were unlabeled phenetole.

***n*-Propyl Phenyl Ether.**—A mixture of 2 g. (0.021 mol.) of phenol and 1 ml. of 12 N hydrochloric acid in 6 g. (0.1 mol.) of *n*-propyl alcohol was sealed in a tube. After the solution had been heated at 180°C for 48 hr., the sealed tube was broken and treated as has been described above. *n*-Propyl phenyl ether (0.75 g.) was obtained (yield 55.1%). The infrared spectrum was found to be identical within the range of experimental error with that of the authentic sample. B. p. 188—189°C, n_D^{20} 1.5056. Found: C, 79.41; H, 8.89%. Meanwhile, the authentic sample of *n*-propyl phenyl ether was prepared by reacting sodium phenolate with *n*-propyl bromide in a 95.6% yield.

***p*-Tolyl Ethyl Ether.**—A mixture of 2.2 g. (0.02 mol.) of *p*-cresol and 1 ml. of 12 N hydrochloric acid in 5 g. (0.109 mol.) of ethyl alcohol was sealed in a tube.

9) V. Gold and D. P. N. Satchell, *J. Chem. Soc.*, **1955**, 3619.
10) A. J. Kresge, G. W. Barry, K. R. Charles and Y. Chiarry, *J. Am. Chem. Soc.*, **80**, 4343 (1962).

After the mixture had been heated at 180°C for 52 hr. the sealed tube was broken and treated as has been described above. *p*-Tolyl ethyl ether (0.9 g.) was obtained (yield 33.3%). The infrared spectrum was identical with that of an authentic sample. B. p. 188—189°C, n_D^{20} 1.5038. Found: C, 79.39; H, 8.86%. Meanwhile, an authentic sample of *p*-tolyl ethyl ether was prepared in a 100% yield by reacting sodium *p*-methyl phenolate with ethyl bromide.

***p*-Nitrophenyl Ethyl Ether.**—A mixture of 1.4 g. (0.01 mol.) of *p*-nitrophenol and 1 ml. of 12 N hydrochloric acid in 2.3 g. (0.05 mol.) of ethyl alcohol was sealed in a tube. After the tube had been heated at 180°C for 48 hr., it was broken and treated as above. Only a small amount of yellow crystals of *p*-nitrophenyl ehtyl ether was obtained; this was recrystalized from ethanol. M. p. 60°C. Found: C, 57.48; H, 5.41%. Most of the reactants were decomposed. Meanwhile, an authentic sample of *p*-nitrophenyl ethyl ether was prepared in a 24% yield by reacting sodium *p*-nitro phenolate with ethyl bromide. M. p. 59—60°C.

Analysis for Oxygen-18.—The experimental procedure and method of calculation were similar to those described in the previous paper.[11]

11) S. Oae, T. Kitao and Y. Kitaoka., *J. Am. Chem. Soc.*, **84**, 3359 (1962).

BULLETIN OF THE CHEMICAL SOCIETY OF JAPAN VOL. 39 614—617 (1966)

The Reaction of Diphenyl Sulfoxide with Bromine in Aqueous Acetic Acid[1],*

By Waichiro TAGAKI,† Kunihiko KIKUKAWA,†† Norio KUNIEDA† and Shigeru OAE†

† *Department of Applied Chemistry, Faculty of Engineering, Osaka City University, Sumiyoshi-ku, Osaka*

†† *Department of Applied Chemistry, Osaka Institute of Technology, Asahi-ku, Osaka*

(Received August 5, 1965)

When diphenyl sulfoxide was allowed to react with bromine in a mixture of acetic acid and ^{18}O-enriched water, the sulfoxide was recovered, together with a small amount of diphenyl sulfone. The sulfoxide recovered incorporated a very small amount of ^{18}O from the water. Meanwhile, diphenyl sulfoxide was found to undergo a facile oxygen exchange reaction with water in the presence of hydrobromic acid. Possible mechanisms for these reactions have been discussed.

Previously, we found that oxygen exchange takes place when sulfoxide is dissolved in ^{18}O-enriched concentrated sulfuric acid.[2] The mechanism suggested, on the basis of the several observations, was the nucleophilic attack of the sulfur atom of sulfoxide on sulfuric acid (Eq. 1). A similar oxygen exchange reaction is conceivable between sulfoxides and other acids, such as hypobromous acid. Hypobromous acid is known to be an equilibrium species in a bromine-water solution. Therefore, it seems that it would be interesting to examine the possibility of the oxygen exchange reaction of sulfoxide in a bromine-water mixture, although the reaction in this mixture may be expected to be somewhat complex, as will be explained later.

This paper will describe a preliminary investigation of the reactions of diphenyl sulfoxide in a bromine - water - acetic acid solution; the products were analyzed, and the oxygen exchange reaction was studied.

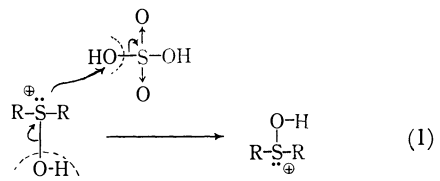

(1)

Reaction Products.—Diphenyl sulfoxide was found to be recovered almost quantitatively when the reaction mixture was quenched with water after the solution of diphenyl sulfoxide had been kept for 24 hr. in bromine - water - acetic acid at around room temperature (Table I). It is interesting to note, however, that a small amount of diphenyl sulfone (1—0.5%) was always isolated. Since the starting sulfoxide was prepared by the oxidation of diphenyl sulfide with hydrogen peroxide, the inclusion of a trace of sulfone in the starting sulfoxide is conceivable; in fact, the presence of a trace of sulfone was always shown by the characteristic infrared spectra near 1150 cm^{-1}, even in a pure diphenyl sulfoxide which had been obtained after repeated recrystallizations and which had the constant m. p. of 70°C. However, such a trace of the sulfone could be completely removed by purification through alumina-column

1) This work was supported by the Petroleum Reseasch Fund, administered by the American Chemical Society.

* Paper VIII on Sulfoxides.

2) a) S. Oae, T. Kitao and Y. Kitaoka, *Chem. & Ind.*, **1961**, 291; b) S. Oae, T. Kitao, Y. Kitaoka and S. Kawamura, This Bulletin, **38**, 546 (1965).

Table I. The products obtained in the reaction of diphenyl sulfoxide with bromine in water - acetic acid (1: 15, v/v)

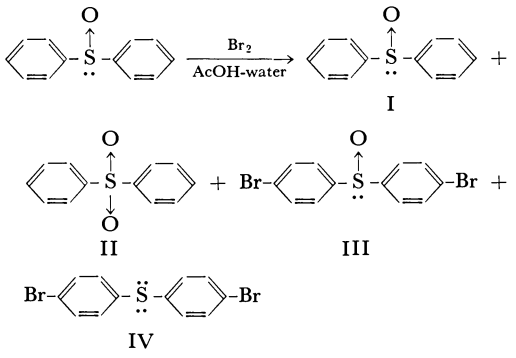

Reaction temp., °C	Yield of the products, %			
	I	II	III	IV
25	98.5—99	1—0.5	—	—
60	98—99	1—0.5	trace	—
100	—	—	—	90

chromatography using a mixture of *n*-hexane and benzene as the solvent. When the sulfoxide thus purified was used, a small amount of the sulfone was found in the quenched product described above. Therefore, the oxidation of the sulfoxide to the sulfone undoubtedly took place in this bromine - water - acetic acid solution. The yield of diphenyl sulfone increased up to 5% when the reaction mixture was quenched with aqueous sodium carbonate.

Two pathways are conceivable for the oxidation of the sulfoxide to the sulfone. One is the direct oxidation of sulfoxide by hypobromous acid (Eq. 2); the other involves the incipient formation of the bromosulfonium intermediate, which is subsequently hydrolyzed by water to give the sulfone (Eqs. 3a and 3b).

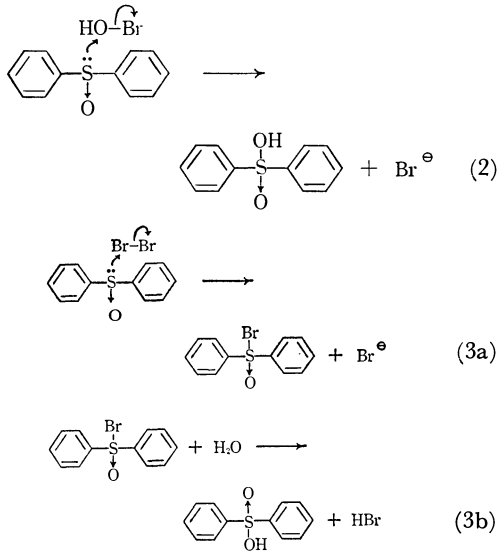

At a higher temperature, the bromination of the benzene ring and the reduction of S–O bond were observed (Table I). Thus practically all the diphenyl sulfoxide was quantitatively converted to bis-(*p*-bromophenyl) sulfide (IV) by the action of a one-mole equivalent of bromine at around 100°C.

The Oxygen Exchange Reaction of Diphenyl Sulfoxide.—The oxygen exchange reactions were carried out at 25°C for two different systems. In one system diphenyl sulfoxide with a natural oxygen- and ^{18}O-enriched water were used, while in the other the ^{18}O-labeled sulfoxide and the natural water were applied. The solvent was the same as that shown in Table I. The ^{18}O-enriched sulfoxide was prepared by the oxidation of diphenyl sulfide with *N*-bromosuccinimide in ^{18}O-enriched water,[3] since the sulfoxide thus prepared is known to be completely free from the sulfone. The results of oxygen exchange are shown in Table II.

It is interesting to note that there was a definite incorporation of ^{18}O in the recovered sulfoxide, though the amount of incorporation was very small, as can be seen from the runs 1—5 in Table II. The small decrease in ^{18}O content (except in the run 4) observed when the "crude sulfoxide" was purified to "pure sulfoxide" by alumina column chromatography, is due to the removal of the sulfone. Since at least one of the two oxygen atoms of the sulfone originates in the ^{18}O-enriched water, the ^{18}O content of the sulfone should be higher than that of the sulfoxide when the extent of the exchange reaction is low. The same conclusion can be derived more definitely by the use of the ^{18}O-labeled sulfoxide (run 6). Here, contrary to the cases in the runs 1—5, the removal of the sulfone increased the ^{18}O content of the pure sulfoxide.

The mechanism of the oxygen exchange reaction by bromine water is not clear. Although the oxygen exchange could take place between the sulfoxide and hypobromous acid much as with sulfuric acid (cf. Eq. 1), there is no definite evidence to substantiate the mechanism, nor is there any concrete evidence to exclude other possibilities. However, if one assumes that hypobromous acid causes the oxygen exchange, the accompanying oxidation of the sulfoxide to the sulfone can be nicely fit in the same reaction scheme. Another likely possibility is that the exchange reaction is due to hydrobromic acid, since hydrobromic acid is formed during the formation of diphenyl sulfone, as is illustrated in Eqs. 2 and 3. Although hydrogen chloride was recently found to be an effective catalysis for the concurrent oxygen exchange and racemization reaction of sulfoxides,

3) W. Tagaki, K. Kikukawa, K. Ando and S. Oae, *Chem. & Ind.*, **1964**, 1624.

TABLE II. OXYGEN EXCHANGE REACTIONS OF DIPHENYL SULFOXIDE IN A BROMINE - ACETIC ACID - WATER MIXTURE

^{18}O-concentration (atom.%) of the starting sulfoxide	Run No.	Reaction temp., °C	^{18}O-concentration (atom.%) of Crude sulfoxide[b]	^{18}O-concentration (atom.%) of Pure sulfoxide[c]
0.21[a]	1	25	0.27	0.25
	2	25	0.28	0.26
	3	25	0.35	0.32
	4	60	0.25	0.28
	5	60	0.25	0.24
0.85	6	25	0.71	0.77

a) 1.5% ^{18}O-enriched water.
b) The recovered sulfoxide containing a trace of sulfone.
c) The sulfoxide completely free from the sulfone.

hydrobromic acid was found to cause the decomposition of sulfoxide.[4] However, we have found that, in a low concentration in aqueous acetic acid, hydrobromic acid can cause the oxygen exchange of diphenyl sulfoxide with a quantitative recovering of the sulfoxide, as is shown in Table III. In this alternative mechanism, the sulfone formation is an independent process, probably caused by the oxidation with hypobromous acid.

TABLE III. OXYGEN EXCHANGE REACTIONS OF DIPHENYL SULFOXIDE IN AN AQUEOUS HYDROBROMIC ACID - ACETIC ACID MIXTURE
(22°C, 24 hr.)

Run No.	Sulfoxide	^{18}O-Concentration (atom.%)
	Starting sulfoxide from the solutions: HBr[a]: water (v/v)	0.98
1	1:3	0.83
2	1:7	0.76
3	1:15	0.84

a) Commercial hydrobromic acid solution, 47.9%.

Experimental

Diphenyl Sulfoxide. — This was prepared by the oxidation of diphenyl sulfide with hydrogen peroxide in acetic acid.[5] The product was recrystallized from *n*-hexane - benzene to give the sulfoxide with a constant m. p. of 70—71°C. This sulfoxide, however, was shown by the infrared spectral band near 1150 cm^{-1} to include a trace of the sulfone. Therefore, this apparently pure sulfoxide was further purified by alumina column chromatography using *n*-hexane - benzene (1 : 9 v/v) as the developing solvent. Diphenyl sulfone was eluted first; then, after the elution of a few fractions of the mixture of the sulfone and the sulfoxide, the fractions of pure sulfoxide were eluted. Usually one or two chromatographic purifications were enough to obtain the spectroscopically-pure sulfoxide.

The Reaction of Diphenyl Sulfoxide with Bromine Aqueous Acetic Acid.—Diphenyl sulfoxide (1.4 g.) (0.0069 mol.) was dissolved in 15 ml. of glacial acetic acid; to this there were added 1.0 ml. of water and an equimolar amount of bromine (1.1 g.). The reaction mixture was then left at 25°C for 24 hr. in a constant temperature bath. The initial orange color of the reaction mixture did not disappear within 24 hr. The reaction mixture was then dissolved in benzene (15—20 ml.), washed with water containing sulfur dioxide to remove free bromine, washed with a dilute sodium carbonate solution, and dried. The benzene was removed to give a colorless product (1.27 g.). The product was analyzed by the alumina column chromatography described above. In the case of the reaction at 100°C, over 90% of the product was bis-(*p*-bromophenyl) sulfide, m. p. 111—112°C (lit., 109—111°C)[6]; it was difficult to detect other products. At 60°C, a minute but definite formation of bis-(*p*-bromophenyl) sulfoxide was observed in the last fractions of the elution chromatography; this showed the melting point of 150—151°C (lit., 151°C)[7] here, and the same melting point when mixed with an authentic sample. All these results are sohown in Table I.

The Preparation of ^{18}O-Labeled Diphenyl Sulfoxide.—The method of labeling was based on our previous communication,[3] where the experimental details were not, however, described.

Diphenyl sulfoxide (5 g.) (0.027 mol.) was suspended in a solution of 5 ml. of methanol and 1 g. of ^{18}O-enriched water. Into this there was vigorously stirred, portion by portion, 5 g. (0.028 mol.) of *N*-bromosuccinimide over a 10 min. period. The reaction was very rapid and over within 10 min. When *N*-bromosuccinimide was added, a red color appeared and then faded very rapidly. The reaction mixture was stirred for an additional 20 min. and then taken up in ether. The ether solution was washed with water, dilute aqueous sodium carbonate, and water, and then dried. The ether was removed, and the residue was recrystallized from *n*-hexane - benzene to give ^{18}O-labeled diphenyl sulfoxide, 3 g.; m. p. 70—71°C; atom% of ^{18}O: 0.85 (Table II), and 0.98 (Table III). Further purification by alumina column chromatography was found to be unnecessary.

The Oxygen Exchange Reaction of Diphenyl Sulfoxide.—*With Bromine in Aqueous Acetic Acid.*—The reaction conditions and the procedures for the isolation of the products were the same as have been described for the reactions in Table I. The crude sulfoxide

4) K. Mislow, T. Simmons, J. T. Melillo and L. Ternay, Jr., *J. Am. Chem. Soc.*, **86**, 1452 (1964).
5) S. Oae and S. Kawamura, This Bulletin, **36**, 163 (1963).
6) F. Kraft, *Ber.*, **7**, 1164 (1874).
7) G. Leandri, A. Mangini and R. Passerini, *J. Chem. Soc.*, **1957**, 1386.

was obtained by the recrystallization of the crude product from *n*-hexane - benzene. The pure sulfoxide was obtained by the purification of the crude sulfoxide by alumina column chromatography, as has been described above. In a separate experiment, it was confirmed that the chromatography did not change the ^{18}O content of the sulfoxide. Analyses of ^{18}O content were made by the same procedure as has been reported elsewhere. The results are shown in Table II.

With Hydrobromic Acid in Aqueous Acetic Acid.— Volumes of commercial hydrobromic acid (48%) were diluted with 3, 7 and 15 volumes of water respectively. Each 5 ml. of these hydrobromic acid solutions was dissolved in 10 ml. of glacial acetic acid, and to this diphenyl sulfoxide (0.001 mol.) was added. The reaction mixtures were then left at room temperature (22°C) for 24 hr., poured into benzene, and washed with water, dilute aqueous sodium carbonate and water; the benzene layer was then dried over anhydrous sodium sulfate. The benzene was then removed to give the recovered sulfoxide. The yield of the sulfoxide was over 95% in each case, and the purity of the sulfoxide after one recrystallization from *n*-hexane - benzene was enough for the ^{18}O-analyses. The results are shown in Table III.

Summary

The reactions of diphenyl sulfoxide in dilute solutions of bromine in acetic acid - water mixtures have been investigated. The formation of diphenyl sulfone, bis-(*p*-bromophenyl) sulfoxide or bis-(*p*-bromophenyl) sulfide has been observed, depending on the reaction temperatures. Minutely but definitely, the oxygen exchange has been observed for the recovered diphenyl sulfoxide from this bromine solution. The oxygen exchange of diphenyl sulfoxide has also been found to take place in a dilute solution of hydrobromic acid in an acetic acid - water mixture. The mechanisms of these oxygen exchange reactions have been discussed.

NOTES

The Asymmetric Synthesis of (−)-Menthol and (−)-Isomenthol by the Hydroboration of (±)-3-*p*-Menthene

By Jun KATSUHARA, Hajime WATANABE, Komei HASHIMOTO and Masahisa KOBAYASHI

Research Laboratory, Sun Star Dentifrice Co., Takatsuki, Osaka

(Received February 24, 1965)

Brown and Zweifel[1] recently reported that the hydroboration of olefins with diisopinocampheylborane resulted in a nearly complete asymmetric synthesis of the corresponding alcohols. On the basis of the steric course proposed,[2] it should be possible to perform an asymmetric synthesis of (−)-menthol and (−)-isomenthol by means of the hydroboration of (±)-3-*p*-menthene with (+)-monoisopinocampheylborane derived from (−)-(1S : 5S)-α-pinene.

We wish here to report such a synthesis.

Because of the feeble reactivity of the trisubstituted ethylene bond in 3-*p*-menthene toward dialkylborane, the monoisopinocampheylborane was preferred here as the asymmetric hydroboration reagent to the usual diisopinocampheylborane. 2.1 g. of (−)-α-pinene ($[\alpha]_D^{20}$ −34.7°; 68% optical purity), (0.015 mol.)), and 0.8 g. of sodium borohydride were dissolved in 15 ml. of dry diglyme at room temperature; to this solution there was then stirred, drop by drop, 3.0 g. of boron trifluoride etherate (47% BF_3 content) under a nitrogen stream over a 30-min. period. The disappearance of pinene was checked from time to time by g. l. c. (±)-3-Menthene (2.1 g.) (0.015 mol.) was added to the isopinocampheylborane, and, after the completion of the reaction (2 hr.), the reaction mixture was treated with 3 N sodium hydroxide and a 30% hydrogen peroxide solution. After 16 hr., this was worked up as usual. The separation of the product by g. l. c. yielded (−)-menthol, $[\alpha]_D^{20}$ −6.9° (chloroform), optical purity 14%, 0.57 g. (24.4% based on 3-menthene), (−)-isomenthol, $[\alpha]_D^{20}$ −13.4° (chloroform), optical purity 56%, 1.03 g. (44.0%) and (+)-isopinocampheol, $[\alpha]_D^{20}$ +22.1° (chloroform), 1.82 g. Both (−)-menthol and (−)-isomenthol were identified by a comparison of their n_D, IR,

1) H. C. Brown and G. Zweifel, *J. Am. Chem. Soc.*, **83**, 486 (1961).

2) H. C. Brown, N. R. Ayyanger and G. Zweifel, ibid., **86**, 397 (1964).

and R^t values with those of authentic specimens.

Of the various conceivable anti-Markownikoff-*cis*-additions of the boron-hydrogen bond of (+)-monoisopinocampheylborane (I) to the double bond in both (1S)-3-menthene (II) and (1R)-3-menthene (III), the attack of I, with the less bulky C_4-methylene grouping of the isopinocampheyl moiety oriented in the front, as is illustrated, to the rear sides of both II and III should be sterically more favored than those occurring in the opposite direction. This accounts for the experimental results which show that (−)-(1S : 3R : 4S)-isomenthol and (−)-(1R : 3R : 4S)-menthol were obtained preponderantly over their respective dextrorotatory enantiomers, which would be expected from the attack of I on the front side of III and II. Moreover, an inspection of the Stuart model of III reveals considerable steric interference between the (1R)-methyl group of III and the C_4-methylene grouping of the (+)-isopinocampheyl moiety, while this is not the case with II', where the (1S)-methyl group is kept away from the C_4-methylene of I. The situation is just reversed in the less favored attack occurring on the rear side of I. This accounts for the higher optical yield of (−)-isomenthol (IV) and the lower optical purity of (−)-menthol (V).

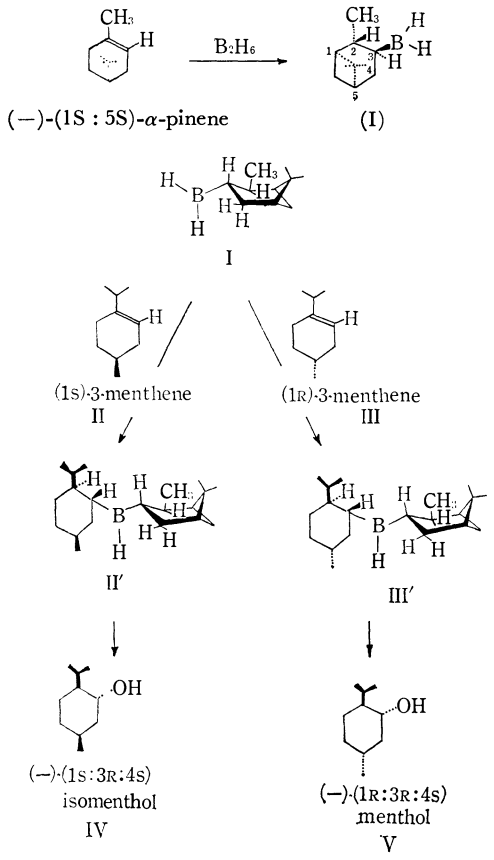

In carrying out the conversion of (±)-3-*p*-menthene to racemic menthol by hydroboration with diborane, Ascoli[3] observed that the total yield of hydroxylic compounds was lower, the larger the ratio of menthol to isomenthol. This was ascribed to the higer oxidation-hydrolysis rate of menthylborane as compared with that of isomenthylborane. However, the (−)-menthol/(−)-isomenthol ratio (1 : 1.8) observed in our asymmetric synthesis, in which oxidation-hydrolysis was completely effected, may also be interpreted in terms of the rate of the formation of the intermediates, II' and III', from II and III respectively.

Studies of the asymmetric hydroboration of other monoterpeneolefins are currently in progress in our laboratories; they will be described elsewhere in detail.

We wish to thank Dr. Yuzo Inoue for his many helpful discussions and suggestions.

3) F. Ascoli, A. M. Liquori and B. Pispia, *Chem. Ind.*, **1964**, 1579.

The Preparation of Several Triphenylsiloxysilanes

By Toshio TAKIGUCHI, Minoru ABE, Katsutoshi TAKAHASHI[1] and Kōji URANO

Department of Synthetic Chemistry, Kiryu College of Technology, Gunma University, Tenjin-cho, Kiryu

(Received April 30, 1965)

The reaction of an excess of sodium triphenylsilanolate with triorganochlorosilanes (trimethyl- and triphenylchlorosilane), diorganodichlorosilanes (dimethyl-, diphenyl-, methylphenyl- and vinylphenyldichlorosilane), organotrichlorosilanes (methyl-, phenyl- and vinyltrichlorosilane) and silicon tetrachloride gave the corresponding triphenylsiloxysilanes (hexaorganodisiloxanes, octaorganotrisiloxanes, organo-tris-triphenylsiloxysilanes and tetrakistriphenylsiloxysilane respectively).

The products obtained, including octaphenyltrisiloxane, 3 - vinylheptaphenyl - trisiloxane, 3-methylheptaphenyltrisiloxane, vinyl-tris-triphenylsiloxysilane and phenyl-tris-triphenylsiloxysilane, the new compounds were all crystalline substances of a high chemical stability; they were obtained in consistent yields of 63—67%. The siloxanes were all well defined and were characterized by means of their infrared absorption spectra.

Experimental

Sodium Triphenylsilanolate.—Sodium triphenylsilanolate neut. equiv. 294—297 was prepared according to the method of Hyde et al.[2]

Organolchlorosilanes.—Trimethylchlorosilane, b.p 58°C, dimethyldichlorosilane, b. p. 70—71°C, methyltrichlorosilane, b. p. 66—67°C phenyltrichlorosilane, b. p. 202—203°C, diphenyldichlorosilane, b. p. 130—133°C/2 mmHg and vinyltrichlorosilane, b. p. 90—92°C were obtained from the Shin-etsu Chemical Industrial Co. in commercial grades. All were further purified by distillation immediately before use. Triphenylchlorosilane, m. p. 97—98°C was isolated from a high boiling residue[3] of the direct synthesis of phenylchlorosilane. Vinylphenyldichlorosilane, b. p. 87—88°C/10 mmHg and methylphenyldichlorosilane, b. p. 197—199°C were synthesized by the Grignard process.[4] Reagent-grade silicon tetrachloride, b. p. 56—57°C was used after a single distillation.

Phenyl-tris-triphenylsiloxysilane.—A mixture of phenyltrichlorosilane (4 g., 0.0 2mol.), sodium triphenylsilanolate (30 g. 0.1 mol.) and a small portion of sodium ethylate in 300 ml. of toluene was heated to reflux. After this mixture had been refluxed for 15 hr., the jelly-like precipitate formed was centrifuged and the clear liquid was concentrated to about 50 ml., which in turn gave a white precipitate when added to a large excess of methanol. The precipitate was then recrystallized from 1, 4-dioxane to give 12 g. (67%) of elongated platelets, phenyl-tris-triphenylsiloxysilane, melting at 339—340°C (measured in molten *p*-diphenylbenzene as a medium), together with a small amount of hexaphenyldisiloxane.

Found: C, 76.7; H, 5.1; Si, 12.2; mol. wt., 895, 926 (in benzene). Calcd. for $C_{60}H_{50}O_3Si_4$: C, 77.4; H, 5.4; Si, 12.1%; mol. wt., 931.

Other Siloxanes.—The following siloxanes were obtained by substantially the same procedure: *Octaphenyltrisiloxane*, m. p. 153°C. Found: C, 77.7; H, 5.1; Si, 11.1; mol. wt., 720, 727. Calcd. for $C_{48}H_{40}O_2Si_3$: C, 78.8; H, 5.5; Si, 11.5%; mol. wt., 732.

3-Vinylheptaphenyltrisiloxane, m. p. 122—123°C.

Found: C, 77.0; H, 5.2; Si, 12.2; mol. wt., 659, 677. Calcd. for $C_{44}H_{38}O_2Si_3$: C, 77.4; H, 5.6; Si, 12.3%; mol. wt., 682.

3-Methylheptaphenyltrisiloxane, m. p. 119—120°C.

Found: C, 76.1; H, 5.4; Si, 12.5; mol. wt., 666, 663. Calcd. for $C_{43}H_{38}O_2Si_3$: C, 77.0; H, 5.7; Si, 12.5%; mol. wt., 670.

Vinyl-tris-triphenylsiloxysilane, m. p. 211—212°C.

Found: C, 75.8; H, 5.2; Si, 12.4; mol. wt., 894, 890. Calcd. for $C_{56}H_{48}O_3Si_4$: C, 76.4; H, 5.5; Si, 12.8%; mol. wt., 880.

Methyl-tris-triphenylsiloxysilane, m. p. 224°C (lit.[5] m. p. 224—225°C).

Found: Si, 13.2; mol. wt., 844—853. Calcd. for $C_{55}H_{48}O_3Si_4$: Si, 13.0%; mol. wt., 868.

3, 3-Dimethylhexaphenyltrisiloxane, m. p. 147—149°C (lit.[5] m. p. 155—156°C).

Found: Si, 13.6; mol. wt., 610—617. Calcd. for $C_{38}H_{36}O_2Si_3$: Si, 13.9%; mol. wt., 608.

Tetrakis-triphenylsiloxysilane, m. p. 231—232°C (lit.[6] m. p. 235°C).

Found: Si, 12.2; mol. wt., 1117, 1127. Calcd. for $C_{72}H_{60}O_4Si_5$; Si, 12.4%; mol. wt., 1130.

1, 1, 1-Trimethyltriphenyldisiloxane, m. p. 49°C (lit. m. p. 48°C[2], 51°C[7]).

Found: Si, 15.6; mol. wt., 339. Calcd. for $C_{21}H_{24}OSi_2$: Si, 16.1%; mol. wt., 348.

Hexaphenyldisiloxane, m. p. 230—231°C (lit.[7] m. p. 226°C).

Found: Si, 9.7; mol. wt., 522—528. Calcd. for $C_{36}H_{30}OSi_2$: Si, 10.5%; mol. wt., 535.

X-ray powder patterns recorded by using Cu$K\alpha$ radiation filtered by Ni are given for purposes of their rapid identification.

$C_6H_5Si[OSi(C_6H_5)_3]_3$

d, *kX*	11.33	9.94	8.93	5.68	4.90	4.70	4.46	4.19	3.92	3.36	3.28

1) Present address: Dai-Nippon Ink Chemical Industrial Co., Itabashi, Tokyo.

2) J. F. Hyde, O. K. Johannson, W. H. Daudt, R. F. Fleming, H. B. Laudenslager and M. P. Roche, *J. Am. Chem. Soc.*, **75**, 5615 (1953).

3) T. Takiguchi and M. Abe, *J. Chem. Soc. Japan, Ind. Chem. Sect.* (*Kogyo Kagaku Zassi*), **68**, 679 (1965).

4) T. Takiguchi and M. Abe, ibid., **66**, 625 (1963); M. Momonoi and J. Suzuki, *J. Chem. Soc. Japan, Pure Chem. Sect.* (*Nippon Kagaku Zasshi*), **78**, 581 (1957).

5) V. S. Chugunov, *Izvest. Akad. Nauk S. S. S. R., Otdel. Khim. Nauk*, **1957**, 1368.

6) V. A. Zeitler and C. A. Brown, *J. Am. Chem. Soc.*, **79**, 4616 (1957).

7) W. H. Daudt and J. F. Hyde, ibid., **74**, 386 (1952).

I/I_0	1.00	0.27	0.20	0.29	0.20	0.48	0.25	0.30	0.20	0.20 0.18
	$(C_6H_5)_2Si[OSi(C_6H_5)_3]_2$									
d, *kX*	10.91	9.31	7.83	5.40	5.04	4.72	4.51	4.35	4.27	4.04 3.90 3.20 2.96
I/I_0	0.43	0.86	0.51	0.50	0.50	1.00	0.95	0.70	0.91	0.54 0.53 0.29 0.29
	$CH_2{:}CH{\cdot}C_6H_5Si[OSi(C_6H_5)_3]_2$									
d, *kX*	9.41	7.50	7.25	5.54	5.37	5.10	4.93	4.70	4.51	4.23 3.83 3.59 3.45
I/I_0	1.00	0.31	0.34	0.25	0.22	0.24	0.28	0.39	0.44	0.50 0.20 0.26 0.19
	$CH_3{\cdot}C_6H_5Si[OSi(C_6H_5)_3]_2$									
d, *kX*	8.85	6.86	5.22	4.85	4.48	4.33	4.23	4.10	3.93	3.87 3.63 3.31
I/I_0	0.84	0.36	0.51	0.61	1.00	0.45	0.46	0.27	0.24	0.24 0.27 0.23
	$CH_2{:}CHSi[OSi(C_6H_5)_3]_3$									
d, *kX*	10.40	6.92	5.40	4.77	4.40	4.15				
I/I_0	0.63	0.23	0.23	0.91	1.00	0.47				
	$CH_3Si[OSi(C_6H_5)_3]_3$									
d, *kX*	9.94	9.31	4.77	4.33	4.10	3.27				
I/I_0	0.35	0.19	0.22	1.00	0.19	0.29				
	$(CH_3)_2Si[OSi(C_6H_5)_3]_2$									
d, *kX*	9.21	8.42	8.19	7.17	6.81	6.20	4.72	4.46	4.19	3.83
I/I_0	0.15	0.26	0.33	0.30	0.20	0.55	0.83	1.00	0.17	0.14
	$[(C_6H_5)_3SiO]_4Si$									
d, *kX*	19.64	9.94	4.96	4.75	4.40	3.79	3.29	3.25		
I/I_0	0.28	0.27	1.00	0.15	0.63	0.22	0.50	0.25		
	$(CH_3)_3SiOSi((C_6H_3)_3$									
d, *kX*	8.85	6.93	5.68	4.87	4.37	3.68	3.44	2.69		
I/I_0	0.35	0.26	0.22	1.00	0.31	0.51	0.27	0.20		
	$[(C_6H_5)_3Si]_2O$									
d, *kX*	9.94	8.51	7.76	7.57	6.92	5.47	4.96	4.75	4.60	4.46 4.21 3.79 3.29
I/I_0	0.19	0.19	0.25	0.23	0.22	0.19	1.00	0.33	0.33	0.51 0.32 0.33 0.18

The authors are grateful to the Shin-etsu Chemical Industrial Co. for the supply of organochlorosilanes used in the present work.

Some Azo-compounds which form Spherical Micro-particles

By Hiroshi MIDORIKAWA, Heinosuke YASUDA, Hiroe ASABA and Tatsuo TAKESHIMA

The Institute of Physical and Chemical Research, Bunkyo-ku, Tokyo;
Department of Chemistry, Faculty of Science, Shizuoka University, Shizuoka

(Received May, 10 1965)

The present investigation will be concerned with 5-phenylazoresorcylaldehyde (I) and related compounds. I has been synthesized by Borsche.[1] He reported that the substance is prone to resinify when recrystallized, thereby preventing isolation. When he conducted the recrystallization from ethanol under a microscope, he first observed the separation of yellow needles, but they were soon covered with red-yellow resinous droplets. I was thus isolated only in the form of its phenylhydrazone.

We observed a peculiar property of the cyanoacetic ester derivative of I; it was obtained in the form of dark red spherical micro-particles and reflected the incident light fairly accurately in the opposite direction.

The present work was undertaken in order to explore the related behavior of the hydroxy derivatives of azobenzene.

I was prepared from resorcylaldehyde and, after being separated from the accompanying 3, 5 - bisphenylazoresorcylaldehyde (II), was recrystallized to yield long orange plates, m. p. 149.5—50°C. The compound, however, was apt to form spherical micro-particles in the case of recrystallization. The particles, once formed, exhibited a nature different from that of the original substance. It has no melting point and begins to carbonize, for example, above ca. 160°C and, unlike I, is hardly soluble in ethanol.

In the coupling reaction to prepare I, the 3- or 5-position of resorcylaldehyde is available for the entering phenylazo group. The assignment of the I structure is based on the following facts. I was submitted to hydrogenolysis in dioxane containing acetic anhydride. The resulting acetamidoresorcylaldehyde was identical with the acetamidoresorcylaldehyde (IV) obtained from 5-nitroresorcylaldehyde (V). However, since no rigorous determination[2] of the structure of V prepared by the nitration of resorcylaldehyde has been carried out, we methylated the nitro compound and then compared the resulting dimethoxynitrobenzaldehyde with that prepared by the nitration of 2, 4-dimethoxybenzaldehyde, which was considered to afford the 5-nitro derivative (VI) because of steric hindrance. These two specimens, prepared via alternate routes, were identical.

I, on treatment with ethyl cyanoacetate, also gave the characteristic dark red micro-particles, the composition of which varied to a certain extent;

1) W. Borsche and L. E. Bolser, *Ber.*, **34**, 2098 (1901).

2) L. Gattermann, *Ann.*, **357**, 337 (1907)

for example, the substance was composed of a ratio of one mole of I to two moles of the ester.

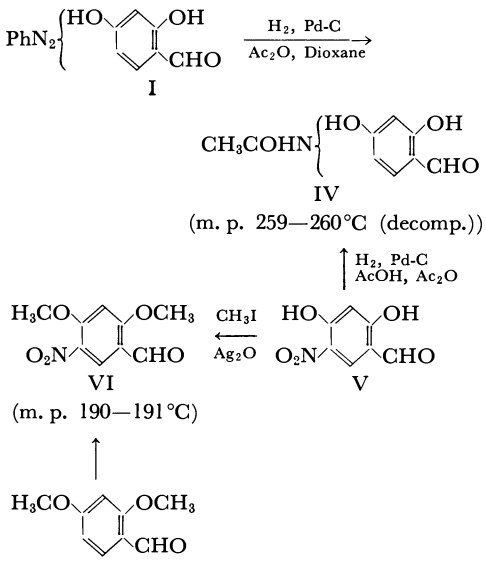

The particles in this case seemed more stable than the preceding ones and began to carbonize above ca. 200°C without melting. When I was treated with the cyanoacetate a crystalline substance, brown needles, was obtained in addition to the particles. It seems from the analysis, the mode of reaction, and an analogy reported by Matsumura that this crystalline substance is of the III enamine structure.

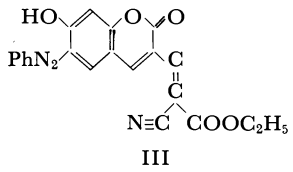

3, 5-Bisphenylazoresorcylaldehyde (II), which is produced along with I in the coupling reaction, showed no tendency to form particles.

Experimental*

5-Phenylazoresorcylaldehyde (I).—Into a solution of 5 g. (0.036 mol.) of resorcylaldehyde, 3.1 g. (0.033 mol.) of aniline, and 30 ml. of concentrated hydrochloric acid in 1500 ml. of water was added portionwise 4 g. of sodium nitrite over period of ca. 10 min. at ca. 7°C with stirring. After the mixtrue had stirred for an additional 20 min., 30 g. of sodium acetate was added, and then a solution of 20 g. of potassium carbonate (anhydrous) in 100 ml. of water was added over a period of 30 min. at the same temperature. Stirring was continued for further 3 hr. and then kept overnight in an ice-box. The precipitates were collected, washed with water, and dried in a desiccator. The product, which weighed ca. 7 g., consisted of a mixture of I and 3, 5-bisphenylazoresorcylaldehyde (II). The crude product was then treated with ca. 250 ml. of hot ethanol or, bester, with the same volume of cold acetone, and filtered. From the filtrate, upon the addition of water, this was obtained ca. 3.8 g. of I, which, on repeated recrystallization from acetone containing water, formed orange long plates, m. p. 149.5—150°C (slow heating) and 156°C (rapid heating).

Found: C, 64.48; H, 4.08; N, 11.60. Calcd. for $C_{13}H_{10}O_3N_2$: C, 64.46; H, 4.16; N, 11.57%.

The 2, 4-Dinitrophenylhydrazone: brownish red plates, m. p. 275°C (decomp.).

Found: C, 57.51; H, 3.76; N, 19.58. Calcd. for $C_{24}H_{19}O_6N_7$: C, 57.48; H, 3.82; N, 19.55%.

The Semicarbazone: brown needles or long plates; m. p. above 300°C.

Found: N, 21.48. Calcd. for $C_{14}H_{13}O_2N_5+C_2H_5OH$: N, 21.27%.

3, 5-Bisphenylazoresorcylaldehyde (II). — From the acetone-insoluble fraction, red needles or long plates, m. p. 253°C (decomp.), were obtained.

Found: C, 65.81; H, 4.10; N, 16.28. Calcd. for $C_{19}H_{14}O_3N_4$: C, 65.89; H, 4.07; N, 16.18%.

The 2, 4 - Dinitrophenylhydrazone: lustrous black-purple crystals, m. p. ca. 277°C (decomp.).

Found: C, 57.36; H, 3.67; N, 21.28. Calcd. for $C_{25}H_{18}O_6N_8$: C, 57.03; H, 3.45; N, 21.29%.

The Treatment of I with Ethyl Cyanoacetate.—To a solution of 0.1 g. (0.00041 mol.) of I in 5 ml. of ethanol were added 0.1 g. (0.00089 mol.) of ethyl cyanoacetate and one drop of piperidine; the resulting solution was then warmed on a water bath for a while. The red or dark-red micro-particles (apparently a powder) produced were more stable than those obtained in the aforesaid treatment, carbonizing at a higher temperature, e. g., above 200°C. The other properties, on the whole, were similar to those of the particles described immediately above.

The Hydrogenolysis of I to 5-Acetamidoresorcylaldehyde (IV).—Into a mixture of 2 ml. of acetic anhydride and 15 ml. of dioxane, 0.16 g. of I was dissolved. The resulting solution was shaken with hydrgen in the presence of palladium-on-charcoal. The yellowish solid obtained was recrystallized from acetic acid to give yellowish crystals which melted at 259—260°C (decomp.).

Found: N, 7.23. Calcd. for $C_9H_9O_4N$: N, 7.18%.

The Reduction of 5-Nitroresorcylaldehyde (V) to IV.—A solution of 3.5 g. of V in a mixture of 100 ml. of acetic acid and 10 ml. of acetic anhydride was shaken with hydrogen in the presence of palladium-on-charcoal. Three grams of yellowish crystals, m. p. 259—260°C (decomp.), was obtained. The melting point was undepressed on admixture with the specimen obtained by the hydrogenolysis of I.

Found: C, 55.38; H, 4.63; N, 7.18. Calcd. for $C_9H_9O_4N$: C, 55.38; H, 4.65; N. 7.18%.

The 2, 4-Dinitrophenylhydrazone of IV.—This melted above 300°C.

Found: C, 48.04; H, 3.19; N, 18.40. Calcd. for $C_{15}H_{13}O_7N_5$: C, 48.00; H, 3.49; N, 18.66%.

The Preparation of 2, 4-Dimethoxy-5-nitrobenzaldehyde (VI) from V.—Into a mixture of 1.2 g. of V, 15 ml. of dioxane and 2 g. of silver oxide was added

3) S. Matsumura, This Bulletin, **34**, 995 (1961).

* All melting points are uncorrected.

dropwisw a solution of 11.5 g. of methyl iodide in 5 ml. of dioxane with stirring. The product was recrystallized from methanol to yield 0.15 g. of brownish yellow short needles; m. p. 190—191°C, reported 188—189°C.[4]

Found: C, 50.91; H, 4.28; N, 6.63. Calcd. for $C_9H_9O_5N$: C, 51.19; H, 4.30; N, 6.63%.

The Preparation of VI from 2, 4-Dimethoxybenzaldehyde.—The method used was that described by Rao al.[4] M. p. 190—191°C; reported 188—189°C[4] A mixed melting point with the preceding specimen from V was not depressed.

We are indebted to Miss Kazue Takamura and Mr. Norimichi Koizumi for their kind assistance.

4) M. G. S. Rao, C. Srikantia and M. S. Iyenger, *J. Chem. Soc.*, **127**, 558 (1925).

The Stereochemistry of 2-Hydroxyisoflavanones

By Shozo YAMAGUCHI, Shoei ITO, Asao NAKAMURA and Naoto INOUE

College of General Education, Tohoku University, Kawauchi, Sendai

(Received July 5, 1965)

2-Hydroxyisoflavanones are often isolated as unstable intermediates in the course of the syntheses of isoflavones by means of the reactions of 2-hydroxyphenyl benzyl ketones with ethyl formate in the presence of sodium.[1,2,4]

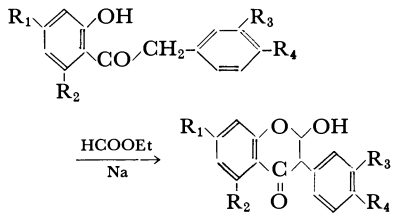

(I): $R_1=R_2=R_3=R_4=H$
(II): $R_1=OMe$; $R_2=R_3=R_4=H$
(III): $R_1=R_2=OMe$; $R_3, R_4 = O{>}CH_2$

The stereochemistry of 2-hydroxyisoflavanones has been discussed previously by Whalley,[3] who reported that 2-hydroxyisoflavanones have a trans configuration with equatorial C_2 hydroxyl and equatorial C_3 phenyl groups.

In order to confirm his assignment, the NMR spectra of 2-hydroxyisoflavanones were investigated; the results will be reported in this paper.

2-Hydroxyisoflavanone (I) and 2-hydroxy-7-methoxyisoflavanone (II) were synthesized, and the NMR spectra of I, II and 2-hydroxy-5, 7-dimethoxy - 3', 4' - methylenedioxy - isoflavanone (III)[4] were measured in $CDCl_3$, $CHCl_3$ (containing a trace of water or hydrochloric acid) or pyridine, depending on their solubilities. The spectra were determined with a Varian A-60 spectrometer at 60 mc., using tetramethylsilane as an internal reference, the results obtained are summerized in Table I.

In the NMR spectra of I in $CDCl_3$, the broadenings of the doublet with its center at 248.4 c. p. s. and of the triplet with its center at 348.3 c. p. s. seem to be due to the slow exchange of the C_2-hydroxyl proton. In order to confirm this consideration, the NMR spectrum of I was measured in $CHCl_3$ containing a trace of water. The broad doublet at 248.4 c. p. s. became extremely broad and almost unrecognizable; however, the integration curve showed the presence of one proton between 248 and 287 c. p. s. The triplet at 348.3 c. p. s. became a sharp doublet with its center at the same position. Furthermore, in the NMR spectrum of I in $CHCl_3$ containing a trace of hydrochloric acid, the triplet at 348.3 c. p. s. observed in $CDCl_3$ became a sharper doublet than that in the spectra measured in $CHCl_3$ containing a trace of water.

From these observations, it may be concluded that the signals of I at 233.1, 248.4 and 348.3 c. p. s. are to be attributed to the C_3-proton, hydroxyl proton and C_2-proton respectively; the coupling constant between the C_2-proton and the C_3-proton has been determined to be 4.2 c. p. s.

The NMR spectrum of III was measured in a pyridine solution because of its low solubility in $CDCl_3$. As a result of the solvent effect caused by pyridine, the signals of III were shifted to a considerably low field as compared with the corresponding signals of I in $CDCl_3$; however, the complete assignments for the signals of III could be made with reference only to those of I measured in pyridine.

---

* Present address: The Ajinomoto Co., Ltd., Kawasaki, Japan.

1) W. B. Whalley, *J. Am. Chem. Soc.*, **75**, 1059 (1953); W. B. Whalley, *J. Chem. Soc.*, **1953**, 3366; A. Robertson and Whalley, ibid., **1954** 1440.

2) N. Narasimhachari, D. Rajanparan and T. R. Seshadri, *J. Sci. Ind. Research (India)*, **12**, 287 (1954).

3) W. B. Whalley, "The Chemistry of Flavonoid Compounds," Ed. by T. A. Geisman, Pergamon Press, Oxford (1962), p. 462.

4) N. Inoue, *J. Chem Soc. Japan, Pure Chem. Sect.* (*Nippon Kagaku Zasshi*), **79**, 222 (1958).

Table I. NMR Spectra of 2-hydroxyisoflavanones

Isoflavanones	Position of peaks in c.p.s.	No. of protons	Assignment	Remarks	Configuration
2-OH*(I)	233.1	1	3-H	Doublet, $J_{2,3}=4.2$ c.p.s.	
	248.4	1	Hydroxyl proton	Broad doublet	
	348.3	1	2-H	Broad triplet	
2-OH**(I)	233.1	1	3-H	Doublet	$J_{2,3}=4.2$ c.p.s. 2(eq), 3(ax) cis
	348.3	1	2-H	Doublet	
2-OH, 7-MeO*(II)	236.5	1	3-H	Partly screened by methyl signal	
	351.0	1	2-H	Doublet, $J_{2,3}=4.0$ c.p.s.	2(eq), 3(ax) cis
2-OH***(I)	265.9	1	3-H	Doublet	$J_{2,3}=3.7$ c.p.s.
	280.3	1	2-H	Doublet	
2-OH, 5,7-di-MeO-3′,4′-methylenedioxy***(III)	255.2	1	3-H	Doublet	$J_{2,3}=3.5$ c.p.s. 2(eq), 3(ax) cis
	269.9	1	2-H	Doublet	

* $CDCl_3$ was used as solvent.
** $CHCl_3$ + trace H_2O or trace HCl was used as solvent.
*** Pyridine was used as solvent.

Since 2-hydroxyisoflavanones have the hemiacetal structure, the coupling constant of glucopyranose can be used for determining the configurations of the compounds I, II and III.

Considering Karplus' calculated results,[5] the coupling constant of glucopyranose[6] and the observed $J_{2,3}$, of I, II and III (4.2 c.p.s., 4.0 c.p.s. and 3.5 c. p. s., respectively), it may be concluded that the 2-hydroxyisoflavanones obtained as the intermediates in the syntheses of isoflavones have cis configurations.

2-Hydroxyisoflavanones are generally converted to the corresponding isoflavones through dehydration by heating or treatment with acid.[3] However, I and II were found to give the corresponding isoflavones in a quantitative yield even when treated with ethanol or benzene under the mild conditions described in Table II.

Table II. Transformations of 2-hydroxyisoflavanones to isoflavones

(a)*—Ethanol (10 ml.), reflux 30 min.
(b)*—Pyridine (0.5 ml.) in benzene (5 ml.), 50°C, 20 min.
(c)*—Ethanolic potassium hydroxide (5% 10 ml.), room temperature, 20 hr.

* In each case 50 mg. of the sample (I or II) was employed.

5) M. Karplus, *J. Chem. Phys.*, **30**, 11 (1959).
6) R. V. Lemieux, R. K. Kulling, H. J. Bernstein and W. G. Schneider, *J. Am. Chem. Soc.*, **80**, 6098 (1958).

Experimental

2-Hydroxyisoflavanone (I).—Into 3 g. of sodium dust there was stirred, drop by drop, over a period of 40 min. under cooling with ice, a mixture of 60 ml. of ethyl formate and 6 g. of 2-hydroxyphenyl benzyl ketone. After had been stirred the mixture three more hours, it was allowed to stand overnight under cooling with ice. To the reaction mixture there was then added ice water. The separated crystals were filtered, dried, and washed with hot petroleum ether and then with a small amount of ethanol. Recrystallization from benzene - petroleum ether (1: 1) gave 2-hydroxyisoflavanone (ν_{OH} 3600 cm^{-1}, 3400 cm^{-1}; $\nu_{C=O}$ 1695 cm^{-1}; $CHCl_3$ solution), m. p. 110—111°C (decomp.), 2.2 g. (32%).

Found: C, 74.95; H, 5.26. Calcd. for $C_{15}H_{12}O_3$: C, 74.99; H, 5.03%.

One gram of isoflavone, m. p. 132—133°C, was obtained from the mother liquor of I.

2-Hydroxy-7-methoxyisoflavanone (II).—2-Hydroxy-4-methoxyphenyl benzyl ketone was treated with ethyl formate and sodium in a manner similar to that used for the formation of I. The crude crystals were recrystallized from benzene yielding II (ν_{OH} 3350 cm^{-1}, 3460 cm^{-1}; $\nu_{C=O}$ 1688 cm^{-1}; $CHCl_3$ solution) m. p. 145—146°C (decomp.)[2] in a 43% yield. By refluxing II in acetic acid for 20 min., it was quantitatively converted to 7-methoxyisoflavone, m. p. 154—155°C.

Separation of ^{90}Sr and ^{90}Y by Paper Electrophoresis with Very Dilute Hydrochloric Acid Background Electrolyte

By Shoichi KAWAMURA and Masami IZAWA

Chemistry Division, National Institute of Radiological Sciences, Anagawa-cho, Chiba

(Received July 12, 1965)

Many methods have been employed for the separation of ^{90}Sr and ^{90}Y. One of them is paper electrophoresis, by which ^{90}Sr-^{90}Y have been separated by using lactic acid, ammonia,[1] ammonium acetate or ammonium citrate[2] as background electrolytes. The present paper will report on the successful use of 10^{-3} N hydrochloric acid as the background electrolyte for the separation of ^{90}Sr and ^{90}Y. The use of hydrochloric acid eliminates the trouble of removing the organic ingredient after the extraction of the ^{90}Sr or ^{90}Y fraction from the filter paper.

Experimental

The sample without a carrier was prepared by diluting ^{90}Sr-^{90}Y, obtained from the Oak Ridge National Laboratory, with redistilled water, while the one with a carrier was prepared by adding ^{90}Sr-^{90}Y to Sr or Y ($SrCl_2$ or YCl_3) to make 0.05 M solution. The filter paper used was Tokyo filter paper No. 3 (2×40 cm.) supplied by the Tokyo Roshi Kaisha, Ltd. The sample to be separated was applied at 10 cm. from an end of the paper. After the paper was sandwiched between plastic plates,[3] a d. c. potential of 20 V./cm. was applied to it for 30 min. After drying, the paper was cut into strips 1 cm. in length, and the activity of each strip was determined by a G. M. counter.

The relative distance, R_D, was also determined according to a slight modification of Bermes method.[4] The filter paper was sandwiched between plastic plates and arranged as is shown in Fig. 1. The background electrolyte was allowed to soak through the paper until it reached point B. When the background electrolyte reached this point, the sample to be determined was applied to point A through a hole above A. The background electrolyte was then permitted to continue its flow without the application of a d. c. current until it almot reached the other end of the paper strip, B'. Meanwhile, the sample moved to point A'. R_D was calculated from the following equation.

$$\text{Relative distance, } R_D = \frac{\text{Migrant movement}}{\text{Solvent movement}}$$

The electrosmotic flow was determined by using glucose as an indicator under the same conditions as were employed for the separation of ^{90}Sr and ^{90}Y.

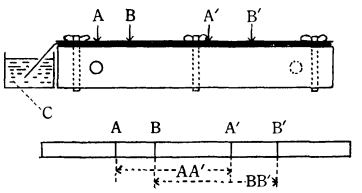

Fig. 1. Arrangement for measuring relative distance, R_D of ^{90}Sr.

$$\text{Relative distance, } R_D = \frac{AA'}{BB'} = \frac{^{90}Sr \text{ movement}}{10^{-3}\text{ N HCl movement}}$$

where A : initial ^{90}Sr position, A' : final ^{90}Sr position, B : initial 10^{-3} N HCl front, B' : final 10^{-3} N HCl front, C : 10^{-3} N HCl

Results and Discussion

As is shown in Fig. 2A, the separation of ^{90}Sr and ^{90}Y was accomplished by using 10^{-3} N hydrochloric acid as the background electroyte.

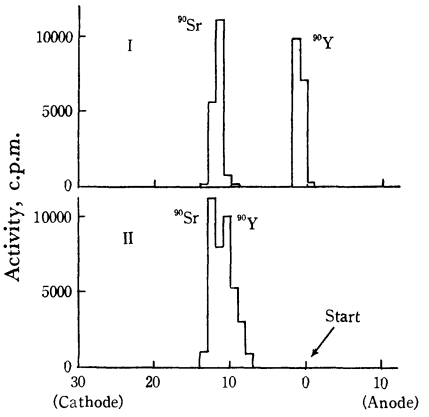

Fig. 2. Electrophoregram (20 V./cm., 30 min.) of ^{90}Sr and ^{90}Y.
I 10^{-3} N HCl II 10^{-2} N HCl

It was difficult to separate ^{90}Sr and ^{90}Y in 10^{-2} N hydrochloric acid, in which Sr and Y migrate at almost the same speed (Fig. 2B). The use of 10^{-1} N hydrochloric acid as the background electrolyte made it impossible to carry out the experiment because of the over-heating of the filter paper. When the hydrochloric acid concentration is

1) T. R. Sato, W. P. Norris and H. H. Strain, *Anal. Chem.*, **26**, 267 (1954).
2) S. Kawamura, *Japan Analyst (Bunseki Kagaku)*, **10**, 975 (1961).
3) S. Kawamura, ibid., **11**, 814 (1962).
4) E. W. Bermes, Jr., and H. J. McDonald, *J. Chromatog.*, **4**, 34 (1960).

reduced to 10^{-4} N, the current through the paper strip becomes negligible; therefore, the use of 10^{-4} N hydrochloric acid made it impossible to carry out the experiment.

In these experiments, the behavior of ^{90}Sr and ^{90}Y without a carrier was almost identical with those of the substances with a carrier. Sr and Y immersed in a filter paper strip migrate toward the cathode against the barrier effect due to the filter paper. In order to determine this effect, the relative distances suggested by Bermes were determined; the results are shown in Fig. 3.

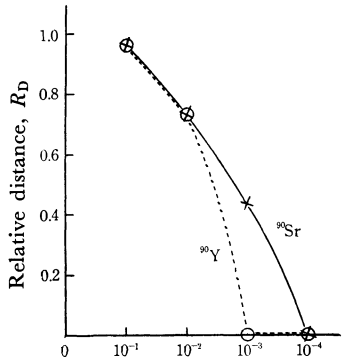

Fig. 3. Relation between relative distance and concentration of hydrochloric acid.

The results shown in Fig. 2A may be explained by the fact that the R_D value of ^{90}Y in 10^{-3} N hydrochloric acid is 0; therefore, the ^{90}Y in the solution remains at the starting point, being absorbed by the filter paper, while ^{90}Sr, on the other hand, migrates to the cathode. The migration distance of ^{90}Sr in a free solution of 10^{-3} N hydrochloric acid at 20 V./cm. was calculated from the above data as follows:

$$A = \frac{B - C}{R_D} = \frac{11 - 2.5}{0.45} = 19 \text{ (cm.)} \quad (1)$$

where

A: the migration distance of ^{90}Sr in a free solution of 10^{-3} N hydrochloric acid

B: the migration distance of ^{90}Sr in 10^{-3} N hydrochloric acid by paper electrophoresis 11 cm.

C: the migration distance due to electrosmosis 2.5 cm.

The migration distance of ^{90}Sr in a free solution is calculated as follows:

$$D = \frac{l_{Sr} \times V \times t}{F} = 22 \text{ (cm.)} \quad (2)$$

where

l_{Sr}: the ionic conductance of Sr, 59.5 coulomb, cm./V.sec.

V: the applied voltage, 20 V./cm.

t: the migration time, 30 min.

F: the Faraday constant

The migration distance in a free solution as calculated from Eq. 1 agreed fairly well with the one obtained from Eq. 2. This means that Sr migrates in the form of a divalent cation in a 10^{-3} N hydrochloric acid-background electrolyte, and that the value of R_D determined is reasonable.

The Infrared Spectra of Sublimed Methylsuccinic Acid

By Yoshiko TAKEOKA

Research Laboratory of Resources Utilization, Tokyo Institute of Technology, Ookayama, Tokyo

(Received August 4, 1965)

It was noted by Duncanson[1] that the infrared spectrum of sublimed methylsuccinic acid was different from that of the one recrystallized from water and that this change produced by sublimation was consistent with the occurence of rotational isomers involving the central carbon-carbon bond. He proposed that, if recrystallized methylsuccinic acid from water had a form similar to that of succinic acid,[2] namely, a trans form with respect to two carboxyl groups (Fig. 1 (a)), as is suggested by its dipole measurements and its infrared spectrum, the sublimed one would probably possess a gauche form, as is shown in Fig. 1 (b). Since the infrared spectrum of *os*-dimethylsuccinic acid did not change upon sublimation, such a molecule seemed to display a fairly strong resistance of the carbonyl group to the rotation passing near a β-methyl group.

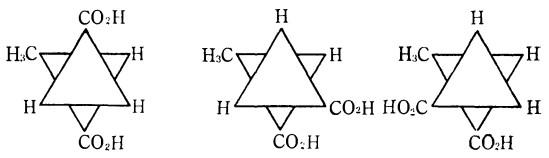

Fig. 1. Rotational isomers of methylsuccinic acid.

1) L. A. Duncanson, *J. Chem. Soc.*, **1952**, 1753.
2) J. D. Morrison and J. M. Robertson, ibid., **1949**, 980.

We have found that, when the infrared spectra of methylsuccinic acid sublimed at 70—80°C/ 1×10^{-1} mmHg and condensed on the surface of copper held at 30°C, 0°C and −145°C, were measured immediately after sublimation, some new bands appeared which did not exist in Duncanson's spectrum (Fig. 2). From these measurements, it has been shown that, with a decrease in the temperature at the copper surface, the new bands increased in intensity. Three hours after sublimation, the intensity of these bands decreased while that of some neighbouring bands increased. The spectra became very similar to those given by Duncanson in the course of two days, but after that it remained almost unchanged, even for as long as half a year. When the sublimed sample was recrystallized from water, it gave the same spectrum as that observed before sublimation. The bands of the O–H and C–O stretching vibrations almost did not change at all, and no band characteristic to anhydride appeared near 1800 cm^{-1} after sublimation. These facts suggest that succinic anhydride was not produced. In the region below 1350 cm^{-1}, most bands are modified by sublimation, as is shown in Fig. 2; some strong bands disappeared and some others appeared. Such large variations in spectra may be well explained by assuming the existence of rotational isomers, as has been pointed out by Duncanson.

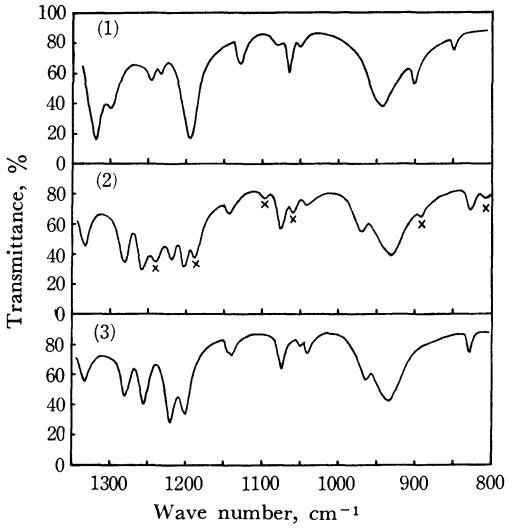

Fig. 2. Infrared spectra of methylsuccinic acid. (solid; Nujol mull)
(1) before sublimation (recrystallized from water)
(2) immediately after sublimation, condensed on Cu surface held at −145°C (×; disappeared during two days)
(3) two days after sublimation

It has been well-known that the rotational isomers of ethane derivatives possess mutually different infrared spectra. In many cases, two or more isomers coexist in the liquid or gas state, but only one isomer exists in the solid state. In the present case, the sublimed sample, condensed on the copper surface at −145°C, showed the largest spectral change, after sublimation, and many bands, even the strong band found at 1320 cm^{-1} before sublimation, did not appear in the spectrum of the sublimed sample. These facts suggest that rotational isomers, produced by sublimation in the state and possessing different configurations, might have produced unstable crystals when rapidly cooled.

As has been mentioned above, the spectra of the sublimed product changed gradually. The intensity of some bands increased and that of some others decreased; the former bands disappeared completely in two days, after which none of the spectra showed any more variation. From such behavior it may be supposed that the sublimed sample probably has at least two rotational isomers. Since the energy difference is small, the unstable form is transformed into the stable one in two days. The spectral change occured in the solid state, so it seems that the potential barrier between one isomer and another is not so high.

These observations can be well explained by the following considerations. If we assume, as did Duncanson, that the molecule of methylsuccinic acid before sublimation has a form similar to that of succinic acid, such as a trans form, the configurations of its probable rotational isomers can be represented as in Fig. 1 (b) and (c). It is known that, at low pressures and at high temperatures, the vapor of carboxylic acids consists to a large extent of the monomeric form. Therefore, in the present case, many molecules in the gas state exist, perhaps as monomers after sublimation. They probably prefer to be in a gauche form, for they could be stabilized in this form only as a result of forming an intramolecular hydrogen bond. The b form seems to be more stable than c, because in the former the methyl group is not situated near carboxyl groups. The transformation from the a form into the b can be realized by the rotation in which methyl and carboxyl groups pass only near the hydrogen atom. In the changes from the a or b form to the c, the carboxyl groups may find it difficult to pass near the β-methyl group, as has been indicated by Duncanson; however, we consider the transformation from the b form to the c to be possible by means of the following assumptions. In the b form, this molecule is probably stabilized in the gas state by the formation of an intramolecular hydrogen bond consisting of a seven-membered ring. By the inversion of this seven-membered ring, as in the case of cyclohexane ring, the b form may then be transformed into the c rather easily, leaving the intramolecular hydrogen bond unchanged. Therefore, it may be supposed that the

sublimed molecules immediately after sublimation have the b and c forms as a result of the rapid cooling and that the spectral change in the sublimed solid is due to the transformation from the c form to the b. However, in the solid state the intermolecular hydrogen bond can be formed in either the b or the c form, so the situation is more complicated than in the gas state.

The band at 945 cm^{-1} in the solid spectrum before sublimation becomes extremely broad in the liquid; it can be assigned to the O–H out-of-plane deformation vibration, much as in the case of succinic acid.[3] The frequency of this band is greatly lowered (934 cm^{-1}) by sublimation, showing a weaker hydrogen bond. However, in the sublimed solid spectrum, this band shows only a small shift (936 cm^{-1}) in two days. This fact suggests that the isomers coexisting in the sublimed solid are similar to each other in the strength of their hydrogen bonds. The band of the O–H stretching vibration shifts to a higher frequency upon sublimation; this fact shows as in the case of the O–H out-of-plane deformation vibration mentioned above, that the molecule before sublimation has a stronger hydrogen bond than the sublimed molecule.

For many ethane derivatives, such as 1, 2-dichloroethane or 1, 2-dibromoethane, a trans form is generally more stable than a gauche form in the gas state. However, the more stable form of ethylene chlorohydrin in the gas state is a gauche form, for stabilization by the formation of the intramolecular hydrogen bond is possible only in the gauche form.[4] Similarly, it may well be assumed that methylsuccinic acid also possesses a gauche form in the gas state, as it is more stable configuration.

The author wishes to express her thanks to Professor Shiro Maeda for his valuable discussions.

3) T. Takenishi, *J. Chem. Soc. Japan, Pure Chem. Sect.* (*Nippon Kagaku Zasshi*), **82**, 319 (1961).

4) S. Mizushima, T. Shimanouchi, T. Miyazawa, K. Abe and M. Yasumi, *J. Chem. Phys.*, **19**, 1477 (1951).

The Absorption Spectra of 2, 4, 6-Trinitroanisole in Methanolic Sodium Methoxide

By Takehiro ABE

The College of General Education, Tohoku University, Kawauchi, Sendai

(Received August 4, 1965)

It has been reported that the absorption spectrum of a colored methanolic solution of 2, 4, 6-trinitroanisole in the presence of sodium methoxide is due to the Meisenheimer complex I.[1-4] In the present work, an attempt has been made to investigate the further interaction of 2, 4, 6-trinitroanisole with the methoxide ion at very high methoxide concentrations. For this purpose, the author measured the spectra of the colored solutions at various methoxide concentrations, using a Hitachi EPU-2A spectrophotometer at room temperature. The solutions were left to stand for half an hour before

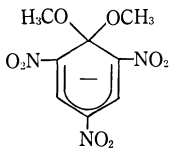

I

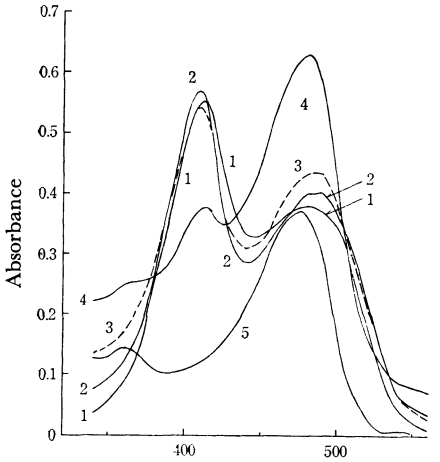

Fig. 1. Absorption spectra of 2, 4, 6-trinitroanisole (2.15×10^{-5} M) in methanol in the presence of sodium methoxide (path-length of cells, 1 cm.).
Concentrations of sodium methoxide:
1) 1.01×10^{-2} M; 2) 1.23 M; 3) 2.46 M; 4) 3.94 M; 5) 4.92 M

1) R. Foster, *Nature*, **176**, 746 (1955); **183**, 1042 (1959).
2) V. Gold and C. H. Rochester, *J. Chem. Soc.*, **1964**, 1687.
3) T. Abe, This Bulletin, **37**, 508 (1964).
4) T. Abe, T. Kumai and H. Arai, ibid., **38**, 1526 (1965).

the measurements, because it took at least several minutes for the equilibrium needed for the formation of the first complex to be attained.[2,4] In the present wavelength region, 2, 4, 6-trinitroanisole at a low concentration and the methoxide ion did not absorb. The results are shown in Fig. 1.

Absorption curve 1, with two maxima at ca. 485 and 410 mμ for the solution at the methoxide concentration of 1.01×10^{-2} M in Fig. 1, may be ascribed to the complex I.[1-4] The sbsorption intensity of the band at 410 mμ is stronger than that at 485 mμ. When the concentration of the methoxide is increased, the absorption intensity of the band at ca. 480 mμ is stronger than that at ca. 410 mμ at the methoxide concentration of 3.94 M. From those results, the absorption maximum at 480 mμ in the curve 4 can be attributed to a second complex, one formed by a further reaction between the first complex I and the methoxide, as was suggested by Gold and Rochester.[2] They suggested that the second complex is likely to involve two methoxide ions per methyl picrate molecule. At the very much higher methoxide concentration of 4.92 M, the absorption intensity at ca. 480 mμ decreases and the absorption maximum at ca. 410 mμ disappears. This can be interpreted in terms of the formation of a third complex between the second complex and the methoxide, a complex with no absorption in the visible region. The above results lead to the conclusions that the Meisenheimer complex I has two bands, at ca. 485 and 410 mμ; that the second complex has a band at ca. 480 mμ, and that the third complex has no bands in the visible region.

Assuming that the second and the third complex are II and III respectively, the present author calculated the energy levels of the molecular orbitals of π-electrons in the three complexes I, II and III, using the same parameters as in the previous paper[3] by means of the simple LCAO MO method. The results are shown in Fig. 2. The predictions for the transitions in the complexes, indicated in Fig. 2, agree qualitatively with the experimental results in Fig. 1. Accordingly, it is likely that the second complex II with the absorption maximum at ca. 480 mμ and the third complex III with no absorption in the visible region are formed as the concentration of sodium methoxide increases.

II III

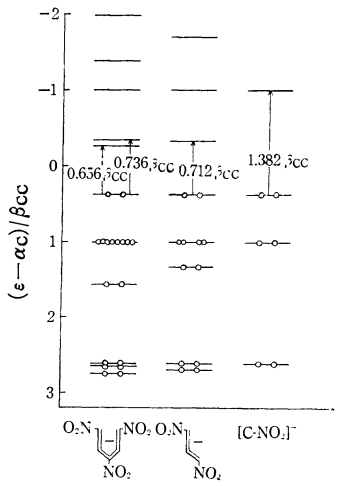

Fig. 2. The energy levels and transitions of π-electrons in the complexes I, II and III.

The Fundamental Fragmentation of Several Fulvenes upon Electron Impact

By Yoshio KITAHARA, Ichiro MURATA and Kunikatsu SHIRAHATA*

Department of Chemistry, Faculty of Science, Tohoku University, Katahira-cho, Sendai

(Received August 16, 1965)

A few papers have appeared concerning the mass spectral fragmentation patterns of non-benzenoid aromatic compounds.[1,2] Here we will report, in a preliminary form, as the behavior of several simple fulvene derivatives upon electron impact.

The fragmentation of 6-methylfulvene by electron impact was first observed by Hanus and Dolejsek[3] in relation to their study of the series of hydrocarbons which have the molecular formula of C_7H_8, e. g., toluene, cycloheptatriene, spiro-[2, 4] - heptadiene - 2, 4, ethinylcyclopentene - 1, ethinylcyclopentene-2, etc. The most important step of the fragemtation is the formation of the tropylium ion by the expulsion of hydrogen from the molecular ion. The feature is common to all of the C_7H_8 isomers.

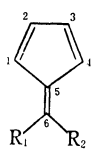

(1) : $R_1=R_2=CH_3$
(2) : $R_1=CH_3$, $R_2=C_2H_5$
(3) : $R_1=CH_3$, $R_2=CH_2CH(CH_3)_2$
(4) : $R_1-R_2=(CH_2)_5$
(5) : $R_1=H$, $R_2=C_6H_5$
(6) : $R_1=CH_3$, $R_2=C_6H_5$
(7) : $R_1=R_2=C_6H_5$

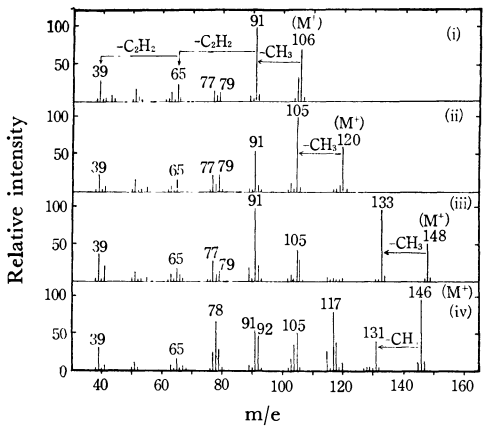

Fig. 1. Mass spectra of 6,6-dialkylfulvenes.
(i) 6,6-Dimethylfulvene
(ii) 6-Methyl-6-ethylfulvene
(iii) 6-Methyl-6-isobutylfulvene
(iv) 6,6-Pentamethylenefulvene

In the mass spectra of the 6, 6-dialkyl derivatives, such as dimethyl- (1), methyl-ethyl- (2) and methyl-isobutylfulvene (3) [see Fig. 1], the base peaks [*m/e* 91, 105, and 133] produced by the elimination of a fragment of 15 mass units from the corresponding parent ions may safely be assumed to be the tropylium, methytropylium, and isopropyltropylium ions (a: R=H, CH_3, *i*-C_3H_7) respectively. The formation of these ions is probably associated with the loss of the methyl radicals from the 6-position of the fulvenes. In the low mass region of the spectra of these fulvenes, a group of peaks, *m/e* 79, 77, 65 and 39, is characteristic of all isomers of the hydrocarbons of C_7H_8; the peaks may reasonably be interpreted as indicating the ions of benzonium (b), phenyl (c), cyclopentadienyl (d), and cyclopropenylium (e) respectively.

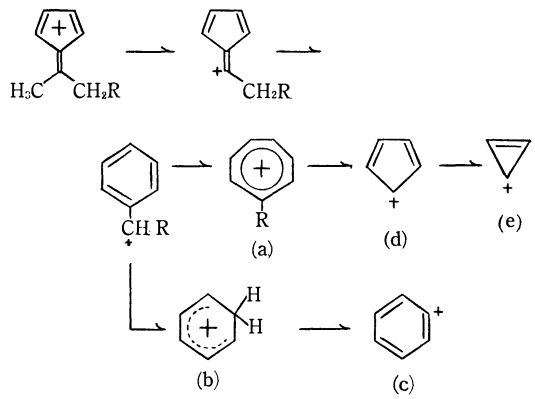

(1′) : R=H
(2′) : R=CH_3
(3′) : R=$CH(CH_3)_2$

6, 6-Pentamethylenefulvene (4), however, showed a peculiar fragmentation pattern. In spite of the fact that compound 4 has no methyl substituent on the 6-position, the first step of the fragmentation is the loss of a methyl radical [*m/e* 131, M^+-15]. The process is confirmed by the existence of an appropriate metastable ion peak at *m/e* 117.5. This suggests that the first step of the fragmentation is the well-known β-fission of the aliphatic moiety, with a simultaneous expulsion of the methyl radical, thus leading to the ion of *m/e* 131 (f). The mechanism of the appearance of peaks at *m/e* 92 and 78 [Fig. 1, (iv)] with a considerable intensity still remains in question.

* Present address: Takasago Perfumary Co., Ltd., Kamata, Tokyo.

1) J. M. Willson, M. Ohashi, H. Budzikiewicz, C. Djerassi, S. Ito and T. Nozoe, *Tetrahedron*, **19**, 2247 (1963).
2) Y. Kitahara and T. Kato, *Chem. and Pharm. Bull.*, **12**, 916 (1963).
3) V. Hanus and Z. Dolejsek, *Coll. Czech, Chem. Comm.*, **28**, 652 (1963).

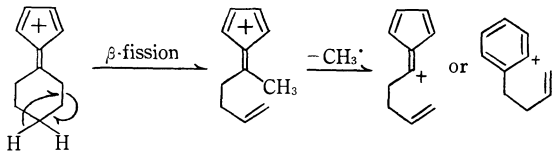

(4′) (f)

The base peaks from 6-phenyl- (5) and 6-methyl-6-phenylfulvene (6) [see Fig. 2] are ions of *m/e* 153 (g); they correspond to the loss of the hydrogen and the methyl radicals [M^+-1 and M^+-15] respectively.

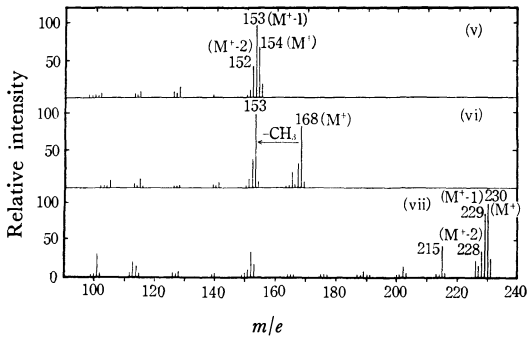

Fig. 2. Mass spectra of 6-arylfulvenes.
(v) 6-Phenylfulvene
(vi) 6-Methyl-6-phenylfulvene
(vii) 6,6-Diphenylfulvene

The moderately intense peak at *m/e* 152 in both compounds is presumably a biphenylene ion (h) produced by the further loss of hydrogen. This is supported by the fact that the spectra in the low mass region [less than *m/e* 153] of the compounds 5 and 6 were similar to that of biphenyl.

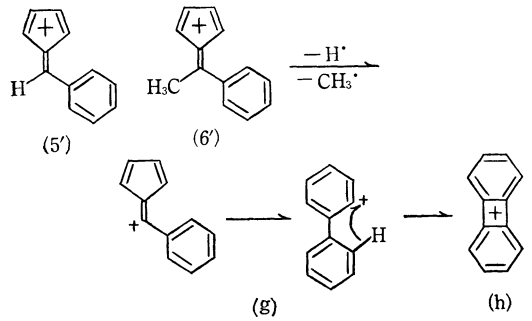

(5′) (6′) (g) (h)

6,6-Diphenylfulvene (7) does not show any tendency to eliminate the phenyl radical from the 6-position, but it does show very intense peaks at *m/e* 229 [M^+-1] (i) and at *m/e* 228 [M^+-2] (j). In this case, the interaction of two sterically crowded phenyl groups probably plays an improtant role in the fragmentation process of this compound. Thus, the formation of a [M^+-2] ion through an intramolecular abstraction of a hydrogen atom from the ortho position of the phenyl group is conceivable. This [M^+-2] ion may naturally by represented as a dibenzofulvalene ion (j). Furthermore, the prominent metastable ion peak at *m/e* 101.5 suggests that the next fragmentation step is the formation of the biphenylene ion.

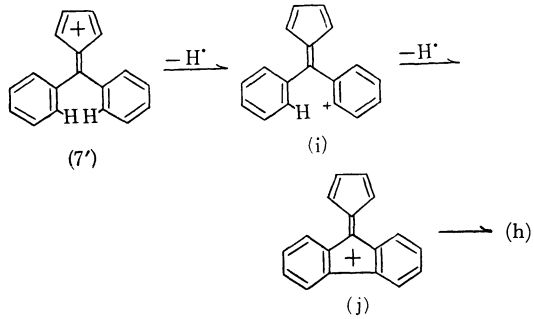

(7′) (i) (j)

Finally, it should be pointed out that the most fundamental fragmentation of 6-substituted fulvenes is initialed by the fission of hydrogen or substituents at the 6-position, thus forming stable aromatic ions except in the case of 6,6-diphenylfulvene (7).

The mass spectra were taken with a Hitachi Mass Spectrometer, Model RMU-5B, using an all-glass inlet system. The ionizing potential was kept at 75 eV., and the ionizing current, at 80 μamp.

The authors are grateful to Messers. Tamotsu Noda, Yasuo Nakajima and Hiroshi Sato of the Naka Works, Hitachi Co. Ltd., Katsuta, Ibarki, for their kind measurement of the mass spectra.

SHORT COMMUNICATIONS

A Novel Deacylation of the γ-Oxoacyl Amino Acid and Peptide

By Fumio SAKIYAMA, Michiyo MORISHITA, Tsuneo SOWA and Kozo NARITA

Institute for Protein Research, Osaka University, Kita-ku, Osaka

(Received September 7, 1965)

Several attempts to effect the cleavage of a specified peptide bond by a chemical reagent have been reported, and some of them are widely utilized for the sequential analysis of protein.[1] For the tyrosyl and tryptophyl bond cleavage, the NBS[2] method has successfully been used. Recently Shaltiel and Patchornik[3] effected an histidyl bond cleavage by using the same principle.

The present aughors have exploited another principle to cleave the histidyl and the tryptophyl bonds. This principle is based, first, on the formation of the γ-oxo group which can be derived from the above residues by the proper reactions: namely, Bamberger's degradation[4] and the subsequent mild hydrolysis of the γ-benzamino group for the histidine residue and peroxide or ozone oxidation[5] for the tryptophan residue. Secondly, the elimination of the γ-oxoacyl group by tetrahydropyridazone formation with hydrazine leads to an exposure of the amino group, which is bonded with the carboxyl side of the amino acid residue in question.

N-Laevuloyl-, *N*-(3-benzoyl-propionyl)- and *N*, *N'*-dibenzoyl-γ-oxoornithyl-L-phenylalanine and *N*-(3-benzoylpropionyl)-L-leucylglycine have been prepared as model compounds for the reaction of the second step.[6] The deacylation of *N*-laevuloyl-L-phenylalanine was performed by the following procedure. *N*-Laevuloyl-L-phenylalanine dicyclohexylamine salt (m. p., 155—156°, 20 μmol.) was heated to a boil in 2 ml. of a 2.0 M acetate buffer (pH 3.6) containing hydrazine (100 μmol.). An aliquot was examined by paper chromatography,[7] and the amino acid released was determined by densitometry after Cd-ninhydrin colorization[8] (Fig. 1). The phenylalanine, quantitatively released after half an hour, was identified as both free amino acid and the DNP[9] derivative by paper and thin-layer chromatography.[10] The cyclization product obtained from the laevuloyl group and hydrazine was shown to be identical with 6-methyl-2, 3, 4, 5-tetrahydropyridaz-3-one[11] by paper and thin layer chromatography[12] and by infrared spectroscopy.

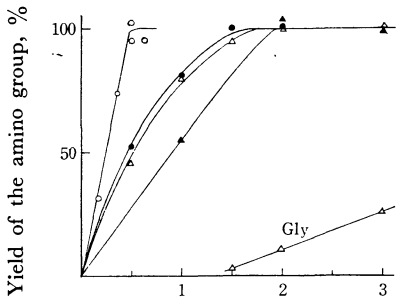

Fig. 1. The release of the amino group from the γ-oxoacyl amino acid and peptide.
○: *N*-laevuloyl-L-phenylalanine
●: *N*-(3-benzoylpropionyl)-L-phenylalanine
△: *N*-(3-benzoylpropionyl)-L-leucylglycine
▲: *N*-(*N*, *N'*-dibenzoyl-γ-oxoornithyl)-L-phenylalanine
Determination of the amino group was performed after paper chromatographic separation of the reaction mixture.

The rate of the release of the amino group depends mainly on the nature of the γ-oxoacyl group, as is shown in Fig. 1. The *N*, *N'*-dibenzoyl-γ-oxoorinthyl group, a descendant of the histidyl residue, was most resistant to cyclization under the present conditions. Prolonged heating caused an appreciable hydrolysis of the peptide bond.

Deacylation from the acetoacetyl derivative of amino acid and peptide can be accomplished by the reaction with phenylhydrazine.[13] A detailed description of this study will be presented elsewhere.

1) Cf. B. Witkop, *Adv. Protein Chem.*, **16**, 221 (1961).
2) NBS, *N*-Bromosuccinimde.
3) S. Shaltiel and A. Patchornik, *J. Am. Chem. Soc.*, **85**, 2799 (1963).
4) E. Bamberger and A. Berle, *Ann.*, **273**, 342 (1893).
5) B. Witkop, *Ann.*, **556**, 103 (1944); A. Previero, E. Scoffone, P. Pajetta and C. A. Benassi, *Gazz. chim. Ital.*, **93**, 841 (1963); A. Previero, M. A. Colletti and L. Galzigna, *Biochem. Biophys. Res. Comm.*, **16**, 195 (1964).
6) The details of the preparation of these new γ-oxoacyl derivatives will be presented later.
7) Solvent system: butan-1-ol-acetic acid-water, 4:1:1 by volume.
8) R. C. Canfield and C. B. Anfinsen, "The Proteins, Vol. I, Ed. by H. Neurath, Academic Press, New York. (1963), p. 318.
9) DNP: 2, 4-Dinitrophenyl. Solvent system, 2-methyl butan-2-ol saturated with 0.1 M phthalate buffer (pH 6.0).
10) Solvent system for phenylalanine, see Ref. 7.
11) L. Wolff, *Ann.*, **394**, 98 (1912).
12) The Ehrlich reagent was used for detection of the pyridazone derivatives after chromatography. Solvent system, see Ref. 7.
13) F. D'Angeli, F. Filia and E. Scoffone, *Tetrahedron Letters*, **1965**, 605.

Totalsynthese der Racemischen Aspergillsäure

Von Yasuhiro CHIGIRA, Mitsuo MASAKI und Masaki OHTA

Laboratorium für Organische Chemie, Tokyo Institut für Technologie, Ookayama, Tokyo

(Eingegangen am 20. November, 1965)

Über die Aspergillsäure, die 1943 von White und Hill[1] aus dem Kulturfiltrat von Aspergillus flavus isoliert wurde, wurde geschlossen, dass die Substanz 3-Isobutyl-6-*sek*-butyl-2-hydroxypyrazin-1-oxyd oder dessen tautomere Hydroxamsäure (I-a)[2] darstellt. Vier weitere eng verwandte Antibiotika—Hydroxyaspergillsäure (I-b),[3] Mutaaspergillsäure (I-c),[4] Neoaspergillsäure (I-d)[5] und Neohydroxyaspergillsäure (I-e)[7]—sind auch wahrscheinlich 3, 6-Disubstituierte-2-hydroxypyrazin-1-oxyd, obwohl Synthese dieser Antibiotika bisher noch nicht berichtet worden sind.

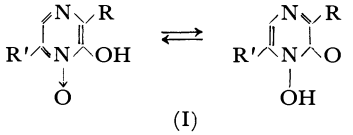

(I)

R = $C_3H_7{}^iCH_2$–

R' = a, $C_2H_5(CH_3)CH$–
b, $C_2H_5(CH_3)(OH)C$–
c, $(CH_3)_2(OH)C$–
d, $C_3H_7{}^iCH_2$–
e, $C_3H_7{}^i(OH)CH$–

Kürzlich gelang uns die Synthese von Neoaspergillsäure,[7] indem man das Verfahren, das zur Herstellung von Pyrazin Hydroxamsäure in unserem Laboratorium ergeben worden ist,[8] anwendet.

In analoger Weise konnten wir nun ja weiter die racemische Aspergillsäure totalsynthetisch herstellen (Formelschema 1).

Umsetzung von 1-Chlor-3-methyl-2-oximinopentan (II)[9] mit *N*-Leucyl-*O*-benzylhydroxylamin (III)[8] in Tetrahydrofuran beim Zimmertemperatur führte zu *N*-[4-Methyl-2-(3-methyl-2-oximinopentylamino)valeryl]-*O*-benzylhydroxylamin (IV), welches mit Salzsäure in Methanol bei 42—45°C zu 2-Ketopentylamino-körper (V) verseift wurde. Beim Reduktiv-Debenzylierung ergab V 4-Methyl-2-(3-methyl-2-oxopentylamino)valerohydroxamsäure (VI) vom Schmp. 134°C (Zers.) (Gef.: C, 59.25; H, 10.15; N, 11.65. Ber. für $C_{12}H_{24}N_2O_3$: C, 58.99; H, 9.90; N, 11.47%.).

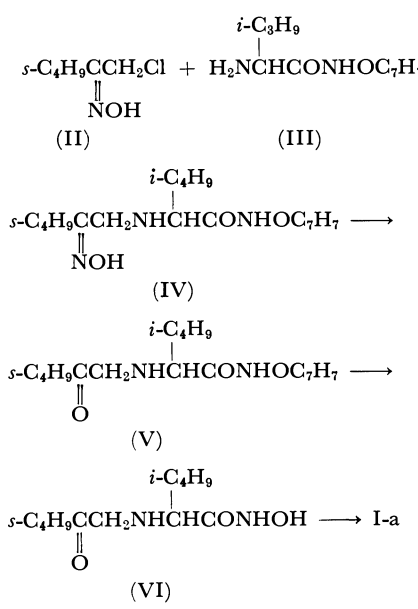

Formelschema 1

Durch die direkte Cyclisierungsreaktion konnten wir VI zu 3-Isobutyl-6-*sek*-butyl-2-hydroxypyrazin-1-oxyd (I-a) (60 mg) überführen, indem man VI (0.7 g) ammoniakalischem Methanol (20 ml) bei Zimmertemperatur behandelt. Die letzte Stufe der Synthese ist die Luft-Oxydation, die in den meisten Pyrazinsynthesen allgemein ist.[10] Die racemische Aspergillsäure (gelbliche Nadeln vom Schmp. 97.5—98.0°C aus 60 proz. Methanol) ergab mit Ferrichlorid in Methanol eine rote Färbung und liess sich durch Elementaranalyse (Gef.: C, 64.21; H, 9.17; N, 12.56. Ber. für $C_{12}H_{20}N_2O_2$: C, 64.25; H, 8.99; N, 12.49%.) und durch Ultraviolet-Spektrum [λ_{max}^{EtOH} 233 mμ (ε=7600) und 328 mμ (ε=8700)] sowie durch Infrarot-Spektrum [scharfe Banden bei 2050, 2870, 2950 und 3130 cm^{-1} und breite Banden bei 2300—2800 und 3300—3600 cm^{-1}] charakterisieren. [Lit. der Aspergillsäure[11] Schmp. 97—99°C, UV-Spektrum λ_{max}^{EtOH} 234 mμ (ε=6500) und 328 mμ (ε=8300)].

1) E. C. White und T. H. Hill, *J. Bacteriol.*, **45**, 433 (1943).
2) J. D. Dutcher, *J. Biol. Chem.*, **171**, 321 (1947); G. T. Newbold, W. Sharp und F. S. Spring, *J. Chem. Soc.*, **1951**, 2679.
3) A. E. O. Menzel, O. Winterstein und G. Rake, *J. Bacteriol.*, **46**, 109 (1943); J. D. Dutcher, *J. Biol. Chem.*, **232**, 785 (1958).
4) S. Nakamura, *Bull. Agr. Chem. Soc. (Japan)*, **23**, 65 (1959), **24**, 629 (1960); S. Nakamura, *Agr. Biol. Chem.*, **25**, 74, 658 (1961).
5) R. G. Micetich und J. C. MacDonald, *J. Chem. Soc.*, **1964**, 1507.
6) U. Weiss, F. Strelitz, H. Flow und I. N. Asheshov, *Arch. Biochem. Biophys.*, **74**, 150 (1958).
7) M. Masaki, Y. Chigira, M. Sugiyama und M. Ohta, *Tetrahedron letters*, **1965**, 4837
8) M. Masaki und M. Ohta, *J. Org. Chem.*, **29**, 3165 (1964).
9) Y. Chigira, M. Masaki und M. Ohta, Dieses Bulletin, im Druck.
10) M. Masaki und M. Ohta, ebenda, **36**, 1177 (1963).
11) G. Dunn, J. J. Gallagher, G. T. Newbold und F. S. Spring, *J. Chem. Soc.*, **1949**, S126.

Studies of Purine *N*-Oxides. I. The Synthesis of Hypoxanthine 1-*N*-Oxide

By Hideaki KAWASHIMA, Takashi MEGURO and Izumi KUMASHIRO

Central Research Laboratories, Ajinomoto Co., Inc., Suzuki-cho, Kawasaki

(Received December 16, 1965)

Hypoxanthine 1-*N*-oxide has been synthesized by the orthoformate ring closure of 4-amino-imidazole-5-hydroxamic acid.[1] However, this method is not applicable to a large scale synthesis, because 4-aminoimidazole-5-hydroxamic acid cannot be obtained easily.

Hypoxanthine is not convertible to hypoxanthine 1-*N*-oxide by direct oxidation. However, adenine has been readily oxidized with hydrogen peroxide in aqueous acetic acid to give adenine 1-*N*-oxide.[2,3]

The present paper will deal with the deamination of adenine 1-*N*-oxide with nitrous acid to give hypoxanthine 1-*N*-oxide. Five grams of adenine 1-*N*-oxide were treated with 23 g. of sodium nitrite in 350 ml. of 29% acetic acid solution at room temperature. After it had stood for four days, the precipitate was collected and washed with water. Light yellow crystals of hypoxanthine 1-*N*-oxide were obtained in a 90% yield (4.5 g.). The crystals showed a single spot on chromatography.[1] After being recrystallized several times, colorless crystals were obtained (Found: C, 39.92; H, 3.07; N, 37.14. Calcd. for $C_5H_4O_2N_4$: C, 39.48; H, 2.65; N, 36.84%).

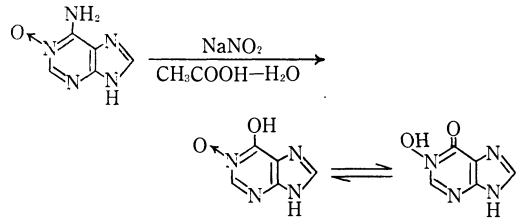

The crystals were identified by means of a study of their paper chromatographic behavior and by a comparison of their ultraviolet and infrared absorption spectra with those of an authentic sample.[1] The catalytic reduction of this product with hydrogen (10 kg./cm^2) afforded hypoxanthine in the presence of Adams' catalyst at 60°C for 24 hr.

After the present work, had been finished, adenosine 1-*N*-oxide and AMP-5' 1-*N*-oxide were found to be deaminated with nitrosyl chloride, yielding inosine 1-*N*-oxide and IMP-5' 1-*N*-oxide respectively.[4]

1) E. C. Taylor, C. C. Cheng and O. Vogl, *J. Org. Chem.*, **24**, 2019 (1959).
2) M. A. Stevens, D. I. Magrath, H. W. Smith and G. B. Brown, *J. Am. Chem. Soc.*, **80**, 2755 (1958).
3) M. A. Stevens and G. B. Brown, ibid., **80**, 2759 (1958).
4) H. Sigel and H. Brintzinger, *Helv. Chim. Acta*, **48**, 433 (1965).

π-Allyl-cycloocta-1, 5-diene-rhodium (I)

By Akira KASAHARA and Keiko TANAKA

Department of Chemistry, Faculty of Liberal Arts and Science, Yamagata University, Yamagata

(Received December 16, 1965)

Recently a number of organometallic π-complexes of π-allyl systems have been reported,[1] and the first π-allylic complex of rhodium(III), π-cyclododeca-1, 5, 9-trienyl-rhodium(III)-dichloride, has been isolated.[2] However, no report on an example of the π-allyl complexes of rhodium(I) has yet been published. In this paper we wish to describe the preparation of π-allyl-cycloocta-1, 5-diene-rhodium(I).

The treatment of a solution of bis-(cyclooct-1, 5-diene)-μ, μ'-diiodo - dirhodium[3] in anhydrous tetrahydrofuran with a four-equivalent amount of allyl magnesium bromide in ether at 0°C under nitrogen, followed by hydrolysis with aqueous ammonium chloride and chromatography on alumina, resulted in the formation of pale yellow crystals of π-allyl-cycloocta-1, 5-diene-rhodium(I), (yield, 30%; m. p. 108—112°C (decomp.). Found: C, 51.93; H, 6.97; mol. wt. (in benzene), 248. Calcd. for $C_{11}H_{17}Rh$: C, 52.39; H, 6.79%; mol. wt., 252).

The π-allylic sandwich structure for this compound is supported by its proton magnetic resonance in deuteriochloroform. The spectrum has a peak at 6.04τ of a relative intensity of 4 for the olefin hydrogens of the cyclooctadiene ring; a peak at 6.95τ of a relative intensity of 8 for the methylene hydrogens of the cyclooctadiene ring, and a multiline pattern at 4.83τ of a relative intensity of 1 for the central hydrogen atom of the π-allyl group. The characteristic doublets for the π-allyl group are present at 7.35τ and 8.38τ with J=6 c. p. s. and J=10 c. p. s. respectively, and with relative intensities of 2 : 2.

π-Allyl-cycloocta-1, 5 - diene - rhodium(I), was found to be diamagnetic, stable enough to be handled in air and soluble in most organic solvents, although it was poorly soluble in cyclohexane and decomposed slowly in hot cyclohexane. The treatment of π-allyl-cycloocta-1, 5-diene-rhodium with hydrochloric acid (in dichloromethane at room temperature) caused a cleavage of the compound at the π-allyl group; bis-(cycloocta-1, 5-diene)-μ, μ'-dichloro-dirhodium[3] was thus isolated. A similar result was obtained when the π-allyl rhodium complex was reacted with anhydrous aluminum chloride in dichloromethane at 0°C.

1) a) R. G. Guy and B. L. Shaw, "Advances in Inorganic Chemistry and Radiochemistry," Vol. IV, Academic Press Inc., New York (1963), p. 77; b) E. O. Fischer and H. Werner, *Z. Chem.*, 2, 174 (1962); c) M. L. Green and P. L. I. Nagy, "Advances in Organometallic Chemistry," Vol. II, Academic Press Inc., New York (1964), p. 325.

2) G. Pajaro and R. Palumbo, *Angew. Chem.*, **75**, 861 (1963).

3) J. Chatt and L. M. Venanzi, *J. Chem. Soc.*, **1957**, 4735.

The Reaction of Benzenesulfonyl Azide with Phenylmagnesium Bromide

By Suketaka Ito

Department of Industrial Chemistry, Faculty of Engineering, Shinshu University, Nagano

(Received December 27, 1965)

Diazocyclopentadiene has been prepared by the reaction of cyclopentadienyllithium with *p*-toluenesulfonyl azide,[1] and some active methylene compounds have been diazotized by *p*-toluenesulfonyl azide in the presence of a base.[2]

This communication will report that benzenesulfonyl azide reacts with phenylmagnesium bromide to yield the salt of 3-benzenesulfonyl-1-phenyltriazene, which then decomposes to give phenyl azide and the salt of benzenesulfinic acid.

$$C_6H_5MgBr + C_6H_5SO_2N_3 \longrightarrow C_6H_5\text{-}N{=}N\text{-}N(MgBr)\text{-}SO_2C_6H_5$$

$$\longrightarrow C_6H_5N_3 + C_6H_5SO_2MgBr$$

Benzenesulfonyl azide was prepared by a modification of the procedure of Curtius,[3] by means of the action of sodium nitrite on benzenesulfonhydrazide in dilute hydrochloric acid. The almost colorless oily sulfonyl azide (n_D^{25}: 1.5488) was stored over anhydrous sodium carbonate in a dark place.

Into a stirred solution of 9.2 g. (0.05 mol.) of benzenesulfonyl azide in 60 ml. of dry ether, there was added over a period of 30 min., a solution of phenylmagnesium bromide (prepared from 1.5 g. (0.064 mol.) of magnesium and 9.4 g. (0.06 mol.) of bromobenzene in the usual way) in 60 ml. of ether at −18—−15°C; hereupon white precipitates separated simultaneously and the reaction mixture turned slightly yellow. The mixture was then separated by filtration into a yellow ether solution and a slight yellow solid, which was then washed with ether and dried in a vacuum desiccator. The yield was 21.4 g.

From the filtrate, 0.9 g. of unreacted sulfonyl azide was recovered.

In a 300 ml. round-bottomed flask 21.0 g. of the powdered solid was placed; the flask was then connected to a series of traps and a vacuum system. The flask was heated to 50°C (0.1 mmHg) to effect a final drying and then to 120—130°C (0.1—3.0 mmHg) in an oil bath for an hour.

Yellow crude phenyl azide was condensed at −70°C (4.9 g.; 82% of the theoretical amount); distillation in vacuo (4 mmHg) gave purified pale yellow azide (n_D^{25}: 1.5593), the infrared spectrum of which was spectroscopically identical with that of an authentic sample.

The reduction of the product with sodium and ethanol gave aniline, which was then acetylated with ketene to yield acetanilide, m. p. 114.0—114.5°C.

The residual powder obtained after the pyrolysis was dissolved in alkaline water and filtered; the filtrate was then acidified with hydrochloric acid. The resulting precipitate was filtered and dried to give 4.0 g. of benzenesulfinic acid, the infrared spectrum of which was spectroscopically identical with that of an authentic sample.

By the treatment of the sodium salt of the sulfinic acid with benzyl chloride in ethanol, phenyl benzyl sulfone was obtained, m. p. 147.0—148.0°C, its infrared spectrum was spectroscopically identical with that of an authentic sample.

1) W. von E. Doering and C. H. DePuy, *J. Am. Chem. Soc.*, **75**, 5955 (1953).
2) M. Regitz, *Ann.*, **676**, 101 (1964); M. Regitz and G. Heck, *Chem. Ber.*, **97**, 1482 (1964); M. Regitz, ibid., **98**, 1210 (1965).
3) T. Curtius, *J. prakt. Chem.* [2], **58**, 174 (1898); "Beilsteins Handbuch der Organischen Chemie," Bd. XI (1928), p. 53.

The Anodic Oxidation of Ethylenediaminetetraacetic Acid and Its Divalent Metal Chelates at the Carbon Paste Electrode

By Toyokichi KITAGAWA and Syōichirō TSUSHIMA

Department of Chemistry, Faculty of Science, Osaka City University, Sumiyoshi-ku, Osaka

(Received January 14, 1966)

Recent works in voltammetry[1,2] have shown the existence of oxide films on platinum electrodes after they had been anodized at highly positive potentials. Therefore, it is not suitable to use a platinum electrode as an indicator electrode at a positive potential region. A carbon paste electrode (graphite intimately mixed with Nujol) has been reported to possess unique advantages and to be very precise in anodic voltammetry.[3]

A single anodic wave of EDTA is observed in the pH range from 1.8 to 2.5, with $E_{P/2}$ of +0.93 V. (vs. SCE) varying slightly with the pH. A second wave appears in the pH range from 4 to 6. The second wave shifts to less positive potentials with an increase in the pH and merges into the first wave.

The peak current - concentration relationship is linear for the first wave in the range from 10^{-2} mM to 1 mM at any pH less than 5 and is reproducible within ±2 to 3%.

The anodic oxidation of metal-EDTA complexes containing a slight excess of metal ions in a 0.1 M HOAc - 0.1 M NaOAc buffer solution with 0.005% polyacrylamide was also investigated at the carbon paste electrode. According to the anodic oxidation potential of metal-EDTA complexes, the following four situations arise, as is shown in Fig. 1: (a) Co(II)EDTA is oxidized more easily than EDTA. The anodic oxidation of Co(II)EDTA to Co(III)EDTA was confirmed by chronopotentiometry. (b) Ni(III)EDTA shows an anodic wave at almost the same potential as that of EDTA. The peak current is, however, about one-half that of EDTA. (c) The anodic wave of Cu(II)EDTA appears at a potential less negative than that of EDTA. This peak current is also about one-half that of EDTA at the same concentration. (d) Cd(II)EDTA does not show any anodic wave until the final increase in the background current appears. Pb(II)EDTA and Zn(II)EDTA behave the same way.

The details of the mechanisms of these electrode reactions will be reported later.

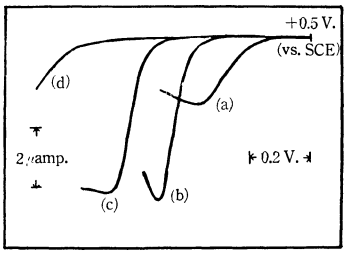

Fig. 1. Current-voltage curves for the oxidation of metal-EDTA complexes in 0.1 M HOAc - 0.1 M NaOAc buffer solution.
1 mM metal EDTA, 0.005% polyacrylamide
(a) Co(II)EDTA (b) Ni(II)EDTA
(c) Cu(II)EDTA (d) Cd(II)EDTA
Scanning rate 0.2V./min.,
Electrode area 0.0853 cm^2

1) I. M. Kolthoff and N. Tanaka, *Anal. Chem.*, **26**, 623 (1954).
2) H. A. Laitinen and C. G. Enke, *J. Electrochem. Soc.*, **107**, 773 (1960).
3) C. Olson and R. N. Adams, *Anal. Chim. Acta*, **22**, 582 (1960).

The Proton Magnetic Resonance Spectra of Hydrogen Selenide and HDSe

By Kensuke TAKAHASHI and Genjiro HAZATO

The Chemical Research Institute of Non-Aqueous Solutions, Tohoku University, Katahira-cho, Sendai

(Received January 17, 1966)

The proton magnetic resonance spectrum of HDSe has not yet been observed. Our interest has been drawn to comparing the proton-deuteron coupling constant of HDSe with such other hydrides as HDS[1]. After we had reported the multiplet structure of HDS in gas in a previous paper,[1] we observed the multiplet structures of both HDS and HDSe in liquid. Aluminum selenide[2] was placed in a bottle connected with a vacuum line and was treated with D_2O in a vacuum. In this case the impurity, H_2O, in D_2O was used as a source of the proton for HDSe. The D_2Se evolved, containing HDSe to a minor extent, was then introduced into a 5-mm. glass tube in a vacuum, with a small amount of TMS added as an internal reference. This liquid mixture of HDSe and D_2Se gave only a triplet signal of HDSe 0.85_5 p. p. m. upfield from that of TMS, as is shown in Fig. 1. The observed proton-deuteron coupling constant is 2.04 ± 0.05 c. p. s. The proton-proton coupling constant for hydrogen selenide thus obtained is 13.28 ± 0.33 c.p.s.; this magnitude is almost the same as that of HDS.[1]

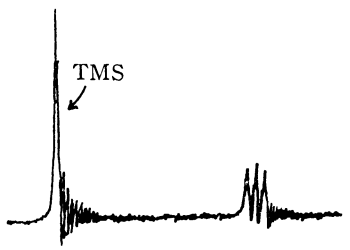

Fig. 1. The proton magnetic resonance spectrum of a liquid mixture of D_2Se and HDSe at 24°C in a sealed glass tube. The applied magnetic field increases from left to right.

Many factors may be considered to contribute to the coupling constants between two protons. In a way, it can be expressed as follows:

$$J_{ij}=A(r,\ \theta)\ \rho(i)\ \rho(j)$$

where $A(r, \theta)$ will be a function defined by the bond length, r, and the bond angle, θ, in a molecule, and where $\rho(i)$ and $\rho(j)$ express the electron densities around the protons in question, i and j respectively. In the case of the simple hydrides, H_nX, $\rho(H)$ will decrease with an increase in the electronegativity of X. Now we can compare the coupling constants of some simple hydrides, H_2O,[3] NH_3,[4] CH_4,[5] H_2S[1] and H_2Se. The order of the magnitudes of their coupling constants is approximately parallel to that of the decreasing electronegativities of the center atoms.

The isotope shift of HDSe with reference to H_2Se was also observed in the spectrum of the sample prepared by using a mixture of H_2O and D_2O as a reactant for aluminum selenide. The triplet of HDSe was centered 0.036 ± 0.003 p. p. m. upfield from the hydrogen selenide resonance, which overlapped with one of the triplet lines of HDSe. Two satellites were observed on both sides of the center band; they may be due to the isotope of selenium-77, the natural abundance of which is 7.5%. The observed proton - selenium-77 coupling constant for hydrogen selenide is 60.5 ± 0.5 c. p. s. As far as we know, this is the first case of a coupling constant observed in the direct H-Se^{77} bond. The signal of hydrogen selenide was also observed in the gaseous phase 1.78 p. p. m. upfield from TMS in contact with the liquid phase at 24°C,

The equilibrium constant of the following exchange reaction:

$$H_2Se + D_2Se \rightleftarrows 2HDSe$$

was estimated to be approximately 0.8 in liquid at 24°C by the use of the intensity measurement of the absorption signal of H_2Se and HDSe, and by the use of some approximations concerned with the initial concentration of hydrogen and deuterium. The rate of the above exchange reaction in liquid can be estimated to be slower than $0.5\ sec^{-1}$ at 24°C. Details will be given later elsewhere.

1) K. Takahashi and G. Hazato, This Bulletin, **38**, 1807 (1965).
2) H. S. Booth, "Inorganic Syntheses", **2**, 183 (1939).
3) J. R. Holmes, D. Kivelson and W. C. Drinkard, *J. Chem. Phys.*, **37**, 150 (1962).
4) R. A. Bernheim and H. B.-Hernandez, *J. Chem. Phys.*, **40**, 3446 (1964).
5) R. A. Bernheim and B. J. Lavery, ibid., **42**, 1464 (1965).

The Spectrophotometric Determination of Fluorine with a PAC-Th Complex

By Kyoji Tōei, Tadashi Hayami,* Haruo Miyata and Yasuaki Shimoishi

Department of Chemistry, Faculty of Science, Okayama University, Tsushima, Okayama

(Received January 24, 1966)

In the course of our studies of the thorium complex formed with ortho-substituted phenylazochromotropic acid, it was found that the thorium complex of PAC, [2-(1, 8-dihydroxy-3, 6-disulfo-2-naphthylazo)-phenoxy acetic acid],[1] can be used in the spectrophotometric determination of microgram quantities of fluoride ions, and that the sensitivity of the thorium complex towards fluoride ions was almost twice that of the thorium Neo-thorin complex.[2]

The principle of the determination of fluoride ions with the thorium complex was the same as the case of the thorium Neo-thorin complex; it was based on the bleaching effect of the fluoride ions on the thorium complex.

Figure 1 shows the absorption spectra of the reagent and its thorium complex. The color of the reagent is pink, while the thorium complex is a bluish violet.

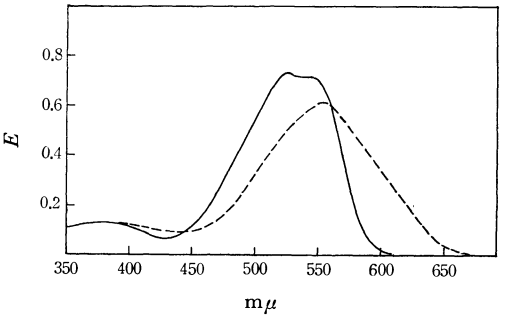

Fig. 1. Absorption spectra of the reagent and its thorium complex (broken line) at pH 2.7.
—— 2.0×10^{-5} M
---- Thorium concn. to the reagent concn. =0.68 : 1

Figure 2 shows the effect of pH on the absorbances of the thorum complex and the reagnet at 610 mμ. The absorbance of the thorium complex remains constant between the pH values of 2.5 and 4.0.

According to the mole ratio method, the thorium complex in the pH range was a 1 : 1 complex[1] formed completely by adding less than 0.75 mol. thorium to one mole of the reagent in the molar ratio cited. Therefore, the reagent used in the present experiment was composed of a 0.68 : 1 mixture of thorium and PAC (on the molar basis).

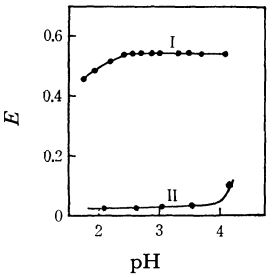

Fig. 2. Effect of pH on the absorbance of the thorium complex at 610 mμ.
I The thorium complex (the reagent concn.$=4.0\times10^{-5}$ M)
II The reagent

Figure 3 shows the calibration curve of fluoride ions: Five milliliters of the reagent (2×10^{-4} M), 0.3 ml. of the thorium nitrate solution (2.27×10^{-3} M), varying amounts (0—1.2 ml.) of the standard sodium fluoride solution (1.91×10^{-3} M) and 0.2 ml. of a 0.2 N perchloric acid solution were mixed in order to adjust the pH and then diluted to 25 ml. with distilled water. The absorbance was measured at 610 mμ in a 1 cm. cell against a water blank.

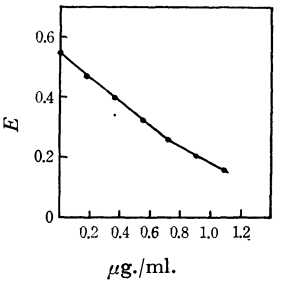

Fig. 3. Calibration curve of fluoride ion.

Beer's law is obeyed over the range from 0 to 0.6 μg. per ml. of fluoride ions.

Further, detailed studies are now in progress.

* Present address: Liberal Arts and Science, Okayama University, Tsushima, Okayama.

1) K. Tōei, H. Miyata, T. Shibata and S. Miyamura, This Bulletin, **38**, 334 (1965).

2) K. Emi and T. Hayami, *J. Chem. Soc. Japan, Pure Chem. Sect.* (*Nippon Kagaku Zassi*), **76**, 1291 (1955).

BULLETIN OF THE CHEMICAL SOCIETY OF JAPAN VOL. 39 639—642 (1966)

Effects of Pressure on the Chemical Properties of the Solid Surface. II. The Surface Acidity and the Catalytic Activity of Compressed Potassium Bisulfate

By Yoshisada OGINO, Takeshi KAWAKAMI and Kazuyuki TSURUMI

Department of Chemical Engineering, Faculty of Engineering, Tohoku University, Sakura-koji, Sendai

(Received April 13, 1965)

Experimental studies of the chemical properties of the surface of potassium bisulfate samples which had been subjected to compressions of 0—3750 kg./cm^2 at room temperature were carried out. Namely, on the compressed sample, the surface acidity at room temperature was measured by the indicator method, while the catalytic activity for the conversion of acetaldehyde to metaldehyde was measured at the temperature of a dry ice - methanol mixture by the bulk polymerization technique. Experimental results showed that the compression of the bisulfate resulted in an increase in the surface acidity at $H_0=1.5$ and in a reduction of the acidity at $H_0=4.0$. Further, it was found that the increase in the compressing pressure resulted in an increase in the catalytic activity of the sample. Thus, the existence of a close relation between the catalytic activity and the surface acidity at $H_0=1.5$, and the effectiveness of the pressure in the improvement of the catalytic activity through changing the acid strength distribution on the sample surface were experimentally demonstrated.

Little attention has been directed to the effect of compacting pressure on the chemical properties of solid surfaces. In view of this, the present authors started to study the surface properties of compressed solids; they have found[1] that the surface acidity of various metal sulfates can be varied by varying the compression. The present research is an extension of the finding to the field of surface catalysis.

According to the current theory[2] of catalysis, the surface acidity of a solid has a close relation to the catalytic properties of the solid; thus, an increase in the surface acidity is a useful way to improve the catalytic activity. A common way to increase the surface acidity is to heat the solid at a suitable temperature.[3] The compression of the solid has not yet been attempted.

In the present research, potassium bisulfate was chosen as the sample material, and the effects of compacting pressure on the surface acidity and the catalytic activity of the bisulfate in the conversion of acetaldehyde to metaldehyde were studied. The experimental results showed that the compression was effective in improving the catalytic activity. Further, the acid strength distribution, which is related to the catalytic activity, was found to vary upon compression.

Experimental

Sample.—About 0.5 g. of potassium bisulfate was compressed by essentially the same apparatus as that described in a previous paper.[1] Samples compressed at 0, 1250, 2500 and 3750 kg./cm^2 were prepared. The pelleted material was ground and pulverized in an agate mortar and stored for 6 hr. in a desiccator containing granules of freshly-dried silica gel. Immediately after the drying, the acidity measurement or the activity test was carried out.

Surface Acidity.—The acidity was determined by Benesi's method[4] with the following four indicators; phenylazonaphthylamine ($pK_a = 4.0$), *p*-dimethylaminoazobenzene ($pK_a = 3.3$), benzeneazodiphenylamine ($pK_a=1.5$), and dicinnamalacetone ($pK_a=-3.0$).

Catalytic Activity.—As a measure of the catalytic activity of the sample material, the conversion of acetaldehyde to metaldehyde was measured with the apparatus indicated in Fig. 1.

After the purified acetaldehyde (containing only traces of water) had been distilled in vacuo from Tube

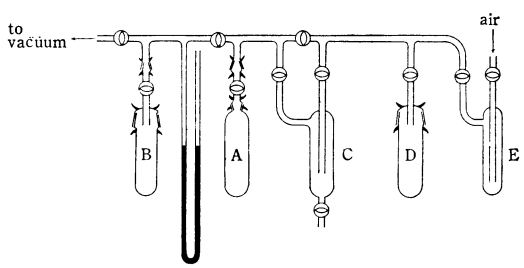

Fig. 1. The apparatus for activity tests.

A: An acetaldehyde container
B: The reaction tube (purified aldehyde)
C: A trap used for the distillation of acetaldehyde
D: An acetaldehyde container (crude aldehyde)
E: A trap containing granules of silica gel

1) Y. Ogino and T. Kawakami, This Bulletin, **38**, 972 (1965).
2) N. M. Chirkov, M. I. Vinnik, S. G. Entelis and V. I. Tsvetkov, *Intern. Chem. Eng.*, **3**, 112 (1963).
3) K. Tanabe and R. Ohnishi, *J. Research Inst. Catalysis, Hokkaido University*, Vol. X, 229 (1962).
4) H. A. Benesi, *J. Phys. Chem.*, **61**, 970 (1957).

D into Tube A, which was kept at −76°C, Tube A was weighed and the temperature was brought to 0°C. Then the aldehyde was distilled again in vacuo, at the rate of 10 g./hr., into the reaction tube, B, which was kept at −76°C and which contained 0.2 g. of catalyst powder. Finally, Tube A, containing residual aldehyde, was reweighed. This enabled us to evaluate the quantity of aldehyde monomers charged in the reaction tube. Usually the ratio of the monomer to the catalyst (by weight) was adjusted to 80.

The reaction was started by shaking the reaction tube; it was interrupted after 30 hr. by adding 20 ml. of a 1% solution of β-naphthylamine in acetone into the reaction tube. After the interruption of the reaction, the mixture in the reaction tube was filtered by suction. The solid product obtained on the filter paper was thoroughly washed with distilled water and, after it had been dried in vacuo, weighed. The conversion was estimated from the ratio of the weight of the product to that of the initial charge of the acetaldehyde monomer.

The solid product was identified by means of an infrared spectrometer and an X-ray diffractometer.

Results

Surface Acidity.—The relation between the surface acidity of potassium bisulfate and the compacting pressure is given in Fig. 2. As may be seen in this figure, the acidity at H_0*1=4.0 diminishes on compression, while the acidity at H_0=1.5 increases on compression. On the other hand, the acidity at H_0=3.3 varied in an irregular manner, and the acidity at H_0=−3.0 was essentially zero.

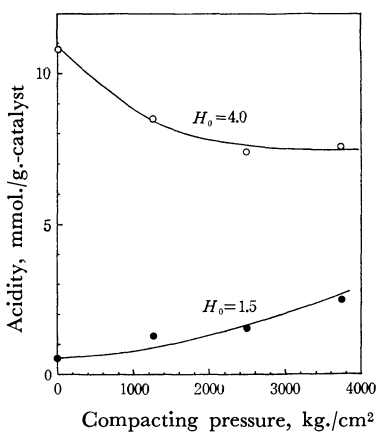

Fig. 2. Relations between the compacting pressure and the surface acidity.

Catalytic Activity.—The conversion of acetaldehyde to the solid product is given in Fig. 3 as a function of the compacting pressure. The figure shows that the catalytic activity of potassium bisulfate increases almost linearly with the compacting pressure.

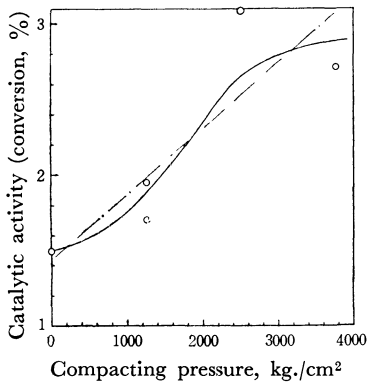

Fig. 3. The relation between the compacting pressure and the catalytic activity.

The reaction product was a white, non-tacky solid. This solid was found to decompose at 110—120°C, and it was insoluble in ordinary organic solvents. From the infrared absorption spectra given in Fig. 4 and the powder X-ray diffraction patterns given in Fig. 5, the reaction product was identified as metaldehyde. The other products, such as paraldehyde or high polymers, were found to be negligible.*2

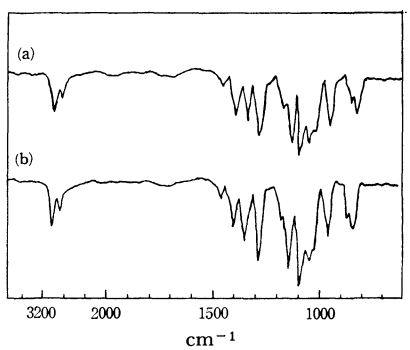

Fig. 4. Infrared absorption spectra of the solid product (a) and metaldehyde (b).

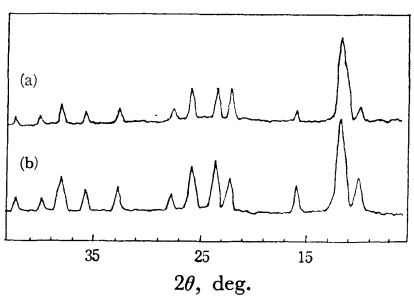

Fig. 5. X-Ray diffraction patterns of the solid product (a) and pure metaldehyde (b).

*1 H_0 means Hammett's acidity function (*J. Am. Chem. Soc.*, **54**, 2721 (1932)).

*2 By adopting some different methods of reaction, an amorphous high polymer of acetaldehyde could be formed using potassium bisulfate as a catalyst.

Discussion

One of the most important facts which were established in the present research is that the distribution of acid strength on the surface of potassium bisulfate varied upon compression. Calculations based on the experimental results indicated in Fig. 2 show that the total acidity, as defined by the acidity at $H_0=4.0$, was diminished to about 70% of the original value by the compression at 3750 kg./cm^2. On the other hand, the percentage of the acidity at $H_0=1.5$ against the total acidity was increased from 5% (original value) to 32% by the compression at 3750 kg./cm^2. These results show that the quantity of weak acid on the surface was reduced by the compression, while the quantity of the strong acid, which has a H_0 value between 1.5 and -3.0, was increased by the compression.

Although the detailed mechanisms of the change in the acid strength distribution have not yet been clarified, some important roles played by the crystal imperfections formed through the dehydration[1] of potassium bisulfate to potassium pyrosulfate may be supposed. According to high-pressure chemistry,[5] dehydration due to compression can occur. However, the same sort of dehydration may also occur when the sample is heated. In fact, Tanabe and his cowerkers[6] considered that the surface acidity of nickel sulfate is due to the crystal imperfection contained in an unstable phase produced by heating the sulfate. Thus, it must be suspected that the compression of the sample might cause a rise in the temperature of the sample.

According to a preliminary experiment*3 in the present work, the temperature of the sample was raised only 3°C by the compression at about 3000 kg./cm^2. Therefore, increases in the temperature on compression might not be the cause of the acidity change; the main cause of the change might be the formation of the crystal imperfection due to the compression.

As may be seen in Fig. 3, the catalytic activity of potassium bisulfate was increased by the compression. This experimental fact may be explained in terms of the acidity change on compression. The relations between the catalytic activity and the surface acidity at $H_0=4.0$ and at $H_0=1.5$ are given in Fig. 6. The figure reveals that the increase in the surface acidity at $H_0=4.0$ results in the reduction of the catalytic activity, whereas the increase in the surface acidity at $H_0=1.5$ makes the surface more active for the reaction. In the previous paragraph it was shown that the compression of potassium bisulfate was effective in increasing the surface acidity at $H_0=1.5$. Accordingly, it can be understood that the compression makes the surface richer in strong acids, whereby the surface of the bisulfate is brought to a more active state.

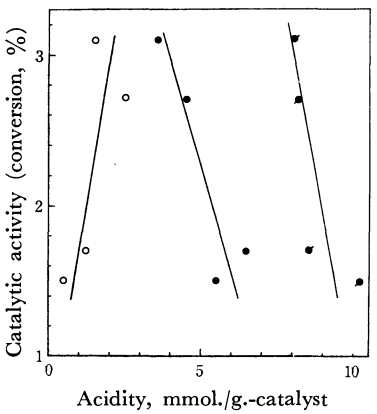

Fig. 6. Relations between the catalytic activity and the surface acidities at $H_0=4.0$ (◉), $H_0=3.3$ (●), and $H_0=1.5$ (○).

It is an important fact that the compression is effective in improving the catalytic activity through changing the acid strength distribution. Although the possibility of cases where the catalytic activity is independent of the total acidity can not be completely denied, many experimental results which support an intimate relation between the catalytic activity and the surface acidity at a given H_0 value can be seen in the literature. For instance, Takida and Noro[7] described how the catalytic activity of metal sulfates in the polymerization of acetaldehyde to an amorphous high polymer was dependent on the surface acidity at $H_0=3.3$. Thus, in order to improve the catalytic activity of acidic solids, some suitable procedures which can adjust the acid strength distribution on the solid surface are required. The experiments in the present research were confined to the case of potassium bisulfate, but it seems that the knowledge obtained here can make some contribution toward this requirement.

Summary

The acidic nature of the potassium bisulfate surface varied with the compression. Namely,

5) S. D. Hamann, "Physico-Chemical Effects of Pressure," Butterworths Scientific Publications, London (1957), p. 208.

6) T. Takeshita, R. Ohnishi, T. Matsui and K. Tanabe, *J. Catalysts Soc. Japan* (*Shokubai*), **6**, 270 (1964).

*3 The temperature of the compressed sample was measured in the following way. The same apparatus as that described in the previous paper was used. A small hole, 3 mm. in diameter, was drilled at the center of the bottom cover of the apparatus. The inside opening of the hole was covered with a copper disk which was sufficiently thick to create an internal pressure of below 3000 kg./cm^2. Then the sample material was packed into the sample room of the apparatus, and it was compressed to about 3000 kg./cm^2. Thus, the disk was broken. At the instant of the breaking, the temperature of the sample which was flowing out from a hole opened in the disk was measured with a thermocouple.

7) H. Takida and K. Noro, *Chemistry of High Polymers* (*Kobunshi Kagaku*), **21**, 23 (1964).

the total acidity, as defined by the acidity at $H_0=4.0$, is reduced, while the acidity at $H_0=1.5$ is increased by the compression. These facts have been considered to show that the acid strength distribution on the surface of potassium bisulfate can be adjusted by the compression.

The catalytic activity of the bisulfate in the reaction of acetaldehyde to metaldehyde is increased by compressing the material. This increase in the catalytic activity can be related to the increase of acidity at $H_0=1.5$. On the basis of the experimental results, it has been suggested that the compression might be effective in improving the catalytic activity of acidic solids.

BULLETIN OF THE CHEMICAL SOCIETY OF JAPAN VOL. 39 642—644 (1966)

The Spectrophotometric Determination of Thiophene in Petroleum Naphtha with α-Nitroso-β-naphthol

By Masayuki KASHIKI and Kazuyoshi ISHIDA

Research Center, Maruzen Oil Co., Ltd., Shimotsu-Cho, Kaiso-Gun, Wakayama

(Received April 14, 1965)

A colorimetric method for the direct estimation of thiophene in petroleum naphtha without interference from the other sulfur compounds present has been worked out. The test is based on the blue-green color produced by the reaction between thiophene and α-nitroso-β-naphthol in the presence of sulfuric acid. The procedure accounted for from 10.0 mg./ml. of thiophene sulfur down to a mere trace of thiophene, of the order of 0.01 mg./ml. thiophene sulfur.

In the preceding paper[1] we have reported a s. w. polarographic determination of mercaptan compounds and free sulfur in petroleum naphtha. This paper will describe an investigation of α-nitroso-β-naphthol as a colorimetric reagent in concentrated sulfuric acid for the determination of thiophene. A survey of the literature revealed that α-nitroso-β-naphthol has not been reported on previously for the colorimetric determination of thiophene. The absorption curves of the reaction products are given in the visible region. Isosbestic absorption occurs at 640 mμ, where Beer's law is obeyed, and the color is stable for at least 4 hr. Thiophene can be determined in petroleum naphtha at concentrations as low as 0.01 mg. per ml., with a percentage error of 16.0%.

The effects on the absorbance of a reagent solution by many of the more common sulfur compounds were studied; the following compounds did not interefere at the concentrations tested: elemental sulfur (1.0 mg./ml.), di-*n*-butyldisulfide (1.0 mg./ml.), di-*n*-butylmercaptan (1.0 mg./ml.), and di-*n* butyltrisulfide (1.0 mg./ml.).

The reagent, which consists of α-nitroso-β-naphthol dissolved in concentrated sulfuric acid, reacts quantitatively with thiophene compounds, producing a stable blue-green color. The color formation, like that of the Indofenin reaction,[2-4] is believed to be due to the formation of dehydrocondensation compounds by the concentrated sulfuric acid in the reaction mixture.

Experimental

Reagents.—A thiophene (Tokyo Kasei Organic Chemicals) stock solution was prepared by dissolving thiophene of an analytical grade in petroleum naphtha free from sulfur compounds. It was then diluted with that same petroleum naphtha to a desired concentration. An α-nitroso-β-naphthol (Wako Chemicals) was dissolved in concentrated sulfuric acid (Ishizu Chemicals) to give a concentration of 5×10^{-5} mol./l.

Apparatus. — Spectrophotometric measurements were made with a Shimazu, model SV-50A, spectrophotometer, using 5 cm. transmission cells. All experiments were carried out at 25±0.5°C.

Procedure.—Pipet 2.5 ml. of 1×10^{-3}M α-nitroso-β-naphtohol solution and 10 ml. of the sample solution into a 100 ml. separatory funnel. Stopper the funnel and shake vigorously for at least 60 sec. Allow the two phases to separate, and draw off the lower sulfuric acid layer into a clean, dry, 50 ml. volumetric flask. Add 10 ml. of sulfuric acid, stopper the funnel, and shake for 30±5 sec. Again allow the layers to separate. Draw off the lower layer and combine it with the first extract in the 50 ml. volumetric flask. Dilute to volume with sulfuric acid and mix well.

Read the absorbance at 640 mμ, using a 5-cm. cell and using the reagent blank as the reference material.

Results and Discussion

The intensity and stability of the colored complex formed are not influenced by the temperature

1) M. Kashiki and K. Ishida, *Rev. of Polarography*, **12**, 169 (1964).
2) G. Heller, *Angew. Chem.*, **37**, 1017 (1924).
3) G. Heller, *Chem. Ztg.*, **54**, 585 (1930); **57**, 74 (1933).
4) W. Steinkopf et al., *Ann.*, **541**, 238 (1939); **546**, 211 (1941).

of the solvents, the photochemical reaction, or the presence of impurities in the reaction mixture at 640 mμ. To illustrate the influence of each variable and to find the best conditions for obtaining reproducible results, each variable was considered separately.

Absorption Spectra.—The absorption spectrum of the reagent was studied from 380 to 720 mμ. The absorbance was negligible above 380 mμ, but it showed a steady increase at lower wavelengths without reaching a maximum. The absorption spectrum of the complex was studied from 380 to 720 mμ. No study was made below 380 mμ because of the high absorbance of the reagent in this range. Two absorption maxima occur in the spectrum of the complex between 380 and 720 mμ. The working portion of the curve is shown in Fig. 1. All the absorbance measurements for this investigation were made at 640 mμ in order to minimize the interfering absorbance of the α-nitroso-β-naphthol - thiophene complex, which is lower at this wavelength than at 430 mμ.

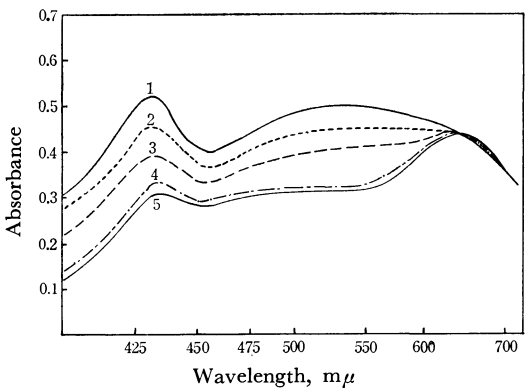

Fig. 1. Absorption spectrum of the reaction product of thiophene and α-nitroso-β-naphthol, and the effect of time.
1: 25 min. 2: 45 min. 3: 90 min. 4: 150 min.
5: 180 min. Thiophen: 0.85 mg./ml.

The Effect of Reagent Concentration.—In order to study the effect of the concentration of α-nitroso-β-naphthol, a series of absorbances was measured at various concentrations of α-nitroso-β-naphthol, using standard petroleum naphtha and reagent blanks of the same concentration as points of reference. Figure 2 gives the effect of the concentration of α-nitroso-β-naphthol in the reaction mixture on the absorbance of solution. It is apparent that a concentration of 5×10^{-5} mol./l. α-nitroso-β-naphthol is necessary in order to obtain a maximum color with this reaction. The absorbance at the isosbestic point of 640 mμ is affected by the amount of α-nitroso-β-naphthol below 5×10^{-5} mol./l. In the thiophene determination, therefore, a 5×10^{-5} mol./l. reagent solution was used, and the absorbance

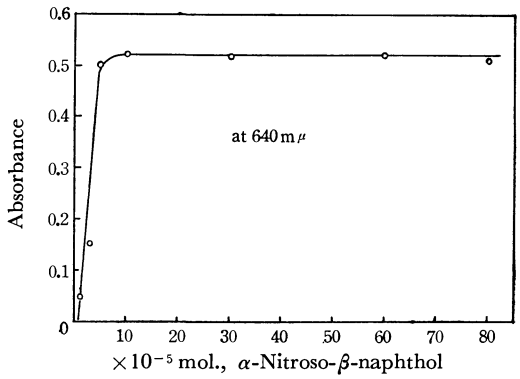

Fig. 2. The effect of addition of α-nitroso-β-naphthol. Thiophene: 1.0 mg./ml.

measurements were made at 640 mμ.

Shaking.—The maximum absorptivity was obtained when the α-nitroso-β-naphthol - concentrated sulfuric acid and petroleum naphtha (sample) were shaken vigorously for at least 60 sec. Procedure is recommended in order to minimize any variations resulting from differences in the rate of shaking.

The Effect of the Temperature on Color Formation.—The absorbance of the solution of the α-nitroso-β-naphthol - thiophene complex at 430 mμ gradually decreased with the time of standing at 10 to 35°C. About 15% of its intensity diminished within the first 2 hr., then it

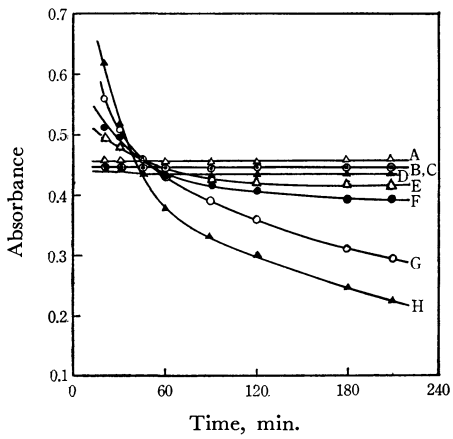

Fig. 3. Effect of temperature and time on color development.
A, B, C, D: 640 mμ, E, F, G, H: 430 mμ
△: 10°C, ●: 15°C, ○: 25°C, ▲: 35°C
Thiophene: 0.85 mg./ml.

remained constant for an additional 2 hr. However, the absorbance at the isosbestic point (see Fig. 1) of 640 mμ remained constant for several hours (see Fig. 3).

The Effect of the Photochemical Reaction.—The authors have found that ordinary room

light (from 100 W. tungsten bulbs) catalyzes the undesired reaction. Fig. 4 shows that the spectrum of the α-nitroso-β-naphthol - thiophene complex is stable if the solutions are kept in the dark or are exposed to light at 640 mμ, but that a change occurs at 430 mμ. The authors find that the absorbance at 430 mμ decreased appreciably in a few minutes if exposed to light, but it decreased much more slowly if kept in the dark.

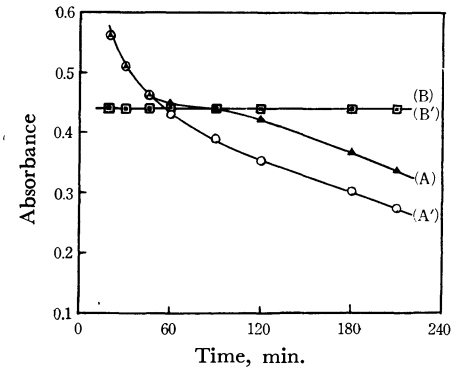

Fig. 4. Effect of light on spectra of α-nitroso-β-naphthol - thiophene complex.
Thiophen: 0.85 mg./ml.
(A): in Dark, (A'): in Light } 430 mμ, (B): in Dark, (B'): in Light } 640 mμ

Conformity to Beer's Law.—Measurements of the absorbance were made with a number of colored solutions containing varying amounts of thiophene. The straight-line calibration curve (see Fig. 5) showed a conformity to Beer's law for the concentration range studied. The useful range for a 5 cm. cell is 0.01 to 0.12 mg. per ml.

The Determination of the Formula of the Complex.—The methods of continuous variation[5] were employed in order to determine spectrophotometrically the reagent-to-thiophene ratio of the complex. The continuous-variations method was performed by mixing $4-X$ ml. of a 0.01 M solution of α-nitroso-β-naphthol and X ml. of a thiophene solution of the same concentration. Absorbance measurements were made at 640 mμ for the eight solutions. The continuous-variation plot using corrected absorbance values is shown in Fig. 6. The maximum absorbance occured at about a 0.5 mol. fraction of thiophene, indicating that one mole of α-nitroso-β-naphthol coordinated with one mole of thiophene.

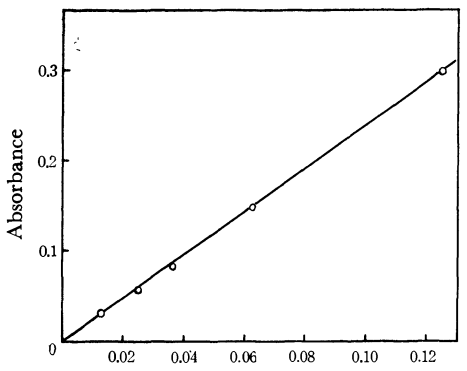

Fig. 5. Calibration curve.

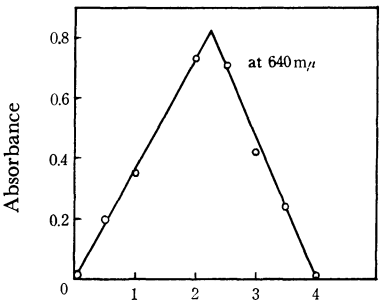

Fig. 6. Continuous variation method.
Continuous variation method applied to α-nitroso-β-naphthol - thiophene complex, X ml. of reagent added to $4-X$ ml. of thiophen solution.

Relative Error in the Determination of Thiophene.—The method seems to be the most favorable one for thiophene determination. The results obtained by the proposed procedure are shown in Table I.

TABLE I. RELATIVE ERROR IN THE DETERMINATION OF THIOPHENE

Concn. mg./ml.	Percentage error %
0.01	16.0
0.02	10.5
0.03_8	5.0

The authors wish to express their gratitude to Dr. Shigeru Oae of Osaka City University for his kind guidance, to Dr. Kiichiro Sugita of Ritsumeikan University for his helpful discussion, and to Mr. Tsunehide Kozuma, General Manager of the Maruzen Oil Co., Ltd., Research Center, for his encouragement throughout the work.

5) J. H. Yoe and A. L. Jones, *Ind. Eng. Chem., Anal.-Ed.*, **16**, 111 (1944).

BULLETIN OF THE CHEMICAL SOCIETY OF JAPAN VOL. 39 645—650 (1966)

Calculation of the Three π—π^* Absorptions of Conjugated Systems by Hückel MO Method

By Kichisuke NISHIMOTO†

Mellon Institute, Pittsburgh, Pennsylvania, U. S. A.

(Received April 22, 1965)

Correlation relations between the Hückel molecular orbital energies and the absorption wavelengths of the ^1L_a, ^1L_b, and ^1B_b species of an alternant hydrocarbon are presented. After a small modification, the present relations are applied fairly well to the calculations of the electronic spectra of α-substituted hydrocarbon and *N*-heterobenzenes. This shows us that the nature of the electronic spectra of these compounds are very similar with those of parent hydrocarbon. On the other band, the calculation for β-substituted derivatives does not give good results, although the agreement between the calculated and observed values is semi-quantitatively satisfactory. This should be attributed to the complicated configuration interaction scheme between the lower excited configurations of the molecule.

It is widely recognized that the Hückel molecular orbital theory[1] (HMO theory) provides very useful theoretical information for the prediction of the various ground state properties of the conjugated molecules, such as bond distances, reactivity, resonance energy, and dipole moment, in spite of its appalling simplicity. However, only a few attempts[2] made to positively treat the electronic spectra of the aromatic compounds by HMO theory, because this theory does not explicitly, but only implicitly, take the electron repulsions into account. It would be, however, very convenient when we can calculate the electronic spectra of these compounds in the framework of HMO theory.

The present paper shows that there is a possibility for the prediction of the main three absorptions of a given aromatic compound in the near ultraviolet or visible region by HMO theory, when we set up an appropriate HMO transition energy - absorption wavelength relationship, just as in the case of the bond length calculation for which we usually use Coulson's bond order - bond length relation.[3] In this paper, first of all, we will provide some relationships between HMO transition energies and the absorption wavelengths of ^1L_a, ^1L_b, and ^1B_b species for the alternant hydrocarbon. Secondly, we will apply these relations to some *N*-heterocycles and aromatic derivatives. All of the HMO calculations are carried out by the IBM 7090 computer of the University of Pittsburgh.

HMO Energy - Absorption Wavelength Relations

Alternant Hydrocarbons.—The spectra of an aromatic hydrocarbon in the longer wavelength region has usually three absorption maxima: weak, medium, and intense bands, which on an empirical basis Clar[4] classified as α-, *p*-, and β-bands, respectively. However, on a theoretical point of view, a spectroscopic symbolism developed by Platt[5] on the basis of free electron model is more convenient for the classification of the absorption bands. According to this nomenclature, the ^1L_a band (Clar's *p*-band) is associated with a transition from the highest occupied MO, ψ_1, to the lowest vacant MO, $\psi_{1'}$. A convention given in the previous paper[6] is used for numbering of MO. In HMO theory, the MO energy associated with *i*th MO, ψ_i, is expressed by

$$\psi_i; \quad \varepsilon_i = \alpha + m_i\beta \tag{1}$$

where α and β are conventional Coulomb and resonance integrals, respectively. The eigenvalue m_i is a root of the secular determinant. The HMO transition energy associated with ^1L_a absorption is, therefore, given by

$$E(^1L_a) = (m_1 - m_{1'})\beta$$

or

$$\Delta m = E(^1L_a)/\beta = m_1 - m_{1'} \tag{2}$$

For the convenience, an excited configuration associated with one electron transition from an

† Visiting Fellow, April 1964 to April 1965. Permanent Address: Department of Chemistry, Faculty of Science, Osaka City University, Osaka.

1) A. Streitwieser, Jr., "Molecular Orbital Theory for Organic Chemists," John Wiley & Sons, Inc., New York (1961).

2) For example, Ref. 1, p. 202.

3) C. A. Coulson, *Proc. Roy. Soc.*, **A169**, 413 (1939).

4) E. Clar, "Aromatische Kohlenwasserstoffe," Springer-Verlag, Berlin (1952).

5) J. R. Platt, *J. Chem. Phys.*, **17**, 484 (1949); *J. Opt. Soc. Am.*, **43**, 252 (1953).

6) K. Nishimoto and R. Fujishiro, This Bulletin, **37**, 1660 (1964).

TABLE I. CALCULATED AND OBSERVED ABSORPTION WAVELENGTHS FOR HYDROCARBONS (in mμ)

	$\lambda(^1L_a)$		$\lambda(^1L_b)$		$\lambda(^1B_b)$	
	Calcd.	Obs.	Calcd.	Obs.	Calcd.	Obs.
Acetylene	161	166*	—	—	—	—
Ethylene	174	174[1]	—	—	—	—
Benzene	190	190[2],*	264	264[2]	179	179[2]
Naphthalene	283	285[2]	316	315[2]	221	221[2]
Anthracene	380	375[2]	352	—	253	252[2]
Tetracene	478	471[2]	378	—	276	274[2]
Pentacene	579	582[2]	396	428[2]	294	303[2]
Phenanthrene	286	293[2]	361	345[2]	261	251[2]
Chrysen	320	319[2]	374	360[2]	273	267[2]
Picene	328	329[2]	406	376[2]	303	287[2]
3, 4-Benzphenanthrene	320	315[2]	394	372[2]	273	281[2]
Benzanthracene	354	359[2]	411	385[2]	307	390[2]
Pyrene	358	334[2]	372	372[2]	270	272[2]

1) P. G. Wilkinson and H. L. Johnston, *J. Chem. Phys.*, **18**, 190 (1950).
2) E. Clar, "Polycyclic Hydrocarbons," Vols. 1 and 2, Academic Press, New York (1964).
* See text.

occupied orbital, ϕ_i, to a vacant orbital, ϕ_j, is represented by χ_{i-j} in this paper. In an alternant hydrocarbon, the two excited configurations, $\chi_{1-2'}$ and $\chi_{2-1'}$ are degenerate, namely

$$\Delta m = m_1 - m_{2'} = m_2 - m_{1'} \qquad (3)$$

and interact each other by the first order configuration interaction, as shown in Fig. 1. This configuration interaction gives rise to a highly allowed intense ^1B_b band (Clar's β band) and a very weak ^1L_b band (Clar's α-band). According to the Pariser-Parr-Pople theory,[7] in which the electron repulsions are explicitly taken into account, the energy associated with a singlet electronic transition $^1\chi_{i-j}$ is given by:

$$\Delta E_{i-j} = \varepsilon_j^F - \varepsilon_j^F - [ii|jj] + 2[ij|ij] \qquad (4)$$

where ε_i^F and $[ij|kl]$ are the Hartree-Fock orbital energy associated with ϕ_i and the electron repulsion integral over MO's, respectively. The peculiar degeneracy in an alternant hydrocarbon,

$$\Delta E_{1-2'} = \Delta E_{2-1'}$$

is still valid in Pariser-Parr-Pople treatment. However, the comparison of Eq. 2 with Eq. 4 makes clear that in the discussion of electronic spectra, the conventional resonance integral β does not have its original meaning, which is a characteristic integral for a given carbon-carbon bond, but it is a complicated function of electron repulsion integrals and core integrals over atomic orbitals. The value should, therefore, depend on the molecular shape and varies from molecule to molecule. However, as shown in the previous paper,[6] in linear polyacene series the value of ε_i and $[ij|kl]$ monotonously decreases with increase in the molecular size.

7) K. B. Wiberg, "Physical Organic Chemistry," John Wiley & Sons, Inc., New York (1963), p. 116.

This suggests that in a linear polyacene series there are some relationships between the wavelengths of three main absorptions, $\lambda(^1L_a)$, $\lambda(^1L_b)$, and $\lambda(^1B_b)$, and the corresponding Δm values of Eqs. 2 and 3. The plot of the absorption wavelength against the $1/\Delta m$ in Fig. 2 shows excellent correlations. The correlations are satisfactorily represented by:

$$\lambda(^1L_a) = 474(\Delta m)^{-1/2} - 145 \text{ m}\mu \qquad (5)$$

$$\lambda(^1L_b) = 428(\Delta m)^{-1} + 50 \text{ m}\mu \qquad (6)$$

$$\lambda(^1B_b) = 358(\Delta m)\text{m}\mu \qquad (7)$$

respectively. Rather similar relations have been found by Streitwieser,[1] except for ^1L_a species. The calculated wavelengths for various hydrocarbons are compared with the experimental data in Table I. The agreement between the calculated and observed values is satisfactory in the whole. From Eq. 5, the conventional resonance integrals for ethylene and acetylene are estimated as $\beta_{C=C}=1.1\beta$ and $\beta_{C\equiv C}=1.2\ \beta$, respectively. In benzene and acetylene, the configurations $\chi_{1-1'}$ and $\chi_{2-2'}$ are degenerate and interact each other. This gives rise to a weak ^1L_a and strong ^1B_a absorptions. Therefore, the calculated $\lambda(^1L_a)$ should be compared with the harmonic mean of the observed $\lambda(^1L_a)$ and $\lambda(^1B_a)$.

The correlation equations, 5 and 7, have the following noteworthy features; that is, the transition energy associated with the ^1B_b species is proportional to the corresponding HMO energy ($\beta=-3.46$ eV.), whereas $\lambda(^1L_a)$ varies linearly with the inverse square root of Δm. This seems to suggest us that when we use the valence bond language the excitation from the ground state to the ^1L_a state may be described by the change in the covalent structure and that to ^1B_b state may be represented by the change from covalent to

charge resonance structure. Indeed, every ^1L_a absorption of a hydrocarbon is accompanied with the vibrational fine structure which is resulted from a vibronic coupling. Whereas, the ^1B_b absorption is usually consisted of only one sharp and high peak, as the absorption band in a charge resonance system, e. g. cyanine analogs[8] and some organic ions.[9] In polyacene series, the ^1L_a absorption is polarized to the direction of the molecular short axis.[10] On the other hand, the ^1L_b and ^1B_b absorptions are polarized in the direction of the molecular long axis. Consequently, the electron displacement in the ^1L_a species is limited at the largest in 2.78 A, however in the latter species the largest electron displacement will be proportional to the number of benzene rings. This situation may partly be responsible to such characteristic shifts as represented by the correlation equations.

α-Substituted Hydrocarbons.—In an aromatic derivative, the peculiar degeneracy of the two excited configurations, $\chi_{1-2'}$, and $\chi_{2-1'}$, of the parent hydrocarbon is removed by the perturbation of the substituent. Furthermore, this perturbation leads to an interaction between all configurations. However, as pointed out in the previous paper,[6] in α-substituted hydrocarbon which has an auxochromic substituent in the α-position, such as α-naphthol, $\chi_{1-2'}$ strongly interacts with $\chi_{2-1'}$, but only slightly with $\chi_{1-1'}$, so that the nature of the π—π^* absorption is practically the same as that of the parent hydrocarbon. We will, therefore, be able to calculate the $\lambda(^1L_a)$ of an α-derivative from Eq. 5. On the other hand, the calculations of the $\lambda(^1L_b)$ and $\lambda(^1B_b)$ are very difficult, because there is no means of estimating the interaction energy between the configurations χ_{1-2} and χ_{2-1}. The configurational energy associated with χ_{1-2} is approximately given by a harmonic mean of the hypothetical $\lambda(^1B_b)$ and $\lambda(^1L_b)$, which are calculated from Eqs. 6 and 7, using $\Delta m = m_1 - m_{2'}$. Similarly, the energy of $\chi_{2-1'}$ is estimated. One approximation is that a geometric mean of Δm_{1-2} and Δm_{2-1} is assigned to Δm. However, this approximation has not any theoretical background, but only an intuitive analogy with a well-known approximation for the interaction energy between two different molecules.[11] In summarizing, the three absorption wavelengths of an α-substituted hydrocarbon are calculated from the following equations;

$$\lambda(^1L_a) = 474(\Delta m_1)^{-1/2} - 145\ \mathrm{m}\mu \quad (8)$$

$$\lambda(^1L_b) = 428(\Delta m_2)^{-1} + 50\ \mathrm{m}\mu \quad (9)$$

$$\lambda(^1B_b) = 358(\Delta m_2)^{-1}\mathrm{m}\mu \quad (10)$$

where

$$\Delta m_1 = m_1 - m_{1'}$$

$$\Delta m_2 = \sqrt{(m_1 - m_{2'})(m_2 - m_{1'})}$$

Table II. Parameterr for HMO calculation

Atom core (X)	δ_X	Bond (XY)[a]	k_{XY}
C^+	0	C=C	1
N^+	0.5	C=N	1.05
N^{2+}	1.0	N=N	1.10
O^{2+}	1.5	C-NH_2	0.8
F^{2+}	2.0	C-OH	0.7
		C-F	0.6

a) = means an aromatic bond.

The HMO calculations are carried out using the parameters given in Table II. In Table II, the conventional Coulomb and resonance integrals are expressed as follows;

$$\alpha_X = \alpha + \delta_X\beta$$

$$\beta_{XY} = k_{XY}\beta$$

where δ_X and k_{XY} are the characteristic constants for atom core X and bond X-Y, respectively. It would be reasonable to compare α_X with the diagonal element of the Hartree-Fock operator, F_{XX}, over the π-AO of atom X. F_{XX} should be considered as the effective electronegativity of atom X in the molecule.[12] To a first approximation, α_X is, therefore, given by the valence state electronegativity, which was circumstantially investigated by Prichard and Skinner[13] and Hinze and Jaffé[14]. According to their study, the electronegativity in a given valence state increases almost linearly with the atomic number in the same period. The δ_X values given in Table II are in accord with their results. The calculated absorption wavelengths for some α-derivatives are compared with the experimental values in Table III. Table III shows that the simple correlations are still applicable to the prediction of the three main absorptions of these compounds.

Benzene Derivatives and *N*-Heterobenzenes.—In the calculation of benzene's $\lambda(^1L_a)$, we have used the harmonic mean of observed $\lambda(^1L_a)$ and $\lambda(^1B_b)$ as the reference, because they come from two degenerated configurations $\chi_{1-1'}$ and $\chi_{2-2'}$. In benzene derivatives and *N*-heterobenzenes, we can not neglect the configuration interaction between $\chi_{1-1'}$ and $\chi_{2-2'}$. Fortunately, this configuration interaction energy has, however, practically the same value with that of benzene.[6,12,15] So that, in good approximation, the $\lambda(^1L_a)$ of a benzene derivative or a *N*-heterobenzene is given by

8) L. G. S. Brooker, *Revs. Modern Phys.*, **14**, 275 (1942).
9) H. P. Leftin, *J. Phys. Chem.*, **64**, 1714 (1964).
10) R. Pariser, *J. Chem. Phys.*, **24**, 250 (1956).
11) M. Kurata, "Polymer Physics," Ed. by Phys. Soc. Japan, Asakura Shoten, Tokyo (1963), p. 71.
12) N. Mataga and K. Nishimoto, *Z. Physik. Chem.* (*Frankfult*), **13**, 140 (1957).
13) H. O. Pritchard and H. A. Skinner, *Chem. Revs.*, **55**, 745 (1955).
14) J. Hinze and H. H. Jaffé, *J. Am. Chem. Soc.*, **84**, 540 (1962).
15) K. Nishimoto and R. Fujishiro, This Bulletin, **31**, 1036 (1958).

TABLE III. CALCULATED AND OBSERVED ABSORPTION WAVELENGTHS FOR α-SUBSTITUTED HYDROCARBONS (in mμ)

Hydrocarbon	Substituent	λ(¹L$_a$) Calcd.	λ(¹L$_a$) Obs.	λ(¹L$_b$) Calcd.	λ(¹L$_b$) Obs.	λ(¹B$_b$) Calcd.	λ(¹B$_b$) Obs.
Naphthalene	NH_2	305	317[3]	327	332[3]	231	242[3]
	OH	291	289[3]	320	322[3]	225	230[3]
	F	285	291[4]	318	316[4]	223	—
Anthracene	NH_2	394	397[5]	358	368[5]	258	260[5]
	OH	382	389[3]	354	—	255	253[3]
	F	378	—	353	—	254	—

3) H. Baba and S. Suzuki, This Bulletin, **34**, 82 (1961); **35**, 683 (1962).
4) T. Iredale and J. W. White, *Trans. Faraday Soc.*, **56**, 1719 (1960).
5) S. Suzuki and H. Baba, This Bulletin, **37**, 519 (1964).

TABLE IV. CALCULATED AND OBSERVED ABSORPTION WAVELENGTHS OF BENZENE DERIVATIVES AND *N*-HETEROBENZENES (in mμ)

Parent compound	Substituent	λ(¹L$_a$) Calcd.	λ(¹L$_a$) Obs.	λ(¹L$_b$) Calcd.	λ(¹L$_b$) Obs.	λ(¹B$_b$) Calcd.	λ(¹B$_b$) Obs.
Benzene	NH_2	227	234[6]	285	286[6]	196	197[6]
	OH	213	213[6]	273	272[6]	186	190[6]
	F	207	204[7]	268	266[7]	182	—
	H	204	204[2]	264	264[2]	179	179[2]
Pyridine	2-OH	209	205[8]	269	269[8]	183	—
	3-OH	212	216[8]	273	276[8]	186	—
	4-OH	212	222[8]	272	235[8]	185	—
	H	201	—	261	251[8]	177	—
Pyridazine	—	200	—	259	246[8]	177	—
Pyrimidine	—	198	—	255	243[8]	175	—
Pyrazine	—	198	—	257	260[8]	172	—
s-Triazine	—	189	—	247	222[8]	174	—
s-Tetrazine	—	191	—	251	252[8]	166	—

6) H. Baba, This Bulletin, **34**, 76 (1961).
7) K. Bowden and F. A. Braude, *J. Chem. Soc.*, **1952**, 1068.
8) S. F. Mason, ibid., **1959**, 1247, 1253; **1957**, 5010.

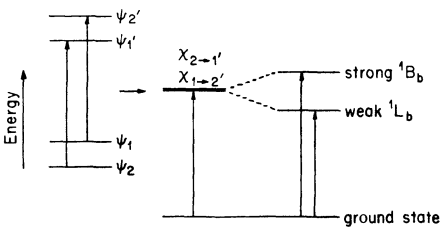

Fig. 1. First order configuration interaction in an alternant hydrocarbon.

$$\lambda(^1L_a) = 2\left/\left[\frac{1}{\lambda_1}+\frac{1}{\lambda_2} - \sqrt{\left(\frac{1}{\lambda_1}-\frac{1}{\lambda_2}\right)^2+(0.701)^2\times 10^{-6}}\right]\right. \text{ m}\mu$$

where

$$\lambda_1 = 474(\Delta m_3)^{-1/2} - 145$$
$$\lambda_2 = 474(\Delta m_4)^{-1/2} - 145$$
$$\Delta m_3 = m_1 - m_{1'}$$
$$\Delta m_4 = m_2 - m_{2'}$$

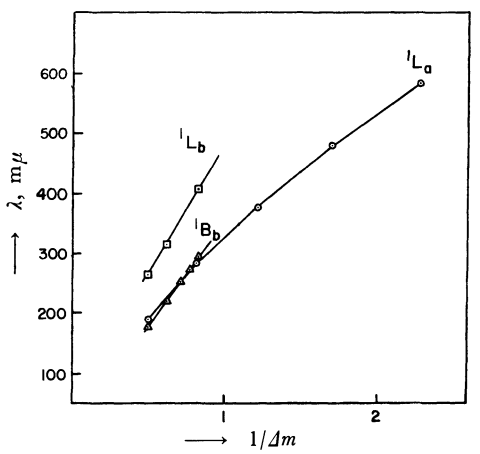

Fig. 2. Absorption spectra of linear polyacenes and the inverse of HMO energy differences :
— : Calculaled line.
○, □, △: Experimental data

Table V. Calculated and observed absorption wavelengths of miscellaneous compounds (in mμ)

Parent compound	Substituent	$\lambda(^1L_a)$ Calcd.	$\lambda(^1L_a)$ Obs.	$\lambda(^1L_b)$ Calcd.	$\lambda(^1L_b)$ Obs.	$\lambda(^1B_b)$ Calcd.	$\lambda(^1B_b)$ Obs.
Quinoline	H	279	275[9]	314	315[9]	220	232[9]
	2-OH	278	270[10]	321	324[10]	227	224[10]
	3-OH	287	270[10]	325	330[10]	230	—
	4-OH	283		316		222	—
	5-OH	292	—	321	323[10]	226	242[10]
	6-OH	291	—	316	—	230	227[10]
	7-OH	285	263[10]	325	333[10]	229	227[10]
	8-OH	295	—	321	305[10]	226	242[10]
Isoquinoline	H	282	280[9]	314	320[9]	220	217[9]
	1-OH	286	—	317	—	222	—
	3-OH	293	—	321	—	226	—
	4-OH	293	295[10]	320	330[10]	225	230[10]
	5-OH	294	303[11]	321	328[11]	226	234[11]
	6-OH	285	286[11]	328	300[11]	232	229[11]
	7-OH	290	301[11]	326	333[11]	230	224[11]
	8-OH	291	304[11]	318	334[11]	224	233[11]
Phenanthrene	H	286	293[2]	361	345[2]	261	251[2]
	1-OH	295	308[12]	367	335[12]	267	245[12]
	2-OH	286	292[12]	368	355[12]	268	255[12]
	3-OH	292	305[12]	364	355[12]	264	248[12]
	4-OH	292	302[12]	368	340[12]	268	245[12]
	9-OH	295	305[12]	366	355[12]	266	248[12]
Azulene	—	361	352[13]	389	659[13]	286	279[13]

9) R. Muller and F. Dorr, *Z. Elektrochem.*, **63**, 1150 (1959).
10) S. F. Mason, *J. Chem. Soc.*, **1957**, 5010.
11) K. Nakanishi, M. Ohashi and H. Koike, This Bulletin, **34**, 533 (1961).
12) C. Djerassi, H. Bendes and P. Sengupta, *J. Org. Chem.*, **20**, 1046 (1955).
13) J. F. Tilney-Bassett and W. A. Waters, *J. Chem. Soc.*, **1959**, 3123.

In Table IV, the calculated absorption wavelengths of a number of benzene compounds are shown and compared with the experimental data. Generally speaking, the agreement between them is satisfactory, except for the $\lambda(^1L_b)$'s of *s*-triazine and 4-OH pyridine.

Micellaneous Compounds.—As pointed out in the previous paper,[6] in β-substituted derivatives, such as β-naphthol, all of the lower excited configurations interact strongly each other, so that the transition characteristics of the parent hydrocarbon are completely lost. Namely, we can not represent the ^1L_a species by $\chi_{1-1'}$ and so on. In attempts to explain the electronic spectra of a β-derivative, we have therefore to consider the interaction among all configurations. It would be, however, desirable to examine to what extent we can expect the electronic spectra of a β-derivative, making the same assumption with an α-derivative. In Table V, the calculated absorption wavelengths for quinoline, isoquinoline, phenanthrene, and their hydroxy derivatives, using Eqs. 8—10 are given and compared with the experimental values. Generally speaking, although the agreement between calculated and observed values is semiquantitatively satisfactory, it is not quite so good as that of α-derivative.

In order to explain the electronic spectra of a β-derivative by HMO theory, we have to set up other correlation equations considering the complicated configuration interactions. The present correlation equations predict fairly well the $\lambda(^1L_a)$ and $\lambda(^1B_b)$ of azulene as shown in Table V. The scheme of configuration interaction in a derivative having a chromophor, such as $-NO_2$, $-NO$, $-COR$, etc., is an intricate problem. However, the preliminary calculation shows that the ^1L_a absorptions of such derivatives are satisfactorily calculated by Eq. 8.

Conclusion

The results of this study indicate that the HMO method is applicable to the prediction of the three π-π^* absorptions of conjugated systems, when we set up the appropriate relationships. Simple correlation equations provided in the present study are particularly useful for the alternant hydrocarbons and their α-derivatives having an auxochromic group and also for some *N*-heterocycles. In order

to predict the electronic spectra of β-derivatives and the derivatives having a chromophor, we have to set up other relationships considering the complicated configuration interaction scheme.

The author gratefully wishes to acknowledge the many kindneses and the most generous financial support of the Mellon Institute which has made his extremely enjoyable stay at the Institute possible.

BULLETIN OF THE CHEMICAL SOCIETY OF JAPAN VOL. 39 650—654 (1966)

Polyesters Containing Carbazole Rings in the Main Chain. III. Syntheses of New Polyesters from Carbazole-dibasic Acids

By Yoshio NAGAI and Chin-Chuan HUANG

Institute of Industrial Science, The University of Tokyo, Azabu, Tokyo

(Received May 18, 1965)

Several new polyesters were synthesized by the reaction of ethylene glycol with such carbazoledicarboxylic acids as carbazole-3, 6-dicarboxylic, 9-ethylcarbazole-3, 6-dicarboxylic, carbazole-3, 6-dibutanoic and 9-methylcarbazole-3, 6-dibutanoic acid in the presence of various catalysts.

Several new polyesters were prepared from ethylene glycol and acids of the general formula HO_2C-$(CH_2)_n$ 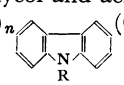 $(CH_2)_nCO_2H$,[1,2] in which n is 0 or 3, and R indicates –H or alkyl groups (–CH_3 or –C_2H_5). With respect to the polymer-melt temperature, intrinsic viscosity, color, and resistance to organic solvents, the new polyesters have, in general, better properties than those derived from ethylene glycol and carbazole keto acids HO_2C-$(CH_2)_2OC$ 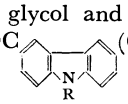 $(CH_2)_2CO_2H$, in which R indicates –H or –CH_3 group.

Experimental

Preparation of Monomers.—The syntheses of carbazole - 3, 6 - dicarboxylic acid (CDA), diethyl carbazole - 3, 6 - dicarboxylate (diEtCD), 9 - ethylcarbazole-3, 6-dicarboxylic acid (9-EtCDA), diethyl 9-ethylcarbazole - 3, 6 - dicarboxylate (diEt 9 - EtCD), carbazole-3, 6-dibutanoic acid (CDBA), and 9-methylcarbazole-3, 6-dibutanoic acid (9-MeCDBA) were described in previous papers.[1,2] Ethylene glycol was purified according to the previous method.[2]

Polycondensation. — *Preparation of Poly(ethylene carbazole-3, 6-dibutanoate) (PECB) and Poly(ethylene 8 - Methylcarbazole - 3, 6 - dibutanoate) (9-MePECB).* — A highly polymeric PECB or 9-MePECB can be made by heating ethylene glycol with CDBA or 9-MeCDBA, in which the molar ratio of ethylene glycol and CDBA or 9-MeCDBA is 2 : 1. Preferably the higher molar ratios of ethylene glycol for the simple ester of the acid or the acid are used. During the ester interchange period the temperature advantageously approaches the boiling point of the glycol. In the first stage, in the preparation of β-hydroxyethyl carbazole-3, 6-dibutanoate or β-hydroxyethyl 9-methylcarbazole-3, 6-dibutanoate, there is no particular need to add the catalysts. Once all of the acid has reacted with glycol, the temperature is raised and the excess glycol is removed from the reaction mixture in the presence of various catalysts by distillation under reduced pressure. During this process of heating the viscosity of reaction mixture gradually increases. The heating may be effected in an inert atmosphere, for instance, in a stream of nitrogen gas.

Preparation of Poly(ethylene Carqazole-3, 6-dicarboxylate) (PECC) and Poly(ethylene 8-Ethylcarbazole-3, 6-dicarboxylate) (9-EtPECC).—Since CDA and 9-EtCDA sparingly dissolve in most organic solvents, diEtCD and diEt 9-EtCD are used in the polycondensation. The reaction is carried out under conditions in which the displaced ethanol can be removed by distillation. At least two moles of ethylene glycol per mole of diEtCD or diEt 9-alkylCD should be used. Preferably the heating is effected in an inert atmospher, and is continued until the distillation of the displaced ethanol ceases.

The low polymeric product can be converted into the highly polymeric polyester by heating it above 280°C for several hours under reduced pressure.

Examples of Polycondensation.—*PX-11*—One gram of ethylene glycol and 2.5 g. of CDBA were heated in the presence of 0.0026 g. of germanium dioxide in a stream of oxygen-free nitrogen for about 2 hr. at 194°C. The resulting β-hydroxyethyl carbazole-3, 6-dibutanoate was further heated in a stream of nitrogen for three hours at 237°C, and finally at 285°C for 30 min. The low polymeric product was then heated at 285°C for an additional 30 min. under reduced pressure (0.2 mmHg). The polycondensation product showed an intrinsic viscosity of 0.54 in *m*-cresol at

* A part of this paper was presented at the 13th Annual Meeting of the Society of High Polymers of Japan, June, 1964.

1) Y. Nagai and C.-C. Huang, This Bulletin, **38**, 951 (1965).

2) Y. Nagai and C.-C. Huamg, ibid., **38**. 1136 (1965).

30°C; the color of the polymer was light yellow and transparent.

Found: C, 71.97; H, 6.39; O, 17.75. Calcd. for $-(C_{22}H_{23}O_4N)-$ or $-OC(CH_2)_3-C_{12}H_7N-(CH_2)_3CO_2-(CH_2)_2O-$, where $C_{12}H_9N$ is the carbazole ring: C, 72,23; H, 6.3; O, 17.53%.

9-MePECB.—A mixture consisting of 2.0 g. of 9-MeCDBA, 1.0 g. of ethylene glycol, and 0.003 g. of germanium dioxide was heated in a hard glass flask under the same conditions as in the previous example, thus giving a polyester which is light amber color and shows an intrinsic viscosity of 0.41 in *m*-cresol at 30°C.

Found: C, 72.01; H, 6.73; O, 17.20. Calcd. for $-(C_{23}H_{25}O_4N)-$ or $-OC(CH_2)_3-C_{13}H_9N-(CH_2)_3CO_2-(CH_2)_2O-$, where $C_{13}H_9N$ is the 9-methylcarbazole ring: C, 72.83; H, 6.59; O, 16.89%.

PX-5.—Two grams of diEtCD, 1.0 g. of ethylene glycol, and a blended catalyst of 0.005 g. of cobaltous acetate and 0.003 g. of calcium hydride were heated in a hard glass flask at 194°C for 1 hr. in a stream of oxygen-free nitrogen. The resulting β-hydroxyethyl carbazole-3, 6-dicarboxylate was heated at 235°C for 2 hr. in the same inert atmosphere and finally at 285°C for 30 min., while the pressure of the system was gradually reduced to 0.2 mmHg. Heating at 285°C was then continued for an additional hour under the same pressure. The product was a light yellowish-white opaque solid showing an intrinsic viscosity of 0.51 in *m*-cresol at 30°C; the polymer-melt point was above 210°C.

Found: C, 63.52; H, 4.08; O, 23.21. Calcd. for $-CO-C_{12}H_7N-CO_2(CO)_2O-$: C, 64.77; H, 3.91; O, 22.81%.

9-EtPECC.—A mixture consisting of 2.0 g. of diEt 9-EtCD, 1.0 g. of ethylene glycol, 0.005 g. of cobaltous acetate, and 0.002 g. of calcium hydride was allowed to react under the same conditions and over the same period as in the synthesis of PECC. The polycondensation product showed an intrinsic viscosity of 0.34 in *m*-cresol at 30°C.

Found: C, 69.57; H, 4.95; O, 21.48. Calcd. for $-(C_{18}H_{15}O_4N)-$ or $-OC-C_{14}H_{11}N-CO_2(CH_2)_2O-$, in which $C_{14}H_{11}N$ is the 9-ethylcarbazole ring: C, 69.90; H, 4.85; O, 20.71%.

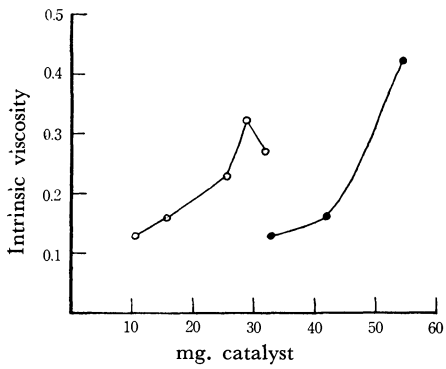

Fig. 1. Intrinsic viscosity of poly(ethylene carbazole-3,6-dibutanoate) vs. catalysts.
○ $Ca(CH_3CO_2)\cdot H_2O$ and Sb_2O_3
● $Ca(CH_3CO_2)_2\cdot H_2O$

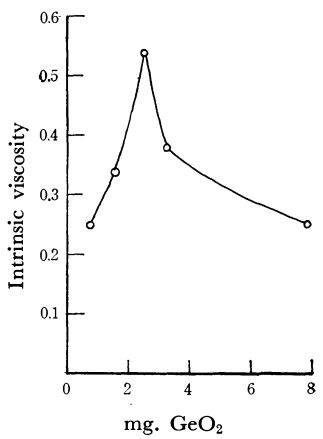

Fig. 2. Intrinsic viscosity of poly(ethylene carbazole-3,6-dibutanoate) vs. weight of GeO_2.

Results and Discussion

As has been described previously[2] polyesters obtained from ethylene glycol and diethyl carbazole-3, 6-γ, γ'-diketobutanoate, diEtCDKB, or diethyl 9-methylcarbazole-3, 6-γ, γ'-diketobutanoate, diEt 9-MeCDKB, suffer from the defects of dark color

Table I. Relation between weight of catalyst and intrinsic viscosity

Polymer code	Catalyst		Intrinsic[a] viscosity
	Fromula	Wt., g.	
PX-1	$Ca(CH_3CO_2)_2\cdot H_2O$	0.042	0.16
PX-2	$Ca(CH_3CO_2)_2\cdot H_2O$	0.033	0.13
PX-3	$Ca(CH_3CO_2)_2\cdot H_2O$	0.055	0.42
PX-4	$Ca(CH_3CO_2)_2\cdot H_2O$	0.011	0.13
	Sb_2O_3	0.003	
PX-5	$Ca(CH_3CO_2)_2\cdot H_2O$	0.016	0.16
	Sb_2O_3	0.004	
PX-6	$Ca(CH_3CO_2)_2\cdot H_2O$	0.026	0.23
	Sb_2O_3	0.006	
PX-7	$Ca(CH_3CO_2)_2\cdot H_2O$	0.029	0.32
	Sb_2O_3	0.007	
PX-8	$Ca(CH_3CO_2)_2\cdot H_2O$	0.032	0.27
	Sb_2O_3	0.003	
PX-9	GeO_2	0.0008	0.25
PX-10	GeO_2	0.0016	0.34
PX-11	GeO_2	0.0026	0.54
PX-12	GeO_2	0.0033	0.38
PX-13	GeO_2	0.0079	0.25
PX-14	Mg	0.0473	0.22
PX-15	B_2O_3	0.0025	0.27
PX-16	ZnO	0.007	0.31
	B_2O_3	0.005	
PX-17	Sb_2O_3	0.0057	0.13
PX-18	Sb_2O_3	0.0053	0.29
	CaH_2	0.0610	
PX-19	Control	—	0.11

a) Viscosity was measured with Cannon-Fenske viscometer in *m*-cresol at 30°C.

TABLE II. COLOR AND SOFTENING TEMPERATURE OF POLY(ETHYLENE CARBAZOLE-3,6-DIBUTANOATE)

Polymer code	Color[a)]	Softening temp.[b)]
PX-1	IIIa	80 (285)
PX-2	IIIa	82 (285)
PX-3	IIIb	100 (293)
PX-4	IIIa	83 (290)
PX-5	IIIa	85 (290)
PX-6	IIIa	80 (285)
PX-7	IV	98 (290)
PX-8	IV	85 (290)
PX-9	II	83 (290)
PX-10	II	110 (293)
PX-11	II	122 (295)
PX-12	II	112 (295)
PX-13	IIIa	83 (285)
PX-14	V	80 (285)
PX-15	IV	82 (290)
PX-16	IV	90 (292)
PX-17	IIIa	80 (285)
PX-18	IV	90 (290)
PX-19	IIIa	80 (285)

a) Color of crude product was classified in six grades as follows: I, water white; II, light yellow (transparent); IIIa, light amber (transparent); IIIb, light amber (opaque); IV, amber; V, dark amber.

b) Temperature at which polyester becomes rubbery or soften without melting. Numbers in parentheses are temperatures above which the polymer decomposed.

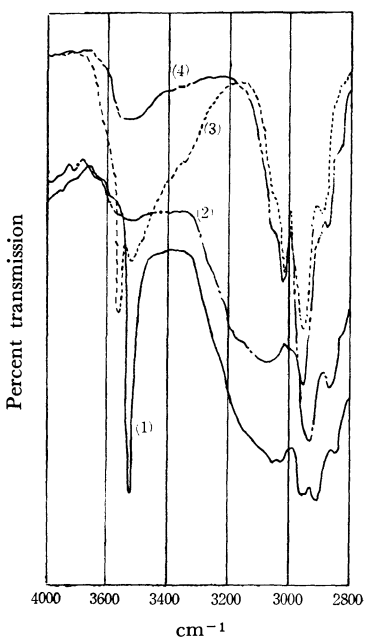

Fig. 3. Infrared spectra of 1, CDBA (——); 2, 9-MeCDBA (—·—); 3, low polymeric PECB (·····, in $CHCl_3$); and 4, low polymeric 9-MePECB (----, in $CHCl_3$).

and brittleness, though they have rather good resistance to many organic solvents. It seems that the dark color of poly(ethylene CDKB) or poly(ethylene 9-MeCDKB) can be partly ascribed to carbonyl groups which attach directly to two benzene rings of the carbazole molecule and which may serve as possible chromophores, because PECB or 9-MePECB, which has no such groups, is in general a lighter color. Such catalysts as lead and cobaltous acetate or alkali metals can also exert a marked effect on the color of PECKB and PECB when added in large amounts. Blended catalysts

TABLE III. SOLUBILITY PROPERTIES[a)] OF POLY(ETHYLENE CARBAZOLE-3,6-DIBUTANOATE) AND POLY(ETHYLENE CARBAZOLE-3,6-DICARBOXYLATE)

Polymer solvent	PX-3	PX-7	PX'-5	PX-14	PX-16
Benzene	4	4	4	4	4
Cyclohexane	4	4	4	4	4
Dioxane	4	4	4	4	4
Toluene	6	4	4	4	4
Pyridine	1	3	4	3	4
n-Butyl acetate	4	4	4	4	4
Phenol	3	3	4	6	6
o-Cresol	1	1	1	1	1
m-Cresol	1	1	1	1	1
Nitrobenzene	2	2	4	2	6
Dichlorobenzene	3	2	4	6	6
DMF	2	2	4	6	3

a) The solubility is indicated by the numbers as follows[2)]: 1, soluble in hot solvent and remains soluble when the solution becomes cold; 2, very low solubility, or little solvent action on solute; 3, absorption of solvent produces gelling; 4, insoluble; 5, soluble in hot solvent, precipitated when the solution becomes cold; 6, melted or sticky in hot solvent.

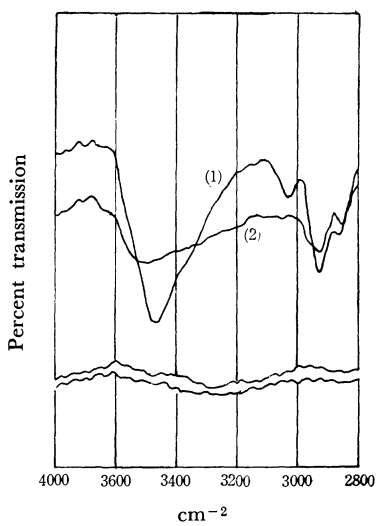

Fig. 4. Infrared spectra of 1, PECB (in KBr); and 2, N MePECB (in KBr).

Table IV. Relation between catalysts and intrinsic viscosity of poly(ethylene carbazole-3,6-dicarboxylate)

Polymer code	Catalyst: Formula	Catalyst: Wt., g.	Intrinsic viscosity[a]
PX'-1	Control	—	0.06[p]
PX'-2	Na_2CO_3	0.005	0.08[p]
PX'-3	$Pb(C_2H_3O_2)_2 \cdot 3H_2O$	1) 0.005	0.08[p]
		2) 0.013	0.15[c]
PX'-4	$Pb(C_2H_3O_2)_2 \cdot 3H_2O$	0.005	
	CaH_2	0.003	0.23[c]
PX'-5	$Co(CH_3CO_2)_2 \cdot 4H_2O$	0.005	
	CaH_2	0.003	0.51[c]
PX'-6	Sb_2O_3	0.005	
	CaH_2	0.001	0.50[c]

a) Viscosity was measured with Cannon-Fenske viscometer and intrinsic viscosity obtained by plotting inherent viscosity numbers vs. concentration and extrapolating to zero concentration.
c) In *m*-cresol at 30°C.
p) In pyridine at 30°C.

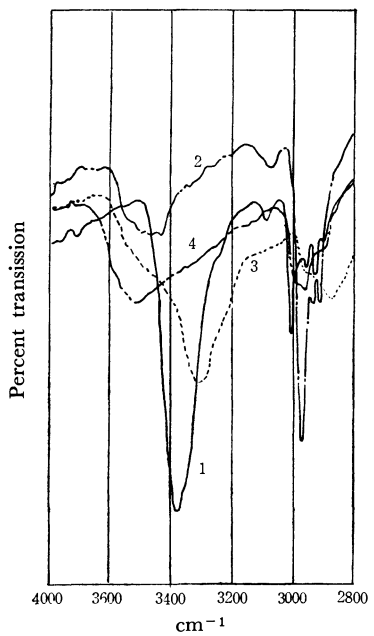

Fig. 5. Infrared spectra of 1, diEtCD (——); 2, diEt9-EtCD (—·—); 3, PECC (·····); 4, 9-Et PECC (– – –).

are prone to give a darker polycondensation products, as is shown in Table II.

Numerous PECB by adding different amount of germanium dioxide, ranging from 0.03 to 0.32% by weight of CDBA, exhibited a light yellow color, and the crude product was transparent. Figure 2 shows that the viscosity of the resulting PECB tended to decrease when more than 0.13% of germanium dioxide (based on the weight of CDBA) was added in a polycondensation. As is shown in Fig. 1, calcium acetate, used singly, was equally as effective as the combined catalyst ($Ca(CH_3CO_2)_2 \cdot H_2O/Sb_2O_3=4/1$). The antimony trioxide in combination with calcium hydride exerted a good effect, whereas it did not enhance the marked catalyst effect when used together with calcium acetate, as is shown in Table I.

Table V. Dependence of polymer-melt temperature on structure of acid component (acid or simple ester of general formula

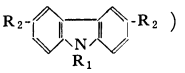

		R_2	PMT (°C)
A	$R_1=-H$	-COEt	above 200
		$-(CO_2)_3COOH$	below 100*
		$-CO(CH_2)_2COOEt$	above 165
B	$R_1=-CH_3$	$-(CH_2)_3COOH$	below 120*
		$-CO(CH_2)_2COOEt$	above 190
C	$R_1=-C_2H_5$	-COOEt	above 280

* Polymer softening temperature

The catalysts effective in the syntheses of PECKB and PECB were mostly ineffective in the preparation of PECC (for instance, calcium acetate or germanium dioxide). In the absence of calcium halide, the reaction of diEtCD and ethylene glycol at the early stage did not proceed smoothly, so that β-hydroxyethyl carbazole-3, 6-dicarboxylate was obtained in only a low yield. On the other hand the reaction proceeded readily in the presence of calcium hydride.

In the synthesis of PECC, calcium acetate as a single catalyst proved to be ineffective, whereas lead acetate was suitable. Under the influence of blended catalysts, such as lead acetate and antimony trioxide, an infusible and insoluble PECC was obtained. However, a mixture of lead acetate and calcium hydride or cobaltous acetate and calcium hydride was revealed to be a good catalyst blend in preparing PECC.

The polymer melt temperature or the polymer softening temperature depends greatly on the structure of the acid component, as is shown in Table V. In contrast to PECB, which was more susceptible to deformation by heat, PECC showed a fairly high polymer melt temperature.

The infrared spectra of the starting monomers and the polyesters (PECC, 9-EtPECC, PECB, and 9-MePECB) were compared in order to establish the structures of polycondensation products. Figures. 3, 4 and 5 show the characteristic N–H stretching absorptions. As is illustrated in the figures, these absorptions are apparently absent in the spectra of 9-MeCDBA, 9-MePECB, 9-EtCDA, and 9-EtPECC. The presence of an aromatic-type structure is also evidenced by the absorption near 3030 cm^{-1}, as shown in Figs. 3, 4, and 5. These characteristic absorptions, as

well as other absorptions in the lower regions of the charts (arising from the C=O and C=C groups), together with the data of the elementary analyses of the polyesters, indicated that PECB and PECC are linear polyesters with the following recurring units:

PECB, $-(OCOC_3H_6-C_{12}H_7N-C_3H_6CO_2C_2H_4O)-$, in which $-C_{12}H_7N-$ is the carbazole ring; PECC, $-(OC-C_{12}H_7N-CO_2C_2H_4O)-$. in which $-C_{12}H_7N-$ is the carbazole ring.

BULLETIN OF THE CHEMICAL SOCIETY OF JAPAN VOL. 39 654—664 (1966)

Single Stage Oxidation of *p*-Xylene with Ozonized Air

By Tsuguo TAKAYA, Tadashi KOGA and Tadashi HARA

Department of Chemical Engineering, Faculty of Engineering, Doshisha University, Kamikyo-ku, Kyoto

(Received May 22, 1965)

A new method has been found by which terephthalic acid can easily be obtained by a single-stage oxidation of *p*-xylene in glacial acetic acid. *p*-Xylene was oxidized with ozonized oxygen or air at 90°C in the presence of cobaltous acetate, ammonium bromide and an unsaturated aliphatic compound such as tetrachloroethylene. The effects of various factors on the oxidation rate were examined by measuring the absorption rates of oxygen. The reaction rates were measured for two steps, i. e., *p*-xylene to *p*-toluic acid and *p*-toluic acid to terephthalic acid, in the presence and absence of ozone respectively. The reaction mechanisms for each step have been discussed. It seems that the role of ozone and tetrachloroethylene in the present oxidation reaction can be attributed to the formation of ozonide which is transformed to hydroperoxide and which then participates in the chain reaction.

Many attempts have been made to obtain terephthalic acid by the oxidation of *p*-xylene with nitric acid,[1] air,[2] or oxygen gas,[3] sulfur in ammonium hydroxide[4] or ammonium sulfide,[5] and their combinations,[6] etc. Most of these attempts have been carried out under drastic reaction temperature and pressure conditions. The method developed by Brill[3] gives terephthalic acid in a good yield by the single-stage oxidation of *p*-xylene under the following conditions: oxidizing agent: oxygen gas; pressure: 1 atm.; solvent: glacial acetic acid; temperature: 90°C; catalysts: cobaltous acetate tetrahydrate; activator: a ketone containing an α-methylene group; and reaction time: 24 hr. However, the reaction does not proceed with air instead of oxygen. The present experiment was, therefore, carried out with the objectives of finding a catalyst with which the oxidation reaction of *p*-xylene is allowed to proceed under conditions milder than those in the conventional method, and of clarifying the reaction mechanism.

As a result of experiments, a new method was developed, and crude terephthalic acid was obtained in an about 95% yield under the following conditions: temperature: 90°C; pressure: 1 atm.; reaction time: 6 hr.; catalysts: cobaltous acetate, ammonium bromide, and a small amount of unsaturated aliphatic compound; oxidant: ozonized oxygen or air; and solvent: glacial acetic acid.

Though the ozone[8] has been reported to be effective as an initiator for the liquid-phase oxidation of *p*-xylene, no method has been reported in detail. According to the present procedure, the methyl groups bonded directly to the benzene ring are easily oxidized to the carboxyl groups, and crude terephthalic acid is obtained in a 83—85% yield by the single-stage oxidation of *p*-xylene using air which contains about 0.5% ozone. Unsaturated aliphatic compounds are effective as the promotor; upon their use the yield of terephthalic acid increases more than 10%.

Though the rate equation in the oxidation stage from *p*-toluic acid to terephthalic acid has been given by Ravens,[7] no rate equation has been reported with the *p*-xylene → *p*-toluic acid, and *p*-xylene → *p*-toluic acid and *p*-toluic acid → tetrephhalic acid oxidations using ozonized oxygen. Therefore, the rate equation was studied by measuring the absorption rate of oxygen gas, and the reaction mechanism was considered.

Experimental

Reagents.—*p*-Xylene (98.5% purity) presented by the Maruzen-Sekiyu Co., Ltd., was treated with sulfuric acid, sodium hydroxide, and water in that order,

1) U. S. Pat. 2636899 (1953).
2) U. S. Pat. 2833816 (1958).
3) W. F. Brill, *Ind. Eng. Chem.*, **52**, 837 (1960).
4) U. S. Pat. 2762839 (1956).
5) W. A. Pryor, *J. Am. Chem. Soc.*, **80**, 6481 (1958).
6) For example, U. S. Pat. 2653165 (1954).
7) D. A. S. Ravens, *Trans. Faraday Soc.*, **55**, 1768 (1959).

dehydrated, and distilled; the distillate was then purified by fractional crystallization. Acetic acid containing 0.38 wt.% water was used. The cobaltous acetate and ammonium bromide were of the reagent grade. The tetrachloroethylene was treated with sulfuric acid, sodium hydroxide, and water in that order, and distilled. The other reagents were used after purification.

Apparatus.—A Siemens-type ozonizer was built up with Pyrex glass, and about 10 kV. of voltage was applied to it through a transformer. The ozonized air was washed with a 10% sodium hydroxide solution in order to remove the oxides of nitrogen, dehydrated with concentrated sulfuric acid and calcium chloride (anhydride), and introduced into a reaction vessel. A 500 ml. reaction vessel attached with four holes to a thermometer, a stirrer, a condenser, and a gas-inlet was used. The reaction vessel was heated by a mantled heater. The oxidants were introduced into the reaction vessel through the ozonizer from an oxygen bomb or after the compressed air had been dehydrated with concentrated sulfuric acid and silica gel. The reaction rate was measured by the apparatus shown in Fig. 1. F is thermostatted at 90°C in an oil-bath, and A, B, and C at 25°C. *p*-Xylene is made to react with oxygen in the cell, F, and the solution is stirred by a magnetic stirrer. The manostat, B, operates by the absorption of oxygen gas, and then the electrolyzer, D, operates until the oxygen pressure in the system becomes equal to the original. The gas evolved by D is sent to the left-hand side of the gas-burette, A, and the meniscus of the right-hand side is raised. The amount of oxygen gas absorbed is read on the right-hand side of A. To operate this apparatus, all the cocks except the cocks 3, 7, 8, and 12 are opened, and the system is evacuated. Then the cocks 1 and 4 are closed in that order, and more than 1 atm. of oxygen gas is introduced into the balloon through the cock 3. The cock 4 is opened, and the system is filled with oxygen gas. The cocks 4 and 2 are closed in that order, and the cock 1 is opened. The cock 7 is gradually opened. For a measurement, the cock 8 is opened, and the cocks 5, 6, 7, 9, 10, and 11 are closed, followed by the opening of the cock 12. When the meniscus of A on the right-hand side has risen up to the top, the cocks 6, 9, and 11 are opened after the closure of the cock 12 and the opening of the cocks 10 and 7, and the measurement is continued as before. F is dipped into the oil-bath when the cock 15 is opened, and the cock is closed just before the measurement. Since the vapor pressure of acetic acid at 90°C is 300 mmHg, the vapor pressure of air at the same temperature is given by 760−300=460 mmHg. By assuming the composition of the air to be $O_2 : N_2 = 1 : 4$, the partial pressure of oxygen gas at 90°C is found to be approximately 92 mmHg through all the experiments.

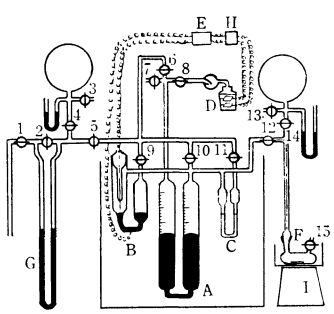

Fig. 1. An apparatus for the measurement of oxidation rate.
A: Gas burette B: Manostat
C: Manometer (charged with dibutyl phthalate)
D: Electrolyzer E: Relay
F: Reaction cell
G: Manometer (charged with mercury)
H: Stabileizr I: Magnetic stirrer

The Analysis of the Oxidation Products.—After the reaction had finished, the products were filtered, washed with glacial acetic acid and water, dried, and weighed, and the yields of crude terephthalic acid were calculated. When an aliquot amount of crude terephthalic acid was esterified with methanol and sulfuric acid, the ester showed a m. p. of 140.2—140.9°C. The aldehyde content was determined by dissolving a sample in an excess silver nitrate/ammonium hydroxide solution, by filtering the deposits off, and by estimating the remaining silver by the Volhard method. The carboxyl group content was also determined conductometrically by dissolving an aliquot amount of the sample in ammonium hydroxide and by titrating it with a standard lithium hydroxide solution. According to this procedure, each acid is determined graphically, since the mixture consisting of mono- and di-basic acids gives two inflection points on the titration curve.

The Determination of the Ozone.—The apparatus shown in Fig. 2 was devised. In Fig. 2, I is the inlet for the sample gas, and II, the outlet. In order to determine the ozone content, the gas sample is passed through the flask, III, and then the cock, IV, and the flask are turned to take a definite volume of the sample. The vessel, V, is filled with an excess potassium iodide solution, and most of the solution is dropped into III by compressed air, after which IV is closed. Then the apparatus is shaken for a minute, and the flask is taken off. The inside of the upper part is washed down with water, and the combined solution is titrated with a standard sodium thiosulfate solution. The results obtained by this procedure agreed with those obtained by the conventional method; the ozone contents in the ozonized oxygen gas and air used in this experiments were approximately 1.0 and 0.5 vol.% respectively.

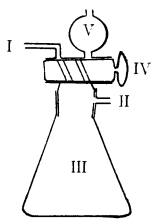

Fig. 2. An apparatus for determination of ozone in ozonized gases.
I: Gas inlet IV: Cock
II: Gas outlet V: KI tank
III: Flask

The Measurement of the Reaction Rate and Order.—The sample is put in the reaction cell, and the

cell is heated at 90°C for 5 min. After exactly 5 min., or after 10 minutes' passage of the ozonized oxygen containing approximately 0.8 vol.% ozone, the measurement is started, and the oxygen amount absorbed is read at definte intervals. The reaction rate was expressed as the mean value obtained by dividing the total oxygen amount absorbed by the reaction time.

In order to determine the reaction order of a certain component, the oxygen amount absorbed was measured under conditions in which the concentration of the component was varied, and the reaction rate was plotted against the concentration of the component. The reaction order of the component was found from the slope of a straight line on the graph.

Results and Discussion

The Oxidation of *p*-Xylene with Ozonized Oxygen.—In order to examine the effect of ozone on the oxidation of *p*-xylene, the reaction was carried out under the following conditions: acetic acid: 200 ml.; *p*-xylene: 25.0 ml.; cobaltous acetate tetrahydrate: 4.982 g.; ammonium bromide: 0.1 g.; tetrachloroethylene: 1.0 ml.; reaction temp.: 90°C; ozone content: 1.0 vol.%; gas flow rate: 140 l./hr.; and reaction time: 6 hr. The results obtained are shown in Table I.

TABLE I. THE EFFECT OF OZONE ON THE YIELDS OF TEREPHTHALIC ACID

No.	Yield %	No.	Yield %
1	77.1	4	82.4
2	68.7	5	93.5
3	72.1	6	95.6

No. 1: Ozonized oxygen until the deposit of terephthalic acid, and then oxygen alone
No. 2: Oxygen alone until the deposit of terephthalic acid, and then ozonized oxygen
No. 3: Oxygen alone
No. 4: Ozonized oxygen for 2 hr., and then oxygen for 4 hr.
No. 5: Ozonized oxygen for 3 hr., and then oxygen for 3 hr.
No. 6: Ozonized oxygen for 6 hr.

It has been reported that ozone is effective as an initiator,[8] but it is not always necessary after the solution has become dark green. However, it may be seen from Table I that ozone is effective not only as an initiator but also as an activator during the reaction. In order to examine the effect of aliphatic unsaturated compounds on the yields of terephthalic acid, the oxidation was carried out under the same conditions as before except in the presence of various unsaturated compounds. The results obtained are shown in Table II. As can be seen from Table II, the yields increase in the presence of aliphatic unsaturated compounds. This seems to be because of the interaction between the ozone and the double bond.

TABLE II. THE EFFECT OF ALIPHATIC UNSATURATED COMPOUNDS ON THE YIELDS

Compound	Added	NH_4Br g.	Yield %
Maleic anhydride	7.845 g.	0.1	94.5
Allyl bromide	4.6 ml.	—	84.6
Tetrachloroethylene	1.0 ml.	0.1	95.0
Hexachloro-1,3-butadiene	10.43 g.	0.1	92.5
None	—	0.1	75.0

It has been also reported[9] that *p*-xylene could be oxidized into terephthalic acid under these conditions: catalysts: Co^{2+}, Mn^{2+}, Cl^-, and Br^-; solvent: propionic acid; reaction temp.: 137°C; and reaction time: 5.1 hr. It may, however, be supposed from Table II and the data that the double bond may affect the yields of terephthalic acid more than chloride ions. The product is white in the presence of chloride ions, while yellow in their absence. Therefore, tetrachloroethylene was used as the aliphatic unsaturated compound in the experiments below. The experiments were also designed to examine the effects of cobaltous acetate, bromide, and tetrachloroethylene on the yields of terephthalic acid; the results obtained are shown in Tables III and IV.

Judging from the results shown in Tables III and IV, the following conditions are recommended for the oxidation of *p*-xylene: acetic acid: 200 ml.; *p*-xylene: 25.0 ml.; cobaltous acetate tetrahydrate: 4.982 g.; ammonium bromide: 0.1 g.; tetrachloroethylene: 1.0 ml.

Cobaltous acetate and ammonium bromide had the main effects on the yields. In the case of the oxidation with ozonized oxygen, no interaction was found among cobaltous acetate, ammonium bromide, and tetrachloroethylene, while the reverse was true in the case of the oxidation with oxygen alone. It may, therefore, be supposed that cobalt, bromide, and tetrachloroethylene may be separately activated with ozone to take part in the oxidation reaction. The relationships between the reaction time, or the reaction temperature, or the water content, and the yields were also examined by carrying out the oxidation under the optimum conditions mentioned above; the yields were 35.2, 64.9, 89.6, 94.7 95.6, 96.8, and 97.3% for 2, 3, 4, 5, 6, 8, and 10 hours' reactions respectively; 0, 56.3, 63.3, 69.2, 96.1, and 83.5% at 50, 60, 70, 80, 90, and 100°C respectively; and 92.4, 89.8, 90.1, 90.6, 87.0, 81.2, 78.2, and 22.9% in 0, 1.0, 2.0, 3.0, 4.0, 10.0, 15.0, and 20.0 ml. of waters respectively.

The oxidation products were analyzed by the above mentioned procedures; the results are

8) Brit. Pat. 798619 (1958); A. S. Hay and J. W. Eustance, *J. Org. Chem.*, **25**, 616 (1960).

9) Japanese Pat. 5472 (1960).

Table III. The effects of catalysts on the yields of terephthalic acid

No.	$Co(OAc)_2 4H_2O$ g.	NH_4Br g.	Tetrachloroethylene g.	Recovery, % Series I	Series II
1	4.982	0.1	1.0	96.1	88.0
2	4.982	0.5	3.0	92.1	93.5
3	4.982	0.5	1.0	96.5	90.5
4	4.982	0.1	2.0	83.3	86.2
5	2.491	0.1	2.0	76.6	78.3
6	4.982	0.1	3.0	89.9	83.4
7	2.491	0.5	3.0	77.5	86.5
8	2.491	0.5	1.0	84.2	88.9
9	2.491	0.5	2.0	89.9	79.8
10	2.491	0.1	1.0	80.3	74.3
11	4.982	0.5	2.0	92.3	89.8
12	2.491	0.1	3.0	75.0	77.5

Table IV. Analysis of variance

SS: variation, ϕ: degree of freedom, V: unbiased variation

Factor	SS	ϕ	V	F_0	F 0.01	0.05
A	522	1	522	30	9.33	4.75
B	241	1	241	13.9	9.33	4.75
C	42	2	21	1.2	6.93	3.89
A × B	11	1	11	—		
A × C	26	2	13	—		
B × C	1	2	0.5	—		
A × B × C	18	2	9	—		
E (error)	209	12	17.4			
Total	1070	23				

A: Cobaltous acetate, B: Ammonium bromide, C: Tetrachloroethylene

Table V. Analysis of the oxidation products

Sample No.	Terephthalic acid, %	*p*-Toluic acid, %	*p*-Formylbenzoic acid, %
1	85.0	4.6	9.3
2	88.6	2.9	8.6
3	87.2	5.8	6.8

shown in Table V. *p*-Toluic acid and *p*-formylbenzoic acid were found as the impurities. *p*-Formylbenzoic acid was easily oxidized into terephthalic acid with Tollen's reagent, and terephthalic acid was recovered with a purity of ca. 99%. Since the contamination with *p*-formylbenzoic acid as an impurity is a serious obstacle to obtaining highly-pure terephthalic acid, an effort is being made to prepare the terephthalic acid free from *p*-formylbenzoic acid.

The present method was further applied to the oxidation of alkylbenzenes; the yields of benzoic acid from toluene, isophthalic acid from *m*-xylene, and phthalic acid from *o*-xylene in 6 hours' reaction were 97.4, 93.3, and 48.8% respectively. However, the yield of phthalic acid increased to 95.2% in 10 hours' oxidation.

The oxidation rate of *o*-xylene is smaller than those of *m*- and *p*-xylene; this shows a close relation with the average reaction rate,[10] $o < m \fallingdotseq p$,

Table VI. The effects of ammonium bromide on the yields

(Reaction temp.: 90°C)

NH_4Br added, g. First	Second	Yield %	Product
0.1960	0.1960	67.5	White*
0.0490	0.0490	70.5	White
0.0980	0.0980	82.4	White
0.0980	0.1960	83.9	White
0.0980	0.2940	84.3	White
0.0980	0.4900	83.2	Slightly yellow

* Reaction temp.: 80°C

in the xylene isomers. It has been reported that the smaller reaction rate of *o*-xylene seems to be based on the chelation between cobaltous ions and phthalic acid, and on the fact that the acidity[10] of phthalic acid is stronger than that of the others.

The Oxidation of *p*-Xylene with Ozonized Air.—The oxidation procedure with ozonized air differs from that with ozonized oxygen in the following points; 1) Ozonized air is blown into the solution; 2) The ozone content is

10) N. Ohta, E. Takahashi and H. Kinase, *Yuki Gosei Kagaku*, **21**, 536 (1963).

TABLE VII. ORIGINAL DATA FOR THE ANALYSIS OF VARIANCE

HOAc: 25.0 ml., *p*-xylene: 1.0 ml., reaction time: 100 min.

Exp. No.	$Co(OAc)_2 4H_2O$ g.	NH_4Br g.	$Cl_2C=CCl_2$ ml.	O_2 absorbed, cc. 1st	2nd
1	0.20	0.01	0	49.70	47.40
2	0.20	0.02	0.20	9.90	6.60
3	0.20	0.02	0	30.80	30.20
4	0.20	0.01	0.10	23.90	30.20
5	0.10	0.01	0.10	27.20	31.60
6	0.20	0.01	0.20	37.90	39.00
7	0.10	0.02	0.20	50.80	54.00
8	0.10	0.02	0	46.10	52.40
9	0.10	0.02	0.10	40.40	43.30
10	0.10	0.01	0	39.50	37.40
11	0.20	0.02	0.10	16.80	18.30
12	0.10	0.01	0.10	29.20	30.80

TABLE VIII. ANALYSIS OF VARIANCE

Factor	SS	ϕ	V	F_0	F 0.01	0.05	0.10
K	828	1	828	135.7	9.33	4.75	3.13
L	26	1	26	4.3	9.33	4.75	3.13
M	694	2	347	56.9	6.93	3.89	2.81
K × L	1752	1	1752	287.1	9.33	4.75	3.13
K × M	190	2	95	15.6	6.93	3.89	2.81
L × M	34	2	17	2.8	6.93	3.89	2.81
K × L × M	263	2	132	21.6	6.93	3.89	2.81
E (error)	74	12	6.1				
Total	3861	23					

K: Cobaltous acetate, L: Ammonium bromide, M: Tetrachloroethylene

about 0.5%; 3) The flow rate is about 300 l. per hour; 4) Two portions of ammonium bromides are added, one at the beginning of the reaction and the other at just one-half the time from the deposit of terephthalic acid to the end, and 5) Chloroacetic acid is added as a co-catalyst.

The effects of ammonium bromide on the yields are shown in Table VI.

It was found that the yields in the presence of tetrachloroethylene increase by 10—13%. The yields were 70.9, 74.5, 75.6, 81.3, 81.1, 79.0, and 57.1%, respectively in the presence of each 0.1, 0.2, 0.3, 0.5, 0.8, 0.9, and 0 g. of chloroacetic acids. Since terephthalic acid was obtained in a high yield in the case of ozonized oxygen, the effects of chloroacetic acid could not be discriminated from its yield. Chloroacetic acid has been reported[11] to be effective for the oxidation of *p*-xylene; this coincides well with the present results. In the coming experiments, chloroacetic acid is always added in 0.5 g. portions until otherwise stated.

The yields were 58.9, 69.3, 81.3, 70.0, 67.9, and 63.6%, respectively, with each 2.491, 4.982, 7.473, 9.964, 12.455, and 14.946 g. of cobaltous acetate tetrahydrate. As may be seen from these results, up to a definite concentration Co^{2+} behaves positively, while it behaves negatively with a greater concentration. Since it has been established that the metal ions showing reversibly changeable valencies often behave as inhibitors in the radical chain reaction,[12,13] the negative behavior of cobaltous ions seems to be based on a similar mechanism.

The yields were 84.3, 87.6, 87.8, and 90.3%, respectively, in 6, 7, 8, and 10 hours' reactions. Since some *p*-xylene was lost, together with some air, it was difficult to raise the yields higher, even by making the reactions last more than 10 hr. When the oxidation products were analyzed, they were found to be composed of 76.9—79.6% terephthalic acid, 10.5—11.97% *p*-toluic acid, and 10—14.8% *p*-formylbenzoic acid. It was also noted that the contents of *p*-toluic acid and *p*-formylbenzoic acid are larger than those in the ozonized oxygen.

The Reaction Rate from *p*-Xylene to *p*-Toluic Acid.—At first, the reaction rate was measured under an oxygen pressure of 92 mmHg without allowing the solution to come in contact

11) N. Ohta, K. Sunaoka and N. Nitanai, *J. Chem. Soc. Japan, Ind. Chem. Sect.* (*Kogyo Kagaku Zasshi*), **63**, 768 (1960).

12) N. Ohta and S. Maruge, ibid., **58**, 798 (1955).

13) K. Kagami, *Yuki Gosei Kagaku*, **20**, 284 (1962).

with the ozone. The amounts of the oxygen absorbed were measured on the basis of the design of the experiments in which cobaltous acetate, ammonium bromide, and tetrachloroethylene are looked upon as factors; duplicate experiments are planned at the level of $2\times2\times3$. Tables VII and VIII show the original data and the analysis of the variance respectively.

When the significant level is adopted as 10% by taking the reproducibility and the error in measurement into account, the effects are found in all the factors. However, the main effect of cobalt, and the interaction between cobaltous ions and bromide, are predominant among them. The reaction shows an independence of the concentration of *p*-xylene. The reaction also shows a first-order dependence on the concentration of cobaltous acetate at $[Co^{2+}]\leqq0.024$ mol./l.; thereafter the rate decreases with an increase in $[Co^{2+}]$. The reaction shows a one-fourth-order dependence on the concentration of ammonium bromide at $NH_4Br\leqq10.0$ mg., and a negative one-half-order dependence on the concentration of tetrachloroethylene. The negative effect of tetrachloroethylene in the absence of ozone seems to be based on the facts that tetrachloroethylene can be only activated with difficulty and that it consumes the radical in the radical chain reaction. Because 1) the reaction mixture does not become dark green at all, just as in the presence of a considerable amount of bromide, and 2) the interactions among cobalt, bromide, and tetrachloroethylene are found in the design of experiments, it may be supposed that tetrachloroethylene not only consumes the radical but also accelerates the reaction from cobaltic to cobaltous ions in accordance with the following mechanism:

$$Co^{3+} + HBr \rightleftharpoons Co^{2+} + Br\cdot + H^+$$

$$Cl_2C{=}CCl_2 + Br\cdot \cdots\longrightarrow \text{inactives}$$

The reaction shows a first-order dependence on the concentration of chloroacetic acid at $[ClCH_2COOH]\leqq0.13$ mol./l.

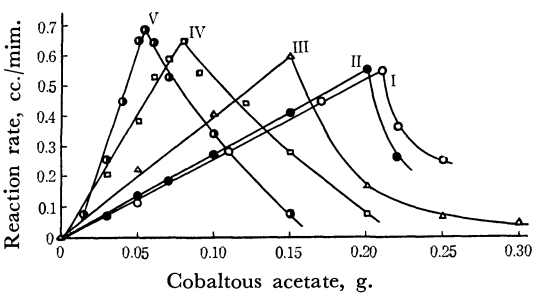

Fig. 3. Relationship among the amounts of cobaltous acetate and ammonium bromide, and the reaction rate.
I: NH_4Br 0.005 g. IV: NH_4Br 0.030 g.
II: NH_4Br 0.010 g. V: NH_4Br 0.040 g.
III: NH_4Br 0.020 g.

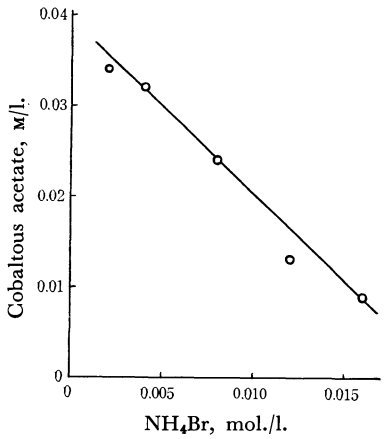

Fig. 4. Relationship between the amounts of cobaltous acetate and ammonium bromide at the maximum reaction rates.

The relationship among the reaction rate and the concentrations of cobaltous acetate and ammonium bromide is given in Fig. 3. The relationship between the concentrations of cobaltous acetate and ammonium bromide at the maximum absorption rate is further shown in Fig. 4, where it is given by a straight line. On the basis of Fig. 4, the relationship is expressed as follows:

$$[Co^{2+}] + 2[NH_4Br] \leqq 0.04 \text{ mol./l.}$$

By combining the above results, the reaction rate at $[Co^{2+}] + 2[NH_4Br] \leqq 0.04$ mol./l. and $[ClCH_2COOH]\leqq0.13$ mol./l. is expressed by the following equation:

$$R_1 = k_1[Co^{2+}][NH_4Br]^{1/4}\cdot [ClCH_2COOH][Cl_2C{=}CCl_2]^{-1/2}$$

With the objective of examining the effect of ozone on the initial reaction, the absorption rate of oxygen after 10 minutes' passage of ozonized oxygen was measured. Though the reaction rates in the above experiments were measured under an oxygen pressure of 92 mmHg, those after the passage of the ozonized oxygen were measured under an oxygen pressure of 460 mmHg. The reaction shows one-half-order, three-second-order, one-half-order at $[NH_4Br]/[Co^{2+}]\leqq5/4$ or first-order at $[NH_4Br]/[Co^{2+}] > 5/4$, zero-order, and zero-order dependences on the concentrations of *p*-xylene, cobaltous acetate, ammonium bromide, tetrachloroethylene, and chloroacetic acid, respectively.

It may be noted that tetrachloroethylene has a negative effect on the progress of the reaction in the absence of ozonized oxygen, while the reaction rate after 10 minutes' passage of ozonized oxygen is independent of the concentration of tetrachloroethylene. Therefore, ozone may be expected to exert a positive effect on the reaction when it is passed through during the experiment.

This is consistent with an increase of the yield of terephthalic acid in the presence of ozone.

To summarize the above results, the initial rates after 10 minutes' passage of ozonized oxygen are as follows:

$$R_2 = k_{II}[p\text{-xylene}]^{1/2}[Co^{2+}]^{3/2}[NH_4Br]^{1/2} \quad \text{at } [NH_4Br]/[Co^{2+}] \leqq 5/4$$

$$R_3 = k_{III}[p\text{-xylene}]^{1/2}[Co^{2+}]^{3/2}[NH_4Br] \quad \text{at } [NH_4Br]/[Co^{2+}] > 5/4$$

The Reaction Rate from *p*-Toluic Acid to Terephthalic Acid.—At first, the absorption rate of oxygen in the absence of ozone was measured much as in the above experiment. The reaction shows an independence of the concentration of *p*-toluic acid, and a first-order dependence on that of cobaltous acetate. The reaction shows a one-half-order dependence on the concentration of ammonium bromide at $[NH_4Br] \leqq 0.04$ mol./l. and $[NH_4Br]/[Co^{2+}] \leqq 5/4$. The reaction rate increases ca. 12.5% upon the addition of any tetrachloroethylene, while it shows independences of the concentrations of chloroacetic acid and tetrachloroethylene. To summarize the above results, the reaction rate may be given as follows:

$$R_4 = 1.125k_{IV}[Co^{2+}][NH_4Br]^{1/2}$$
at $[NH_4Br] \leqq 0.04$ mol./l.
and $[NH_4Br]/[Co^{2+}] \leqq 5/4$

Then the absorption rate of oxygen after 10 minutes' passage of ozonized oxygen was measured much as before. The reaction shows an independence of the concentration of *p*-xylene, and three-second-order and one-fourth-order dependences on the concentrations of cobaltous acetate at $[Co^{2+}] \leqq 0.024$ mol./l. and $([Co^{2+}]+[NH_4Br]) \leqq 0.028$ mol./l., and at $[Co^{2+}] > 0.024$ mol./l. and $([Co^{2+}]+[NH_4Br]) > 0.028$ mol./l., respectively. The reaction also shows a one-half-order or second-order dependence on the concentrations of ammonium bromide at $[NH_4Br] \leqq 0.012$ mol./l. and $([Co^{2+}]+[NH_4Br]) \leqq 0.028$ mol./l., and at $[NH_4Br] > 0.012$ mol./l. and $([Co^{2+}]+[NH_4Br]) > 0.028$ mol./l. Further, the reaction shows an independence of the concentration of tetrachloroethylene. To summarize the above results, the reaction rate may be given as follows;

$$R_5 = k_V[Co^{2+}]^{3/2}[NH_4Br]^{1/2}$$

at $[NH_4Br] \leqq 0.012$ mol./l. and $([Co^{2+}]+[NH_4Br]) \leqq 0.028$ mol./l.

$$R_6 = k_{VI}[Co^{2+}]^{1/4}[NH_4Br]^{2.0}$$

at $[NH_4Br] > 0.012$ mol./l. and $([Co^{2+}]+[NH_4Br]) > 0.028$ mol./l.

Reaction Mechanism.—Since no reaction mechanism has been reported with regard to the oxidation of *p*-xylene to *p*-toluic acid, it has been considered first. It is supposed in glacial acetic acid that the following reaction occurs easily, and that [HBr] is directly proportional to $[NH_4Br]$, since hydrogen bromide does not dissociate so much.[14]

$$NH_4Br + CH_3COOH \rightleftharpoons HBr + CH_3COONH_4$$

Thus the reaction rate obtained experimentally may be expressed as a dependence on $[HBr]^{1/4}$. Hydrogen bromide is thus made to react with oxygen to produce the radical in accordance with the reaction 1:

$$HBr + O_2 \xrightarrow{k_1} Br\cdot + HO_2\cdot \qquad v_1 \quad (1)$$

By expressing $-\langle\bigcirc\rangle-CH_3$ with ϕ, reactions 2 and 3 are given as:

$$\phi CH_3 + Br\cdot \xrightarrow{k_2} \phi CH_2\cdot + HBr \qquad v_2 \quad (2)$$

$$\phi CH_2\cdot + O_2 \xrightarrow{k_3} \phi CH_2O_2\cdot \qquad v_3 \quad (3)$$

The absence of *p*-xylene from the rate equation establishes that it does not enter into the propagation steps; the reaction 3a, which would involve a first-order dependence on [*p*-xylene], is therefore excluded:

$$\phi CH_3 + \phi CH_2O_2\cdot \rightarrow \phi CH_2OOH + \phi CH_2\cdot \quad (3a)$$

The replacement of 3a by an electron-transfer reaction between a cobaltous ion and a hydroperoxy-radical may be suggested; 4 represents the sum of two possible courses, 4a—4b and 4c—4d:

$$\phi CH_2O_2\cdot + Co^{2+} \xrightarrow{k_4} \phi CHO + OH^- + Co^{3+} \qquad v_4 \quad (4)$$

(i) $\phi CH_2O_2\cdot \rightarrow \phi CHO + OH\cdot$ (thermal) (4a)

$$OH\cdot + Co^{2+} \rightarrow Co^{3+} + OH^- \quad (4b)$$

(ii) $\phi CH_2O_2\cdot + Co^{2+} \rightarrow \phi CH_2O_2^- + Co^{3+}$ (4c)

$\phi CH_2O_2^- \rightarrow \phi CHO + OH^-$ (very fast) (4d)

Of these mechanisms, it is the more probable, since it is unlikely that the thermal decomposition of a hydroperoxyradical would produce an aldehyde exclusively. The regeneration of the cobaltous ion by the reaction 5 is suggested:

$$Co^{3+} + HBr \underset{k_{-5}}{\overset{k_{+5}}{\rightleftharpoons}} Co^{2+} + Br\cdot + H^+ \qquad \begin{matrix} v_{+5} \\ v_{-5} \end{matrix} \quad (5)$$

The concentration of Co^{3+} appears to be much smaller than that of Co^{2+}, since the color of the solution during an oxidation shows none of the deep green usually associated with the cobaltic state. The reaction 5 is considered to be reversible and in an equilibrium under a steady state. Since $[Co^{3+}]$ is much smaller than $[Co^{2+}]$, v_{+5} is

14) I. M. Kolthoff and A. Willman, *J. Am. Chem. Soc.*, **56**, 1007 (1934).

thought to be very large compared to v_{-5}; therefore, the apparent rate of the reaction 5 may be approximately given by v_{+5}.

The reaction accompanying tetrachloroethylene is thought to proceed in accordance with the reaction 6, 6a, 6b, and 6c on the basis of the mechanism proposed by Schumacher et al.[15] with regard to the reaction-between Cl· and tetrachloroethylene:

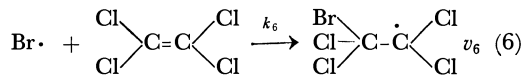
(6)

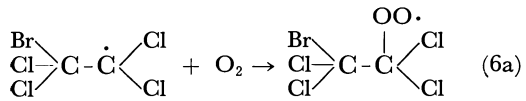
(6a)

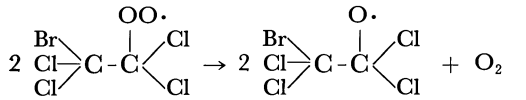
(6b)

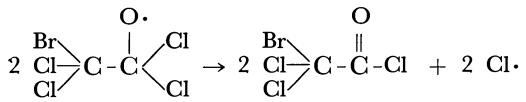
(6c)

On the basis of the data* obtained by the present authors, the Br· in 6 might be replaced by an increasing amount of Cl· in 6c, and there might be a chain reaction consisting of 6—6c. Though a small amount of oxygen is consumed through the reactions 6—6c, the consumption of Br· in 6 would involve a retardation of 2 in the principal chain reaction and would, therefore, allow tetrachloroethylene to behave negatively. By considering further that the velocity of the propagation reaction in the *p*-xylene → *p*-toluic acid reaction is larger than that in the *p*-toluic acid → terephthalic acid reaction, it may be understood that the rate in the former is independent of the concentration of tetrachloroethylene, but that it increases by ca. 12.5%. It is further assumed that the reaction 6 is a rate-determining step in 6—6c, and that, therefore, v_6 is approximately equal to the apparent rate.

By assuming that $v_3 \gg v_4$** even under an oxygen pressure of 92 mmHg, the chain-termination is expressed by the reaction 7:

$$2\ \phi CH_2O_2\cdot \xrightarrow{k_7} \text{inactives} \qquad v_7 \quad (7)$$

When the reaction has reached a steady state, the rate of initiation is equal to the sum of v_6 and v_7.

$$k_1[HBr][O_2] = k_7[\phi CH_2O_2\cdot]^2 + k_6[Cl_2C{=}CCl_2][Br\cdot] \qquad (a)$$

By assuming $v_7 \gg v_6$, since a considerable amount of tetrachloroethylene was recovered after the oxidation of *p*-xylene, Eq. a is given by b and c:

$$k_1[HBr][O_2] = k_7[\phi CH_2O_2\cdot]^2 \qquad (b)$$

$$\text{hence:}\quad [\phi CH_2O_2\cdot] = \{(k_1/k_7)[HBr][O_2]\}^{1/2} \qquad (c)$$

By supposing that v_6 is constant, since [Br·] ≪ [tetrachloroethylene] and both are approximately constant at a steady state, Eqs. d and e are obtained:

$$v_6 = k_6[Cl_2C{=}CCl_2][Br\cdot] = K_I \qquad (d)$$

$$\text{therefore:}\quad [Br\cdot] = (K_I/k_6)[Cl_2C{=}CCl_2]^{-1} \qquad (e)$$

Under a steady state, the radical and Co concentrations may be considered stationary; i. e., $d[Co^{3+}]/dt = d[\phi CH_2\cdot]/dt = d[\phi CH_2O_2\cdot]/dt = 0$. The following relations are then obtained:

$$v_3 = v_2 = v_4 + v_7, \qquad v_4 = v_{+5},$$

$$v_1 = v_5 + v_6 \fallingdotseq v_7$$

and
$$-d[O_2]/dt = v_1 + v_3 = 2\ v_1 + v_4$$
$$= 2k_1[HBr][O_2] + k_4[\phi CH_2O_2\cdot][Co^{2+}]$$

If it is further assumed that the propagation chains are long compared to the initiation reaction, the oxygen absorption by the initiation reaction may be neglected, and Eq. f is obtained:

$$-d[O_2]/dt = k_4[\phi CH_2O_2\cdot][Co^{2+}] \qquad (f)$$

From $v_4 = v_{+5}$, Eq. g is obtained:

$$[\phi CH_2O_2\cdot] = (k_{+5}/k_4)\{[Co^{3+}][HBr]/[Co^{2+}]\} \qquad (g)$$

By introducing v_{+5}/v_{-5} = constant, h is derived:

$$[Co^{3+}] = (k_{-5}K_{II}/k_{+5})\{[Co^{2+}][Br\cdot][H^+]/[HBr]\} \qquad (h)$$

By combining g and h:

$$[\phi CH_2O_2\cdot] = (k_{-5}K_{II}/k_4)[Br\cdot][H^+] \qquad (i)$$

By multiplying c by i, and by taking its square root, j is derived:

$$[\phi CH_2O_2\cdot] = (k_1/k_7)^{1/4}(k_{-5}K_{II}/k_4)^{1/2}\cdot [HBr]^{1/4}[O_2]^{1/4}[Br\cdot]^{1/2}[H^+]^{1/2} \qquad (j)$$

By substituting e for [Br·]:

$$[\phi CH_2O_2\cdot] = (k_1/k_7)^{1/4}(k_{-5}K_{II}/k_4)^{1/2}(K_I/k_6)^{1/2}\cdot [HBr]^{1/4}[O_2]^{1/4}[Cl_2C{=}CCl_2]^{-1/2}[H^+]^{1/2} \qquad (k)$$

By combining f and k, Eqs. l and m are derived:

$$-d[O_2]/dt = (k_4k_{-5}K_IK_{II}/k_6)^{1/2}(k_1/k_7)^{1/4}\cdot [Co^{2+}][HBr]^{1/4}[O_2]^{1/4}\cdot [Cl_2C{=}CCl_2]^{-1/2}[H^+]^{1/2} \qquad (l)$$

15) H. J. Schumacher and W. Thurauf, *Z. Physik. Chem.*, **A189**, 183 (1941).

* Y. Sakuyama and T. Hara, unpublished. The amount of bromide and chloride in the reaction mixtures during the oxidation were investigated potentiometrically by using a glass electrode-silver (silver chloride) electrode combination, and by titrating this with a silver acetate solution in glacial acetic acid. The amount of bromide decreased at the beginning of the reaction, while the amount of chloride increased gradually. There was a considerable amount of chloride at the end of oxidation. These results give an indirect certification for the reactions 6-6c.

** Though this relation generally holds when the oxygen pressure is above ca. 100 mmHg, it is also assumed in the present case, since a similar rate equation, as will be shown later, was obtained at oxygen pressures 92 mmHg or higher pertaining to the oxidation of *p*-toluic acid. Cf. L. Bateman, G. Gee, A. L. Morris and W. F. Watson, *Discussions Faraday Soc.*, **10**, 250 (1951); F. Mashio, *J. Chem. Soc. Japan, Ind. Chem. Sect.* (*Kogyo Kagaku Zasshi*), **63**, 699 (1960).

$$-d[O_2]/dt = k_p[Co^{2+}][HBr]^{1/4}[Cl_2C{=}CCl_2]^{-1/2} \quad (m)$$

where

$$k_p = (k_4 k_{-5} K_I K_{II}/k_6)^{1/2}(k_1/k_7)^{1/4}[O_2]^{1/4}[H^+]^{1/2}$$

Since the present experiment was carried out under a definite oxygen pressure and since the reaction orders of all the factors except chloroacetic acid were examined in the absence of chloroacetic acid, $[H^+]$ may be considered constant and the term of chloroacetic acid in the experimental rate may be independent. Thus Eq. m agrees in form with the rate equation found by the experiment.

Though chloroacetic acid has been reported to act in three ways:[11] 1) enhancing the reactivity of alkylbenzenes, 2) increasing the activity of catalyst, and 3) offering a radical in itself, its behavior in the present reaction still remains unknown.

Since it seemed to be very difficult technically to oxidize *p*-xylene with oxygen of air containing a definite amount of ozone and to analyze the reaction mechanism, the effect of ozone on the reaction rate was examined by comparing it with one in oxygen alone. The reaction showed a negative one-half-order dependence on the concentration of tetrachloroethylene in the absence of ozone, but a zero-order dependence after 10 minutes' passage of ozone. It is, therefore, supposed in the latter case that the reaction 6 does not occure, but the reactions 8 and 9, which were proposed by Rieche[16] and Criegee,[17] do.

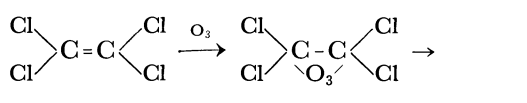

(8)

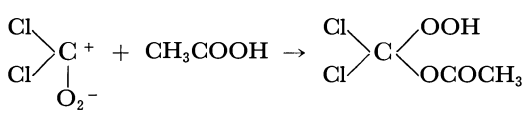

(9)

Judging from the experimental results, it may further be supposed that the formation of ozonide is not so slow as to consume Br· markedly, and that the hydroperoxide produced in 9 takes part in the propagation reaction, which results in an increase of the yield. By accepting these assumption, it is understandable that the reaction shows an independence of the concentration of tetrachloroethylene. By passing ozonized oxygen into the reaction mixture for 10 min. at 90°C, the cobalt-peroxy-radical shown in the reaction 10 can be produced, as has been proposed by several persons.[18]

$$Co^{2+} + O_2 \underset{k_{-10}}{\overset{k_{+10}}{\rightleftharpoons}} Co^{2+}\cdot O_2\cdot \qquad \begin{matrix} v_{+10} \\ v_{-10} \end{matrix} \quad (10)$$

The reaction 10 is assumed to be reversible and in an equilibrium. Therefore, Eq. 10-1 and 10-2 are derived:

$$K_{III} = \frac{k_{+10}[Co^{2+}][O_2]}{k_{-10}[Co^{2+}\cdot O_2\cdot]} \quad (10\text{-}1)$$

$$[Co^{2+}\cdot O_2\cdot] = (k_{+10}/K_{III}\cdot k_{-10})[Co^{2+}][O_2] \quad (10\text{-}2)$$

The chain reaction is supposed to be initiated by the reactions 11 and 12, followed by the propagation reactions, 13, 14, 15, 16, and the termination reaction, 17.

$$Co^{2+}\cdot O_2\cdot + HBr \xrightarrow{k_{11}} Co^{3+} + HO_2\cdot + Br\cdot \qquad v_{11} \quad (11)$$

$$Co^{2+}\cdot O_2\cdot + \phi CH_3 \xrightarrow{k_{12}} Co^{2+} + HO_2\cdot + \phi CH_2\cdot \qquad v_{12} \quad (12)$$

$$\phi CH_3 + Br\cdot \xrightarrow{k_{13}} \phi CH_2\cdot + HBr \qquad v_{13} \quad (13)$$

$$\phi CH_2\cdot + O_2 \xrightarrow{k_{14}} \phi CH_2O_2\cdot \qquad v_{14} \quad (14)$$

$$\phi CH_2O_2\cdot + Co^{2+} \xrightarrow{k_{15}} \phi CHO + OH^- + Co^{3+} \qquad v_{15} \quad (15)$$

$$Co^{3+} + HBr \xrightarrow{k_{16}} Co^{2+} + H^+ + Br\cdot \qquad v_{16} \quad (16)$$

$$2\ \phi CH_2O_2\cdot \xrightarrow{k_{17}} \text{inactives} \qquad v_{17} \quad (17)$$

By introducing a steady state, $v_{17} = v_{11} + v_{12}$, and Eq. n is derived:

$$k_{17}[\phi CH_2O_2\cdot]^2 = (k_{+10}k_{11}/K_{III}k_{-10})[Co^{2+}][O_2][HBr] + (k_{+10}k_{12}/K_{III}k_{-10})[Co^{2+}][O_2][\phi CH_3] \quad (n)$$

By assuming $v_{11}/v_{12} = K_{IV}$,

$$k_{11}[Co^{2+}\cdot O_2\cdot][HBr]/k_{12}[Co^{2+}\cdot O_2\cdot][\phi CH_3] = K_{IV}$$

Hence, $k_{11}[HBr] = K_{IV}k_{12}[\phi CH_3]$, and

$$k_{12}[\phi CH_3] = (k_{11}/K_{IV})[HBr]$$

By substituting these values into Eq. n, Eqs. o and o' are obtained:

$$[\phi CH_2O_2\cdot] = (k_{10}k_{12}/K_{III}k_{-10}k_{17})^{1/2}\cdot (K_{IV}+1)^{1/2}[Co^{2+}]^{1/2}[O_2]^{1/2}[\phi CH_3]^{1/2} \quad (o)$$

or:

$$[\phi CH_2O_2\cdot] = (k_{10}k_{11}/K_{III}k_{-10}k_{17})^{1/2}\cdot (1+1/K_{IV})^{1/2}[Co^{2+}]^{1/2}[O_2]^{1/2}[HBr]^{1/2} \quad (o')$$

Consequently, Eqs. p and p' are derived:

$$-d[O_2]/dt = v_{14} + v_{10} = v_{15} + v_{17} + v_{10} \fallingdotseq v_{15} = k_{15}[\phi CH_2O_2\cdot][Co^{2+}]$$

16) A. Rieche, *Angew. Chem.*, **70**, 251 (1958).
17) R. Criegee and M. Lederer, *Ann.*, **583**, 29 (1953).
18) P. George and A. Robertson, *Trans. Faraday Soc.*, **42**, 217 (1946); G. Wittig, *Angew. Chem.*, **60**, 169 (1948); N. Uri, *Nature*, **177**, 1177 (1956); H. Kropf, *Ann.*, **637**, 73 (1960).

$$= k_{15}(k_{10}k_{12}/K_{III}k_{-10}k_{17})^{1/2}(K_{IV}+1)^{1/2}\cdot [Co^{2+}]^{3/2}[O_2]^{1/2}[\phi CH_3]^{1/2} \quad (p)$$

or:

$$-d[O_2]/dt = k_{15}(k_{10}k_{11}/K_{III}k_{-10}k_{17})^{1/2}\cdot (1+1/K_{IV})^{1/2}[Co^{2+}]^{3/2}[O_2]^{1/2}[HBr]^{1/2} \quad (p')$$

Under a definite oxygen pressure, the initial rate is expressed as Eq. q:

$$-d[O_2]/dt = k_q[Co^{2+}]^{3/2}[HBr]^{1/2}[\phi CH_3]^{1/2} \quad (q)$$

Equation q agrees in form with the rate obtained experimentally. Though the reaction showed a first-order dependence on the concentration of hydrogen bromide at $[HBr]/[Co^{2+}]>5/4$, this is considered to be due to the increase in v_{11} and to the velocities in the coming reactions.

Though the reaction conditions from *p*-toluic acid to terephthalic acid in the present experiment are different in temperature and oxygen pressure from those used by Ravens, the reaction rate has been obtained in a form similar to that obtained by Ravens. The reaction rate by Ravens is shown by:

$$-d[O_2]/dt = k_r[Co^{2+}][NaBr]^{1/2}[O_2]^{1/2} \quad (r)$$

while that of the present authors is given by:

$$-d[O_2]/dt = 1.125k_s[Co^{2+}][NH_4Br]^{1/2} \quad (s)$$

In the latter, the reaction shows independences of the concentrations of both chloroacetic acid and tetrachloroethylene. Therefore, the reaction is considered to proceed by the following mechanism, which is similar to that proposed by Ravens:

$$NH_4Br + CH_3COOH \rightleftharpoons HBr + CH_3COONH_4 \quad (18)$$

$$HBr + O_2 \rightarrow Br\cdot + HO_2\cdot \quad (19)$$

$$\phi'CH_3 + Br\cdot \rightarrow \phi'CH_2\cdot + HBr \quad (20)$$

$$\phi'CH_2\cdot + O_2 \rightarrow \phi'CH_2O_2\cdot \quad (21)$$

$$\phi'CH_2O_2\cdot + Co^{2+} \rightarrow \phi'CHO + OH^- + Co^{3+} \quad (22)$$

$$Co^{3+} + HBr \rightarrow Co^{2+} + Br\cdot + H^+ \quad (23)$$

$$2\,\phi'CH_2O_2\cdot \rightarrow \text{inactives} \quad (24)$$

where ϕ' means -COOH.

Though the reaction showed an independence of the concentration of tetrachloroethylene, the rate always increased by 12.5% in the presence of any amount of it. This phenomenon has already been explained. Chloroacetic acid was effective in the $\phi CH_3 \rightarrow \phi'CH_3$ reaction, but not in the $\phi'CH_3 \rightarrow \phi'COOH$ reaction. The reason for this remains unknown.

By assuming that the reaction mechanism in the oxidation of *p*-toluic acid to terephthalic acid after the passage of ozonized oxygen is similar to that of *p*-xylene to *p*-toluic acid, a rate which is the same as that obtained experimentally is derived; it is shown by Eq. t:

$$-d[O_2]/dt = k_t[Co^{2+}]^{3/2}[NH_4Br]^{1/2} \quad (t)$$

The facts that the reaction shows one-fourth- and second-order dependences on the concentrations of cobaltous ion and ammonium bromide respectively at $([Co^{2+}]+[NH_4Br])>0.028$ mol./l. may be attributed to a decrease in the velocity in the reaction corresponding to 12 and to an increase in the concentration of bromide radicals by another reaction, e. g., the direct reaction between oxygen and hydrogen bromide.

Summary

It has been found that terephthalic acid can be obtained by single-stage oxidation in the liquid phase under certain conditions such as the following: *p*-xylene: 25.0 ml.; $Co(OAc)_2\cdot 4H_2O$: 4.982 g.; NH_4Br: 0.1 g.; tetrachloroethylene: 1.0 ml.; solvent: 200 ml. HOAc; reaction temp.; 90°C; oxidant: ozonized oxygen or air; chloroacetic acid: 0.5 g. (used only in the case of ozonized air); and reaction time: 6 hr.

The yields as crude terephthalic acid were 95% with oxygen and 84% with air. The individuality of the present method consists in the use of the ozonized oxygen or air, together with an aliphatic unsaturated compound.

The reaction rates have been examined by measuring the absorption rate of oxygen; they may be expressed as follows:

1) From *p*-xylene to *p*-toluic acid:

a) Ozone-free (under an oxygen pressure of 92 mmHg)

$$R_1 = k_1[Co^{2+}][NH_4Br]^{1/4}\cdot [ClCH_2COOH][Cl_2C=CCl_2]^{-1/2}$$

where $[Co^{2+}]+2[NH_4Br] \leqq 0.04$ mol./l. and $[ClCH_2COOH] \leqq 0.13$ mol./l.

b) Ozone present (under an oxygen pressure of 460 mmHg)

$$R_2 = k_{II}[p\text{-xylene}]^{1/2}[Co^{2+}]^{3/2}[NH_4Br]^{1/2}$$ at $[NH_4Br]/[Co^{2+}] \leqq 5/4$

$$R_3 = k_{III}[p\text{-xylene}]^{1/2}[Co^{2+}]^{3/2}[NH_4Br]$$ at $[NH_4Br]/[Co^{2+}]>5/4$

2) From *p*-toluic acid to terephthalic acid:

a) Ozone-free (under an oxygen pressure of 92 mmHg)

$$R_4 = 1.125k_{IV}[Co^{2+}][NH_4Br]^{1/2}$$ at $[NH_4Br] \leqq 0.04$ mol./l. and $[NH_4Br]/[Co^{2+}] \leqq 5/4$

b) Ozone present (under an oxygen pressure of 460 mmHg)

$$R_5 = k_V[Co^{2+}]^{3/2}[NH_4Br]^{1/2}$$

at $[NH_4Br] \leqq 0.012$ mol./l.

and $([Co^{2+}]+[NH_4Br]) \leqq 0.028$ mol./l., and

$R_6 = k_{VI}[Co^{2+}]^{1/4}[NH_4Br]^{2.0}$

at $[NH_4Br] > 0.012$ mol./l.

and $([Co^{2+}]+[NH_4Br]) > 0.028$ mol./l.

The reaction mechanism has been further discussed, and the rate equations have been derived by assuming the steady state.

The authors wish to express their hearty thanks to Mr. Sadao Hoshizake, Mr. Yasuo Hayano, Mr. Hiroshi Yamamoto, Mr. Kazuhiro Kashima, Mr. Yasuo Matsumura, Mr. Hitoshi Matsubayashi, and Mr. Ryohei Matsumoto for their help in the experiment. Their thanks are also due to the Maruzen Sekiyu Co., Ltd., which provided the *p*-xylene.

BULLETIN OF THE CHEMICAL SOCIETY OF JAPAN VOL. 39 664—672 (1966)

The Oxidation of Acetylacetone in the Presence of Cobaltous Ions

By Tadashi KOGA and Tadashi HARA

Department of Chemical Engineering, Faculty of Engineering, Doshisha University, Kamikyo-ku, Kyoto

(Received May 22, 1965)

Concerning the oxidation of toluene and *p*-xylene with atmospheric oxygen at 90°C in glacial acetic acid in the presence of cobaltous acetate and acetylacetone (HAAH), it was found that the reaction proceeds smoothly only at the mole ratio of $[HAAH]/[Co^{2+}]=2$. When the absorption rate of oxygen was then measured for acetic acid solutions containing cobaltous ions and HAAH, the following results were obtained:

at $[HAAH]/[Co^{2+}] \leqq 3$, $-d[O_2]/dt = K_a[HAAH]^{1/2}[Co^{2+}]^{-1/3}$

at $[HAAH]/[Co^{2+}] \geqq 4$, $-d[O_2]/dt = K_b[HAAH][Co^{2+}]^{1/4}$

These rates agree well with those derived by means of elementary equations in the radical chain reactions. It was further supposed, on the basis of the elementary equations, that active intermediates, such as Co^{3+}, $[Co^{3+}(AAH^-)_2]^+$, and some radicals, were produced smoothly at the mole ratio of $[HAAH]/[Co^{2+}]=2$. However, ketones, such as acetonylacetone and ethyl acetoacetate, were still active even at the mole ratio of $[ketone]/[Co^{2+}]=3$. This seems to stem from the differences in complex stabilities between cobalt and HAAH or other ketones.

It was reported by Brill[1] in 1960 that alkylbenzenes are effectively oxidized when an alkylbenzene in glacial acetic acid in the presence of cobaltous acetate tetrahydrate and ethyl methyl ketone (a ketone containing an α-methylene group) is allowed to contact with oxygen while being sufficiently stirred at 90°C under an atmospheric pressure. This report attracted the present authors, since it enabled us to anticipate some effects based on the chelate formation between cobalt and such a ketone as acetylacetone, and provided a clue as to the nature of the oxidation mechanism.

p-Xylene was then oxidized under the same conditions as were used in Brill's method, except for the utilization of acetylacetone in its various mole ratios to cobalt; it was thus found that terephthalic acid could be obtained only at the cobalt: acetylacetone mole ratio of 1 : 2. Since this fact was very interesting to the present authors, a study was primarily made of the oxidation of acetylacetone in the presence of cobaltous ions by measuring the absorption rate of oxygen.

With a view to identifying the final products in the oxidation of acetylacetone, acetylacetone was oxidized in propionic acid much as in glacial acetic acid, and the oxidation products were examined by gas chromatography.

Experimental

Reagents.—The *p*-xylene obtained from the Maruzen Sekiyu Co., Ltd., was treated with sulfuric acid, sodium hydroxide and water, and recrystallized twice; the distillate with a b. p. of 138.5°C was used. Toluene was treated much as was *p*-xylene, but the distillate with a b. p. of 110.5°C was used. The cobaltous acetate tetrahydrate and the glacial acetic acid were both of an analytical reagent grade. Acetylacetone was distilled, and the distillate with a b. p. of 137°C was used. Cobaltous propionate was synthesized from propionic acid and cobaltous carbonate, and recrystallized from ethanol and diethyl ether. The cobalt was determined chelatometrically by using ethylenediaminetetraacetic acid and murexide. The distillate with a b. p. of 141°C was used for propionic acid.

1) W. F. Brill, *Ind. Eng. Chem.*, **52**, 837 (1960).

Table I. Relationship between the mole ratios of charged ketones to cobalt and the oxidation products

No.	Ketones containning α-methylene group	mol./l.	*p*-Xylene mol./l.	$Co(OAc)_2 \cdot 4H_2O$ mol./l.	Terephthalic acid
1	Ethyl methyl ketone* ($CH_3CH_2COCH_3$)	0.2	1	0.1	(yield** about 65%)
2	Acetylacetone ($CH_3COCH_2COCH_3$)	0.1	1	0.1	impossible
		0.2	1	0.1	(yield about 75%)
		0.3	1	0.1	impossible
		0.4	1	0.1	impossible
		0.5	1	0.1	impossible
3	Acetonylacetone ($CH_3COCH_2CH_2COCH_3$)	0.2	1	0.1	yield 40% (toluic acid about 40%)
		0.3	1	0.1	yield 40% (toluic acid about 40%)
4	Ethyl acetoacetate ($CH_3COCH_2COOC_2H_5$)	0.2	1	0.1	yield 40% (toluic acid about 20%)
		0.3	1	0.1	yield 40% (toluic acid about 20%)
			Toluene mol./l.		Benzoic acid
5	Acetylacetone	0.2	1	0.1	possible
		0.3	1	0.1	impossible

* The same conditions as in Brill's experiment.
** The yields are given by the mole per cent of the oxidation products to charged *p*-xylene.

The Oxidation of *p*-Xylene and Toluene.—To 200 ml. of glacial acetic acid, 0.02 mol. of cobaltous acetate tetrahydrate, 0.2 mol. of *p*-xylene or toluene, and 0.02—0.1 mol. of a ketone such as acetylacetone, acetonylacetone, ethyl acetoacetate and ethyl methyl ketone are added. The solution is then placed in contact with oxygen for 24 hr. at 90°C, 1 atm., and 800—1000 r. p. m.

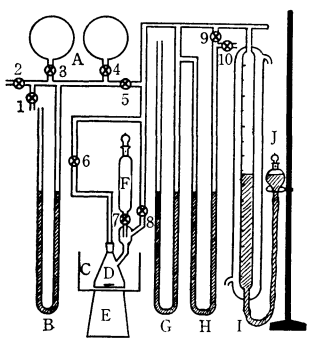

Fig. 1. An apparatus for the measurement of oxygen absorption rate.
A: gas storage B: manometer (charged with mercury) C: thermostat D: reaction vessel E: magnetic stirrer F: funnel for supplying sample G: manometer (charged with mercury) H: manometer (charged with dibuthylphthalate) I: gas burette J: mercury pool

The Absoption Rate of Oxygen.—The absorption rate of oxygen was measured by the apparatus shown in Fig. 1. The apparatus was operated as follows: all the cocks except the cocks 2, 7 and 10 are opened after J has been lowered, and the system is made completely vacuous through the cock 1. The cocks 1 and 5 are then closed, and A is filled with more than 1 atm. of oxygen through the cock 2. Then the cock 2 is closed, and the oxygen gas pressure is adjusted to the atmospheric pressure by opening the cock 5 and reading the manometer, G, charged with mercury. The cock 9 is closed, and the cock 10 is opened. To the reaction vessel, D, 50 ml. of glacial acetic acid and cobaltous acetate are added, and the solution is heated at 60±0.2°C, The liquid surfaces of the manometer, H, charged with dibutyl phthalate are adjusted to the same level by moving J vertically. Acetylacetone is added through the cock 7, and the reaction is started.

During the reaction, the liquid surfaces of the manometer, H, are held on the same level by moving J; thereby the oxygen gas pressure is always maintained at 1 atm. The absorption rate of oxygen is measured by reading the gas burette, I, at definite intervals. Oxygen is supplied to the system by closing the cocks 6 and 8, lowering J, and introducing oxygen through the cock 5 until the liquid surfaces of H reach just the same level. I is read at once, and measurement is continued after the opening of the cocks 6 and 8.

The Identification of the Oxidation Products of Acetylacetone.—Since the absorption rate of oxygen in propionic acid was confirmed to be quite similar to

Table II. Oxygen absorption in various mole ratios of acetylacetone to cobalt

No.	Co^{2+}		HAAH		Mole ratios Co^{2+} : HAAH	O_2 absorbed		Induction period
	mol./l.	mol.*	mol./l.	mol.*		ml.**	mol.	min.
1	0.1	0.005	0.05	0.0025	1 : 0.5	93.5	0.0038	1
2	0.1	0.005	0.10	0.005	1 : 1	177.2	0.0072	2
3	0.1	0.005	0.20	0.010	1 : 2	275.4	0.0113	6
4	0.1	0.005	0.30	0.015	1 : 3	319.7	0.0131	15
5	0.1	0.005	0.40	0.020	1 : 4	370.7	0.0155	26
6	0.1	0.005	0.50	0.025	1 : 5	444.2	0.0187	47
7	0.1	0.005	0.60	0.030	1 : 6	499.1	0.0210	79
8	0.1	0.005	0.70	0.035	1 : 7	545.3	0.0229	148
9	0.01	0.0005	0.20	0.010	1 : 20	274.0	0.0111	90
10	0.02	0.001	0.20	0.010	1 : 10	286.6	0.0117	35
11	0.04	0.002	0.20	0.010	1 : 5	296.2	0.0125	18
12	0.05	0.0025	0.20	0.010	1 : 4	273.9	0.0115	11
13	0.07	0.0035	0.20	0.010	1 : 3	282.0	0.0118	7
14	0.10	0.005	0.20	0.010	1 : 2	275.4	0.0113	6
15	0.20	0.010	0.20	0.010	1 : 1	263.2	0.0111	2

* Mol. in 50 ml. HOAc. ** ml. at 25°C

that in glacial acetic acid, except for a slight elongation of the induction period, the oxidation products of acetylacetone were identified as follows: Acetylacetone in 1.5×10^{-2} mol. and cobaltous propionate in 5×10^{-3} mol. are dissolved in 50 ml. propionic acid, and the solution is placed in contact with oxygen for 3 hr. at 60°C, 1 atm. Then the solution is distilled by introducing the vapor of methanol or ethanol, and the acids in the distillate are directly converted into their esters. After esterification, the esters are distilled, and the residues are diluted with water and then extracted with ether. Both the extract and the distillate are examined by gas chromatography.

Results

The Oxidation of *p*-Xylene and Toluene.— For the oxidation of *p*-xylene in the presence of 0.02 mol. of cobaltous acetate and 0.04 mol. of acetylacetone, the solution gradually changed its color from violet to brown, and finally to dark green after about 6 hours' reaction, whereupon a small amount of terephthalic acid began to deposit.

In any mole ratios other than acetylacetone: cobalt=2 : 1, terephthalic acid was not identified in 24 hours' reaction, and the unreacted *p*-xylene was found in the oily phase after the reaction mixture had been diluted with water.

When the mole ratios of acetonylacetone or ethyl acetoacetate to cobaltous acetate were 2 : 1 and 3 : 1 respectively, however, terephthalic acid was identified after 7 hours' reaction.

For the oxidation of toluene, benzoic acid was obtained in a good yield at only the mole ratio of acetylacetone : cobalt=2 : 1.

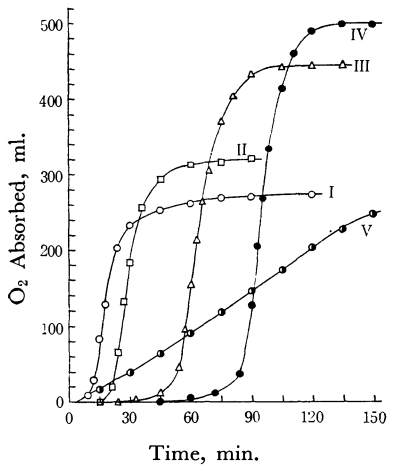

Fig. 2. Relationships between the amount of oxygen absorbed and the reaction time.
Reaction temp.: 60±0.2°C, [Co^{+2}]: 0.1 mol./l.
I: 0.2 mol. HAAH/l. II: 0.3 mol. HAAH/l.
III: 0.5 mol. HAAH/l. IV: 0.6 mol. HAAH/l.
V: 0.2 mol. HAAH/l. + 0.5 mol. *p*-xylene/l.

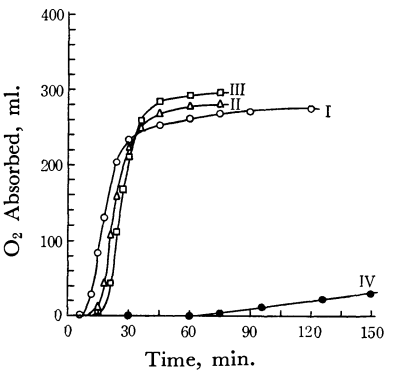

Fig. 3. Relationships between the amount of oxygen absorbed and the reaction time.
Reaction temp.: 60±0.2°C, [HAAH]: 0.2 mol./l.
I: 0.1 mol. Co^{2+}/l. II: 0.05 mol. Co^{2+}/l.
III: 0.04 mol. Co^{2+}/l.
IV: 0.1 mol. $Co^{3+}(AAH^{-})_3$

The Oxidation of Acetylacetone.—The absorption rate of oxygen was measured for the oxidation of acetylacetone in the absence of alkylbenzene; the results obtained are shown in Table II. As can be seen from Experiments Nos. 1—8 in Table II, the amount of oxygen gas absorbed increases with the concentration of HAAH at 0.1 mol./l. cobaltous acetate; the relationship between the amount of oxygen gas absorbed and the concentration of HAAH is shown in Fig. 4. Here,

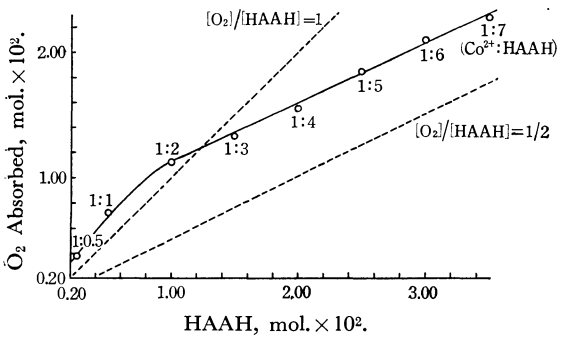

Fig. 4. Relationships between the mole ratio of [HAAH]/[Co^{2+}] and the amount of O_2 absorbed; [Co^{2+}]: 0.1 mol./l.

HAAH, HAA· and AAH^- are given by the following:

HAAH: $CH_3-\overset{\overset{O}{\|}}{C}-CH_2-\overset{\overset{O}{\|}}{C}-CH_3$, HAA·: $CH_3-\overset{\overset{O}{\|}}{C}-\dot{C}H-\overset{\overset{O}{\|}}{C}-CH_3$, and AAH^-: $CH_3-\overset{\overset{O^-}{|}}{C}=CH-\overset{\overset{O}{\|}}{C}-CH_3$

Figure 4 shows that the mole ratios of the [HAAH] to the [O_2] absorbed are equal to 1 and 2 at [HAAH]/[Co^{2+}]<2 and [HAAH]/[Co^{2+}]>3 respectively.

In Experiments Nos. 9—15, the concentration of cobaltous ions was varied against 0.2 mol./l. HAAH, but the amounts of oxygen gas absorbed were almost constant. These results are shown in Fig. 5. The straight line in Fig. 5 is represented by $t=k([HAAH]^2/[Co^{2+}])K^{1/4}$, where t is referred to the induction period and K, to the [HAAH]/[Co^{2+}]. It may be seen from the above equation that t does not only depend on the mole ratio of HAAH to Co^{2+}, but also on their concentrations.

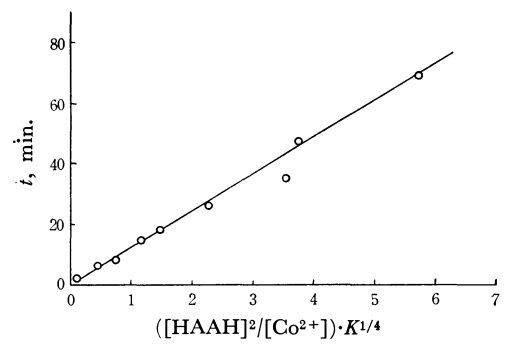

Fig. 5. Relationships between the introduction period, t, and $([HAAH]^2/[Co^{2+}])\cdot K^{1/4}$.

After the induction period, the temperature of the reaction mixture increased in accordance with the changes in color from pink to dark green. This color change is considered to be due to the formation of cobaltic ions. After the absorption of oxygen had finished, the solution was red at the mole ratio of [HAAH]/[Co^{2+}]<3, but dark green at [HAAH]/[Co^{2+}]>4. When the dark-green substance was extracted into the benzene layer, the aqueous layer remained wine-red. The spectrophotometric absorption curves of the benzene and aqueous layers showed their maximum absorptions at 600 and 510 mμ respectively; they were compared with those of $Co^{2+}(OAc^-)_2$, $Co^{2+}(AAH^-)_2$, and $Co^{3+}(AAH^-)_3$.

The Oxidation Rate of Acetylacetone.—The relationship between the absorption rate of oxygen and the concentrations of HAAH or Co^{2+} are shown in Tables III and IV. Since there are linear relations between $\log(d[O_2]/dt)$ and log-[HAAH], and $\log(d[O_2]/dt)$ and $\log[Co^{2+}]$ respectively, the absorption rates of oxygen are given

Table III. The concentration of acetylacetone and the oxygen absorption rate

Reaction temp.: 60±0.2°C

Oxygen pressure: 1 atm., [Co^{2+}]: 0.1 mol./l.

No.	$d[O_2]dt$* ml. sec^{-1}	log-$(d[O_2]/dt)$	[HAAH] mol. l^{-1}	log-[HAAH]	Apparent rate constant
1	8.56	0.9325	0.05	−1.3009	17.8
2	11.64	1.0660	0.1	−1.0000	17.1
3	16.13	1.2076	0.2	−0.6990	16.8
4	19.56	1.2914	0.3	−0.5229	16.6
5	15.33	1.1852	0.4	−0.3979	68.0
6	19.73	1.2952	0.5	−0.3010	70.0
7	23.52	1.3715	0.6	−0.2218	69.5
8	24.36	1.3867	0.7	−0.1549	61.6

Table IV. The concentration of cobalt and the oxygen absorption rate

Reaction temp.: 60±0.2°C

Oxygen pressure: 1 atm., [HAAH]: 0.1 mol./l.

No.	$d[O_2]/dt$* ml. sec^{-1}	log-$(d[O_2]/dt)$	[Co^{2+}] mol. l^{-1}	log-[Co^{2+}]	Apparent rate constant
9	13.45	1.1287	0.01	−2.0000	212
10	15.67	1.1951	0.02	−1.6990	208
11	18.31	1.2627	0.04	−1.3979	205
12	20.92	1.3220	0.05	−1.3010	221
13	19.71	1.2947	0.07	−1.1549	18.1
14	16.13	1.2076	0.10	−1.0000	16.8
15	14.25	1.1538	0.20	−0.6990	18.6

* These values were obtained by differentiating the oxygen absorption curves at 25°C.

as follows:

at $[HAAH]/[Co^{2+}] \leq 3$,

$$-d[O_2]/dt = k_a[HAAH]^{1/2}[Co^{2+}]^{-1/3}$$

at $[HAAH]/[Co^{2+}] \geq 4$,

$$-d[O_2]/dt = k_b[HAAH][Co^{2+}]^{1/4}$$

Since the concentration of HAAH is enough in Experiments Nos. 5—8, the dissolution velocity of oxygen into the solution is considered to be rate-determining; therefore, their apparent rate constants are supposed to be smaller than those in Nos. 9—12. That the apparent rate constants in Nos. 5—8 are much smaller than those in Nos. 9—12 is due to the facts that the dissolution velocity of oxygen into the solution is rate-determining and that it is smaller than the consumption velocity of oxygen in the oxidation reaction. It may, therefore, be supposed that the apparent rate constants in the case of $[HAAH]/[Co^{2+}] \geq 4$ are equal to those in Nos. 9—12.

The Identification of the Oxidation Products of HAAH.—The sample distilled with the vapor of methanol was analyzed by gas chromatography under the following conditions: carrier gas: hydrogen; flow rate: 30 ml./min.; column: dioctyl phthalate, and column temperature: 50°C. It was confirmed from the gas chromatogram that there were aldehydes, methyl formate, methanol (solvent), methyl acetate or acetone, and methyl propionate. The distillate with the vapor of ethanol and the extracts with ether from the residues after esterification were also analyzed, under the same conditions as above except for the column temperature, which was here 60°C or 100°C respectively. The following substances were confirmed: ethyl formate, ethanol (solvent), ethyl acetate, and ethyl propionate for the former, in which acetone was negative; and ether (solvent), ethyl propionate, and ethyl pyruvate for the latter. On the basis of the gas chromatographic data and the detection of aldehyde with an ammoniacal silver nitrate solution, it was concluded that the oxidation products of HAAH were composed of acetic acid and formic acid as the major constituents, and of formaldehyde, acetaldehyde and pyruvic acid as the minor constituents.

Discussion

The oxidation mechanism of HAAH in glacial acetic acid in the presence of cobaltous ions is considered to be as follows:

In the Case of $[HAAH]/[Co^{2+}] \leq 3$:

It is assumed that the reaction proceeds in accordance with the following radical chain reaction, in which the rate constants are given by the k_1—k_{10} value:

Initiation

$$\begin{cases} Co^{2+} + AAH^- \underset{k_{-1}}{\overset{k_1}{\rightleftarrows}} Co^{2+}(AAH^-) & V_1,\ V_{-1}\ (1) \\ Co^{2+}(AAH^-) + O_2 \xrightarrow{k_2} Co^{2+} + HAA\cdot + \cdot O_2^- & V_2\ (2) \end{cases}$$

Propagation

$$\begin{cases} HAA\cdot + O_2 \xrightarrow{k_3} HAAO_2\cdot & V_3\ (3) \\ HAAO_2\cdot + HAAH \xrightarrow{k_4} HAAO_2H + HAA\cdot & V_4\ (4) \\ \begin{cases} HAAO_2\cdot + \{Co^{2+}(AAH^-)_2\}\cdots O_2 \xrightarrow{k_5} \text{complex} & V_5\ (5) \\ \text{Complex} \xrightarrow{k_6} 2Co^{2+}(AAH^-)_2O_2 + HAA\cdot & V_6\ (6) \end{cases} \end{cases}$$

Branched propagation

$$\begin{cases} Co^{2+} + HAAO_2H \xrightarrow{k_7} Co^{3+} + HAAO\cdot + OH^- & V_7\ (7) \\ Co^{3+} + HAAH \xrightarrow{k_8} Co^{2+} + HAA\cdot + H^+ & V_8\ (8) \\ HAAO\cdot + HAAH \xrightarrow{k_9} HAAOH + HAA\cdot & V_9\ (9) \end{cases}$$

Termination

$$\{2HAAO_2\cdot \xrightarrow{k_{10}} \text{Inactive products} \qquad V_{10}\ (10)$$

In the initiation reaction, the 1 : 1 cobaltous chelate is made to react with oxygen to produce HAA·, while the HAA· induced the propagation reactions, which consist of two courses: 3—4, and 3—5—6. The hydroperoxide produced in the reaction 4 induces the reaction 7—9. It seems to be reasonable to suppose the branched reaction, since the solution during the oxidation shows the dark green usually associated with the cobaltic state. It is considered that in the reaction 5 the bridged compound, $\{(AAH^-)_2Co^{2+}\cdots O_2\cdots Co^{2+}(AAH^-)_2\}$,[2] in which each cobalt has a vacant position on the coordination sphere, is coordinated of with $HAAO_2\cdot$ to produce a complex compound.[3]

The absorption rate of oxygen is given by Eq. a·1:

$$-d[O_2]/dt = V_3 = k_3[HAA\cdot][O_2] \qquad (a\cdot1)$$

Under a steady state, the following i—iii are assumed:

i) By assuming $d[HAAO_2\cdot]/dt = 0$, $V_3 = V_4 + V_5 + V_{10}$:

Here, V_{10} is neglected, since the chain is long enough and since $V_{prop.} \gg V_{term.}$.

By assuming that the ratio, C, of V_5 to V_4 is constant and that the reaction 5 is the rate-determining step in the course 5—6, Eq. a·1 is rewritten by Eq. a·2:

2) A. Werner and A. Mylius, *Z. Anog. Chem.*, **16**, 1245 (1898).

3) For example, P. George and A. Robertson, *Trans. Faraday Soc.*, **42**, 217 (1946).

$$-d[O_2]/dt = (1+C)V_4$$
$$= (1+C)k_4[HAAO_2\cdot][HAAH] \quad (a\cdot2)$$

ii) By assuming $V_{\text{Inlt.}} = V_{\text{term.}}$, Eq. b·1 is obtained:

$$k_2[Co^{2+}(AAH^-)][O_2] = k_{10}[HAAO_2\cdot]^2 \quad (b\cdot1)$$

By supposing $k_1/k_{-1} = K_m$ in the reaction 1:

$$[Co^{2+}(AAH^-)] = K_m[Co^{2+}][AAH^-]$$

By introducing $HAAH \overset{Ka}{\rightleftarrows} AAH^- + H^+$, in which K_a is referred to the dissociation constant, $K_a = [AAH^-][H^+]/[HAAH]$; therefore, $[AAH^-] = K_a^{1/2}[HAAH]^{1/2}$.

Hence, Eq. b·1 is expressed by b·2:

$$[HAAO_2\cdot]^2 = (k_2\cdot K_m\cdot K_a^{1/2}/k_{10})\cdot [Co^{2+}][O_2][HAAH]^{1/2} \quad (b\cdot2)$$

iii) By assuming $d[HAAO_2\cdot]/dt = 0$ and $d[\{Co^{2+}(AAH^-)_2\}\cdots O_2]/dt = 0$* in the reaction 5, Eq. c·1 is obtained:

$$k_5[\{Co^{2+}(AAH^-)_2\}\cdots O_2][HAAO_2\cdot] = K_c \quad (c\cdot1)$$

By introducing $[\{Co^{2+}(AAH^-)_2\}\cdots O_2] = K_1^2\cdot K_m^2\cdot K_a^2\cdot[Co^{2+}]^2[HAAH]^2[O_2]$ into Eq. c·1, Eqs. c·2 and c·3 are obtained:

$$k_5\cdot K_1^2\cdot K_m^2\cdot K_a^2[Co^{2+}]^2[HAAH]^2\cdot [O_2][HAAO_2\cdot] = K_c \quad (c\cdot2)$$

Hence,

$$[HAAO_2\cdot] = K_c(k_5\cdot K_1^2\cdot K_m^2\cdot K_a^2)^{-1}\cdot [Co^{2+}]^{-2}[HAAH]^{-2}[O_2]^{-1} \quad (c\cdot3)$$

By mutiplying c·3 by b·2, Eq. d is derived:

$$[HAAO_2\cdot]^3 = \{(k_2\cdot K_c)/(k_5\cdot k_{10}\cdot K_1^2\cdot K_m\cdot K_a^{3/2})\}\cdot [Co^{2+}]^{-1}[HAAH]^{-3/2}$$

hence:

$$[HAAO_2\cdot] = \{(k_2\cdot K_c)/(k_5\cdot k_{10}\cdot K_1^2\cdot K_m\cdot K_a^{3/2})\}^{1/3}[Co^{2+}]^{-1/3}[HAAH]^{1/2} \quad (d)$$

By substituting d into a·2, Eq. e is obtained and rewritten as Eq. f:

$$-d[O_2]/dt = k_4\{(k_2\cdot K_c)/(k_5\cdot k_{10}\cdot K_1^2\cdot K_m\cdot K_a^{3/2})\}^{1/3}\cdot [Co^{2+}]^{-1/3}[HAAH]^{1/2} \quad (e)$$

or: $$-d[O_2]/dt = k_a[Co^{2+}]^{-1/3}[HAAH]^{1/2} \quad (f)$$

where $k_a = k_4\{(k_2\cdot K_c)/(k_5\cdot k_{10}\cdot K_1^2\cdot K_m\cdot K_a^{3/2})\}^{1/3}$.

In the Case of [HAAH]/[Co²⁺]≧4:

It is assumed that the chain reaction proceeds by way of Eqs. 11—19:

Initiation

$$\begin{cases} Co^{2+} + O_2 \overset{k_{11}}{\underset{k_{-11}}{\rightleftarrows}} Co^{2+}\cdots O_2{}^{6)} \text{ (or } Co^{3+}\cdots O_2{}^-)^{6)} & V_{11},\ V_{-11} \quad (11) \\ Co^{2+}\cdots O_2 + HAAH \overset{k_{12}}{\rightarrow} Co^{2+} + HAA\cdot + HO_2\cdot & V_{12} \quad (12) \end{cases}$$

Propagation

$$\begin{cases} HAA\cdot + O_2 \overset{k_{13}}{\rightarrow} HAAO_2\cdot & V_{13} \quad (13) \\ HAAO_2\cdot + HAAH \overset{k_{14}}{\rightarrow} HAAO_2H + HAA\cdot & V_{14} \quad (14) \end{cases}$$

Branched propagation

$$\begin{cases} Co^{2+}(AAH^-)_2 + HAAO_2H \overset{k_{15}}{\rightarrow} \{Co^{3+}(AAH^-)_2\}^+ + HAAO\cdot + OH^- & V_{15} \quad (15) \\ \{Co^{3+}(AAH^-)_2\}^+ + HAAH \overset{k_{16}}{\rightarrow} Co^{2+}(AAH^-)_2 + HAA\cdot + H^+ & V_{16} \quad (16) \\ HAAO\cdot + HAAH \overset{k_{17}}{\rightarrow} HAAOH + HAA\cdot & V_{17} \quad (17) \end{cases}$$

Termination

$$\begin{cases} 2HAAO_2\cdot \overset{k_{18}}{\rightarrow} \text{Inactive products} & V_{18} \quad (18) \\ Co^{3+}(AAH^-)_2O_2{}^- + HAA\cdot \overset{k_{19}}{\underset{k_{19}}{\rightleftarrows}} Co^{3+}(AAH^-)_3 + O_2 & V_{19},\ V_{-19} \quad (19) \end{cases}$$

In this case, the reaction is initiated by the action of cobaltous peroxide on HAAH, since the concentration of HAAH is higher than that in the preceding case, and the HAA· produced induces the propagation reaction. The hydroperoxide produced in the reaction 14 induces the branched propagation reaction. The reactions 18 and 19, in which the former belongs to the conventional self-termination while the latter belongs to the exchange reaction between the ligands, is supposed to be the termination stage. By assuming $V_{18} \gg V_{19}$ on the basis of the experimental conditions, the reaction 18 may be expected to be predominant in the termination stage. The reaction 19 is supposed to be reversible, since the solution was dark

* The bridged compound, $(AAH^-)_2Co^{2+}\cdots O_2\cdots Co^{2+}(AAH^-)_2$, is formed as follows:[4]

$$Co^{2+}(AAH^-) + HAA\cdot \text{ (or } HAAO\cdot, HAAO_2\cdot) \overset{K_d}{\rightleftarrows} Co^{3+}(AAH^-)_2$$
$$Co^{3+}(AAH^-)_2 + O_2 \overset{K_e}{\rightleftarrows} Co^{3+}(AAH^-)_2O_2 \overset{K_f}{\rightleftarrows} Co^{2+}(AAH^-)_2O_2\cdot$$
$$2Co^{2+}(AAH^-)_2O_2\cdot \overset{K_g}{\rightleftarrows} \{Co^{2+}(AAH^-)_2\}_2\cdots O_2 + O_2$$

Hence:

$$K_d\cdot K_e\cdot K_f\cdot K_g = K = [\{Co^{2+}(AAH^-)_2\}_2\cdots O_2]/[Co^{2+}(AAH^-)]^2[HAA\cdot]^2[O_2]$$

Since HAA· (or HAAO·, $HAAO_2\cdot$) is constant at a steady state and since $Co^{2+}(AAH^-)$ is approximately constant at $[HAAH]/[Co^{2+}] \leq 3$ on the basis of the Bjerrum's assumption,[5] the $\{Co^{2+}(AAH^-)_2\}_2\cdots O_2$ value is almost constant also. Since HAA· is formed through the reaction accompanying HAAH or AAH^-, at a steady state it may be proportional to $[AAH^-]$.

Therefore, $[HAA\cdot] = K_1\cdot[AAH]$, and:

$$K = [\{Co^{2+}(AAH^-)_2\}_2\cdots O_2]/K_1^2\cdot K_m^2\cdot[Co^{2+}]^2[AAH^-]^4[O_2]^{-1} = [\{Co^{2+}(AAH^-)_2\}_2\cdots O_2]/K_1^2\cdot K_m^2\cdot K_a^2\ [Co^{2+}]^2[HAAH]^2[O_2]^{-1}$$

4) Cf. E. M. Arnett and M. A. Mendelsohn, *J. Am. Chem. Soc.*, **84**, 3828 (1962).

5) J. Bjerrum, "Metal Ammine Formation in Aqueous Solution," P. Hasse Son, and Copenhagen (1941).

6) N. Uri, *Nature*, **177**, 1177 (1956); H. Hock and H. Kropf, *Angew. Chem.*, **69**, 313 (1957).

green even after the completion of the oxidation reaction, and green cobaltic chelates, $Co^{3+}(AAH^-)_3$, were extracted into the benzene layer. The absorption rate of oxygen is shown by Eq. A·1.

$$-d[O_2]/dt = V_{13} = k_{13}[HAA\cdot][O_2] \quad (A\cdot1)$$

i—iii below are assumed under a steady state.

i) By assuming $d[HAAO_2\cdot]/dt=0$, $V_{13}=V_{14}+V_{18}$. Since the chain is long enough and since $V_{prop.} \gg V_{term.}$, V_{13} is approximately equal to V_{14} and Eq. B is obtained:

$$k_{13}[HAA\cdot][O_2] = k_{14}[HAAO_2\cdot][HAAH] \quad (B)$$

Therefore, A·1 is expressed by A·2:

$$-d[O_2]/dt \fallingdotseq V_{14}=k_{14}[HAAO_2\cdot][HAAH] \quad (A\cdot2)$$

ii) The rate of the initiation reaction, $V_{init.}$, should be equal to the rate of the termination reaction, $V_{term.}$, in order that the propagation reaction may proceed under a steady state. Therefore, $k_{12}[Co^{2+}\cdots O_2][HAAH]=k_{18}[HAAO_2\cdot]^2$.

By introducing $k_{11}/k_{-11}=K_n$ and $[Co^{2+}\cdots O_2]=K_n[Co^{2+}][O_2]$, Eq. C·1 is obtained:

$$k_{12}\cdot K_n[Co^{2+}][O_2][HAAH] = k_{18}[HAAO_2\cdot]^2 \quad (C\cdot1)$$

By substituting $[AAH^-]=K_a^{1/2}[HAAH]^{1/2}$ into C·1, Eq. C·2 is obtained:

$$[HAAO_2\cdot]=(k_{12}\cdot K_n\cdot K_a/k_{18})^{1/2}\cdot [Co^{2+}]^{1/2}[O_2]^{1/2}[AAH^-] \quad (C\cdot2)$$

iii) By assuming $V_{19}/V_{-19}=K_h$, in which K_h is constant, Eq. D·1 is obtained:

$$K_h = (k_{19}[Co^{3+}(AAH^-)_2O_2^-][HAA\cdot])/(k_{-19}[Co^{3+}(AAH^-)_3][O_2]) \quad (D\cdot1)$$

The cobaltic chelates are formed in accordance with the following reactions:

$$\{Co^{3+}(AAH^-)_2\}^+ + AAH^- \overset{Ki}{\rightleftarrows} Co^{3+}(AAH^-)_3$$

$$\{Co^{3+}(AAH^-)_2\}^+ + O_2^- \overset{Kj}{\rightleftarrows} Co^{3+}(AAH^-)_2\cdot O_2^-$$

By using these relations, Eq. D·1 may be rewritten as Eq. D·2:

$$[HAA\cdot] = (k_{-19}\cdot K_h\cdot K_i/k_{19}\cdot K_j)\cdot [AAH^-][O_2][O_2^-]^{-1} \quad (D\cdot2)$$

By combining B and D·2, Eq. E is obtained:

$$[HAAO_2\cdot]=(k_{13}\cdot k_{-19}\cdot K_h\cdot K_i/k_{14}\cdot k_{19}\cdot K_j\cdot K_a^{1/2})\cdot [AAH^-]^{-1}[O_2]^2[O_2^-]^{-1} \quad (E)$$

By multiplying C·2 by E, Eq. F is obtained:

$$[HAAO_2\cdot]^2= (k_{12}\cdot K_n/k_{18})^{1/2}(k_{13}\cdot k_{-19}\cdot K_h\cdot K_i/k_{14}\cdot k_{19}\cdot K_j)\cdot [Co^{2+}]^{1/2}[O_2]^{5/2}[O_2^-]^{-1}$$

Hence:

$$[HAAO_2\cdot]= (k_{12}\cdot K_n/k_{18})^{1/4}(k_{13}\cdot k_{-19}\cdot K_h\cdot K_i/k_{14}\cdot k_{19}\cdot K_j)^{1/2}\cdot [Co^{2+}]^{1/4}[O_2]^{5/4}[O_2^-]^{-1/2} \quad (F)$$

By substituting F into A·2, Eq. G is obtained:

$$-d[O_2]/dt= k_{14}(k_{12}\cdot K_n/k_{18})^{1/4}(k_{13}\cdot k_{-19}\cdot K_h\cdot K_i/k_{14}\cdot k_{19}\cdot K_j)^{1/2}\cdot [Co^{2+}]^{1/4}[HAAH][O_2]^{5/4}[O_2^-]^{-1/2} \quad (G)$$

Since the oxygen pressure is definite and since the $[O_2^-]$ value is approximately constant under a steady state, G is expressed briefly by Eq. H:

$$-d[O_2]/dt = k_b[Co^{2+}]^{1/4}[HAAH] \quad (H)$$

By taking the following equilibrium into consideration, Eq. 1 is obtained:

$$Co^{2+}(AAH^-)_2 + O_2 \overset{K_p}{\rightleftarrows} Co^{2+}(AAH^-)_2\cdots O_2 \overset{K_q}{\rightleftarrows} Co^{3+}(AAH^-)_2\cdots O_2^- \overset{K_j^{-1}}{\rightleftarrows} \{Co^{3+}(AAH^-)_2\}^+ + O_2^- \quad (20)$$

$$Co^{2+} + 2AAH^- \overset{K_s}{\rightleftarrows} Co^{2+}(AAH^-)_2, \text{ and}$$

$$Co^{3+} + 2AAH^- \overset{K_t}{\rightleftarrows} \{Co^{3+}(AAH^-)_2\}^+$$

$$[O_2^-]=\{(K_p\cdot K_q\cdot K_j^{-1}\cdot K_s)/K_t\}\cdot [O_2][Co^{2+}]/[Co^{3+}] \quad (I)$$

Since the $[Co^{2+}]/[Co^{3+}]$ is considered to be approximately constant under a steady state, the $[O_2^-]$ may also be expected to be almost constant.

The Relationship among the Induction Period, [HAAH] and the Total Amount of Oxygen Absorbed.—The induction period is supposed to depend on the time interval in which the amount of HAA· necessary for the progress of the reaction 3 or 13 could be accumulated in the solution. In the reaction using a definite amount of Co^{2+}, the concentration of Co^{2+} decreases with an increase in the mole ratio of [HAAH]/$[Co^{2+}]$, since Co^{2+} is more or less consumed in the formation of the chelate. The induction period is, therefore, considered to become longer with an increase in the mole ratio of [HAAH]/$[Co^{2+}]$.

It may also be supposed, on the basis of the experimental results, that the liberated HAAH can be oxidized more easily than the chelated HAAH. When the amount of HAAH increases in proportion to a definite amount of cobalt, the increases in the liberated HAAH is not so large as the increase in the HAAH added, since some parts of HAAH are consumed in the formation of the chelate.

Therefore, the total amount of the oxygen absorbed is not considered to increase markedly in comparison with the increase in the [HAAH] added. In the case of $[HAAH]/[Co^{2+}]>3$, about one-half of the increment in the HAAH added is considered to take part in the chelate formation.

The Oxidation of *p*-Xylene and Toluene Using the Co-HAAH System.—At the beginning of the radical chain reaction, the formation of

the radicals by withdrawing the hydrogen atom from the hydrocarbons is induced with tervarent cobalt,[1,7] including the metal peroxide.[6,8] Though the formation of Co^{3+} in an aqueous solution is not easy, since $E°=-1.84$ V., the cobalt in the activated state seems to be easily formed in glacial acetic acid in the presence of such ketones as ethyl methyl ketone, HAAH, acetonylacetone and ethyl acetoacetate.

It is easily ascertained spectroscopically that Co^{2+} is converted with oxygen into the higher valency state or the activated state in the presence of HAAH.

Therefore, the formation of the radicals from *p*-xylene and toluene seems to be reduced to the action of $HAAO_2\cdot$, Co^{3+} and $\{Co^{3+}(AAH^-)_2\}^+$, etc., against them. As is shown in Fig. 2, the absorption rate of oxygen in the presence of 0.5 mol./l. *p*-xylene is slower than that in the absence of *p*-xylene.

This shows that the active species produced in the solution might be consumed by reacting with *p*-xylene. However, the formation of the radical seems to be based on the action of Co^{3+} and $\{Co^{3+}(AAH^-)_2\}^+$, since the concentration of $HAAO_2\cdot$ is not as high as is necessary for Eq. 21 to hold:

$$RH + HAAO_2\cdot \rightarrow R\cdot + HAAO_2H \qquad (21)$$

It is clear from Fig. 3 that the cobaltic acetylacetonate, $Co^{3+}(AAH^-)_3$, could be almost stable for the oxidation with oxygen. Though the co-existence of a suitable amount of HAAH is necessary for the oxidation of *p*-xylene and toluene, the formation of $Co^{3+}(AAH^-)_3$ becomes easier with an increase in the mole ratio of [HAAH]/[Co^{2+}], while the formation of the activated species of Co^{2+} becomes more difficult with a decrease in the mole ratio of [HAAH]/[Co^{2+}]. Therefore, the optimum conditions for the oxidation of *p*-xylene and toluene are when [HAAH]/[Co^{2+}]=2.

In the cobaltous acetylacetonate, $Co^{2+}(AAH^-)_2$, four co-ordination positions are already occupied with AAH^-, but there are still two vacant positions which can be easily co-ordinated with water, acetic acid, oxygen molecules, etc.

In the case of a co-ordination with O_2 as is shown in the reaction 20, it is supposed that Co^{2+} and O_2 are converted into Co^{3+} and O_2^- respectively; these activated species make the withdrawing of hydrogen atoms from hydrocarbon easier. Since the ease of the formation of the negatively charged oxygen species are generally in the order of $O_2^->O^->O^{2-}$,[9] the oxygen in the activated species is assumed to be O_2^-.

Since such ketones as ethyl acetoacetate and acetonylacetone show a smaller co-ordination ability to cobalt ions than HAAH, the cobalt chelates with these ligands are expected to be too unstable to resist oxidation.

When the authors write the structure of the chelate of the acetoacetic ester:

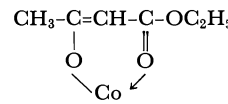

it may be seen that the enolate (or benzenoid) resonance involving the cobalt is greatly interferred with by the participation of one of the C=O groups in the very strong ester resonance, thus accounting for the very large decrease in the stability of the chelate.[10]

Since it is generally accepted that a six-membered chelate ring is much more stable than a seven-membered one,[11] the cobalt chelate of acetonlylacetone with a seven-membered ring is not expected to be more stable than that of HAAH with a six-membered ring.

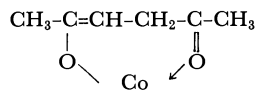

Hence, the equilibrium concentrations of the unbound acetoacetic ester and acetonylacetone

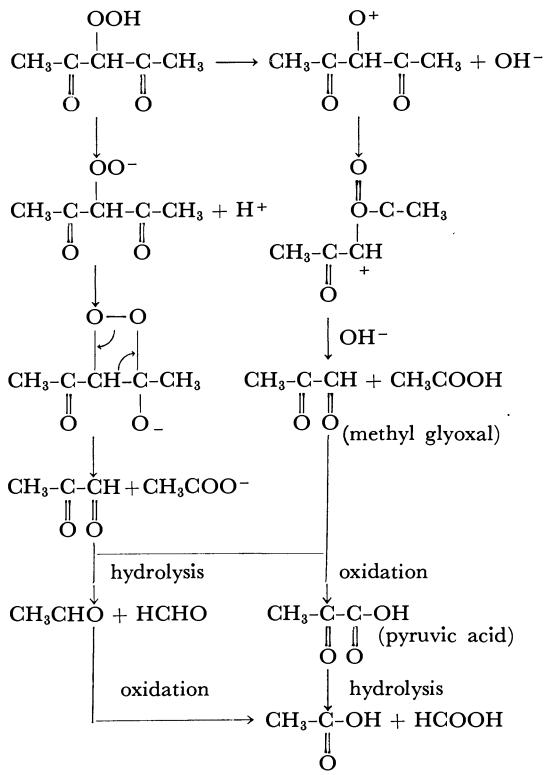

7) C. E. H. Bawn and J. E. Jolley, *Proc. Roy. Soc.*, **237**, 297 (1956), etc.

8) H. Kropf, *Ann.*, **637**, 73, 93, 111 (1960).

9) N. Ohta et al., "Shokubai Kōgaku Kōza (Catalytic Engineering)," Vol. 7, Catalysts Society of Japan, Chijinshokan & Co. Ltd., Tokyo (1964), p. 11.

10) M. Calvin and K. W. Wilson, *J. Am. Chem. Soc.*, **67**, 2007 (1945).

11) For example, D. P. Graddon, "An Introduction to Co-ordination Chemistry," Pergamon Press, Oxford (1961), Chap. 4.

are expected to be higher than that in HAAH.

It is, therefore, considered that the oxidation of hydrocarbons in the presence of the above ketones proceeds favorably even when the mole ratio is [ketone]/[Co^{2+}]=3.

Oxidation Products of Acetylacetone. — The oxidation products identified by gas chromatography are considered to come from $HAAO_2H$ or $HAAO_2\cdot$ by the mechanisms as show in page 671.

Summary

Acetylacetone is oxidized in a glacial acetic acid solution containing bi-valent cobalt to produce α-hydroperoxyacetylacetone, by which Co^{2+} is further oxidized to Co^{3+}.

At the end of the oxidation, acetylacetone is converted into formic acid, acetic acid, and small amounts of aldehydes.

Under a definite pressure of oxygen, the oxidation rates are as follows; at [HAAH]/[Co^{2+}]$\leq$3,

$$-d[O_2]/dt = k_a[HAAH]^{1/2}[Co^{2+}]^{-1/3}$$

and at [HAAH]/[Co^{2+}]$\geq$4,

$$-d[O_2]/dt = k_b[HAAH][Co^{2+}]^{1/4}$$

In order to oxidize toluene and *p*-xylene in the glacial acetic acid solution containing Co and HAAH catalysts, the formation of Co^{3+} and $\{Co^{3+}\text{-}(AAH^-)_2\}^+$ in the solution is indispensable. Since the [HAAH] is insufficient for the formation of Co^{3+} at the mole ratio of [HAAH]/[Co^{2+}]$<$2, and since the stable chelate, $Co^{3+}(AAH^-)_3$, is easily produced at the mole ratio of [HAAH]/[Co^{2+}]$>$3, the Co-HAAH systems are considered to be active only at the mole ratio of [HAAH]/[Co^{2+}]=2 for the oxidation of *p*-xylene and toluene. However, such ketones as acetonylacetone and ethyl acetoacetate are still active at the mole ratio of [ketone]/[Co^{2+}]=3, since these ligands form less stable complexes than the complex with HAAH.

12) W. Pritzkow, *Chem. Ber.*, **87**, 1668 (1954); **88**, 482 (1955).

BULLETIN OF THE CHEMICAL SOCIETY OF JAPAN VOL. 39 672—674 (1966)

The NMR Analysis of the Water of Crystallization in Beryl

By Yoshinori SUGITANI, Kozo NAGASHIMA and Shizuo FUJIWARA

Department of Chemistry, Faculty of Science, The University of Tokyo, Hongo, Tokyo

(Received May 26, 1965)

The existence of two types of protons in beryl was proved by the proton magnetic resonance technique; one is as a molecular form of water in the channel of the crystal, while the other is as a hydroxyl-ion replacing O^{2-} ion of the crystal lattice. The proton-proton line of the water was found to be parallel to the c-axis of the crystal.

There are many minerals which contain an indefinite amount of the water of crystallization. Beryl, $Be_3Al_2Si_6O_{18}\cdot nH_2O$, is one of them; it usually contains about one to three weight per cent of water.

Some studies have been carried out concerning the water in beryl by thermogravimetric analysis (TGA), infrared spectroscopy, differential thermal analysis (DTA), and so on. According to Matsuda's finding,[1] two abrupt changes in the ignition loss of water were observed in TGA, and also two endothermic peaks in DTA.

Furthermore, after a detailed consideration using the ordinary methods mentioned above, Sugiura[2] proposed the presence of two types of water in cordierite and beryl - one, a molecular form in the tubular channel of the crystal, and the other, an OH^- ion form replacing the O^{2-} ion of the lattice point. In the present paper, the structure of water in beryl will be investigated by the broad-line NMR technique.

The crystal structure of beryl is shown in Fig. 1. Its crystal system is hexagonal, with a space group 6/m 2/m 2/m. A unit cell contains two molecules; the lattice parameters are $a=9.215$ Å and $c=9.17$ Å. As can be seen in the figure, there are holes about 4.5 Å in diameter, and they line up in a row along the c-axis, making tubular channels which serve to accomodate water molecules, occluded gases and alkali ions. The holes are 4.59 Å apart from each other. If a water molecule is placed in each of these holes, the n number in the chemical formula is equal to 1; if they are placed in every other hole, n is equal to 0.5.

Experimental

A single crystal of the prismatic form, which was obtained in Saga,* was cut into a size proper for being

1) S. Matsuda, *J. Min. Soc. Japan* (*Kobutsugaku Zasshi*), **6**, 40, 53 (1963).

2) K. Sugiura, *Tokyo Kôgyô Daigaku Gakuho, Ser.-B*, **1**, 1 (1959).

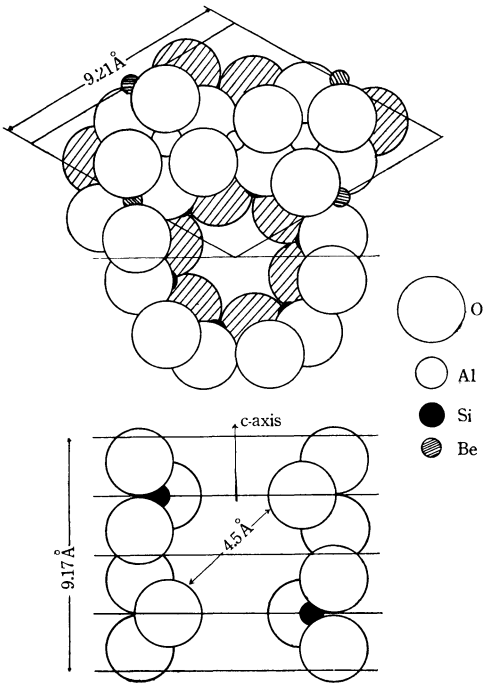

Fig. 1. The structure of beryl.

inserted into an rf coil. The water content of this sample is determined to be 3.05% by means of the ignition-loss method. A simple calculation shows that the n number in the chemical formula of this sample is nearly equal to 1.

The spectra were measured at 30 Mc and in the $-100 \leftrightarrow +150$°C temperature range by using an NMR spectrometer, type JNM-W-30, manufactured by the Japan Electron Optics Laboratory Co., Ltd.

Results and Discussion**

First, the sample was placed in a probe with the c-axis perpendicular to the main magnetic

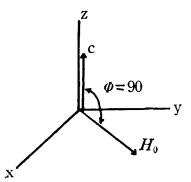

Fig. 2. The c-axis is fixed parallel to the z-axis, and the H_0 field rotates around the origin, O, with the Φ angle always kept 90°.

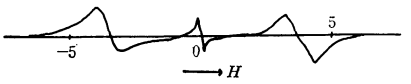

Fig. 3. One of the NMR spectra observed. The other spectra closely resemble this fugure.

field, H_0. The crystal was then rotated and measured at 15° intervals about the c-axis. The line shape of the spectrum did not change with this rotation. One of the spectra obtained is given in Fig. 3. Next, the crystal was placed with the c-axis parallel to H_0, and rotated about the g_1- or $[2\bar{1}\bar{1}0]$-axis, so as to change the angle, Φ, between the c-axis and the magnetic field H_0. The line shape varied with the angle Φ, as is shown in Fig. 5. Similar results within the range of experimental errors were obtained for rotations about five other axes, g_2, g_3, g_4, g_5, and g_6; these are shown in Fig. 6.

As may be seen in Fig. 5, each observed spectrum is composed of three parts, one very narrow, and two broad. The two broad parts are always symmetrically shifted from the center of the narrow part.

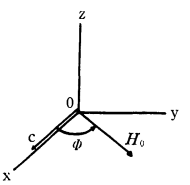

Fig. 4. The angle, Φ, between the c-axis and the H_0 field varies as H_0 rotates around the origin, O, in the xy plane.

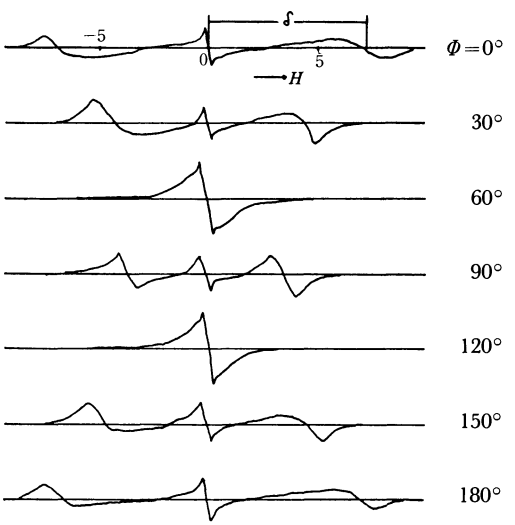

Fig. 5. NMR spectra observed at various angles. The spectra were measured at 15° intervals between 0° and 180°; however, only the spectra observed at 30° intervals are shown in this figure.

* Sugiyama in Saga prefecture. The sample is hexagonal prismatic, about 1.5 cm. long, 0.7 cm. in diameter, and pale green in color.

** After we finished our work, the following paper has come to our attention: X. Parè and P. Ducros, Bull. Soc. Franç. Minér. Crist. (1964) LXXXVII, 429—433. While their results are in accordance with ours, they do not indicate the presence of two types of protons.

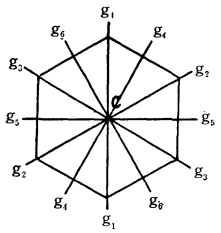

Fig. 6. The hexagon represents the (0001) plane of the single crystal of beryl, while the line perpendicular to this plane at point c is the six-fold axis of the crystal.

From the results obtained above, the protons which contribute to the observed NMR spectra may be classified into two types. The narrow component may be ascribed to either protons which are very easy to move, such as the water molecules in the liquid state, or to protons which are isolated from each other nd which so have negligible dipolar interactions.

The former possibility can be eliminated for two reasons: i) The water molecule in beryl can not be removed easily by heating it up to several hundred degrees, and therefore, it cannot be in a liquid state; ii) we could not find any fluid inclusion in our sample under a microscope.

Therefore, we may assume that the narrow part of the spectrum is due to the protons of the OH^- ions which occupy the position of the O^{2-} ions in the crystal. This conclusion coincides with the results obtained by the IR and other methods by Sugiura.

The remaining two broad parts may be interpreted in terms of the dipolar interactions between two protons belonging to the same water molecule. This means assuming a two-spins system. The magnetic field provided by one of the two water protons is given by[3]:

$$H = H_0 \pm \alpha(3\cos^2\theta - 1), \quad \alpha = \frac{3}{4}\frac{\gamma\hbar}{r^3}$$

where θ is the angle between the line connecting the two protons and the H_0 field; γ, the proton gyromagnetic ratio; $\hbar$, Planck's constant divided by 2π, and r, the distance between two interacting protons in a water molecule.

3) G. E. Pake, *J. Chem. Phys.*, **16**, 327 (1948).

In Fig. 7, the open circles are the observed shifts, δ, of the broad part from the center of the narrow part, while the solid lines represent the plots of the function, $\pm\alpha(3\cos^2\theta - 1)$, fitted to the experimental value at $\Phi = 90°$. The agreement between the two plots is fairly good.

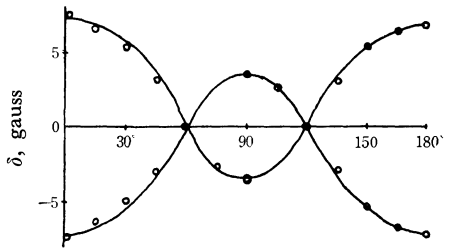

Fig. 7. The solid lines are the calculated lines of the functions, $\pm\alpha(3\cos^2\theta - 1)$, while the open circles are the observed values of δ.

From these results, it can be concluded that the angle, θ, between the proton-proton line and the H_0 field indicates the angle, Φ, between the c-axis and the H_0 field; that is, the proton-proton line of a water molecule is parallel to the c-axis of the crystal. (The position of the oxygen atom of the water molecule has not been determined by the present experiment).

Measurements of the temperature dependence of the line shapes were taken in the $-100 \leftrightarrow +150$°C range. In this experiment, the crystal was placed in the probe with the c-axis perpendicular to the H_0 field. The separation, 2δ, of the two broad parts varied slightly with the temperature, as is shown in Fig. 8. The explanation of this temperature dependence will be the subject of a future study.

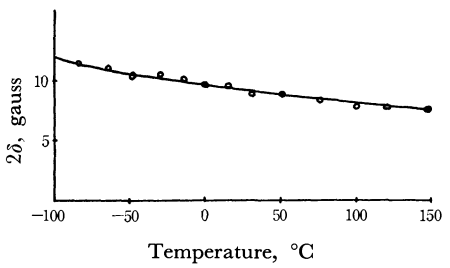

Fig. 8. Temperature dependence of the separation 2δ between the two broad parts.

BULLETIN OF THE CHEMICAL SOCIETY OF JAPAN VOL. 39 675—680 (1966)

A Kinetic Study of the γ-Radiation-Induced Polymerization of Ethylene at a Normal Temperature*

By Sueo MACHI, Miyuki HAGIWARA, Masao GOTODA and Tsutomu KAGIYA

Japan Atomic Energy Research Institute, Takasaki Radiation Chemistry Research Establishment, Takasaki, Gunma

(Received May 31, 1965)

The gamma-radiation-induced polymerization of ethylene was carried out in the intermediate pressure region from 70 to 400 kg./cm^2 with a dose-rate from 5×10^3 to 4.3×10^5 rad./hr. and at a temperature of 30°C. An overall G-value of the 10^4 order was usually obtained. No induction period for polymerization was observed. The polymerization rate and the molecular weight of the polymer formed were shown to increase almost proportionally with the reaction time and with the pressure of ethylene. The dose-rate exponents of the rate and the molecular weight were found to be 0.9 and 0 respectively. These results indicate that the stationary-state hypothesis, i. e., that the rate of initiation is equal to that of termination, is not realized in this polymerization. From the kinetic discussion of the initial stage of polymerization, where the concentration of monomer remains essentially constant, it was concluded that the rates of termination and transfer reaction are very small; the life of polymer radicals is, therefore, quite long and the growing of polymer radicals proceeds successively under irradiation.

Several studies[1-7] of the γ-radiation-induced polymerization of ethylene have been published during the past ten years. Hayward and Bretton,[1] for instance, reported that the reaction consisted of two parts; the one was strongly inhibited by a trace of oxygen, and the other was not. Laird et al.[2] reported that the rate of polymerization depended on the ethylene pressure (P) and the radiation intensity (I), as the rate$=kP^{2.6}I^{0.9}$, with the overall activation energy of 3.3 kcal./mol. at lower temperatures of 20 to 125°C and at pressures from 473 to 1185 atm., while at higher temperatures (from 100 to 200°C) the rate$=kP^{3.1}I^{0.8}$, with the activation energy of 13.6 kcal./mol. Medvedev et al.[5] observed that the rate of polymerization increased with the reaction time, and that the maximum rate was proportional to the ethylene concentration to the power of 4—5 and to the 0.3 th power of the dose rate. More recently, Steinberg et al.[7] reported the rate equation to be rate$=kP^{1.02}I^{0.42}$ and that the G-value was very high.

We are now undertaking a series of investigations of the γ-radiation-induced polymerization of ethylene in order to find its mechanism. We have already communicated briefly[8,9] that the polymerization rate and the molecular weight of the polymer increase with the reaction time, and that the life of the growing polymer radical is long at 30°C under irradiation. In the present work, the polymerization rate and the molecular weight have been measured in the pressure range from 70 to 400 kg./cm^2, at the temperature of 30°C, and at dose-rates from 5000 to 430000 rad./hr. using ethylene of a high purity. The main topic of this paper is a kinetic discussion of the polymerization at normal temperature.

Experimental

A scheme of the experimental equipment is shown in Fig. 1. The reaction vessel was an unstirred stainless-steel (SUS-27) autoclave with a capacity of 100 ml. The pressure measurements were made by a Bourdon tube gauge. A chromel-alumel thermocouple with a recorder was used for the continuous temperature measurements. The reaction temperature was regulated within 2°C by an automatic controller. The reactions were carried out by the batch stysem.

Before the vessel was filled with ethylene, the system was evacuated and swept out with ethylene three times; then ethyene was introduced from a reservoir to the vessel, which had been cooled in a methanol - dry ice

* Presented at the 17th Annual Meeting of the Chemical Society of Japan, Tokyo, April, 1964, and at the 6th Japan Conference on Radioisotopes, Tokyo, November, 1964.

1) J. C. Hayward, Jr. and R. H. Bretton, *Chem. Eng. Progr., Symp. Ser.*, **50** (13), 73 (1954).

2) R. K. Liard, A. G. Morrel and L. Seed., *Discussions Faraday Soc.*, **22**, 126 (1956).

3) J. G. Lewis, J. J. Martin and L. C. Anderson, *Chem. Eng. Progr., Symp. Ser.*, **50** (5), 249 (1954).

4) B. G. Bray, R. A. Carstens, O. A. Larson, J. J. Martin and K. K. G. Sikchi, ibid., **55** (27), 33 (1959).

5) S. S. Medvedev, A. D. Abkin, P. M. Khomikovskii, G. N. Gerasimov, V. F. Gromov, Yu. A. Chikin, V. A. Tsingister, A. L. Auer, M. K. Yalovleva, L. P. Mezhirova, A. V. Matveeva and Z. G. Bezzubuik, *Polymer Sci. (USSR) (English Transl.)*, **2**, 457 (1961).

6) Y. Hosaka, M. Takehisa, Y. Urano and M. Yasumoto, *Tokyo Kogyo Shikensho Hokoku*, **56**, 225 (1961).

7) M. Steinberg, P. Colombo, L. Kukacka, R. N. Chapman and G. Alder, *Proc. Intern. Symp. Radiation Induced Polymerization Copolymerization*, Battelle Memorial Institute, 70 (Nov. 29—30, 1962).

8) S. Machi, M. Hagiwara, M. Gotoda and T. Kagiya, *J. Polymer Sci.*, **B2**, 765 (1964).

9) S. Machi, M. Hagiwara, M. Gotoda and T. Kagiya, ibid., **3A**, 2931 (1965).

TABLE I. EFFECT OF REACTION PRESSURE AND TIME ON POLYMER YIELD AND MOLECULAR WEIGHT

Ethylene*			Reaction time	Polymer yield	Molecular weight	*G*-value molecule/ 100 eV.
Pressure kg./cm²	Fugacity kg./cm²	Concn. mol./l.	hr.	g.	$\times 10^{-4}$	$\times 10^{-3}$
400	116	16.4	0.26	0.03	7.0	3.4
400	116	16.4	0.53	0.14	14.7	8.0
400	116	16.4	1.0	0.74	26.6	22.4
384	112	16.0	2.6	2.62	31.5	31.5
405	117	16.4	4.0	5.52	33.2	42.5
400	116	16.4	8.0	11.72	31.2	43.3
388	113	16.1	20.8	22.79	24.0	34.2
295	90	15.4	0.70	0.16	13.3	7.4
295	90	15.4	1.0	0.27	17.4	8.8
300	91	15.4	1.7	0.71	26.5	13.5
300	91	15.4	4.0	2.52	32.0	20.4
296	90	15.4	20.2	14.84	26.0	23.7
200	70	14.4	0.70	0.08	5.9	4.0
200	70	14.4	1.2	0.12	6.6	3.5
200	70	14.4	2.5	0.50	12.7	7.0
201	70	14.4	4.0	1.50	17.2	13.0
200	70	14.4	8.0	3.89	24.1	16.9
203	71	14.4	20.0	11.42	23.2	19.9
152	61	13.4	1.7	0.19	6.3	4.2
152	61	13.4	2.5	0.31	8.8	4.6
152	61	13.4	4.0	0.79	16.4	7.4
154	61	13.4	8.0	2.29	19.4	10.7
150	60	13.3	20.3	6.79	22.3	12.4
70	45	7.2	15.0	0.39	2.1	1.8
70	45	7.2	20.7	0.50	1.6	1.7
70	45	7.2	44.6	3.07	4.3	4.8

Reaction temperature, 30°C; Dose-rate, 2.5×10^4 rad./hr.
* at initial condition

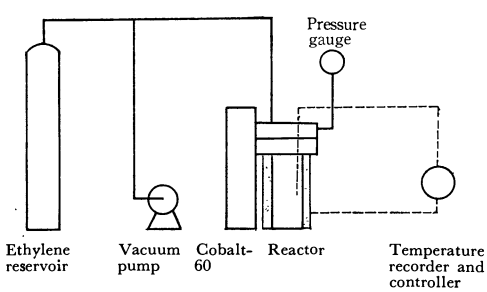

Fig. 1. Experimental equipment.

bath. The vessel was then brought to the desired reaction temperature and pressure. As a source of γ-ray, 400-curie and 12000-curie cobalt-60 were used. The radiation intensity inside the reaction vessel was measured by ferrous sulfate dosimetry. At the end of the irradiation period, the unpolymerized ethylene was purged and the vessel was opened in the air. The amount of polymer formed was determined by direct weighing.

The ethylene used was commercially available and was 99.9% pure (free of CO and H_2S), containing 48 p. p. m. acetylene and 3 p. p. m. oxygen. The density and fugacity of ethylene at a given pressure and temperature are known from Benzler's pressure-enthalpy diagram.[10]

The solution viscosity of the polyethylene formed was measured in tetralin at 130°C. The number-average molecular weight of polymer was estimated by Tung's formula[11]:

$$[\eta] = 4.60 \times 10^{-4} \overline{M}_n^{0.725}$$

Results

The results are summarized in Tables I and II.

The polymer yield is plotted against the reaction time in Fig. 2. In these experiments there is no induction period in which no polymer is formed. The yield of the polymer formed increases rapidly with the reaction time in the early stage, while in the stage of higher conversion, the increasing rate is gradually reduced because of the drop in pressure.

10) H. Benzler and A. V. Koch, *Chem. Ingr. Tech.*, **27** (2), 71 (1955).
11) L. H. Tung, *J. Polymer Sci.*, **24**, 333 (1957).

Table II. Effect of dose-rate on polymer yield and molecular weight

Dose-rate rad./hr. $\times 10^{-4}$	Reaction time hr.	Polymer yield g.	Molecular weight $\times 10^{-4}$	G-Value molecule/100 eV. $\times 10^{-3}$
43	1.0	0.91	4.4	1.8
21	1.0	0.55	5.5	2.2
12	1.0	0.36	5.8	2.6
5.6	1.0	0.25	6.6	3.8
2.5	1.2	0.12	6.6	3.5
1.3	5.0	1.08	24.5	14.2
0.77	4.0	0.54	25.5	15.0
0.50	5.0	0.57	26.0	19.5

Ethylene pressure, 200 kg./cm²
Reaction temperature, 30°C

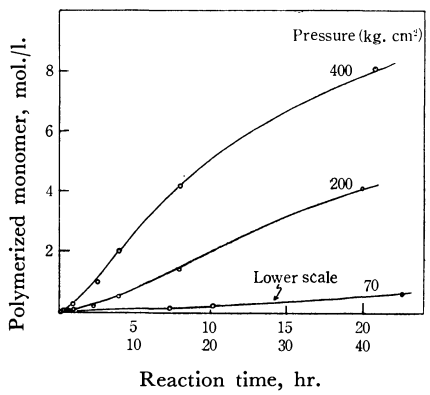

Fig. 2. The amount of ethylene polymerized vs. reaction time.
(Reaction temperature, 30°C; dose-rate, 2.5× 10^4 rad./hr.)

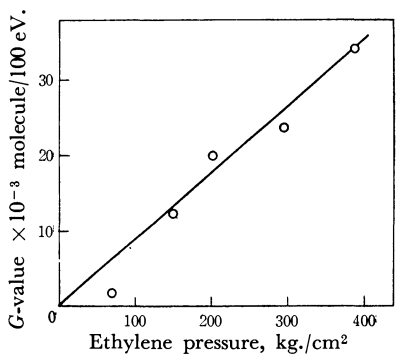

Fig. 3. G-value vs. initial ethylene pressure.
(Reaction temperature, 30°C; dose-rate, 2.5× 10^4 rad./hr.; reaction time, ca. 20 hr.)

The G-value (molecules of ethylene polymerized per 100 eV. absorbed in the mass of the monomer and the polymer) is also shown in Tables I and II. The G-value depends on the reaction time, the ethylene pressure, the dose-rate and the reaction temperature; it lies between 1.8×10^3 and 4.3×10^4. Figure 3 indicates that the overall G-value is proportional to the initial pressure of ethylene.

Polymerization under a Low Conversion.—The experiments concerned with kinetic study were carried out under conditions in which the conversion of ethylene to polymer was low and the pressure remained essentially constant during the course of the reaction.

Polymer Yield.—The polymer yield, with a dose rate of 2.5×10^4 rad./hr. under various pressures, is plotted against the time in Fig. 4. No induction period was observed in our experiments. As is shown in Table I, at a pressure of 400 kg./cm² under 30°C, 0.03 g. of polymer is formed in only 16 min. in a 100 ml. reactor. On the other hand, an induction period of more than several hours, as a result of oxygen, was reported in the case of the polymerization of ethylene containing over 60 p. p. m. oxygen by Steinberg et al.[7] and by Hayward et al.[1] The reason for the difference between these results and ours is not clear,

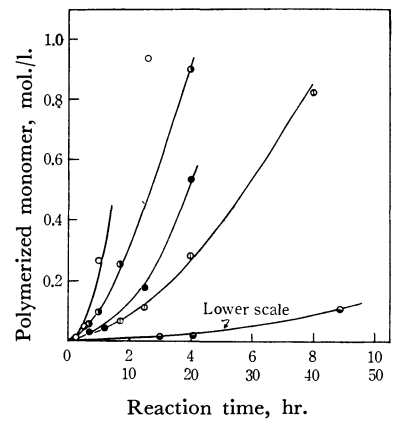

Fig. 4. The amount of polymerized monomer vs. reaction time.
(Reaction temperature, 30°C; dose-rate, 2.5×10^4 rad./hr.; ethylene pressure, 70 (◒), 150 (◐), 200 (●), 300 (◑), 400 kg./cm² (○))

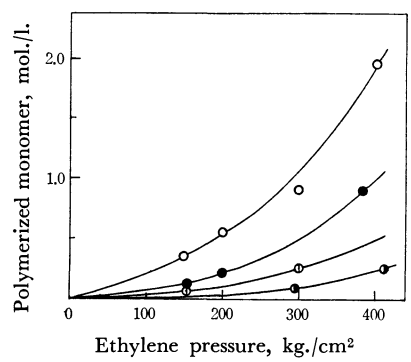

Fig. 5. The amount of polymerized monomer vs. ethylene pressure.
(Reaction temperature, 30°C; dose-rate, 2.5×10^4 rad/hr.; reaction time, 1.0 (◑), 1.7 (◐), 2.5 (●.), 4.0 hr. (○))

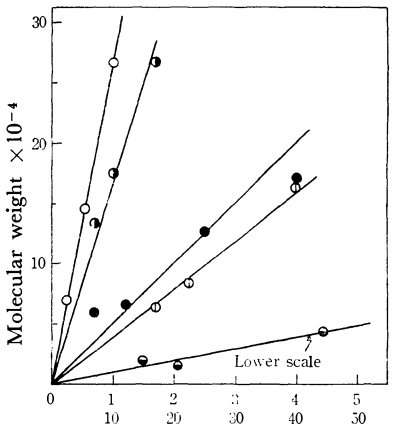

Fig. 6. Molecular weight vs. reaction time. (Reaction conditions and notes are the same as Fig. 4.)

but it may be ascribed to the difference in the amounts of oxygen; i. e., the ethylene used in our experiments contains only 3 p. p. m. oxygen, plus other impurities.

Since the polymer yield increases rapidly with the reaction time, as is shown in Fig. 4, it should be noted that a rate acceleration is observed in this polymerization.

The effect of the intensity was investigated over the dose-rate range from 0.5×10^4 to 43×10^4 rad./hr.; a hundred-fold range was thus covered. In Table II, it is shown that the amount of polymer formed increases with the dose-rate. Figure 5 indicates that the polymer yield at a constant time increases rapidly with the pressure.

Molecular Weight.—In these experiments, the molecular weight falls in the wide range from 20000 to 300000, depending on the reaction conditions.

The molecular weight of the polymer formed in the early stage of less than ca. 3% conversion is plotted against the reaction time at each respective pressure (but these pressures are almost constant during the reaction) in Fig. 6. It is a characteristic phenomenon that the molecular weight of the polymer formed increases proportionally with the reaction time. The increase in ethylene pressure obviously gives the increase in the molecular weight of the polymer.

The dependence of the molecular weight of the polymer on the radiation dose-rate is seen in Table II. It is interesting that the molecular weight at the unit reaction time is almost independent of the dose rate.

Discussion

From the characteristic features—(1) the reaction rate increases with the reaction time; (2) the molecular weight of the polymer formed increases with the reaction time, and a polymer of a very high molecular weight is easily obtained, and (3) the radiation dose-rate has little effect on the molecular weight of the polymer, it can be concluded that the stationary-state hypothesis, that the rate of initiation is equal to that of termination, is not realized in this polymerization.

In our kinetic study experimental results are, therefore, treated without using the stationary-state hypothesis.

Polymerization Rate.—The following elementary reactions are assumed for the γ-radiation-induced polymerization of ethylene in bulk; the respective rate expressions are also shown at the right.

1. Initiation $\quad M \xrightarrow{k_i} R_1\cdot \quad R_i=k_i\rho_M I \quad (1)$
2. Ethylene excitation $\quad M \rightleftarrows M^*$
$$M+M^* \rightleftarrows M_2^* \quad f_{M_2^*}=K_e f_M^2 \quad (2)$$
3. Propagation $\quad R_1\cdot+M_2^* \xrightarrow{k_p} R_3\cdot$
$$R_{n-2}\cdot+M_2^* \xrightarrow{k_p} R_n\cdot$$
$$R_p=k_p[R\cdot]f_{M_2^*} \quad (3)$$
4. Termination $\quad R_m\cdot+R_n\cdot \xrightarrow{k_{t1}} P_{m+n}$
$$R_n\cdot+Z \xrightarrow{k_{t2}} P_n$$
$$R_t=k_{t_1}[R\cdot]^2+k_{t_2}[R\cdot][Z] \quad (4)$$
5. Transfer $\quad R_n\cdot+Y \xrightarrow{k_{tr}} P_n+Y\cdot$
$$R_{tr}=k_{tr}[R\cdot][Y] \quad (5)$$

where M represents the ethylene monomer; $R_n\cdot$, an active polymer chain composed of n monomers; $[R\cdot]$, the total concentration of all the active polymer chains, irrespective of size (i. e., $\sum_{n=1}^{\infty}[R\cdot_n]$); M*, the excited ethylene monomer; M_2^*, the excited ethylene dimer; Y, the substance to which the activity of $R\cdot_n$ is transferred; Z, the substance by which $R\cdot_n$ is deactivated; P_n, a dead polymer composed of n monomers; R_i, R_p, R_{tr}, and R_t, the rates of initiation, propagation, transfer, and termination; k_i, k_p, k_{tr}, and k_t, the rate constants of these reactions; ρ_M the density of ethylene; I, the dose rate; f_M, the fugacity of ethylene; $f_{M_2^*}$ the fugacity of the excited ethylene dimer, and K_e, the equilibrium constant of the 2nd step.

Since the initiation step is brought about by the absorption of the radiation energy by the monomer, the rate of the initiation reaction may be considered to be proportional to the density of ethylene presented in the reactor and to the intensity of radiation. The rate expression 1 is, therefore, given for the initiation reaction. The 2nd step is characteristic in this scheme. The step of the formation

of the excited dimer from the monomer with radiation is introduced because of the following facts; (1) as was reported before,[9] the propagation reaction does not take place without radiation, though it takes place with a radiation of a very low dose rate, and (2) the rate of propagation is proportional to the 2nd power of ethylene fugacity, as will be described later. It is well known that the rates of excitation and energy transfer are very fast in the radiation chemistry. The 2nd step is, therefore, very fast compared with the 3rd step and is in equilibrium.

In the propagation step, the excited dimer adds to the propagating chain. Ordinary chain termination and transfer are assumed. The overall rate of polymerization is approximately equal to the rate of propagation; accordingly, it becomes:

$$R=\mathrm{d}M_p/\mathrm{d}t\simeq R_p=k_p[\mathrm{R}\cdot]f_{\mathrm{M}}^*, \qquad (6)$$

where R represents the overall polymerization rate, and M_p, the amount of monomer polymerized. Here, without the assumption of stationary-state, [R·] is given by:

$$[\mathrm{R}\cdot]=k_i\rho_{\mathrm{M}}It-\int R_t\mathrm{d}t \qquad (7)$$

From the facts that the rate of polymerization and the molecular weight of the polymer increase with the reaction time, it can be assumed that no termination reaction occurs, that, namely, R_t is zero. Equation 7 then becomes:

$$[\mathrm{R}\cdot]=k_i\rho_{\mathrm{M}}It \qquad (8)$$

From the combination of Eqs. 2, 6 and 8, the overall rate of polymerization can be expressed by the following equation:

$$R=\mathrm{d}M_p/\mathrm{d}t\simeq R_p=k_pk_iK_e\rho_{\mathrm{M}}f_{\mathrm{M}}^2It \qquad (9)$$

By integrating Eq. 9, the amount of the monomer polymerized is expressed as a function of the density and the fugacity of ethylene, the dose rate, and the reaction time; namely,

$$M_p=(1/2)\cdot k_pk_iK_e\rho_{\mathrm{M}}f_{\mathrm{M}}^2It^2 \qquad (10)$$

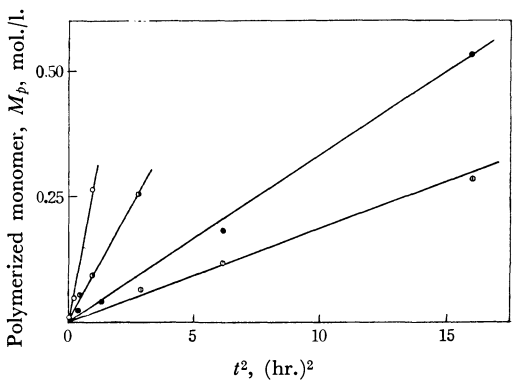

Fig. 7. The amount of polymerized monomer vs. square of reaction time.
(Reaction conditions and notes are the same as Fig. 4.)

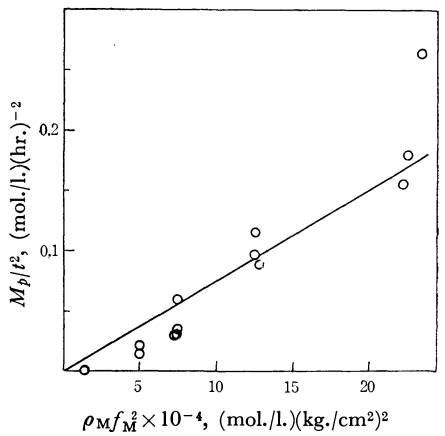

Fig. 8. M_p/t^2 vs. $\rho_{\mathrm{M}}\cdot f^2{}_{\mathrm{M}}$.
(Reaction temperature, 30°C; dose-rate, 2.5×10^4 rad./hr.; ethylene pressure, 70 to 400 kg./cm^2).

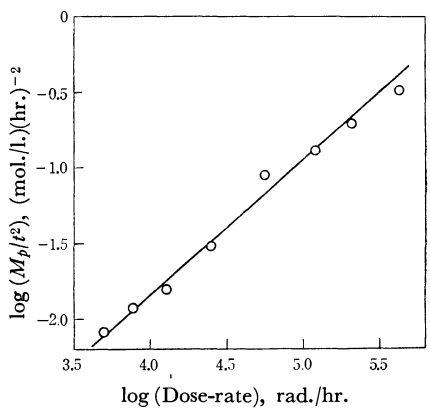

Fig. 9. Logarithmic plots of M_p/t^2 vs. dose-rate.
(Reaction temperature, 30°C; ethylene pressure, 200 kg./cm^2)

A distinct linear relation exists between the amount of monomer polymerized and the square of the reaction time at each respective pressure, as is indicated in Fig. 7. The plot of $\rho_{\mathrm{M}}f_{\mathrm{M}}^2$ versus M_p/t^2 also gives the straight line in Fig. 8. The logarithmic plot of the dose-rate against M_p/t^2 is shown in Fig. 9, from which the dose-rate exponent of M_p/t^2 may be seen to be 0.9.

The results are combined and an empirical expression of amount of monomer polymerized is obtained as:

$$M_p=k_1\rho_{\mathrm{M}}f_{\mathrm{M}}^2I^{0.9}t^2 \qquad (11)$$

The approximate agreement of the empirical expression with the theoretical one (10), derived from the elementary reactions presumed above, is thus shown.

The Degree of Polymerization.—The number-average degree of polymerization at a given reaction time is written for the polymerization with no termination by recombination as follows:

$$\overline{DP}=(\int R_p\mathrm{d}t)/(\int R_i\mathrm{d}t+\int R_{tr}\mathrm{d}t) \qquad (12)$$

where $\overline{DP}$ represents the number-average degree of polymerization, and $\int R_p\mathrm{d}t$ is as given in Eq. 10 ($\int R_i\mathrm{d}t$ is also obtained from Eq. 1); accordingly:

$$\overline{DP}=\frac{(1/2)\cdot k_p k_i K_e \rho_M f_M^2 I t^2}{k_i \rho_M I t+(k_{tr}/k_p K_e)\cdot([Y]/f_M^2)\cdot M_p} \qquad (13)$$

then;

$$1/\overline{DP}=(2/k_p K_e f_M^2 t)+(k_{tr}/k_p K_e)\cdot([Y]/f_M^2) \qquad (14)$$

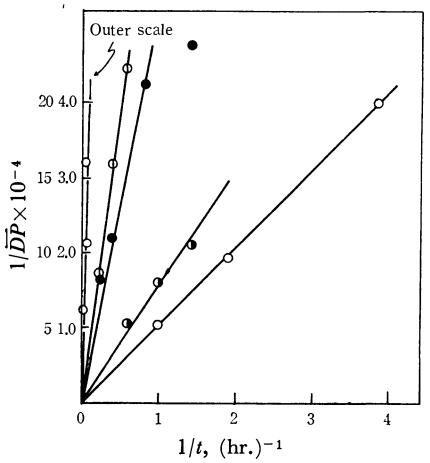

Fig. 10. Reciprocal of degree of polymerization vs. reciprocal of time.
(Reaction conditions and notes are the same as Fig. 4.)

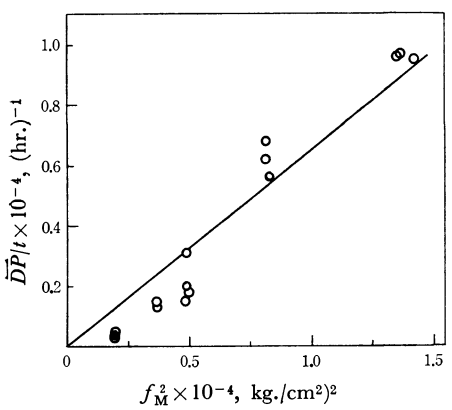

Fig. 11. $\overline{DP}/t$ vs. square of ethylene fugacity.
(Reaction temperature, 30°C; dose-rate, 2.5×10^4 rad./hr.; ethylene pressure, 70 to 400 kg./cm^2)

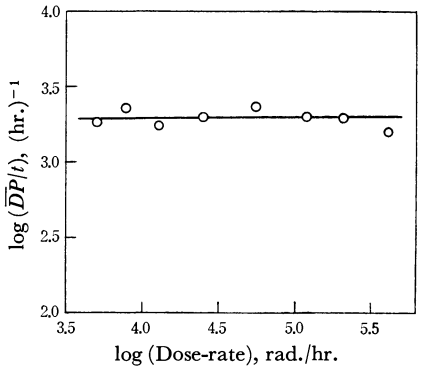

Fig. 12. Logarithmic plots of $\overline{DP}/t$ vs. dose-rate.
(Reaction temperature, 30°C; ethylene pressure, 200 kg./cm^2)

The plot of the reciprocal of $\overline{DP}$ against the reciprocal of the reaction time gives a straight line through the origin, as is shown in Fig. 10. The fact that the line goes through the origin indicates that there is no transfer reaction in the polymerization; Eq. 14 thus becomes:

$$\overline{DP}=(1/2)\cdot k_p K_e f_M^2 t \qquad (15)$$

The linear relation between $\overline{DP}$ and the time has previously been shown in Fig. 6. In Fig. 11, it is shown that the ratio of the degree of polymerization to the reaction time is approximately proportional to the square of ethylene fugacity. Figure 12 shows that the dose rate does not influence $\overline{DP}/t$. By combining these results, the following empirical expression of the degree of polymerization is obtained:

$$\overline{DP}=k_2 f_M^2 t \qquad (16)$$

The empirical expression is shown to agree with theoretically derived Eq. 15.

In the view of fact that the experimental results on both polymerization rate and the degree of polymerization coincide with the equation theoretically derived, the proposed elementary reaction and the assumption that the termination is essentially eliminated, and that the stationary state is not realized in this polymerization, may be accepted. In other words, the propagation, proceeds successively, and a long-lived active polymer chain may exist under irradiation. The long life-time of the active chain has been proved by a kind of post polymerization experiment.[9]

BULLETIN OF THE CHEMICAL SOCIETY OF JAPAN VOL. 39 681—684 (1966)

The Combustion-Gas Chromatographic Determination of Minute Quantities of Sulfur in Metals

By Jiro KASHIMA and Takuo YAMAZAKI

The Castings Research Laboratory, Waseda University, Shinjuku-ku, Tokyo

(Received June 7, 1965)

The determination of minute quantities of sulfur in metals is an important problem in refinery processing. This paper will describe a combustion-gas chromatographic method which gives precise results. This method is applicable to various metals, including iron and steels. Standard samples containing 0.011% of sulfur show a standard deviation of 0.0001%. Titanium and copper containing from 0.004 to 0.008% of sulfur show a mean deviation of 0.0003%. The limit of detection is 10 μg. (0.001%) of sulfur in a 1.0 g. sample. It takes about 10 min. to determine the sulfur content by this method.

Because of the adverse effect of sulfur on the physical properties of pure metals, steel and cast iron, a method for controlling the sulfur content during refining is desirable. The determination of sulfur in metals is generally performed by a chemical method which measures the concentration of SO_4^{2-} or SO_3^{2-} ions formed by bubbling the combustion products (carbon dioxide, sulfar dioxide, water, etc.) through an aqueous solution of hydrogen peroxide. Several other methods[1-7] have been proposed for the determination of minute quantities, i. e., several micrograms, of sulfur. Colorimetric,[1-3] conductometric[4,5] and chromatographic - gravimetric[7] methods are available for the determination of extremely small amounts of sulfur in metals. For rapid analysis, a neutron-activation analysis[6] is used. Recently, a combustion-gas chromatographic method[8] has been proposed to determine carbon and sulfur simultaneously in ferrous metals.

This paper will describe a combustion-gas chromatographic method which is capable of determining sulfur accurately in various metals. The method is a simplification in the following three ways: a gas chromatograph was used for the analysis of the combustion gases; a simple chromatographic concentration technique[9] was used for isolating sulfur dioxide and pure copper powder or foil was used as the bedding material to burn titanium, silicon, etc., in a commercially-available H-F combustion furnace. Minute amounts of sulfur can be accurately determined by this method within ten minutes.

Experimental

Apparatus.—A simple schematic diagram is shown in Fig. 1. The apparatus is simlar in principle to that described[8] elsewhere by the present authors and used for the determination of small amounts of carbon in pure iron and steel; it consists of a commercially-available combustion funace to ignite the sample and a gas chromatograph connected to the concentration column to isolate sulfur dioxide in the combustion products. Some changes have, however, been made in the apparatus and in the procedure used previously for the determination of carbon. A silica gel column

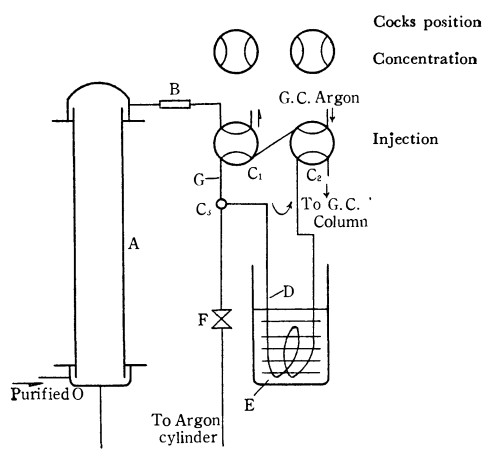

Fig. 1. Schematic diagram of apparatus and the basic flow system.
A. Combustion system, B. Drierite, C_1. Hard glass four-way cock, C_2. Four-way gas sampling cock. C_3. Three-way cock, D. Concentration column packed with silica gel, E. Warming bath of potassium carbonate, F. Needle valve, G. Glass capillary tube

1) A. I. Ponomarew and A. A. Astanina, *Tr. Inst. Met. im A. A. Baikava*, **10**, 231 (1962).
2) K. E. Burke and C. M. Davis, *Anal. Chem.*, **34**, 1747 (1962).
3) O. H. Kriege and A. L. Wolfe, *Talanta*, **9**, 673 (1962).
4) E. Pell and H. Malissa, ibid., **9**, 1056 (1962).
5) I. Fujishima and T. Takeuti, *J. Chem. Soc. Japan, Ind. Chem. Sect.* (*Kogyo Kagaku Zasshi*) **66**, 775 (1963).
6) P. Bouten and J. Hoste, *Anal. Chim. Acta.*, **27**, 315 (1962).
7) S. Bertddi, D. Grosso and F. Casalvolone, *Chim. Anal.* (*Paris*), **45**, (11), 560 (1963).
8) W. K. Stuckey and J. M. Walker, *Anal. Chem.*, **35**, 2015 (1963).
9) J. Kashima and T. Yamazaki, *Japan Analyst* (*Bunseki Kagaku*), **13**, 775 (1964).

was used instead of an activated charcoal column, and accelerator was added.

Oxygen gas of a commercially-pure grade was introduced from a gas cylinder through the reducing valve. The gas was further purified by passing it through tubes of granular potassium hydroxide and of phosphorus pentoxide, thus removing the sulfur dioxide and water.

The combustion was carried out by the use a of Kokusai Denki H-F combustion furnace; the oxygen stream was regulated by means of a reducing valve attached to the gas cylinder.

The combustion products were led into concentration column, D, by stainless steel tubing (2 mm. in diameter.) through a Drierite, B, and a silica wool plug.

C_1 is a four-way cock which connects the concentration column, D, and the gas-sampling cock, C_2, of the gas chromatograph, as is shown in Fig. 1.

The Flikentite cuplets (crucibles) and the caps (made by the Nihon Kagaku Kogyo Co.) were prebaked for 3 hr. at a temperature of about 1500°C in a hydrogen stream; the cuplets were then baked for 4—5 more min. in the same manner as in the ordinary combustion procedure.

Gas Chromatography.—A Yanagimoto gas chromatograph, Model GCG 100, and a Minneapolis-Honeywell recorder, Model SY 153, with a full-scale sensitivity of 50 mV. were used. In order to measure a minute quantity of sulfur dioxide, the recorder was connected with an Ohkura DC. amplifier, Model AM 101, and employed at a full-scale sensitivity of 500 μV. The detector was a thermal conductivity cell with a pair of tungsten filaments; the current supply to the bridge circuit was adjusted to 150 mamp.

The argon gas, which was less than 0.01% impure, was used as the carrier gas at a flow rate of 50 ± 2 ml./min.

The chromatographic column was a copper tube 50 cm. long and 6 mm. in diameter. It was packed with 30—64 mesh Celite 545 containing 30% tricresyl phosphate and was kept at the temperature of 40°C in a thermostat chamber.

The concentration column was a copper tube 10 cm. long and 6 mm. in diameter.; it was packed with 30—64 mesh silica gel. This column was used for concentrating only sulfur dioxide at room temperature. The concentrated gas was injected into the chromatograph at the temperature of 120°C.

Procedure.—The concentration column, D, was heated in a salt bath, with the argon gas allowed to flow through for several minutes, until the water absorbed in the silica gel had been removed. In order to remove the water from the combustion system, it was heated in oxygen gas.

The sample (approximately 1.0 g.) was weighed into a cuplet, together with the analytical-grade accelerators, i. e., 100 mg. of tin shot and 50 min. of chromium(III) oxide powder. The sample was placed in position, and then agron gas was passed through the apparatus for 2 min. The column, D, was connected with the combustion tube by turning cocks C_1, C_2 and C_3 to the positions shown in Fig. 1; the rate of oxygen flow was adjusted to 150 ml./min., and then the combustion was started.

The products of the combustion were collected in the column at room temperature for 3—5 min. while the sample was being burned. The three-way cock, C_3, was then turned 90° to cut off the oxygen flow. The sample cuplet was removed from the combustion tube to avoid overheating the silicone gaskets. By opening the needle valve, the oxygen in the column was expelled in 20—30 sec. by the argon stream at a flow rate of 50 ml./min. C_3 was then returned to the previous position, and the column was immersed in a potassium carbonate bath at 120—130°C. By turning C_2, the gases in the column were then injected into the gas chromatograph. A typical chromatogram is shown in Fig. 3.

The blank value for this method was obtained from the data derived from the ordinary results. The blank value was about 12 μg. of sulfur; this was very low in comparison with the amounts of sulfur in 1—2 g. samples of steel. A fluctuation of the blank values was, however, found between various kinds of crucibles used. The measurement of a peak area of sulfur dioxide was carried

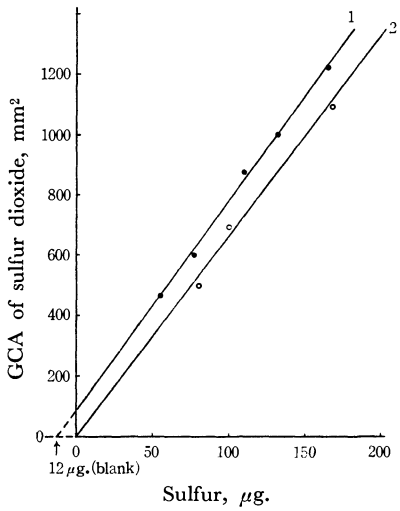

Fig. 2. Calibration curve for determining sulfur contents.
1. Values obtained using the samples of 0.5—1.5 g. 2. Values obtained by the use of a standard sulfur dioxde gas, under conditions such as 20°C, 758 mmHg.

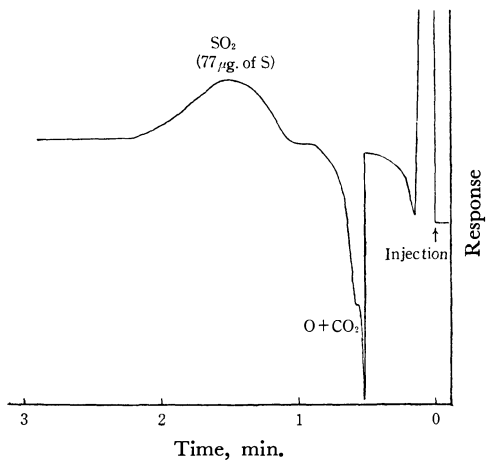

Fig. 3. A typical chromatogram.

out by the use of a planimeter or by the conventional appoximate method, while the sulfur content in the sample was obtained by the following equation:

$$\text{Sulfur, } \% = (a_t - a_b)/w \cdot K$$

where a_t: the area of the chromatogram of sulfur dioxide in sq. mm. for the sample; a_b: the area of the chromatogram of sulfur dioxide in sq. mm. for the blank test; w: the sample weight in mg. and K: the constant = 0.15 (μg. sulfur per sq. mm.), which was determined by using standard samples of known compositions or standard gas.

Table I. Accuracy and agreement with JISS value of the proposed method

Sample designation	Sulfur, μg. Taken	Found	Sulfur content wt. %	Standard deviation %
JISS No. 11 (tungsten steel, 0.011%S)	110	118	0.0118	
		118	0.0118	
		114	0.0114	
		118	0.0118	
		122	0.0122	
		112	0.0112	
		116	0.0116	
		116	0.0116	
	mean	116	0.011_6	0.0001_3
	165	161	0.0108	
		163	0.0109	
		170	0.0113	
		164	0.0109	
	mean	164	0.010_9	0.0001_2
JISS No. 5 (d) (basic open hearth steel, 0.023%S)	*230*	*230*	*0.0230*	
		230	0.0230	
		235	0.0235	
		230	0.0230	
		222	0.0222	
		233	0.0233	
		230	0.0230	
		228	0.0228	
		228	0.0228	
	mean	230	0.023_0	0.0003_6
	115	115	0.0230	
		118	0.0236	
		115	0.0230	
		116	0.0232	
		118	0.0236	
		121	0.0242	
		121	0.0242	
	mean	118	0.023_5	0.0005_1

Table II. Sulfur contents in electrolytic irons

Sample designation	No. of determinations	Sulfur %	Standard deviation %
SP-1 (plate, 0.006%S*)	7	0.0059_4	0.00034
HP-1 (powder, 0.010%S*)	9	0.0096_1	0.00048
HP-2 (powder, 0.010%S*)	5	0.0087_6	0.00055

* Sulfur content obtained by a combustion-conductometry.

The calibration was carried out with three samples measured manometrically using a standard gas of sulfur dioxide in the 1.0-ml. sampling cell used for quantitative gas analysis, where the system for sampling was evacuated to 10^{-3} mm. Hg by means of a rotary oil pump. The calibrated value was obtained from the relationship between the concentration and the chromatogram area. However, when the calibration was carried out by using the standard steel sample, this value was different from that obtained by using the gas.

Results

The accuracy of this method and agreement of the results with those shown in JISS were tested by determining the sulfur content of JISS No. 11 and No. 5(d) and of the electrolytic iron samples; the results are shown in Tables I and II. The data were obtained from 1—2 g. samples to which suitable accelerators had been added.

The usefulness of this method was proved by determining the sulfur contents of cast iron, titanium, silicon, copper, chromium and manganese; the results are given in Tables III and IV. In these metals only copper was effectively burnt by the H-F combustion technique; commercial copper powder or foil could be used as the bedding material in place of iron powder. The data were obtained with 0.3—1.0 g. samples, with 1—1.5 g. of copper and with 0.1 g. of chromium(III) oxide used as the accelerators.

Discussion

The use of a highly-sensitive gas chromatograph for the analyses of combustion gases enables us to determine sulfur contents as low as 10 μg. in pure metals; in this case, the blank value of this method can be kept below 3 μg. of sulfur by using the Leco. 528-31 cuplet. The determination of sulfur contents below 100 μg. is difficult in the conventional method. By using the Leco. cuplet, this method can also be applied to non-ferrous pure metals by the addition of special purified copper foil and some accelerators. It is of a great advantage to be able to use the Flikentite or the Leco. cuplet, since they require no complicated pretreatment, unlike as in the other combustion method. If the Flikentite cuplet prepared for carbon analysis was used for the determination of the sulfur content in cast iron, however, a lower value was obtained. For this reason, the study of the modification of refractory materials for the crucible is now being continued with the cooperation of other laboratories.

The sulfur contents in the silica gel column as found by the actual combustion are given in Table V. The data were obtained with an oxygen stream with a flow rate of 150 ml./min. at room temperature. From this table, it is clear that an oxygen flow of 6 min. is sufficient.

TABLE III. DETERMINATION OF SULFUR CONTENTS IN CRAY CAST IRON

Sample designation	No. of determinations	Sulfur %	Deviation from mean, %	Accelerator
P-732 (0.019%S*)	3	0.0176	±0.0007	Cr_2O_3 0.1 g. shot Sn 0.5 g.
P-733 (0.019%S*)	4	0.0163	0.0003	
P-506 (0.045%S*)	5	0.0440	0.0020	
P-507 (0.064%S*)	6	0.0613	0.0047	

* Sulfur content obtained by a combustion-conductometry.

TABLE IV. SULFUR CONTENTS OF METALS

Designation	No. of determinations	Sulfur %	Deviation from mean, %	Accelerator
Titanium rod	4	0.0085_4	$\pm 0.0003_2$	(bedding metal SP copper 1—1.5 g. Cr_2O_3 0.1 g.
Lump silicon	3	0.0057_7	0.001_2	
Electrolytic copper	6	0.0041_5	0.0001_9	
Electrolytic chromium	4	0.0508	0.006_4	
Electrolytic manganese	5	0.0135	0.001_2	

TABLE V. COLLECTION OF SULFUR DIOXIDE BY SILICA GEL COLUMN*

Collection time min.	Chromatogram area, sq.mm.	Sulfur, μg. Taken	Found
1.9	192	59	—
2.5	334	59	—
3.1	438	59	54
6.1	465	59	59
10	459	59	58
20	468	59	59
3.5	764	100	101
6.0	762	100	101
10	742	100	99
15	736	100	98

* The seize is of 4 mm. in diameter and 10 cm. long.

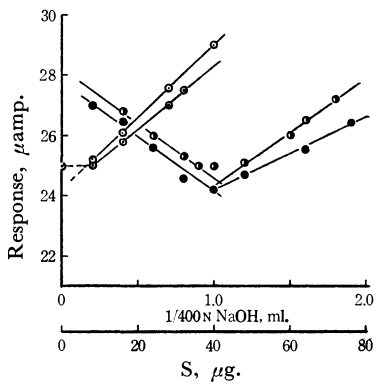

Fig. 4. A typical titration of SO_4^{2-} by H-F conductometry.
-◑- -●- plots on 1.0 ml. of 1/400 N sulfuric acid
—⊙— plots on the solution washed sulfur trioxide absorbed in the concentration column with a little neutral water

Some investigators[2,9,10] have described how materials with sulfur contents of above 90% were converted into sulfur dioxide by the complete combustion of the metal. Similar results seem to be obtained by the present experiment. If sulfur trioxide is formed in the combustion products, the results obtained are erratic, because sulfur trioxide is absorbed in the concentration column. The experiment was carried out to measure the concentration of SO_4^{2-} ions by means of highly-sensitive conductometry using a Shimadzu H-F titrator. The above-mentioned SO_4^{2-} ions were present in the 20 ml. of water used to wash the column. The titration curves of an aqueous solution containing 1.0 ml. of 1/400 N standard sulfulic acid and those of this washed solution are shown in Fig. 4. The sulfur content as SO_3 was below 8 μg.; this quantity is below the limit of detection by conductometry.

Combustion times of 5—6 min. were found to be effective in the oxidation of metals. Copper, used as the bedding material in these experiments, burned smoothly at high temperatures (above 1600°C). In the reaction it was dissolved in crucible materials; copper is one of the metals with the lowest sulfur content. When it is then used together with the Leco. crucible, which shows a small blank value, the correction becomes small.

Because a small amount of lump silicon was available for performing the complete combustion, 200—300 mg. of the samples was used with 2 g. of the foil copper; satisfactory burnings were still obtained with titanium, however, when only 1 g. samples and 1—1.5 g. of copper powder were used.

10) R. C. Rooney and F. Scott, *J. Iron Steel Inst.*, **195**, 417 (1960).
11) A. Kaya and Y. Kakita, *J. Japan Inst. Met.* (*Nippon Kinzoku Gakkaishi*), **26**, 522 (1962).

BULLETIN OF THE CHEMICAL SOCIETY OF JAPAN VOL. 39 685—694 (1966)

Colloid Chemical Studies of Phase Diagrams of Binary Polyoxyethylene Nonylphenyl Ether - Water Systems

By Kazutoshi KENJO

Takahashi Toyodo Co., Ltd., Shinogawa-machi, Shinjuku-ku, Tokyo

(Received June 26, 1965)

Colloid chemical studies of the phase diagrams of binary systems of aqueous polyoxyethylene nonylphenyl ethers with different degrees of the polymerization of ethylene oxide, n, have been undertaken. The phase diagrams obtained have been divided into the heterogeneous region I, existing in the range of temperature higher than cloud points; the homogeneous phase region II; the heterogeneous region III, existing below the II region; and the solid phase region IV. The II region contains a gel-like hardening region. The III region has been further divided into two sub-regions, on the higher and lower concentration sides; these subregions contain one hardening region each. The molecular and micellar structure models of these hardening regions have been presented. An unusual zone has been found in the phase diagram of the system for $n=7.5$; its state has also been discussed. Further, the mechanisms of the phase separation and phase inversion have been proposed, and three different types distinguished for the phase separation at the cloud point. A functional relationship has been found between the cloud point, the water content of an aqueous solution at the cloud point (the water affinity), and the n value. A linear relation has also been found between the solidification points of 100% surfactants and the ethylene oxide contents of the surfactants.

Owing to their stability against hydrolysis, heavy metal ions and pH change, and their rapid progress in chemical synthesis, the non-ionic surfactants are finding wide use in various industries. However, as for their chemical nature and fundamental properties, relatively few studies have been reported compared with the studies of the ionic surfactants.[1-4]

The present author has previously studied[5] ternary systems consisting of decaoxyethylene nonylphenyl ether, essential oils and water, and found some unusual phenomena, such as the existence of two cloud points in the same system, a discontinuity in the curve of the cloud point vs. the concentration, and a gel-like hardening.

The first phenomenon is very similar to the so-called "double cloud point" already reported,[6] which afterwards turned out to be due to the presence of impurities.[7] However, it is worth studying the phenomena in further detail since they have much to do with the practice of surfactant application. To facilitate the understanding of the phenomena shown by the ternary systems, it is pertinent first to get much information about the more simple binary systems, composed of the nonionic surfactants and water. As for such studies of binary systems, we have a few, but only a few reports, on, for instance, a possible phase diagram,[8,9] on the viscosity,[10-12] on the gel formation,[1,10,11,13] and especially on concentrated systems, for the variation of viscoelastic properties with the temperature,[14] the concentration,[15] and the frequency.[16]

Under such circumstances, the present author has taken up a binary system of aqueous nonionic surfactants of the polyoxyethylene nonylphenyl ether type, which are now widely used in practice, at temperatures ranging between -10°C and 100°C, constructed phase diagrams, and made colloid chemical studies by observing the change in the diagrams with the change in the degree of polymerization of ethylene oxide.

Materials

Polyoxyethylene nonylphenyl ether (abbreviation; NP-n, n being the degree of the polymerization of

1) N. Schönfeldt, "Oberflächenaktive Anlagerungs Produkte des Äthylenoxyds," Wissenschaftliche Verlagsges, Stuttgart (1959), pp. 100, 102.
2) T. Nakagawa, K. Shinoda, "Colloidal Surfactants," Academic Press, New York and London (1963), p. 97.
3) P. Becher, Fourth International Congress of Surface Activity, B/IV 20 (1964).
4) R. A. Hudson and B. A. Pethica, ibid., B/IV 21 (1964).
5) K. Kenjo, Unpublished.
6) C. D. Weston, *Hexagon Digest*, No. 13, 3 (1953).
7) T. Sagano, *J. Chem. Soc. Japan, Pure Chem. Sect.* (*Nippon Kagaku Zasshi*), **84**, 520 (1963).
8) R. R. Balmbra, J. S. Clunie, J. M. Corkill and J. F. Goodman, *Trans. Faraday Soc.*, **58**, 1661 (1962).
9) B. A. Mulley and A. D. Metcalf, *J. Colloid Sci.*, **19**, 501 (1964).
10) K. Boedeker, *Kolloid-Z.*, **94**, 161 (1941).
11) L. Marcou, *Teintex*, **17**, 421 (1952).
12) G. Böhme and R. Heusch, *Fette, Seifen, Anstrich Mittel*, **62**, 87 (1960).
13) H. L. Greenwald and G. L. Brown, *J. Phys. Chem.*, **58**, 825 (1954).
14) S. Kuroiwa, *J. Chem. Soc. Japan, Ind. Chem. Sect.* (*Kogyo Kagaku Zasshi*), **63**, 2065 (1960).
15) S. Kuroiwa, ibid., **63**, 1384 (1960).
16) S. Kuroiwa, ibid., **65**, 2032 (1962).

ethylene oxide) made by Nikko Chemicals and polyethylene glycol (abbreviation; PEG-n', n' being the mean molecular weight) made by Sanyo Kasei were used after drying to a constant weight at 105°C. Some of their properties are shown in Table I. The NP-8.5 P in Table I was a sample derived from NP-7.5 by extracting it repeatedly, first with *n*-hexane at room temperature and then with water at temperatures higher than the cloud point. Thus, from 20 g. of NP-7.5, there were obtained 14.5 g. of a non-ionic agent, 5.1 g. of a *n*-hexane-soluble matter, and 0.2 g. of a hot water-soluble matter. Here, NP-8.5P denotes that the substance is purified from NP-7.5; the degree of the polymerization of ethylene oxide was found from its hydroxyl value to be about 8.5.

TABLE I. PROPERTIES OF MATERIALS USED

Material	Hydroxyl value	Solidification point, °C
NP-5	125	
NP-7.5	103	−11.8
NP-8.5	93.0	−1.8
NP-10	87.1	7.3
NP-12.5	76.8	14.0
NP-15	70.0	19.0
NP-18	58.3	25.2
NP-20	53.4	31.6
NP-25	45.9	35.0
NP-30	34.0	37.0
NP-50	25.8	43.5
PEG-1000	110	35.0
PEG-2000	54.5	47.2
NP-8.5P	94.5	−9.0

Experimental

Turbidity and Viscoelasticity Measurement.—Aqueous solutions or heterogeneous mixtures of water and non-ionic surfactants were taken in test tubes; the contents were heated to 100°C, and then cooled gradually. The change in the turbidity and viscoelastic appearance up to the solidification of the system was observed visually for rising and falling temperatures. The cooling curve was further constructed, and from it the solidification point was obtained.

Thus, the temperatures showing abrupt changes in turbidity and viscoelastic properties were plotted against the concentration of surfactant; the phase diagrams consisting of different dispersion states were thus obtained

The Observation of the Phase Separation.—The appearance of phase separation was visually observed for NP-7.5-surfactant solutions of 6, 8, 15, 33, 42 and 57% concentrations at varying temperatures (±0.2°C), and the volume fraction of the lower phase separated was measured.

Notations of the States of the System.—The turbid states were divided into five patterns, of the following increasing order of turbidity, on the phase diagrams:

transparent, half-transparent,

slightly turbid, turbid,

strongly turbid

Here "half-tranaparent" corresponded to a TiO_2 (R-820 TiO_2, made by Ishihara Sangyo) aqueous dispersion below 0.0015%, "slightly turbid" to 0.0015—0.005%, "turbid" to 0.005—0.02%, and "strongly turbid" to above 0.02%-by-weight TiO_2.

The viscous states were divided into four gradations of "liquid" (S_1), "slightly viscous" (S_2), "viscous" (S_3) and "heavily viscous" (S_4) in the order of increasing viscosity. Here, S_1, S_2, S_3 and S_4 corresponded approximately to the viscosities below 0.5, 0.5—3, 3—12 and 12—50 poises respectively.

The hardened states were divided into four gradations of "weak paste" (P_1), "paste" (P_2), "strong paste" (P_3) and "rigid paste" (P_4) in the order of increasing consistency; they were qualitatively detected by the flow resistance of the paste. The "weak paste" was distinguished from the "heavily viscous" liquid in that the former did not deform perceptibly for at least ten seconds when the test tube used was kept horizontal. Here P_1, P_2, P_3 and P_4 corresponded approximately to 100—200, 200—600, 600—2000 and above 2000 poises respectively.

The Curves of the Diagrams.—CP-curve: cloud point curve; TP-curve; the curve of transparent points dividing the upper transparent and lower turbid regions; SP-curve: solidification point curve, and HP-curve: hardening point curve.

Results

Phase Diagrams.—The phase diagrams of NP-5 to NP-50 are shown in Figs. 1 to 11, and those of PEG·1000, PEG·2000 and NP-8.5P, in Figs. 12 to 14.

Symbols used in Figs. 1—14.

Regions

I: Region of two phase system
II: Region of homogeneous phase system
IV: Region of solid phase
R_{TP_1}, R_{TP_2}: Region of microheterogeneous system
R_{HP_1}, R_{HP_2}, R_{HP_3}: Region of hardening system
Ru: Unusual zone

Curves

SP: Solidification point curve
CP: Cloud point curve
TP_1, TP_2: Transparent point curve
HP_1, HP_2, HP_3: Hardening point curve
FP: Freezing point curve
T_I: Line of phase inversion

States of systems

Viscosity: Liquid (S_1), slightly viscous (S_2), viscous (S_3), and heavily viscous (S_4).

Consistency: Weak paste (P_1), paste (P_2), strong paste (P_3), and rigid paste (P_4)

Turbidity: Transparent

half-transparent

slightly turbid

turbid

strongly turbid

//////////: Part of region showing fluorescence near minimum of CP-curve.

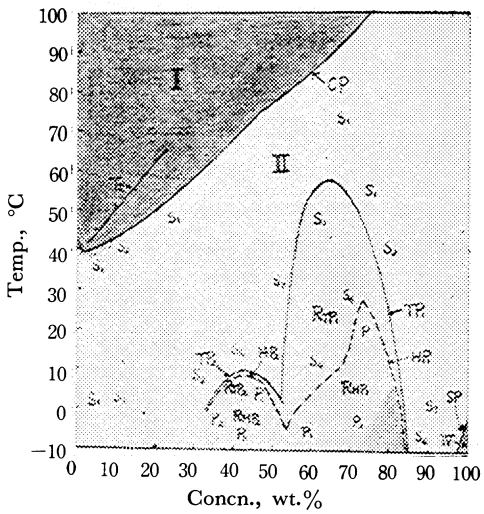

Fig. 3. Phase diagram of NP-8.5 - water system.

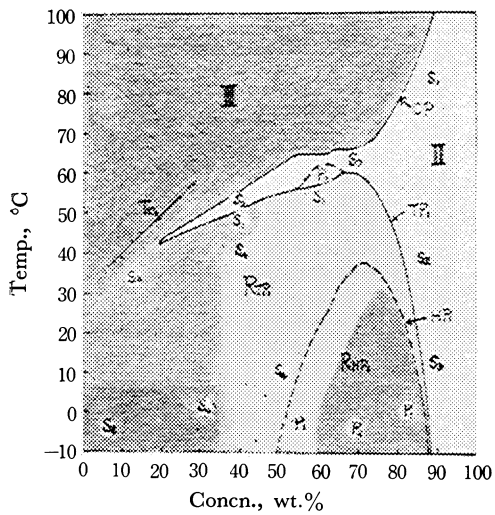

Fig. 1. Phase diagram of NP-5 - water system.

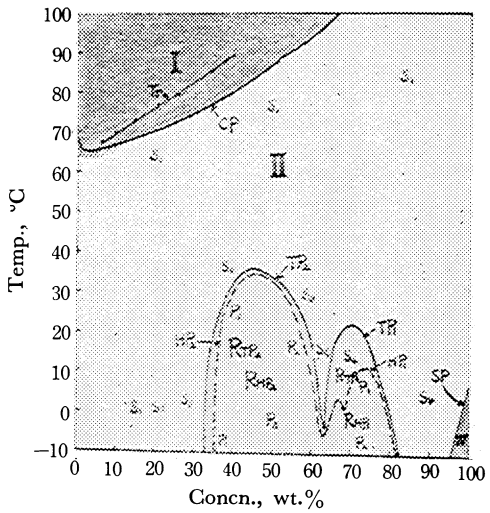

Fig. 4. Phase diagram of NP-10 - water system.

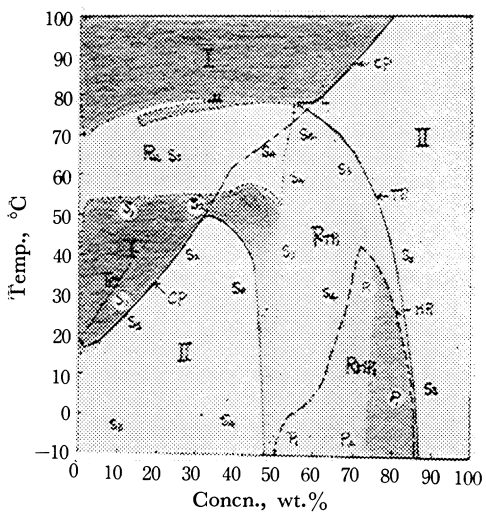

Fig. 2. Phase diagram of NP-7.5 - water system.

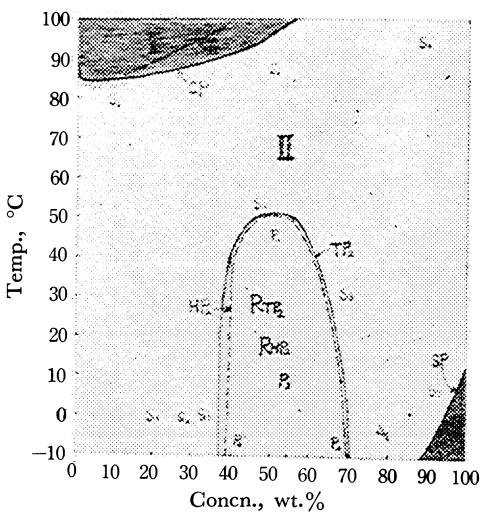

Fig. 5. Phase diagram of NP-12.5 - water system.

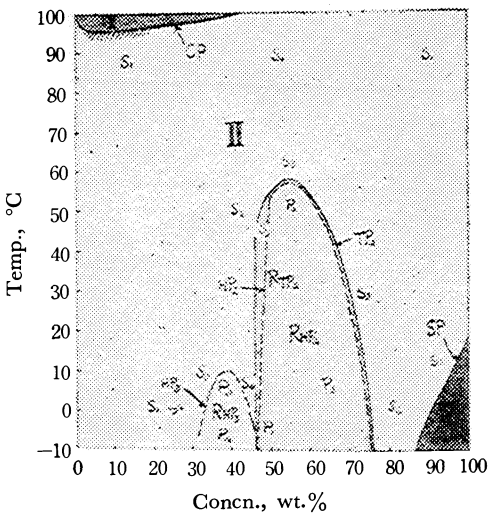

Fig. 6. Phase diagram of NP-15 - water system.

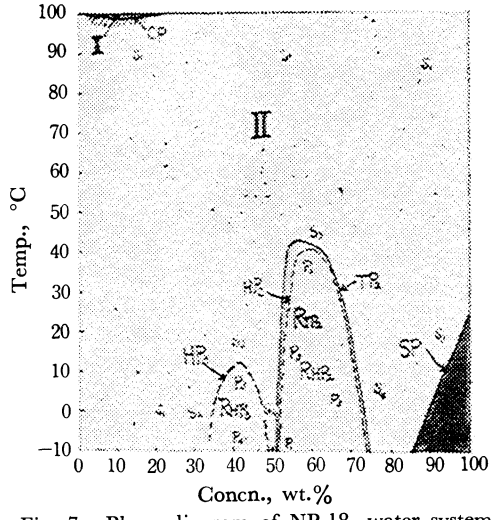

Fig. 7. Phase diagram of NP-18 - water system.

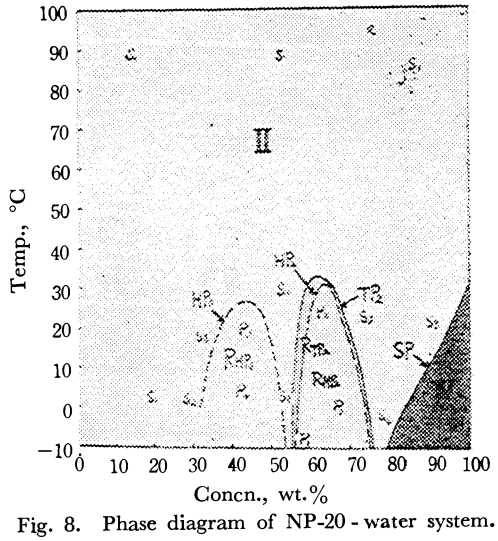

Fig. 8. Phase diagram of NP-20 - water system.

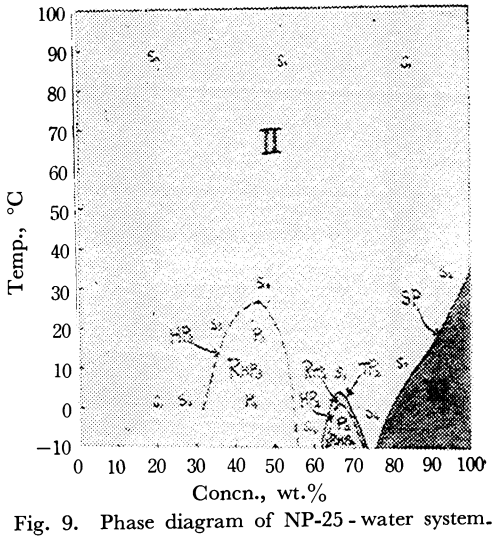

Fig. 9. Phase diagram of NP-25 - water system.

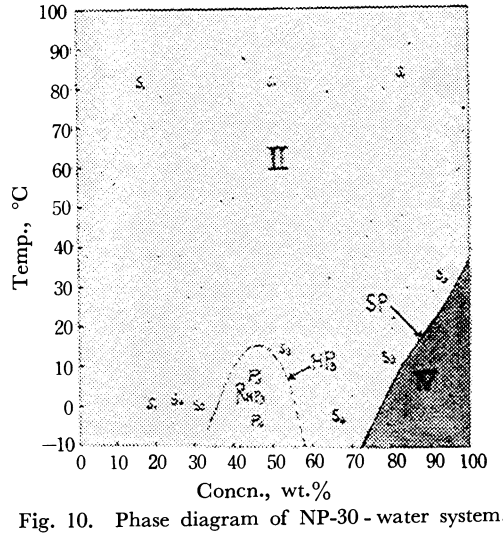

Fig. 10. Phase diagram of NP-30 - water system.

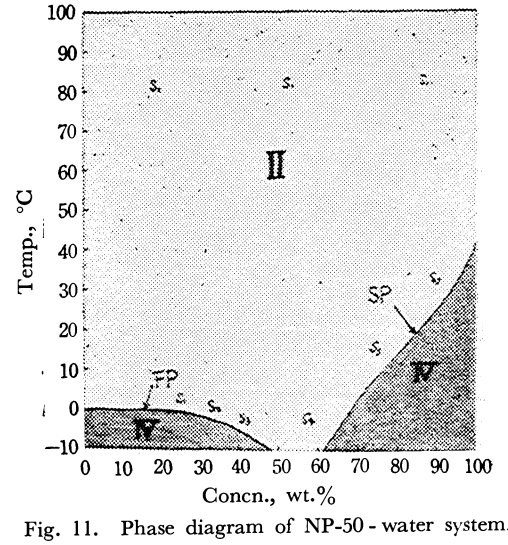

Fig. 11. Phase diagram of NP-50 - water system.

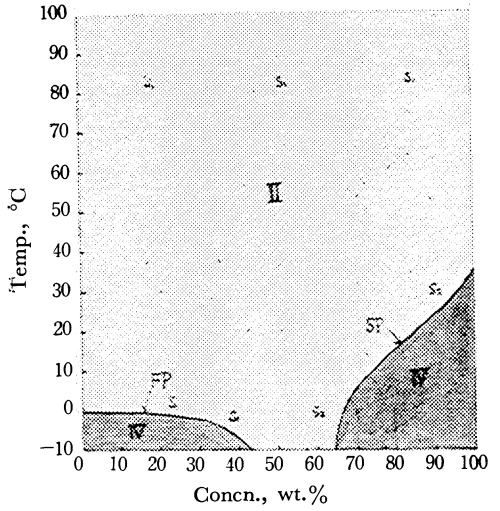

Fig. 12. Phase diagram of PEG-1000 - water system.

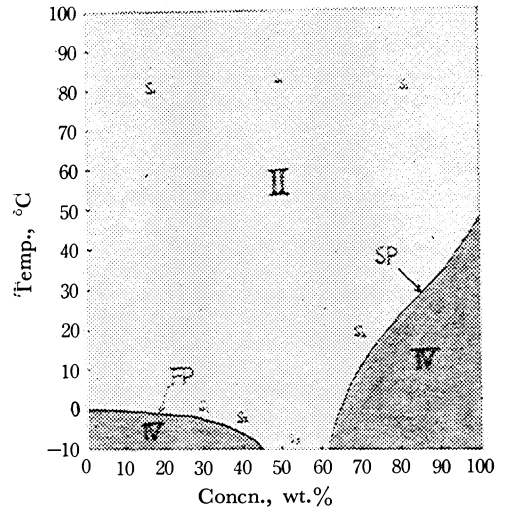

Fig. 13. Phase diagram of PEG-2000 - water system.

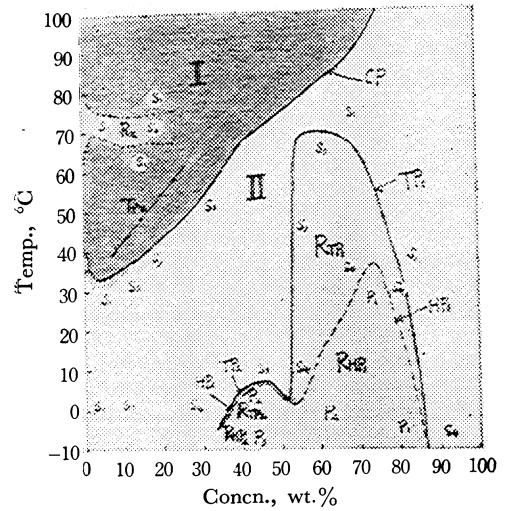

Fig. 14. Phase diagram of NP-8.5P - water system.

All the phase diagrams obtained were divided into four regions: I (a two-phase system existing above the CP-curve), II (a homogeneous phase system), III(a microheterogeneous or dispersed system below the TP-cruve) and IV (a solid phase system). For n values above 15, there was a region of clear paste, R_{TP_3}. The III region was further divided into two sub-regions, R_{TP}, and R_{TP_2}. containing R_{TP_1} and R_{TP_2} paste regions respectively, The phase diagram of PEG-2000 ($n \fallingdotseq 45$) system resembled that of the NP-50 system, but at lower temperatures the former system was much less biscous than the latter; at -20°C it remained in S_3 states, while the NP-50 system hardened at this temperature and in a concentration of about 52%.

A peculiarity was noted in the region I of the NP-7.5 system, which was divided into two parts by an "unusual zone" (Fig. 2). In this unusual zone the system did not separate into macroscopic phases, even after prolonged standing.

Phase Separation.—The results for the phase-separation experiments in the case of a 6% aqueous solution of NP-7.5, for instance, showed that, at the temperatures slightly above 76°C and 28°C, the lower phase considered as the dispersed phase sedimented in the upper phase of the dispersion medium, while slightly below these temperatures the lower phase changed into the dispersion medium and the upper phase creamed up and separated from the lower one.

Therefore, 28°C and 76°C are considered to be the temperatures of the phase inversions in this system. The volume fraction of the lower phase after the complete separation into two layers and the time required for it are plotted against the temperature in Fig. 15.

Usually, the lower phase after complete separation became turbid when the temperature was slightly raised, while it suffered no change when the temperature was lowered. However, somewhat different features were seen near 76°C; namely, the

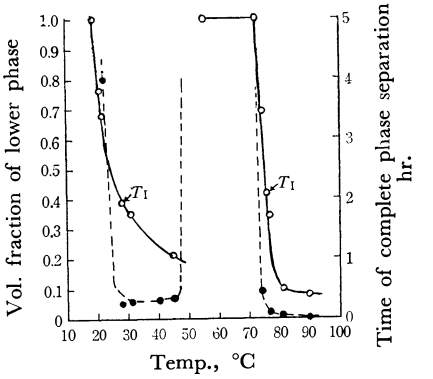

Fig. 15. Relative phase volume (solid line) and time of complete phase separation (broken line) vs. temperature for 6% aqueous solution of NP-7.5.
T_I indicates the temperature of phase inversion.

lower phase separated at 76°C, became transparent between 74.5°C and 76°C, and turbid below 74.5°C and above 76°C, while the upper phase suffered no change upon such a slight change of temperature. From these facts it follows that a narrow region, presumably belonging to the region II, may exist close to the upper limit of the unusual zone.

Calculating from the concentrations and the volume fractions of the lower phases, the concentration of NP-7.5 in the upper phase was found to be almost zero within the range of experimental errors for all cases; this can also be expected from the phase diagram (Fig. 2), and it is also in agreement with the result obtained by Nakagawa et al.[17] Figure 15 shows that there are two phase-inversion temperatures and that the volume fractions, of the lower phase at these two temperatures are nearly equal (0.42 and 0.39 respectively). This would mean that the volume ratio of the phase inversion is distinctly fixed for a given concentration of the surfactant. Results in the case of 8% and 15% solutions of NP-7.5 were similar to that of the 6% solution.

In the case of a 33% solution at 77.5°C, corresponding to the system in the narrow projected region I, the turbid liquid gradually turned into fluorescent heterogeneous state, but it did not separate into two phases, even after prolonged standing; this was presumably due to the small difference between the compositions of these two phases. In the case of a 42% solution at 79°C, the system rapidly separated into two phases, and the volume fraction of the lower phase was 0.35. From this result, the two phases separated are considered to have compositions corresponding to the U (33.3%) and L (60.5%) points in Fig. 2, the upper and the lower phases respectively. The upper phase, U, should then further separate very rapidly into two phases when the temperature is further raised slightly, since they are quite different in composition but are nearly equal in volume, while the lower phase, L, is expected to show only a slight turbidity. Such was actually proved to be the case. Thus it was confirmed that the point U in Fig. 2 is the extreme point of the narrow projection of the unusual zone, as is shown in Fig. 2. In the case of a 57% solution, the appearance of phases separated above the cloud point (78.5°C) was similar to that of the 6% solution, but below 77°C in the R_{TP_1} region the system did not separate into two phases, even after standing for 24 hr.

The temperatures of phase inversion obtained above were also plotted against the concentration in the phase diagrams, which can be expressed approximately by the following equation:

$$T_I = Ac + B \quad (1)$$

where T_I denotes the temperature of the phase inversion; and c, the concentration by weight % of the surfactants, and A and B are constants depending only on n. The values of A and B obtained are shown in Table II, while the straight lines obtained are indicated on the phase diagrams by the line T_I.

Table II. The values of A and B

Surfactant	A	B
NP-5	0.96	30.2
NP-7.5	1.48	18.4
NP-8.5	1.15	38.7
NP-10	0.69	62.3
NP-12.5	0.46	80.2
NP-8.5P	1.21	29.9

Discussion

Solidification Point.—The solidification points of 100% surfactants shown in Table I first rose markedly, and then gradually, with the increase in n. However, plotting the 100% solidification points, S, against the weight content, E, of ethylene oxide in a surfactant molecule (Fig. 16) gives:

$$S = 168E - 106 \quad (2)$$

where $E = 44n/(220+44n)$.

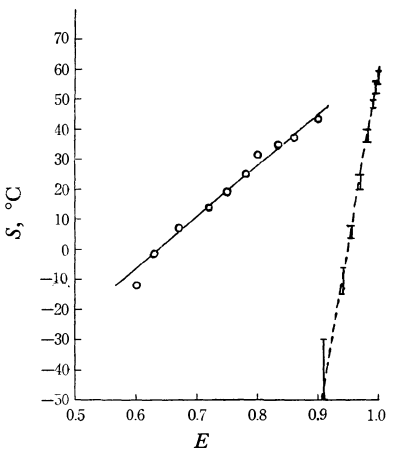

Fig. 16. Solidification point vs. weight content of ethylene oxide in NP-series (solid line) and PEG series (broken line).
S : Solidification point of 100% substances
E : Weight content of ethylene oxide in a molecule

The deviation of the solidification point of NP-7.5 from the straight line in Fig. 16 is considered to be due to its being a lower member.

A similar linear relation (Fig. 16) is obtained for polyethylene glycol homologues (F-4772 of the Union Carbide Chemical Co., U. S. A.) as follows:

$$S = 1200E - 1139.5 \quad (3)$$

17) T. Nakagawa, K. Tori, *Kolloid-Z.*, **168**, 132 (1960).

where S denotes the solidification point of 100% polyethylene glycol, and E, the weight content of ethylene oxide calculated from $44n/(18+44n)$.

Equations 2 and 3 indicate that the solidification is affected mainly by the polyoxyethylene chain and that the solidification point rises linearly with the ethylene oxide content of the molecule. The larger the weight of the part of the molecule to which ethylene oxides are attached, the smaller the slope of the straight line which may result, presumably because of their stronger resistance against the solidification.

It may be seen from the phase diagrams obtained that the smaller the n value of the surfactants, the greater the slope of the SP curves near 100% surfactants becomes, and that the slopes near 100% are smaller for PEG systems than for NP systems. This is because the weight fraction of the polyoxyethylene chain mainly responsible for solidification becomes smaller with the decrease in n for the NP series and is smaller for the surfactant than for polyethylene glycol possessing an approximately equal n value for an equal solute concentration.

Recently, Iino et al.[18] measured the solidification points of polyoxyethylene fatty acid esters, the fatty acid radical of C_6—C_8 chain length and the polyoxyethylene of n=2—30 mol. ethylene oxide. If the solidification points they obtained are plotted against the ethylene oxide content in the esters given above, linear relations are obtained for the esters of fatty acids of C_6 and C_8 possessing polyoxyethylene chains longer than the one corresponding to the minimum point, but not for those of fatty acids above C_{10}. This again confirms the above solidification effect of polyoxyethylene, while too long a fatty acid chain interferes with, and causes anomalies in, solidification.

Cloud Point.—In Fig. 17 the minima of CP-curves, CP_m, and the corresponding concentration, m, are plotted against n, the latter being linear, as is shown. The CP_m and m values NP-8.5P, which are shown by circles in the figure, correspond approximately to those of n=8 and n=11.5 respectively. Thus it is shown that the removal of lesser hydrophilic compounds such as the lower homologues results in a little increase in CP_m but a large increase in m when expressed in terms of n.

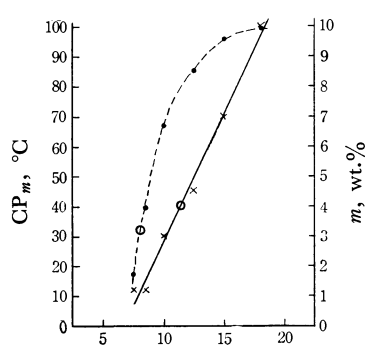

Degree of polymerization of ethylene oxide, n

Fig. 17. Change of temperature (●: CP_m) and concentration (×: m) of minimum in CP-curve with n.
Circles indicate the value for NP-8.5 P.

Such minima of CP curves in relatively dilute solutions were also found for the series of polyoxyethylene isooctylphenyl ethers.[19]

Phase Separation and Phase Inversion.—The heterogeneous system above the CP curve (Fig. 18) is composed of an upper layer of water or a dilute aqueous solution and a lower layer of a surfactant-rich solution. The line MN in the figure shows the line of the phase inversion.

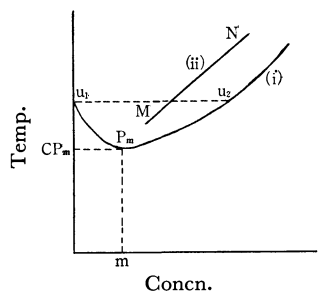

Fig. 18. CP-curve (i) and line of phase inversion (ii).

The heterogeneous region left to the line MN forms an emulsion of the surfactant-in-water type, while the heterogeneous region to the right of the line MN forms the opposite type of emulsion. The line MN passes through the minimum point P_m of the CP curve. Therefore, the heterogeneous system with a surfactant concentration larger than that of the point P_m shows the phase inversion phenomena when the system above the line MN is cooled, while the heterogeneous system with a concentration less than that of P_m shows no indication of a phase inversion under similar treatment. The clouding behavior of the heterogeneous system at the cloud point when heated also differs according as the concentration is below that of P_m, between P_m and U_2 in Fig. 18 (namely, the lowest possible concentration at which pure water separates at the cloud point), and above U_2. The results of the experiments showed that the first system separated minute droplets of a relatively-concentrated surfactant solution; the second, a dilute aqueous solution, and the third, pure water. The first case mentioned above is in agreement with the findings of Nakagawa et al.[20] that very large micelles

18) S. Iino, K. Tagawa and N. Oba, *J. Chem. Soc. Japan, Ind. Chem. Sect.* (*Kogyo Kagaku Zasshi*), **65**, 2047 (1962).

19) M. Aoki and Y. Iwayama, *J. Pharm. Soc. Japan*, **79**, 516 (1959).

20) T. Nakagawa, K. Kuriyama and H. Inoue, Symposium on Colloid Chem., (Chem. Soc. Japan) 12th symposium, p. 29 (1959).

suddenly appear at the cloud point.

Shinoda et al.[21] have regarded the cloud point as the temperature of the pseudo-phase inversion in veiew of the fact that the micelle formation is a phenomenon similar to a phase separation and because it is considered that, upon being heated, the systems of aqueous non-ionic detergent are altered from a detergent-in-water type to a water-in-detergent type at the cloud point. As has been mentioned above, not the region II below the CP curve but the region I above the CP curve is regarded in the present study as a dispersion or a heterogeneous system in the usual sense, one in which phase inversion occurs. Thus, the concept of the phase inversion is different in the present study from the concept of pseudo-phase inversion of Shinoda et al.

Water Affinity.—In the case of the concentration range above the minimum m of the CP curve, when a system has reached the CP curve by the repeated addition of water to the surfactant at a certain temperature, the system became turbid because of the deposit of a slight excess of water. Therefore, we call the weight ratio, x, of water to surfactant at the cloud point the "water affinity" of the surfactant at that temperature. By plotting the logarithm of the water affinity against the cloud point, as in Fig. 19, a linear relation is found between them in the surfactant-rich region of the CP curve measured; this is shown by the following general equation:

$$\log x = \log X + K(100-t) \tag{4}$$

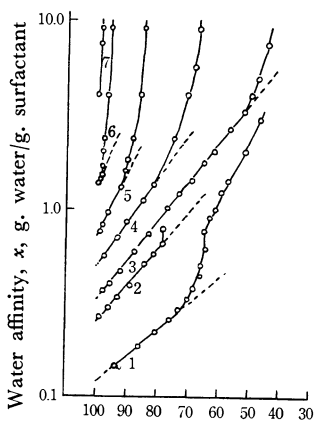

Fig. 19. Relation between the water affinity and cloud point.

1	NP-5	4	NP-10	7	NP-18
2	NP-7.5	5	NP-12.5		
3	NP-8.5	6	NP-15		

where t represents the cloud point; X, the water affinity of the surfactant at 100°C, and K, a constant.

21) K. Shinoda and H. Arai, *J. Phys. Chem.*, **68**, 3485 (1964).

In Eq. 4, the constants, X and K, are found to be expressed as a function of n, as is shown by the following equations:

$$\log X = \log 0.0320 + 0.117n \tag{5}$$

$$K = 0.00257n \quad (n<12.5) \tag{6}$$

From Eqs. 4, 5 and 6 we obtain for $n<12.5$, and $t\approx100$°C:

$$\log x = \log 0.0320 + 0.117n + 0.00257n(100-t) \tag{7}$$

The Transparent Point, the Hardening Point and Their Regions.—In the hardening region, the molar ratio of water to ethylene oxide units in a surfactant is considered to be more significant than the concentration. Thus, for instance, the relationship of such a molar ratio for three hardening regions and n at 20°C is as is shown in Fig. 20. This figure shows that every surfactant of the NP-n series possesses no, one or two hardening regions, according to the variation in n value.

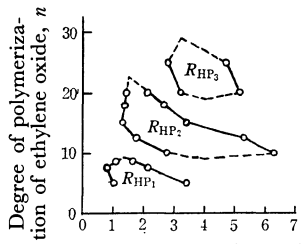

Fig. 20. Relation between n and molar ratio of water to ethylene oxide unit in surfactants in each hardening region at 20°C.
Broken lines indicate the ranges presumed from diagrams.

The relation between n and the nature of the hardening regions at various temperatures is shown in Table III.

The maxima of the viscosity of the aqueous solutions of non-ionic surfactants have been reported,[10] and the gel formation of such systems have also been found.[11-13,15] The systems showed a single concentration region in most cases, but the existence of two concentration regions of gel formation was reported in a few special cases.[1,12] Thus, for instance, Schönfeldt[1] measured the viscosity of the aqueous solutions of the NP-n series and found a single gel region for each surfactant in the range of n between 8.0 and 36.0, with two exceptions (the n values of 9.0 and 17.2 showed two gel regions each).

Comparing our hardening regions (in Table III) with those of Schönfeldt, the hardening regions of his $n=9.0$ value correspond to our R_{HP_1} and R_{HP_2} regions, while those of his $n=17.2$ value correspond to our R_{HP_2} and R_{HP_3} regions.

Several explanations have been given for the maximum of the viscosity versus the concentration

TABLE III. THE RANGES OF n FOR VARIOUS HARDENING REGIONS AND TEMPERATURE

Number of hardening regions	0	1			2	
Type of hardening regions		R_{HP_1}	R_{HP_2}	R_{HP_3}	R_{HP_1} and R_{HP_2}	R_{HP_2} and R_{HP_3}
5°C	>37.0	5.0—8.0	11.0—13.5	24.0—37.0	8.0—11.0	13.5—24.0
15°C	>31.5	5.0—9.0	9.0—18.5	23.0—31.5	9.0— 9.5	18.5—23.0
20°C	>29.0	5.0—9.0	9.3—19.0	22.5—29.0	9.0— 9.3	19.0—22.5
25°C	9.0— 9.3, >28.0	5.0—9.0	9.3—19.3	22.0—28.0	—	19.3—22.0
35°C	8.0—10.0, >19.5	5.0—8.0	10.0—19.0	—	—	—

curve and for the gel formation: (1) the interlocking of incompletely-hydrated surfactant molecules to form a network,[5] (2) a phenomenon resembling the phase inversion in the emulsion consisting of water as one phase, and hydrated surfactants assumed to be composed of one water molecule per ether linkage as another phase,[12] and (3) the immobilization of the water in the network by the entanglement of the hydrophilic groups of surfactants because of their spacious properties.[15] Kuroiwa[15] has further suggested that the decrease in viscoelasticity at the higher concentrations is produced by the formation of inverse micelles in the system.

However, these explanations can not well be applied to the system showing two or more maxima in viscoelastic properties, as was found in the present NP-8.5, 10, 15, 18, 20, and 25 systems.

The phenomena observed in the present experiments may, however, be appropriately explained as follows.

As the concentration of a surfactant is increased at a constant temperature, the micelles increase, while, at a certain concentration, depending upon the n and on the temperature, the system hardens because of the network composed of micelles and water acting as adhesives between micelles by means of hydrogen bonding with polyoxyethylene groups of the surfaces of micelles and by means of the immobilization of the aqueous solution with a monomolecular dispersion. The ability of water to act as an adhesive is considered to have an optimum range of compositon depending on the temperature, the n value, and the nature of the surfactant molecule. As is clear from such an explanation, this hardening region should be the one appearing in the region II; it is considered to correspond to R_{HP_3} or R_{HP_2}.

On a further increase in the concentration, micelles further increase in number, but the water molecules combining them become insufficient; accordingly, each individual micelle is rendered relatively free in motion. This state coincides with the part of the region II, between two hardening region in the phase diagrams.

A further increase in the concentration results in the approach of micelles more closly, and the inverse micelles appear with a saturated aqueous phase inside. The region of the concentartion where such an iversion of micelle type occurs and where both types of micelles coexist is considered to correspond to another hardening region, R_{HP_2} or R_{HP_1}. The systems of these hardening regions are more or less turbid because they are mixtures of two phases. The smaller the value of n becomes, the greater the difference between the two types of micelles may be expected to grow because of the more hydrophobic property of the surfactant. This results in the increasing turbidity and the decreasing viscosity of the system in R_{HP}. On the contrary, the system of the surfactant with a larger n value is considered to be somewhat similar in structure between the two phases. This hardening system would be something like the lamellar structure of micelles with sandwiched water;[22] therefore, it results in a much less turbid and more rigid state, as in R_{HP_2}.

Upon the further addition of the surfactant, the system eventually turns into a single-phase system composed of the inverse micelle type or the surfactant, with water dissolved in it, which is transparent and low in viscosity.

The above explanation of the two maxima of viscoelasticity in the nonionic surfactant-water system coincides approximately with those suggested by Kuroiwa[15] for the hardening region in the lower concentration and by Greenwald et al.[13] for the hardening region in the higher concentration. In the former mechanism of the hardening, of course, the polyoxyethylene group must be long enough to exhibit an effective adhesive field for hydration. The adequate chain length is considered to correspond to $n=22$ for R_{HP_3} and $n=15$ for R_{HP_2} in the NP-n series.

The appearance of the R_{TP_1} and R_{TP_2} regions is explained somewhat similarly to that of R_{HP_1} but all the regions, except for R_{HP}, were out of the range of the suitable ratio between water and surfactant for the hardening or the higher temparature range, showing no hardening due to the reduced hydration. The fact that R_{TP_1} had quite a wide range at temperatures higher than R_{HP_1} can be explained by the fact that the system of this region contains relatively little water and appears

22) S. S. Marsden and J. W. McBain, ibid., **52**, 110 (1948).

only in the case of surfactant with a low n value. Therefore, it should be cooled to a temperature sufficiently low in order for hydrogen bonding to harden the system.

Unusual Zone.—Sugano[7] found an unusual zone such as is shown in Fig. 2 above the cloud point in the aqueous solution of crude hexaoxyethylene lauryl ether. He ascribed the appearance of this phenomenon to such impurities as the higher alcohols or non-ionic surfactants of a low hydrophilic property. Since his unusual zone indicated an unusually high viscosity and a double refraction, he concluded that the zone was similar to the liquid crystalline state formed when amphiphilic compounds were added to the aqueous solution of ionic surfactants.[23] It has been further referred to the G-phase obtained by Winsor[24] and to the optical anisotropic state found in concentrated solutions of sodium laurate and hexanolamine oleate.[25]

If the unusual zone found in the present study is considered to be the liquid crystalline state, this zone can well be explained as that formed by the extension of the R_{TP_1} region in the direction of higher temperatures and lower concentrations, as may be seen from its contact with R_{TP_1}, which is considered to be optically anisotropic.[8] This also explains the discontinuity in the CP cruve.

If the unusual zone appears because of the existence of R_{TP_1}, it would not appear in any aqueous system of the surfactant with an n value above 12.5, but in fact it may appear even in such a system because of the possible transition of R_{TP_2} into R_{TP_1} by the addition of the lower homologues, as in the change of the NP-8.5P to the NP-7.5 system.

Although the NP-5 system (Fig. 1) seems not to show the unusual zone, it shows considerable anomalies below a 70% surfactant solution. The narrow transparent zone is somewhat similar to the narrow transparent part of the unusual zone of the NP-7.5 system (Fig. 2). The slopes of the CP curve below 70% of a surfactant and the slopes of the line of the phase inversion were smaller than those of NP-7.5. Further, the transparent hardening region found above the TP_1 curve is simialr to the part at the highest concentration of the unusual zone in the NP-7.5 system. In veiw of these points, the NP-5 system below 70% of the surfactant may be considered to show an unusual zone except for the region I.

The author wishes to express his deep gratitude to Professor Tsunetaka Sasaki of Tokyo Metropolitan University for his valuable advice and for his inspection of this report; to Mr. Tsunetaro Matsumoto, Manager of the Laboratory of Takahashi Toyodo Co., Ltd., for his encouragement throughout this investigation, and to the President of the Takahashi Toyodo Co., Ltd., for permission to publish this research. He is also grateful to Miss Sadako Usui for her aid in preparing this paper.

23) A. J. Hyde, D. M. Langbudge and A. S. C. Lawrence, *Discussions Faraday Soc.*, **18**, 239 (1954).
24) P. A. Winsor, *J. Phys. Chem.*, **56**, 391 (1952).
25) E. Gonick and J. W. McBain, *J. Am. Chem. Soc.*, **68**, 683 (1946).

BULLETIN OF THE CHEMICAL SOCIETY OF JAPAN VOL. 39 694—697 (1966)

The Stereoselectivity of Catalysts in Hydrogenation. I. The Catalytic Hydrogenation of 2-Cyclopentylidene-cyclopentanol and 2-Benzylidene-1-tetralol

By Sekio MITSUI, Yasuhisa SENDA and Hideyo SAITO

Department of Applied Science, Faculty of Engineering, Tohoku University, Sendai

(Received July 9, 1965)

2-Cyclopentylidenecyclopentanol (I) was hydrogenated over Raney Ni to produce a mixture of 95% of *trans*- and 5% of *cis*-2-cyclopentylcyclopentanol (III). However, over a Pd catalyst I gave a mixture of 2-cyclopentylcyclopentanone (IV), cyclopentylcyclopentane (V) and *trans*- and *cis*-III. In the hydrogenation of I over PtO_2, *trans*-III was a predominant product (93%) in ethanol, whereas in acetic acid a mixture of 2 parts of *trans*- and 1 part of *cis*-III was obtained, and in acetic acid with one drop of hydrochloric acid, the ratio of trans and cis was one to two. A large amount of V was also obtained in cases of both acetic acid. The hydrogenation of 2-benzylidene-1-tetralol (II) resulted in 2-benzyl-1-tetralols (VI), the yields of *trans*- and *cis*-VI being as follows: over Raney Ni, 78% and 19%; over Pd, 33% and 63%; and over PtO_2 in ethanol, 58% and 34%, respectively. From these results, it was found that, in the cases of Raney Ni and PtO_2 in ethanol, the directive effect of the hydroxyl group is very efficient, but that it is small over Pd, while in acetic acid, especially with hydrochloric acid, such an effect decreases over PtO_2.

Recent communications[1,2] reporting that the catalytic hydrogenation of 2-cyclopentylidenecyclopentanol and its methyl ether over Raney nickel gave *trans*-2-cyclopentylcyclopentanol and its methyl ether respectively, have prompted us to report our observations of stereoselectivity of the catalysts in the hydrogenation of some allyl-type alcohols.

We have investigated to see whether such a directive effect of the hydroxyl group may be found in the hydrogenation of allyl-type alcohols as has been observed in the hydrogenolysis of some optically-active benzyl-type alcohols.[3-6]

2-Cyclopentylidenecyclopentanol (I) and 2-benzylidene-1-tetralol (II) have been hydrogenated over Raney nickel, palladium-charcoal and platinum oxide at room temperature and atmospheric pressure (Tables I and II). The Raney nickel hydrogenation of I had already been done by Howard,[1] who obtained mainly a single entity, *trans*-2-cyclopentylcyclopentanol (III). Similar results were obtained in the present work. III was formed in a ratio of 95% trans and 5% cis. The palladium-charcoal hydrogenation of I gave a mixture containing cis and trans isomers of III, along with 2-cyclopentylcyclopentanone (IV) and cyclopentylcyclopentane (V). The products were analyzed by vapor phase chromatography (Hitachi model F-6, P. E. G. 45 m. Golay column).

2-Benzylidene-1-tetralol (II) (m. p. 72°C) was hydrogenated to give 78% *trans*-2-benzyl-1-tetralol (VI) (m. p. 119°C) over Raney nickel, but a 63% cis isomer (m. p. 72°C) over palladium-charcoal. The products were separated by fractional recrystallization from petroleum benzine and confirmed by elementary analysis. An authentic sample of the trans isomer of VI was synthesized by the hydroboration[7] of 3-benzyl-1, 2-dihydronaphthalene, which had been prepared by the dehydration of VI with *p*-toluenesulfonic acid in benzene, followed by oxidation with alkaline hydrogen peroxide.

It may be considered from the results that, if it is accepted that hydrogen adds cis from the catalyst surface, the unsaturated alcohols are preferentially adsorbed with the hydroxyl group directed toward the surface of the Raney nickel catalyst by the interaction of the lone pair of oxygen as well as of the π-electrons of the double bond, with the catalyst, and that the addition of hydrogen to the compounds in these adsorbed states will give the trans alcohols[1] (Fig. 1). On the other hand, in the case of the palladium catalyst, the adsorbed states where the hydroxyl group is directed away from the catalyst surface are assumed to increase in the course of the reaction (Fig. 1).

The formation of IV and V on the palladium catalyst may also be explained from the adsorbed state shown in Fig. 1 (see Figs. 2 and 3). 2-Cyclopentyl-1-cyclopentene-1-ol, the enol form of IV, may be obtained by the same kind of isomerization as was observed in the isomerization reported by Henbest et al.[8] (Fig. 2). Since it was reported that the hydrogenolysis of the optically-active benzyl-type alcohols over the palladium catalyst proceeds with an inversion of the configuration,[3-6] the allylic alcohol such as I may also be hydrogenolyzed with inversion to give cyclopentylidenecyclopentane, which is then hydrogenated to V (Fig. 3). It may be argued from these considerations that the favored adsorbed state on the palladium catalyst is the one in which the hydroxyl group is directed away from the catalyst surface, especially on palladium-charcoal-A.[9]

On the hydrogenation of II over palladium-charcoal, the cis isomer of VI was obtained preferably.

Since it has been reported that the hydrogenolysis of the C–O bonds of benzyl-type alcohols and alkyl ethers takes different courses of reaction according to the kind of catalyst used,[3-6] it may be suggested that the difference in the affinity of nickel and palladium for the oxygen atom controls not only the stereochemistry of the hydrogenolysis of benzyl-type alcohols, but also that of the hydrogenation of the double bond of allyl-type alcohols. Therefore, the composition of the products is affected by the difference in this affinity with the kind of catalyst. The platinum oxide hydrogenation of I in ethanol gave the trans isomer as the predominant product (trans : cis=23 : 1). It may be presumed that this is because of the directive effect of the hydroxyl group, as was observed in the Raney nickel hydrogenation. In acetic acid, I was hydrogenated to give a mixture containing 22% *trans*- and 10% *cis*-III (trans : cis=2 : 1), 3% IV and 50% V. The hydrogenation in acetic acid containing one micro drop of concentrated hydrochloric acid gave more than 90% hydrocarbon (V), 3% *trans*- and 6% *cis*-III (trans : cis=1 : 2). These results show that the presence of acid increases the percentage of the cis product.

On the hydrogenolysis of optically-active 2-phenyl-2-butanol in ethanol over platinum oxide, which usually contains a trace of alkaline substances,

* A part of this study was presented at the 18th Annual Meeting of the Chemical Society of Japan, Suita, Osaka, April, 1965.

1) T. J. Howard, *Chem. & Ind.*, **1963**, 1899.
2) T. J. Howard, *Rec. Trav. Chim.*, **83**, 992 (1964).
3) S. Mitsui, Y. Senda and K. Konno, *Chem. & Ind.*, **1963**, 1354.
4) S. Mitsui, K. Iijima and T. Masuko, *J. Chem. Soc. Japan, Pure Chem. Sect.* (*Nippon Kagaku Zasshi*), **84**, 833 (1963).
5) S. Mitsui and K. Iijima, ibid., **85**, 682, 687 (1964).
6) S. Mitsui and Y. Kudo, *Chem. & Ind.*, **1965**, 381.
7) H. C. Brown, "Hydroboration," W. A. Benjamin, Inc., New York, N. Y. (1962).
8) J. B. Bream, D. C. Eaton and H. B. Henbest, *J. Chem. Soc.*, **1957**, 1974.
9) S. Mitsui and H. Saito, *J. Chem. Soc. Japan, Pure Chem. Sect.* (*Nippon Kagaku Zasshi*), **82**, 890 (1961).
10) M. C. Dart and H. B. Henbest, *J. Chem. Soc.*, **1960**, 3563.
11) S. Nishimura and K. Mori, This Bulletin, **36**, 318 (1963).

a slight excess of a configurationally inverted product (55%) was obtained, but upon the addition of two micro drops of concentrated hydrochloric acid to the solvent, the reaction proceeded predominantly with an inversion of the configuration (80%).[5] Consequently, it may be assumed that, in an acidic solvent, the hydrogenolysis of a benzyl- or allyl-type alcohol such as I takes place mainly, with an inversion of the original configuration over platinum oxide. These results are in line with the present observations that, on platinum oxide which contains a trace of basic substances, the directive effect of the hydroxyl group is observed in ethanol to be as on Raney nickel,[10] while in acetic acid this effect decreases,[11] that the attack of hydrogen on the double bond or the carbon atom to which the hydroxyl group is attached, occurs from the less hindered side, and that it seems that this trend is promoted by the presence of hydrochloric acid.

As III was not acetylated by letting it stand with acetic acid, the III-acetate obtained (in Experimental Runs 5 and 6 in Table I) seems to be the hydrogenated product of I-acetate formed by the acetylation of I during the course of the reaction.

TABLE I. CATALYTIC HYDROGENATION OF 2-CYCLOPENTYLIDENECYCLOPENTANOL[a]

	Catalyst	Products, %			
		Compound III		IV	V
		Trans	Cis		
1	Raney nickel	95	5	—	—
2	5% Palladium Charcoal-A[b] (contains a trace of acid)	14	10	11	65
				86	
3	5% Palladium charcoal-B[b] (contains a trace of base)	71	23	5	1
				29	
4	Platinum oxide	92	4	3	1
5	Platinum oxide[c]	22	10	3	50
6	Platinum oxide[d,e]	3	6	—	90

a) Runs 1—4: in ethanol, Runs 5 and 6: in acetic acid. b) Reference 9. c) In addition to these products, 9% *cis*-III-acetate and 6% *trans*-III-acetate were also obtained. d) With one micro drop of concentrated hydrochloric acid. e) In addition to these products, III-acetate was also obtained.

TABLE II. CATALYTIC HYDROGENATION OF 2-BENZYLIDENE-1-TETRALOL IN ETHANOL

	Catalyst	Products (%)		
		Compound VI		Unidentified component
		Trans	Cis	
7	Raney nickel	78	19	3
8	5% Palladium charcoal-B (contains a trace of base)	33	63	4
9	Platinum oxide	58	34	8

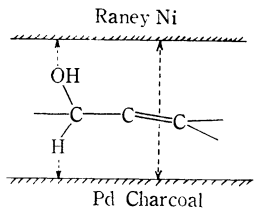

Fig. 1

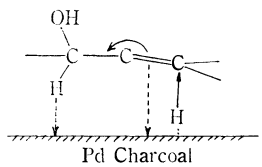

Fig. 2

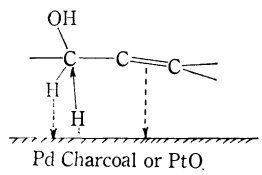

Fig. 3

Experimental

2 - Cyclopentylidenecyclopentanone. — 2 - Cyclopentylidenecyclopentanone was prepared by the method of Hückel et al.,[12] by the self-condensation of cyclopentanone. From 84 g. of cyclopentanone and 4 g. of sodium hydroxide in 250 ml. of 30% aqueous ethanol, there was obtained 30.4 g. (40%) of the product, b. p. 96—101°C/5.0 mmHg.

2-Cyclopentylidenecyclopentanol (I).—I was prepared by the method of Le Guillanton[13] by the reduction of 2-cyclopentylidenecyclopentanone with lithium aluminum hydride in ether at 0——10°C. The distilled substance (b. p. 91—101°C/1.0 mmHg) was partly solidified, and the oily part, which was expected to be the saturated alcohol, was removed by absorption on a porous plate. The solid was recrystallized from petroleum ether to give pure I, m. p. 57—59°C; yield 12 g. (39%).

The Catalytic Hydrogenation of I.—I (1.5 g.), a catalyst and 50 ml. of solvent were stirred with hydrogen at an ordinary temperature and at atmospheric pressure. After the hydrogenation was over, the catalyst was filtered and the products were analyzed by V. P. C. The experimental data are summarized in Table III.

2-Benzylidene-1-tetralone.—Benzaldehyde (17 g.) was added drop by drop to a mixture of 20 g. of 1-tetralone in 300 ml. of 60% aqueous ethanol and 9.5 g. of sodium hydroxide. The reaction mixture was stirred at room temperature for 4 hr., and then 250 ml. of water was added. The yellow solid which separated was filtered, washed with water, and recrystallized from ethanol, m. p. 107°C; yield 27.5 g. (85%).

Found: C, 87.04; H, 5.78. Calcd. for $C_{17}H_{14}O$: C, 87.15; H, 6.02%.

12) W. Hückel, M. Marier and E. Jordan, *Ann.*, **616**, 46 (1958).
13) G. Le Guillanton, *Bull. Soc. Chim. France*, **1963**, 611.
14) R. Adams, "Organic Reactions," Vol. 13, 1 (1963).

Table III. Experimental data of catalytic hydrogenation

1) 2-Cyclopentylidenecyclopentanol (1.5 g.)

Catalyst	Weight of catalyst, g.	Hydrogen Uptake ml. (mol.)	Solvent
Raney nickel	0.4	220 (1.0)	Ethanol
5% Palladium charcoal-A	0.1	380 (1.7)	Ethanol
5% Palladium charcoal-B	0.1	225 (1.0)	Ethanol
Platinum oxide	0.1	273 (1.2)	Ethanol
Platinum oxide	0.1	295 (1.3)	Acetic acid
Platinum oxide	0.1	477 (2.1)	Acetic acid with one micro drop of HCl

2) Benzylidene-1-tetralol (1.4 g.)

Catalyst	Weight of catalyst, g.	Hydrogen Uptake ml. (mol.)	Solvent
Raney nickel	0.5	146 (1.1)	Ethanol
5% Palladium charcoal-B	0.2	139 (1.0)	Ethanol
Platinum oxide	0.04	160 (1.2)	Ethanol

2-Benzylidene-1-tetralol (II).—Sodium borohydride (0.4 g.) was added gradually to a solution of 4.5 g. of 2-benzylidene-1-tetralone in 150 ml. of methanol at room temperature. The reaction mixture was then stirred at room temperature for 4 hr.; about 100 ml. of methanol was removed by distillation, and then an equal volume of water was added. The white solid which separated was filtered, washed with water, and recrystallized from petroleum benzine, m. p. 71—72°C; yield 3.9 g. (85%).

Found: C, 86.59; H, 6.99. Calcd. for $C_{17}H_{16}O$: C, 86.40; H, 6.83%.

3-Benzyl-1, 2 - dihydronaphthalene. — 2-Benzyl -1-tetralol (1.5 g.) was heated with 0.5 g. of *p*-toluenesulfonic acid in 200 ml. of benzene for 15 hr. Water was successively removed by azeotropic distillation; the benzene layer was washed with a sodium bicarbonate solution and water, and the benzene was distiled off under reduced pressure. 1.2 g. of 3-benzyl-1, 2-dihydronaphthalene was thus obtained. This compound was checked by a study of its infrared spectrum and V. P. C.

The Hydroboration[14] of 3-Benzyl-1, 2-dihydronaphthalene.[12]—To a solution of 0.4 g. of sodium borohydride in 10 ml. of diglyme containing 1.1 g. of 3-benzyl-1, 2-dihydronaphthalene, there was added 0.76 ml. of boron trifluoride etherate at room temperature. The mixture was stirred for 3 hr. before the excess hydride was decomposed with water. The organoborane was oxidized at room temperature by the addition of 4 ml. of a 3 N solution of sodium hydroxide, followed by the drop-by-drop addition of 4 ml. of 30% hydrogen peroxide. The reaction mixture was extracted with ether, and the extract was washed five times with equal volumes of a saturated salt solution in order to remove the diglyme. The extract was then dried over anhydrous sodium sulfate. The residue left after the solvent had been removed, was recrystallized from petroleum benzine. The yield of *trans*-2-benzyl-1-tetralol was 0.95 g. (80%), m. p. 119°C.

Found: C, 85.95; H, 7.82. Calcd. for $C_{17}H_{18}O$: C, 85.67; H, 7.61%.

The Catalytic Hydrogenation of II.—The following general procedure was used. 1.4 g. of II, a catalyst, and 50 ml. of ethanol were stirred with hydrogen at an ordinary temperature and at atmospheric pressure. The hydrogen uptake ceased after one mole of hydrogen had been absorbed; the catalyst was then filtered and, the ethanol distilled off.

Over Raney Nickel.—The residue was recrystallized from petroleum benzine to give the trans isomer of VI, m. p. 119°C. The yield was 1.09 g., 78%.

Found: C, 85.23; H, 7.71. Calcd. for $C_{17}H_{18}O$: C, 85.67; H, 7.61%.

When the mother liquor was concentrated, the cis-isomer of VI was obtained, 0.27 g.; 19%. The melting point was 72°C.

Found: C, 85.37; H, 7.78. Calcd. for $C_{17}H_{18}O$: C, 85.67; H, 7.61%.

Over Palladium Charcoal-B.—The residue was recrystallized from petroleum benzine to give *trans*-VI, m. p. 119°C. The yield was 0.47 g., 33%. When the mother liquor was concentrated, *cis*-VI was obtained, m. p. 72°C. The yield was 0.88 g., 63%.

Over Platinum Oxide.—The residue was recrystallized from petroleum benzine to give *trans*-VI, m. p. 119°C. The yield was 0.81 g., 58%. When the mother liquor was concentrated, *cis*-VI was obtained, m. p. 72°C. The yield was 0.48 g., 34%. The products of the hydrogenation over palladium charcoal-B and platinum oxide were, by means of a mixed fusion and a comparison of the infrared spectra, identified with the samples obtained by the hydrogenation of II over Raney nickel.

The experimental details are summarized in Table III.

BULLETIN OF THE CHEMICAL SOCIETY OF JAPAN VOL. 39 698—702 (1966)

Catalytic Asymmetric Benzaldehyde Cyanohydrin Synthesis with Synthetic Optically Active Polymer. III. *N*-Substituted Poly-(s)-isobutylethylenimine

By Sei Tsuboyama

Laboratory of Polymer Chemistry, The Institute of Physical and Chemical Research, Komagome, Bunkyo-ku, Tokyo

(Received July 10, 1965)

Asymmetric syntheses of benzaldehyde cyanohydrin in the presence of polymers of *N*-methyl-, *N*-ethyl- and *N*-benzyl-(s)-2-isobutylethylenimine as catalysts have been studied. The selectivity of these polymers was poor (optical yield of (−)-isomer obtained; 0—1%) compared with that of a non-*N*-substituted polymer (20%). It seems that the large difference in the optical yield can be ascribed to their conformation. As to the polymer being capable of promoting the reaction asymmetrically, it is assumed that the isobutyl group and a helical form are the responsible factors. On the basis of these findings, a model for the addition step has been suggested in order to explain the observed result.

In asymmetric syntheses of benzaldehyde cyanohydrin using poly-(s)-isobutylethylenimine (I) and its cross-linked polymer (II) as catalysts, the signs of the optical rotation of cyanohydrin produced were unexpectedly opposite to each other,

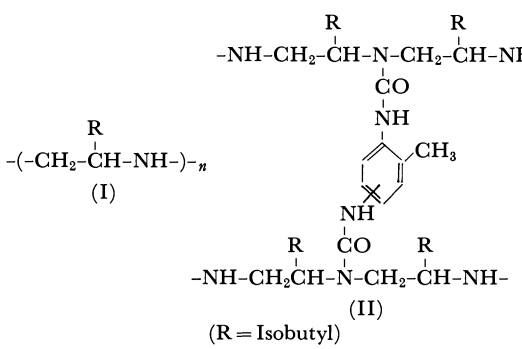

(I)

(II)

(R = Isobutyl)

though the two polymers are of the same configuration.[1,2] The cause of this was found to be due, not to the cross-linking of the polymer, but to the contribution of –NH–CO–N= group, for when linear and soluble polymers containing –NH–CO–N= group were used the (+)-isomer was obtained as well as when the insoluble polymer II was used. This suggests that the configuration of the product is not necessarily controlled by the configuration but rather by the conformation of the catalyst.

This paper will describe the results of a similar asymmetric synthesis using *N*-substituted poly-(s)-isobutylethylenimine as the catalyst, it will attempt to elucidate in detail how the reactions proceed stereochemically.

The selectivity of the polymer I in the asymmetric reaction may be attributed to the steric effect of the regularly-arranged isobutyl group adjacent to the catalytic center and to the conformation effect of the polymer. For conformation of this, we have so far no data with which to draw any conclusion, yet if we assume a helical form for it, the reaction can be explained. In the *N*-substituted polymer, we can imagine that the pitch of the presumed helix becomes elongated by the steric hindrance of *N*-substituent and by the disappearance, in consequence of tertiarization, of hydrogen atom that might otherwise form hydrogen bonding between nitrogen atoms. Therefore, the said steric effect of the isobutyl group will be reduced by the unfavorable conformation, and a low selectivity may be expected.

Synthesis of Polymer.—Polymers of *N*-methyl- (XIII), *N*-ethyl- (XIV) and *N*-benzyl-(s)-isobutylethylenimine (XV) were prepared by the following process:

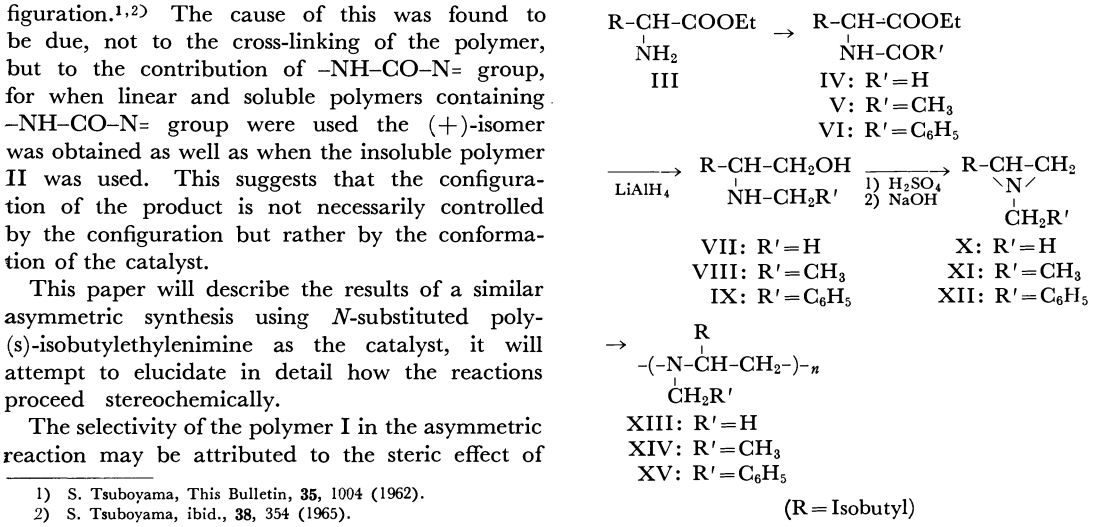

(R = Isobutyl)

1) S. Tsuboyama, This Bulletin, **35**, 1004 (1962).
2) S. Tsuboyama, ibid., **38**, 354 (1965).

Table I. Asymmetric synthesis of benzaldehyde cyanohydrin with *N*-substituted poly-(*s*)-isobutylethylenimine

Catalyst		Cyanohydrin			
Polymer	$[\alpha]_D$ of polymer*1 degree	Yield %	α_D, degree	$[\alpha]_D$*2, degree	P%
Original (I)	+59.70*3	50.0	−1.81	−7.07	16.1
Original (I)	+66.70	51.5	−2.28	−8.57	19.6
N-Methyl (XIII-1)	−46.03	82.0	−0.08	0	0
N-Methyl (XIII-2)	−10.60	61.1	−0.33	−1.01	2.3
N-Methyl (XIII)	−52.88*3	72.9	−0.04	0	0
N-Methyl (XIII)	−70.00	87.8	−0.09	0	0
N-Ethyl (XIV)	−144.8*3	64.2	0.00	0	0
N-Ethyl (XIV)	−207.4	91.2	0.00	0	0
N-Benzyl (XV)	−219.0	64.8	−0.20	−0.59	1.3

*1 *c* 0.5—2 in benzene. *2 *c* 1—5 in benzene.
*3 Lower molecular weight fraction. Molecular weight of polymer I: 1020, 5000.

Optically active *N*-substituted imine monomers, which were prepared from acylated amino acid esters through the corresponding amino alcohols, were polymerized by boron trifluoride-etherate under nitrogen. They became tacky low-molecular-weight polymers when heated at 100—120°C for a day or two; heating at higher temperatures causes thermal degradation.[3] Several fractionations in acetone gave *N*-ethyl and *N*-benzyl polymers of a fairly high degree of crystallinity but with the low molecular weights of 1300—1600. For reference, the polymer I was treated with formaldehyde and formic acid (XIII-1) or methyl iodide (XIII-2) in order to introduce the *N*-methyl group into it. According to the analytical data and the infrared spectra, XIII-1 seemed to be partly acylated, and the amino groups of XIII-2 were partially quarternarized. In both cases, various treatments failed to remove the groups involved. The infrared spectra and optical rotatory dispersion curves of these polymers are shown in Figs. 1 and 2.

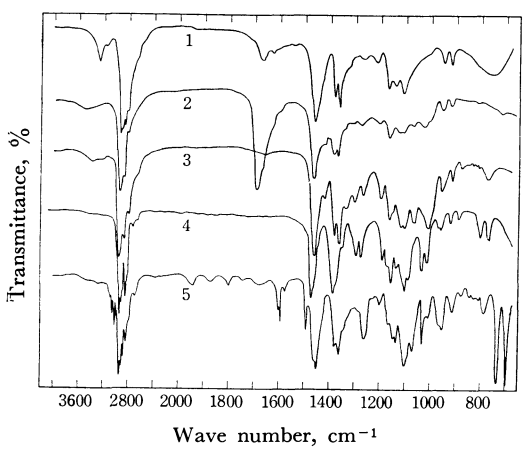

Fig. 1. Infrared absorption spectra.
1. polymer I; 2. polymer XIII-1 (*N*-methyl); 3. polymer XIII (*N*-methyl); 4. polymer XIV (*N*-ethyl); 5. polymer XV (*N*-benzyl).

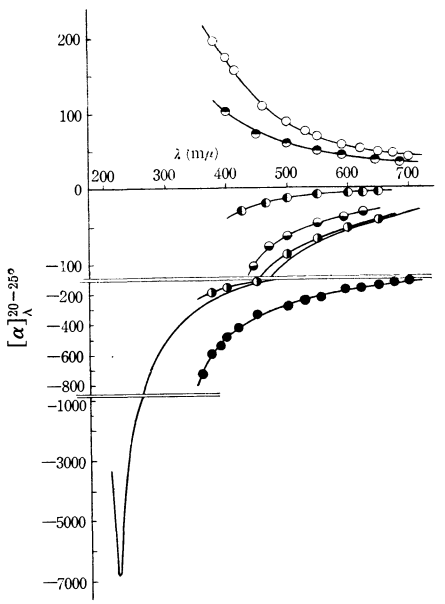

Fig. 2. Optical rotatory dispersion curves.
○, polymer I in benzene; ◓, polymer I in dioxane; ◐, polymer XIII-2 (*N*-methyl) in benzene; ◒, polymer XIII-1 (*N*-methyl) in dioxane; ◑, polymer XIII (*N*-methyl) in dioxane; ●, polymer XIV (*N*-ethyl) in benzene; —, polymer XV (*N*-benzyl) in isooctane

Asymmetric Synthesis.—The asymmetric synthesis and analysis of the product were carried out in the manner described in a previous paper.[1] The results are summarized in Table I.

The selectivity of these polymers for the asymmetric reaction was quite low or non-existent and was independent of their molecular weight. As regards the *N*-methyl polymer XIII-2, NH group capable of promoting the asymmetric reaction

3) W. G. Barb, *J. Chem. Soc.*, **1955**, 2577.

seemed still to remain in it. The rates of cyanohydrin formation with the polymers XIII and XIV indicated that the reactions did not proceed asymmetrically from the beginning (Fig. 3). These findings justify the expectation mentioned above; nevertheless, some other causes might produce a similar result. For instance, if the racemization rate of cyanohydrin is faster than the rate of formation during the reaction, the selectivity of the reaction will become hardly observable. In confirmation of this, the racemization of optically active cyanohydrin in the presence of the polymer XIV was examined; we thus found that the optical rotation of cyanohydrin is not affected by the presence of the polymer.

There still remains the problem of the stereoregularity of these polymers. Though there is no suitable method for the direct determination of the regularity, it seems likely that, in acid-catalyzed polymerization, a preferential break

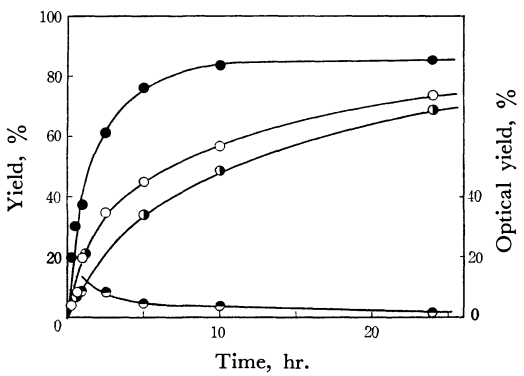

Fig. 3. Time dependence of cyanohydrin formation and its optical yield: ○, polymer XIII (*N*-methyl); ●, polymer XIV (*N*-ethyl); ◑, polymer XV (*N*-benzyl); ◓, optical yield with polymer XV.

in the cyclic imine ring at CH_2–N bond occurs independently of the asymmetric carbon, giving rise to polymers with an unaffected asymmetry.[4-6] Consequently, the configuration of the asymmetric atoms in the polymer must be identical to those of the monomer. This matter will be discussed in another paper on the ring-opening orientation of (R) (+)-ethylethylenimine. Furthermore, the optical rotatory dispersion data may account for the configurational regularity, though the following is not necessarily a proper comparison because it contains an involved group, as has been described above. As is shown in Fig. 2, the curve of the polymer I is positive, whereas when the polymer is *N*-methylated, the curve becomes negative, similar to that found in the case of the polymer XIII prepared from monomers already containing *N*-methyl groups. Therefore, the regularity of these polymers may be considered to be similar despite the large difference in selectivity. This again seems to suggest that the variances in the contributions of these polymers to asymmetric synthesis as catalysts are ascribable, not to their configurational regularity, but to their overall molecular arrangement—conformation. As regards the *N*-benzyl polymer, it may be different from *N*-alkylated polymers with a slight selectivity as a result of a favorable conformation resulting from interaction between aromatic rings in the side chain of the polymer.

Previously it was postulated that the amine catalyst in this asymmetric synthesis should have not only one steric group in a monomeric unit, but also one more obstructive factor with regard to the mobile catalytic center. However effective the steric group may be, because of the ability of trivalent nitrogen to undergo rapid inversion,[7] and since the catalytic center in a monomeric unit may also be converted into their conformers and since asymmetric reactions occur on two sides of the conformer, the products that arise there are enantiomers of equal amounts; hence, there will be no optical rotation. Therefore, only when the accessibilities of the reagent to the catalytic center are different on the two sides of the amine does an asymmetric reaction become possible. In the polymer I, the isobutyl group and the helical conformation are likely to be responsible for the asymmetric reaction. In the *N*-substituted polymer, however, the contribution of the conformation to the reaction is smaller than in the polymer I; this will cause the reagent to approach the active site equivalently, and therefore the optical yield will be lowered.

In the early stage of the reaction, the carbonyl reagent and the amine catalyst form a stereospecific transition complex, to which cyanide ion is then added.[8] Accordingly, the conformation of the transition intermediate should be the most important factor in controlling the steric course of the reaction. In the model of the polymer I shown in Fig. 4, it is assumed that the conformation is helical, even in such a solvent. The isobutyl group will be found on the outside of the helix, with its axis perpendicular to the plane of the paper. In the transition state, the carbonyl reagent will approach the least-hindered site of the conformation of the catalyst as a result of the

4) J. D. Jones, A. Langsjoen, M. M. C. Neumann and J. Zomlefer, *J. Org. Chem.*, **9**, 125 (1944); J. D. Jones, ibid., **9**, 484 (1944).
5) L. B. Clapp, *J. Am. Chem. Soc.*, **70**, 184 (1948).
6) Y. Minoura, M. Takebayashi and C. C. Price, ibid., **81**, 4689 (1959).
7) J. Meisenheimer, L. Angermann, O. Finn and E. Veiweg, *Ber.*, **57**, 1747 (1924); A. T. Bottini and J. D. Roberts, *J. Am. Chem. Soc.*, **80**, 5203 (1958).
8) V. Prelog and M. Wilhelm, *Helv. Chim. Acta*, **37**, 1634 (1954).

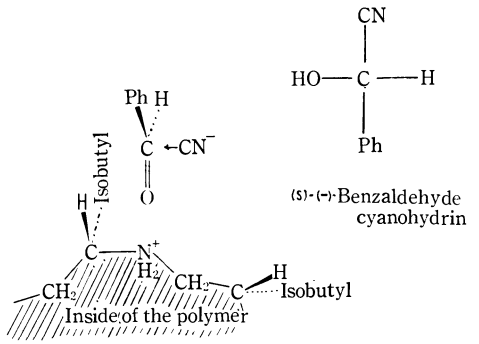

Fig. 4. Asymmetric synthesis of benzaldehyde cyanohydrin with polymer I.

steric group. Hence, the product may be expected to be of the s-configuration. Cyanohydrin was found by observation to be negative in sign, which means that it has the s-configuration and that the assumption of a steric course is justified. For the cross-linked polymer II, some other model must be constructed.

Experimental

***N*-Formyl-L-leucine Ethyl Ester (IV).** — The procedure proposed by du Vegneaud and Meyer for the formylation of phenylalanine[9] was used with a slight modification. To a solution of L-leucine ethyl ester (III) (32 g., 0.2 mol.) in 88% formic acid (360 g., 7 mol.) was added dropwise acetic anhydride (122 g., 1.2 mol.) at room temperature with vigorous stirring. The reaction mixture was then kept at 70°C for 15 min. After the excess of the reagents had been removed in vacuo, the residual liquid was distilled under reduced pressure to give 36 g. (96%) of a colorless liquid, b. p. 124—125°C/3 mmHg, n_D^{27} 1.4459, $[\alpha]_D^{27}$ −31.90° (*c* 2.539, ethanol).

Found: C, 57.72; H, 8.99; N, 7.32. Calcd. for $C_9H_{17}NO_3$: C, 57.73; H, 9.15; N, 7.48%.

***N*-Acetyl-L-leucine Ethyl Ester (V).**—This was prepared according to the method of the literature.[10] The acetylated ester V was obtained in 94% yield, b. p. 138—139°C/6 mmHg, n_D^{20} 1.4470, $[\alpha]_D^{20}$ −42.07° (*c* 2.686, ethanol). (Found: C, 59.62; H, 9.19; N, 6.87%.)

***N*-Benzoyl-L-leucine Ethyl Ester (VI).**—The ester was prepared by the method given by Bergmann and Zervas.[11] Recrystallization from petroleum ether afforded 25 g. (95%) of fine needle crystals (from 16 g., 0.1 mol. of ester), m. p. 66.5—67.5°C, $[\alpha]_D^{25}$ −22.47° (*c* 1.112, ethanol). (Found: C, 68.18; H, 8.03; N, 5.24%)

***N*-Methyl-L-leucinol (VII).**—The amino alcohol was obtained from IV (18.7 g., 0.1 mol.) by refluxing with lithium aluminum hydride for 24 hr. in ether. The yield of VII was 10.6 g. (81%), and it had b. p. 84.5—85°C/8 mmHg, n_D^{27} 1.4425, $[\alpha]_D^{23}$ +47.33° (*c* 1.627, ethanol).

Found: C, 64.08; H, 13.46; N, 10.93. Calcd. for $C_7H_{17}NO$: C, 64.07; H, 13.06; N, 1.68%.

Monooxalate: crystallized from ethanol in needles, m. p. 143—143.5°C, $[\alpha]_D^{30}$ +12.45° (*c*, 0.964, ethanol).

Found: C, 48.68; H, 8.49; N, 6.22. Calcd. for $C_9H_{19}NO_5$: C, 48.85; H, 8.66; N, 6.33%.

***N*-Ethyl-L-leucinol (VIII).**—The amino alcohol was prepared in 77% yield (8.3 g.) from V (15 g., 0.075 mol.) according to the procedure described above. The product had b. p. 82—83°C/6 mmHg, m. p. 38—39°C, $[\alpha]_D^{18}$ +48.01° (*c* 2.084, ethanol).

Found: C, 66.11; H, 13.10; N, 9.50. Calcd. for $C_8H_{19}NO$: C, 66.15; H, 13.19; N, 9.64%.

***N*-Benzyl-L-leucinol (IX).**—This compound also was prepared from VI (17 g., 0.064 mol.) and lithium aluminum hydride in tetrahydrofuran. The solution of the ester was refluxed for 3 hr. A silky crystal (10.9 g., 81%) was obtained by recrystallization from petroleum ether, m. p. 73—74°C, $[\alpha]_D^{26}$ +23.44° (*c* 1.024, benzene).

Found: C, 75.46; H, 10.19; N, 6.66. Calcd. for $C_{13}H_{21}NO$: C, 75.31; H, 10.21; N, 6.76%.

***N*-Methyl-(s)-isobutylethylenimine (X).** — The procedure followed was Leighton's method.[12] Redistillation over sodium gave 4.5 g. (40%) of a volatile liquid which odored of imine from VII (13 g., 0.1 mol.), b. p. 116—117°C, $n_D^{31.5}$ 1.4063, $[\alpha]_D^{31.5}$ +30.18° (*c* 0.994, benzene). The infrared specturm showed the presence of an imine ring (3050 cm^{-1}) and of the N–CH_3 group (2785 cm^{-1}).

Found: C, 73.85; H, 13.11; N, 12.43. Calcd. for $C_7H_{15}N$: C, 74.27; H, 13.36; N, 12.37%.

The reaction product of X with hydrogen chloride in ether was recrystallized from ether-ethanol, m. p. 149—150°C, $[\alpha]_D^{21}$ +23.32° (*c* 2.745, ethanol). It is probably 1-chloro-4-methyl-2-methylaminopentane hydrochloride.

Found: C, 45.11; H, 9.08; N, 7.33; Cl, 38.65. Calcd. for $C_7H_{17}NCl_2$: C, 45.17; H, 9.21; N, 7.53; Cl, 38.10%.

***N*-Ethyl-(s)-isobutylethylenimine (XI).**—This also was prepared by Leighton's method. From VIII (18 g., 0.12 mol.), the imine was obtained as a colorless liquid (7.5 g., 48%), b. p. 135—136°C, n_D^{20} 1.4161, $[\alpha]_D^{20}$ +22.67° (*c* 1.147, benzene). The infrared spectrum showed the presence of an imine ring at 3060 cm^{-1}.

Found: C, 75.41; H, 13.23; N, 10.98. Calcd. for $C_8H_{17}N$: C, 75.52; H, 13.47; N, 11.01%.

The reaction product of XI with hydrogen chloride in ether was white flakes and had m. p. 141—142.5°C, $[\alpha]_D^{25}$ 0.00° (*c* 0.2132, ethanol), after several recrystallizations from ether-ethanol.

Found: C, 48.17; H, 9.28; N, 6.75; Cl, 35.61. Calcd. for $C_8H_{19}NCl_2$: C, 48.01; H, 9.57; N, 7.00; Cl, 35.43%.

From the mother liquor another crystal was obtained, m. p. 204—205°C, $[\alpha]_D^{28}$ +8.48° (*c* 1.061, ethanol).

Found: C, 48.20; H, 9.37; N, 7.23; Cl, 35.11. Calcd. for $C_8H_{19}NCl_2$: C, 48.01; H, 9.57; N, 7.00; Cl, 35.43%.

It is probable that the former is 2-chloro-1-ethylamino-4-methylpentane hydrochloride and that the latter is 1-chloro-2-ethylamino-4-methylpentane hydrochloride, because the latter, which has an optical activity, seems to be produced by breaking at the primary

9) V. du Vigneaud and C. E. Meyer, *J. Biol. Chem.*, **98**, 295 (1932).
10) E. Fischer, *Ber.*, **34**, 433 (1901).
11) M. Bergmann and L. Zervas, *J. Biol. Chem.*, **133**, 341 (1936).
12) P. A. Leighton, *J. Am. Chem. Soc.*, **69**, 1540 (1947).

carbon of the cyclic imine ring, regardless of the asymmetric carbon, and so the asymmetry is maintained.

***N*-Benzyl-(s)-isobutylethylenimine (XII).**—The imine was produced in 46% yield (3.1 g.) from IX (7 g., 0.034 mol.) by the procedure described above. The product had b. p. 98.5—99.5°C/6 mmHg, n_D^{23} 1.4975, $[\alpha]_D^{23}$ +9.74° (*c* 1.129, benzene). The infrared spectrum indicated an imine band at 3030 cm^{-1}.

Found: C, 82.35; H, 9.93; N, 7.97. Calcd. for $C_{13}H_{19}N$: C, 82.48; H, 10.12; N, 7.40%.

Poly-(s)-*N*-methylisobutylethylenimine (XIII).—The polymerization of the imine was carried out as described previously,[1] and the product obtained was refined by fractionation in cold acetone. The product was a light-yellow tacky solid which was soluble in common organic solvents but insoluble in water, and which exhibited no crystallinity. The infrared specturm of film evaporated from a benzene solution showed an N-CH_3 band at 2785 cm^{-1}, while the band at 3050 cm^{-1} disappeared; $[\alpha]_D^{20}$ −70.00° (*c* 1.000, benzene), molecular weight, 1330 (cryoscopic method with benzene).

Found: C, 72.44; H, 13.13; N, 12.15. Calcd. for $(C_7H_{15}N)_n$: C, 74.27; H, 13.36; N, 12.37%.

Poly-(s)-*N*-ethylisobutylethylenimine (XIV).—After fractionation using acetone, the precipitate was freeze-dried to give a white powder, m. p. 146°C, $[\alpha]_D^{15}$ −207.4° (*c* 1.176, benzene), molecular weight, 1340; it had a high crystallinity.

Found: C, 75.71; H, 13.19; N, 10.99. Calcd. for $(C_8H_{17}N)_n$: C, 75.52; H, 13.47; N, 11.01%.

Poly-(s)-*N*-benzylisobutylethylenimine (XV).—The polymer obtained had m. p. 118—121°C, $[\alpha]_D^{22}$ −219.0° (*c* 0.950, benzene), molecular weight, 1645. Although the infrared spectrum still showed the band near 3050 cm^{-1} despite treatment several times with various methods, it seems not to be the absorption band of the imine ring but that of the C-H stretching of the aromatic ring. An X-ray examination of the polymer showed a fairly high degree of orientation.

Found: C, 82.12; H, 10.16; N, 7.30. Calcd. for $(C_{13}H_{19}N)_n$: C, 82.48; H, 10.12; N, 7.40%.

***N*-Methylation of Polymer I.**—*By Eschweiler-Clarke's Method (XIII-1).*—Attempts to prepare a product which had no carbonyl group were unsuccessful. The polymer I (200 mg.) was added to a solution of 35% formaldehyde (1 g.) and 88% formic acid (0.25 g.) with a slight warming. The mixture was heated gently until the evolution of carbon dioxide ceased, and then it was refluxed on a steam bath for 5 hr. The solution obtained was cooled and saturated with solid potassium hydroxide. The organic layer was separated, diluted with benzene, and washed with water until it was neutral. After freeze-drying, the benzene solution gave 170 mg. of a pale yellow powder, m. p. 132—140°C, $[\alpha]_D^{25}$ −46.03° (*c* 1.035, benzene). In the infrared specturm, the band of the N-CH_3 group is observed instead of the disapperance of the N-H band near 3285 cm^{-1}. Besides, a strong peak near 1700 cm^{-1} appears even after various purifications. It perhaps indicates a carbonyl group coming from alkylating agents.

Found: C, 72.35; H, 12.04; N, 10.46. Calcd. for $(C_7H_{15}N)_n$: C, 74.27; H, 13.36; N, 12.37%.

By Methyl Iodide (XIII-2).—The polymer I (300 mg.) was dissolved in 10 g. of methyl iodide and then allowed to stand at 50°C for 48 hr. After the excess of the reagent had been removed, the residue was added to benzene and washed by alcoholic potash, 3 N potassium nitrate, N sodium chloride, N sodium hydroxide solution, and water successively. A yellow, powdery polymer was obtained by freeze-drying. The yield was 310 mg., $[\alpha]_D^{31}$ −6.20° (*c* 1.000, benzene). Although the reaction and treatment were repeated, the alkylation of the polymer was not sufficient and no halogene could be removed: $[\alpha]_{30}^{D}$ −10.62° (*c* 2.730, benzene).

Found: C, 68.20; H, 12.05 N, 11.78; Halogene as iodide, 6.86. Calcd. for $(C_5H_{19}NO)_n$: C, 66.15; H, 13.19; N, 11.02%.

A similar polymer was obtained by the quaternarization of polymer XIII with methyl iodide, but it was more difficult to obtain it in a pure state than in the case of XIII-2.

Asymmetric Synthesis.—A catalyst polymer (0.5 mmol.) in benzene was added to a solution of refined benzaldehyde (5 ml.) and anhydrous hydrogen cyanide (2 ml.) in benzene at 20°C; then the mixture was made up to 25 ml. with benzene. After this solution had been allowed to stand at 20°C for 20 hr., the reaction mixture was quenched by 10% sulfuric acid solution; the unchanged hydrogen cyanide was then removed in vacuo in the presence of one drop of phosphoric acid. The residue was decanted or filtered off, and the resulting solution was again made up to 25 ml. with benzene. The optical rotation of the solution was measured in a 2 dm. tube. Whenever the rotatory power was very small, distillation was carried out and the optical rotation was checked by a photoelectric instrument. The concentration of the solution was determined by titration with 0.1 N silver nitrate solution by a method described previously.[1]

Rate of Cyanohydrin Formation.—A polymer was dissolved in a mixture of benzene and 20 ml. of refined benzaldehyde. To the solution, hydrogen cyanide (8 ml.) was then added, and the mixture was made up to 100 ml. with benzene at 20°C. The solution was kept at 20°C. At intervals, 5 ml. portions were withdrawn and treated in a way similar to that described above except that the sample was made up to 10 ml.

Racemization of Cyanohydrin by Polymer XIV.—The polymer XIV (63.6 mg.) was added to (+)-cyanohydrin ($[\alpha]_D^{25}$ +1.49°, *c* 9.340) benzene solution at 20°C. The mixture was then kept at 20°C for 105 min. Distillation gave (+)-isomer with $[\alpha]_D^{25}$ +1.47° (*c* 20.400, benzene). When the distillation was carried out in the presence of the polymer XIV and one drop of phosphoric acid, no racemization of the cyanohydrin occurred. Before distillation, $[\alpha]_D^{25}$ −0.52° (*c* 21.24, benzene); after distillation, $[\alpha]_D^{25}$ −0.52° (*c* 3.09, benzene).

Optical Rotatory Dispersion.—This was measured by Rudolph spectro-polarimeter. Model 200-S-80 and Nihon Bunko, Jasco ORD/UV-5 type.

The author wishes to thank Dr. Masaya Yanagita for his stimulating discussion.

BULLETIN OF THE CHEMICAL SOCIETY OF JAPAN VOL. 39 703—708 (1966)

The Determination of Micro Amounts of Polythionates. V.* A Photometric Method for the Determination of Polythionates When Two Species of Them, Tetra-, Penta- and Hexathionate, are Present Together[1]

By Tomozo KOH and Iwaji IWASAKI

Laboratory of Analytical Chemistry and Geochemistry, Tokyo Institute of Technology, Ookayama, Tokyo

(Received July 28, 1965)

In the previous papers of this series, the present authors have found the conditions under which all three polythionates (n=4, 5 and 6) are quantitatively converted into thiocyanate. When one mole of polythionate undergoes cyanolysis, one mole of thiosulfate and ($n-3$) moles of thiocyanate are formed. The thiosulfate formed from polythionate is then converted into thiocyanate by the addition of a cupric chloride solution. A photometric method for the determination of polythionate when two species of polythionates, tetra-, penta- and hexathionate, are present toghther has been devised; it depends upon the determination of the different amounts of thiocyanate formed from the cyanolysis of polythionates both in the presence of cupric ions and in their absence. The mean number of sulfur atoms, n, in the formula, $S_nO_6^{2-}$, for polythionate, was determined; the polythionate composition of the solution was also evaluated from the n value

In the previous papers[2-4] of this series, the present authors have established excellent methods for the determination of polythionates, tetra-, penta- and hexathionate. These methods are based on the reaction:

$$S_nO_6^{2-} + (n-1)CN^- + H_2O = S_2O_3^{2-} + SO_4^{2-} + 2HCN + (n-3)SCN^- \quad (A)$$
(n=4, 5 and 6)

followed by the photometric determination of the thiocyanate thus formed with ferric iron when tetra-, penta- or hexathionate is present by itself alone. They also have found the conditions under which all these polythionates are quantitatively converted into thiocyanate.

Iwasaki and his co-worker[5] have proposed a method for the determination of tetrathionate by means of its decomposition with sulfite.

It would be important and interesting, from the analytical and the geochemical viewpoints, to determine micro quantities of polythionates mixed with one another, but no satisfactory method has yet been devised for when they are present together. In the present paper, an attempt has been made, as the initial step, to determine polythionate when two species of polythionates, tetra-, penta- and hexathionate, are present together. It has been stated in the literature[6] that cupric ion has a catalytic effect on the conversion of thiosulfate into thiocyanate. Consequently, if the cupric chloride is added after the above Eq. A has been completed, then the thiosulfate formed from polythionate is further converted into thiocyanate. The overall reaction of polythionates, accordingly, is as follows:

$$S_nO_6^{2-} + nCN^- + H_2O = SO_3^{2-} + SO_4^{2-} + 2HCN + (n-2)SCN^- \quad (B)$$
(n=4, 5 and 6)

Urban[7] has evaluated n in the formula, $S_nO_6^{2-}$, for polythionates by means of the photometric determination of different amounts of the thiocyanate formed in accordance with Eq. A and B. However, penta- and hexathionate, as has been pointed out in the previous papers,[2,3] are not quantitatively converted into thiocyanate under the conditions of Urban's method,[7] because of the partial alkaline decomposition arising from the higher pH value caused by the addition of a sodium cyanide solution. Therefore, Urban's method is inapplicable to the evaluation of n in the formula, $S_nO_6^{2-}$, for polythionates.

The present authors will here investigate, in greater detail, a photometric method for the determination of thiosulfate which is based on the formation of thiocyanate from thiosulfate by reaction with cyanide in the presence of cupric ions; they will propose a method for the determination of micro amounts of polythionates when two species of them are present together by means of the photometric determination of different amounts

* Part IV: This Bulletin, **39**, 576 (1966).

1) Presented at the 18th Annual Meeting of the Chemical Society of Japan, Osaka, April, 1965.

2) T. Koh, This Bulletin, **38**, 1510 (1965).

3) T. Koh and I. Iwasaki, ibid., **38**, 2135 (1965).

4) T. Koh and I. Iwasaki, ibid., **39**, 352 (1966).

5) I. Iwasaki and S. Suzuki, ibid., **39**, 576 (1966).

6) B. Sörbo, *Biochim. Biophysica Acta*, **23**, 412 (1957).

7) P. J. Urban, *Z. anal. Chem.*, **180**, 110 (1961).

of the thiocyanate formed in accordance with Eqs. A and B. They will also determine n, the mean number of sulfur atoms in the formula, $S_nO_6^{2-}$, for polythionates above trithionate, and, at the same time, will evaluate the polythionate composition of the solution from the n values.

Experimental

Apparatus and Materials.—Unless stated otherwise, the apparatus and materials used in this investigation were the same as those described in previous papers.[2-4]

The Standard Thiosulfate Solution.—The stock solution of thiosulfate was prepared by dissolving guaranteed sodium thiosulfate pentahydrate in freshly-boiled and cooled redistilled water containing a small amount of sodium carbonate; it was then standardized with a standard potassium iodate solution. The working thiosulfate solutions were prepared by diluting the stock solution properly.

The Cupric Chloride Solution.—The working cupric chloride solutions were prepared by diluting a 1 M solution properly.

Buffer Solution.—The solutions of acetic acid - sodium acetate (0.1 M), sodium dihydrogen phosphate-sodium hydroxide (0.2 M), borax - hydrochloric acid (0.2 M—0.1 N) and disodium phosphate - sodium hydroxide (0.1 M) were mixed with each other, at various ratios, in order to obtain buffer solutions from pH 3.2 to 5.0, from pH 6.0 to 8.0, from pH 8.8 to 10.0, and from pH 11.2 to 12.0 respectively.

Procedure A.—A sample solution of 10.0 ml. is placed in a 25 ml. volumetric flask. To this solution are added, first, 4.0 ml. of a phosphate buffer solution of pH 7.0, and then 2.5 ml. of a 0.1 M sodium cyanide solution; the pH of the solution is thereby brought to 8.7. The volumetric flask is kept in the thermostat at 40°C for 30 min.; polythionates are thereby quantitatively converted into thiocyanate according to Eq. A. Then 3.0 ml. of a 1.5 M ferric nitrate - perchloric acid solution is added. After the flask has been filled with redistilled water to the mark, the contents are mixed well. The absorbancy of the solution of the ferric-thiocyanate complex thus formed is measured at the wavelength of 460 mμ, using the reagent blank as a reference.

Procedure B.—To 10.0 ml. of a sample solution in a 25-ml. volumetric flask there are added, first, 4.0 ml. of a buffer solution of pH 7.0, and then 2.5 ml. of a 0.1 M sodium cyanide solution. After the volumetric flask has been kept in the thermostat at 40°C for 30 min., 1.5 ml. of a 0.05 M cupric chloride solution is added; the pH of the solution is thereby brought to 7.1. The mixture is shaken vigorously, whereupon polythionates are converted into thiocyanate quantitatively in accordance with Eq. B. Then 3.0 ml. of a perchloric acid solution of ferric nitrate is added; after filling the flask with redistilled water to the mark, the contents are mixed well. The absorbancy of the solution of the ferric-thiocyanate formed is measured at 460 mμ against the reagent blank.

Results and Discussion

Calibration Curves.—The calibration curves shown in Fig. 1 were obtained by the procedure B, using the standard solutions of thiosulfate and thiocyanate.

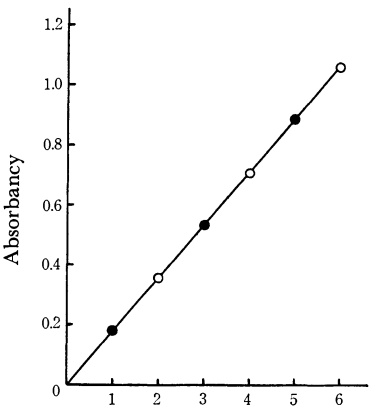

Concn. of $S_2O_3^{2-}$ and SCN^-, $\times 10^{-4}$ M

Fig. 1. Calibration curves.

○ Thiosulfate, ● Thiocyanate

When one ion of thiosulfate undergoes cyanolysis, one ion of thiocyanate is formed. Therefore, if thiosulfate is converted into thiocyanate quantitatively and completely, the calibration curve of thiosulfate should be in full accord with that of thiocyanate when plotted by the mole concentrations for thiosulfate and thiocyanate. Figure 1 shows that the reaction of thiosulfate with cyanide in the presence of cupric ions is stoichiometric and goes well to completion under the conditions mentioned above.

The standard solutions containing various amounts of tetra-, penta-, hexathionate and thiocyanate were treated by the procedure B described above; the experimental results are plotted in Figs. 2 and 3.

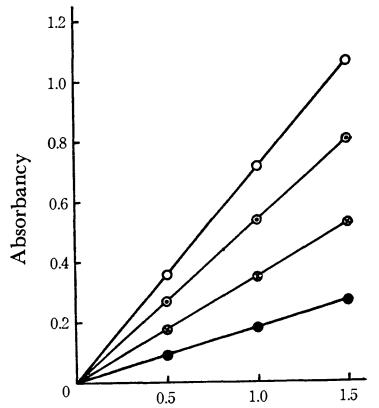

Concn. of SCN^-, $S_4O_6^{2-}$, $S_5O_6^{2-}$, and $S_6O_6^{2-}$, $\times 10^{-4}$ M

Fig. 2. Calibration curves.

● Thiocyanate, ⊗ Tetrathionate
⊙ Pentathionate, ○ Hexathionate

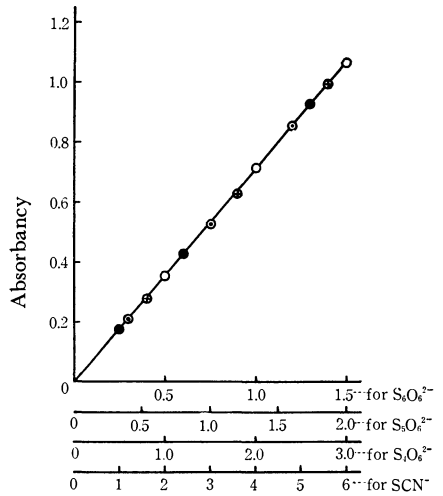

Concn. of SCN^-, $S_4O_6^{2-}$, $S_5O_6^{2-}$, and $S_6O_6^{2-}$, $\times 10^{-4}$ M

Fig. 3. Calibration curves.

● Thiocyanate, ⊗ Tetrathionate
⊙ Pentathionate, ○ Hexathionate

According to Eq. B, when one ion of polythionate, $S_nO_6^{2-}$ (n=4, 5 and 6), undergoes cyanolysis, ($n-2$) ions of thiocyanate are formed. As a matter of fact, Fig. 2 shows that the calibration curves of tetra-, penta- and hexathionate are, respectively, twice, three times and four times as sensitive as that of thiocyanate when plotted by the molar concentration.

As can also be seen in Fig. 3, their calibration curves are in exact accordance with that of thiocyanate when the scales of the concentrations of thiocyanate, tetrathionate and pentathionate are made to one-fourth, two-fourths and three-fourths of the hexathionate concentration, demonstrating that all three of these polythionates are quantitatively converted into thiocyanate according to Eq. B.

The Effect of the pH.—In order to study the effect of the pH on the cyanolysis, the reaction of thiosulfate with cyanide in the presence of cupric ions was carried out at various pH values. Figure 4 shows that the optimum pH value for the complete and stoichiometric reaction is within a range from 5.0 to 9.0 under the conditions of the procedure B described above.

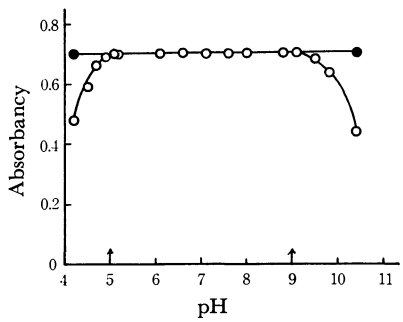

Fig. 4. The effect of the pH.

● 4.0×10^{-4} M SCN^-, ○ 4.0×10^{-4} M $S_2O_3^{2-}$

The pH of the solution, after the cyanolysis of polythionates in accordance with Eq. A, was brought from 8.7 to 7.1 by the addition of a 0.05 M cupric chloride solution in the procedure B.

The decreases in absorbancy below the pH value of 4.9 and above pH 9.1 may be attributed to the decrease in the concentration of cyanide ions with the lowering of the pH, and to the decrease of the concentration of cupric ions due in all probability to the formation of the cuprous-cyanide complex[8] which might result from the increase in the concentration of cyanide ions with the elevation of the pH.

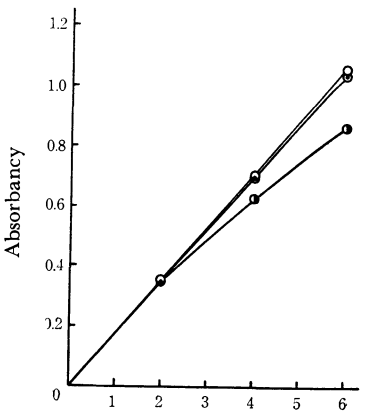

Concn. of thiosulfate, $\times 10^{-4}$ M

Fig. 5. The effect of the amount of sodium cyanide. The pH was adjusted to the range from 5.0 to 9.0 in all cases.

○ 0.1 M NaCN 1.2, 1.5, and 2.5 ml. (III)
◑ 0.1 M NaCN 0.5 ml. (I)
⊙ 0.1 M NaCN 1.0 ml. (II)

The Effect of the Amount of Sodium Cyanide.—In measuring the effect of the amount of sodium cyanide on the conversion of thiosulfate into thiocyanate, a volume of from 0.5 to 2.5 ml. of 0.1 M sodium cyanide was employed; in all cases the solution was buffered to the optimum pH range. The resulting effect is shown in Fig. 5.

The calibration curves with 0.5 and 1.0 ml. do not form straight lines (see I and II), indicating that the conversion of thiosulfate is not quantitative because of insufficient amounts of cyanide. Figure 5 shows that 1.2 ml. of a 0.1 M sodium cyanide solution is sufficient for the quantitative conversion and that the amount of sodium cyanide does not have any effect on the method as long as

8) E. P. Treadwell and W. T. Hall, "Analytical Chemistry," Vol. II, John Wiley & Sons, New York (1935), p. 667.

Table I. The effect of the amount of cupric chloride

Time min.	Sample	Absorbancy: 4.0×10^{-4} M 0.05 M $CuCl_2$ 0.5 ml.	4.0×10^{-4} M 0.05 M $CuCl_2$ 1.0 ml.	4.0×10^{-4} M 0.05 M $CuCl_2$ 1.5 ml.	4.0×10^{-4} M 0.05 M $CuCl_2$ 2.0 ml.	6.0×10^{-4} M 0.05 M $CuCl_2$ 0.5 ml.	6.0×10^{-4} M 0.05 M $CuCl_2$ 1.0 ml.	6.0×10^{-4} M 0.05 M $CuCl_2$ 1.5 ml.	6.0×10^{-4} M 0.05 M $CuCl_2$ 2.0 ml.
	SCN^-	0.705	0.705	0.705	0.705	1.055	1.055	1.055	1.055
0.5	$S_2O_3^{2-}$	0.150	0.328	0.705	0.696	0.231	0.530	1.053	1.053
1	$S_2O_3^{2-}$	0.158	0.335	0.699	0.703	0.236	0.519	1.058	1.053
3	$S_2O_3^{2-}$	0.149	0.348	0.701	0.698	0.236	0.522	1.053	1.053
60	$S_2O_3^{2-}$	0.163	0.348	0.704	0.697	0.232	0.510	1.054	1.054

it is sufficient and the pH is adjusted to an optimum value. From a consideration of the cyanolysis of polythionate prior to the cyanolysis of the thiosulfate formed from the reaction of polythionate with cyanide, 2.5 ml. of a 0.1 M sodium cyanide solution was added in the present work.

The Effect of the Amount of Cupric Chloride.—In order to investigate the effect of the quantity of cupric ions, a solution of from 0.5 to 2.0 ml. of 0.05 M cupric chloride was employed; in all cases the solution was buffered to a pH value from 5.0 to 9.0. The results listed in Table I show that 1.5 ml. of a 0.05 M cupric chloride solution is sufficient for quantitative cyanolysis and that thiosulfate is instantly converted into thiocyanate in the pre- sence of cupric ions.

The Effect of Shaking on the Cyanolysis of Thiosulfate.—Table II shows that the shaking has to be made after the addition of a cupric chloride solution in order that the cyanolysis of thiosulfate may be stoichiometric and may go well to completion; otherwise the quantitative reaction does not occur.

Table II. Effect of shaking on cyanolysis of thiosulfate

Sample	Concn., $\times10^{-4}$ M	Absorbancy: No shaking	No shaking	Shaking	Shaking
SCN^-	4.0	0.704	0.706	0.705	0.705
$S_2O_3^{2-}$	4.0	0.592	0.538	0.705	0.705

The Evaluation of n in $S_nO_6^{2-}$ for Polythionates.—Suppose A and B are the absorbancies obtained by the two procedures, A and B, described above, then:

$$A/B = (n-3)/(n-2)$$

When rearranged:

$$n = A/(B-A)+3 \quad \text{or} \quad n = (3B-2A)/(B-A)$$

The former, being the simpler for determining the n value, was used in this work. The results obtained when applied to solutions of tetra-, penta- and hexathionate are listed in Table III.

Table III. The evaluation of n in $S_nO_6^{2-}$ for polythionates

Sample	Concn. $\times10^{-4}$ M	Absorbancy: A	B	n
$S_4O_6^{2-}$	1.5	0.268	0.525	4.04
$S_5O_6^{2-}$	1.5	0.522	0.801	4.87
$S_6O_6^{2-}$	1.5	0.801	1.063	6.06

Urban[7] has pointed out that polythionates, with the exception of tetrathionate, are mixtures containing the other polythionates; he deduced this from the n values, which he estimated to be from 4.29 to 4.34 for pentathionate and from 4.87 to 5.35 for hexathionate. However, his results do not seem reasonable, because these polythionates, as has been mentioned above, undergo a partial alkaline decomposition besides cyanolysis under the conditions of Urban's method.

From Table III, it may be seen that the n value, the mean number of sulfur atoms in the formula, $S_nO_6^{2-}$, for polythionate, could be sufficiently accurately determined by the present method.

The Evaluation of the Composition of Polythionates Simultaneously Present.—The composition of polythionates can be easily evaluated from the n value and Figs. 6 and 7 when two species of polythionates from among tetra-, penta- and hexathionate are simultaneously present. The experimental results are given in Table IV.

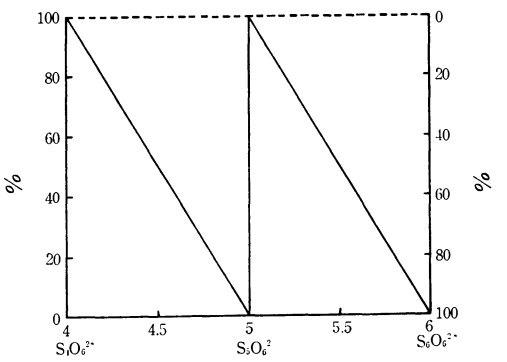

Fig 6.

Table IV. Evaluation of composition of polythionates present together

Concn. $\times 10^{-4}$ M		Composition calcd., %		n	Composition evaluated, %		Difference %	
$S_4O_6^{2-}$	$S_5O_6^{2-}$	$S_4O_6^{2-}$	$S_5O_6^{2-}$		$S_4O_6^{2-}$	$S_5O_5^{2-}$	$S_4O_6^{2-}$	$S_5O_6^{2-}$
1.5	0.5	75	25	4.21	79	21	+4	−4
1.0	1.0	50	50	4.44	56	44	+6	−6
0.5	1.0	33.3	66.7	4.60	40	60	+6.7	−6.7
$S_5O_6^{2-}$	$S_6O_6^{2-}$	$S_5O_6^{2-}$	$S_6O_6^{2-}$		$S_5O_6^{2-}$	$S_6O_6^{2-}$	$S_5O_6^{2-}$	$S_6O_6^{2-}$
1.0	0.6	62.5	37.5	5.33	67	33	+4.5	−4.5
0.8	0.8	50	50	5.44	56	44	+6	−6
0.4	1.2	25	75	5.73	27	73	+2	−2
$S_4O_6^{2-}$	$S_6O_6^{2-}$	$S_4O_6^{2-}$	$S_6O_6^{2-}$		$S_4O_6^{2-}$	$S_6O_6^{2-}$	$S_4O_6^{2-}$	$S_6O_6^{2-}$
1.4	0.2	87.5	12.5	4.24	88	12	+0.5	−0.5
1.0	0.6	62.5	37.5	4.75	62.5	37.5	0	0
1.0	1.0	50	50	5.09	45.4	54.6	−4.6	+4.6
0.5	1.0	33.3	66.7	5.29	35.8	65.2	+2.5	−2.5

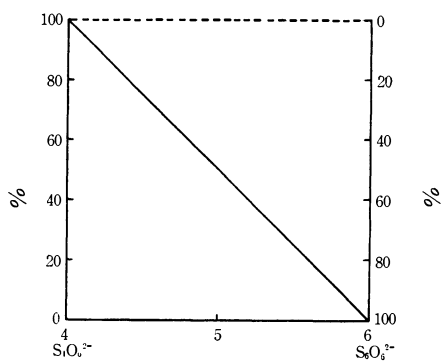

Fig. 7.

As may be seen in Table IV, there is a remarkable agreement between the experimental and the calculated compositions.

The Determination of Tetrathionate and Pentathionate Simultaneously Present.—The method consists of the determination of the different amounts of thiocyanate formed from Eqs. A and B on two separate aliquots of the sample; one is treated by the procedure A, and the other, by the procedure B. Then:

$$(S_4O_6^{2-}) = 2B-3A \text{ and } (S_5O_6^{2-}) = 2A-B,$$

where $(S_4O_6^{2-})$ and $(S_5O_6^{2-})$ indicate the absorbancy corresponding to the same concentration of thiocyanate as those of tetrathionate and pentathionate; A and B are the absorbancies obtained by the procedures A and B.

Tetrathionate and pentathionate simultaneously present can be readily determined by reference to the calibration curve in Fig. 1. The results listed in Table V show that this method can be accurately applied to the determination of tetrathionate and pentathionate simultaneously present at various ratios.

The Determination of a Tetrathionate-Hexathionate Mixture and a Pentathionate-Hexathionate Mixture.—The following equations can also be obtained: for a tetrathionate-hexathionate mixture, $(S_4O_6^{2-})=(3B-4A)/2$ and $(S_6O_6^{2-})=(2A-B)/2$; for a pentathionate-hexathionate mixture, $(S_5O_6^{2-})=3B-4A$ and $(S_6O_6^{2-})=3A-2B$. These polythionates can be determined in the same way as that used for a tetrathionate-pentathionate mixture, by using the above equations when two species of polythionates are simultaneously present. The results of the deter-

Table V. Determination of tetrathionate and pentathionate present together

Polythionates taken, $\times 10^{-4}$ M		Polythionates found, $\times 10^{-4}$ M		Difference $\times 10^{-4}$ M	
$S_4O_6^{2-}$	$S_5O_6^{2-}$	$S_4O_6^{2-}$	$S_5O_6^{2-}$	$S_4O_6^{2-}$	$S_5O_6^{2-}$
0.50	1.00	0.63	0.91	+0.13	−0.09
0.50	1.60	0.57	1.54	+0.07	−0.06
1.00	1.00	1.14	0.91	+0.14	−0.09
1.00	1.50	1.02	1.45	+0.02	−0.05
1.50	0.50	1.56	0.45	+0.06	−0.05
1.50	1.00	1.56	0.92	+0.06	−0.08
2.00	0.60	2.04	0.54	+0.04	−0.06

Table VI. Determination of tetrathionate and hexathionate present together

Polythionates taken, $\times 10^{-4}$ M		Polythionates found, $\times 10^{-4}$ M		Difference $\times 10^{-4}$ M	
$S_4O_6^{2-}$	$S_6O_6^{2-}$	$S_4O_6^{2-}$	$S_6O_6^{2-}$	$S_4O_6^{2-}$	$S_6O_6^{2-}$
0.50	0.50	0.56	0.46	+0.06	−0.04
0.50	1.00	0.58	0.96	+0.08	−0.04
0.50	1.20	0.52	1.18	+0.02	−0.02
1.00	0.50	0.96	0.51	−0.04	+0.01
1.00	0.60	0.99	0.60	−0.01	0
1.00	1.00	0.92	1.02	−0.08	+0.02
1.50	0.50	1.54	0.47	+0.04	−0.03
1.50	0.70	1.66	0.73	+0.16	+0.03
2.00	0.40	1.96	0.40	+0.04	0

Table VII. Determination of pentathionate and hexathionate present together

Polythionates taken, $\times 10^{-4}$ M		Polythionates found, $\times 10^{-4}$ M		Difference $\times 10^{-4}$ M	
$S_5O_6^{2-}$	$S_6O_6^{2-}$	$S_5O_6^{2-}$	$S_6O_6^{2-}$	$S_5O_6^{2-}$	$S_6O_6^{2-}$
0.30	0.50	0.41	0.40	+0.11	−0.10
0.30	1.00	0.39	0.93	+0.09	−0.07
0.30	1.20	0.28	1.19	−0.02	−0.01
0.40	1.20	0.42	1.16	+0.02	−0.04
0.50	0.50	0.68	0.36	+0.18	−0.14
0.50	1.00	0.65	0.88	+0.15	−0.12
0.50	1.20	0.36	1.28	−0.14	+0.08
0.80	0.80	0.90	0.72	+0.10	−0.08
1.00	0.40	1.18	0.26	+0.18	−0.14
1.00	0.60	1.08	0.54	+0.08	−0.06
1.00	0.80	0.98	0.80	−0.02	0
1.50	0.40	1.54	0.37	+0.04	−0.03

mination of polythionates mixed in various ratios are given in Tables VI and VII.

As will be seen in Tables V, VI and VII, the results are reproducible within an error of $\pm 0.2 \times 10^{-4}$ M of polythionates.

Summary

The photometric method for the determination of a small amount of thiosulfate has been investigated in greater detail; it is based on the formation of thiocyanate from the reaction of thiosulfate with cyanide in the presence of cupric ions, and on the determination of the thiocyanate with an excess of ferric iron.

The polythionates are first converted into thiocyanate with cyanide; one ion of thiosulfate is also thereby formed. The thiosulfate formed is then converted into thiocyanate by the addition of a cupric chloride solution. A method for the determination of micro amounts of polythionates mixed with each other has been devised; it is based on the determination of the different amounts of thiocyanate formed from the cyanolysis of polythionates in the presence of cupric ions and in their absence.

The present method was reproducible to $\pm 0.2 \times 10^{-4}$ M of polythionates when applied to the determination of polythionates simultaneously present at various ratios.

The authors wish to express their gratitude to Dr. Satori Utsumi of Nihon University, and to Mr. Takejiro Ozawa and Dr. Minoru Yoshida of the Tokyo Institute of Technology, for their valuable advice during this study.

BULLETIN OF THE CHEMICAL SOCIETY OF JAPAN VOL. 39 708—713 (1966)

The Reactions of Amido Phosphites. A New Synthesis of Oxazolidine, Imidazolidone and Thiazolidine Derivatives

By Oyo MITSUNOBU[†], Takashi OHASHI[††] and Teruaki MUKAIYAMA[†]

[†]*Laboratory of Organic Chemistry, Tokyo Institute of Technology, Ookayama, Tokyo*
[††]*Technical Research Department, Bridgestone Tire Co., Ltd., Ogawa Higashi-cho, Kodaira-shi, Tokyo*

(Received July 28, 1965)

A new method for the preparation of various 2, 3-disubstituted oxazolidine, 2, 3-disubstituted thiazolidine and 1, 3-disubstituted imidazolidone derivatives from β-aminoethyl phosphites and either phenyl isocyanate or phenyl isothiocyanate has been developed. When 1 mol. of ethyl bis(β-anilinoethyl) phosphite, resulting from the reaction of ethyl bis(diethylamido) phosphite with *N*-phenyl ethanolamine, was treated with 2 mol. of phenyl isocyanate, 2-phenylimino-3-phenyl-1,3-oxazolidine was obtained in a 57% yield, along with an oily product. This oily product afforded a 36% yield of *N*, *N'*-diphenyl-2-imidazolidone when it was treated with sodium ethoxide. On the other hand, the pentavalent phosphorus compound, ethyl bis(β-*N*-phenyl-ureidoethyl) phosphate, did not afford an oxazolidine derivative but was converted to imidazolidone in the presence of sodium ethoxide. The reaction of β-anilinoethyl propylene phosphite with an equimolar amount of phenyl isocyanate gave only *N*, *N'*-diphenyl-2-imidazolidone in a 32% yield; 2-phenylimino-3-phenyl-1, 3-oxazolidine could not be obtained. These reactions were then extended to the preparation of exo-imino-thiazolidines. The reactions of β-aminoethyl phosphites with phenyl isothiocyanate resulted in the formation of 2-phenylimino-3-phenyl-1, 3-thiazolidine in fairly good yields.

It has been found in a previous paper[1] that bis(β-anilinoethyl) phenyl phosphonite reacts with phenyl isocyanate to form 2-phenylimino-3-phenyl-1, 3-oxazolidine in a fairly good yield. Exo-imino cyclic compounds, such as ethylene iminocarbonates, 2-iminotetrahydrofuranes and 2-imino-1, 3-oxazolidines, have been known to polymerize in the presence of cationic catalysts, giving polyurethanes, polyamides and polyureas respectively.[2-5]

Concerning the preperation of exo-imino oxazolidine and thiazolidine, several methods have been reported.[6-10]

In the present investigation, a new method for the preparation of various exo-imino oxazolidine and thiazolidine derivatives from β-aminoethyl phosphite and either phenyl isocyanate or phenyl isothiocyanate has been studied. When 1 mol. of ethyl bis(β-anilinoethyl) phosphite(I), the result of the reaction of 1 mol. of ethyl bis(diethylamido) phosphite with 2 mol. of *N*-phenyl ethanolamine, was treated with 2 mol. of phenyl isocyanate in benzene at room temperature, a considerable heat liberation was observed. After the reaction mixture had been refluxed for 3 hr., a highly viscous substance (II) was formed. Its infrared spectrum showed an absorption at 1670 cm^{-1} which was due to a carbonyl group of an urea linkage or to an exo-imino group of a five-membered ring, while the absorption peak at 2280 cm^{-1} which was due to an isocyanate group had disappeared. When this substance (II) was left to stand for a few days at room temperature, a crystalline product was obtained; this was identified as 2-phenylimino-3-phenyl-1, 3-oxazolidine (III) by a comparison of its infrared spectrum with that of an authentic sample[5] and by an elemental analysis. A 57% yield of the 2-phenylimino-3-phenyl-1, 3-oxazolidine was obtained by filtration. The infrared absorption spectrum of the filtrate showed characteristic bands attributed to P–H (2350 cm^{-1}) and to P=O (1260—1280 cm^{-1}). When the substance IV was treated with sodium ethoxide in benzene and *N*, *N'*-diphenyl-2-imidazolidone (V), cyclic urea was obtained in a 36% yield according to the following equation (1):

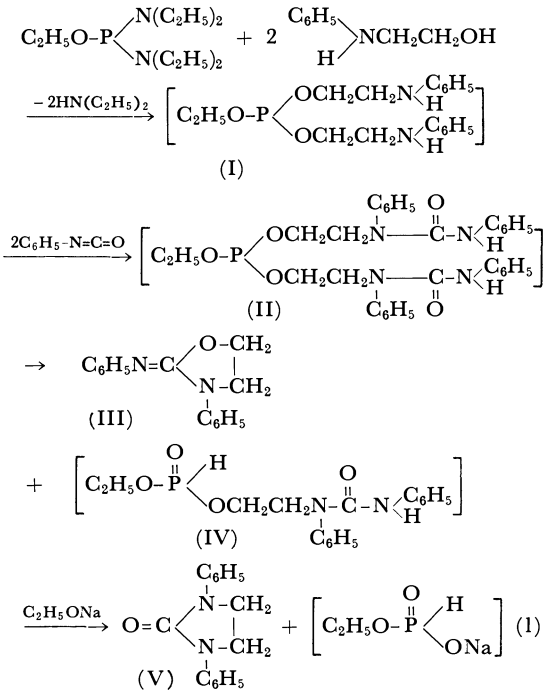

(1)

Similarly, the other substituted exo-imino oxazolidines and imidazolidones were obtained in fairly good yields (see Tables I and II).

Ethyl bis(β-anilinoethyl) phosphite, which had been obtained from the reaction of 2-ethoxy-3-phenyl-1, 3, 2-oxazaphospholidine (VI) and an equimolar amount of *N*-phenyl ethanolamine, was treated with phenyl isocyanate* to give 52.1% of the oxazolidine and 48.8% of the imidazolidone. On the other hand, the exo-imino compound could not be obtained by the reaction of β-anilinoethyl propylene phosphite (VII) with an equimolar amount of phenyl isocyanate under the same conditions. *N*, *N'*-Diphenyl-2-imidazolidone (V) resulted in a 40% yield when the above-mentioned reaction mixture VIII was treated with sodium ethoxide (Eq. 2):

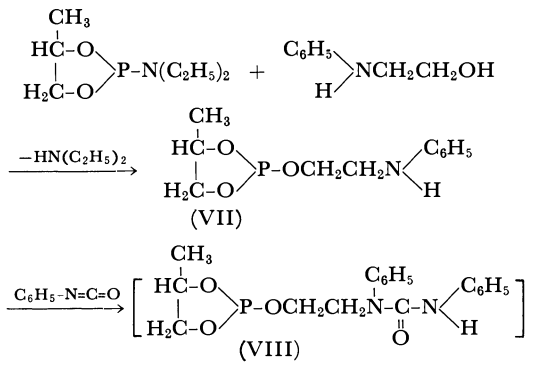

1) O. Mitsunobu, T. Ohashi, M. Kikuchi and T. Mukaiyama, This Bulletin, **39**, 214 (1966).
2) T. Mukaiyama, T. Fujisawa, H. Nohira and T. Hyugaji, *J. Org. Chem.*, **27**, 3337 (1962).
3) T. Mukaiyama and K. Sato, This Bulletin, **36**, 99 (1963).
4) T. Fujisawa, Y. Tamura and T. Mukaiyama, ibid., **37**, 793 (1964).
5) H. Nohira, Y. Nishikawa and T. Mukaiyama, ibid., **37**, 797 (1964).
6) F. B. Dains, R. Q. Brewster, J. S. Blair and W. C. Thompson, *J. Am. Chem. Soc.*, **44**, 2637 (1922).
7) F. B. Dains, R. Q. Brewster, I. L. Malm, A. W. Miller, R. V. Maneval and J. A. Sultzaberger, *J. Am. Chem. Soc.*, **47**, 1981 (1925).
8) B. Adcock, A. Lawson and D. H. Miles, *J. Chem. Soc.*, **1961** 5120.
9) R. W. Luckenbaugh, U. S. Pat. 2902356 (1959).
10) J. T. Thurston, U. S. Pat. 2479525 (1949).

* It has been proved that the isomerization reaction of 2-phenylimino-3-phenyl-1, 3-oxazolidine to *N*, *N'*-diphenyl-2-imidazolidone does not occur when the oxazolidine is treated with sodium ethoxide in refluxing ethanol for 1 hr. Eighty per cent of the oxazolidine is recovered.

TABLE I. THE SYNTHESIS OF 2-PHENYLIMINO-3-ARYL-1,3-OXAZOLIDINE

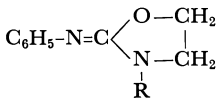

R	Yield %	M. p. °C		Analysis, % C	H	N	IR absorption cm^{-1}	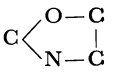
C_6H_5	57.0	115—116	Found	75.65	5.96	11.74	1670	1410
			Calcd.	75.63	5.88	11.76		
p-CH_3-C_6H_4	69.5	142—144	Found	76.12	6.15	11.39	1673	1410
			Calcd.	76.16	6.39	11.10		
p-CH_3O-C_6H_4	57.4	108—109	Found	71.65	6.19	11.04	1670	1415
			Calcd.	71.62	6.01	10.44		
p-Cl-C_6H_4	46.3	136—138	Found	65.95	4.77	10.00	1675	1407
			Calcd.	66.00	4.77	10.02		

TABLE II. THE SYNTHESIS OF 1-PHENYL-3-ARYL-IMIDAZOLIDONE-2

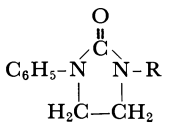

R	Yield %	M. p. °C		Analysis, % C	H	N	IR absorption cm^{-1} 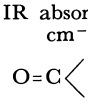	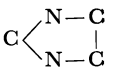
C_6H_5-	35.9	216—218	Found	76.06	5.97	11.86	1690	1420
			Calcd.	75.63	5.88	11.76		
p-CH_3-C_6H_4-	50.8	191—193	Found	75.86	6.58	11.15	1692	1430
			Calcd.	76.16	6.39	11.10		
p-CH_3O-C_6H_4-	69.7	212—213	Found	71.77	6.23	10.57	1690	1420
			Calcd.	71.62	6.01	10.44		1436
p-Cl-C_6H_4-	11.2	200—202	Found	65.81	4.72	10.27	1688	1427
			Calcd.	66.00	4.77	10.02		

TABLE III. THE SYNTHESIS OF 2-PHENYLIMINO-3-ARYL-1,3-THIAZOLIDINE

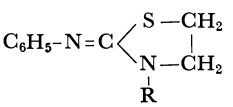

R	Yield %	M. p. °C		Analysis, % C	H	N	IR absorption cm^{-1}	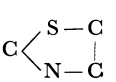
C_6H_5-	70.7	134—135	Found	70.96	5.71	11.28	1617	1374
			Calcd.	70.87	5.51	11.02		
p-CH_3-C_6H_4-	81.2	122—123	Found	71.89	6.15	10.72	1630	1378
			Calcd.	71.70	5.96	10.46		
p-CH_3O-C_6H_4-	97.7	117—118	Found	67.44	5.53	10.07	1615	1388
			Calcd.	67.60	5.63	9.85		
p-Cl-C_6H_4-	56.0	105—106	Found	62.08	4.66	9.87	1615	1385
			Calcd.	62.30	4.50	9.69		

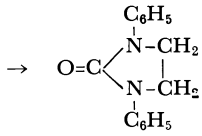

(2)

Also, it was found that 2-phenylimino-3-phenyl-1, 3-oxazolidine (III) could not be obtained by the treatment of either 2-ethoxy-3-phenyl-1,3,2-oxazaphospholidine or *N*-phenyl ethanolamine with phenyl isocyanate (Eq. 3):

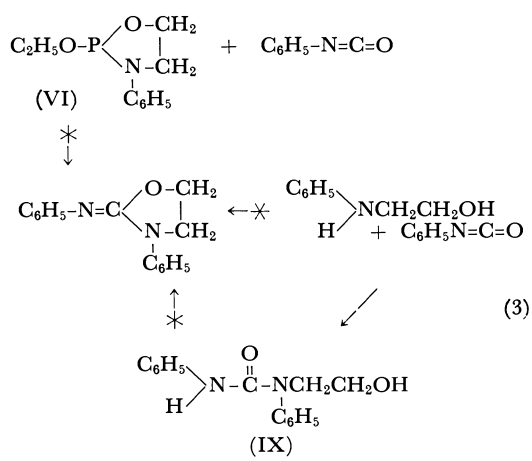

(3)

These results suggest that ethyl bis(β-*N*-phenylureidoethyl) phosphite (II) may be a necessary intermediate for the formation of oxazolidine. The proposed intermediate (II) may be expected to be analogously formed by the reaction of *N*-(β-hydroxyethyl)-*N*, *N'*-diphenyl urea (IX) with amido phosphite. Indeed, when the urea alcohol was treated with ethyl bis(diethylamido) phosphite, nearly quantitative yields of 2-phenylimino-3-phenyl-1, 3-oxazolidine and an oily product were formed. The oily product gave a 26.9% yield of *N*, *N'*-diphenyl-2-imidazolidone upon treatment with sodium ethoxide (Eq. 4):

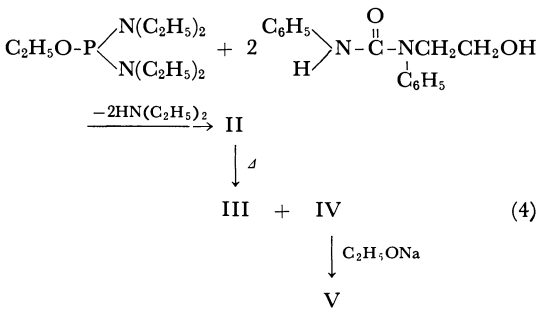

(4)

On the basis of these results, it can be considered that the reaction proceeds through a key intermediate II, which, on heating, is decomposed into IV and oxazolidine by an internal nucleophilic displacement of carbonyl oxygen to α-carbon (as is shown in Eq. 5):

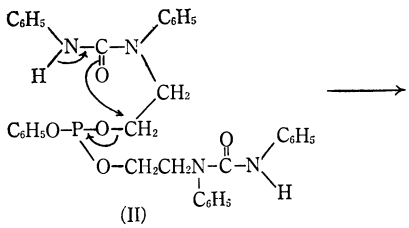

(5)

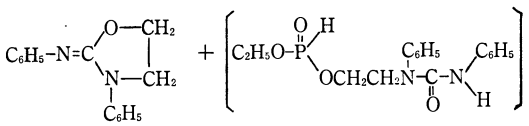

On the other hand, imidazolidone was formed by an internal nucleophilic attack of nitrogen on α-carbon when IV or VIII was treated with sodium ethoxide, as is shown in the following equation (Eq. 6):

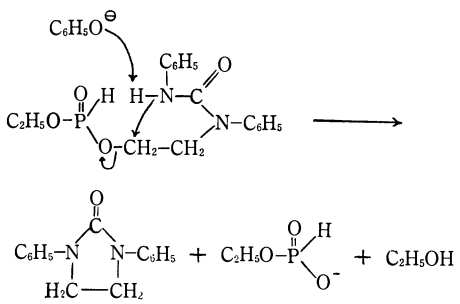

(6)

It must be noted that when ethyl bis(β-*N*-phenylureidoethyl) phosphate (X) was used in place of the trivalent phosphorus compound, exo-imino oxazolidine could not be obtained, but a 85.7% yield of imidazolidone was obtained by treatment with sodium ethoxide (Eq. 7):

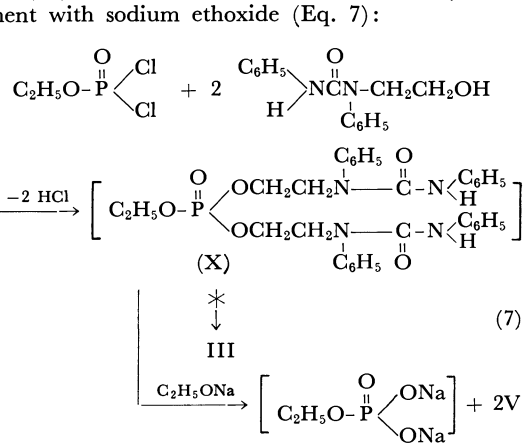

(7)

Further, for the purpose of extending the reaction to the preparation of exo-imino thiazolidine derivatives, 3.48 g. of ethyl bis(β-anilinoethyl) phosphite (I) was treated with 2.70 g. of phenyl isothiocyanate; 3.59 g. of 2-phenylimino-3-phenyl-1, 3-thiazolidine (XII) was thus obtained. Similarly, the other exo-imino thiazolidine derivatives

were obtained in good yields by the treatment of *N*-substituted ethanolamines with amido phosphite and phenyl isothiocyanate (see Table III).

Contrary to the case of ethyl bis(β-*N*-phenylureidoethyl) phosphite (II), this result shows that the decomposition of 1 mol. of ethyl bis(β-*N*-phenylthioureidoethyl) phosphite (XI) affords 2 mol. of thiazolidine (Eq. 8):

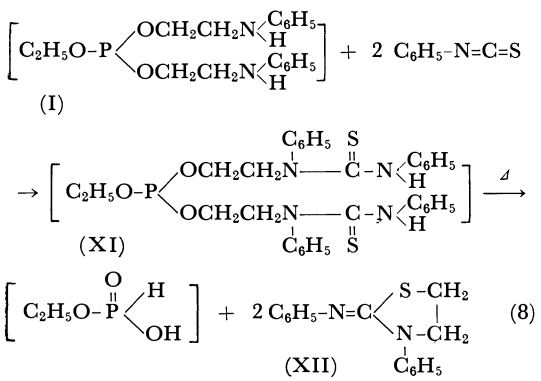

(8)

In this connection, it is interesting to note that the reaction of β-anilinoethyl propylene phosphite (VII) with an equimolar amount of phenyl isothiocyanate resulted in the formation of exo-imino thiazolidine (XII) in a fairly good yield (Eq. 9):

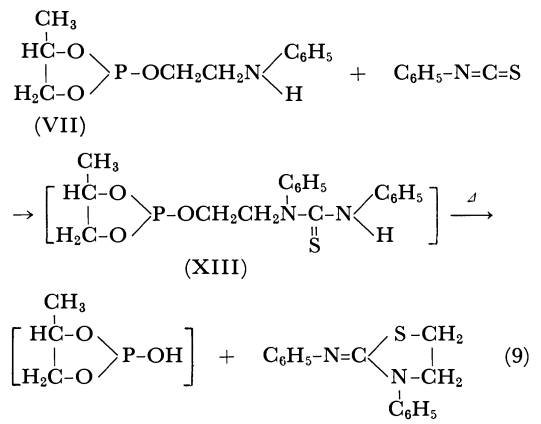

(9)

The predominant formation of thiazolidine from mono or bis(β-*N*-phenylthioureidoethyl) phosphite (XIII or XI) may be attributed to the high nucleophilicity of the sulfur.

Experimental

Materials. — Commercially - available *N* - phenyl ethanolamine, phenyl isocyanate and phenyl isothiocyanate were purified by distillation. *p*-Tolyl ethanolamine, *p*-anisyl ethanolamine and *p*-chlorophenyl ethanolamine were prepared from the corresponding aromatic amines, ethylenechlorohydrine and triethylamine. Ethyl bis(diethylamido) phosphite (b. p. 81—83°C/9 mmHg) was prepared in a manner analogous to that reported by Burgada.[11] *N*-(β-Hydroxyethyl)-*N*, *N'*-diphenyl urea[12] and ethyl phosphorodichloridate[13] were prepared according to literature procedures. Bis(β-anilinoethyl) phenyl phosphonite, ethyl bis(β-anilinoethyl) phosphite and β-anilinoethyl propylene phosphite were prepared as has been previously described.[1] The purification of ethyl bis(β-anilinoethyl) phosphite was difficult since it decomposes into *N*, *N'*-diphenyl piperazine during distillation. Therefore, the reaction mixture resulting from the reaction of 1 mol. of ethyl bis(diethylamido) phosphite with 2 mol. of *N*-phenyl ethanolamine was used as the starting material, ethyl bis(β-anilinoethyl) phosphite, in the following experiments.

The Reaction of Ethyl Bis(β-anilinoethyl) Phosphite with Phenyl Isocyanate.—A solution of phenyl isocyanate (2.38 g.; 0.02 mol.) in 10 ml. of dry toluene was added, drop by drop, into a solution of ethyl bis(β-anilinoethyl) phosphite, which had resulted from the reaction of 2.20 g. (0.01 mol.) of ethyl bis(diethylamido) phosphite with 2.74 g. (0.02 mol.) of *N*-phenyl ethanolamine, in 20 ml. of dry toluene at room temperature. After an exothermic reaction had ceased, the reaction mixture was refluxed for 3 hr. The solvent was then removed under reduced pressure, and a viscous oily substance was obtained. When the substance had been left standing for several days at room temperature, a small amount of a colorless crystalline compound appeared. After 5 ml. of 99.5% ethanol had been added to the mixture, a colorless crystalline compound, 1.35 g. (57%), m. p. 111-116°C, was obtained by filtration. After recrystallization from ethanol, the melting point rose to 115—116°C.

The infrared spectrum of the product was identical with that of authentic 2-phenylimino-3-phenyl-1, 3-oxazolidine.[5] (Found: C, 75.65; H, 5.96; N, 11.74%).

The filtrate was then concentrated to give an oily substance. A slurry of sodium ethoxide (from 0.23 g. of sodium) in 10 ml. of dry benzene was added to the oily substance, and the mixture was stirred at room temperature until it became homogeneous. After it had stood for a few days, a crystalline compound, *N*, *N'*-diphenyl-2-imidazolidone, was precipitated. This precipitate was filtered and washed well with benzene, 0.86 g. (35.9%); m. p. 208—211°C. After it had been recrystallized from ethyl acetate, the melting point rose to 216—218°C. The infrared absorption bands are at 1690 (s), 1420(s), 1230(s), 1100(m) and 893(m) cm^{-1}.

Found: C, 76.07; H, 5.97; N, 11.86. Calcd. for $C_{15}H_{14}N_2O$: C, 75.63; H, 5.88; N, 11.76%.

By an analogous procedure, the other oxazolidines and the corresponding imidazolidones were obtained. Their yields, melting points, analyses and infrared absorptions are summarized in Tables I and II.

The Reaction of 2-Ethoxy - 3 - Phenyl-1, 3, 2-Oxazaphospholidine with *N*-Phenyl Ethanolamine and Phenyl Isocyanate.—A mixture of 2-ethoxy-3-phenyl-1, 3, 2-oxazaphospholidine (2.11 g., 0.01 mol.) and *N*-phenyl ethanolamine (1.37 g., 0.01 mol.) in 5 ml. of dry toluene was refluxed for 3 hr. Then a solution of phenyl isocyanate (2.38 g., 0.02 mol.) in 15 ml. of dry toluene was added, drop by drop, into

11) R. Burgada, *Ann. Chim.*, 347 (1963).

12) H. C. Beachell and C. P. Ngoc Son, *J. Polymer Sci.*, Part A, **2**, 4773 (1964).

13) B. C. Saunders, G. J. Stacey, F. Wild and I. G. E. Wilding, *J. Chem. Soc.*, **1948**, 699.

the reaction mixture at room temperature. When the reaction mixture was treated as in the above experiments, 2-phenylimino-3-phenyl-1, 3-oxazolidine 1.24 g. (52.1%); m. p. 111—114°C (after recrystallization from ethanol, the melting point rose to 116—118°C) and *N, N'*-diphenyl-2-imidazolidone 1.16 g. (48.8%); m. p. 208—210°C (after recrystallization from ethyl acetate, the melting point rose to 215—217°C) were obtained.

The Reaction of *N*-Phenyl Ethanolamine with Phenyl Isocyanate.—A solution of phenyl isocyanate (1.19 g.; 0.01 mol.) in 10 ml. of dry toluene was added, drop by drop, into a solution of *N*-phenyl ethanolamine (1.37 g., 0.01 mol.) in 10 ml. of dry toluene at room temperature. A slight heat liberation was observed. The reaction mixture was then refluxed for 3 hr. After the solvent had been completely removed under reduced pressure, the residue was solidified, 2.76 g.; m. p. 80—83°C. The infrared spectrum of this solid was identical with that of an authentic *N*-(β-hydroxyethyl)-*N, N'*-diphenyl urea.[12] Recrystallization from ethyl actate gave 1.50 g. (58.7%); m. p. 88—89°C. (Found: C, 69.92; H, 6.42; N, 11.23%).

The Reaction of Ethyl Bis(diethylamido) Phosphite with *N*-(β-Hydroxyethyl)-*N, N'*-diphenyl Urea.—A of ethyl bis(diethylamido) phosphite mixture (2.20 g.; 0.01 mol.) and *N*-(β-hydroxyethyl)-*N, N'*-diphenyl urea (5.12 g., 0.02 mol.) in 20 ml. of dry toluene was refluxed for 3 hr., by which time the theoretical amount of diethylamine had been distilled off. Then the reaction mixture was refluxed for an additional 7 hr. After the solvent had been completely removed, the residue was almost solidified. When 5 ml. of 99.5% ethanol was added to the mixture, a white crystalline compound was precipitated 2.31 g. (97%); m. p. 111—114°C. Recrystallization from ethanol gave 2-phenylimino-3-phenyl-1, 3-oxazolidine, m. p. 115—116°C. *N, N'*-Diphenyl-2-imidazolidone was obtained from the oily residue by treating it with sodium ethoxide as in the foregoing experiment, 0.56 g. (23.4%); m. p. 202—206°C. After recrystallization from ethyl acetate, the melting point rose to 217—218°C.

The Reaction of β-Anilinoethyl Propylene Phosphite with Phenyl Isocyanate.—A solution of phenyl isocyanate (1.19 g.; 0.01 mol.) in 10 ml of dry toluene was added drop by drop to a solution of β-anilinoethyl propylene phosphite (2.41 g.; 0.01 mol.) in 10 ml. of dry toluene at room temperature. After an initial slight exothermic reaction had ceased, the reaction mixture was refluxed for 3 hr. When the solvent was then removed under reduced pressure, an oily substance was obtained. The infrared absorption bands of the substance are at 3420(w), 1655(s), 1070(m) and 990(m) cm^{-1}. Although this oily substance was kept standing in a refrigerator for a few days, 2-phenylimino-3-phenyl-1, 3-oxazolidine could not be obtained. Then a solution of sodium ethoxide (from 0.23 g. of sodium) in 10 ml. of ethanol was added to the oily subtance and the mixture was refluxed for one hour. After the reaction mixture had cooled, a crystalline compound was precipitated, 0.77 g. (32.2%), m. p. 185—190°C. The crystalline compound was recrystallized from ethyl acetate, m. p. 218—219°C. The infrared spectrum and elemental analysis of this crystalline compound were identical with those of *N, N'*-diphenyl-2-imidazolidone.

Found: C, 75.76; H, 6.10; N, 11.76%.

The Reaction of Ethyl Phosphorodichloridate with *N*-(β-Hydroxyethyl)-*N, N'*-diphenyl Urea.—A solution of ethyl phosphorodichloridate with (1.63 g., 0.01 mol.) in 20 ml. of dry benzene was vigorously added, drop by drop, into a solution of *N*-(β-hydroxyethyl)-*N, N'*-diphenyl urea (5.12 g., 0.02 mol.) in 30 ml. of dry benzene at room temperature. After the addition had been completed, the mixture was refluxed for 7 hr. Hydrogen chloride was evolved copiously. When the solvent was removed under reduced pressure, an oily residue was obtained. When 99.5% of ethanol was added to the mixture, as has been mentioned in the above experiments, oxazolidine could not be obtained. On the other hand, when sodium ethoxide (0.46 g. of sodium in 15 ml. of ethanol) was added to the mixture, it was solidified with an evolution of heat, 4.66 g., m. p. 208—243°C. This solid was then recrystallized from ethyl acetate, 3.99 g. (84.0%), m. p. 209—210°C. The infrared spectrum of this crystalline compound was identical with that of authentic *N, N'*-diphenyl-2-imidazolidone (see Experimental Section, Part 1).

The Reaction of Ethyl Bis(β-anilinoethyl) Phosphite with Phenyl Isothiocyanate.—A solution of phenyl isothiocyanate (2.70 g.; 0.02 mol.) in 10 ml. of dry toluene was added, drop by drop, into a solution of ethyl bis(β-anilinoethyl) phosphite (3.48 g.; 0.01 mol.) in 10 ml. of dry toluene at room temperature. In this case an exothermic reaction was not observed. When the reaction mixture was refluxed for 3 hr., a red liquid was obtained. After the solvent had been removed, a yellow crystalline compound was precipitated, 3.59 g. (70.7%), m. p. 126—128°C. Recrystallization from ethanol gave white needles, m. p. 134—135°C. Its infrared spectrum shows 1620(s), 1375(m), 1307(s), 1140(m) and 1080(m) cm^{-1}. This crystalline compound was found to be identical with 2-phenylimino-3-phenyl-1, 3-thiazolidine by means of elemental analysis.

Found: C, 70.96; H, 5.71; N, 11.28. Calcd. for $C_{15}H_{14}N_2S$: C, 70.78; H, 7.51; N, 11.02%.

By a similar procedure, the other thiazolidines were obtained. Their yields, melting points, analyses and infrared absorptions are listed in Table III.

The Reaction of β-Anilinoethyl Propylene Phosphite with Phenyl Isothiocyanate.—A solution of phenyl isothiocyanate (1.35 g., 0.01 mol.) in 10 ml. of dry toluene was added drop by drop to a solution of β-anilinoethyl propylene phosphite (2.14 g., 0.01 mol.) in 10 ml. of dry toluene at room temperature. After the reaction mixture had been refluxed for 5 hr., a red color, accompanied by a slight isonitrile smell, appeared. The solvent was removed under reduced pressure, and a crystalline compound was precipitated.

The precipitate was filtered off, giving 1.0 g. (39.4%) m. p. 126—128°C of 2-phenylimino-3-phenyl-1, 3-thiazolidine. After recrystallization from ethanol, the melting point rose to 131—132°C.

The authors wish to thank Mr. Kunio Yasutake of the Bridgestone Tire Co., Ltd., for permission to publish this work, and also to acknowledge their gratitude to Mr. Yoshitake Kubota and the late Mr. Koshiro Fujiwara for much helpful advice given during this work.

BULLETIN OF THE CHEMICAL SOCIETY OF JAPAN VOL. 39 714—716 (1966)

Organic Syntheses by Means of Noble Metal Compounds. XVIII. Friedel-Crafts Reaction Catalyzed by Rhenium Pentachloride[1]

By Jiro Tsuji, Tatsuo Nogi and Masanobu Morikawa

Basic Research Laboratories, Toyo Rayon Company, Kamakura

(Received July 30, 1965)

Rhenium pentachloride has been found to be a Lewis acid with an efficient Friedel-Crafts catalytic property. Aromatic rings have been alkylated smoothly with olefins or alkyl halides. By the reaction of ethylene with benzene in the presence of rhenium pentachloride, *s*-butylbenzene has been obtained as the main product. In the Friedel-Crafts acylation, a quantitative amount of the catalyst has been consumed in the reaction at a low temperature. On the other hand, the acylation reaction at a high temperature can proceed catalytically. Rhenium pentachloride is also active in the oligomerization of olefins, and in the cyclization and oligomerization of acetylenes.

Numerous metal halide-type Lewis acids, of which aluminum chloride is the most frequently used, are known as Friedel-Crafts catalysts. Until the present time, however, no definite report has appeared on the catalytic activity of group VII metal halides in the Friedel-Crafts reaction.[2] We have found, in the course of our studies of the catalytic activity of noble metal compounds, that rhenium pentachloride is a Lewis acid and that it is an efficient, though mild Friedel-Crafts catalyst, as has already been reported briefly.[3]

Experimental

Gas chromatographic analyses were carried out on a Silicone DC 550 on a Celite column, 2 m. in length, at 180°C or at 100°C. Molecular weights were determined in benzene by using a Mechrolab vapor pressure osmometer. Commercially-available rhenium pentachloride (purchased from Kanto Kagaku) was used without further purification.

Most of the products were purified by preparative gas chromatography and identified by infrared spectra (Hitachi infrared spectrometer, model EPI-S2, in a solution of carbon tetrachloride) and NMR spectra (Varian high resolution spectrometer, models DP 60 and HR 100). The boiling points and melting points were uncorrected.

Alkylation and Acylation.—The reaction conditions and results obtained are summarized in Tables I, III and IV.

The Isomerization of Alkylbenzenes.—The results obtained are summarized in Table II.

Oiligomerization and Cyclization.—The reaction conditions and results are given in Table V.

Results and Discussion

The Alkylation Reaction with Alkenes and Alkyl Halides.

—The alkylation reaction with olefins proceeded smoothly in the presence of a small amount of the catalyst, and in general a mixture of products was obtained, as is shown in Table I. The most characteristic feature of the catalytic action of rhenium pentachloride can be seen in the alkylation with ethylene. At 75°C and at an ethylene pressure of 47 kg./cm^2, a rapid pressure drop was observed, and ethylbenzene, *s*-butylbenzene and hexaethylbenzene were obtained in the ratio of 1 : 2 : 1. It is interesting to notice that *s*-butylbenzene was obtained as the main product, showing that the dimerization of ethylene to form *s*-butyl carbonium ions competes favorably with the direct attack of ethyl carbonium ions on the benzene ring. From anisole, only *p*- and *m*-*s*-butylanisoles were obtained. When a large excess of olefin was used, a considerable amount of the polymer was obtained. This means that the oligomerization of the olefin catalyzed by rhenium pentachloride is quite rapid.

When the reaction of propylene with benzene was carried out at 75°C for 24 hr., a mixed product composed of mono-, di-, tri- and tetraisopropylbenzenes was isolated. On the other hand, when the reaction was carried out with a large excess of benzene, cumene was the main product. It seems likely that some of these products were formed by the isomerization of the initial alkylation products. In order to test the isomerization of alkylbenzene catalyzed by rhenium pentachloride, several alkylbenzenes were heated with a catalytic amount of rhenium pentachloride. Table II indicates that rhenium pentachloride is active in the isomerization, as may be expected for a Friedel-Crafts catalyst.

Alkylation with alkyl halides also proceeded smoothly, as is shown in Table III. Isopropyl bromide gave the same distribution of products as that obtained from propylene.

1) Part XVII: J. Tsuji, H. Takahashi and M. Morikawa, *Tetrahedron Letters*, **1965**, 4387.
2) G. A. Olah, "Friedel-Crafts and Related Reactions," Vol. I, Interscience Pub., New York (1963), p. 201.
3) J. Tsuji, M. Morikawa and T. Nogi, *Chem. Ind.*, **1964**, 543.

Table I. Alkylation with olefin

Aromatic compound g.	Olefin	Product (g.)
Benzene 45	Ethylene (47 kg./cm²)	Ethylbenzene (0.8), *s*-Butylbenzene (1.5), Hexaethylbenzene (0.8)
Benzene 25	Propylene 30 ml.	Cumene (5.0), *m*- and *p*-Diisopropylbenzenes (4.0), 1,2,4-, and 1,3,5-Triisopropylbenzenes (3.5), 1,2,4,5-Tetraisopropylbenzene (1.5)
Benzene 25	1-Butene 30 ml.	*s*-Butylbenzene (11.5), *m*- and *p*-Di-*s*-butylbenzenes (5.0), 1,3,5-Tri-*s*-butylbenzene (1.0)
Ethylbenezene 45	Ethylene (50 kg./cm²)	*m*- and *p*-*s*-Butylethylbenezenes (2.5)
Anisole 25	Ethylene (50 kg./cm²)	*m*- and *p*-*s*-Butylanisoles (3.0)

The reactions were carried out in the 200 ml. autoclave for 24 hr. at 75°C. 1 g. of $ReCl_5$ was used.

Table II. Isomerization reaction

Aromatic compound g.	$ReCl_5$ g.	Product (%)
Cumene (5)	1	Benzene (44), Cumene (44), Diisopropylbenzene (10), Triisopropylbenzene (2)
1,2,4-Triisopropylbenzene (2)	0.5	Benzene (25), Cumene (30), Diisopropylbenzene (20), Triisopropylbenzene (25)
1,2,4-Triisopropylbenzene (2) and Benzene (10)	1	Cumene (85), Di- and Tri-isopropylbenzene (15)
o-Diethylbenzene (2)	0.5	Benzene (10), Ethylbenzene (20), Diethylbenzene (60), Triethylbenzene (10)

The reactions were carried out at 50°C for 8 hr.

Table III. Alkylation with alkyl halide

Aromatic compound g.	Alkyl halide ml.	Product (g.)
Benzene 12	Ethyl bromide 30	Ethylbenzene (2.5), *m*- and *p*-Diethylbenzenes (1.5)
Benzene 12	Isopropyl bromide 30	Cumene (3.0), *m*- and *p*-Diisopropylbenzene (2.0), 1,2,4- and 1,3,5-Triisopropylbenzenes (2.0), 1,2,4,5-Tetraisopropylbenzene (0.5)
Benzene 12	Cyclohexyl bromide 30	Cyclohexylbenzene (8.0), *p*-Dicyclohexylbenzene (2.5)
Benzene 25	Benzyl bromide 40	Diphenylmethane (21.0)

The reactions carried out at 50°C for 8 hr. 1 g. of $ReCl_5$ was used.

Acylation Reaction.—In the Friedel-Crafts acylation, it is generally known that an amount of catalyst equivalent to acyl halide is consumed as a result of the formation of a complex of metal halide with a ketonic compound formed by the acylation. The stability of the complex seems to vary with the kind of metal halide used. If the complex can be dissociated under certain conditions, especially by heating, then it might be possible to carry out the acylation reaction as a catalytic reaction. Actually this has been proved to be possible. For example, the benzoylation of toluene was found to be carried out in the presence of a catalytic amount of ferric chloride when the reaction temperature was kept between 135 and 150°C.[4] From this standpoint, the catalytic activity at a rather high temperature was compared by using chlorides of aluminum, iron(III), molybdenum and rhenium; the results are shown in Table IV.

Table IV. Benzoylation of toluene

Cayalyst	Temp.[a]	Yield 1[b]%	Yield 2[c]%
$ReCl_5$	125	850	10.5
$MoCl_5$	135	2300	29.0
$FeCl_3$	150	5000	60.0
$AlCl_3$	127	600	7.7

a) Maximum temperature, reached at the end of the reaction.
b) mol. %, based on the amount of the catalyst.
c) Based on benzoyl chloride.

As is apparent from the table, ferric chloride was the most efficient catalyst from this standpoint. As for rhenium pentachloride, the catalyst can not be recycled at 80°C; it then gives only 85%

4) A. Noguchi, T. Ikawa and Y. Shimada, *J. Soc. Org. Syn. Chem. Japan*, **21**, 377 (1963).

Table V. Oligomerization and cyclization

Olefin	Solvent ml.	Reaction		Product (g.)
		Temp., °C	Time, hr.	
Ethylene 50 kg./cm^2	Cyclohexane 30	70	20	C_4 olefins (1.5), C_6 (0.5), Higher than C_8 (0.5)
Propylene 20 ml.	Cyclohexane 20	70	20	C_6 olefin (2.0), C_9 olefin (4.5), C_{12} olefin (3.0), Higher olefins (2.0)
1-Butene 20 ml.	Cyclohexane 20	70	20	C_8-olefin (3.0), Higher olefins (2.0)
Propyne 20 ml.	*n*-Pentane 30	80	24	1,2,4- and 1,3,5-Trimethylbenezenes (1.0)

The reactions were carried out in the 200 ml. autoclave. 1 g. of $ReCl_5$ was used.

of the acylation product (based on rhenium chloride). On the other hand, a yield of 850% was obtained in the reaction carried out at 120—125°C. These results clearly show that the dissociation of the complex formed from certain metal halides and ketonic products is temperature-dependent, that at higher temperatures it is possible to carry out the acylation reaction in the presence of a catalytic amount of the metal halides.

The Oligomerization of Olefins and Acetylene.—It is known that Lewis acids can catalyze the oligomerization of olefins; rhenium chloride was tested for this activity. As is shown in Table V, a mixture of oligomers was obtained, but no selectivity was observed under the reaction conditions adopted. Therefore, no further studies were carried out. Acetylenes were found to be cyclized to form benzene derivatives in addition to a certain quantity of linear oligomers. For example, 1, 2, 4- and 1, 3, 5-trimethylbenzenes were obtained from propyne heated with rhenium pentachloride.

BULLETIN OF THE CHEMICAL SOCIETY OF JAPAN VOL. 39 716—720 (1966)

Studies of the Synthetic Inorganic Ion Exchanger. V.[1] The Separation of Zirconium-95 and Niobium-95 by Means of a Stannic Phosphate Cation Exchanger

By Akiko SATŌ, Yasushi INOUE and Shin SUZUKI

The Research Institute for Iron, Steel and Other Metals, Tohoku University, Katahira-cho, Sendai

(Received July 31, 1965)

With the aim of developing a method for the separation of ^{95}Zr and ^{95}Nb, various eluants were investigated, a sulfuric acid solution was found to be most suitable for this purpose. After the stannic phosphate exchanger column had been conditioned with 1 N nitric acid, the sample solution was passed through it to adsorb ^{95}Zr and ^{95}Nb. By using a 2 N sulfuric acid solution and a 3 N sulfuric acid - 0.01 N hydrofluoric acid solution as eluants, ^{95}Zr and ^{95}Nb could be eluted respectively. The separation was not quantitative, however, because of the unfavorable tailing of the elution curves. On the basis of the above results, the posibility of the total radiochemical separation of a long-lived fission product and the mechanism of the adsorption of these ions were discussed.

As one of the inorganic ion exchangers which may be expected to have radiation and thermal stability, stannic phosphate has previously been prepared[2,3] and its fundamental properties, such as its composition, its ion exchange capacity, its chemical stability,[2] its radiation and thermal stability, the nature of its ion exchange equilibrium, its exchange rate and its structure, were investigated.[3] Furthermore, this exchanger has been used for the separation of alkali metals,[2] the separation of individual nuclide contained in the fission products,[4] and the separation of uranium

1) Y. Inoue, S. Suzuki and H. Gotô, This Bulletin, **37**, 1547 (1964).
2) Y. Inoue, *J. Inorg. Nucl. Chem.*, **26**. 2241 (1964).
3) Y. Inoue, This Bulletin, **36**, 1316 (1963).
4) Y. Inoue, ibid., **36**, 1324 (1963).

and fission products,[1] the results have been so successful that it was found to be an excellent material for the cation exchange separation.

In a nitric acid solution, this exchanger shows high distribution coefficients of zirconium and niobium, $2—4\times10^3$ ml./g., over a wide range of acidity. Therefore, in the process of the separation of fission products, these ions once adsorbed on the exchanger bed are not eluted at all with such eluants as ammonium chloride and nitric acid.[4]

With the aim of developing a method for the separation of ^{95}Zr and ^{95}Nb, various eluants, such as hydrochloric acid, hydrofluoric acid, sulfuric acid, oxalic acid, a mixture of hydrochloric acid and hydrofluoric acid and one of sulfuric acid and hydrofluoric acid, were investigated. Of those, oxalic acid, concentrated hydrochloric acid and hydrofluoric acid in a high acidity were not applicable because stannic phosphate could not resist these media. Sulfuric acid solution was found to be the most suitable for this purpose. Then the separation of zirconium and niobium with sulfuric acid eluants was investigated in detail. The results are described below.

Experiments

Reagents.—*Ion Exchanger.*—Stannic phosphate prepared by a method described previously was used.[2]

^{95}Zr-^{95}Nb Equilibrium Mixture.—This was obtained from the Oak Ridge National Laboratories (U. S. A.) and from the N. H. Philips-Roxane-Pharmaceutisch-Chemische Industries "Duphar" (Holland) as an about 1% oxalate solution. Prior to use, concentrated nitric acid was added to this solution and it was evaporated almost to dryness. This process was repeated several times in order to convert the nuclides into their nitrate forms completely. When either ^{95}Zr or ^{95}Nb was in need individually, they were separated from one another by the acetylacetone - benzene extraction method[5] immediately before use.

The other chemicals, such as sulfuric acid, hydrofluoric acid and acetyl acetone, were of the highest purity grade.

Apparatus.—The measurements of the β and γ activities were made by a Hitachi G. M. counter and Kobe Kogyo well-type scintillation counter respectively. For making elution curves in the column operation, a fraction collector, Toyo Kagaku Sangyo Model SF-200A, was used.

Procedures.—The experimental procedures were as follows, except otherwise noted.

The Determination of the Distribution Coefficients.—The batch distribution coefficients were determined after equilibrating 500 mg. of the ion exchanger (100—200 mesh or 200—350 mesh) in hydrogen form with 50 ml. of a suitable solution for about 100 hr. in a thermostat kept at 25°C. An aliquot of the supernatant liquid was then taken out in order to measure the radioactivity. The radioactivity on the exchanger was estimated from the difference between the total activity initially taken and that found finally in the solution.

In each case, the distribution coefficient was calculated by the following equation:

$$K_d=\frac{\text{Radioactivity on exchanger/g. of exchanger}}{\text{Radioactivity in solution/ml. of solution}}$$

Column Operation.—Into 2 g. of an air-dried exchanger in hydrogen form (100—200 mesh) a sufficient amount of distilled water was well stirred in order to expel any adhering air bubbles. After mixing, the slurry was poured into a glass column tube 7 mm. in internal diameter, in which glass wool had been put as a column support. The column thus prepared was 40 mm. high. Then the exchanger bed was conditioned by 1 N nitric acid, the sample solution was loaded on the bed to adsorb zirconium and niobium, and an elution was started. The flow rate of the influent was kept nearly constant, at 0.2—0.3 ml./min., throughout this experiment.

Results and Discussion

Distribution Coefficients. — In order to contribute to the establishment of the method of separation, the distribution coefficients of ^{95}Zr and ^{95}Nb were determined in sulfuric acid media; the results are shown in Table I. In contrast with the case of a nitric acid solution,[4] the distribution coefficients of these ions decrease with the increase in the acidity and a remarkable difference between zirconium and niobium is observed; that is to say, zirconium shows a distribution coefficient lower than niobium by one order. This indicates the possibility of separating zirconium

Table I. Distribution coefficient of zirconium and niobium in sulfuric acid solution

Concn. of H_2SO_4 N	Particle size Mesh	Distribution coefficient Zr	Nb
0.5	100—200	1.18×10^2	10.9×10^2
1.0	100—200	0.37×10^2	4.65×10^2
1.5	200—350	7.48×10^2	16.6×10^2
2.0	200—350	4.61×10^2	14.4×10^2
2.5	200—350	3.59×10^2	12.6×10^2
3.0	100—200	0.10×10^2	1.10×10^2
6.0	100—200	0.02×10^2	0.17×10^2

from niobium. However, the distribution coefficients of these ions vary with the particle size of the exchanger used. This phenomenon offers one reason for the ill-defined elution peak; it may also be considered to depend on the nature of the ion exchange reaction. This will be discussed in detail later.

The Separation of ^{95}Zr and ^{95}Nb.—In order to seek some good conditions for the selective elution of ^{95}Zr, the elution of zirconium and niobium by sulfuric acid solutions of various concentrations was carried out. The results are shown in Fig. 1. Although the elution curves of zirconium show remarkable tailing under any of the conditions

5) T. Shigematsu, M. Tabushi and M. Matsui, *Bull. Inst. Chem. Res., Kyoto Univ.*, **41**, 212 (1963).

examined, the higher the acidity, the sharper the elution curve. Corresponding to the shape of the elution curve, the yield of zirconium increases with the increase in the acidity of eluant. When the acidity is 1 N, the yield is only 20% with 100 ml.

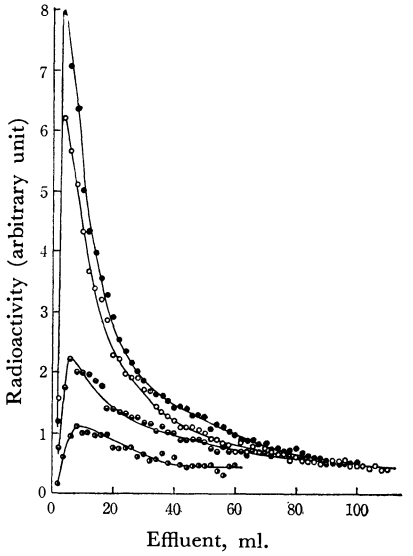

Fig. 1. The elution curves of zirconium and niobium.
—◒—: Zr, 1 N H_2SO_4;
—●—: Zr, 2.5 N H_2SO_4;
—○—: Zr, 2 N H_2SO_4;
—◑—: Nb, 2.5 N H_2SO_4.

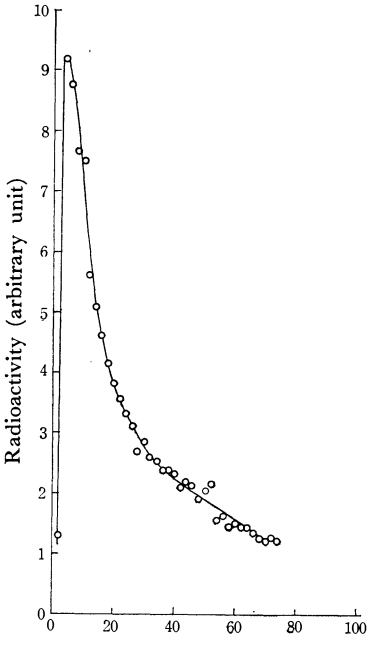

Fig. 2. The elution curve of niobium by 3 N sulfuric acid - 0.01 N hydrofluoric acid.

of the eluant; when the acidity is 2 N, the yield is about 80% with 110 ml.; when the acidity is 2.5 N, the yield is about 90% with 100 ml. Niobium, however, is eluted a little with 2.5 N sulfuric acid solution, so this acid concentration is not desirable for the separation of zirconium from niobium, although the yield of zirconium is indeed high. From the above fact, a 2 N sulfuric acid solution seems to be most adequate for the selective elution of zirconium. In order to confirm this, the zirconium solution obtained after the elution was submitted to the drawing of a β-ray absorption curve by aluminum absorbers; it was confirmed that this solution contained a monoenergetic nuclide with a maximum energy of 0.40 MeV. This fact establishes the complete separation of zirconium from niobium.

From the values of the distribution coefficients, the sulfuric acid solution seems to be ineffective in the elution of niobium. Therefore, its elution was performed with a sulfuric acid solution containing a small amount of hydrofluoric acid. In this case the hydrofluoric acid concentration should be kept as low as possible because too many fluoride ions may dissolve the exchanger. As is shown in Fig. 2, the 3 N sulfuric acid - 0.01 N hydrofluoric acid mixture was effective in the elution of niobium. Tailing was observed in this curve as in the case of zirconium, but the shape of elution curve is comparatively sharp and the yield is about 80% with 75 ml. of the eluant.

As has been mentioned above, the separation of zirconium and niobium can be achieved by using a 2 N sulfuric acid solution at first for zirconium, and then a 3 N sulfuric acid - 0.01 N hydrofluoric acid solution for niobium. The niobium fraction, however, is partially contaminated with

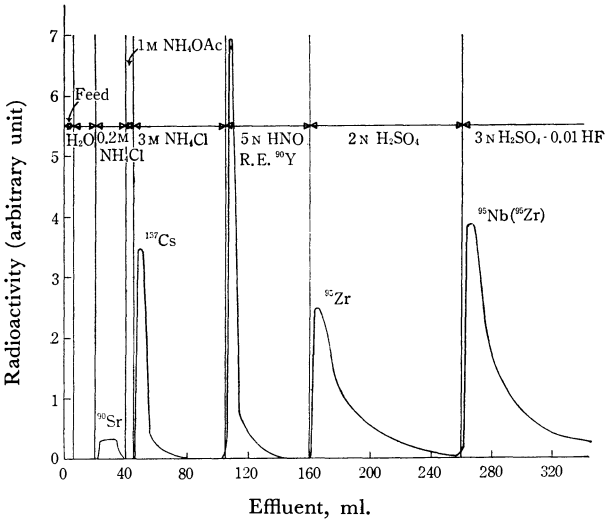

Fig. 3. Schematic representation of the separation of fission products.

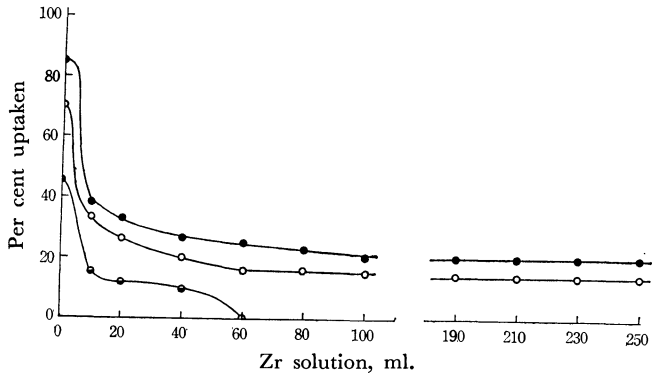

Fig. 4. Adsorption of zirconium from 1 N nitric acid solution.
Concn. of Zr: 0.01 M; —◒—: −100 mesh; —○—: 100—200 mesh; —●—: 200—350 mesh

zirconium because of the incomplete elution of the latter.

Discussion.—As has been stated in a preceding report,[4] in the separation of long-lived fission products, ^{95}Zr and ^{95}Nb in the nitric acid solution were not quantitatively adsorbed on the exchanger, but they could not be eluted at all by any eluants when they were once adsorbed. From the results of the present investigation, it may be considered that they can be separated from other fission products by eluting them with the eluants mentioned above after rare earths have been eluted according to the procedure described in the third part of this series.[4] This process is shown schematically in Fig. 3. It should be borne in mind that zirconium contaminates niobium to some extent because of the unfavorable tailing of its elution curve.

Many peculiar aspects of the behavior of zirconium and niobium in response to this ion exchanger have been observed. One of these aspects is the independency of the distribution coefficients on the concentration of nitric acid solution, as has been stated earlier.[4] It is clear from this observation that the adsorption of zirconium cannot be explained by the simple cation exchange reaction for which the mass action law holds. The other aspects are the intense tailing of the elution curve and the difference in the distribution coefficients obtained with the ion exchanger as its particle size varies. This behavior has not been observed in the case of the other ions, so it seems to characterize zirconium and niobium. In order to clarify this point, the adsorption of zirconium from 1 N nitric acid was examined by the column operation of the above-mentioned experimental procedure with the exchanger having various particle sizes, as is shown in Fig. 4. These curves do not show a S-shape, as is usually observed in an ion-exchange resin; rather, they composed of two parts, one of which represents rapid adsorption, while the other is a part of the long tailing. The effect of the particle size is remarkable; namely, when it is greater than 100 mesh, the exchanger is saturated with the passage of only 60 ml. of a 0.01 M zirconium solution. On the other hand, when the particle size is smaller than this, the exchange is not saturated with even more than 250 ml. of a 0.01 M solution. If we assume that one molecule of zirconium corresponds to four equivalents, the break-through capacity of the exchanger coarser than 100 mesh is calculated to be 0.096 meq./g. When the exchanger is 100—200 mesh, the amounts of zirconium adsorbed after the passage of 250 ml. of a 0.01 M solution is 0.44 meq./g. These values are extremely low compared with the hydrogen absorption capacity and the hydrogen liberation capacity of 1.3—1.4 meq./g. as defined in the first part of this series.[2] The tailing encountered in the elution step and the incomplete uptake of zirconium seem to be attributable to the slow rate of the adsorption-desorption reaction. This can also be reasonably explained by the fact that when adsorption is continued after an interruption of 10 hr. or more, the adsorption curve comes to be as if it were obtained with a new exchanger. From the above results it may reasonably be postulated that there are two kinds of adsorption sites. One is on the surface of the exchanger particle, while the other is in the inner part. On the surface, zirconium is adsorbed rapidly and reversibly, whereas in the inner part of the particle the adsorption is slow and irreversible. The adsorption in the inner part of the particle may proceed by one of the following two mechanisms. One is the formation of stable zirconium compounds with the phosphate because the presence of a lot of free phosphate groups close to each other in the inner part of the particle, unlike such a grouping on the surface of the materials, may facilitate the reaction. This argument is consistent with the property of zirconium, which easily forms sparingly-soluble compounds with phosphate, even in a strong acid solution. Another possibility is the exchange of tin, one of the elements constructing the exchanger net work, for the zirconium ion. At present it

cannot be decided conclusively which is the correct mechanism. Therefore, further investigations must be carried out.

Summary

The separation of zirconium and niobium has been carried out by means of a stannic phosphate cation exchanger. By using a 2 N sulfuric acid solution and a 3 N sulfuric acid-0.01 N hydrofluoric acid solution as eluants, zirconium and niobium could be eluted respectively. However, the separation was not quantitative because of the unfavorable tailing of the elution curves. From the above results, the possibility of the total radiochemical separation of long-lived fission products and the mechanism of the adsorption of these ions have been discussed.

Part of the expenses for this investigation have been defrayed by a grant-in-aid by the Ministry of Education.

BULLETIN OF THE CHEMICAL SOCIETY OF JAPAN VOL. 39 720—725 (1966)

The Heats of Mixing for Binary Mixtures. III. The Intermolecular Energy of Hydrogen Bonding between Alcohol and Several Other Polar Molecules

By Sachio MURAKAMI and Ryoichi FUJISHIRO

Department of Chemistry, Faculty of Science, Osaka City University, Sumiyoshi-ku, Osaka

(Received July 31, 1965)

Calorimetric measurements of the heat of mixing have been made at 25.0±0.01°C for binary mixtures of *n*-butanol with polar liquids (acetonitrile, acetone, *n*-butyl ether, and *n*-butyl amine), and for binary mixtures of polar liquids with *n*-hexane. The calorimeter for measuring the heats of mixing was of twin type, and a thermomodule, HTM 0516 type (Sharp Electric Co., Ltd., Osaka) was used as the temperature-sensing device. By plotting the values of the heat of mixing, $\Delta H^{M}_{x_1}$, against the mole fraction of component 1, x_1, and by extrapolating the curve to an infinite dilution ($x_1 \rightarrow 0$) for each system, the heats of mixing per mole of component 1 at an infinite dilution ($\lim_{x_1 \rightarrow 0} \Delta H^{M}_{x_1}$) were obtained graphically. By using the values of $\lim_{x_1 \rightarrow 0} \Delta H^{M}_{x_1}$ obtained for these systems and by using the same treatment as that described in a previous paper [S. Murakami, K. Amaya and R. Fujishiro, This Bulltein, **37**, 1776(1964)], the intermolecular hydrogen bond energies between alcohol and polar molecules were estimated; it was found that the strength of the hydrogen bond was in the following order: *n*-butyl amine > *n*-butyl ether > acetone > acetonitrile. This agrees with the results obtained from the spectroscopic study.

In previous papers,[1,2] the heats of mixing for alcohol+ketone and alcohol+hexane solutions have been measured, and from these data the hydrogen bond energy between alcohol and ketone molecules has been estimated.

In the present paper, the same treatment will be applied to the *n*-butanol+polar liquid+hexane systems, and the hydrogen bond energies between butanol and polar molecules will be estimated. Acetonitrile, acetone, *n*-butyl ether and *n*-butyl amine will be used as the polar liquids.

Experimental

The apparatus for measuring the heats of mixing is the same as that used in the previous papers,[1,2] except for replacing a 7-junction copper-constantan

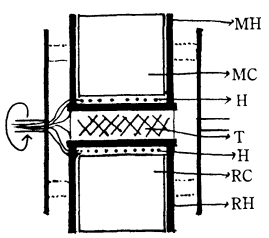

Fig. 1. Calorimeter.

MH: Mixing holder
MC: Mixing cell
H : Heater
T : Thermomodule (temperature-sensing device)
RC: Reference cell
RH: Reference holder

1) S. Murakami, K. Amaya and R. Fujishiro, This Bulletin, **37**, 1776 (1964).
2) M. Takami, S. Murakami and R. Fujishiro, ibid., **38**, 291 (1965).

thermocouple with a thermomodule, type HTM 0516 (Sharp Electric Co., Ltd., Osaka), in order to detect a smaller temperature change. The mixing cell and other modifications are shown schematically in Fig. 1.

The experimental procedure was similar to that described in the previous papers.[1,2]

In order to check the accuracy of our calorimeter, the heat of mixing was measured for the benzene+carbon tetrachloride system, on which the fairly accurate data of the heat of mixing had previously been obtained by Larkin and McGlashan.[3] The results obtained are shown in Fig. 2, together with those obtained by Larkin and McGlashan; here x_1 is the mole fraction of carbon tetrachloride, and ΔH^M is the heat of mixing expressed in joule per mole of the mixture. Our results are found to agree with those of Larkin and McGlashan within an error of only a few percent.

Alcohol, acetone, and *n*-hexane were purified in the way described previously. *n*-Butyl ether was shaken with concentrated sulfuric acid, with a dilute aqueous solution of sodium carbonate, further with water and with mercury for a long time, and finally distilled

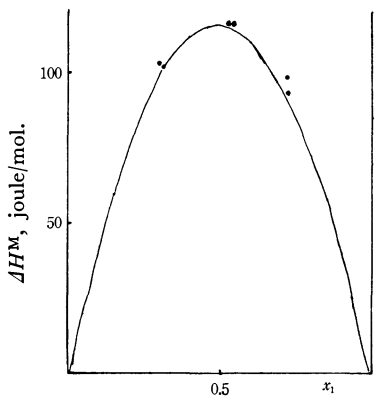

Fig. 2. Heats of mixing curve for carbon tetrachloride+benzene system.
—— Larkin and McGlashan
● This work

twice in a long column. A commercial *n*-butyl amine was fractionally distilled twice with sodium in a long column covered with aluminum foil in order to protect the amine from decomposition by light. The gas chromatographs of all the samples on polyethylene glycol and d-nonyl phthalate substrates showed a single peak.

Results and Discussion

The measurements of heats of mixing were carried out on the polar liquid+*n*-hexane systems and *n*-butanol+polar liquid systems at 25.0±0.01°C. The results obtained are given in Tables I to VIII and in Figs. 3 to 5, where x_1 is the mole fraction of component 1, and ΔH^M and $\Delta H^M_{x_1}$ are the heats of mixing expressed in cal. per mole of mixture and

3) J. A. Larkin and M. L. McGlashan, *J. Chem. Soc.*, **1961**, 3425.

Table I. Heat of mixing of *n*-butanol (1) and *n*-hexane (2)

Mole fraction of the component 1, x_1	ΔH^M, cal./mol. of mixture	$\Delta H^M_{x_1}$, kcal./mol. of the component 1
0.0241	59.2	2.462
0.0543	80.1	1.475
0.1372	115.1	0.840
0.2150	137.6	0.640
0.2803	137.1	0.489
0.2830	143.1	0.506
0.2890	142.2	0.492
0.4765	129.1	0.271
0.4823	130.5	0.271
0.4913	126.1	0.257
0.5863	112.9	0.193
0.7133	85.5	0.120
0.8234	57.0	0.069_3
0.9001	35.9	0.039_8

Table II. Heat of mixing of *n*-butyl ether (1) and *n*-hexane (2)

Mole fraction of the component 1, x_1	ΔH^M, cal./mol. of mixture	$\Delta H^M_{x_1}$, kcal./mol. of the component 1
0.0304	2.5_7	0.084_5
0.0366	3.1_8	0.087_0
0.0469	4.2_4	0.090_4
0.0866	8.7_9	0.101
0.0934	11.2	0.117
0.2348	18.7	0.085_2
0.2594	18.5	0.071_3
0.3746	19.3	0.051_4
0.3787	19.0	0.050_3
0.5846	20.2	0.034_6
0.6764	15.9	0.023_5
0.8705	7.8_7	0.009

Table III. Heat of mixing of *n*-butyl amine (1) and *n*-hexane (2)

Mole fraction of the component 1, x_1	ΔH^M, cal./mol. of mixture	$\Delta H^M_{x_1}$, kcal./mol. of the component 1
0.0466	54.8	1.176
0.1105	118.1	1.069
0.1613	153.0	0.949
0.2794	215.6	0.772
0.3917	237.6	0.607
0.4905	233.1	0.475
0.6069	225.5	0.372
0.7037	196.4	0.279
0.8197	132.6	0.162
0.8987	80.4	0.089

Table IV. Heat of mixing of acetonitrile (1) and *n*-hexane (2)

Mole fraction of the component 1, x_1	ΔH^M, cal./mol. of mixture	$\Delta H^M_{x_1}$, kcal./mol. of the component 1
0.0205	56.4	2.75
0.0236	69.4	2.93
0.0256	57.3	2.24
0.0292	71.5	2.45

TABLE V. HEAT OF MIXING OF *n*-BUTANOL (1) AND ACETONITRILE (2)

Mole fraction of the component 1, x_1	ΔH^M, cal./mol. of mixture	$\Delta H^M_{x_1}$, kcal./mol. of the component 1
0.0306	64.5	2.105
0.544	107.4	1.975
0.1056	190.5	1.808
0.2065	325.7	1.577
0.2793	381.0	1.364
0.3748	419.6	1.119
0.4906	437.3	0.891
0.4968	437.4	0.881
0.5154	436.2	0.846
0.5708	425.0	0.745
0.7009	360.4	0.514
0.7721	278.5	0.361
0.9067	149.7	0.165

TABLE VI. HEAT OF MIXING OF *n*-BUTANOL (1) AND ACETONE (2)

Mole fraction of the component 1, x_1	ΔH^M, cal./mol. of mixture	$\Delta H^M_{x_1}$, kcal./mol. of the component 1
0.0341	53.4	1.566
0.0599	88.1	1.471
0.1266	163.0	1.288
0.2209	244.5	1.107
0.2486	268.4	1.080
0.3584	305.4	0.852
0.4121	311.9	0.757
0.4841	328.8	0.675
0.4904	326.7	0.666
0.4906	327.5	0.660
0.5475	328.3	0.600
0.6843	297.9	0.435
0.6937	296.5	0.427
0.8086	200.8	0.248
0.8448	180.6	0.214
0.8997	111.4	0.124

TABLE VII. HEAT OF MIXING OF *n*-BUTANOL (1) AND *n*-BUTYL ETHER (2)

Mole fraction of the component 1, x_1	ΔH^M, cal./mol. of mixture	$\Delta H^M_{x_1}$, kcal./mol. of the component 1
0.0202	24.4	1.210
0.0626	70.2	1.121
0.1205	124.4	1.032
0.1627	145.7	0.896
0.2026	175.2	0.865
0.2940	189.4	0.644
0.3828	191.7	0.501
0.4038	191.6	0.480
0.4412	188.9	0.410
0.4741	191.9	0.405
0.5665	172.7	0.305
0.6858	145.5	0.212
0.7901	106.8	0.135
0.9153	42.4	0.045

TABLE VIII. HEAT OF MIXING OF *n*-BUTANOL (1) AND *n*-BUTYL AMINE (2)

Mole fraction of the component, 1, x_1	ΔH^M, cal./mol. of mixture	$\Delta H^M_{x_1}$, kcal./mol. of the component 1
0.0348	65.8	1.891
0.0590	111.7	1.893
0.1013	190.2	1.894
0.1027	197.6	1.923
0.2118	375.5	1.773
0.3013	487.5	1.619
0.3935	566.7	1.440
0.4781	599.6	1.254
0.5848	564.8	0.966
0.6864	497.2	0.724
0.8031	437.1	0.494
0.8910	212.1	0.238

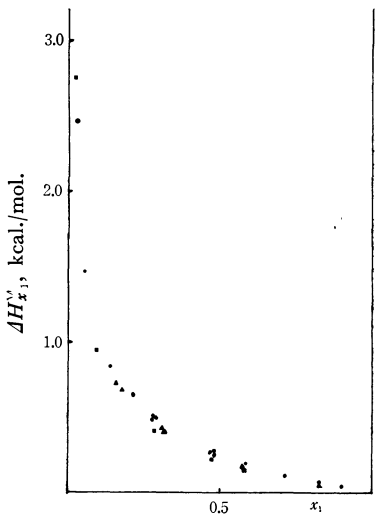

Fig. 3. Heats of mixing for *n*-butanol+*n*-hexane system.
■: Wolf, Pahlke and Wehage
▲: Brown, Fock and Smith
●: This work

those expressed in kcal. per mole of component 1 respectively.

In Fig. 3, the results we obtained for the *n*-butanol+*n*-hexane system are compared with those reported by Brown, Fock and Smith,[4] and also those reported by Wolf, Pahlke and Wehage.[5] A fairly good agreement is found between the present results and the previously published ones.

Plotting ΔH^M_x against x_1 and extrapolating the curve to an infinite dilution ($x_1 \to 0$) for each system, as is shown in Figs. 3 to 5, we can obtain the heats of mixing per mole of component 1 at the infinite dilution ($\lim_{x_1 \to 0} \Delta H^M_x$). They are as follows:

4) I. Brown, W. Fock and F. Smith, *Aust. J. Chem.*, **17**, 1106 (1964).
5) Landolt-Börnstein, "Physikalishe-Chemischen Tabellen," Springer, Berlin (1936).

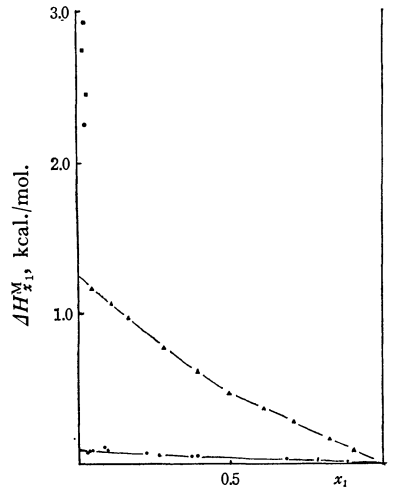

Fig. 4. Heats of mixing for polar liquid+ *n*-hexane system.
■: Acetonitrile+*n*-hexane
▲: *n*-Butyl amine+*n*-hexane
●: *n*-Butyl ether+*n*-hexane

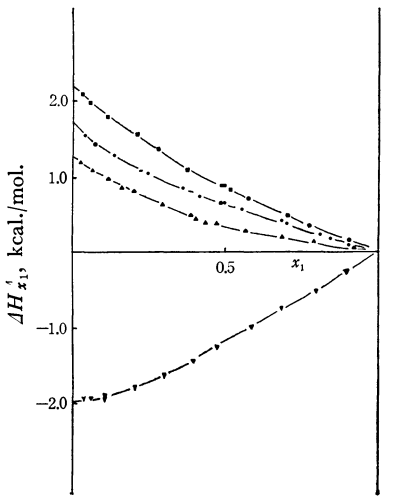

Fig. 5. Heats of mixing for *n*-butanol+polar liquid system.
■: *n*-Butanol+acetonitrile
●: *n*-Butanol+acetone
▲: *n*-Butanol+*n*-butyl ether
▼: *n*-Butanol+*n*-butyl amine

2.25 kcal. for the *n*-butanol(1)+acetonitrile(2)

1.70 kcal. for the *n*-butanol(1)+acetone(2)

1.26 kcal. for the *n*-butanol(1)+*n*-butyl ether(2)

−1.98 kcal. for the *n*-butanol(1)+*n*-butyl amine (2)

1.27 kcal. for the *n*-butyl amine(1)+*n*-hexane(2)

0.10 kcal. for the *n*-butyl ether(1)+*n*-hexane(2)

For the *n*-butanol+*n*-hexane system, as is shown in Fig. 3, however, the extrapolation to $x_1=0$ is very difficult because the curve is very steep at small x_1 values and the measurements are accompanied with considerable errors at these concentration ranges. Fortunately, the value of $\lim_{x_1\to 0} \Delta H^{M}_{x_1}$ had been found by Pahlke[5] for this system to be 5.50 kcal. Therefore, we have adopted 5.50 kcal. for the $\lim_{x_1\to 0} \Delta H^{M}_{x_1}$ of this system.

Measurements of the acetonitrile+*n*-hexane system were also very difficult, because only a slight amount of acetonitrile dissolves into *n*-hexane at room temperature. The $\Delta H^{M}_{x_1}$ values obtained for this system have scattered from 2.2 to 2.9 kcal./mol. at $x_1\simeq 0.02$. The extrapolation to $x_1=0$, using only experimental data in the limited concentration range, gives 3 kcal., but its error may amount to ± 0.5 kcal.

In pure alcohol, all the molecules form hydrogen bonding with each other, while each alcohol molecule in the infinite dilution of alcohol in hexane is surrounded by hexane molecules and the hydrogen bonds are broken. Therefore, the value of 5.50 kcal. represents the energy sufficient to break the hydrogen bonds of pure alcohol. Similarly, the $\lim_{x_1\to 0} \Delta H^{M}_{x_1}$ values for the alcohol+polar liquid systems correspond to the energy change from the pure alcohol state to that in which each alcohol molecule makes a hydrogen bond with a polar molecule and in which such complexes are surrounded with a large amount of the polar-liquid medium. Roughly speaking, the difference between the $\lim_{x_1\to 0} \Delta H^{M}_{x_1}$ values for the alcohol + polar liquid systems and that for the alcohol + hexane system may correspond to the measure of the alcohol + polar liquid intermolecular hydrogen bonding. The results are as follows:

−2.25 kcal. for *n*-butanol+acetonitrile

−3.80 kcal. for *n*-butanol+acetone

−4.24 kcal. for *n*-butanol+*n*-butyl ether

−7.48 kcal. for *n*-butanol+*n*-butyl amine

It may be seen from these values that butanol forms the strongest hydrogen bond with *n*-butyl amine, while it forms the weakest hydrogen bond with acetonitrile. Strictly speaking, in the values mentioned above, the dipolar stabiiization energy must be included, because alcohol + polar liquid complex molecules are embedded in the polar medium.

In order to estimate the hydrogen bond energy more properly, we carried out the treatment described in previous papers,[1,2] applying the thermochemical cycle depicted in Fig. 6. The intermolecular hydrogen bond energy, ΔH_5, between alcohol and polar-liquid molecules is given by:

$$\Delta H_5 = -\Delta H_1 - x\Delta H_2 + \Delta H_3 + \Delta H_4 \qquad (1)$$

TABLE IX. PHYSICAL CONSTANTS OF ALCOHOL-POLAR LIQUID COMPLEXES NECESSARY FOR CALCULATION OF DIPOLAR ENERGIES AND CALCULATED VALUES OF ΔG_i AND ΔH_i

	μ D	t °C	α $\times 10^{23}$	a^3 $\times 10^{23}$ cc.	$-\Delta G_p$ kcal./mol.	$-\Delta H_p$ kcal./mol.	$-\Delta G_H$ kcal./mol.	$-\Delta H_H$ kcal./mol.
		15	1.3189	5.6793	4.0964		1.3565	
A-CN	5.11	20	1.3192	5.7101	4.0639	5.97	1.3413	2.23
		25	1.3194	5.7414	4.0310	5.99	1.3261	2.23
					Average	5.98	Average	2.23
		15	1.5187	6.5045	2.3106		0.79489	
A-K	4.19	20	1.5192	6.5422	2.2890	3.55	0.78567	1.32
		25	1.5194	6.5794	2.2676	3.55	0.77659	1.32
					Average	3.55	Average	1.32
		15	2.5035	10.295	0.32774		0.19493	
A-E	2.60	20	2.5034	10.344	0.32157	0.68	0.19289	0.313
		25	2.5039	10.399	0.31518	0.70	0.19072	0.319
					Average	0.69	Average	0.32
		15	1.8309	7.5211	0.56774		0.25443	
A-NH_2	2.54	20	1.8282	7.5403	0.55873	1.09	0.25231	0.37
		25	1.8254	7.5598	0.54935	1.11	0.25019	0.37
					Average	1.10	Average	0.37

Dielectric constant;

t°C	15	20	25
Acetonitrile	38.3	37.5	36.7
Acetone	(21.7)	21.2	20.7
n-Butyl ether	(3.18)	(3.12)	3.06
n-Butyl amine	(5.52)	5.34	5.16
n-Hexane	1.897	1.890	1.883

* μ, α and a are dipole moment, the polarizability and the molecular radius of the A-polar liquid complex, respectively. They are estimated in the same way as that described in the previous paper.[1]

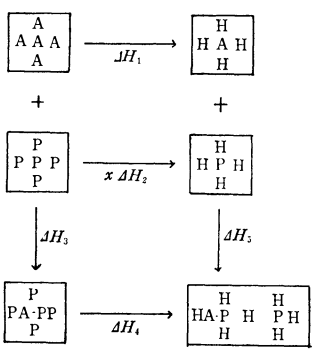

Fig. 6. The thermochemical cycle.

Here ΔH_1 is the energy of breaking the hydrogen bonds of pure alcohol by adding a large quantity of hexane; $x\Delta H_2$, the heat of the dilution of x mol. of polar liquid by a large amount of hexane and ΔH_3, the energy change accompanied by the dilution of the pure alcohol by a large amount of polar liquid; ΔH_4 consists of two parts; the first one is equal to $(x-1)\Delta H_2$, while the second one is due to the difference in the dipolar stabilization energy of a complex dipole arising from the reaction field by different media. This part of the energy change in ΔH_4 may be calculated by the previously-described method.[1,2] The results obtained are summarized in Table IX, together with the data necessary for this calculation.

By using the ΔH_4 value calculated above and the other measured values, the intermolecular hydrogen bond energies between the alcohol and polar molecules, ΔH_5, are found from Eq. 1 to be:

for *n*-butanol+acetonitrile (A-CN):

$$\Delta H_5 = -5.50 - 3x + 2.25 + 3.75 + 3(x-1)$$
$$= -2.50 \text{ kcal.}$$

for *n*-butanol+acetone (A-K):

$$\Delta H_5 = -5.50 - 2.15x + 1.70 + 2.23 + 2.15(x-1)$$
$$= -3.72 \text{ kcal.}$$

for *n*-butanol+*n*-butyl ether (A-E):

$$\Delta H_5 = -5.50 - 0.10x + 1.26 + 0.37 + 0.10(x-1)$$
$$= -3.97 \text{ kcal.}$$

for *n*-butanol+*n*-butyl amine (A-NH_2):

$$\Delta H_5 = -5.50 - 1.27x - 1.98 + 0.72 + 1.27(x-1)$$
$$= -8.03 \text{ kcal.}$$

The strength of the hydrogen bond between alcohol and polar molecules is in the following order:

A-NH_2>A-E>A-K>A-CN.

It is known from the spectroscopic study[6] that the shift in the frequency of the O–H bands, $\Delta\nu_s$, of alcohol in a variety of polar liquids is arranged in the order of:

$$A\text{-}NH_2 > A\text{-}E > A\text{-}K > A\text{-}CN.$$

Therfore, if $\Delta\nu_s$ is correlated with the energy of a hydrogen bond, the above-estimated intermolecular hydrogen bond energies agree with the results obtained from the spectroscopic study.

Summary

The heats of the mixing of *n*-butanol with polar liquids (acetonitrile, acetone, *n*-butyl ether, and *n*-butyl amine) and those of polar liquids with *n*-hexane have been measured calorimetrically. The results obtained for these systems have been compared with one another, and it has been found that the intermolecular hydrogen bond energies between alcohol and polar molecules are as follows:

−2.5 kcal. for *n*-butanol+acetonitrile

−3.7 kcal. for *n*-butanol+acetone

−4.0 kcal. for *n*-butanol+*n*-butyl ether

−8.0 kcal. for *n*-butanol+*n*-butyl amine

The authors wish to thank Dr. Ko Kimura for his kind advice. The expenses of this work have been partly defrayed by a grant from the Ministry of Education.

6) W. Gordy, *J. Chem. Phys.*, **7**, 93 (1939).

BULLETIN OF THE CHEMICAL SOCIETY OF JAPAN VOL. 39 725—728 (1966)

Spectroscopic Studies of Dialkylaluminum Alkoxides and the Trialkylaluminum-Ether Complex. I. Structures and Symmetries*1

By Ryokichi TARAO

Research Center, Chisso Co., Ltd., Kanazawa-ku, Yokohama

(Received August 2, 1965)

The infrared and Raman spectra of $[Al(CH_3)_2OCH_3)]_3$, $[Al(C_2H_5)_2OCH_3]_3$, $[Al(C_2H_5)_2 \cdot OC_2H_5]_2$, and $Al(CH_3)_3 \cdot (CH_3)_2O$ have been measured in the 3000—300 cm^{-1} region, and the infrared absorption bands and the Raman lines in the skeletal vibration region (720—300 cm^{-1}) have been compared. For $[Al(CH_3)_2OCH_3]_3$ and $[Al(C_2H_5)_2OCH_3]_3$, the results are consistent with trimeric structures with symmetry D_{3h}. For $[Al(C_2H_5)_2OC_2H_5]_2$, the results are consistent with a dimeric structure with symmetry V_h. Thus, the structures with the oxygen bridge proposed by Hoffmann for these polymeric compounds have been confirmed by spectroscopic measurements. The structures with alkyl bridges are very unlikely. For $Al(CH_3)_3 \cdot (CH_3)_2O$, the results do not contradict the postulated structure, with symmetry C_s.

It has been suggested, although there has been no direct experimental evidence, that dimethylaluminum methoxide $[Al(CH_3)_2OCH_3]_3$, diethylaluminum methoxide $[Al(C_2H_5)_2OCH_3]_3$, and diethylaluminum ethoxide $[Al(C_2H_5)_2OC_2H_5]_2$ have the molecular structures of the dimeric or trimeric bridge forms represented by[1,2]:

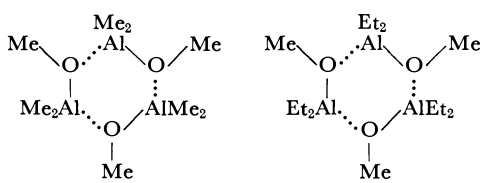

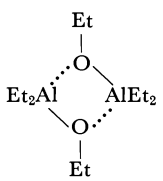

and that the trimethylaluminum - dimethyl ether complex, $Al(CH_3)_3 \cdot (CH_3)_2O$, has the structure with symmetry C_s represented by[3]:

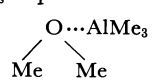

Structures with the alkyl bridges, as in the case of trimethylaluminum, however, also appear to be possible for these three dialkylaluminum alkoxides. In the present study, in order to

*1 Presented in part at the 18th Annual Meeting of the Chemical Society of Japan, Osaka, April, 1965.

1) E. G. Hoffmann, *Ann.*, **629**, 104 (1960).

2) N. Davidson and H. C. Brown, *J. Am. Chem. Soc.*, **64**, 316 (1942).

3) S. Takeda and R. Tarao, This Bulletin, **38**, 1567 (1965).

TABLE I. DIALKYLALUMINUM ALKOXIDES AND THE TRIMETHYLALUMINUM - DIMETHYL ETHER COMPLEX

Compond	B.p., °C/mmHg	Al %		Mol. wt.	
		Calcd.	Found*1	Calcd.	Found*2
$(AlMe_2OMe)_3$*3	75.6—76.8/4	30.7	30.3	264.2	294.7
$(AlEt_2OMe)_3$	70.5—72.0/5	23.2	23.0	348.4	361.1
$(AlEt_2OEt)_2$*4	59.0/1.5	20.7	20.4	260.3	278.7
$AlMe_3 \cdot Me_2O$*4	41.5/10	22.8	22.7	118.2	121.6

*1 Analysis was carried out by volumetric method (oxine complex salt method).
*2 Molecular weights were determined by measuring freezing point depression of benzene solution; values listed are mean values of several measurements.
*3 Me=CH_3, Et=C_2H_5. These abbreviations are used throughout Tables I—II.
*4 Cited from Ref. 3.

obtain some positive evidences of these proposed structures, the infrared and Raman spectra of these three dialkylaluminum alkoxides and the trimethylaluminum - dimethyl ether complex have been measured, and the infrared absorption bands and the Raman lines in the skeletal vibration region (720—300 cm^{-1}) have been compared. Some conclusions have been reached from these spectra as to the structures of these compounds.

The infrared spectra of diethylaluminum ethoxide and the trimethylaluminum-dimethyl ether complex were reported in the previous paper,[3] but those of dimethylaluminum methoxide and diethylaluminum methoxide and the Raman spectra of these four compounds have not yet been reported as far as the author is aware.

Experimental

Dimethylaluminum methoxide was prepared by the reaction of trimethylaluminum with methanol. Diethylaluminum methoxide was prepared by the reaction of triethylaluminum with methanol. Diethylaluminum ethoxide was prepared by the reaction of triethylaluminum with ethanol. The trimethylaluminum - dimethyl ether complex was prepared by the reaction of trimethylaluminum with dimethyl ether. Table I shows the boiling points, aluminum contents, and molecular weights of these four compounds.*2

The infrared spectra were measured in the 3000—300 cm^{-1} region in the liquid state with a Japan Spectroscopic Co., Model DS-402G infrared spectrophotometer. The procedure described in the previous paper was used.[3] The Raman spectra were measured in the same region and in the liquid state with a Shimadzu GRS Raman spectrophotometer. All the samples were distilled into Raman tubes, which were then sealed off under reduced pressure to prevent contamination with air or moisture. Figure 1 shows the Raman spectra observed. The Raman spectrum of dimethylaluminum methoxide was also measured in a 10 volume per cent benzene solution. The spectrum obtained was merely a superposition of the spectrum of pure dimethylaluminum methoxide on that of benzene. No Raman line of dimethylaluminum methoxide shifted to either a higher or a lower frequency.

*2 The author is indebted to Mr. Hitoshi Shinkoda for his aluminum analysis.

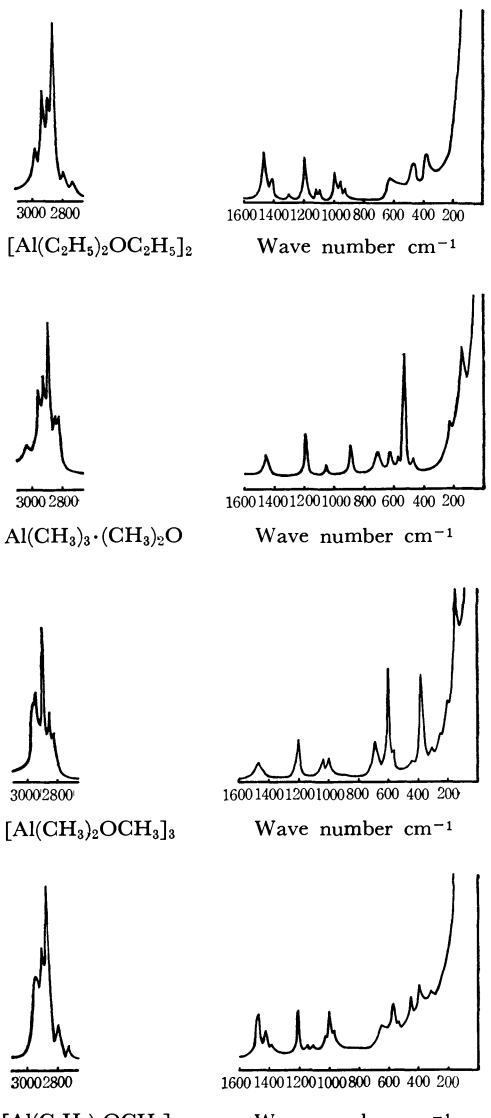

Fig. 1. The Raman spectra of dialkylaluminum-alkoxides and the trimethylaluminum - dimethyl ether complex.

Table II. Observed frequencies of dialkylaluminum alkoxides and the trimethylaluminum-dimethyl ether complex in cm^{-1}

$(AlMe_2OMe)_3$		$(AlEt_2OMe)_3$		$(AlEt_2OEt)_2$		$AlMe_3 \cdot Me_2O$	
Raman	IR	Raman	IR	Raman	IR*	Raman	IR*
						3035w	3028w
	2988 sh		2989 sh	2974w	2977m	2989 vw	2983m
2953m	2954 sh					2957m	2953 sh
2935m	2934 s	2937m	2941 s	2930m	2939 s	2926m	2925 s
2894 s	2895w	2897w	2901 s	2898w	2901 s	2887 s	2889m
2854m	2853m	2865 s	2865 s	2865 s	2864 s	2842m	2847w
2828w	2829 vw					2820m	2820 vw
		2792m	2796m	2791w	2791w		
		2730 vw	2731w	2729w	2727w		
					1482w		
			1467m		1462 sh		
1458w	1457m	1464 s	1454m	1458 s	1451 s	1460m	1462 s
		1414m	1411m	1410m	1409 s		
		1381 vw	1376w		1394 s		
				1295w	1288m		
	1256 vw		1254w		1254w		1250w
			1223w		1222w		
1201m	1200 vs	1195 s	1197 s	1193 s	1193 s	1190m	1185 vs
		1134 vw		1118w			1153m
		1099w		1084w	1100 s		
1018m	1019 vw	1016 vw	1019 vw		1058 vs	1052w	1046 vs
994w	987 vs	988 s	984 vs	990m	985 s		
		962 vw	956w	955w	948m		
			918m	928w	914w		
			885w		894 s	894m	891 s
			848w		806 s		
687m	686 vs	650m	655 vs		652 vs	716m	710 s
	642 s		632m	634m		625m	622m
596 s		568 s				576w	
569 vw	567 vw	536 vw	540 vw			525 vs	525m
					481w		
440 vw	437m	449w	460m	462m		470w	473m
380 s		393 s		380m			
309 vw	305m	339 vw	351m				

* Data in the 2000—300 cm^{-1} region are cited from Ref. 3.

Dimethylaluminum Methoxide

Hoffmann found that this compound takes a trimeric structure in the benzene solution.[1] The similarity between the Raman spectrum in the liquid state and that in the benzene solution described above shows that the same trimeric structure remains also in the liquid state.

In the liquid state this compound has five infrared absorption bands and six Raman lines in the 720—300 cm^{-1} region; of those, four are both infrared and Raman active, as is shown in Table II.

There are two possible structural formulas, I and II, for this trimeric compound;

Formula I, with symmetry D_{3h}, has an oxygen bridge which would be formed by the coordination of lone-pair electrons in oxygen atoms with aluminum. Formula II, with symmetry C_{3v} or

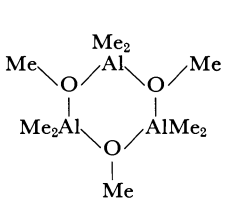

I

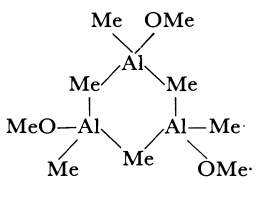

II

C_s, has an alkyl bridge which would be formed by the half bonds, as in the case of trimethylaluminum. Here the following postulations are made: the six atoms which constitute the oxygen bridge ring (model I) or the alkyl bridge ring (model II) are on a plane and occupy the six apices of a hexagon with D_{3h} symmetry; three methoxyl groups (model I) or three bridging alkyl groups (model II) lie on the ring plane, and

the plane containing two terminal alkyl groups (model I) or terminal methoxyl and alkyl groups (model II) and an aluminum atom is perpendicular to the ring plane. Model II requires that all skeletal vibrations be both infrared and Raman active. On the other hand, model I requires the skeletal vibrations of the species E' to be both infrared and Raman active, those of the species A_2'' to be infrared active and Raman inactive, and those of the species A_1' and E'' to be infrared inactive and Raman active. The results described above support model I.

Diethylaluminum Methoxide

In the liquid state this trimeric compound has five infrared absorption bands and six Raman lines in the 720—300 cm^{-1} region; of these four are both infrared and Raman active, as is shown in Table II. These results are quite similar to those of dimethylaluminum methoxide. Analogous considerations lead to the conclusion that this compound is represented by the oxygen bridge model III:

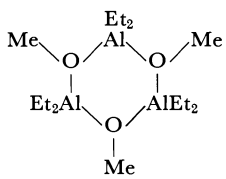

III

Diethylaluminum Ethoxide

For this dimeric compound two infrared absorption bands and three Raman lines are observed in the liquid state in the 720—300 cm^{-1} region: the rule of mutual exclusion holds for these infrared absorption bands and Raman lines, as is shown in Table II. There are three possible structural formulas, IV, V, and VI, for this dimeric compound:

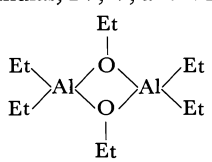

IV

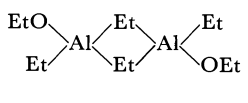

V

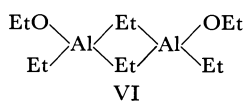

VI

Formula IV, with symmetry V_h, has an oxygen bridge. For diethylaluminum chloride, bromide, and iodide, a dimeric bridge structure over the halogen atoms with symmetry V_h (which corresponds to model IV) has been established by Yamamoto.[4] Formula V, with symmetry C_{2h}, corresponds to the "trans" form, in which two ethoxyl groups are present on opposite sides of the bridge plane, while formula VI, with symmetry C_{2v}, corresponds to the "cis" form, where the ethoxyl groups are on the same side of the bridge plane. In the latter two formulas, the alkyl bridge would be formed by the half bonds. Here the following postulation is made: the plane containing two terminal ethyl groups (model IV) or terminal ethoxyl and ethyl groups (models V and VI) and an aluminum atom is perpendicular to the bridge plane, as in the case of diethylaluminum halides (see also Ref. 4). The results described above eliminate the possibility of model VI, because model VI would require a majority of skeletal vibrations species (A_1, B_1, and B_2) to be both infrared and Raman active. The spectral data cannot be used to determine which of the remaining two forms, model IV and model V, exist in the liquid state, because the rule of mutual exclusion should hold for the skeletal vibrations in either case. If, however, we consider the conclusion of the preceding section that dimethylaluminum methoxide is represented by the oxygen bridge model I, model IV seems preferable.

The Trimethylaluminum - Dimethyl Ether Complex

For this complex four infrared absorption bands and five Raman lines are observed in the 720—300 cm^{-1} region; all of them are both infrared and Raman active, with the exception of a weak Raman line at 576 cm^{-1} which does not agree with any infrared band, as is shown in Table II. Though the possibility of the structure with a lower symmetry can not be eliminated, these results at least do not contradict the postulated structure with symmetry C_s.

Summary

The infrared and Raman spectra of dimethylaluminum methoxide, diethylaluminum methoxide, diethylaluminum ethoxide and the trimethylaluminum - dimethyl ether complex have been measured in the 3000—300 cm^{-1} region. For the three dialkylaluminum alkoxides, the results are consistent with the dimeric or trimeric structures with the oxygen bridge proposed by Hoffmann. For the trimethylaluminum - dimethyl ether complex, the results do not contradict the postulated structure with symmetry C_s.

The author is indebted to Professor Takehiko Shimanouchi of the University of Tokyo and to Mr. Saburo Takeda for their valuable discussions throughout this work, and to Dr. Hiroshi Suzuki of the University of Tokyo for reading the manuscript and for advice.

4) O. Yamamoto, This Bulletin, **35**, 619 (1962).

BULLETIN OF THE CHEMICAL SOCIETY OF JAPAN VOL. 39 729—733 (1966)

The Copolymerization of the Vinyl Monomer with a Cyclic Compound. III. The Cationic Copolymerization of Styrene with Substituted Ethylene Oxides*

By Shuzo AOKI, Kazuo FUJISAWA, Takayuki OTSU and Minoru IMOTO

Faculty of Engineering, Osaka City University, Sumiyoshi-ku, Osaka

(Received August 7, 1965)

The copolymerization of styrene with substituted ethylene oxides catalyzed by boron trifluoride - diethyl ether has been investigated. In all cases, rather low-molecular-weight copolymers were obtained. The copolymerization reactivity of the substituted ethylene oxides with styrene varied with the substituents, in the order of: isobutene oxide>propylene oxide> styrene oxide>epichlorohydrin. This has been explained in terms of cross-propagation or the reaction of the growing oxide cation with styrene.

The styrene unit content of the copolymer of styrene and epichlorohydrin increases with an increase in the solvent polarity and with an increase in the temperature. It has been concluded from the experimental results that the copolymerizability of alkylene oxide toward styrene is increased by the introduction of electron-releasing substituents into the oxide and by the use of a polar solvent at a moderate temperature.

Recently the investigations of the cationic copolymerizations of some vinyl monomers with 3, 3-bis(chloromethyl)oxetane[1] and with β-propiolactone[2] have been reported. During the course of these investigations, it has been suggested that the structure of a growing terminal cation arising from the cyclic compound in its copolymerization reactivity is significant.

This work was undertaken in order to obtain information regarding the effect of the substituents in cyclic ethers on their cationic copolymerizations with styrene. Styrene (St) was copolymerized with substituted ethylene oxides, such as epichlorohydrin (ECH), propylene oxide (PO), isobutene oxide (IBO) and styrene oxide (StO), in the presence of a boron trifluoride - diethyl ether catalyst. The effects of the solvent and the temperature were also investigated.

Experimental

Materials.—Isobutene oxide was prepared from methallyl chloride through the corresponding chlorohydrin by the method described by Ishida.[3] B. p. 52°C, n_D^{20} 1.3732; lit.[3] b. p. 50.2—50.5°C, n_D^{20} 1.3730.

Styrene oxide was prepared from styrene through the corresponding iodohydrin, following the procedure used by Golumbic and Cottle.[4] B. p. 87°C/23 mmHg, n_D^{25} 1.5329; lit.[4] b. p. 87—88°C/23 mmHg, n_D^{25} 1.5331.

Epichlorohydrin, propylene oxide and styrene were obtained commercially. All of the monomers were distilled over calcium hydride before use.

The purifications of boron trifluoride - diethyl ether and methylene chloride were carried out as has been described in a previous paper.[1] Toluene and nitromethane were also purified by the usual methods.

Copolymerization Procedure.—The copolymerization was carried out in a glass stoppered-test tube. The initial concentrations of the total monomers and the catalyst in the copolymerization were kept constant at 3.0 and 0.07 mol./l. respectively. The reaction was stopped at a given time by the addition of ammoniacal methanol. Then the mixture was washed by pure water in order to remove the residual catalyst, and the volatile substances were evaporated under reduced pressure at a somewhat elevated temperature until the weight of residue became constant. The other procedures were the same as in a previous paper.[1]

The Analysis of the Resulting Polymer.—The copolymer composition was determined from the ele-

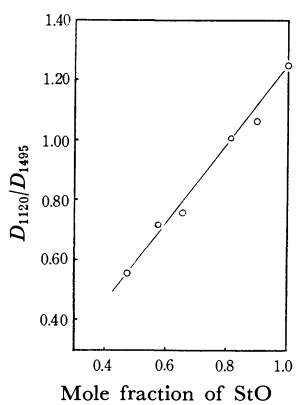

Fig. 1. Calibration curve for the composition of the styrene-styrene oxide copolymer.

* Vinyl Polymerization. CXXXII.

1) S. Aoki, Y. Harita, T. Otsu and M. Imoto, This Bulletin, **38**, 1922 (1965).

2) S. Aoki, Y. Harita, T. Otsu and M. Imoto, ibid., **38**, 1928 (1965).

3) S. Ishida, ibid., **33**, 924 (1960).

4) C. Golumbic and D. L. Cottle, *J. Am. Chem. Soc.*, **61**, 996 (1939).

Table I. Copolymerization of styrene with substituted ethylene oxides*

Substituted ethylene oxide	Reaction time min.	Conversion %	Polymer obtained: Anal. %	Polymer obtained: St mole fraction	Polymer obtained: Mol. wt.	Polymer obtained: Appearance	Hot methanol-insoluble fraction: Wt. %	Hot methanol-insoluble fraction: Anal. %	Hot methanol-insoluble fraction: St mole fraction	Hot methanol-insoluble fraction: Mol. wt.	Hot methanol-insoluble fraction: Appearance
ECH	5	5.5	Cl: 28.34	0.25	590	Viscous liquid	17.0	Cl: 13.24	0.63	3240	Glassy solid
PO	5	5.1	C: 83.71	0.64	1270	Resinous solid	84.2	C: 87.41	0.78	2340	Colorless powder
IBO	7	4.9	C: 88.75	0.81	3760	Resinous solid	93.2	C: 89.49	0.85	4210	Colorless powder
StO	1	18.9	$\frac{D_{1120}}{D_{1495}}$: 0.668	0.44	420	Waxy solid	24.5	$\frac{D_{1120}}{D_{1495}}$: 0.485	0.57	1060	Glassy solid

* Initial mole ratio of styrene and substituted ethylene oxide was 9/1, in methylene chloride at 0°C.

Table IV. Effects of solvents and temperature on the composition of styrene-epichlorohydrin copolymer*

Solvent**	Reaction temp. °C	Reaction time min.	Conversion %	Polymer obtained: Cl content %	Polymer obtained: St mole fraction	Polymer obtained: Appearance	Hot methanol-insoluble fraction: Wt. %	Hot methanol-insoluble fraction: Cl content %	Hot methanol-insoluble fraction: St mole fraction	Hot methanol-insoluble fraction: Mol. wt.	Hot methanol-insoluble fraction: Appearance
Toluene (2.38)	−30	3.3	3.0	33.60	0.11	Viscous liquid	11.6				Rubbery substance
	0	2.2	5.1	32.66	0.13		3.4				
	30	1.3	7.4	31.21	0.17		2.0				
Methylene chloride (9.08)	−30	4.0	4.1	30.18	0.19	Viscous liquid	21.0	21.03	0.42		Rubbery substance
	0	5.0	5.5	28.34	0.25		17.0	13.24	0.63	3240	
	30	2.2	6.4	24.68	0.38		33.0	12.23	0.66	1380	Glassy solid
Nitromethane (35.87)	−30	2.0	1.8	15.45	0.57	Resinous solid	43.2	5.70	0.84	2040	
	0	1.3	3.3	11.41	0.68		44.5	4.84	0.86	1780	Glassy solid
	30	0.8	5.2	8.42	0.76		70.5	4.87	0.86	1300	

* $[\text{Styrene}]_0/[\text{Epichlorohydrin}]_0=9/1$.

** Figures in parentheses are the dielectric constant.

mentary analysis of the resulting polymer, except in the case of the styrene oxide copolymer. The composition of the styrene - styrene oxide copolymer was determined from its infrared spectrum, using the ratio of the optical densities at 1120 and 1495 cm^{-1}, which are the characteristic frequencies of the ether linkage and the benzene nucleus respectively. The calibration curve is shown in Fig. 1.

The copolymer formation was confirmed by the fractional extraction of the resulting polymer with hot methanol, in which the homopolyethers were soluble, while polystyrene was insoluble.

The molecular weight of the resulting polymer was determined with a Mechrolab. vapor pressure osmometer Model 301-A.

Results and Discussion

The Effect of the Substituents of the Oxides. —Styrene was copolymerized with the substituted ethylene oxides in the initial monomer mole ratio of 9/1 in methylene chloride at 0°C. The results are given in Table I, while the infrared spectra of the resulting polymers are shown in Fig. 2.

The polymers obtained above were separated by fractional extraction with hot methanol into soluble and insoluble fractions in order to confirm the copolymer formation. The data on hot methanol-insoluble fractions are also given in Table I.

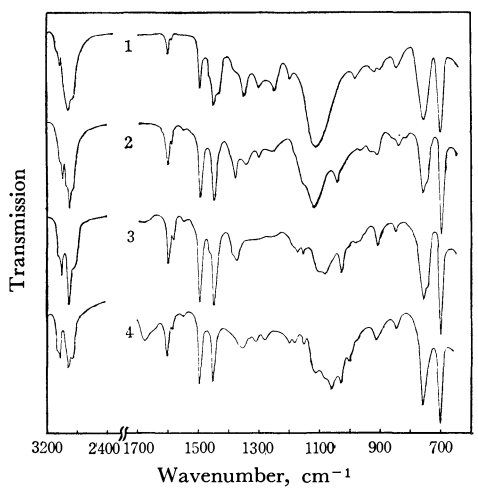

Fig. 2. Infrared spectra of the copolymer of styrene and substituted ethylene oxides.
1: St-ECH; 2: St-PO; 3: St-IBO; 4: St-StO

Furthermore, the copolymerizations of styrene with epichlorohydrin and with styrene oxide were carried out at different monomer mole ratios in methylene chloride at 0°C. The results are given in Tables II and III, while the monomer-copolymer composition curves are shown in Fig. 3.

From the infrared spectra (Fig. 2) and the elementary analyses (Table I), it was found that the

Table II. Copolymerization of styrene with epichlorohydrin*

St mole fraction in monomer mixture	Reaction time min.	Conversion %	Cl in copolymer %	St mole fraction in copolymer
0.90	3	5.4	29.57	0.20
0.80	1	8.2	34.76	0.07
0.70	5	13.8	36.33	0.03
0.60	5	18.6	36.49	0.03
0.50	5	23.7	—	—
0.00	1	54.4	37.75**	0.00

* In methylene chloride at 0°C.
** Calculated value for C_3H_5OCl is 38.32.

Table III. Copolymerization of styrene with styrene oxide*

St mole fraction in monomer mixture	Reaction time sec.	Conversion %	D_{1120}/D_{1495}	St mole fraction in monomer mixture
0.90	60	18.9	0.668	0.44
0.80	45	25.6	0.739	0.39
0.70	45	30.9	0.889	0.27
0.60	45	29.9	0.923	0.24
0.50	30	30.8	1.091	0.12
0.40	30	35.5	1.074	0.13
0.00	15	33.3	1.250	0.00

* In methylene chloride at 0°C.

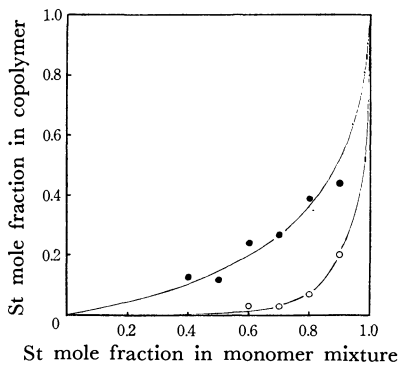

Fig. 3. Monomer-copolymer composition curves.
-○-: St-ECH; -●-: St-StO

polymers obtained in the systems of styrene-substituted ethylene oxides contained both monomer units. The hot methanol-insoluble fractions of the resulting polymers also contained both monomer units (Table I). This indicates that the copolymers were obtained under the present conditions in every case.

Table I makes it clear that the cationic copolymerizability of the substituted ethylene oxides by styrene varied with their substituents, in the order of:

isobutene oxide > propylene oxide > styrene oxide > epichlorohydrin

The contents of the methanol-insoluble fraction in these copolymers and of styrene units in this fraction were also found to increase in the order given above (Table I).

The real values of the monomer reactivity ratios could not be evaluated in this work, because the molecular weights of the resulting copolymers were low. However, the following propagation reactions may reasonably be the most significant in determining the resulting copolymer composition, even though the initiation and the termination reactions have an influence on them:

$$\text{-St}^+ + \text{St} \xrightarrow{k_{11}} \text{-St·St}^+ \quad (1)$$

$$\text{-St}^+ + \text{Oxide} \xrightarrow{k_{12}} \text{-St·Oxide}^+ \quad (2)$$

$$\text{-Oxide}^+ + \text{Oxide} \xrightarrow{k_{22}} \text{-Oxide·Oxide}^+ \quad (3)$$

$$\text{-Oxide}^+ + \text{St} \xrightarrow{k_{21}} \text{-Oxide·St}^+ \quad (4)$$

The k_{11} value is essentially constant as compared with the other constants. When both k_{12} and k_{22} decrease and k_{21} increases, the formation of a copolymer containing a large quantity of styrene units is encouraged. The values of k_{12} and also probably of k_{22} depend on the nucleophilicity of the oxides, which is to be expected from their basicity.[5] Thus the reactivity in their reaction is:

propylene oxide > styrene oxide > epichlorohydrin

This order is the reverse of that used to explain the experimental results given above. Therefore, the results should be explained by an increase in the value of the residual k_{21}.

It has been discussed in the previous papers[1,2] how, in the cationic copolymerization of vinyl monomers with cyclic compounds, the structure of the growing terminal cation arising from the cyclic compound has a significant effect on the copolymer formation; a growing carbonium ion could react with a vinyl monomer, but an oxonium ion could not. Therefore, it is assumed that the substituted ethylene oxides which copolymerize with styrene give a carbonium ion in the propagation reaction, and that hence the cross-propagation becomes favorable.

In the cationic copolymerization of the substituted ethylene oxides and 3, 3-bis(chloromethyl)oxetane,[6] we proposed an intermediate structure (I) of both carbonium and oxonium ions for the growing oxide cation in the transition state. A similar structure:

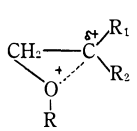

(I)

was postulated for the β-propiolactone growing cation.[2] The carbonium ion character of the ion I may be increased by the electron-releasing substituents and the ring strain. Thus, it may be assumed that, in this work, the oxides copolymerized with styrene in the order mentioned above, according to the following scheme:

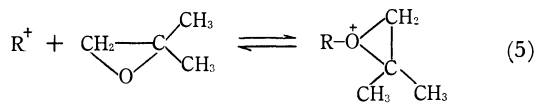

(5)

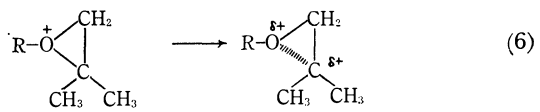

(6)

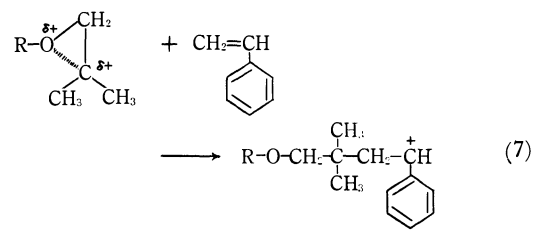

(7)

Pritchard and Long[7] have reported on the hydrolysis of the substituted ethylene oxides in aqueous perchloric acid. The rate constant of this reaction, which proceeds through an S_N1-type mechanism, varied with the substituents, in the order of:

isobutene oxide > propylene oxide > epichlorohydrin

This order agrees with that of their copolymerization reactivities given above; it indicates the enhanced significance of carbonium ion participation in their propagations in the cationic copolymerization with styrene.

The Effects of the Solvent and the Temperature.—It may be expected that the extent of the partial charge distribution in the growing ion of the oxide I may be affected by both the solvent polarity and the temperature. The copolymerization of styrene and epichlorohydrin was carried out in the monomer mole ratio of 9/1 in toluene, methylene chloride and nitromethane at −30, 0 and 30°C. The results are given in Table IV.

The styrene unit content of the resulting polymer increased with an increase in the polarity of the solvent and with an increase in the temperature. This can be explained from the enhanced carbonium

5) S. Iwatsuki, N. Takigawa, M. Okada, Y. Yamashita and Y. Ishii, *J. Chem. Soc. Japan, Ind. Chem. Sect.* (*Kogyo Kagaku Zasshi*), **67**, 1236 (1964).

6) S. Aoki, K. Fujisawa, T. Otsu and M. Imoto, ibid., **69**, 131 (1966).

7) J. G. Pritchard and F. A. Long, *J. Am. Chem. Soc.*, **78**, 2667 (1956).

ion character of the growing oxide cation I. However, if the k_{11} in Eq. 1 increases in a polar solvent and at a higher temperature more than the k_{22} in Eq. 3, this also affects the copolymer composition.

The authors wish to thank Mr. Yoshiaki Tanaka for his experimantal assistance.

BULLETIN OF THE CHEMICAL SOCIETY OF JAPAN VOL. 39 733—735 (1966)

Studies of the Solution Properties of Co-polymer. I. Styrenepolysulfone*

By Ryūichi ENDŌ, Tomoyuki MANAGŌ and Masatami TAKEDA

Tokyo College of Science, Department of Chemistry, Faculty of Science, Kagurazaka, Shinjuku-ku, Tokyo

(Received August 9, 1965)

Styrenepolysulfone was polymerized and then, for its fractionation, tetrahydrofuran and methanol were used as solvent and precipitant respectively. The viscosities and osmotic pressures of fractions of this co-polymer were examined in tetrahydrofuran. The relation between the intrinsic viscosity and the molecular weight, $[\eta]=0.38_9\times10^{-4}\overline{M}_n^{0.78}$, was thus obtained. The unperturbed molecular dimension was calculated by the Fixman-Stockmayer method. The results were then compared with the calculated end-to-end distance of the hypothetical freely-rotating chain. The steric parameter, $\sigma=1.53$, was also obtained and compared with that of polystyrene.

The polymerization of styrene and sulfur dioxide has been reported by Staudinger[1] and others[2]; the co-polymers obtained were called styrenepolysulfones. The synthesis of the co-olymer was examined with various compositions of styrene and sulfur dioxide, and the form of combination of the monomeric units was studied in terms of the head-to-head or head-to-tail combination.[3] However, the solution properties of this co-polymer have not been examined as yet.

Recently, the solution properties of hexene-1 polysulfone were examined by Ivin et al.,[4] and the unperturbed molecular dimensions of this co-polymer were obtained by using two kinds of θ-solvents. Considerably different values of the unperturbed dimensions were obtained in the two θ-solvents. This was a new finding, in contrast to the prevailing view that the unperturbed dimension of flexible polymer chains was practically independent of the solvent nature; the solvent effect observed was interpreted as arising from the dipolar interaction between polar groups contained in the main chain of this molecule.

In the present work, the unperturbed molecular dimensions of styrenepolysulfone and polystyrene will be studied. The viscosities and osmotic pressures of fractions of this co-polymer and those of polystyrene will be examined in tetrahydrofuran as the solvent. The relations between the intrinsic viscosity and the molecular weight will be determined for both styrenepolysulfone and polystyrene. The unperturbed molecular dimensions will be calculated by the Fixman-Stockmayer method.[5] The results will be compared with the calculated end-to-end distance of the hypothetical freely-rotating chain.

Experimental

Materials and Fractionation.—Styrenepolysulfone was polymerized, with α, α'-azobis-isobutyronitrile as the catalyzer, from styrene and sulfur dioxide (mole ratio 1 : 1) at 30°C. On the basis of the chemical analysis, the composition of styrenepolysulfone was determined to be $(\text{Styrene})_2SO_2$. For the fractionation of styrenepolysulfone, tetrahydrofuran and methanol were used as the solvent and the precipitant respectively. The solvent and the precipitant were purified and distilled before use. Ten fractions were obtained by fractional precipitation from a tetrahydrofuran solution (concentration: 10 g./l.) upon the addition of methanol as the precipitant, with the system kept at 40°C. For the fractionation of polystyrene (commercial name: Styron 666), benzene and methanol were used as the solvent and the precipitant respectively. About ten fractions of polystyrene were prepared by fractional precipitation.

Viscosity and Osmotic Pressure Measurements.—Tetrahydrofuran was used as the solvent for viscosity and osmotic pressure measurements. The viscosity measurements were carried out with a dilution-type Ubbelohde viscometer at 30±0.005°C. Solutions with a wide variety of concentration were prepared from an

* Presented at the 13th Annual Meeting of the Society of High Polymer of Japan, Kyoto, June, 1964.

1) H. Staudinger and B. Ritzenthaler, *Ber.*, **68**, 455 (1935).

2) W. W. Crouch and J. E. Wicklatz, *Ind. Eng. Chem.*, **47**, 160 (1955).

3) F. J. Glavis, L. L. Ryden and C. S. Marvel, *J. Am. Chem. Soc.*, **59**, 707 (1937).

4) K. J. Ivin, H. A. Ende and G. Meyerhoff, *Polymer*, **3**, 129 (1962).

5) W. H. Stockmayer and M. Fixman, *J. Polymer Sci.*, Part C, **1**, 137 (1963).

original stock solution by successive dilution with a definite volume of solvent and were then used in the measurements. The concentration of the original stock solution was determined by the evaporation method. The osmotic pressure measurements were made at 30±0.005°C by the semi-dynamic method with a modified Zimm-Meyerson-type osmometer fitted with gelcellophane. The intrinsic viscosities and molecular weights were determined by extraporating the viscosity and osmotic pressure data to zero concentration by the least-square method. The solution density measurements were made with an Ostwald-Sprengel pycnometer.

Results and Discussion

The Relation between Intrinsic Viscosities and Molecular Weights.—The results of the viscosity and osmotic pressure measurements for styrenepolysulfone and polystyrene fractions are collected in Table I. The intrinsic-viscosity-vs.-molecular-weight relationship is illustrated in Fig. 1, where the open circles represent log $[\eta]$ for polystyrene fractions plotted against log $\overline{M}_n$, and the closed circles those for styrenepolysulfones. Using these data, the Mark-Houwink equations were calculated by the least-square method. The results are shown by the straight lines in Fig. 1; they are:

$$[\eta] = 1.16_0 \times 10^{-4} \overline{M}_n^{0.73} \quad (1)$$

for polystyrene, and:

$$[\eta] = 0.38_9 \times 10^{-4} \overline{M}_n^{0.78} \quad (2)$$

for styrenepolysulfone.

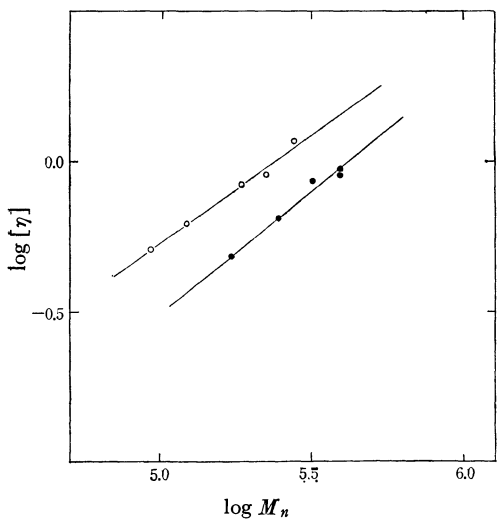

Fig. 1. Relationship between intrinsic viscosity and molecular weight.
○ Polystyrene fractions
● Styrenepolysulfone fractions

The Estimation of Unperturbed Molecular Dimension Parameters.—The unperturbed end-to-end distance, r_0, may be estimated from the $[\eta]$-vs.-M relationship with the aid of the Fixman-Stockmayer method. We first calculate $[\eta]M^{-1/2}$ and $M^{1/2}$ for each fraction. Then the values of $[\eta]M^{-1/2}$ are plotted against $M^{1/2}$, as is shown in Fig. 2, and a straight line is obtained for each polymer-solvent system.

Table I.

Polymer	Fraction	$[\eta]$	$\overline{M}_n \times 10^{-4}$
Styron 666	F_2	1.170	26.3
	F_4	0.902	22.3
	F_6	0.853	18.5
	F_8	0.618	12.1
	F_9	0.508	9.2
Styrenepoly-sulfone	F_1	0.939	39.0
	F_2	0.902	38.9
	F_3	0.861	31.8
	F_6	0.646	24.3
	F_7	0.480	17.1

According to Stockmayer and Fixman, the $[\eta]M^{-1/2}$ ratio is given by:

$$[\eta]M^{-1/2} = K + BM^{1/2} \quad (3)$$

where K and B are constant, relating to the unperturbed molecular dimension parameter and to the polymer and solvent interaction respectively. Thus, the value of K can be readily determined from the intercept of the straight line shown in Fig. 2. The results are given in Table II. As the value of K for polystyrene in a mixed θ-solvent is essentially identical with our data obtained with the Fixman-Stockmayer method, it seems most reasonable to assume that the value of K for styrenepolysulfone is accurate. The unperturbed end-to-end distance, r_0, for styrenepolysulfone and polystyrene can be calculated from

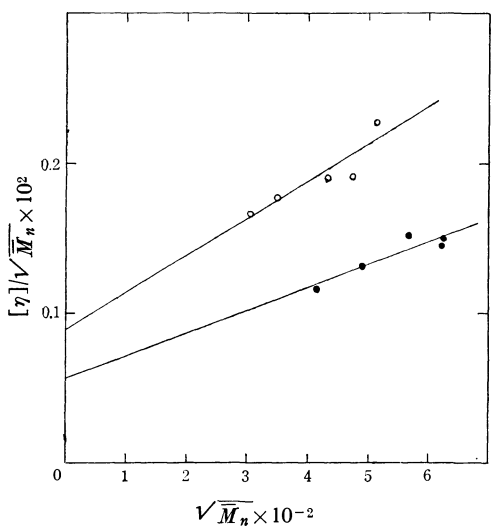

Fig. 2. Relationship between $[\eta]M^{-1/2}$ and $M^{1/2}$.
○ Polystyrene fractions
● Styrenepolysulfone fractions

TABLE II.

Polymer	Solvent	Temp., °C	$K\times10^4$	$(\bar{r}^2_0/M)\times10^{11}$	$(\bar{r}^2_0/\bar{r}^2_{0f})^{1/2}$	$\Phi\times10^{21}$
PS[a]	A	30	8.6(θ)	735	2.44	2.1
	THF	30	8.99	754	2.49	2.1
SPS[b]	THF	30	5.74	649	1.53	2.1
HPS[c]	B	27	4.8(θ)		1.61	2.6
	C	13	3.3(θ)		2.1	1.8

Polymer : a) Polystyrene, b) Styrenepolysulfone c) Hexene-1-polysulfone
Solvents : A Toluene (0.476)-*n*-Heptane (0.524)
B Ethyl methyl ketone (0.37)-Isopropylalcohol (0.63)
C *n*-Hexyl chloride
T. H. F. Tetrahydrofuran

the experimental values of K by the following equation:

$$K = \Phi(\bar{r}^2_0/M)^{3/2} \tag{4}$$

where Φ is the universal viscosity constant. The results are also given in Table II, with other data given for the sake of comparison.

Table II shows that the molecular dimension of styrenepolysulfone is smaller than that of polystyrene in a tetrahydrofuran solution.

According to the results of chemical analysis and other evidence,[6] the molecular formula, $-CH_2CH(C_6H_5)SO_2CH_2CH(C_6H_5)-$, seems appropriate for the repeating units of styrenepolysulfone. To the distance from phenyl-to-phenyl groups in this molecule is larger than that in polystyrene, the steric interaction between phenyl groups, and consequently the hindrance to the rotation of the main chain, would be less significant than with the polystyrene chain. With the model defined by the above molecular formula or shown in Fig. 3, the mean-square end-to-end distance of free rotation for the monomer unit of styrenepolysulfone may be calculated by Flory's method as:[7]

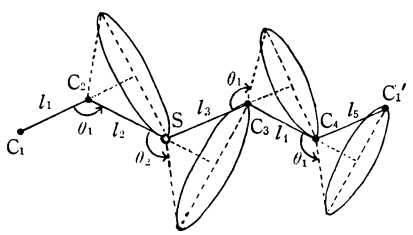

Fig. 3. Spatial representation of styrenepolysulfone monomer for free rotation.
l_1, l_4, l_5: C-C bond length 1.54 Å
l_2, l_3: C-S bond length 1.82 Å
θ_1: ∠C-C-C, ∠C-C-S 109.5°
θ_2: ∠C-S-C 115°

$$(\bar{r}^2_m) = \begin{vmatrix} \overline{l_1\cdot l_1} + \overline{l_1\cdot l_2} + \cdots\cdots + \overline{l_1\cdot l_5} \\ + \overline{l_2\cdot l_1} + \overline{l_2\cdot l_2} + \cdots\cdots + \overline{l_2\cdot l_5} \\ + \overline{l_3\cdot l_1} + \overline{l_3\cdot l_2} + \cdots\cdots + \overline{l_3\cdot l_5} \\ + \cdots\cdots\cdots\cdots\cdots\cdots \\ + \cdots\cdots\cdots\cdots\cdots\cdots \end{vmatrix} \tag{5}$$

where l_1, l_4 and l_5 are the bond lengths of C–C, and l_2 and l_3 are the bond lengths of C–S. The result is:

$$\begin{aligned}(\bar{r}^2_m) &= l_1^2[1+2(1-\cos\theta_1)(1-\cos^2\theta_1\cdot\cos\theta_2)] \\ &\quad +2l_2^2(1-\cos\theta_2) \\ &\quad -2l_1l_2\cos\theta_1(2-\cos\theta_1)(1-\cos\theta_2)\end{aligned} \tag{6}$$

where θ_1 is the bond angles of C–C–C and C–C–S, and θ_2 is the bond angle of C–S–C. For the polymer with the polymerization degree of x, the mean-square end-to-end distance of free rotation in the main chain is obtained as:

$$(\bar{r}^2_{0f}) = x\cdot(\bar{r}^2_m)(1-\cos\theta_1)/(1+\cos\theta_1) \tag{7}$$

where θ_1 is the bond angle of C–C–C (monomer)–(monomer). On the other hand, for the freely-rotating state of polystyrene, $\bar{r}^2_{0f}$ is given as:

$$(\bar{r}^2_{0f}) = n\cdot l^2(1-\cos\theta_1)/(1+\cos\theta_1) \tag{8}$$

where l is the bond length of C–C. Therefore, the steric parameter, $(\bar{r}^2_0/\bar{r}_{0f})^{1/2}$, can be calculated for styrenepolysulfone and for polystyrene by using Eq. 7 and Eq. 8 respectively. The results are shown in Table II. It is notable that the values of $(\bar{r}^2_0/M)$ and $(\bar{r}^2_0/\bar{r}^2_{0f})^{1/2}$ for styrenepolysulfone are considerably smaller than those of polystyrene. This clearly shows that the internal rotation around the bond axis in the main chain can occur with less hindrance in styrenepolysulfone than in polystyrene. Finally, if it is compared with that for hexen-1-polysulfone, the steric parameter for styrenepolysulfone is approximately identical with that for hexen-1-polysulfone obtained from mixed θ-solvent (ethyl methyl ketone and isopropylalcohol).

6) N. Tokura and M. Matsuda, *J. Chem. Soc. Japan, Ind. Chem. Sect* (*Kogyo Kagaku Zasshi*), **64**, 501 (1961).
7) P. J. Flory, Principles of Polymer Chemistry," Cornell University Press, Ithaca, N. Y. (1953).

BULLETIN OF THE CHEMICAL SOCIETY OF JAPAN VOL. 39 736—741 (1966)

The Band Structure of Tetramethylammonium Pentaiodide*

By Shigekazu KUSABAYASHI** and Hiroshi MIKAWA**

The Institute of Scientific and Industrial Research, Osaka University, Sakai-shi, Osaka

(Received August 12, 1965)

The iodine framework in the crystal is constructed by repeated translations of a group of two pentaiodide ions (repeating unit). The wave function of a repeating unit is calculated by Hückel's approximation, the resonance integrals between iodine 5 p orbitals being estimated empirically from the data for the gaseous iodine molecule. The wave functions of the crystal are set up in the form of Bloch functions from the wave functions of the repeating unit. The energy is calculated by a tight-binding approximation, the values of the resonance integrals between nearest neighboring repeating units being estimated from the wave functions of the repeating unit. The band-gap energy thus calculated is 1.26 eV., satisfactorily near the experimental value of 1.36 eV. This finding supports our conclusion (This Bulletin, **37**, 811 (1964)) that the iodine framework is primarily important in the electrical conductivity. It is also supposed that the band model may satisfactorily be applied to the conduction mechanism. The interactions of the Bloch functions of different energies being very slight, the band-gap energy is influenced at most in the order of 10^{-2} eV. even when level interactions are taken.

In previous papers,[1] it was shown that the specific resistivities (20°C) and the band-gap energies of organic polyiodides decreased with the number of iodine atoms in the polyiodide anion. It was also shown that the iodine framework in the crystal structure was of primary importance in determining the electrical conductivity of polyiodides.

On the basis of the above discussion, we will now attempt to calculate the band structure of the tetramethylammonium pentaiodide crystal by the so-called tight-binding approximation, in order to see whether the band theory is applicable to the conduction mechanism of tetramethylammonium pentaiodide.

According to the X-ray analyses,[2,3] the tetramethylammonium pentaiodide crystal is end-centered monoclinic with a space group C2/c and with $a_0=13.34$, $b_0=13.59$, $c_0=8.90$ Å, $\beta=107°50'$, and $Z=4$. The coordinates of the iodine atoms and the tetramethylammonium cations are also reported. Five iodine atoms as a group form a planar V-shaped pentaiodide ion. Pentaiodide anions are arranged nearly parallel to (001). Thus, the layer structure of iodine atoms exists in the crystal, as is shown in Figs. 1 and 2.

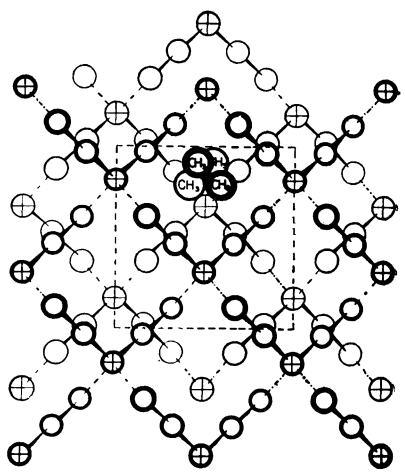

Fig. 1. Projection of the structure of tatramethylammonium pentaiodide along the c_0-axis onto the plane (001), showing the nets of iodine atoms in the upper plane and that in the lower plane. Nets are stacked so as to leave large holes for the cations. Only one is shown, upper center, though every hole is filled. The dashed line outlines the unit cell. (From Ref. 2)

The iodine framework in the crystal can be looked upon as being constructed simply by repeated translations of a group of two pentaiodide ions, as in Fig. 2. In order to calculate the band structure by tight-binding approximation, this repeating unit is first looked upon as a molecule and the wave function of the repeating unit is calculated as usual by the method of simple LCAO MO, the values of the resonance integrals between iodine atoms being estimated empirically from the data reported for the gaseous iodine molecule.

* Presented at the 18th Annual Meeting of the Chemical Society of Japan, Osaka, April, 1965.

** Present address: Department of Chemical Technology, Faculty of Engineering, Osaka University, Miyakojima-ku, Osaka.

1) a) S. Kusabayashi, H. Mikawa, S. Kawai, M. Uchida and R. Kiriyama, This Bulletin, **37**, 811 (1964); b) S. Kawai, R. Kiriyama, M. Uchida, S. Kusabayashi and H. Mikawa, ibid., **38**, 799 (1965); c) S. Kusabayashi and H. Mikawa, ibid., **38**, 1410 (1965).

2) R. J. Hach and R. E. Rundle, *J. Am. Chem. Soc.*, **73**, 4321 (1951).

3) J. Broekema, E. E. Havinga and E. H. Wiebenga, *Acta Cryst.*, **10**, 596 (1957).

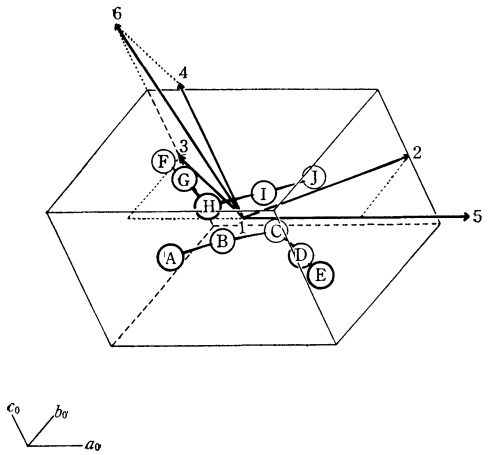

Fig. 2. Repeating unit consisting of two pentaiodide anions. Five vectors 2—6 connecting nearest neighboring repeating unit.

As the whole crystal is made up of simple repetitions of the three-dimensional translations of the repeating unit with the "molecular" wave functions thus calculated, the wave functions of the crystal can easily be set up in the form of Bloch functions from the "molecular" wave functions of the repeating unit. The energy band structure is next calculated by a tight-binding approximation as usual, the values of the resonance integrals between nearest neighboring repeating units needed for calculation being estimated from the "molecular" wave functions of the repeating unit.

The band structure thus calculated is shown in Fig. 4, the lower band being occupied and the upper vacant. The estimated band-gap energy is 0.455 β or 1.26 eV. This value is satisfactorily near to the experimental value of 1.36 eV.

Calculation

The Use of Only p Orbitals.—Several previous attempts have been made to explain the bonds in polyhalides by assuming the spd hybridization of the iodine atomic orbitals, the delocalization of the outer p orbital of the iodine atoms and so on.[4]

Pimentel[5] and Hach and Rundle[2] suggested the use of only the 5p orbitals; they based their argument on the linear form of triiodide ions. Havinga and Wiebenga[4] reviewed the structure of polyiodide ions and explained the observed configurations of atoms by means of the delocalization of the 5p orbitals, the valency angles being very close to 90° or 180° in all cases. Bersohn[6] and Rosenberg[7] have worked out the band structure of iodine on the assumption that only p orbitals are involved.

In such circumstances, only the 5p orbitals were used in the present calculation of the pentaiodide ion.

The Coordinates of the Iodine Atoms.—In our calculation of the band structure, the coordinates of the iodine atoms were estimated by the parameter reported in Ref. 3.

In order to set up the Bloch functions of an electron in a periodic field of the crystal, the repeating unit, which consists of two neighboring anions in a direction parallel to the c_0-axis, as has been stated before, must be examined first. The relation between neighboring repeating units in the crystal is drawn in Fig. 2; the numbers, 1, 2, ...,6, denote the nearest neighboring repeating units in the crystal. The ten iodine atoms in a repeating unit were named A, B, C,.., I and J. The distances between each two atomic centers were estimated as follows:

(a) Distances within the 1 repeating unit:
$A_1B_1=D_1E_1=F_1G_1=I_1J_1=2.81$ Å, $B_1C_1=C_1D_1=G_1H_1=H_1I_1=3.17$ Å, $B_1D_1=G_1I_1=4.67$ Å, $A_1G_1=D_1J_1=4.40$ Å, $A_1H_1=C_1J_1=4.73$ Å, $B_1G_1=D_1I_1=4.48$ Å, $B_1H_1=C_1I_1=4.74$ Å, $B_1I_1=4.68$ Å.

(b) Distances between the 1 and 2 repeating units:
$C_1A_2=J_1H_2=3.62$ Å, $D_1A_2=J_1G_2=4.91$ Å, $J_1A_2=4.59$ Å.

(c) Distances between 1 and 3:
$B_1E_3=F_1I_3=4.91$ Å, $C_1E_3=F_1H_3=3.62$ Å.

(d) Distances between 1 and 4:
$F_1B_4=I_1E_4=4.40$ Å, $F_1C_4=H_1E_4=4.73$ Å, $G_1B_4=I_1D_4=4.48$ Å, $G_1C_4=H_1D_4=4.74$ Å, $G_1D_4=4.68$ Å.

(e) Distances between 1 and 5:
$E_1A_5=J_1F_5=4.92$ Å.

(f) Distances between 1 and 6:
$F_1E_6=4.59$ Å.

Any distances between two atomic centers larger than 5.0 Å may be disregarded, for the overlap integrals decrease exponentially with the distance of two atomic centers.

The "Molecular Orbital" of a Repeating Unit.—The "molecular" orbital function of a repeating unit, φ, was approximated with a linear combination of 30 Slater-type 5p atomic orbitals, χ, belonging to the 10 iodine atoms in the unit. The energy and the coefficients of the "molecular" orbitals of the repeating unit were calculated by applying the variation principle and Hückel's approximation in the usual manner.

If χ_i is the wave function of the ith atomic orbital, the explicit parameters which enter the secular determinant are the Coulomb integral, $\alpha_i=\int\chi_i^*\boldsymbol{H}\chi_i d\tau$, and the resonance integral between adjacent orbitals, $\beta_{ij}=\int\chi_i^*\boldsymbol{H}\chi_j d\tau$, the overlap integrals being neglected. If all the orbitals are

4) E. E. Havinga and E. H. Wiebenga, *Rec. Trav. Chim.*, **78**, 724 (1959).
5) G. C. Pimentel, *J. Chem. Phys.*, **19**, 446 (1951).
6) R. Bersohn, ibid., **36**, 3445 (1962).
7) J. L. Rosenberg, ibid., **40**, 1707 (1964).

equivalent, the Coulomb integral will become an additive constant. $\boldsymbol{H}$ is a one-electron Hamiltonian. It is, therefore, necessary to evaluate the resonance integrals.

The resonance integrals were estimated by the familiar relation:

$$\beta' = \beta\frac{S'/(1+S')}{S/(1+S)} \qquad (1)$$

where β' and S' are, respectively, resonance and overlap integrals between the interesting orbitals, and β and S are, respectively, the resonance and overlap integrals for some standard. In our present calculation, β and S are the values for $(5p\sigma, 5p\sigma)$ at the interatomic distance, 2.68 Å, of an iodine molecule. The estimation of the numerical value of the basic parameter of our calculation, β, will be discussed later in detail.

The values of $S(5p\sigma, 5p\sigma)$ and $S(5p\pi, 5p\pi)$ between two iodine 5p atomic orbitals were calculated by Mulliken's special formulas[8] for Slater-AO overlap integrals for $t=0$. The formulas may be given as follows:

$$S(5p\sigma, 5p\sigma) = e^{-p}[-1-p-(29/70)p^2-(17/210)p^3 - (1/735)p^4+(1/294)p^5+(67/66150)p^6 + (13/66150)p^7+(1/33075)p^8]$$

$$S(5p\pi, 5p\pi) = e^{-p}[1+p+(33/70)p^2+(29/210)p^3 + (41/1470)p^4+(1/245)p^5 + (29/66150)p^6+(1/33075)p^7]$$

where $p=(\mu_a+\mu_b)R/2a_H$, $t=(\mu_a-\mu_b)/(\mu_a+\mu_b)$, R is the interatomic distance, a_H is the Bohr radius, and the $\mu_a=\mu_b$ value is 1.90 for the iodine-pair.

Next, in order to ascertain the overlap integral, S'_{ab}, between any two 5p iodine orbitals, $\boldsymbol{A}_a$ and $\boldsymbol{A}_b$, new orthogonal coordinates (X, Y, Z), in which the Z axis is parallel to the direction of the internuclear vector, are set up, and the interesting overlap integral, S'_{ab}, is estimated as follows:

$$S'_{ab} = -A_{az}\cdot A_{bz}\cdot S(5p\sigma, 5p\sigma) + (A_{ax}\cdot A_{bx} + A_{ay}\cdot A_{by})\cdot S(5p\pi, 5p\pi)$$

where $A_{ax}, A_{ay}, .., A_{bz}$ are the X, Y and Z components of the vectors of the atomic orbitals, $\boldsymbol{A}_a$ and $\boldsymbol{A}_b$.

In order to calculate the energy of the repeating unit, it is first assumed that the V-shaped pentaiodide ion is planar, that the I_B–I_C–I_D angle is 90° and that the arms are linear, the pentaiodide ion reported in Ref. 3 being planar within±0.09 Å, the I_B–I_C–I_D angle, 95°, and the angle of arms, 174.5°.

The sign and the numbering of the atomic p orbitals are as shown in Fig. 3. Thus, all the resonance integrals between any pairs of iodine atoms from A to J were estimated in β untis. Using these resonance integrals, a 30-order secular determinant was set up and solved by a computor. The energy levels of a repeating unit and the orbital coefficients for some levels are shown in Fig. 4 and Table I. The levels from 1 to 26 are filled; the levels from 27 to 30, lying much higher, are vacant.

TABLE I. THE ORBITAL COEFFICIENTS FOR SOME LEVELS OF A REPEATING UNIT

Number of level	Coefficients*				
28	−0.009	0.025	−0.211	0.351	−0.287
	−0.008	0.028	−0.212	0.349	−0.286
	0.005	0.006	−0.002	−0.006	0.002
	−0.008	0.028	−0.212	0.349	−0.286
	−0.009	0.025	−0.211	0.351	−0.287
	−0.002	0.006	0.002	−0.006	−0.005
27	−0.006	0.029	−0.213	0.349	−0.287
	−0.007	0.026	−0.211	0.349	−0.287
	−0.004	−0.005	0.001	0.004	−0.001
	0.007	−0.026	0.211	−0.349	0.287
	0.006	−0.029	0.213	−0.349	0.287
	−0.001	0.004	0.001	−0.005	−0.004
26	−0.047	0.019	−0.002	−0.001	0.003
	−0.098	0.129	−0.014	−0.010	0.012
	0.272	−0.403	0.298	−0.304	0.231
	0.098	−0.129	0.014	0.010	−0.012
	0.047	−0.019	0.002	0.001	−0.003
	0.231	−0.304	0.298	−0.403	0.272
25	0.072	−0.041	0.013	0.004	−0.008
	0.102	−0.132	0.021	0.011	−0.013
	0.295	−0.299	0.288	−0.358	0.277
	0.102	−0.132	0.021	0.011	−0.013
	0.072	−0.041	0.013	0.004	−0.008
	−0.277	0.358	−0.288	0.299	−0.295

* Orbital number from left to right, up to down.

Band Structure. — The band structure is calculated by the tight-binding approximation. We denote the unit cell vector by $\boldsymbol{a}_0$, $\boldsymbol{b}_0$ and $\boldsymbol{c}_0$, and define the new vector by $\boldsymbol{a}=(\boldsymbol{a}_0+\boldsymbol{b}_0)/2$, $\boldsymbol{b}=(-\boldsymbol{a}_0+\boldsymbol{b}_0)/2$ and $\boldsymbol{c}=\boldsymbol{c}_0$; therefore, $\boldsymbol{a}$, $\boldsymbol{b}$ and $\boldsymbol{c}$ connect the centers of the nearest-neighbor repeating units (Fig. 2).

The one-electron crystal wave functions, Ψ_k, are constructed from the linear combination of one-electron wave functions of the repeating unit, φ_j; since we are dealing with an electron in a periodic field, the wave function must be a Bloch function:

$$\Psi_k(\boldsymbol{r}) = \sum_{j=1}^{N}\exp(i\boldsymbol{k}\boldsymbol{r}_j)\varphi_j(\boldsymbol{r}-\boldsymbol{r}_j)$$

Here $\boldsymbol{r}_j$ locates the center of a repeating unit, j, and the sum extends over N repeating units in the crystal.

The application of periodic boundary conditions defines an elementary cell in $\boldsymbol{k}$ space, whose volume

8) R. S. Mulliken, C. A. Rieke, D. Orloff and H. Orloff, *J. Chem. Phys.*, **17**, 1248 (1949).

is given by the conditions:

$$-\pi < \boldsymbol{ka},\ \boldsymbol{kb},\ \boldsymbol{kc} \leq \pi$$

The energy of one-electron with the wave vector $\boldsymbol{k}$ is calculated by the following expression:

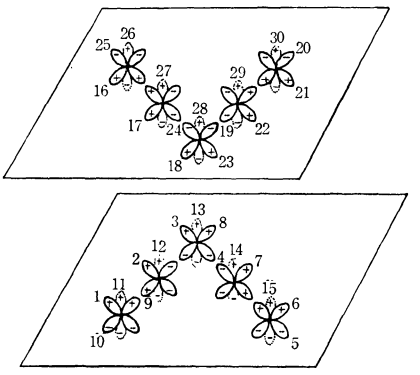

Fig. 3. The sign and the numbering of the atomic p-orbitals. 1—15 make a lower layer and 16—30 an upper layer. Lobes shown with dotted lines are perpendicular to each layer.

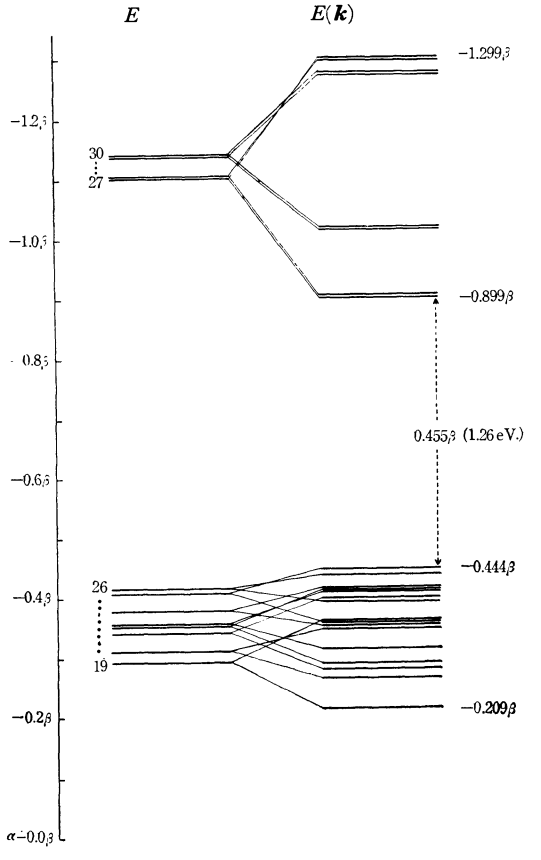

Fig. 4. Energy levels of a repeating unit, E, and energy bands of solid pentaiodide, $E(\boldsymbol{k})$. (Among 30 energy levels of a repeating unit only the levels 19—30 are shown.)

$$E(\boldsymbol{k}) = \frac{\int \Psi_k^* \boldsymbol{H} \Psi_k d\tau}{\int \Psi_k^* \Psi_k d\tau} = E_0 + 2\sum E_s \cdot \cos \boldsymbol{k r_s}$$

where $\boldsymbol{H}$ is the Hamiltonian for one electron in the crystal; E_0 is the molecular orbital energy of a repeating unit, and $\boldsymbol{r_s}$ is the primitive translation vector. The structure of the band is determined by the resonance integrals between repeating units, E_s. Each resonance integral between repeating units is a sum of the interatomic resonance integrals. Of the two-center atomic integrals in each E_s, only those involving a small interatomic distance and a large Hückel coefficient of a repeating unit are important.

The resonance integrals fall off rapidly with the distance between repeating units; only five nearest-neighbor interactions are found to be important. They are E_a, E_b, E_c, E_{a-b} and E_{b+c}, corresponding to $\boldsymbol{r_s} = \boldsymbol{a}$, $\boldsymbol{b}$, $\boldsymbol{c}$, $\boldsymbol{a}-\boldsymbol{b}$ and $\boldsymbol{b}+\boldsymbol{c}$ respectively.

The one-electron energy for each band is, therefore, given by:

$$E(\boldsymbol{k}) = E_0 + 2[E_a \cos \boldsymbol{ka} + E_b \cos \boldsymbol{kb} + E_c \cos \boldsymbol{kc} + E_{a-b} \cos \boldsymbol{k}(\boldsymbol{a}-\boldsymbol{b}) + E_{b+c} \cos \boldsymbol{k}(\boldsymbol{b}+\boldsymbol{c})] \quad (2)$$

The values of E_a, E_b,..., and E_{b+c} for the band corresponding to each nth "molecular" orbital are listed in Table II.

Table II. Resonance integrals between repeating units (β unit)

Number of level	E_a	E_b	E_c	E_{a-b}	E_{b+c}
30	−0.032	−0.031	0.000	−0.003	−0.001
29	−0.031	−0.032	0.000	−0.003	0.001
28	−0.048	−0.049	0.000	0.003	0.001
27	−0.050	−0.049	0.000	0.003	−0.001
26	0.005	0.006	0.000	0.000	0.000
25	0.009	0.008	0.006	0.000	0.003
24	0.008	0.007	−0.004	−0.002	−0.004
23	0.009	0.009	0.006	−0.002	0.000
22	−0.001	0.010	−0.017	0.004	−0.003
21	0.010	0.009	−0.011	0.002	0.000
20	0.008	0.008	0.005	0.002	0.001
19	0.015	0.005	0.013	0.004	0.004

Results and Discussion

Using Eq. 2, the total width of each band was calculated. The energy levels of a repeating unit and the total width of each band are represented in Fig. 4.

As is shown in Fig. 4, the bands from 19 to 26 are all occupied by electrons and as a whole form a hole band, while the bands from 27 to 30 are all vacant and form an electron band. The band-gap energy is found to be 0.455 β.

In order to estimate the numerical value of β, as Rosenberg suggested,[7] the following assumption was made:

$$\beta(5p\sigma,\ 5p\sigma)-\beta(5p\pi,\ 5p\pi)=-1.71\ \text{eV}. \quad (3)$$

where β is the value for the interatomic distance, 2.68 Å, for the iodine molecule. This is the average value of T_e,[9] the pure electronic excitation, of the first two excited states, A and B, relative to the ground state, X, in the gaseous iodine molecule. The $X \rightarrow A$ and $X \rightarrow B$ transitions are the two spectroscopically-observed transitions of the vapor phase iodine corresponding to the orbital jump from π-antibonding to σ-antibonding orbitals.

The substitution of $\beta(5p\pi,\ 5p\pi)=0.381\beta$ from Eq. 1 into Eq. 3 gives $\beta=-2.76$ eV.

The band-gap energy is, therefore, calculated to be 1.26 eV. This value is in good agreement with the experimental value of 1.36 eV., reported in the previous papers,[1a,1b] for the band-gap energy of tetramethylammonium pentaiodide from the conductivity measurements.

As described before, the calculations have been performed on the assumptions that the V-shaped pentaiodide ion is planar, the I_B–I_C–I_D angle is rectangular, and the arms are linear. The calculations were also carried out with the pentaiodide ion, which has a more complicated geometry; the band gap energy thus calculated was found, however, to be almost the same as the above value (the difference was within 0.1 eV).

Although the treatment of the calculation is semiquantitative, this result may offer additional evidence in support of our previous conclusion that the iodine framework in the tetramethylammonium pentaiodide crystal structure is of primary importance in determining the electrical conductivity. It may also be supposed that the band model is satisfactorily applied for the conduction mechanism. Thereby, the experimental energy gap may be supposed to be the one of intrinsic conduction.

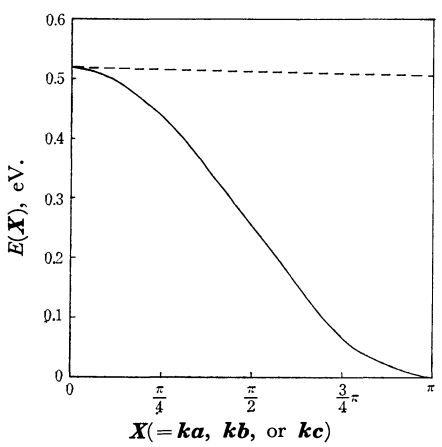

Fig. 5. The 27 band structure in the a^{-1} (solid line), b^{-1} (the same line as a^{-1}) and c^{-1} (dashed line) directions.

9) L. Mathieson and A. L. G. Rees, *J. Chem. Phys.*, **25**, 753 (1956).

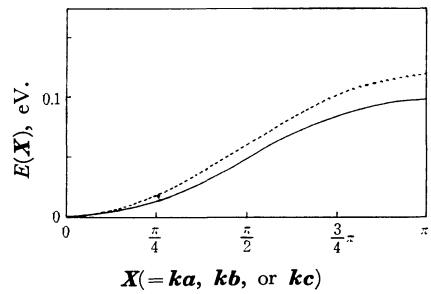

Fig. 6. The 25 band structure in the a^{-1} (solid line), b^{-1} (dotted line) and c^{-1} (the same line as a^{-1}) directions.

On examining the Hückel coefficients of the wave functions of the repeating unit, one finds that the electron band is mainly σ in character. No. 25 and 26 bands located at the top of the hole band are mainly π in character, perpendicular to the planar V-shaped pentaiodide ion.

In the reduced zone scheme given by $-\pi < ka, kb, kc \leq \pi$, the 27 and 25 band structures in the reciprocal crystal axis direction are as shown in Figs. 5 and 6. The origins of the energy scales are arbitrarily taken in both figures. The values of the bandwidths in the a^{-1}, b^{-1}, and c^{-1} directions are shown in Table III.

Table III. Bandwidths of 27 and 25 (eV.)

	27	25
a^{-1}	0.519	0.099
b^{-1}	0.519	0.121
c^{-1}	0.011	0.099

So far no mutual interactions of the Bloch functions of different energy have been taken into consideration; the interactions between the levels with different energies have thus been neglected.

In order to calculate the electron band, it is desirable to mix four vacant levels 27—30. The usual way to do this is to make a linear combination of these four functions and, next, set up a 4th order secular determinant by variation. It is, however, very difficult to solve the determinant thus obtained. To calculate the hole band in this way, it is desirable to interact eight levels at one time, leading to the 8th order secular determinant; these interactions are, however, impossible to solve.

We therefore attempted to see if there were pairs of levels which interact so strongly that the value of the energy gap estimated hitherto without level interactions must be changed. As will be shown below the level interactions were found to be so slight that the value of the energy gap changes at most in the order of 10^{-2} eV.

The interaction between two different Bloch functions, Ψ_p and Ψ_t, has been examined on the basis of a linear combination;

Table IV. E_s' from a pair of different Bloch functions

p, t	E_a'	E_b'	E_c'	E'_{a-b}	E_{b+c}'	cos or sin
27, 30	0.082	−0.080	0.000	0.000	−0.002	cos
27, 29	0.018	−0.016	0.000	−0.006	−0.002	sin
27, 28	0.000	0.000	0.000	0.000	0.002	sin
25, 26	0.000	0.000	0.004	−0.002	0.002	sin
24, 25	0.014	0.012	0.000	−0.002	0.008	sin
19, 25	0.014	−0.010	−0.014	−0.002	−0.008	cos

$$\Phi = c_1\Psi_p + c_2\Psi_t$$

By applying the variation principle, the secular determinant of the following form is obtained:

$$\begin{vmatrix} \int\Psi_p^*\boldsymbol{H}\Psi_p d\tau - E & \int\Psi_p^*\boldsymbol{H}\Psi_t d\tau \\ \int\Psi_t^*\boldsymbol{H}\Psi_p d\tau & \int\Psi_t\boldsymbol{H}\Psi_t d\tau - E \end{vmatrix} = 0$$

In solving the determinant, the band energy is written in explicit form as:

$$E_{p,t}(\boldsymbol{k}) = \frac{E_p(\boldsymbol{k}) + E_t(\boldsymbol{k})}{2} \pm \sqrt{\left(\frac{E_p(\boldsymbol{k}) - E_t(\boldsymbol{k})}{2}\right)^2 + |B|^2}$$

where

$$E_p(\boldsymbol{k}) = \int\Psi_p^*\boldsymbol{H}\Psi_p d\tau,\ E_t(\boldsymbol{k}) = \int\Psi_t^*\boldsymbol{H}\Psi_t d\tau,$$

$$B = \int\Psi_p^*\boldsymbol{H}\Psi_t d\tau = \int\varphi_p(\boldsymbol{r})\boldsymbol{H}\varphi_t(\boldsymbol{r})d\tau + \sum\{\exp(-i\boldsymbol{k}\boldsymbol{r}_s)\int\varphi_p^*(\boldsymbol{r})\boldsymbol{H}\varphi_t(\boldsymbol{r}-\boldsymbol{r}_s)d\tau - \exp(i\boldsymbol{k}\boldsymbol{r}_s)\int\varphi_p^*(\boldsymbol{r})\boldsymbol{H}\varphi_t(\boldsymbol{r}+\boldsymbol{r}_s)d\tau\}$$

$$B^* = \int\Psi_t^*\boldsymbol{H}\Psi_p d\tau,\ |B|^2 = (\sum E_s'\cos\boldsymbol{k}\boldsymbol{r})^2 \text{ or } (\sum E_s'\sin\boldsymbol{k}\boldsymbol{r})^2$$

Since $\varphi_p(\boldsymbol{r})$ and $\varphi_t(\boldsymbol{r})$ are orthogonal, $\int\varphi_p(\boldsymbol{r})\boldsymbol{H}\cdot\varphi_t(\boldsymbol{r})d\tau$ vanishes. The sum, $\sum$, is taken over the nearest-neighboring repeating units located in the five directions, $\boldsymbol{a}$, $\boldsymbol{b}$, $\boldsymbol{c}$, $\boldsymbol{a}-\boldsymbol{b}$ and $\boldsymbol{b}+\boldsymbol{c}$. One finds that, for some p, t pairs, $|B|^2$ contains only sine terms, $(\sum E_s'\sin\boldsymbol{k}\boldsymbol{r}_s)^2$ and for some other pairs, only cosine terms, $(\sum E_s'\cos\boldsymbol{k}\boldsymbol{r}_s)^2$. The E_s' values are listed in Table IV for several p, t pairs.

E_a' and E_b' in cosine terms are large but are opposite in sign. E_a and E_b are large and have the same sign. Hence, it is clear that when $\cos\boldsymbol{k}\boldsymbol{a} \fallingdotseq \cos\boldsymbol{k}\boldsymbol{b} \fallingdotseq \pm 1$, i. e., near the top and bottom of these bands, $|B|^2$ must be small, the interaction between p and t levels being very small for these $\boldsymbol{k}$ values. For the $E_{p,t}(\boldsymbol{k})$ bands with only sine terms in $|B|^2$, $|B|^2$ remains very small, irrespective of $\boldsymbol{k}$, very small interactions existing between p and t levels here also.

It may, therefore, be inferred that the position of the bottom of the electron band, as well as the position of the top of the hole band, will not change very much even when corrected for the interactions of the levels with different energies. Consequently, the band-gap energy will also remain unchanged, or will change at most in the order of 10^{-2} eV.

The authors wish to express their thanks to Professor Junjiro Kanamori of Osaka University for his kind discussion. They also wish to thank Professor Kenzo Jo of Osaka University and the members of his laboratory for their help in performing the calculations with an electronic computer.

BULLETIN OF THE CHEMICAL SOCIETY OF JAPAN VOL. 39 742—749 (1966)

The Vibrational Spectra and Vibrational Assignments of Isotactic Polybutene-1

By Minoru UKITA

Government Industrial Research Institute, Osaka, Oyodo-ku, Osaka

(Received August 17, 1965)

The polarized infrared spectra of isotactic polybutene-1 in a hexagonal form will be measured in the region from 4000 to 700 cm^{-1}. The normal vibrations of this polymer, which takes a three-fold helical conformation, will be calculated by the use of the ***GF***-matrix method, with the modified Urey-Bradley force field. It will be found that the parallel and perpendicular bands correspond reasonably well to the calculated frequaencies of the A and E($2\pi/3$) symmetry species respectively. In accordance with these correspondences, the assignments of these bands will be made and their vibrational modes discussed.

In recent years, it has been reported that isotactic polybutene-1 exhibits three polymorphs, namely, a stable hexagonal form,[1-5,8] a stable orthorhombic form,[4,5,7-9] and an unstable tetragonal form,[2,4-9] and that these three crystalline forms exhibit significantly different infrared spectra in the region from 2000 to 400 cm^{-1}.[10-12] The spectral difference may depend upon the molecular conformations of the polymer, but the vibrational analysis of the correlation between the spectral difference and molecular conformations has not yet been dealt with.

On the other hand, the polarized infrared spectra of isotactic vinyl polymers, including the isotactic polybutene-1, were measured by Tadokoro et al.[13] in order to examine whether or not the bands associated with helical structures appear; the 1217 cm^{-1} band of isotactic polybutene-1 in the hexagonal form was proposed as the band to be associated with the helical conformation. Thereafter, the correlations of the infrared spectra with the crystallinity and the stereoregularity of the polybutene-1 samples were studied by Nishioka and Yanagisawa.[14] These studies showed that the absorption band at 1221, 1208, 1098, 1059, 1029, 922, 849, and 816 cm^{-1} in the hexagonal crystals are related to the crystallinity, while the absorption bands at 1220, 972, and 917 cm^{-1} in a carbon disulfide solution of the polymer are directly related to the stereoregularity. However, these bands have scarcely been assigned at all because of the complexity of this molecule.

Thus, in order to obtain some information about these problems, the normal vibrations for the isotactic polybutene-1 molecule of a three-fold helical conformation (hexagonal form) were calculated, using the force constants transferred from simple aliphatic hydrocarbons. The calculated frequencies will be compared with the observed frequencies, and the assignments of bands based on the calculated potential energy distributions will be given for the fundamental bands observed from 4000 to 700 cm^{-1}. The vibrational modes of the absorption bands characteristic of the three-fold helical conformation and other bands will also be discussed.

Experimental

A sample of isotactic polybutene-1 was prepared, with titanium-mercaptide as the catalyst, in the laboratory of the Toyo Soda Industrial Company. The sample was extracted with ethyl ether, and the insoluble part (ca. 75%) was used in this work. The film specimens for the measurement of the infrared spectra were obtained at about 40°C by casting a one percent solution in carbon tetrachloride on glass plates. The oriented film specimens were prepared by annealing the film at 90°C and by then elongating the film at 60°C. The polarized infrared spectra in the regions from 4000 to 2700 cm^{-1} and from 2700 to 700 cm^{-1} were taken

1) G. Natta, P. Pino, P. Corradini, F. Danusso, E. Mantica, G. Mazzanti and G. Moraglio, *J. Am. Chem. Soc.*, **77**, 1708 (1955).
2) G. Natta, P. Corradini and I. W. Bassi, *Atti. accad. naz. Lincei Rend., Classe Sci. fis. mat. e nat.*, **19**, 404 (1955).
3) G. Natta, P. Corradini and I. W. Bassi, *Makromol. Chem.*, **21**, 20 (1956); *Nuovo Cimento Suppl.*, **15**, 52 (1960).
4) R. Zanetti, P. Manaresi and G. C. Buzzoni, *Chim. Ind. (Milan)*, **43**, 735 (1961).
5) F. Dannuso and G. Gianotti, *Makromol. Chem.*, **61**, 139 (1963).
6) A. Turner-Jones, *J. Polymer Sci.*, **B1**, 445 (1963).
7) C. Geacintov, R. S. Schotland and R. B. Miles, ibid., **B1**, 587 (1963).
8) R. L. Miller and V. F. Holland, *Polymer Letters*, **2**, 519 (1964); V. F. Holland and R. L. Miller, *J. Appl. Phys.*, **35**, 3241 (1964).
9) J. Boor, Jr., and E. A. Youngman, *Polymer Letters*, **2**, 903 (1964).
10) G. Natta, *Makromol. Chem.*, **35**, 94 (1960).
11) H. Yasuda and M. Takayanagi, *Repts. Progr. Polym. Phys. Japan*, **7**, 245 (1964).
12) J. P. Luongo and R. Salovey, *Polymer Letter*, **3**, 513 (1965).
13) H. Tadokoro, T. Kitazawa, S. Nozakura and S. Murahashi, This Bulletin, **34**, 1209 (1961).
14) T. Nishioka and K. Yanagisawa, *Chem. High Polymer (Kobunshi Kagaku)*, **19**, 667, 671 (1962).

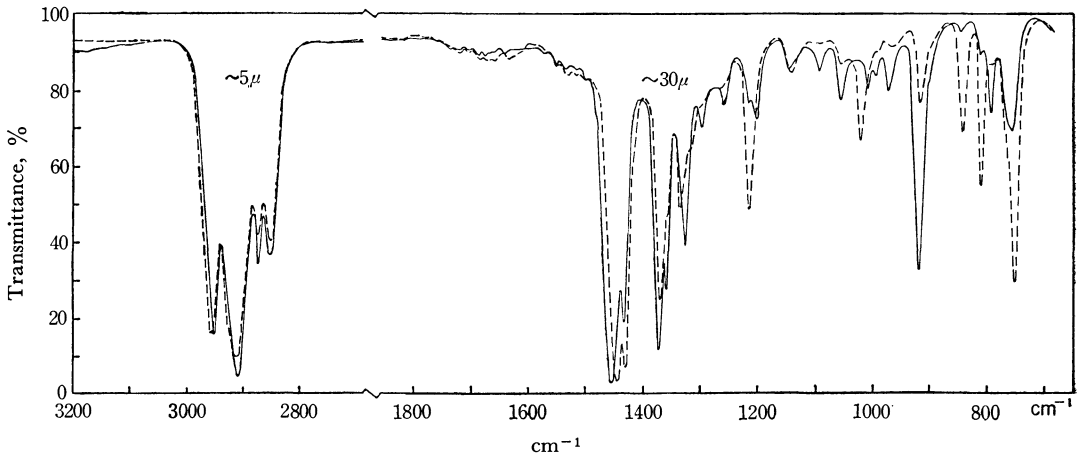

Fig. 1. Polarized infrared spectra of crystalline isotactic polybutene-1 (hexagonal form).
Solid curve: electric vector perpendicular to the direction of stretch
Broken curve: electric vector parallel to this direction.

TABLE I. SYMMETRY SPECIES, NUMBERS OF NORMAL MODES, SELECTION RULES, AND DICHROISM FOR ISOTACTIC POLYBUTENE-1 MOLECULE UNDER THE GROUP $C(2\pi/3)$*1

	E	C_3^1	C_3^2	Numbers*2	Infrared*3	Raman*4
A	1	1	1	36-2 ($T_\parallel$, $R_\parallel$)	A($\parallel$)	A(p)
E	$\begin{Bmatrix}1\\1\end{Bmatrix}$	$\begin{matrix}\varepsilon^1\\ \varepsilon^{-1}\end{matrix}$	$\begin{matrix}\varepsilon^2\\ \varepsilon^{-2}\end{matrix}$	$\begin{matrix}\text{36-1 } (T_\perp)\\ \text{36-1 } (T_\perp)\end{matrix}\Big\}$	A($\perp$)	A(dp)

*1 $\varepsilon=\exp(2\pi i/3)$.
*2 $T_\parallel$ and $T_\perp$, pure translations; $R_\parallel$, pure rotation.
*3 A, active; $\parallel$ or $\perp$ indicates that the dipole moment is parallel or perpendicular to the helical axis.
*4 p, polarized; dp, depolarized.

TABLE II. INTERNAL COORDINATES

Bond length	Bond angle	Bond angle	Bond length	Bond angle	Bond angle
$R_1=C_1\text{-}C_2$	$\Theta_1=\angle C_2''\text{-}C_1\text{-}C_2$	$\varphi_3=\angle H_1\text{-}C_1\text{-}C_2$	$r_3=C_2\text{-}H_3$	$\theta_2=\angle H_4\text{-}C_3\text{-}H_5$	$\varphi_9=\angle C_2\text{-}C_3\text{-}H_5$
$R_2=C_2\text{-}C_1'$	$\Theta_2=\angle C_1\text{-}C_2\text{-}C_1'$	$\varphi_4=\angle H_2\text{-}C_1\text{-}C_2$	$r_4=C_3\text{-}H_4$	$\theta_3=\angle H_6\text{-}C_4\text{-}H_7$	$\varphi_{10}=\angle H_4\text{-}C_3\text{-}C_4$
$R_3=C_2\text{-}C_3$	$\Phi_1=\angle C_1\text{-}C_2\text{-}C_3$	$\varphi_5=\angle C_1\text{-}C_2\text{-}H_3$	$r_5=C_3\text{-}H_5$	$\theta_4=\angle H_6\text{-}C_4\text{-}H_8$	$\varphi_{11}=\angle H_5\text{-}C_3\text{-}C_4$
$R_4=C_3\text{-}C_4$	$\Phi_2=\angle C_3\text{-}C_2\text{-}C_1'$	$\varphi_6=\angle H_3\text{-}C_2\text{-}C_1'$	$r_6=C_4\text{-}H_6$	$\theta_5=\angle H_7\text{-}C_4\text{-}H_8$	$\varphi_{12}=\angle C_3\text{-}C_4\text{-}H_6$
$r_1=C_1\text{-}H_1$	$\Phi_3=\angle C_2\text{-}C_3\text{-}C_4$	$\varphi_7=\angle H_3\text{-}C_2\text{-}C_3$	$r_7=C_4\text{-}H_7$	$\varphi_1=\angle C_2''\text{-}C_1\text{-}H_1$	$\varphi_{13}=\angle C_3\text{-}C_4\text{-}H_7$
$r_2=C_1\text{-}H_2$	$\theta_1=\angle H_1\text{-}C_1\text{-}H_2$	$\varphi_8=\angle C_2\text{-}C_3\text{-}H_4$	$r_8=C_4\text{-}H_8$	$\varphi_2=\angle C_2''\text{-}C_1\text{-}H_2$	$\varphi_{14}=\angle C_3\text{-}C_4\text{-}H_8$

TABLE III. THE LOCAL SYMMETRY COORDINATES

S_1	$2^{-1/2}\Delta(r_1+r_2)$	$\nu_s(CH_2)_m$
S_2	$2^{-1/2}\Delta(r_1-r_2)$	$\nu_a(CH_2)_m$
S_3	Δr_3	$\nu(CH)$
S_4	$2^{-1/2}\Delta(r_4+r_5)$	$\nu_s(CH_2)_s$
S_5	$2^{-1/2}\Delta(r_4-r_5)$	$\nu_a(CH_2)_s$
S_6	$3^{-1/2}\Delta(r_6+r_7+r_8)$	$\nu_s(CH_3)$
S_7	$6^{-1/2}\Delta(2r_6-r_7-r_8)$	$\nu_a(CH_3)$
S_8	$2^{-1/2}\Delta(r_7-r_8)$	$\nu_a'(CH_3)$
S_9	$2^{-1/2}\Delta(R_1+R_2)$	$\nu_s(CC)_m$
S_{10}	$2^{-1/2}\Delta(R_1-R_2)$	$\nu_a(CC)_m$
S_{11}	$2^{-1/2}\Delta(R_3+R_4)$	$\nu_s(CC)_s$
S_{12}	$2^{-1/2}\Delta(R_3-R_4)$	$\nu_a(CC)_s$
S_{13}	$2^{-1}\Delta(\varphi_1-\varphi_2+\varphi_3-\varphi_4)$	$r(CH_2)_m$
S_{14}	$2^{-1}\Delta(\varphi_1+\varphi_2-\varphi_3-\varphi_4)$	$w(CH_2)_m$
S_{15}	$2^{-1}\Delta(\varphi_1-\varphi_2-\varphi_3+\varphi_4)$	$t(CH_2)_m$
S_{16}	$20^{-1/2}\Delta(4\theta_1-\varphi_1-\varphi_2-\varphi_3-\varphi_4)$	$\delta(CH_2)_m$
S_{17}	$30^{-1/2}\Delta(5\Theta_1-\varphi_1-\varphi_2-\varphi_3-\varphi_4-\theta_1)$	$\delta(CC)_m$
S_{18}	$6^{-1/2}\Delta(2\varphi_7-\varphi_5-\varphi_6)$	$\delta(CH)$
S_{19}	$2^{-1/2}\Delta(\varphi_5-\varphi_6)$	$w(CH)$
S_{20}	$6^{-1/2}(\varphi_5+\varphi_6+\varphi_7-\Phi_1-\Phi_2-\Theta_2)$	$\delta_s(CC)$
S_{21}	$6^{-1/2}(2\Theta_2-\Phi_1-\Phi_2)$	$\delta'(CC)_m$
S_{22}	$2^{-1/2}(\Phi_1-\Phi_2)$	$\delta(CC)_s$
S_{23}	$2^{-1}(\varphi_8-\varphi_9+\varphi_{10}-\varphi_{11})$	$r(CH_2)_s$
S_{24}	$2^{-1}(\varphi_8+\varphi_9-\varphi_{10}-\varphi_{11})$	$w(CH_2)_s$
S_{25}	$2^{-1}(\varphi_8-\varphi_9-\varphi_{10}+\varphi_{11})$	$t(CH_2)_s$
S_{26}	$20^{-1/2}(4\theta_2-\varphi_8-\varphi_9-\varphi_{10}-\varphi_{11})$	$\delta(CH_2)_s$
S_{27}	$30^{-1/2}(5\Phi_3-\varphi_8-\varphi_9-\varphi_{10}-\varphi_{11}-\theta_2)$	$\delta'(CC)_s$
S_{28}	$6^{-1/2}(2\varphi_{12}-\varphi_{13}-\varphi_{14})$	$r_a(CH_3)$
S_{29}	$2^{-1/2}(\varphi_{13}-\varphi_{14})$	$r_a'(CH_3)$
S_{30}	$6^{-1/2}(\varphi_{12}+\varphi_{13}+\varphi_{14}-\theta_3-\theta_4-\theta_5)$	$\delta_s(CH_3)$
S_{31}	$6^{-1/2}(2\theta_5-\theta_3-\theta_4)$	$\delta_a(CH_3)$
S_{32}	$2^{-1/2}(\theta_3-\theta_4)$	$\delta_a'(CH_3)$
S_{33}	$6^{-1/2}(\varphi_1+\varphi_2+\varphi_3+\varphi_4+\theta_1+\Theta_1)$	redundant coordinates
S_{34}	$6^{-1/2}(\varphi_5+\varphi_6+\varphi_7+\Phi_1+\Phi_2+\Theta_2)$	
S_{35}	$6^{-1/2}(\varphi_8+\varphi_9+\varphi_{10}+\varphi_{11}+\theta_2+\Phi_3)$	
S_{36}	$6^{-1/2}(\varphi_{12}+\varphi_{13}+\varphi_{14}+\theta_3+\theta_4+\theta_5)$	

TABLE IV. FORCE CONSTANTS OF ISOTACTIC POLYBUTENE-1*1

$K(CH)(CH_3)$	4.350 mdyn./Å.	F(HC)	0.540*2 mdyn./Å
$K(CH)(CH_2)$	4.050*2	F(CC)	0.335*2
$K(CH)(CH)$	3.900*2	$\kappa(CH_3)$	0.008*2 mdyn.·Å
K(CC)	2.000	$\kappa(CH_2)$	0.033*2
H(HCH)	0.431*2	κ(CH)	0.063*2
H(HCC)	0.186*2	T	0.118*2
H(CCC)	0.275*2	G	−0.030
F(HH)	0.080*2	F'	−0.1 F

*1 K, stretching; H, bending: F, repulsion; T, trans coupling; G, gauche coupling; κ, intramolecular tension.
*2 Transferred from Ref. 16.

TABLE V. THE C-H STRETCHING VIBRATIONS (IN cm^{-1}) OF ISOTACTIC POLYBUTENE-1

Obsd.*1	Calcd.		Assignment
2961 (∥, vs)	2949 (A)	ν_1	CH_3 asym. stretching, $\nu_a(CH_3)$
	2948 (E)		
2958 (⊥, vs)	2947 (E)	ν_2	CH_3 asym. stretching, $\nu_a'(CH_3)$
	2947 (A)		
2914 (⊥, vs)	2920 (E)	ν_3	CH stretching, ν(CH)
	2919 (A)		
	2909 (E)	ν_4	CH_2 antisym. stretching, $\nu_a(CH_2)_m$
	2910 (A)		
	2908 (E)	ν_5	CH_2 antisym. stretching, $\nu_a(CH_2)_s$
	2907 (A)		
2874 (⊥, s)	2897 (E)	ν_6	CH_3 sym. stretching, $\nu_s(CH_3)$
	2899 (A)		
2851 (⊥, s)	2878 (E)	ν_7	CH_2 sym. stretching, $\nu_s(CH_2)_m$
	2875 (A)		
	2869 (E)	ν_8	CH_2 sym. stretching, $\nu_s(CH_2)_s$
	2867 (A)		

*1 vs, very strong; s, strong

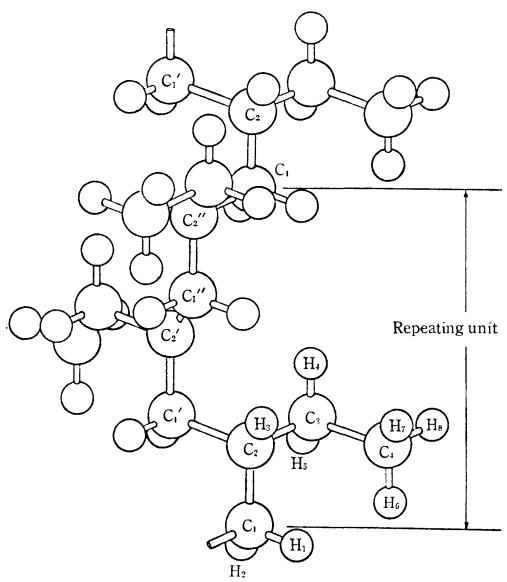

Fig. 2. Unit cell for three-fold helical structure of isotactic polybutene-1.

by using a Perkin-Elmer, model 221, grating spectrophotometer and a Hitachi Ltd., model EPI-S2, spectrophotometer respectively. The polarization measurements were carried out with a silver chloride polarizer. The observed spectra are shown in Fig. 1.

Normal Coordinate Treatment

The molecule of isotactic polybutene-1 in the hexagonal crystals contains three chemical unit, $-CH_2-CH(-CH_2-CH_3)-$, in one turn of the fiber identity period of 6.50 Å.[1-3] The unit cell for this structure is shown in Fig. 2. This model corresponds to the right-handed helix. This infinitely-extended helical structure belongs to the factor group, $C(2\pi/3)$, isomorphous with the point group, C_3; therefore, the molecular vibrations can be treated under the factor group $C(2\pi/3)$. The results of this treatment are given in Table I. Thirty-four of the modes listed in Table I belong to A species and are totally symmetric to the three-fold helical axis. Accordingly, the dipole-moment change for an A mode is parallel to the helical axis. On the other hand, the thirty-five degenerate modes belong to the E species, and the phase difference between adjacent chemical units is $2\pi/3$. The resultant dipole-moment change for an E mode is perpendicular to the helical axis.

TABLE VI. THE OBSERVED AND CALCULATED FREQUENCIES OF ISOTACTIC POLYBUTENE-1 IN THE REGION FROM 1500 TO 700 cm^{-1}

Obsd.*1	Calcd.		Potential energy distributions (%)*2
1463 (⊥, s)	1478 (E)	ν_9	$\delta_a'(CH_3)$ (66), $\delta_a(CH_3)$ (24)
	1478 (A)		$\delta_a'(CH_3)$ (67) − $\delta_a(CH_3)$ (23)
1458 (∥, s)	1476 (A)	ν_{10}	$\delta_a(CH_3)$ (68) + $\delta_a'(CH_3)$ (23)
	1476 (E)		$\delta_a(CH_3)$ (66), $\delta_a'(CH_3)$ (24)
1441 (∥, s)	1475 (A)	ν_{11}	$\delta(CH_2)_m$ (64) − $\delta(CH_2)_s$ (31)
	1475 (E)		$\delta(CH_2)_m$ (90)
1439 (⊥, s)	1473 (E)	ν_{12}	$\delta(CH_2)_s$ (93)
	1473 (A)		$\delta(CH_2)_s$ (65) + $\delta(CH_2)_m$ (31)
1380 (⊥, s)	1407 (E)	ν_{13}	$\delta_s(CH_3)$ (91)
	1407 (A)		$\delta_s(CH_3)$ (92)
1366 (⊥, s)	1378 (E)	ν_{14}	$w(CH_2)_s$ (23), w(CH) (21), δ(CH) (13), $w(CH_2)_m$ (11)
	1372 (A)		$w(CH_2)_s$ (41) + w(CH) (23) + δ(CH) (11)
1342 (∥, m)	1380 (A)	ν_{15}	$w(CH_2)_m$ (36) − δ(CH) (23) + w(CH) (15)
1331 (⊥, m)	1368 (E)		δ(CH) (31), $w(CH_2)_m$ (18), w(CH) (18)
	1341 (E)	ν_{16}	$w(CH_2)_s$ (47), $w(CH_2)_m$ (16)
1321 (∥, w)	1331 (A)		$w(CH_2)_s$ (42) − w(CH) (30) − δ(CH) (11)
1302 (⊥, w)	1312 (E)	ν_{17}	$w(CH_2)_m$ (46), w(CH) (13), δ(CH) (11)
	1299 (A)		$w(CH_2)_m$ (61) + δ(CH) (13)
1263 (⊥, w)	1262 (E)	ν_{18}	$t(CH_2)_s$ (50), $r_a(CH_3)$ (16)
	1280 (A)		$t(CH_2)_s$ (49) + $t(CH_2)_m$ (30)
1222 (∥, m)	1235 (A)	ν_{19}	$t(CH_2)_m$ (30) − δ(CH) (15) + $r(CH_2)_s$ (15) + $r_a'(CH_3)$ (10)
1207 (⊥, w)	1180 (E)		$t(CH_2)_m$ (33), w(CH) (13)
1150 (⊥, w)	1140 (E)	ν_{20}	ν(CC) (36)
	1124 (A)		ν(CC) (43) − $r_a(CH_3)$ (11)
1096 (⊥, w)	1090 (E)	ν_{21}	ν(CC) (32), $r_a(CH_3)$ (13)
1062 (⊥, w)	1027 (E)	ν_{22}	ν(CC) (39), $t(CH_2)_m$ (14)
	1048 (A)	ν_{21}	$r_a'(CH_3)$ (25) + $\nu(CC)_s$ (23)
1028 (∥, w)	1015 (A)	ν_{22}	$\nu_a(CC)_s$ (43) + $\nu_a(CC)_m$ (10)
1015 (⊥, w)	993 (E)	ν_{23}	$\nu_a(CC)_s$ (37), $\nu_s(CC)_s$ (21), $\nu_a(CC)_m$ (17)
	998 (A)		$\nu_a(CC)_m$ (36) − $\nu_a(CC)_s$ (23)
977 (⊥, w)	961 (E)	ν_{24}	$r_a(CH_3)$ (21), $\nu_a(CC)_m$ (19), $\nu_s(CC)_m$ (18)
	966 (A)		$\nu_s(CC)_m$ (25) + $r_a(CH_3)$ (20) − $\nu_s(CC)_s$ (12)
924 (⊥, s)	918 (E)	ν_{25}	$r_a'(CH_3)$ (23), $r(CH_2)_m$ (20), $\nu_s(CC)_m$ (13), $\nu_s(CC)_s$ (10)
848 (∥, w)	874 (A)		$r_a'(CH_3)$ (25) − $\nu_s(CC)_s$ (16) − $\nu_s(CC)_s$ (16) − $\nu_s(CC)_m$ (10)
816 (∥, m)	796 (A)	ν_{26}	$r(CH_2)_m$ (65) − $\nu_s(CC)_s$ (11)
798 (⊥, w)	796 (E)		$r(CH_2)_m$ (30), $\nu_s(CC)_s$ (17), $\nu_s(CC)_m$ (17)
764 (⊥, w)	742 (E)	ν_{27}	$r(CH_2)_s$ (51), $r_a(CH_3)$ (21)
758 (∥, s)	738 (A)		$r(CH_2)_s$ (55) − $r_a(CH_3)$ (24)

*1 vs, very strong; s, strong; m, medium; w, weak.

*2 δ_a and δ_a', asymmetric deformations; δ_s, symmetric deformation; ν_s, symmetric stretching; ν_a, antisymmetric stretching; δ, bending; w, wagging; t, twisting; r, r_a, and r_a', rockings. The $(CH_2)_m$ and $(CH_2)_s$ represent methylene units of the main chain and the ethyl group, respectively.

The internal coordinates of a unit cell are expressed in vector notations, as in Eq. 1:

$$q = \begin{Vmatrix} q(j) \\ q(j') \\ q(j'') \end{Vmatrix} \quad (1)$$

where q(j), q(j'), and q(j'') represent the coordinates of unprimed, single-primed, and double-primed atoms, as is shown in Fig. 2. Table II lists the elements of the internal coordinate q(j). For the present coordinates, the freedom of internal rotation about CC bonds is ignored. These internal coordinates, q, were transformed into the local symmetry coordinates, S, as expressed in Eq. 2:

$$S = \begin{Vmatrix} S(j) \\ S(j') \\ S(j'') \end{Vmatrix} \quad (2)$$

The elements of the local symmetry coordinates, S(j), together with four redundant coordinates, are listed in Table III.

The $\boldsymbol{G}$ or $\boldsymbol{F}$ matrix based on the local symmetry coordinates may be factored into three matrices by the unitary transformation;[15] $\boldsymbol{G}$(A), $\boldsymbol{G}$(E), and

15) H. Tadokoro, *J. Chem. Phys.*, **33**, 1558 (1960); **35**, 1050 (1961).

TABLE VII. THE L MATRIX ELEMENTS OF ISOTACTIC POLYBUTENEPOLYBUTENE-9 (A SPECIES)*1

	1478	1476	1475	1473	1408	1380	1372	1331	1299
$\nu_s(CC)_m$	0	0	0	0	0	0	0	0	0
$\nu_a(CC)_m$	0	0	0	0	0	−1	1	0	0
$\nu_s(CC)_s$	0	0	0	0	0	0	0	0	0
$\nu_a(CC)_s$	0	0	0	0	0	0	1	0	0
$r(CH_2)_m$	0	0	0	0	0	0	2	−2	1
$w(CH_2)_m$	0	0	0	0	0	8	0	0	9
$t(CH_2)_m$	0	0	0	0	0	−3	0	2	3
$\delta(CH_2)_m$	1	−1	−12	8	0	0	0	0	0
$\delta(CH)$	0	0	0	0	1	−6	−4	4	4
$w(CH)$	0	0	0	0	0	5	−6	6	−3
$r(CH_2)_s$	0	0	0	0	0	1	0	0	0
$w(CH_2)_s$	−1	0	0	0	2	0	−8	−7	0
$t(CH_2)_s$	0	0	0	0	0	2	0	0	−3
$\delta(CH_2)_s$	0	1	8	12	0	0	0	0	0
$r_a(CH_3)$	1	3	0	0	0	0	0	1	0
$r_a'(CH_3)$	3	−1	0	0	0	0	1	1	0
$\delta_s(CH_3)$	0	0	0	0	13	0	3	0	0
$\delta_a(CH_3)$	7	12	−1	0	0	0	−1	0	0
$\delta_a'(CH_3)$	−12	7	−1	0	0	0	1	1	0

	1280	1235	1124	1048	1015	998	966	874	796	738
$\nu_s(CC)_m$	0	0	−1	0	−1	0	−1	−1	0	0
$\nu_a(CC)_m$	0	0	−2	−1	1	−2	0	0	0	0
$\nu_s(CC)_s$	0	0	1	−1	0	−1	1	−1	1	0
$\nu_a(CC)_s$	0	0	0	−1	2	1	0	0	0	0
$r(CH_2)_m$	0	0	1	−1	0	0	2	−1	−6	0
$w(CH_2)_m$	0	0	0	1	0	0	−1	0	0	0
$t(CH_2)_m$	6	−6	−1	−3	−2	1	0	−1	0	0
$\delta(CH_2)_m$	0	0	0	0	0	0	0	0	0	0
$\delta(CH)$	0	4	2	2	2	−1	0	0	0	0
$w(CH)$	0	0	−1	−1	0	0	1	0	−2	0
$r(CH_2)_s$	0	−4	2	1	1	−1	0	0	0	−5
$w(CH_2)_s$	0	0	0	−2	0	0	−1	1	0	0
$t(CH)_s$	8	2	1	2	2	−3	−2	−2	0	0
$\delta(CH_2)_s$	0	0	0	0	0	0	0	0	0	0
$r_a(CH_3)$	−3	−3	3	0	1	−2	−4	0	0	3
$r_a'(CH_3)$	0	3	2	−5	−2	0	−2	4	0	−1
$\delta_s(CH_3)$	0	0	0	0	0	0	0	0	0	0
$\delta_a(CH_3)$	1	1	−1	0	0	0	1	0	0	0
$\delta_a'(CH_3)$	0	−1	0	−1	0	0	0	1	0	0

*1 The first row represents the calculated frequencies.

G(E*) or F(A), F(E), and F(E*). The resultant matrix, G(A) or F(A), is a real symmetric matrix of Order Thirty-two, while G(E) or F(E) is an Hermitian matrix of Order Thirty-two. G(E*) or F(E*) is the complex conjugated matrix of G(E) or F(E). Therefore, the symmetry coordinates of this helical structure are expressed as in Eq. 3:

$$\begin{aligned} S(A) &= 3^{-1/2}[S(j)+S(j')+S(j'')] \\ S(E) &= 3^{-1/2}[S(j)+S(j')e^{i\omega}+S(j'')e^{2i\omega}] \\ S(E^*) &= 3^{-1/2}[S(j)+S(j')e^{-i\omega}+S(j'')e^{-2i\omega}] \end{aligned} \quad (3)$$

where $\omega=2\pi/3$.

The force constants used in this work were transferred from the values of ethane, propane, and isobutane;[16] they are shown in Table IV. In the calculations, the bond lengths of R(C–C) and r(C–H) were taken as 1.54 and 1.09 Å respectively, and all the bond angles were assumed to be tetrahedral (109°28′) for the sake of simplicity. As an analytical method of calculating the normal vibrations, the GF-matrix method of Wilson was used.[17] The calculations of normal frequencies, L matrices, potential energy distributions, and phase angles were made with an OKITAC 5090A electronic digital compurter

16) H. Takahashi, *J. Chem. Soc. Japan, Pure Chem. Sect.* (*Nippon Kagaku Zasshi*), **83**, 976, 978, 980 (1962).
17) E. B. Wilson, *J. Chem. Phys.*, **7**, 1047 (1939); **9**, 76 (1941).

TABLE VIII. THE L MATRIX ELEMENTS OF ISOTACTIC POLYBUTENE-1 (E SPECIES)*1

	1478	1476	1475	1473	1407	1378	1368	1341	1312	1262	1180	1140	1090	1027	993	961	918	796	742
$\nu_s(CC)_m$	0	0	0	0	0	0	0	0	0	0	0	1 (64)	0	1 (−53)	0	1 (−13)	1 (43)	1 (22)	0
$\nu_a(CC)_m$	0	0	0	0	0	1 (53)	1 (27)	0	0	0	0	1 (−18)	2 (−8)	0	1 (0)	1 (−34)	0	0	0
$\nu_s(CC)_s$	0	0	0	0	0	0	0	0	0	0	0	1 (25)	1 (14)	0	1 (2)	0	1 (−76)	1 (12)	0
$\nu_a(CC)_s$	0	0	0	0	0	1 (28)	0	0	0	0	0	1 (16)	0	2 (−37)	2 (8)	0	0	0	0
$r(CH_2)_m$	0	0	0	0	0	1 (−78)	1 (16)	0	1 (23)	1 (−44)	3 (72)	2 (80)	0	1 (76)	1 (−11)	0	4 (−70)	4 (−22)	1 (5)
$w(CH_2)_m$	0	0	0	0	0	4 (8)	5 (82)	5 (−26)	8 (−41)	2 (−12)	2 (87)	0	1 (−10)	1 (29)	0	0	0	0	0
$t(CH_2)_m$	0	0	0	0	0	3 (1)	2 (56)	3 (−61)	3 (−17)	0	6 (−5)	3 (24)	2 (81)	3 (−48)	1 (5)	0	1 (45)	0	0
$\delta(CH_2)_m$	1 (−56)	2 (6)	14 (0)	2 (68)	0	0	0	0	0	0	0	0	0	0	0	0	0	0	0
$\delta(CH)$	0	0	0	0	1 (1)	4 (19)	7 (16)	3 (53)	3 (−71)	3 (−5)	1 (79)	2 (74)	0	2 (61)	1 (83)	1 (24)	1 (−31)	0	1 (10)
$w(CH)$	0	0	0	0	1 (0)	6 (41)	5 (28)	3 (−28)	4 (0)	1 (−80)	4 (8)	2 (22)	3 (−50)	2 (−8)	1 (41)	0	1 (70)	0	0
$r(CH_2)_s$	0	0	0	0	0	0	1 (11)	0	0	2 (2)	2 (−64)	2 (−48)	2 (−3)	1 (64)	0	0	0	1 (−73)	5 (−4)
$w(CH_2)_s$	1 (0)	0	0	0	2 (0)	6 (32)	3 (−74)	8 (−3)	3 (−18)	0	0	0	1 (14)	1 (13)	1 (40)	2 (−52)	1 (−45)	0	0
$t(CH_2)_s$	0	0	0	0	0	0	4 (14)	1 (−77)	3 (−52)	8 (5)	0	2 (−32)	1 (−9)	2 (58)	1 (−80)	3 (−9)	2 (−28)	0	1 (−5)
$\delta(CH_2)_s$	0	1 (14)	2 (−70)	14 (0)	0	0	0	0	0	0	0	0	0	0	0	0	0	0	0
$r_a(CH_3)$	1 (0)	3 (0)	0	0	0	0	0	1 (−3)	1 (−29)	4 (3)	1 (−41)	2 (−76)	3 (4)	1 (−71)	1 (−48)	4 (−29)	0	1 (−40)	3 (−8)
$r_a'(CH_3)$	3 (0)	1 (1)	0	0	0	0	0	1 (−5)	0	2 (4)	3 (−80)	2 (0)	2 (13)	3 (33)	1 (67)	3 (−73)	4 (−43)	1 (35)	2 (6)
$\delta_s(CH_3)$	0	0	0	0	13 (0)	3 (30)	0	0	0	0	0	0	0	0	0	0	0	0	0
$\delta_s(CH_3)$	7 (0)	12 (0)	2 (10)	0	0	0	0	0	0	2 (3)	0	0	1 (4)	0	0	1 (−29)	0	0	0
$\delta_a'(CH_3)$	12 (0)	7 (1)	1 (−78)	0	0	1 (31)	0	1 (−3)	0	0	1 (−78)	0	0	0	0	0	1 (−43)	0	0

*1 The first row represents the calculated frequencies.

(4000 core locations) using the programs described previously.[18,19] The calculated frequencies are shown in Tables V and VI, where they are compared with the observed frequencies. The vibrational assignments based on the potential energy distributions are shown in the last columns of Tables V and VI. The $\boldsymbol{L}$ matrix elements for the A and E symmetry species are listed in Tables VII and VIII respectively. In Table VII, the phase relations among the symmetry coordinates are represented by the signs plus and minus, which stand for in-phase and out-of-phase respectively. In Table VIII, each element for the E species is expressed by the amplitude, $|L_{jk}|$, and the phase angle (in parentheses), δ_{jk}, in degrees. The phase relations among the symmetry coordinates in a certain normal vibration are represented by the difference in phase angles (see Ref. 18).

Discussion

The factor group analysis shows that the vibrational modes belonging to the A and E symmetry species have parallel ($\parallel$) and perpendicular ($\perp$) dichroisms respectively when the molecular chain is oriented along the stretching direction of the film specimen. As Tables V and VI show, the observed frequencies of parallel and perpendicular bands correspond reasonably well to the calculated frequencies of the A and E species respectively. The average deviations in this work are 1.29 (A species) and 1.12 (E species) %.

C–H Stretching Vibtations.—In the region from 3000 to 2800 cm^{-1} four perpendicular bands, at 2958, 2914, 2874, and 2851 cm^{-1}, and one parallel band at 2961 cm^{-1}, are observed. The assignments of these bands are given in Table V. All bands in this region are assigned to the overlapped modes of the A and the E species for each C–H stretching vibration. In addition to that, the CH_2 stretching vibrations for the main chain and the ethyl group are assigned to the same bands (see Table V).

CH_2 Bending and CH_3 Deformation Modes.—In the region from 1500 to 1370 cm^{-1}, three perpendicular bands, at 1463, 1439, and 1380 cm^{-1}, and two parallel bands, at 1458 and 1441 cm^{-1}, are observed. The strong bands at 1463 and 1458 cm^{-1} are assigned to the CH_3 asymmetric deformation modes, namely, $\delta'_a(CH_3)$(A, E) and $\delta_a(CH_3)$(A, E). The strong perpendicular band at 1380 cm^{-1} is easily assigned to the CH_3 symmetric deformation mode, $\delta_s(CH_3)$(A, E). The assignments of these bands related to the methyl group are consistent with those of isotactic polypropylene.[18,20-22]

The intense parallel band at 1441 cm^{-1} and the medium intensity band at 1439 cm^{-1} are assigned together to the CH_2 bending modes, but the CH_2 bending modes of the main chain and the ethyl group couple with each other in this polymer. The schematic representations of these CH_2 bending modes are shown in Figs. 3(a) and 3(b). On the basis of these normal modes, it may reasonably be understood that the 1441 cm^{-1} band has an intense parallel dichroism.

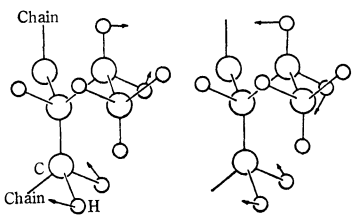

(a) (b)

Fig. 3. Vibrational modes for a chemical unit of the parallel band at 1441 cm^{-1} (a) and the 1439 cm^{-1} band (b).

CH_2 Wagging, CH_2 Twisting, CH Bending, and CH Wagging Modes.—In the region from 1370 to 1200 cm^{-1}, five perpendicular bands, at 1366, 1331, 1302, 1263, and 1207 cm^{-1}, and three parallel bands, at 1342, 1321, and 1222 cm^{-1}, are observed. As is shown in Table VI, all the bands observed from 1370 to 1300 cm^{-1} are assigned to the mixed modes of the CH_2 wagging, the CH bending, and the CH wagging. In this region, the medium intensity bands at 1331 and 1342 cm^{-1} appear in the spectra of a hexagonal form and are either extremely weak or do not appear in other crystalline forms.[12] The character of these bands may be due to the coupling of the CH_2 wagging (main chain), the CH bending, and the CH wagging modes (see Table VI).

The parallel band at 1222 cm^{-1} closely related to stereoregularity and crystallinity is observed in three crystalline forms.[12] This fact indicates that the 1222 cm^{-1} band is not affected by the molecular conformations. Therefore, it may easily be understood that this band is characteristic of stereoregularity. According to the present work, this band corresponds to the ν_{19}(A) vibration of the calculated frequency at 1235 cm^{-1}. The ν_{19}(A) vibration is associated with the CH_2 twisting, the CH bending, and the ethyl rocking modes. For this band, Tadokoro et al.[13] suggested that, in the mode assignable, the vibration

18) H. Tadokoro, M. Kobayashi, M. Ukita, K. Yasufuku, S. Murahashi and T. Torii, *J. Chem. Phys.*, **42**, 1432 (1965).
19) M. Ukita, *Bul. Gov. Ind. Res. Inst., Osaka (Osaka Kogyo Gijitsu Shikensho Kiho)*, **16**, 42 (1965).
20) T. Miyazawa and Y. Ideguchi, This Bulletin, **36**, 1125 (1963); **37**, 1065 (1964).
21) C. Y. Liang, M. R. Litton and C. J. Boone, *J. Polymer Sci.*, **54**, 523 (1961).
22) R. G. Snyder and J. H. Schatschneider, *Spectrochim. Acta*, **20**, 853 (1964).

in the main chain would couple with that of the side group. This suggestion is clearly confirmed by the present work. The 1207 cm^{-1} band related to crystallinity appears only in the hexagonal form.[12] The character of this band may be due to the coupling of the CH_2 twisting (main chain) and the CH wagging modes.

CC Stretching, CH_2 Rocking, and CH_3 Rocking Modes.—In the region from 1200 to 1000 cm^{-1}, four perpendicular bands, at 1150, 1096, 1062, and 1015 cm^{-1}, and one parallel band, at 1028 cm^{-1}, are observed. The weak bands in this region are mainly assigned to the CC stretching modes, except for the 1062 cm^{-1} band, which is assigned to the coupling vibration of the CH_3 rocking and the CC stretching modes of the ethyl group. The CC stretching modes which are not localized in several CC symmetry coordinates are represented by ν(CC) in Table VI.

In the region from 1000 to 700 cm^{-1} five perpendicular bands, at 999,* 977, 924, 798, and 764 cm^{-1}, and three parallel bands, at 848, 816, and 758 cm^{-1}, are observed. The weak band at 977 cm^{-1} is assigned to the overlapped vibration (A and E species) of ν_{23}, which is associated with the coupling of the CC stretching modes of the main chain with the CH_3 rocking mode. The crystalline sensitive band at 924 cm^{-1} corresponds to the ν_{25}(E) vibration, which is associated with the coupling of the CH_2 rocking mode in the main chain with the CH_3 rocking mode. The schematic representation of this mode for a chemical unit is shown in Fig. 4(a). This mode has a transition moment perpendicular to the helical axis; therefore, the E vibration of this mode should have an intense perpendicular dichroism. This calculated result shows a good agreement with the observed result. The crystalline sensitive band at 848 cm^{-1} is assigned to the coupling vibration of the CH_3 rocking and the CC stretching modes. The medium intensity band at 816 cm^{-1} and the weak band at 798 cm^{-1} are assigned to the coupling vibration of the CH_2 rocking (main chain) and the CC stretching modes. Similar bands associated with the CH_2 rocking and the CC stretching modes have been observed at 841 ($\parallel$, medium) and 809 ($\perp$, weak) cm^{-1} in isotactic polypropylene.[18,20,22] It should be noted that similar bands are observed in this region.

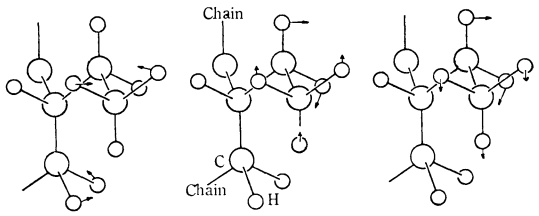

(a) (b) (c)

Fig. 4. Vibrational modes for a chemical unit of the perpendicular bands at 924 cm^{-1} (a) and at 764 cm^{-1} (b), and the parallel band at 758 cm^{-1} (c).

With respect to ethyl rocking vibrations, Havey and Ketley[23] observed the infrared spectra for seven polymers with an ethyl group, and found that the ethyl rocking vibrations appear in the region from 785 to 760 cm^{-1}. According to the present work, the perpendicular band at 764 cm^{-1} and the parallel band at 758 cm^{-1} are to be assigned to the ethyl rocking modes, namely, ν_{27}(E) and ν_{27}(A) respectively. Therefore, the assignments by Havey et al. are consistent with the calculated results. The schematic representations of these modes for a chemical unit are shown in Figs. 4(b) and 4(c).

The dichroic properties of the observed bands can reasonably be explained by the normal modes. The molecular vibrations in the far infrared region will be reported on in the near future.

The author wishes to thank Professor Hiroyuki Tadokoro of Osaka University, and Dr. Isao Shiihara and Dr. Kazuo Nagai of this laboratory, for their kind guidance throughout the course of this work. He also wishes to thank Mr. Hiroshi Tamaoki of the Toyo Soda Industrial Company for supplying the sample, and Mr. Kiyohisa Imada of Kyushu University and Mr. Toshihide Ishikawa of this laboratory for supplying the routine programs.

* The weak perpendicular band at 999 cm^{-1} is observed in the spectra of three crystalline forms, and it is difficult to obtain a reasonable correspondence with a calculated frequency. Therefore, this band may be associated with the vibration of the atactic part or the end group of isotactic polybutene-1.

23) M. C. Havey and A. D. Ketley, *J. Appl. Polym. Sci.*, **5**, 246 (1961).

BULLETIN OF THE CHEMICAL SOCIETY OF JAPAN VOL. 39 750—757 (1966)

Dipole Moment and Molecular Structure of Copolymers. III. Dipole Moment of *p*-Methoxystyrene - Styrene Copolymers and *p*-Chlorostyrene - Styrene Copolymers

By Akira KOTERA, Keizo SUZUKI, Kimiyoshi MATSUMURA, Mikiko SHIMA and Etsuro JOKO

Department of Chemistry, Faculty of Science, Tokyo Kyoiku University, Otsuka, Bunkyo-ku, Tokyo

(Received August 18, 1965)

The *p*-methoxystyrene monomer has been synthesized from anisole through *p*-methoxyacetophenone and *p*-methoxyphenyl methyl carbinol. Then copolymers of *p*-methoxystyrene and styrene have been prepared. The dielectric properties of the copolymers in a benzene solution have been measured, and it has been found that the value of the dipole moment, μ, of the *p*-methoxystyrene monomer unit in the copolymers increases with an increase in the styrene content, e. g., from 1.21 D (for poly-*p*-methoxystyrene) to 1.32 D (for the copolymer in which the mole fraction of *p*-methoxystyrene is 0.175) at 20°C. The variation in the value of μ has been discussed in view of the detailed arrangement of polar monomer units. The theory concenring the relation between the dielectric polarization and the detailed structure of the copolymer molecule developed in the preceding paper, Part I, has been applied to the experimental results. In addition, a similar analysis has been made for the dielectric polarizations of the *p*-chlorostyrene - styrene copolymers which had been measured previously by one of the authors.

The properties of copolymers should depend on the detailed arrangement of the monomer units as well as on their composition. For instance, there are three different arrangements that can be considered for a copolymer which contains equimoles of A and B monomer units:

(1) —AAAAAABBBBBBAAAAABBBBB—

(2) —ABABABABABABABABABAB—

(3) —AABBBAAABABAABBBABBAAA—

(1) The block arrangement, in which long sequences predominate. A copolymer having this structure is usually called a block copolymer.

(2) The regular alternating arrangement, in which the sequence length is always 1.

(3) The random arrangement, in which short sequences of A units alternate with short sequences of B units in an essentially random fashion. This arrangement may be considered the molecular structure of a normal copolymer.

The copolymers with these three structures can be expected to have different properties: they may be considered to be different chemical species, even though they have the same overall composition. The copolymer which has a structure of type 1 might be expected to resemble, in many respects, a simple mixture of the homopolymers of A and B. A short-sequence copolymer, on the other hand, would be expected to be unlike a mixture of the two homopolymers.

The reaction mechanism of copolymerization has been discussed in detail more than once.[1,2] From the basic theory of copolymerization, it is possible to calculate the number-average sequence length of monomer units and, hence, a statistically probable arrangement of individual monomer units in the copolymer molecular chain, the monomer reactivity ratios of which are known. However, as has already been mentioned,[3,4] there has yet been no convincing experimental evidence of the distribution of sequence lengths of individual monomer units in the copolymer molecule. A number of methods have been proposed in attempts to gain information about the detailed arrangement of individual monomer units in copolymers. They include the dechlorination of the vinyl chloride - vinyl acetate copolymer with zinc by Marvel et al.,[5] the intramolecular gamma-lactone formation in vinyl alcohol - acrylic acid copolymers,[6] and a study of the solution properties of partially-acetylated polyvinyl alcohol.[7] Recently developed methods have include the study of the dielectric properties of *p*-chlorostyrene-styrene copolymers in the solid state[8] and the

1) F. R. Mayo and C. Walling, *Chem. Revs.*, **46**, 191 (1950).
2) T. Alfrey, Jr., J. Bohrer and H. Mark, "Copolymerization," Interscience Publishers, Inc., New York (1952).
3) M. Shima, *J. Polymer Sci.*, **56**, 213 (1962).
4) M. Shima and A. Kotera, *Makromol. Chem.*, **64**, 172 (1963).
5) C. S. Mervel, G. D. Jones, T. W. Mastin and G. L. Schertz, *J. Am. Chem. Soc.*, **64**, 2358 (1942).
6) T. Matsumoto, *Kobunshi Kagaku*, **7**, 142 (1950); I. Sakurada and K. Kawasaki, ibid., **8**, 142 (1951).
7) I. Sakurada and O. Yoshizaki, ibid., **10**, 306 (1953); H. Matsuda, K. Naraoka, S. Ishiguro and A. Kotera, ibid., **12**, 10 (1955).
8) R. N. Work and Y. M. Trehu, *J. Appl. Phys.*, **27**, 1003 (1956).

Table I. Dielectric polarization and dipole moments of *p*-methoxystyrene monomer unit in *p*-methoxystyrene - styrene copolymers

Temp., °C	x*a	α	β	p_2	P_{Av}, cc.	μ, Debye	P_{Calc}, cc.
20	1.0000	1.407	−0.268	0.5223	70.1	1.21	
	0.8347	1.289	−0.274	0.5388	71.2	1.23	71.2
	0.5799	1.026	−0.251	0.4991	72.8	1.26	73.0
	0.4075	0.839	−0.237	0.4259	74.5	1.29	74.3
	0.1749	0.554	−0.222	0.3772	76.0	1.32	76.1
	(0.0000*b	0.323	−0.213	0.3370	35.1	0.28)	
50	1.0000	1.309	−0.310	0.5123	68.8	1.24	
	0.8347	1.147	−0.303	0.4901	69.9	1.26	69.6
	0.5799	0.952	−0.289	0.4478	70.9	1.28	71.1
	0.4075	0.789	−0.277	0.4185	72.2	1.31	72.2
	0.1749	0.529	−0.254	0.3738	73.8	1.34	73.7
	(0.0000*b	0.343	−0.255	0.3364	35.0	0.29)	

*a x is the mole fraction of *p*-methoxystyrene in the copolymer. $\alpha=\left(\frac{\varepsilon_{12}-\varepsilon_1}{w_2}\right)$ and $\beta=\left(\frac{v_{12}-v_1}{w_2}\right)$ where ε is the dielectric constants, and v is the specific volume. The suffixes 1, 2, and 12 refer to solvent (benzene), solute (copolymer), and solution. p_2 is the specific polarization of the copolymer. P_{Av} is the average molecular polarization of a *p*-methoxystyrene unit in the copolymer molecule. μ is the dipole moment calculated from the equation

$$\mu = 0.0128 \times [\{P_{Av} - (\mathrm{MR})_D\}T]^{1/2}$$

in which 39.7 cc. was used as the value of $(\mathrm{MR})_D$ for the *p*-methoxystyrene monomer unit.

*b Polystyrene

infrared spectroscopic study of acrolein-acrylonitrile copolymers.[9] One of the present authors previously measured the dielectric properties of copolymers of methyl methacrylate - styrene[3] and methyl acrylate - styrene[4] in benzene solution, and developed a theory which connects the average dielectric polarization of copolymers with the detailed arrangement of monomer units in the copolymer molecule.

In this paper, we will work on the dielectric properties of copolymers of *p*-methoxystyrene and styrene, and will discuss the experimental results by applying the theory described in a preceding paper, Part I.[3] In addition, we will describe the results of a similar analysis for the *p*-chlorostyrene - styrene copolymers, the dielectric polarizations of which were measured previously by one of the present authors.[10]

Experimental

The Synthesis of the *p*-Methoxystyrene Monomer.—The *p*-methoxystyrene monomer was synthesized through the following three processes:

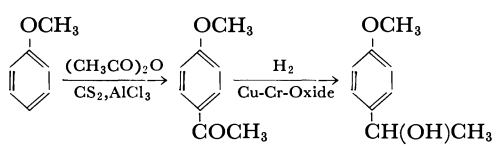

(I) (II)

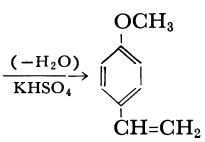

(III)

p-Methoxyacetophenone (I) was prepared, by means of the Friedel-Craft reaction, from anisole and acetic acid anhydride in carbon disulfide, in the presence of anhydrous aluminum chloride.[11] *p*-Methoxyphenyl methyl carbinol (II) was obtained by the reduction of *p*-methoxyacetophenone with copper-chromium-oxide and hydrogen; this was carried out in an autoclave under a high pressure of more than 100 atm.[12,13] The reaction of the dehydration was carried out by heating *p*-methoxyphenyl methyl carbinol with acid potassium sulfate, and then distilling the *p*-methoxystyrene.

Copolymerization.—The *p*-methoxystyrene monomer was dried with anhydrous sodium sulfate and distilled three times under reduced pressure prior to polymerization; the b. p. was 84—86°C/8 mmHg. The styrene monomer used in these experiments was a commercial one, which was washed with a 10% aqueous solution of sodium hydroxide and water, dried with anhydrous sodium sulfate, and distilled under reduced pressure; the b. p. was 45—46°C/17 mmHg.

Monomer mixtures which total about 25 g. and which contain no catalyst were prepared over a whole range of composition and sealed in glass tubes. The polymerizations were carried out thermally by holding the tubes in an oil-bath at 100°C for about 120 hr. The

9) R. C. Schultz, H. Cherdon and W. Kern, *Makromol. Chem.*, **29**, 190 (1959).

10) A. Kotera, *J. Chem. Soc. Japan, Pure Chem. Sect.* (*Nippon Kagaku Zasshi*), **63**, 364 (1942).

11) "Organic Syntheses," **1**, 109; C. R. Noller and R. Adams, *J. Am. Chem. Soc.*, **46**, 1889 (1937).

12) J. H. Brown and C. R. Marvel, ibid., **59**, 1176 (1937).

13) H. Adkins, "Reaction of Hydrogen with Organic Compounds over Copper-Chromium-Oxide and Nickel Catalysts," Japanese translation, Kawaide Shobō, Tokyo (1937).

polymers were precipitated from a benzene solution into methanol and dried in a high vacuum.

Measurements of the Dielectric Polarization of Copolymers.—The experimental determination of the dielectric polarization of copolymers was carried out in the usual way by measuring the dielectric constants and the specific volumes of the copolymer solutions. The apparatus was similar to that described in Part I.[3] The cell is composed of three concentric platinum cylinders in a glass tube, and its capacity is about 35 $\mu\mu$F. The cell capacitance measurements were made by the heterodyne-beat method at a frequency of 500 kilocycles per second. The specific volumes were measured by "the mess-flask type" pycnometer, the volume of which was about 10 cc. The extrapolated values of the specific polarization of the copolymer at an infinite dilution were calculated according to the Halverstadt-Kumler equation[14]:

$$p_2 = \frac{3\alpha v_1}{\varepsilon_1+2} + (v_1 + \beta)\frac{\varepsilon_1-1}{\varepsilon_1+2} \qquad (1)$$

where ε_1 and v_1 are the dielectric constant and the specific volume of the solvent (benzene) respectively. α and β, denoting the dielectric constant and the specific volume of solution, ε_{12} and v_{12} respectively, are given as:

$$\varepsilon_{12} = \varepsilon_1+\alpha w_2, \quad v_{12} = v_1+\beta w_2$$

where w_2 is the weight fraction of the solute (the copolymer).

The dielectric constants and the specific volumes were measured on four solutions of different concentrations, from 1% to 9%, for each copolymer sample. The values of α and β obtained are given in Table I.

The specific polarization of copolymer, p_2, can be expressed as follows:

$$p_2 = w_A p_{MeO}+(1-w_A)p_{St} \qquad (2)$$

where w_A is the weight fraction of *p*-methoxystyrene in the copolymer, and p_{MeO} and p_{St} are the effective specific polarizations associated with *p*-methoxystyrene and styrene monomer units, respectively, in the copolymer molecule. As the styrene monomer is nonpolar, the value of p_{St} may not be very greatly influenced by the neighboring groups. Therefore, it was assumed that the value of p_{St} is the same as that of polystyrene. The average molecular polarization of *p*-methoxystyrene monomer units in the copolymer molecule, $P_{Av}(=M_A p_{MeO}$: M_A is the molecular weight of the *p*-methoxystyrene monomer unit) was calculated from Eq. 2. Further, the sum of electronic polarization and atomic polarization was assumed to be equal to the molecular refraction for the D line calculated from the atomic refractions of the constituent atoms. The dipole moment of the *p*-methoxystyrene unit was calculated by the equation:

$$\mu = 0.0128\times\{(P_{Av}-[MR]_D)T\}^{1/2} \qquad (3)$$

$[MR]_D$; the molecular refraction for the D line.

Results and Discussion

Experimental Results for *p*-Methoxystyrene-Styrene Copolymers.—The results of experiments are summarized in Table I. The tendency found in the cases of the copolymers of methyl methacrylate - styrene and methyl acrylate - styrene is also observed in the variation in μ value with the composition of the copolymers. The value of the effective dipole moment of the *p*-methoxystyrene monomer unit in the copolymers increased with an increase in the styrene content; i. e., the value of μ increased from 1.21 D for poly *p*-methoxystyrene ($x=1.000$) to 1.32 D for the copolymer of $x=0.1749$ at 20°C and from 1.24 D to 1.34 D at 50°C. This may be interpreted qualitatively as follows: the value of the dipole moment of the *p*-methoxystyrene monomer unit obtained from the measurement of the homopolymer is not the value of the isolated unit. Rather, it includes the effect of intramolecular interactions between the neighboring polar units along the chain, i. e., the influence of dipole-dipole interactions, steric hindrance, and so on. Because of the influence of these interactions, the value of μ in the poly-*p*-methoxystyrene should be smaller than that of the isolated equivalent unit. In the copolymer molecule, the influence of the dipole-dipole interactions may be reduced by the nonpolar styrene units separating the polar units. The increase in the styrene content should increase the isolated *p*-methoxystyrene units in the copolymer molecule, and, accordingly, the value of μ will approach that of the isolated unit.

The Relation between the Dielectric Polarization and a Detailed Arrangement of Polar Monomer Units in the Copolymer Molecule.—By applying the theory described in Part I,[3] to the experimental results, we shall attempt to treat quantitatively the relation between the dielectric polarization and the detailed arrangement of *p*-methoxystyrene units in the copolymer molecule. If it is assumed that the polar monomer units in a polar (A) - nonpolar (B) copolymer molecule can be classified into three types:

(1) two neighbors along the chain are the same polar units, A and A:

~~~ A Ⓐ A ~~~

(2) one neighbor is the polar unit A, and the other is the nonpolar unit B:

~~~ A Ⓐ B ~~~

(3) both neighbors are nonpolar units, B and B:

~~~ B Ⓐ B ~~~

and that these three types have different values of molecular polarization, P_{AA}, P_{AB} and P_{BB} respectively, then the average molecular polarization of the monomer unit, A, in the copolymer molecule, P_{Av}, may be given by the equation:

$$P_{Av} = P_{AA}F_{AA}+P_{AB}F_{AB}+P_{BB}F_{BB} \qquad (4)$$

where F_{AA}, F_{AB} and F_{BB} are the fractions of the polar monomer units A in the states of (1), (2) and (3) respectively. This equation can be transformed as follows, provided that f_{AA} is the

14) I. F. Halverstadt and W. D. Kumler, *J. Am. Chem. Soc.*, **64**, 2988 (1942).
~~~

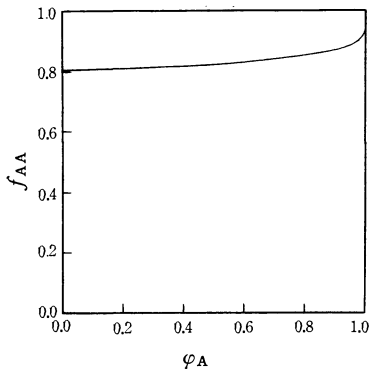

Conversion of *p*-methoxystyrene monomer

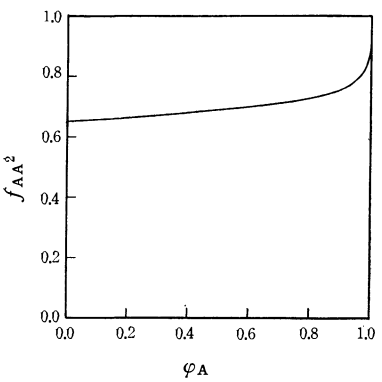

Conversion of *p*-methoxystyrene monomer

Fig. 1. Up, probability of AA sequence arising in copolymer; under, probability of double AA sequence arising in copolymer. $x_0=0.8347$

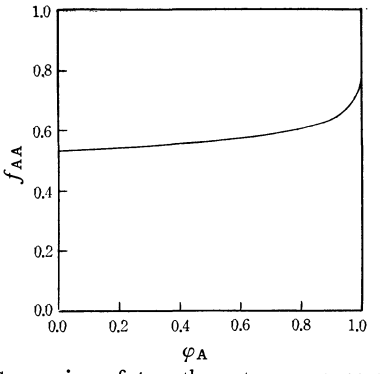

Conversion of *p*-methoxystyrene monomer

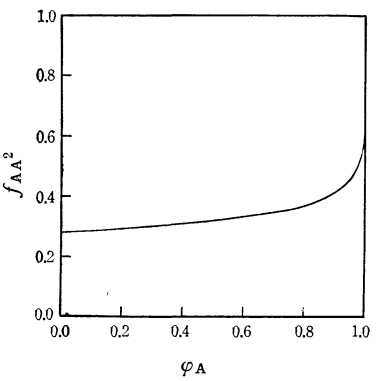

Conversion of *p*-methoxystyrene monomer

Fig. 2. Up, probability of AA sequence arising in copolymer; under, probability of double AA sequence arising in copolymer. $x_0=0.5799$

probability that a neighbor of the polar monomer unit A is polar:

$$P_{Av}=P_{AA}\overline{f_{AA}^2}+2P_{AB}(\overline{f_{AA}}-\overline{f_{AA}^2})+P_{BB}(1-2\overline{f_{AA}}+\overline{f_{AA}^2}) \quad (5)$$

The averages of f_{AA} and f_{AA}^2 can be calculated from the equations:

$$\overline{f_{AA}}=\frac{\int_0^{\varphi_A} f_{AA}\,d\varphi_A}{\int_0^{\varphi_A} d\varphi_A} \quad \text{and} \quad \overline{f_{AA}^2}=\frac{\int_0^{\varphi_A} f_{AA}^2\,d\varphi_A}{\int_0^{\varphi_A} d\varphi_A} \quad (6)$$

where φ_A is the conversion of the monomer A. f_{AA} and φ_A are related to each other through the mole fraction, x, of the A monomer in the monomer mixture, as is given by the equations:[1]

$$f_{AA}=\frac{r_1x}{r_1x+1-x} \quad \text{and}$$

$$(1-\varphi_A)=\left(\frac{x}{x_0}\right)^{1/(1-r_2)}\left(\frac{1-x}{1-x_0}\right)^{r_1/(1-r_1)}\times\left\{\frac{(r_1+r_2-2)x-(r_2-1)}{(r_1+r_2-2)x_0-(r_2-1)}\right\}^{r_1r_2-1/(1-r_1)(1-r_2)}$$

where x_0 is the x of the initial monomer mixture, and r_1 and r_2 are the monomer reactivity ratios. As f_{AA} and f_{AA}^2 can not be expressed as an explicit function of φ_A, we calculated the values of $\overline{f_{AA}}$ and $\overline{f_{AA}^2}$ by the numerical integrations of Eq. 6.

The Results of Calculation for Copolymers of *p*-Methoxystyrene - Styrene and *p*-Chlorostyrene - Styrene.—Figures 1—4 show f_{AA} and f_{AA}^2 as functions of the conversion, φ_A, of the A monomer for each sample of *p*-methoxystyrene - styrene copolymers. In this experiment, the monomers A and B referred to *p*-methoxystyrene and styrene respectively, and the values of $r_1=0.82$ and $r_2=1.16$[15] were employed in the calculation of f_{AA}. The values of $\overline{f_{AA}}$ and $\overline{f_{AA}^2}$ were obtained from the evaluation of the areas under the curves in these figures: they are given in Table III.

One of the present authors previously measured the dielectric properties of *p*-chlorostyrene - styrene copolymers in a benzene solution. Table II gives the results of these measurements.[16] We

15) C. Walling, E. R. Briggs, K. B. Wolfstein and F. R. Mayo, ibid., **70**, 1537 (1948).
16) A. Kotera, *Kobunshi Kagaku*, **1**, 1 (1949).

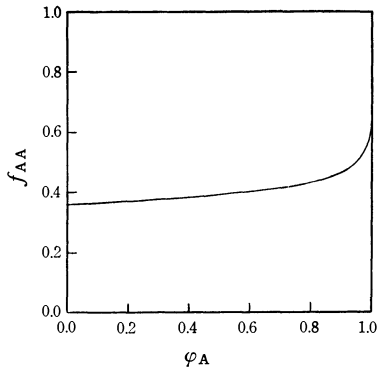

Conversion of *p*-methoxystyrene monomer

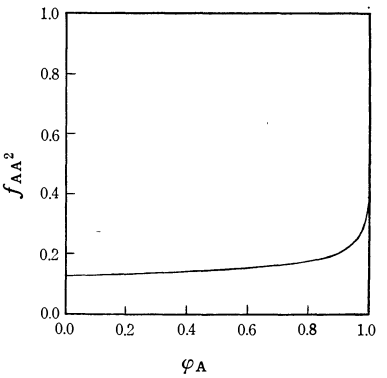

Conversion of *p*-methoxystyrene monomer

Fig. 3. Up, probability of AA sequence arising in copolymer; under, probability of double AA sequence arising in copolymer. $x_0=0.4075$

TABLE II. DIELECTRIC POLARIZATIONS AND DIPOLE MOMENT OF *p*-CHLOROSTYRENE MONOMER UNIT IN *p*-CHLOROSTYRENE - STYRENE COPOLYMERS

Temp. °C	w_A*a	p_2	P_{Av}, cc.	μ Debye	P_{Calc} cc.
25	1.0000	0.5605	76.7	1.39	
	0.8247	0.5535	83.0	1.48	83.1
	0.6668	0.5372	88.2	1.56	87.2
	0.5621	0.5128	89.8	1.59	89.8
	0.4665	0.4890	91.5	1.61	92.1
	0.2601	0.4306	95.7	1.68	96.3
	0.0000	0.3392*b			
50	1.0000	0.5503	76.3	1.42	
	0.8247	0.5418	81.1	1.51	81.0
	0.6668	0.5230	85.2	1.58	84.9
	0.5621	0.5025	87.3	1.61	87.2
	0.4665	0.4795	88.7	1.64	89.4
	0.2601	0.4267	93.6	1.71	93.4
	0.0000	0.3392*b			

*a w_A is the weight fraction of *p*-chlorostyrene in the copolymer. p_2 is the specific polarization of the copolymer. P_{Av} is the average molecular polarization of a *p*-chlorostyrene monomer unit in the copolymer molecule. μ is the dipole moment calculated from the equation

$$\mu=0.0128\times[\{P_{Av}-(MR)_D\}T]^{1/2}$$

in which 38.2 cc. was used as the value of $(MR)_D$ for the *p*-chlorostyrene monomer unit.

*b The value of p_{St} for polystyrene.

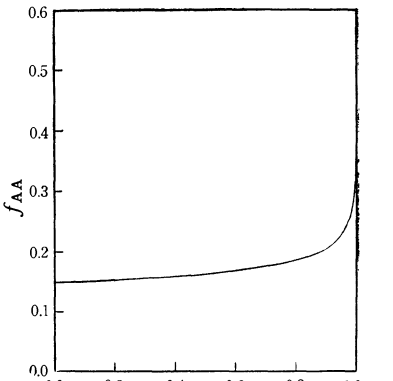

Conversion of *p*-methoxystyrene monomer

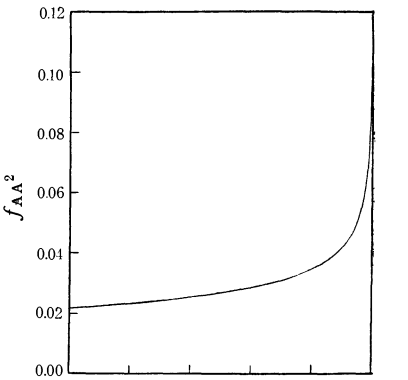

Conversion of *p*-methoxystyrene monomer

Fig. 4. Up, probability of AA sequence arising in copolymer; under, probability of double AA sequence arising in copolymer. $x_0=0.1749$

TABLE III. PROBABILITIES OF AN AA SEQUENCE AND A DOUBLE AA SEQUENCE ARISING IN THE COPOLYMERS

p-Methoxystyrene - styrene copolymers

x	$\overline{f_{AA}}$	$\overline{f_{AA}^2}$
1.0000	1.0000	1.0000
0.8347	0.8344	0.6997
0.5799	0.5780	0.3361
0.4075	0.4050	0.1659
0.1749	0.1730	0.0303
0.0000	0.0000	0.0000

p-Chlorostyrene - styrene copolymers

x	$\overline{f_{AA}}$	$\overline{f_{AA}^2}$
1.0000	1.0000	1.0000
0.7795	0.7911	0.6261
0.6007	0.6186	0.3826
0.4910	0.5113	0.2615
0.3966	0.4048	0.1749
0.2039	0.2175	0.0507
0.0000	0.0000	0.0000

x is the mole fraction of the polar monomer A in the copolymer.

may treat the experimental results of the *p*-chlorostyrene - styrene copolymers in the way described above. Figures 6—10 give the f_{AA} and f_{AA}^2 values for the copolymers of *p*-chlorostyrene and styrene

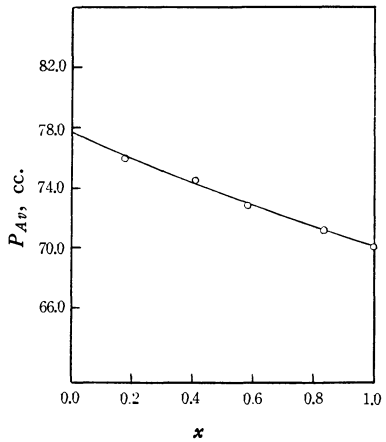

Mole fraction of *p*-methoxystyrene in copolymer

Fig. 5. Average dielectric polarization vs. composition.
——; theoretical curve from Eq. 5
○ ; experimental values (at 20°C)

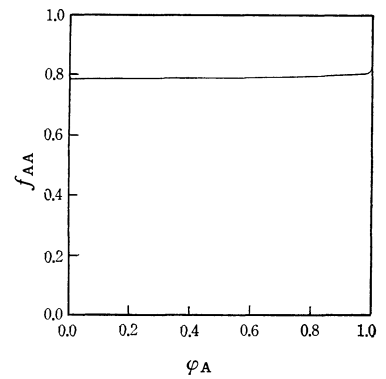

Conversion of *p*-chlorostyrene monomer

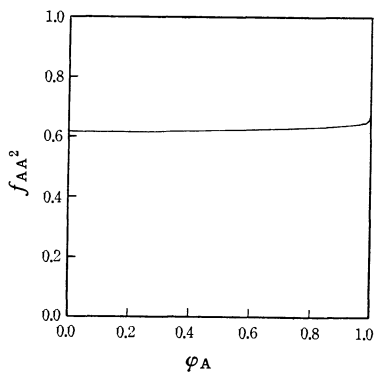

Conversion of *p*-chlorostyrene monomer

Fig. 6. Up, probability of AA sequence arising in copolymer; under, probability of double AA sequence arising in copolymer. $x_0=0.7795$

as functions of the conversion of the *p*-chlorostyrene monomer. The monomer reactivity ratios for this copolymer system, $r_1=1.038$ and $r_2=0.786$, were employed[17]: the values of $\overline{f_{AA}}$ and $\overline{f_{AA}^2}$ calculated from these figures are shown in Table III.

By substituting the values of $\overline{f_{AA}}$ and $\overline{f_{AA}^2}$ and the experimental data of P_{Av} into Eq. 5, the values of P_{Av} and P_{BB} were obtained by the method of least squares. The last columns in Table I and Table II give the theoretical values of the average

Table IV. Values of molecular polarization and dipole moment for the three types of polar monomer unit assumed in Eq. 4

Temp. °C	P_{AA} cc.	P_{AB} cc.	P_{BB} cc.	μ_{AA} Debye	μ_{AB} Debye	μ_{BB} Debye
p-Methoxystyrene - styrene copolymers						
20	70.1	73.2	77.7	1.21	1.27	1.35
50	68.8	71.2	75.1	1.24	1.29	1.37
p-Chlorostyrene - styrene copolymers						
25	77.7	90.8	100.8	1.39	1.60	1.75
50	76.3	87.8	97.8	1.42	1.62	1.78

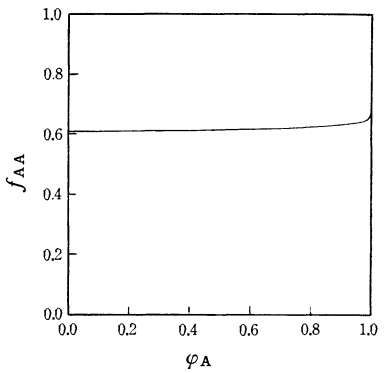

Conversion of *p*-chlorostyrene monomer

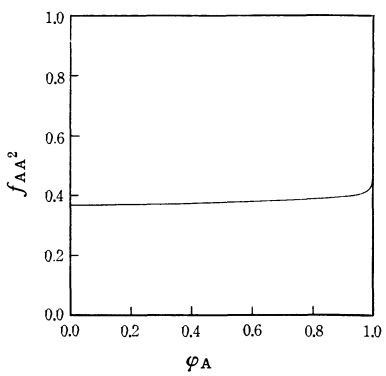

Conversion of *p*-chlorostyrene monomer

Fig. 7. Up, probability of AA sequence arising in copolymer; under, probability of double AA sequence arising in copolymer. $x_0=0.6007$

17) F. M. Lewis, C. Walling, W. Cummings, F. R. Briggs and F. R. Mayo, *J. Am. Chem. Soc.*, **70**, 1519 (1948).

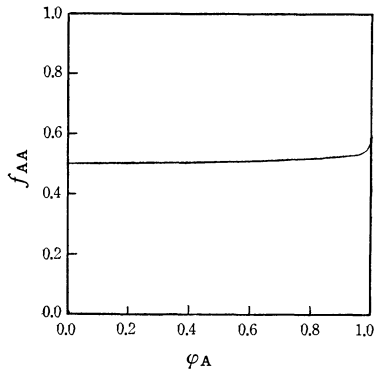

Conversion of *p*-chlorostyrene monomer

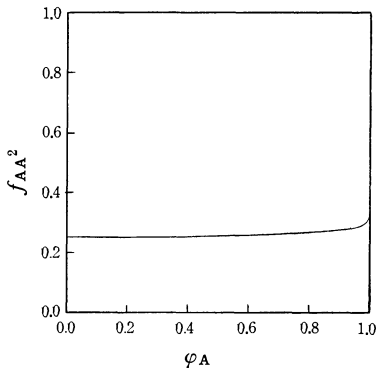

Conversion of *p*-chlorostyrene monomer

Fig. 8. Up, probability of AA sequence arising in copolymer; under, probability; of double AA sequence arising in copolymer. $x_0=0.4910$

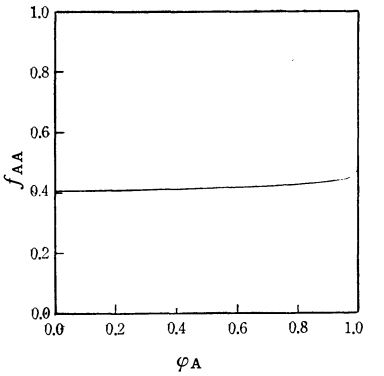

Conversion of *p*-chlorostyrene monomer

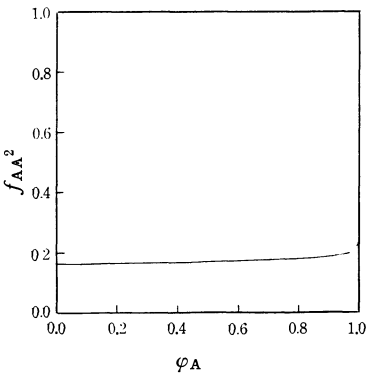

Conversion of *p*-chlorostyrene monomer

Fig. 9. Up, probability of AA sequence arising in copolymer; under, probability of double AA sequence arising in copolymer. $x_0=0.3966$

molecular polarization obtained by Eq. 5 for the polar monomer unit in the copolymers. These values are also shown in Fig. 5 and Fig. 11 as a function of the composition of copolymers and compared with the experimental values. The good agreement of these results with the experimental values over the whole range of composition implies that the values of P_{AA}, P_{AB} and P_{BB} are practically constant and that the assumptions made in the theory are reasonable in the case of the copolymers of both *p*-methoxystyrene - styrene and *p*-chlorostyrene - styrene. The values obtained for P_{AA}, P_{AB} and P_{BB} are given in Table IV. The values of μ_{AA}, μ_{AB} and μ_{BB} were calculated by using Eq. 3.

The difference in the values of μ at 20°C and 50°C may be interpreted in terms of the internal rotation in the polymer molecule. It is known that in a chain molecule of polymer, the internal rotation around the C–C bonds of the chain skeleton is not free and that three energetically-favored positions persist, i. e., one "trans" and two "gauche" configurations.[18] The temperature dependence of the potential energy for the restricted rotation may explain the difference in values of μ at 20°C and 50°C.

It was noticed that the shape of the curves in Figs. 5 and 11 is not similar to that for the methyl methacrylate - styrene copolymers or methyl acrylate - styrene copolymers; i. e., in Figs. 5 and 11, the curve of P_{Av} seems to be almost linear with respect to x. This may be because, in the case of *p*-methoxystyrene - styrene copolymers and *p*-chlorostyrene - styrene copolymers, the difference between the values of P_{AA} and P_{BB} is rather small, the value of P_{AB} is close to the average of P_{AA} and P_{BB}, and the value of f_{AA} is almost equal to that of the mole fraction, x, therefore, Eq. 5 can be regarded as approximately a linear function of x.

According to the definition of P_{BB}, μ_{BB} is the dipole moment of the polar group which is separated by nonpolar groups from the influence of the interactions of the other polar groups in the same copolymer molecule; its value may be compared with that of the dipole moment of the polar group in an isolated state, which can be obtained from measurements in a nonpolar solvent. The experimental value of the dipole moment of *p*-methoxyethyl-benzene is not knwon, but by taking the

18) P. J. Flory, "Principles of Polymer Chemistry," Cornell University Press, Ithaca, New York (1953).

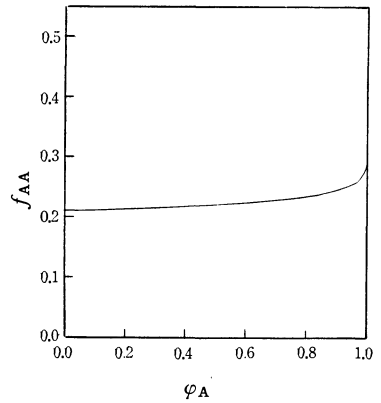

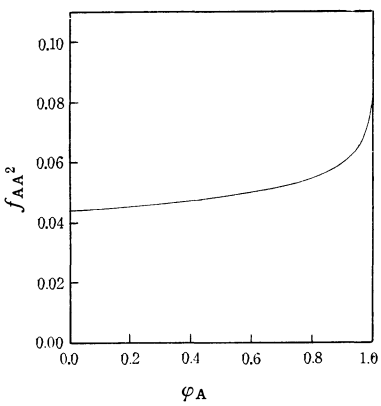

Fig. 10. Up, probability of AA sequence arising in copolymer; under, probability of double AA sequence arising in copolymer. $x_0=0.2039$

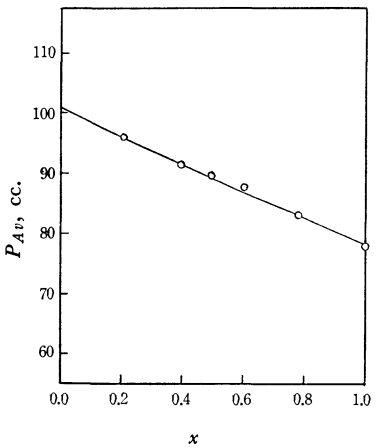

Fig. 11. Average dielectric polarization vs. composition.
——; theoretical curve from Eq. 5
○ ; experimental values (at 25°C)

vector sum of the moment of anisole, 1.25 D,[19] and that of toluene, 0.37 D,[19] we can obtain 1.16 D as the calculated value. The value of μ_{BB} in the *p*-methoxystyrene - styrene copolymer was 1.35—1.37 D. The dipole moment of *p*-chlorotoluene is known to be 1.94 D,[19] which may be compared with the μ_{BB} values of 1.75—1.78 D in the *p*-chlorostyrene - styrene copolymer. In the above comparison, it can be seen that the values of μ_{BB} are always a little smaller than those of the moments of the polar groups in the isolated state. These differences may be due to the effect of the induced moments of the neighboring styrene monomer units, which are induced on benzene nuclei by the polar group under consideration. A comparison of the μ_{BB} value of the *p*-methoxystyrene unit with that of the *p*-chlorostyrene unit suggests that the inductive effect may be a little larger in the *p*-methoxystyrene - styrene copolymer than in the *p*-chlorostyrene - styrene copolymer, and that the average of the angle between the dipole moment of the polar group and the induced dipole moment may be nearer to 180° in the former than in the latter.

It was noticed that the values of μ_{AB} are very near the average value of μ_{AA} and μ_{BB} in both copolymers. The value of $(\mu_{BB}-\mu_{AB})/(\mu_{AB}-\mu_{AA})$ is 0.08/0.06 at 20°C and 0.08/0.05 at 50°C in the *p*-methoxystyrene - styrene copolymer, and 0.15/0.21 at 25°C and 0.16/0.20 at 50°C in the *p*-chlorostyrene - styrene copolymer. The difference between μ_{BB} and μ_{AB} gives the decrease in the moment caused by the interaction effect of one neighboring polar group, which was introduced as a neighbor instead of the nonpolar styrene group, while the difference between μ_{AB} and μ_{AA} is the further decrease in the moment caused by the replacement of the neighboring styrene with a polar group. It appears that, in the *p*-methoxystyrene - styrene copolymer, the first decrease in the moment is a little larger than the second decrease, while the reverse is true in the *p*-chlorostyrene - styrene copolymer. However, the difference between $(\mu_{BB}-\mu_{AB})$ and $(\mu_{AB}-\mu_{AA})$ is so small in these copolymers that these two values may be considered to be almost equal to each other. In the copolymer in which there is a possibility of internal rotation within the polar group, the value of $(\mu_{BB}-\mu_{AB})$ should be much larger than that of $(\mu_{AB}-\mu_{AA})$, which was found in previous considerations of the methyl methacrylate - styrene copolymer and the methyl acrylate - styrene copolymer.

19) C. P. Smyth, "Dielectric Behavior and Structure," McGraw-Hill Book Company, Inc., New York (1955).

BULLETIN OF THE CHEMICAL SOCIETY OF JAPAN VOL. 39 758—761 (1966)

Copolymerization Characteristics of Methyl Acrylate and Methyl Methacrylate. II. Analysis of Methyl Acrylate-Methyl Methacrylate Copolymers by Infrared Spectroscopy

By Akira KOTERA, Mikiko SHIMA, Katsuo AKIYAMA, Masako KUME and Machiko MIYAKAWA

Department of Chemistry, Faculty of Science, Tokyo Kyoiku University, Otsuka, Bunkyo-ku, Tokyo

(Received August 18, 1965)

The infrared absorption spectra of polymers and copolymers of methyl acrylate and methyl methacrylate have been measured, and then used as the basis of a spectrophotometric method for the analysis of the copolymers. The 6.73 μ band, which may be due to methyl (–C–CH_3) vibration, was selected as the key band for measuring the methyl methacrylate component, while the 6.89 μ band was used as the standard. The monomer reactivity ratios for copolymerization of methyl acrylate - methyl methacrylate system have been determined to be $r_1=0.5\pm0.1$, and $r_2=2.3\pm0.4$ (M_1; methyl acrylate, M_2; methyl methacrylate) at 130°C. These values are in good agreement with those previously obtained by the deuterium tracer method. It has also been shown that the procedure used in this study is appropriate for the analyses of methyl acrylate - methyl methacrylate copolymers.

In a preceeding paper,[1] we have investigated the copolymerization kinetics of the methyl acrylate-methyl methacrylate system by using monomers containing deuterium as a tracer. As we mentioned in that paper, it is difficult to determine the composition of the copolymers of methyl acrylate and methyl methacrylate by using the conventional combustion analysis because of the similarity of the component monomers in chemical composition. In such a case, the spectrophotometric method may be useful.

When the infrared absorption spectra of the polymers and the copolymers of methyl acrylate and methyl methacrylate were measured, it was found that the ratio of the optical density of the absorption band at 6.73μ, which may be due to methyl (–C–CH_3) vibration, to that of the band at 6.89μ, which is probably due to methylene (–CH_2–) vibration, changes linearly with the change in the composition of copolymers. By using these two bands as the key bands for the analysis of the copolymer, the composition of the copolymers were determined; we also attempted to determine the monomer reactivity ratios for the copolymerization of this system.

Experimental

Copolymerization.—The methyl acrylate and methyl methacrylate monomers used in these experiments were supplied by the Mitsubishi Rayon Company. They were distilled twice under a reduced nitrogen atmosphere; the b. p.'s were 28°C/110 mmHg and 35.5°C/70 mmHg respectively. The polymerizations were carried out thermally in sealed pyrex tubes, each of which contained about 0.2 mol. of the monomer mixture and no catalyst. The tubes were kept in an oil-bath at 130°C and removed when the desired degree of conversion ($\leq 10\%$) had been reached. The polymers were precipitated from a benzene solution into methanol and dried in a high vacuum to a constant weight.

Measurements of Infrared Absorption Spectra.—The infrared spectra of the samples were measured by using a Nippon Bunko, Model SDl0l, double-beam spectrometer with a NaCl prism. All the samples were in the form of a solid film approximately 0.01 mm. thick; these films were prepared on a surface of mercury from the chloroform solution. The infrared spectra of polymethyl acrylate, polymethyl methacrylate, and copolymers are shown in Figs. 1—3.

In the 6—7 μ region, the spectra of polymethyl methacrylate and the copolymer show two absorption bands. The absorption band at 6.73 μ, which may be due to a methyl (–C–CH_3) deformation vibration,[2] decreases as the methyl methacrylate component in the copolymer decreases, and disappears in polymethyl acrylate. On the other hand, the intense band at 6.89 μ, which is probably due to a methylene (–CH_2–) vibration,[3] doesn't change appreciably with the change in the composition of the copolymers.

These two bands were used as a measure of methyl (–C–CH_3) groups and methylene (–CH_2–) groups respectively. The optical density at 6.73 μ, D_1 is, expressed as follows from the Beer-Lambert law:[4]

$$D_1=\log\frac{I_0^1}{I_1}=k_1^1c_1t+k_1^2c_2t \qquad (1)$$

1) M. Shima and A. Kotera, *J. Polymer Sci.*, Part A, **1**, 1115 (1963).

2) U. Baumann, H. Schreiber and K. Tessmar, *Makromol. Chem.*, **36**, 81 (1959).

3) W. Fuchs and D. Louis, ibid., **22**, 1 (1957).

4) E. J. Slowinski, Jr., H. Walter and R. L. Miller, *J. Polymer Sci.*, **19**, 353 (1956).

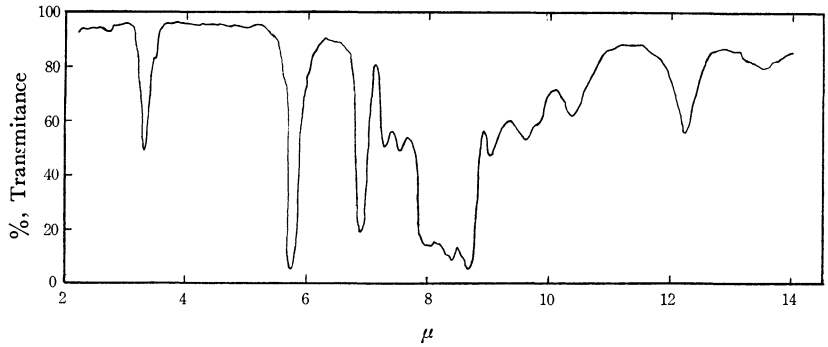

Fig. 1. Infrared spectra of polymethyl acrylate for ca. 0.01 mm. solid film.

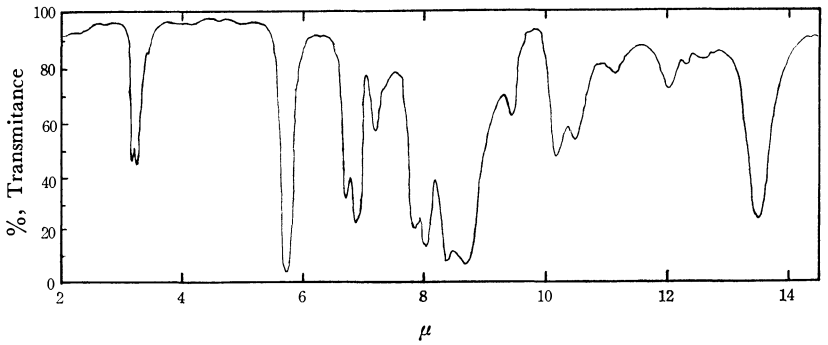

Fig. 2. Infrared spectra of polymethyl methacrylate for ca. 0.01 mm. solid film.

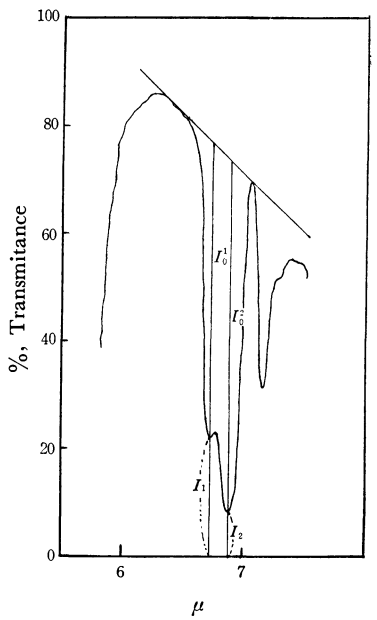

Fig. 3. The 6 to 7 μ region of a typical copolymer of methyl acrylate and methyl methacrylate.

where I is the transmission measured by the height of the absorption peak; k_1^1 and k_1^2 are the extinction coefficients of the 6.73 μ band and of the 6.89 μ band at 6.73 μ respectively; c_1 and c_2 are the number of methyl ($-C-CH_3$) groups and methylene ($-CH_2-$) groups per gram respectively, and t is the thickness of the film. The optical density at 6.89 μ, D_2, is given as:

$$D_2=\log\frac{I_0^2}{I_2}=k_2^2c_2t \tag{2}$$

where k_2^2 is the extinction coefficient of the 6.89 μ band at 6.89 μ. In order to eliminate the necessity of making an accurate measurement of the thickness of each sample, the ratio of the optical density of the 6.73 μ band, D_1, to that of the 6.89 μ band, D_2, was employed:

$$\frac{D_1}{D_2}=\frac{k_1^1c_1}{k_2^2c_2}+\frac{k_1^2}{k_2^2} \tag{3}$$

Therefore, if it is assumed that the Beer-Lambert law is valid in these samples and that the effect of methyl groups at chain ends can be neglected, a linear relationship should exist between D_1/D_2 and the mole fraction of methyl methacrylate in the copolymer, $f_2(=c_1/c_2)$.

The calibration curve was obtained from the measurements of the samples of a mixture of polymethyl acrylate and polymethyl methacrylate. All the samples were optically-uniform films which had been prepared from the chloroform solution of polymethyl acrylate and polymethyl methacrylate. The measurements for D_1/D_2 were repeated three to five times on each sample; the mean values of the measurements are shown in Table I. The data in this table are plotted in Fig. 4, where they prove the linear relation between D_1/D_2 and f_2. A least-square treatment of the points gives the following equation:

$$\frac{D_1}{D_2}=0.744(\pm0.0018)f_2+0.053(\pm0.012) \tag{4}$$

Using this equation, the composition of the copolymers in Table III was calculated.

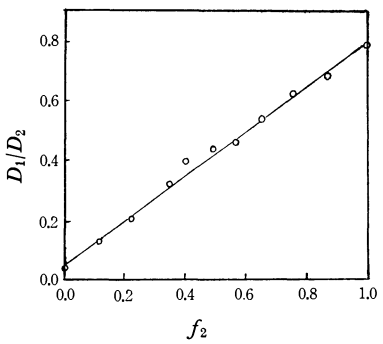

Fig. 4. Calibration curve for the composition of copolymers.

TABLE I. DATA FOR CALIBRATION CURVE

Sample	f_2	D_1/D_2
PMA	0.0000	0.0297
1	0.1133	0.129
2	0.2190	0.198
3	0.3531	0.319
4	0.3965	0.407
5	0.4886	0.445
6	0.5687	0.460
7	0.6487	0.540
8	0.7542	0.626
9	0.8736	0.678
PMMA	1.0000	0.783

f_2 is the mole fraction of methyl methacrylate in the sample. D_1 and D_2 are the optical densities of the absorption band at 6.73 μ and of the absorption band at 6.89 μ, respectively. The measurements for D_1/D_2 were repeated three to five times on each sample, and the mean values of the measurements are shown.

Results

The results of the experiments are summarized in Table II and Table III. The monomer reactivity ratios were determined by the method of Fineman and Ross.[5] The ratio of the molar concentrations of two monomers in the copolymer formed may be given by the following relation,[6]

TABLE II. COPOLYMERIZATION CONDITION

Expt. No.	F_2	Monomer g.	Polymer g.	Time min.	Conversion %
C1	1.0000	20.05	0.8066	60	4.02
C2	0.7915	19.557	0.8605	50	4.40
C3	0.5912	19.272	1.2256	55	6.36
C4	0.3971	18.392	0.9242	45	5.03
C5	0.1998	17.867	1.1491	45	6.43
C6	0.0000	29.758	16.1247	50	54.19

F_2 is the mole fraction of methyl methacrylate in the initial monomer mixture.

5) M. Fineman and S. D. Ross, *J. Polymer Sci.*, **5**, 259 (1950).
6) T. Alfrey, Jr., J. J. Boher and H. Mark, "Copolymerization," Interscience Publishers, New York (1952), p. 10.

TABLE III. COMPOSITIONS OF COPOLYMERS

Sample	F_2	D_1/D_2	f_2
C2	0.7915	0.7047	0.876
C3	0.5912	0.5913	0.724
C4	0.3971	0.4732	0.565
C5	0.1998	0.2619	0.281

F_2 is the mole fraction of methyl methacrylate in the initial monomer mixture, and f_2 is the mole fraction of methyl methacrylate in the copolymer.

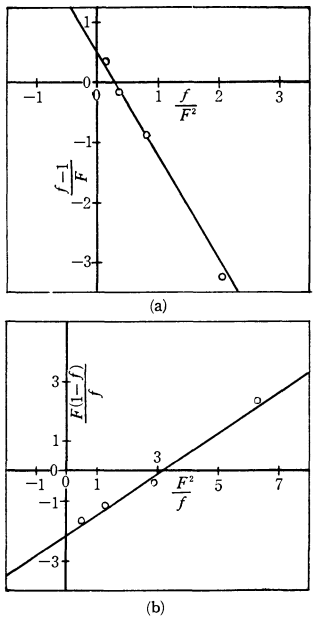

Fig. 5. Treatment of copolymer composition data by the method of Fineman and Ross. (a) using Eq. (5), (b) using Eq. (6).

provided the conversion is low;

$$\frac{m_1}{m_2}=\frac{M_1}{M_2}\cdot\frac{r_1M_1+M_2}{r_2M_2+M_1}$$

where M_1 and M_2 represent the molar concentrations of the respective monomers in the initial monomer mixture, and where r_1 and r_2 are the monomer reactivity ratios. Fineman and Ross made the $F=M_1/M_2$ and $f=m_1/m_2$ substitutions in the above equation, and so obtained the following equations:

$$\frac{f-1}{F}=\frac{-r_2f}{F^2}+r_1 \qquad (5)$$

$$\frac{F(f-1)}{f}=\frac{r_1F^2}{f}-r_2 \qquad (6)$$

Thus, a plot of $(f-1)/F$ against f/F^2 yields a straight line with a slope of r_2 and an intercept of r_1, while the latter equation yields r_1 as the slope and r_2 as the intercept. The data of Table III are plotted in Fig. 5 using both Eqs. 5 and 6.

A least-square treatment of the points yields:

$r_1 = 0.5 \pm 0.1$ using Eq. 5

$r_2 = 2.3 \pm 0.4$ using Eq. 6

(M_1: methyl acrylate; M_2: methyl methacrylate)

These values agree with those previously obtained by the deuterium tracer method, $r_1 = 0.47 \pm 0.09$ and $r_2 = 2.3 \pm 0.5$. This means that the procedure used in these experiments is quite appropriate for the analysis of methyl acrylate - methyl methacrylate copolymers.

BULLETIN OF THE CHEMICAL SOCIETY OF JAPAN VOL. 39 761—766 (1966)

The Rotatory Dispersion and Stereochemistry of Organic Compounds. IX.[1] The Nitrates of Glucose

By Yojiro Tsuzuki, Koko Tanabe and Kikuhiko Okamoto

Department of Chemistry, Tokyo College of Science, Kagurazaka, Shinjuku-ku, Tokyo

(Received August 23, 1965)

We have measured the rotatory dispersion (RD) and the ultraviolet absorption of twelve nitrates of glucopyranosides carrying a nitrate chromophore, $-O-NO_2$, in the position of the carbon atoms 1, 2, 3, 4, and 6. On the basis of the experimental results and of those results already reported concerning four nitrates,[1] studies have been made as to the correlation between the configuration and the Cotton effect. The sign of the Cotton effect has been determined by the RD curve as well as by the dispersion constant as computed from the dispersion data. A regular relation has been found, namely, irrespective of the position of the nitrate group on the carbon atom, α-glucosides with a nitrate chromophore in the α- or (D)-configuration show negative Cotton effects, while the sign of the Cotton effects of the corresponding β-glucosides is positive. On the contrary, α-glucosides with a nitrate chromophore in the β- or (L)-configuration show positive Cotton effects, while the sign of the Cotton effects of the corresponding β-glucosides is negative.

In a previous preliminary report[1] it has been shown, with some nitrates of glucose, that the $-C-ONO_2$ (nitrate) chromophore has a feeble optically active absorption around 270 mμ ($\varepsilon \sim 20$) and gives rise to a Cotton effect at a region nearly 20 mμ longer than that of the ultraviolet absorption.

In this paper further studies will be reported; these studies were carried out with various nitrates of glucose (Table I) with the object of elucidating the correlation between the configuration and the sign of the Cotton effect, especially the optical rotatory contribution of the functional group attached to each asymmetric center.

Results and Discussion

Figure 1 shows the RD curves of the α- and β-anomers of C_1-nitrates (2, 3, 4, 6-tetraacetyl-α-D-glucopyranose-1-nitrate (I) and the β-anomer (II)). The compound I exhibits a positive Cotton effect which has a peak at 285 mμ, while the compound II shows a negative one, the trough of which lies at 298 mμ. The curve I is positively increased more than the background RD curve XVII (pentaacetyl-α-D-glucopyranose), indicating that the α-C_1-ONO_2 chromophore makes a larger positive rotatory contribution that the C_1-OH group, which is usually expected to make a positive rotatory contribution. (It should, however, be remarked that the C_1-xanthate chromophore has been found to exhibit a distinctly negative Cotton effect,[2] just the opposite effect.)

In a similar, inverse way, the β-C_1-ONO_2 group contributes to the negative rotation of the compound II (Fig. 1), just opposite in sign to the positive effect of the β-C_1-xanthate group.[2]

The compound I, with 1α-$C-ONO_2$, is of the R-configuration according to the rule of Cahn et al.[3]; this is in harmony with the positive Cotton effect, and the absolute configuration of the compound II with β-C_1-ONO_2 is s, in accordance negative effect.

Figure 2 gives the RD curves of a number of various anomers with a nitrate group at the C_2-position. The compounds III and IV in the α-configuration show a weak negative Cotton effect, as has already

1) Y. Tsuzuki, K. Tanabe and K. Okamoto, This Bulletin, **38**, 274 (1965).

2) Y. Tsuzuki, K. Tanabe, M. Akagi and S. Tejima, ibid., **37**, 162 (1964).

3) R. S. Cahn, C. K. Ingold and V. Prelog, *Experientia*, **12**, 81 (1956).

Table I. Nitrates of glucose

Compound			Compound		
I	2,3,4,6-Tetra-*O*-acetyl-1-*O*-nitro-α-D-glucopyranose	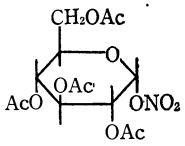	X	Methyl 4:6-*O*-ethylidene-α-D-glucopyranoside 2:3-dinitrate	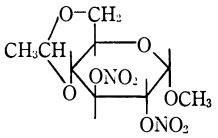
II	2,3,4,6-Tetra-*O*-acetyl-1-*O*-nitro-β-D-glucopyranose	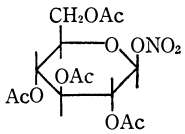	XI	Methyl 4:6-*O*-ethylidene-β-D-glucopyranoside 2:3-dinitrate	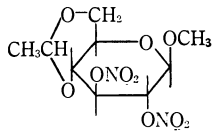
III[1]	1,3,4,6-Tetra-*O*-acetyl-2-*O*-nitro-α-D-glucopyranose	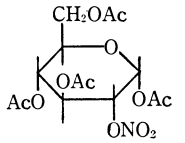	XII[1]	Methyl 4:6-*O*-benzylidene-α-D-glucopyranoside 2:3-dinitrate	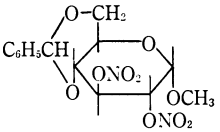
IV[1]	3,4,6-Tri-*O*-acetyl-2-*O*-nitro-α-D-glucopyranosyl chloride	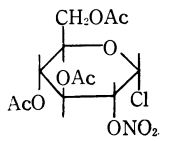	XIII	Methyl 4:6-*O*-benzylidene-β-D-glucopyranoside 2:3-dinitrate	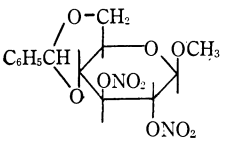
V	1,3,4,6-Tetra-*O*-acetyl-2-*O*-nitro-β-D-glucopyranose	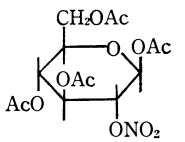	XIV	Methyl 2,3,6-tri-*O*-acetyl-4-*O*-nitro-β-D-glucopyranoside	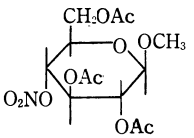
VI	3,4,6-Tri-*O*-acetyl-2-*O*-nitro-β-D-glucopyranosyl chloride	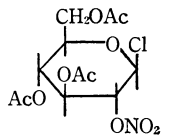	XV	Methyl 2,3-di-*O*-acetyl-4,6-di-*O*-nitro-β-D-glucopyranoside	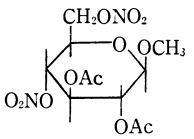
VII	Methyl 4:6-*O*-ethylidene-β-D-glucopyranoside 2-nitrate	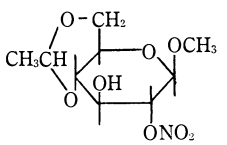	XVI	Methyl 2,3,4-tri-*O*-acetyl-6-*O*-nitro-α-D-glucopyranoside	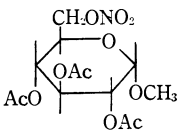
VIII[1]	Methyl 4:6-*O*-benzylidene-α-D-glucopyranoside 3-nitrate	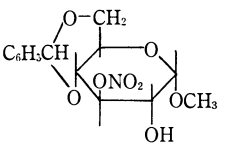	XVII[1]	Pentaacetyl-α-D-glucopyranose	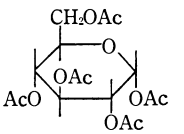
IX	Methyl 4:6-*O*-ethylidene-β-D-glucopyranoside 3-nitrate	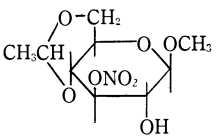	XVIII	Pentaacetyl-β-D-glucopyranose	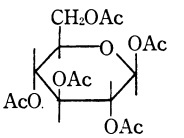

been reported,[1] while the corresponding β-anomers (compounds V and VI) show positive Cotton effects, with peaks at 295 and 300 mμ respectively. The ethylidene derivative (VII) of the β-configuration likewise exhibits a positive Cotton effect, with a peak at 300 mμ.

As may be seen from Fig. 2, all the β-anomers show relatively low rotations as a result of the background laevorotatory contribution of the β-glucosidic type (XVIII); this is consistent with the fact that the C_1–OH far surpasses the C_2–OH in rotatory contribution to glucose. A similar interpretation can be made of the RD curves of the nitrates of the α-form (III and IV) and the background α-pentaacetate (XVII), where the discrepancy in rotation is very little except the

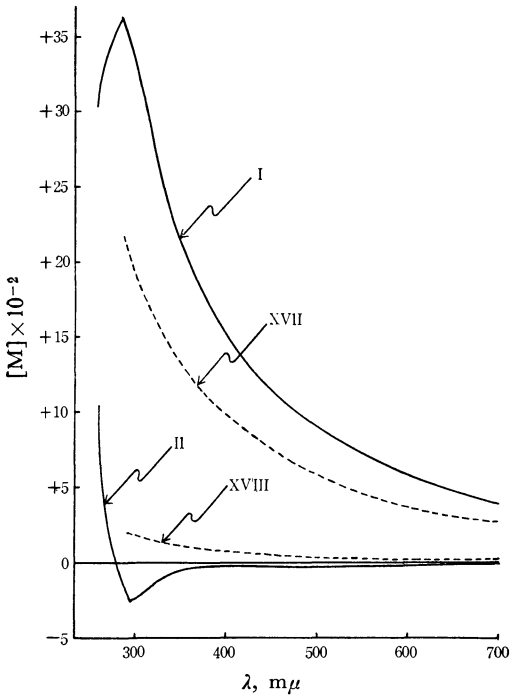

Fig. 1. RD of α- and β-1-nitrates of glucose.

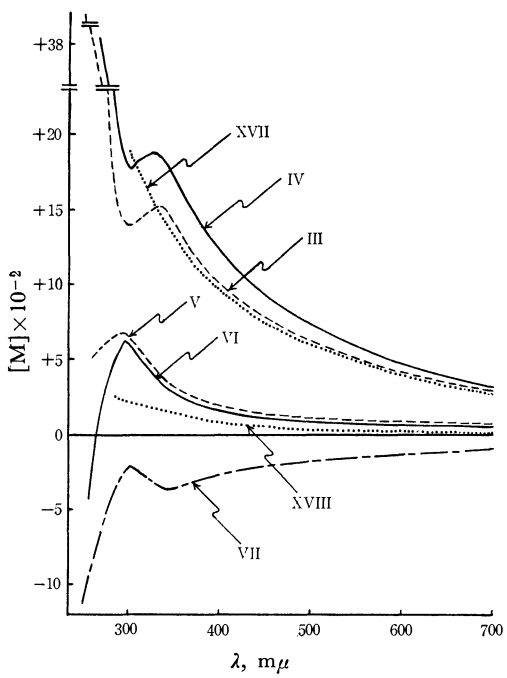

Fig. 2. RD of α- and β-2-nitrates of glucose.

feeble Cotton effects of the former due to the nitrate chromophore.

The rule of Cahn et al. does not appear to hold with the C_2-nitrates(R), since the α-forms (III and IV) show negative Cotton effects.

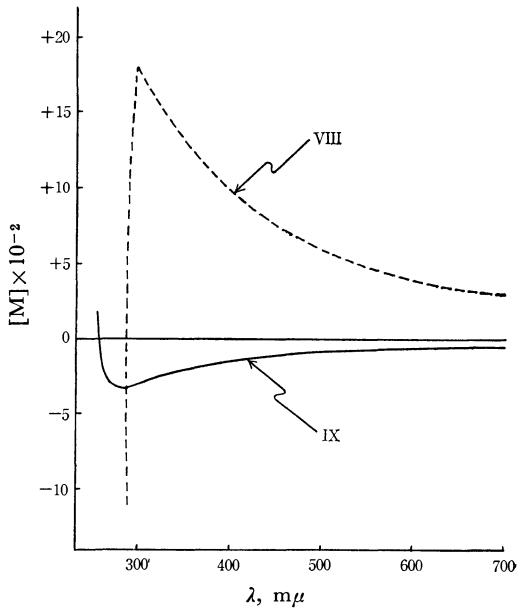

Fig. 3. RD of α- and β-3-nitrates of glucose.

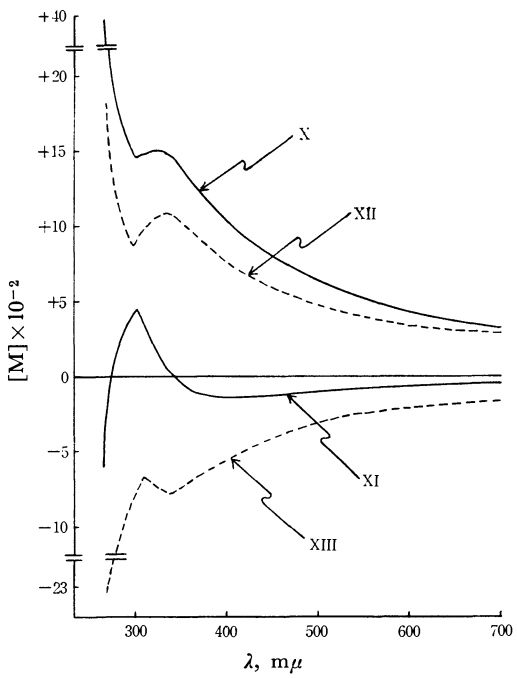

Fig. 4. RD of α- and β-2:3-dinitrates of glucose.

Figure 3 shows the RD curves of the anomers of the C_3-nitrates of glucose. While the α-anomer (VIII) clearly exhibits a positive Cotton effect,[1] quite in harmony with the R-configuration of the carbon 3, the β-glucoside (IX) shows an anomalous RD curve, and the Cotton effect with a trough at 290 mμ is indistinct in sign,

Figure 4 gives the RD curves of the 2 : 3-dinitrates

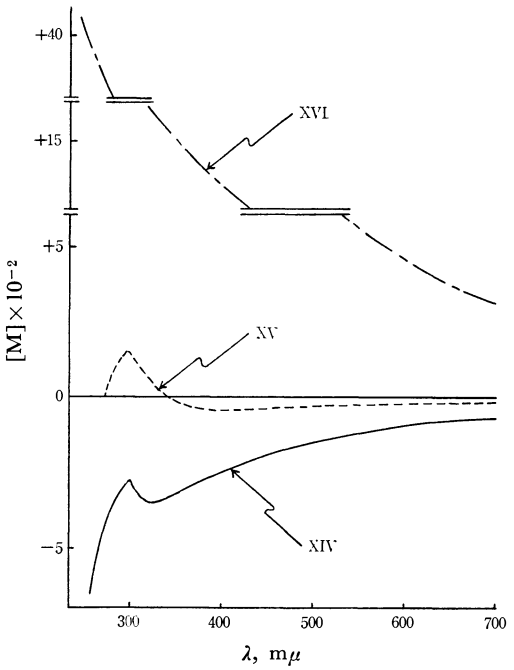

Fig. 5. RD of 4-, 6- and 4:6-dinitrates of glucose.

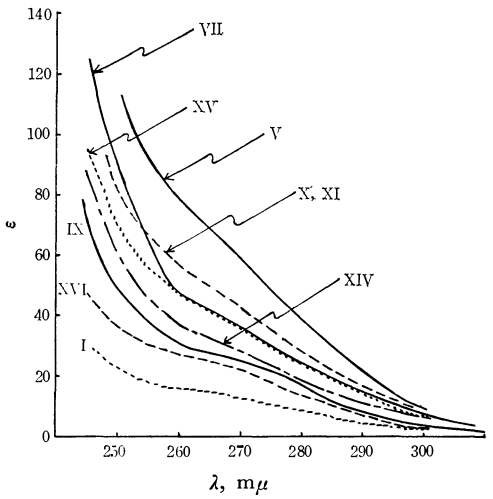

Fig. 6. UV absorption spectra of nitrates of glucose.

(X–XIII). The benzylidene derivatives (XII) show a negative Cotton effect, as has already been reported.[1] Here the rotatory contribution of the carbon 2 is greater than that of the carbon 3, so a negative Cotton effect results in the compound XII.

On the contrary, the β-anomer (XIII) shows a positive Cotton effect, indicating that the C_2-nitrate group also predominates over the C_3-chromophore. This is reasonable when we consider that the C_2-nitrates of the β-form (V–VII) all show positive Cotton effects.

A similar contrast in RD between the α- and β-

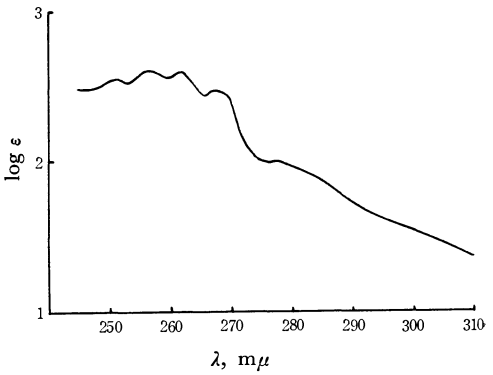

Fig. 7. UV absorption spectrum of XIII.

anomers can be seen in the α- and β-ethylidene derivatives (X and XI). It may, however, be seen in Fig. 4 that the ethylidene derivatives show more distinct Cotton effects than the benzylidene derivatives. Mention should also be made of how the sharper contrast between the former anomers can be used as a means of identification.

Figure 5 shows the RD curves of C_4-nitrate (XIV), 4, 6-dinitrates (XV) and 6-nitrate (XVI). The 4-nitrate exhibits a distinctly positive Cotton effect, even though in the negative domain, the peak of which is located at 300 mμ. The negative background rotation of IV undoubtedly arises from the β-methylglucoside. The RD curve of the compound XV shows a more strongly positive Cotton effect, thus showing the effect of the C_4–ONO_2 group. The 6-nitrate (XVI) does not appear to exhibit any Cotton effect, presumably because the carbon 6 is not asymmetric. The strongly positive background rotation is, naturally, due to the α-form of the glucoside.

The ultraviolet absorption spectra of these nitrates are assembled in Fig. 6, except for the spectrum of XI, which is shown in Fig. 7. As may be seen in Fig. 6, all the spectra show slightly visible shoulders in a region from 265 to 280 mμ, though they are not as distinct as those of alkyl nitrates.[4]

As in the case already elucidated,[1] in these cases a red shift of 5 to 25 mμ is also observed between the ultraviolet absorption and the peak of the Cotton effect. The ultraviolet absorption spectrum of the compound XI shows exceptionally a fine structure and relatively large extinction coefficients (Fig. 7), but it exerts almost no influence on the position of the Cotton effect.

Dispersion Constants

The dispersion data have been found to conform more suitably to the simplified two-term equation of Drude (1), than to the normal two-term equation (2).

4) H. E. Ungade and R. A. Smiloy, *J. Org. Chem.*, **21**, 993 (1956).

Table II. Dispersion data

$$[M] = \frac{A}{\lambda^2-\lambda_0^2} + \frac{B}{\lambda^2}$$

Compound	Drude's equation			λ_{RD}, μ	Sign of Cotton effect	Configuration of C_1
	A	B	λ_0, μ			
I	+20.75	+172.9	0.285	0.285	+	α
II	− 2.58	+ 2.37	0.287	0.298	−	β
III	− 2.35	+159.1	0.298	0.300	−	α
IV	− 2.83	+186.0	0.295	0.295	−	α
V	+ 7.60	+ 17.22	0.265	0.295	+	β
VI	+ 3.62	+ 20.66	0.277	0.300	+	β
VII	+ 2.05	− 45.54	0.283	0.300	+	β
VIII	+20.18	+108.4	0.259	0.300	+	α
IX	−0.565	− 24.16	0.271	0.290	−	β
X	−6.69	+162.8	0.306	0.300	−	α
XI	+5.43	− 28.00	0.291	0.2975	+	β
XII	−3.72	+124.7	0.291	0.295	−	α
XIII	+1.40	− 77.30	0.278	0.308	+	β
XIV	+0.185	− 36.22	0.290	0.300	+	β
XV	+3.45	− 18.43	0.291	0.295	+	β

$$[M] = \frac{A}{\lambda^2-\lambda^2_0} + \frac{B}{\lambda^2} \quad (1)$$

$$[M] = \frac{A_1}{\lambda^2-\lambda^2_1} + \frac{A_2}{\lambda^2-\lambda^2_2} \quad (2)$$

The results of the computation are given in Table II, together with the sign of the Cotton effect.

As may be seen in Table II, the term A invariably agrees with the Cotton effect in sign, indicating that A represents the Cotton effect indeed, the values of λ_0 nearly coincide with the values of λ_{RD}, the optically active absorption maxima observed from the RD, although in some cases the former are 10 to 30 mμ shorter.

The term B without doubt represents the rotatory strength of the non-chromophoric contributions; its value is in general far greater than the corresponding A value. This means that the nitrate chromophore is a feeble contributor to the Cotton effect and, hence, to the optical rotation, and that the dominant rotation originates in the residue of the molecule, mainly in the asymmetry of the carbon 1.

As may be seen in Table II, the values of B are always positive with the α-anomers, while with the β-anomers they are negative in sign, with a few exceptions. However, even with these exceptions (II, V and VI), the positive values are comparatively small.

Conclusion

The results of the above studies are summarized in Table III, where some regular correlations can be seen between the configurations of the carbon atom carrying the nitrate chromophore, as well as the glucosidic carbon atom C_1, and the sign of the Cotton effect.

Table III. The Configurations and signs of the Cotton effect of nitrates

Configuration of C-O-NO_2	C_1-Configuration	Sign of the Cotton effect
D or α	α-anomer	negative
D or α	β-anomer	positive
L or β	α-anomer	positive
L or β	β-anomer	negative

Experimental

The nitrates of glucose were prepared according to the literature. The rotatory dispersion was measured with a Rudolph spectropolarimeter over the region from 250 to 700 mμ. The ultraviolet absorption was measured with a self-recording spectrophotometer of the Hitachi EPU-II type. The dispersion constants of the Drude equation were calculated from the data by means of the least-square method with an electronic computer of the Fuji FACOM 201 type.

2, 3, 4, 6-Tetra-*O*-acetyl-1-*O*-nitro-α-D-glucopyranose (Compound I).[5]—Colorless prisms and plates; m. p. 150.5—151°C. The RD was measured at 21°C in chloroform (c 1.0100). $[\alpha]^{21}_{700}$ +103°, $[\alpha]_{589}$ +151°, $[\alpha]_{500}$ +222°, $[\alpha]_{400}$ +382°, $[\alpha]_{300}$ +832°, $[\alpha]_{285}$ +921° (peak), $[\alpha]_{270}$ +844°, $[\alpha]_{260}$ +790°.

2, 3, 4, 6-Tetra-*O*-acetyl-1-*O*-nitro-β-D-glucopyranose (Compound II).[5]—Colorless needles; m. p. 86°C. The RD was measured at 21°C in chloroform (c 1.142). $[\alpha]^{21}_{650}$ −0.110°, $[\alpha]_{589}$ −1.37°, $[\alpha]_{500}$ −1.52°, $[\alpha]_{400}$ −4.50°, $[\alpha]_{300}$ −60.4° (trough), $[\alpha]_{280}$ +2.63°, $[\alpha]_{260}$ +262°.

1, 3, 4, 6-Tetra-*O*-acetyl-2-*O*-nitro-β-D-glucopyranose (Compound V).[6]—Colorless needles; m. p. 121—122°C. The RD was measured at 21°C in chloroform (c 1.3930). $[\alpha]^{21}_{700}$ +13.2°, $[\alpha]_{600}$ +19.1°, $[\alpha]_{589}$ +20.2°, $[\alpha]_{500}$ +27.6°, $[\alpha]_{400}$ +48.9°, $[\alpha]_{300}$ +165°, $[\alpha]_{290}$ 173° (peak), $[\alpha]_{270}$ +149°.

5) E. Fischer and E. F. Armstrong, *Ber.*, **34**, 975 (1901).
6) M. L. Wolfrom, A. Thompson and O. R. Lineback, *J. Org. Chem.*, **28**, 1930 (1963).

3,4,6-Tri-*O*-acetyl-2-*O*-nitro-β-D-glucopyranosyl Chloride (Compound VI).[7]—Colorless needles; m. p. 138°C. The RD was measured at 21°C in chloroform (*c* 0.9006). $[\alpha]_{700}^{21}$ +14.0°, $[\alpha]_{589}$ +19.1°, $[\alpha]_{500}$ +27.9°, $[\alpha]_{400}$ +49.3°, $[\alpha]_{300}$ +159°, $[\alpha]_{295}$ +165°(peak), $[\alpha]_{270}$ +5.55°, $[\alpha]_{260}$ −100°.

Methyl 4:6-*O*-Ethylidene-β-D-glucopyranoside 2-Nitrate (Compound VII).[8]—Colorless needles; m. p. 143—144°C. The RD was measured at 21°C in chloroform (*c* 0.5880). $[\alpha]_{700}^{21}$ −34.1°, $[\alpha]_{589}$ −44.6°, $[\alpha]_{400}$ −101°, $[\alpha]_{340}$ −131° (broad extreme), $[\alpha]_{305}$ −83.7°(peak), $[\alpha]_{280}$ −183°, $[\alpha]_{265}$ −402°.

Methyl 4:6-*O*-Ethylidene-β-D-glucopyranoside 3-nitrate (Compound IX).[8]—Colorless needles; m. p. 145.5—146°C. The RD was measured at 21°C in chloroform (*c* 0.8740). $[\alpha]_{700}^{21}$ −19.3°, $[\alpha]_{589}$ −26.0°, $[\alpha]_{500}$ −37.9°, $[\alpha]_{400}$ −61.2°, $[\alpha]_{300}$ −111°, $[\alpha]_{290}$ −118°(trough), $[\alpha]_{260}$ −44.6°.

Methyl 4:6-*O*-Ethylidene-α-D-glucopyranoside 2:3-Dinitrate (Compound X).[9]—Colorless needles; m. p. 100—101°C. The RD was measured at 21°C in chloroform (*c* 2.492). $[\alpha]_{700}^{21}$ +98.6°, $[\alpha]_{589}$ +141°, $[\alpha]_{500}$ +201°, $[\alpha]_{400}$ +330°, $[\alpha]_{320}$ +494° (broad extreme), $[\alpha]_{300}$ +477°, (peak), $[\alpha]_{270}$ +1261°.

Methyl 4:6-*O*-Ethylidene-β-D-glucopyranoside 2:3-Dinitrate (Compound XI).[9]—Colorless prisms; m. p. 88—89°C. The RD was measured at 20.5°C in chloroform (*c* 1.0182). $[\alpha]_{700}^{20.5}$ −15.3°, $[\alpha]_{589}$ −21.6°, $[\alpha]_{500}$ −28.5°, $[\alpha]_{400}$ −38.7°(broad extreme), $[\alpha]_{330}$ +8.15°, $[\alpha]_{297.5}$ +142°(peak), $[\alpha]_{280}$ +19.6°, $[\alpha]_{270}$ −189°.

Methyl 4:6-*O*-Benzylidene-β-D-glucopyranoside 2:3-Dinitrate (Compound XIII).—This compound was obtained by the same procedure as was used in the case of compound XII,[1] but the reaction temperature was from −5 to −10°C. The compound was identified by means of its ultraviolet spectrum, its infrared spectrum and its analytical value. Colorless prisms; m. p. 163°C. The RD was measured at 21°C in tetrahydrofuran (*c* 1.2756). $[\alpha]_{700}^{21}$ −40.3°, $[\alpha]_{589}$ −59.0°, $[\alpha]_{500}$ −80.2°, $[\alpha]_{400}$ −140°, $[\alpha]_{337.5}$ −201° (broad extreme), $[\alpha]_{308}$ 178° (peak), $[\alpha]_{300}$ −192°, $[\alpha]_{270}$ −772°.

Methyl 2,3,6-Tri-*O*-acetyl-4-*O*-nitro-β-D-glucopyranoside (Compound XIV).[9]— Colorless needles; m. p. 113.5°C. The RD was measured at 20.8°C in chloroform (*c* 1.0644). $[\alpha]_{700}^{20.8}$ −19.8°, $[\alpha]_{589}$ −26.3°, $[\alpha]_{500}$ −39.8°, $[\alpha]_{400}$ −64.3°, $[\alpha]_{325}$ −90.5° (broad extreme), $[\alpha]_{300}$ −76.1°(peak), $[\alpha]_{280}$ −106°, $[\alpha]_{265}$ −181°.

Methyl 2,3-Di-*O*-acetyl-4,6-di-*O*-nitro-β-D-glucopyranoside (Compound XV).[10]—Colorless needles; m. p. 116°C. The RD was measured at 21°C in chloroform (*c* 1.7118). $[\alpha]_{700}^{21}$ −8.00°, $[\alpha]_{589}$ −10.2°, $[\alpha]_{500}$ −13.4°, $[\alpha]_{420}$ −16.2°(broad extreme), $[\alpha]_{350}$ −5.26°, $[\alpha]_{300}$ +77.7°, $[\alpha]_{295}$ +82.4°(peak), $[\alpha]_{275}$ +3.51°.

Methyl 2,3,4-Tri-*O*-acetyl-6-*O*-nitro-α-D-glucopyranoside (Compound XVI)[11]—Colorless prisms; m. p. 112—113°C. The RD was measured at 21°C in chloroform (*c* 1.1437). $[\alpha]_{700}^{21}$ +89.9°, $[\alpha]_{589}$ +131°, $[\alpha]_{500}$ +190°, $[\alpha]_{400}$ +316°, $[\alpha]_{300}$ +589°, $[\alpha]_{250}$ +1159°.

Pentaacetyl-β-D-glucopyranose (Compound XVIII).[12]—Colorless needles; m. p. 132°C. The RD was measured at 21°C in chloroform (*c* 2.1320). $[\alpha]_{700}^{21}$ +4.36°, $[\alpha]_{589}$ +6.47°, $[\alpha]_{500}$ +9.05°, $[\alpha]_{400}$ +16.8°, $[\alpha]_{300}$ +44.2°.

7) M. L. Wolfrom and I. C. Gillam, *Science*, **130**, 1424 (1959).
8) K. S. Ennor and J. Honeyman, *J. Chem. Soc.*, **1958**, 2586.
9) J. Honeyman and J. W. W. Morgan, ibid., **1955**, 3669.
10) D. J. Bell and R. L. M. Synge, ibid., **1937**, 1715.
11) E. K. Gladding and C. B. Purres, *J. Am. Chem. Soc.*, **66**, 153 (1944).
12) E. Fischer, *Ber.*, **49**, 584 (1916).

BULLETIN OF THE CHEMICAL SOCIETY OF JAPNA VOL. 39 766—771 (1966)

The Electronic Structures and Electronic Spectra of Some Aliphatic Nitroso Compounds

By Masashi TANAKA*, Jiro TANAKA* and Saburo NAGAKURA

The Institute for Solid Physics, The University of Tokyo, Azabu, Tokyo

(Received August 28, 1965)

The electronic structures and electronic spectra of 1-chloro-1-nitrosocyclohexane, nitrosyl chloride, methyl nitrite and dimethylnitrosoamine were studied by making molecular orbital calculations and by measuring the electronic absorption spectra. Concerning 1-chloro-1-nitrosocyclohexane, the $n\rightarrow\pi^*$ and $\pi\rightarrow\pi^*$ bands were observed at 650 and 160 mμ respectively. The conjugation effect of electron donors such as Cl, OCH_3 and $N(CH_3)_2$ upon the electronic spectrum of the nitroso group was studied. The intramolecular charge-transfer bands characteristic of the donor-acceptor interaction were found at 190, 210 and 230 mμ for nitrosyl chloride, methyl nitrite and *N*, *N*-dimethylnitrosoamine respectively. This shows that the intramolecular charge-transfer bands appear at longer wavelengths in the order of the increasing ability of the electron donors, $Cl<OCH_3<N(CH_3)_2$. On the other hand, the $n\rightarrow\pi^*$ bands shift to shorter wavelengths in the same order.

* Present address: Department of Chemistry, Faculty of Science, Nagoya University, Chikusa-ku, Nagoya.

In a previous paper which studied the electronic absorption spectra of nitrosobenzene[1] and its derivatives, it was shown that the nitroso group is a strong electron acceptor, and that their ultraviolet absorption spectra are greatly different from that of benzene. Nitrosobenzene exhibits a new band characteristic of the charge-transfer interaction between the benzene ring as an electron donor and the nitroso group as an electron acceptor. Moreover, the maximum wavelength of the band is longer than the corresponding band of nitrobenzene. This seems to mean that the electron affinity of the nitroso group is greater than that of the nitro group. In view of the large electron-accepting ability of the nitroso group, the electronic structures of aliphatic nitroso compounds have been studied in the present paper by combining the experimental data of the absorption spectra with the theoretical results based on the molecular orbital calculations.

The electronic absorption spectra of aliphatic nitroso compounds have been studied by several workers from both experimental[2-7] and theoretical[8,9] points of view. In the present study, the electronic absorption spectrum of 1-chloro-1-nitrosocyclohexane was measured in order to obtain fundamental knowledge about the electronic structure of the nitroso group itself. Then the charge-transfer interaction of the nitroso group with electron donors such as Cl, OCH_3 and $N(CH_3)_2$ has been studied by the aid of the electronic absorption spectra in the vacuum ultraviolet region.

Experimental

Materials.—*Methyl Nitrite.*[2]—A sulfuric acid (12 N) solution was dropped on a mixture of methanol and a 45% aqueous sodium nitrite solution. The crude product was dried over calcium chloride and was purified by repeated low-temperature distillations in vacuo.

N, N-Dimethylnitrosoamine.[10]—A mixture of dimethylamine and sodium nitrite was heated for several hours. The oil layer was separated and the aqueous portion was extracted with benzene. The benzene was removed by distillation and the residue was fractionally distilled under reduced pressure. The nitrosoamine was obtained as a light yellow liquid; b. p. 104°C/ca. 10mmHg.

1-Chloro-1-nitrosocyclohexane.[5]—Cyclohexanone oxime was dissolved in diluted hydrochloric acid and the solution was cooled by ice water.

A fairly rapid stream of chlorine was passed through the solution until no more gas was absorbed. The separated blue oil was extracted with ether and then washed with an aqueous sodium bicarbonate solution and with water. After the extract had been dried with anhydrous sodium sulfate, the ether was removed. The nitroso compound was then distilled under reduced pressure as a purple oil with a very unpleasant smell; (b. p. 58°C/13 mmHg).

Measurements.—The absorption spectra of the

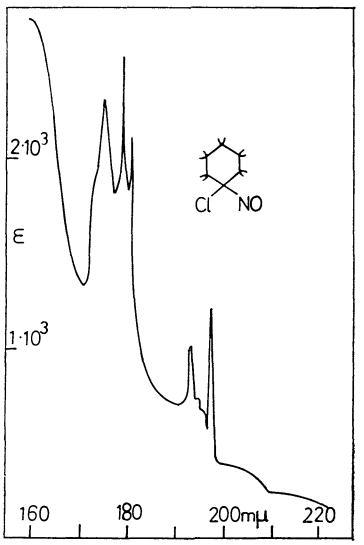

Fig. 1. The ultraviolet absorption spectrum of 1-chloro-1-nitrosocyclohexane.

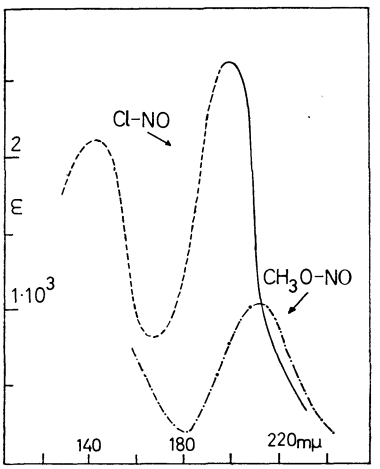

Fig. 2. The ultraviolet absorption spectra of methyl nitrite and nitrosyl chloride.
—— nitrosyl chloride, measured by Goodeve and Katz
---- nitrosyl chloride, measured by Price and Simpson
-·— methyl nitrite, measured by the present authors

1) K. Tabei and S. Nagakura, This Bulletin, **38**, 965 (1965).
2) P. Tarte, *J. Chem. Phys.*, **20**, 1570 (1955).
3) R. N. Haszeldine and B. J. H. Hattinson, *J. Chem. Soc.*, **1955**, 4172.
4) J. Mason, ibid., **1957**, 3904.
5) D. L. Hammick and M. W. Lister, ibid., **1937**, 489.
6) C. F. Goodeve and S. Katz, *Proc. Roy. Soc.*, **A172**, 437 (1939).
7) W. C. Price and D. M. Simpson, *Trans. Faraday Soc.*, **37**, 106 (1941).
8) J. Tanaka, *J. Chem. Soc. Japan, Pure Chem. Sect.* (*Nippon Kagaku Zassi*), **78**, 1647 (1957).
9) K. L. McEwen, *J. Chem. Phys.*, **34**, 546 (1961).
10) M. Kotake, "Daiyuki Kagaku-Organic Chemistry-III," Asakura, Tokyo (1959), p. 126.

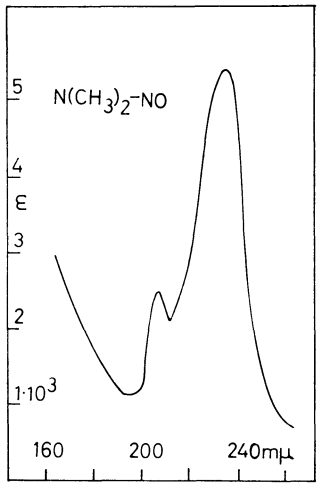

Fig. 3. The ultraviolet absorption spectrum of *N*, *N*-dimethylnitrosoamine.

above-mentioned samples were measured in the gaseous states. The ultraviolet absorption measurements down to 190 mμ were made with a Cary recording spectrophotometer, model 14 M, a quartz cell 10 cm. long being used. A vacuum ultraviolet spectrophotometer constructed in our laboratory was used for the measurements in the vacuum ultraviolet region. In this case, a gas cell 0.7 cm. long and equipped with lithium fluoride windows was used.

The results are shown in Figs. 1—3, together with the absorption spectrum of nitrosyl chloride, which was measured by Goodeve and Katz[6] down to 190 mμ and by Price and Simpson[7] down to 130 mμ.

The peak wavelengths and molar extinction coefficients are tabulated in Table I.

Table I. The Observed peak wavelengths and molar extinction coefficients for various aliphatic nitroso compounds

Sample	λ_{max}, mμ	ε_{max}
1-Chloro-1-nitroso-cyclohexane	(750	0.6)*[5]
	197	1200
	179	2800
	~160	>2600
Nitrosyl chloride[6,7]	(615	0.7)*
	197	2550
	145	2000
Methyl nitrite	(386	10)*
	212	1050
N, *N*-Dimethyl nitrosoamine	(377	50)*
	227	5200
	205	2350

* These absorptions have vibrational structures. The wavelengths given in this table are those for the longest wavelength bands which may be assigned to the 0—0 band.

Theoretical

The π-electron structures of nitrosyl chloride, methyl nitrite and *N*, *N*-dimethylnitrosoamine have been studied theoretically on the basis of the geometrical structures shown in Fig. 4. The geometrical structures of nitrosyl chloride and methyl nitrite were studied by Ketelaar and Palmer[11] and by Rogowski[12] respectively. However, the geometrical structure of *N*, *N*-dimethylnitrosoamine has not yet been studied experimentally. Therefore, we assume its structure to be as is shown in Fig. 4.

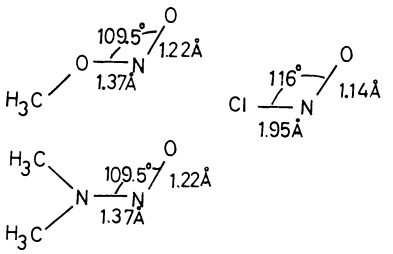

Fig. 4. The geometrical structures of nitrosyl chloride, methyl nitrite and *N*, *N*-dimethylnitrosoamine.

Calculation of the MO of the Nitroso Group. —First of all, the LCAO SCF MO's ϕ_i of the π-electron system of the nitroso group were evaluated by means of the usual equation[13]:

$$F\phi_i = \varepsilon_i\phi_i, \quad \phi_i = a\chi_N + b\chi_O$$

where χ_N and χ_O indicate the $2p\pi$ atomic orbitals of the nitrogen and the oxygen atoms of the nitroso group respectively. The details of the calculation will be given in the Appendix.

The resultant molecular orbitals, ϕ_i, and orbital energies, ε_i, are given below:

$$\varepsilon_1 = -17.70 \text{ eV.}, \quad \phi_1 = 0.5963\chi_N + 0.8028\chi_O$$

$$\varepsilon_2 = -0.61 \text{ eV.}, \quad \phi_2 = 0.8028\chi_N - 0.5963\chi_O$$

It is clear from these results that the μ-electron distribution in the ϕ_1 orbital of the nitroso group inclines toward the oxygen atom, and that the electron affinity of the nitroso group, $-\varepsilon_2 = 0.61$ eV., is larger than those of the nitro and carbonyl groups, 0.40 eV.[14] and −1.20 eV.[15] respectively.

The transition energy, $\Delta E(N \rightarrow V)$, and oscillator strength, f, were calculated as follows:

$$\Delta E(N \rightarrow V) = 7.96 \text{ eV.}$$

$$f = 0.475$$

For the purpose of checking the theoretical results,

11) J. A. Ketelaar and K. J. Palmer, *J. Am. Chem. Soc.*, **59**, 2629 (1937).
12) F. Rogowski, *Ber.*, **75**, 244 (1942).
13) C. C. J. Roothaan, *Rev. Mod. Phys.*, **23**, 69 (1951).
14) J. Tanaka, *J. Chem. Soc. Japan, Pure Chem. Sect.* (*Nippon Kagaku Zassi*), **78**, 1643 (1957).
15) S. Nagakura, *Mol. Phys.*, **3**, 105 (1960).

we measured the absorption spectrum of 1-chloro-1-nitrosocyclohexane. As may be seen in Table I, 1-chloro-1-nitrosocyclohexane shows absorption bands at 750, 197, 179 and ~160 mμ. The 750 mμ band may safely be regarded as the $n\rightarrow\pi^*$ transition band. The peak at about 160 mμ (7.75 eV.) may correspond to the N→V ($\pi\rightarrow\pi^*$) transition of the nitroso group, while the other two peaks, at 179 mμ and 197 mμ, seem to correspond to an $n\rightarrow\pi^*$ transition or a band of the Rydberg series.

Configuration Interaction Calculation.—The π-electron energy levels and the wave functions of nitrosyl chloride, methyl nitrite and *N*, *N*-dimethylnitrosoamine were calculated by taking into account the configurational interaction among several electron configurations. The respective molecules were separated into the two components, the electron donor, Cl–, CH_3O– or $(CH_3)_2N$– and the electron acceptor, NO–. The interaction between them was considered by means of the configurational interaction among π electron configurations which were constructed by putting the four π electrons into the appropriate orbitals of the components.

The electron configurations actually taken up in the present calculation are shown in Fig. 5.

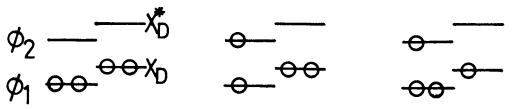

ground config. | locally excited config. | charge-transfer config.

Fig. 5. The electron configurations of the nitroso compounds.

In addition to the ground configuration, G, a charge-transfer configuration, CT, caused by an electron transfer from the electron donor toward the electron acceptor, and a locally excited configuration, LE, were considered. The energy of the ground configuration, H_G, was taken as the standard. The energy of the locally excited configuration, H_{LE}, was set equal to 7.96 eV., the N→V transition energy of the nitroso group as evaluated theoretically by the present authors. The energy of the charge-transfer configuration, H_{CT}, was calculated by the following equation:

$$H_{CT} = I_D - A_{NO} - 0.5963^2(\mathrm{NN/DD}) - 0.8028^2(\mathrm{OO/DD})$$

Here the I_D's are the ionization potentials of the electron-donating groups, i. e., Cl–, CH_3O– and $(CH_3)_2N^-$. They were taken to be 12.84, 10.85 and 8.24 eV. for the chloro, methoxy and *N*, *N*-dimethylamino groups respectively from the ionization potentials of hydrochloric acid,[16] methanol[17] and dimethylamine[18]. A_{NO} is the electron affinity of the electron-accepting group, –NO; it was calculated to be 0.61 eV. by the present authors. D indicates the $2p\pi$ or $3p\pi$ atomic orbital for the lone pair electrons of the donor.

Two center Coulomb repulsion integrals like (NN/DD) were evaluated nonempirically, using Slater orbitals except for (NN/ClCl) and (OO/ClCl), which were calculated by Pariser and Parr's method.[19] The energies and wave functions of the configurations used in the present calculations are tabulated in Table II.

Table II. The energies and wave functions of the electron configurations

Energy, eV.	Wave function
$H_G=0$	$\Phi_G=\lvert\phi_1\bar{\phi}_1\mathrm{D}\bar{\mathrm{D}}\rvert$
$H_{LE}=7.96$	$\Phi_{LE}=1/\sqrt{2}\{\lvert\phi_1\bar{\phi}_2\mathrm{D}\bar{\mathrm{D}}\rvert + \lvert\phi_2\bar{\phi}_1\mathrm{D}\bar{\mathrm{D}}\rvert\}$
$H_{CT}=5.77$(NOCl) 2.58(CH_3ONO) −0.04($(CH_3)_2NNO$)	$\Phi_{CT}=1/\sqrt{2}\{\lvert\phi_1\bar{\phi}_1\phi_2\bar{\mathrm{D}}\rvert + \lvert\phi_1\bar{\phi}_1\mathrm{D}\bar{\phi}_2\rvert\}$

Table III. The off-diagonal elements used in the present calculation

$H_{GLE}=0$ $\quad H_{G\,CT}=\sqrt{2}\,b\beta_{ND}$ $\quad H_{LE\,CT}=-a\beta_{ND}$

$$\beta_{NCl}=\int\chi_N\boldsymbol{H}^{core}\chi_{Cl}d\tau=-1.40\ \mathrm{eV}.$$

$$\beta_{NO}=\int\chi_N\boldsymbol{H}^{core}\chi_{Cl}d\tau=-2.20\ \mathrm{eV}.$$

$$\beta_{NN}=\int\chi_N\boldsymbol{H}^{core}\chi_{Cl}d\tau=-2.10\ \mathrm{eV}.$$

The off-diagonal matrix elements of the total electronic Hamiltonian, each of which represents the magnitude of the interaction between two different configurations, were evaluated by the aid of the formulations by Pople[20] and by Longuet-Higgins and Murrell.[21] They are given in Table III in terms of the core resonance integrals, β_{NCl}, β_{NO} and β_{NN}. By solving the determinants constructed by the matrix elements given in Tables II and III with an electronic computer, Facom 202, in our Institute, the π electron energy levels and the wave functions for nitrosyl chloride, methyl nitrile and *N*, *N*-dimethylnitrosoamine were evaluated. The results are shown in Table IV. From these results, the dipole moments due to the π electrons in the ground state, the transition energies and the oscillator strengths were calculated for these nitroso compounds. The results are shown Table V, together with the observed results.

16) W. C. Price, *Proc. Roy. Soc.*, **A167**, 216 (1938).
17) K. Watanabe, *J. Chem. Phys.*, **26**, 542 (1957).
18) K. Watanabe, ibid., **26**, 1773 (1957).
19) R. Pariser and R. G. Parr, ibid., **21**, 466, 767 (1953); R. Pariser, ibid., **24**, 250 (1956).
20) J. A. Pople, *Trans. Faraday Soc.*, **49**, 1375 (1953).
21) H. C. Longuet-Higgins and J. N. Murrell, *Proc. phys. Soc.*, **A68**, 601 (1955).

TABLE IV. THE ENERGY LEVELS AND WAVE FUNCTIONS FINALLY OBTAINED WITH NITROSYL CHLORIDE, METHYL NITRITE AND *N*,*N*-DIMETHYLNITROSOAMINE

	Energy, eV.	Wave function
Nitrosyl chloride	$W_0 = -0.41$	$\Psi_0 = 0.9673\Phi_G - 0.0251\Phi_{LE} + 0.2522\Phi_{CT}$
	$W_1 = 5.86$	$\Psi_1 = -0.2442\Phi_G - 0.3588\Phi_{LE} + 0.9009\Phi_{CT}$
	$W_2 = 8.28$	$\Psi_2 = -0.0679\Phi_G + 0.9330\Phi_{LE} + 0.3533\Phi_{CT}$
Methyl nitrite	$W_0' = -1.57$	$\Psi_0' = 0.8441\Phi_G - 0.0731\Phi_{LE} + 0.5312\Phi_{CT}$
	$W_1' = 3.80$	$\Psi_1' = -0.5308\Phi_G - 0.2551\Phi_{LE} + 0.8082\Phi_{CT}$
	$W_2' = 8.30$	$\Psi_2' = -0.7644\Phi_G + 0.9641\Phi_{LE} + 0.2542\Phi_{CT}$
N,*N*-Dimethyl-nitrosoamine	$W_0'' = -2.48$	$\Psi_0'' = 0.6900\Phi_G - 0.0862\Phi_{LE} + 0.7187\Phi_{CT}$
	$W_1'' = 2.23$	$\Psi_1'' = 0.7222\Phi_G + 0.1477\Phi_{LE} - 0.6757\Phi_{CT}$
	$W_2'' = 8.17$	$\Psi_2'' = -0.0479\Phi_G + 0.9853\Phi_{LE} + 0.1642\Phi_{CT}$

TABLE V. THE OBSERVED AND CALCULATED DIPOLE MOMENTS, TRANSITION ENERGIES AND OSCILLATOR STRENGTHS

	Dipole moment in the ground state (DU)		Transition	Transition energy eV.		Oscillator strength	
	Obs.	Calcd.		Obs.	Calcd.	Obs.[a]	Calcd.
Nitrosyl chloride	1.83[22]	1.91	$W_0 \rightarrow W_1$	6.28	6.28		0.263
			$W_0 \rightarrow W_2$	8.55	8.69		0.263
Methyl nitrite	3.84[23]	3.90	$W_0' \rightarrow W_1'$	5.90	5.38	0.052	0.272
			$W_0' \rightarrow W_2'$	7.5	9.88		0.270
N,*N*-Dimethyl-nitrosoamine	3.98[24]	5.50	$W_0'' \rightarrow W_1''$	5.47	4.71	0.150	0.253
			$W_0'' \rightarrow W_2''$	7.5	10.65		0.194

a) Observed oscillator strengths are uncertain.

Discussion

Nitrosyl Chloride.—As is shown in Fig. 2 and Table I, nitrosyl chloride shows three absorption bands in the visible and ultraviolet regions. The 615 mμ band may be ascribed to the $n \rightarrow \pi^*$ transition. The 197 mμ band can be assigned to the W_0-W_1 transition. From the wave function, Ψ_1, given in Table IV, it may be seen that the band has the character of the intramolecular charge-transfer band. The band at about 145 mμ is due to the W_0-W_2 transition, which has the property of the local excitation within the nitroso group. Therefore, the 160 mμ band of the nitroso group shifts to 145 mμ by conjugation with the nonbonding electrons of the chlorine atom.

It may be seen from Ψ_0 given in Table IV that the contribution of the charge-transfer configuration in the ground state of this compound is only 6%. The calculated dipole moment due to the π-electrons can explain the observed value satisfactorily (see Table V).

Methyl Nitrite.—Methyl nitrite shows two absorption peaks, at 386 mμ and 212 mμ. In addition, a strong band appears below 160 mμ (see Fig. 2). The 386 mμ band may be assigned to the $n \rightarrow \pi^*$ band of the nitroso group. The 212 mμ band, which corresponds to the $W_0' \rightarrow W_1'$ transition of methyl nitrite, may be regarded as an intramolecular charge-transfer band. This is because, as may be seen from Ψ_1' in Table V, the contribution of the charge-transfer configuration in the W_1' state amounts to 65%. The shorter wavelength band, the maximum of which does not appear until 160 mμ, may be ascribed to the $W_0' \rightarrow W_2'$ transition. This band may be interpreted as the blue-shifted band of the 170 mμ band of the nitroso group. It is known from Ψ_0' given in Table IV that the contribution of the charge-transfer configuration in the ground state is 28%.

***N*, *N*-Dimethylnitrosoamine.** — The absorption spectrum of *N*, *N*-dimethylnitrosoamine is similar to that of methyl nitrite. The 377 mμ band may be regarded as an $n \rightarrow \pi^*$ transition band, as may be the 386 mμ band of methyl nitrite. The strong band at 227 mμ corresponds to the 212mμ band of the methyl nitrite and may be interpreted as an intramolecular charge-transfer band. The absorption tail below 190mμ may be due to the local excitation within the NO group. A similar absorption tail was also observed with methyl nitrite. The peak at 205 mμ may be thought to be an extra band in the sense that the corresponding band was not observed with methyl nitrite. This may be regarded as the $n \rightarrow \pi^*$ transition band of the dimethylamino group.[25]

As may be seen from Table IV, the contribution of the charge-transfer configuration in the ground state

22) J. A. Ketelaar, *Rect. trav. chim.*, **62**, 289 (1943).
23) T. Chiba, This Bulletin, **28**, 505 (1955).
24) E. G. Cowley and J. R. Rartington, *J. Chem. Soc.*, **1933**, 1255.
25) H. Tsubomura, K. Kimura, K. Kaya, J. Tanaka and S. Nagakura, This Bulletin, **37** 417 (1964).

decreases in the following order; *N*, *N*-dimethylnitrosoamine>methyl nitrite>nitrosyl chloride. This means that the electron-donating power of the substituents decreases in the order of $N(CH_3)_2$> OCH_3>Cl.

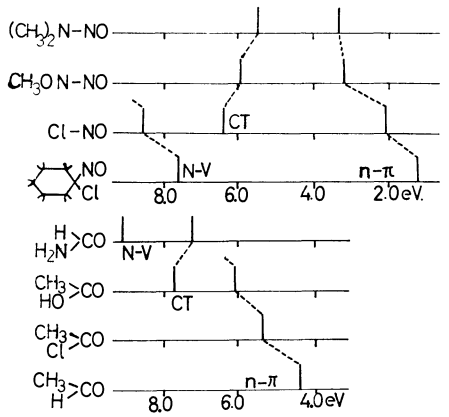

Fig. 6. The relation between the transition energy and the electron-donating ability of Cl, OCH_3 and $N(CH_3)_2$.

The Effect of the Electron-donating Group upon the Absorption Spectrum of the Nitroso Compounds.—The results obtained by the present authors are summarized in Fig. 6. This figure shows that the absorption spectra of XNO change regularly with the electron-donating power of X. That is, with the increasing electron-donating power of X, the $n\rightarrow\pi^*$ band shifts toward the shorter wavelengths, and the charge-transfer band toward the longer wavelengths. As is shown in Fig. 6, the same tendency was observed with the carbonyl compounds, O=CRX. The $n\rightarrow\pi^*$ transition band which appears at 280 mμ for acetaldehyde shifts to 232 mμ and to 205 mμ for acetylchloride and acetic acid respectively[26]. The band of acetamide shifts to a shorter wavelength than 200 mμ. On the other hand, the intramolecular charge-transfer band appears at 171.7 mμ and at 160 mμ for formamide and acetic acid respectively[15,27].

The authors' thanks are due to Dr. Michiya Itoh for his kind advice in preparing 1-chloro-1-nitrosocyclohexane, and also to Mr. Koji Kaya for his kind help in measuring the vacuum ultraviolet absorption spectra.

Appendix

The molecular orbital energies ε_i are solutions of the following secular determinant

$$\begin{vmatrix} F_{NN}-\varepsilon & F_{NO} \\ F_{NO} & F_{OO}-\varepsilon \end{vmatrix}=0$$

By the aid of the Pariser-Parr method,[19] the F_{NN}, F_{OO} and F_{NO} are given in the following

$$F_{NN} = \alpha_N + a^2(NN/NN) + 2b^2(NN/OO)$$
$$F_{OO} = \alpha_O + 2a^2(NN/OO) + b^2(OO/OO)$$
$$F_{NO} = \beta_{NO} - ab(NN/OO)$$

In this expression, one-center Coulomb repulsion integrals (NN/NN) and (OO/OO) are estimated by the aid of Pariser's approximation, namely averaging the I_p—A of the $2p\pi$ electron at various valance states, where I_p is the appropriate valence state ionization potential[28] and A the appropriate valence state electron affinity.[28] The two-center Coulomb repulsion integral was calculated by the use of the Slater orbitals[29] at the bond length r_{NO}=1.22 Å. Following the Pariser-Parr theory, the core integral β_{NO} was left as an adjustable parameter, and α_N and α_O were given by the following equations.

$$\alpha_N = -I_p(N) - (NN/OO)$$
$$\alpha_O = -I_p(O) - (NN/OO)$$

The above-mentioned various quantities are presented in Table VI.

Table VI. Integrals involving π-atomic orbitals (eV.)

$\alpha_N=-23.15$	$\alpha_O=-28.41$
$I_p(N)=14.51$	$I_p(O)=17.79$
$(NN/NN)=13.38$	$(OO/OO)=14.33$
$(NN/OO)=10.62$	
$\beta_{NO}=-3.10$	

26) S. Nagakura, ibid., **25**, 164 (1952).
27) S. Nagakura, K. Kaya and H. Tsubomura, *J. Mol. Spect.*, **13**, 1 (1964).
28) G. Pilcher and H. A. Skinner, *J. Inorg. Nucl. Chem.*, **24**, 937 (1962).
29) C. C. J. Roothaan, *J. Chem. Phys.*, **19**, 1445 (1951).

BULLETIN OF THE CHEMICAL SOCIETY OF JAPAN VOL. 39 772—776 (1966)

The Cation Effect on the Polarographic Reduction of *cis*-Dioxalatodiaquochromate(III) and Trioxalatochromate(III) Ions

By Nobuyuki TANAKA, Eiki ITABASHI* and Reita TAMAMUSHI**

Department of Chemistry, Faculty of Science, Tohoku University, Katahira-cho, Sendai

(Received September 3, 1965)

The cation effect on the polarographic reduction of *cis*-dioxalatodiaquochromate(III) and trioxalatochromate(III) ions has been reported. *cis*-Dioxalatodiaquochromate(III) ions give an irreversible wave corresponding to a three-electron reduction in the solutions of univalent electrolytes, while they give a double wave in the solutions of bivalent electrolytes, the first wave being of a one-electron reduction and the second wave, of a two-electron reduction. Trioxalatochromate(III) ions are reduced to chromium(0) in the univalent and the bivalent electrolyte solutions at more negative potentials than *cis*-dioxalatodiaquochromate(III) ions. The reduction potentials of these complex anions depend on the nature and the concentration of cations of electrolytes present in the solution, and shift to less negative potentials with increasing ionic charges of the cation and, at the constant ionic charge, with decreasing radii of the hydrated ion and increasing concentrations of the cation present. The cation effect was explained by taking into consideration of both the structure of the electrical double layer and the formation of ion-pairs.

In the previous papers[1-3] evidences have been presented that *cis*-dioxalatodiaquochromate(III) ions gave an irreversible wave corresponding to three-electron reduction with a half-wave potential of -1.52 V. vs. SCE in a 0.3 M potassium chloride solution,[1] and that trioxalatochromate(III) ions gave no reduction wave in a 0.1 M solution of tetramethylammonium bromide,[2] but gave a well-defined reduction wave in the solutions of other electrolytes such as potassium chloride or barium chloride.[3] This result seemed to differ from that of Pamfilov and his co-workers,[4] who reported trioxalatochromate(III) ions gave two irreversible waves with the half-wave potentials of -1.315 and -1.450 V. vs. NHE in a 1.0 N potassium chloride solution.

In the present paper are reported the detailed results of the effects of the nature and the concentration of supporting electrolytes on the polarographic reduction of *cis*-dioxalatodiaquochromate(III) and trioxalatochromate(III) ions. The cation effect is discussed on the basis of the formation of ion-pairs and the change in the structure of the electrical double layer.

Experimental

Current-potential curves were recorded with a pen-recording polarograph, a Yanagimoto Galvarecorder Model PR-2 with an automatic potential scanner. A Yanagimoto Y-GR 2 Galvarecorder was used for recording alternating current (a.c.) polarograms. Kalousek polarograms were recorded with the same circuit as has been described previously.[5] To determine the integral capacity in the double layer, the capacitance was measured using the same circuit as given in the previous report.[6]

The dropping mercury electrode had an m value of 1.84_7 mg./sec., and a drop time, t_d, of 3.1 sec. being measured in an air-free 1 M potassium chloride solution containing 0.005% galatin at -1.70 V. vs. SCE at 45 cm. of the mercury reservoir.

The cell equipment was the same as has been reported previously.[7] The potentials were referred to a saturated calomel electrode (SCE). The dissolved oxygen in the solution was removed by bubbling pure nitrogen gas through the solution. All measurements were carried out in a thermostat of 25.0°C. All current-potential curves presented in this paper are corrected for the residual current and the ohmic drop (iR) across the electrolysis cell.

Potassium *cis*-dioxalatodiaquochromate(III)[8] and potassium trioxalatochromate(III)[9] were prepared with the procedures given in the literatures. All other chemicals used were of a guaranteed reagent grade. In the case of lithium chloride, it was dissolved in redistilled water, a small amount of insoluble substance was

* Present address: Department of Chemistry, Faculty of Science, Osaka University Toyonaka, Osaka.

** Present address: The Institute of Physical and Chemical Research, Komagome, Bunkyo-ku, Tokyo.

1) N. Tanaka, E. Itabashi, R. Tamamushi and G. Satô, This Bulletin, **37**, 226 (1964).

2) N. Tanaka, E. Itabashi and E. Kyuno, ibid., **36**, 917 (1963).

3) N. Tanaka, E. Itabashi and R. Tamamushi, ibid., **37**, 762 (1964)

4) A. V. Pamfilov, O. I. Lopushans'ka and T. S. Zueva, *Ukr. Khim. Zh.*, **29**, 299 (1963); *Chem. Abstr.*, **59**, 3543 (1963).

5) N. Tanaka, R. Tamamushi and M. Kodama, This Bulletin, **33**, 14 (1960).

6) R. Tamamushi and N. Tanaka, *Z. physik. Chem. N. F.*, **21**, 89 (1959); **28**, 158 (1961).

7) N. Tanaka, K. Ebata and G. Satô, This Bulletin, **36**, 912 (1963).

8) A. Werner, W. J. Bowis, A. Hoblik, H. Schwarz and H. Surker, *Ann.*, **406**, 261 (1914).

9) A. Rosenheim, *Z. anorg. Chem.*, **11**, 196, 225 (1892).

removed by decantation and pH of the solution was adjusted to about 7.0 by adding hydrochloric acid. Redistilled water was used to prepare the cell solution.

Results

The current-potential curves of *cis*-dioxalatodiaquochromate(III) and trioxalatochromate(III) ions were obtained in the solutions of various supporting electrolytes and at various concentrations of the electrolytes in the presence of 0.005% gelatin added as a maximum suppressor. The typical current-potential curves of *cis*-dioxalatodiaquochromate(III) ions are given in Figs. 1 and 2. Figure 1 shows the current-potential curves obtained in the solutions of univalent electrolytes.

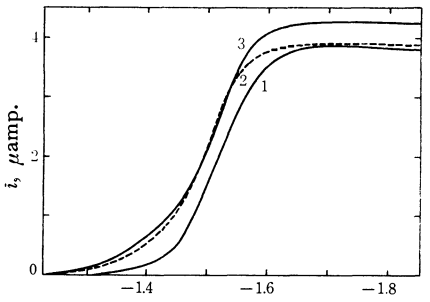

Fig. 1. Current-potential curves of 0.5 mM *cis*-dioxalatodiaquochromate(III) ions in the univalent electrolyte solutions containing 0.005% gelatin: (1) 1.0 M LiCl, (2) 1.0 M NaCl, (3) 1.0 M KCl.

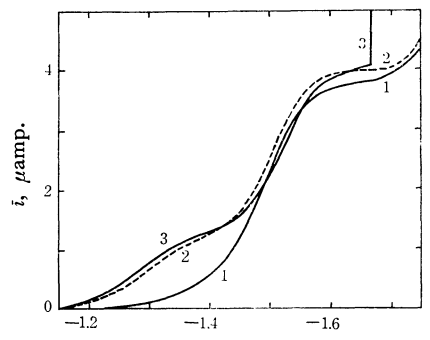

Fig. 2. Current-potential curves of 0.5 mM *cis*-dioxalatodiaquochromate(III) ions in the bivalent electrolyte solutions containing 0.005% gelatin: (1) 0.5 M $MgCl_2$, (2) 0.5 M $SrCl_2$, (3) 0.5 M $BaCl_2$.

The limiting current was found to be diffusion-controlled and proportional to the concentration of the complex ions. The current-potential curves obtained in the bivalent electrolyte solutions are reproduced in Fig. 2. In a solution of strontium chloride or barium chloride, especially, the wave was found to split into two steps; the first wave was observed in the potential range from −1.2 to −1.45 V. vs. SCE, which was not observed in the univalent electrolyte solutions. The limiting currents of both the first and the second wave are diffusion-controlled and proportional to the concentration of the complex ions. The gradual increase in the current was observed in the bivalent electrolyte solutions at more negative potentials than −1.75 V. vs. SCE. A maximum was observed at the potentials of the limiting current plateau when the measurement was made in a barium chloride solution, and the height of the maximum increases with increasing concentrations of barium chloride. The maximum was not suppressed by the addition of relatively high concentrations of gelatin, but suppressed by the addition of a small amount of hydrogen ion.

The diffusion current constants and the reduction potentials at $\bar{i}=\bar{i}_l/6$ and $\bar{i}=2\bar{i}_l/3$ on the reduction of *cis*-dioxalatodiaquochromate(III) ions which were obtained in the solutions of various electrolytes and at various concentrations of the electrolytes in the presence of 0.005% gelatin are given in Table I. The half-wave potential was not used because of the irregular shapes of the waves.

Table I. Diffusion current constants and reduction potentials oe *cis*-dioxalatodiaquochromate(III) ions obtained in various electrolyte solutions containing 0.005% gelatin

Electrolyte soluiton	$I_{obs.}$*	$I_{corr.}$*	$E_{1/6}$** V. vs. SCE	$E_{2/3}$** V. vs. SCE
1.0 M LiCl	4.26	4.47	−1.46	−1.54
1.0 M NaCl	4.24	4.41	−1.41	−1.52
0.1 M KCl	4.30	4.30	−1.47	−1.55
0.5 M KCl	4.58	4.59	−1.44	−1.53
1.0 M KCl	4.61	4.60	-1.40_5	−1.52
2.0 M KCl	4.58	4.58	−1.38	−1.53
0.5 M $MgCl_2$	4.15	4.55	−1.41	−1.51
0.1 M $SrCl_2$	4.63	4.68	−1.35	−1.51
0.3 M $SrCl_2$	4.48	4.66	−1.32	−1.51
0.5 M $SrCl_2$	4.37	4.63	−1.30	−1.51
0.5 M $BaCl_2$	4.35	4.61	−1.29	−1.52

* $I_{obs.}$ and $I_{corr.}$ represent the obserbed diffusion current constant and the diffusion current constant corrected for the relative viscosity of the electrolyte solutions, respectively.

** $E_{1/6}$ and $E_{2/3}$ represent the reduction potentials at $\bar{i}=\bar{i}_l/6$ and $\bar{i}=2\bar{i}_l/3$, respectively.

Figure 3 shows the current-potential curves of trioxalatochromate(III) ions obtained in 1.0 M solutions of univalent electrolytes containing 0.005 % gelatin. The typical current-potential curves obtained in 1.0 M solutions of bivalent electrolytes containing 0.005% gelatin are reproduced in Fig. 4.

The limiting current was found to be diffusion-controlled and proportional to the concentration of trioxalatochromate(III) ions. The overall

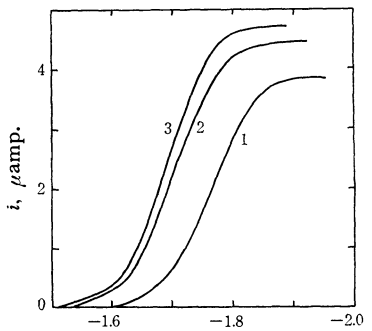

Fig. 3. Current-potential curves of 0.5 mM trioxalatochromate(III) ions in the univalent electrolyte solutions containing 0.005% gelatin: (1) 1.0 M LiCl, (2) 1.0 M NaCl, (3) 1.0 M KCl.

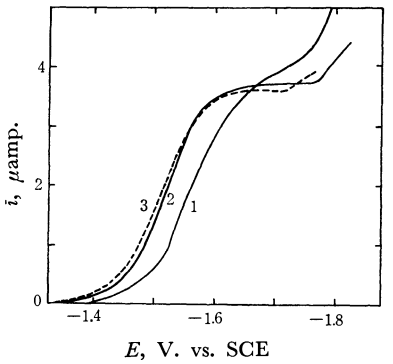

Fig. 4. Current-potential curves of 0.5 mM trioxalatochromate(III) ions in the bivalent electrolyte solutions containing 0.005% gelatin: (1) 1.0 M $MgCl_2$, (2) 1.0 M $SrCl_2$, (3) 1.0 M $BaCl_2$.

TABLE II. DIFFUSION CURRENT CONSTANTS AND HALF-WAVE POTENTIALS OF TRIOXALATOCHROMATE(III) IONS OBTAINED IN VARIOUS ELECTROLYTE SOLUTIONS CONTAINING 0.005% GELATIN

Electrolyte solution	$I_{obs.}$	$I_{corr.}$	$E_{1/2}$ V. vs. SCE	Reciprocal slope of log-plot, mV.
1.0 M LiCl	4.34	4.48	−1.76	85
1.0 M NaCl	4.93	5.16	−1.70	85
0.1 M KCl	4.97	4.97	−1.83	90
0.3 M KCl	5.07	5.07	−1.76	87
1.0 M KCl	5.19	5.17	-1.68_5	85
3.0 M KCl	5.07	5.14	−1.64	80
1.0 M $MgCl_2$	4.25	4.80	−1.56	—
1.0 M $SrCl_2$	4.11	4.59	-1.51_5	75
0.1 M $BaCl_2$	4.69	4.73	−1.55	70
0.3 M $BaCl_2$	4.42	4.57	−1.53	69
1.0 M $BaCl_2$	4.04	4.56	-1.50_5	72

electrode process was considered to be of a three-electron reduction of chromium(III) to chromium(0), being compared with the reduction wave of *cis*-dioxalatodiaquochromate(III) ions previously reported.[1] The relation between E and $\log \bar{i}/(\bar{i}_l - \bar{i})$, Kalousek polarograms and a. c. polarograms indicated the electrode processes of trioxalatochromate(III) ions to be irreversible.

Table II shows the diffusion current constants, the half-wave potentials and the reciprocal slopes of log-plots obtained in the solutions of various supporting electrolytes and at various concentrations of the electrolytes.

Discussion

The polarographic reduction of *cis*-dioxalatodiaquochromate(III) and trioxalatochromate(III) ions was affected by the nature and the concentration of the cation of electrolyte present in the solution.

The reduction of *cis*-dioxalatodiaquochromate(III) ions at the DME in the solutions of univalent electrolytes proceeds irreversibly according to the equation,

$$cis\text{-}[Cr(ox)_2(H_2O)_2]^- + 3e \rightarrow Cr(0) + 2\,ox^{2-} + 2H_2O$$

In the solutions of bivalent electrolytes, on the other hand, two waves are observed as mentioned above. The electrode processes of these waves are considered as follows:

The first wave is of a one-electron reduction corresponding to the reaction,

$$cis\text{-}[Cr(ox)_2(H_2O)_2]^- + 2pH_2O + e \rightarrow [Cr(ox)_{2-p}(H_2O)_{2p+2}]^{(2-2p)-} + p\,ox^{2-}$$

The second wave is of a two-electron reduction, which proceeds as,

$$cis\text{-}[Cr(ox)_{2-p}(H_2O)_{2p+2}]^{(2-2p)-} + 2e \rightarrow Cr(0) + (2-p)ox^{2-} + (2p+2)H_2O$$

In the case of trioxalatochromate(III) ions, an irreversible wave corresponding to the reduction from chromium(III) to chromium(0) was found to appear at more negative potentials than those of *cis*-dioxalatodiaquochromate(III) ions in the solutions of both univalent and bivalent electrolytes. The result seems to contradict the result obtained by Pamfilov and his co-workers.[4]

The shifts of the reduction potential and the changes in the diffusion current constants given in Tables I and II indicate that the effect of the cations of electrolytes on the reduction potentials increases with the increase in the ionic charge, and at constant ionic charge, with the increase in the radius of the hydrated cation and the increase in the concentration of the electrolytes present in the solution. These facts may be explained by taking into account of both the structure of the

electrical double layer and the formation of ion-pairs.[10-12]

Since both *cis*-dioxalatodiaquochromate(III) and trioxalatochromate(III) ions are reduced at the negative side of electrocapillary maximum, the reduction of these complex anions are more difficult at lower concentrations of electrolytes because of greater electrostatic repulsion between the electrode surface and the electroactive complex anions. Trioxalatochromate(III) ions gave actually no reduction wave at lower concentrations of the univalent electrolytes in the solution.

If the potential difference across the diffuse double layer is decreased with increasing concentrations of electrolyte or by changing the nature of the cation of electrolyte, the electrostatic repulsion, which hinders the approach of the electroactive complex anions to the electrode surface, decreases so that the surface concentration of the complex anions increases. This and an increase in the effective potential difference in the Helmholtz double layer facilitate the reduction of the complex anions, as pointed out by Vlček[13] on the reduction of hexacyanocobaltate(III) ions. He reported that the reduction potential of hexacyanocobaltate(III) ions at the DME shifted to less negative potentials with increasing concentrations of potassium chloride and increasing radii of the univalent cation in the solution.

The shifts of the half-wave potential, $\Delta E_{1/2}$, with the change in the concentration of electrolyte is approximately given by the relationship,[14,15]

$$\Delta E_{1/2}=\frac{\alpha n_a - z_O}{\alpha n_a}\Delta(\phi_H-\phi_S)_{1/2} \qquad (1)$$

where α is the transfer coefficient, n_a the number of electron involved in the electron-transfer process, z_o the valency, with sign, of the reducible species and $\Delta(\phi_H-\phi_S)_{1/2}$ the change in the potential difference across the diffuse double layer at the half-wave potential of the reduction wave.

The relation between the electrode potential, E, and the value of $(\phi_H-\phi_S)$ can be calculated on the basis of the classical Gouy-Chapmann theory for the z-z type electrolyte,

$$K_i[(E-E_z)-(\phi_H-\phi_S)]=\left(\frac{2\boldsymbol{R}T\varepsilon C_t}{\pi}\right)^{1/2}\sinh\left\{\frac{|z|\boldsymbol{F}(\phi_H-\phi_S)}{2\boldsymbol{R}T}\right\} \qquad (2)$$

where K_i is the integral capacity of the Helmholtz double layer, E_z the potential at zero charge of the electrode, ε the dielectric constant, C_t the bulk concentration of ions with valence z.

In the calculation of Eq. 2, E_z and K_i which were determined from the electrocapillary curve and the capacitance measurements, respectively. The value of αn_a in Eq. 1 was obtained from the plot of E vs. $\log \bar{i}/(\bar{i}_d-\bar{i})$. The values of E_z and K_i obtained at varied concentrations of potassium chloride are given in Table III.

Table III. The potential of zero charge of the electrode (E_z) and the integral capacity in the Helmholtz double layer (K_i) obtained at varied concentrations of potassium chloride

Concn. of KCl in the solution* M	E_z V. vs. SCE	K_i μF/cm^2
0.1	-0.510	16.7_4
0.3	-0.51_5	18.0_5
1.0	-0.52_0	19.3_3
2.0	-0.55_0	20.4_8
3.0	-0.60_0	20.7_5

* All solutions contain 0.005% gelatin.

Equation 1 was not able to apply to the electrode process of *cis*-dioxalatodiaquochromate(III) ions because no straight line was obtained in the log-plot analysis.

The experimental and the calculated values for the shift of the half-wave potential on the reduction of 0.5 mM trioxalatochromate(III) ions with varied amounts of potassium chloride are given in Table IV. The calculation was made with three different values of the valency of the complex anion participating in the electron-transfer process. Table IV shows that the experimental shifts of the half-wave potential agree to the calculated ones which were obtained with $z_O=-1$. This suggests that the species which is involved in the electron-transfer process is probably a $K_2[Cr(ox)_3]^-$ ion.

The concentration of the species, $K_2[Cr(ox)_3]^-$, in the bulk of the solution is estimated to be much smaller than that of the species, $K[Cr(ox)_3]^{2-}$, from the calculation with the association constants of these ion-pairs. Consequently, it is presumed that the species, $K_2[Cr(ox)_3]^-$ is present predominantly only at the electrode surface, and that one of the potassium ions of $K_2[Cr(ox)_3]^-$ plays a role of bridging the electrode surface and the electroactive species at the electron-transfer process. The formation of ion-pairs lessens the ionic charge of trioxalatochromate(III) ions, so that it facilitates their approach to the electrode surface. The electrode process for the reduction of trioxalatochromate(III) ions, therefore, may be written as follows:

10) P. Delahay and A. Aramata, *J. Phys. Chem.*, **66**, 1194 (1962).
11) L. Gierst, "Transactions of the Symposium on the Electrode Processes," Ed. by E. Yeager, John Wiley & Sons, Inc., N. Y. (1961), p. 109.
12) A. N. Frumkin and N. Nikolaeva-Fedrovich, "Progress in Polarography," Vol. 1, Ed. by P. Zuman and I. M. Kolthoff, Interscience Publishers, N. Y. (1962), p. 223.
13) A. A. Vlček, "Progress in Inorganic Chemistry, Vol. 5, Ed. by F. A. Cotton, Interscience Publishers, N. Y. (1963), p. 211.
14) M. Breiter, M. Kleinerman and P. Delahay, *J. Am. Chem. Soc.*, **80**, 5111 (1958).
15) P. Delahay, "Progress in Polarography," Vol. 1, Ed. by P. Zuman and I. M. Kolthoff, Interscience Publishers, N. Y. (1962), p. 43.

Table IV. Experimental and calculated shifts of the half-wave potential for the reduction of 0.5 mM trioxalatochromate(III) ions in the solutions of various concentrations of potassium chloride containing 0.005% gelatin

Concn. of KCl, M	$E_{1/2}$ V. vs. SCE	$\Delta E_{1/2obs.}$ V.	$(\phi_H - \phi_S)_{1/2}$ V.	$\Delta E_{1/2calc.}$, V.		
				$z_O = -3$	$z_O = -2$	$z_O = -1$
0.1	−1.83	—	-0.12_2	—	—	—
0.3	−1.76	0.07	-0.09_7	0.13_3	0.09_7	0.06_1
0.5	−1.73	0.10	-0.08_6	0.19_2	0.14_0	0.08_8
1.0	-1.68_5	0.14_5	-0.06_8	0.28_7	0.20_9	0.13_1
2.0	−1.65	0.18	-0.05_5	0.35_6	0.25_9	0.16_3
3.0	−1.64	0.19	-0.04_5	0.40_9	0.29_8	0.18_3

$$K[Cr(ox)_3]^{2-} + K^+ \rightleftarrows K_2[Cr(ox)_3]^-$$

$$K_2[Cr(ox)_3]^- + 3e \longrightarrow Cr(0) + 3ox^{2-} + 2K^+$$

In conclusion, it may be said that the reduction processes of *cis*-dioxalatodiaquochromate(III) and trioxalatochromate(III) ions depend on the nature and the concentration of the cation of the electrolyte in the solution and that this cation effect may be understood by the consideration of the formation of ion-pairs as well as the change in the electrical double layer.

The authors wish to thank the Ministry of Education for the financial support granted for this research.

BULLETIN OF THE CHEMICAL SOCIETY OF JAPAN VOL. 39 776—778 (1966)

The Rheological Behavior of Suspensions of Ion-exchange Resin Particles

By Manabu SENŌ and Takeo YAMABE

The Institute of Industrial Science, The University of Tokyo, Azabu, Tokyo

(Received September 6, 1965)

The flow properties of the suspensions of ion-exchange resin particles, the highly-crosslinked polyelectrolyte gel particles, were examined, especially in relation to their charged state. The steady viscosities and the dynamic viscoelasticities of these suspensions were measured, and the results were interpreted in terms of the dispersion state of the suspended particles. The flow system of the highly-charged particles, such as Na-form resin particles, exhibits a high viscoelasticity and is in a well-dispersed state. On the contrary, the flow system of the lower-charged particles, such as Ba-form particles, is not viscoelastic, but viscous and dilatant. This behavior may be attributed to the variation in the electrical double layers around the suspended particles.

Ion-exchange resin particles are excellent model substances of the colloidal system for investigating its behavior in relation to the structure, because they have a well-defined polyelectrolyte structure and vary in the surface state according to the kind of counter-ions in their fixed dissociation groups. We have previously investigated the aggregation behavior of these particles[1] and measured their electro-kinematic potential.[2] As one extention of these investigations, we will now report on the rheological behavior of a suspension of these particles. This investigation will reveal how the rheological behavior of the suspension is affected by the charged state of the suspended particles.

1) M. Senō and T. Yamabe, This Bulletin, **34**, 1002 (1961).
2) M. Senō and T. Yamabe, *Nature*, **202**, 1110 (1964).

Experimental

The ion-exchange resin particles used were composed of Amberlite resin (Rohm & Haas), IR-120. This is a strongly-dissociated cation-exchange resin which had been prepared from polystyrene sulfonic acid crosslinked with divinylbenzene. The resin particles from commercial sources were ground in a wet state in a ball mill and sieved in water. The part which

TABLE I. THE CHARACTERIZATION OF SAMPLES OF SUSPENDING PARTICLES, AMBERLITE IR-120

Ionic form	Real density g./cm^3	Water content %	Apparent density g./cm^3
H	1.55	48.4	1.22
Na	1.64	46.2	1.26
Ca	1.60	42.8	1.27
Ba	1.88	36.3	1.56

had settled after 1—10 hr. was collected and washed thoroughly after conditioning; from this part the sample in various ionic forms was prepared. The ionic forms were the H–, Na–, Ca, and Ba–form. They are 2—20μ in size; their water contents and real densities were as shown in Table I.

The viscosity of the dilute suspensions was measured with an Ostwald-type capillary viscometer. The viscosity and the dynamic visco elasticity were measured with a rotational viscometer (McMichael type) and with a rheometer which was described in a preceding paper.[3]

Results and Discussion

The viscosities of the ion-exchange resin particle suspension in the range of relatively small concentrations are shown in Fig. 1 as a function of the volume fraction of particles. The rate of the increase in the viscosity with the increasing concentration is larger in the order; H->Na->Ca->Ba-form. The relationship between the relative viscosity and the volume fraction is ruled regularly by the following equation, proposed by Asbeck et al.[4]:

$$\ln \eta_{rel} = \frac{K\varphi}{\varphi_c - \varphi}$$

The linear relation of $1/\log \eta_{rel}$ and $1/\varphi$ is shown in Fig. 2, from which the parameters, K and φ_c, are obtained. The former is a shape factor, while the latter is a crowding factor which represents the extent of the packing of suspended particles or that of the immobilization of the dispersing media.[5] The results are shown in Table II.

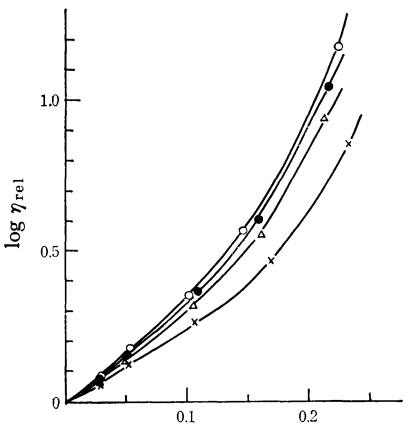

Fig. 1. Viscometric behavior of suspensions of ion-exchange resin particles.
○ H-form particles
● Na-form particles
△ Ca-form particles
× Ba-form particles

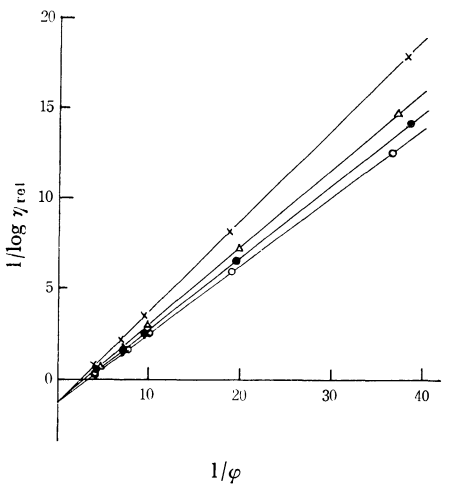

Fig. 2. Plots of $1/\log \eta_{rel}$ vs. $1/\varphi$. Symbols are the same as in Fig. 1.

From this table, the following important finding is derived. The shape factor, K, is identical for all suspensions, independently of their ionic forms, and approximately equals 2.5, which is the value for the spherical particles. On the contrary, the crowding factor, φ_c, is greatly dependent on the ionic forms of the suspending particles. This value is 0.502 for the Ba-form, which is the value for the cubic packing, the loosest closed-packing. The values for the other ionic forms are smaller than that for the Ba-form. This indicates either that these suspensions are in the looser packing state, or that the suspending medium is immobilized by the particles to a greater extent.

Table II. The analysis of the relation of viscosity and concentration by the equation $\ln \eta_{rel} = K\varphi/(\varphi_c - \varphi)$

Ionic form	K	φ_c
H	2.56	0.377
Na	2.56	0.391
Ca	2.56	0.427
Ba	2.56	0.502

This finding may be interpreted reasonably. For the sulfonate group, hydrogen and sodium ions are highly dissociated counterions, calcium ions are hardly dissociated, and barium ions are undissociated. The order of the degree of dissociation is in accordance with that of the interfacial electro-kinematic potential of the particles. That is, the ion-exchange resin particles of highly-dissociated counterions are accompanied by a highly-extended interfacial electrical double-layer. The same particles with a well-established electrical double-layer do not approach nearer to each other, since the electrical repulsion force is exerted between the double-layers with charges of the same sign. Therefore, such a suspending particle takes a loose packing state, accompanied

3) T. Nakagawa and M. Senō, This Bulletin, **29**, 471 (1956).

4) W. K. Asbeck and G. A. Scherer, *Ind. Eng. Chem.*, **47**, 1472 (1955).

5) J. Robinson, *J. Phys. & Colloid Chem.*, **53**, 1042 (1949); M. Mooney, *J. Colloid Sci.*, **6**, 162 (1951).

by the immobilization of the suspending medium.

The rheological properties of the suspension exhibit a more characteristic feature in the higher concentration region according to the variation in the charged state of the particles. One of the results is provided by the measurements using the rheometer of the forced-oscillation type. The coefficients of the dynamic viscoelasticity are given in Table III. The suspensions in which the particles have highly-dissociated counter-ions show large values of the dynamic viscosity and rigidity, and the suspension of the undissociated barium-ion form particles is nearly viscous. This establishes that the viscoelasticity of this suspension

TABLE III. THE DYNAMIC VISCOSITY AND RIGIDITY OF THE CONCENTRATED SUSPENSIONS
(30°C and 30—35 sec./cycle)

Ionic form	Volume fraction of particles	Dynamic viscosity poise	Dynamic rigidity dyn./cm^2
H	0.291	25.06	8.23
Na	0.295	9.91	3.70
Ca	0.304	3.06	0.44
Ba	0.328	0.76	0.09

results from the repulsion forces between the double-layers established around the suspending particles. The same has been proposed by Bolt.[6]

Another characteristic of the concentrated suspensions is revealed by the observation on the dilatancy behavior. It was clearly observed that the dilatancy of the suspensions the suspending particles of which have more undissociated counter-ions is more remarkable. Although no exact method for the estimation of the dilatancy has yet been established, an estimate is provided by the measurements using a rotational viscometer. The results are shown in Fig. 3.

TABLE IV. THE PROPERTIES OF THE SUSPENSIONS OF ION-EXCHANGE RESIN PARTICLES

Ionic form	Concentration range of characteristic flow	Characteri-zation	Volume fraction at settling
H	0.26~0.295	Viscoelastic	0.295
Na	0.27~0.30	Viscoelastic	0.302
Ca	0.27~0.31	Viscoelastic	0.315
Ba	0.28~0.33	Dilatant-viscous	0.394

No anomalous behavior is detected in the suspensions of H–, Na–, and Ca–form particles in the region of the measuring conditions, but, for the suspension of the Ba-form particles, an abrupt increase in the viscosity is observed, accompanied by the occurence of a turbulent flow, over the radial viscosity of 7.2 sec^{-1}. This value corresponds to values of 1.80 sec^{-1} for the rate of shear and of 3.0 for the Reynolds number. The latter is very small compared to the critical Reynolds number (about 1200—2000); therefore, it may be said that this suspension exhibits the anomalous turbulent flow which occurs at a very small Reynolds number. However, no exact interpretation of the relation of the dilatancy and the anomalous turbulent flow has yet been established, altough their intimate relation is recognized.[7] This suggests that the interfacial electrical double-layer reduces the friction between the particles as a result of the repulsive interaction of the double-layers, and that the Ba-form particle suspension, of which the double-layers are infant, is dilatant, while the H- and Na-form particle suspensions, the double-layers of which are well-established, are not dilatant. These characteristics are summarized in Table IV.

The suspensions of H- and Na-form particles are viscoelastic, the suspension of Ba-form particles is dilatant-viscous, and the suspension of Ca-form particles is intermediate in nature, in the characteristic concentration range covered in Table IV. In the lower concentration range, all the suspensions are purely viscous, while in the higher concentration range they are powdery solids.

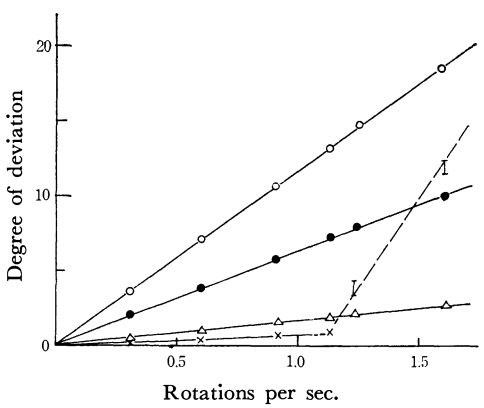

Fig. 3. Measurements using a rotational viscometer. Symbols are the same as in Fig. 1.

Table IV also shows the concentration of the sedimentation state of these suspensions. It is clear that the dispersed system with the lower-charged particles is in the more compact state at the settling; this accords with the generally accepted concept.

6) G. H. Bolt, *Geotechnique*, 6, (6) (1956).

7) G. V. Vinogradov, A. Ya. Malkin and A. I. Leonov, *Koll.-Z.*, **191**, 25 (1963).

BULLETIN OF THE CHEMICAL SOCIETY OF JAPAN VOL. 39 779—784 (1966)

The Automatic Measurement of the Ohmic and Capacitive Components of the Impedance on a Platinum Electrode in Transient States

By Shigeo SHIBATA

Department of Chemistry, Faculty of Liberal Arts and Science, Yamagata University, Koshirakawa-cho, Yamagata

(Received September 6, 1965)

A new technique with an electronic circuit is described in which the ohmic and the capacitive components of the impedance of the electrode-solution interface may be registered simultaneously and continuously as a function of the time at a given frequency during polarization with a constant anodic or cathodic current. Impedance measurements were made on a smooth platinum in 2 N perchloric acid, 2 N sodium perchlorate and 2 N sodium hydroxide solutions in the region of oxygen deposition. According to the observed behavior of the impedance of the electrode, the oxide film on the electrode surface may be completed anodically through three stages; first, the adsorption of the hydroxyl radical; second, the formation of oxide (II), and finally, the conversion of this oxide to one of a higher grade. The dependence of the value of the electrode capacity at the first stage on the pH of the solution is discussed on the basis of the ion-exchange adsorption of cations and anions on the electrode surface covered by the hydroxyl radicals.

Much effort has been expended in the past on the study of platinum surface oxidation.[1-26] A chief concern of early investigations was the nature and the extent of surface coverage with oxygen species under a variety of conditions and using a variety of techniques. Early conclusions were based largely on the shape of the charging curve and on the value of the transition time between the onset of surface oxidation and the oxygen evolution.[10-26]

Measurements of the impedance of the electrode-solution interface yield information on the structure of the interface and on the kinetics of electrode reaction.[27-33] Therefore, it is useful in making clear the mechanism of the surface oxidation to measure the impedance change of the electrode during the anodic polarization.

Many methods for the quick measurement of the impedance have been reported.[34-40] All of them, however, appear to suffer from certain disadvantages for the continuous measurement of the impedance, which changes with time. Recently, a new technique has been described by Breiter,[41] in which the impedance of the electrode-solution interface may be obtained as a function of the potential during the anodic and the cathodic sweep of the electrode potential, which changes linearly with time. Baddy and Sundburg[42] and Krischer and Osteryoung[43] have also developed

1) I. M. Kolthoff and N. Tanaka, *Anal. Chem.*, **26**, 623 (1954).
2) F. C. Anson and J. J. Lingane, *J. Am. Chem. Soc.*, **79**, 4901 (1957).
3) F. G. Will and C. A. Knorr, *Z. Elektrochem.*, **64**, 258 (1960).
4) W. Böld and M. Breiter, *Electrochim. Acta*, **5**, 145 (1961).
5) A. Kozawa, This Bulletin, **35**, 1051 (1962).
6) A. Kozawa, *J. Electrochem. Soc. Japan (Denki Kagaku)*, **30**, 720 (1962); **31**, 183, 315, 618 (1963).
7) E. Lange, *Z. phys. Chem.*, **226**, 209 (1964).
8) W. Visscher and M. A. V. Devanathan, *J. Electroanal. Chem.*, **8**, 127 (1964).
9) R. L. Every and R. L. Grimsley, ibid., **9**, 165 (1965).
10) F. P. Bowden, *Proc. Roy. Soc.*, **A125**, 446 (1929).
11) J. A. V. Butler and G. Armstrong, *J. Chem. Soc.*, **1934**, 743.
12) J. A. V. Butler and G. Armstrong, *Proc. Roy. Soc.*, **A137**, 605 (1932).
13) A. L. Ferguson and M. B. Towns, *Trans. Electrochem. Soc.*, **83**, 271, 285 (1943).
14) A. Hickling, *Trans. Faraday Soc.*, **41**, 333 (1945).
15) B. V. Ershler, *Discussions Faraday Soc.*, **1**, 269 (1947).
16) A. Hickling and W. H. Wilson, *J. Electrochem. Soc.*, **98**, 425 (1951).
17) S. E. S. Wakked and S. H. Emara, *J. Chem. Soc.*, **1951**, 461.
18) M. Breiter, C. A. Knorr and W. Volkl, *Z. Elektrochem.*, **59**, 681 (1955).
19) M. Becker and M. Breiter, ibid., **60**, 1080 (1956).
20) G. Radlein, ibid., **61**, 727 (1957).
21) K. J. Vetter and D. Berndt, ibid., **62**, 378 (1958).
22) J. Giner, ibid., **63**, 386 (1959).
23) J. Giner, ibid., **64**, 491 (1960).
24) H. A. Latinen and C. G. Enke, *J. Electrochem. Soc.*, **107**, 773 (1960).
25) S. W. Ferdberg, C. G. Enke and C. E. Briker, ibid., **110** 826 (1963).
26) J. S. Mayell and S. H. Langer, ibid., **111**, 438 (1964).
27) C. Falk and E. Lange, *Z. Elektrochem.*, **54**, 132 (1950).
28) H. Gerischer, *Z. phys. Chem.*, **198**, 286 (1951); **201**, 55 (1952).
29) D. C. Graham, *J. Electrochem. Soc.*, **99**, 370 (1952).
30) W. Lorenz, *Z. phys. Chem., N. F.*, **19**, 377 (1959).
31) J. Llopis, J. Fernandez-Biarge and M. P. Fernandez, *Electrochim. Acta*, **1**, 130 (1959).
32) K. Franke, C. A. Knorr and M. Breiter, *Z. Elektrochem.*, **63**, 226 (1959).
33) R. G. Hoey and M. Cohen, *J. Electrochem. Soc.*, **106**, 776 (1959).
34) J. E. B. Randles, *Discussions Faraday Soc.*, **1**, 11 (1947).
35) B. Breyer and F. Gutman, ibid., **1**, 19 (1947).
36) M. Breiter, H. Kammermaier and C. A. Knorr, *Z. Elektrochem.*, **60**, 37 (1956).
37) H. H. Bauer, *Anal. Chem.*, **30**, 334 (1958).
38) B. D. Cahan and P. Rüetschi, *J. Electrochem. Soc.*, **106**, 543 (1959).
39) J. S. Rivey, G. M. Schmid and N. Hackerman, *Rev. Scientific Instruments*, **32**, 588 (1961).
40) S. Schuldiner and R. M. Roe, *J. Electrochem. Soc.*, **110**, 332 (1963).
41) M. W. Breiter, *J. Electroanal. Chem.*, **7**, 38 (1964).
42) P. J. Boddy and W. J. Sundburg, *J. Electrochem. Soc.*, **110**, 1170 (1963).
43) C. C. Krischer and R. A. Osteryoung, ibid., **112**, 735 (1965).

methods for measuring the capacity continuously and rapidly.

A technique in which both the ohmic and the capacitive components of the impedance as a function of time during the galvanostatic polarization can be registered immediately and simultaneously on a suitable recorder has been developed and will be reported on this paper.

The technique will be applied to the determination of the impedance of a bright platinum electrode in the region of oxygen deposition in acid, neutral and alkaline solutions.

Principle of the Method

The impedance of the electrode-solution interface may be regarded as equivalent to a resistance, R_s, and a capacitacne, C_s, in series governed by the relation;

$$Z = R_s + 1/jwC_s \tag{1}$$

where Z is the impedance of the circuit. The a. c. current, i, passed through the circuit and the voltage drop, e, across a and b in Fig. 1 are represented as follows:

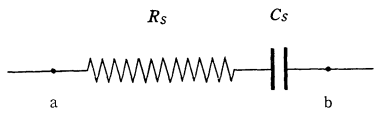

Fig. 1. Equivalent circuit of the electrode.

$$i = I\sin(\omega t+\theta) \tag{2}$$

$$e = E\sin\omega t \tag{3}$$

where I and E are the maximum values of the current and the voltage of the a. c. respectively; ω is the angular frequency, and θ, the phase difference between the current and the voltage. The values of the resistance and the capacitive reactance can be calculated by the following equations:

$$R_s = |Z|\cos\theta = |Z|\sin(\pi/2-\theta) \tag{4}$$

$$1/\omega C_s = |Z|\sin\theta \tag{5}$$

where $|Z|$ is the absolute value of the impedance. If the intensity of the current passed through the circuit is constant, the value of the potential drop, E, is proportional to the magnitude of $|Z|$. Consequently,

$$R_s \sim E\sin(\pi/2-\theta) \tag{6}$$

$$1/\omega C_s \sim E\sin\theta = E\sin(\pi-\theta) \tag{7}$$

The values of R_s and $1/\omega C_s$ are proportional to the instantaneous value of e at the times of $\omega t = \pi/2-\theta$ and $\pi-\theta$ respectively.

In measuring the value of the ohmic component, R_s, the phase of the current, i, was first shifted by $\pi/2$, as is shown in Fig. 2. The a. c. thus shifted is converted to a square-wave current and differentiated in order to make pulses. The sine wave voltage, e, from the cell is sampled with these positive pulses, which are generated at $\omega t = \pi/2-\theta$ in every half cycle. The peak voltage of the pulses thus sampled is proportional to the value of R_s. The value of the capacitive component, $1/\omega C_s$, can be obtained by sampling the value of e with pulses which are generated at $\omega t = \pi-\theta$, as is shown in Fig. 2.

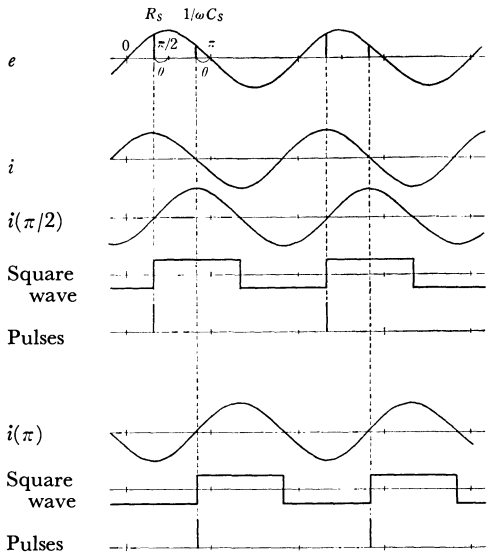

Fig. 2. Principle of the impedance measurement by sampling the signal, e, from the cell with pulses.

Apparatus

The measurements were carried out with an electronic circuit which was designed on the basis of a principle described earlier and constructed in this laboratory. A block diagram of the impedance meter is shown in Fig. 3. For the measurement of R_s, the signal of a given constant frequency from an oscillator is fed through a cathode-follower amplifier to the phase shifter, in which the phase of the signal is shifted by exactly $\pi/2$. The signal from this shifter is then converted with a Schmitt trigger circuit to square-wave a. c. with the same phase and frequency as the input sine wave signal. The rise time in the square wave a. c. was 0.2 μsec. The square wave is differentiated with a resistor and a capacitor in series, and the pulses thus obtained are rectified with a germanium diode. The signal, e, from the cell is sampled with these pulses using a vacuum tube, 6AS6, which has two separate control grids. The signal, e, is fed to one of these grids, while the vacuum tube is gated by the pulses introduced into the other grid. The peak voltage of the pulses from the sampler is proportional to the value of R_s. The

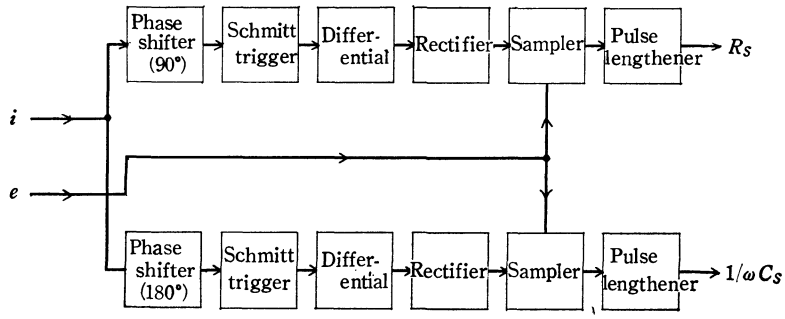

Fig. 3. Block diagram of the impedance measurement.

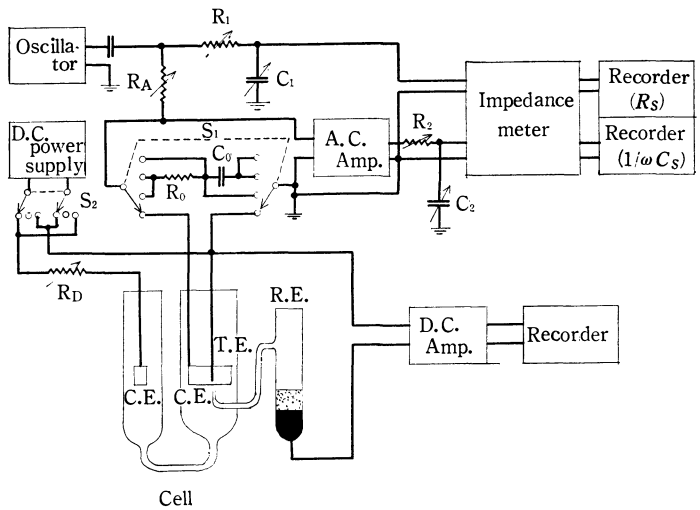

Fig. 4. Circuit diagram.

T. E., test electrode. C. E., counter electrode. R. E., reference electrode.

width of the pulses is broadened and made smooth through a pulse lengthener, because the width of the original pulse is so narrow that the direct measurement of its peak voltage is impossible with a usual recorder. The smoothed signal is amplified with a differential amplifier and then introduced to a pen recorder.

In order to measure the capacitive component, $1/\omega C_s$, the signal from the oscillator is fed, after its phase has shifted by π, to the square-wave converter. The subsequent electronical treatment of the signal is quite similar to that for the measurement of the ohmic component described above. The values of R_s and $1/\omega C_s$ as a function of the time are registered continuously and simultaneously on one chart of a two-pen recorder.

Procedure

A simplified schematic diagram of the measurement circuit is shown in Fig. 4. A constant a. c. of a small amplitude which is controlled by a variable resistor, R_A, in series with the cell was superimposed on the constant d. c. The output voltage from the oscillator was 20 V. p-p, while the d. c. voltage from the regulated power supply was 135 V. The intensity of the a. c. passed through the cell was so adjusted that the amplitude of the polarization voltage of the electrode resulting from its a. c. was below 2 mV. The a. c. signal from the cell was amplified with a high-gain a. c. amplifier and then introduced into the impedance meter. The phase of the a. c. signal was shifted through the a. c. amplifier; this is because of the small time constant or the stray inductance of the amplifier. In order to correct this phase shift, the cell in the measuring circuit was replaced with a noninductive standard resistor, and the variable resistor and capacitor, R_1, and C_1, or R_2 and C_2, were so adjusted that the difference in phase between the input signals of i and of e into the impedance meter was eliminated. The elimination of this phase difference was then checked by means of cathode-ray oscilloscopic observation. The impedance meter was calibrated with standard resistors, R_0, and capacitors, C_0, in series. When the applicability of the indicator was checked in the frequency range from 20 to

20000 c. p. s., the accuracy of the indicator was found to be ±2%.

The d. c. potential of the electrode was referred to a 1 N sulfuric acid - mercurous sulfate - mercury electrode for acid electrolytes or to a saturated calomel electrode for neutral and alkaline electrolytes. The values of the potential described in this paper are referred to the standard hydrogen scale. The stop-cock separating the reference electrode from the Luggin capillary was kept close in order to prevent any appreciable diffusion of the electrolyte of the reference electrode to the test electrode. Charging curves with the d. c. were registered by another pen recorder through a d. c. amplifier of a high-input impedance at the same time as the impedance measurement.

Experimental

The conductivity water was prepared by redistilling laboratory-distilled water from an alkaline permanganate solution in a Pyrex still, followed by triple redistillation with a quartz still. The electrolyte solutions used were 2 N perchloric acid, 2 N sodium perchlorate and 2 N sodium hydroxide solutions, all of which were prepared from guaranteed-grade reagents by appropriate dilution with the conductivity water. The electrolyte solutions were freed from dissolved oxygen by passing pure nitrogen gas through.

The test electrode was a platinum wire, 0.5 mm. in diameter and 10 mm. long. The counter electrode for the impedance measurement was a platinum gauze in the shape of a cylinder, 20 mm. high and 25 mm. in diameter, which was placed around the test electrode. A platinum plate in the other chamber of the cell served as a counter electrode for the d. c. galvanostatic polarization. The measurement was made in an all-glass vessel described previously[44] at the room temperature of 15±2°C. The test vessel had been in constant use for one year; it was, therefore, well aged. A hot chromic acid was used in order to clean the vessel at the beginning of this series of measurements, and the vessel was soaked in a test electrolytic solution for several days.

The correctness of the elimination of the ohmic potential drop which is caused by the electrolytic resistance between the test and the counter electrode in the a. c. measurement was checked with an R_s curve at 10000 c. p. s., according to the method described by Breiter.[45]

Results and Discussion

Figure 5 represents typical charging curves for each solution; the regions of β, γ and δ are attributed to the charging of the double layer, to the formation of oxygen layer, and to the evolution of oxygen respectively. The shapes of these curves have been discussed extensively. The quantities of electricity consumed in the γ regions of the solutions are nearly equal to one another. Figure 6 shows the curves of the corresponding ohmic component, R_s, while Fig. 7 shows those of the capacitive component, $1/\omega C_s$, of the impedance at 540 c. p. s. The three characteristic regions, i. e., γ', γ'' and γ''', are marked for these impedance curves corresponding to the γ region of the charging curves. The quantity of electricity consumed for each of those three regions is nearly the same, about 0.43 millicoulombs/cm².

In a previous paper,[45] it was suggested that the first step of the surface oxidation in acid solutions

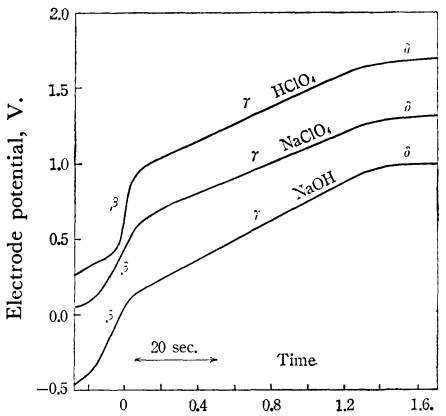

Fig. 5. Anodic charging curves.
i_a=22 μamp./cm²

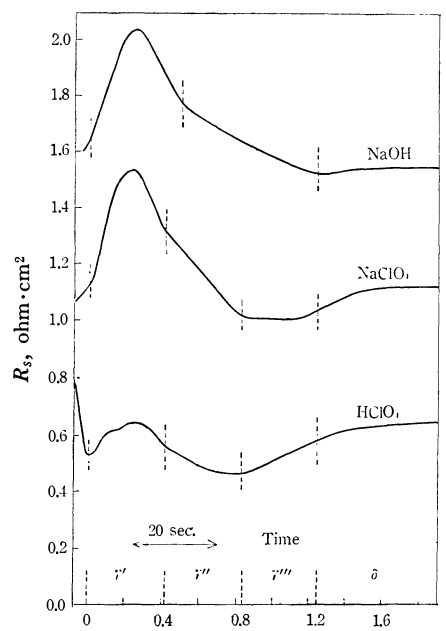

Fig. 6. Ohmic component of the interfacial impedance at 540 c. p. s. as a function of time during the constant current anodic polarization.
i_a=22 μamp./cm²

44) S. Shibata, This Bulletin, **37**, 410 (1964).
45) M. W. Breiter, *J. Phys., Chem.*, **68**, 2254 (1964).

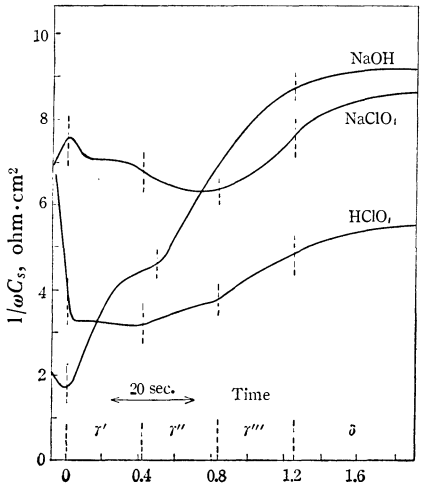

Quantity of electricity passed through the electrode in the region of γ, millicoulombs/cm²

Fig. 7. Capacitive component of the interfacial impedance at 540 c. p. s. as a function of time during the constant current anodic polarization.
i_a=22 μamp./cm²

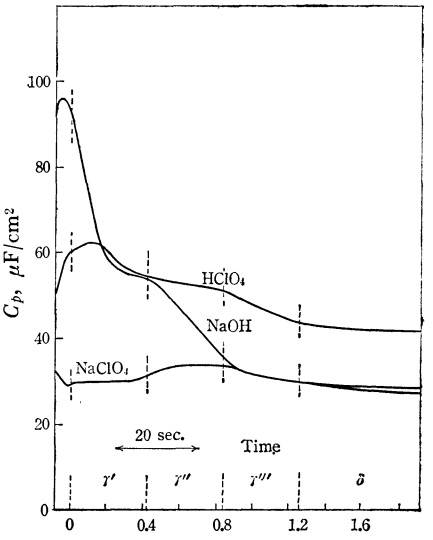

Quantity of electricity passed through the electrode in the region of γ, millicoulombs/cm²

Fig. 8. Capacity of the electrode at 4000 c. p. s. as a function of time during the constant current anodic polarization.
i_a=22 μamp./cm²

is the formation of a layer of hydroxyl radicals adsorbed on the surface; this reaction takes place in the region from the initial potential of the region, γ, to 1.15 V. in the charging curve, which corresponds to the γ' region described here. If was also suggested that in the region above 1.15 V. definite oxide films are formed. If this suggestion is correct, the mechanism of the surface oxidation in acid solutions may be proposed as being by the following three stages in terms of the equal amount of electricity required in each of three regions.

The first stage, γ', is the adsorption of hydroxyl radicals on the platinum surface:

$$Pt+H_2O \rightarrow Pt\text{–}OH+H^+ +e \qquad (8)$$

The formation of Pt–OH species is reasonable, since it requires the transfer of only one electron.

In the second stage, γ'', the definite oxide layer is formed by the further oxidation of Pt–OH:

$$Pt\text{–}OH \rightarrow PtO+H^+ +e \qquad (9)$$

where the symbol PtO is used for the oxygen film instead of Pt–O, because it seems to be a monolayer of true oxide rather than an adsorbed layer of oxygen atoms.

The oxide layer thus formed is converted to a higher oxidized state in the final stage, γ''':

$$PtO+H_2O \rightarrow PtO_2H+H^+ +e \qquad (10)$$

Reactions in the neutral and the alkaline solutions may be similar to the reaction in the acid solution, except that not water molecules but hydroxyl ions are discharged.

Figure 8 shows the capacity, C_p, of the interfacial impedance in a parallel circuit as a function of the time for 4000 c. p. s. during the anodic polarization of each solution. The value of C_p was computed in the usual way from the measured values of R_s and $1/\omega C_s$. The values of C_p measured with such a high frequency may represent mainly the differential capacity of the ionic double layer, because these C_p curves resemble in shape the capacity curve[45] which was measured by the short pulse technique. In the acid solution the capacity exhibits a maximum value in the first region, γ'. The appearance of such a maximum is frequently explained in terms of an additional capacity in the inner double layer,[46-48] and it is assumed that the change in the double-layer capacity is brought about by the presence of an additional charge or dipolar species in the inner double layer.[48]

Various metal oxides with a hydrated surface generally have an ion-exchange property. The hydroxyl group which exists on a metal surface in aqueous solutions usually dissociates in one of two ways, depending on the pH of the solution[49]:

$$MOH \rightleftarrows M^+ +OH^- \text{ (in acid solutions)} \qquad (11)$$

$$MOH \rightleftarrows MO^- +H^+ \text{ (in alkaline solutions)} \qquad (12)$$

where M represents a metal atom on the surface. These OH^- or H^+ ions are held near the M^+ or OM^- ions respectively.

In order to understand the marked dependence of the capacity value of the platinum electrode in

46) D. C. Graham, *Chem. Revs.*, **41**, 441 (1947).
47) A. N. Frumkin, *J. Electrochem. Soc.*, **107**, 461 (1960).
48) G. M. Schmid and R. N. O'Brien, ibid., **111**, 832 (1964).
49) C. B. Amphlett, L. A. Donald and M. J. Redman, *J. Inorg. and Nucl. Chem.*, **6**, 236 (1958).

the γ' region on the pH of the solution, the anion adsorption in acid solutions and the cation adsorption in alkaline solutions due to the ion exchange are assumed in the inner double layer:

$$Pt^+OH^- + ClO_4^- \rightleftarrows Pt^+ClO_4^- + OH^- \quad (13)$$

$$PtO^-H^+ + Na^+ \rightleftarrows PtO^-Na^+ + H^+ \quad (14)$$

The lower value of the capacity in the γ' region for the neutral solution is explained in terms of a small dissociation of Pt–OH on the surface. The large capacity value which appears in the first half of the γ' region in the alkaline solution is not fully understood, but it is not probably caused by the ion-exchange but by a specific adsorption of sodium ions. The capacity behavior resulting from the ion-exchange outlined above can be expected to hold for the formation of a Pt–OH surface, but it will not hold for surface oxidation to PtO and PtO_2H.

BULLETIN OF THE CHEMICAL SOCIETY OF JAPAN VOL. 39 784—790 (1966)

The Synthesis of Glycidylferrocenes and Related Compounds

By Hamao WATANABE, Izumi MOTOYAMA and Kazuo HATA

Department of Chemistry, Faculty of Science, Tokyo Metropolitan University, Setagaya-ku, Tokyo

(Received September 10, 1965)

Ferrocene derivatives with one or two glycidyl substituents, desired for the formation of polymeric ferrocene compounds, were synthesized by the epoxidation of chlorohydrin compounds obtained from the products of the addition of ferrocenyllithium to epichlorohydrin at −40——78°C. In the course of this synthesis, mono- and di-chlorohydrin compound and a disubstituted ferrocene with a 3-chloro-2-hydroxypropyl and a glycidyl substituent were isolated. All of them are stable liquid compounds. The investigation of the relationship between the reaction conditions and the yield of glycidylferrocenes revealed that the larger molar ratio of each reactant to ferrocene at each reaction step causes a higher conversion into glycidylferrocenes. In the epoxidation reaction of chlorohydrins with caustic alkali, a small amount of ethers, formed by the reaction of epoxides and the solvent ethanol, was obtained under some reaction conditions. In all cases, a small amount of biferrocenyl was isolated; the formation of this compound was considered to be attributable to the Wurtz-type coupling reaction of ferrocenyl radicals. The structures of all these products were confirmed by their infrared absorption spectra and, in part, by the NMR spectra.

In a previous communication[1] it was briefly reported that ferrocene derivatives with one or two glycidyl substituents were obtained by the epoxidation of chlorohydrins which had been derived from the products of the addition of ferrocenyllithium to epichlorohydrin. It seemed that these epoxy derivatives are promising monomers for the formation of various types of polymers. The present paper will deal with the synthesis of glycidylferrocenes and the related compounds in full detail.

The reaction of phenyllithium with epichlorohydrin has been reported by Gilman and his coworkers.[2] However, no reaction of this type on the ferrocene derivatives has yet been reported. In the present study a similar reaction was applied to the addition of ferrocenyllithium to epichlorohydrin in order to obtain the compounds which can lead to epoxy compounds.

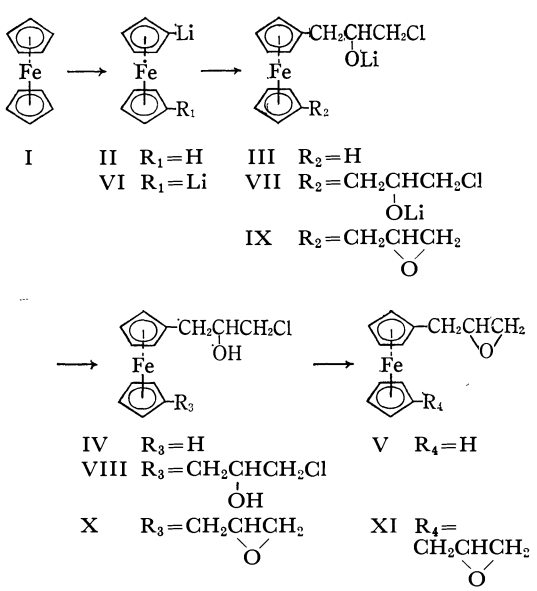

1) K. Hata, I. Motoyama and H. Watanabe, This Bulletin, **36**, 1698 (1963).

2) H. Gilman, B. Hofferth and J. B. Honeycutt, *J. Am. Chem. Soc.*, **74**, 1594 (1952).

Table I. The reaction conditions and the products

Exp. No.	Lithiation: Mol. ratio *n*-BuLi/FcH[a]	Lithiation: Time, hr. Temp., °C	Addition reaction: Mol. ratio EpCl[b]/FcH	Addition reaction: Time, hr. Temp., °C	Product and yield, %[c]: V	XI	XII
207	2.14	$64^{2}/_{3}$ −20 to room temp.	5	4 −65 to −45	12.8	ca. 0.3	0.2
208	1	$2^{3}/_{4}$ −15 to room temp.	2	$3^{1}/_{4}$ −70 to −55	1.2	0	0.1
210	2	114 −30 to room temp.	5	$23^{2}/_{3}$ −65 to −40	14.6	16.3	0.3

a) Ferrocene
b) Epichlorohydrin
c) Total summation of the final products which were obtained by the procedures described in the experimental part.

Table II. A result obtained by chromatographic separation of the reaction product (Exp. No. 210)

Order of the elution	Eluent	Product	Band color in the column	Composition of the product, %
1st	Benzene	I	Orange	—
2nd	Benzene	XII	Light orange	1.1
3rd	Benzene	V	Orange yellow	16.7
4th	Benzene	XI	Orange yellow	10.0
5th	Benzene	IV	Orange yellow	18.0
6th	Benzene-ether (1 : 1)*	X	Orange yellow	20.0
7th	Ether-methanol (9 : 1)*	VIII	Orange yellow	32.2
8th (last)	Methanol	Mixture	—	1.1

* Ratio by volume

Results and Discussion

The route and the products of the reactions are as follows:

Ferrocene (I) was converted into lithium derivatives (II and VI) by treatment with *n*-butyllithium in anhydrous ether under an atmosphere of nitrogen.[3] When a suspension of ferrocenyllithium was treated with epichlorohydrin at −40 to −78°C, a mixture of addition products (III, VII and IX) was obtained. The mixture was hydrolyzed to give chlorohydrin derivatives (IV, VIII and X). The chlorohydrin compounds were separated from the reaction mixture by adequate procedures, and each chlorohydrin compound was separated by means of vacuum distillation and/or chromatography on alumina. Each chlorohydrin was then epoxidized in an ethanol solution[4] by treatment with a 30% aqueous solution of potassium hydroxide. Monoglycidylferrocene (V) and diglycidylferrocene (XI) were thus obtained as dark red liquids. These epoxides were also obtained by a direct epoxidation of the chlorohydrin mixture (IV, VIII and X) without the previous separation of each chlorohydrin. Glycidylferrocenes (V and XI) were isolated from the reaction mixture by chromatography on alumina.

The Reaction of Ferrocenyllithium and Epichlorohydrin.—The preparation of ferrocenyllithium from ferrocene, followed by the addition reaction with epichlorohydrin, was attempted under various conditions, and the resultant lithium compounds were hydrolyzed. The reaction conditions and the results are listed in Table I, in which the yields of the final products are calculated on the basis of the ferrocene used. The addition reaction of ferrocenyllithium to epichlorohydrin could be accomplished at a low temperature, but not at an ordinary temperature, as has been shown by Gliman and his co-workers.[2] A similar reaction was also attempted with ferrocenylsodium[5] and epichlorohydrin. In this attempt also, no successful reaction

3) R. A. Benkeser, D. Goggin and G. Schroll, ibid., **76**, 4025 (1954); M. D. Rausch, M. Vogel and H. Rosenberg, *J. Org. Chem.*, **22**, 900 (1957).
4) S. Winstein, T. L. Jacobs, G. B. Linden, D. Seymour, E. F. Levy, B. F. Day, J. H. Robson, R. B. Henderson and W. H. Florsheim, *J. Am. Chem. Soc.*, **68**, 1831 (1946).
5) A. N. Nesmeyanov, E. G. Perevalova and Z. A. Bienoravichute, *Doklady Akad. Nauk S. S. S. R.*, **112**, 439 (1957); *Chem. Abstr.*, **51**, 13855 (1957); S. I. Goldberg, D. W. Mayo, M. Vogel, H. Rosenberg and M. D. Rausch, *J. Org. Chem.*, **24**, 824 (1959); M. Okawara, Y. Takemoto, H. Kitaoka, E. Haruki and E. Imoto, *J. Chem. Soc. Japan, Ind. Chem. Sect.* (*Kogyo Kagaku Zasshi*), **65**, 685 (1962).

occurred without cooling, or when the mixture was heated in toluene, but the reaction may be expected to occur here also if it is undertaken at a low temperature. The conversion of ferrocene into ferrocenyllithium and its addition reaction with epichlorohydrin was facilitated by the increase in the molar ratios of *n*-butyllithium and of epichlorohydrin to ferrocene, and by the elongation of each reaction time. The reaction products were separated by vacuum distillation or chromatography on alumina. Besides two chlorohydrin compounds (IV and VIII), two epoxy compounds (V and XI) and a mixed epoxy-chlorohydrin compound (X) were isolated in significant amounts. These results indicate that the epoxy-ring formation from the compounds III, VII and IX occurred at least in part in the course of the addition reaction. When each step of the reaction was cut to a shorter reaction time (Exp. Nos. 207 and 208), however, the product was found to consist mainly of chlorohydrin derivatives.

Monochlorohydrin IV could be separated by vacuum distillation from the reaction product. It was found, however, that the reaction product was apt to decompose during the distillation, so the temperature must be carefully controlled under a high vacuum. Therefore, the method for separation and purification by means of alumina chromatography was recommended. A typical example is shown in Table II. Each product was successively eluted with benzene and other solvents.

In the separation procedure of the chromatography, a small amount of orange crystals was isolated from the early-eluted fraction next to the ferrocene recovered. This compound was identified as biferrocenyl (XII), as has been reported in another communication by the present authors.[6] The mechanism of the formation of biferrocenyl in the course of the reaction was inferred to be as follows: ferrocenyllithium was subjected to homolytic fission between the ferrocenyl group and lithium to afford ferrocenyl radical, which then coupled to give biferrocenyl. Further investigations of this problem will be reported in a following paper.[7]

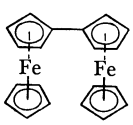

XII

By a comparison of the rate of elution in the chromatography, the adsorbability to alumina was estimated to be in the following order: I< XII<V<XI<IV<X<VIII.

Epoxidation Reaction.—*The Separate Epoxidation of Each Chlorohydrin.*—Each chlorohydrin separated by the chromatography was dissolved in ethanol and treated with a 30% aqueous solution of potassium hydroxide under cooling with ice water and high-speed stirring. After the epoxidation reaction was over, a large quantity of water and ether was added, and the crude epoxide (V or XI) was obtained from the ethereal layer and purified by alumina chromatography. The epoxidation of the chlorohydrin derivatives gave, in general, good yields of the corresponding glycidylferrocenes. In some exceptional instances, it was found that the reaction mixture was contaminated by a small amount of a liquid compound other than epoxy compound. These compounds were isolated after the separation of each product from the epoxidized mixture and purification by alumina chromatography. From the various analytical results, the compounds were found to be addition products of the glycidylferrocenes and ethanol used as the solvent.

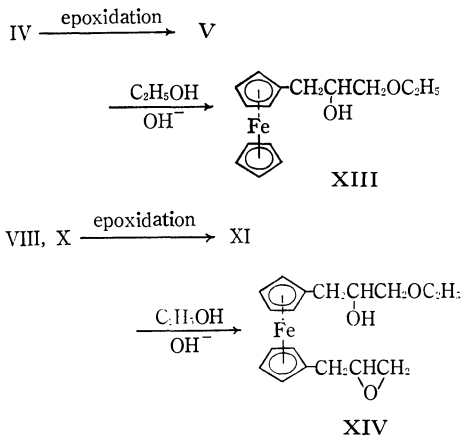

Compounds XIII and XIV were supposed to be formed by the addition of ethanol to glycidylferrocenes during the epoxidation reaction in the presence of potassium hydroxide. This presumption was proved by an experiment, in which epoxide(XI) dissolved in ethanol was treated with a potassium hydroxide solution by a work-up similar to that described above; a part of the epoxide (XI) was converted into XIV, while most of it was recovered unchanged.

The yield of compound XIII or XIV was increased by the prolonged reaction time of epoxidation, as is shown in Table III. Compounds XIII and XIV are dark red liquids (n_D^{20} 1.5796 and 1.5711 respectively), the former being more viscous than the latter. It was shown that these compounds have slightly higher adsorbabilities than the corresponding epoxides.

The Direct Epoxidation of the Chlorohydrin Mixture.—The reaction product obtained by the reaction of ferrocenyllithium and epichlorohydrin was dissolved in ethanol without any further separation process, and directly epoxidized by treatment with

6) K. Hata, I. Motoyama and H. Watanabe, This Bulletion, **37**, 1719 (1964).
7) K. Hata, I. Motoyama and H. Watanabe, ibid., **39**, 790 (1966).

Table III. Epoxidation reactions and the products

Compound	Mol. ratio C_2H_5OH : KOH : EpCl[a]	Reaction temp., °C	Reaction time min.	Product and yield, % V	XIII	XI	XIV
IV	70 : 10 : 1	0—10	10	91.0	+[c]	—	—
			25 (+35)[b]	87.6	++[c]	—	—
VIII	50 : 10 : 1	0—10	12	—	—	92.0	0
			30 (+45)[b]	—	—	66.9	++[c]
X	70 : 10 : 1	0—10	25 (+35)[b]	—	—	77.3	+[c]

a) Epichlorohydrin substituent $-CH_2CH(OH)CH_2Cl$
b) Time in parentheses is additional stirring period without cooling.
c) + trace, ++ small amount

Table IV. A result obtained by chromatographic separation of the epoxidation product
(Sample obtained from Exp. No. 210)

Order of the elution	Eluent	Product	Band color in the column	Composition of the product, %*
1st	Benzene	XII	Light orange	0.6
2nd	Benzene	V	Deep yellow	35.8
3rd	Benzene	Unknown	Light pink	2.3
4th	Benzene	XI	Light yellow	53.2
5th (last)	Methanol	Mixture	Orange red	8.0

* Calculated after the exclusion of recovered ferrocene.

Table V. Physical properties of the liquid products

Product	Color	B. p., °C/mmHg	n_D^{20}	Relative viscosity
IV*	Dark red	156—158/0.80—0.90 or 144/0.52—0.53	1.6102	High
V	Dark red	111—115/0.17—0.18	1.6093	Low (very fluid)
VIII	Dark red	—	1.6069	High
X	Dark red	—	1.6014	Medium
XI	Dark red	160—161/0.09—0.12	1.5968	Low (very fluid)

* Epoxy equivalent, 0.99 (HCl - dioxane method)

potassium hydroxide under the reaction conditions similar to those described in the above section. When the reaction mixture was submitted to a vacuum distillation, compounds V and XI were obtained, boiling at 111—115°C under 0.17—0.18 mmHg and at 160—161°C under 0.09—0.12 mmHg respectively. A small amount of biferrocenyl was also isolated from the residue of the vacuum distillation.

The chromatography to separate the products into each compound gave the results shown in Table IV. By the chromatographic separation, biferrocenyl was again isolated besides another unknown substance.

The Assignment of the Structures of the Products.—Compounds IV, V, VIII, X, XII, XIII and XIV were stable in air. These compounds were identified by means of their elemental analyses, infrared spectra and NMR spectra, and by a study of their chemical natures.

The physical properties of the various products are summarized in Table V. All of these products are dark red liquids. Mono- and di-chlorohydrin derivatives (IV and VIII) have higher viscosities than those of the corresponding glycidylferrocenes, which are fairly fluid. The viscosity of the compound X falls between those of VIII and XI. As a whole, the order of the viscosity of these compounds as determined by visual observation is: VIII$\geqq$IV$>$X$>$XI$>$V. The epoxy equivalent of monoglycidylferrocene (V) was determined by the hydrochloric acid - dioxane method,[8] using cresol red as an indicator, to be 0.99; this value agrees well with the theoretical value (1.00).

It has been shown in the previous paper[1] that when a mixture of glycidylferrocenes was treated with a hydrochloric acid - dioxane mixture in order to obtain the corresponding chlorohydrin mixture, only bischlorohydrin (VIII) was isolated by chromatography on alumina, and it was reconverted into diglycidylferrocene with potassium hydroxide. A similar ring-opening reaction was observed in the measurement of the epoxy equivalent of the

8) G. King, *Nature*, **164**, 706 (1949); "Organic Analysis," Vol. 1, 135; "Kobunshi Jikkengaku Koza," Vol. 9, Kyoritsu Shuppan, Tokyo (1958), p. 259.

compound V: a dark red, viscous liquid material obtained after the measurement was found to be identical with an authentic chlorohydrin compound IV. From these results it is obvious that a reversible epoxy-ring closure and opening reaction was effected between these compounds by alkali and hydrochloric acid.

It was substantiated that the disubstituted ferrocenes described above are heteroannularly-substituted compounds, from the fact that their infrared absorption spectra lack the absorption bands at 1100 and 1000 cm^{-1}. This assignment has been designated as the 9—10 rule.[9]

The infrared spectra of two chlorohydrins (IV and VIII) and two glycidylferrocenes (V and XI) exhibit essentially identical absorption bands in each pair, except for the region between 1100 and 1000 cm^{-1}. The characteristic peaks for the chlorohydrin group in IV and VIII appear at 3400 (ν_{C-H}), 1090—1050 (ν_{C-O}) and 760—690 cm^{-1} (ν_{C-Cl}), while the characteristic peaks for the epoxy group in V and XI appear at 3050 and 2970 cm^{-1} (ν_{C-H}) and at 1256, 960—900, and 845 cm^{-1} (epoxy ring). Compound X shows the absorption bands due to both the chlorohydrin group and the epoxy group.

Further confirmation was obtained by the examination of the NMR spectra of two glycidylferrocenes (V and XI). In the spectrum of the monoglycidylferrocene a singlet signal was observed at τ 6.[10] This is attributable to the overlapping of the signal of unsubstituted ring protons (5H) and that of monosubstituted ring protons (4H) because of the close resemblance of their chemical shifts. The signal was yet a sharp peak in spite of the overlapping. On the other hand, the NMR spectrum of diglycidylferrocene showed a singlet signal at τ 5.96 assignable to the heteroannularly-disubstituted ring protons (8H), and no other signals assignable to any homoannularly-disubstituted ring protons were observed. Two other complex signals, centered at τ7.0 and τ7.4, were assigned to the protons of glycidyl groups, the former due to the methine proton in the oxide group, and the latter to the two protons of methylene and two protons of oxide methylene.

Experimental

The temperatures in the reactions and measurements were uncorrected. The infrared spectra were determined on a Model EPI-S2 recording spectrometer (Hitachi Co.), and the NMR spectra were determined at 60 Mc. on a Model JNM-C-60 spectrometer (Japan Electron Optics Laboratory Co.), employing a room-temperature method in deuteriochloroform containing tetramethylsilane as an internal standard and ca. 30% (by volume) of the sample.

All column chromatographies were performed on Sumitomo Chemicals' activated alumina (150—250 meshes) which had previously been exposed to air for eigtht hours in order to diminish its adsorption ability. A benzene solution of the sample was placed on the alumina and developed with the same solvent.

1. The Reaction of Ferrocenyllithium and Epichlorohydrin.—The lithiations of ferrocene with *n*-butyllithium and the subsequent reactions of ferrocenyllithium with epichlorohydrin were carried out with stirring in anhydrous ether under an atmosphere of nitrogen. Three runs of the reaction were accomplished by essentially identical procedures except for the molar ratios of the reactants and the reaction times (Table I). A typical procedure for the preparation of ferrocenyllithiums and their reaction with epichlorohydrin is as follows (Exp. No. 210).

A solution of 0.6 mol. of *n*-butyllithium was prepared, according to the method described in the literature,[11] from 82.8 g. (0.6 mol.) of *n*-butyl bromide in 120 ml. of ether and 10.35 g. (1.5 g.-atom) of suspended lithium, cut into pieces as small as possible, in 240 ml. of ether, the temperature being kept at −30°C by cooling in a dry ice - acetone bath. In another vessel 55.8 g. (0.3 mol.) of ferrocene was dissolved in 650 ml. of ether and cooled to −20——30°C in a dry ice - acetone bath. The solution of *n*-butyllithium previously prepared was added to the ferrocene solution through a siphon, the inlet tube of which was covered with glass wool in order to filter off solid impurities. After the addition was complete, the mixture was allowed to warm up to room temperature with stirring over a 20-hr. period. Further stirring was continued for 94 hr. Since the spontaneous evaporation of the solvent under a stream of nitrogen was observed during this period, 400 ml. of ether was added in two portions (150 and 250 ml.).

The orange suspension of ferrocenyllithium thus obtained was cooled to ca. −65°C in a dry ice - acetone bath, and 138.8 g. (1.5 mol.) of epichlorohydrin (b. p. 115.0—115.4°C) in 100 ml. of ether was then added to the suspension during a 2-hr. period so as to maintain the temperature at −60°C or below. After the addition was complete, the mixture was kept at this temperature for 7 hr., and then allowed to warm up to −40°C over a 16.5-hr. period. Then, the cooling bath was removed and the mixture was allowed to come to room temperature, after which the contents were poured into a large amount of ice water in order to hydrolyze the lithium compounds.

The ethereal layer was separated, and the aqueous layer was extracted with ether. The combined ethereal solution was dried over magnesium sulfate and evaporated in order to remove the ether and the remaining epichlorohydrin. On concentration, a large quantity of unreacted ferrocene separated out as orange crystals; it was removed by filtration. The filtrate was placed in a Claisen-type flask fitted with a Vigraux-column and evaporated under 1.5 mmHg at 130°C on an oil bath, thus removing materials of a lower boiling point and/or a higher vapor pressure (the remaining ferrocene

9) K. L. Rinehart, Jr., K. L. Motz and S. Moon, *J. Am. Chem. Soc.*, **79**, 2749 (1957); M. Rosenblum and R. B. Woodward, ibid., **80**, 5443 (1958); A. N. Nesmeyanov, L. A. Kazitzyna, B. V. Lokshin and V. D. Vil'chevskaya, *Doklady Akad. Nauk S. S. S. R.*, **125**, 1037 (1959); *Chem. Abstr.*, **53**, 21857 (1959).

10) Y. Nagai, J. Hooz and R. A. Benkeser, This Bulletin, **37**, 53 (1964).

11) "Organic Reactions," Vol. 6, 352 (1951).

sublimed inside the Vigraux-column). After the vacuum evaporation, 36.8 g. of the reaction product was obtained as a dark red, very viscous liquid.

2. The Separation of Each Compound from the Reaction Mixture.—*a) Vacuum Distillation.*—As has been reported in a previous communication,[1] a vacuum distillation of the reaction product (Exp. No. 207) gave a very viscous dark red liquid which was identified as the monochlorohydrin compound IV; b. p. 156—158°C/0.8—0.9 mmHg, or 144°C/0.52—0.53 mmHg; n_D^{20} 1.6102.

Found: C, 56.09; H, 5.33. Calcd. for $C_{13}H_{15}FeClO$: C, 56.05; H, 5.43%.

b) Separation by Means of Chromatography.—In order to make a more delicate separation, 9.2 g. of the reaction product described above (Exp. No. 210) was dissolved in a small amount of benzene and chromatographed on alumina using benzene as a developer. Elution was performed by successively changing the eluent. The results of the chromatography are shown in Table II.

The first elution with benzene gave ferrocene (0.03 g.).

The second elution with benzene yielded orange crystals (0.10 g.), which were then recrystallized from a mixture of benzene and petroleum ether; m. p. 233.8—234.5°C (in a sealed capillary). The compound was identified as biferrocenyl (XII); NMR spectrum, τ 5.68 (triplet), 5.85 (triplet), and 6.03 (singlet). These signals will be discussed in a following paper.[7]

Found: C, 64.78; H, 5.05. Calcd. for $C_{20}H_{18}Fe_2$: C, 64.91; H, 4.90%. Mol. wt. Found: 370(Rast) and 330 (vapor pressure osmometer method). Calcd. 370.

The third elution with benzene gave rise to monoglycidylferrocene (V, 1.48 g.; n_D^{20} 1.6093), whose identification was established as will be described below (3-a).

The fourth elution with benzene yielded diglycidylferrocene (XI, 0.90 g.) as a slightly viscous, dark red liquid; n_D^{20} 1.5968. The identification was established as will be described below (3-b).

A very viscous, dark red liquid obtained from the fifth band was the monochlorohydrin compound (IV, 1.80 g.). It was identified as the same compound as had been described above (2-a).

The sixth elution, with benzene-ether (1 : 1), gave a relatively viscous, dark red liquid (1.79 g.) which gave a pure material upon rechromatography. The compound was identified as a heteroannularly-substituted ferrocene (X); n_D^{20} 1.6014.

Found: C, 57.31; H, 5.12. Calcd. for $C_{16}H_{19}\cdot FeClO_2$: C, 57.43; H, 5.72%.

The seventh elution, with ether-methanol (9 : 1), gave rise to the dichlorohydrin compound (VIII, 1.89 g.); n_D^{20} 1.6069.

Found: C, 51.83; H, 5.26. Calcd. for $C_{16}H_{20}\cdot FeCl_2O_2$: C, 51.79; H, 5.43%.

The product from the last elution with methanol was presumed to be a mixture of many compounds (0.10 g.), but their separation and the identification were not attempted.

3. Epoxidation.—The separate epoxidation of each chlorohydrin (IV, VIII, X) was effected under common reaction conditions; 50 or 70 mol. of ethanol (used as solvent) and 10 mol. of potassium hydroxide were used per mole of the chlorohydrin function. The reaction conditions of epoxidation are shown in Table III.

a) The Epoxidation of IV to V.—A solution of 0.82 g. (2.94 mmol.) of IV in 80 g. (0.208 mol.) of ethanol was cooled to 0—10°C in an ice-water bath. Into the cold solution 5.6 g. of a 30% aqueous solution of potassium hydroxide (containing 29.4 mmol. of potassium hydroxide) was added with vigorous stirring. After the addition, the stirring was continued for 8 min., after which large amounts of water and ether were added. The ethereal layer was separated, and the aqueous layer was repeatedly extracted with ether. The combined ethereal solution was filtered and evaporated to give a crude epoxy compound (0.77 g.). The crude product was dissolved in benzene and chromatographed on alumina, using the same solvent as a developer. Elution with benzene yielded pure epoxide V (0.65 g., 91% yield); n_D^{20} 1.6093.

Found: C, 64.41; H, 5.57. Calcd. for $C_{13}H_{14}FeO$: C, 64.50; H, 5.83%. Epoxy equivalent, 0.99 (HCl-dioxane method).[8]

Vacuum distillation revealed the purity of the epoxide; b. p. 107-—113°C/0.13—0.16 mmHg: n_D^{20} 1.6093.

When a similar epoxidation reaction of the same chlorohydrin (IV) was carreid out for a elongated stirring period, as is shown in Table III, a subsequent fraction was obtained by elution with benzene-ether (1 : 1). This fraction gave rise to a small amount of a dark red, relatively viscous liquid, which was found to be an addition product (XIII) between V and ethanol; n_D^{20} 1.5796.

Found: C, 62.85; H, 6.97. Calcd. for $C_{15}H_{20}FeO_2$: C, 62.52; H, 7.00%.

b) The Epoxidation of VIII to XI.—The epoxidation reaction was accomplished according to the procedure described above. A solution of 1.34 g. (7.22 mmol.) of VIII in 16 g. (0.348 mol.) of ethanol was treated with 15 g. of a 30% aqueous solution of potassium hydroxide (containing 72.2 mmol. of potassium hydroxide). After the addition of the alkaline solution under cooling in an ice-water bath had been complete, a vigorous stirring was continued without cooling so as to allow the temperature of the mixture to rise from 10 to 25°C in 45 min. The reaction mixture was then extracted with ether. After the evaporation of the ether, a slightly viscous, dark red liquid (1.11 g.) remained. It was separated by alumina chromatography much as in procedure 3-a.

Elution with benzene yielded diglycidylferrocene (XI, 0.72 g., 66.9%); n_D^{20} 1.5968.

Found: C, 64.40; H, 6.18. Calcd. for $C_{16}H_{18}FeO_2$: C, 64.45; H, 6.09%.

The attempted purification of XI by vacuum distillation resulted in its boiling at 160—161°C/0.09—0.12 mmHg; n_D^{20} 1.5968.

Elution with benzene-ether (1 : 1) gave rise to a dark red, slightly viscous liquid (0.16 g.) which was identified as compound XIV; n_D^{20} 1.5711.

Found: C, 62.68; H, 6.91. Calcd. for $C_{18}H_{24}FeO_3$: C, 62.81; H, 7.03%.

When the epoxidation of VIII was accomplished in a short reaction time (Table III, 12 min. at 0—10°C), the yield of XI increased to 92%, while the compound XIV was not detected.

c) The Epoxidation of X to XI.—A solution of 0.84 g. (2.51 mmol.) of X in 8 g. (0.17 mol.) of ethanol was treated with 4.3 g. of a 30% aqueous solution of potassium hydroxide (containing 22.6 mmol. of potassium hydroxide). The products were separated by the

procedure described in 3-b.

Elution with benzene gave diglycidylferrocene (XI, 0.58 g., 77.3% yield) and compound XIV (0.10 g.).

d) The Reaction of Diepoxide XI with Alkali in Ethanol. —A solution of 1.27 g. (8.54 mmol.) of XI in 18 g. (0.348 mol.) of ethanol was vigorously stirred with 15 g. of a 30% aqueous solution of potassium hydroxide (containing 72.2 mmol. of potassium hydroxide) at 0—10°C for 25 min. The stirring was continued for further 40 min. without cooling. The following procedure was similar to that adopted for the epoxidation of chlorohydrin compounds. The product was chromatographed on alumina and eluted with benzene and benzene-ether.

Elution with benzene gave 1.03 g. of the recovered XI (81.1% recovery).

Elution with benzene-ether (1 : 1) gave a dark red, relatively viscous liquid (0.18 g.). The liquid was rechromatographed and identified as compound XIV by a comparison of its infrared spectrum and refractive index with those of an authentic material.

e) The Direct Epoxidation of the Chlorohydrin Mixture. —In the direct epoxidation of a mixture of chlorohydrins, it must be noted that a molar ratio calculation of the reactants was established on the basis of a composition analysis of the various components, which were determined from the results of alumina chromatography. The following example shows the epoxidation of the sample obtained by Exp. No. 210 (Table I); the composition of the sample is listed in Table II.

To a solution of 16.21 g. of the sample (containing 48.5 mmol. of chlorohydrin function) in 141 g. (3.06 mol.) of ethanol, 77.5 g. of a 30% aqueous solution of potassium hydroxide (containing 0.485 mol. of potassium hydroxide) was added under cooling in an ice-water bath, and the mixture was stirred for 10 min. After a treatment similar to that described above (3-a), 14.13 g. of a dark red liquid was obtained. The product was chromatographed on alumina. Five fractions were successively eluted with benzene and methanol, as is shown in Table IV.

The first elution with benzene gave rise to a mixture of ferrocene and biferrocenyl. Ferrocene (ca. 0.10 g.) was removed by vacuum sublimation, and the remaining red-brown solid material was purified by recrystallization from a mixture of benzene and petroleum ether to give 80 mg. of biferrocenyl (XII); m. p. 231.0—232.0°C (in a sealed capillary).

The second elution with benzene yielded 4.96 g. of monoglycidylferrocene (V).

The third elution with benzene gave a slightly viscous, dark red liquid (1.24 g.) on which no further analysis was attempted.

The fourth elution with benzene yielded 6.44 g. of diglycidylferrocene (XI).

The last elution, with methanol, gave a mixture (1.12 g.). Although it was supposed that the mixture might contain several compounds, such as XIII and XIV, no further attempt was made to separate and identify them.

Finally, as has been shown in a previous paper,[1] the epoxidized crude product was also purified by vacuum distillation to give V; b. p. 111—115°C/0.17—0.18 mmHg; n_D^{20} 1.6093. A small amount of biferrocenyl was separated as orange crystals by filtration from the residue of the vacuum distillation.

Thanks are due to the Ministry of Education for the financial support granted for this research.

BULLETIN OF THE CHEMICAL SOCIETY OF JAPAN VOL. 39 790—801 (1966)

The Direct Formation of Biferrocenyl and Polyferrocenyls from Ferrocenyllithium

By Hamao WATANABE, Izumi MOTOYAMA and Kazuo HATA

Department of Chemistry, Faculty of Science, Tokyo Metropolitan University, Setagaya-ku, Tokyo

(Received September 10, 1965)

In the presence or absence of *n*-butyl bromide, ferrocenyllithium and cobaltous chloride reacted to give various polyferrocenyls and butylated polyferrocenyls. They were isolated, mainly by alumina chromatography, and their structures were established, principally from the NMR spectra, to be heteroannularly-bonded ones. The formation of these compounds is considered to be due to the coupling reactions of the ferrocenyl radical, the ferrocenylene biradical and the butyl radical, which were formed by homolytic fissions of some reactive intermediate and butyl halide. The presence of the alkyl halide greatly affected the sorts and yields of the products. No cyclic polyferrocenylene was obtained. The "9—10 rule" concerning the infrared spectra of ferrocene derivatives was found not to apply to di-substituted biferrocenyls. It was found, by a study of the X-ray diffraction patterns and the infrared spectra, that terferrocenyl crystallizes in polymorphic forms according to the method and the solvent of crystallization. The polymorphism may be attributable to the rotational isomerism around the central ferrocene nucleus.

In connection with the synthesis of glycidylferrocenes and the related compounds,[1,2] the direct formation of biferrocenyl from ferrocenyllithium was previously reported by the present authors.[3] It was supposed that the formation of biferrocenyl is attributable to the Wurtz-type reaction,[4] in which the coupling of ferrocenyl radicals, produced by the homolytic fission of ferrocenyllithium molecules, gives rise to biferrocenyl. It has been shown by Kharasch and his co-workers[5] that small quantities of cobaltous chloride favor the formation of biphenyl from phenyllithium. Wittig and Lehmann[6] have also reported the coupling reaction of biphenyldilithium in the presence of cobaltous chloride. With reference to their experiments, the present authors attempted the reaction of ferrocenyllithium and cobaltous chloride in order to establish the radical mechanism. The mechanism has already been presumed from the results of the reaction which partly reported in a previous paper.[3]

Just after the present experiment was finished, Spilners and Pellegrini[7] reported a similar reaction of lithiated ferrocene and cobaltous chloride in ether-tetrahydrofuran. The reaction of ferrocenyl magnesium halide and cobaltous chloride to give biferrocenyl has also been reported by Shechter and Helling.[8] These investigators proposed the radical mechanism. However, no detailed description of a reaction of this type affording many sorts of polyferrocenyls has ever appeared.

The present paper will deal in full detail with the direct formation of biferrocenyl and polyferrocenyls from ferrocenyllithium. The reaction of ferrocenyllithium and cobaltous chloride was accomplished in dry ether under an atmosphere of nitrogen, in the presence or absence of an equimolar amount of alkyl halide, such as *n*-butyl bromide, to the ferrocene used. After the reaction of ferrocenyllithium and cobaltous chloride, the reaction mixture was poured into ice water in order to quench the reactive compounds. The organic layer was then separated from the inorganic aqueous layer. After the solvent has been removed from the organic layer, many products were isolated from the solid mixture by various procedures. The isolated crude products were then purified by rechromatography or recrystallization.

Results and Discussion

The reaction scheme and the products are as follows:

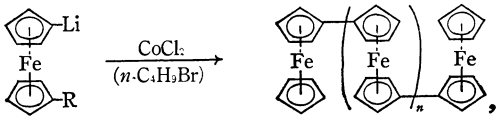

R=H or Li

I $n=0$
II $n=1$
III $n=2$
IV $n=3$
V $n=4$

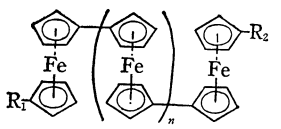

VI $n=0$, $R_1=n\text{-}C_4H_9$, $R_2=H$
VII $n=0$, $R_1=R_2=n\text{-}C_4H_9$
VIII $n=1$, $R_1=n\text{-}C_4H_9$, $R_2=H$
IX $n=2$, $R_1=n\text{-}C_4H_9$, $R_2=H$

The reaction products in the presence of *n*-butyl bromide were found to be biferrocenyl (I), terferrocenyl (II), quaterferrocenyl (III), quinqueferrocenyl (IV), sexiferrocenyl (V), monobutyl-biferrocenyl (VI), dibutyl-biferrocenyl (VII), monobutyl-terferrocenyl (VIII), and monobutyl-quaterferrocenyl (IX). In the reaction without the halide, however, it was found that biferrocenyl, terferrocenyl and monobutyl-terferrocenyl were the main products. All of these products except biferrocenyl were confirmed to be hetero-annularly-bonded compounds. Their structures were established by means of their infrared, NMR and ultraviolet spectra, molecular weight determinations, elemental analyses, and by the behavior of these compounds in the chromatographic separation.

The Reactions of Ferrocenyllithium and Cobaltous Chloride.—The reaction conditions and the rate of the conversion of ferrocene into the condensation products are shown in Table I. The conversion rate in Run A was 36.2%, while in Run B it was 4.8%, in spite of the longer reaction period. This indicates that the presence of alkyl halide greatly affected the conversion of ferrocenyllithium into the condensation products. The reaction products, separated by chromatography, are listed in Table II.

In the reaction without the halide the present authors observed the formation of orange-red crystals which are apparently different from ferrocene and may be suspected to be an intermediate compound. Moreover, it is noticeable that, after the reaction was complete, a fine, almost black solid was found in the bottom of the flask. This solid was proved to be so sensitive to water that it rapidly changed

1) K. Hata, I. Motoyama and H. Watanabe, This Bulletin, **36**. 1698 (1963).
2) K. Hata, I. Motoyama and H. Watanabe, ibid., **39**, 784 (1966).
3) K. Hata, I. Motoyama and H. Watanabe, ibid., **37**, 1719 (1964).
4) D. Bryce-Smith, *J. Chem. Soc.*, **1956**, 1603.
5) M. S. Kharasch, D. W. Lewis and W. R. Reynolds, *J. Am. Chem. Soc.*, **65**, 498 (1943).
6) G. Wittig and G. Lehmann, *Chem. Ber.*, **90**, 875 (1957).
7) I. J. Spilners and J. P. Pellegrini; The 148th National Meeting of the American Chemical Society, Division of Organic Chemistry, Chicago, Illinois, August 31 to September 4, 1964; *Chem. & Eng. News*, **42**, 47 (1964); *J. Org. Chem.*, **30**, 3800 (1965).
8) H. Shechter and J. F. Helling, *J. Org. Chem.*, **26**, 1034 (1961).

TABLE I. THE REACTION CONDITIONS AND THE RESULTS

Run	Lithiation		Reaction with $CoCl_2$		Conversion rate of ferrocene %
	Mol. ratio *n*-BuLi/FcH	Time, hr. Temp., °C	Mol. ratio *n*-BuBr : $CoCl_2$: FcH	Time, hr. Temp., °C	
A	2	73 1/6 −30 to room temp.	1 : 0.23 : 1	45 5 to 35	36.2
B	2	71 1/12 −30 to room temp.	0 : 0.23 : 1	72 room temp. to 33	4.8

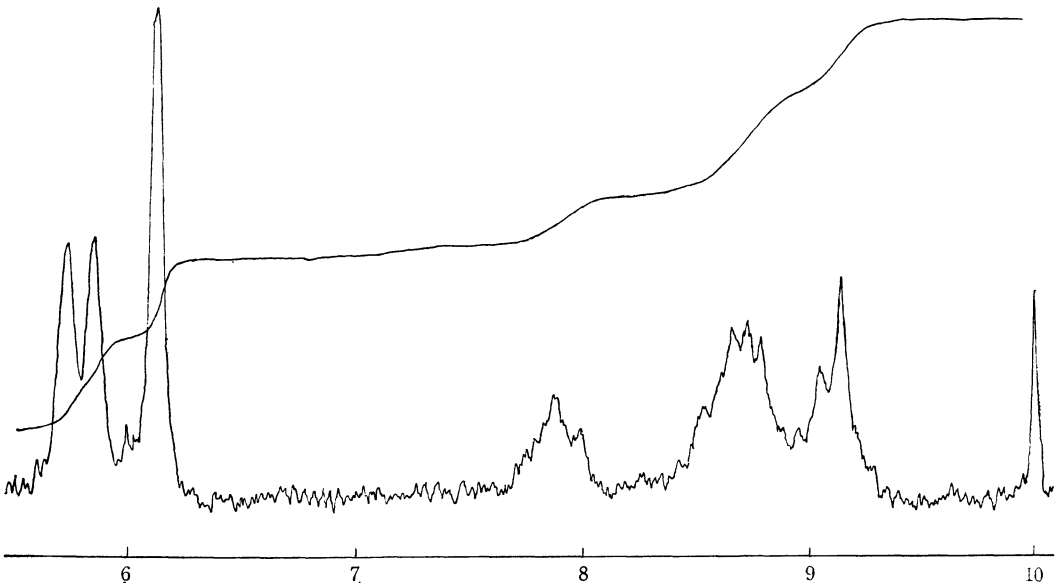

τ, p. p. m.

Fig. 1. NMR spectrum of dibutyl-biferrocenyl (VII).

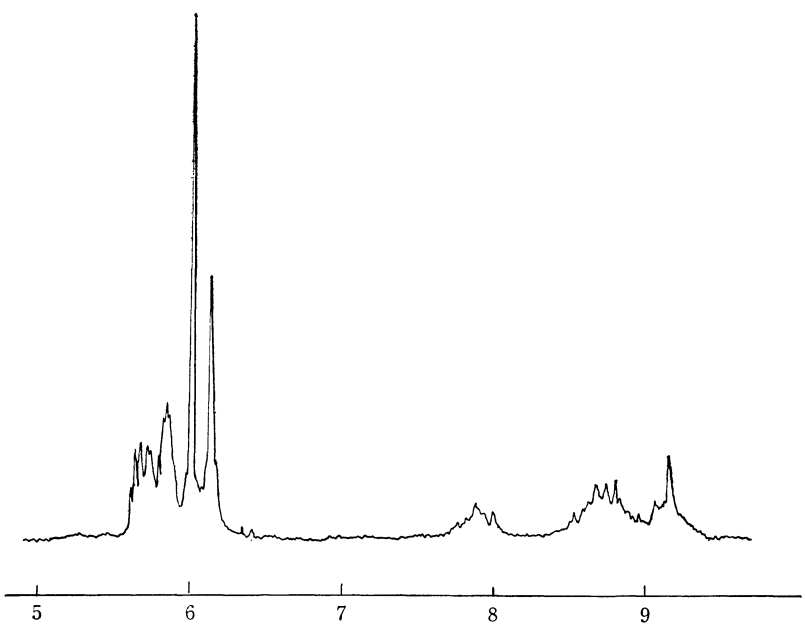

τ, p. p. m.

Fig. 2. NMR spectrum of monobutyl-biferrocenyl (VI).

TABLE II. THE PRODUCTS OBTAINED BY CHROMATOGRAPHIC SEPARATION AND THE ANALYTICAL RESULTS

Order of the elution	Product	M. p., °C[a]	Composition[b] and yields,[c] %	
			Run A	Run B
1st	Dibutyl-biferrocenyl (VII)	52.0—53.0	1.0 (0.3)	±
2nd	Monobutyl-biferrocenyl (VI)	68.2—70.2	11.0 (3.4)	16.1 (0.5)
3rd	Biferrocenyl (I)	233.8—234.5	27.9(11.2)	45.5 (1.9)
4th	Monobutyl-terferrocenyl (VIII)	113.0—115.0	2.5 (0.8)	±
5th	Terferrocenyl (II)	226.5—227.2	11.9 (5.7)	5.9 (0.2)
6th	Monobutyl-quaterferrocenyl (IX)	177.4—179.4	0.7 (0.2)	0
7th	Quaterferrocenyl (III)	280	17.9 (4.0)	±
—	Quinqueferrocenyl (IV)	240—245	0.2 (0.1)	±
—	Sexiferrocenyl (V)	252—256	2.8 (1.1)	±

a) All melting points were measured in sealed capillary.
b) Percentage composition of the products, any unidentified products being excluded in the table.
c) The yields, calculated on the basis of used ferrocene, are shown in parentheses.

into a fine orange solid, which seemed to be ferrocene, upon contact with water. Since ferrocenyllithium is yellow or orange, this reactive substance may be inferred to be an intermediate compound, something like X or XI, derived from ferrocenyllithium and cobaltous chloride. Probably, the homolytic fission of the intermediate affords the ferrocenyl radical (XII) and the ferrocenylene biradical (XIII), as has been reported in connection with phenyl derivatives by Kharasch and his co-workers[5] and by Wilds and McCormack.[9]

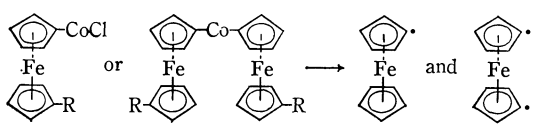

X XI XII XIII

R=H, Li or CoCl R=H, Li, CoCl, or -Co-

In the present experiment, however, it could not be elucidated from which intermediate, X or XI, the ferrocenyl and ferrocenylene radicals were derived. Nevertheless, it may be concluded that the formation of many polynuclear ferrocenes is attributable to the coupling reactions of these radicals, and that the presence of alkyl halide in the reaction system facilitates the formation of these radicals. Besides, alkyl halide itself is subjected to homolytic fission to give the alkyl radical, which then couples with ferrocenyl and ferrocenylene radicals to afford alkylated polyferrocenyls. The formation of some cyclic product was expected from the radical mechanism, as has been reported by Wittig and Lehmann[6] on biphenyl series, but no cyclic compounds such as biferrocenylene and polyferrocenylene were isolated at all from the reaction product. This is probably due to the steric inhibition of the radical coupling reaction and/or to the termination of the chain coupling by the ferrocenyl or the butyl radical.

Spectroscopic Behavior of the Products.— The structures of the products which were soluble in organic solvents were mainly assigned by means of their NMR spectra.

In the chromatographic separation of the products (Table II), the first elution gave rise to a red-orange compound (VII; m. p. 52.0—53.0°C), the NMR spectra of which is shown in Fig. 1. Three multiplet signals of eighteen protons, centered at τ 7.89, 8.73 and 9.14, are apparently due to the two butyl groups on the biferrocenyl nuclei. Nagai and his co-workers[10] pointed out that, in general, the four protons of the cyclopentadienyl ring with an alkyl group are subjected to the shielding effect from the alkyl group, and that a singlet signal appears at

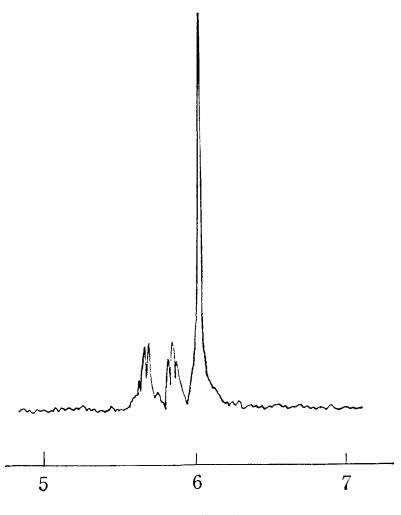

Fig. 3. NMR spectrum of biferrocenyl (I).

9) A. L. Wilds and W. B. McCormack, *J. Org. Chem.*, ibid., **14**, 45 (1949).

10) Y. Nagai, J. Hooz and R. A. Benkeser., This Bulletin, **37**, 53 (1964).

TABLE III. THE CHEMICAL SHIFTS OF THE PRODUCTS[1] (τ value)

Compound	$H_{u.r.}$[2]	$H_{\alpha,\beta}$[3]	$H_{s.r.}$[4]	$H_{b.}$[5]
FcH	5.85(10)	—	—	—
I	6.03(10)	5.68 (4); 5.85 (4)	—	—
II	6.03(10)	5.79 (8); 5.88 (8) 5.84[6]	—	—
VI	6.02 (5)	5.70 (4); 5.85 (4)	6.14 (4)	7.87, 8.85, 9.15 (9)
VII	—	5.73 (4); 5.85 (4)	6.13 (8)	7.89, 8.73, 9.14(18)
VIII	6.06 (5)	5.86[6](16)	6.18 (4)	7.95, 8.75, 9.18 (9)
IX	6.07 (5)	5.91[6](24)	6.18 (4)	8—9.5 (9)

1) The values in parentheses are relative intensities.
2) Unsubstituted ring protons.
3) Alpha and beta protons on directly bonded rings.
4) Protons on the ring substituted with one butyl group.
5) Protons of butyl group.
6) Value of the center of multiplet signal.

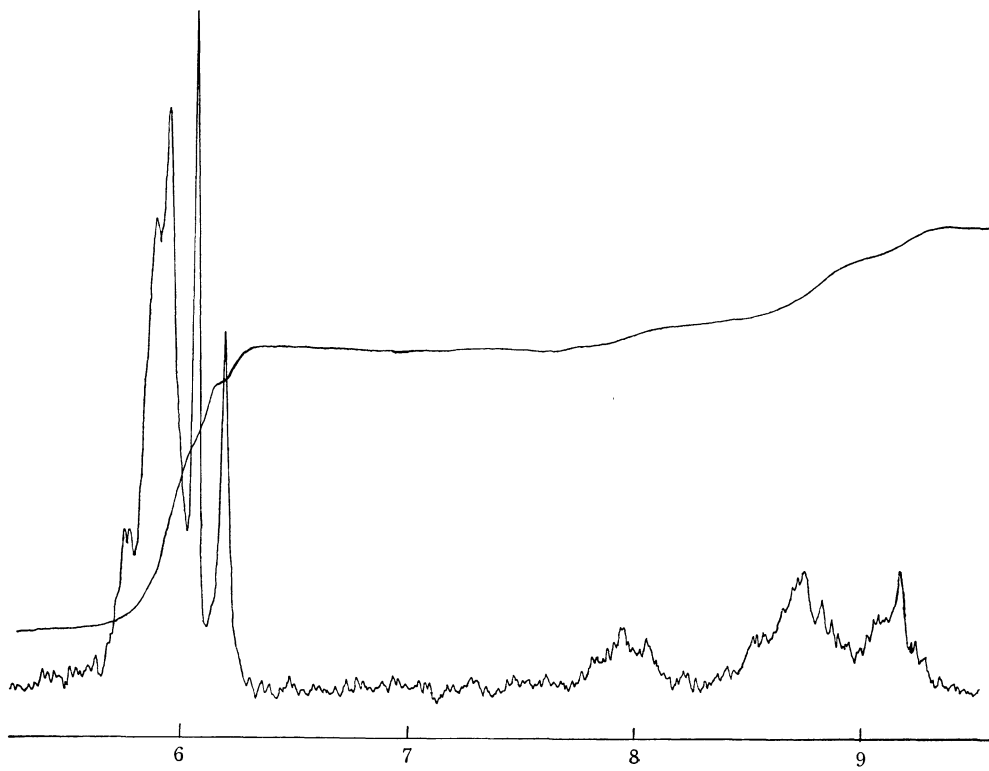

Fig. 4. NMR spectrum of monobutyl-terferrocenyl (VIII).

a higher field than that of the protons of the unsubstituted ring. Further, it is known that two directly-bonded ferrocene nuclei in biferrocenyl or its derivatives exert a strong mutual deshielding effect on the α and β protons in the bonded ring. From these facts, and by a comparison with the spectrum of monobutyl-biferrocenyl (Fig. 2. see below), the eight-proton singlet signal at τ 6.13 may be said to be due to the protons on the two rings respectively substituted with one butyl group, while the remaining two signals of four protons, centered at τ 5.73 and 5.85, are assignable to the α and β protons respectively. Therefore, this compound was determined to be heteroannularly-dibutylated biferrocenyl (VII).

The second elution gave a compound (VI; m. p. 68.2—70.2°C), the NMR spectrum of which is shown in Fig. 2. The singlet signal at τ 6.14 is due to the four protons on the substituted ring with a butyl group. The singlet signal at τ 6.02 is due to the five protons on an unsubstituted ring, and the two four-proton multiplet signals at τ 5.70 and

5.85 respectively to the α and β protons on the two directly-bonded rings. The signals of a butyl group appear at a higher field (centered at τ 7.87, 8.85 and 9.15). From these analyses this compound was identified as heteroannularly-monobutylated biferrocenyl (VI).

The NMR spectrum of biferrocenyl (I), obtained from the fraction of the third elution, shows only three signals (Fig. 3), as has been reported by Goldberg.[11] A singlet signal at τ 6.03 is attributable to ten protons on the two unsubstituted rings, and two triplet signals at τ 5.68 and 5.85 respectively to the α and β four protons on the directly-bonded rings.

The orange-red compound VIII melting at 113.0—115.0°C, obtained from the fraction of the fourth elution, shows a spectrum similar to that of monobutyl-biferrocenyl (see Fig. 4). By a compraison of the τ values of the signals and the intensities of the resonance peaks in Fig. 4 and Fig. 2, the compound VIII was identified as heteroannularly-bonded monobutyl-terferrocenyl.

The compound II, m. p. 226.5—227.2°C, obtained from the fraction of the fifth elution, was identified as terferrocenyl. Its NMR spectrum is shown in Fig. 5. A singlet signal at τ 6.03 is assignable to the ten protons on the two unsubstituted rings, while a multiplet signal centered at τ 5.84 is assignable to the sixteen protons on the four directly-bonded rings.

The orange-red compound IX melting at 177.4—179.4°C, obtained from the fraction of the sixth elution, exhibits the NMR spectrum shown in Fig. 6. By a treatment similar to that of monobutyl-terferrocenyl (VIII), the compound IX was presumed to be monobutylated quaterferrocenyl.

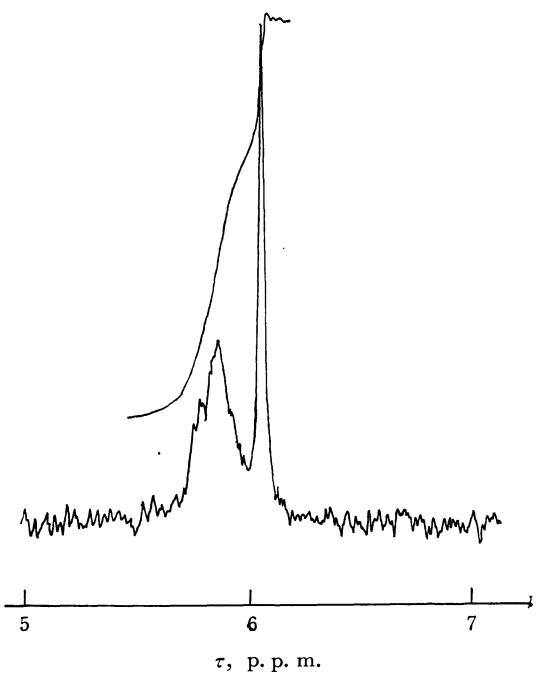

Fig. 5. NMR spectrum of terferrocenyl (II).

All of the peaks of the NMR spectra described above are summarized in Table III.

The NMR spectra of the remaining products, III, IV and V, were not available, for these compounds were insoluble in the solvent necessary for the observation of the spectra. The structures of these compounds were determined by other means to be heteroannularly-bonded quaterferrocenyl, quinqueferrocenyl and sexiferrocenyl.

As is shown in Figs. 7 and 8, the infrared absorption spectra of five polyferrocenyls (I—V) and of four butylated polyferrocenyls (VI—IX) are respectively very similar, while slight differences appeared mainly in the regions near 1100 and 900—800 cm^{-1}.

It is well known that the 9 and 10 μ bands are, respectively, due to unsubstituted ring breathing and to C–H bending in the plane. These absorption bands are very useful in distinguishing monosubstitution and heteroannular disubstitution in mononuclear ferrocene derivatives.[12] However, in the absorption spectra of heteroannularly-disubstituted biferrocenyl VII (Fig. 8), both 9 and 10 μ bands are observed in spite of the lack of an unsubstituted ring. Similar observations have been reported by several investigators.[13] Thus, it is obvious that the 9—10 rule is only applicable to mononuclear ferrocene derivatives.

By a careful comparison of the spectrum of compound VII with those of polyferrocenyls I—V, however, slight differences are found; there are two absorption bands in the latter in the 9 μ region (1105 and 1100 cm^{-1}). The band at 1105 cm^{-1} may be attributable to the directly-bonded ring breathing, and the band at 1100 cm^{-1}, to the unsubstituted ring breathing.

The ultraviolet absorption spectra of ferrocene, biferrocenyl (I) and terferrocenyl (II) in cyclohexane are shown in Fig. 9. As may be seen in the figure, the latter two compounds display the K-band at 220 and 225 mμ and the B-band in the region near 300 mμ, while ferrocene is inferred to show the K-band in a shorter wavelength region. The bathochromic shifts in this band are due to the increase in the conjugation in these polyferrocenyls. It is interesting that the position and the intensity of the absorption maxima of biferrocenyl are so

11) S. I. Goldberg, D. W. Mayo and J. A. Alford., *J. Org. Chem.*, **28**, 1708 (1963).

12) K. L. Rinehart, Jr., K. L. Motz and S. Moon, *J. Am. Chem. Soc.*, **79**, 2749 (1957); M. Rosenblum and R. B. Woodward, ibid., **80**, 5443 (1958); A. N. Nesmeyanov, L. A. Kazitzyna, B. V. Lokshin and V. D. Vil'chevskaya, *Doklady Akad. Nauk S. S. S. R.*, **125**, 1037 (1959); *Chem. Abstr.*, **53**, 21857 (1959).

13) S. I. Goldberg and J. S. Crowell, *J. Org. Chem.*, **29**, 996 (1964); A. N. Nesmeyanov, V. N. Drotz, V. A. Sazonova, V. I. Romanenko, A. K. Prokophiev and L. A. Nikonova, *Izvestia Akad. Nauk S. S. S. R.*, **1963**, 667; K. Yamakawa, N. Ishibashi and K. Arakawa, *Chem. Pharm. Bulletin*, **12**, 119 (1964).

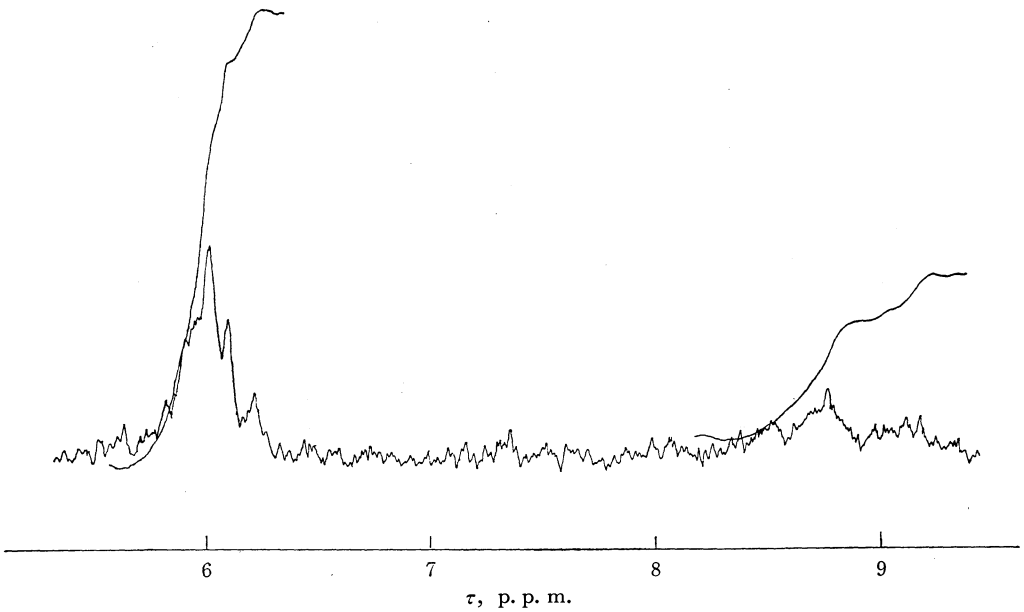

Fig. 6. NMR spectrum of monobutyl-quaterferrocenyl (IX).

similar to those of terferrocenyl that the effect of the accumulation of ferrocene nuclei on the spectra can hardly be recognized, while it is distinguished in para-polyphenyls.[14]

Chromatographic Behavior and Solubilities of the Products.—The order of the elution of the reaction products in the chromatographic separation (Table II) suggests that, in the series of polynuclear ferrocenes, the adsorbability on alumina increases according to the increase in the molecular weight, and that the increase in the number of butyl substituents on the polynuclear ferrocene nuclei causes a decrease in the adsorbability. Thus, as a whole, the order of the adsorbability on alumina is as follows: dibutyl-biferrocenyl < monobutyl-biferrocenyl < biferrocenyl < monobutyl-terferrocenyl < terferrocenyl < monobutyl-quaterferrocenyl < quaterferrocenyl < other polyferrocenyls (IV and V).

Among these compounds, alkylated polynuclear ferrocenes are soluble in common organic solvents, but polyferrocenyls without any alkyl group are less soluble than those of alkylated compounds. The solubilities of the series of polynuclear ferrocenes decrease with the increase in the molecular weight; quaterferrocenyl is almost insoluble, and quinque- and sexiferrocenyl are quite insoluble. Therefore, the latter two compounds could not be purified by the recrystallization method. In contrast, terferrocenyl was purified by recrystallization and chromatography on alumina.

The Polymorphism of Terferrocenyl.—It was found that, when the sample of terferrocenyl was crystallized from different solvents, the crystals were obtained in polymorphic forms, although no remarkable difference was observed between their melting points (around 226°C). The crystals obtained from benzene, ethanol, and ethyl acetate solution showed identical infrared absorption bands (Fig. 10). On the other hand, the spectrum of the crystals obtained by the crystallization from a large amount of petroleum ether (Fig. 11) was quite different in the region of the finger print from those of the former. The sample crystallized from the mixture of benzene and petroleum ether again showed a different spectrum (Fig. 12). The X-ray diffraction pattern of each crystal was also observed; the results were consistent with those of the infrared spectra, as is shown in Figs. 10—12. It was also found from the infrared spectra and X-ray diffraction patterns that the crystals obtained by the rapid cooling method in the crystallization are mixtures of the polymorphic forms described above, even when the same solvents were used.

The polymorphism of terferrocenyl may be accounted as a rotational isomerism (which belongs to the molecular polymorphism) about the central ferrocene nucleus, caused by rotation around the axis connecting the two cyclopentadienyl rings through an iron atom. It is also probable that the polymorphism is due to the variation in the arrangement of molecules in the crystal lattice caused by any hydrogen bonding possibly present.

Experimental

General.—Ferrocene was prepared according to the method previously reported by the present authors.[15]

14) A. E. Gillam and D. H. Hey, *J. Chem. Soc.*, **1939**, 1170.

15) H. Watanabe, I. Motoyama and K. Hata, This Bulletin, **38**, 853 (1965).

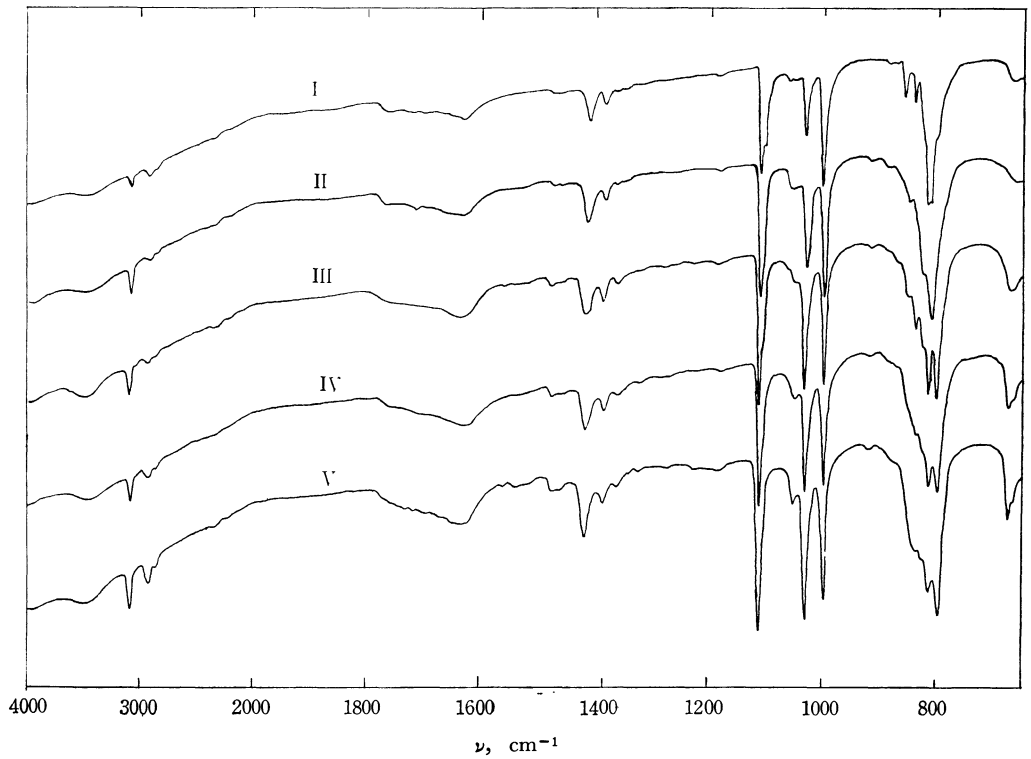

Fig. 7. Infrared spectra of polyferrocenyls (KBr disk method).

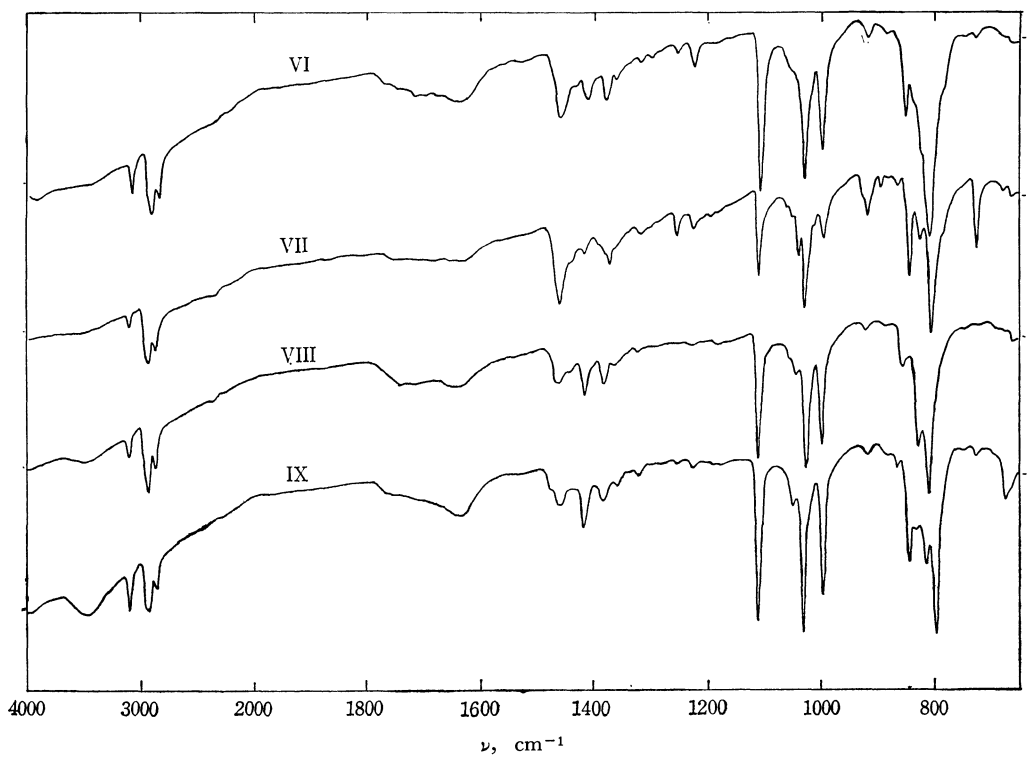

Fig. 8. Infrared spectra of butylated polyferrocenyls (KBr disk method).

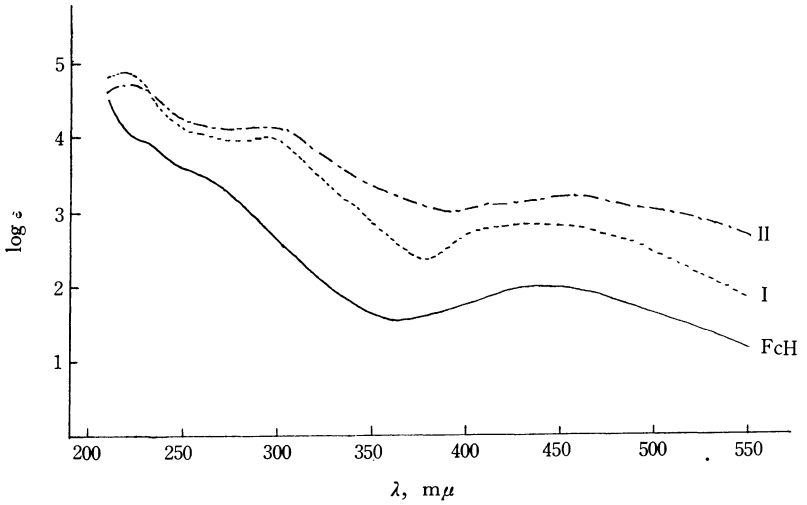

Fig. 9. Ultraviolet spectra of ferrocene, biferrocenyl (I) and terferrocenyl (II) in cyclohexane.

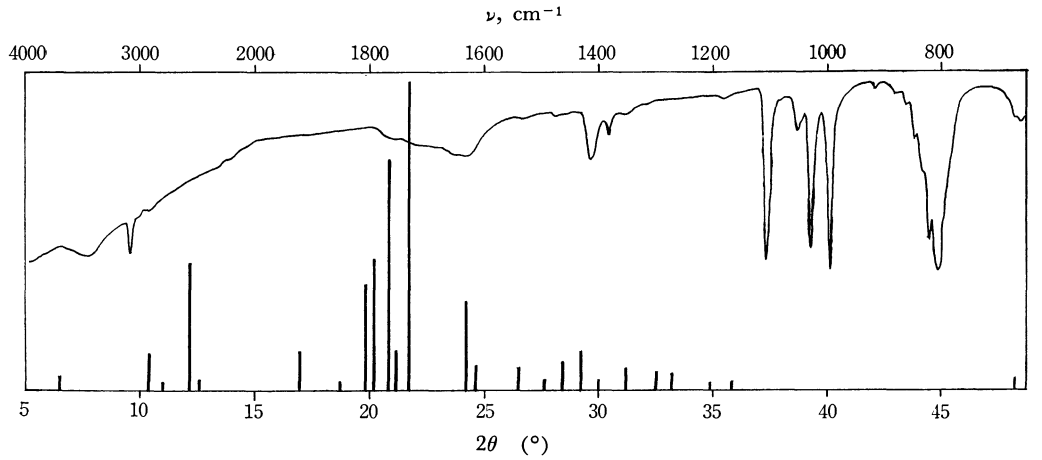

Fig. 10. Infrared spectrum and X-ray diffraction pattern of terferrocenyl from benzene, ethanol, or ethyl acetate.

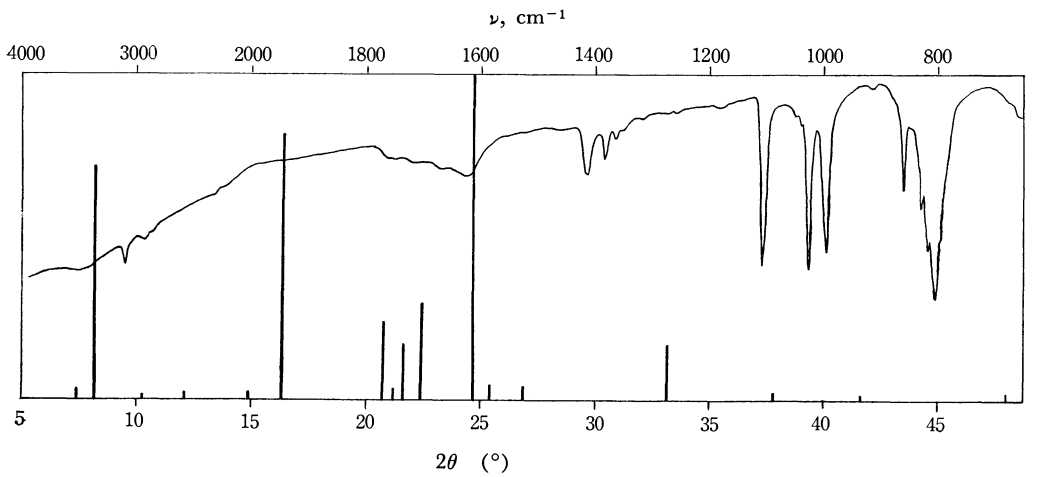

Fig. 11. Infrared spectrum and X-ray diffraction pattern of terferrocenyl from petroleum ether.

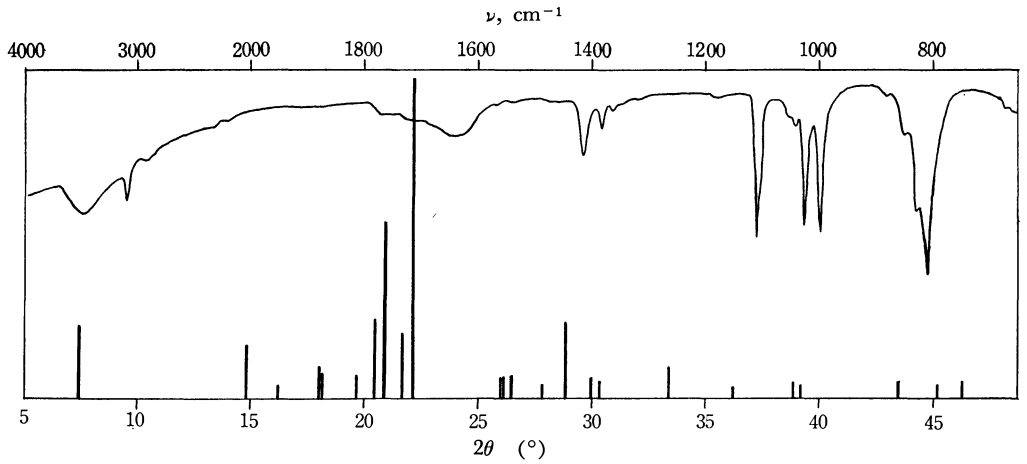

Fig. 12. Infrared spectrum and X-ray diffraction pattern of terferrocenyl from a mixture of benzene and petroleum ether.

The temperatures in the reactions and measurements were uncorrected, and each melting point was determined in a sealed capillary except for the case of the particular description. The NMR spectra were determined at 60 Mc. on a Model JNM-C-60 spectrometer (Japan Electron Optics Laboratory Co.) and a Model A-60 spectrometer (Varian Associates) in deuteriochloroform, containing tetramethylsilane as the internal standard. Molecular weight measurements with a vapor pressure osmometer were carried out on a Model 301-A (The Mechrolab Inc.). The infrared spectra were obtained on a Model EPI-S2 spectrometer (Hitachi Co.) by means of potassium bromide disks. The ultraviolet spectra were determined on a Model EPS-3 recording spectrometer (Hitachi Co.) in cyclohexane. Chromatographies were performed on Sumitomo Chemicals' activated alumina (150—250 meshes). After benzene solutions of the samples had been placed on alumina packed into a column with hexane, each component was developed and eluted with the appropriate solvent, as described below. The X-ray diffraction patterns[16] of terferrocenyl were obtained on a Model ADX-103 spectrometer (Toshiba Electric Co.) by the powder method. The differences among polymorphic forms from various crystallization methods were determined by a study of the X-ray diffraction patterns and infrared spectra.

The Reaction of Ferrocenyllithium and Cobaltous Chloride in the Presence of *n*-Butyl Bromide (Run A).—According to the method described in a previous paper,[2] a suspension of ferrocenyllithium was prepared by stirring 55.8 g. (0.3 mol.) of ferrocene and 0.6 mol. of *n*-butyllithium in anhydrous ether under an atmosphere of nitrogen. In this experiment, the lithiation took 72 hr. at room temperature.

Anhydrous cobaltous chloride (9.1 g., 0.07 mol.), obtained from its hydrate,[17] was added to the oragne suspension of ferrocenyllithium in an atmosphere of nitrogen, and then 14.4 g. (0.105 mol.) of *n*-butyl bromide was added at room temperature through a dropping funnel. An exothermic reaction took place with an evolution of gas and a vigorous refluxing, but the latter subsided when the flask was immersed into an ice-water bath. Then, the additional main part (26.70 g.; 0.195 mol.) of *n*-butyl bromide was added at one time. Immediately the vigorous refluxing of ether broke out again; it was again suppressed by cooling. After the mixture had been stirred for 44 hr. at room temperature, it was heated to reflux for another hour. The dark brown suspension thus obtained was poured into a large amount of ice water in order to hydrolyze the reactive compounds. On filtration, the reaction mixture was separated into two parts: (1) the filtrate, consisting of an ethereal layer and an aqueous layer, and (2) the residue on the filter. The following is the work-up for the two parts:

1) The ethereal layer was separated, and the aqueous layer was repeatedly extracted with ether. After the complete evaporation of ether from the combined ethereal solutions, the residue was submitted to sublimation in order to collect the unreacted ferrocene (35.6 g. recovery; the percentage of converted ferrocene: ca. 36.2%). After the sublimation, 15.5 g. of an orange-red solid (Substance A) remained; this was chromatographed on alumina.

2) The residue on the filter was washed with a sufficient amount of water and ether, and then left stand until it almost reached dryness in vacuo (water-jet pump). After it had been extracted with ether in a Soxhlet apparatus for ca. 100 hr., 14.7 g. of brown powder remained. This was further triturated with boiling benzene several times (total volume: 1.5 l.). After the trituration, 6.6 g. of a gray residue remained; this was interpreted as being an inorganic material derived from cobaltous chloride. Fine glittering orange-red crystals (0.67 g., Substance B), which separated when the hot benzene solution was cooled, were collected on a filter. The dark red mother liquor was evaporated to dryness in vacuo, and the solid was again dissolved in 600 ml. of boiling benzene. The undissolved material (0.44 g., Substance C) was collected by filtration while hot. After the hot solution had been cooled, 0.55 g. of an orange-red powder (Substance D) separated; this was collected on a filter. The filtrate was concentrated to about 200 ml. and cooled in order to separate

16) The present authors wish to express their thanks to Dr. M. Ichikuni for taking the X-ray patterns and his kind suggestion.
17) "Inorganic Syntheses," Vol. 5, 153 (1957).

additional crystals. Upon filtration, 0.98 g. of another orange-red powder (Substance E) was obtained. Finally the filtrate was evaporated to remove the benzene; 2.05 g. of a dark red-brown solid (Substance F) was thus obtained.

When the ethereal solution obtained by the Soxhlet-extraction described above was left to stand, 0.33 g. of an orange-red solid material (Substance G) separated. After the filtration, the mother liquor was evaporated to give rise to a red-orange solid material (1.79 g., Substance H).

The Chromatographic Separation and the Identification of Each Product.—*Substance A* (15.5 g.).—After the development with hexane, the elutions of the colored bands in the column were successively performed in the following order.

1) The first elution, with petroleum-benzene (3:1 by volume), yielded 1.0 g. of a yellow-orange liquid, which was then rechromatographed with the same eluent to afford two fractions. The first was an orange liquid (0.22 g.) which solidified to orange crystals upon standing. It was found to be dibutyl-biferrocenyl (VII), which is very soluble in common organic solvents; m. p. 52.0—53.0°C.

Found: C, 70.35; H, 6.96. Calcd. for $C_{28}H_{34}Fe_2$: C, 69.74; H, 7.11%.

The second fraction (0.22 g.) also solidified by itself, upon standing, to orange crystals, which were identified as monobutyl-biferrocenyl (VI) (see below).

2) The second elution, with the same solvent as in 1), yielded 1.95 g. of red-orange crystals which were very soluble in common organic solvents. This compound was identified as monobutyl-biferrocenyl (VI); m. p. 68.0—70.0°C.

Found: C, 67.61; H, 5.95%; mol. wt., 446 (Rast), 400 (vapor pressure osmometer method). Calcd. for $C_{24}H_{26}Fe_2$: C, 67.64; H, 6.19%; mol. wt. 426.

3) The third elution, also with the same solvent as in 1), yielded 5.78 g. of biferrocenyl (I), which melted at 225—234°C under decomposition (in an open capillary).

4) The fourth elution, with petroleum ether - benzene (1 : 1), yielded monobutyl-terferrocenyl (VIII, 0.34 g.), which was purified by rechromatography; m. p. 113.0—115.0°C.

Found: C, 67.07; H, 5.49%; mol. wt., 565 (v. p. o. method). Calcd. for $C_{34}H_{34}Fe_3$: C, 66.93; H, 5.62%; mol. wt., 610.

5) The fifth elution, with the same solvent as in 4), yielded orange crystals of terferrocenyl (II, 1.54 g.). The pure compound, recrystallized from a mixture of benzene and petroleum ether, had a m. p. of 226.5—227.2°C.

Found: C, 65.03; H, 4.73%; mol. wt., 554 (Rast). Calcd. for $C_{30}H_{26}Fe_3$: C, 64.89; H, 4.81%; mol. wt., 554.

6) The last elution, with methanol, gave rise to ca. 1.0 g. of a dark red glassy material. It was supposed to be still a mixture, but no attempt was made to separate and identify the components.

Substance B (0.67 g.).—Substance B melted at 252—256°C and was almost insoluble in common organic solvents. From the various analytical results, this compound was identified as sexiferrocenyl (V).

Found: C, 65.23; H, 4.87%; mol. wt., 1089 (Rast). Calcd. for $C_{60}H_{50}Fe_6$: C, 65.15; H, 4.56%; mol. wt., 1106.

Substances C, D and E (1.97 g. in total).—These substances are in fact the same compound, as is revealed by the identity of their infrared absorption spectra (Fig. 7). From the various analytical results, it was identified as quaterferrocenyl (III). It was insoluble in most common organic solvents, but it could be recrystallized from a large amount of hot benzene; m. p. 280°C.

Found: C, 65.76, 65.84, 65.63; H, 4.83, 4.84, 4.53%; mol. wt., 717, 729 (Rast; perylene being used instead of camphor because of the high melting point of this compond).[6] Calcd. for $C_{40}H_{34}Fe_4$: C, 65.09; H, 4.64%; mol. wt., 738.

Substance F (2.05 g.).—This substance was separated by chromatography into the following six fractions.

1) The first elution, with petroleum ether - benzene (1 : 1), yielded 0.2 g. of crude biferrocenyl; this was recrystallized from a mixture of benzene and petroleum ether to give a pure compound (I); m. p. 228.0—231.0°C.

2) The second elution, with the same solvent as in 1), gave ca. 90 mg. of monobutyl-terferrocenyl (VIII).

3) The third elution, with benzene, provided 0.57 g. of crude terferrocenyl (II, m. p. 214—220°C). The pure compound was obtained by the recrystallization from a mixture of benzene and petroleum ether.

4) The fourth elution, also with benzene, gave orange-red crystals (0.14 g., m. p. 170—173°C). The pure compound, obtained by recrystallization from a mixture of benzene and petroleum ether, had a m. p. of 177.0—179.0°C and was soluble in common organic solvents. The compound was found from the various analytical results to be monobutyl-quaterferrocenyl (IX).

Found: C, 66.24; H, 5.30. Calcd. for $C_{44}H_{42}Fe_4$: C, 66.54; H, 5.33%. The ultraviolet absorption spectrum (in cyclohexane) showed λ_{max} 228 ($\log \varepsilon$ 4.89), 305 (4.29) and 450 mμ (3.25).

5) The fifth elution, also with benzene, gave rise to quaterferrocenyl (III) as an orange-red powder (0.3 g., m. p. 280°C). This was found to be the same compound as Substances C, D and E.

6) The last elution, with methanol, yielded 0.29 g. of a dark red glassy solid. It was supposed to be a mixture, but further treatments were not attempted.

Substance G (0.33 g.).—This substance was repeatedly triturated with a sufficient amount of hot benzene. After the trituration, 55 mg. of a light brown powder remained; m. p. 240—245°C. From various analytical results this compound was identified as quinqueferrocenyl (IV). It is insoluble in common organic solvents.

Found: C, 61.83; H, 4.59%; mol. wt., 903 (Rast: perylene being used). Calcd. for $C_{50}H_{42}Fe_5$: C, 65.11; H, 4.59%; mol. wt., 922.

On the other hand, the evaporation of the benzene solution after the trituration gave 0.254 g. of a red-orange powder. This was dissolved in a small amount of benzene, and then chromatographed on an alumina column.

1) The first elution, with benzene - petroleum ether (4 : 1), yielded biferrocenyl (I) as orange leaflets (10 mg., m. p. 218.0—222.0°C).

2) The second elution, with the same solvent as in 1), gave rise to terferrocenyl (II) as orange crystals (0.77 g.).

3) The third elution, also with the same solvent as

in 1), yielded monobutyl-quaterferrocenyl (IX) as orange-red crystals (20 mg.).

4) The fourth elution, with benzene, gave rise to quaterferrocenyl (III) as orange-red crystals (56 mg., m. p. 278.0—279.5°C, recrystallized from a large amount of benzene).

5) The last elution, with methanol, afforded a dark red glassy solid (47 mg.). This was assumed to be a mixture of many compounds, but their separation and identification were not attempted.

Substance H (1.79 g.).—This substance was dissolved in a small amount of benzene and placed on alumina. The following is the work-up of the elution:

1) The first elution, with petroleum ether - benzene (3 : 1), gave rise to orange crystals (leaflets, 0.25 g.) which were found to be biferrocenyl (I).

2) The second elution, with petroleum ether - benzene (1 : 1), yielded 0.13 g. of fine yellow-orange crystals; these were rechromatographed by using petroleum ether - benzene (3 : 1) to give a pure substance. The compound had a m. p. of 113.0—115.0°C and was identified as monobutyl-terferrocenyl (VIII).

3) The third elution, with the same solvent as in 2), gave terferrocenyl (II, 0.78 g.).

4) A dark red glassy solid was obtained from the fraction of the last elution, but no further treatments were attempted.

The Reaction of Ferrocenyllithium and Cobaltous Chloride (Run B).—To an orange suspension of ferrocenyllithium, prepared from 55.8 g. (0.3 mol.) of ferrocene and 0.6 mol. of *n*-butyllithium according to the method described above, 9.1 g. (0.07 mol.) of anhydrous cobaltous chloride was added at one time. After the addition, a gentle refluxing occurred because of the exothermic reaction, but no cooling procedure was applied. The mixture was allowed to cool to room temperature over a period of 3 hr. The dark brown suspension was then stirred for 70 hr. under a stream of nitrogen at room temperature, and then for an additional hour under refluxing on a water bath. After cooling, the suspension was poured into a large amount of ice water in order to hydrolyze the reactive compounds. The total mixture was filtered to separate it into a solid and a liquid part.

The solid material which remained on the filter was repeatedly washed with a sufficient amount of water and benzene, dried in vacuo at room temperature, and extracted with ether for 8 hr. in a Soxhlet apparatus. The residual gray-black powder (7.77 g.) was conceived to be an inorganic substance derived from cobaltous chloride.

On the other hand, the liquid part from the reaction mixture consisted of an ethereal layer and an aqueous layer. The liquid part was combined with the washings of the solid part and the ethereal solution from the Soxhlet extraction. The combined organic layer was separated from the aqueous layer, and the aqueous layer was repeatedly extracted with ether. All the parts of the organic solution were combined, dried over magnesium sulfate, filtered, and evaporated to obtain an orange-red crystalline substance. It was submitted to vacuum sublimation at 100—120°C under 0.5 mmHg to collect the unreacted ferrocene (53.4 g., 95.5% recovery). The remaining dark red-brown solid (2.33 g.) was dissolved in a small amount of benzene and chromatographed on alumina. The solution of the sample was placed on alumina packed into a column with benzene - pertroleum ether (1 : 1), and the same solvent was used as the developer. Elution was performed as follows:

1) The first elution, with petroleum ether - benzene (1 : 1), gave rise to monobutyl-biferrocenyl (VI, 0.38 g., m. p. 67.0—69.0°C).

2) The second elution, with the same solvent as in 1), yielded biferrocenyl (I, 1.06 g., m. p. 228.5—233.0°C).

3) The third elution, also with the same solvent as in 1), gave an orange solid (59 mg.) which was found to be butyl-polyferrocenyl by a comparison of its infrared spectrum with those of other butyl-polyferrocenyls, such as monobutyl-biferrocenyl and monobutyl-terferrocenyl. It might be crude monobutyl-terferrocenyl, but no further treatments were attempted.

4) The fourth elution, with benzene, yielded terferrocenyl (II, 0.14 g., m. p. 215.0—218.0°C).

5) A dark red-brown glassy solid (0.20 g.) was obtained from the fraction of the elution with methanol. This was inferred to be a mixture which might contain some polyferrocenyls of a greater molecular weight than that of terferrocenyl. However, no further investigation was undertaken.

Thanks are due to the Ministry of Education for the financial support granted for this research.

BULLETIN OF THE CHEMICAL SOCIETY OF JAPAN VOL. 39 802—803 (1966)

Organic Sulfur Compounds. I. Reactions of Arylsulfinic Acids with Alkyl Chlorosulfites

By Michio KOBAYASHI, Miki TERAO and Asami YAMAMOTO

Department of Chemistry, Yokohama City University, Mutsuura-machi, Kanazawa-ku, Yokohama

(Received September 14, 1965)

The salts of arylsulfinic acids were found to react with alkyl chlorosulfite to form alkyl sulfinates. *p*-Toluenesulfinic acid-^{18}O was synthesized and treated with ethyl chlorosulfite to give ethyl *p*-toluenesulfinate-^{18}O, which retained half of the oxygen atoms existing in the original sulfinic aicd. A mechanism for this novel reaction was proposed.

The formation of carboxylic esters from the salts of carboxylic acids and chlorosulfites has previously been known.[1,2] The possibility of an analogous preparation of the sulfinic esters from the salt of sulfinic acids and chlorosulfites has now been investigated; the results will be described in this paper.

Ethyl chlorosulfite was added to the suspension of sodium *p*-toluenesulfinate in acetonitrile; this reaction mixture then warmed at 60°C for 2 hr. to form *p*-toluenesulfinate, as expected, in a 59% yield. When this reaction was carried out without a solvent, sulfur dioxide evolved vigorously and ethyl sulfinate was obtained in a 42% yield. Sodium *p*-bromobenzenesulfinate gave the ethyl ester in a 34% yield by a similar treatment.

A solution of *p*-toluenesulfinic acid in pyridine reacted rapidly with ethyl chlorosulfite to give ethyl *p*-toluenesulfinate in a 21% yield. Since alkyl chlorosulfites are known to decompose very rapidly to alkyl chlorides and sulfur dioxide in the presence of pyridine, the above result suggests that the rate of the reaction of the sulfinate anion with alkyl chlorosulfite is also very high.

The formation of the mixed anhydride of sulfinic acid and monoalkyl sulfite (I) is suggested by these reactions, although the actual isolation of the intermediate was not possible.

$$RSO_2Na + ClS\text{-}OR' \rightarrow \underset{\underset{O}{\downarrow}}{R\text{-}S\text{-}O\text{-}S\text{-}OR'}_{\underset{O}{\downarrow}\quad\underset{O}{\downarrow}} \qquad (1)$$

(I)

There are two possibilities for the decomposition of the mixed anhydride (I), namely, the alkyl-oxygen cleavage (path a) and alkoxy-sulfur cleavage (path b):

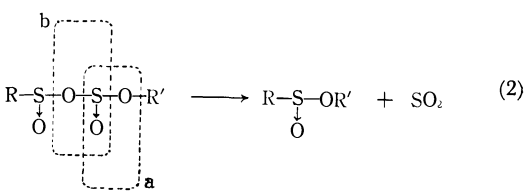

(2)

When sodium *p*-toluenesulfinate-^{18}O, which had been prepared from *p*-toluenesulfinyl chloride and ^{18}O water, was treated with ethyl chlorosulfite, the resultant ethyl *p*-toluenesulfinate-^{18}O was found to contain about a half of the heavy oxygen atoms originally incorporated in the starting sulfinic acid. Therefore, the alkoxy-sulfur splitting (path b) may be chosen.

$$CH_3C_6H_4\text{-}S\text{-}Cl + H_2{}^{18}O \rightarrow \underset{\underset{O}{\downarrow}}{CH_3C_6H_4S^{18}O_2H} \qquad (3)$$

$$CH_3C_6H_4S^{18}O_2Na + \underset{\underset{O}{\downarrow}}{ClS\text{-}OC_2H_5} \rightarrow \underset{\underset{{}^{18}O}{\downarrow}\quad\underset{O}{\downarrow}}{CH_3C_6H_4\text{-}S\text{-}{}^{18}O\text{-}S\text{-}OC_2H_5} \qquad (4)$$

(Ia)

$$Ia \rightarrow CH_3C_6H_4S\text{-}OC_2H_5 + \underset{\underset{{}^{18}O}{\downarrow}}{SO} \qquad (5)$$

Between the following two mechanisms, a four-center mechanism (6) and a base-catalyzed ionic chain mechanism (7, 8, 9), which fit the above results equally well, there is no evidence to make a choice possible at present.

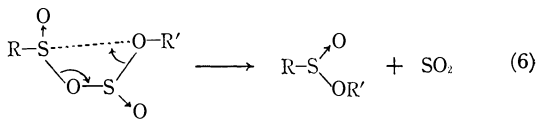

(6)

$$R\text{-}S\text{-}O\text{-}S\text{-}OR' + :B$$

$$\underset{O}{\downarrow}\quad\underset{O}{\downarrow}$$

(I)

1) P. Carré and D. Libermann, *Bull. soc. chim. France*, [4], **53**, 1050 (1933).
2) M. S. Newman and W. S. Fones, *J. Am. Chem. Soc.*, **69**, 1046 (1947).

$$\rightarrow [R\text{-}SO\cdots B]^+ + \left[R'O\text{-}S\begin{matrix}O\\O\end{matrix}^-\right] \quad (7)$$

(II)

$$II \rightarrow R'O^- + SO_2 \quad (8)$$

$$R'O^- + I \rightarrow R\text{-}S\text{-}OR' + II \quad (9)$$
$$\downarrow$$
$$O$$

(:B indicates the base catalyst)

Experimental

Ethyl *p*-Toluenesulfinate.—*Reaction in Acetonitrile.*—Sodium *p*-toluenesulfinate dihydrate[3] was dehydrated by heating it at 130°C for a few hours in a vacuum to anhydrous salt. To a suspension of 5.8 g. of the fine powder of this salt in 20 ml. of acetonitrile there was added 4.5 g. of ethyl chlorosulfite (b. p. 45°C/55 mmHg) drop by drop. The reaction mixture was warmed at 60°C for 2 hr. and kept overnight. Extraction with ether and distillation in a vacuum gave ethyl *p*-toluenesulfinate (b. p. 115°C/5 mmHg) (3.6 g.) in a 59% yield of the theoretical.

Reaction without a Solvent.—When ethyl chlorosulfite was added to the fine powder of sodium *p*-toluenesulfinate at room temperature, sulfur dioxide evolved quickly (about 70% of the theoretical yield). The reaction mixture became jelly-like after being heated at 60°C for 2 hr. A work up similar to that above gave 2.8 g. of ethyl *p*-toluenesulfinate from 5.8 g. of the sodium salt in a 42% yield of the theoretical.

Ethyl *p*-Bromobenzenesulfinate.—To 8.0 g. of the finely-powdered sodium *p*-bromobenzenesulfinate there was added 6.0 g. of ethyl chlorosulfite. When the first exothermic reaction accompanying the evolution of 350 ml. (45%) of sulfur dioxide subsided, the reaction mixture was extracted with petroleum ether. Vacuum distillation gave ethyl *p*-bromobenzenesulfinate (2.8 g.) (b. p. 132°C/2 mmHg) in a yield 34% of the theoretical yield.

Ethyl *p*-Toluenesulfinate.—*Reaction in Pyridine.*—Four grams of *p*-toluenesulfinic acid was dried in a vacuum overnight and dissolved in 20 ml. of anhydrous pyridine. When 3.5 g. of ethyl chlorosulfite was added to this solution drop by drop, the reaction proceeded with the evolution of heat. After it had stood overnight, the mixture was diluted with water, acidified, and extracted with petroleum ether. The yield of ethyl *p*-toluenesulfinate was 1.0 g., 21% of the theoretical.

***p*-Toluenesulfinyl Chloride.**—Prepared from 15 g. of *p*-toluenesulfinic acid and 20 g. of thionyl chloride. The yield was 13.3 g (116°C/5 mmHg).

Sodium *p*-Toluenesulfinate-^{18}O.—To 13.3 g. of *p*-toluenesulfinyl chloride there was added 1.8 g. of $H_2{}^{18}O$ (^{18}O: 1.5 atom %) with cooling in an ice bath. The reaction started immediately, and white crystals of sulfinic acid were deposited. These crystals were vigorously stirred into an ice-cooled solution of sodium hydroxide (7 g.) in 30 ml. of water. The mixture was warmed to ensure a complete dissolution and then cooled in an ice bath in order to precipitate the sodium sulfinate. The salt filtrated was recrystallized once from the distilled water to give 9.0 g. of sodium *p*-toluenesulfinate-^{18}O dihydrate. The concentration of the mother liquid gave 6 g. of the second crop. The dehydration of the first crop in a vacuum afforded 7.5 g. of the anhydrous salt. It was confirmed in a separate experiment that no exchange of oxygen atoms occurred between sulfinic acid and water in neutral or basic conditions. The ^{18}O content of the anhydrous salt was 0.69, 0.70 atom %.

Ethyl *p*-Toluenesulfinate-[sulfinyl-^{18}O].—In 25 ml. of acetonitrile, 5.8 g. of sodium *p*-toluenesulfinate-^{18}O was treated with 4.5 g. of ethyl chlorosulfite. The mixture was then warmed at 60°C for one hour and left at room temperature for 2 days. A precipitated powder was filtered off, and the filtrate was evaporated under reduced pressure. The residue was extracted with petroleum ether, and the extract was washed with water and dried over magnesium sulfate. Vacuum distillation gave 2.4 g. of ethyl *p*-toluenesulfinate-^{18}O in a yield 41% of the theoretical. The ^{18}O atom % of this ester was 0.41%. The calculated ^{18}O atom %, based on the retention of half of the oxygen atoms, was 0.46%.

The infrared spectra of all the products in the above experiments were superimposable with those of an authentic specimen.

Thanks are due to Professor Shigeru Oae of Osaka City University for the donation of the heavy oxygen water. The authors are also grateful to Drs. Teijiro Kitao and Reiko Kiritani of the Radiation Center of Osaka Prefecture for their analyses of ^{18}O, and to Mr. Tadao Ohkusa of the Central Research Laboratories, Chisso Co., for his infrared measurements.

3) "Organic Syntheses," Coll. Vol. 1, 492 (1941).

BULLETIN OF THE CHEMICAL SOCIETY OF JAPAN VOL. 39 804—809 (1966)

The Magnetic Properties of Several *Pseudo*-Jahn-Teller Nonbenzenoid Aromatic Hydrocarbons

By Takeshi NAKAJIMA and Susumu KOHDA

Department of Chemistry, Ibaraki University, Mito

(Received September 15, 1965)

The effect of bond length alternation on the magnetic properties of several *pseudo*-Jahn-Teller nonbenzenoid aromatic hydrocarbons with 4ν carbon atoms will be investigated. The magnetic moment and the susceptibility of a cyclic polyene will first be formulated in terms of the bond alternation parameter. Appropriate cross-links for forming nonbenzenoid aromatic hydrocarbons, such as pentalene and heptalene, will then be treated as perturbations. It will be shown that the anomalously large paramagnetic susceptibilities of these molecules predicted by Pullman et al. ("Les Théories Electroniques de la Chimie Organique," Masson, Paris (1952), p. 527) arise mainly from the neglect of the bond alternation inherent in them. It will then be concluded that the magnetic susceptibility is a very sensitive indicator of the bond alternation, and that the diamagnetically-induced ring currents in these molecules are very much impeded.

The diamagnetic anisortopy of an aromatic hydrocarbon, attributable to induced ring currents in its π-electron network, is one of the important indications of π-electron delocalization. London[1] has developed a technique for calculating diamagnetic susceptibilities on the basis of the Hückel LCAO MO theory, and this method has since been used extensively for a variety of aromatic hydrocarbons.[2,3] The calculated diamagnetic anisotropies of benzenoid aromatic hydrocarbons are usually in quite good agreement with the experimental values.

As for nonbenzenoid aromatic hydrocarbons, on the other hand, the direct application of London's technique often brings about quite unsatisfactory results; Mayot et al.[4] and Pullman et al.[5] have, for instance, pointed out that the contribution to the magnetic susceptibility due to π-electron delocalization in the nonbenzenoid aromatic hydrocarbons with 4ν carbon atoms, such as pentalene and heptalene, turns out to be paramagnetic instead of diamagnetic. Wagnière and Gouterman[6] have recently interpreted such an anomalously-reduced diamagnetism as a quenched paramagnetism.

It has recently been shown that, as the result of a *pseudo*-Jahn-Teller distortion,[7] there exists a significant alternation in length in the peripheral C–C bonds of these nonbenzenoid aromatic hydrocarbons, the skew structure (C_{2h}) being more favorable energetically than the conventional symmetric structure (D_{2h}).[8-15] It is very probable that the unusually high paramagnetic susceptibilities obtained by the French authors are due mainly to the neglect of the bond alternation characteristic of these molecules.

The aim of this paper is to investigate the effect of bond length distortion on the magnetic susceptibilities of *pseudo*-Jahn-Teller nonbenzenoid aromatic hydrocarbons, such as pentalene, heptalene, *s*-indacene, and dibenzpentalene. The magnetic moment and the susceptibility of a cyclic polyene will first be formulated in terms of the bond alternation parameter, an external magnetic field being treated as a complex perturbation. The formulae will then be tested for cyclooctatetraene and [24]annulene. The formation of cross-links to yield the nonbenzenoid aromatic hydrocarbons will be considered further as a perturbation. The effect of this perturbation on the magnetic properties will then be investigated.

The Cyclic Polyenes, $C_{2n}H_{2n}$

In the presence of an external magnetic field, **H** assumed to be normal to the molecular plane,

1) F. London, *J. Phys. Radium*, **8**, 397 (1937).
2) B. Pullman and A. Pullman, "Les Théories Electroniques de la Chimie Organique," Masson, Paris (1952).
3) R. McWeeny, *Proc. Phys. Soc.*, **A64**, 261, 921 (1951); ibid., **A65**, 839 (1952); ibid., **A66**, 714 (1953).
4) M. Mayot, G. Berthier and B. Pullman, *J. Phys. Radium*, **12**, 652 (1951); *J. Chim. Phys.*, **50**, 176 (1953).
5) B. Pullman, A. Pullman, E. D. Bergmann, G. Bertheir, E. Fischer, Y. Hirshberg and J. Pontis, ibid., **49**, 24 (1952).
6) G. Wagnière and M. Gouterman, *Mol. Phys.*, **5**, 621 (1962).
7) C. A. Coulson, *Chem. Soc.* (*London*) *Spec. Publ.*, No. 12 (1958), p. 85.
8) P. C. Boer-Veenendaal and D. H. W. Boer, *Mol. Phys.*, **4**, 33 (1961).
9) P. C. Boer-Veenendaal, J. A. Vliegenthart and D. H. W. Boer, *Tetrahedron*, **18**, 1325 (1962).
10) L. C. Snyder, *J. Phys. Chem.*, **66**, 2299 (1962).
11) T. Nakajima and S. Katagiri, *Mol. Phys.*, **7**, 149 (1963).
12) T. Nakajima, Y. Yaguchi, R. Kaeriyama and Y. Nemoto, This Bulletin, **37**, 272 (1964).
13) T. Nakajima, "Molecular Orbitals in Chemistry, Physics, and Biology," Ed. by P. O. Löwdin and B. Pullman, Academic Press, New York (1964), p. 451.
14) T. Nakajima, T. Saijo and H. Yamaguchi, *Tetrahedron*, **20**, 2119 (1964).
15) P. C. Boer, D. H. W. Boer, C. A. Coulson and T. H. Goodwin, ibid., **19**, 2163 (1963).

the MO's of the π-electrons are constructed from the AO's, χ_r^m, given by:

$$\chi_r^m = \chi_r \exp\{-2\pi i(e/hc)\mathbf{A}_r \cdot \rho\} \tag{1}$$

where χ_r is the $2p\pi$ atomic orbital for the rth atom and $\mathbf{A}_r$ is the value of the magnetic vector potential at the rth atom. For a uniform magnetic field, $\mathbf{A}$ is given by $-(1/2)\rho \times \mathbf{H}$, while at the rth atom we have $\mathbf{A}_r = -(1/2)\mathbf{R}_r \times \mathbf{H}$. According to London, the secular problem for the MO's is different from that without the field merely in the form of the resonance integrals, which now include the field-dependent phase factor:

$$\beta_{rs}^m = \beta_{rs} \exp\{\pi i(e/hc)(\mathbf{A}_r - \mathbf{A}_s) \cdot (\mathbf{R}_r + \mathbf{R}_s)\} \tag{2}$$

Using simple geometry, Eq. 2 may be rewritten as:

$$\beta_{rs}^m = \beta_{rs} \exp\{2\pi i(e/hc) S_{rs} H\} \tag{3}$$

where S_{rs} is the singed area of a triangle formed by the origin (where $A=0$) and the bond $r \rightarrow s$ (S_{rs} is positive if the direction $r \rightarrow s$ is right-handed about the direction of the magnetic field). By expanding the exponential function and writing $(e/hc)S_{rs}H = f_{rs}$, we obtain the change in the resonance integral due to the presence of the field as:

$$\Delta_{rs} = \beta_{rs}(2\pi i f_{rs} - 2\pi^2 f_{rs}^2 + \cdots) \tag{4}$$

The total perturbation due to the presence of the field is represented by:

$$\Delta = \sum_{r<s} \Delta_{rs} \tag{5}$$

It is assumed that $\beta_{rs}=0$ if the atoms r and s are not bonded in a conventional structure.

Now let us consider a cyclic polyene, $C_{2n}H_{2n}$, the MO's of which are assumed to be expressed in the following form:

$$\left.\begin{aligned} \varphi_l &= a_l \varphi_l^o + b_l \varphi_l^e \quad (l=0, \pm 1, \pm 2, \cdots, n) \\ \varphi_l^o &= \frac{1}{\sqrt{n}} \sum_{r=1}^{n} \chi_{2r-1} \exp\{i\theta_l(r-1)\} \\ \varphi_l^e &= \frac{1}{\sqrt{n}} \sum_{r=1}^{n} \chi_{2r} \exp\left\{i\theta_l\left(r-\frac{1}{2}\right)\right\} \end{aligned}\right\} \tag{6}$$

where:

$$\theta_l = 2\pi l/n \tag{7}$$

Allowing for the possibility of a two-fold bond length alternation, we denote by β the resonance integrals for bonds between atoms $2r-1$ and $2r$, and by $k\beta$ ($k \leqq 1$), those for bonds between atoms $2r$ and $2r+1$, including the bond between the $2n$th atom and the first atom. Then we have:

$$\left.\begin{aligned} \int \varphi_l^{o*} \mathbf{H} \varphi_l^e dv &= (e^{i\theta_l/2} + k e^{-i\theta_l/2})\beta = \gamma_l \beta \\ \int \varphi_l^{e*} \mathbf{H} \varphi_l^o dv &= (e^{-i\theta_l} + k e^{i\theta_l/2})\beta = \gamma_l^* \beta \end{aligned}\right\} \tag{8}$$

$$\left.\begin{aligned} \int \varphi_l^{o*} \mathbf{H}_l^o dv &= \int \varphi_l^{e*} \mathbf{H} \varphi_l^e dv = \alpha \end{aligned}\right\}$$

By solving the quadratic secular equation, we obtain, for the orbital binding energies:

$$\begin{aligned} x_l^{(0)} &= (\varepsilon_l - \alpha)/\beta = \pm(1 + 2k\cos\theta_l + k^2)^{1/2} \\ &= \pm(\gamma_l^* \gamma_l)^{1/2} \end{aligned} \tag{9}$$

where + and − should be taken for the bonding and antibonding orbitals respectively.

The partial π-bond orders for the $2r-1$—$2r$ bonds (double bonds) and the $2r$—$2r+1$ bonds (single bonds) are given respectively by the forms[16]:

$$\left.\begin{aligned} p_{l,d} &= \frac{1}{n}(a_l^* b_l e^{i\theta_l/2} + a_l b_l^* e^{-i\theta_l/2}) \\ &= \pm \frac{1 + k\cos\theta_l}{n(1 + 2k\cos\theta_l + k^2)^{1/2}} \\ p_{l,s} &= \frac{1}{n}(a_l b_l^* e^{i\theta_l/2} + a_l^* b_l e^{-i\theta_l/2}) \\ &= \pm \frac{k + \cos\theta_l}{n(1 + 2k\cos\theta_l + k^2)^{1/2}} \end{aligned}\right\} \tag{10}$$

In order to take account of the imaginary perturbation due to an external magnetic field, we define in this connection the imaginary partial π-bond orders, which are given by:

$$\left.\begin{aligned} \bar{p}_{l,d} &= \frac{1}{n}(a_l^* b_l e^{i\theta_l/2} - a_l b_l^* e^{-i\theta_l/2}) \\ &= \pm \frac{ik\sin\theta_l}{n(1 + 2k\cos\theta_l + k^2)^{1/2}} \\ \bar{p}_{l,s} &= \frac{1}{n}(a_l b_l^* e^{i\theta_l/2} - a_l^* b_l e^{-i\theta_l/2}) \\ &= \pm \frac{i\sin\theta_l}{n(1 + 2k\cos\theta_l + k^2)^{1/2}} \end{aligned}\right\} \tag{11}$$

According to the LCAO perturbation theory, the first-order change in the energy of the lth MO due to the presence of a magnetic field is expressed in terms of bond orders. Using Eqs. 10 and 11, we obtain:

$$\begin{aligned} \delta x_l^{(1)} &= \langle \psi_l^* | \Delta | \psi_l \rangle \\ &= -2\pi i f n(\bar{p}_{l,d} + k\bar{p}_{l,s}) \\ &\quad -2\pi^2 f^2 n(p_{l,d} + k p_{l,s}) \\ &= \pm \left\{ \frac{2}{n} \frac{k\sin\theta_l}{(1 + 2k\cos\theta_l + k^2)^{1/2}} \omega \right. \\ &\quad \left. -\frac{1}{2n}(1 + 2k\cos\theta_l + k^2)^{1/2} \omega^2 \right\} \end{aligned} \tag{12}$$

where:

$$\omega = 2n\pi f = (e/hc)\pi SH \tag{13}$$

in which S is the total area of the molecular plane.

16) Y. Ooshika, *J. Phys. Soc. Japan*, **12**, 1246 (1957).

TABLE I. MO ENERGIES, MAGNETIC MOMENTS, AND MAGNETIC SUSCEPTIBILITIES OF C_8H_8

	$x_l^{(0)}$		λ_l		μ_l	
l	$k=1$	$k<1$	$k=1$	$k<1$	$k=1$	$k<1$
-2	0.0000	$k-1$	-0.5000	0.0000	0.0000	$1/32\{(1-k)-(1+k)^2(1-k)^{-1}\}$
2	0.0000	$1-k$	0.5000	0.0000	0.0000	$-1/32\{(1-k)-(1+k)^2(1-k)^{-1}\}$ $(\geqq 0)$
-1	1.4142	$(1+k^2)^{1/2}$	-0.3536	$-k/2(1+k^2)^{1/2}$	-0.0442	$-1/32\{(1+k^2)^{1/2}-(1-k^2)^2(1+k^2)^{-3/2}\}$ $(\leqq 0)$
1	1.4142	$(1+k^2)^{1/2}$	0.3536	$k/2(1+k^2)^{1/2}$	-0.0442	$-1/32\{(1+k^2)^{1/2}-(1-k^2)^2(1+k^2)^{-3/2}\}$ $(\leqq 0)$
0	2.0000	$1+k$	0.0000	0.0000	-0.0625	$-1/32\{(1+k)-(1-k)^2(1+k)^{-1}\}$ $(\leqq 0)$
$2\sum_l{}^*$	9.6568	$4+4(1-k^2)^{1/2}$	1.0000	0.0000	-0.3018	$(k^2/2)\{(1-k^2)^{-1}-(1+k^2)^{-3/2}\}$ $(\geqq 0)$
$2\sum_l{}^{2-}{}^\dagger$	9.6568	$2(1+k)+4(1+k^2)^{1/2}$	0.0000	0.0000	-0.3018	$-(k/4)\{(1+k)^{-1}+2k(1+k^2)^{-3/2}\}$ $(\leqq 0)$

* The summation is over $l=0, \pm 1, 2$.
† The summation is over $l=0, \pm 1, \pm 2$.

McWeeny[17] has already shown that the second-order energy change of the lth MO due to complex perturbations is related to the imaginary partial mutual bond polarizability defined as:

$$\bar{\pi}_{l,rs,tu} = \pi_{l,rs,tu} - \pi_{l,rs,ut} + \pi_{l,sr,ut} - \pi_{l,sr,tu} \tag{14}$$

where:

$$\pi_{l,rs,tu} = \sum_{m(\neq l)} \frac{c_{rl}^* c_{sm} c_{tm}^* c_{ul}}{x_l^{(0)} - x_m^{(0)}} \tag{15}$$

The zero-field MO's are assumed to be $\psi_l = \sum_r c_{rl}\chi_r$. The second-order energy change in the lth MO due to the presence of a magnetic field is thus given by:

$$\begin{aligned}\delta x_l^{(2)} &= \sum_{m(\neq l)} \frac{\langle\psi_l^*|\Delta|\psi_m\rangle\langle\psi_m^*|\Delta|\psi_l\rangle}{x_l^{(0)} - x_m^{(0)}} \\ &= -4\pi^2 f^2 n(\bar{\pi}_{l,d,d} + k\bar{\pi}_{l,d,s} \\ &\quad + k\bar{\pi}_{l,s,d} + k^2\bar{\pi}_{l,s,s}) \\ &= \pm\frac{1}{2n^2}\left\{\frac{(1-k^2)^2}{(1+2k\cos\theta_l+k^2)^{3/2}}\right. \\ &\quad \left. + (n-1)(1+2k\cos\theta_l+k^2)^{1/2}\right\}\omega^2 \end{aligned} \tag{16}$$

We can now formulate the magnetic moment and the magnetic susceptibility associated with the lth MO. The shifts in orbital energies due to the magnetic field being very small, we may in general expand the energy of a given MO as a function of H in Taylor's series in H:

$$x_l = x_l^{(0)} + \lambda_l\omega + \mu_l\omega^2 + \cdots \tag{17}$$

where, using Eqs. 12 and 16 respectively, λ_l and μ_l are given by (in β units):

$$\lambda_l = \mp\frac{2}{n}\frac{k\sin\theta_1}{(1+2k\cos\theta_l+k^2)^{1/2}} \tag{18}$$

$$\mu_l = \pm\frac{1}{2n^2}\left\{(1+2k\cos\theta_l+k^2)^{1/2} - \frac{(1-k^2)^2}{(1+2k\cos\theta_l+k^2)^{3/2}}\right\} \tag{19}$$

The magnetic moment and the susceptibility, χ_l, associated with the lth MO are given, by $-\lambda_l(\omega/H)$ and $-2\mu_l(\omega/H)^2$, respectively. For the bonding MO's, the first term of Eq. 19 represents the pure diamagnetism (negative in β units), while the second term, which arises from the second-order perturbation, represents the induced paramagnetism (positive in β units).

Salem[18] has derived a formula similar to Eq. 19 for the effect of a bond alternation on the magnetic susceptibility of a cyclic polyene. However, the pure diamagnetic term and the second-order paramagnetic term are not separated in his expression, and the origin of the paramagnetic susceptibility is not clearly explained.

The usefulness of Eqs. 18 and 19 may also be demonstrated for cyclooctatetraene and [24]-annulene.

Cyclooctatetraene (C_8H_8).—The orbital energies and the magnetic contributions, λ_l and μ_l, calculated using Eqs. 9, 18, and 19 are presented in Table I. When $k=1$, all the MO's except for the lowest and the highest (vacant) ones are doubly degenerate. The bond alternation lifts the degeneracy of the nonbonding orbitals (with $l=\pm 2$), the top two electrons being both placed in the lower level. As we are concerned with the effect of the bond length distortion on the magnetic properties, we adopt for the case when $k=1$ the electron configuration in which the top two electrons are both placed into one of the degenerate nonbonding orbitals. This gives rise to a molecular paramagnetic moment due to the non-compensating orbital angular

17) R. McWeeny, *Mol. Phys.*, **1**, 311 (1958).

18) L. Salem, *Proc. Cambridge Phil. Soc.*, **57**, 353 (1961); H. C. Longuet-Higgins and L. Salem, *Proc. Roy. Soc.*, **A257**, 445 (1960).

momentum.* The magnetic moment of the occupied nonbonding orbital disappears if the bond alternation is introduced, and, at the same time, the magnetic susceptibility turns out to be paramagnetic. In other words, the first-order paramagnetism is quenched by the bond length distortion and transferred to the susceptibility as an induced paramagnetism. This second-order paramagnetism greatly predominates over the diamagnetism originating from all other, lower-lying electrons, giving rise to a molecular paramagnetic susceptibility. The molecular susceptibility is very sensitive to the value of k; the value of $2\sum_l \mu_l$ varies from ∞ to 0 as k varies from 1 to 0.

In the dianion of cyclooctatetraene that forms a closed electron shell when $k=1$, no such an anomalous paramagnetic susceptibility is predicted.

Hoarau[19] has recently made improvements on the London method by refining the calculation of the gauge factors. According to him, the molar magnetic anisotropy is given by:

$$\Delta K = (1/3)\Delta K_{\text{London}} + \text{A}\times 10^{-18}R \qquad (20)$$

where $\Delta K_{\text{London}}=N\chi_\pi$, in which N is Avogadro's number and $\chi_\pi=2\sum_l \chi_l$; R is the π-electron delocalization energy as calculated using the Hückel-type MO method. The value adopted for the proportionality constant, A, is 0.940.**

The magnetic susceptibilities as a function of the k of C_8H_8 calculated using Eq. 20 indicate that, within the range $0.2\geq k>0$, the susceptibility turns out to be diamagnetic, if only slightly so. Actually, it has been shown that the molecule exhibits a marked bond length alternation, as revealed by its tub form, and that it has a weak diamagnetism.[20] On the other hand, the $C_8H_8^{2-}$ dianion has been known to show the normal diamagnetism, as in benzenoid aromatic hydrocarbons, and no bond length alternation.[21]

[24]annulene ($C_{24}H_{24}$).—The molecule, if the molecular symmetry group is D_{3h}, possesses an open-shell electronic configuration in the sense that the top two degenerate MO's are filled with two electrons. The bond length distortion lifts the degeneracy of these MO's and results in the achievement of a closed electron shell, the situation being quite similar to the case of C_8H_8.

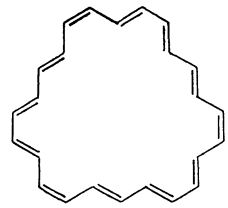

$C_{24}H_{24}$

In order to determine the equilibrium bond length alternation, we employ the minimum energy method, in which the effects of σ-bond compression are taken into account.[11] The total binding energies, V, taken to be the sum of the π-bond energy and the σ-bond energy, are calculated for a series of k values (1–0), and then the equilibrium bond alternation, $k_{\min}$, is given by the minimum of the V-k curve. The $k_{\min}$ value thus calculated for [24]annulene turns out to be 0.61, which indicates that in this molecule there exists a significant bond length alternation, one which is comparable in extent to that in butadiene (with $k_{\min}=0.55$).

The molar anisotropy, $\Delta K/\Delta K_{\text{benzene}}$, calculated for the skew form with $k=0.61$ turns out to be 0.012. This indicates that the induced diamagnetic ring current in this molecule is highly impeded. It has recently been shown that the proton NMR spectrum of this molecule consists of one single band at 3.16 τ, which is close to that observed for the olefinic protons of linear-conjugated polyenes, showing an absence of the ring current as in the benzenoid aromatic hydrocarbons.[22]

The Introduction of Cross-Links

Now let us consider a cata-condensed aromatic hydrocarbon formed by the introduction of certain cross-links into a cyclic polyene, the formation of cross-links being treated as a perturbation.

Let us consider the formation of a cross-link between the odd-numbered atoms, $2r-1$ and $2r'-1$, of a cyclic polyene, and let us denote the change in the π-electron Hamiltonian by $\mathbf{H}^o$. We then have:

$$\langle \varphi_l^{o*}|\mathbf{H}|\varphi_l^o\rangle = (2k^o\beta/n)\cos\theta_l(r'-r) = \delta_l^o\beta \qquad (21)$$

where we set $\int \chi_{2r-1}\mathbf{H}^o\chi_{2r'-1}dv=k^o\beta$. Similarly, for the cross-link between the even-numbered atoms, $2r$ and $2r'$, we have:

$$\langle \varphi_l^{e*}|\mathbf{H}^e|\varphi_l^e\rangle = (2k^e\beta/n)\cos\theta_l(r'-r) = \delta_l^e\beta \qquad (22)$$

where $\int \chi_{2r}\mathbf{H}^e\chi_{2r'}dv=k^e\beta$. Further, for the cross-

* We may place alternatively each of the top two electrons in one of the degenerate levels. This gives rise to a triplet spin paramagnetism.

19) J. Hoarau, *Ann. Chim.*, **1**, 544 (1956).

** The value of A has been determined so that the $\Delta K/\Delta K_{\text{benzene}}$ values calculated using Eq. 20 fit the experimental ones. Hoarau has proposed a value of 0.776 calculated using the experimental anisotropies of a number of aromatic hydrocarbons, including biphenyl and stilben, which show a remarkable bond length variation. We have re-examined the value using the experimental values of benzene, naphthalene, anthracene, phenanthrene, and naphthacene, which do not exhibit any significant bond length variation.

20) S. Shida and S. Fujii, This Bulletin, **24**, 173 (1951).

21) T. J. Katz, *J. Am. Chem. Soc.*, **82**, 3784 (1960); T. J. Katz and H. L. Strauss, *J. Chem. Phys.*, **32**, 1873 (1960).

22) L. M. Jackman, F. Sondheimer, Y. Amiel, D. A. Ben-Efraim, Y. Gaoni, R. Wolovsky and A. A. Bothner-By, *J. Am. Chem. Soc.*, **84**, 4307 (1962).

TABLE II. MO ENERGIES, MAGNETIC MOMENTS, AND MAGNETIC SUSCEPTIBILITIES OF PENTALENE*

	x_l		λ_l		μ_l	
l	$k=k^o=1$	$k=k^o=0.55$	$k=k^o=1$	$k=k^o=0.55$	$k=k^o=1$	$k=k_o=0.55$
−2	0.0000	−0.3330	0.0000	0.0000	−0.5000	−0.1461
2	0.5000 (0.4707)	0.6080 (0.5950)	0.0000 (0.0000)	0.0000 (0.0000)	0.5000 (0.4968)	0.1461 (0.1423)
−1	1.1861 (1.0000)	1.0120 (0.8989)	−0.3482 (0.0000)	−0.2392 (0.0000)	−0.0422 (−0.3333)	−0.0249 (−0.2605)
1	1.1861 (1.4142)	1.0120 (1.1413)	0.3482 (0.0000)	0.2392 (0.0000)	−0.0422 (0.2500)	−0.0249 (0.2111)
0	2.0000 (2.3429)	1.6936 (1.7247)	0.0000 (0.0000)	0.0000 (0.0000)	−0.0620 (−0.0549)	−0.0442 (−0.0412)
$2\sum_l$	9.7444 (10.4556)	8.6512 (8.7198)	0.0000 (0.0000)	0.0000 (0.0000)	0.7072 (0.7172)	0.1042 (0.1034)

* The values in parentheses for x_l are calculated by solving the secular equation, and those for λ_l and μ_l are calculated by using London's method.

link between an odd-numbered atom, $2r-1$, and an even-numbered atom, $2r'$, we have:

$$\langle\varphi_l^{o*}|\mathbf{H}'|\varphi_l^{e}\rangle = (k'\beta/n)e^{i\theta_l(r'-r+1/2)} = \delta_l'\beta \quad (23)$$

where $\int \chi_{2r-1}\mathbf{H}'\chi_{2r'-1}dv = k'\beta$.

Assuming the perturbations due to the three types of cross-links to be additive, and solving the quadratic secular equation, we then obtain the energy of the $l$the MO as (in β units):

$$x_l = \frac{1}{2}\left[\left(\delta_l^o+\delta_l^e\right) \pm\left\{\delta_l^2+4\left(\gamma_l^*+\delta_l'^*\right)\left(\gamma_l+\delta_l'\right)\right\}^{1/2}\right] \qquad \left(\delta_l=\delta_l^o-\delta_l^e\right) \quad (24)$$

Using the LCAO perturbation theory generalized to take account of the imaginary perturbation due to a magnetic field, as described in the preceding chapter, we obtain the magnetic contributions, λ_l and μ_l, as:

$$\lambda_l = \pm\{4k\sin\theta_l - i(e^{i\theta_l/2}-ke^{-i\theta_l/2})\delta_l'^* + i(e^{-i\theta_l/2}-ke^{i\theta_l/2})\delta_l'\}/n\{\delta_l^2 + 4(\gamma_l^*+\delta_l'^*)(\gamma_l+\delta_l')\}^{1/2} \quad (25)$$

$$\mu_l = \pm\frac{1}{2n^2}\left[\frac{2\gamma_l^*\gamma_l+\gamma_l^*\delta_l'+\delta_l'^*\gamma_l}{\{\delta_l^2+4(\gamma_l^*+\delta_l'^*)(\gamma_l+\delta_l')\}^{1/2}} - \frac{2}{\{\delta_l^2+4(\gamma_l^*+\delta_l'^*)(\gamma_l+\delta_l')\}^{3/2}} \times\{4(1-k^2)^2+(1-2k\cos\theta_l+k^2) \times(\delta_l^2+2\gamma_l^*\delta_l'+2\delta_l'^*\gamma_l+2\delta_l'^*\delta_l') + (e^{i\theta_l}-2k+k^2e^{-i\theta_l})(2\gamma_l^*\delta_l'^*+\delta_l'^{*2}) + (e^{-i\theta_l}-2k+k^2e^{i\theta_l})(2\gamma_l\delta_l'+\delta_l'^2)\}\right] \quad (26)$$

For the bonding MO's, the first term in the bracket of Eq. 26 represents the pure diamagnetism, while the second term, which arises from the second-order perturbation due to the magnetic field, represents the induced paramagnetism. Equations 25 and 26 will first be tested for pentalene, and then applied to heptalene, *s*-indacene, and dibenzpentalene.

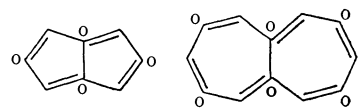

(I) (II)

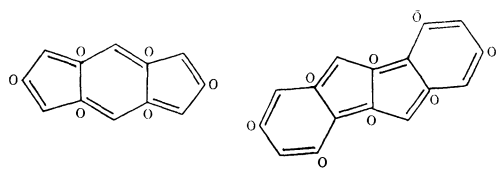

(III) (IV)

Pentalene (I).—The molecule is formed from cyclooctatetraene by the introduction of a cross-link between the atoms of a like parity with $r'-r=4$. The perturbation is given by $\delta_l^o=(k^o/2)-\cos\pi l$, the cross-linked atoms being assumed to be odd-numbered. The values of x_l, λ_l, and μ_l calculated using Eqs. 24—26 are presented in Table II. By comparing Table II with Table I, we can see how the introduction of the cross-link influences these quantities. By examining the figures of the case when $k(=k^o)=1$, it may be seen that the cross-link perturbation lifts the degeneracy of the non-bonding orbitals of the parent cyclic polyene. At the same time, the magnetic moment of the non-bonding orbitals is quenched and reproduced as the second-order susceptibility; namely, the first-order magnetic moment, λ_2, of the parent polyene is transferred to the second term of μ_2 as an induced paramagnetism. This paramagnetism greatly overshadows the diamagnetism from all other, lower-lying orbitals, giving rise to a large molecular paramagnetic susceptibility.

Table II includes the values of x_l, λ_l, and μ_l

for the case when $k(=k^0)=0.55$, which is the k_{min} value of the parent polyene. It may be seen that the susceptibility is very senstive to the value of k.

The values of x_l calculated by solving the secular equation, and those of λ_l and μ_l calculated by the direct use of London's method, are also included in Table II. For the molecular susceptibility, $2\sum_l \mu_l$, there is a good agreement between the present perturbation calculations and the complete MO calculations, though as to μ_1 and μ_{-1} there is a large difference.

Pentalene has not yet been synthesized.

Heptalene (II).—The k_{min} value of the perimeter of this molecule, dodecahexaene, was calculated to be 0.59. The cross-link perturbation used to yield heptalene from the cyclic polyene is $\delta_l^0=(k^0/3)\cos\pi l$. Assuming $k^0=0.59$ and using Eq. 26, one obtains $\chi_\pi=0.803\times10^{-17}\,\beta$. The $\Delta K/\Delta K_{benzene}$ value turns out to be -0.15 (cf. $\Delta K/\Delta K_{benzene}=-5.65$ when $k=k^0=1$). This indicates that, in heptalene, the magnetically-induced ring currents should be impeded considerably. A part of evidence for this conclusion is given by the proton NMR spectrum of this molecule, which exhibits the proton signals in the vinyl region (4–5τ).[23]

s-Indacene (III).—The cross-link perturbations used to form this molecule from the corresponding cyclic polyene are $\delta_l{}^0=(k^0/3)\cos(2\pi l/3)$. Assuming $k=k^0=0.59$, we obtain $\chi_\pi=0.377\times10^{-17}\,\beta$, which in turn yields $\Delta K/\Delta K_{benzene}=0.007$. The magnetically-induced ring currents should be considerably impeded in this molecule also. Comparing the $\Delta K/\Delta K_{benzene}$ values of heptalene and *s*-indacene, it may be expected that the NMR proton signals of the latter should appear at lower fields than do those of the former. It has experimentally been shown that *s*-indacene exhibits signals between 2.4 and 3.7 τ.[24]

Dibenzpentalene (IV).—The k_{min} value of the perimeter of this molecule, the 16-membered cyclic polyene, is calculated to be 0.60. The cross-link perturbations used to form dibenzpentalene from the cyclic polyene are $\delta_l^0=(k^0/4)\cos\pi l$ for the central cross-link (between atoms of a like parity) and $\delta_l'=(k'/8)\exp(5\pi il/8)$ for the other two cross-links (between atoms of a different parity). Assuming $k^0=k=0.60$ and $k'=(1+k)/2=0.80$, we obtain $\Delta K/\Delta K_{benzene}=0.99$. The calculated value is in good agreement with the observed value, 0.87, for dimethyldibenzpentalene.[19] The introduction of a methyl substituent would result in the reduction of the diamagnetic anisotropy.

In conclusion, it may be said that, in these catacondensed nonbenzenoid aromatic hydrocarbons with 4 ν carbon atoms, magnetically-induced ring currents are considerably impeded by the bond length alternation inherent in them, and that, hence, the π-electron delocalization is fairly restricted. In this sense these molecules can not be considered to belong to the "aromatic" category. They should have, rather, characteristics of a cyclic polyolefin.

23) H. J. Dauben and D. J. Bertelli, ibid., **83**, 4659 (1961).

24) K. Hafner, K. H. Häfner, C. König, M. Kreuder, G. Ploss, G. Schulz, E. Sturm and K. H. Vöpel, *Angew. Chem.*, **75**, 35 (1963); K. Hafner, ibid., **75**, 1041 (1963).

BULLETIN OF THE CHEMICAL SOCIETY OF JAPAN VOL. 39 809—813 (1966)

The Intramolecular Interaction between the N–H Group and π-Electrons. IV.[1] The Energetics of the Interaction[2]

By Michinori Ōki and Kiyoshi Mutai

Department of Chemistry, Faculty of Science, The University of Tokyo, Hongo, Tokyo

(Received September 17, 1965)

The thermodynamic parameters for the intramolecular interaction between the N–H group and the π-electrons in *N*-benzylanilines were determined from the temperature dependence of the N–H stretching absorptions. A comparison of the $-\Delta H$'s with those for the O–H···π interaction indicates that there is no appreciable difference between the interactions involving the N–H and the O–H groups. The $-\Delta H$'s are less than 2 kcal./mol., this figure being considered to be a borderline differentiating the X–H···π interaction from the ordinary hydrogen bond. The wave number shift accompanying the interaction cannot be a measure of the $-\Delta H$ in the N–H group, nor be indicative of the difference between two groups. The $-\Delta H$ was found to be closely related with the equilibrium constant in these derivatives.

1) Part III of this series: This Bulletin, **38**, 393 (1965).

2) M. Ōki and K. Mutai, Presented at the 14th Annual Meeting of the Chemical Society of Japan, Tokyo, April, 1961.

In the previous papers of this series,[1),3)] the existence of the interaction of the N–H group with π-electrons in *N*-(ω-phenylalkyl)anilines has been confirmed. A comparison of the chain lengths which permit the X–H$\cdots\pi$ interaction has shown that the N–H$\cdots\pi$ interaction is favored over the O–H$\cdots\pi$ interaction, contrary to the general expectation. Although this was presumed to be due mainly to the steric requirement of the phenyl group attached to the N–H nitrogen, it seemed that it would be interesting to compare the other characteristics of the interactions which involve the O–H and the N–H groups. The thermodynamic parameters are the most directly connected, and so they are most appropriate objects of comaprison. Thus the present paper is concerned with the determination of such parameters, on the basis of which the differences or the similarities of the two interactions may be discussed.

Experimental

Spectral Measurements.—A Perkin-Elmer, model 112G, double-pass high-precision grating infrared spectrometer, as has been described previously,[3)] was used. A carbon tetrachloride solution of a sample (ca. 0.004 mol./l.) was placed in a quartz cell (2 cm. long) covered with a heating coil protected with asbestos. The temperature of the solution was controlled by varying the current through the heating coil; the temperature was kept at each equilibrated temperature within an accuracy of 0.3°C and was read by a thermometer dipped in the solution. The spectrometer being of a single-beam type, a background trace was recorded every time immediately before or after scanning with the solution.

Calculation.—The band obtained was separated into its components and their integral intensities were calculated in a manner described before.[3)] The observed system can be regarded as being in the equilibrium expressed by Eq. 1, where K is an equilibrium constant:

$$\text{Free form} \overset{K}{\rightleftarrows} \text{Interacting form} \qquad (1)$$

Therefore, the well-known van't Hoff equation (2) can be used to obtain the energy difference between the two forms:

$$\ln K = \frac{\Delta H}{RT} + \frac{\Delta S}{R} \qquad (2)$$

K is given by spectral measurements:

$$K = \frac{c_i}{c_f} = \frac{A_i/a_i}{A_f/a_f} = \frac{a \cdot A_i}{A_f} \qquad (3)$$

where a_i and a_f represent the intensities per molecule for the interacting and the free N–H group respectively; a, their ratio, and the A's, the integrated intensities of each form.

By combining Eq. 2 with Eq. 3, Eq. 4 is obtained:

$$\ln\frac{A_i}{A_f} = \frac{-\Delta H}{RT} + \left(\frac{\Delta S}{R} - \ln a\right) \qquad (4)$$

Assuming that a_i and a_f, or their ratio, a, are independent of the temperature, at least within the 20—70°C range, the interaction energy ($-\Delta H$) can be determined from the slope of the $\ln(A_i/A_f)$ vs. $1/T$ polt by the least-squares treatment.

Results and Discussion

The effect of the temperature on the N–H stretching frequencies and the intensities of *N*-benzylanilines are summarized in Table I through V.

Some slight changes in the spectral characteristics with the temperature are observed. For instance, $\Delta\nu_{max}$ (the wave number shift accompanying the interaction) has a tendency to decrease with an increase in the temperature, though the shift is indefinite. The total integral intensity (A_i+A_f) also decreases. The latter phenomenon may be mainly due to the thermal expansion of the solvent, the effect resulting in a decrease of the concentration.

The spectrum of the *p*-nitro derivative (Table V) behaves unusually; the $\log(A_i/A_f)$ changes irregularly with the temperature, and a new, third band appears at a higher temperature, as shown in Fig. 1.[4)] The experiment was repeated twice for this case; the results were qualitatively similar, as is shown in Fig. 2 (the data given in Table V are those of one case). It may be supposed that the compound which is rather unstable in a solution would react with the solvent carbon tetrachloride, and that the product at this reaction would be the origin of the new band. However, the room temperature spectrum of the solution which had been heated to a high temperature showed no appreciable difference from that before heating.

For the origin of the new band at the high temperature, there are several possibilities: 1) the appearance of a new conformer, one which is unstable at room temperature; 2) the existence of a new product from the solute and the solvent which is

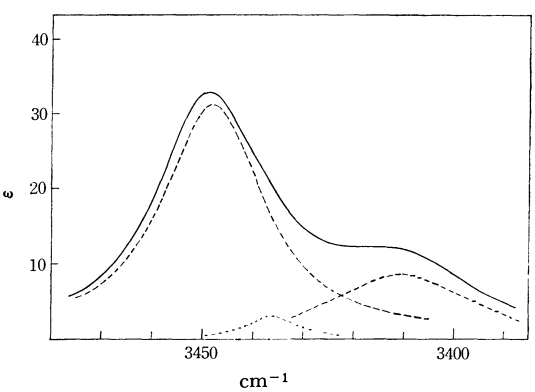

Fig. 1. ν_{N-H} Absorption of *N*-(*p*-nitrobenzyl)aniline at 74°C.

3) M. Ōki and K. Mutai, This Bulletin, 38, 387 (1965).

4) It is assumed that the curves are expressed by Lorentzian equation. This assumption is hold throughout this paper.

THE EFFECT OF THE TEMPERATURE ON ν_{N-H}'S OF BENZYLANILINES

TABLE I. *N*-(*p*-DIMETHYLAMINOBENZYL)ANILINE

Temperature $1/T\times10^3$ (°K^{-1})	ν_{max} cm^{-1}	$\Delta\nu_{max}$ cm^{-1}	$\Delta\nu^a{}_{1/2}$ cm^{-1}	$A\times10^{-3}$ mol^{-1} l. cm^{-2}	$\ln(A_i/A_f)$
3.38	3448.7 3418.2	30.5	24.2 27.6	1.30 3.14	0.878
3.18	3450.8 3419.8	31.0	26.6 24.8	1.43 2.86	0.695
3.03	3449.5 3418.8	30.7	26.4 24.4	1.53 2.64	0.548
2.90	3448.8 3419.5	29.3	31.4 26.6	1.60 2.58	0.475

TABLE II. *N*-(*p*-METHOXYBENZYL)ANILINE

Temperature $1/T\times10^3$ (°K^{-1})	ν_{max} cm^{-1}	$\Delta\nu_{max}$ cm^{-1}	$\Delta\nu^a{}_{1/2}$ cm^{-1}	$A\times10^{-3}$ mol^{-1} l. cm^{-2}	$\ln(A_i/A_f)$
3.34	3450.2 3418.6	31.6	28.6 29.2	2.16 2.70	0.223
3.18	3449.7 3418.5	31.2	26.6 26.4	1.87 2.19	0.161
3.03	3449.1 3418.4	30.7	27.6 24.8	1.87 1.99	0.079
2.91	3448.1 3417.9	30.2	30.8 26.2	1.94 1.98	0.018

TABLE III. *N*-BENZYLANILINE

Temperature $1/T\times10^3$ (°K^{-1})	ν_{max} cm^{-1}	$\Delta\nu_{max}$ cm^{-1}	$\Delta\nu^a{}_{1/2}$ cm^{-1}	$A\times10^{-3}$ mol^{-1} l. cm^{-2}	$\ln(A_i/A_f)$
3.34	3449.4 3417.7	31.7	26.4 27.0	2.03 1.99	−0.018
3.22	3448.9 3417.4	31.5	25.8 26.0	2.18 2.07	−0.055
3.10	3448.5 3417.3	31.2	27.4 26.2	2.22 2.02	−0.092
3.01	3448.1 3418.0	30.1	27.2 24.0	2.10 1.77	−0.154
2.89	3448.2 3417.2	31.0	28.4 24.0	2.18 1.81	−0.186

TABLE IV. *N*-(*m*-CHLOROBENZYL)ANILINE

Temperature $1/T\times10^3$ (°K^{-1})	ν_{max} cm^{-1}	$\Delta\nu_{max}$ cm^{-1}	$\Delta\nu^a{}_{1/2}$ cm^{-1}	$A\times10^{-3}$ mol^{-1} l. cm^{-2}	$\ln(A_i/A_f)$
3.35	3449.0 3413.2	35.8	28.2 34.2	2.93 2.11	−0.324
3.18	3448.4 3413.5	34.9	26.8 29.8	2.63 1.84	−0.354
3.06	3448.3 3413.3	35.0	27.6 30.2	2.66 1.83	−0.370
2.92	3448.4 3413.3	35.1	28.8 30.4	2.61 1.74	−0.405

TABLE V. *N*-(*p*-NITROBENZYL)ANILINE

Temperature $1/T\times10^3$ (°K^{-1})	ν_{max} cm^{-1}	$\Delta\nu_{max}$ cm^{-1}	$\Delta\nu^a{}_{1/2}$ cm^{-1}	$A\times10^{-3}$ mol^{-1} l. cm^{-2}	$\ln(A_i/A_f)$
3.32	3448.9 3410.5	38.4	24.6 36.0	3.57 1.25	−1.04
3.18	3448.9 3410.9	38.0	24.6 37.0	3.32 1.24	−0.984
3.06	3448.4 3432.1 3410.3	38.1	23.4 18.0 32.4	3.21 0.12 1.10	−1.10 (−1.07)*
2.88	3448.2 3436.3 3410.2	38.0	24.4 12.6 33.0	2.75 0.13 1.03	−1.03 (−0.981)*

* The values in parentheses are those calculated by ignoring the intensity of a new band at ca. 3432—3436 cm^{-1}.

Table VI. Thermodynamic parameters of *N*-benzylanilines. $RC_6H_4CH_2NHC_6H_5$

Substituent, R	$-\Delta H$, kcal./mol.	$\Delta S/R-\ln a$	$\Delta\nu_{max}$,[a] cm^{-1}	$\ln(A_i/A_f)$[c] (at 300°K)
p-Me_2N	1.69±0.07	−2.01±0.12	30.4	0.828
p-MeO	0.96±0.03	−1.38±0.05	30.9	0.226
H	0.77±0.04	−1.31±0.07	31.1	−0.014
m-Cl	0.35±0.03	−0.93±0.04	35.2	−0.331
p-NO_2	0.02±0.12[b]	−1.06±0.19[b]	38.1	−1.028

a) Average of the values at various temperatures.
b) Calculated from the data of two runs.
c) Read from the line of $\ln(A_i/A_f)$ vs. $1/T$ plot drawn by least-squares treatment.

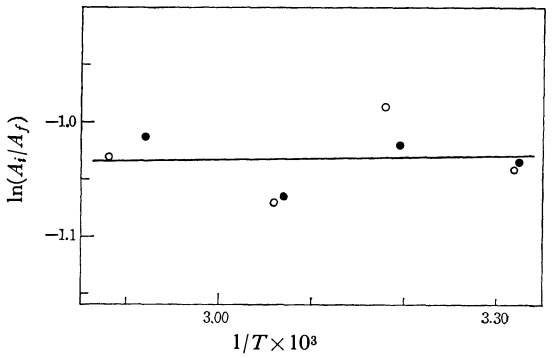

Fig. 2 Intensity ratios of *N*-(*p*-nitrobenzyl)aniline at various temperatures. Filled and open circles show the values of two runs.

only present at the higher temperature; 3) a change in the absorption curve shape which allows a third band to find its place as a result of the somewhat indefinite calculation method (the trial and error method), etc. The band intensity, however, is very small, the position of its maximum is uncertain, and its existence is much limited by the compound and the temperature. Therefore, the authors have not yet tried to make a choice among the possibilities. It is difficult to determine whether the third band should be classified as the interacting or the free form, but it was temporarily assumed to be the free form. At any rate, the classification matters little to the intensity ratio.

Table VI summarizes the thermodynamic parameters obtained by applying Eq. 4 to the data in Tables I through V.

In Table VI it may be seen that the $-\Delta H$ values are all smaller than that for the ordinary hydrogen bond, which is more than 2 kcal./mol. In this connection it is interesting and significant that the N–H group is similar to the O–H group[5),6)] in the intramolecular interaction with π-electrons. The interaction energy ($-\Delta H$) of both groups is generally less than 2 kcal./mol., this small ΔH value may be the best criterion for differentiating the X–H···π interaction from the ordinary hydrogen bonding, not only for the O–H group but also for the N–H group.

In this connection, it would be interesting to examine the thermodynamic data for the intermolecular N–H···π interaction. Recently Whetsel and Lady[7)] reported that the energies of the intermolecular N–H···π interactions in *N*-methylaniline - benzene and aniline - benzene systems were 1.5 and 1.6 kcal./mol. respectively, the value being again in the range for X–H···π interaction. They also reported that the C–H···π interaction energy in a chloroform - benzene system was 2 kcal./mol. In conclusion, all the data so far available confirm the above criterion to be reliable. The small $-\Delta H$ values are probably due to the weak electron-donating power of the π-electron system of benzene.

With these values in mind, it may be easily explained why Moritz[8)] could not find any detectable change in the N–H stretching bands of *N*-benzylaniline with a varying temperature. Generally a small intensity change accompanying a small $-\Delta H$ is difficult to detect, especially when it is not the extinction coefficient but the half-band width that determines the value of the integral intensity.

In view of the $-\Delta H$ values and the frequency shifts ($\Delta\nu_{max}$) in Table VI, it is evident that there is no generally supposed linear relationship between the two. On the contrary, a large $-\Delta H$ value is accompanied by a small $\Delta\nu_{max}$ value (for instance, the $-\Delta H$ of the *p*-dimethylamino derivative is 1.7 kcal./mol. and the $\Delta\nu_{max}$, 30.4 cm^{-1}, whereas the $-\Delta H$ and $\Delta\nu_{max}$ of *p*-nitro derivatives are nearly zero and 38.1 cm^{-1} respectively). It should be emphasized that this anomaly is observed in a group of substituted benzylanilines, since in this group of compounds steric, electronic and other factors are nearly equal, and it may generally be expected that the stretching frequency of the N–H group would be predominantly affected by the strength of the interaction, namely, the energy of the interaction, $-\Delta H$. Considering this anomaly, it sould not be safe to discuss the interaction energies by using the $\Delta\nu_{max}$ value only.

On the other hand, the energy is closely related to the intensity ratio. As may be seen in Fig. 3,

5) M. Ōki and H. Iwamura, This Bulletin, **33**, 717 (1960).
6) M. Ōki and H. Iwamura, ibid., **33**, 1600 (1960).
7) K. B. Whetsel and J. H. Lady, *J. Phys. Chem.*, **69**, 1596 (1965).
8) A. G. Moritz, *Spectrochim. Acta*, **16**, 1176 (1960).

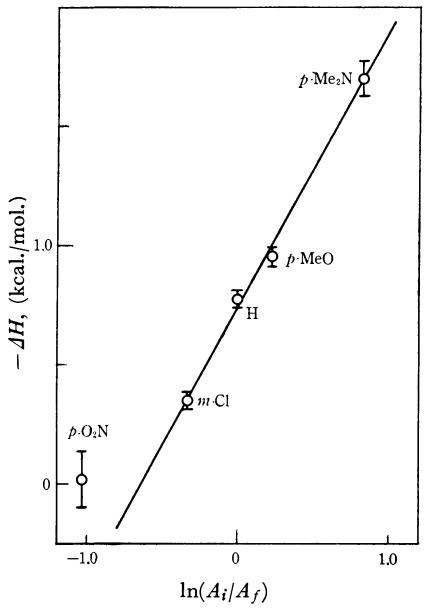

Fig. 3. Relation of $\ln(A_i/A_f)$ with interaction energy $(-\Delta H)$.

a plot of $-\Delta H$ against $\ln(A_i/A_f)$ shows a linear correlation, except for the value for the *p*-nitro derivative. In this group of compounds, it may safely be said that the equilibrium constant, K, is affected mainly by $-\Delta H$, with some part compensated for by the entropy.

The entropy change of the interaction (ΔS) could not be determined, because we do not know the a value. Strictly speaking, for the calculation of the entropy change another standard band, common in frequency and in molecular absorption coefficient with both interacting and free forms, must be used together with these two bands.[9] The value, $\Delta S/R - \ln a$, obtained as an intercept from the plot is, therefore, only a rough measure of the true ΔS, and no fruitful discussion can be expected from these data.

The $-\Delta H$ value of *p*-nitro derivative is nearly zero, and there remains a possibility of its being negative (ΔH is positive). This possibility is also supported by extending the line of the $-\Delta H$ vs. $\ln(A_i/A_f)$ plot (see Fig. 3), though the value obtained is obscured by large errors. Taking this into account, together with the N–H$\cdots\pi$ interaction which will cause some stability, it is suggested that there are some factors other than the N–H$\cdots\pi$ interaction which affects the total energy. The problem seems to be closely connected with the conformations of the two forms. An explanation for this phenomenon will be published in a forthcoming paper.

The authors are indebted to Professor Yoshiyuki Urushibara and Professor Takehiko Shimanouchi for their valuable discussions and encouragement. They are also indebted to the Ministry of Education for a grant-in-aid for Fundamental Scientific Research.

9) S. Mizushima, T. Shimanouchi, K. Kuratani and T. Miyazawa, *J. Am. Chem. Soc.*, **74**, 1378 (1952).

BULLETIN OF THE CHEMICAL SOCIETY OF JAPAN VOL. 39 813—817 (1966)

Intramolecular Interaction between Hydroxyl Group and π-Electrons. XX.[1] Conformationally-fixed *o*-Vinylphenols

By Michinori Ōki, Hiizu Iwamura, Takeru Onoda and Michiko Nishida

Department of Chemistry, Faculty of Science, The University of Tokyo, Hongo, Tokyo

(Received September 17, 1965)

1, 2-Dihydro-5-hydroxy-8-methoxy-3-methylnaphthalene (III) was prepared, starting from 5, 8-dimethoxy-α-tetralone, via 8-hydroxy-5-methoxy-2-methyl-1-keto-1, 2, 3, 4-tetrahydronaphthalene. The O–H stretching absorptions (ν_{O-H}) and the ultraviolet absorptions of III, 1, 17 β-dihydroxy-4-methylestra-1, 3, 5(10), 9(11)-tetraene (IV), and the related naphthols were measured and compared with those of *o*-isobutenylphenol. IV showed a ν_{O-H} at 3532 cm^{-1} which is assigned to the hydroxyl group taking part in the strong interaction with the π-electrons on the ethylenic group; it corresponds well in its location to the lowest frequency band of *o*-isobutenylphenol. The previous assignment of this band to the conformer II with the double bond *syn* to the hydroxyl was thus confirmed. III showed only a symmetric band at 3618 cm^{-1}, which was assigned to the free ν_{O-H}, and could not be a model for the conformer with a ν_{O-H} at 3576 cm^{-1}, presumably because of the more planar structure for the overlap between the orbitals of the hydroxyl group and the ethylenic group.

In the foregoing paper,[1] the doublet O–H stretching absorption bands (ν_{O-H}) at 3576 and 3539 cm^{-1} of *o*-isobutenylphenol were assigned to the hydroxyl groups interacting with the π-electrons in conformations expressed approximately by I and II respectively. In an attempt to verify this tentative assignment, the model compounds conformationally fixed as in I and II have now been prepared and their ν_{O-H} absorptions examined. They are α-naphthol, 5-hydroxy-1, 2-dihydronaphthalene,[2] 1, 2-dihydro-5-hydroxy-8-methoxy 3-methylnaphthalene (III), and 1, 17-β-dihydroxy-4-methylestra-1, 3, 5(10), 9(11)-tetraene(IV)[3];

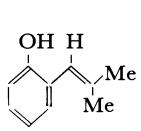

I

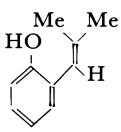

II

all are known compounds except III, whose preparation started from 5, 8-dimethoxy-α-tetralone and was analogous to the route to equilenin developed by Bachman et al.[4]

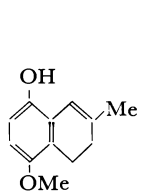

III

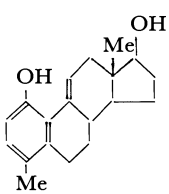

IV

The α-tetralone (V) was condensed with methyl oxalate by the action of sodium methoxide under nitrogen, and the methoxalyl derivative (VI) was heated in order to effect decarbonylation and to give the 2-methoxycarbonyl derivative (VII) of the α-tetralone. The sodio-derivative of the latter was methylated with methyl iodide. Saponification, followed by decarboxylation, gave 5, 8-dimethoxy-2-methyl-α-tetralone (IX). Gentle refluxing with constant boiling hydroiodic acid demethylated the 8-methoxyl group preferentially. The hydroxy-ketone (X) was reduced to the corresponding diol (XI) with lithium aluminum hydride. Refluxing with acetic anhydride, followed by saponification, gave III with a m. p. of 92—93°C.

The Diels-Alder reaction between toluquinone and isoprene has been shown to afford 3, 4-dihydro-

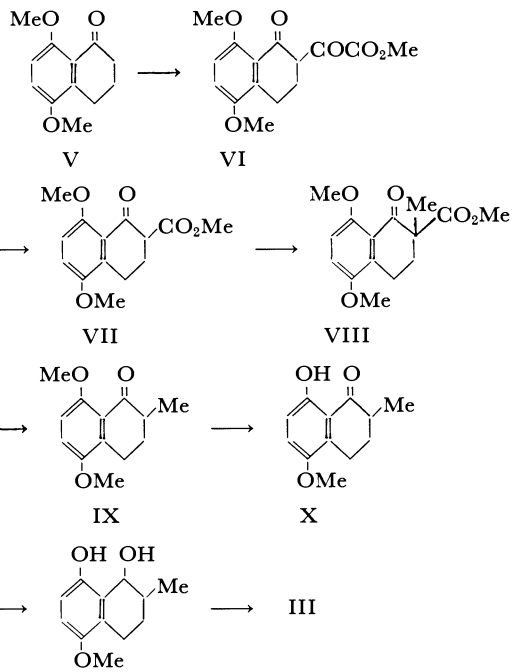

V VI VII VIII IX X XI III

5, 8-dihydroxy-2, 7-dimethylnaphthalene after acid-catalyzed rearrangement.[5] The diol (XII) similarly obtained from the reaction between benzoquinone and isoprene was dissolved in aqueous sodium hydroxide and partially methylated with dimethyl sulfate. Through chromatography on alumina, a fraction of a mono-methyl ether was obtained. Recrystallization gave pure mono-methyl ether, which was different from III. Since further methylation afforded the common dimethyl ether (XIV), the latter mono-methyl ether must be the 5-methoxy-8-hydroxy isomer (XIII).

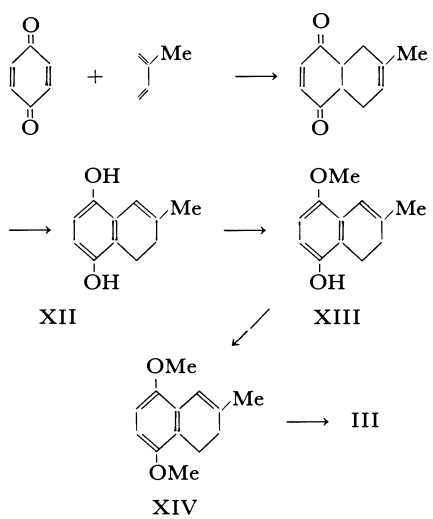

XII XIII XIV III

1) Part XIX: M. Ōki and H. Iwamura, This Bulletin, **39**, 470 (1966).

2) J. F. Eastham and D. R. Larkin, *J. Am. Chem. Soc.*, **80**, 2887 (1958).

3) The sample was generously offered by Professor R. M. Dodson of the University of Minnesota, to whom the authors' thanks are due.

4) W. E. Bachman, W. Cole and A. L. Wilds, *J. Am. Chem. Soc.*, **62**, 824 (1940).

5) H. Inoue and T. Arai, *Chem. Pharm. Bull.*, **12**, 533 (1964).

Experimental

Spectral Measurements.—Those were carried out as described previously.[1]

Materials.

Methyl 5, 8-Dimethoxy-1-keto-1, 2, 3, 4-tetrahydronaphthalene-2-glyoxalate (VI).—In 100 ml. of anhydrous methanol was dissolved 9.2 g. of sodium and the excess methanol was evaporated to dryness at 100°C under diminished pressure. To the white solid were added 47.2 g. of dimethyl oxalate and 200 ml. of dry benzene. The mixture was refluxed under dry nitrogen for half an hour in order to dissolve the solid. To the cooled solution was added 41.2 g. (0.2 mol.) of 5, 8-dimethoxy-α-tetralone (V)[6] dissolved in 300 ml. of benzene. After it had stood for four hours at room temperature with occasional shaking, the mixture was hydrolyzed with 500 ml. of water. The aqueous layer was then drawn off, the benzene layer was extracted twice with 100 ml. of a 5% sodium hydroxide solution, and the combined aqueous solution was carefully acidified with dilute hydrochloric acid. The yellow crystalline deposit was collected and recrystallized from methanol to give 50.5 g. of the glyoxalate (VI), m. p. 108—109°C, corresponding to a yield of 95%.

Found: C, 61.83; H, 5.63. Calcd. for $C_{15}H_{16}O_6$: C, 61.64; H, 5.52%.

Methyl 5, 8-Dimethoxy-1-keto-1, 2, 3, 4-tetrahydro-2-naphthoate (VII).—The methyl glyoxalate (VI) (26.7 g.) was mixed with 20g. of 200 mesh glass powder in a Claisen flask, and the mixture was carefully heated under diminished pressure. A vigorous evolution of carbon monoxide commenced at about 160°C. After half an hour at 180°C, the evolution of the gas stopped and, as the pressure inside the flask dropped, refluxing took place. The temperature of the oil bath was then raised to 240°C and an oil boiled at 180—190°C under ca. 3 mmHg was collected. The viscous oil was dissolved in benzene and recrystallized to give colorless prisms (20.5 g.; yield, 85%), m. p. 86°C.

Found: C, 63.54; H, 6.28. Calcd. for $C_{14}H_{16}O_5$: C, 63.63; H, 6.10%.

Methyl 5, 8-Dimethoxy-1-keto-2-methyl-1, 2, 3, 4-tetrahydro-2-naphthoate (VIII).—To 23 g. of sodium dissolved in 500 ml. of anhydrous methanol was added 23.9 g. of VII dissolved in 200 ml. of benzene. After this mixture had been refluxed for fifteen minutes on a water bath, 50 ml. of methyl iodide was added over a five-minute period. Another 50 ml. of methyl iodide was added after an exothermic reaction had ceased, and the mixture was refluxed for an hour. After neutralization with acetic acid, the solvents were evaporated nearly to completion, and the residue was treated with 500 ml. of benzene and 300 ml. of water. The organic layer was washed with 5% sodium hydroxide and then with water, and dried over sodium sulfate. After the solvent had then been evaporated, the residue was crystallized from carbon tetrachloride (yield, 20 g.; 80%) m. p., 63—63.5°C.

Found: C, 64.92; H, 6.73. Calcd. for $C_{15}H_{18}O_5$: C, 64.74; H, 6.52%.

5, 8-Dimethoxy-2-methyl-1-keto-1, 2, 3, 4-tetrahydronaphthalene (IX).—A mixture of 100 ml. of 45% aqueous potassium hydroxide and 300 ml. of methanol was mixed with 30 g. of VIII, refluxed on a water bath for two hours, and diluted with water in order to collect the resulting solid. Recrystallization from methanol gave colorless prisms, m. p. 69°C.

Found: C, 70.99; H, 7.46. Calcd. for $C_{13}H_{16}O_3$: C, 70.89; H, 7.32%.

8-Hydroxy-5-methoxy-2-methyl-1-keto-1, 2, 3, 4-tetrahydronaphthalene (X).—IX (20 g.) was heated under reflux with 200 ml. of 52% hydroiodic acid for 2 hr. The mixture was then diluted with water, and the product was triturated with a 20% aqueous sodium hydroxide solution to give the insoluble sodium salt, which was collected and washed with aqueous alkali and then with water. The residue was then suspended in 50 ml. of water and acidified with 1 N hydrochloric acid. The oil was extracted with ether, and the solution was dried over anhydrous sodium sulfate. After evaporation, the residue was crystallized from methanol to give pale yellow needles (yield, 16 g.; 85.4%), m. p. 46.5—47°C.

Found: C, 69.93; H, 6.84. Calcd. for $C_{12}H_{14}O_3$: C, 69.88; H, 6.84%.

The NMR spectra[7] of 5% $CDCl_3$ solution consisted of the following signals; 1.26 ($C_{(2)}$'-Me, doublet), 1.8—3.1 (aliphatic, multiplet), 3.81 (O'Me), 6.70, 6.85, 7.01 and 7.16 (the AB quartet of the aromatic protons), and 11.99 (chelated OH).

1, 8-Dihydroxy-5-methoxy-2-methyl-1, 2, 3, 4-tetrahydronaphthalene (XI).—To a slurry of 4 g. of lithium aluminum hydride in 100 ml. of ether was added, drop by drop, a solution of 10.3 g. of the hydroxyketone (X) in 70 ml. of ether. After the reaction had subsided, the mixture was refluxed for an hour. The excess reagent was decomposed with ethyl acetate and then treated with 2 N sulfuric acid. The combined ether extracts were washed with 1 N sodium bicarbonate and dried over anhydrous potassium carbonate. The solvent was evaporated, and the residue was recrystallized from carbon tetrachloride to give needles, m. p. 125°C (yield, 9.5 g.; 91.3%).

Found: C, 68.91; H, 8.02. Calcd. for $C_{12}H_{16}O_3$: C, 69.21; H, 7.74%.

1, 2-Dihydro-5-hydroxy-8-methoxy-3-methylnaphthalene (III).—A solution of 5 g. of the above diol (XI) in 50 ml. of acetic anhydride was refluxed for an hour. When, after the solvent had been evaporated, the dehydrated acetate was distilled under diminished pressure, a fraction boiling at 120—130°C/1.5 mmHg was collected. The distillate was dissolved in 50 ml. of 5% ethanolic sodium ethoxide, and the mixture was refluxed for thirty minutes. The volume of the solvent was reduced to half, and the residue was diluted with water. The solution was treated with a small portion of active charcoal and filtered while hot. The filtrate was acidified and the product crystallized from carbon tetrachloride to give needles, m. p., 92—93°C; the yield was 2.8 g. (61.3%).

Found: C, 75.78; H, 7.66. Calcd. for $C_{12}H_{14}O_2$: C, 75.76; H, 7.42%.

1, 2-Dihydro-5, 8-dihydroxy-3-methylnaphthalene (XII).—A solution of 12 g. of *p*-benzoquinone and 7 g.

6) M. Crawford and V. R. Supaneka, *J. Chem. Soc.*, **1960**, 1985.

7) Determined at 60 Mc./sec. on a model A-60 spectrometer (Varian Associates, Palo Alto, Calif., U. S. A.) at the normal operating temperature (36.5°C) and reported in units of δ in p.p.m., from the signal of TMS used as the internal standard.

of isoprene in 50 ml. of acetic acid was kept at room temperature for 24 hr. The solid was then collected on a Buchner funnel and washed several times with water. To a suspension of the crude adduct in 50 ml. of chloroform, 20 ml. of concentrated hydrochloric acid was added, and the mixture was heated under reflux for 12 hr. The solid mass was filtered when it had cooled, washed several times with chloroform, and finally recrystallized from chloroform-acetone to give needles, m. p. 175°C.

Found: C, 75.10; H, 6.99. Calcd. for $C_{11}H_{12}O_2$: C, 74.97; H, 6.86%.

1, 2-Dihydro - 8 - hydroxy - 5 - methoxy-3-methylnaphthalene (XIII).—To a solution of 8.8 g. of the diol (XII) in 200 ml. of 10% aqueous sodium hydroxide was added, drop by drop, 7 g. of dimethyl sulfate with cooling and shaking. The dark solution was washed twice with ether, and the aqueous layer was acidified with dilute hydrochloric acid. The heavy oil was dissolved in ether, and the ether solution was dried over anhydrous sodium sulfate. After the solvent had evaporated, the residue was dissolved in benzene - petroleum ether (b. p. —60°C) (1 : 1 in volume) and chromatographed on alumina. Following a fraction of an oil, a series of fractions was obtained and found to be homogeneous. The residue obtained after the evaporation of the solvent was recrystallized from carbon tetrachloride to give needles (1.2 g.; 12%), m. p. 124.5—125°C.

Found: C, 76.01: H, 7.34. Calcd. for $C_{12}H_{14}O_2$: C, 75.76; H, 7.42%.

The ethereal layer yielded a small amount of a dimethyl ether which was identical with the specimen whose preparation is described below.

1, 2-Dihydro - 5, 8 -dimethoxy -3 - methylnaphthalene (XIV).—To a solution of 3.8 g. of III in 50 ml. of 10% aqueous sodium hydroxide, 3 g. of dimethyl sulfate was added; the mixture was then shaken for ten minutes. The oil was extracted in ether, and the ether solution was dried over anhydrous potassium carbonate. The residue obtained after the evaporation of the solvent was recrystallized from petroleum ether to give needles (3.8 g.; 93%), m. p. 66°C.

Found: C, 76.56; H, 8.10. Calcd. for $C_{13}H_{16}O_2$: C, 76.44; H, 7.90%.

Results and Discussion

In Fig. 1 are shown the apparent ν_{O-H} absorptions of III and IV, while in Table I all of the ν_{O-H} data concerned are collected.

The band at the highest frequency of IV is due to the secondary alcoholic hydroxyl group at the 17-position of the steroid skeleton; it is outside the present discussion. Judging from its location, the absorption maximum at 3606 cm^{-1} can be assigned to the free ν_{O-H} of the phenolic hydroxyl group.[1,8] The lowest-frequency band, at 3532 cm^{-1}, may consequently be assigned to the phenolic hydroxyl group interacting with π-electrons on the ethylenic group. Compared with the interacting ν_{O-H}'s of *o*-isobutenylphenol, the location of the

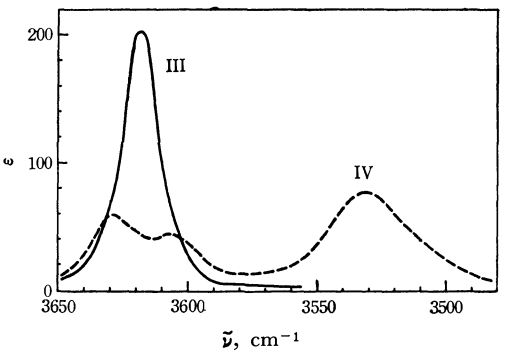

Fig. 1. ν_{O-H} absorptions of 1, 2-dihydro-5-hydroxy-8-methoxy-3-methylnaphthalene (III) and 1, 17β-dihydroxy-4-methylestra-1, 3, 5(10), 9(11)-tetraene (IV).

last band of IV corresponds well to the lower one at 3539 cm^{1-} of *o*-isobutenylphenol; therefore, it may be concluded that this band should be assigned to the hydroxyl group in conformation II. The Dreiding model of IV suggests that the angle between the benzene ring and the plane made by the ethylenic linkage is ca. 10°. Table II lists the ultraviolet absorption maxima of these *o*-vinylphenol derivatives. The K-band in *n*-hexane of IV is shifted to the red side by 20 mμ from that of *o*-isobutenylphenol, and it is even comparable to those of the more planar *o*-vinylphenol and *o*-(*trans*-propenyl)phenol.[1] Although a part of the effect may be attributed to the auxochromic effect in IV of the additional alkyl groups attached to the chromophore, the UV data indicate that the benzene ring and the ethylenic group in IV are mutually more co-planar than those of *o*-isobutenylphenol. It is not yet clear why this molecule shows a strong interaction despite its near co-planarity, but it is interesting to note that the compound IV and *o*-isobutenylphenol show essentially the same ν_{O-H} values at the lower frequencies. It is possible that the ν_{O-H} in conformation II is rather insensitive to the angle between the benzen ring and the plane of the ethylenic group.

The ν_{O-H}'s of 5-hydroxy-1, 2-dihydronaphthalene and III are, contrary to the expectation, singlets, like those of α-naphthol and XIII. The apparently unusually high ν_{O-H} of III and XIII is due to the electronic effect of the methoxyl substitution.[8] No absorption of any degree indicative of the presence of intramolecular interaction between the hydroxyl group and the π-electrons was detected. It is not unreasonable to assume, however, that there is no interaction in α-naphthol and XIII, since there is no π-electron available for the interaction in the latter, and since in the former the hydroxyl group must point to the node of the π-orbitals. The Dreiding models of 5-hydroxy-1, 2-dihydronaphthalene and III suggest that the angle between the benzene

8) K. U. Ingold and D. R. Taylor, *Can. J. Chem.*, **39**, 471 (1961).

Table I. ν_{O-H} Absorptions of o-vinylphenols

	ν_{max} cm^{-1}	$\Delta\nu^{a}_{1/2}$ cm^{-1}	A×10^{-4} l.mol^{-1} cm^{-2}	$\Delta\nu_{max}$ cm^{-1}
o-Isobutenylphenol	3609.8	14.6	0.12	33.7
	3576.1	37.0	0.40	70.5
	3539.3	26.8	0.81	
α-Naphthol	3609.2	18.3	1.46	0
5-Hydroxy-1,2-dihydronaphthalene	3613.2	17.8	1.42	0
III	3618.5	16.1	1.23	0
IV	3606.1	—	—	74.4
	3531.7	38.4	1.05	
XIII	3618.2	17.4	1.18	0

Table II. Ultraviolet absorptions of o-vinylphenols

	Solvent	K-band mμ (log ε)	B-band mμ (log ε)
o-Isobutenylphenol	H	235.0 (3.79)	282.0 (3.41)
	A	242.0 (3.96)	287.5 (3.57)
5-Hydroxy-1,2-dihydronaphthalene	H	—	—
	A	267.0 (3.83)	298.0 (3.45), 308 (3.41)
III	H	267 (s), 273.5 (3.96) 285 (s)	317 (3.68), 330 (s)
	A	266 (s), 272.0 (3.97) 283 (s)	320 (3.72)
IV	H	255.5 (—)	302 (—)
	A	249 (s), 257.5 (4.01) 265 (s)	301 (3.49), 310 (s)
XIII	H	264.5 (s), 273.5 (4.05)	317 (3.78)
	A	264.5 (s), 274 (4.08)	319 (3.75)

H; n-Hexane; A; 95% Ethanol; s; shoulder

ring and the plane made by the ethylenic group is ca. 25°. Since there is no interaction even in III, in which the proton-accepting power of the ethylenic group is enriched by methyl substitution, it may be concluded that III does not reflect the conformation I of o-isobutenylphenol, but that the dihedral angle made by the plane of the ethylenic group and the plane of the benzene ring must be much larger than that in III in order to have interaction with the hydroxyl group.

The effects of conformations, including the dihedral angles made by the benzene ring and the ethylenic linkage and the relative location of the double bond, remain to be fully explored. However, one possible reason for the poor interaction in the compound III may be that two *p*-orbitals are available for the interaction in conformation II, while only one is available in conformation I. The former is expected to be the preferable interacting form, on analogy with the benzene-silver ion complex.[9,10]

9) W. von Doering, M. Saunders, H. G. Boyton, H. W. Earhart, E. F. Wadley, W. R. Edwards and G. Laber, *Tetrahedron*, **4**, 178 (1958).

10) M. Ōki and H. Iwamura, This Bulletin, **32**, 1135 (1959).

BULLETIN OF THE CHEMICAL SOCIETY OF JAPAN VOL. 39 818—826 (1966)

The Crystal Structure of 1, 2, 3, 4-Tetrachlorobenzo[g]sesquifulvalene

By Yoriko NISHI, Yoshio SASADA, Tamaichi ASHIDA and Masao KAKUDO

Institute for Protein Research, Osaka University, Joancho, Kita-ku, Osaka

(Received September 20, 1965)

The molecular structure of 1, 2, 3, 4-tetrachlorobenzo[g]sesquifulvalene has been ascertained by X-ray crystal analysis. The crystal of this substance is monoclinic, with four molecules in a unit cell of dimensions: $a=21.31$, $b=16.88$, $c=3.83$ Å, and $\beta=93.3°$, the space group being $P2_1/a$. The crystal structure was determined by the Harker-Kasper inequality and the Sayer's method. The atomic coordinates and the anisotropic temperature factors of each atom were refined by the block-diagonal-matrix least-squares method. The average length of the C–Cl bonds is 1.705 Å, a value which is in good agreement with those of several chlorobenzenes. In the sesquifulvalene skeleton, longer and shorter bonds are disposed as may be expected from the conventional chemical formula. The average length of the longer bonds is 1.461 Å, while that of the shorter ones is 1.354 Å. The mean C–C bond length in the benzene ring is 1.413 Å. The whole molecule is not on a plane, although the component ring systems are nearly planar. The five-membered ring and the seven-membered ring twist to each other by an angle of about 31° around the bond connecting these two rings. This might be due to the repulsion forces between chlorine and hydrogen atoms which approach each other closely. The plane of the seven-membered ring makes an angle of about 5° with that of the six-membered ring.

In attempting to synthesize some derivatives of sesquifulvalene (cycloheptatrienylidenecyclopentadiene), Kitahara, Murata, Funamizu and Asano[1] have found that there action of tropone with 1, 2, 3, 4-tetrachlorocyclopentadiene (I) in methanol results in a mixture of 1, 2, 3-trichloro-6-(*o*-methoxyphenyl)fulvene and the corresponding para-isomer. This is an entirely new type of rearrangement reaction, in which the methoxy group enters the seven-membered ring (a six-membered ring after the rearrangement) and in which a chlorine atom in the five-membered ring is liberated. This chemical conclusion was confirmed by an independent crystal structure determination of an analogous product containing bromine atoms.[2]

Such a kind of rearrangement could be avoided by using benzo[d]tropone (II) instead of tropone; the product, in the form of fine violet needles, may be supposed to be 1, 2, 3, 4-tetrachlorobenzo-[g]sesquifulvalene (III).[3]

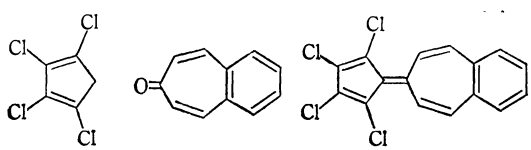

(I) (II) (III)

The results of the elementary analysis of the substance also supported this formula. For an independent verification of the structure by means of X-ray analysis, a sample of the compound was supplied to us by Professor Yoshio Kitahara of Tohoku University.

The stereochemistry of this compound is also interesting. If the molecule is planar, or nearly so, as may be expected from the chemical formula, much steric hindrance should be exerted between Cl(1) and the hydrogen atom bonded to C(10), and between Cl(4) and the hydrogen bonded to C(5). In addition to the establishment of the chemical formula, this investigation has been carried out in order to clarify the molecular configuration and the features of the steric hindrance.

The present paper will describe the structure determination of this compound by the three-dimensional Fourier and least-squares methods.

Experimental

The crystals of 1, 2, 3, 4-tetrachlorobenzo[g]sesquifulvalene are deep violet needles elongated along the c axis.

The crystallographic and physical data found are as follows:

1, 2, 3, 4-Tetrachlorobenzo[g]sesquifulvalene, $C_{16}H_8Cl_4$.

M.p.: 234°C.

Monoclinic: $a=21.31\pm0.05$, $b=16.88\pm0.03$, $c=3.83\pm0.02$ Å, $\beta=93.3\pm0.3°$.

Volume of the unit cell: 1375.3 Å^3.

Density observed by the floatation method; 1.64 g.cm^{-3}

Density calculated; 1.65 g.cm^{-3}

Number of molecules in the unit cell: 4

1) Y. Kitahara, I. Murata, M. Funamizu and T. Asano, This Bulletin, **37**, 1399 (1964).

2) Y. Kato, Y. Sasada and M. Kakudo, ibid., **38**, 1761 (1965).

3) Y. Kitahara, I. Murata and S. Katagiri, *Angew. Chem.*, **77**, 345 (1965).

Absent spectra: $(h0l)$ when h is odd,
$(0k0)$ when k is odd
Space group: $P2_1/a$.

The crystal was found to be twin; the X-ray photographs showed that the twinning occurred with a common (100) plane. The crystals were so thin along the c axis that it was impossible to obtain a single crystal. Therefore, we selected a few crystals in which one component of the twin was as small as possible.

Copper $K\alpha$ radiation was used with a nickel filter. The intensity data were collected only for the $(hk0)$, $(hk1)$ and $(hk2)$ zones by means of equi-inclination Weissenberg photographs. In order to correlate strong and weak reflections, the multiple-film technique was applied, the relative intensities being ranged between 3300 and 1 for $(hk0)$, between 5000 and 1 for $(hk1)$, and between 350 and 1 for $(hk2)$. The maximum $(2\sin\theta)$'s of the observed reflections were 1.98, 1.66 and 1.75 for $(hk0)$, $(hk1)$ and $(hk2)$ respectively. 277 independent reflections out of 418 possible $(hk0)$, and 428 out of 935 $(hk1)$ and $(hk2)$, were observed within the above-mentioned ranges.

Precession photographs were also taken for the $(h0l)$ zone in order to determine the relative scale factors among the three layers of the Weissenberg photographs. The crystal used had a cross section of about 0.1×0.03 mm.

The intensities were estimated visually by comparison with a standard intensity scale prepared using the same crystal. Corrections for Lorentz and polarization factors were applied as usual, while the absorption effect was neglected because of the small size of the crystal used in the experiment. The observed structure factors were then put onto a tentative absolute scale by means of Wilson's statistics.[4]

Structure Determination

Structure Projected along the c Axis.— Since the c axis of the crystal is short, the molecule was supposed to be approximately planar and almost parallel to the (001) plane. In order to locate the four chlorine atoms, the sharpened Patterson projections on the (001) plane were synthesized with several degrees of sharpening. It was difficult to interpret the maps so obtained, however, because of the heavy overlappings of peaks due to chlorine-chlorine and chlorine-carbon interactions.

In the next attempt, the direct sign-determination methods were applied to $F(hk0)$'s. The Harker-Kasper inequality[5] was used;

$$(U_{\mathrm{H}}\pm U_{\mathrm{H}'})^2 \leq (1\pm U_{\mathrm{H}+\mathrm{H}'})(1\pm U_{\mathrm{H}-\mathrm{H}'})$$

where U_{H} etc., are the unitary structure factors for the $(hk0)$ plane. Signs for 76 out of 277 observed reflections were obtained by this method. Further sign-determinations were made by using Sayre's relation,[6]

$$S_{\mathrm{H}}=S_{\mathrm{H}'}S_{\mathrm{H}+\mathrm{H}'}$$

where S_{H} denotes the sign of F_{H}. The relation gave signs of 50 more reflections. After the final refinement of the structure, it was found that only two out of the 126 signs determined by the direct methods were incorrect.

The projection of the electron-density distribution along the c axis was then synthesized using these 126 reflections. The map showed not only the four chlorine atoms, but also a rough layout of the carbon skeleton, as may be seen from Fig. 1. The structure was then refined by the usual Fourier technique, after which the anisotropic temperature factors in the form of $\exp\{-(h^2B_{11}+k^2B_{22}+hkB_{12})\}$ were assigned to each non-hydrogen atom, and the least-squares refinement method was applied with a block-diagonal-matrix approximation. The atomic scattering factors given by Berghuis, Haanappel, Potters, Loopstra, MacGillavry and Veenendaal[7] for carbon and chlorine and by McWeeny[8] for hydrogen were used throughout this structure determination. After three cycles of refinement, the discrepancy factor, $R=\sum||F_o|-|F_c||/\sum|F_o|$, decreased to 0.091 for all the observed reflections ($R=0.145$ if unobserved reflections were included).

Using the coordinates so determined, the (F_o-F_c) synthesis was computed. Several peaks of residual electron density were observed, as is shown in Fig. 2; some of these might be due to the hydrogen atoms. Among them, two peaks corresponding to H(5) and H(10) were also included; those two hydrogen atoms are involved in the steric hindrance mentioned above. Therefore, all the hydrogen atoms were located geometrically at a distance of 1.0 Å outward from the carbon atoms.

Three more least-squares refinement cycles, including those hydrogen atoms with isotropic temperature factors, were carried out. The final discrepancy factor was 0.081 for all the observed reflections ($R=0.133$ including the unobserved reflections). The final x- and y-coordinates and temperature factors are given in Tables I and II respectively, while the observed and calculated structure factors, $F(hk0)$, are listed in Table III. The final electron density projection along the c axis is shown in Fig. 3.

The Determination of the z-Coordinates.— Although no complete three-dimensional intensity data were collected, the Harker section, $P(u, 1/2, w)$, was synthesized, using $F(hk0)$, $F(hk1)$ and $F(hk2)$, in order to obtain the z-coordinates of the atoms. The peaks on the Harker section, as is shown in Fig. 4, were interpreted rather easily by assuming that the chlorine atoms attached to the five-membered ring are coplanar. As the y-coordinates of Cl(2) and Cl(4) are nearly

4) H. Lipson and W. Cochran, "The Determination of Crystal Structure," Bell, London (1953), p. 61.
5) Ibid., p. 250.
6) Ibid., p. 269.
7) J. Berghuis, IJ. M. Haanappel, M. Potters, B. O. Loopstra, C. H. MacGillavry and A. L. Veenendaal, *Acta Cryst.*, 8, 478 (1955).
8) R. McWeeny, *Acta Cryst.*, 4, 513 (1951).

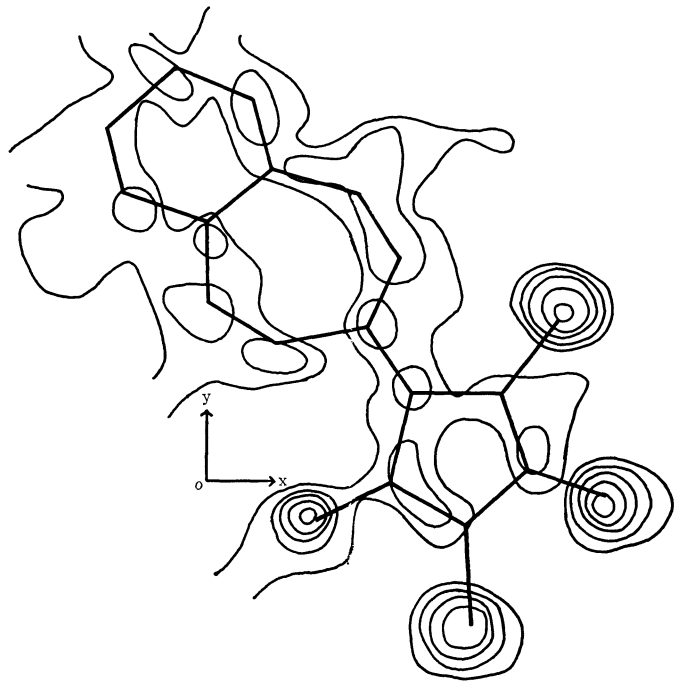

Fig. 1. The first electron density projection along the c axis. In Fourier summation, 126 reflections are included whose signs have been obtained by the direct methods. Contours are drawn at equal intervals on an arbitrary scale. The final skeleton of the molecule is superimposed.

TABLE I. THE FINAL ATOMIC COORDINATES

Atom	x/a	y/b	z/c
Cl(1)	0.2693	0.1691	0.0109
Cl(2)	0.3192	−0.0155	−0.0310
Cl(3)	0.2066	−0.1394	0.2110
Cl(4)	0.0793	−0.0364	0.3927
C (1)	0.2276	0.0882	0.1284
C (2)	0.2476	0.0139	0.0873
C (3)	0.1982	−0.0382	0.1680
C (4)	0.1443	0.0031	0.2154
C (5)	0.0509	0.1378	0.1426
C (6)	0.0008	0.1804	0.1874
C (7)	−0.0049	0.2594	0.3513
C (8)	0.0459	0.3089	0.4791
C (9)	0.1127	0.2921	0.4430
C (10)	0.1429	0.2267	0.3381
C (11)	0.1613	0.0895	0.1830
C (12)	0.1190	0.1511	0.2437
C (13)	−0.0684	0.2868	0.3777
C (14)	−0.0798	0.3583	0.5557
C (15)	−0.0298	0.4043	0.6876
C (16)	0.0306	0.3839	0.6453

TABLE II. THE FINAL TEMPERATURE FACTORS, USED FOR THE CALCULATION OF $F(hk0)$.

Atom	B_{11}	B_{22}	B_{12}
Cl(1)	0.00199	0.00399	−0.00084
Cl(2)	0.00238	0.00484	0.00160
Cl(3)	0.00369	0.00305	0.00040
Cl(4)	0.00238	0.00346	−0.00105
C (1)	0.00214	0.00365	−0.00152
C (2)	0.00267	0.00458	0.00280
C (3)	0.00247	0.00322	0.00124
C (4)	0.00283	0.00425	−0.00051
C (5)	0.00316	0.00367	−0.00152
C (6)	0.00314	0.00333	−0.00023
C (7)	0.00281	0.00237	−0.00158
C (8)	0.00186	0.00359	−0.00183
C (9)	0.00274	0.00445	0.00099
C (10)	0.00217	0.00389	−0.00017
C (11)	0.00187	0.00338	0.00053
C (12)	0.00267	0.00386	0.00230
C (13)	0.00225	0.00389	0.00056
C (14)	0.00301	0.00400	0.00051
C (15)	0.00335	0.00359	−0.00063
C (16)	0.00257	0.00328	0.00105

equal, the non-Harker peak due to these atoms should be placed at the mid-point of their Harker peaks,[9] the Harker peak of each chlorine being indicated in Fig. 4. Near this non-Harker peak, the Harker peak of Cl(3) appears accidentally. This is the reason why the peak corresponding to Cl(3) is higher than those of the other chlorine atoms.

A three-dimensional Fourier synthesis was carried out using the structure factors based on the four chlorine atoms. The electron density

9) G. Albrecht and R. B. Corey, *J. Am. Chem. Soc.*, **61**, 1087 (1939).

TABLE III. OBSERVED AND CALCULATED STRUCTURE FACTORS, $F(hk0)$

K	10FO	10FC
H,L= 0,		
2	101	92
4	0	-1
6	264	283
8	110	107
10	45	-45
12	0	1
14	0	-6
16	40	-43
18	37	-38
20	8	-1
H,L= 1,		
2	70	-73
3	110	111
4	150	148
5	0	-3
6	55	51
7	70	72
8	123	121
9	108	-102
10	158	162
11	62	-60
12	0	2
13	0	-15
14	62	-58
15	9	-19
16	52	52
17	15	-25
18	0	-4
19	14	-13
20	21	-24
21	13	8
H,L= 2,		
0	119	-103
1	38	-39
2	177	-177
3	87	88
4	23	15
5	0	-7
6	186	-192
7	77	73
8	48	-44
9	96	88
10	19	17
11	11	-23
12	81	-76
13	33	-39
14	49	-48
15	32	-33
16	0	12
17	22	-25
18	0	-4
19	32	-31
20	8	9
21	21	-22
H,L= 3,		
1	103	-102
2	0	2
3	133	135
4	36	40
5	183	186
6	197	207
7	64	61
8	38	42
9	60	-59
10	80	-83
11	76	72
12	107	104
13	23	-19
14	9	16
15	0	-7
16	64	-67
17	10	15
18	0	-5
19	0	5
20	8	10
21	31	-30
H,L= 4,		
0	178	172
1	72	-68
2	97	-90
3	42	43
4	168	-177
5	325	322
6	55	55
7	39	43
8	22	-22
9	0	11
10	0	-15
11	85	83
12	59	58
13	76	75
14	43	-42
15	29	32
16	10	22
17	10	-19
18	0	-3
19	0	3
20	17	-18
21	0	0
H,L= 5,		
1	104	-100
2	69	-73
3	218	-238
4	77	76
5	109	-114
6	0	12
7	33	-28
8	36	-35
9	0	12
10	41	44
11	38	-41
12	13	-10
13	0	18
14	45	-43
15	77	76
16	0	-10
17	25	-28
18	0	-15
19	0	-5
20	23	-22
21	18	18
H,L= 6,		
0	77	-74
1	208	214
2	31	29
3	0	-4
4	54	75
5	88	-90
6	69	-65
7	56	55
8	93	96
9	65	64
10	79	76
11	53	53
12	61	58
13	24	-32
14	25	22
15	29	28
16	42	38
17	19	-24
18	0	3
19	23	-16
20	0	7
21	15	-13
H,L= 7,		
1	91	-85
2	128	132
3	132	-135
4	71	-69
5	125	125
6	0	-3
7	41	-43
8	146	139
9	0	-9
10	8	13
11	117	115
12	36	37
13	37	46
14	38	33
15	14	-8
16	0	18
17	40	39
18	34	31
19	30	26
20	18	16
21	14	-23
H,L= 8,		
0	103	-101
1	226	-230
2	208	-204
3	92	-89
4	15	-34
5	76	75
6	38	-31
7	119	-116
8	50	-55
9	115	-116
10	17	20
11	0	-2
12	102	94
13	0	0
14	0	-17
15	0	0
16	0	22
17	0	0
18	41	38
19	0	5
20	0	-3
H,L= 9,		
1	62	59
2	168	-167
3	37	44
4	113	-104
5	0	7
6	118	-109
7	45	47
8	142	-139
9	50	46
10	71	-70
11	0	-0
12	14	-18
13	0	-1
14	48	-54
15	49	51
16	0	-5
17	10	-15
18	0	8
19	0	-3
20	23	23
H,L= 10,		
0	13	23
1	0	-3
2	0	5
3	0	-5
4	0	-3
5	78	-81
6	0	12
7	0	6
8	49	33
9	0	-9
10	86	-86
11	27	-35
12	47	-48
13	56	54
14	0	-1
15	0	14
16	0	-4
17	24	20
18	29	-27
19	31	27
H,L= 11,		
1	14	-14
2	111	110
3	112	-110
4	72	-73
5	0	6
6	40	-41
7	53	-53
8	8	-9
9	122	-126
10	23	21
11	0	13
12	32	-25
13	61	-71
14	10	-13
15	48	-45
16	30	30
H,L= 12,		
0	37	33
1	53	-48
2	101	93
3	15	10
4	146	145
5	44	39
6	0	2
7	112	-109
8	9	-18
9	23	-38
10	9	14
11	14	-23
12	20	22
13	30	-34
14	41	-43
15	0	-6
H,L= 13,		
1	87	87
2	11	-24
3	152	154
4	0	14
5	15	18
6	44	43
7	61	-58
8	0	-0
9	70	64
10	14	17
11	14	29
12	9	13
13	53	-49
14	0	10
15	12	-7
H,L= 14,		
0	48	41
1	72	70
2	55	-51
3	12	-22
4	8	-18
5	15	-19
6	13	-12
7	105	92
8	0	-6
9	14	22
10	59	-65
11	9	-8
12	14	-24
13	10	27
14	0	-4
15	0	-14
H,L= 15,		
1	94	91
2	0	3
3	52	-53
4	29	34
5	63	57
6	33	-27
7	64	67
8	43	50
9	20	-36
10	9	17
11	0	0
12	25	-23
13	13	-11
14	37	-30
15	9	-17
H,L= 16,		
0	9	11
1	35	40
2	19	13
3	69	69
4	84	85
5	39	41
6	34	38
7	14	14
8	14	12
9	60	59
10	0	5
11	47	47
12	0	-7
13	26	-27
14	0	2
15	22	23
H,L= 17,		
0	0	15
1	80	-79
2	27	37
3	9	-14
4	56	59
5	87	-91
6	9	-26
7	48	53
8	0	6
9	0	2
10	0	15
11	9	18
12	0	-4
H,L= 18,		
0	14	-13
1	28	34
2	69	-70
3	20	-29
4	35	-39
5	0	-4
6	0	3
7	0	18
8	0	-16
9	31	-34
10	10	19
11	0	-9
12	39	41
13	9	11
H,L= 19,		
1	41	41
2	54	-53
3	50	-53
4	17	22
5	0	-5
6	0	10
7	47	53
8	10	-16
9	19	4
10	29	22
11	15	20
12	9	9
13	19	18
H,L= 20,		
0	39	-44
1	0	-7
2	32	-33
3	0	-13
4	0	-0
5	0	9
6	15	24
7	21	-19
8	0	5
9	15	19
10	10	-2
11	21	17
12	0	-10
H,L= 21,		
2	0	20
3	0	6
4	40	-44
5	0	-7
6	34	-34
7	12	-14
8	0	-3
9	29	26
10	37	-34
11	0	-3
12	0	-21
H,L= 22,		
0	33	31
1	0	1
2	0	-0
3	19	-14
4	0	17
5	9	-24
6	30	29
7	0	-6
8	0	-12
9	16	-20
11	15	-13
12	29	28
H,L= 23,		
1	0	-4
2	30	-30
3	29	-22
4	0	17
5	0	-4
6	0	-0
7	13	-14
8	0	-17
H,L= 24,		
0	9	-3
1	0	-12
2	0	12
3	0	-6
4	9	-3
5	0	-10
6	0	-7
7	20	-26
H,L= 25,		
1	41	34
2	22	21
3	31	27
4	12	-23
5	11	10
6	0	-3
H,L= 26,		
0	49	37
2	0	-4
5	16	13
6	16	8
H,L= 27,		
2	17	-15

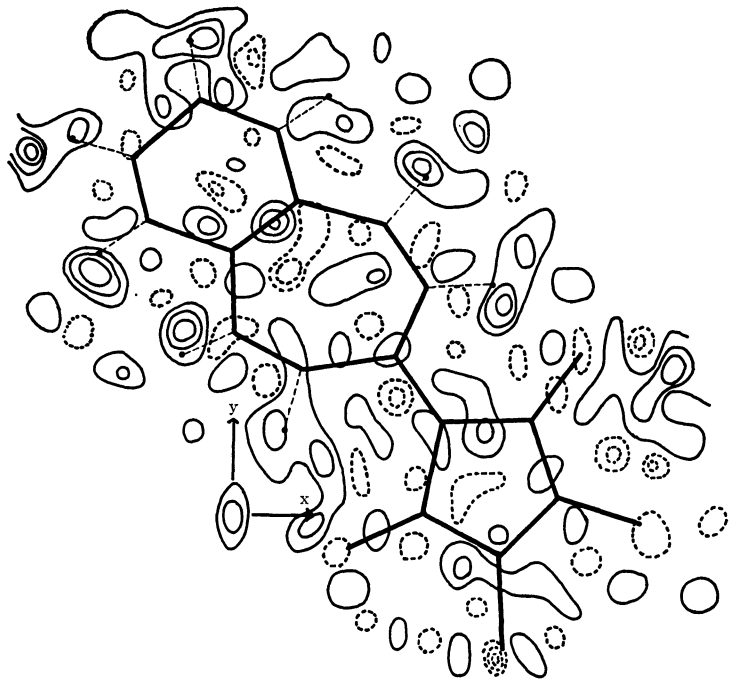

Fig. 2. The (F_o-F_c) synthesis projected along the c axis. Contours are drawn at intervals of 0.3 e. Å^{-2}. Negative contours are broken. The skeleton of the molecule is superimposed and the estimated positions of hydrogen atoms are shown by black circles.

TABLE IV. THE FINAL TEMPERATURE FACTORS USED FOR THE CALCULATION OF $F(hk1)$ AND $F(hk2)$

For chlorine atoms, temperature factors are in form of

$$\exp\{-(B_{11}h^2+B_{22}k^2+B_{33}l^2+B_{12}kh+B_{23}kl+B_{31}lh)\}$$

Atom	B_{11}	B_{22}	B_{33}
Cl(1)	0.0026	0.0045	0.1294
Cl(2)	0.0031	0.0056	0.1298
Cl(3)	0.0046	0.0034	0.1730
Cl(4)	0.0030	0.0036	0.1303
Atom	B_{12}	B_{23}	B_{31}
Cl(1)	−0.0007	0.0039	0.0046
Cl(2)	0.0010	0.0008	0.0028
Cl(3)	0.0004	0.0008	0.0008
Cl(4)	−0.0010	0.0014	0.0032

Atom	B(Å^2)	Atom	B(Å^2)
C (1)	3.93	C (9)	5.17
C (2)	5.62	C (10)	6.04
C (3)	5.80	C (11)	4.49
C (4)	4.81	C (12)	5.25
C (5)	5.35	C (13)	6.25
C (6)	5.47	C (14)	6.79
C (7)	5.23	C (15)	6.01
C (8)	6.07	C (16)	6.25

distribution so obtained showed up all the carbon atoms clearly. After one more three-dimensional Fourier synthesis, the structure was subjected to the least-squares refinement. Since the three-dimensional intensity data were incomplete, not only in number but also in their accuracy, only the z-coordinates and temperature factors of non-hydrogen atoms were refined, while anisotropic temperature factors for chlorine and isotropic temperature factors for carbon atoms were assigned. The final R factor for the set of $F(hk1)$ and $F(hk2)$ is 0.136 for the observed reflections.

The final z-coordinates of all the atoms are included in Table I, while the final temperature factors are listed in Table IV. The observed and calculated structure factors, $F(hk1)$ and $F(hk2)$, are tabulated in Table V.

All the numerical computations in this study were done on the NEAC-2101 of the Institute, the NEAC-2206 of the Computing Center of Osaka University and the IBM 7090 of the "UNICON" project, with programmes written by the authors and their collaborators.

A Description of the Structure and Discussion

From the first electron density distribution, which was obtained without any assumption regarding the structure, it was concluded exclusively that the chemical formula deduced from the synthetic process was valid as a whole. This conclusion was confirmed by the subsequent refinement, which gives a fairly good agreement between the observed and calculated structure factors

TABLE V. OBSERVED AND CALCULATED STRUCTURE FACTORS, $F(hk1)$ and $F(hk2)$

K	10FO	10FC
H,L=	0,	1
0	192	103
2	150	157
3	190	178
4	26	-40
5	30	-38
6	180	174
7	23	22
9	94	96
12	112	106
13	29	-46
H,L=	1,	1
2	220	-207
3	187	-161
4	107	105
5	22	-27
6	97	93
7	102	-95
10	144	127
11	54	59
16	21	30
H,L=	2,	1
0	531	-796
1	58	-76
2	161	-165
3	20	-28
4	21	-36
5	26	20
6	172	-170
7	40	-56
8	38	-49
9	143	-130
H,L=	3,	1
1	98	98
2	56	-69
3	53	-63
4	89	-92
5	39	40
6	22	-12
7	54	68
8	88	-92
9	34	-26
10	97	-106
11	43	46
14	65	63
H,L=	4,	1
0	326	306
1	38	-37
2	59	-54
4	42	-47
6	82	94
7	78	-83
H,L=	5,	1
1	39	-40
2	71	-85
3	32	38
4	35	-40
5	92	-106
6	155	-145
7	68	-71
12	106	-99
H,L=	6,	1
2	77	83
4	189	188
5	169	-155
9	17	-42
10	47	45
H,L=	7,	1
1	56	72
2	58	-71
3	84	87
5	66	84
6	41	55
9	64	-60
11	35	39
14	37	41
15	57	-55
H,L=	8,	1
0	65	76
1	129	-126
4	98	-93
5	41	64
6	49	51
7	57	-53
8	48	-49
10	78	-71
12	36	-39
H,L=	9,	1
1	48	60
2	29	-43
3	120	109
4	61	55
11	56	-57
12	30	-39
H,L=	10,	1
1	146	147
2	42	55
3	74	78
4	33	46
7	115	104
9	89	93
H,L=	11,	1
1	60	-62
2	53	60
3	38	-56
4	98	89
H,L=	-3,	1
10	54	63
15	21	-35
H,L=	12,	1
1	133	127
2	148	-144
3	36	52
4	130	130
5	162	172
6	132	128
8	34	-43
9	15	15
H,L=	-4,	1
0	65	78
1	133	143
3	62	72
5	90	-101
6	100	91
8	122	-108
9	68	69
10	25	-36
11	18	32
13	47	-56
14	53	-53
H,L=	-5,	1
2	184	165
3	34	38
4	58	-75
5	94	-84
8	181	164
11	76	-80
10	31	43
13	57	-61
H,L=	-6,	1
0	182	169
1	58	-66
2	243	210
5	33	33
6	43	43
7	68	-72
8	23	41
11	18	39
12	72	-78
16	29	-17
18	51	-46
H,L=	-7,	1
6	82	94
7	78	-83
H,L=	5,	1
1	39	-40
2	71	-85
3	32	38
4	35	-40
5	92	-106
6	155	-145
7	68	-71
12	106	-99
H,L=	6,	1
2	77	83
4	189	188
5	169	-155
9	17	-42
10	47	45
H,L=	7,	1
1	56	72
2	58	-71
3	84	87
5	66	84
6	41	55
9	64	-60
11	35	39
14	37	41
15	57	-55
H,L=	8,	1
0	65	76
1	129	-126
4	98	-93
5	41	64
6	49	51
7	57	-53
8	48	-49
10	78	-71
12	36	-39
H,L=	9,	1
1	48	60
2	29	-43
3	120	109
4	61	55
11	56	-57
12	30	-39
H,L=	10,	1
1	146	147
2	42	55
3	74	78
4	33	46
7	115	104
9	89	93
H,L=	11,	1
1	60	-62
2	53	60
3	38	-56
4	98	89
H,L=	-3,	1
10	54	63
15	21	-35
H,L=	12,	1
1	133	127
2	148	-144
3	36	52
4	130	130
5	162	172
6	132	128
8	34	-43
9	15	15
H,L=	-4,	1
0	65	78
1	133	143
3	62	72
5	90	-101
6	100	91
8	122	-108
9	68	69
10	25	-36
11	18	32
13	47	-56
14	53	-53
H,L=	-5,	1
2	184	165
3	34	38
4	58	-75
5	94	-84
8	181	164
11	76	-80
10	31	43
13	57	-61
H,L=	-6,	1
0	182	169
1	58	-66
2	243	210
5	33	33
6	43	43
7	68	-72
8	23	41
11	18	39
12	72	-78
16	29	-17
18	51	-46
H,L=	-7,	1
2	209	-205
6	145	-129
8	143	-133
9	45	-45
H,L=	-15,	1
1	48	51
7	45	41
10	41	-40
H,L=	4,	2
0	112	123
2	98	97
3	34	47
6	49	61
7	32	24
H,L=	-17,	1
9	126	115
2	42	-59
H,L=	5,	2
1	89	-79
4	61	58
5	29	-30
6	35	37
7	65	-68
10	42	43
11	26	-14
H,L=	6,	2
0	161	-152
2	56	58
3	12	-12
4	42	45
5	38	40
7	23	31
13	26	14
14	37	-2
H,L=	7,	2
2	44	31
3	61	-56
4	26	37
6	59	61
7	50	39
12	38	41
H,L=	8,	2
0	61	-59
2	63	-65
4	64	-62
5	41	40
6	38	-34
7	36	-39
9	42	41
H,L=	9,	2
1	58	-52
2	36	33
3	23	26
5	34	-31
6	36	-44
8	18	-0
9	42	41
12	26	-31
14	24	-17
H,L=	10,	2
0	53	-44
4	30	43
10	38	46
13	25	23
14	23	16
H,L=	11,	2
1	17	-22
3	57	-55
H,L=	12,	2
0	36	36
1	44	-53
2	17	20
3	41	-36
4	31	-30
7	70	-72
9	33	-27
14	31	22
H,L=	13,	2
11	40	-32
H,L=	14,	2
1	42	47
10	44	-36
H,L=	15,	2
2	18	-23
4	26	27
5	18	29
6	18	-7
H,L=	17,	2
8	38	28
H,L=	-1,	2
2	31	28
3	24	5
4	55	-59
5	89	-95
H,L=	-7,	2
6	128	-121
10	31	-41
H,L=	-2,	2
0	57	-49
1	20	-25
3	77	-67
4	57	-62
5	54	62
6	40	-39
8	46	46
14	42	48
H,L=	-3,	2
1	34	44
2	100	-116
3	15	-28
4	103	105
6	46	-49
7	77	73
8	85	-86
13	47	47
H,L=	-4,	2
1	37	-35
2	106	-118
3	31	-44
4	31	-29
9	56	-39
11	37	-35
H,L=	-11,	2
2	13,	2
1	70	-75
2	92	103
3	21	-33
5	31	-45
6	34	39
7	22	-29
8	92	89
9	25	26
10	37	43
12	18	9
H,L=	-6,	2
1	35	41
2	25	33
3	60	58
5	44	50
6	14	-19
8	60	54
9	93	89
12	22	-31
H,L=	-7,	2
2	12	-26
3	79	-79
4	36	39
5	20	-38
9	55	-54
10	18	35
11	18	-35
H,L=	-8,	2
4	25	-34
7	38	44
9	25	25
10	18	-26
11	18	-4
12	26	-19
13	33	31
H,L=	-9,	2
1	47	54
2	14	-11
3	152	153
5	15	33
9	25	41
12	33	22
H,L=	-10,	2
2	66	77
6	30	-29
7	61	-65
11	18	10
13	25	-27
H,L=	-11,	2
3	44	-58
6	25	38
9	26	-40
H,L=	-12,	2
0	45	57
1	15	34
2	15	42
6	45	52
7	18	-14
8	38	40
10	26	-36
H,L=	-13,	2
2	25	-54
4	52	-63
10	26	-29
H,L=	-14,	2
0	52	-68
2	17	-30
6	38	-52
7	51	-60
H,L=	-15,	2
11	39	40
H,L=	-16,	2
11	33	-27
H,L=	-17,	2
5	38	-26
H,L=	-18,	2
5	46	47

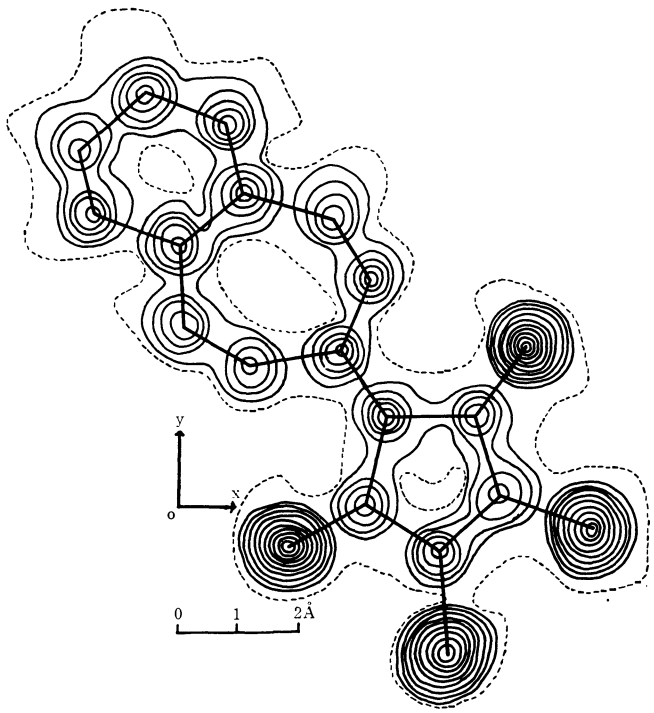

Fig. 3. The final electron density projection along the c axis. Contours are drawn at intervals of 1 e. Å^{-2} with broken contour of 1 e. Å^{-2}. For chlorine atoms, contours are drawn at intervals of 2 e. Å^{-2} beginning with 2 e. Å^{-2}.

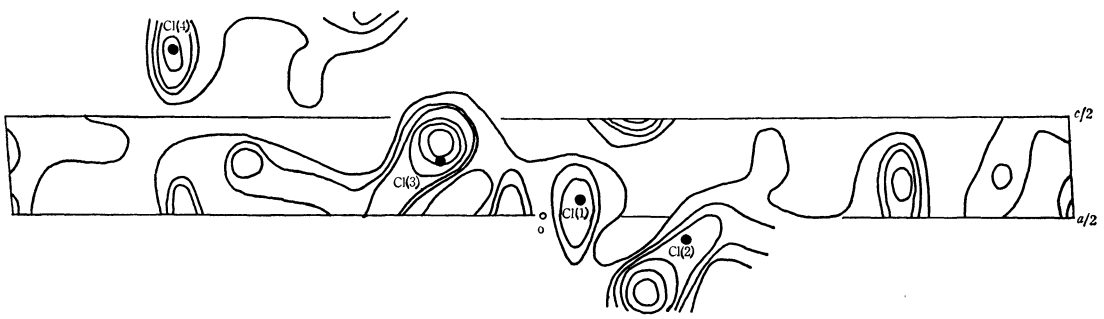

Fig. 4. Harker section $P(u, 1/2, w)$. Contours are drawn at equal intervals on an arbitrary scale. Harker peaks corresponding to the chlorine atoms are indicated.

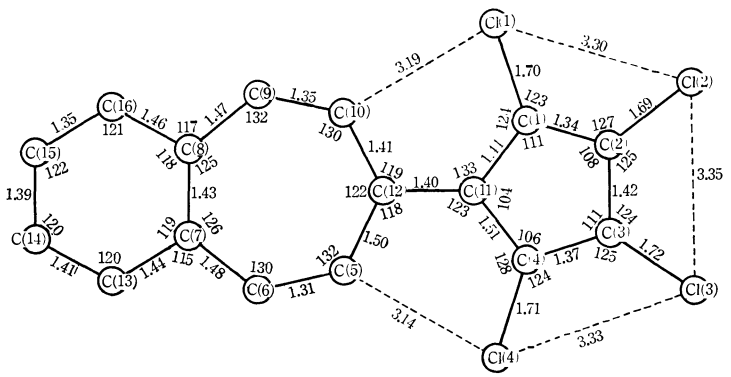

Fig. 5. Bond lengths (Å) and bond angles (°) in the molecule of 1,2,3,4-tetrachlorobenzo[g]-sesquifulvalene.

and which results in quite reasonable intra- and intermolecular distances.

All the bond lengths and angles are shown in Fig. 5. The average standard deviations of the atomic coordinates are 0.011 and 0.036 Å for chlorine and carbon atoms respectively. Therefore, the estimated standard deviation of a C–C bond length is 0.05 Å, while that of a C–Cl bond length is 0.04 Å.

The mean length of C–Cl bonds is 1.705 Å, a value which is in good agreement with the average value of those in several chlorobenzenes (1.70 Å).[10] In the benzene ring of the present molecule, the mean C–C length is 1.413 Å.

In the sesquifulvalene skeleton, longer and shorter bonds are disposed alternately, as could be expected from the chemical formula (III). The average of the longer bond lengths is 1.461 Å, while that of the shorter is 1.354 Å. These values may be compared with those observed in some similar compounds; 1.451 and 1.373 Å in 8, 8-dicyanoheptafulvene,[11] 1.446 and 1.358 Å in 7, 7, 8, 8-tetracyanoquinodimethane,[12] 1.477 and 1.322 Å in *p*-benzoquinone,[13] 1.477 and 1.342 Å in tetrachloro-*p*-benzoquinone,[14] and 1.470 and 1.322 Å in cyclooctatetraenecarboxylic acid.[15]

Murata[16] deduced the bond orders in benzo[g]-sesquifulvalene from a molecular orbital treatment by assuming the planarity of the molecule and the presence of a mirror plane perpendicular to the molecular plane through C(11)-C(12). Table VI shows the theoretical bond lengths converted from the bond orders. It can be said that the observed lengths of the bonds related to each other by the mirror do not differ significantly in the present molecule. Therefore, the average lengths of the equivalent bonds (Table VI) may be compared with the theoretical values. The agreement between them is fairly good, although the assumption of the planarity of the molecule does not hold, as will be described below .

Table VI. Theoretical and observed bond lengths (Å)

Bonds	Theoretical	Observed
C(1)-C(2) and C(3)-C(4)	1.36	1.355
C(2)-C(3)	1.46	1.420
C(1)-C(11) and C(4)-C(11)	1.45	1.475
C(11)-C(12)	1.37	1.400
C(10)-C(12) and C(5)-C(12)	1.46	1.455
C(9)-C(10) and C(5)-C(6)	1.36	1.330
C(8)-C(9) and C(6)-C(7)	1.46	1.475
C(7)-C(8)	1.41	1.430
C(8)-C(16) and C(7)-C(13)	1.46	1.450
C(15)-C(16) and C(13)-C(14)	1.39	1.380
C(14)-C(15)	1.40	1.390

The equations of the best planes of the five-, seven- and six-membered rings (A, B and C respectively) were derived by the least-squares method. In the final evaluation of the coefficients of the equations, the C(1) and C(12) atoms were excluded, because they were significantly off the planes. The equations of these best planes are:

$$-4.786X-Y-16.984Z+26.139=0 \quad (A)$$

$$-0.002X-Y+2.238Z+1.342=0 \quad (B)$$

$$-0,008X-Y+1.842Z+1.947=0 \quad (C)$$

where $X=x\sin\beta$, $Y=y$, and $Z=z+x\cos\beta$.

The perpendicular displacements of the atoms from each mean plane are shown in Table VII. The C(1) atom is shifted from the mean plane by 0.12 Å. Except for this, the five-membered ring might be thought to be planar. Some of the chlorine atoms are significantly off from the five-membered ring. In the seven-membered ring, the C(12) atom which is linked to the five-membered ring deviates from the mean plane by 0.22 Å. The other atoms in the ring lie on the plane. The six-membered ring also seems to be planar within the limit of error.

Table VII. Deviation of the atoms from the mean planes (Å)

Atoms	From the plane A (The five-membered ring)	From the plane B (The seven-membered ring)	From the plane C (The six-membered ring)
Cl(1)	0.04		
Cl(2)	0.14		
Cl(3)	−0.11		
Cl(4)	−0.30		
C (1)	−0.12		
C (2)	0.01		
C (3)	−0.01		
C (4)	0.02		
C (11)	−0.02	0.39	
C (12)	−0.11	0.22	0.39
C (5)		0.04	0.24
C (6)		−0.04	0.11
C (9)		−0.04	−0.06
C (10)		0.01	0.08
C (7)		−0.01	0.03
C (8)		0.04	0.00
C (13)		−0.03	−0.03
C (14)		0.11	0.01
C (15)		0.20	0.02
C (16)		0.12	−0.03

10) "Tables of Interatomic Distances and Configuration in Molecules and Ions," The Chemical Society, London (1958), p. 15.
11) H. Shimauchi, T. Ashida, Y. Sasada, M. Kakudo, I. Murata and Y. Kitahara, This Bulletin, **38**, 1230 (1965).
12) R. E. Long, R. A. Sparks and K. N. Trueblood, *Acta Cryst.*, **18**, 932 (1965).
13) J. Trotter, *Acta Cryst.*, **13**, 86 (1960).
14) S. S. C. Chu, G. A. Jefferey and T. Sakurai, *Acta Cryst.*, **15**, 661 (1962).
15) D. P. Shoemaker, H. Kinder, W. G. Sly and R. C. Srivastave, *J. Am. Chem. Soc.*, **87**, 482 (1965).
16) I. Murata, Private Communication (1964).

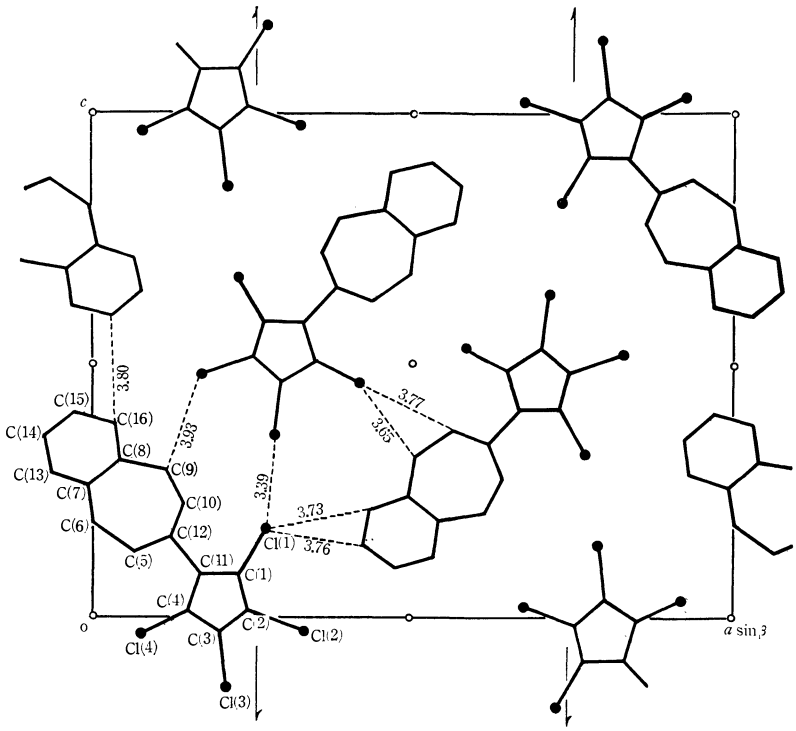

Fig. 6. Arrangement of the molecules in the crystal viewed along the c axis. Short intermolecular distances are indicated.

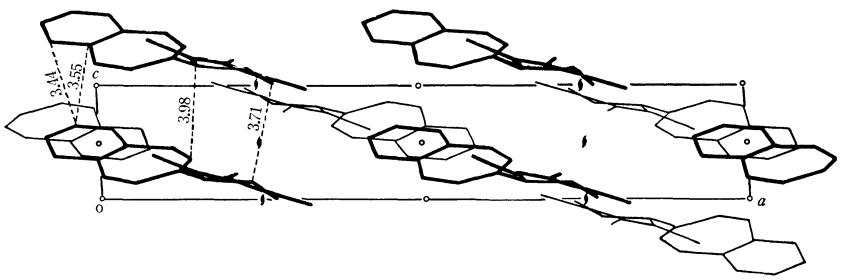

Fig. 7. Arrangement of the molecules in the crystal viewed along the b axis. Short intermolecular distances are indicated.

The five- and seven-membered rings twist around the C(11)–C(12) bond by an angle of about 31° to each other. This might be due to repulsion forces between Cl(1) and H(10) and between Cl(4) and H(5). If the hydrogen atoms are assumed so as to be located at a distance of 1.0 Å outward from the carbon atoms, the distances between the chlorine and hydrogen atoms may be computed to be 2.45 Å for the former and 2.57 Å for the latter.

The seven- and six-membered rings are not coplanar; these two planes make slight angles (of about 5°).

The arrangement of the molecules in the crystal is shown in Figs. 6 and 7, where the short intermolecular distances are given. There is observed one short intermolecular approach, 3.39 Å between Cl(1) in a molecule and Cl(3) in the neighboring molecule related by the screw axis to it. All the other intermolecular separations are equal to or larger than the sums of the van der Waals radii of the corresponding atoms.

As may be seen from Figs. 6 and 7, two molecules related by a center of symmetry to each other make a pair; the dipole moment of this compound (5.20 D)[3] is compensated for by this pairing. Such pairs are packed together in the manner found in the crystals of typical aromatic molecules.

The authors would like to express their deep thanks to Professor Yoshio Kitahara and Dr. Ichiro Murata of Tohoku University for supplying material and for their continued interest. Thanks are also due to the staff of the University Computing Center for their kind help. The computing time of the IBM 7090 was made available to the authors through the "UNICON" project.

BULLETIN OF THE CHEMICAL SOCIETY OF JAPAN VOL. 39 827—828 (1966)

The Oxidation of Chloromethyl Compounds with Lead Tetraacetate

By Yasuhide YUKAWA and Mitsuru SAKAI

Institute of Scientific and Industrial Research, Osaka University, Sakai, Osaka

(Received September 20, 1965)

In studying the reaction of styrene, olefins, vinyl ethers and vicinally-substituted compounds with lead tetraacetate, it was shown that the methyl group of 9-chloro-9-methylfluorene was easily acetoxylated with lead tetraacetate. This novel reaction was then applied to 1, 1-diphenylethyl chloride, 1-phenylethyl chloride and *t*-butyl chloride. In every case the methyl group of chlorides with an α-methyl group was acetoxylated preferentially.

The authors have, in recent years, been studying the reactions of lead tetraacetate with various unsaturated compounds, such as styrene, olefins, vinyl ethers and vicinally-substituted compounds.[1] In this paper we wish to report the novel acetoxylation of a methyl group with lead tetraacetate. It has been found that the methyl group of 9-chloro-9-methylfluorene, 1, 1-diphenylethyl chloride, 1-phenylethyl chloride and *t*-butyl chloride is preferentially acetoxylated by the reactions with lead tetraacetate. Table I shows the results of these reactions.

The yield of the acetoxylated products has been slightly raised by the addition of a small amount of anhydrous sodium acetate. The formation of tarry by-products has been suppressed when the reaction is carried out at a moderate temperature, below 70°C.

The lead tetraacetate could be used without any special precautions for its purification, since it has been found that these acetoxylation reactions are not influenced by the presence of the 10 to 15% of lead dioxide which could be a major impurity of lead tetraacetate.

The structures of the products were assigned by their conversion to the respective glycols. The hydrolysis of the 2-chloro-acetate was carried out by sodium hydroxide in methanol. The resulting glycols were shown to be III, VI, IX and XII by a comparison of these infrared spectra and the retention times in gas chromatography (on two different columns, silicon grease and apiezon grease on firebrick) with those of the authentic samples. The migration of the chlorine atom was rejected in the oxidation of IV. The structures for the two isomers of V and XIII were assigned by Summerbell.[2] The melting points of V and XIII were 76 and 30°C respectively. XIII was synthesized from ethyl chloroacetate and phenylmagnesium bromide, followed by acetylation with acetic anhydride. The product in the oxidation of IV showed a marked depression of melting point when mixed with XIII.

$$\begin{matrix} Ph_2\text{-}C\text{-}CH_2Cl \\ | \\ OAc \end{matrix}$$
(XIII)

Neither 2-phenylethyl halide nor cyclohexyl halide was acetoxylated, even under more drastic conditions. Bromides with an α-methyl group gave similarly acetoxylated products. Iodides gave mainly tarry products. Thus it has been demonstrated that chlorides and bromides in which the methyl group and halogen atoms are joined to the same carbon atom react with lead tetraacetate to give halohydrin acetates in fairly good yields.

Although the mechanism of this reaction has not yet been settled, there can be little doubt, in view of the radical mechanism in lead tetraacetate oxidation, that the reaction involves a one electron-transfer from chlorine to lead (Pb^{IV}) and a concurrent hydrogen abstraction from the methyl group by an acetoxyl radical. The following mechanism is tentatively suggested:

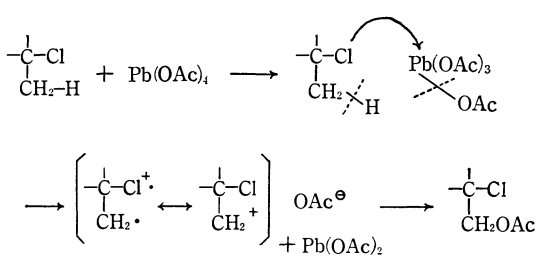

The oxidation of chloromethyl compounds with lead tetraacetate in acetic acid provides a useful route for the synthesis of pure chlorohydrin acetate.

Experimental

The melting points were determined on a Yanagimoto hot bench melting point apparatus and are corrected. The elementary analyses were performed by the Microanalytical Laboratories of Osaka University. The

1) Y. Yukawa and M. Sakai, This Bulletin, **36**, 761 (1963); Y. Yukawa and M. Sakai, *J. Chem. Soc. Japan, Pure Chem. Sect.* (*Nippon Kagaku Zasshi*), **87**, 79, 81, 84 (1966).

2) R. K. Summerbell and M. J. Kland-English, *J. Am. Chem. Soc.*, **77**, 5095 (1955).

TABLE I. THE REACTION BETWEEN α-METHYL CHLORIDES AND LEAD TETRAACETATE

Starting material	Product	Yield	Glycol
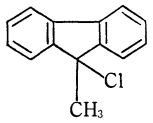	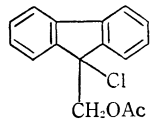	50%	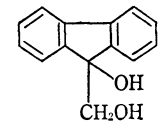
(I)	(II)		(III)
Ph_2-C-CH_3 Cl	Ph_2-C-CH_2OAc Cl	50%	Ph_2-C-CH_2OH OH
(IV)	(V)		(VI)
$(CH_3)_3$-C-Cl	$(CH_3)_2$-C-CH_2OAc Cl	45%	$(CH_3)_2$-C-CH_2OH OH
(VII)	(VIII)		(IX)
Ph-CH-CH_3 Cl	Ph-CH-CH_2OAc Cl	45%	Ph-CH-CH_2OH OH
(X)	(XI)		(XII)

infrared spectra were determined using a Hitachi double-beam spectrophotometer.

Materials.—Lead tetraacetate was prepared from red lead oxide and acetic acid.[3] The following reagents were commercial materials and were redistilled before use; acetic acid, butanol, *t*-benzaldehyde, β-phenylethyl alcohol and ethyl chloroacetate. The following commercial reagents were used without further purification; benzophenone, fluorenone, cyclohexanol and methyl iodide. 9-Chloro-9-methylfluorene,[4] 1, 1-diphenylethyl chloride,[5] *t*-butyl chloride[6] and 1-phenylethyl chloride[7] were prepared by the methods described in the literature.

General Procedure.—In order to avoid needless repetition, the experimental conditions for carrying out these reactions have been generalized. A stirred solution of 0.1 mol. of the substituted chloride and 0.1—0.12 mol. of lead tetraacetate in 100 ml. of a solvent, under a slight pressure of dry nitrogen, was maintained at 60 to 70°C for about 0.5—1 hr. From the resulting clear solution, about a half of the acetic acid was removed under a vacuum below 65°C. The residue was then dissolved in ethyl ether (100 ml.) and washed with water (80 ml.) three times in order to remove the inorganic lead compounds. The etheral solution was treated with anhydrous sodium sulfate filtered, and vacuum-distilled.

9-Acetoxymethyl-9-chlorofluorene (II).—Under the general procedure, with acetic acid as the solvent, 9-chloro-9-methylfluorene and lead tetraacetate gave a 50% yield of II, m. p. 118°C (from ethanol).

Found: C, 70.17; H, 4.76; Cl, 13.16. Calcd. for $C_{16}H_{13}O_2Cl$: C, 70.46; H, 4.80; Cl, 13.00%.

The hydrolysis of II gave 9-hydroxymethyl-9-fluorenol (III), m. p. 105—106°C (from benzene), lit.[8] m. p. 105—108°C.

Found: C, 79.31; H, 5.84, Calcd. for $C_{14}H_{12}O_2$: C, 79.22; H, 5.70%.

2-Chloro-2, 2-diphenylethyl Acetate (V).—Under the general procedure, with acetic acid as the solvent, 1, 1-diphenylethyl chloride and lead tetraacetate gave a 50% yield of V, m. p. 75—76°C (from ethanol).

Found: C, 69.85; H, 5.61; Cl, 13.07. Calcd. for $C_{16}H_{15}O_2Cl$: C, 69.95; H, 5.50; Cl, 12.90%.

The hydrolysis of V gave asym-diphenylethylene glycol (VI), m. p. 122°C (from benzene); lit.[9] m. p. 121°C.

2-Chloro-2, 2-dimethylethyl Acetate (VIII).—Under the general procedure, with acetic acid as the solvent, *t*-butyl chloride and lead tetraacetate gave a 45% yield of VIII, b. p. 95—97°C/35 mmHg.

Found: Cl, 23.83. Calcd. for $C_6H_{11}O_2Cl$: Cl, 23.54%.

The hydrolysis of VIII gave asym-dimethylethylene glycol (IX) (diphenylurethan, m. p. 140°C).

2-Chloro-2-phenylethyl Acetate (XI).—Under the general procedure, with acetic acid as the solvent, 1-phenylethyl chloride and lead tetraacetate gave a 45% yield of XI, b. p. 110°C/4.0 mmHg.

Found: Cl, 17.54. Calcd. for $C_{10}H_{11}O_2Cl$: Cl, 17.85%.

The hydrolysis of XI gave styrene glycol (XII), m. p. 67°C.

3) O. Dimroth and R. Schweizer, *Ber.*, **56**, 1375 (1923).
4) H. Wieland, *Ann.*, **433**, 135 (1925).
5) S. Kawamatsu, K. Oikawa and T. Inoue, *J. Chem. Soc. Japan, Ind. Chem. Sect.* (*Kōgyō Kagaku Zassi*), 53 **357** (1950).
6) H. Stone and H. Shechter, *J. Org. Chem.*, **15**, 491 (1950).
7) G. L. Goerner and W. G. Hines, *J. Am. Chem. Soc.*, **70**, 3511 (1948).
8) T. Mole, *J. Chem. Soc.*, **1960**, 2132.
9) F. N. Peters, Jr., and E. Griffith, *J. Am. Chem. Soc.*, **47**, 453 (1925).

BULLETIN OF THE CHEMICAL SOCIETY OF JAPAN VOL. 39 829—833 (1966)

The Electrical Resistivity of Carbon Black under Compression

By Tokiti NODA, Hajime KATO, Toshihiko TAKASU, Akihide ŌKURA and Michio INAGAKI

Department of Applied Chemistry, Faculty of Engineering, Nagoya University, Chikusa-ku, Nagoya

(Received September 21, 1965)

The electrical resistivity of carbon blacks was measured under compression (up to 9 kilobars) at room temperature using a pressure vessel of the piston-cylinder type. The slope of the log ρ vs. log P relation was about -0.5 for all the carbon black specimens except the original channel black. For the thermal blacks heat-treated above 2100°C, i. e., the graphitized thermal blacks, the linear relation between logarithms of resistivity, ρ, and of pressure, P, broke at about 2.5—4.5 kilobars. After the break the slope of the log ρ vs. log P relation for the graphitized thermal blacks had the same value as that for natural graphite. The original channel black had a value of the slope as high as -0.9, but the 1300°C-treated channel black had a value similar to that of the other samples. This was probably due to the removal of the high-resistance film on the particle surface by the heat treatment. The first stage of the decrease in electrical resistivity with an increase in the pressure seems to be due to the yielding deformation of carbon black particles caused by the increased packing of the particles, while the second stage may be due mainly to the increase in the contact of crystallites in the particles by the elastic deformation, accompanied by a change in the preferred orientation of crystallites with the pressure.

The measurement of the electrical resistivity of carbon black under compression has been carried out by a number of investigators with both technical and scientific interests. However, the measurements under pressures above 2 kilobars (kb) have been very few. According to Adelson and Austin,[1] the resistance versus pressure curves of a number of carbon blacks broke relatively sharply at approximately 30 kb; this break was assumed to be caused by the change from the elastic to the yielding deformation of carbon black particles. In their work, however, there might have been a considerable pressure gradient in the radial direction of the compressed specimen, because they used opposed anvils of a flat face as the pressure apparatus.

In the present work, the electrical resistivity of carbon black under compression was investigated under a pressure of up to 9 kb at room temperature using a pressure vessel of the piston-cylinder type. In this pressure vessel, the gradient of the pressure is negligibly small, in both the radial and the longitudinal directions of the compressed specimen, if the specimen is appropriately thin, as will be described below. Not only original carbon blacks but also heat-treated carbon blacks were used as samples.

Experimental

The materials used in the present work were two kinds of thermal black, a channel black, their heat-treated specimens and a pulverized natural graphite. The thermal blacks have no "structure"; the particle size of one of them is quite uniform, about 1000 Å on the average, while the other's is not so uniform, its average particle size being 3000 Å. The carbon blacks were heat-treated in an induction furnace at various temperatures under a reduced pressure of 10^{-2} Torr for 30 min. The natural graphite powder was also heated at 2700°C for 10 min. under 10^{-2} Torr in the same furnace. The polyhedral form of the particles of thermal blacks heat-treated above 2100°C was observed in their electron micrographs.

The density measured by the pycnometric method,[2] d_p; the density calculated from lattice constants, d_x, and the porosity, 100 $(d_x-d_p)/d_p$, of the carbon blacks are given in Table I.

The pressure vessel of the piston-cylinder type is shown schematically in Fig. 1. The piston and the cylinder were made of tool steel. The surfaces of the upper and lower pistons were plated with copper and silver in order to decrease the contact resistance between the piston and the specimen. This vessel could be used under pressures of up to 10 kb. The dimensional change of the cylinder by the elastic compression at the pressure of 10 kb was found to be negligible for the measurement of the resistivity. As an insulator between the pistons and the cylinder, a polyethylene sheet, a phenol resin pipe and a pipe made of epoxy resin reinforced with glass fibre were tested. A polyethylene sheet 0.04 mm. thick was proved to be the best among them and could be used for the measurement of the resistivity under pressures of up to 10 kb. The phenol and reinforced epoxy resin pipes, which were 2.5 mm. thick, fractured when the specimen was compressed to about 6 kb. Also, the dimensional

1) E. Andelson and A. E. Austin, presented at the Sixth Biennial Conference on the Carbon (1963), Pittsburgh, Pa.

2) M. Mizutori, S. Hagiwara, K. Kawazohe and Y. Fukuda, *J. Chem. Soc. Japan, Ind. Chem. Sect.* (*Kogyo Kagaku Zasshi*), **66**, 1757 (1963).

Table I. The densities and porosity of carbon black particles

Specimen	d_p	d_x	Porosity
Channel black			
(Spheron-9) original	1.789±0.009	—	—
1270°C HT	1.857±0.004	2.23	19.8
2020°C HT	1.933±0.002	2.24	16.1
2610°C HT	1.951±0.004	2.24	14.9
Thermal black			
(Miike #20) original	1.739±0.009	—	—
1340°C HT	1.860±0.002	2.24	20.2
2120°C HT	2.014±0.006	2.24	10.9
2680°C HT	2.014±0.006	2.24	9.7
Thermal black			
(Nippon Gas Chem.)			
original	1.693±0.004	—	—
2500°C HT	2.143±0.006	2.24	7.2
3000°C HT	2.167±0.006	2.24	3.2
Natural graphite	2.254±0.006	2.26	—

change in the resin pipes by compression could not be neglected in the measurement of the resistivity when the thick pipes were used. In the case of the polyethylene sheet, however, its dimensional change was negligible because it was very thin compared with the diameter of the compressed specimen. The pressure applied to a specimen was calibrated by the measurement of the volume change of NH_4F transition (3.8 kb.) The pressure loss for friction between the piston and the cylinder was found to be 5%.

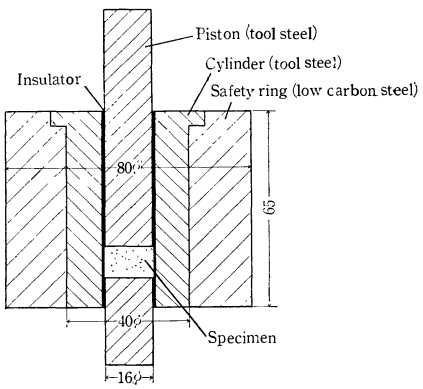

Fig. 1. The pressure vessel of piston-cylinder type.

The electrical resistance under compression was measured as a function of the thickeness of the specimen by a Kelvin bridge using the pistons as electrodes. The very good linear relation between the measured resistance and the thickness of specimen was observed, as is shown in Fig. 2. When the thickness of the specimen became too high, the measured resistance of the specimen deviated upwards from this line as a result of the non-uniformity of the pressure in the specimen. Accordingly, the thickness of the specimen was limited to about 4 mm. The electrical resistivity was determined from the inclination of this line using the least-squares calculation.

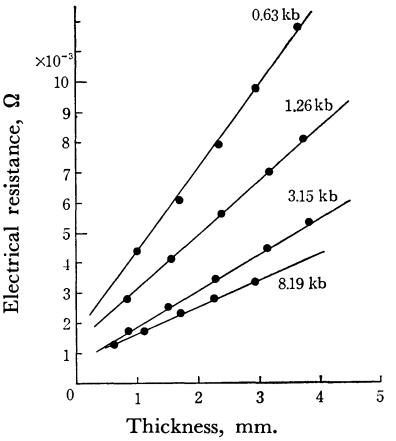

Fig. 2. Dependence of the measured electrical resistance on the thickness of the 2680°C-treated thermal black (Miike #20).

Results

The changes in the electrical resistivity, ρ, of the thermal blacks (Miike #20) and of the natural graphite with the pressure, P, are shown on logarithmic plots in Fig. 3; that of the channel black (Spheron-9), in Fig. 4 and that of the thermal black (N. G. C.), in Fig. 5.

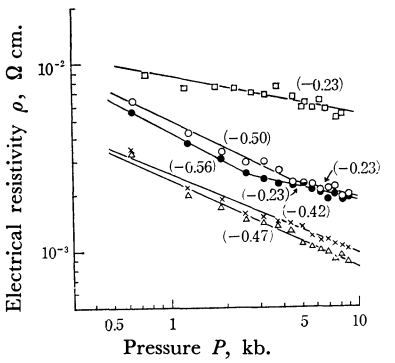

Fig. 3. Dependence of electrical resistivity ρ of carbon black on pressure P.
□: natural graphite (NG)
×: original thermal black (TBM)
△: 1340°C-treated thermal black (TBM-1300)
○: 2120°C-treated thermal black (TBM-2100)
●: 2680°C-treated thermal black (TBM-2700)
Figures in parentheses along lines are slopes of these lines.

The relation between $\log \rho$ and $\log P$ can be said to be linear. For the 2100°C-, 2700°C- and 3000°C-treated thermal blacks, the $\log \rho$ vs. $\log P$ relations break relatively sharply at the pressure of about 4.5—3.0 kb. The pressure of the break point decreases with the increase in the heat treatment temperature. However, the original and 1300°C-treated thermal blacks do not show

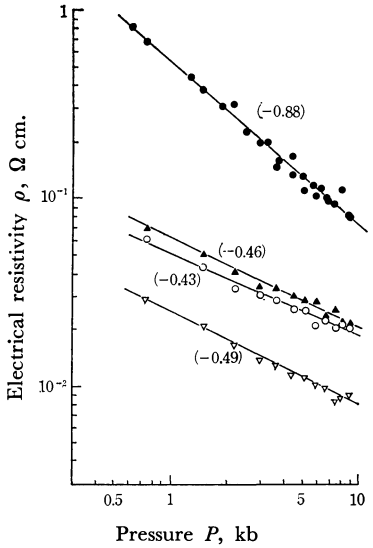

Fig. 4. Dependence of electrical resistivity ρ of carbon black on pressure P.
●: original channel black
▽: 1270°C-treated channel black (CB-1300)
○: 2020°C-treated channel black (CB-2000)
▲: 2610°C-treated channel black (CB-2600)
Figures in parentheses along lines are slopes of these lines.

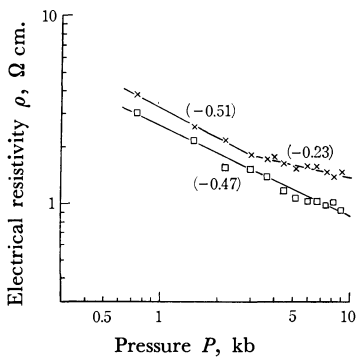

Fig 5. Dependence of electrical resistivity ρ of carbon black on pressure P.
□: original thermal black (NGC)
×: 3000°C-treated thermal black (NGC-3000)

any break within the limits of the pressure applied in the present work. In other words, the 2100°C-, 2700°C- and 3000°C-treated or graphitized thermal blacks show the change in resistivity with the pressure in two stages, while the original and 1300°C-treated thermal blacks show only the first stage of the change in resistivity. The slopes of the thermal blacks at the first stage are about −0.5, scattering somewhat from specimen to specimen. At the second stage, the relation between $\log \rho$ and $\log P$ has almost the same slope, −0.23, for all graphitized thermal blacks. This value of slope agrees with that for natural graphite.

The relation between $\log \rho$ and $\log P$ for the channel black shows no break. The original channel black has quite a high resistivity and a high slope of the $\log \rho$ vs. $\log P$ relation.

Discussion

The change in the electrical resistivity with the pressure results from the process of packing the carbon black particles. Takahashi[3] reported the dependence of the electrical resistivity of carbon black on pressures up to 200 kg./cm² to be $\rho = A/P + B$ for hard spheres and $\rho = C/P^{1/2} + D$ for deformable particles as derived from Holm's contact resistance theory. Akamatu and Inokuchi[4] observed the relation $\rho = a/P + b$ (3) for various carbon blacks in the 11—160 kg./cm² pressure range. Honda, Ouchi and Toyoda[5] reported that there was, in general, the relation $\rho = AP^{-2} + B$, where $n \approx 1$—2 for heat-treated coals, cokes and charcoals in the 400—2000kg./cm² pressure range. They also derived the relation from the relations of the void ratio to the pressure and of the void ratio to the resistivity, and deduced $n = 2$ for plastically-undeformable particles. Ōtani[6] found $n = 1$—0.5 for various carbons in the 500—2200 kg./cm² pressure range. According to Mrozowski,[7] the electrical resistivity of the powder

$$\rho \cong 0.34\bar{\rho}E^{1/3}/(P^{1/3}\varphi^{1.0})$$

for a purely elastic deformation (4)

and

$$\rho \cong 0.445\bar{\rho}H^{1/2}/(P^{1/2}\varphi^{3/4})$$

for a purely yielding deformation (5)

where $\bar{\rho}$ = the real resistivity; E = the elastic modulus, H = the hardness of the material of the particles, and φ = the fraction of the volume occupied by the particle. From the experimentally-established relation for the volume of a definite amount of material, $\log V = -m \log P$[7] and $\varphi \cong 1/V$,

$$\rho = k_1/(P^{(1/3+m)}) \text{ for elastic deformation} \quad (4')$$

and

$$\rho = k_2/P^{(1/2+3m/4)} \text{ for yielding deformation} \quad (5')$$

The pressure dependence of the resistivity caused by the change in packing is very small and leads to a small correction in the slope of the $\log \rho$ vs. $\log P$ relation. The slopes of the first stage of all the curves for $\log \rho$ vs. $\log P$ are alsmost equal to −0.5 except for the original channel black. Therefore, the first stage of the $\log \rho$ vs. $\log P$

3) H. Takahashi, *J. Chem. Soc. Japan, Pure Chem. Sect.* (*Nippon Kagaku Zasshi*), **71**, 361 (1950).
4) H. Akamatu and H. Inokuchi, ibid., **70**, 185 (1949).
5) H. Honda, K. Ouchi and S. Toyoda, ibid., **76**, 364 (1955).
6) S. Ōtani, *J. Chem. Soc. Japan, Ind. Chem. Sect.* (*Kogyo Kagaku Zasshi*), **60**, 407 (1957).
7) S. Mrozowski, Proc. Third Conf. Carbon, Pergamon (1959), p. 495.

relation may mainly correspond to the yielding deformation process of the packing of the particles, although the elastic deformation process may play some part. One can see a slight increase in the slope for the thermal black with the increase in the heat treatment temperature. As can be seen from Table I, carbon black particles are porous and are, therefore, deformable, especially when they are heat-treated at higher temperatures and become softer. The slope of the $\log \rho$ vs. $\log P$ relation for the original channel black is -0.9. This is due to the surface film on the carbon black particles.[7,8] The film on the particle surface can be removed by heat treatments at high temperatures. Therefore, the 1300°C-treated channel black has a slope similar to those of the other samples.

The pressure of the break point of the $\log \rho$ vs. $\log P$ relation for the graphitized thermal blacks conincided with the pressure at which the bulk density of the compressed mass is almost equal to the density of carbon black particles; i. e., the void ratio is almost zero (Fig. 6).

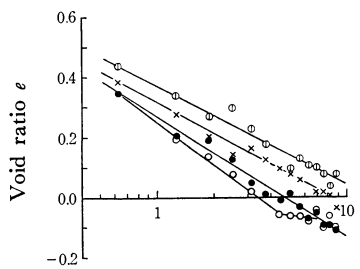

Fig. 6. Dependence of void ratio e of thermal black on pressure P.
⦶: original thermal black (TBM)
×: 1340°C-treated thermal black (TBM-1300)
●: 2120°C-treated thermal black (TBM-2100)
○: 2680°C-treated thermal black (TBM-2700)

From this point on, the particles themselves are compressed and the bulk density of particles finally reaches almost the same density as that calculated from the lattice constants, d_x. In the case of the channel black and the original and calcined (1370°C treated) thermal blacks, the bulk densities never exceeded their particle densities (Figs. 6 and 7). The plots $\log \rho$ vs. $\log P$ for these blacks had only the first stage, and not the second stage. In the second stage the dependence of the electrical resistivity on the pressure may mainly be represented by the elastic deformation mechanism, although the experimental slope, -0.23, is rather smaller than the predicted value, -0.33. There may be an increase in the preferred orientation of crystallites in the compressed

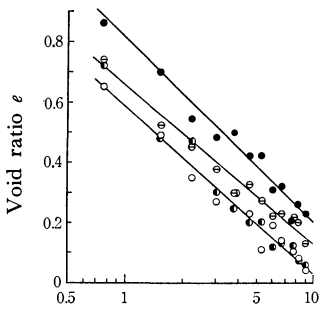

Fig. 7. Dependence of void ratio e of channel black on pressure.
●: original channel black
⊖: 1270°C-treated channel black (CB-1300)
◐: 2020°C-treated channel black (CB-2000)
○: 2610°C-treated channel black (CB-2600)

mass with the increase in compression. When the distribution function of crystallite orientation is assumed to be $\sin^n \Phi$,[9] where Φ is the angle between the normal to the basal plane of crystallite and the normal to the direction of compression, the resistivity, $\bar{\rho}$, can be taken to be approximately $\rho_{\parallel c} \sin^n \Phi$, because $\rho_{\parallel c} \gg \rho_{\perp c}$, where $\rho_{\parallel c}$ and $\rho_{\perp c}$ are the resistivities of single crystals of graphite parallel to and perpendicular to the c-axis respectively. The distribution function may be related to the pressure of compression as $\sin^n \Phi = a P^b$; therefore,

$$\bar{\rho} = a \cdot \rho_{\parallel c} \cdot P^b \tag{6}$$

From Eqs. (4) or (4′) and (6)

$$\bar{\rho} \cong 0.34a \cdot \rho_{\parallel c} E^{1/3}/(P^{1/3-l}\varphi^{1.0}) \cong k_3/(P^{1/3+m-l}) \tag{7}$$

Thus the increase in the preferred orientation decreases the slope of the $\log \rho$ vs. $\log P$ relation.

From Eq. 5 one can calculate the hardness, H, from the applied pressure, P, and the bulk density of the carbon black powder at the pressure. The resistivity at 9 kb was taken as $\bar{\rho}$, because the change in the resistivity with the increase in the pressure in the high pressure range was very small. Mrozowski[7] obtained 8×10^5 lb/in^2 = 56×10^3 kg./cm^2, which is an unreasonably high value for calcined soft carbons of coarse powder. However, he suggested the use of the calculated hardness in estimating relative values. Our results were about the same order as his value, i. e., very high. For example, the hardness was estimated to be 51×10^3 kg./cm^2 for the original thermal black, 38×10^3 kg./cm^2 for the 1340°C-treated thermal black, 28×10^3 kg./cm^2 for the 2120°C-treated thermal black, and 24×10^3 kg./cm^2 for the 3000°C-treated thermal black.

8) S. Mrozowski, A. Chaberski, F. E. Loebner and H. T. Pinnick, ibid., p. 211.

9) G. E. Bacon, *J. Appl. Chem.* (*London*), **6**, 477 (1956).

The original carbon blacks have about the same hardness as calcined soft carbons, and the hardness of the carbon blacks decreases to about half when they are graphitized, i. e., heat treated above 2000°C. Therefore, the graphitized carbon black particles deform easier than the original and calcined particles. In the case of the graphitized thermal black, all space in the compressed mass is filled up with material of the density of the carbon black particle at about 3—5 kb. At higher pressures the compression can be achieved only by increasing the density of the particle material, thus increasing the contact between crystallites in the particle by the elastic deformation mechanism. At the final stage of compression, the density reached 2.2 g./cm^3. This value is very near to the true density, d_x=2.24. The shape of the carbon black particles did not change even when the particles were compressed at pressures of 9 kb or above, where the bulk density of the carbon black was 2.2 g./cm^3 or above. The shapes of the carbon black particles before and after the compression are shown in Plate 1.

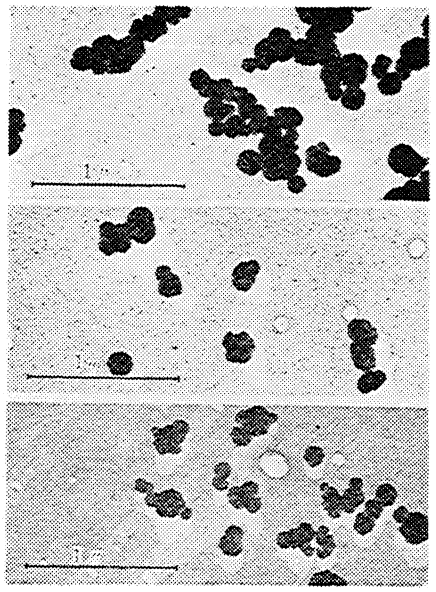

Plate 1. Electron micrographs of 2680°C-treated thermal black (Miike #20) Al-shadowed.
(a) before compression
(b) after compression at 8.8 kb
(c) after compression at 25 kb

In conclusion, the change in the electrical resistivity of carbon black particles with the pressure proceeds in three stages. In the lower pressure range, where the packing proceeds by filling voids by the rearrangement of carbon black particles, the resistivity changes with the number of contact points between particles. It has been reported that the resistivity changes with $1/P$—$1/P^{1/2.3,4}$. However, the dependence of the resistivity of carbon black on the pressure seems to be proportional to $1/P^{1/2}$, even in a very low pressure range.[10] In the medium and high pressure ranges, where the contact area increases with an increase in the deformation of the particles, the resistivity, ρ, changes with $1/P^{1/2}$. In the very high pressure range, the elastic deformation, accompanied by the change in the preferred orientation with the pressure, is the main process in determining the change in the resistivity with the pressure, $\rho \propto 1/P^{1/3-t}$. No change in the shape of carbon black particles after compression under a very high pressure could be observed.

Thanks are due to Mr. Etsuro Kato for his discussion. The authors are also indebted to the Tokai Electrode Mfg. Co. for the supply of specimens, and to the Mitsubishi Chem. Co. and the Onoda Cement Co. for taking electron micrographs.

10) E. Kato, Private communication, to be published in *J. Chem. Soc. Japan, Ind. Chem. Sect.* (*Kogyo Kagaku Zasshi*).

BULLETIN OF THE CHEMICAL SOCIETY OF JAPAN VOL. 39 833—837 (1966)

Kinetic Studies of the Oxidation of Aldopentoses: L-Arabinose and D-Xylose Oxidized by Hexacyanoferrate(III) in an Alkaline Medium

By Rajendra Kumar SRIVASTAVA, Narendra NATH and M. P. SINGH

Department of Chemistry, University of Allahabad, Allahabad, India

(Received May 13, 1965)

The kinetic studies of the oxidation of L-arabinose and D-xylose have been carried out using potassium ferricyanide in the presence of sodium hydroxide and sodium carbonate. The order of the reaction has been found to be zero with respect to ferricyanide and first with respect to the reducing sugar. The reaction rate is also directly proportional to the hydroxide ion concentration. The reaction also has a very small induction period.

Kinetic studies of reactions in solutions have achieved commendable importance during the last few decades, especially in explaining the mechanism of the reactions. So far as the kinetics of oxidation of these reducing sugars is concerned, however, this field has not been studied for several years. Most of the works in this direction were first carried out by using halogens[1] as oxidising agents in alkaline and acidic media. Ingels and Israel[2] studied the kinetics of the oxidation of simple monosaccharides as well as of disaccharides by alkaline hypoiodide; they reported the order of the reaction with respect to each reactant to be unity. They also observed that the rates of the oxidation of D-galactose and D-arabinose are greater than those of D-glucose and D-xylose respectively.

Systematic studies of the kinetics of oxidation of several hexoses and pentoses by cupric tartrate and cupric citrate in the presence of sodium hydroxide were made in this laboratory by Singh, Krishna and Ghosh.[3,4] They reported that the reaction is of the first order with respect to the cupric complex and that it is catalysed by the free hydroxide ion. There is also an autocatalysis due to the cuprous oxide produced in the system. Recently Nath and Singh[5,6] studied the kinetics of the oxidation of several aldo and keto hexoses by potassium ferricyanide in an alkaline medium. The advantage of taking potassium ferricyanide as the oxidant lies in the value of its redox potential, which is large compared to that of copper. They have observed that the reaction rate is of the zero order with respect to ferricyanide and of the first order with respect to reducing sugar. Further, the reaction rate is directly proportional to the concentration of hydroxide ions, and the reaction has a small induction period, which is probably due to the presence of oxygen. The present work will deal with the kinetics of the oxidation of L-arabinose and D-xylose by potassium ferricyanide in an alkaline medium; such a study will give more evidence on the mechanism.

Experimental

Potassium ferricyanide was of B. D. H. (AnalaR)-grade sample. The standard solution of reducing sugar was prepared just before starting the reaction. The sugar and the sodium hydroxide used were of E. Merck grade.

The volumetric procedure developed by Lang[7] which depends upon the precipitation of complex zinc-ferrocyanide to complete the reaction between potassium ferricyanide and iodine is not very accurate because it does not give a very clear end point due to the appearance of a bluish colour in the end. Therefore, the present method of estimating ferricyanide was slightly modified by increasing the overall strength of potassium iodide to a great extent instead of by adding zinc sulphate.

The mixture of potassium ferricyanide and alkali was kept in a black-coated jena bottle at a constant temperature (±0.1°C); the fresh solution of reducing sugar was kept separately in the same bath. When the solutions have attained the temperature of the bath, the requisite quantity of reducing sugar was added to a solution containing potassium ferricyanide and alkali. The progress of the reaction was followed by sucking out an aliquot (10 or 5 ml.) and pouring it into a beaker containing 10 ml. of a strong fresh solution of potassium iodide (40%) and 5 ml. of 4 N sulphuric acid of B. D. H. (AnalaR) grade. The function of the sulphuric acid was to check the reaction by neutralising the alkali as well as to help in the liberation of iodine. The liberated iodine was immediately titrated by a standard solution of sodium thiosulphate (hypo), using starch as an indicator and with the help of micro-burette.

Results

The Determination of the Order of Reaction with Respect to Ferricyanide Ions.—In order to find out the order of the reaction with respect to ferricyanide ions, the concentration of the reducing sugar was kept high. If the concentration of the reducing sugar is in a large excess as compared to the concentration of ferricyanide ions, the variation in the velocity of the reaction will mainly be determined by the concentration of the latter. The results given below consistently show that the reaction is of the zero order with respect to ferricyanide ions.

TABLE I

Temp.: 30°C Total vol.: 200 ml.
Aliquot sucked out: 10 ml.
Overall concn.:
$K_3Fe(CN)_6$, 0.0025 M; NaOH, 0.02 N;
L-Arabinose, 0.01 M

Time min.	Vol. of N/420 hypo ml.	$k_0=\frac{\Delta x}{\Delta t}$
0	10.30	—
15	9.45	0.056
30	8.25	0.080
45	7.05	0.080
75	4.90	0.072
90	3.90	0.067
105	2.90	0.067
120	1.75	0.070
∞	0.00	—
	Mean k_0	0.072
	(Neglecting the first constant)	
	k_s	1.71×10^{-5}
	(mol. l^{-1} min^{-1})	

1) J. W. Green, *Advan. Carbohydrate Chemistry*, **3**, 129 (1948).
2) O. G. Ingels and E. C. Israel, *J. Chem. Soc.*, **1948**, 810.
3) M. P. Singh, B. Krishna and S. Ghosh, "Proceedings of the National Academy of Sciences, India, Section A, Vol. XXVIII, Part I (1959), pp. 21—29; Section A, Vol. XXVIII, Part I, (1959), pp. 39—42.
4) M. P. Singh, B. Krishna and S. Ghosh, *Z. physik. Chem.*, **204**, 1 (1955); **205**, 285 (1956); **208**, 265 (1958).
5) N. Nath and M. P. Singh, ibid., **221**, 204 (1962).
6) N. Nath and M. P. Singh, ibid., **224**, 419 (1963).
7) R. Lang, *Z. anal. Chem.*, **79**, 161 (1929); **93**, 21 (1937).

Table II

Temp.: 40°C Total vol.: 200 ml.
Aliquot sucked out: 10 ml.
Overall concn.:
$K_3Fe(CN)_6$, 0.0025 M; Na_2CO_3, 0.5 N;
L-Arabinose, 0.01 M

Time min.	Vol. of N/374 hypo ml.	$k_0=\frac{\Delta x}{\Delta t}$
0	9.10	—
5	8.25	0.170
10	7.70	0.110
20	6.60	0.110
30	5.50	0.110
40	4.50	0.100
50	3.40	0.110
70	1.25	0.108
∞	0.00	—
	Mean k_0	0.110
	(Neglecting the first constant)	
	k_s	2.96×10^{-5}
	(mol. l^{-1} min^{-1})	

Table III

Temp.: 30°C Total vol.: 100 ml.
Aliquot sucked out 5 ml.
Overall concn.:
$K_3Fe(CN)_6$, 0.0025 M; NaOH, 0.01 N;
D-Xylose, 0.01 M

Time min.	Vol. of N/740 hypo ml.	$k_0=\frac{\Delta x}{\Delta t}$
0	9.70	—
10	8.92	0.078
20	7.74	0.118
30	6.54	0.120
40	5.40	0.114
50	4.18	0.122
60	2.92	0.126
70	1.80	0.112
∞	0.00	—
	Mean k_0	0.119
	(Neglecting the first constant)	
	k_s	3.21×10^{-5}
	(mol. l^{-1} min^{-1})	

A perusal of the above tables will show that the zero order velocity constants assume practically constant values after a certain induction period. Below each table the mean value of standard zero order velocity constant (k_s) has been given; each has been calculated by taking the mean zero order velocity constant (k_0) and multiplying it by the factor S/V, where S is the strength of the hypo used in the estimation and V, the volume of the aliquot taken;

$$k_s = k_0 \times (S/V)$$

A further confirmation of the order of reaction with respect to ferricyanide can be seen from Tables V and VI.

Table IV

Temp.: 35°C Total vol.: 100 ml.
Aliquot sucked out: 5 ml.
Overall concn.:
$K_3Fe(CN)_6$, 0.0025 M; Na_2CO_3, 0.20 N
D-Xylose, 0.01 M

Time min.	Vol. of N/880 hypo ml.	$k_0=\frac{\Delta x}{\Delta t}$
0	11.00	—
10	10.00	0.100
20	8.30	0.170
30	6.80	0.150
40	5.20	0.160
50	3.90	0.130
60	2.40	0.150
70	0.90	0.150
∞	0.00	—
	Mean k_0	0.150
	(Neglecting the first constant)	
	k_s	3.408×10^{-5}
	(mol. l^{-1} min^{-1})	

Table V

Temp.: 30°C
Overall concn.:
NaOH, 0.048 N; L-Arabinose, 0.001 M

Concn. of ferricyanide M	Rate const. $k_s\times10^5$ mol. l^{-1} min^{-1}
0.0025	3.5
0.0033	3.7
0.0050	3.7
0.0100	3.7

Table VI

Temp.: 30°C
Overall concn.:
NaOH, 0.05 N; D-Xylose 0.001 M

Concn. of ferricyanide M	Rate const. $k_s\times10^5$ mol. l^{-1} min^{-1}
0.0025	15.4
0.0033	15.4
0.0050	15.4
0.0066	15.4

The Effect of Varying the Ferrcyanide Ion Concentration—From Table V, it is evident that though the concentration has been varied from 25×10^{-4} M to 100×10^{-4} M, with the concentrations of other reactants kept the same, the zero order rate constants are practically the same. Table VI confirms the above statement in the case of D-xylose. Thus Tables V and VI also confirm that the reaction is of the zero order with respect to potassium ferricyanide in the concentration range of alkali and potassium ferricyanide studied.

The Determination of the Order of Reaction with Respect to Reducing Sugar. — In order

Table VII

Overall concn. of $K_3Fe(CN)_6$: 0.0025 M

	Temp., °C	Overall concn. of NaOH N	Overall concn. of sugar M	Rate const. $k_s \times 10^6$ mol. l^{-1} min^{-1}	$\frac{k_s}{[sugar]} \times 10^4$
L-Arabinose	30	0.02	0.0200	32.40	16.20
			0.0125	20.10	16.08
			0.0066	11.30	16.95
			0.0050	8.50	17.00
D-Xylose	30	0.02	0.0200	111.6	55.80
			0.0125	75.0	60.00
			0.0066	40.3	60.40
			0.0050	30.5	60.00

Table VIII

Overall concn. of $K_3Fe(CN)_6$: 0.0025 M

	Temp., °C	Overall concn. of sugar	Overall concn. of NaOH N	Rate const. $k_s \times 10^6$ mol. l^{-1} min^{-1}	$\frac{k_s}{[NaOH]} \times 10^4$
L-Arabinose	30	0.01 M	0.0200	17.10	8.55
			0.0125	10.70	8.55
			0.0100	8.33	8.33
			0.0050	4.12	8.24
D-Xylose	30	0.01 M	0.0200	61.00	30.50
			0.0125	39.20	31.36
			0.0100	32.10	32.10
			0.0066	21.00	31.50

to determine the order of reaction with respect to reducing sugar, the concentration of reducing sugar was varied, while the concentration of other reactants was kept constant. It has been shown that the reaction is of the zero order with respect to ferricyanide ions; therefore, the average velocity ($\Delta x/\Delta t$), the instantaneous velocity (dx/dt), and the specific rate constant are identical. If, therefore, the average velocity (the velocity in the case of a zero order reaction) increases in direct proportionality with the increase in the concentration of reducing sugar, it proves that the reaction is of the first order with respect to reducing sugar. The table given below shows the effect of varying the reducing sugar concentration on the zero order velocity constant.

From Table VII it is evident that k_s/[sugar] gives practically a constant value, which indicates that the reaction rate is directly proportional to the reducing sugar concentration. Thus, it is evident that the order of reaction with respect to reducing sugar is unity.

The Effect of Varying the Hydroxyl Ion Concentration.—A perusal of Table VIII will show that the zero-order velocity constant increases proportionally with the increase in the concentration of hydroxide ions.

Discussion

A careful study of the kinetics of the oxidation of the above sugars shows that the rate of expression is of the form:

$$-\frac{d[Fe(CN)_6^{3-}]}{dt} = k[sugar][OH^-]$$

which implies that the rate of reaction is independent of the concentration of ferricyanide ions, while the reaction is of the first order both with respect to reducing sugar as well as to alkali. In cases where the concentration of the sugar as well as of alkali is large as compared to the concentration of ferricyanide, the rate expression takes the form:

$$-\frac{d[Fe(CN)_6^{3-}]}{dt} = k_s = \frac{\Delta\chi}{\Delta t}$$

where $k_s = k[sugar][OH^-]$

Further, on the basis of the above experimental results, it appears that the first slow step involves a reaction between hydroxide ions and the reducing sugar, leading to the formation of an intermediate reactive form:

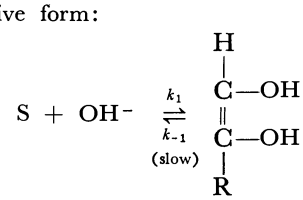

(1st step)

(1, 2 enediol)

where S represents the reduing sugar. The fact that this step is slow explains how the order of the reaction is unity with respect to reducing sugar. Further, this intermediate reactive form, which

is called "1, 2 enediol," is subsequently oxidised by ferricyanide to give ferrocyanide and other reaction products:

$$\text{en} + [Fe(CN)_6^{3-}] \xrightarrow[\text{fast}]{k_2} [Fe(CN)_6^{4-}] + \text{other reaction product}$$

(2nd step)

where "en" represents "1, 2 enediol." The fact that the second step is fast explains the zero order of the reaction with respect to ferricyanide ions. Further work on the kinetics of the oxidation of several more reducing sugars is now in progress; the details will be published later.

NOTES

Amperometric Titrations of Thorium with Alkali Tungstate

By C. M. GUPTA

Department of Chemistry, University of Rajasthan Jaipur, India

(Received March 29, 1965)

In view of the interesting results reported[1] in the amperometric studies of rare metal molybdates and tungstates, it was considered that it would be of interest to make a detailed study of the similar reaction between thorium nitrate and alkali tungstate from an analytical point of view. A perusal of the literature, however, revealed that no amperometric investigation seems to have been carried out on the thorium nitrate - alkali tungstates system. Only the preparation of thorium tungstate has been described long ago by Berzelius,[2] who mixed a solution of each of these salts.

Reagent-grade thorium nitrate and sodium tungstate were used. The strengths of these solutions were checked by the standard gravimetric methods.

Much anomalous polarographic behaviour of thorium at d. m. e. has been reported.[3] Amperometric titrations of thorium have also been described.[4,5] In view of this, it was considered worthwhile to investigate for analytical purposes the nature of the reduction wave produced by Th^{4+}. In this investigation the current voltage curves were obtained as usual by means of a manual polarograph with a lamp and scale galvanometre. The capillary had the following characteristics: ($m=2.416$ mg./sec., $t=3.6$ and $m^{2/3}\ t^{1/6}=2.235$ at -1.0 V.). Polarograms were run on 0.2 to 2 mM Th^{4+} solutions in a supporting electrolyte (1 M with respect to LiCl). Gelatin (0.01%) was used as a maximum suppressor. After making a correction for the residual current, the value of the limiting current at each concentration was determined at an applied potential $=-1.60$ versus SCE. The values of i_e/C were calculated; it was found that these values are fairly constant from a 1 mM to a 2 mM concentration of Th^{4+}. Though the wave seems to be catalytic, it may serve our purpose for carrying out amperometric titrations between a thorium salt and an alkali tungstate in this narrow range of Th^{4+} concentrations.

Twenty-five milliliters of a solution containing 1 mM of thorium as thorium nitrate is pipetted into the supporting electrolyte, 1 M lithium chloride, contained in the titration vessel. Oxygen is removed by passing nitrogen through for ten minutes. A standard solution of sodium tungstate is then added in small increments, and nitrogen is bubbled through the solution for one minute. The current is read at a potential value of -1.60 V. one minute after being diverted over the tip of the solution. The readings thus obtained are then plotted against the volume of the titrant after correcting for the volume added. The equivalence point is obtained in the usual manner from the point where the straight lines interesect.

In direct titration, where sodium tungstate is used as the titre, it is noted that at $E_{de}=-1.60$ V. versus SCE the WO_4^{2-} ion yields no measurable diffusion current, because, as is well known, this ion gives no polarographic wave in a neutral or an alkaline medium.[6] Little change in the value of current was observed on the addition of

1) C. M. Gupta, *J. Inorg. Nucl. Chem.*, **14**, 297 (1960); *Naturwissenchaften*, **50**, 545 (1963); *Z. anal. Chem.*, **204**, 3, 181 (1964); *Ind. J. Chem.*, **2**, (1965); This Bulletin, in press.

2) Berzelius, *Pogg. Ann.*, **16**, 385 (1829).

3) J. H. Paterson and C. V. Banks, *Anal. Chem.*, **20**, 897 (1948); Masek, *Chem. Listy*, **52**, 7 (1958).

4) A. Langer, *Ind. Eng. Chem. (Anal. Ed.)*, **12**, 511 (1940).

5) V. P. Vasilenko, *Zhur. Anal. Khim.*, **16**, 433 (1961).

6) I. M. Kolthoff and J. Lingane, "Polarography," Part II (1952), p. 461.

thorium salt until the stoichiometric end point is reached; after this point, however, it is found to increase linearly with the addition of the titrant. In the case of inverse titrations, the current falls. It falls as more of the precipitant is added; this continues until all of the Th^{4+} in the test solution is precipitated. Beyond the equivalence point, it reaches the residual current value. The amperometric titration curves have an L shape and feature a break at the point where the molecular ratio of Th:W is 1 : 2; this corresponds to the formation of normal tungstate of thorium $ThO_2 \cdot 2WO_3$ in the pH range from 3.5 to 7.5.

The accuracy and reproducibility of these titrations are found to be quite satisfactory, even at low concentrations of thorium salt (1 mM) or alkali tungstate. The titrations can be easily completed in twenty minutes. Cations which form a precipitates with alkali tungstate, e. g., silver, cadmium, cerium, mercury(I) and mercury-(II), and anions which react with Th^{4+}, e. g., vanadate, chromate, molybdate, tellurite, selenite and oxalate, interfere and so must be excluded.

The above results have been corroborated by making pH measurements on a battery-operated Cambridge pH meter. Direct and reverse pH titrations show a sharp break at the 1 : 2 (Th : W) ratio. The pH titrations indicate a sharp change in pH value from the acidic to the neutral side of the end point. These titrations suggest the possibility of estimating metal thorium within a 2% error.

Grateful thanks are due to Dr. R. C. Mehrotra, D. Phil, Ph. D. (London), F. R. I. C., F. N. I., Professor and Head of the Department of Chemistry, University of Rajasthan, Jaipur, for his encouragement and for providing the necessary facilities, and to Dr. M. L. Mital for his help.

The Racemization of Optically Active α-Phenylethyl Alcohol in Liquid Sulfur Dioxide

By Niichiro TOKURA and Fuminori AKIYAMA

Chemical Research Institute of Non-Aqueous Solutions, Tohoku University, Katahira-cho, Sendai

(Received April 23, 1965)

It has been reported that optically active α-phenylethyl alcohol is racemized in an aqueous solution by the catalysis of perchloric acid; carbonium ion is presumed to be formed during the reaction.[1] In the present communication we should like to report on the racemization of the alcohol in liquid sulfur dioxide in the absence of any proton donor; this is supposedly a somewhat different kind of racemization.

As may be seen in Fig. 1, the optical rotation of the solution first increases, reaches a maximum, and then tends to decrease very slowly, thus resulting in the complete racemization. Such a phenomenon may be presumed to be typical of the series of consecutive reactions involving an intermediate formation:

$$\underset{[A]}{ROH} + SO_2 \underset{k_{-1}}{\overset{k_1}{\rightleftarrows}} \underset{[C]}{\text{Intermediate}} \xrightarrow{k_2} \underset{[R]}{\text{Racemic ROH}}$$

There are three possible intermediates, I, II and III.

$$ROH + H^+ \rightarrow \underset{I}{ROH_2^+} \rightarrow R^+ + H_2O \qquad (1)$$

$$ROH + SO_2 \rightarrow \underset{II}{ROH\cdot SO_2} \rightarrow R^+ + {}^-OH\cdot SO_2 \qquad (2)$$

$$ROH + SO_2 \rightarrow \underset{III}{ROSO_2H} \rightarrow R^+ + {}^-HSO_3 \qquad (3)$$

They are a protonated alcohol (I), a SO_2–ROH complex (II), and an ester of sulfurous acid (III), respectively.

It might be considered that the trace of water present in liquid sulfur dioxide is the source of a proton which could combine with the alcohol as I and racemize via the route 1. This mechanism is unlikely, however, since the acid- or proton-catalyzed racemization ordinarily results in a smooth descending curve vs. the time plot, with no maximum of the rotation at all, as has been shown in the literature.[1] Moreover, the water content in dehydrated (by phosphorus(V) oxide) liquid sulfur dioxide is as low as 48 p. p. m., thus showing practically no effect of the catalyst.

As for the interaction between an alcohol and liquid sulfur dioxide, several papers have appeared lately. Hoyer[3] has observed that the sulfur dioxide molecule can neither permit hydrogen bonds among alcohol molecules themselves nor make hydrogen bridges with the hydrogen atoms of the alcohol by

1) E. Grunwald, A. Heller and F. S. Klein, *J. Chem. Soc.*, **1957**, 2604.
2) N. Tokura and F. Akiyama, This Bulletin, **37**, 1723 (1964).
3) H. Hoyer, *Angew. Chem.*, **72** 269 (1960).

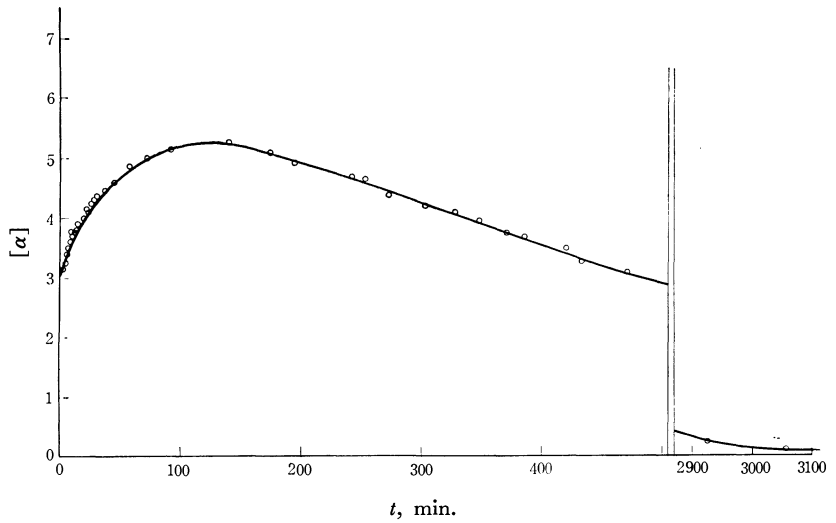

Fig. 1. Optical rotation of *l*-α-phenylethyl alcohol in liquid sulfur dioxide.

using oxygen atoms of the sulfur dioxide molecules. Only a very small amount of $RO{\cdot}SO_2H$ has been found in the mixture of ethyl alcohol and sulfur dioxide,[4] and Guss[5] has revealed that, by the colorimetric titration, a sulfite or an ester like III might partly be formed from the alcohol and sulfur dioxide.

Since the optical rotaion of an alcohol is generally enhanced when it is converted to an ester, as is the case in *l*-menthol,[2] the rise in the rotation might be suspected to result from an ester-formation such as III. The recovered residue of the racemization was not the sulfurous acid ester of the α-phenylethyl alcohol, but the racemized alcohol itself. However, the present authors are not sure whether the intermediate of the reaction is the complex II or the sulfite III, the stoichiometry of the two being the same. A complex formation like II has already been indicated by Dietzel and Galanos.[6] However, we cannot distinguish the complex from the ester like III, since the ester is also very unstable, as was reported by Zimmermann.[7]

The over-all racemization process may be deemed to be the result of the consecutive reactions, the reversible formation of the intermediate and the dissociative racemization of the intermediate, II or III.

Actually, the experimental curve in Fig. 1 has a maximum of rotation, α_{max}; this fact may be fairly reconciled with the consecutive (series) reaction mechanism consisting of intermediate formation and racemization, where $k_2 \gg k_{-1}$. The alternative route, viz., a preliminary reversible formation of the intermediate C, $k_2 \ll k_{-1}$, may thus be ruled out, as will be elucidated below. I $k_2 \gg k_{-1}$, for the A→C→R series,

$$-d(A)/dt = k_1(A) \quad (4)$$

$$d(C)/dt = k_1(A) - k_2(C) \quad (5)$$

$$d(R)/dt = k_2(C) \quad (6)$$

and $(C)_0$ and $(R)_0$ are zero, where the suffix zero indicates the initial concentration. The solution of the series reactions is:

$$(C) = \frac{(A)_0 k_1}{k_2 - k_1}(e^{-k_1 t} - e^{-k_2 t}) \text{ and } (A) = (A)_0 e^{-k_1 t} \quad (7)$$

and a variable vs. time plot should be a curve with a maximum.[8] Since $\alpha = [\alpha]_A \cdot (A) + [\alpha]_C \cdot (C)$, where $[\alpha]_A$ and $[\alpha]_C$ are the specific rotations of the alcohol and the intermediate, respecively, in liquid sulfur dioxide at the temperature, by rearranging and substituting Eq. 8 one gets:

$$\alpha = (A)_0 \left\{ [\alpha]_A e^{-k_1 t} + [\alpha]_C \frac{k_1}{k_2 - k_1}(e^{-k_1 t} - e^{-k_2 t}) \right\} \quad (8)$$

By differentiating Eq. 8 and putting $d\alpha/dt = 0$ at α_{max} and t_{max} on the curve in Fig. 1, the value of $[\alpha]_C$ can be estimated; this will give the ultimate equation with regard to α.

As a first approximation, the complication of the calculation may be alleviated by the following procedures. The expressions are derived from the above discussion as:

$$d(C)/dt = k_1(A)_0 \left\{ e^{-k_1 t} - \frac{1}{1 - k_1/k_2} e^{-k_1 t}(1 - e^{(k_1 - k_2)t}) \right\} \quad (9)$$

4) A. Simon and R. Paetzold, *Z. anorg. und allgem Chem.*, **303**, 53 (1960).
5) L. S. Guss, *Chem. Abstr.*, **39**, 4278 (1945).
6) R. Dietzel and S. Galans, *Z. Elektrochem.*, **31**, 466 (1925).
7) M. R. Zimmermann, *Angew. Chem.*, **15**, 898 (1902).
8) A. A. Frost and R. G. Pearson, *Kinetics and Mechanism*, John Wiley, New York (1953), pp. 153—154.

and:

$$d(R)/dt = k_2 \frac{(A)_0}{k_2/k_1 - 1} e^{-k_1 t}(e^{(k_2-k_1)t} - 1) \quad (10)$$

where (R) is the concentration of the racemized alcohol. In the region where t is zero to t_{max}, especially when t is very small, i. e. at the initial stage of the reaction, $e^{(k_1-k_2)t}$ is approximately unity and $1/e^{k_1 t} < 1$, so the second term in parentheses in Eq. 9 may be eliminated;

$$d(C)/dt = k_1(A)_0 e^{-k_1 t} \quad (11)$$

Since, in the reaction stage from t_{max} to t, $k_2/k_1 \fallingdotseq 0$, and $e^{(k_2-k_1)t} = 0$, Eq. 10 reduces to:

$$d(R)/dt = k_2(A)_0 e^{-k_2 t} \quad (12)$$

Consequently, the rate constants, k_1 and k_2, can be estimated from the ascending and the descending parts of the curves in Fig. 1 respectively:

$$\ln \frac{\alpha_{max} - \alpha_0}{\alpha_{max} - \alpha} = k_1 \cdot t \quad (13)$$

$$\ln \frac{\alpha_{max}}{\alpha} = k_2 \cdot t \quad (14)$$

where α, α_0 and α_{max} are the optical rotations of the reaction mixture at time t, at time zero, and at the time when the rotation was at the maximum respectively. Both plots were linear, as may be seen in Figs. 2 and 3, and both obey the first-order rate law derived in the above discussion.

The constants, k_1 and k_2, are estimated to be as in Table I.

Table I

Concn. of the alcohol mol./l.	$k_1 \times 10^4 \mathrm{sec}^{-1}$	$k_2 \times 10^5 \mathrm{sec}^{-1}$
0.327	6.26	2.89
0.223	6.41	2.86
Mean	6.34	2.88

Experimental

Materials.—Liquid sulfur dioxide was dehydrated by phosphorus(V) oxide and distilled. Optically active α-phenylethyl alcohol was prepared by the fractional crystallization of the brucine-complex salt of hydrogen monophthalate of the alcohol; b. p. 76.5°C/6 mmHg, $[\alpha]_D^{25} = -45°$ degree. $dm^{-1}g^{-1}ml.$ in benzene.[1]

Polarimetry.—A Shimadzu-Lippich type, model II, polarimeter equipped with a glass pressure cell coupled with an inlet joint was used.[6]

A Typical Run of the Racemization of α-Phenylethyl Alcohol in Liquid Sulfur Dioxide.—Into 18.2 ml. of liquid sulfur dioxide in a pressure cell (the length of which was 22 cm.[2]) there was dissolved 0.503 g. of optically-active *l*-α-phenylethyl aclohol; the solution was then allowed to stand for over 10 hr.

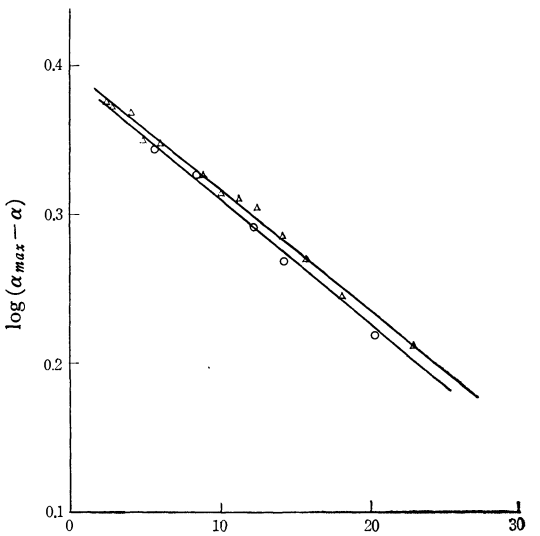

Fig. 2

△ 0.327 mol./l ○ 0.233 mol./l

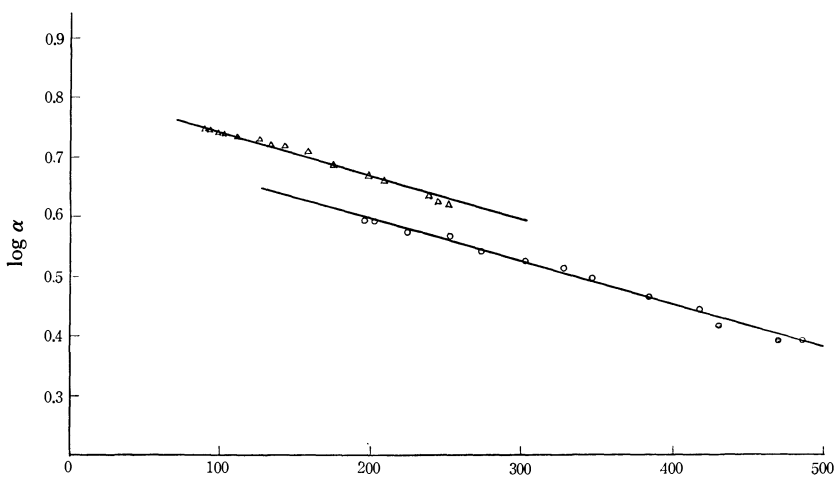

Fig. 3

△ 0.327 mol./l. ○ 0.223 mol./l.

in a thermostat the temperature of which was kept at 25± 0.2°C.

The plot of the change in the optical rotation, α, of the solution vs. the time is visualized in Fig. 1.

The Recovery of the Racemized Material from the Solution.—The sulfur dioxide solution, consisting of optically active α-phenylethyl alcohol (2.9 g.) in liquid sulfur dioxide (50 ml.), was allowed to stand for 60 hr. at 25°C. The residue was then further aerated with dried nitrogen, leaving a transparent oil (2.6 g.) which showed no reaction as an acid. The oil was the racemic α-phenylethyl alcohol; b. p. 76.5°C/6 mmHg, $[\alpha]_D^{25}=0$, benzene.

Found; C, 78.46; H, 8.23. Calcd. for $C_8H_{10}O$: C, 78.65; H, 8.25%.

The infrared spectrum of the sample was superimposable upon that of a synthetic specimen.

The Reactions of Hydrogen Atoms with Methylamine Initiated by Ionizing Radiation

By Setsuo TAKAMUKU and Hiroshi SAKURAI

The Institute of Scientific and Industrial Research, Osaka University, Sakai-shi, Osaka

(Received June 30, 1965)

In a previous paper[1] dealing with the radiolysis of methylamine in the gas phase, it has been shown that the main volatile products are hydrogen, ammonia and methane, and that the most important primary process is the formation of hydrogen atoms by the dissociation of the N–H bond, though there is a small amount of unscavengeable hydrogen formation. Even after the study, however, there was still uncertainty concerning the position of the abstractable hydrogen atoms (the N–H and C–H hydrogen) in the secondary process. It became desirable, therefore, to clarify this step by an investigation using isotopic methylamines (CH_3ND_2 and CD_3NH_2) or by the measurement of the activation energy of the process.

The activation energy of the hydrogen abstraction from ethyleneimine by methyl radicals produced photochemically was found to be 4.8 kcal./mol. by Brinton and Volman;[2] this value is much lower than the values for any C–H type abstraction, found by Trotman-Dickenson and Steacie.[3] Therefore, they suggested that it is the N–H hydrogen atoms which are active in methane formation. Thynne[4] has also studied the reaction of methyl radicals with a deuterated methylamine, CH_3ND_2; he observed a very low activation energy (5.7 kcal./mol.) for the N–H abstraction, while the value was 9.0 kcal./mol. for the C–H abstraction.

The present paper is concerned with the activation energy of the reaction of hydrogen atoms with methylamine; we used ethylene as a hydrogen atom scavenger in the radiolysis of methylamine.

Experimental

The preparation and purification of methylamine and ethylene have been previously described.[1] Gaseous samples, involving 300 mmHg of methylamine and various amounts of ethylene, were irrradiated in a 500 ml. Pyrex cyrindrical vessel fitted with a breakable seal and graphite-coated electrodes in order to measure the saturation ion current during γ-irradiation.

Irradiations were carried out using a 5000-curie ^{60}Co source at various temperatures up to 152°C. The conversion was kept lower than 0.1%. A conventional vacuum line was used to degas the irradiation samples and to analyze the products.

The other experimental details have been described previously.[1]

Results and Discussion

On the basis of the mechanism elucidated for the radiolysis of methylamine at room temperature,[1] the following main reactions appear to be acceptable representations of the initial steps:

$$CH_3NH_2 \xrightarrow{\sim\sim} H + CH_3NH\cdot \quad (1)$$

$$\xrightarrow{\sim\sim} H_2 + CNH_3 \quad (2)$$

$$\xrightarrow{\sim\sim} \cdot CH_3 + \cdot NH_2 \quad (3)$$

$$H + CH_3NH_2 \rightarrow H_2 + CNH_4 \quad (4)$$

$$2CNH_4 \rightarrow NH_3 + C_2NH_5 \quad (5)$$

Reaction 3 was supposed not to be important at room temperature, because of the low yields of methane and ethane.

The yield of methane, however, increased at higher temperatures, as is shown in Fig. 1 while the ion-pair yield of hydrogen decreased. These temperature dependencies of the products may be interpreted as showing that the precursors, which will give hydrogen atoms or molecules at lower temperatures, prefer to dissociate to amino and methyl radicals (reaction 3), thus leading to

1) S. Takamuku and H. Sakurai, This Bulletin, **38**, 791 (1965).
2) R. K. Brinton and D. H. Volman, *J. Chem. Phys.*, **20**, 25 (1952).
3) A. F. Trotφanm-Dickenson and E. W. R. Steacie, ibid., **18**, 1097 (1950); **19**, 163, 169, 329 (1951).
4) J. C. J. Thynne, *Proc. Chem. Soc.*, **145** (1963).

Table I. Ion-pair yields of the products and the rate constant ratios (k_4/k_6)

Temp. °C	$(M/N)_{H_2}$	$(M/N)_{H_2(1)}$	Radical %	$(M/N)_{CH_4}$	$(k_4/k_6)\times 10^2$
20	3.10	2.50	81	0.10	1.05
50	2.91	2.30	79	0.14	1.51
80	2.64	2.11	80	0.27	1.71
152	2.46	2.02	82	0.68	3.60

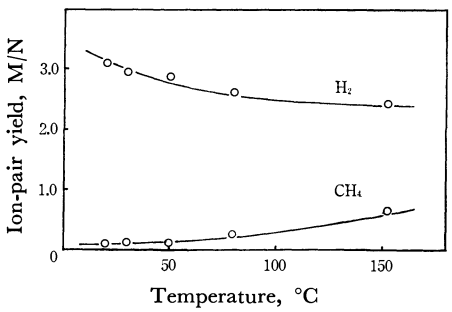

Fig. 1. Ion-pair yields of hydrogen and methane as a function of temperature (methylamine, 300 mmHg at a room temperature).

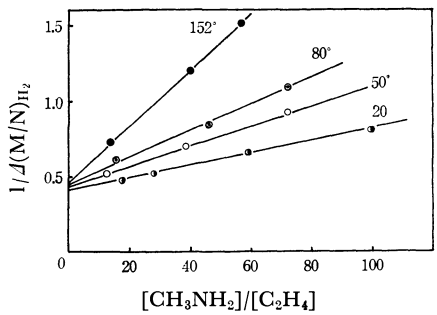

Fig. 2. Kinetic plot of the data from experiments with added ethylene at various temperatures (The total pressure 300 mmHg at a room temperature).

the formation of methane at high temperatures. Another possibility is that the precursors are collisionally deactivated as the pressure increases at a high temperature (the pressure of the irradiation sample was kept constant, 300 mmHg, at room temperature). The increase in methane yield may be explained as due to the thermal degradation of the primary radicals, thus producing methyl radicals.

As was pointed out earlier,[1,5-7] when a radical scavenger (C_2H_4) is present in the system, it competes with methylamine (reaction 4) for hydrogen atoms:

$$H + C_2H_4 \rightarrow C_2H_5\cdot \qquad (6)$$

The following equation was obtained by the steady-state kinetic treatment of hydrogen atom production:

$$\frac{1}{\Delta(M/N)_H} = \frac{1}{(M/N)_{H(1)}} \cdot \frac{k_4[CH_3NH_2]}{k_6[C_2H_4]} + \frac{1}{(M/N)_{H(1)}} \qquad (I)$$

where $\Delta(M/N)_{H_2}$ is the difference in the ion-pair yield of hydrogen, without and with ethylene, and $(M/N)_{H(1)}$ is the ion-pair yield of hydrogen produced by reaction 1. Figure 2 shows that the results here obtained obey Eq. 1, even at high temperatures.

The rate constant ratios, k_4/k_6 and $(M/N)_{H(1)}$, calculated from these straight lines are summarized in Table I. From these results it is obvious that the relative importance of the radical process in the hydrogen formation is independent of the temperature, though the total hydrogen yield decreases slightly with the temperature.

Arrhenius plots of the rate constant ratios, k_4/k_6, give a fairly good straight line, as is shown in Fig. 3. This result is expressed by the equation:

$$\frac{k_4}{k_6} = 3.2 \exp(-2.3/\boldsymbol{R}T) \qquad (II)$$

By assuming the activation energy of the reaction 6 to be 1.9 kcal./mol.[7] and the log A value to be 12.9,[7] the following relation is obtained:

$$k_4 = 10^{13.4} \exp(-4.2/\boldsymbol{R}T) \qquad (III)$$

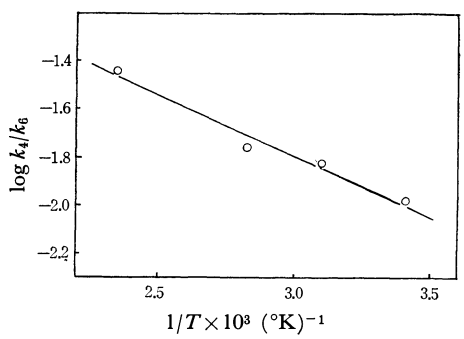

Fig. 3. Arrhenius plot of values of k_4/k_6.

The activation energy, 4.2 kcal./mol., estimated for the reaction 4 is considerably lower than the others reported for the C–H type abstractions. For example, the activation energies of the hydrogen abstraction from methane, ethane, propane and neopentane by hydrogen atoms were reported by

5) R. A. Back, *J. Phys. Chem.*, **64**, 124 (1960).
6) T. J. Hardwick, ibid., **65**, 101 (1961).
7) K. Yang, *J. Am. Chem., Soc.*, **84**, (1961).

Steacie[8] to be 13, 9.5, 8.5 and 9.3 kcal./mol. respectively.

The present observation, therefore, supports the suggestion that the N–H bond is the acitive participant in the reaction 4, on analogy to the low activation energy for the abstraction of N–H hydrogen by methyl radicals.

Summary

The radiolysis of methylamine with and without ethylene has been investigated at various temperatures up to 152°C.

The relative importance of the radical process (80%) in the hydrogen formation is independent of the temperature, though there are a slight decreases in the total hydrogen formation at high temperatures.

The thermal hydrogen atoms thus formed in the primary process may be supposed to abstract mainly the N–H hydrogen atoms of methylamine, because the activation energy for the process has been observed to be 4.2 kcal./mol., much lower than any C–H type abstraction.

8) E. W. R. Steacie and W. R. Trost, *J. Chem. Phys.*, **16**, 361 (1948); E. W. R. Steacie and R. E. Rebbert, ibid., **21**, 1723 (1953).

A Relationship between the Binding Energy and the Scattering Intensity of Electrons from Gas Molecules

By Takao Iijima

Department of Chemistry, Faculty of Science, Hokkaido University, Sapporo, Hokkaido

(Received August 3, 1965; in revised form November 24, 1965)

The effect of chemical bond formation on the scattering intensity has been investigated in several recent theoretical and experimental studies[1-8] of the scattering of fast electrons from gas molecules. The results of these studies have indicated that the intensity of electrons scattered by molecules shows a decrease, or at least a difference, from the calculated intensity based on *the independent atom model*[6] in the region of small scattering angles. This decrease in intensity has been attributed to a change in the effective volume occupied by a fixed percentage of electrons due to chemical binding, and thus qualitatively related to the binding energy of the system.[6-8] The present communication is intended to show that this decrease in intensity is directly and quantitatively related to the binding energy of the molecule. The theoretical prediction of the binding effect for the H_2 molecule[6] has been found to be consistent with this relationship. Also, a preliminary value of the binding energy of methane has been obtained by the use of the same relationship.

Tavard and Roux[4] have recently presented the following suggestive integral formula:

$$\left\langle \psi \left| \sum\sum_{i<j} \frac{Z_i Z_j}{r_{ij}} - \sum\sum_{i,\mu} \frac{Z_i}{r_{i\mu}} + \sum\sum_{\mu<\nu} \frac{1}{r_{\mu\nu}} \right| \psi \right\rangle = \frac{1}{\pi} \int \mathrm{d}s [s^4 I^T(s) - \sum_i Z_i^2 - \sum_i Z_i] \quad (1)$$

where Z_i is the atomic number of the ith atom, and r_{ij}, $r_{i\mu}$, $r_{\mu\nu}$ are the nuclear-nuclear, nuclear-electron and electron-electron distances respectively. The electronic wave function of the system is denoted by ψ; s is the scattering parameter $(4\pi/\lambda)\sin(\theta/2)$, and $I^T(s)$ is the total intensity of electrons scattered by the system involved in the first Born approximation. By noting that the left-hand side of Eq. 1 is the potential energy and by using the virial theorem, the total molecular energy, E_M, may be related to the total intensity of the electrons scattered by the molecule $I_M{}^T(s)$ through the expression:

$$E_M = \frac{1}{2\pi} \int_0^\infty \mathrm{d}s [s^4 I_M{}^T(s) - \sum_i Z_i^2 - \sum_i Z_i] \quad (2)$$

When all the internuclear distances, r_{ij}, are infinitely large, Eq. 1 is reduced to:

$$E_A = \frac{1}{2\pi} \int_0^\infty \mathrm{d}s [s^4 I_A{}^T(s) - \sum_i Z_i^2 - \sum_i Z_i] \quad (3)$$

where E_A is the sum of the atomic energies and $I_A{}^T(s)$ is the atomic background. By subtracting Eq. 2 from 3, the binding energy, E_b, is obtained as:

$$E_b = \frac{1}{2\pi} \int_0^\infty \mathrm{d}s [s^4 I_A{}^T(s) - s^4 I_M{}^T(s)] \quad (4)$$

1) C. Tavard, M. Rouault, M. Roux and M. Cornille, *J. Chem. Phys.*, **39**, 2390 (1963).
2) C. Tavard, *Cah. Phys.*, **17**, 165 (1963).
3) C. Tavard, M. Rouault, M. Roux and M. Cornille, *J. chim. phys.*, **61**, 1324, 1330 (1964).
4) C. Tavard and M. Roux, *Compt. rend.*, **260**, 4460, 4933 (1965).
5) J. Geiger, *Z. f. Physik*, **181**, 413 (1964).
6) R. A. Bonham and T. Iijima, *J. Phys. Chem.*, **67**, 2266, 2769 (1963).
7) R. A. Bonham and T. Iijima, *J. Chem. Phys.*, **42**, 2612 (1965).
8) T. Iijima, R. A. Bonham, C. Tavard, M. Roux and M. Cornille, This Bulletin, **38**, 1757 (1965).

This relationship can be rewritten in a more convenient form by using the intensity calculated by the independent atom model, $I_{IAM}{}^{T}(s)$:

$$E_b=\frac{1}{2\pi}\int_0^\infty ds[s^4I_{IAM}{}^{T}(s)-s^4I_M{}^{T}(s)] + \frac{1}{2\pi}\int_0^\infty ds[s^4I_A{}^{T}(s)-s^4I_{IAM}{}^{T}(s)] \quad (5)$$

The integrand of the first term corresponds to the decrease in intensity discussed earlier,[6-8] while the second integrand is simply the molecular term calculated by the independent atom model.*

For the H_2 molecule, the right-hand side of Eq. 5 was evaluated by the use of the $I_M{}^{T}(s)$ value which was calculated with the Weinbaum(ionic) wave function and reported previously.[6,7] Because the calculated $I_M{}^{T}(s)$ values were available only up to $s=10$, the integration of the first term had to be terminated at $s=10$. The second integration was evaluated with a simple analytical expression:

$$\frac{1}{2\pi}\int_0^\infty ds[s^4I_A{}^{T}-s^4I_{IAM}{}^{T}(s)] = -\frac{e^{-2D}}{D}\left[1+\frac{5}{8}D-\frac{3}{4}D^2-\frac{1}{6}D^3\right] \quad (6)$$

(D: the H-H distance)

for the case of H_2.[9] The first term amounted to 0.267 Ry (Rydberg), and the second term, to 0.002 Ry; thus total binding energy was calculated to be 0.269 Ry, while the binding energy of the Weinbaum(ionic) function is 0.296 Ry. The discrepancy may reasonably be understood as due to the termination error, which may be estimated to be 0.03 Ry by the graphical extrapolation of the $s^4(I_{IAM}{}^{T}-I_M{}^{T})$ curve.

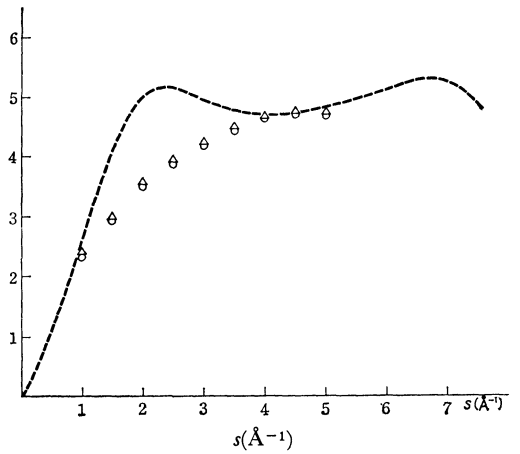

Fig. 1. The $s^3I_{IAM}{}^{T}(s)$ (--) and the observed scattering intensity with an s^3-sector of methane in an arbitrary scale. The results from two different plates are indicated by ○ and △. The difference in the scattering intensity shown in this figure which corresponds to the first integrand of Eq. 5, must be multiplied by s prior to integration.

The relationship given by Eq. 5 was used to analyze the diffraction data for methane** reported elsewhere.[8] Because of the lack of the sufficiently accurate experimental data in the region of large s values, there remains some ambiguity in the choice of a normalizing factor to make $I_M{}^{T}(s)$ fit the $I_{IAM}{}^{T}(s)$ intensity at large s values. On the assumption that no appreciable binding effect would appear in the range beyond $s=5$, the plausible normalization shown in Fig. 1 was made***; the intergration of Eq. 5 for this choice gave 1.06 Ry† as the binding energy of CH_4, a value which is in good agreement with the reported value of E_b, 1.34 Ry.[10] Both the first and the second term were integrated numerically.

It appears possible that a careful diffraction experiment could give the total binding energy of many molecules. This might be especially useful in cases where the determination of E_b by ordinary methods is difficult. Moreover, the known value of the binding energy might be used with the experimental intensity data to help provide estimates of such higher order effects on the scattering intensity as polarization and multiple scattering, by taking advantage of the relationship between the tatal intensity and the binding energy.

The author is greatly indebted to Professors Masao Kimura, Kimio Ohno, Kozo Kuchitsu and Russell A. Bonham, and also to Dr. Claude Tavard for reading the manuscript and giving helpful comments.

* The formulae equivalent to Eqs. 4 and 5 have also been obtained by Tavard; private communication via Professor R. A. Bonham; C. Tavard, to be published.

9) C. Tavard, private communication.

** The diffraction patterns for CH_4 were obtained in the Electron Diffraction Laboratory of Indiana University, Bloomington, Indiana. The author wishes to thank Professor R. A. Bonham for letting him use his apparatus.

*** The data beyond $s=5$, although not shown on the figure, are not in coincidence with the $s^3I_{IAM}{}^{T}$ curve. The inconsistency in this portion of data must be due to experimental error. A project to obtain more accurate intensity data is under way.

† The coherent and incoherent scattering factors used in the present calculation are based on the Hartree-Fock SCF wave functions.[11] Accordingly the value (1.37 Ry) thus obtained by Eq. 5 should be corrected for by the amount of the difference between the true atomic energy and the Hartree-Fock energy of carbon, namely, by about 0.31 Ry.[12,13]

10) G. Glockler, *J. Chem. Phys.*, **21**, 1242 (1953). The value reported by Glockler, 1.25 Ry, was corrected for the zero point energy by 0.09 Ry.

11) "International Tables for X-Ray Crystallogaphy," Vol. III, The Kynoch Press, Birmingham, England (1962).

12) C. E. Moore, "Atomic Energy Levels," National Bureau of Standards, USA (1949).

13) E. Clementi, *J. Chem. Phys.*, **38**, 996 (1963).

The Dipole Moments and Polarizabilities in the Excited States of Naphthalene from Spectral Solvent Shifts

By Takehiro ABE,

College of General Education, Tohoku University, Kawauchi, Sendai

and

Yoshito AMAKO, Tadashi NISHIOKA and Hiroshi AZUMI

Department of Chemistry, Faculty of Science, Tohoku University, Katahira-cho, Sendai

(Received August 23, 1965)

Several attempts have been made to estimate dipole moments in excited states of aromatic compounds on the basis of the solvent effects on their electronic spectra.[1-5] Recently Abe[6] has evolved a theory for solvent effects by means of the application of the van der Waals interaction and has estimated the dipole moment and polarizability in the excited state of nitrobenzene. In the present paper, the dipole moments and polarizabilities in the $^1B_{1u}$- and $^1B_{2u}$-excited states of naphthalene will be estimated by the application of the general expression derived by Abe to the solvent shifts for naphthalene.

The general expression presented by Abe can be written as:

$$\{(\mu_i^u)^2-(\mu_0^u)^2\} + A\cdot\alpha_i^u = B \qquad (1)$$

where:

$$A = \left\{\frac{2}{3kT}\cdot(\mu_0^v)^2+\alpha_0^v\right\}^{-1} \times\left\{(\mu_0^v)^2+\frac{3}{2}\cdot(\alpha_0^v)\cdot I_0^v\cdot\frac{I_0^u-hc\nu^0_{i0}}{I_0^v+I_0^u-hc\nu^0_{i0}}\right\}$$

and:

$$B = \left\{\frac{2}{3kT}\cdot(\mu_0^v)^2+\alpha_0^v\right\}^{-1} \times\left[\left\{(\mu_0^v)^2+\frac{3}{2}\cdot(\alpha_0^v)\cdot I_0^v\cdot\frac{I_0^u}{I_0^v+I_0^u}\right\}\cdot(\alpha_0^u) -\left\{1.007\times10^{65}(\mathrm{erg^{-1}cm^{-1}})\times\left(\frac{d^v}{M^v}\right)^{2/3}\right\}^{-1} \times\left\{\left(\left(\frac{M^u}{d^u}\right)^{1/3}+\left(\frac{M^v}{d^v}\right)^{1/3}\right)^{-4} +\left(\left(\frac{M^u}{d^u}\right)^{1/3}+3\left(\frac{M^v}{d^v}\right)^{1/3}\right)^{-4} +\left(\left(\frac{M^u}{d^u}\right)^{1/3}+5\left(\frac{M^v}{d^v}\right)^{1/3}\right)^{-4}\right\}^{-1}\times(\nu_{i0}-\nu^0_{i0})\right]$$

Here ν^0_{i0} and ν_{i0} are the maximum wave numbers in the vapor and in the solution respectively in an absorption transition from the ground state to the ith excited state of an isotropic solute molecule. All the notations refer to Abe's original paper. The notations of μ_i^u and α_i^u are the dipole moment and the polarizability in the ith excited state. The values of A and B can be calculated from the observed values, so the plot of B against A should be linear; the slope of the straight line will be equal to α_i^u, and the intersection of the line at $A=0$ will be equal to $\{(\mu_i^u)^2-(\mu_0^u)^2\}$.

Experimental

Measurements were made with a Hitachi EPS-2 recording spectrophotometer or a Shimazu GE-100

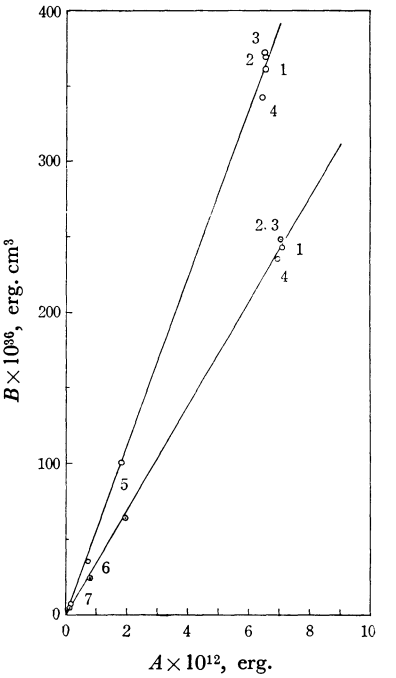

Fig. 1. Plots of B against A.

○ $^1B_{1u}$
◉ $^1B_{2u}$

1) E. G. McRae, *J. Phys. Chem.*, **61**, 562 (1957).
2) M. Ito, K. Inuzuka and S. Imanishi, *J. Am. Chem. Soc.*, **82**, 1317 (1960).
3) K. Semba, This Bulletin, **34**, 722 (1961).
4) A. Kawski, *Naturwissenschaften*, **51**, 82 (1964).
5) W. W. Robertson, A. D. King, Jr., and O. E. Weigang, Jr., *J. Chem. Phys.*, **35**, 464 (1961).
6) T. Abe, This Bulletin, **38**, 1314 (1965).

TABLE I. THE $^1B_{1u}$ AND $^1B_{2u}$ TRANSITIONS IN NAPHTHALENE AND THE DATA USED

No.	Solvent	ν_{i0}, cm^{-1}		μ_0[8] D, gas	α_0[8] $\times 10^{25}$ cm^3	I_0 eV.
		$^1B_{1u}$	$^1B_{2u}$			
	Vapor	32456[7]	35919[7]	0	175.2*	8.12[9]
1	*n*-Pentane	32198[7]	35049[7]	0	99.5	10.55[10]
2	*n*-Hexane	32168[7]	35007[7]	0	117.8	10.43[10]
3	*n*-Heptane	32169[7]	35002[7]	0	136.1	10.35[10]
4	Cyclohexane	32160[7]	34965[7]	0	108.7	9.88[9]
5	Ethyl ether	32220	35000	1.18	87.3	9.53[9]
6	Ethanol	32200	34940	1.68	53.1*	10.50[10]
7	Acetonitrile	32190	34730	3.94	44.166**	12.39[11]

* These values were calculated by the use of the observed values[8] for deformation polarizations.
** This value was calculated from the sum of bond refractions.

grating spectrophotograph at room temperature. The results of the measurements of the $^1B_{1u}$ and $^1B_{2u}$ bands of naphthalene in polar solvents are given in Table I. Usually the first reasonably intense vibration band of a transition was measured.

Naphthalene was purified by sublimation after being recrystallized four times, alternately from ethyl ether and from ethanol. Ethanol was twice distilled after being refluxed with 12 N sulfuric acid and with potassium hydroxide and silver nitrate, dried over calcium chloride, and fractionated. Ethyl ether was refluxed with 10% sodium carbonate, distilled, dried over calcium chloride, and distilled over sodium. Acetonitrile was of spectroscopic grade and had been obtained from the Eastman Co.

Results

The first intense vibration bands of the $^1B_{1u}$ and $^1B_{2u}$ transitions in naphthalene and the other data used are listed in Table I. The densities of d at 20°C taken from Lange's table[12] and from another source were used. On the assumption that the temperature is 20°C, that is, that $2/3kT$ is 1.647×10^{13} erg^{-1}, the present authors calculated the values of A and B and plotted B against A, as is shown in Fig. 1. It may be seen in Fig. 1 that the points fall close to the straight lines which approximately pass through the point of origin. The values of $\{(\mu_i^u)^2-(\mu_0^u)^2\}$ are, therefore, estimated to be zero. Accordingly, both the dipole moments in the $^1B_{1u}$- and $^1B_{2u}$-excited states of naphthalene are estimated to be zero, because the observed value of μ_0^u is zero. From the slopes of the lines in Fig. 1, the polarizabilities in the $^1B_{1u}$- and $^1B_{2u}$-excited states of naphthalene are found to be 345.8×10^{-25} and 556.2×10^{-25} cm^3 respectively.

7) O. E. Weigang, Jr., *J. Chem. Phys.*, **33**, 892 (1960).
8) Landolt-Börnstein, "Physikalische-chemische Tabellen," 6th Ed., Springer, Berlin (1951), pp. 386, 393, 509.
9) K. Watanabe, *J. Chem. Phys.*, **26**, 542 (1957).
10) R. E. Honig, ibid., **16**, 105 (1948).
11) J. D. Morrison and A. J. C. Nicholson, ibid., **20** 1021 (1952).
12) N. A. Lange, "Handbook of Chemistry," 10th Ed., McGraw-Hill Book Co., New York (1961), p. 1277.

The Electron Spin Resonance Spectra of Nitrobiphenyl Radical Anions

By Yasuto NAKAI, Katsuyuki KAWAMURA, Kazuhiko ISHIZU, Yasuo DEGUCHI and Hideo TAKAKI

Department of Chemistry, Kyoto University, Sakyo-ku, Kyoto

(Received August 30, 1965)

In a study of series of substituted biphenyls, several nitro derivatives have been synthesized and the ESR spectra of their anion radicals investigated. The analysis of the spectra is quite straightforward for the mononitrobiphenyls. Although the hyperfine splitting constant for the nitrogen atom is distinct, those for the hydrogen atoms can not be assigned unequivocally. These splittings can, however, be assigned with reasonable certainty, as shown in Table I, by using the theoretical estimates of the spin density distribution and by comparing the splitting constants of a related series of radicals, including halogenated nitrobenzene and hydrogenated nitrobiphenyl. The results seem to sustain the view that the frame-work of mononitrobiphenyls is similar to that of nitrobenzene as far as the frontier electronic orbital level is concerned. Although they are phenylated, the effect of the conjugation of ortho- and meta-substituents is small because of the sterically-induced decoupling and the small spin density respectively. This observation is contrary to that made of alkyl-[1], methoxyl-,[2] or cyanobiphenyls.[3] For paraphenylnitrobenzene, however, the electron-withdrawing nitro group does not entirely dominate the mesomeric interaction effect of the additional aromatic ring; this results in somewhat smaller splitting constants for the main ring atoms.

Table I. Hyperfine splitting constants of nitrobiphenyl anions and related compounds

Anion	a^N	a_o^H	a_p^H	a_m^H	
o-Nitrobiphenyl	9.85	3.21	3.99	1.17	
	8.7	3.9	3.9	0.9	
m-Nitrobiphenyl	9.80	3.28	3.78	1.15	
	9.55	3.28	3.36	1.04	
p-Nitrobiphenyl	—	—		—	
	8.79	2.84		0.93	3.34(b) 0.4(c)
o,*o'*-Dinitrobiphenyl	9.28	1.42	3.25	1.28	
	4.28	1.45	1.84	0.38	
m,*m'*-Dinitrobiphenyl	9.49	3.34	3.75	1.09	
	4.00	2.92	2.29	1.21	
p,*p'*-Dinitrobiphenyl	—	—	—	—	
	3.54	1.38	(a)		
p-Cyclohexylnitrobenzene	8.90	3.20		1.25	

Upper row: reduced by potassium in 1,2-dimethoxyethane
Lower row: reduced electrolytically in *N*,*N*-dimethylformamide
(a) No discrete structure was evident
(b) Interaction with a proton
(c) Interaction with two protons

Dinitrobiphenyls all give substantially different spectra depending upon the method of reduction used to produce anion radicals. The spectra of electrolytically-generated radicals could be readily interpreted on the basis of symmetry considerations alone. When reduced by alkali metals, the contiguity of the small cation to the nitro group seems to destroy the molecular symmetry, so the unpaired electron tends to localize exclusively only one of the two nitrogens in a molecule, as in the case of dinitrobenzene.[4] A striking feature of the spectra exhibited in Fig. 1(a) and (b) is that the spectrum of metadinitrobiphenyl closely resembles that of metanitrobiphenyl.

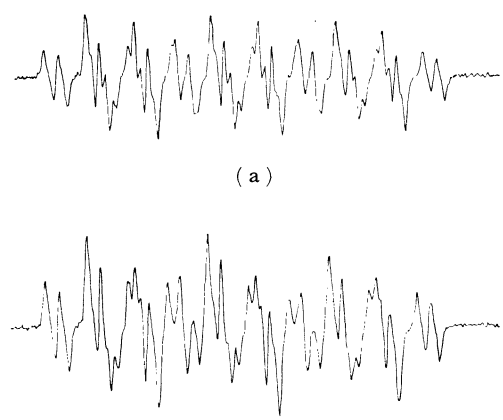

(a)

(b)

Fig. 1. The electron spin resonance spectra of *m*-nitrobiphenyl (a) and *m*,*m'*-dinitrobiphenyl (b) anion radicals.

When the spin density calculations based on the simple Hückel LCAO approximation for these compounds are compared with the experimental data, we find that the internal rotation rather than the cation-induced polarization of the nitro group in dinitrobiphenyl is the more probable model. The *o*,*o'*-dinitrobiphenyl anion forms a

1) K. Ishizu, This Bulletin, **36**, 938 (1964); **37**, 1093 (1964).

2, 3) Y. Nakai and H. Shikata, unpublished data.

4) R. L. Ward, *J. Chem. Phys.*, **36**, 1405 (1962).

stable ion-pair[5] with the alkali metal cation. The metal hyperfine splittings are 0.35 gauss for lithium and 0.18 gauss for sodium. Since one of the benzene rings possesses most of the unpaired spin during the formation of a stable ion pair, the nitrogen in the other ring shows a very small hyperfine splitting, 0.38 gauss.

We have not been able to detect anion radicals with alkali metals in *p,p'*-dinitrobiphenyl.

5) H. Nishiguchi, Y. Nakai, K. Nakamura, K. Ishizu, Y. Deguchi and H. Takaki, ibid., **40**, 241 (1964); *Mol. Phys.*, **9**, 153 (1965).

Sterol Constituents of *Daedalea quercina* L. (Fr.)

By Yoshiaki TANAHASHI and Takeyoshi TAKAHASHI

Department of Chemistry, Faculty of Science, The University of Tokyo, Hongo, Tokyo

(Received September 7, 1965)

In the course of our studies of higher terpenoids, we have examined the ethyl acetate extract of *Daedalea quercina* L. (Fr.) and isolated a mixed crystal of ergosterol and 5-dihydroergosterol, together with 5-dihydroergosterol (ergosta-7, 22-dien-3β-ol) and ergosterol peroxide (5, 8-epidioxyergosta-6, 22-dien-3β-ol).[1]

The sources of *D. quercina* were as follows; (1) Commercially supplied; living on beech; 380 g. (2) Commercially supplied; generally called "Baikisei" and used as a herb medicine; living on Prunus Mume Sieb. et Zucc.; 2.5 kg. (3) Living on beech. Collected in April and May, 1962, at Tanzawa in Kanagawa Prefecture; 15 kg.

The first sample gave a neutral alcoholic compound, named DQ-ol A_1. The ultraviolet spectrum of DQ-ol A_1 was very similar to that of ergosterol, but its intensities were slightly weaker. The concentrated extract of the second, "Baikisei," gave DQ-ol A_2, which was found to be identical with DQ-ol A_1. The mother liquor furnished, on chromatographic separation, DQ-ol B and DQ-ol C, which were later identified as 5-dihydroergosterol and ergosterol peroxide respectively. The third sample afforded DQ-ol A_3 which showed much weaker absorptions in the ultraviolet spectrum than those of DQ-ol A_1.

The constants of DQ-ol A_1 were found to be very similar to those of "neosterol," which was first considered by Wieland et al.[2] to be a new sterol isolated from yeast fat. Barton et al.[3] have established, however, that neosterol consists of 75.5% of ergosterol and 24.5% of 5-dihydroergosterol, and have found that "synthetic neosterol" and its benzoate can not be separated by recrystallization. Table I shows the constants of neosterol, "synthetic neosterol", DQ-ol A_1, and ergosterol.

From these data, it seems probable that DQ-ol A_1 is a mixed crystal of ergosterol and 5-dihydroergosterol, as in the case of neosterol, and that DQ-ol A_3 contains much more 5-dihydroergosterol. The chemical evidence for these conclusions is as follows:

a) On catalytic hydrogenation over platinum oxide in acetic acid, DQ-ol A_1 absorbed 1.89 mol. of hydrogen, while ergosterol absorbed 2.01 mol. of hydrogen under the same conditions.

b) DQ-ol A_3 acetate gave only 5-dihydroergosteryl acetate on hydrogenation over Raney nickel in benzene; 0.49 mol. of hydrogen was absorbed.

c) The photosensitized oxidation of DQ-ol A_3 afforded 5-dihydroergosterol in a 60% yield and a small amount of ergosterol peroxide.

d) 3β-Acetoxy-Δ^7- and -$\Delta^{5,7}$-steroids are well known to show their C-18 methyl signals at τ 9.43 and τ 9.37 respectively.[4] The NMR spectrum of DQ-ol A_3 acetate consisted of two signals of an approximately equal intensity at τ 9.36 and 9.46,*1 and the whole spectrum could be interpreted as the sum of those of ergosteryl acetate and of 5-dihydroergosteryl acetate.

e) The infrared spectra of DQ-ol A_1 and A_3 may be well interpreted as a sum of the spectra of ergosterol and 5-dihydroergsoterol.

Table II shows the estimated compositions of DQ-ol A_1 and of DQ-ol A_3.

TABLE I. CONSTANTS OF NEOSTEROL, "SYNTHETIC NEOSTEROL," DQ-OL A_1 AND ERGOSTEROL

Substance	M. p. °C	$[\alpha]_D$	ε at λ_{max} 271 mμ	282 mμ	293 mμ
Neosterol[2]	164—165	−105°	11400	11400	6900
"Synthetic neosterol"[3]	164—165	−107°	9500	10100	5000
DQ-ol A_1	160—161	−103°	9100	9450	5300
Ergosterol	162—163	−119°	11500	12100	7050

1) Cf. L. F. Fieser and M. Fieser, "Steroids," Reinhold Publishing Corporation, New York (1959), Chap. 4.

2) H. Wieland and M. Asano, *Ann.*, **473**, 300 (1929); H. Wieland, F. Rath and H. Hesse, ibid., **548**, 34 (1941).

3) D. H. R. Barton and D. J. Cox, *J. Chem. Soc.*, **1948**, 1357.

4) R. F. Zürcher, *Helv. Chim. Acta*, **46**, 2054 (1963).

*1 Run on a Japan Electron Optics Model 3H-60 high-resolution spectrometer at 60 Mc. in a $CDCl_3$ solution, using TMS as the internal standard.

Table II. Ergosterol in DQ-ol A*2

Estimated from the data in:	DQ-ol A_1	DQ-ol A_3	DQ-ol A_3 acetate
$[\alpha]_D$	74%	30%	—
UV	79%	35%	50%
Hydrogenation	80%	—	49%

Experimental*3

Isolation.—*DQ-ol A_1*.—Chopped, air-dried fungus (100 g.) was extracted with ethyl acetate (800 cc.). After filtration, the ethyl acetate extract was concentrated to a small volume and crude crystals (330 mg.), m. p. 153—160°C, were separated out; these gave white needles after filtration through the column of alumina, m. p. 160—161°C (from ethyl acetate), $[\alpha]_D$ −103° (*c* 1.72), λ_{max}^{EtOH} 271 mμ (ε 9100), 282 mμ (ε 9450) and 293 mμ(ε 5300), ν_{OH} 3622.1 cm^{-1} *4 (in CCl_4 soln., secondary hydroxyl group), ν^{Nujol} (cm^{-1}) 1664, 1605, 1050, 968, 846(sh.), 835, 802.

Found: C, 82.93, 83.06, 82.09; H, 11.39, 11.41, 11.18. Calcd. for $C_{28}H_{44}O\cdot\frac{1}{2}H_2O$: C, 82.90; H, 11.18: for $C_{28}H_{46}O\cdot\frac{1}{2}HO$: C, 82.61; H, 11.62%.

DQ-ol A_2.—Powdered, air-dried fungus "Baikisei" (2.5 kg.) was extracted with ethyl acetate (10 l.). The extract, worked up as above, gave crude crystals; these in turn yielded DQ-ol A_2 (11 mg.), as white needles, m. p. 160—161°C, virtually identical with that of DQ-ol A_1.

The dark brown residue of the mother liquor was dissolved in benzene and adsorbed on alumina (600 g.). The column was eluted with (i) benzene, (7 l.), (ii) benzene-ether (9 : 1) (7 l.), (iii) benzene-ether (3 : 1) (5 l.), (iv) benzene-ether (1 : 1) (3 l.) and (v) ether (4 l.). Fraction (ii) gave 400 mg. of DQ-ol B (characterized as its acetate; m. p. 172—174°C, identical with that of 5-dihydroergosteryl acetate). Fraction (v) gave 80 mg. of DQ-ol C, m. p. 171—173°C, identical with that of an authentic sample of ergosterol peroxide.

DQ-ol A_3.—Fifteen kilograms of *Daedalea quercina* L. (Fr.) was extracted by the same method. After purification, DQ-ol A_3 (4.51 g.), m. p. 162—163°C, $[\alpha]_D$ −54° (*c* 1.53), λ_{max}^{EtOH} 271 mμ (ε4550), 282 mμ (ε 4600) and 293 mμ(ε 2700) was obtained. (Mixed m. p. with DQ-ol A_1: 158—162°C). The infrared spectrum of DQ-ol A_3 is virtually identical with that of DQ-ol A_1, except for the two peaks at 835 and 802 cm^{-1}, which are weaker than in the case of A_1.

On acetylation DQ-ol A_3 gave its acetate, m. p. 172—174°C (from methanol), λ_{max}^{EtOH} 271 mμ (ε 6100), 282 mμ(ε 6400) and 293 mμ(ε 3800).

The Photosensitized Oxidation of DQ-ol A_3.—A hot solution (about 60°C) of DQ-ol A_3 (500 mg.) in 95% ethanol (200 cc.), containing eosin (3 mg.), was aerated with a dry air-stream for 9 hr. under irradiation by a 200-watt lamp. After cooling, white crystals (305 mg.) were separated from the reaction mixture. Recrystallization from ethanol gave 5-dihydroergosterol, m. p. 172—173.5°C; identified with an authentic sample prepared by the hydrogenation of ergosterol.

After the concentration of the mother liquor, a small amount of the crystalline product was obtained. Its infrared spectrum was completely superimposable upon that of ergosterol peroxide.

The Hydrogenation of DQ-ol A_3 Acetate.—DQ-ol A_3 acetate (440 mg.) in thiophene-free benzene was hydrogenated over Raney nickel at room temperature. Within 10 min., 13.2 cc. of hydrogen was absorbed. The reaction mixture was then worked up in the usual manner, and the crystallization of the product from ethyl acetate gave 5-dihydroergosteryl acetate (350 mg.), m. p. 173°C, $[\alpha]_D$ −17.6° (*c* 2.7)

Under the same conditions, ergosteryl acetate (440 mg.) absorbed 27.2 cc. of hydrogen to yield 5-dihydroergosteryl acetate (320 mg.), m. p. 174°C, $[\alpha]_D$ −16.2° (*c* 1.85).

We are greatly indebted to Dr. Hiizu Iwamura of The University of Tokyo for his IR and NMR measurements.

*2 The other component is 5-dihydroergosterol.

*3 All the m.p.'s are measused in the capillary and are uncorrected. The specific rotations are for chloroform solutions.

*4 Run on a Perkin-Elmer 112G spectrometer.

The Electric Properties of Metallocenes and Their Derivatives

By Hamao WATANABE, Izumi MOTOYAMA and Kazuo HATA

Department of Chemistry, Faculty of Science, Tokyo Metropolitan University, Setagaya-ku, Tokyo

(Received September 10, 1965)

It is well known that electron acceptors, such as tetracyanoethylene, tetracyanoquinodimethane, and *p*-chloranil, form various types of charge transfer complexes with many donor compounds, and that some of these complexes have the properties of semiconductors. Although a great number of ferrocene derivatives have already been synthesized and their chemical properties have been elucidated, only a few reports on the properties of semiconductors in the field of metallocene derivatives have appeared.[1] As has been reported by the present authors,[2] ketazine polymers derived from diacetylferrocene and hydrazine have an interesting property, i. e., their electric resistivities are near to those of organic semiconductors.

Now the present authors wish to report on the electric properties of some metallocenes, polyferrocenyls, and two sorts of charge transfer complexes which consist of one mole of metallocene and two moles of *p*-chloranil.

Samples.—Ferrocene and nickelocene were prepared by the method reported in a previous paper.[3] Terferrocenyl, quater-ferrocenyl and sexiferrocenyl are products of the reaction of ferrocenyllithium and cobaltous chloride reported in previous papers.[4]

The Nickelocene-*p*-chloranil (1 : 2) Charge Transfer Complex.—This complex was prepared by the method reported by Goan and his co-workers.[5] A solution of 2.6 g. of *p*-chloranil in 250 ml. of dry benzene and a solution of 1.0 g. of nickelocene in 10 ml. of dry benzene (2 : 1 in mole ratio) were mixed; the complex immediately precipitated as a crystalline solid. After it had stood for several minutes, it was collected on a filter, washed with benzene, and dried in vacuo at room temperature. Thus 1.7 g. of the complex was obtained (ca. 47% yield) as dark brown glittering fine needles which did not melt at 300°C in air (on Kofler apparatus) nor at 250°C in nitrogen (in a sealed capillary). The ESR observation in acetonitrile gave no signal in the spectrum. (Found: C, 38.72; H, 1.75; Cl, 41.74, 41.69. Calcd. for $(C_{10}H_{10}Ni)(C_6Cl_4O_2)_2$: C, 38.82; H, 1.47; Cl, 41.67%).

The Cobaltocene-*p*-chloranil (1 : 2) Charge Transfer Complex.—According to a method similar to that described above, ca. 1.9 g. of the complex was obtained by mixing a solution containing 2.6 g. of *p*-chloranil in 250 ml. of benzene and a solution of cobaltocene (ca. 1.0 g.) in 50 ml. of benzene under an atmosphere of nitrogen in a dry box. This complex was a brown solid which melted at 150—155°C in nitrogen in a sealed capillary. It decomposed at 125—128°C in air and also after standing for a long period at room temperature. The solution of this complex in acetonitrile gave a sharp ESR signal corresponding to one spin per formula weight, the *g* value being estimated to be 2. (Found: C, 38.64; H, 2.19; Cl, 38.83, 38.78. Calcd. for $(C_{10}H_{10}Co)(C_6Cl_4O_2)_2$: C, 38.81; H, 1.49; Cl, 41.66%).

As is shown in Fig. 1, the infrared spectra of the two complexes show very similar absorption bands, while both are vastly different from that of *p*-chloranil.

Specific Resistivity.—The specific resistivities of the samples were measured in a vacuum with pellets prepared by pressing them at more than 7000 kg./cm^2. For the pellets of the three polyferrocenyls, aluminum foils prepared by vacuum evaporation on thier surfaces were used as electrodes. For the pellets of ferrocene, nickelocene and the two complexes, the electrodes were prepared with an electroconductive paint, "Dotite paint, Type S-1",[6] because of the failure of the application of the aluminum evaporation method. In the latter cases, after the painting of the electrodes on the surfaces of the pellets, they were evacuated under a high vacuum in order to exclude any solvent which might have remained in them.

The relationship between the logarithm of the specific resistivity and the reciprocal of the temperature is shown for three polyferrocenyls in Fig. 2. The specific resistivities at room temperature are listed in Table I. The energy gap, ΔE_g, was determined from the temperature dependence of the resistivity according to the following equation:

1) a) L. R. Melby, R. J. Harder, W. R. Hertler, W. Mahler, R. E. Benson and W. E. Mochel, *J. Am. Chem. Soc.*, **84**, 3374 (1962); b) I. M. Pauskin, L. S. Polak, T. P. Vishnyakova, I. I. Patalakh, F. F. Machus and T. A. Sokolinskaya, *Doklady Akad. Nauk S. S. S. R.*, **149**, 856 (1963); *J. Polymer Sci.*, Part C, No. 4, 1481 (1964).

2) K. Hata, I. Motoyama and K. Azuma, to be published in this Bulletin; read before the 16th Annual Meeting of the Chemical Society of Japan, Tokyo, April, 1963.

3) H. Watanabe, I. Motoyama and and K. Hata, This Bulletin, **38**, 853 (1965).

4) K. Hata, I. Motoyama and H. Watanabe, ibid., **37**, 1719 (1964); **39**, 790 (1966).

5) J. C. Goan, E. Berg and H. E. Podall, *J. Org. Chem.*, **29**, 975 (1964).

6) A product of Fujikura Kasei Co.

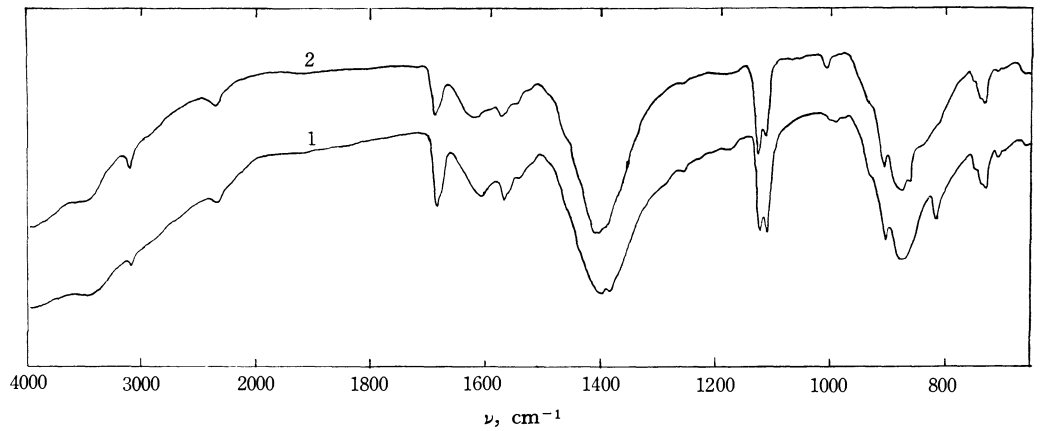

Fig. 1. Infrared spectra of the charge transfer complexes in KBr disk.
1: $(C_{10}H_{10}Ni)(C_6Cl_4O_2)_2$ 2: $(C_{10}H_{10}Co)(C_6Cl_4O_2)_2$

$$\rho = \rho_0 \exp(\Delta E_g/2kT)$$

All of these metallocene derivatives have higher electric conductivities than those of the original metallocenes. The two metallocene-*p*-chloranil complexes have especially high electric conductivities, but they are apt to decompose during the measurements. The electric resistivity shows a minimum at 40—45°C, indicating decomposition at this temperature. Therefore, the energy gaps could not be determined for these substances.

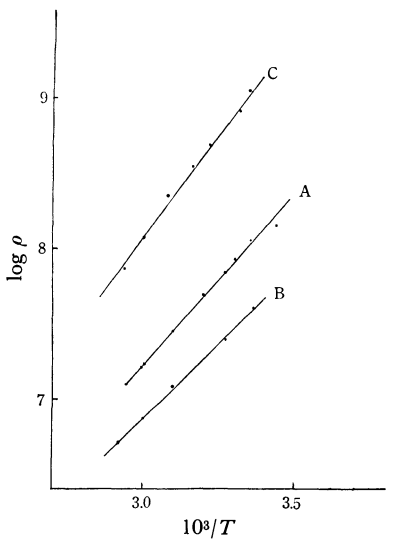

Fig. 2. Temperature dependence of the resistivity.
A: terferrocenyl B: quaterferrocenyl
C: sexiferrocenyl

Table I. Electric properties of the samples

Sample	Specific resistivity at room temperature, Ω·cm.	Energy gap ΔE_g, eV.
Ferrocene	10^{12}	—
Nickelocene	10^{11}	—
Terferrocenyl	10^{8}	0.8
Quaterferrocenyl	10^{7}	0.9
Sexiferrocenyl	10^{9}	1.1
Nickelocene-*p*-chloranil complex	10^{5}	—
Cobaltocene-*p*-chloranil complex	10^{6}	—

A solution of the cobaltocene-*p*-chloranil complex in acetonitrile gave a sharp ESR signal, while the nickelocene-*p*-chloranil complex gave no signal. From these facts it may be concluded that the former is present in the form of a charge transfer anion radical, $[C_{10}H_{10}Co^+][C_6Cl_4O_2]_2^{\cdot-}$, in the solution, and the latter, in the form of a charge transfer anion, $[C_{10}H_{10}Ni^{2+}][C_6Cl_4O_2]_2^{2-}$, as has been pointed out by Goan and his coworkers,[1a,5] and by other investigators.[7] Finally, it can be concluded that these polyferrocenyls and charge transfer complexes have the properties of semiconductors.

The authors are indebted to Professor Shu Kambara of the Tokyo Institute of Technology for his measurement of the specific resistivities. Thanks are also due to the Ministry of Education for the financial support granted for this research.

7) O. W. Webster, W. Mahler and R. E. Benson, *J. Am. Chem. Soc.*, **84**, 3678 (1962); M. Rosenblum, R. W. Rish and C. Bennett, ibid., **86**, 5166 (1964).

SHORT COMMUNICATIONS

The Catalytic Hydrolysis of Esters by Amidines

By Eiichi HARUKI, Toshikazu FUJII and Eiji IMOTO

Department of Applied Chemistry, College of Engineering, University of Osaka Prefecture, Sakai, Osaka

(Received December 20, 1965)

It has been well recongnized that α-chymotrypsine catalyzes the hydrolyses of esters and that its esteratic activity is due to the imidazolyl group of the histidine residue in α-chymotrypsine. In fact, imidazoles effectively hydrolyze many kinds of esters.

We have now found that amidines, which are considered to be a part of the imidazole ring, catalyze the hydrolyses of esters more effectively than do imidazole and its derivatives. For example, ethyl acetate and γ-butyrolactone were hydrolyzed very easily with benzamidine or acetamidine, but they were not hydrolyzed with imidazole. When a solution of an ester in ethanol-water was mixed with a solution of an amidine in the same solvent at room temperature, the ester was quickly hydrolyzed to the corresponding acid and the acid did form the salt with free amidine, although the salts of amidines do not catalyze the reaction. The kinetics of the reaction were followed by measuring the amount of the residual amidine, which was determined by titration with hydrochloric acid, using phenolphthalein as an indicator. Kinetic studies were carried out starting with about 0.02 mol. solutions of both amidines and esters in a 85% ethanol-water solvent. The reactions were of the second order; the initial second-order rate constants, which were determined from the data for the first 40% of the reaction, are summarized in Table I.

TABLE I. RATE CONSTANTS FOR HYDROLYSIS OF VARIOUS ESTERS BY FORMAIDINE, ACETAMIDINE, BENZAMIDINE AND GUANIDINE IN 85% ETHANOL-WATER AT 30°C

Ester	Catalyst	Second order rate constant $1\ mol^{-1}\ sec^{-1}$
Ethyl acetate	Formamidine	1.82×10^{-2}*
	Acetamidine	2.82×10^{-3}*
	Guanidine	3.75×10^{-3}
	Hydroxide ion	1.09×10^{-2}
γ-Butyrolactone	Formamidine	very fast
	Acetamidine	5.42×10^{-3}*
	Benzamidine	1.43×10^{-3}
	Guanidine	2.90×10^{-2}
Phenyl acetate	Formamidine	very fast
	Acetamidine	3.40×10^{-2}
	Benzamidine	2.37×10^{-2}
	Imidazole	1.80×10^{-3}**
p-Cresyl acetate	Benzamidine	2.44×10^{-2}
	Imidazole	8.83×10^{-3}**

* These values include the rate of the self-decomposition of amidines.

** Determined in a 60% acetone-water solvent at 25°C by T. C. Bruice and G. L. Schmir, *J. Am. Chem. Soc.*, **79**, 1663 (1957).

N-Substituted amidines seem to be very weak catalysts. The relations between the reactivities and the structures of amidines and of esters will be reported on later. However, it must be noted here that the glycidic esters are hydrolyzed without opening the epoxide ring to form the amidinium salts of the glycidic acids.

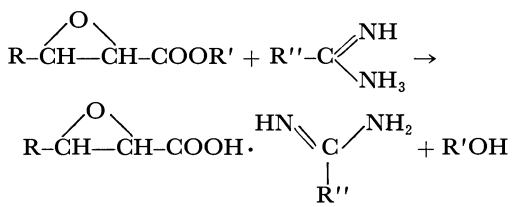

Further study is now in progress.

The Rearrangement of Acid Anhydride by a *t*-Amine. The Preparation of Glycylglycine from *N*-Benzyloxycarbonylglycine Anhydride

By Hiroshi KOTAKE and Tomoo SAITO

Department of Chemistry, Faculty of Science, Kanazawa University, Kanazawa, Ishikawa

(Received January 7, 1966)

In a previous paper,[1] it was reported that β-hydroxy-α-amino acid *N*-carboxy anhydrides rearrange to 2-oxazolidone-4-carboxylic acid 5-derivatives in the presence of triethylamine. The reaction presumes the possibility of an analogous rearrangement reaction between other acid anhydrides and a *t*-amine.

In this communication, a new method for the preparation of dipeptide via the rearrangement reaction of *N*-benzyloxycarbonylamino acid anhydride with *t*-amine, followed by reduction, will be described. *N*-Benzyloxycarbonylglycine anhydride (I) (m. p. 122—123°C, IR: $\nu_{C=O}$ 1825 cm^{-1} and 1765 cm^{-1}), prepared from *N*-benzyloxycarbonylglycine (m. p. 120°C) by the use of dicyclohexylcarbodiimide,[2,3] was rearranged by the reaction of a *t*-amine, e. g., triethylamine in an inactive solvent such as dioxane or tetrahydrofuran at room temperature, to *N'*-(*N*-benzyloxycarbonylglycyl) *N'* - benzyloxycarbonylglycine (II) (yield 85%; m. p. 135°C, IR: $\nu_{C=O}$ 1685 cm^{-1}, 1720 cm^{-1}, and 1745 cm^{-1}. Found: C, 60.00; H, 4.94; N, 6.91; equiv. wt. 398, Calcd. for $C_{20}H_{20}O_7N_2$: C, 59.99; H, 5.04; N, 7.00%; equiv. wt. 400.4).

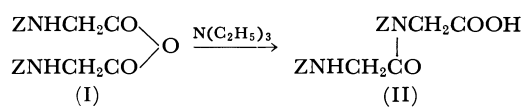

(I) (II)

1) T. Saito, *J. Chem. Soc. Japan, Pure Chem. Sect.* (*Nippon Kagaku Zasshi*), **84**, 441 (1963); T. Saito, This Bulletin, **37**, 624 (1964).

2) I. Muramatsu, *J. Chem. Soc. Japan, Pure Chem. Sect.* (*Nippon Kagaku Zasshi*), **82**, 83 (1961).

3) H. Schüssler and H. Zahn, *Chem. Ber.*, **95**, 1076 (1962).

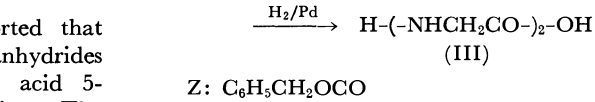

(III)

Z: $C_6H_5CH_2OCO$

Even if the amount of the base added was less than the equivalent of I (1—1/10 mol. per mol. of I), the reaction gave satisfactory yields (about 85%). This result indicates that the base reacted with I as a catalyst. Since II has the molecular formula, $C_{20}H_{20}O_7N_2$, which agreed with that of I, it should be an isomer of I. The product II dissolved when a portion of it was heated with aqueous sodium hydrogen carbonate. On acidification, a crystalline product, which was found to be identical with the starting material (II) by means of a mixed melting point procedure (m. p. 135°C), was deposited from the solution. Therefore, II must contain a free carbonyl group. The fact mentioned above led us to conclude that II must be a rearranged product. Another piece of evidence relating to the II structure was also obtained by the reduction producing glycylglycine (III) (yield 97%; m. p. 215—220°C (decomp.), Found: C, 36.51; H, 5.99; N, 21.03; equiv. wt. 134, Calcd. for $C_4H_8O_3N_2$: C, 36.36; H, 6.10; N, 21.20%; equiv. wt. 132.1) from II with palladium black in ethanol.

The infrared spectrum of III was identical with that of an authentic sample in all regions. Thus, this reaction will be extended as a new method of preparing dipeptides. One further investigations of the rearrangement reaction will be reported in the future.

The Synthesis of Nitriles From Aldehydes

By Akira MISONO, Tetsuo OSA and Seiichiro KODA

Department of Industrial Chemistry, Faculty of Engineering, The University of Tokyo, Hongo, Tokyo

(Received January 14, 1966)

Recently, the ammoxidation reaction in a liquid phase has attracted interest because it may be carried out under mild conditions. While studying some aspects of liquid-phase ammoxidation reactions, we have discovered a one-step method of synthesizing nitriles from aldehydes and ammonia in the presence of iodine.

Previously-reported methods for the production of nitriles from the corresponding aldehydes involve the application of a thoria catalyst at about 440°C to a mixture of aldehyde and ammonia,[1] the reaction of phenyl-imidophosgene with benzaldoxime,[2] or other methods using such selective reagents as *O*, *N*-bis-(trifluoroacetyl)-hydroxylamine,[3] hydroxylamine and sodium formate,[4] hydroxylamine and sodium acetate,[5] or nitropropane and ammonium dibasic phosphate.[6] Brackman and Smit[7] obtained nitriles by stirring a methanolic solution of aldehydes, ammonia, a complexed copper salt, and a strong base under oxygen. Parameswaran and Friedman[8] found a method using lead tetraacetate as an oxidizing agent.

It was found in the present study that iodine is a more convenient oxidizing agent than oxygen and a copper complex or lead tetraacetate. By this method, benzonitrile (reaction time: 1.5 hr.; yield: 50%), heptanenitrile (0.15 hr.; 26%), cinnamonitrile (1.5 hr.; 10%) anisonitrile (2 hr., 50%), and *p*-chlorobenzonitrile (1.5 hr., 68%) can be prepared from the corresponding aldehydes at room temperature.

A typical procedure is the preparation of benzonitrile.

Benzonitrile.—Thirty-two grams (0.3 mol.) of benzaldehyde and 16 g. (0.3 mol.) of sodium methoxide were added to 400 ml. of methanol saturated with ammonia. After the sodium methoxide had been dissolved 76 g. (0.3 mol.) of iodine (in 100 ml. of methanol) was added to the solution. Ammonia gas was continuously bubbled into the mixture during the reaction at room temperature. When the color of the solution became a light yellow (in 1.5 hr.), the bubbling in of ammonia gas was stopped. After the volatile reactants had then been removed from the reaction solution in vacuo, the residual oil was extracted with ether. The ethereal solution was treated with an aqueous solution of sodium bisulfite and distilled. Benzonitrile was thus obtained in a yield of 50% (16 g.); b. p. 83°C/20 mmHg; n_D^{20} 1.526.

When hydrobenzamide was used as the starting material in place of benzaldehyde, benzonitrile was again obtained, though in a small yield. This fact supports the theory that benzilideneimine is a possible intermediate.

The simplicity, rapidity, and mildness of this method make it apparent that it can be a convenient method for the preparation of nitriles,[9] especially aromatic nitriles.

Detailed results and a discussion of the possible mechanism will be published in the near future.

1) A. Maihle and De Godon, *Bull. Soc. Chim. France*, **23**, 238 (1918).
2) T. Mukaiyama, T. Fujisawa and O. Mitsunobu, This Bulletin, **35**, 1104 (1962).
3) J. H. Pomeroy and C. A. Craig, *J. Am. Chem. Soc.*, **81**, 6340 (1959).
4) T. Van Es., *J. Chem. Soc.*, **1965**, 1564.
5) J. H. Hunt, *Chem. Ind.*, **1961**, 1873.
6) H. M. Blatter, H. Lukaszewski and G. Stevens, *J. Am. Chem. Soc.*, **83**, 2203 (1961).
7) W. Brackman and P. J. Smit, *Rec. Trav. Chim.*, **82**, 757 (1963).
8) K. N. Parameswaran and O. M. Friedman, *Chem. Ind.*, **1965**, 988.
9) D. T. Mowry, *Chem. Revs.*, **42**, 189 (1948).

Rearrangement in the Substitution Reaction of 3-Keto-4β-bromo-5β-steroids

By Yasuo SATOH, Masaaki MUKOH, Yuichi OGAKI, Tomoyoshi TAKAHASHI
Takako KIMURA, Hiromitsu AOKI and Akira HAGITANI

Department of Chemistry, St. Paul's University (Rikkyo Daigaku), Toshima-ku, Tokyo

(Received January 18, 1966)

The authors wish to report on a new rearrangement in the substitution reaction of 3-keto-4β-bromo-5β-steroids with potassium acetate.

4β-Bromo-5β-chloestan-3-one (8 g.) in acetic acid (280 ml.) was refluxed with potassium acetate (56 g.) in a nitrogen atmosphere for 6 hr. The reaction mixture was then evaporated under reduced pressure, and the residue was extracted with ether. The ethereal extracts were washed with an aqueous sodium bicarbonate solution and water, dried, and evaporated. Two crystallizations of the residue from ethanol gave needles (2.6 g.), m. p. 149—151°C. Found: C, 78.37; H, 10.85. Calcd. for $C_{29}H_{48}O_3$: C, 78.33; H, 10.88%. IR (KBr disk): 1765 ($\nu_{C=O}$), 1743 ($\nu_{C=O}$) and 1224 cm^{-1} (ν_{C-O-C}); ORD in dioxane (*c* 1.00) at 18°, $[\alpha]_{589}$ +8.0°, $[\alpha]_{400}$ +8.0°, $[\alpha]_{308}$ −195.0°, $[\alpha]_{285}$ +205.0°; NMR δ: 5.24 (one proton, quartet) (=C_2H–OAc), 2.15 (three protons, singlet) (C_2–OOCCH_3).

By treating a mixture of methyl 4β-bromo-3-ketocholanate (2 g.), potassium acetate (11 g.) and acetic acid (55 ml.) as described above, needles (1.3 g.), m. p. 168.5—170°C were obtained. Found: C, 72.68; H, 9.50. Calcd. for $C_{27}H_{42}O_5$: C, 72.61; H, 9.48%. IR (KBr disk): 1750 ($\nu_{C=O}$), 1722 ($\nu_{C=O}$), 1227 (ν_{C-O-C}), 1150 cm^{-1} (ν_{C-O-C}); ORD in dioxane at 19°: $[\alpha]_{589}$ +5.5°, $[\alpha]_{380}$ +9.0, $[\alpha]_{309}$ −190.0°, $[\alpha]_{285}$ +230.0°; NMR δ: 5.24 (one proton, quartet) (=C_2H–OAc), 3.68 (three protons, singlet) (C_{23}–COOCH_3), 2.15 (three protons, singlet) (C_2–OOCCH_3).

Both products of this reaction are 2β-acetoxy-3-keto-5β-steroids, not 4-substituted isomers. This has been confirmed by the signs of the Cotton effect and its specific rotations in ORD, and by the patterns of the splitting and its coupling constants in NMR spectra (Fig. 1).[1,2]

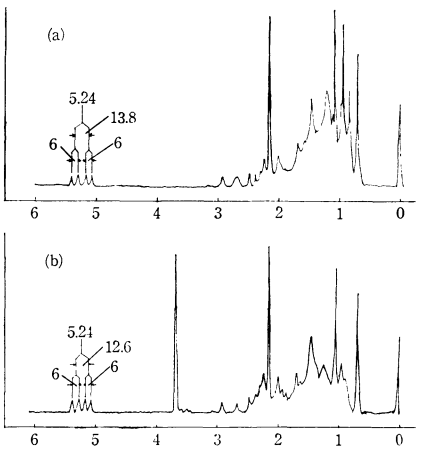

Fig. 1. Nuclear magnetic resonance spectra.
(a) 2β-Acetoxy-5β-cholestan-3-one
(b) Methyl 2β-acetoxy-3-ketocholanate

We may conclude that the substitution reaction of 4β-Br in 3-keto-5β-steroids with potassium acetate is accompanied by the rearrangement of C_4 to C_2.

This result is contrary to that reported by Fieser and Romero concerning the C_2—C_4 rearrangement of 2α-bromo-5α-chloestan-3-one with potassium acetate.[3]

Further details will be published later.

1) W. Moffitt, R. B. Woodward, C. Djerassi and W. Klyne, *J. Am. Chem. Soc.*, **83**, 4013 (1961).
2) K. L. Williamson and W. S. Johnson, ibid., **83**, 4623 (1961).
3) L. F. Fieser and M. A. Romero, ibid., **75**, 4716 (1953).

Medium-sized Cyclophanes. II. The Stereoselective Synthesis and Optical Resolution of 4, 14-Dimethyl[2.2]metacyclophane[1]

By Takeo SATO,† Sadatoshi AKABORI,† Masatsune KAINOSHO†† and Kazuo HATA†

†*Department of Chemistry, Faculty of Science, Tokyo Metropolitan University, Setagaya-ku, Tokyo*

††*The Ajinomoto Co., Ltd., Kawasaki*

(Received January 25, 1966)

Among the medium-sized ring compounds, [2.2]metacyclophane (I) is unique in that it represents one of the few examples in which the conformations have been elucidated by X-ray measurements.[2] It has a step-like structure, containing two distorted benzene rings arranged in two parallel planes. The structural features of compound I have also been shown to be reflected in the NMR spectra.[3] In addition to an AB_2-type absorption of aryl protons at δ 7.18 and 6.97, a triplet appeared at δ 4.23; it is assignable to the intraannular aryl protons at C_8 and C_{16}, which are shifted to a higher magnetic field as they are extended over the ring current of the opposite benzene rings. An A_2B_2-type absorption centered at δ 2.55 indicates the presence of non-equivalent methylene protons. Since the ten-membered ring in compound I exists in a chair conformation, it is quite natural to assign these to axial and equatrial protons.

Our interest in the possible inversion of compound I prompted us to study the high-temperature NMR spectra. The spectra determined at 67 (in CCl_4), 126 and 190°C (both in hexachloro-1, 3-butadiene) were compared with those taken at room temperature and at a low temperature (ca. −80°C). It was not possible, however, to find any appreciable temperature dependence in the spectra. Especially, the A_2B_2 absorption was surprisingly held unchanged throughout the range of the temperature studied, indicating that the molecule is frozen in the chair conformation (e. g., IIa, b: R=H).

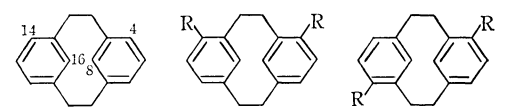

I II III

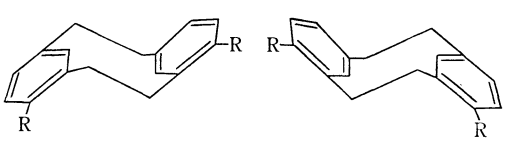

IIa IIb

These results were taken as an indication that there is a substantial conformational barrier between the inverted isomers. It is, then, to be expected that suitably-substituted cyclophanes, such as II, would become optically resolvable, IIa and IIb being the optical antipodes. The Wurtz reaction of 2, 4-bis(chloromethyl)toluene using disodium tetraphenylethane as a condensing agent in tetrahydrofuran afforded 4, 14-dimethyl-[2.2]metacyclophane, m. p. 68—69°C (Found: C, 91.34; H, 8.34%; mol. wt., 235 in a 21% yield. High-dilution conditions were realized by the combination of a slow addition (68 hr.) and a low reaction temperature (−60—70°C). The generation of the metacyclophane structure was confirmed by the NMR spectra, which consisted of four sets of absorption and which were consistent with the structure II (R=CH_3); an AB-type absorption of aryl protons at δ 6.90, a doublet for intraannular aryl protons at δ 4.18, A_2B_2 patterns centered around δ 2.43, and a singlet for the methyl group at δ 2.31.

The preferential formation of the II-type compound over the III-type compound, which should be the *meso* compound, due to the extremely mild reaction conditions used, was also encountered in the preparation of the methoxyl analog. By the coupling reaction described above, 2, 4-bis-(chloromethyl)anisole afforded compound II (R=OCH_3), m. p. 132—134°C (Found: C, 80.65; H, 7.45%; mol. wt., 260, as a major product, together with a small amount of a higher melting isomer, possibly II (R=OCH_3), m. p. 182°C (Mol. wt. Found: 278). The structure was determined by a comparison of the NMR spectra of methylene signals.

The optical resolution of compound II (R=CH_3) was achieved by using (−)-α-(2, 4, 5, 7-tetranitro-9-fluorenylideneaminooxy)-propionic acid[4] as a complex-forming reagent. A levorotatory isomer, $[\alpha]_{578}^{26}$ −3.4, and a dextrorotatory isomer, $[\alpha]_{578}^{26}$ +4.2 (ethanol), both with identical infrared spectra with a racemic compound, were obtained by the liberation of hydrocarbon by passing through an alumina column.

1) Part I: T. Sato, E. Yamada, Y. Okamura, T. Amada and K. Hata, This Bulletin, **38**, 1049 (1965).

2) C. J. Brown, *J. Chem. Soc.*, **1953**, 3278.

3) Cf. D. J. Wilson, V. Boekelheide and R. W. Griffin, Jr., *J. Am. Chem. Soc.*, **82**, 6302 (1960).

4) M. S. Newman and W. B. Lutz, ibid., **78**, 2469 (1956).

A Delayed Excimer Fluorescence of Acriflavine Stretched PVA Sheet

By Masao SATO, Tohru AZUMI and Hiroshi AZUMI

Department of Chemistry, Faculty of Science, Tohoku University, Sendai

(Received January 29, 1966)

A delayed excimer fluorescence of (the excimer fluorescence of long-lived) acriflavine has been observed. Acriflavine, absorbed into a stretched polyvinylalcohol (PVA) sheet, was irradiated by a high-pressure xenon lamp; the long-lived emission was then observed by means of a Shimadzu spectrograph. At a dilute concentration, the long-lived emission is composed of α-phosphorescence and β-phosphorescence.[1] At a high concentration, a new, previously-unobserved band arises about 1400 cm^{-1} to the red of the α-phosphorescence; this band increases in intensity as the concentration increases. (See Fig. 1.) The absorption spectra of these samples as recorded by a Hitachi EPU-2 absorption spectrometer exhibit no change in spectral distribution. On this ground, the newly-observed long-lived emission may be ascribed to an excimer species.

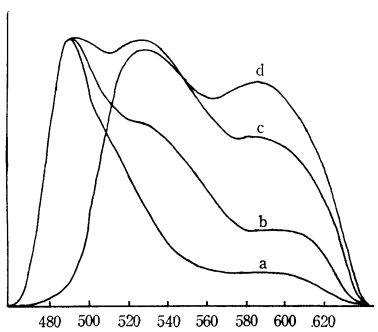

Fig. 1. Microphotometer tracings of the long-lived emission of acriflavine in streched PVA sheets. Samples were prepared by immersing PVA sheets in solutions of acriflavine at concentrations of: a: 5×10^{-5}; b: 9×10^{-5}; c: 4.6×10^{-3}; 10^{-2} mol./l. The ordinates are approximately normalized.

A long-lived excimer fluorescence has previously been observed for a limited number of polyacenes in liquid solutions[2,3] and in solid solutions.[4] In all the cases investigated, the delay of the emission has been ascribed to triplet-triplet annihilation. In the present case, however, the delayed excimer fluorescence is interpreted to be the excimer α-phosphorescence, consisting of thermal excitation from the triplet state to the excimer state followed by emission. The mechanism can be represented by the following reaction scheme:

$$S_0 + S_1 \rightleftarrows E \rightarrow 2S_0 + \text{(excimer fluorescence)}$$
$$\downarrow \quad T_1 \rightarrow S_0 + \text{(phosphorescence)}$$
$$S_0 + \text{(fluorescence)}$$

where S_0 and S_1 are, respectively, the ground state and the first-excited singlet state, and where T_1 is the lowest triplet state. The parentheses indicate that there are both radiative and radiationless transitions. No distinction is made between the triplet state of the monomer and that of the excimer, since the exciton band width of the triplet state may very well be equated with zero. According to this reaction scheme, the Arrhenius plots of ϕ_f/ϕ_p and ϕ_e/ϕ_p should yield the activation energies for the $T_1\rightarrow S_1$ and $T_1\rightarrow E$ processes, respectively, where ϕ_f, ϕ_p, and ϕ_e are the quantum yields of the monomer α-phosphorescence, the β-phosphorescence, and the delayed excimer fluorescence, respectively. The experiments were performed between -20°C and -44°C; the activation energies obtained were 10 and 4.5 kcal./mol. for the $T_1\rightarrow S_1$ and $T_1\rightarrow E$ processes, respectively. These values are in agreement with the energy differences of the corresponding peaks of emission spectra. These kinetic treatments substantiate the above identification of the newly-observed band is being the excimer α-phosphorescence.

The fact that the spectrum of dimeric species is observed in a stretched PVA sheet is another point of interest. This will facilitate the polarization measurements of dimeric species, which has not hitherto been attempted.

2) C. A. Parker and C. G. Hatchard, *Proc. Roy. Soc.*, **A269**, 574 (1962).

1) The terminology is those of G. N. Lewis, D. Lipkin and T. T. Magel, *J. Am. Chem. Soc.*, **63**, 3005 (1941).

3) C. Tanaka, J. Tanaka, E. Hutton and B. Stevens, *Nature*, **198**, 1192 (1963).

4) T. Azumi and S. P. McGlynn, *J. Chem. Phys.*, **39**, 3533 (1963); F. Smith and S. P. McClynn, ibid., **42**, 4308 (1965).

The Synthesis of 3-Isopropylidene-2, 5-dioxopiperazines

By Chung-gi SHIN, Mitsuo MASAKI and Masaki OHTA

Laboratory of Organic Chemistry, Tokyo Institute of Technology, Ookayama, Tokyo

(Received February 16, 1966)

Albonoursin, isolated from the culture filtrates of Streptomyces noursei and Streptmyces albus var. fungatus, has been concluded to be 3-benzylidene-6-isobutylidene-2, 5-dioxopiperazine (I) by Khokhlov et al.,[1] Vondráček et al.,[2] and Brown et al.[3]

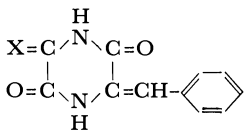

X: CH_3>CH_3>CHCH= (I)

CH_3>CH_3>C= (II)

Dioxopiperazine has been known to condense with aromatic aldehyde in the presence of acetic anhydride and sodium acetate, yielding mono- or di-benzylidene derivatives.[4,5] However, the synthesis of 3-alkylidene or 3, 6-dialkylidene derivatives of dioxopiperazine has never been reported.

In connection with a program directed toward a total synthesis of albonoursin, we have sought a method of synthesizing of 3-alkylidene dioxopiperazine. We wish to report in the present paper a synthesis of 3-isopropylidene dioxopiperazine and a homolog of albonoursin, 3-benzylidene-6-isopropylidene-2, 5-dioxopiperazine (II) by a new method.

Methyl α-amino-β, β-dimethylacrylate (III), obtained by the reduction of the corresponding nitro compound, was treated in an aqueous solution of sodium bicarbonate with phthaloylglycyl chloride; it thus gave methyl α-phthaloylglycylamino-β, β-dimethyl acrylate (IV) as colorless needles with a m. p. of 234—235°C in a quantitative yield (Found: C, 60.50; H, 5.38; N, 8.95. Calcd. for $C_{16}H_{16}N_2O_5$: C, 60.75; H, 5.10; N, 8.86%). The hydrolysis of IV with 1 N sodium hydroxide afforded α-phthaloylglycylamino-β, β-dimethyl acrylic acid (V) in a 31.8% yield, colorless fibrous needles from methanol, m. p. 258—259°C (decomp.) (Found: C, 59.21; H, 4.82; N, 9.44. Calcd. for $C_{15}H_{14}N_2O_5$: C, 59.60; H, 4.67; N, 9.27%). By treatment with hydrazine hydrate, V was converted into α-glycylamino-β, β-dimethylacrylic acid (VI) in an almost quantitative yield, colorless prisms with a m. p. of 232—234°C (decomp.) from a 50% aqueous ethanol (Found: C, 49.05 H, 7.09; N, 16.31. Calcd. for $C_7H_{12}N_2O_3$: C, 48.83; H, 7.03; N, 16.27%), which was then esterified with methanol - hydrogen chloride to give the corresponding methyl ester hydrochloride (VII) as colorless prisms with a m. p. of 178—180°C (Found: N, 12.58. Calcd. for $C_8H_{14}N_2O_3 \cdot HCl$: N, 12.58%).

When VII was heated with an aqueous solution of an equivalent mole of sodium bicarbonate on a boiling water bath for 30 min., a cyclization reaction occured and 3-isopropylidene-2, 5-dioxopiperazine (VIII) was obtained in a 70% yield. Recrystallization form boiling water afforded colorless prismatic needles with a m. p. of 260—261°C (decomp.) (Found: C, 54.52; H, 6.83; N, 18.16. Calcd. for $C_7H_{10}N_2O_2$: C, 54.53; H, 6.54; N, 18.17%), λ_{max}^{EtOH} 230 mμ (ε=22800), 240 mμ (ε=23000), ν_{max}^{KBr} 3200, 3050, 1680, 1665 and 1625 cm^{-1}. VIII was also obtained in a 54% yield by heating IV with hydrazine hydrate in a small amount of methanol.

The condensation reaction of VIII with benzaldehyde was carried out by heating it in acetic anhydride in the presence of sodium acetate at 120—130°C for 8 hr.; II was thus obtained in a 77% yield. Recrystallization from boiling acetic acid afforded colorless needles with a m. p. of 283—284°C (decomp.) (Found: C, 69.45; H, 5.72; N, 11.81. Calcd. for $C_{14}H_{14}N_2O_2$: C, 69.40; H, 5.83; N, 11.56%), λ_{max}^{DMF} 321 mμ (ε=21600), ν_{max}^{KBr} 3250, 3050, 1680 and 1635 cm^{-1}. These data of the ultraviolet and infrared absorption spectra are very similar to those of albonoursin.

III was heated in a sealed tube at 180—190°C for 48 hr.[6] to yield 3, 6-diisopropylidene-2, 5-dioxopiperazine in a 27% yield, colorless needles with a m. p. of 264—265°C (decomp.) (Found: N, 14.43. Calcd. for $C_{10}H_{14}N_2O_2$: N, 14.42%).

The details of the present communication and the methods of preparing the starting meterials will be described shortly in a further publication.

1) A. S. Khokhlov and G. B. Lokshin, *Tetrahedron Letters*, **1963**, 1881.
2) M. Vondráček and Z. Vaněk, *Chem. Ind.*, **1964**, 1686.
3) R. Brown, C. Kelley and S. E. Wiberley, *J. Org. Chem.*, **30**, 277 (1965).
4) T. Sasaki, *Ber.*, **54**, 163 (1921).
5) T. Sasaki and T. Hashimoto, ibid., **54**, 168 (1921).
6) E. Fischer, ibid., **34**, 433 (1901).

BULLETIN OF THE CHEMICAL SOCIETY OF JAPAN VOL. 39 859—863 (1966)

Effects of Pressure on the Chemical Properties of the Solid Surface. III. The Catalytic Activity and the Structure of the Compressed Tungstic Acid

By Yoshisada OGINO, Takeshi KAWAKAMI and Toru MATSUOKA

Department of Chemical Engineering, Faculty of Engineering, Tohoku University, Sakura-koji,, Sendai

(Received May 14, 1965)

In order to investigate the surface properties of tungstic acid samples which had been compressed at pressures of 640—3840 kg./cm^2, experimental studies concerning the catalytic activity for the vapor-phase hydration of propylene, the specific surface area, the pore structures, the surface acidities and the crystal structures were carried out. According to the experimental results, both the catalytic activity and the surface acidity became higher as the compressing pressure of the sample was increased, whereas the specific surface area remained practically constant. Further, a relation between the surface acidity and the crystal structure was deduced from X-ray diffraction studies. Namely, the crystal structure of the reduced sample approached the structure of $H_{0.1}WO_3$ from a WO_3-like structure as the compressing pressure was increased. In other words, samples with higher compressing pressures had crystal structures of a higher proton content. In addition to the above results, the total pore volume, the mean pore radius, the apparent activation energy, and the frequency factor became smaller as the compressing pressure was increased. On the basis of these experimental results, it was deduced that the catalytic activities of the compressed samples are affected by intra-particle diffusion.

The previous works[1,2] in this series have shown the special effects of pressures on the surface acidity of several metal sulfates. Further, by the use of potassium bisulfate as a sample it has been revealed that both acid strength distributions and catalytic acitvities varied with the degree of compression. These findings seem to suggest that the surface properties of other substances might be altered by manipulating the compression; this might then be a useful procedure for improving catalytic activities.

In the present research, tungstic acid was used as the sample material in order to test the surface property and the structure in the compressed state. In testing the catalytic activity, the yields of isopropanol from water and propylene were measured. The surface acidity was measured by a conventional indicator method. Information about pore structures and crystal structures in the compressed state was also obtained. This paper will present the detailed results of the present work; these results will demonstrate the actual occurrence of the anitcipated effect.

Experimental

The Preparation of the Sample.—Powders of commercial tungstic acid were packed into the sample space of the apparatus shown in Fig. 1. Then the apparatus was sandwiched between the stationary bed and the moving bed of an oil press, by which means a desired amount of load was applied on the piston head for 10 min. period. Thus cylindrical pellets of 4×4 mm. were prepared. The compacting pressures,

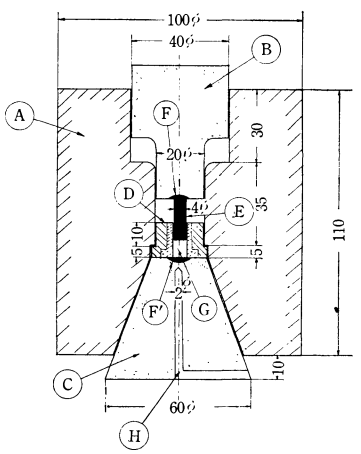

Fig. 1. The apparatus for the preparation of the sample pellet.
A: Body (stainless steel), B: The larger piston (stainless steel), C: Bottom cover (stainless steel), D: Cylinder (the inner part made from Cr-Mo steel was shrinkaged into the outer part made from Cr steel), E: The smaller piston (stellite), F, F': Mounted stellite, G: Sample room, H: Thermo-couple well

1) Y. Ogino and T. Kawakami, This Bulletin, **38**, 972 (1965).
2) Y. Ogino, T. Kawakami and K. Tsurumi, ibid., to be published.

which were estimated by a conventional means of calculation,[1] were 640, 1280, 1920, 2560, 3200 and 3840 kg./cm^2.

Catalytic Activity.—The vapor-phase hydration of propylene over 5 ml. of sample pellets was carried out with the apparatus shown in Fig. 2. Prior to the activity test, catalyst pellets were reduced during a 0.5 hr. period with a mixed vapor of water and propylene ($H_2O/C_3H_6=2.0$, S.V.$=4.8\times10^3$ hr^{-1}) at 200°C and 1 atm. After the reduction, the temperature of the catalyst bed was adjusted to a desired value, and, after the stationary state had been reached, liquid products were collected. Except for the temperature, the reaction conditions were the same as those of the reduction. The isopropanol content in the liquid products was determined by the gas chromatographic analysis.

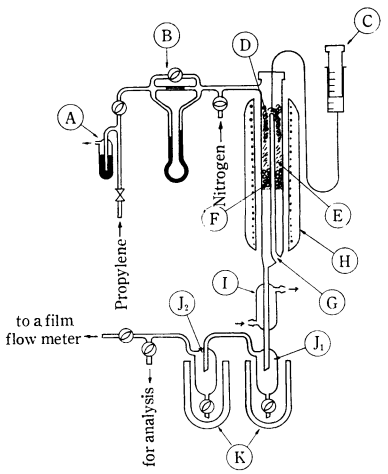

Fig. 2. The apparatus for the activity test.
A: Buffer, B: Flow meter, C: Water injector, D: Glass wool, E: Copper granules, F: Catalysts, G: Thermo-couple well, H: Electric furnace, I: Condenser, J_1, J_2: Separators, K: Ice bath

The conversion (x%) of propylene to isopropanol was evaluated from simple material-balance considerations based on the assumptions that no side reaction occurs and that the vapors of water and isopropanol are completely condensed in the separator.

After the activity test, the residual propylene was purged from the catalyst bed by the water vapor; then dry nitrogen was passed through the bed untill the reactor was cooled to room tmperature. The catalyst pellets which were taken out from the reactor were stored in an evacuated ampule.*

Surface Area, Pore Volume, Pore Radius and Particle Diameter.—The specific surface area (S, m^2./g.) was measured by means of a B. E. T. adsorption isotherm with n-butane at 0°C. The mercury displacement valume (V_{Hg}, ml./g.), as well as the water displacement volume (V_w, ml./g.), were also measured by a simple pycnometric method.[3] The difference between these volumes, $V_{Hg}-V_w$, was defined as the total pore volume (V_g, ml./g.) of the sample pellet.

The mean pore radius, $\bar{r}$, was evaluated by Eq. 1[4]

$$\bar{r} = 2V_g/S \quad (1)$$

while the mean particle diameter, $\bar{d}$, was evaluated by Eq. 2

$$\bar{d} = 6V_w/S \quad (2)$$

All the experiments described in this section were carried out with the reduced sample.

Surface Acidity.—Pellets of the reduced sample were pulverized and dried for 6 hr. in a desiccator; immediately after the drying, the surface acidity of the powder was measured. Essentially the same method as that of Benesi[5] was adopted in this measurement. Since the blue color of the sample powder masks that of the indicator adsorbed on the sample surface, a given weight (W, g.) of silica-alumina powder of a known acidity (A_0, mmol./g.) was mixed with the sample, and the total quantity of n-butylamine (A, mmol.) needed to neutralize the acid on the mixture was determined. Then, the surface acidity (A_s, mmol./g.) of the sample powder was evaluated by Eq. 3

$$A_s = (A-A_0W)/W_s \quad (3)$$

where W_s is the weight of the sample powder.

In the present work, three indicators, i. e., p-dimethylaminoazobenzene ($pK_a=3.3$), benzeneazodiphenylamine ($pK_a=1.5$) and dicinnamalacetone ($pK_a=-3.0$), were used.

Crystal Structure.—Powder X-ray diffraction patterns of the reduced sample as well as of the unreduced sample were obtained with an X-ray diffractometer. The Cu$K\alpha$ radiation (Ni filter) at 30 kV. and at 15 mamp. was adopted.

Results

Catalytic Activity.—The relations between the conversion of propylene to isopropanol per unit weight of the catalyst pellet and the reaction temperature are given in Fig. 3. As may be seen in this figure, the conversion increases with the compacting pressure of the catalyst.

Surface Area, Pore Structure.—The values of the specific surface area of the compressed samples (reduced samples) are given in Table I. In the

Table I. Specific surface areas of compressed samples

Compacting psess., kg./cm^2	640	1920	3200	3840
Surface area, m^2/g.	21.5	23.7	21.8	22.6

table, no systematic dependency of the surface area upon the compacting pressure can be seen, and the surface area seems to be roughly constant.

In Fig. 4, the total pore volume, the mean pore radius and the mean particle diameter are given as functions of the compacting pressure. It may be seen that the pore volume and the pore radius decrease with the compacting pressure, while the mean particle diameter stays at a constant

* In this paper, samples which were treated in this manner will be called reduced samples.

3) A. J. Juhola and E. O. Wiig, *J. Am. Chem. Soc.*, **71**, 2078 (1949).

4) A. Wheeler, "Catalysis," Vol. II, Ed. by P. H. Emmett, Reinhold Publishing Corporation, New York (1955), p. 105.

5) H. A. Benesi, *J. Phys. Chem.*, **61**, 970 (1957).

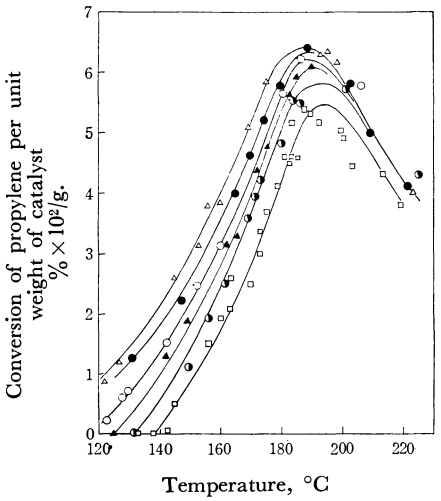

Fig. 3. Catalytic activities of the catalysts compressed at 640 (□), 1280 (◑), 1920 (▲), 2560(○), 3200 (●), 3840 kg./cm² (△).

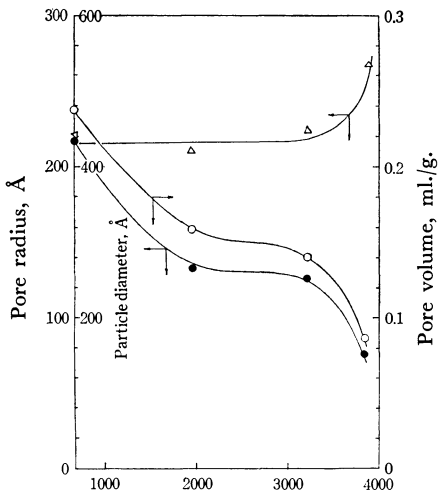

Fig. 4. Variations of the mean pore radius (●), the total pore volume (○) and the mean particle diameter (△) on compression.

level.

Surface Acidity.—The relations between the compacting pressure and the surface acidity at various H_0 values[6] are given in Fig. 5. As may be seen in this figure, the surface acidity increases with the compacting pressure.

Crystal Structure.—The powder X-ray diffraction patterns of reduced samples compressed at different pressures are given in Fig. 6(a)—(c). These patterns are supplemented by Miller's notations of WO_3 and $H_{0.1}WO_3$.[7] They show

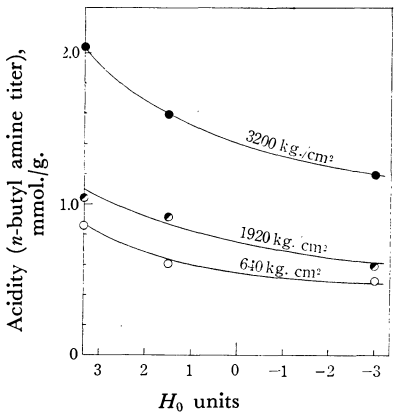

Fig. 5. Variations of the surface acidity on compression.

that, at the lower compacting pressure, the crystal structure of the sample closely approximates the structure of WO_3, while at the higher compacting pressure it approximates the structure of $H_{0.1}WO_3$.

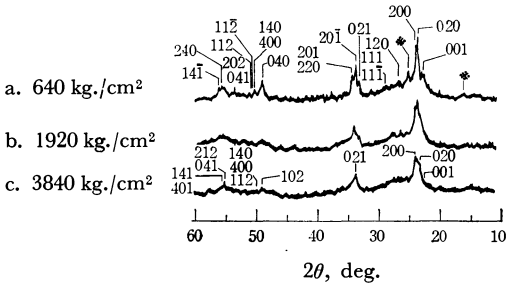

Fig. 6. X-ray diffraction patterns of reduced samples, together with Miller's notations for WO_3 (a) and $H_{0.1}WO_3$ (c).
The symbol * in (a) indicates residual peaks of H_2WO_4.

On the contrary, few changes due to the compression were observed in the X-ray diffraction patterns of unreduced samples.

Discussion

Catalytic Activity and Surface Acidity.—One of the most important results obtained in the present work may be the fact that the catalytic activity of tungstic acid can be increased by the compression of the catalyst (cf. Fig. 3). From this fact, it may be said that the effect of compression suggested in the previous paper has actually appeared.

The activity increase on compression might be due to the increase in the surface acidity. It is well known[8] that the hydration of propylene is catalyzed by acidic solids, and that increases

6) L. P. Hammett and A. J. Deyrup, *J. Am. Chem. Soc.*, **54**, 2721 (1932).
7) O. Glemser and C. Naumann, *Z. anorg. u. allgem. Chem.*, **265**, 287 (1951).
8) N. M. Chirkov, M. I. Vinnik, S. G. Entelis and V. I. Tsvetkova, *Intern. Chem. Eng.*, **3**, 112 (1963).

in the surface acidity make the catalyst more active. Therefore, from Fig. 5, which shows the acidity increase on compression, the increase in the catalytic activity can be understood.

Further effects of the compression on the catalytic activity were revealed by analyzing the conversion-temperature relationship with a rate equation which had been derived by one of the present authors[9] under the assumption that the rate-controlling step is a surface reaction on a sparsely-covered surface. The results of the analysis are given in Fig. 7 and Table II. These results show

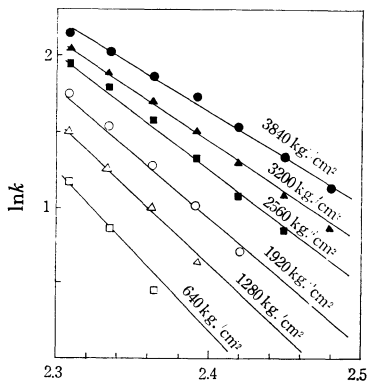

Fig. 7. Arrhenius plots.

TABLE II. FREQUENCY FACTORS AND APPARENT ACTIVATION ENERGIES FOR VARIOUS CATALYSTS COMPRESSED AT DIFFERENT PRESSURES

Compacting pressure kg./cm²	Frequency factor* ml./hr.g.-cat.	Activation energy kcal./mol.
640	1.39×10^{11}	21.2
1280	1.22×10^{10}	18.6
2560	2.88×10^{8}	15.1
3200	4.14×10^{7}	13.3
3840	1.02×10^{7}	12.1

* The rate constant whose frequency factor is given in this table was defined by the following equation

$$k=(273\boldsymbol{R}C_{\mathrm{m}}P^2/1\ \mathrm{atm.})\{(m)/(1+n+m)^2\}k_0$$

where R is gas constant, C_{m} is the mean compressibility factor of the mixed vapor at the standard state (N. T. P.), $m=C_3H_6/H_2O$ (mole ratio), $n=$inert gas/H_2O (mole ratio) and k_0 is the rate constant defined by the following rate equation

$$r(\text{rate of reaction, mol./hr. g.-cat.})=k_0p_{H_2O}p_{C_3H_6}-k_*p_{C_3H_7OH}$$

where k_* is the rate constant of the reverse reaction.

that both the frequency factor of the rate constant and the apparent activation energy were decreased by the compression. In other words, the so-called compensation effect holds among the activities of catalysts compressed at different pressures. This shows that the effect of compression on the catalytic activity is not a simple one.

At first sight, it seems possible to explain the compensation effect on the basis of the theory[10] of the inhomogeneity in active centers. Since the experimental results indicated in Fig. 5 showed the existence of acid centers of different strength, if it is assumed that all acid centers are effective as active centers, the theory might be applicable. However, it has previously been shown[9] that the rate of the hydration of propylene is nearly proportional to the acidity of a limited strength. Therefore, the application of the theory upon the basis of the present data is inadequate.

The Catalytic Activity and Pore Structure. —The interferences of the intra-particle diffusion of reactants and products with the intrinsic activity, which is considered to be dependent purely on the surface acidity, seem to be a cause of the compensation effect. Generally, the interference becomes more evident when the intrinsic activity is higher and when the pore radius is smaller. The experimental results show the higher surface acidity and the smaller pore radius at the higher compacting pressure. Therefore, when a highly-compressed catalyst is used for the activity test, retardations due to the diffusion process should be serious in the over-all reaction process. Further, the size of the catalyst pellet used in the present work was quite large, i. e., 4×4 mm. This would enhance the retardation. Thus, the low activation energy and the low frequency factor, both of which were found when a highly-compressed catalyst was used, might be attributed to the low activation energy of the diffusion process and to the retardation due to the diffusion respectively.

According to the explanation presented above of the compensation effect, it is necessary to consider that both the surface reaction and the intra-particle diffusion control the rate of the over-all reaction. Usually, in such cases, the experimental rate constant, k_{exp}, is regarded as a product of the true rate constant, k_{t}, and the effectiveness factor, E_{f}. Although details of the pore structure of the sample are not yet clear and although a rigorous evaluation of E_{f} is not possible, a rough estimation under suitable assumptions showed that the E_{f} value for the catalyst compressed at 3840 kg./cm² is about 0.8* at 435°K. This shows that the effect of the intra-particle diffusion on the over-all reaction is considerable. Further, if it is assumed that, at the lowest reaction temperature, the reaction is purely kinetic, the activation energy for the catalyst compressed at 3840 kg./cm² is corrected to 16 kcal./mol. Although this

9) Y. Ogino, *J. Catalysis Soc. Japan* (Shokubai), **4**, 73 (1962).

10) S. Glasstone, K. J. Laidler and H. Eyring, "The Theory of Rate Process," McGraw-Hill Book Company, New York and London (1941) p. 394.

value of activation energy is yet lower than the value for the catalyst compressed at a lower pressure, e. g., 640 kg./cm^2, the simple consideration described above seems sufficient to show that, if the pore structure of the compressed sample is clarified and the effect of intra-particle diffusion is correctly taken into account, the observed compensation effect might be explained.

Crystal Structure. — Among many works concerning the crystal structure of the reduced tungsten oxide, the work of Glemser[11] seems to contain much information relevant to the present work. Glemser observed that the reduction of WO_3 with atomic hydrogen resulted in a systematic change in the crystal structure. Namely, the crystal structure of H_xWO_3, which is the formula employed to express the composition of the reduced tungsten oxide, was varied by the reduction from the skewed structure of WO_3 (monoclinic) to the symmetrical structure of $H_{0.5}WO_3$ (cubic) by way of $H_{0.1}WO_3$ (orthorhombic) and $H_{0.33}WO_3$ (tetragonal). These results were explained by him as follows. Namely, hydrogen atoms in the crystal of H_xWO_3 are protonized; the contrapolarization effect of these protons then releases repulsions among oxygen ions in the crystal, and, as a consequence of this release, a closer packing of oxygen ions in the crystal becomes possible.

The experimental results obtained in the present work seem to be consistent with the results of Glemser. The acidity increase, which was thought to be the main cause of the activity increase on compression, seems to be related to the change in the crystal structure of the reduced tungstic acid. In the present work, it was found that the crystal structure of the reduced sample was transformed from a WO_3-like structure to a $H_{0.1}WO_3$-like structure by the compression. Therefore, the sample would contain many more protons in the highly-compressed state than in the less-compressed one. Further, the surface-area measurement showed that, irrespective of the compacting pressure, the surface area remained constant. Therefore, the probability of the appearance of protons on the surface of the sample might be higher in the highly-compressed state than in the less-compressed state. Thus, the acidity increase on compression can be understood.

The observed effect of the compression on the crystal structure might be attributed mainly to pressures.* According to high-pressure chemistry,[12] some orderings resulting from compression can be expected in microscopic structures of substances. By applying this principle to the present case, it might be expected that pressures would make some contributions to the progress of the following reactions:

$$H_2WO_4 \rightarrow WO_3 + H_2O \qquad (I)$$

$$WO_3 \xrightarrow{+H} H_{0.1}WO_3 \xrightarrow{+H} H_{0.33}WO_3 \xrightarrow{+H} H_{0.5}WO_3 \qquad (II)$$

(A loose packing of oxygen ions→ A closer packing of oxygen ions)

Indications showing the occurrence of some of these reactions have appeared in X-ray diffraction patterns of reduced samples, while they have not appeared in the patterns of unreduced samples.

These results seem to show that, in addition to the compression, the subsequent reduction of the sample was a necessary condition for the occurrence of those reactions. This is reasonable, because the progress of the reaction II may be assumed to require some proton donors. Further, the incomplete progress of the reaction II, i. e., the occurrence of the reaction $WO_3 \rightarrow H_{0.1}WO_3$ only, may be attributed mainly to the existence of water in the reducing vapor (propylene and water). According to the work of Glemser et al.,[7] highly-reduced oxides of tungsten, e. g., $H_{0.5}WO_3$ are oxidized very easily by water.

Summary

It has been established that the compression of tungstic acid is effective in increasing the catalytic activity in the vapor-phase hydration of propylene. The activity increase on compression is thought to be dependent upon the acidity increase resulting from the compression. The increase in the surface acidity has been attributed to the change in the crystal structure. Namely, it is thought that the compression and the subsequent reduction of the catalyst force the crystal structure to transform from a WO_3-like structure to a $H_{0.1}WO_3$-like structure, which is capable of containing many protons and so giving the high surface acidity.

On the other hand, the increase in the compacting pressure resulted in a considerable decrease in the pore radius of the catalyst. This fact supports the explanation that the observed compensation effect among catalytic activities of compressed catalysts is due to the interference of the intra-particle diffusion with the intrinsic activity.

* The estimation was carried out by the method of Kubota et al. (*Chem. Eng., Japan* (Kagaku Kōgaku), **23**, 284 (1959).) under the following assumptions:

1. Since the conversion is low, reverse reaction can be neglected, and the concentration of the reactant approximates to the inlet value.
2. The diffusion coefficient of the reactant is approximated by the value of the Knudsen diffusion coefficient of propylene at 435°K.
3. The mean pore radius, $\bar{r}$, is 80 Å, and the porosity, θ, is 0.3.
4. The labyrinth factor, χ, for the uncompressed catalyst is 0.1, but by the compression of 3840 kg./cm^2 the value of χ is reduced to 0.01. (This assumption is based on the experimental result of D. van Zoonen et al. (*J. Inst. Petrol.*, **49**, 383 (1963)), who showed that, by the pelleting pressure, the diffusivity of the Co-Mo-Al_2O_3 is reduced to about 1/10 of the initial value.)

11) O. Glemser, *Angew. Chem.*, **73**, 785 (1961).

* The increase in temperature due to the compression was less than 5°C, which might have little influences on the surface property of the sample. In this measurement, a thermocouple was inserted directly into the sample.

12) S. D. Hamann, "Physico-Chemical Effects of Pressure," Butterworths Scientific Publications, London (1957), p. 4.

BULLETIN OF THE CHEMICAL SOCIETY OF JAPAN VOL. 39 864—867 (1966)

A Phase Study of the Iron(III) Sulfate, Sodium Sulfate and Sodium Chloride System

By Kohzoh SUGIYAMA and Takehiko TAKAHASHI

Department of Applied Chemistry, Faculty of Engineering, Nagoya University, Chikusa-ku, Nagoya

(Received June 8, 1965)

A phase diagram was drawn by using the results of a differential thermal analysis of the samples sealed in vicolglass and X-ray diffraction techniques undertaken in connection with the study of chlorine formation by the reaction of sodium chloride with sulfur dioxide and oxygen in the presence of iron compounds. In the two-component sodium sulfate - iron(III) sulfate system, the eutectic point was found at 562°C, the peritectic point, at 780°C, and the peritectoid point, at about 380°C. The former two values differ from those found by K. A. Bol' shakov et al. (*Zhur. Neorg. Khim.*, **8**, 2577 (1963)). In the trigonal diagram, two eutectic points were found, one at 465°C with a composition of about 13.5 mol.% iron sulfate, 53.5 mol.% sodium chloride and 33.0 mol.% sodium sulfate, and the other at 454°C with 15.0 mol.% iron(III) sulfate on the line of sodium chloride - iron(III) sulfate. It was confirmed that the peritectic point corresponding to the $Fe_2(SO_4)_3+Na_2SO_4(l)=2NaFe(SO_4)_2$ reaction shifted from 780°C on the line of sodium sulfate - iron(III) sulfate to 680°C on that of sodium chloride - iron(III) sulfate. From the diagram, the retarding tendency of the reaction rate of the final period of chlorine formation was attributed to diffusion control coming from the formation of solid phases.

The formation reaction of chlorine represented by the equation $2NaCl+SO_2+O_2=Na_2SO_4+Cl_2$ has previously been studied by the authors of this paper.[1] It was observed that the presence of iron compounds extremely accelerated the reaction rate and easily converted the system into the melt. This paper will give information about the phase change as the reaction proceeds. The phase diagram of the titled system is also expected to give fundamental data on the deposits produced at the medium temperature range in an oil furnace.

The titled system is a half of the four-component system iron(III) sulfate - sodium sulfate - sodium chloride - iron(III) chloride, which must be considered in the above-mentioned formation reaction of chlorine.

In order to draw the phase diagram, the differential thermal analysis (DTA) was performed in sealed cells, as it was inevitable in open apparatus for the composition of samples to change spontaneously, as a result of the decomposition, to form sulfur dioxide, sulfur trioxide and chlorine at temperatures above 600°C.

Apparatus and Experimental Methods

Reagents.—Chemically-pure sodium sulfate and sodium chloride were used after drying, while iron(III) sulfate was prepared from chemically-pure $Fe_2(SO_4)_3 \cdot xH_2O \cdot yH_2SO_4$ by double drying processes; the first process involved drying at 180°C for two or three hours in an open vessel, and the second, drying at 450°C for an hour in a test tube, in which the dead space over the reagent was made as small as possible. The composition of the reagent prepared by these methods corresponded to $Fe_2(SO_4)_3 \cdot 0.016Fe_2O_3$, and the X-ray diffraction pattern accorded with that in the literature.[2] The DTA cells were made of vicolglass; they were 40 mm. long, 4.7 mm. in inner diameter, and 0.7 mm. thick. Alumel-chromel thermocouples were used for the measurement of the differential temperature, and alumina powder was used as the standard substance. The temperature scale was calibrated at three points: the melting point of sodium chloride (801°C), the α, β transition point of potassium sulfate (583°C), and the transition point of silver chloride from $\alpha+\beta$ to γ (143°C). The ascending and descending speeds of the temperature were adjusted to 3°C per min. by the use of a photoelectric programmer. Generally, the first ascending curves were abandoned, and after holding at 900°C for an hour, the descending curves were recorded. From the temperatures under 150°C, the ascending curves were recorded again. Some samples which had the composition of iron(III) sulfate above 40 mol.% were heated up to 1000°C on account of their hard melting properties.

The compositions of samples were selected on the lines of 0, 3.3, 6.6, 10, 15, 20, 30, 40 and 50 mol.% iron(III) sulfate in the triangular diagram; these lines are close enough in composition that the nearest two compositions have difference of less than 10 mol.% for every component. Many samples were also taken up on the lines of sodium chloride - iron(III) sulfate and sodium sulfate - iron(III) sulfate.

1) K. Sugiyama and T. Takahashi, *J. Chem. Soc. Japan, Ind. Chem. Sect.* (*Kogyo Kagaku Zasshi*), **66**, 1773 (1963).

2) J. V. Smith, A. S. Beward, L. G. Berry, B. Post, S. Weissmann and M. B. Lotz, "Index to the Powder Diffraction File," American Society for Testing and Materials, Philadelphia (1964), p. 605.

The analysis of DTA was carried out as usual; the temperature of the phase change was decided by the point of intersection of the build-up tangent and the corresponding ground line. After the DTA measurements, the samples were analyzed to give X-ray diffraction diagrams by Co K_α at room temperature.

Results and Discussion

The Sodium Sulfate and Iron(III) Sulfate System.—From the results shown in Fig. 1, the eutectic point B is found to be 562°C at 17.5 mol.% of iron(III) sulfate. The peritectic point, DF, at which the $Fe_2(SO_4)_3+Na_2SO_4(l)=2NaFe\cdot(SO_4)_2$ reaction occurs, is about 780°C, and the peritectoid point, KMN, is also found to be about 380°C (here the $NaFe(SO_4)_2+Na_2SO_4(l)=Na_3Fe(SO_4)_3$ reaction occurs).

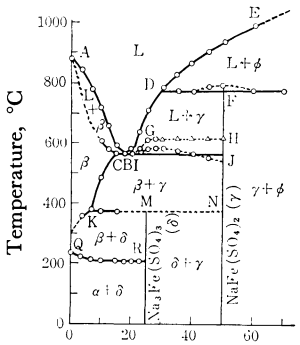

Fig. 1. The system Na_2SO_4-$Fe_2(SO_4)_3$.
GH and IJ lines refer to irreversible changes, and α, β refer to α and β sodium sulfate solid solutions respectively.

On the line of GH, the peaks of DTA curve were observable only in the run of ascending temperature, except for a few points near G. On the contrary, the peaks of the DTA curve on the line of IJ were observed only in the run of descending temperature, except for a few points near I.

According to Bol'shakov et al.,[3] who have reported on the same system, this system has the eutectic point at 620°C, the peritectic point at 680°C, the peritectoid point at 420°C, and the α, β transition point of a sodium sulfate solid solution at 220—228°C. Considerable discrepancies are found between Bol'shakov's results and those of the present paper. Though little description of the apparatus and experimental methods appeared in Bol'shakov's report, it is likely that the discrepancies arise from the dependence of the phase transition temperature on the pressure in the present experiment, or from the change in the composition of the sample on account of the decomposition in Bol'shakov's experiment.

In Fig. 2, the X-ray diffraction diagrams of the sodium sulfate - iron(III) sulfate system are drawn. The patterns of tri-sodium iron(III) tri-sulfate are found above 6.6 mol.% iron(III) sulfate; they increase in intensity up to 25 mol.%, above which the patterns of sodium iron(III) di-sulfate gradually increase to 50 mol.% iron-(III) sulfate.

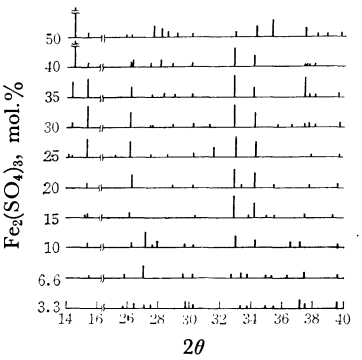

Fig. 2. X-ray diffraction diagrams of the system Na_2SO_4-$Fe_2(SO_4)_3$.

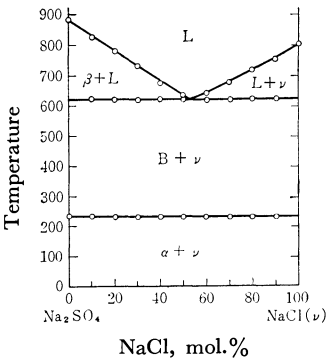

Fig. 3. The system Na_2SO_4-NaCl.

The Sodium Chloride and Sodium Sulfate System.—The phase diagram of this system, indicated in Fig. 3, is in good accordance with the results reported by Fedorov et al.[4]

The Inner Territory of the Sodium Sulfate, Sodium Chloride and Iron(III) Sulfate System.—To represent variations in temperature as well as in composition, the sectional diagrams, which are cut along various mol.%'s of iron(III) sulfate, are indicated in Figs. 4 to 10. The phase boundary between the phase containing β-sodium sulfate, tri-sodium iron(III) tri-sulfate and sodium chloride and the phase containing tri-sodium iron(III) tri-sulfate, sodium iron(III) di-sulfate and sodium chloride was determined from the peaks of the

3) K. A. Bol'shakov, P. I. Fedorov and N. I. Iliena, *Zhur. Neorg. Khim.*, 8, 2577 (1963).

4) P. I. Fedorov and K. A. Bol'shakov, ibid., 4, 893 (1959).

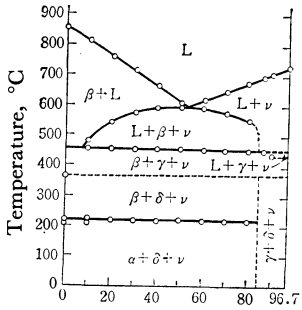

Fig. 4. Sectional diagram cut along the composition of 3.3 mol.% $Fe_2(SO_4)_3$.

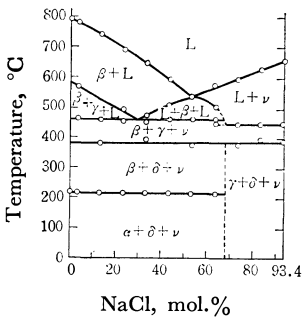

Fig. 5. Sectional diagram cut along the composition of 6.6 mol.% $Fe_2(SO_4)_3$.

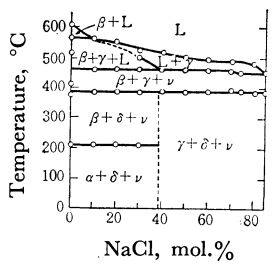

Fig. 6. Sectional diagram cut along the composition of 15 mol.% $Fe_2(SO_4)_3$.

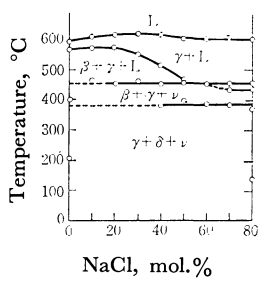

Fig. 7. Sectional diagram cut along the composition of 20 mol.% $Fe_2(SO_4)_3$.

α, β transition of sodium sulfate in DTA curves, as is shown in Figs. 4 to 6 by vertical dotted lines. The presence of iron(III) sulfate, tri-sodium iron-

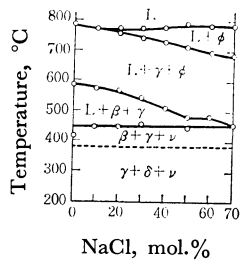

Fig. 8. Sectional diagram cut along the composition of 30 mol.% $Fe_2(SO_4)_3$.

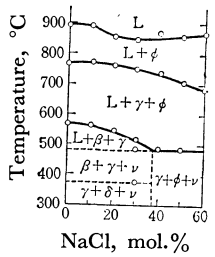

Fig. 9. Sectional diagram cut along the composition of 40 mol.% $Fe_2(SO_4)_3$.

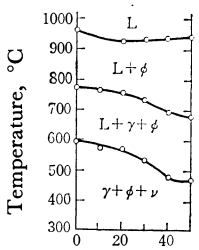

Fig. 10. Sectional diagram cut along the composition of 50 mol.% $Fe_2(SO_4)_3$.

(III) tri-sulfate and sodium iron(III) di-sulfate was detected by X-ray diffraction, in which the most distinct peaks by which to identify the respective compounds were found at 2θ values of 16.9°, 15.1° and 14.3° respectively.

From Figs. 7 to 10, it seems that the liquidus planes of the samples containing above 20 mol.% of iron(III) sulfate are influenced slightly by the variation in the mixing ratio of sodium sulfate and sodium chloride. The phase containing iron(III) sulfate is found over 30 mol.% of iron(III) sulfate at a high temperature and over 40 mol.% at room temperature, as is shown in Figs. 8 to 10. It may clearly be seen in Figs. 8 and 9 that the peritectic point, where the $Fe_2(SO_4)_3 + Na_2SO_4 = 2NaFe(SO_4)_2$ reaction occurs, varies from the sodium sulfate and iron(III) sulfate side to the sodium chloride and iron(III) sulfate side, and that the maximum temperature difference of the both sides reaches about 100°C.

The first solid phase which separates on cooling

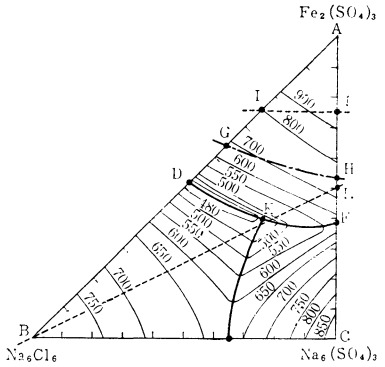

Fig. 11. Liquidus plane indicated by contour method.

is indicated by thick lines (DK, KF and KE) and a broken line (GH) in Fig. 11, in which the corners of the triangle are taken as 6 equivalent compounds—for example, Na_6Cl_6 instead of NaCl. The inner zone of AGH corresponds to the phase separating iron(III) sulfate first; GDKFH, to that separating sodium iron(III) di-sulfate; DBEK, to that separating sodium chloride, and EKFC, to that separating a β-sodium sulfate solid solution.

In Fig. 11, the dotted lines indicate the phase boundaries which are stable at room temperature; the inner zone of AJI corresponds to the phase containing sodium chloride, iron(III) sulfate and sodium iron(III) di-sulfate; IBHJ, to that containing sodium chloride, tri-sodium iron(III) tri-sulfate and sodium iron(III) di-sulfate; and LBC, to that containing sodium chloride, tri-sodium iron(III) tri-sulfate and α-sodium sulfate. The slender zone near the line of Na_6Cl_6 - $Fe_2(SO_4)_3$ is inferred to contain iron(III) chloride because of the stoichiometric discrepancy, but its presence could not be detected by DTA and X-ray diffraction.

In Fig. 11, the liquidus plane is also indicated by the method of the isothermal contour, and thick lines correspond to the ternary eutectic curves. It is found that the eutectic point, K, is 465°C, with a composition of about 13.5 mol.% iron(III) sulfate, 53.5 mol.% sodium chloride and 33 mol.% sodium sulfate. Another eutectic is also found at 454°C on the line of Na_6Cl_6-$Fe_2(SO_4)_3$, which has about 15 mol.% iron(III) sulfate. The characteristic low melting zone (450—490°C) distributes from the central region of the triangle to the Na_6Cl_6-$Fe_2(SO_4)_3$ line.

In the reaction of sodium chloride with sulfur dioxide, 20 to 40 wt.% pyrite was effectively added to sodium chloride in order to accelerate the reaction rate. When the composition containing 30 wt.% pyrite is considered, it corresponds to the liquidus point of about 660°C on the Na_6Cl_6-$Fe_2(SO_4)_3$ line in Fig. 11. In the course of the reaction, the composition will vary from the Na_6Cl_6-$Fe_2(SO_4)_3$ to the $Na_6(SO_4)_3$-$Fe_2(SO_4)_3$ line, parallel with the Na_6Cl_6-$Na_6(SO_4)_3$ line. If the temperature of the reaction is above 560°C, the whole system will be changed into the melt as the reaction proceeds. However, the system will have deposits of the β-sodium sulfate solid solution in the final step of the reaction if a temperature below 600°C is selected. These deposits of β-sodium sulfate are susceptible to interference with the diffusion of gas and liquid, as has been established by the previous data of the present authors.[1] On the other hand, the higher concentration of iron compounds will spread the attainable extent of the reaction, since the eutectic point of the $Na_6(SO_4)_3$-$Fe_2(SO_4)_3$ system is as low as 562°C. This is again supported by the previous results of the present authors.

As a whole, the state of the reaction system may be explained as being in close relation to the attainable extent and the velocity of the formation reaction of chlorine through the oxidation of sodium chloride and sulfur dioxide in the presence of iron compounds.

The authors wish to thank Mr. Katsuhiko Kitagawa for his assistance in the experimental work.

BULLETIN OF THE CHEMICAL SOCIETY OF JAPAN VOL. 39 868—874 (1966)

The Charge-transfer Complex and the Photochemical Reactions of Anthracene with Sulfur Dioxide in Various Solvents

By Toshikazu NAGAI, Kenichi TERAUCHI and Niichiro TOKURA

Department of Applied Chemistry, Faculty of Engineering, Osaka University, Higashinoda, Miyakojima-ku, Osaka

(Received June 26, 1965)

The equilibrium constant, K, of the 1 : 1 charge-transfer complex formation of anthracene with sulfur dioxide has been estimated by spectrophotometric measurements to be 0.33 in carbon tetrachloride at 15°C. The values of ΔH (-4.8 kcal.mol^{-1}) and $\Delta S°$ (-19 cal.deg^{-1}mol^{-1}) have been derived. The K value is nearly zero when estimated in the longer wavelength region, indicating that a contact charge-transfer complex is involved. A sort of contact charge-transfer complex of anthracene-SO_2 is also observed in benzene. Irradiations by a high-pressure mercury lamp of anthracene with sulfur dioxide in various solvents have been carried out. In solvents such as *n*-hexane and carbon tetrachloride, which have no interaction with sulfur dioxide, anthracene gives sulfur-containing substances, such as anthracene-9-sulfonic acid (I) and dianthranyl-(9.9')-sulfonic acid-(10) (II). On the contrary, in benzene or in carbon disulfide, no product such as the sulfonic acid, the dimer or the endoperoxide of anthracene is produced, indicating that the interaction of anthracene with sulfur dioxide is diminished by the solvent - sulfur dioxide interaction. A suggestion was made that the activated intermediate which induced the formation of I and II was of a singlet character.

Comprehensive studies have been made of the photochemical reactions of anthracene, especially of dimerization and oxidation in solutions.[1-3] According to these studies, in such hydrocarbon solvents as benzene and hexane anthracene affords its dimer through an excited singlet state ($^1A^*$), whereas in a heavy atom containing such solvents as carbon tetrachloride, chloroform and carbon disulfide, a transition from $^1A^*$ to ^3A (a triplet state) results in the formation of a cyclic endoperoxide in the presence of oxygen.

Such behavior of anthracene in various solvents has prompted the present authors to investigate the solvent effects of a photochemical reaction in the presence of sulfur dioxide, since the interaction of anthracene and sulfur dioxide has been the subject of considerable interest lately.[4,5]

Weiss[4] has concluded that the complex between anthracene and sulfur dioxide is an ion pair as the result of a complete electron transfer. Lichtin et al.,[5] however, have found that the complex in liquid sulfur dioxide is not a very good conductor, and no evidence has been provided for the ionic nature of the complex, either by conductometry or ultraviolet spectrometry.

In this paper, the electronic spectra of anthracene in various solvent systems involving liquid sulfur dioxide have been examined in order to obtain a greater understanding of the nature of the charge-transfer complex of anthracene - sulfur dioxide, our results will be discussed, together with the photochemical outcomes of the reaction of anthracene with sulfur dioxide in various solvents.

Experimental

Materials.—Liquid sulfur dioxide was dehydrated with phosphorus pentoxide and distilled. Carbon tetrachloride, benzene, *n*-hexane, and ethanol were purified by ordinary methods. A chromatographically-purified anthracene, m. p. 215—215.5°C, was used.

The Measurement of Electronic Spectra. — A Hitachi EPU 2 A-type spectrophotometer equipped with a thermostat was used. A pressure cell made of quartz was used to ensure the measurement in a sulfur dioxide solution; the width of the cell could be adjusted to 0.706 mm. by the insertion of a spacer. Lambert-Beer's law was satisfactorily obeyed throughout the range of the measurements.

The Calculation of the Equilibrium Constant of the Complex-Formation.—The Benesi-Hildebrand equation[6] was used for the estimation of the equilibrium constant.

Since the formation of the complex is shown as:

$$A + SO_2 \rightleftarrows A{\cdot}SO_2 \text{ (Complex)} \qquad (1)$$

the equilibrium constant can be expressed as:

$$K = \frac{[A{\cdot}SO_2]}{([A]_0-[A{\cdot}SO_2])([SO_2]_0-[A{\cdot}SO_2])} \qquad (2)$$

where $[A{\cdot}SO_2]$ = the molar concentration of the complex, $[A]_0-[A{\cdot}SO_2]$ = the molar concentration of free anthracene, and $[SO_2]_0-[A{\cdot}SO_2]$ = the mole fraction of

1) R. M. Hochstrasser and G. B. Porter, *Quarterly Rev.*, **XIV 2**, 146 (1960).
2) E. J., *Discussions. Faraday Soc.*, **14**, 143 (1953).
3) E. J. Bowen and D. W. Tanner, *Trans. Faraday Soc.*, **51**, 475 (1955).
4) J. Weiss, *J. Chem. Soc.*, **1942**, 250.
5) N. N. Lichtin, R. E. Weston, Jr., and J. D. White, *J. Am. Chem. Soc.*, **74**, 4715 (1952).
6) H. A. Benesi and J. H. Hildebrand, ibid., **71**, 2703 (1949).

free sulfur dioxide. [A·SO_2] in the last term is expressed in terms of the mole fraction.

Under the experimental conditions,

$$[SO_2]_0 \gg [A\cdot SO_2]$$

and

$$[SO_2]_0 - [A\cdot SO_2] \fallingdotseq [SO_2]_0$$

The Benesi-Hildebrand equation is derived as:

$$\frac{l[A]_0}{D} = \frac{1}{\varepsilon_c \cdot K[SO_2]_0} + \frac{1}{\varepsilon_c} \qquad (3)$$

where ε_c, D and l are the molecular extinction coefficient of the complex, the optical density of the solution, and the light-path length of the cell respectively. A linear plot of $l[A]_0/D$ vs. $1/[SO_2]_0$ will give $1/\varepsilon_c \cdot K$ and $1/\varepsilon_c$ by the slope and the intercept of the line respectively. K can thus be estimated.

The Estimation of $\Delta G°$, ΔH and $\Delta S°$. — The thermodynamic values, $\Delta G°$ (free energy change), ΔH (enthalpy change), and $\Delta S°$ (entropy change), were calculated by the following relation:

$$R \ln K = \Delta S° - \frac{\Delta H}{T}$$

Apparatus.—The vessel used for the reaction is illustrated in Fig. 1.

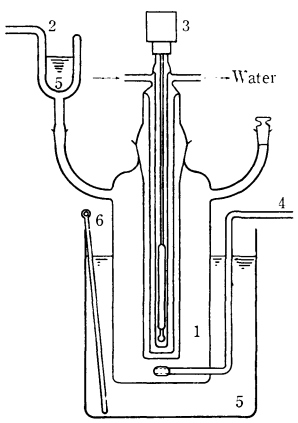

Fig. 1. Reaction vessel.

(1) reaction vessel, (2) cooler, (3) high pressure mercury lamp (which is equipped with double layered surrounding tubes made of quartz to be useful for low temperature experiment), (4) gas-inlet tube, (5) dry ice-trichloroethylene, (6) thermometer

A reaction vessel (1), equipped with a dry ice cooler (2), a 300-Watt high-pressure mercury lamp (3) inside the vessel and an inlet tube for nitrogen or oxygen gas (4), was chilled with dry ice - triclene bath in a Dewar vessel (5) equipped with thermometer (6).

The Procedure of the Reaction.—Anthracene (0.11—1.5 g.) was dissolved in a solvent (liquid sulfur dioxide, carbon tetrachloride, benzene, *n*-hexane or ethanol) in the reaction vessel; then a measured amount of liquid sulfur dioxide was charged into this solution. The atmosphere in the vessel was replaced by pure nitrogen gas several times, under cooling with the dry ice - triclene bath, the temperature of the vessel being kept at −25°C. The mixture was then irradiated for a definite time (1.5—8 hr.) by the mercury lamp. After the reaction, the solvent and /or liquid sulfur dioxide was distilled, and the residue was triturated with ethanol.

The ethanol-soluble part was evacuated to dryness and extracted with benzene in order to remove the unreacted anthracene. The residual part was added and digested with alcoholic sodium hydroxide until the pH of the solution became 7. The precipitated sodium salt was filtered and dried; thus it was identified as the sodium salt of I.

The ethanol-insoluble part was again extracted with benzene, since the extracts still contained some unreacted anthracene. The benzene-insoluble substance was in the form of dark brown crystals (II).

The Identification of the Products.—*Anthracene-9-sulfonic Acid (I).*—I was a hygroscopic substance containing sulfur; it was insoluble in a non-polar solvent

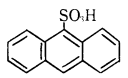

(I)

and soluble in methanol, ethanol and aqueous alkali, and it formed alkaline salts readily. The properties are coincident with the results described in the literature[7] for anthracene-9-sulfonic acid. IR (KBr disk), 3400 cm^{-1} (ν_{OH}), 1140—1220 cm^{-1} ($\nu_{as.SO_2}$ of SO_2OH) and 1040 cm^{-1} ($\nu_{s.SO_2}$ of SO_2OH). An authentic specimen was synthesized by the method of Minajew and Fedorow[8] by the following scheme:

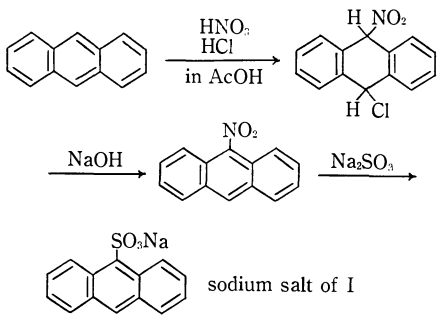

The ultraviolet spectra of the sodium salt of I and the authentic sample in an aqueous solution were entirely superimposable upon each other: λ_{max} 256 ($\log \varepsilon$ = 4.61), 335 (3.12), 351 (3.37), 370 (3.55) and 390 mμ (3.52). The R value of the salt as determined by thin-layer chromatography (adsorbent, Wako-silica gel B-5, 0.63 mm., elution with water), R=0.56., was coincident with that of the authentic specimen.

Dianthranyl-(9.9)'-sulfonic Acid-(10) (II). — II had a m. p. above 300°C and was sparingly soluble in ordinary solvents. Its infrared spectrum was almost identical with that of anthracene-9-sulfonic acid.

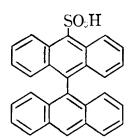

(II)

7) Beilstein's "Handbuch," **EII 11**, 110 (1950).
8) W. Minajew and B. Fedorow, *Ber.*, **62**, 2489 (1929).

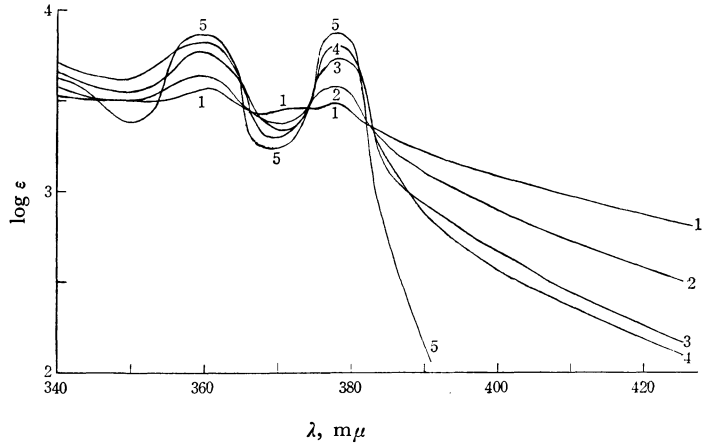

Fig. 2. The electronic spectra of anthracene, CCl_4-SO_2 system, 30°C.

ν_{max}^{KBr} 3400 cm^{-1} (ν_{OH}), 1160—1220 cm^{-1} and 1030 cm^{-1} (sulfur dioxide stretching of sulfonic acid), which disappeared when this compound was heated in a crucible. The sulfur content, 7.36% (calcd., 7.36%), shows that the molar ratio of the SO_3H group to the anthracene ring is 1 : 2. This ratio was confirmed by the alkali titration of II (neutral equivalent 409; calcd., 434). Moreover, the mass spectrum shows the presence of a dianthranyl ring, *m/e*, 354, 178, 127, 80, 64 and 48. The properties obtained here are coincident with the results described in the literature,[9] and so II was confirmed to be dianthranyl-(9.9')-sulfonic acid-(10).

An authentic specimen was synthesized by the following method:[10]

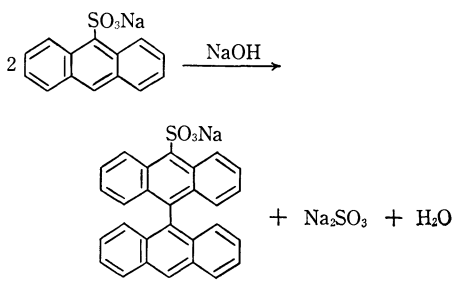

The infrared spectrum and *R*-value (0.81) as determined by the thin-layer chromatography (adsorbent, Wako-silica gel B-5, 0.30 mm.; elution with 1 : 1 ethanol-water) of the sodium salt of II were coincident with those of the authentic specimen.

9, 9', 10, 10'-Dianthracene(III).—This compound was sparingly soluble in an organic solvent, m. p. 255—257°C, and a mixed melting point determination with

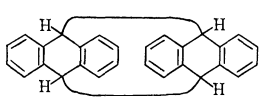
(III)

an authentic dianthracene[11] showed no depression. At the melting point, this compound dissociated to the anthracene-monomer (m. p. 211—212°C). These properties are coincident with those of the photodimers of anthracene derivatives reported by Greene et al.[12] The 725 cm^{-1} band due to the out-of-plane C–H deformation vibration of *ortho*-di-substituted aromatics which is observed in anthracene itself is replaced by a band at 760 cm^{-1} in this compound similar to that proposed for 9.10-dihydroanthracene.[13]

Found: C, 94.26; H, 5.52. Calcd. for $C_{28}H_{20}$: C, 94.38; H, 5.63%.

III was thus confirmed to be 9, 9', 10, 10'-dianthracene.

9.10-Anthracene-endo-cyclicperoxide (IV).—IV decomposed at 120°C (reported, m. p. (decomp.) 120°C[14]). The active oxygen was analyzed by the spectrophotometric determination of iodine which had been liberated

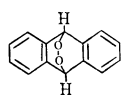
(IV)

from the ethanolic solution of IV by the addition of potassium iodide. The infrared spectrum showed no absorption at 3450 cm^{-1} due to the ν_{OH} of hydroperoxide. This compound was confirmed by reexamining the method of Bowen and Tanner[8] in the absence of sulfur dioxide.

Results and Discussion

The Interaction of Anthracene with Liquid Sulfur Dioxide. Solvent Effects.—In Fig. 2, the electronic spectra of the anthracene - liquid sulfur dioxide - carbon tetrachloride system are compared at different molar ratios of sulfur dioxide vs. carbon tetrachloride, where a constant amount of anthracene (6.3 mg.) was dissolved in 10 ml. of carbon tetrachloride.

As is shown in Fig. 2, the characteristic fine structure of the absorption of anthracene disappears

9) Beilstein's "Handbuch," **EII 11**, 112 (1950).
10) W. Minajew and B. Fedorow, *Ber.*, **62**, 2493 (1929).
11) E. Funakubo, Y. Matsumoto and T. Nagai, *Technol. Repts. of Osaka Univ.*, **11**, 409 (1961).
12) F. D. Greene, S. L. Misrock and J. R. Wolfe, *J. Am. Chem. Soc.*, **77**, 3852 (1955).
13) L. J. Bellamy, "The Infrared Spectra of Complex Molecules," 2nd Ed., Methuen, London (1958), p. 77.
14) E. H. Rodd (Editor) "Chem. of Carbon Compound," **IIIB** Elsevier Publishing Co., New York (1956), p. 1365.

as the molar fraction of sulfur dioxide increases, while the absorption of the longer-wave-length region (as far as 470 mμ) of the broad absorption increases. The absorption bands above 400 mμ may obviously be identified as a charge-transfer complex[15] between anthracene and sulfur dioxide, since the absorptions of both anthracene and sulfur dioxide are below 400 mμ in carbon tetrachloride.

Figure 3 shows the Benesi-Hildebrand plot at 0°C; it indicates a 1 : 1 complex formation. This complex formation is also confirmed from the linear Benesi-Hildebrand plots at 15 and 30°C, and by the linear plot in Fig. 4, where a linear correlation between $\ln K$ vs. $1/T$ is visualized.

The equilibrium constants, K, for the complex formation estimated at various wavelengths are listed in Table I.

Table I. Equilibrium constant of the complex formation

Wavelength	0°C	15°C	30°C
400 mμ	0.581	0.327	0.216
410 mμ	0.188	0	0
420 mμ	0	0	0

The K values are different depending on the wavelengths. The null-values of the K's at the higher wavelengths are of some interest, because these values mean that the interactions are principally due to the contact charge-transfer complex[16] and that the effects of many complexes with different orientations are overlapping to show a broad absorption band.

The small values of the equilibrium constants, K, are due to the fact that there are various mixtures, from the loose forms of the 1 : 1 complexes to the contact-type form. In contrast to this, the K value for the A–I_2 complex in carbon tetrachloride is estimated to be $K_c=52$ (1./mol.)[17] and $K_c=3.7$ (1./mol.).[18] The same tendency is also shown in the K's at 15 and 30°C.

The apparent enthalpy and entropy changes calculated from these K values at 400 mμ are as follows:

$\Delta G^\circ=0.64$ kcal. mol^{-1}, $\Delta H=-4.8$ kcal. mol^{-1} and $\Delta S^\circ=-19$ cal. deg^{-1} mol^{-1}.

The spectra of liquid sulfur dioxide in various solvents indicate the interaction of the solvents with sulfur dioxide. The maximum of the absorption of sulfur dioxide is observed at 290 mμ (ε 383)[19]; the λ_{max} and ε were almost the same in such solvents as *n*-hexane and carbon tetrachloride,

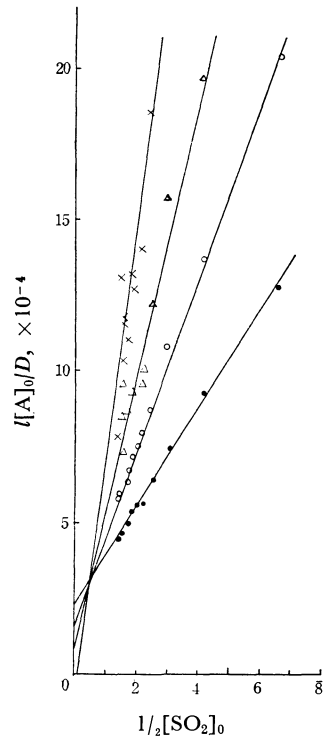

Fig. 3. Benesi-Hildebrand plot, anthracene-SO_2 in CCl_4 at 0°C.
●—● 390 mμ △—△ 410 mμ
○—○ 400 mμ ×—× 420 mμ

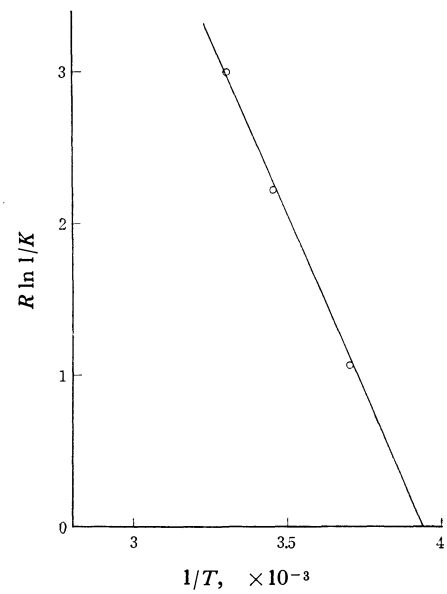

Fig. 4. $R \ln 1/K$ vs. $1/T$ plot. Anthracene-SO_2 in CCl_4

which show no interaction with sulfur dioxide. However, in benzene, ethanol and methanol the λ_{max} of sulfur dioxide shifts to a shorter wavelength

15) R. S. Mulliken, *J. Phys. Chem.*, **56**, 801 (1952).
16) L. E. Orgel and R. S. Mulliken, *J. Am. Chem. Soc.*, **71**, 4839 (1957).
17) B. Bhattacharya and S. Basu, *Trans. Faraday Soc.*, **54**, 1286 (1958).
18) J. Peters and W. B. Person, *J. Am. Chem. Soc.*, **86**, 10 (1964).
19) D. Booth, E. S. Dainton and K. J. Ivin, *Trans. Faraday Soc.*, **55**, 1293 (1959).

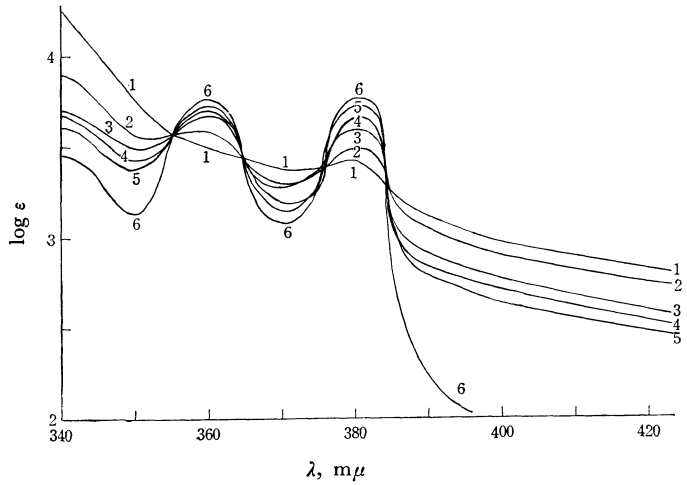

Fig. 5. The electronic spectra of anthracene, benzene-SO_2 system, 30°C.

TABLE II. THE RESULTS OF PHOTOCHEMICAL REACTION

No.	Anthracene $\times 10^{-2}$ mol./l.	Solvent	ml.	Temp. °C	Time hr.	Product %
1	1.33	liq.SO_2	380	−25	3	I (53.1)
						II (9.3)
2	0.43	*n*-Hexane	350	−25	3	I (75.2)
		liq.SO_2	20			II (14.9)
3	1.35	CCl_4	221			I (25.9)
		liq.SO_2	195	−25	3	II (46.6)
4	0.16	Ethanol	450			I trace
		liq.SO_2	40	−25	3	II (39.0)
5	6.48	Benzene	130	20	3	III (31.7)
6	6.39	Benzene	130			
		liq.SO_2	2	20	3	no reaction
7	1.69	Benzene	107			
		liq.SO_2	60	20	8	no reaction
8	1.40	Benzene	222			
		liq.SO_2	180	−25	3	no reaction
9*	1.94	CS_2	233	−10	1.5	IV (9.7)
10*	1.91	CS_2	233	−10	1.5	trace of sulfur
		liq.SO_2	4			compound**
11	1.91	CS_2	233			
		liq.SO_2	4	−10	1.5	no reaction
12*	1.47	liq.SO_2	320	−10	1.5	I (84.4)
						II (4.7)

The yields of the products are in mole percent.

* O_2 was bubbled into the solution.

** m. p. >300°C (sinters at ca. 135°C), IR, 1680 cm^{-1} ($\nu_{C=O}$), 1160 and 1310—1340 cm^{-1} (ν_s and ν_{as} SO_2), UV, λ_{max} 252 mμ. Sulfur content 14.88%. The yield was very small and the structure was not identified.

(280—274 mμ) and the molecular extinction coefficient, ε, also increases (for example, 1390 in benzene),[20] indicating an interaction of some extent. In carbon disulfide, an absorption which might be due to a charge-transfer complex with sulfur dioxide appears. The same trend is seen in benzene, as is shown in Fig. 5, which indicates that the anthracene-sulfur dioxide complex is affected by benzene. The Benesi-Hildebrand plot is scattered, indicating that the anthracene-sulfur dioxide interaction in benzene results in a sort of contact charge-transfer complex.

In ethanol, despite the supposed EtOH - sulfur

20) L. J. Andrews and R. N. Keefer, *J. Am. Chem. Soc.*, **73**, 4169 (1951).

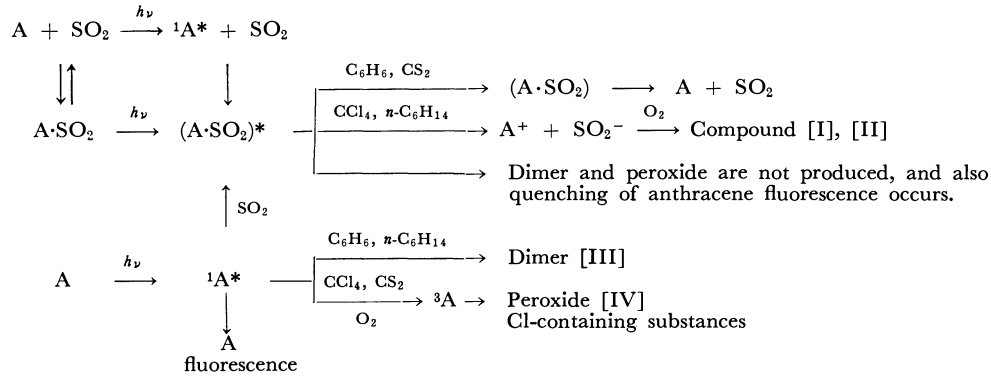

Fig. 6. Reaction schemes.

dioxide interaction, a linear Benesi-Hildebrand plot was observed, indicating that either a loose 1 : 1 complex or a complicated, anthracene - sulfur dioxide - EtOH (for example, a 1:1:1 complex) complex might be formed. Moreover, the absorptions at 610—680 mμ of anthracene due to the S–T transition[21] of anthracene in an approximately saturated solution were not observed in such systems as carbon tetrachloride, carbon disulfide and carbon disulfide - oxygen.

The Irradiation of Anthracene - Sulfur Dioxide Solutions by a High-pressure Mercury Lamp.—In order to obtain further information about the effects of solvents on the interaction between sulfur dioxide and anthracene, irradiation by a high-pressure mercury lamp was attempted. The results are listed in Table II.

The yields of I and II were higher in the presence of *n*-hexane and carbon tetrachloride. According to the findings of Bowen et al., the irradiation of anthracene in carbon tetrachloride gave chlorine-containing compounds,[22] whereas in this anthracene - sulfur dioxide - carbon tetrachloride system sulfur-containing compounds were produced in place of chlorinated compounds.

It has been already established that, in benzene, anthracene dimerizes by an irradiation through an excited singlet state (Exp. No. 5). By the addition of a small amount of sulfur dioxide, regardless of its quantity or the reaction time, the dimerization reaction was inhibited (Exp. No. 6, 7 or 8). In addition, no sulfur compounds were found in the reaction mixture. The results are interpreted as being the consequence of the formation of an anthracene - sulfur dioxide - benzene contact complex. In an ethanol solution (Exp. No. 4), the sulfur content in the products was greatly decreased. In carbon disulfide (Exp. No. 11), also, no sulfur-containing compound was found in the reaction mixture. The previously-recognized formation of endocyclic peroxide through a triplet state by the bubbling of oxygen gas into a carbon disulfide solution of anthracene (Exp. No. 9) was inhibited by the addition of sulfur dioxide in the presence of oxygen; it was replaced by the formation of a small amount of a sulfur compound.

With regard to the influence of oxygen addition to sulfur dioxide (Exp. No. 12), it was demonstrated that formation of I and II was not affected. Thus, it can be assumed that the activated intermediate which induces the formation of I and II is of a singlet character. This assumption is supported by the following facts. i) Neither the disulfone nor the disulfonic acid of anthracene was produced, though expected, if the intermediate was of a triplet state as a result of its radical character. In fact, Squire et al.[23] obtained diphenyl disulfone by the thermal reaction of benzene and sulfur dioxide in the presence of a radical source such as benzoyl peroxide. ii) As has been described above, the sulfur-containing substances were produced in preference to chlorinated compounds in the anthracene - sulfur dioxide - carbon tetrachloride system, though a Cl-radical-abstracting reaction might be expected if the intermediate had a triplet character. Actually, under irradiation by a low-pressure mercury lamp (2537 Å), chlorinated compounds were produced in preference to sulfur-containing compounds, even in the anthracene - sulfur dioxide - carbon tetrachloride system which is similar to that of the photoreaction of anthracene in carbon tetrachloride without sulfur dioxide undertaken by Bowen et al.[22] (A low-pressure mercury lamp does not emit the radiation of the wavelength required for the excitation of anthracene-sulfur dioxide complex.) This behavior differs from the behavior under the irradiation of a high-pressure mercury lamp. iii) Moreover, the absorption at 610—680 mμ of anthracene due to S–T transition was not observed.

21) In a $CHCl_3$ solution of anthracene containing acetylacetonate of Fe^{3+}, the absorptions at 610—680 mμ due to the S–T transition of anthracene have been recognized by Chaudhuri et al. (J. N. Chaudhuri and S. Basu, *Trans. Faraday Soc.*, **54**, 1605 (1958)).

22) E. J. Bowen and K. K. Rohatgi, *Discussions Faraday Soc.*, **14**, 146 (1953).

23) J. M. Squire and W. A. Waters, *J. Chem. Soc.*, **1962**, 2068.

As has been described above, the photochemical reactions in solutions, the reaction of anthracene with sulfur dioxide are seriously influenced by the solvents used, the interaction between the solvent and sulfur dioxide being of the greatest importance. The reaction schemes are illustrated in Fig. 6. As is shown in the scheme, the various reaction courses in the photochemical influence are presumably founded on the excited anthracene - sulfur dioxide complex $(A \cdot SO_2)^*$, which may be produced by the photo-activation of a charge-transfer complex or by the interaction of sulfur dioxide with photoactivated anthracene rather than by the photoactivated sulfur dioxide.[24]

Dimerization in a benzene solution is thus inhibited, and the quenching[25-28] of anthracene fluorescence occurs by the addition of a small amount of sulfur dioxide. Moreover, in benzene or a carbon disulfide solution, in the presence of sulfur dioxide, I and II are not formed, indicating that the interaction of anthracene with sulfur dioxide is diminished by the solvent-sulfur dioxide interaction.

On the contrary, in a *n*-hexane or in carbon tetrachloride solution, which has no interaction with sulfur dioxide, anthracene interacts with sulfur dioxide as much as in liquid sulfur dioxide, where the electron - transferred complex is stabilized in the excited state by solvation with the surrounding sulfur dioxide. The sulfur-containing compounds, such as sulfonic acid of the aromatic compound, will thus be produced from the excited anthracene-sulfur dioxide complex and an atmospheric oxygen which is probably present slightly in the reaction system. The photochemical formation of sulfonic acid of the aromatic compound gives a new synthetic method.

The authors wish to express their thanks to Mr. Hiroshi Takeuchi of our laboratory for his help in the experimental work.

24) In the photochemical gas-phase reactions between sulfur dioxide and olefin or paraffin, the formation of sulfinic acids due to the excitation of sulfur dioxide has been reported by Dainton and Ivin (F. S. Dainton and K. J. Ivin, *Trans. Faraday Soc.*, **46**, 374, 382 (1950)). Thereby, the photochemical products, such as dibenzyl disulfone and benzyl-sulfinic acid, may be expected from sulfur dioxide and toluene if sulfur dioxide is excited, but no photochemical formation is observed under the present conditions. Therefore, the interaction of the photo-activated free anthracene with sulfur dioxide is predominant, rather than that by photo-activated sulfur dioxide, since greater amounts of anthracene than the quantity of the complexed anthracene expected from the calculated value of the equilibrium constant, *K*, are brought into the reaction or inhibition for dimerization. It would be very interesting to know if there is a possibility of a singlet-triplet intersystem crossing of the photo-activated anthracene by sulfur dioxide, due to the spin-orbit coupling. However, no evidence for such a conversion has been obtained.

25) W. S. Metcalf, *J. Chem. Soc.*, **1954**, 2485.
26) B. Stevens, *Trans Faraday Soc.*, **51**, 610 (1955).
27) H. W. Malherbe and J. Weiss, *J. Chem. Soc.*, **1944**, 541.
28) E. J. Bowen and W. S. Metcalf, *Proc. Roy. Soc.*, **A206**, 437 (1951).

BULLETIN OF THE CHEMICAL SOCIETY OF JAPAN VOL. 39 874—879 (1966)

The Electron Spin Resonance of Oxovanadium Sulfate Dispersed on Porous Materials

By Hazime TANAKA and Akira MATSUMOTO

The Central Research Laboratory, Showa Denko K.K., Haramati, Ohta-ku, Tokyo

(Received August 18, 1965)

Oxovanadium sulfate was fixed on silica and alumina gel bases as a model of the oxidation catalyst. On silica gel the ESR spectra showed an exchange narrowing without hyperfine lines as a result of the formation of small crystallites. In this case, axially-symmetrical g factors were obtained: $g_{\perp}=1.969\pm0.001$ and $g_{\parallel}=1.915\pm0.005$. When sulfuric salts of alkali metals were added to the system, the dispersion of VO^{2+} ions became homogeneous and a hyperfine structure was observed in the ESR spectra. On an alumina gel base the spectrum resembled that of the frozen aqueous solution of $VOSO_4$ and showed the hyperfine structure, $A_{\perp}=(7.0\pm0.2)\times10^{-3}cm^{-1}$ and $A_{\parallel}=(1.85\pm0.05)\times10^{-2}\,cm^{-1}$. It may be considered that VO^{2+} ions are distributed homogeneously in the surfase layer of alumina. In the alumina gel and silica gel with alkali sulfate, the decrease in the V^{4+} ions with heat treatment was slower than in the silica gel system.

Vanadium complexes which are fixed on various base materials have been used for oxidation catalysts. The mechanism of their catalytic reaction and the effects of added materials have been investigated

by many authors from the point of view of kinetics or of structure.[1-10]

Recently some investigators[11-14] have analyzed the electronic structure of V^{4+} or VO^{2+} in the catalyst system. The V^{4+} ion has a single unpaired electron in the 3d orbital and shows the ESR spectrum with eight hyperfine lines as a result of V^{51} ($I=7/2$). Fortunately, the studies about V^{4+} and VO^{2+} have been stored up from the theoretical point of view in the relation of the ESR spectra from various states.[15-24]

In this paper, the circumstances of the VO^{2+} ions in a catalytic system with silica or alumina gel bases will be investigated by the ESR method. The interaction between oxovanadium sulfate and base materials will be discussed, as well as the effects of the addition of the sulfates of alkali metals.

Experimental

Sample Preparation. — Oxovanadium sulfate, $VOSO_4 \cdot 3H_2O$, was prepared by the reduction of vanadium(V) oxide with sulfur dioxide. Silica and alumina gels were immersed in an aqueous solution at varying concentrations of oxovanadium sulfate and sulfuric acid. They were then dried and kept in an air bath at 120°C for 10 hr. Five kinds of alkali sulfate, lithium sulfate, sodium sulfate, potassium sulfate, cesium sulfate and ammonium sulfate, were added to aqueous solutions of $VOSO_4$.

Table I. Samples

Base material	$VOSO_4$ content	Alkali sulfates added to the system
Silica gel Alumina gel	5—40% of base materials	Li_2SO_4; Na_2SO_4; K_2SO_4; Cs_2SO_4; $(NH_4)_2SO_4$

ESR Measurements. — The ESR spectra were measured at two frequencies, the X and K bands. The K-band spectrometer was a super-heterodyne type constructed by the Oyo Denki (Applied Electric) Laboratory Co., Ltd., while the X-band spectrometer was made in the authors' laboratory. The magnetic field was monitored with the proton resonance at an accurately known frequency. As a standard of the signal intensity, a small ruby crystal and calcium oxide powder containing Mn^{2+} were employed.

Results and Discussion

The ESR of VO^{2+} in Aqueous Solutions.— The ESR signals of the VO^{2+} ions in aqueous solutions were measured as a function of the concentrations of VO^{2+} and sulfuric acid in order to examine the ionic configuration of VO^{2+}. In the concentration range from 0.1 to 3 mol./l. of VO^{2+}, a typical hyperfine structure of eight lines was observed. The width of the hyperfine components changed with the nuclear spin quantum number, m_I. At a more concentrated solution of VO^{2+}, it became impossible to observe the separate hyperfine structure. When sulfuric acid was added to the solutions where the hyperfine components were distinguished, however, the individual hyperfine width became broad, probably because of an increase in the viscosity. The addition of alkali metal ions did not affect the spectra.

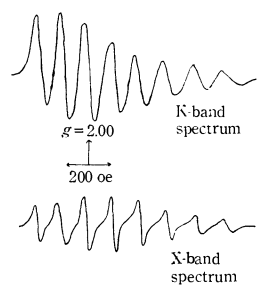

Fig. 1. ESR spectrum of $VOSO_4$ in aqueous solution (0.1 mol./l.).

Kivelson,[15] Rogers and Pake[16] have given the following equation for the width of the hyperfine components of VO^{2+} in solutions:

$$\Delta H = a_0 + a_1 m_I + a_2 m_I^2 \qquad (1)$$

where ΔH is the width, m_I is the nuclear spin quantum number, and a_0, a_1, a_2 are as follows:

1) J. K. Dixon and J. E. Longfield, "Catalysis," Vol. VII, Reinhold Publishing Corporation, New York (1960), p. 183.
2) K. Tarama and K. Oda, "Shokubai Kogaku Kôza," Vol. VII, Tizin Syobo, Tokyo (1964), pp. 21, 80.
3) T. Kawaguchi, *Ryusan*, **5**, 79 (1952); *Chem. & Chem. Ind. (Kagaku to Kogyo)*, **13**, 811 (1960).
4) K. Tarama, S. Teranishi, K. Hattori, A. Yasui, T. Miyazaki, K. Yamaguchi and T. Nishibori, *Ryusan*, **6**, 241 (1953); *J. Chem. Soc. Japan, Ind. Chem. Sect. (Kogyo Kagaku Zassi)*, **55**, 68 (1952), **56**, 302, 661 (1953), **57**, 490 (1954); *J. Chem. Soc. Japan, Pure Chem., Sect. (Nippon Kagaku Zasshi)*, **81**, 1034, 1038 (1961), **82**, 438 (1962).
5) G. L. Simard, J. F. Steger, R. J. Arnott and L. A. Siegel, *Ind. Eng. Chem.*, **47**, 1424 (1955).
6) R. Matsuura, *J. Chem. Soc. Japan, Pure Chem. Sect. (Nippon Kagaku Zasshi)*, **82**, 276, 281, 417, 419, 421 (1961).
7) H. Kakinoki, N. Sahara, I. Kamata and Y. Aigami, *Shokubai (Catalyst)*, **4**, 113 (1962).
8) V. B. Bibin and L. A. Kasatkina, *Kin. i Kat.*, **5**, 734 (1964).
9) V. Ya. Volfson, Ya. V. Zhigailo, E. F. Totzkaya and V. V. Raksha, ibid., **6**, 162 (1965).
10) B. Dmuchovsky, M. C. Freerks, E. D. Pierron, R. H. Munch and F. B. Zienty, *J. Catalysis*, **4**, 291 (1965).
11) K. Tarama, S. Teranishi, S. Yoshida, N. Tamura and H. Yoshida *Shokubai (Catalyst)*, **3**, 187 (1961), **4**, 346 (1962); This Bulletin, **34**, 1195 (1961).
12) V. B. Kazanskii, Z. I. Ezhkova, A. G. Lyubarskii, V. V. Voevodskii and I. I. Ioffe, *Kin. i Kat.*, **2**, 783 (1961).
13) Z. I. Ezhkova, I. I. Ioffe, V. B. Kazanskii, A. V. Krylova, A. G. Lyubarskii and L. Ya. Margolis, ibid., **5**, 861 (1964).
14) V. Ya. Volfson and L. N. Ganyuk, ibid., **6**, 306 (1965).
15) D. Kivelson, *J. Chem. Phys.*, **33**, 1094 (1960).
16) G. Pake and R. Rogers, ibid., **33**, 1107 (1960).
17) D. Kivelson and S.-K. Lee, ibid., **41**, 1896 (1964).
18) R. Faber and M. T. Rogers, *J. Am. Chem. Soc.*, **81**, 1849 (1959).
19) H. R. Germann and J. D. Swalen, *J. Chem., Phys.*, **36**, 3221 (1962).
20) D. E. O'Reilly, ibid., **29**, 1188 (1958).
21) E. M. Roberts and W. S. Koski, ibid., **34**, 591 (1961).
22) I. Bernal and P. Reiger, *Inorg. Chem.*, **2**, 256 (1963).
23) M. B. Palma-Vittorelli, M. U. Palma, D. Palumbo and F. Sgarlata, *Nuovo Cimento*, **3**, 718 (1956).
24) C. J. Ballhausen and H. B. Gray, *Inorg. Chem.*, **1**, 111 (1962).

$$a_0=\alpha+\tau_c[4/45(\Delta\gamma H_0)^2+3/40I(I+1)b^2] \quad (2a)$$

$$a_1=\tau_c[4/15(b\Delta\gamma H_0)] \quad (2b)$$

$$a_2=\tau_c[1/8b^2] \quad (2c)$$

where α is the contribution from unspecified sources, τ_c is correlation time, $H_0=\omega_0/\gamma$, $\Delta\gamma=\beta(g_\perp-g_\parallel)$, and $3b=2(A_\parallel-A_\perp)$. In Eqs. 2a, 2b and 2c the small terms are neglected.

The values of α and the $\Delta\gamma H_0/b$ ratio have been calculated; they are listed in Table III. The values of α are not in good agreement, as the line shapes of the hyperfine components are not symmetric and the theory is not sufficient to describe the broadening mechanism. The $\Delta\gamma H_0/b$ ratio should be 2.5 times larger in the K-band spectra than in the X-band spectra. Actually, however, the results obtained are from 1.9 to 2.8 times larger in the former.

TABLE II. VARIATION IN THE WIDTHS OF HYPERFINE LINES IN THE ESR SPECTRA OF VO^{2+} IN AQUEOUS SOLUTIONS

Concentration		Width parameters[1]			
VO^{2+} mol./l.	H_2SO_4 N	a_0 œ.	a_1 œ.	a_2 œ.	
3.0	0	63.5	4.7	1.2	k)
		19.7	2.3	1.7	x)
1.0	0	57.6	10.5	2.2	k)
		13.1	1.4	0.6	x)
0.1	0	29.5	7.2	1.4	k)
		6.6	0.6	0.2	x)
0.1	0.1	26.2	6.3	1.3	k)
0.1	1.0	25.9	6.0	1.3	k)
		7.9	1.0	0.4	x)
0.1	3.0	26.0	6.0	1.3	k)
		8.7	0.7	0.3	x)
0.1	10	35.0	8.0	1.5	k)

1) The meanings of a_0, a_1 and a_2 are given in Eq. 1.
k) K-band measurement.
x) X-band measurement.

It may be considered from these data that the electronic structure around VO^{2+} does not change greatly in the solution at from 0.1 to 1.0 mol./l. VO^{2+} concentration nor upon the addition of up to 3 N of sulfuric acid. A distorted octahedral structure of $VO(OH_2)_5$, which has been proposed for dilute aqueous solutions of VO^{2+} ions, can be considered.[24] When the concentration of VO^{2+} ions or that of sulfuric acid increases, not only the change in viscosity but also the change in the structure of coordination around VO^{2+} must occur.

VO^{2+} Ions on Silica Gel Base.—Oxovanadium

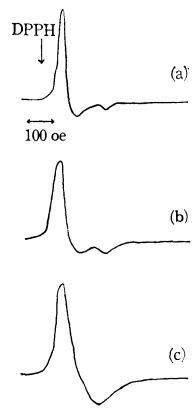

Fig. 2. (a) ESR spectrum of powdered $VOSO_4$·$3H_2O$. (b) ESR spectrum of $VOSO_4$ on silica gel base; $VOSO_4$ content: 10 mol.%. (c) ESR spectrum of $VOSO_4$ on silica gel with Na_2SO_4; Na_2SO_4: 10 mol.%.

sulfate dispersed on silica gel shows an ESR spectrum of an axial symmetrical g anisotropy without a hyperfine structure (Fig. 2), which resembles the ESR spectra of $VOSO_4$·$3H_2O$ and of $VOSO_4$·H_2SO_4 in powder. In these systems, the exchange narrowing becomes dominant and the hyperfine interaction is negligible as compared with the g

TABLE III. ESR CONSTANTS OF VO^{2+} IN AQUEOUS SOLUTIONS

Concentration		g Factor $\langle g\rangle$	Hyperfine constant $\langle A\rangle\times10^2$, cm^{-1}	α œ.	$\Delta\gamma H_0/b$	
VO^{2+}, mol./l.	H_2SO_4, N					
3.0	0	1.962		52	1.8	k)
			1.16	3.4	0.64	x)
1.0	0	1.962	1.20	45	2.2	k)
			1.17	7.0	1.1	x)
0.1	0	1.962	1.22	15	2.4	k)
			1.19	4.3	1.2	x)
0.1	0.1	1.960	1.22	13	2.3	k)
0.1	1.0	1.962	1.21	13	2.2	k)
			1.19	4.2	1.2	x)
0.1	3.0	1.966		13	2.2	k)
			1.2	5.8	1.2	x)
0.1	10	1.962	1.2	19	2.4	k)

k) K-band measurement. x) X-band measurement.

anisotropy for the K-band measurements. The VO^{2+} ions seem to form small crystallites of $VOSO_4 \cdot nH_2O$. Therefore, if each individual csystallite is distributed in random orientation and gives Lorentzian line shape, the ESR spectrum may be expressed approximately as follows:[25]

$$I(H) = \int K \sin\theta \cdot \frac{d\theta}{(H-H_0)^2+b^2} \qquad (3)$$

where H_0 is the resonance field, θ is the angle between the applied field H and the crystal axis, $K=1/8\, g_\perp{}^2[(g_\parallel/g_\perp)^2+1]$, and b is the half-width at the half-power of each crystallite.

The values of $g_\perp$, $g_\parallel$ and b can be estimated from the experimental data, if b remains constant throughout the θ range. The results are listed in Table IV.

Table IV. ESR constants of $VOSO_4$ on silica gel base

Additional material	g Factor $g_\perp$	g Factor $g_\parallel$	g Factor $\langle g \rangle$	Width ΔH_{msl}
none	1.969	1.915		36
			1.963*	64*
10%LiSO	1.965	1.90		55
	1.968*	1.91*		50*
10%Na_2SO_4			1.967	46
10%K_2SO_4			1.956	60—70
10%Cs_2SO_4			1.955	80—90
10%$(NH_4)_2SO_4$	1.970	1.912		31
$VOSO_4 \cdot 3H_2O$**	1.976	1.913		26
	1.974*	1.90*		28*
$VOSO_4 \cdot H_2SO_4$**	1.976	1.90		20

The quantity of $VOSO_4$: 10 mol.% of base material.

The quantity of alkali sulfate: 10 mol.% of base material.

* Measured after heat treatment at 300°C.

** Without base material.

When the sample was heated in a stream of air, the ESR signal decreased in intensity, while the width was increased. As the symmetry of the spectrum increased, only an apparent value of g could be obtained. The exchange narrowing, therefore, seems to become weak as a result of the decrease in the concentration of VO^{2+} ions, while the ill-resolved hyperfine structure seems to cause the inhomogeneous broadening.

When alkali sulfates were added to the system, the hyperfine structure appeared in the ESR spectrum. This effect was influenced by the quantity of alkali sulfate as well as by its kind. In Fig. 4 the change in the hyperfine splitting of the system with various concentrations of cesium sulfate is shown. When the mole ratio of cesium sulfate to the silica gel base reached about 0.4, the width of each individual hyperfine component was about

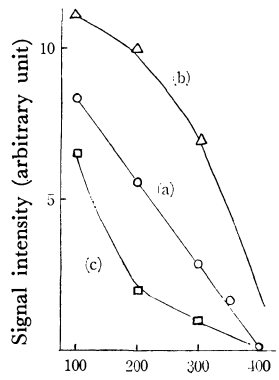

Fig. 3. The Variation of the ESR intensity of $VOSO_4$ on silica gel with heat treatment; (a) without additional material, (b) with Na_2SO_4, (c) with $(NH_4)_2SO_4$. The content of $VOSO_4$ and of additional materials are 10 mol.% to base.

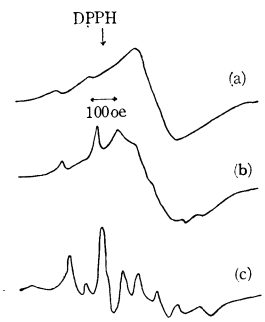

Fig. 4. The variation of ESR spectra of $VOSO_4$ on silica gel as a function of the additional quantity of Cs_2SO_4; 1) 10 mol.%, 2) 20 mol.%, and 3) 40 mol.%. $VOSO_4$ content is about 10 mol.%.

40 oe. and the splitting between the components had the value noted.

The samples containing alkali sulfate gave complicated spectra as a result of the anisotropy of g as well as that of the hyperfine structure. From the figure of the narrowing spectrum, it may be assumed that the axial symmetry exists for both g and hyperfine tensors, with $g_\perp > g_\parallel$ and with $A_\perp < A_\parallel$. Some hyperfine components which appear in the low magnetic field have highly-distorted signal shapes in the K-band measurements. On the other hand, in the X-band measurements, it is easy to obtain the value of $A_\parallel$, but difficult to determine $g_\perp$, $g_\parallel$ and $A_\perp$.

If both g and hyperfine tensors have an axial symmetry and if each ion is distributed at rondom, the ESR spectrum may be expressed as follows:[26]

25) J. A. Ibers and D. Swalen, *Phys. Rev.*, **127**, 1914 (1962).

26) T. Vänngard and R. Aasa, *Proc. First Int. Conf. Paramagnetic Resonance*, Jerusalem, 1962, Academic Press, New York (1963), p. 509.

$$I(H) = \frac{1}{(2I+1)} \sum_{m_I=-7/2}^{7/2} \int_0^1 K(\theta) \cdot S(H-H_0)^2 \cdot dz \tag{4}$$

where $z=\cos\theta$, θ and $K(\theta)$ have meanings given in Eq. 3, $S(x)$ is the shape function, and $S(H-H_0)=1/\{(H-H_0)^2+b^2\}$ for Lorentzian. Including the magnetic hyperfine interaction to the second order, the resonance field is given approximately by:

$$\begin{aligned} H_0 = {} & H_c - Km_I/g\beta - (4H_c)^{-1}(g\beta)^{-2}A_\perp{}^2 \\ & \times (A_\parallel{}^2 + K^2)K^{-2}[I(I+1) - m_I{}^2] \\ & - (2H_c)^{-1}(g\beta)^{-2}(A_\parallel{}^2 - A_\perp{}^2)^2 \\ & \times K^{-2}g_\perp{}^2g_\parallel{}^2g^{-4}z^2(1-z^2)m_I{}^2 \end{aligned} \tag{5}$$

where $H_c = h\nu/g\beta$, $g^2 = g_\perp{}^2 + (g_\parallel{}^2 - g_\perp{}^2)z^2$ and

$$K^2g^2 = A_\parallel{}^2g_\parallel{}^2z^2 + A_\perp{}^2g_\perp{}^2(1-z^2)$$

$A_\perp$ and $A_\parallel$ are hyperfine-structure constants in energy units.

By comparing the K-band spectra to the above expressions, we can obtain $g_\perp$, $A_\perp$, and $A_\parallel$, because the K-band spectra shows the characteristic signal from those crystallites which have orientations perpendicular to the magnetic field. When $z=0$, Eq. 5 becomes:

$$\begin{aligned} H_0(m_I) = {} & H_\perp - A_\perp m_I/g_\perp\beta - (4H_\perp)^{-1}(g_\perp\beta)^{-2} \\ & \times (A_\perp{}^2 + A_\parallel{}^2)(63/4 - m_I{}^2) \end{aligned}$$

where $H_\perp = h\nu/g_\perp\beta$. The results are listed in Table V.

When the quantity of alkali sulfate remains only ten percent of the base materials, the values of $g_\perp$ and $g_\parallel$ can not be determined separately, but they give an apparent value of $g : \langle g\rangle = (2g_\perp + g_\parallel)/3$. When the hyperfine splitting is so large that Eq. 5 is applicable, the values of g obtained are slightly greater than those of the sample without alkali sulfate, The values of $A_\perp$ appear to be 6.3×10^{-3} cm^{-1} for the sample with 20% cesium sulfate, and 7.5×10^{-3} cm^{-1} for that with 40% cesium sulfate.

The decrease in the ESR intensity with heat treatment is slower for the systems containing alkali sulfates than for the system without them, except for the case of ammonium salt. Alkali sulfates make the ESR of VO^{2+} insensitive to the heat treatment. They prevent the oxidation of vanadium ions from 4+ to 5+ and the formation of crystallites of vanadium(V) oxide,

VO^{2+} on an Alumina Gel Base.—Oxovanadium sulfate on an alumina gel base showed ESR spectra closely resembling those of the system of a silica base with alkali sulfate in the concentration range from 5 to 10 percent of $VOSO_4$. The addition of alkali sulfates did not have any remarkable effects. Table V shows the results obtained by the method described in the preceding section. As the concentration of $VOSO_4$ increased, the width of each hyperfine component exceed the hyperfine splitting. The ESR spectrum was observed as a broad single line which had a good symmetry.

TABLE V. ESR CONSTANTS OF $VOSO_4$ IN ALUMINA GEL AND IN SILICA WITH ALKALI SULFATES

Sample		g	Hyperfine constant	
Base	Additional material		$A_\parallel\times10^2$ cm^{-1}	$A_\perp\times10^3$ cm^{-1}
Silica	20% Cs_2SO_4			6.26
Silica	40% Cs_2SO_4	1.978	2.2	7.52
Silica	40% $(NH_4)_2SO_4$	1.980	2.0	7.52
Alumina	none	1.967	1.92	6.41
Alumina	10% Li_2SO_4	1.968	1.86	6.58
Alumina	10% Na_2SO_4	1.968	1.86	5.95
Alumina	10% $(NH_4)_2SO_4$	1.964	1.92	5.95
		1.965*		6.85*

$VOSO_4$ content: 10 mol.% of bsse material
* Measured after heat treatment at 300°C.

VO^{2+} Ions in an Aqueous Solution at 77°K.—The ESR spectra of $VOSO_4$ in aqueous solution at 77°K are shown in Fig. 5. In aqueous solutions

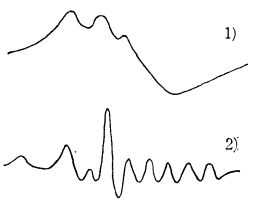

Fig. 5. ESR spectra of $VOSO_4$ in aqueous solutions observed at 77°K. 1) VO^{2+}: 0.1 mol./l., 2) VO^{2+}: 0.1 mol./l., H_2SO_4: 1 N.

containing under 0.1 N sulfulic acid, the hyperfine lines show a broadening in spite of the low concentration of $VOSO_4$. In the solutions containing over 1.0 N sulfuric acid, on the contrary, the sharp hyperfine components were clearly separated. This system can be considered to be a typical model of the random distribution of VO^{2+} ions. The values of $g_\perp$, $A_\perp$, $A_\parallel$ can be calculated by using Eq. 5; they are listed in Table VI. They are in good agreement with the results obtained from the data on an alumina gel base.

From the variation in spectra with the different concentrations of sulfuric acid, the existence of

TABLE VI. ESR CONSTANTS OF $VOSO_4$ IN AQUEOUS SOLUTIONS AT 77°K

Concentration		g	Hyperfine constant	
VO^{2+} ion mol./l.	H_2SO_4 N		$A_\parallel\times10^2$ cm^{-1}	$A_\perp\times10^3$ cm^{-1}
0.1	0.3			7.28
0.1	1.0		2.9	7.37
0.1	3.0	1.965	2.3	7.05
0.1	10.0	1.966	2.3	7.16

excess SO_4^{2-} ions may be considered to change the circumstances around VO^{2+} ion, or the coordination state of VO^{2+}.

The Effects of Base Materials and Alkali Sulfates.—Silica gel has a weaker interaction with transition metal oxides dispersed on it than has alumina gel.[27] Oxovanadium sulfate is deposited as small crystallites on silica gel, and so the ESR of VO^{2+} on silica shows the exchange narrowing.

When alkali sulfates are added to the system, double salts, $M_2 \cdot V_2O_2(SO_4)_3$, are formed[28] and the exchange between VO^{2+} ions is prevented. An excess addition of alkali sulfates bring about a dilution of the double salt and a decrease in the width of the hyperfine lines in the ESR spectrum. If the random dispersion of VO^{2+} ions is realized at an adequate concentration, an ESR with a hyperfine structure can be observed. Frozen sulfuric acid solutions of VO^{2+} are good models for this state. The spectra obtained with an alumina base are similar to those of the frozen sulfuric acid solutions. VO^{2+} ions may be considered to be combined strongly with an alumina base and to be dispersed homogeneously in the surface layers of almuina.

27) A. Matsumoto, H. Tanaka and N. Goto, This Bulletin, **38**, 45 (1965).

28) H. Remy, "Treatise on Inorganic Chemistry," Vol. II, (transland into English), Elsevier Publishing Company, Amsterdam (1956), p. 101.

Summary

The electron spin resonance spectra of oxovanadium sulfate has shown an exchange narrowing on a silica gel base as a result of the formation of small crystallites. In this case, the g factor has an axial symmetry of $g_\perp = 1.969 \pm 0.001$ and $g_\parallel = 1.915 \pm 0.005$. When alkali sulfates are added to the system, the dispersion of VO^{2+} ions on the base materials becomes homogeneous and ESR spectra with hyperfine lines appear.

On an alumina gel base, VO^{2+} ions seems to be dispersed homogeneously in the surface layers of the base, and ESR spectra show the hyperfine structure with the parameter of $A_\perp = (7.0 \pm 0.2) \times 10^{-3}\,cm^{-1}$ and $A_\parallel = (1.85 \pm 0.05) \times 10^{-2}\,cm^{-1}$. These values are slightly smaller than the value of $\langle A \rangle$, $(1.20 \pm 0.03) \times 10^{-2}\,cm^{-1}$ which has been obtained from aqueous solutions of VO^{2+}.

The authors are indebted to Messieurs Nobuhisa Goto, Kunihiko Nakamura and Hiroshi Fukunaga for their kind help in the ESR measurements and for their discussions.

BULLETIN OF THE CHEMICAL SOCIETY OF JAPAN VOL. 39 879—882 (1966)

The Reactions of the Benzil - Triethyl Phosphite Adduct

By Teruaki MUKAIYAMA and Takanobu KUMAMOTO

Tokyo Institute of Technology, Ookayama, Tokyo

(Received August 26, 1965)

The decomposition of benzil - triethyl phosphite adduct in the presence of copper powder or cupric sulfate has been studied. When benzil, triethyl phosphite and cupric sulfate were treated in boiling toluene, *cis*-dibenzoylstilbene and triethyl phosphate were obtained. When the reaction was carried out in the presence of active hydrogen compounds, such as alcohol, carboxylic acid and amine, the corresponding benzoin derivatives were obtained. Further, when the adduct was decomposed in the presence of phenyl isocyanate or dicyclohexylcarbodiimide, 3, 4, 5-triphenyl-4-oxazoline-2-one or 2-cyclohexylimino-3-cyclohexyl-4, 5-diphenyl-4-oxazoline was obtained, along with triethyl phosphate.

It has recently been found that the decomposition of the adducts of α-diketones and triethyl phosphite[2] gives disubstituted acetylenes and triethyl phosphate in good yields.[1] The reactions take place at a comparatively high temperature, that is, above 215°C.

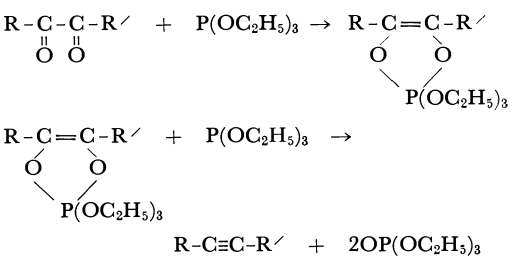

In the present experiment, several catalysts, such as copper powder and cupric sulfate, were

1) T. Mukaiyama, H. Nambu and T. Kumamoto, *J. Org. Chem.*, **29**, 2243 (1964).

2) a) F. Ramirez, R. B. Mitra and N. B. Desai, *J. Am. Chem. Soc.*, **82**, 2651 (1960). b) F. Ramirez and N. B. Desai, ibid., **85**, 3252 (1963). c) V. A. Kukhtin, K. M. Kirillora and R. R. Shagidulline, *J. Gen. Chem. USSR*, **32**, 640 (1962).

TABLE I. THE DECOMPOSITION OF BENZIL-TRIETHYL PHOSPHITE ADDUCT IN THE PRESENCE OF ACTIVE HYDROGEN COMPOUNDS

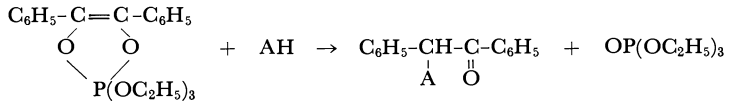

AH	Catalyst	Yield, %	C_6H_5-CH(A)-C(=O)-C_6H_5 B. p., °C (mmHg)	M. p. °C	$OP(OC_2H_5)_3$ Yield, %
CH_3OH	$CuSO_4$	11*	118—121 (0.1)	49—51	70
C_2H_5OH	$CuSO_4$	30*	141—144 (0.4)	60—61	69
n-C_3H_7OH	$CuSO_4$	24*	114—118 (0.03)	53	80
iso-C_3H_7OH	$CuSO_4$	40*	130—134 (0.2)	58	80
C_6H_5OH	$CuSO_4$	47*	160—166 (0.2)	85	96
C_6H_5COOH	$CuSO_4$	29		124—125	85
$C_6H_5NH_2$	Cu	63		97—98	71

* As the isolation of ethers of benzoin from reaction mixture was difficult, the yields of the ethers were comparatively low.

examined in order to carry out the decomposition of the adduct of benzil and triethyl phosphite at a lower temperature.

When a mixture of benzil and triethyl phosphite was refluxed in anhydrous toluene for five hours under nitrogen in the presence of anhydrous cupric sulfate, disubstituted acetylene could not be obtained, contrary to the case of the decomposition of the adduct in the absence of a catalyst. Instead, *cis*-dibenzoylstilbene and triethyl phosphate were obtained in 41% and 81% yields respectively, along with a small amount of tetraphenyl furan (18% yield).

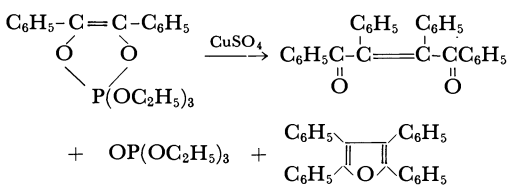

Similarly, when copper powder or mercuric chloride was used as a catalyst, *cis*-dibenzoylstilbene was obtained in a 32% or a 14% yield respectively.

These results may be explained by considering an initial formation of triethyl phosphate and phenyl benzoyl carbene[3] by the decomposition of the adduct. The carbene thus formed may in turn dimerize to form dibenzoylstilbene.

Usually, α-ketocarbene[4] is known to be unstable and to yield disubstituted ketene by a Wolff rearrangement. On the other hand, Yater[5] reported that α-ethoxy acetophenone was produced when α-diazoacetophenone was decomposed in the presence of alcohol and copper powder, but the rearranged product, the ester of phenylacetic acid, could not be obtained.

The intermediate of the decomposition of the adduct, carbene, may be demonstrated by the formation of benzoin derivatives when the adduct is decomposed in the presence of active hydrogen compounds.

Indeed, when a mixture of benzil, triethyl phosphite and ethanol was refluxed in toluene for five hours under nitrogen in the presence of anhydrous cupric sulfate, benzoin ethyl ether (30% yield) and triethyl phosphate (69% yield) were obtained, along with a small amount of *cis*-dibenzoylstilbene (5% yield) and dibenzoyldiphenyl ethane (3% yield).

Similar reactions were observed in the cases of the other alcohols and phenol (see Table I).

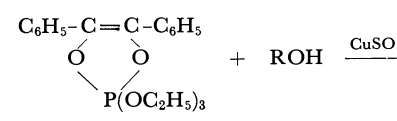

By the same method, anilino desoxybenzoin (63% yield) and benzoin benzoate (29% yield) were obtained when the adduct was treated with aniline and benzoic acid respectively.

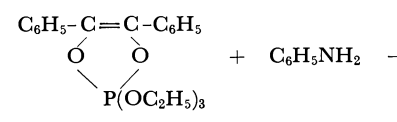

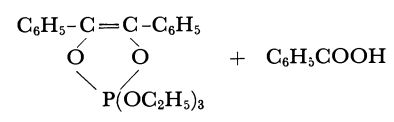

In connection with the reaction of the α-diketone - tertiary phosphite adduct with active hydrogen compounds, Ramirez et al. have

3) a) F. Ramirez, H. Yamanaka and O. H. Basedow, *J. Am. Chem. Soc.*, **83**, 173 (1961). b) P. J. Bunyan and J. I. G. Cadogan, *J. Chem. Soc.*, **1963**, 42.

4) F. Weygand and H. J. Bestmann, *Angew. Chem.*, **72**, 535 (1960).

5) P. Yater, *J. Am. Chem. Soc.*, **74**, 5376 (1952).

Table II. Reactions of 2-cyclohexylimino-3-cyclohexyl-4, 5-diphenyl-4-oxazoline and protonic acid

Acid	Yield, %	Salt of oxazoline: Formula of salt	Analysis Found (Calcd.) C	H	N	M. p., °C (Decomp. p.)
Hydrogen chloride	100	$C_{27}H_{32}N_2O \cdot HCl$	73.66 (74.11	7.82 7.56	6.26 6.41)	(234—236)
Phenylphosphonic acid	86	$C_{27}H_{32}N_2O \cdot C_6H_5PO(OH)_2$			4.90 (5.02)	191—192
p-Toluenesulfonic acid	89	$C_{27}H_{32}N_2O \cdot C_7H_7SO_3H$	70.84 (71.30	7.30 6.99	5.01 4.89)	178—180
Monochloroacetic acid	81	$C_{27}H_{32}N_2O \cdot ClCH_2CO_2H \cdot H_2O$	67.24 (67.85	7.45 7.22	5.68 5.47)	(115—120)

reported[6] that α-ketol-monophosphates resulted when α-diketone - trimethyl phosphite adducts reacted with hydrogen chloride. On the other hand, desyl chloride was obtained when the benzil - triphenyl phosphite adduct was treated with hydrogen chloride.

Also, it has recently been reported[7] by Ramirez et al. that the hydrolysis of the biacetyl - trimethyl phosphite adduct in boiling benzene gave trimethyl phosphate.

The carbene, 1, 3-dipolar intermediate, was further demonstrated by the formation of 3, 4, 5-triphenyl-4-oxazoline-2-one when benzil, triethyl phosphite and phenyl isocyanate were allowed to react in the presence of copper powder. By the above reaction, 3, 4, 5-triphenyl-4-oxazoline-2-one and triethyl phosphate were obtained in 23% and 79% yields respectively, as expected.

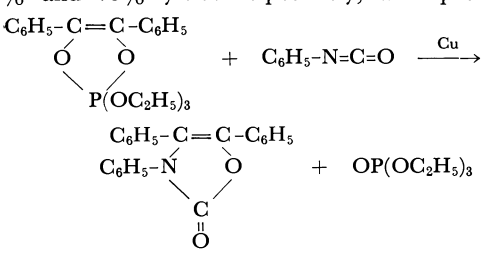

Furthermore, when the adduct was treated with dicyclohexylcarbodiimide in boiling toluene in the presence of copper powder under nitrogen, 2 - cyclohexylimino - 3 - cyclohexyl - 4, 5 - diphenyl - 4 - oxazoline (72% yield) and triethyl phosphate (89% yield) were obtained.

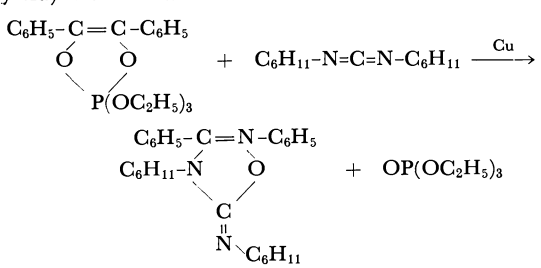

6) F. Ramirez, R. B. Mitra and N. B. Desai, ibid., **82**, 2652 (1960).

7) F. Ramirez, O. P. Madan and C. P. Smith, ibid., **87**, 670 (1965).

Next, several reactions of the oxazoline were studied. 2-Cyclohexylimino-3-cyclohexyl-4, 5-diphenyl-4-oxazoline reacts with protonic acids, such as hydrogen chloride, *p*-toluenesulfonic acid, monochloroacetic acid and phenylphosphonic acid, to form the corresponding salts in high yields (see Table II).

On the other hand, 2-cyclohexylimino-3-cyclohexyl-4, 5-diphenyl-4-oxazoline is very stable towards hydrolysis in both basic and acidic media. Further study of the reaction of the oxazoline is now in progress.

Experimental

The Decomposition of the Benzil - Triethyl Phosphite Adduct in the Presence of Cupric Sulfate.—A mixtrue of benzil (4.20 g., 0.02 mol.), triethyl phosphite (3.32 g., 0.02 mol.) and cupric sulfate (2.00 g.) was refluxed in anhydrous toluene (15 cc.) under nitrogen for 5 hr. The removal of the solvent gave a white precipitate. Its recrystallization from benzene gave *cis*-dibenzoylstilbene, 1.12 g., m. p. 215—217°C.

Found C, 86.37; H, 5.24. Calcd. for $C_{28}H_{20}O_2$: C, 86.57; H, 5.19%.

The fractional distillation of filtrate gave triethyl phosphate, 2.89 g. (81%); b. p. 113—115°C/28 mmHg. The addition of a small amount of ether to the residue also gave *cis*-dibenzoylstilbene. It was recrystallized from benzene, 0.48g., m. p. 214—216°C. The total yield of *cis*-dibenzoylstilbene was 41%.

Further, a crystalline was isolated from the residue. Its recrystallization from acetic acid gave tetraphenyl furan, 0.66 g. (18%), m. p. 173—174°C.

Found C, 90.03; H, 5.38. Calcd. for $C_{28}H_{20}O$: C, 90.29; H, 5.41%.

The Decomposition of the Benzil - Triethyl Phosphite Adduct in the Presence of Ethanol and Cupric Sulfate.—A mixture of benzil (2.10 g., 0.01 mol.), triethyl phosphite (1.66 g., 0.01mol.), ethanol (0.46 g., 0.01mol.) and cupric sulfate (1.00 g.) was refluxed in toluene (10 cc.) for 5 hr. under nitrogen. After the cupric sulfate had then been filtered off, the solvent was removed. Then a white precipitate was obtained. Recrystallization from benzene gave dibenzoyldiphenyl ethane, 0.05 g. (3%), m. p. 253—254°C. The residue was distilled in vacuo giving triethyl phosphate, 1.25 g. (69%), 114—116°C/30

mmHg, and another fraction, 1.45 g., 141—144°C/0.4 mmHg. This was a mixture of benzil and benzoin ethyl ether. By the addition of a small amount of petroleum ether, benzil was recovered, along with benzoin ethyl ether; recrystallization from ligroin gave 0.72 g. (30%); m. p. 59—61°C.

Found C, 79.63; H, 6.98. Calcd. for $C_{16}H_{16}O_2$: C, 79.97; H, 6.71%.

When to the residue of fractional distillation there was added a small amount of diethyl ether, a white precipitate was obtained. It was recrystallized from benzene to give *cis*-dibenzoylstilbene, 0.10 g. (5%); m. p. 213—215°C.

By a similar procedure, various benzoin ethers were obtained from the reactions of benzil, triethyl phosphite and alcohols.

Analogously, anilino desoxybenzoin or benzoin benzoate was obtained from the reaction of benzil, triethyl phosphite and corresponding aniline or benzoic acid (see Table I).

The Decomposition of the Benzil-Triethyl Phosphite Adduct in the Presence of Phenyl Isocyanate and Copper Powder.—A mixture of benzil (2.10 g., 0.01 mol.), triethyl phosphite (1.66 g, 0.01 mol.), phenyl isocyanate (1.19 g., 0.01 mol.) and copper powder (0.50 g.) was refluxed in toluene for 5 hr. under nitrogen. The removal of the solvent gave a white precipitate. This was recrystallized from benzene to give 3, 4, 5-triphenyl-4-oxazoline-2-one, 0.73 g. (23%); m. p. 212—213°C; mixed m. p. 213°C. The filtrate was distilled in vacuo to give triethyl phosphate, 1.43 g. (79%), b. p. 103—105°C/20 mmHg.

The Decomposition of the Benzil-Triethyl Phosphite Adduct in the Presence of Dicyclohexylcarbodiimide and Copper Powder.—A mixture of benzil (4.20 g., 0.02 mol.), triethyl phosphite (3.32 g., 0.02 mol.), dicyclohexylcarbodiimide (4.12 g., 0.02 mol.) and copper powder (1.00 g.) was refluxed in toluene (15 cc.) for 5 hr. under nitrogen. After copper powder was filtered, the solvent was removed.

The fractional distillation of the residue gave triethyl phosphate, 3.24 g. (89%); b. p. 103—106°C/18 mmHg. The addition of a small amount of ethanol to the residue gave a white precipitate. Recrystallization from ethanol gave 2-cyclohexylimino-3-cyclohexyl-4, 5-diphenyl-4-oxazoline, 5.76 g. (72%); m. p. 133—134°C.

Found C, 80.73; H, 8.28; N, 7.10. Calcd. for $C_{27}H_{32}N_2O$: C, 80.96; H, 8.05; N, 6.99%. ν_{max}^{KBr} 2925, 2855, 1673, 1648, 1595, 1500, 1444, 1363, 1342, 1047, 1020, 984, 736, 698 and 683 cm^{-1}.

The Reaction of 2-Cyclohexylimino-3-cyclohexyl-4, 5-diphenyl-4-oxazoline with Hydrogen Chloride.—Anhydrous hydrogen chloride was passed through a solution of 2-cyclohexylimino-3-cyclohexyl-4, 5-diphenyl-4-oxazoline (2.00 g., 0.005 mol.) in anhydrous ether. A white precipitate was thus obtained. This was recrystallized from ethyl acetate giving 2-cyclohexylimino-3-cyclohexyl-4, 5-diphenyl-4-oxazoline hydrochloride, 3.83 g. (100%); m. p. 234—236°C (decomp.).

By a similar procedure, various salts of 2-cyclohexylimino-3-cyclohexyl-4, 5-diphenyl-4-oxazoline were obtained from the oxazoline and *p*-toluenesulfonic acid, phenylphosphonic acid and monochloroacetic acid respectively (see Table II).

The authors wish to express their hearty thanks to Mr. Takenori Nagaoka for his help during the course of this experiment.

BULLETIN OF THE CHEMICAL SOCIETY OF JAPAN VOL. 39 882—888 (1966)

The Syntheses of Peptides Related to the *N*-Terminal Structure of Corticotropin. VII. The Synthesis of Peptide Derivatives Corresponding to Positions 11 to 18 in the Corticotropin Molecule

By Hideo Otsuka, Ken Inouye, Makoto Kanayama and Fusako Shinozaki

Biochemistry Division, Shionogi Research Laboratory, Shionogi & Co., Ltd., Fukushima-ku, Osaka

(Received August 27, 1965)

The derivatives of lysyl-prolyl-valyl-glycyl-arginyl-arginine, lysyl-prolyl-valyl-glycyl-lysyl-arginyl-arginine and lysyl-prolyl-valyl-glycyl-lysyl-lysyl-arginyl-arginine, which correspond to the amino acid sequences in positions 11—14 plus 17—18, 11—14 plus 16—18, and 11—14 plus 11—18 of the corticotropin molecule respectively, have been obtained as intermediates for the synthesis of adrenocorticotropically active peptides.

As a step toward our synthesis of the adrenocorticotropically active peptides involving a hexadecapeptide $\alpha^{1-14,17-18}$-Gly^{1}-ACTH,[1] a heptadecapeptide $\alpha^{1-14,16-18}$-Gly^{1}-ACTH-18-amide,[2] and octadecapeptides α^{1-18}-ACTH and α^{1-18}-ACTH-18-amide,[3] we prepared the peptide intermediates

1) H. Otsuka, K. Inouye, M. Kanayama and F. Shinozaki, This Bulletin, **38**, 679 (1965).

2) H. Otsuka, K. Inouye, M. Kanayama and F. Shinozaki, ibid., **38**, 1563 (1965).

3) H. Otsuka, K. Inouye, F. Shinozaki and M. Kanayama, *J. Biochem.*, **58**, 512 (1965).

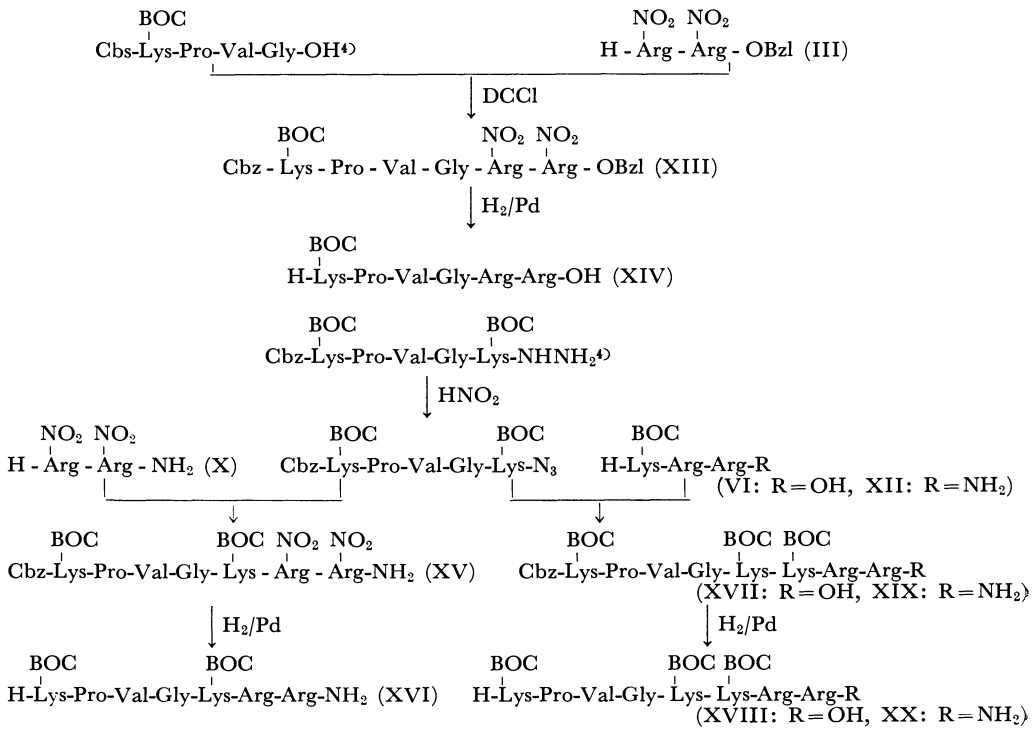

Fig. 1. Outline of the synthetic procedure for the hexapeptide, heptapeptide and octapeptide derivatives. Cbz, carbobenzoxy; BOC, *t*-butyloxycarbonyl; Bzl, Benzyl; DCCl, *N*, *N'*-dicyclohexylcarbodiimide.

corresponding to the natural and the partially-altered sequences of positions 11 to 18 in the corticotropin (ACTH) structure; namely, N^{ε}-*t*-butyloxycarbonyl - lysyl - prolyl-valyl-glycyl-arginyl-arginine (XIV), N^{ε}-*t*-butyloxycarbonyl-lysyl-prolyl-valyl-glycyl - N^{ε} - *t* - butyloxycarbonyl- lysyl-arginyl-arginine amide (XVI), and N^{ε}-*t*-butyloxycarbonyl-lysyl - prolyl - valyl - glycyl - N^{ε}- *t* -butyloxycarbonyl-lysyl -N^{ε}- *t* - butyloxycarbonyl -lysyl-arginyl-arginine (XVIII) and its amide (XX).*1

An outline of the synthetic procedure is shown in Fig. 1. The heptapeptide (XV) and the octapeptides (XVII and XIX) were built by the idea of the coupling of Lys-Pro-Val-Gly-Lys with Arg-Arg and with Lys-Arg-Arg respectively, while the hexapeptide (XIII) was prepared from Lys-Pro-Val-Gly and Arg-Arg. The synthesis of the sequences of Lys-Pro-Val-Gly and Lys-Pro-Val-Gly-Lys has already been reported.[4] Therefore, we wish to describe here the synthesis of arginyl-arginine and lysyl-arginyl-arginine fragments. We wish also to describe in detail the procedures for preparing the longer peptides from them.

The Synthesis of the Hexapeptide Derivative (XIV).—Attempts to synthesize the nitroarginine benzyl ester were made by three different methods as follows:

(1) H-Arg(NO_2)-OH + $C_6H_5CH_2OH$
$\xrightarrow{CH_3C_6H_4SO_3H}$ H-Arg(NO_2)-OBzl·$CH_3C_6H_4SO_3H$

(2) BOC-Arg(NO_2)-OH + $C_6H_5CH_2Cl$
$\xrightarrow{\text{triethylamine}}$ BOC-Arg(NO_2)-OBzl
$\xrightarrow{CF_3COOH}$ H-Arg(NO_2)-OBzl·CF_3COOH

(3) Cbz-Arg(NO_2)-OH
$\xrightarrow[\text{in dioxane}]{PCl_5}$ NH-Arg(NO_2)-CO (CO—O)
$\xrightarrow{HCl/C_6H_5CH_2OH}$ H-Arg(NO_2)-OBzl·HCl

In each case, no salt of the ester was crystallized. Of these methods, the first one was found to be the most convenient and to give a moderate yield. The *t*-butyloxycarbonyl-nitroarginine benzyl ester, which was obtained as an intermediate in the second method, was homogeneous in thin-layer chromatography (R_f=0.61, ethyl acetate - methanol (95 : 5)), but it also resisted all attempts at crystallization. In the third method, it seemed that the nitroguanidino function did not decompose upon the treatment with phosphorus pentachloride.

The nitroarginine benzyl ester *p*-toluenesulfonate (I) was, after having been converted into the free

*1 All amino acid residues are of the L-configuration, with the exception of glycine.

4) H. Otsuka, K. Inouye and Y. Jono, This Bulletin, **37**, 1471 (1964).

base, combined with *t*-butyloxycarbonyl-nitroarginine to give the *t*-butyloxycarbonyl-nitroarginyl-nitroarginine benzyl ester (II), which failed to crystallize. Compound II was, however, found by thin-layer chromatography to be homogeneous. The *t*-butyloxycarbonyl group was removed with the trifluoroacetic acid treatment; the nitroarginyl-nitroarginine benzyl ester trifluoroacetate (III) was thus obtained. This was then coupled with N^{α}-carbobenzoxy-N^{ε}-*t*-butyloxycarbonyl-lysyl-prolyl-valyl-glycine[4] by the *N*, *N'*-dicyclohexylcarbodiimide (DCCl) procedure, thus affording a hexapeptide derivative, the N^{α}-carbobenzoxy-N^{ε}-*t*-butyloxycarbonyl-lysyl-prolyl-valyl-glycyl-nitroarginyl-nitroarginine benzyl ester (XIII). Compound XIII crystallized with a 90 per cent yield. The catalytic hydrogenolysis of XIII gave a partially protected hexapeptide N^{ε}-*t*-butyloxycarbonyl-lysyl-prolyl-valyl-glycyl-arginyl-arginine diacetate (XIV), which was homogeneous in paper chromatography.

The Synthesis of the Heptapeptide Amide Derivative (XVI).—Carbobenzoxy-nitroarginine was treated with ethylchloroformate and tri-*n*-butylamine in a tetrahydrofuran solution in order to convert it into a mixed anhydride, which was then allowed to react with a small excess of aqueous ammonia to produce carbobenzoxy-nitroarginine amide (VII) in an 81 per cent yield. Compound VII crystallized readily from aqueous ethanol and had a melting point of 220—221°C. Van Orden and Smith gave a m. p. of 219—220°C for the same compound.[5] The treatment of VII with hydrogen bromide in acetic acid gave the crystalline monohydrobromide of nitroarginine amide (VIII) in an 85 per cent yield. Carbobenzoxy-nitroarginine and VIII were coupled by the mixed anhydride procedure to produce carbobenzoxy-nitroarginyl-nitroarginine amide (IX), which crystallized from dimethylformamide, combining two molecules of the solvent. The carbobenzoxy group was removed from compound IX by hydrogen bromide in acetic acid. The resultant dipeptide amide nitroarginyl-nitroarginine amide monohydrobromide (X) failed to crystallize, but it was found by paper chromatography to be homogeneous. Compound X was then added to an aqueous tetrahydrofuran solution of N^{α}-carbobenzoxy-N^{ε}-*t*-butyloxycarbonyl-lysyl-prolyl-valyl-glycyl-N^{ε}-*t*-butyloxycarbonyl-lysine azide, which was derived from the corresponding hydrazide;[4] they were then allowed to react in the presence of sufficient triethylamine to produce a hyptapeptide derivative N^{α}-carbobenzoxy-N^{ε}-*t*-butyloxycarbonyl-lysyl-prolyl-valyl-glycyl-N^{ε}-*t*-butyloxycarbonyl-lysyl-nitro-arginyl-nitroarginine amide (XV). A pure sample of compound XV, which was easily obtained by reprecipitation from *n*-butanol in a moderate yield (66%), was found by thin-layer chromatography to be homogeneous. The catalytic hydrogenolysis of XV yielded the partially protected heptapeptide amide N^{ε}-*t*-butyloxycarbonyl-lysyl-prolyl-valyl-glycyl-N^{ε}-*t*-butyloxycarbonyl-lysyl-arginyl-arginine amide triacetate (XVI), which had no absorption in the 250—390 mμ region and which gave a single ninhydrin and Sakaguchi reactive spot on paper.

In our previous communication, N^{α}-carbobenzoxy-N^{ε}-*t*-butyloxycarbonyl-lysyl-prolyl-valyl-glycyl-N^{ε}-*t*-butyloxycarbonyl-lysine methyl ester was synthesized from the carboxyl terminal by a step-by-step procedure.[4] Now this protected pentapeptide has also been obtained in an excellent yield (86%) by the DCCl-mediated condensation from N^{α}-carbobenzoxy-N^{ε}-*t*-butyloxycarbonyl-lysyl-prolyl-valyl-glycine[4] and the N^{ε}-*t*-butyloxycarbonyl-lysine methyl ester.[5] The product was found to be identical with that obtained previously.

The Synthesis of the Octapeptide Derivatives (XVIII and XX).—The N^{α}-carbobenzoxy-N^{ε}-*t*-butyloxycarbonyl-lysine *N*-hydroxysuccinimide ester (XI), which had been prepared from the diacyllysine and *N*-hydroxysuccinimide by the DCCl-mediated reaction,[6] was utilized for the synthesis of the Lys-Arg-Arg sequence. Compound XI was allowed to react with III and with X, each of which had been neutralized with triethylamine, in aqueous tetrahydrofuran to yield, respectively, the benzyl ester (V) and the amide (XI) of N^{α}-carbobenzoxy-N^{ε}-*t*-butyloxycarbonyl-lysyl-nitroarginyl-nitroarginine in 70 per cent yields. Compound XI was also obtained by the mixed anhydride procedure, and the product was identical in optical rotation to that obtained by the active ester method. Compounds V and XI were hydrogenolyzed to obtain the partially deblocked tripeptides, N^{ε}-*t*-butyloxycarbonyl-lysyl-arginyl-arginine diacetate (VI) and N^{ε}-*t*-butyloxycarbonyl-lysyl-arginyl-arginine amide triacetate (XII) respectively. Both of these were found by paper chromatography to be homogeneous.

The reaction of the pentapeptide azide with the partially deblocked tripeptide VI or XII proceeded smoothly, affording an octapeptide, N^{α}-carbobenzoxy-N^{ε}-*t*-butyloxycarbonyl-lysyl-prolyl-valylglycyl-N^{ε}-*t*-butyloxycarbonyl-lysyl-N^{ε}-*t*-butyloxycarbonyl-lysyl-arginyl-arginine (XVII) or its amide (XIX). The octapeptides XVII and XIX, which were purified by simple extraction (see "Experimental") were, found to be homogeneous to ninhydrin and Sakaguchi reagent in thin-layer chromatography. Judging from the number of positive charges, compounds XVII and XIX would form the monoacetate and the diacetate, respectively, if they were isolated from the aqueous acetic acid solutions. It was, however, a fact that compound XVII combined with one molecule of acetic acid, whereas the acid was not detected in XIX, when

5) H. van Orden and E. L. Smith, *J. Biol. Chem.*, **208**, 751 (1954).

6) G. W. Anderson, J. E. Zimmerman and F. M. Callahan, *J. Am. Chem. Soc.*, **86**, 1839 (1964); **85**, 3039 (1963).

they had been dried ordinarily (at 60°C in vacuo). Compounds XVII and XIX were then submitted to catalytic hydrogenolysis, which gave N^{ε}-*t*-butyloxycarbonyl-lysyl-prolyl-valyl-glycyl-N^{ε}-*t*-butyloxycarbonyl-lysyl-N^{ε}-*t*-butyloxycarbonyl-lysyl-arginyl-arginine (XVIII) and its amide (XX) respectively. Compound XX was obtained as the triacetate, but XVIII did not contain so much acetic acid as had been expected theoretically. This anomalous phenomenon, which has been observed only with the octapeptides, may suggest that they possess a certain kind of unusual conformation within their molecules. Compound XX was homogeneous in paper chromatography, but XVIII was found to be contaminated by a trace of impurity, which had a little higher R_f value than that of XVIII.

Table I. Compositions of basic amino acids in acid hydrolysates of the hexapeptide (XIV), heptapeptide(XVI) and octapeptides (XVIII and XX)

Acid hydrolysate of	Molar ratio of basic amino acids		
	Lys	Arg	NH_2
Compound XIV	1.00 (1)	1.99 (2)	0.17 (0)
Compound XVI	2.00 (2)	1.96 (2)	1.13 (1)
Compound XVIII	3.00 (3)	1.96 (2)	0.33 (0)
Compound XX	3.00 (3)	2.11 (2)	1.23 (1)

Numbers in parentheses are theoretical values.

The compositions of basic amino acids in the acid hydrolysates of the synthesized peptide derivatives (XIV, XVI, XVIII and XX) were determined by an automatic analyzer.[7] The results are shown in Table I, where it may be found that the heptapeptide (XVI) and the octapeptide (XX) each contain one amide group per molecule, as was expected.

Experimental

All melting points are uncorrected.

Nitroarginine Benzyl Ester *p*-Toluenesulfonate (I).—A mixture of 10.96 g. (0.05 mol.) of nitroarginine and 14.25 g. (0.075 mol.) of *p*-toluene-sulfonic acid monohydrate in 100 ml. of benzyl alcohol was stirred at 100°C. To this solution 50 ml. portions of carbon tetrachloride were added at about 40-min. intervals and then allowed to distill out. After five hours the reaction mixture was cooled, and 500 ml. of anhydrous ether was introduced. The supernatant was removed by decantation, and the sirupy residue was thoroughly washed with ether and dried in vacuo, thus affording 25.3 g. of the crude ester *p*-toluenesulfonate.

A 5 g. sample of the crude product was dissolved in 20 ml. of *n*-butanol, which had been saturated with water, and the solution was washed three times with water and evaporated at 45°C in vacuo to give an oily residue. The pure material was precipitated by the addition of ether; 4.36 g. (91.7% based on nitroarginine used); a highly hygroscopic powder, $[\alpha]_D^{25.5}$ $-1.4\pm1°$ (*c* 1.970, methanol). A single ninhydrin reactive spot was visible on paper, at $R_f=0.83$ (BAPW).*2

Found: C, 49.98; H, 5.71; N, 12.77; S, 7.06. Calcd. for $C_{13}H_{19}N_5O_4\cdot C_7H_8O_3S$: C, 49.89; H, 5.65; N, 14.54; S, 6.65%.

***t*-Butyloxycarbonyl-nitroarginyl-nitroarginine Benzyl Ester (II).**—Compound I (4.10 g., 8.5 mmol.) in water-*n*-butanol-ethyl acetate (1 : 1 : 4) was cooled in an ice-bath; to this 5 ml. of ice-cold 50% potassium carbonate was added, and the mixture was shaken vigorously. The aqueous phase was extracted again with *n*-butanol-ethyl acetate (1 : 4). The organic extracts were combined, washed with water, dried over anhydrous sodium sulfate, and concentrated in vacuo. The nitroarginine benzyl ester (free base) was precipitated by the addition of ether; 1.88 g. (71.6%).

This free ester (1.88 g.) and 1.815 g. (5.0 mmol.) of *t*-butyloxycarbonyl-nitroarginine[9] were dissolved in 10 ml. of dimethylformamide. To this solution there was then added 1.03 g. (5.0 mmol.) of *N*, *N'*-dicyclohexylcarbodiimide (DCCl), dissolved in 15 ml. of methylene chloride, and the reaction mixture was allowed to stand in a refrigerator overnight. After the *N*, *N'*-dicyclohexylurea (DCU) had been removed, the filtrate was evaporated at 40—45°C in vacuo. The resultant sirupy residue was dissolved in *n*-butanol-ethyl acetate (1 : 2), and the solution was washed successively with water, ice-cold N hydrochloric acid, M sodium bicarbonate and water, dried over anhydrous sodium sulfate, and evaporated in vacuo. The desired dipeptide was then precipitated from *n*-butanol as an amorphous solid; 2.42 g. (79.2%), $[\alpha]_D^{25}$ $-18.1\pm1°$ (*c* 2.487, methanol). A single spot was visible in thin-layer chromatography, at $R_f=0.40$ (Silica-gel G, methanol-ethyl acetate (15 : 85)).

Found: C, 47.68; H, 6.78; N, 21.42. Calcd. for $C_{24}H_{38}N_{10}O_9$: C, 47.21; H, 6.27; N, 22.94%.

Nitroarginyl-nitroarginine Benzyl Ester-Trifluoroacetate (III).—Compound II (0.916 g., 1.5 mmol.) was dissolved in trifluoroacetic acid, and the solution was allowed to stand at room temperature for 60 min., after which time the dipeptide ester trifluoroacetate was precipitated by the addition of anhydrous ether; 0.892 g. (95.2%).

Found: C, 40.76; H, 5.80; N, 21.57. Calcd. for $C_{19}H_{30}N_{10}O_7\cdot CF_3COOH$: C, 40.39; H, 5.00; N, 22.43%.

***N*$^{\alpha}$-Carbobenzoxy-*N*$^{\varepsilon}$-*t*-butyloxycarbonyl-lysine *N*-Hydroxysuccinimide Ester (IV).**—To a solution of N^{α}-carbobenzoxy-N^{ε}-*t*-butyloxycarbonyl-lysine (prepared from 5.62 g. (0.01 mol.) of the dicyclohexylamine-salt)[4] and 1.15 g. (0.01mol.) of *N*-hydroxy-succinimide in acetonitrile 2.06 g. (0.01 mol.) of DCCl was added, and the mixture was kept in a refrigerator overnight. After the urea had been removed by filtration, the filtrate was evaporated in vacuo to give a sirupy residue. An ethyl acetate solution of the residue was washed succesively with ice-cold N hydrochloric acid, water, M sodium bicarbonate and water, and dried over anhydrous sodium sulfate. The removal of the solvent yielded a sirupy residue, which crystallized from ethyl

7) D. H. Spackman, W. H. Stein and S. Moore, *Anal. Chem.*, **30**, 1191 (1958).

*2 BAPW = *n*-butanol-acetic acid-pyridine-water (30 : 6 : 20 : 24 by volume).[8]

8) S. G. Waley and J. Watson, *Biochem. J.*, **55**, 328 (1953).

9) K. Inouye, This Bulletin, **38**, 1148 (1965).

acetate - isopropyl ether; 4.58 g. (95.8%), m. p. 91—94°C. Recrystallization from the same solvent gave 4.00 g. (83.7%); m. p. 94.5—95.5°C, $[\alpha]_D^{27.5}$ −14.8 ±1° (*c* 1.770, dioxane).

Found: C, 57.73; H, 6.73; N, 8.93. Calcd. for $C_{23}H_{31}N_3O_8$: C, 57.85; H, 6.54; N, 8.80%.

N^{α}-Carbobenzoxy-N^{ε}-*t*-butyloxycarbonyl-lysyl-nitroarginyl-nitroarginine Benzyl Ester (V).—The dipeptide ester trifluoroacetate (III, 0.843 g., 1.35 mmol.) was dissolved in 10 ml. of 90% tetrahydrofuran, and then 0.38 ml. (2.7 mmol.) of triethylamine was added. After this solution had been cooled in an ice bath, 0.645 g. (1.35 mmol.) of IV was added, and the mixture was kept in a refrigerator overnight. After the solvent had been removed, the residue was redissolved in *n*-butanol - ethyl acetate - water (3 : 2 : 1) and the organic phase was washed successively with ice-cold N hydrochloric acid, water, 5% sodium bicarbonate and saturated sodium chloride, dried over anhydrous sodium sulfate, and evaporated in vacuo to give a gelatinous mass. This was reprecipitated from hot acetonitrile to give the desired tripeptide as an amorphous solid; 0.88 g. (74.5%), $[\alpha]_D^{24}$ −20.3 ± 1° (*c* 2.112, methanol).

Found: C, 51.99; H, 6.84; N, 19.00. Calcd. for $C_{38}H_{56}N_{12}O_{12}$: C, 52.28; H, 6.47; N, 19.26%.

N^{ε}-*t*-Butyloxycarbonyl-lysyl-arginyl-arginine Diacetate (VI).—Compound V (0.740 g.) was hydrogenolyzed in a 90% acetic acid solution in the presence of palladium catalyst at room temperature and at atmospheric pressure for 6.5 hr. After the catalyst had been removed by filtration, the filtrate was evaporated in vacuo to give a sirupy residue, which was lyophilized to afford a colorless powder; 0.578 g., $[\alpha]_D^{24}$ +5.3±1° (*c* 2.132, 50% acetic acid). A single ninhydrin and Sakaguchi reactive spot was visible on paper, at R_f= 0.51 (BAPW).

Carbobenzoxy-nitroarginine Amide (VII).—Carbobenzoxy-nitroarginine (17.67 g., 0.05 mol.) and 13.1 ml. (0.055 mol.) of tri-*n*-butylamine were dissolved in 130 ml. of anhydrous tetrahydrofuran. To this solution 5.3 ml. (0.055 mol.) of ethyl chloroformate was added drop by drop at an ice-salt bath temperature. After 10 min. aqueous 28% ammonia (9.6 ml.) was introduced, and the mixture was stirred for 2 hr. at 0°C. The precipitates which formed were filtered off, washed with tetrahydrofuran and ether, and dried in vacuo (19.31 g.). These precipitates crystallized from aqueous ethanol to give pure VII; 14.26 g. (80.9%), m. p. 217—219°C. A sample was recrystallized from the same solvent for analyses; there was a recovery of 92.4%, m. p. 220—221°C, $[\alpha]_D^{24}$ +4.9 ± 1° (*c* 1.946, dimethylformamide). The lit.[5] m. p. 219—220°C, $[\alpha]_D$ not given.

Found: C, 47.40; H, 5.75; N, 24.10. Calcd. for $C_{14}H_{20}N_6O_5$: C, 47.72; H, 5.72; N, 23.85%.

Nitroarginine Amide Hydrobromide (VIII).—To 1.06 g. of VII there was added 8 g. of 40% (w/w) hydrogen bromide in acetic acid; the mixture stood at room temperature for 30 min., after which time anhydrous ether (30 ml.) was introduced. The resultant precipitates were filtered off, washed with anhydrous ether, and dried to give the dihydrobromide as a hygroscopic powder (1.18 g.), which changed to the monohydrobromide upon crystallization from aqueous ethanol; 0.764 g. (85.2%), m. p. 237—239°C. Recrystallization from the same solvent did not alter the melting point; $[\alpha]_D^{26}$ +13.7±0.5° (*c* 2.550, water). A single ninhydrin reactive spot was visible on paper, at R_f=0.38—0.39 (BAPW).

Found: C, 24.09; H, 5.22; N, 28.21; Br, 26.83. Calcd. for $C_6H_{14}N_6O_3$·HBr: C, 24.09; H, 5.05; N, 28.10; Br, 26.71%.

Carbobenzoxy-nitroarginyl-nitroarginine Amide (IX).—Carbobenzoxy-nitroarginine (7.07 g., 0.02 mol.) was converted into the mixed anhydride in a tetrahydrofuran solution by the same procedure as was employed for the preparation of compound VII. After 20 min. an ice-cold solution of 5.99 g. (0.02 mol.) of VIII and 4.77 ml. (0.02 mol.) of tri-*n*-butylamine in 20 ml. of water and 140 ml. of dioxane was added, and the mixture was stirred for 2 hr. at 0°C. The separated precipitates were filtered off, washed with dioxane and ether, and dried in vacuo to give 13.2 g. (92.1%) of the crude dipeptide amide; m. p. 116—119°C. Recrystallization from hot dimethylformamide gave fine needles which seemed to combine two molecules of dimethylformamide as the crystallization solvent; 9.49 g. (66.1%), m. p. 115—115.5°C, $[\alpha]_D^{25}$ −6.2±1° (*c* 2.165, 50% acetic acid).

Found: C, 43.40; H, 6.75; N, 25.42. Calcd. for $C_{20}H_{31}N_{11}O_8$·2HCON$(CH_3)_2$·H_2O: C, 43.51; H, 6.60; N, 25.37%.

Nitroarginyl-nitroarginine Amide Hydrobromide (X).—To 5.74 g. (8.0 mmol.) of compound IX there was added 70 g. of 40% (w/w) hydrogen bromide in acetic acid; the mixture stood at room temperature for 40 min., after which time anhydrous ether (150 ml.) was introduced. The resultant precipitates, which were highly hygroscopic, were reprecipitated from aqueous ethanol; 4.21 g. (96.4%), m. p. 147—155°C (decomp.). Reprecipitation from the same solvent gave 3.95 g. (90.5%) of a colorless powder; m. p. 153.5—156°C (decomp.), $[\alpha]_D^{23.5}$ +14.1±1° (*c* 2.026, water). A single ninhydrine reactive spot was visible in paper chromatography, at R_f=0.33 (BAPW).

Found: N, 28.83; Br, 14.24. Calcd. for $C_{12}H_{25}N_{11}O_6$·HBr·C_2H_5OH: N, 28.25; Br, 14.65%.

N^{α}-Carbobenzoxy-N^{ε}-*t*-butyloxycarbonyl-lysyl-nitroarginyl-nitroarginine Amide (XI).—*By the N-Hydroxysuccinimide Ester.*[6]—To a solution of 1.41 g. (2.5 mmol.) of compound X and 1.16 ml. (6.25 mmol.) of tri-*n*-butylamine in a mixture of 3.5 ml. of water and 9 ml. of tetrahydrofuran, 1.19 g. (2.5 mmol.) of the *N*-hydroxysuccinimide ester (IV) was added ; the mixture was then left to stand at room temperature for 4 hr. The solvent was removed by evaporation in vacuo, and the residue was dissolved in a mixture of water, *n*-butanol and ethyl acetate (2 : 1 : 2). The organic phase was washed successively with ice-cold N hydrochloric acid, water, and M sodium bicarbonate, and dried over anhydrous sodium sulfate. After the solvent had been removed by evaporation, a sirupy residue was redissolved in hot *n*-butanol. The protected tripeptide, which separated upon cooling, was collected, washed with cold *n*-butanol and ether, and dried; 1.75 g. (87.4%). Reprecipitation from hot *n*-butanol gave 1.44 g. (71.8%) of a pure material; m. p. 111—114°C, $[\alpha]_D^{25.5}$ −15.4±1° (*c* 2.092, methanol). Thin-layer chromatography gave a single ninhydrin reactive spot when the chromatographed plate had been treated with hydrochloric acid, at R_f=0.45

(Silica-gel G, methanol - ethyl acetate (25 : 75)).

Found: C, 46.83; H, 6.88; N, 22.51. Calcd. for $C_{31}H_{51}N_{13}O_{11}\cdot H_2O$: C, 46.55; H, 6.68; N, 22.77%.

By the Mixed Anhydride Procedure.—To a solution of N^{α}-carbobenzoxy-N^{ε}-*t*-butyloxycarbonyl-lysine (prepared from 1.12 g. (2.0 mmol.) of the dicyclohexylamine salt)[4] and 0.48 ml. of tri-*n*-butylamine in 10 ml. of anhydrous tetrahydrofuran, 0.19 ml. (2.0 mmol.) of ethyl chloroformate was added at an ice-salt bath temperature (ca. −10°C). After the mixture had been stirred for 15 min., a solution of nitroarginyl-nitroarginine amide hydrobromide and 0.57 ml. (2.4 mmol.) of tri-*n*-butylamine in 2 ml. of water and 14 ml. of tetrahydrofuran was added. The reaction mixture was stirred for one hour at 0°C and then allowed to stand at room temperature for 3 hr. The solvent was removed by evaporation in vacuo to give a sirupy residue, to which were added 5 ml. of *n*-butanol, 10 ml. of ethyl acetate and 5 ml. of water. The aqueous phase was extracted twice with *n*-butanol - ethyl acetate (1 : 2). The organic extracts were combined, washed successively with ice-cold N hydrochloric acid, M sodium bicarbonate and water, dried quickly over anhydrous sodium sulfate, and evaporated in vacuo at 40—45°C. The residue was reprecipitated from hot *n*-butanol to give the desired tripeptide; 1.05 g. (65.6%), m. p. 110—120°C, $[\alpha]_D^{24.5}$ −15.5±1° (*c* 2.046, methanol), homogeneous in thin-layer chromatography.

Found: C, 46.19; H, 6.74; N, 22.27. Calcd. for $C_{31}H_{51}N_{13}O_{11}\cdot H_2O$: C, 46.55; H, 6.68; N. 22.77%.

N^{ε}-*t*-Butyloxycarbonyl-lysyl-arginyl-arginine Amide Triacetate (XII).—Compound XI (1.00 g.) in 90% acetic acid was hydrogenolyzed in the presence of a palladium catalyst at room temperature and at atmospheric pressure for 5 hr. After the catalyst had been removed by filtration, the filtrate was evaporated in vacuo and the residue was lyophilized to give a colorless powder; 0.913 g., $[\alpha]_D^{23.5}$ +2.7±2° (*c* 1.318, 50% acetic acid). A single ninhydrin and Sakaguchi reactive spot was visible on paper, at R_f=0.51 (BAPW).

Found: C, 46.73; H, 8.06; N, 19.99; CH_3CO. 16.24. Calcd. for $C_{23}H_{47}N_{11}O_5\cdot 3CH_3COOH\cdot 2H_2O$: C, 45.01; H, 8.21; N, 19.91; CH_3CO, 16.69%.

N^{α}-Carbobenzoxy-N^{ε}-*t*-butyloxycarbonyl-lysyl-prolyl-valyl-glycyl-nitroarginyl-nitro-arginine Benzyl Ester (XIII).—The dipeptide benzyl ester trifluoroacetate (III) (1.29 g., 2.0 mmol.) in *n*-butanol - methylene chloride (1 : 1) was treated with 50% potassium carbonate at 0°C. The organic phase was, after being dried over anhydrous sodium sulfate, concentrated in vacuo. The free ester of the dipeptide solidified upon the addition of ether. The dipeptide ester thus obtained and 1.11 g. (1.75 mmol.) of N^{α}-carbobenzoxy-N^{ε}-*t*-butyloxycarbonyl-lysyl-prolyl-valyl-glycine[4] were dissolved in dimethylformamide, and to this solution there was added a methylene chloride solution of 0.361 g. (1.75 mmol.) of DCCl at 0°C. The reaction mixture was then allowed to stand in a refrigerator for 40 hr. The DCU which formed was filtered off and the filtrate was evaporated in vacuo. The residue was dissolved in 2 ml. of *n*-butanol and 20 ml. of ethyl acetate, and the solution was washed with ice-cold N hydrochloric acid, water, M sodium bicarbonate and with saturated sodium chloride, dried over anhydrous sodium sulfate, and evaporated in vacuo at 40—45°C. The resultant foamy residue crystallized from acetonitrile and ethyl acetate; 1.62 g. (92.8%), m. p. 113—115°C. Recrystallization from the same solvent system gave the pure hexapeptide derivative; 1.49 g. (85.2%), m. p. 114—115°C, $[\alpha]_D^{25}$ −49.4±1° (*c* 1.986, methanol). A single spot was detected in thin-layer chromatography, at R_f=0.36 (Silica-gel G, methanol - ethyl acetate (15 : 85)).

Found: C, 52.54; H, 6.49; N, 18.52. Calcd. for $C_{50}H_{75}N_{15}O_{15}\cdot H_2O$: C, 52.48; H, 6.78; N, 18.36%.

N^{ε}-*t*-Butyloxycarbonyl-lysyl-prolyl-valyl-glycyl-arginyl-arginine Diacetate (XIV).—Compound XIII (0.687 g.) was hydrogenolyzed in 90% acetic acid in the usual manner for 8 hr. After the catalyst had been removed, the solvent was removed by evaporation in vacuo, and the residue was then lyophilized; 0.586 g. (100%), $[\alpha]_D^{26.5}$ −50.1±1.5° (*c* 1.565, 50% acetic acid).

Found: N, 19.51; CH_3CO, 9.68. Calcd. for $C_{35}H_{65}N_{13}O_9\cdot 2CH_3COOH$: N, 19.54; CH_3CO, 9.24%.

N^{α}-Carbobenzoxy-N^{ε}-*t*-butyloxycarbonyl-lysyl-prolyl-valyl-glycyl-N^{ε}-*t*-butyloxycarbonyl-lysyl-nitroarginyl-nitroarginine Amide (XV).—A solution of 0.876 g. (1.0 mmol.) of N^{α}-carbobenzoxy-N^{ε}-*t*-butyloxycarbonyl-lysyl-prolyl-valyl-glycyl-N^{ε}-*t*-butyloxycarbonyl-lysine hydrazide[4] in 10 ml. of 90% tetrahydrofuran was chilled in an ice-salt bath, and to this 2.5 ml. of ice-cold N hydrochloric acid and 0.55 ml. of ice-cold 2M sodium nitrite were added. After five minutes the mixture was made neutral by the addition of 0.35 ml. of triethylamine. To this mixture there was then added an ice-cold solution o 0.569 g. (1.0 mmol.) of compound X and 0.168 ml. (1.2 mmol.) of triethylamine in 1.5ml. of water and 7.5 ml. of tetrahydrofuran; the reaction mixture was stirred at 0—4°C for 40 hr. After most of the solvent had been removed by evaporation at 30°C, 10ml. of water, 10 ml. of ethyl acetate and 5 ml. of *n*-butanol were added and the mixture was shaken vigorously. The organic phase which separated was cooled in an ice-bath, washed successively with ice-cold N hydrochloric acid, water, and M sodium bicarbonate, dried quickly over anhydrous sodium sulfate, and evaporated at 40—45°C in vacuo. The residue was dissolved in about 20 ml. of hot *n*-butanol, and the solution was refrigerated overnight. The precipitates which separated were collected, washed with cold *n*-butanol, ethyl acetate and ether, and dried in vacuo to give the pure heptapeptide derivative; 0.856 g. (65.6%), m. p. 133—135°C, $[\alpha]_D^{25.5}$ −40.4±1° (*c* 1.751, methanol). A single spot was detected in thin-layer chromatography, at R_f= 0.42 (Silica-gel G, methanol - ethyl acetate (25 : 75)).

Found: C, 49.76; H, 7.29; N, 19.31. Calcd. for $C_{54}H_{90}N_{18}O_{17}\cdot 2^1/_2H_2O$: C, 49.57; H, 7.32; N,19.27.

N^{ε}-*t*-Butyloxycarbonyl-lysyl-prolyl-valyl-glycyl-N^{ε}-*t*-butyloxycarbonyl-lysyl-arginyl-arginine Amide Triacetate (XVI).—Compound XV (0.75 g.) was hydrogenolyzed in 90% acetic acid in the presence of palladium black for 8 hr. After the catalyst had been removed, the filtrate was evaporated in vacuo to give an oily residue. In order to remove the remaining acetic acid, this residue was dissolved in *n*-butanol and evaporated again in vacuo. The resultant residue was dissolved in water, and the aqueous solution was concentrated to a small volume in order to remove a trace of *n*-butanol, and then lyophilized to give a colorless fluffy powder; 0.747 g. (100%), $[\alpha]_D^{24}$ −44.8

$\pm 1°$ (c 1.530, 50% acetic acid). A single ninhydrin and Sakaguchi reactive spot was visible on paper, at $R_f=0.69$ (BAPW).

Found: N, 17.79; CH_3CO, 11.10. Calcd. for $C_{46}H_{86}N_{16}O_{11}\cdot 3CH_3COOH\cdot 2H_2O$: N, 17.85; CH_3CO, 10.29%.

N^{α}-Carbobenzoxy-N^{ε}-*t*-butyloxycarbonyl-lysyl-prolyl-valyl-glycyl-N^{ε}-*t*-butyloxycarbonyl-lysyl-N^{ε}-*t*-butyloxycarbonyl-lysyl-arginyl-arginine Monoacetate (XVII).—To a solution of the protected pentapeptide azide (prepared from 0.876 g. (1.0 mmol.) of N^{α}-carbobenzoxy-N^{ε}-*t*-butyloxycarbonyl-lysyl-prolyl-valyl-glycyl-N^{ε}-*t*-butyloxycarbonyl-lysine hydrazide[4] by the procedure described in the synthesis of compound XV) there was added an ice-cold solution of 0.527 g. (0.76 mmol.) of compound VI, which had been dissolved in 1.5 ml. of water and 6.0 ml. of tetrahydrofuran containing 0.21 ml. (1.52 mmol.) of triethylamine. The reaction mixture was then stirred at 0—4°C for 56 hr. After the solvent had been removed by evaporation, the residue was dissolved in 10 ml. of N acetic acid, and the solution was extracted four times with ethyl acetate. The ethyl acetate extracts were then combined and concentrated to about 20 ml. in vacuo. The resultant concentrate was extracted four times with N acetic acid. The equeous extracts were combined and concentrated to about 10 ml. at 40—45°C in vacuo. The resultant aqueous solution was extracted four times with *n*-butanol which had been saturated with water. The butanol extracts were pooled, dried over anhydrous sodium sulfate, and evaporated at 40—45°C in vacuo. The foamy residue was then lyophilized to give a colorless fluffy powder; 0.587 g. (52.8%), $[\alpha]_D^{25.5}$ $-46.1\pm 2°$ (c 1.044, 50% acetic acid). Paper chromatography, $R_f=0.92$ (BAPW).

Found: C, 50.66; H, 8.32; N, 15.32; CH_3CO, 2.80. Calcd. for $C_{65}H_{111}N_{17}O_{17}\cdot CH_3COOH\cdot 7H_2O$: C, 50.65; H, 8.18; N, 14.99; CH_3CO, 2.71%.

N^{ε}-*t*-Butyloxycarbonyl-lysyl-prolyl-valyl-glycyl-N^{ε}-*t*-butyloxycarbonyl-lysyl-N^{ε}-*t*-butyloxy-carbonyl-lysyl-arginyl-arginine Acetate (XVIII).—Carbobenzoxy octapeptide (XVII) (0.300 g.) was hydrogenolyzed in 15 ml. of 90% acetic acid over a palladium black catalyst for 4.5 hr. in the usual manner. The catlyst was then filtered off, and the filtrate was evaporated at 40—45°C in vacuo. The residue was treated as was compound XVI in order to remove the remaining acetic acid, and then lyophilized; 0.275 g. (98.9%), $[\alpha]_D^{25.5}$ $-41.6\pm 2°$ (c 1.007, 50% acetic acid). Paper chromatography gave a main spot and a faint minor one reactive to both ninhydrin and Sakaguchi reagents, at $R_f=0.86$ (BAPW) and 0.94 (BAPW) respectively.

Found: C, 47.44; H, 8.54; N, 16.71; CH_3CO, 2.42. Calcd. for $C_{57}H_{105}N_{17}O_{15}\cdot {}^3/_4CH_3COOH\cdot 7H_2O$: C, 48.80; H, 8.54; N, 16.54; CH_3CO, 2.24%.

N^{α}-Carbobenzoxy-N^{ε}-*t*-butyloxycarbonyl-lysyl-prolyl-valyl-glycyl-N^{ε}-*t*-butyloxycarbonyl-lysyl-N^{ε}-*t*-butyloxycarbonyl-lysyl-arginyl-arginine Amide (XIX).—To a solution of the protected pentapeptide azide (prepared from 1.313 g. (1.5 mmol.) of the hydrazide[4] by the procedure described in the synthesis of compound XV) there was added a solution of 0.756 g. (1.0 mmol.) of compound XII, which had been dissolved in 2.0 ml. of water and 8.0 ml. of tetrahydrofuran, together with 0.28 ml. (2.0 mmol.) of triethylamine. The reaction mixture was then stirred at 0—4°C for 40 hr., and evaporated at 30°C in vacuo. The residue was purified exactly as was compound XVII. The purified product was then lyophilized to give a colorless fluffy powder; 1.292 g. (84.2%), $[\alpha]_D^{22.5}$ $-43.7\pm 1°$ (c 1.745, 50% acetic acid). Thin-layer chromatography gave a Sakaguchi reactive spot, at $R_f=0.76$ (Silica-gel G, dimethylformamide - ethyl acetate - acetic acid (15 : 10 : 2)).

Found: C, 50.85; H, 8.54; N, 16.33; CH_3CO, 0.0%. Calcd. for $C_{65}H_{112}N_{18}O_{16}\cdot 7{}^1/_2H_2O$: C, 50.80; H, 8.33; N, 16.41; CH_3CO, 0.0%.

N^{ε}-*t*-Butyloxycarbonyl-lysyl-prolyl-valyl-glycyl-N^{ε}-*t*-butyloxycarbonyl-lysyl-N^{ε}-*t*-butyloxycarbonyl-lysyl-arginyl-arginine Amide Triacetate (XX).—A sample of carbobenzoxy-octapeptide amide (XIX) was hydrogenolyzed for 3 hr. in 15 ml. of 90% methanol containing 0.1 ml. of acetic acid in the presence of palladium black. The catalyst was then removed by filtration, and the filtrate was evaporated in vacuo. The lyophilization of the resultant residue gave a colorless fluffy powder; $[\alpha]_D^{24}$ $-41.0\pm 2°$ (c 1.210, 50% acetic acid). A single ninhydrin and Sakaguchi reactive spot was visible on paper, at $R_f=0.80$ (BAPW).

Found: C, 50.22; H, 8.22; N, 16.83; CH_3CO, 8.37. Calcd. for $C_{57}H_{106}N_{18}O_{14}\cdot 3CH_3COOH\cdot 2H_2O$: C, 51,00; H, 8.29; N, 16.99; CH_3CO, 8.70%.

N^{α}-Carbobenzoxy-N^{ε}-*t*-butyloxycarbonyl-lysyl-prolyl-valyl-glycyl-N^{ε}-*t*-butyloxycarbonyl-lysine Methyl Ester.—N^{α}-Carbobenzoxy-N^{ε}-*t*-butyloxycarbonyl-lysyl-prolyl-valyl-glycine (3.17 g., 5.0 mmol.)[4] and the N^{ε}-*t*-butyloxycarbonyl-lysine methyl ester (prepared from 1.76 g. (5.5 mmol.) of the acetate)[4] were dissolved in methylene chloride, and to this solution a methylene chloride solution of 1.135 g. (5.5 mmol.) of DCCl was added. The mixture was then allowed to stand in a refrigerator overnight. After the DCU which separated had been removed, the filtrate was evaporated in vacuo and the residue was redissolved in ethyl acetate. This solution was then washed successively with ice-cold N hydrochloric acid, 5% sodium bicarbonate and water, and dried over anhydrous sodium sulfate. The gelatinous precipitates separated from the concentrated ethyl acetate solution upon the addition of ether; 4.14 g. (94.6%), m. p. 92—94°C. The amorphous solid was reprecipitated from acetone-ether to give fine crystals with a m. p. of 101—104°C; 3.75 g. (85.5%), $[\alpha]_D^{25}$ $-56.6\pm 1°$ (c 2.017, methanol). Lit.[4] m. p. 105—107°C, $[\alpha]_D^{25}$ $-55.2\pm 1°$ (c 2.126, methanol).

Found: C, 58.72; H, 7.98; N, 11.13. Calcd. for $C_{43}H_{69}N_7O_{12}$: C, 58.95; H, 7.94; N, 11.19%.

Grateful acknowledgement is made to Dr. Mitsuo Ebata and staff for amino acid analyses, to Dr. Kaoru Kuriyama and staff for optical rotation measurements, and to Dr. Satoshi Mizukami and staff for elemental microanalyses.

BULLETIN OF THE CHEMICAL SOCIETY OF JAPAN VOL. 39 889—892 (1966)

The Attempted Cationic Polymerization of 1, 1-Dimethylcyclopropane and Phenylcyclopropane

By Shuzo AOKI, Yoshiyuki HARITA, Takayuki OTSU and Minoru IMOTO

Faculty of Engineering, Osaka City University, Sumiyoshi-ku, Osaka

(Received August 30, 1965)

1, 1-Dimethylcyclopropane and phenylcyclopropane gave the oligomer by aluminum bromide-catalyzed polymerization in *n*-hexane or in methylene chloride at 0°C. The polymerization reactivity of 1,1-dimethylcyclopropane was lower than that of styrene, and the content of cyclopropane units in their copolymers was decreased by a lowering of the temperature. The polymerization of 1,1-dimethylcyclopropane in the presence of polystyrene gave a graft polymer by chain transfer reaction. The polymerization of the cyclopropanes by a coordinated catalyst, $C_2H_5AlCl_2/TiCl_3$, in *n*-heptane at room temperature gave polymers with molecular weights of above 1200. The results are discussed in comparison with those of the polymerization of the corresponding vinyl monomers.

Cyclopropyl compounds polymerize in the presence of Lewis acids to give an oligomer.[1-3] The polymerizations of 1, 1-dimethylcyclopropane and phenylcyclopropane catalyzed by Lewis acids and a coordinated catalyst will be attempted in this work as an experiment preliminary to the copolymerization of the vinyl monomer with a cyclopropyl compound. 1, 1-Dimethylcyclopropane will be referred to isobutene in terms of their structures, especially, as growing terminal cations, while phenylcyclopropane will be referred to styrene. The results will be discussed in comparison with those of the polymerization of the corresponding vinyl monomers.

Experimental

Materials.—1, 1-Dimethylcyclopropane was prepared from 1, 3-dibromo-2, 2-dimethylpropane according to the method given by Shortridge et al.[4] B. p. 20.8°C; lit.[4] b. p. 20.63°C.

Phenylcyclopropane was obtained following the method of Dale et al.[5] B. p. 68.5—69.0°C/12 mmHg, n_D^{20} 1.5320; lit.[5] b. p. 69°C/12 mmHg, n_D^{20} 1.5320.

The monomers and solvents were carefully purified by the usual methods. Boron trifluoride - diethyl etherate, and stannic and titanic chlorides were distilled prior to use. The other catalysts, obtained commercially, were used without further purification.

Procedure.—*Polymerization by Lewis Acid.*—Into a glass stoppered test tube the monomer and solvent were taken and chilled to a given temperature. Then the catalyst solution was added. After a given time, ammoniac or acidic methanol was added to the reaction system in order to stop the polymerization. The resulting product was precipitated by the addition of a large amount of methanol, or, in some cases, it was fractionally distilled from the reaction system.

Polymerization by Coordinated Catalyst.—The polymerization was carried out in *n*-heptane in a sealed tube at room temperature, using a catalyst which had been aged for an hour. After a given time, the contents of the tube were poured into a large amount of isopropanol containing hydrochloric acid in order to precipitate the resulting polymer and remove the residual catalyst. The polymer was washed several times with pure methanol, and then dried under reduced pressure.

Results

The Polymerization of 1, 1-Dimethylcyclopropane.—In order to examine the catalytic activity, 1, 1-dimethylcyclopropane was polymerized in methylene chloride at 0°C by using various Lewis acids, such as aluminum bromide, aluminum chloride, stannic chloride, titanic chloride and boron trifluoride - diethyl etherate. Aluminum bromide-catalyzed polymerization afforded an oligomer with the molecular weight of 390, whereas no product was obtained by using the other Lewis acids.

The effects of the solvents are shown in Table I. In alkane (*n*-hexnane) the reaction proceeded very fast and gave an oligomer. The fast reaction in toluene, however, gave a liquid product. The infrared spectra of the products obtained in *n*-hexane and in toluene are shown in Fig. 1. The spectrum of the product obtained in *n*-hexane agreed with that of poly-1, 1-dimethylcyclopropane,[3] whereas the spectrum of the product obtained in toluene contained aromatic absorption bands. The absorptions at 1890, 1780 and 810 cm^{-1} indicated that the para-substitution of toluene by attacking the alkyl cation. Thus aromatic compounds

1) H. Pines, W. D. Huntsman and V. N. Ipatieff, *J. Am. Chem. Soc.*, **75**, 2315 (1953).
2) C. F. H. Tipper and D. A. Walker, *J. Chem. Soc.*, **1959**, 1352.
3) A. D. Ketley, *J. Polymer Sci.*, **B1**, 313 (1963).
4) R. W. Shortridge, R. A. Craig, K. W. Greenlee, J. M. Derfer and C. E. Boord, *J. Am. Chem. Soc.*, **70**, 946 (1948).
5) W. J. Dale and P. E. Swartzentruber, *J. Org. Chem.*, **24**, 955 (1959).

Table I. Aluminum bromide-catalyzed polymerization of 1,1-dimethylcyclopropane*1

Solvent	Reaction time min.	Conversion %	Mol. wt.	Appearance
n-Hexane	0.5	>90	370	Viscous liquid
Methylene chloride	16	1.2	—	Viscous liquid
Toluene	1	>40*2	170*3	Liquid

*1 $[Monomer]_0=3.0$ mol./l. $[AlBr_3]_0=0.007$ mol./l., 0°C

*2 Separated from the reaction mixture by distillation. It boiled at 145—149°C under slightly reduced pressure. The yield was calculated as C_5H_{11}- -CH_3.

*3 Calcd. value for C_5H_{11}- 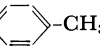 -CH_3 is 162.

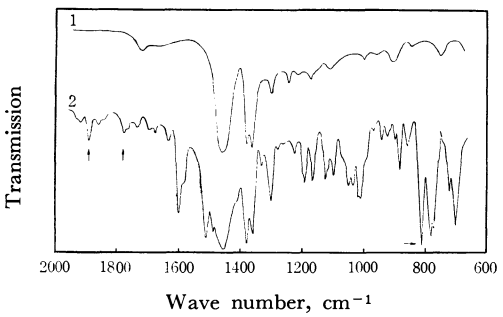

Fig. 1. Infrared spectra of the reaction products from 1,1-dimethylcyclopropane in *n*-hexane (1) and toluene (2).

seem to be unsuitable as solvents for the cyclopropane polymerization.

The Copolymerization of 1, 1-Dimethylcyclopropane with Styrene.—The copolymerization of 1, 1-dimethylcyclopropane with styrene was attempted in the presence of aluminum bromide. The results are given in Table II.

The rate of the polymerization of 1, 1-dimethylcyclopropane was markedly lower than that of styrene, and the copolymer containing the higher concentration of styrene units resulted from the equimolar mixture of the monomers. The cyclopropane unit content of this copolymer decreased with a lowering of the temperature.

The infrared spectrum of the copolymer agreed with that of polystyrene, and no evidence for the presence of the para-substituted styrene units was obtained.

The Graft Polymerization of 1, 1-Dimethylcyclopropane onto Polystyrene.—1, 1-Dimethylcyclopropane was polymerized in the presence of polystyrene to produce a graft polymer by the attack of the growing cyclopropane cation on the benzene nucleus of polystyrene. Table III shows the results of the graft polymerization. *n*-Hexane-insoluble polystyrene, obtained by radical polymerization, was used as the backbone. The entire polymer recovered after the polymerization of cyclopropane was soluble in *n*-hexane. This indicates that the high-molecular-weight polystyrene initially used was modified. The rubbery polymer recovered was fractionated by the *n*-hexane - isopropanol system (Table III). The infrared spectra

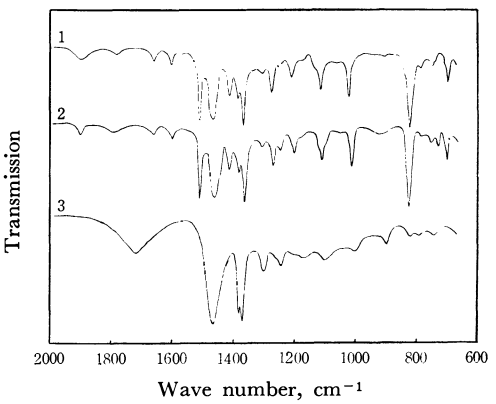

Fig. 2. Infrared spectra of the graft polymer 1: first fraction, 2: second fraction, 3: third fraction.

Table II. Copolymerization of styrene with 1,1-dimethylcyclopropane*

Monomer composition: 1,1-Dimethylcyclopropane	Monomer composition: Styrene	Solvent	Reaction temp. °C	Reaction time min.	Conversion %	Carbon content in polymer %	Polymer composition: Cyclopropane	Polymer composition: Styrene	Mol. wt.
0	100	CH_2Cl_2	0	0.25	97.1				
50	50	CH_2Cl_2	0	1.0	28.0	91.68	23	87	1320
100	0	CH_2Cl_2	0	16	1.2				
0	100	CH_2Cl_2	−15	0.25	95.9				
50	50	CH_2Cl_2	−15	1.0	21.6	91.87	8	92	—
100	0	CH_2Cl_2	−15	20	0.4				
0	100	CH_2Cl_2	−30	0.25	93.0				
50	50	CH_2Cl_2	−30	0.5	14.8	91.94	7	93	2400
100	0	CH_2Cl_2	−30	25	0.2				
50	50	*n*-C_6H_{14}	0	20	11.9	90.46	35	65	1890
50	50	*n*-C_6H_{14}	−15	20	10.4	91.72	12	88	—

* $[M_1+M_2]_0=3.0$ mol./l., $[AlBr_3]_0=0.007$ mol./l.

Table III. Polymerization of 1,1-dimethylcyclopropane in the presence of polystyrene

Polymerization condition and result:

Polystyrene: 0.1170 g., 1,1-Dimethyl cyclopropane: 5.0 ml., CH_2Cl_2: 8.0 ml., $AlBr_3$: 0.49 g., Reaction time: 75 hr., Reaction temp.: 0°C. Whole polymer recovered: 0.4200 g., Content of polystyrene in the polymer: 27.9%.

Fractionation of the polymer recovered:

Sample initially used: 0.3963 g.

First fraction (Precipitate in *n*-hexane 20 ml. - isopropanol 30 ml.): 0.1510 g. (38.1%). Rubbery substance.

Second fraction (Precipitate in *n*-hexane 20 ml. - isopropanol 40 ml.): 0.0544 g. (13.7%). Rubbery substance.

Third fraction (Methanol insoluble): 0.1819 g. (45.9%). Viscous liquid.

of the first and the second fractions contained a strong absorption at 820 cm^{-1} (Fig. 2). This indicates the presence of the para-substituted styrene units, an evidence of grafting. The third fraction was found from its infrared spectrum to be the homopolycyclopropane (Fig. 2).

The Polymerization of Phenylcyclopropane.—The polymerization of phenylcyclopropane (3.0 mol./l.) was attempted in the presence of aluminum bromide (0.07 mol./l.) in *n*-hexane at 0°C. After 15 sec., the exothermic reaction gave a viscous liquid at about a 90% conversion. About 60% of the product was distilled off below 200°C/1.5 mmHg. The molecular weight of the distillate at 200°C/1.5 mmHg was 320. The infrared spectrum of this fraction is shown in Fig. 3. The absorptions at 2000—1700 cm^{-1} indicated the presence of 1,2-disubstituted benzene units. The

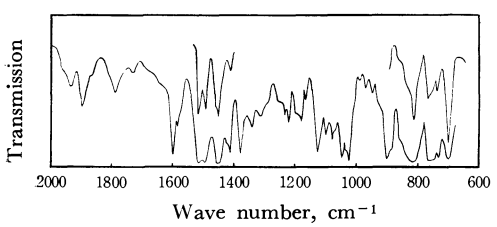

Fig. 3. Infrared spectrum of the reaction product from phenylcyclopropane.

presence of 1,4-disubstituted benzene units was also confirmed by the absorption at 810 cm^{-1}.

Thus the reaction scheme may be expressed as follows:

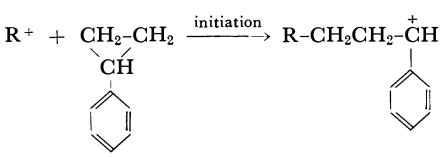

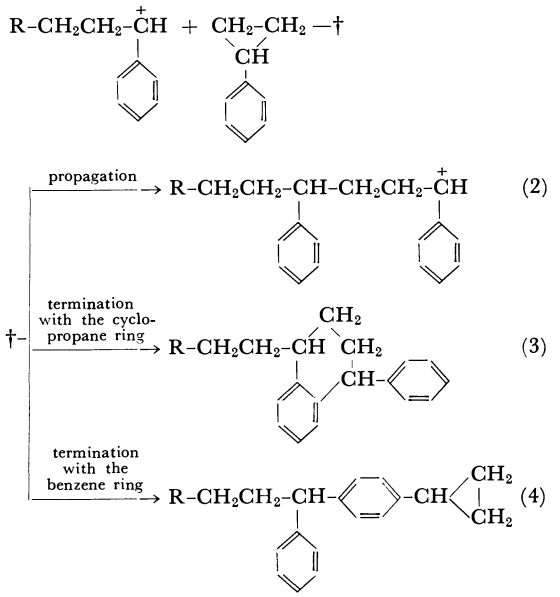

The Coordinated Polymerization of Cyclopropanes.—The polymerization of 1,1-dimethylcyclopropane with $C_2H_5AlCl_2/TiCl_3$ catalyst (Al/Ti=2) in *n*-heptane at room temperature for 18 days gave a waxy polymer with the molecular weight of 1240 in a 66% conversion. Phenylcyclopropane also gave a resinous polymer, this one with the molecular weight of 1480 in a 45% conversion. The other catalyst systems, $(C_2H_5)_2AlCl/TiCl_3$ and $(C_2H_5)_3Al/TiCl_3$, did not show any catalytic activity for the cyclopropane polymerization.

The degradation temperature of the polyphenylcyclopropane was found by the differential thermal analysis to be 430°C. If the polyphenylcyclopropane has the following structure (I), the thermal degradation of this polymer may give styrene and ethylene in the ratio of 2/1;

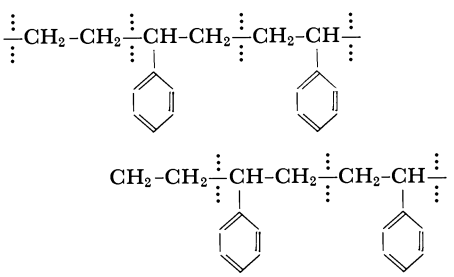

(I)

Styrene and ethylene in the degradation products at 450°C of this polymer were detected on a gas chromatogram, though the quantitative analysis was unsuccessful because of the complexity of the by-products.

The infrared spectrum of this polymer, shown in Fig. 4, contained the absorption band at 820 cm^{-1}, showing the presence of 1,4-disubstituted benzene

units arising from chain transfer reaction, besides the structure I.

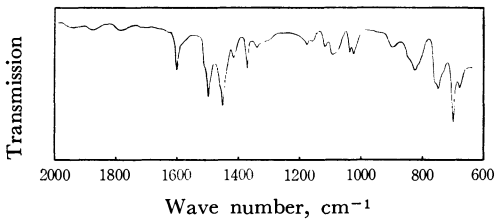

Fig. 4. Infrared spectrum of polyphenylcyclopropane.

Discussion

Dainton, Devlin and Small,[6] using the semi-empirical method, evaluated the heat of polymerization as 13.7 kcal./mol. for isobutene and 20.4 kcal./mol. for 1, 1-dimethylcyclopropane. These values suggest that the reactivity of 1, 1-dimethylcyclopropane is higher than that of isobutene. However, the results of the Lewis acid-catalyzed polymerizations of the cyclopropanes mentioned above indicate that the polymerization reactivity of the cyclopropanes is lower than that of the corresponding vinyl monomers.

1, 1-Dimethylcyclopropane was less reactive than styrene in the homopolymerization and in the copolymerization (see Table II), though, in general, isobutene was more reactive than styrene.[7] The content of cyclopropane units in the 1, 1-dimethylcyclopropane-styrene copolymer was influenced by the reaction temperature, for it decreased with a lowering of the temperature. This may be explained by the difference in the activation energies of the propagation reaction, as in the other copolymerization.[8,9]

The graft polymer was obtained in the polystyrene-1, 1-dimethylcyclopropane system, though the polystyrene-isobutene system did not give the graft polymer.[10] If the reactivities of the growing terminal cations of 1, 1-dimethylcyclopropane and isobutene are similar because of the similarity in the structure of their cations, this also indicates the lower reactivity of the cyclopropane monomer as compared with that of the vinyl monomer.

Phenylcyclopropane did not afford a high polymer under the conditions under which styrene gives a high polymer. This can be explained by the fact that the termination proceeds much further than the propagation in this polymerization because of the lower reactivity of the cyclopropane.

The cationic polymerization of vinylcyclopropane gave results which indicate that the cyclopropyl group has a lower reactivity than the vinyl group.[11]

A more quantitative study will be published later.

The authors wish to thank the Osaka Research Laboratory of the Japan Gas Chemical Co. for supplying the raw material and for the differential thermal analysis and the gas chromatographic measurements.

6) F. S. Dainton, T. R. E. Devlin and P. A. Small, *Trans. Faraday Soc.*, **51**, 1710 (1955).
7) J. P. Kennedy, "Copolymerization," Ed. by G. E. Ham, Interscience Publishers, New York (1964), p. 306.
8) K. Saotome and M. Imoto, *J. Chem. Soc. Japan, Ind. Chem. Sect.* (*Kogyo Kagaku Zassi*), **61**, 1500 (1958).
9) G. R. Brown and D. C. Pepper, *J. Chem. Soc.*, **1963**, 5930.
10) H. C. Haas, P. M. Kamath and N. W. Schuler, *J. Polymer Sci.*, **24**, 85 (1957).
11) T. Takahashi and I. Yamashita, *J. Chem. Soc. Japan, Ind. Chem. Sect.* (*Kogyo Kagaku Zasshi*), **68**, 869 (1965).

BULLETIN OF THE CHEMICAL SOCIETY OF JAPAN VOL. 39 892—898 (1966)

The Radiation-Induced Addition of Hydrogen Chloride to Ethylene

By Akira TERAKAWA, Jun NAKANISHI and Toru HIRAYAMA

Central Research Laboratory, Showa Denko K. K., Ota-ku, Tokyo

(Received August 31, 1965)

In a stainless steel autoclave, ethylene and hydrochloric acid or dried hydrogen chloride were irradiated with cobalt-60 gamma-rays. *n*-Butyl chloride and ethyl chloride were thus produced efficiently, unlike as when an ultraviolet light or catalyst was used. The products were quantitatively analyzed by gas chromatography. This reaction was supposed to be a vapor-phase radical chain reaction; the proposed reaction mechanism agreed well with our results. The selectivity of ethylene to the products was considered to be practically 100%. The *G* values of ethyl chloride, *n*-butyl chloride and the ethylene consumed, using the ratio of the total absorbed dose to ethylene, were calculated to be 16000, 10000 and 35000 respectively at 50°C and at a dose rate of 1.10×10^4 r./hr. The ratios of the rate constants for ethyl chloride and *n*-butyl chloride were 366, 499 and 580 at 50, 40 and 15°C respectively, and the apparent activation energies for ethyl chloride and *n*-butyl chloride were calculated from the reaction rates to be 6.94 and 8.95 kcal./mol. respectively.

Although the chain addition of hydrogen bromide to olefins is readily brought about by peroxide[1] or by radiation,[2] it has been generally recognized that the analogous reaction of hydrogen chloride is much less likely. There are only a few articles which are concerned with this reaction. One of them is by Ford and Hanford,[3,4] who reported the formation of mixtures of straight-chain primary alkyl chlorides, ranging from ethyl chloride to greases and waxes, by the reaction between ethylene and hydrogen chloride in the presence of catalysts and water at a high temperature and a high pressure.

Another article is that by Raley, Rust and Vaughan,[5] who recognized that the vapor-phase addition of hydrogen chloride to ethylene, as initiated by ultraviolet light or di-*t*-butyl peroxide, yielded ethyl chloride and small amounts of hydrogen and ethane (both 0.1% or less).

The general methods of preparing alkyl chlorides include one working from corresponding *n*-alcohol using zinc chloride and concentrated hydrochloric acid,[6] and one working from the chlorination of the corresponding alkyl hydrocarbons with hydrogen chloride.[7] However, it is generally considered that the selective preparation of *n*-alkyl chlorides from the chlorination of olefins is rather difficult; besides, there is no report on such a reaction using actinic radiation. The authors found that both *n*-butyl chloride and ethyl chloride were efficiently formed from a gamma-ray-induced reaction between ethylene and hydrogen chloride; the results of this process will be given in the present paper.

Experimental

Materials.—Ethylene and dried hydrogen chloride were obtained from the Nihon Sekiyu Kagaku Co., Ltd. (Kawasaki), and the Dow Chemical Co. (Matheson Co., Inc., U. S. A.) respectively, and were used without further purification. Reagent-grade concentrated hydrochloric acid (sp. gr. 1.184, 20°C) was obtained from the Kanto Kagaku Co., Ltd. (Tokyo), or the Wako Junyaku Co., Ltd. (Osaka), and all chemicals and materials used for analysis and identification were guaranteed reagents.

Apparatus and Procedures.—Dried hydrogen chloride or 15 ml. of concentrated hydrochloric acid in a glass vessel was introduced into a stainless steel autoclave with a capacity of 50 ml. After that, ethylene was compressed at pressures ranging from 25 to 65 kg./cm^2 and irradiated with cobalt-60 gamma-rays at a does rate of 1.10×10^4 r./hr. or 3.82×10^4 r./hr. After irradiation for 0—160 hr., the gaseous components in the autoclave were absorbed in toluene. The absorbants, as well as the liquid components, were then stored in a refrigerator for analysis. The autoclave was washed and cleaned with ethyl alcohol and ethyl ether after each reaction in order to avoid the effects of any impurities.

Dosimetry.—The intensity of the cobalt-60 source used was about 230 curies. The dose rates were determined with a Fricke dosimeter, using $G(Fe^{3+})=15.6$. The does absorbed by ethylene was calculated by the following equation[8]:

$$D_{C_2H_4} = D_{H_2O}\times\frac{(a/\rho)_{C_2H_4}}{(a/\rho)_{H_2O}} = D_{H_2O}\times\frac{(Z/A)_{C_2H_4}}{(Z/A)_{H_2O}}$$

where $D_{C_2H_4}$ and D_{H_2O} represent the doses absorbed by ethylene and by water in the system. (a/ρ) denotes the mass energy absorption coefficient, and Z and A represent the atomic number and the molecular weight of the substances in the system respectively.

Analytical.—The products, ethyl chloride and *n*-butyl chloride, were identified by comparing them with pure materials, by flame tests, by boiling point and refractive index measurements, by examining the infrared spectrum, and by gas chromatography. Hydrogen and chlorine were identified by gas chromatography. The products were quantitatively analyzed by gas chromatography using Kotaki Gu-12 model equipment. A 5-m. column of tri-*m*-cresyl phosphate on cerite was used at an operating temperature of 65°C and at a flow rate of 80 ml./min. of helium (Southern Oxygen Co.).

A known volume of the toluene absorbant of the gaseous products was taken for gas chromatography. As to the liquid products, known volumes of the toluene phase from the product of the extraction and of the aqueous hydrochloric acid phase were analyzed by gas chromatography.

Results

Products and *G* Values.—Table I shows the results obtained without irradiation and with and without the addition of the $AlCl_3$ catalyst, which is commonly employed in the production of ethyl chloride. No ethyl chloride, or only a small amount of it, was produced, and no *n*-butyl chloride was detected in any case. The pressure of hydrochloric acid in Table I represents the partial pressure of

Table I. Yields of ethyl chloride and *n*-butyl chloride in the case of non-irradiation

Temp. °C	Reaction time hr.	Initial pressure HCl mmHg	Initial pressure C_2H_4 mmHg $\times10^{-2}$	Yield C_2H_5Cl mol. $\times10^3$	Yield *n*-C_4H_9Cl mol.
28.5	66.0	207.0	441.3	0	0
50.0	66.0	573.0	470.7	1.48	0
50.0*	111.0	573.0	470.7	2.61	0

* 0.276 wt.% of $AlCl_3$ added to aqueous hydrochloric acid.

1) F. R. Mayo and C. Walling, *Chem. Revs.*, **27**, 351 (1940).
2) W. E. Vaughan, F. F. Rust and T. W. Evans, *J. Org. Chem.*, **7**, 477 (1942)
3) U. S. Pat. 2418832, April 15 (1947).
4) T. A. Ford, W. E. Hanford and J. H. Harman, *J. Am. Chem. Soc.*, **74**, 4323 (1952).
5) J. H. Raley, F. F. Rust and W. E. Vaughan, ibid., **70**, 2767 (1948).
6) A. M. Whaley and J. E. Copenhaver, ibid., **60**, 2497 (1938).
7) G. Egloff and M. Alexander, *Oil Gas J.*, **41**, No. 15—18 (1942).
8) J. W. T. Spinks and R. J. Woods, "An Introduction to Radiation Chemistry," John Wiley & Sons, New York (1964), p. 88.

hydrogen chloride over the aqueous hydrochloric acid.

A comparison of the reactions of ethylene with dried hydrogen chloride gas and with the aqueous hydrochloric acid are given in Table II. The products, yields and quantities expected from our postulated reaction mechanism agreed with each other in these two cases. Furthermore, Raley and

TABLE II. COMPARISON OF REACTION OF ETHYLENE WITH HYDROGEN CHLORIDE GAS AND AQUEOUS HYDROCHLORIC ACID

Reaction temp., 15°C Dose rate: 3.82×10^4 r./hr.

	Time hr.	Initial pressure		Yield		Selectivity of C_2H_4 %
		C_2H_4 mmHg$\times10^{-3}$	HCl mmHg	C_2H_5Cl mol.$\times10^3$	n-C_4H_9Cl mol.$\times10^3$	
Hydrogen chloride	15.5	368	760	3.98	0.10	92.9
Hydrogen chloride	16.0	368	83	1.23	0.61	98.9
Aqueous hydrochloric acid	15.0	368	83	1.14	0.61	95.1

TABLE III. RELATION BETWEEN YIELDS AND INITIAL PRESSURE OF ETHYLENE

Temp. °C	Initial pressure of C_2H_4 kg./cm^2	Pressure ratio $\frac{HCl}{C_2H_4}\times10^2$	Yield		Conversion of C_2H_4 %	Selectivity of C_2H_4 %	Mole ratio $\frac{C_2H_5Cl}{n\text{-}C_4H_9Cl}$	G value of C_2H_4 consumed
			C_2H_5Cl mol.$\times10^3$	n-C_4H_9Cl mol.$\times10^3$				
50	157.0	1.7						
50	64.0	1.21	31.30	19.32	60.8	89.4	1.11	25500
50	60.0	1.29	34.74	12.40	40.3	100.0	2.80	23900
50	49.6	1.56	18.67	3.41	24.4	95.4	5.42	11200
50	33.1	2.34	13.83	1.49	25.1	100.0	9.28	7800
20	55.0	0.30	7.12	7.27	8.2	98.0	0.98	7300
20	45.0	0.36	3.96	2.08	12.0	68.5	1.90	3100
20	35.0	0.47	3.33	1.19	9.4	78.2	2.80	2300
20	25.0	0.65	1.94	0.56	6.0	92.2	3.46	1300

TABLE IV. DEPENDENCY OF YIELDS ON TIME AND G VALUES

Initial pressure of C_2H_4: 471×10^2 mmHg (64 kg./cm^2)
Initial pressure of HCl: 573 mmHg
Reaction temperature: 50°C
Dose rate: 1.10×10^4 r.hr.

Time hr.	Conversion of C_2H_4 %	Selectivity of C_2H_4 %	Yield		G Values			$\frac{C_2H_5Cl}{n\text{-}C_4H_9Cl}$
			C_2H_5Cl mol.$\times10^3$	n-C_4H_9Cl mol.$\times10^3$	C_2H_5Cl	n-C_4H_9Cl	$-C_2H_4$	
14.0	9.7	82.6	7.55	1.37	13400	2440	18280	5.53
16.0	11.7	85.3	8.89	1.98	14100	3140	20380	4.49
40.5	24.2	83.2	19.10	5.90	13400	4130	21660	3.24
67.0	54.4	89.4	31.30	19.32	15500	9540	34580	1.62
73.0	58.2	92.9	33.08	20.81	15600	9800	35200	1.59
90.0	67.5	94.1	34.96	23.39	14700	9870	34440	1.49
161.5	80.8	91.2	40.45	26.82	13100	8680	30460	1.51

TABLE V. DEPENDENCY OF YIELDS ON TIME AND G VALUES

Initial pressure of C_2H_4: 435×10^2 mmHg (59.2 kg./cm^2)
Initial pressure of HCl: 351 mmHg
Reaction temperature: 40°C
Dose rate: 1.10×10^4 r./hr.

Time hr.	Conversion of C_2H_4 %	Selectivity of C_2H_4 %	Yield		G Values			$\frac{C_2H_5Cl}{n\text{-}C_4H_9Cl}$
			C_2H_5Cl mol.$\times10^3$	n-C_4H_9Cl mol.$\times10^3$	C_2H_5Cl	n-C_4H_9Cl	$-C_2H_4$	
15.5	6.3	81.9	4.01	1.14	6530	1850	10230	3.52
37.0	16.4	84.2	10.43	3.26	7660	2390	12440	3.20
65.0	31.7	98.3	20.70	9.22	9600	4270	18140	2.24
87.0	40.8	99.5	23.13	13.16	8500	4830	18160	1.76
114.0	41.9	99.0	23.83	15.48	7100	4610	16320	1.54

Table VI. Dependency of yields on time and G values

Initial pressure of C_2H_4: 383×10^2 mmHg (52 kg./cm^2)
Initial pressure of HCl: 83 mmHg
Reaction temperature: 15°C
Dose rate: 1.10×10^4 r./hr.

Time hr.	Conversion of C_2H_4 %	Selectivity of C_2H_4 %	Yield		G Values			$\frac{C_2H_5Cl}{n\text{-}C_4H_9Cl}$
			C_2H_5Cl mol.$\times10^3$	n-C_4H_9Cl mol.$\times10^3$	C_2H_5Cl	n-C_4H_9Cl	$-C_2H_4$	
42.0	8.7	91.2	3.69	2.77	2360	1770	5900	1.33
48.0	10.0	97.3	4.02	3.28	2260	1850	5960	1.23
65.0	21.1	90.9	7.49	7.51	3440	3450	10340	0.997
93.0	23.1	97.9	7.99	9.03	2500	2830	8160	0.885
156.5	28.9	87.7	7.94	9.68	1560	1900	5360	0.820

Table VII. Dependency of yields on time and G values

Initial pressure of C_2H_4: 368×10^2 mmHg (50 kg./cm^2)
Initial pressure of HCl: 83 mmHg
Reaction temperature: 15°C
Dose rate: 3.82×10^4 r./hr.

Time hr.	Conversion of C_2H_4 %	Selectivity of C_2H_4 %	Yield		G Values			$\frac{C_2H_5Cl}{n\text{-}C_4H_9Cl}$
			C_2H_5Cl mol.$\times10^3$	n-C_4H_9Cl mol.$\times10^3$	C_2H_5Cl	n-C_4H_9Cl	$-C_2H_4$	
15.0	2.6	84.6	1.14	0.17	607	357	1321	1.70
22.0	3.6	95.1	1.34	1.28	498	476	1450	1.03
42.0	18.4	86.5	4.95	6.50	968	1270	3508	0.761
65.0	30.0	96.2	8.73	11.89	1200	1640	4480	0.734

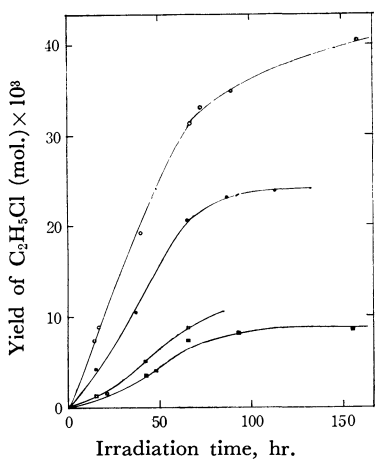

Fig. 1. The relation between irradiation time and yields of C_2H_5Cl at 50, 40 and 15°C.
○: 50°C, Dose rate 1.10×10^4 r./hr.
●: 40°C, Dose rate 1.10×10^4 r./hr.
■: 15°C, Dose rate 1.10×10^4 r./hr.
□: 15°C, Dose rate 3.82×10^4 r./hr.

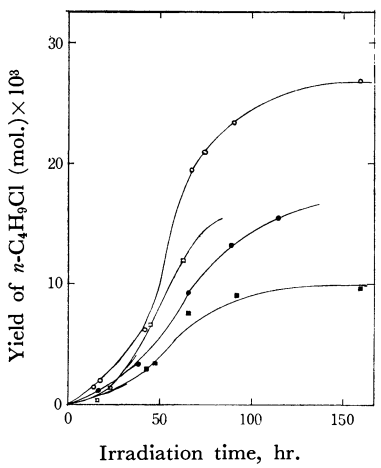

Fig. 2. The Relation between irradiation time and yields of n-C_4H_9Cl at 50, 40 and 15°C.
○: 50°C, Dose rate 1.10×10^4 r./hr.
●: 40°C, Dose rate 1.10×10^4 r./hr.
■: 15°C, Dose rate 1.10×10^4 r./hr.
□: 15°C, Dose rate 3.82×10^4 r./hr.

his co-workers[5] reported that their synthesis of ethyl chloride by ultraviolet light was a vapor-phase reaction. From these results, it is reasonable for us to conclude that the present reaction, using aqueous hydrochloric acid, is a vapor-phase radical reaction rather than a liquid one. G values were calculated on the basis of the assumption that this reaction is vapor-phase one, using total dose absorbed by ethylene.

Table III shows the relation between the yields and the initial pressure of ethylene. The reaction time was 66 hr. 15 ml. of aqueous hydrochloric acid were used in this series. It is evident from these relations that the mole ratios of the products are

controlled by the temperature and by the ratio of the initial pressures of ethylene to hydrogen chloride.

The relation between the irradiation time by cobalt-60 gamma-rays and the yields at 50, 40 and 15°C are shown in Figs. 1 and 2. Tables IV, V and VI show the G values against the total dose absorbed. The results obtained when the dose rate is changed are given in Table VII.

Since the energy absorbed during the induction period is included, the G values in the above results are naturally small when the conversion rate is low. Above $1—2\times10^6$ r., a wax-like or a solid polymer was produced; these were confirmed to be polyethylene by means of a study of their infrared spectra.

When the reaction temperature was above 60°C, viscous decomposition products were found in addition to ethyl chloride and *n*-butyl chloride. This is considered to be attributable to the fact that the reaction, being due to a high temperature, makes the walls of the autoclave tend to corrosion.

Although the selectivity of ethylene to ethyl chloride and *n*-butyl chloride is not quite 100% in some cases in Tables V, VI and VII, it is considered to be practically 100% in all cases, because no product other than ethyl chloride and *n*-butyl chloride was observed. Furthermore, the mole ratio of ethyl chloride to *n*-butyl chloride becomes smaller with an increase in the reaction time. This observation indicates that the partial pressure of hydrogen chloride with respect to the total pressure is decreased more rapidly than that of ethylene in spite of the feeding of hydrogen chloride from the aqueous hydrochloric acid.

The after-effects of the irradiation on yields were practically negligible in the case of 15°C.

The Effect of the Dose Rate on G Values.—Effects of the dose rate on the yields can be seen by comparing Tables VI and VII or Figs. 1 and 2. According to the curves in the figures, the G values of the consumed ethylene depend on the reaction time. If the logarithm $G(-C_2H_4)$ is plotted against the logarithm of the dose rate at each time, we find that G values are proportional to -0.54 powers of the dose rate, as is shown in Fig. 3.

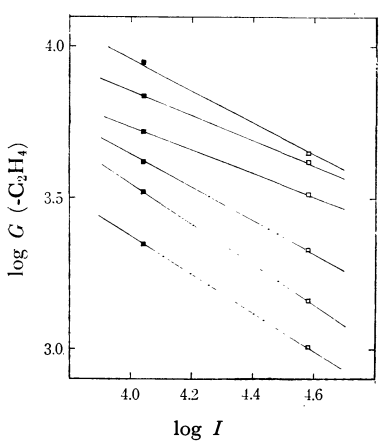

Fig. 3. Dependency of $G(-C_2H_4)$ on dose rate (I).

Discussion

Reaction Mechanism.—Since the investigated reaction is guessed to be a vapor-phase radical reaction, it may be presumed that hydrogen and chlorine radicals are initially formed from hydrogen chloride by irradiation and that the reaction proceeds in accordance with the following chain mechanism:

$$HCl \xrightarrow{f(I)} H\cdot + Cl\cdot \quad (1)$$

$$C_2H_4 + Cl\cdot \xrightarrow{k_2} C_2H_4Cl\cdot \quad (2)$$

$$C_2H_4Cl\cdot + HCl \xrightarrow{k_3} C_2H_5Cl + Cl\cdot \quad (3)$$

$$C_2H_4Cl\cdot + C_2H_4 \xrightarrow{k_4} C_4H_8Cl\cdot \quad (4)$$

$$C_4H_8Cl\cdot + HCl \xrightarrow{k_5} C_4H_9Cl + Cl\cdot \quad (5)$$

$$C_4H_8Cl\cdot + C_2H_4 \xrightarrow{k_6} C_6H_{12}Cl\cdot \quad (6)$$

$$C_6H_{12}Cl\cdot + HCl \xrightarrow{k_7} C_6H_{13}Cl + Cl\cdot \quad (7)$$

$$Cl\cdot + Cl\cdot \xrightarrow{k_8} Cl_2 \quad (8)$$

$$H\cdot + C_2H_4 \xrightarrow{k_9} C_2H_5\cdot \quad (9)$$

$$C_2H_5\cdot + HCl \xrightarrow{k_{10}} C_2H_6 + Cl\cdot \quad (10)$$

The addition reaction of the $C_6H_{12}Cl$ radical to C_2H_4 in this reaction mechanism need not be considered, since no products beyond *n*-butyl chloride were obtained.

By applying the stationary-state method, the following equation is obtained:

$$\frac{d(C_2H_5Cl)}{d(n\text{-}C_4H_9Cl)} = \frac{k_3(HCl)}{k_4(C_2H_4)} + \frac{k_3k_6}{k_4k_5} = m \quad (11)$$

This equation shows that the ratio of the reaction rate (m) of ethyl chloride to that of *n*-butyl chloride is proportional to the pressure ratio of hydrogen chloride to that of ethylene; that its slope is equal to the ratio of rate constants, k_3/k_4, and that k_6/k_5 is derived from the intercept of the line.

The rates of formation were calculated on the basis of the differential of the formation curves in Figs. 1 and 2, while the depression of ethylene pressure was measured with a gauge. The partial pressure of hydrogen chloride, not being subjectable to direct measurement, was calculated by the use of both Perry's data[9] and the concentration of

9) J. H. Perry, "Chemical Engineering Handbook," McGraw-Hill, New York (1950), pp. 166—167.

hydrogen chloride, which in turn was calculated from the yields of ethyl chloride and *n*-butyl chloride. The relation represented by Eq. 11 is illustrated in Fig. 4; the values of k_3/k_4 obtained with a dose rate of 1.10×10^4 r./hr. at 50, 40 and 15°C were 366, 499 and 580 respectively. In the case of a dose rate of 3.82×10^4 r./hr. at 15°C, a value of 568 was obtained.

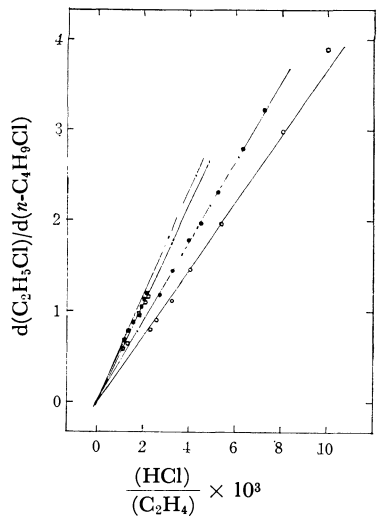

Fig. 4. The relation between ratio of reaction rate (m) and pressure ratio $(HCl)/(C_2H_4)$.
○: 50°C, Dose rate 1.10×10^4 r./hr.
●: 40°C, Dose rate 1.10×10^4 r./hr.
■: 15°C, Dose rate 1.10×10^4 r./hr.
□: 15°C, Dose rate 3.82×10^4 r./hr.

From the fact that these straight lines practically pass through the origin, the value of k_3k_6/k_4k_5 is practically zero; thus, k_6/k_5 approximately equals zero. This calculation agrees well with the fact that nothing beyond *n*-butyl chloride was actually obtained. The logarithms of k_3/k_4 against $1/T$ (T: absolute temperature) gave a straight line according to the Arrhenius equation, as is shown in Fig. 5. From its slope, the difference between activation energies, E_4-E_3, was calculated; its value was 2.29 kcal./mol.

In the case of a dose rate of 1.10×10^4 r./hr., the energies absorbed by ethylene were nearly equal in all cases up to the reaction time of 30 hr.; at this point, a value of 7×10^{19} eV. was obtained. After the pressures of hydrogen chloride and ethylene had been equalized in three cases, the relation between the reaction rates of ethyl chloride and *n*-butyl chloride was found to be as shown in Fig. 6. From the slopes of these straight lines, the apparent activation energies for ethyl chloride and *n*-butyl chloride were calculated to be 6.94 and 8.95 kcal./mol. respectively. The difference between them is 2.01 kcal./mol., which is in good agreement with $E_4-E_3=2.29$ kcal./mol. Evans[10] calculated the

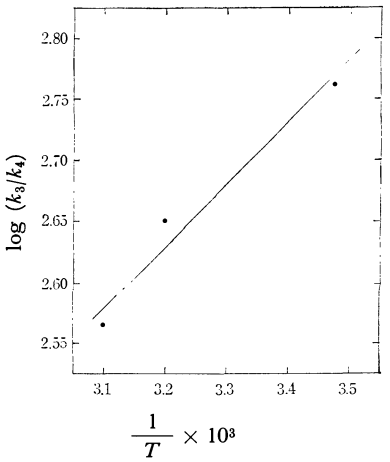

Fig. 5. Logarithms of k_3/k_4 against $1/T$°K.

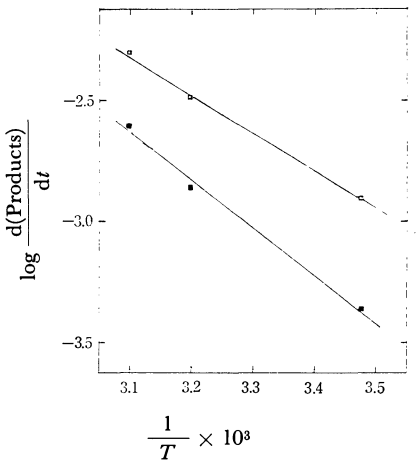

Fig. 6. Logarithms of reaction rates of C_2H_5Cl or n-C_4H_9Cl against $1/T$°K.
□: C_2H_5Cl, Dose rate 1.10×10^4 r./hr.
■: n-C_4H_9Cl, Dose rate 1.10×10^4 r./hr.

activation energy, $E_2=4.5$ kcal./mol., from the distance between atomic centers. Walling and his co-workers[11] calculated the ΔH values in Eqs. 2 and 3 to be −26 and +5 kcal./mol. respectively, and suggested that the value of E_3 is a little greater than +5 kcal./mol. Our results agree fairly well with these data.

Although Vaughan[5] established the formation of ethane, we could not find ethane under our experimental conditions as long as the reaction temperature was kept below 60°C. However, above the reaction temperature of 60°C, small amounts of ethane were observed.

Since the activation energies for the reactions between the H radical and chlorine gas or hydrogen

10) M. G. Evans, J. Gergely and E. C. Seaman, *J. Polymer Sci.*, **3**, 866 (1948).
11) C. Walling, "Free Radicals in Solution," John Wiley & Sons, New York (1957), p. 241.

chloride are rather small, the following equations, 12 and 13, may have occured in the system:

$$H\cdot + Cl_2 \cdots\cdots HCl + Cl\cdot \quad (12)$$

$$H\cdot + HCl \cdots\cdots H_2 + Cl\cdot \quad (13)$$

Usually no products from the reaction between ethylene and ethyl chloride and *n*-butyl chloride except polymers were observed, but there were a few cases where small amounts of *s*-butyl chloride were observed. This is presumably due to the isomerization of *n*-butyl chloride to *s*-butyl chloride.

Summary

Ethyl chloride and *n*-butyl chloride have been selectively prepared by the cobalt-60 gamma-ray-induced addition of hydrogen chloride to ethylene. The *G* values of consumed ethylene reached 35000. This reaction has been presumed to be a vapor-phase radical chain reaction, and the proposed reaction mechanism show a good agreement with our experimental results. The activation energies for the production of ethyl chloride and *n*-butyl chloride have been calculated from the rate constants to be 6.94 and 8.95 kcal./mol. respectively.

BULLETIN OF THE CHEMICAL SOCIETY OF JAPAN VOL. 39 898—901 (1966)

The Barium Content of Barite-forming Hydrothermal Waters as Exemplified by Tamagawa Hot Spring Waters

By Masami ICHIKUNI

Faculty of Science, Tokyo Metropolitan University, Setagaya-ku, Tokyo

(Received September 3, 1965)

An estimation of the barium concentration in Tamagawa Hot Spring water was made on the basis of the partition of lead between spring waters and barite deposits precipitated from the waters. As the lead content of the waters and the chemical composition of the deposits are already known, the barium concentration can be computed by the use of the following relation:

$$D=\left(\frac{\mathrm{Pb}}{\mathrm{Ba}}\right)_{\mathrm{S}}\Big/\left(\frac{\mathrm{Pb}}{\mathrm{Ba}}\right)_{\mathrm{L}}$$

where D is the partition coefficient of lead, and where S and L denote the solid and liquid phases respectively. A value of 2 ± 1 mg./l. was obtained for the barium concentration in the water issuing from the vents. It was pointed out that the water is supersaturated with barium sulfate. This supersaturation may be due to the addition of a considerable amount of sulfates, probably formed by supergene processes, to the original thermal water. The genesis of hydrothermal barite deposits was also discussed.

The determination of the barium content of thermal waters presents a considerable difficulty, its concentration being in general very small. The accumulation of data on the barium concentration in natural waters, especially of hydrothermal origin, will therefore provide useful information on the genesis of ore deposits containing barium minerals. It is of particular importance to define the range of its concentration in various hydrothermal waters producing barite or related minerals.

As one spring indicating a high barium content, we may refer to the Tamagawa Hot Springs, where a continuous deposition of plumbian barite, or so-called hokutolite, occurs on the bed of the stream. The barite originates from the principal spring, called "Obuki," and from other small springs located nearby.

In the studies of the genesis of plumbian barite, Suganuma[1] gave a value of 1.1 mg./l. as the barium sulfate content of Obuki Spring water. This value is, however, very questionable, as compared with the lead content of the same spring water, which has recently been reported by Minami et al.[2] Admittedly, Watanuki,[3] assuming the saturation of the spring water with barium sulfate, recommended a value of 1 mg./l. as its barium concentration. However, this value is possibly a lower limit of barium content, because the water issuing from the vents may be supersaturated with barium sulfate. On the other hand, Minami et al.[4] gave the following values for the barium concentration in the same spring water: 2.9 mg./l.

1) I. Suganuma, This Bulletin, **3**, 69 (1928).
2) E. Minami, G. Sato and K. Watanuki, *J. Chem. Soc. Japan, Pure Chem. Sect.* (*Nippon Kagaku Zassi*), **78**, 1096 (1957).
3) K. Watanuki, *Onsen Kagaku*, **14**, 88 (1963).
4) E. Minami, Y. Oyagi and M. Suzuki, reference cited in E. Minami, G. Sato and K. Watanuki, *J. Chem. Soc. Japan, Pure Chem. Sect.* (*Nippon Kagaku Zassi*), **79**, 860 (1958).

(sample collected on May 5, 1954) and 5.7 mg./l. (collected on July 14, 1956). It is obvious that more extensive works must be done in order to obtain a reliable value for the barium content.

This report will propose another approach to estimating the concentration of this element. It is a method developed on the basis of the partition equilibrium of a minor element between the liquid and solid phases. As we have a useful review on this subject,[5] it would be unnecessary to give the full details of this method. Minami et al.[6] outlined the same approach, but they did not make any accurate calculations.

Method of Calculation

From the experiments on the partition of lead between the solution and the barium sulfate precipitate, Kolthoff and Noponen[7] determined the partition coefficient, D, to be as follows: 0.027 at 95°C, and 0.026 at 26°C. The coefficient D is defined by Eq. 1:

$$D=\left(\frac{\mathrm{Pb}}{\mathrm{Ba}}\right)_{\mathrm{S}}\Big/\left(\frac{\mathrm{Pb}}{\mathrm{Ba}}\right)_{\mathrm{L}} \qquad (1)$$

where (Pb/Ba) designates the weight ratio of the two elements, and the subscripts S and L refer to the solid and liquid phases respectively. They examined the precipitates with compositions ranging from 0.025 to 0.302 in a Pb/Ba ratio. The composition of plumbian barites from the Tamagawa Hot Springs falls entirely within this range. It was also shown that perchloric acid had no effect upon the partition coefficient; thus, the value is not affected by a high acidity of spring water. The presence of chloride ions in spring water may modify the coefficient slightly as a result of the complex-formation of lead, but as a first approximation, the reported value can be used here without correction.

In the Tamagawa Hot Springs, the plumbian barite precipitates from waters ranging in temperature from 90°C to 40°C; therefore, a partition coefficient of 0.027 may be accepted in this calculation. Special emphasis must be placed on a small variability of the coefficient with the temperature. From Eq. 1, the barium concentration in the solution $(\mathrm{Ba})_{\mathrm{L}}$ is given by the following equation:

$$(\mathrm{Ba})_{\mathrm{L}}=\frac{0.027(\mathrm{Pb})_{\mathrm{L}}}{\left(\frac{\mathrm{Pb}}{\mathrm{Ba}}\right)_{\mathrm{S}}} \qquad (2)$$

where $(\mathrm{Pb})_{\mathrm{L}}$ is the lead concentration in the stream water from which the plumbian barite is precipitating. Since the lead concentration appears to be roughly constant in the stream, a value of 1.2 mg./l. for the stream water[2] is inserted into Eq. 2. In reality this is not true, however, it will be seen later that the correction due to a decrease in lead concentration does not affect the results of calculation. The lowering of the lead concentration resulting from the confluence of some streamlets with the main stream can be equally neglected, their discharge being small compared with that of the latter.

Results and Discussion

Table I indicates the chemical composition of several plumbian barites[8,9] and the calculated barium contents of the waters which are in equilibrium with these minerals. Figure 1 represents the locality of the barites. It is well known that the deposits formed in the lower course of the stream are rich in lead, while those formed in the upper course are deficient in this element. The change in chemical composition can be attributed to the selective incorporation of barium into the deposits. Thus, the Pb/Ba ratio in the

Table I. Composition of some plumbian barites and calculated barium concentrations in solution

No.	Locality (distance from Obuki spring, m.)	PbO %	BaO %	$(\mathrm{Pb/Ba})_{\mathrm{S}}$	$(\mathrm{Ba})_{\mathrm{L}}$ mg./l.
1	30	—	—	0.035*	0.92
2	50	0.75	64.25	0.0121	2.68
3	50	4.61	62.18	0.0768	0.42
4	100	7.17	53.57	0.139	0.23
5	700	15.17	48.14	0.327	0.10
6	700	16.83	47.67	0.366	0.088

* Estimated from the refractive index α.

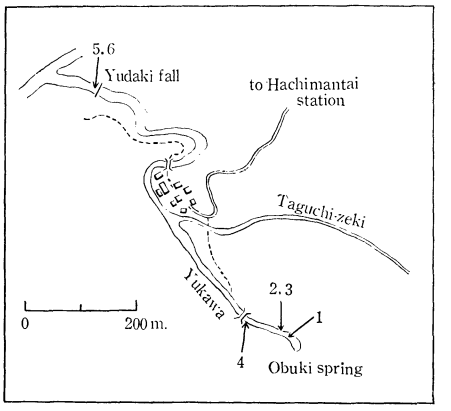

Fig. 1. General map of the Tamagawa Hot Springs and localities of barite samples

5) W. L. McIntire, *Geochim. et Cosmochim. Acta*, **27**, 1209 (1963).
6) E. Minami, G. Sato and K. Watanuki, *J. Chem. Soc. Japan, Pure Chem. Sect.* (*Nippon Kagaku Zassi*), **79**, 860 (1958).
7) I. M. Kolthoff and G. E. Noponen, *J. Am. Chem. Soc.*, **60**, 197 (1938).
8) E. Minami, "Geochemistry of the Tamagawa Hot Springs," Tokyo (1963), p. 108.
9) S. Misumi, ibid., p. 146.

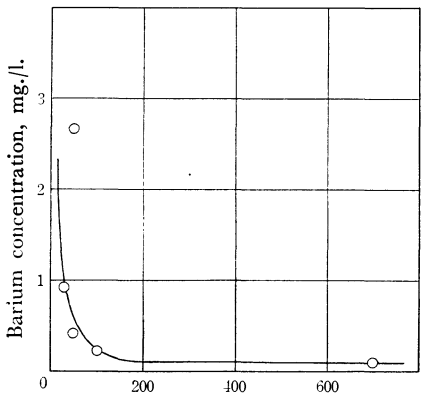

Fig. 2. Plot of calculated barium concentrations against distance from Obuki Spring.

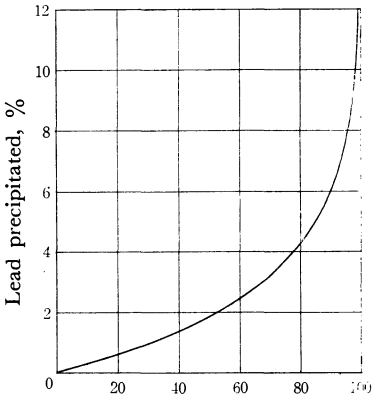

Fig. 3. Relation between the portion of barium precipitated and that of lead precipitated.

waters is evidently the lowest at the vents of the springs, and increases gradually with the flowing of the stream. In Fig. 2, the calculated barium concentration in the stream water is plotted against the distance from the Obuki Spring. The figure shows that 2 ± 1 mg./l. may be a reasonable value for the barium concentration in the water issuing from the vent of the Obuki Spring. This leads to the rather surprising conclusion that the major portion of the barium contained in the original water precipitates within 100 m. of the Obuki Spring.

The quantity of lead coprecipitated with barium can be computed if we assume that the precipitate once formed has no further interaction with the solution. Starting from Eq. 1, we have:

$$\frac{-(\Delta\mathrm{Pb})}{-(\Delta\mathrm{Ba})} = D\frac{(\mathrm{Pb})}{(\mathrm{Ba})} \tag{3}$$

where $(\Delta\mathrm{Pb})$ and $(\Delta\mathrm{Ba})$ represent small portion of these elements incorporated into the precipitate, and where (Pb) and (Ba) refer to their concentrations in the solution from which the precipitate was formed. The integration of the above equation gives:

$$\frac{(\mathrm{Pb})}{(\mathrm{Pb})_0} = \left\{\frac{(\mathrm{Ba})}{(\mathrm{Ba})_0}\right\}^D \tag{4}$$

where $(\mathrm{Pb})_0$ and $(\mathrm{Ba})_0$ denote their initial concentrations. Equation 4 indicates the relation between lead and barium concentrations in the solution during the formation of the precipitate. From Eq. 4, the portion of lead coprecipitated is given by:

$$1 - \frac{(\mathrm{Pb})}{(\mathrm{Pb})_0} = 1 - \left\{\frac{(\mathrm{Ba})}{(\mathrm{Ba})_0}\right\}^D$$

Figure 3 shows the relation between the portion of barium precipitated and the corresponding value for lead. In order to calculate the total amount of plumbian barite deposited on the bed of the stream extending over 700 m. from the Obuki Spring to the Yudaki Fall, we need only the lead and the barium concentrations in the water at both points and the discharge of the stream in this area. As is shown in Fig. 2, the amount of barium precipitated on the bed under consideration corresponds to approximately 95% of its initial amount. In this case, a value of 8% may be expected for the coprecipitated portion of lead. Consequently, one liter of spring water may precipitate 1.9 mg. of barium and 0.096 mg. of lead, or 3.37 mg. of mixed sulfate (Ba, Pb) SO_4. Using a discharge value of 75.4 l./sec. or 2.4×10^9 l./yr. (both as given by Miura[10]), we can estimate the annual production of deposits as 8.09×10^9 g.

If the bed of the stream between the Obuki Spring and the Yudaki Fall were covered with crustal deposits of a uniform thickness, the rate of the growth of the crustal deposits would be of 0.86 mm./yr.* This value is extremely high compared with the results obtained by Saito et al.[11] A spectrochemical investigation by Nakagawa[12] showed that some sulfurous sinters occuring in the Tamagawa Hot Springs contain a considerable amount of barium and lead, so the above-mentioned disagreement means simply that the precipitate exists mainly in the form of minute crystals buried in sulfurous sinters, and not in the form of crustal deposits.

The formation of abundant microcrystals of plumbian barite presents a direct evidence that the spring water issuing from the vents is supersaturated with barium sulfate. It is well known that the greater the degree of supersaturation,

* This calculation was made on the assumption that the bed occupies an area of 2100 m^2 and that the barite deposits have a density of 4.5 g./cm^3.

10) H. Miura, "Geochemistry of the Tamagawa Hot Springs," Tokyo (1963), p. 83.

11) N. Saito, Y. Sasaki and H. Sakai, ibid., p. 182.

12) R. Nakagawa, *J. Chem. Soc. Japan, Pure Chem. Sect.* (*Nippon Kagaku Zasshi*), **86**, 46 (1965).

the greater will be the number of nuclei formed. We will discuss here briefly the possible causes of this phenomenon. It may be attributed to a rapid decrease in the temperature or to an abrupt change in the chemical composition of the original thermal water. As a cause of the decrease in the temperature, the mixing of the original water with some groundwater of a low temperature may be considered. However, the addition of groundwater of a low mineralization cannot always result in the precipitation of barium sulfate, for the water may be effective not only in cooling the original solution, but also in diluting it. Therefore, no separation of solid barium sulfate takes place unless the water is accompanied by a considerable quantity of sulfates. It may be generally admitted that the increase in sulfate concentration is indispensable for the formation of barite deposits. This hypothesis is in accord with the present author's interpretation of the formation of the Tamagawa Hot Springs.[13]

From the foregoing discussion, we can schematize the genesis of hydrothermal barite deposits as follows: the original ore solutions are relatively deficient in sulfate ions and contain at least 1 mg. of barium per liter. When the ore solutions encounter some subsurface waters which are rich in sulfates, the precipitation of barite will take place because of the decrease in the solubility of the barium sulfate. The sulfates may be formed by the oxidation of sulfides contained in the same ore solutions or by some other supergene processes.

The author wishes to express his gratitude to the Matsunaga Science Foundation for its support of this study.

13) M. Ichikuni, *Geochim. et Cosmochim. Acta*, **17**, 6 (1959).

BULLETIN OF THE CHEMICAL SOCIETY OF JAPAN VOL. 39 901—909 (1966)

Electronic Spectra of Trivalent Metal Complexes of 3-Phenyl- and 3-Benzyl-2, 4-pentanedione*

By Yukito MURAKAMI and Katsuyuki NAKAMURA

Department of Organic Synthesis, Faculty of Engineering, Kyushu University, Hakozaki, Fukuoka

(Received September 3, 1965)

The 3-phenyl- and 3-benzyl-2, 4-pentanedione complexes of trivalent aluminum, chromium, iron and cobalt were prepared, and their electronic absorption spectra measured in the 220—900 mμ range. The spectral data were interpreted in detail in terms of the $\pi_3 \rightarrow \pi_4$, the electron transfer ($d_\varepsilon \rightarrow \pi_4$) and the $d \rightarrow d^*$ transitions of the various components. In this series of complexes, an inter-ring π-interaction between a phenyl ring and a chelate ring is expected to remain to a limited extent in the metal complexes of 3-phenyl-2, 4-pentanedione, although the twist of both rings from the coplanarity is significant. For the aluminum complexes, π-electrons in the ligand part remain delocalized in a manner similar to that which holds in the corresponding enolate ion. On the other hand, each kind of $\pi_3 \rightarrow \pi_4$ transition in the transition metal complexes of the 2, 4-pentanedione derivatives was found to depend on the number of d_ε electrons of the central metal ion and to appear in this increasing order of energy: Cr < Fe < Co. In addition, the metal-ligand π-interaction has a major effect on the $\pi_3 \rightarrow \pi_4$ transition, and it seems to increase with respect to the ligands in the order: 2, 4-pentanedione, 3-phenyl-2, 4-pentanedione, and 3-benzyl-2, 4-pentanedione. The two major substituent (at the 3-position of 2, 4-pentanedione) effects which may affect the $\pi_3 \rightarrow \pi_4$ transitions were identified.

Much work has been done on the interpretation of the absorption spectra of 2, 4-pentanedione complexes from various aspects.[1-6] In two of these studies, Barnum applied the Hückel LCAO-MO calculation to the 2, 4-pentanedione chelate systems in order to estimate the effect of metal-ligand π-bonding on the electronic transition energies; he also successfully analyzed $\pi_3 \rightarrow \pi_4$ and $d_\varepsilon \rightarrow \pi_4$ transition bands.[4,5]

In the present study, the 3-phenyl- and 3-benzyl-2, 4-pentanedione complexes of trivalent aluminum, chromium, iron and cobalt have

* Contribution No. 93 from the Department of Organic Synthesis, Faculty of Engineering, Kyushu University.

1) K. Sone, I. Miyake, H. Kuroya and K. Yamasaki, *J. Chem. Soc. Japan, Pure Chem. Sect.* (*Nippon Kagaku Zassi*), **69**, 70 (1948).

2) R. L. Belford, A. E. Martell and M. Calvin, *J. Inorg. Nucl. Chem.*, **2**, 11 (1956).

3) R. H. Holm and F. A. Cotton, *J. Am. Chem. Soc.*, **80**, 5658 (1958).

4) D. W. Barnum, *J. Inorg. Nucl. Chem.*, **21**, 221 (1961).

5) D. W. Barnum, ibid., **22**, 183 (1961).

6) J. P. Fackler, Jr., F. A. Cotton and D. W. Barnum, *Inorg. Chem.*, **2**, 97 (1963).

Table I. Analyses and melting points of trivalent metal complexes of 3-substituted 2,4-pentanediones

3-Substituent	Complex	Carbon,* %	Hydrogen,* %	Metal,* %	M.p., °C
Phenyl	$Al(C_{11}H_{11}O_2)_3$	71.40(71.73)	6.21(6.02)	—	268
	$Cr(C_{11}H_{11}O_2)_3$	68.59(68.62)	5.78(5.76)	—	272—273 (decomp.)
	$Fe(C_{11}H_{11}O_2)_3$	67.74(68.17)	5.85(5.72)	—	259—259.5 (decomp.)
	$Co(C_{11}H_{11}O_2)_3$	66.03(67.81)	5.68(5.69)	—	183—184 (decomp.)
Benzyl	$Al(C_{12}H_{13}O_2)_3$	72.61(72.71)	6.75(6.61)	—	165.7—166.3
	$Cr(C_{12}H_{13}O_2)_3$	70.06(69.78)	6.35(6.34)	—	174.5—175.0 (decomp.)
	$Fe(C_{12}H_{13}O_2)_3$	69.38(69.34)	6.58(6.30)	8.95(8.96)	160—161.5 (decomp.)
	$Co(C_{12}H_{13}O_2)_3$	68.74(69.00)	6.44(6.27)	9.42(9.41)	142—143.5 (decomp.)

* Calculated values for the specified formula are given in parentheses.

Table II. Ultraviolet absorption bands of 2,4-pentanediones

β-Diketone	λ_{max}(mμ); log ε		
	n-Hexane	Ethanol	Ethanol and sodium ethoxide*
3-Phenyl-2,4-pentanedione		(227—243)	
	284; 3.98	286; 3.95	306.5; 4.26
3-Benzyl-2,4-pentanedione	(262)	(261)	
	(269)	(269)	
	287; 3.80	289; 3.58	309; 4.29
3,3-Dibenzyl-2,4-pentanedione	(248)	248.5; 2.47	
	253.5; 2.56	253.3; 2.57	
	259.4; 2.68	258.9; 2.68	
	265.0; 2.62	264.7; 2.60	
	269.0; 2.44	(268.0)	
	301; 2.08	294; 2.09	
2,4-Pentanedione		274.0	294.0; 4.43
	268.8; 4.08†	272.5; 4.02†	

Shoulder bands or indistinct bands are enclosed in parentheses.

* Ethanol contains 0.022 to 0.11 N sodium exthoxide.

† The values are cited from J. B. Conant and A. F. Thompson, Jr., *J. Am. Chem. Soc.*, **54**, 4039 (1952).

been prepared, and their electronic spectra interpreted in terms of the $\pi_3 \rightarrow \pi_4$ transition which is characteristic of the ligand molecules and of the electron transfer transition in the chromium, iron and cobalt complexes. The $d \rightarrow d^*$ transitions characteristic of the nuclear metals have also been assigned for the transition metal complexes.

Experimental

Preparation of Materials. — 3-Phenyl-2,4-pentanedione was prepared from phenylacetone and acetic anhydride in the presence of boron trifluoride and of *p*-toluenesulfonic acid in the 0—5°C temperature range, following the method described in the literature[7]; b. p. 110—115°C at 17 mmHg; m. p. 58.0—59.0°C (reported[7] b. p. 116—118°C at 20 mmHg; m. p. 58.5—59.5°C). 3-Benzyl-2,4-pentanedione was obtained by the reaction of sodium acetylacetonate with excess benzyl chloride[8]; b. p. 115—118°C at 4 mmHg; n_D^{25} 1.5236 (reported b. p. 140—146°C,[8] 143—146°C[9] at 10 mmHg; n_D^{25} 1.5250[9]); a yield of 43%.

The methods of preparation employed for the trivalent metal complexes of acetylacetonate were used in this study with some modification for the syntheses of 3-phenyl- and 3-benzyl-2,4-pentanedione complexes of the corresponding trivalent metals. The procedure has been described in detail elsewhere.[10] The results of analysis, along with the values of the melting point, are listed in Table I.

7) C. R. Hauser, F. W. Swamer and J. T. Adams, "Organic Reactions," Vol. 8, 133 (1954).

8) G. T. Morgan, *J. Chem. Soc.*, **1925**, 797.

9) R. P. Dryden and A. Winston, *J. Phys. Chem.*, **62**, 635 (1958).

10) K. Nakamura and Y. Murakami, *Tech. Reports Kyushu Univ.* (*Kyushu Daigaku Kogaku Shuho*), **38**, 329 (1965).

TABLE III. ABSORPTION BANDS IN METAL COMPLEXES OF 2,4-PENTANEDIONES

Metal complex	λ_{max}(mμ); log ε			
	3-Phenyl-2,4-pentanedione		3-Benzyl-2,4-pentanedione	
	Ethanol	Chloroform	Ethanol	Chloroform
Al(III) complex	231.5; 4.10			
			(264)	(265)
			(270)	(272)
	299.0; 4.51	301.5; 4.54	301.5; 4.48	305.0; 4.57
	(314)	(314)	(318)	(318)
Cr(III) complex	(258; 4.18)	(260; 4.23)	(257; 3.98)	
			265; 4.05	266; 4.06
			270; 4.06	271; 4.06
	(289; 4.02)	(291; 4.04)	(285; 4.00)	288.5; 4.02
	(310; 3.93)	(312; 4.02)	(318; 3.92)	(320; 3.95)
	348.0; 4.10	351.0; 4.14	352; 4.11	355.5; 4.13
	(395)	(395)	(400)	(400)
	(410—440)	(410—440)	(420—445)	(420—445)
	575	575.0; 2.06	565; 2.01	565.0; 2.00
Fe(III) complex	247.0; 4.36		(240; 4.16)	
			(263)	(265)
			(270)	(271)
	284.0; 4.39	284.0; 4.36	286.0; 4.33	286.5; 4.38
			(310)	
	368.0; 3.58	372.0; 3.58	372.5; 3.56	378.0; 3.58
	445.0; 3.55	457.0; 3.65	450.0; 3.50	462.0; 3.63
Co(III) complex	228.5; 4.54		(227; 4.52)	
	253.0; 4.51	256.5; 4.71	248.5; 4.55	
	(263.5)	(264.5)	(262.5)	(264)
	(270)	(271)	(269)	(270)
	(308)	(308)	(300)	(300)
	(338; 3.82)	(340; 3.88)	341; 3.84	343; 3.88
	(410—470)	(410—470)	(410—460)	(410—460)
	608; 2.2	608; 2.35	595; 2.28	596; 2.28

Shoulder or indistinct bands are enclosed in parentheses.

Spectral Measurements.—The ultraviolet and visible spectra of the metal complexes were measured by standard methods, using a Hitachi ESP-2 type recording spectrophotometer. Ethanol, *n*-hexane and chloroform were used as solvents in this study.

Results and Assignments

The absorption spectra of 3-phenyl- and 3-benzyl-2, 4-pentanedione and of the corresponding enolate ions are illustrated in Fig. 1, along with that of 3, 3-dibenzyl-2, 4-pentanedione. The spectra of the trivalent metal complexes of 3-phenyl- and 3-benzyl-2, 4-pentanedione are shown in Figs. 2 through 5. It may be seen that these absorption spectra of metal complexes are generally similar to the corresponding 2, 4-pentanedione complexes. The significant peaks of the absorption spectra of the ligands and the metal complexes are listed in Tables II and III respectively.

Ligands.—The $\pi_3 \rightarrow \pi_4$ transition band of acetylacetone was observed to shift to a longer wavelength upon replacement of the γ-hydrogen with either phenyl or benzyl group. Besides this profound band, several indistinct shoulders, which are due to $\pi \rightarrow \pi^*$ transitions in a benzene ring system, were observed. Among several shoulders which appeared in the 249—274 mμ range in the spectrum of 3-benzyl-2,4-pentanedione, 263 and 269 mμ bands were noticed as being most intense. On the other hand, in 3, 3-dibenzyl-2, 4-pentanedione there are three distinct bands, of nearly identical intensity, at 253.3, 258.9 and 264.7 mμ in ethanol; this is because of the absence of its enol form. These $\pi \rightarrow \pi^*$ bands are located on the longer wavelength side relative to the secondary bands (^1L_b) of benzene itself.

Although 3-phenyl-2, 4-pentanedione seems to demonstrate shoulder bands due to a similar electronic transition in approximately the same range, the definite position of these bands could not be detected clearly. In 3-phenyl-2, 4-pentanedione, several indistinct shoulders were also observed in the 227—243 mμ range; they may

Table IV. Absorption bands in 2,4-pentanedione complexes and their assignments

Metal complex	λ_{max}(mμ) Ethanol This work	Ethanol Literature (4)	Ethanol Literature (3)	Chloroform This work	Chloroform Literatuer (3)	Assignment of transition
Al(III)	287.0* (300)		288			$\pi_3 \rightarrow \pi_4$
Cr(III)	256.5	255				$\pi_3(e) \rightarrow \pi_4(a_1)$
	272	270				$\pi_3(e) \rightarrow \pi_4(e)$, $\pi_3(a_2) \rightarrow \pi_4(a_1)$
	(295)	(295)				$\pi_3(a_2) \rightarrow \pi_4(e)$
	335	332	336			$d_\varepsilon(a_1) \rightarrow \pi_4(e)$, $d_\varepsilon(e) \rightarrow \pi_4(a_1)$
		380		376	374	$d_\varepsilon(e) \rightarrow \pi_4(e)$
		388		384	382	
				391	388	
		(410)		(412), (435)	410	$^4A_{2g} \rightarrow {}^4T_{1g}$
		560		560	560	$^4A_{2g} \rightarrow {}^4T_{2g}$
Fe(III)	237	235	237			$\pi_3(e) \rightarrow \pi_4(a_1)$
	274	272	274		273	$\pi_3(e) \rightarrow \pi_4(e)$, $\pi_3(a_2) \rightarrow \pi_4(a_1)$
	(295)					$\pi_3(a_2) \rightarrow \pi_4(e)$
	354	351	354[1]		353	$d_\varepsilon(a_1) \rightarrow \pi_4(e)$, $d_\varepsilon(e) \rightarrow \pi_4(a_1)$
	437	431	435[1]		437	$n \rightarrow d^*$
					725	$^6A_{1g} \rightarrow {}^4T_{2g}$
					975	$^6A_{1g} \rightarrow {}^4T_{1g}$
Co(III)	230	228	228			$\pi_3(e) \rightarrow \pi_4(a_1)$
	258	256	257			$\pi_3(e) \rightarrow \pi_4(e)$, $\pi_3(a_2) \rightarrow \pi_4(a_1)$
	(295)	(295)				$\pi_3(a_2) \rightarrow \pi_4(e)$
	326	323				$d_\varepsilon(a_1) \rightarrow \pi_4(e)$, $d_\varepsilon(e) \rightarrow \pi_4(a_1)$
				(405—440)	(400)	$d_\varepsilon(e) \rightarrow \pi_4(e)$, $^1A_{1g} \rightarrow {}^1T_{2g}$
				595	592	$^1A_{1g} \rightarrow {}^1T_{1g}$

Shoulder bands are given in parentheses.
* log ε, 4.61

be attributed to the primary bands (^1L_a) in the benzene π-system.

The $n \rightarrow \pi^*$ forbidden transition in the ketonic forms of the present ligands is expected to appear on a longer wavelength side of the $\pi \rightarrow \pi^*$ transition band. Nevertheless, this band of a rather low intensity seems to be hidden by the intense $\pi \rightarrow \pi^*$ bands. On the other hand, the $n \rightarrow \pi^*$ band with a maximum at 301 mμ in *n*-hexane was clearly observed in 3, 3-dibenzyl-2, 4-pentanedione, and it demonstrated a significant solvent effect, which resulted in a blue shift to 294 mμ in ethanol.

In the presence of sodium ethoxide, the enolate ions are formed, and the $\pi \rightarrow \pi^*$ transition bands shift to longer wavelengths, i. e., to 306.5 mμ in the 3-phenyl derivative and to 309 mμ in the 3-benzyl; also, their intensities increase.

Aluminum Complexes.—The general appearance of the absorption spectra is quite similar to that of the respective free ligand species. The $\pi_3 \rightarrow \pi_4$ band upon chelation shifts to a wavelength shorter by 850 cm^{-1} with respect to the enolate ion. Also, the γ-substituent tends to shift the $\pi_3 \rightarrow \pi_4$ transition band to a longer wavelength with respect to the acetylacetonate complex; 1670 cm^{-1} with a benzyl group and 1400 cm^{-1} with a phenyl, while the benzyl group obviously has a greater effect on the π-energy level. The secondary bands (^1L_b) of the benzene ring appear in the 3-benzyl-2, 4-pentanedione complex as shoulders located at 264 and 270 mμ, while the phenyl derivative demonstrates in its spectrum the first primary band (^1L_a) of a phenyl substituent at 231.5 mμ.

Chromium Complexes.—The general appearance of the absorption spectra of transition metal complexes is quite different from those of non-transition metal complexes, such as aluminum complexes. The splittings of the $\pi \rightarrow \pi^*$ band

caused by the π-interaction between metal and ligand, and the appearance of electron transfer bands ($d_\varepsilon \rightarrow \pi^*$) and of $d_\varepsilon \rightarrow d_\gamma$ bands brought about by a ligand field are characteristic of the absorption spectra of transition metal complexes. The general trend of the absorption spectra of trivalent metal complexes of the present ligands is quite similar to that of the corresponding acetylacetonate complexes. Therefore, the results of

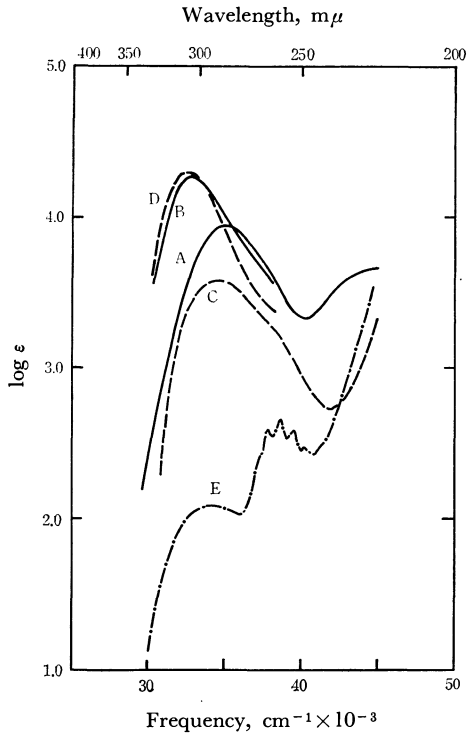

Fig. 1. Absorption spectra of 2,4-pentanediones in ethanol: A, 3-phenyl-2,4-pentanedione; B, 3-phenyl-2,4-pentanedione with sodium ethoxide; C, 3-benzyl-2,4-pentanedione; D, 3-benzyl-2,4-pentanedione with sodium ethoxide; E, 3,3-dibenzyl-2,4-pentanedione.

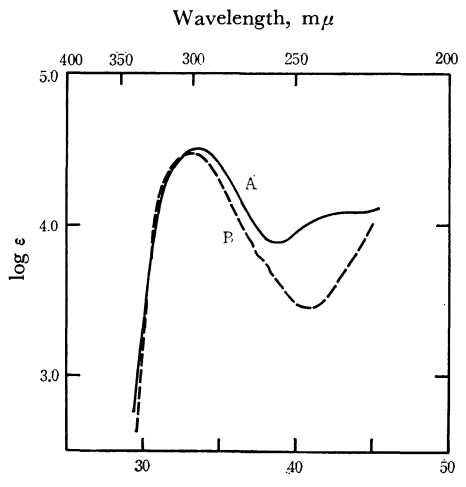

Fig. 2. Absorption spectra of aluminum(III) complexes in ethanol: A, tris(3-phenyl-2,4-pentanediono)aluminum(III); B, tris(3-benzyl-2,4-pentanediono)aluminum(III).

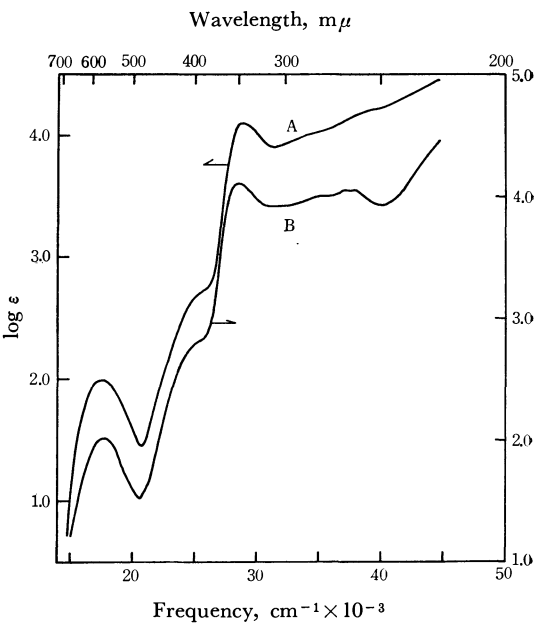

Fig. 3. Absorption spectra of chromium(III) comlexes in ethanol: A, tris(3-phenyl-2,4-pentanediono)chromium(III); B, tris(3-benzyl-2,4-pentanediono)chromium(III).

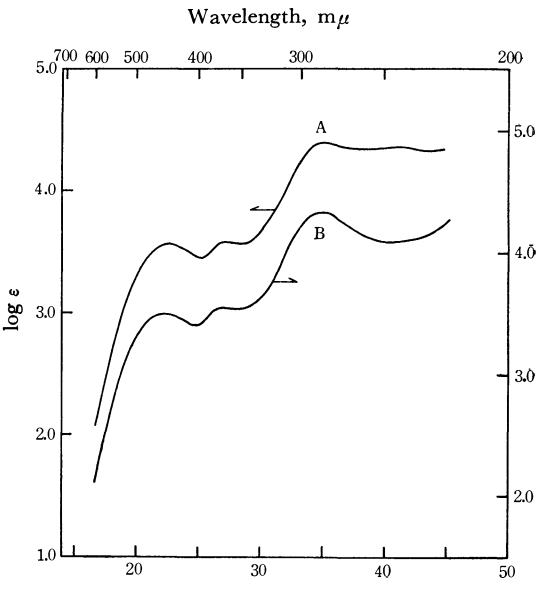

Fig. 4. Absorption spectra of iron(III) complexes in ethanol: A, tris(3-phenyl-2,4-pentanediono)-iron(III); B, tris(3-benzyl-2,4-pentanediono)iron-(III).

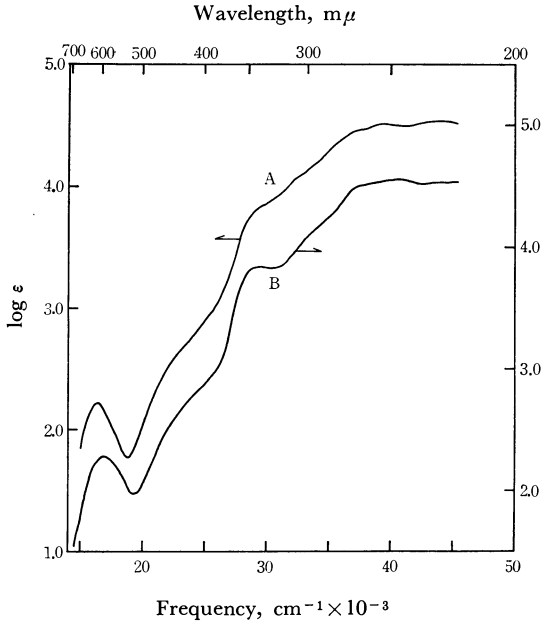

Fig. 5. Absorption spectra of cobalt(III) complexes in ethanol: A, tris(3-phenyl-2,4-pentanediono)cobalt(III); B, tris(3-benzyl-2,4-pentanediono)cobalt(III).

the Hückel LCAO-MO calculation carried out by Barnum[5] are referred to in the assignment of absorption bands in this work.

The 3-phenyl derivative shows extremely broad bands in the ultraviolet region of its electronic spectrum due to the presence of $\pi\rightarrow\pi^*$ transition bands of a phenyl ring. Thus, the assignment of $\pi_3\rightarrow\pi_4$ bands would involve some uncertainty due to the lack of an exact resolution of absorption bands. The 258 mμ band in ethanol is tentatively assigned to the $\pi_3(e)\rightarrow\pi_4(a_1)$ transition. In the range of $\pi_3(e)\rightarrow\pi_4(a_1)$ transition for the 3-benzyl-2,4-pentanedione complex, three absorption bands appeared at 257, 265 and 270 mμ; of these, the first one was found to be a weak shoulder. Some of these bands (most likely the latter two) are presumably due to the $\pi\rightarrow\pi^*$ secondary bands (^1L_b) of the benzene ring. The 289 and the 310 mμ bands in the phenyl derivative, and the 285 and the 318 mμ bands in the benzyl (when ethanol is used as a solvent), all of which appeared as shoulders, were assigned to the $\pi_3(e)\rightarrow\pi_4(e)$ overlapped with $\pi_3(a_2)\rightarrow\pi_4(a_1)$ and the $\pi_3(a_2)\rightarrow\pi_4(e)$ transitions respectively. All these $\pi_3\rightarrow\pi_4$ bands shifted to longer wavelengths upon replacement at the 3-position, with reference to those of the 2,4-pentanedione complex.

Electron transfer ($d_\varepsilon\rightarrow\pi_4$ transition) bands were also observed to shift to longer wavelengths upon replacement of the 3-position, relative to the parent complex. The overlapping $d_\varepsilon(a_1)\rightarrow\pi_4(e)$ and $d_\varepsilon(e)\rightarrow\pi_4(a_1)$ transitions are attributed to the 348 mμ band and the 352 mμ band, while the $d_\varepsilon(e)\rightarrow\pi_4(e)$ transition are attributed to the 395 mμ shoulder band and the 400 mμ shoulder band in the phenyl and the benzyl derivative respectively.

The first $d\rightarrow d^*$ ($^4A_{2g}$—$^4T_{2g}$) transition lies at 575 and 565 mμ in the phenyl and the benzyl derivative respectively. On the other hand, a shoulder lying in 410—440 mμ for the phenyl derivative and one in 420—445 mμ for the benzyl are assigned to the second $d\rightarrow d^*$ band. Since 2,4-pentanedione has been shown to be placed in the spectrochemical series[11] in the neighborhood of oxalate and water, the second $d\rightarrow d^*$ ($^4A_{2g}\rightarrow{}^4T_{1g}$) transition is expected to lie close to the 416 mμ band of the oxalate complex[12] or to the 407 mμ band of the aqueous complex.[12] In addition, Sone[13] suggested that the following relationship holds among the first and the second bands for the chromium(III) complex:

$$\nu_2 = 1.117\,\nu_1 + 13.06$$

where ν_1 and ν_2 represent the first and the second bands in the frequency unit (10^{13} sec^{-1}) respectively. From this equation, the second bands for both the phenyl and benzyl derivatives may be expected to appear in the vicinity of 420 mμ. Thus, the above assignment for the second $d\rightarrow d^*$ band seems reasonable.

Cobalt Complexes.—The $\pi_3(e)\rightarrow\pi_4(a_1)$, $\pi_3(e)\rightarrow\pi_4(e)$ overlapped with $\pi_3(a_2)\rightarrow\pi_4(a_1)$, and the $\pi_3(a_2)\rightarrow\pi_4(e)$ transitions are believed to lie, respectively, at 228.5, 253, and 308 mμ (as a slight shoulder) in the phenyl derivative, and at 227, 248.5, and 300 mμ (as a slight shoulder) in the benzyl derivative. The first and second transition bands are shifted to shorter wavelengths with reference to those of the 2,4-pentanedione complex. On the longer wavelength side of the $\pi_3(e)\rightarrow\pi_4(e)$ and $\pi_3(a_2)\rightarrow\pi_4(a_1)$ bands in both complexes, there exist several shoulder bands, among which the 263 mμ and the 270 mμ band are most likely to be ascribed to the secondary band (^1L_b) of a benzene.

The $d_\varepsilon\rightarrow\pi_4$ ($a_1\rightarrow e$, $e\rightarrow a_1$) band in the phenyl and benzyl derivatives shifted to longer wavelengths, at 338 (shoulder) and 341 mμ respectively, with reference to that in the 2,4-pentanedione complex. On the longer wavelength side of these $d_\varepsilon\rightarrow\pi_4$ bands, there were observed very broad shoulders in which the $d_\varepsilon(e)\rightarrow\pi_4(e)$ charge transfer band and the second $d\rightarrow d^*$ ($^1A_{1g}\rightarrow{}^1T_{2g}$) band are expected to be involved. According to the LCAO-MO calculation for the 2,4-pentanedione complex,[5] the $d_\varepsilon(e)\rightarrow\pi_4(e)$ band for this complex

11) Y. Shimura and R. Tsuchida, This Bulletin, **29**, 311 (1956).
12) J. S. Griffith, "The Theory of Transition Metal Ions," Cambridge University Press, Cambridge (1961), p. 425.
13) K. Sone, *J. Chem. Soc. Japan, Pure Chem. Sect.* (*Nippon Kagaku Zassi*), **71**, 271, 316 (1950).

is expected to lie around 400 mμ, although only a shoulder was observed in this range. Meanwhile, Shimura and Tsuchida[11] assigned the 405 mμ band in the 2, 4-pentanedione complex to the second $d \rightarrow d^*$ transition. On the other hand, Sone[13] has proposed a relationship which may correlate the first $d \rightarrow d^*$ band with the second:

$$\nu_2 = 1.189\,\nu_1 + 13.31$$

(ν_1 and ν_2: frequency in $10^{13}\,\mathrm{sec}^{-1}$ unit)

The first band ($^1A_{1g} \rightarrow {}^1T_{1g}$) for the 2, 4-pentanedione complex, and the 3-phenyl- and 3-benzyl-2, 4-pentanedione complexes were observed at 595, 608 and 596 mμ (in chloroform) respectively. Thus, the second bands for these complexes are expected to lie in the 410—420 mμ range. Nevertheless, no unambiguous assignment was made because of the broadness of the absorption spectra in this range, as has been mentioned above.

Iron Complexes.—All the absorption bands in the 3-phenyl- and the 3-benzyl-2, 4-pentanedione complexes were observed to shift to longer wavelengths with reference to the corresponding bands in the 2, 4-pentanedione complex, as is shown in Table III and Fig. 4. The $\pi_3(e) \rightarrow \pi_4(a_1)$ and the $\pi_3(e) \rightarrow \pi_4(e)$ and $\pi_3(a_2) \rightarrow \pi_4(a_1)$ bands are believed to be located at 247 and 284 mμ in the phenyl derivative, and at 240 (shoulder) and 286 mμ in the benzyl derivative, respectively. Two distinct bands appear in the visible region for each iron complex of 2, 4-pentanedione derivatives. The absorption bands lying around the 370 mμ range are assigned to the $d_\varepsilon(a_1) \rightarrow \pi_4(e)$ and $d_\varepsilon(e) \rightarrow \pi_4(a_1)$ transitions. Barnum[4,5] has not made any assignment for the 437 mμ band in the 2, 4-pentanedione complex. The corresponding bands in the phenyl and benzyl derivatives are, respectively, at 445 and 450 mμ in ethanol. The magnitudes of these spectral shifts from the corresponding band in the 2, 4-pentanedione complex are 400 and 700 cm^{-1} for the phenyl and the benzyl derivatives respectively. Although the direction of the band shift is the same as that of the $d \rightarrow \pi^*$ bands, its magnitude is smaller than that of the latter (1100 cm^{-1} for the phenyl derivative, and 1400 cm^{-1} for the benzyl). In addition, as the polarity of a solvent increases, the band tends to shift to a shorter wavelength; there is also a decrease in its intensity. This solvent effect seems to be, in general, characteristic of an electronic transition involving a nonbonding electron, while $d \rightarrow \pi$ bands do not show such a strong solvent-dependency. Thus, a band appearing in the 450 mμ range is considered to be due to the $n \rightarrow d_\gamma$ transition, in which oxygen n-electrons are involved.

The $d \rightarrow d^*$ transitions ($^6A_{1g} \rightarrow {}^4T_{1g}$, and $^6A_{1g} \rightarrow {}^4T_{2g}$) are expected to lie in a region with much longer wavelengths; they were not observed in the present measurements.

Discussion

Ligands.—An absorption band characteristic of β-diketones is generally subject to the solvent effect which controls their keto-enol isomerism. This absorption band consists of two components: a $\pi \rightarrow \pi^*$ transition of an enol form, and a $n \rightarrow \pi^*$ forbidden transition of the corresponding keto-form, which appears on the longer-wavelength side of the former. 3-Phenyl-2, 4-pentanedione shows an absorption band at 284 mμ in n-hexane which shifts to a slightly longer wavelength with a somewhat decreased intensity in ethanol. As far as the spectral shift is concerned, the same solvent-dependency was observed for 3-benzyl-2, 4-pentanedione. However, the absorption intensity for this ligand decreases in ethanol to a greater extent than for 3-phenyl-2, 4-pentanedione. This suggests that the enol component of the latter diketone may be predominant in ethanol,* though in general polar solvents stabilize a keto-form. On the other hand, the 3-benzyl derivative increases its keto component when the solvent is changed from n-hexane to ethanol.

$\pi \rightarrow \pi^*$ Bands.—The spatial configuration of a phenyl ring relative to the chelate ring in a 3-phenyl-2, 4-pentanedione complex seems to control the extent of π-interaction among these groups. Such a π-interaction among these two groups would not be as strong as among the two phenyl groups in biphenyl, or as among olefinic and phenyl groups in styrene, since the latter two molecules show an absorption band in the range around 250 mμ,[14] while in a 3-phenyl-2, 4-pentanedione complex no such band exists in that range. In 2,6-dimethyl-biphenyl the inter-ring resonance may be reduced to a certain extent by the twist of both rings from coplanarity. Such a diminished π-interaction makes the absorption band appear in the 240 mμ range[15] as a shoulder, which is assigned to the first primary band (^1L_a) of a benzene ring in this substituted biphenyl. Meanwhile, in the aluminum complex of 3-phenyl-2, 4-pentanedione the steric interaction among a phenyl ring and two methyl groups on the chelate ring tends to twist both phenyl and chelate rings. However, such a fairly large deviation from coplanarity will not destroy all of the inter-ring resonance interaction, since the aluminum complex shows a $\pi \rightarrow \pi^*$ transition band at 231.5 mμ. In other transition metal complexes of the same ligand, absorption bands are broad and intense in the 240—250 mμ range in comparison with those of the corresponding metal complexes of 2, 4-pentanedione and of 3-benzyl-2, 4-pentanedione. The breadth of absorption bands in such a range

* This keto-enol isomerism was studied in this laboratory by means of infrared and NMR spectroscopies. These results will be described in a forthcoming paper.

14) H. E. Ungnarde, Ed., "Organic Electronic Spectral Data," Vol. II, Interscience Publishers, New York (1957), pp. 130, 295.

may be ascribed to the existence of the primary band (^1L_a) of a benzene ring in addition to the $\pi \rightarrow \pi^*$ bands of the chelate ring. From the observations mentioned above, the inter-ring π-interaction remains to a limited extent in the metal complexes of 3-phenyl-2, 4-pentanedione. Meanwhile, this inter-ring π-interaction may help to raise the π_3 orbital of the chelate ring to a higher energy, thus shifting the $\pi_3 \rightarrow \pi_4$ band to a longer wavelength.

In the metal complexes of 3-benzyl-2, 4-pentanedione, both the hyperconjugation and inductive effects of the methylene group may raise the π_3 level to a higher energy.

The enolate ions of β-diketones decrease their delocalization energy upon chelation with either hydrogen or aluminum. The enol-forms of β-diketones show their $\pi \rightarrow \pi^*$ band at shorter wavelengths relative to the corresponding enolate ions. The magnitude of such a spectral shift follows the sequence:

2, 4-pentanedione ($2700\ cm^{-1}$) > 3-phenyl-2, 4-pentanedione ($2400\ cm^{-1}$) > 3-benzyl-2, 4-pentanedione ($2250\ cm^{-1}$)

Such a great loss of delocalization energy in the enol forms of β-diketones (structure I) is consistent

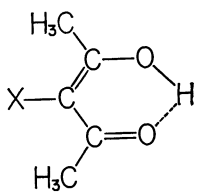

(I)

X = H, phenyl, benzyl

with the fact that an enolic proton is located closer to one oxygen than the other, that the two C–C bonds are not equivalent to each other in bonding character, and that neither are the two C–O bonds. Meanwhile, an identical bond character is expected for the C–C bonds and also for the C–O bonds in the enolate ion, as is illustrated by structure II.

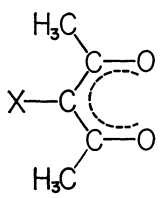

(II)

X = H, phenyl, benzyl

On the other hand, upon chelation with the aluminum ion, the $\pi \rightarrow \pi^*$ band shifts to a wavelength lower by $850\ cm^{-1}$ than that of the corresponding enolate ion, regardless of the ligand species. The substituent effect on the chelate ring, therefore, seems parallel to that on the enolate ion. This leads one to the conclusion that π-electrons in the ligand part remain delocalized much like those in the corresponding enolate ion, even when the coordinate bonds are formed among an aluminum ion and carbonyl oxygens. The structure of such a chelate ring of the aluminum complexes may be represented by III.

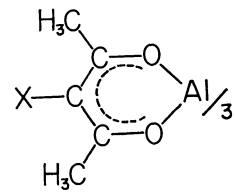

(III)

X = H, phenyl, benzyl

The metal-ligand π-interaction in transition metal complexes results in a splitting of the $\pi_3 \rightarrow \pi_4$ band, and in a shift of these $\pi_3 \rightarrow \pi_4$ transitions to higher energies. The magnitude of the spectral shift to a lower wavelength was found to depend on the number of d_ε electrons that the central metal ion possesses, as has been observed in the 2, 4-pentanedione complexes.[4,5] Thus, the $\pi_3 \rightarrow \pi_4$ transitions in the trivalent metal complexes of the present 2, 4-pentanedione derivatives have been found to appear in this increasing order of energy:

$$Cr < Fe < Co$$

In the iron and chromium complexes, each $\pi_3 \rightarrow \pi_4$ transition band was observed to shift to a longer wavelength as the ligand varies in this order: 2,4-pentanedione, 3-phenyl-2, 4-pentanedione, and 3-benzyl-2, 4-pentanedione. On the other hand, both the $\pi_3(e) \rightarrow \pi_4(a_1)$ band, and the $\pi_3(e) \rightarrow \pi_4(e)$ combined with $\pi_3(a_2) \rightarrow \pi_4(a_1)$ band in the cobalt complexes shift in the reverse direction in the same order. In the transition metal complexes, the metal-ligand π-interaction has a major effect on the $\pi_3 \rightarrow \pi_4$ transition, and it seems to increase with respect to the ligands in this order: 2, 4-pentanedione, 3-phenyl-2, 4-pentanedione, and 3-benzyl-2, 4-pentanedione. As each $\pi_3 \rightarrow \pi_4$ transition band in a complex shifts to a shorter wavelength with reference to the enolate ion of the correspond ing ligand, the comparison of the size of these spectral shifts may give the extent of metal-ligand π-interaction. Thus, a 3-benzyl-2, 4-pentanedione complex in general shows the greatest spectral shift among the corresponding metal complexes of three different 2, 4-pentanediones, while a metal complex of the 3-phenyl derivative comes next. For example, the $\pi_3(e) \rightarrow \pi_4(a_1)$ band in cobalt complexes shifts to a wavelength shorter from the

15) G. H. Beaven, "Steric Effects in Conjugated Systems," Butterworths, London (1958), Chapter 3.

enolate ion by 9500 cm^{-1} with 2, 4-pentanedione as the ligand, by 11000 cm^{-1} with 3-phenyl-2, 4-pentanedione, and by 12000 cm^{-1} with the 3-benzyl derivative.

It may be concluded that the $\pi_3 \rightarrow \pi_4$ transition is affected by either or both of the two major effects of a substituent at the 3-position of 2, 4-pentanedione:

(1) A substituent tends to raise the π_3 level of the chelate π-orbitals to a higher energy, either through the π-interaction with the chelate ring or its inductive effect on the chelate ring. As a result, a $\pi_3 \rightarrow \pi_4$ band shifts to a longer wavelength.

(2) Such π_3-orbitals that were raised to a higher energy may interact with the d_ε-orbitals. This interaction lowers the energy of the π_3-orbitals on the one hand and raises that of the d_ε-orbitals on the other. This effect results in a shift of the $\pi_3 \rightarrow \pi_4$ transition to a higher energy.

In the transition metal complexes, both of the substituent effects may come into play in the $\pi_3 \rightarrow \pi_4$ transitions, while the first effect is expected to be predominant in the aluminum complexes and the enolate ions. Upon substitution at the 3-position of 2, 4-pentanedione, the spectral shift toward a longer wavelength was observed to be greater in the aluminum complexes and the enolate ions than in the transition metal complexes. This experimental fact can be understood from the above point of view.

Meanwhile, the greatest metal-ligand π-interaction is expected in the cobalt complexes as a result of the presence of the largest number of d_ε electrons. In this instance, the second substituent effect may prevail over the first one and $\pi_3 \rightarrow \pi_4$ transition bands may tend to shift to a lower wavelength upon substitution.

In general, the solvent effect tends to shift the $\pi \rightarrow \pi^*$ band to a longer wavelength in a solvent with a higher polarity. In fact, the $\pi \rightarrow \pi^*$ bands of the ligands (the enol form) appear on the longer wavelength side in ethanol relative to those measured in *n*-hexane, as is shown in Table II. On the other hand, it is interesting to note that the reverse spectral shifts were observed in the metal complexes when the solvent was changed from chloroform to ethanol.

$d_\varepsilon \rightarrow \pi_4$ Bands.—These transition bands tend to shift to lower energies upon substitution at the 3-position of 2, 4-pentanedione. The magnitudes of such spectral shifts in metal complexes are approximately 1100 cm^{-1} with a phenyl group and 1350—1450 cm^{-1} with a benzyl with reference to the corresponding bands in 2, 4-pentanedione complexes, regardless of the metal ions employed. These phenomena are most likely caused by electronic interaction among d_ε and π_3 orbitals, which raises d_ε orbitals to a higher energy. As for the metal species concerned, the $d_\varepsilon \rightarrow \pi_4$ transition energy is greatest for the cobalt complexes and least for the iron complexes.

$d \rightarrow d^*$ Bands.—From the first $d \rightarrow d^*$ bands observed for the cobalt and chromium complexes, 2, 4-pentanedione and its 3-benzyl derivative may be inferred to occupy a higher position relative to 3-phenyl-2, 4-pentanedione in the spectrochemical series. However, the strength of the coordinate bonds may not be directly related to the value of Δ, the energy difference between the d_ε and the d_γ orbitals, as the crystal field theory would predict. Since the metal-ligand π-interactions are involved[4,5] in these transition metal complexes, it is rather difficult to estimate the hypothetical crystal field effects of these ligands which may be expected in the absence of π-interaction.

Infrared and NMR studies of these trivalent metal complexes, as well as similar spectroscopic studies of some divalent metal complexes, are now in progress in this laboratory; these results will be described in a forthcoming paper.

BULLETIN OF THE CHEMICAL SOCIETY OF JAPAN VOL. 39 910—916 (1966)

Asymmetric Synthesis with Sugar Derivatives. I. The Conjugate Additions of Grignard Reagents to α, β-Unsaturated Esters of Sugar Derivatives

By Masajiro KAWANA and Sakae EMOTO

The Institute of Physical and Chemical Research, Komagome, Bunkyo-ku, Tokyo

(Received September 3, 1965)

Partial asymmetric syntheses were carried out in the reaction of Grignard reagents with crotonic and cinnamic esters of 1, 2 : 5, 6-di-*O*-cyclohexylidene-D-glucose, 1, 2 : 5, 6-di-*O*-isopropylidene-D-glucose, 1, 2-*O*-isopropylidene-5-deoxy-D-xylose and (−)-menthol. The reaction of 3-*O*-crotonyl-1, 2 : 5, 6-di-*O*-cyclohexylidene-D-glucose (Ic) with phenylmagnesium bromide, followed by the hydrolysis of the resulting ester, gave (−)-3-phenylbutyric acid (III) in 33% optical and 12% synthetic yields, while in the presence of cuprous chloride as a catalyst, III was obtained in 74% and 58% yields respectively. The reaction of 3-*O*-crotonyl-1, 2-*O*-isopropylidene-5-deoxy-D-xylose (Ie) with phenylmagnesium bromide gave (+)-acid (III) without cuprous chloride in 16% optical and 32% synthetic yields and (−)-acid (III) with cuprous chloride, in 58% and 61% yields respectively. The reaction of 3-*O*-cinnamoyl-1, 2 : 5, 6-di-*O*-cyclohexylidene-D-glucose (IVc) with benzylmagnesium chloride, followed by the saponification of the resulting ester, gave (−)-3, 4-diphenylbutyric acid (VI) in 18% optical and 62% synthetic yields without cuprous chloride, and in 17% and 58% yields with cuprous chloride. In the formation of acid (VI), cuprous chloride seemed to have no effect on optical and synthetic yields nor on the change in the sign of optical rotation. The steric courses of these reaction are discussed.

Numerous partial asymmetric syntheses have been made in an attempt to introduce a new asymmetric center into a carbon chain of organic acid under the influence of an optically active alkoxy group on the carbonyl carbon of the carboxylic ester. For example, 2-hydroxy-2-phenylpropionic acid (atrolactic acid) was asymmetrically synthesized by Grignard reaction from (−)-menthyl,[1] (+)-1-(2′, 4′, 6′-tricyclohexylphenyl) - ethyl[2] and (+)-α-phenyldihydrothebaine-isomethine[3] phenylglyoxylates, respectively, in 17, 66 and 91% optical yields. In these asymmetric syntheses, it is evident that the esters' asymmetric centers derived from the naturally-occurring terpenes or alkaloids play an important role in making one transient comformation of esters predominant over the others. However, sugar derivatives have been utilized as the alcohol to only a negligible extent in this field. Many oxygens on the asymmetric carbons of a sugar derivative are supposed to show a particular stereoselectivity in such reactions when organometallic compounds or metal catalysts are used. Thus, the authors were interested in the stereoselective addition of metallic compounds to the α, β-unsaturated esters of sugar derivatives.

Recently, Inouye and Walborsky[4] reported that a partial asymmetric synthesis of (+)-3-phenylbutyric acid (III) was achieved (5.4% optical yield) by the addition of phenylmagnesium bromide to (−)-menthyl crotonate (Ia), followed by the hydrolysis of the adduct (IIa) (Eq. 1); moreover, when the catalytic amount of cuprous chloride was added to the reaction mixture, the optical rotation of the acid III obtained had an opposite sign and its synthetic yield was somewhat increased, compared with the case of the absence of cuprous catalyst. However, the stereochemical course of the reactions has never been established. As to the conjugate addition of Grignard reagent to

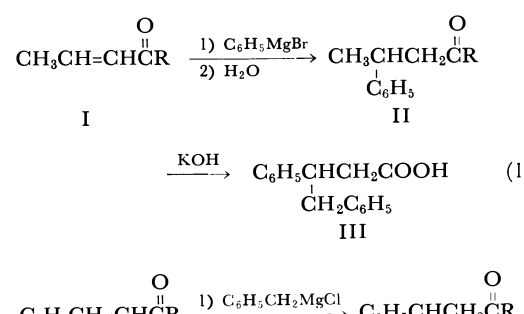

(1)

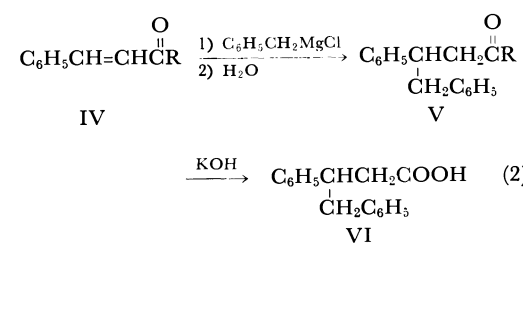

(2)

1) A. McKenzie, *J. Chem. Soc.*, **1904**, 1249.
2) V. Prelog, Eva Phillin, E. Watanabe and M. Wilhelm, *Helv. Chim. Acta*, **39**, 1086 (1956).
3) J. A. Berson and M. A. Greenbaum, *J. Am. Chem. Soc.*, 80, 445 (1958).
4) Y. Inouye and H. M. Walborsky, *J. Org. Chem.*, **27**, 2706 (1962).

R= a, (−)-Menthoxy
b, (±)-*sec*-Butoxy
c,

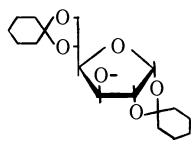

d,

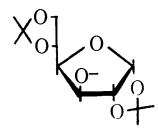

e,

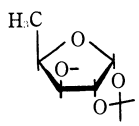

crotonate, Munch-Petersen[5] described that (±)-*s*-butyl crotonate (Ib) with phenylmagnesium bromide gave (±)-*s*-butyl 3-phenylbutyrate (IIb) in a 67% yield in the presence of cuprous chloride, which had been known to catalyze predominantly a 1, 4-addition over a 1, 2-addition in the α, β-unsaturated carbonyl system (Eq. 1). He and his co-workers[6] also found that (—)-*s*-butyl cinnamate (IVb) with benzylmagnesium chloride gave (±)-*s*-butyl 3, 4-diphenylbutyrate (Vb) in a 63% yield; in this case, cuprous chloride has no catalytic effect (Eq. 2).

The present authors have studied[7] the partial asymmetric syntheses achieved by the 1, 4-addition of phenylmagnesium bromide to crotonic esters (Ic, Id and Ie) and of benzylmagnesium chloride to cinnamic esters (IVc, IVd and IVe), using three kinds of sugar derivatives, 1, 2 : 5, 6-di-*O*-cyclohexylidene-D-glucose (VII),[8] 1, 2 : 5, 6-di-*O*-isopropylidene-D-glucose (VIII)[9] and 1, 2-*O*-isopropylidene-5-deoxy-D-xylose (IX),[10] in the presence or absence of a cuprous catalyst.

Procedure and Results

The crotonic ester of each sugar derivative (Ic, Id and Ie) was prepared by the addition of crotonyl chloride to a solution of the sodium alcoholate of each sugar derivative in toluene, according to a modification of the method of Otey et al.[11] This method gave a better yield than the general reaction of the free hydroxy-group of a sugar with crotonyl chloride in pyridine-chloroform. The cinnamic ester of each sugar derivative (IVc, IVd and IVe) was obtained in a fairly good yield by the reaction of each sugar derivative with cinnamoyl chloride in pyridine-chloroform.

Their yields, physical properties and analyses are listed in Table III.

The Grignard reactions were carried out in ether at temperature from −17°C to −15°C by a method based on the procedure of Munch-Petersen.[12] A catalytic amount of cuprous chloride was added in four portions at regular intervals during the addition of the esters to the Grignard reagents. The adducts were not purified but were completely saponified by refluxing them with a large excess of potassium hydroxide in aqueous alcohol for 16 hr. The racemization of the asymmetric carbon atoms of 3-phenylbutyric acid (III) and 3, 4-diphenylbutyric acid (VI) did not occur during saponification (See Ref. 4 and the Experimental Section). 1, 2 : 5, 6-Di-*O*-cyclohexylidene-D-glucose (VII) and 1, 2 : 5, 6-di-*O*-isopropylidene-D-glucose (VIII) were recovered in 60—85% yields, but the recovery of 1, 2-*O*-isopropylidene-5-deoxy-D-xylose (IX) was poorer because the compound was readily soluble in water.

The 3-phenylbutyric acid (III) obtained was identified by a comparison of its infrared spectrum with that of an authentic sample.[4] Elemental analysis of the crystalline anilide of III was performed. The optical[13] and synthetic yields of III are shown in Table I.

In this reaction, Ic gave (−)-acid (III) in 33% optical and 12% synthetic yields without cuprous chloride (Exp. 3), while in the presence of cuprous chloride, it gave III with the same sign of optical rotation as that in the case of no catalyst in increased optical and synthetic yields, 74% and 58% respectively (Exp. 4). The effect of cuprous chloride on the reaction of Id (Exp. 6 and 7) showed a same tendency as that on the reaction of Ic. On the contrary, it is noteworthy that the reaction of Ie (Exp. 8) gave (+)-acid (III) in 16% optical and 32% synthetic yields without cuprous chloride, but (−)-acid (III) was afforded in much better optical (58%) and synthetic (61%) yields with cuprous chloride (Exp. 9). However, Ia gave (+)-acid (III) without cuprous catalyst in poor optical yields under the conditions of both Inouye[4] and us.

The 3, 4-diphenylbutyric acid (VI) obtained by the reaction of each sugar ester (IVc, IVd and IVe) or (−)-menthyl cinnamate (IVa) with benzylmagnesium chloride was identified by a comparison

5) J. Munch-Peterson, ibid., **22**, 170 (1957).
6) J. Munch-Peterson, P. Møller Jørgensen and S. Refn, *Acta Chem. Scand.*, **13**, 1955 (1959).
7) Most of the results and assumptions presented in this paper were reported at the 18th Annual Meeting of the Chemical Society of Japan, Osaka, April, 1965.
8) R. C. Hockett, R. E. Miller and A. Sacttergood, *J. Am. Chem. Soc.*, **71**, 3072 (1949).
9) W. L. Glen, G. S. Myers and G. A. Grant, *J. Chem. Soc.*, **1951**, 2568.
10) P. A. Levene and J. Compton, *J. Biol. Chem.*, **111**, 325 (1935).
11) F. H. Otey and C. L. Mehltretter, *J. Am. Oil. Chemists' Soc.*, **35**, 455 (1958).
12) J. Munch-Petersen and V. K. Andersen, *Acta Chem. Scand.*, **15**, 271 (1961).
13) Calculated on $[\alpha]_D$ −57°: H. Rupe (*Ann.*, **369**, 311 (1909)) reported $[\alpha]_D^{20}$ −57.23° (α = −5.03, benzene).

TABLE I. ASYMMMETRIC SYNTHESES OF 3-PHENYLBUTYRIC ACID (III)

Ester	Exp. No.	Cat.	Optical yield %	Synthetic yield %	$[\alpha]_D$ Crude	$[\alpha]_D$ Pure (concn. in benzene)	Temp., °C	B. p. (0.5—1 mmHg) °C
Ia	1	no	9	51	+4°	+5° (7.61)	18	100—102
	2	Cu_2Cl_2	5	42	−0.0°	−3° (10.2)	18	98—103
	*1	no	5	46.1	—	+3.1 (10.3)	25	113—115*4
	*1	Cu_2Cl_2	10	63.5	—	−5.9°(—)	25	—
Ic	3	no	33	12	−14°	−19° (5.05)	20	98—100
	4	Cu_2Cl_2	74	58	−35°	−42° (4.01)	20	97— 99
Id	5	no	32	12	−14°	−18° (5.49)	20	97—100
	6	Cu_2Cl_2	68	50	−29°	−39° (5.11)	20	102—105
	7*2	Cu_2Cl_2	70	44	−36°	−40° (3.99)	16	104—106
Ie	8	no	16	32	+ 4°	+ 9° (5.54)	20	103—107
	9	Cu_2Cl_2	58	61	−22°	−33° (4.55)	18	97—100

Anilides of III

Ester	Exp. No.	n_D	Temp. °C	M. p. °C	$[\alpha]_D$ (concn. in acetone) Temp. °C	Anal.*3 (Found) % C	H	N
Ia	1	1.5153	17	135—137	+2° (5.48) 28	80.62	7.17	5.69
	2	1.5161	18	136—138	−1° (5.87) 25	80.15	7.25	5.82
	*1	1.5150	25	—	— — —	—	—	—
	*1	—	—	—	— — —	—	—	—
Ic	3	1.5179	19	134—135	−12° (5.47) 25	80.39	7.08	5.56
	4	1.5182	16	131—141	−25° (5.89) 18	80.13	6.80	5.82
Id	5	1.5179	19	134—136	−12° (5.56) 25	80.54	7.22	5.67
	6	1.5180	20	133—137	−24° (5.48) 28	80.58	7.05	5.65
	7*2	1.5189	16	133—140	−25° (3.52) 28	80.23	7.12	5.69
Ie	8	1.5168	20	132—136	+ 5° (5.83) 18	80.67	6.99	5.71
	9	1.5160	18	133—140	−22° (5.24) 18	80.10	6.86	5.83

*1 Data of Inouye et al. Ref. 4
*2 Alkaline saponification for 5 hr.
*3 Calcd. for $C_{16}H_{17}NO$: C, 80.36; H, 7.16; N, 5.85%
*4 3 mmHg

TABLE II. ASYMMETRIC SYNTHESES OF 3,4-DIPHENYLBUTYRIC ACID (VI)

Ester	Exp. No.	Cat.	Optical yield %	Synthetic yield %	$[\alpha]_D$ Crude	$[\alpha]_D$ Pure (concn. in benzene)	Temp., °C	B. p. (0.5—1 mmHg) °C	M. p. °C	Anal.*2 (Found) % C	H
IVa	10	no	32	59	−25°	−19° (6.04)	20	155—162	81—92	80.15	6.51
	11	Cu_2Cl_2	27	61	−24°	−16° (6.06)	20	155—160	81—91	80.01	6.64
IVc	12	no	18	62	− 9°	−11° (8.03)	20	150—158	84—93	80.27	6.47
	13*1	no	17	62	−10°	−10° (5.39)	20	155—165	89—93	80.23	6.78
	14	Cu_2Cl_2	17	58	− 8°	−10° (6.23)	18	155—158	86—93	79.89	6.50
IVd	15	no	18	49	−12°	−11° (9.63)	20	150—158	85—93	80.08	6.65
	16	Cu_2Cl_2	22	40	−12°	−13° (6.20)	15	148—153	84—92	79.99	6.41
IVe	17	no	18	53	− 7°	−11° (3.78)	20	147—149	84—94	79.70	6.34
	18	Cu_2Cl_2	17	56	− 8°	−10° (6.04)	20	158—167	80—89	80.05	6.95

*1 Alkaline saponification for 5 hr.
*2 Calcd. for $C_{16}H_{16}O_2$: C, 79.97; H, 6.71%

TABLE III. SUGAR ESTERS OF CROTONIC AND CINNAMIC ACIDS

Ester	Yield %	M. p. °C	$[\alpha]_D$ (concn. in benzene) Temp. °C	IR $\nu_{max}^{cm^{-1}}$ (in $CHCl_3$) C=O	C=C	Molecular formula	C, % Found	Calcd.	H, % Found	Calcd.
Ic	76	glass	−18° (4.97) 18	1725	1660	$C_{22}H_{32}O_7$	64.61	64.68	8.06	7.90
Id	52	64—66	−36° (2.83) 18	1729	1661	$C_{16}H_{24}O_7$	58.70	58.52	7.14	7.37
Ie	28	47—49	+31° (2.80) 18	1723	1661	$C_{12}H_{18}O_5$	59.79	59.49	7.25	7.49
IVc	39	132—134	−54° (4.96) 22	1717	1641	$C_{27}H_{34}O_7$	68.84	68.92	6.87	7.28
IVd	76	glass	−70° (3.28) 18	1715	1639	$C_{21}H_{26}O_7$	64.84	64.60	6.52	6.71
IVe	84	73—75	+44° (4.72) 22	1715	1640	$C_{17}H_{20}O_5$	66.68	67.09	6.40	6.22

of its infrared spectrum with the sample prepared from an authentic ester (Vb).[6] Optically pure VI, $[\alpha]_D -60°$, was obtained for the first time by the resolution of quinine salt in the present experiment. The optical[14] and synthetic yields of VI are shown in Table II. The reactions of IVc, IVd and IVe all gave (−)-acid (VI) in a 18% optical yield in the absence of cuprous chloride (Exp. 12, 15 and 17) and in 17, 22 and 17% yields respectively in the presence of cuprous chloride (Exp. 14, 16 and 18). The reaction of IVa gave (−)-acid (VI) in a 32% optical yield without cuprous chloride (Exp.10). It is interesting that cuprous chloride seems to have no effect on the optical and synthetic[6] yields in the reactions of cinnamates with benzylmagnesium chloride.

Discussion

Recently Munch-Petersen et al.[15] suggested that there were two types of mechanisms in the addition of Grignard reagents to conjugated esters, depending on the natures of the substrate and the Grignard reagent, i. e., the carbanion mechanism, A, and the cyclic mechanism, B. These mechanisms have

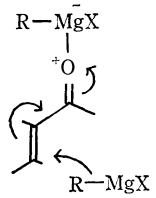

A

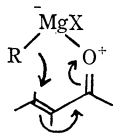

B

been considered to be irreversible. They also reported that the mode of the catalytic action of cuprous chloride was still obscure, but that it exerted its effect by way of complex formation between the cuprous ion and the carbon-carbon double bond.

The results may be explained by the following

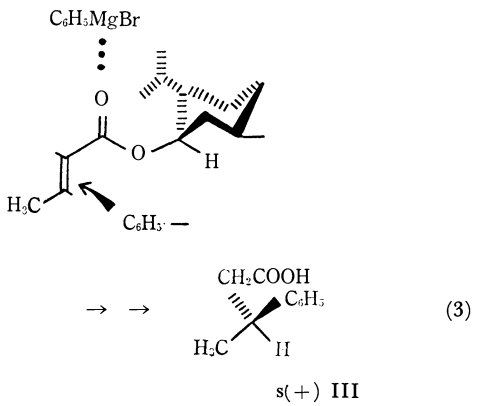

(3)

s(+) III

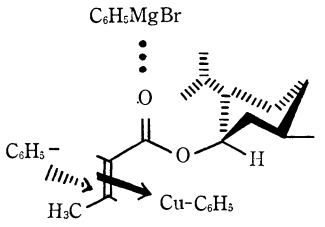

X

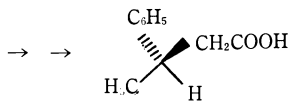

(4)

R(−) III

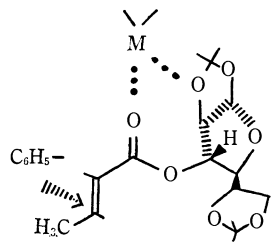

XI

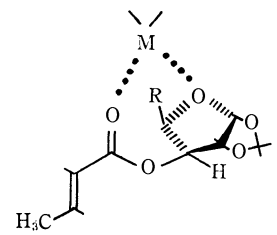

XII

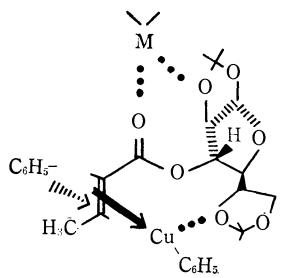

XIII

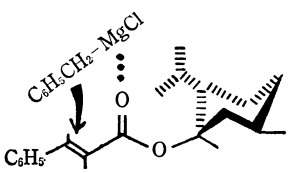

XIV

14) Calculated on $[\alpha]_D$ −60°.

15) S. Jacobsen, A. Jart, T. Kindt-Larsen, I. G. K. Andersen and J. Munch-Petersen, *Acta Chem. Scand.*, **17**, 2423 (1963).

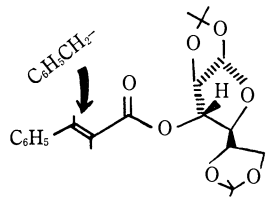

XV

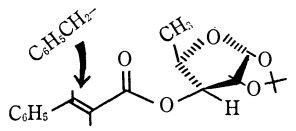

XVI

M=Mg or Cu

assumptions. If Prelog's rule[16] can be applied to these asymmetric syntheses, on the reaction of (−)-menthyl crotonate (Ia) the phenyl group in the Grignard reagent would preferrably enter from the least-hindered side of the double bond in the mechanism A to give s-(+)-acid (III) predominantly, as is shown in Eq. 3, because the absolute configurations of (−)-menthol[17] and III[18] have been established to be as depicted in Eqs. 3 and 4. In the presence of cuprous chloride, the initial attack of the phenyl copper[15,19] prepared from cuprous chloride and the Grignard reagent would be towards the least hindered side of the double bond to form a complex (X); then the phenyl group of the Grignard reagent or phenyl copper would enter from the other side to give R-(−)-acid (III) predominantly (Eq. 4).

On the reaction of both the sugar esters, Ic and Id, the model XI is expected to be most stable, since Prelog's model XII has the steric hindrance of the substituent at C-4 of the furan ring against the ester carbonyl. Furthermore, magnesium or copper could coordinate[20] with the unshared electron pairs of oxygen to make this model XI more rigid. This force is very useful in preventing free rotation between the sugar part and the acid part. Consequently, the attack of the phenyl group from the front side of the double bond according to the mechanism A would be sterically hindered by the 5, 6-*O*-cyclohexylidene group of Ic or the 5, 6-*O*-isopropylidene group of Id, and R-(−)-acid (III) would be more predominantly produced. When cuprous chloride is present, the oxygen at C-5 of glucose would contribute to form a copper complex which would fix the conformation as is shown in XIII.[21] This model (XIII) predicts not only that R-(−)-acid (III) will predominate, but that the optical yield will be high.

On the reaction of Ie, it is considered that the model XII (R=CH_3) would be rather stable because of the decrease of the bulkiness of the substituent at C-4 of the furan ring. Thus, the phenyl group would attack from the front side of the double bond, as a result of the steric effect of the methyl group, to give s-(+)-acid (III) predominantly by the mechanism A. Although the mode of action of cuprous chloride is not clear in this case, the increase in the optical yield with cuprous chloride suggests that the oxygen at C-2 of the furan ring participates in the formation of the similar chelation, as is shown in XIII. The acid III obtained, therefore, has a R-(−)-configuration in a good optical yield.

Meanwhile, the absence of any catalytic effect of cuprous chloride on the formation of 3, 4-diphenylbutyric acid (VI) suggests that the esters of cinnamic acid would react with the Grignard reagent according to the mechanism B. Though the absolute configuration of VI has not yet been established, the formation of VI, which has the same sign of optical rotation in every synthesis, may be attributed to the steric effect of the isopropyl group in (−)-menthol (XIV: Prelog's model), the 1, 2-*O*-cyclohexylidene or the 1, 2-*O*-isopropylidene group (XV: the most stable model) in IVc and IVd, and the methyl group (XVI: Prelog's model) in IVe, which block the backside-attack of the benzyl group on the double bond. In these models, the optical yields of VI prepared from the sugar esters would be lower than that of VI prepared from (−)-menthyl cinnamate (IVa), because there is no fixation between the ester carbonyl and the sugar part.

Experimental[22]

The Sugar Ester of Crotonic Acid.—The esters were prepared by a modification of the method of Otey et al.[11] Into a solution of 0.075 mol. of the sugar derivative, 1, 2 : 5, 6-di-*O*-cyclohexylidene-D-glucose (VII), 1, 2 : 5, 6-di-*O*-isopropylidene-D-glucose (VIII) or 1, 2-*O*-isopropylidene-5-deoxy-D-xylose (IX), in 100 ml. of dry toluene, there was stirred 6.0 g. of sodium powder in three portions over a 2 hr. period at room temperautre; the stirring was then continued overnight. To the solution, decanted from excess sodium, there was then stirred, drop by drop, a solution of 0.075 mol. of crotonyl chloride in 20 ml. of toluene

16) V. Prelog, *Helv. Chim. Acta*, **36**, 308 (1953).
17) A. J. Birch, *Ann. Reports*, **47**, 192 (1950); A. Fredga and J. K. Miettine, *Acta Chem. Scand.*, **1**, 371 (1947); J. Read and W. J. Grubb, *J. Chem. Soc.*, **1939**, 1779.
18) V. Prelog and H. Scherrer, *Helv. Chim. Acta*, **42**, 2227 (1959).
19) H. Gilman, R. G. Jones and L. A. Woods, *J. Org. Chem.*, **17**, 1630 (1952).
20) M. L. Wolfrom and S. Hanessian, ibid., **27**, 1800 (1962).
21) H. B. Henbest and B. Nicholls (*J. Chem. Soc.*, **1959**, 227) reported a similar phenomenon in the methoxy-mercuration of 4-substituted cyclohexenes.
22) All melting points and boiling points are uncorrected. The infrared spectra were taken with a Perkin-Elmer 521 grating infrared spectrophotometer. The optical rotations were performed with a Hitachi No. 070-1 polarimeter, using a 1 dm. tube. Elemental analyses were performed by the Institute of Physical and Chemical Research.

at 0—5°C until the reaction mixture became acidic, a large excess of crotonyl chloride being avoided. Saturated aqueous sodium bicarbonate (ca. 40 ml.) was then added immediately with vigorous stirring to the reaction mixture, which was then extracted with ether and the ether layer was washed with water, dried over sodium sulfate and distilled. The residue was dissolved in chloroform-ligroin (1 : 1 v./v.) and chromatographed on a column of activated alumina. Elution with the same solvents first gave the pure sugar ester. The yield, physical properties and analytic results are recorded in Table III.

The Sugar Ester of Cinnamic Acid.—Into a solution of 0.20 mol. of the sugar ester, 1, 2 : 5, 6-di-*O*-cyclohexylidene-D-glucose (VII), 1,2 : 5,6-di-*O*-isopropylidene-D-glucose (VIII) or 1, 2-*O*-isopropylidene-5-deoxy-D-xylose (IX) in a mixture of 100 ml. of dry pyridine and 100 ml. of dry benzene, there was stirred a solution of 0.22 mol. of cinnamoyl chloride in 50 ml. of dry benzene for about 0.5 hr. at −5—0°C. After it had been stirred for 1 hr., the reaction mixture was allowed to stand overnight at room temperature and then poured into ice water. The mixture was then extracted with ether (or chloroform for VII). The extract was washed with ice water, mixed with ice, washed succesively with iced 3% aqueous sulfuric acid, cold water, saturated aqueous sodium bicarbonate and water, and dried over sodium sulfate. After the solvent had been removed, the residue was dissolved in chloroform-ligroin (1 : 1 v./v.) and chromatographed on a column of activated alumina. Elution with the same solvents first gave the pure sugar ester, except for IVc, which was recrystallized from ligroin. The yield, the physical properties and the analytical results are recorded in Table III.

The Asymmetric Synthesis of 3-Phenylbutyric Acid (III).—A solution of Grignard reagent was prepared from 1.82 g. (0.075 g.-atom) of magnesium and 11.8 g. (0.075 mol.) of bromobenzene in 60 ml. of dry ether. Into this solution of phenylmagnesium bromide, there was added, drop by drop, a solution of 0.03 mol. of the ester Ia,[13] Ic, Id or Ie, in 60 ml. of dry ether (dry tetrahydrofuran for Ic) at −17——15°C for 1 hr. After the addition had been completed, the stirring was continued at the same temperature for 0.5 hr. and then at room temperature for 0.5 hr. The reaction mixture was poured into saturated aqueous ammonium chloride (250 ml.) with vigorous shaking. The ether layer was separated, and the water layer was extracted with ether. The combined ether layers were washed with water, dried over sodium sulfate, and removed. The residual oil, the infrared spectrum of which did not show the presence of the starting ester, was not purified but was hydrolyzed by reflux with 16.8 g. (0.3 mol.) of potassium hydroxide in a solution of 10 ml. of water and 70 ml. of ethanol for 16 hr. After the ethanol had been removed, the resulting solution, diluted with 50 ml. of water, was extracted with 100 ml. of ether and then with 100 ml. of chloform. The combined ether-chloroform extracts were treated as will be descrived below. The water layer was acidified with 6 N hydrochloric acid on cooling and extracted with ether. After the ether had been removed, 50 ml. of saturated aqueous sodium bicarbonate was added with vigorously shaking. The resulting solution was extracted with ether, and the water layer was acidified with 6 N hydrochloric acid and extracted with ether. The ether layer was washed with water, dried over sodium sulfate and then removed. The residue, the optical rotation of which had been measured, was distilled to give pure 3-phenylbutyric acid (III). Its infrared spectrum was identified with that of an authentic sample.[4] The yield and physical properties for III are recorded in Table I.

The ether-chloroform extracts were washed with water, dried over sodium sulfate, and removed. The residue, which had no absorption of ester carbonyl in the infrared spectrum, gave 1, 2 : 5, 6-di-*O*-cyclohexylidene-D-glucose (VII) or 1, 2 : 5, 6-di-*O*-isopropylidene-D-glucose (VIII) by recrystallization from ligroin in a 60—85% yield. 1, 2-*O*-Isopropylidene-5-deoxy-D-xylose (IX) was recovered in a 30—50% yield by extracting the residue with 23 ml. of water, and then extracting it with 150 ml. of ether.

In the case of the addition of cuprous chloride to the reaction mixture, the experiment was carried out similarly except that when the ester (0.03 mol.) was added, 107 mg. (1.4 mol. percent with respect to Grignard reagent) of cuprous chloride was added concurrently in four portions at the interval of 15 min., the first portion being added just before the addition of the ester and the last one, just after.

The Anilide of 3-Phenylbutyric Acid (III). — A mixture of 500 mg. (0.0030 mol.) of the acid III obtained by each of the above asymmetric syntheses and 1.0 g. (0.0084 mol.) of thionyl chloride was refluxed for 0.5 hr. To the solution there was added a solution of 2.0 g. (0.0215 mol.) of aniline in 15 ml. of dry benzene on cooling, and the mixture was refluxed for 2 min. After cooling, 20 ml. of ether was added and the mixture was washed successively with 5 ml. of water, 5 ml. of 6 N hydrochloric acid, 5 ml. of water, 5 ml. of 3 N sodium hydroxide, and 10 ml. of water. The organic solvents were removed, and the residue was recrystallized once from 50% aqueous ethanol, with treatment of charcol, to give anilide in a 80—95% yield. The physical properties and the results of the analysis for anilide are recorded in Table I.

(±)-3, 4-Diphenylbutyric Acid (VI).[23] — (±)-*s*-Butyl-3, 4-diphenylbutyrate (Vb), b. p. 150—155°C/1 mmHg, n_D^{20} 1.5356 (lit.[6] b. p. 157°C/1 mmHg, n_D^{20} 1.5333) was prepared by the method described by Munch-Petersen et al.[6] A mixture of 2.0 g. (0.0067 mol.) of Vb, 20 ml. of ethanol and 5.0 g. (0.089 mol.) of potassium hydroxide in 5.0 ml. of water was refluxed for 3 hr. After it had then been concentrated, 50 ml. of water was added and the solution was extracted with chloroform. The water layer was acidified with 6 N hydrochloric acid and extracted with ether. The ether which dried over sodium sulfate was removed, and the resulting product was recrystallized from ligroin - ethyl acetate (1 : 1 v./v.), with treatment of charcol, to give 1.2 g. of (±)-acid (VI), m. p. 94—96°C (lit.[23] m. p. 95—96°C).

Found: C, 79.70; H, 6.60. Calcd. for $C_{16}H_{16}O_2$: C, 79.97; H, 6.71%.

IR λ_{max}^{KBr}: 3030, 2920, 1709, 1435, 1414, 1245 cm^{-1}.

IR ν_{max}^{CHCl}: 3033, 2916, 1708, 1413 cm^{-1}.

The Asymmetric Synthesis of 3, 4-Diphenylbutyric Acid (VI).—A solution of Grignard reagent was prepared from 1.82 g. (0.075 g.-atom) of magnesium

23) S. Ruhemann, *J. Chem. Soc.*, **1910**, 460.

and 9.5 g. (0.075 mol.) of benzylchloride in 60 ml. of dry ether. Into this solution of benzylmagnesium chloride there was then stirred, drip by drop, a solution of 0.03 mol. of the ester IVa,[24] IVc, IVd or IVe in 60 ml. of dry ether (dry tetrahydrofuran for IVc) at −17——15°C for 1 hr; the stirring was then continued at the same temperature for 0.5 hr. and then at room temperature for an additional 0.5 hr. The reaction mixture was poured into saturated aqueous ammonium chloride (250 ml.) with vigorous shaking. The ether layer was separated, and the water layer was extracted with ether. The combined ether layer were washed with water, dried over sodium sulfate, and removed. The residual oil, the infrared spectrum of which did not show the presence of the starting ester, was not purified but was hydrolyzed by refluxing it with 6.2 g. (0.11 mol.) of potassium hydroxide in 5 ml. of water and 75 ml. of ethanol for 16 hr. After the ethanol had been removed and water had been added, the solution was extracted with 100 ml. of ether and 100 ml. of chloroform. The removal of organic solvents gave 1, 2 : 5, 6-di-*O*-cyclohexylidene-D-glucose (VII), 1, 2 : 5, 6-di-*O*-isopropylidene-D-glucose (VIII) or 1, 2-*O*-isopropylidene-5-deoxy-D-xylose (IX) in 80%, 70%, and 55% yields respectively, in the same manner described in the asymmetric synthesis of 3-phenylbutyric acid. The water layer acidified with 6 N hydrochloric acid on cooling and extracted with ether. The ether was washed with water, dried over sodium sulfate, and removed. The residue, the optical rotation of which had been measured, was distilled to give pure 3, 4-diphenylbutyric acid (VI). Its infrared spectrum (in chloroform) was identified with that of a racemic sample prepared from an authentic ester (Vb).[6] The yield, the physical properties and the results of the analysis for VI are recorded in Table II.

In the case of addition of cuprous chloride, the experiment was carried out in the same way described as asymmetric synthesis of 3-phenylbutyric acid (III).

The Resolution of 3, 4-Diphenylbutyric Acid (VI).—A mixture of 4.8 g. (0.02 mol.) of VI, m. p. 89—95°C, $[\alpha]_D^{28}$ −9° (*c* 2.25, benzene) which had been obtained by the above asymmetric synthesis, 6.5 g. (0.02 mol.) of quinine, and 70 ml. of ethanol was boiled until dissolution was complete. After the mixture had stood overnight at 0°C, the crystalline product was separated and washed with small quantities of ethanol. Weight of the dried product, 4.0 g.; $[\alpha]_D^{25}$ −95° (*c* 1.82, chloroform), m. p. 160—162°C. Three further recrystallizations from the same solvent gave 1.8 g. of quinine salt as needles, m. p. 165—166°C, $[\alpha]_D^{25}$ −101° (*c* 1.72, chloroform), as was indicated by its constant rotation when subjected to further recrystallization.

Found: C, 76.61; H, 7.07; N, 4.96. Calcd. for $C_{36}H_{40}N_2O_4$: C, 76.56; H, 7.14; N, 4.96%.
Decomposition in the usual manner gave a specimen of (−)-acid (VI) with a m. p. of 84—86°C, $[\alpha]_D^{28}$ −67° (*c* 0.81, chloroform), which after four recrystallizations from ligroin, had a m. p. of 87—88°C, $[\alpha]_D^{28}$ −60° (*c* 1.92, benzene). Yield, 280 mg. Further recrystallization led to no change in the optical rotation.

Found: C, 80.03; H, 6.50. Calcd. for $C_{16}H_{16}O_2$: C, 79.97; H, 6.71%.

The mother liquors containing the (+)-acid were concentrated and allowed to stand overnight at room temperature. After the precipitate had been filtered out, the filtrate was concentrated to dryness. The re-resulting solid (4.0 g.), which had a m. p. of 65—100°C, $[\alpha]_D^{25}$ −57° (*c* 1.63, chloroform), was recrystallized three times from 50% aqueous ethanol to give quinine salt of (+)-acid (VI) as needles, m. p. 110—111°C, $[\alpha]_D^{25}$ −66° (*c* 1.47 chloroform).

Found: C, 75.13; H, 7.14; N, 4.75. Calcd. for $C_{36}H_{40}N_2O_4 \cdot 1/2H_2O$: C, 75.36; H, 7.20; N, 4.88%.
Decomposition gave (+)-acid (VI) with a m. p. of 82—88°C, $[\alpha]_D^{27}$ +46° (*c* 1.24, benzene), which, after three recrystallizations from ligroin, had a m. p. of 86—88°C, $[\alpha]_D^{28}$ +59° (*c* 1.85, benzene). Yield, 200 mg. Further recrystallization led to no change in the optical rotation.

Found: C, 80.25; H, 6.64. Calcd. for $C_{16}H_{16}O_2$: C, 79.97; H, 6.71%.

IR_{max}^{KBr}: 3023, 2914, 1711, 1659, 1407, 1279 cm^{-1}.
Its infrared spectrum (in chloroform) was identified with that of racemic acid (VI).

Examination for the Optical Stability of (—)-3, 4-Diphenylbutyric Acid (VI) in an Alkaline Solution.—A mixture of 253 mg. of VI, m. p. 87—88°C, $[\alpha]_D^{28}$ −60° (*c* 1.92, benzene), 200 mg. of potassium hydroxide in 0.1 ml. of water and 2.5 ml. of ethanol was treated under the same conditions as that of saponification in the asymmetric synthesis of VI. (−)-Acid (VI) was recovered in a 93% yield; it had a m. p. of 86.5—89.0°C, $[\alpha]_D^{28}$ −61° (*c* 1.61, benzene).

Found: C, 80.24; H, 6.65. Calcd. for $C_{16}H_{16}O_2$: C, 79.97; H, 6.71%.
The infrared spectrum was identical in every respect with that of the starting material.

The authors wish to express their thanks to Dr. Hiroyoshi Kuzuhara for his useful suggestions, to Dr. Haruo Homma and his co-workers for microanalyses, and to Mr. Teruo Kurihara for measurement of infrared spectra. The authors also wish to thank Miss Kimiko Noda and Miss Suzue Ishikawa for their helpful assistance.

24) J. B. Cohen and C. E. Weiteley, *J. Chem. Soc.*, **1901**, 1308; T. P. Hilditch, ibid., **1908**, 6.

BULLETIN OF THE CHEMICAL SOCIETY OF JAPAN VOL. 39 917—920 (1966)

A Preliminary Study of the Carboxylation and Decarboxylation of Some Sulfides[1)]

By Waichiro TAGAKI, Kenji UEYAMA, Isao MINAMIDA, Yong He KIM
Yoshinori IKEDA and Shigeru OAE

Department of Applied Chemistry, Faculty of Engineering, Osaka City University, Sumiyoshi-ku, Osaka

(Received September 3, 1965)

Some sulfides with benzylic hydrogen have been carboxylated by carbonating the respective carbanions generated with dimsylsodium in dimethyl sulfoxide. The resulting mercaptocarboxylic acids have then been found to have considerably-enhanced rates of decarboxylation reaction.

The ability of divalent sulfide groups to stabilize the α-carbanion has been disclosed in a number of reactions.[2)] The Dieckmann condensation of α, β-dicarboxy methyl ethyl sulfide, the tautomeric double-bond migration between vinyl and allyl sulfides, the alkylation at the α-carbon of mercaptal, and the hydrogen isotopic exchange reaction, are a few typical examples of these reactions. Recently we have suggested that the electron-accepting 3d orbital resonance of the divalent sulfur atom is the major factor in the facile base-catalyzed D–H hydrogen isotopic exchange reactions of a number of mercaptals and related compounds.[2b,3)]

$$R\text{-}\ddot{S}\text{-}\overset{\ominus}{\underset{|}{C}}\text{-} \leftrightarrow R\text{-}\overset{\ominus}{\ddot{S}}\text{=}C\text{-} \qquad (1)$$

Base-catalyzed decarboxylation is also considered to be a reaction involving the carbanion intermediate which is similar to the base-catalyzed hydrogen exchange reaction.[4)] However, no systematic investigation of the decarboxylation reaction of α-substituted mercapto-carboxylic acids has been known. If the carbanion is relatively stable and if, hence, its equilibium concentration is substantial in a basic solution, it would not be difficult to trap the carbanion by reacting it with carbon dioxide. In the case of the hydrogen exchange or the decarboxylation reaction, a rapid reaction does not necessarily mean a high equilibrium concentration of carbanion. Only a few examples are known which indicate an appreciable concentration of the carbanion of divalent sulfide in an equilibrating system. Fröling and Arens found that mercaptals were metalated in liquid ammonia, and they observed an increased electrical conductivity in the reaction mixture.[5)] Truce and Roberts found that benzaldehyde diphenylmercaptal was readily metalated in dimethylformamide, and that the resulting carbanion was alkylated with alkyl halide.[6)] Therefore, the study of the decarboxylation of mercapto-carboxylic acids and the carboxylation of sulfides is quite significant for the evaluation of the effects of the divalent sulfide group on the stabilization of the carbanion.

$$R\text{-}\ddot{S}\text{-}\overset{|}{C}\text{-}CO_2^{\ominus} \rightarrow R\text{-}\ddot{S}\text{-}\overset{\ominus}{\underset{|}{C}}\text{-} + CO_2 \qquad (2)$$

$$R\text{-}\ddot{S}\text{-}\overset{\ominus}{\underset{|}{C}}\text{-} + BH^{\oplus} \rightarrow R\text{-}\ddot{S}\text{-}\overset{|}{C}\text{-}H + B \qquad (3)$$

During the course of the investigations aimed at finding some appropriate base and solvent systems for the generation of carbanions of various sulfides at an appreciable equilibrium concentration, we have found that some sulfides with benzylic hydrogen can be successfully carboxylated by quenching, with carbon dioxide, solutions of the sulfides in dimsylsodium - dimethyl sulfoxide. The resulting carboxylic acids have all been found to have enhanced rates of decarboxylation. This paper will describe the preliminary results of these carboxylation and decarboxylation reactions.

Results and Discussion

Carboxylation Reactions.—A sulfide was dissolved in an excess of 0.5 N dimsylsodium in dimethyl sulfoxide[7)] under an air-free nitrogen atmosphere. When a sulfide was dissolved, the initial brilliant red color of the dimsylsodium solution due to the addition of an indicator amount of triphenylmethane turned a dark yellowish brown, dark green, or dark purple depending on the kind of sulfide dissolved.

1) a) Paper VIII: 3d-Orbital Resonance in Divalent Sulfides. b) This work was supported by the Petroleum Research Fund, administered by the American Chemical Society.

2) a) C. C. Price and S. Oae, "Sulfur Bonding," Ronald Press, New York (1962); b) S. Oae, "3d Orbital Resonance Involving the Sulfur Atoms in Organic Sulfides," in "Organic Sulfur Compounds," Ed. by N. Kharasch, Vol. IV, Pergamon Press, in press.

3) S. Oae, W. Tagaki and A. Ohno, *Tetrahedron*, **20**, 427 (1964), and the preceding papers.

4) a) B. R. Brown, *Quart. Revs.*, **5**, 137 (1951); b) J. Hine, "Physical Organic Chemistry," 2nd ed., McGraw-Hill, New York, (1962).

5) A. Fröling and J. F. Arens, *Rec. trav. chim.*, **81**, 1009 (1962).

6) W. E. Truce and F. E. Roberts, *J. Org. Chem.*, **28**, 961 (1963).

7) E. J. Corey and M. Chaykovsky, *J. Am. Chem. Soc.*, **84**, 866 (1962).

The carboxylation was then performed by quenching the reaction mixture with or an ether suspension of solid carbon dioxide. The results are shown in Table I.

As is indicated in Table I, none of the carboxylic acids were obtained from the sulfides, VI and VII, with only the aliphatic C–S bonds. In the case of 1, 3-dithian (VI), the starting sulfides was largely recovered alone with a small amount of resinous product. The bicyclic sulfide (VII) also gave mainly a resinous product. These resinous products were probably formed by the cleavage of C–S bonds, similar to the cases where mercaptals were cleaved by some such metalating agents as Grignard reagents, phenyllithium, or *n*-butyllithium.[2a,8,9]

Although qualitative, it seems that the yield of the carboxylic acid in Table I can be explained on the basis of the stability of the carbanion formed by the dissociation of the α-proton of sulfide. The rates of hydrogen exchange reaction have been found to increase dramatically with the increase in the number of the substitution of the mercapto group at the α-carbon atom.[3] Similarly, Table I indicates that the yield of the carboxylic acid from benzaldehyde diethylmercaptal (II) is much higher than that from the benzyl ethyl sulfide (I). Table I also indicates that the yield of the carboxylic acid from benzyl phenyl sulfide (III) is much higher than that from benzyl ethyl sulfide (I). This appears to indicate that the phenylmercapto group is more effective than the ethylmercapto group in the stabilization of carbanion, this is confirmed by the results of the subsequent decarboxylation reactions shown in Table II.

Decarboxylation Reaction.—As Table I shows, the acids, XII and XI, obtained from the sulfides, II and IV, were readily decomposed when their crystals were heated at around 140°C in a glass tube, there was also a vigorous evolution of carbon dioxide. The corresponding sulfides, II and IV, were quantitatively obtained. The acids from the III and V sulfides, are relatively stable, and their decomposition was not observed below 200°C. These acids were then subjected to the base-catalyzed decarboxylation reaction. The results are shown in Table II, although the methods of the kinetics will be reported in detail elsewhere.

Table II appears to disclose the following three points: (1) The rate of diethyl mercapto acetic acid (VIII) is much smaller than those of the other acids. (2) The rates of the decarboxylation of the disubstituted acids, IX and X, are smaller than those of the trisubstituted acids, XI and XII. (3) The rates of the decarboxylation of phenylmercapto-substituted acids (XI and IX) are greater than that of ethylmercapto-substituted acids, (XII and VIII). These observations can be explained by assuming that the ability to stabilize α-carbanion is greater for phenyl and phenylmercapto groups than for the aliphatic mercapto (RS) group, and that the stability of the carbanion is increased with the increasing substitution of mercapto groups.

The products of the decarboxylation reaction were analyzed, the results are shown in Table III. The most plausible mechanism for the present decarboxylation reaction is the formation of carbanion at the rate determining slow step, followed by the fast protonation of the carbanion. However, such other mechanisms as the formation of a methylene intermediate are also possible, in which different kinds of products may be expected.[10] Although the analyses were preliminary and were not thoroughly enough to exclude the formation of a very small quantity of unknown products, it was found that more than 90% of the mercapto acids were decomposed to give carbon dioxide and that the corresponding mercaptals were obtained in high yields; the direct analyses of the reaction mixtures by gas chromatography did not indicate the formation of products other than dimethyl sulfoxide and the mercaptals. The products of the decomposition of diphenoxyacetic acid other than carbon dioxide are not clear. The infrared spectra of the product, however, showed the presence of phenol. This suggests a possibility that the mechanism of the decarboxylation of RO-substituted acid is different from that of RS-substituted acetic acids.

Experimental

The Preparation of Sulfides.—Benzyl ethyl sulfide (I) and benzyl phenyl sulfide (III) were prepared by the reaction of benzyl chloride with the corresponding sodium mercaptide in ethanol (I, b. p. 110°C/20 mmHg; II, b. p. 167—168°C/15 mmHg, m. p. 40—42°C). Benzaldehyde diphenylmercaptal (IV) was prepared by saturating the mixture of benzaldehyde and phenyl mercaptan with dry hydrogen chloride (b. p. 183—184°C/1 mmHg; m. p. 50—51°C). Similarly, formaldehyde diphenylmercaptal (V) was prepared by the acid (HCl)-catalyzed condensation of formaldehyde with phenylmercaptan (b. p. 164—167°C/3 mmHg). The preparations and the properties of benzaldehyde diethylmercaptal (II) and the cyclic mercaptals, VI and VII, have been reported in previous papers.[11]

Carboxylation Reaction.—Commercial dimethyl sulfoxide was dried with calcium hydride under 50°C and vacuum-distilled (below b. p. 55°C). Sodium hydride (7 g.) in a 50% oily suspension was dissolved in 590 ml. of the above dimethyl sulfoxide below 60°C under an air-free nitrogen atomosphere to give a pale brown dimsylsodium solution,[7] the solution was then

8) E. E. Reid, "Organic Chemistry of Bivalent Sulfur," Vol. III, Chemical Publishing Co., New York, N. Y. (1960), p. 332.
9) A. Schönberg and L. V. Vagha, *Ber.*, **64**, 2577 (1931).
10) J. Hine, "Divalent Carbon," Ronald Press, New York (1964).
11) S. Oae, W. Tagaki and A. Ohno, *Tetrahedron*, **20**, 417, 427, 437 (1964).

Table I. Carboxylation of some sulfides in dimsylsodium - dimethyl sulfoxide (room temperature, 17 hr.)

$$RH \xrightarrow{CH_3SOCH_2^{\ominus}Na^{\oplus}} [R^{\ominus}] \xrightarrow[2)\ H^{\oplus}]{1)\ CO_2} RCO_2H$$

RH		Color of the reaction mixture	Recovered RH, %	RCO_2H Yield %	RCO_2H M. p., °C	RCO_2H Thermal decomp., °C
$PhCH_2$-S-C_2H_5	(I)	Dark purple	83	trace[a]	—	—
$PhCH(SC_2H_5)_2$	(II)	Dark green-purple	38	31	79—81[b]	>140
$PhCH_2SPh$	(III)	Dark orange-red	35	58	101—101[c]	>270
$PhCH(SPh)_2$	(IV)	Dark orange-red	42	49	140—141[d]	>140
$H_2C(SRh)_2$	(V)	Dark yellow	25	51	104—105[e]	>205
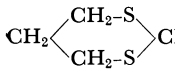	(VI)	Dark green	85	none	—	—
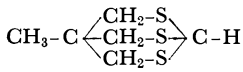	(VII)	Dark green	—	none[f]	—	—

a) Not identified. b) Lit., 81°C[13] c) Lit., 101—102°C[14] d) Lit., 143°C[15]
e) Lit., 104—106°C[16] f) Mainly a resinous product

Table II. The amine-catalyzed decarboxylation of some mercapto-carboxylic acids in dimethyl sulfoxide

Acid		Temp., °C	k_1, sec^{-1}	Rec. rate.
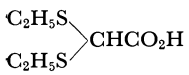	(VIII)[a]	160	4.85×10^{-5}	1
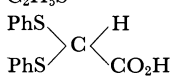	(IX)[a]	90	1.95×10^{-4}	2.80×10^{3}
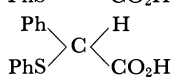	(X)[a]	90	3.71×10^{-4}	5.33×10^{3}
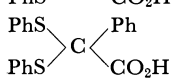	(XI)[b]	18.5	3.20×10^{-3}	9.57×10^{7}
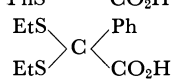	(XII)[b]	80	1.65×10^{-3}	7.47×10^{4}

a) 0.5×10^{-3} mol. of acid and 5×10^{-3} mol. of triethanol amine in 50 ml. D. M. S. O.
b) 1.5×10^{-3} mol. of acid and 1.5×10^{-3} mol. of triethylamine in 29 ml. D. M. S. O.

Table III. Decarboxylation products

$$RCO_2H \xrightarrow{\text{in } CH_3SOCH_3} RH + CO_2$$

RCO_2H	Temp., °C	Time hr.	Yield, % of CO_2[a]	Yield, % of RH
$(C_2H_5S)_2CHCO_2H$	150	30	93	90±5[b]
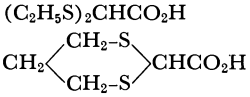	150	25	97	90±5[b]
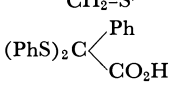	80	10 min.	95	57
$(PhO)_2CHCO_2H$	150	35	100	—[c]

a) Trapped as barium carbonate.
b) Determined by gas chromatography.
c) Unidentified, but the product was shown to contain phenol from the infrared spectra.

12) E. Baumgarten and C. R. Hauser, *J. Am. Chem. Soc.*, **66**, 1039 (1944).
13) F. Weygand, W. Steglich and H. Janner, *Ann.*, **658**, 128 (1962).
14) Z. J. Vejdelek, O. Nemecek and A. Simek, *Collection Czech, Chem. Commun.*, **28**, 2618 (1963); *Chem. Abstr.*, **59**, 15269a (1963).
15) R. Escales and E. Baumann, *Ber.*, **19**, 1787 (1886).
16) R. Otto and J. Troeger, ibid., **25**, 3425 (1892).

connected to an air-tight automatic buret.[12] Sulfide (2.0 g.) was weighed in a glass tube, dissolved in 25 ml. of a dimsylsodium solution which had been transferred from the above automatic buret, and sealed under an air-free nitrogen atmosphere. The reaction mixture was then left at room temperature for 17 hr., after which the tube was opened and the contents poured into an excess suspension of solid carbon dioxide in ether to give a salt suspension. Water was added to the salt suspension, and the water layer was extracted with ether twice. The ether layers were combined, washed with water, dried and concentrated, and the residue was vacuum-distilled to give the unreacted sulfide. The water layer was acidified with hydrochloric acid and then extracted with ether three times. The ether extract was dried and concentrated to give the mercapto acid. The results are shown in Table I. An air-free nitrogen atomsphere is not necessarily required for the purpose of the carboxylation, and the reaction time can be shortened by increasing the reaction temperature to 50°C.

Decarboxylation Reaction.—*Kinetics.*—The carboxylic acid and triethylamine or triethanolamine were dissolved in anhydrous dimethyl sulfoxide and heated in a constant temperature bath under an air-free nitrogen stream. Carbon dioxide was absorbed in dilute solutions of sodium hydroxide and back-titrated with dilute sulfuric acid. While the kinetic procedures will be reported in detail elsewhere, the results are shown in Table II. The relative rates were calculated from the apparent activation energy of the decarboxylation reaction of the acid (X) (29.2 kcal./M) obtained from Arrhenius plot.

The Product Analysis of the Decarboxylation.—In a 100-ml. two-necked flask with a nitrogen gas inlet tube and a reflux condenser there was placed 0.01 mol. of an acid and 50 ml. of dimethyl sulfoxide. The reaction mixture was then heated on an oil bath under the bubbling of air-free nitrogen gas. The carbon dioxide evolved was led through a dry ice - cooled trap to an absorbing trap containing 0.2 M barium hydroxide. The heating was then continued, by replacing the absorbing trap with another one, until the evolution of carbon dioxide was no more observed. The reaction mixture was cooled and analyzed by gas chromatography and finally subjected to a fractional distillation. The results are shown in Table III.

BULLETIN OF THE CHEMICAL SOCIETY OF JAPAN VOL. 39 920—925 (1966)

Chronopotentiometry of Tris(ethylenediamine)chromium(III) Ions in Various Supporting Electrolyte Solutions

By Nobuyuki TANAKA and Akifumi YAMADA

Department of Chemistry, Faculty of Science, Tohoku University, Sendai

(Received September 8, 1965)

The reduction of tris(ethylenediamine)chromium(III) ions at the dropping mercury electrode has been studied chronopotentiometrically in various supporting electrolyte solutions. The electrolysis at constant cathodic current in an acid solution gives a well-defined chronopotentiogram which corresponds to the one-electron reduction of chromium(III) to chromium(II). The anodic chronopotentiogram which is obtained by the current-reversal techniques is clearly separated from the cathodic one. Two cathodic steps are obtained in alkaline ethylenediamine solutions, and two anodic steps, at the current reversed. No chemical reaction involving hydrogen ions or ethylenediamine takes place prior to the electron transfer. The presence of very small amount of surface-active substances was found to improve the shape of chronopotentiograms. In the presence of EDTA, the one-electron cathodic chronopotentiogram splits into two steps.

In a previous paper,[1] the present authors reported on the chromopotentiometric behavior of hexamminechromium(III) ions in acetate buffer solutions. Since only a little work has been reported on the electroreduction of tris(ethylenediamine)-chromium(III) ions,[2-4] it seems worthwhile to carry out the polarographic or chronopotentiometric study of this complex.

The present paper is concerned with the chronopotentiometry of tris(ethylenediamine)chromium-(III) ions in various supporting electrolyte solutions. The observations in the cathodic chronopotentiometry and in the anodic chronopotentiometry by the current-reversal techniques will be presented, and the mechanism of the electrode processes will be discussed.

Experimental

Tris(ethylenediamine)chromium(III) chloride was

1) N. Tanaka, A. Yamada and R. Tamamushi, This Bulletin., **37**, 1821 (1964).
2) N. Maki, Y. Shimura and R. Tsuchida, ibid., **31**, 413 (1958).
3) J. A. Friend and P. W. Smith, *J. Phys. Chem.*, **63**, 314 (1959).
4) E. Fischerová and O. Fischer, *Chem. Zvesti*, **16**, 306 (1962).

prepared according to the method of Pfeiffer[5]; the chromium and nitrogen contents were determined by the usual methods.

Found: Cr, 12.79; N, 20.4. Calcd. for $[Cr(en)_3]Cl_3 \cdot 3^1/_2\ H_2O$: Cr, 12.94; N, 20.9%.

As the complex is sensitive to light and not very stable in aqueous solutions[6-9] precautions were taken when it was used. All other chemicals used were of analytical reagent grade. Redistilled water was used for the preparation of the solutions of desired concentrations. Polyoxyethylene laulyl ether (LEO), $C_{12}H_{25}O(C_2H_4O)_n$-OH (n=ca. 15), was used for a maximum suppressor. The contamination of the solution with surface-active substance was carefully avoided.

Chronopotentiometric measurements were carried out in general by following the procedure given in the previous paper.[1] A dropping mercury electrode of a long drop time was used for the working electrode; it had an m value of 0.1164 mg./sec. and a drop time, t_d, of 61 sec., being measured in a deaerated solution containing 0.1 M acetate buffer and 0.9 M ammonium chloride at open circuit at 25 cm. of the mercury reservoir. The auxiliary electrode was a platinum wire, which was isolated in a compartment provided with a sintered glass disk. A saturated calomel electrode (SCE) was used for the reference electrode. Dissolved oxygen in the electrolytic solution was removed by bubbling purified nitrogen gas through the solution. All measurements were carried out at 25±0.1°C.

Results

In the polarographic measurements, tris(ethylenediamine)chromium(III) was found not to give a well-defined polarographic wave in neutral unbuffered solutions, but to give a well-defined wave in acetate buffer or acid solutions.[10] Similar observations were made in the chronopotentiometric measurements. Typical examples are shown in Fig. 1.

The characteristics of the potential-time curve for the reduction of tris(ethylenediamine)chromium-(III) ions in neutral media were studied in a 1 M ammonium chroride solution. No linear relation was found between the concentration and the square root of the transition time. An example of the potential-time curves, which were obtained by the electrolysis at a constant cathodic current followed by the electrolysis at the constant anodic current of the same magnitude is given in Fig. 2. The values of τ_c/τ_a, $E^c_{t=0}$ and $E^a_{t=0}$ were determined to be 3.2, −0.94 V. vs. SCE and −0.75 V. vs. SCE respectively, where τ_c and $E^c_{t=0}$ mean the transition time and the potential at t=0 of the cathodic chronopotentiogram respectively, and τ_a and $E^a_{t=0}$, those of the anodic chronopotentiogram obtained by the current-reversal techniques respectively.

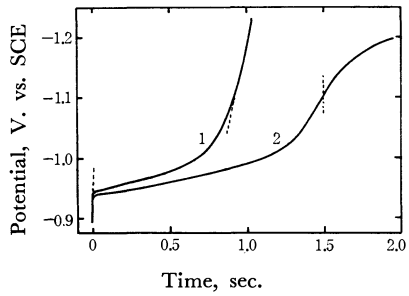

Fig. 1. Chronopotentiograms of 1 mM $[Cr(en)_3]Cl_3 \cdot 3^1/_2H_2O$ (1) in 0.9 M NH_4Cl+0.1 M acetate buffer (pH 4.6) and (2) in 1 M NH_4Cl at 25°C at current densities of (1) 0.231_4 and (2) 0.165_5 mamp.cm^{-2}. The measurements were started at 40 sec. after the beginning of the growth of mercury drop.

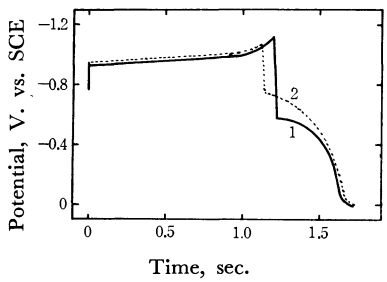

Fig. 2. Chronopotentiograms for the reduction and the subsequent reoxidation of 1 mM $[Cr(en)_3]Cl_3 \cdot 3^1/_2H_2O$ (1) in 0.9 M NHCl+0.1 M acetate buffer (pH 4.6) and (2) in 1 M NH_4Cl at 25°C. Current densities are (1) 0.181_7 mamp. cm^{-2} and (2) 0.186_0 mamp.cm^{-2}.

In acetate buffer solutions, well-defined chronopotentiograms were observed (see curve 1 in Figs. 1 and 2). The transition time (τ) was determined at various current densities (i) ranging from 0.179 to 0.508 mamp. cm^{-2}. The results showed that the product $i\tau^{1/2}$ was independent of the current density, indicating clearly that tris(ethylenediamine)chromium(III) ions are directly reduced at the electrode without any preceding chemical reaction prior to the electron-transfer process. The average value of $i\tau^{1/2}/C_O$, where C_O represents the concentration of the complex in the bulk of the solution, was obtained to be 0.211 mamp. sec$^{1/2}$ cm^{-2} mM^{-1}.

Measurements were also made at various concentrations of the complex. The results showed that the square root of the transition time was proportional to the concentration of the complex up to 1.5 mM, but at higher concentrations the transition time abnormally increased. The average value of $i\tau^{1/2}/C_O$ was obtained to be 0.211 mamp.

5) P. Pfeiffer, P. Koch, G. Lando and A. Trieschman, *Ber.*, **37**, 4255 (1904).
6) S. Egashira, *J. Chem. Soc. Japan, Pure. Chem. Sect.* (*Nippon Kagaku Zasshi*), **79**, 301 (1958).
7) H. L. Schäfer and O. Kling, *Z. anorg. Chem.*, **287**, 296 (1956).
8) H. L. Schäfer and O. Kling, *J. Inorg. Nucl. Chem.*, **8**, 320 (1958).
9) H. L. Schäfer and O. Kling, *Z. Physik. Chem. N. F.*, **16**, 14 (1958).
10) N. Sato, B. S. thesis, Tohoku University (1962).

Table I. Effect of ionic strength on the chronopotentiogram of 1mM $[Cr(en)_3]Cl_3 \cdot 3^1/_2\ H_2O$ obtained at current density of 0.301_7 mamp. cm^{-2} in solutions containing 0.1 M acetate buffer

Ionic strength*	$E_{t=0}$ V. vs. SCE	τ sec.	$i\tau^{1/2}/C_O$ mamp. $sec^{1/2}\,cm^{-2}\,mM^{-1}$	Slope of log-plot mV.
0.1	−0.917	0.465	0.206	32
0.5	−0.929	0.475	0.208	47
1.0	−0.948	0.496	0.212	55
1.5	−0.962	0.502	0.214	59
2.0	−0.972	0.517	0.217	64

* Adjusted with NH_4Cl.

Table II. Effect of supporting electrolyte on the chronopotentiogram of 1 mM$[Cr(en)_3]Cl_3 \cdot 3^1/_2\ H_2O$ obtained in solutions containing 0.1 M acetatebuffer at ionic strength of 1.0

Supporting electrolyte	$i\tau_c^{1/2}/C_O$ mamp. $sec^{1/2}\,cm^{-1}mM^{-1}$	τ_c/τ_a	$E^c_{t=0}$ V. vs. SCE	$E^a_{t=0}$ V. vs. SCE	Slope of log-plot, mV.
0.9M NH_4Cl	0.211	2.9_9	−0.94	−0.57	55
0.9M NaBr	0.205	3.0_2	−0.93	−0.62	65
0.9M KNO_3	0.204	varied*	−0.93	−0.53	not linear
0.3M en·2HCl	0.206	2.9_1	−0.96	−0.59	65
0.3M $(NH_4)_2SO_4$	0.182	3.0_3	−0.95	−0.48	not linear
0.3M $CaCl_2$	0.204	3.0_0	−0.91	−0.58	55

* See text and Table IV.

$sec^{1/2}\,cm^{-2}\,mM^{-1}$ in the range of the concentration up to 1.5 mM. According to Sand[11] the value of $i\tau^{1/2}/C_O$ is expressed as

$$i\tau^{1/2}/C_O = \frac{\pi^{1/2}}{2} nFD_O^{1/2} = 85.51nD_O^{1/2} \qquad (1)$$

where F is the Faraday, C_O the bulk concentration expressed in mM, D_O the diffusion coefficient expressed in $cm^2\,sec^{-1}$, i the current density expressed in mamp. cm^{-2} and n the number of electrons involved in the electrode reaction. The transition time constant $i\tau^{1/2}/C_O$ is correlated to the polarographic diffusion current constant I, which is given by the equation,

$$I = 607\,nD_O^{1/2} \qquad (2)$$

when the original form of the Ilkovic equation and the average current during the life of a mercury drop are employed. Hence, one obtains

$$i\tau^{1/2}/C_O = 0.1409\,I \qquad (3)$$

Introducing 1.47 μamp. $sec^{1/2}\,mg^{-2/3}\,mM^{-1}$ for I, which was determined by the polarographic measurement, the theoretical value of $i\tau^{1/2}/C_O$ was caluclated to be 0.207 mamp. $sec^{1/2}cm^{-2}mM^{-1}$. This value was in a satisfactory agreement with the experimental one.

The potential at $t=0$ ($E_{t=0}$) was found to be dependent on the current density and to change linearly with log i as shown in Fig. 3. Chronopotentiograms were obtained at various pH's in acetate buffer solutions, when the potential at $t=0$, the slope of the log-plot (log $(\tau^{1/2}-t^{1/2})$ vs. E) and the transition time constant were found to be independent of pH of the solution. The transition time constant, the potential at $t=0$ and the slope of the log-plot which were obtained at varied ionic strengths and in various supporting electrolyte solutions are given in Tables I and II, respectively. The effect of LEO on the chronopotentiogram of tris(ethylenediamine)-chromium(III) ions is shown in Table III. The transition time was not affected unless the concentration of LEO exceeded 5×10^{-4} M, whereas the potential at $t=0$ is affected by the addition of 5×10^{-6} M LEO.

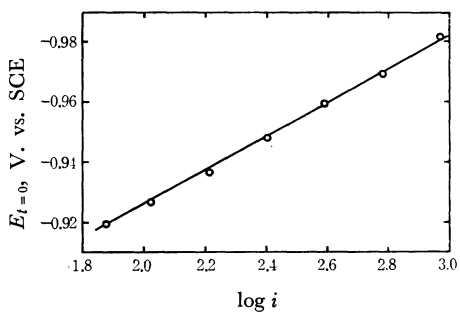

Fig. 3. Relation of $E_{t=0}$ with log i for the reduction of 1 mM $[Cr(en)_3]Cl_3 \cdot 3^1/_2H_2O$ in 0.9 M NH_4Cl+0.1 M acetate buffer. Ohmic drop is corrected.

When a small amount of disodium ethylenediaminetetraacetate (EDTA) is added to the solution, the one-electron cathodic chronopotentiogram of the tris(ethylenediamine)chromium(III) ions split into two steps. A typical example of the

11) H. J. S. Sand, *Phil. Mag.*, **1**, 45 (1901).

Table III. Effect of LEO on the chronopotentiogram of 1 mM $[Cr(en)_3]Cl_3 \cdot 3^1/_2H_2O$ obtained at current density of 0.214_7 mamp.sec$^{1/2}$ in solutions containing 0.9M NH_4Cl and 0.1M acetate buffer

Concn. of LEO, M	τ sec.	$E_{t=0}$ V. vs. SCE	$i\tau^{1/2}/C_O$ map.sec$^{1/2}$ cm^{-2} mM^{-1}
0	0.980	−0.932	0.212
5×10^{-9}	0.978	−0.931	0.212
5×10^{-8}	0.978	−0.931	0.212
5×10^{-7}	0.982	−0.932	0.212
5×10^{-6}	0.979	−0.955	0.212
5×10^{-5}	0.980	−1.210	0.212
5×10^{-4}	0.960	−1.244	0.211

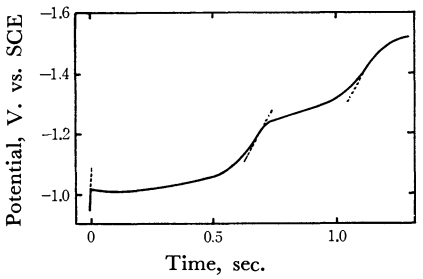

Fig. 4. Chronopotentiogram of 0.99 mM $[Cr(en)_3]Cl_3 \cdot 3^1/_2H_2O$ obtained in the presence of 0.203 mM EDTA at current density of 0.223_6 mamp. cm^{-2} in the solution (pH 4.6) containing 0.9 M NH_4Cl and 0.1 M acetate buffer.

chronopotentiogram is shown in Fig. 4.

Chronopotentiograms in alkaline ethylenediamine solutions were not so simple as in acid solutions. As shown in Fig. 5, two cathodic steps were observed in a solution containing 0.5 M ethylenediamine dihydrochloride and 1 M sodium hydroxide, and two anodic steps at the current reversed.

Discussion

Tris(ethylenediamine)chromium(III) ion gives no well-defined chronopotentiogram in neutral unbuffered solutions, because it contains basic ligands and, when reduced, it forms an insoluble film on the surface of the electrode, as has already been reported in the case of the polarographic reduction of some chromium(III) complexes.[12-14] In an acid solution the ethylenediamine molecules which the reduced chromium(II) species liberate are neutralized by hydrogen ions diffusing from the bulk of the solution; consequently, the formation of an insoluble film is prevented. It may be concluded from the results obtained at various current densities and at various concentrations of the complex that tris(ethylenediamine)chromium-(III) ions are directly reduced at the dropping mercury electrode without any preceding chemical reaction prior to the electron-transfer process. The anodic chronopotentiograms obtained by the current-reversal techniques indicate that the overall process of the reduction of tris(ethylenediamine)chromium(III) to chromium(II) species proceeds irreversibly at the dropping mercury electrode:

$$[Cr(en)_3]^{3+} + e + 2p\ H_3O^+ \rightarrow [Cr(H_2O)_{2p}(en)_{3-p}]^{2+} + p\ H_2en^{2+} \quad (4)$$

In alkaline ethylenediamine solutions, the first cathodic and the first anodic chronopotentiogram appeared in approximately the same potential region. This observation agrees with the result which was obtained by Fischerovâ and Fischer[4] in their oscillograph-polarographic study on the reduction of the same complex.

The potential of the cathodic chronopotentiogram is dependent on the ionic strength of the solution; the potential at $t=0$ ($E^c_{t=0}$) shifts to more negative potentials as the ionic strength increases (Table I). Such a shift is also observed in the reduction of other chromium(III) complexes.[13-15]

A plot of $E_{t=0}$ versus log i yielded a straight line with a slope of 55 mV. The plot of $\log(\tau^{1/2}-t^{1/2})$ versus E in various supporting electrolyte solutions, however, did not always yield a straight line as given in Table II. This makes the theoretical analysis of the potential-time curve less feasible. According to the theoretical treatment of potential-time curves reported previously,[1] the slope of these plots is equal to $2.3\,\boldsymbol{R}T/n\boldsymbol{F}$ for a reversible electron-transfer and $2.3\,\boldsymbol{R}T/\alpha n\boldsymbol{F}$ for an irreversible electron-transfer, where α represents the transfer coefficient and $\boldsymbol{R}$ the gas constant. At the moment, however, it seems impossible to decide, from the experimental results, by which process the reduction of tris(ethylenediamine)chromium(III) ions takes place, because of the insufficient knowledge on

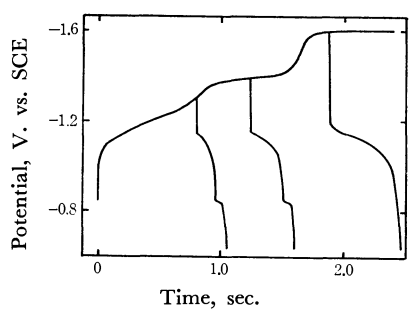

Fig. 5. Chronopotentiograms for the reduction and the subsequent reoxidation of 1 mM $[Cr(en)_3]Cl_3 \cdot 3^1/_2H_2O$ at current density of 0.223_6 mamp. cm^{-2} in the solution containing 0.5 M en·2HCl and 1 M NaOH (pH 7.9).

12) N. Tanaka and G. Satô, *Nature*, **197**, 176 (1963).
13) N. Tanaka, K. Ebata and G. Satô, This Bulletin, **36**, 912 (1963).
14) N. Tanaka, Y. Sato, R. Tamamushi and G. Satô, ibid., **36**, 1193 (1963).
15) N. Tanaka, E. Itabashi, R. Tamamushi and G. Satô, ibid., **37**, 226 (1964).

the reactivity of chromium(II) complexes.

The ratio of τ_c/τ_a fluctuates around 3, i. e., the theoretical value that is expected when the reduced species is soluble and the current densities at the forward and the reverse process are equal in magnitude.[16] The value of τ_c/τ_a in potassium nitrate solutions was found to increase as τ_c increased, as seen in Table IV. This suggests the interaction between the reduced chromium(II) complex and nitrate ions.

TABLE IV. TRANSITION TIME FOR THE REOXIDATION PROCESS OF 1mM $[Cr(en)_3]Cl_3 \cdot 3^1/_2H_2O$ RECORDED AT CURRENT DENSITY OF 0.182_0 mamp.cm^{-2} IN 0.9M KNO_3+0.1M ACETATE BUFFER

τ_c sec.	τ_a sec.	τ_c/τ_a	$E_t^c=0$ V. vs. SCE	$E_t^a=0$ V. vs. SCE
1.2_8	0.30_0	4.2_7	−0.93	−0.53
1.0_8	0.28_0	3.8_6		
0.88_0	0.25_0	3.5_2		
0.68_0	0.25_0	3.4_0		

The transition time constant of tris(ethylene diamine)chromium(III) ions (0.211 mamp.sec$^{1/2}$ cm^{-2}mM^{-1}) obtained in the solution containing 0.1 M acetate buffer and 0.9 M ammonium chloride was smaller by 20 per cent than that of hexammine-chromium(III) ions obtained under the same condition. The difference is considered to be due to a larger size of the ethylenediamine complex ion. The transition time constant obtained in the ammonium sulfate solution was found to be smaller by some 10 per cent than that obtained in other supporting electrolytes. This is considered as due to the ion-pair formation of tris(ethylene-diamine)chromium(III) with sulfate ions, the details of which will be reported elsewhere.

It is known that the transition time decreases more or less markedly when a strongly adsorbable substance is present in the solution.[17-19] In the case of the reduction of tris(ethylendiamine)-chromium(III) ions, in contrast, the addition of a very low concentration of surface-active substances improved the shape of the potential-time curves (see Fig. 6). In the absence of surface-active substance, no satisfactory chronopotentiogram was obtained; a sudden change or a drift in potential occurred, immediately before the transition time is attained. Table III indicates that the addition of LEO up to 5×10^{-7} M in concentration gives satisfactory chronopotentiograms of tris(ethylene-diamine)chromium(III) ions. A similar example of the improvement of a chronopotentiogram by the addition of a small amount of surface-active substance has been reported for the reduction of copper(II) ions in the presence of polyacrylamide.[19]

In the presence of EDTA, the cathodic chrono-potentiogram of tris(ethylenediamine)chromium-(III) ions splits into two steps; the potential of the first step is almost the same as that of the chronopotentiogram obtained in the absence of EDTA, while the potential of the second step corresponds to the oxidation-reduction potential of chromium(II)- and chromium(III)-EDTA complexes. The first step decreases in the transition time with the increase in the EDTA concentration, and it vanishes when the EDTA concentration exceeds a critical value. A plot of $\tau_1^{1/2}$ versus [EDTA]/C_O yields a nearly straight line as is seen in Fig. 7, where τ_1 is the transition time of the first step, [EDTA] the concentration of EDTA and C_O the concentration of the complex. These phenomena were considered as being caused by the electrode process given as follows [20,21]:

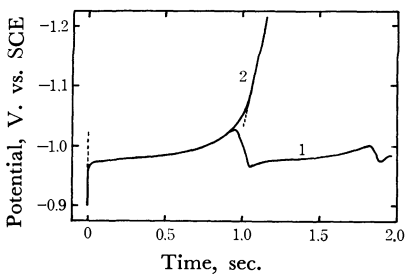

Fig. 6. Chronopotentiograms of 1 mM $[Cr(en)_3]Cl_3 \cdot 3^1/_2H_2O$ obtained at current density of 0.238_6 mamp.cm^{-2} in the solution containing 0.9 M KSCN and 0.1 M acetate buffer (1) in the absence and (2) in the presence of 5×10^{-9} M of LEO.

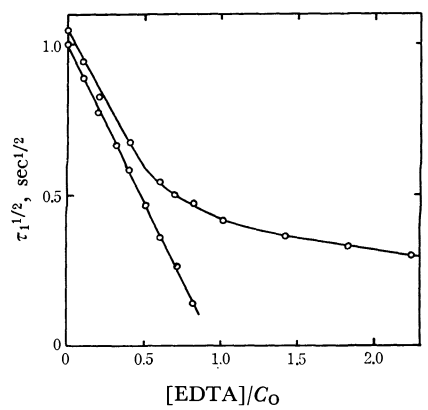

Fig. 7. Relation of $\tau_1^{1/2}$ with [EDTA]/C_O obtained at various concentrations of $[Cr(en)_3]Cl_3 \cdot 3^1/_2H_2O$ in the solution containing (1) 0.1 M acetate buffer and 0.9 M NH_4Cl and (2) 0.1 M acetate buffer and 0.3 M $CaCl_2$. Current densities are (1) 0.211_6 mamp.cm^{-2} and (2) 0.195_7 mamp.cm^{-2}.

16) A. C. Testa and W. H. Reinmuth, *Anal. Chem.*, **32**, 1512 (1960).
17) T. Murayama, *Sci. Repts. Tohoku Univ., Ser. I*, **45**, 84 (1961).
18) L. Gierst and A. Juliard, *J. Phys. Chem.*, **57**, 701 (1953).
19) T. Nagai, *J. Chem. Soc. Japan, Pure Chem. Sec.* (*Nippon Kagaku Zasshi*), **81**, 93 (1960).
20) N. Tanaka and K. Ebata, *J. Electroanal. Chem.*, **8**, 120 (1964).
21) K. Ebata, *Sci. Repts. Tohoku Univ., Ser. I*, **47**, 191 (1964).

$$[Cr(en)_3]^{3+} + e \rightarrow [Cr(en)_3]^{2+}$$

$$[Cr(en)_3]^{2+} + EDTA \rightleftharpoons Cr(II)\text{-}EDTA + 3en \quad (5)$$

$$Cr(II)\text{-}EDTA \rightarrow CrY(H_2O)^- + e$$

where Y^{4-} represents a quadrivalent EDTA anion and Cr(II)-EDTA, either $[CrYH_2O]^{2-}$ or $[Cr(HY)(H_2O)]^-$ according to the pH of the solution.[22] As is seen in Fig. 7, when a large excess of calcium ions is present in the solution, the decrease in transition time of the first step is much smaller than that observed in the absence of calcium ions. This is considered to be due to the decrease in the activity of free EDTA anions because a large excess of calcium ions reacts with free EDTA anions to form stable calcium-EDTA complexes. The details will be reported elsewhere.

The authors wish to thank the Ministry of Education for the financial support granted for this research.

22) R. L. Pecsok, L. D. Shields and W. P. Schaeffer, *Inorg. Chem.*, **3**, 114 (1964).

BULLETIN OF THE CHEMICAL SOCIETY OF JAPAN VOL. 39 925—928 (1966)

Chemical Studies of Minerals Containing Rarer Elements from the Far East District. LX.*,[1] Thalenite from Suishoyama, Kawamata-machi, Fukushima Prefecture, Japan

By Kozo NAGASHIMA**

Department of Chemistry, Faculty of Science, The University of Tokyo, Hongo, Tokyo

and Akira KATO

Department of Geology, National Science Museum, Ueno Park, Taito-ku, Tokyo

(Received September 10, 1965)

Chemical studies of thanlenite from Suishoyama pegmatite, Fukushima Prefecture, showed its composition to be very close to the ideal formula, $Y_2Si_2O_7$, and to a selective distribution pattern of rare earths belonging to the thortveitite-type as defined by Goldschmidt and Thomassen. The X-ray powder studies disclosed a metamict state hitherto unknown in this species, and the original state could be recovered by thermal treatment. Optical and other properties: color, colorless to light gray; luster, resinous; optical properties, $\alpha=1.709\pm0.002$, $\beta=1.716\pm0.002$, $\gamma=1.723\pm0.002$, $(-)2V\sim70°$, $\rho<v$; specific gravity, 4.16, hardness; $6^1/_2$. Chemical analysis: SiO_2, 30.68%; Al_2O_3, 0.10%; Fe_2O_3, 0.17%; $\sum Y_2O_3$, 64.89%; UO_2, 1.12%; ThO_2, 0.20%; CaO, 0.35%; MnO, 0.38%; MgO, 0.33%; Na_2O, 0.02%; $H_2O(+)$, 1.56%; $H_2O(-)$, 0.11%; total, 99.91%.

The rare yttrium sorosilicate mineral thalenite, $Y_2Si_2O_7$, was first described by Benedicks[2] in 1898 on the basis of a specimen from a granite pegmatite at Österby, Sweden; then it was described on the basis of samples found at Askagen, Sweden,[3] and from Hundholmen and other places, Norway.[4] The localities of this mineral added thereafter include Kofu, Japan,[5] Arizona[6] and Colorado[7], U. S. A., and Siberia, U. S. S. R.[8]

Suishoyama pegmatite, Kawamata-machi, Fukushima Prefecture, is found in a Mesozoic biotite granite body, which also contains several other pegmatites, smaller than the Suishoyama one. This pegmatite has a well-developed zonal arrangement of felsic minerals and has been worked for quartz and feldspar for many years. It is also very famous for the occurrences of many rare element-bearing minerals, such as abukumalite

* This paper was read at the 18th Annual Meeting of the Chemical Society of Japan, held at Kansai University, April, 1965.

1) Part LIX: K. Nagashima, A. Kato and M. Chiba, *J. Chem. Soc. Japan, Pure Chem. Sect.* (*Nippon Kagaku Zasshi*), **86**, 913 (1965).

** Present address: Department of Chemistry, Faculty of Science, Tokyo Kyoiku University, Otsuka, Tokyo.

2) C. Benedicks, *Geol. Fören. Förn.*, **20**, 308 (1898).

3) H. Sjögren, ibid., **28**, 93 (1906).

4) W. C. Brøgger, Th. Vogt and J. Schetelig, *Vid.-Selsk. Skrifter*, Kristiania, 1. Mat-Nat., Kl. No. 1 (1922).

5) K. Nagashima, *J. Chem. Soc. Japan, Pure Chem. Sect.* (*Nippon Kagaku Zasshi*), **73**, 600 (1952).

6) F. W. Galbraith and D. J. Brennan, *Univ. Arizona Bull.*, **30**, No. 2, 116 (1959); "Minerals of Arizona," 3rd Ed.

7) J. W. Adams, F. A. Hildebrand and R. G. Havens, "U. S. Geol. Survey Professional Paper," No. 450-D, 6 (1962).

8) T. I. Stolyrova, *Doklady Acad. Nauk. U. S. S. R.*, **155**, 100 (1964).

(type locality),[9] yttrialite,[10] fergusonite,[11] tengerite,[12] thorogummite,[13] allanite,[14,15] uraninite,[16] zircon,[17] gadolinite,[18] keilhauite[19] and some secondary uranium minerals, such as autunite, torbernite and zeunerite.[20] Most of these minerals are found in aggregates of large blades of a lepidomelane containing a small amount of lithium.[21] Abukumalite, allanite, a fergusonite-uraninite mixture and zircon also occur as larger crystals in the intermediate zone composed of large crystals of microcline, albite and quartz. It is in this zone that the thalenite here described was found together with a fergusonite-uraninite mixture. The largest thalenite crystals are fist-size and weigh about 1 kg. Some of them display a few crystal faces, though they are not goniometrically measurable due to their ruggedness.

The mineral thalenite also provides an example of the selective assemblage of rare earth elements in which dysprosium is dominant and which is known under the name "thalenite-type", by Goldschmidt and Thomassen.[22] The mode of the distribution of rare earth elements in the thalenite we have studied is not of the "thalenite-type" but rather of the "thortveitite-type," in which the maximum content of rare earth is in ytterbium. It is worthy to note that another Japanese thalenite, from Kofu, Yamanashi Prefecture, shows the same tendency.

Physical Properties

The outer parts of the thalenite grains are white and have a clouded, porcelain-like appearance, while the inner parts range from colorless to a very light gray or are transparent. The X-ray powder studies showed the former to be a mixture of more or less metamictized thalenite and tengerite, and the latter, to be thalenite itself, but more metamictized than the former. The physical properties, including the optical properties, of the core part are given in Table I. Among them, the refractive indices which are lower than those of thalenite from other localities are so significant as to constitute one of the characteristics of the metamictized minerals (e. g., $\alpha=1.725$, $\beta=1.746$, and $\gamma=1.762$ for thanlenite from Kofu, Japan[5]). However, the conoscopic figure is unexpectedly sharp irrespective of the broader and weaker X-ray diffraction peaks, as will be established in the succeeding.

Table I. Optical and other prorerties

Color	colorless
Luster	resinous to glassy
X-Ray powder diffractions	broad and weak
Optical property	α 1.709±0.002
	β 1.716±0.002
	γ 1.723±0.002
	$(-)2V\sim70°$, $\rho<v$
Specific gravity	4.16
Hardness	$6\,1/2$

X-Ray Powder Studies

The X-ray powder studies were made on unheated and heated materials from the inner parts using a Norelco X-ray Diffractometer. The former gives a few, broad diffraction peaks, as is shown in Table II. After the material has been heated for one hour at about 900°C in the air, the diffraction peaks become very sharp and the powder data are very similar to those for thalenite (non-metamict) obtained from Snowflake pegmatite,[7] Colorado, U. S. A., as is shown in Table II. The positions of all the diffraction peaks of the unheated material shift to the high angle side when heated, without any significant changes in their relative intensities. This means a complete recovery from the metamict to the crystalline state after thermal treatment up to about 900°C; the recovered crystalline state is crystallographically identical with that of ordinary nonmetamict thalenite. Also, the metamictization of this mineral yields the expansion of the unit cell, which is substantially responsible for the lowering of the refractive indices.

Chemical Composition

Chemical analyses were carried out on hand-picked material from the inner part. The average atomic weight of the rare earth elements was determined by titrating the weighed mixed oxides with EDTA after first dissolving them in hydrochloric acid. The water content was determined by igniting the sample and by then absorbing the liberated water in calcium chloride. Sodium and potassium were determined by flame-photometry.

The results of the chemical analyses are given in Table III, together with the molecular ratios of the components. The higher uranium content and the presence of thorium that characterize

9) S. Hata, *Sci. Pep. Inst. Physic. Chem. Research*, **34**, 1018 (1938).
10) S. Hata, ibid., **34**, 455 (1938).
11) S. Iimori and S. Hata, ibid., **34**, 504 (1938).
12) T. Iimori, ibid., **34**, 832 (1938).
13) S. Iimori and S. Hata, ibid., **34**, 447 (1938).
14) S. Hata, ibid., **36**, 112 (1939).
15) T. Iimori, ibid., **36**, 53 (1939).
16) T. Iimori, ibid., **39**, 208 (1941).
17) S. Hata, ibid., **34**, 619 (1938).
18) S. Hata, *Reports of the Scientific Research Institute*, **29**, 488 (1953) (in Japanese).
19) K. Kimura, T. Kawai, K. Morinaga, K. Nagashima and H. Shibata, *J. Chem. Soc. Japan, Pure Chem. Sect.* (*Nippon Kagaku Zasshi*), **74**, 692 (1953).
20) K. Hemmi, *Min. Jour.*, **2**, 134 (1957).
21) H. Hamaguchi and N. Shimoda, *J. Chem. Soc. Japan, Pure Chem. Sect.* (*Nippon Kagaku Zassi*), **74**, 879 (1953).
22) V. M. Goldschmidt and L. Thomassen, *Vidensk. Skrift. I. Mat. Naturv. Klasse*, No. 5 (1924).

TABLE II. X-RAY DIFFRACTIONS OF THALENITES*

Teller County[7]		Suishoyama heated		Suishoyama unheated		Teller County[7]		Suishoyama heated		Suishoyama unheated	
d(Å)	Intensity	d(Å)	Intensity	d(Å)	Intensity	d(Å)	Intensity	d(Å)	Intensity	d(Å)	Intensity
6.3	5	6.36	10			1.977	4	1.979	10		
6.07	4	6.11	5			1.953	2	1.947	5		
5.57	2	5.57	30	5.59	mb	1.922	0.7	1.922	5		
5.50	20	5.51	30					1.901	5		
5.16	3	5.16	5			1.895	3	1.893	5		
4.98	1	5.02	5 b			1.873	7	1.872	15		
4.67	5					1.859	0.7				
4.44	5	4.43	10			1.845	3	1.844	10		
4.17	4	4.17	15			1.817	4	1.816	10		
3.95	1	3.95	5			1.797	3	1.798	5		
3.79	25	3.79	40	3.83	w	1.781	2	1.779	5 b		
3.63	5	3.65	5 b			1.768	1				
3.49	4	3.50	20			1.746	0.7				
3.44	11	3.47	20 b	3.49	w	1.740	0.7	1.737	5		
3.31	2	3.30	5			1.728	1				
3.27	18	3.27	80	3.31	s	1.716	4	1.715	10		
3.16	18	3.17	40	3.16	w	1.704	2	1.711	5		
3.13	11	3.14	20			1.681	1	1.682	5		
3.10	100	3.10	100	3.13	s	1.670	5	1.670	30		
3.05	4	3.04	5			1.658	2	1.659	30		
2.96	1	2.964	10			1.645	5	1.645	10		
2.86	6	2.864	5			1.631	5	1.631	10		
2.81	40	2.812	30			1.616	4	1.617	5		
2.75	30	2.754	30			1.603	1				
		2.715	5			1.583	0.5				
		2.670	5			1.570	5	1.567	20		
2.61	2	2.605	5			1.558	2				
2.57	5	2.577	20			1.547	2	1.545	5		
2.51	4	2.520	5			1.523	1	1.531	5 b		
2.46	3	2.460	5 b			1.510	2	1.514	5 b		
2.42	1	2.428	5			1.497	0.7				
2.40	3	2.409	15			1.478	2				
2.37	1	2.368	5			1.465	2				
2.34	3	2.332	5			1.455	3	1.455	10		
2.30	2	2.306	5			1.445	1				
		2.254	5			1.429	0.7				
2.24	30	2.240	50	2.26	w	1.425	1				
2.21	1					1.415	0.7				
2.20	1					1.408	1	1.409	10		
2.18	9	2.176	60			1.404	1				
2.127	6	2.120	15			1.391	0.7				
2.103	0.7	2.110	15			1.382	0.7				
2.076	0.7					1.370	2	1.369	10		
2.053	3	2.047	5								
2.027	2	2.032	5								
1.994	3	1.994	5								

*b ……broad m……medium
s ……strong w……weak

this material are responsible for the metamict state.

As is shown in Table III, the experimental formula of the thalenite from Suishoyama is $(Y, Yb, Er, Dy, U, Ca, etc.)_{2.012}(Si, Al)_{2.009}O_{7.000}\cdot 0.38H_2O$, which is very close to the ideal formula, $(Y, Yb)_2Si_2O_7$, except for an additional 0.38 mol. of H_2O.

The crystallochemical nature of the water in thalenite is still unknown. In Doelter's handbook,[23] the formula is given as $Y_2Si_2O_7\cdot{}^1/_2H_2O$; this has lately been revised to $Y_2Si_2O_7$. However, judging from the results of a survey of the literature concerned, no significant study has hitherto been made of the water in this mineral.

23) C. Doelter, "Handbuch der Mineralchemie," Band II, 2 Hälfte, Teodor Steinkopff, Dresden und Leipzig (1917), s. 170.

Table III. Chemical analysis

		%/F.W.	No. of oxygens	No. of metal atoms	No. of metal atoms×3.919	
SiO_2	30.68	0.5106	1.0212	0.5106	2.0010	2.009
Al_2O_3	0.10	0.0010	0.0030	0.0020	0.0078	
Fe_2O_3	0.17	0.0011	0.0033	0.0022	0.0086	2.012
*$\sum Y_2O_3$	64.89	0.2430	0.7290	0.4860	1.9046	
UO_2	1.12	0.0041	0.0082	0.0041	0.0160	
ThO_2	0.20	0.0008	0.0016	0.0008	0.0031	
CaO	0.35	0.0062	0.0062	0.0062	0.0243	
MnO	0.38	0.0054	0.0054	0.0054	0.0212	
MgO	0.33	0.0082	0.0082	0.0082	0.0321	
Na_2O	0.02	0.0003	0.0003	0.0006	0.0024	
$H_2O(+)$	1.56	0.0975			0.3819	
$H_2O(-)$	0.11					
	99.91		1.7864			

* Average atomic weight 109.5
Specific gravity 4.16

Proton magnetic resonance studies[24] of water molecules in this material proved that they are not in a merely absorbed state, but that they combine with the mineral rather tightly at room temperature, and that they (more precisely, the protons) do not exist as isolated OH^- ions, either. Nearly 10% water (by weight) has been found in the white outer part of the mineral, which is in a less metamictized state than the inner part, according to the X-ray powder study. Even though the presence of a small amount of tengerite in the outer part is taken into consideration, a considerable amount of water should be in thalenite itself; it is responsible for the less metamictized state.

The Distribution Pattern of Rare Earth Elements

The distribution pattern of rare earth elements was determined by the X-ray fluorescent method; yttrium, neodymium, samarium, gadolinium, terbium, dysprosium, erbium and ytterbium were thus found. Lutetium may be present, but its presence was not confirmed due to the overlapping diffractions of other spectra with stronger intensities. A quantitative estimation is given in Table IV, in which the total of the detected oxides is calculated to be 100% and is compared with those for the Siberia thalenite.[8] The present material has predominances of dysprosium, erbium and ytterbium among the lanthanides, and a very high concentration of yttrium in rare earths. The concentration of cerium-group lanthanides is too low to be detected. The average atomic weight calculated by adopting the values rendered by the X-ray fluorescent analysis was 108, which coincides rather well with that determined by the ordinary chemical method shown in Table III.

Table IV. Composition of rare earth elements

	Siberia[8]	Suishyoyama
$\sum Ce_2O_3$	1.1	
Nd_2O_3		0.3
Sm_2O_3		0.2
Gd_2O_3	1.1	1.2
Tb_2O_3	0.6	0.2
Dy_2O_3	6.4	4.3
Ho_2O_3	2.4	
Er_2O_3	9.1	5.9
Tu_2O_3	2.9	
Yb_2O_3	9.1	11.6
Lu_2O_3	0.9	
Y_2O_3	67.5	76.4
	100.1	100.1

The authors wish to express their thanks to Professor Takeo Watanabe, Geological Institute, Faculty of Science, the University of Tokyo, for making the X-ray diffraction and fluorescent analysis instruments available for their present work, and to Mr. Hideo Katagiri, the Manager of the Suishoyama quarry, for his help in collecting the minerals studied.

24) K. Nagashima and Y. Sugitani, 18th Annual Meeting of the Chemical Society of Japan, Osaka, 1965.

BULLETIN OF THE CHEMICAL SOCIETY OF JAPAN VOL. 39 929—932 (1966)

The Structure of a Yellow Pigment from the Mutant *lemon* of *Bombyx mori*

By Miki GOTO, Masaki KONISHI and Katsura SUGIURA

Department of Chemistry, Gakushuin University, Mejiro, Toshima-ku, Tokyo

and Motoo TSUSUE

Department of Biology, Tokyo Metropolitan University, Setagaya-ku, Tokyo

(Received September 11, 1965)

The structure of N_8-methylsepiapterin was previously postulated for a new pteridine from *Bombyx mori lemon* (This Bulletin, **38**, 503 (1965)). This structure must, however, be modified on the basis of some new experiments. We will now present the 7, 8-dihydro-6-lactyllumazine structure for this compound.

Hirata, Nakanishi and Kikkawa[1] have reported the isolation of a yellow pigment, named xanthopterin-B, from the epidermis of the mutant *lemon* of *Bombyx mori*. Nawa and Taira[2] have reported that xanthopterin-B is indistinguishable from a yellow compound found in comparatively large quantities in the eyes of the *sepia* mutant of *Drosophila melanogaster*. Aruga, Kawase and Akino[3] have shown, by chromatographic techniques, the presence of two yellow, yellow-fluorescent compounds (xanthopterin-B_1 and xanthopterin-B_2) in the epidermis of *B. mori lem.* Tsusue and Akino[4] have succeeded in isolating a small amount of xanthopterin-B_1, which is by far the major component, in a pure state and have demonstrated that it has the same structure as sepiapterin, i. e., 2-amino-4-hydroxy-7, 8-dihydro-6-lactylpteridine I.[5] The second component, xanthopterin-B_2, is present in extremely small amounts, and it is very sensitive to light. In a preliminary report,[6] we described some degradations of this compound and postulated a structure for it. This structure must, however, be modified in the light of some new experiments which will be described here. We now wish to propose the structure II for this compound.

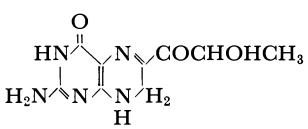

(I)

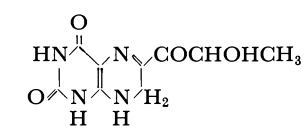

(II)

Experimental

The Isolation of Xanthopterin-B_2.—The epidermis of silkworms (*B. mori*, mutant *lemon*) was treated with acetone, filtered, and pulverized. The pteridines were extracted by boiling the epidermis (100 g., wet) with 800 ml. of 50% ethanol for 20 min.; the solution was then filtered. The extraction with 50% ethanol was repeated twice, after which the yellow filtrates were combined and evaporated to dryness in vacuo. The residue was dissolved in water, and the solution was passed through an Ecteola cellulose column (7×12 cm.). The yellow fluorescent material (xanthopterin-B_2) was concentrated in a band at the top of the column; after the column had been throughly washed with water, this band was eluted with 0.01 N acetic acid. The eluate was concentrated, and the solution was again passed through an Ecteola cellulose column (3×10 cm.). The yellow eluate obtained by washing this with a 1% ammonium chloride solution was evaporated to a small bulk. The extract was then passed through a Filtrol (grade 58) column (2×7 cm.). After the column had been thoroughly washed with water, the band was eluted with 10% aqueous acetone. The eluate was concentrated to dryness in vacuo. All the above procedures were carried out in the dark in order to avoid photolysis. Four hundred grams of the epidermis gave 15 mg. of the crude product in a repetition of this procedure. From this about 2 mg. of the pure material was obtained by crystallization from methanol and water. The ultraviolet absorption spectra of the compound are shown in Fig. 1.

Air Oxidation in a Borax Solution.[5]—A small amount of the compound was dissolved in 5% aqueous borax and then shaken at 35°C for 24 hr. in the dark in order to avoid photodecomposition; the yellow color of the solution thereby gradually changed to a weak yellowish green, and the yellow fluorescence, to green. The product was purified by paper chromatography using as solvents *n*-propanol - 1% ammonia (2 : 1) and *n*-butanol - acetic acid - water (4 : 1 : 1). The absorption spectra, R_f-values and electrophoretic behavior

1) Y. Hirata, K. Nakanishi and H. Kikkawa, This Bulletin, **23**, 76 (1950).
2) S. Nawa and T. Taira, *Proc. Japan Acad.*, **30**, 632 (1954).
3) H. Aruga, S. Kawase and M. Akino, *Experientia*, **14**, 182 (1958).
4) M. Tsusue and M. Akino, *Zool. Magazine Japan*, **74**, 91 (1965).
5) S. Nawa, This Bulletin, **33**, 1555 (1960).
6) M. Goto, M. Kinishi and M. Tsusue, ibid., **38**, 503 (1965).

Table I. Paper chromatography and electrophoresis of xanthopterin-B_2 and its degradation products

Substance	Paper chromatography solvent					Electrophoresis*
	1	2	3	4	5	
Xanthopterin-B_2	0.24	0.54	0.42	0.50	0.43	0
Air oxidation product (in borax solution)	0.36	0.51	0.62	0.60	0.60	10
6-Hydroxylumazine	0.36	0.51	0.62	0.60	0.60	10
$KMnO_4$ oxidation product	0.15	0.28	0.32	0.35	0.58	48
Lumazine-6-carboxylic acid	0.15	0.28	0.32	0.35	0.58	48
$NaBH_4$ reduction product	0.31	0.45	0.45	0.55	0.59	0
Lumazine	0.31	0.45	0.45	0.55	0.59	0

Solvents: 1, *n*-butanol, acetic acid, water (4 : 1 : 1)
2, isopropanol, 1% ammonia (2 : 1)
3, *s*-butanol, formic acid, water (8 : 2 : 5)
4, *n*-propanol, 2% ammonium acetate (1 : 1)
5, 3% ammonium chloride

* Distance (in mm.) to anode after electrophoresis at pH 4.65 (sodium acetate buffer) for 1 hr. at 36 V./cm.

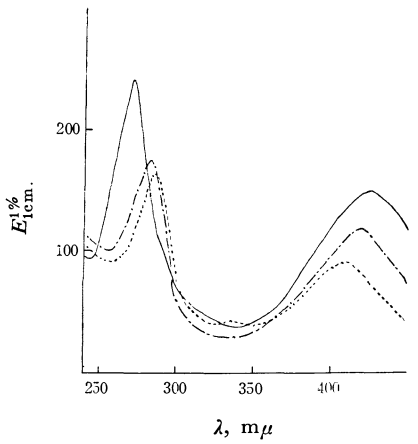

Fig. 1. The ultraviolet absorption spectra of xanthopterin-B_2: ——, at pH 12; —·—·, at pH 6.0; and ·····, at pH 1.0.

of the product were identical with those of an authentic sample of 6-hydroxylumazine[7] (Table I).

The Characterization of Lactic Acid.[8]—An aqueous solution of the compound (xanthopterin-B_2) (0.28 ml., c=41.0 μg./ml.) was treated with 5% borax (0.1 ml.) and shaken at 35°C for 24 hr. in the dark. The solution was then diluted with water to 1 ml. and heated at 100°C for 5 min. with 6 ml. of sulfuric acid and 0.05 ml. of 2% copper(II) sulfate. After cooling, 0.1 ml. of a 1.5% *p*-hydroxybiphenyl reagent was added; the mixture was allowed to stand at 30°C for 30 min. and then heated at 95°C for 1—2 min. The color which developed was estimated at 570 mμ (Hitachi spectrophotometer EPS-3). From a standard curve obtained with known amounts of lithium lactate, 41.0 μg. (1 ml. of the reaction mixture) was estimated to give 13.1 μg. of lactic acid (84% of the theoretical yield).

Potassium Permanganate Oxidation.—An aqueous solution of the sample (0.04 ml., c=5 mg./ml.) was treated with a saturated solution of potassium permanganate in 0.1 N sodium hydroxide (0.08 ml.) at 95°C for 30 min. The excess permanganate was then destroyed with alcohol, and the solution was filtered

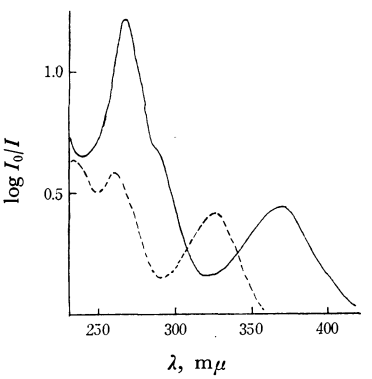

Fig. 2. The ultraviolet absorption spectra of the pteridine obtained by permanganate oxidation of xanthopterin-B_2: ——, at pH 12; and ·····, at pH 1.

in order to remove the manganese(IV) oxide. The product was identical with lumazine-6-carboxylic acid[9] (Table I and Fig. 2).

Periodate Oxidation.—A small amount (enough for paper chromatography) of an aqueous solution of the sample was treated with sodium metaperiodate at 30°C for 24 hr. and then submitted to paper chromatography and electrophoresis. The product was identical with lumazine-6-carboxylic acid.

Reduction with Sodium Borohydride.—An aqueous solution of the compound (xanthopterin-B_2) (0.1 mg./10 ml.) was treated with sodium borohydride (1 mg.); the greenish yellow fluorescence of the solution

7) A. Albert, J. H. Lister and C. Pedersen, *J. Chem. Soc.*, **1965**, 4621.
8) S. B. Barker and W. H. Summerson, *J. Biol. Chem.*, **138**, 535 (1941).
9) R. B. Angier, J. H. Boothe, J. H. Mowat, C. W. Waller and J. Semb. *J. Am. Chem. Soc.*, **74**, 408 (1952).

thereby almost disappeared. When the reaction mixture was shaken in air, its fluorescence became blue. The paper chromatography of this solution showed the presence of three fluorescent compounds. The major spot was lumazine-6-carboxylic acid and the intermediate lumazine; this was confirmed by the ultraviolet absorption spectra and the electrophoretic migration (Table I).

The Reaction of 2, 5-Diamino-4-hydroxy-6-methylaminopyrimidine with Glyoxal.—2-Amino-4-hydroxy-6-methylamino-5-nitropyrimidine was prepared from 2-amino-6-chloro-4-hydroxy-5-nitropyrimidine and aqueous methylamine.[10] The product (6.0 g.) was purified by dissolution in 8% aqueous ammonia (100 ml.) (charcoal) and by reprecipitation with hydrochloric acid (6 N).

Found: C, 27.6; H, 3.3; N, 30.6. Calcd. for $C_5H_7N_5O_3 \cdot HCl$: C, 27.3; H, 3.6; N, 31.5%.

The pyrimidine hydrochloride (2 g.) in hot 3% ammonia (5 ml.) was treated with sodium dithionite. The solution was neutralized with acetic acid (pH 6), 8 ml. of glyoxal (40%) was added, and the whole was refluxed for 30 min. under nitrogen. The precipitate was collected by centrifugation and purified by chromatographic methods using a cellulose column (9×50 cm.; developer: isopropanol/1% ammonia=2 : 1) and a Dowex 1X8 column (5×24 cm.; $HCOO^-$; developer: 0.03 M formic acid/ammonia, the pH value being changed continuously from 9.4 to 7.0). The effluent containing the main fluorescent band was acidified with hydrochloric acid (pH 2—3), and the compound was adsorbed on Darco G-60, which was then washed well with water. The pteridine was eluted with 2% ammonium hydroxide-ethanol (3 : 1), the eluate evaporated to dryness in vacuo, and the residue crystallized from water to give a faint yellow product (20 mg.).

Found: C, 43.3; H, 2.3; N, 33.9. Calcd. for $C_6H_4N_4O_2$: C, 43.9; H, 2.5; N, 34.1%.

The product was indistinguishable from synthetic lumazine on the basis of ultraviolet, infrared and mass spectral data and R_f-values.

The Reaction of 2, 5-Diamino-4-hydroxy-6-methylaminopyrimidine with Monochloracetone.—2-Amino-4-hydroxy-6-methylamino-5-nitropyrimidine hydrochloride (2 g.) in hot 16% ammonia (50 ml.) was treated with sodium dithionite (8 g.), and then the solution was adjusted to pH 5 with acetic acid. After the addition of monochloracetone (6.0 ml.) it was refluxed for 1 hr. and concentrated to a small bulk in vacuo. By the use of a Dowex 1X8 column ($HCOO^-$), two main products (A and B) were separated from the reaction mixture.

Product A (24 mg.): colorless needles; m. p. 246—248°C (decomp.).

Found: C, 47.5; H, 3.3; N, 31.2. Calcd. for $C_7H_6N_4O_2$: C, 47.2; H, 3.4; N, 31.5%. λ_{max} mμ ($E^{1\%}_{1cm.}$) 248 (842), 360 (408) in 0.1 N sodium hydroxide and 327 (560) in 0.1 N hydrochloric acid.

Product B (14 mg.): faint yellow needles; m. p. 266—268°C (decomp.).

Found: N, 31.7. Calcd. for $C_7H_6N_4O_2$: N, 31.5%. λ_{max} mμ ($E^{1\%}_{1cm.}$) 256 (995), 368—372 (349) in 0.1 N sodium hydroxide and 232 (724), 333 (480) in 0.1 N hydrochloric acid.

Product A was indistinguishable from authentic 7-methyllumazine, while product B was identical with 6-methyllumazine, as determined by a study of the ultraviolet, infrared and mass spectral data and the R_f values. On oxidation compounds A and B gave lumazine-7-carboxylic acid and lumazine-6-carboxylic acid respectively.

Discussion

The new naturally-occurring compound described above gives ultraviolet spectra similar to those of sepiapterin. The presence of the parent lumazine ring system was demonstrated by reduction with $NaBH_4$ and by the reoxidation of the reduction product. This yielded lumazine. The production of lumazine-6-carboxylic acid by oxidation (potassium permanganate and sodium periodate) showed that there was a substituent on the 6-position, while its nature was demonstrated by the fact that the pteridine, on air oxidation in a borax solution, yielded 6-hydroxylumazine and lactic acid. From these findings, it may be concluded that the compound is a 6-lactyllumazine. No direct evidence for the presence of the reduced ring system was obtained; however, the similarity of the chemical properties and ultraviolet spectra (in basic, acidic and neutral media) to those of sepiapterin strongly suggests that it is 7, 8-dihydro-6-lactyllumazine. The 7, 8-dihydro structure of sepiapterin was proved by its nuclear magnetic resonance spectrum*.

In 1962 Kaufman[11] reported that sepiapterin functions as a cofactor in the enzymatic transformation of phenylalanine to tyrosine (the activity is 25 times that of folic acid). The activity of the compound (xanthopterin-B_2) as the cofactor was, however, only one-fourth that of sepiapterin.**

The question then arises as to the origin of this compound. A possible explanation is that it is produced enzymatically from reduced lumazine in exactly the same way that sepiapterin or isosepiapterin can be synthesized from reduced 2-amino-4-hydroxypteridine and an active C_3-compound.[12,13] Current theory supposes that the pteridine ring arises from guanosine or guanosine-5'-phosphate. The first step of the reaction involves the opening of the imidazole ring of the guanine moiety and the elimination of the carbon-8 of the purine.[14] The resulting 2, 5-diamino-4-hydroxy-6-D-ribofuranosylaminopyrimidine could then undergo transformation to lumazine in the presence of a two-carbon unit in just the same way

10) R. Lohrmann and H. S. Forrest, *J. Chm. Soc.*, **1964**, 460.

* Unpublished.

** M. Matsubara, personal communication.

11) S. Kaufman, *J. Biol. Chem.*, **237**, PC 2712 (1962).

12) S. Nawa and H. S. Forrest, *Nature*, **196**, 169 (1962).

13) F. I. Maclean, H. S. Forrest and J. Myers. *Biochem. Biophys. Res. Commun.*. **18**, 623 (1965).

14) F. Weygand, H. Simon, G. Dahms, M. Waldschmidt, H. J. Schliep and H. Wacker, *Angew. Chem.*, **73**, 402 (1961).

as lumazine can be synthesized from 2, 5-diamino-4-hydroxy-6-methylaminopyrimidine and glyoxal in vitro. Attempts to obtain 6-lactyl-7, 8-dihydrolumazine from reduced lumazine and α-keto-β-hydroxybutyric acid in the presence of thiamine, were, however, fruitless. An alternative pathway, in which xanthopterin-B_2 is derived enzymatically from xanthopterin-B_1, is more probable. The presence of sepiapterin-deaminase in *B. mori lem* was actually demonstrated by one of us (M. T.). This finding will be reported on elsewhere.

In a preliminary communication,[6] we reported that the oxidation product of the compound (xanthopterin-B_2) (potassium permanganate and potassium poriodate) is indistinguishable from the synthetic "2-amino-4-hydroxy-8-methyl 4, 8-dihydropteridine-6-carboxylic acid" obtained by the condensation of 2, 5-diamino-4-hydroxy-6-methylamino-pyrimidine with β-bromopyruvic acid, and that a reduction product ($NaBH_4$) is identical with the "2-amino-4-oxo-8-methyl 4, 8-dihydropteridine" prepared by the condensation of the pyrimidine with glyoxal.[15] From these observations and its behavior upon air-oxidation in a borax solution, the N_8-methylsepiapterin structure was tentatively postulated. However, the present investigation has proved that the condensation of 2, 5-diamino-4-hydroxy-6-methylaminopyrimidine with β-bromopyruvic acid or glyoxal under the conditions described here does not give the desiredp roducts, but, that unexpectedly, lumazine-6-carboxylic acid or lumazine is formed. In the same way, the condensation of the pyrimidine with monochloracetone yields 6-methyllumazine and its 7-isomer. Previously, we were not aware of this unusual reaction; this led to an incorrect formulation of xanthopterin-B_2. We now wish to present the structure II for this compound.

15) D. J. Brown and N. W. Jacobsen, *J. Chem. Soc.*, **1961**, 4413.

Summary

On the basis of degradative experiments, the structure of 7, 8-dihydro-6-lactyllumazine has been postulated for a yellow pigment from *Bombyx mori lem.*

The authors wish to express their thanks to Dr. Jeanne M. Lagowski for her survey of the manuscript. Thanks are also due to Professor Teinosuke Kobayashi for his encouragement.

BULLETIN OF THE CHEMICAL SOCIETY OF JAPAN VOL. 39 932—935 (1966)

The Chemiluminescence of Acyl Luminols

By Yoshimori OMOTE, Takeo MIYAKE, Seiya OHMORI and Noboru SUGIYAMA

Department of Chemistry, Tokyo Kyoiku University, Otsuka, Tokyo

(Received September 11, 1965)

From a study of the chemiluminescence spectra of acyl luminols (e. g., 3-acetylaminophthalhydrazide, 3-propanoylaminophthalhydrazide and 3-undecenoylaminophthalhydrazide) and of the corresponding fluorescence spectra of the reaction products, it is tentatively assumed that the emitting species of the chemiluminescence of acyl luminols in dimethylformamide-water (3 : 1 in vol.) is the corresponding 3-acylaminophthalate ion in the excited state.

Since Albrecht[1] first described the bright chemiluminescence of luminol (3-aminophthalhydrazide) (I), the synthetic approach to a clarification of the mechanism of the chemiluminescence had been attempted by several groups of workers.[2] Recently White et al.[3] showed that the 3-aminophthalate ion might be the light emitting species in the chemiluminescent reaction of luminol in water or in dimethylsulfoxide.

As a part of the investigation of the synthesis of chemiluminescent polymers,[4] the present authors have studied the synthesis and chemiluminescence of acyl luminols. The object of this paper is to present a convenient modified method for the acylation of luminol and to describe the relation between the chemiluminescence spectra of acylated luminols and the corresponding fluorescence spectra of the chemiluminescent reaction products.

1) H. O. Albrecht, *Z. Phys. Chem.*, **136**, 321 (1928).

2) a) H. D. K. Drew and R. F. Garwood, *J. Chem. Soc.*, **1937**, 1841. b) H. D. K. Drew and R. F. Garwood, ibid., **1938**, 791. c) E. H. White, O. Zafiriou, H. H. Kägi and J. H. M. Hill, *J. Am. Chem. Soc.*, 86, 940 (1964). d) M. A. Bernanose, *Bull. soc. chim. France*, **18**, 329 (1951).

3) E. H. White and M. M. Bursey, *J. Am. Chem. Soc.*, **86**, 941 (1964).

4) N. Sugiyama et al., to be published.

Results and Discussion

The Acylation of Luminol.—It has been found in this laboratory that dimethylformamide is a suitable solvent for the acylation of luminol, which is sparingly soluble in most organic solvents. Monoacyl derivatives of luminol were prepared by the action of several acyl chlorides on luminol dissolved in dimethylformamide in the presence of pyridine.

The ultraviolet absorption spectra of luminol and its three acyl derivatives, 3-acetylaminophthalhydrazide (II), 3-propanoylaminophthalhydrazide (III) and 3-undecenoylaminophthalhydrazide (IV), are shown in Fig. 1. The absorption maximum about 330 nm* was useful for the identification of the acyl derivatives.

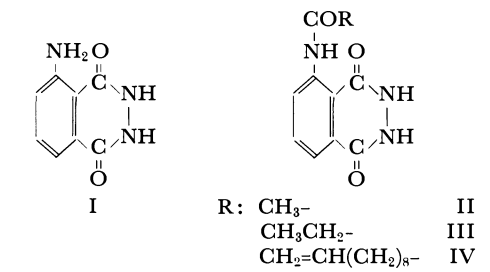

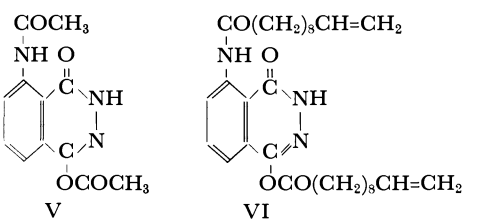

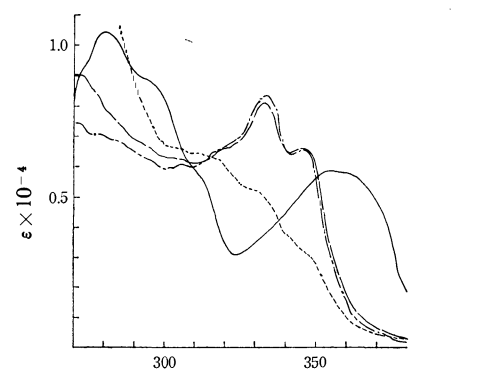

Fig. 1. Ultraviolet absorption spectra of luminol and acyl luminols.
luminol (I) ——, 3-acetylaminophthalhydrazide - — -, 3-propanoylaminophthalhydrazide — —, 3-undecenoylaminophthalhydrazide ---- in dimethylformamide.

* Following the IUPAC rule, the new notation nm (nanometer) is used instead of mμ.

When luminol was treated with an excess of several acyl chlorides, diacyl derivatives of luminol were obtained. Those were tentatively deduced to be V and VI from their infrared absorption spectra, which have the strong absorption at 1760 cm^{-1} characteristic of the carbonyl group of the enol ester type.

The Chemiluminescence Spectra of Luminol and Acyl Luminols.—The color of the chemiluminescence of luminol was bright blue, with a spectral maximum at 470 nm, while acyl derivatives showed a greenish blue chemiluminescence, with a maximum at about 480 nm. The chemiluminescent spectra spread over a broad region between about 400 nm and 600 nm.

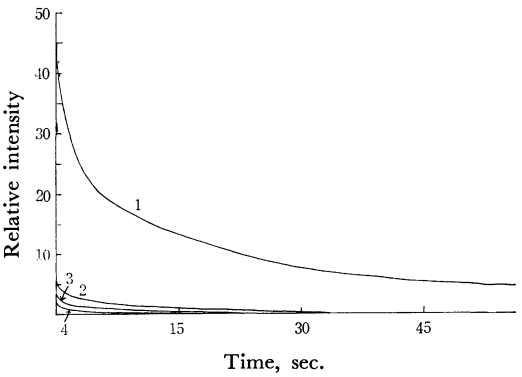

Fig. 2. Change of chemiluminescence intensity at the emission maximum.
luminol (I) (470 nm) ····· 1, 3-acetylaminophthalhydrazide (II) (480 nm) ····· 2, 3-propanoylaminophthalhydrazide (III) (480 nm) ····· 3, 3-undecenoylaminophthalhydrazide (IV) (480 nm) ····· 4
Concn.: 7.5×10^{-4} mol. in DMF-water mixture (vol. 3 : 1) respectively.

Figure 2 shows the change in chemiluminescence intensity with time. The chemiluminescence intensity strikingly decreases with the acylation of the amino group of luminol. This suggests that both the inductive and steric effects of the acylamino group serve to decrease the chemiluminescence of luminol, as has been reported by earlier investigators.[5] The spectra of the chemiluminescence of acyl luminols show the emission maximum at a little longer wavelength than luminol, as is shown in Table I. This fact is likely to show that the energy difference between the emitting species and the emission products of acyl derivatives is smaller than that of luminol. Moreover, a comparison of the wavelengths and intensities at the maximum of emission spectra of

5) a) H. D. K. Drew and F. H. Pearman, *J. Chem. Soc.*, **1937**, 586. b) C. N. Zellner and G. Dougherty, *J. Am. Chem. Soc.*, **59**, 2580 (1937). c) B. E. Cross and H. D. K. Drew, *J. Chem. Soc.*, **1949**, 638. d) K.-D. Gundermann and M. Drawert, *Chem. Ber.*, **95**, 2018 (1962).

TABLE I. FLUORESCENCE AND CHEMILUMINESCENCE OF LUMINOL (I), 3-ACETYLAMINOPHTHALHYDRAZIDE (II), 3-PROPANOYLAMINOPHTHALHYDRAZIDE (III), 3-UNDECENOYLAMINOPHTHALHYDRAZIDE (IV)

Compound		Fluorescence λ_{max},nm(*)		Chemiluminescence λ_{max},nm(*)		Ultraviolet absorption λ_{max},nm
Luminol(I)	A	410	(100)	470	(100)	353
	B	475				358
2-Acetylaminophthalhydrazide(II)	A	412	(3)	480	(10)	333
	B	500				344
3-Propanoylaminophthalhydrazide(III)	A	412	(3)	480	(8)	333
	B	500				344
3-Undecenoylaminophthalhydrazide(IV)	A	412	(5)	480	(5)	300(sh.)
	B	495				346

* Relative intensity
A Fluorescence in dimethylformamide.
B Fluorescence after chemiluminescent reaction in dimethylformamide water-mixture (Vol. 3 : 1).

II, III and IV shows that the acylamino group with a longer alkyl chain is more unfavorable to the emission than that with a shorter one (Table I and Fig. 2).

The Relation of Chemiluminescence and Fluorescence.—The fluorescence spectra in various conditions are useful in deciding the emitting species in the chemiluminescent reaction.[6] First, the authors have examined the fluorescence spectra of luminol and its acyl derivatives in dimethylformamide or in the mixed solvent of dimethylformamide and water (3 : 1 in vol.). The results are summarized in Table I. During the measurement of the fluorescence spectrum of luminol, it was found that the intensity at the maximum of 410 nm decreased with the increase in the intensity at the new maximum, 470 nm, as is shown in Fig. 3. The spectral change seemed to be accelerated by adding water. Also, acyl luminols showed a similar phenomenon, which is likely to be related to the photochemical reaction with oxygen in the solvent.[6d] A more precise experiment investigating this phenomenon is now in progress.

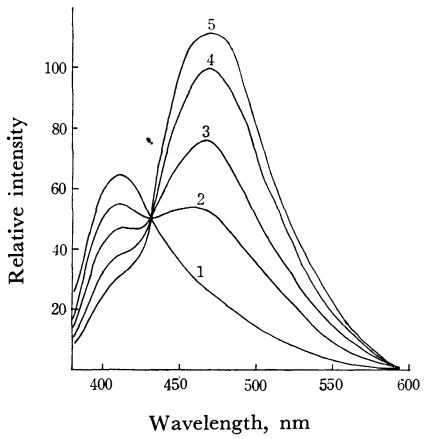

Fig. 3. The change of fluorescence spectrum of luminol in dimethylformamide with time 1—5, 5 min. interval.

Next, the fluorescence spectrum of the total reaction product of the chemiluminescent reaction of each compound was measured after chemiluminescence. The results are summarized in Table I, while the typical chemiluminescence spectra of I and II are shown in Figs. 4 and 5 respectively.

White et al.[3] reported, that in the chemiluminescence of luminol in dimethylsulfoxide and also in water, a good match had been found in the wavelength distribution in chemiluminescence, the

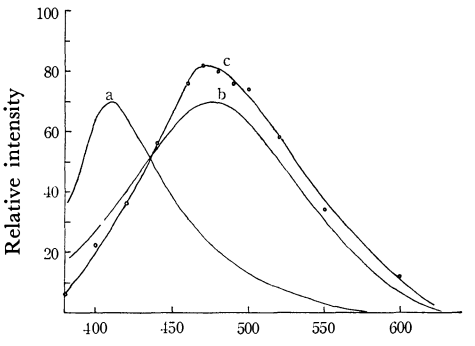

Fig. 4. Fluorescence and chemiluminescence spectra of luminol.
a. Fluorescence in DMF, 2×10^{-7} mol.
b. Fluorescence after chemiluminescent reaction, 7.5×10^{-6} mol.
c. Chemiluminescence in DMF-water (3:1 in vol.) in 7.5×10^{-4} mol.

6) In addition to luminol (cf. Ref. 3), other chemiluminescent compounds, such as lucigenin (a), lophine (b, c, d) and 7-dialkylamino-naphthalin-1, 2-dicarboxylic acid hydrazide (e) have been recently treated by the similar approach. a) F. McCapra and D. G. Richardson, *Tetrahedron Letter*, **1964**, 3167. b) J. Sonnenberg and D. M. White, *J. Am. Chem. Soc.*, **86**, 5686 (1964). c) E. H. White and M. J. C. Harding, ibid., **86**, 5686 (1964). d) K. Maeda, H. Ojima and T. Hayashi, This Bulletin, **38**, 76 (1965). e) K.-D. Gundermann and W. Horstmann, *Ann.*, **684**, 127 (1965).

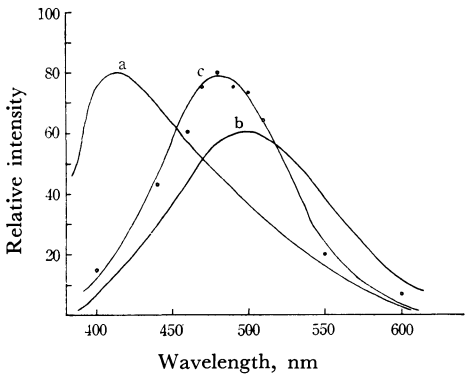

Fig. 5. Fluorescence and chemiluminescence spectra of 3-acetylaminophthalhydrazide.
a. Fluorescence in DMF, 1.4×10^{-5} mol./l.
b. Fluorescence after chemiluminescent reaction, 7.5×10^{-6} mol.
c. Chemiluminescence in DMF-water (3 : 1 in vol.), 1.5×10^{-2} mol./l.

fluorescence of the total reaction product, and the fluorescence of sodium aminophthalate. The present observation of luminol in a dimethylformamide-water mixture (3 : 1 in vol.), shown in Fig. 4, led to the same conclusion as that of White et al.,[3] who concluded that the 3-aminophthalate ion is the light-emitting species.

In the case of acyl luminols a rough coincidence between the maximum of the chemiluminescence spectrum and the fluorescence maximum after chemiluminescence was observed (Table I). Considering that the wavelength distribution of the chemiluminescence spectrum is similar to that of the corresponding fluorescence spectrum after chemiluminescence, the authors tentatively assume that 3-acylaminophthalate ion in the excited state is mainly the light emitting species of the chemiluminescent reaction of 3-acylaminophthalhydrazide.

Experimental*

3-Acetylaminophthalhydrazide (II).—To the solution of luminol (0.9 g.) in dimethylformamide (20 ml.), pyridine (0.4 ml.) was added; then acetyl chloride (0.4 ml.) in dimethylformamide (1 ml.) was slowly stirred in under cooling. After the reaction mixture had been allowed to stand overnight, water was carefully poured into the mixture. The fine crystals which formed were collected, washed with water, and recrystallized from dimethylformamide and water successively to give faint yellow needle crystals, m. p. 315°C. The authentic sample, which was synthesized from 3-acetylaminophthalic anhydride and hydrazine, showed a m. p. of 320°C (decomp.).[2a]

Found: C, 54.38; H, 4.32; N, 19.20. Calcd. for $C_{10}H_9O_3N_3$: C, 54.79; H, 4.14; N, 19.17%.

UV: λ_{max}^{DMF} 333 nm (ε=8400), IR: ν^{KBr} 3420, 1530 cm^{-1} (-NH).

3-Acetylamino-*O*-acetylphthalhydrazide (V). — When the treatment as described in the preparation of II was carried out with an excess of acetyl chloride (4 ml.), 3-acetylamino-*O*-acetylphthalhydrazide was obtained. The compound was soluble in dimethylformamide to a much smaller extent than luminol, and was reprecipitated from dimethylformamide and water as light yellow crystals, m. p. 251°C (decomp.).

Found: C, 54.75; H, 4.22; N, 16.16. Calcd. for $C_{12}H_{11}O_4N_3$: C, 55.17; H, 4.21; N, 16.09%.

UV: λ_{max}^{DMF} 332 nm (ε=9600), IR: ν^{KBr} 3420, 1760, 1530 cm^{-1}.

3-Propanoylaminophthalhydrazide (III).—Luminol (0.9 g.) in dimethylformamide (20 ml.), pyridine (0.4 ml.), and propanoyl chloride (0.5 ml.) were treated as in the case of II. The product formed was then reprecipitated from dimethylformamide and water as a pale yellow powder, m. p. 278°C (decomp.).

Found: C, 56.18; H, 4.74; N, 18.21. Calcd. for $C_{11}H_{11}O_3N_3$: C, 56.55; H, 4.75; N, 18.02%.

UV: λ_{max}^{DMF} 333 nm (ε=8200), IR: ν^{KBr} 3420, 1530 cm^{-1}.

3-Undecenoylaminophthalhydrazide (IV). — Luminol (0.9 g.) and undecenoyl chloride (0.6 ml., prepared from undecenoic acid and thionyl chloride) brought to reaction according to the procedure used in the preparation of II. A light yellow powder resulted, m. p. 275°C.

Found: C, 66.73; H, 7.13; N, 12.22. Calcd. for $C_{19}H_{25}O_3N_3$: C, 66.45; H, 7.34; N, 12.24%.

UV: λ_{max}^{DMF} 300 nm (ε=6700, shoulder), IR: ν^{KBr} 3420, 2925, 2850, 1530 cm^{-1}.

3-Undecenoylamino-*O*-undecenoylphthalhydrazide (VI).—The procedure used in the preparation of IV but with an excess of undecenoyl chloride (about 6 ml.) gave a diundecenoyl derivative as a faint yellow powder, m. p. 142°C.

Found: C, 70.56; H, 8.22; N, 8.30. Calcd. for $C_{30}H_{43}O_4N_3$: C, 70.69; H, 8.50; N, 8.25%.

UV: λ_{max}^{DMF} 329 nm (ε=8300), IR: ν^{KBr} 3420, 2950, 2850, 1760, 1540 cm^{-1}.

The Chemiluminescence Spectra.—The chemiluminescence spectra of luminol and its acyl derivatives in the dimethylformamide-water system were measured with an Hitachi recording spectrophotometer, EPS-2 type. The procedure for the measurement of the chemiluminescence spectrum was as follows: To a 10^{-3} mole. solution of luminol or acyl luminols in dimethylformamide (3 ml.), 1 ml. of a 1 *N* sodium hydroxide solution containing potassium ferricyanide (10^{-2} mole./l.) was added. The final concentrations of the components in the chemiluminescent system were: luminol or acyl luminols, 7.5×10^{-4} mol., the hydroxide ion, 2.5×10^{-1} mol., and the ferricyanide ion, 2.5×10^{-3} mol./l. The mixture gave a brilliant chemiluminescence. The decrease in the chemiluminescence of luminol and acyl luminol with time was measured in a dimethylformamide-water mixture (3 : 1 in vol.), at the maximum of the chemiluminescence spectrum at 38—40°C.

The Fluorescence Spectra.—The fluorescence spectra were measured at 30°C with a spectrophotometer equipped with an attachment for measuring the fluorescence spectrum. The 365 nm line of a high-pressure mercury lamp was used for excitation, and the spectra were measured at concentrations of 10^{-5}—10^{-4} mol./l.

* All melting points are uncorrected.

BULLETIN OF THE CHEMICAL SOCIETY OF JAPAN VOL. 39 936—939 (1966)

The Dipole Moment and Polarizability in the n-π^* Excited State of Acetone from Spectral Solvent Shifts

By Takehiro ABE

College of General Education, Tohoku University, Kawauchi, Sendai

(Received September 11, 1965)

This paper has presented the expression for the frequency shift, including the solvent refractive index and the dielectric constant; the expression has been determined on the basis of a previous paper (This Bulletin, **38**, 1314 (1965)). According to the present theory and E. G. McRae's theory (*J. Phys. Chem.*, **61**, 562 (1957)), the excited state dipole moment of acetone has been estimated to be 0.86 and 1.84 *D* respectively, both being smaller than the ground state value. The results calculated by the present theory show that the excited state polarizability is 163.1×10^{-25} cm^3 and that the solvation energies in the solvents of *n*-heptane, cyclohexane, carbon tetrachloride, ethyl ether, and methyl acetate are less in the ground states than in the excited states.

McMurry[1] has identified the 280 mμ band of acetone as a forbidden n-π^* transition involving the excitation of a non-bonding electron of the oxygen atom to an anti-bonding π-orbital between the carbon and oxygen atoms of the carbonyl group. The band shifts to the blue in polar solvents compared with the case in non-polar solvents.[2,3] Bayliss and McRae[3,4] have stated that the transfer of the electronic charge away from the oxygen will cause the permanent dipole moment to be decreased in the excited state, since the acetone molecule has a dipole with the negative end directed toward the oxygen.

In the present paper, an attempt has been made to estimate the dipole moment and isotropic polarizability in the n-π^* excited state of acetone by the applications of McRae's expression[5] and of a new expression, which has derived by the same procedure as in the previous paper,[6] to the frequency shifts of the n-π^* transition of acetone.

Theoretical

On the assumption that there are no strong dipole orientation strains among the spherical solute and the spherical solvent molecules, one may obtain the expression for the frequency shift of an absorption spectrum in a very dilute solution by the same procedure as was used in a previous paper[6] as follows: Considering an unperturbed solute molecule and the solvent molecules already interacting with one another in the zeroth order approximation, one may write the solvation energy in erg in the ith excited state of the solute as:

$$E'_i = -2.378\times10^{25}\times\left(\frac{M^v}{d^v}\right)^{1/3}\times\left[\left\{\left(\frac{M^u}{d^u}\right)^{1/3}+\left(\frac{M^v}{d^v}\right)^{1/3}\right\}^{-4}+\left\{\left(\frac{M^u}{d^u}\right)^{1/3}+3\left(\frac{M^v}{d^v}\right)^{1/3}\right\}^{-4}+\left\{\left(\frac{M^u}{d^u}\right)^{1/3}+5\left(\frac{M^v}{d^v}\right)^{1/3}\right\}^{-4}\right]$$
$$\times\left[\frac{2}{3}\cdot\frac{\{\varepsilon^v-(n^v)^2\}\{2\varepsilon^v+(n^v)^2\}}{\varepsilon^v\{(n^v)^2+2\}^2}\cdot(\mu_i^u)^2+1.380\times10^{-16}(\mathrm{erg\cdot deg^{-1}})\times T\times\frac{\{\varepsilon^v-(n^v)^2\}\{2\varepsilon^v+(n^v)^2\}}{\varepsilon^v\{(n^v)^2+2\}^2}\cdot(\alpha_i^u)+\frac{1}{3}\cdot\frac{(n^v)^2-1}{(n^v)^2+2}\cdot(\mu_i^u)^2+\frac{1}{2}\cdot\frac{(n^v)^2-1}{(n^v)^2+2}\cdot\frac{I_i^u\times I_0^v}{I_i^u+I_0^v}\cdot(\alpha_i^u)\right] \quad (1)$$

where M is the molecular weight; d, the liquid density; ε, the dielectric constant; n, the refractive index; I, the ionization potential; T, the absolute temperature; μ, the permanent dipole moment, and α, the isotropic polarizability. Throughout this paper the notations u and v will refer to the solute and the solvent respectively. Here E'_i is taken as negative if the ith excited state energy of the solute is decreased in solution. The solvation energy for the ground state of the solute is obtained by replacing i by 0 in Eq. 1. It is obvious from Fig. 1 that the frequency shift $\Delta\nu_{i0}=\nu_{i0}(\mathrm{soln})-\nu^0_{i0}$ (gas) is given by $\Delta\nu_{i0}=E'_i-E'_0$, as is found by Bayliss and McRae.[3] The frequency shift in cm^{-1} is given by:

$$\Delta\nu_{i0} = -1.198\times10^{41}(\mathrm{erg^{-1}cm^{-1}})\times\left(\frac{M^v}{d^v}\right)^{1/3}\times\left[\left\{\left(\frac{M^u}{d^u}\right)^{1/3}+\left(\frac{M^v}{d^v}\right)^{1/3}\right\}^{-4}\right.$$

1) H. L. McMurry, *J. Chem. Phys.*, **9**, 231 (1941).
2) H. Baba, *J. Chem. Soc. Japan, Pure Chem. Sect.* (*Nippon Kagaku Zassi*), **72**, 411 (1951).
3) N. S. Bayliss and E. G. McRae, *J. Phys. Chem.*, **58**, 1006 (1954).
4) N. S. Bayliss and E. G. McRae, ibid., **58**, 1002 (1954).
5) E. G. McRae, ibid., **61**, 562 (1957).
6) T. Abe, This Bulletin, **38**, 1314 (1965).

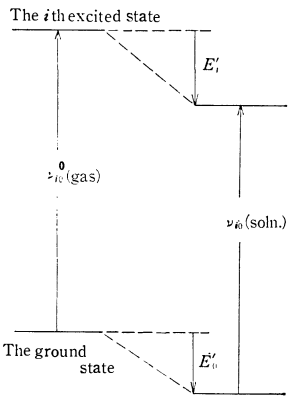

Fig. 1. Formal diagram of the effect of the solvation energies E_0' and E_i' on the relation between the absorption frequencies in the gas state and in solution.

$$+\left\{\left(\frac{M^u}{d^u}\right)^{1/3}+3\left(\frac{M^v}{d^v}\right)^{1/3}\right\}^{-4}$$
$$+\left\{\left(\frac{M^u}{d^u}\right)^{1/3}+5\left(\frac{M^v}{d^v}\right)^{1/3}\right\}^{-4}\Bigg]$$
$$\times\Bigg[\frac{2}{3}\cdot\frac{\{\varepsilon^v-(n^v)^2\}\{2\varepsilon^v+(n^v)^2\}}{\varepsilon^v\{(n^v)^2+2\}^2}\cdot\{(\mu_i^u)^2-(\mu_0^u)^2\}+\boldsymbol{k}T$$
$$\times\frac{\{\varepsilon^v-(n^v)^2\}\{2\varepsilon^v+(n^v)^2\}}{\varepsilon^v\{(n^v)^2+2\}^2}\cdot\{(\alpha_i^u)-(\alpha_0^u)\}$$
$$+\frac{1}{3}\cdot\frac{(n^v)^2-1}{(n^v)^2+2}\cdot\{(\mu_i^u)^2-(\mu_0^u)^2\}$$
$$+\frac{1}{2}\cdot\frac{(n^v)^2-1}{(n^v)^2+2}\cdot I_0^v\cdot\left\{\frac{I_0^u-\boldsymbol{hc}\nu_{i0}^0}{I_0^v+I_0^u-\boldsymbol{hc}\nu_{i0}^0}\cdot(\alpha_i^u)-\frac{I_0^u}{I_0^v+I_0^u}\cdot(\alpha_0^u)\right\}\Bigg] \quad (2)$$

where $\boldsymbol{h}$ is the Planck constant; $\boldsymbol{c}$, the velocity of light, and $\boldsymbol{k}$, the Boltzmann constant. For a non-polar solvent the first and second terms in the second square brackets in Eq. 2 are zero. Equation 2 can be further written in the following form:

$$\{(\mu_i^u)^2-(\mu_0^u)^2\}+(\alpha_i^u)\cdot A=B \quad (3)$$

where

$$A=3\times\left[\frac{2\{\varepsilon^v-(n^v)^2\}\{2\varepsilon^v+(n^v)^2\}}{\varepsilon^v\{(n^v)^2+2\}^2}+\frac{(n^v)^2-1}{(n^v)^2+2}\right]^{-1}$$
$$\times\left[\boldsymbol{k}T\cdot\frac{\{\varepsilon^v-(n^v)^2\}\{2\varepsilon^v+(n^v)^2\}}{\varepsilon^v\{(n^v)^2+2\}^2}+\frac{1}{2}\cdot\frac{(n^v)^2-1}{(n^v)^2+2}\cdot\frac{I_0^v(I_0^u-\boldsymbol{hc}\nu_{i0}^0)}{I_0^v+I_0^u-\boldsymbol{hc}\nu_{i0}^0}\right]$$

and

$$B=3\times\left[\frac{2\{\varepsilon^v-(n^v)^2\}\{2\varepsilon^v+(n^v)^2\}}{\varepsilon^v\{(n^v)^2+2\}^2}+\frac{(n^v)^2-1}{(n^v)^2+2}\right]^{-1}$$
$$\times\left[\boldsymbol{k}T\cdot\frac{\{\varepsilon^v-(n^v)^2\}\{2\varepsilon^v+(n^v)^2\}}{\varepsilon^v\{(n^v)^2+2\}^2}+\frac{1}{2}\cdot\frac{(n^v)^2-1}{(n^v)^2+2}\cdot\frac{I_0^v\times I_0^u}{I_0^v+I_0^u}\right]\cdot(\alpha_0^u)$$
$$-8.351\times10^{-42}(\text{erg}\cdot\text{cm.})\times\left(\frac{d^v}{M^v}\right)^{1/3}\times\Delta\nu_{i0}$$
$$\times\left(\left\{\left(\frac{M^u}{d^u}\right)^{1/3}+\left(\frac{M^v}{d^v}\right)^{1/3}\right\}^{-4}+\left\{\left(\frac{M^u}{d^u}\right)^{1/3}+3\left(\frac{M^v}{d^v}\right)^{1/3}\right\}^{-4}+\left\{\left(\frac{M^u}{d^u}\right)^{1/3}+5\left(\frac{M^u}{d^u}\right)^{1/3}\right\}^{-4}\right)^{-1}\Bigg]$$

The values of A and B can be calculated from the observed values, so the plot of B against A should be linear; the slope of the straight line will be equal to α_i^u, and the intersection of the line at $A=0$ will be equal to $\{(\mu_i^u)^2-(\mu_0^u)^2\}$.

The general expression derived by McRae is written in the approximate form:[5]

$$\Delta\nu_{i0}=(aL_0+b)\cdot\frac{(n^v)^2-1}{2(n^v)^2+1}+c\left[\frac{\varepsilon^v-1}{\varepsilon^v+2}-\frac{(n^v)^2-1}{(n^v)^2+2}\right] \quad (4)$$

where a, b and c are constants characteristic of the solute molecule. Assuming that Onsager's reaction radius is equal to $(3M^u/4\pi\boldsymbol{A}_0d^u)^{1/3}$, where $\boldsymbol{A}_0$ is the Avogadro number, one may have:

$$c=2.541\times10^{40}(\text{erg}^{-1}\text{cm}^{-1})\times(d^u/M^u)\cdot\mu_0^u(\mu_0^u-\mu_i^u) \quad (5)$$

Therefore, one can obtain the value of μ_i^u from Eq. 5 by the same procedure that Robertson, King and Weigang have used for azulene.[7] By taking L_0 to be approximately a constant characteristic of the solute molecule, they first found the value of (aL_0+b) from the plot of $\Delta\mu_{i0}$ against $\{(n^v)^2-1\}/\{2(n^v)^2+1\}$ in the case of non-polar solvents, because the second term in Eq. 4 is zero in this case. Then, in the case of polar solvents they found the value of c that best reproduced the observed value of $\Delta\nu_{i0}$.

In Eqs. 2 and 4, the important effect of hydrogen bonding found by Nagakura and Baba[8] has not been considered.

7) W. W. Robertson, A. D. King and O. E. Weigang, Jr., *J. Chem. Phys.*, **35**, 464 (1961).
8) S. Nagakura and H. Baba, *J. Am. Chem. Soc.*, **74**, 5693 (1952).

Table I. The n-π^* transition bands of acetone and the data used

No.	Solvent	n^{v}(20°C)	ε^{v}(20C°)	$\mu_0(D, \text{gas})$[9]	I_0, eV.	ν_{i0}, cm^{-1}
	Vapor			2.84	9.92[10]	36200[3]
1	n-Heptane	1.388	1.924	0	10.35[11]	35840[3]
2	Cyclohexane	1.426	2.023	0	9.24[10]	35740[3]
3	Carbon tetrachloride	1.460	2.238	0	11.0[9]	35710[3]
4	Ethyl ether	1.356	4.335	1.18	9.72[10]	36090[13]
5	Methyl acetate	1.362	6.68	1.67	10.51[12]	36290[13]
6	Acetonitrile	1.344	37.5	3.94	12.39[10]	36500[13]

Results and Discussion

The n-π^* transition bands of acetone in several solvents and the other data to be used are listed in Table I. The observed value of α_0^u for acetone is 63.3×10^{-25} cm^3.[9]

Assuming that the temperature is 20°C, the author has applied Eq. 3 to acetone. The plot of B against A is shown in Fig. 2. It may be

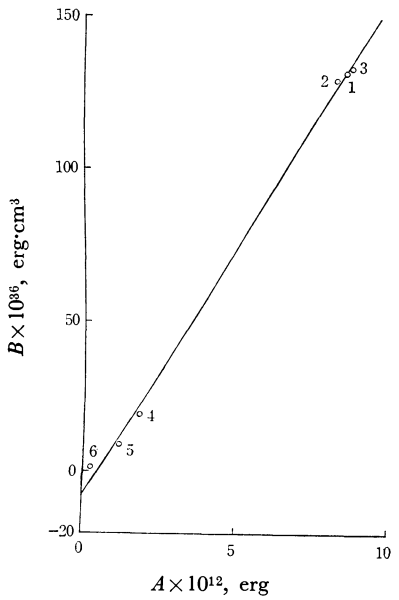

Fig. 2. The plot of B against A.

seen in Fig. 2 that all the points except for the point 6 fall close to the straight line. It may be expected that there are strong orientation strains between the acetone and the acetonitrile molecules, because acetonitrile has the large dipole moment of 3.94 D. Equations 1—3 are limited for use in solutions in which no strong dipole orientation strains occur between solutes and solvent molecules. Equation 3, therefore, will not hold sufficiently for the case of acetonitrile. On account of the strain, the point 6 is likely to deviate from the line. From the intersection of the line in Fig. 2 the value of $\{(\mu_i^u)^2-(\mu_0^u)^2\}$ is estimated to be -7.3267×10^{-36} erg·cm^3. Accordingly, the dipole moment in the excited state due to the n-π^* transition is estimated to be 0.86 D, because the observed value of μ_0^u is 2.84 D. From the slope of the line the excited state polarizability is estimated to be 163.1×10^{-25} cm^3.

By applying Eq. 4 in the way mentioned above, the author has obtained the values of -2156 and 983 cm^{-1} for (aL_0+b) and c respectively. From Eq. 5, then, the excited-state dipole moment is obtained as 1.84 D. The frequency shifts calculated are compared with the observed shifts in Fig. 3.

The excited state dipole moment of 0.86 D obtained by Abe's method is considerably smaller than that obtained by McRae's method. This seems to be due to the inclusion of the ground

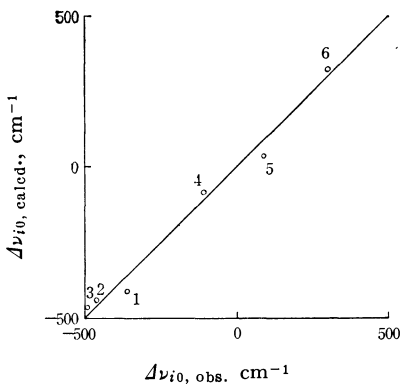

Fig. 3. Calculated vs. observed frequency shifts in n-π^* band of acetone (McRae's method)

and excited state polarizabilities in the Abe expressions, while the polarizabilities have not been considered explicitly in McRae's expression. The excited state polarizability plays an important role in the frequency shift, because the polarizability is much larger than that for the ground state.

According to the above two methods, the n-π^*

9) Landolt-Börnstein, "Physikalisch-chemische Tabellen," Vol. 1, Part 3, 6th Ed., Springer, Berlin (1951), pp. 386, 395, 509.
10) J. D. Morrison and A. J. C. Nicholson, *J. Chem. Phys.*, **20**, 1021 (1952).
11) R. E. Honig, ibid., **16**, 105 (1948).
12) K. Higasi, I. Omura and H. Baba, *Nature*, **178**, 652 (1956).
13) M. Ito, K. Inuzuka and S. Imanishi, *J. Am. Chem. Soc.*, **82**, 1317 (1960).

excited-state dipole moment of acetone is considerably smaller than that for the ground state. On the basis of McRae's theory, Ito, Inuzuka and Imanishi[13] have also mentioned that the excited-state dipole moments of ketones are much smaller than their ground-state values. In the ground state of acetone the π electronic charges are distributed more at the oxygen atom than at the carbon in the carboxyl group, because the absolute value of the Coulomb integral for the oxygen atom is larger than that for the carbon atom. The n–π^* transition in acetone transfers a non-bonding electron of the oxygen atom to a π^* orbital distributed over C=O,[3] especially at the carbon atom. The transition is probably represented by:

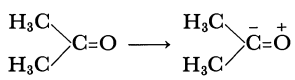

Consequently, the dipole moment is considerably decreased in the excited state, since the ground-state dipole has the negative end directed toward the oxygen atom.

By putting the above values of $\mu_i^u=0.86\,D$ and $\alpha_i^u=163.1\times10^{-25}$ cm^3 into Eq. 1, the author has calculated the solvation energies and transition energies of acetone in all the solvents except acetonitrile; they are listed in Table II. The calculated frequency shifts in Table II are in good agreement with the observed shifts in Table I. The differences between the theoretical and the observed values are greater for the polar solvents than for the non-polar solvents. This is probably due to the use of Onsager's approximate expression[14] for the polar-solvent dipole moments. Table II shows that the excited states of acetone are more stabilized than the ground states in the non-polar solvents. These results are contrary to those obtained by Bayliss and McRae's theory.[3,4] According to their theory, the solvation energy in the excited state of acetone is less than the ground-state energy in a non-polar solvent, since the solute dipole moment decreases as a result of the transition. The discrepancy between the present results and Bayliss and McRae's theory seems to be due to the exclusion of the ground- and excited-state polarizabilities in their theory.

Table II. The results of calculation of solvation energies and transition energies

Solvent	E'_0 cm^{-1}	E'_i cm^{-1}	ν_{i0}, calcd. cm^{-1}
1	− 559	− 921	35840
2	− 695	−1165	35730
3	− 790	−1294	35700
4	− 802	−1007	36000
5	−1118	−1201	36120

14) L. Onsager, ibid., **58**, 1486 (1936).

BULLETIN OF THE CHEMICAL SOCIETY OF JAPAN VOL. 39 939—944 (1966)

The Flotation of Cation by Cationic and Anionic Surfactants

By Norichika Aoki* and Tsunetaka Sasaki

Department of Chemistry, Faculty of Science, Tokyo Metropolitan University, Fukazawa-cho, Setagaya-ku, Tokyo

(Received September 11, 1965)

The ion flotation of a cation by a cationic surfactant with the aid of an anionic chelating agent was studied for the system of Fe^{3+} - ethylenediaminetetraacetic acid (EDTA) - octadecyldimethylammonium chloride (ODAC). The systems of Fe^{3+}-EDTA and Fe^{3+}-ODAC were also studied for purposes of comparison. The effects of the concentration of the above three components, the pH and the gas-flow time on the flotation efficiency were measured. The diagram of the flotation efficiency vs. the pH showed a W-shaped curve for the Fe^{3+}-EDTA-ODAC system, which was explained by the formation of Fe^{3+}-EDTA, Fe^{3+}-ODAC and Fe^{3+}-EDTA-ODAC complexes, each of which has a different optimum pH region of its formation. The flotation of a cation by an anionic surfactant was also studied using ferric, ferrous, silver and Malachite Green ions as cations and sodium dodecylsulfate (SDS) as an anionic surfactant. The flotation efficiency increased with the time of the gas flowing, except for the system of Fe^{3+}-SDS. Such an increase was explained by the relatively insoluble nature of the corresponding SDS salts.

* Present address: Technical Laboratory, Central Research Institute of Electric Power, 1229, Iwato, Komae-machi, Kitatama- gun, Tokyo.

Recently, the technique of the ion flotation or the foam fractionation** has been receiving increasing attention, from both the practical and the theoretical points of view,[1] due chiefly to their remarkable efficiency in ion separation and concentration in dilute aqueous solutions. In the usual practice of ion flotation, ions in a solution are collected by the foam produced by an ionic surfactant of the charge opposite to that of the ion to be floated.[2] Thus, metallic cations are floated, for instance, by sodium dodecylsulfate (SDS). However, the possibilities have not yet been fully studied of floating ions by an ionic surfactant of the same sign, with or without the addition of a chelating agent or "collector" electrolyte which has the electric charge opposite in sign to both of them and so acts as a bridging ion between the surfactant and the metallic ions.

The present paper will describe the results of an ion flotation study from such a point of view, a study chiefly of the Fe^{3+} - ethylendiaminetetraacetic acid (EDTA) - octadecyldimethylammonium chloride (ODAC) system. The ordinary ion flotation of a cation by an anionic surfactant will also be studied for the sake of comparison.

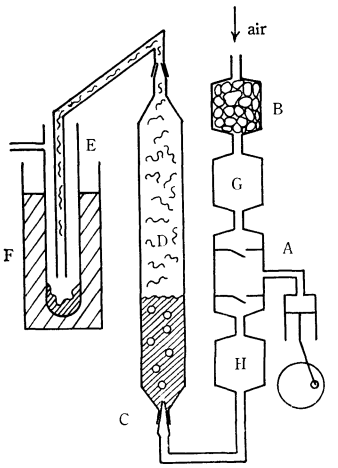

Fig. 1A. Ion flotation apparatus for stable foam.
A, circulation pump; B, chamber filled with wet cotten wool; C, glass tip; D, ion flotation column; E, foam liquid receiver; F, freezing mixture; G and H, empty chambers.

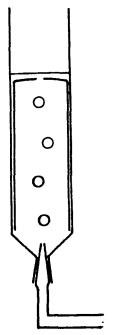

Fig. 1B. Ion flotation apparatus for unstable foam.

Experimental

Materials.—Cations used for separation: ferric and ferrous ions as sulfates, silver ion as nitrate, and Malachite Green ion as the corresponding dye salt.

Chelating agent used as a collector: ethylenediaminetetraacetic acid (EDTA).

Foaming agents: octadecyldimethylammonium chloride (ODAC) and sodium dodecylsulfate (SDS).

The ferric, ferrous and silver salts were purified by recrystallization, while the rest of the reagents of chemically-pure grade were used without purification.

Apparatus and Procedure.—The apparatus used in the foam separation experiment is shown in Fig. 1A. By means of a circulation pump, A, air moistened by passing it through the chamber, B, filled with wet cotton wool was introduced, at room temperature (20—25°C) into 50 cc. of the sample solution contained in the cell, D (32 cm. long and 2.5 cm. in diameter), from the the tip, C, about 0.3 mm. in diameter. The rate of gas flow was kept at 1.04 cc./sec. The gas-flow time was kept at 10 min. unless otherwise stated. The foam thus produced was made to overflow and was collected in the chamber, E, where it was cooled by a freezing mixture, F, to about −8°C and thus collapsed. The volume of the collapsed foam was usually about 0.7 cc. for 10 mins' foaming. The concentration of the cation in this solution was determined as follows.

Ferric and ferrous ions: Concentrated sulfuric acid and nitric acid were added to the liquid, and the mixture was heated to destroy the organic matter. The ferric ion was then reduced to the ferrous ion by hydroquinone, and after o-phenanthroline had been added, the ferrous ion concentration was determined at a pH value of about 4.5 by the light absorption at 508 Å, using a Beckmann spectrophotometer.

Malachite Green ion: The light absorption was measured at 615 Å, using a Beckmann spectrophotometer.

Silver ion: The concentration was determined by potentiometry using a cell consisting of a calomel electrode and a silver electrode. The foaming agent present did not interfere with the measurement.

The Efficiency of Ion Flotation.—The efficiency of ion flotation may be differently expressed according to whether we refer to the separation, the purification, the extraction or the concentration of ions in question. In the present case, we are chiefly interested in the concentration of cations. Therefore, the efficiency may be conventionally expressed by the ratio:

$$R = X/Y$$

where X is the concentration of ions in the solution obtained by collapsing the foam, and Y, the concentration of the same ions in the initial sample solution.

Results and Discussion

Numerous factors, such as the nature and concentration of the collector, the foaming agent, the ions to be floated and other additives, the time and rate of gas-flow, the temperature of the solution and the construction of the flotation cell, influence the efficiency of ion flotation. Of these,

** Some authors distinguish these two processes according to whether the separation or fractionation of the solutes occurs exclusively on bubbles in a solution or chiefly on films of foam upon a solution. In the present paper, however, the term "ion flotation" will be used for the sake of the brevity and convenience, though the process adopted is actually a case of foam fractionation.

1) F. Sebba, "Ion Flotation," Elsevier Publisher, Amsterdam, London, New York (1962); H. Kishimoto, *Kolloid-Z.*, **192**, 66 (1963); C. A. Brunner and D. G. Stephan, *Ind. Eng. Chem.*, **57** No. 5, May, 40 (1965).

2) F. Sebba, *Nature*, **184**, 1062 (1959).

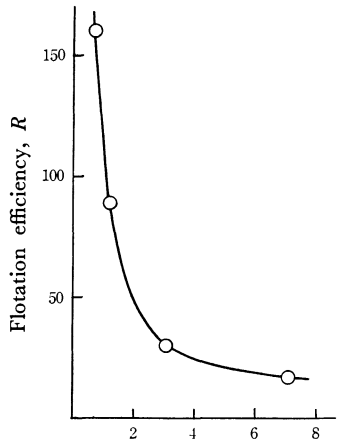

Fig. 2. Flotation efficiency vs. concn. of Fe^{3+} for Fe^{3+}-EDTA-ODAC system.
ODAC 3.02×10^{-4} mol./l.
EDTA 1.102×10^{-4} mol./l.
Time of gas flow, 10 mim.

several factors have been taken up and studied.

The Flotation of Ferric Ions by ODAC.—*The Effect of the Ferric Ion Concentration.*—Figure 2 shows the effect of the ferric ion concentration upon the flotation efficiency, R, for the Fe^{3+}-EDTA-ODAC system at constant ODAC and EDTA concentrations, and at a constant rate and time (10 min.) of gas-flow. It may be seen that R increased from 16 to 160 with the decrease in the ferric sulfate concentration from 7×10^{-5} mol./l. to 7×10^{-6} mol./l. This is in accord with the general trend of ion flotation.[3] By 10 mins' gas flowing, about 54% of the ferric ions in 50 cc. of the 7×10^{-6} mol./l. initial solution was removed and concentrated in about 0.17 cc. of foam.

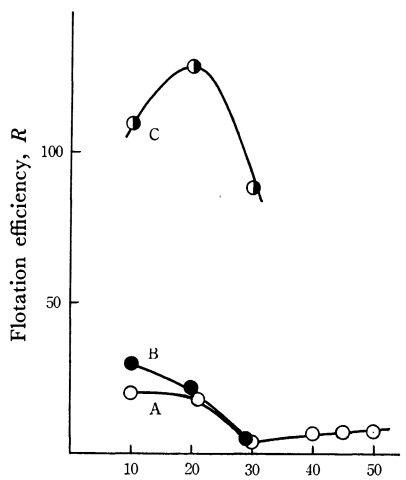

Fig. 3. Flotation efficiency vs. gas flowing time for Fe^{3+}-EDTA-ODAC system.
ODAC, 3.16×10^{-4} mol./l.; EDTA, 1.70×10^{-4} mol./l.; Fe^{3+} conc.: A, 6.4×10^{-4}; B, 6.8×10^{-4}; C, 5.0×10^{-6} mol./l.

The Effect of the Time of the Gas-Flow.—Figure 3 shows the relation between the time of gas-flow and R at constant concentrations of ODAC, EDTA and ferric ions. We can see in this figure that the overall (integrated) value of R decreased with the increase in the gas-flow time. Further, a marked increase in R with the dilution of ferric ions can be confirmed. The value of $R=150$ for 20 mins' gas flowing in a 5×10^{-6} mol./l. ferric sulfate solution corresponds to a complete removal of ferric ions from the solution by foaming. These facts again agree with the general tendency of the ion flotation.[3]

The Effect of the Collector Concentration.—Figure 4 shows the effect of the collector concentration of

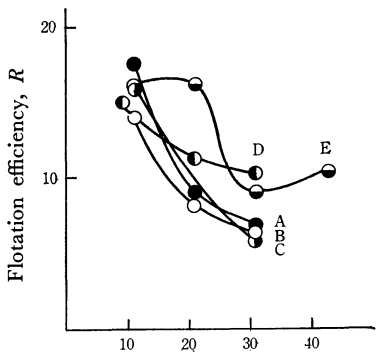

Fig. 4. Flotation efficiency vs. gas flowing time for Fe^{3+}-EDTA-ODAC system.
ODAC 3.3×10^{-4} mol./l., Fe^{3+} 6.4×10^{-5} mol./l.
EDTA A 0, B 3.6×10^{-6}, C 7.2×10^{-6}, D 3.6×10^{-5}, E 1.7×10 mol./l.

R when the rest of the conditions were held constant. As may be seen in this figure, the effect of the EDTA concentration is not very distinct at 10 mins' gas flowing, while the increase in R can be confirmed with increasing concentrations of EDTA at 30 mins' gas flowing. Here, it should be noticed that no small value of R is confirmed even when the concentration of EDTA is zero. This is rather unexpected, since it is a case of cation flotation by a cationic surfactant, just the opposite of the usual case of ion flotation by an oppositely charged surfactant. This will be discussed in detail in a later section.

The Effect of the Surfactant Concentration.—Since the existence of EDTA did not seem to be essential, measurements were made for the effect of the surfactant concentration on the flotation of ferric

3) H. Schoen and G. Gazzella, *Industrial Water Wastes*, May—June, 71 (1961).

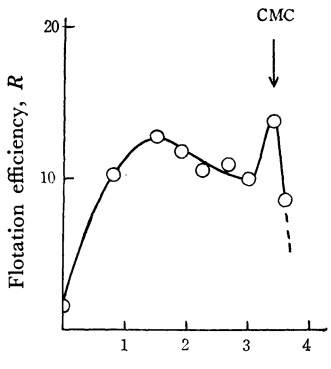

Fig. 5. Flotation efficiency vs. ODCA concn. for Fe^{3+}-ODAC system.
Time of gas flowing, 10 min.; Fe^{3+}, 6.4×10^{-5} mol./l.

ions from the solution without the addition of EDTA. The results are shown in Fig. 5. We can see in this figure that R does not change appreciably over a wide range of ODAC concentration, except for a zero concentration, and presumably beyond the critical micelle concentration, where R steeply falls to a small value. In the case of the measurement at a zero concentration of ODAC, a flotation cell as is shown in Fig. 1B was used, since the foam produced was very unstable. This cell separated the surface zone of the solution from its bulk by a diaphragm with a small opening in its center which allowed the passage of bubbles. The bubbles bursted on the surface of the solution, leaving the surface layer rich in the solute, which was then prevented from mixing with the interior of the solution. After the gas had flowed, the surface layer was taken for the determination of the concentration,

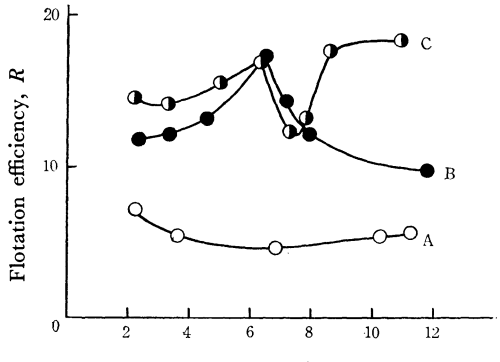

Fig. 6. Flotation efficiency vs. pH for Fe^{3+}-EDTA-ODAC, Fe^{3+}-EDTA and Fe^{3+}-ODAC system.
A: EDTA, 1.0×10^{-4}mol./l.; Fe^{3+}, 6.4×10^{-5}mol./l.
B: ODAC, 2.99×10^{-4}mol./l.; Fe^{3+}, 6.4×10^{-5}mol./l.
C: ODAC, 3.02×10^{-4}mol./l.; EDTA, 1.0×10^{-4}mol./l.; Fe^{3+} 6.4×10^{-5} mol./l.

and the R value was calculated. Thus the value of 1.5 was obtained. Strictly speaking, the value obtained here cannot be plotted on the same scale as those obtained by the former method, but it may be used for the purpose of comparison with other data as a whole.

The Effect of the pH.—In all the above experiments, the pH of the solution was not especially controlled: it was about 4. Now, aqueous ferric sulfate solutions containing ODAC and/or EDTA varying in pH value were studied. The results are shown in Fig. 6. In this experiment, the pH of the solution was controlled by using hydrochloric acid and sodium hydroxide.
The measurement of the R value for the Fe^{3+}-EDTA system was made by using the apparatus shown in Fig. 1B.

It may be seen in Fig. 6 that the systems containing both EDTA and ODAC show R values larger than those containing ODAC alone in the regions of pH higher than about 8 and lower than 6. Between pH 6 and 8, the difference in R value between both systems is not distinct. The latter system shows a maximum R value at about pH 6. This maximum may be explained as the optimum pH region of the formation of a coordination compound consisting of ferric ions and free octadecyldimethylamine, as was pointed out by Sebba.[4] The system containing EDTA alone shows a smaller value of R than these two systems, though the comparison is somewhat qualitative in this case.

Let us now attempt to explain the change in flotation efficiency with the pH value for the Fe^{3+}-EDTA-ODAC system. It can readily be seen from the coincidence of the maximum of R between the Fe^{3+}-ODAC system and the Fe^{3+}-EDTA-ODAC system in Fig. 6, that the flotation of Fe in the latter system near pH 6 is mainly due to the formation of the Fe^{3+}-ODAC complex, while the flotation of Fe in a low pH region is considered to be due to the formation of both Fe^{3+}-ODAC and Fe^{3+}-EDTA complexes, as is expected from the R values of these systems. As for the explanation of the large increase in R for the Fe^{3+}-EDTA-ODAC system in an alkaline region, the flotation of Fe by Fe^{3+}-ODAC and Fe^{3+}-EDTA interaction seems insufficient. Here, we may conceivably take account of Fe^{3+}-EDTA-ODAC linkage, since the interaction between EDTA and ODAC is expected to show a broad optimum in an alkaline region, considering the rather strongly basic nature of ODAC.

Thus, we can explain the total flotation effect of Fe over a wide range of pH by the above three interactions of Fe^{3+}-ODAC, Fe^{3+}-EDTA and Fe^{3+}-EDTA-ODAC. The so-called sublate salt formation insisted on by Sebba[4] is not marked in this system, since the interaction between Fe

4) F. Sebba, "Ion Flotation," Elsevier Publisher, London, New York (1962), p. 71.

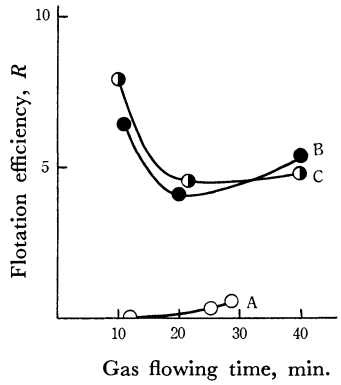

Fig. 7. Flotation efficiency vs. gas flowing time for Fe^{3+}-SDS system.
SDS: 3.0×10^{-3} mol./l.
Fe^{3+}: A, 1.7×10^{-5} mol./l.; B, 6.1×10^{-5} mol./l.; C, 1.8×10^{-4} mol./l.

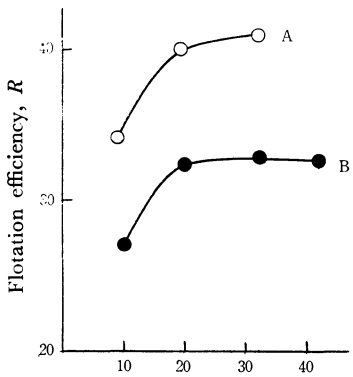

Fig. 8. Flotation efficiency vs. gas flowing time for Fe^{2+}-SDS system.
A: SDS, 2.99×10^{-3}mol./l.; Fe^{2+}, 1.58×10^{-4}mol./l.
B: SDS, 3.10×10^{-3}mol./l.; Fe^{2+}, 2.58×10^{-4}mol./l.

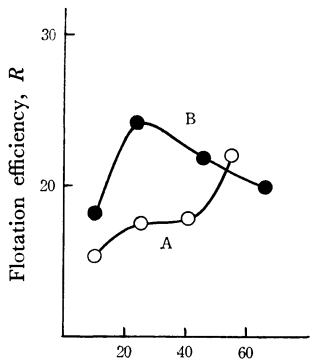

Fig. 9. Flotation efficiency vs. gas flowing time for Ag^{+}-SDS and Malachite Green ion - SDS systems.
A: SDS, 3.03×10^{-3}mol./l.; Ag^{+}, 6.7×10^{-5}mol./l.
B: SDS, 5.69×10^{-3}mol./l.;
Malachite Green ion, 1.8×10^{-5} mol./l.

and the surfactant is rather weak in a low pH region, contrary to his case. A slight increase in R in the acid region may be due to the formation of a simple compound of Fe^{3+}-ODAC, together with Fe^{3+}-EDTA, as has been mentioned above. The co-operating action of ODAC and EDTA in the flotation, especially in the alkaline region, would correspond to the action of polyaminopolycarboxylic acid, which is known to be effective in ion flotation.[5] This may suggest that the functional radicals of the collecting and frothing actions need not coexist in a single molecule, but that they can exist in separate molecules in a mixed solution, to show an effective ion flotation. This would open many possibilities in the practice of the choice of flotation agents.

The Flotation of Ferric, Ferrous, Silver and Malachite Green Ions by SDS.—The effect of the gas-flow-time on aqueous Fe^{3+}-SDS, Fe^{2+}-SDS, Ag^{+}-SDS and Malachite Green - SDS systems is shown in Figs. 7, 8 and 9. It may be seen in these figures that the values of R do not decrease, but rather increase, with time, except for the case of Fe^{3+}-SDS, which exhibits a decrease similar to that of the Fe^{3+}-ODAC system (cf. Fig. 4). This increase may come from the relatively insoluble nature of the corresponding SDS salts, the flotation of which is largely independent of the concentration of the cation to be floated. The increase in R with the gas-flow time is especially marked in the case of the Ag^{+}-SDS system, which forms an insoluble salt and an unstable foam. The effect of the concentration of the cation to be floated upon R was examined for ferric and ferrous ions, as may be seen in Figs. 7 and 8. The

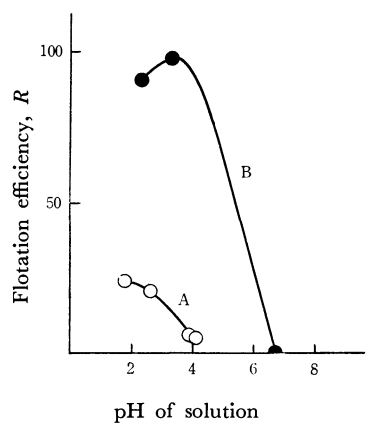

Fig. 10. Flotation efficiency vs. pH for Fe^{3+}-SDS and Fe^{2+}-SDS systems.
A: gas flowing time, 20 min.
SDS, 3.00×10^{-3} mol./l.; Fe^{3+}, 7.5×10^{-5} mol./l.
B: gas flowing time, 10 min.
SDS, 2.99×10^{-3} mol./l.; Fe^{2+}, 3.2×10^{-5} mol./l.

5) R. W. Schnepf, E. L. Garden, Jr., E. Y. Mirocznik and E. Schonfeld, *Chem. Eng. Prog.*, **55**, 42 (1959).

results were somewhat irregular for ferric ions, but a trend similar to that in the case of the Fe^{3+}-EDTA-ODAC system was seen for ferrous ions.

The effects of the pH on Fe^{3+}-SDS and Fe^{3+}-SDS systems are shown in Fig. 10. The values of *R* for both systems are large in the region of low pH, but they decrease rapidly with an increase in the pH value, reaching zero near pH 4—5 in the former system and near pH 7 in the latter system. This fact was also inferred by Sebba.[6] It may be explained by the lower solubility of ferric than that of ferrous hydroxide. In fact, in the solutions near the above pH's, white precipitates appeared and the foam became very unstable.

The authors wish to express their thanks to Mr. M. Nakamura of our laboratory for his assistance in this work. They also thank the Ministry of Education for the Scientific Research Expenditure Grant given to facilitate the present work.

6) Ref. 4, p. 109.

BULLETIN OF THE CHEMICAL SOCIETY OF JAPAN VOL. 39 944—947 (1966)

Photo-induced Reactions. III.[1),*1] The Synthesis of Biphenyls from Aromatic Bromo-Compounds

By Teruo MATSUURA and Kanji OMURA

Department of Synthetic Chemistry, Faculty of Engineering, Kyoto University, Sakyo-ku, Kyoto

(Received September, 13, 1965)

Various bromobenzene derivatives were irradiated in benzene with a low-pressure mercury lamp. The corresponding biphenyl derivatives were formed as the main products. A mechanism for the reaction has been discussed.

In 1961, Wolf and Kharasch briefly reported that, when aromatic iodo-compounds were irradiated with ultraviolet light (2537 Å) in aromatic solvents, the corresponding biphenyl derivatives were obtained in synthetically useful yields.[2)] This reaction has since been applied to various iodo-compounds, including some aliphatic iodides. The primary reaction in the irradiation of iodo-compounds is now recognized to be a homolytic cleavage of the carbon-iodine bond.[3-7)] Such a homolytic cleavage also occurs in the photolysis of aromatic bromo-compounds.[7-10)] However, no synthetic applications have yet been undertaken.

We have carried out the photolysis of bromobenzene derivatives under conditions similar to those used by Wolf and Kharasch. When a 0.05 molar solution of bromobenzene in benzene was irradiated with a low-pressure mercury lamp (quartz) under bubbling nitrogen, biphenyl was obtained in a 40% yield, in addition to a non-volatile material which was assumed to be a mixture of polymers. Various bromobenzene derivatives were also photolyzed under the same conditions, and the products were either analyzed by vapor-phase chromatography or isolated. The results are summarized in Table I. In Experiments 1, 2, 5, 6, 7 and 10, the corresponding biphenyl derivatives were obtained in 30—40% yields, while *p*-bromoacetophenone (Exp. 9) gave 4-acetylbiphenyl in a lower yield. This is probably due to the presence of a carbonyl group which is photochemically reactive and which gives rise to side reactions.

The photolysis of *p*-bromoaniline (Exp. 8) and *m*- and *p*-bromonitrobenzene (Exps. 11 and 12) in benzene yielded no biphenyl derivative, but a large amount of the starting substance was recovered unchanged; also a small amount of a non-volatile material was formed.

The photolysis of *p*-bromophenol, *p*-bromoacetophenone and methyl *p*-bromobenzoate resulted in the reduction of the carbon-bromine bond, in addition to the formation of the corresponding biphenyls. Phenol, acetophenone, and methyl benzoate were respectively, detected in the reaction

1) Part II: T. Matsuura, K. Omura and R. Nakashima, This Bulletin, **38**, 1358 (1965).

*1 This work was presented at the 18th Annual Meeting of the Chemical Society of Japan, Osaka, April, 1965.

2) W. Wolf and N. Kharasch, *J. Org. Chem.*, **26** 283 (1961).

3) N. Kharasch, W. Wolf, T. J. Erpelding, P. G. Naylor and L. Tokes, *Chem. Ind.*, **1962**, 1720.

4) N. Kharasch and Göthlich, *Angew. Chem.*, **74**, 651 (1962).

5) N. Kharasch and P. Friedman, Abstract of Papers of 148th ACS Meeting, August, 1964, p. 27S.

6) J. A. Kampmeier and E. Hoffmeister, *J. Am. Chem. Soc.*, **84**, 3787 (1962).

7) S. M. Kupchan and H. C. Wormer, *Tetrahedron Letters*, No. 6, 359 (1965).

8) Z. R. Grabowski, *Z. Physik. Chem.*, **27**, 239 (1961).

9) J. Szychlinski and L. Litwin, *Roczniki Chem.*, **37**, 670 (1963); *Chem. Abstr.*, **95**, 13521 (1963).

10) T. Latowski and A. Basinski, *Roczniki Chem.*, **37**, 341 (1963); *Chem. Abstr.*, **59**, 3460 (1963).

Table I. Photolysis of bromobenzene derivatives in benzene[a)]

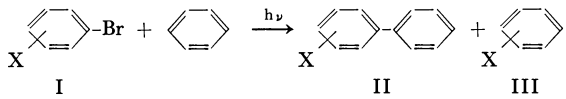

I II III

Expt. No.	X in I	Irradiation period, hr.	Recovered I, %	Yield of II,[b)] %	Yield of III,[b)] %	Non-volatile products, g.
1	H	20	8	40	—	0.39
2[c)]	H	20	8	38	—	0.29
3[d)]	H	20	14	0.6	—	0.27
4[e)]	H	10.5	45	4.7	—	0.15
5	*p*-OH	22	39	31	10	0.44
6	*p*-OCH_3	40	9	37	—	0.39
7	*p*-CH_3	40	16	38	—	0.36
8	*p*-NH_2	40	57	—	—	0.16
9	*p*-$COCH_3$	20	5	23	8	0.98
10	*p*-$COOCH_3$	20	0	34	26	0.56
11	*p*-NO_2	24	73	—	—	0.08
12	*m*-NO_2	20	89	—	—	0.06

a) A solution of I (0.01 mol.) in benzene (200 ml.) was irradiated with a 40 W. low-pressure mercury lamp (quartz) under bubbling nitrogen, unless otherwise indicated.
b) Yields were based on the reacted I.
c) Irradiation was made with a 40 W. low-pressure mercury lamp (Vycor).
d) During irradiation oxygen was bubbled instead of nitrogen.
e) A solution of bromobenzene (0.02 mol.) in benzene (450 ml.) was irradiated with a 450 W. high-pressure mercury lamp with a pyrex jacket.

mixture. On the other hand, the corresponding reduction products could not be detected in the photolysis of bromobenzene, *p*-bromoanisole, or *p*-bromotoluene. In the case of bromobenzene the detection of benzene, which may be formed in the course of the reaction, is not possible. It is assumed that, in other cases, the corresponding reduction products might be formed in such small quantities that they could not be detected.

When the photolysis of bromobenzene in benzene was carried out with a low-pressure mercury lamp made of a Vycor tube in order to cut off short wavelength lights below about 220 mμ, biphenyl was obtained in a similar yield and the yield of the non-volatile products was slightly depressed. On the other hand, when the irradiation was made with a high-pressure mercury lamp using a pyrex filter which cut off lights below about 290 mμ, the reaction proceeded much more slowly and biphenyl was formed in only a small yield. The above results show that the reaction is initiated mainly by light near 2537 Å, which is known to be the most effective point of the light of a low-pressure mercury lamp.

A possible mechanism for the formation of biphenyls from bromobenzenes and benzene is shown by Eqs. 1—4.

The starting bromo-compound dissociates into a corresponding phenyl radical and a bromine atom by an ultraviolet light of 2537 Å (Eq. 1). The phenyl radical then attacks the solvent, benzene, to form a radical intermediate (IV) (Eq. 2). The last step of the reaction involves a hydrogen abstraction from the intermediate (IV) by either the bromine atom or the phenyl radical (Eqs. 3 and 4). Thus, a biphenyl derivative is formed simultaneously with the formation of a benzene derivative or hydrogen bromide respectively. This mechanism is supported by the findings that corresponding benzene derivatives were isolated in the photolysis of *p*-bromophenol (Exp. 5), *p*-bromoacetophenone (Exp. 9) and methyl *p*-bromobenzoate (Exp. 10), and that the liberation of hydrogen bromide was observed only when biphenyl derivatives were formed. In fact, hydrogen bromide was obtained in a 20% yield in the photolysis of bromobenzene in benzene.

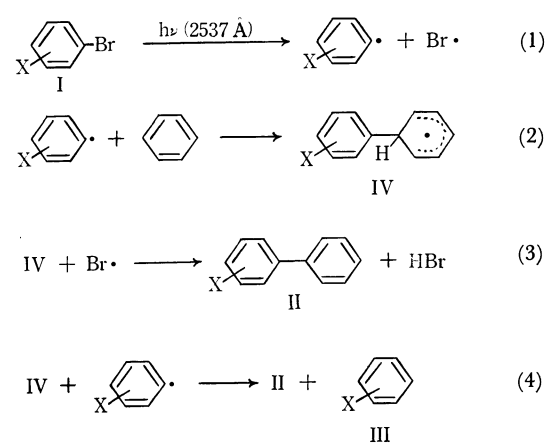

Experimental

The melting points were determined in capillary tubes and were uncorrected. The infrared spectra were taken with a Nihon Bunko spectrophotometer, Model IR-S. The starting materials were commercially available, unless otherwise indicated, and their purities were checked by a melting point determination or by vapor-phase chromatography. The products were analyzed by vapor-phase chromatography under the following conditions: stationary phase, silicone DC 550 on celite; carrier gas, helium; gas pressure, 0.8 kg./cm^2.

The Photolysis of Bromobenzene.—Exp. 1.—A solution of 1.57 g. (0.01 mol.) of bromobenzene in 200 ml. of benzene was placed in a cylindrical vessel, into which a 40 W. low-pressure mercury lamp (quartz-made, unless otherwise indicated) was then inserted. During irradiation, a stream of nitrogen was bubbled through a sintered-glass disk jointed at the bottom of the vessel, which was cooled with tap water. The exhausted gas was then passed through ice-cooled water in order to trap the hydrogen bromide liberated from the reaction mixture. The aqueous solution was neutralized with 18.20 ml. of an aqueous 0.1 N sodium hydroxide solution. The yield of hydrogen bromide was calculated as 19.8% on the basis of the reacted bromobenzene. After being irradiated for 20 hr., the solvent was removed under reduced pressure and the residual liquid was distilled to yield 0.79 g. of a semi-solid, which boiled below 110°C/14 mmHg, and 0.39 g. of a non-volatile material. Vapor-phase chromatography of the semi-solid showed that it consisted of 0.13 g. (8.3%) of the starting material recovered, 0.57 g. (40%) of biphenyl, and 0.09 g. of an unknown product. The recrystallization of the semi-solid from methanol gave colorless crystals, m. p. 66—68°C, whose infrared spectrum was identical with that of an authentic sample of biphenyl.

Exp. 2.—Brombenzene was irradiated with a 40 W. low-pressure mercury lamp (Vycor), and the reaction mixture was treated in the way described in Exp. 1. The results are shown in Table I.

Exp. 3.—Bromobenzene was photolyzed as has been described in Exp. 1, except that the solution was bubbled with oxygen instead of nitrogen. The results are shown in Table I.

Exp. 4.—A solution of 3.14 g. (0.02 mol.) of bromobenzene in 450 ml. of benzene was irradiated for 10.5 hr. with a 450 W. high-pressure mercury lamp surrounded with a water-cooled pyrex jacket. The results are shown in Table I.

The Photolysis of *p*-Bromophenol (Exp. 5).—A solution of 1.73 g. of *p*-bromophenol in 200 ml. of benzene was photolyzed. The distillation of the products yielded three fractions; (i) 0.74 g. of a liquid, b. p. 40—78°C/28 mmHg, which was found by vapor-phase chromatography to consist of 0.68 g. of *p*-bromophenol and 0.06 g. of phenol; (ii) 0.33 g. of a solid, b. p. 90—110°C/16 mmHg, and (iii) 0.44 g. of a non-volatile material. The recrystallization of the fraction ii from benzene and cyclohexane gave 4-hydroxybiphenyl as crystals, m. p. 163—164°C. Lit. m. p. 163°C.[11]

The Photolysis of *p*-Bromoanisole (Exp. 6).—A solution of 1.88 g. of *p*-bromoanisole in 200 ml. of benzene was irradiated. The distillation of the products yielded three fractions: (i) 0.49 g. of a liquid, b. p. 30—70°C/6 mmHg, a preparative vapor phase chromatography of which, gave 0.16 g. of *p*-bromoanisole (ii) 0.64 g. of a solid, b. p. 72—105°C/6 mmHg, which showed only one peak in its vapor-phase chromatography and which was recrystallized from ethanol to give 4-methoxybiphenyl as colorless crystals, m. p. 86—87.5°C (lit. m. p. 89°C[12]), and (iii) 0.39 g. of a non-volatile material.

The Photolysis of *p*-Bromotoluene (Exp. 7).—A solution of 1.71 g. of *p*-bromotoluene in 200 ml. of benzene was irradiated. The distillation of the products yielded three fractions: (i) 0.32 g. of a liquid, b. p. 52—80°C/9 mmHg, which was found by vapor-phase chromatography to contain 0.27 g. of *p*-bromotoluene; (ii) 0.55 g. of a semi-solid, b. p. 82—102°C/9 mmHg, which was recrystallized from methanol to give 4-methylbiphenyl, m. p. 44—50°C (lit. m. p. 47.7°C[13]), and (iii) 0.36 g. of a non-volatile material.

The Photolysis of *p*-Bromoaniline (Exp. 8).—A solution of 1.73 g. of *p*-bromoaniline in 200 ml. of benzene was irradiated. During this irradiation brown materials were deposited on the surface of the lamp tube. The reaction mixture was then washed with an aqueous sodium hydroxide solution, dried over anhydrous sulfate, and evaporated. The distillation of the residual liquid yielded two fractions: (i) 0.99 g. of a solid, b. p. 90—106°C/15 mmHg, whose infrared spectrum was identical with that of *p*-bromoaniline, and (ii) 0.16 g. of a non-volatile material.

The Photolysis of *p*-Bromoacetophenone (Exp. 9).—A solution of 1.99 g. of *p*-bromoacetophenone in 200 ml. of benzene was irradiated. The distillation of the products yielded three fractions; (i) 0.24 g. of a semi-solid, which was found by vapor-phase chromatography to consist of 87 mg. of acetophenone and 105 mg. of *p*-bromoacetophenone; (ii) 0.44 g. of colorless crystals, which showed one peak in its vapor-phase chromatography and which were recrystallized from benzene and methanol to give 4-acetylbiphenyl as crystals, m. p. 119—121°C (lit. m. p. 120.5°C[14]), and (iii) 0.98 g. of a non-volatile material.

The Photolysis of Methyl *p*-Bromobenzoate (Exp. 10).—A solution of 1.50 g. (0.007 mol.) of the methyl ester[15] in 200 ml. of benzene was irradiated. The distillation of the products yielded three fractions: (i) 0.24 g. of a yellow liquid, whose infrared spectrum was identical with that of methyl benzoate; (ii) 0.52 g. of a solid, m. p. 98—114°C, which was recrystallized from ethanol to give methyl *p*-phenylbenzoate as colorless crystals, m. p. 115—116°C (lit. m. p. 117.5°C[16]), and (iii) 0.56 g. of a non-volatile material.

The Photolysis of *p*-Bromonitrobenzene (Exp. 11).—A solution of 2.02 g. of *p*-bromonitrobenzene in 200 ml. of benzene was irradiated. The distillation of the products yielded two fractions: (i) 1.48 g. of crystals, b. p. below 66°C/ca. 1 mmHg and m. p. 117—123°C, which were recrystallized from methanol to give

11) Chas. Raiford and J. C. Colbert, *J. Am. Chem. Soc.*, **47**, 1456 (1925).

12) M. Busch and W. Schmidt, *Ber.*, **62**, 2612 (1929).

13) M. Gomberg and J. C. Pernert, *J. Am. Chem. Soc.*, **48**, 1372 (1926).

14) H. C. Gull and E. E. Turner, *J. Chem. Soc.*, **1929**, 491.

15) The ester was prepared by esterification of the parent acid with methanol and concentrated sulfuric acid, m. p. 77—79°C.

16) W. Schlenk, *Ann.*, **368**, 295 (1909).

p-bromonitrobenzene as colorless crystals, m. p. 123—125°C, and (ii) 82 mg. of a non-volatile material.

The Photolysis of *m*-Bromonitrobenzene (Exp. 12).—A solution of 2.00 g. of *m*-bromonitrobenzene in 200 ml. of benzene was irradiated. The distillation of the products yielded two fractions: (i) 1.77 g. of colorless crystals, b. p. 87°C/7 mmHg and m. p. 52—56°C, whose infrared spectrum was identical with that of *m*-bromonitrobenzene, and (ii) 0.06 g. of a non-volatile material.

BULLETIN OF THE CHEMICAL SOCIETY OF JAPAN VOL. 39 947—951 (1966)

t-Amyloxycarbonyl as a New Protecting Group in Peptide Synthesis. II. Synthesis of a Hexapeptide Amide Related to Eledoisin by the *t*-Amyloxycarbonyl Method

By Shumpei SAKAKIBARA and Masahiko FUJINO*

Peptide Center, Institute for Protein Research, Osaka University, Kita-ku, Osaka

(Received September 17, 1965)

The synthesis of a hexapeptide amide, L-lysyl-L-phenylalanyl-L-isoleucylglycyl-L-leucyl-L-methionine amide, has been carried out as a demonstration of the *t*-amyloxycarbonyl method. This peptide is known to possess strong biological activity which is similar to that of eledoisin and bradykinin. During the synthesis, no complication occurred involving the *t*-amyloxycarbonyl group, and the final product had the expected activity. Therefore, it is considered that the *t*-amyloxycarbonyl method is useful for the synthesis of complicated peptides.

In the preceding paper,[1] the syntheses and properties of *t*-amyloxycarbonyl (AOC) amino acids were reported, and it was suggested that the use of the AOC *N*-protecting group should be valuable in peptide synthesis, because this group has similar properties to the *t*-butoxycarbonyl (BOC) group and preparation of AOC-amino acids is as easy as that of carbobenzoxy derivatives. In the present work, a hexapeptide amide (X), L-lysyl-L-phenylalanyl-L-isoleucylglycyl-L-leucyl-L-methionine amide, was synthesized to test the efficiency of the AOC-method, and a part of the compound was also synthesized by the classical method for comparison.

The syntheses of eledoisin and its analogues have already been reported by many workers,[2,3] and the hexapeptide amide X was found by Bernardi et al.[3] to possess high biological activity. In those works, mentioned above, the BOC-method was used for the synthesis together with the carbobenzoxy group to avoid an undesirable side reaction with the methionine residue. In the present work, di-AOC-lysyl-phenylalanyl-isoleucyl-glycine (IV) was first prepared from glycine benzyl ester by the stepwise elongation method[4] as shown in Scheme 1.

AOC-Ileu-OH + H-Gly-OBz
→ (67%, DCCD in THF+$CHCl_3$)
AOC-Ileu-Gly-OBz (Ia)
→ (81%, 1) CF_3COOH 2) AOC-Phe-ONP)
AOC-Phe-Ileu-Gly-OBz (IIa)
→ (88%, 1) CF_3COOH 2) di-AOC-Lys-ONP in DMF)
di-AOC-Lys-Phe-Ileu-Gly-OBz (IIIa)
→ (98%, H_2/Pd in MeOH)
di-AOC-Lys-Phe-Ileu-Gly-OH (IVa)

Scheme 1.

The classical method for synthesizing this compound is shown in Scheme 2.

* Present address: Chemical Research Laboratories, Takeda Chemical Industries, Ltd., Higashiyodogawa-ku, Osaka.

1) S. Sakakibara, M. Shin, M. Fujino, Y. Shimonishi, N. Inukai and S. Inouye, This Bulletin, **38**, 1522 (1965).

2) E. Sandrin and R. A. Boissonnas, *Experientia*, **18**, 59 (1962); B. Camerino, G. De Caro, R. A. Boissonnas, E. Sandrin and E. Stürmer, ibid., **19**, 339 (1963); E. Sandrin and R. A. Boissonnas, *Helv. Chim. Acta*, **46**, 1637 (1963); E. Schröder and K. Lübke, *Experientia*, **20**, 19 ((1964); E. Stürmer, E. Sandrin and R. A. Boissonnas, ibid., **20**, 303 (1964); E. Sandrin and R. A. Boissonnas, *Helv. Chim. Acta*, **47**, 417 (1964); K. Lübke, E. Schröder, R. Schmiechen and H. Gibian, *Ann.*, **679**, 195 (1964); F. Chillemi, *Gazz. Chim. Ital.*, **93**, 1079 (1963); L. Bernardi, G. Bosisio, R. De Castiglione, O. Goffredo and F. Chillemi, ibid., **94**, 853 (1964); F. Chillemi and O. Goffredo, ibid., **94**, 866 (1964); R. De Castiglione, F. Chillemi, L. Bernardi and O. Goffredo, ibid., **94**, 875 (1964); F. Chillemi, L. Bernardi and G. Bosisio, ibid., **94**, 891 (1964); E. Schröder, K. Lübke and R. Hempel, *Experientia*, **21**, 70 (1965).

3) L. Bernardi, G. Bosisio, F. Chillemi, G. De Caro, R. De Castiglione, V. Erspamer, A. Claesser and O. Goffredo, *Experientia*, **20**, 306 (1964).

4) M. Bodanszky and V. du Vigneaud, *J. Am. Chem. Soc.*, **81**, 5688 (1959).

Z-Ileu-ONP + H-Gly-OEt
87% ↓ in $CHCl_3$
Z-Ileu-Gly-OEt (Ib)
78% ↓ 1) HBr in AcOH 2) Z-Phe-ONP in DMF
Z-Phe-Ileu-Gly-OEt (IIb)
73% ↓ 1) HBr in AcOH 2) di-AOC-Lys-ONP in DMF
di-AOC-Lys-Phe-Ileu-Gly-OEt (IIIb)
82% ↓ NaOH in pyridine
di-AOC-Lys-Phe-Ileu-Gly-OH (IVb)

Scheme 2.

During the synthesis shown in Scheme 1, no complications occurred in relation to the AOC-group; that is, removal of the AOC-groups with trifluoroacetic acid was almost quantitative, as was expected, and the crystallizability of the product at each step was quite satisfactory. On the other hand, trouble arose over the last stage of Scheme 2, and saponification of the ester group in the AOC-tetrapeptide ethyl ester (IIIb) gave only a colored product with a low melting point. Further, AOC-leucyl-methionine amide (VI) was prepared without any trouble by the active ester method, as shown in Scheme 3, and then compound VI was converted to leucyl-methionine amide (VII) using 2N hydrogen chloride in acetic acid. Condensation of the AOC-tetrapeptide IV with dipeptide amide VII was carried out using *p*-nitrophenyl trifluoroacetate as the condensing reagent according to the description of Sakakibara and Inukai.[5] In this case, AOC-tetrapeptide *p*-nitrophenylester was isolated and then coupled with compound VII (Scheme 3). Finally, the protected hexapeptide amide IX obtained was treated with 2 N hydrogen chloride in acetic acid to get the hexapeptide amide X, and it was confirmed that the removal of the AOC-groups was as smooth as that of BOC groups.

The homogeneity of the resulting hexapeptide amide X was judged by paper chromatography and by paper electrophoresis, and no contamination was detected by those procedures. The amino acid ratio in the acid hydrolyzate of compound X was determined using an automatic amino acid analyzer, and the result was also quite satisfactory. Furthermore, it was found that this compound was completely digestible by leucine aminopeptidase to give the expected amount of each amino acid, indicating that no racemization occurred during the synthesis. The biological activity of compound X was determined by the contraction test with guinea-pig ileum,[6] and the activity was 2.5 times higher than that of bradykinin which was prepared in this laboratory.[7] In conclusion, it can be asserted that the AOC method is useful in place of the BOC method for synthesis of complicated peptides.

Incidentally, during the course of the synthesis, carbobenzoxy-L-isoleucine was obtained as crystals for the first time in this laboratory.[8] Of the many carbobenzoxy derivatives of common L-amino acids, carbobenzoxy-L-leucine and this material were thought not to be crystallizable and, moreover, commercially available L-isoleucine used to be contaminated with *allo*-isoleucine and with leucine. Therefore, the crystallization of carbobenzoxy-L-isoleucine is a great advantage in the

AOC-Leu-ONP + H-Met-OMe
89% ↓ in DMF
AOC-Leu-Met-OMe (V)
72% ↓ NH_3 in MeOH
AOC-Leu-Met-NH_2 (VI)
92% ↓ 2N HCl in AcOH
H-Leu-Met-NH_2·HCl (VII)

IVa IVb
98% 65%
↓ CF_3COONP
di-AOC-Lys-Phe-Ileu-Gly-ONP (VIII)

83.6% ↓ in DMF
di-AOC-Lys-Phe-Ileu-Gly-Leu-Met-NH_2 (IX)
↓ 2 N HCl in AcOH
2HCl·Lys-Phe-Ileu-Gly-Leu-Met-NH_2 (X)

Scheme 3.

5) S. Sakakibara and N. Inukai, This Bulletin, **34**, 1979 (1965).
6) T. Suzuki, Y. Mizushima, T. Sato and S. Iwanaga, *J. Biochem.* (*Japan*), **57**, 14 (1965).
7) S. Sakakibara and N. Inukai, This Bulletin, in preparation.
8) S. Inoue, "The 3rd Symposium on Peptide Chemistry (Japan)," Inst. for Protein Research, Osaka University, Osaka (1964), p. 89.

purification of this compound. The purity of the crystallized product and an oily material which was obtained from the mother liquor after recrystallization were tested with an automatic amino acid analyzer after removal of the *N*-protecting group, and only a trace of contamination was detected in the crystallized product, whereas the *allo*-isoleucine and leucine contaminating the original material were both found to be concentrated in the oily residue.

Experimental*

Crystallization of Carbobenzoxy-L-isoleucine.[8] —Crude carbobenzoxy-L-isoleucine, which was prepared from L-isoleucine[9] (131 g., 1 mol.) by the usual procedure, was purified once by sodium bicarbonate extraction, and then the oily material was treated with petroleum ether (60—80°C) at −20°C. After each extraction the upper layer was discarded, and the inside-surface of the vessel was scratched with a glass bar under fresh petroleum ether at −20°C. Then the mixture was stored in a deep freezer for about one week and a small crop of crystals were obtained in the syrup. The remaining oil was then crystallized completely by triturating the crystals thoroughly and then storing them again in the deep freezer for two or three more days. If crystal-seed is available, crude material can be crystallized directly by triturating it with the seeds at −20°C. The crude crystals thus obtained were collected by filtration at −20°C using a pre-cooled funnel. Then, the product was dissolved in a mixture of toluene (250 ml.) and petroleum ether (250 ml.), and the solution was seeded with a few crystals and kept in a deep freezer. After one or two days, about 30% of the compounds separated as crystals, while the rest separated as an oil. Then, the mixture was gradually warmed to room temperature to re-dissolve the oily part, the crystals were triturated well, and the mixture was restored in the deep freezer. After two more days, this procedure was repeated, and finally the crystals formed were collected by filtration. Filtration, washing and drying procedures in vacuo were carried out at below 10°C, and the yield of dried crystals was about 60% (157 g.); m. p. 44—46°C, $[\alpha]_D^{26}$ +6.5° (*c* 6, ethanol).

Found: C, 63.48; H, 7.24; N, 5.25. Calcd. for $C_{14}H_{19}O_4N$: C, 63.38; H, 7.22; N, 5.28%.

***t*-Amyloxycarbonyl-L-isoleucylglycine Benzyl Ester (Ia).**—A solution of *t*-amyloxycarbonyl-L-isoleucine (4.92 g., 0.02 mol.) in tetrahydrofuran (40 ml.) was cooled to −5°C, and dicyclohexylcarbodiimide (4.12 g., 0.02 mol.) was added to the solution with stirring. After about 10 min., a solution of glycine benzyl ester tosylate (6.74 g., 0.02 mol.) and triethylamine (2.8 ml., 0.02 mol.) in chloroform (20 ml.) was added to the reaction mixture. The mixture was allowed to react for one hour at −5°C, and then for additional 10 hr. at 10°C. Dicyclohexylurea formed was removed by filtration, and the filtrate was concentrated to syrup which was dissolved again in ethyl acetate (100 ml.). Then, the solution was washed thoroughly with 0.5 N hydrochloric acid, 5% sodium bicarbonate and water, and the washed solution was dried over anhydrous sodium sulfate. The dried solution was then concentrated to syrup, and the residue was redissolved to a mixture of ethyl acetate (5 ml.) and petroleum ether (60—80°C, 40 ml.) to precipitate a small amount of insoluble materials which was filtered off. The final solution was concentrated to dryness, and the residue was crystallized gradually as colorless needles. Recrystallization from a mixture of ether (1 ml.) and petroleum ether (30 ml.) gave 5.0 g. (67%) of product; m. p. 68—70.5°C, $[\alpha]_D^{22}$ −25.7° (*c* 2.0, methanol).

Found: C, 64.28; H, 8.32; N, 7.09. Calcd. for $C_{21}H_{32}O_5N_2$: C, 64.26; H, 8.22; N, 7.14%.

Carbobenzoxy-L-isoleucylglycine Ethyl Ester (Ib).—Carbobenzoxy-L-isoleucine *p*-nitrophenyl ester[4] (3.86 g., 0.01 mol.) was dissolved in a solution of glycine ethyl ester hydrochloride (1.39 g., 0.01 mol.) and triethylamine (1.4 ml., 0.01 mol.) in chloroform (20 ml.), and the mixture was allowed to react at room temperature for 20 hr. The solvent was distilled off in vacuo, and the residue was dissolved in ethyl acetate. The ethyl acetate solution was washed well with N ammonia, N hydrochloric acid and water. After drying it over anhydrous sodium sulfate, the solvent was removed by distillation under reduced pressure and the product was obtained as crystals; wt. 3.20 g. (91%), m. p. 150—152°C. Recrystallization from ethyl acetate (25 ml.) gave 2.8 g. (87%) of product; m. p. 153.5—154.5°C, $[\alpha]_D^{24}$ −26.0° (*c* 1, acetic acid); Bernardi et al.[10] reported m. p. 156—159°C.

Found: C, 62.01; H, 7.38; N, 8.06. Calcd. for $C_{18}H_{26}O_5N_2$; C, 61.70; H, 7.48; N, 8.00%.

***t*-Amyloxycarbonyl-L-phenylalanyl-L-isoleucylglycine Benzyl Ester (IIa).**—Compound Ia (4.32 g., 0.011 mol.) was dissolved in anhydrous trifluoroacetic acid (10 ml.) and the solution was allowed to stand at room temperature for 20 min. The trifluoroacetic acid was then evaporated off in vacuo, and the remaining oil was dried by flushing with toluene followed by storage over sodium hydroxide in vacuo. The residue was dissolved in dimethylformamide (25 ml.), neutralized with triethylamine (1.6 ml., 0.011 mol.) and subjected to reaction with AOC-L-phenylalanine *p*-nitrophenyl ester[1] (4.4 g., 0.011 mol.). After standing overnight at room temperature, the solution was diluted with water (60 ml.) to precipitate the product as crystals which were separated by filtration, washed well with N ammonia and with water, and dried; wt. 5.84 g. (98%). The crude material was recrystallized from 60% methanol; wt. 4.85 g. (81%), m. p. 142—144°C, $[\alpha]_D^{22}$ −13.8° (*c* 1.9, dimethylformamide), −33.3° (*c* 2, methanol.)

Found: C, 66.65; H, 7.82; N, 7.87. Calcd. for $C_{30}H_{41}O_6N_3$: C, 66.77; H, 7.66; N, 7.79%.

Carbobenzoxy-L-phenylalanyl-L-isoleucylglycine Ethyl Ester (IIb).—Compound Ib (3.5 g., 0.01 mol.) was treated with 31% hydrogen bromide in acetic acid (10.8 g.) for 40 min., and the product was precipitated by adding dry ether (150 ml.) to the reaction mixture. The separated product was washed with ether by decantation, and dried over sodium hydroxide in vacuo.

* All melting points given are uncorrected.

9) This material was obtained from Tanabe Pharmaceutical Co., Ltd., Osaka.

10) L. Bernardi, G. Bosisio, R. De Castiglione, O. Goffredo and F. Chillemi, *Gazz. Chim. Ital.*, 853 **94**, (1964).

The dried powder was dissolved in dimethylformamide, and triethylamine (1.80 ml.) was added to the solution. The triethylamine hydrobromide formed was filtered off, and the filtrate was subjected to reaction with carbobenzoxy-L-phenylalanine *p*-nitrophenyl ester (4.0 g., 0.01 mol.) for 24 hr. at room temperature. Water (100 ml.) was added to the mixture, and crystalline precipitates which appeared were filtered, washed well with N ammonia, and dried. The product was recrystallized from ethanol; wt. 3.9 g. (78%), m. p. 179.5—180.5°C, $[\alpha]_D^{24}$ −21.0° (*c* 1.7, acetic acid). Bernardi et al.[10] reported m. p. 175—176°C.

Found: C, 65.31; H, 6.90; N, 8.31. Calcd. for $C_{27}H_{33}O_6N_3$: C, 65.44; H, 6.71; N, 8.48%.

Di-*t*-amyloxycarbonyl-L-lysyl-phenylalanyl-L-isoleucylglycine Benzyl Ester (IIIa).—Compound IIa (3.78 g., 0.007 mol.) was dissolved in anhydrous trifluoroacetic acid (8 ml.), and the solution was allowed to stand at room temperature for 25 min. The trifluoroacetic acid was then evaporated to dryness in vacuo, and the residue was treated with a mixture of ether and petroleum ether to obtain crystals. The supernatant was removed by decantation, and the product was dried over sodium hydroxide in vacuo at room temperature; wt. 3.75 g., m. p. 202—203°C. This material was dissolved in dimethylformamide (30 ml.), neutralized with triethylamine (0.93 ml.) and then subjected to reaction with di-AOC-L-lysine *p*-introphenyl eater[1] (3.22 g., 0.0065 mol.). After standing overnight at room temperature, the solution was diluted with water (50 ml.) to precipitate the product, which was separated by filtration, washed well with N ammonia and with water, and dried. The product was recrystallized from 60% ethanol; wt. 4.47 g. (88%), m. p. 151—152°C, $[\alpha]_D^{22}$ −17.5° (*c* 2, dimethylformamide).

Found: C, 64.78; H, 8.13; N, 8.85. Calcd. for $C_{42}H_{63}O_9N_5$: C, 64.50; H, 8.12; N, 8.95%.

Di-*t*-amyloxycarbonyl-L-lysyl-L-phenylalanyl-L-isoleucylglycine Ethyl Ester (IIIb).—Compound IIb (1.25 g., 0.0025 mol.) was treated with 31% hydrogen bromide in acetic acid (2.6 g.) for 40 min., and the product was precipitated by adding dry ether (70 ml.) to the reaction mixture. It was separated by decantation, washed well with dry ether and dried over sodium hydroxide in vacuo. The dried powder was dissolved in dimethylformamide, and then triethylamine (0.38 ml.) was added to the solution. The triethylamine hydrobromide formed was filtered off, and the filtrate was subjected to reaction with di-*t*-amyloxycarbonyl-L-lysine *p*-nitrophenyl ester[1] (1.24 g., 0.0025 mol.) for 24 hr. at room temperature. Water (40 ml.) was added to the reaction mixture, and the precipitate which appeared was filtered, washed well with N ammonia and dried; wt. 1.64 g. (91%). This material was recrystallized from 60% ethanol; wt. 1.31 g. (73%), m. p. 162—163°C, $[\alpha]_D^{21}$ −18.5° (*c* 1.5, dimethylformamide).

Found: C, 61.71; H, 8.46; N, 9.75. Calcd. for $C_{37}H_{61}O_9N_5$: C, 61.72; H, 8.54; N, 9.73%.

Di-*t*-amyloxycarbonyl-L-lysyl-L-phenylalanyl-L-isoleucylglycine (IV).—a) Hydrogen was passed through a solution of IIIa (3.13 g., 0.004 mol.) in methanol (150 ml.) containing a small amount of palladium black for about 3 hr. The catalyst was then removed by filtration, and the filtrate was concentrated to dryness under reduced pressure. The residue was dissolved in a mixture of methanol and ethyl acetate (30 ml. each), and the product was precipitated as crystals by adding petroleum ether (60—80°C, 60 ml.). Recrystallization of the crude product from 50% methanol gave 2.74 g. (98%) of product which was dried over phosphorus pentoxide in vacuo at 60°C for 8 hr.; m. p. 127—133°C (decomp.), $[\alpha]_D^{21.5}$ −17.2° (*c* 2, dimethylformamide).

Found: C, 59.93; H, 8.48; N, 9.98. Calcd. for $C_{35}H_{57}O_9N_5 \cdot 1/2\ H_2O$: C, 59.99; H, 8.34; N, 9.99%.

b) A solution of IIIb (0.94 g., 0.0013 mol.) in pyridine (5 ml.) was treated with N sodium hydroxide solution (1.5 ml.) at room temperature for 3 hr., and then the solution was neutralized with N hydrochloric acid (1.5 ml.). The solvent was evaporated out under reduced pressure, and the residue was washed with ether and then with water. Then, the residue was dissolved in hot ethanol (10 ml.) and reprecipitated by adding water (30 ml.). It was collected by filtration and reprecipitated again from hot 50% methanol: wt. 0.74 g. (82%) after drying in vacuo at 60°C for 8 hr., m. p. 123—131°C (decomp.).

Found: C, 60.48; H, 8.41; N, 10.29. Calcd. for $C_{35}H_{57}O_9N_5 \cdot 1/2H_2O$: C, 59.99; H, 8.34; N, 9.99%.

***t*-Amyloxycarbonyl-L-leucyl-L-methionine Methyl Ester (V).**—Triethylamine (1.1 ml.) was added to a solution of L-methionine methyl ester hydrochloride (1.39 g., 0.007 mol.) in dimethylformamide (15 ml.), and the crystals formed were filtered off. The *p*-nitrophenyl ester of *t*-amyloxycarbonyl-L-leucine[1] (2.56 g., 0.007 mol.) was added to the filtrate prepared as described above, and the mixture was allowed to stand at room temperature for 20 hr. Water (120 ml.) was then added to the reaction mixture, and an oil separated which was extracted well with ethyl acetate (about 100 ml.). The ethyl acetate extract was washed thoroughly in succession with N ammonia, 0.5 N hydrochloric acid and water, and dried over anhydrous sodium sulfate. On removal of the solvent a crystalline residue was obtained, which was recrystallized from a mixture of ethyl acetate and petroleum ether; wt. 2.73 g. (89%), m. p. 92—93°C, $[\alpha]_D^{22}$ −39.5° (*c* 2.1, methanol).

Found: C, 55.53; H, 8.89; N, 7.29; S, 8.15. Calcd. for $C_{18}H_{34}O_5N_2S$: C, 55.35; H, 8.78; N, 7.17; S, 8.21%.

***t*-Amyloxycarbonyl-L-leucyl-L-methionine Amide (VI).**—A solution of V (2.0 g., 0.0051 mol.) in methanol (50 ml.) was saturated with dry ammonia gas at 0°C, and the solution was allowed to stand for 24 hr. at room temperature. The reaction mixture was concentrated to dryness under reduced pressure, and the residue was crystallized from a mixture of aqueous ethanol and acetone. The yield of product was 1.38 g. (72%); m. p. 104—106°C, $[\alpha]_D^{22}$ −37.8° (*c* 1.1, methanol).

Found: C, 54.50; H, 8.90; N, 11.36; S, 8.53. Calcd. for $C_{17}H_{33}O_4N_3S$: C, 54.37: H, 8.85; N, 11.19; S, 8.53%.

Di-*t*-amyloxycarbonyl-L-lysyl-L-phenylalanyl-L-isoleucylglycyl-L-leucyl-L-methionine Amide (IX).—Compound IVa (1.038 g., 0.0015 mol.) was dried over phosphorus pentoxide in vacuo at 80°C for 8 hr. and then dissolved in dry pyridine (3.0 ml.). *p*-Nitrophenyl trifluoroacetate (0.494 g., 0.0021 mol.) was added to the solution and the mixture was allowed to react overnight at room temperature. Then ice-cold water (20 ml.) was added to the mixture, and the precipitate

formed was separated by filtration. The product was then resuspended in water (20 ml.), collected by filtration, and dried in vacuo over phosphorus pentoxide; wt. 1.20 g. (98%), m. p. 171—173°C (decomp.). This material VIIIa was used in the following reaction without further purification. The same type compound VIIIb was prepared from IVb in 90% yield; m. p. 165—168°C (decomp.) which had to be recrystallized from 60% methanol for the following reaction; yield 65%, m. p. 176—179°C (decomp.). Compound VI (0.563 g., 0.0015 mol.) was treated with 2 N hydrogen chloride in acetic acid (5 ml.) at room temperature for 40 min., and then the reaction product was precipitated by adding ice-cold ether (30 ml.). The precipitate was collected by filtration, washed well with ether and dried over sodium hydroxide in vacuo. The product which corresponded to leucylmethionine amide hydrochloride VII (0.44 g.) was added to a solution of VIIIa (1.2 g., 0.0015 mol.) in dimethylformamide (5 ml.) together with triethylamine (0.21 ml.), and the mixture was allowed to react overnight at room temperature. Water was added in the reaction mixture to precipitate the product, which was then collected by filtration, washed well with N ammonia and with water, and dried. Repeated precipitation from dimethylformamide - ethyl acetate and then from dimethylformamide-water gave 1.16 g. (82%) of product; m. p. 233—234°C, $[\alpha]_D^{21.5}$ −26.5° (*c* 1, dimethylformamide).

Found: C, 58.91; H, 8.36: N, 12.10; S, 3.24. Calcd. for $C_{46}H_{78}O_{10}N_8S$: C, 59.07; H, 8.41; N, 11.98; S, 3.43%.

Compound VIIIb was also subjected to the same reaction with VII, and the same product was finally obtained in 85% yield; m. p. 233—234°C, $[\alpha]_D^{21.5}$ −25.9° (*c* 0.9, dimethylformamide).

L-Lysyl-L-phenylalanyl-L-isoleucylglycyl-L-leucyl-L-methionine Amide Dihydroc hloride Dihydrate (X).—Compound IX (0.2 g.) was dissolved in 2 N hydrogen chloride in acetic acid (5 ml.), and the solution was allowed to react at room temperature for 40 min. The product was precipitated by adding ice-cold ether (20 ml.) at 0°C, and the precipitate was collected by filtration washed well with ether and dried over sodium hydroxide in vacuo. The residue was dissolved in 60% methanol (4 ml.), and insoluble material was filtered off. The filtrate was concentrated to dryness over phosphorus pentoxide in vacuo to obtain the final product; wt. 0.17 g., m. p. 240—243°C (decomp.), $[\alpha]_D^{23}$ −16.8° (*c* 0.8, acetic acid); Bernardi et al. reported[3] m. p. 240—243°C (decomp.), $[\alpha]_D^{21}$ −17° (*c* 0.8, 95% acetic acid).

Found:* C, 50.00; H, 7.96; N, 13.63. Calcd. for $C_{34}H_{58}O_6N_8S \cdot 2HCl \cdot 2H_2O$: C, 50.05; H, 7.91; N, 13.73%.

The R_f values of the product in *n*-butanol : acetic acid : water (4 : 1 : 1) and *n*-butanol : pyridine : water (1 : 1 : 1) were 0.62 and 0.74 respectively (R_f values of an authentic leucine in the same solvent systems were 0.61 and 0.54 respectively); paper electrophoresis showed this compound to be homogeneous at pH 2.3 and 4.75, respectively. The amino acid ratios in the acid hydrolyzate were Lys 1.03, Phe 1.00, Ileu 0.98, Gly 1.06, Leu 1.01, Met 0.87. The amino acid ratios in the leucine-aminopeptidase digest were Lys 1.06, Phe 0.97, Ileu 0.98, Gly 1.06, Leu 1.00,Met 1.00. The biological activity, determined by the contraction test with guineapig ileum[6] was 2.5 times more than that of bradykinin prepared in this laboratory.[7]

The authors wish to express their thanks to Professor Tomoji Suzuki for determining the biological activity of the synthetic material.

* This material was dried over phosphorus pentoxide in vacuo for 10 hr. at 80°C.

BULLETIN OF THE CHEMICAL SOCIETY OF JAPAN VOL. 39 951—955 (1966)

The Radiolysis of Aqueous Solutions of Potassium Iodide

By Takeshi SAWAI, Yoshiharu SHINOZAKI and Gisuke MESHITSUKA

Tokyo Metropolitan Isotope Research Center, Fukazawa-cho, Setagaya-ku, Tokyo

(Received September 17, 1965)

The radiolysis of potassium iodide aqueous solutions has been studied in order to elucidate the contribution of the hydrated electrons to the radiolysis mechanisms. The deaerated and aerated solutions were irradiated by ^{60}Co γ-rays under various conditions, and the yields of iodine, hydrogen peroxide, hydrogen and oxygen were determined. The pH dependences of the initial yields of iodine and hydrogen peroxide in the deaerated solutions are different from the results obtained in the aerated solutions. These results can be reasonably explained by assuming the hydrogen atoms and hydrated electrons to be the reducing species. From an examination of the results, the radiolysis mechanisms of the potassium iodide aqueous solutions have been discussed. The rate constant of the reaction of hydrated electrons for iodine has been calculated to be 5.9×10^{10} M^{-1} sec^{-1}.

The radiolysis of aqueous solutions containing iodide ions has already been studied by several

workers,[1-5] and it is known that the yields of the products, iodine, hydrogen peroxide, hydrogen and oxygen, depend upon the concentrations of iodide ions, hydrogen ions and oxygen in the solution. Allen et al.[3] observed that the yield of iodine from the radiolysis of the deaerated iodide solution was very low in a neutral and high in a 0.8 N sulfuric acid solution. The radiolysis of an iodide ion solution is known to be an oxidation-reduction reaction, but this system has not yet been completely examined.

Most of the radiation chemical reactions of aqueous solutions have been explained by assuming hydrogen atoms and hydroxyl radicals as the primary intermediates. Recently the existence of two forms of the reducing species has been reported by many authors, and it has been shown that one is a hydrogen atom and the other, a hydrated electron.[6-19]

In the present work, the radiolysis of potassium iodide aqueous solutions has been investigated under various conditions in order to elucidate the contribution of the hydrated electrons to the radiolysis mechanisms.

Experimental

The Preparation of Samples and the Irradiation.—All the materials used were of GR grade, and the solutions were prepared using triply-distilled water. The aerated and deaerated solutions (20 ml.) of various concentrations of potassium idodide, from 5×10^{-4} to 0.1 M, and of various pH values, from 0.5 to about 7, were irradiated by ^{60}Co γ-rays at room temperature. The air-free neutral solutions were obtained by bubbling in nitrogen gas filtered with triply-distilled water and by degassing them using the standard freezing-pumping technique. For the determination of the variation in the oxygen concentration in the irradiated aerated solutions, an irradiation vessel similar to one described by Boyle[20] was used. The pH value was controlled with sulfuric acid and was measured in a nitrogen stream by using a Horiba, model 3, pH meter.

To avoid the thermal oxidation of iodide ions at low pH values, the irradiations were made immediately after mixing the degassed potassium iodide solution with the degassed sulfuric acid solution.

The doses employed were from 1.0×10^{18} to 1.5×10^{19} eV./ml. Dosimetry was carried out by using an aerated solution of 5×10^{-3} M ferrous ammonium sulfate in 0.8 N sulfuric acid.

Analysis.—Iodine was determined from the absorption of tri-iodide ions at 305 mμ by using a Shimadzu QR-50 spectrophotometer and hydrogen peroxide, by Ghormley's method.[21] The gaseous products were collected by means of a Toepler pump, and hydrogen and oxygen were analyzed by gas chromatography (Shimadzu GC-2B) by using a Molecular Sieve 13X column at room temperature. As a carrier gas, argon or hydrogen was used. The hydrogen was also determined by a mass spectrometer (Hitachi RMU-5G).

Results

The Yields of Products in Air-free Neutral Potassium Iodide Solutions.—The formation of iodine, hydrogen peroxide, hydrogen, and oxygen in deaerated neutral solutions of potassium iodide (pH 6.5—6.7) is shown in Fig. 1. The

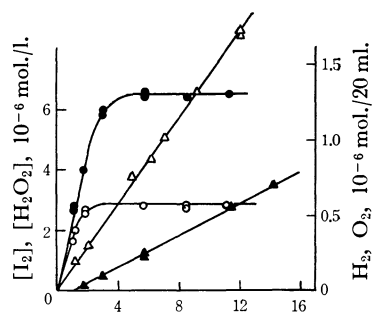

Fig. 1. Yields of products from deaerated potassium iodide aqueous solutions irradiated by ^{60}Co γ-rays.
[KI] : 5×10^{-4} M, pH : 6.5—6.7
● : H_2O_2, ○ : I_2, △ : H_2, ▲ : O_2

concentrations of iodine and hydrogen peroxide increase with an increase in the dose and reach the steady-state concentrations at about 2×10^{18} eV./ml. The initial G-values of iodine and hydrogen peroxide are 0.10 and 0.13 respectively. The amount of hydrogen produced increases linearly with the dose, and $G(H_2)$ is calculated to be 0.45, which is in good agreement with the "molecular hydrogen yield." Oxygen is formed at doses higher

1) F. Fricke and E. J. Hart, *J. Chem. Phys.*, **3**, 596 (1935).
2) E. R. Johnson, ibid., **21**, 1417 (1953).
3) A. O. Allen, J. P. Jr. Losee and H. A. Schwarz, *J. Am. Chem. Soc.*, **76**, 4693 (1954).
4) E. J. Hart and C. B. Senvar, *Proceedings of the International Conference on the Peaceful Uses of Atomic Energy*, **29**, 19 (1958).
5) S. Gordon and E. J. Hart, ibid., **29**, 13 (1958).
6) E. Hayon, O. Armstrong, E. Collinson, F. S. Dainton, D. M. Donaldson, N. Miller and J. Weiss, ibid., **29**, 80 (1958).
7) J. Weiss, G. Scholes and J. Holian, *Nature*, **191**, 1386 (1961).
7) J. Weiss, G. Scholes and J. Holian, *Nature*, **191**, 1386 (1961).
8) A. O. Allen and E. Hayon, *J. Phys. Chem.*, **65**, 2181 (1961).
9) G. Czapski and H. A. Schwarz, ibid., **66**, 471 (1962).
10) E. Collinson, F. S. Dainton, D. R. Smith and S. Tazuké, *Proc. Chem. Soc.*, 140 (1962).
11) J. T. Allan and G. Scholes, *Nature*, **187**, 218 (1960).
12) J. Rabani and G. Stein, *J. Chem. Phys.*, **37**, 1865 (1962).
13) J. T. Allan and C. M. Beck, *J. Am. Chem. Soc.*, **86**, 1483 (1964).
14) J. T. Allan, *J. Phys. Chem.*, **68**, 2697 (1964).
15) G. E. Adams, J. W. Boag and B. D. Michael, *Trans. Faraday Soc.*, **61**, 492 (1965).
16) E. Hayon, ibid., **61**, 723 (1965).
17) E. J. Hart and J. W. Boag, *J. Am. Chem. Soc.*, **84**, 4090 (1962).
18) S. Gordon, E. J. Hart, M. S. Matheson, J. Rabani and J. K. Thomas, ibid., **85**, 1375 (1963).
19) J. P. Keene, *Nature*, **197**, 47 (1963).
20) J. W. Boyle, *Rad. Res.*, **17**, 450 (1962).
21) A. O. Allen, C. J. Hochanadel, J. A. Ghormley and T. W. Paris, *J. Phys. Chem.*, **56**, 575 (1952).

than 1×10^{18} eV./ml., and the $G(O_2)$ value is 0.17. In the deaerated solution of pH 5.3, the G-values of iodine, hydrogen peroxide, and oxygen are 0.14, 0.27, and 0.22 respectively.

The Effects of the Potassium Iodide Concentration on the Initial Yields of Iodine and Hydrogen Peroxide.—The initial G-values of iodine and hydrogen peroxide in the aerated and deaerated solutions are shown in Fig. 2 as a function of the potassium iodide concentration. With an increase in the iodide ion concentration, the yield of iodine increases and the hydrogen peroxide yield decreases, the formation of hydrogen peroxide reaches a very low steady-state concentration ($\sim1\times10^{-6}$ M) at the higher concentration of iodide ion ($\sim$0.1 M).

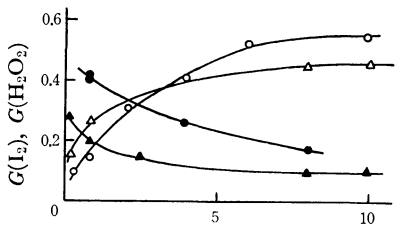

Fig. 2. Effects of potassium iodide concentrations on the initial yields of products in aerated and deaerated solutions at pH 5.3.

○ : I_2 in aerated, ● : H_2O_2 in aerated,
△ : I_2 in deaerated, ▲ : H_2O_2 in deaerated

The Dependence of the Initial Yields on the pH Values.—The pH dependences of the initial yields in the deaerated and aerated iodide solutions of 8.5×10^{-3} M are shown in Figs. 3 and 4. In the deaerated systems, the hydrogen yield decreases with an increase in the pH and becomes constant at about pH 2.5. The iodine yield shows a minimum in the range of pH 2.0—2.5. On the contrary, the yield of hydrogen peroxide shows a maximum in the same pH range. From the results in Fig. 3, it can be seen that, at pH values lower than 2, the change in the $G(I_2)$ with the pH is equal to the sum of the changes in $G(H_2O_2)$ and $G(H_2)$, and that in the higher pH range the change in $G(I_2)$ is equal to the change in $G(H_2O_2)$.

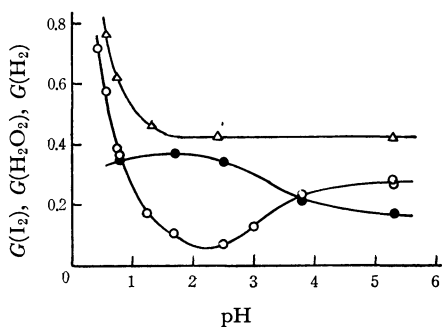

Fig. 3. Effects of pH on the initial yields of I_2, H_2O_2 and H_2 in the radiolysis of deaerated aqueous potassium iodide solutions.

[KI] : 8.5×10^{-3} M
△ : H_2, ○ : I_2, ● : H_2O_2

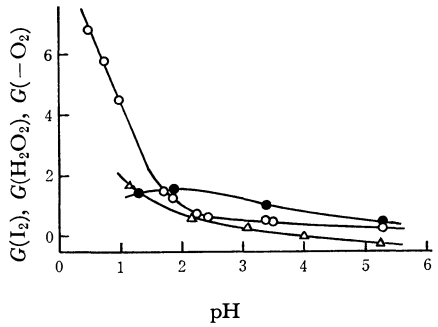

Fig. 4. Effects of pH on the initial yields of I_2, H_2O_2 and $-O_2$ in the radiolysis of aerated aqueous potassium iodide solutions.

[KI] : 8.5×10^{-3} M
○ : I_2, ● : H_2O_2, △ : $-O_2$

In the aerated systems, $G(I_2)$ decreases smoothly with an increase in the pH, as is shown in Fig. 4. $G(H_2O_2)$ shows behavior similar to that of the deaerated systems. With irradiation, the amount of dissolved oxygen increases at pH 5.3 but decreases at pH values lower than 4, while $G(-O_2)$ increases with a decrease in the pH.

Discussion

The Dependence of Initial Yields on the pH.—The radiolysis mechanisms of the aerated iodide solution were proposed by Allen.[22] For the deaerated system, however, no definite mechanisms have been given. In the radiolysis of aqueous solutions, hydrogen atoms and hydroxyl radicals have so far been assumed to be the primary intermediates, but the results obtained in these experiments, for example, the pH dependence of $G(I_2)$ or $G(H_2O_2)$, can not be explained only in terms of hydrogen atoms and hydroxyl radicals.

As to the formation of iodine from iodide ions, the following reactions can be postulated:

$$OH + I^- \rightarrow OH^- + I \quad (1)$$

$$2I^- + H_2O_2 \xrightarrow{H^+} 2I + 2H_2O \quad (2)$$

$$I + I \rightarrow I_2 \qquad I + I^- \rightarrow I_2^- \quad (3)$$

$$I_2^- + I_2^- \rightarrow I_3^- + I^- \qquad I_2 + I^- \rightleftarrows I_3^- \quad (4)$$

By assuming a hydrated electron as an intermediate, the results can be explained by the following competitive reactions:

22) A. O. Allen, "The Radiation Chemistry of Water and Aqueous Solutions," D. Van Nostrand Co., New York (1961).

$$e^-_{aq} + H^+ \rightarrow H \quad (5)$$

$$e^-_{aq} + H_2O_2 \rightarrow OH + OH^- \quad (6)$$

$$e^-_{aq} + I \rightarrow I^- \quad (7)$$

In a strongly acidic medium, hydrated electrons are converted to hydrogen atoms by the reaction 5, followed by the reaction 8, which forms hydrogen and iodine:

$$H + I^- + H^+ \rightarrow H_2 + I \quad (8)$$

As the pH increases, the reaction 8 decreases and the reaction 5 is followed by the reaction 9, and thus $G(I_2)$ and $G(H_2)$ decrease:

$$H + I \rightarrow H^+ + I^- \quad (9)$$

From the fact that $G(H_2)$ shows an almost constant value at pH higher than 2.5, it is clear that the reaction 8 is negligible in this pH range and that the hydrogen atoms produced reduce iodine atoms by means of the reaction 9. These facts agree with the results of the reaction of iodide ions with atomic hydrogen presented by Stein et al.[23] The oxidation reaction by hydrogen peroxide, which can occur in a strongly acidic medium, also decreases with an increasing pH, resulting in a slight increase in $G(H_2O_2)$:

$$2I^- + H_2O_2 \xrightarrow{H^+} 2I + 2H_2O \quad (2)$$

With a further increase in pH, the reaction 6 becomes important in giving more iodine by the reaction of the hydroxyl radical produced by the reaction 6, and thus $G(I_2)$ increases and $G(H_2O_2)$ decreases. From these mechanisms, the relations between the changes in $G(I_2)$ and $G(H_2O_2)$ with the pH (Fig. 3) can be explained reasonably.

In the aerated solutions, the following reactions are added to the reactions in the deaerated solutions:

$$e^-_{aq} + O_2 \rightarrow O_2^- \quad (10)$$

$$O_2^- + I \rightarrow O_2 + I^- \quad (11)$$

$$O_2^- + H^+ \rightarrow O_2 + H \quad (\text{or } HO_2) \quad (12)$$

$$H + O_2 \rightarrow HO_2 \quad (13)$$

$$HO_2 + I^- + H^+ \rightarrow H_2O_2 + I \quad (14)$$

$$HO_2 + HO_2 \rightarrow H_2O_2 + O_2 \quad (15)$$

With an increasing pH, the reactions 10 and 11 increase and 12, 13, and 14 decrease; thus $G(I_2)$, $G(H_2O_2)$, and $G(-O_2)$ fall smoothly, as is shown in Fig. 4. At pH 5.3 oxygen is formed, as will be described later.

The Dependence of Hydrogen Peroxide Formation on the Potassium Iodide Concentration.—From the dependence of $G(I_2)$, $G(H_2O_2)$ and the stationary concentration of iodine and hydrogen peroxide on the iodide ion concentration, it may be concluded that the hydrogen peroxide oxidizes iodide ions, presumably by the reaction 2. The fact that in the aerated solutions $G(H_2O_2)$ and the steady concentration of hydrogen peroxide are higher than those in the dearated solution, may be explained by the reactions 10, 12, 13, and 14.

Reactions in Deaerated Neutral Solutions.—The reactions 1, 5, 6, 7, and 9 can be assumed in the deareated neutral solution of potassium iodide 5×10^{-4} M, because the concentrations of hydrogen ion and iodide ion are very low. The oxidation reaction by hydrogen peroxide can be neglected in the low concentration range of potassium iodide in a neutral solution.

Oxygen is formed secondarily by the reaction of hydrogen peroxide with iodine. The following mechanisms were suggested by Anbar et al.[24] for the formation of oxygen in the radiolysis of potassium iodide solutions saturated with nitrous oxide:

$$I_2^- + H_2O_2 \rightarrow 2I^- + H^+ + HO_2 \quad (16)$$

$$I_3^- + H_2O_2 \rightarrow 3I^- + 2H^+ + O_2 \quad (17)$$

$$I_2 + HO_2 \rightarrow I_2^- + H^+ + O_2 \quad (18)$$

$$I_2^- + HO_2 \rightarrow 2I^- + H^+ + O_2 \quad (19)$$

Since the pK of HO_2 is 4.5 ± 0.2,[25] oxygen may also be produced by the following reactions:

$$HO_2 \rightleftarrows O_2^- + H^+ \quad (20)$$

$$O_2^- + (I, I_2, I_2^-, I_3^-) \rightarrow O_2 \quad (11')$$

The iodine produced is present in the forms of I_2 and I_3^-. If hydrogen peroxide is oxidized by I_2 or I_3^- to oxygen, the variations in the concentrations of hydrogen peroxide and iodine have to be observed as post-irradiation effects. However, the effects do not occur in dilute solutions. The iodine which can oxidize hydrogen peroxide to give oxygen seems to be I or I_2^-. Under the experimental conditions, all the hydroxyl radicals are scavenged by iodide ions and the following reactions, 21 and 22, do not occur, because the rate constants of these reactions are relatively slow (k_{21} and $k_{22}=4\times10^7$ M^{-1} sec^{-1}):[26,27]

$$OH + H_2O_2 \rightarrow HO_2 + H_2O \quad (21)$$

$$H + H_2O_2 \rightarrow OH + H_2O \quad (22)$$

From the results of the stationary concentrations of iodine and hydrogen peroxide in Fig. 1 and from the mechanisms proposed above, the following equations can be derived. As to the stationary state of iodine concentration:

$$G_{OH} + G e^-_{aq} \frac{k_6[H_2O_2]}{k_5[H^+]+k_6[H_2O_2]+k_7[I_2]}$$

23) G. Czapski, J. Jortner and G. Stein, *J. Phys. Chem.*, **63**, 1769 (1959).

24) M. Anbar, D. Meyerstein and P. Neta, ibid., **68**, 2967 (1964).

25) G. Czapski and L. M. Dorfman, ibid., **68**, 1169 (1964).

26) H. A. Schwarz, ibid., **66**, 255 (1962).

27) J. K. Thomas, ibid., **67**, 2593 (1963).

$$= G_{H} + Ge^{-}_{aq}\frac{k_5[H^+]+k_7[I_2]}{k_5[H^+]+k_6[H_2O_2]+k_7[I_2]} + 2G(O_2) \quad (23)$$

As to that of hydrogen peroxide:

$$G_{H_2O_2}=Ge^{-}_{aq}\frac{k_6[H_2O_2]}{k_5[H^+]+k_6[H_2O_2]+k_7[I_2]} + G(O_2) \quad (24)$$

From Eqs. 23 and 24, the following relations can be obtained:

$$G_{OH} + 2G_{H_2O_2} = G_{H} + Ge^{-}_{aq} + 4G(O_2) \quad (25)$$

In the potassium iodide solution of 5×10^{-4} M, most of the iodine produced is present in the form of I_2:

$$I_2 + I^- \rightleftarrows I_3^- \qquad (K = 7.2\times10^2)^{28)}$$

The values of k_5 and k_6 reported by Hart et al.[29] and $Ge^{-}_{aq}=2.8$ being used,[13,14,30] the rate constant of the reaction of hydrated electrons with iodine, $k_{e^-_{aq}+I_2}$, can be calculated from Eq. 24 to be 5.9×10^{10} M^{-1} $sec.^{-1}$ a value which is in good agreement with the value obtained by Hart et al.[31] using the pulse radiolysis technique.

On the other hand, in the deaerated solution of pH 5.3, $G(I_2)$ $G(H_2O_2)$ and $G(O_2)$, and the stationary concentrations of iodine and hydrogen peroxide are a little higher than those in the neutral solution. This may be due to the additional reaction of carbon dioxide with hydrated electrons.

$$CO_2 + e^-_{aq} \rightarrow CO_2^- \quad (26)$$

28) L. I. Grossweiner and M. S. Matheson, ibid., **61**, 1089 (1957).

29) S. Gordon, E. J. Hart, S. Matheson, J. Rabani and J. K. Thomas, *Discussions Faraday Soc.*, **36**, 193 (1963).

30) T. Sawai, unpublished data.

31) J. K. Thomas, S. Gordon and E. J. Hart, *J. Phys. Chem.*, **68**, 1524 (1964).

BULLETIN OF THE CHEMICAL SOCIETY OF JAPAN VOL. 39 955—960 (1966)

Radical Yields in the Radiolysis of Neutral Aqueous Solutions

By Takeshi SAWAI

Tokyo Metropolitan Isotope Research Center, Fukazawa-cho, Setagaya-ku, Tokyo

(Received September 17, 1965)

The determination of the yields of the two reducing species and the OH radical in the radiolysis of neutral aqueous solutions was undertaken, using deaerated 2-propanol aqueous solutions containing potassium nitrate or hydrogen peroxide as electron scavengers. Irradiation was carried out with ^{60}Co γ-rays, and the hydrogen, nitrite ion, acetone, hydrogen peroxide and pinacol so produced were analyzed. The hydrogen yield decreases upon the addition of hydrogen peroxide or nitrate ions. The yield of hydrogen atoms is found to be 0.61 ± 0.03 by subtracting the molecular yield of hydrogen from the total hydrogen yield in the solutions containing enough scavengers. The yield of nitrite ions increases with an increase in the concentration of nitrate ions, and decreases with an increase in the concentration of acetone and with a decrease in the pH value. The acetone yield increases sharply with an increase in the quantity of nitrate ions and reaches a plateau value in the concentration range of nitrate ions higher than 1×10^{-2} M. In the presence of potassium nitrate of 1×10^{-2} M, pinacol is not formed, and the yield of hydrogen peroxide is less than the molecular yield of hydrogen peroxide. On the basis of these results, radiolysis mechanisms are elucidated and the yields of the hydrated electron and the OH radical of a neutral solution are found to be 2.77 ± 0.03 and 3.0 respectively. The relative rate constants, $k_{H+NO_3^-}/k_{H+(CH_3)_2CHOH}$ and $k_{e^-_{aq}+(CH_3)_2CO}/k_{e^-_{aq}+NO^-_3}$, are found to be 0.18 and 0.78.

Recent experimental evidence obtained by many investigators[1-5] in radiation chemical studies of dilute aqueous solutions has indicated that two forms of reducing species are produced in irradiated aqueous solutions. From chemical

1) E. Hayon and J. Weiss, *Proceedings of the International Conference on the Peaceful Uses of Atomic Energy*,, **29**, 80 (1958).
2) N. F. Barr and A. O. Allen, *J. Phys. Chem.*, **63**, 928 (1959).
3) J. Weiss, *Nature*, **186**, 751 (1960).
4) J. Weiss, G. Scholes and J. Holian, ibid., **191**, 1386 (1961).
5) A. O. Allen and E. Hayon, *J. Phys. Chem.*, **65**, 2181 (1961).

and physical investigations[6-17] it has been established that the major part of the reducing species is a hydrated electron, which is referred to as e^-_{aq}. The other reducing species is presumed to be a hydrogen atom. The yields of the two reducing species, $G e^-_{aq}$ and G_H, have been measured using different aqueous systems.[6,8,10] Allan and Beck,[11] using deaerated 2-propanol solutions containing nitrous oxide, found the yields to be 2.80 ± 0.1 and 0.6 ± 0.1. More recently, however, from the radiolysis of aqueous methanol - sodium nitrate solutions, Allan[12] obtained $G e^-_{aq}=2.80\pm0.15$ and $G_{OH}=2.95$, while Adams et al.,[13] calculating the primary radical yields in neutral and alkaline solutions from the results of the pulse radiolysis of ferrocyanide solutions, obtained $G_{OH}=3.2$, $G_{e^-_{aq}}=3.16$, and $G_H=0.6$ to 0.8.

The present investigation was undertaken in order to determine the yields of the two reducing species and of the OH radical under neutral conditions in the gamma radiolysis of deaerated 2-propanol aqueous solutions containing potassium nitrate or hydrogen peroxide.

Experimental

The Preparation of Samples and the Irradiation.—2-Propanol was distilled, and the middle fraction was checked by gas chromatography prior to use. Other reagents of the GR grade were used without further purification. Solutions were prepared using water triply-distilled from acidic permanganate, dichromate and alkaline permanganate. The pH of the solutions was in the range between 5.6 and 5.7. In some experiments the pH of solutions was varied by adding sulfuric acid, sodium bicarbonate or sodium hydroxide. Solutions (20 ml.) degassed by the standard freezing-pumping technique were irradiated by ^{60}Co γ-rays at room temperature. The meansurements were made at least three times. The dose rate mainly employed was 2.42×10^{17} eV./ml.hr. Dosimetry was carried out with a usual ferrous dosimeter.

Analysis.—The hydrogen was analyzed by gas chromatography (Yanagimoto GCG-220) by using a molecular sieve 5A column (2m.) at room temperature and by using argon as the carrier gas. The acetone was determined by the spectrophotometric method[18] (Shimadzu QR-50 and Cary Model 14). The analysis of nitrite ion was made on the basis of the absorption at 525 mμ by using the method of sulfanilic acid and α-naphthylamine.[19] For the 2-propanol - hydrogen peroxide system, hydrogen peroxide was determined by the method developed by Ghormley,[20] while for the potassium nitrate - 2-propanol system the reduction of ceric ion was used for the determination of hydrogen peroxide. Pinacol was identified by a hydrogen-flame ionization detector using glycerol and PEG-6000 columns, and was determined from acetone obtained by the reaction with lead tetraacetate.[21]

Results

Deaerated 2-Propanol Aqueous Solutions Containing Hydrogen Peroxide.—Deaerated aqueous solutions containing various concentrations of hydrogen peroxide were irradiated and the amounts of hydrogen, acetone and hydrogen peroxide produced were determined. As for the organic product, only acetone was determined.

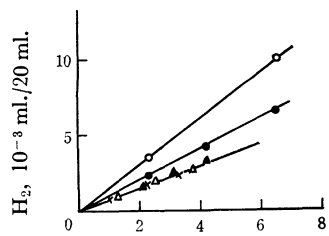

Fig. 1. Yields of H_2 in the radiolysis of deaerated aqueous solutions of 2.5×10^{-2} M 2-propanol containing various concentrations of H_2O_2 at pH 5.6.
$[H_2O_2]$, ○ : 0, ● : 1.0×10^{-4} M,
△ : 5.0×10^{-4} M, ▲ : 1.0×10^{-3} M,
× : 2.4×10^{-3} M

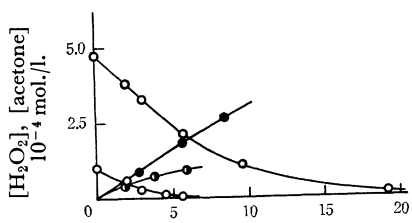

Fig. 2. Yields of acetone and disappearance of H_2O_2 in the radiolysis of deaerated aqueous solutions of 2.5×10^{-2} M 2-propanol containing H_2O_2 at pH 5.6.
○ : H_2O_2,
◑ : Acetone in 1×10^{-4} M H_2O_2 soln.
● : Acetone in 4.8×10^{-4} M H_2O_2 soln.

6) J. T. Allan and G. Scholes, *Nature*, **187**, 218 (1960).
7) E. Collinson, F. S. Dainton, D. R. Smith and S. Tazuké, *Proc. Chem. Soc.*, 140 (1962).
8) G. Czapski and A. O. Allen, *J. Phys. Chem.*, **66**, 262 (1962).
9) J. Rabani, *J. Am. Chem. Soc.*, **84**, 868 (1962).
10) J. Rabani and G. Stein, *J. Chem. Phys.*, **37**, 1865 (1962).
11) J. T. Allan and C. M. Beck, *J. Am. Chem. Soc.*, **86**, 1483 (1964).
12) J. T. Allan, *J. Phys. Chem.*, **68**, 2697 (1964).
13) G. E. Adams, J. W. Boag and B. D. Michael, *Trans. Faraday Soc.*, **61**, 492 (1965).
14) E. Hayon, ibid., **61**, 723 (1965).
15) G. Czapski and H. A. Schwalz, *J. Phys. Chem.*, **66**, 471 (1962).
16) E. J. Hart and J. W. Boag, *J. Am. Chem. Soc.*, **84**, 4090 (1962).
17) J. P. Keene, *Nature*, **197**, 47 (1963).
18) S. Berntsson, *Anal. Chem.*, **28**, 1337 (1956).
19) F. D. Snell and C. T. Snell, "Colorimetric Method of Analysis," Vol. II, D. Van Nostrand Co., New York (1961), p. 802.
20) A. O. Allen, C. J. Hochanadel, J. A. Ghormley and J. W. Paris, *J. Phys. Chem.*, **56**, 575 (1952).
21) E. Bear, J. M. Grosheintz and H. O. L. Fischer, *J. Am. Chem. Soc.*, **61**, 1384 (1939).

The formation of hydrogen is linear with the dose, as is shown in Fig. 1. Figure 2 shows the plots of the production of acetone and the disappearance of hydrogen peroxide versus the dose. They are dependent on the hydrogen peroxide concentration below 1×10^{-4} M. The variations in G-values with hydrogen peroxide concentration are given in Fig. 3. As the hydrogen peroxide

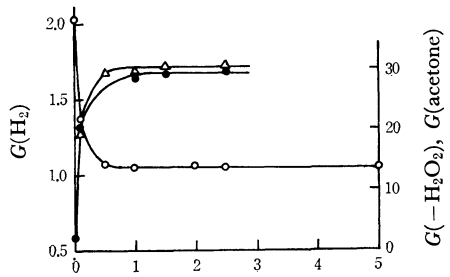

Fig. 3. Effects of H_2O_2 concentration on $G(H_2)$, G(acetone) and $G(-H_2O_2)$ in the radiolysis of deaerated aqueous solutions of 2.5×10^{-2} M 2-propanol at pH 5.6.

○: H_2, ●: acetone, △: $-H_2O_2$

concentration increases, the hydrogen yield decreases and the yields of acetone formation and of the disappearance of hydrogen peroxide increase, while at higher concentrations of hydrogen peroxide, these yields reach constant values. The constant $G(H_2)$ is 1.06 ± 0.02, a value which is in agreement with the results obtained by Allan et al.[6,11] and Stein et al.[10]

Deaerated 2-Propanol Aqueous Solutions Containing Potassium Nitrate.—The deaerated 2-propanol aqueous solutions containing nitrate ions were irradiated under various conditions, and the amounts of hydrogen, nitrite ion, acetone, pinacol and hydrogen peroxide produced were determined.

The formations of the H_2, NO_2^- and $(CH_3)_2CO$ are linear with the dose up to 2.5×10^{17} eV./ml. Above this dose, however, the rate of nitrite ion formation becomes slightly slower. The initial yields were obtained from the slopes of the straight lines.

The effects of potassium nitrate, 2-propanol and pH on the yields of hydrogen, nitrite ion and acetone are shown in Fig. 4 and in Tables I and II.

As the potassium nitrate concentration increases, the hydrogen yield decreases from 2.05 to 0.79 at the nitrate concentration of 6×10^{-2} M, while, on the other hand, the nitrite yield increases from 2.20 to 2.89. The acetone yield increases sharply at first and then decreases slowly. At the constant concentration of nitrate of 1×10^{-2} M, the nitrite yield slightly decreases with an increase in the amount of 2-propanol and reaches a constant value at 2.77 ± 0.03. These yields are independent of

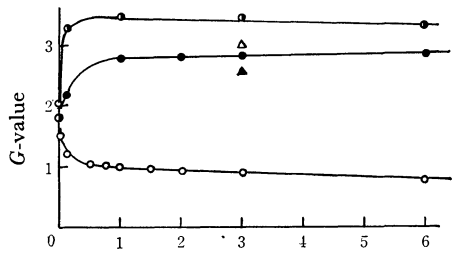

Fig. 4. Effects of KNO_3 concentration on $G(H_2)$, $G(NO_2^-)$ and G(acetone) in the radiolysis of deaerated aqueous solutions of 2×10^{-2} M 2-propanol at pH 5.6.

○: H_2, ●: NO_2^-, ◑: acetone,
▲: NO_2^- in aerated, △: acetone in aerated

Table I. Effects of 2-propanol concentration on $G(NO_2^-)$ in the radiolysis of deaerated solutions of 1×10^{-2} M KNO_3 at pH 5.6

2-Propanol concn., M	$G(NO_2^-)$
2×10^{-2}	2.80 ± 0.02
4×10^{-2}	2.81 ± 0.02
6×10^{-2}	2.77 ± 0.02
10×10^{-2}	2.77 ± 0.03

Table II. Effects of pH on $G(H_2)$, $G(NO_2^-)$ and G(acetone) in the radiolysis of deaerated solutions of 2×10^{-2} M 2-propanol and 1×10^{-2} M KNO_3

pH	$G(H_2)$	$G(NO_2^-)$	G(acetone)
3.0	1.25 ± 0.02	1.39 ± 0.01	4.5 ± 0.2
4.0		2.45 ± 0.02	3.8 ± 0.2
5.0	1.00 ± 0.02	2.77 ± 0.02	3.6 ± 0.2
5.6	1.02 ± 0.02	2.80 ± 0.04	3.5 ± 0.1
6.5—6.7	1.02 ± 0.02	2.80 ± 0.02	3.4 ± 0.1
7.3		2.80 ± 0.02	3.4 ± 0.1
9.5	1.00 ± 0.02	2.79 ± 0.05	3.4 ± 0.1
11	0.99 ± 0.03	3.36 ± 0.08	

pH 3—5, $KNO_3=2\times10^{-2}$ M

the pH from 5.6 to 9.5; at pH 11 the nitrite yield shows a higher value, below pH 5.0 it shows a lower value, and the hydrogen and acetone yields decrease with an increase in the pH. The nitrite yield also decreases in the presence of such other electron scavengers as oxygen and acetone as is shown in Fig. 4 and Table III. The hydrogen peroxide

Table III. Effects of acetone concentration on $G(H_2)$ and $G(NO_2^-)$ in the radiolysis of deaerated solutions of 2×10^{-2} M 2-propanol and 1×10^{-2} M KNO_3 at pH 5.6

$(CH_3)_2CO$, M	$G(H_2)$	$G(NO_2^-)$
0	1.02 ± 0.02	2.80 ± 0.04
2.8×10^{-3}		2.20 ± 0.03
4.3×10^{-3}		2.03 ± 0.05
8.5×10^{-3}	1.00 ± 0.03	1.58 ± 0.01

yield is plotted as a function of the dose in Fig. 5. It is very low in the absence of nitrate ions, but in the presence $G(H_2O_2)=0.5$. Pinacol and acetone are detected in the absence of nitrate ions by means of a hydrogen-flame ionization detector, whereas in solutions containing nitrate ions, pinacol can not be detected. The formation of pinacol is shown in Fig. 6, from which the yield is found to be about 0.2.

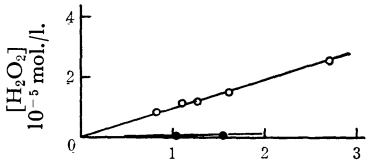

Dose, 10^{18} eV./ml.

Fig. 5. Yields of H_2O_2 in the radiolysis of deaerated aqueous solutions of 2×10^{-2} M 2-propanol at pH 5.6.

●: KNO_3 not added, ○: KNO_3 1×10^{-2} M

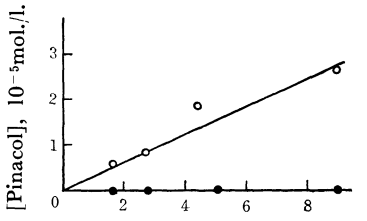

Dose, 10^{18} eV./ml.

Fig. 6. Yields of pinacol in the radiolysis of deaerated aqueous solutions of 2×10^{-2} M 2-propanol at pH 5.6.

○: KNO_3 not added, ●: KNO_3 1×10^{-2} M

Discussion

Deaerated 2-Propanol Aqueous Solutions Containing Hydrogen Peroxide.—The radiolysis of water can be expressed as follows:

$$H_2O \longrightarrow H,\ e^-_{aq},\ OH,\ H_2,\ H_2O_2, \quad (1)$$

In the presence of 2-propanol, H atoms and OH radicals react with the solute, mainly according to 2 and 3:

$$(CH_3)_2CHOH + H \rightarrow (CH_3)_2COH + H_2 \quad (2)$$

$$(CH_3)_2CHOH + OH \rightarrow (CH_3)_2COH + H_2O \quad (3)$$

The rate constant for the reaction of the H atom with 2-propanol is 2×10^7 M^{-1} sec^{-1},[22] and that of OH is 1.74×10^9 M^{-1} sec^{-1}.[23] Acetone is formed by the following reactions:[10,11]

$$(CH_3)_2COH + H_2O_2 \rightarrow (CH_3)_2CO + OH + H_2O \quad (4)$$

$$2(CH_3)_2COH \rightarrow (CH_3)_2CO + (CH_3)_2CHOH \quad (5)$$

Dimerization was also suggested by Stein et al.[10] as the possible disappearance reaction of the organic radical.

It is well known that hydrogen peroxide is a good electron scavenger. In the presence of hydrogen peroxide, it reacts with the hydrated electron in competition with the hydrogen ions:

$$H_2O_2 + e^-_{aq} \rightarrow OH + OH^- \quad (6)$$

$$H^+ + e^-_{aq} \rightarrow H \quad (7)$$

Both reactions, 6 and 7, are very fast; the rate constants of these reactions have been determined by Hart et al.[24] to be 1.2×10^{10} M^{-1} sec^{-1} and 2.3×10^{10} M^{-1} sec^{-1} respectively. On the other hand, hydrogen peroxide reacts with the hydrogen atom and the hydroxyl radical according to:

$$H_2O_2 + H \rightarrow OH + H_2O \quad (8)$$

$$H_2O_2 + OH \rightarrow HO_2 + H_2O \quad (9)$$

Both reactions, however, are relatively slow, and the rate constants, k_8 and k_9, are 4×10^7 [25] and 4.5×10^7 M^{-1} sec^{-1} [26] respectively. Therefore, the reactions 7, 8 and 9 can be ignored in systems which contain 2-propanol of 2.5×10^{-2} M and hydrogen peroxide of the 1×10^{-3} M-5×10^{-3} M range, and the hydrogen yield can be expressed by the following equation:

$$G(H_2) = G_{H_2} + G_H \quad (10)$$

The yield of the hydrogen atom, G_H, in the radiolysis of water can be calculated from the values of the total hydrogen yield, $G(H_2)$, and the molecular yield of hydrogen, G_{H_2}. From the results of Fig. 3, G_H is caluculated to be 0.61 ± 0.02 by using the value of $G_{H_2}=0.45$.[27,28]

The G values of acetone formation and of the disappearance of hydrogen peroxide are higher in the presence of higher concentrations of hydrogen peroxide. It seems that the chain reactions 3 and 4 occur, as suggested by Rabani et al.[10] The decrease in the rates of acetone formation and of hydrogen peroxide disappearance in the dilute solutions of hydrogen peroxide may be due to the competition of the reactions 4 and 5.

Deaerated Aqueous 2-Propanol Solutions Containing Potassium Nitrate.—*Hydrogen Yield.*—It is known that nitrate ion is a good electron scavenger; the rate constant of the scavenging was found by Hart et al.[29] to be 1.1×10^{10} M^{-1} sec^{-1}.

22) $k(H+NO_3^-)=1\times10^7$ M^{-1} sec^{-1} (G. Navon and G. Stein, *J. Phys. Chem.*, **69**, 1384 (1965)), k(H+2-propanol)/k(H+NO_3^-) =2 (Ref. 31).

23) J. K. Thomas, *Trans. Faraday Soc.*, **61**, 702 (1965).

24) S. Gordon, E. J. Hart, M. S. Matheson, J. Rabani and J. K. Thomas, *Discussions Faraday Soc.*, **36**, 193 (1963).

25) J. K. Thomas, *J. Phys. Chem.*, **67**, 2593 (1963).

26) H. A. Schwarz, ibid., **66**, 255 (1962).

27) A. O. Allen, "The Radiation Chemistry of Water and Aqueous Solutions," D. Van Nostrand Co., New York (1961).

28) T. Sawai, Y. Shinozaki and G. Meshitsuka, *Tokyo Metropolitan Isotope Res. Center, Ann. Report*, **3**, 65 (1964).

29) J. K. Thomas, S. Gordon and E. J. Hart, *J. Phys. Chem.*, **68**, 1524 (1964).

The nitrate ion is reduced to the nitrite ion by reaction with the hydrated electron, but the details are not clear:

$$e^-_{aq} + NO_3^- \rightarrow NO_2^- \quad (11)$$

The hydrated electron reacts also with the hydrogen ion to give the H atom (reaction 7). In the presence of higher concentrations of nitrate ions, on the other hand, the reaction of the H atom with NO_3^- should be considered. It has been proposed that the H atom reduces the nitrate ion to the nitrite ion by the reactions 12 and 13:[30]

$$H + NO_3^- \rightarrow NO_2 + OH^- \quad (12)$$

$$2NO_2 + H_2O \rightarrow NO_3^- + NO_2^- + 2H^+ \quad (13)$$

The decrease in $G(H_2)$ with an increase in the nitrate ion concentration (Fig. 4) can be explained by the competition of the reactions 7, 11, 2 and 12.

The hydrogen yield in this system will be given by:

$$G(H_2) = G_{H_2} + \left(G_H + Ge^-_{aq}\frac{k_7[H^+]}{k_7[H^+]+k_{11}[NO_3^-]}\right) \times \frac{k_2[ROH]}{k_2[ROH]+k_{12}[NO_3^-]} \quad (14)$$

In the range of $k_7[H^+] \ll k_{11}[NO_3^-]$,

$$G(H_2) = G_H + \frac{G_H}{1+\dfrac{k_{12}[NO_3^-]}{k_2[ROH]}} \quad (15)$$

According to the Eq. 15, $G(H_2)$ is plotted versus $(G(H_2)-G_{H_2})[NO_3^-]/[ROH]$ in Fig. 7. A straight

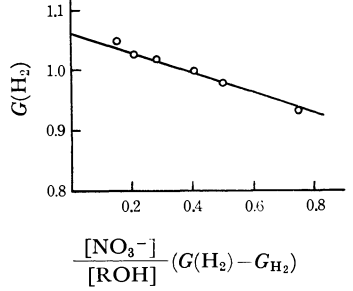

Fig. 7. Dependences of KNO_3 concentration on $G(H_2)$ in the radiolysis of deaerated aqueous solutions of 2×10^{-2} M 2-propanol at pH 5.6.

line is obtained, and from the intercept $G_H + G_H$ is found to be 1.06 ± 0.03, a value in good agreement with the results in the 2-propanol-hydrogen peroxide system. The ratio of the rate constants, k_{12}/k_2, is also calculated from the slope to be 0.18; this value is a little lower than the value, 0.5, given by Scholes et al.[31]

Nitrite Yield.—The radiolysis of aqueous nitrate solutions has been studied, but the reaction mechanisms are not clear.[30,32,33] As for the reaction of the hydrated electron with the nitrate ion, the following reactions, 16 and 17, have been examined:

$$e^-_{aq} + NO_3^- \rightarrow NO_2 + 2OH^- \quad (16)$$

$$e^-_{aq} + NO_3^- \rightarrow NO_2^- + OH + OH^- \quad (17)$$

If the reaction 16 is predominant, $G(NO_2^-)$ has to be approximately equal to 1/2 Ge^-_{aq}. However, the present result shows $G(NO_2^-)=2.8$, which is near the reported values of Ge^-_{aq} instead of half of them. From the studies of the radiolysis of sodium nitrate ice, Kevan[34] has shown that NO_2 is not formed via a reaction with the electron. If a nitrite ion is produced directly by the reaction 17, the increase in $G(H_2)$ and the decrease in $G(NO_2^-)$, with the decrease in pH equal one other. As Table II shows, however, this is not the case.

As possible reactions, the followings were suggested by Allan:[12]

$$e^-_{aq} + NO_3^- \rightarrow NO_3^{2-} \quad (18)$$

$$NO_3^{2-} + (CH_3)_2COH \rightarrow (CH_3)_2CO + NO_2^- + OH^- \quad (19)$$

The NO_3^{2-} radical ion has been tentatively identified by electron paramagnetic resonance studies of the radical species produced in the irradiated potassium nitrate crystal.[35]

In neutral solutions containing high concentrations of 2-propanol and nitrate ions, all hydrated electrons are scavenged by nitrate ions and the reaction 12 can be ignored; $G(NO_2^-)$ is equal to Ge^-_{aq}, on the basis of the reactions 18 and 19. From the results noted in Table I, the value of the hydrated electron yield is given as $Ge^-_{aq}=2.77\pm0.03$, which is in good agreement with the finding of Allan et al.[11,12] $G(NO_2^-)$ does not change with the pH value from 5.0 to 9.5; therefore, Ge^-_{aq} is constant in this pH range. The changes in $G(NO_2^-)$ with the variation in the nitrate ion concentration is about half that of $G(H_2)$, as is shown in Table IV. The nitrite ion formation by the

Table IV. Effects of KNO_3 concentration on $\Delta G(NO_2^-)$ and $-\Delta G(H_2)$ in the radiolysis of deaerated solutions of 2×10^{-2} M 2-propanol at pH 5.6

KNO_3 concn., M	$\Delta G(NO_2^-)$	$-\Delta G(H_2)$
1.0×10^{-2}	0	0
1.5×10^{-2}		0.02
2.0×10^{-2}	0.03	0.07
3.0×10^{-2}	0.05	0.10
6.0×10^{-2}	0.09	0.23

30) J. Bednar, "Proc. Titany Symposium Rad. Res. Chem.," Akademiai Kiado, Budapest (1964), p. 325.
31) A. Appleby, G. Scholes and M. Simic, *J. Am. Chem. Soc.*, **85**, 2891 (1963); G. Scholes and M. Simic, *J. Phys. Chem.*, **68**, 1738 (1964).
32) H. A. Mahlman and J. W. Boyle, *J. Chem. Phys.*, **27**, 1434 (1957).
33) H. A. Mahlman, ibid., **32**, 601 (1960).
34) L. Kevan, *J. Phys. Chem.*, **68**, 2590 (1964).
35) J. Cunningham, ibid., **66**, 972 (1962).

reaction of the H atom with nitrate may arise via the reactions 12 and 13.

In the presence of acetone, $G(NO_2^-)$ decreases by the following competitive reactions:

$$e^-_{aq} + NO_3^- \rightarrow NO_3^{2-} \quad (18)$$

$$e^-_{aq} + (CH_3)_2CO \rightarrow (CH_3)_2CO^- \quad (20)$$

In terms of the reaction kinetics, the yield of nitrite is written as follows:

$$G(NO_2^-) = Ge^-_{aq}\frac{k_{18}[NO_3^-]}{k_{18}[NO_3^-]+k_{20}[R_2CO]} + 1/2\,G_H\frac{k_{12}[NO_3^-]}{k_{12}[NO_3^-]+k_2[ROH]} \quad (21)$$

By introducing the numerical values of $G_H=0.6$, $k_{12}/k_2=0.18$, $[NO_3^-]=1.0\times10^{-2}$ M, and $[ROH]=2.0\times10^{-2}$ M, one can obtain the following relation:

$$\frac{1}{G(NO_2^-)-0.02} = \frac{1}{Ge^-_{aq}}1+\left(\frac{k_{20}[R_2CO]}{k_{18}[NO_3^-]}\right) \quad (22)$$

In Fig. 8, $1/G(NO_2^-)-0.02$ is plotted as a function of $[R_2CO]$, and $G(NO_2^-)$ and k_{20}/k_{18} are found from the intercept and the slope of the straight line to be 2.8 and 0.78 respectively. The ratio of the rate constants, k_{20}/k_{18}, is in agreement with the results obtained using the pulse radiolysis technique.[36,37]

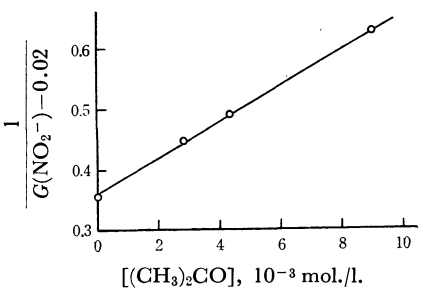

Fig. 8. Variations of $G(NO_2^-)$ with $(CH_3)_2CO$ concentration in the radiolysis of deaerated aqueous solutions of 2×10^{-2} M 2-propanol, 1×10^{-2} M KNO_3.

Acetone Yield.—In the potassium nitrate 1×10^{-2} M-2-propanol 2×10^{-2} M system, all the H atom and OH radicals react with 2-propanol to give organic radicals, and all the hydrated electrons are scavenged by nitrate ions. The yield of hydrogen peroxide is slightly lower than that of the molecular hydrogen peroxide in water radiolysis (Fig. 5); the results of Fig. 6 indicate that the dimerization of organic radicals can be neglected.

The mechanisms of the acetone formation can be written as follows:

$$(CH_3)_2COH + NO_3^{2-} \rightarrow (CH_3)_2CO + NO_2^- + OH^- \quad (19)$$

$$(CH_3)_2COH + H_2O_2 \rightarrow (CH_3)_2CO + OH + H_2O \quad (4)$$

$$2(CH_3)_2COH \rightarrow (CH_3)_2CO + (CH_3)_2CHOH \quad (5)$$

On the basis of the reactions, 2, 3, 4, 5 and 19, G(acetone) is given by:

$$\begin{aligned} G(\text{acetone}) &= G(NO_2^-)+G_{H_2O_2}-G(H_2O_2)+ \\ &\quad 1/2[G_H+G_{OH}+G_{H_2O_2}-(G(NO_2^-)+ \\ &\quad G_{H_2O_2}-G(H_2O_2))] \\ &= 1/2[G(NO_2^-)+G_H+G_{OH}] \\ &\quad +G_{H_2O_2}-G(H_2O_2) \end{aligned} \quad (23)$$

By using the numerical values of $G_{H_2O_2}-G(H_2O_2)=0.2$, $G(NO_2^-)=2.8$, $G_H=0.6$ and G(acetone)$=3.4$, G_{OH} can be calculated from Eq. 23 to be 3.0.

Radical Yields.—From the radiolysis of the deaerated neutral solutions of 2-propanol containing hydrogen peroxide or potassium nitrate, the primary radical yields have been obtained:

$$G_{OH}=3.0,\ Ge^-_{aq}=2.77\pm0.03,$$
$$G_H=0.61\pm0.03$$

These values are relatively high. Recently Hayon[14] obtained $G_{OH}=2.25$, $Ge^-_{aq}=2.3$ and $G_H=0.55$ from the radiolysis of dilute solutions containing various solutes, and suggested that the radical scavenger concentration was important in the measurement of the radical yields. Since relatively higher concentrations of scavengers were used in the present experiments, the higher values obtained may be due to reactions similar to those postulated by Dainton et al.[38] to account for the increase in radical yields at high and low pH values:

$$(H_2O^+ + H_2O^-) + NO_3^- \rightarrow NO_3^{2-} + OH + H^+ + H_2O \quad (24)$$

The author is indebted to Dr. Gisuke Meshitsuka and Dr. Yoshiharu Shinozaki for many helpful discussions.

36) E. J. Hart, S. Gordon and J. K. Thomas, ibid., **68**, 1271 (1964).

37) J. H. Baxendale, E. M. Fielden, C. Capellos, J. M. Francis, J. V. Davies, M. Ebert, C. W. Gilbert, J. P. Keene, E. J. Land, A. J. Swallow and J. M. Nosworthy, *Nature*, **201**, 468 (1964).

38) F. S. Dainton and W. S. Watt, ibid., **195**, 1294 (1962).

BULLETIN OF THE CHEMICAL SOCIETY OF JAPAN VOL. 39 961—967 (1966)

Organic Sulfur Compounds. II. The Formation and Thermal Decomposition of Carboxylic Sulfurous Anhydrides

By Michio KOBAYASHI and Asami YAMAMOTO

Department of Chemistry, Yokohama City University, Mutsuura-machi, Kanazawa-ku, Yokohama

(Received November 1, 1965)

Mixed anhydrides of carboxylic acids and monoalkyl sulfites have been prepared, and their thermal decomposition has been studied. Some of these mixed anhydrides can be distilled without decomposition. Disproportionation to carboxylic anhydride and dialkyl sulfite is the main pathway of the thermal decomposition.

A mixed anhydride of carboxylic acid and sulfurous acid (I) has been postulated as an intermediate in the reaction of carboxylic acid salts and chlorosulfites to form the carboxylic esters,[1-3] but it has not been isolated or identified. The formation of the carboxylic esters by the above method has been thought to proceed by the following reaction sequence:

$$RCO_2Na + ClSOOR' \rightarrow R\text{-}\underset{\underset{O}{\|}}{C}\text{-}O\text{-}\underset{\underset{O}{\downarrow}}{S}\text{-}OR' + NaCl \quad (1)$$

(I)

$$I \rightarrow RCO_2R' + SO_2 \quad (2)$$

In the analogous decomposition of carboxylic carbonic anhydride (II),[4] the disproportionation reaction 4 takes place along with the reaction 3, which has a formal similarity to the reaction 2:

$$R\text{-}\underset{\underset{O}{\|}}{C}\text{-}O\text{-}\underset{\underset{O}{\|}}{C}\text{-}OR' \rightarrow RCO_2R' + CO_2 \quad (3)$$

(II)

$$II \rightarrow {}^1/_2(RCO)_2O + {}^1/_2(R'O)_2CO + {}^1/_2CO_2 \quad (4)$$

On the other hand, the nitric ester formation is the sole decomposition mode in the pyrolysis of the nitric carbonic anhydride (alkyl nitratocarbonate) (III):[5]

$$R'O\text{-}\underset{\underset{O}{\|}}{C}\text{-}ONO_2 \rightarrow R'ONO_2 + CO_2$$

(III)

In the present paper, the preparation of several compounds of this little known class of carboxylic sulfurous anhydride and studies of their reactions, including thermal decomposition, will be described.

Results and Discussion

Methyl chlorosulfite was found to react with the anhydrous sodium acetate to give methyl acetoxysulfinate (Ia) (I: $R=R'=CH_3$) as a colorless mobile liquid which can be distilled without decomposition in vacuo. This anhydride is extremely sensitive to moisture, by which it is decomposed to acetic acid and sulfur dioxide. The determination of sulfur by oxidation with hydrogen peroxide as barium sulfate indicated the presence of approximately the calculated amount of sulfur atoms in this compound. Its infrared spectrum exhibited a strong carbonyl band at 1757 cm^{-1} which disappeared in contact with moisture, to be replaced by the absorption of acetic acid at 1712 cm^{-1}.

In a similar manner, ethyl acetoxysulfinate (Ib) (I: $R=CH_3$, $R'=C_2H_5$) was prepared from ethyl chlorosulfite and sodium acetate. The observed value of the sulfur content was close to the calculated figure. The high sensitivity of these anhydrides to moisture made the analysis very difficult. In the infrared spectrum, a strong carbonyl band at 1752 cm^{-1} and a S–O stretching band at 1190 cm^{-1} were observed.

Both the methyl ester and the ethyl ester were rather more stable than expected; they could be stored in a refrigerator for several days without any appreciable decomposition, provided strict caution was taken to avoid moisture.

The carbon tetrachloride solution of Ib was also stable; no change of its infrared spectrum was observed after one day. When refluxed for several hours, this solution produced acetic anhydride and ethyl sulfite, while it produced ethyl acetate on prolonged boiling. There was estimated to be a 40% decomposition in 3 hr. and a 55% decomposition in 6 hr.

When triethylamine was added to a solution of

1) P. Carré and D. Liberman, *Bull. soc. chim. France*, [4] **53**, 1050 (1933).
2) M. S. Newman and W. S. Fones, *J. Am. Chem. Soc.*, **69**, 1046 (1946).
3) M. S. Newman and C. Courduvelis, *J. Am. Chem. Soc.*, **86**, 2942 (1964).
4) a) T. B. Windholz, *J. Org. Chem.*, **23**, 2044 (1958); **25**, 1703 (1960); b) D. S. Tarbell and F. J. Longosz, ibid., **24**, 774 (1959); c) F. J. Longosz and D. S. Tarbell, ibid., **26**, 2161 (1961); d) C. J. Michejda, D. S. Tarbell and W. H. Saunders, Jr., *J. Am. Chem. Soc.*, **84**, 4113 (1962); d) C. J. Michejda and D. S. Tarbell, *J. Org. Chem.*, **29**, 1168 (1964).
5) R. Boschan, *J. Am. Chem. Soc.*, **81**, 3341 (1959); G. A. Mortimer, *J. Org. Chem.*, **27**, 1876 (1962); D. N. Kevill and G. H. Johnson, *J. Am. Chem. Soc.*, **87**, 928 (1965).

benzoic acid and ethyl chlorosulfite in carbon tetrachloride, an exothermic reaction took place, with the precipitation of triethylamine hydrochloride. The filtered solution showed strong infrared absorptions at 1724 cm^{-1} (C=O) and at 1222 cm^{-1} (S–O) (Fig. 1). The concentration of this solution under reduced pressure gave a pale sirup. The infrared spectrum of this liquid was the same as that of the carbon tetrachloride solution, suggesting the formation of ethyl benzoyloxysulfinate (Ic) (I: $R=C_6H_5$, $R'=C_2H_5$). This compound was also very sensitive to moisture, which caused its decomposition to benzoic acid.

The reaction mixture of sodium benzoate and ethyl chlorosulfite was extracted with carbon tetetrachloride after the initial vigorous reaction had finished, and the insoluble powder was then filtered off. The infrared spectrum of the filtrate was superimposable upon that of the specimen obtained by the triethylamine method, showing the formation of Ic in this reaction, too. This fact seems to justify the postulation in the literature[2] which assumed the formation of I in the reaction 1.

The carbon tetrachloride solution of Ic was stable; 61% of it remained unchanged after 18 days. When this solution was heated under reflux in the presence of benzoic acid, a 42% decomposition in 6 hr. and a nearly complete decomposition in 14 hr. were observed. The products were benzoic anhydride and ethyl sulfite, both in yields 98% of the theoretical, and 2 mol. % of ethyl benzoate. Ether or benzene can be used as the solvent instead of carbon tetrachloride in the preparation of the mixed anhydride Ic.

n-Butyl benzoyloxysulfinate (Id) (I: $R=C_6H_5$, $R'=n\text{-}C_4H_9$) was obtained as a solution from sodium benzoate and *n*-butyl chlorosulfite by a manner similar to that which produces Ic. In its infrared spectrum (Fig. 2), strong C=O and S–O absorption bands appear. This anhydride gave ethyl *n*-butyl sulfite in a 54% yield when treated with anhydrous ethanol at room temperature, but no ethyl benzoate. This seems to indicate the preferable attack on sulfinyl sulfur by the anionoid reagent (reaction 5) rather than to the carbonyl group (reaction 6).

$$C_6H_5\text{–}\underset{\underset{O}{\|}}{C}\text{–O–S–}OC_4H_9 + C_2H_5OH \rightarrow$$

(Id)

$$C_6H_5CO_2H + C_2H_5O\text{–}\underset{\underset{O}{\downarrow}}{S}\text{–}OC_4H_9 \qquad (5)$$

$$Id + C_2H_5OH \rightarrow C_6H_5CO_2C_2H_5 + SO_2 + C_2H_5OH \qquad (6)$$

When a solution of Id in carbon tetrachloride was refluxed, a slow decomposition took place with the evolution of sulfur dioxide. This reaction was accelerated in the presence of triethylamine, resulting in a complete decomposition within a few hours. The products were benzoic anhydride and di-*n*-butyl sulfite, both in yields 98% of the theoretical; there was only a 2% yield of *n*-butyl benzoate.

So far, no carboxylic sulfurous anhydride has been obtained in the pure crystalline state. In an attempt to get one, we attempted to prepare *p*-nitrobenzoyloxysulfinate (Ie) (I: R = *p*-nitrophenyl, $R'=C_2H_5$) repeatedly. The reaction of *p*-nitrobenzoic acid, ethyl chlorosulfite, and pyridine in ether, and the reaction of sodium *p*-nitrobenzoate with ethyl chlorosulfite, were examined. Both gave a solution whose infrared evidence strongly suggested the presence of the expected mixed anhydride (Fig. 3). However, the separated crystals, after the evaporation of the solvent in a vacuum at room temperature, exhibited almost the same infrared spectrum as that of *p*-nitrobenzoic acid in a KBr disk, although the melting point of the product was 85—90°C (with decomposition), far below the 242°C of *p*-nitrobenzoic acid. Probably this compound was so sensitive to the presence of moisture that a complete hydrolysis by atmospheric moisture took place during the preparation of the KBr disk. When these crystals were shaken with carbon tetrachloride and the insoluble powder (*p*-nitrobenzoic acid) was filtered off, the infrared spectrum of the filtrate was superimposable upon Fig. 3, indicating the presence of Ie in this specimen.

Although the formation of the carboxylic ester over the postulated mixed anhydride I in a good yield has been reported in the literature,[1,2] most of the thermal decomposition of the carboxylic sulfurous anhydrides studied in this paper in carbon tetrachloride proceeded according to the disproportionation reaction 7, analogous to the reaction 4 observed in the carboxylic carbonic anhydride (II):

$$R\text{–}\underset{\underset{O}{\|}}{C}\text{–O–S–OR}' \rightarrow$$

(I)

$$^1/_2(RCO)_2O + {}^1/_2(R'O)_2SO + {}^1/_2SO_2 \qquad (7)$$

The pyrolysis of I without a solvent was also investigated. When the reaction of sodium benzoate and ethyl chlorosulfite was carried out without the solvent and when the resulting mixture was distilled under reduced pressure, the main products were again benzoic anhydride (50% of the theoretical yield) and ethyl sulfite (42% of the theoretical), while the yield of ethyl benzoate was only 5%. The pyrolysis of the reaction mixture of sodium benzoate and *n*-butyl chlorosulfite at 140—160°C gave benzoic anhydride and di-*n*-butyl sulfite as the main products, plus *n*-butyl benzoate in a 5% yield. With a 2 molar equivalent of butyl chlorosulfite, the yield of butyl benzoate was 10%, in comparison to yield of 43% for benzoic anhydride

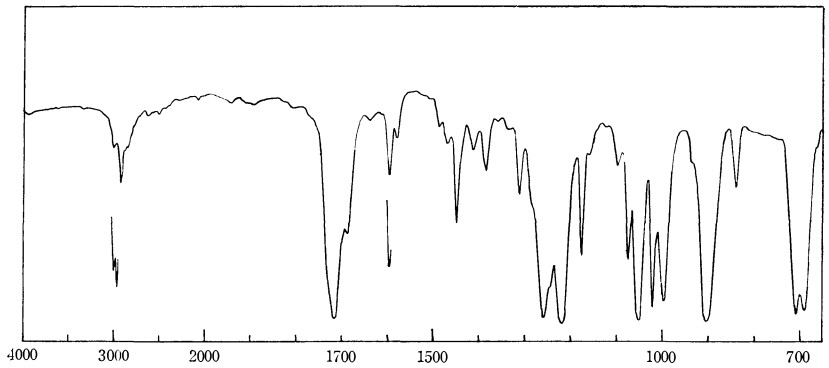

Fig. 1. Infrared spectrum of ethyl benzoyloxysulfinate (Ic) in CCl_4.

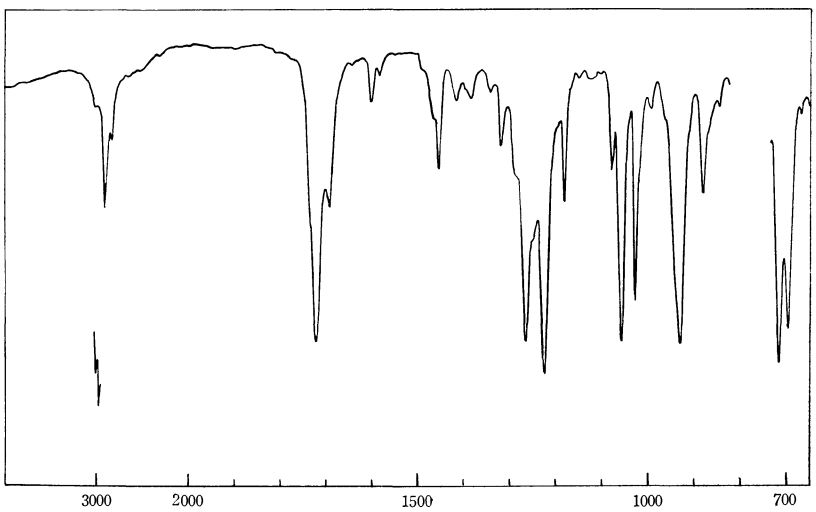

Fig. 2. Infrared spectrum of *n*-butyl benzoyloxysulfinate in CCl_4.

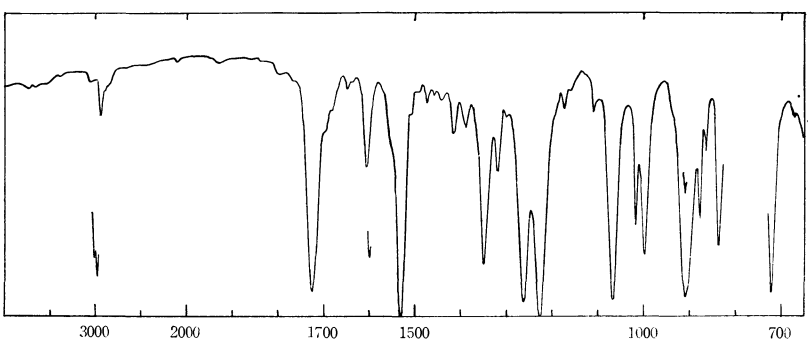

Fig. 3. Infrared spectrum of ethyl *p*-nitrobenzoyloxysulfinate (Ie) in CCl_4.

and 56% for di-*n*-butyl sulfite. When the reaction mixture of sodium *p*-nitrobenzoate and ethyl chlorosulfite was heated at 125°C for one hour and treated with water and ether, an insoluble powder remained in either solvent; it was identified as *p*-nitrobenzoic anhydride. The yield was 17% of the theoretical. No ethyl nitrobenzoate was detected.

In conclusion, the thermal decomposition of the carboxylic sulfurous anhydride at a comparatively low temperature results in the disproportionation 7 as the main reaction. With elevation of the reaction temperature, the yield of the carboxylic ester shows a tendency to increase, but it is rather doubtful whether this ester is the direct result of the reaction 2. There is a good chance that this

carboxylic ester is formed by the interaction of carboxylic anhydride with dialkyl sulfite, both being the main products of the primary reaction 7. Several examples of this type of the reaction 8 have been reported[6]:

$$(RCO)_2O + (R'O)_2SO \rightarrow 2RCO_2R' + SO_2 \quad (8)$$

In the case of Ib in carbon tetrachloride, ethyl acetate appeared only in the later stage of the reaction, in cost of acetic anhydride, clearly indicating the occurrence of the reaction expressed by the formula 8.

Mixed anhydride I could be formed from acyl chloride and sodium monoalkyl sulfite, besides the reaction 1. For example, Ic may be prepared by the interaction of benzoyl chloride and sodium ethyl sulfite (IV), as shown below:

$$C_6H_5COCl + NaO\text{-}\underset{\underset{O}{\downarrow}}{S}\text{-}OC_2H_5 \rightarrow Ic + NaCl \quad (9)$$

(IV)

When IV, prepared from sodium ethylate and sulfur dioxide, was treated with benzoyl chloride without the solvent, the reaction proceeded very slowly at room temperature. At a higher temperature, benzoic anhydride in a 53% yield, ethyl sulfite in a 50% yield and ethyl benzoate in a 10% yield were obtained, suggesting the expected formation of the intermediate Ic according to the reaction 9. When both reactants were left in carbon tetrachloride at room temperature for 3 days, 80% of the starting materials remained unchanged. Benzoic anhydride was formed in an amount 20% of the theoretical yield, while no indication of Ic itself was observed, even in the infrared spectrum. Only a slight amount of ethyl benzoate was there at first, but about 12 mol. % of it was detected when the filtrate from the unchanged IV was kept at room temperature for one week. Most probably it arises from the interaction of benzoyl chloride and ethyl sulfite, one of the primary products. This type of the reaction, 10, has also been known to occur with some acyl chlorides[6]:

$$2RCOCl + (R'O)_2SO \rightarrow 2RCO_2R' + SO_2 \quad (10)$$

The failure to detect the intermediate Ic may be attributable to the slowness of the reaction 9, during which the disproportionation 7 of the once-formed Ic proceeds (probably by a catalytic acceleration of IV itself as a base).

The disproportionation (7) may be concluded to be a base catalytic from the effect of triethylamine to accelerate the decomposition of Id, as has been described above, and also on the basis of the following evidence. Ethyl chlorosulfite was added to a solution of benzoic acid in pyridine, and the reaction mixture was warmed at 70°C for half an hour, diluted with water, and extracted with ether to give benzoic anhydride in a 55% yield, ethyl sulfite in a 27% yield, and a trace of ethyl benzoate. This experiment showed that Ic was decomposed even under these mild conditions, while refluxing for more than 10 hr. was necessary to complete the decomposition of Ic in carbon tetrachloride in the absence of a base. The above experiment also suggests that the rate of the reaction between the carboxylate anion and alkyl chlorosulfite is very fast, since the chlorosulfites are known to be decomposed by pyridine to form alkyl chlorides and sulfur dioxide with great ease.[7]

On the other hand, the decomposition of Ic in the presence of benzoic acid in carbon tetrachloride caused the disproportionation 7, although at a much slower rate than the base-catalytic one.

The following mechanism may be proposed for the disproportionation 7, where B means base catalyst:

$$R\text{-}\underset{\underset{O}{\|}}{C}\text{-}O\text{-}\underset{\underset{O}{\downarrow}}{S}\text{-}OR' + :B \longrightarrow$$

I

$$RCO_2^- + \left[B\text{----}\underset{\underset{O}{\|}}{S}\text{-}OR'\right]^+ \quad (11)$$

$$I + RCO_2^- \longrightarrow (RCO)_2O + \left[RO'\text{-}S\overset{O}{\diagdown\!\diagup}O\right] \quad (12)$$

$$[R'O\text{-}SO_2^-] \longrightarrow R'O^- + SO_2 \quad (13)$$

$$R'O^- + I \longrightarrow (R'O)_2SO + RCO_2^- \quad (14)$$

The anionoid attack on I occurred on the sulfinyl sulfur preferentially, not on carbonyl, as shown in the reaction of Id with ethanol. The attraction of an anionoid reagent to the positive center on sulfur atom, the linkage of which to the sulfinyl oxygen bears a strong semipolar character,[8] may be the reason for this difference in reactivity. The attack by the carboxylate anion on I also could take place on the sulfur atom, but it would form another I (15), with the net result of no apparent reaction:

$$I + RCO_2^- \longrightarrow RCO_2^- + I \quad (15)$$

Therefore, the only fruitful attack is the one expressed in 12, giving acyl anhydride.

Decomposition in the presence of the carboxylic acid was considered to proceed as is shown below:

$$I + RCO_2H \longrightarrow \left[R\text{-}\underset{\underset{O}{\|}}{C}\text{-}O\text{-}\underset{\underset{O}{\|}}{S}\text{-}OR'\right]^+ + RCO_2^- \quad (16)$$

6) R. Levaillant, *Compt. rend.*, **190**, 55 (1930).

7) J. Kenyon, H. Phillips and F. M. H. Taylor, *J. Chem. Soc.*, **1931**, 382; C. E. Boozer and E. S. Lewis, *J. Am. Chem. Soc.*, **75**, 3182 (1953).

8) C. C. Price and S. Oae, "Sulfur Bonding," Ronald Press Co., N. Y. (1962).

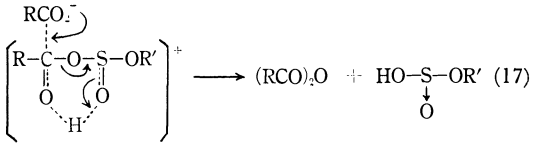

$$HO\text{-}S\text{-}OR' \longrightarrow SO_2 + R'OH \qquad (18)$$

$$I + R'OH \longrightarrow RCO_2H + (R'O)_2SO \qquad (19)$$

Infrared Spectra of the Carboxylic Sulfurous Anhydride.—The wave numbers of the C=O and S-O stretching bands of several derivatives of I are shown in Table I.

Table I

R	R'	Peak position[a] C=O, cm^{-1}	S-O, cm^{-1}
Methyl	Methyl	1757	1196
Methyl	Ethyl	1752	1190
Phenyl	Ethyl	1724	1222
Phenyl	*n*-Butyl	1723	1223
Phenyl	Phenyl[b]	1729	1230
p-Nitrophenyl	Ethyl	1730	1227

a) In CCl_4.
b) In ether. This compound will be described in detail later.

The wave numbers of the C=O absorptions of these compounds are close to those of the carboxylic carbonic anhydrides (for example, 1755 cm^{-1} for II: R=methyl, R'=ethyl; 1739 cm^{-1} for II: R=phenyl, R'=ethyl,[9] and they lie in a lower frequency region than that of the carboxylic sulfonic anhydride V[10] (1780 cm^{-1} for V: R=phenyl, R'=phenyl; 1800 cm^{-1} for V: R=ethyl, R'=phenyl).

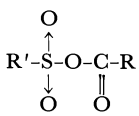

(V)

Experimental

1. Methyl Acetoxysulfinate (Ia).—When, to 4.5 g. of a fine powder of sodium acetate (VI) which had been dehydrated at 200°C in vacuum for a few hours, there was added 6.5 g. of methyl chlorosulfite drop by drop, with constant shaking and good cooling, the reaction started at once, and heat was evolved. After 5 hr. at room temperature, the jelly-like reaction mixture was distilled in vacuo to give 4.5 g. of a colorless, mobile liquid at 37—39°C/1 mmHg in a 60% yield of the theoretical; infrared spectrum, 1752 (C=O), 1210 (S-O), 940, and 690 cm^{-1} (neat). This compound reacted with water very rapidly. In a small vial with a ground glass stopper there was weighed 365.0 mg. of this ample, which had been stored for 2 weeks in a refrigerator; the sample was then hydrolyzed with a solution of 2 g. of sodium hydroxide in 20 ml. of water in a closed vessel. The oil dissolved in less than one minute, thus forming a clear solution, which was then oxidized with 6 ml. of 30% hydrogen peroxide for 2 hr. Diluted hydrochloric acid was added to this solution, and the sulfate anion was precipitated as barium sulfate (551.9 mg.).

S: Found: 20.8%. Calcd. for $C_3H_6O_4S$: 23.3%.

2. Ethyl Acetoxysulfinate (Ib). — *2.1. Reaction without a Solvent.* — From 12.5 g. of ethyl chlorosulfite (VII) and 8.0 g. of VI, 8.3 g. of Ib was obtained as a colorless liquid (b. p. 44°C/1 mmHg) by a manner similar to that used for Ia. The yield was 56% of the theoretical. This sample (169.7 mg.) gave 249.5 mg. of barium sulfate.

S: Found: 20.2%. Calcd. for $C_4H_8O_4S$: 21.1%.

2.2. Reaction in Carbon Tetrachloride.—A solution of 3.0 g. of VII in 50 ml. of carbon tetrachloride was added to 2.2 g. of VI, shaken well for 30 min., and filtered through a fritted glass funnel. The infrared spectrum of the filtrate was almost entirely superimposable upon that of the specimen obtained in 2.1. IR: 1752, 1190, 1000, 898, 700 cm^{-1}. After one day, no change was observed in the infrared spectrum.

2.3. The Decomposition of Ib.—A carbon tetrachloride solution of Ib (4.7×10^{-1} mol./l.) was refluxed to produce acetic anhydride in a 40% yield in 3 hrs, and in a 55.5% yield in 6 hr. When it was boiled for another 6 hr., the concentration of acetic anhydride was decreased to 11% and replaced by ethyl acetate in a 27.5% yield. (The determinations were made by the infrared spectroscopic method.)

3. Ethyl Benzoyloxysulfinate (Ic).—*3.1. Preparation.*—Benzoic acid (6.9 g.) and VII (7.3 g.) were dissolved in 180 ml. of carbon tetrachloride; no change was observed. When 6.8 g. of triethylamine was added drop by drop to this solution cooled in an ice bath, a vigorous reaction occurred, with the precipitation of white crystals; these crystals were identified as triethylamine hydrochloride. The infrared spectrum of the filtrate is shown in Fig. 1. When this filtrate was evaporated under reduced pressure at room temperature, with precaution taken to avoid moisture, it gave a pale sirup which solidified to a glassy mass at −70°C. When it came in contact with moisture, this sirup formed crystals of benzoic acid rapidly. After a carbon tetrachloride solution of Ic (3.14×10^{-1} mol./l. as 100% pure) had been refluxed for 6 hr., an aliquot of it was washed with a diluted potassium carbonate solution and water successively, and then dried over magnesium sulfate. By its infrared spectrum the presence of 5.73 $\times10^{-2}$ mol./l. of benzoic anhydride and 5.72×10^{-2} mol./l. of ethyl sulfite was detected. At this stage of the reaction, the yield of two products was 34% of the theoretical and in an equimolecular ratio. The main portion of the solution of Ic was refluxed for another few hours and finally evaporated to expel the solvent, after which the residue was heated in an oil bath for one hour to complete the decomposition. After it had been diluted with carbon tetrachloride, this residue was analyzed by infrared spectroscopy and so found to contain benzoic anhydride and ethyl sulfite in a 1.15 : 1.00 molar ratio. A few grams of aniline were added to this solution to remove benzoic anhydride as almost insoluble

9) D. S. Tarbell and N. A. Leister, *J. Org. Chem.*, **23**, 1149 (1958); 4b.
10) C. Overberger and E. Sarlo, *J. Am. Chem. Soc.*, **85**, 2446 (1963).

benzanilide (identified by melting point and infrared spectrum); The filtrate was then washed repeatedly with a potassium carbonate solution and dried over magnesium sulfate. The infrared spectrum of this solution revealed the presence of a small amount of ethyl benzoate, which was masked by benzoic anhydride before the treatment with aniline. The yields of benzoic anhydride, ethyl sulfite and ethyl benzoate were 94%, 82%, and 6% of the theoretical yield respectively.

3.2. The Decomposition of Ic in the Presence of Acid. When a solution of Ic (1.90×10^{-1} mol./l.) and benzoic acid (8.45×10^{-2} mol./l.) in carbon tetrachloride was refluxed, the yield of benzoic anhydride was 42% of the theoretical in 3 hr, and 98% in 14 hr. The corresponding yield of ethyl sulfite was also 98% in 14 hr. By treatment with aniline as described in 3.1, the yield of ethyl benzoate was estimated to be 2.4%. Therefore, 98% of the decomposition of Ic in this condition was shown to proceed according to the reaction 7, leaving only 2% at most for the reaction 2. The slightly higher yield of ethyl benzoate in 3.1 may be attributable to the high reaction temperature in the last stage of the reaction without the solvent, during which stage some of benzoic anhydride may react with ethyl sulfite to give ethyl benzoate following the reaction 8.

3.3. Formation from Sodium Benzoate.—Two grams of sodium benzoate and 1.7 g. of VII were mixed and extracted with 100 ml. of carbon tetrachloride after the initial exothermic reaction was over. The infrared spectrum of this extract was almost identical with that shown in Fig. 1, indicating the formation of the same mixed anhydride Ic. After 18 days, this solution was found by infrared analysis still to contain 61% of original Ic.

3.4. Decomposition without a Solvent.—Nine grams of VII was added to 10.0 g. of sodium benzoate, and the resultant gel-like mixture was distilled under reduced pressure. The redistillation of the total distillate gave the forerun, consisting of 2.0 g. of ethyl sulfite (42% of the theoretical yield), 0.5 g. of ethyl benzoate (4.8 mol.%), and 4.0 g. of benzoic anhydride (51% of the theoretical yield), b. p. 170—171°C/5 mmHg.

3.5. Reaction with Ethanol.—To a reaction mixture of 5.5 g. of sodium benzoate and 5.0 g. of VII 5 ml of ethanol (absolute) was added, after the initial vigorous reaction had subsided. The work-up of this mixture gave 2.0 g. of ethyl sulfite (38%), with no ethyl benzoate. The amount of benzoic acid recovered was 4.0 g. (82%). Therefore, ethanol attacked Ic on the sulfur atom, not on carbonyl.

3.6. The Reaction in Pyridine.—Benzoic acid (6.5 g.) was dissolved in 20 ml. of dry pyridine and cooled in an ice bath. When 7.0 g. of VII was added to this solution, no gas evolved and no precipitate appeared. After it had been heated in an oil bath for 30 min. at 70°C, the solution was diluted with a lot of water, made acidic with hydrochloric acid, and extracted with ether. The usual work-up gave 0.7 mol. % of ethyl benzoate, ethyl sulfite in 27.2% of the theoretical yield, and benzoic anhydride in a yield 55% of the theoretical.

4. *n*-Butyl Benzoyloxysulfinate.—*4.1. Preparation in Carbon Tetrachloride.*—When 2.5 g. of triethylamine was added to a solution of 2.8 g. of benzoic acid and 3.5 g. of *n*-butyl chlorosulfite (VIII) (b. p. 70°C/13 mmHg) in 62 ml. of carbon tetrachloride, triethylamine hydrochloride was precipitated at once. The infrared spectrum of the filtrate is shown in Fig. 2; it has a close similarity to that of the ethyl analog. (i) Anhydrous ethanol (5 ml.) was added to 10 ml. of this solution, and the mixture was warmed, washed with water and aqueous sodium hydrogen carbonate successively, and dried over magnesium sulfate. The infrared spectrum of the filtrate coincided with that of ethyl *n*-butyl sulfite. The yield was estimated by infrared analysis to be 54% of the theoretical. No ethyl benzoate was detected. (ii) Triethylamine (0.5 g.) was added to the remaining solution of the mixed anhydride Id; this mixture was then refluxed for a few hours, during which the evolution of sulfur dioxide was completed. The formation of benzoic anhydride and di-*n*-butyl sulfite, each in a 98% yield of the theoretical, was confirmed by the infrared spectroscopy. After treatment with aniline, *n*-butyl benzoate in a 2.1% yield was detected.

4.2. Reaction without a Solvent.—(i) A reaction mixture of 7.5 g. of sodium benzoate and 10.0 g. of VIII (equimolecular) was heated at 140—160°C for 2 hr. and diluted with water. The deposited oil was washed with aqueous sodium hydrogen carbonate, dried over magnesium sulfate, and distilled under reduced pressure to give a forerun consisting of 1.5 g. (31% of the theoretical yield) of di-*n*-butyl sulfite and 0.5 g. of butyl benzoate (5%) at 119—126°C/26 mmHg and 1.5 g. of benzoic anhydride (26% of the theoretical yield) at 207°C/25 mmHg. (ii) The reaction of 6.0 g. of sodium benzoate and 12 g. (1.9 mol.) of VIII was carried out as above. After they had been heated at 140—180°C for one and a half hours, the products were extracted with ether. Vacuum distillation gave 2.2 g. of di-*n*-butyl sulfite (56% of the theoretical yield), 0.7 g. of butyl benzoate (10 mol.%) and 2.0 g. of benzoic anhydride (43% of the theoretical yield).

5. Ethyl *p*-Nitrobenzoyloxysulfinate (Ie). — *5.1. Formation in Carbon Tetrachloride.*—VII (3 g.) was added to a suspension of 4.5 g. of sodium *p*-nitrobenzoate, which had been finely ground and dehydrated in a vacuum at 140°C for 3 hr., in 50 ml. of carbon tetrachloride. The reaction mixture was shaken occasionally and filtered, after 1.5 hrs., through a fritted glass funnel. The infrared spectrum of the filtrate (Fig. 3) exhibited strong C=O and S–O absorptions. With caution taken to avoid moistrue, this filtrate was concentrated under reduced pressure; this left almost colorless crystals (m. p. 85—90°C) (with decomposition). Its infrared spectrum in a KBr disk was almost the same as that of *p*-nitrobenzoic acid. When 2.7 g. of this specimen was shaken with 20 ml. of carbon tetrachloride, 2 g. remained undissolved, and the filtrate showed an infrared spectrum identical with that in Fig. 3, indicating the presence of Ie in the above specimen, probably contaminated with nitrobenzoic acid.

5.2. Formation in Toluene.—Sodium *p*-nitrobenzoate (10.0 g.) was suspended in 40 ml. of toluene, which had been dehydrated by boiling it over molten sodium, and treated with 8.5 g. of VII. The gel-like white precipitate was filtered off, and the filtrate was cooled in a dry ice - ethanol bath at −66°C to deposit pale crystals. About 50 ml. of petroleum ether was then added to decrease the solubility, and the supernatant was removed by decantation, thus leaving 5 g. of crystals (m. p. 85—90°C). Its infrared spectrum in

a KBr disk again coincided with that of *p*-nitrobenzoic acid.

5.3. Decomposition without a Solvent.—A reaction mixture of 7.3 g. of sodium *p*-nitrobenzoate and 10.5 g. of VII (2.1 molar equivalent) was heated in an oil bath at 125°C for one hour. Ether and water were added to the mass after it had been cooled. One gram of the white powder, identified as *p*-nitrobenzoic anhydride, remained undissolved. The yield was 17% of the theoretical yield. A lot of nitrobenzoic acid was recovered, but no ethyl *p*-nitrobenzoate was detected. The low yield of the acid anhydride may be attributed to the too mild reaction conditions, insufficient to bring about the complete decomposition of the mixed anhydride Ie.

6. Reaction between Benzoyl Chloride and Sodium Ethyl Sulfite.—*6.1. Without a Solvent.*—Sodium ethyl sulfite (IV) was prepared by passing dry sulfur dioxide into sodium ethoxide in ethanol and by evaporating the mixture to dryness under reduced pressure; it was finally dried in a vacuum for 3 hr. To 6.5 g. of this salt there was then added 7.0 g. of benzoyl chloride. After one hour at room temperature, the mixture was subjected to vacuum distillation to recover most of the starting materials unchanged. When the same amounts of the reactants were, in another experiment, heated at 120°C for few hours, 500 ml. of sulfur dioxide (about 40 mol.%) evolved. The vacuum distillation of the remaining mass gave 3.0 g. of the forerun at 50—70°C/80 mmHg and 3.0 g. of benzoic anhydride (52% of the theoretical yield), m. p. 41°C. The forerun was found by the infrared analysis to contain 1.75 g. of ethyl sulfite (50% of the theoretical) and 0.75 g. of ethyl benzoate (10 mol.%).

6.2. *Reaction in Carbon Tetrachloride.*—To a suspension of 1.5 g. of IV 1.5 g. of benzoyl chloride was added; the mixture was kept in a desiccator and occasionally shaken over a 4-day period, and then filtered from the insoluble powder. The infrared specturm of the filtrate showed that 10.1 mol.% (20.2% of the theoretical yield) of benzoic anhydride was produced, although a large part of the benzoyl chloride remained unaltered. The key bands of ethyl benzoate were weak in this filtrate at first, and those of ethyl sulfite were masked by benzoyl chloride. After 6 days, benzoyl chloride and benzoic anhydride were decomposed by aniline to benzanilide and filtered off. The filtrate was washed by diluted hydrochloric acid, aqueous potassium carbonate and water successively, and found by the infrared spectroscopy to contain 12.2 mol.% of ethyl benzoate and 4.3 mol.% of ethyl sulfite. If the same molar (10.1 mol.%) of ethyl sulfite as benzoic anhydride was assumed to have existed in the first filtrate, the difference (5.8 mol.%) may be considered to have converted into 11.6 mol.% of ethyl benzoate, in accordance with the observed value, probably by the reaction 9.

BULLETIN OF THE CHEMICAL SOCIETY OF JAPAN VOL. 39 967—970 (1966)

Organic Sulfur Compounds. III. The Reactions of Toluenesulfinic Acid with Acyl Chlorides

By Michio KOBAYASHI

Department of Chemistry, Yokohama City University, Mutsuura-machi, Kanazawa-ku, Yokohama

(Received September 21, 1965)

Sodium *p*-toluenesulfinate reacts with acetyl chloride to form acetic anhydride, *p*-toluenesulfinyl chloride, thiolsulfonate, and sodium *p*-toluenesulfonate. A reaction with benzoyl chloride gives benzoic anhydride in a good yield. A mixed anhydride of sulfinic acid and carboxylic acid is postulated as an intermediate, one which survives for a few hours at −60°C. The reaction mechanism is discussed.

The literature contains three reports on the reactions between arylsulfinic acid and carboxylic chloride. The reaction of sodium *p*-toluenesulfinate (I) and benzoyl chloride has been claimed[1] to form a ketosulfone, $C_6H_5COSO_2C_6H_4CH_3$, but this was questioned in a later paper.[2] The reaction of the same salt as a dihydrate with benzoyl chloride was reported in the second paper to give benzoic acid in a quantitative yield and *p*-tolyl *p*-toluenethiolsulfonate (IVa) in 20 mol.%,[2] but the exact material balance was not examined, nor was the reaction mechanism considered. On the other hand, the reaction of the anhydrous salt (I) and benzoyl chloride in xylene or in ether gave sodium *p*-toluenesulfonate, IVa, and an oil, which reacted with aniline to form benzanilide. A reaction mechanism involving a mixed anhydride of sulfinic acid and carboxylic acid was suggested.[3]

In this paper, studies of the mechanism of the reaction of *p*-toluenesulfinic acid with acetyl chloride and benzoyl chloride will be described.

1) E. P. Kohler and M. B. MacDonald, *Am. Chem. J.*, **22**, 219 (1899).

2) H. T. Hookway, *J. Am. Chem. Soc.*, **71**, 3240 (1949).

3) L. Panizzi and R. A. Nicolaus, *Gazz. chim. ital.*, **80**, 431 (1950).

Results and Discussion

The reaction of anhydrous sodium *p*-toluenesulfinate (I) with an equimolar amount of benzoyl chloride (II) was carried out at room temperature, and the reaction mixture was extracted with carbon tetrachloride. Infrared analysis revealed the formation of about 50 mol.%, namely 100% of the theoretical yield, of benzoic anhydride (III), and thiolsulfonate (IVa) in a 20 mol.% yield. The insoluble products in carbon tetrachloride contained sodium *p*-toluenesulfonate (25 mol.%). Therefore, the fate of the 100% portion of the benzoyl group and that of the 65% portion of $CH_3C_6H_4S$ group were clarified. The formation of benzoic anhydride was confirmed by the preparation of benzanilide in a yield 84% of the theoretical. The amount of the unchanged sulfinic acid was very small.

When the reaction mixture of I and acetyl chloride (V) was treated with anhydrous methanol, methyl *p*-toluenesulfinate was obtained in a low yield.

In another experiment, I was treated with acetyl chloride, and the reaction mixture was distilled in a vacuum to give acetic anhydride in a yield 68% of the theoretical. The residue gave 15.8 mol.% of the thiolsulfonate (IVa) and 14.2 mol.% of *p*-toluenesulfonate as *S*-benzylthiuronium salt (VI). The fact that sulfonic acid existed in the original residue as sodium salt was confirmed by the infrared spectrum in KBr disk, where a by-product, sodium chloride, did not interfere at all.

There remained at least one-fourth of the sulfur atoms, which fate had still not been explained. Since sulfonic acid was formed as sodium salt, it was clear that not all the chlorine atom could exist as sodium chloride in equimolar reaction conditions. This suggests that some of the sulfur compounds might be formed as chloride, such as sulfonyl chloride or sulfinyl chloride.

The reaction mixture of I and V was subjected to vacuum distillation as in the foregoing experiment. After the acetic anhydride had been collected, the distillation was continued and an orange-yellow high-boiling distillate was obtained. By its infrared spectrum and by the rapid reaction with water to give *p*-toluenesulfinic acid, this liquid was identified as *p*-toluenesulfinyl chloride, VII. The yield was 18.3 mol.% From the residue, 22.2 mol.% of *p*-toluenesulfonic acid was again isolated as VI.

On the basis of the above results, it was concluded that almost 100% of the acyl group was converted into the acyl anhydride, and that about 1/4 of the sulfur was recovered as sulfonic acid salt, another 1/4 as sulfinyl chloride, and 1/2 as thiolsulfonate. This means that the overall reaction can be expressed by the following formula 1:

$$\begin{aligned} RSO_2Na + R'COCl \rightarrow\ & {}^1/_2(R'CO)_2O + {}^1/_4\ RSO_2SR \\ & + {}^1/_4\ RSO_3Na + {}^1/_4\ RSOCl \\ & + {}^3/_4\ NaCl \end{aligned} \quad (1)$$

The formation of methyl *p*-toluenesulfinate in the reaction of methanol with the reaction mixture between I and V is explained by the interaction of methanol with the VII produced in reaction 1.

As the first step of the reaction of sulfinic acid salt with carboxylic chloride, either of the following two reactions could take place:

$$RSO_2Na + R'COCl \rightarrow R\text{-}\underset{\underset{O}{\downarrow}}{S}\text{-}O\text{-}\underset{\underset{O}{\|}}{C}\text{-}R' + NaCl \quad (2)$$

(VIII)

$$RSO_2Na + R'COCl \rightarrow R\text{-}\overset{\overset{O}{\uparrow}}{\underset{\underset{O}{\downarrow}}{S}}\text{-}\underset{\underset{O}{\|}}{C}\text{-}R' + NaCl \quad (3)$$

Although the usual alkyltion of sulfinate anion results in the formation of a *S*-alkyl derivative, not of a *O*-alkyl compound, the formation of carboxylic sulfurous anhydride[4] indicates the possibility of the formation of the VIII type. This class of compound, a mixed anhydride of sulfinic acid and carboxylic acid has been suggested[3] as described above, but never been isolated, and not expected to be stable compound.

The following experiments were carried out to determine whether the transitory formation of VIII in the reaction between sulfinate and acyl chloride could be verified.

A solution of free sulfinic acid and II in ether was cooled at −66°C and treated with triethylamine. An aliquot of the reaction mixture was then filtered, and its infrared spectrum was measured at once, in order to determine if any carbonyl band was present which could be attributed to VIII. Surprisingly, there was already strong absorption of benzoic anhydride; its yield was estimated to be almost theoretical. This must mean that the reaction is completed at −66°C or within several minutes at room temperature, the time interval needed to filter the solution and to inject the filtrate into the infrared cell. Anhydrous ethanol was added to the main portion of the above reaction mixture kept at −66°C. The usual work-up of this mixture gave benzoic anhydride in 29 mol.% yield, not in the 50 mol.% estimated above, and ethyl *p*-toluenesulfinate (IX) in a 35 mol.% yield, with a slight amount of ethyl benzoate. Therefore, the intermediate VIII may be considered to survive at a low temperature such as −66°C for some time, and to be converted into sulfinic ester by reaction 5, which proceeds along with the disproportionation 4:

4) Part 2 of this series.

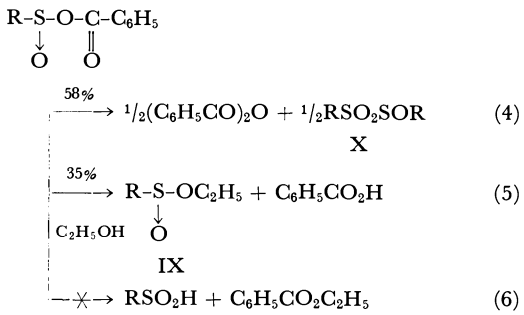

Ethyl sulfinate IX could be formed by the reaction of sulfinyl chloride (VII), which might be formed in a reaction analogous to reaction 1, with ethanol, but in such a case the yield would not exceed 25 mol.%. The preferential attack of ethanol on VIII on the sulfur atom (reaction 5), rather than on the carbonyl group of VIII (reaction 6), may be explained by the attraction of the nucleophilic reagent to the positive center of the sulfinyl sulfur.

The fact that the sulfinyl anion rapidly reacted with benzoyl chloride, even at −66°C, suggested the possibility of preparing IX by reacting I with II in the presence of ethanol; here the sulfinyl anion would react with II ahead of ethanol to form VIII, and then this VIII would react with ethanol according to the reaction 5 prior to the decomposition by the disproportionation 4. Indeed, I suspended in absolute ethanol reacted with II at 0°C to give the mixture, which consisted of IX in a 74 mol.% yield, III in a yield 19% of the theoretical, and ethyl benzoate in a 6 mol.% yield. These results showed that the rate of the reaction 5 was slightly higher than that of the disproportionation 4. It should be noticed that no thiolsulfonate (IVa) was detected in this experiment, although III was formed in yields as high as 10 mol.%. This indicated that thiolsulfonate was not the primary product of the disproportionation 4.

The variety of the products formed in the overall reaction 1 implies the complicated nature of this reaction. After the first step 2, the disproportionation 7 of VIII could proceed by the following mechanism 8 and 9:

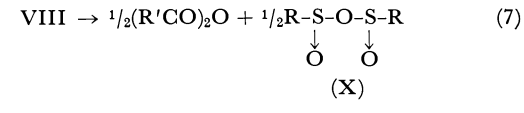

The sulfinic anhydride (X) has been considered to be very unstable, and it is expected to be isomerized to the sulfinyl sulfone XI, which has been prepared from the sulfinic acid by the dehydration with acetic anhydride.[5-7]

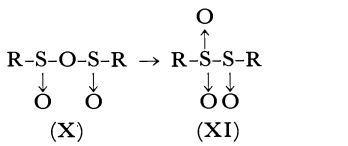

XI would further rearrange to a mixed sulfenic sulfonic anhydride XII[8]:

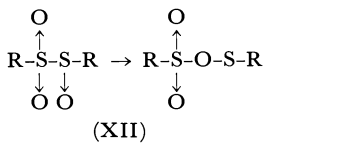

The formation of the thiolsulfonate IV could be explained by the reaction 12, which is similar to the proposed reaction for the formation of IV in the disproportionation of the sulfinic acid under acidic conditions.[8]

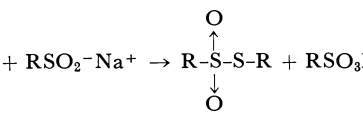

The formation of the sulfinyl chloride would then be the result of one of the following two reactions, of which the former is our choice:

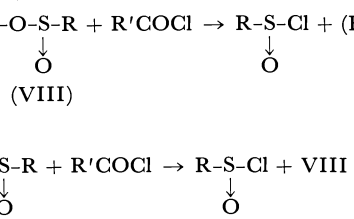

Therefore, the following reaction sequences would lead to the net reaction 13:

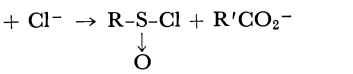

By combining (2), (7), $^1/_2$(11) and $^1/_2$(12), the following formula 17 was obtained:

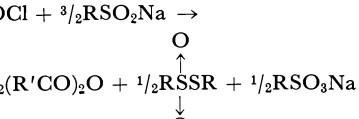

while, by combining $^1/_2$(2) and $^1/_2$(13), Formula (18) was given:

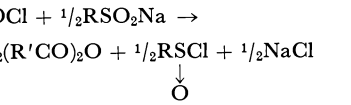

5) H. Bredereck, A. Wagner, E. H. Beck, H. Herlinger and K. G. Kottenhahn, *Angew. Chem.*, **70**, 268 (1958).
6) F. Knoevenagel and L. Polack, *Ber.*, **41**, 3323 (1908).
7) H. Bredereck, A. Wagner, H. Beck and R. J. Klein, *Chem. Ber.*, **93**, 2736 (1960).
8) J. L. Kice and K. W. Bowers, *J. Am. Chem. Soc.*, **84**, 605 (1962).

Finally, we get the overall reaction formula 1 by adding 17 to 18 and by dividing by 2.

Experimental

The Reaction of Sodium *p*-Toluenesulfinate and Benzoyl Chloride without a Solvent.—To 7.0 g. of II there was added 9.0 g. (equimolecular) of a fine powder of I (dried in a vacuum at 140°C for a few hours) with cooling; exothermic reaction then started. After 30 min., 80 ml. of carbon tetrachloride was added to the jelly-like reaction mixture, and the insoluble white powder was filtered off. An aliquot of the filtrate was taken, diluted to 10 times of its volume, and its infrared specturm was measured. The formation of 50 mol.% of III, and 19.8 mol.% of IVa was observed, and trace of the II was unchanged. Into the main portion of the filtrate 6 g. of aniline were then stirred in order to precipitate the white crystals of benzanilide, 4.2 g. (84% of the theoretical yield), which was identified by its infrared spectrum. The filtrate of benzanilide was evaporated, and the residue was recrystallized from petroleum ether to give 2.3 g. of IVa (16.6 mol.%). The mother liquid was chromatographed through an alumina column, and 0.2 g. (4 mol.%) of *p, p'*-ditolyl disulfide was obtained as colorless crystals from the first eluant. A part of the white powder, insoluble in carbon tetrachloride, was examined by means of the infrared spectrum in a KBr disk and so found to contain *p*-toluenesulfonic acid as sodium salt, not as a free form. The main part of the salt residue was taken up in water, where a negligible amount remained undissolved. The addition of *S*-benzylthiuronium chloride gave 4.0 g. (25 mol.%) of the precipitate of *S*-benzylthiuronium *p*-toluenesulfonate (VI). To a part of the aqueous solution there was then added a ferric chloride solution, where the characteristic red color of ferric sulfinate was observed but no precipitate[9] was separated after one night.

The Reaction of *p*-Toluenesulfinic Acid with Benzoyl Chloride in Ether.—*p*-Toluenesulfinic acid was liberated from its sodium salt and dried in a vacuum. A solution of 3.0 g. of this acid in 70 ml. of anhydrous ether was then cooled in a dry ice - ethanol bath at −66°C. Three grams of the freshly-distilled II were dissolved in 20 ml. of ether, added to the above solution, and cooled; most part of the sulfinic acid was crystallized out. A solution of 2.0 g. of triethylamine in 20 ml. of ether was then added to the above suspension drop by drop over a 20 min. period. When the white precipitate filled the solution, one milliliter of the reaction mixture was taken out by suction, filtered through a fritted-glass funnel, and its infrared spectrum measured at once. The strong C=O absorption bands of benzoic anhydride were observed at 1790 and 1728 cm^{-1}; from their intensities, the yield of III was estimated to be 49.5 mol.%. To the main portion of the reaction mixture, kept at −66°C, 10 ml. of anhydrous ethanol was added in small portions. The mixture was cooled for 2 hr. at this temperature, allowed to warm to room temperature, and left overnight. The precipitate was filtered off and identified as triethylamine hydrochloride. The filtrate was washed by water, aqueous sodium carbonate and water successively, and dried over magnesium sulfate. On the evaporation of the filtrate, 3.2 g. of a colorless oil was obtained as a residue. Infrared analysis showed that this oil contained 1.3 g. of III (29 mol.%) and 1.3 g. of IX (35 mol.%). Actually, on vacuum distillation, 0.8 g. of IX (b. p. 115—117°C/4 mmHg) and 1.1 g. of III (b. p. 170°C/4 mmHg) were isolated. Ethyl benzoate was detected by infrared analysis, but its yield was too low to allow its isolation.

The Reaction of *p*-Toluenesulfinate with Benzoyl Chloride in Ethanol.—A suspension of 9.0 g. of I in 100 ml. of anhydrous ethanol was boiled once and cooled in ice water, whereby most of the I was separated as a fine powder. Into this ice-cooled suspension, 7.0 g. of II was stirred, and the reaction mixture was kept for 2 hr. in an ice bath. A lot of water was added to the mixture, and the heavy oil precipitated was extracted with 40 ml. of carbon tetrachloride. The infrared analysis of this extract showed the presence of 73.8 mol.% of IX, 9.6 mol.% of III and 6.1 mol.% of ethyl benzoate, with no thiolsulfonate IVa.

The Reaction of Sodium *p*-Toluenesulfinate with Acetyl Chloride (V).—i) To 9.0 g. of I 13.0 g. of freshly-distilled V were added with cooling. Heat was evolved, and a gel-like mixture resulted. After one hour, the whole mixture was vacuum-distilled to give 1.7 g. of a low boiling liquid, which was identified as acetic anhydride. Ether (40 ml.) was added to the residue, and an insoluble powder (3.4 g.) was filtered off. Ether was expelled from the extract, and 3.7 g. of the residue was treated with petroleum ether to give 1.7 g. of IVa. A white powder, insoluble in ether, was taken up in water and the insoluble matter was removed by filtration. The latter was also identified as IVa, the total yield of which reached 2.2 g. (63% of the theoretical). The yield of *p*-toluenesulfonic acid in the aqueous solution was determined as VI to be 14.2 mol.% (56.8% of the theoretical). A part of this aqueous solution again showed a red color with a ferric chloride solution, but it gave no precipitate of ferric sulfinate.

ii) To 5.3 g. of I 3.0 g. of V were added; then, after the initial exothermic reaction was over, 1 ml. of anhydrous methanol was added to the jelly-like mixture, whereby heat was evolved again. The mixture was diluted with water and extracted with petroleum ether to give 0.3 g. of methyl *p*-toluenesulfinate (6%).

iii) The reaction mixture of 9.0 g. of I and 5.0 g. of V was vacuum-distilled as in i). Three milliliter of a low boiling fraction was collected; it was found to contain 1.6 g. (63% of the theoretical) of acetic anhydride on redistillation. After it, a trace of a green-colored liquid came out, and finally 1.6 g. of an orange-yellow liquid at 100—110°C/3 mmHg (mostly at 110°C) was obtained. This oil formed colorless crystals of *p*-toluenesulfinic acid upon coming in contact with water. The infrared specturm of this liquid also confirmed it to be *p*-toluenesulfinyl chloride. The yield was 18 mol.% (73% of the theoretical yield, based upon formula 1). When the residue in the vacuum distillation was treated with water, the yield of *p*-toluenesulfonic acid was estimated to be 22.2 mol.% (89% of the theoretical yield) by precipitation as VI (3.63 g.).

9) J. Mitchel, I. M. Kolthoff, E. S. Proskauer and A. Weissberger, "Organic Analysis," Vol. I, Interscience Publisher, Inc., New York, N. Y. (1953), p. 378.

BULLETIN OF THE CHEMICAL SOCIETY OF JAPAN VOL. 39 971—980 (1966)

The Liquid-Liquid Extraction of Alkaline Earth Metals with TTA (2-Thenoyltrifluoroacetone)

By Ikuko AKAZA

Department of Chemistry, Faculty of Science, Kanazawa University, Kanazawa

(Received September 21, 1965)

The liquid-liquid extraction of alkaline earth metals was investigated with a TTA-MIBK solvent and a NH_4OAc-AcOH-NH_4OH aqueous solution in the presence of relatively large amounts of the metals. The extractability of the metal ions was in the decreasing order of magnesium, calcium, strontium and barium, while their distribution ratios were too close to one another for them to be separated from each other. Critical studies were made on several factors affecting the distribution of each metal, such as the amount of metal in the aqueous solution, the concentration of TTA in the organic solvent, and the pH of the solution. It was noticed that the concentration of TTA in MIBK played a principal role in this extraction and that the log *D*-log(TTA) relation was shown as a curve, not a straight line. The relation in other similar cases had usually been shown as a straight line, but the new results were obtained by compensating pH-change, the extent of which was variable with the concentration of TTA in the system. Among the metal ions, calcium and magnesium could be separated from each other by carrying out the extraction from their solution in the presence of EDTA. A further extention of this extraction to a reversed-phase partition chromatography will be undertaken and reported on in another paper.

The chelating agent 2-thenoyltrifluoroacetone (usually abbreviated as TTA) has proved to be a valuable reagent for the solvent extraction of many metal ions. It has the property of accomplishing the extraction from stronger acid solutions than other chelating agents. Thus, there is a wide range of metal ions that may be extracted without interference from hydrolysis. A considerable amount of work has been done on the use of TTA[1] alone or with other chelating agents.[2] However, there have been few works on the extraction of alkaline earth metal ions except for the determination of the stability constant of their chelates with TTA.[3] Khym, Tompkins and Cohen[4] have reported the separation of the calcium-45 produced by the Sc(d, 2p) reaction from the target by solvent extraction with 0.5 M TTA in benzene from a solution of pH 9. Kiba and Mizukami[5] have studied the rapid separation of radioactive strontium by solvent extraction with 0.05 M TTA in methyl isobutyl ketone (abbreviated as MIBK) from a solution of pH 8. Although TTA was believed to cleave to trifluoroacetic acid and acetylthiophen when the pH of its aqueous solution was in excess of 9,[6] their intuitive choice of the solvent surmounted a difficulty of using TTA in a basic medium, for MIBK was later proved as to be a good retardent for the decomposition of TTA,[7] as well as a good polar solvating agent to facilitate the chelate formation and extraction. After this study, alkaline earth metals and heavier alkali metals such as cesium became the objects of quantitative extraction with TTA in MIBK from their aqueous solutions of higher pH values, especially in the preparation of radio-isotopes, the processing of irradiated reactor fuel, and the analysis of fission products.[8] However up to the present there have been no systematic studies of the liquid-liquid extraction of alkaline earth metals with TTA-MIBK in relatively large amounts of the metals.

The present author studied critically the extraction from aqueous solutions over a wide range of pH values, and determined the distribution ratio of each individual ion with relation to the concentration of TTA in the solvent and the pH of the aqueous phase. It was noticed that the distribution ratio between two phases varied remarkably with the concentration of TTA in the organic phase, and that the extraction mechanism is not as simple as it had been considered to be. As a result, the distribution ratios of the metals are too close together for them to be separated easily. The author aims to separate these metal ions by later extending this extraction method to the reversed-phase partition chromatography, which will be described in another paper.

1) A. M. Poskamzer and B. M. Foreman, Jr., *J. Inorg. Nucl. Chem.*, **16**, 323 (1961).
2) T. Sekine and D. Dyrssen, ibid., **26**, 1727 (1964).
3) R. A. Bolomfy and L. Wish, *J. Am. Chem. Soc.*, **72**, 4483 (1950).
4) J. X. Kyhm, P. C. Tompkins and W. E. Cohen, U.S.A.E.C. **MDDC-1214** (1958).
5) T. Kiba and S. Mizukami, This Bulletin, **31**, 1007 (1958).
6) E. H. Cook and R. W. Taft, Jr., *J. Am. Chem. Soc.*, **74**, 6103 (1952).
7) P. Crowther and F. L. Moore, *Anal. Chem.*, **35**, 2081 (1963).
8) T. Kiba, S. Ohashi and T. Maeda, This Bulletin, **38**, 818 (1960).

Experimental

Reagents and Apparatus. — *TTA (2-Thenoyltrifluoroacetone).*—Dotite TTA, prepared by the Dōjindō Research Laboratories, was used without further purification. It was dissolved in MIBK (methyl isobutyl ketone) of an analytical reagent grade to make a 0.2 M TTA-MIBK solution in most cases.

Buffer Solution.—A buffer solution consisting of ammonium acetate - ammonia - acetic acid was employed to keep constant the pH of the aqueous solution. In consideration of its buffer capacity, a 6 M-solution was usually employed for adding to the sample solution, and the final concentration of the buffer solution was made 3 M by diluting the test solution to twice the volume of the initial buffer solution. Sometimes a 1.0 M buffer solution was also used to make the final concentration of the test solution 0.5 M.

Salt Solution.—Barium chloride dihydrate, strontium nitrate tetrahydrate, calcium nitrate tetrahydrate, and magnesium chloride hexahydrate, all of analytical grades, were dissolved in water to make solutions containing 10^4 p. p. m. of the metal ion. The concentration of each solution was standardized by titration with EDTA (ethylenediaminetetraacetic acid disodium salt). The stock solutions thus prepared were diluted with water to suitable concentrations before use.

Radioactive strontium-90 - yttrium-90 as nitrate and barium-140 - lanthanum-140 as chloride were employed in order to examine their behavior in the extraction, after their daughter nuclides had been separated by the usual method.

EDTA Solution.—Analytical-grade disodium salt of ethylenediaminetetraacetic acid (Dotite 2 Na) was dissolved in water to make a 0.01 M solution, the concentration of which was then standardized with standard calcium carbonate.

Buffer Solution of pH 10.—The buffer solution used for titration by EDTA was prepared by dissolving 7 g. of ammonium chloride in 57 ml. of aqueous ammonia and then diluting it to 100 ml.; it was adjusted to pH 10 by adding an ammonium chloride solution or aqueous ammonia.

Eriochrome Black T, the indicator, and a 0.1 M magnesium-EDTA solution were prepared as usual.

Separating Funnel.—A 85 ml., spindle-type separating funnel was used.

pH Meter.—A pH meter with a glass electrode and a saturated calomel electrode, Model M-3 Horiba Manufacturing Co., was employed.

Flame Photometer. — A spectrophotometer, Hitachi Model EPU-2A, provided with an accessory flame burner, H-2, was used to determine the quantity of metal ions in a solution, using hydrogen gas as the fuel.

Radioactivity Counter.—A G-M counting set of the Kōbe Kōgyō Co., consisting of a No. 131-G-M tube and a "100 scalor," was used for β-counting.

Shaker.—The shakng of the separating funnel was effected by a vertical electric shaker, Iwaki Model 3, operating at 300 strokes per minute.

Experimental Procedure. — In the separating funnel 10 ml. of a 0.2 M TTA-MIBK solution, 5 ml. of a sample solution and 5 ml. of a 6 M buffer solution were put together. The funnel was then shaken for ten minutes with the electric shaker. After the two phases had separated the aqueous solution was taken out through the stem and its pH was measured. The sample solution adhering to the glass electrode of the pH meter and to the inside wall of the funnel was washed down into a beaker. On the other hand, the organic phase remaining in the funnel was treated with 5 ml. of 1 M hydrochloric acid in order to back-extract the metal ion in the organic phase. The back extraction was repeated twice, and the acid washing was submitted to the determination of the metal ions contained in the organic phase. The original aqueous phase was also submitted to the determination, according to the following methods.

Titration Method.—The aqueous solution was nearly neutralized with a 1 M sodium hydroxide solution or 3 M aqueous ammonia, and 2 ml. of a buffer solution with a pH of 10 was added; then 2 ml. of a magnesium-EDTA solution was pipetted into the solution. The solution was titrated with a 0.01 M EDTA solution and two or three drops of a BT indicator solution. The acetate ion, which interferes with the clear exhibition of this color change, should be completely eliminated by evaporating the aqueous solution to dryness with a strong acid before the titration.

Flame Photometry. — The original aqueous phase contained various amounts of acetate, so it was difficult to re-establish the same conditions in a series of reference solutions and so draw the working curve. Therefore, the back-extract was submitted to flame photometry. However, in the solution some acetic acid, ammonia and TTA - methyl isobutyl ketone were present, together with the metal ion to be tested. These substances were removed by the following treatment before the flame-photometric determination. A half-volume of ethyl ether was added to the solution in a separating funnel, and the contents shaken for a while; then the aqueous phase was transferred into another funnel and shaken with ether again. The aqueous solution separated from ether was warmed to 50°C, and air was passed through the solution for about thirty minutes in order to expel the ether. Then the solution was submitted to the determination. As references for the determination a series of solutions were prepared containing definite amounts of the respective metals in 1 N hydrochloric acid.

Results and Discussion

Preliminary Experiments.—*The Behavior of Individual Ions.*—In order to examine the behavior of individual ions in larger amounts, some preliminary experiments were undertaken under the same conditions as had been done in its trace scale by Kiba and Mizukami.[5] In a separating funnel there were placed together 5 ml. of a 1.0 M buffer solution of pH 8.0, 5 ml. of a 0.02 M solution of the metal ion, and 10-ml. of a TTA-MIBK solvent of varying concentrations, from 0.05 M to 0.5 M. The recovery of each ion in the organic phase is shown in Fig. 1, from which it may be found that the percent extraction decreases in the order of magnesium, calcium, strontium and barium, and increases with the concentration of TTA in methyl isobutyl ketone. Extraction was also carried out with strontium and barium in varying amounts

from a trace to 0.005 M; the recovery is shown in Figs. 2 and 3.

In each case the increase in the concentration of TTA promoted the extraction of metal ions, and the larger the quantity of metal ion present, the lower was the percentage of extraction. When the quantity of metal ions was minute, methyl isobutyl ketone containing 0.2 M or more of TTA was very useful in effecting a satisfactory recovery of the metal. The extraction behavior was much the same in these four metals, as is shown by the closeness of the extraction curves in Fig. 1.

The Use of a Mixed Solvent.—Because of the similar behavior of the metal ions, the separation from one another seemed to be very difficult. Therefore, the mixed solvent was used in an attempt to effect a separation of the metals. Ten milliliters

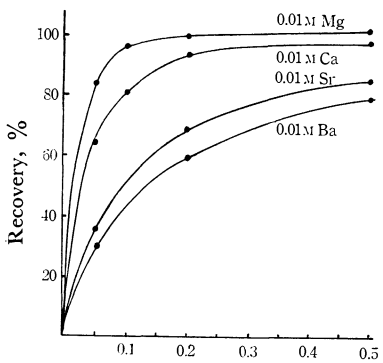

Fig. 1. Recovery of metal ions from 10 ml. of aqueous phase consisting of 0.5 M buffer solution of pH 8.0 and 0.01 M solution of metal ion by extraction with 10 ml. of MIBK containing various amounts of TTA.

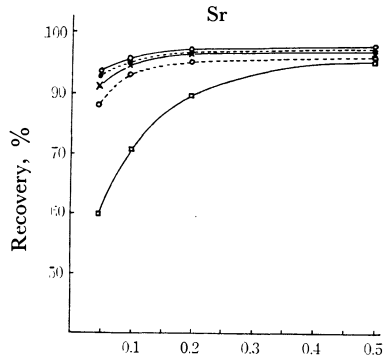

Fig. 2. Recovery of strontium by 10 ml. of MIBK containing various amounts of TTA from 10 ml. of aqueous phase consisting of 0.5 M buffer solution of pH 8.0 containing various amounts of strontium.

○—○ Carrier free ●--● 0.0001 M
×—× 0.0005 M ○--○ 0.001 M
□—□ 0.005 M

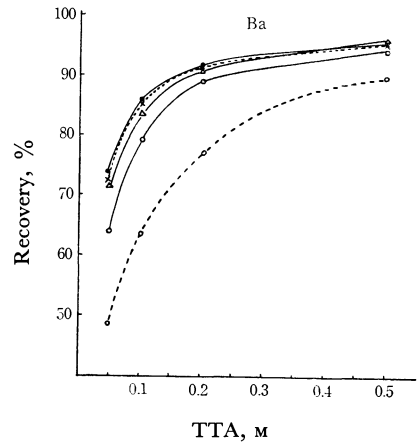

Fig. 3. Recovery of barium by 10 ml. of MIBK containing various amounts of TTA from 10 ml. of aqueous phase consisting of 0.5 M buffer solution of pH 8.0 containing various amounts of barium.

●—● Carrier free ×--× 0.0001 M
△—△ 0.0005 M ○—○ 0.001 M
○--○ 0.005 M

of a mixed solvent consisting of 0.1 M TTA - benzene and 0.1 M TTA - MIBK in various ratios was used for extraction from a solution composed of 5 ml. of a 1.0 M buffer solution of pH 8.0 and 5 ml. of a 0.02 M solution of metal ions. The results obtained with mixed solvents of various compositions are shown in Fig. 4, which reveals that though the percentage extraction of each metal increases with the volume of TTA-MIBK, no better separation from one another can be expected. It also reveals that benzene does not play any role in the attainment of selectivity. Thereafter, MIBK was exclusively employed in this method.

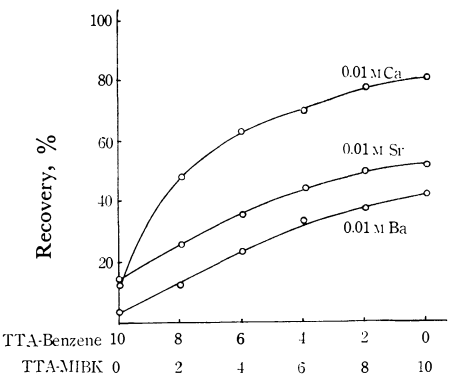

Fig. 4. Recovery of metal using mixed solvent.
Aqueous phase: 10 ml. of 0.5 M buffer solution of pH 8.0
Organic phase: 10 ml. of mixed solvent of 0.1 M TTA - MIBK and 0.1 M TTA - Benzene

The Change in pH During Extraction.—When a 1.0 M buffer solution was used in an aqueous phase, the pH, which was 8.0 initially, became 6.8 after the extraction. Since TTA can be considered to be a weak acid, its dissolution into the aqueous phase during the extraction and the release of protonized hydrogen from it by the metal ion may have caused the increase in hydrogen ions in the aqueous phase. In order to keep the pH nearly constant during the extraction, a 6 M buffer solution was preferred because of its large buffer capacity. In the subsequent experiments 5 ml. of the buffer solution was taken and diluted to 10 ml. with the sample solution and water in order to make the buffer concentration in the aqueous phase 3 M. The concentration of TTA in MIBK was also kept at 0.2 M in the subsequent experiments.

The Mechanism of Extraction.—The equation for the extraction of a metal ion with the charge $+z$, M^{z+}, and with a monobasic chelating agent, HT, can be simply written as:

$$M^{z+}_{(a)} + zHT_{(o)} \rightleftharpoons MT_{z(o)} + zH^{+}_{(a)}$$

where the subscripts a and o refer to the aqueous and organic phases respectively. A thermodynamic extraction constant for this process can be written most simply as:

$$K=(MT_z)_o(H^+)_a^z/(M^{z+})_a(HT)_o^z$$

and:

$$K=D(H^+)_a^z/(HT)_o^z$$

where D is the extraction coefficient (the total concentration of metal in the organic phase/the total concentration of metal in the aqueous phase).

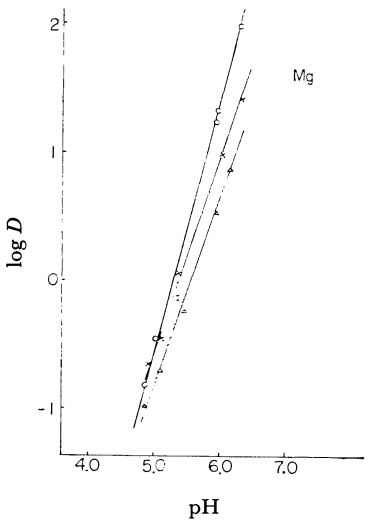

Fig. 5. Dependence of distribution ratio, D upon the pH of the solution in case of magnesium.
Aqueous phase: 3 M Buffer solution
Organic phase: 0.2 M TTA - MIBK
○ 0.125 mmol./10 ml. × 0.25 mmol./10 ml.
△ 0.50 mmol./10 ml.

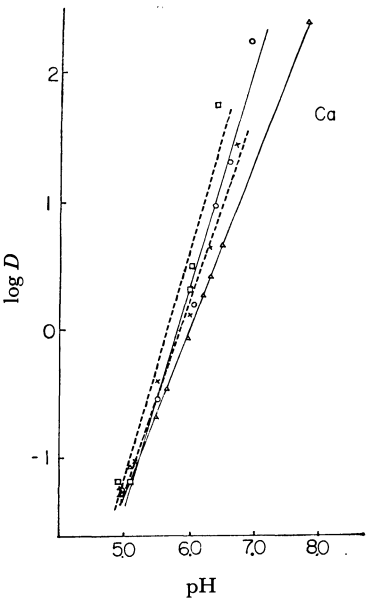

Fig. 6. Dependence of distribution ratio, D upon the pH of the solution in case of calcium.
Aqueous phase: 3 M buffer solution
Organic phase: 0.2 M TTA - MIBK
□ 0.031 mmol./10 ml. ○ 0.125 mmol./10 ml.
× 0.252 mmol./10 ml. △ 0.508 mmol./10 ml.

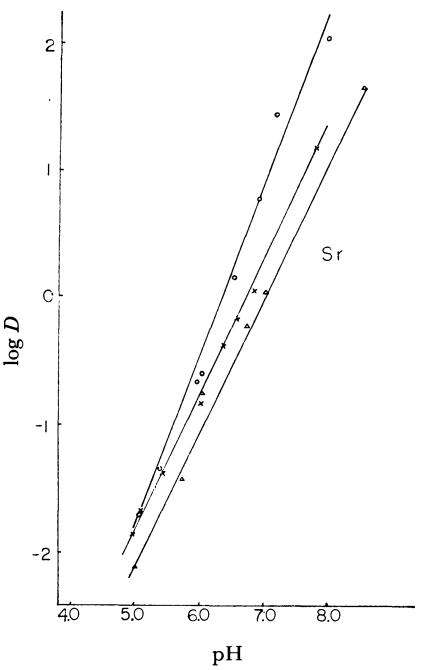

Fig. 7. Dependence of distribution ratio, D upon the pH of the solution in case of strontium.
Aqueous phase: 3 M buffer solution
Organic phase: 0.2 M TTA - MIBK
○ 0.143 mmol./10 ml. × 0.573 mmol./10 ml.
△ 0.286 mmol./10 ml.

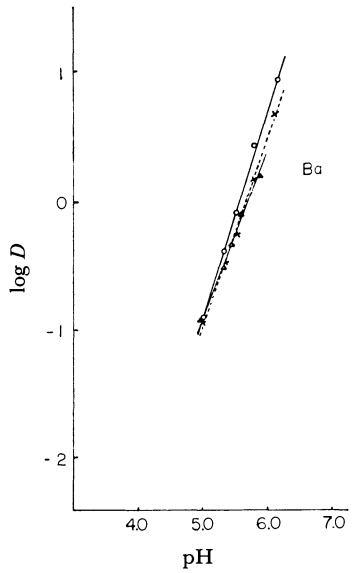

Fig. 8. Dependence of distribution ratio, D upon the pH of the solution in case of barium.

Aqueous phase: 3 M buffer solution
Organic phase: 0.2 M TTA - MIBK
○ 0.125 mmol./10 ml. × 0.25 mmol./10 ml.
△ 0.498 mmol./10 ml.

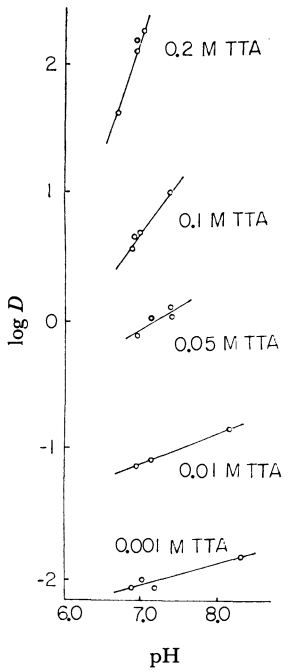

Fig. 9. Dependence of distribution ratio, D upon the pH of the solution.

Aq. phase: 3 M buffer solution containing 0.125 mmol. of calcium
Org. phase: MIBK containing varying amounts of TTA

D can also be written as:

$$D=K(\mathrm{HT})_o^z/(\mathrm{H}^+)_a^z \quad (1)$$

Therefore, the distribution ratio depends on the activity of both the chelating agent and the hydrogen ions. The values of D, determined in various concentrations of the chelating agent while the pH is kept constant, and at varying pH values at a definite concentration of the chelating agent, may clarify the extraction mechanism.

First the dependence of D on the pH of an aqueous solution after the extraction was examined by the following experiments. The distribution ratios were estimated in a series of extractions between 10-ml. portions of organic and aqueous phases, the former being 0.2 M TTA - MIBK and the latter consisting of various amounts of a metal ion in a 3 M buffer solution of varying pH values. The relations between log$D$ and pH after the extraction are shown as straight lines having slopes of unity to two for magnesium, calcium, strontium and barium, respectively, in Figs. 5, 6, 7 and 8. The slope becomes sharper as the quantity of the metal ions decreases and as the stability of the metal chelate increases.[1] The dependence of D on the concentration of TTA in methyl isobutyl ketone was also examined in the extraction between 10-ml. portions of organic and aqueous phases, the former being MIBK containing various amounts of TTA, and the latter consisting of 5 ml. of a 0.025 M solution of calcium ion and 5 ml. of a 6 M buffer solution of varying pH values. The results are summarized in Fig. 9, in which the pH noted is, of course, that of the aqueous phase after the extraction.

Next, the author attempted the extraction at a constant pH value of 7.0 of the aqueous phase and at the constant concentration of calcium of 0.125 mmol. between 10 ml. of the aqueous phase and 10 ml. of MIBK containing varying amounts of TTA. However, the author failed in the attempt to make the pH of the solution exactly 7.0 after each extraction, since the pH of the aqueous phase was liable to be made lower by mere contact with the organic phase, probably because of the partial transfer of the TTA from the organic to the aqueous phase. Even when a buffer solution with a higher capacity, such as a 6 M solution, is used, the pH of the aqueous solution cannot be guaranteed to remain strictly constant. Moreover, when an organic solvent containing a still larger amount of TTA is employed, the distribution of calcium is enormously affected by even a slight change in the pH, as is shown in Fig. 9. The proper distribution ratio should be estimated at the constant pH, but it is difficult to maintain the constant pH over all the estimation of log D - log(TTA). Therefore, the relation of the distribution ratio to the concentration of TTA at pH 7.0 was constructed from the data in Fig. 9. A noteworthy fact was thereby

found about the extraction mechanism. As Fig. 10 shows, the concentration of TTA, noted as (TTA) in the figure, has the relation with the distribution ratio given in the curve of log D vs. log(TTA). The curve seems to illustrate the true behavior of the extraction at pH 7.0. Nevertheless, a number of researchers who investigated the extraction of the TTA-chelates of other metals have described how the relation between log D and log(TTA) is usually represented by a straight line with a slope of an integral value, the integer being the number of TTA molecules attached to the metal. In many cases they seem to have overlooked the facts that the pH of the aqueous solution is lowered not only by the hydrogen ion exchanged with the metal, but also by the dissociation of TTA in the aqueous phase; that a lowering of the pH is remarkable when the concentration of TTA is high, and that, therefore, the higher the concentration of TTA, the larger the decrease in the extent of the distribution ratio. Such a change in the pH will be slight in an acidic solution, but it will be remarkable in a neutral or alkaline solution.

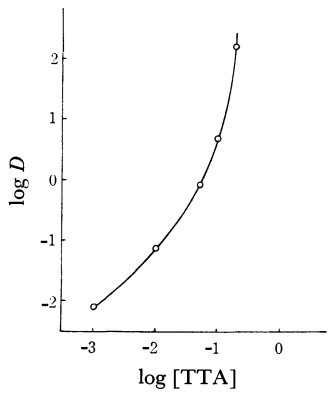

Fig. 10. Dependence of log [TTA] at pH 7.0, same data as in Fig. 9.

The curve drawn by the present author appears as a smooth one in Fig. 10, but it is suspected that it is really composed of a large number of short lines, with their slopes increasing from unity to large integers. This suggests that various species of metal-chelate are formed with the increase in the concentration of TTA in the organic phase. When the concentration of TTA is large, the number of TTA radicals attached to the calcium atom increases and, as a matter of fact, the distribution of the metal into the organic phase is enhanced. In addition, the distribution of metal usually depends upon the following factors: the time required for the attainment of equilibrium, the temperature, the kind and concentration of the metal ion and of the chelating agent, the pH of the aqueous phase, the other chelating agents present, the adduct-forming agent, and the organic solvent used.[9]

9) G. K. Schweitzer, *Anal. Chim. Acta*, **30**, 68 (1964).

The extraction between an aqueous phase containing a divalent ion as calcium and an organic phase containing TTA can be written as follows:

$$M^{2+}_{(a)} + 2HT_{(o)} \rightleftharpoons MT_{2(o)} + 2H^{+}_{(a)} \quad (2)$$

$$D = K(HT)^2_o/(H^+)^2_a \quad (3)$$

Therefore, D is inversely proportional to the square of (H^+). As has been described above, the author has found that the relation between log D and pH is linear, with the slope between unity and two. Therefore, Eq. 3 can explain the phenomenon where the slope is two, but not where it is unity. Similar behavior of alkaline earth metals has already been cited in the description by Cerrai et al.,[10] who investigated the liquid-liquid extraction of alkaline earth metals with di-(2-ethylhexyl)orthophosphoric acid (abbreviated as HDEHP). In their study they considered that this fitful phenomenon was caused by the acetate ions present. Thorium has been proved to be a metal subject to the same effect of acetate,[11] even in extraction with TTA from acidic solutions. The present author wishes to take this effect into account in clarifying the above phenomenon.

If a divalent metallic cation, M^{2+}, is present in a large excess of acetate ions in the buffer solution, a competition may occur between HT and the acetate ion for co-ordinating to the metal ion in the following manner:

$$M(CH_3COO)^{+}_{(a)} + HT_{(o)} \rightleftharpoons M{\cdot}CH_3COO{\cdot}T_{(o)} + H^{+}_{(a)} \quad (4)$$

In this case the dependence of the distribution ratio of metal on the hydrogen ion concentration may be written as a first-power dependence. On the

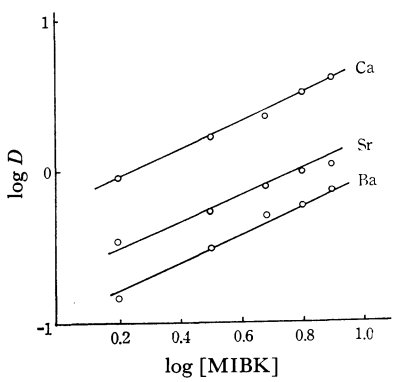

Fig. 11. Dependence of log D to log [MIBK].
Org. phase: 10 ml. of mixed solvent of 0.1 M TTA-MIBK and 0.1 M TTA-benzene in various ratio
Aq. phase: 10 ml. of 0.5 M buffer solution of pH 8.0 containing 0.1 mmol. metal ions

10) E. Cerrai and G. Ghersini, *J. Chromatog.*, **13**, 211 (1964).
11) G. Goldstein, O. Menis and D. L. Manning, *Anal. Chem.*, **32**, 400 (1960).

Table I. Some aspects of the behavior of the extraction of calcium

pH	TTA in organic phase, initial m	Metal ion in aqueous phase, initial, n	x	m/n calcd.	m/n tangent of the curve in Fig. 10
	M	M			
7.0	0.2	0.0125	1.74	16	8.7
7.0	0.1	0.0125	0.81	8	3.1
7.0	0.05	0.0125	0.36	4	1.95
7.0	0.01	0.0125	0.24	0.8	1.15

other hand, the methyl isobutyl ketone used as an extracting solvent may also participate in the extraction mechanism, because of its polarity. Log D and log(MIBK) have a linear relation with a slope of unity, as is shown in Fig. 11, when methyl isobutyl ketone of various concentrations in benzene is used in the extraction of alkaline earth metal from an aqueous solution kept at pH 8 by a 1.0 M buffer solution. This shows that methyl isobutyl ketone can co-ordinate to the alkaline earth metal as a monodentate ligand; therefore, Eqs. 2 and 4 should be revised to 5 and 6, respectively, in such a case:

$$M^{2+}_{(a)} + 2HT_{(o)} + L_{(o)} \rightleftharpoons MT_2 \cdot L_{(o)} + 2H^+_{(a)} \quad (5)$$

$$M(CH_3COO)^+_{(a)} + HT_{(o)} + L_{(o)} \rightleftharpoons MT \cdot CH_3COO \cdot L_{(o)} + H^+_{(a)} \quad (6)$$

where L is methyl isobutyl ketone as a non-charged ligand.

From these equations, the dependence of the distribution ratio on the concentration of TTA is considered to be only linear or quadratic, but the phenomena shown in Fig. 10, in which the distribution ratio increases with the concentration, even by the power of three, cannot be explained unless undissociated TTA is regarded as participating in the equilibrium. Equations 5 and 6, then will become 7 and 8 respectively:

$$M^{2+}_{(a)} + (2+m-2)HT_{(o)} + L_{(o)} \rightleftharpoons MT_2(HT)_{m-2} \cdot L_{(o)} + 2H^+_{(a)} \quad (7)$$

$$M(CH_3COO)^+_{(a)} + (1+m-1)HT_{(o)} + L_{(o)} \rightleftharpoons MT(HT)_{m-1} \cdot CH_3COO \cdot L_{(o)} + H^+_{(a)} \quad (8)$$

where m is the mole number of TTA in the organic phase participating in the extraction and varies with the concentration of TTA added to the system. These equations show the general scheme of the extraction with TTA from an aqueous solution containing metal ions; they satisfactorily explain the phenomena show in Fig. 10. The numerical value 2 noted in Eq. 7 resulted from the extractions carried out in the range of 0.2 M TTA - MIBK and 0.125 mmol. of calcium (cf. Figs. 5—9). Under different conditions each term in Eqs. 7 and 8 may vary with the circumstance and other types of metal chelates may be formed.

In higher concentrations of TTA, the molecules are supposed to associate around the chelate and the distribution of metal may increase remarkably. The acetate ion and methyl isobutyl ketone may be displaced from the chelate by TTA as its concentration increases. For all that, the concentration of TTA plays a principal role in the extraction.

If all of the TTA added in the system reacts with the metal, the equilibrium may be written as follows:

$$nM + (xn+m-xn)HT \rightleftharpoons n(NT_x \cdot (HT)_{m/n-x}) + nxH^+ \quad (9)$$

where n is the moles of metal ion, m is the moles of HT added in the system, and x is the moles of hydrogen ion displaced by the combined HT. From the experimental data on which Figs. 9 and 10 are based, some systematic relations can be derived for the equilibrium of the extraction. These relations are shown in Table I. If all of the TTA present in the system (m) participates in the extraction of all the metal ions (n), the m/n value shown in the fifth column will indicate the number of TTA attachable to a metal ion schematically, but the tangent at any point on the curve in Fig. 10 will indicate the actual number of TTA radicals participating in the extraction of the metal ion at the definite concentrations of TTA and metal ions (sixth column). The number of TTA radicals combined by their ionic linkage in the chelate is given in the column under x. It can be obtained from the slope of the line in the log$D$-pH graph. The conspicuous difference between the values in the fifth and sixth columns from the assumption arbitrarily made in calculating the m/n (the fifth column) that all the TTA is capable of attaching to the metal ion. Therefore, the m in Eq. 9 is not the total concentration of TTA in the system; rather, it should be m, that of the TTA participating in the extraction with the metal. Therefore, the TTA molecules other than those functionally attached seem to be left out of the extraction process. Then, however, the distribution ratio will reach a steady value when the concentration of TTA exceeds some definite value.

However, the distribution ratio shown in Fig. 10 increases boundlessly with the increase in TTA. Therefore, it may be assumed that all the TTA added to the system participates in the extraction in various forms. Then, another equilibrium may be present between the total amount of TTA and the functional amount:

$$\text{total (HT)} \rightleftharpoons m(\text{HT}) \qquad (10)$$

To confirm the above assumption, the following experiment was undertaken. Methyl isobutyl ketone containing 1.48 mol. of TTA per liter was equilibrated with a 0.5 M buffer solution of pH 5.5 of the same volume. The buffer solution thus treated was then used to prepare a solution containing a definite amount of calcium. Each variation in the volume of this solution was taken in a separating funnel, and the total volume was made up to 7.3 ml. with the pre-equilibrated buffer solution. The extraction was carried out between 7.3 ml. of this aqueous solution and the methyl isobutyl ketone pre-equilibrated as above. After the extraction, the amount of calcium ion remaining unextracted was determined by flame-photometry. The ratio of the amount of TTA to that of calcium in the organic phase was calculated from the data obtained over all the range. It was found that when the amount of calcium in the aqueous solution was increased, the calcium in the organic phase reached a saturation point with the molar ratio of calcium to TTA at 1 : 34. In other words, at least thirty-four molecules of TTA were required to extract an ion of calcium. Even this minimum number is larger than the number evaluated from the tangents of the curve of log D-log(TTA) obtained under the same conditions as in this experiment. The number obtained from the curve is considered to be the number of TTA molecules attached to the chelate; apparently, no additional molecules seem to be necessary for the extraction. This is, however, not correct. Since the saturation of calcium occured in the organic solvent when it contained 34 molecules of TTA to one calcium ion and since the distribution ratio of calcium increased boundlessly with the increase in the concentration of TTA, the extra TTA molecules must be regarded as necessary for the extraction. Therefore, it may be supposed that a relatively large number of TTA molecules besides those attached to the chelate are required for the complete extraction of calcium. Consequently, Eq. 10 seems to hold for the equilibrium of the extraction system.

The Separation of Magnesium from Calcium, Strontium and Barium.—The distribution ratios of alkaline earth metals are so close to one another that it seems difficult to separate one from the others, even by multiple-batch extraction. However, if another chelating agent such as EDTA is present in an aqueous solution, calcium may be separated from the others by taking advantage of the greater stability of its EDTA-chelate.

The Behavior of Individual Ions in the Extraction in the Presence of EDTA.—The extraction procedure is based on the principle of competition between TTA and EDTA in the formation of the chelate. To an aqueous solution containing magnesium, calcium, strontium and barium ions and a suitable amount of EDTA, aqueous ammonia was added to make the solution almost neutral; then extraction with TTA-MIBK was carried out as has been previously described. After the extraction the aqueous phase was transferred to a beaker and evaporated nearly to dryness. The residue was dissolved in a mixture of 2 ml. of 6 N hydrochloric acid and 10 ml. of 30% hydrogen peroxide, and then the solution was evaporated nearly to dryness. In order to destroy the EDTA completely, the successive additions of 10 ml. of 30% hydrogen peroxide and evaporations were repeated. After the treatment, some water was added to dissolve the residue; the solution thus obtained was neutralized with sodium hydroxide and then titrated with a standard solution of EDTA, using BT as an indicator, at pH 10.

The extraction with 0.2 M TTA - MIBK was carried out for solutions containing about 0.5 mmol. of each metal ion at varying pH values, in the presence of EDTA in an amount equivalent to the metal. The recovery of the metals, especially calcium and magnesium, in the organic phase is shown in Fig. 12. The result shows that magnesium is very easily extractable, but calcium is not, their separation factor, β, being 139. Further experiments were made in order to examine the behavior of each alkaline earth metal in the presence of as much as four equivalents of EDTA. Table II shows the results obtained in the extraction of magnesium, calcium, strontium and barium at varying pH values. This method was found suitable for separating magnesium from other alkaline earths. EDTA-chelate of calcium has a large stability, but the other metals have a smaller stability. From this fact it may be expected that magnesium, strontium and barium can be extracted all together with TTA; however, this is not the case except for magnesium. This anomalous behavior of strontium and barium may come from the fact that their TTA-chelates have a relatively lower stability than that of magnesium.

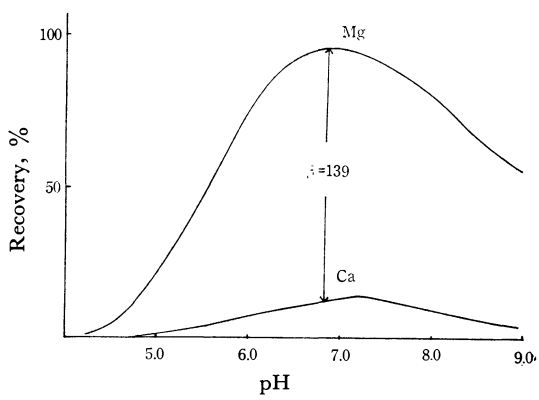

Fig. 12. Behavior of calcium and magnesium in extraction in presence of EDTA.
Taken: Ca 0.52 mmol., Mg 0.42 mmol.
EDTA: 1 : 1 molar ratio to each metal.

Table II. Behavior of the alkaline earth metal ions in extraction with TTA-MIBK in presence of four equivalents of EDTA

Metal ion, taken in 10 ml. of soln.	Final pH	D	% extraction
Mg : 0.42 mmol.	5.6	0.36	26.5
	8.8	0.13	11.9
	6.8	2.71	73.0
	7.4	1.44	59.1
	8.0	0.43	30.4
	8.7	0.17	14.8
Ca : 0.52 mmol.	5.8	0.03	3.6
	6.8	0.03	3.1
	7.8	0.03	3.3
	8.1	0.03	3.0
	8.5	0.02	2.2
	8.7	0.02	2.1
Sr : 0.52 mmol.	5.6	0.04	3.8
	6.1	0.03	3.2
	6.7	0.04	3.9
	7.0	0.03	3.7
	7.5	0.04	4.1
	8.6	0.01	1.5
Ba : 0.50 mmol.	5.5	0.00	0.3
	6.7	0.01	1.0
	8.4	0.01	1.3
	8.9	0.01	1.3

The Separation of Magnesium from Calcium by Extraction with TTA in the Presence of EDTA.—An aqueous solution containing a total amount of magnesium and calcium of 0.5 mmol. was subjected to extraction with 0.2 M TTA - MIBK in the presence of four equivalents of EDTA. The extraction was then repeated two more times with new batches of the organic solvent in order to make a satisfactory separation. The organic phases were then put together into another separating funnel. The back extraction of the organic phase was carried out with 1 N hydrochloric acid. The solution thus obtained was evaporated with the addition of 30% hydrogen peroxide in order to decompose the EDTA. The hydrochloric acid solution was first adjusted to pH 10 by adding a buffer solution of aqueous ammonia and ammonium chloride; then it was titrated with a standard solution of EDTA, using BT as an indicator. The volume of the EDTA solution required was equivalent to the sum of the amounts of calcium and magnesium extracted in the organic phase. Then, another part of the back-extracted solution was treated in the same way, and its pH was adjusted to 12 by adding potassium hydroxide and it was titrated with a standard solution of EDTA, using Dotite NN (calcon) as an indicator. The volume of the EDTA solution required in the latter titration represented the amount of calcium extracted in the organic phase. The recovery of calcium and magnesium from their mixture in various ratios is shown in Table III, from which it may be found that magnesium can be separated largely in the organic phase, while calcium remains in the aqueous phase, although there is some mutual contamination.

Table III. Separation of calcium from magnesium by extraction with TTA-MIBK in presence of EDTA

Molar ratio in sample soln. Mg : Ca	Recovery in organic phase, % Mg	Ca
Mg alone	95.2	—
2 : 1	95.8	8.7
1 : 2	98.9	8.5
1 : 3	99.5	7.0
Ca alone	—	6.2

Summary

The liquid-liquid extraction of alkaline earth metal ions with 2-thenoyltrifluoroacetone dissolved in methyl isobutyl ketone has been investigated with a view of separating them. The extractability of the ions decreases in the order of magnesium, calcium, strontium and barium; moreover, the distribution ratios between the organic solvent and the aqueous solution are too close to one another for a satisfactory separation. Critical studies have been made on some factors affecting the distribution ratio (hereafter denoted by D) of each metal, such as the amount of metal ion in the aqueous solution, the concentration of TTA in the organic solvent, and the pH of the solution. Among these factors the concentration of TTA in MIBK was found to play a principal role in this extraction, and the relation between $\log D$ and log(TTA) was shown as a curve, not a straight line, in the range of TTA concentration from 0.001 to 0.2 M in MIBK, while another investigators had previously stated that the relation could be shown in many other cases as a straight line with a slope of 2. The slope of the straight line representing the relation between $\log D$ and log (TTA) had usually been believed to show the number of molecules of the chelating agent attached to the metal extracted, i. e., the extracted species; however, the curve obtained by the present author indicates that the extraction process is not so simple but is, rather, very complicated. The difference may be caused by a fact overlooked by the other investigators: the pH of the aqueous solution is lowered enormously by contact with the organic phase, and the distribution ratio is thereby remarkably decreased.

In the author's experiment with 1.48 M TTA-MIBK, the number of TTA molecules attached to a calcium ion is enormously large, at least thirty-four. This phenomenon can be explained

by assuming that, in a lower concentration of TTA, the metal ion is bonded not only by TTA but by the acetate ion present in the buffer solution or by MIBK, a polar solvent, while, on the other hand, in a higher concentration of TTA, the acetate ion and the MIBK do not participate the chelate formation but only the TTA can be attached to the metal, and a network of TTA, which will increase the distribution of metal into the organic solvent, may be produced surrounding the metal.

Among the metal ions, calcium and magnesium could be separated from each other by carrying out the extraction in the presence of EDTA, by virtue of the competition between EDTA and TTA for chelate formation. The author has extended this extraction method to a reversed-phase partition chromatography in a column; this will be described in a following paper.

The author wishes to express her thanks to Professor Toshiyasu Kiba for his kind advice and encouragement.

BULLETIN OF THE CHEMICAL SOCIETY OF JAPAN VOL. 39 980—989 (1966)

The Separation of Alkaline Earth Metals as Their TTA-Complexes by Reversed-Phase Partition Chromatography

By Ikuko AKAZA

Department of Chemistry, Faculty of Science, Kanazawa University, Kanazawa

(Received September 21, 1965)

The author's preceding work, the liquid-liquid extraction of alkaline earth metals with TTA-MIBK, has now been extended to a reversed-phase partition chromatography in order to attain a good separation of the metal ions. The method was carried out with relatively large amounts of the metals through a column of Kel-F on which the organic phase of 1.5 M TTA - MIBK was supported. Elution was performed with 0.5 M buffer solutions, of various pH values, consisting of acetic acid, ammonium acetate and aqueous ammonia. The actual separation of each metal ion from the mixture of alkaline earth metals was achieved; the results are shown in several figures. The dependence of the distribution ratio on the pH of the solution and on the concentration of TTA in the stationary phase was examined from the elution curves; it might be considered that the same relation held as in the case of the liquid-liquid extraction system. Other experiments were then carried out in order to clarify the behavior of the TTA-chelates in the presence of a large amount of TTA; it was found that all of the TTA in the system participated in the effective extraction of the metal ion. The steps in the formation of the higher TTA-chelate in the column are depicted by the break-through curve of the chromatographic process.

Previously the present author studied the liquid-liquid extraction of alkaline earth metal ions with TTA (2-thenoyl trifluoroacetone) in methyl isobutyl ketone (abbreviated as MIBK); the details of that investigation have been described in a preceding paper.[1] As a consequence of that study it was found that the separation of alkaline earth metals from one another by batch extraction was very difficult because the distribution ratios of the TTA-chelates of the metals between methyl isobutyl ketone and an aqueous solution of a different pH value were so close together. The lower separation factors among the metal ions induced the author to seek other more convenient and efficient methods based upon extraction with TTA - MIBK. Reversed-phase partition chromatography is closely related to liquid-liquid extraction, except that in the former the water-immisible extractant is immobilized on a stationary inert support. In the column extraction of this type an aqueous solution containing the solute to be extracted is always in contact with the fresh organic solvent on the column, and multiple extraction may be carried out throughout the process; therefore, effective separation may be achieved between the substances of a lower separability. Moreover, a larger quantity of metal ions may be treated by this method.

In this investigation Kel-F (polytrifluorochloroethylene), presented by Hamlin et al.,[2] was chosen as the inert solid support from among the

1) I. Akaza, This Bulletin, **39**, 971 (1966).

2) A. G. Hamlin, B. J. Roberts, W. Laughlin and S. G. Walker, *Anal. Chem.*, **33**, 1547 (1961).

various kinds of material that had been recommended. Reversed-phase partition chromatography has never been applied for the separation of alkaline earth metals in the column method, excepting the work by O'Laughlin and Banks[3] who separated barium, magnesium and calcium from each other using bis(di-*n*-hexyl-phosphinyl)-methane. Recently, however, Cerrai and Ghersini[4] attempted the paper chromatographic method with di-(2-ethylhexyl)orthophosphoric acid, HDEHP; the R_f value for each metal showed a capability of separation.

This paper will describe a column method of reversed-phase chromatography in which the stationary phase is a solution of TTA in MIBK supported on Kel-F, and the mobile phase is a 0.5 M buffer solution consisting of acetic acid, ammonium acetate and aqueous ammonia. The results of the liquid-liquid extraction of TTA-chelates of alkaline earth metals described in a preceding paper[1] will be fully utilized. The elution of the individual ions and the isolation of each metal could be achieved successfully by the column method. The relation of the chromatography to the liquid-liquid extraction will be discussed in detail.

Experimental

Apparatus.—The column, the fraction collector and the flame photometer were the same as those described in previous paper,[6] but the inner diameter of the column tube was 1.2 cm. and the length was 20 cm.

Reagents and Materials.—Kel-F (polytrifluorochloroethylene), TTA (2-thenoyltrifluoroacetone) and MIBK (methyl isobutyl ketone) were the same as those used by the author in previous investigations.[1,6]

The Organic Solvent Solution Used for The Stationary Phase.—In 20 ml. of MIBK placed in a separating funnel, dissolve 8.888 g. of TTA; the volume of the solution thereby becomes 27 ml. Adjust the pH of a 0.5 M ammonium acetate solution saturated with MIBK to the value which is preferred for each eluting process. Put 27 ml. of this solution into the separating funnel, and shake the vessel until the two phases are equilibrated enough. Use the organic phase for adsorbing on Kel-F powder, as will be described below. This method of preparation was employed in many cases in this research and is referred to as the 1.48 M TTA-MIBK solvent solution. In some cases, however, MIBK solutions with different amounts of TTA were also used.

Eluting Solution.—The eluting solution in each case should have a composition similar to that of an aqueous solution which has been equilibrated with the organic solvent solution it comes in contact with in the column. To save the trouble of actually equilibrating the two phases, the following method should be employed: First, prepare a solution containing a definite amount of TTA in MIBK. Next, prepare a 0.5 M ammonium acetate - acetic acid or aqueous ammonia buffer solution of a definite pH which is saturated with MIBK. Place equal volumes of the TTA-MIBK solution and the buffer solution in a separating funnel, and equilibrate the two phases by shaking. Take out a definite volume of the organic phase and pour it on the Kel-F powder in order to prepare a stationary phase of the column. Determine the amount of TTA present in the aqueous phase by the author's method.[5] Weigh the appropriate amount of TTA as calculated from the value and dissolve it in the buffer solution in the manner shown below.

Eluting Solution of pH 5.5.—Put into a 1-l. separating funnel 3.15 g. of a TTA reagent and 900 ml. of a 0.5 M ammonium acetate solution which has been saturated with MIBK; then shake the vessel for 30 min. in order to dissolve the reagent completely. Then adjust the pH of the solution to 5.5 by adding 0.5 M acetic acid. Make the total volume of the solution to 1 l. with a solution of 0.5 M ammonium acetate saturated with MIBK. Employ this solution for elution.

The amounts of TTA in the various buffer solutions which have been determined are as follows; the same amount of TTA should be dissolved for the preparation of each eluting solution:

Organic phase contacted	pH of the buffer solution	TTA g./l.
1.48 M TTA - MIBK	5.5	3.15
1.48 M TTA - MIBK	6.5	3.2
0.2 M TTA - MIBK	5.5	0.2
0.2 M TTA - MIBK	6.5	0.42
0.2 M TTA - MIBK	7.5	0.59

These eluting solutions can be stored without decomposition for a month in a dark place between 0°C and 3°C.

In the above case the amount of TTA to be dissolved in each eluting solution differs with the temperature, so the temperature during the preparation of the eluting solution and the elution of a solute from the column should be kept constant. Changes in temperature affect the solubility of MIBK in the eluting solution; therefore, the solubility of TTA also varies.

Sample Solution.—Barium chloride dihydrate, strontium nitrate tetrahydrate, calcium chloride dihydrate, and magnesium chloride hexahydrate, all of which are analytically-pure reagent grade materials, were employed. It is desirable, but not in all cases, that the sample solution have a composition like to that of the eluting solution. Three-milliliter portions of the sample solution were used for the column experiment.

Experimental Procedure.—*Preparation of the Stationary Phase.*—In a glass-stoppered Erlenmyer flask, put 8.0 g. of the Kel-F powder which has been dried at 80°C and stored in a calcium chloride desiccator; pour on it 7.3 ml. of an organic solvent solution prepared as above. After stoppering the flask, shake it by hand in order to homogenize the contents, and leave it in an ice-box for at least three hours. Add a small volume of a suitable eluting solution, and pour the slurry little by little into the chromatographic column, taking care not to let any air bubbles in, and gently pressing the slurry down with a glass rod each time. After pouring in all

3) J. W. O'Laughlin and C. V. Banks, U.S.A.E.C. Rep., IS-737, 145 (1963).
4) E. Cerrai and G. Ghersini, *J. Chromatog.*, **13**, 211 (1964).
5) I. Akaza, M. Kosaka and T. Imamura, *Bunseki Kagaku (Japan Analyst)*, **14**, 825 (1965).
6) I. Akaza, This Bulletin, **39**, 585 (1966).

the slurry, press the column bed with a glass rod in order to make it height about 18 cm. The upper surface of the column should be covered by the eluting solution.

The Elution, Separation and Determination of Metals.—Pour 3 ml. of the sample solution on the upper surface of the column and allow it to percolate into the column at the rate of 0.2 ml. per minute; then twice pour in little portion of the eluting solution in order to wash inside of the glass tube above the upper surface of the column, letting it flow down the column at the same rate. Set on the top of the glass tube a separating funnel from which the eluting solution of a definite composition is allowed to flow through the column, and carry out the elution at the rate of 0.5 ml. per minute. Collect the effluent in suitable fractions by a fraction collector, and determine the amount of metal in each fraction by flame-photometer. In order to get a satisfactory separation of an ion from the others with reasonable speed, a different eluting solution should be used for each ion.

Results and Discussion

The Characteristic Behavior of the Column.—*The Choice of Column Material.*—The author preferred Kel-F moulding powder for the same reason as was stated in a preceding paper.[6]

The Amount of Methyl Isobutyl Ketone that can be adsorbed by Kel-F.—In a glass-stoppered Erlenmyer flask 10 g. of Kel-F powder was placed; 50 ml. of MIBK was then poured on the powder, and the vessel was put aside for overnight after having been gently shaken. The unadsorbed solvent was drained through a small glass filter into a measuring cylinder under a slight suction. The inside wall of the flask was washed with 1 ml. of a fresh solvent in order to transfer all the Kel-F powder to the filter. The difference between the volume taken and that measured in the cylinder indicated the volume of the solvent adsorbed on Kel-F. It came to 9.0 ml. of the solvent for 10 g. of Kel-F powder.

The Volume of the Mobile Phase in the Column.—The column bed was prepared as follows: On to 8.0 g. of Kel-F powder, 7.2 ml. of MIBK saturated with water was poured. The ratio of these amounts was fixed at that obtained in the above experiment. The powder was then allowed to adsorb the liquid by standing overnight. A 0.1 M sodium chloride solution saturated with MIBK was added to the powder, and the resulting slurry was poured into the glass tube in order to make a column bed 18 cm. deep. Plenty of 0.1 M sodium chloride solution-saturated MIBK was allowed to flow down until the effluent showed the same concentration of sodium chloride as the original solution. After careful washing, with water, the inside of the tube below the fritted glass filter, water-saturated MIBK was poured on the column in order to wash down the 0.1 M sodium chloride solution occupying the pores of the column. The amount of sodium chloride was determined in the washing liquor by titrating it with a 0.1 M silver nitrate solution as usual; the volume of the pores of the column was then obtained from this value. That turned out to be 7.27 ml; hence, the volume ratio of the stationary phase to the mobile phase was found to be 1 : 1 in this case. This showed that the elution process consisted of multiple extractions between equal volumes of the two phases.

The pre-equilibration between the organic solvent and eluting solution of equal volumes, described in the preceding section, was necessary to maintain the condition of actual equi-volume extraction. However, they were not always prepared by the actual equilibration of the two phases, but usually by putting a calculated amount of the reagent in an aqueous solution.

Column Life and Stability.—After loading 0.09 mmol. of calcium on the column, elution with a solution of pH 5.5 was carried out; the elution curve was thus obtained as usual. The same experiment was repeated three more times in succession with the same column. The volume of eluent spent before the emergence of the calcium ion at a maximal concentration, as denoted by E, in each case is shown in Table I. In these experiments the temperature was kept at about 12°C, and the column was kept covered with black paper in order to exclued sunlight. In each elution about 420 ml. of the eluent was used, so the total volume came to as much as 1.7 l. On the other hand, two elutions carried out under the same conditions with the same column at an interval of two weeks gave a satisfactory result each time. Therefore, the column seems to remain capable of satisfactory use for a week, if the temperature is kept below 12°C and if light is excluded.

Table I. Column life revealed by the shifting of elution peak

Experiment in order	Date	Volume of effluent before peak of maximum elution
1	April 22	158.9 ml.
2	April 23	161.9 ml.
3	April 24	174.9 ml.
4	May 1	126.8 ml.

The Recovery of Kel-F.—The Kel-F powder could be recovered from the degraded column by the following method: The powder used was washed with water repeatedly, and with 1 M hydrochloric acid several times. It was then put in water containing 40% alcohol, which had been found to be a good wetting solvent for Kel-F, and stirred well in order to remove the MIBK from the powder. This treatment was repeated several times until the solution became neutral and the powder, pure white. The powder was

then washed again with 99% alcohol and the washings were removed with a glass filter under suction. Some ethyl ether was poured on the powder. The powder was dried under strong suction in order to remove the ether completely. The powder of Kel-F thus treated could be used again after drying at 80°C for one hour.

Column Capacity.—The capacity of the column prepared as described in the procedure was estimated by loading it with a calcium salt of a known concentration. The breakthrough curve obtained was not as sharp nor as smooth as usual. This may be due to the mechanism of the extraction described in a foregoing paper[1]; the meaning of an irregular curve will be discussed later.

The Chromatographic Behavior of Alkaline Earth Metals.—The chromatographic behavior of each alkaline earth metal ion can be predicted from the previously-descrived results obtained in the liquid-liquid extraction of their TTA-chelates with MIBK.[1] Their distribution ratios were found to depend on the hydrogen ion concentration of the aqueous phase, the concentration of TTA in the organic phase, and the quantity of metal ion to be treated. At any definite pH value of the aqueous phase, the distribution ratio of each metal ion was in the desending order: magnesium, calcium, strontium and barium. From these results it was expected that, in the column chromatography, barium could be eluted from the column faster than the others. Taking each extraction curve obtained previously into account, the elution curves of each metal ion were obtained at pH 6.5 and 5.5.

The Elution Curve of Individual Ions.—To examine quantitatively the retention on, and the elution from, the column, 0.025 mmol. of each metal ion was placed in the column and eluted with an eluting solution of pH 6.5. The results are shown in Fig. 1, which shows that the elution at this condition may be useful for the separation of the two metals. When a similar elution was carried out at pH 5.9, the two curves overlapped with each

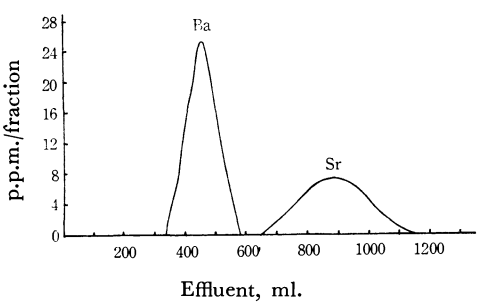

Fig. 1. Elution curves of barium and strontium.
(Experiments with Ba and Sr conducted separately)
Loaded: 0.025 mmol. of the element
Eluting solution: pH 6.5

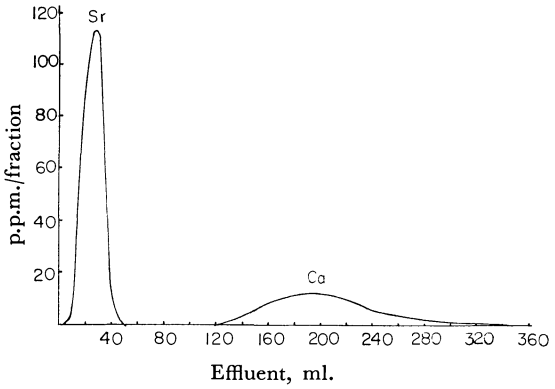

Fig. 2. Elution curves of strontium and calcium, individually.
Loaded: 0.025 mmol. of the element
Eluting solution: pH 5.5

other. The elution curves of strontium and calcium at pH 5.5 are shown in Fig. 2. They show the possibility of using this condition for the separation of the above two metals. Magnesium, however, was precipitated as the insoluble TTA-chelate over the pH range mentioned above.

The Separation of Metal Ions.—a) The Separation of Barium and Strontium.—Various amounts of

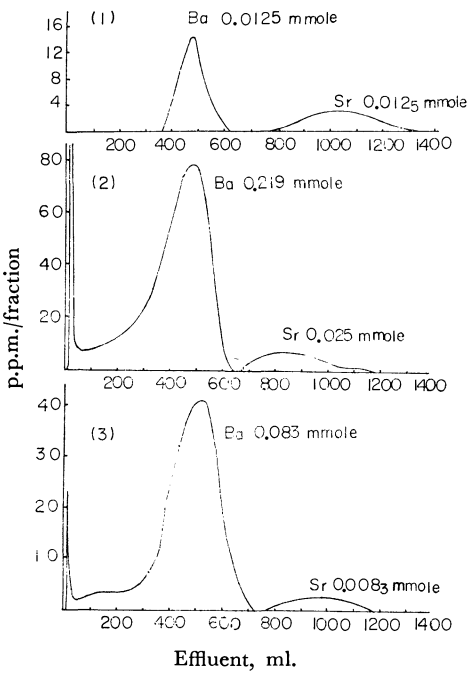

Fig. 3. Separation of barium from strontium.
Loaded: (1) 0.0125 mmol. Ba and 0.0125 mmol. Sr
(2) 0.219 mmol. Ba and 0.025 mmol. Sr
(3) 0.083 mmol. Ba and 0.008_3 mmol. Sr
Eluting solution: pH 6.5

barium and strontium ions were mixed in an eluting solution of pH 6.5 to make three kinds of a sample solution: (i) 0.0125 mmol. barium and 0.0125 mmol. strontium; (ii) 0.219 mmol. barium and 0.025 mmol. strontium and (iii) 0.083 mmol. barium and 0.0083 mmol. strontium, each in 3 ml. portions. Three milliliters of each sample solution were placed in the column, and the elution was carried out with the eluting solution of pH 6.5. The results obtained are shown in Fig. 3, from which it may be seen that the two metals could be separated from one another, even if they were present in widely different ratios.

b) The Separation of Strontium and Calcium.—In the column prepared as described in the procedure there was placed 3 ml. of a sample solution containing 0.333 mmol. strontium and 0.005 mmol. calcium and then another 3 ml. containing 0.005 mmol. strontium and 0.15 mmol. calcium. The elution was carried out with an eluting solution of pH 5.5. A satisfactory separation could be achieved, as is shown in Fig. 4.

c) The Separation of Barium, Strontium, Calcium and Magnesium.—A 3 ml. sample solution containing 0.0125 mmol. barium, 0.0125 mmol. strontium, 0.025 mmol. calcium and 0.0125 mmol. magnesium was employed. The TTA was left out, for it would precipitate magnesium as the chelate. Elution was carried out at first with an eluting solution of pH 6.5 until the volume of the effluent reached 700 ml. During the elution barium was eluted down as is shown in Fig. 5. Then the elution was continued with 400 ml. of an eluting solution of pH 5.5. Strontium and calcium

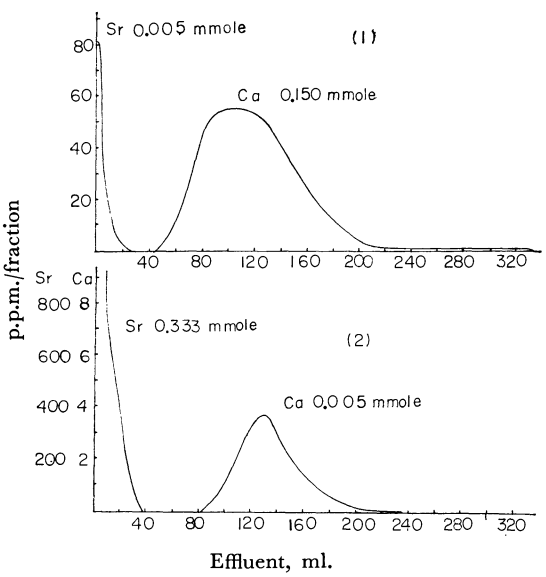

Fig. 4. Separation of strontium from calcium.
Loaded: (1) 0.005 mmol. Sr and 0.15 mmol. Ca
(2) 0.333 mmol. Sr and 0.005 mmol. Ca
Eluting solution: pH 5.5

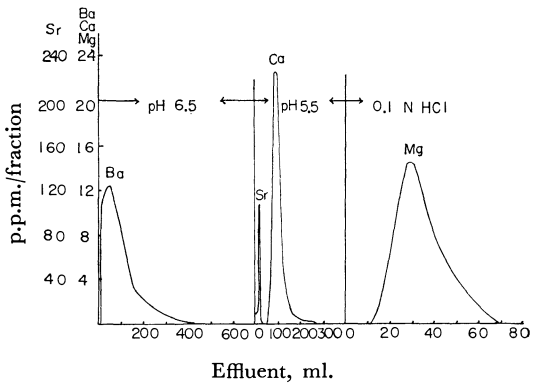

Fig. 5. Separation of barium, strontium, calcium and magnesium.
Loaded: 0.0125 mmol. Ba, 0.0125 mmol. Sr, 0.025 mmol. Ca and 0.0125 mmol. Mg
Eluting solution: As mentioned in the graph

appeared in the effluent. At last the magnesium retained on the column was eluted down with 0.1 M hydrochloric acid. Thus the separation of alkaline earth metals from their mixture was achieved.

A Blank Test with the Solvent without TTA.—If the absence of the chelating agent TTA in MIBK causes a retention of alkaline earth metal ions by the stationary phase on the column, the method will be unsatisfactory for the separation of these ions. To test whether such retention really occurs, 7.3 ml. of MIBK which had been equilibrated with a 0.5 M buffer solution of pH 6.5 saturated with MIBK was allowed to be adsorbed on 8.0 g. of Kel-F powder and then the column was prepared. The elution of calcium ions was then carried out. Calcium ions appeared as early as in the first fraction of the effluent, and reached a maximum in the third. Therefore, the calcium ions placed in the column could not be retained at all without the presence of TTA in the organic solvent.

Some Relation to the Liquid-liquid Extraction.—*The Dependence of the Distribution of Metal Ions on the pH of the Solution.*—In a preceding paper[1] the present author stated that the dependence of the distribution ratio upon the hydrogen ion concentration of the aqueous phase could be represented by a straight line with a slope of about one to two in the graph of log$D$ vs. pH. The slope of the line was sharper when the quantity of metal ions was smaller, as well as when the stability of the chelate of the metal was higher; a higher concentration of TTA in the organic phase also made the slope sharper. In the present study, the relation between the distribution ratio of metal and the pH was investigated in the extraction process in the column. Each 3-ml. portion of sample solutions of varying pH values contained 0.005 mmol.

of strontium. This 3 ml.-portion was placed in the column; elution was then carried out with eluting solutions of the same pH. The elution curve was obtained as usual, and the distribution ratio of the metal in each case was calculated by Eq. 1, which is identical with the one generally used in partition chromatorgraphy:

$$D = (E - F)/B \qquad (1)$$

where

D: distribution ratio; E: the volume of the effluent before the emergence of the solute in a maximal concentration; B: the volume of the stationary phase, and F: the volume of the mobile phase, viz., the pores in the column.

The value of D calculated in each case is plotted in a graph of log D vs. pH in Fig. 6. In these experiments the pH of the eluting solution scarcely varied from the initial value. The relation between log D and pH is shown as a straight line with a slope of 2.3.

For comparison with the above results, a series of liquid-liquid extractions was carried out with 7.3 ml. of the same organic solvent as had been adsorbed on Kel-F powder and 21.9-ml.* portions of several eluting solutions containing 0.1 mmol. of calcium ions; the calcium ion content in the aqueous phase was determined by flame-photometry. This was repeated with samples of different pH values; the distribution ratio of calcium was calculated as usual. The data obtained are shown

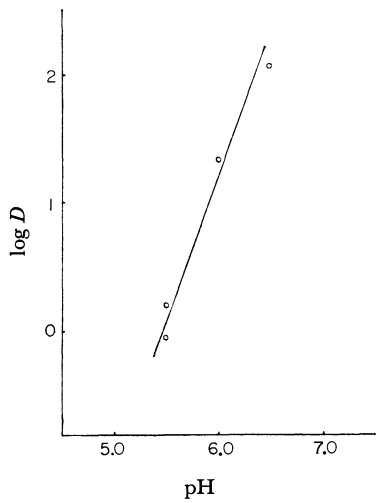

Fig. 6. Dependence of distribution ratio upon pH of the solution.
The values of D were calculated from respective elution curves.

* The reason for taking 21.9-ml. portions of the solution is as follows: If equal volumes (7.3 ml. each) of the solution and the organic solvent were used, the volume would be too small to separate the aqueous phase from the extraction system in the batch extraction with the organic solvent adsorbed on Kel-F described below. The author carried out the extraction at the volume ratio of 3 : 1.

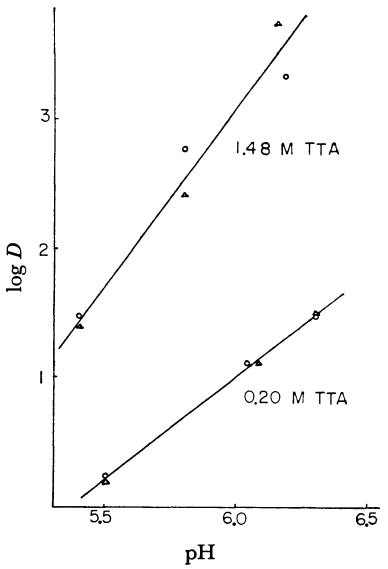

Fig. 7. Dependence of distribution ratio of calcium upon pH of the solution. Obtained from a batch extraction between each 7.3 ml. of solvent and 21.9 ml. of aqueous solution.
Loaded 0.1 mmol. Ca
△ Liq.-liq.(on Kel-F) batch extraction
○ Liq.-liq. batch extraction

in Fig. 7 as a graph of log D vs. pH.

Another series of extractions was carried out with the organic solvent solution adsorbed on Kel-F powder. The organic solution and the aqueous solution, as well as their volumes, were identical in this experiment and in that described just above. In a 100-ml. glass-stoppered Erlenmyer flask 8.0 g. of Kel-F powder was placed, and then an organic solvent solution was poured in. After the vessel had stood for more than three hours, each eluting solution containing calcium ions was introduced into it. The vessel was gently shaken for a while under tightly-stoppered conditions. The content was poured on a coarse glass filter, and the aqueous phase was allowed to drain by gravity into another vessel. The calcium ion content in the solution was determined by flame-photometry. The data obtained are shown in Fig. 7, in which the pH is that of the aqueous solution after the extraction.

The data obtained from the liquid-liquid batch extraction and those from the batch extraction between the liquid and a stationary phase on Kel-F are in good agreement. This shows that Kel-F did not affect the extraction. The slope of the line in log D vs. pH is 2.7 in the case of 1.48 M TTA-MIBK and 1.5 in the case of 0.2 M TTA. As in Fig. 9 of a preceding paper,[1] in which similar behavior of the relation log D vs. pH had been shown in this case the slope of the line increased with the concentration of TTA.

The column extraction and the batch extraction of metal ions were found to give lines of the same

slope, as is shown in Fig. 6 and Fig. 7, though the ion treated was strontium in the former and calcium in the latter. However, the slopes of the lines were 2.3 and 2.7 respectively; that is, they were larger than the slope (2.0) of the lines illustrated in a preceding paper,[1] in which a 0.2 M TTA solvent solution was used. Since the number of TTA attachable to a calcium ion with ionic linkage is two, the slope must also be two. In this case, however, the excess over two seems to indicate the formation of some anionic species of chelate in a higher concentration of TTA, such as 1.48 M.

The Dependence of the Distribution Ratio on the Concentration of TTA in the Solvent.—The relation of log$D$ to log(TTA) was obtained by the column chromatographic method, with a stationary solvent phase containing varying amounts of TTA. A definite volume of MIBK containing various amounts of TTA was equilibrated with an equal volume of the eluting solution of pH 5.5. The organic phase was used for the stationary phase on Kel-F powder. Several eluting solutions were prepared in accordance with the amounts of TTA in the organic phase in each case. Then, 0.02 mmol. of the calcium ion was loaded to the column and elution was carried out with the proper eluting solution. The dependence of log D on log (TTA) was obtained from the effluent volume of E. The results are shown in Fig. 8.

In a glass-stoppered centrifugal tube, liquid-liquid extraction was carried out with 7.3 ml. of the same organic solvent used in each stationary phase in the column chromatography, and with 21.9 ml. of the same eluting solution, which contained 0.1 mmol. of calcium ion. After centrifugation in order to separate the phases, the aqueous phase was taken out for the determination of calcium. The distribution ratio of calcium was calculated as usual.

Another batch extraction was carried out with the same organic solvent placed on Kel-F powder and with each eluting solution used in the above extraction. In a 100 ml.-Erlenmyer flask 7.3 ml. of the organic solvent solution was poured onto 8.0 g. of Kel-F powder. After the vessel had stood more than three hours, 21.9 ml. of the eluting solution, containing 0.1 mmol. of calcium ion, was poured onto the powder. The vessel was then stoppered and shaken gently for ten minutes. Calcium ion content in the aqueous phase was determined. This was repeated with solvents containing different amounts of TTA. The data obtained are shown in Fig. 9 as a graph of log$D$ vs. log(TTA). The data obtained from the liquid-liquid extraction and those from the batch extraction with the stationary phase placed on Kel-F are found to be in good agreement on the curve. This shows again that Kel-F powder does not affect the extraction mechanism.

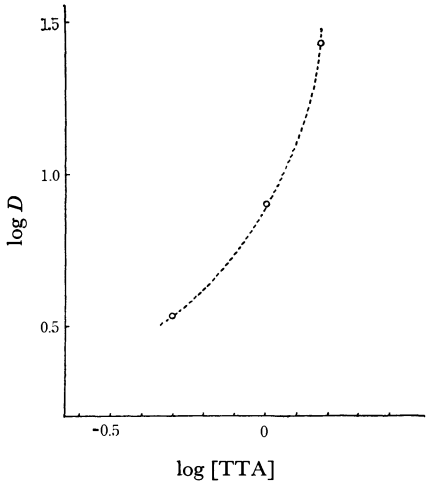

Fig. 8. Dependence of distribution ratio of calcium upon the concentration of TTA in the organic phase. The values of D were obtained from the elution curves for different concentrations.
Loaded: 0.02 mmol. Ca
Eluting solution: pH 5.5

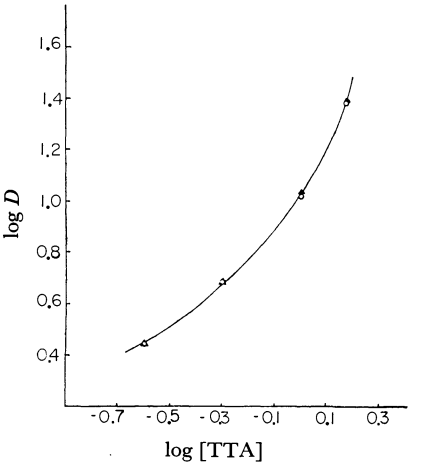

Fig. 9. Dependence of distribution ratio of calcium upon the concentration of TTA in the organic solvent.
○: D was obtained from liq.-liq. extraction.
▲: D was obtained from batch extraction with Kel-F.
Taken: 7.3 ml. of organic solvent, 21.9 ml of aqueous solution of pH 5.5, and 0.1 mmol. Ca

The column extraction and batch extraction resemble each other, as is shown in Figs. 8 and 9. In the former, however, the distribution ratio is a little lower in the low concentration of TTA. Because when the concentration of TTA is low the rate of chelate formation may be very small, in the column fresh eluting solution seems to be running through without reaching a satisfactory

equilibrium. But in the batch extraction complete equilibrium of the two phases is achieved upon longstanding contact.

The Variation in the Elution Curve due to the Variation in the Quantity of Metal Ions in the System.—It was described in a preceding paper[1] that, in the liquid-liquid extraction of the TTA-chelate of metal, the distribution of the metal ion decreases with the increase in the metal-ion content in the aqueous phase. Now the author has tried to ascertain if this is also the case in column extraction.

A sample solution, 3 ml., of pH 5.5, containing a known quantity of calcium ions, was placed on the column, and elution was carried out with the same eluting solution. This was then repeated with different amounts of calcium. The results are summarized in Table II, which shows that the

Table II. Distribution ratio obtained from the elution curves at various concentration of calcium

Amount of calcium loaded mmol.	Effluent volume before maximum elution, ml. (E)	Distribution ratio calculated (D)	Number of plates (N)
0.0125	220.0	29.1	39.6
0.03	204.7	27.0	22.2
0.09	174.9	22.9	20.1
0.15	170.9	22.4	19.2

peak of the elution curve is displaced forward with the increase in the quantity of metal ions loaded. This phenomenon seems to be caused by the decrease in the distribution ratio of the metal, as has been described previously.[1] The number of theoretical equivalent plates, N, was also calculated from the usual equation:

$$N = E(E - F)/s^2 \qquad (2)$$

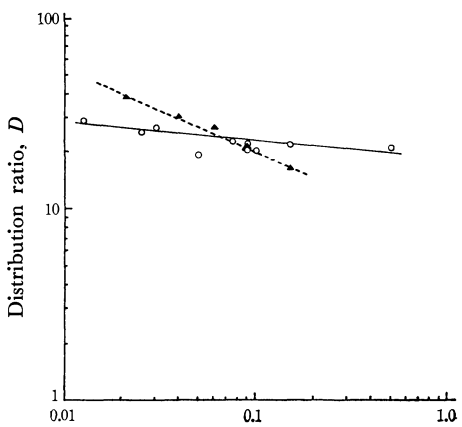

Fig. 10. Dependence of distribution ratio of calcium upon the concentration of calcium taken.
○ Obtained from elution through the column
▲ Obtained from liq.-liq. extraction

For comparison with the above column extraction, batch extraction was carried out between 7.3 ml. of the organic solvent and eluting solutions of pH 5.5 containing various quantities of calcium ions. The organic solvent was exactly the same as that held on Kel-F powder in the column. The relation observed in the batch extraction is shown in Fig. 10 with ▲ marks. In the batch extraction the decrease in the distribution ratio due to the increase in metal ion content appeared remarkably larger than in the column extraction. This inequality may be caused by the differences in the contact times of the two phases.

The Breakthrough Curve and the Capacity of the Column.—A column was prepared as described in

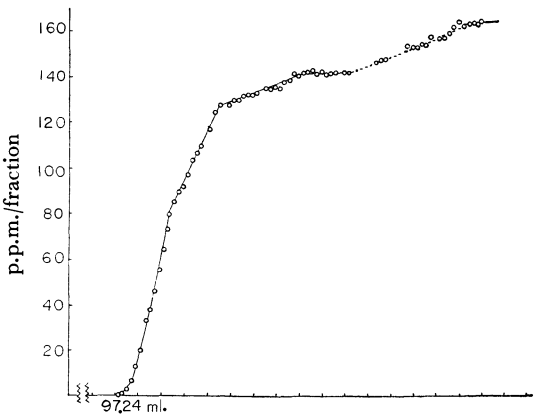

Fig. 11. Breakthrough curve of calcium.
With eluting solution of pH 5.5 containing 0.0040_6 mmol. Ca per ml.

the procedure; 500 ml. of a feed solution containing 0.00406 mmol. of calcium per ml. was also prepared by diluting 8 ml. of a stock solution of calcium salt with an eluting solution of pH 5.5 in a 500-ml. measuring flask. The solution was then fed on the column continuously at the rate of 0.05 ml. per minute. The breakthrough curve obtained is very irregular, as is shown in Fig. 11. It is neither sharp nor smooth over the whole range of the effluent, unlike most other breakthrough curves. The part of the curve shown by the dotted line merely shows the tendency of the curve, because the deviation of the measured results was too large for a perfect curve to be drawn. Let us attempt to account for the irregularity of the breakthrough curve. The calcium ion coming into the column at first forms its lowest TTA-chelate on the stationary phase, and then it changes to a higher TTA-chelate, which has a higher distribution ratio. Therefore, the increase in the amount of calcium in the effluent becomes slower, and the curve becomes less steep. When the stationary phase is saturated with calcium chelate of the highest distribution ratio, higher chelates begin to be degraded

to lower ones by the influx of new calcium ions into the phase, followed by a gradual decrease in the distribution ratio. The curve thus begins to become steeper again, and eventually the concentration in the calcium ion in the effluent reaches the constant value possessed by the initial feed solution. It may be assumed that in the column process, unlike as in the batch extraction, a solution passes through the column without reaching a satisfactory state of phase-equilibrium because of the small formation rate of the higher TTA-chelate. Consequently, the breakthrough curve may be thought to depict the steps of the formation of TTA-chelates as they really are. The amount of calcium retained on the column from the beginning to the breakthrough point was estimated to be 0.36 mmol., while the amount of calcium retained on the column throughout the interval represented in the curve was estimated to be 0.58 mmol.

In order to clarify the above picture, liquid-liquid extraction was carried out. In particular, the saturation of calcium in the organic phase was examined under conditions similar to those used in the column process. Each 7.3 ml. of an organic solution and an aqueous solution of pH 5.5 containing various amounts of calcium ion were shaken for ten minutes and then centrifuged. The amount of calcium remaining unextracted in the aqueous phase was then determined. The ratio of the amount of calcium extracted from each sample to the amount of TTA in the organic phase was plotted against the total amount of calcium taken. In this case the amount of TTA had been estimated to be 10.7 mmol. by the author's method.[5] The relation is shown in Fig. 12, in which the graph is a curve, not a straight line. This may be due

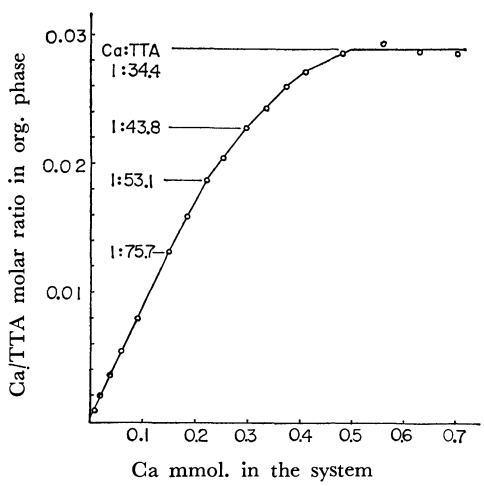

Fig. 12. Saturation of calcium in the organic phase.

Shown in the relation between the composition of the phase and the amount of calcium taken in the system.

to the step-by-step change in the species of metal-chelate with varying amounts of metal ions, followed by the variation in the distribution ratio. With the increase in the amount of calcium taken into the system, the quantity of TTA attached to a calcium ion decreases steadily. The distribution ratio of the metal-chelate formed at that time may be assumed to be lower. Finally, the organic phase is saturated with calcium, and the calcium chelate begins to separate out. This behavior of saturation corresponds to that of the breakthrough curve in Fig. 11; moreover, the saturation of calcium ion is maintained when about 0.5—0.6 mmol. of calcium is present in the system, while the amount of calcium in the organic phase is estimated to be 0.31 mmol.

When the elution is carried out, the amount of calcium loadable may be estimated to be approximately 0.3 mmol., that is, the value of the breakthrough point, though it is dependent on the flow rate, the concentration of metal ions, the particle size of Kel-F, the temperature, and so on. When 0.5 mmol. of calcium ion is fed into the column, the ion makes its appearance as early as in the first fraction, as has been confirmed by the author's experiment.

The picture of the process taking place in the column seems to be endorsed by these experiments.

Some Consideration of the Mechanism of the Extraction on the Column.—In liquid-liquid extraction the distribution ratio of alkaline earth metals depends upon the pH of the aqueous phase and on the concentration of TTA in the organic phase, as has been described in a preceding paper.[1] The behavior of the column extraction seems to be similar to that of the liquid-liquid extraction described in the same paper, in view of the group of facts clarified by the author's experiments. In the column extraction, as well as the other experiments described in this paper, an organic solvent containing as high a concentration of TTA as 1.48 M was used. At higher concentrations of TTA, calcium ions combine substantially with TTA, but not with acetate ions or MIBK. Among these, the number of TTA molecules involved in the ionic linkage is two; the number attached to calcium, including the above number, increases remarkably, as shown in Figs. 8 and 9, with the increase in the concentration of TTA in the solvent. However, as is shown in Fig. 12, the molar ratio of TTA to a calcium ion is thirty-four at the saturation of calcium in the organic phase; this number is the minimum ratio of TTA to calcium ion. Even this minimum number seems to be far larger than the number of TTA molecules which, we may expect from the relation of $\log D$ vs. $\log(\mathrm{TTA})$, are required by a calcium ion. Almost all the TTA in the system should be considered to participate in the extraction of calcium ions directly or indirectly, just as was described in a preceding paper.[1]

Summary

The author has extended the liquid-liquid extraction process of alkaline earth metal ions to a reversed-phase partition column chromatography, taking advantage of the results described in a preceding paper.[1] In the column, a methyl isobutyl ketone solution of TTA held on Kel-F powder has been used as a stationary phase. The separation of each metal ion from its mixture has been successfully achieved by carrying out the elution with eluting solutions of various pH values. It is noteworthy that as large an amount as several milligrams of a sample can be treated by this method. The relation between the method and the liquid-liquid extraction has been examined; no fundamental difference could be discovered between them. However, in the column chromatography, as well as in the batch extraction, described in this paper the organic phase contains a higher concentration of TTA than it does in the batch extraction in the liquid-liquid extraction described in a preceding paper. The experiments have also confirmed several facts which the batch method of the liquid-liquid extraction in a preceding paper[1] had seemed to suggest, regarding the behavior of TTA chelates in the presence of large amounts of TTA. Since the formation of TTA-chelate usually seems to require considerable time, in the column the eluting solution may pass through each plate while in an incomplete state of extraction equilibrium. The total distribution ratio of a metal ion as calculated from an elution curve is not much affected by the concentration of the metal in the system. The breakthrough curve of the column is thought to reflect the process taking place on the column.

The author wishes to express her thanks to Professor Toshiyasu Kiba for his kind advice and encouragement.

BULLETIN OF THE CHEMICAL SOCIETY OF JAPAN VOL. 39 989—994 (1966)

The Intramolecular Hydrogen Bond of the Diol Ethers as Model Compounds of the Diols*[1]

By Hazime SAITÔ,*[2] Teijiro YONEZAWA, Shinichi MATSUOKA† and Kenichi FUKUI

Faculty of Engineering, Kyoto University, Sakyo-ku, Kyoto
† *Faculty of Science, Kanazawa University, Kanazawa*

(Received September 24, 1965)

The intramolecular and intermolecular hydrogen bonds of the diol ethers are examined as model compounds of the diols by means of a study of their infrared and NMR spectra. The hydrogen bond shift and the intramolecular hydrogen bond shift are obtained. The value of the intramolecular hydrogen bond shift is discussed in terms of the electric field effect due to lone-pair electrons of the proton acceptor.

In a previous paper,[1] the free OH proton shifts of the diols have been estimated from a theoretical treatment, and their hydrogen bond shifts have been determined using both experimental and theoretical OH proton shifts. It has been pointed out that the hydrogen bond shift obtained arises predominantly from the intermolecular hydrogen bond, but the contribution of the intramolecular hydrogen bond can not be ignored.

The intramolecular hydrogen bond of the diols was investigated by Kuhn and others[2-9] with infrared spectra. Kuhn reported[2] that its strength is related to the number of methylene groups between two hydroxyl groups. That is to say, 1, 4-butanediol, which has four methylene groups, forms the strongest intramolecular hydrogen bond of the diols, making a stable seven-membered ring. Trimethylene glycol, which has three methylene groups, forms a stronger intramolecular hydrogen bond than ethylene glycol, with two methylene groups, and a weaker one than 1, 4-butanediol.

For the investigation of the intramolecular hydrogen bond with NMR, the measurements

*1 Presented at the 15th Annual Meeting of the Chemical Society of Japan, April, 1962.

*2 Present address: Basic Research Laboratories, Toyo Rayon Co., Ltd., Kamakura.

1) T. Yonezawa, H. Saitô, S. Matsuoka and K. Fukui, This Bulletin, **38**, 1431 (1965).

2) L. P. Kuhn, *J. Am. Chem. Soc.*, **74**, 2492 (1952).

3) L. P. Kuhn, ibid., **76**, 4323 (1954).

4) L. P. Kuhn, ibid., **80**, 5950 (1958).

5) M. St. C. Flett, *Spectrochim. Acta*, **10**, 21 (1957).

6) P. von. R. Schleyer, *J. Am. Chem. Soc.*, **83**, 1368 (1961).

7) F. V. Brutcher, Jr., and W. Bauer, Jr., ibid., **84**, 2236 (1962).

8) H. Kwart and W. G. Vosburgh, ibid., **76**, 5400 (1954).

9) L. P. Kuhn, P. von R. Schleyer, W. F. Baitinger, Jr., and L. Eberson, ibid., **86**, 650 (1964).

Table I. Comparison of intramolecular hydrogen bond of the diols with the diol ethers

The diols[a]	Free OH stretching cm^{-1}	Intramolecular hydrogen bonded OH stretching cm^{-1}	$\Delta\nu$ cm^{-1}	The diol ethers	Free OH stretching cm^{-1}	Intramolecular hydrogen bonded OH stretching cm^{-1}	$\Delta\nu$ cm^{-1}
$HOCH_2CH_2OH$	3644	3612	32	$HOCH_2CH_2OCH_3$	—[b]	3605(3600)	35[c]
				$HOCH_2CH_2OC_2H_5$	—[b](3632)	3607(3600)	33[c]
				$HOCH_2CH_2OC_4H_9$	—[b](3632)	3607(3601)	33[c]
$HOCH_2CH_2CH_2OH$	3636	3558	78	$HOCH_2CH_2CH_2OCH_3$	3640	3547	93
$HOCH_2CH_2CH_2CH_2OH$	3634	3478	156	$HOCH_2CH_2CH_2CH_2OCH_3$	3640	3456	184

a) Results by L. P. Kuhn.[2]
b) In our experiment, this value is not obtained. Values in parenthesis are results by M. St. C. Flett.[5]
c) The value assumed that free OH stretching is 3640 cm^{-1} as same as the value of trimethylene glycol monomethyl ether and 1,4-butanediol monomethyl ether.

should be carried out with as low a concentration as possible in a non-polar solvent such as carbon tetrachloride. The solubility of the diols in carbon tetrachloride, however, is lower than 0.005 mol./l., and NMR spectra cannot be obtained at such a low concentration.

Therefore, the diol monoalkyl ethers (diol ethers) are used as model compounds to investigate the natures of intramolecular hydrogen bond of the diols. The intramolecular hydrogen bond of the diol ether has also been studied, by means of infrared spectra, by Kuhn and Wires[10]; they reported the energy of the intramolecular hydrogen bond.

As model compounds for the diols, 1, 4-butanediol monomethyl ether, trimethylene glycol monomethyl ether, ethylene glycol monomethyl ether, ethylene glycol monoethyl ether, and ethylene glycol monobuthyl ether are used. From the measurement of the NMR spectra, the hydrogen bond shift due to the formation of an intramolecular hydrogen bond is obtained. The hydrogen bond shift is about 4.8 p. p. m. for the diol ethers; this value is found to be smaller than those of the diols and alcohols.

The intramolecular hydrogen bond shift referred to the free OH shift is 1.21 p. p. m. for ethylene glycol monomethyl ether and larger than 1.65 p. p. m. and 1.67 p. p. m. for trimethylene glycol monomethyl ether and 1, 4-butanediol monomethyl ether, respectively. This value is interpreted in terms of the electrostatic nature of the hydrogen bond using the Marshall-Pople formula.[11]

Experimental

Ethylene glycol monomethyl ether, ethylene glycol monoethyl ether, ethylene glycol monobutyl ether and carbon tetrachloride of guaranteed-grade reagent are used. Trimethylene glycol monomethyl ether and 1, 4-butanediol monomethyl ether are prepared from the corresponding diols by Smith's method.[12] The diol ethers are used after vacuum distillation after having been dried over barium oxide.

The NMR spectra are usually measured with a JNM-3 40 mc spectrometer; however, a Varian DP-60 60 mc spectrometer is used for lower concentrations, and a sample tube 15 mm. in diameter is used for the lowest concentration. Benzene is used as an external standard.

The infrared spectra for the diol ethers are measured with a Perkin-Elmer 12-C spectrometer equipped with a LiF prism and using a 3 mm.—20 mm. cell.

Results and Discussion

Infrared Spectra.—The infrared spectra for the diol ethers were measured in carbon tetrachloride (0.005 mol./l.) in order to compare the strength of the intramolecular hydrogen bond of the diol ethers with that of the diols. Table I gives our results, together with those of Kuhn,[2] on the diols.

Since no free OH stretching bands of ethylene glycol monomethyl- monoethyl- and monobutyl-ethers are observed in this concentration, the free OH proton may be said not to be present.

Then the shift of the OH stretching frequency, $\Delta\nu$, due to the intramolecular hydrogen bond in the infrared spectra of the diols is compared with that of the corresponding diol ethers, there is a distinct parallelism between the $\Delta\nu$ values of the diols and those of the diol ethers, though the $\Delta\nu$ values of the diol ethers are about twenty percent greater than those of the diols.

Therefore, it may be reasonable to adopt the diol ethers as a model compound of the diols so long as the fact that the $\Delta\nu$ values in the diol ethers are larger than those of the diols is kept in mind. In order to obtain information on the intramolecular hydrogen bond, the results of infrared spectra measured at various concentrations are shown in Fig. 1. Figure 1 shows that there is no free OH proton of ethylene glycol monomethyl ether in the range of the concentration between 0.005 to 0.5 mol./l., and that all OH protons make intramolecular hydrogen bonds

10) L. P. Kuhn and R. A. Wires, ibid., **86**, 2161 (1964).
11) T. W. Marshall and J. A. Pople, *Mol. Phys.*, **1**, 199 (1958).
12) L. Smith and J. Sprung, *J. Am. Chem. Soc.*, **65**, 1276 (1943).

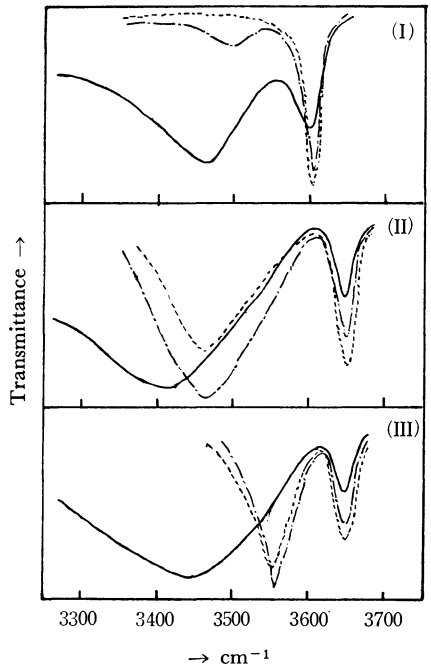

Fig. 1. Infrared spectra of diol ethers.
(I) Ethylene glycol monomethyl ether
(II) 1,4-Butanediol monomethyl ether
(III) Trimethylene glycol monomethyl ether
---- 0.005 mol./l. ----- 0.05 mol./l.
—— 0.5 mol./l.

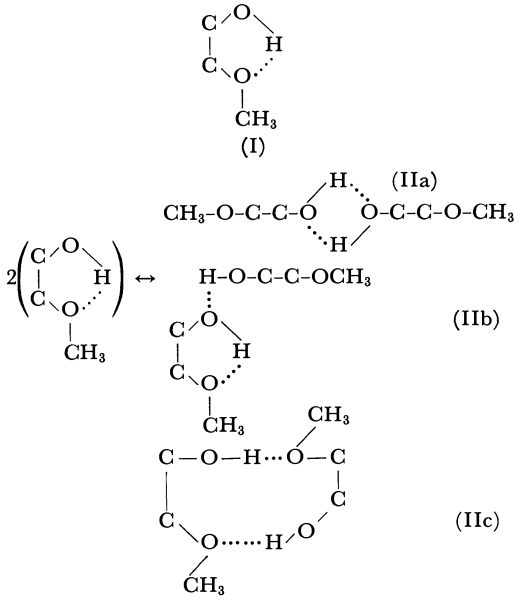

Fig. 2. Intra- and intermolecular hydrogen bond of ethylene glycol monomethyl ether in the lower concentration.

forming five-membered rings (Fig. 2 (I)). Now, in the concentration near 0.05 mol./l., the absorption band due to the intermolecular hydrogen bond is present in addition to the intramolecular bond itself, so it seems that there is an equilibrium between the monomer and the dimer, as is shown in Fig. 2 (II). The structure shown in Fig. 2 may be adequate, though we can consider other structures. This consideration is confirmed by the fact that no free OH absorption is observed in the infrared spectra of the diol ethers. Of the three structures, II-b is expected to be preferable.

Figure 3 is obtained by making the plot of the molecular extinction coefficient, $\varepsilon=(1/cd)\log(I_0/I)$, vs. the mole fraction of ethylene glycol monomethyl ether, where c is the concentration (mol./l.) and d, the thickness of the cell. If we use the ε_0 value, which is the value obtained by extrapolating the curve to an infinite dilution, the $\varepsilon/\varepsilon_0$ value is the fraction of the OH group which makes the intramolecular hydrogen bond. As is shown in Fig.

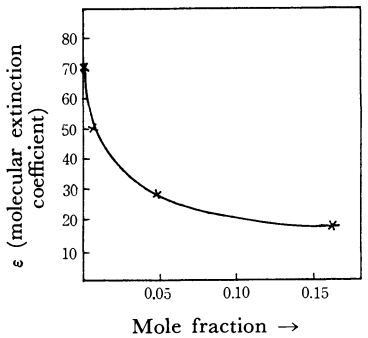

Fig. 3. A plot of ε vs. mole fraction of ethylene glycol monomethyl ether.

3, the OH shift of ethylene glycol monomethyl ether in an infinitely-diluted solution seems to indicate the intramolecular hydrogen bond shift. However, in trimethylene glycol monoethyl ether and 1, 4-butanediol monomethyl ether, there are free OH protons at the concentration of 0.005 mol./l., and so the value obtained by the extrapolation of the curve to an infinite dilution cannot always be expected to correspond with that resulting from a completely intramolecular hydrogen-bonded state. Namely, there seems to be an equilibrium in the infinite dilution as is shown in Fig. 4. It seems curious at first sight that trimethylene glycol monomethyl ether and 1, 4-butanediol monomethyl ether, which make stable

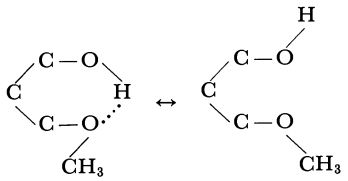

Fig. 4. Equilibrium between free and intramolecular hydrogen bonded state in infinitely diluted solution.

six- and seven-membered rings, respectively, in the intramolecular hydrogen bond, are in the equilibrium shown in Fig. 4, while ethylene glycol monomethyl ether, which makes a weaker hydrogen bond than they, is not in such an equilibrium. Because of the hindered rotation around the C-C and C-O bond axes, the probability of breaking the OH···O intramolecular hydrogen bond might increase as the number of C-C and C-O bonds between two hydroxyl groups becomes greater. Therefore, it may be understood that a free OH proton exists in 1, 4-butanediol monomethyl ether and trimethylene glycol monomethyl ether.

NMR Spectra.—NMR spectra at various concentrations of a carbon tetrachloride solution were measured, using benzene as an external standard. The plots of the OH proton shift vs. the mole fraction of the diol ethers are given in Fig. 5 and Fig. 6 for concentrations lower than 0.03 mol./l. The same plot for ethanol, as reported by Becker et al.,[13] is reproduced in Fig. 5 using the same scale. It may be seen in Fig. 5 that the change in the OH proton shift against the concentration in the diol ethers is smaller than that in ethanol. This is probably because there are a number of intramolecular hydrogen bonds in place of free OH protons in the ethanol at these concentrations.

The Hydrogen Bond Shift and the Intramolecular Hydrogen Bond Shift.—*Free OH Proton Shift.* — The free OH proton shift was calculated by the procedure reported in the previous paper,[1] using a simple LCAO MO method for the sigma electron system reported. The parameters used are the same as those in the previous paper. The sigma electron density for the OH proton of the diol ethers is given in Table II. The observed OH proton shifts referred to the benzene proton are shown in Table III. The bulk susceptibility correction is made in a usual way. The volume susceptibility needed for the correction is measured by Gouy's balance.

TABLE II. σ-ELECTRON DENSITY OF THE DIOL ETHERS

	OH	αCH_2
$HOCH_2CH_2OCH_3$	0.8073	0.9158
$HOCH_2CH_2OC_2H_5$	0.8069	0.9126
$HOCH_2CH_2OC_4H_9$	0.8069	0.9126
$HOCH_2CH_2CH_2OCH_3$	0.8074	0.9167
$HOCH_2CH_2CH_2CH_2OCH_3$	0.8074	0.9169

The hydrogen bond shift is calculated as follows; the observed OH proton shift in a neat liquid state at room temperature* is corrected

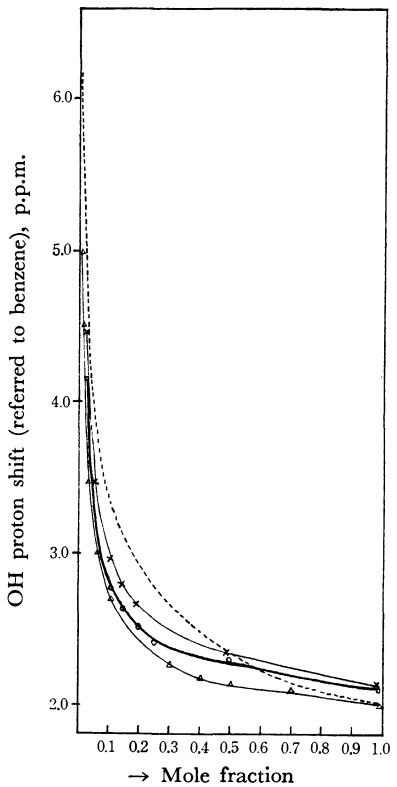

Fig. 5. A plot of OH proton shift vs. mole fraction of diol ethers (uncorrected).
------ Ethanol
—×— Ethylene glycol monomethyl ether
—○— Trimethylene glycol monomethyl ether
—△— 1,4-Butanediol monomethyl ether

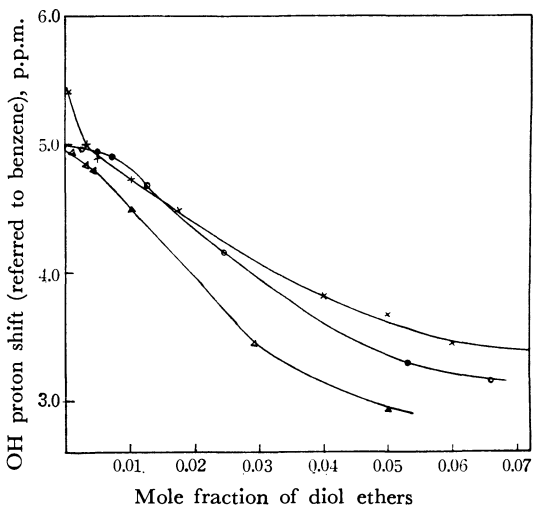

Fig. 6. A plot of OH proton shift (referred to benzene) vs. mole fraction of diol ethers (uncorrected).
—×— Ethylene glycol monomethyl ether
—○— Trimethylene glycol monomethyl ether
—△— 1,4-Butanediol monomethyl ether

13) E. D. Becker, U. Liddel and J. N. Shoolery, *J. Mol. Spectry.*, **2**, 1 (1958).

* As the term "hydrogen bond shift" corresponds to the maximum hydrogen bond, measurements must be carried out just above freezing point. However, we here extend the definition of this term to the measurement at room temperature in comparison to the hydrogen bond between the diols and the diol ethers.

Table III. Hydrogen bond shift of the diols referred to benzene

	OH proton shift (obs.) p.p.m.	Volume susceptibility[a] $-\chi_v \times 10^6$	Bulk susceptibility correction	OH proton shift (corrected) p.p.m.	Free OH proton shift[b] p.p.m.	Hydrogen bond shift p. p. m.
$HOCH_2CH_2OCH_3$	2.12	0.660	+0.07	2.19	6.77	4.58
$HOCH_2CH_2OC_2H_5$	2.18	0.644	+0.04	2.22	6.76	4.54
$HOCH_2CH_2OC_4H_9$	2.18	0.660	+0.06	2.34	6.76	4.52
$HOCH_2CH_2CH_2OCH_3$	2.07	0.630	+0.01	2.08	6.77	4.69
$HOCH_2CH_2CH_2CH_2OCH_3$	2.00	0.657	+0.06	2.06	6.77	4.71

a) Measured by present authors.
b) Free OH proton shift referred to benzene.

Table IV. Intramolecular hydrogen bond shift (unit: p.p.m.)

	OH proton shift (extrapolated to infinite dilution)	OH proton shift (corrected)	Free OH proton shift (calcd.)	Intramolecular hydrogen bond shift
$HOCH_2CH_2OCH_3$	5.44	5.56	6.77	1.21
$HOCH_2CH_2CH_2OCH_3$	5.00	5.12	6.77	>1.65
$HOCH_2CH_2CH_2CH_2OCH_3$	4.98	5.10	6.77	>1.67

by the bulk susceptibility correction and subtraction from the calculated free OH proton shift. The results are given in Table III. Table III shows that the hydrogen bond shift of the diol ethers is smaller than that of ethanol, 4.8 p. p. m., and that of the diols, about 5.4 p. p. m.** The reason why the hydrogen bond shift of the diol ethers is smaller than that of the diols may be that the diols have two hydroxyl groups and both of them may be both proton acceptors and donners, while in the diol ethers the methoxy group replaced by the hydroxyl group may only be a proton acceptor. Therefore, the association of the diols is easier than that of the diol ethers.

It may be found by comparing Table III with Table I that the hydrogen bond shift of the diol ethers becomes larger as the intramolecular hydrogen bond is stronger.

The Intramolecular Hydrogen Bond Shift of the Diol Ethers.—In the case of ethylene glycol monomethyl ether, the intramolecular hydrogen bond shift is obtained by extrapolating the curve of the OH proton shift to an infinitely-diluted solution, as was described in the previous section. In the cases of 1, 4-butanediol monomethyl ether and trimethylene glycol monomethyl ether, however, the extrapolated values are not precisely correspondent to the intramolecular hydrogen bond shift, as has been mentioned in connection with the results of the infrared spectra. If free OH protons are present, the extrapolated value of the intramolecular hydrogen bond shift is smaller than the genuine intramolecular hydrogen bond shift, because the proton shift in an infinitely-diluted solution, δ, referred to the free OH proton shift is expressed as;

$$\delta = (1-\omega_f)\delta_{intra} \quad (1)$$

where δ_{intra} is an intramolecular hydrogen bond shift and ω_f the fraction of the free OH proton. Thus, $\delta < \delta_{intra}$ is concluded to hold in the case of $\omega_f > 0$. The intramolecular hydrogen bond shifts thus obtained are listed in Table IV.

The hydrogen bond shift of the diols seems to be a little larger than that of the diol ethers, considering that the $\Delta\nu$ values of the diol ethers are somewhat larger than those of the diols, as is shown in Table I.

A Theoretical Consideration of the Intramolecular Hydrogen Bond Shift.—It was reported by Kuhn that there is the following relation between the bond length, L, of OH···O and the shift of the wave number, $\Delta\nu$, for the intramolecular hydrogen bond of the diols[2]:

$$\Delta\nu = 250/L - 74 \quad (2)$$

Assuming that the above relation is valid for the diol monomethyl ethers, the OH···O bond lengths of the intramolecular hydrogen bond of the diol ethers and the diols may be evaluated from the above equation.

By using the value obtained above and the electrostatic model for the hydrogen bond described by Pople,[14] the intramolecular hydrogen bond shift can be evaluated. The electrostatic model is shown below, where L is the length of H···O and l, the length of the lone-pair dipole of the oxygen atom.

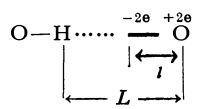

The variation in shift due to the electric field, E, was found by Marshall-Pople[11] to be as follows:

** Values at room temperature; see Ref. 1.

14) J. A. Pople, "Hydrogen Bonding," Ed. by Hadzi, Pergamon Press, New York (1959), p. 71.

TABLE V. CALCULATED INTRAMOLECULAR HYDROGEN BOND SHIFT BASED ON THE MARSHALL'S FORMULA

	$\Delta\nu$ cm^{-1}	L Å	Intramolecular hydrogen bond shift p. p. m. Calcd. l=0.11Å	Calcd. l=0.29Å	Obs.
$HOCH_2CH_2OH$	32	1.99	0.06	1.39	
$HOCH_2CH_2OCH_3$	35	1.99	0.06	1.39	1.56
$HOCH_2CH_2CH_2OH$	78	1.64	0.18	2.00	
$HOCH_2CH_2CH_2OCH_3$	93	1.49	0.35	3.74	>1.65
$HOCH_2CH_2CH_2CH_2OH$	156	1.40[a]	0.52	5.70	>1.67
$HOCH_2CH_2CH_2CH_2OCH_3$	184				

a) As Eq. 2 is applied in the range of $1.6<L<3.3$, this value is estimated referring the crystal data.[16]

$$\delta_E = -\frac{881}{216}\frac{a^3}{mc^2}E^2 \qquad (3)$$

In this equation, the intramolecular hydrogen bond shift is calculated by using the E value due to the dipolar field of lone-pair electrons of the proton acceptor, where L is estimated by means of Eq. 2 and where l is assumed to be 0.11 Å[14] and 0.29 Å[15] in the two cases. The calculated bond lengths and intramolecular hydrogen bond shifts are listed in Table V, along with the hydrogen bond shifts of the diol ethers obtained in the experiments. The results of the calculation depend greatly on the length of the lone-pair dipole, l. The calculated values in the case of l=0.29 Å can explain the experimental value, while the values corresponding to l=0.11 Å are too small to explain it. Although the intramolecular hydrogen bond shift cannot be discussed precisely because of the uncertainty of our knowledge of the lone-pair dipole and the OH···O bond length, this hydrogen bond shift may be understood in terms of the electric field effect of the proton acceptor.*

The authors are grateful to Drs. Tanekazu Kubota and Yoshiki Matsui of the Shionogi Research Laboratory, Shionogi & Co., Ltd., for their measurements of the infrared spectra, and to Drs. Kenkichi Nukada (present address; Basic Research Laboratories, Toyo Rayon Co., Ltd.) and Osamu Yamamoto of the Government Chemical Industrial Research Institute, Tokyo, for their measurements of the NMR spectra.

15) W. G. Schneider, *J. Chem. Phys.*, **23**, 26 (1955).
16) G. C. Pimentel and A. L. McClellan, "The Hydrogen Bond," W. H. Freeman and Company, San Francisco (1960), p. 260.

* Other contributions such as that of the charge transfer structure to the hydrogen bond has been studied by ^{14}N NMR for the OH···N system (H. Saitô, K. Nukada, H. Kato, T. Yonezawa and K. Fukui, *Tetrahedron Letters*, **1965**, 111).

BULLETIN OF THE CHEMICAL SOCIETY OF JAPAN VOL. 39 994—1002 (1966)

Nickel(II) and Copper(II) Complexes of β-Ketoamines Derived from β-Diketones and Aromatic Amines[1)]

By Shoichiro YAMADA, Hiroaki NISHIKAWA* and Emiko YOSHIDA

Institute of Chemistry, College of General Education, Osaka University, Toyonaka, Osaka

(Received September 24, 1965)

Nickel(II) and copper(II) complexes of β-ketoamines derived from acetylacetone or benzoylacetone and aromatic amines have been newly synthesized and characterized. The aromatic amines included aniline, *o*-, *m*- and *p*-toluidine, *o*, *o'*-dimethylaniline, *o*, *o'*-diethylaniline, *o*-, *m*- and *p*-chloroaniline, and α- and β-naphthylamine. The configurations of these complexes in pyridine have been examined and compared with those in non-donor solvents. All these complexes are considered to be square-planar in non-donor solvents and in the solid state. The nickel(II) complexes of the *o*, *o'*-disubstituted derivatives do not combine with pyridine molecules, whereas the corresponding copper(II) complexes readily combine with the pyridine molecule. The difference between nickel(II) and copper(II) ions is discussed in terms of the bonding nature of the metal ions. The β-ketoamines and salicylideneimines are also compared.

* Present address: Department of Chemistry, Faculty of Science, Kanazawa University, Kanazawa.

1) Presented in part at the 8th International Conference on Co-ordination Chemistry (8th ICCC), Vienna, September, 1964; The Proceedings, 8th ICCC (1964), p. 373.

Studies of nickel(II) and copper(II) complexes of Schiff bases derived from salicylaldehyde have so far been carried out by a number of investigators, yielding many conclusions which are of significance to the co-ordination chemistry of these metal ions. At that stage, it was thought to be interesting to compare the complexes of salicylideneimines with the corresponding complexes of β-ketoamines, such as acetylacetone- and benzoylacetoneamines (Fig. 1).[2,3] However, no systematic study has been carried out on the synthesis and characterization of these complexes.

In the present work, a series of new copper(II) and nickel(II) complexes have been synthesized with the β-ketoamines derived from aromatic amines and β-diketones. Then their configurations in pyridine have been examined and compared with the configurations in non-donor solvents, in order to establish the ability of the metal ions to combine with additional ligands at the residual co-ordination sites of the quadri-co-ordinate complexes. Copper(II) and nickel(II) have also been compared as the central metal ion, as the β-ketoamines and the salicylideneimines have been compared as the ligand. This kind of examination is particularly significant for the *N*-*o*, *o*'-disubstituted phenyl-derivatives, since these complexes might behave differently from the *N*-monosubstituted phenyl derivatives due to the steric condition, and so a comparison would yield important information about the co-ordination chemistry of these metal ions. Several new complexes of nickel(II) and copper(II) with salicylideneimines have also been synthesized in the present work.

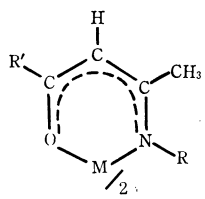

Fig. 1. Metal(II) complexes of β-ketoamines with R'=CH_3 or C_6H_5.

Experimental

Materials.—Bis(*N*-substituted acetylacetoneaminato)-nickel(II) complexes were prepared by the general method given below. Into a warm solution of nickel(II) acetate (0.01 mol.) and the ligand (0.012—0.013 mol.) in ethanol (15—20 ml.), a solution of potassium ethanolate was stirred drop by drop; this solution had been prepared, in advance, by adding potassium metal (0.022—0.024 g. atom) into ethanol (15—20 ml.). The reaction was then continued at about 70°C for two to six hours, depending upon the ligands used.

Table I. Elemental analyses of bis(*N*-substituted acetylacetoneaminato)nickel(II) and copper(II), $(CH_3\cdot CO\cdot CH\cdot C\cdot NR)_2M$ (with CH_3 on C)

R	Calcd. %			Found, %		
M=Ni(II)	C	H	N	C	H	N
C_6H_5	64.93	5.90	6.88	64.36	5.81	6.84
o-$CH_3C_6H_4$	66.27	6.44	6.44	66.70	6.66	6.57
p-$CH_3C_6H_4$				66.63	6.47	6.54
o, *o*'-$(CH_3)_2C_6H_3$**	67.41	6.96	6.05	67.70	6.83	6.22
o, *o*'-$(C_2H_5)_2C_6H_3$	69.40	7.71	5.40	68.01	7.72	6.09
o-ClC_6H_4	54.50	4.62	5.89	55.57	4.72	5.93
m-ClC_6H_4*				55.79	4.77	5.90
p-ClC_6H_4				55.43	4.77	5.90
α-Naphthyl	71.03	5.56	5.52	71.06	5.71	5.55
β-Naphthyl				70.84	5.72	5.61
M=Cu(II)						
p-$CH_3C_6H_4$	65.52	6.37	6.37	64.95	6.45	6.20
o, *o*'-$(CH_3)_2C_6H_3$	66.71	6.89	5.99	66.10	7.00	6.21
o, *o*'-$(C_2H_5)_2C_6H_3$	69.03	7.29	5.31	68.31	7.74	5.39
o-ClC_6H_4	54.94	4.58	5.83	54.71	4.73	5.45
m-ClC_6H_4*				54.97	4.68	5.81
p-ClC_6H_4				55.02	4.72	5.75
α-Naphthyl	70.38	5.57	5.34	70.36	5.51	5.47

* Recrystallized from ethyl ether.

** Recrystallizable from ethanol, according to Ref. 4b. However, the complex is scarcely soluble in ethanol, and the recrystallization has been carried out from benzene in the present work.

2) As a matter of convenience, these ligands will be referred to as β-ketoamines in the present paper.

3) Abbreviated in this paper as M(Sal. R)$_2$, M(Aca. R)$_2$, and M(Bza. R)$_2$ respectively.

TABLE II. ELEMENTAL ANALYSES OF BIS(*N*-SUBSTITUTED BENZOYLACETONEAMINATO)NICKEL(II) AND COPPER(II), $(C_6H_5\cdot CO\cdot CH\cdot C\cdot NR)_2M$ (CH_3)

R / M=Ni(II)	Calcd. % C	Calcd. % H	Calcd. % N	Found, % C	Found, % H	Found, % N
C_6H_5	72.37	5.27	5.27	71.66	5.23	5.17
o-$CH_3C_6H_4$	73.03	5.73	5.01	72.15	5.82	4.85
p-$CH_3C_6H_4$				72.98	5.86	4.95
o, *o'*-$(CH_3)_2C_6H_3$*	73.63	6.14	4.77	73.82	6.37	4.77
o, *o'*-$(C_2H_5)_2C_6H_3$	74.68	6.84	4.36	74.90	6.97	4.47
o-ClC_6H_4	64.03	4.34	4.67	64.22	4.42	4.58
m-ClC_6H_4				63.67	4.26	4.62
p-ClC_6H_4				64.24	4.52	4.73
M=Cu(II)						
o-$CH_3C_6H_4$	72.40	5.68	4.97	72.43	5.83	4.99
m-$CH_3C_6H_4$				72.30	5.70	4.92
p-$CH_3C_6H_4$				72.12	5.86	4.90
o, *o'*-$(CH_3)_2C_6H_3$	73.03	6.09	4.73	71.54	6.21	4.56
o, *o'*-$(C_2H_5)_2C_6H_3$	74.13	6.80	4.32	73.67	6.91	4.43
o-ClC_6H_4	63.52	4.30	4.63	63.00	4.41	4.52
m-ClC_6H_4				62.95	4.28	4.47
p-ClC_6H_4				63.09	4.31	4.50

* Yellow-brown (light green, according to Ref. 4b)

TABLE III. ELEMENTAL ANALYSES OF BIS(*N*-SUBSTITUTED SALICYLIDENEIMINATO)NICKEL(II) AND COPPFR(II), $(Sal.NR)_2M$

R / M=Ni(II)	Calcd. % C	Calcd. % H	Calcd. % N	Found, % C	Found, % H	Found, % N
o, *o'*-$(CH_3)_2C_6H_3$	67.41	6.96	6.05	67.70	6.83	6.22
o, *o'*-$(C_2H_5)_2C_6H_3$	72.52	6.39	4.97	71.59	6.25	4.90
α-Naphthyl	71.03	5.56	5.52	71.06	5.71	5.55
β-Naphthyl				70.84	5.72	5.61
p-ClC_6H_4	55.50	4.66	5.88	55.43	4.77	5.90
o, *p*, *o'*-$Cl_3C_6H_2$	47.46	2.15	4.26	47.81	2.16	4.15
o, *p*, *o'*-$Br_3C_6H_2$	33.77	1.53	3.03	33.81	1.60	3.15
M=Cu(II)						
o, *m*-$(CH_3)_2C_6H_3$	70.36	5.51	5.47	70.30	5.44	5.71
o, *p*-$(CH_3)_2C_6H_3$				70.39	5.54	5.52
o, *o'*-$(CH_3)_2C_6H_3$				70.30	5.50	5.40
o, *o'*-$(C_2H_5)_2C_6H_3$	71.91	6.34	4.93	71.84	6.35	4.91
o, *p*, *o'*-$Cl_3C_6H_2$	47.12	2.13	4.23	47.34	2.10	4.23
o, *p*, *o'*-$Br_3C_6H_2$	33.60	1.52	3.01	33.78	1.66	3.13

When the solution was cooled, crude crystals of the compound separated out. Pure crystals of the compound were obtained by the recrystallization of the crude product from suitable solvents. Prior to the above procedure, the ligand had generally been prepared by refluxing a mixed solution of the *β*-diketone and the amine on a water-bath for many hours. The elemental analyses of these compounds are given in Table I. These complexes are green.

Bis(*N*-substituted acetylacetoneaminato)copper(II) complexes were prepared in the same way as were the corresponding nickel(II) complexes, except that the reaction period with the copper(II) complexes was generally longer. The crystals which separated out were quickly filtered, washed, generally with ethanol, and dried in a vacuum desiccator. The elemental analyses of these compounds are shown in Table I. Most of these complexes are dark-brown or dark-green.

Bis(*N*-substituted phenyl-benzoylacetoneaminato)-nickel(II) complexes were prepared in a way similar to that used for the corresponding bis(acetylacetoneaminato)nickel(II) complexes. The elemental analyses are shown in Table II. These complexes are green or brownish green.

Bis(*N*-substituted phenyl-benzoylacetoneaminato)-copper(II) complexes were prepared in a way similar to that used for the corresponding bis(benzoylacetoneaminato)nickel(II) complexes. The elemental analyses are shown in Table II. These complexes are dark-brown.

Table IV. Absorption maxima of bis(*N*-substituted acetylacetoneaminato)nickel(II), $(CH_3\cdot CO\cdot CH\cdot \underset{\displaystyle CH_3}{\overset{\displaystyle |}{C}}\cdot NR)_2Ni$

R	Solvent	ν $10^3\,cm^{-1}$	log ε	ν $10^3\,cm^{-1}$	log ε
o-$CH_3C_6H_4$	$CHCl_3$	16.7	1.54	sh*	
	py**	10.0	0.90	17.0	1.25
p-$CH_3C_6H_4$	$CHCl_3$	17.0	1.63	sh	
	py	10.4	1.19	17.3	1.17
o, *o'*-$(CH_3)_2C_6H_3$	$CHCl_3$	16.6	1.70	20.5	1.96
	py	16.5	1.68	20.9	1.96
o, *o'*-$(C_2H_5)_2C_6H_3$	$CHCl_3$	16.6	1.57	20.7	1.89
	py	16.6	1.62	20.8	1.89
α-Naphthyl	$CHCl_3$	16.4	1.74	20.5	2.05
	py	9.9	1.22	16.8	1.27
β-Naphthyl	$CHCl_3$	16.4	1.71	sh	
	py	10.4	1.29	17.6	1.59
o-ClC_6H_4	$CHCl_3$	16.6	1.69	20.7	1.90
	py	10.4	1.18	17.2	1.20
m-ClC_6H_4	$CHCl_3$	16.6	1.68	20.8	1.91
	py	10.5	1.25	17.4	1.18
p-ClC_6H_4	$CHCl_3$	16.4	1.70	20.7	1.94
	py	10.1	1.26	17.0	1.17

* sh: shoulder ** pyridine=py

Table V. Absorption maxima of bis(*N*-substituted benzoylacetoneaminato)nickel(II), $(C_6H_5\cdot CO\cdot CH\cdot \underset{\displaystyle CH_3}{\overset{\displaystyle |}{C}}\cdot NR)_2Ni$

R	Solvent	ν $10^3\,cm^{-1}$	log ε	ν $10^3\,cm^{-1}$	log ε
o-$CH_3C_6H_4$	$CHCl_3$	16.2	1.81	sh*	
	py**	10.6	1.20	17.4	1.74
p-$CH_3C_6H_4$	$CHCl_3$	16.1	1.76	sh	
	py	10.3	1.11	17.6	1.39
o, *o'*-$(CH_3)_2C_6H_3$	$CHCl_3$	16.6	1.78	sh	
	py	16.4	1.70	sh	
o, *o'*-$(C_2H_5)_2C_6H_3$	$CHCl_3$	16.3	1.75	sh	
	py	16.1	1.70	sh	
o-ClC_6H_4	$CHCl_3$	16.0	1.80	sh	
	py	10.3	1.19	17.6	1.46
m-ClC_6H_4	$CHCl_3$	16.0	1.78	sh	
	py	16.5	1.24	17.6	1.68
p-ClC_6H_4	$CHCl_3$	16.5	1.82	sh	
	py	10.8	1.16	17.7	1.18

* sh: shoulder ** pyridine=py

The solvents used for the recrystallization of all the above complexes were mostly benzene and ethanol, although acetone and chloroform were occasionally employed.

The following complexes were reported previously[4]: Ni(Aca. *o*, *o'*-$(CH_3)_2C_6H_3)_2$, Ni(Bza. $C_6H_5)_2$, Cu(Aca. $C_6H_5)_2$, Cu(Aca. *o*, *o'*-$(CH_3)_2C_6H_3)_2$ and Cu(Bza. $C_6H_5)_2$. The methods of the preparation in the present work are different from that employed previously, except for that for the first complex. A paper has recently been presented describing the *N*-alkyl substituted β-ketoamine complexes of nickel(II).[5]

Bis(*N*-substituted phenyl-salicylideneiminato)complexes were prepared by reactions between the bis(salicylaldehyde)metal complex and one of the aromatic amines in ethanol or methanol. These complexes are dark-brown or dark-green.

For the preparation of *o*, *p*, *o'*-trichlorophenyl-substituted complexes of this series, a solution of the Schiff base, which had been prepared in advance, was added to copper acetate or nickel acetate in ethanol,

4) a) A. S. Kudryavtsev and I. A. Savich, *Vestn. Moskow Univ. Ser. II. Khim.*, **18** (4), 61 (1963). b) T. M. Hseu, D. F. Martin and T. Moeller, *Inorg. Chem.*, **2**, 587 (1963).

5) G. W. Everett, Jr., and R. H. Holm, *J. Am. Chem. Soc.*, **87**, 2117 (1965).

and then the solid sodium hydrogen carbonate was added. The reaction was continued at 60—70°C for several hours. The elemental analyses are shown in Table III. These complexes are all brown or green.

The other complexes discussed in the present paper were prepared according to the methods previously reported. Elemental analyses for carbon, hydrogen and nitrogen agreed with the formulae given previously.

Measurements.—The electronic absorption spectra of the complexes in solution were determined with a Shimadzu QR 50 spectrophotometer and a Beckman DU spectrophotometer. Pyridine for a solvent was purified by distillation after it had been boiled for some hours over barium oxide.

The diamagnetism of the nickel(II) complexes in the solid state was detected by Gouy's method.

Results and Discussion

The Nickel(II) Complexes of β-Ketoamines and Salicylideneimines Derived from Aromatic Amines.—Numerous new nickel(II) complexes of the ketoamines have been prepared in the present work; they are shown in Tables I, II and III, together with several new complexes of salicylideneimines. In general, the preparation of the metal complexes of the β-ketoamines was found to be more difficult in many ways than the preparation of the corresponding complexes of the salicylideneimines.

The fact that all these nickel(II) complexes of the β-ketoamines are diamagnetic in the solid state indicates the planar configuration of these complexes. It is now well known that the electronic spectrum of a nickel(II) complex varies remarkably according as the nickel(II) complex is square-planar, tetrahedral or octahedral.[6,7] Consequently, the spectrum may be regarded as symptomatic of the configuration of the nickel(II) complex. Thus, the present measurements clearly indicate that the electronic spectra of the complexes of $Ni(Aca.aryl)_2$ and $Ni(Bza.aryl)_2$ types in chloroform or benzene are characteristic of the square-planar nickel(II) complex (Figs. 2 and 3).[8] There is controversy about the assignment of the absorption bands of square-planar nickel(II) complexes,[9] but a tentative assignment may be ^1A_g—$^1B_{1g}$ and ^1A_g—$^1B_{3g}$ for the absorption bands at about 16.5 and 20.5×10^3 cm^{-1} respectively. These complexes show no absorption at about 900—1000 mμ, where the tetrahedral or the octahedral nickel(II) complexes are expected to absorb. Hence, both the presence of the monomeric, tetrahedral species and the association of the square-planar complexes may be excluded, at least near room temperature. The same conclusion was obtained with a solution of a very high concentration. Comparison clearly shows that the tendency of the square-planar complexes to form associated polymers in solution is much lower with the β-ketoamine complexes than with the corresponding salicylideneimine complexes, since the previous studies[6] have shown that bis(*N*-monosubstituted phenylsalicylideneiminato)-nickel(II) complexes in non-donor solvents consist of the square-planar monomer, the associated polymer with the sexa-co-ordinated nickel(II), and the tetrahedral monomer, the former two being in equilibrium with each other near room temperature. This difference between the β-ketoamine and the salicylideneimine complexes may be due to the stronger ligand field produced by the β-ketoamines, since the stronger ligand field will increase the energy difference between the $d_{x^2-y^2}$ orbital and the next highest orbital of the nickel(II) ion, making the highest $d_{x^2-y^2}$ orbital less readily occupied in the formation of the sexa-co-ordinated nickel-(II).[10]

In order to examine the effect of the two substituents at the *o*- and *o'*-carbon atoms on the residual co-ordination sites, the electronic absorption spectra of the compounds were examined in pyridine, and compared with the results for the corresponding complexes with monosubstituted radicals. With the exception of the *o*, *o'*-disubstituted complexes, all the nickel(II) complexes examined were found to take up two pyridine molecules, as may be seen from their electronic spectra (Figs. 2 and 3, and Tables IV and V). The absorption bands at about 10 and 16.5×10^3 cm^{-1} are tentatively identified as $^3A_{2g}\rightarrow{}^3T_{2g}$ and $^3A_{2g}\rightarrow{}^3T_{2g}$ (F) for the octahedral nickel(II) complexes. The spectra obtained, which are remarkably different from the spectra of the tetrahedral and the square-planar complexes of nickel(II), have the main features characteristic of the sexa-co-ordinated nickel(II) complexes.[6,7,11] Since Beer's law is generally obeyed, an equilibrium between the octahedral complex and another species may be excluded. It should be noted that even the *o*-monosubstituted complexes form sexa-co-ordinated complexes by taking up two pyridine molecules for the complexes of the $Ni(Sal.R)_2$, $Ni(Aca.R)_2$ and $Ni(Bza.R)_2$ types. This is also found to be the case with the complexes having α-naphthyl for R.

On the contrary, the spectra of the *o*, *o'*-disubstituted nickel(II) complexes of salicylideneimines, acetylacetoneamines and benzoylacetoneamines in pyridine are very similar to the spectra of the same compounds in chloroform (Figs. 2 and 3, and Tables IV and V). It is clear that

6) L. Sacconi, "Essays in Co-ordination Chemistry" (Eds. W. Schneider, G. Anderegg and R. Gut), Birkhauser Verlag, Basel (1964), p. 148; R. H. Holm and K. Swaminathan, *Inorg. Chem.*, **1**, 599 (1962).

7) S. Yamada and H. Nishikawa, This Bulletin, **36**, 755 (1963).

8) In general, the electronic spectra of these complexes in benzene or ethanol are essentially the same as those in chloroform.

9) G. Maki, *J. Chem. Phys.*, **29**, 1129 (1958); J. Ferguson, ibid., **34**, 611 (1961). Another assignment is given by A. D. Liehr and C. J. Ballhausen, *J. Am. Chem. Soc.*, **81**, 538 (1959).

10) A. B. P. Lever, The Proceedings, 8th ICCC (1964), p. 123.

11) A pyridine adduct of bis(*N*-phenyl-salicylideneiminato)-nickel(II) was reported previously. L. Sacconi and M. Ciampolini, *J. Am. Chem. Soc.*, **85**, 1750 (1963).

the square-planar configuration of these complexes is held in pyridine as well as in chloroform. Neither the sexa-co-ordinated form combining the two pyridine molecules nor the tetrahedral form is present, since there is no absorption in the frequency region lower than 700 mμ, except for a very feeble absorption band which may be ascribed to the singlet-triplet(spin-forbidden) transition of

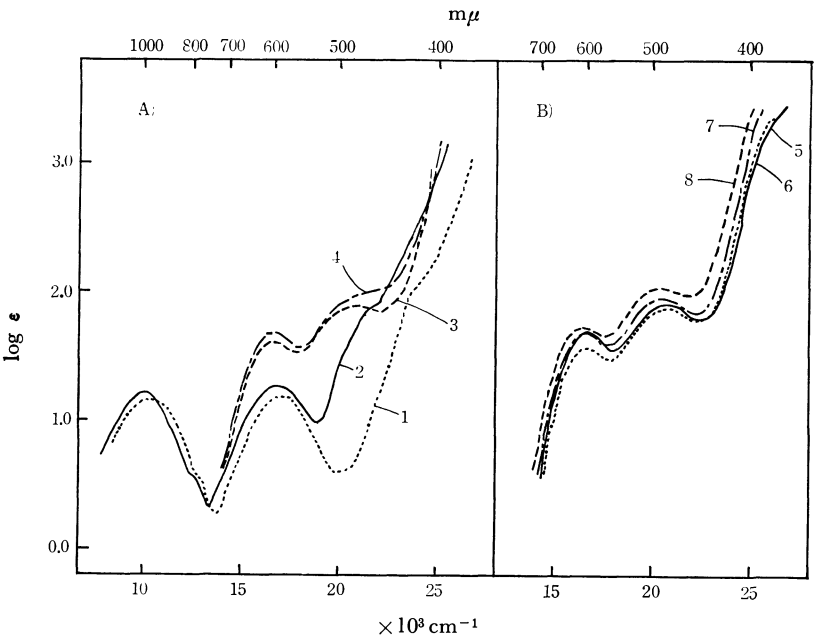

Fig. 2. Electronic absorption spectra of $Ni(Aca.R)_2$. (A) In pyridine : 1, R=*o*-ClC_6H_4 (---------); 2, R=α-naphthyl (——); 3, R=*o*,*o*'-$(C_2H_5)_2C_6H_3$ (— — —); 4, R=*o*,*o*'-$(CH_3)_2C_6H_3$(— · — · —); and (B) in chloroform: 5, R=*o*-ClC_6H_4 (——); 6, R=*o*,*o*'-$(C_2H_5)_2C_6H_3$ (---------); 7, R=*o*,*o*'-$(CH_3)_2C_6H_3$ (— · — · —); 8, R=α-naphthyl (— — —).

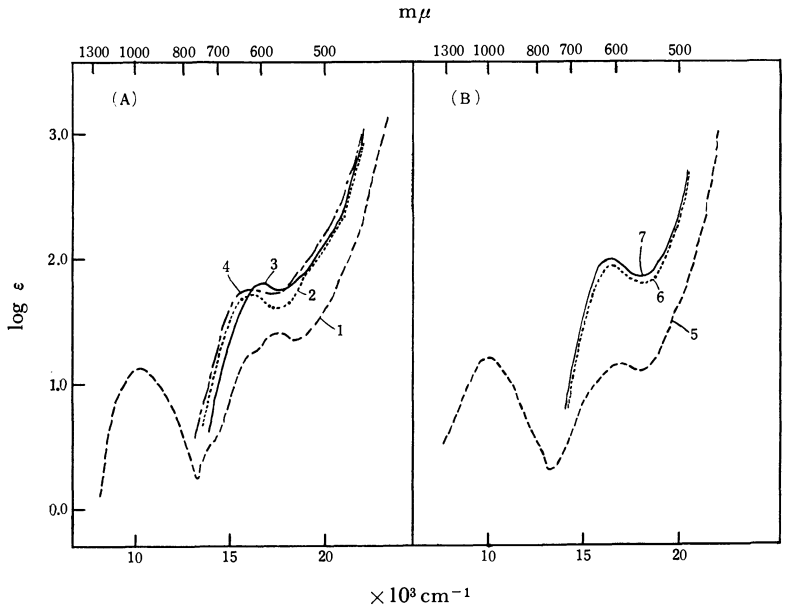

Fig. 3. Electronic absorption spectra of (A) $Ni(Bza.R)_2$: 1, R=*p*-$CH_3C_6H_4$ in pyridine (— — —); 2, R=*o*,*o*'-$(C_2H_5)_2C_6H_3$ in pyridine (---------); 3, R=*o*,*o*'-$(CH_3)_2C_6H_3$ in chloroform (——); 4, R=*p*-$CH_3C_6H_4$ in chloroform (— · — · —) and (B) $Ni(Sal.R)_2$: 5, R=*p*-$CH_3C_6H_4$ in pyridine (— — —); 6, R=*o*,*o*'-$(C_2H_5)_2C_6H_3$ in pyridine (---------); 7, R=*o*,*o*'-$(C_2H_5)_2C_6H_3$ in chloroform (——).

the square-planar complex. The fact that no association of the square-planar complexes takes place may be interpreted on the basis of the steric hindrance due to the two methyl or ethyl groups at the *o*- and *o'*-positions.

The Copper(II) Complexes of β-Ketoamines and Salicylideneimines Derived from Aromatic Amines.—Many new copper(II) complexes

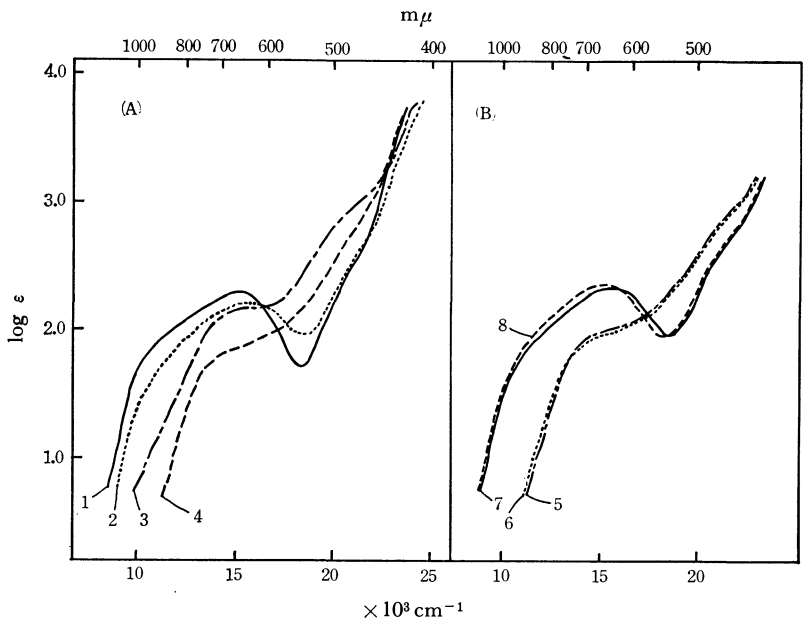

Fig. 4. Electronic absorption spectra of (A) Cu(Sal.R)$_2$: 1, R=*o*,*p*,*o'*-$Cl_3C_6H_2$ in pyridine(——); 2, R=*o*-$CH_3C_6H_4$ in pyridine (---------); 3, R=*o*-$CH_3C_6H_4$ in chloroform (—·—·—); 4, R=*o*,*p*,*o'*-$Cl_3C_6H_2$ in chloroform (— — —) and (B) Cu(Sal.R)$_2$: 5, R=*o*,*o'*-$(C_2H_5)_2C_6H_3$ in chloroform (— — —); 6, R=*o*,*o'*-$(CH_3)_2C_6H_3$ in chloroform (---------); 7, R=*o*,*o'*-$(CH_3)_2C_6H_3$ in pyridine (——); 8, R=*o*,*o'*-$(C_2H_5)_2C_6H_3$ in pyridine(— — —).

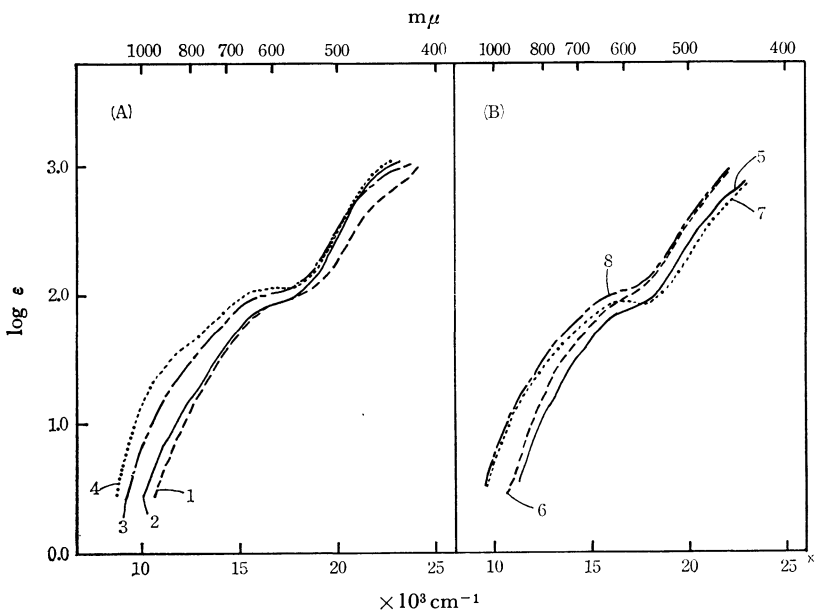

Fig. 5. Electronic absorption spectra of (A) Cu(Aca.R)$_2$: 1, R=*o*,*o'*-$(C_2H_5)_2C_6H_3$ in chloroform (---------); 2, R=*o*,*o'*-$(CH_3)_2C_6H_3$ in chloroform (——); 3, R=*o*,*o'*-$(C_2H_5)_2C_6H_3$ in pyridine (— — —); 4, R=*o*,*o'*-$(CH_3)_2C_6H_3$ in pyridine (---------); and (B) Cu(Bza.R)$_2$: 5, R=*o*,*o'*-$(CH_3)_2C_6H_3$ in chloroform (——); 6, R=*o*,*o'*-$(C_2H_5)_2C_6H_3$ in chloroform (— — —); 7, R=*o*,*o'*-$(CH_3)_2C_6H_3$ in pyridine (---------); 8, R=*o*,*o'*-$(C_2H_5)_2C_6H_3$ in pyridine (— — —).

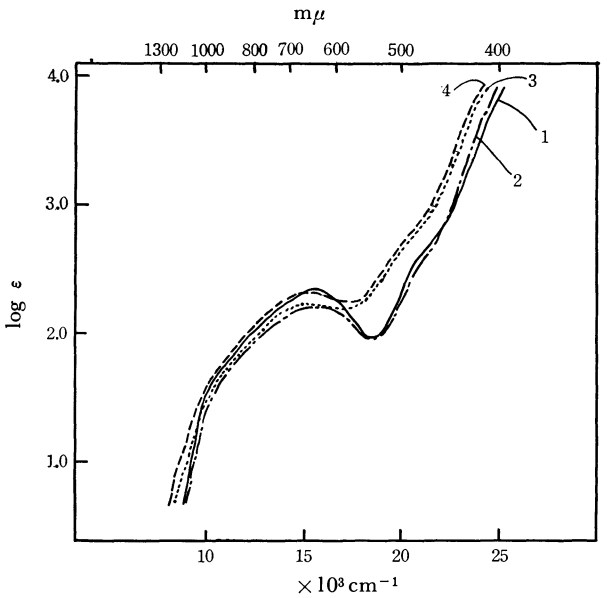

Fig. 6. Electronic absorption spectra of $Cu(Sal.R)_2$ in pyridine : 1, R=*o*, *o*'-$(CH_3)_2C_6H_3$ (——); 2, R=*o*-$CH_3C_6H_4$ (—·—·—); 3, R=*p*-$CH_3C_6H_4$ (·····); 4, R=*m*-$CH_3C_6H_4$ (—··—··—).

of the β-ketoamines and salicylideneimines, which are shown in Tables I, II and III, have been prepared in the present work. The planar configuration is most likely for the copper(II) complexes, since the tendency of the copper(II) complex to take the square-planar configuration is known to be very great. The square-planar configuration can not be rejected, even for the *o*, *o*'-disubstituted complexes of copper(II), on the steric ground alone, since the corresponding complexes of nickel(II) have been found to be square-planar. It is reasonable to presume that the *o*, *o*'-disubstituted and the monosubstituted complexes of copper(II) take a square-planar configuration. This presumption seems to be consistent with the present observation that the *o*, *o*'-disubstituted and the monosubstituted complexes of copper(II) show ligand field bands at a nearly identical frequency, and that the whole pattern of the spectra is also quite similar among these complexes (Fig. 4). It was previously shown that the ligand field band was shifted toward a considerably lower frequency when the cupric complex was distorted appreciably from the square-planar configuration.[6,7]

The change in the ligand field band of these copper(II) complexes on going from chloroform to pyridine, the change shown in Figs. 4 and 5, is similar to the change observed previously when the quadri-co-ordinated complex of copper(II) takes up one or two additional ligands to form a quinque- or sexa-co-ordinated complex.[12] It may be concluded, therefore, that all the cupric complexes examined in the present work are combined with one or two pyridine molecules in the pyridine solution. The change in the spectrum of the complex on going from chloroform to pyridine is more pronounced for the salicylideneimine complexes than for the corresponding β-ketoamine complexes.

Judging from the steric effect due to the two substituents, it is most likely that the *o*, *o*'-disubstituted complexes are able to take only one molecule of pyridine to form a quinque-co-ordinated configuration. It should be noted that the spectral behavior of the *o*, *o*'-disubstituted complexes of copper(II) in pyridine is quite similar to that of the corresponding monosubstituted complexes, and that the monosubstituted complexes of copper(II) in pyridine show spectra almost superposable on those of the corresponding disubstituted complexes (Figs. 5 and 6). The spectral change on going from chloroform to pyridine is also similar for these complexes. It is most likely that all these copper(II) complexes, therefore, take an identical configuration in pyridine. This seems to be in agreement with a previous finding concerning the ability of bis(acetylacetonato)copper(II) to combine with another ligand such as pyridine.[13]

Comparison of Nickel(II) with Copper(II). —It has been found in the present work that, in the binding of the additional pyridine molecule, the *o*, *o*'-disubstituted complexes of copper(II) are different from the corresponding complexes of nickel(II); the nickel(II) complexes combine

12) See, for example, M. Honda and G. Schwarzenbach, *Helv. Chim. Acta*, **40**, 27 (1957); R. L. Belford and T. S. Piper, *Mol. Phys.*, **5**, 251 (1962).

13) D. P. Graddon, *J. Inorg. Nucl. Chem.*, **17**, 222 (1961); D. Gillard and G. Wilkinson, *J. Chem. Soc.*, **1963**, 5885.

with no additional pyridine molecule. This difference between copper(II) and nickel(II) may be interpreted in terms of the bonding nature of the metal ions and in terms of the steric condition of the ligands. In the complexes of copper(II) with a d^9 configuration, the copper-ligand bond distance along the z-direction is generally found to be appreciably longer, due to the Jahn-Teller effect, than the corresponding bond distance in the xy-plane, that is, the complex-plane. Moreover, quinque-co-ordinated complexes are not rare for the copper(II) ion. On the other hand, the six bonds between the nickel(II) ion and ligands are essentially equivalent in the sexa-co-ordinated complexes of nickel(II) with a d^8 configuration. It is, therefore, reasonable to expect that the two substituents at the o- and o'-positions may prevent the pyridine molecule from combining with the nickel(II) ion, whereas the copper(II) ion in the corresponding complex may combine with the pyridine molecule at a little farther distance in spite of the possible steric hindrance.

The present work was supported in part by the Ministry of Education.

BULLETIN OF THE CHEMICAL SOCIETY OF JAPAN VOL. 39 1002—1006 (1966)

Infrared Spectra of Urea Complexes of Copper(II) *n*-Alkanoates

By Yoko KURODA, Akira SASANO and Masaji KUBO

(*Department of Chemistry, Nagoya University Chikusa, Nagoya*)

(*Received September* 25, 1965)

The infrared absorption spectra of various urea complexes of copper(II) carboxylates were recorded and the assignments of observed frequencies have been carried out to various modes of vibration. On the basis of comparison of the observed spectra with those of related compounds, it is concluded that copper(II) carboxylate monoureas and hemiureas form dimer molecules in crystals as in copper(II) acetate monohydrate, that copper(II) formate bisurea dihydrate has a crystal structure bearing resemblance to that of copper(II) formate tetrahydrate, and that urea molecules in these urea complexes are involved in bonding by electrostatic forces or hydrogen bondings instead of being bonded to copper atoms by coordination bonds.

Urea forms various addition compounds with copper(II) *n*-alkanoates.[1,2] The most general types of the urea complexes are copper(II) *n*-alkanoate monoureas, $Cu(C_nH_{2n+1}CO_2)_2\cdot(NH_2)_2CO$ (n=0—3, 5), and copper(II) *n*-alkanoate hemiureas, $Cu(C_nH_{2n+1}CO_2)_2\cdot 0.5(NH_2)_2CO$ (n=4—9). In addition, the hydrated urea complexes of copper(II) formate and acetate, $Cu(HCO_2)_2\cdot 2(NH_2)_2CO\cdot 2H_2O$ and $Cu(CH_3CO_2)_2\cdot(NH_2)_2CO\cdot H_2O$, can be prepared in the crystalline state. We have observed the magnetic moments of these copper(II) compounds and found that except for copper(II) formate bisurea dihydrate, they show subnormal magnetic moments, 1.40±0.03 Bohr magnetons, per copper atom at room temperature, suggesting the existence of paired copper atoms in crystals. Undoubtedly, urea molecules in the monourea complexes occupy the same positions about copper atoms as do water molecules in the crystals of copper(II) acetate monohydrate.[3] However, the structures of the hemiurea complexes and the hydrated urea complexes are open to speculation so long as the magnetic data alone are taken into account. The present investigation has been undertaken in order to gain some information from infrared spectroscopy about the role of urea molecules possibly participating in coordination on copper atoms.

Experimental

Materials tested were prepared by methods described in a previous paper.[2] Infrared absorptions were recorded over a wave number range from 4000 to 200 cm^{-1} using a Model DS-402G grating infrared spectrophotometer from Japan Spectroscopic Company. In the frequency range above 400 cm^{-1}, all samples were run as potassium bromide disks and checked in Nujol mulls. Below 430 cm^{-1}, spectra were obtained using Nujol mulls. Potassium bromide plates and thin polyethylene films were used as cell windows for Nujol mulls in the two regions, respectively.

Results

Copper(II) Acetate Monourea.—The absorptions of copper(II) acetate monourea are compared

1) M. Kishita and M. Kubo, *Naturwissenschaften*, **49**, 230 (1962).
2) M. Kishita, M. Inoue and M. Kubo, *Inorg. Chem.*, **3**, 237 (1964).
3) J. N. van Niekerk and F. R. L. Schoening, *Acta Cryst.*, **6**, 227 (1953).

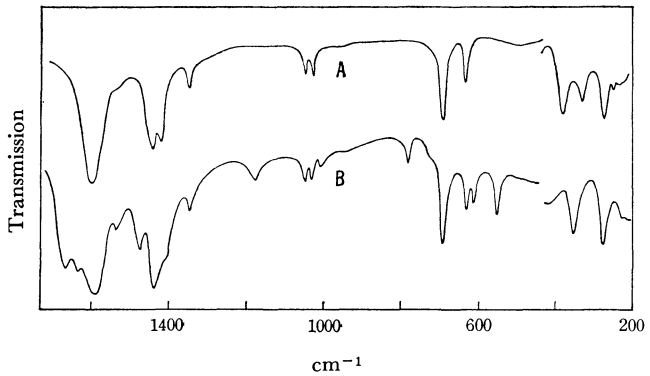

Fig. 1. Infrared spectra of (A) copper(II) acetate monohydrate and (B) copper(II) acetate monourea.

Table I. Infrared absorptions (cm^{-1}) of copper(II) acetate, copper(II) acetate monohydrate, and copper(II) acetate monourea*

Copper(II) acetate	Copper(II) acetate monohydrate	Copper(II) acetate monourea
		1670 s
		1635 sh
1590 vs	1602 vs	1595 vs
hump	hump	1535m
		1475 s
1441 vs	1441 vs	1440 vs
1412 vs	1418 vs	1415 sh
1352m	1351m	1355m
		1178m
1051m	1051m	1050m
1038 sh	1032m	1032m
		1006m
945w	hump	hump
		782m
		725w
692 s	690 s	687 s
625m	629m	627m
		614m
		550m
382m	375m	
340m	330w	350m
284m	274m	274m
	254w	
~240w	~235w	~233w

* vs, very strong. s, strong. m, medium. w, weak. sh, shoulder.

Table II. Infrared absorptions (cm^{-1}) of copper(II) caproate, copper(II) caproate monourea, and copper(II) caproate hemiurea*

Copper(II) caproate	Copper(II) caproate monourea	Copper(II) caproate hemiurea
	1675 s	1675 s
	1655 s	1660 s
	1625 s	1626 s
		1614 s
1585 vs	1585 vs	1586 vs
1510m	1535m	1535m
1432m	1465 s	1460 s
1416 s	1430 s	1427 s
1378—1191 p	1380—1230 p	1380—1194 p
	1170m	1175 sh
1113w	1114m	1115m
	1000w	
895w	890w	892w
848w	850w	853w
	778 sh	
	772m	778w
	737m	740 sh
725m	722 sh	720m
664m	651m	670m
		645w
	605m	599m
	541m	532m
	443m	
385m	389m	400m
342w	334m	352m
303w		
245m	260m	270m

* p, band progression.

with those of copper(II) acetate and copper(II) acetate monohydrate[4] in Table I. In the wave number range 1800—400 cm^{-1}, all absorption peaks characteristic of anhydrous copper(II) acetate, which shows practically the same spectrum as that of copper(II) acetate monohydrate in this frequency range, appear in the spectrum of copper(II) acetate monourea without any appreciable change in the position, the intensity, and the shape of absorption bands as shown in Fig. 1. Accordingly, additional absorptions appearing in the spectrum of copper(II) acetate monourea can be assigned to vibrations involving urea molecules. On the other hand, no such clear correspondence can be made below

4) Y. Kuroda. *J. Chem. Soc. Japan, Pure Chem. Sect.* (*Nippon Kagaku Zasshi*), **82**, 1624 (1961).

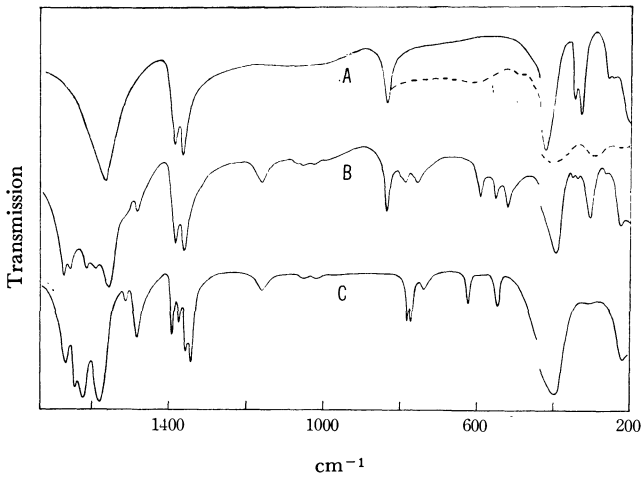

Fig. 2. Infrared spectra of (A) anhydrous copper(II) formate (full curve), copper(II) formate tetrahydrate (broken curve), (B) copper(II) formate bisurea dihydrate, and (C) copper(II) formate monourea.

400 cm^{-1}, probably because lattice vibrations, librations, etc. are involved in the spectra. In a region beyond 1800 cm^{-1}, only NH stretching vibrations are observable as intense bands.

Other copper(II) *n*-alkanoate monoureas were tested and yielded analogous results.

Copper(II) Caproate (*n*-Hexanoate) Hemiurea.—Table II shows the absorptions of copper(II) caproate, copper(II) caproate monourea, and copper(II) caproate hemiurea. In the region of band progressions (about 1350—1200 cm^{-1}), the spectra are complicated and no definite correspondence of absorption peaks can be found between the spectra of these compounds, presumably owing to difference in the interactions of methylene chains in crystals. However, major peaks of copper(II) caproate appearing in the wave number range 1800—400 cm^{-1} can be found in the spectra of the monourea and hemiurea complexes also without any appreciable shifts. In particular, a very strong peak at 1585 cm^{-1} is practically unaltered in its wave number and band shape. Below 400 cm^{-1}, no definite correspondence of absorption peaks can be made between these spectra for the same reason as given for copper(II) acetate and its derivatives. By taking into account relative intensities and band shapes, peaks attributable to urea molecules were selected from the spectra of copper(II) caproate monourea and hemiurea in the wave number range 1800—400 cm^{-1}.

The absorption spectra of other copper(II) carboxylate hemiureas were recorded and absorptions characteristic of urea molecules were determined.

Copper(II) Formate Bisurea Dihydrate and Copper(II) Formate Monourea.—The absorptions of copper(II) formate, copper(II) formate tetrahydrate, copper(II) formate bisurea dihydrate, and copper(II) formate monourea are shown in Table III. In the wave number range 1800—830 cm^{-1}, the spectrum of anhydrous copper(II) formate is practically identical with that of the tetrahydrate, although they differ markedly from each other below about 700 cm^{-1}. The absorptions of the tetrahydrate appearing in the wave number range 1800—400 cm^{-1} can be found in the

TABLE III. INFRARED ABSORPTIONS (cm^{-1}) OF COPPER(II) FORMATE AND ITS DERIVATIVES*

Copper(II) formate (pale blue modification)	Copper(II) formate tetrahydrate	Copper(II) formate bisurea dihydrate	Copper(II) formate monourea
		1675 s	1668 s
		1656 s	1645 s
		1614 s	1621 s
		1592 s	
1562 vs	1562 vs	1562 vs	1581 vs
			1513w
		1485m	1485m
1384 s	1384 s	1379m	1389m
			1369w
			1355m
1366 s	1366 s	1361 s	1343 s
		1160w	1161w
		1020 vw	1048 vw
834m	834m	834m	779m
		787w	772m
		757w	738w
	800—550 br	591w	618m
		550w	
		512m	542m
423m	~390m	392m	~395m
343, 330m	~308w	305w	
~216m	~250w	~227m	~225m

* vw, very weak. br, broad.

TABLE IV. VIBRATIONAL FREQUENCIES OF UREA MOLECULES IN PURE CRYSTALS AND VARIOUS UREA COMPLEXES

Vibrational mode	Urea (tetragonal)	Urea adducts (hexagonal)	Copper(II) carboxylate monoureas	Copper(II) carboxylate hemiureas	Copper(II) formate bisurea dihydrate
NH_2 stretchings	3449 3436 3362 3342	3420 3360 3240 3190	3420—3500*	~3475*	3440 3375 3240
CO stretching NH_2 scissoring	1681 1629 1603	1684 1656 1626 1597	~1670 ~1620	1677 1661 1626 ~1612	1675 1656 1614 1592
Antisym. CN stretching	1466	1486	1468—1485	~1470	1485
NH_2 rocking	1156	1157	1160—1178	1170—1175	1160
Sym. CN stretching	1004	1015	~1000—1015		~1020
Out-of-plane skel. deformation	789	794	~780	~775	787
NH_2 wagging	715	720	~725—738		757
In-plane CO bending	571	608	605—618	599	591
NCN scissoring	558	608	535—550	534	550
NH_2 twisting	530	610			512

* Additional weaker bands appearing beyond 3000 cm^{-1} are omitted.

spectrum of copper(II) formate bisurea dihydrate also without any appreciable shift and change in the band contour as shown in Fig. 2.

Discussion

The absorptions characteristic of carboxylate ions appearing in the wave number range 1800—400 cm^{-1} are almost unaltered by the addition of urea to copper(II) carboxylates except for copper(II) formate and by the substitution of water in copper(II) acetate monohydrate with urea to form copper(II) carboxylate monoureas and hemiureas. In addition, the frequency of absorptions at about 1585 cm^{-1} attributable to the antisymmetric COO stretching vibration is shifted to some extent from the corresponding frequencies observed for sodium, potassium, and silver salts.[4,5] These facts lend additional support to the presumption already suggested by magnetic measurements[1,2] that copper(II) carboxylate monoureas and hemiureas form dimer molecules in crystals.

In the wave number range 1800—400 cm^{-1}, the spectrum of copper(II) formate bisurea dihydrate has all absorptions of copper(II) formate tetrahydrate without any appreciable change, in addition to bands attributable to urea molecules. This indicates that the compound forms crystals consisting of two-dimensional network structures as observed by X-ray crystal analysis for the tetrahydrate.[6] On the other hand, copper(II) formate monourea shows a spectral feature quite different from those of copper(II) formate tetrahydrate and bisurea dihydrate. In the first place, the antisymmetric COO stretching frequency at 1581 cm^{-1} is higher than the corresponding frequencies of the tetrahydrate and the bisurea dihydrate by about 20 cm^{-1}. Secondly, the COO scissoring vibration appearing at 779 cm^{-1} is lower by about 55 cm^{-1}. Lastly, marked splittings of bands are observed in the wave number region of 1389—1343 cm^{-1}. These results suggest that the structure of copper(II) formate monourea is basically different from those of copper(II) formate bisurea dihydrate and copper(II) formate tetrahydrate in conformity with a conclusion from magnetic studies[2] that among copper(II) formate and its derivatives, only copper(II) formate monourea forms dimer molecules analogous to those in copper(II) acetate monohydrate in crystals.

The normal vibrations of urea have been calculated and the assignment of observed frequencies has been made by Yamaguchi et al.[7,8] Kutzelnigg et al.[9] have discussed the vibrational spectra of urea molecules in pure crystals and solutions and those constituting the host lattice of urea adducts in relation to intermolecular forces. Based on the results of these investigations, frequencies observed for the urea complexes of copper(II) carboxylates have been assigned to various modes of vibration as shown in Table IV. The frequency observed for copper(II) carboxylate monoureas depends on the kind of carboxylate ions to some extent, whereas that of copper(II) carboxylate hemiureas is almost independent of the chain length of the carboxylate ions.

A urea molecule has an oxygen atom and two nitrogen atoms capable of being coordinated on a

5) Y. Kuroda and M. Kubo, *J. Phys. Chem.*, **64**, 759 (1960).
6) R. Kiriyama, H. Ibamoto and K. Matsuo, *Acta Cryst.*, **7**, 482 (1954).
7) A. Yamaguchi, *J. Chem. Soc. Japan, Pure Chem. Sect. (Nippon Kagaku Zasshi)*, **78**, 1319, 1467 (1957).
8) A. Yamaguchi, T. Miyazawa, T. Shimanouchi and S. Mizushima, *Spectrochim. Acta*, **10**, 170 (1957).
9) W. Kutzelnigg, R. Mecke, B. Schrader, F. Nerdel and G. Kresse, *Z. Electrochem.*, **65**, 109 (1961).

metal atom. It is expected that coordination affects the vibrational frequencies of urea, especially those of NH_2 stretching and CO stretching vibrations. In fact, Penland et al.[10] have found that dichloro(bisurea)platinum(II) and dichloro(bisurea)palladium(II) show a decrease in the frequencies of NH_2 stretchings and antisymmetric CN stretching as well as an increase in the frequencies of CO stretching coupled with NH_2 scissoring and concluded that nitrogen is involved as donor atoms in coordination. On the other hand, Table IV shows that no marked differences can be found in the NH_2 stretchings, the CO stretching mixed with the NH_2 scissoring, the antisymmetric CN stretching, etc. between tetragonal or hexagonal urea and the urea complexes of copper(II) carboxylates. Accordingly, it is concluded that urea molecules in these urea complexes are not bonded to copper atoms by coordination bonds having a covalent character but that they are involved in bonding by electrostatic forces or hydrogen bondings as in the tetragonal or hexagonal crystals of urea. Penland et al.[10] have presumed that oxygen-to-metal bonds are formed in the dichloro(bisurea) complexes $M(NH_2CONH_2)_2Cl_2$ of zinc(II) and copper(II) showing no such marked shifts of bands as observed for the platinum(II) and palladium(II) complexes and that two chlorine atoms and two oxygen atoms occupy coordination sites at the corners of a square with a metal atom at its center. However, it is very likely that in dichloro(bisurea)-copper(II), for instance, all the coordination sites of copper are occupied by chlorine, the coordination squares being arranged in a one-dimensional array by sharing their edges as in the crystals of dichloro-(1, 2, 4-triazole)copper(II)[11] and that urea molecules are not directly involved in the square coordination of copper.

This paper is dedicated to Professor Masao Kotani of the University of Tokyo in commemoration of his sixtieth birthday.

10) R. B. Penland, S. Mizushima, C. Curran and J. V. Quagliano, *J. Am. Chem. Soc.*, **79**, 1575 (1957).

11) J. A. J. Jarvis, *Acta Cryst.*, **15**, 964 (1962).

BULLETIN OF THE CHEMICAL SOCIETY OF JAPAN VOL. 39 1006—1008 (1966)

The NMR Signal Shape of Identical Nuclei Exchanging between Two Different Environments*

By Toshio NAKAGAWA

Shionogi Research Laboratory, Shionogi & Co., Ltd., Fukushima-ku, Osaka

(Received September 28, 1965)

The Gutowsky-Holm equation has been transformed into a formula which expresses the signal as a function of dimensionless parameters ($a=2\pi\tau|\nu_A-\nu_B|$, $r=1/2\pi T_2|\nu_A-\nu_B|$ and p_B) and a dimensionless variable ($f=(\nu-\nu_A)/(\nu_B-\nu_A)$). The shape function in this form is convenient for graphic representation and can be easily calculated for a desired combination of the parameters by using a suitable computer. The exchange rate can be determined by searching for a theoretical curve that agrees with the shape of the experimental signal.

When an assembly of identical nuclei are exchanging in a random statistical manner between two environments with different chemical shifts, the signal takes on various shapes, depending on the exchange rate, the fractional populations, and the transverse relaxation times. In this report we shall neglect all coupling, and examine the signal shape observed under these circumstances.

This problem has already been solved mathematically by Gutowsky and Holm for the case where the two transverse relaxation times, T_{2A} and T_{2B}, are equal.[1] The equation thus obtained is, however, inconvenient for a general discussion of signal shape because it is formulated in terms of dimensional quantities. The main purpose of the present report is to transform it into a formula which expresses the shape of a signal as a function of dimensionless parameters, and then to discuss its application to the determination of exchange rates.

Theoretical Consideration

First of all we shall define the dimensionless parameters:

$$a = 2\pi\tau|\nu_A-\nu_B| = 2\pi p_B\tau_A|\nu_A-\nu_B| = 2\pi p_A\tau_B|\nu_A-\nu_B| \quad (1)$$

$$r = 1/2\pi T_2|\nu_A-\nu_B| = w/|\nu_A-\nu_B| \quad (2)$$

* Presented at the International Symposium on Nuclear Magnetic Resonance, Tokyo, September, 1965.

1) H. S. Gutowsky and C. H. Holm, *J. Chem. Phys.*, **25**, 1228 (1956).

and a dimensionless variable:

$$f = (\nu_A-\nu)/(\nu_A-\nu_B) = (\nu-\nu_A)/(\nu_B-\nu_A) \quad (3)$$

By substituting them into the Gutowsky-Holm equation, we get a general formula:

$$\begin{aligned} v = C\times[&(1+ar)\{-af(f-1)+r(1+ar)\} \\ &+a(f+p_B-1)(f+2arf-ar-p_B)] \\ &\div[\{-af(f-1)+r(1+ar)\}^2 \\ &+(f+2arf-ar-p_B)^2] \end{aligned} \quad (4)$$

where $C = -\gamma H_1 M_0/2\pi\,|\nu_A-\nu_B|$

Here v describes the transverse component of the resultant magnetic moment, which is perpendicular to the rotating field, H_1, and which is proportional to the absorption intensity. The same symbol, v, will be used hereafter to represent the absorption intensity. C is a constant, dependent on the apparatus sensitivity. The other notations, other than w, have their usual meanings. The parameter, r, is one half of the half-height-width of the A (or B) signal, w, divided by the separation between the A and B signals, in the absence of exchange effects and with no overlap of signals.

Equation 4 is convenient for graphic representation because this formula gives the relative intensity as a function of the relative position, f, with respect to the signal positions of the A and B states. The shape function can be easily calculated for a desired combination of a, r, and p_B by using a suitable computer. An IBM-1620 computer performed the calculation in a quarter of an hour. The Fortran program is shown in Table I. In this program, the maximum signal height is made equal to unity by choosing automatically a proper value of C.

Table I. Fortran program for Eq. 4

```
C       SHAPE FUNCTION
        DIMENSION F(301), V(301)
        READ 1, A, R, PB
        AR=A*R
        AR1=1.+AR
        RAR1=R*AR1
        HIST=0.
        D0 20 I=1, 301
        P=I+99
        F(I)=P/100.-2.
        B=RAR1-A*F(I)*(F(I)-1.)
        C=F(I)+PB-1.
        D=F(I)+2. *AR*F(I)-AR-PB
        V(I)=(AR1*B+A*C*D)/(B*B+D*D)
        IF (V(I)-HIST) 20, 20, 10
   10   HIST=V(I)
   20   CONTINUE
        D0 30 I=1, 301
        V(I)=V(I)/HIST
   30   TYPE 2, F(I), V(I)
    1   FORMAT (E12.8, E12.8, F4.2)
    2   FORMAT (F5.2, 5X, F8.5)
        END
```

In several limiting cases, Eq. 4 becomes simpler and is reduced to the familiar relations, 5 to 9.

$$v_{(p_B=0)} = C\times\{r/(r^2+f^2)\} \quad (5)$$

$$v_{(p_A=0)} = C\times[r/\{r^2+(f-1)^2\}] \quad (6)$$

$$v_{(a\to\infty)} = C\times[rp_A/(r^2+f^2)+rp_B/\{r^2+(f-1)^2\}] \quad (7)$$

$$v_{(a=0)} = C\times[r/\{r^2+(f-p_B)^2\}] \quad (8)$$

$$v_{(r\to\infty)}=0 \quad (9)$$

$$\begin{aligned} v_{(r=0)} &= C\times[ap_Ap_B/\{a^2f^2(f-1)^2+(f-p_B)^2\}] \\ &= C'\times[1/\{a^2f^2(f-1)^2+(f-p_B)^2\}] \end{aligned} \quad (10)$$

The last equation (10) has previously been derived by the author and presented graphically for many combinations of a and p_B.[2)]

A one-to-one correspondence can be shown to hold between the signal shape (expressed in the relative intensity as a function of f) and the set of parameters (a, r, and p_B). One important exception, however, is the case where r equals zero, and where a tends to infinity. In this case, two lines appear, at $f=0$ and at $f=1$. The ratio of their heights varies from p_A/p_B to p_A^2/p_B^2, depending on the product of a and r, or, in other words, on the ratio of τ to T_2. Both times are infinitely large compared with $1/|\nu_A-\nu_B|$, but their ratio may be finite.

$$v_{(\text{at } f=0)}/v_{(\text{at } f=1)} = p_A(p_A+ar)/p_B(p_B+ar) \quad (11)$$

The following two cases may also be considered as rather exceptions. As is shown by Eq. 9, no signal appears for an infinitely large r value, regardless of the values of a and p_B. The same Lorentzian curve is obtained for sets of parameters which have r's all equal, a's all different, and $p_B=0$ (or 1). A detailed discussion of these cases seems unnecessary, however, since no information of practical importance could be derived from such a discussion.

The most important application of Eq. 4 is probably to the case where $p_A=p_B=1/2$. Except for the last paragraph, we shall be concerned exclusively with this case in the remainder of this section. Equation 4 can be reduced to Eq. 12, which is symmetrical with respect to $f=1/2$:

$$\begin{aligned} v = C\times&\{a^2rf(f-1)+r(1+ar)^2+a(1+2ar)/4\} \\ &\div\{a^2f^2(f-1)^2+(1+2ar+2a^2r^2)f(f-1) \\ &+r^2(1+ar)^2+(1+2ar)^2/4\} \end{aligned} \quad (12)$$

The signal shapes have been calculated and presented graphically for all combinations of $a=\infty$, 32, 8, 4, $2\sqrt{2}$, 2, 1.7, $\sqrt{2}$, 1.2, 1, $1/\sqrt{2}$, 1/2,

2) T. Nakagawa, *Ann. Rept. Shionogi Lab.*, **13**, 60 (1963).

1/4, 1/16, 0 and $r=0$, 1/20, 1/10, 1/5, 1/3, 1/2.** Both the life-time, τ_A $(=\tau_B)$, and the transverse relaxation time, T_2, can be determined by searching for a figure that agrees with the shape of the experimental signal.

Provided one of the signal positions of the components, ν_A, or ν_B, is known on the chart by some means, the comparison is easy. The scale of f can be determined from the center of symmetry ($f=1/2$) and from the position of ν_A or ν_B ($f=0$ or 1). Because of the one-to-one correspondency, both a and r can be determined unequivocally.

In most cases, however, we cannot scale f by a glance at the chart. Equation 12 has two independent parameters, a and r; therefore, it is necessary to use at least two shape parameters in order to compare the experimental and theoretical curves. The ratios of maximum to minimum height, of quarter-height-width to half-height-width, of half-height-width to three-quarter-height-width, etc., may be used as such parameters. A more precise comparison can be achieved by dividing the signal peak into many equal heights, and by comparing the relative widths of the experimental and theoretical curves at corresponding heights.

Provided $a=0$, the signal displays a Lorentzian curve for any r value; the value of r cannot be determined from the signal shape. Even in this case, however, we are able to evaluate T_2 from the half-height-width ($T_2=1/2\pi w$), and deduct τ_A $(=\tau_B)=0$ from the Lorentzian shape of the signal. The signal position of the components, ν_A and ν_B, cannot be determined. For $a\neq 0$, there is only one theoretical curve that accurately coincides with the signal obtained experimentally, thus, a, r, ν_A, and ν_B can all be determined.

** Duplicates are available on microfilm on request to the author.

Life-times have frequently been estimated by ignoring the effect of T_2. In more rigorous analysis, T_2 has been evaluated from the line width at high temperatures, where the signal narrows into a sharp peak. Then the life-time can be evaluated, for example, by comparing the peak separations at a temperature in the transition region and at a temperature sufficiently low to stop the exchange. The temperature independency of T_2, ν_A, and ν_B is assumed in this analysis.

The advantage of the present method is that it is free from these assumptions. At least in principle, τ, T_2, ν_A, and ν_B can be determined uniquely and simultaneously from a single experiment at any temperature in the transition region. The applicability to an actual system depends on the adequacy of the assumption that $T_{2A}=T_{2B}$, and on the accuracy of the apparatus used.

For the case where $T_{2A}\neq T_{2B}$[3] a more general formula:

$$v=C\times[\{(1+ar_Ap_B+ar_Bp_A)K+a(f+p_B-1)L\}/(K^2+L^2)] \quad (13)$$

where

$$K=(r_Ap_A+r_Bp_B)+a\{r_Ar_B-f(f-1)\}$$
$$L=f(1+ar_A+ar_B)-(ar_A+p_B)$$
$$C=-\gamma H_1M_0/2\pi\,|\nu_A-\nu_B|$$
$$a=2\pi\tau\,|\nu_A-\nu_B|$$
$$r_A=1/2\pi T_{2A}\,|\nu_A-\nu_B|$$
$$r_B=1/2\pi T_{2B}\,|\nu_A-\nu_B|$$
$$f=(\nu-\nu_A)/(\nu_B-\nu_A)$$

is derived. It is easy to design a program similar to that shown in Table I.

3) M. T. Rogers and J. C. Woodbrey, *J. Phys. Chem.*, **66**, 540 (1962).

BULLETIN OF THE CHEMICAL SOCIETY OF JAPAN VOL. 39 1009—1014 (1966)

Studies of the Cage Effect of Solvents. V. The Photolysis of Azoethane in *n*-Heptane

By Sukeya KODAMA, Shin'ichi FUJITA, Junsuke TAKEISHI and Osamu TOYAMA

Department of Applied Chemistry, College of Engineering, University of Osaka Prefecture, Sakai, Osaka

(Received September 29, 1965)

The effect of a solvent cage on the photolysis of azoethane in *n*-heptane was investigated at 366 mμ in the temperature range from −75 to 99°C. Among the gaseous products, nitrogen served as a measure of the azoethane decomposed. The other gaseous products were *n*-butane, ethane and ethylene; these three hydrocarbons accounted for ninety per cent of the decomposition at 0°C. The quantum yield of nitrogen was found to decrease with a lowering of the temperature. The value obtained at 0°C was 0.021. In the presence of a sufficient amount of styrene, which was used as a scavenger for ethyl radicals, the yields of the gaseous hydrocarbons were more or less reduced to constant values; from these the ratio of rate constants for the combination and disproportionation of the geminate ethyl radicals formed by the photolysis in a solvent cage was determined to be $k_{comb}/k_{disp}=11.5\exp(-371/\boldsymbol{R}T)$. The fraction of ethyl radicals that reacted in these ways in the solvent cage, before escaping it, was dependent on the temperature; it decreased from 0.838 at −75°C to 0.467 at 99°C. In the absence of styrene, the reactions for ethyl radicals that escaped the original solvent cages were inferred to be hydrogen abstraction, addition, combination and disproportionation.

In previous papers of the present series,[1] the effect of a solvent cage on the geminate methyl radicals formed by the photolysis of azomethane in various solvents was reported on. This paper will report on a similar study of the ethyl radicals obtained by the photolysis of azoethane in *n*-heptane.

The cage effect in the photolysis of azoethane in solution has been investigated by Szwarc and his co-workers[2] in an attempt to determine the ratio of disproportionation to combination of the geminate ethyl radicals in a solvent cage, and in an attempt to compare the results with those obtained in the gas phase. The present work will provide quantitative data that will enable us to discuss the reactions in the solvent cage in relation to the other reactions involved in the photolysis.

Experimental

Materials.—Azoethane was prepared by the thermal decomposition of the azoethane - cuprous chloride obtained from diethyl hydrazine di-hydrochloride and then purified and stored in a way similar to that used for azomethane.[1a] The solvent used in this work was *n*-hepane. It was chosen for various reasons: *n*-butane, a major product in the photolysis, is separated with ease from *n*-heptane by fractional distillation; the ethyl radicals formed in the photolysis would not be consumed in the addition reaction to solvent molecules if the latter had no double bonds; and the rate of the photolysis of azoethane would be reduced if the solvent were polar.[3] *n*-Heptane, obtained as a commercial sample, was found to be gas chromatographically pure. It was, however, further purified by vacuum distillation before use.

The scavenger used in this work for ethyl radicals was styrene, which was used in the previous work for methyl radicals. Commercial styrene was purified by vacuum distillation.

Apparatus and Procedure.—The photolysis was carried out with a solution of about 0.05 M azoethane in *n*-heptane at 366 mμ, using a high-pressure mercury lamp of 100 W. (Mazda SHL-100UV) and a glass filter (Mazda UV-Dl). In a few experiments, the filter was removed to obtain a high-intensity light. In experiments with varied light intensity, screens were used to reduce the light intensity. The reaction cell was a glass cylinder of 3.6 cm. in diameter and 1.0 cm. long, with a capacity of about 10 ml. The other details about the apparatus and the procedure have been described in a previous paper.[1a]

The gaseous products were nitrogen, ethylene, ethane and *n*-butane. These were separated from the solution by thrice-repeated bulb-to-bulb distillation at the dry ice - acetone temperature. For *n*-butane, an automatic fractional distillation vessel was used. Undecomposed azoethane, heptane vapor and by-products were separated by a column of cuprous chloride crystals at −120°C. This column reduced the vapor pressure of azoethane by forming an addition compound in the way opposite to that described above for preparing azoethane and enabled us to separate butane from azoethane at −120°C. The addition and release processes of azoethane on the column were reversible at a reduced pressure. *n*-Butane was condensed at

1) a) S. Kodama, This Bulletin, **35**, 652 (1962); b) ibid., **35**, 658 (1962); c) ibid., **35**, 824 (1962); d) ibid., **35**, 827 (1962).

2) a) M. Matsuoka, P. S. Dixon, A. P. Stefani and M. Szwarc, *Proc. Chem. Soc.*, 304 (1962); b) P. S. Dixon, A. P. Stefani and M. Szwarc, *J. Am. Chem. Soc.*, **85**, 2551 (1963).

3) Such tendency has been found for the photolysis of azomethane (Refs. 1b and 1c).

TABLE I. PHOTOLYSIS OF AZOETHANE IN *n*-HEPTANE AT 366 mμ

Temp.	$\frac{[C_6H_5C_2H_3]}{[C_7H_{16}]}$	Reac. time	Rate of formation × 10^{11} mol. cc^{-1} sec^{-1}				$\frac{C_2H_4}{N_2}$	$\frac{C_2H_6}{N_2}$	$\frac{C_4H_{10}}{N_2}$	$\frac{1/2(C_2H_4+C_2H_6)+C_4H_{10}}{N_2}$	$\left(\frac{C_4H_{10}+C_2H_4}{N_2}\right)_S$	$\frac{C_2H_4}{C_4H_{10}}$
°C	%	min.	R_{N_2}	$R_{C_2H_4}$	$R_{C_2H_6}$	$R_{C_4H_{10}}$	%	%	%	%	%	%
0	0	240	7.86	0.91	3.44	4.84	11.6	43.8	61.6	89.3		18.8
0	0	125[a]	18.1	1.96	7.61	11.3	10.8	42.0	62.3	88.7		17.3
0	0	120	19.3	2.12	8.01	12.2	11.0	41.5	63.0	89.3		17.4
0	0	80[a]	39.6	4.87	15.6	25.5	12.3	39.4	64.3	90.2		19.1
0	0	75[a]	46.7	5.60	17.5	30.8	12.0	37.6	66.0	90.8		18.2
0	0.116	120	17.9	1.95	2.90	—	10.9	16.2	—		—	—
0	0.348	120	16.7	1.75	2.14	9.95	10.5	12.8	59.6		70.1	17.6
0	1.15	120	19.9	2.05	2.29	—	10.3	11.5	—		—	—
0	2.38	120	19.8	2.12	2.12	11.9	10.7	10.7	60.3		71.0	17.8
0	4.22	120	18.4	1.95	1.97	11.1	10.6	10.7	60.1		70.6	17.6
0	6.05	95[a]	40.2	4.10	4.34	24.2	10.2	10.8	60.2		70.4	17.0
0	6.05	135	19.3	2.05	2.05	11.6	10.6	10.6	60.1		70.7	17.6
−75	6.0	190	12.1	1.84	1.90	8.29	15.2	15.7	68.5		83.8	22.2
−50	6.0	180	11.8	1.57	1.64	7.81	13.3	13.9	66.2		79.8	20.1
−25	6.0	180	13.9	1.63	1.72	8.74	11.7	12.4	62.8		74.5	18.6
25	6.0	121	16.6	1.53	1.69	9.40	9.2	10.2	56.6		65.8	16.3
50	6.0	120	12.9	1.04	1.20	6.66	8.1	9.3	51.7		59.8	15.6
62	6.0	170	20.5	1.57	1.69	10.1	7.7	8.3	49.5		57.1	15.4
75	6.0	120	7.20	0.50	0.61	3.37	7.0	8.4	46.8		53.7	14.8
87	6.0	170	25.8	1.61	2.03	—	6.2	7.9	—		—	—
90	6.0	170	15.9	1.09	1.25	6.87	6.5	7.9	43.2		49.7	15.0
99	6.0	120	23.5	1.36	1.70	9.62	5.8	7.2	40.9		46.7	14.2

a) Without filter

−165°C, while ethane and ethylene were condensed at −210°C. The noncondensed nitrogen was determined by a Toepler gauge. The ethane and ethylene were determined by the Toepler gauge and a gas chromatograph with a column of 2% squalane on activated alumina (2 m.) and ethylene glycol saturated with silver nitrate on celite (2 m.) at room temperature. The Toepler gauge was also used to determine the *n*-butane.

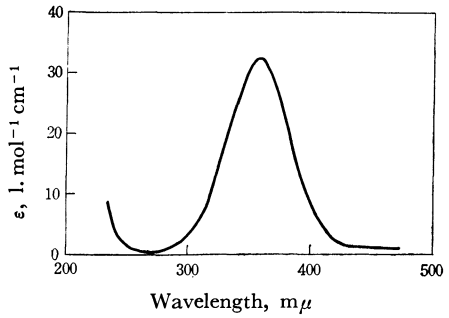

Fig. 1. Absorption curve of azoethane in *n*-heptane.

The molecular extinction coefficient of azoethane in *n*-heptane was determined to be as shown in Fig. 1. The quantum yield of nitrogen formation was measured by using a potassium ferrioxalate actinometer[4] and a quartz reaction cell. The value obtained at 366 mμ was 0.021 at 0°C.

Results

Table I summarizes the results obtained. The rates of the formation of the various products given in the table refer to the initial conversion of a small percentage. The $[1/2(C_2H_4+C_2H_6)+C_4H_{10}]/N_2$ column represents the material balance which takes only these products into account, since one molecule of azoethane gives one molecule of nitrogen and two ethyl radicals, the latter of which combine to butane or produce ethylene and ethane. The $[(C_2H_4+C_4H_{10})/N_2]_s$ column represents the sum of the yields of ethylene and butane relative to that of nitrogen in the presence of a sufficient amount of styrene; it gives, as is shown below, the fraction of ethyl radicals that undergo cage reactions.

Figure 2 shows the dependence of the yields of butane, ethane and ethylene and the material balance on the rate of photolysis, i. e., on the light intensity, in the absence of styrene at 0°C. Figure 3 shows the effect of the addition of styrene in increasing amounts at 0°C. Figures 2 and 3 both show that the result of photolysis is scarcely influenced at all by removing the light filter. This indicates that the most effective mercury line is 366 mμ, as would be expected from the absorption curve given in Fig. 1 and from the absorption property of the glass reaction cell.

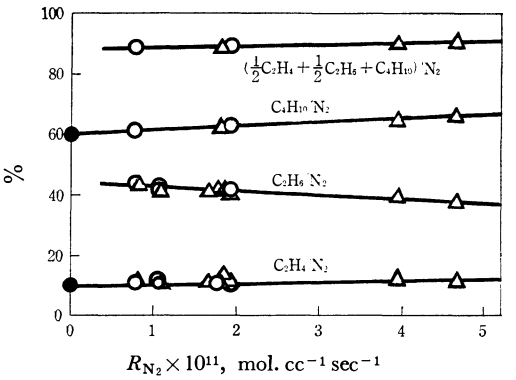

Fig. 2.
○, at 366 mμ; △, without filter; ●, in presence of styrene

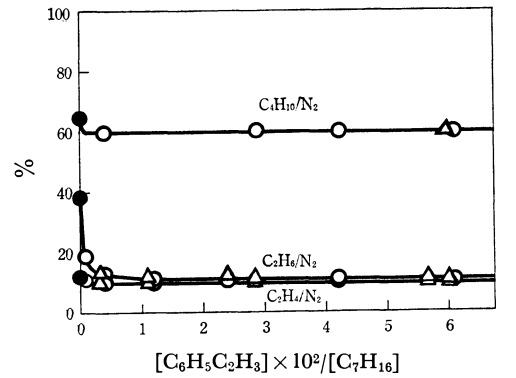

Fig. 3. Effect of styrene on the photolysis at 0°C.
○, at 366 mμ; △, without filter; ●, in absence of styrene, at $R_{N_2}=4\times 10^{-11}$ mol. cc^{-1} sec^{-1}

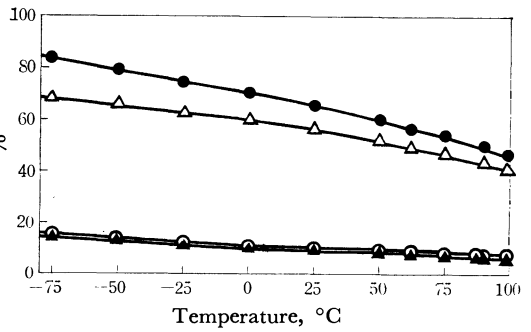

Fig. 4. Effect of temperature on the photolysis in the presence of styrene.
●, $[(C_4H_{10}+C_2H_4)/N_2]_s$; △, $(C_4H_{10}/N_2)_s$;
○, $(C_2H_6/N_2)_s$; ▲, $(C_2H_4/N_2)_s$

Figure 4 shows the effect of the temperature on the photolysis in the presence of styrene. Figure 5 shows the effect of the temperature on the quantum yield of nitrogen at 366 mμ. This curve was

4) C. A. Parker, *Proc. Roy. Soc.*, **A220**, 104 (1953); C. G. Hatchard and C. A. Parker, ibid., **235**, 518 (1956).

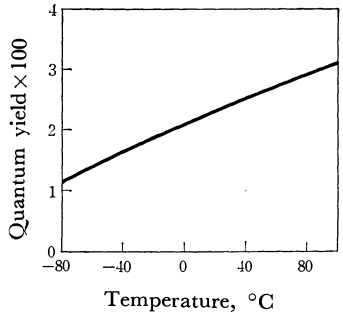

Fig. 5. Dependence of quantum yield on temperature.

drawn by comparing the rates of nitrogen formation at various temperatures, keeping the azoethane concentration and light intensity constant and normalizing them to the quantum yield value of 0.021 at 0°C.

Discussion

Primary Processes.—Previous studies of the photolysis of azoethane in the gas phase[5] and of azomethane in solution[1] suggest that the probable processes in the initial stage of the present photolysis may be:

$$C_2H_5N_2C_2H_5 + h\nu \rightarrow C_2H_5N_2C_2H_5^* \quad (1)$$

$$C_2H_5N_2C_2H_5^* + M \rightarrow C_2H_5N_2C_2H_5 + M \quad (2)$$

$$C_2H_5N_2C_2H_5^* \rightarrow [2C_2H_5 + N_2] \quad (3)$$

Here the asterisk denotes the excited state; M, a solvent molecule, and the bracketed species, those formed together in a solvent cage.

Cerfontain and Kutschke[5c] have shown that, in the gas phase photolysis of azoethane as well as in that of azoisopropane, the excited molecules of the substrate are deactivated by collision, while such deactivation is absent in the case of azomethane. Reaction 2, therefore, cannot be omitted in the present case, though a corresponding deactivation process was previously neglected in the photolysis of azomethane in solution.[1]

Reaction 2 appears to account for the result that the quantum yield of nitrogen is considerably less than unity. However, the quantum yield falls off with a lowering of the temperature, as is shown in Fig. 5, while the studies of the yield of fluorescence in solution show that the quenching by deactivation usually increases with the temperature.[6] If reaction 2 is the only process involved in reducing the quantum yield, the decomposition of the excited azoethane must require an appreciable energy of activation.

The decomposition of the excited molecules of azoethane is represented in reaction 3 as a one-step act. If, however, they decompose in two stages, as $C_2H_5N_2C_2H_5^* \rightarrow C_2H_5N_2 + C_2H_5$ followed by $C_2H_5N_2 \rightarrow C_2H_5 + N_2$, the recombination reaction, $C_2H_5N_2 + C_2H_5 \rightarrow C_2H_5N_2C_2H_5$, in a solvent cage may provide an alternative explanation for the low quantum yield of nitrogen. Such a possibility can not be ruled out, though the decomposition of the $C_2H_5N_2$ radicals has been inferred to be considerably exothermic[7] and the flash photolysis technique has as yet given no evidence for the formation of this species as a transient intermediate.[5d,5f]

The short-lived $C_2H_5N_2$ radicals, if formed, would not survive to take part in reactions other than the decomposition and recombination considered above. So far as the secondary reactions to be discussed below are concerned, therefore, the decomposition of the excited azoethane may virtually be represented by reaction 3.

Cage Reactions.—In view of the reactions between ethyl radicals in the gas phase, the probable reactions for the geminate ethyl radicals formed by reaction 3 may be :

$$[2C_2H_5 + N_2] \rightarrow C_4H_{10} + N_2 \quad (4)$$

$$\rightarrow C_2H_6 + C_2H_4 + N_2 \quad (5)$$

$$\rightarrow 2C_2H_5 + N_2 \quad (6)$$

Reactions 4 and 5 are, respectively, the combination and disproportionation of the geminate ethyl radicals in the original solvent cage, while reaction 6 represents the separation of the radicals from each other by their escaping the cage before they combine or disproportionate.

Figure 3 shows that, in the presence of a sufficient amount of styrene as a scavenger for ethyl radicals, almost all the butane, ethane and ethylene are formed by the cage reactions 4 and 5.[8] However, in Fig. 3 as well as in Fig. 4, the yield of ethane in the presence of styrene is slightly higher than that of ethylene, whereas they should be equal to each other according to reaction 5. It seems possible that this slight difference arises from the hydrogen atom abstraction by hot ethyl radicals from the solvent molecules constituting the cages, since the excess energy released by the decomposition of azoethane amounts to 62 kcal./mol. at 366 mμ.

The fraction of the geminate ethyl radicals that react in the solvent cage as represented in reactions 4 and 5 may be computed from the sum of the

5) a) J. L. Weiniger and O. K. Rice, *J. Am. Chem. Soc.*, **74**, 6216 (1953); b) P. Ausloos and W. R. Steacie, *Bull. soc. chim. Belges.*, **63**, 87 (1954); c) H. Cerfontain and O. K. Kutschke, *Can. J. Chem.*, **36**, 344 (1958); d) B. C. Roquitte and J. H. Futrell, *J. Chem. Phys.*, **37**, 378 (1962); e) H. Cerfontain and O. K. Kutschke, *J. Am. Chem. Soc.*, **84**, 4017 (1962); f) D. P. Dingledy and J. G. Calvert, ibid., **85**, 856 (1963).

6) For example, E. J. Bowen and J. Sahn, "Photochemistry in the Liquid and Solid States," Ed. by F. Daniels, John Wiley & Sons, Inc., New York and London (1960), p. 55.

7) B. G. Gowenlock, J. R. Majer and D. R. Snelling, *Trans. Faraday Soc.*, **58**, 670 (1962).

8) The direct formation of these compounds from azoethane by a molecular rearrangement has been shown to be negligible (Refs. 5e and 5f).

relative yields $(C_4H_{10}+C_2H_4)/N_2$ in the presence of styrene. Figure 4 shows that this fraction is greater than 0.8 below $-50°C$, but that it decreases with a rise in the temperature, reflecting the fact that the escape of the ethyl radical from the solvent cage by diffusion is favored at high temperatures.

The Reactions of Ethyl Radicals That Have Escaped the Original Cages.—The results obtained in the present work, together with those obtained previously in the photolysis of azomethane in solution,[1] suggest that the probable reactions for the ethyl radicals that have escaped the original cages are:

$$C_2H_5 + C_2H_5 \rightarrow C_4H_{10} \quad (7)$$

$$C_2H_5 + C_2H_5 \rightarrow C_2H_6+C_2H_4 \quad (8)$$

$$C_2H_5 + RH \rightarrow C_2H_6+R \quad (9)$$

$$C_2H_5+(C_2H_5)_2N_2 \rightarrow (C_2H_5)_3N_2 \quad (10)$$

RH in reaction 9 represents a molecule of *n*-heptane, the solvent. The hydrogen atom abstraction from azoethane molecules by ethyl radicals may not be important, because its rate constant may be of the same order of magnitude as that for reaction 9, while the concentration of azoethane in the present experiment is as low as 0.05 mol./l.

The difference between the results obtained with and without styrene is accounted for by reactions 7—10. Figures 2 and 3 show that ethane formed in other ways than reaction 5 is largely due to reaction 9. Figure 2, however, shows that, as the rate of nitrogen formation increases, i. e., as the concentration of ethyl radicals increases, the yield of ethane falls off, while those for butane and ethylene increase. These observations may be explained as follows. As the concentration of ethyl radicals increases, the rates of combination and disproportionation increase; both of these rates are second-order with respect to ethyl radicals and have very low activation energies. This, in turn, reduces the fraction of ethyl radicals consumed in reaction 9, which is first-order in the ethyl radical and which has a considerable activation energy.[9] For a similar reason, the fraction of ethyl radicals consumed in reaction 10 is also reduced; this improves, though slightly, the material balance given in Fig. 2 as the concentration of ethyl radicals increases.

It cannot be concluded from the present work that only reaction 10 is responsible for the material balance less than unity, represented by $[1/2(C_2H_4+C_2H_6)+C_4H_{10}]/N_2$. Another possibility may be $C_2H_5+R\rightarrow C_2H_5R$. However, a combination $R+R\rightarrow R_2$ is also a probable reaction for the solvent radical R. It will, however, be tentatively assumed below that the loss in material balance arises mostly from reaction 10.

In the previous studies with azomethane,[1] the combination of methyl radicals corresponding to reaction 7 was found to be negligible compared to the hydrogen atom abstraction reaction similar to reaction 9. This difference probably reflects the lower ability of ethyl radicals in solution to abstract hydrogen atoms from solvent molecules.

The Evaluation of the Rate Constant Ratios.—A steady-state treatment of reactions 1—3, combined with the dependence of the quantum yield of nitrogen on the temperature (Fig. 5), yields:

$$k_3/k_2 = 0.5 \exp(-650/\boldsymbol{R}T)\,\text{mol.}\,l^{-1} \quad (I)$$

A corresponding expression for the gas-phase photolysis has been obtained as:[10]

$0.25 \exp(-2000/\boldsymbol{R}T)\,\text{mol.}\,l^{-1}$

Reactions 4—6, when regarded as ordinary elementary steps, lead to:

$$k_4/k_5 = (C_4H_{10})_s/(C_2H_4)_s \quad (II)$$

$$k_6/k_4 = [(N_2)_s - (C_4H_{10})_s - (C_2H_4)_s]/(C_4H_{10})_s \quad (III)$$

$$k_6/k_5 = [(N_2)_s - (C_4H_{10})_s - (C_2H_4)_s]/(C_2H_4)_s \quad (IV)$$

where the suffix s denotes the presence of styrene. The Arrhenius plots of these rate constant ratios are shown in Fig. 6. The plot for Eq. II is linear and yields:

$$k_4/k_5 = 11.5 \exp(-371/\boldsymbol{R}T) \quad (V)$$

The rate constant ratio for the disproportionation and combination of ethyl radicals as given

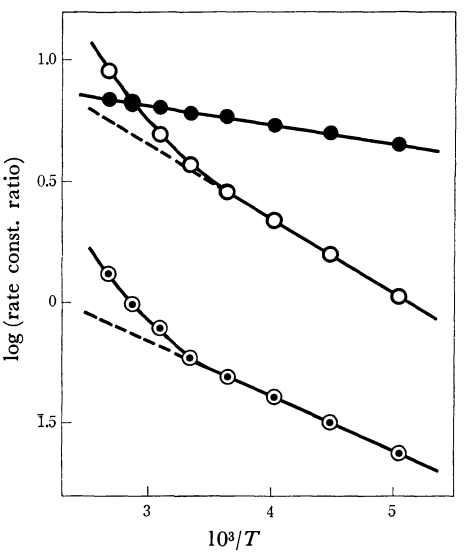

Fig. 6. Arrhenius plots of rate constant ratio.
●, k_4/k_5; ○, k_6/k_5; ⊙, k_6/k_4

9) A reported value in the gas phase is 10.6 kcal./mol. (D. G. L. James and E. W. R. Steacie, *Proc. Roy. Soc.*, **A244**, 289 (1958)).

10) Calculated from the results obtained by Cerfontain and Kutschke (Ref. 5c).

by the C_2H_4/C_4H_{10} ratio of yields has been investigated by many workers in the gas phase. The most reliable value given by these studies is 0.13 ± 0.02; it is independent of the temperature in the 50—250°C range.[2b,5f] All the values of $(C_2H_4)_s/(C_4H_{10})_s$ given in Table I are greater than 0.13, and Eq. V shows that k_4/k_5 is slightly dependent on the temperature. Similar results have been obtained and discussed in detail by Szwarc and his co-workers.[2]

Figure 6 shows that the plots for Eqs. III and IV are not linear above room temperature. Similar deviations at high temperatures were observed in the photolysis of azomethane in solution.[1d] The Arrhenius plots for the self-diffusion in such liquids as *n*-pentane and *n*-heptane also show anomalies at high temperatures.[11] As was described in a previous paper on the photolysis of azomethane,[1d] the crude representation for the escape of a radical from a solvent cage given in reaction 6 seems to break down at high temperatures, giving rise to these deviations.

The linear portions of the plots for k_6/k_4 and k_6/k_5 below room temperature yield:

$$k_6/k_4 = 3.40 \exp(-1050/\boldsymbol{R}T) \quad \text{(VI)}$$

$$k_6/k_5 = 39.0 \exp(-1420/\boldsymbol{R}T) \quad \text{(VII)}$$

The significance of these expressions will be discussed in a later paper, together with the results obtained in the photolysis of $CH_3N_2C_2H_5$ in solution.

The yields of butane, ethane and ethylene formed by reactions 7—9 are given by comparing each yield in the presence of and in the absence of styrene. The yield for reaction 10 is obtained as $2-(2C_4H_{10}+C_2H_6+C_2H_4)/N_2$. By combining these quantities, we obtain the following values at 0°C:

$$k_9/k_7^{1/2} = 1.2\times 10^{-4}\ l^{1/2}\ mol^{-1/2}\ sec^{-1/2}$$

$$k_{10}/k_7^{1/2} = 1.1\times 10^{-2}\ l^{1/2}\ mol^{-1/2}\ sec^{-1/2}$$

$$k_{10}/k_9 = 93$$

11) E. Fishman, *J. Phys. Chem.*, **59**, 469 (1955)

BULLETIN OF THE CHEMICAL SOCIETY OF JAPAN VOL. 39 1014—1016 (1966)

The Synthesis of Deoxyaspergillic Acid and Tetrahydrodeoxyaspergillic Acid

By Yasuhiro CHIGIRA, Mitsuo MASAKI and Masaki OHTA

Laboratory of Organic Chemistry, Tokyo Institute of Technology, Ookayama, Tokyo

(Received September 30, 1965)

Deoxyaspergillic acid (I) and tetrahydrodeoxyaspergillic acid (II) were synthesized. 1-Chloro-3-methyl-2-pentanone was directly oximinated with hydroxylamine, and then the oxime was treated with L-leucine ethyl ester to yield *N*-(3-methyl-2-oximinopentyl)-L-leucine ethyl ester (III), which, on alkali-hydrolysis, followed by acid-hydrolysis, gave *N*-(3-methyl-2-oxopentyl)-L-leucine (IV). The treatment of the methyl ester of IV with ammonia gave I, and the hydrogenation of III on Raney nickel gave II.

The antibiotic aspergillic acid has been concluded to be 1-hydroxy-3-isobutyl-6-*sec*-butyl-2-pyrazinone or its tautomeric 1-oxide of the 2-hydroxypyrazine.[1] The reduction of aspergillic acid with hydrazine yields deoxyaspergillic acid, i. e., 3-isobutyl-6-*sec*-butyl-2-hydroxypyrazine (I), while reduction with zinc in acetic acid gives tetrahydrodeoxyaspergillic acid, i. e., 3-isobutyl-6-*sec*-butyl-2-piperazinone (II).[2]

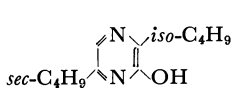

(I)

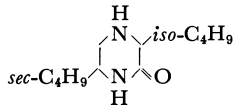

(II)

Two routes for the synthesis of racemic deoxyaspergillic acid have been reported. The first, reported by Newbold et al.,[1] consists of the reaction of 3-methyl-2-oximinovaleraldehyde with leucine nitrile to give 2-aminopyrazine-1-oxide derivative, which is then converted into I by treatment with sodium dithionite, followed by hydrolysis. The second synthesis consists of the treatment of DL-leucyl-DL-isoleucine anhydride with phosphoryl chloride.[3] On the other hand, tetrahydrodeoxyaspergillic acid has never been synthesized. The present paper will describe an alternative route for the synthesis of racemic deoxyaspergillic acid and the synthesis of racemic tetrahydrodeoxyaspergillic acid.

It has been previously reported in our laboratory that 3, 6-disubstituted 2-hydroxypyrazines[4] and 2-piperazinones[5] can be synthesized starting from

1) G. T. Newbold, W. Sharp and F. S. Spring, *J. Chem. Soc.*, **1951**, 2679.
2) J. D. Dutcher, *J. Biol. Chem.*, **171**, 321 (1947).
3) J. J. Gallagher, G. T. Newbold, W. Sharp and F. S. Spring, *J. Chem. Soc.*, **1952**, 4870.
4) M. Masaki and M. Ohta, This Bulletin, **36**, 1177 (1963).
5) M. Masaki and M. Ohta, ibid., **36**, 922 (1963).

N-(2-oximinoalkyl)-amino acid esters. In an application of this method to the synthesis of I and II, however, 1-chloro-3-methyl-2-pentanone oxime (III) is required. Aliphatic α-halooxime is generally prepared by the reduction of nitroolefine with stannous chloride.[6] The direct oximination of aliphatic α-haloketones with hydroxylamine has been successfully reported only in the case of α-bromo- and α-chloro-acetone,[7] because the reaction of α-haloketone with amines is very complex.[8]

The reaction of 1-chloro-2-pentanone with hydroxylamine was, therefore, studied under various conditions; finally a 43% yield of 1-chloro-2-pentanone oxime was obtained by stirring a suspension of the ketone in an aqueous hydroxylamine solution at 0°C for 4 hr. In a similar manner, 1-chloro-3-methyl-2-pentanone was converted into the corresponding oxime (III) in a 50% yield.

The treatment of 1-chloro-3-methyl-2-pentanone oxime (III) with L-leucine ethyl ester in ether at room temperature yielded *N*-(3-methyl-2-oximinopentyl)-L-leucine ethyl ester (IV) as a yellow oil which was characterized by saponifying it to the corresponding carboxylic acid (V). *N*-(3-Methyl-2-oximinopentyl)-L-leucine (V) was treated with benzaldehyde in hydrochloric acid - methanol to give *N*-(3-methyl-2-oxopentyl)-L-leucine (VI), which was then converted into the methyl ester hydrochloride (VII) by esterification with methanol and hydrogen chloride. When treated with ammonia in methanol, this ester hydrochloride yielded 3-isobutyl-6-*sec*-butyl-2-hydroxypyrazine (I). The last stage of this reaction involves air oxidation, which is common to most pyrazine syntheses.[4] The product was confirmed by a comparison of its melting point, as well as its infrared and ultraviolet absorption spectra, with those of the deoxyaspergillic acid derived from aspergillic acid[2] or that synthesized by Newbold et al.[1,3]

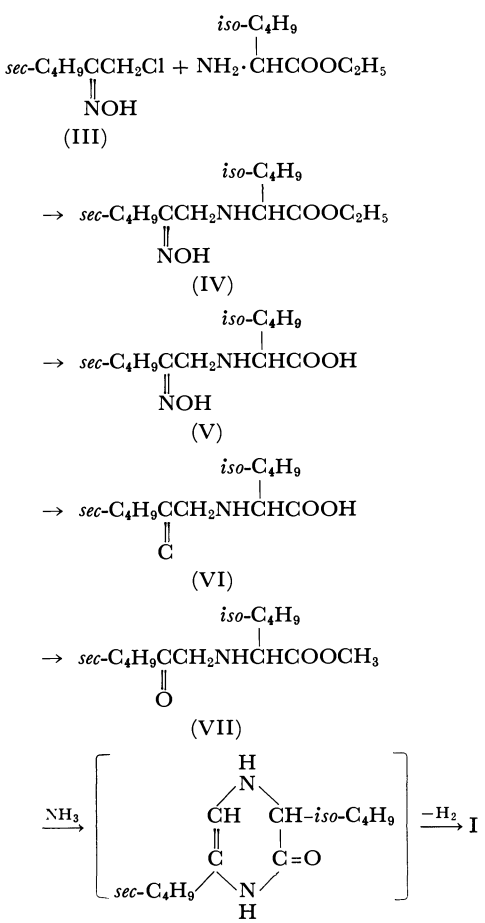

The oximino ester (IV) was hydrogenated in the presence of Raney nickel at 80°C in an autoclave; thereby the initially-produced amino ester cyclized spontaneously to yield 3-isobutyl-6-*sec*-butyl-2-piperazinone (II), which was isolated as its hydrochloride. The hydrochloride showed the same melting point as that of tetrahydrodeoxyaspergillic acid hydrochloride and showed the absorption bands at 3200, 1660 and 1470 cm^{-1} characteristic of 3, 6-disubstituted 2-piperazinones.[5] These data, as well as the results of the elementary analysis, support the assigned structure.

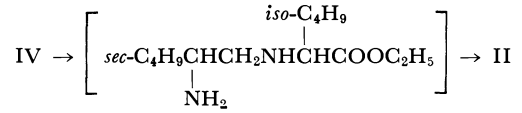

Experimental

The Oximination of 1-Chloro-2-pentanone.—An aqueous solution of hydroxylamine [from the hydrochloride (3 g.) in water (2.5 g.) and sodium carbonate decahydrate (6 g.) in water (10 ml.)] was stirred, drop by drop, into 1-chloro-2-pentanone (5.0 g.) at 0°C; then, after the addition was complete, the stirring was continued for another 4 hr. The mixture was extracted with ether, and the ethereal layer was washed twice with water and dried over anhydrous sodium sulfate. The evaporation of the ether and the distillation of the residue yielded 2.3 g. of 1-chloro-2-pentanone oxime, b. p. 62—70°C/3 mmHg (lit.[5] 78—82°C/7 mmHg.)

Found: N, 10.32. Calcd. for $C_5H_{10}NOCl$: N, 10.33%.

1-Chloro-3-methyl-2-pentanone Oxime (III).—In an analogous manner to that used for 1-chloro-2-pentanone, 1-chloro-3-methyl-2-pentanone[9] (20 g.) was treated with an aqueous solution of hydroxylamine hydrochloride (10 g.) and sodium carbonate decahydrate (20 g.); 1-chloro-3-methyl-2-pentanone oxime (12 g.) was thus obtained as a colorless oil, b. p. 74—78°C/2.5 mmHg.

Found: C, 48.06; H, 8.19; N, 9.20. Calcd. for $C_6H_{12}NOCl$: C, 48.16; H, 8.13; N, 9.36%.

6) A. Dornow, H. D. Jordan and A. Müller, *Chem. Ber.*, **94**, 67 (1961).
7) R. Scholl and G. Matthaiopoilos, ibid., **29**, 1552 (1896).
8) C. L. Stevens, P. Blumbergs and M. Munk, *J. Org. Chem.*, **28**, 331 (1963).
9) G. T. Newbold and F. S. Spring, *J. Chem. Soc.*, **1947**, 375.

The reaction of the product with piperidine afforded 1-piperidino-3-methyl-2-pentanone oxime as a colorless oil, b. p. 108—110°C/0.15 mmHg.

Found: N, 14.41. Calcd. for $C_{11}H_{22}N_2O$: N, 14.14%.

***N*-(3-Methyl-2-oximinopentyl)-L-leucine Ethyl Ester (IV).**—To a solution of leucine ethyl ester (15.5 g.) in absolute ether (50 ml.) there was added a solution of 1-chloro-3-methyl-2-pentanone oxime (6.4 g.) in absolute ether (25 ml.); the mixture was then allowed to stand at room temperature for a week. After the crystals of leucine ethyl ester hydrochloride (4.5 g.) had been removed, the ethereal solution was washed several times with water and extracted with 3 N hydrochloric acid (3×50 ml.). The combined extracts were neutralized with an aqueous solution of sodium carbonate to give a yellow oil, which was then extracted with ether. The ethereal extracts were washed twice with water and dried over anhydrous sodium sulfate. The evaporation of the ether yielded IV as a yellow oil (10 g.), which was characterized by saponifying it to the corresponding carboxylic acid (V), as is shown below.

***N*-(3-Methyl-2-oximinopentyl)-L-leucine (V).**—The crude IV (4.5 g.) was added to a solution of potassium hydroxide (4.5 g.) in water (20 ml.). When the mixture was allowed to stand at room temperature overnight, the mixture became nearly clear. The solution was diluted with water (20 ml.), treated with activated charcoal, and then neutralized with a 20% aqueous acetic acid to give colorless needles, which were recrystallized from methanol, m. p. 168—169°C (decomp.). Yield, 2.2 g.

Found: N, 11.18. Calcd. for $C_{12}H_{24}N_2O_3$: N, 11.47%.

***N*-(3-Methyl-2-oxopentyl)-L-leucine (VI).**—To a mixture of V (2 g.) and 3 N hydrochloric acid (20 ml.), benzaldehyde (2 g.) and methanol (20 ml.) were added the resultant clear solution was allowed to stand at room temperature. After a week the mixture was concentrated to about 20 ml. under reduced pressure. The residue was washed three times with ether and neutralized with a saturated solution of sodium carbonate. The precipitated crystals (0.9 g.) were recrystallized from methanol to yield colorless microscopic needles, m. p. 164.5—165.5°C (decomp.).

Found: N, 6.41. Calcd. for $C_{12}H_{23}NO_3$: N, 6.11%.

***N*-(3-Methyl-2-oxopentyl)-L-leucine Methyl Ester Hydrochloride (VII).**—A suspension of VI (0.8 g.) in methanol was refluxed for 2 hr., while dry hydrogen chloride was passed continuously through the mixture; then the mixture was allowed to stand overnight. The solution was evaporated under reduced pressure to give an oily residue, which was dried in a desiccator over potassium hydroxide under reduced pressure. Crystallization from ethyl acetate afforded colorless plates, m. p. 145°C (after half melting at 134°C). Yield, 0.4 g.

Found: N, 5.24. Calcd. for $C_{13}H_{25}NO_3 \cdot HCl$: N, 5.01%.

3-Isobutyl-6-*sec*-butyl-2-hydroxypyrazine (I).—A solution of VII (0.3 g.) in methanol (20 ml.) was saturated with ammonia. After three days the solution was evaporated to afford a brown oily residue, to which ethyl acetate (5 ml.) was then added. After the insoluble ammonium chloride had been removed, the filtrate was again concentrated under reduced pressure, and the residue was extracted with 6 N hydrochloric acid. After treatment with activated charcoal, the solution was neutralized with 2 N sodium hydroxide, yielding pale brown crystals (0.1 g.). Recrystallization from aqueous methanol gave colorless needles with a m. p. of 99.5—100.5°C. λ_{max}^{EtOH} 228 mμ (ε=7900) and 325 (8400). (Found: C, 69.22; H, 9.98; N, 13.68).

These constants are essentially identical with those of the racemic deoxyaspergillic acid derived from aspergillic acid [m. p. 103—104°C, λ_{max}^{EtOH} 228 mμ (ε=7000) and 325 (8400)][2] or that synthesized by Newbold et al. [m. p. 100.5—101.5°C, λ_{max}^{EtOH} 227 mμ (ε=8000) and 324 (8000)].[1] The infrared spectrum of the product was also essentially identical with that[10] of deoxyaspergillic acid.

3-Isobutyl-6-*sec*-butyl-2-piperazinone (II) Hydrochloride.—A solution of crude IV (4 g.) in ethanol (150 ml.) was shaken with Raney nickel (2 g.) at an initial pressure of 90 kg./cm² of hydrogen at 80°C. After the hydrogen absorption had ceased, the catalyst was removed and the solution was concentrated under reduced pressure. The residue was dissolved in ether (100 ml.) and treated with dry hydrogen chloride to give a yellow oil, which was, after being washed several times with ether, left in absolute ether in a refrigerator. After two days, small needles crystallized out. They were collected and recrystallized twice from *n*-butanol to yield 0.5 g. of colorless needles, which melted at 260°C (decomp.) after darkening at 230°C. ν_{max}^{KBr} 3200, 2950, 1660, 1470, 1280 and 1000 cm⁻¹. (Found: C, 58.15; H, 9.95; N, 11.26.)

According to Dutcher,[2] the tetrahydrodeoxyaspergillic acid hydrochloride derived from aspergillic acid by reduction with zinc and acetic acid melts at 260°C after darkening at 235°C.

10) S. Nakamura, *Agr. Biol. Chem.*, **25**, 658 (1961).

BULLETIN OF THE CHEMICAL SOCIETY OF JAPAN VOL. 39 1017—1019 (1966)

The Surface Adsorption of Sodium Alkyl Sulfates from Dioxane-Water Mixtures

By Keishiro SHIRAHAMA, Kiyoshi NAKAO, Hiroko ENDO and Ryohei MATUURA

Department of Chemistry, Faculty of Science, Kyushu University, Hakozaki

(Received October 4, 1965)

The surface adsorptions of three sodium alkyl sulfates (C_{12}, C_{14}, C_{16}) from dioxane-water mixtures have been measured by using ^{35}S-labeled surfactants; it has been found to decrease with an increase in the dioxane concentration. This decrease has been explained in terms of the following factors; (1) the variation in the standard chemical potential of the surfactant in the bulk phase, or the free energy of transfer, (2) the surface tension of the solution, and (3) the dielectric constant of the solvent. In a solvent containing more dioxane than 40 wt.%, it has been shown, both by experiment and by theory, that these alkyl sulfates lose their surface activities.

The air/solution interface reflects the properties of the bulk phase. Thus, in the case of a surfactant solution, the surface excess may be correlated to the chemical potential of the surfactant in the solution by Gibbs' equation.

If the nature of a solvent in the bulk phase is changed by adding to it a third substance, the surface properties should correspondingly be altered; therefore, it is informative to study the surface phenomena in relation to the nature of the solvent in the bulk phase.

The surface adsorption of an ionic surfactant from an aqueous solution has been shown to be affected very much by the addition of extraneous salts, and this has been explained by considering only the electrical double layer produced just below the surface.[1]

In a previous paper, such properties as the micelle formation and solubility of sodium alkyl sulfates in the dioxane-water mixed solvent were discussed in detail.[2]

The present work will describe the surface adsorption of sodium hexadecyl (SHS), tetradecyl (STS) and dodecyl (SDS) sulfates from their solution in a dioxane-water mixture, and will attempt to explain the decrease in the surface adsorption in terms of the variation, with the dioxane concentration, of the standard chemical potential of the surfactant, of the dielectric constant of the solvent, and of the surface tension of the solution.

Experimental

The surfactants used, i. e., SHS, STS and SDS, were synthesized and purified as described in the previous work.[2] The surface adsorption measured by the radiotracer method in the same way as has already been reported.[3] The surface tension of the solutions was measured by the drop-weight method with the Harkins-Brown corrections applied.[4] The solvents used were the same as were used in the previous work.[2] The experiments were carried out at 25°C.

Results and Discussion

The surface adsorption of the three alkyl sulfates is shown in Fig. 1 as a function of the dioxane concentration. The general feature is the decrease in the adsorption with the increase in the dioxane concentration; the adsorption becomes undetectable when the dioxane concentration increases beyond 30 wt.% for SDS and STS, and 45 wt.% for SHS. This trend may be explained in the following manner.

The chemical potential of the surfactant ion in the surface phase is expressed as:

$$\mu^s = \mu^{os} + \boldsymbol{k}T \ln a^s - \gamma A + e\psi \qquad (1)$$

and that in the bulk phase as:

$$\mu = \mu^o + \boldsymbol{k}T \ln a \qquad (2)$$

where the superscript s refers to the surface, μ^o and a are the standard chemical potential and the activity, respectively, of the surfactant ion; γ is the surface tension of the solution; A is the surface area of a surfactant molecule; e is a unit charge, and ψ is the surface potential. The other notations have the ordinary meanings. According to Gouy's theory,

$$\psi = (2\boldsymbol{k}T/e)\sinh^{-1}\{(\sigma/C^{1/2})(500\pi/D\boldsymbol{R}T)^{1/2}\} \qquad (3)$$

In this equation, C is the total electrolyte concentration in mol./l.; D is the dielectric constant of the solvent, and $\sigma = e\Gamma$, where Γ is the surface excess of a surfactant in mol./cm^2.

1) R. Matuura, H. Kimizuka and K. Yatsunami, This Bulletin, **32**, 646 (1959); R. Matuura, H. Kimizuka and A. Matsubara, ibid., **34**, 1512 (1961); R. Matuura, H. Kimizuka, A. Matsubara, K. Matsunobu and T. Matsuda, ibid., **35**, 552 (1962).

2) K. Shirahama and M. Matuura, ibid., **38**, 373 (1965).

3) R. Matuura, H. Kimizuka, S. Miyamoto and R. Shimozawa, ibid., **31**, 532 (1958).

4) W. D. Harkins and F. E. Brown, *J. Am. Chem. Soc.*, **38**, 288 (1916); **41**, 499 (1919).

When $\psi \geqq 100$ mV., Eq. 3 reduces to:

$$\psi = (2\boldsymbol{k}T/e)\ln\{(2e\Gamma/C^{1/2})(500\pi/D\boldsymbol{R}T)^{1/2}\} \quad (4)$$

The activities a^s and a in Eqs. 1 and 2 can be replaced by concentrations when the solutions are sufficiently dilute. Using Eq. 4 and the relation $C^s = 1000\Gamma/d$, where C^s is the surface concentration expressed in mol./l., and d, the surface thickness,[5] we obtain from equating Eqs. 1 and 2, after rearrangment:

$$3\boldsymbol{k}T \ln \Gamma = \mu^o - \mu^{os} + \gamma A + \boldsymbol{k}T \ln D + K \quad (5)$$

where $K = 2\boldsymbol{k}T \ln C - \boldsymbol{k}T \ln(10^6 e^2\pi/2d\boldsymbol{R}T)$. Here, we are primarily interested in the relative adsorption, Γ_x/Γ_0, where the subscripts 0 and x refer to the water and dioxane-water mixtures, respectively. Hence at a constant surfactant concentration in the bulk phase, we have:

$$\log(\Gamma_x/\Gamma_0) = \frac{1}{3}\{(\mu_x^o - \mu_0^o)/2.3\boldsymbol{R}T + (\gamma_x - \gamma_0)A/2.3\boldsymbol{R}T + \log(D_x/D_0)\} \quad (6)$$

The first term of the right hand side of Eq. 6 can be estimated from the solubility data shown in the previous paper,[2] while the other terms can easily be calculated from the data of the surface tension and the dielectric constant of the solution and the solvent (Table I). The calculated values are shown by the solid lines in Fig. 1. The rather good agreement with experimental values may show the validity of Eq. 6. In order to see what term of the three in the R.H.S. of Eq. 6 is the most effective in effecting the decrease in the surface adsorption with the dioxane concentration, the magnitude of each term is shown in Table II.

TABLE I. VARIOUS PROPERTIES OF THE SOLUTION

Dioxane wt. fraction	Surface tension (dyne/cm)			Dielectric constant*
	SHS	STS	SDS	
0.0	66.0	71.6	70.8	78.5
0.1	54.5	54.1	56.5	70.0
0.2	52.0	49.0	49.0	61.6
0.4	48.9	43.0	48.0	42.8
Surfactant concn. (mol./l.)	10^{-5}	5×10^{-5}	10^{-4}	

* Dielectric constant was quoted from Ref. 6.

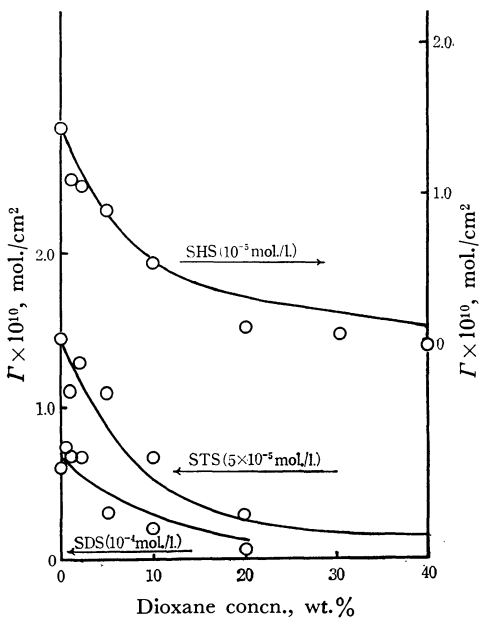

Fig. 1. Surface adsorption vs. dioxane concentration.
Circles are the measured points at 25°C.

TABLE II. THE CALCULATION OF EACH TERM OF Eq. 6

Dioxane wt. fr.	$-(\mu_x^o - \mu_0^o)/2.3\boldsymbol{R}T$*	$-(\gamma_x - \gamma_0)A/2.3\boldsymbol{R}T$**	$-\log(D_x/D_0)$
	SHS $C = 10^{-5}$ mol./l.		
0.1	0.974	0.238	0.0496
0.2	1.59	0.292	0.106
0.4	2.58	0.356	0.263
	STS $C = 5\times10^{-5}$ mol./l.		
0.1	0.898	0.364	
0.2	1.45	0.468	
0.4	2.01	0.594	
	SDS $C = 10^{-4}$ mol./l.		
0.1	0.800	0.300	
0.2	1.31	0.468	

* Calculated on the molar concentration basis, while in the previous paper the free energy of transfer was calculated on the mole fraction basis.

** γA was calculated in kcal. with A taken as 20Å^2.

It is evident that the free energy of transfer term, $(\mu_x^o - \mu_0^o)$, is the major factor. This means that the surfactant becomes more solvophilic as the dioxane concentration increases, and that it is pulled down from the surface to the bulk phase. As to the surface tension term, it also contributes, although not dominantly, to the decrease in the surface adsorption. Finally, the low dielectric constant of the mixed solvent affects the surface adsorption so as to strengthen the electric field due to the ions in the diffuse layer, and in turn, to increase the surface electrical energy. Thus, the bulk phase becomes more favorable for the surfactant to escape from the surface, and, in the region of dioxane concentration greater than 40 wt.%, the surfactant is no longer "surface-active."

5) J. T. Davies and E. K. Rideal, "Interfacial Phenomena," Academic Press, London (1961), p. 154.

6) J. B. Hasted. G. H. Haggis and P. Hutton, *Trans. Faraday Soc.*, **47**, 577 (1951).

This corresponds to the fact that no micelle formation was detected in this region.[2] In spite of the larger bulk concentration in the case of SDS and STS, the surface adsorptions disappear at a dioxane concentration smaller than that in the case of SHS. This, however, may easily be understood. The shorter hydrocarbon chain would become readily solvophilic upon the addition of a smaller amount of dioxane.

The approximation made in the derivation of Eq. 4 from Eq. 3 was checked; it was found to be satisfied at all points measured. The other assumption is the complete dissociation of the adsorbed surfactant. In an aqueous medium, an almost complete dissociation has been suggested by a comparison of the surface excess measured by the radiotracer method with the one calculated from the surface tension measurement.[3] In a dioxane-rich solvent, there should be an appreciable ionic association, but such a solvent is outside our present area of interest.

BULLETIN OF THE CHEMICAL SOCIETY OF JAPAN VOL. 39 1019—1027 (1966)

The Reaction between Phenol and Formaldehyde in Non-Aqueous Media. I. The Kinetics of the Reaction Catalyzed by Boron Trifluoride-Etherate

By Shin'ichi MURAYAMA

Central Research Laboratory, Sumitomo Bakelite Co., Ltd., Totsuka-ku, Yokohama

(Received October 16, 1965)

The papers of this series are kinetic studies of the reaction between phenol and formaldehyde in non-aqueous media; this reaction has, however, not been investigated as thoroughly as the reactions in aqueous media. During the course of the reaction, the reactants and products have been determined by gas chromatography. Within the range of low conversion, the overall reaction between phenol and methylal may be represented by:

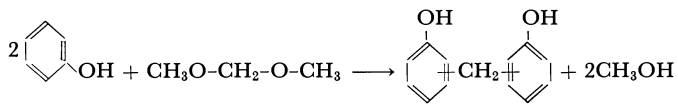

Moreover, the kinetic equation and the apparent activation energy have been estimated as follows :

$$\frac{\mathrm{d[methyl\ alcohol]}}{\mathrm{d}t} = -\frac{\mathrm{d[phenol]}}{\mathrm{d}t} = \frac{k[\mathrm{phenol}]^2[\mathrm{methylal}]^0[\mathrm{catalyst}]^1}{[\mathrm{methyl\ alcohol}]^3}$$

$$E \fallingdotseq 18.6 \text{ kcal./mol.}$$

At the same time, methyl phenyl formal is detected as an intermediate in the reaction system. Judging from these experimental results, it seems that the acetal exchange reaction, and the substitution on aromatics proceed concurrently and consecutively in the complex system.

The reaction between phenol and aldehydes has been investigated intensively over the past fifty years, and the mechanisms of the reaction in aqueous media have been almost established.[1,2] However, very little is known concerning the reaction in non-aqueous media.

Since formaldehyde in aqueous media exists as a mixture of methylene glycol, polymethylene glycol, their hemiacetals and acetals (when an alcohol is present),[3] the reactions in aqueous media may be very complicated, especially when such a solvent as alcohol or dioxane is present in the system.[4]

1) M. Imoto, H. Kakiuchi and M. Oiwa, *Kobunshi Kagaku*, **6**, 67, 385, 398 (1949); ibid., **8**, 29, 33 (1951); *Kobunshi Tenbo*, **4**, 60 (1951); ibid., **8**, 30 (1952); *J. Chem. Soc. Japan, Ind. Chem. Sect.* (*Kogyo Kagaku Zassi*), **61**, 1646 (1958); K. Oshima and E. Imoto, *Kobunshi Kagaku*, **3-4**, 51, 57, 60, 65 (1946—47); K. Manaka, ibid., **8**, 276 (1951); ibid., **10**, 346 (1953); ibid., **11**, 34, 421 (1954); R. Inoue and T. Minami, ibid., **9**, 179, 191 (1952); *J. Chem. Soc. Japan, Ind. Chem. Sect.* (*Kogyo Kagaku Zassi*), **61**, 1340 (1958); K. Hultzch, *Ang. Chem.*, **A60**, 179 (1948).

2) S. Seto and H. Horiuchi, *J. Chem. Soc. Japan, Ind. Chem. Sect.* (*Kogyo Kagaku Zassi*), **57**, 842 (1954); ibid., **58**, 378 (1955); ibid., **61**, 1387 (1958); ibid., **66**, 139 (1963).

3) M. Tsuge, 18th Annual Meeting of the Chemical Society of Japan, Osaka, April, 1965.

4) T. Tanigaki and M. Imoto, *J. Chem. Soc. Japan. Ind. Chem. Sect.* (*Kogyo Kagaku Zassi*), **59**, 712 (1956); ibid., **61**, 144 (1958); K. Manaka, ibid., **59**, 1436 (1956); ibid., **60**, 346 (1957); H. Horiuchi, ibid., **66**, 155 (1963).

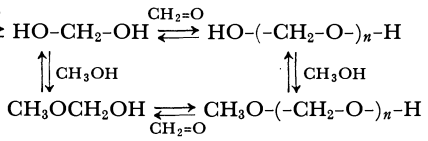

(1)

Several years ago, Uenaka, Naokawa and Yoshino[5] developed a new technique of producing phenol resins; this was one of the earliest examples of the reaction in non-aqueous media. They used paraformaldehyde as the source of formaldehyde, butyl alcohol as the solvent, and calcium hydroxide as the catalyst; then the water produced was removed from the reaction system by azeotropic distillation during the course of the reaction. It was shown by their results that both the rates and the products of the reaction in the non-aqueous media differed remarkably from those of the reaction in the aqueous media. It was also found that the presence of butyl phenyl formal in the reaction system had a significant effect on the rate of reaction.[6]

Recently, Horiuchi[7] found, by means of gas chromatography, that a small amount of methyl phenyl formal was present only at the early stage of the reaction between phenol and the formaldehyde solution containing water and methyl alcohol. However, the alkyl phenyl formal produced at an earlier phase of the reaction was subsequently decomposed by hydrolysis and the rate of the overall reaction may not be appreciably influenced by this intermediate in aqueous media.

More recently, Heslinga and Schors[8] developed a new type of phenolic resin, one prepared by curing novolac with cyclic formals in the presence of an acid as the catalyst at room temperature and under atmospheric pressure. Although the preparation,[8] the processing and the physical properties[9] of the phenol formal resins were studied extensively, however, the mechanism of the reaction between phenol (or novolac) and cyclic formals was not fully investigated.

Meerwein[10] has reviewed recent research on the reactions of acetals including the syntheses, the decomposition, the acetal exchange, the hydrolyses, and the alcoholyses. In this review, some aspects of the behavior of alkyl aryl formals are described, especially those of methyl phenyl formal.

Since acetals are relatively stable in alkaline media, but not in acidic media, almost all the reactions of acetals can be catalyzed by a small amount of an acid, for example, hydrochloric acid, sulfuric acid, phosphoric acid, ferric chloride, calcium chloride, ammonium chloride, boron trifluoride, hydrogen sodium sulfate, monochloroacetic acid, *p*-touenesulfonic acid or the acidic forms of ion exchange resins.

It seems probable that the principal reactions between phenol and formals in non-aqueous media are the acetal exchange[10,11] and the substitution on the aromatic ring; the former is reversible, while the latter is irreversible.

If formaldehyde is added to the system as a formal, the acid-catalyzed phenol-formaldehyde reactions in non-aqueous media may be simpler than those in aqueous media.

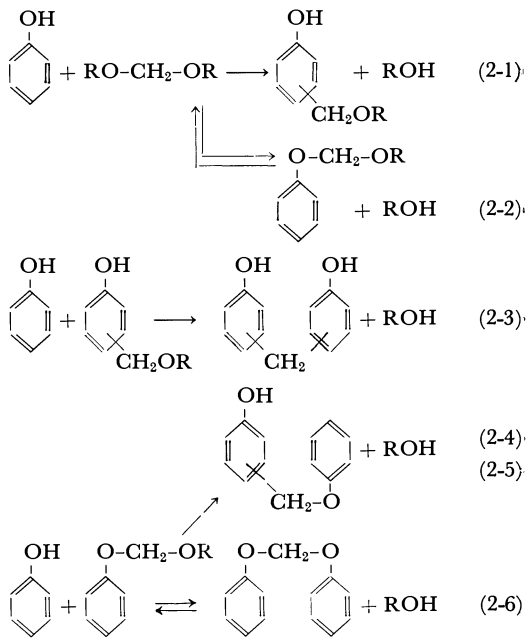

If the reaction is fully represented by Eqs. 2-1—2-6, if that is, the products of the reaction are only the mono-substituted phenols and the unsubstituted binuclear compounds, the amount of phenol consumed must be equivalent to the amount of methyl alcohol produced. By actual measurements, the above condition was found to hold at conversions up to 30%; this experimental evidence simplifies the kinetic treatment.

Even though the phenol-formaldehyde reaction in non-aqueous media is one of the most important problems in the field of phenol resins, no kinetic studies have been done on this reaction, as has been mentioned earlier. From this point of view, this investigation has been undertaken, therefore, first to deduce the kinetic equation for the reaction between phenol and methylal in non-aqueous media; second, to elucidate the reaction mechanism,

5) M. Uenaka, T. Naokawa and S. Yoshino, Japanese Pat. 232910 (1957); ibid., 236930 (1957); ibid., 242652 (1958).
6) K. Ishikawa, T. Naokawa and Y. Okada, ibid., 275695 (1960).
7) H. Horiuchi, *J. Chem. Soc. Japan, Ind. Chem. Sect.* (*Kogyo Kagaku Zasshi*), **66**, 150 (1963).
8) A. Heslinga and A. Schors, *J. Appl. Polym. Sci.*, **8**, 1921 (1964).
9) L. K. H. Von Beek, ibid., **8**, 2843 (1964).
10) H. Meerwein, "Methoden der Organischen Chemie," Ed. by E. Müller, Georg Thieme Verlag, Stuttgart, **VI/3**, (1965), pp. 204—207, 272—278.
11) W. J. Croxall, *J. Am. Chem. Soc.*, **71**, 2736, 2741 (1949).

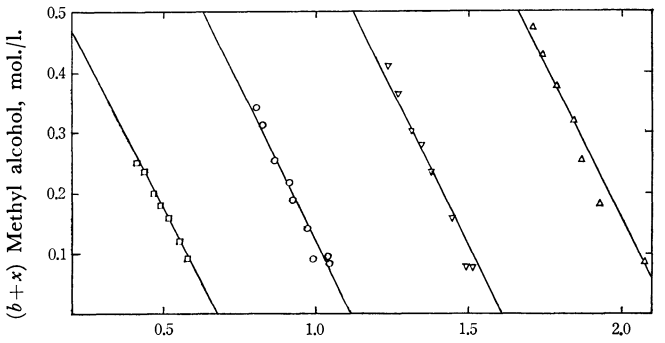

Fig. 1. The rate of production of methyl alcohol and the rate of consumption of phenol.
Methylal 1.0 mol./l., Methyl alcohol 0.1 mol./l., BF_3OEt_2 0.01 mol./l. at 30°C in nitromethane.
Phenol △ : 2.07 mol./l. ▽ : 1.50 mol./l. ○ : 1.00 mol./l. □ : 0.57 mol./l.

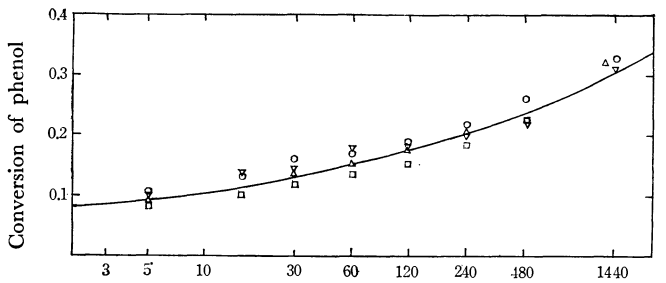

Fig. 2. The effect of methylal on rate.
Phenol 2.0 mol./l., $BF_3 \cdot OEt_2$ 0.02 mol./l. at 30°C in nitromethane.
Methylal □ : 0.5 mol./l. ○ : 1.0 mol./l. △ : 2.0 mol./l. ▽ : 3.0 mol./l.

and third, to point out several interesting problems incident to these results.

Investigations of the mechanism of the reaction in non-aqueous media should be based on exact and detailed experimental results with many kinds of reactants, catalysts and solvents over a wide range of reaction conditions; consequently, the present work should be considered as a mere attempt in this direction.

Experimental

Materials.—The reactants, solvents and catalysts used are purified by conventional methods and, their purity is checked by gas chromatography.[12] Methyl phenyl formal, an important intermediate, is prepared from monochloromethyl methyl ether and potassium phenolate in dioxane,[13] and checked by gas chromatography.[7] Diphenyl formal is prepared from diiodomethane and potassium phenolate in xylene,[14] and checked by gas chromatography.[15]

The Determination of the Concentration of Reactants by Gas Chromatography.—*Apparatus.*—A Kotaki Model GU-21 vapor fractiometer was used with a hot wire detector. The column used for methylal and methyl alcohol was 3 meters long, formed of 4.5 mm.ϕ copper tubing packed with 30% of polyethylene glycol 1500 on diabase A, and the gas chromatography was carried out at 100°C with a helium flow of 40 ml. per minute as measured at the column exit.[12] The column used for phenol and methyl phenyl formal was 1.5 m. long, formed of 4.5 mm.ϕ copper tubing packed with 20% of dilauryl phthalate on diabase A, and the gas chromatography was carried out at 155°C with a helium flow of 40 ml. per minute as measured at the column exit.[7] The correction for the differences in the amounts of samples injected was made by using carbon tetrachloride, toluene and *p*-chlorotoluene as internal markers for methylal, methyl alcohol and phenol (methyl phenyl formal) respectively.

Procedure.—The reactants, the catalyst ($BF_3 \cdot OEt_2$) and the solvent (nitromethane) were mixed, and then the mixture was placed, without stirring, in a water bath regulated at a constant temperature (usually

12) M. Tsuge, private communication.
13) S. Seto and K. Ozaki, *J. Chem. Soc Japan, Ind. Chem. Sect.* (*Kogyo Kagaku Zassi*), **56**, 936 (1953).
14) H. Meerwein, "Methoden der Organischen Chemie," Ed. by E. Müller, Georg Thieme Verlag, Stuttgart, **VI/3**, (1965), p. 240.
15) F. Fujiwara, 12th Annual Meeting on Thermosetting Resin, Osaka, 1962; H. Horiuchi, *J. Chem. Soc. Japan, Ind. Chem. Sect.* (*Kogyo Kagaku Zasshi*), **66**, 146 (1964).

30±0.1°C). During the course of the reaction, two milliliters of the solution were withdrawn, and these samples were added to a dioxane solution (0.5 ml.) containing the internal markers (CCl_4, CH_3–C_6H_5, and p-CH_3–C_6H_4–Cl) and the reaction stopper (tribenzyl amine). Then they were subjected to gas chromatographic analysis in order to determine the amounts of methylal, methyl alcohol and sometimes phenol.

The Detection of the Intermediates by Paper Chromatography.—The following intermediates in the reaction system are examples of the intermediates detected by the two-dimensional paper chromatography developed by Seto and Ozaki:[16] mononuclear compounds (*o*-, or *p*-methoxymethyl phenol), dinuclear compounds (*o*-*o*' *o*-*p*' and *p*-*p*' dioxydiphenyl methane, and their derivatives containing methoxymethyl group), and trinuclear compounds. On the other band, intermediates such as methyl phenyl formal are detected by gas chromatography.[7,15]

Results and Discussion

Before a detailed discussion of the experimental results is undertaken, it is advantageous to consider the overall processes of the reaction in non-aqueous media, as determined by gas chromatography. The overall reaction between phenol and methylal may be represented as follows:

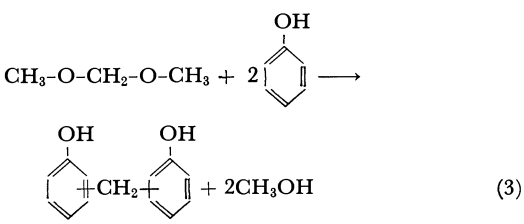

$$CH_3\text{-}O\text{-}CH_2\text{-}O\text{-}CH_3 + 2\,C_6H_5OH \longrightarrow HO\text{-}C_6H_4\text{-}CH_2\text{-}C_6H_4\text{-}OH + 2CH_3OH \quad (3)$$

This equation shows a stoichiometric relationship in which the rate of consumption of phenol is equal to the rate of the production of methyl alcohol, or twice the rate of the consumption of methylal. In the actual reactions these relationships were examined as is shown in Fig. 1. When the conversion is low (up to 30%), these quantitative relationships hold among the reactants and the products. This equation does not, however, show the details of the kinetics; they will be discussed later.

The characteristic features of the reaction are as follows: 1) The reaction rate is very fast at earlier stages, becomes considerably slower later, but does not reach an equilibrium even after 24 hr. or more (cf. Figs. 2 and 5).

2) As the initial concentration of phenol is increased, the rate of conversion is decreased. Accordingly, it seems clear that the overall reaction order is a minus value (cf. Figs. 10 and 15).

3) Because of the facts described in 1) and 2), the reaction order may not be determined by the use of only conventional methods, such as the half-lives, the initial rates or the integration.

4) The reaction products, such as methyl alcohol or methyl phenyl formal, have significant effects on the reaction order.

5) The above experimental results suggest that the reaction rate is very much contributed to by rapid reactions, such as acetal exchange, which are more probable in non-aqueous media than in aqueous media.

On the basis of these considerations, the experimental determination of kinetic equation of the reaction can be carried out. To start with, the following expression will represent the kinetic equation:

$$\frac{dx}{dt} = \frac{d[\text{methyl alcohol}]}{dt} = -\frac{d[\text{phenol}]}{dt} = k[\text{phenol}]^{\alpha}[\text{methylal}]^{\beta}\cdot[\text{methyl alcohol}]^{\gamma}[\text{catalyst}]^{\delta} \quad (4)$$

The Effect of Methylal.—As is shown in Fig. 2, the reaction rates do not depend upon the initial concentration of methylal over the range of 0.5—3.0 mol./l., when the initial concentrations of phenol and the catalyst are kept constant. Accordingly, the order with respect to methylal, β, can be estimated to be about zero; this implies the presence of a very fast opposing reaction involving methylal. Because of this experimental fact, the further kinetic examination was considerably simplified.

The Effect of Phenol.—In this experiment, a small amount of methyl alcohol is added into each reaction system in order to retard the initial reaction

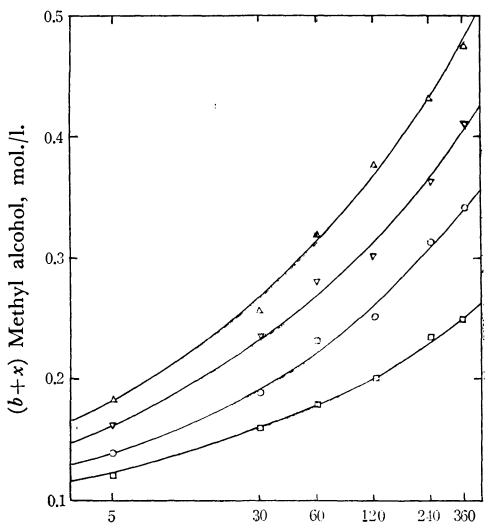

Fig. 3. The effect of phenol on rate.
Methylal 0.5 mol./l., methyl alcohol 0.1 mol./l.
$BF_3 \cdot OEt_2$ 0.01 mol./l. at 30°C in nitromethane
Phenol ▽ : 2.07 mol./l. ▽ : 1.50 mol./l.
○ : 1.00 mol./l. □ : 0.57 mol./l.

16) G. A. Olah and M. W. Meyer, "Friedel-Crafts and Related Reactions," Vol. 1, Interscience Publishers, New York (1963), pp. 230—235, pp. 686—688.

rate. The effect of the initial concentrations of phenol is shown in Fig. 3, at constant initial concentrations of methyl alcohol, methylal and catalyst. As is shown in Fig. 3, the higher the initial concentration of phenol, the lower the rate of conversion becomes. The reaction rates at various phenol concentrations were compared after negating the influence of methyl alcohol. When $\beta=0$, and the concentrations of methyl alcohol and the catalyst are kept constant, Eq. 4 will be simplified to:

$$\Delta x/\Delta t = K_1[\text{phenol}]^{\alpha} \quad (4')$$

$$\log \Delta t = (\log \Delta x - \log K_1) - \alpha \log[\text{phenol}] \quad (5)$$

The values of Δx are kept constant as 0.0125 mol./l. and the values of Δt are calculated from the curves of Fig. 3. Then, $\log \Delta t$ is plotted against log-[phenol] to be as is shown in Fig. 4.

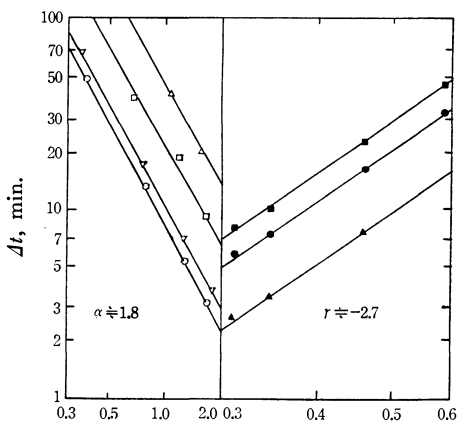

Fig. 4 Fig. 5

Fig. 4. Reaction order of phenol.
$\Delta x/\Delta t=k_1[\text{phenol}]^{\alpha}$

Fig. 5. Reaction order of methyl alcohol.
$\Delta x/\Delta t=k_2[\text{methyl alcohol}]^{\gamma}$
$\Delta x=0.0125$ mol./l.
Methyl alcohol
△ : 0.389 mol./l. □ : 0.306 mol./l.
▽ : 0.231 mol./l. ○ : 0.206 mol./l.
Phenol
■ : 1.0 mol./l. ● : 1.2 mol./l.
▲ : 1.8 mol./.l

If Eq. 5 is applicable to this system, the relationship between $\log \Delta t$ and log[phenol] should be linear, and the slope of the straight line must correspond to the reaction order of phenol. From the slopes of straight lines in Fig. 4, the order of phenol, α, is estimated to be about two for the period of low conversion (up to about 30%).

The Effect of Methyl Alcohol.—The effect of methyl alcohol can be deduced by negating the influence of the phenol remaining according to a method similar to the one used in the earlier section. The time intervals, Δt, which elapsed for the production of methyl alcohol, Δx, at the same concentrations of phenol are calculated from the results of Fig. 4. As is shown in Fig. 5, parallel straight lines are obtained. From the slopes of these lines, the order of methyl alcohol is estimated by the relation of Eq. 5' to be about minus three;

$$\log \Delta t \fallingdotseq (\log \Delta x - \log K_2) - \gamma[\text{methyl alcohol}] \quad (5')$$

Thus, the reaction order with respect to methyl alcohol, γ, can be determined experimentally by considering the effect of methyl alcohol on the reaction rates.

Thus, the kinetic equation obtained over the range of low conversion is as follows:

$$\frac{\mathrm{d}[\text{methyl alcohol}]}{\mathrm{d}t} = k\frac{[\text{methylal}]^0[\text{phenol}]^2}{[\text{methyl alcohol}]^3} \quad (6)$$

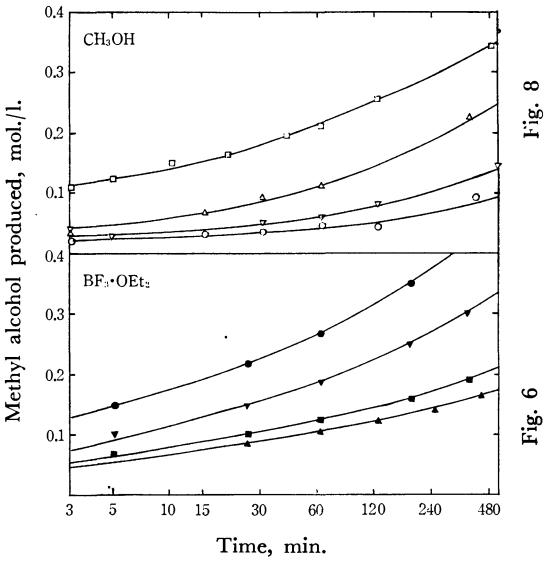

Fig. 8

Fig. 6

Fig. 6. Effect of methyl alcohol added on rate.
Phenol 1 mol./l., Methylal 0.6 mol./l., $BF_3\cdot OEt_2$ 0.02 mol./l. in nitromethane at 30°C.
Methyl alcohol
□ : 0 mol./l. △ : 0.14 mol./l.
▽ : 0.30 mol./l. ○ : 0.50 mol./l.

Fig. 8. The effect of catalyst on rate.
Phenol 0.5 mol./l., methylal 0.5 mol./l. in nitromethane at 30°C
$BF_3\cdot OEt_2$
● : 0.02 mol./l. ▼ : 0.05 mol./l.
■ : 0.001 mol./l. ▲ : 0.005 mol./l.

The Effect of the Methyl Alcohol Added.—In order to confirm the appropriateness of the kinetic equation obtained in the earlier section, the following supplementary experiments were undertaken. Figure 6 shows the relationship between the reaction rates and the initial concentrations of methyl alcohol over the range of 0.15—0.5 mol./l., when the initial concentrations of phenol, methylal and catalyst are kept constant.

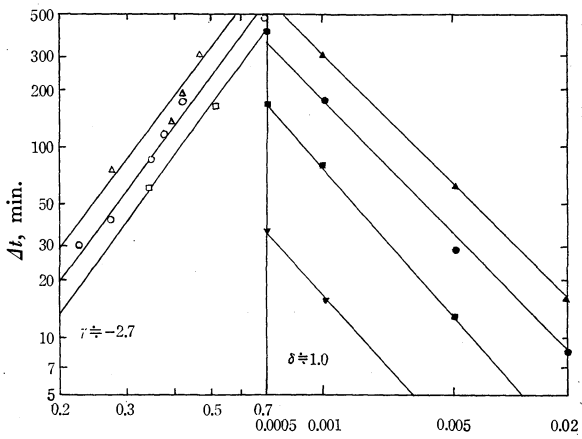

Fig. 7 Fig. 9

Fig. 7. Reaction order of methyl alcohol.
$\Delta x/\Delta t = k_3[\text{methyl alcohol}]^{\gamma}$
Methyl alcohol
△ : 0.175 mol./l. □ : 0.05 mol./l.
○ : 0.125 mol./l.

Fig. 9. Reaction order of catalyst
$\Delta x/\Delta t = k_4[\text{catalyst}]^{\delta}$
Methyl alcohol
▲ : 0.250 mol./l. ■ : 0.150 mol./l.
● : 0.200 mol./l. ▼ : 0.100 mol./l.

As was expected, the order of methyl alcohol is about minus three (Fig. 7). This confirms the reaction order of methyl alcohol determined in the earlier section.

The Effect of the Catalyst.—The effect of the concentration of the catalyst on the reaction rate is shown in Fig. 8. In a similar way, the concentration of the catalyst is plotted against the time intervals in Fig. 9. From the slopes of the straight lines in Fig. 9, the order of the catalyst is estimated to be about one. The catalyst used is $BF_3 \cdot OEt_2$, which easily reacts with one or two moles of water or alcohol to produce complex compounds. If a large amount of methyl alcohol is present in the reaction system, the activity of the catalyst is considerably decreased as a result of the formation of a relatively inactive complex compound, such as $BF_3 \cdot [CH_2OH]_2$.[17] The interaction between the catalyst and methyl alcohol may be one of the reasons why the reaction order of methyl alcohol has a minus value in this reaction system:

$$[BF_3 \cdot \text{solvent}] + 2CH_3OH \rightleftarrows [BF_3 \cdot CH_3OH] + CH_3OH + \text{solvent} \rightleftarrows [BF_3 \cdot 2CH_3OH] + \text{solvent} \quad (7)$$

The Integral Form of Kinetic Equation.—In general, kinetic studies should be conducted in two or more ways, for example, differential or integration methods. After a number of attempts, the following integral form of the kinetic equation, with certain initial conditions, has been found to be most satisfactory for the reaction between phenol and methylal in nitromethane. The differential form;

$$\frac{dx}{dt} = \frac{k(a-x)^2}{(b+x)^3}$$

The integral form:

$$kt = \frac{(a+b)^2}{2}[(1-p)^2 - 6(1-p) + 6\ln(1-p) + 6\ln(a+b) + 2/(1-p)] - C_0 \quad (9)$$

where

x : the concentration of CH_3OH produced
b : the initial concentration of CH_3OH
a : the initial concentration of HO-ϕ
p : a variable depending upon the conversion

that is:

$$p = (b+x)/(a+b) \quad (10)$$

C_0: integral constant
x/a: the conversion of phenol
$(b+x)$: the concentration of CH_3OH present
$(a-x)$: the concentration of HO- remaining

The initial conditions:

at $t = 0$,

$$x = 0.035a,\ p = (b + 0.035a)/(a + b) \quad (11)$$

Therefore,

$$C_0 = \frac{(a+b)^2}{2}\left[\left(\frac{0.965a}{a+b}\right)^2 - 6\left(\frac{0.965a}{a+b}\right) + 6\ln(0.965a) + 2\frac{(a+b)}{0.965a}\right] \quad (12)$$

In Figs. 10 and 11, the solid lines are the calculated values, while the points plotted are the measured values. There is a good agreement between them within the range of low conversion up to 30%. If x is assumed to be zero at $t=0$ as the initial condition of Eq. 9, the calculated values differ significantly from the measured values, especially in Fig. 11, which corresponds to a system containing a relatively high concentration of methyl alcohol. Careful examination shows that the kinetic equation obtained above is good enough to explain any experimental results over a wide range of conditions.

The Reaction Rate over the Range of High Conversion.—When no methyl alcohol is added to the system, the overall reaction rate is remarkably fast at an early stage of the reaction, and the conversion often reaches 30% or more within a few minutes, especially in the case of a low initial concentration of phenol, as is shown in Fig. 12. Over the range of high conversion, the estimated

values of the reaction orders of phenol and methyl alcohol are about 1 and −2.5 respectively; these values differ significantly from the values in a low conversion, as Figs. 13—15 show.

The differential form:

$$\frac{dx}{dt} = \frac{k(a-x)^1}{(b+x)^{2.5}}$$

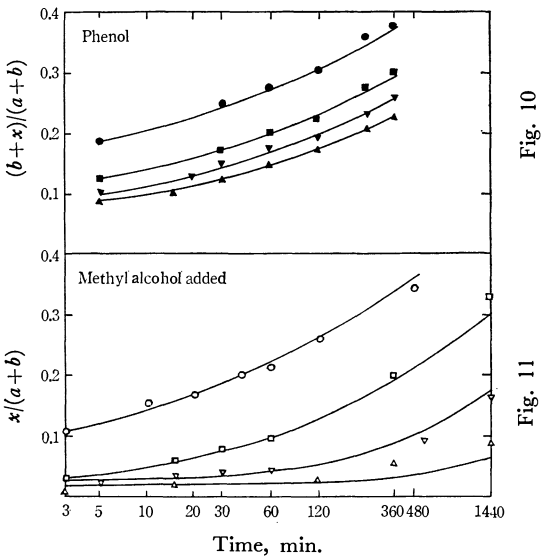

Fig. 10

Fig. 11

Fig. 10, 11 Comparison of calculated values and experimental values.

$kt=((a+b)^2/2)\{(1-p)^2-6(5p)+6\ln(1-p)+2/(1-p)+6\ln(a+b)\}+C_0$

at $t=0$, $x=0.035a$, $p=(b+x/a+b)$

Phenol

● : 0.57 mol./l. ■ : 1.0 mol./l.
▼ : 1.5 mol./l. ▲ : 2.0 mol./l.

Methyl alcohol

○ : 0.0 mol./l. □ : 0.14 mol./l.
▽ : 0.30 mol./l. △ : 0.02 mol./l.

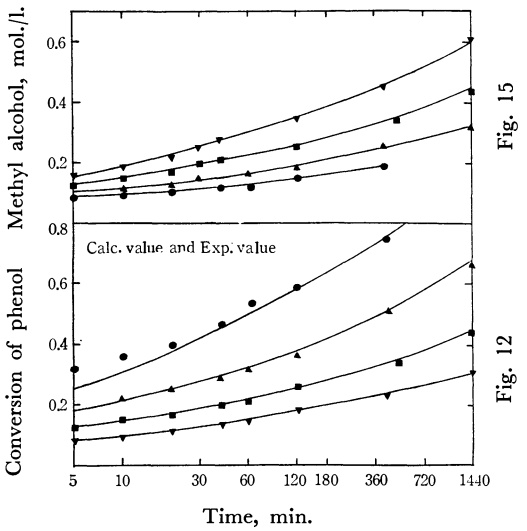

Fig. 15

Fig. 12

Fig. 12. The effect of phenol on rate (high conversion).

Fig. 15. Comparison of calculated values and experimental values.

Methylal 0.6 mol./l., catalyst 0.02 mol./l. in nitromethane at 30°C.

Phenol

● : 0.25 mol./l. ▲ : 0.50 mol./l.
■ : 1.00 mol./l. ▼ : 2.00 mol./l.

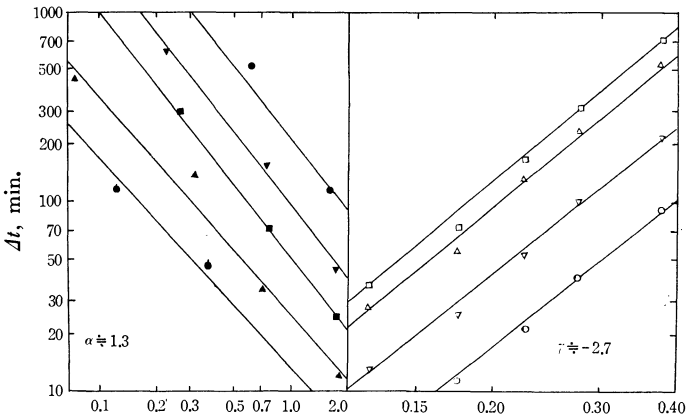

Fig. 13

Fig. 14

Fig. 13. Reaction order of phenol (high conversion).

$\Delta x/\Delta t = k'[\text{phenol}]^{\alpha'}$, $\Delta x = 0.05$ mol./l.

Methyl alcohol ● : 0.40 mol./l. ■ : 0.25 mol./l. ◆ : 0.15 mol./l.
▼ : 0.30 mol./l. ▲ : 0.20 mol./l.

Fig. 14. Reaction order of methyl alcohol (high conversion).

$\Delta x/\Delta t = k'[\text{methyl alcohol}]^{\gamma'}$, $\Delta x' = 0.05$ mol./l.

Phenol ○ : 0.4 mol./l. △ : 0.5 mol./l. ▽ : 1.0 mol./l. ○ : 2.0 mol./l.

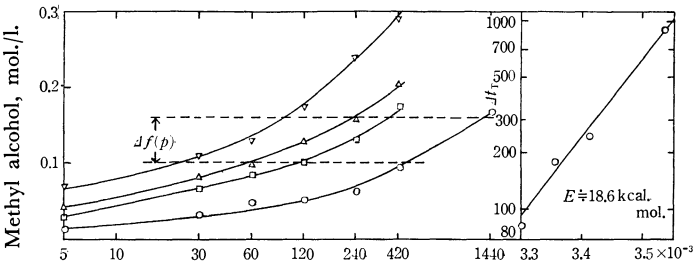

Fig. 16 Fig. 17

Fig. 16. Rates of production of methyl alcohol at various temperatures.
Phenol 10 mol./l., methylal 0.5 mol./l., methyl alcohol 0.1 mol./l., $BF_3 \cdot OEt_2$ 0.01 mol./l. in nitromethane at 30°C.
Temperature ▽ : 30°C △ : 25°C □ : 20°C ○ : 10°C
Fig. 17. Activation energy of the reaction.
$k_T t_T = f(p)_T$ if $\Delta f(p)_T$ = const., $\log k_T = -K'_T \log \Delta t_T$

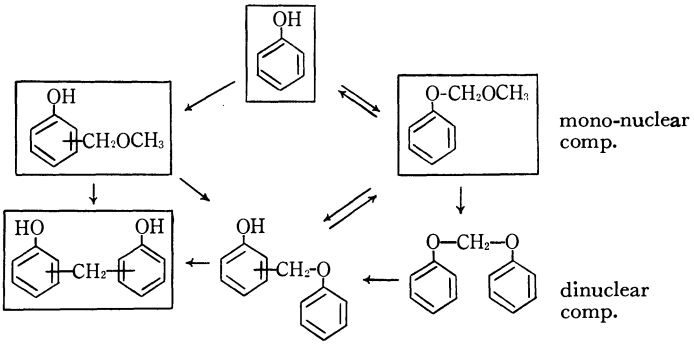

Fig. 18. Probable scheme of the reaction between phenol and methylal.

The integral form:

$$kt = 2(a+b)^{2.5}\{\ln|\tan(1/2 \cdot \sin^{-1}p^{1/2} + \pi/4)| - p^{1/2} - 1/3 \cdot p^{3/2} - 1/5 \cdot p^{5/2} - C_0\} \quad (14)$$

where

x: the concentration of CH_3OH produced

a: the initial concentration of phenol

b: the initial concentration of CH_3OH added

p: a variable depending upon the conversion, that is,

$$p = (b+x-0.035a)/(a+b) \quad (15)$$

The initial conditions:

$$x = 0$$

$$x = 0.035a,\ p = \frac{b}{a+b}$$

C_0: integral constant

As is shown in Fig. 15, although there is a fair agreement between the experimental and the calculated values over the range of high conversion, still the stoichiometric relation in Eq. 3 does not hold in this system. Consequently, it seems probable that the reaction mechanism changes gradually, depending upon the degree of conversion, particularly in the range of conversion beyond 30%.

The Temperature Dependence of the Reaction Rate.—A comparison of reaction rates at various temperature (30, 25, 20, 10°C) is shown in Fig. 16. The time intervals, Δt, which elapse for the production of a certain amount of methanol at each temperature are measured from Fig. 16. The relation between a logarithm of the time interval and a reciprocal temperature is a straight line, as Fig. 17 shows. From the slope of Fig. 17, the apparent activation energy in this non-aqueous medium can be said to be about 18.6 kcal./mol., which is comparable to that in aqueous media.[1] Nevertheless, the overall rate of the reaction in non-aqueous media is faster than that in aqueous media. The kinetic system is too complicated for the entropy of activation to be discussed. However, the difference in overall reaction rate between non-aqueous and aqueous media may be ascribed to the entropy of activation rather than to the energy of activation.

The Estimation of the Reaction Scheme.—

The reaction in non-aqueous media is very complex; it involves substitution on aromatics, acetal exchange by methyl alcohol or phenol, and interaction between methyl alcohol and $BF_3 \cdot OEt_2$, etc.. A probable reaction scheme is shown in Fig. 18.

Phenol and methyl phenyl formal can be identified by gas chromatography, while *p*-methoxymethylphenol and dioxydiphenylmethane (*pp'* and *op'*) can be identified by paper chromatography; however, the other intermediate can not be detected so definitely. Therefore, it seems probable that the process passing through methyl phenyl formal is important in non-aqueous media. A detailed discussion of the reaction mechanism will be given in the following reports.

The author is indebted to Professor Hiromu Murata of the Faculty of Science of Hiroshima University for his helpful discussions and encouragement throughout this work. He also wishes to express his gratitude to Dr. Keiji Oshima, Managing Director of Sumitomo Bakelite Co., Ltd. and Director of the Central Research Laboratory of the same company for permission to publish this paper, and to Dr. Ryuzo Nakatsuka and Mr. Mitsuo Niwa of this Laboratory for valuable assistance.

BULLETIN OF THE CHEMICAL SOCIETY OF JAPAN VOL. 39 1027—1031 (1966)

The Reaction between Phenol and Formaldehyde in Non-Aqueous Media. II. The Behavior of Methyl Phenyl Formal in the Reaction Catalyzed by Boron Trifluoride - Etherate

By Shin'ichi MURAYAMA

Central Research Laboratory, Sumitomo Bakelite Co., Ltd., Totsuka-ku, Yokohama

(Received October 16, 1965)

Methyl phenyl formal (MPF) is one of the most important intermediates in the acid-catalyzed reaction between phenol and methylal in non-aqueous media. On the acidic decomposition of MPF itself, phenol and methylal are mainly produced, along with a small amount of methyl alcohol at the first step; at the same time, there exists an equilibrium state between the reactants and the products. At the second step, the phenol produced is gradually consumed, and the reaction eventually yields methyl alcohol and such condensation products of phenol as methoxymethylphenol and dioxydiphenylmethane. Thus, the acetal exchange proceeds faster than the substitution on aromatics. On the other hand, the acidic decomposition of MPF is retarded remarkably by methyl alcohol, considerably by methylal, and fairly much by phenol. This behavior of MPF can be explained by its interaction with the catalyst and the opposing reactions with it. As a result, the reaction of MPF can better be understood.

The previous paper reported on the kinetics of the phenol-formaldehyde reaction in non-aqueous media, but it was confined to the experimental characterization of the complex system.[1] This paper will deal with several intermediates of the reaction, such as methyl phenyl formal, methoxymethylphenols and dioxydiphenylmethanes, which were detected in the reaction system. It seems probable that methyl phenyl formal is one of the most important intermediates in the reaction of non-aqueous media; an understanding of its behavior is the key to an elucidation of the reaction mechanism.

Therefore, the objects of this investigation are: (1) to examine the reaction of methyl phenyl formal with and without other reactants, and then (2) to establish a reaction scheme for these reactions.

There have been only a few reports on the reaction of alkyl aryl formal, especially in non-aqueous media. In the presence of a trace of an acid, alkyl aryl formal may change at once partly to symmetric formals, and probably also to nuclear-substituted compounds.[2] Though a small amount of methyl phenyl formal has been obtained in the acid-catalyzed phenol-formaldehyde reaction in aqueous media by Horiuchi,[3] the role of the formal as an active intermediate has been not thorouglhy studied in aqueous media, because

1) Part I of this Series: S. Murayama, This Bulletin, **39**, 1019 (1966).

2) H. Meerwein, "Methoden der Organishen Chemie," **VI/3**, Ed. by E. Müller, Georg Thieme Verlag, Stuttgrart pp. 237—238 (1965); P. Hoering and F. Baum, German Pat. 209, 608 (1907); *Chem. Zentr.*, **1909** I, 1681.

3) H. Horiuchi, *J. Chem. Soc. Japan, Ind. Chem. Sect.* (*Kogyo Kagaku Zasshi*), **66**, 150 (1963).

the formal is easily hydrolyzed in acidic aqueous media. The extensive studies of the kinetics and the mechanisms of the reactions of acetals have been performed with regard only to the hydrolysis[4] or the alcoholysis.[5]

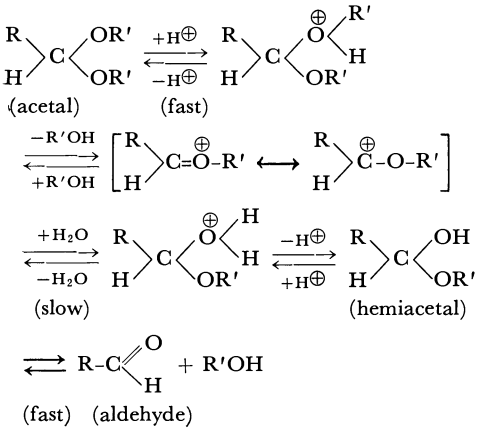

According to this mechanism, the rate of the acid-catalyzed hydrolysis of an acetal depends mainly on either the stability of the carbonium ion produced or on the electron density on the oxygen atom, while the rate of the hydrolysis of a hemiacetal is very rapid, even in the absence of an acid catalyst.[4]

On the other hand, the acetal-exchange reaction with an alcohol or an aldehyde also proceeds in the presence of an acid catalyst, such as HCl, H_2SO_4, $FeCl_3$ or BF_3.[5,6]

$$RCH(OR')_2 + R''(OH) \rightleftarrows RCH(OR')(OR'') + R'(OH)$$

$$RCH(OR')(OR'') + R''(OH) \rightleftarrows RCH(OR'')_2 + R'(OH)$$

$$RCH(OR')_2 + R'''CHO \rightleftarrows R'''CH(OR')_2 + RCHO$$

The rates and the equilibrium constants of the hydrolyses of acetals have been studied systematically. Dimethyl formal is one of the most stable acetals, while alkyl aryl formals are unstable; diaryl formals are stable.[6]

The catalytic action of boron trifluoride-etherate is very complex, but it may be regarded as the action of hydrogen ions produced by the reaction between the catalyst and a trace of water present in the reaction system. It is known that boron trifluoride - etherate easily forms complex compounds with alcohols, ether, nitromethane or phenol.[7]

$$[BF_3 \cdot OEt_2] + H_2O \rightleftarrows [BF_3 \cdot H_2O] + OEt_2 \overset{+H_2O}{\rightleftarrows}$$

$$[BE_3 \cdot 2H_2O] \rightleftarrows [BF_3 \cdot OH]^{\ominus} + H_3O^{\oplus}$$

$$[BF_3 \cdot H_2O] \rightleftarrows [BF_3 \cdot OH]^{\ominus} + H^{\oplus}$$

As for the acid-catalyzed phenol-formaldehyde reaction in aqueous media, the reaction mechanism has been established by Imoto et al.[8] to be:

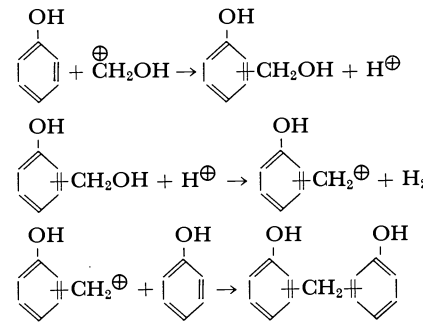

etc.

The ratio of the amounts of *o*- and *p*-derivatives produced mainly depends upon the reaction temperature and upon the catalyst (or pH) in an aqueous media.[9]

Therefore, it seems that the main reactions of methyl phenyl formal in the presence of boron trifluoride - etherate include the following two types of reactions:

(A) Acetal exchange

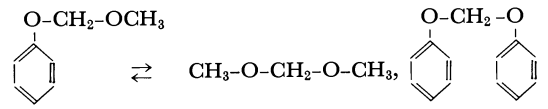

(B) Substitution on aromatics

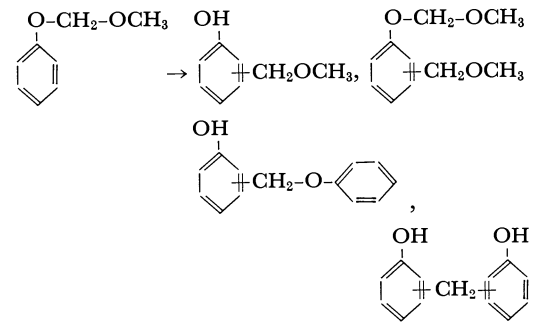

4) M. M. Kreevoy and R. W. Taft, *J. Am. Chem. Soc.*, **77**, 3146, 5590 (1955).

5) N. B. Lorette and W. L. Howard, *J. Org. Chem.*, **25**, 521 (1960); W. J. Croxall, *J. Am. Chem. Soc.*, **71**, 2736, 2741 (1949).

6) H. Meerwein, "Methoden der Organishen Chemie," **VI/3**, Ed. by E. Müller, Georg Thieme Verlag, Stuttgart, (1965), pp. 272—276.

7) N. N. Greenwood and R. L. Martin, *J. Chem. Soc.*, **1953**, 1427.

8) M. Imoto, *Kobunshi Tenbo*, **4**, 60 (1951); ibid., **8**, 29, 33 (1952).

9) H. Horiuchi, *J. Chem. Soc. Japan, Ind. Chem. Sect.* (*Kogyo Kagaku Zasshi*), **66**, 1379 (1963); H. L. Bender *Modern Plastics*, **30**, 136 (Feb. 1953); ibid., **31**, 115 (Mar. 1954); S. R. Finn and J. W. G. Musty, *J. Soc. Chem. Ind.*, **69**, S49 (1950); H. L. Bender, A. G. Farnham, J. W. Guyer, F. N. Apel and T. B. Gibb, Jr., *Ind. Eng. Chem.*, **44**, 1619 (1952); D. A. Flaser, R. W. Hall and A. J. Raum, *J. Appl. Chem.* (*London*), **7**, 676, 689 (1957), R. Inoue and T. Minami, *J. Chem. Scc. Japan, Ind. Chem. Sect.* (*Kogyo Kagaku Zasshi*), **61**, 1340 (1958).

By analogy with the reaction in aqueous media, the following reaction scheme may be postulated. (1) The Activation of MPF by $H^{\oplus}$ (MPF= methyl phenyl formal):

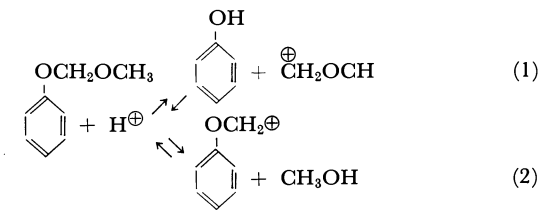

(2) The Reactions of the methoxymethyl cation:

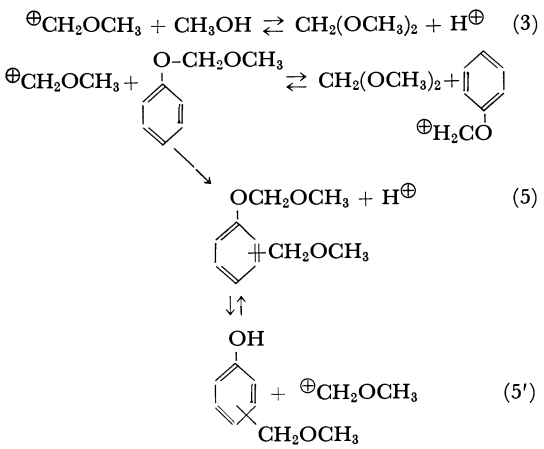

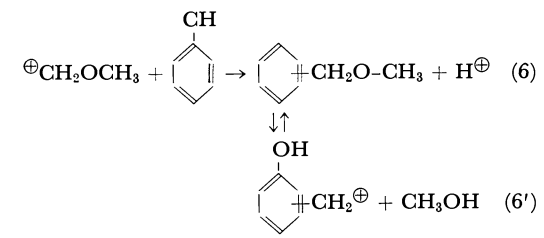

(3) The Reactions of the phenoxymethyl cation:

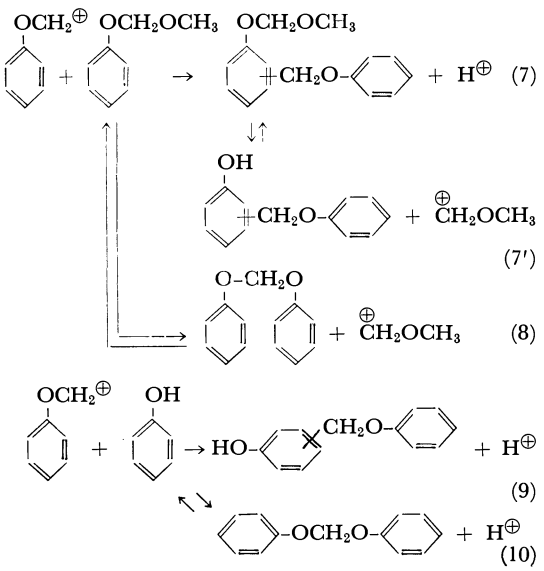

(4) The Reactions of the oxybenzyl cation:

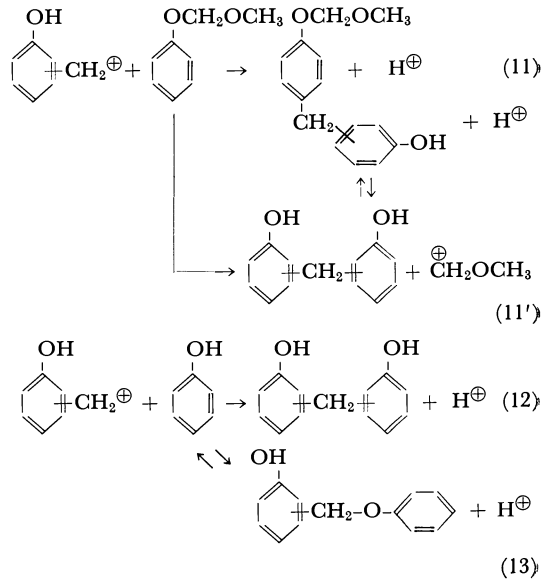

The scheme postulated above will now be examined through experiments on the reactions of the intermediates. It is expected that the effects of the other reactants, catalysts and solvents can be understood better through these experiments.

Experimental

Materials.—The reagents, the solvent and the catalyst used were purified by the conventional methods and were checked by gas chromatography.[1)]

Analytical Method.—The amounts of methyl phenyl formal, phenol, methyl alcohol and methylal were measured quantitatively by gas chromatography.[1)]

Procedure.—Conventional techniques were used throughout this study. In every experiment, nitromethane was used as the solvent and boron trifluoride - etherate was used as the catalyst.

Results and Discussion

The Decomposition of Methyl Phenyl Formal (MPF).—In order to investigate the decomposition of MPF (1 mol./l.) in the presence of the boron trifluoride - etherate catalyst (0.001—0.00025 mol./l.), the amounts of MPF, phenol, methylal and methyl alcohol were determined during the course of the reaction, as is shown in Fig. 1.

At the first step of the acidic decomposition of MPF, the amount of phenol produced is almost equal to that of the methylal produced, while only a small amount of methyl alcohol is produced.

It follows from this fact that the two reactions activating MPF by proton (Eqs. 1 and 2) are very fast and of almost equal rates. This means that the methoxy-methyl cation, methyl alcohol, phenol and the phenoxymethyl cation are produced

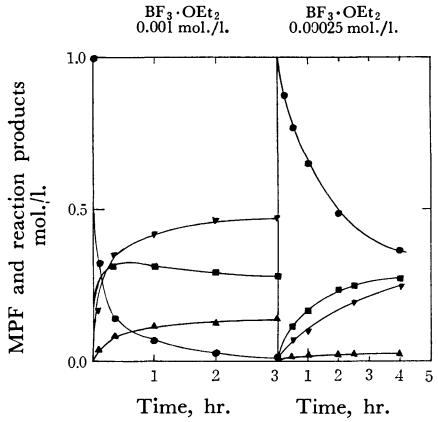

Fig. 1. The effect of the catalyst on the reaction of M.P.F.

M.P.F. 1 mol./l. in nitromethane at 30°C
●: MPF; ■: Phenol; ▼: Methylal;
▲: Methyl alcohol

in amounts almost equivalent to one another. Then, the methoxymethyl cation reacts with methyl alcohol at once to produce methylal, while the phenoxymethyl cation reacts with MPF to form various condensation products by Eqs. 7, 7', 8, etc.

After the reaction has proceeded to some extent, the amount of phenol in the system becomes so great that the reactions of phenol, such as Eqs. 6 and 6', take place significantly. Then the amounts of methyl alcohol and methylal remarkably increase, while the amount of phenol decreases gradually after passing through a maximum; at the same time, the amount of MPF decreases rapidly toward zero.

The reactions of the earlier stage (such as Eqs. 1, 2 and 3) proceed rapidly in the presence of a very low concentration of the catalyst, but the rates of the reactions of the later stage (such as 6 and 6') depend markedly upon the concentration of the catalyst, as is shown in Fig. 1.

It seems probable that the unstable assymmetric acetal (MPF) is changed to the stable symmetric acetal (methylal) by the acetal exchange in the presence of a trace of an acidic catalyst, until an equilibrium is established between them.

Diphenyl formal was not detected in the reaction mixture under these conditions, contrary to our expectation; this fact may have something to do with the stability or the rate of formation of the diaryl formal.

The substitution reactions on aromatics may easily accompany the acetal exchange reactions at relatively high concentrations of the catalyst, and the amounts of methyl alcohol produced may indicate the amounts of the di- or polynuclear compounds produced.

The Reaction of MPF with Phenol.—The reaction between MPF (1 mol./l.) and phenol (1 mol./l.) in the presence of $BF_3 \cdot OEt_2$ (0.00025 mol./l.) was also investigated. Figure 2 shows the amounts of the reactants and the products produced during the course of the reaction.

The reaction of MPF with phenol is very similar to the decomposition of MPF alone, but it has the following distinctive characteristics : 1) The amount of phenol produced is certainly smaller than that of methylal.

2) The overall reaction rate is slightly decreased by the addition of phenol to the reaction system.

The condensation reactions of phenol, such as Eqs. 6, 9, 10, 12, and 13, will proceed markedly to consume phenol in the presence of a considerable amount of phenol, and thus, the overall reaction rate might be increased by these reactions. On the other hand, phenol may form relatively stable complexes with catalysts such as $[BF_3 \cdot$ $-OH]$

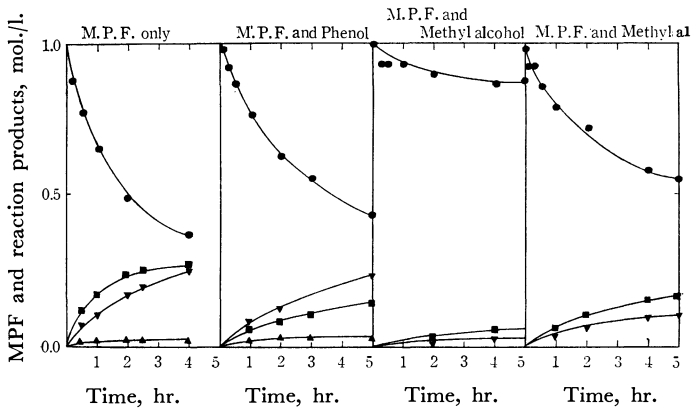

Fig. 2. The effect of reactants on the reaction of MPF
MPF 1 mol./l., $BF_3 \cdot OEt_2$ 0.00025 mol./l. in nitro methane at 30°C other reactant 1 mol./l. (if present)
●: MPF., ■: Phenol; ▼: Methylal; ▲: Methylalcohol

or $[BF_3 \cdot 2C_6H_5OH]$; the formation of these complexes should result in the decrease of the overall reaction rate. These two effects of phenol on the reaction rate compensate each other, and the net effect of the addition of phenol was a slight decrease in the overall reaction rate, while a relatively large amount of the nuclear-substituted compounds are produced.

The Reaction of MPF with Methylal.—The reaction between MPF (1 mol./l.) and methylal (1 mol./l.) in the presence of $BF_3 \cdot OEt_2$ (0.00025 mol./l.) was investigated by measuring the amounts of the reactants and products during the course of the reaction; the results are shown in Fig. 2. In this case, the overall reaction rate is considerably lower than that of MPF by itself, and methyl alcohol is not produced at all, while phenol and methylal are produced as in the case of MPF alone. These results indicate that, in the presence of a considerable amount of methylal, the reaction of methylal with the phenoxymethyl cation (the back reaction of Eq. 4) is very fast and produces the methoxymethyl cation, which then consumes methyl alcohol (by Eq. 3) and probably phenol (by the back reaction of Eq. 1). Thus, the presence of methylal inhibits the overall rate of the reaction by promoting various opposing reactions, though the interaction of methylal with the catalyst may be negligibly small.

The Reaction of MPF with Methyl Alcohol.—In the presence of methyl alcohol (1 mol./l.), the reaction of MPF (1 mol./l.) with $BF_3 \cdot OEt_2$ (0.00025 mol./l.) as a catalyst is significantly inhibited, and both MPF and methyl alcohol are consumed very gradually; this fact shows that methyl alcohol may promote the opposing reaction. The catalyst readily changes to a stable complex by reacting with methyl alcohol. Since the two types of effects in the presence of methyl alcohol are additional, methyl alcohol decreases the overall reaction rate remarkably.

Summary

The acidic decomposition of MPF in nitromethane has been studied, and the reaction mechanism has been investigated. 1) There must exist an equilibrium between MPF, methylal, phenol and methyl alcohol through acetal exchange reactions, but the actual equilibrium state is changed successively by substitution reactions on aromatics.

2) The acetal exchange reactions proceed very fast, even in the presence of a very low concentration of the catalyst, while the substitution reactions on aromatics proceed more slowly under the same conditions.

3) The formation of complex compounds between the catalyst and such reactants as phenol, methylal and methyl alcohol results in various decreases in the overall reaction rate according to the stabilities of the various complexes.

4) The acidic decomposition of MPF may be significantly inhibited by methylal and methyl alcohol as a result of the opposing reactions, but not inhibited by phenol, if the effects of complex formations on reaction rates are eliminated. The reaction using sulfuric acid as the catalyst may prove this fact more clearly.[10]

5) The behavior of MPF can be explained by supposing that the reaction proceeds through some reactive intermediates, such as the methoxymethyl cation, the phenoxymethyl cation and the oxybenzyl cation.

6) Diphenyl formal is not formed during the disproportionation reactions of MPF, contrary to our expectation. This experimental evidence suggests a difference in reactivity between the methoxymethyl cation and the phenoxymethyl cation.

7) From the results of this experiments, the mechanism of the reaction between phenol and methylal in non-aqueous media can be better understood.

The author is indebted to Professor Hiromu Murata of the Faculty of Science of Hiroshima University for his helpful discussions and encouragement throughout the work. He also wishs to express his gratitude to Dr. Keiji Oshima, Managing Director of the Sumitomo Bakelite Co., Ltd., and Director of the Central Research Laboratory of the same company for permission to publish this paper, and to Dr. Ryuzo Nakatsuka and Mr. Mitsuo Niwa of this Laboratory for their valuable assistance.

10) S. Murayama, M. Niwa and R. Nakatsuka, 18th Annual Meeting of the Chemical Society of Japan, Osaka, April, 1965.

BULLETIN OF THE CHEMICAL SOCIETY OF JAPAN VOL. 39 1032—1035 (1966)

The Reaction between Phenol and Formaldehyde in Non-Aqueous Media. III. The Mechanism of the Reaction Catalyzed by Boron Trifluoride-Etherate

By Shin'ichi MURAYAMA

Central Research Laboratory, Sumitomo Bakelite Co., Ltd., Totsuka-ku, Yokohama

(Received October 16, 1965)

In the previous papers of this series, the reaction between phenol and methylal in non-aqueous media has been investigated by means of the experimental characterization of the kinetic system; a plausible reaction scheme has thus been presented. The object of the present paper is to make a mathematical characterization of the kinetic system, a kinetic equation has been obtained by calculation based on the probable reaction scheme; it has been found to be in good agreement with the kinetic equation obtained experimentally.

There are only few reactions which lend themselves to a simple kinetic description in terms of the reaction order in the field of the resin-forming condensation reactions. Since there are many processes by which the reaction proceeds, the author has expected to find a concomitant difficulty in expressing the rates of phenol-formaldehyde reactions in simple terms. Since the phenol-formaldehyde reactions involve the opposing, concurrent and consecutive reactions, their kinetic studies have been established only in aqueous media.[1] Unfortunately, the mechanism of the reactions in aqueous media is not suitable for explaining the behavior of the reactions in non-aqueous media. The series of works conducted at this laboratory have aimed at clarifying the differences between the reactions in non-aqueous media and those in aqueous media.

The previous papers of this series have dealt with the kinetics of the reaction between phenol and formaldehyde in nitromethane catalyzed by boron trifluorideetherate. The course of the reaction was followed by the quantitative gas chromatographic analysis of the reactants and products.

After the experimental characterization of this reaction system, the following kinetic equation was obtained:[2]

$$\frac{\mathrm{d[methyl\ alcohol]}}{\mathrm{d}t} = \frac{k[\mathrm{catalyst}][\mathrm{phenol}]^2[\mathrm{methylal}]^0}{[\mathrm{methyl\ alcohol}]^3}$$

Methyl phenyl formal was detected as one of the reactive intermediates in this reaction system; the behavior of methyl phenyl formal was therefore studied as a means of estimating the reaction scheme.[3] The objects of the present paper are: (1) to perform a mathematical characterization of the kinetic system, and (2) to gain detailed information about the mechanism of the phenol-formaldehyde reaction in non-aqueous media.

Results and Discussion

Reaction Scheme.—The reaction between phenol and methylal in nitromethane catalyzed by boron trifluoride-etherate may be represented in the following simplified form:

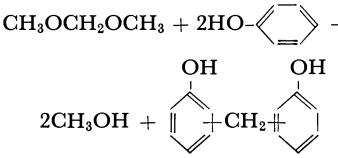

(1)

The stoichiometric relations of Eq. 1 are in accordance with the experimental findings[2] that the rate of phenol consumed is almost equal to the rate of methyl alcohol produced, and that the ratio of the rates of the consumption of methylal and phenol is 1 : 2, when the conversion is low (up to 30%).

On the other hand, the acidic decomposition of methyl phenyl formal can be explained by using an ionic mechanism, which involves the formation of such active intermediates as the methoxymethyl cation, the phenoxymethyl cation and the oxybenzyl cation.

From the experimental evidence, it seems that the reaction between phenol and methylal in non-aqueous media should be regarded as a complex kinetic system consisting of two series of consecutive reactions passing through methoxymethylphenols or methyl phenyl formal, and that each of the two series involves such concurrent

1) M. Imoto et al., *Kobunshi Tenbo*, **4**, 60 (1951); ibid., **8**, 29, 33 (1952).

2) Part I of this Series: S. Murayama, This Bulletin, **39**, 1019 (1966).

3) Part II of This Series: S. Murayama, ibid., **39**, 1027 (1966).

reactions as the acetal exchange and the substitution on aromatics. Nevertheless, from the analogy of acidic reactions in aqueous media, the formation of di- or tri-methoxymethylphenols may also be neglected in non-aqueous media so as to simplify the mathematical calculation. The differences in the reactivities of the ortho- and para-positions of phenol is not taken into consideration.

The following reaction scheme may, then, be presented for the phenol-formaldehyde reaction in non-aqueous media:

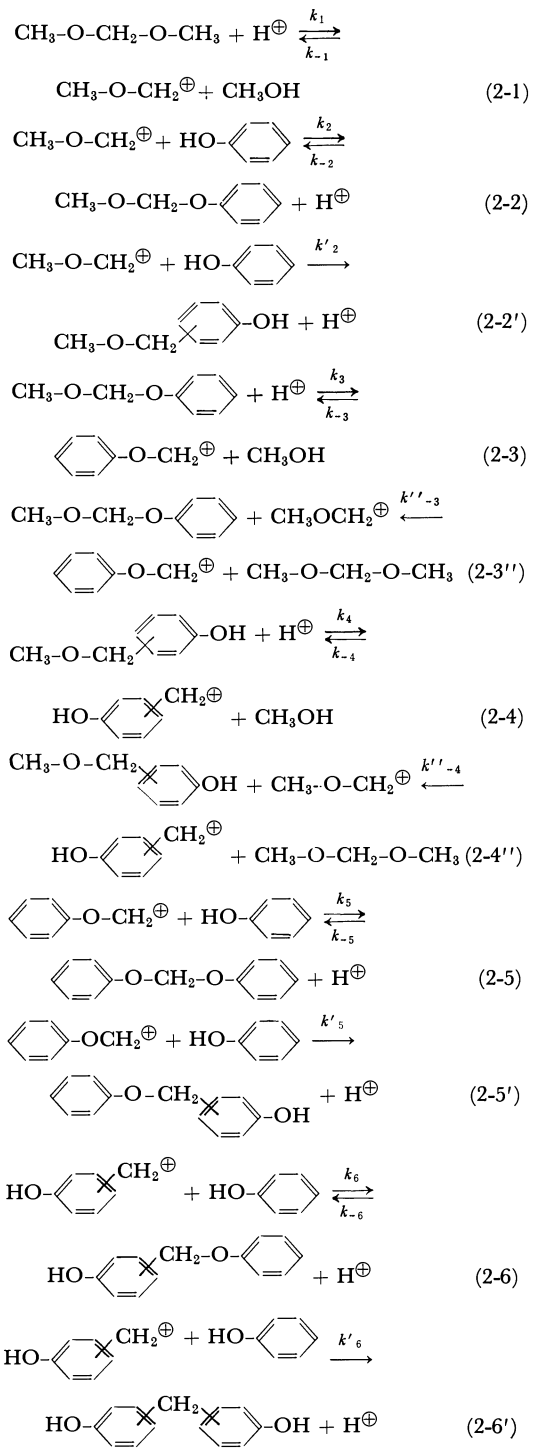

Fig. 1. Reaction scheme.

The Mathematical Calculation of the Reaction Rate.—On the basis of the reaction scheme shown in Fig. 1, the rate of the methyl alcohol produced is calculated by using the stoichiometric relations and the stationary-state hypothesis.

First, the terms and the rate of production (or consumption) of reactants and intermediates are represented as follows:

m: methylal
p: phenol
a: methyl alcohol
c^*: the effective concentration of catalyst
α: the methoxymethyl cation
β: methylphenyl formal
γ: methoxymethylphenol
δ: the phenoxymethyl cation
ε: the oxybenzyl cation
ρ: phenoxymethylphenol
φ: diphenyl formal

$$\frac{d\alpha}{dt} = -(k_{-1}a+k_2p+k'_2p)\alpha + k_{-2}c^*\beta + k''_{-3}m\delta + k''_{-4}m\varepsilon + k_1mc^* \quad (3\text{-}1)$$

$$\frac{d\beta}{dt} = k_2p\alpha + (k_{-3}a + k''_{-3}m)\delta - (k_3c^* + k_{-2}c^*)\beta \quad (3\text{-}2)$$

$$\frac{d\gamma}{dt} = k'_2p\alpha + (k_{-4}a + k''_{-4}m)\delta - k_4c^*\gamma \quad (3\text{-}3)$$

$$\frac{d\delta}{dt} = k_3c^*\beta + k_{-5}c^*\varphi - (k_{-3}a + k''_{-3}m + k_5p + k'_5p)\delta \quad (3\text{-}4)$$

$$\frac{d\varepsilon}{dt} = k_4c^*\gamma + k_{-6}c^*\rho - (k_{-4}a + k''_{-4}m + k_6p + k'_6p)\varepsilon \quad (3\text{-}5)$$

$$\frac{d\varphi}{dt} = k_5p\delta - k_{-5}c^*\varphi \quad (3\text{-}6)$$

$$\frac{d\rho}{dt} = k'_5p\delta + k_6p\varepsilon - k_{-6}c^*\rho \quad (3\text{-}7)$$

$$-\frac{dp}{dt} = (k_2 + k'_2)p\alpha - k_{-2}c^*\beta + (k_5 + k'_5)p\delta + (k_6 + k'_6)p\varepsilon - k_{-5}c^*\varphi - k_{-6}c^*\rho \quad (3\text{-}8)$$

$$\frac{da}{dt} = k_1c^*m - k_{-1}a\alpha + k_3c^*\beta - k_{-3}a\delta + k_4c^*\gamma - k_{-4}a\varepsilon \quad (3\text{-}9)$$

$$\frac{dm}{dt} = -k_1a\alpha + k''_{-3}m\delta + k''_{-4}m\varepsilon + k_1mc^* \quad (3\text{-}10)$$

Second, we have two conditions:

Conditions (A):

(i) Stoichiometric relations:

$$-\frac{dp}{dt} = \frac{da}{dt} = -2\frac{dm}{dt} \tag{4}$$

(ii) Stationary-state hypothesis:

$$\frac{d\alpha}{dt}=\frac{d\beta}{dt}=\frac{d\gamma}{dt}=\frac{d\delta}{dt}=\frac{d\varepsilon}{dt}=\frac{d\varphi}{dt}=\frac{d\rho}{dt}=0 \tag{5}$$

From these conditions, we can obtain the solution of each variable as follows:

$$\alpha = k_1k'_6Fmc^*/\Delta_0 \tag{6-1}$$

$$\beta = k_1k_2k'_6m[k''_{-3}m + k_{-3}a + k'_5p]/\Delta_0 \tag{6-2}$$

$$\gamma = k_1[k_2k_3k'_5D + k'_2(D+k'_6)F]mp/k_4\Delta_0 \tag{6-3}$$

$$\delta = k_1k_2k_3k'_6mc^*/\Delta_0 \tag{6-4}$$

$$\varepsilon = k_1(k_2k_3k'_5+k'_2F)mc^*/\Delta_0 \tag{6-5}$$

$$\rho = k_1k_2k_3k_5k'_6mp/k_{-5}\Delta_0 \tag{6-6}$$

$$\varphi = k_1\{k_2k_3k'_5(k_6+k'_6) + k'_2k_6F\}mp/k_{-6}\Delta_0 \tag{6-7}$$

where:

$$\Delta_0 = k_{-1}k'_6Fa + \{k_2k_3k''_{-3}k'_6-k''_{-4}(k_2k_3k'_5 + k'_2F)\}m+(k_2k_3k'_5+k'_2F)k'_6p \tag{6'-1}$$

$$F = k_3k'_5 + k_{-2}k'_5 + k_{-2}(k_{-3}a/p + k''_{-3}m/p) \tag{6'-2}$$

$$D = k_{-4}a/o + k''_{-4}m/p \tag{6'-3}$$

Lastly, the general equation for the rate of the production of methyl alcohol is obtained as follows:

$$\frac{da}{dt} = 2[k_2k_3k'_5 + k'_2F]k_1k'_6mpc^*[k_{-1}k'_6Fa + (k''_{-3}k_2k_3k'_6 - k_2k_3k''_{-4}k'_5 - k'_2k''_{-4}F)m + (k_2k_3k'_5 + k'_2F)k_6'p]^{-1} \tag{7}$$

When further plausible assumptions are added to Eq. 7, a simple form of the kinetic equation is deduced.

Assumptions (B):

$$k''_{-3} \gg k_{-3}$$

$$k''_{-3} \gg k'_5$$

$$k_{-2}k''_{-3} \gg k_3k'_5$$

$$k_2k_3k'_5 \gg k_2'k_{-2}k''_{-3} \quad (\text{or } k_2 \rangle\rangle\rangle k_2') \tag{8'}$$

$$k_{-1}k_{-2} \gg k_2k_3$$

$$k_{-1}k_{-2}k''_{-3}k'_6 \gg k_2k_3k''_{-4}k'_5 \quad (\text{or } k''_{-3}k'_6 \geq k''_{-4}k'_5)$$

$$\frac{da}{dt} = \frac{2k_1k_2k_3k'_5}{k_{-1}k_{-2}k''_{-3}}\frac{p^2c^*}{a} \tag{8}$$

On the other hand, we assume that the effective concentration of the catalyst, c^*, can be estimated from the consideration of the equilibrium of the reaction forming the complex with methyl alcohol:

$$[BF_3\cdot\text{solvent}] + 2CH_3OH \overset{K}{\rightleftarrows} [BF_3\cdot 2CH_3OH] + \text{solvent} \tag{9}$$

where the equilibrium constant, K, is very large,

$$[BF_3\cdot\text{solvent}] = \frac{[BF_3\cdot 2CH_3OH][\text{solvent}]}{K[CH_3OH]^2} \tag{10}$$

$$\therefore \quad c^* = \frac{k_0\cdot c}{a^2} \tag{11}$$

From Eqs. 8 and 11, the kinetic equation 12 is deduced.

The calculated equation:

$$\frac{da}{dt} = \frac{2k_0k_1k_2k_3k'_5}{k_{-1}k_{-2}k''_{-3}}\frac{m^0p^2c^1}{a^3} \tag{12}$$

The experimental equation:

$$\frac{d[\text{methyl alcohol}]}{dt} = \frac{k[\text{methylal}]^0[\text{phenol}]^2[\text{catalyst}]^1}{[\text{methyl alcohol}]^3} \tag{12'}$$

Thus, the kinetic equation obtained by calculations based on the reaction scheme of Fig. 1 is in good agreement with the kinetic equation obtained experimentally. This fact indicates that the reaction scheme of Fig. 1 represents the reactions actually taking place. Therefore, our attempt to elucidate the mechanism of the reaction may be regarded as satisfactory.

The Probable Reaction Paths.—The probable paths of the reaction between phenol and methylal in non-aqueous media are shown in Fig. 2. In Fig. 2, the assumptions used for the deduction of Eq. 8 from Eq. 7 are presented in relation to the behavior of intermediates.[3]

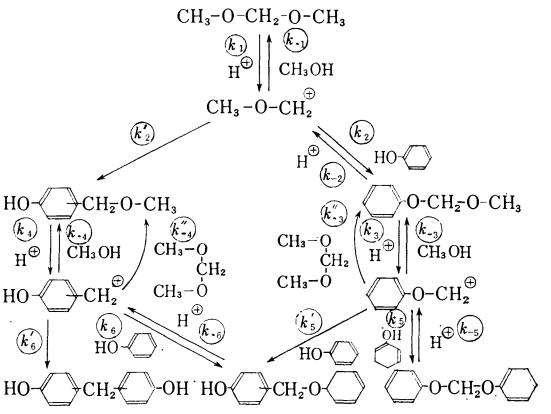

Fig. 2. Reaction scheme.

The assumption, that $k_2 \gg k'_2$ means that the reaction passes mainly through methyl phenyl formal instead of methoxymethylphenol, that is, that the methoxymethyl cation reacts more easily with the phenolic OH group than with the aromatic nuclei of phenol. The assumption that $k''_{-3} \gg k_{-3}$ or that $k_3'' \gg k'_5$ means that the phenoxymethyl cation reacts more easily with methylal than with methyl alcohol or phenol

The assumptions that $k_{-1}/k_2 \gg k_3/k_{-2}$, that $k''_{-3}/k'_5 \geq k''_{-4}/k'_6$ and that $k''_{-3}/k'_5 \gg k_3/k_{-2}$ are connected with the reactivities of the methoxymethyl cation, the phenoxymethyl cation, the oxybenzyl cation and methyl phenyl formal.

The assumptions used in the calculation are plausible and are not contradictory to the actual behavior of the reactants and the intermediates.[3)]

The probable reaction path from methylal to dioxydiphenylmethane in this system is estimated to be as follows:

The Activation of Methylal.—In the first step of the reaction, methylal is activated by the proton to produce methyl alcohol and the methoxymethyl cation in a reversible manner.

The proton is produced by the reaction of the BF_3· solvent with a trace of water in the reaction system; therefore, the affinities of BF_3 toward the solvent, the reactants, and the products have a remarkable effect on the activity of the catalyst. Particularly, the activity of the catalyst depends upon the concentration of methyl alcohol because of the formation of stable complexes from the catalyst and methyl alcohol.

The Reaction of the Methoxymethyl Cation with Phenol.—The methoxymethyl cation readily attacks the oxygen atom of phenol, instead of the benzene ring, to produce methyl phenyl formal in a reversible manner. Consequently, the main path passes through methyl phenyl formal, instead of methoxymethylphenols. The reaction of the methoxymethyl cation with phenol is considerably inhibited by the competing reactions with methyl alcohol.

The Activation of Methyl Phenyl Formal by Proton.—The acidic decomposition of methyl phenyl formal yields the methoxymethyl cation and the phenoxymethyl cation in a reversible manner.

The Reaction of the Phenoxymethyl Cation with Phenol.—Phenoxymethylphenols are produced slowly in the irreversible reaction of phenoxymethyl cations with the nuclei of phenol; this reaction may be the rate-determining step of this reaction system.

At the same time, the phenoxymethyl cation easily attacks the oxygen atom of methylal to reproduce the methoxymethyl cation and methyl phenyl formal; accordingly, methylal inhibits the reaction rate in this reaction step. Though it was expected that the phenoxymethyl cation would rapidly attack the oxygen atom of phenol, not even a trace of diphenyl formal was detected in the reaction system.

Phenoxymethylphenols change in the presence of proton to dioxydiphenylmethane, passing through the oxybenzyl cation in a similar manner; at the same time, methoxymethylphenols are formed as by-products.

The Reaction Rate at Higher Conversions.—As has been mentioned above, the reaction mechanism can be explained when the conversion is low (up to 30%). If the B asumptions and Eq. 8′ are changed slightly, then the calculated equation, Eq. 8, is modified as follows:

Modified assumptions C:

$$k''_{-3} \gg k_{-3}$$
$$k_3'' \gg k_6'$$
$$k_{-2}k''_{-3} \gg k_3k'_5$$
$$k_2k_3k'_5 \gg k'_2k_{-2}k''_{-3} \quad (\text{or } k_2 \rangle\rangle\rangle k'_2) \qquad (13')$$
$$k''_{-3}k'_6 \gg k''_{-4}k'_5$$
$$k_{-1}k_{-2} \geq k_2k_3$$

Modified calculated equation:

$$\frac{da}{dt} = \frac{2k_1k_2k_3k'_5 \cdot pc}{(k_{-1}k_{-2}k''_{-3} \cdot a/p + k_2k_3k''_{-3})a^2} \qquad (13)$$

Experimental equation at higher conversions[2)]:

$$\frac{d[\text{methyl alcohol}]}{dt} = \frac{k[\text{phenol}]^1[\text{methylal}]^0[\text{catalyst}]^1}{[\text{methyl alcohol}]^{2.5}} \qquad (14)$$

The calculated equation, Eq. 13, may be almost equal to the experimental equation, Eq. 14. Equations 13 and 14 are applicable only for the systems of a high conversion.

It seems probable that there are few differences between Eqs. 12 and 13 with respect to the mathematical characterization of the kinetic system, while the stoichiometric relations, Eq. 4, and the stationary state hypothesis, Eq. 5, may not be used so exactly in systems of a higher conversion.

Summary

By the mathematical calculation of the reaction system, a kinetic equation has been deduced, and it has been found to represent satisfactorily the experimental findings of the phenol-formaldehyde reaction in non-aqueous media.

The reaction mechanism has then been elucidated from both the experimental and the mathematical points of view.

The most important difference between the aqueous and non-aqueous media is the contribution of formals as reactive intermediates.

Moreover, several interesting information regarding the effects of the solvent or the catalyst on the reaction mechanism have been obtained.

The author is indebted to Professor Hiromu Murata of the Faculty of Science of Hiroshima University for his helpful discussions and encouragement throughout the work. He also wishes to express his gratitude to Dr. Keiji Oshima, Managing Director of the Sumitomo Bakelite Co., Ltd., and Director of the Central Research Laboratory of the same company, for permission to publish this paper, and to Dr. Ryuzo Nakatsuka and Mr. Mitsuo Niwa of this Laboratory for their valuable assistance.

BULLETIN OF THE CHEMICAL SOCIETY OF JAPAN VOL. 39 1036—1039 (1966)

The Conversion of Cellulose into Soluble Glucose Polymers in a Sulfur Dioxide Solution of Sulfur Trioxide

By Yoshio SAKAI

Faculty of Agriculture, Tokyo University of Education, Komaba, Meguro-ku, Tokyo

(Received October 18, 1965)

The conversion of cellulose into soluble glucose polymers was shown to be composed of a set of irreversible reactions in series: $A \xrightarrow{k_1} B \xrightarrow{k_2} C$, where A is cellulose; B, a soluble glucose polymer, and C, the decomposition product, which does not give reducing sugar under further hydrolysis by dilute acid. The first-order rate constants, k_1 (hr^{-1}) and k_2 (hr^{-1}), were given in 0.32 to 3.3% sulfur dioxide solutions of sulfur trioxide:

$$k_1 = 2.64 \times 10^{11} C^{1.63} \exp[-16700/(RT)] \quad \text{(for 0—50°C)},$$

and

$$k_2 = 8.99 \times 10^{15} C^{1.63} \exp[-24500/(RT)] \quad \text{(for 25—50°C)}.$$

From k_1 and k_2, the sulfur trioxide concentration, C, and temperature, T, the maximum yields of the soluble glucose polymer and the time required to attain a maximum yield were obtained. It was shown that the application of the technique to wood saccharification is possible.

In a sulfur dioxide solution of sulfur trioxide, cellulose reacts with sulfur trioxide to form water-soluble cellulose sulfate.[1] The product and the cellulose residue are insoluble in the solution. This is interesting from the viewpoint of wood saccharification. After the treatment of wood in a liquid sulfur dioxide solution of sulfur trioxide, the insoluble product can be easily separated from the solution. The product is water-soluble and ready for hydrolysis in a dilute acid. The recovered sulfur dioxide solution, fortified by sulfur trioxide, is readily adaptable for repeated use. If this reaction takes the place of the mainhydrolysis in wood saccharification, it is possible to regard it as a new process which can be carried out with a minimum consumption of sulfuric acid.

Materials and Methods

Materials.—*Cellulose.*—Filter paper (Tôyô Roshi, No. 2) ground to small flakes with a grater was used.

Wood.—Sawdust of Yachidamo wood (*Fraxinus mandshurica*, Rupr.) passed through a 20-mesh sieve was used. Before use the sawdust was prehydrolyzed in 10% sulfuric acid at 100°C for 3 hr., washed with water, and dried at 105°C. The prehydrolyzed wood contained 69.9% potential reducing sugar, 1.7% potential pentose, and 32.4% lignin.

Sulfur Trioxide.—An asbestos-like sulfur trioxide was redistilled before use.

Sulfur Dioxide.—Liquid sulfur dioxide distilled from the gas cylinder was used.

Procedure.—The pressure glass vessels[2] were used. The bottle containing a cellulose and sulfur dioxide solution of sulfur trioxide was shaken in a water-bath at different temperatures for various periods. After the reaction, the product was filtered off and the residue was washed five times with sulfur dioxide. The sulfur dioxide adsorbed on the washed product was stripped off overnight by suction. The water-insoluble part was then centrifuged and washed with water. The reducing sugar and the potential reducing sugar in the soluble and the insoluble parts were determined. The soluble part was easy to hydrolyze in dilute acid. The insoluble part was, however, as difficult to as cellulose.

Analytical Methods.—The reducing sugar was determined by Somogyi's new reagent.[3]

The potential reducing sugar in the insoluble part was determined by the method of Saeman, Bubl and Harris.[4] From the result, the amount of unreacted cellulose was obtained.

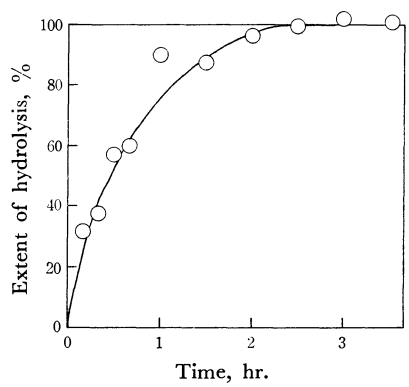

Fig. 1. Hydrolysis of soluble glucose polymer obtained in SO_2 solution of SO_3, in 2.5% HCl at 100°C.

1) R. Asami and N. Tokura, *J. Chem. Soc. Japan, Ind. Chem. Sect.* (*Kogyo Kagaku Zasshi*), **62**, 1953 (1959).

2) M. Amagasa and H. Yamaguchi, *Tohoku Daigaku Hisuiyoeki Kagaku Kenkyusho Hokoku* (*Bull. Chem. Research Inst. Non-Aqueous Soln., Tohoku Univ.*), **1**, 181 (1951); **2**, 75, 179 (1952).

3) M. Somogyi, *J. Biol. Chem.*, **160**, 16 (1945).

4) J. F. Saeman, J. L. Bubl and E. E. Harris, *Ind. Eng. Chem., Anal. Ed.*, **17**, 35 (1945).

The determination of the potential reducing sugar in the soluble part was carried out by Somogyi's method after hydrolysis in 2.5% hydrochloric acid at 100°C for 3 hr. (Fig. 1). From the result, the amount of the soluble glucose polymer was obtained.

In this paper, the soluble glucose polymer and the unreacted and initial celluloses are expressed in terms of the potential reducing sugar.

Results and Discussion

Reaction Mechanism.—After treating cellulose in a liquid sulfur dioxide solution of sulfur trioxide for different times at 0, 25 and 50°C, the unreacted cellulose was determined. The extent of cellulose degradation was indicated by the ratio of the residual cellulose to the initial cellulose (Fig. 2). Figure 2 shows the progress of the reaction according to the equation of the first-order reaction, with reference to cellulose degradation. At the same time, the produced soluble glucose polymer was also determined as is shown in Fig. 3. The soluble glucose polymer rose to a maximum and then fell. The amount of decomposition product (the difference between the initial cellulose and the sum of the soluble and insoluble glucose polymers) rose continuously (Fig. 3). These findings suggest that the reaction belongs to a set of irreversible reactions in series:

$$A \xrightarrow{k_1} B \xrightarrow{k_2} C \qquad (1)$$

where A is cellulose; B, the soluble glucose polymer; C, the decomposition product which does not give reducing sugar under further hydrolysis by dilute acid; k_1, the first-order rate constant which governs the A→B reaction, and k_2, the constant for B→C. The amounts of A and B at any time, t, are given for such a system by:

$$c_A = a \exp(-k_1 t) \qquad (2)$$

$$c_B = a k_1 [\exp(-k_1 t) - \exp(-k_2 t)]/(k_2 - k_1) \qquad (3)$$

where a is the initial amount of cellulose and c_A and c_B are the amounts of A and B at time t. Equation 2 fits in with the present data, as has been described above (Fig. 2). The values of k_1 found at 30°C in a 2.2% sulfur trioxide concentration and at 50°C in a 1.1% concentration were 0.375 and 1.88 hr^{-1}. Using these k_1 values, the reaction times, t, and the corresponding amounts of the soluble glucose polymer produced, c_B, k_2 can be calculated according to Eq. 3 to be 0.0327 hr^{-1} at 30°C in 1.1% sulfur trioxide and 0.335 hr^{-1} at 50°C in 2.2% sulfur trioxide. The c_B-time curves calculated from k_1 and k_2 agreed with the observed data, as is shown in Fig. 3. These facts prove that, with reference to cellulose, the present reaction progresses according to the mechanism described by the successive first-order reactions 1.

The Rate Constant of Cellulose Degradation.—Because it was previously found that the degradation of cellulose took place as a first-order reaction, the rate constants, k_1, were determined, using Eq. 2 and the c_A/a values observed in sulfur trioxide concentrations ranging from 0.32 to 3.3% at 0, 25, and 50°C for various times. The k_1's (hr^{-1}) are shown in Table I. When the logarithm of the reaction rate constant was plotted against the logarithm of the percentage concentration of sulfur trioxide in a liquid sulfur dioxide solution, the parallel straight lines were obtained at intervals depending on the temperature (Fig. 4). The slope of the lines is 1.63. The plotting of the logarithm of k_1 at a 1% sulfur trioxide concentration (Fig. 4) against the reciprocal of the absolute temperature

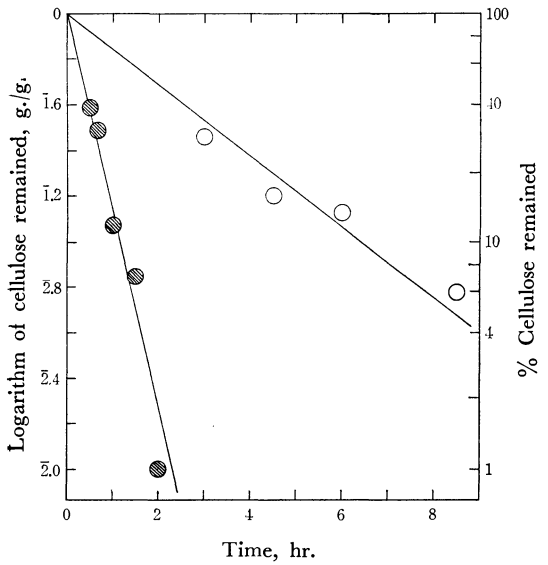

Fig. 2. Rates of cellulose degradation in SO_2 solution of SO_3.
▨ 50°C, SO_3 concn.: 1.1%, SO_3/cellulose: 1.1
○ 25°C, SO_3 concn.: 2.2%, SO_3/cellulose: 1.5

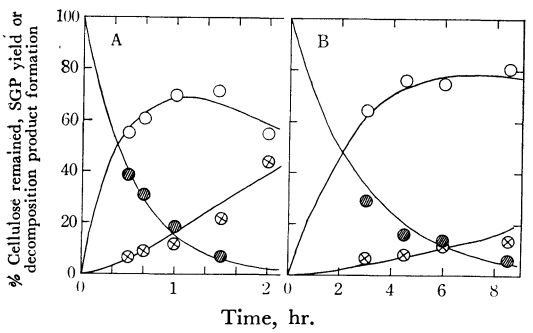

Fig. 3. Cellulose degradation to soluble glucose polymer (SGP) and simultaneous decomposition of SGP.
A 50°C, SO_3 concn.: 1.1%, SO_3/cellulose: 1.1
B 25°C, SO_3 concn.: 2.2%, SO_3/cellulose: 1.5
▨ Cellulose remained, g. PRS/100 g. cellulose
○ SGP yield, g. PRS/100 g. cellulose
⊗ Decomposition product formation, g. loss of PRS/100 g. of cellulose

Table I. First-order reaction rate constants of cellulose degradation (k_1) and soluble glucose polymer destruction (k_2)

Temp. °C	SO_3 concn. %	SO_3/cellulose g./g.	k_1 Obsd. hr^{-1}	k_1 Calcd. hr^{-1}	k_2 Obsd. hr^{-1}	k_2 Calcd. hr^{-1}
0	0.44	0.17	0.00281	0.00304		
	0.60	0.17	0.00674	0.00502		
	1.22	0.55	0.0345	0.0159		
	1.90	0.84	0.0272	0.0329		
	2.07	1.11	0.0672	0.0378		
	2.50	0.71	0.0341	0.0515		
25	0.32	0.64	0.0762	0.0225	0.00173	0.00161
	0.50	0.49	0.0400	0.0466	0.00394	0.00334
	0.50	1.10	0.124	0.0466	0.00491	0.00334
	0.93	1.00	0.102	0.128	0.00695	0.00917
	2.20	1.50	0.412	0.521	0.0550	0.0373
	2.20	1.50	0.403	0.521	0.0348	0.0373
	2.20	1.50	0.333	0.521	0.0373	0.0373
	2.20	1.50	0.332	0.521	0.0260	0.0373
	2.96	1.87	0.768	0.844	0.0250	0.0578
	3.30	2.26	1.00	1.01		
50	0.45	0.80	0.810	0.347	0.0508	0.0593
	0.48	0.49	0.439	0.388	0.0275	0.0661
	0.91	0.53	0.487	1.10	0.128	0.188
	0.92	0.53	0.532	1.12	0.203	0.191
	0.97	1.42	1.42	1.22	0.435	0.208
	1.05	1.10	1.88	1.39	0.388	0.237
	1.05	1.10	1.76	1.39	0.351	0.237
	1.05	1.10	2.24	1.39	0.360	0.237
	1.05	1.10	1.72	1.39	0.243	0.237
	1.05	1.10	2.30	1.39	0.237	0.237
	1.20	1.64	1.82	1.72	0.487	0.293
	1.28	0.63	1.16	1.94		

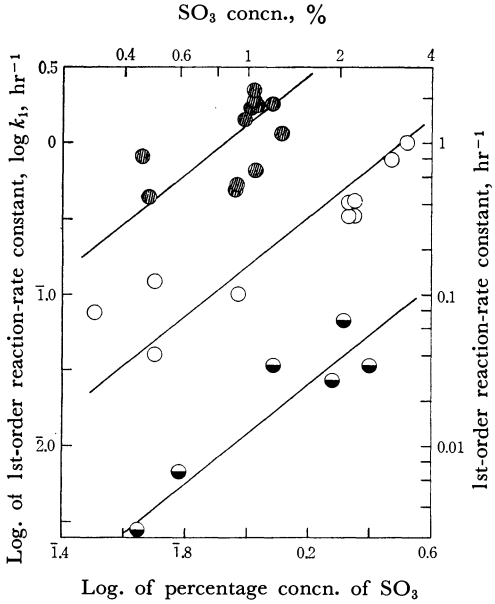

Fig. 4. First-order reaction-rate constants of cellulose degradation in various concentrations of SO_3 solution of SO_3 at 0, 25, and 50°C.
◍ 50°C, ○ 25°C, ◒ 0°C

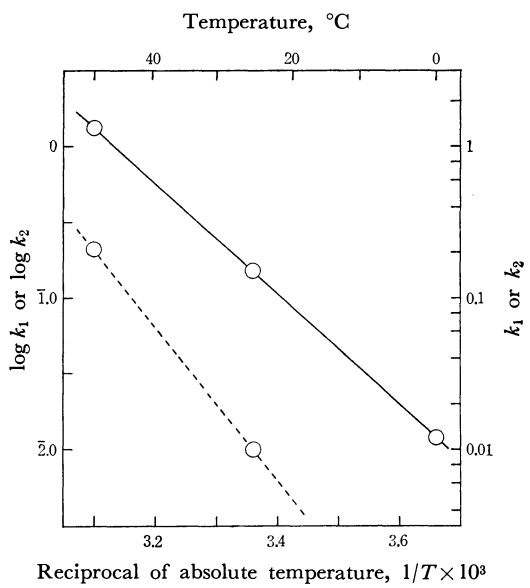

Fig. 5. First-order reaction-rate constants of celulose degradation (——) and soluble glucose polymer decomposition (----) in 1% SO_3 solution of SO_3 at different temperatures.

gives the straight line shown in Fig. 5. The slope of the line is −3650°K. Using these two values, the following experimental equation, which fits the observed k_1 (hr^{-1}) values (Table I), was obtained:

$$\log k_1 = 11.4215 + 1.63 \log C - 3650(1/T)$$

or $$k_1 = 2.64 \times 10^{11} C^{1.63} \exp[-16700/(\mathbf{R}T)] \quad (4)$$

where C is the sulfur trioxide concentration in liquid sulfur dioxide; T, the absolute temperature (273—323°K), and $\boldsymbol{R}$, the gas constant (cal./deg.).

The Rate Constant of the Decomposition of the Soluble Glucose Polymer to Substances Other than Reducing Sugar.—The soluble glucose polymer yield, c_B, at the time t and the corresponding k_1 (hr^{-1}) value gave the k_2 (hr^{-1})

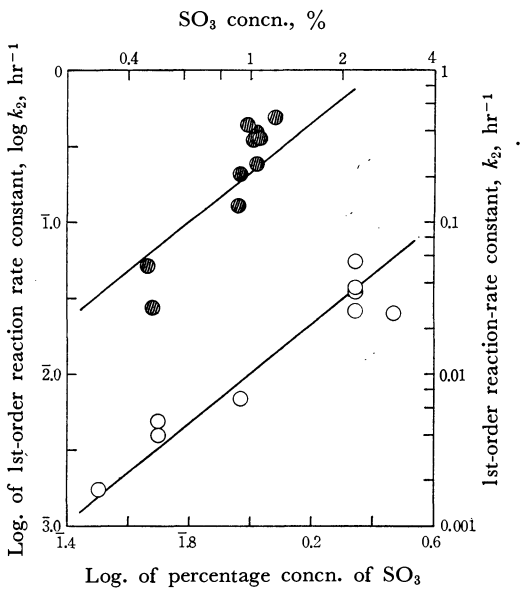

Fig. 6. First-order reaction-rate constants of soluble glucose polymer decomposition in various concentrations of SO_2 solution of SO_3 at 25 and 50°C.
▨ 50°C, ○ 25°C

value according to Eq. 3. The values are shown in Table I. The values at 0°C were so small that they could be taken as zero. The equation describing k_2 (hr^{-1}) as a function of the temperature and of the sulfur trioxide concentration was obtained in the same manner as the equation describing k_1 (Figs. 5 and 6):

$$\log k_2 = 15.953 + 1.63 \log C - 5380(1/T)$$

or $$k_2 = 8.99 \times 10^{15} C^{1.63} \exp[-24600/(\mathbf{R}T)] \quad (5)$$

Maximum Yield.—The yield of the soluble glucose polymer at the maximum is given by:

$$c_B = K^{1/(1-K)}$$

where $K = k_1/k_2 = 2.94 \times 10^{-5} \exp(3990/T)$ (6)

For example, the maximum yields are 84 and 72% at 25 and 50°C. At a lower temperature, such as 0°C, the yield must be higher than that given by the equation, because scarcely any sugar decomposition occured.

The yield of the soluble glucose polymer reaches a maximum at the time, t_m (hr.), given by Eq. 7.

$$t_m = 2.303(\log k_1 - \log k_2)/(k_1 - k_2) \quad (7)$$

where k_1 and k_2 are given by Eqs. 4 and 5. For example, a reaction time of 1.7 hr. is necessary to obtain the maximum yield at 50°C, and 6.6 hr, at 25°C.

Application to Wood Saccharification.—The prehydrolyzed sawdust of hardwood was treated by a sulfur dioxide solution of sulfur trioxide. The results are shown in Fig. 7. Although a portion of lignin was dissolved in the solution, it precipitated again after the dilute acid hydrolysis.

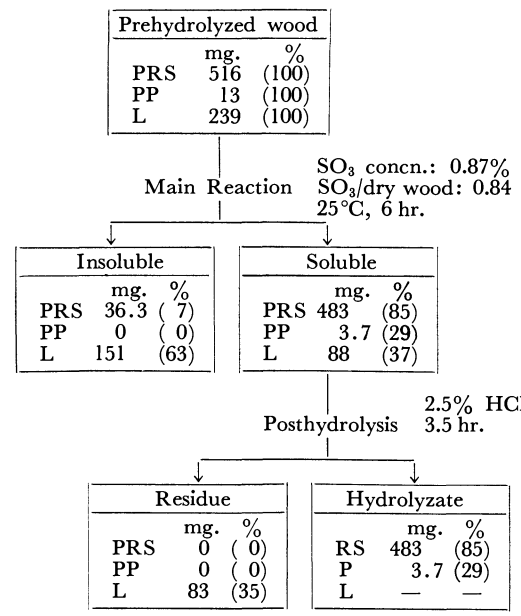

Fig. 7. Saccharification of prehydrolyzed hardwood using sulfur dioxide solution of sulfur trioxide.
PRS: potential reducing sugar, RS: reducing sugar, PP: potential pentose, P: pentose, L: lignin

The author thanks Professor Tatsuyoshi Kobayashi for his guidance and Mr. Yoshi Kamiyama for his assistance.

BULLETIN OF THE CHEMICAL SOCIETY OF JAPAN VOL. 39 1040—1042 (1966)

The Phosphorylation of Alcohols by the Reaction of Monobromocyanoacetamide with Monobenzyl Phosphite or Inorganic Phosphorous Acid

By Teisuke OBATA, Masaaki UEKI and Teruaki MUKAIYAMA

Laboratory of Organic Chemistry, Tokyo Institute of Technology, Ookayama, Tokyo

(Received October 19, 1965)

This paper describes a successful method of preparing monoalkyl phosphates by the reaction of monobromocyanoacetamide with monobenzyl phosphite or inorganic phosphorous acid in the presence of alcohols. When equimolar amounts of monobromocyanoacetamide and either of the above-mentioned phosphorus compounds in alcohols were heated at about 100°C, the corresponding monoalkyl dihydrogen phosphates were obtained as anilinium salts in fairly good yields, together with cyanoacetamide and benzyl bromide or hydrogen bromide. The reaction can be interpreted in terms of a mechanism in which the initially-formed enol-phosphonium salts of cyanoacetamide are easily transformed to the second phosphonium salts by the action of the alcohols present from the salts, alkyl dihydrogen phosphates are produced.

A previous paper[1] presented a successful method of oxidizing various triesters of phosphorous acid or phosphines to triesters of phosphoric acid or phosphine oxides by means of monobromocyanoacetamide, along with either benzyl or allyl alcohol. In a similar way, dialkyl phosphates were prepared from the corresponding dialkyl phosphites.[2] The reaction was then further extended to the synthesis of monoalkyl dihydrogen phosphates (IV) by the oxidation of dibenzyl phosphite (I) with monobromocyanoacetamide (II) in alcohols and by subsequent catalytic debenzylation.[2]

$$\underset{\text{(I)}}{(C_6H_5CH_2O)_2\overset{O}{\overset{\|}{P}}H} + \underset{\text{(II)}}{NCCHBrCONH_2} \xrightarrow{ROH} \underset{\text{(III)}}{C_6H_5CH_2O-\overset{O}{\overset{\|}{P}}\begin{matrix}OR\\OH\end{matrix}}$$

$$\text{III} \xrightarrow{H_2/PdO} \underset{\text{(IV)}}{RO-\overset{O}{\overset{\|}{P}}\begin{matrix}OH\\OH\end{matrix}} + C_6H_5CH_3 \qquad (1)$$

In the present paper, a similar type of the phosphorylation of alcohols was attempted, employing monobenzyl phosphite or inorganic phosphorous acid and monobromocyanoacetamide.

First the reaction of monobenzyl phosphite with monobromocyanoacetamide in the presence of an equimolar amount of benzyl alcohol was attempted; a 27% yield of monobenzyl dihydrogen phosphate was thus obtained.

The result can be explained in terms of the following mechanism involving a quaternary phosphonium salt (VI), which is similar to that shown in the preceding paper[2]:

$$C_6H_5CH_2O-\overset{O}{\overset{\|}{P}}\begin{matrix}H\\OH\end{matrix} \rightleftarrows C_6H_5CH_2O-P\begin{matrix}OH\\OH\end{matrix}$$

$$\xrightarrow{NCCHBrCONH_2} \underset{\text{(V)}}{\left[\begin{matrix}NCCH{=}C{-}NH_2\\ \vdots\\ C_6H_5CH_2O\end{matrix}\!\!>\!\overset{+}{P}\!<\!\begin{matrix}OH\\OH\end{matrix}\right)Br^-\Big]}$$

$$V + ROH \longrightarrow \underset{\text{(VI)}}{\left[\left(\begin{matrix}C_6H_5CH_2O\\HO\end{matrix}\!\!>\!\overset{+}{P}\!<\!\begin{matrix}OH\\OR\end{matrix}\right)Br^-\right]}$$

$$\longrightarrow RO-\overset{O}{\overset{\|}{P}}\begin{matrix}OH\\OH\end{matrix} + C_6H_5CH_2Br \qquad (2)$$

In order to elucidate the proposed mechanism and examine the possibility of its application to the phosphorylation of alcohols, the reaction of ethanol with monobenzyl phosphite and monobromocyanoacetamide was attempted. In this case, it was expected that monoethyl dihydrogen phosphate would primarily be formed, since benzyl bromide, rather than the other alkyl or hydrogen bromide, is preferentially eliminated from the proposed quaternary phosphonium salt (VI, R= C_2H_5); thus, the phosphorylation of alcohols would be successful, and alkyl dihydrogen phosphates could be synthesized by a one-step procedure.

Indeed, when a mixture of monobenzyl phosphite and monobromocyanoacetamide in dry ethanol was refluxed for two hours, monoethyl phosphate and benzyl bromide were obtained in 46% and 63% yields respectively.

Similarly, *n*-propyl, isopropyl and *n*-butyl dihydrogen phosphates were obtained as anilinium salts when the phosphite and monobromocyanoacetamide were treated in the corresponding alcohols.

However, this procedure is not applicable to the phosphorylation of long-chain solid alcohols or those available in only small amounts, because the

1) T. Mukaiyama, O. Mitsunobu and T. Obata, *J. Org. Chem.*, **30**, 101 (1965).
2) O. Mitsunobu, T. Obata and T. Mukaiyama, ibid., **30**, 1071 (1965).

reaction should be carried out in a large excess of alcohol (usually in alcohol solvents); probably, the initially-formed quaternary phosphonium salt (V) is very unstable and the spontaneous decomposition takes place before it reacts with alcohols, giving several kinds of phosphorus compounds, some of which are not well characterized by paper chromatography.

Next, this type of reaction was further extended to a selective phosphorylation of alcohols, starting from inorganic phosphorous acid.

The reaction proceeds through the formation of quaternary phosphonium salt (VII), which is similar in structure to V. Therefore, the subsequent elimination of hydrogen bromide from VIII will result in the formation of alkyl dihydrogen phosphates.

When an equimolar amount of phosphorous acid and monobromocyanoacetamide in ethanol were refluxed for two hours, monoethyl dihydrogen phosphate was obtained in a 78% yield as chromatographically-pure anilinium salt.

Similarly, methyl, *n*-propyl, and *n*-butyl dihydrogen phosphates were obtained from the corresponding alcohols as the anilinium salts in 87, 82 and 64% yields respectively (see Table II).

As is the case with dialkyl or monoalkyl phosphite, inorganic phosphorous acid is expected to react with monobromocyanoacetamide in its tautomeric trivalent structure, giving enol-phos phonium salt of cyanoacetamide (VII), which is in turn transformed to the second quaternary phosphonium salt (VIII) by the action of the alcohols present.

This assumption was confirmed by the following experiments. Phosphoric acid was exclusively produced when water or benzyl alcohol was treated with monobromocyanoacetamide and phosphorous acid; in either case, hydrogen bromide or benzyl bromide was also detected.

$$(HO)_2\overset{\overset{O}{\|}}{P}H \rightleftarrows (HO)_3P + NCCHBrCONH_2$$

$$\longrightarrow \left[\begin{pmatrix} NCCH{=}C{-}NH_2 \\ | \\ HO\diagdown \\ HO\diagup P\diagdown O \\ \quad\quad\diagup OH \\ + \end{pmatrix} Br^- \right]$$

(VII)

$$VIII + ROH \longrightarrow \left[\begin{pmatrix} HO\diagdown \\ RO\diagup P\diagdown OH \\ \quad\quad\diagup OH \\ + \end{pmatrix} Br^- \right]$$

(VIII)

$$\longrightarrow RO{-}\overset{\overset{O}{\|}}{P}\begin{matrix} OH \\ \diagup \\ OH \end{matrix} + HBr \qquad (3)$$

(R=H or alkyl)

Monoalkyl phosphates could not be isolated as pure anilinium salts when an equimolar amount of alcohol was to be phosphorylated by this method; at the same time, several uncharacterized phosphorus compounds were also produced, thus making the purification much more difficult.

Experimental

Materials.—Monobromocyanoacetamide[3] and monobenzyl phosphite[4] were prepared by the method given in the literature. Inorganic phosphorous acid was obtained from a commercial source and dried over phosphorus pentoxide under a high vacuum. The alcohols and solvents used were purified by ordinary procedures. Phosphorus compounds were identified by paper chromatography; solvent system: *n*-propyl alcohol : conc. NH_4OH : H_2O=6 : 3 : 1.

The Oxidation of Monobenzyl Phosphite by Means of Monobromocyanoacetamide and Benzyl Alcohol.—A solution of equimolar amounts of monobenzyl phosphite (1.54 g., 0.01 mol.), monobromocyanoacetamide (1.63 g., 0.01 mol.) and benzyl alcohol (1.08 g., 0.01 mol.) in 20 ml. of dry peroxide-free tetrahydrofuran was refluxed for 2 hr. under a nitrogen atmosphere. After the solvent had then been removed under reduced pressure, 10 ml. of dry ether was added to separate the cyanoacetamide (0.57 g., 68%). The filtrate was concentrated and distilled to give benzyl bromide (b. p. 32—36°C/0.15 mmHg; 0.93 g., 54%). The oily residue was dissolved in 99% ethanol (10 ml.), and aniline (4 g., 0.04 mol.) was added. Precipitated anilinium salt of monobenzyl phosphate was filtered, washed twice with 99% ethanol (2 ml.) and dried over phosphorus pentoxide in a desiccator (0.89 g., 24%). Paper chromatography showed one spot (R_f: 0.57); this was identical with that of an authentic specimen. One recrystallization from 95% ethanol gave an analytical sample, m. p. 149—152°C.

Found: N, 7.56, Calcd. for $C_{19}H_{18}N_2O_4P$: N, 7.48%.

The Phosphorylation of Ethanol by the Reaction of Monobenzyl Phosphite and Monobromocyanoacetamide.—A solution of equimolar amounts of monobenzyl phosphite (1.54 g., 0.01 mol.) and monobromocyanoacetamide (1.63 g., 0.01 mol.) in absolute ethanol (10 ml.) was refluxed for an hour under a nitrogen atmosphere. The reaction mixture was concentrated and 10 ml. of chloroform was added to separate the cyanoacetamide (0.78 g., 92%). From the filtrate, benzyl bromide (b. p. 46—47°C/2 mmHg, 1.08 g., 63%) was obtained by fractionation. The residue was dissolved in 99% ethanol (10 ml.), and aniline (1.7 g.) was added. After the mixture had been cooled to −20°C, anilinium salt of monoethyl phosphate (m. p. 132—149°C, 1.02 g., 46%) was filtered. One recrystallization from acetonitrile-water gave an analytically-pure sample (m. p. 160—164°C; lit.[2] 164—165°C).

Found: N, 6.30, Calcd. for $C_8H_{14}NO_4P$: N, 6.39%.

The R_f-value shown by paper chromatography was identical with that of an authentic specimen.[2]

Similarly, the other alkyl phosphates were prepared and characterized by comparison with authentic samples[2] (see Table I).

The Phosphorylation of Ethanol by the Reaction of Phosphorous Acid and Monobromocyanoacetamide.—Equimolar amounts of phosphorous acid (0.82 g., 0.01 mol.) and monobromocyanoacetamide (1.63 g., 0.01 mol.) were dissolved in absolute ethanol

3) T. Hata and T. Mukaiyama, This Bulletin, **35**, 1106(1962).
4) J. Baddiley, V. M. Clark, J. J. Michalshi and A. R. Todd, *J. Chem. Soc.*, **1949**, 815.

TABLE I. PHOSPHORYLATION OF ALCOHOLS BY MEANS OF MONOBENZYL PHOSPHITE AND MONOBROMOCYANOACETAMIDE

Alcohol	Product: Phosphate (anilinium salt)	Yield %	M. p. °C	Anal. (N, %) Found	Anal. (N, %) Calcd.	R_f*
ROH	$RO-P(=O)(OH)(O^-)$					
C_2H_5OH	$C_2H_5O-P(=O)(OH)(O^-)$	46	160—165	6.30	6.39	0.37
n-C_3H_7OH	*n*-$C_3H_7O-P(=O)(OH)(O^-)$	49	142—145	6.13	6.01	0.44
iso-C_3H_7OH	*iso*-$C_3H_7O-P(=O)(OH)(O^-)$	68	158—162	6.18	6.01	0.42
n-C_4H_9OH	*n*-$C_4H_9O-P(=O)(OH)(O^-)$	50	144—147	5.74	5.67	0.50

* Solvent system : *n*-propyl alcohol : conc. NH_4OH : H_2O=6 : 3 : 1.

TABLE II. PHOSPHORYLATION OF ALCOHOLS BY MEANS OF INORGANIC PHOSPHOROUS ACID AND MONOBROMOCYANOACETAMIDE

Alcohol	Product: Phosphate (anilinium salt)	Yield %	M. p. °C	Anal. (N, %) Found	Anal. (N, %) Calcd.
ROH	$RO-P(=O)(OH)(O^-)$				
CH_3OH	$CH_3O-P(=O)(OH)(O^-)$	87	163—165	6.69	6.80
C_2H_5OH	$C_2H_5O-P(=O)(OH)(O^-)$	82	162—164	6.37	6.39
n-C_3H_7OH	*n*-$C_3H_7O-P(=O)(OH)(O^-)$	76	148—150	6.23	6.02
n-C_4H_9OH	*n*-$C_4H_9O-P(=O)(OH)(O^-)$	64*	145—152	6.03	5.67

* A trace of phosphorous acid is contaminated in the product.

ml.), and then the mixture was refluxed for 2 hr. under a nitrogen atmosphere. After the excess ethanol had been evaporated, cyanoacetamide (0.79 g., 92%) was filtered out. The filtrate was dissolved in 99% ethanol (5 ml.) and then aniline (2 ml.) was added. After the mixture had stood for 30 min., monoethyl dihydrogen phosphate (1.67 g., 82%) was filtered out. Recrystallization from 15 ml. of 95% ethanol gave an analytical sample (m. p. 162—164°C; 1.15 g.; lit.[2] 164—165°C).

Found: N, 6.37. Calcd. for $C_8H_{14}NO_4P$: N, 6.39%. Paper chromatography showed one spot, R_f: 0.37 (lit.[2] 0.36—0.37).

The other alkyl dihydrogen phosphates were prepared by a similar method. The yields and the physical constants are summarized in Table II.

The Reaction of Phosphorous Acid with Monobromocyanoacetamide in the Presence of Water or Benzyl Alcohol.—A solution of equimolar amounts of phosphorous acid (0.41 g.) and monobromocyanoacetamide (0.82 g.) in acetonitrile (15 ml.) and water (2 ml.) was refluxed for an hour. The paper chromatography of the reaction mixture showed only one yellow spot of inorganic phosphoric acid (R_f: 0.17—0.18); the strong blue spot of inorganic phosphorous acid (R_f: 0.28) had completely disappeared. This shows that the phosphorylation of water or the oxidation of phosphorous acid has taken place. The same result was also observed when benzyl alcohol was employed in place of water in the above reaction. In this case, a good deal of benzyl bromide was formed; it was characterized by distillation and by its lachrymatory odor.

The authors wish to express their hearty thanks to Dr. Oyo Mitsunobu for his helpful suggestions and to Miss Keiko Nakamura for her microanalysis.

BULLETIN OF THE CHEMICAL SOCIETY OF JAPAN VOL. 39 1043—1048 (1966)

The Polarographic Investigation on the Reaction between Chromium(II)-ethylenediaminetetraacetate and Nitrate Ions

By Nobuyuki TANAKA and Tasuku ITO

Department of Chemistry, Faculty of Science, Tohoku University, Sendai

(Received October 19, 1965)

The effect of nitrate ions on the polarographic waves of ethylenediaminetetraacetatoaquochromate(III) ions has been studied in acetate buffer solutions and acid potassium chloride solutions. Nitrate ions are chemically reduced in the vicinity of the mercury drop of the electrode by chromium(II)-EDTA complexes which are formed by the electroreduction of chromium(III)-EDTA complexes. The chromium(III)-EDTA complexes thus formed are reduced again at the DME and the intermediate products of nitrate ions are reduced further chemically with chromium(II)-EDTA complexes or electrochemically, resulting in the enhancement of the current. The nature of the limiting current is investigated and compared with that predicted from the theoretical treatment. The reaction between chromium(II)-EDTA and nitrate ions has also been investigated in acetate buffer solutions and its rate constant, 35 l. mol^{-1} sec^{-1} at nearly 0°C, $\mu=0.1$, has been compared with 30 l. mol^{-1} sec^{-1}, the value obtained from the polarographic catalytic current under almost the same condition.

Catalytic poloargraphic currents due to the presence of nitrate have been observed in several electrolytic reductions. The effect of nitrate ions on the reduction waves of uranyl ions,[1-5] molybdate ions[6-8] and chromium complexes[9-11] has been reported. In the last case, it has been known that the reduction of chromium complexes with glycine,[9] alanine[10] thiourea[11] and oxalate give peculiar maximum waves in the presence of nitrate ions. This was attributed to the induced reaction of nitrate ions.

In addition, another kind of polarographic catalytic wave due to nitrate ions was found in the course of a systematic investigation of the chromium complexes in this laboratory. It was considered as due to the reaction between nitrate ions and chromium(II)-EDTA complexes taking place at the electrode surface, the latter being formed by the electroreduction of ethylenediaminetetraacetatoaquochromate(III) ions at the electrode.

In this communication the polarographic investigation on this reaction taking place in the solution and at the electrode surface is presented; the stoichiometry and the rate constant of the reaction are determined and the reaction mechanisms are discussed.

Experimental

Hydrogen ethylenediaminetetraacetatoaquochromate(III), H[Cr(H_2O)edta], was prepared according to the procedure of Hamm.[12] It was identified by the measurement of the absorption spectra and by the determination of hydrogen, nitrogen and carbon contents.

Found: C, 33.05; N, 7.82; H, 4.26. Calcd. for H[Cr(H_2O)edta]: C, 33.40; N, 7.80; H, 4.21%.

All the chemicals used were of a guaranteed reagent grade.

Current-potential curves were obtained with a pen-recording polarograph, Yanagimoto Galvarecorder Model GR-103, with an automatic potential scanner. The same polarograph but without an automatic potential scanner was used for the automatic recording of limiting current-time curves of the reactions in the solution. The dropping mercury electrode (DME) used had a rate of mercury flow, m, of 1.65_7 mg./sec. and a drop time, t_d, of 5.22 sec., when measured in an air-free solution containing 0.1 M acetate buffer (pH 4.9) at −0.5 V. vs. SCE and at 50 cm. of height of a mercury reservoir. The potential of the DME was referred to the saturated calomel electrode (SCE). The temperature of the electrolytic solution was maintained by means of a water thermostat at 25°C, unless otherwise stated. The dissolved oxygen in the electrolytic solution was removed by bubbling pure nitrogen gas through the solution. No maximum suppressor was used.

The measurements were made in 0.1 M acetate buffer

1) I. M. Kolthoff, W. E. Harris and C. Matsuyama, *J. Am. Chem. Soc.*, **66**, 1782 (1944).
2) J. Koryta, *Collection Czech. Chem. Commun.*, **20**, 667 (1955).
3) B. Kelin and J. W. Otvos, *J. Am. Chem. Soc.*, **68**, 2665 (1946).
4) T. Murata, *J. Chem. Soc. Japan, Pure Chem. Sect.* (*Nippon Kagaku Zasshi*), **81**, 1240 (1960).
5) J. Collat and J. J. Lingane, *J. Am. Chem. Soc.*, **76**, 4214 (1954).
6) M. Johnson and R. Robinson, *Anal. Chem.*, **24**, 366 (1952).
7) D. Chow and R. Robinson, ibid., **25**, 1493 (1953).
8) I. M. Kolthoff and I. Hodara, *J. Electroanal. Chem.*, **5**, 2 (1963).
9) R. E. Hamm and C. D. Withrow, *Anal. Chem.*, **27**, 1913 (1955).
10) H. Hamaguchi, J. Hashimoto and N. Fukushi, *J. Chem. Soc. Japan, Pure Chem. Sect.* (*Nippon Kagaku Zassi*), **79**, 1482 (1958).
11) K. Nakano, K. Morinaga and Y. Narusawa, Presented at the 8th Annual Symposium on polarography, the Chemical Society of Japan Fukuoka (1961), Abstracts, p. 95.
12) R. E. Hamm, *J. Am. Chem. Soc.*, **75**, 6570 (1953).

solutions (pH 4.9), unless otherwise stated. The experimental conditions were in most cases such as those postulated in the theoretical treatment so that it was possible to compare the experimental results with the theoretical ones.

The controlled potential electrolysis was carried out with a Yanagimoto automatic potentiostat, Model VE-3. The working electrode was a mercury pool and the auxiliary electrode was platinum wire which was connected to the electrolytic solution through a potassium chloride agar bridge. The potential of the working electrode was controlled against the saturated calomel electrode (SCE). The solution was stirred by means of a magnetic stirrer. Nitrogen gas was bubbled through the solution continuously to provide stirring and to remove atmospheric oxygen.

Results

Polarographic Characteristics of Ethylenediaminetetraacetatoaquochromate(III) Ions in the Presence of Nitrate.—Ethylenediaminetetraacetatoaquochromate(III) ions, $[Cr(H_2O)edta]^-$, gave a well-defined polarographic reduction wave in a 0.1 M acetate buffer solution. This wave was found to correspond to the one-electron reduction of chromium(III) to chromium(II). The half-wave potential, $E_{1/2}$, was -1.24 V. vs. SCE and the diffusion current constant, I, was 1.48 μamp. $sec^{1/2}$ mM^{-1} $mg^{-2/3}$, both of which were in accord with the values obtained by Pecsok, Shields and Schaeffer.[13]

The addition of nitrate caused the exaltation of the limiting current, although the solutions with or without nitrate ion gave the identical current-potential curves in the absence of $[Cr(H_2O)edta]^-$ (Fig. 1). The exaltation phenomenon was so sensitive that the effect of nitrate ion on the d. c. polarograms could be observed at the concentration as low as 10^{-6} M of $[Cr(H_2O)edta]^-$.

The effect of nitrate ions on the polarograms of $[Cr(H_2O)edta]^-$ was found to be of the catalytic nature, as will be proved later. The polarographic characteristics of the solution containing $[Cr(H_2O)edta]^-$ and nitrate ions were examined and compared with those predicted from the theoretical studies on the catalytic polarographic current.[14,15]

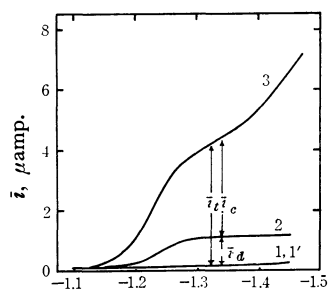

E, V. vs. SCE

Fig. 1. Polarograms obtained with the solutions containing (1) 0.1 M acetate buffer, (1′) (1)+19.6 mM KNO_3, (2) (1)+0.36$_4$ mM $H[Cr(H_2O)edta]$, and (3), (2)+19.6 mM KNO_3.

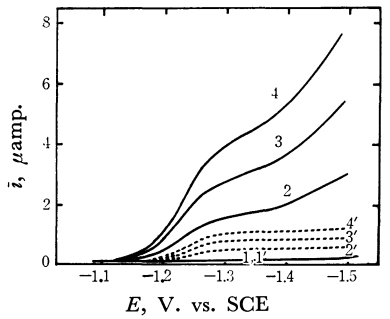

E, V. vs. SCE

Fig. 2. Polarograms of 0 (1, 1′), 0.12_2 (2, 2′), 0.25_3 (3, 3′), and 0.36_4 (4, 4′) mM of $H[Cr(H_2O)edta]$ in the solutions containing 0.1 M acetate buffer in the presence (1, 2, 3, 4) and the absence (1′, 2′, 3′, 4′) of 19.6 mM KNO_3.

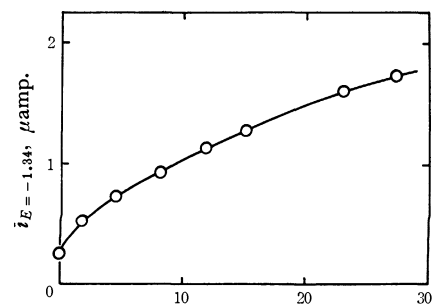

$[KNO_3]$, mM

Fig. 3. The limiting currents (at -1.34 V.) obtained with 0.1 mM $H[Cr(H_2O)edta]$ in 0.1 M acetate buffer solutions containing varied concentrations of nitrate.

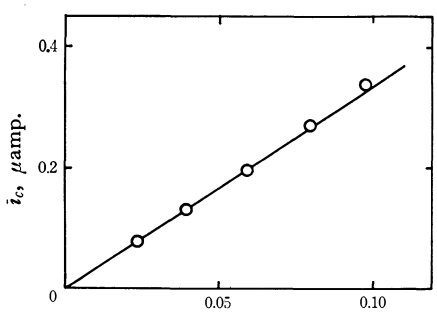

$[KNO_3]$, mM

Fig. 4. The relation between the catalytic current and the concentration of nitrate, obtained with 1.2_4 mM $H[Cr(H_2O)edta]$ in 0.1 M acetate buffer solutions containing varied concentrations of nitrate.

13) R. L. Pecsok, L. D. Shields and W. P. Schaeffer, *Inorg. Chem.*, **3**, 114 (1964).

14) P. Delahay and G. L. Stiehl, *J. Am. Chem. Soc.*, **74**, 350 (1952).

15) J. Koutecký, *Collection Czech. Chem. Commun.*, **18**, 311 (1953).

The polarograms obtained at various concentrations of $[Cr(H_2O)edta]^-$ and at the given concentration of nitrate are shown in Fig. 2. The limiting current at -1.34 V. was found to be almost proportional to the concentration of $[Cr(H_2O)edta]^-$.

Figure 3 indicates a relation between the limiting current and the concentration of nitrate, which was obtained at the given concentration of $[Cr(H_2O)edta]^-$. When the concentration of nitrate was relatively small, in other words, when the experimental condition was not that postulated in the theoretical study on the catalytic current, the catalytic current, $\bar{i}_c$, (the additional portion on the limiting current caused by the presence of nitrate, cf. Fig. 1) was almost proportional to the concentration of nitrate (Fig. 4). The presence of nitrate did not bring about the plateau but the rather inclined limiting current, even after the residual current was corrected. The inclination of the limiting current became larger with increasing concentrations of nitrate.

The catalytic currents obtained at various heights of the mercury reservoir are given in Table I. The total limiting currents are almost proportional to the square root of the height of the mercury reservoir under the conditions where $\bar{i}_c$ is proportional to the concentration of nitrate.

Table I. Limiting currents of $[Cr(H_2O)edta]^-$ obtained in the presence of nitrate ions at various heights of the mercury reservoir (h) in acetate buffer solutions

h cm.	Solution 1*		Solution 2**	
	$\bar{i}_t$, μamp.	$\bar{i}_c$, μamp.	$\bar{i}_t$, μamp.	$\bar{i}_t/h$
65	3.1	2.4	5.1	1.6
60	3.0	2.3	4.9	1.6
55	2.9	2.3	4.8	1.5
50	2.8	2.2	4.6	1.5
45	2.7	2.1	4.5	1.5
40	2.6	2.1	4.3	1.5

* Solution 1 contains 0.2 mM $[Cr(H_2O)edta]^-$ and 19.6 mM KNO_3.

** Solution 2 contains 1.0_3 mM $[Cr(H_2O)edta]^-$ and 0.8_3 mM KNO_3.

The measurements were also made at various pH's of the solution (Fig. 5). The lower the pH value was, the larger the catalytic waves were obtained in acetate buffer solutions. However, the further increase in hydrogen ion concentration with hydrochloric acid decreased the height of the catalytic waves. At lower pH of the solution, chromium(II) ion is no longer Cr(II)-EDTA, but some other aquated species which are considered less or least effective in the catalytic process.*

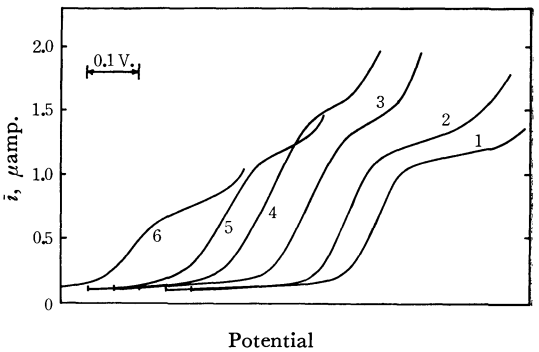

Fig. 5. Polarograms of 0.2 mM $[Cr(H_2O)edta]^-$, obtained in the presence of 2.0 mM KNO_3 in 0.1 M acetate buffer solutions of pH 5.5_0 (1), 4.8_8 (2) and 3.4_0 (3) and in 0.1 M potassium chloride solutions of pH 2.9_5 (4), 2.6_8 (5) and 2.0_2 (6). Each curve starts at -0.90 V. vs. SCE. Residual currents are not corrected.

The Reaction between Cr(II)-EDTA and Nitrate Ions in Solutions.—The presence of nitrate has no effect unless the potential is negative enough so that the reduction of $[Cr(H_2O)edta]^-$ occurs (Fig. 1). The fact strongly suggests that Cr(II)-EDTA formed at the electrode surface reacts with nitrate ion. In order to find the mechanism of the reaction taking place at the electrode surface, the characteristics of the reaction between Cr(II)-EDTA and nitrate ions in solutions were studied.

Cr(II)-EDTA was prepared by reducing the corresponding chromium(III) complex, $[Cr(H_2O)edta]^-$, at a mercury pool cathode, whose potential was controlled at -1.3 V. vs. SCE using an automatic potentiostat. The electrolysis cell used was shown in Fig. 6. Polarograms obtained after the electrolysis are of the typical reversible oxidation-reduction wave of chromium(II)- and chromium-

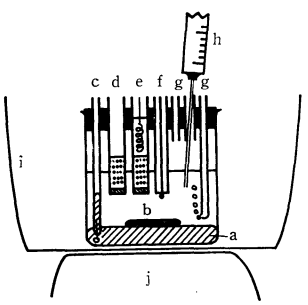

Fig. 6. Electrolysis cell: a, Hg-pool served as working electrode; b, stirrer; c, contact of working electrode; d, KCl-agar bridge connected to SCE; e, Pt-wire electrode; f, DME; g, N_2 gas disperser; h, syringe used for adding reagent after electrolysis; i, water thermostat; j, magnetic stirrer.

* According to Pecsok et al., the Cr(II)-EDTA complex has 13.61 of logarithmic stability constant and -3.00 of logarithmic acidity constant.[13] From these values, the percentage of the species Cr(II)edta, Cr(II)edtaH and Cr^{2+} which are in equilibrium in the solution are calculated to be 0, 0, ~100% at pH 2, 19, 19, 62% at pH 3, 82, 8, 10% at pH 4 and 98, 1, 1% at pH 5, respectively.

Table II. Stoichiometry of the reaction between Cr(II)-EDTA and nitrate ions, obtained in acetate buffer solutions at room temperature

Run	Initial concn. of Cr(II)-EDTA mM	Concn. of KNO_3 mM	Cr(II)-EDTA reacted with nitrate, mM	Reaction ratio, Cr(II)-EDTA/KNO_3	Temp. °C
1	0.68_9	0.049_5	0.39_1	7.9_2	27.0
2	0.69_6	0.049_5	0.39_4	7.9_6	27.0
3	0.57_6	0.049_5	0.39_8	8.0_4	26.5
4	0.70_9	0.049_5	0.39_2	7.9_4	26.5
5	0.74_5	0.049_5	0.39_9	8.0_4	25.5
6	0.64_4	0.049_5	0.39_4	7.9_6	25.5

(III)-EDTA complexes.* The concentration of Cr(II)-EDTA formed was determined by the measurement of the decrease in the reduction wave of $[Cr(H_2O)edta]^-$ at −1.4 V. vs. SCE or by the measurement of the height of the oxidation wave of Cr(II)-EDTA at −0.55 V. vs. SCE. In all experiments at pH 4.9 the sum of the height of the reduction wave at −1.4 V. and that of the oxidation wave at −0.55 V. after the electrolysis was approximately equal to the height of the reduction wave at −1.4 V. before the electrolysis. However this did not hold at lower pH, because the dissociation of Cr(II)-EDTA complex takes place. The anodic current observed at −0.55 V. results from the oxidation of Cr(II)-EDTA, but not from the oxidation of the aquated species.

When nitrate ions were added to this solution, the oxidation wave was decreased or sometimes completely obliterated according to the quantities of nitrate added. The formation of $[Cr(H_2O)edta]^-$ was at first confirmed spectrophotometrically. The stoichiometry was then ascertained at room temperature (ca. 25—27°C). The consumption of Cr(II)-EDTA by the addition of a known quantity of nitrate ions showed that one mole of nitrate reacted with eight moles of Cr(II)-EDTA (Table II).

This stoichiometry seems to show that the reaction proceeds as,

$$8\,Cr(II)\text{-}EDTA + NO_3^- + 10H^+ + 5H_2O = 8[Cr(H_2O)edta]^- + NH_4^+ \quad (1)$$

and that the final product in the reduction of a nitrate ion is an ammonium ion. The fact well accords with the results which were obtained by Lingane and Pecsok[16,17] on the reaction between chromium(II) and nitrate ions in sulfuric acid solutions.

In order to clarify the kinetics of the reaction, the decrease in the concentration of Cr(II)-EDTA by the addition of nitrate was pursued at approximately 0°C; the change in height of the oxidation wave of Cr(II)-EDTA at −0.55 V. was followed with time. Figure 7 shows an example of the wave height-time relationship. The rate constant was calculated with the assumption that the reaction is of second order. This assumption was not proved strictly but seemed to be most probable. Let a and b represent the initial concentrations of Cr(II)-EDTA and nitrate, respectively. At a given time t, x moles of nitrate react with $8x$ moles of Cr(II)-EDTA, and then we have

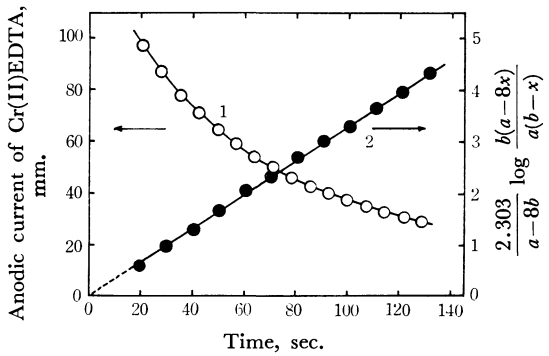

Fig. 7. The relation of the anodic limiting current with time (1) and that of the right-hand side of Eq. 4 with time (2), of the Cr(II)EDTA-nitrate reaction, obtained in a 0.1 M acetate buffer solution at nearly 0°C. The current was measured at −0.55 V. vs. SCE. The initial concentrations of Cr(II)-EDTA and KNO_3 were 0.24_6 and 0.06_1 mM, respectively.

$$-\frac{1}{8}\frac{d(a-8x)}{dt} = -\frac{d(b-x)}{dt} = k(a-8x)(b-x) \quad (2)$$

$$\frac{dx}{dt} = k(a-8x)(b-x) \quad (3)$$

Integrating and using the boundary values, the following relation is obtained:

$$kt = \frac{1}{a-8b}\ln\frac{b(a-8x)}{a(b-x)} \quad (4)$$

The rate constant can be determined from the slope of the straight line which is obtained from the plot of t against the right-hand side of Eq. 4. The value of $(a-8x)$ can be found by the measurement of the polarogram. As an example, the

* It was impossible to reduce completely, even though the dissolved and the atmospheric oxygen was sufficiently removed. Therefore, the sample solution of Cr(II)-EDTA always contained Cr(III) species, $[Cr(H_2O)edta]^-$.

16) J. J. Lingane and R. L. Pecsok, *Anal. Chem.*, **21**, 622 (1949).

17) H. A. Laitinen, "Chemical Analysis," McGraw-Hill Book Company, New York (1960), p. 449.

Table III. The rate constant of the reaction between Cr(II)-EDTA and nitrate ions, obtained in 0.1M acetate buffer solutions of various pH's at nearly 0°C

pH	Initial concentration Cr(II)-EDTA mM	Initial concentration KNO_3 mM	Rate constant l.mol^{-1}sec^{-1}
5.0_4	0.27_0	0.060_5	35
4.9_0	0.33_3	0.024_8	37
4.8_8	0.28_1	0.024_8	35
4.7_7	0.37_0	0.060_5	34
4.0_2	0.26_9	0.060_5	38
3.4_1	0.21_6	0.060_5	35

relation mentioned above is also given in Fig. 7. The rate constants thus obtained at various pH's are given in Table III.

According to the stability constant obtained by Pecsok et al., the acid complex Cr(II)edtaH is formed at lower pH.[13] Nevertheless, the kinetic studies at various pH's yielded approximately the same rate constant. This seems to indicate that Cr(II)edtaH reacts with nitrate ion as fast as Cr(II)edta dose.

Discussion

The experimental results clearly show that the effect of nitrate ions on the polarographic reduction waves of $[Cr(H_2O)edta]^-$ is of a catalytic nature and that the initiation of the catalytic process is the reaction of Cr(II)-EDTA with nitrate ions. The reoxidized $[Cr(H_2O)edta]^-$ is reduced again at the DME, resulting in an exaltation of the current. The reaction product of nitrate is again reduced by Cr(II)-EDTA or it may be reduced electrochemically, until it is reduced to the final product.

The reaction between Cr(II)-EDTA and nitrate ions at the vicinity of the electrode surface proceeds regardless of the electrode potential. The presence of EDTA causes the decrease of the limiting current of $[Cr(NCS)_6]^{3-}$ over some potential range to split a one-electron reduction wave into two steps. This is caused by the electro-oxidation of Cr(II)-EDTA wich is formed at the electrode surface through the chemical reaction following the electron transfer.[18-20] When nitrate is added to this solution, the decrease of the limiting current of $[Cr(NCS)_6]^{3-}$ becomes smaller, because some of the Cr(II)-EDTA formed were not oxidized electrochemically but chemically by the reaction with nitrate ions (Fig. 8). This indicates that the exaltation phenomena described in this paper are entirely different from those obtained in the reduction of nitrate ions in the presence of multi-

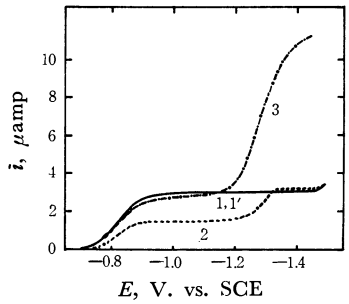

Fig. 8. Polarograms of 1.0 mM $K_3[Cr(NCS)_6]$, obtained in the solutions containing 0.9 M KSCN, 0.1 M acetate buffer and 0.005% gelatin without (1) and with (1') 5.0 mM KNO_3 and also after the addition of 0.5 mM EDTA without (2) and with (3) 5.0 mM KNO_3.

valent cations.[21]

In the case of catalytic currents, substance O is reduced to substance R, and the latter is oxidized again to substance O by the reaction with substance Z:

$$O + ne \rightarrow R \quad (5)$$

$$R + Z \xrightarrow{k} O \quad (6)$$

In the following discussion, the currents denoted by $\bar{i}_d$, $\bar{i}_c$ and $\bar{i}_t$ represent the diffusion current of substance O, the catalytic current due to the presence of substance Z and the total limiting current, respectively (Fig. 1.). The symbol k means the rate constant of the reaction 6.

The polarographic characteristics of the catalytic currents and the relation between k and $\bar{i}_c$ were reported by Delahay and Stiehl[14] and Koutecký[15]. The experimental results concerned with the dependency of the current on the concentration of $[Cr(H_2O)edta]^-$ (Fig. 2) and nitrate ion (Fig. 3) and the height of the mercury reservoir (Table I) are consistent, although not satisfactorily, with the theoretical prediction.

The results given in Fig. 4 and the last two columns of Table I were obtained under the condition where the concentration of nitrate is relatively small. Under this condition, it seems that the rate of the catalytic process is determined by the rate of the diffusion of nitrate ions, as was observed by Kolthoff et al. in the study of the catalytic current of the uranyl ions.[1]

The effect of pH on the catalytic waves was observed as given in Fig. 5. The decrease of the limiting current at pH 2 is explained, as mentioned before, by considering the dissociation of Cr(II)-EDTA complexes.

Collat and Lingane[5] studied by means of the controlled potential coulometric analysis the

18) N. Tanaka, T. Ito and R. Tamamushi, This Bulletin, **37**, 1430 (1964).
19) N. Tanaka, K. Ebata, *J. Electroanal. Chem.*, **8**, 120 (1964).
20) K. Ebata, *Sci. Repts. Tohoku Univ. Ser.*, I, **47**, 191 (1964).
21) I. M. Kolthoff and J. J. Lingane, "Polarography", Interscience Publishers, New York (1952), p. 533.

reduction product of nitrate which was formed in the electrode reaction of uranyl ions taking place in the presence of nitrate. From the consumption of electricity and that of hydrogen ion and the chemical analysis, they concluded that nitrate ions were primarily reduced to hydroxylamine. They also reported that the reduction of nitrate ion was accompanied by the reduction of hydrogen ion and that a considerable fraction of the electricity was evidently consumed for the reduction of hydrogen ions.

In the present case, similar reactions may take place. The phenomenon that the limiting current increased with decreasing pH in acetate buffer solutions may be attributed to the change in the quantity of the reduction of hydrogen ions. The formation of acid complex, $[CredtaH]^-$, does not seem to bring about the larger limiting current, because the $[CredtaH]^-$ was found to react with nitrate ion at almost the same rate as $[Credta]^{2-}$.

From the above discussions, the catalytic reduction of nitrate ion in the electrode reaction of $[Cr(H_2O)edta]^-$ is considered as follows. The reduction of nitrate ion is initiated by the reaction with Cr(II)-EDTA, which is followed by a series of rapid consecutive reactions, presumably both electrochemical and chemical. That the electrochemical and the chemical reactions are both involved might be the cause for the inconsistency of the polarographic characteristics with the prediction of the theoretical study on the catalytic polarographic current. There may be some possibilities that a nitrate ion is reduced to a product different from that in the homogeneous reaction. Hydroxylamine, which is formed by the six-electron reduction of nitrate ion, can react with Cr(II)-EDTA in solution, but the rate is not so large as that of the reaction of nitrate. Hydroxylamine can be reduced also at the DME and gives the polarographic wave as shown in Fig. 9.

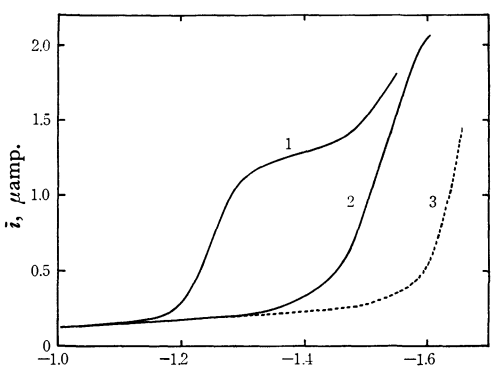

Fig. 9. Polarograms of (1) 0.2 mM $[Cr(H_2O)edta]^-$ with 2.0 mM KNO_3 and (2) 0.2 mM $NH_2OH \cdot HCl$, obtained in 0.1 M acetate buffer solutions of pH 4.8_8. Curve 3 represents the residual current.

The rate constant of the reaction between Cr(II)-EDTA and nitrate ion given by Eq. 1 or 6 was calculated from the catalytic polarographic current, using the Koutecký's equation with the assumption that the reaction occurring in the vicinity of the electrode surface proceeds in the same way as the homogeneous reaction does. In other words, nitrate ions were assumed to be reduced chemically, but not electrochemically. With a further assumption that the backward reaction is negligible, the ratio $\bar{i}_t/\bar{i}_d$ is written in the form,

$$\frac{\bar{i}_t}{\bar{i}_d} = 0.812\chi^{-1/2} + 1.92\chi^{-7/6} \quad (7)$$

with

$$\chi = \alpha k C_Z t_d \quad (8)$$

where t_d represents the drop time and α is the stoichiometry of the reaction 6($\alpha=8$ in the present case).[15,22] Using the numerical relation between χ and $\bar{i}_t/\bar{i}_d$ calculated by Koutecký,[15,23] the rate constant in the present case was determined, from the current at −1.34 V. vs. SCE to be approximately 30 $l.mol^{-1}sec^{-1}$ at 0°C and 70 $l.mol^{-1}sec^{-1}$ at 25°C, $\mu=0.1$, pH 4.9 (Table IV). It should be noted that only a small portion, if any, of the measured catalytic current is considered to be due to the reduction of hydrogen ions.

TABLE IV. THE RATE CONSTANT OBTAINED FROM THE CATALYTIC CURRENT AT −1.34 V. VS. SCE IN 0.1 mM $[Cr(H_2O)edta]^-$ SOLUTIONS CONTAINING 0.1M ACETATE BUFFER AND VARIOUS AMOUNTS OF KNO_3 AT NEARLY 0°C

Temp. °C	Concn. of KNO_3 mM	$\bar{i}_d$ μamp.	$\bar{i}_t$ μamp.	Rate constant $l.mol^{-1}sec^{-1}$
0	11.7_3	0.1_7	0.4_6	28
0	15.0	0.1_7	0.5_2	28
0	23.2_6	0.1_7	0.6_6	28
0	31.4	0.1_7	0.7_9	30
25	15.0	0.2_5	1.2_7	72
25	19.1_5	0.2_5	1.5_5	64
25	23.2_6	0.2_5	1.5_9	73
25	27.3_8	0.2_5	1.7_2	73

The rate constant obtained from the catalytic current is in good agreement with the one obtained in the homogeneous reaction. However this agreement seems to be rather fortuitous, if the complication of the reaction at the electrode surface is considered. A more precise comparison between the result from the homogeneous reaction and that from the electrode reaction seems less feasible, unless the reaction mechanisms are clarified on both kinds of the reactions.

The authors wish to thank the Ministry of Education for the financial support granted for this research.

22) J. Koutecký, *Collection Czech. Chem. Commun.*, **22**, 160 (1957).
23) P. Delahay, "New Instrumental Methods in Electrochemistry," Interscience Publishers, New York (1954), p. 105.

BULLETIN OF THE CHEMICAL SOCIETY OF JAPAN VOL. 39 1049—1054 (1966)

The Chemistry of Polyazanes. II. 1, 8-Di-*p*-tolyl-3, 6-diphenyl-1, 4, 7-octaaztriene

By Hiroshi MINATO, Masayoshi OKU* and Samuel Hung-Pui CHAN

Department of Chemistry, International Christian University, Mitaka, Tokyo

(Received October 19, 1965)

1, 8-Di-*p*-tolyl-3, 6-diphenyl-1, 4, 7-octaaztriene (DTDPO) was prepared by the potassium permanganate oxidation of 1-*p*-tolyl-3-phenyl-1-tetraazene (TPT), and the kinetics and the products of the decomposition of DTDPO were investigated. The experimental results can best be explained by assuming a mechanism in which DTDPO decomposes homolytically to yield a nitrogen molecule and two triazenyl radicals, which then combine to form 1, 3, 4, 6-tetraaryl-1, 5-hexaazdiene; the latter is very unstable and decomposes quickly to yield substituted azobenzenes and phenyl and *p*-tolyl radicals. The rather slow rate of decomposition of DTDPO was also discussed.

Except for carbon, very few elements are capable of forming compounds with chains of the same atoms linked linearly. Nitrogen is one of these few exceptions, and the polyazanes appear to be very interesting compounds. Our laboratories have been investigating the chemistry of various polyazanes; in this paper the chemistry of 1, 8-di-*p*-tolyl-3, 6-diphenyl-1, 4, 7-octaaztriene (DTDPO) will be described.

Wohl and Schiff[1] reported on the synthesis of DTDPO by the oxidation of 1-*p*-tolyl-3-phenyl-1-tetraazene (TPT) with an aqueous potassium permanganate solution at 0°C. Although they reported that DTDPO was very unstable, no precise kinetic measurements were made, nor were the products of the decomposition studied. Therefore, this investigation was undertaken in order to determine the rates of decomposition, the activation parameters, and the products of the decomposition of DTDPO.

Results and Discussion

1, 8-Di-*p*-tolyl-3, 6-diphenyl-1, 4, 7-octaaztriene (DTDPO) was synthesized by the potassium permanganate oxidation of 1-*p*-tolyl-3-phenyl-1-tetraazene (TPT), which had been prepared from the coupling of *p*-toluenediazonium chloride with phenylhydrazine.

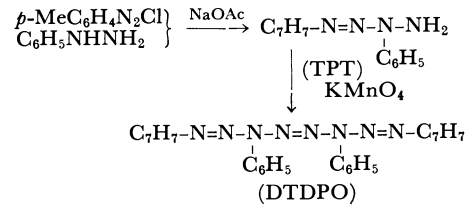

In the reaction between *p*-toluenediazonium chloride and phenylhydrazine, the fact that the α-nitrogen, not the β-nitrogen, receives the electrophilic attack of the diazonium ion is worthy of attention. However, this fact should not be interpreted to mean that α-nitrogen is more basic than β-nitrogen. The analysis of the side products of this coupling reaction indicated the presence of aniline, *p*-toluidine, phenyl azide and *p*-tolyl azide, which are the decomposition products of 1, 4-diaryl-1-tetraazenes, the latter being formed by the attack of the diazonium ion on the β-nitrogen atom of the phenylhydrazine. Undoubtedly both the α- and β-nitrogens are attacked by electrophilic diazonium ions. The TPT formed is susceptible to the attack of a proton and goes back to the diazonium ion and phenylhydrazine when the medium is acid. 1, 4-Diaryl-1-tetraazenes are also susceptible to the attack of a proton, but for these compounds three reactions are possible; one is the back reaction, the

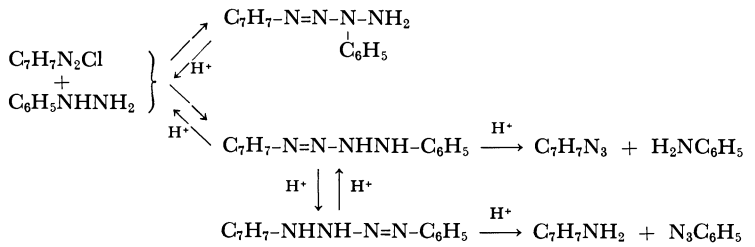

* American Chemical Society-Petroleum Research Fund Scholar.

1) A. Wohl and H. Schiff, *Ber.*, **33**, 2741 (1900).

second is the isomerization by the transfer of the double bond on the nitrogen chain, and the third is decomposition to yield an azide and an amine. The only irreversible products formed from the various reactions described above are the azides and the amines. When the medium was sufficiently acid, the only products isolated were azides and amines, and no TPT was obtained. Even when a quantity of sodium acetate sufficient for the neutralization of the diazonium chloride was present, the formation of some azides and amines was unavoidable.

The crude TPT containing some moisture changed into azides and amines in three days, even at −17°C, whereas the recrystallized TPT remained unchanged for at least two weeks at −17°C. The pure TPT decomposed into only azides and amines when it was allowed to stand in the open air at room temperature for 50 hr. The crude TPT smoked and then exploded when allowed to stand at 30°C for ten minutes.

TPT is very soluble in benzene or toluene, and slightly soluble in methanol or ethanol. In all of these solvents, however, TPT gradually decomposed at room temperature, and the color of the solution changed into brownish red and then into dark brown. Apparently the backward reaction yielded some diazonium compounds which reacted further to produce the coloration. TPT is very soluble in methylene chloride and slightly soluble in carbon tetrachloride, but TPT decomposed very fast in these chlorinated hydrocarbons and the solutions became dark brown within five minutes.

DTDPO was prepared by oxidizing TPT with potassium permanganate below 0°C. The crude DTDPO could be purified by the recrystallization in ether at −73°C. The pure yellow crystals of DTDPO were rather stable at room temperature when no mechanical shock was applied. However, they violently exploded when scratched or rubbed. DTDPO crystals must be handled with extreme caution.

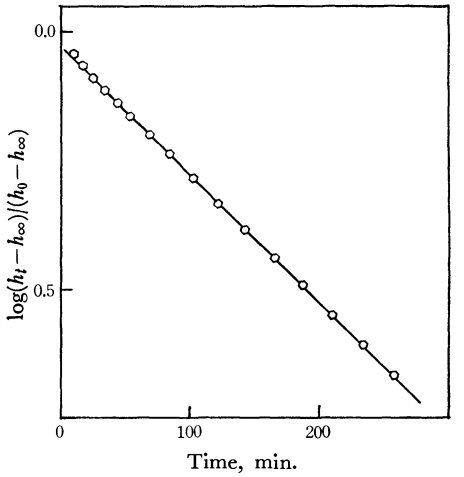

Fig. 1. Rate of decomposition of DTDPO in cumene at 30.0°C.
h_0, h_t and h_∞ are the difference of the mercury heights at $t=0$, $t=t$ and $t=\infty$, repectively.

TABLE I. RATES OF DECOMPOSITION OF DTDPO IN CUMENE

Temp. °C	$10^5 k_1$ sec^{-1}	Half life min.
10.0	0.417	2760
20.0	1.90	605
30.0	9.35	123

The spontaneous decomposition of DTDPO was investigated by dissolving about one gram of DTDPO in about 40 ml. of cumene at lower temperatures and by warming up the solution to 10.0°C, 20.0°C and 30.0°C and keeping it there. The decomposition followed good first-order kinetics, as is seen in Fig. 1. The first-order rate constants at these three temperatures are shown in Table I, together with the half-lives. When $\ln(k/T)$ was plotted against $1/T$, a straight line was obtained, as is seen in Fig. 2. The values of the activation parameters obtained from the slope of Fig. 2 were $\Delta H^{\ddagger}=25.1$ kcal./mol. and $\Delta S^{\ddagger}=5.8$ e.u. Table II lists the products obtained

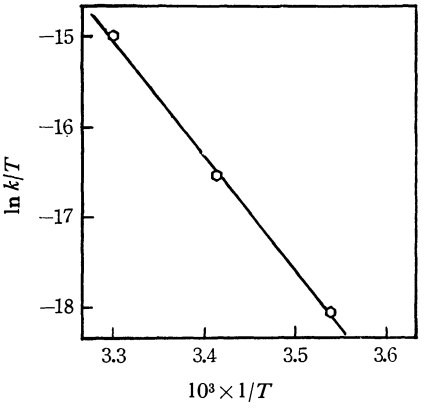

Fig. 2. $\ln k/T$ vs. $1/T$ for the decomposition of DTDPO.

TABLE II. PRODUCTS OF DECOMPOSITION OF DTDPO IN CUMENE AT 30.0°C*

Product	mmol.	mol./mol. DTDPO
N_2	6.47	2.94
$C_6H_5N{=}NC_6H_5$	0.968	0.44
$MeC_6H_4N{=}NC_6H_5$	0.880	0.40
$MeC_6H_4N{=}NNHC_6H_5$	0.176	0.08
C_6H_6	1.45	0.66
C_6H_5Me	3.10	1.41
$(C_6H_5CMe_2)_2$	1.12	0.51

* 0.9878 g. of DTDPO (2.20 mmol.) was dissolved in 39.0 ml. of degassed cumene, and decomposed at 30.0°C for 24 hr.

from the decomposition of DTDPO at 30°C.

It is plausible that the initial step of the decomposition of DTDPO in inert solvents may be represented as follows:

$$MeC_6H_4\text{-}N{=}N\text{-}\underset{\displaystyle C_6H_5}{N}\text{-}N{=}N\text{-}\underset{\displaystyle C_6H_5}{N}\text{-}N{=}N\text{-}C_6H_4Me \xrightarrow{(1)} MeC_6H_4\text{-}N{=}N\text{-}\dot{\underset{\displaystyle C_6H_5}{N}} + N_2 + \dot{\underset{\displaystyle C_6H_5}{N}}\text{-}N{=}N\text{-}C_6H_4Me$$

The production of toluene, bezene, azobenzenes, and about three moles of nitrogen from a mole of DTDPO cannot be explained by the reaction 1. Obviously further consideration and refinement of the mechanism is necessary.

Theilacker and Fintelmann[2] oxidized 1, 3-diaryl-triazenes with potassium permanganate, thus obtaining unstable crystals of 1, 3, 4, 6-tetraaryl-1, 5-hexaazdienes from the triazenes substituted with electron-withdrawing groups on the arene rings.

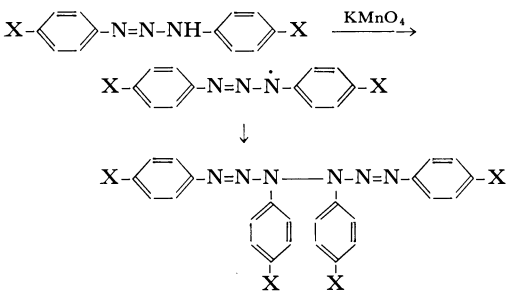

When there are no substituents or when there are electron-releasing substituents on the arene rings, no hexaazdienes were obtained, only such decomposition products as azobenzenes. Even the hexaazdienes substituted with electron-withdrawing groups were rather unstable; they were found to decompose gradually, even in cold, yielding substituted azobenzenes.

$$Ar\text{-}N{=}N\text{-}\underset{\displaystyle Ar'}{N}\text{-}\underset{\displaystyle Ar'}{N}\text{-}N{=}N\text{-}Ar \rightarrow 2Ar\text{-}N{=}N\bullet + Ar'\text{-}N{=}N\text{-}Ar' \rightarrow 2Ar\bullet + 2N_2$$

These facts appear to be quite relevant to the decomposition of DTDPO in cumene. It is likely that the diaryltriazenyl radicals formed by the reaction 1 combine to form 1, 3, 4, 6-tetraaryl-1, 5-hexaazdienes, which then rapidly decompose to yield substituted azobenzenes, toluene, benzene, and bicumyl. Since these arene rings are either nonsubstituted or substituted with electron-releasing groups, it is understandable that no hexaazdienes were found as the intermediates in the decomposition of DTDPO.

Table II shows that only a small amount of 1-*p*-tolyl-3-phenyltriazene was formed; one has therefore to assume that the majority of the triazenyl radicals combine with each other. This assumption is supported by the formation of almost three moles of nitrogen and considerable amounts of azobenzenes, benzene, toluene, and bicumyl. It is reasonable that the triazenyl radicals do not react with the solvent molecules and do not survive long enough to recombine with each other, since the triazenyl radical is more stable than the 1-methyl-1-phenylethyl radical, which is formed by hydrogen-abstraction from cumene by the triazenyl radical.

Since the triazenyl radical formed by the abstraction of a hydrogen atom from 1-*p*-tolyl-3-phenyltriazene is stabilized by the resonance:

$$MeC_6H_4\text{-}N{=}N\text{-}\dot{N}\text{-}C_6H_5 \leftrightarrow MeC_6H_4\text{-}\dot{N}\text{-}N{=}N\text{-}C_6H_5$$
(A) (B)

there are three possible combinations of these radicals: A and A, A and B, and B and B. Upon decomposition, A-A would yield azobenzene, the *p*-tolyl radical and nitrogen; A-B would yield 4-methylazobenzene, *p*-tolyl and phenyl radicals and nitrogen; B-B would yield 4, 4-dimethylazobenzene, the phenyl radical and nitrogen. Since no 4, 4-dimethylazobenzene was found in the decomposition products of DTDPO, the

$$2MeC_6H_4\cdot + 2N_2 + C_6H_5\text{-}N{=}N\text{-}C_6H_5 \xleftarrow{(3)} MeC_6H_4\text{-}N{=}N\text{-}\underset{\displaystyle C_6H_5}{N}\text{-}N{=}N\text{-}C_6H_4Me \text{ (A)-(A)}$$

$$\xleftarrow{(2)} \boxed{MeC_6H_4\text{-}N{=}N\text{-}\dot{\underset{\displaystyle C_6H_5}{N}} + \dot{\underset{\displaystyle C_6H_5}{N}}\text{-}N{=}N\text{-}C_6H_4Me} \xrightarrow{(4)} MeC_6H_4\text{-}N{=}N\text{-}\underset{\displaystyle C_6H_5}{\overset{\displaystyle C_6H_4Me}{N}}\text{-}N{=}N\text{-}C_6H_5 \text{ (A)-(B)}$$

$$\xrightarrow{(5)} MeC_6H_4\cdot + 2N_2 + C_6H_5\text{-}N{=}N\text{-}C_6H_4Me' + \cdot C_6H_5$$

$$MeC_6H_4\cdot + C_6H_5CHMe_2 \xrightarrow{(6)} MeC_6H_5 + C_6H_5\dot{C}Me_2$$

$$C_6H_5\cdot + C_6H_5CHMe_2 \xrightarrow{(7)} C_6H_6 + C_6H_5\dot{C}Me_2$$

$$2C_6H_5\dot{C}Me_2 \xrightarrow{(8)} (C_6H_5CMe_2)_2$$

2) W. Theilacker and E-C. Fintelmann, *Chem. Ber.*, **91**, 1597 (1958).

combination between B and B did not occur to any measurable extent. Both phenyl and *p*-tolyl radicals would abstract hydrogen atoms from cumene molecules, and the cumyl radicals thus produced would combine to form bicumyl molecules.

The reactions 1—8 are consistent with the experimental results and can account for all the products shown in Table II.

However, the formation of the 1, 3, 4, 6-tetraarylhexaazdienes, A-A and A-B, is possible by another route, namely, the heterolytic decomposition of DTDPO:

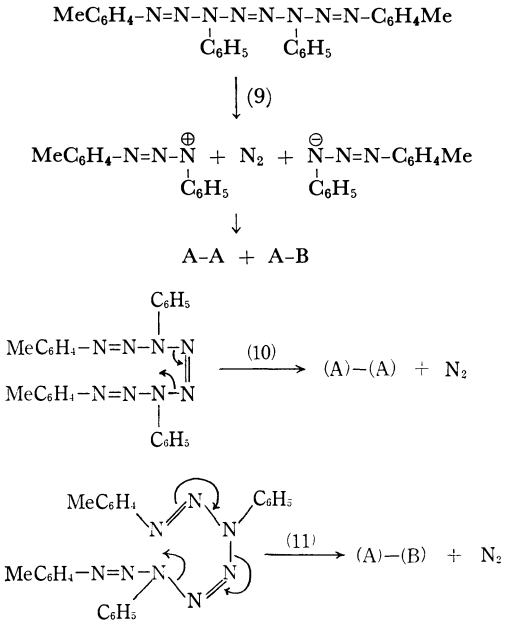

Although B-B was not found in the decomposition products, the formation of B-B is also possible by a similar cyclic route:

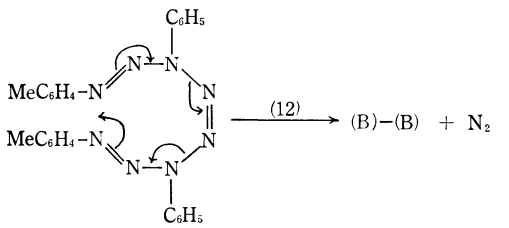

The heterolytic decomposition of DTDPO and the subsequent decomposition of hexaazdienes (i. e., the reactions 9, 10, 11, 3, 5, 6, 7, and 8) can account for all the products shown in Table II.

The choice between the homolytic mechanism and the heterolytic mechanism for the decomposition of DTDPO cannot be made easily. However, the homolytic mechanism (Reactions 1—8) seems more plausible than the heterolytic mechanism (Reactions 9, 10, 11, 3, 5, 6, 7 and 8), in view of the facts that: (a) the activation parameters

TABLE III. RATES OF DECOMPOSITION OF VARIOUS AZO COMPOUNDS

Azo compound	Solvent	Temp. °C	$10^4 k_1$ sec^{-1}	Ref.
Me–N=N–Me	(Gas)	300	5.6	5
$Me_2(NC)C$–N=N–$C(CN)Me_2$	Xylene	80	1.53	6
Ph–N=N–$CHPh_2$	Decalin	54	1.01	7
Ph–N=N–CPh_3	Toluene	53	2.25	8
	Benzene	25	0.042	9
DTDPO	Cumene	20	0.190	
C_7H_7–N=N–$N(C_7H_7)$–N=N–C_7H_7	Cumene	25.8	12.9	4

($\Delta H^{\ddagger}$=25.1 kcal./mol., $\Delta S^{\ddagger}$=5.8 e. u.) are consistent with a homolytic decomposition rather than a heterolytic decomposition, and (b) the symmetric azo compounds or peroxides rarely undergo heterolytic decomposition.

In Table III, the rate of the decomposition of DTDPO is compared with the rates of the decomposition of several azohydrocarbons. The fact that DTDPO is more stable than 1, 3, 5-tri-*p*-tolyl-1, 4-pentaazdiene is rather surprising. This fact should be discussed further.

The lone-pair electrons of 3- and 6-nitrogen atoms of DTDPO are in resonance with the *p*-orbitals of azo linkages; hence, these orbitals

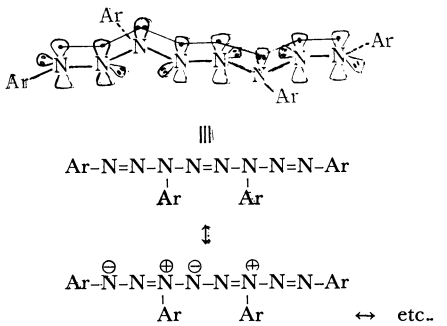

Fig. 3(a)

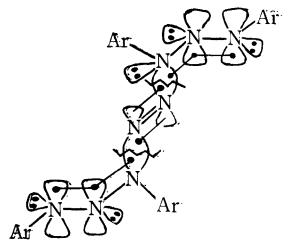

Fig. 3(b)

3) A. Wohl and H. Schiff, *Ber.*, **26**, 1587 (1893).
4) H. Minato and M. Oku, This Bulletin, **38**, 1529 (1965).
5) O. K. Rice and D. V. Sickman, *J. Chem. Phys.*, **4**, 239, 242, 608 (1936).
6) C. G. Overberger, M. T. O'Shaughnessy and H. Shalit, *J. Am. Chem. Soc.*, **71**, 2661 (1949).
7) S. G. Cohen and C. H. Wang, ibid., **77**, 3628 (1955).
8) S. G. Cohen and C. H. Wang, ibib., **75**, 5504 (1953).
9) M. G. Alder and J. E. Leffler, ibid., **76**, 1425 (1954).

are probably parallel with one another, as is shown in Fig. 3(a). When the molecule of DTDPO with the structure shown in Fig. 3(a) is to decompose, the $MeC_6H_4N{=}N{-}\dot{N}{-}C_6H_5$ radical to be formed in the transition state does not have the resonance energy which is available to the molecules with the 3(b) structure. The rotation of the groups in 3(a) to obtain 3(b) is possible in solution. However, the molecule of DTDPO possesses four bulky arene rings on the chain of eight nitrogen atoms; it is very rare for the molecule of DTDPO with so much freedom to have the orientation represented in Fig. 3(b). Thus, the extremely small possibility of attaining a transition state stabilized with the resonance represented in Fig. 3(b) may be the reason for the rather slow rate of decomposition of DTDPO.

Experimental

Materials.—Tokyo Kasei Co. G. R. cumene was shaken with portions of concentrated sulfuric acid until the acid layer no longer became colored on long shaking. After washing with water, a sodium bicarbonate solution, and water again, the cumene was dried with calcium chloride and distilled from sodium through a 90-cm. column packed with glass helices. The center fraction, boiling at 152—153.2°C, was stored under nitrogen atmosphere and used.

All the other chemicals were those of the best grade commercially available, and were used without further purification.

The Synthesis of 1-*p*-Tolyl-3-phenyl-1-tetraazene (TPT).—The method of Wohl and Schiff[3] was modified a little. Into a mixture of 22 g. of *p*-toluidine (0.2 mol.) and 30 ml. of water, 52 ml. of concentrated hydrochloric acid (0.6 mol.) was added. The mixture was heated to dissolve its elements, and then the solution was cooled thoroughly by adding cracked ice to it and by placing it in an ice bath. The diazotization was carried out at 0°C by adding a solution of 14 g. of sodium nitrite (0.2 mol.) in 40 ml. of water the toluidine hydrochloride solution drop by drop.

Into a mixture of 22 g. of phenylhydrazine (0.2 mol.), 50 ml. of water, and 12 g. of acetic acid (0.2 mol.), a solution of 82 g. of sodium acetate (1 mol.) in 20 ml. of acetic acid and 120 ml. of water was added all at once; the mixture was then cooled to 0°C. Into this phenylhydrazine mixture the *p*-toluenediazonium chloride solution was stirred in portions at temperatures between 0 and 2°C. A light yellow substance was formed at once and floated on the surface of the water layer. It changed to a yellowish brown after one hour of stirring in an ice bath. The crude brown product was then collected by filtration; 22 g. (50%). The melting point of the crude product was 63—67°C, but when 22 g. of the crude product was recrystallized in ether at −73°C, 9.8 g. of fine yellow crystals was obtained, melting at 74.5°C with gas evolution (reported by Wohl and Schiff, 66—67°C).[1]

The Synthesis of 1,8-Di-*p*-tolyl-3,6-diphenyl-1,4,7-octaaztriene (DTDPO).—The method of Wohl and Schiff[1] was modified a little. After two grams of TPT had been dissolved in 25 ml. of ether cooled at 0°C, the solution was cooled to −12°C. Into this cold TPT solution, 50 ml. of a 1% potassium permanganate solution was added slowly over a 20-min. period A pale yellow substance gradually appeared and floated at the top of the upper ethereal layer, and the violet color of potassium permanganate changed to dark brown. The mixture was stirred for 30 min. at −4—1°C after the potassium permanganate solution had been added.

The two layers were then separated with a separatory funnel, and the pale yellow product, contaminated with some black manganese dioxide, was filtered from the ethereal layer. Fifteen milliliters of a 3% sulfurous acid solution cooled to 0°C was added to the residue in the funnel in order to wash away the black manganese dioxide. The crude DTDPO was then washed well with cold water. The yield of the crude DTDPO was 0.6 g.; m. p. 61.5—64°C (with an evolution of gas).

The slightly wet DTDPO (0.6 g.) was dissolved in 5 ml. of ether at room temperature, and the solution was cooled to −73°C. The ice formed was removed by decantation. After 10 min. at −73°C, light yellow needles were formed and collected by filtration. The yield was 0.3 g.; m. p. 65.5—66.0°C (reported by Wohl and Schiff[1], 64—67°C).

The crystals of DTDPO are extremely sensitive to mechanical shock. After the crystals had been dried by an aspirator for about four minutes at room temperature, and the rubber tubing had then been taken off, the stream of air suddenly flowing into the vessel was a shock sufficient to cause an explosion of DTDPO crystals. DTDPO also exploded when it was rubbed in a mortar, or when it was dropped into concentrated hydrochloric or sulfuric acid.

When crystals of DTDPO were dissolved in carbon tetrachloride, dichloromethane, ether or toluene at room temperature, they quickly decomposed, with an evolution of gas. However, the solid DTDPO was rather stable when there was no mechanical shock. The crystals of DTDPO did not decompose at all when kept at −17°C in darkness for at least three weeks; the melting point of crystals decreased by only 1—2°C when they were placed in the open air for two days. The fact that it is rather stable as a solid but unstable in a solution is reminiscent of the behavior of 1, 3, 5-tri-*p*-tolyl-1, 4-pentaazdiene.[4]

Kinetic Procedure.—About 1 g. of DTDPO was placed in a glass vessel attached to an end of a U-shaped tube, and then about 40 ml. of cumene was

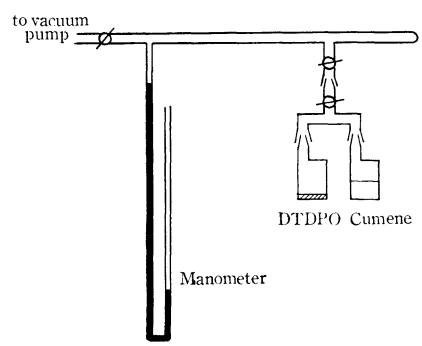

Fig. 4

placed in a glass vessel attached to the other end of the U-shaped tube, as is shown in Fig. 4. These two were degassed and then mixed at −78°C. Then this U-tube was attached to a vacuum system of a known volume with the mercury manometer. The U-tube was immersed in a small bath of a constant temperature by elevating the bath with a lab-jack. By turning a stopcock, the U-tube was opened to the evacuated system, and the increase in the pressure of the system was measured versus the time. After the U-tube had been warmed to the temperature of the bath, the plots of the increase in the pressure showed good first-order behavior. The infinity point was taken after about ten half-lives.

Procedure for Product Studies.—The DTDPO solution used for kinetic studies was analyzed for the products of decomposition. The amount of nitrogen was determined from the data on the pressure, the volume and the temperature of the system. The cumene solution was distilled to yield brownish solids and a distillate. When the distillate was investigated by a Shimadzu Gas Chromatograph GC-2B, the peaks corresponding to benzene and toluene were observed, in addition to the peak of cumene. The amounts of benzene and toluene were determined by using ethanol as the internal standard.

The infrared spectrum of the brownish residue showed the absorptions of bicumyl (2, 3-dimethyl-2, 3-diphenylbutane), azobenzene, 4-methylazobenzene, and 3-phenyl-1-*p*-tolyltriazene. The elution chromatography of these brownish solids on alumina yielded bicumyl as the first fraction, a mixture of azobenzene and 4-methylazobenzene as the second fraction, and 3-phenyl-1-*p*-tolyltriazene as the last fraction. The identity of bicumyl and 3-phenyl-1-*p*-tolyltriazene was established by comparing their melting points and infrared spectra with those of authentic samples. The amounts of azobenzene and 4-methylazobenzene were determined by comparing the infrared spectrum of the mixture with those of authentic samples, and finally by preparing a synthetic mixture of azobenzene and 4-methylazobenzene; the infrared spectrum of this synthetic mixture was identical with that of the mixture derived from the reaction products.

Grateful acknowledgment is made to the donors of The Petroleum Research Fund, administered by the American Chemical Society, for support of this research.

BULLETIN OF THE CHEMICAL SOCIETY OF JAPAN VOL. 39 1054—1058 (1966)

The Chemistry of Polyazanes. III. The Reaction of Nitrosobenzene with Hydrazine and Phenylhydrazine

By Hiroshi MINATO and Takiko FUJISAWA

Department of Chemistry, International Christian University, Mitaka, Tokyo

(Received October 19, 1965)

The reaction between nitrosobenzene and hydrazine was studied. Aniline and nitrogen were found to be the products, but it was not certain whether or not phenyltriazene existed as an intermediate. Then the reaction between nitrosobenzene and phenylhydrazine was studied. The products were azoxybenzene, diphenylamine, benzene and nitrogen. The reaction between *p*-nitrosotoluene and phenylhydrazine yielded 4, 4′-azoxytoluene, 4-methyldiphenylamine, benzene and nitrogen. The mechanisms of these reactions were discussed on the basis of these findings.

It has been of interest to seek for the initiators which form free radicals at low temperatures. *t*-Butyl triphenylperacetate is an unstable perester, decompositing at lower temperatures to yield free radicals, but this compound cannot be used as an initiator, since one of the free radicals produced, the triphenylmethyl radical, is so stable that it does not initiate polymerization.

The possibility of producing two carbon dioxide molecules to further hasten decomposition while still producing highly-reactive radicals has been explored in the study of di-*t*-butyl peroxalate,[1,2] but later work[3,4] has suggested that in decomposing these peroxalates form only one molecule of carbon dioxide in the transition state.

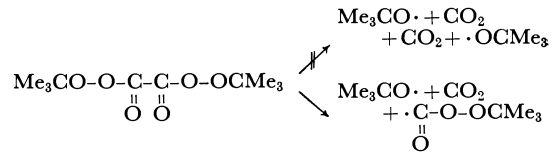

In view of the fact that the attempt to produce two carbon dioxide molecules at the transition state failed, it seemed of great interest to attempt to prepare the 1, 4-disubstituted tetraazdienes, which might decompose with a concerted breakage

1) P. D. Bartlett, E. P. Benzing and R. E. Pincock, *J. Am. Chem. Soc.*, **82**, 1762 (1960).
2) P. D. Bartlett and R. E. Pincock, ibid., **82**, 1769 (1960).
3) P. D. Bartlett and H. Sakurai, ibid., **84**, 3269 (1962).
4) P. D. Bartlett, B. A. Gontarev and H. Sakurai, ibid., **84**, 3101 (1962).

TABLE I. PRODUCTS OF THE REACTION BETWEEN NITROSOBENZENE AND HYDRAZINE

Run	Reactants,* mmol.		Other additives	$\frac{(C_6H_5NO)}{(N_2H_4)}$	Solvent	Products, mmol.			%C_6H_5 Accounted for
	C_6H_5NO	N_2H_4				$C_6H_5NH_2$	C_6H_5NO	$C_6H_5N{=}NC_6H_5$	
1	1.00	1.60		0.625	CH_2Cl_2 2 ml.	0.855	0	0.0697	99.4
2	9.99	9.94		1.00	CH_2Cl_2 20 ml.	7.73	2.67	0	104
3	22.3	8.92		2.50	MeOH 20 ml.	5.16	7.79	1.92	75.5
4	20.8	10.8	MeONa 2.0 mmol	1.93	MeOH 20 ml.	8.00	0	4.90	85.6

* Reactants were mixed below −30°C, and then the mixture was gradually warmed up to room temperature.

of three bonds, with the expulsion of two molecules of nitrogen. It is known that nitrosobenzene reacts with aniline to yield azobenzene, and it seemed plausible that the reaction between nitrosobenzene and hydrazine might yield a tetraazdiene. Therefore, the reaction between nitrosobenzene and hydrazine has been investigated:

$$C_6H_5NO + H_2NC_6H_5 \rightarrow C_6H_5\text{-}N{=}N\text{-}C_6H_5$$

$$2C_6H_5NO + N_2H_4 \overset{?}{\rightarrow} C_6H_5\text{-}N{=}N\text{-}N{=}N\text{-}C_6H_5$$

During the investigation of various polyazanes, we have come across a paper, written by Mills, reporting that the reaction between nitrosobenzene and phenylhydrazine yields nitrogen and azobenzene.[5]

$$C_6H_5NO + H_2NNHC_6H_5 \rightarrow N_2 + C_6H_5\text{-}N{=}N\text{-}C_6H_5$$

Since the reaction between nitrosobenzene and aniline yields azobenzene, one would expect that the reaction between nitrosobenzene and phenylhydrazine would yield 1, 3-diphenyltriazene, which is a well-characterized, stable compound:

$$C_6H_5NO + H_2NNHC_6H_5 \overset{?}{\rightarrow} C_6H_5\text{-}N{=}N\text{-}NH\text{-}C_6H_5$$

Obviously the reaction of nitrosobenzene and phenylhydrazine yielding azobenzene is not straightforward; it therefore calls for further investigation. Therefore, the reaction between nitrosobenzene and phenylhydrazine and the reaction between *p*-nitrosotoluene and phenylhydrazine have been investigated and will be described in this paper.

Results and Discussion

The Reaction between Nitrosobenzene and Hydrazine.—When nitrosobenzene was mixed with hydrazine in dichloromethane at −50——78°C most of the nitrosobenzene remained as a solid due to its low solubility at low temperatures, unless a great amount of the solvent was used. However, when the solution was warmed up to about −30°C, a homogeneous solution with a light green color was obtained; the color did not appear to change when the solution was kept at this temperature. Apparently, nitrosobenzene and hydrazine do not react at this temperature. When however, the solution was further warmed up to about −8°C, the green color of nitrosobenzene began to change to a yellowish brown, with an evolution of nitrogen. The evolution of nitrogen was complete after the solution had been kept at room temperature for three hours. Besides the nitrogen evolved, the products of the reaction were aniline, azobenzene and unreacted nitrosobenzene, as is shown in Table I. In any case, the gas chromatographic analysis showed the absence of benzene, which is a product likely to be formed if 1, 4-diphenyl-1, 3-tetraazdiene was formed. Apparently, one mole of hydrazine reacted with only one mole of nitrosobenzene, and aniline and nitrogen were produced. It is not certain whether or not phenyltriazene was present as the intermediate.

$$C_6H_5NO + N_2H_4 \rightarrow (C_6H_5\text{-}N{=}N\text{-}NH_2\ ?) \rightarrow C_6H_5NH_2 + N_2$$

Dimroth prepared phenyltriazene by reducing phenyl azide with stannous chloride and dry hydrogen chloride in absolute ether at −20°,C and then by purifying the phenyltriazene through its copper derivative, which was then decomposed with aqueous potassium cyanide at a low temperature:[6]

$$C_6H_5\text{-}N{=}N^+{=}N^- \xrightarrow{SnCl_2} C_6H_5\text{-}N{=}N\text{-}NH_2$$

Phenyltriazene was found to be in the form of colorless leaflets melting at 50°C, and it was very unstable. It rapidly decomposed into aniline anp nitrogen n all solvents at room temperature:

5) C. Mills, *J. Chem. Soc.*, **67**, 925 (1895).

6) O. Dimroth, *Ber.*, **40**, 2378 (1907).

$$C_6H_5\text{-}N{=}N\text{-}NH_2 \rightarrow C_6H_5NH_2 + N_2$$

It seemed of interest to determine whether or not the phenyltriazene was the intermediate at the reaction between hydrazine and nitrosobenzene. Attempts have been made to find experimental conditions where nitrosobenzene and hydrazine react and yet the product (presumably phenyltriazene) does not decompose to yield nitrogen. Whether nitrosobenzene has reacted or not can be determined from the loss of the light green color. However, it was found that the loss of the green color was always accompanied by the evolution of nitrogen, even though the solution was warmed up very slowly. In an attempt to facilitate the reaction between the hypothetical phenyltriazene and another mole of nitrosobenzene, sodium methoxide was added to the reaction mixture, but there was no essential difference in the products.

These experimental findings can be explained by either of the following two assumptions:

(A) Nitrosobenzene reacts with hydrazine to form phenyltriazene, which is so unstable that it immediately decomposes before reacting with another mole of nitrosobenzene.

(B) Nitrosobenzene reacts with hydrazine to yield aniline and nitrogen, without going through phenyltriazene as the intermediate.

The mechanism B may best be described in the following scheme:

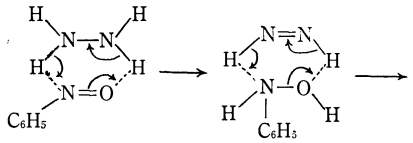

$$C_6H_5NH_2 + N_2 + H_2O$$

The experimental findings described so far are not sufficient for us to make a choice between these two mechanisms, but the experimental evidence to be described below for the reaction between nitrosobenzene and phenylhydrazine seems to indicate that the reaction between nitrosobenzene and hydrazine is best described by the mechanism B.

The Reaction between Nitrosobenzene and Phenylhydrazine.—Phenylhydrazine was added drop by drop to a stirred solution of nitrosobenzene in dichloromethane at room temperature until no more evolution of nitrogen occurred. The products of the reaction were then identified by the use of elution chromatography and by a study of the infrared spectra; the results are summarized in Table II.

TABLE II. PRODUCTS OF THE REACTION BETWEEN NITROSOBENZENE AND PHENYLHYDRAZINE

Reactant	Nitrosobenzene	10.0 mmol.
	Phenylhydrazine	3.95
Product	Benzene	1.90 mmol.
	Azoxybenzene	3.59
	Diphenylamine	1.38
$\%C_6H_5$ of C_6H_5NO	accounted for	81.7%
$\%C_6H_5$ of $C_6H_5N_2H_3$	accounted for	83.0%

The formation of benzene, azoxybenzene and diphenylamine can be explained by either of the following two mechanisms, C and D:

(C)

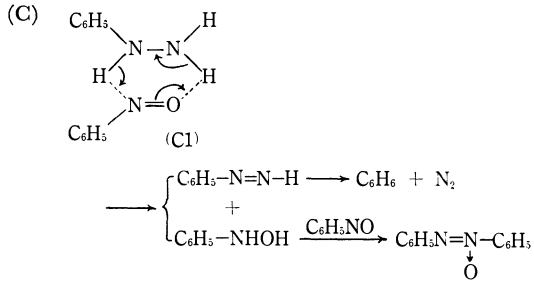

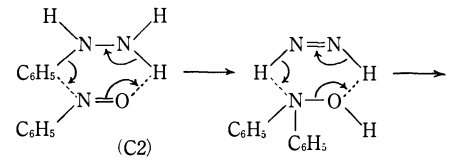

$$(C_6H_5)_2NH + N_2 + H_2O$$

(D)

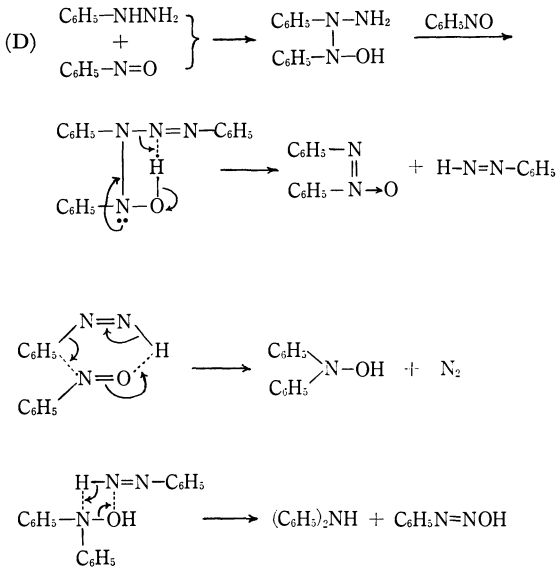

Although the mechanism C looks more attractive than the mechanism D, the products of the reaction are consistent with the mechanism D as well. Therefore, the reaction between *p*-nitrosotoluene and phenylhydrazine was investigated in order to find out which of these two mechanisms is better applicable to these reactions.

The Reaction between *p*-Nitrosotoluene and Phenylhydrazine.—*p*-Nitrosotoluene and phenylhydrazine were allowed to react in the same manner

as in the case of nitrosobenzene and phenylhydrazine. The rate of the evolution of nitrogen was less vigorous than in the case of nitrosobenzene. The products of the reaction are summarized in Table III.

Table III. Products of the reaction between *p*-nitrosotoluene and phenylhydrazine

Reactant	*p*-Nitrosotoluene	10.0 mmol.
	Phenylhydrazine	4.37
Product	Benzene	1.63 mmol.
	4, 4'-Azoxytoluene	3.37
	4-Methyldiphenylamine	0.79
	Phenylhydrazine	0.63
$\%CH_3C_6H_4$ of $CH_3C_6H_4NO$ accounted for		75.3%
$\%C_6H_5$ of $C_6H_5N_2H_3$ accounted for		69.8

If the mechanism C is right, the products should be 4, 4'-azoxytoluene, 4-methyldiphenylamine and benzene. On the other hand, if the mechanism D is right, the products should be 4-methylazoxybenzene, 4, 4'-dimethyldiphenylamine and toluene:

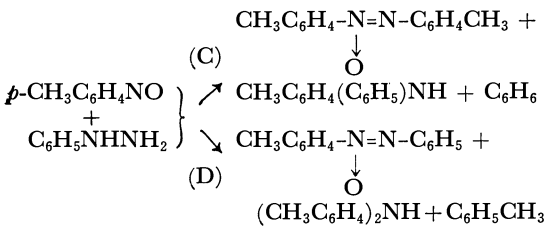

The products of the reaction shown in Table III contradict the mechanism D, but they are consistent with the mechanism C.

The mechanism C assumes both phenylhydroxylamine and diphenylhydroxylamine as intermediates. However, a modified mechanism, C', is possible, which assumes only phenylhydroxylamine as an intermediate:

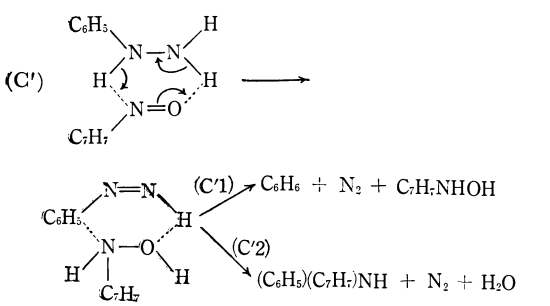

According to the mechanism C', combined phenyldiimide and *p*-tolylhydroxylamine either depart from each other to yield benzene and nitrogen according to the step C'1, or react further in a solvent cage to yield 4-methyldiphenylamine according to the step C'2. The ratio of C'1 to C'2 can be calculated from the yields of benzene and 4-methyldiphenylamine to be 2.06; in other words, 67% of the reaction proceeds by C'1, while 33% proceeds by C'2. In th ecase of nitrosobenzene, the ratio of C'1 to C'2 is 1.38; in other words, 58% of the reaction proceeds by C'1, while 42% proceeds by C'2.

In the case of the reaction between nitrosobenzene and hydrazine, we assumed a combination of intermediates, diimide and phenylhydroxylamine similar to that in the mechanism B. In this case, however, all the phenylhydroxylamine must have been reduced with diimide in a solvent cage, because if some phenylhydroxylamine departs from diimide without being reduced further, it should react with nitrosobenzene to yield azoxybenzene; the latter was not, however, found in any products studies of the reaction. These findings show the stronger reducing power of diimide compared with that of phenyldiimide.

As for the choice between the mechanisms C and C', no experimental evidence is available which favors one over the other, although C' appears a little more attractive than C.

Experimental

Materials.—Nitrosobenzene and *p*-nitrosotoluene were prepared by the reduction of nitrobenzene and *p*-nitrotoluene respectively.[7] Commercial hydrazine hydrate was dehydrated by refluxing it with sodium hydroxide.

4, 4'-Azoxytoluene was prepared by heating 500 mg. of 4, 4'-azotoluene in 2.5 ml. of acetic acid containing 0.1 ml. of 30% hydrogen peroxide in a water bath.[8] The yellow crystals obtained were recrystallized from ethanol, m. p. 70°C.

All the other chemicals were of the best grade commercially available and were used without further purification.

The Reaction between Nitrosobenzene and Hydrazine.—*Run. 1.*—To a solution of hydrazine (0.0512 g., 1.60 mmol.) in dichloromethane (2.587 g.), nitrosobenzene (0.1069 g., 1.00 mmol.) was added at −30°C. The transparent, light green solution thus obtained did not change when kept at −30°C. When it was gradually warmed up, the color changed to a yellowish green at −10°C, and nitrogen gas started to evolve at −8°C. The evolution of nitrogen ceased when the solution was kept for three hours at room temperature, and the color of the solution changed to a yellowish brown. The infrared specturm of the solution was completely accounted for by the absorption of aniline and azobenzene. 0.855 mmol. of aniline and 0.0697 mmol. of azobenzene were found to be present by the use of the absorptions at 1620 cm^{-1} (for aniline) and 1073 cm^{-1} (for azobenzene.).

Run 2.—The procedure was essentially the same as in Run 1, except that about equimolar amounts of

7) E. C. Horning, "Organic Syntheses," Coll. Vol. I, 668 (1955).

8) T. Parsons, Jr., and J. C. Bailar, Jr., *J. Am. Chem. Soc.*, **58**, 269 (1936).

nitrosobenzene and hydrazine were used and the reactants solutions were degassed before mixing. The infrared specturm of the dichloromethane solution of the products was completely accounted for by the absorption of aniline and undecomposed nitrosobenzene. The amount of nitrosobenzene was determined by the use of an absorption at 1120 cm^{-1}.

Run 3.—A solution of hydrazine (0.286 g., 8.92 mmol.) in 20 ml. of methanol was placed in a container attached to one end of a U-shaped tube; solid nitrosobenzene (2.388 g., 22.3 mmol.) was placed in a container attached to the other end of the U-shaped tube. After these two had been degassed by the usual technique on a vacuum system, they were mixed at −78°C and then gradually warmed up. The evolution of gas started at −10°C, it became vigorous when the mixture was further warmed up to room temperature. The reaction had been completed in about three hours at room temperature. After the mixture had been kept at room temperature for one day, it was distilled in a vacuum; a greenish distillate and a brownish residue were thus obtained. The greenish distillate was found to be a methanol solution, with small amounts of nitrosobenzene and water, by a study of its infrared spectrum and by vapor-phase chromatography. No benzene was found in the distillate. The infrared spectrum of the brownish residue was completely accounted for by the absorption of aniline, nitrosobenzene and azobenzene.

Run 4.—The procedure was essentially the same as the one used for Run 3, except that sodium methoxide (2.0 mmol.) was added to the mixture.

The Reaction between Nitrosobenzene and Phenylhydrazine.—Phenylhydrazine was stirred, drop by drop, into a solution of nitrosobenzene (1.072 g., 10.0 mmol.) in dichloromethane (3.0 ml.) at room temperature. Reaction occurred with a vigorous evolution of nitrogen upon the addition of each drop of phenylhydrazine. When 0.4273 g. (3.95 mmol.) of phenylhydrazine was added, no more reaction occurred upon the addition of another drop of phenylhydrazine. When the dark red solution obtained was distilled, a colorless distillate and a dark red oil were obtained.

The colorless distillate was viewed against pure dichloromethane in the infrared region, and the spectrum was superimposable upon that of pure benzene. 1.90 mmol. of the benzene was found to be present by a comparison of the specturm with that of a solution containing a known amount of benzene.

1.1548 g. of dark red oil was chromatographed on about 25 g. of alumina. Fractions 1—6, eluted with petroleum ether - benzene, were in the form of light yellow crystals (0.6377 g.), melting at 34.5—35.5°C. Its infrared spectrum was identical with that of azoxybenzene. When recrystallized from ethanol, the crystals melted at 36°C; the melting point was not depressed when authentic azoxybenzene (m. p. 36°C) was mixed with these yellow crystals.

Fractions 8—11, eluted with benzene-ether, were in the form of colorless crystals (0.1770 g.), melting at 52—53°C. The infrared spectrum was identical with that of diphenylamine. When recrystallized, the crystals melted at 54°C, and the melting point was not depressed when authentic diphenylamine (m. p. 54°C) was mixed with these crystals. Fraction 7, eluted with benzene, was a mixture of azoxybenzene and diphenylamine; the amounts of the compounds were determined by a comparison of the infrared spectrum of the mixture with the spectra of authentic samples.

The Reaction between *p*-Nitrosotoluene and Phenylhydrazine.—Phenylhydrazine was stirred drop by drop into a solution of *p*-nitrosotoluene (1.2109 g., 10.0 mmol.) in dichloromethane (5.0 ml.) at room temperature. The evolution of nitrogen occurred less vigorously than in the case of nitrosobenzene and phenylhydrazine. When 0.4720 g. (4.37 mmol.) of phenylhydrazine was added, no more reaction occurred upon the addition of another drop of phenylhydrazine. When the dark orange solution was distilled, a colorless distillate and a brown solid were obtained.

The colorless distillate was viewed against pure dichloromethane in the infrared region; the spectrum was identical with that of pure benzene. 1.63 mmol. of benzene was found to be present by comparison with the spectrum of a solution containing a known amount of benzene.

1.1924 g. of a brown solid was chromatographed on about 25 g. of alumina. Fractions 1—9, eluted with petroleum ether - benzene, were light yellow crystals (0.7135 g.), melting at 69—70°C. Its infrared spectrum was identical with that of 4, 4'-azoxytoluene. The melting point was not depressed when authentic 4, 4'-azoxytoluene (m. p. 69—70°C) was mixed with these light yellow crystals.

Fractions 11—13, eluted with benzene - ether, were colorless needles (0.0729 g.), melting at 79—86°C. Its infrared spectrum was very similar to that of diphenylamine. When recrystallized from ligroin, the colorless needles melted sharply at 88—89°C, the melting point of authentic 4-methyldiphenylamine. Since diphenylamine melts at 54°C and 4,4'-dimethyldiphenylamine, at 79°C, this colorless crystalline amine can be identified with 4-methyldiphenylamine.

Fraction 10, eluted with benzene, weighed 0.0493 g. and was a mixture of 4, 4'-azoxytoluene and 4-methyldiphenylamine. The amounts of each compound were determined by a comparison of the infrared spectrum of the fraction 10 with the spectra of pure compounds.

Fractions 14 and 15, eluted with ether and methanol, were a black oil, weighing 0.1286 g., which was found to contain 0.0678 g. of unreacted phenylhydrazine.

Acknowledgment is made to the donors of The Petroleum Research Fund, administered by the American Chemical Society, for support of this research.

BULLETIN OF THE CHEMICAL SOCIETY OF JAPNA VOL. 39 1059—1063 (1966)

The Pyrolysis and Thermochromism of the Crystalline Powder of Dianthraquinone

By Haruo KURODA and Ryoichi SUDO*

Department of Chemistry, Faculty of Science, The University of Tokyo, Hongo, Tokyo

(Received November 15, 1965)

The crystalline powder of dianthraquinone changes its color from yellow to green when it is heated above 250°C. A heat-treated powder of a green color exhibits an ESR absorption, the line width of which is about 7 gauss, and the *g*-value, 2.0032. The intensity of the ESR absorption was studied as a function of the temperature of heat-treatment and the heating time. The activation energy for the formation of the paramagnetic species is estimated to be 74 kcal./mol. The X-ray diffraction patterns of heat-treated specimens indicate that a marked disorder is produced in the crystal structure by the heat treatment and that, finally, the dianthraquinone crystal becomes an amorphous solid. A close correlation can be found between the intensity of ESR absorption and the structural change. Polymerization occurs at higher temperatures and results in the formation of a dark green solid insoluble in organic solvents. It is suggested that the initial process of these thermal changes is associated with the thermochromism of dianthraquinone.

It is well known that a solution of dianthraquinone shows a thermochromism, namely, a reversible change of color from yellow to green, as its temperature is raised.[1-3] Nielsen and Fraenkel found that the solution shows an electron-spin-resonance (ESR) absorption when it is in the green-colored state at an elevated temperature.[4] Thus, it is suggested that the thermochromism of dianthraquinone is due to the thermal equilibrium between two isomeric forms of the molecule, in which the high energy form is in a biradical state or a triplet state. The molecular structure of this high energy form has been a matter of discussion for a long time, different models have been proposed by several investigators.[5-8]

A crystalline powder of dianthraquinone shows a similar color change at elevated temperatures.[1] The color changes from yellow to green when it is heated to about 250°C. In this case, however, the change is not reversible, and the powder remains in the green colored state as the temperature is lowered. According to Mayer,[1] the original color can be completely recovered by recrystallization. Matsunaga[9] showed that the diamagnetic susceptibility of the dianthraquinone powder appreciably decreases when it is treated for about 1 hr. at temperatures above 240°C. This suggests the formation of paramagnetic species, which is in agreement with the observation of ESR absorption by Nielsen and Fraenkel.[4] According to Matsunaga,[9] however, the change caused by the heat treatment is by no means reversible, and some kind of polymerization seems to occur during the heat treatment, which makes it hard to dissolve the heat-treated solid in organic solvents. He concluded, therefore, that the color change of the dianthraquinone powder is not due to the thermochromism, but to a chemical reaction or a pyrolysis.

Extensive investigations have been made into the evolution of paramagnetism in the process of the pyrolysis of various organic materials.[10-13] When we compare the behavior of dianthraquinone with the pyrolysis of a usual organic compound, the initial variation in ESR absorption with the heat-treatment at temperatures below 300°C is considerably different. It seems of interest to see, therefore, whether this peculiarity in the thermal change of dianthraquinone powder is associated with the thermochromism or not. In the present study we have investigated the ESR absorption and the X-ray diffraction on the heat-treated powder of dianthraquinone in order to elucidate the nature of the thermal change.

* Present address: Hitachi, Ltd., Yokohama Works, Yokohama.

1) H. Meyer, *Monatsh. Chem.*, **30**, 165 (1909).
2) W. T. Grubb and G. B. Kistiakowsky, *J. Am. Chem. Soc.*, **72**, 419 (1950).
3) W. Theilacker, G. Kortüm and G. Frieheim, *Chem. Ber.*, **83**, 508 (1950).
4) W. G. Nielsen and G. K. Fraenkel, *J. Chem. Phys.*, **21**, 1619 (1953).
5) Y. Hirschberg and E. Fischer, *J. Chem. Soc.*, **1953**, 629.
6) G. Kortüm, *Angew. Chem.*, **70**, 14 (1958).
7) W. Wassermann and R. Davis, *J. Chem. Phys.*, **30**, 1367 (1959).
8) S. L. Matlow, ibid., **23**, 152 (1955).
9) Y. Matsunaga, This Bulletin, **29**, 582 (1956).
10) F. H. Winslow, W. O. Baker and W. A. Yager, *J. Am. Chem. Soc.*, **77**, 4751 (1955).
11) D. J. E. Ingram, *Proc. Third Carbon Conf.*, Pergamon Press (1959), p. 93.
12) H. Akamatu, S. Mrozowski and D. Wobschall, ibid., p. 135.
13) L. S. Singer, *Proc. Fifth Carbon Conf.*, Pergamon Press (1963), Vol. II, p. 37.

Experimental

Dianthraquinone was synthesized from the commercial anthraquinone,[9] and purified by recrystallization repeated three times.* The dianthraquinone powder was heat-treated in an atmosphere of ambient nitrogen by means of a small electric furnace. The heat-treatment temperature (HTT) was varied in the 200—300°C range. The powder was heat-treated while sealed in a glass capillary to facilitate ESR measurement. The X-ray diffraction was examined by using a X-ray diffractometer, Geigerflex (Rigaku Denki Co.), with Cu$K\alpha$ radiation, and the ESR spectrum, by means of a Hitachi MPS-1 ESR Spectrometer. All measurements were made at room temperature.

Results and Discussion

At a low HTT, below 200°C, the dianthraquinone powder changes little in color, even if it is heated for several hours. No ESR absorption can be detected with a heat-treated powder in this case. The color change becomes appreciable, however, as the HTT exceeds 240°C. After a 25 min. treatment, the color becomes pale green at 250°C and green at 270°C. The ESR absorption can be observed with a green-colored powder, as has been reported by Nielsen and Fraenkel. Its intensity increases parallel with the color change, the absorption being weak for a pale green powder and strong for a green one. The spectrum consists of one broad line without a structure, the line width being about 7 gauss and the g-value, 2.0032. The spin concentration estimated from the intensity of the ESR absorption is given in Table I for the powders treated for 25 min. at several temperatures. In the 200—300°C, range, the spin concentration increases as the temperature is raised, but it decreases in the 300—400°C range. If the HTT is raised above 400°C, a carbonaceous solid of a black color is formed, and the intensity of ESR absorption increases again. The change which occurs above 500°C is not different from the one found for the pyrolysis of usual organic solids.

Table I. The spin concentrations of the heat-treated powder of dianthraquinone

HTT °C	Spin concn., spins/g. Heated for 15 min. in nitrogen	Heated for 15 min. in air
230	0.84×10^{17}	1.06×10^{17}
240	1.73×10^{17}	1.85×10^{17}
252	1.11×10^{18}	1.72×10^{18}
270	7.6×10^{18}	1.36×10^{19}

The spin concentration is dependent not only on the HTT but also on the length of heat treatment. Its variation with time is shown in Fig. 1. The spin concentration increases at first linearly with time, but reaches a maximum and decreases afterward. The results shown in Fig. 1 evidently suggest that two different processes are involved in the thermal change observed here. The one is the formation of paramagnetic species, while the other is a reaction that results in the disappearance of the paramagnetism.

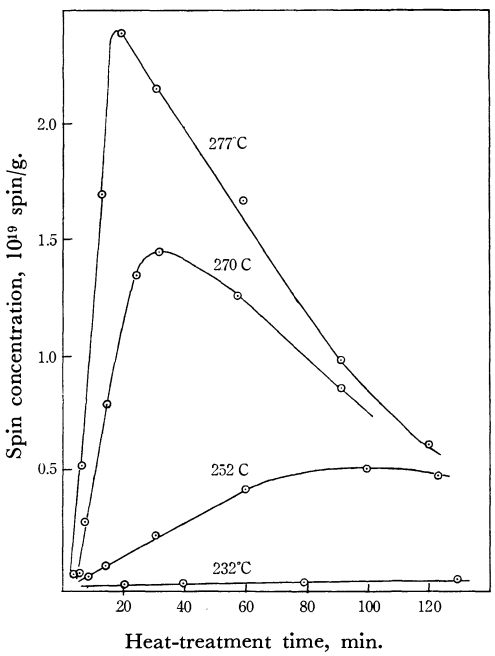

Fig. 1. The variation of spin concentration on heat-treatment of the dianthraquinone powder.

The pyrolysis of an aromatic compound usually begins at a temperature about 400°C. The paramagnetism appears at the same time, and increases with the progress of the carbonization. When the starting material contains some free radicals, however, the pyrolysis begins at lower temperatures because of the instability of the free radicals. This causes an initial decrease in the spin concentration at temperatures about 300°C.[12] In the region of much higher HTT values, however, the dependence of the spin concentration on the HTT is similar to that for the pyrolysis of usual organic compounds. The behavior of dianthraquinone powder seems similar to the case described above except that the free radicals are not present from the beginning, but are formed in the first step of the thermal change.

It should be mentioned here that the ESR absorption of the heat-treated dianthraquinone is little affected by the oxygen. No appreciable change can be found in the intensity as well as in the line width of the ESR spectrum when a specimen prepared in vacuo or in nitrogen is exposed to air. The difference in the spin concentration

* Solvesso-100 (Standard Vacuum Oil Co.) was used as the solvent.

is quite small even if dianthraquinone is heat-treated in air instead of in nitrogen, as is shown in Table I.

The X-ray diffraction patterns of several heat-treated specimens are shown in Fig. 2. The diffraction peaks due to the dianthraquinone crystal are reduced in their intensity by the heat-treatment, and a diffuse scattering appears in the background. The intensity of the diffuse scattering increases with the progress of the thermal change. A dark green solid formed by the one-hour treatment at 270°C shows a diffraction pattern consisting only of diffuse scattering, like amorphous carbons. No diffraction peak associated with a new crystalline phase appears in the HTT range studied here. We can conclude that the heat treatment causes a marked disorder in the crystal lattice of dianthraquinone, finally resulting in the formation of an amorphous solid.

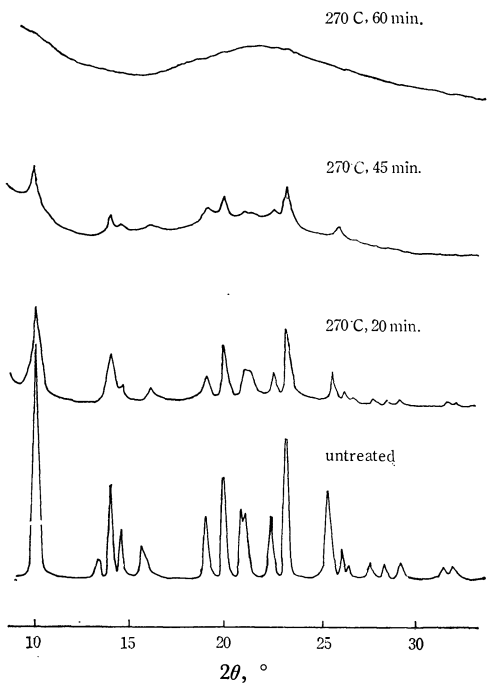

Fig. 2. The X-ray diffraction patterns of the heat-treated powders of dianthraquinone.

The ratio of the intensity of the crystalline diffraction to that of the diffuse scattering can be a measure of the crystallinity. For the value to represent the crystallinity of a heat-treated powder of dianthraquinone, we shall define here a quantity, K, by the following equation;

$$K = \int_{15°}^{30°} I_C \mathrm{d}(2\theta) \Big/ \int_{15°}^{30°} I_D \mathrm{d}(2\theta) \qquad (1)$$

where I_C is the intensity of the crystalline diffraction; I_D, that of the diffuse scattering, and 2θ, the diffraction angle. The variation of K with the heat-treatment time is shown in Fig. 3.

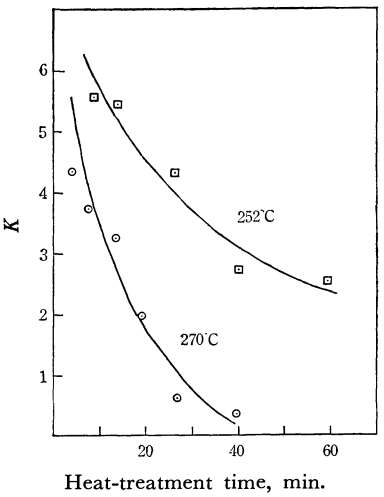

Fig. 3. The change in the crystallinity of dianthraquinone powder on heat-treatment.

In Fig. 4, the spin concentration, as determined from the ESR absorption, is plotted against the value of K. Interestingly, the points fall on a single curve in spite of the difference in the HTT. This means that the formation of the paramagnetic species and the change in the crystal structure are directly related to each other.

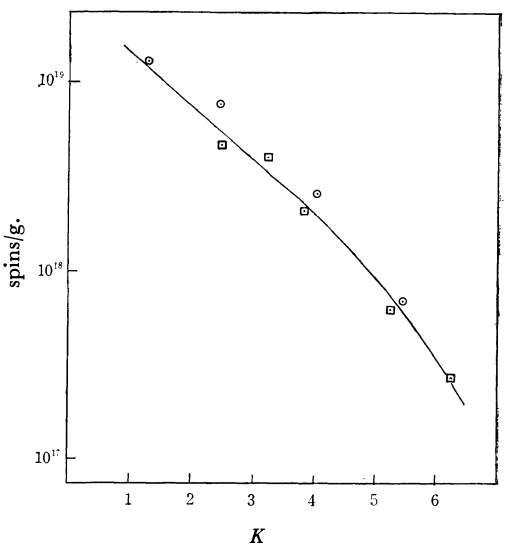

Fig. 4. The relation between the spin concentration and the crystallinity.
⊡ 252°C ⊙ 270°C

The pale green powder obtained by a short heat treatment at a low HTT can be dissolved in several organic solvents, and the original yellow color can be recovered by the recrystallization. However, a dark green powder prepared by a long treatment at 270° is insoluble in organic solvents; this is in agreement with the observation

reported by Matsunaga. Between these two extremes, there is an intermediate state where the heat-treated powder is partialy soluble. We can extract unreacted dianthraquinone from a green specimen by treating it with a solvent. In this stage of thermal change, the dianthraquinone powder gives a diffraction pattern consisting of the diffraction peaks due to dianthraquinone and a diffuse scattering, but if dianthraquinone is extracted from it, the residue shows only a diffuse scattering similar to that of the dark green solid. Therefore, the main part of the insoluble component seems to be the product of polymerization. Suppose that the evolution of the paramagnetism is entirely due to the polymerization of dianthraquinone; the residue of the extraction may then be expected to have a higher spin concentration. However, the spin concentration after the extraction of dianthraquinone is a little smaller than that before the extraction. For example, the powder treated for 25 min. at 270°C originally has 13×10^{18} spins/g., but it has 4×10^{18} spins/g. after the extraction of the unreacted dianthraquinone. It seems that the paramagnetism is associated not only with the products of polymerization, but also with dianthraquinone molecules. Presumably the initial evolution of the paramagnetism is due to the formation of dianthraquinone molecules in a metastable triplet state, as it is in the case of thermochromism in the solution.

We can estimate the activation energy required for the formation of the paramagnetic species in the dianthraquinone crystal by using the experimental data obtained on the ESR absorption. As is shown in Fig. 1, the spin concentration of the heat-treated dianthraquinone at first increases linearly with the heat-treatment time. This can be fitted to a kinetic equation of the first-order reaction. We estimated the apparent rate constant, k, at several HTT value by assuming Eq. 2:

$$dn/dt = kN \qquad (2)$$

where n is the spin concentration, and N, the number of molecules per gram. If the logarithm of k is plotted against the reciprocal of HTT, a straight line can be obtained, as is shown in Fig. 5; the activation energy can thus be estimated to be 74 kcal./mol. On the other hand, the energy difference between the two isomeric forms has been experimentally determined to be 3.4 kcal./mol. for the thermochromism in the solution. Therefore, the observed activation energy for the formation of paramagnetic species in the solid state is too large to be simply attributed to the energy difference between the two isomeric forms of the thermochromism.

According to the model given by Hirschberg and Fischer or that by Wassermann, the shape of a dianthraquinone molecule is not greatly different between the two isomeric forms. If this is the case, a molecule can be transformed from the one form to the other in the crystal without a drastic change in the crystal structure; accordingly, the energy required for this ought to be of the same order as that for a free molecule. On the other hand, Gruff and Kistiakowsky[2] supposed that anthrone halves are perpendicular to each other in the high-energy form of the thermochromism, Matlow[8] also showed later, by the molecular orbital treatment, that a triplet state is lower than the lowest singlet state for the conformation of the molecule mentioned above, and that the energy difference between this state and the ground state, in which anthrone halves are parallel to each other, is 3.3 kcal./mol., in good agreement with the observed energy difference between the two isomeric forms of the thermochromism. For the high-energy form, Kortüm and his collaborators also proposed a model in which anthrone halves are considerably twisted.[3,6] If we assume models of this type, we must consider that the transformation of a dianthraquinone molecule to the high-energy form can not occur without producing quite a large distortion in the crystal lattice; consequently, the energy necessary for this transformation must be very large compared with that for a free molecule. This seems compatible with our experimental results, since we have actually observed that the formation of paramagnetic species is accompanied by the introduction of a marked disorder into the crystal lattice, and since the activation energy for the

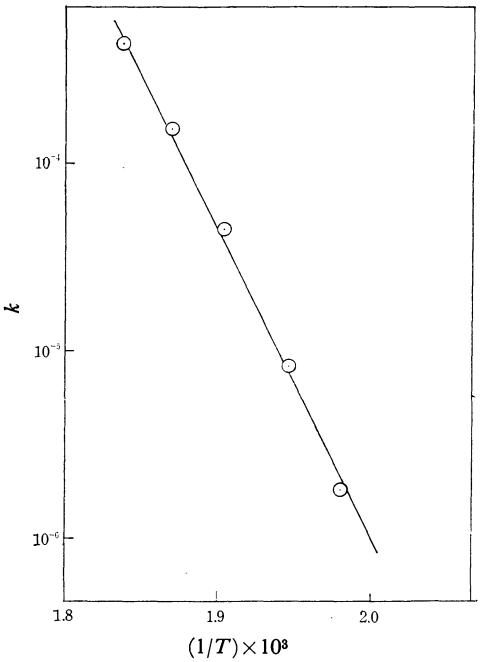

Fig. 5. The plot of $\log k$ against $(1/T)$.

formation of the paramagnetic species in the crystal is large enough to assume such a process. In conclusion, we may suppose that the initial changes in the color and in the ESR absorption are due to the excitation of molecules to the state corresponding to the high-energy form of the thermochromism. In the solid state, however, once a molecule is transformed to such a state at an elevated temperature, it remains in that state even after the temperature is lowered, since a large activation energy is also required in the reverse process because of the necessary rearrangements of the neighboring molecules.

Naturally a molecule in the metastable triplet state is rather unstable, and can be expected to take part in the second process of the thermal change, a polymerization. The X-ray diffraction pattern of the heat-treated powder gives, however, little information on the structure of the polymerization product. The infrared absorption spectrum of the dark green solid of an amorphous structure prepared by 60 min. treatment at 270°C is shown in Fig. 6, together with the spectrum of the dianthraquinone powder. A sharp and strong absorption at 1650 cm^{-1} in the spectrum of dianthraquinone can be attributed to the C=O stretching vibration. Since this band changes little between the two spectra shown in Fig. 6, we can consider that the C=O group of dianthraquinone remains in the pyrolysis product. The absorption bands in the 1400—1600 cm^{-1} region, which are associated with the skeletal vibrations of the aromatic nucleus, are broadened a little. A remarkable change is found in the 650—950 cm^{-1} region, associated with the C–H bending vibrations.

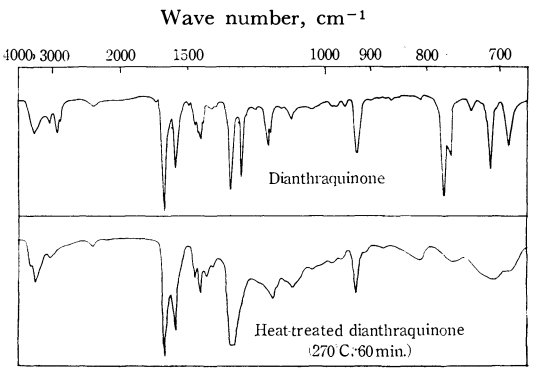

Fig. 6. The change in the infrared absorption spectrum of the dianthraquinone powder on heat-treatment.

These results seem to suggest that, in the polymerization product, the neighboring dianthraquinone molecules are connected by a bridge formed at the periphery of the anthrone halves, presumably at the expense of hydrogen atoms. Interestingly, the char obtained from the pyrolysis of dianthraquinone in the solid state is a non-graphitizing carbon. If the pyrolysis of dianthraquinone in the solid state proceeds in the manner suggested in the present paper, the orientations of aromatic nuclei may be expected to be quite random in the dianthraquinone-char. This might be what makes the char hard to be graphitized in heat treatment at high temperatures.

The authors wish to thank Professor Hideo Akamatu for his valuable discussions, and Dr. Minoru Kinoshita for his advise given on the ESR absorption experiment.

NOTES

A High Frequency Titrimetric Study of the Reaction between Thorium and Alkali Molybdate

By M. L. MITTAL* and S. S. DUBE*

Department of Chemistry, Government College, Kota (Rajasthan), India

(Received March 19, 1965)

The reaction between Th^{4+} and MoO_4^{2-} ions has been investigated by means of high frequency titrations of thorium nitrate with sodium molybdate, by both the direct and reverse methods, in 30% ethanolic media. The end-points obtained from the well-defined breaks in titration curves provide cogent evidence for the formation of normal thorium molybdate, $ThO_2 \cdot 2MoO_3$, in the pH range from 4.2 to 5.8. The precipitation of the compound has been found to be quantitative. The reaction offers a simple, rapid, and accurate method for the determination of thorium as molybdate.

One of the present authors, Mittal,[1-3] has made a detailed study of this reaction by several electrometric methods. The present investigation has been undertaken with a view of substantiating the previous results and studying the possibility of developing a reaction for the analytical determination of thorium. There is, however, no reference in the literature to any high-frequency titrimetric study of this reaction.

Anal. R. (BDH) reagents, thorium nitrate, and sodium molybdate were used; their solutions were prepared in air-free conductivity water. A high-frequency titrimeter of the HFT 30 C type (WTW Germany) with a working frequency of 10 Mc./s. ±1% and a capacity range of 0.25 pF was used; all the high-frequency titrations were carried out by adopting the deflection method. One hundred milliliters of a 30% ethanolic solution of titre was taken into the cell each time. After each addition of a titrant, the cell solution was stirred by an electrically-driven stirrer and the corresponding scale reading was noted and plotted against the volume of titrant added. Only one figure has been given for the sake of brevity (Fig. 1).

Using different concentrations of reactants, thorium nitrate and sodium molybdate a series of high-frequency titrations were carried out by both the direct and inverse methods. Table I illustrates the concentrations employed and the results of study.

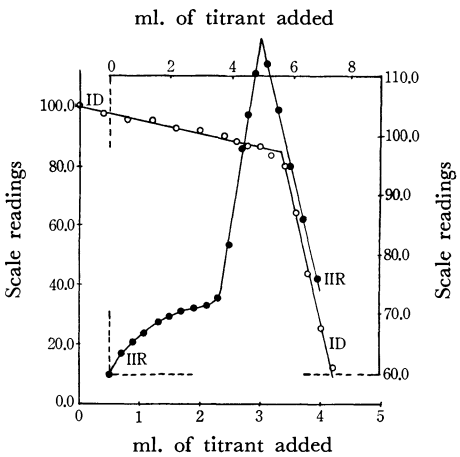

Fig. 1. Direct (curve ID; M/10 $Th(NO_3)_4$ vs. M/150 Na_2MoO_4) and reverse (curve IIR; M/10 Na_2MoO_4 vs. M/400 $Th(NO_3)_4$) high frequency titrations between thorium nitrate and sodium molybdate.

In direct titrations, when sodium molybdate is used as the titre (Fig. 1, curve ID), it may be noted that, on the addition of the titrant (thorium

Table I. A SUMMARY OF THE RESULTS OF HIGH FREQUENCY TITRATIONS

Concentrations		Calcd.	Equivalence points (ml.)	
$Th(NO_3)_4$	Na_2MoO_4		Obs.	Direct titrations Fig. 1, curve ID
M/10	M/150	3.33	3.35	
M/40	M/500	4.00	4.00	
M/75	M/750	5.00	5.05	
M/100	M/1254	4.00	3.95	
Na_2MoO_4	$Th(NO_3)_4$			Reverse titrations Fig. 1, curve IIR
M/10	M/400	5.00	5.00	
M/20	M/1000	4.00	4.02	
M/25	M/1500	3.33	3.30	
M/40	M/2000	4.00	4.05	

1) R. S. Saxena and M. L. Mittal, *J. Sci. Ind. Res. (India)*, **21B**, 92 (1962).
2) R. S. Saxena and M. L. Mittal, *Z. Phys. Chem. (N. F.)*, **34**, 319 (1962).
3) R. S. Saxena and M. L. Mittal, *Naturwissenschaften*, **50**, 373 (1963).

* Present address: Department of Chemistry, Malaviya Regional Engg. College, Jaipur (Rajasthan), India.

nitrate), the scale reading decreases slightly until the stoichiometric end-point is reached; then, when all the MoO_4^{2-} ions have been removed by precipitation as thorium molybdate, there is a sudden decrease in the scale reading. In the case of reverse titrations when thorium nitrate solutions were used as titre, upon the addition of sodim molybdate the scale reading first increases slightly and then, in the vicinity of the end-point, appreciably until the point corresponding to the $ThO_2 : MoO_3$ ratio of 1:2 is reached, after which there is a rapid decrease. Both direct and reverse titrations yield well-defined breaks and suggest the formation of normal thorium molybdate, $ThO_2 \cdot 2MoO_3$. The accuracy and reproducibility of these titrations have been found to be excellent, even at considerably low dilutions of thorium salt (0.5 mM). In view of the accuracy of the method and its applicability to dilute solutions, this reaction can be recommended for the quantitative determination of thorium as molybdate.

The results of high-frequency titrations fully support those obtained with other electrometric methods (loc. cit.).

The authors are indebted to Professor Dr. R. S. Saxena, Malaviya Regional Engineering College, Jaipur, India, for his invaluable help.

The Synthesis of Several Gold Chelates[1)]

By Takahiko INAZU

Department of Chemistry, Faculty of Science, Kyushu University, Hakozaki, Fukuoka

(Received May 24, 1965)

Very few papers have, until recently, been published reporting on the synthesis of gold chelates.[2,3)] In this paper, the synthesis of several gold chelates will be reported. In each case, the gold chelate was obtained by the addition of an ethanolic or an aqueous solutions of chloroauric acid to an ethanolic solution of a ligand. Seven chelates were obtained in a crystalline state, and two as powder.

The first group

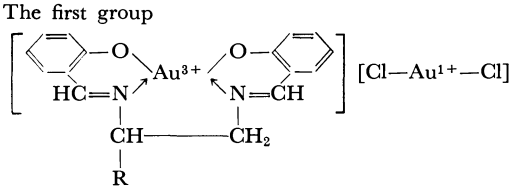

A R=H, CH_3

The second group

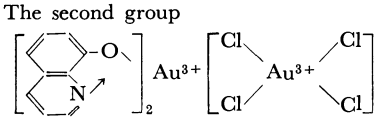

B cis and trans.

The third group

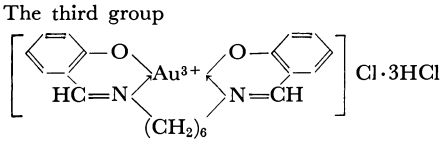

C

They may be classed roughly into three groups (see Fig. 1). It is well known that aurous gold always appears to be two-covalent, while auric gold is always four-convalent and the four valencies are coplanar with the gold atom.[4,5)] Considering the above facts, and the results of paper ionophoresis and the analytical data, it seems most reasonable to assume that one of two gold atoms in the chelate

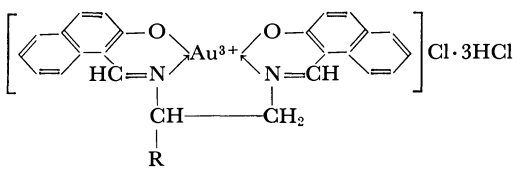

D R=H, CH_3

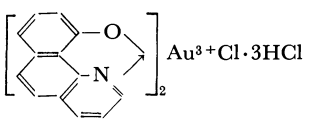

E

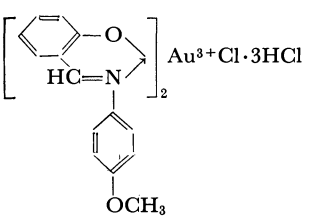

F

Fig. 1

1) Presented at the Kyushu, Shikoku and Chugoku Local Meeting of the Chemical Society of Japan, Miyazaki, December, 1961.
2) R. E. Rundle, *J. Am. Chem. Soc.*, **76**, 3101 (1954).
3) P. Rothemund and A. R. Menotti, ibid., **70**, 1808 (1948).
4) E. G. Cox and K. C. Webster, *J. Chem. Soc.*, **1936**, 1635.
5) D. P. Graddon, "An Introduction to Coordination Chemistry," Pergamon Press, London (1961), p. 42.

TABLE I

Chelate[a]	Appearance[b]	Analysis, % Found C	H	N	Cl	Au	Calcd. C	H	N	Cl	Au
A[c] R=H	Orange y. n.	26.06	2.24	3.84	10.09	53.0	26.25	2.06	3.83	9.70	53.9
A[d] R=CH_3	Pale y. n.	27.57	2.30	3.23		52.11	27.40	2.16	3.76		52.86
B[e]	Dark g. c.	26.26	1.59	3.58		47.81	26.24	1.47	3.40		47.80
B[e]	Amber n.	26.41	1.69	3.53		47.70	26.24	1.47	3.40		47.80
C[f]	Y. brown n.	36.17	3.96	3.92		29.47	36.16	3.79	4.22		29.66
D[g] R=H	Brown p.	40.03	3.16	4.09		27.89	40.07	2.99	3.96		27.81
D[h] R=CH_3	Brown p.	41.73	3.35	3.54		27.20	41.57	3.21	3.88		27.27
E[i]	Dark v. c.	42.35	3.64	3.52	17.70	24.1	42.30	3.52	3.52	17.85	24.8
F[j]	Dark v. n.	42.61	2.50	3.80	19.72	27.2	42.70	2.60	3.84	19.42	27.0

a) Percentages were calculated according to the formula; c) $C_{16}H_{14}O_2N_2Cl_2Au_2$, d) $C_{17}H_{16}O_2N_2Cl_2Au_2$, e) $C_{18}H_{12}O_2N_2Cl_4Au_2$, f) $C_{20}H_{25}O_2N_2Cl_4Au$, g) $C_{24}H_{21}O_2N_2Cl_4Au$, h) $C_{25}H_{25}O_2N_2Cl_4Au$, i) $C_{28}H_{27}O_4N_2Cl_4Au$, j) $C_{26}H_{19}O_2N_2Cl_4Au$.
b) c=crystals, g=green, n=needles, p=powder, v=violet, y=yellow

molecule of the first group is in a reduced univalent state.[6] In the case of 8-hydroxyquinoline chelates, which belong to the second group, two kinds of crystals, of different colors, were obtained. They may be cis and trans isomers each other. In these chelates, the oxidation states of both golds in the cationic and the anionic parts might be considered to be tervalent[7] on the basis of the analytical data and the paper ionophoresis (Fig. 2, No. 2). The chelates of the third group contain one tervalent gold atom and three molecules of hydrogen chloride in each chelate molecule. All the chelates decomposed spontaneously within a year.

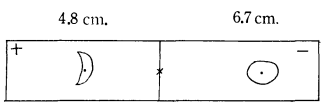

No. 1

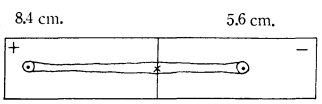

No. 2

Fig. 2. Paper ionophoresis of gold chelates.

Experimental

The following examples represent the methods of preparing the chelates obtained.

Bis(8-quinolinolato)gold (III) - tetrachloroaurate-(III) (B).—A solution of 210 mg. of 8-hydroxyquinoline in 25 ml. of ethanol was mixed with a solution of 300 mg. of chloroauric acid tetrahydrate in 15 ml. of ethanol. After this mixture had stood overnight, a mixture of green crystals and amber needles was obtained. Each of the separated crystals was then collected and washed with a little ethanol. They were slightly soluble in acetone and insoluble in water.

Bis[10-benzo-(h)-quinolinolato]gold(III) - chloride Trihydrogen Chloride (E).—A solution of 85 mg. of chloroauric acid tetrahydrate in 10 ml. of ethanol was mixed with a solution of 127 mg. of a chelating agent[8] in 10 ml. of ethanol. Dark violet needles were immediately formed; these were collected and washed with a little ethanol. They were slightly soluble in acetone and chloroform and insoluble in water.

Paper Ionophoresis.—Tôyô Roshi No. 51 filter paper was used, with a solvent system of acetone - acetic acid - water (1 : 1 : 1 by vol.) (500 V., 2 hr.). The papers were dried in an oven at 120°C, and then left standing overnight. Without further treatment, gray spots of reduced gold were obtained.

N, N' -Disalicylidene-ethylenediaminato-gold(III) - dichloroaurate(I).—(Fig. 2, No. 1).—Two spots were obtained; one spot in the plus region due to $Au(I)Cl_2^-$, and one spot in the minus region due to $Au(III)Ln^+$. (Ln =ligand).

Bis (8 - quinolinolato) gold (III) - tetrachloroaurate(III).—(Amber needles, Fig. 2, No. 2).—Two spots with long tailings were obtained; one spot in the plus region due to $Au(III)Cl_4^-$, and one spot in the minus region due to $Au(III)Ln_2^+$.

The author withes to thank Professor Tokuichi Tsumaki, Professor Tamotsu Yoshino and Dr. Masaru Yamaguchi for their kind direction of this work.

6) As an example of this type, there is the dimethylglyoxime gold complex, confirmed by X-ray diffraction analysis; cf. Ref. 2.
7) The $\alpha, \beta, \gamma, \delta$-tetraphenyl porphine gold complex also belongs to this type; cf., Ref. 3.
8) T. Yoshino, *J. Chem. Soc. Japan, Pure Chem. Sect.* (*Nippon Kagaku Zasshi*), **78**, 108 (1957).

Infrared Absorption Spectral Studies of the Complexes with Substituted 2-Thioureas. I. Bis(1-phenyl-2-thiourea)copper(I) Chloride

By M. A. NABAR

Department of Chemical Technology, University of Bombay, Bombay 19, India

(Received May 31, 1965)

Several co-ordinated complexes in which the ligands are urea and 2-thiourea have been reported. Quagliano and his co-workers[1] have established that, among the urea complexes, some are co-ordinated through one of the nitrogen atoms, and the others, through the oxygen atom of the urea molecule. They have then extended these studies to 2-thiourea and 1-methyl-2-thiourea complexes,[2,3] and have concluded that although the co-ordination takes place either through the sulphur atom or one of the nitrogen atoms when 1-methyl-2-thiourea is a ligand, the sulphur atom is exclusively involved in the co-ordination in the 2-thiourea complexes. Rivest[4] came to a similar conclusion from his studies of the co-ordinate complexes of titanium(IV) chloride with alkyl and aryl substituted 2-thioureas. More recently Berni and others[5] have studied the properties of the metal ion complexes of ethylene urea (2-imidazolidinone).

The present investigations were undertaken in order to examine the influence of substituents such as alkyl, aryl and acyl[6] groups on the relative donor abilities towards co-ordination of either the sulphur or the nitrogen atom of the 2-thiourea.

Cuprous salts form many complexes with ligands such as 1-phenyl- and 1-acetyl-2-thioureas in different mole-ratios.[7] This note will present the results of the infrared absorption studies of $CuCl \cdot 2C_6H_5NHCSNH_2$.

Experimental

Preparation of the Compound—Eastman-Kodak white-label 1-phenyl-2-thiourea was used without further purification. The $CuCl_2 \cdot 2H_2O$ used was of the reagent grade. Bis(1-phenyl-2-thiourea)copper(I) chloride was prepared according to the method of Banerjee and Sukthankar[7]; it was recrystallised from acetone and dried in a vacuum desiccator for a constant analysis.

Absorption Measurements—The spectra were obtained with a Perkin-Elmer recording infrared spectrophotometer, model 21. A sodium chloride prism was used over the complete infrared region to be reported on. As a routine, polystyrene film was used for the wave number calibration. The spectra were taken using the KBr disc technique and were checked using Nujol and fluorolube mulls. The spectra obtained are illustrated in Fig. 1, while the experimental results, along with the corresponding assignments of the frequencies, are given in Table I.

Results and Discussion

As a necessary prerequisite, the assignments required for this analysis were made on a comparative basis, mainly with 2-thiourea and 1-methyl-2-thiourea,[2,3] since there are no adequate published assignment data on 1-phenyl-2-thiourea.[8] For phenyl-ring and ring-hydrogen vibrations, the assignments of Randle and Whiffen[9] were used.

The absence in the 2500—2600 cm^{-1} region of the absorption band characteristic of the SH group in the spectra of the complex and the ligand (1-phenyl-2-thiourea) indicates that the ligand is in its thiocarbonyl resonance form.

The formation of S→M bonds is expected to result in an increased double-bond character for the carbon-to-nitrogen bond and a lowering of it for the carbon-to-sulphur bond.

A comparison of the spectrum of 1-phenyl-2-thiourea with that of the copper(I) complex shows that the general spectral profile of the complex in the 3 μ region is almost unchanged. These bands, which can be assigned to N–H absorptions, are neither shifted to significantly lower frequencies not split into groups with a decrease in intensity, on the formation of the complex. This indicates the absence of nitrogen-to-metal bonds; therefore, the bonding must be between sulphur and the metal atoms. The broadening of these bands can be attributed to a considerable amount of hydrogen bonding, perhaps a Cl···H–N type of hydrogen bonding, in the complex.[10]

1) R. B. Penland, S. Mizushima, C. Curran and J. V. Quagliano, *J. Am. Chem. Soc.*, **79**, 1575 (1957).
2) A. Yamaguchi, R. B. Penland, S. Mizushima, T. J. Lane, C. Curran and J. V. Quagliano, ibid., **80**, 527 (1958).
3) T. J. Lane, A. Yamaguchi, J. V. Quagliano, J. A. Ryan and S. Mizushima, ibid., **81**, 3824 (1959).
4) R. Rivest, *Can. J. Chem.*, **40**, 2234 (1962).
5) R. J. Berni, R. R. Benerito, W. M. Ayres and H. B. Jonassen, *J. Inorg. Nucl. Chem.*, **25**, 807 (1963).
6) M. A. Nabar, unpublished results.
7) S. N. Banerjee and A. C. Sukthankar, *J. Indian Chem. Soc.*, **39**, 197 (1962); **40**, 385 (1963).
8) H. G. Mautner and W. D. Kumler, *J. Am. Chem. Soc.*, **78**, 97 (1956).
9) R. R. Randle and D. H. Whiffen, "Molecular Spectroscopy" (Inst. Petroleum, E. Thornton, ed.), Pergamon Press, New York (1955), p. 111.
10) W. Kutzelnigg and R. Mecke, *Spectrochim. Acta*, **17**, 530 (1961).

Table I. Infrared frequencies (cm^{-1}) and assignments for 1-phenyl-2-thiourea and bis(1-phenyl-2-thiourea)copper(I) chloride

$C_6H_5NHCSNH_2$	$CuCl{\cdot}2C_6H_5NHCSNH_2$	Assignment
3440 s	3450 ms	NH stretching
3280 s	3285 s	
3180 vs	3180 s	
3025 mw	~3040 sh	CH sym. stretching
1614 vs	1616 vs	NH_2 bending
1593 ms	1596 s	CC stretching
	1546 sh	
1527—1522 s, b	1536 vs	NH deformation + CN antisym. stretching
1490 m		CC stretching
1465 m	1498 s	NCN stretching + CC stretching
1451 s	1452 s	CC stretching
	1420 mw	
1316 ms	1321 ms	CC stretching
1295 m	1298 m	CN antisym. stretching + NH deformation
1274 m	1265—1260 m, b	CH in-plane deformation + X sensitive*
1259 m	1253 sh	
1231 m	1243—1233 m, b	
1168 vw	1173 vw	CH in-plane deformation
1153 vw	1155 vw	CH in-plane deformation
1073 mw	1081 sh	CH in-plane deformation
1062 m	1066 mw	CS stretching + CN sym. stretching + NH_2 rocking
1025 vw	1027 vw	CH in-plane deformation
998 vw	1004 vw	Ring breathing
918 vw	910 vw	CH out-of-plane deformation
855 vw	853 vw	CH out-of-plane deformation
811 mw	795 mw	CS stretching + CN sym. stretching and X sensitive*
750 ms	747 ms	CH out-of-plane deformation and NH out-of-plane bending
~ 707 sh		Ring out-of-plane deformation
693 ms	692 ms	Ring out-of-plane deformation

* In monosubstituted benzenes (C_6H_5X) there are six fundamental frequencies, out of the possible thirty, sensitive to the mass and the nature of X, the substituent (-$NHCSNH_2$ in the present case). These are classified as X sensitive. The two bands observed here are mainly CX stretching vibrations with some contribution from one of the ring breathing vibrations and CX in-plane deformation vibration.[9]

Abbreviations : s=strong ; m=medium ; w=weak ; sh=shoulder ; b=broad ; v=very.

The strong broad band at 1522—1527 cm^{-1} can be explained as an "hydrid" band due to N–H deformation and C–N antisymmetric stretching vibrations. On co-ordination, this band is shifted to a higher frequency, indicating the increased double-bond character of the C–N bond and, hence, co-ordination through the sulphur atom. Similar behaviour was observed in complexing in the case of 2-thiourea and 1-methyl-2-thiourea.[2,3]

The N–C–N stretching band at 1465 cm^{-1} in the 1-phenyl-2-thiourea corresponds to the 1470 cm^{-1} band of 2-thiourea. The frequency of this band is increased by about 33 cm^{-1} on complexing, again indicating an increased double-bond character of the carbon-to-nitrogen bond.* A similar shift has been observed by Kutzelnigg and Mecke[10] in the $CuCl{\cdot}4CH_3CSNH_2$ complex.

A marked difference in the spectrum of the free ligand and its metal complex appears in at about 1100 cm^{-1}. A sharp absorption band at 1062 cm^{-1} of 1-phenyl-2-thiourea, corresponding to the 1083 cm^{-1} and 972 cm^{-1} bands of 2-thiourea and 1-methyl-2-thiourea[2,3] respectively, is very much broadened and weakened. The contribution of the C=S vibration and, hence, the intensity of this band is decreased on co-ordination through the sulphur atom. The symmetric N–C–N stretching

* It seems likely that this band corresponds to the "thioureide" band assigned by Randall and others[11] between 1613—1471 cm^{-1}, by Ettlinger,[12] at 1508 cm^{-1} and by Mann,[13] at 1495 cm^{-1}.

11) H. M. Randall, R. G. Fowler, N. Fuson and J. R. Dangl, "Infrared Determination of Organic Structures," D. Van Nostrand Co., Inc., New York (1949).

12) M. G. Ettlinger, *J. Am. Chem. Soc.*, **72**, 4699 (1950).

13) J. Mann, *Trans. Inst. Rubber Ind.*, **27**, 232 (1951).

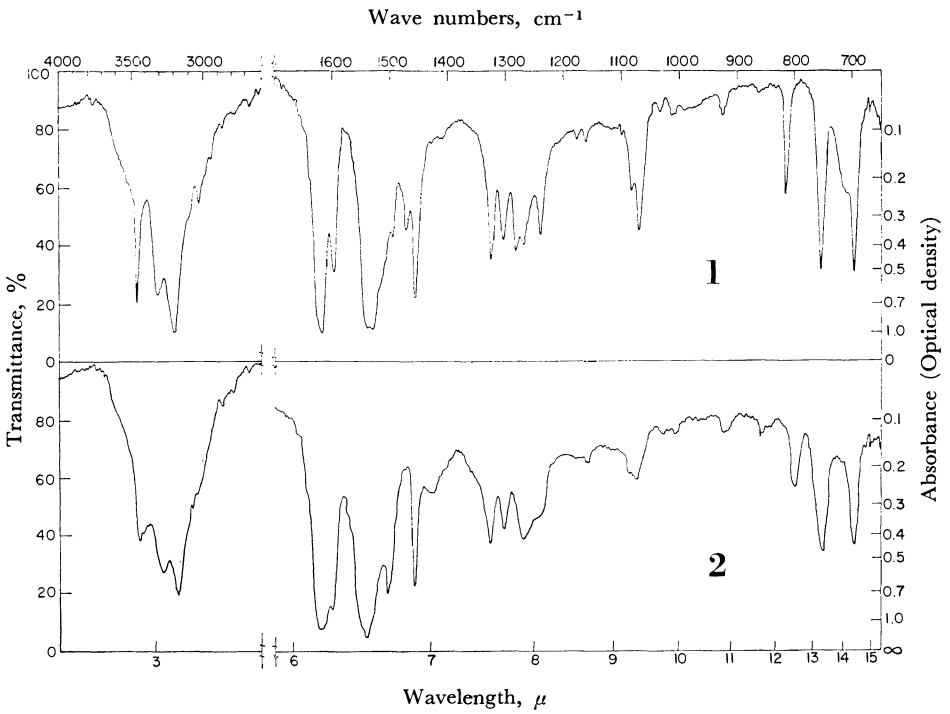

Fig. 1. Infrared spectra in KBr disk.
1. 1-phenyl-2-thiourea 2. Bis(1-phenyl-2-thiourea)copper(I) chloride

vibration can not contribute much to this band, as has been shown for the spectra of urea and 2-thiourea; this explains the overall decrease in intensity. A similar weakening or complete disappearance of a band was observed in co-ordination through sulphur in the case of 2-thiourea and 1-methyl-2-thiourea.[2,3]

The band at 811 cm^{-1} of 1-phenyl-2-thiourea is considered to correspond to the 731 cm^{-1} and 774 cm^{-1} bands in 2-thiourea and 1-methyl-2-thiourea respectively,[2,3] bands arising mainly from the C=S stretching vibration, though with a little contribution from the symmetric C–N stretching vibration. The lowering of this frequency by about 16 cm^{-1} can be attributed to the reduced double-bond character of the carbon-to-sulphur bond.

The above-mentioned three bands could also be identified as "–N–C=S" I, III and IV bands respectively, according to Rao.[14] However in the region to which he assigned the "–N–C=S"–II band, no definite conclusions could be drawn, mainly because of the other overlapping regions.

No significant changes have been observed in the remaining bands of the spectra of the ligand on complexing; this is not unexpected, as these could be identified as arising from the presence of the phenyl ring and from the ring hydrogen vibrations.[9]

The co-ordination of 1-phenyl-2-thiourea to copper(I) shifts certain infrared absorption frequencies, notably at about 1450, 1100 and 800 cm^{-1}; these shifts can be correlated with the changes in the double-bond character of the C–S and C–N bonds. Such a situation suggests a considerable covalent character of the sulphur-copper bonds, indicating a ligation through the sulphur atom in a complex.

The author wishes to thank Mr. R. Ironside of the Analytical Section, Applied Chemistry Division, National Research Council, Canada, for repeating some spectral work, and also the National Research Council, Canada, for a post-doctoral Fellowship, during the tenure of which this paper was written.

14) C. N. R. Rao, "Chemical Applications of Infrared Spectroscopy," Academic Press., New York and London (1963), p. 303.

The Formation Constants of 1 : 1 and 1 : 2 Complexes of Ethyl Acetate and Phenyl Acetate with Phenol

By S. Sriraman and V. Shanmugasundaram

Department of Physics, Annamalai University, Annamalainagar, South India

(Received July 19, 1965)

The detection of complex formation is convincingly accomplished by the study of infrared spectra. A complete survey of the literature wherein infrared spectroscopy is used as an analytical tool for the detection of such complexes has been made by Pimentel and McClellan.[1] Several recent studies[2-4] of the hydrogen bonding of phenols to different proton-acceptor groups have indicated the existence of at least two different types complexes in most of the systems over a wide range of concentration. A large number of values of the equiliarium constants for the formation of 1 : 1 complexes is available for many systems, but no quantitative values are available for the 1 : 2 complexes. The main purpose of this work is to obtain the formation constants for such complexes, along with the formation constants for 1 : 1 complexes; these values will make possible the determination of the concentrations of different molecular species in the system under consideration.

The formation constants, K_{11} and K_{12}, of 1 : 1 and 1 : 2 complexes of ethyl acetate and phenyl acetate with phenol in carbon tetrachloride were determined by studying the infrared absorption in the hydroxyl and carbonyl regions. The measurements were made with a Hilger H 800 double-beam spectrophotometer equipped with sodium chloride optics; approximately 0.04 M solutions of phenyl acetate and ethyl acetate 0.25 mm. thick were placed in a variable-path-length micrometer cell supplied by the Hilger. The temperature of the cell was maintained at 22°C.

The modified method of Brown and Kubota[5] developed by Whetsel and Kagarise[4] was used for the calculation of the equilibrium constants for the formation of the complexes of the $A+B \rightleftarrows AB$ and $AB+B \rightleftarrows AB_2$ types, where A represents the ester and B, the monomeric phenol. This method, given in detail by those authors, involves the calculation of a set of K_{11} values for different assumed values of K_{12}. A plot of the values of K_{11} against the concentration of the phenol results in a series of lines with different slopes and intercepts (Fig. 1). The value of K_{12} which gave a line of zero slope was taken as the best value, and the intercept of this line was taken as K_{11}. The formation constants of 5.9±1 l./mol. and 13.5±2 l./mol. were obtained for the 1 : 1 and 1 : 2 phenyl acetate and phenol complexes respectively. For the ethyl acetate - phenol system, values of 8.6±1 l./mol. and 25±2 l./mol. were obtained for K_{11} and K_{12} respectively.

The formation constants for the 1 : 1 complexes were also obtained by the method suggested by Nash.[6] This method, derived by Nash, utilises the $Y=X(K-\alpha)-K$ relation, where Y is the reciprocal of the concentration of monomeric phenol at equilibrium and

$$X = \frac{1}{1-A/A_0}$$

where A_0 and A are the absorbances of the ester at a given frequency in the absence and in the presence of the donor respectively. The equilibrium concentrations of phenol required were determined from the hydroxyl absorption, and A and A_0 were taken in the carbonyl region near the characteristic frequency of the 1 : 1 complex. The intercept of the plot of Y against X is the negative value of the formation constant for the 1 : 1 complex.

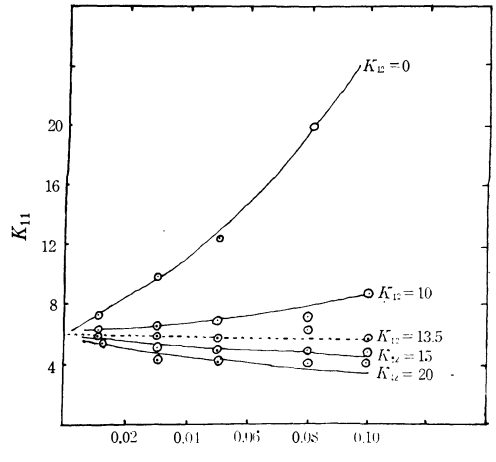

Fig. 1. Formation constants for 1:1 and 1:2 complexes of phenyl acetate and phenol in CCl_4 solution.

1) G. C. Pimentel and A. L. McClellan, "The Hydrogen Bond," W. H. Freeman & Co., London (1960), p. 67.
2) E. Gray, *Ann. Chim.*, (12) **3**, 355 (1948).
3) J. Lascombe, Thesis, University of Bordeaux (1960).
4) R. E. Kagarise and K. B. Whetsel, *Spectrochim. Acta*, **18**, 315 (1962).
5) T. L. Brown and M. Kubota, *J. Am. Chem. Soc.*, **83**, 331 (1961).
6) C. P. Nash, *J. Phys. Chem.*, **64**, 950 (1960).

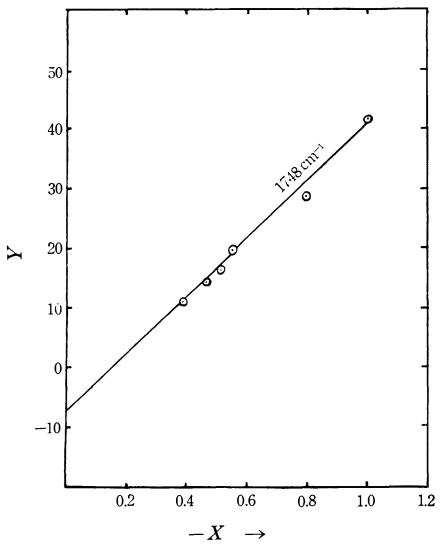

Fig. 2. Formation constant for 1:1 complex phenyl acetate with phenol determined by Nash method.

Figure 2 shows such a plot for the phenyl actate - phenol system. A value of 6.5 l./mol. was obtained for the formation constant K_{11} for the phenyl acetate - phenol system. In a similar manner, a value of 8 l./mol. was obtained for K_{11} for ethyl acetate - phenol system. The values of the formation constants of 1 : 1 complexes obtained by the two methods agree well.

The values of K_{11} obtained in the present investigation compare favourably with the value of 8.68 l./mol. at 27.85°C obtained by Powell and West[7] for the phenol - ethyl acetate system. Also, the value of 7.1 l./mol. at 30°C for the same system reported by Nagakura[8] from his ultraviolet studies agrees closely with the results of our present investigation.

7) D. L. Powell and R. West, *Spectrochim. Acta*, **20**, 983 (1964).
8) S. Nagakura, *J. Am. Chem. Soc.*, **76**, 3070 (1954).

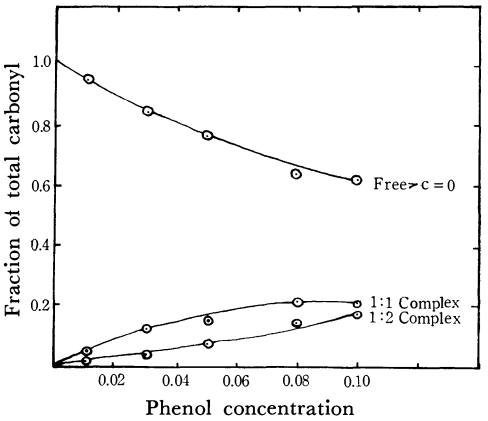

Fig. 3. Relative abundance of free and complexed phenyl acetate in mixtures of phenol and CCl_4.

It should be noted that the K_{11} and K_{12} values obtained in the present investigation for the phenyl acetate - phenol system are relatively lower than those for the ethyl acetate - phenol system. This may be due to the molecular complexity of phenyl acetate, which may hinder the possibility of the formation of specific complexes.

From the knowledge of the formation constants K_{11} and K_{12} the relative abundance of 1 : 1 and 1 : 2 complexes can be easily determined. Figure 3 shows that a high fraction of the complexed ester is present as 1 : 2 species and that at higher concentrations of phenol the 1 : 2 complex may predominate.

The authors wish to express their thanks to Dr. M. G. Krishna Pillai, Reader in Spectroscopy, Annamalai University, and to Dr. K. Ramaswamy, Infrared Division, National Physical Laboratory, New Delhi, for their kind and valuable suggestions throughout the progress of this work.

The NMR of Benzene/Water Emulsion

By Toshiro OKAMURA, Iwao SATAKE and Ryohei MATUURA

Department of Chemistry, Faculty of Science, Kyushu University, Hakozaki, Fukuoka

(Received August 7, 1965)

To date, no paper has reported the application of the high-resolution NMR technique to the investigation of emulsion except that of Cratin and Robertson.[1] Since the emulsion state is heterogeneous and thermodynamically-metastable, its complete analysis is very difficult. In this communication, some information obtained with the NMR technique concerning the benzene/water emulsion will be reported.

1) P. D. Cratin and B. K. Robertson, *J. Phys. Chys. Chem.*, **69**, 1087 (1965).

Experimental

The emulsions were prepared by shaking portions of benzene with equal amounts of water containing an emulsifier in various concentrations. As the emulsifier sodium dodecyl sulfate (SDS) was used. The emulsions thus obtained were of the o/w type. The freshly-prepared emulsion was left to stand for about 24 hr. before the NMR investigation was started in order to secure the state of the emulsion which was stable enough during the NMR measurement.

The chemical shifts of the proton in water, benzene and SDS were measured at constant temperatures, but the shifts of the latter two were so small as to fall within the range of experimental error; therefore, the final measurements were made solely with the water proton peaks. The shifts were measured by using a Japan Electron Optics JNM-3 high-resolution NMR spectrometer, with dioxane as the external reference. The experimental error was less than 0.5 c. p. s.

Results and Discussion

Figure 1 shows the water proton chemical shifts in SDS solutions of various concentrations and temperatures. The water proton gave a single but somewhat broad resonance line; this line shifted towards the higher applied field with an increase in the SDS concentration and temperature. The single line in this case represents the rapid proton exchange between different species, and the higher field shift is assumed to show that the structure of water is increasingly destroyed by the increase in the concentration of SDS, as well as by the rise in temperature, the shift per mole of SDS nearly corresponding to that per ten degrees of temperature. There should be a kink at the critical micelle concentration (CMC) on the curve of the shift vs. SDS concentration, as was shown by Pethica,[2] but in this experiment the range of the SDS concentration is so high that the kink at the CMC is not clear. However, it may be said from Fig. 1 that the slope of the curve below the CMC decreases with the temperature, while that above the CMC is independent of the temperature.

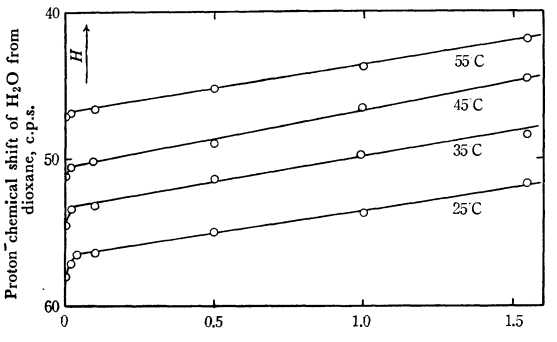

Fig. 1. Proton chemical shift of H_2O vs. SDS concentration at various temperatures.

The concentration of the SDS solution used for preparing the emulsion in this experiment was far above the CMC, and the amount of benzene added was large enough so that the bulk solution should have been saturated with benzene (solubilization). The chemical shift of the water proton in the SDS solution saturated with benzene was, therefore, measured. The results are shown in Fig. 2. In the presence of solubilized benzene, the water proton shifts to a higher field than in the absence of benzene; this shift increases with the amount of benzene solubilized. When Wiedmann's theory is applied, the chemical shift due to the change in bulk susceptibility is less than 0.4 c. p. s. at the SDS concentration of 1.0 mol./l. The observed value is much larger than this. Therefore, the higher field shift due to solubilized benzene may be attributed to the magnetic anisotropy of benzene. If the solubilized benzene is only in the central part of micelles, this effect can not be expected. It is, therefore, reasonable to consider that the solubilized benzene is, as Eriksson[3] proposed, near the micelle surface, or that, as Nakagawa et al.[4] showed, benzene molecules in the micelle exchange with those in the bulk solution.

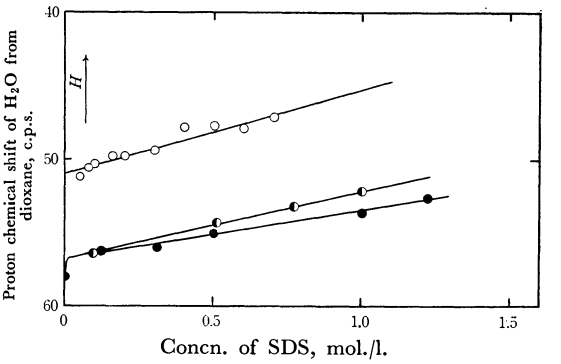

Fig. 2. Proton chemical shift of H_2O vs. SDS concentration at 25°C.
○ In emulsion ● In SDS solution
◐ In SDS solution saturated with benzene

Also in Fig. 2, the chemical shift of the water proton in the benzene/water emulsion is plotted against the SDS concentration, the latter being determined after the destruction of the emulsion. It may be seen that the shift of the water proton in the emulsion state containing SDS as an emulsifier is further towards the higher magnetic field than in the case of the SDS solution containing solubilized benzene. This higher field shift can not be due to the magnetic anisotropy of benzene, since we found a similar shift in the case of the cyclohexane/water

2) J. Clifford and B. A. Pethica, *Trans. Faraday Soc.*, **60**, 1483 (1964).

3) J. C. Eriksson, *Acta Chem. Scand.*, **17**, 1478 (1963).

4) T. Nakagawa and K. Tori, *Kolloid-Z. u. Z. Polymere*, **194**, 143 (1964).

emulsion. The observed difference between the chemical shift of the water proton in the SDS solution, which has solubilized benzene, and that in the benzene/water emulsion state is to be attributed to the surface effect of the emulsion particles.

At the oil/water interface the SDS molecules are considered to form an adsorbed layer. Accordingly, the water molecules near the interface are different in structure from those of the bulk water due to the charge as well as to the dipole effect of the adsorbed SDS molecules. It is difficult to distinguish the true interface effect (without an adsorbed emulsifier) from the effect of the adsorbed layer of the emulsifier, but it would be natural to consider that the higher field shift of the water proton in the emulsion state over the shift of that in the bulk solution containing benzene is caused chiefly by the breaking of the hydrogen bond structure of water at the interface. Again, it is assumed that the exchange of water between the surface and the bulk is rapid. When the chemical shifts of water protons in the emulsion state, at the interface, and in the bulk solution, are denoted by δ_e, δ_s, and δ_b respectively, then:

$$\delta_e = X_s\delta_s + (1 - X_s)\delta_b \quad (1)$$

where X_s is the mole fraction of water near the interface causing δ_s. From Eq. 1 we have:

$$\Delta\delta/X_s = \delta_s - \delta_b \quad (2)$$

where $\Delta\delta = \delta_e - \delta_b$. We have attempted to determine the particle-size distribution of the benzene droplets in the emulsion by microscopic observations as a function of the SDS concentration. From this we can estimate the value corresponding to X_s at each SDS concentration, assuming that X_s is proportional to the interfacial area between benzene droplets and water. For δ_b the chemical shift of the water proton in the SDS solution saturated with benzene can be used. From these data the $\Delta\delta/X_s$ vs. δ_b plot can be obtained. Unfortunately, due to errors accompanying the particle-size distribution of the emulsion, we could only roughly confirm the linear relationship between $\Delta\delta/X_s$ vs. δ_b. We are expecting to reach a more precise conclusion after the particle-size distribution has been improved.

An Anomalous Electric Property Found in Grain and at the Grain Boundary of the Barium Titanate Ceramic Doped with Bismuth

By Masato YANASE and Katsuhiro OHNO

The Central Research Laboratories, Mitsubishi Electric Corporation, 80 Nakano, Minamishimizu, Amagasaki, Hyogo

(Received August 26, 1965)

It has been reported[1-3] that the resistivity of the polycrystalline barium titanate ceramic doped with bismuth increased anomalously above its Curie point. It is generally considered that this increase is due to the existence of a particular barrier at the grain boundary of the ceramic. However, the experimental results obtained with a single crystal do not seem to support this view. For example, Brown and Taylar[4] recently indicated that the single crystal of barium titanate doped with niobium prepared by the zone-melting process showed the same anomaly. Also, Kawabe and Inuishi[5] reported that a similar increase in resistivity could be found in the semiconductor obtained by reducing the barium titanate single crystal with hydrogen.

These results may suggest that the polycrystalline and single crystals of this ceramic have different electric properties.

A large-grained ceramic with an anomalous increase in resistivity was prepared, and the potential changes in the grain and at the grain boundary were studied (see Fig. 1).

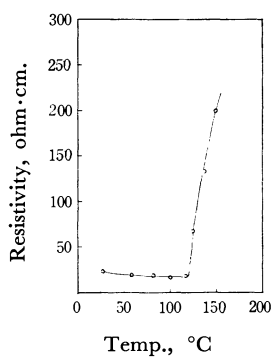

Fig. 1. Resistivity-temperature dependence of specimens used this experiment.

1) H. A. Sauer and S. S. Flaschen, Proc. Electron. Com. Sym. 7th, Washington D. C. May, 1956.
2) O. Suburi, *J. Phys. Soc. Japan*, **14**, 1159 (1959).
3) W. Heywang, *Solid State Electron*, **3**, 51 (1961).
4) F. Brown and C. E. Taylor, *J. Appl. Phys.*, **35**, 2554 (1964).
5) K. Kawabe and Y. Inuishi, *Japanese J. Appl. Phys.*, **2**, 590 (1963).

Experimental

Specimens of barium titanate ceramic doped with bismuth were prepared from barium titanyl oxalate[6] as the starting substance. This powder was mixed with 0.1 mol.% bismuth sesquioxide using a ball mill and was calcined at 1000°C in air. It was then pressed into disks 50 mm. in diameter and 3 mm. thick and was sintered at 1400°C in air. The mean grain diameter was found under a mecroscope to be about 500 μ. This was cut into plates 1 mm. thick, 20 mm. long and 5 mm. wide, pasted into glass plates, lapped to a thickness below 300 μ in order to obtain a single grain layer, and etched in order to make it possible to see the grain boundary. The electrodes were made at both sides of the specimen by utilizing the special nickel plating shown in Fig. 2.

The potential change produced in the specimen was measured by the two-points method using a sharp-headed probe made of tungsten wire 0.3 mm. in diameter. The head was wet with liquid indium-mercury alloy[7] in order to obtain an ohmic contact.

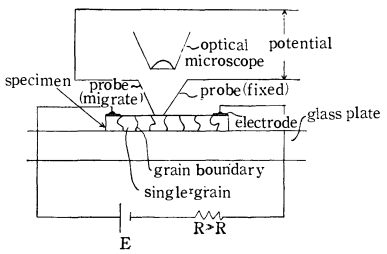

Fig. 2. Scheme of specimen and measure method.

Results and Discussion

Figure 3 shows the variation in the electrical potential between two probes. The one was fixed at the side of the specimen, while the other was moved on the surface on the grain. A large potential difference was always observed across the grain boundary. This shows that a barrier exists at the grain boundary, but its magnitude is different according to the specimen. This may indicate that the amount of barrier existing at the grain boundary varies and that the property of this barrier may be affected by the grain.

It is clear that the grain boundaries of the barium titanate ceramic doped with bismuth have a particular potential barrier. However, it is not clear whether the height of this potential barrier depends on the temperature above the Curie point. Therefore, the temperature-dependence of the potential drop should be measured. For this purpose, the resistivity of the grain was measured at various temperatures. The specimen was heated and its temperature was measured by a 0.1 mm.-in-diameter copper-constantan thermocouple pasted on the glass plate attached to the specimen.

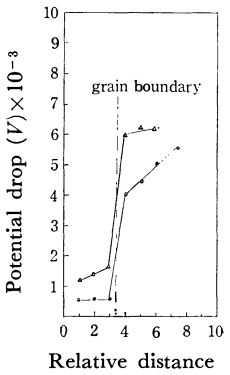

Fig. 3. Potential drop variation in case that crossed a grain boundary.

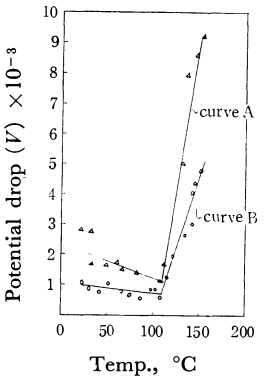

Fig. 4. Potential drop-temperatures dependence of the inside of grain.

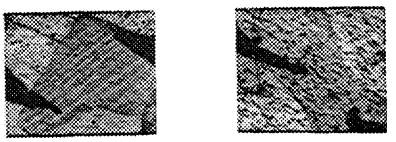

Fig. 5. Measured grains correspond with Curves A and B.

The potential change was found to be at about 110°C (see Figs. 4 and 5). In Fig. 4, the anomalous increase in resistivity in the grain is shown. This suggests that the anomalous increase of resistivity can not be attributed only to the barrier at the grain boundary. However, it was not possible to determine separately the temperature-dependent resistivity in the grain and that due to the barrier existing at the grain boundary.

The results obtained from this experiment may be summarized as follows: (1) A particular barrier causing a large potential change would exist at the grain boundary of the barium titanate ceramic doped with bismuth. (2) An anomalous increase in resistivity was observed in the grain of the barium titanate ceramic doped with bismuth, but it is

6) W. S. Clabaugh, E. M. Swiggard and R. Gilchrist, *J. Res. Natl. Bur. Stands.*, **56**, 286 (1956).

7) S. S. Flaschen and L. G. von Uitert, *J. Appl. Phys.*, **27**, 190 (1956).

not clear whether the mechanism of the increase of the resistivity of this material is to be attributed to the barrier at the grain boundary or to that in the grain.

The authors wish to acknowledge many valuable discussions with Dr. Sumiaki Ibuki of their laboratory.

The Absolute Configuration of *trans*-2-Methylcyclopropanecarboxylic Acid[1]

By Toshio SUGITA and Yuzo INOUYE

Institute for Chemical Research, Kyoto University, Takatsuki, Osaka

(Received August 30, 1965)

In the course of our studies of asymmetric syntheses in Simmons-Smith reactions, it was necessary to establish the absolute configuration of *trans*-2-methylcyclopropanecarboxylic acid.[2] We wish, at this time, to report the absolute assignment of the configuration of this acid by means of a direct chemical transformation. In a previous paper[3], the absolute configurations of (−)-*trans*-1, 2-cyclopropanedicarboxylic acid and (+)-*trans*-2-phenylcyclopropanecarboxylic acid were established as 1*R* : 2*R* and 1*S* : 2*S* respectively by an unequivocal correlation with *trans*-1, 2-dimethylcyclopropane of a known configuration. This provides us with the mean of correlating *trans*-2-methylcyclopropanecarboxylic acid with *trans*-2-phenylcyclopropanecarboxylic acid.

Methyl *trans*-2-phenylcyclopropanecarboxylate, $[\alpha]_D^{12}$ −171.9°, of a 51.3% optical purity, which had resulted from the quantitative esterification with diazomethane of the corresponding (−)-acid, was reduced with lithium aluminum hydride to the carbinol, $[\alpha]_D^{12}$ −46.6°. The carbinol was then converted with methanesulfonyl chloride in lutidine into the mesylate; then due to the instability of the mesylate, it was immediately reduced with lithium aluminum hydride to 1-methyl-2-phenylcyclopropane, $[\alpha]_D^{16}$ −57.7°. The ozonolysis of the laevorotatory hydrocarbon produced (−)-*trans*-2-methylcyclopropanecarboxylic acid, $[\alpha]_D^{19}$ −42.9° (chloroform), $[\alpha]_D^{19}$ −39.7° (ethanol). On the basis of this chemical conversion, (−)-*trans*-2-methylcyclopropanecarboxylic acid can be assigned the 1*R* : 2*R* absolute configuration.

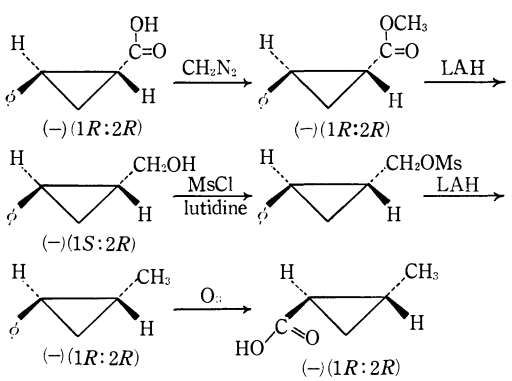

The predictions of the direction and the magnitude of rotation by the Brewster calculation of conformational asymmetry[4] show a good agreement with the observed values of (−)-(1*R* : 2*R*)-1-methyl-2-phenylcyclopropane, $[M]_D$ −148.7° (Found; chloroform), $[M]_D$ −140° (Calcd.) and (−)-(1*R* : 2*R*) - 2 - methylcyclopropanecarboxylic acid, $[M]_D$ −83.7° (Found; chloroform), $[M]_D$ −90° (Calcd.).

Experimental

Methyl (—)-*trans*-2-Phenylcyclopropanecarboxylate.—(−)-*trans*-2-Phenylcyclopropanecarboxylic acid ($[\alpha]_D^{22}$ −200.8° (*c* = 3.168, 1 dm., ethanol); optical purity 64.4% based on $[\alpha]_D$ 311.7°[3]; 6.8 g.) was esterified by the standard method with diazomethane to give the methyl ester, b. p. 128—131°C/10 mmHg; n_D^{20} 1.5292; $[\alpha]_D^{12}$ −215.7° (*c* 3.786, 1 dm., ethanol). Yield, 7.1 g. (95%).

(—) - *trans* - 1-Hydroxymethyl-2-phenylcyclopropane.—Methyl (—)-*trans*-2-phenylcyclopropanecarboxylate, $[\alpha]_D^{12}$ −171.9°; of a 51.3% optical purity, 12.4 g.; 0.07 mol., was stirred drop by drop into a slurry of lithium aluminum hydride (1.9 g.; 0.05 mol.) in 200 ml. of dry ether at room temperature. After the addition had been completed, the reaction mixture was gently refluxed by stirring it for 30 min. To the reaction mixture chilled in ice water, there was then added enough dilute hydrochloric acid (*ca.* 30 ml. of concentrated hydrochloric acid in 200 ml. of ice water) to effect a clear solution. The acidic solution was extracted with ether, and the ethereal extract was washed with aqueous sodium bicarbonate and sodium chloride solutions and dried over sodium sulfate. After ether had been removed, the residue was distilled under reduced pressure to give the carbinol, b. p. 133—135°C/10 mmHg; n_D^{21} 1.5502;

1) This work was supported by Grant 1240-A4 from the Petroleum Research Fund, administered by the American Chemical Society.

2) Asymmetric syntheses of this acid have been achieved by Simmons-Smith reactions in our laboratory and will be described in detail later elsewhere.

3) Y. Inouye, T. Sugita and H. M. Walborskv, *Tetrahedron*, **20**, 1695 (1964).

4) J. H. Brewster, *J. Am. Chem. Soc.*, **81**, 5483 (1959).

$[\alpha]_D^{13}$ −46.6° (c=2.640, 1 dm., ethanol). Yield, 10.4 g. (quantitative).

***trans*-1-Mesyloxymethyl-2-phenylcyclopropane.**—Into a solution of the (−)-carbinol (10.4 g.; 0.07 mol.) in 40 g. of dry lutidine (freshly distilled over barium oxide) methanesulfonyl chloride (10 g.; 0.096 mol.) was effectively stirred under a nitrogen atmosphere so as to maintain the reaction temperature at −10—0°C. After the addition had been completed, stirring was continued for an additional 3 hr. under cooling. The pasty product was then poured onto a mixture of concentrated hydrochloric acid (35 ml.) and crushed ice. The oily product which separated was collected with ether and dried over anhydrous magnesium sulfate. The ether was removed in vacuo and an oily product was obtained which solidified on dry-ice cooling. Because of the instability, no further purification of the crude mesylate (16.8 g.; 106%) was attempted. The infrared spectrum of the crude mesylate indicated SO_3-bands at 1172 and 1350 cm^{-1}, while the OH-band originally present in the carbinol had disappeared.

(—)-*trans*-1-Methyl-2-phenylcyclopropane.—The mesylate (16.8 g.) in 100 ml. of dry ether was stirred into a slurry of lithium aluminum hydride (7.6 g.; 0.2 mol.) in dry ether (500 ml.) at room temperature. The reaction mixture was then gently refluxed for an additional 3 hr. After ice water containing 70 ml. of concentrated hydrochloric acid had been added to the chilled reaction mixture, the ethereal solution was separated and the aqueous layer was extracted with ether. The combined extract was washed with an aqueous sodium bicarbonate solution and dried over sodium sulfate. Upon distillation, a crude hydrocarbon was obtained, b. p. 184—192°C; (6.7 g.) Since this product was colored a dark wine-red, it was percolated through an alumina column using petroleum ether as the eluent. The colorless effluent was redistilled under reduced pressure to give the (−)-hydrocarbon, b. p. 77—78°C/18 mmHg; n_D^{20} 1.5181; $[\alpha]_D^{13}$ −49.2° (c 3.432, 1 dm., ethanol); $[\alpha]_D^{13}$ −52.8° (c 1.60, 1 dm., chloroform). Yield, 6.69 g. (72% based on the carbinol). Since the v. p. c. analysis of the product indicated contamination by a by-product, the product was fractionated by means of preparative v. p. c. to give pure (−)-*trans*-1-methyl-2-phenylcyclopropane, b. p. 74—76°C/18 mmHg; n_D^{21} 1.5185; $[\alpha]_D^{16}$ −57.7° (c 3.676, 1 dm., chloroform) (lit.[5] b. p. 78—79°C/20 mmHg; n_D^{25} 1.5204 for a racemic sample). Yield, 3.2 g. The infrared spectrum of the contaminant fraction showed a nonconjugated C=C band at 1641 cm^{-1} and CH_2=CH– bands at 911, 995 and 1414 cm^{-1}; these bands suggested 3-phenylbutene-1 and/or 4-phenylbutene-1, but no further investigation was attempted.

(—)-*trans*-2-Methylcyclopropanecarboxylic Acid.—A stream of crude ozone was passed through a solution of the (−)-hydrocarbon (2.8 g.; 0.021 mol.) in carbon tetrachloride (70 ml.) at 40°C for 29 hr. After the reaction mixture had been allowed to stand still overnight at room temperature with 30 ml. of 10% hydrogen peroxide, another 10 ml. of 30% hydrogen peroxide was added and the mixture was gently refluxed for 1 hr. The acid was taken up a dilute sodium hydroxide solution and the alkaline solution, free from neutral substances, was acidified with dilute hydrochloric acid and distilled in steam. The distillate was thoroughly extracted with ether and dried over sodium sulfate. The distillation of the extract under reduced pressure gives (−)-*trans*-2-methylcyclopropanecarboxylic acid, b. p. 97—100°C/18 mmHg; n_D^{20} 1.4331; $[\alpha]_D^{19}$ −42.9° (c 3.625, 2 dm., chloroform); $[\alpha]_D^{19}$ −39.4° (c 3.060, 2 dm., ethanol); (lit.[6] b. p. 96.0—97.0°C/16 mmHg; n_D^{25} 1.4348 for a racemic sample). Yield, 1.0 g. (47%). The infrared spectrum was identical in every respect with that of an authentic specimen.[6] *p*-Phenylphenacylester, m. p. 105—106°C, laths (from methanol) $[\alpha]_D^{14}$ −33.4° (c 1.065, 2 dm., chloroform).

Found: C, 77.25; H, 6.22, Calcd. for $C_{19}H_{18}O_3$: C, 77.53; H, 6.16%.

(±)-*trans*-2-Methylcyclopropanecarboxylic acid prepared from (±)-*trans*-2-phenylcyclopropanecarboxylic acid by the same route as above had a b. p. of 96—102°C/18 mmHg, n_D^{21} 1.4350, and was identified by means of its infrared spectrum as well as by its amide, m. p. 108—108.5°C, needles (from chloroform and petroleum ether) (lit.[6] m. p. 111.3—112.0°C).

Found: C, 60.35; H, 9.26. Calcd. for C_5H_9ON: C, 60.59; H, 9.15%.

Since the starting material used in the correlation work was of a 51.3% optical purity, the maximum rotations of (−)-*trans*-2-methylcyclopropanecarboxylic acid and (−)-*trans*-1-methyl-2-phenylcyclopropane should be $[\alpha]_D$ −83.6° and $[\alpha]_D$ −112.5° respectively in chloroform.

5) H. D. Simmons and R. D. Smith, *J. Am. Chem. Soc.*, **81**, 4256 (1959).

6) D. E. Applequist and A. H. Peterson, ibid., **82**, 2372 (1960).

The Interaction of Thorium(IV) with Pyrocatechol-3, 5-disulfonate at a 1 : 1.5 Molar Ratio

By Yukito MURAKAMI and Arthur E. MARTELL

Department of Organic Synthesis, Faculty of Engineering, Kyushu University, Hakozaki, Fukuoka and Department of Chemistry, Illinois Institute of Technology, Chicago 16, Illinois, U.S.A.

(Received September 3, 1965)

In a previous paper[1] potentiometric measurements were reported on the chelating behavior of pyrocatechol-3, 5-disulfonate toward thorium(IV) ion at various molar ratios of ligand to metal ion. For ligand to metal ratios of 1.5 : 1 or higher the formation of a unique chelate of 1.5 : 1 ratio was observed, regardless of the amount of excess ligand present. The nature of this chelate was established by spectrophotometric measurements as well as by extraction[2] and ultracentrifugation[3] studies. The present work consists of a detailed study of the 1 : 1.5 thorium(IV) - pyrocatechol-3, 5-disulfonate system by means of potentiometric measurements to clarify the nature of the dinuclear thorium chelate.

Experimental

Materials.—Disodium pyrocatechol-3, 5-disulfonate (Tiron) was purchased from LaMotte Chemical Products Co., Baltimore, Md., U. S. A. and used without further purification. An aqueous stock solution of this ligand was standardized by potentiometric titration with standard base. Reagent grade thorium nitrate tetrahydrate, $Th(NO_3)\cdot 4H_2O$, purchased from Allied Chemical and Dye Corp., N. Y., was standardized gravimetrically and used to make up a stock solution for use in potentiometric titration.

Potentiometric Measurements. — A Beckman Model GS pH meter equipped with extension glass and calomel electrodes was used to measure hydrogen ion concentration directly. Calibration of the pH meter was performed by the aid of acetic acid buffer as well as standard hydrochloric aicd and sodium hydroxide. Measurements were carried out at 25.0± 0.05°C in a jacketed titration cell fitted with a magnetic stirrer, nitrogen inlet and outlet tubes, microburet delivery tube and electrodes. In all titrations the ionic strength was maintained at approximately 0.10 M with potassium nitrate, and a nitrogen atmosphere was maintained.

Results and Discussion

Potentiometric titration curves obtained at three different concentrations for the thorium(IV) - pyrocatechol-3, 5-disulfonate chelate system of a 1.5 : 1 molar ratio of ligand to metal ion are shown in Fig. 1. A sharp inflection region was observed at $m=3.0$ as has been previously observed for chelate systems of higher ligand to metal ratio.[1] On the basis of the rapid equilibria observed in the first buffer region, a simple reaction process is proposed for this range. Since the value of $([H^+]+T_{OH})/T_M$, the number of protons liberated per mole of total thorium species, already exceeds 2.0 at the start of titration, it may be concluded that the 1 : 1 metal chelate is nearly completely formed at this point. Thus, the predominant reaction, which proceeds in the buffer region lying below $m=3.0$, may be represented as:

$$2ThL + H_2L \rightleftarrows Th_2L_3 + 2H^+$$

$$K_D = \frac{[Th_2L_3][H^+]^2}{[ThL]^2[H_2L]} \quad (1)$$

The stoichiometric relations involved in this system*1 are:

$$T_M = [ThL] + 2[Th_2L_3] \quad (2)$$

$$T_L = [ThL] + 3[Th_2L_3] + [H_2L] \quad (3)$$

$$T_{OH} + [H^+] = 2[ThL] + 6[Th_2L_3] \quad (4)$$

where T_M and T_L represent the total analytical concentration of the metal species and of the ligand species present in a solution, while T_{OH} is the analytical concentration of the hydroxide ions added to a solution during the titrations. Combination and rearrangement of Eqs. 2 through 4 gives expressions for $[Th_2L_3]$, $[ThL]$ and $[H_2L]$ in terms of the measurable or known quantities m, $[H^+]$ and T_M. When these relations are introduced into Eq. 1, the equilibrium constant K_D may be expressed as:

$$K_D = \frac{\{(m-2)T_M+[H^+]\}[H^+]^2}{\{(3-m)T_M-[H^+]\}^3} \quad (5)$$

The logarithm of this equilibrium constant (log K_D) was calculated as 0.89.

In contrast to the first buffer region, the rate of attaining equilibrium was found to be extremely slow in the second buffer region ranging from 3.0 to 4.0. In addition, from the appearance of a second inflection at around $m=4.0$, it is assumed that a simple intramolecular olation reaction takes place

1) Y. Murakami and A. E. Martell, *J. Am. Chem. Soc.*, **82**, 5605 (1960).
2) R. F. Bogucki, Y. Murakami and A. E. Martell, ibid., **82**, 5608 (1960).
3) R. L. Gustafson and A. E. Martell, ibid., **82**, 5610 (1960).

*1 Recently, a probable structural formula was presented for the 2 : 3 thorium(IV) - pyrocatechol-3, 5-disulfonate chelate by Martell at the Symposium on Coordination Chemistry, held at Tihany, Hungary, Sept. 14—17, 1964. In his structure the phenoxide groups of Tiron act as bridging components with the retention of high symmetry of a molecule.

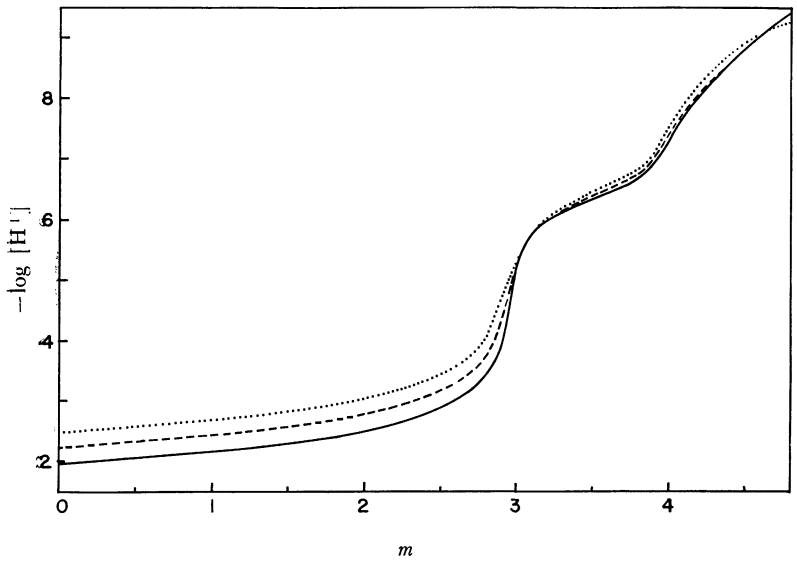

Fig. 1. Potentiometric titration of thorium(IV)-pyrocatechol-3, 5-disulfonate chelate system in 0.10 M KNO_3 at 25°C, with 1.5 : 1 molar ratio of ligand to metal ion at total thorium concentrations of: A, 5.15×10^{-3} M; B, 2.58×10^{-3} M; C, 1.29×10^{-3} M; m=moles of base added per gram-ion of metal. —— A; ---- B; ···· C

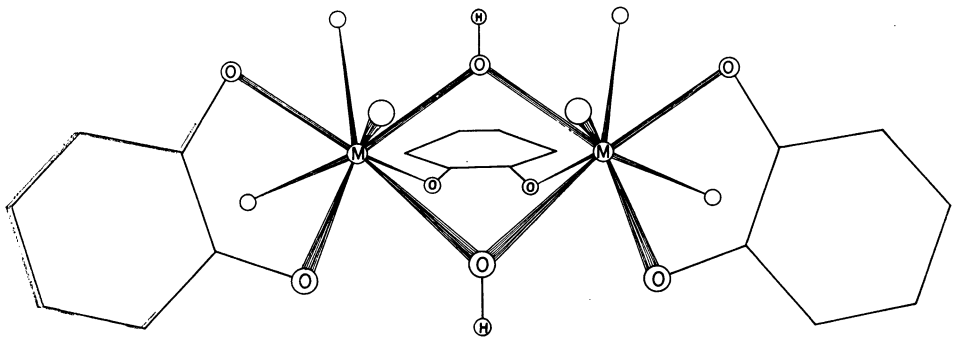

I ○, H_2O; Ⓜ, Th

Table I. Equilibrium relationships for Th(IV) chelates at 25°C, μ=0.10 (KNO_3)

Ligand	Type formula	Equilibrium constant: Quotient	Log K
EDTA[4]	H_4L	$[ThL]/[ThL(OH)][H^+]$	7.04±0.05
		$[ThL]^2/[Th_2L_2(OH)_2][H^+]^2$	9.82±0.05
		$[Th_2L_2(OH)_2]/[ThL(OH)]^2$	4.3±0.1
CDTA[4]	H_4L	$[ThL]/[ThL(OH)][H^+]$	7.58±0.05
		$[ThL]^2/[Th_2L_2(OH)_2][H^+]^2$	10.84±0.05
		$[Th_2L_2(OH)_2]/[ThL(OH)]^2$	4.3±0.1
Tiron	H_2L	$[Th_2L_3]/[Th_2L_3(OH)_2][H^+]^2$	12.8±0.1
		$[ThL]^2[H_2L]/[Th_2L_3(OH)_2][H^+]^4$	11.9±0.1

EDTA: ethylenediaminetetraacetic acid
CDTA: 1, 2-diaminocyclohexanetetraacetic acid

in the second buffer region.*2 Thus, the simple dissociation type reaction assumed for this region is:

$$Th_2L_3 \rightleftarrows Th_2L_3(OH)_2 + 2H^+$$

$$K_{D(OH)_2} = \frac{[Th_2L_3(OH)_2][H^+]^2}{[Th_2L_3]} \quad (6)$$

Stoichiometric relations consistent with Eq. 6 are:

$$T_M = 2[Th_2L_3(OH)_2] + 2[Th_2L_3] \quad (7)$$

$$T_{OH} + [H^+] - [OH^-] = 2[Th_2L_3(OH)_2] \quad (8)$$

Since $[H^+]-[OH^-]$ may be neglected in this pH region, the expression for the equilibrium constant $K_{D(OH)_2}$ simplifies to:

$$K_{D(OH)_2} = m'[H^+]^2/(1 - m') \quad (9)$$

where $m' = m - 3$.

At the half-neutralization point ($m' = 1/2$), the equilibrium constant becomes equal to the square of the hydrogen ion concentration. Although the present titration data do not provide an equilibrium constant of high accuracy for the above-assumed reaction, an approximate value has been obtained by use of Eq. 9. The estimated constant is given in Table I together with values for the EDTA and the CDTA chelate systems.[4] The dimeric thorium-(IV) - pyrocatechol-3, 5-disulfonate chelate may be considered at least qualitatively to show an olation tendency similar in magnitude to the other thorium chelates listed in Table I. A probable structure for the reaction product (I) is quite similar to that proposed for the ethylenediaminetetraacetate and the 1, 2-diaminocyclohexanetetraacetate chelates of thorium.[4]

In the second inflection region lying beyond $m = 4.0$, reaction equilibrium was reached extremely slowly. Therefore, further rearrangement and disproportionation reactions of the chelate formed in the second buffer region presumably take place with the participation of hydroxide ions.

*2 These experimental data do not eliminate the possibility of olation-polymerization through which the 2 : 3 Th(IV) - pyrocatechol-3, 5-disulfonate chelate further polymerize with hydroxide ions as bridging components. Further detailed studies on the 1 : 1.5 titration curve in much wider concentration range would help to clarify such an interaction.

4) R. F. Bogucki and A. E. Martell, *J. Am. Chem. Soc.*, **80**, 4170 (1958).

The Condensation of Methyl β-Chlorovinyl Ketone with Aromatic Diamines

By Yoshimori OMOTE, Katsumi KURIHARA, Yumiko KURABAYASHI and Noboru SUGIYAMA

Department of Chemistry, Tokyo Kyoiku University, Otsuka, Tokyo

(Received September 11, 1965)

The condensation of methyl β-chlorovinyl ketone (I) with amines such as aniline and *p*-aminophenol has previously been reported from this laboratory,[1] while the reaction of monoamines with I has been reported by Yakubovich.[2] While the reaction of α, β-unsaturated ketone with aromatic diamine is well known,[3] no example involving the condensation of I, an α, β-unsaturated ketone with chlorine on the β-position, with a diamine is found in the literature. During the course of a synthetic investigation of cyclic-conjugated compounds containing nitrogen it, however, became desirable to prepare new condensation products of I with aromatic diamines. This paper is concerned with the reaction of I with aromatic diamines, e. g., *o*-, *m*-, and *p*-phenylenediamines.

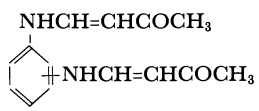

II: *o*-
III: *m*-
IV: *p*-

The reaction of two moles of I with one mole of *o*-phenylenediamine in the presence of potassium carbonate afforded a resinous substance which was sparingly soluble in ether. By the chromatographical fractionation of the resinous substance, a small quantity of crystals was obtained and identified with V on the basis of its elementary analysis and its ultraviolet and infrared absorption spectra. V showed an ultraviolet absorption spectrum

1) G. Inoue, *J. Chem. Soc. Japan, Pure Chem. Sect.* (*Nippon Kagaku Zasshi*), **79**, 1233 (1958); **80**, 1061 (1959).
2) A. Ya. Yakubovich and E. N. Merkulova, *J. Gen. Chem.* (USSR), **16**, 55; *Chem. Abstr.*, **41**, 91 (1947).
3) a) W. Ried and P. Stahlhofen, *Chem. Ber.*, **90**, 815 (1957). b) J. Davoll, *J. Chem. Soc.*, **1960**, 308. c) G. Bryant and L. V. Heisey, *J. Am. Chem. Soc.*, **71**, 1985 (1949). d) W. Ried and Urlass, *Chem. Ber.*, **86**, 1101 (1953). e) W. Ried and W. Hohne, ibid., **87**, 1181 (1954). f) F. B. Wigton and M. M. Joullie, *J. Am. Chem. Soc.*, **81**, 5212 (1959). g) W. R. Benson and A. E. Pohland, *J. Org. Chem.*, **29**, 385 (1964). h) F. Scotti and E. J. Frazza, ibid., **29**, 1800 (1964).

analogous to that of 2-methylbenzimidazol[4] and, as its infrared absorption maxima, 3400 (ν_{N-H}) and 2950 (ν_{C-H}) cm^{-1}. The formation of V might be explained as follows.

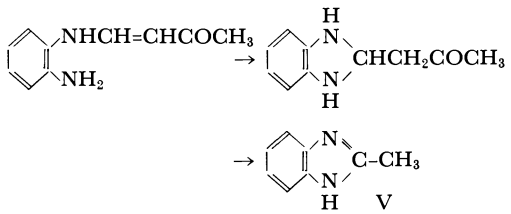

The reaction of two moles of I with one mole of *m*-phenylenediamine or *p*-phenylenediamine in the presence of potassium carbonate gave the expected condensation products, III and IV respectively. The ultraviolet absorption maximum of III appeared at 352 mμ in a neutral solution and at 351 mμ in an acid solution. If the nitrogen atom in the conjugated system of III had been protonated in an acid solution, the maximum of the absorption should move to the shorter wavelength. The preceeding observation that the absorption did not show the hypsochromic shift means that the protonation on the oxygen atom of the acetyl group in III is preferable to that on the nitrogen atom. The similar discussion will be supported by the fact that the ultraviolet absorption maximum of IV was 386 mμ in neutral and 395 mμ in acid solution. The infrared absorption maxima were found at 3400 (ν_{N-H}) and 1640 ($\nu_{C=O}$) cm^{-1} for III and at 3400 (ν_{N-H}) and 1630 ($\nu_{C=O}$) cm^{-1} for IV. These spectral data are consistent with structures III and IV.

The reactivity of III or IV with formaldehyde or benzaldehyde in the presence of piperidine acetate was so small that the aldol condensation products could not be formed. Both III and IV were found to be reasonably stable to sunlight, ultraviolet ray or γ-ray irradiation.

Experimental

All the melting points are uncorrected.

The Reaction of *o*-Phenylenediamine with Methyl β-Chlorovinyl Ketone.—Freshly-distilled methyl β-chlorovinyl ketone (10 g., 0.1 mol.) and *o*-phenylenediamine (5 g., 0.05 mol.) were dissolved in water (50 ml.); to this mixture potassium carbonate (27 g., 0.2 mol.) was then gradually added. The reaction product was resinous and insoluble in ether. The ethanol solution of the product was chromatographed on alumina. From the elution a trace of colorless crystals (V) was obtained; m. p. 176°C.

Found: C, 71.29; H, 5.37; N, 21.07. Calcd. for $C_8H_8N_2$: C, 72.70; H, 6.10; N, 21.20%.

UV: λ_{max}^{EtOH} (ε) 245 (6100), 273 (5900), 279 (6800) mμ, λ_{max}^{acid} 240, 268, 274 mμ, IR: ν_{N-H} 3400, ν_{C-H} 2950, 2850, ν_{C-H} 1360 cm^{-1}.

It was difficult to crystallize most of the resinous substance whose ultraviolet absorption maximum was near 390 mμ. This suggested the formation of II, but the resinous substance could not be sublimed in vacuo (10^{-3}—10^{-4} torr.) with a molecular still. Consequently, this substance must not be II but must be composed of polymers containing a conjugation similar to that of II.

***N, N'*-Di-(2-acetylvinyl)-*m*-phenylenediamine (III).**—To the mixture of methyl β-chlorovinyl ketone (10 g., 0.1 mol.) and *m*-phenylenediamine (5 g., 0.05 mol.) in water (50 ml.), potassium carbonate (27 g., 0.2 mol.) was gradually added. The reaction product was extracted with ether, and the ether layer was concentrated and kept in a refrigerator; brown fine cyrstals, 1.35 g., m. p. 195°C, were thus afforded.

Found: C, 68.89; H, 6.46; N, 11.52. Calcd. for $C_{14}H_{16}O_2N_2$: C, 68.83; H, 6.60; N, 11.47%.

UV: λ_{max}^{EtOH} (ε) 352 (41000) mμ, λ_{max}^{acid} 351 mμ.

IR: ν_{N-H} 3400, $\nu_{C=O}$ 1640, ν_{C-H} 1350 cm^{-1}.

***N, N'*-Di-(2-acetylvinyl)-*p*-phenylenediamine (IV).**—The reaction mixture of methyl β-chlorovinyl ketone (10 g., 0.1 mol.) and *p*-phenylene diamine (5 g., 0.05 mol.) in the presence of potassium carbonate (27 g., 0.2 mol.) was extracted with ether, dissolved in hot ethanol, and kept at room temperature. After recrystallization, fine orange-yellow needle crystals were obtained, m. p. 193°C.

Found: C, 68.72; H, 6.56; N, 11.48. Calcd. for $C_{14}H_{16}O_2N_2$: C, 68.83; H, 6.60; N, 11.47%.

UV: λ_{max}^{EtOH} (ε) 386 (47000) mμ, λ_{max}^{acid} 395 mμ.

IR: ν_{N-H} 3400, $\nu_{C=O}$ 1630, ν_{C-H} 1360 cm^{-1}.

The Attempted Condensation of III or IV with Aldehydes.—Equimolecular mixtures of III or IV and formaldehyde or benzaldehyde were kept at room temperature or heated under reflux in the presence of piperidine acetate or piperidine. From each reaction mixture III or IV and aldehyde were recovered.

The Change of III or IV with Sunlight, Ultraviolet Ray or γ-Ray Irradiation.—III and IV were stable to sunlight for a week, and to the ultraviolet rays of a high-pressure mercury lamp for two days. The γ-ray irradiation of III and IV, with a total dose of 5×10^7 r./hr. and a dose rate of 1.5×10^7 r./hr. showed little change in the ultraviolet absorption spectrum. The precise results will be reported elsewhere.[5]

4) R. Huisgen and H. Rist, *Ann.* **594**, 161 (1955).

5) Y. Kurabayashi, K. Kurihara, Y. Omote, *J. Vacuum Chem. Soc. Japan* (*Shinku Kagaku*), in press.

The Determination of Dissolved Oxygen by the Use of Its Stoichiometric Reaction with Metallic Lead

By Yūsuke UJIHIRA, Hideo WATANABE* and Eiji NIKI

Department of Industrial Chemistry, Faculty of Engineering, The University of Tokyo, Hongo, Tokyo

(Received September 15, 1965)

The study of the quantitative determination of minute amounts of dissolved oxygen is receiving particular attention, with special regard being paid to the control of the oxygen content of feeding water to a high-pressure boiler plant, or to the biochemical processes.

Among the many techniques proposed for the estimation of oxygen dissolved in water,[1] the method based on the oxidation and dissolution of metal is thought to be most promising.

The oxidation of metallic thallium to a thallous ion and subsequent determination by means of the electric conductivity,[2] the radioactive ^{204}Tl tracer technique,[3,4] or by polarography[4] have been investigated recently; also a several p. p. m. concentration of oxygen has been measured by the oxidation of zinc amalgam[5] or copper metal[6,7].

The authors, in the course of a study of the reaction of metal and dissolved oxygen, noticed a stoichiometry in lead-aqueous oxygen system.

The resultant of the reaction was lead hydroxide, which can be dissolved with an acetic acid and sodium acetate solution, whereas lead metal is not bitten by the acetate mixture. The reaction is conjectured to be:

$$Pb + 1/2O_2 + H_2O \rightarrow Pb(OH)_2$$

$$Pb(OH)_2 + 2CH_3COOH \rightarrow Pb(CH_3COO)_2 + 2H_2O$$

or

$$Pb + 1/2O_2 + 2CH_3COOH \rightarrow Pb(CH_3COO)_2 + H_2O$$

The eluted plumbous ion was determined directly by a. c. polarography. Useful information was obtained thus for designing a method of determining the oxygen dissolved in water.

Experimental, Results and Discussion

The sample solution was prepared by boiling pure water in an atmosphere of nitrogen, and the dissolved oxygen content was calibrated by the amperometric titration with two polarized electrodes, as reported by Potter and White.[8] The standardized sample solution was fed to the reaction column (diam. 1.2 cm., height 7.0 cm.), which had been filled with metallic lead grain (diam. 2—3 mm.), together with a 50% acetic acid solution, saturated with sodium acetate. The schematic diagram of the experimental system is shown in Fig. 1.

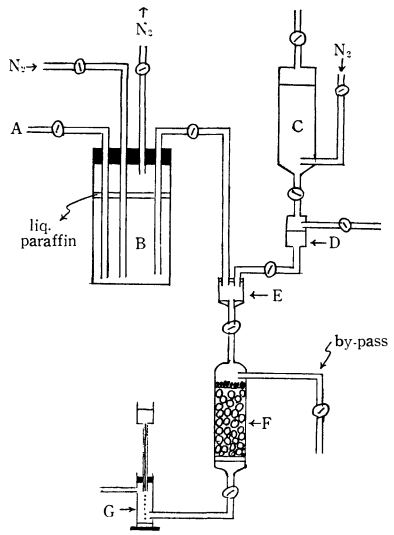

Fig. 1. Schematic diagram.

A: To the amperometric titration
B: Sample preparation and storage tank
C: Deaerated acetate buffer and storage tank
D: Constant head device
E: Mixing cell
F: Lead column
G: Polarograph cell for continuous measurement

The volume ratio of the acetic acid - sodium acetate mixture to the sample solution was 1.43 to 0.01. The eluted solution was received directly in

* Present address: Research Division, Toyo Soda Mgf. Co., Ltd., Tsuno-gun, Yamaguchi Pref.

1) "Symposium on Dissolved Oxygen," *Japan Analyst*, **13**, 567 (1964).

2) W. T. Lindsay, Jr., *Anal. Chem.*, **35**, 408 (1963).

3) H. G. Richier and A. S. Gillespie, Jr., ibid., **34**, 1116 (1962).

4) E. Niki, Y. Ujihira and H. Watanabe, *Japan Analyst*, **15**, 360 (1966).

5) T. Takahashi, H. Sakurai and T. Sakamoto, ibid., **13**, 627 (1964).

6) A. D. Klerk and B. B. Neurs, *Anal. Chim. Acta*, **16**, 296 (1957).

7) H. Imai, S. Chaki and Y. Tanaka, *Japan Analyst*, **10**, 191 (1961).

8) E. C. Potter and J. F. White, *J. Appl. Chem.*, **17**, 309 (1957).

a electrolytic cell, the quantity of lead was determined by measuring the wave height of the a. c. polarogram.

The results of this experiment are shown in Table I.

TABLE I. THE STOICHIOMETRY OF $Pb+1/2O_2+2CH_3COOH \rightarrow Pb(CH_3COO)_2+H_2O$ REACTION

Oxygen content in sample sol. (p.p.m.)	Quantities of lead dissolved per ml. calcd. (μg.)	Dissolved quantities of lead. obsd. (μg.)	Obsd./Calcd.
7.50	97.5	96.0	0.98
4.86	63.2	65.7	1.04
3.14	40.8	37.5	0.92
2.80	36.4	38.0	1.04
1.51	19.6	22.5	1.15
0.34	4.4	7.2	1.64

The stoichiometry of the $Pb+1/2O_2+2CH_3COOH \rightarrow Pb(CH_3COO)_2+H_2O$ reaction above the p.p.m. region could be confirmed because the ratio of the observed to the calculated quantity of dissolved lead was approximately one.

Accordingly, the linearity of the aqueous oxygen content vs. the dissolved lead is perfect in the 1—10 p.p.m. range.

The completeness of the reaction of a metallic lead and aqueous oxygen was confirmed by the fact that no oxygen reduction wave was detected in the polarogram. Though a marked departure from the stoichiometrical linearity was observed for the extremely low oxygen content solution, this seems to result from the leakage of air into the sample and the acetate buffer solution, through polyvinyl tubings or through the interstice between polyvinyl and glass tubings in the course of the experiments. The advantages of the lead column method over the other methods (especially the thallium column method) will be outlined below:

(1) A lead column can be used effectively for a weak acidic sample, whereas the thallium method results in a serious positive error due to the dissolution of metallic thallium by a sample solution.

(2) A lead column can be readily prepared by filling the commercially-available lead grain in a glass tubing.

(3) The lead is more immune to oxidation by air than is the thallium.

(4) The dissolved quantities of lead can be determined by the use of the radioactivity, as ^{210}Pb is readily available.

(5) The lead-column method is readily applicable to the continuous measurement of the aqueous oxygen content.

A Semiempirical Unrestricted SCF Calculation of the *trans*-Stilbene Anion Radical

By Keiji MOROKUMA, Takashi KAWAMURA, Shoichi MATSUNAMI and Teijiro YONEZAWA

Faculty of Engineering, Kyoto University, Sakyo-ku, Kyoto

(Received September 27, 1965)

In recent electron spin resonance studies of the anion radicals of *trans*-stilbene,[1] azobenzene,[2] benzaldehyde and acetophenone,[3] it has been found that the isotropic coupling constants of the protons of two *ortho*-positions, and also that of two *meta*-positions in the phenyl ring, differ from each other. These differences can not be interpreted by either the Hückel molecular orbital (HMO) method or the McLachlan procedure,[4] because in these methods the resonance integrals between non-bonded atoms are not taken into account.

Hence, we will make an semiempirical unrestricted SCF calculation, as proposed by Pople and Nesbet[5] and developed by Brickstock and Pople,[6] for the *trans*-stilbene anion radical. It will be shown in the present treatment that the difference between spin densities at two *ortho*-positions and also that at two *meta*-positions appear in accordance with the experimental results.

The Method of Calculation

In the semiempirical unrestricted SCF method, two sets of LCAO coefficients, $\chi_{i\mu}{}^{\alpha}$ and $\chi_{i\mu}{}^{\beta}$, are calculated as follows:

$$\sum_{\nu} F^{\alpha}_{\mu\nu}\chi^{\alpha}_{i\nu} = E^{\alpha}_{i}\chi^{\alpha}_{i\mu}; \quad \sum_{\nu} F^{\beta}_{\mu\nu}\chi^{\beta}_{i\nu} = E^{\beta}_{i}\chi^{\beta}_{i\mu} \qquad (1)$$

where:

1) R. Chang and C. S. Johnson, Jr., *J. Chem. Phys.*, **41**, 3272 (1964).
2) E. T. Strom, G. A. Russell and R. Konaka, ibid., **42**, 2033 (1865).
3) N. Steinberger and G. K. Fraenkel, ibid., **40**, 723 (1960).
4) A. D. McLachlan, *Mol. Phys.*, **2**, 233 (1960).
5) J. A. Pople and R. K. Nesbet, *J. Chem. Phys.*, **22**, 571 (1954).
6) A. Brickstock and J. A. Pople, *Trans. Faraday Soc.*, **50**, 901 (1954).

Table I. Calculated and experimentally found[1] spin distributions in the *trans*-stilbene anion radical

Position	a_H[a]	$\mid \rho_{exp} \mid$[9]	ρ_{SCF}	$\rho_{McL.}$	ρ_{HMO}
1	2.90	0.132	+0.1230	+0.1232	+0.0750
2	0.81	0.036	−0.0672	−0.0804	+0.0063
3	3.89	0.173	+0.1747	+0.1436	+0.0984
4	0.30	0.013	−0.0651	−0.0804	+0.0063
5	1.90	0.0844	+0.1168	+0.1232	+0.0750
6	—	—	+0.0205	−0.0031	+0.0472
7	4.37	0.194	+0.1974	+0.2739	+0.1919

a) From Ref. 1), in units of gauss. The assignment of the coupling constants of two sets of *ortho*-protons and of *meta*-protons is made based on our calculation.

$$\left.\begin{aligned} F^{\alpha}_{\mu\mu} &= U_{\mu\mu} + P^{\beta}_{\mu\mu}\gamma_{\mu\mu} + \sum_{\sigma(\neq\mu)}(P_{\sigma\sigma} - 1)\gamma_{\mu\sigma} \\ F^{\beta}_{\mu\mu} &= U_{\mu\mu} + P^{\alpha}_{\mu\mu}\gamma_{\mu\mu} + \sum_{\sigma(\neq\mu)}(P_{\sigma\sigma} - 1)\gamma_{\mu\sigma} \\ F^{\alpha}_{\mu\nu} &= \beta_{\mu\nu} - P^{\alpha}_{\nu\nu}\gamma_{\mu\nu} \quad (\mu \neq \nu) \\ F^{\beta}_{\mu\nu} &= \beta_{\mu\nu} - P^{\beta}_{\mu\nu}\gamma_{\mu\nu} \quad (\mu \neq \nu) \end{aligned}\right\} \quad (2)$$

$$\left.\begin{aligned} P^{\alpha}_{\mu\nu} &= \sum_{i}^{occ} \chi^{\alpha}_{i\mu}\chi^{\alpha}_{i\nu}; \quad P^{\beta}_{\mu\nu} = \sum_{i}^{occ} \chi^{\beta}_{i\mu}\chi^{\beta}_{i\nu} \\ P_{\mu\nu} &= P^{\alpha}_{\mu\nu} + P^{\beta}_{\mu\nu} \end{aligned}\right\} \quad (3)$$

In Eq. 1, 2 and 3, all the notations are the same as Brickstock and Pople's.[6] The spin density at the carbon atom μ, ρ_μ, is obtained from Eq. 4:

$$\rho_\mu = P^{\alpha}_{\mu\mu} - P^{\beta}_{\mu\mu} \quad (4)$$

As the penetration integral is neglected, $U_{\mu\mu}$ becomes a constant over all the carbon atoms. $\gamma_{\mu\nu}$ is calculated by means of the approximation of Pariser and Parr.[7] The resonance integral, $\beta_{\mu\nu}$, is calculated by means of Eq. 5:

$$\beta_{\mu\nu} = \begin{cases} -10.44\, S_{\mu\nu}\ \text{eV.} & (R_{\mu\nu} < 3.0\text{Å}) \\ 0 & (R_{\mu\nu} \geq 3.0\text{Å}) \end{cases} \quad (5)$$

where $R_{\mu\nu}$ is the distance between the μth and νth atoms, and $S_{\mu\nu}$ is the overlap between two $2P_Z$ Slater-type atomic orbitals with $Z^* = 3.25$.

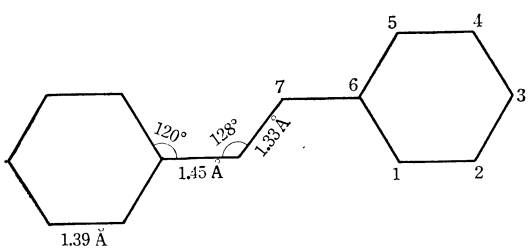

Fig. 1. Structure and numbering of positions of *trans*-stilbene.

The structure[8] and the numbering of the positions in *trans*-stilbene are shown in Fig. 1.

Results and Discussion

The spin distribution calculated with the semiempirical unrestricted SCF method and the observed coupling constants[1] and the spin densities[9] are tabulated in Table I.

Chang and Johnson[1] assigned coupling constants of 2.96 gauss and 1.90 gauss, which correspond to the spin densities of 0.132 and 0.0844 respectively,[9] to the *ortho*-protons, but they did not make clear which of these coupling constants is due to the proton in the C–H bond at the carbon atom 1 (1-proton) and which to that at the carbon atom 5 (5-proton). We obtained $\rho_1 = +0.1230$ and $\rho_5 = +0.1168$ as the spin densities at the *ortho*-carbons by means of our SCF calculation. Through a comparison of these coupling constants and calculated spin densities, we could assign the coupling constant of 2.96 gauss to the 1-proton and that of 1.90 gauss to the 5-proton. By then comparing the coupling constants of the *meta*-protons and the calculated spin densities at the *meta*-carbons, we could assign the coupling constant of 0.81 gauss to the 2-proton and that of 0.30 gauss to the 4-proton. The values in the second and in the third columns in Table I are written according to the above-mentioned assignment. The agreement between the observed spin distribution and the spin distribution calculated by means of the SCF method seems fairly good.

Spin distributions calculated by means of the HMO method and by means of the McLachlan procedure with $\lambda = 1.00$ are also listed in Table I for the sake of comparison.

The SCF and HMO calculations were carried out on the KDC-I digital computer of Kyoto University.

7) R. Pariser and R. G. Parr, *J. Chem. Phys.*, **21**, 466, 767 (1953).

8) J. M. Robertson and I. Woodward, *Proc. Roy. Soc.*, **A162**, 568 (1937).

9) To calculate the spin density from the coupling constant, we used the following equation; $a_{\mu\text{-H}} = 22.5 \mid \rho_\mu \mid$. H. M. McConnell and D. B. Chesnut, *J. Chem. Phys.*, **28**, 107 (1958).

Bis[cyclopentadienyl(cyclohexyl isocyanide)nickel]

By Yasuhiro YAMAMOTO and Nobue HAGIHARA

The Institute of Scientific and Industrial Research, Osaka University, Sakai, Osaka

(Received October 4, 1965)

It has already been well established that isocyanides, analogous to carbon monoxide, produce various isocyanide complexes of transition metals. Pauson and Stubbs[1] have prepared bis[cyclopentadienyl(phenyl isocyanide)nickel] by means of the reaction of nickelocene with tetrakis(phenyl isocyanide)nickel; they have suggested the sturucture I on the basis of the peak of the infrared spectrum at 2175 cm^{-1}.

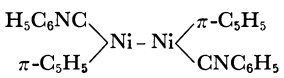

(I)

Recently, Pauson and his co-workers[2] have reported an iron complex with a bridging isocyanide group and have also established that bis[cyclopentadienyl(phenyl isocyanide)nickel] has a bridged structure in a solid state, but these points have not been discussed in detail.

We wish to report the direct preparation of a similar compound from nickelocene by means of cyclohexyl isocyanide. During the studies of the polymerization of cyclohexyl isocyanide using various metallocenes as catalysts, we found that the use of nickelocene as a catalyst was very favorable to the polymerization; in this case bis[cyclopentadienyl(cyclohexyl isocyanide)nickel] (II) was isolated as an intermediate of the polymerization reaction.

When nickelocene was treated with cyclohexyl isocyanide at room temperature, the reaction took place instantaneously, as was shown by the rapid color change from green to red brown, and gave a 38% yield of bis[cyclopentadienyl(cyclohexyl isocyanide)nickel] as red brown needles. The infrared spectrum of this compound in Nujol mull showed two peaks, at 1870 and 1830 cm^{-1}; these peaks were analogous to those of bis[cyclopentadienyl(carbonyl-nickel] with bridging carbonyl groups. The spectrum in benzene showed a strong peak at 2140 cm^{-1} and two weak peaks, at 1880 and 1840 cm^{-1}, while in *n*-hexane it showed only a strong peak at 2140 cm^{-1}.

It was concluded from the infrared spectrum that bis[cyclopentadienyl(cyclohexyl isocyanide)nickel] had a bridged isocyanide structure II-a in a solid state and that it existed in an equilibrium between a bridged isocyanide structure II-a and a terminal isocyanide structure II-b in solutions, in which the former should make a greater contribution than the latter.

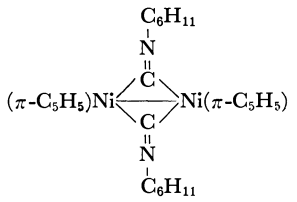

(II-a)

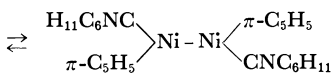

(II-b)

The reaction of cyclohexyl isocyanide with bis[cyclopentadienyl(carbonyl)nickel] took place readily at room temperature, and it also gave a 15% yield of bis[cyclopentadienyl(cyclohexyl isocyanide)nickel]. Analogously, dicyclopentadienyl(acetylene)dinickel gave a 12% yield of the same compound.

Experimental

Materials.—Cyclohexyl isocyanide,[3] nickelocene,[4] bis[cyclopentadienyl(carbonyl)nickel],[5] and dicyclopentadienyl(acetylene)dinickel[6] were prepared by methods described in the literature.

The Reaction of Cyclohexyl Isocyanide with Nickelocene. — A solution of 1.0 g. (5.3 mmol.) of nickelocene in 40 ml. of a benzene - *n*-hexane mixture (1 : 1) was treated with 0.6 g. (5.5 mmol.) of cyclohexyl isocyanide at room temperature and then kept for 3 hr. The reaction mixture was evaporated to about 10 ml. under reduced pressure and chromatographed on alumina. Eluting with a benzene - *n*-hexane mixture gave raw products, from which bis[cyclopentadienyl(cyclohexyl isocyanide)nickel] was obtained as red brown needles by recrystallization from the benzene - *n*-hexane mixture (1 : 5). (Yield. 38%; m. p. 155—156°C (decomp.)) This compound was sensitive to air, so all the procedures mentioned above were performed under a nitrogen atmosphere.

1) P. L. Pauson and W. H. Stubbs, *Angew. Chem.*, **74**, 466 (1962).
2) K. K. Joshi, O. S. Mills, P. L. Pauson, B. W. Shaw and W. H. Stubbs, *Chem. Comm.*, **1965**, 181.
3) I. Ugi and R. Mayr, *Chem. Ber.*, **93**, 239 (1960).
4) J. F. Cordes, ibid., **95**, 3084 (1962).
5) E. O. Fischer and C. Palm, ibid., **91**, 1725 (1958).
6) M. Dubeck, *J. Am. Chem. Soc.*, **82**, 502 (1960).
* By the cryoscopic benzene method.

Found: C, 61.59; H, 7.01. Calcd. for $[Ni(C_5H_5)(CNC_6H_{11})]_2$ C, 61.85; H, 6.87%. M. w. 451* (466).

The Reaction of Cyclohexyl Isocyanide with Bis[cyclopentadienyl(carbonyl)nickel] (III) or Dicyclopentadienyl(acetylene)dinickel (IV) $(C_5H_5)Ni(HC{\equiv}CH)Ni(C_5H_5)$.—The procedure was similar to the reaction described above except that dry benzene was used as the solvent. The working-up of the reaction mixture gave bis[cyclopentadienyl(cyclohexyl isocyanide)nickel]. The yields of II from III and IV were 12% and 15% respectively.

The Reduction of Styrene Derivatives with the Commercial Sodium-Lead Alloy

By Katsumi TABEI, Hidetoshi HIRANUMA and Norio AMEMIYA

Tokyo College of Pharmacy, Kashiwagi, Shinjuku-ku, Tokyo

(Received October 26, 1965)

Recently a sodium-lead alloy was marketed as a drying agent of organic solvents.[1] A sodium-lead alloy had previously been used in the reduction of multivalent metal ions, such as titanium(IV), vanadium(V), and chromium(III),[2] but the alloy has not yet been used in organic reduction.

The present authors have tried the commercial sodium-lead alloy, "Drynap," as a reducing agent in place of sodium amalgam for the reduction of cinnamic acid in an aqueous sodium hydroxide solution according to the method of Erlenmeyer[3]; hydrocinnamic acid was thus obtained in a 87% yield. From this successful result, the Drynap reduction of several styrene derivatives was also attempted; a little of the information so obtained will be reported here.

The reduction was carried out in an ethanol solution by using the commercial sodium-lead alloy and acetic acid as in the method of amalgam reduction.[4,5] Under these conditions, benzylideneacetone, dibenzylideneacetone, benzylideneacetophenone, piperonylideneacetone, and methyl-cinnamate were not reduced to the corresponding di- or tetra-hydrogenated compound, but were dimerized to 4, 5-diphenyl-2, 7-octanedione, 1, 5, 6, 10-tetraphenyl-1, 9-decadiene-3, 8-dione, 1, 3, 4, 6-tetraphenyl-1, 6-hexanedione, 4, 5-di-(3, 4-methylenedioxyphenyl)-2, 7-octanedione, and dimethyl 2, 4-diphenyladipate respectively. ω-Nitrostyrene was also reduced with Drynap and acetic acid in an ethanol solution to phenylacetaldoxime in about a 60% yield.

In the above reactions, the yield generally increased at higher temperatures, but decreased above 60°C because of the increase in polymerization. The yield also decreased in the reaction on a larger scale.

On the other hand, styrene, isosafrol, and cinnamyl alcohol were not affected by the sodium-lead alloy under the above conditions; the reaction then resulted in the recovery of the starting material. Cinnamaldehyde was also not reduced with sodium-lead alloy and acetic acid, and was easily polymerized, even at low temperatures.

On the basis of the above results, the authors recommend the use of sodium-lead alloy as the mild reducing agent; however, it has the disadvantage of being expensive.

Experimental

The Reduction of Cinnamic Acid with the Sodium-Lead Alloy.—Ten grams of cinnamic acid

TABLE I. THE PRODUCTS OF DRYNAP REDUCTION

Material	Product	M. p., °C	Yield, %
Ph-CH=CH-$COCH_3$	[Ph-CH-CH_2-$COCH_3$]$_2$	116	10—35
Ph-CH=CH-CO-CH=CH-Ph	[Ph-CH-CH_2-CO-CH=CH-Ph]$_2$	210	58
Ph-CH=CH-CO-Ph	[Ph-CH-CH_2-CO-Ph]$_2$	193	45
$(H_2C\langle^{O}_{O}\rangle C_6H_3)$-CH=CH-$COCH_3$*	[$(H_2C\langle^{O}_{O}\rangle C_6H_3)$-CH-$CH_2$-$COCH_3$]$_2$	228	25—30
Ph-CH=CH-$COOCH_3$	[Ph-CH-CH_2-$COOCH_3$]$_2$	178	~5
Ph-CH=CH-NO_2	Ph-CH_2-CH=N-OH	103	~60

* $(H_2C\langle^{O}_{O}\rangle C_6H_3)$- is 3,4-methylenedioxyphenyl group.

1) H. Soroos, *I. E. C., Anal. Ed.*, **11**, 657 (1939).
2) R. A. Edge and G. W. Fowles, *Anal. Chim. Acta*, **32**, 191 (1965).
3) A. Erlenmeyer, *Ann.*, **121**, 375 (1862); **137**, 334 (1866).
4) L. Gattermann, Die Praxis des organischen Chemikers, 40 Aufl., 203 (1961).
5) C. Harries and G. Eschenbach, *Ber.*, **29**, 383 (1896); R. Kuhn and M. Hoffer, ibid., **65**, 170 (1932)

was dissolved in 70 ml. of a 5% sodium hydroxide solution. Into the solution, 50 g. of the commercial sodium-lead alloy "Drynap" (contains more than 9.5% of active sodium metal) was vigorously stirred in small portions at 55—60°C. After one hour, the alkaline mixture was acidified with hydrochloric acid; 9.0 g. of hydrocinnamic acid, m. p. 49°C, was thus obtained in a 87% yield.

The General Procedure of the Reduction with Drynap and Acetic Acid.—Into an ethanol solution of 0.02 mol. of material described in Table I, 20 g. of Drynap (corresponding to 0.08 atom of sodium metal) and 5 ml. of gracial acetic acid were vigorously stirred in small portions. The reaction temperature was maintained below 60°C.

After 1 or 1.5 hr., the reaction mixture was separated from the residual spongy lead, and the filtrate was evaporated in order to remove the solvent. The residue was extracted with benzene.

The extract was washed with 5% sodium hydrogen carbonate solution and water, and dried over sodium sulfate. The crude product was dissolved in benzene, passed through an alumina column, and recrystallized with benzene or ligroin.

The materials and reduced products are listed in Table I.

The authors wish to thank Dr. Akio Nara for his microanalyses, and the Wako Pure Chemical Co., Ltd., for its gift of Drynap.

SHORT COMMUNICATIONS

Asymmetric Hydrogen with Modified Raney Nickel. VII

By Yoshiharu IZUMI, Susumu TATSUMI and Masami IMAIDA

Division of Organic Chemistry, Institute for Protein Research, Osaka University, Kita-ku, Osaka

(Received December 24, 1965)

It has been reported from our laboratory[1] that Raney nickel catalyst, modified with aqueous solutions of optically active 2-amino and 2-hydroxycarboxylic acids, shows an asymmetric hydrogenation activity in the hydrogenation of methyl acetoacetate to methyl 3-hydroxybutyrate, and that optically-active dihydroxy dicarboxylic acids, such as D- or L-tartaric acid, and their *C*-alkyl-substituted derivatives are very effective in the asymmetric modification.

The present paper will describe the asymmetric activity of Raney nickel modified with (+)-1, 2-dihydroxycyclohexane-1, 2-dicarboxylic acid,* which is a sort of *C, C'*-disubstituted tartaric acid. The asymmetric activity of the catalyst in the hydrogenation of methyl acetoacetate to methyl 3-hydroxybutyrate was measured as described in a previous paper.[1]

When Raney nickel was modified at 0°C with an aqueous solution of the acid, its asymmetric activity was greatly influenced by the pH of the modifying solution, as is shown in Fig. 1, this influence being quite different from those of catalysts obtained on modifications with tartaric acid, *C*-methyl- and *C, C'*-dimethyltartaric acid.[1] Optimum asymmetric activities were observed at pH 5—7; this pH range approximately corresponds to the pH-jumping region of the neutralization curve of the acid, as is shown in Fig. 2. However, there was a very great diminution in activity at pH values below pH 5. It is likely that both carboxyl groups of the modifying reagent are adsorbed upon the nickel metal under acidic conditions, while at pH 5—7, one of them is desorbed completely from the metal and forms a massive steric hindrance, which then regulates the approach of methyl acetoacetate to the catalyst. Further details will be reported in the near future.

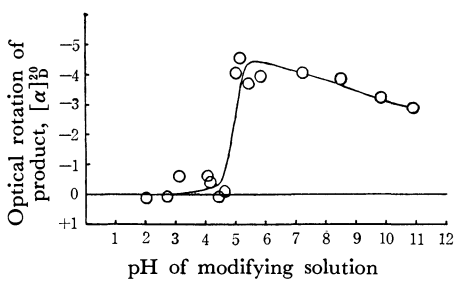

Fig. 1. Modification with (+)-1,2-dihydroxycyclohexane-1,2-dicarboxylic acid.

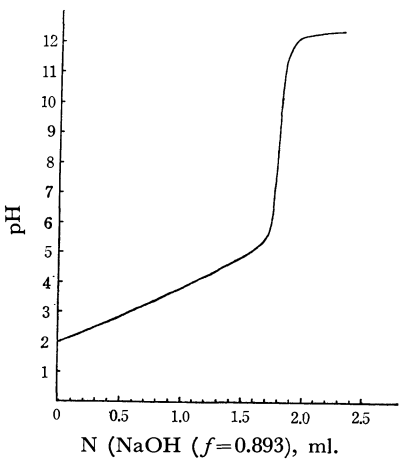

Fig. 2. Neutralization curve of 1% acid solution with N NaOH.

* The preparation of this hydroxy acid will be reported in this Bulletin in the near future.

1) Part V; Y. Izumi, S. Tatsumi, M. Imaida, Y. Fukuda and S. Akabori, This Bulletin, **38**, 1206 (1965); Part VI; Y. Izumi, S. Tatsumi, M. Imaida, Y. Fukuda and S. Akabori, ibid., in press.

The Preparation of Polymeric Fine Powder with Crosslinkage and Its Application as a Mordant

By Yukio MIZUTANI

Tokuyama Soda Co., Ltd., Tokuyama, Yamaguchi

(Received November 29, 1965)

It has been well known that a polymeric fine powder can be prepared by emulsion polymerization; no other method of preparation has yet been reported. A new method of preparing a polymeric fine powder with crosslinkage (PFPC) and its application as a mordant for poorly dyeable fibers will be reported in this paper. Vinyl monomers and divinyl benzene (DVB) were polymerized in some specified solvents (for example, an aliphatic hydrocarbon or an aliphatic alcohol) with stirring using benzoyl peroxide (BPO) as a polymerization initiator; PFPC was thus obtained. Table I shows examples of the polymerization at 80 ±5°C. The usefulness of these solvents may be attributed to the behavior of these solvents, in which the monomers are soluble but the polymer is insoluble. Furthermore, DVB should be effective in promoting the separation of the polymer from the solvent and in making the polymer very fine powdery. The PFPC prepared by this new method was a spherical powder with a diameter of about 0.1 μ or less; accordingly, its application as a mordant for poorly dyeable fibers could be expected.

Also, it has been known that the blend of some dyeable polymers, such as polymethyl methacrylate[1] or polyvinylpyridine[2], is effective in improving the polypropylene dyeability; the dyeable polymer is thus finely dispersed[1] because of its immiscibility to the fiber substrate.[3] The dyeable polymers thus blended can easily be extracted by acetone, but the newly-developed PFPC was inextractable because of its crosslinked structure. A common disadvantage of these blend systems, however, is that the dye in the substrate is not fixed perfectly by the chemical bond, and so can easily be extracted by acetone. Following the general idea mentioned above to improve the dyeability of a polymer-blended system, the author finally decided to apply the glycidyl group to PFPC as a reactive functional group; this proved to be very useful not only in dyeability but also in resistance to the the solvent extraction of the dyeings. Some of the results are shown in Table II.

Table II. The dyeing result with celliton blue extra type*3

Sample blended*1	Color after dyeing	Color after acetone-extraction*2
A	medium colored	none
B	medium colored	none
C	medium colored	medium colored

*1 The quantity of PFPC added: 3.8% by weight.

*2 The extraction was carried out for 8 hr. by the use of a Soxhlet extractor.

*3 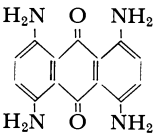

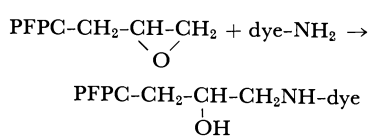

In conclusion, we recommend using PFPC with a reactive functional group which may behave as a mordant in the dyeing of polypropylene fiber. The details will be reported soon.

Table I. Preparation and properties of PFPC

Sample	Polymerization conditions: Monomer, g.	DVB g.	Solvent, cc.	BPO g.	Yield g.	Grain size of PFPC, μ
A	MA, 20	2	K, 150	0.1	9	0.1—0.2
B	VAc, 20 AA, 5	5	B, 150	0.3	—	0.1
C	GMA, 44	7	K, 400	0.3	38	0.1

MA: methyl acrylate, VAc: vinyl acetate, AA, acrylamide, GMA: glycidyl methacrylate, K: kerosene, B: *n*-butanol

1) Y. Mizutani, S. Matsuoka and K. Yamamoto, This Bulletin, **38**, 2045 (1965).

2) P. Ginstiani, G. Natta and G. Mazzanti, U. S. Pat. 3115478.

3) H. Hatakeyama and Y. Arata, Japanese Pat. 25788 (1964).

The Relationship between Allylic or Homoallylic-coupling Constants and Electron Localization on C=N Double Bonds in Some Schiff Bases and Their *N*-Oxides

By Kazuo TORI, Masako OHTSURU and Tanekazu KUBOTA

Shionogi Research Laboratory, Shionogi & Co. Ltd., Fukushima-ku, Osaka

(Received February 17, 1966)

It is well known that the magnitude of an allylic or a homoallylic coupling constant[1] depends upon the degree of σ-π overlaps[1,2] and the amount of electron localization on the intervening double bond.[1,3,4] A similar situation is also seen when the central double bond is C=N.[1,3,5,6]

We have recently observed the PMR spectra of benzal-*N*-methylamine (I),[7] its *N*-oxide (II),[7] methylbenzal-*N*-methylamine (III),[8] and its *N*-oxide (IV).[9] The spectral data obtained by the first-order approximation are listed in Table I.

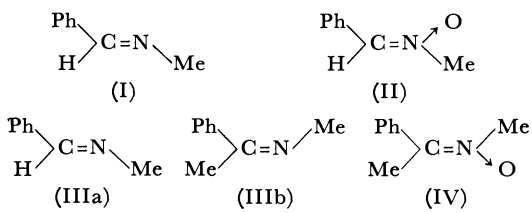

The introduction of the N→O bond into I extends the conjugation and causes an electron delocalization on the C=N double bond, as our previous study by ultraviolet absorption spectroscopy proved.[7] Therefore, it may readily be expected that the allylic or the homoallylic coupling constants vary from compound to compound and with the protonation occurring in such an acid solvent as trifluoroacetic acid. The fairly large $|J_{H,CH_3}|$ value in I becomes smaller in a deuterotrifluoroacetic acid solution and much smaller in II, in spite of the increase in the electronegativity of the nitrogen atom by the protonation to I and also by introducing an N→O group into I. These decreases in the $|J_{H,CH_3}|$ value should, accordingly, be attributed to the decreasing double-bond character of the C=N bond. In fact, π-bond orders calculated by Hückel MO method[10] are consistent with these results (Table I). However, the J_{CH_3,CH_3} value in IV, which is considerably larger than the $|J_{H,CH_3}|$ value in II, does not decrease appreciably in comparison with the J_{CH_3,CH_3} value in IIIb. These facts can be ascribed to the steric hindrance of the phenyl group with the methyl groups, which interrupts the conjugation of the benzene ring with the C=N bond. These conclusions are consistent with the results obtained by the earlier ultraviolet absorption spectroscopic study.[7] A study of the solvent effects and a theoretical study of the chemical shifts of these and other related compounds in connection with electron densities and other factors are now in progress.

TABLE I. PMR SPECTRAL DATA*1 AND RESULUS OF HÜCKEL MO CALCULATION*2

Compound	Chemical shift (τ)		Coupling constant*3, (c.p.s.)		π-Bond order of C=N
	=CH or =C-CH_3	=N-CH_3	J_{H,CH_3}	J_{CH_3,CH_3}	
I	1.81 (1.18)*4	6.53 (6.03)*4	−1.6 (−1.1)*4	—	0.873 (0.529)*5
II	2.76	6.21	−0.5	—	0.732
IIIa	7.82 (7.06)*4	6.69 (6.33)*4	—	+0.8 (+0.6)*4	
IIIb	7.82 (~7.05)*4	7.03 (6.42)*4	—	+1.4 (+0.9)*4	
IV	7.69	6.45	—	+1.2	

*1 The spectra were recorded on a Varian A-60 spectrometer by using solutions in CCl_4 containing Me_4Si as an internal reference, unless otherwise noted.
*2 See, Ref. 10.
*3 For the signs of these coupling constants, see Refs. 1, 2 and 11.
*4 Observed in CF_3COOD solutions.
*5 Calculated for $-C=N^+$ system.

1) For a review, see S. Sternhell, *Rev. Pure Appl. Chem.*, **14**, 15 (1964).
2) M. Barfield, *J. Chem. Phys.*, **41**, 3825 (1964).
3) H. Rottendorf and S. Sternhell, *Australian J. Chem.*, **17**, 1315 (1964).
4) P. M. Nair and G. Gopakumar, *Tetrahedron Letters*, **1964**, 709.
5) G. O. Dudek, *J. Am. Chem. Soc.*, **85**, 694 (1963); G. O. Dudek and G. F. Volpp, ibid., **85**, 2697 (1963).
6) H. A. Staab, F. Vögtle and A. Mannschreck, *Tetrahedron Letters*, **1965**, 697.
7) T. Kubota, M. Yamakawa and Y. Mori, This Bulletin, **36**, 1552 (1963).
8) We have obtained this compound as a mixture of *syn*- (IIIa) and *anti*- (IIIb) isomers in a ratio of 18 : 1. The assignment of each isomer in the spectra was made according to Ref. 6.
9) Y. Mori, unpublished results; we are also indebted to Dr. Mori for supplying us with a specimen of IV.
10) T. Kubota and M. Yamakawa, This Bulletin, **36**, 1564 (1963).
11) D. Gagnaire, A. Rouseau and P. Servoz-Gavin, *J. Chim. Phys.*, **61**, 1207 (1964).

The Configuration of Verarine[1]

By Tadashi MASAMUNE, Iwao YAMAZAKI and Mitsuo TAKASUGI

Department of Chemistry, Faculty of Science, Hokkaido University, Sapporo

(Received March 7, 1966)

Tomko and Bauer have recently isolated a steroid alkaloid named verarine from *Veratrum album subsp. lobelianum*. From a chemical and spectroscopic investigation of this substance, they have concluded that the alkaloid is 23-desoxy-veratramine,[2] but until now no details have been available of its steric configuration. Our present study confirms their structural formula and, in addition, provides the stereochemistry of the compound.

The treatment of veratramine (I) with acetic anhydride (6 mol.) in pyridine at −10°C, followed by chromatography, afforded, in a 44% yield, 3, *N*-diacetylveratramine[3] (II), m. p. 161—163°C; IR,[3] ν_{max} 1027 cm^{-1}. On oxidation with Jones' reagent, II was converted to 23-dehydro-3, *N*-diacetylveratramine (III) in a 73% yield, m. p. 196—198°C; UV,[3] λ_{max} 302 mμ (ε 250); ORD,[3] a strong negative Cotton effect. The treatment of III with sodium methoxide in refluxing methanol and subsequent acetylation led to an isomeric ketone (IV), m. p. 246—248°C; UV, λ_{max} 303 mμ (ε 290); ORD, a weak negative Cotton effect. III and IV were isolated in the ratio of 1 : 10 from an equilibrium mixture in an alkaline solution. As the benzyl part at C-22 and the 26-methyl group in the piperidine ring are *cis*-oriented in III,[4] those groups in IV must have a *trans*-configuration.

III was treated with ethane-1, 2-dithiol in methanol saturated with hydrogen chloride at 0°C. The product showed two main spots on a thin-layer chromatogram on silica gel. The fraction with the large R_f value yielded 23-ethylene thioketal (V), m. p. 155—156°C, while the product

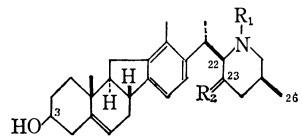

I R_1=H, R_2=-H, ···OH
VI R_1=Ac, R_2=H_2

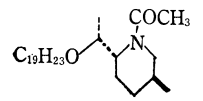

VII

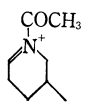

VIII

obtained from the fraction with the small R_f value again showed the same two spots. Having available the facile isomerization of the latter, V was isolated in a 73% yield. The treatment of V with Raney nickel in refluxing ethanol resulted in desulfurization, giving *N*-acetyl-23-desoxy-veratramine (VI) in a 60% yield, m. p. 195—197 °C; $[\alpha]_D$[3] −21°; UV, λ_{max} 267 mμ (ε 930) and 275 (900); IR, ν_{max} 3410, 1610, 1068 and 808 cm^{-1}. On the other hand, the Huang-Minlon reduction of III led to the removal of the 23-oxygen, with a concomitant epimerization at C-22, and gave an isomeric 23-desoxy compound (VII) in a good yield, m. p. 240—242°C; $[\alpha]_D$ −28°; UV, λ_{max} 269 mμ (ε 870) and 278 (810); IR, ν_{max} 3419, 1622, 1060 and 810 cm^{-1}. Both VI and VII showed strong peaks at *m/e* 140 due to a fragment, VIII, in the mass spectra.[5] In view of the process of the Huang-Minlon reaction, it is apparent that VI has the same configuration as III. Through the kindness of Dr. J. Tomko, VI was proved to be identical with *N*-acetylverarine in all respects. Since the configurations of all the asymmetric carbon atoms in I have already been established,[6] the present transformation completes the stereochemistry of verarine.

1) Part V of "*C*-Nor-D-homosteroids and Related Alkaloids"; Part IV : T. Masamune et al., This Bulletin, **38**, 1374 (1965).

2) J. Tomko and S. Bauer, *Coll. Czech. Chem. Comm.*, **29**, 2570 (1964).

3) Satisfactory analyses were obtained for all the new compounds described herein. The optical rotations, ORD curves, UV and IR spectra were measured in chloroform, in methanol, in ethanol and in Nujol respectively.

4) J. Sicher and M. Tichy, *Tetrahedron Letters*, **1956**, 6; R. L. Augustine, *Chem. & Ind (London)*, **1961**, 1448.

5) H. Budzikiewicz, *Tetrahedron*, **20**, 2267 (1964).

6) T. Masamune, M. Takasugi and Y. Mori, *Tetrahedron Letters*, **1965**, 489; O. Wintersteiner and M. Moore, *Tetrahedron*, **20**, 1947 (1964), and the references cited therein.

An X-Ray Analysis of Blasticidin S Monohydrobromide

By Shigeki ONUMA, Yoshiharu NAWATA and Yoshihiko SAITO

The Institute for Solid State Physics, The University of Tokyo, Azabu, Tokyo

(Received March 16, 1966)

Blasticidin S is an antibiotic isolated[1] from *Streptomyces griseochromogenes*. In cooperation with the organic chemical investigation of Yonehara et al.,[2] blasticidin S monohydrobromide has now been subjected to X-ray analysis in order to elucidate its molecular structure.

Small plate-like crystals were kindly supplied by Professor H. Yonehara and Professor N. Otake. They are orthorhombic, of the space group $P2_12_12_1$, with four molecules of $C_{17}H_{26}O_5N_8 \cdot HBr$ in a unit cell with dimensions of $a=20.39$, $b=21.34$ and $c=4.81$Å.

The intensities were estimated visually from equi-inclination Weissenberg photographs of the $hk0$–$hk3$ layers; the multiple-film technique was employed. The relative values of the observed structure amplitudes of 1653 reflections were collected by means of Cu $K\alpha$ radiation. The exposures were such that the various layers were approximately on the same relative scale; the absolute scale of each layer was obtained at a later stage by correlation with the calculated structure amplitudes. No absorption correction was applied.

At first the analysis proceeded directly on the basis of the usual two-dimensional sign-determining heavy-atom method, because the c-axis is fairly short. The initial coordinates of the bromide ion were determined by calculating the Patterson projection. With the signs determined by only the bromide ion and with the observed 354 $hk0$ amplitudes, the first two-dimensional electron-density distribution was calculated; however, it was hard to interpret. The heavy atom did not seem to be powerful enough for the signs to be determined correctly. Many cycles of iterative Fourier syntheses had to be carried out until a structure was found plausible enough for further refinement. At later stages of the analysis, the structure was refined by the difference syntheses and by the isotropic least-squares method. The final R index for $hk0$ reflections was about 0.15.

The final two-dimensional electron-density distribution and the corresponding molecular framework are shown in Fig. 1. The topography of the final difference synthesis is flat, even in the neighborhood of the bromide ion, within the range of ± 1 e/Å^2. The individual isotropic temperature factors, B, refined by the least-squares method are reasonable values of 4.3 for the bromide ion and 2.5—3.9 for the carbon, nitrogen and oxygen atoms; the light atoms were assigned correctly. The resulted molecular structure is consistent with the modified structure reported by the chemical group.

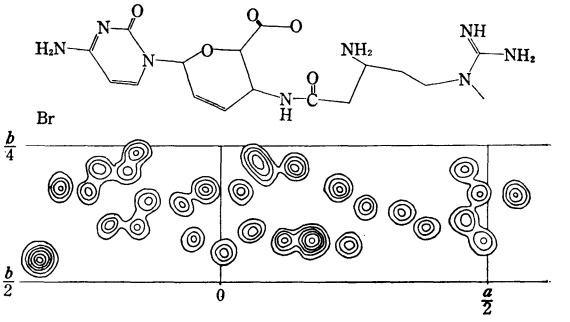

Fig. 1

A three-dimensional analysis is now in progress; the results will be published elsewhere.

1) S. Takeuchi, K. Hirayama, K. Ueda, H. Sakai and H. Yonehara, *J. Antibiotics*, **11a**, 1 (1958).
2) N. Otake, S. Takeuchi, T. Endo and H. Yonehara, *Tetrahedron Letters*, **1965**, 1405, 1411.

The Photo-Ionization of Molecules in Solutions. II. Electron Transfer from Aromatic Diamine to Pyrene

By Hiroshi TSUBOMURA, Naoto YAMAMOTO and Yoshihiro NAKATO

Department of Chemistry, Faculty of Engineering Science, Osaka University, Toyonaka, Osaka

(Received March 23, 1966)

We have found that the process of the photo-ionization of *N*, *N*, *N'*, *N'*-tetramethyl-*p*-phenylenediamine (TMPD) in solutions shows interesting differences depending on the nature of the solvent and on the temperature.[1]

The deoxygenated rigid matrix at 77°K composed of 1 part methylcyclohexane and 1 part isopentane (hereafter called MP), which contained 10^{-4} mol./l. TMPD and various concentrations of pyrene (Pyr) (10^{-2}—10^{-4}mol./l.), was illuminated by a Hg lamp at wavelengths between 3000—4000 Å. It showed not only the absorption spectrum of $TMPD^+$, but also that of Pyr^-. The latter is identical with the spectrum obtained by Hoijtink and others by the reduction of Pyr with sodium.[2] The spectrum persists for a long time at 77°K. As there is no sign of complex formation between TMPD and Pyr at either 77°K or 20°C, as may be seen from the absorption spectra, it may reasonably be assumed that they are distributed randomly. Then, we can estimate the mean distances between TMPD and Pyr, which should be proportional to $[Pyr]^{-1/3}$ under conditions where $[Pyr^-] \gg [TMPD^+]$. (Here [ ] means the concentration.) The ratio ω defined by $[Pyr^-]/[TMPD^+]$ can be determined experimentally by the use of the molecular extinction coefficients of both species. The ω values thus obtained are plotted against [Pyr] in curve b, Fig. 1. Here, for instance, $\omega=0.5$ means that one half the electrons ejected from TMPD are trapped in the matrix, while the rest of them reach Pyr. From a simple statistical treatment, we can conclude that, in MP, some of the electrons can travel at least 80 Å away from TMPD. This result may be the first definite proof that the photo-ejected electrons can migrate a considerable distance away from the molecule.

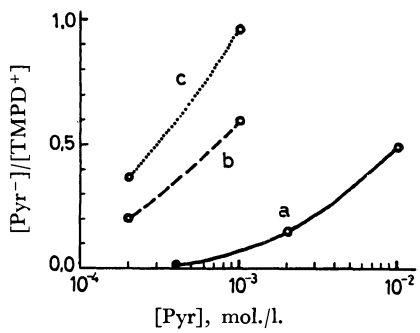

Fig. 1. Formation of ions by ultraviolet excitation of TMPD: a) in EPA matrix, b) in MP matrix, c) the same, illuminated with infrared light. (With prolonged ultraviolet excitation the ratio ω decreases in all three cases.)

By the illumination in the infrared (0.7—5 μ) region, the MP matrix containing $TMPD^+$ and Pyr^- emits light. At the same time, $[TMPD^+]$ slightly decreases and $[Pyr^-]$ largely increases (curve c, Fig. 1). This shows that the electrons trapped in the matrix are excited by the infrared light and migrate randomly in the matrix. The emission is probably due to the fluorescence and phosphorescence of TMPD.[3] By pulling the sample cell in which the ionized species are contained out of the Dewar, a thermoluminescence was observed; when this was measured photographically, it was seen that there is only one band, with a maximum at 476 mμ. We may assume that this emission is due to the transition from the charge transfer state formed by the encounter of $TMPD^+$ and Pyr^- in the half-melting matrix to the ground state.[4]

In degassed EPA matrices at 77°K containing TMPD and Pyr, $TMPD^+$ and Pyr^- are also formed by the ultraviolet excitation. This time, however, the ratio ω is much smaller than that for the MP matrix, showing that more electrons are trapped in the solvent (curve a, Fig. 1). The illumination in the infrared region and down to 6000 Å does not change $[TMPD^+]$ and $[Pyr^-]$, nor does it stimulate the emission. Illumination in the range of the absorption spectrum of Pyr^-, ($\lambda<5000$ Å), lowers the $[Pyr^-]$ value. The color of the solution fades instantaneously as the matrix is warmed, although a small amount of the cation remains for some time. However, no thermoluminescence is observed.

1) H. Tsubomura, N. Yamamoto, K. Kimura, T. Sato, H. Yamada, M. Kato, G. Yamaguchi and Y. Nakato, This Bulletin, **38**, 2021 (1965). The spectrum shown by curve a in Fig. 1 was later concluded to be the T—T' absorption of TMPD. The details for this will be published in a near future.

2) P. Balk, S. deBruijtink and C. J. Hoijtink, *Rec. trav. chim.*, **76**, 907 (1957).

3) Some related phenomena are obtained: K. D. Cadogan and A. C. Albrecht, *J. Chem. Phys.*, **43**, 2550 (1965); J. D. W. Van Voorst and G. J. Hoijtink, ibid., **42**, 3395 (1965).

4) Luminescence from the recombination of organic cations and anions are also reported. E. A. Ckandros, J. W. Longworth and R. E. Visco, *J. Am. Chem. Soc.*, **87**, 3259 (1965).

BULLETIN OF THE CHEMICAL SOCIETY OF JAPAN VOL. 39 1093—1094 (1966)

Potentiometric Studies of the Reaction between Mercury(I) Nitrate and Sodium Arsenate

By C. S. BHATNAGER

Department of Chemistry, Government College, Kota (Rajasthan), India

(Received May 1, 1965)

The reaction between mercury(I) nitrate and sodium arsenate has been studied potentiometrically at various concentrations, by both the direct and reverse methods, employing bright platinum foil as an indicator electrode in conjunction with a saturated calomel electrode. The end-points obtained from the sharp inflections in titration curves and pronounced maxima in dE/dV provide cogent evidence for the formation and precipitation of mercury(I) arsenate, Hg_3AsO_4, in the 8.2—9.4 pH range. The precipitation of the compound is almost quantitative. The reaction can be successfully used for the determination of Hg_2^{2+} or AsO_4^{3-} ions in solutions at suitable concentrations and pH ranges.

The formation of mercury(I) arsenate has been studied earlier analytically. Coloriano[1] and Gognet[2] obtained mercury(I) arsenate (Hg_3AsO_4) by heating arsenic(V) oxide and mercury in a sealed tube at 230°C for 60 hr., and Haack,[3] by treating meraury(I) nitrate with an excess of sodium arsenate, while Simon[4] prepared it by adding a solution of mercury(I) nitrate into a concentrated solution of arsenic acid and redissolving the white precipitate so formed in an excess of acid, which had the composition of $HgHAsO_4 \cdot 1/2H_2O$. Recently Guerin and Boulitrop[5] studied the arsenic(III) oxide - mercury(I) oxide - water system at 60°C and reported the formation of Hg_3AsO_4. There is, however, no reference in the literature concerning its study by electrometric techniques. The H^+ ion concentration plays an important role in the formation of such compounds.

Because of the complexity of reaction equilibria between alkali metal arsenates as a result of the appreciable tendency for hydrated forms to be concerted into higher aggregated products, which causes the precipitation of heavy metal salts of varying compositions, belonging some times to one type and some times to another,[6] the conclusions of the reports on analytical investigations on this reaction seem to be overstrained and require a further approach using recent electrometric methods, which provide more conclusive evidence.[7] The present investigation has, therefore, been undertaken with a view to study the reaction between mercury(I) nitrate and alkali arsenate more precisely.

Experimental

Merck's guaranteed extra-pure reagents, mercury(I) nitrate and Na_3AsO_4 were used; their solutions were prepared in air-free conductivity water. The sodium arsenate solution was standardised by the method given by Williams.[8] The mercury(I) nitrate solution was prepared in the minimum quantity of nitric acid and was then estimated by titrating it against a standard sodium chloride solution potentiometrically.

The E. M. F. measurements of the cells, which consisted of a bright platinum electrode, acting as an indicator electrode, in conjuction with a saturated calomel electrode dipped into a titre solution, were carried out with a Backmann pH meter. Twenty milliliters of the titre solution was taken in the cell each time, the cell was kept immersed in an electrically-maintained thermostat, and the solution was stirred by an electrical stirrer. The observed values of E. M. F. were plotted against the volume of the titrant added, and the end-points were located graphically; the locations were then checked further by determining the maximum value of dE/dV.

Using different concentrations of the reactants, mercury(I) nitrate and $NaAsO_4$, a series of potentiometric titrations were carried out with each of the reagents, using them alternately as titrants. The reaction was also followed in the presence of 15% and 30% ethanolic media. The results of this study have been tabulated below (Table I); only one figure (Fig. 1) illustrating direct and reverse titrations has been given, in the interests of brevity.

1) A. Coloriano, "Sur des arseniates crystallises," Paris, **49**, (1886); *Bull. Soc. Chem.*, **2**, 45, 707 (1886); *Compt. Rend.*, **103**, 275 (1886).

2) H. Gognet, "Contribution a l'stendedes arsenates et des antimonites crystallises prepares par voie humide," Paris, **49**, 1896.

3) K. Haack, Veber Arsenate and Phosphate des Quecksilvers, Halle, **35**, 1890; *Leibigs Ann.*, **262**, 190 (1891).

4) G. F. Simon, *Pogg. Ann.*, **40**, 442 (1837); **41**, 424 (1837).

5) H. Guerin and R. Boulitrop, *Compt. Rend.*, **2**, 53 (1888).

6) "Inorganic Chemistry," Ed. by P. C. L. Thorne and E. R. Roberts (1949), p. 745.

7) R. S. Saxena and C. S. Bhatnagar, *J. Indian Chem. Soc.*, **31**, 157 (1954); *Z. anorg. Chem.*, **285**, 95 (1956); *Naturwissenschaften*, **6**, 128 (1958); **18**, 438 (1958); *Z. anal. Chem.*, **165**, 95 (1959); *J. Nucl. & Inorg. Chem.*, **12**, 38 (1960); *Z. anorg. Chem.*, **303**, 1 2 (1960).

8) H. E. Williams, *J. Soc. Dyres. Col.*, **12**, 86 (1896).

Table 1. A SUMMARY OF THE RESULTS OF POTENTIOMETRIC TITRATIONS

Molarity of solutions		Equivalence point (ml.)				Formula supported
			Obs. in presence of Alc.			
Na_3AsO_4	$HgNO_3$	Calcd.	0.0%	15.0%	30.0%	
			Direct titrations : Fig. 1, curve I			
M/9	M/10	6.00	5.95	5.96	6.02	Hg_3AsO_4
M/24	M/40	4.00	3.90	3.94	3.98	
M/120	M/160	5.00	4.90	4.94	4.96	
			Reverse titrations : Fig. 1, curve II			
M/180	M/15	5.00	4.94	4.96	4.96	Hg_3AsO_4
M/250	M/25	6.00	5.9	5.92	5.95	
M/750	M/50	4.00	3.9	3.92	3.96	

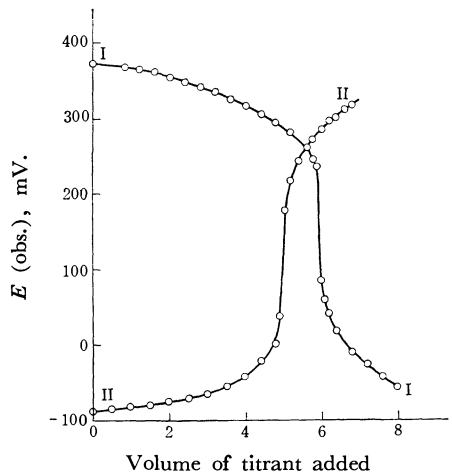

Fig. 1. Direct (curve I, M/9 Na_3AsO_4 vs. M/10 $HgNO_3$) and reverse (curve II, M/15 $HgNO_3$ vs. M/180 Na_3AsO_4) potentiometric titrations between mercury(I) nitrate and sodium arsenate in the absence of ethanol.

Discussion

Figure 1 illustrates the direct and reverse potentiometric titrations between mercury(I) nitrate and Na_3AsO_4. In the case of inverse titrations, when the mercury(I) nitrate solution is added to the Na_3AsO_4 solution, the arsenate ions are removed from the solution by precipitation and the E. M. F. gradually rises up to the addition of about 2.5 mol. of mercury(I) nitrate per mole of Na_3AsO_4, but at the stoichiometric end-point which corresponds to the formation of Hg_3AsO_4 a sharp upward jump in potential is noted, after which the E.M.F. becomes practically constant. In direct titration (curve I), i. e., when Na_3AsO_4 solution was added to the mercury(I) nitrate solution taken into a cell, the E. M. F. of the cell gradually decreases up to the vicinity of the end-point which is indicated by a sharp fall in E. M. F.; after this the E. M. F. assumes a practically constant value. Both the direct and reverse potentiometric titrations yield a sharp inflection at the point where the molecular ratio of mercury(I) and AsO_4^{3-} is 3 : 1, corresponding to the formation of mercurous arsenate, Hg_3AsO_4, in the 8.2—9.4 pH range. The accuracy and reproducibility of these titrations have been found to be excellent, and the precipitation of the compound is almost quantitative.

It has been noted that each titration takes about half an hour for completion, and that a thorough stirring in the vicinity of the end-point has a favourable effect. The presence of ethanol increases the sharpness of the end-point and, consequently, the magnitude of the dE/dV, as it reduces the solubility of the precipitates formed and decreases the hydrolysis and adsorption of AsO_4^{3-}.

It is apparent from the above study that, when mercury(I) nitrate reacts with Na_3AsO_4, the formation of mercury(I) arsenate, Hg_3AsO_4, takes place in the 8.2—9.4 pH range. As the precipitation of the compound is quantitative, the reaction can be successfully utilised for the determination of Hg_2^{2+} or AsO_4^{3-} ions in solutions at suitable concentrations and pH range.

The author is thankful to Professor Dr. R. S. Saxena, D. Sc., Professor of Chemistry, Malaviya Regional Engineering College, Jaipur, India, for his kind help.

BULLETIN OF THE CHEMICAL SOCIETY OF JAPAN VOL. 39 1095—1101 (1966)

The Autoxidation of α-Methylstyrene in the Presence of Metal Salt[1)]

By Etsuo NIKI and Yoshio KAMIYA

Department of Fuel Engineering, The University of Tokyo, Hongo, Tokyo

(Received May 14, 1965)

The azobisisobutyronitrile-initiated autoxidation of α-methylstyrene in the presence of metal salt was studied from the viewpoints of rate and products. The over-all activation energy was found to be 19.7 kcal./mol. In most cases, metal salts had a retarding effect on the rate of oxidation. With manganese and copper salts, an increase in the concentration of the metal decreased the rate of oxidation monotonously. However, cobalt naphthenate had an accelerating effect within a limited range of concentration, although it also had an inhibiting effect at higher concentrations. The products were acetophenone, formaldehyde, α-methylstyrene oxide and α-methylstyrene polyperoxide. Metal salt had little effect on the products of oxidation, with the exception of cobalt salt, which gave α-methylstyrene oxide in considerable yield even at 760 mmHg of oxygen pressure, where little α-methylstyrene oxide was formed in the presence of other metal salts or in the absence of catalysts.

The initiated and metal-catalyzed oxidation of hydrocarbons has received considerable attention in recent years.[2)] The functions of the metal salts in the autoxidizing systems are not yet, however, fully understood in detail. Most of the previous work on the metal-catalyzed autoxidation of unsaturated hydrocarbons has been concerned with compounds that have relatively unreactive double bonds. The metal-catalyzed oxidation of unsaturated compounds with reactive and polymerizable double bonds has received little attention. In view of these circumstances, it is a matter of theoretical as well as technological interest to study the autoxidation of olefins with reactive double bonds in the presence of the metal salts.

The purpose of this work is to study the azobisisobutyronitrile-initiated autoxidation of α-methylstyrene in the presence of metal naphthenate from the viewpoints of rate and products.

Mayo, Miller and Russell[3)] studied the oxidation of unsaturated compounds with reactive double bonds in the presence of azobisisobutyronitrile as a free radical initiator, although in the absence of metal catalysts. They showed that the autoxidation of α-methylstyrene by a free radical mechanism gives two simultaneous reactions, a copolymerization of α-methylstyrene with oxygen and a cleavage reaction to form acetophenone, formaldehyde and α-methylstyrene oxide.

Experimental

Materials.—α-Methylstyrene was obtained from Allied Chemical; it was more than 99.8 mol.% pure. Prior to the experiment it was washed with alkali to remove the inhibitor, passed through activated alumina, and stored under nitrogen. Guaranteed reagent-grade azobisisobutyronitrile (hereafter designated as ABN) was stored in an ice box. Metal salt catalysts were obtained from the Dainippon Printing Ink Mfg. Co. and the Nihon Kagaku Sangyo Co. The metals used were cobalt, manganese, copper, lead, zinc, iron, and nickel (10.0, 8.2, 10.2, 30.3, 10.6, 10.0, and 8.0% respectively). The catalysts were used as metal naphthenates. The purity of the oxygen and the nitrogen was more than 99% (as determined by gas chromatography).

Procedures.—Two procedures were employed, one for measuring the oxidation rate of the monomer (R_M) and the rate of formation of the products, and the other for measuring the rate of oxygen absorption ($-dO_2/dt$). In the former procedure, a catalyst was dissolved in 65 ml. of α-methylstyrene in advance; then this solution and ABN were added to a 300-ml., 4-necked flask equipped with ground glass joints. The mixture was stirred vigorously by a Teflon paddle using a magnetic stirrer. All of the reaction was performed under one atmosphere. The reaction gas was sometimes diluted with nitrogen to make a fixed-oxygen partial pressure and was fed in at the rate of 4 cc./sec. The exhaust gas was taken out through a reflux condenser and then a trap cooled by methanol and dry ice to −50°C. The reaction mixture was sampled periodically and analyzed. The rate of oxygen absorption was measured by a manometer in a constant-pressure closed system.

Analyses.—The oxidation rate of the monomer was measured by following the disappearance of the monomer by gas chromatography A (Apiezon-L column;

1) Presented in part at 18th Annual Meeting of the Chemical Society of Japan, Osaka, April, 1965.

2) a) J. L. Bolland, *Quart. Revs.*, **3**, 1 (1949); b) L. Bateman, ibid., **8**, 147 (1954); c) H. S. Blanchard, *J. Am. Chem. Soc.*, **82**, 2014 (1960); d) Y. Kamiya and K. U. Ingold, *Can. J. Chem.*, **41**, 2020, 2034 (1963), **42**, 1027, 2424 (1964).

3) a) A. A. Miller and F. R. Mayo, *J. Am. Chem. Soc.*, **78**, 1017 (1956); b) G. A. Russell, ibid., **78**, 1035 (1956); c) F. R. Mayo, ibid., **80**, 2465 (1958); d) F. R. Mayo and A. A. Miller, ibid., **80**, 2480 (1958); e) F. R. Mayo, ibid., **80**, 2497 (1958); f) F. R. Mayo, A. A. Miller and G. A. Russell, ibid., **80**, 2500 (1958).

column temperature, 180°C; nitrogen carrier gas, 30 cc./min.). The oxidation products were analyzed by gas chromatography A, a study of the infrared spectra and by chemical analysis. The internal standard method was employed for the gas chromatographic analyses of the reaction mixture, using styrene as an internal standard. Infrared spectra analyses were made as well, because there was some possibility that peroxide decomposed in the gas chromatography to form the decomposition products. It was found, however, that the decomposition of peroxides in the gas chromatographic column was negligible. Acetophenone was sometimes determined gravimetrically with 2, 4-dinitrophenylhydrazine. In a few experiments, formaldehyde was measured as a dimethone derivative. However, its quantitative analysis was extremely difficult since most of the formaldehyde formed in the oxidation became attached to the wall as paraformaldehyde. Several iodometric methods were employed in an attempt to determine the peroxide, but no satisfactory procedure could be found. Carbon monoxide and carbon dioxide were measured by gas chromatography with a column of Molecular Sieve-13X and Acetonyl Acetone-S respectively. The formation of both gases was found to be negligible. The water content was measured by Karl Fisher titration; its formation was very small, below 0.1% of the products. Moreover, no other products could be detected either by gas chromatography or by a study of the infrared spectra. It was assumed, therefore, that formaldehyde was formed in an amount equivalent to acetophenone and that the only product other than acetophenone, formaldehyde and α-methylstyrene oxide was α-methylstyrene polyperoxide.

The Preparation of α-Methylstyrene Oxide.—α-Methylstyrene oxide was prepared as follows for use as the standard of the gas chromatographic analyses. A mixture of 102 g. of acetic anhydride and 2.4 g. of sulfuric acid was vigorously stirred into 57 g. of 30% hydrogen peroxide at room temperature and then reacted for an hour. Fifty grams of α-methylstyrene was then dropped into the solution, with the temperature kept at 0°C, and stirred for two hours. After the reaction, *t*-butylcathecol, an inhibitor, was added, the reaction mixture was extracted with benzene, and acetic acid was removed by 5% sodium bicarbonate, washed with water and dehydrated. The products thus obtained were distilled in vacuo.

The Preparation of α-Methylstyrene Polyperoxide.—The reaction was carried out like the other experiments. The final reaction mixture was poured into twice as much cold methanol to precipitate the methanol-insoluble polyperoxide. The polymer was then washed with methanol until it became stiff. It was dissolved in benzene, precipitated, and washed with methanol. This operation was repeated twice. Finally it was dried in vacuo to remove the methanol.

Results and Discussion

The products of the oxidation of α-methylstyrene are acetophenone, formaldehyde, α-methylstyrene oxide and α-methylstyrene polyperoxide. A typical example of the reaction of α-methylstyrene with oxygen is shown in Fig. 1.

The Effect of ABN on the Rate and Products of Oxidation.—The rates of oxygen absorption at 0.003, 0.005 and 0.010 mol./l. of ABN were 0.29, 0.36 and 0.51 mol./l./hr. respectively, when α-methylstyrene was oxidized at 70°C in the absence of the metal salt. These results show that the rate of oxidation is proportional to the square root of the ABN concentration. This suggests that, at a sufficiently high oxygen pressure, termination is a bimolecular reaction of two radicals. The reaction sequence must be as follows[2a,b]:

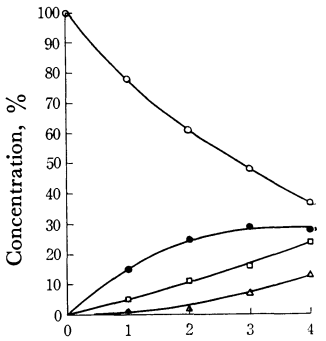

Fig. 1. Oxidation of α-Methylstyrene at 70°C, ABN 0.030 mol./l., Co-N 3.4×10^{-3} mol./mol. and oxygen pressure 760 mmHg.
○: α-methylstyrene
●: α-methylstyrene polyperoxide
□: acetophenone
△: α-methylstyrene oxide

$$\mathrm{ABN} \xrightarrow{k_i} 2\mathrm{R'}\cdot \rightarrow 2e\mathrm{M}\cdot \quad (1)$$

$$\mathrm{M}\cdot + \mathrm{O_2} \rightarrow \mathrm{MOO}\cdot \quad (2)$$

$$\mathrm{MOO}\cdot + \mathrm{M} \rightarrow \mathrm{M}\cdot \quad (3)$$

$$2\mathrm{MOO}\cdot \rightarrow \text{non-radical products} \quad (4)$$

where R'· is the dimethylcyanomethyl radical, e is the efficiency of ABN, and M is the α-methylstyrene monomer. M· and MOO· represent free radicals of an unspecified length and ending in monomer and peroxide units respectively. In this paper, M· and MOO· correspond to $\sim CH_2C(CH_3)(C_6H_5)\cdot$ and $\sim CH_2C(CH_3)(C_6H_5)OO\cdot$. In fact, this mechanism is simplified; for example, the alkoxy radical MO·, i. e., $\sim CH_2C(CH_3)(C_6H_5)O\cdot$, which may arise from the depolymerization of the polyperoxy radical, is left out of consideration, and also consumption of oxygen in reaction 1 is disregarded. Under steady state conditions, the rate of oxidation is given by Eq. 5;

$$-\mathrm{d}[\mathrm{O_2}]/\mathrm{d}t = \frac{k_3}{(2k_4)^{1/2}}[\mathrm{M}](R_i)^{1/2} \quad (5)$$

where $R_i=2ek_i[\mathrm{ABN}]$. The experimental data coincide with this rate equation provided e is constant independent of the concentration of the initiator. It was also confirmed that the rate was first-order with respect to α-methylstyrene

Table I. Oxidation of α-methylstyrene at 70°C, ABN 0.030 mol./l. and oxygen pressure 760 mmHg

Catalyst		Conv.[a]	Rate (R_M)[b]	Products Yields in mol. %[c]		
	mol./mol.	%	mol./l./hr.	AcC_6H_5	$C_9H_{10}O$	$(C_9H_{10}O_2)_n$
Ni-N[d]	3.0×10^{-4}	65	1.93	52	—	48
Zn-N	3.0×10^{-4}	61	1.74	53	—	47
Pb-N	4.2×10^{-4}	60	1.69	53	—	47
Fe-N	3.1×10^{-4}	57	1.66	43	—	57
Co-N	3.4×10^{-4}	53	1.39	55	7	38
Mn-N	3.0×10^{-4}	38	0.89	26	—	74
Cu-N	3.2×10^{-4}	32	0.71	43	—	57
None	—	62	1.79	56	—	44

a) (Reacted α-methylstyrene/initial α-methylstyrene)$\times10^2$ Reactions were carried out for 4 hr.
b) Observed rate of oxidation of monomer.
c) Based on α-methylstyrene reacted.
d) N represents naphthenate.

(shown in Fig. 5).

Nitrogen evolution by the decomposition of the initiator must be taken into consideration in some cases. The fragments from ABN are assumed to either take up oxygen to produce the dimethylcyanomethyl peroxy radical or recombine in the "cage." The resulting peroxy radicals can initiate the chains. This situation is indicated by the following eqautions;

$$\mathrm{ABN} \xrightarrow{k_t} 2\mathrm{R'}\cdot + \mathrm{N_2} \qquad (1')$$

$$2\mathrm{R'}\cdot \xrightarrow{\mathrm{O_2}} 2e\mathrm{R'OO}\cdot + (1-e)(\mathrm{R'-R'}) \qquad (1'')$$

$$2e\mathrm{R'OO}\cdot \xrightarrow{\mathrm{M}} 2e\mathrm{M}\cdot \qquad (1''')$$

Hence, the net oxygen absorption by the monomer is given by the observed value plus $(1-e)k_i$[ABN]. However, the kinetic chains in this reaction are long enough so that the consumption of oxygen and the monomer, and the nitrogen evolution in reaction 1 may be disregarded. As a matter of fact, $(1-e)k_i$[ABN] is equal to 1.5×10^{-3} mol./l./hr. at 70°C and with 0.030 mol./l. of ABN, assuming e to be 0.7. This value is less than 1% of the observed value.

As for the products, an increase in the concentration of ABN increases the cleavage products, acetophenone, formaldehyde and α-methylstyrene oxide. These results may probably be attributed to the increase in the rate of termination.

The Effect of Metal Salt on the Rate and Products of Oxidation.—The rates and the products of the oxidation of α-methylstyrene in the presence and in the absence of various metal salts are shown in Table I.

As Table I shows, manganese and copper salts retard the oxidation significantly. However, the activity of the catalyst cannot be compared directly in Table I, since it depends on the concentration of the catalyst. The effect of the concentration of the metal salts on the rate of oxidation is shown in Fig. 2. Manganese and copper naphthenates act as retarders independent of their concentrations, and an increase in the concentration of these salts decreases the rate of oxidation monotonously. The inhibiting effect of metal salt catalysts is observed in some cases at a high concentration of catalysts,[4] but it is seldom observed that manganese and copper salts show an inhibiting effect independent of their concentrations. The effect of the cobalt naphthenate catalyst differs from that of manganese and copper catalysts.

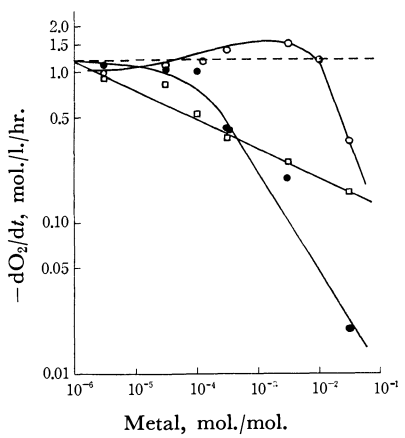

Fig. 2. Effect of the metal concentration on the rate of oxidation at 70°C, ABN 0.030 mol./l. and oxygen pressure 760 mmHg.
○: Co, ●: Mn, □: Cu
The broken line illustrates the rate of oxidation in the absence of metal catalysts.

The rate of oxidation increases gradually with an increase in the concentration of the cobalt salt catalyst, reaches a maximum at 3.4×10^{-3} mol./mol. of cobalt naphthenate, and then falls rapidly with a further, small increase in the catalyst.

It is assumed that these inhibiting effects of

4) For example, N. Ohta, *J. Chem. Soc. Japan, Ind. Chem. Sect.* (*Kogyo Kagaku Zasshi*), **65**, 1353 (1962).

TABLE II. EFFECT OF TEMPERATURE ON RATE OF OXIDATION OF α-METHYLSTYRENE WITH ABN 0.030 mol./l., Co-N 3.4×10^{-3} mol./mol. AND OXYGEN PRESSURE 760 mmHg

Expt. No.	Reaction temp., °C	R_i[1] mol./l./hr.	Rate const. sec^{-1}	R_M mol./l./hr.	Chain length[2]
242	60	0.0018	3.20×10^{-5}	0.85	470
214	70	0.0070	7.00×10^{-5}	1.85	260
241	80	0.024	1.85×10^{-4}	4.90	200
228	90	0.068	3.56×10^{-4}	9.43	140

1) Rate of initiation. Calculated from Ref. 5. $R_i=2ek_i[ABN]$ e was assumed to be 0.7.
2) Chain length$=R_M/R_i$

the catalyst may be attributed to the direct termination and/or the deactivation of active radicals, for example, the transfer reaction between radicals and metal ions or the formation of an inactive complex, by the metal salt catalyst.

One of the authors previously proposed the following chain termination in the oxidation of tetralin[2d];

$$ROO\cdot + Me \rightarrow \text{inactive products} \quad (6)$$

or, alternatively:

$$ROO\cdot + Me^{2+} \rightarrow (ROO^-Me^{3+}) \quad (7)$$

$$(ROO^-Me^{3+}) + ROO\cdot \rightarrow \text{inactive products} \quad (8)$$

If the chain termination is assumed to be reaction 6, or reactions 7 and 8 instead of reaction 4, they give the following rate equations:

$$-d[O_2]/dt = \frac{k_3[M](R_i)}{k_8[Me]} \quad (9)$$

or

$$-d[O_2]/dt = \frac{k_3[M](R_i)^{1/2}}{(2K_8k_9[Me])^{1/2}} \quad (10)$$

respectively. Indeed, these chain terminations by the catalyst are competitive with the reaction 4, but at a sufficiently high concentration of the metal salt the former reactions may well be predominant, while at the utmost limit Eq. 5 must be replaced by Eq. 9 or 10.

In Fig. 2 it may be seen that the rate of oxidation is approximately inversely proportional to $[Cu\text{–}N]^{0.2}$. In the presence of manganese naphthenate, the rate decreases slowly as the metal concentration is increased, but when it exceeds 10^{-4} mol./mol., the rate decreases sharply and is inversely proportional to $[Mn\text{-}N]^{0.7}$. These results may well be attributed to the chain termination reaction by metal salt in addition to reaction 4; probably in the case of copper salt, reactions 7 and 8, and in the case of manganese salt, reaction 6.

Cobalt showed quite a different effect, as has been stated above, which must now be discussed in connection with the products. The yields of the products are shown in Table I. A distinctive feature is that a considerable amount of α-methylstyrene oxide is formed in the presence of the cobalt naphthenate catalyst, although in the presence of other salts, as well as in the absence of the metal salt, little epoxide was formed under these reaction conditions. The effect of the concentration of cobalt salt on the yield of α-methylstyrene oxide was found to be analogous to that on the rate of oxidation. The results, shown in Fig. 3, indicate that the increase in the

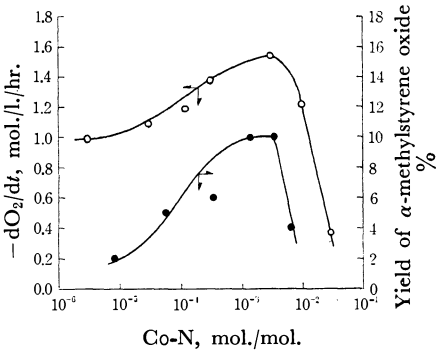

Fig. 3. Effect of Co-N concentration on the rate of oxidation and the yield of α-methylstyrene oxide (at conv.=50%) at 70°C, ABN 0.030 mol./l. and oxygen pressure 760 mmHg.

rate of oxidation and the formation of epoxide are closely related. Cobalt naphthenate, unlike manganese and copper salts, is assumed to be able to increase the rate of oxidation and to form α-methylstyrene oxide as well. However, it also terminates chains as it is increased above a critical concentration, i. e., 3.4×10^{-3} mol./mol. The decrease in the rate of oxidation is very sharp, and, in Fig. 2, it may also be seen that the rate is inversely proportional to $[Co\text{-}N]^{1.0}$, suggesting that the reaction 4 is replaced by the reaction 6.

The apparent order of the oxidation on the metal, however, is complex. Moreover, the proportions of the two valence states of the metal and the nature of the ligands probably change during the oxidation, further complicating the apparent order.

Other metal naphthenate catalysts had little effect on the products of the oxidation.

The Effect of the Temperature on the Rate and Products of Oxidation.—Reactions were carried out over the temperature range from 50 to 90°C. The results are summarized

in Table II. From Table II the over-all activation energy of the oxidation of α-methylstyrene in the presence of ABN and cobalt naphthenate may be found to be 19.7 kcal./mol. The effect of the temperature on the formation of acetophenone is shown in Fig. 4. Polyperoxide was supposed

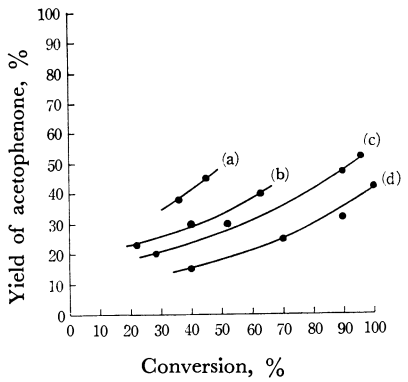

Fig. 4. Effect of temperature on the yield of acetophenone in the oxidation of α-methylstyrene with ABN 0.030 mol./mol., Co-N 3.4×10^{-3} mol./mol. and oxygen pressure 760 mmHg. (a) 60°C, (b) 70°C, (c) 80°C, (d) 90°C

to decompose more rapidly at higher temperatures, causing an increase in the yields of the cleavage products. On the contrary, the yield of acetophenone became lower as the reaction temperature rose. The new broad band near 3500 cm^{-1}, probably due to the polymeric hydroxy group, appeared in the infrared spectrum of the products more significantly at higher temperatures.

The Effect of the Oxygen Pressure on the Rate and Products of Oxidation.—This effect had been studied in detail by Mayo and Miller[3d] in the absence of the metal catalysts. We obtained similar results in the presence of catalysts. At low oxygen pressures, the rate of oxidation increased with the oxygen pressure, becoming independent of it above 365 mmHg. These results indicate that, at low oxygen pressures, chain termination reactions involve the monomer radicals in addition to the peroxy radicals. The yield of α-methylstyrene oxide varied considerably with the oxygen pressure, although the formation of acetophenone was not influenced so much. The yields of α-methylstyrene oxide under 175, 365, and 760 mmHg of oxygen pressure were 20, 13, and 9%, while those of acetophenone were 30, 33, and 33%, respectively, when 50% of the initial α-methylstryene was oxidized at 70°C with 0.030 mol./l. of ABN and 3.4×10^{-3} mol./mol. of cobalt naphthenate. An increase in the oxygen partial pressure decreases the yield of α-methylstyrene oxide.

Three mechanisms have been proposed for the formation of epoxides[6]; (a) the direct addition of oxygen to a double bond via a cyclic peroxide; (b) the addition of hydroperoxide to a double bond, and (c) the addition of peroxy radicals to a double bond.

(a) $\rangle C{=}C\langle + O_2 \rightarrow \rangle C(-O-O-)C\langle \rightarrow \rangle C(-O-)C\langle$ (11)

(b) $\rangle C{=}C\langle + ROOH \rightarrow \rangle C(-\overset{+}{C}-)\langle \rightarrow \rangle C(-O-)C\langle + ROH$ (12)

(c) $\rangle C{=}C\langle + ROO\cdot \rightarrow \rangle C(-\dot{C}-)\langle \rightarrow \rangle C(-O-)C\langle + RO\cdot$ (13)

The effect of oxygen pressure on the yield of α-methylstyrene oxide supports the reaction 13. The decomposition of the intermediate radical, in this case a free radical of an unspecified length ending in the monomer unit $ROOCH_2C(CH_3)(C_6H_5)\cdot$, into epoxide and alkoxy radical is competitive with reaction 2, the addition of oxygen to the monomer radical. Therefore, the more

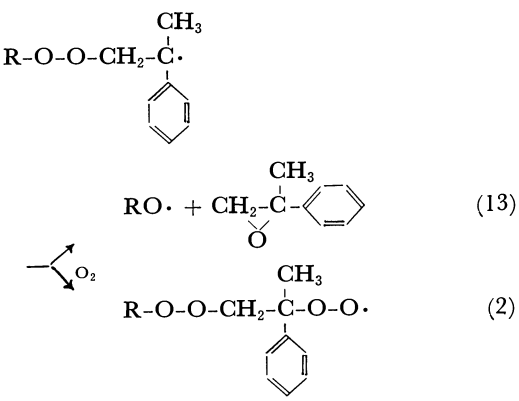

slowly the intermediate β-peroxy alkyl radical reacts with oxygen, the more chance the radical has to decompose unimolecularly.[3d,7] The formation of epoxide is thereby increased by lowering the oxygen partial pressure.

The Effect of the Reaction Time on Rate and Products of Oxidation.—As is shown in Fig. 5, the rate of oxidation is first-order with respect to α-methylstyrene, confirming Rate Eq. 5. The yield of the products depends on the time; the yield of polyperoxide decreases, and that of the cleavage products increases, with time. As will be discussed later, α-methylstyrene polyperoxide is quite stable under the reaction conditions employed; hence, these results do not arise from the

5) C. Walling, "Free Radicals in Solution," John Wiley & Sons, Inc., New York (1957).

6) Reviewed in the paper by G. H. Twigg, *Chem. & Ind.*, 4 (1962); W. F. Brill, *J. Am. Chem. Soc.*, **85**, 141 (1963).

7) G. A. Russell, *J. Chem. Educ.*, **36**, 111 (1959).

TABLE III. α-METHYLSTYRENE POLYPEROXIDE[a]

	C, %	H, %	O, %[b]	N, %	mol. wt.
Calcd.[c]	71.98	6.71	21.31	0	
Found	73.37	6.75	19.88	0.0	1530[d]
	73.35	6.54	20.11	0.0	
$H-(C_9H_{10}O_2)_{10}-H$	71.90	6.79	21.31	0	1502
$H-(C_9H_{10}O_2)_{10}-CH=C(CH_3)(C_6H_5)$	73.42	6.80	19.78	0	1618

a) Prepared at 70°C, ABN 0.010 mol./l. and oxygen pressure 760 mmHg.
b) Calcd. by the difference.
c) Calcd. for $(C_9H_{10}O_2)_n$.
d) Determined by osmometry.

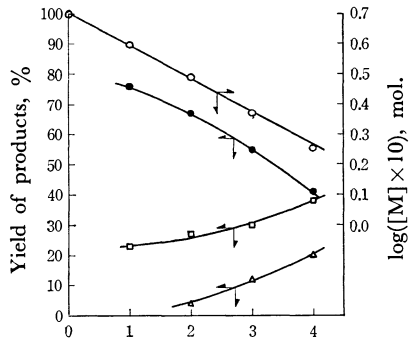

Fig. 5. Effect of the reaction time on the rate and products of oxidation at 70°C, ABN 0.030 mol./l., Co-N 3.4×10^{-3} mol./mol. and oxygen pressure 760 mmHg.
○: α-methylstyrene
●: α-methylstyrene polyperoxide
□: acetophenone
△: α-methylstyrene oxide

decomposition of polyperoxide. The reason for this is not definitely known. One possibility is the decrease in the concentration of α-methylstyrene, a strong radical scavenger itself. The peroxy radical reacts competitively in two ways; one is the addition to the double bond of α-methylstyrene (reaction 3), while the other is the cleavage reaction to form the cleavage products (reaction 14):

$$RO_2CH_2C(CH_3)(C_6H_5)O_2\cdot \rightarrow RO_2\cdot + CH_2O + C_6H_5C(O)CH_3 \qquad (14)$$

This must be also applied to the alkoxy radical. The decrease in the concentration of α-methylstyrene, as a result, presumably increases the life time of peroxy and alkoxy radicals and gives these radicals more chance to decompose into the cleavage products.

α-Methylstyrene Polyperoxide.—The polymer prepared by the method described in the experimental part was colorless, transparent and a little gummy. The composition of methanol-insoluble α-methylstyrene polyperoxide was determined by elementary analyses. The results are illustrated in Table III.

The effects of the end groups are not taken into consideration in the values calculated from $(C_9H_{10}O_2)_n$. The difference between the data obtained and the calculated value is evidently due to the end groups. Mayo and Miller[3d] reported that $HO_2CH_2C(CH_3)(C_6H_5)-$, $O=CHC(CH_3)(C_6H_5)-$ and H- were good possibilities. However, the data indicate that the end groups do not contain oxygen. Here two end groups, H- and $(C_6H_5)(CH_3)C=CH-$, are presumed; the values calculated from these end groups are also listed in Table III.

From these data $H-(C_9H_{10}O_2)_{10}-CH=C(CH_3)-(C_6H_5)$ may be expected to be most plausible. The infrared spectra show the disappearance of the double bond and the formation of peroxide (at 1030 cm^{-1}). α-Methylstyrene polyperoxide is believed to be rather clear compared with styrene polyperoxide. In the absence of oxygen, no reaction at all was observed. This absence of the homopolymerization of α-methylstyrene practically eliminates the excess monomers from the polymer and reduces irregularities in the polymer. It may be presumed, however, that the composition of α-methylstyrene polyperoxide is not always uniform but has some irregularities, and that the molecular weight has a wide distribution.

Mayo and Miller[3d] reported that the structure of α-methylstyrene polyperoxide was substantially $(-OOCH_2C(CH_3)(C_6H_5))_n-$; they based their conclusion on the experimental findings that the pyrolysis of it gave acetophenone and formaldehyde in yields up to 93% and its reduction to α-methylstyrene glycol in a 60% yield. On the other hand, Hock and Siebert[8] proposed the following structure:

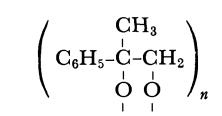

They also proposed the reaction mechanism shown in Fig. 6. However, the effect of oxygen pressure on the yield of α-methylstyrene oxide cannot be illustrated in this sequence.

The decomposition of α-methylstyrene polyperoxide in the presence of a metal salt catalyst

8) H. Hock and M. Siebert, *Chem. Ber.*, **87**, 546 (1954).

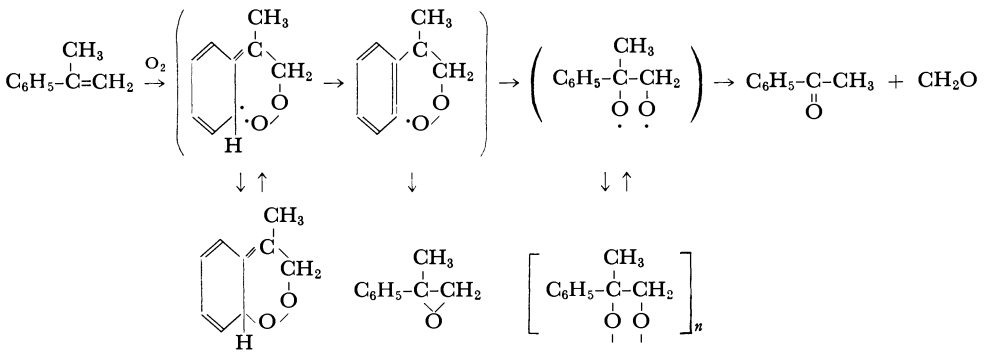

Fig. 6. Reaction mechanism by Hock and Siebert.[8]

was also studied. Some examples of the experiments are given blow.

Expt. A.—The product of oxidation at 70°C, ABN 0.030 mol./l. and oxygen pressure 760 mmHg was distilled in vacuo in order to remove both unreacted α-methylstyrene and cleavage products. The residue was dissolved in chlorobenzene (a guaranteed reagent was shaken with sulfuric acid, washed with water, and distilled). Cobalt naphthenate was added to the solution, and the reaction was carried out for 2 hr.

Expt. B—The oxidation of α-methylstyrene was carried out for 2 hr. at 70°C, ABN 0.030 mol./l., and oxygen pressure 760 mmHg, and in the absence of a metal salt catalyst. Then the stream was converted from oxygen to nitrogen, cobalt naphthenate was added to the reaction mixture, and the reaction was continued for another 3 hr.

These experiments demonstrated that α-methyl styrene polyperoxide is surprisingly stable under these reaction conditions, and no depolymerization was observed. After all, the cleavage products are expected to be formed not by the depolymerization of polyperoxide, but by the decomposition of the peroxy radicals and/or alkoxy radicals which are produced from peroxy radicals or by reaction 13, the splitting off of epoxide from a polyperoxy radical ending in a monomer unit.

The authors take this opportunity to express their thanks to Professor Shingo Ando and Dr. Nobuto Ohta for their continuing encouragement and discussions.

BULLETIN OF THE CHEMICAL SOCIETY OF JAPAN VOL. 39 1101—1103 (1966)

The Amperometric Determination of Thallium(III) and Silver(I) with Ascorbic Acid Using Two Polarized Indicator Electrodes

By D. SINGH and Uma BHATNAGAR

Department of Chemistry, Banaras Hindu University, Varanasi, India

(Received May 15, 1965)

Amperometric determinations of thallium(III) and silver(I) with ascorbic acid have been carried out with two polarized electrodes at 100 mV. and 50 mV. respectively. A simple method for the successive determination of thallium(III) and silver(I) has been developed. At an acidity of 0.1 to 1.0 N with respect to sulphuric acid, only thallium(III) is reduced; silver (I) remains unaffected. After the completion of the reaction with thallium(III), the pH of the solution is adjusted to 6.5 to 7.0 and the silver(I) is titrated with ascorbic acid.

In recent studies in this laboratory, it has been shown that the amperometric method using two polarized electrodes (biamperometric titration) can be applied with success to the successive determination of cerium and iron,[1] iron and vanadium[2] and a number of other elements.[3,4]

This paper will report the results of the biamperometric titration of thallium(III) and silver(I)

1) D. Singh, A. Varma and V. S. Agarwala, *Z. analyt. Chem.*, **183**, 172 (1961).
2) D. Singh and A. Varma, *J. Sci. Res., B. H. U.*, **11**, 127 (1960—61).
3) D. Singh and A. Varma, ibid., **11**, 202 (1960—61).
4) D. Singh and A. Varma, ibid., **12**, 320 (1961—62).

separately and also together in a mixture, with a standard ascorbic acid solution used as the titrant.

Of the various methods employed to determine thallium(III), a few gravimetric and volumetric methods are important. The most useful titrimetric method was developed by Hollens and Spencer,[5] who reduced thallium(III) ion with iodide and titrated the liberated iodine with thiosulphate or arsenite. Smith[6] determined thallium(III) gravimetrically by precipitating it with tetraphenyl arsonium chloride in the presence of a considerable amount of hydrochloric acid. Busev et al.[7] estimated thallium(III) by complexometric titration, and Berka and Busev[8] determined it potentiometrically. Majumdar and Bhatnagar[9] used the same method to determine thallium(III) with chromium(II).

Experimental and Results

A thallium(III) sulphate solution was prepared by dissolving thallium(III) oxide in 20.0 N sulphuric acid, and then making up the volume in a 100-ml. standard flask with distilled water; the solution was standardized iodimetrically. A stock solution of silver nitrate (A. R.) was prepared and standardized as usual. A weighed quantity of ascorbic acid, sold for medical purposes, was dissolved in water, and then a few milliliters of 25% formic acid was added as a stabilizer. The ascorbic acid solutions to be used were obtained by the accurate dilution of a more concentrated stock solution, which was standardized every day before use against a standard potassium iodate solution. All the other chemicals used were of C. P. grade.

Amperometric titrations at a constant voltage with two platinum electrodes were carried out with a circuit similar to those described by Foulk and Bawden[10] and Stone and Scholten.[11] The titration vessel was a 100 ml. beaker, covered with a tight-fitting rubber stopper provided with holes for the platinum electrodes, an inlet and an outlet for nitrogen, and a burette; a constant voltage of 50 mV. or 100 mV. was applied between the platinum electrodes, and the variations in the current were measured by a sensitive-mirror galvanometer with a lamp and scale arrangement. The galvanometer was shunted by a variable resistance so as to obtain the desired deflexions on the scale. The solution was uniformly stirred during the titration by a magnetic stirrer. The titration mixture, usually 20 ml. in the desired medium, was taken into the titration cell, and then the titrant was added from a 2.0-ml. semi-microburette with 0.01-ml. divisions. Equivalence points were obtained graphically by the plot of the galvanometer deflexion against the volume of the titrant added. A few typical titration curves are shown in Figs. 1 and 2. A large number of experiments were carried out, and each determination was repeated several times in order to obtain good and satisfactory results. The results of the determinations of thallium(III) and silver(I) are summarized in Tables I and II respectively.

Table I. Determination of thallium(III) at 100 mV.
Volume of the titration mixture: 20 ml.
Medium: 0.1 to 1.0 N sulphuric acid

Determinations made	Amount of Tl(III) mg.		Experimental error %	
	Taken	Found	Average	Maximum
2	11.1725	11.140	−0.09	−0.25
2	4.469	4.474	+0.11	+0.11
3	2.2345	2.230	−0.18	−0.34
5	0.7918	0.7995	+1.00	+2.00
4	0.3959	0.3919	±0.00	−1.01
5	0.1980	0.1970	+0.09	+1.10
6	0.0792	0.0839	+2.22	+5.0

Table II. Determination of silver(I) at 50 mV.
Volume of the titration mixture: 20 ml.
Medium: pH: 6.5—7.0

Determinations made	Amount of Ag(I) mg.		Experimental error %	
	Taken	Found	Average	Maximum
2	25.80	25.84	+0.03	+0.15
3	9.98	9.99	+0.02	+0.11
4	5.12	5.13	+0.07	+0.35
6	1.259	1.266	+0.09	+0.4
9	1.079	1.085	+0.55	+3.1
5	0.5395	0.5340	−1.00	−2.1
4	0.2158	0.2114	−2.00	−4.2

The successive determinations of thallium(III) and silver(I) present together in test solutions were carried out, taking special care to maintain the acidity of the solution. Into a 0.1 N to 1.0 N medium with respect to sulphuric acid, ascorbic acid is an excellent reducing agent for thallium(III); silver(I) is, however, not reduced in this medium. Tervalent thallium has thus been successfully titrated with two polarized electrodes at an applied voltage of 100 mV. After the completion of the reduction of thallium(III), as established by a fall in the galvanometer deflexion to a constant value, a 6.0 N ammonia solution was added drop by drop until the pH of the solution became 6.5 to 7.0. The mixture was then titrated again at 100 mV. against

5) W. R. A. Hollens and J. F. Spencer, *Analyst*, **60**, 673 (1935).
6) Wm. T. Smith, Jr., *Anal. Chem.*, **20**, 937 (1948).
7) A. I. Busev, L. L. Talipova and V. M. Ivanov, *Zh. Vses. Khim. Obschestva im D. I. Mendeleeva*, **6**, 598 (1961).
8) A. Berka and A. I. Busev, *Anal. Chim. Acta*, **27**, 493 (1962).
9) R. Majumbar and M. L. Bhatnagar, ibid., **25**, 203 (1961).
10) C. W. Foulk and A. T. Bawden, *J. Am. Chem. Soc.*, **48**, 2045 (1926).
11) K. G. Stone and H. G. Scholton, *Anal. Chem.*, **24**, 671 (1952).

the standard ascorbic acid until the galvanometer deflexion approached a constant value.

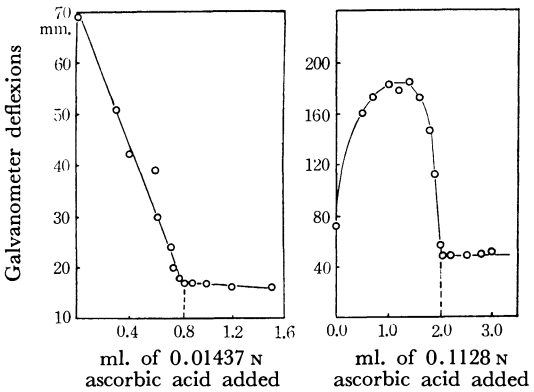

Fig. 1. Amperometric titrations of (a) 2.289 mg. of thallium(III) and (b) 25.84 mg. of silver(I) with two polarized electrodes.

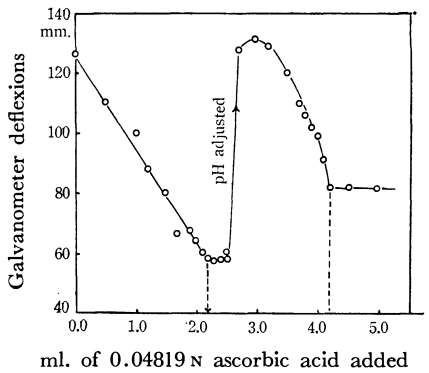

Fig. 2. Amperometric titrations of 6.027 mg. thallium(III) and 3.038 mg. silver(I) present together in solution with two polarized electrodes.

TABLE III. DETERMINATION OF THALLIUM(III) AND SILVER(I) PRESENT TOGETHER IN SOLUTION AT 100 mV.

Volume of the titration mixture: 20 ml.

Amount of Tl(III), mg.			Amount of Ag(I), mg.		
Taken	Found	Difference	Taken	Found	Difference
12.054	12.08	+0.026	6.18	6.20	+0.02
6.04	6.027	−0.013	3.09	3.067	−0.023
5.608	5.615	+0.007	2.162	2.133	−0.029
1.120	1.088	−0.032	1.081	1.078	−0.003
0.415	0.4535	+0.038	0.432	0.464	+0.032

The graphical method was employed to determine the equivalence point of these estimations, as is shown in Fig. 2; the results of the successive determinations of thallium(III) and silver(I) in various mixtures are presented in Table III.

Discussion

The normal oxidation-reduction potential of the Tl^{3+}/Tl^{+} system is $E_0=1.21$ V., while that of Ag^{+}/Ag^{0} couple is $E_0=0.7991$ V. As the normal redox potential of ascorbic acid is 0.40 V. at $[H^{+}]=1$, it can be used for the quantitative determination of thallium(III) in 0.1 N to 1.0 N sulphuric acid in the presence of univalent silver, since the latter is reduced only at pH 6.5 to 7.0.

In the present investigation reversible Tl^{3+}/Tl^{+}, Ag^{+}/Ag^{0} couples are titrated by an irreversible system, with an appreciable current flowing through the cell before the end point. In the determination of thallium(III), the current is the greatest at the very beginning of the titration, since there is a considerable quantity of thallium(III) ions in the the sample taken for estimation. The concentration of the thallium(III) ions diminishes with the addition of the titrant, and thus there is a rapid decrease in the galvanometer deflexion; on the other hand, as the concentration of Ag^{+} diminishes, the galvanometer deflexion reaches a maximum when the titration has proceeded by 50%, and then falls on the further addition of ascorbic acid; this is in essential agreement with the earlier findings.[1-3,11] At the equivalence point and thereafter in both cases, no thallium(III) or silver(I) ions are left in the solution, and the limiting current for the couples, Tl^{3+}/Tl^{+} or Ag^{+}/Ag^{0}, is virtually zero. Although both components of the ascorbic acid/dehydroascorbic acid system are present in the solution, practically no current flows through the titration cell since the couple is irreversible. The current will, therefore, attain a constant value depending upon the resistance of the circuit, and the curves have the shape shown in Figs. 1 and 2.

The authors' thanks are due to the authorities of Banaras Hindu University for providing the facilities for the work. The financial assistance of the Government of India in the form of a Research Training Scholarship to one of the authors, Miss Uma Bhatnagar, is also gratefully acknowledged.

BULLETIN OF THE CHEMICAL SOCIETY OF JAPAN VOL. 39 1104—1107 (1966)

The Decomposition of Formic Acid on the Intermetallic Compounds of 3d-Transition Metals

By Chiyoko SUZUKI and Ikuya MATSUURA

Department of Chemistry, Faculty of Engineering, Kansai University, Senriyama, Suita, Osaka

(Received July 3, 1965)

The catalytic behavior of the intermetallic compounds of Cr-Co, Fe-Cr, Fe-Mo, Ni-V and Fe-V systems on the decomposition reaction of formic acid was studied by the usual static method and compared with that of some alloys and manganese. A zeroth-order decomposition reaction was observed throughout the catalysts employed and the adsorption of formic acid on the catalysts during the decomposition reaction approched to the saturation value under the experimental condition, i. e., under the pressure range of 10—20 mmHg, and at the temperature of 200—300°C. The activation energy of the reaction varied from 13.5 to 20.7 kcal./mol. for various catalysts. It has been also found that the activation energy of the reaction catalyzed by the intermetallic compounds increased with the ratio of the electrons in d- and s-bands to atom of the catalyst.

The low catalytic activity of an intermetallic compounds as compared with the corresponding alloy is generally attributed to the presence of some linkage of covalent nature in the compound.

The catalytic behavior of alloys of silver, gold, and copper with other metals has been studied by Schwab,[1] and it has been revealed that the activation energy of the catalytic decomposition of formic acid on copper-tin alloy catalyst became higher with increasing content of tin in the alloy from about 24 kcal./mol., making a very distinct maximum (33 kcal./mol.) at the phase (20 atomic % of tin) which has a deformed body-centered cubic lattice. Then, the energy falls again with the increasing content of tin in the alloy.

On the other hand, the binary alloys of the 3d-transition metals, chromium-cobalt, iron-chromium, iron-molybdenum, nickel-vanadium and iron-vanadium, have sigma phases, and the sigma phase of the crystals of these alloys are intermetallic compounds having the deformed body-centered cubic lattice. The 3d-transition metals have partially filled *d* electron levels, and the ratio of electron to atom in these compounds is around seven.

The present work deals with the catalytic behavior of some intermetallic compounds of 3d-transition metals on the decomposition reaction of formic acid, was compared with some alloys and with metallic manganese having seven electrons in the d- and s-bands of the atom.

Experimental

Apparatus.—The experiment was carried out by a usual static method. The volume of the system corresponded to 702.3 ml. at 30°C, with the reaction vessel held at 250°C.

Material.—A certified reagent grade formic acid (98—100%) obtained from Merck was dried over anhydrous cupric sulfate, and distilled under a reduced pressure at room temperature. The purified acid was stored in a cold and dark place.

Catalysts.—The metallic manganese used was prepared from manganese oxide. The oxide was reduced at 250°C for 300 hr. by circulating hydrogen. The alloy catalysts, chromium-cobalt, iron-chromium, iron-molybdenum, nickel-vanadium and iron-vanadium were prepared by the fusion of the components having the suitable composition for the formation of the sigma phases, as is shown in Table I, followed by a heat-treatment at about 1000°C for a week in a reaction vessel in an atmosphere of argon. All the catalysts were used as 100 mesh powder. The phase composition and the lattice constant in the sigma phase of each alloy are summarized in Table I, together with the temperatures of the heat-treatment used in the preparation of the intermetallic compound. The specimens of the catalysts prepared were subjected to the X-ray diffraction measurements to confirm the formation of intermetallic compounds, and the lattice constants of these catalysts were found to be in agreement with the reported values for the corresponding intermetallic compounds. The surface areas of these catalysts

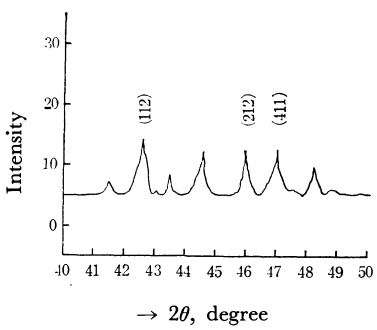

Fig. 1. X-Ray diagram of Fe-Cr powder with Cu$K\alpha$ radiation and Ni filter.

1) G. M. Schwab, *Trans. Faraday Soc.*, **17**, 689 (1946).

Table I. Catalysts

	A	B	B atomic-%	Heat-treat. temp., °C	Lattice const. a	Lattice const. c
	Mn				3.774	3.533
σ phase	Cr	Co	37	1200	8.750	4.540
	Fe	Cr	50	800	8.790	4.559
	Fe	Mo	50	800	9.188	4.812
	Ni	V	33	1200	8.966	4.641
	Fe	V	50	1100	8.930	4.660
$\alpha+\sigma$ phase	Fe	Cr	42	—	—	
	Fe	Mo	49	—	—	
	Fe	V	42	—	—	

Table II. The relationship between the activation energies and the ratios of electron to atom of catalysts

Catalyst		Surface area $m^2/g.$	Electron : atom* ratio	Activation energy, kcal./mol.
Mn		0.76	7.00	26.8
Intermetallic compound	Cr-Co	0.87	7.12	20.7
	Fe-Cr	0.95	7.02	18.0
	Fe-Mo	1.87	7.00	20.0
	Ni-V	1.10	6.65	15.5
	Fe-V	1.51	6.47	13.5
Alloy	Fe-Cr	1.07	7.16	7.2
	Fe-Mo	1.75	7.02	10.0
	Fe-V	1.35	6.74	4.4

* P. A. Beck, "Electronic Structure and Alloy Chemistry of the Transition Elements," John Wiley & Sons, New York and London (1963), p. 106

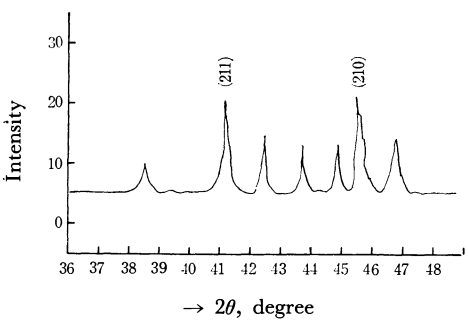

Fig. 2. X-Ray diagram of Ni-V powder with Cu-$K\alpha$ radiation and Ni filter.

were determined by the B. E. T. method by using nitrogen gas at the temperature of liquid nitrogen (cf. Table II).

Procedure.—The alloy or the intermetallic compound (approximately 10 g.) placed in the reaction vessel was maintained at 350°C for 20 hr. under a pressure of less than 10^{-6} mmHg, and reduced with hydrogen (1 atm.) at 350°C for 48 hr. Then the reaction vessel was kept at the same temperature under a vacuum overnight. After this treatment, a known amount of the purified formic acid was introduced into the reaction system and the decomposition reaction was followed by measuring the pressure of the reaction system at suitable time intervals. The composition of the reaction products was determined by mass spectrometry. In most cases, the products were found to be carbon dioxide and hydrogen. The decomposition reaction was carried out over the range of temperatures from 200 to 300°C and the range of the pressures from 10 to 20 mmHg.

Results

The catalytic decomposition of formic acid was carried out in the presence of carbon dioxide or hydrogen to find out the influence of the reaction products on the decomposition reaction. No

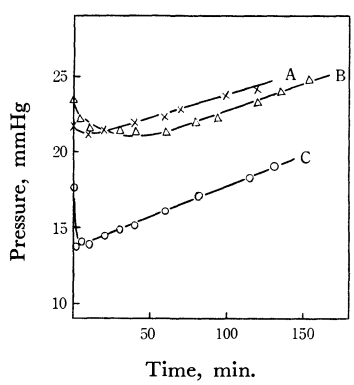

Fig. 3. The decomposition of formic acid on Mn at 225°C in the presence of H_2 and CO_2.
A: with 6.98 mmHg H_2, B: with 7.05 mmHg CO_2, C: pure formic acid

appreciable effect on the reaction rate is observed, as is shown in Fig. 3.

The pressure-time curve of the reaction on a manganese catalyst at 250°C gave a characteristic S shape, as is shown in Fig. 4. The rapid decrease of the pressure of the reaction system in the first few minutes can be reasonably attributed to the adsorption of the acid on the catalyst surface. After about 100 min., the slight decreace in activity due to the influence of poisoning of the catalyst caused by a negligible amount of water which was produced by a side decomposition reaction became appreciable. However, the S curve has a good linear part at reaction times between 20 and 100 min.

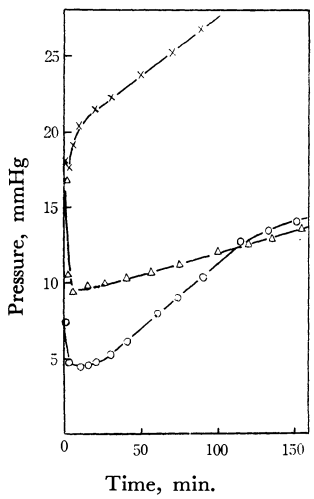

Fig. 4. The pressure-time curves for the decomposition of formic acid, on Mn.
—×— at 250°C, P_0 18.13 mmHg
—○— at 250°C, P_0 7.44 mmHg
—△— at 225°C, P_0 17.32 mmHg

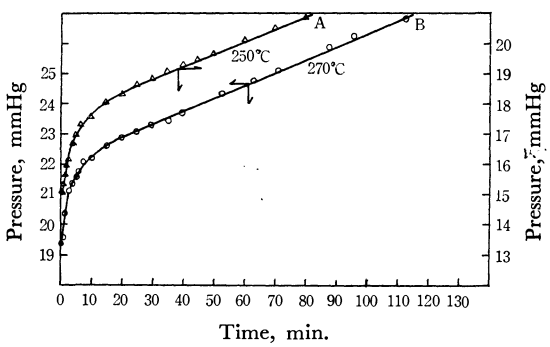

Fig. 5. The pressure-time curves for the decomposition of formic acid.
A. Fe-V intermetallic compound, B. Fe-Mo alloy

The change in pressure in the decomposition of formic acid on the iron-vanadium intermetallic compound and the iron-molybdenum alloy are indicated in Fig. 5. In both experiments, the time-pressure curve clearly indicates the presence of an inflection point, the first part with a steeper slope, ending at the reaction time of about 5 min., and the second part with a flatter slope. This fact suggests that the reaction first occurs at the most active points of the surface of the catalyst, after which the activity remained almost constant.

The rate constants of the zeroth-order decomposition reactions at different temperatures were obtained, their logarithms are plotted against $1/T$, i. e., the reciprocal of the absolute temperature (Fig. 6). The curve in Fig. 7 indicates how the values of the activation energies on the intermetallic compounds are correlated with the ratios of the electrons in the d- and s-bands to the atom of the catalysts.

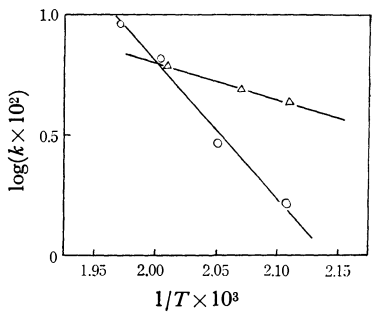

Fig. 6. Arrhenius plots for the decomposition of formic acid.
○ Mn 26.8 kcal./mol.
△ Cr-Co 20.7 kcal./mol.

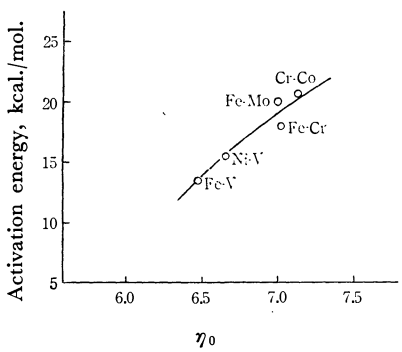

Fig. 7. The drop of the activation energy of the decomposition of formic acid by intermetallic compound is plotted against the ratio of electron in s- and d-bands to atom of catalyst.

Discussion

In the present work every effort has been made to prepare intermetallic compound catalysts which are homogeneous both in bulk and on surface. The homogeneity of the catalysts was confirmed by the X-ray diffraction measurements.

Although the decomposition of formic acid has

been much studied,[2-4] it has often proved difficult to elucidate its mechanism. Recently, it has been confirmed that the formic acid is adsorbed on the surface of metal as formate ions which are observed by means of infrared spectra.[5,6]

In the case of the present work, the following scheme was presented as the mechanism of the decomposition of formic acid on a 3d-transition metal catalyst.

$$M + HCOOH \rightleftarrows M/H^+ + HCOO^- \quad (1)$$

$$M + HCOO^- \rightleftarrows M/HCOO^- \quad (2)$$

$$M/HCOO^- \rightarrow M^-/H + CO_2 \quad (3)$$

$$M/H^+ \rightleftarrows M^+/H \rightleftarrows M^+ + H \quad (4)$$

$$M^-/H + M^+ + H \rightarrow 2M + H_2 \quad (5)$$

In the initial step, the formic acid molecule is dissociated by chemisorption, yielding formate ions, $HCOO^-$, and adsorbed hydrogen, M/H^+; the measurement of the heat of the adsorption of formic acid on a catalyst made it clear that the catalyst was covered completely by the formic acid at a pressure of about 10 mmHg at 150°C. It can, therefore, be assumed that the decomposition of adsorbed ions is the rate-determining step; in this stage the adsorbed formate ions donate electrons to the catalyst, resulting in the decomposition of the formate ions into carbon dioxide and chemisorbed hydrogen. According to the above-stated mechanism, the reaction should be of the zeroth-order. In fact, the present results indicate that the reaction is of the zeroth-order in all the cases under the experimental conditions (see Figs. 3 and 4).

The activation energy was found to increase with the ratio of electrons in the d- and s-bands to the atom of the intermetallic compounds excepting the case of the iron-molybdenum catalyst. The relatively high activation energy in the case of iron-molybdenum catalyst might be due to a larger d character of molybdenum, though it was expected to be the same or lower than that of the case of iron-chromium from the ratio of the electrons in d- and s-bands to the atom.

The decrease of the heat of adsorption of hydrogen on metals or intermetallic compounds with the increase in the ratio of electrons in d- and s-bands to the atom of the catalyst was reported by one of the present authors (I. M.)* (see Fig. 8).

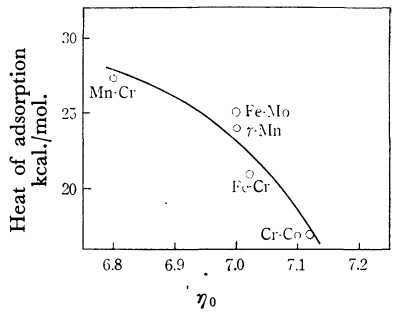

Fig. 8. The drop of the heat of adsorption of hydrogen with the degree of coverage of 0.3 is plotted against the ratio of electron in s- and d-bands to atom of catalyst.

Accordingly, an intermetallic compound having low electron concentration should be effective as the catalyst in an electron-donating reaction as in the case of the decomposition of formic acid via formate ion, on the other hand, an intermetallic compound having high electron concentration should be a good catalyst in an electron-accepting reaction as in the case of the above-mentiond adsorption of hydrogen.

It is also evident from Table II that the catalytic activity of an intermetallic compound is poorer than that of an alloy, though they have the same reaction order in the decomposition of formic acid. The detailed discussion about this point will be published in a following paper.

The authers are grateful to Professor Kiyoshi Kamei for his helpful advice.

2) H. C. Tingey and C. N. Hinshelwood, *J. Chem. Soc.*, **121** 1668 (1922).
3) G. Renecker and J. Volter, *Z. Anorg. Chem.*, 300 (1959).
4) K. Tamaru, *Trans. Faraday Soc.*, **55**, 824 (1959).
5) W. M. H. Sachtler and J. Fahrenfort, "Proc. Inter. Cong. on Catalysis, 2nd Paris, 1960," **1**, 831.
6) K. Hirota, K. Kuwata, T. Otaki and S. Assai, ibid., 809.

* Ikuya Matsuura, Presented before the 16th Anuual Meeting of the Chemical Society of Japan, April, 1962, Tokyo.

BULLETIN OF THE CHEMICAL SOCIETY OF JAPAN VOL. 39 1108—1113 (1966)

Normal Coordinate Analysis of Trigonal Bipyramidal XY_5 Type Molecules*

By Robert A. CONDRATE** and Kazuo NAKAMOTO

Department of Chemistry, Illinois Institute of Technology, Technology Center, Illinois 60616, U. S. A.

(Received July 12, 1965)

Normal coordinate analysis has been carried out for trigonal bipyramidal XY_5 molecules such as PF_5, SbF_5, PCl_5 and $SbCl_5$. It has been found that the simple Urey-Bradley force field does not provide satisfactory results for the bending modes of these molecules. The results have been improved considerably by introducing an interaction constant between equatorial and axial angle coordinates. In carrying out normal coordinate analysis, the repulsive force constants were first estimated from a Lennard-Jones type potential. Then the stretching and bending force constants were adjusted to fit the observed frequencies. Finally, the new interaction constant was introduced to minimize the errors in the bending frequencies. The force constants thus obtained are consistent through the four molecules studied. Some conflicting band assignments made by previous investigators have been discussed on the basis of the present calculations.

The vibrational spectra of trigonal bipyramidal XY_5 type molecules have already been studied extensively. Although the band assignments for antimony pentachloride and phosphorous pentafluoride are consistent among several investigators, no difinite band assignments are yet available for antimony pentafluoride and phosphorus pentachloride. In the present investigation, we have carried out a systematic normal coordinate analysis of the four molecules mentioned above. The present work differs from the previous normal coordinate analyses in the following respects: (1) The most recent spectral data which were not available in previous investigations have been used. (2) A modified Urey-Bradley force field has been developed to express the potential energy. (3) All the force constants have been selected so that their values are consistent for the four molecules studied and are reasonable in view of their electronic structure.

Experimental

Most of the spectral data used for the normal coordinate analyses were taken from the literature. The Raman spectrum of phosphorus pentachloride was obtained, however, to confirm some of the calculated frequencies. A saturated benzene solution of phosphorus pentachloride (Baker Analyzed Reagent) was analyzed in a Hilger E-612 two-prism Raman spectrograph. Mercury light of wavelength 4358 Å was used for exciting the Raman transitions. A solution of Dupont rhodamine 5 GDN-Extra dye mixed with an ethanol solution of *p*-nitrotoluene was used to filter out the other mercury lines. Eastman 103a-J plates were employed to record the spectra. In addition to a number of Raman lines due to benzene, the following lines were observed for phosphorus pentachloride 585cm^{-1}(medium strong), 394 cm^{-1} (very strong), 282 cm^{-1} (strong), 273 cm^{-1} (strong), 264 cm^{-1} (medium strong). The transitions below 200 cm^{-1} could not be observed because of strong background scattering. Figure 1 shows the microdensitometer reading plotted against the frequency in the range between 430 and 200 cm^{-1}.

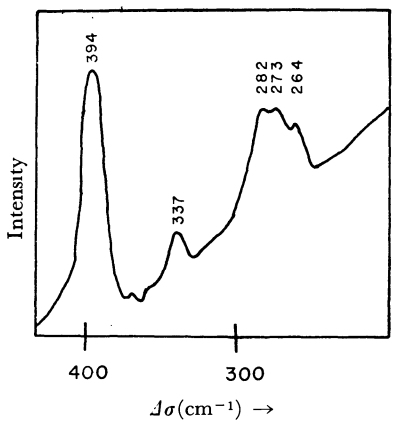

Fig. 1. Microdensitometer tracing vs. frequency for PCl_5.

Procedure of Calculation

The trigonal bipyramidal XY_5-type molecule shown in Fig. 2 belongs to the point group D_{3h}, and its twelve normal modes of vibration are grouped into the four species A_1', A_2'', E', and E''. The appropriate symmetry coordinates used are given in Table I, and the elements of the $\boldsymbol{G}$ and $\boldsymbol{F}$ matrices are listed in Tables II and III. The $\boldsymbol{G}$ matrix elements were calculated using the bond distances reported in the literature.† The matrix secular

* This work was partly supported by the U. S. Army Research Office (Contract No., DA-31-124-ARO(D)-38).

** Supported by a Public Health-Service predoctoral fellowship (1-Fl-GM-24, 175-01). To be submitted by Robert A. Condrate to the faculty of Illinois Institute of Technology in partial fulfillment of the requirements for the degree of Doctor of Philosophy.

† $SbCl_5$: r=2.31Å, d=2.43Å (Ref. 1a); PCl_5 : r=2.04Å, d=2.19Å (Ref. 1a); SbF_5: $r \approx d \approx$2.00Å(Ref. 13); PF_5 : $r \approx d \approx$ 1.57Å (Ref. 1b).

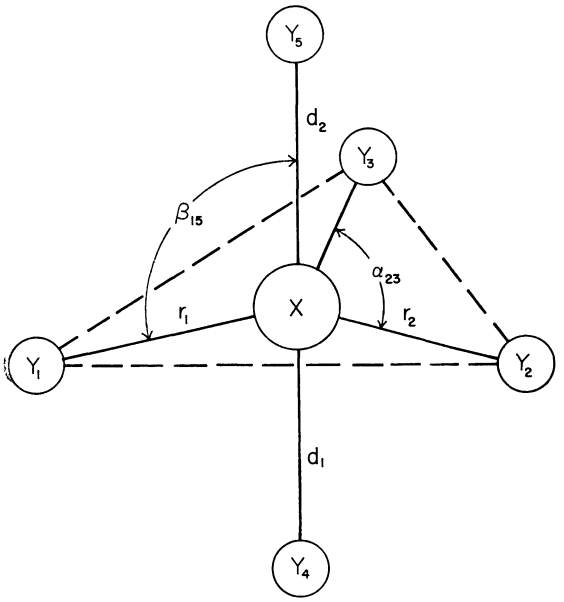

Fig. 2. Structure and internal coordinates of the trigonal bipyramidal XY_5 type molecule.

TABLE I. SYMMETRY COORDINATES FOR TRIGONAL BIPYRAMIDAL XY_5 TYPE MOLECULES

A_1'-species

$S_1 = (1/\sqrt{3})(\Delta r_1+\Delta r_2+\Delta_3)$

$S_2 = (1/\sqrt{2})(\Delta d_1+\Delta d_2)$

$S_a = (1/\sqrt{3})(\Delta\alpha_{12}+\Delta\alpha_{23}+\Delta\alpha_{31}) \equiv 0$

$S_b = (1/\sqrt{6})(\Delta\beta_{14}+\Delta\beta_{24}+\Delta\beta_{34}+\Delta\beta_{15}+\Delta\beta_{25}+\Delta\beta_{35}) \equiv 0$

A_2''-species

$S_3 = (1/\sqrt{2})(\Delta d_1-\Delta d_2)$

$S_4 = (1/\sqrt{6})(\Delta\beta_{14}+\Delta\beta_{24}+\Delta\beta_{34}-\Delta\beta_{15}-\Delta\beta_{25}-\Delta\beta_{35})$

E'-species

$S_{5a} = (1/\sqrt{6})(2\Delta r_1-\Delta r_2-\Delta r_3)$

$S_{5b} = (1/\sqrt{2})(\Delta r_2-\Delta r_3)$

$S_{6a} = (1/\sqrt{6})(2\Delta\alpha_{23}-\Delta\alpha_{12}-\Delta\alpha_{31})$

$S_{6b} = (1/\sqrt{2})(\Delta\alpha_{31}-\Delta\alpha_{12})$

$S_{7a} = (1/\sqrt{12})(2\Delta\beta_{14}-\Delta\beta_{24}-\Delta\beta_{34}+2\Delta\beta_{15}-\Delta\beta_{25}-\Delta\beta_{35})$

$S_{7b} = (1/2)(\Delta\beta_{24}-\Delta\beta_{34}+\Delta\beta_{25}-\Delta\beta_{35})$

E''-species

$S_{8a} = (1/\sqrt{12})(2\Delta\beta_{14}-\Delta\beta_{24}-\Delta\beta_{34}-2\Delta\beta_{15}+\Delta\beta_{25}+\Delta\beta_{35})$

$S_{8b} = (1/2)(\Delta\beta_{24}-\Delta\beta_{34}-\Delta\beta_{25}+\Delta\beta_{35})$

equations of the form $|GF-E\lambda|=0$ were solved for each species using an IBM 7094 electronic computer.

In order to express the potential energy, the simple Urey-Bradley force (SUBF) field[2] of the following type was first employed:

1) a) M. Rouaut, *Ann. Phys.*, **14**, 78 (1940); 1b) L. O. Brockway and J. Y. Beach, *J. Am. Chem. Soc.*, **60**, 1836 (1938).
2) T. Shimanouchi, *J. Chem. Phys.*, **17**, 245 (1949).

TABLE II. *G*-MATRIX ELEMENTS*

A_1'-species

$G_{11} = \mu_y$, $G_{12}=G_{21}=0$, $G_{22}=\mu_y$

A_2''-species

$G_{33} = 2\mu_x+\mu_y$, $G_{34} = G_{43} = -2\sqrt{3}\,\rho_r\mu_x$,

$G_{44} = 6\rho_r^2\mu_x+2\rho_r^2\mu_y$

E'-species

$G_{55} = \mu_y+(3/2)\mu_x$, $G_{56} = G_{65} = 3(\sqrt{3}/2)\rho_r\mu_x$,

$G_{57} = G_{75} = -(3/\sqrt{2})\mu_x\rho_d$,

$G_{66} = 3\rho_r^2\mu_y+(9/2)\rho_r^2\mu_x$,

$G_{67} = G_{76} = -3(\sqrt{3}/\sqrt{2})\mu_x\rho_r\rho_d$,

$G_{77} = 3\rho_d^2\mu_x+(3/2)\rho_d^2\mu_y$

E''-species

$G_{88} = 2\rho_r^2\mu_y+(3/2)\rho_d^2\mu_y$

* μ_x and μ_y are the reciprocal masses of X and Y, while ρ_r and ρ_d are the reciprocals of the bond distances, r and d, respectively.

TABLE III. *F*-MATRIX ELEMENTS

A_1'-species

$F_{11} = K_r+4s^2_{rr}F_{rr}+2t^2_{rd}F'_{dr}+2s^2_{rd}F_{dr}$,

$F_{12} = F_{21} = \sqrt{6}(-t_{dr}t_{rd}F'_{dr}+s_{dr}s_{rd}F_{dr})$,

$F_{22} = K_d+3t^2_{dr}F'_{dr}+3s^2_{dr}F_{dr}$

A_2''-species

$F_{33} = K_d+3t^2_{dr}F'_{dr}+3s^2_{dr}F_{dr}$,

$F_{34} = F_{43} = \sqrt{3}\,r(t_{dr}s_{rd}F'_{dr}+t_{rd}s_{dr}F_{dr})$,

$F_{44} = rd(H_\beta-s_{rd}s_{dr}F'_{dr}+t_{rd}t_{dr}F_{dr})$

E'-species

$F_{55} = K_r+3t^2_{rr}F'_{rr}+s^2_{rr}F_{rr}+2t^2_{rd}F'_{dr}+2s^2_{rd}F_{dr}$,

$F_{56} = F_{65} = -r(t_{rr}s_{rr}F'_{rr}+t_{rr}s_{rr}F_{rr})$,

$F_{57} = F_{75} = \sqrt{2}\,d(t_{rd}s_{dr}F'_{dr}+t_{dr}s_{rd}F_{dr})$,

$F_{66} = r^2(H_\alpha-s^2_{rr}F'_{rr}+t^2_{rr}F_{rr})$,

$F_{67} = F_{76} = -\sqrt{2}\,r^{3/2}d^{1/2}H_{\alpha\beta}$,

$F_{77} = rd(H_\beta-s_{rd}s_{dr}F'_{dr}+t_{rd}t_{dr}F_{dr})$

E''-species

$F_{88} = rd(H_\beta-s_{rd}s_{dr}F'_{dr}+t_{rd}t_{dr}F_{dr})$

* Here

$s_{dr}=t_{rd}=d/q_{dr}$, $s_{rd}=t_{dr}=r/q_{dr}$, $s_{rr}=\sqrt{3}/2$, $t_{rr}=1/2$,

where

$q^2_{dr}=r^2+d^2$.

$$V=\sum_i [K_r'r(\Delta r_i)+1/2K_r(\Delta r_i)^2]$$
$$+\sum_i [K'_d d(\Delta d_i)+1/2K_d(\Delta d_i)^2]$$
$$+\sum_{i<j} [H'_\alpha r_\alpha^2(\Delta\alpha_{ij})+1/2H_\alpha(r_\alpha\Delta\alpha_{ij})^2]$$
$$+\sum_{i<j} [H'_\beta r_\beta^2(\Delta\beta_{ij})+1/2H_\beta(r_\beta\Delta\beta_{ij})^2]$$
$$+\sum_{i<j} [F'_{rr}q_{rr}(\Delta q_{ij})+1/2F_{rr}(\Delta q_{ij})^2]$$
$$+\sum_{k<j} [F'_{dr}q_{dr}(\Delta q_{jk})+1/2F_{dr}(\Delta q_{jk})^2]$$

where Δr_i, Δd_i, $\Delta\alpha_{ij}$, $\Delta\beta_{ij}$, Δq_{ij}, and Δq_{jk} are, respectively, the change in the bond lengths r and d, the change in the bond angles α and β, and the change in the distances q_{rr} and q_{dr} between

TABLE IV. UREY-BRADLEY FORCE CONSTANTS OF VARIOUS TRIGONAL BIPYRAMIDAL MOLECULES (md./Å)

	K_r	K_d	H_α	H_β	F_{rr}	F_{dr}	$H_{\alpha\beta}$
$SbCl_5$	2.20	1.83	0.06	0.085	0.08	0.13	0.043
PCl_5	2.10	1.00	0.07	0.15	0.10	0.55	0.07
SbF_5	5.30	4.60	0.095	0.12	0.07	0.10	0.07
PF_5	5.50	3.85	0.37	0.48	0.15	0.80	0.09

TABLE V. FUNDAMENTAL FREQUENCIES OF $SbCl_5$ (cm^{-1})*

	Siebert[4]	Wilmshurst[5]	Carlson[6]	Present work		
				Observed	Calculated SUBF	Calculated MUBF
A_1' σ_1	356(R)	356	356(R)	356	358	353
σ_2	307(R)	307	307(R)	307	307	307
A_2'' σ_3	((390))	387(IR) 380(IR)	371(IR)	387 380	384	384
σ_4	((131))	(156)	154(IR)	154	156	156
E' σ_5	399(R)	398(IR)	395(IR, R)	398	399	402
σ_6	182(R)	182	172(IR, R)	172	140	172
σ_7	74(R)	74	72(R)	74	107	74
E'' σ_8	166(R)	166	165(R)	165	163	163

* In Tables V to VIII, the following abbreviations were used: frequencies followed by IR (gaseous or matrix-phase infrared spectra) or R (Raman spectra) were actually observed by the investigator reporting the data; frequencies taken from a previous investigator are denoted by numbers only; frequencies calculated from overtones or combination bands are in single parentheses ( ), and those obtained from normal coordinate analysis are in double parentheses (( )). The values calculated in the present investigation are compared in the tables with what we consider the best reported values.

TABLE VI. FUNDAMENTAL FREQUENCIES OF PCl_5 (cm^{-1})

	Siebert[4]	Wilmshurst and Bernstein[7]	Carlson[6]	Taylor and Woodward[9]	Present work		
					Observed	Calculated SUBF	Calculated MUBF
A_1' σ_1	392(R)	394(R)	393(R)	395	394(R)	394	394
σ_2	271(R)	394(R)	?	370	264(R)	261	261
A_2'' σ_3	449(R)*	465(IR)	446(IR)	441	465	470	470
σ_4	((124))	(176)	299(IR)	301	299	303	303
E' σ_5	495(R)	592(IR, R)	580(IR, R)	581	592	562	588
σ_6	190(R)	335(IR, R)	273(IR, R)	281	273(R)	247	278
σ_7	100(R)	100	100(R)	100	100	132	100
E'' σ_8	190(R)	280(R)	289(R)	261	282(R)	277	277

* Although this mode is only infrared active, Siebert[4] claims that he observed it in the Raman spectrum, and he attributes the origin of this band to the distortion of the trigonal bipyramidal structure.

TABLE VII. FUNDAMENTAL FREQUENCIES OF SbF_5 (cm^{-1})

	Akers[12]		Gaunt and Ainscough[13]	Present work		
				Observed	Calculated SUBF	Calculated MUBF
A_1' σ_1	397(R)	718(R)	667(R)	718	709	709
σ_2	265(R)	672(R)	264(R)	672	649	649
A_2'' σ_3	758(IR)	758(IR)	(294)	724	743	743
σ_4	708(IR)	708(IR)	(212)	212	206	206
E' σ_5	718(R) 724(IR)	397(R)	710(IR) 716(R)	758	772	774
σ_6	672(R)	265(R)	498(IR)	265	199	258
σ_7	224(R)	224(R)	ca. 90(R)	93	167	92
E'' σ_8	187(R)	187(R)	228(R)	224	234	234

TABLE VIII. FUNDAMENTAL FREQUENCIES OF PF_5 (cm^{-1})

		Gutowski and Liehr[16]	Pemsler and Planet[17]	Griffiths et al.[18]	Present work		
					Observed	Calculated SUBF	Calculated MUBF
A_1'	σ_1	—	—	817(R)	817	801	801
	σ_2	—	—	640(R)	640	628	628
A_2''	σ_3	948(IR)	948(IR)	945(IR)	945	958	958
	σ_4	576(IR)	576(IR)	576(IR)	576	542	542
E'	σ_5	1025(IR)	1029(IR) 1026(IR)	1026(IR, R)	1029 1026	1039	1055
	σ_6	534(IR)	534(IR)	533(IR, R)	534	495	535
	σ_7	—	—	301(IR)*	301	339	302
E''	σ_8	—	—	514(R)	514	536	536

* See Ref. 19.

nonbonded atoms. The symbols K, H, and F represent stretching, bending, and repulsive force constants, respectively. The primed letters donote first derivatives; r, d, r_α, r_β, q_{rr}, and q_{dr} are the values of the distances at equilibrium; they are inserted to make the dimensions of the force constants the same. The quantities K' and H' vanish in the final result, since they can be expressed in terms of F' using the equilibrium condition. F' was taken as $-0.1F$ by assuming that the repulsive energy between the nonbonded atoms is proportional to r^{-9}.

In adjusting the force constants, we first estimated the reasonable values for the repulsive force constants from a Lennard-Jones type potential. Figures III and IV illustrate the repulsive force constants which are derived from the 6-12 Lennard-Jones potentials for Ne···Ne and Ar···Ar repulsions, respectively. Then, we have adjusted these values to obtain the best fit to the observed frequencies. The final repulsive force constants thus obtained are plotted in the same figures together with those used

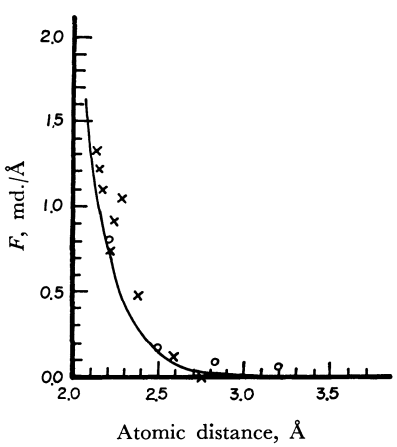

Fig. 3. Repulsive force constants derived from 6-12 Lennard-Jones potential for Ne···Ne repulsion and F···F repulsive force constants (×, Shimanouchi et al.; ○, present work)

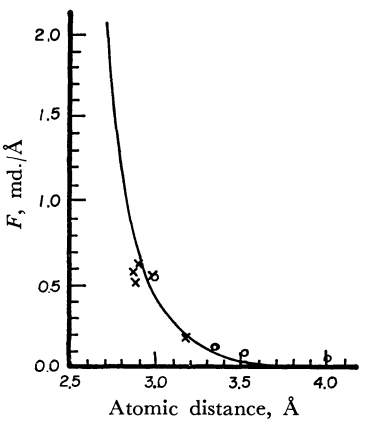

Fig. 4, Repulsive force constants derived from 6-12 Lennard-Jones potential for Ar···Ar repulsion and Cl···Cl repulsive force constants (×, Shimanouchi et al.; ○, present work)

by Shimanouchi and his coworkers[3] for other molecules. It is seen that our values are quite close to those predicted from the Lennard-Jones potentials. Table IV lists the final sets of force constants thus obtained. Tables V to VIII compare the observed frequencies with those calculated for each molecule. It is seen immediately that the two bending modes (σ_6 and σ_7) belonging to the E' species show marked deviation from the observed frequencies. Evidently, the SUBF field is not satisfactory for trigonal bipyramidal XY_5 type molecules.

In order to improve these results, we have introduced an additional force constant to the SUBF field. After several trials, we have found that the addition of a term, $\sum_{k\neq i<j} [H_{\alpha\beta}(r_\alpha \Delta\alpha_{ij})(r_\beta \Delta\beta_{ik})]$ to the potential energy improves the results considerably. Here, $H_{\alpha\beta}$ denotes an angle-angle interaction constant between α and β which lie in planes perpendicular to each other and share

3) J. Hiraishi, I. Nakagawa and T. Shimanouchi, *Spectrochim. Acta*, **20**, 819 (1964).

a common bond. The last columns in Tables V to VIII indicate the calculated frequencies obtained by using this modified Urey-Bradley force (MUBF) field. It is seen that the agreement between calculated and observed frequencies becomes quite satisfactory; the average deviation for 32 frequencies is 1.1%, and the maximum deviation is 34 cm^{-1}.

Results and Discussion

Antimony Pentachloride.—Table V compares the calculated frequencies with those observed by Siebert (Raman),[4] Wilmshurst (gaseous-phase IR),[5] and Carlson (Raman and matrix-phase IR).[6] All the band assignments made by these investigators are consistent with each other, and the calculated frequencies are in perfect agreement with those observed.

Phosphorus Pentachloride.—As is seen in Table VI, the previous band assignments differ seriously among the investigators. Siebert[4] assigned a Raman line at 271 cm^{-1} to σ_2, whereas Carlson assigned it to σ_6 (E' species) because an infrared band was observed at 273 cm^{-1}. Wilmshurst and Bernstein[7] assigned a Raman line at 394 cm^{-1} to both σ_2 and σ_1 on the assumption of accidental degeneracy. However, this assignment seems highl unlikely because, with this assumption, the stretching force constants for both the axial and the equatorial bonds would have to be of the same magnitude. On the contrary, an electron diffraction[1] and a tracer study[8] show that the axial and the equatorial bonds are not equivalent. Although Taylor and Woodward[9] assigned a Raman line at 370 cm^{-1} to σ_2, it is rather weak as is seen in Fig. 2. The corresponding line for antimony pentachloride is relatively strong. We, therefore, assigned it to a combination band ($\sigma_6+\sigma_7$ or $\sigma_2+\sigma_7$).

According to our normal coordinate analysis, σ_2 should be around 260 cm^{-1}. As is shown in Fig. 2, we have observed three Raman lines in the region 290—260 cm^{-1} using the photographic method. Therefore, the line at 264 cm^{-1} which is closest to our calculated frequency, is assigned to the σ_2 mode. It should be mentioned that Wilmshurst and Bernstein[7] also observed a Raman line at 264 cm^{-1} which they attributed to a combination band. However, one of the fundamentals (176 cm^{-1}), which was assumed to be a component of this combination band, was not observed by Carlson[6] in his infrared spectrum. Therefore, the Raman line at 264 cm^{-1} cannot be a combination band.

The calculated frequency for σ_4 (303 cm^{-1}) is in good agreement with that observed by Carlson (299 cm^{-1})[6] in the infrared spectrum. The frequencies predicted by Wilmshurst and Bernstein (176 cm^{-1})[7] and by Siebert (124 cm^{-1})[4] are too low for this mode. Furthermore, Carlson did not observe any infrared band arount 176 or 124 cm^{-1}. The calculated frequency for σ_5 (588 cm^{-1}) is in good agreement with that observed by Wilmshurst and Bernstein (592 cm^{-1}), and is fairly close to that observed by Carlson (580 cm^{-1}). Although Siebert assigned it to a Raman line at 495 cm^{-1}, it was found that this line is due to phosphorus oxychloride contaminated in a solution of phosphorus pentachloride.

The calculated frequency for σ_6 (278 cm^{-1}) is in good agreement with that observed by Carlson (273 cm^{-1})[6] and by the present investigators (273 cm^{-1}). Carlson observed this mode both in the infrared and Raman spectra. Therefore, it must belong to the E' or A'' species. Although Taylor and Woodward[9] assigned σ_6 to a Raman line at 281 cm^{-1}, no infrared band was observed at this frequency. On the other hand, Wilmshurst and Bernstein[7] assigned it at 335 cm^{-1}. However, Taylor and Woodward did not observe any Raman line near 335 cm^{-1}.

The calculated frequency for σ_8 (277 cm^{-1}) is close to the Raman line observed at 282 cm^{-1} in the present work. This line was also observed by Wilmshurst and Bernstein and by Calrson, and was assigned by both to the σ_8 mode.

Recently, Radhakrishnan[10] and Krynauw et al.[11] have carried out normal coordinate analysis of phosphorus pentachloride using the band assignments made by Wilsmshurst and Bernstein[7] and by Carlson[6], respectively. Our results are different from those of previous workers since our band assignments and force field are different from theirs.

Antimony Pentafluoride. — The infrared and Raman spectra of antimony pentafluoride were observed by Akers[12] and by Gaunt and Ainscough,[13] but their band assignments are in complete disagreement, as is seen in Table VII. Furthermore, Akers presented two different sets of band assignments both of which differ from that of Gaunt and Ainscough. Nagarajan,[14] and Haarhoff and Pistorius[15] have carried out normal coordinate analysis using the band assignments by

4) H. Siebert, *Z. anorg. u. allgem. Chem.*, **265**, 303 (1951).
5) J. K. Wilmshurst, *J. Mol. Spectry*, **5**, 343 (1960).
6) G. L. Carlson, *Spectrochim. Acta*, **19**, 1291 (1963).
7) J. K. Wilmshurst and H. J. Bernstein, *J. Chem. Phys.*, **27**, 661 (1957).
8) J. Downs and R. E. Johnson, ibid., **22**, 143 (1954).
9) M. J. Taylor and L. A. Woodward, *J. Chem. Soc.*, **1963**, 4670.
10) M. Radhakrishnan, *Indian J. Pure Appl. Phys.*, **1**, 437 (1963).
11) G. N. Krynauw, C. W. F. T. Pistorius and M. C. Pistorius, *Z. Physik. Chem.*, **43**, 213 (1964).
12) L. K. Akers, Univ. Microfilms (Ann Arbor, Michigan), Pub. No. 12965 (1955).
13) J. Gaunt and J. B. Ainscough, *Spectrochim. Acta*, **10**, 57 (1957).
14) G. Nagarajan, *Bull. soc. chim. Belg.*, **72**, 563 (1963).
15) P. C. Haarhoff and C. W. F. T. Pistorius, *Z. Naturforsch.*, **14A**, 972 (1959).

Gaunt and Ainscough, and have obtained a large negative interaction force constant between two axial bond stretching coordinates in the general valence force field. They suggested that this might be due to incorrect assignments for σ_2 and σ_3 made by Gaunt and Ainscough.

In order to solve these conflicting band assignments, it is useful to consider the frequency order observed in antimony pentachloride and phosphorus pentachloride. From Table V and VI, it is seen that the stretching frequencies (σ_1, σ_2, σ_3, and σ_5) are much higher than the bending frequencies (σ_4, σ_6, σ_7, and σ_8), and the order of the stretching frequencies is always σ_5(asym. in-plane) > σ_3(asym. out-of-plane) > σ_1(sym. in-plane) > σ_2-(sym. out-of-plane) the six fundamental observed by Akers[12] and the two fundamentals observed by Gaunt and Ainscough[13] were rearranged with this trend in mind. The four bending frequencies were also rearranged so as to obtain the frequency order $\sigma_6 > \sigma_8 > \sigma_4 > \sigma_7$, which was found to hold for antimony pentachloride. As is seen in Table VII, the agreement between the calculated and observed frequencies is quite satisfactory. It should be mentioned that the set of the fundamentals selected by the present investigators can account for all the other observed frequencies on the assumption that they are overtones and combination bands.

Phosphorus Pentafluoride.—Table VIII compares the calculated frequencies with those observed by Gutowski and Liehr (infrared),[16] by Pemsler and Planet (infrared),[17] and by Griffith et al. (infrared and Raman).[18,19] All the band assignments made by these investigators are consistent with one another and agree quite well with the calculated frequencies.

Trends in Force Constants.—The force constants listed in Table IV have several interesting implications. First of all, the stretching force constants involving the fluorine atoms are much larger than those involving the chlorine atoms. This is consistent with the fact that the heat of formation of phosphorus pentafluoride (−290 kcal./mol.) is much larger than that of phosphorus pentachloride (−95.35 kcal./mol.). Secondly, the stretching force constants for the equatorial bonds (K_r) are larger than those for the axial bonds (K_d) in all the four molecules studied. This trend is consistent with the results of X-ray[20] and electron diffraction[1] studies which indicate that the equatorial bonds are shorter than the axial bonds.

Table IV also indicates that the bending force constants of the fluorides are always larger than those of the corresponding chlorides, and that the bending force constants of the phosphorus compounds are always larger than those of the corresponding antimony compounds. All these changes which occur upon the replacement of either the central or the halogen atom can be explained satisfactorily in terms of the electron pair repulsion theory developed by Gillespie.[21] His theory also predicts that the bending force constants for the axial bond angle (H_β) should be larger than that for the equatorial bond angle (H_α). As is seen in Table IV, this was found to be the case.

As stated previously, the repulsive force constants follow the trends predicted from the 6—12 Lennard-Jones potential. Therefore, their values increase progressively as the bond distances decrease. Thus, we have the following orders:

$$F_{rr}(SbF_5) < F_{dr}(SbF_5) < F_{rr}(PF_5) < F_{dr}(PF_5)$$

$$F_{rr}(SbCl_5) < F_{rr}(PCl_5) < F_{dr}(SbCl_5) < F_{dr}(PCl_5)$$

It has already been shown that the introduction of an angle-angle interaction constant, $H_{\alpha\beta}$, improves the calculated frequencies for the σ_6 and σ_7 modes considerably. It is interesting to note that these two vibrations are responsible for "pseudorotation" which was proposed by Berry[22] for trigonal bipyramidal XY_5 type molecules. Since the angles α and β must be interchanged during pseudorotation, it is reasonable to introduce such an interaction term in the potential energy.

16) H. S. Gutowsky and A. D. Liehr, *J. Chem. Phys.*, **20**, 1652 (1952).
17) J. P. Pemsler and W. G. Planet ibid., **24**, 920 (1956).
18) J. E. Griffith, R. P. Carter and R. R. Holms, ibid., **41**, 863 (1964).
19) J. E. Griffith, ibid., **42**, 2632 (1965).
20) S. M. Ohlberg, *J. Am. Chem. Soc.*, **81**, 811 (1959); *Acta Cryst.*, **7**, 640 (1954).
21) R. J. Gillespie, *J. Chem. Soc.*, **1963**, 4672.
22) R. S. Berry *J., Chem. Phys.*, **32**, 933 (1960).

BULLETIN OF THE CHEMICAL SOCIETY OF JAPAN VOL. 39 1114—1119 (1966)

The Coprecipitation Behavior of Rare Earth Elements with Calcium Oxalate upon Precipitation from a Homogeneous System

By Masakazu MATSUI

Institute for Chemical Research, Kyoto University, Sakyo-ku, Kyoto

(Received July 19, 1965)

The effects of the pH value, the concentration of organic acid and several other variables upon the distribution coefficient were studied for the coprecipitation process of the calcium-lanthanide oxalate system. The logarithmic distribution law was followed in all cases of the coprecipitation of rare earth elements. Of the several variables studied which affected the logarithmic distribution coefficient, the most important were the pH value and the concentration of an organic acid. The coefficient decreased as the acid anion content increased. This can be attributed to the fact that the acid anion formed complex compounds with lanthanide and calcium. The distribution coefficients of several rare earth elements in producing the precipitate from a similar solution were closely related to their basicity or to the solubility of their oxalate salts. The order of the magnitude of the distribution coefficient was as follows: Lu>Y>Eu>Ce; this was in the reverse order of the basicity of rare earth elements or of the solubility of their oxalate salts.

Coprecipitation has often been used for the chemical concentration or enrichment of trace elements from dilute solutions and for the chemical separation of radioisotopes. Furthermore, coprecipitation phenomena are observed in the precipitation method of gravimetric analysis and in geochemical processes.

When a macro component is precipitated, micro components in the solution are distributed between the solid and liquid phases. The initial distribution may be quite random, but structural transformation must occur in the recrystallization process of the precipitate. As equilibrium conditions are reached, an orderly rearrangement is achieved. For such a system, macro and micro components distribute themselves to obey the following equation, which was introduced by Chlopin[1] and by Henderson and Kracek[2]:

$$\left(\frac{\text{tracer}}{\text{carrier}}\right)_{\text{crystal}} = D\left(\frac{\text{tracer}}{\text{carrier}}\right)_{\text{solution}} \qquad (1)$$

where D is the homogeneous distribution coefficient and is constant for a given system. This homogeneous distribution law represents a true thermodynamic equilibrium.

Beside the homogeneous distribution in crystals, there are many possible heterogeneous arrangements. Only one of these was given by Doerner and Hoskins' distribution equation.[3] It is called the logarithmic distribution law and is expressed as follows:

$$\log\left(\frac{\text{initial quantity}}{\text{quantity left in soln.}}\right)_{\text{tracer}} = \lambda \log\left(\frac{\text{initial quantity}}{\text{quantity left in soln.}}\right)_{\text{carrier}} \qquad (2)$$

where λ is the logarithmic distribution coefficient and is also constant for a given system. It is postulated in the logarithmic law that a distribution equilibrium is attained between the ions in the solution and the ions on the solid surface as each new crystal layer is formed. A crystal formed under such circumstances retains a radial gradient of the concentration of the tracer component distributed in a logarithmic manner. If λ is larger than unity, the tracer component is enriched in the crystal and the concentration of the tracer component is the highest at the center of each crystal, decreasing gradually toward the outer part of the crystal. When λ is smaller than unity, the tracer component is enriched in the solution, and the radial concentration gradient in the crystal becomes the reverse of that of the case of values of λ greater than unity.

The coprecipitation method using calcium oxalate as a carrier is often used for the enrichment of strontium, scandium and rare earth elements from dilute solutions for the separation of those radioisotopes from the other elements.

Some attempts have been made to reveal the distribution behavior of macro and micro components. In general, due to the low solubility of oxalates, coprecipitation from a homogeneous system was used. This also gave rise to the more reproducible results.

1) W. Chlopin, *Z. anorg. u. allgem. Chem.*, **143**, 97 (1925).
2) L. M. Henderson and F. C. Kracek, *J. Am. Chem. Soc.*, **49**, 738 (1927).
3) H. A. Doerner and W. M. Hoskins, ibid., **47**, 662 (1925).

Feibuch, Rowly and Gordon[4] reported that the coprecipitation of pairs of rare earth oxalates obeyed the logarithmic distribution law. Purkayastha and Bhattacharyya[5] showed that the coprecipitation of yttrium and europium with calcium oxalate also followed the logarithmic distribution law. Previously, Shigematsu et al. had studied the coprecipitation behavior of scandium[6] and yttrium ions[7] with calcium oxalate from a homogeneous system and found that there were distinct differences between the two cases. In the calcium-yttrium system, the logarithmic distribution law was followed, regardless of the composition of the solutions, while the distribution of scandium deviated gradually from the logarithmic law with an increase in the pH value, and under similar conditions yttrium gave larger distribution coefficients than did scandium. On the basis of the above results, it was deduced that yttrium was more stable than scandium in the calcium oxalate crystal, because the ionic radius of bivalent calcium is closer to that of tervalent yttrium than to that of tervalent scandium.

In this research, the coprecipitation of rare earth elements with calcium oxalate was investigated. The effects of the pH values, the concentration of acetate used as the buffer solution and several other variables on the distribution coefficient were studied, using cerium-144, yttrium-91, europium-152, 154 and lutetium-177 as the radiotracers. The distribution coefficients of rare earth elements coprecipitated under the same conditions were compared.

Experimental

Apparatus and Reagents.—Radioactivity countings were made with a Phillips halogen-quenched G-M tube connected to a dekatron scaler (Metro Model D-5), and with a NaI (Tl) ($1^3/_4' \times 2'$) well-type scintillation counter (Kobe Kogyo Model PS-300) connected to a scaler (Model SA-230). A Hitachi-Horiba pH meter, Model M-3, was used for the pH measurements.

Radioisotopes were supplied as chloride in hydrochloric acid from The Radio Chemical Centre, Amersham, England. Reagent-grade dimethyl oxalate was purified by recrystallization from anhydrous methanol and was stored in a dry atmosphere to prevent it from hydrolysis by moisture. Stock solutions of rare earth elements were prepared by dissolving their reagent-grade oxides in hydrochloric acid. The calcium solution was prepared by dissolving reagent-grade calcium carbonate in hydrochloric acid. The EDTA solution (0.01 M) containing a Mg-EDTA complex was standardized with a standard calcium solution.

The other chemicals were chemically pure or were reagent-grade materials.

Procedure.—A representative procedure adopted in the homogeneous coprecipitation is as follows.

Twenty milliliters of a calcium chloride stock solution (2.0 M) and a suitable volume of a rare earth solution, with an appropriate amount of radioactive isotopes, are placed in a 250-ml. Erlenmeyer flask. Twenty milliliters of 10 M acetic acid or formic acid (as a buffer solution), a suitable volume of a sodium hydroxide solution, and 2.36 g. of dimethyl oxalate dissolved in water are added, the resulting solution is diluted to 200 ml., and the pH of the solution is measured. Then the flask, equipped with a reflux condenser, is placed in a thermostat, and the solution is stirred continuously with a mechanical stirrer to prevent it from supersaturation.

When the temperature of the solution rises to 60°C, 2 ml. of the solution is pipetted out into a glass counting dish 25 mm. in diameter for beta counting or into a polyethylene counting tube 12 mm. in diameter for gamma counting. After calcium ions begin to be precipitated by the oxalate ions released from dimethyl oxalate, 2.0 ml. of the solution is pipetted out from the reacting solution through a sintered glass filter into a counting vessel at appropriate intervals of time, and 0.2 ml. of concentrated hydrochloric acid is added immediately to stop any precipitation which may occur in cooling. The radioactivities of the liquid samples in the dish or tube are measured to determine the amount of rare earth elements in the solution phase. This solution is then washed out into a beaker with 5 N hydrochloric acid, dried slowly, and ashed by fuming it repeatedly with perchloric acid on a hot plate. After dilution with water and the addition of a buffer solution, the calcium ion is titrated with a 0.01 M EDTA standard solution containing its magnesium chelate, using Eriochrome Black T as an indicator. The homogeneous and logarithmic distribution coefficients, D and λ, are calculated from Eqs. 1 and 2.

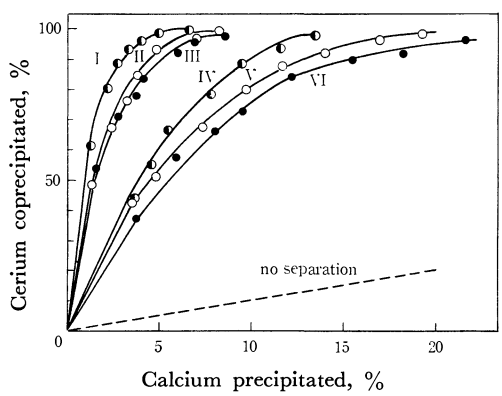

Fig. 1. Coprecipitation of cerium with calcium oxalate at several pH values.

Ca^{2+}: 0.2 M, Ce^{3+}: 10^{-6} M, Dimethyloxalate: 0.1 M, Temp: 60°C,
1 M formate: I, pH 2.92; II, pH 3.50, III, pH 4.06,
1 M acetate: IV, pH 4.08; V, pH 4.42; VI, pH 4.90

4) A. M. Feibuch, K. Rowley and L. Gordon, *Anal. Chem.*, **30**, 1605 (1958).
5) B. C. Purkayastha and S. N. Bhattacharyya, *J. Inorg. Nucl. Chem.*, **10**, 103 (1959).
6) T. Shigematsu, M. Tabushi and M. Matsui, *Bull. Inst. Chem. Res., Kyoto Univ.*, **40**, 381 (1962).
7) T. Shigematsu, M. Tabushi and M. Matsui, This Bulletin, **37**, 1610 (1964).

Results and Discussion

The effect of the pH value on the coprecipitation was studied. The results in the calcium-cerium(III) system are shown in Fig. 1, in which the percentages of coprecipitated cerium at several pH values are plotted against the fractions of calcium precipitated. The diagram shows that the cerium ion is enriched in the precipitate in the pH range investigated, with the extent of enrichment increasing as the pH decreases. This is a similar case to that of yttrium.

The logarithmic and homogeneous distribution coefficients, λ and D, were calculated from these data, and λ was plotted against the percentage of the precipitation of a macro component (cf. Figs. 2 and 3). As Fig. 2 shows cerous ion coprecipitates obey the logarithmic law regardless of pH, and the value of λ increases with the decrease in pH, when the precipitation occurs in a 1 M formate solution. The value of λ which was obtained in a 1 M acetate solution is affected by the pH value in a similar manner, as is shown in Fig. 3. In the experiment made at a lower pH, λ does not seem to be constant; instead, it increases as the precipitation proceeds. The fact that deviation is more influenced in the more weakly-buffered pH range can be explained from the fact that the pH value is lowered and the value of λ increases as the oxalates are formed. Considering the shift of pH during the reaction progress, there is no doubt that the distribution in a 1 M acetate solution also follows the logarithmic distribution law.

Europium and lutetium ions behave in the same way as a cerous ion does. In Fig. 4, the logarithmic distribution coefficients are plotted against the pH in calcium-cerium and calcium-lutetium systems. Although λ increases as the pH decreases, in the pH range studied these systems obey the logarithmic law. It should be pointed out that a difference was found between the distribution curves obtained in acetate and formate buffer solutions. The coefficients change monotonously with the change in pH and gradually approach a constant value in each buffer solution, though as different curves, depending upon the species of organic acid used as the buffer substance. This can be interpreted in terms of the complex formation of metal ions with those acids. The coefficients of lutetium are somewhat higher than cerium throughout the pH range investigated in Fig. 4.

The effect of the organic acid concentration on the coefficient was examined in the calcium-cerium system. The precipitations were carried out on solutions containing 2.0, 1.0 and 0.5 M of acetate at pH 4.50, a value which was suitable

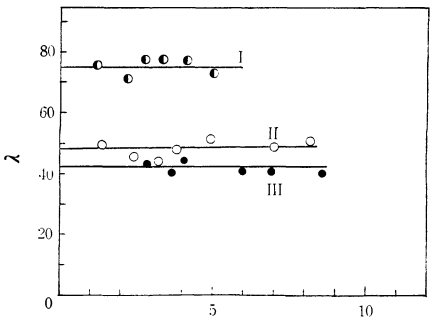

Fig. 2. Effect of pH on distribution coefficient for calcium-cerium oxalate system.
Ca^{2+}: 0.2 M, Ce^{3+}: 10^{-6} M, formate: 1 M, dimethyloxalate: 0.1 M, temperature: 60°C,
I: pH 2.92, λ=75, II: pH 3.50, λ=48,
III: pH 4.06, λ=42

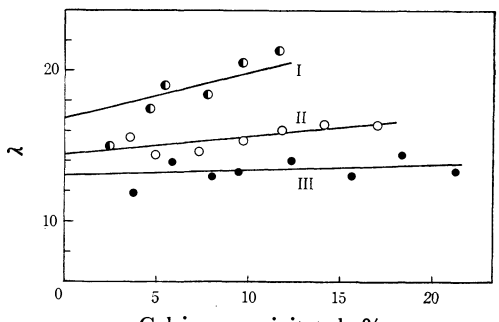

Fig. 3. Effect of pH on distribution coefficient for calcium-cerium oxalate system.
Acetate: 1 M,
I: pH 4.08, λ=16.7, II: pH 4.42, λ=13.8,
III: pH 4.90, λ=12.8,
Others are the same as in Fig. 1.

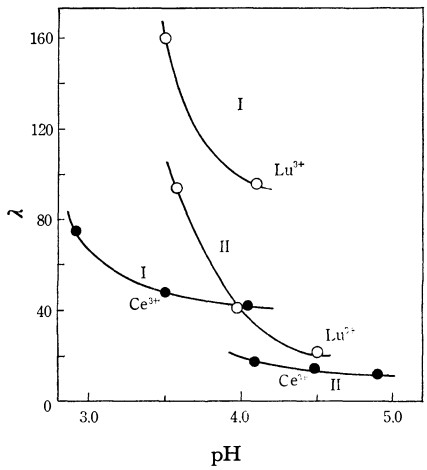

Fig. 4. Effect of pH on distribution coefficient.
I: 1 M formate, II: 1 M acetate,
Others are the same as in Fig. 1.

for the estimation of λ. Although the coefficient increases slightly in the process of the precipitation, much as in Fig. 3, the distribution must obey the logarithmic law, taking account of shift in pH mentioned above.

The values extrapolated to zero percent of calcium on the coefficient-precipitated calcium curve are taken as the exact coefficient at pH 4.50. The results are represented in Fig. 5, where it is evident that the coefficient is remarkably increased by the decrease in the acetate concentration.

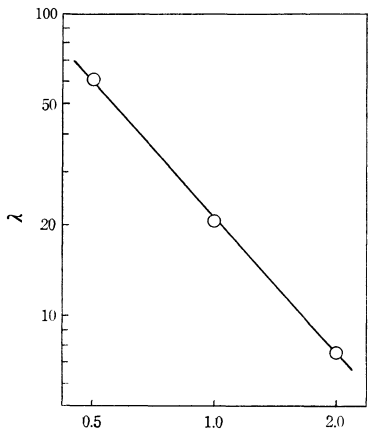

Fig. 5. Effect of acetate concentration on distribution coefficient for calcium-cerium system.
pH: 4.50, Others are the same as in Fig. 1.

The effects of other such variables as the concentration of coexisting ions and the concentration of micro component will be discussed below, although they are not so evident. To examine the effect of the ionic concentration, sodium chloride was added to make the final concentration nil, 1.0 and 2.0 M at pH 4.50 in the calcium-lutetium system. The experiment was performed in a 0.5 M acetate solution, which was selected as being suitable in respect to ionic concentration and buffer action. The results shown in Fig. 6 indicate that the coefficient is scarcely influenced by the ionic concentration. The influence of the concentration of a micro component was also hardly recognized in the calcium-lutetium system. The value of λ at pH 4.50 in 1 M acetate was 19.3 at 10^{-7} M and 19.5 at 10^{-5} M of lutetium ions respectively. As has been mentioned above, it is obvious that the factors influencing the coefficient are the pH of the solution and the concentration of a coexisting organic acid.

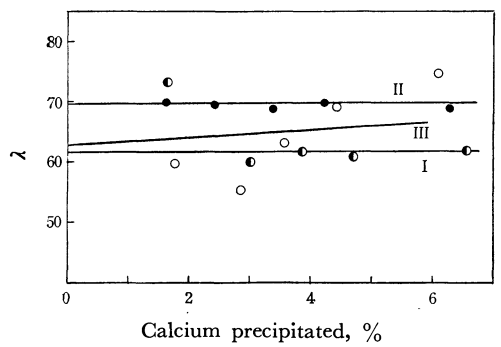

Fig. 6. Effect of ion concentration on distribution coefficient for calcium-lutetium system.
NaCl added: I, none, II, 1 M, III, 2 M,
Acetate: 0.5 M, pH: 4.50,
Others are the same as in Fig. 1.

Chlopin[8] offered the following explanation for the relation between the composition of a solution and the homogeneous distribution coefficient, D: if the ratio of the ionic concentration of a micro component to that of a macro component does not vary, even when the composition of the solution varies, the value of D will practically not change. When a complex or an insoluble compound is formed with a change in the composition of the solution, or when the ionic concentration of a macro or micro component undergoes a change separately, the value of D will increase if the ionic concentration of a macro component decreases more rapidly than that of a micro component, and vice versa.

This explanation can be applied to the system studied, which obeyed the logarithmic distribution law. When the pH becomes higher or when the concentration of organic acid used as a buffering agent becomes higher, the ionic concentration of the organic acid increases. The acid anion forms complex compounds with rare earth and calcium, the former complex being more stable than the latter. Then, as the ionic concentration of the acid anion increases, the decrease in the concentration of calcium ions will be less than that of rare earth ions, although the situation is complicated by the formation of a hydroxo complex or by other factors which should also be taken into consideration. Therefore, the logarithmic coefficient will gradually decrease.

The coprecipitation of several rare earth elements was examined by conducting the precipitation under identical conditions; the distribution coefficient of these elements were then compared. The results are summarized in Figs. 7 and 8. Figure 7 shows the relationship between the ionic radii of several rare earth ions and their distribution coefficients obtained at pH 3.50 in a 1 M formate solution. The coefficients of several elements in Fig. 8 are obtained in the same way at pH 4.50 in 1 M acetate. The ionic radii of tervalent rare earth ions are quoted from the numerical values obtained by Goldschmidt. A

8) I. E. Starik, "Hoshakagaku no Kiso" (Fundamental Radiochemistry), translated from Russian by F. Ichikawa, H. Okashita and R. Ishiwatari, Nankodo, Tokyo (1962), p. 174.

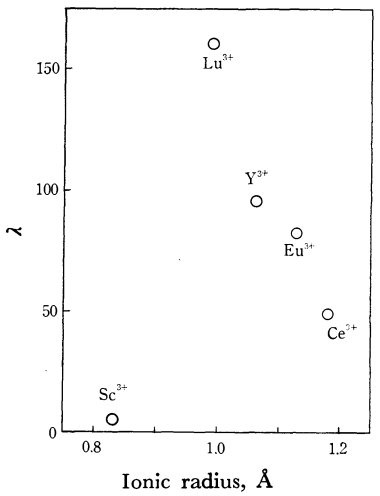

Fig. 7. Relation between ionic radius and λ at pH 3.50.

Formate: 1.0 M, Others are the same as in Fig. 1.

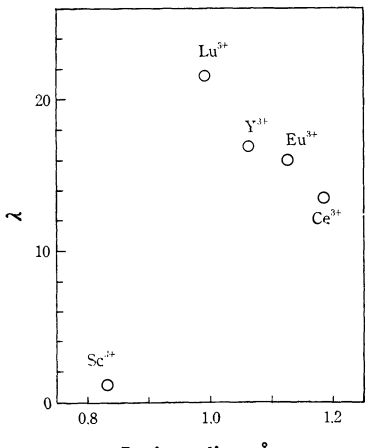

Fig. 8. Relation between ionic radius and distribution coefficient at pH 4.50.

Acetate: 1.0 M, Others are the same as in Fig. 1.

divalent calcium ion is equal in ionic radius to a tervalent yttrium ion. The limiting distribution coefficient of the calcium-scandium system in these figures was cited from the previous paper[6] for the sake of comparison. As is shown in the figures, the distribution coefficients of rare earth ions, the ionic radii of which come closer to that of divalent calcium, are closely related to their basicity or to the solubility of their oxalate salts. The order of the basicity of rare earth elements or of the solubility of their oxalate salts is as follows: Ce>Eu>Y>Lu, which is the reverse of the order of the distribution coefficients found in the present work.

Scandium ion constitutes an exception. Although it has a weaker basicity than rare earth elements, scandium is rather unstable in a calcium oxalate crystal and shows a smaller coefficient. This may be caused by the fact that the difference between the ionic radius of tervalent scandium and that of divalent calcium is quite large. This fact is a typical example showing that the ionic radius plays an important role in the coprecipitation process.

Gordon has questioned whether the logarithmic distribution equation (Eq. 2) can be justifiably applied to coprecipitation systems in which the charges of the ions are different; he has thus proposed an equation in which the charges of ions were taken into account.[9,10]

The present system is an example of the coprecipitation of the tervalent cation with divalent calcium salt. The equilibrium is represented by the following equation:

$$3Ca^{2+}_{cryst.} + 2M^{3+}_{aq.} = 3Ca^{2+}_{aq.} + 2M^{3+}_{cryst.}$$

The equilibrium constant, D^1, is defined as follows:

$$D' = \frac{[Ca^{2+}]^3_{aq.}[M^{3+}]^2_{cryst.}}{[M^{3+}]^2_{aq.}[Ca^{2+}]^3_{cryst.}}$$

When the equation proposed by Gordon[9] is applied to the above system, the following equation is obtained:

$$\log \frac{M_{initial}}{M_{final}} = 0.8686\ \lambda_g (Ca_{final}^{-1/2} - Ca_{initial}^{-1/2}) \quad (3)$$

Table I. Effect of the initial carrier concentration on λ and λ_g

Eu^{3+}: 10^{-5} M, acetic acid: 2 M, pH: 4.50, Temp.: 60°C

Ca pptd. %	Eu coppted. %	λ	λ_g
(A) Ca^{2+}: 0.1 M, dimethyloxalate 0.05 M			
5.86	42.07	9.04	2.81
6.91	56.57	11.65	3.62
10.12	71.50	11.77	3.62
13.47	82.25	11.92	3.64
19.68	90.51	10.75	3.22
23.79	92.82	9.70	2.86
	Average	10.81	3.30
(B) Ca^{2+}: 0.4 M, dimethyloxalate 0.2 M			
12.77	49.40	5.00	3.05
17.91	62.33	4.95	2.98
23.77	75.12	5.12	3.03
29.40	84.64	5.39	3.12
35.79	91.58	5.59	3.16
39.85	94.22	5.60	3.11
	Average	5.28	3.07

9) L. Gordon, M. L. Sulutsky and H. H. Willard, "Precipitation from Homogeneous Solution," John Wiley & Sons, New York (1959), p. 132.

10) J. Block and L. Gordon, *Talanta*, **10**, 351 (1963).

where $M_{initial}$ and $Ca_{initial}$ represent the initial concentrations in a solution; M_{final} and Ca_{final} represent the final concentrations in a solution, and λ_g is the distribution coefficient of this system.

Equation 3 suggests that when the ions have different charges the distribution coefficient is dependent upon the initial calcium concentration. Therefore, the effect of the initial calcium concentration on λ and λ_g was examined. It is represented in Table I. The results show that λ and λ_g are about equally constant throughout the reaction process, and λ is more extensively affected than λ_g by the initial calcium concentration. However, it is doubtful from these data whether Eq. 3 is valid for the present system. Further research is needed to justify the applicability of Eq. 3 to systems involving differently-charged ions.

In this paper, λ was calculated by means of the logarithmic distribution equation of Doerner and Hoskins (Eq. 2), because the coprecipitation behavior shows the same tendency, whichever coefficient is used, and also because the applicability of λ_g still remains to be studied.

The author wishes to thank Professor Tsunenobu Shigematsu and Dr. Masayuki Tabushi for their kind and valuable advice throughout this study.

BULLETIN OF THE CHEMICAL SOCIETY OF JAPAN VOL. 39 1119—1124 (1966)

Reactions of 2-Chlorocycloalkanone Oximes. I. Their Preparations and Conversion to 2-Alkoxy-, 2-Acyloxy- and 2-Alkylthiocycloalkanone Oximes[1]

By Masaji OHNO, Norio NARUSE, Seiichi TORIMITSU and Masaru OKAMOTO

Basic Research Laboratories, Toyo Rayon Co., Ltd., Tebiro, Kamakura

(Received July 22, 1965)

The preparation of 2-chlorocycloalkanone oximes has been investigated in detail. 2-Chlorocyclooctanone oxime is prepared in an excellent yield by the reaction of cyclooctene with nitrosyl chloride under the irradiation of light from a high-pressure mercury lamp. 2-Chlorocyclododecadienone oxime, 2-chlorocyclohexanone oxime and 3-chloronorcamphor oxime are prepared in good yields by the addition of nitrosyl chloride to *cis*, *trans*, *trans*-1, 5, 9-cyclododecatriene, cyclohexene and norbornene respectively in the presence of hydrochloric acid. Their displacement reactions with such nucleophilic reagents as sodium alkoxides, sodium ethanethiolate and sodium salts of carboxylic acids have been studied, and the syntheses of 2-alkoxy-, 2-ethylthio- and 2-acyloxycycloalkanone oximes have been successfully achieved.

The addition of nitrosyl chloride to olefins has been of considerable importance in the developement of cyclic terpene chemistry.[2,3] It has mainly played an important role in unsaturation tests of natural products by affording dimers of nitrosochlorides, which are very easily obtained in crystalline forms if the formation of bimolecular compounds is not prevented from steric hindrance (Eq. 1):

$$>C=C< + NOCl \rightarrow ON-\underset{|}{\overset{|}{C}}-\underset{|}{\overset{|}{C}}-Cl \rightleftarrows (ON-C-C-Cl)_2 \qquad (1)$$

The first synthetic application of the reaction was studied by Wallach[4] and Deussen[5] on exo double bonds of cyclohexane derivatives and on a sesquiterpene, caryophyllene, as is expressed in Eqs. 2 and 3 respectively:

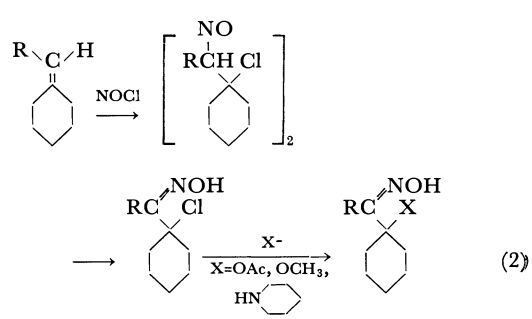

(2)

1) Presented at the 17th and 18th Annual Meeting of the Chemical Society of Japan, Tokyo, April, 1964 and Osaka, April, 1965, respectively.

2) W. A. Tilden, *J. Chem. Soc.*, **1875**, 514.

3) L. J. Beckham, W. A. Fessler and M. A. Kise, *Chem. Revs.*, **48**, 369 (1951).

4) O. Wallach, *Ann.*, **332**, 305 (1904); **360**, 26 (1908); **374**, 198 (1910); **389**, 185 (1912); **414**, 257 (1918).

5) E. Deussen, ibid., **369**, 41 (1909).

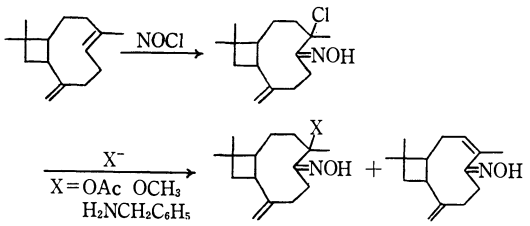

(3)

However, these reactions were limited to trisubstituted olefins, and later investigations have shown that stable adducts nitrosochlorides can be formed only from tetra and trisubstituted olefins,[3] while disubstituted olefins have been considered to afford unstable or tarry materials.

Another way[6,7] of preparing α-chlorooximes is based on ketones, as is expressed in Eq. 4:

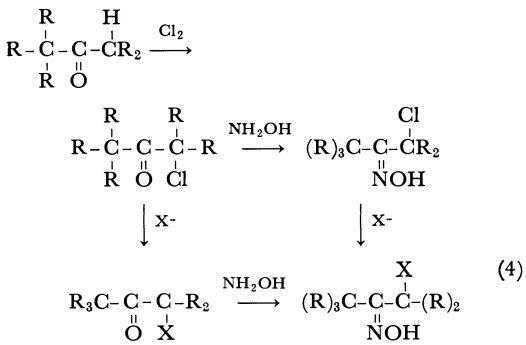

(4)

This method has been chiefly applied to steroidal ketones; it obviously requires many steps and affords by-products.

Recently, Dornow[8] reported the new method of preparing α-chlorooxime from nitroolefins expressed in Eq. 5:

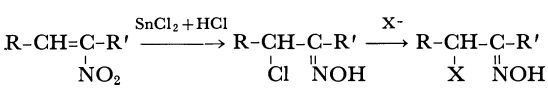

(5)

The method is limited to acyclic olefins.

In this report, we have first investigated the reactions of cyclohexene, cyclooctene, cyclododecatriene and norbornene with nitrosyl chloride, since these disubstituted olefins are now easily available as a result of the recent progress in petroleum chemistry but have not been treated with nitrosyl chloride in detail. Secondly, the successful preparation of their α-chlorooximes has enabled us to investigated their displacement reactions with nucleophilic reagents.

6) C. L. Stevens, P. Blumbergs and M. Munk, *J. Org. Chem.*, **28**, 331 (1963).
7) B. Tchoubar, *Bull. Soc. Chim. France*, **1955**, 1363.
8) A. Dornow, H. D. Jordan and A. Müller, *Chem. Ber.*, **94**, 67 (1961).

Results

When cyclohexene was treated with nitrosyl chloride in liquid sulfur dioxide, an isomer of bis(1-chloro-2-nitrosocyclohexane) was isolated in a 60—90% yield.[9] Another isomer of bis(1-chloro-2-nitrosocycolhexane) was obtained from the reaction in trichloroethylene.[10] These adducts were, however, found to be unsatisfactory as starting materials for displacement reactions. Therefore, the hydrochloride of 2-chlorocyclohexanone oxime, prepared from a reaction of cyclohexene and nitrosyl chloride in the presence of hydrochloric acid,[11] has been used in this research.

2-Chlorocyclooctanone oxime was obtained in an excellent yield when cyclooctene was treated with nitrosyl chloride under the irradiation of light from a high-pressure mercury lamp. The usual addition method affords 2-chlorocyclooctanone oxime in a poor yield,[12,13] and the product of the addition in the presence of hydrochloric acid is accompanied by a considerable amount of 2-chlorocyclooctanone when it is converted into the free oxime with a base.

2-Chlorocyclooctanone oxime is very stable at room temperature, while 2-chlorocyclohexanone oxime is very unstable to air and heat; the extreme instability of the latter might be the main reason why synthetic reactions for such a simple system have not yet been investigated.

The reaction of *cis, trans, trans*-1, 5, 9-cyclododecatriene with nitrosyl chloride in the presence of hydrochloric acid afforded 2-chlorocyclododecadienone oxime in nearly quantitative yields.[14] It should be mentioned that the product is obtained in a free oxime state simply by recrystallization from such organic solvents as ligroin and ethanol. Furthermore, the double bond preferentially attacked by nitrosyl chloride was found to be one of the *trans* double bonds of *cis, trans, trans*-1, 5, 9-cyclododecatriene. This method provides the most convenient way to prepare α-chlorooxime of a 12-membered ring system, since the starting material is now easily available from the trimerization of butadiene.[15]

The addition of nitrosyl chloride to norbornene in the presence of hydrochloric acid afforded 3-chloronorcamphor oxime hydrochloride in a good yield and did not involve molecular rearrangement. Previously, Miller[16] showed that the dimeric

9) R. K. Allison, U. S. Pat. 2485180 (1949).
10) M. Ohno, M. Okamoto and K. Nukada, *Tetrahedron Letters*, **1965**, 4047.
11) O. von Schickh and H. Metzger, U. S. Pat. 3078306 (1963).
12) L. E. Craig, U. S. Pat. 2890248 (1959).
13) O. von Schickh and H. Metzger, German Pat. 1068708 (1959).
14) M. Ohno, M. Okamoto and N. Naruse, *Tetrahedron Letters*, **1965**, 1971.
15) G. Wilke, *Angew. Chem.*, **75**, 10 (1963).
16) J. B. Miller, *J. Org. Chem.*, **26**, 4905 (1961).

nitrosochloride of norbornene can be converted into α-chlorooxime with neither hydrochloric acid nor heat, but with urea; therefore, our method presents a simple method for the preparation of 3-chloronorcamphor oxime.

The methods of preparing 2-chlorocycloalkanone oximes are shown in the following schemes:

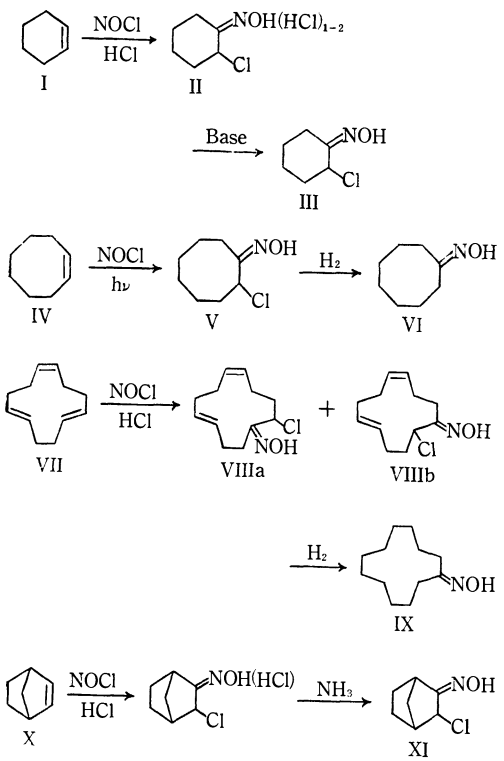

Displacement reactions of 2-chlorocyclooctanone and 2-chlorocyclododecadienone oximes with sodium alkoxides, sodium ethanethiolate, and sodium salts of carboxylic acids were investigated first, and then the investigation was extended to unstable 2-chlorocyclohexanone oxime.

α-Chlorooximes were treated with sodium alkoxides in the corresponding alcohol or in tetrahydrofuran at 40—60°C. Methanol, ethanol, 2-propanol, *t*-butyl alcohol and phenol were used for the displacement reactions. The best yields were generally obtained when more than two mole equivalents of sodium alkoxide were used. In each reaction, a blue color was always observed at the beginning, but it always disappeared soon, strongly suggesting the formation of nitroso compounds during the reaction. The reaction with 2-propanol and *t*-butyl alcohol afforded products only in the case of the 8-membered ring.

It has been shown that the yields of α-alkoxyoximes of the 8- and 12-membered rings are better than those of the 6-membered ring and that no appreciable amount of an unsaturated oxime was detected in these reactions, contrary to the cases of trisubstituted olefins.[4]

Treatments of α-chlorooximes with sodium ethanethiolate were carried out in tetrahydrofuran with vigorous stirring. The expected α-ethylthiooximes were obtained in good yields from the 8- and 12-membered rings, but not from the 6-membered ring. In these cases, too, a blue color was observed during the reactions.

α-Chlorooximes were treated with sodium salts of various carboxylic acids in tetrahydrofuran or acetone, affording α-acyloxyoximes in good yields.

The yields of these reactions are summarized in Table I.

Table I. Displacement reactions with RONa, EtSNa, and RCOONa

Reagent	2-Substituted-cyclohexanone oxime %	2-Substituted-cyclooctanone oxime %	2-Substituted-cyclododecadienone oxime %
MeONa	77	97.5	90
EtONa	55	90	88
i-PrONa	*	40—58	*
t-BuONa	*	60—80	*
PhONa	*	80	*
EtSNa	*	72	84.6
HCOONa	*	80	*
CH_3COONa	86	80	81
PhCOONa	65	72	65

* Only a tarry material was obtained; the isolation of the expected products was unsuccessful.

The mechanism of these reactions seems not to be a simple S_N2-type, but a Michael-type, addition of nucleophiles to the α, β-unsaturated nitroso compound formed during the reaction, since a freshly-prepared solution of 2-chlorocyclooctanone oxime and *n*-butyllithium in tetrahydrofuran possessed a deep blue color with maximum absorptions at 258 mμ (ε, 3300) and 645 mμ (ε, 10).

Experimental

2-Chlorocyclohexanone Oxime (III).[11]—Cyclohexene (100 g.) was placed in a 300-ml. three-necked round-bottom flask equipped with a stirrer, a gas inlet and gas outlet tubes; then at the bottom of the flask a two-way stop cock was fitted in order to remove the products. A mixed gas of nitrosyl chloride (1.3 mole equivalent) and hydrogen chloride was passed through cyclohexene, and the reaction temperature was kept at about −10°C. The oily product which was gradually formed at the bottom of the flask was removed through the stopcock. The oily product (62 g.) solidified on standing at room temperature and was confirmed to be the hydrochloride of 2-chlorocyclohexane oxime from its infrared spectrum and from its conversion into cyclohexanone oxime by catalytic reduction. Free 2-chlorocyclohexanone oxime was obtained by neutralizing the hydrochloride with aqueous ammonia, followed by extraction with ether and the removal of the solvent.

It was immediately used for displacement reactions.

2-Chlorocyclooctanone Oxime (V).—Nitrosyl chloride (13 g.) was passed through a solution of cyclooctene (10 g.) in a mixed solvent of methylene chloride (100 ml.) and methanol (15 ml.) under the irradiation of light from a high-pressure mercury lamp (200 W.) for 70 min. After the reaction, and after the solvent had been removed under reduced pressure, a colorless solid (17 g.) was obtained, along with a very small amount of an oily material. The solid material was washed with ligroin and recrystallized from methanol. It melted at 98—99°C and showed infrared absorptions at 3200 cm^{-1} for the hydroxy group and 1650 cm^{-1} for the C=N group. The NMR spectrum showed a triplet signal at τ 5.48; thus the structure proved to be 2-chlorocyclooctanone oxime.

Found: C, 54.70; H, 8.06; N, 8.07; Cl, 20.24. Calcd. for $C_8H_{14}NOCl$: C, 54.71; H, 8.05; N, 8.01; Cl, 20.21.

2-Chlorocyclododecadienone Oxime (VIIIa and VIIIb). — *cis, trans, trans*-1, 5, 9-Cyclododecatriene (200 g.) dissolved in 1 l. of trichloroethylene was placed in a 2-l. three-necked flask equipped with a stirrer and an inlet tube for nitrosyl chloride. A mixed gas of nitrosyl chloride (81 g.) and hydrogen chloride was bubbled into the solution over 3 hr, while the reaction temperature was kept below 12°C. After the addition of nitrosyl chloride, hydrogen chloride was passed through the solution for another hour. After the reaction, the solvent was removed under aspirator pressure; a pale-yellow crude product (287 g.) was thus obtained. It was crystallized from ligroin, showing a m. p. of 127—129°C.

Found: C, 63.15; H, 7.85; N, 5.85; Cl, 15.99. Calcd. for $C_{12}H_{18}NOCl$: C, 63.29; H, 7.92; N, 6.16; Cl, 15.60.

Its infrared spectrum showed absorptions at 980 cm^{-1} characteristic of a *trans* double bond and at 707 cm^{-1} characteristic of a *cis* double bond, thus showing that one of the *trans* double bonds was preferentially attacked by nitrosyl chloride. Besides the above absorptions, an absorption for the hydroxyl group was observed at 3210 $cm.^{-1}$ No skeletal change or transannular reaction was observed, since its hydrogenation with palladium charcoal afforded cyclododecanone oxime in a quantitative yield. Therefore, the product must be a mixture of 2-chloro-*cis*-5, *trans*-9-cyclododecadienone oxime (VIIIa) and 2-chloro-*trans*-5, *cis*-9-cyclododecadienone oxime (VIIIb), which were used for displacement reactions without separation.

Similar reactions using methylene chloride, chloroform, and carbon tetrachloride showed that there was no essential change in the product, which always afforded 2-chlorocyclododecadienone oxime in yields of 60—90%.

3-Chloronorcamphor Oxime (XI).—A mixed gas of nitrosyl chloride (17.5 g.) and hydrogen chloride was introduced into a solution of norbornene (25 g.) in 120 ml. of trichloroethylene over a 2-hr. period, During the reaction, the temperature was kept at 0—5°C. The reaction mixture became green at the beginning, and then colorless precipitates were formed. After the reaction, a solid fraction (60 g.) was separated by filtration. It was treated with a 2 N ammonia solution to neutralize it and extracted with ether. The ethereal solution afforded colorless needle crystals (38 g.), m. p. 117—119°C, which were recrystallized from ethanol.

Found: C, 52.95; H, 6.21; N, 8.41; Cl, 22.36; M. W.=161.3. Calcd. for $C_7H_{10}NOCl$: C, 52.68; H, 6.32; N, 8.74; Cl, 22.22%; M. W.=159.6.

The NMR spectrum showed a signal (singlet, 1H) at 0.38τ for the hydroxyl proton and a signal (doublet J=3 c. p. s., 1H) at 5.60τ for the endo hydrogen on C-3.

2-Methoxycyclooctanone Oxime.—Sodium metal (3 g.) was dissolved in 100 ml. of methanol. 2-Chlorocyclooctanone oxime (10 g.) dissolved in 50 ml. of methanol was then added to the solution over a 1 hr. period. The reaction temperature was kept at 50—60°C. A blue color was observed immediately after chlorooxime was added, but it soon disappeared. After another hour, the solvent was removed under reduced pressure. When the residue was treated with water and then ether, the ethereal solution afforded a pale-yellow solid (9.5 g.). It was recrystallized from *n*-hexane and melted at 65—67°C. The infrared spectrum showed absorptions at 3,300 cm^{-1}(-OH), 1640 cm^{-1}(-C-N-), and 1085 cm^{-1}(-C-O-C).

Found: C, 60.14; H, 10.06; N, 7.60. Calcd. for $C_9H_{17}NO_2 \cdot 1/2H_2O$: C, 59.97; H, 10.07; N, 7.77%.

2-Methoxycyclododecadienone Oxime. — 2-Chlorocyclododecadienone oxime (10 g.) dissolved in 100 ml. of methanol was treated with a sodium methoxide solution, prepared from 2 g. of sodium and 100 ml. of methanol, at 40—50°C for 3 hr. After the reaction, the methanol was removed under reduced pressure, and the residue was treated with water and then ether. The ethereal solution afforded a colorless, oily product. The infrared spectrum showed absorptions at 3300 cm^{-1}(-OH), 1650 cm^{-1}(>C=N-), and 1080—1090 cm^{-1}(-C-O-C). The 2, 4-dinitrophenylhydrazone showed a m. p. of 191—193°C.

Found: C, 57.97; H, 7.20; N, 14.23. Calcd. for $C_{19}H_{28}O_5N_4$: C, 58.14; H, 7.19; N, 14.28%.

2-Methoxycyclohexanone Oxime. — Crude 2-chlorocyclohexanone oxime (10 g.), freshly prepared from its hydrochloride by treatment with ammonium hydroxide, was dissolved in a methanol solution (100 ml.) of sodium methoxide prepared from 4 g. of sodium. It was then heated to 40—50°C for 2 hr. After usual treatments, a brown oily material was obtained. The chromatography on alumina using ether as an eluent afforded a pale-yellow oil (6.2 g.). An attempt to distill the oil was unsuccessful, since it decomposed readily at 80°C. Therefore, it was hydrolyzed to 2-methoxycyclohexanone, b. p. 70—72°C/12 mmHg (reported b. p. 72—73°C/14 mmHg[17]), according to the procedure of DePuy and Ponder.[18] The phenylhydrozone showed a m. p. of 92—94°C (reported m. p. 94—96°C[17]).

Found: C, 71.42; H, 8.21; N, 12.52. Calcd. for $C_{13}H_{18}ON_2$: C, 71.51; H, 8.32; N, 12.84%.

2-Ethoxycyclooctanone Oxime.—Sodium (2.6 g.) was dissolved in ethanol (50 ml.), and then 2-chlorocyclooctanone oxime (10 g.) dissolved in ethanol (50 ml.) was added to the solution. After one hour at 40—50°C, the reaction mixture was treated as usual. The

17) M. Bergmann and M. Gierth, *Ann.*, **448**, 64 (1926).
18) C. H. DePuy and B. W. Ponder, *J. Am. Chem. Soc.*, **81**, 4629 (1959).

ethereal extract was washed with water, dried, and evaporated to dryness to give 9.5 g. of a yellow solid. It was recrystallized from aqueous ethanol, giving an analytical sample, m. p. 84.5—85.5°C.

Found: C, 65.11; H, 10.34; N, 7.78; O, 17.14. Calcd. for $C_{10}H_{19}O_2N$: C, 64.83; H, 10.34; N, 7.56; O, 17.27%.

2-Ethoxycyclododecadienone Oxime.—2-Chlorocyclododecadienone oxime (20 g.) was treated with a sodium ethoxide solution prepared from sodium (4.5 g.) and ethanol (100 ml.). A pale yellow oily product (18.5 g.) was obtained after the usual work-up, described above. The 2, 4-dinitrophenylhydrazone showed a m. p. of 143—145°C.

Found: C, 59.22; H, 7.60; N, 13.80. Calcd. for $C_{20}H_{30}O_5N_4$: C, 59.09; H, 7.44; N, 13.79%.

2-Ethoxycyclohexanone Oxime. — According to procedures similar to those described above, 2-ethoxycyclohexanone oxime (8.2 g.), an oily product, was obtained from the reaction of 2-chlorocyclohexanone oxime (10 g.) with sodium ethoxide (14.1 g.). The infrared spectrum showed abosrptions at 3300 cm^{-1} (–OH), 1660 cm^{-1}(–C=N–), and 1100 cm^{-1}(–C–O–C). It was distilled under reduced pressure to give an oily material, b. p. 87—88°C/1.3 mmHg.

Found: C, 61.02; H, 9.41; N, 9.00. Calcd. for $C_8H_{15}O_2N$: C, 61.12; H, 9.62; N, 8.91%.

2-*t*-Butoxycyclooctanone Oxime.—According to procedures similar to those described above, 2-*t*-butoxycyclooctanone oxime (9.8 g.), an oily product, was obtained from the reaction of 2-chlorocyclooctanone oxime (20 g.) with sodium *t*-butoxide (7.1 g.). IR: 3300, 1645, 1100 cm^{-1} (KBr). NMR: 6.14 τ (1H, triplet). The dinitrophenylosazone showed a m. p. of 205—207°C.

Found: C, 48.24; H, 4.22; N, 22.01. Calcd. for $C_{20}H_{20}N_8O_8$: C, 48.64; H, 4.02; N, 22.39%.

2-Isopropoxycyclooctanone Oxime.—According to procedures similar to those described above, 2-isopropoxycyclooctanone oxime (6.7 g.), an oily product, was obtained from the reaction of 2-chlorocyclooctanone oxime (10 g.) with sodium isopropoxide (5.2 g.). IR: 3300, 1650, 1110 cm^{-1} (KBr). NMR: 6.18 (1H, triplet), 6.32 (1H, multiplet), 8.66 τ (6H, doublet). It formed the same osazone as has been described above.

2-Phenoxycyclooctanone Oxime.—Sodium phenoxide was prepared from sodium (4 g.) and phenol (25 g.) in tetrahydrofuran (100 ml.). To the solution was added a solution of 2-chlorocyclooctanone oxime (10 g.) in tetrahydrofuran (50 ml.) over a 30 min. period. The reaction mixture was kept at 50°C while being stirred for 2 hr. The solvent was then removed under reduced pressure. The ethereal extract was washed with water, dried, and evaporated to dryness to give 21.2 g. of a pale-yellow solid. It was recrystallized from ligroin, giving an analytical sample with a m. p. of 76—78°C.

Found: C, 72.31; H, 8.26; N, 5.88. Calcd. for $C_{14}H_{19}NO_2$: C, 72.07; H, 8.21; N, 6.00%. IR: 3250(–OH), 1650(–C=N–), 1600(–C_6H_5), 1030 (–C–O–C), 750(–O–C_6H_5)cm^{-1} (KBr).

2-Ethylthiocyclooctanone Oxime.—Sodium ethanethiolate was prepared in tetrahydrofuran from ethanethiol (30 ml.) and sodium (3.5 g.). 2-Chlorocyclooctanone oxime (20 g.) dissolved in tetrahydrofuran (50 ml.) was added to the solution over a 1 hr. period. A blue color was observed immediately after the addition, but it soon disappeared. The reaction was continued for 3 hr. with stirring. Sodium chloride was removed by filtration, and the solvent of the filtrate was removed under reduced pressure. The ethereal extract of the residue was washed with water, dried, and evaporated to dryness to give 16.5 g. of pale yellow needle crystals. They were recrystallized from ligroin, giving an analytical sample with a m. p. of 95—96.5°C.

Found: C, 59.75; H, 9.56; N, 6.67; S, 15.90. Calcd. for $C_{10}H_{19}NOS$: C, 59.66; H, 9.51; N, 6.96; S, 15.93%.

IR: 3200(–OH), 1640(–C=N–) cm^{-1} (KBr).

2-Ethylthiocyclododecadienone Oxime.—According to procedures similar to those described above, an oily product (31 g.) was obtained from the reaction of 2-chlorocyclododecadienone oxime (35 g.) and sodium ethanethoilate (20 g.) in tetrahydrofuran. This product was chromatographed on silica gel and eluted with chloroform. A homogeneous oily product (27 g.) was thus obtained, showing the presence of an ethyl group in the NMR spectrum; this was consistent with 2-ethylthiocyclododecadienone oxime.

Found: C, 66.69; H, 9.44; N, 5.93. Calcd. for $C_{14}H_{23}NOS$: C, 66.37; H, 9.15; N, 5.53%.

The Reaction of 2-Chlorocyclohexanone Oxime with Sodium Ethanethiolate. — 2-Chlorocyclohexanone oxime (6 g.) was treated with sodium ethanethiolate (a 2.13 mole equivalent) at 40—50°C for 2 hr. The reaction product was chromatographed on silica gel and eluted with chloroform, but an attempt to isolate a homogeneous fraction was unsuccessful.

2-Formyloxycyclooctanone Oxime.—Acetone (100 ml.) and sodium formate (6.8 g.) were placed in a 300 ml. three-necked round-bottom flask equipped with a stirrer, a condenser, and a separatory funnel. 2-Chlorocyclooctanone oxime (8.8 g.) dissolved in acetone (50 ml.) was added to the sodium formate solution over a 15 min. period. The reaction mixture was refluxed for 3 hr. and the precipitates were removed by filtration. The filtrate was evaporated under reduced pressure; the residue afforded a solid product (8.2 g.) when triturated with cyclohexane. It was recrystallized from cyclohexane, giving an analytical sample with a m. p. of 82—83°C.

Found: C, 58.48; H, 8.25; N, 7.54. Calcd. for $C_9H_{15}O_3N$: C, 58.36; H, 8.16; N, 7.56%.

2-Acetoxycyclooctanone Oxime.—2-Chlorocyclooctanone oxime (8.8 g.) dissolved in tetrahydrofuran (50 ml.) was added to a solution of sodium acetate (8.2 g.) in tetrahydrofuran, over a 15 min. period, using the reaction vessel which has been described in the case of the formyloxylation. It was refluxed for 2 hr. A blue color was observed during the reaction and disappeared in 30 min. After the reaction, sodium chloride was removed, and the filtrate was evaporated under reduced pressure. The residue was triturated with a small amount of cyclohexane, affording 8.0 g. of a solid. It was recrystallized from cyclohexane, giving an analytical sample with a m. p. of 92—93°C. The infrared spectrum showed the absorptions at 1740 cm^{-1} and 1210—35 cm^{-1} characteristic of the acetoxyl group.

Found: C, 60.14; H, 8.54; N, 6.95. Calcd. for $C_{10}H_{17}O_3N$: C, 60.28; H, 8.60; N, 7.03%.

2-Benzoyloxycyclooctanone Oxime. — 2-Chlorocyclooctanone oxime (8.8 g.) dissolved in acetone (70 ml.) was added to a solution of sodium benzoate (14.5 g.) in acetone (100 ml.) over a 15 min. period and heated to 50°C for 2 hr. with stirring, using the reaction vessel described in the case of the formyloxylation. After a similar treatment, a solid (9.5 g.) was obtained. It was recrystallized from cyclohexane, giving an analytical sample with a m. p. of 93—94°C. The infrared spectrum showed the absorptions at 1725 cm^{-1} and 1210 cm^{-1} characteristic of the benzoyloxy group.

Found: C, 68.97; H, 7.24; N, 5.35. Calcd. for $C_{15}H_{19}O_3N$: C, 68.94; H, 7.33; N, 5.36%.

2-Acetoxycyclododecadienone Oxime.—2-Chlorocyclododecadienone oxime (10 g.) dissolved in acetic acid (50 ml.) was added to a solution of sodium acetate (25 g.) in acetic acid (100 ml.) over a 15 min. period and then heated to 70°C for 2 hr. After the reaction, water (300 ml.) was added to the reaction mixture, and a solid (9 g.) was deposited. This solid was recrystallized from cyclohexane and shown to have a m. p. of 117—119°C. The infrared spectrum showed the absorptions at 1740 and 1230 cm^{-1} characteristic of the acetoxyl group.

Found: C, 67.07; H, 8.49; N, 5.73. Calcd. for $C_{14}H_{21}O_3N$: C, 66.90; H, 8.42; N, 5.57%.

A part of the 2-acetoxycyclododecadienone oxime (2.5 g.) was hydrogenated with 10% palladium charcoal in acetic acid, absorbing two mole equivalents of hydrogen and affording 2.3 g. of a colorless product. This product, when recrystallized from cyclohexane, showed a m. p. of 111—112°C.

The infrared spectrum showed no absorption of a double bond; thus, the structure of the hydrogenated product was consistent with that of 2-acetoxycyclododecanone oxime.

Found: C, 65.77; H, 9.77; N, 5.44. Calcd. for $C_{14}H_{25}O_3N$: C, 65.85; H, 9.87; N, 5.49%.

2-Benzoyloxylcyclododecadienone Oxime.—2-Chlorocyclododecadienone oxime (10 g.) dissolved in acetone (100 ml.) was stirred into a solution of sodium benzoate (23 g.) in acetone (100 ml.) over a 15 min. period and then refluxed for 3 hr.

The sodium chloride formed was removed by filtration immediately after the reaction, and the filtrate was evaporated to dryness to give a solid material (9.1 g.).

When this solid material was recrystallized from ethanol, it showed a m. p. of 163—164°C. The infrared spectrum showed the absorptions at 1725 and 1210 cm^{-1} of the benzoyloxy group, besides those at 980 cm^{-1} and 707 cm^{-1} for *trans* and *cis* double bonds respectively.

Found: C, 72.69; H, 7.40; N, 4.44. Calcd. for $C_{19}H_{23}O_3N$: C, 72.82; H, 7.40; N, 4.47%.

The unsaturated product (3.2 g.) was further hydrogenated in methanol with 10% palladium charcoal. Two mole equivalents of hydrogen were absorbed, and a colorless material was quantitatively obtained, with a m. p. of 125—126°C after recrystallization from ethanol.

The infrared spectrum showed no double-bond absorption.

Found: C, 71.81; H, 8.51; N, 4.34. Calcd. for $C_{19}H_{27}O_3N$: C, 71.89; H, 8.57; N, 4.41%.

2-Acetoxycyclohexanone Oxime.—2-Chlorocyclohexanone oxime hydrochloride (9.5 g.) suspended in acetone (100 ml.) was stirred into a solution of sodium acetate (24.6 g.) in acetone (100 ml.) and heated at 50°C for 2 hr. A colorless solid (7.2 g.) was obtained after treatment similar to that described above. It was recrystallized from cyclohexane, giving an analytical sample with a m. p. of 103—104°C. IR: 3200(-OH), 1725(-$OCCH_3$), 1660(-C=N-), 1230—1260(-$OCCH_3$), cm^{-1} (KBr).

Found: C, 55.99; H, 7.45; N, 8.06. Calcd. for $C_8H_{13}O_2N$: C, 56.12; H, 7.65; N, 8.15%.

2-Benzoyloxycyclohexanone Oxime.—2-Chlorocyclohexanone oxime hydrochloride (19 g.) dissolved in acetone (100 ml.) was added to a suspension of sodium benzoate (57.6 g.) and sodium carbonate (20 g.) in acetone (200 ml.) over 30 min. and then heated at 50°C for 2 hr. while being stirred. After a usual work-up, a solid (16 g.) was obtained. It showed a m. p. of 118—119°C after recrystallization from cyclohexane.

Found: C, 67.10; H, 6.50; N, 5.96. Calcd. for $C_{13}H_{15}O_3N$: C, 66.93; H, 6.48; N, 6.01%. IR: 3450 (-OH), 1705 (-OCC_6H_5), 1660(-C=N-), 1280 (-OCC_6H_5), 720(-C_6H_6) cm^{-1} (KBr).

BULLETIN OF THE CHEMICAL SOCIETY OF JAPAN VOL. 39 1125—1128 (1966)

Reactions of 2-Chlorocycloalkanone Oximes. II.[1] Syntheses of 3-Aminocycloalka[C]isoxazoles[2]

By Masaji OHNO and Norio NARUSE

Basic Research Laboratories, Toyo Rayon Co., Ltd., Tebiro, Kamakura

(Received July 22, 1965)

The displacement reactions of α-chlorocycloalkanone oximes with sodium cyanide in dimethyl sulfoxide or ethanol have been studied. It has been shown that 3-aminocycloalka[C]-isoxazoles can be obtained in excellent yields. α-Chlorooximes of cyclohexanone, cyclooctanone, cycloocten-5-one, cyclododecanone, and cyclododecadien-5, 9-one have been subjected to the reaction, affording the corresponding isoxazole derivatives in 48, 96, 89, 95, and 90% yields respectively. The application of the method to 3-chloronorcamphor oxime and α-chlorooximes from acyclic olefins afforded cyanooximes; it failed to give isoxazole derivatives. The hydrogenation of 3-aminocycloocta[C]isoxazole gave 2-amino-1-cyclooctanecarbonamide by the hydrogenolysis of the nitrogen-oxygen bond of the isoxazole ring system. The amino-carbonamide was treated with either the base or acid to give 2-oxycyclooctanecarboxylic acid.

Various methods of synthesizing isoxazole derivatives have been extensively investigated, and excellent reviews have been published by Quilico[3] and by Kochetkov and Sokolov.[4] The known synthetic plans of an isoxazole ring can be expressed by the following three general schemes, indicated by I, II, and III:

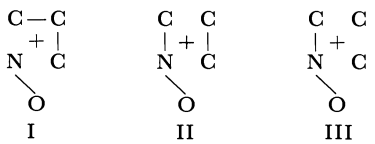

I II III

The reaction of 1, 3-dicarbonyl compounds with hydroxylamine is the method which has been used most widely for the synthesis of isoxazoles; it belongs to type I (Eq. 1);

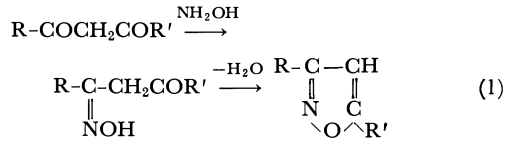

(1)

The isoxazole synthesis from nitrile oxides is another interesting method; it belongs to type II (Eq. 2):

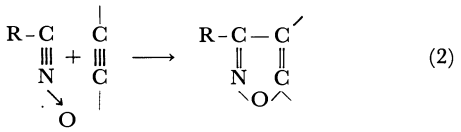

(2)

A special method for the formation of trisubstituted isoxazoles, one which starts from primary nitro derivatives, belongs to type III (Eq. 3):

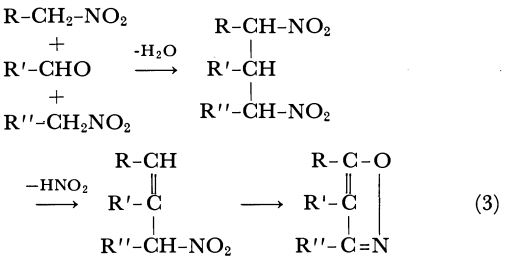

(3)

During the investigation of the displacement reaction of 2-chlorocycloalkanone oximes with various nucleophilic reagents,[1] we have found a new method of synthesizing cycloalka[C]isoxazoles, one which is different from any of the methods mentioned above; it belongs to a new type, IV:

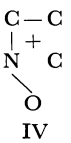

IV

In this report, the scope and limitations of the new synthesis and some reactions of 3-aminocycloalka[C]isoxazoles will be described.

2-Chlorocycloalkanone oximes were prepared readily by the reaction of cycloalkenes with nitrosyl chloride.[1] The reaction of 2-chlorocyclohexanone oxime with potassium or sodium cyanide in dimethyl sulfoxide or ethanol afforded a colorless crystalline material in a 48% yield. The infrared spectrum showed no absorption due to a nitrile group, but it did show absorptions at 3310 and 3160 cm^{-1} due to a primary amino group, and

1) Part I: M. Ohno, N. Naruse, S. Torimitsu and M. Okamoto, This Bulletin, **39**, 1119 (1966).

2) Presented at the 17th Annual Meeting of the Chemical Society of Japan and for a preliminary communication, see M. Ohno and N. Naruse, *Tetrahedron Letters*, **1964**, 2151.

3) A. Quilico, "The Chemistry of Heterocyclic Compounds," Vol. 17th, Interscience Pubishers, New York (1962), p. 1.

4) N. K. Kochetkov and S. D. Sokolov, "Advances in Heterocyclic Chemistry," Vol. 2, Academic Press, New York (1963), p. 365.

Table I. Yields and physical properties of 3-aminocycloalka[C]isoxazoles

Cycloalkene	Formula	Yield, %	M. p., °C	3-Aminocycloalka[C]isoxazoles UV, mμ	IR, cm^{-1}
Cyclohexene	V	48	117—118	243 (ε, 7400)	3310 3160 1655 1640 1500
Cyclooctene	VI	96	77— 78	252 (ε, 9700)	3380 3210 1650 1610 1500
Cyclooctadiene	VII	89	81.5—82.5	251 (ε, 8230)	3310 3180 1645 1610 1500
Cyclododecene	VIII	95	119—121	253 (ε, 7960)	3430 3280 3120 1650 1610 1495
cis, trans, trans-1,5,9-Cyclododecatriene	IX	95	148—150	244 (ε, 8000)	3420 3310 3180 1645 1615 1500
trans, trans, trans-1,5,9-Cyclododecatriene	X	90	131—134	256 (ε, 7900)	3420 3310 3180 1645 1915 1500

absorptions at 1655, 1640, and 1500 cm^{-1} due to a conjugated double bond system. The ultraviolet spectrum showed an absorption at 243 mμ (ε, 7400).

These spectral data, together with those of the elementary analysis, show that the structure of this compound can be identified as 3-amino-4, 5, 6, 7-tetrahydrocyclohexa[C]isoxazole (V). This has been confirmed further by a comparison of the melting point and spectra with those of an authentic sample.[5]

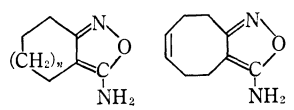

V $n=1$ VII
VI $n=3$
VIII $n=7$

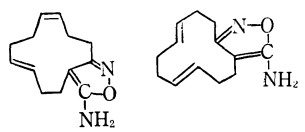

IX X

The formation of an isoxazole ring can be easily explained in terms of the displacement of an active chlorine atom with a cyanide anion, followed by an instantaneous ring closure between the oxime and the cyano groups.

This method has now been extended to α-chlorooximes of cyclooctanone, 5-cyclooctenone, and cyclododecanone, and to those[1] from *cis, trans, trans*-1, 5, 9-cyclododecatriene, and *trans, trans, trans*-1, 5, 9-cyclododecatriene. The corresponding 3-aminocycloalka[C]isoxazoles, VI, VII, VIII, IX, and X, have been obtained in excellent yields.

5) K. v. Auwers, Th. Bahr and E. Frese, *Ann.*, **441**, 68 (1925).

The results are summarized in Table I, and the synthetic method is expressed in the following successive formulae:

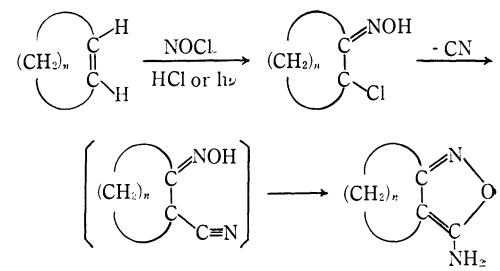

In order to clarify the scope and limitations of the reaction, the method was applied to norbornene, which is an example of the more strained olefins. The treatment of 3-chloronorcamphor oxime[1] with sodium cyanide in dimethyl sulfoxide afforded a mixture of two stereoisomers (XI and XII) of 3-cyanonorcamphor oxime, which did not form isoxazole.

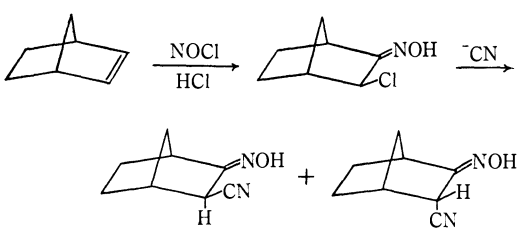

XI XII

This result suggests that the increase in ring strain is unfavorable for the formation of an isoxazole ring, but that the formation from 8- and 12-membered rings can be achieved easily because of no substantial ring strain. The application of this reaction to acyclic α-chlorooximes, which can be formed from isobutylene and butene-2,

also failed to give the isoxazole compounds, but did give the corresponding cyano-compounds.

The hydrogenation of 3-aminocycloocta[C]-isoxazole and the chemical degradation of the hydrogenated product were investigated with a view to ascertaining some properties of the system. Just one-mole equivalent of hydrogen was absorbed by the catalytic hydrogenation of 3-aminocycloocta[C]isoxazole, using 5% palladium charcoal under atmospheric pressure; a crystalline product was thus obtained in a 98% yield. The infrared spectrum showed absorptions at 3400, 3300, and 3150 cm^{-1} due to a primary amino group, and absorptions at 1642 and 1610 cm^{-1} due to an amide group. The ultraviolet spectrum showed a maximum absorption at 242 mμ (ε, 8000), suggesting the presence of a conjugated amide. The spectral evidence is very consistent with 2-amino-1-cyclooctenecarbonamide (XIII). The hydrogenated product (XIII) was treated with either hydrochloric acid or potassium hydroxide to form 2-oxo-cyclooctylcarbonamide (XV). The prolonged treatment of the compound XIV with alkali gave 2-oxo-cyclooctylcarboxylic acid (XV), together with a small amount of cyclooctanone (XVI). The β-ketocarboxylic acid, XV, has been proved to be identical with an authentic sample prepared by the reaction of cyclooctanone with sodium hydride - ethyl carbonate and by subsequent hydrolysis. Therefore, the structure of the hydrogenated product (XIII) has been proved to be correct.

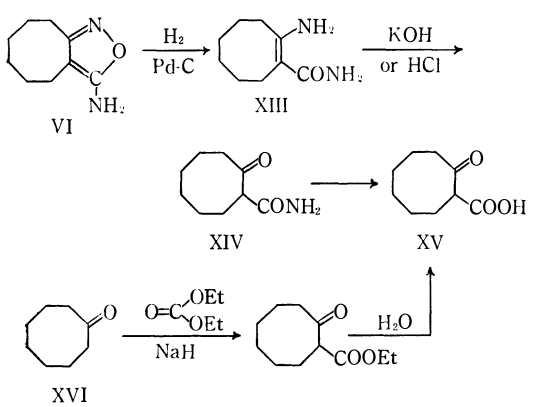

Experimental

3 - Amino - 4, 5, 6, 7-tetrahydrocyclohexa [C] iso - xazole (V).—Freshly-prepared 2-chlorocyclohexanone oxime[1] (10 g., 0.068 mol.) was treated with sodium cyanide (5 g., 0.10 mol.) in 50 ml. of ethanol under reflux for 2.5 hr. After the reaction, the sodium chloride formed and the unreacted sodium cyanide were removed by filtration and ether was added to the filtrate to remove the insoluble fraction. After the etherael solution had been evaporated, a brown solid was obtained. It was recrystallized from a mixed solvent of ether and petroleum ether to give a colorless crystalline material (4.5 g., 48%), m. p. 117—118°C. The infrared and ultraviolet spectra are shown in Table I.

Found: C, 61.19; H, 7.42; N, 20.23. Calcd. for $C_7H_{10}N_2O$: C, 60.85; H, 7.30; N, 20.28%.

This substance was shown to be completely identical with an authentic sample[5,6] by a mixed melting point determination and by a study of the spectral evidence. The authentic sample was prepared in the following way. Chlorocyan (7 g.) dissolved in 20 ml. of dioxane was added drop by drop to a solution of morpholine enamine (16 g.) of cyclohexanone in 130 ml. of dioxane at 0—5°C over a 2 hr. period. The reaction mixture was then allowed to stand overnight at room temperature. The reaction mixture was poured into ice-water and extracted with ether. After it had been dried and the ether had been evaporated, a yellow oil was obtained. It was distilled under reduced pressure to give a colorless oil, b. p. 120—130°C/1 mmHg, which was confirmed to be 2-cyanocyclohexanone. The cyano-ketone was treated with hydroxylamine, generated from hydroxylamine hydrochloride and sodium carbonate, for 1 hr. After it had then been extracted with ether, the ethereal solution afforded colorless crystalline 3 - aminocyclohexa[C]isoxazole, m. p. 115—116°C, after recrystallization from ether - petroleum ether.

Found: C, 60.75; H, 7.30; N, 20.27. Calcd. for $C_7H_{10}N_2O$: C, 60.85; H, 7.30; N, 20.28%.

3 - Amino - 4, 5, 6, 7, 8, 9 - hexahydrocycloocta[C]-isoxazole (VI).—2-Chlorocyclooctanone oxime (10 g., 0.056 mol.) dissolved in 30 ml. of dimethyl sulfoxide was vigorously stirred, over a 20 min. period, into a suspended solution of sodium cyanide (4 g., 0.081 mol.) in 40 ml. of dimethyl sulfoxide at 80—95°C. The reaction was continued for further 1.5 hr. at the same temperature. The reaction mixture was then treated with water and ether. The ethereal solution was dried and evaporated to give a pale yellow product (8.2 g., 96%). It was recrystallized from ether - petroleum ether to give a colorless analytical sample, m. p. 77—78°C.

Found: C, 65.26; H, 8.46; N, 16.70; O, 10.01. Calcd. for $C_9H_{14}N_2O$: C, 65.03; H, 8.49; N, 16.85; O, 9.63%.

The infrared and ultraviolet spectra are shown in Table I.

3 - Amino - 4, 5, 8, 9 - tetrahydrocycloocta [C] iso-xazole (VII).—2-Chlorocyclooctenone oxime (2 g., 0.01 mol.) was treated with sodium cyanide (1 g., 0.02 mol.), in a manner similar to that described above, and a crystalline material, m. p. 81.5—82.5°C, was obtained in a 89% yield.

Found: C, 65.63; H, 7.41; N, 17.10. Calcd. for $C_9H_{12}N_2O$: C, 65.83; H, 7.37; N, 17.06%.

3 - Amino - 4, 5, 6, 7, 8, 9, 10, 11, 12, 13 - decahydro-cyclododeca[C]isoxazole (VIII).—2-Chlorocyclododecanone oxime (3.0 g.) was treated with sodium cyanide (2 g.) in dimethyl sulfoxide in a manner similar to that described above; after the usual work-up, a crystalline product, m. p. 119—121°C, was obtained in a 95% yield.

Found: C, 70.14; H, 9.96; N, 12.56. Calcd. for $C_{13}H_{22}N_2O$: C, 70.23; H, 9.97; N, 12.60%.

6) M. E. Kuehine, *J. Am. Chem. Soc.*, **81**, 5400 (1959).

3-Amino-4, 5, 8, 9, 12, 13-hexahydrododeca[C]-isoxazole (IX).—2-Chlorocyclododecadienone oxime (3.5 g., 0.015 mol.), prepared by the reaction of *cis, trans, trans*-1, 5, 9-cyclododecatriene with nitrosyl chloride, was treated with sodium cyanide (2 g., 0.04 mol.) suspended in dimethyl sulfoxide at 80—90°C for 3 hr. After the usual treatment of the reaction mixture, a pale-yellow solid (3.2 g., 95%) was obtained; it was recrystallized from ether-petroleum ether to give an analytical sample, m. p. 148—150°C.

Found: C, 71.32; H, 8.31; N, 12.83. Calcd. for $C_{13}H_{18}N_2O$: C, 71.52; H, 8.31; N, 12.83%.

3-Amino-4, 5, 8, 9, 12, 13-hexahydro-*trans*-6, *trans*-10-cyclododeca[C]isoxazole (X).—2-Chlorocyclododecadienone oxime (5 g., 0.022 mol.), prepared by the reaction of *trans, trans, trans*-1, 5, 9-cyclododecatriene with nitrosyl chloride, was treated with sodium cyanide (3 g., 0.06 mol.) under the conditions described above. After usual treatment, a solid (4.2 g., 90%) was obtained; an analytical sample showed a m. p. of 131—134°C.

Found: C, 71.90; H, 8.31; N, 12.84. Calcd. for $C_{13}H_{18}N_2O$: C, 71.52; H, 8.31; N, 12.83%.

The Reaction of 3-Chloronorcamphor Oxime with Sodium Cyanide.—3-Chloronorcamphor oxime (10 g.) was treated with two mole equivalents of sodium cyanide in dimethyl sulfoxide under the conditions described above. A solid product was obtained in a 90% yield, one showing a m. p. of 107—130°C after recrystallization from ether-petroleum ether. The infrared spectrum showed an absorption at 2245 cm^{-1} characteristic of a saturated nitrile group, besides those characteristic of the oxime group, and no absorption characteristic of an isoxazole ring system.

The NMR spectrum showed signals for the hydrogen next to the oxime group at τ 6.76 and τ 6.56, with coupling constants of 2.7 c. p. s. and 4.7 c. p. s. respectively. Therefore, the product must be a mixture of two stereoisomers (XI and XII) of 3-cyanonorcamphor oxime.

Found: C, 63.71; H, 6.71; N, 18.51. Calcd. for $C_8H_{10}N_2O$: C, 63.98; H, 6.71; N, 18.65%.

The Hydrogenation of VI with Palladium Charcoal.—3-Aminocycloocta[C]isoxazole (VI, 1.0 g.) was hydrogenated in ethanol with 5% palladium charcoal (0.25 g.) under atmospheric pressure while being stirred. Hydrogen (131 ml.) was absorbed during a 3 hr. period; this is in accord with the calculated amount (129 ml. for one mole equivalent of hydrogen). After filtration the alcoholic solution was evaporated to dryness to give a colorless solid (1.0 g.). This was recrystallized from ethanol to give an analytical sample, m. p. 111—113°C.

Found: C, 64.01; H, 9.46; N, 16.16. Calcd. for $C_9H_{16}N_2O$: C, 64.25; H, 9.59; N, 16.35%.

The infrared spectrum showed absorptions at 3400 (s), 3300 (w), 3150, 1642 (s), 1610 (s), and 1535 (m) cm^{-1}.

The ultraviolet spectrum showed a maximum at 242 mμ (ε, 8000). Therefore, the structure was identified as 2-amino-1-cyclooctene carbonamide (XIII).

The Hydrolysis of XIII with Potassium Hydroxide.—Compound XIII (3 g.) was added to a solution of potassium hydroxide (0.3 g.) dissolved in a mixture of water (25 ml.) and ethanol (25 ml.), the reaction mixture was then refluxed for 8 hr. After the ehanol had been evaporated, the residue was treated with hydrochloric acid and then extracted with ether-chloroform. The organic layer was dried and evaporated to dryness to give a pale-yellow solid (1.24 g., 42%). It was chromatographed on silica gel, using chloroform as an eluent; a crystalline substance, m. p. 106—108°C, was thus obtained. The infrared spectrum showed absorptions at 1710 cm^{-1} of carbonyl group, and 1670 and 1630 cm^{-1} of an amide group. The NMR spectrum showed signals at τ 6.48 for tertiary hydrogen. Therefore, the product was identified as 2-oxocyclooctanecarbonamide (XIV); it proved to be identical with an authentic sample prepared by the reaction of cyclooctanone and diethylcarbonate in the presence of sodium hydride and by subsequent hydrolysis.

Found: C, 64.07; H, 8.83; N, 8.34. Calcd. for $C_9H_{15}NO_2$: C, 63.88; H, 8.94; N, 8.28%.

The prolonged treatment of XIII with potassium hydroxide afforded cyclooctanone as a by-product.

The Hydrolysis of XIII with Hydrochloric Acid.—Compound XIII (1.0 g.) was added to a mixture of ethanol (30 ml.) and 1 N hydrochloric acid (20 ml.); then the reaction mixture was refluxed for 2 hr. The oil obtained by the extraction with ether-methylene chloride was chromatographed on silica gel using chloroform. The solid (0.78 g., 80%) obtained was identical with that obtained from treatment with potassium hydroxide.

BULLETIN OF THE CHEMICAL SOCIETY OF JAPAN VOL. 39 1129—1134 (1966)

Reactions of 2-Chlorocycloalkanone Oximes. III.[1] Displacement Reactions with Various Nucleophilic Reagents[2]

By Masaji OHNO, Seiichi TORIMITSU, Norio NARUSE, Masaru OKAMOTO and Ikuo SAKAI

Basic Research Laboratories, Toyo Rayon Co., Ltd., Tebiro, Kamakura

(Received July 22, 1965)

The displacement reactions of 2-chlorocycloalkanone oximes with various nucleophilic reagents, such as ammonia, primary and secondary amines, silver and sodium nitrite, sodium azide, Grignard reagents, and carbanions derived from acetylacetone and ethyl malonate, have been investigated. α-Alkylamino, α-nitro, α-azido, and α-alkyloximes of the 8- and 12-membered rings have been prepared in excellent yields, and those of the 6-membered ring, in moderate yields. It has been shown that 2-chlorocyclohexanone oxime hydrochloride can be treated directly with a large excess of the nucleophilic reagents. 2-Chlorocyclooctanone oxime was used in the free state, and 2-chloro-5, 9-cyclododecadienone oxime was first treated with nucleophilic reagents; the resulting α-substituted oximes of the 12-membered ring were hydrogenated to the corresponding saturated oximes with palladium charcoal. These reactions have shown that α-chlorocycloalkanone oximes have a potential synthetic utility.

In previous papers[1,3] of this series, we have described the preparation of 2-chlorocycloalkanone oximes by the reaction of disubstituted olefins or cycloolefins with nitrosyl chloride, i. e., the syntheses of 2-alkoxy-, 2-acyloxy-, and 2-alkylthio-cycloalkanone oximes. We have also described a simple way of preparing 3-aminocycloalka[C]isoxazoles. These results have clearly shown that α-chlorooximes obtained by the addition of nitrosyl chloride to cycloolefins have a potential synthetic utility besides the potential testing reagent for the unsaturation of natural products.[4]

In this report, we will investigate the displacement reactions of 2-chlorocycloalkanone oximes with various nucleophilic reagents, such as ammonia, primary amines, secondary amines, metal nitrite, sodium azide, Grignard reagents, and carbanions derived from acetylacetone and diethyl malonate, in an effort to establish the scope and limitations of the synthetic application of the α-chlorooximes. The general scheme of the reactions is shown by the following equations:

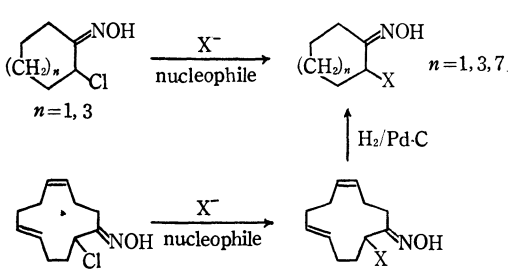

As usual in our procedure, the displacement reactions of 2-chlorocyclooctanone oxime with various amines were first investigated in detail, since this starting material is the most stable to handle and can be prepared easily in a state of free oxime.[3]

The treatment of 2-chlorocyclooctanone oxime with ammonia did not form 2-aminocyclooctanone oxime, but it did give 2, 2'-iminodicyclooctanone oxime in a 30% yield. Reactions with morpholine, piperidine, *n*-butylamine, and hydrazine gave the corresponding α-aminooximes in excellent yields, as had been expected. The same reaction was then applied successfully to 2-chlorocyclohexanone oxime and 2-chlorocyclododecadienone oxime to give the corresponding α-aminooximes. 2-Aminocyclododecadienone oximes obtained were selectively hydrogenated to 2-aminocyclododecanone oximes by catalytic reduction with palladium charcoal.

Since cyclododecene is not easily available[3] and since only *trans*-cyclododecene reacts with nitrosyl chloride, 2-aminocyclododecanone oxime has been prepared conveniently by the reaction of *cis*, *trans*, *trans*-1, 5, 9-cyclododecatriene with nitrosyl chloride. In the case of 2-chlorocyclohexanone oxime, the hydrochloride[3] was treated directly with a large excess of amines. Since the hydrochloride is unstable and is considered to be a mixture of mono- and dihydrochloride,[5] the yields could not be estimated exactly.

1) Part II: M. Ohno and N. Naruse, This Bulletin, **39**, 1125 (1966).

2) Presented at the 18th Annual Meeting of the Chemical Society of Japan, Osaka, April, 1965.

3) Part I: M. Ohno, N. Naruse, S. Torimitsu and M. Okamoto, This Bulletin, **39**, 1119 (1966).

4) L. J. Beckham, W. A. Fessler and M. A. Kise, *Chem. Revs.*, **48**, 369 (1951).

5) H. Saito, K. Nukada and M. Ohno, *Tetrahedron Letters*, **1964**, 2124.

Table I. Displacement reactions with various amines

α-Chlorooxime	Reagent	Product	M. p., °C	Yield, %
2-Chlorocyclooctanone oxime	$NH_3/NaNH_2$	2,2'-Iminodicyclooctanone oxime (I)	182	30
2-Chlorocyclooctanone oxime	Morpholine	2-Morpholinocyclooctanone oxime (II)	133—134	86
2-Chlorocyclooctanone oxime	Pyrrolidine	2-Pyrrolidinocyclooctanone oxime (III)	161—162	93
2-Chlorocyclooctanone oxime	Piperidine	2-Piperidinocyclooctanone oxime (IV)	162—163	81
2-Chlorocyclooctanone oxime	Aniline	2-Anilinocyclooctanone oxime (V)	135—136	91
2-Chlorocyclooctanone oxime	*n*-Butylamine	2-(*n*-Butylamino)-cyclooctanone oxime (VI)	134—135	87
2-Chlorocyclooctanone oxime	Hydroxylamine	2-(Oxyamino)cyclooctanone oxime (VII)	144—145	80
2-Chloro-5,9-cyclododeca-dienone oxime	Morpholine	2-Morpholino-5,9-cyclododecadienone oxime (VIII)	108—110	71
2-Chloro-5,9-cyclododeca-dienone oxime	Pyrrolidine	2-Pyrrolidino-5,9-cyclododecadienone oxime (IX)	112—114	81
2-Chloro-5,9-cyclododeca-dienone oxime	Piperidine	2-Piperidino-5,9-cyclododecadienone oxime (X)	100—103	92
2-Chlorocyclohexanone oxime	Morpholine	2-Morpholino-cyclohexanone oxime (XI)	117—118	80—90
2-Chlorocyclohexanone oxime	Pyrrolidine	2-Pyrrolidinocyclohexanone oxime (XII)	120—121	80—90
2-Chlorocyclohexanone oxime	Piperidine	2-Piperidinocyclohexanone oxime (XIII)	117—118	75—85
2-Chlorocyclohexanone oxime	*n*-Butylamine	2-(*n*-Butylamino)-cyclohexanone oxime (XIV)	79— 80	72—80

Table II. Displacement reactions with nitrite, azide, Grignard reagents, and carbanions

α-Chlorooxime	Reagent(solv.)	Product	M. p., °C	Yield, %
2-Chlorocyclooctanone oxime	$AgNO_2$(ether)	2-Nitrocyclooctanone oxime (XV)	95— 96	89
2-Chlorocyclooctanone oxime	$NaNO_2$(DMSO)	2-Nitrocyclooctanone oxime (XV)	95— 96	66
2-Chlorocyclooctanone oxime	$NaN_3(CH_3CN)$	2-Azidocyclooctanone oxime (XVI)	52— 53	75
2-Chlorocyclooctanone oxime	$H_2C(COOEt)_2$	Ethyl-2-oximmocyclooctylmolonate (XXI)	89— 90	95
2-Chlorocyclooctanone oxime	$H_2C(COCH_3)_2$	2-(Diacetylmethyl)cyclooctanone oxime (XXIV)	155—156	72
2-Chloro-5,9-cyclododecadienone oxime	$AgNO_2$(OMSO)	2-Nitro-5,9-cyclododecadienone oxime (XVI)	115—117	80
2-Chloro-5,9-cyclododecadienone oxime	NaN_3(OHSO)	2-Azido-5,9-cyclododecadienone oxime (XVII)	63— 65	80
2-Chloro-5,9-cyclododecadienone oxime	PhMgBr	2-Phenyl-5,9-cyclododecadienone oxime (XIX)	133—135	52
2-Chloro-5,9-cyclododecadienone oxime	PhC≡CMgBr	2-(Phenylethynyl)-5,9-cyclododecadienone oxime (XX)	120—121	60
2-Chloro-5,9-cyclododecadienone oxime	$H_2C(COOEt)_2$	Ethyl-2-oximinocyclododecadienylmalonate (XXII)	91— 92	96
2-Chloro-5,9-cyclododecadienone oxime	$H_2C(COCH_3)_2$	2-(Diacetylmethyl)cyclododecadienone oxime (XXV)	159—160	98
2-Chlorocyclohexanone oxime	$H_2C(COOEt)_2$	Ethyl-2-oximinocyclohexylmalonate (XXIII)	71— 72	69
2-Chlorocyclohexanone oxime	$H_2C(COCH_3)_2$	2-(Diacetylmethyl)cyclohexanone oxime (XXVI)	154—155	13

As in the case of displacement reactions with sodium salts of alcohols, carboxylic acids and ethanethiol, maximum yields in the present investigation were also obtained when amounts greater than two mole equivalents of amines were used.[6] These results are shown in Table I.

In order to introduce a strong electron-withdrawing substituent to the α-position of the oxime group, 2-chlorocycloalkanone oximes were treated with silver and sodium nitrite. α-Chlorooximes of 8- and 12-membered rings gave the corresponding α-nitrooximes in excellent yields when treated with silver nitrite in dimethylsulfoxide. Since the same reaction with 2-chlorocyclooctanone oxime in ether did not form 2-nitrocyclooctanone oxime at all and since the starting material was then recovered, dimethylsulfoxide is the most effective solvent for this reaction in these cases. This method is thus a new way of preparing α-nitrocycloalkanone oximes, which were formerly prepared by the reaction of cycloolefins with nitric oxide in the presence of oxygen.[7]

6) A. Cornow and H. D. Jordan, *Chem. Ber.*, **94**, 1960 (1961).

7) D. Klamann and W. Koser, *Angew. Chem.*, **76**, 591 (1964).

These results are summarized in Table II.

Next, the displacement reaction with azide ion has been investigated, since the negative charge of the ion is distributed over more than one polarizable atom and the ion is well known as a strong nucleophilic reagent.[8] The treatment of 2-chlorocyclooctanone oxime and of 2-chloro-5, 9-cyclododecadienone oxime with sodium azide in dimethylsulfoxide, ethanol or acetonitrile gave the corresponding α-azidooxime in 75 and 80% yields respectively. The structure is supported by the fact that the infrared spectrum showed a characteristic strong absorption, at 2140 cm^{-1}, of an asymmetric stretching vibration of azide.[9] Both of the α-azidooximes were hydrogenated with palladium charcoal in the presence of moist hydrochloric acid to give hydrochlorides of the corresponding α-aminoketones.

The reactions of α-chlorooximes of the acyclic system with Grignard reagents and carbanions to give higher oximes have been investigated by Dornow.[10] In the case of α-chlorooximes of cyclic systems, however, no investigation has been reported. To check this point, 2-chlorocycloalkanone oximes were treated with various Grignard reagents, such as phenylmagnesium bromide, ethylmagnesium bromide, and phenylethynylmagnesium bromide. The products from the reaction of the oximes of 2-chlorocyclohexanone and 2-chlorocyclooctanone with Grignard reagents were unstable oily materials, and all attempts to isolate pure substances were unsuccessful. However, the reaction of 2-chloro-5, 9-cyclododecadienone oxime with phenylmagnesium bromide and with phenylethynylmagnesium bromide gave the corresponding α-substituted oximes (Table II) successfully. It is of interest to note that 2-(phenylethyl)cyclododecadienone oxime has been converted into an allene derivative with sodium ethoxide.

Finally, displacement reactions with carbanions derived from various active hydrogen compounds were investigated. The treatments of the oximes of 2-chlorocyclohexanone, 2-chlorocyclooctanone, and 2-chloro-5, 9-cyclododecadienone with sodium salts of ethyl malonate and acetylacetone gave the corresponding α-substituted oximes (Table II). The yields of the products of the 8- and 12-membered rings were excellent, but those of the 6-membered ring were rather poor. The reactions of α-chlorocycloalkanone oximes with nitromethane, acetone, and ethyl acetate in the presence of a base did not afford the corresponding α-substituted oximes at all, but rather resinous matters, which might be formed by the polymerization of an α, β-unsaturated nitroso compound.

8) E. S. Gould, "Mechanism and Structure in Organic Chemistry," Henry Holt and Company, New York (1959), p. 250.
9) L. J. Bellamy, "The Infrared Spectra of Complex Molecules," John Wiley & Sons, Inc., New York (1958), p. 273.
10) A. Donow and H. D. Jordan, *Chem. Ber.*, **94**, 76 (1961).

The accumulated evidence of the displacement reactions of 2-chlorocycloalkanone oximes described above have established the following points: (1) Most of the nucleophilic reagents replace the chlorine atoms of 2-chlorocyclolakanone oximes smoothly. (2) No appreciable amounts of unsaturated compounds were formed in the displacement reactions of α-chlorooximes of cycloolefins. (3) α-Chlorooximes of the 8- and 12-membered rings can be transformed into α-substituted oximes in excellent yields, but that of the 6-membered ring affords the product in a moderate yield. These results suggest that the stability of the α, β-unsaturated nitroso compounds formed as intermediates during the reactions is dependent upon the ring size. (4) The α-chlorooximes obtained by the addition of nitrosyl chloride to cycloolefins have a potential synthetic utility.

Experimental[11]

The Reaction of 2-Chlorocyclooctanone Oxime with Ammonia.—2-Chlorocyclooctanone oxime was treated with ammonia in the presence of sodium amide in tetrahydrofuran. A colorless solid was obtained in a 30% yield, m. p. 182—183°C. The infrared spectrum showed an absorption at 1650 cm^{-1} due to an oxime group.

Found: C, 64.81; H, 9.87; N, 14.06. M. W. 298. Calcd. for $C_{16}H_{29}N_3O_2$: C, 65.05; H, 9.90; N, 14.23%. M. W., 295.42.

2-Morpholinocyclooctanone Oxime (II).—Morpholine (19 g.) and ethanol (10 ml.) were placed in a 300-ml. three-necked round bottom flask equipped with a stirrer, a reflux condenser, and a dropping funnel. 2-Chlorocyclooctanone oxime (17.5 g.) dissolved in 70 ml. of ethanol was then added to the solution over a 30-min. period. The reaction mixture was then stirred at room temperature for 3 hr. After the solvent had been removed under reduced pressure, a solid product (19.7 g.) was obtained after washing the residue with water. It was recrystallized from ethanol to give an analytical sample, m. p. 133—134°C.

Found: C, 63.50; H, 9.73; N, 12.32. Calcd. for $C_{12}H_{22}N_2O_2$: C, 63.68; H, 9.80; N, 12.39%. IR: 3300—3000, 1640, 1500, 1115 cm^{-1} (KBr).

2-Pyrrolidinocyclooctanone Oxime (III).—2-Chlorocyclooctanone oxime (17.5 g.) dissolved in 70 ml. of ethanol was treated with pyrolidine (20 g.) in ethanol (100 ml.) for 3 hr. After the solvent had been removed and the residue washed with water, a solid product (17.5 g.) was obtained; this was recrystallized from ethanol to give an analytical sample, m. p. 161—162°C.

Found: C, 68.26; H, 10.46; N, 13.15. Calcd. for $C_{12}H_{22}ON_2$: C, 68.53; H, 10.54; N, 13.32%. IR: 3300—3000, 1650, 1512, 1120, 1095 cm^{-1} (KBr).

2-Piperidinocyclooctanone Oxime (IV).—2-Chlorocyclooctanone oxime (26.3 g.) was treated with piperidine (25 g.) in ethanol. After a work-up similar to that described above, a solid product (28.5 g.) was obtained; it was recrystallized from ethanol to give analytical sample, m. p. 162—163°C.

Found: C, 69.48; H, 10.76; N, 12.51. Calcd. for

11) All melting points are uncorrected.

$C_{13}H_{24}ON_2$: C, 69.60; H, 10.78; N, 12.49%. IR: 3300—3000, 1643, 1500, 1100 cm^{-1} (KBr).

2-Anilinocyclooctanone Oxime (V).—2-Chlorocyclooctanone oxime (17.5 g.) was treated with aniline (37 g.) in ethanol and, after a similar work-up, a solid product (21.2 g.) was obtained; it was then recrystallized from ethanol to give an analytical sample, m. p. 135—136°C.

Found: C, 72.27; H, 8.73; N, 11.86. Calcd. for $C_{14}H_{20}ON_2$: C, 72.38; H, 8.68; N, 12.06%. IR: 3370, 3200—3100, 1610, 1520, 1500, 750 cm^{-1} (KBr).

2-(*n*-Butylamino)cyclooctanone Oxime (VI).—2-Chlorocyclooctanone oxime (17.5 g.) was treated wtih *n*-butylamine (30 g.) in ethanol; after the usual work-up, a solid product (19 g.), m. p. 134—135°C, was obtained.

Found: C, 67.82; H, 11.34; N, 13.27. Calcd. for $C_{12}H_{24}ON_2$: C, 67.88; H, 11.39; N, 13.19%. IR: 3250, 1642, 1500, 1100 cm^{-1} (KBr).

2-(Oxyamino)cyclooctanone Oxime (VII).—In a 500-ml. three necked round bottom flask equipped with a stirrer, a dropping funnel, and a reflux condenser there were placed 200 ml. of ethanol containing hydroxylamine (about 7 g.) and water containing sodium carbonate (10 g.). 2-Chlorocyclooctanone oxime (17.5 g.) dissolved in 70 ml. of ethanol was stirred into the solution over a period of 30 min. The reaction mixture was then refluxed for 2 hr. After the usual work-up, as described in the case of 2-morpholinocyclooctanone oxime (II), a solid product (13.1 g.), m. p. 144—145°C, was obtained

Found: C, 55.64; H, 9.18; N, 16.11. Calcd. for $C_8H_{16}O_2N_2$: C, 55.79; H, 9.36; N, 16.27%. IR: 3250, 1645, 1510, 1110 cm^{-1} (KBr).

2 - Morpholino-5, 9-cyclododecadienone Oxime (VIII).—2-Chlorocyclododecadienone oxime (23 g.) was treated with morpholine (18 g.) in ethanol for 3 hr. After the solvent had been removed under reduced pressure, an oily product was obtained. By adding an excess of water to the product, a solid material (19.7 g.) was obtained and recrystallized from methanol to give an analytical sample, m. p. 106—109°C. The infrared spectrum showed absorptions at 1650, 980, and 707 cm^{-1} characteristic of an oxime group, and of *traus* and *cis* double bonds respectively, and absorptions at 1000—1100 cm^{-1} characteristic of an morpholino group.

Found: C, 68.81; H, 9.36; N, 10.09. Calcd. for $C_{16}H_{26}O_2N_2$: C, 69.03; H, 9.41; N, 10.06%.

The Hydrogenation of VIII.—2-Morpholinocyclododecadienone oxime (VIII, 2.8 g.) dissolved in 100 ml. of acetic acid was hydrogenated with 10% palladium charcoal (1 g.) under atmospheric pressure and at room temperature. Two mole equivalents of hydrogen was absorbed in 3 hr. After the solvent had been removed, the reaction product was treated with a 4 N sodium hydroxide solution to afford a colorless solid. This was recrystallized from methanol to give an analytical sample, m. p. 104—106°C. The infrared spectrum showed no absorption for carbon-carbon double bonds, and it was consistent with 2-morpholinocyclododecanone oxime.

Found: C, 67.89; H, 10.63; N, 9.90. Calcd. for $C_{16}H_{30}O_2N_2$: C, 68.04; H, 10.71; N, 9.92%.

2 - Pyrrolidino-5, 9-cyclododecadienone Oxime (IX).—2-Chlorocyclododecadienone oxime (23 g.) was treated with pyrrolidine (28 g.) in ethanol at 60—70°C for 2 hr. After the usual work-up, a solid product (21 g.) was obtained and recrystallized from methanol, m. p. 112—113°C.

Found: C, 73.13; H, 9.89; N, 10.61. Calcd. for $C_{16}H_{26}ON_2$: C, 73.24; H, 9.99; N, 10.68%. IR 3200, 1660, 1510, 970, 720 cm^{-1} (KBr).

This product (2.6 g.) was then hydrogenated in acetic acid (100 ml.) with 10% palladium charcoal (1 g.). After the absorption of two mole equivalents of hydrogen, the solvent was removed under reduced pressure; the residue was neutralized with a 4 N sodium hydroxide solution to afford a colorless solid in a nearly quantitative yield. It melted at 146—148°C after recrystallization from methanol. The infrared spectrum was consistent with the structure of 2-pyrrolidinocyclododecanone oxime.

Found: C, 72.18; H, 11.35; N, 10.53. Calcd. for $C_{16}H_{30}ON_2$: C, 72.13; H, 11.35; N, 10.52%. IR: 3200, 1650, 1510 cm^{-1} (KBr).

2-Piperidino-5, 9-cyclododecadienone Oxime (X).—2-Chlorocyclododecadineone oxime (24 g.) was treated with piperidine (35 g.) in ethanol at 60—70°C for 3 hr. After the usual work-up, a solid product (22.3 g.) was obtained and recrystallized from methanol to give an analytical sample, m. p. 100—103°C.

Found: C, 73.80; H, 10.20; N, 10.06. Calcd. for $C_{17}H_{28}ON_2$: C, 73.86; H, 10.21; N, 10.14%. IR: 3300, 1660, 1120, 960, 705 cm^{-1} (KBr).

A part of the product (2.8 g.) was hydrogenated in acetic acid (100 ml.) with 10% palladium charcoal (1 g.). Two mole equivalents of hydrogen were absorbed during a 3-hr. period. After a work-up similar to that described in the case of 2-morpholinocyclododecanone oxime, a solid product was obtained in a nearly quantitative yield; this was recrystallized from methanol to give an analytical sample, m. p. 96—97°C.

Found: C, 72.58; H, 11.45; N, 9.95. Calcd. for $C_{17}H_{32}ON_2$: C, 72.80; H, 11.50; N, 9.99%. IR: 3300—3000, 1640, 1110 cm^{-1} (KBr).

2-Morpholinocyclohexanone Oxime (XI).—Hydrochloride of 2-chlorocyclohexanone oxime (25 g.) dissolved in ethanol (100 ml.) was stirred, over a 30-min. period, into a solution of morpholine (50 g.) in ethanol (15 ml.) at 40°C; the reaction was then continued at 70°C for another hour. After the solvent had been removed, the residue solidified and was washed with water. When recrystallized from ether, it showed a m. p. of 117—118°C.

Found: C, 60.39; H, 9.06; N, 14.07. Calcd. for $C_{10}H_{18}O_2N_2$: C, 60.58; H, 9.15; N, 14.13%.

2-Pyrrolidinocyclohexanone Oxime (XII).—The hydrochloride of 2-chlorocyclohexanone oxime (12 g.) was treated with pyrrolidine (23 g.) in ethanol. After the usual work-up, described above, a solid product (10.7 g.) was obtained and recrystallized from ether, m. p. 120—121°C.

Found: C, 65.78; H, 9.92; N, 15.35. Calcd. for $C_{10}H_{18}ON_2$: C, 65.89; H, 9.96; N, 15.37%.

2-Piperidinocyclohexanone Oxime (XIII).—The hydrochloride of 2-chlorocyclohexanone oxime (9.5 g.) was treated with piperidine (25 g.) in ethanol. After the usual work-up, a solid product (8.5 g.) was obtained and recrystallized from ether, m. p. 117—118°C.

Found: C, 67.24; H, 10.23; N, 14.26. Calcd. for $C_{11}H_{20}ON_2$: C, 67.30; H, 10.27; N, 14.27%.

2-(*n*-Butylamino)cyclohexanone Oxime (XIV).—The hydrochloride of 2-chlorocyclohexanone oxime (18.4 g.) was treated with *n*-butylamine (36 g.) in ethanol.

After the usual work-up, a solid product (16 g.) was obtained and recrystallized from ether, m. p. 79—80°C.

Found: C, 65.39; H, 10.88; N, 15.15. Calcd. for $C_{10}H_{20}ON_2$: C, 65.17; H, 10.94; N, 15.20%.

2-Nitrocyclooctanone Oxime (XV).—Silver nitrite (13.2 g.) and ether (100 ml.) were placed in a 500-ml. three-necked round-bottom flask equipped with a stirrer, a condenser, and a dropping funnel. A solution of 2-chlorocyclooctanone oxime (15 g.) dissolved in 150 ml. of ether was then vigorously stirred into the above suspended solution over a 1-hr. period, after which the reaction was continued for 4 hr. at room temperature. The precipitate of silver chloride was removed by filtration, and the filtrate was washed with water. The ethereal solution was dried over sodium sulfate and evaporated to dryness to give a yellow solid (14.2 g., 89.3%). It was dissolved in hot ligroin and treated with activated carbon to give a pale-yellow solid, which was then further recrystallized from ligroin to afford colorless needles, m. p. 95—96°C. The infrared spectrum showed absorptions at 3310 and 1640 cm^{-1} for the oximino group, and at 1550 cm^{-1} (strong) for the nitro group.

Found: C, 51.71; H, 7.66; N, 14.85. Calcd. for $C_8H_{14}O_3N_2$: C, 51.60; H, 7.58; N, 15.04%.

In a separate run, 2-chlorocyclooctanone oxime (5 g.) was treated with silver nitrite (4.5 g.) in dimethylsulfoxide at room temperature for 1 hr. The ether extract of the reaction mixture was dried and evaporated to dryness to give 4.5 g. of a yellow solid, which was confirmed to be identical with the product obtained from the above reaction using ether as the solvent. When sodium nitrite was used in dimethylsulfoxide, 2-nitrocyclooctanone oxime was obtained in about a 66% yield, but in ether no detectable amount of 2-nitrocyclooctanone oxime was obtained.

2-Nitro-5, 9-cyclododecadienone Oxime (XVI).—2-Chlorocyclododecadienone oxime (10 g.) was treated with silver nitrite (7 g.) in dimethylsulfoxide at room temperature for 1 hr. After treatment similar to that described above, a yellow solid (8.4 g.) was obtained; it was recrystallized from ligroin to give a colorless solid, m. p. 115—117°C. The infrared spectrum showed absorptions at 980 and 707 cm^{-1} characteristic of *trans* and *cis* double bonds respectively, at 3320 and 1640 cm^{-1} characteristic of an oximino group, and at 1560 cm^{-1} characteristic of nitro group.

Found: C, 60.54; H, 7.68; N, 11.47. Calcd. for $C_{12}H_{18}O_3N_2$: C, 60.48; H, 7.61; N, 11.76%.

2-Azidocyclooctanone Oxime (XVII).—2-Chlorocyclooctanone oxime (36 g.) was treated with sodium azide (14g.) in acetonitrile while being stirred and heated on a steam bath for 5 hr. To the reaction mixture, water (500 ml.) was added, and the ethereal extract was dried and evaporated to dryness to give a solid product. It was recrystallized from a mixed solvent of ether and petroleum ether to give an analytical sample, m. p. 52—53°C.

Found: C, 52.45 : H, 7.69; N, 30.66. Calcd. for $C_8H_{14}ON_4$: C, 52.73; H, 7.74; N, 30.65%.

The product was hydrogenated in moist ethanol containing hydrochloric acid with 5% palladium charcoal under atmospheric pressure. The infrared spectrum of the hydrogenated product, m. p. 186—188°C (decomp.) showed a strong absorption at 1705 cm^{-1} characteristic of 8-membered ring ketone and one at 3300 cm^{-1} characteristic of an amino group. Thus the structure may be though to be that of the hydrochloride of 2-aminocyclooctanone.

2-Azido-5, 9-cyclododecadienone Oxime (XVIII).—2-Chlorocyclododecadienone oxime (68.25 g.) was treated with sodium azide (23.4 g.) in dimethyl sulfoxide (600 ml.) while being vigorously stirred and heated on a steam bath for 12 hr. After treatment similar to that described above, a solid product (56 g.) was obtained and recrystallized from a mixed solvent of ether and petroleum ether to give a colorless material, m. p. 63—65°C.

Found: C, 61.77; H, 7.85; N, 24.11. Calcd. for $C_{12}H_{18}ON_4$: C, 61.51; H, 7.74; N, 23.91%.

In order to confirm the structure, the product was hydrogenated with 5% palladium charcoal in moist ethanol containing hydrochloric acid. The infrared spectrum of the hydrogenated procuct, m. p. 223°C (decomp.), showed a strong absorption at 1704 cm^{-1} characteristic of 12-membered ring ketone, and one at 3320 cm^{-1} characteristic of an amino group, with neither the absorption at 980 nor that at 707 cm^{-1} characteristic of *trans* and *cis* double bonds respectively.

Found: C, 61.30; H, 10.28; N, 6.06; Cl, 15.30. Calcd. for $C_{12}H_{24}NOCl$: C, 61.20; H, 10.35; N, 5.96; Cl, 15.05%.

2-Phenyl-5, 9-cyclododecadienone Oxime (XIX).—In a 2-l. three necked round-bottom flask equipped with a stirrer, a condenser, and a dropping funnel, magnesium (7.3 g.) was placed. A solution of bromobenzene (47.1 g.) dissolved in tetrahydrofuran (400 ml.) was then vigorously stirred into the reaction vessel. After phenyl magnesium bromide had been made, 2-chlorocyclododecadienone oxime (22.75 g.) dissolved in tetrahydrofuran (100 ml.) was added slowly at 20—25°C and the reaction was continued for 15 hr. at room temperature. The reaction mixture was treated with ice, diluted hydrochloric acid, and extracted with ether. The ethereal extract was treated with a sodium carbonate solution and then with a saturated solution of sodium chloride, dried, and evaporated to dryness to give a crude product (20 g.). This was recrystallized from methanol, m. p. 133—135°C.

Found: C, 80.13; H, 8.54; N, 5.12. Calcd. for $C_{18}H_{23}ON$: C, 80.25; H, 8.61; N, 5.20%. IR: 3300, 1660, 960, 760, 710 cm^{-1} (KBr).

2-(Phenylethynyl)cyclododecadienone Oxime (XX).—2-Chlorocyclododecadienone oxime was treated with phenylethynyl magnesium bromide under conditions similar to those described above. 2-(Phenylethynyl)-5, 9-cyclododecadienone oxime was thus obtained in a 60% yield, m. p. 120—121°C.

Found: C, 81.63; H, 7.90; N, 4.67. M. W., 306. Calcd. for $C_{20}H_{23}ON$: C, 81.87; H, 7.90; N, 4.77%. M. W., 293.

The compound XX was treated with sodium ethoxide to afford an isomer, m. p. 136—139°C. The infrared spectrum showed an absorption at 1930 cm^{-1} characteristic of allene and not the absorption at 2240 cm^{-1} characteristic of the acetylene group observed in the compound XX.

Found: C, 81.92; N, 8.01; N, 4.77%.

Ethyl α-Oximinocyclooctylmalonate (XXI).—Sodium salt of ethyl malonate was prepared by a reaction of sodium (5.3 g.) with ethyl malonate (35 ml.) in ether (200 ml.). To the solution there was added, drop by drop, 2-chlorocyclooctanone oxime (17.5 g.)

dissolved in ether (100 ml.) over a 1-hr. period; the reaction was then continued for an additional 2 hr. The excess of the sodium salts was decomposed with ice water, and the reaction mixture was extracted with ether. The ethereal extract was dried and cooled at 0°C to deposit a colorless solid. After the solid had been separated by filtration, the filtrate was evaporated to remove the ether and the ethyl malonate, thus giving a solid product. The combined solid materials (28.5 g.) were recrystallized from ethanol to give a pure substance, m. p. 89—90°C. The infrared spectrum was consistent with that of ethyl α-oximinocyclooctylmalonate (XXI).

Found: C, 60.35; H, 8.37; N, 4.66. M. W., 300. Calcd. for $C_{15}H_{25}O_5N$: C, 60.18; H, 8.42; N, 4.68%. M. W., 299.

Ethyl α-Oximinocyclododecadienylmalonate (XXII).—According to a procedure similar to that described above, compound XXII (33.8 g.) was prepared by the reaction of 2-chlorocyclododecadienone oxime (22.8 g.) with sodium salt of ethyl malonate. It was recrystallized from ethanol to give an analytical sample, m. p. 91—92°C.

Found: C, 64.93; H, 8.32; N, 3.99. M. W., 359. Calcd. for $C_{19}H_{29}O_5N$: C, 64.95; H, 8.35; N, 3.94%. M. W., 351.

Ethyl α-Oximinocyclohexylmalonate (XXIII).—According to a procedure similar to that described above, compound XXIII (18.8 g.) was prepared by the reaction of hydrochloride of 2-chlorocyclohexanone oxime with sodium salt of ethylmalonate. It was recrystallized from ethanol to give an analytical sample, m. p. 71—72°C.

Found: C, 57.41; H, 7.78; N, 5.07. M. W., 274. Calcd. for $C_{13}H_{21}O_5N$: C, 57.55; H, 7.80; N, 5.16. M. W., 271.

2-(Diacetylmethyl)cyclooctanone Oxime (XXIV).—Sodium salt of acetylacetone was prepared from sodium (5.3 g.) and acetylacetone (50 ml.) in ether (200 ml.). 2-Chlorocyclooctanone oxime (17.5 g.) was then stirred into the above solution at 0—5°C over a 1-hr. period. After 2 hr., the reaction mixture was treated with ice water in ordor to decompose the excess of the sodium salt. A colorless solid (17.2 g.) was thus obtained; it was recrystallized from ethanol, m. p. 155—156°C. IR (cm^{-1}): 3010, 2925, 2850, 2560, 1708, 1605, 1255, 1205, 1160, 1150. UV: λ_{max}^{EtOH} 240 mμ (ε, 10700); NMR(τ), 6.30 (1 H, doublet), 6.77 (1 H, multiplet), 7.65 (6 H, singlet). This spectroscopic evidence shows that the structure is 2-(diacetylmethyl)cyclooctanone oxime (XXIV).

Found: C, 65.31; H, 8.85; N, 5.82. M. W., 249. Calcd. for $C_{13}H_{21}O_3N$: C, 65.24; H, 8.85; N, 5.85%. M. W., 239.

2-(Diacetylmethyl)cyclododecadienone Oxime (XXV).—According to a procedure similar to that described above, compound XXV (29 g.) was obtained by the reaction of 2-chlorocyclododecadienone oxime (22.8 g.) with sodium salt of acetylacetone. It was recrystallized from ethanol to give an analytical sample, m. p. 159—160°C. IR (cm^{-1}): 3000—3100, 1705, 1595; UV: λ_{max}^{EtOH} 241 mμ (ε, 13000). NMR (τ), 4.5 (4H, m), 6.30 (1H, d), 6.9 (1H, m), 7.67 (6H, singlet).

Found: C, 69.90; H, 8.54; N, 4.68. M. W., 308. Calcd. for $C_{17}H_{25}O_3N$: C, 70.07; H, 8.65; N, 4.81%. M. W., 301.

2-(Diacetylmethyl)cyclohexanone Oxime (XXVI).—According to a procedure similar to that described above, compound XXVI (2.8 g.) was prepared by the reaction of hydrochloride of 2-chlorocyclohexanone oxime (18.4 g.) with sodium salt of acetylacetone. It was recrystallized from ethanol, m. p. 154—155°C.

IR (cm^{-1}), 3050, 1710, 1630. UV: λ_{max}^{EtOH} 239.5 mμ (ε, 10000).

Found: C, 62.45; H, 8.19; N, 6.59. M. W., 210. Calcd. for $C_{11}H_{17}O_3N$: C, 62.54; H, 8.11; N, 6.63%. M. W., 211.

BULLETIN OF THE CHEMICAL SOCIETY OF JAPAN VOL. 39 1134—1146 (1966)

The Molecular Structure and Force Constants of Boron Trifluoride and Boron Trichloride

By Shigehiro KONAKA*, Yoshitada MURATA, Kozo KUCHITSU and Yonezo MORINO

Department of Chemistry, Faculty of Science, The University of Tokyo, Hongo, Tokyo

(Received August 4, 1965)

The interatomic distances and the mean amplitudes of BF_3 and BCl_3 have been determined, by the sector-microphotometer method of gas electron diffraction, to be: $r_g(B-F)=1.3156\pm 0.0044$ Å, $r_g(F\cdots F)=2.2733\pm 0.0041$ Å, $l(B-F)=0.0398\pm 0.0029$ Å, and $l(F\cdots F)=0.0541\pm 0.0020$ Å for BF_3 and $r_g(B-Cl)=1.7421\pm 0.0044$ Å, $r_g(Cl\cdots Cl)=3.0134\pm 0.0060$ Å, $l(B-Cl)=0.0505\pm 0.0023$ Å, and $l(Cl\cdots Cl)=0.0700\pm 0.0023$ Å for BCl_3. The force constants have also been determined from the mean amplitudes. Their values are in good agreement with those obtained by the isotopic shifts and by the Urey-Bradley force field. The complex scattering factors for B, F, and Cl have been calculated from the Hartree-Fock potential, and it has been shown that the background intensity and the mean amplitudes of BF_3 and BCl_3 are much better accounted for by these scattering factors than by those calculated from the Thomas-Fermi potential.

The force constants of molecules are usually determined from their vibrational frequencies. In most cases, however, the number of observable frequencies is not sufficient for all the force constants in a general quadratic form of the potential function to be determined. In order to overcome this difficulty, it is a common procedure to assume a simple model such as the Urey-Bradley force field, or to use the isotopic shifts of the vibrational frequencies. A more desirable way for determining the force field directly from experiment is to make use of the phenomena closely connected with the force field of the molecule. The mean amplitudes obtained by electron diffraction have thus been used to measure the force constants of several molecules with the aid of vibrational frequencies.[1-3]

The principal purpose of the present report is to determine the structure of boron trifluoride and boron trichloride as accurately as possible, and also to determine the force constants of these molecules from the experimental mean amplitudes. The resulting force constants will be compared with those obtained by other methods. The theoretical scattering factors will also be critically examined on the basis of the experimental mean amplitudes and backgrounds.

The atomic distances in boron trifluoride and trichloride were formerly determined by the visual method. The results obtained by Lévy and Brockway[4] were: $r(B-F)=1.30\pm0.02$ Å, $r(F-F)=2.25\pm0.03$ Å, $r(B-Cl)=1.73\pm0.02$ Å and $r(Cl-Cl)=2.99\pm0.03$ Å, while the results obtained by Braune and Pinnow[5] and those obtained by Sutton et al.[6] were $r(B-F)=1.31$ Å and $r(B-Cl)=1.76\pm0.02$ Å respectively.

During the course of the analysis of the mean amplitudes, it has been made clear that some property of the *l-l* curve is closely related to an empirical law known in spectroscopy regarding the off-diagonal elements of the $\boldsymbol{L}$ matrix. The results will be discussed in the Appendix.

Experimental

The diffraction photographs were taken with an apparatus equipped with an r^3-sector[7] at the camera length of 11.8 cm. The accelerating voltage (43—49 kV.) was automatically stabilized within 0.1%.

The sample of boron trifluoride was kindly provided by Dr. Ryohei Nakane of the Institute of Physical and Chemical Research, and that of boron trichloride, by the Central Research Institute of the Tokyo Shibaura Electric Co. The gas sample was led into the diffraction chamber through a drum-type nozzle at the temperature of 16°C for BF_3 and at 31°C for BCl_3. KEL-F stopcock grease was used to avoid the erosion of the lubricant. The vacuum of the chamber, initially 1—2 $\times10^{-5}$ mmHg, was kept under 1×10^{-4} mmHg even when the gas was introduced into the chamber. The beam current was about 0.006 μ amp., and the exposure time was about 3 minutes.

The patterns were recorded on Fuji Process Hard plates and were developed at 20°C for 5 min. with an FD-131 developer. The wavelengths of the primary electron beam were measured by using the transmission patterns of gold foil.

In order to make sure that the reference gold foil was placed exactly at the position of the diffraction center, gas patterns were also taken with the nozzle rotated around the nozzle axis by 180° by using the sample of boron trifluoride[8] (Fig. 1).

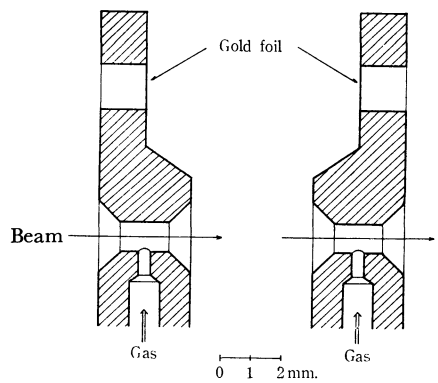

Fig. 1. Cross section of the nozzle used in the present study: normal orientation (left) and reversed orientation (right).

Photographic densities were measured using a Rigaku-Denki MP-3 microphotometer. In order to eliminate undesirable effects of the time lag of this recorder, the plates were scanned along the diameter; the charts thus obtained were measured and averaged on both sides of the center.[8] Four plates at the normal position of the nozzle and three plates at the reversed position were used for the structure analysis of boron trifluoride. Six plates at the normal position were used for the analysis of boron trichloride.

The optical densities of these plates were all between 0.6 and 0.1, where the linear relation between the density and the electron intensity has been confirmed.[9]

Analysis

The molecular intensity curve was obtained by drawing a smooth background line through the intensity curve, which had been corrected for the deviation of the sector shape from an ideal r^3 curve. In order to investigate the effects of atomic scattering factors on the molecular parameters, three

* Present address: Department of Chemistry, Faculty of Science, Hokkaido University, Sapporo, Japan.

1) Y. Morino, Y. Nakamura and T. Iijima, *J. Chem. Phys.*, **32**, 643 (1960).
2) M. Iwasaki and K. Hedberg, ibid., **36**, 594 (1962).
3) Y. Morino and Y. Murata, This Bulletin, **38**, 104 (1965).
4) H. A. Lévy and L. O. Brockway, *J. Am. Chem. Soc.*, **59**, 2085 (1937).
5) H. Braune and P. Pinnow, *Z. physik. Chem.*, **B35**, 239 (1937).
6) A. H. Gregg, G. C. Hampson, G. I. Jenkins, P. L. F. Jones and L. E. Sutton, *Trans. Faraday Soc.*, **33**, 852 (1937).
7) Y. Morino and K. Kuchitsu, *J. Chem. Phys.*, **28**, 175 (1958).
8) Y. Morino and H. Uehara, to be published.
9) Y. Morino and T. Iijima, This Bulletin, **35**, 1661 (1962).

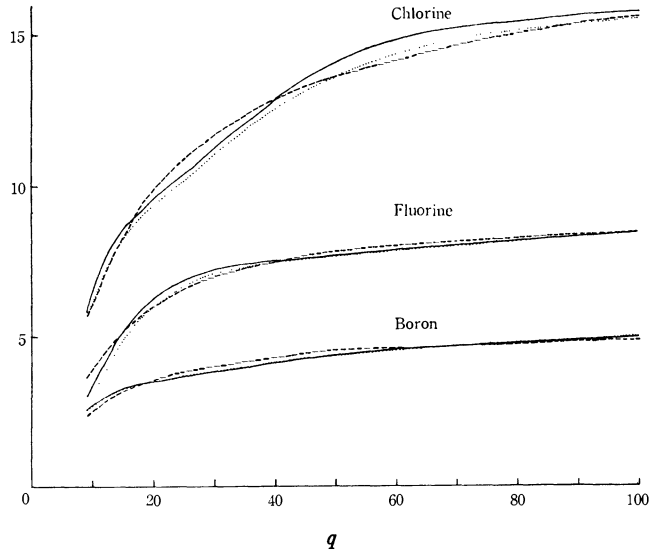

Fig. 2. The atomic scattering factors for electron diffraction.

—— $\frac{h^2s^2}{8\pi^2me^2}f^{B}=Z-f_X$, where f^{B} is the Born scattering factor and f_X is the atomic form factor for X-rays.

---- $\frac{h^2s^2}{8\pi^2me^2}|f|_{T.F.}$, where $|f|_{T.F.}$ is the absolute value of the complex scattering factor calculated from the Thomas-Fermi potential.

..... $\frac{h^2s^2}{8\pi^2me^2}|f|_{H.F.}$, where $|f|_{H.F.}$ is the absolute value of the complex scattering factor calculated from the Hartree-Fock potential.

kinds of atomic scattering factors were used for each atom (Fig. 2). The first, the Born scattering factor, f^{B}, was obtained by taking an appropriate average of the atomic form factors, f_x, calculated by several authors.[10-13] In the first Born approximation, the scattering factor, f^{B}, is equal to $8\pi^2me^2(Z-f_x)/h^2s^2$.[14] The second was the complex atomic scattering factor, $|f|_{T.F.}e^{i\eta_{T.F.}}$, calculated by Ibers and Hoerni using the partial-waves method based on the Thomas-Fermi potential.[15] The phase shift, $\eta_{T.F.}$, was also used, together with the f^{B} of the first set as $f^{B}e^{i\eta_{T.F.}}$. The third was the scattering factor, $|f|_{H.F.}e^{i\eta_{H.F.}}$, calculated by the present authors by using the partial-waves method based on the Hartree-Fock potential[16] (Table I). The inelastic scattering factors were taken from the table given by Bewilogua.[17]

By using the intensity curve from each plate, the molecular structure was analyzed by the method of least squares.[18] The theoretical expression of the molecular intensity is:

$$qM(q) = k\sum_i\sum_j{}' A_{ij}\mu_{ij}\cos\Delta\eta_{ij}\sin\frac{\pi}{10}q\left[r_{aij} - \left(\frac{\pi}{10}q\right)^2\kappa_{ij}\right]\exp\left[-\frac{1}{2}\left(\frac{\pi}{10}q\right)^2 l_{ij}^2\right] \quad (1)$$

$$A_{ij} = \frac{10}{\pi}\frac{1}{r_{aij}}\frac{Z_iZ_j}{\sum_k Z_k(Z_k+1)} \quad (2)$$

$$\mu_{ij} = \frac{|F_i||F_j|}{\sum_k|F_k|^2+\sum_k S_k}\frac{\sum_k Z_k(Z_k+1)}{Z_iZ_j},$$

$$|F| = h^2s^2|f|/8\pi^2me^2 \quad (3)$$

The parameters to be determined by the least-squares analysis were the atomic distances, r_a(B–X) and r_a(X–X), the mean amplitudes, l(B–X) and l(X–X), and the index of resolution, k.

The anharmonicity parameters, κ, were estimated by assuming potential functions of the Morse type for both the bonded B–X and the non-bonded X–X pairs; they were not varied as parameters. The following rough approximation was used:[3,19]

10) J. A. Ibers, *Acta Cryst.*, **10**, 86 (1957).
11) J. Berghuis et al., ibid., **8**, 478 (1955).
12) Y. Tomiie and C. H. Stam, ibid., **11**, 126 (1958).
13) H. Viervoll aad O. Ögrim, ibid., **2**, 277 (1949).
14) P. Debye, *J. Chem. Phys.*, **9**, 55 (1941).
15) J. A. Ibers and J. A. Hoerni, *Acta Cryst.*, **7**, 405 (1954).
16) J. Karle and R. A. Bonham, *J. Chem. Phys.*, **40**, 1396 (1964).
17) L. Bewilogua, *Physik. Z.*, **32**, 740 (1931).
18) Y. Morino, K. Kuchitsu, T. Iijima and Y. Murata, *J. Chem. Soc. Japan, Pure Chem. Sect.* (*Nippon Kagaku Zasshi*), **83**, 803 (1962).
19) K. Kuchitsu and L. S. Bartell, *J. Chem. Phys.* **35**, 1945 (1961).

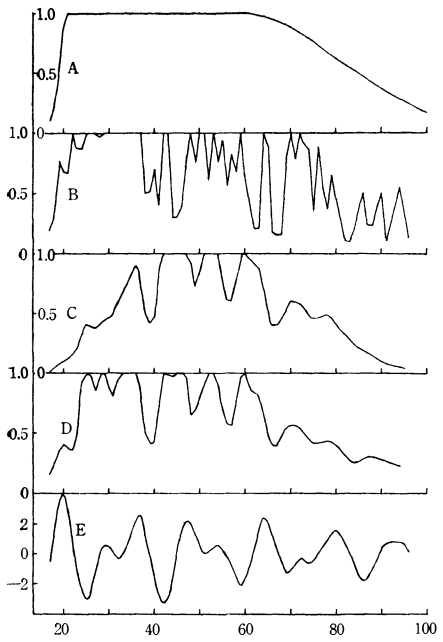

Fig. 3a.

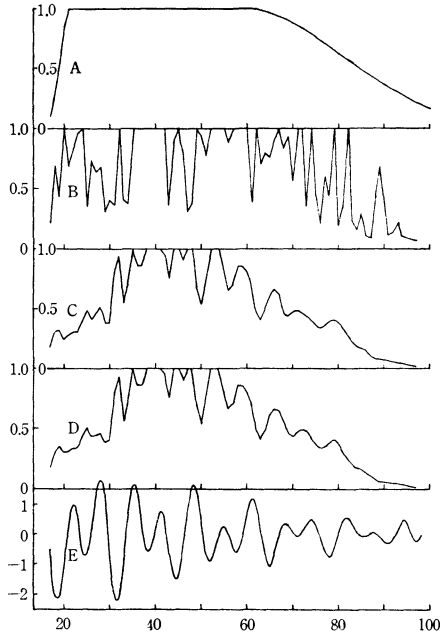

Fig. 3b.

Fig. 3. Weight functions for the least-squares analysis.
(a) Weight functions used for BF_3. (b) Weight functions used for BCl_3.
(A) A conventional weight function. (B) Weights assumed to be inversely proportional to the square of the standard deviation $\sigma(q)$ of the molecular intensities $qM(q)$. (C) Weights estimated from the residuals of the least-squares fitting by the procedure described in Ref. 21. (D) Modification of (C) by the use of σ_m estimated from the standard deviation $\sigma(q)$ of the observed intensity curves. (E) Molecular intensity curves, $qM(q)$.

$$\kappa(\text{B-X}) \simeq \frac{1}{9} l^2(\text{B-X}) \langle \Delta z(\text{B-X}) \rangle \simeq \frac{a}{6} l^4(\text{B-X})$$

$$\kappa(\text{X-X}) \simeq \frac{\sqrt{3}}{9} l^2(\text{X-X}) \langle \Delta z(\text{B-X}) \rangle$$

$$\simeq \frac{\sqrt{3}}{6} a l^2(\text{B-X}) l^2(\text{X-X}) \qquad (4)$$

The anharmonicity constant, a, was estimated to be about 2 $Å^{-1}$.[20]

The initial least-squares analysis was based on a conventional weight function, A, which is shown in Fig. 3. In order to examine the effect of the choice of weight functions on the parameter values, however, three additional weight functions were estimated (Fig. 3). The weight function B was assumed to be inversely proportional to the square of the standard deviation, $\sigma(q)$, of the molecular intensities, $qM(q)$.[9] The other functions, C and D, were calculated by estimating the standard deviation of the population of $qM(q)$, σ_m, which is related to the errors of the measurement of the abscissa and the ordinate of the photometer chart as follows:[21]

$$\sigma_m^2 = G_x^2 \cdot \sigma_x^2 + G_y^2 \cdot \sigma_y^2 \qquad (5)$$

The weight C was obtained in a way similar to that reported previously;[3] that is, σ_m^2 was first estimated from the residuals of the least-squares fitting and was then improved by eliminating the non-essential irregularities of σ_y.

The estimation of σ_m^2 by this procedure is not always reliable, since it tends to put too much weight on the points where the residuals are accidentally very small, while the weights for other points may be severely underestimated. Such effects may be partly compensated for, because the residuals are averaged over several plates and because the weight function is modified by the smoothing of σ_y. It seems to be preferable, however, to estimate σ_m^2 by the variance of the observed intensity curves, $\sigma^2(q)$, and not by the least-squares residuals alone. The weight function D was, accordingly, obtained from $\sigma^2(q)$, with modification by means of Eq. 5. The weight functions were normalized in such a way that about 15% of the observations had the full weight. Figure 4 shows a typical illustration of the observed and smoothed σ_y values which is similar to Fig. 2a of Ref. 21. The σ_y curve was

20) E. R. Lippincott and R. Schroeder, ibid., **23**, 1131 (1955).
21) Y. Morino, K. Kuchitsu and Y. Murata, *Acta Cryst.*, **18**, 549 (1965).

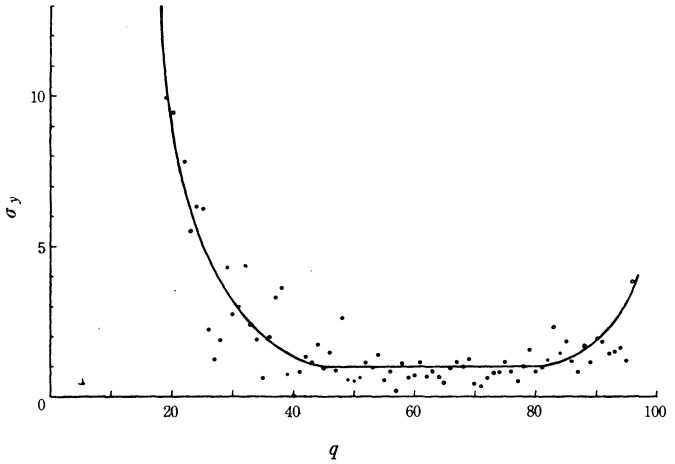

Fig. 4. A typical illustration of the standard error σ_y in the measurement of the ordinate of the photometer chart estimated from the standard error σ_m of $qM(q)$ based on the residuals of the least-squares fitting.

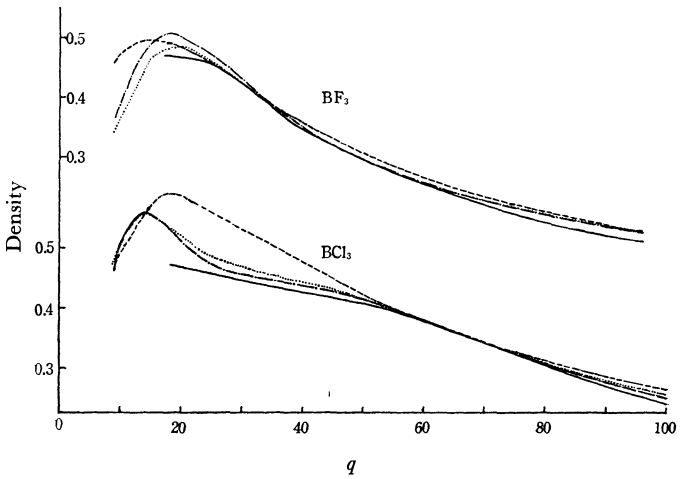

Fig. 5. Comparison of the observed with the theoretical background.

——— Observed.
—·—· f^B
------ $|f|_{T.F.}$
····· $|f|_{H.F.}$
} Theoretical.

TABLE I. COMPLEX SCATTERING FACTORS AT 40 kV. CALCULATED FROM THE HARTREE-FOCK POTENTIALS. ($|f|$ in Å units and η in radians)

$\theta°$	s(Å^{-1})	B		F		Cl	
		$\|f\|$	η	$\|f\|$	η	$\|f\|$	η
0	0	3.06	0.041	1.93	0.087	5.22	0.121
1	1.822	1.98	0.058	1.66	0.098	3.93	0.152
2	3.644	0.912	0.100	1.15	0.129	2.17	0.239
4	7.288	0.273	0.193	0.501	0.227	0.761	0.467
6	10.929	0.134	0.252	0.249	0.334	0.403	0.630
8	14.567	0.082	0.294	0.146	0.425	0.255	0.753
10	18.201	0.055	0.332	0.096	0.496	0.175	0.865
12	21.829	0.040	0.360	0.068	0.554	0.126	0.967
16	29.064	0.023	0.415	0.040	0.643	0.074	1.15
20	36.263	0.015	0.462	0.027	0.715	0.049	1.29
24	43.418	0.011	0.498	0.019	0.777	0.034	1.41
28	50.521	0.008	0.523	0.014	0.828	0.026	1.51

found to be a slowly-varying function of q, while the magnitude of the random experimental errors of the ordinate measurements was comparable with the uncertainty associated with the minimum scale division, as was discussed in Ref. 21.

The results of the least-squares analysis obtained by using the above four kinds of weight functions are listed in Table II. The symbol σ_1 in the table denotes the standard deviation derived by the least-squares fitting, divided by $\sqrt{n}$ so as to represent the

Table II. Results of the least-squares analysis
(r and l in Å units)

(A) Conventional weights

		r_a(B-X)	r_a(X-X)	l(B-X)	l(X-X)	index
BF_3	Average	1.3154	2.2737	0.0410	0.0568	0.983
normal	σ_1	0.0004	0.0005	0.0007	0.0007	0.008
direction	σ_2	0.0016	0.0016	0.0009	0.0008	0.008
BF_3	Average	1.3138	2.2705	0.0412	0.0569	0.974
reversed	σ_1	0.0006	0.0007	0.0009	0.0009	0.010
direction	σ_2	0.0014	0.0016	0.0011	0.0006	0.006
BCl_3	Average	1.7421	3.0143	0.0506	0.0736	1.010
normal	σ_1	0.0006	0.0004	0.0008	0.0006	0.008
direction	σ_2	0.0015	0.0018	0.0008	0.0005	0.016

(B) Weights estimated from the variance in the molecular intensities.

		r_a(B-X)	r_a(X-X)	l(B-X)	l(X-X)	index
BF_3	Average	1.3149	2.2732	0.0395	0.0560	0.969
normal	σ_1	0.0005	0.0006	0.0008	0.0007	0.007
direction	σ_2	0.0013	0.0014	0.0009	0.0005	0.007
BF_3	Average	1.3131	2.2697	0.0389	0.0563	0.959
reversed	σ_1	0.0007	0.0008	0.0010	0.0010	0.010
direction	σ_2	0.0012	0.0013	0.0011	0.0009	0.006
BCl_3	Average	1.7419	3.0140	0.0505	0.0736	1.011
normal	σ_1	0.0005	0.0004	0.0007	0.0005	0.007
direction	σ_2	0.0014	0.0016	0.0006	0.0004	0.013

(C) Weights estimated from the residuals of the least-squares fitting

		r_a(B-X)	r_a(X-X)	l(B-X)	l(X-X)	index
BF_3	Average	1.3154	2.2739	0.0407	0.0567	0.978
normal	σ_1	0.0003	0.0004	0.0006	0.0006	0.007
direction	σ_2	0.0017	0.0016	0.0010	0.0007	0.009
BF_3	Average	1.3138	2.2707	0.0409	0.0566	0.964
reversed	σ_1	0.0004	0.0005	0.0008	0.0007	0.009
direction	σ_2	0.0014	0.0017	0.0010	0.0005	0.004
BCl_3	Average	1.7418	3.0135	0.0503	0.0739	1.009
normal	σ_1	0.0005	0.0004	0.0007	0.0005	0.007
direction	σ_2	0.0014	0.0017	0.0008	0.0006	0.015

(D) Modifications of (C) by the use of the σ_m estimated from the standard deviation $\sigma(q)$ of the observed intensity curves.

		r_a(B-X)	r_a(X-X)	l(B-X)	l(X-X)	index
BF_3	Average	1.3151	2.2736	0.0403	0.0561	0.970
normal	σ_1	0.0004	0.0005	0.0008	0.0007	0.008
direction	σ_2	0.0016	0.0015	0.0010	0.0008	0.009
BF_3	Average	1.3136	2.2704	0.0399	0.0563	0.957
reversed	σ_1	0.0006	0.0007	0.0010	0.0009	0.010
direction	σ_2	0.0014	0.0017	0.0011	0.0008	0.005
BCl_3	Average	1.7417	3.0136	0.0503	0.0738	1.007
normal	σ_1	0.0005	0.0004	0.0007	0.0005	0.007
direction	σ_2	0.0014	0.0017	0.0007	0.0006	0.015

standard deviation for the average value where n is the number of intensity curves. The symbol σ_2 is the standard deviation evaluated by the fluctuation among several sets of the observed values,[3,21] $\sigma_2=\sqrt{\sum(X_i-X)^2/n(n-1)}$. While there are no appreciable differences among the results based on different weights for boron trichloride, the values of the index and the amplitudes differ slightly among one another for boron trifluoride.

The differences between the bond lengths obtained from the plates taken with the normal and the reversed directions of the nozzle were 0.11% for r(B–F) and 0.14% for r(F–F). The average, 0.12%, may be regarded as the difference in the scale factors between the two nozzle directions; the interval between the position of the gold foil and the center of diffraction is, therefore, about 0.06% of the camera length, i. e., about 0.07 mm. This is shorter than the interval of about 0.12 mm. which was determined in a similar way for the asymmetric nozzle used in the study of silicon tetrachloride.[3] The scale factor for boron trichloride must, then, be corrected by 0.06%, since the photographs were taken only for the normal nozzle direction. The results corrected for the difference in the camera lengths due to the different nozzle directions are shown in Table III. The σ_1 and σ_2 values of BF_3 in this table were calculated by the following relation:

$$\sigma=\sqrt{\frac{7}{40}}\,[2\sigma^2_{\text{normal}}+\sigma^2_{\text{reversed}}]^{1/2} \qquad (6)$$

The apparent increases in the mean amplitudes

TABLE III. SUMMARY OF THE RESULTS OF THE LEAST-SQUARES ANALYSIS (r and l in Å units)

Weights - (D)
Atomic scattering factors, $f^{B}e^{i\eta_{T.F.}}$
Corrected for the nozzle asymmetry

		r_a(B–X)	r_a(X–X)	l(B–X)	l(X–X)	index
BF_3	Average	1.3144	2.2720	0.0401	0.0562	0.964
	σ_1	0.0003	0.0004	0.0006	0.0006	0.006
	σ_2	0.0011	0.0011	0.0007	0.0006	0.006
BCl_3	Average	1.7407	3.0118	0.0503	0.0738	1.007
	σ_1	0.0005	0.0004	0.0007	0.0005	0.007
	σ_2	0.0014	0.0017	0.0007	0.0006	0.015

TABLE IV. APPARENT INCREASES IN THE MEAN AMPLITUDES DUE TO THE DISTRIBUTION OF GAS MOLECULES

	f^B	$\lvert f\rvert_{T.F.}$	$\lvert f\rvert_{H.F.}$
l(B–F)	0.0007	0.0009	0.0007
l(F–F)	0.0017	0.0022	0.0017
l(B–Cl)	0.0014	0.0021	0.0017
l(Cl–Cl)	0.0028	0.0042	0.0034

TABLE V. LIMITS OF ERROR OF THE ATOMIC DISTANCES (in Å units)

Source of error	r(B–F)	r(F–F)	r(B–Cl)	r(Cl–Cl)
Random error (2.5 σ)	0.0028	0.0028	0.0035	0.0043
Drift of voltage	0.0007	0.0011	0.0009	0.0015
Calibration of wavelength	0.0009	0.0016	0.0012	0.0021
Inclination of plates	0.0010	0.0017	0.0013	0.0023
Difference in the camera lengths between the sample and the reference			0.0010	0.0017
Effects of κ	0.0030	0.0015	0.0015	0.0015
Total error	0.0044	0.0041	0.0044	0.0060

TABLE VI. LIMITS OF ERROR OF THE MEAN AMPLITUDES AND INDICES (l in Å units)

Source of error	l(B–F)	l(F–F)	index of BF_3	l(B–Cl)	l(Cl–Cl)	index of BCl_3
Random error (2.5σ)	0.0018	0.0015	0.015	0.0018	0.0015	0.038
Sample size (50% of the correction)	0.0004	0.0009		0.0007	0.0014	
Uncertainty in the phase shift	0.0010			0.0010		
Arbitrary choice of the weight function	0.0020	0.0010	0.019	0.0002	0.0002	0.003
Total error	0.0029	0.0020	0.024	0.0022	0.0021	0.038

were determined by measuring the distribution of gas molecules on the basis of the discrepancies in the observed and theoretical backgrounds[22] (Fig. 5) (Table IV). The estimates of these corrections depend on the kind of scattering factors used.

The Estimation of Experimental Errors

The reliability of the observed parameters may be represented by the 99% confidence interval. This interval is equal to 2.5 σ if we assume the normal distribution of errors with a standard deviation, σ.[21] The greater of the σ_1 and σ_2 values of each parameter may safely be taken as the standard deviation, σ, corresponding to random errors. The random errors, 2.5 σ, and various systematic errors (which are considered to correspond to the above confidence interval) are listed in Tables V and VI.

For atomic distances the systematic errors were estimated as follows.[22] The error of the wavelength of the primary electron beam is less than 0.05% because the accelerating voltage was stabilized within 0.1%. When the wavelengths are determined from the reference gold foil, the uncertainty in the lattice constant of the gold foil and the personal errors in the measurement committed by the observer constitute systematic errors which influence the bond distances. The errors associated with the corrections for the inclination of photographic plates were estimated previously.[9]

As the photographs for BCl_3 were taken with only the normal orientation of the nozzle, the errors associated with the correction due to the deviation of the center of diffraction from the position of the gold foil should be taken into consideration. One half of the correction is, therefore, assigned to this source of error in Table V. The errors of the anharmonicity constants, κ, were estimated from the difference in the outputs of the least-squares analyses where the κ constants were either taken as variable parameters or as constants based on the various estimation.

For mean amplitudes, the errors associated with the correction for the distribution of gas molecules around the nozzle were assumed to be 50% of the correction. Errors coming from the arbitrariness of the weights were taken into consideration for both molecules.

The confidence intervals were estimated from the square root of the squared sum of errors, by assuming that these errors occur independently.

Results and Discussion

Atomic Distances and Mean Amplitudes.— The final results of the molecular constants obtained by using the Born scattering factors, $f^{B}e^{i\eta_{T.F.}}$, are given in Table VII. The average interatomic

22) K. Kuchitsu, This Bulletin, **32**, 748 (1959).

Table VII. Molecular constants obtained by using the Born scattering factor f^{B} and the phase shift $\eta_{T.F.}$ (r, l and δ_g in Å units)

BF_3

	B–F	F–F
r_g	1.3156±0.0044	2.2733±0.0041
r_α	1.3130±0.0044	2.2723±0.0041
l	0.0394±0.0029	0.0545±0.0020
index	0.964 ±0.024	
δ_g	0.0054±0.0057 (calcd. 0.0037)	

BCl_3

	B–Cl	Cl–Cl
r_g	1.7421±0.0044	3.0135±0.0060
r_α	1.7387±0.0044	3.0120±0.0060
l	0.0489±0.0022	0.0710±0.0021
index	1.007 ±0.038	
δ_g	0.0039±0.0041 (calcd. 0.0044)	

Table VIII. Molecular constants obtained by using the complex scattering factors for the Thomas-Fermi potential (r, l and δ_g in Å units)

BF_3

	B–F	F–F
r_g	1.3156±0.0044	2.2734±0.0041
r_α	1.3130±0.0044	2.2724±0.0041
l	0.0382±0.0029	0.0528±0.0021
index	0.946 ±0.024	
δ_g	0.0053±0.0058	

BCl_3

	B–Cl	Cl–Cl
r_g	1.7421±0.0044	3.0134±0.0060
r_α	1.7387±0.0044	3.0119±0.0060
l	0.0495±0.0024	0.0687±0.0026
index	0.995 ±0.038	
δ_g	0.0040±0.0041	

Table IX. Molecular constants obtained by using the complex scattering factors for the Hartree-Fock potentials[a] (r, l and δ_g in Å units)

BF_3

	B–F	F–F
r_g	1.3156±0.0044	2.2733±0.0041
r_α	1.3130±0.0044	2.2723±0.0041
l	0.0398±0.0029	0.0541±0.0020
index	0.960 ±0.024	
δ_g	0.0054±0.0057	

BCl_3

	B–Cl	Cl–Cl
r_g	1.7421±0.0044	3.0134±0.0060
r_α	1.7387±0.0044	3.0119±0.0060
l	0.0505±0.0023	0.0700±0.0023
index	1.006 ±0.038	
δ_g	0.0040±0.0041	

a) The parameters listed in this table should be regarded as the final results of this study.

distances, r_g, were calculated from r_a by the relation: $r_g = r_a + l^2/r_a$, and the mean amplitudes were corrected for the finite sample size. The results obtained by the use of the complex scattering factors, $|f|_{T.F.}e^{i\eta_{T.F.}}$ and $|f|_{H.F.}e^{i\eta_{H.F.}}$, are also listed in Tables VIII and IX respectively. For the reason given in the next subsection, the values listed in Table IX should be regarded as the final results of this study.

If the BX_3 molecules were exactly in a rigid planar triangular form, the X–X distance should be equal to $\sqrt{3}$ times the B–X distance. However, when we calculate $\delta_g = \sqrt{3}r_g(\text{B–X}) - r_g(\text{X–X})$, it is not equal to zero, because of the perpendicular amplitudes caused by thermal vibrations.[23] It was found in this experiment that $\delta_g = 0.0054 \pm 0.0057$ Å for BF_3 and $\delta_g = 0.0040 \pm 0.0041$ Å for BCl_3.

The shrinkage mentioned above was calculated by the following relation:

$$\delta_g(\text{calcd.}) = \sqrt{3}\left(\frac{\langle \Delta x^2\rangle + \langle \Delta y^2\rangle}{2r_e}\right)_{B-X} - \left(\frac{\langle \Delta x^2\rangle + \langle \Delta y^2\rangle}{2r_e}\right)_{X-X} \quad (7)$$

where the perpendicular amplitudes, $\langle \Delta x^2\rangle$ and $\langle \Delta y^2\rangle$, can be calculated by using the $\boldsymbol{L}$ and $\boldsymbol{G}$ matrix elements. For the B–X pair,

$$\langle \Delta x^2\rangle = \frac{2}{9}\left(L_{43}^2\langle Q_3^2\rangle + L^2{}_{44}\langle Q_4^2\rangle\right)$$

$$\langle \Delta y^2\rangle = \frac{1}{9}L_{22}^2\langle L_2^2\rangle$$

and for the X–X pair.

$$\langle \Delta x^2\rangle = \frac{1}{6}\{(\sqrt{3}L_{33} - L_{43})^2\langle Q_3^2\rangle + (\sqrt{3}L_{34} - L_{44})^2\langle Q_4^2\rangle\}$$

$$\langle \Delta y^2\rangle = 0$$

The thermal-average distance, r_α, is defined as[24] the sum of the equilibrium distance, r_e, and an anharmonic term, $\langle \Delta z\rangle$; that is, $r_\alpha = r_g - (\langle \Delta x^2\rangle + \langle \Delta y^2\rangle)/2r_e - \delta r$. The centrifugal stretching terms, δr, were calculated to be 0.0003 Å, 0.0006 Å, 0.0005 Å and 0.0009 Å for the B–F, F–F, B–Cl and Cl–Cl pairs respectively.[25] The observed r_α distances are listed in Tables VII, VIII and IX. In this average structure, the nonlinear shrinkage effect should disappear if the molecule is exactly in a planar triangular form. The ratio of the B–X distance to the X–X distance in this structure, $r_\alpha(\text{F–F})/r_\alpha(\text{B–F}) = 1.7306 \pm 0.0045$, $r_\alpha(\text{Cl–Cl})/r_\alpha(\text{B–Cl}) = 1.7323 \pm 0.0023$, is equal to $\sqrt{3}$ within the range of experimental error. It is therefore proved, to within an order of 0.001 Å, that the BF_3 and BCl_3 molecules take a planar triangular form in the average structure, and also in the equilibrium structure.

Although the above results are consistent with those given in previous papers[4-6] within their ranges of experimental error, the present study has provided more direct and confirmative support for the planarity of these molecules.

The thermal average B–F distance, $r_g = 1.3156 \pm 0.0044$ Å, is significantly larger than the effective distance, $r_0 = 1.295_1$ Å, obtained by Nielsen[26] from the rotational constant, B_0, in the analysis of the infrared ν_2 band of BF_3. While a part of this discrepancy stems from the difference in the definition of the internuclear distance, their assignment seems to be questionable. This problem will be studied in more detail in a forthcoming paper.

A Comparison of the Atomic Scattering Factors.—A similar electron diffraction analysis for boron tribromide[27] has revealed that the complex atomic scattering factors, $|f|_{H.F.}e^{i\eta_{H.F.}}$, calculated from the Hartree-Fock potentials provide a value of the mean amplitude, l(B–Br), more reasonable than the other scattering factors, $f^{Be^{i\eta_{T.F.}}}$ and $|f|_{T.F.}e^{i\eta_{T.F.}}$, and that the theoretical background line calculated from $|f|_{H.F.}$ is in better agreement with the observations than those calculated from the scattering factors, f^B and $|f|_{T.F.}$. Accordingly, it seemed desirable to compare the background lines calculated from these atomic scattering factors for the other halides.

The effects of the difference in the scattering factors appear on the mean amplitudes and on the backgrounds, but not appreciably on the atomic distances. The observed mean amplitudes obtained from the three scattering factors are shown in Fig. 6, where the closed areas show the limits of error of the mean amplitudes obtained by using the Hartree-Fock scattering factors, $|f|_{H.F.}e^{i\eta_{H.F.}}$.

As may be seen in Fig. 5, the theoretical backgrounds of boron trifluoride based on the three scatter-ing factors are in good agreement with the observed curve. Slight differences, each within the limits of error, are observed in the mean amplitudes listed in Tables VII—IX however. The results based on $f^{Be^{i\eta_{T.F.}}}$ and $|f|_{H.F.}e^{i\eta_{H.F.}}$ are compatible with the spectroscopic value within the limits of error, while that based on $|f|_{T.F.}e^{i\eta_{T.F.}}$ is in poorer agreement. For the mean amplitudes of boron trichloride, the result based on each scattering factor is in good agreement with the spectroscopic value, with the exception that the $|f|_{T.F.}$ factor gives a poor result for the background. It thus seems that the results based on the $|f|_{T.F.}$ factor are not quite satisfactory. This may be ascribed to the inadequacy of the Thomas-Fermi potential

23) Y. Morino, S. J. Cyvin, K. Kuchitsu and T. Iijima, *J. Chem. Phys.*, **36**, 1109 (1962).
24) Y. Morino, K. Kuchitsu and T. Oka, ibid., **36**, 1108 (1962).
25) M. Iwasaki and K. Hedberg, ibid., **36**, 2961 (1962).
26) A. H. Nielsen, ibid., **22**, 659 (1954).
27) S. Konaka, T. Ito and Y. Morino, This Bulletin, **39**, 1146. (1966).

TABLE XI. FORCE CONSTANTS DETERMINED FROM THE MEAN AMPLITUDES, ISOTOPIC SHIFTS AND THE ASSUMPTION OF THE UREY-BRADLEY FORCE FIELDS WITH $F' = -(1/10)F$ (in md/Å units)

	BF_3			
		Mean amplitudes	Isotopic shifts	U.B.F.F.
F_{11}	8.82 ±0.10			
F_{22}	0.293±0.005			
F_{33}		7.4 ±2.3	7.6 ±1.5	6.675±0.027
F_{34}		−0.9 ±0.9	−0.7 ±0.6	−0.362±0.009
F_{44}		0.58±0.09	0.53±0.03	0.513±0.013
	BCl_3			
		Mean amplitudes	Isotopic shifts	U.B.F.F.
F_{11}	4.63 ±0.10			
F_{22}	0.135±0.003			
F_{33}		3.6 ±1.3	3.4 ±1.4	3.384±0.043
F_{34}		−0.36±0.44	−0.22±0.43	−0.209±0.010
F_{44}		0.26±0.06	0.25±0.10	0.230±0.011

for such light elements as boron, fluorine and chlorine.

Force Constants.—The BX_3 molecules belong to the point group D_{3h} and have four fundamental frequencies. ν_1 is a totally symmetric stretching vibration (A_1' species), ν_2 is an out-of-plane vibration (A_2'' species), and ν_3 and ν_4 are doubly-degenerate vibrations (E' species). Although the force constants of A_1' and A_2'' species can easily be determined from the vibrational frequencies alone, those of E' species cannot be determined uniquely because the number of the force constants (three) exceeds that of the frequencies (two).

So far, several sets of force constants have been calculated by using the frequencies of the boron isotopes as additional observables. Since, however, the mass ratio of ^{10}B to ^{11}B is nearly unity, small experimental errors in the frequencies may lead to large errors in the force constants. The Urey-Bradley force constants of boron trihalides have also been reported.[28,29] The force constants can also be determined more precisely if the Coriolis coupling constants are observed. Thus far, one of the Coriolis constants of boron trifluoride has been determined from the band shape of the ν_4 frequency and used to calculate the force constants.[30] Nevertheless, this finding does not seem to be well-grounded experimentally, since the Coriolis constant was determined only indirectly. For this reason, it seems profitable to calculate the force constants from the mean amplitudes observed by electron diffraction.

The general quadratic potential function, in terms of the internal coordinates for BX_3 molecules, is:

$$2V = \sum f_r(\Delta r_i)^2 + 2\sum f_{rr}(\Delta r_i)(\Delta r_j) + f_\tau(r_0\Delta\tau)^2 + \sum f_\alpha(r_0\Delta\alpha_i)^2 + 2\sum f_{\alpha\alpha}(r_0\Delta\alpha_i)(r_0\Delta\alpha_j) \sum f_{r\alpha}(\Delta r_i)(r_0\Delta\alpha_i) + 2\sum f'_{r\alpha}(\Delta r_i)(r_0\Delta\alpha_j) \quad (8)$$

The internal coordinates are Δr_1, Δr_2, Δr_3, $r_0\Delta\alpha_1$, $r_0\Delta\alpha_2$, $r_0\Delta\alpha_3$ and $r_0\Delta\tau$, where Δr_i is the change in the length of the ith bond, $\Delta\alpha_i$ is the change in the bond angle opposite to r_i, and r_0 is the bond distance. $\Delta\tau$ is the change in the angle between any one of the bonds and the molecular plane.*

The following symmetry coordinates are used:

$$\begin{aligned}
&A_1' \text{ species}, && S_1 = \frac{1}{\sqrt{3}}(\Delta r_1 + \Delta r_2 + \Delta r_3)\\
&A_2'' \text{ species}, && S_2 = r_0\Delta\tau\\
&E' \text{ species}, && S_3 = \frac{1}{\sqrt{6}}(2\Delta r_3 - \Delta r_1 - \Delta r_2)\\
& && S_4 = \frac{1}{\sqrt{6}} r_0(2\Delta\alpha_3 - \Delta\alpha_1 - \Delta\alpha_2)\\
& && S_3' = \frac{1}{\sqrt{2}}(\Delta r_1 - \Delta r_2)\\
& && S_4' = \frac{1}{\sqrt{2}} r_0(\Delta\alpha_1 - \Delta\alpha_2) \quad (9)
\end{aligned}$$

The elements of the $\boldsymbol{F}$ matrix in the symmetry coordinates have the following relations to the constants in Eq. 8:

$$\begin{aligned}
&A_1' \text{ species}, && F_{11} = f_r + 2f_{rr}\\
&A_2'' \text{ species}, && F_{22} = f_\tau\\
&E' \text{ species}, && F_{33} = f_r - f_{rr}\\
& && F_{34} = f_{r\alpha} - f'_{r\alpha}\\
& && F_{44} = f_\alpha - f_{\alpha\alpha} \quad (10)
\end{aligned}$$

When the above transformation (9) is expressed in

28) G. J. Janz and Y. Mikawa, *J. Mol. Spectry.*, **5**, 92 (1960).
29) E. Meisingseth, *Acta Chem. Scand.*, **16**, 1601 (1962).
30) J. L. Duncan, *J. Mol. Spectry.*, **13**, 338 (1964).

* If the displacements of the Cartesian coordinates perpendicular to the molecular plane are denoted as y, they are related to $\Delta\tau$ as $r_0\Delta\tau = y_1 + y_2 + y_3 - 3y_0$, while the $\boldsymbol{G}$ matrix for A_2'' species is given by $G_{22} = 3/m_X + 9/m_B$.

a matrix form:

$$\boldsymbol{S}=\boldsymbol{UR}, \tag{11}$$

the mean amplitudes of vibration are given by[31]:

$$\langle \boldsymbol{R}\tilde{\boldsymbol{R}} \rangle = \tilde{\boldsymbol{U}}\boldsymbol{L}\langle \boldsymbol{Q}\tilde{\boldsymbol{Q}} \rangle \tilde{\boldsymbol{L}}\boldsymbol{U} \tag{12}$$

where $\langle \boldsymbol{Q}\tilde{\boldsymbol{Q}} \rangle$ is a diagonal matrix having the elements of:

$$\langle Q_i^2 \rangle = \frac{h}{8\pi^2\nu_i} \coth\left(\frac{h\nu_i}{2kT}\right) \tag{13}$$

From Eq. 12 the mean square amplitudes for the BX_3 molecules are found to be:

$$\begin{aligned} l^2(\text{B-X}) &= \frac{1}{3} L_{11}^2\langle Q_1^2 \rangle + \frac{2}{3}\{L_{33}^2\langle Q_3^2 \rangle \\ &\quad + L_{34}^2\langle Q_4^2 \rangle\} \\ l^2(\text{X-X}) &= L_{11}^2\langle Q_1^2 \rangle + \frac{1}{6}\{(\sqrt{3}L_{33} \\ &\quad - L_{43})^2\langle Q_3^2 \rangle + (\sqrt{3}L_{34} - L_{44})^2\langle Q_4^2 \rangle\} \end{aligned} \tag{14}$$

In a rigorous sense, the normal frequencies, ν_e, should be used in the calculation of the force field, but at present we do not have enough knowledge of vibrational anharmonicities to convert the fundamental frequencies, ν, to ν_e for boron trihalide.[32] Table X shows the fundamental frequencies used for the calculation[26,33,34] and the uncertainties of the frequencies which are estimated by analogy with other simple polyatomic molecules. When these observed ν values are used, the force constants have only one degree of freedom, and the two mean amplitudes, l(B–X) and l(X–X), cannot be independent. The curve of l(X–X) versus l(B–X) is illustrated in Fig. 6. The spread of the curves corresponds to the errors in the frequencies estimated above. Any one point on the curve corresponds to a set of the force constants. The ranges of the observed mean amplitudes based on the scattering factors, $|f|_{\text{H.F.}}e^{i\eta_{\text{H.F.}}}$, are within the ellipses drawn in solid lines in Fig. 6, while the overlapping regions of the curves indicate reasonable sets of the force constants. The observed value of l(B–F) is smaller than that to be expected from vibrational frequencies by about 0.003 Å, possibly because of some unknown systematic error. The uncertainties in the force constants of boron trifluoride were estimated from the overlapping region of the l-l curve and an ellipse displaced by 0.003 Å parallel to the l(B–F) axis. The displaced ellipse is shown by a dashed line in Fig. 6. The force constant, F_{34}, was determined from the corresponding region in the curve of F_{34} versus (B–X) in Fig. 7, while the other constants, F_{33} and F_{44}, were obtained from the value of F_{34}. The force constants obtained in this way are shown in Table XI.

It is found that the force constants determined from the mean amplitudes are in good agreement with those obtained by the isotopic shifts and the Urey-Bradley force fields (Table XI). The errors

TABLE X. FUNDAMENTAL FREQUENCIES USED FOR THE CALCULATION OF FORCE CONSTANTS
(in cm^{-1} units)

	$^{11}BF_3$	$^{10}BF_3$	Uncertainty[d]
ν_1[a]	888	888	±5
ν_2[b]	691.45	718.23	±1.5
ν_3[c]	1453.9	1504.8	±6
ν_4[a]	480.4	482.0	±5
	$^{11}BCl_3$	$^{10}BCl_3$	Uncertainty[d]
ν_1[a]	471	471	±5
ν_2[a]	454.9	474.3	±5
ν_3[a]	954.2	993.7	±5
ν_4[a]	243	243	±5

a) Ref. 33
b) Ref. 26
c) Ref. 34
d) Limits of uncertainty estimated in the present study.

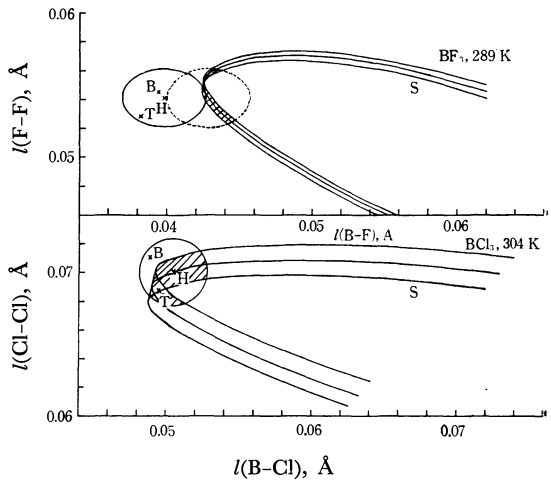

Fig. 6. Correlation curve of the mean amplitudes.
B, T, H: Observed values obtained by using the scattering factors, $f^{\text{B}}e^{i\eta_{\text{T.F.}}}$, $|f|_{\text{T.F.}}e^{i\eta_{\text{T.F.}}}$ and $|f|_{\text{H.F.}}e^{i\eta_{\text{H.F.}}}$, respectively.
S: Calculated values from spectroscopic data.
The small ellipses drawn in solid lines show the limits of error of the mean amplitudes obtained by using the Hartree-Fock complex scattering factors, $|f|_{\text{H.F.}}e^{i\eta_{\text{H.F.}}}$. The dashed curve was used to estimate the uncertainties in the force constants of boron trifluoride (see text). The shaded areas indicate the regions in which the diffraction and spectroscopic data are thought to be compatible.

31) Y. Morino, K. Kuchitsu and T. Shimanouchi, *J. Chem. Phys.*, **20**, 726 (1952); Y. Morino and E. Hirota, ibid., **23**, 737 (1955).
32) C. W. F. T. Pistorius, ibid., **29**, 1174 (1958). He has reported anharmonicity corrections for boron trihalides, but his corrections are questionable.
33) L. P. Lindeman and M. K. Wilson, ibid., **24**, 242 (1956).
34) J. Vanderryn, ibid., **30**, 331 (1959).

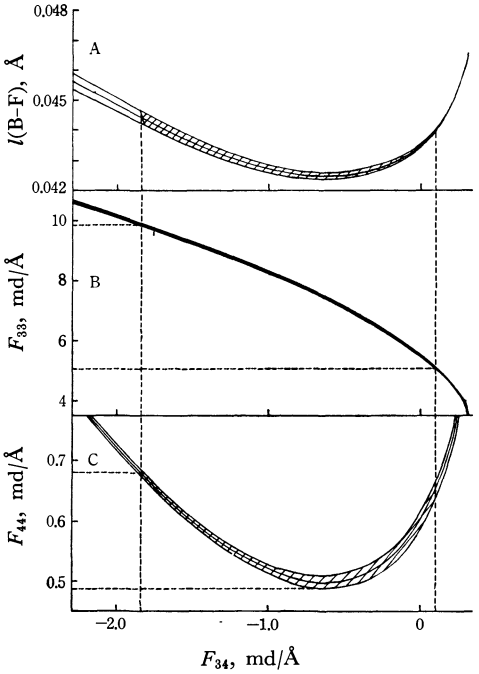

Fig. 7a.

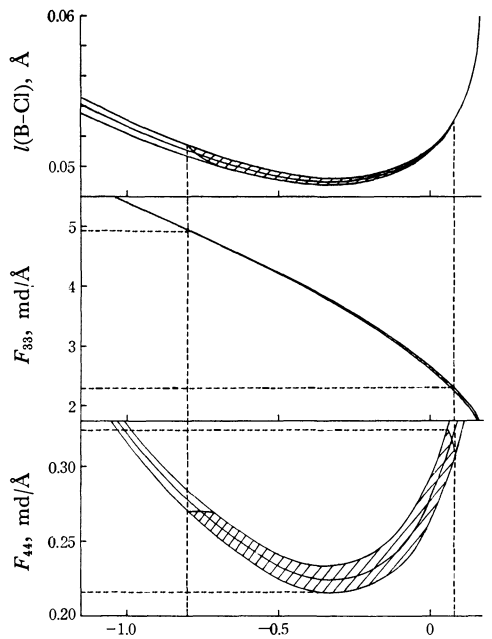

Fig. 7b.

Fig. 7. Determination of the force constants.
(a) BF_3, (b) BCl_3.
(A) Correlation curves of l(B–X) and F_{34}.
(B) Correlation curves of F_{33} and F_{34}.
(C) Correlation curves of F_{44} and F_{34}.
The shaded area indicates reasonable sets of the force constants.

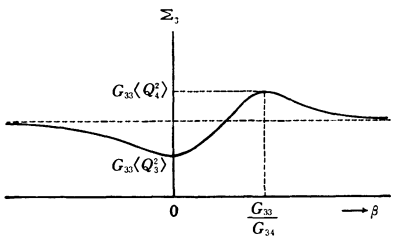

Fig. 8. Dependence of the mean amplitudes Σ_3 on the parameter β.

in the force constants derived from the mean amplitudes are similar in magnitude to those of the force constants obtained by the isotopic shifts. Nevertheless, the force constants are now considered to have been confirmed, since the two different experimental methods have given coincident results.

As is shown in Fig. 6, the positions of the observed mean amplitudes of BF_3 and BCl_3 are at the left-hand edge of the l-l curve. Similar phenomena have also been observed in the CCl_4, $GeCl_4$[1], $SiCl_4$[3], $TiCl_4$[8] and BBr_3[27] molecules which have previously been studied in our laboratory. It, therefore, seems unlikely that this is merely a coincidence. An analysis to be shown in the Appendix will prove that the physical meaning of this effect is related to a well-known empirical rule that the normal modes of stretching vibrations have essentially no dependence on the bending coordinates.[35]

Summary

The atomic distances and the mean amplitudes of boron trifluoride and boron trichloride have been determined by the sector-microphotometer method of gas electron diffraction (Table IX). The force constants determined from the mean amplitudes and the vibrational frequencies are in good agreement with those obtained by the isotopic shifts and by the Urey-Bradley force field.

It has been found that the Born scattering factors and the complex scattering factors for boron trifluoride and boron trichloride calculated from the Hartree-Fock potential give more reasonable mean amplitudes and theoretical backgrounds than the complex scattering factors calculated from the Thomas-Fermi potential.

The authors wish to express their gratitude to Dr. Ryohei Nakane for providing the boron trifluoride, and to the Central Research Institute of the Tokyo Shibaura Electric Co. for supplying the boron trichloride. They are also grateful to of the Ministry Education for a research grant.

35) T. Oka and Y. Morino, *J. Mol. Spectry.*, **11**, 349 (1963).

Appendix

A simple relation has been observed empirically between the observed mean amplitudes of the X-Y and Y-Y distances for the tetrahedral XY_4 molecules (CCl_4, $GeCl_4$[1], $SiCl_4$[3] and $TiCl_4$[8]) and for the planar trigonal XY_3 molecules (BF_3, BCl_3 and BBr_3[27]). Without exception, the observed values of l(X-Y) and l(Y-Y) fall close to the left-hand edge of the l-l ellipse, as is shown in Fig. 6.

We will here show that this phenomenon can be explained quite simply with relation to the characteristic modes of molecular vibrations, that is, by the empirical rule $L_{ij}(i<j) \fallingdotseq 0$, where the normal coordinates and the symmetry coordinates are numbered from the higher to the lower frequencies. According to the following argument, the mean amplitudes of a bonded pair, X-Y, takes a minimum value when $L_{34}=0$.

The l(X-Y) amplitude is related to the $\boldsymbol{L}$ matrix elements as follows:

$$l^2(\text{X-Y}) = \frac{1}{3}\Sigma_1 + \frac{2}{3}\Sigma_3 \qquad \text{for } XY_3 \qquad \text{(A1)}$$

$$= \frac{1}{4}\Sigma_1 + \frac{3}{4}\Sigma_3 \qquad \text{for } XY_4 \qquad \text{(A2)}$$

$$\Sigma_1 = L_{11}^2\langle Q_1^2\rangle \qquad \text{(A3)}$$

$$\Sigma_3 = L_{33}^2\langle Q_3^2\rangle + L_{34}^2\langle Q_4^2\rangle \qquad \text{(A4)}$$

where Σ is the mean amplitude matrix defined by Cyvin.[36] The first terms of Eqs. A1 and A2 have definite values, because $L_{11}^2=G_{11}=1/m_Y$, while the second terms depend on the choice of the force constants, because L_{33} and L_{34} change with the force constants. Therefore, it is sufficient to prove that Σ_3 takes a minimum value in order to prove that the l(X-Y) takes a minimum. Using the relation $\boldsymbol{G}=\boldsymbol{L}\tilde{\boldsymbol{L}}$, we obtain the following formulas:

$$G_{33} = L_{33}^2 + L_{34}^2$$

$$G_{34} = L_{33}L_{43} + L_{34}L_{44}$$

$$G_{44} = L_{43}^2 + L_{44}^2$$

$$\therefore\ (G_{33} - L_{34}^2)(G_{44} - L_{44}^2) = L_{33}^2L_{43}^2 = (G_{34} - L_{34}L_{44})^2 \qquad \text{(A5)}$$

From these equations, we can express L_{34} in terms of the $\boldsymbol{G}$ matrix elements and a parameter, β, where $\beta=L_{34}/L_{44}$:

$$L_{34}^2 = \frac{\beta^2 G_{44}|\boldsymbol{G}|}{(\beta G_{44}-G_{34})^2 + |\boldsymbol{G}|}, \quad |\boldsymbol{G}| = G_{33}G_{44} - G_{34}^2 \qquad \text{(A6)}$$

Then Σ_3 can also be expressed in terms of the parameter β:

$$\Sigma_3 = L_{33}^2\langle Q_3^2\rangle + L_{34}^2\langle Q_4^2\rangle = G_{33}\langle Q_3^2\rangle + L_{34}^2(\langle Q_4^2\rangle - \langle Q_3^2\rangle) = G_{33}\langle Q_3^2\rangle + \frac{\beta^2 G_{44}|\boldsymbol{G}|}{(\beta G_{44}-G_{34})^2 + |\boldsymbol{G}|} \times (\langle Q_4^2\rangle - \langle Q_3^2\rangle) \qquad \text{(A7)}$$

Since $|\boldsymbol{G}|$ and $(\langle Q_4^2\rangle - \langle Q_3^2\rangle)$ are both positive, it is clear that Σ_3 takes a minimum when $\beta=0$, that is, when $L_{34}=0$, and takes a maximum when $\beta=G_{33}/G_{34}$, that is, when $L_{33}=0$. The curve of Σ_3 is shown in Fig. 8.

For molecules of the bent XY_2 type, l(X-Y) takes the minimum value when $L_{12}=0$, since the following relation is the same as those for the planar XY_3 and tetrahedral XY_4 molecules.

$$l^2(\text{X-Y}) = \frac{1}{2}(\Sigma_1 + \Sigma_3) \qquad \text{(A8)}$$

$$\Sigma_1 = L_{11}^2\langle Q_1^2\rangle + L_{12}^2\langle Q_2^2\rangle \qquad \text{(A9)}$$

$$\Sigma_3 = L_{33}^2\langle Q_3^2\rangle \qquad \text{(A10)}$$

36) S. J. Cyvin, *Spectrochim. Acta*, **15**, 828 (1959).

BULLETIN OF THE CHEMICAL SOCIETY OF JAPAN VOL. 39 1146—1154 (1966)

The Mean Amplitudes and Atomic Scattering Factors of Boron Tribromide

By Shigehiro KONAKA*, Tetsuzo ITO* and Yonezo MORINO

Department of Chemistry, Faculty of Science, The University of Tokyo, Hongo, Tokyo

(Received August 4, 1965)

The mean amplitudes and the interatomic distances of BBr_3 have been determined by the sector-microphotometer method of gas electron diffraction. The B–Br and Br–Br distances (r_g) have been found to be 1.8932 ± 0.0054 Å and 3.2830 ± 0.0053 Å respectively. The values of the mean amplitudes are dependent on the atomic scattering factors used in the analysis. The complex scattering factors for B and Br, as calculated on the basis of the Hartree-Fock potential, have given mean amplitudes which are consistent with the vibrational frequencies observed by spectroscopy, while the mean amplitudes derived from the use of other scattering factors are less reasonable. It has been shown that the Hartree-Fock function for the Br atom is a better representation of the atomic potential function than the Thomas-Fermi function. The utility of the method of gas electron diffraction for the study of atomic scattering factors and atomic potential functions in some favorable cases has been pointed out.

Although the difference between the absolute values $|f|$ of the complex atomic scattering factor and the Born scattering factor, f^B, is large for atoms of large atomic numbers, it does not necessarily cause serious trouble in the analysis of usual molecules by gas electron diffraction, since in the calculation of the molecular intensity the difference which appears in the numerator (the total intensity) compensates for that in the denominator (the background).

For boron tribromide, however, the difference in the scattering factors has a serious effect on the observed value of the mean amplitude, l(B–Br). This suggests that information about the atomic scattering factors may be obtained from gas electron diffraction; it is possible to make a critical examination of the theoretical scattering factors by comparing the value of l(B–Br) estimated from the observed vibrational frequencies with the observed values of l(B–Br), which depend on the scattering factors used in the analysis. The experimental backgrounds should provide additional information about the theoretical scattering factors.

It also seems important to determine the molecular structure of boron tribromide as accurately as possible by taking into consideration the effect of the scattering factors. One electron diffraction study of boron tribromide has been carried out, by the visual method, by Lévy and Brockway.[1] Their results were: r(B–Br)$=1.87\pm0.02$ Å and r(Br–Br)$=3.25\pm0.03$ Å.

Experimental

The diffraction apparatus used in this study was the same as that reported on in a previous paper.[2] The diffraction patterns were taken on Fuji Process Hard plates by using an r^3 sector. The camera distances were either 11.8 cm. (short camera distance), which covered the region from $q=17$ to $q=98$, or 27.9 cm. (long camera distance), which covered the region from $q=6$ to $q=36$. The accelerating voltage (43 kV.) was automatically stabilized within 0.1% during the experiment. The sample of a commercial grade was purified by distillation. KEL-F stopcock grease was used to avoid the erosion of the lubricant by the sample. The gas sample was led into the diffraction chamber through a drum-type nozzle (the same as that reported on in a preceding paper)[3] at the temperature of 17°C. The beam current was about 0.005 and 0.002 μamp., and the exposure times were about 3 and 5 min. for the short and long camera distances respectively. The wavelengths of the primary electron beam were measured by making use of the transimission patterns of gold foil.

The densities of the photographs developed at 20°C for 5 minutes with an FD-131 developer were measured using a Rigaku-Denki MP-3 microphotometer. The undesirable effects of the time lag of the recorder were eliminated by the method described in a preceding paper.[3] Seven plates for each camera distance were used for analysis. The optical densities (0.1—0.6) of these plates were all within the range where the linearity between density and intensity has been established by experiment.[4]

Analysis

A molecular intensity curve was obtained by drawing a smooth background line through the undulation of the intensity curve corrected for imperfections in the sector shape. The background line was corrected according to the criterion of minimum ghosts in the radial distribution curve.[5]

Two sets of atomic scattering factors were used to calculate the radial distribution curves: the Born scattering factors, f^B, as calculated by several authors[6-8], and the absolute value, $|f|$, of the complex scattering factors as calculated by Ibers and Hoerni[9] (Fig. 1). The phase shifts, $\Delta\eta_{BBr}=\eta_{Br}-\eta_B$, taken from their table were used for both sets. The inelastic scattering factors were taken from the table of Bewilogua.[10]

The expression of molecular intensity is given by[11]:

$$qM(q)=k\sum A_{ij}\mu_{ij}\cos\Delta\eta_{ij} \times \sin\left(\frac{\pi}{10}qr_{ij}\right)\exp\left(-\alpha_{ij}q^2\right) \quad (1)$$

where:

$$\alpha_{ij}=\frac{1}{2}\left(\frac{\pi}{10}\right)^2 l_{ij}^2 \quad (2)$$

$$\mu_{ij}=\frac{\sum_k Z_k(Z_k+1)}{Z_iZ_j}\frac{|F_i||F_j|}{\sum_k|F_k|^2+\sum_k S_k}$$

$$|F|=\boldsymbol{h}^2s^2|f|/8\pi^2\boldsymbol{m}\boldsymbol{e}^2 \quad (3)$$

The curves of the μ-factors $\mu_{BBr}\cos\Delta\eta_{BBr}$ and μ_{BrBr} are shown in Fig. 2. Since the values of $1-\mu_{BBr}\cos\Delta\eta_{BBr}$ are not small for a small q region ($q<17$) or for a large q region ($q>50$), the usual corrections[12] for non-nuclear scattering, $1-\mu_{ij}\cos\Delta\eta_{ij}$, are not suitable. The molecular intensity for the short camera distance was, therefore, modified into the following $qM(q)_c$ by adding the correction term of $\Delta qM(q)$ to Eq. 1, taking into account the apparent splitting of the B–Br distance because of the failure of the Born approximation:[11]

* Present address: Department of Chemistry, Faculty of Science, Hokkaido University, Sapporo (S. K.), and the Institute for Physical and Chemical Research, Tokyo (T. I.).

1) H. A. Lévy and L. O. Brockway, *J. Am. Chem. Soc.*, **59**, 2085 (1937).
2) Y. Morino and K. Kuchitsu, *J. Chem. Phys.*, **28**, 175 (1958).
3) S. Konaka, Y. Murata, K. Kuchitsu and Y. Morino, This Bulletin, **39**, 1134 (1966).
4) Y. Morino and T. Iijima, This Bulletin, **35**, 1661 (1962).
5) J. Karle and I. L. Karle, *J. Chem. Phys.*, **18**, 957 (1950).
6) J. A. Ibers, *Acta Cryst.*, **10**, 86 (1957).
7) H. Viervoll and O. Ögrim, ibid., **2**, 277 (1947).
8) L. H. Thomas and K. Umeda, *J. Chem. Phys.*, **26**, 293 (1957).
9) J. A. Ibers and J. A. Hoerni, *Acta Cryst.*, **7**, 405 (1954).
10) L. Bewilogua, *Physik. Z.*, **32**, 740 (1931).
11) R. Glauber and V. Schomaker, *Phys. Rev.*, **89**, 667 (1953).
12) L. S. Bartell, L. O. Brockway and R. H. Schwendeman, *J. Chem. Phys.*, **23**, 1854 (1955).

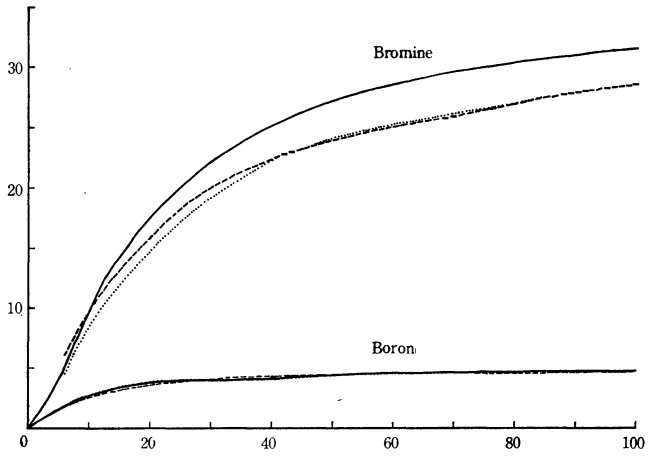

Fig. 1. Atomic scattering factors for the boron and bromine atoms.
—— $\frac{h^2s^2}{8\pi^2me^2}f^B=Z-f_x$, where f^B is the Born scattering factor and f_x is the atomic form factor for X-rays.
---- $\frac{h^2s^2}{8\pi^2me^2}|f|_{T.F.}$, where $|f|_{T.F.}$ is the absolute value of the complex scattering factor calculated from the Thomas-Fermi potential.
····· $\frac{h^2s^2}{8\pi^2me^2}|f|_{H.F.}$, where $|f|_{H.F.}$ is the absolute value of the complex scattering factor calculated from the Hartree-Fock potential.

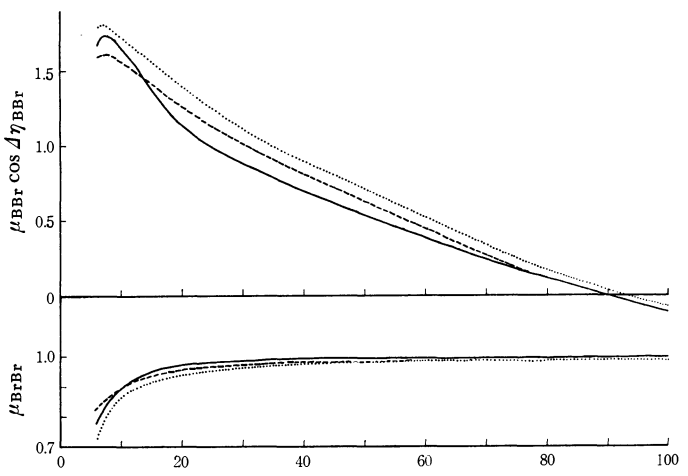

Fig. 2. μ-factors of boron tribromide.
—— $f^Be^{i\eta_{T.F.}}$, ---- $|f|_{T.F.}e^{i\eta_{T.F.}}$, ····· $|f'|_{H.F.}e^{i\eta_{H.F.}}$

$$qM(q)_c=k\frac{A_{BBr}}{2}\left\{\sin\left(\frac{\pi}{10}q(r_{BBr}+\Delta r)\right)+\sin\left(\frac{\pi}{10}q(r_{BBr}-\Delta r)\right)\right\}e^{-\alpha_{BBr}q^2}+kA_{BrBr}\sin\left(\frac{\pi}{10}qr_{BrBr}\right)e^{-\alpha_{BrBr}q^2} \quad (4)$$

$$\Delta qM(q)=kA_{BBr}\left\{\cos\left(\frac{\pi}{10}q\Delta r\right)-\mu_{BBr}\cos\Delta\eta_{BBr}\right\}\times\sin\left(\frac{\pi}{10}qr_{BBr}\right)e^{-\alpha_{BBr}q^2}+kA_{BrBr}(1-\mu_{BrBr})\sin\left(\frac{\pi}{10}qr_{BrBr}\right)e^{-\alpha_{BrBr}q^2} \quad (5)$$

The molecular intensity for the long camera distance, on the other hand, was obtained by adding to Eq. 1 the correction term of $\Delta qM(q)$,

TABLE I. RESULTS OF THE LEAST-SQUARES ANALYSIS (r, l in Å units)

(A) The Born scattering factor f^B and the phase shift $\eta_{T.F.}$

	r_a(B-Br)	r_a(Br-Br)	l(B-Br)	l(Br-Br)	index
Average	1.8930	3.2832	0.0145*	0.0779	1.029
σ_1	0.0018	0.0005	0.0086	0.0006	0.007
σ_2	0.0016	0.0009	0.0029	0.0004	0.011

(B) The complex scattering factor, $|f|_{T.F.}e^{i\eta_{T.F.}}$, calculated from the Thomas-Fermi potential

	r_a(B-Br)	r_a(Br-Br)	l(B-Br)	l(Br-Br)	index
Average	1.8926	3.2833	0.0356*	0.0776	1.035
σ_1	0.0017	0.0005	0.0039	0.0006	0.007
σ_2	0.0017	0.0009	0.0022	0.0004	0.011

(C) The complex scattering factor, $|f|_{H.F.}e^{i\eta_{H.F.}}$, calculated from the Hartree-Fock potential

	r_a(B-Br)	r_a(Br-Br)	l(B-Br)	l(Br-Br)	index
Average	1.8929	3.2832	0.0526*	0.0778	1.042
σ_1	0.0015	0.0004	0.0024	0.0005	0.006
σ_2	0.0017	0.0009	0.0017	0.0004	0.011

* The minimum l(B-Br) value allowed by spectroscopic data is 0.0502 Å

which takes into account the apparent increase in the B-Br mean amplitude because of the slight deviation from the Born formula:[13]

$$qM(q)_c = k\gamma A_{BBr}\sin\left(\frac{\pi}{10}qr_{BBr}\right)e^{-\alpha'_{BBr}q^2} + kA_{BrBr}\sin\left(\frac{\pi}{10}qr_{BrBr}\right)e^{-\alpha_{BrBr}q^2} \quad (6)$$

$$\Delta qM(q) = k\gamma A_{BBr}\left\{1-\frac{\mu_{BBr}\cos\Delta\eta_{BBr}}{\gamma\exp(-\beta q^2)}\right\}\times\sin\left(\frac{\pi}{10}qr_{BBr}\right)e^{-\alpha'_{BBr}q^2} + kA_{BrBr}(1-\mu_{BrBr})\times\sin\left(\frac{\pi}{10}qr_{BrBr}\right)e^{-\alpha_{BrBr}q^2} \quad (7)$$

where:

$$\alpha'_{BBr} = \alpha_{BBr} + \beta \quad (8)$$

and where γ is a constant.

As a result of the above modifications, the $\Delta qM(q)$ values, shown in Fig. 3, were made much smaller than the conventional correction terms, $1-\mu_{ij}\cos\Delta\eta_{ij}$.

When the backgrounds were revised by the non-negativity criterion of the radial distribution curve,[5] the molecular intensity for the long camera distance (q=6—36) agreed with that for the short distance (q=17—98), especially over the region q=18—25 (Fig. 4).

Seven molecular intensity curves were obtained by combining each one of the molecular intensity curves for the short camera distance with any one of those for the long distance in the above q region (18—25). The molecular parameters were determined by the least-squares fitting of the observed molecular intensity to the following theoretical expression,[14] including the anharmonicity parameters κ, which were neglected in the above treatment of the radial distribution curves:

$$qM(q) = k\sum A_{ij}\mu_{ij}\cos\Delta\eta_{ij}\times\sin\frac{\pi}{10}q\left[r_{aij}-\left(\frac{\pi}{10}q\right)^2\kappa_{ij}\right]\times\exp\left[-\frac{1}{2}\left(\frac{\pi}{10}q\right)^2 l_{ij}^2\right] \quad (9)$$

The anharmonicity parameters, κ, were estimated in the way reported on in a preceding paper[3]; they were not varied as parameters. The results of the least-squares analysis are listed in Table I.

Results and Discussion

Mean Amplitudes and Atomic Scattering Factors.—According to the scattering theory of partial waves, the atomic scattering factors, $f(\theta)$, which are required in the analysis of gas electron diffraction are given by:

$$f(\theta) \equiv |f(\theta)|e^{i\eta(\theta)} = (2ik)^{-1}\sum_{l=0}^{\infty}(2l+1)(\exp[2i\delta_l]-1)P_l(\cos\theta) \quad (10)$$

for the elastic scattering of electrons by a central potential, $V(r)$. Here k is the wave number of the electron, and δ_l is the phase shift of the lth partial wave. The complex scattering factors, $|f|e^{i\eta}$, were calculated by Ibers and Hoerni by this formula.[9]

The atomic scattering factors given by the first Born approximation is:

$$f(\theta) \simeq f^B(\theta) = -\frac{8\pi^2 m}{h^2}\int_0^\infty V(r)\frac{\sin sr}{sr}r^2dr \quad (11)$$

13) L. S. Bartell, and L. O. Brockway, *Nature*, **171**, 978 (1953).

14) Y. Morino, K. Kuchitsu, T. Iijima and Y. Murata, *J. Chem. Soc. Japan, Pure Chem. Sect.* (*Nippon Kagaku Zasshi*), **83**, 803 (1962).

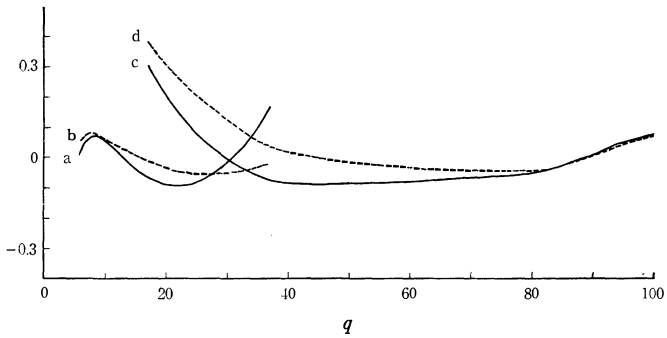

Fig. 3. Corrections for non-nuclear scattering.
—— $f^{B}e^{i\eta_{T.F.}}$, $|f|_{T.F.}e^{i\eta_{T.F.}}$
a: $\dfrac{\mu_{BBr}\cos\Delta\eta_{BBr}}{\gamma\exp(-\beta q^2)}-1$, ($\gamma=1.68$, $\beta=7.04\times10^{-4}$).
b: $\dfrac{\mu_{BBr}\cos\Delta\eta_{BBr}}{\gamma\exp(-\beta q^2)}-1$, ($\gamma=1.53$, $\beta=4.00\times10^{-4}$).
c, d: $\mu_{BBr}\cos\Delta\eta_{BBr}-\cos((\pi/10)q\Delta r)$, ($\Delta r=0.056$Å).

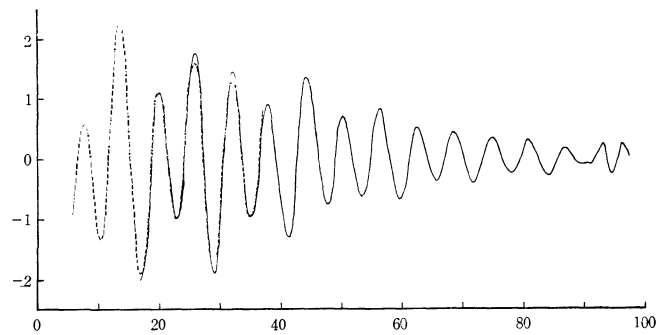

Fig. 4. The molecular scattering intensity observed at the short camera distance (solid line) and at the long camera distance (dashed line).

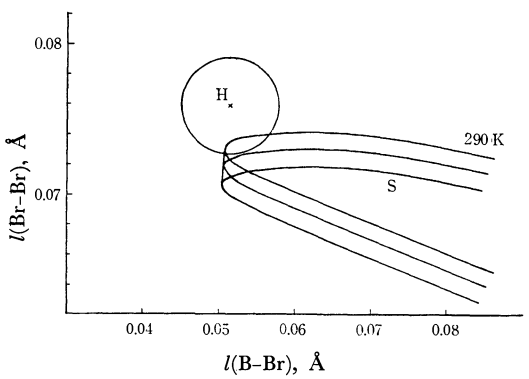

Fig. 5. Correlation curve of two mean amplitudes.
H: The observed values obtained by using the complex scattering factors calculated from the Hartree-Fock potential.
S: Calculated values from spectroscopic data.

which is related to the X-ray form factor, $f_x(\theta)$, by:

$$f^{B}(\theta)=\frac{8\pi^2 me^2}{h^2 s^2}(Z-f_x(\theta)) \qquad (12)$$

where m is the relativistic mass of the incident electron.

While the phase shift, η, calculated by the method of partial waves has been used in most of the recent analysis, the Born scattering factor, f^{B}, has sometimes been used in place of the absolute value, $|f|$. This is possibly due to the fact that f^{B} has been regarded as more reliable than the $|f|$ value as calculated by Ibers and Hoerni, since their partial-waves calculations for most atoms were based on the Thomas-Fermi potential.

The difference between $|f|$ and f^{B} is large for heavy atoms, but its effect is negligible for most molecules in the calculation of the molecular scattering intensity, $qM(q)$, since the scattering factors appear in the numerator and in the denominator of the μ-factor, so the effect is essentially cancelled. Consequently, the difference between the scattering factors, $|f|$ and f^{B}, is large for the bromine atom (Fig. 1), but it has only a negligible effect on the μ-factor of the Br–Br pair (Fig. 2). For the B–Br pair, however, the difference in the scattering factors has a great influence on the μ-factor, as is shown in Fig. 2. This can be easily understood from the following approximate expression of μ_{BBr},

which is obtained by neglecting the $|F|$ of the boron atom and the inelastic scattering factors, S_k, relative to the $|F|$ of the bromine atom in the denominator of f_{BBr}:

$$\mu_{BBr} \propto |F|_B/|F|_{Br} \qquad (13)$$

If the scattering factor $|f|$ is replaced by f^B in this fraction, the denominator changes considerably, while the numerator remains almost unchanged. The value of $\mu_{BBr} \cos \Delta\eta_{BBr}$ then changes the least-squares result of the mean amplitude, l(B–Br), seriously.

In a preceding paper,[3] it was shown that the value of l(B–Br) takes a minimum value when one of the off-diagonal elements of the $\boldsymbol{L}$ matrix, L_{34}, equals zero. The minum value of l(B–Br) allowed by the observed vibrational frequencies is 0.0502 Å at 17°C. Since it is expected, on the basis of the well-known empirical rule stated in the preceding paper,[3] that the value of L_{34} is very nearly zero, the true value of l(B–Br) is expected to be very close to the minimum value, 0.0502 Å. The $l-l$ curve of BBr_3 is shown in Fig. 5, while the vibrational frequencies used in the calculation are listed in Table II.[15]

Table II. Fundamental frequencies used in the calculation[a] (in cm^{-1} units)

	$^{11}BBr_3$	$^{10}BBr_3$	error[b]
ν_1	278	278	±2
ν_2	370	395	±2
ν_3	819.8	856.1	±2
ν_4	148	148	±3

a) Ref. 15.
b) Limits of error assumed in the present study.

The least-squares result of l(B–Br) obtained by using f^B is much smaller than the above minimum value and the values of the mean amplitudes observed for ordinary molecules. The l(B–Br) value obtained by using the $|f|$ value calculated by Ibers and Hoerni is about twice the value given by f^B, but it is still inconsistent with the spectroscopic value. This is possibly to be ascribed to the errors associated with the use of the Thomas-Fermi potential function for the bromine atom in the partial-waves calculation of Ibers and Hoerni.[9]

The complex scattering factors of the bromine atom have recently been calculated by using the Hartree-Fock potential by Bonham and Peacher,[16] but those of the boron atom had never been calculated from the Hartree-Fock potential. The boron-scattering factors were, therefore, calculated in the present study by the method of partial waves by using the Hartree-Fock potential. The results of the calculations are shown in the Appendix.

The values of $|f(\theta)|$ are found to be nearly equal to those obtained from the Thomas-Fermi potential (Fig. 1), whereas the phase shifts $\Delta\eta(\theta)$ are appreciably smaller (Fig. 6); this makes the factor $\mu_{BBr} \cos \Delta\eta_{BBr}$ increase (Fig. 2). The least-squares results obtained by using the new μ-factors are shown in Table I (C). It is noticeable that the standard error of the least-squares analysis for l(B–Br) was made smaller by the use of the revised μ-factors.

The apparent increase in the mean amplitudes due to the sample delocalization was estimated by comparing the observed background line with the theoretical one obtained from the absolute values of the complex atomic scattering factors. The corrections were −0.0012 Å and −0.0019 Å for l(B–Br) and l(Br–Br) respectively.

The estimation of the experimental errors in the mean amplitudes is shown in Table III, while the final results obtained by using the scattering factors calculated from the Hartree-Fock potential

Table III. Limits of error of the mean amplitudes and index (l in Å units)

Source of error	l(B–Br)	l(Br–Br)	index
Random error (2.5σ)	0.0060	0.0013	0.028
Sample size (50% of the correction)	0.0006	0.0010	
Uncertainty in the phase shift	0.0010		
Arbitrary choice of the weight function	0.0010	0.0010	0.021
D-E calibration	0.0015	0.0024	
Total error	0.0063	0.0031	0.035

Table IV. Limits of error of the atomic distances (in Å units)

Source of error	r(B–Br)	r(Br–Br)
Random error (2.5σ)	0.0043	0.0023
Drift of voltage	0.0009	0.0016
Calibration of wavelength	0.0013	0.0023
Inclination of plates	0.0014	0.0025
Difference in the camera lengths between the sample and the reference gold foil	0.0006	0.0010
Arbitrary choice of the weight function	0.0015	0.0003
Effects of κ	0.0020	0.0028
Total error	0.0054	0.0053

Table V. Final results of the molecular constants obtained by using the scattering factor calculated from the Hartree-Fock potential by the method of partial waves (r_g, l and δ_g in Å units)

	B–Br	Br–Br
r_g	1.8932±0.0054	3.2830±0.0053
l	0.0514±0.0063	0.0759±0.0031
index	1.042±0.035	
δ_g	−0.0039±0.0085 (calc. 0.0056)	

15) T. Wentink, Jr. and V. H. Tiensuu, *J. Chem. Phys.*, **28**, 826 (1958).
16) R. A. Bonham and J. L. Peacher, Private communication (1965).

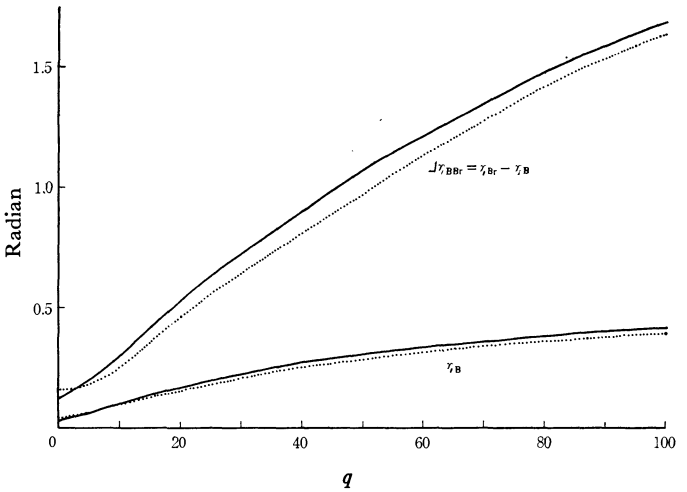

Fig. 6. Phase shift η_B and $\Delta\eta_{BBr}$.
—— Calculated from the Thomas-Fermi potential (Ref. 9).
····· Calculated from the Hartree-Fock potential.

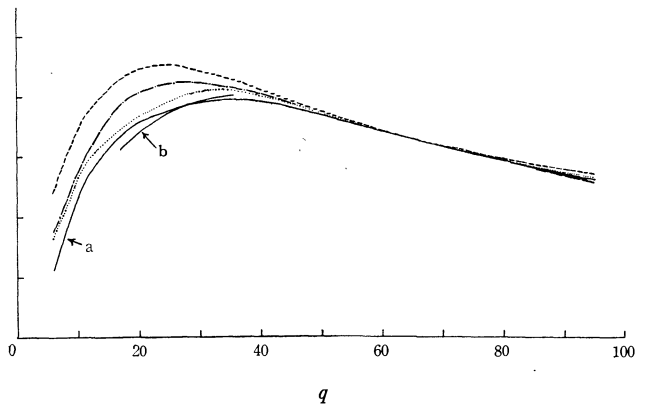

Fig. 7. Comparison of the observed and theoretical background intensities in an arbitrary scale.
—— Observed: (a) long camera distance (b) short camera distance.
—·—·— f^B
-------- $|f|_{T.F.}$ } Theoretical.
····· $|f|_{H.F.}$

by the method of partial waves are listed in Table V.

As is shown in Fig. 5, both the l(B–Br) and l(Br–Br) values are now compatible with those calculated from the observed vibrational frequencies. From the present gas electron diffraction study of boron tribromide, the Hartree-Fock function is, hence, found to be a better representation of the atomic potential function than the Thomas-Fermi function for the bromine atom, which has an intermediate atomic number.

Atomic Distances.—The corrections for the nozzle asymmetry stated in the preceding paper[3] are −0.0011Å and −0.0020 Å for r(B–Br) and r(Br–Br) respectively.

The limits of error of the atomic distances are estimated to be as shown in Table IV. Table V shows the final results obtained by using the scattering factor calculated from the Hartree-Fock potential by the method of partial waves. The results of the atomic distances are consistent with those given in a previous paper.[1]

A Comparison of the Theoretical and Observed Backgrounds.—In Fig. 7, the theoretical backgrounds calculated from the three atomic scattering factors are compared with the observed backgrounds. It is found that the $|f|_{T.F.}$ scattering factors gave a poorer background than the Born scattering factors. This tendency was also encountered in the analysis of boron trichloride.

For boron trifluoride and boron trichloride, the Born scattering factors gave results similar to those obtained from the Hartree-Fock complex scattering factors in the calculations of the mean amplitudes and the backgrounds.[3] For boron tri-

bromide, however, the Born scattering factors were found to give less reasonable backgrounds than the $|f|_{H.F.}$ factors. This gives additional support for the conclusion of the previous subsection that the $|f|_{H.F.}$ scattering factor is superior to f^B for bromine.

Summary

Boron tribromide has been studied by the sector-microphotometer method of electron diffraction in order to make a critical examination of the atomic scattering factors. The complex atomic scattering factors, $|f|_{H.F.}e^{i\eta_{H.F.}}$, calculated from the Hartree-Fock potentials have provided a more reasonable value of the mean amplitude, l(B–Br), than the Born and Thomas-Fermi scattering factors, $f^Be^{i\eta_{T.F.}}$ and $|f|_{T.F.}e^{i\eta_{T.F.}}$. The theoretical background curve calculated from $|f|_{H.F.}$ is also in better agreement with the observed one than are those calculated from the other scattering factors. This indicates that the Hartree-Fock potential function is a better representation of the atomic potential function than the Thomas-Fermi function for the bromine atom. The present study suggests the usefulness of the method of gas electron diffraction for the study of atomic scattering factors and atomic potential functions in some favorable cases.

The authors wish to express their thanks to Professor R. A. Bonham for his advice in the calculation of the complex atomic scattering factors.

Appendix

Partial-waves Calculations of the Scattering Factors of the Boron and Bromine Atoms by the Use of the Hartree-Fock Potential.—The Hartree-Fock potential has been expressed by Bonham[17] in the following analytical expression:

$$V(r)=-\frac{Ze^2}{r}\left(\sum_{i=1}^{2}\gamma_i e^{-\lambda_i r}+r\sum_j \gamma_j e^{-\lambda_j r}\right) \quad \text{(A1)}$$

Table VI. Phases of partial waves δ_l of boron calculated from the Hartree-Fock potential at 40 kV.

l	Born phases calculated by Eq. A2	Asymptotic WKBJ phases calculated by Eq. A3
0	0.4020	0.4133
5	0.1831	0.1832
10	0.1276	0.1277
20	0.0794	0.0794
30	0.0556	0.0556
50	0.0299	0.0299
70	0.0164	0.0164
100	0.0068	0.0068

17) T. G. Strand and R. A. Bonham, *J. Chem. Phys.*, **40**, 1686 (1964).

where j takes the values of 1 and 2 for boron, and 1, 2, and 3 for bromine. The phases of the partial waves[18] have been calculated by the Born phase formula:

$$\delta_l=-\frac{8\pi^2 mk}{h^2}\int_0^\infty V(r)[j_l(kr)]^2r^2dr$$
$$=\alpha\left\{\sum_i \gamma_i Q_l\left[1+\frac{\lambda_i^2}{2k^2}\right]-\sum_j\frac{\gamma_j\lambda_j}{k^2}Q_{l'}\left[1+\frac{\lambda_j^2}{2k^2}\right]\right\} \quad \text{(A2)}$$

where α is $4\pi^2me^2Z/h^2k$, Q_l is the Legendre polynomial

Table VII. Values of complex scattering factors of boron at 40 kV. calculated from the Thomas-Fermi and the Hartree-Fock potentials

($|f(\theta)|$ in Å units and $\eta(\theta)$ in radians)

		Thomas-Fermi[a]		Hartree-Fock[b]	
$\theta°$	s(Å^{-1})	$\|f(\theta)\|$	$\eta(\theta)$	$\|f(\theta)\|$	$\eta(\theta)$
0	0.	7.2	0.03	3.06	0.041
1	1.822	2.08	0.07	1.98	0.058
2	3.644	0.850	0.13	0.912	0.100
4	7.288	0.300	0.20	0.273	0.193
6	10.929	0.145	0.27	0.134	0.252
8	14.567	0.088	0.33	0.082	0.294
10	18.201	0.058	0.36	0.055	0.332
12	21.829	0.040	0.40	0.040	0.360
16	29.064	0.024	0.44	0.023	0.415
20	36.263	0.015	0.48	0.015	0.462
24	43.418	0.011	0.52	0.011	0.498
28	50.521	0.008	0.55	0.008	0.523

a) Interpolated values according to the table of Ibers and Hoerni (Ref. 9).
b) Present calculation.

Table VIII. Complex scattering factors of bromine at 40 kV. calculated from the Thomas-Fermi and the Hartree-Fock potentials

($|f(\theta)|$ in Å units and $\eta(\theta)$ in radians)

	Thomas-Fermi[a]		Hartree-Fock[b]	
	$\|f(\theta)\|$	$\eta(\theta)$	$\|f(\theta)\|$	$\eta(\theta)$
0	13.6	0.16	7.65	0.187
1	7.14	0.27	5.53	0.246
2	3.41	0.48	3.02	0.401
4	1.37	0.82	1·26	0.723
6	0.732	1.11	0.715	0.977
8	0.452	1.37	0.452	1.22
10	0.310	1.60	0.309	1.45
12	0.225	1.79	0.224	1.65
16	0.138	2.11	0.135	1.99
20	0.091	2.39	0.091	2.24
24	0.065	2.61	0.065	2.46
28	0.050	2.80	0.050	2.65

a) Interpolated values according to the table of Ibers and Hoerni (Ref. 9).
b) Ref. 16. Present calculations have given almost identical results.

18) J. Karle and R. A. Bonham, ibid. **40**, 1396 (1964).

of the second kind, and Q_l' is the first derivative of Q_l. When l is large, this formula can be approximated by:

$$\delta_l=\alpha\left\{\sum_i \gamma_i K_0\left[\left(l+\frac{1}{2}\right)\lambda_i/k\right]+\frac{l+(1/2)}{k}\sum_j \gamma_j K_1\left[\left(l+\frac{1}{2}\right)\lambda_j/k\right]\right\} \quad \text{(A3)}$$

where K_0 and K_1 are the modified Bessel functions of the second kind. The phases can also be evaluated by the asymptotic WKBJ formula:

$$\delta_l=\frac{k\alpha}{Ze^2}\int_{(l+\frac{1}{2})/k}^{\infty} V(r)\left[k^2-\left(l+\frac{1}{2}\right)^2/r^2\right]^{-1/2}\mathrm{d}r \quad \text{(A4)}$$

which is reduced to Eq. A3 by using Eq. A1 for the potential $V(r)$.[19,20] Selected values of the δ_l of the boron atom are listed in Table VI.

The sum in Eq. 10 in the text has been taken in the range of $0\leq l\leq 250$ by using the phases of the partial waves given by Eq. A3, which may be good approximations for both the Born phases and the WKBJ phases. The results of the partial-waves calculations are shown in Tables VII and VIII.

19) T. Tietz, ibid., **42**, 2251 (1965).
20) J. A. Hoerni and J. A. Ibers, *Phys. Rev.*, **91**, 1182 (1953).

BULLETIN OF THE CHEMICAL SOCIETY OF JAPAN VOL. 39 1154—1160 (1966)

Studies of Calcichrome as a Spectrophotometric Reagent. I. A New Spectrophotometric Method for the Determination of Copper with Calcichrome and Its Basic Study

By Hajime Ishii and Hisahiko Einaga

Central Research Laboratory, Onoda Cement Co., Ltd., Koto-ku, Tokyo

(Received August 9, 1965)

It was found that Calcichrome, which has been recently established as a reagent for the determination of calcium, forms a stable 1-to-1 complex with copper. Basic studies were carried out, in which the acid dissociation constants of Calcichrome and the apparent formation constant of the complex were determined to be $pK_{a_7}=7.2$, $pK_{a_8}=11.5$, and $K=4.1\times10^8$ respectively. A new method for the determination of copper was also established.

Calcichrome, the self-coupling product of H-acid, was recently suggested by Close and West[1] as a selective metallochromic indicator for the complexometric titration of calcium. As the reagent has several points of excellence, for instance, an easy solubility in water and a stability for storage, it has been used for the determination of calcium in various materials by several investigators.[2-5] It has also been found that the reagent can be used as a spectrophotometric reagent for the determination of calcium.[2-4] The applicability of the reagent to the determination of elements other than calcium as a metallochromic or spectrophotometric reagent has not, however, yet been reported. The authors have recently discovered that the reagent reacts to form complexes with many other metals, such as copper(I and II), iron(II and III), aluminum(III), and titanium(IV). The present paper will describe a direct spectrophotometric method for the determination of copper with Calcichrome and the results of a basic study of it, the outline of this work has already been reported in Short Communication.[6]

1) R. A. Close and T. S. West, *Talanta*, **5**, 221 (1960).
2) A. M. Lukin, K. A. Smirnova and G. B. Zavarikhina, *J. Anal. Chem.* (*U. S. S. R.*), **18**, 389 (1963).
3) M. H.-Lancina and T. S. West, *Anal. Chem.*, **35**, 2131 (1963).
4) P. Pakalns and T. M. Florence, *Anal. Chim. Acta*, **30**, 353 (1964).
5) H. Ishii and H. Einaga, *Japan Analyst* (*Bunseki Kagaku*), **14**, 162 (1965).
6) H. Ishii and H. Einaga, This Bulletin, **38**, 1416 (1965).

Experimental

Reagents.—*Calcichrome Solution.* — A Calcichrome solution (2×10^{-3} M) was prepared by dissolving 0.9909 g. of Calcichrome in distilled water and diluting it to 500 ml. Working solutions were prepared from this solution by dilution. The Calcichrome used in this study was synthesized and purified by the method proposed by Close et al.[1] However, as it contains a small amount of chloride and sodium, furhter purification was carried out as follows for use in potentiometric titrations: Calcichrome was dissolved in distilled water, and the resulting solution was passed through a column packed with cation exchange resin, Amberlite IR-120 (H-form), and then evaporated to dryness on a steam bath, followed by drying at 105°C in an air oven. The Calcichrome thus obtained was free from chloride and sodium.

Standard Cupric Solution.—A standard cupric solution corresponding to 1×10^{-2} mol./l. of copper(II) was prepared by dissolving 2.4969 g. of cupric sulfate penta-hydrate in distilled water, by then adding small amounts of sulfuric acid to prevent any possible hydrolysis, and by diluting the mixture to 1 l. Working solutions of copper(II) were prepared from this solution by dilution.

Standard Cuprous Solution.—A standard cuprous solution corresponding to about 1×10^{-2} mol./l. of copper(I) was prepared by dissolving about 1 g. of cuprous chloride

in distilled water containing small amounts of hydrochloric acid, by then adding about 1 g. of hydroxylamine hydrochloride to prevent any possible oxidation, and by diluting the mixture to 1 l. This solution was standardized by the EDTA titration method, using xylenol orange as an indicator. Working solutions of copper(I) were prepared by diluting the standard solution with distilled water.

Buffer Solutions.—Buffer solutions were prepared by mixing 1 M acetic acid and 1 M sodium acetate in the ratios required.

Apparatus. — A Hitachi automatic recording spectrophotometer, model EPS-2, and a Hitachi spectrophotometer, model 139, were used, together with 1 cm. matched cells, for obtaining absorption curves and for all the other absorbance measurements respectively. A Toa Dempa glass-electrode pH meter, model HM-5A, was used for all the pH measurements.

The Proposed Procedure for the Determination.—To a sample solution containing copper in a 50 ml. volumetric flask, 5 ml. of the Calcichrome solution (4×10^{-4} M) and 10 ml. of the buffer solution (pH 5.2) were added. After the solution had then been diluted with distilled water to the mark, the absorbance of the solution was measured at 535 or 310 mμ against a reagent blank treated in a similar manner.

Results and Discussion

Absorption Curves.—The absorption curves of the copper-Calcichrome complex are shown in

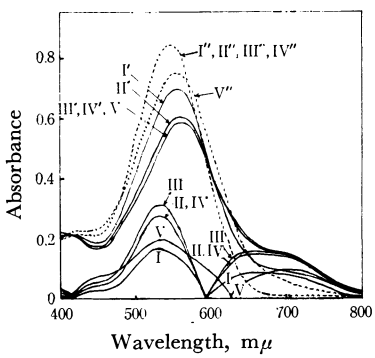

Fig. 1-a. Absorption spectra of Cu(I)-Calcichrome complex and Calcichrome.

I : pH=3.2 Cu(I)-Calcichrome complex
II : pH=4.1 Cu(I)-Calcichrome complex
III : pH=4.9 Cu(I)-Calcichrome complex
IV : pH=5.9 Cu(I)-Calcichrome complex
V : pH=7.2 Cu(I)-Calcichrome complex
} Reference: reagent blank

I' : pH=3.2 Cu(I)-Calcichrome complex
II' : pH=4.1 Cu(I)-Calcichrome complex
III' : pH=4.9 Cu(I)-Calcichrome complex
IV' : pH=5.9 Cu(I)-Calcichrome complex
V' : pH=7.2 Cu(I)-Calcichrome complex
} Reference: water

I'' : pH=3.2 Calcichrome alone
II'' : pH=4.1 Calcichrome alone
III'' : pH=4.9 Calcichrome alone
IV'' : pH=5.9 Calcichrome alone
V'' : pH=7.2 Calcichrome alone
} Reference: water

Calcichrome : 3.2×10^{-5} mol./l.
Cu(I) : 3.2×10^{-5} mol./l.

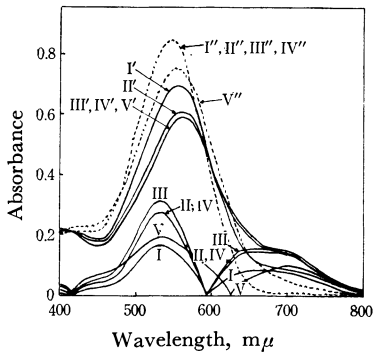

Fig. 1-b. Absorption spectra of Cu(II)-Calcichrome complex and Calcichrome.

I : pH=3.2 Cu(II)-Calcichrome complex
II : pH=4.1 Cu(II)-Calcichrome complex
III : pH=4.9 Cu(II)-Calcichrome complex
IV : pH=5.9 Cu(II)-Calcichrome complex
V : pH=7.2 Cu(II)-Calcichrome complex
} Reference : reagent blank.

I' : pH=3.2 Cu(II)-Calcichrome complex
II' : pH=4.1 Cu(II)-Calcichrome complex
III' : pH=4.9 Cu(II)-Calcichrome complex
IV' : pH=5.9 Cu(II)-Calcichrome complex
V' : pH=7.2 Cu(II)-Calcichrome complex
} Reference: water

I'' : pH=3.2 Calcichrome alone
II'' : pH=4.1 Calcichrome alone
III'' : pH=4.9 Calcichrome alone
IV'' : pH=5.9 Calcichrome alone
V'' : pH=7.2 Calcichrome alone
} Reference: water.

Calcichrome : 3.2×10^{-5} mol./l.
Cu(II) : 3.2×10^{-5} mol./l.

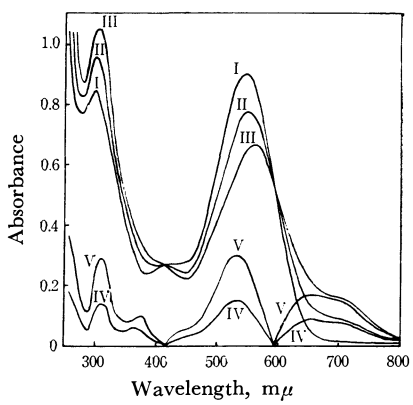

Fig. 1-c. Absorption spectra of Cu(II)-Calcichrome complex.
Calcichrome: 4×10^{-5} mol./l., pH: 5.0

I: Cu=0
II: Cu: Cch=1: 2
III: Cu: Cch=1: 1
} Reference: water

IV: Cu: Cch=1: 2
V: Cu: Cch=1: 1
} Reference: reagent blank

Figs. 1-a, 1-b, and 1-c. By comparing Fig. 1-a with Fig. 1-b, it will be found that these two figures are exactly the same. The copper(I)-Calcichrome complex, therefore, can not be distinguished from the copper(II)-Calcichrome complex, and the

species of the complex formed under the conditions studied are one and the same because the maximum absorption wavelengths of the curves obtained against reagent blanks are identical at 535 mμ. (Although curve V in Fig. 1-a or 1-b differs from the others, this is due to the fact that the absorption curve of Calcichrome itself shifts to the long wavelength side). The ultraviolet and visible absorption curves of the copper(II)-Calcichrome complex at pH 5.0 at various ratios of copper and Calcichrome are shown in Fig. 1-c, from which it may be seen that the complex consisting of a 1-to-1 mixture has two absorption maxima in the ultraviolet (λ_{max} 307 mμ) and visible (λ_{max} 565 mμ) regions, one shoulder at about 700 mμ, and two isosbestic points at 415 and 595 mμ respectively. The curves obtained against a reagent blank have three absorption maxima (λ_{max} 310, 535, and 650 mμ). Although these three wavelengths may be used for the determination of copper(II), the sensitivities at the first two wavelengths are higher than that at the last, and approximately the same sensitivity was obtained at the former.

The ultraviolet and visible absorption curves of the copper(I)-Calcichrome complex under the same conditions were exactly the same as those of the copper(II)-Calcichrome complex; they are therefore omitted here. Judging from the results obtained above, the same considerations can be made of the complex between copper(I) and Calcichrome.

The Effect of pH on the Color Development.—The effect of pH on the color development of the copper(II)-Calcichrome complex was examined by measuring the absorbance of the complex at two wavelengths, 310 and 535 mμ, in which cases the concentrations of copper(II) and Calcichrome were made to 4×10^{-5} mol./l. The results are shown in Fig. 2, from which it can be seen that the maximum color development can be obtained in the pH ranges from 5.0 to 6.5 when measured at 310 mμ and from 5.0 to 5.5 at 535 mμ, and that approximately the same color intensity is obtained in these pH regions.

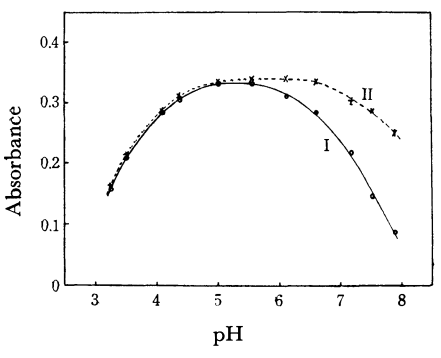

Fig. 2. Effect of pH on absorbance of the Cu(II)-Calcichrome complex.
Concn. of Cu(II): 4×10^{-5} mol./l.
Concn. of Calcichrome: 4×10^{-5} mol./l.
I: at 535 mμ II: at 310 mμ

The effect of pH on the color development of the copper(I)-Calcichrome complex was the same as on that of the copper(II)-Calcichrome complex.

The Effect of the Amount of Calcichrome.—The effect of the reagent concentration on the color development was studied with two series of colored solutions, one of which contained 31.8 μg. of copper(II) (corresponding to 1×10^{-5} mol./l.) and the other, 63.5 μg. of copper(II) (corresponding to 2×10^{-5} mol./l.). The pH values of the solutions were kept constant at 5.2, and the absorbance measurements were carried out at 535 mμ. The results are shown in Fig. 3. For both series, about a 2-fold excess of the reagent over the copper(II) concentration is necessary to obtain the maximum color intensity.

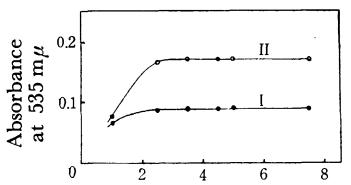

Fig. 3. Effect of amount of Calcichrome.
pH: 5.2, Reference: reagent blank
I: Cu(II), 31.8 μg. II: Cu(II), 63.5 μg.

The same results were obtained when copper(I) was used instead of copper(II). As a compromise between sensitivity and absorbance by the blank solution, 5.0 ml. of a 4×10^{-4} M reagent solution should be used with these copper concentrations.

The Stability of the Color.—The color of the copper(I or II)-Calcichrome complex develops instantaneously at room temperature and is very stable, and there was no change in absorbance over a period of 24 hr.

Adherence to Beer's Law.—The linear relationship between the absorbance and the concentration of copper at 535 mμ was found to be dependent upon the concentration of Calcichrome; Beer's law was obeyed when the molar ratio of copper(II) to Calcichrome was less than about 0.8. The molar extinction coefficient (ε) was about 8×10^3, and the sensitivity was 0.008 μg. Cu(II)/cm^2, which corresponds to log $(I_0/I)=0.001$. Similar results were obtained at 310 mμ.

With the copper(I)-Calcichrome complex, similar results (ε: 8×10^3, sensitivity: 0.008 μg. Cu(I)/cm^2) were obtained.

The Effect of Diverse Ions.—The effect of diverse ions on the determination of copper was examined at pH 5.0. The results are summarised in Table I, from which it can be concluded that aluminum(III), iron(II and III), titanium(IV),

vanadium(V), and zirconium(IV) interfere markedly, even in the smallest amounts, and that nickel(II), oxalate and thiosulfate, also interfere. Among these, the interference by cations seems to be due to the complex formation with Calcichrome under the conditions examined.

Table I. Effect of diverse ions
Cu taken: 75.5 μg.

Diverse ion, added μg.		Cu found μg.	Relative error %
Ag(I)	500	75.5	± 0.0
Al(III)	25	87.6	+16.0
	50	95.8	+26.9
	75	102.3	+35.5
Ba(II)	280	75.5	± 0.0
Ca(II)	500	75.5	± 0.0
Cd(II)	500	75.5	± 0.0
Co(II)	500	75.5	± 0.0
Cr(III)	500	75.5	± 0.0
Cr(VI)	500	75.5	± 0.0
Fe(II)	25	82.0	+ 8.6
	50	87.0	+15.2
	75	91.0	+20.5
Fe(III)	25	119.8	+58.7
Hg(II)	500	75.5	± 0.0
Mg(II)	500	74.2	− 1.7
Mn(II)	500	75.5	± 0.0
Ni(II)	50	78.4	+ 3.8
	500	79.5	+ 5.3
Pb(II)	500	75.5	± 0.0
Si(IV)	500	75.5	± 0.0
Sn(II)	500	75.5	± 0.0
Sr(II)	500	76.0	+ 0.7
Ti(IV)	30	78.5	+ 4.0
	150	85.0	+12.6
	300	87.5	+15.9
V(V)	12.5	80.0	+ 6.0
	37.5	88.5	+17.2
	125	112.5	+49.0
Zn(II)	500	75.5	± 0.0
Zr(IV)	50	78.0	+ 0.7
	250	81.0	+ 7.3
	500	84.0	+11.3
Cl^-	2500	75.5	± 0.0
NO_3^-	2500	75.5	± 0.0
PO_4^{3-}	2500	75.5	± 0.0
$C_2O_4^{2-}$	25	74.5	− 1.3
	75	73.0	− 3.3
	250	70.0	− 6.7
$S_2O_3^{2-}$	50	75.0	− 0.7
	75	72.8	− 3.6
	250	72.3	− 4.2

The Composition of the Complex.—Attempts to obtain the composition of the complex were made by two methods, the continuous variation method and the mole ratio method. These attempts were performed at pH 5.2, and the absorbance measurements were made at three wavelengths between 510 and 545 mμ. Both methods revealed that copper(I or II) forms a 1-to-1 complex with Calcichrome. These findings were further confirmed by the experiments described below. As an example, the results obtained by the application of the continuous variation method to the copper(II)-Calcichrome complex are shown in Fig. 4-a, and those obtained by the application of the mole ratio method to the copper(I)-Calcichrome complex, in Fig. 4-b.

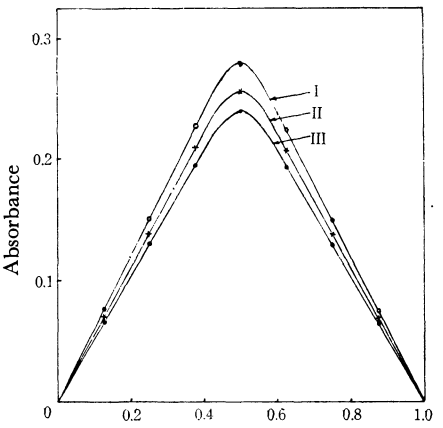

Fig. 4-a. Continuous variation method.
Copper concn. + Calcichrome concn. $=8\times10^{-5}$ mol./l.
pH: 5.2. I: 535 mμ, II: 545 mμ, III: 510 mμ

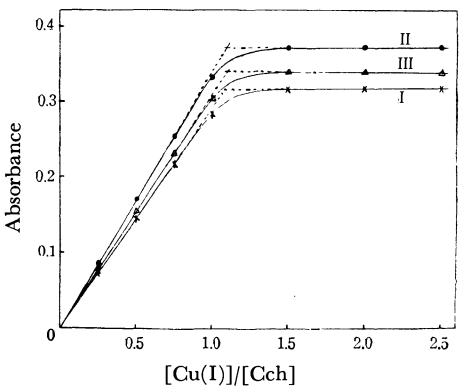

Fig. 4-b. Mole ratio method.
Concn. of Calcichrome: 4.2×10^{-5} mol./l.
I: 510 mμ, II: 535 mμ, III: 545 mμ

The Potentiometric Titration of Calcichrome and Its Copper Complex. — The potentiometric titration of Calcichrome and its copper(II) complex were carried out in order to establish the mechanism of the reaction between Calcichrome and copper, in which case the concentrations of Calcichrome and copper(II) were made to 5×10^{-4} mol./l. the ionic strength was kept constant at 0.1 using a sodium chloride solution and the titration was carried out at 25°C with a 0.3 N potassium hydroxide solution. The results are shown in Fig. 5, in which the curves I and II show the titration curves of Calcichrome and

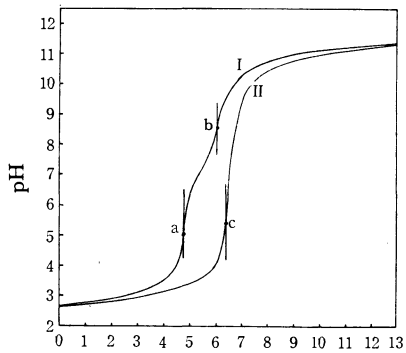

Fig. 5. Potentiometric titration curves of Calcichrome and its copper(II) complex.

Concn. of Copper(II): 5×10^{-4} mol./l.
Concn. of Calcichrome: 5×10^{-4} mol./l.
Ionic strength: 0.1
I: Calcichrome alone
II: Copper(II)-Calcichrome complex

its 1-to-1 copper(II) complex respectively. From Fig. 5 it may be noticed that Calcichrome dissociates to liberate five protons up to about pH 5 (point a) that a) sixth proton is liberated up to about pH 8.5 (point b), and that the sixth proton is also liberated in the complexation. According to the constitutional formula of Calcichrome proposed by Close et al.[1] or Lukin et al.[2], six sulfonic radicals are contained in one molecule of Calcichrome. Taking into consideration of the facts described above, it is considered that sulfonic radical may participate in the complexation. However, the dissociation of sulfonic radicals are generally considered to occur in the lower pH region due to their strongly acidic properties as are seen in the cases of the dissociations of Chromotropic acid and its derivatives. Therefore, there remain some doubts to be concluded directly from the results of the potentiometric titration alone that sulfonic radical may participate in the complexation and further studies should be carried out to solve the problem.

Aside from the experimental results obtained above, the authors considered here on the basis of the general consideration that the group which participate in the complexation is hydroxyl radical rather than sulfonic. Therefore, it may be considered that the dissociation of Calcichrome is shown by Eq. 1, and that copper(II) and/or copper(I) is combined with a hydroxyl radical in the Calcichrome molecule, the reaction in this case being shown by Eq. 2 or 3:

$$H_9Cch^0 \rightleftarrows H_{9-m}Cch^{m-} + mH^+ \quad (1)$$

$$H_3Cch^{6-} + Cu^{2+} \rightleftarrows CuH_2Cch^{5-} + H^+ \quad (2)$$

$$H_3Cch^{6-} + Cu^{+} \rightleftarrows CuH_2Cch^{6-} + H^+ \quad (3)$$

The Effect of pH on the Absorbance of Calcichrome.—The effect of pH on the absorbance of Calcichrome was examined. Here the concentration of Calcichrome was 4×10^{-5} mol./l., the ionic strength was kept constant at 0.25 using a sodium chloride solution, and the absorbance measurements were carried out at 630 mμ. The results are shown in Fig. 6, from which it will be found that three

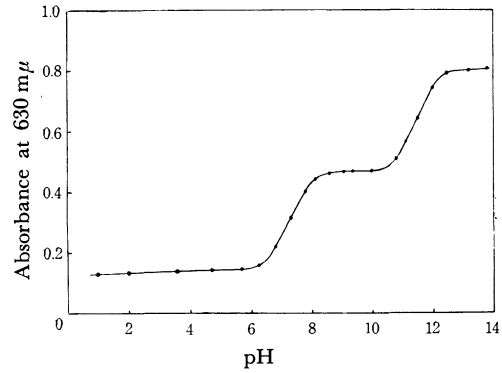

Fig. 6. Effect of pH on absorbance of Calcichrome.

Concn. of Calcichrome: 4×10^{-5} mol./l.
Ionic strength: 0.25

ionic species are present under the conditions examined. Taking account of the discussions described above, these three species are considered to correspond to H_3Cch^{6-}, H_2Cch^{7-}, and $HCch^{8-}$ respectively.

The Acid Dissociation Constant of Calcichrome.—As has been described already, Calcichrome is dissociated as shown by Eq. 1. The seventh and eighth acid dissociation constant, K_{a_7} and K_{a_8}, are:

$$K_{a_7} = [H_2Cch]\,[H]/[H_3Cch] \quad (4)^*$$

$$K_{a_8} = [HCch]\,[H]/[H_2Cch] \quad (5)^*$$

Therefore,

$$pK_{a_7} = pH - \log[H_2Cch]/[H_3Cch] \quad (6)^*$$

$$pK_{a_8} = pH - \log[HCch]/[H_2Cch] \quad (7)^*$$

As the concentrations are proportional to the absorbances, pK_{a_7} and pK_{a_8} are given by the following equations:

$$pK_{a_7} = pH - \log(E_1 - E)/(E - E_2) \quad (8)$$

$$pK_{a_8} = pH - \log(E_2 - E')/(E' - E_3) \quad (9)$$

in which E_1, E_2, and E_3 are the absorbances of H_3Cch^{6-}, H_2Cch^{7-}, and $HCch^{8-}$ respectively at a constant wavelength, and E and E' are the absorbances of the solutions, consisting of H_3Cch^{6-} and H_2Cch^{7-}, and H_2Cch^{7-} and $HCch^{8-}$ respectively, at arbitrary pH values.

The actual examinations were carried out as follows: The concentration of Calcichrome was

* Electronic charges were omitted for the sake of simplicity.

maintained at a constant value, 4×10^{-5} mol./l., and suitable amounts of a disodium hydrogen phosphate - potassium dihydrogen phosphate buffer solution (for the determination of pK_{a_7}) or a 0.1 N sodium hydroxide solution (for the determination of pK_{a_8}) were added to give seven arbitrary pH values between 6.60 and 8.00, or between 10.80 and 11.90, respectively. In both cases, suitable amounts of a sodium chloride solution were added to keep the ionic strength (μ) constant at 0.1. The absorbance measurements were then carried out at 630 mμ. The pK_{a_7} and pK_{a_8} values were calculated from Eqs. 8 and 9 respectively, and the average values of the seven runs are shown in Table II.

TABLE II. pK_{a_7} AND pK_{a_8} OF CALCICHROME

pK_{a_7}	7.2	(μ=0.1, 27°C)
pK_{a_8}**	11.5	(μ=0.1, 23°C)

The Equilibrium Constant.—From the results described above, it seems obvious that copper reacts with Calcichrome to form a 1-to-1 complex and that one proton is liberated as the result of deprotonation during the complex formation. Independent of these facts, on the other hand, the following assumptions and the related examinations were made in order to obtain the equilibrium constant, and also to confirm the facts described above. If the reaction between Calcichrome and copper is obeyed to Eq. 10,

$$Cu^{2+} + H_{9-n}Cch^{n-} \rightleftarrows CuH_{9-(n+m)}Cch^{(n+m)-} + mH^+ \quad (10)$$

the total absorbance at equilibrium, D, is:

$$D = \varepsilon_1(a-x) + \varepsilon_2(b-x) + \varepsilon x \quad (11)$$

where ε_1, ε_2, and ε are the molar extinction coefficients of copper, Calcichrome, and the complex respectively, a and b are the initial concentrations of copper and Calcichrome respectively, and x is the concentration of the complex at equilibrium. As ε_1 is equal to 0, and so may be neglected under these conditions, Eq. 11 can be rearranged to:

$$D = \varepsilon_2(b-x) + \varepsilon x \quad (12)$$

The equilibrium constant, K', may be defined as Eq. 13:

$$K' = [CuH_{9-(n+m)}Cch][H]^m/[Cu][H_{9-n}Cch] = x[H]^m/(a-x)(b-x) \quad (13)^*$$

If the initial concentration of copper, a, is chosen to be equal to that of Calcichrome, Eq. 13 can be rearranged to:

$$K' = x[H]^m/(b-x)^2 \quad (14)$$

By introducing Eq. 12 into Eq. 14, Eq. 15 is obtained:

$$a/(D-D') = 1/(\varepsilon-\varepsilon_2) + \{1/K'(\varepsilon-\varepsilon_2)\}^{1/2}\{[H]^m/(D-D')\}^{1/2} \quad (15)$$

where D' is the absorbance of the reagent blank. When experiments are carried out under suitable conditions and the experimental values of $a/(D-D')$ are plotted against the values of $\{[H]^m/(D-D')\}^{1/2}$, and if the assumption of the value of m is correct, the plots give straight lines with a slope of $\{1/K'(\varepsilon-\varepsilon_2)\}^{1/2}$ and an intercept of $1/(\varepsilon-\varepsilon_2)$.

The actual experiments were carried out under the following conditions. The concentrations of Calcichrome and copper were kept at the same concentration (2×10^{-5} M), the ionic strengths of the solutions were kept at 0.1 with an acetic acid - sodium acetate buffer solution which was added to each solution in order to control the pH value, and the absorbance measurements were carried out at 525, 535, and 545 mμ on six solutions of different pH values between 3.91 and 4.63. The results obtained by plotting the experimental values of

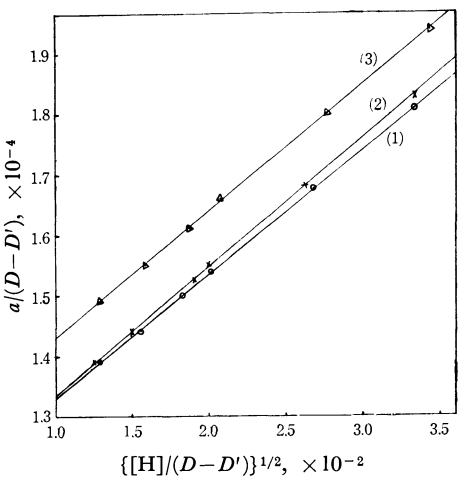

Fig. 7-a. Plots of $a/(D-D')$ vs. $\{[H]/(D-D')\}^{1/2}$ at various wavelengths (in the case of $m=1$). (1): at 535 mμ, (2): at 525 mμ, (3): at 545 mμ

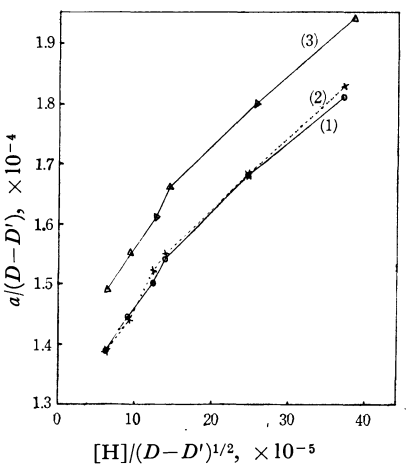

Fig. 7-b. Plots of $a/(D-D')$ vs. $[H]/(D-D')^{1/2}$ at various wavelengths (in the case of $m=2$). (1): at 535 mμ, (2): at 525 mμ, (3): at 545 mμ

Table III. Slope and intercept of lines and equilibrium constant (in the case of $m=1$)

Wavelength	at 535 mμ	at 525 mμ	at 545 mμ	Average
Slope	2.07×10^{-3}	2.12×10^{-3}	2.11×10^{-3}	2.10×10^{-3}
Intercept	1.12×10^{-4}	1.12×10^{-4}	1.22×10^{-4}	1.15×10^{-4}
K'	26.1	24.9	27.4	26.1

$a/(D-D')$ against the values of $\{[H]^m/(D-D')\}^{1/2}$ are shown in Figs. 7-a and 7-b. As may be seen from Fig. 7-a, when the value of m was assumed to be unity, the plots gave straight lines with a slope of 2.10 (on the average). When another value, e. g., two, was assumed for m, however, no straight lines were obtained (shown in Fig. 7-b). Therefore, it may be concluded that one proton is liberated during the complex formation and that the copper-Calcichrome complex formed at the investigated pH value has a molar ratio of 1 to 1. The slopes and the intercepts of lines indicated in Fig. 7-a, which were calculated by the method of least squares, are shown in Table III. The equilibrium constant, K', calculated from these values is also shown in Table III.

The Apparent Formation Constant.—The apparent formation constant, K, was then calculated by Eq. 16 using the values of the acid dissociation constant, pK_{a_7}, and the equilibrium constant, K', already obtained. The value of 4.1×10^8 was obtained as the value of K:

$$K = [CuH_2Cch]/[Cu][H_2Cch] = K'/K_{a_7} \qquad (16)^*$$

which shows a fair stability of the complex.

Summary

The reaction between copper(I or II) and Calcichrome has been studied spectrophotometrically in order to establish the optimum conditions for the determination of copper. In the pH range approximately from 3 to 8, copper(I or II) reacts with Calcichrome to form a stable bluish-violet 1-to-1 complex. The complex has three absorption maxima, at 310, 535, and approximately at 650 mμ, when measured against a reagent blank. Beer's law is obeyed when the molar ratio of copper to Calcichrome is less than about 0.8. The molar extinction coefficient of the complex has been calculated to be 8000. The acid dissociation constants of Calcichrome (pK_{a_7} and pK_{a_8}) and the apparent formation constant (K) were 7.2 and 11.5 ($\mu=0.1$), and 4.1×10^8 respectively. Many other metals, such as aluminum(III), iron(II and III), titanium (IV), vanadium(V) and zirconium(IV), interfere with the determination.

BULLETIN OF THE CHEMICAL SOCIETY OF JAPAN VOL. 39 1160—1163 (1966)

The Behavior of Polonium Evaporated from Fused Salt

By Yuichiro KAMEMOTO and Shigeru YAMAGISHI

Division of Fuel Research and Development, Japan Atomic Energy Research Institute, Tokai, Ibarki, Japan

(Received August 16, 1965)

Studies were made of the evaporation of polonium from a fused potassium chloride - lithium chloride mixture and of the deposition of the evaporated polonium on several metal plates under different temperatures. Approximately 100% of the polonium evaporates, probably as polonium tetrachloride, from the fused salt at the fused salt temperature higher than 500°C when heated for 3 hr. in an argon atmosphere. The evaporated polonium deposited on copper, platinum, palladium and silver plates which were held over the fused salts. The relationship between the percentage of polonium evaporated from these metal plates and the temperature shows that the polonium deposits on these metal plates as elementary polonium or polonide.

Polonium-210 can easily be obtained by separating it from the neutron-irradiated bismuth, the reaction involved being $^{209}Bi\ (n, \gamma)^{210}Bi \xrightarrow{\beta^-\text{-decay}} {}^{210}Po$. The present authors previously studied the extraction of polonium from the irradiated bismuth, using a fused salt, and reported the distribution of polonium between the fused potassium chloride - lithium chloride (eutectic) mixture and the fused bismuth metal.[1] It was found that the polonium in the fused salt was easily evaporated

1) Y. Kamemoto and S. Yamagishi, *J. At. Energy Soc. Japan*, **6**, 500 (1964).

and was removed more rapidly from the fused bismuth metal in contact with fused salt than from that not in contact with fused salt. If the polonium evaporated from the fused salt - fused bismuth system could be collected, this system would be a useful method of separating polonium from the irradiated bismuth.

The evaporation of polonium from the fused potassium chloride - lithium chloride mixture and the deposition of the evaporated polonium on several metal plates were examined under different temperatures, using polonium-210 as the tracer.

Experimental

Reagents.—*Potassium Chloride - Lithium Chloride Eutectic Mixture.*[2]—Potassium chloride and lithium chloride were separately dried by slow heating at 120°C, cooled in a vacuum desiccator, and mixed in the eutectic ratio. The product was fused in an anhydrous hydrogen chloride atmosphere, and the hydrogen chloride was removed from the melt by passing through it purified argon gas. The melt was solidified by pouring it into carbon tetrachloride.

Polonium Tracer.—Polonium-210 was separated by the ion exchange method[3] from a solution of Ra-D, -E and -F extracted from a radon tube. This method involves the adsorption of Ra-D, -E and -F on the anion exchange resin, the elution of Ra-D with a 2 M hydrochloric acid solution, the elution of Ra-E with a 10 M hydrochloric acid solution, and the elution of Ra-F(Po) with a nitric acid solution. The final eluate was evaporated several times with hydrochloric acid, and the residue was dissolved in dilute hydrochloric acid.

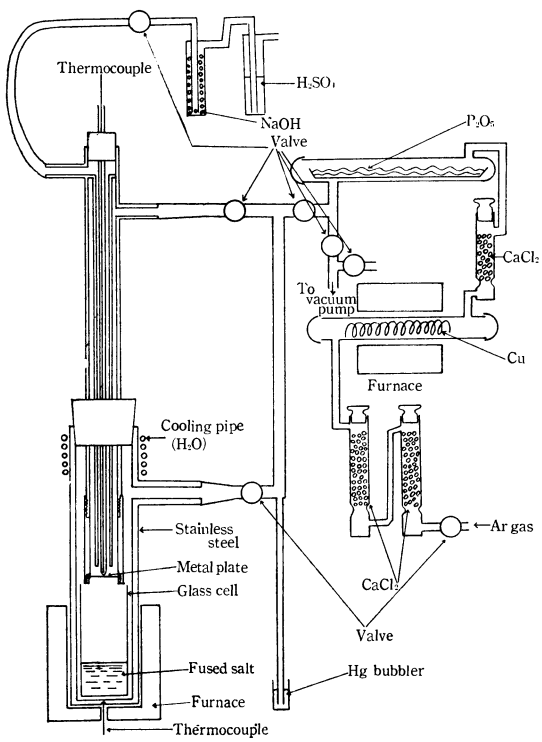

Fig. 1. Experimental apparatus.

Experimental Apparatus.—The apparatus is shown in Fig. 1. The evaporation vessel consists of two cells, an outer, stainless steel cell and an inner, glass cell. The metal plate (24 mm. in diameter) is held over the inner cell with a stainless stell holder. The temperatures of the plate and the fused salt are measured by thermocouples and kept constant by a temperature controller.

Experimental Procedure.—A tenth of a ml. of a polonium tracer solution was added to 10 g. of the potassium chloride - lithium chloride mixture in the inner cell, which was dried by slow heating under reduced pressure. After this inner cell had been placed in the outer cell, as is shown in Fig. 1, the air in the outer and the inner cell was replaced with argon gas, which had been purified by calcium chloride, phosphorus pentoxide, and copper net heated at 350°C. The fused salt, containing polonium-210, was then heated at a certain temperature for 3 hr. under a pressure slightly higher than 1 atm. After cooling, the polonium remaining in the salt was determined and the percentage of polonium evaporated was calculated.

The amount of polonium deposited on the metal plate was also determined, and the percentage of polonium deposited was calculated. The metal plates were disks (24 mm. in diameter) of copper, platinum, palladium and silver.

The metal plate on which polonium had deposited upon the evaporation was held at the middle point in the outer cell with a quartz holder and heated at certain temperatures for 1 hr. in an argon atmosphere; the amount of polonium evaporated was then measured.

Procedure for the Determination of the Polonium.—The amount of polonium deposited on the disk was determined by α-ray counting with a proportional 2π counter.

The polonium remaining in the salt was determined by dissolving the salt in dilute nitric acid, pouring a 10-ml. portion into the cell shown in Fig. 2, depositing spontaneously the polonium on a silver plate by stirring the solution for 1 hr., and counting the alpha activity.

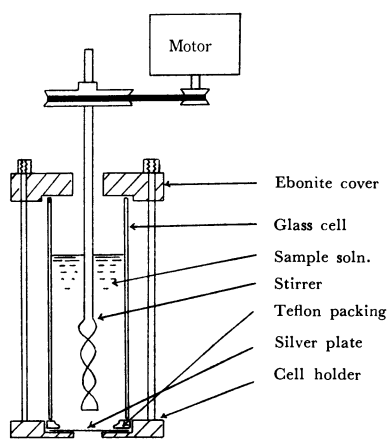

Fig. 2. Apparatus for spontaneous deposition of polonium.

2) S. Yamagishi and Y. Kamemoto, ibid., **5**, 210 (1963).
3) T. Ishimori, This Bulletin, **28**, 432 (1955).

Results

The Evaporation of Polonium from the Fused Potassium Chloride-Lithium Chloride.—The relationship between the temperature of fused salt and the percentage of polonium evaporated is shown in Fig. 3. Approximately 100% of the polonium evaporated from the fused salt at a temperature higher than 500°C within 3 hr. in an argon atmospher.

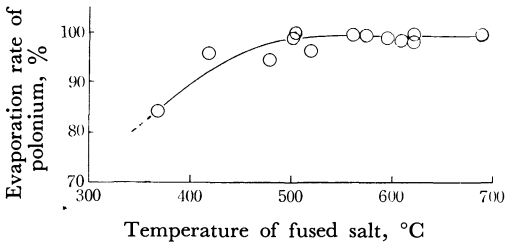

Fig. 3. Evaporation of ^{210}Po from fused salt in argon atmosphere.

The Deposition of Evaporated Polonium on Metal Plates.—The deposition of the polonium evaporated from the fused salt on copper, platinum, palladium and silver plates was determined at various temperatures. The results are shown in Figs. 4—7.

The deposition of polonium on the copper plate decreases with an increase in the temperature of the plate. However, polonium was not deposited on the platinum, palladium and silver plates at temperatures lower than about 290, 300 and 250°C respectively. The amounts of polonium deposited on platinum, palladium and silver plates are constant in the regions between 290—480, 300—400 and 250—425°C respectively, but decrease sharply at higher temperatures.

The Evaporation of the Polonium Deposited on the metal Plates.—The relationship between the amounts of polonium evaporated from metal plates and their temperatures is given in Fig. 8. The evaporation originates at the critical deposition temperatures of polonium (Figs. 4—7). This appears to indicate that the decrease in the percentage of polonium deposited is due to the partial evaporation of polonium from the metal plates.

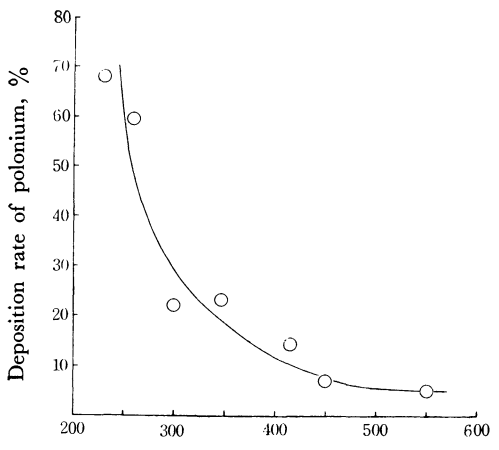

Fig. 4. Deposition of ^{210}Po on copper metal.

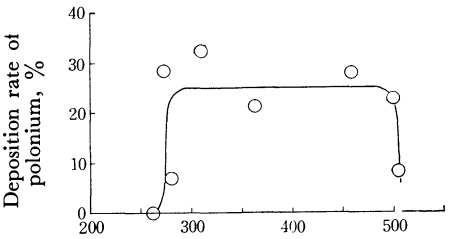

Fig. 5 Deposition of ^{210}Po on platinum metal.

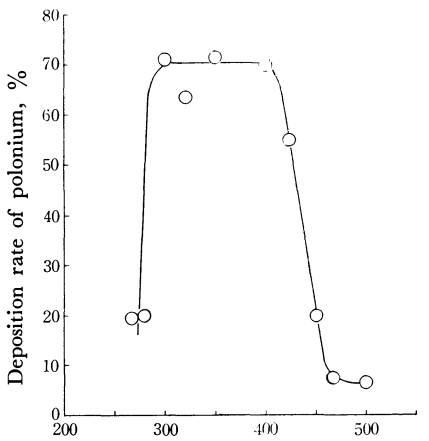

Fig. 6. Deposition of ^{210}Po on palladium metal.

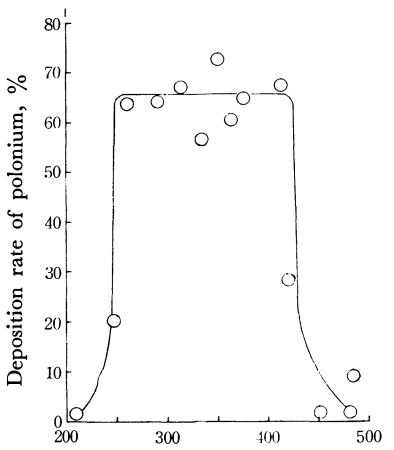

Fig. 7. Deposition of ^{210}Po on silver metal.

Discussion

In the polonium solution extracted from a radon tube, polonium probably exists as tetrachloride,

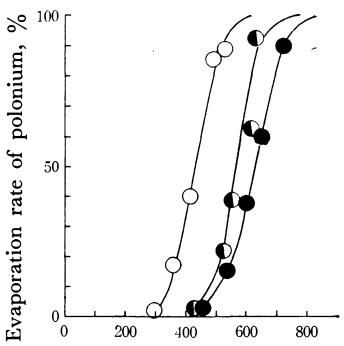

Fig. 8. Evaporation of ^{210}Po from metal plate in argon atmosphere.
○ Cu ● Ag ◐ Pt

because polonium tetrachloride[4-6] is produced by evaporating a solution obtained by dissolving metallic polonium in hydrochloric acid. Thus the fused potassium chloride - lithium chloride mixture, to which this tracer solution has been added, seems to contain polonium in the same form at a low temperature. From this fused salt, polonium is completely evaporated at 500°C in an argon atmosphere under our experimental conditions. The evaporated polonium can not be in the form of polonium dioxide or polonium metal, because neither compound seems to evaporate at this temperature (polonium dioxide sublimes at 885°C and the polonium metal boils at 962°C). The vaporized polonium may be polonium tetrachloride, as its boiling point is 390°C, near to the vaporization temperature experimented with.

Paneth and Hevesy[7-8] reported that almost all the polonium was condensed on a palladium or platinum foil when trace amounts of polonium were distilled in a quartz tube in the flow of a gas and the foil was placed in the cold region of the tube. However, in our experiment, the polonium evaporated from the fused salt was not deposited at a low temperature, but it was deposited at higher temperatures. These results suggest that the polonium evaporated from fused potassium chloride - lithium chloride is not metallic polonium but some polonium compound (probably polonium tetrachloride). This compound seems to be deposited on the metal plate by some reaction and not by adsorption.

Platinum polonide and silver polonide decompose at 450—600°C and approximately 559°C respectively.[7,9] These decomposition temperatures agree with the respective evaporation temperatures of the polonium deposited on platinum and silver metal by our technique using the fused salt. On the other hand, Abe et al. studied the evaporation of polonium-210, at several temperatures and in an argon atmosphere, from certain metal plates on which polonium had spontaneously deposited from a dilute nitric acid solution.[10] Their findings on the relationship between the percentage of polonium evaporated and the temperature of the metal plate are shown in Fig. 9. The evaporation curves of polonium from copper and silver plates, in Figs. 8 and 9, are similar to each other. This shows that the polonium evaporated from the fused salt deposits on the copper and the silver plates in the same form as that spontaneously deposited from a dilute nitric acid solution. It has been thought that the chemical form of the spontaneously-deposited polonium is elementary. From these observations, it seems that the polonium evaporated from the fused potassium chloride - lithium chloride mixture deposits on the metals as elementary polonium or polonide.

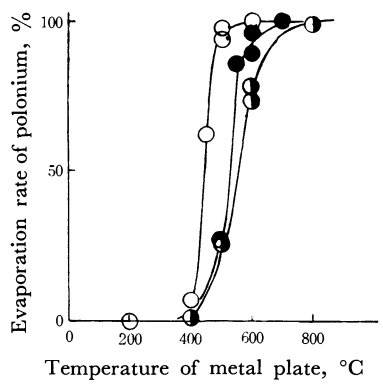

Fig. 9. Evaporation of ^{210}Po deposited spontaneously on metal plate.
○ Cu ● Ag ◑ Ni

On the basis of the arguments presented above, the following explanation can reasonably be made of our results. Polonium is evaporated from the fused potassium chloride - lithium chloride mixture as polonium tetrachloride and deposits on several metals as elementary polonium or polonide.

4) K. W. Bagnall, R. W. H. D'Eye and J. H. Freeman, *J. Chem. Soc.*, **1955**, 2320.
5) J. J. Burbage, *Rec. Chem. Prog.*, **14**, 157 (1953).
6) E. F. Joy, *Amer. Rep.*, M-4123 (1947).
7) K. W. Bagnall, "Chemistry of the Rare Radioelement," Butterworths Scientific Publications, London (1957).
8) F. Paneth and G. Hevesy, *Sitzungsber. Akad. Wiss. Wien. Abt.*, **IIa**, **122**, 1049 (1913).
9) J. M. Goode, *Amer. Rep.*, HLM 677 (1952).
10) S. Abe, S. Yajima and M. Handa, *The 6th Symposium on Radiochemistry, Preprint*, 3B30 (1962).

BULLETIN OF THE CHEMICAL SOCIETY OF JAPAN VOL. 39 1164—1167 (1966)

Studies on the Chemical Decomposition of Simple Sugars. XVII. Pyruvic Acid Formation from D-Glucose-6-^{14}C*

By Sinichi OTANI**

Chemistry Institute, Faculty of Science, Kyoto University, Sakyo-ku, Kyoto

(Received November 29, 1965)

The formation of pyruvic acid from D-glucose-6-^{14}C in a concentrated potassium acid phosphate buffer solution (40%, pH 6.6), was studied. It was found that the C-6 of the glucose was converted into the methyl carbon of pyruvic acid. In view of the formation of pyruvic acid from D-glucose-1-^{14}C, the C-1 and C-6 of the glucose were converted into the methyl carbon of pyruvic acid. This reaction mechanism was similar to that of the formation of acetol (J. Hayami, This Bulletin, **34,** 927 (1961)). The mechanism presented may be summarized as follows: 1) The formation of α-diketose by β-hydroxy-carbonyl elimination after isomerization to 3-ketose or 4-ketose. 2) The formation of acetylformoin by a second β-hydroxy-carbonyl elimination after isomerization to the β-diketose. 3) The hydrolytic cleavage of the acetylformoin.

The formation of pyruvic acid from carbohydrate has never been well studied because of its instability, the low yield, and the difficulty of isolation. Nodzu et al.[1] found pyruvic acid as the 2, 4-dinitrophenylhydrazone in the decomposition of D-glucose, and proposed[2] a mechanism of pyruvic acid formation in which acetylformoin was included as a direct precursor of pyruvic acid. Recently, Hayami et al.[3] effectively used ^{14}C-labeled sugars and methylated sugars for an investigation of the formation of acetol which was formed along with pyruvic acid, and presented a mechanism of the formation of pyruvic acid. In the preceding report,[4] the formation of pyruvic acid from D-glucose-1-^{14}C was examined. The degradation of the alanine which had been derived from pyruvic acid 2, 4-dinitrophenylhydrazine revealed that the C-1 of the D-glucose was converted into the methyl carbon of pyruvic acid.

In the present study, D-glucose-6-^{14}C was decomposed and the relative distribution of a label in the pyruvic acid was determined in order to obtain further evidence of the mechanism of pyruvic acid formation.

Experimental

The Assay Method of Radioactivity.—A sample was converted into barium carbonate by Van Slyke-Folch wet combustion. The barium carbonate was collected on filter paper and counted in an infinite thickness with a 2π-gas flow counter.

The Decomposition of D-Glucose-6-^{14}C.—D-Glucose-6-^{14}C (20 g.) in 200 ml. of a concentrated potassium acid phosphate buffer solution (40%, pH 6.6) was heated and distilled in a way described earlier.[4]

The Isolation of Crude Pyruvic Acid 2, 4-Dinitrophenylhydrazone, and the Reduction of Pyruvic Acid 2, 4-Dinitrophenylhydrazone to Alanine.—These procedures were also carried out in ways described earlier.[4]

The Purification of Alanine.—The crude alanine (16 mg.) was recrystallized from ethanol.

The Degradation of Alanine.—The experiment was carried out in a way described earlier,[4] using 80 mg. of active alanine.

Results and Discussion

In the case of D-glucose-6-^{14}C, radioactivity was mostly found in the methyl carbon of the alanine. This means that the C-6 of D-glucose was converted into the methyl carbon of pyruvic acid. Considering the findings regarding D-glucose-1-^{14}C in the preceding report,[4] it may be concluded

TABLE I. RADIOASSAY DATA OF PYRUVIC ACID*1

Carbon atom(s)	Radioactivity c.p.m./mol.
Total carbons	16*2
CH_3	14*3
C=O	—*4
COOH	1*5

*1 Degraded in the form of alanine.
*2 Probable error was less than 6%.
*3 Probable error was less than 13%.
*4 Not determined.
*5 Probable error was less than 50%.

* The present work was presented at the Symposium on the Mechanism of Organic Chemical Reactions of the Chemical Society of Japan, Nagoya, October, 1964.

** Present address: College of Liberal Arts and Science, Kyoto University, Kyoto.

1) R. Nodzu, K. Matsui, R. Goto and S. Kunichika, *Mem. Coll. Sci. Kyoto Imp. Univ.*, **20**, 197 (1937).

2) R. Nodzu, *J. Biochem. Soc. Japan* (*Nippon Seikagaku Kaishi*), **18**, 237 (1944).

3) R. Goto, J. Hayami, K. Kudo and S. Otani, This Bulletin, **34**, 753 (1961); J. Hayami, ibid., **34**, 924, 927 (1961).

4) S. Otani, ibid., **38**, 1873 (1965).

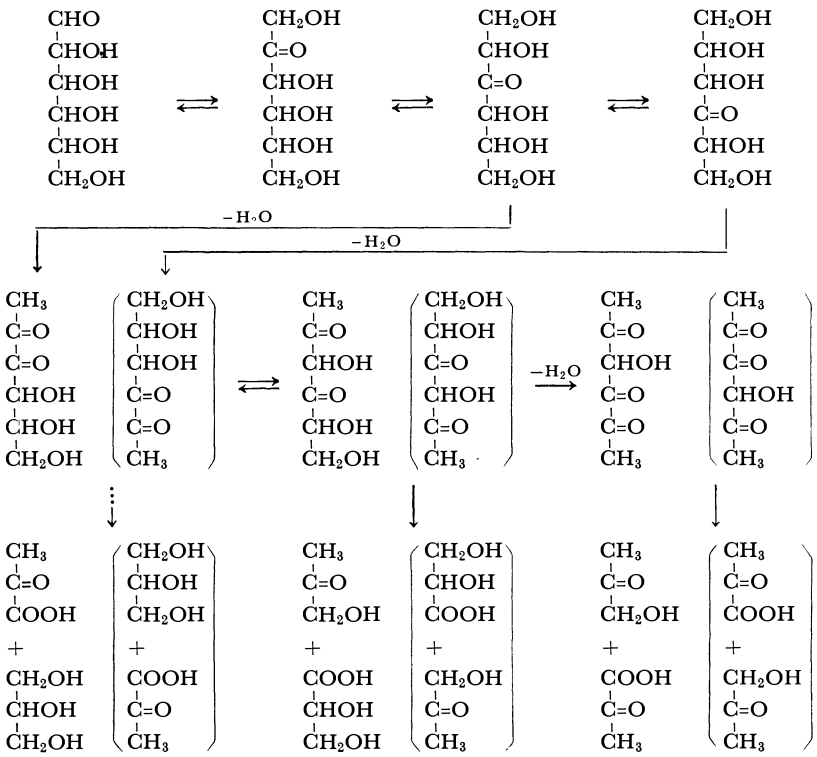

Scheme 1

that the C-1 and C-6 of the glucose were converted into the methyl carbon of pyruvic acid.

In the case of acetol,[3] along with the formation of pyruvic acid, the C-1 and C-6 of the original glucose were converted into the methyl carbon of the acetol, and the C-3 and C-4 of the original glucose were converted into the hydroxymethyl carbon of the acetol. In addition, the acetol-1-^{14}C, which was formed from D-glucose-3, 4-$^{14}C_2$, was found to preserve the molar radioactivity of the original glucose. Therefore, in the formation of acetol, the C-1, 2, 3 and the C-4, 5, 6 portions of the original glucose behaved as units; no skeletal rearrangement in these C_3 units was involved.

Considering the simultaneous formation of acetol and of pyruvic acid from glucose,[1] it seems quite possible that pyruvic acid is formed by a mechanism similar to that of acetol. The mechanism of the pyruvic acid formation can be expressed as shown in Scheme 1.

3-Ketose or 4-ketose, formed by the enolization-ketonization route, is subjected to dehydration by β-hydroxycarbonyl elimination. This conclusion is based on the facts that the methyl carbon of pyruvic acid[4] and of the acetol[3] was found to be converted from the terminal carbon atoms, and that the acetol formation[3] was depressed in the case of 3-*O*-methyl-D-glucose, whereas it was accelerated in the cases of 1-*O*-methyl-D-fructose and 6-*O*-methyl-D-glucose.

The first three steps are known as the Lobry de Bruyn - Alberda van Ekenstein transformation.[5] Since Lobry de Bruyn et al.[6] found the transformation between glucose, mannose and fructose in aqueous alkaline solutions in 1895, the transformation reactions of most reducing sugars have been studied, and the transformation has been recognized to proceed through 1, 2-enediol. Later, transformations by C-3- and C-4-epimerization were observed. For instance, Hough et al.[7] observed the formation of D-psicose from D-glucose by the action of ammonia. Sowden et al.[8] isolated (DL+D)-sorbose from the transformation products of D-glucose in the presence of a strong basic ion-exchange resin.* This means that enolization-ketonization proceeds

5) J. C. Speck, Jr., "Advances in Carbohydrate Chem.," **13**, 63 (1958).

6) C. A. Lobry de Bruyn and W. Alberda van Ekenstein, *Rec. trav. chim.*, **14**, 203 (1895), **15**, 92 (1896), **16**, 257, 262, 274, 282 (1897), **18**, 72 (1899).

7) L. Hough, J. K. N. Jones and E. L. Richards, *J. Chem. Soc.*, **1953**, 2005.

8) M. G. Blair and J. C. Sowden, *J. Am. Chem. Soc.*, **77**, 3323 (1955).

9) W. G. Berl and C. E. Feazel, ibid., **73**, 2054 (1951).

* It was thought that (DL+D)-sorbose could be formed by the aldol condensation of the glyceraldehyde and dihydroxyacetone formed by the fragmentation. In fact, glyceraldehyde gave DL-sorbose and DL-fructose in the presence of alkali.[9] Sowden et al.[10] isolated (DL+D)-sorbose-1-^{14}C from the reaction mixture of D-glucose-1-^{14}C, and from the relative distribution of a label of the enantiomorphs they obtained data showing that the racemic ketose was formed almost exclusively by the enolization-ketonization mechanism, while the fragment-recombination played only a minor role in the isomerization.

through all of the secondary carbon atoms of the chain. Therefore, 1, 2-, 2, 3-, 3, 4-, 4, 5-enediols are possible intermediates in the alkaline isomerization of hexose.

The transformation reaction is usually studied in the presence of bases and placed in the category of alkaline isomerizations, and a sugar is considered to proceed in the form of an anion. However, some instances were found in the presence of acid. This is understandable in view of the facts that the enolization is subjected to a general acid and base catalysis and that the transformation proceeds via enolization.[5] For instance, Ost[11] and Ohno et al.[12] reported the isomerization of D-glucose into D-fructose in dilute sulfuric acid at room temperature. Petuely,[13] observing the isomerization between D-glucose and D-fructose in an acid-catalyzed reaction, considered the protonated sugars to be reaction intermediates. In the formation of the furfural derivatives in the presence of acids, 1, 2-enediol is generally thought to be formed in the first step[14]; in this case, protonation has to be thought of as an important reaction process. Spoehr et al.[15] observed the transformation between D-glucose, D-mannose and D-fructose in a disodium hydrogen phosphate buffer solution (pH 6.69). Ashmarin et al.,[16] using acetate, succinate and formate buffers at pH 4.2, found D-glucose to be transformed to D-fructose. Englis et al.[17] heated D-glucose in a potassium dihydrogen phosphate solution (pH 6.4—6.6) in an autoclave and observed the formation of ketoses the main part of which was D-fructose. Wolfrom et al.[18] obtained (DL+D)-sorbose and (DL+D)-allose from D-fructose in an aconitic acid - potassium hydroxide system (initial pH 8.00; after 24 hr., pH 6.15). In addition to these results, the author observed that D-fructose was formed from D-glucose by heating it in the same medium for one or two hours under the same conditions as those in which pyruvic acid and acetol were formed.[19] From these results, enolization-ketonization can be considered to occur in the present experimental conditions. The mechanism of enolization-ketonization in these nearly neutral solutions has been little discussed. However, Ashmarin et al.[16] proposed that anions of the weak acids were acting as bases, according to Brønsted's conception.

Lobry de Bruyn et al.[6] obtained an unfermentable reducing substance, which they called glutose, as a 3-ketose in an alkali-isomerization mixture of glucose or fructose. Sattler et al.,[20] however, observed that the glutose from D-fructose was a mixture of fructose anhydride and difructose dianhydride. Recently, Sera[21] reported that the so-called "glutosazone" was an impure glucosazone. Thus, 3-ketose has never been proved directly to be formed in an isomerization reaction. When Schaffer synthesized[22] D-manno-3-heptulose and isomerized[23] it in a diluted calcium hydroxide solution at room temperature for a week, he could not detect it in the reaction solution. Stoodley[24] and Sera[25] synthesized a 3-ketopentulose, 3-xylulose. They observed that 3-xylulose was very unstable and that it was easily converted into *erythro*-2-pentulose and *threo*-2-pentulose, even without alkali.* These facts showed that 3-ketose was reactive under the conditions of the Lobry de Bruyn-Alberda van Ekenstein transformation and that the direct detection of 3-ketose in the transformation reaction was impossible.

The next reaction, dehydration by β-hydroxycarbonyl elimination, is generally observed in carbohydrate chemistry. The formation of saccharinic acids[27] in the presence of bases is explained by a benzylic acid-type rearrangement after the dehydration. The formation of furfural derivatives in the presence of acid is also explained by the dehydration.[14,28] Under the present experimental conditions, methylglyoxal was formed from glyceraldehyde by the same type of dehydration.[1]

The α-diketose thus formed isomerizes to the β-diketose without being subjected to the benzylic acid-type rearrangement, and acetylformoin is formed by the second dehydration by β-hydroxycarbonyl elimination. About the isomerization of α-diketone to β-diketone, Hesse et al.[29] recognized that pentane-2-ol-3, 4-dione isomerized

10) J. C. Sowden and R. R. Thompson, ibid., **80**, 1435 (1958).
11) H. Ost, *Angew. Chem.*, **18**, 1170 (1905).
12) Y. Ohno and K. Ward, Jr., *J. Org. Chem.*, **26**, 3928 (1961).
13) F. Tetuely, *Monatsh.*, **84**, 298 (1953).
14) F. H. Newth, "Advances in Carbohydrate Chem.," **6**, 83 (1951).
15) H. A. Spoehr and H. H. Strain, *J. Biol. Chem.*, **85**, 365 (1929).
16) P. A. Ashmarin and Y. S. Belova, *Archi. sci. biol.* (*U. S. S. R.*), **42**, 61 (1936); P. A. Ashmarin and A. D. Braun, ibid., **42**, 53 (1936).
17) O. T. Englis and D. J. Hanahan, *J. Am. Chem. Soc.*, **67**, 51 (1945).
18) M. L. Wolfrom and J. N. Schumacher, ibid., **77**, 3318 (1955).
19) S. Otani, unpublished result.
20) L. Sattler and F. W. Zerban, *Ind. Eng. Chem.*, **37**, 1133 (1945).
21) A. Sera, This Bulletin, **35**, 2031 (1962).
22) R. Schaffer, *J. Am. Chem. Soc.*, **81**, 2838 (1959).
23) R. Schaffer, *J. Org. Chem.*, **29**, 1473 (1964).
24) R. J. Stoodley, *Can. J. Chem.*, **39**, 2593 (1961).
25) A. Sera, This Bulletin, **35**, 2033 (1962).
* Yuen et al.[26] synthesized a 3-ketohexose, DL-*xylo*-3-hexulose, but its transformation reaction has not yet been studied.
26) G. U. Yuen and J. M. Sugihara, *J. Org. Chem.*, **26**, 1598 (1961).
27) J. C. Sowden, "Advances in Carbohydrate Chem.," **12**, 36 (1957); H. S. Isbell, *J. Res. Natl. Bur. Stand.*, **32**, 45 (1944); J. C. Sowden and E. K. Pohlen, *J. Am. Chem. Soc.*, **80**, 242 (1958); J. C. Sowden, M. G. Blair and D. J. Kuenne, ibid., **79**, 6450 (1957); G. Machell and G. M. Richards, *J. Chem. Soc.*, **1960**, 1924, 1932, 1938.
28) J. Kenner and G. N. Richards, ibid., 2921 (1956); W. A. Bonner and M. R. Roth, *J. Am. Chem. Soc.*, **81**, 5454 (1959); T. G. Bonner, E. J. Bourne and M. Ruszkiewicz, *J. Chem. Soc.*, **1960**, 787; M. L. Mednick, *J. Org. Chem.*, **27**, 398 (1962); E. F. L. J. Anet, *J. Am. Chem. Soc.*, **82**, 1502 (1960); *Austral. J. Chem.*, **13**, 396 (1960); **14**, 295 (1961); *Chem. & Ind.*, **1961**, 345; **1962**, 262.
29) G. Hesse and H. S. Stahl, *Chem. Ber.*, **89**, 2414, 2424 (1956).

to pentane-3-ol-2, 4-dione in the presence of proton or hydroxide ion, and reported the isomerization between butane-1-ol-2, 3-dione, butane-2-ol-1, 3-dione, and butane-3-ol-1, 2-dione. Simon,[30] using ^{14}C-labeled sugars, proposed a mechanism including α-diketose $\rightarrow$ β-diketose $\rightarrow$ acetylformoin processes in the formation of 2, 4-dihydroxy-3-piperidino-5-methyl-2-cyclopentanone from 1-deoxy-1-piperidino-D-fructose.

The last step is the hydrolytic cleavage of acetylformoin to form pyruvic acid and acetol. Acetylformoin was synthesized by Nodzu et al.,[31] and found to give pyruvic acid and acetol in a good yield.[32] Compounds with a structure similar to acetylformoin were found to be cleft. For instance, Combes[33] observed the formation of acetol from pentane-3-ol-2, 4-dione by alkali. Blatt et al.[34] and Karrer et al.[35] reported that dibenzoylcarbinol gave benzoylcarbinol and benzoic acid by the use of sodium hydroxide or sodium carbonate. Juni et al.[36] also observed that 3-methylpentane-3-ol-2, 4-dione gave butane-2-ol-3-one and acetic acid by sodium hydroxide. House et al.[37] confirmed the formation of propionic acid and pentane-2-ol-3-one by the sodium hydroxide cleavage of 4-methylheptane-4-ol-3, 5-dione. The hydrolytic cleavage of the carbon-carbon bond between the C-3 and C-4 in the β-diketose stage was the acetol formation process proposed by Hayami et al.[3] The cleavage in the stage of the α-diketose may be conjectured to take place and to give pyruvic acid and glycerin, but there is no experimental data for it. In the case of D-glucose-1-^{14}C,[4] compared with the molar radioactivity of the original labeled glucose and that of the alanine, the lower half of the D-glucose contributed to the formation of the pyruvic acid more than the upper half. The result is compatible with the mechanism in which the acetylformoin is a precursor of pyruvic acid and the acetol, because 3-ketose is thought to be more favorable than 4-ketose in the isomerization reaction.

Thus, the formation of the pyruvic acid can be summarized as follows:

1) The formation of α-diketose by β-hydroxy-carbonyl elimination after isomerization to 3-ketose or 4-ketose.

2) The formation of acetylformoin by a second β-hydroxy-carbonyl elimination after isomerization to the β-diketose.

3) The hydrolytic cleavage of the acetylformoin.

Compared with other carbohydrate reactions in solution, the furfural formation requires neither the transformation nor the benzylic acid - type rearrangement; the saccharinic and the isosaccharinic acid formations need both the *trans*-formation and the rearrangement, and the metasaccharinic acid formation needs the rearrangement, but no transformation. In the present case, it seems probable that the transformation is required without the rearrangement.

The author wishes to express his thanks to Professor Ryozo Goto for his helpful guidance and encouragement, and to Dr. Jun'ichi Hayami for his kind suggestions throughout the course of this work.

30) H. Simon, ibid., **95**, 1003 (1962).
31) R. Nodzu and S. Kunichika, This Bulletin, **15**, 211 (1940).
32) K. Kitamura, Graduation Thesis, Kyoto Imperial University (1938).
33) A. Combes, *Compt rend.*, **111**, 421 (1890).
34) A. H. Blatt and W. L. Hawkins, *J. Am. Chem. Soc.*, **58**, 81 (1936).
35) P. Karrer, J. Kebrle and K. M. Thakkar, *Helv. Chim Acta*, **33**, 1711 (1950).
36) E. Juni and G. A. Heym, *Arch. Biochem. & Biophys.*, **67**, 410 (1957).
37) H. O. House and W. F. Gannon., *J. Org. Chem.*, **23**, 879 (1958).

BULLETIN OF THE CHEMICAL SOCIETY OF JAPAN VOL. 39 1168—1170 (1966)

The Thermal Treatment of Dibenzanthronyls

By Yoshio NAGAI and Kotaro NAGASAWA

The Institute of Industrial Science, The University of Tokyo, Azabu, Tokyo

(Received August 27, 1965)

The ring closure of 3, 3'-dibenzanthronyl to form dibenzanthrone was previously effected by means of homogeneous melting at 430°C in an open vessel or in vacuo (Y. Nagai et al., *J. Chem. Soc. Japan, Ind. Chem. Sect. (Kogyo Kagaku Zasshi)*, **67**, 1977 (1964)). In this report, the thermal treatment of 3, 3'-dibenzanthronyl and its isomers, 3, 4'- and 4, 4'-dibenzanthronyls, in a closed vessel is described. The reaction was carried out in the following way: a glass tube was filled with finely-powdered dibenzanthronyl. The tube was then placed in a stainless-steel bomb and heated to 425—435°C for 25 min. Thus, 3, 3'- or 4, 4'-dibenzanthronyl yielded dibenzanthrone and dibenzanthrene, along with a putative secondary thermal reaction product in the form of a black powder; the nature of this briefly discussed. Similarly, 3, 4'-dibenzanthronyl was converted to isodibenzanthrone and isodibenzanthrene, together with a black powder.

Upon being heated in a closed vessel at 425—435°C, 3, 3'-dibenzanthronyl (I) or 4, 4'-dibenzanthronyl (II) was converted into dibenzanthrone (violanthrone) (III) and dibenzanthrene (IV). Similarly, 3, 4'-dibenzanthronyl (V) was turned into isodibenzanthrone (isoviolanthrone) (IV) and isodibenzanthrene (VII) by the same thermal treatment.

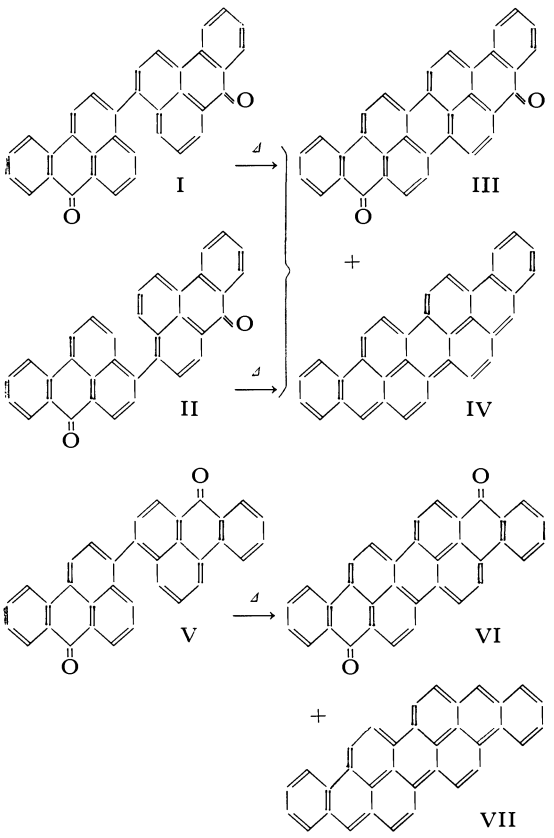

Previously 3, 3'-dibenzanthronyl (m. p. 430°C, uncorr.) was found to suffer from ring closure and to give dibenzanthrone when melted at 430°C in an open vessel under ordinary atmospheric pressure or in vacuo.[1] Its isomers, 3, 4'-dibenzanthronyl (m. p. 330—331°C, uncorr.) and 4, 4'-dibenzanthronyl (m. p. 338—339°C, uncorr.), were, however, not changed by the same treatment, for sublimation prevailed under these conditions. On the other hand, the interference values between hydrogen atoms at the 3- and 4-positions of the benzanthrone residues of these dibenzanthronyls were supposed to be of approximately the same magnitude, and no considerable topochemically-significant differences were found among them. Therefore, further investigations have been made as to whether these dibenzanthronyls give the quinones upon thermal treatment in a vessel closed so as to prevent sublimation. It was thus found, that on separating the pyrolyzed product, the threne was formed unexpectedly, along with the quinone, as has been mentioned above. In addition, when the dibenzanthronyl was heated above 425°C in a closed vessel, a "secondary" thermal reaction product was also obtained as a black powder which dissolved in concentrated sulfuric acid, giving a dark blue color at 50°C. It showed a single, sharp absorption of electron spin resonance, with a spin concentration of the order of 10^{20} spin/g. in the case of 3, 3'-dibenzanthronyl. The shape of the absorption curve indicated that the by-product was not a mere amorphous, graphite-like matter resulting from carbonization. Although further studies of its nature have yet to be carried out, a tentative structure is give in VIII, taking into consideration the fact that the partial reduction product of the quinone, such as that shown in IX, was not separated.

1) Y. Nagai and K. Nagasawa, *J. Chem. Soc. Japan, Ind. Chem. Sect. (Kogyo Kagaku Zasshi)*, **67**, 1977 (1964).

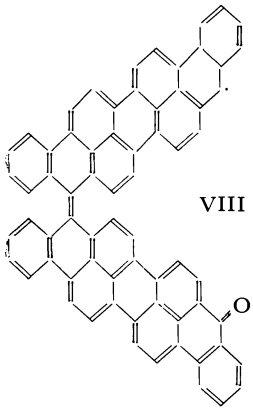

VIII

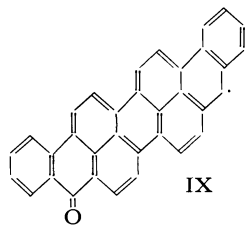

IX

In this connection, dibenzanthrone itself has been reported to be thermally stable up to 475°C,[2] and a dark-red dibenzanthrene was found not to yield any appreciable amount of black matter upon being heated at 450°C. Therefore, it can safely be said that dibenzanthrone and dibenzanthrene are independently unaffected thermally, at least up to 450°C.

Upon being heated above 425°C, with the hydrogen evolved confined in a reaction vessel, 2 mol. of the quinone and 1 mol. of the threne, along with 2 mol. of water, would be produced from 3 mol. of the dibenzanthronyl, if the hydrogen atoms eliminated from the dibenzanthronyl were completely used up in the reduction of carbonyl; this does not take the secondary thermal reaction product into consideration. When the reduction efficiency is taken as unity for this case, the actual efficiencies range from 0.55 to 0.39. The relatively high reduction efficiencies make it probable that the dehydrogenation of the dibenzanthronyl does not proceed by way of molecular hydrogen, but by the step-by-step elimination of the hydrogen radical:

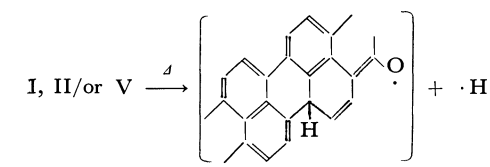

X

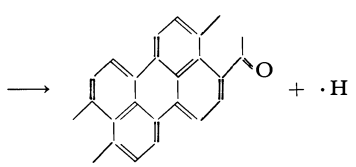

This assumption makes it necessary to consider a radical, such as that shown in **X**, as a presumed transient intermediate for the threne and the secondary thermal reaction product.

The analogous ring closure by means of the thermal treatment of a polynuclear aromatic compound which possesses sterically-hindered C-H bonds is rather sporadic, according to the literature. To cite an example, Clar et al.[3] reported that tetrabenzoperopyrene melts at 482°C, with the evolution of hydrogen, and that it resolidifies with the formation of hexabenzocoronene; the latter can also be obtained from less densely-fused hexaphenylbenzene.[4]

Experimental

The Preparation of Dibenzanthronyls.—*3, 3'-Dibenzanthronyl.*—3, 3'-Dibenzanthronyl was prepared by the condensation of benzanthrone with manganese dioxide in a concentrated sulfuric acid - polyphosphoric acid medium.[5] Purified 3, 3'-dibenzanthronyl, which was negative in its ESR spectum, had a m. p. of 430°C (uncorr.) and was in the form of microscopic yellow needle crystals.

3, 4'-Dibenzanthronyl (II).—3, 4'-Dibenzanthronyl was prepared by cross condensation between 3-chlorobenzanthrone and benzanthrone in sodium anilide at 0°C, following the method of Luttringhaus et al.[6] Purification was carried out with chromatography*1 and recrystallization (m. p. 330—331°C, uncorr.) (331—332°C in the literature), resulting in yellow needle crystals. For the sake of identification, these crystals were then melted with potassium hydroxide; the infrared spectrum of the resultant black violet powder coincided with that of an authentic specimen of isodibenzanthrone.

4, 4'-Dibenzanthronyl.—4, 4'-Dibenzanthronyl was prepared by the alcoholic potash-fusion of benzanthrone at 105°C.[7] With recrystallizations, followed by chromatographic purification, 4, 4'-dibenzanthronyl was obtained as pale yellow plate et crystals (m. p. 338—339°C, uncorr.) (326°C, corr., in the literature). After being subjected to kali-fusion, the resultant black violtet powder was identified from its infrared spectrum as dibenzanthrone.

The Thermal Treatment of Dibenzanthronyls.—*3, 3'-Dibenzanthronyl.* — Finely-powdered 500 mg. of 3, 3'-dibenzanthronyl were charged into a semi-hard glass tube, the open side of which was pulled to a capillary and bent downward. When the tip of the capillary was closed, the glass tube exploded at an elevated temperature in a reaction tube, necessitating the troublesome separation of the glass pieces scattered in the organic matter. The tube was then placed in a stainless-steel reaction tube with a needle bulb mounted on it, and the whole was installed in an electric furnace which had previously been heated to 300°C. Then the temperature was rapidly raised

2) G. Gibson, M. Holohan and H. Riley, *J. Chem. Soc.*, **1946**, 456.

3) E. Clar, C. T. Ironside and M. Zander, ibid., **1959**, 142.

4) A. Halleux, R. H. Martin and G. S. D. King, *Helv. Chim. Acta*, **41**, 1177 (1958).

5) Y. Nagai and K. Nagasawa, *J. Chem. Soc. Japan, Ind. Chem. Sect.* (*Kogyo Kagaku Zasshi*), **68**, 1906 (1965).

6) A. Lüttringhaus and H. Nereshimer, *Ann.*, **473**. 259 (1929).

*1 Commercial alumina for chromatography was deactivated hygroscopically, so that the R_f value (the ratio of development in the radial direction) of the benzanthrone dissolved and developed with benzene lay between 0.6 and 0.7 in disk chromatography. The deactivated alumina is used throughout this report whenever the utilization of alumina or chromatography is described.

7) T. Maki, *J. Chem. Soc. Japan, Ind. Chem. Sect.* (*Kogyo Kagaku Zasshi*), **46**, 1256 (1943).

to 450°C (inner temperature; 430±5°C) (the pressure gauge indicated 2.5 kg./cm² at the maximum). After being kept for 25 min. at that temperature, the reaction tube was immediately taken out of the furnace and cooled to room temperature. By cutting the glass-tube, a dull black-violet mass was obtained. This was pulverized and extracted by refluxing it with 100 g. of *o*-dichlorobenzene. Extraction was repeated as long as a green fluorescence remained in the filtrate. The extracts were then condensed and passed through 5 g. of an alumina layer on a glassfilter (1.5 cm. in diameter). The alumina layer was successively washed with hot *o*-dichlorobenzene until no green fluorescence could be observed in the eluate. *o*-Dichlorobenzene solutions were collected and condensed, then subjected to steam distillation to yield 110 mg. of a dull brownish-red powder, which dissolved in concentrated sulfuric acid with a bluish-green color. After this powder had been sublimed in vacuo, 75 mg. of a dark red crystalline powder were obtained. It did not melt at 450°C, and its infrared spectrum was identical with that of an authentic specimen*2 at the following absorption maxima in the fingerprint region; 735, 742, 784, 818, 840, 870, 938, 1015, and 1198 cm^{-1} (NaCl prism, KBr tablet).

The alumina layer, now free from the reduction product, was impregnated with black violet quinone and the secondary thermal reaction product. It was treated with concentrated sulfuric acid at 50°C, and then the acid was filtered off. The violet filtrate was poured into ice water, and a dark-colored precipitate was collected and washed with water. Then in the form of a dull black slurry, the material was treated with an alkaline sodium dithionite solution at 50—60°C. A red-violet vat was filtered and washed with a warm alkaline sodium dithionite solution to which a small quantity of ethyl alcohol had been added. The vat was then triturated by aeration at room temperature. A black violte precipitate was collected by filtration and dried at 110°C to give 215 mg. of dibenzanthrone (43.4% of the theoretical yield, based on 3, 3'-dibenzanthronyl). This gave a red-fluorescent blue solution with hot *o*-dichlorobenzene and dissolved in concentrated sulfuric acid with a reddish-violet color. Coincidences between its infrared spectrum and that of an authentic specimen were observed at the following absorption maxima; 694, 753, 807, 951, 1034, 1195, 1281, 1298, 1336, 1381, 1450, 1572, and 1642 cm^{-1}.

Unvattable black powder was thoroughly washed with water and dried at 110°C, and then refluxed with 30 g. of nitrobenzene for 1 hr. and filtered while hot. The refluxing was repeated as long as a red fluorescence persisted in the filtrate. Thus, 85 mg. of black powder which was practically insoluble in nitrobenzene were obtained. It became dark blue in warm concentrated sulfuric acid, and when boiled with *asym*-trichlorobenzene, a small quantity of it dissolved and became dark blue. It gave rise to a very sharp ESR signal, corresponding to about 10^{20} spin/g., and showed absorption maxima at $\lambda_{max}^{conc.H_2SO_4}=720$ and 580 mμ. Its infrared spectrum showed an ill-defined absorption at about 1640 cm^{-1}.

When the thermal treatment of 3, 3'-dibenzanthronyl was carried out in a sealed tube at 470°C, no dibenzanthrone was separated, but 70 mg. of dibenzanthrene and 305 mg. of the secondary thermal reaction product were obtained from 500 mg. of the sample.

4, 4'-Dibenzanthronyl.—Under the same conditions as in the case of 3, 3'-dibenzanthronyl, a 100 mg. portion of finely-powdered 4, 4'-dibenzanthronyl was submitted to heating in a sealed tube at 425—435°C for 25 min., yielding 94 mg. of a black powder with a greenish hue. The black powder was then dissolved in 40 cc. of concentrated sulfuric acid at 50°C and poured into ice water. The precipitates were collected and washed until they were neutral. The greenish-black slurry was treated with 50 cc. of a warm alkaline sodium dithionite solution to which 3—4 cc. of pyridine had been added. By filtering and air-oxidizing the red-violet vat, 21 mg. of dibenzanthrone were obtained (21.2% of the theoretical yield). After the unvattable portion had been washed thoroughly with water and then dried, it was refluxed with 50 cc. of nitrobenzene for a few hours. The solution was then passed through 1 g. of alumina on a glass-filter. The eluate was condensed and steam-distilled to give 19 mg. of crude dibenzanthrene, which were recrystallized from *asym*-trichlorobenzene to yield 13 mg. of dibenzanthrene. From the alumina layer, 30 mg. of the secondary thermal reaction product were obtained as a black powder. The infrared spectra of dibenzanthrone and dibenzanthrene were identical with those of the authentic specimens.

3, 4'-Dibenzanthronyl. — Finely-powdered 100 mg. of 3, 4'-dibenzanthronyl were treated at 425—435°C for 25 min. in a sealed tube. The resultant 93 mg. black mass was treated much as in the case of 4, 4'-dibenzanthronyl. From a clear bluish-violet vat, 38 mg. of isodibenzanthrone (38.4% of the theoretical yield) were obtained. This dissolved in concentrated sulfuric acid with a green color, and its infrared spectrum coincided at the following absorption maxima with that of an authentic specimen; 702, 750, 805, 977, 1077, 1281, 1310, 1380, 1474, 1501, 1563, 1588, and 1638 cm^{-1}.

Out of the unvattable portion, 30 mg. of crude isodibenzanthrene were separated; after this had been sublimed in vacuo, 12 mg. of isodibenzanthrene were obtained as a dark red crystalline powder which did not melt at 450°C. Coincidences of the infrared spectrum with that of an authentic specimen at the following maxima in the fingerprint region were observed; 737, 745, 790, 826, 876, 934, 1020, and 1186 cm^{-1}.

Besides the above reaction products, 13 mg. of a black powder were yielded; this powder dissolved in concentrated sulfuric acid at 70°C with a dark color.

The authors are indebted to Professor Shizuo Fujiwara of the Faculty of Science, the University of Tokyo, for providing facilities for measuring the ESR spectra and to Associate Professor Nobuyuki Goto of the Institute of Industrial Science, the University of Tokyo, for his valuable suggestion. They also wish to thank Mr. Osamu Iwayama for his assistance in carrying out the experiments.

*2 The authentic specimens of dibenzanthrene and isodibenzanthrene were prepared by means of the Clar reduction of pure dibenzanthrone and isodibenzanthrone respectively, followed by purification with sublimation in vacuo (E. Clar. *Ber.*, **72**, 1645 (1939); J. Aoki, dissertation, The University of Tokyo, 1964).

BULLETIN OF THE CHEMICAL SOCIETY OF JAPAN VOL. 39 1171—1178 (1966)

Syntheses of Peptides Related to the *N*-Terminal Structure of Corticotropin. VI. The Synthesis of Ser^1- and Gly^1-Decapeptides Corresponding to the First Ten-amino-acid Sequence of Corticotropin

By Hideo OTSUKA, Ken INOUYE, Fusako SHINOZAKI and Makoto KANAYAMA

Biochemistry Division, Shionogi Research Laboratory, Shionogi & Co., Ltd., Fukushima-ku, Osaka

(Received August 27, 1965)

t-Butyloxycarbonyl-seryl-(and-glycyl-)tyrosyl-seryl-methionyl-glutamyl-histidyl-phenylalanyl-arginyl-tryptophyl-glycine have been synthesized as the first step of the synthesis of adrenocorticotropically active peptides. The trifluoroacetic acid treatment of these two compounds afforded the free decapeptides, seryl-tyrosyl-seryl-methionyl-glutamyl-histidyl-phenylalanyl-arginyl-tryptophyl-glycine, which corresponded to the amino-acid sequence of positions 1 to 10 in the corticotropin molecule, and its glycine^1-analog. Concerning the synthesis of serine peptides, a tetrapeptide derivative, corresponding to the first four amino acid residues of corticotropin, was obtained by using *O*-benzyl-serine.

In 1961 Hofmann and Yajima reported that a synthetic tridecapeptide amide, corresponding to the first thirteen amino acid residues of corticotropin (ACTH), exhibited a very low but reproducible ACTH activity.[1] Later Li and his collaborators synthesized a pentadecapeptide which had a sequence corresponding to positions 1—10 plus positions 15—19 of the corticotropin molecule, and the product was found to be active at a low level of potency.[2] From these facts it seemed that the amino terminal decapeptide portion might have a structure functionally essential for the hormonal activity, even if the decapeptide itself did not elicit any appreciable potency.

We have recently completed the synthesis of some biologically-active peptides related to the corticotropin molecule.[3-5] Each of them was obtained by connecting the amino terminal decapeptide fragment with the carboxyl terminal moiety of the molecule. During the course of these syntheses, we prepared the free decapeptide, corresponding to the first ten amino acid residues of corticotropin, and its analog, which had a glycine in place of the amino terminal serine; we prepared, that is, seryl-tyrosyl-seryl-methionyl-glutamyl-histidyl-phenylalanyl-arginyl-tryptophyl-glycine (α-$^{1-10}$-ACTH) (I) and glycyl-tyrosyl-seryl-methionyl-glutamyl-histidyl-phenylalanyl-arginyl-tryptophyl-glycine (α^{1-10}-Gly^1-ACTH) (II).*1 As has been stated above, peptide I may provide a functional core for the ACTH activity, while its protected derivative is a key fragment for the synthesis of adrenocorticotropically-active peptides. In this respect, peptide II may be considered to be the same as peptide I, since the hydroxyl group of the terminal serine has been recognized as being nonessential for the activity.[6] We wish to describe here the synthesis of peptides I and II in detail. Concerning the synthesis of serine peptides, the use of *O*-benzylserine will also be described.

The Synthesis of α^{1-10}-Gly^1-ACTH (II).— Serine was acylated by using 1.1—1.2 equivalent moles of *t*-butyl azidoformate[7,8] to obtain *t*-butyloxycarbonyl-serine (III), which was first isolated in the form of a dicyclohexylamine salt[9] in a 60 per cent yield. The dicyclohexylamine salt was then treated with Dowex-50 (H^+-form) in order to recover compound III, which crystallized as the monohydrate. The crystalline monohydrate became sirupy in a desiccator as a result of the immediate loss of water. When a 100 per cent excess of the azide was used for the above acylation, we could not obtain the crystalline III after all; it appeared most likely that the *O*-acylation of serine had occurred to some extent as a side reaction. The *N*, *N'*-dicyclohexylcarbodiimide (DCCl)-induced coupling[10] of III with the methionine

1) K. Hofmann and H. Yajima, *J. Am. Chem. Soc.*, **83**, 2289 (1961).
2) C. H. Li, J. Ramachandran and D. Chung, ibid., **86**, 2711 (1964); **85**, 1895 (1963).
3) H. Otsuka, K. Inouye, M. Kanayama and F. Shinozaki, This Bulletin, **38**, 679 (1965).
4) H. Otsuka, K. Inouye, M. Kanayama and F. Shinozaki, ibid., **38**, 1563 (1965).
5) H. Otsuka, K. Inouye, F. Shinozaki and M. Kanayama, *J. Biochem.* **58**, 512 (1965).
*1 All amino acid residues are of the L-configuration with the exception of glycine.
6) H. E. Lebovitz and F. L. Engel, *Endocrinol.*, **73**, 573 (1963).
7) L. A. Carpino, *J. Am. Chem. Soc.*, **79**, 98 (1957); L. A. Carpino, C. A. Giza and B. A. Carpino, ibid., **81**, 955 (1959).
8) K. Inouye, M. Kanayama and H. Otsuka, *J. Chem. Soc. Japan, Pure Chem. Sect.* (*Nippon Kagaku Zasshi*), **85**, 599 (1964).
9) E. Klieger, E. Schröder and H. Gibian, *Ann.*, **640**, 157 (1961); F. Weygand and K. Hunger, *Z. Naturforsch.*, **13b**, 50 (1958).
10) J. C. Sheehan and G. P. Hess, *J. Am. Chem. Soc.*, **77**, 1067 (1955).

Table I. Amino acid compositions in the leucine aminopeptidase digests of the decapeptides I and II

Enzyme/substrate ratio (w/w)	Molar ratio (Tyr=1.00)									
	Decapeptide II									
	1 Gly	2 Tyr	3 Ser	4 Met	5 Glu	6 His	7 Phe	8 Arg	9 Try	10 Gly
1/50*	1.00	1.00†	0.90	0.88	0.64	0.59	0.57	0.51	0.41	0.42
1/20**	1.00	1.00	0.91	0.96	(0.78)	0.87	0.86	0·80	0.80	0.77
1/10**	1.00	1.00	0.96	1.00	0.99	0.92	0.89	(0.99)	(0.79)	0.85
	Decapeptide I									
	1 Ser	2 Tyr	3 Ser	4 Met	5 Glu	6 His	7 Phe	8 Arg	9 Try	10 Gly
1/10**	1.00	1.00††	0.93	0.94	0.96	0.94	0.87	0.83	(0.76)	0.86

* In 0.05 M "Tris" buffer (pH 7.85, 0.005 M Mg^{2+}) - dioxane (4 : 1) at 37°C for 24 hr.

** A solution of the substrate (ca. 1 μmol.) in 0.1 ml. of 0.1 N hydrochloric acid was neutralized with 0.1 N sodium hydroxide and to this were quickly added 0.5 ml. of 0.05 M "Tris" buffer (pH 7.85, 0.005 M Mg^{2+}) and the enzyme solution (1 mg./ml. in the same "Tris" buffer as above).*2 The mixture was then incubated at 37°C for 36 hr.

† Recovery 98%. †† Recovery 97%.

methyl ester yielded the *t*-butyloxycarbonyl-seryl-methionine methyl ester (IV) in a good yield (84%). Compound IV was treated with dry hydrogen chloride in ethyl acetate to give seryl-methionine methyl ester hydrochloride as an oil. In this case, it was found that the protective group was not split appreciably, even after 30 min. at room temperature, when anhydrous methanol was used as the solvent in place of ethyl acetate. We previously used a formyl group[11] for the protection of an amino function of the peptide containing a methionine residue.[12] The *t*-butyloxycarbonyl group,[7] which has recently become available, seems to be more advantageous than the formyl group, since the former unlike the latter,[11] usually offers no opportunity for the coupling procedures to be employed. The oily hydrochloride of the seryl-methionine methyl ester was converted into the free base (V), which then crystallized readily from ethyl acetate in a 80 per cent yield based on the IV used. The *t*-butyloxycarbonyl-glycyl-tyrosine methyl ester was easily obtained by the DCCl-mediated condensation of *t*-butyloxycarbonyl-glycine with the tyrosine methyl ester. The amorphous protected dipeptide ester, which was found to be homogeneous in thin-layer chromatography, was converted into the crystalline hydrazide (VI) in a 85 per cent yield based on the *t*-butyloxycarbonyl-glycine used. *t*-Butyloxycarbonyl-glycyl-tyrosine azide, which was derived from compound VI, was made to react with V in acetonitrile to give, in a moderate yield (62%), a crystalline-protected tetrapeptide *t*-butyloxycarbonyl - glycyl - tyrosyl - seryl - methionine methyl ester (VII). Compound VII was then converted into the corresponding hydrazide (VIII).

For the synthesis of a protected decapeptide, *t*-butyloxycarbonyl-glycyl - tyrosyl - seryl - methionyl-γ-*t*-butyl - glutamyl - histidyl - phenylalanyl - arginyl - tryptophyl-glycine (IX), compound VIII was treated with nitrous acid and the resultant azide was allowed to react with the hexapeptide, γ-*t*-butyl - glutamyl - histidyl - phenylalanyl - arginyl - tryptophyl-glycine, the synthesis of which has already been described.[13] The decapeptide (IX) was purified by reprecipitation from dimethylformamide-methanol in a yield of 63 per cent. The purified IX was found to be entirely homogeneous in thin-layer chromatography. The protective group of IX were removed by treatment with trifluoroacetic acid to liberate the decapeptide II (α^{1-10}-Gly^1-ACTH). The synthetic peptide II gave a single spot (R_f=0.36) reactive to ninhydrin, Pauly, Ehrlich, Sakaguchi and methionine (P_tI_6'') reagents on paper in the *n*-butanol - acetic acid - pyridine - water (30 : 6 : 20 : 24 by volume) system.[14] Acid hydrolysis afforded a mixture of the constituent amino acids in the ratios expected by theory, with the exception of the tryptophan, which had partially decomposed with acid.[15] The intact peptide was determined spectrophotometrically to contain tyrosine and tryptophan in a molar ratio of 1 : 1.[16] The peptide II was also submitted to leucine aminopeptidase (LAP) digestion at various enzyme/substrate ratios. The results are presented in Table I, together with those obtained for peptide I. The table shows that the first half of the mol-

*2 Leucine aminopeptidase (LAP) Lot No. 5930, Worthington Biochemical Corporation, Freehold, New Jersey, U. S. A.

11) J. C. Sheehan and D-D. H. Yang, *J. Am. Chem. Soc.*, **80**, 1154 (1958).

12) K. Inouye and H. Otsuka, This Bulletin, **34**, 1 (1961).

13) K. Inouye, ibid., **38**, 1148 (1965).

14) S. G. Waley and J. Watson, *Biochem. J.*, **55**, 328 (1953).

15) D. H. Spackman, W. H. Stein and S. Moore. *Anal. Chem.*, **30**, 1191 (1958).

16) T. W. Goodwin and R. A. Morton, *Biochem. J.*, **40**, 628 (1946); G. H. Beavan and E. R. Holliday, *Advances in Protein Chemistry*, **7**, 319 (1952).

ecules could be digested completely, whereas their carboxyl terminal moieties seemed to be somewhat resistant to the action of the enzyme under the conditions used. The difficulty may have arisen from some inhibition by the accumulated products, since the hexapeptide, which was derived from γ-*t*-butyl-glutamyl-histidyl-phenylalanyl-arginyl-tryptophyl-glycine, an intermediate for the synthesis of peptides I and II, has been found to be completely digestible by the enzyme.[13] Schwyzer and Kappeler[20] described that their preparation of the decapeptide (I) was completely digested by LAP. However, the rate of the hydrolysis by LAP depends partly on the contamination of some endopeptidases, which may promote the digestion. It is, therefore, difficult to compare our results with their directly. The present data may, then, be considered to provide a proof of the optical homogeneity of our decapeptide preparations.

The Synthesis of α^{1-10}-ACTH (I).—*t*-Butyloxycarbonyl-serine (III) was treated with diazomethane in order to obtain the corresponding methyl ester; the resultant oily ester was then converted into *t*-butyloxycarbonyl-serine hydrazide (X) in a yield of 88 per cent based on the III used. Iselin and Schwyzer reported the synthesis of X by another route, starting with the serine methyl ester.[17] The *t*-butyloxycarbonyl-seryl-tyrosine methyl ester (XI) was synthesized by the azide-coupling procedure from compound X and the tyrosine methyl ester in a moderate yield (66%). The melting point of our preparation agrees fairly well with the value reported for XI by Hofmann et al., but the optical rotation differs significantly from theirs.[18] The hydrazide (XII), which was derived from XI, had the same optical rotation as that given by them. Concerning the synthesis of XI, attempts were also made to achieve the DCCl-induced condensation of *t*-butyloxycarbonyl-serine (III) with the tyrosine methyl ester, but the reaction appeared so complicated that it was very difficult to isolate the pure XI from the medium. Concerning this point, it should be noted that Li et al. obtained the carbobenzoxy analog of XI in an excellent yield by the DCCl procedure.[19] *t*-Butyloxycarbonyl-seryl-tyrosine azide, which was derived from XII, was allowed to react with the seryl-methionine methyl ester (V) to yield a tetrapeptide derivative, the *t*-butyloxycarbonyl-seryl-tyrosyl-seryl-methionine methyl ester (XIII). Compound XIII failed to crystallize, but it was found to be homogeneous in thin-laryer chromatography. The optical rotation of our material agrees satisfactorily with the value described for XIII by Iselin and Schwyzer.[17] Compound XIII was then converted almost quantitatively into the crystalline hydrazide (XIV), the melting point and the optical rotation of which coincided fairly well with those reported in the literature.[17]

The protected tetrapeptide hydrazide (XIV) was transformed into the azide, and this was then coupled with γ-*t*-butyl-glutamyl-histidyl-phenylalanyl-arginyl-tryptophyl-glycine[13] to give a protected decapeptide *t*-butyloxycarbonyl-seryl-tyrosyl-seryl-methionyl-γ-*t*-butyl-glutamyl-histidyl-phenylalanyl-arginyl-tryptophyl-glycine (XV), which was found to be homogeneous in thin-layer chromatography after reprecipitation from dimethylformamide-methanol. The yield of the purified XV amounted to 80 per cent when the hydrazide XIV was used in a 50 per cent excess relative to the hexapeptide. Our preparation of XV showed a good agreement in the optical rotation with the substance as prepared by other investigators.[20,21] The free decapeptide I (α^{1-10}-ACTH) was obtained by the trifluoroacetic acid treatment of compound XV. The peptide I was found to be homogeneous to ninhydrin, Pauly, Ehrlich, Sakaguchi and methionine (P_tI_6'') reagents in paper chromatography. Acid hydrolysis gave a mixture consisting of the constituent amino acids in the ratios expected by theory, with the exception of the tryptophan. The intact peptide contained tyrosine and tryptophan in a molar ratio of 1 : 1.[16]

Previously we described the use of *O*-benzyl-serine[22,23] in the synthesis of the *N*-terminal sequence of corticotropin, where the amino function of the *N*-terminal serine was protected by a carbobenzoxy group.[12] An attempt to determine if the *N*-acyl and the *O*-benzyl groups could be removed safely by reduction with sodium in liquid ammonia was made for the protected nonapeptide *N*-carbobenzoxy-*O*-benzyl-seryl-tyrosyl-*O*-benzyl-seryl-methionyl-γ-*t*-butyl-glutamyl-histidyl-phenylalanyl-N^G-tosyl-arginyl-tryptophan methyl ester (m. p. 220—221°C, $[\alpha]_D^{22.5}$ −10.5° (*c* 1.05, dimethylformamide)); it was proved that one of the serine residues, which might be the amino end, was transformed into glycine to an extent of 60—70 per cent upon the treatment.[24] We next synthesized the first tetrapeptide sequence of corticotropin in the form of the *t*-butyloxycarbonyl-*O*-benzyl-seryl-tyrosyl-*O*-benzyl-seryl-methionine methyl ester (XVIII) as an intermediate in the synthesis of corticotropin peptides, in order to test the role of the hydroxyl function of serine in the activity as well as to examine the behavior of the protective groups and the serine residues

17) B. Iselin and R. Schwyzer, *Helv. Chim. Acta*, **44**, 169 (1961).
18) K. Hofmann, J. Rosenthaler, R. D. Wells and H. Yajima, *J. Am. Chem. Soc.*, **86**, 4991 (1964).
19) C. H. Li, J. Meienhofer, E. Schnabel, D. Chung, T-b. Lo and J. Ramachandran, ibid., **83**, 4449 (1961).
20) R. Schwyzer and H. Kappeler, *Helv. Chim. Acta*, **44**, 1991 (1961).
21) R. Geiger, K. Sturm and W. Siedel, *Chem. Ber.*, **96**, 1080 (1963).
22) K. Okawa and H. Tani, *J. Chem. Soc. Japan, Pure Chem. Sect.* (*Nippon Kagaku Zassi*), **75**, 1199 (1954).
23) K. Okawa, This Bulletin, **29**, 486 (1956).
24) H. Otsuka and K. Inouye, unpublished.

in the treatment with sodium in liquid ammonia. We wish to describe here, however, only the synthesis of compound XVIII as an example of serine peptide. The synthetic procedure for XVIII is quite similar to that employed for compound VII. *t*-Butyloxycarbonyl-*O*-benzyl-serine (XVI), which failed to crystallize, was isolated as the dicyclohexylamine salt.[9] The coupling of compound XVI with the tyrosine methyl ester by the DDCI method involved no difficulty other than those encountered with compound XI.

We also tried to obtain *O*-benzyl-D-serine from the *N*-acetyl-*O*-benzyl-D-serine, which could be isolated from the optical resolution medium[23] after *O*-benzyl-L-serine ($[\alpha]_D^{24}$ +7.3° (*c* 2.0, N hydrochloric acid)) had been separated. The treatment of *N*-acetyl-*O*-benzyl-D-serine (m. p. 110—111°C, $[\alpha]_D^{23}$ −46.7° (*c* 2.0, acetic acid)) with 80% hydrazine hydrate at 100°C gave the desired *O*-protected D-serine in a 70 per cent yield, no fission of the *O*-benzyl group was detected. The resultant material had an optical rotation of $[\alpha]_D^{24.5}$ −7.2° (*c* 2.0, N hydrochloric acid); its *N*-*t*-butyloxycarbonyl derivative was also found to be fairly coincident with the L-antipode in optical rotation with an opposite sign.

Experimental

The amino acids used are of the L-configuration, unless otherwise indicated.

All melting points are uncorrected.

***t*-Butyloxycarbonyl-serine Dicyclohexylamine Salt.**—To a solution of 10.51 g. (0.1 mol.) of serine and 22.0 g. (0.24 mol.) of sodium bicarbonate in 200 ml. of water and 200 ml. of dioxane, 17.20 g. (0.12 mol.) of *t*-butyl azidoformate[7,8] was added drop by drop at a bath temperature of 45°C; the mixture was then stirred for 20 hr. at the above temperautre. The reaction mixture was chilled in an ice-bath, neutralized by the addition of 57.5 ml. of ice-cold 4 N hydrochloric acid (pH 4.6—4.8), and concentrated to about 80 ml. at 40°C in vacuo. The concentrated solution was then acidified to below pH 2 with ice-cold 4 N hydrochloric acid in the presence of 200 ml. of ethyl acetate at 0°C. The aqueous phase was extracted three times with 100 ml.-portions of cold ethyl acetate. The organic extracts were then pooled, dried over anhydrous sodium sulfate, and evaporated at 35—40°C in vacuo, thus affording the product as a sirup (13.83 g., 67.5%). The product was dissolved in 100 ml. of ether, and to this was added an ethereal solution of 12.20 g. (0.0675 mol.) of dicyclohexylamine. After the mixture had been stored in a refrigerator overnight, the crystals which separated were filtered off, washed with ether and dried; 23.56 g. (61.0%), m. p. 143—148°C. A 21.8 g.-sample was recrystallized from 220 ml. of hot ethyl acetate to give 19.6 g. of needles; m. p. 142—144°C, $[\alpha]_D^{25.5}$ +13.3±0.5° (*c* 3.044, methanol).

Found: C, 62.17; H, 9.80; N, 7.36. Calcd. for $C_8H_{15}O_5N \cdot C_{12}H_{23}N$: C, 62.15; H, 9.91; N, 7.25%.

***t*-Butyloxycarbonyl-serine Monohydrate (III).**—A solution of 17.40 g. (0.045 mol.) of the dicyclohexylamine salt which was obtained above in 200 ml. of 50% ethanol was shaken in the presence of 45 ml. (wet volume) of Dowex-50WX8 (H^+-form) at room temperature for 30 min. After the resin had been removed by filtration, the filtrate was concentrated to a small volume at 40—45°C in vacuo. The crystalline monohydrate, which separated soon when the mixture was chilled in an ice-bath, was collected and air-dried; 9.81 g. (97.7%), m. p. 45—47°C (sintering at 42°C), $[\alpha]_D^{26}$ −3.0±1° (*c* 2.330, acetic acid), $[\alpha]_D^{25}$ −7.6±0.5° (*c* 2.590, water).

Found: C, 43.25; H, 7.88; N, 6.52; H_2O, 7.19. Calcd. for $C_8H_{15}NO_5 \cdot H_2O$: C, 43.04; H, 7.68; N, 6.28; H_2O, 8.07%.

***t*-Butyloxycarbonyl-serine Hydrazide (X).**—To a solution of 5.58 g. (0.025 mol.) of III in 20 ml. of dioxane there was added, at 0°C, an ethereal solution of diazomethane until the yellow color persisted. After 10 more min. the solvent was removed in vacuo at 30°C. The resultant sirup was dissolved in 25 ml. of anhydrous ethanol; to this was added 3.0 ml. (0.06 mol.) of hydrazine hydrate, and the mixture was kept at room temperature for 24 hr. After the solvent had been removed in vacuo, the sirupy residue was treated with ethyl acetate to afford a crystalline solid. Recrystallization from hot ethyl acetate gave fine needles; 4.82 g. (88.0%), m. p. 109—110°C, $[\alpha]_D^{25.5}$ −9.0±0.5° (*c* 4.127, methanol). Lit.[17] m. p. 112—114°C, $[\alpha]_D^{27}$ −9.4±1° (*c* 4.1, methanol).

Found: C, 43.80; H, 7.91; N, 19.19;. Calcd. for $C_8H_{17}N_3O_4$: C, 43.83; H, 7.82; N, 19.17%.

***t*-Butyloxycarbonyl-seryl-methionine Methyl Ester (IV).** — A mixture of 5.99 g. (0.03 mol.) of methionine methyl ester hydrochloride, 6 ml. of water and 30 ml. of methylene chloride was chilled in an ice-bath and shaken with 15 ml. of ice-cold 50% potassium carbonate. The aqueous phase was then extracted again with cold methylene chloride. The organic extracts were combined, dried over anhydrous sodium sulfate, and evaporated at a bath temperature of 20°C in vacuo, affording the free base as an oil, which was then redissolved in methylene chloride. To this solution there were added 6.13 g. (0.0275 mol.) of compound III and a methylene chloride solution of 5.68 g. (0.0275 mol.) of *N*, *N'*-dicyclohexylcarbodiimide (DCCl); the reaction mixture was then kept in a refrigerator overnight. The *N*, *N'*-dicyclohexylurea (DCU) which formed was removed (5.81 g., 94.1%), and the filtrate was evaporated in vacuo. The residue was dissovled in ethyl acetate, and the solution was washed with ice-cold N hydrochloric acid, M sodium bicarbonate and saturated sodium chloride, dried over anhydrous sodium sulfate, and evaporated in vacuo. The resultant oily residue was dissolved in a small volume of acetonitrile, and the slight amount of the urea which separated upon chilling was removed. The evaporation of the solvent afforded an oily residue which crystallized during storage in a refrigerator. The crystals were washed with ether - petroleum ether and dried; 8.78 g. (91.1%), m. p. 64—66°C. Recrystallization from ethyl acetate - petroleum ether gave a yield of 8.21 g. (83.8%); m. p. 66—67.5°C, $[\alpha]_D^{25.5}$ −29.5±1° (*c* 2.220, methanol).

Found: C, 48.06; H, 7.61; N, 8.20; S, 9.34. Calcd. for $C_{14}H_{26}N_2O_6S$: C, 47.98; H, 7.48; N, 7.99; S,

9.15%.

Seryl-methionine Methyl Ester (V).—To a solution of 1.402 g. (4 mmol.) of IV in 2ml. of ethyl acetate there was added 2.5 ml. of 20% hydrogen chloride in ethyl acetate, the mixture was then allowed to stand at room temperature for 60 min. The solvent was evaporated in vacuo and the resultant oily ester hydrochloride was dissolved in methylene chloride. The solution was then treated with 50% potassium carbonate at 0°C, and the organic phase was dried over anhydrous sodium sulfate and evaporated at a bath temperature of 20°C in vacuo to give a sirupy residue, which crystallized upon the addition of ethyl acetate; 0.825 g. (82.5%), m. p. 84—85°C, $[\alpha]_D^{24.5}$ $-16.3\pm1°$ (*c* 1.791, methanol). Lit.[19] m. p. 86—88°C, $[\alpha]_D^{24}$ $-21°$ (*c* 1, N hydrochloric acid).

Found: C, 43.29; H, 7.29; N, 11.06; S, 12.66. Calcd. for $C_9H_{18}N_2O_4S$: C, 43.18; H, 7.25; N, 11.19; S, 12.81%.

***t*-Butyloxycarbonyl-glycyl-tyrosine Hydrazide (VI).**—To a solution of 2.32 g. of tyrosine methyl ester hydrochloride in 2 ml. of water, 10 ml. of ice-cold 50% potassium carbonate was added at 0°C. The crystalline precipitates which separated were filtered off, washed with cold water, and dried to give the free base of the tyrosine methyl ester; 1.81 g. (93.0%) the free base of the tyrosine methyl ester; 1.81 g. (93.0%), m. p. 134—135°C, $[\alpha]_D^{23.5}$ $+26.9\pm0.8°$ (*c* 2.411, methanol). Lit.[25] m. p. 135°C.

t-Butyloxycarbonyl-glycine (4.85 g., 0.0276 mol.) and 5.40 g. (0.0276 mol.) of the tyrosine methyl ester were dissolved in acetonitrile, and to this solution was added 5.72 g. (0.0276 mol.) of DCCl; the mixture was then kept in a refrigerator overnight. After the DCU which separated had been filtered off, the filtrate was evaporated in vacuo. The residue was dissolved in ethyl acetate, and the solution was washed successively with ice-cold N hydrochloric acid, water, M sodium bicarbonate and water, dried over anhydrous sodium sulfate, and evaporated in vacuo. The resultant amorphous dipeptide, which gave a single spot in thin-layer chromatography (R_f=0.50, Silica-gel G in ethyl acetate), was dissolved in 85 ml. of methanol, and 3.35 ml. of hydrazine hydrate was added. The mixture was then allowed to stand at room temperature for 48 hr. The crystalline precipitates which separated were collected, washed with a mixture of methanol and ether, and then ether, and dried in vacuo to give compound VI; 8.21 g. (84.5%), m. p. 187—188°C. A sample was recrystallized from methanol for analyses; m. p. 189.5—190°C, $[\alpha]_D^{26.5}$ $+0.5\pm1°$ (*c* 2.002, dimethylformamide).

Found: C, 54.56; H, 6.97; N, 15.93. Calcd. for $C_{16}H_{24}N_4O_5$: C, 54.53; H, 6.87; N, 15.93%.

***t*-Butyloxycarbonyl-seryl-tyrosine Methyl Ester (XI).**—Compound X (2.19 g., 0.01 mol.) was dissolved in 20 ml. of ice-cold N hydrochloric acid, and to this was added 6 ml. of ice-cold 2 M sodium nitrite at an ice-salt-bath temperature. After 4 min. the separated azide was taken into ethyl acetate. The organic solution was then washed with ice-cold M potassium carbonate and sodium chloride, and dried over anhydrous sodium sulfate. To this ethyl actate solution 1.95 g. (0.01 mol.) of the tyrosine methyl ester (free base) was added; the mixture was then concentrated to a small volume at a bath temperature of 5—10°C in vacuo, and about 25 ml. of tetrahydrofuran was introduced. The mixture was then left to stand at 0—4°C for 68 hr. The solvent was removed in vacuo, and the residue was redissolved in ethyl acetate. The solution was washed in an ordinary manner with ice-cold hydrochloric acid and sodium bicarbonate and dried. The evaporation of the solvent gave a foamy residue, which crystallized from ether; 2.50 g. (65.5%), m. p. 115—118°C, $[\alpha]_D^{25}$ $-5.0\pm2°$ (*c* 1.036, methanol). Lit.[18] m. p. 117—119°C, $[\alpha]_D^{28}$ $-13.3°$ (*c* 0.97, methanol).

Found: C, 55.94; H, 6.92; N, 7.56. Calcd. for $C_{18}H_{26}N_2O_7$: C, 56.53; H, 6.85; N, 7.33%.

***t*-Butyloxycarbonyl-seryl-tyrosine Hydrazide (XII).**—To a solution of 1.99 g. of compound XI in 20 ml. of anhydrous ethanol 1.3 ml. of hydrazine hydrate was added; the mixture was then allowed to stand at room temperature overnight. The crystalline precipitates which separated were collected, washed with ethanol and ether, and dried; 1.76 g. (88.5%), m. p. 188—190°C (decomp.). A sample was recrystallized from water for analyses; m. p. 193—195°C decomp., $[\alpha]_D^{24}$ $-19.8\pm1°$ (*c* 2.035, 50% acetic acid). Lit.[18] m. p. 199—200°C (decomp.), $[\alpha]_D^{28}$ $-18.6°$ (*c* 1.20, 50% acetic acid).

Found: C, 51.50; H, 7.15; N, 14.97. Calcd. for $C_{17}H_{26}N_4O_6\cdot{}^1/_2H_2O$: C, 52.16; H, 6.95; N, 14.31%.

***t*-Butyloxycarbonyl-glycyl-tyrosyl-seryl-methionine Methyl Ester (VII).**—To a solution of 1.76 g. (5.0 mmol.) of compound VI in 12.5 ml. of ice-cold N hydrochloric acid 3.0 ml. of ice-cold 2M sodium nitrite was added at an ice-salt bath temperature. After 4 min. 10 ml. of saturated sodium chloride was introduced, and the separated azide was placed in 20-ml. portions of ether. The organic extracts were combined, washed with ice-cold M sodium bicarbonate, dried over anhydrous sodium sulfate, and evaporated in vacuo to give a foamy residue, which was then redissolved in cold acetonitirle. To this solution 1.25 g. (5.0 mmol.) of compound V was added and the mixture was left to stand at 0—4°C for two days. The crystalline tetrapeptide VII which separated was filtered off, washed with cold ethyl acetate and ether, and dried; 1.40 g. (61.5%), m. p. 183—185°C (softening at 181°C). A suspension of this slightly-colored material in acetonitrile was boiled for a few minutes and then refrigerated. The treatment gave the colorless crystals with a recovery of 96.7 per cent; m. p. 183—185°C, $[\alpha]_D^{24}$ $-16.5\pm2°$ (*c* 1.15, methanol). A single spot was visible in thin-layer chromatography; R_f=0.48 (Silica-gel G, methanol-ethyl acetate (15:85)).

Found: C, 52.44; H, 7.01; N, 9.98; S, 5.70. Calcd. for $C_{25}H_{38}N_4O_9S$: C, 52.62; H, 6.71; N, 9.82; S, 5.62%.

***t*-Butyloxycarbonyl-glycyl-tyrosyl-seryl-methionine Hydrazide Hemihydrate (VIII).**—Hydrazine hydrate (0.6 mol.) was added to a solution of 1.20 g. of compound VII in 6 ml. of dimethylformamide; the mixture was allowed to stand at room temperature for 40 hr., after which time the hydrazide VIII was precipitated by the addition of 45 ml. of ethyl acetate in the form of a gelatinous mass. This amorphous solid was crystallized from hot water; 1.14 g. (93.9%), m. p. 202—204°C (decomp.), $[\alpha]_D^{23}$ $-17.8\pm1°$ (*c*

25) J. Ramachandran and C. H. Li, *J. Org. Chem.*, **28**, 173 (1963).

1.940, 50% acetic acid).

Found: C, 49.59; H, 6.95; N, 14.39; S, 5.49. Calcd. for $C_{24}H_{38}N_6O_8S \cdot {}^1/_2H_2O$: C, 49.73; H, 6.78; N, 14.50; S, 5.53%.

***t*-Butyloxycarbonyl-seryl-tyrosyl-seryl-methionine Methyl Ester (XIII).**—Compound XII (2.87 g., 7.5 mmol.) was dissolved in 19 ml. of ice-cold N hydrochloric acid containing 2 g. of sodium chloride, and to this was added 4.5 ml. of ice-cold 2M sodium nitrite at an ice-salt bath temperature. After 4 min. the azide was extracted three times with ethyl acetate. The organic extracts were combined, washed with ice-cold M sodium bicarbonate and saturated sodium chloride, and dried over anhydrous sodium sulfate. To this solution 1.33 g. (5.3 mmol.) of V was added, and the resultant suspension was concentrated to about 20—25 ml. at a bath temperature of 5—10°C in vacuo. During the concentration a greater part of the solid disappeared. The mixture was then kept at 0—4°C for 2 days. A little water was added to dissolve the gelatinous precipitates, which had separated, and the resultant clear solution was washed with ice-cold N hydrochloric acid, M sodium bicarbonate and water, dried over anhydrous sodium sulfate, and evaporated in vacuo to give a amorphous solid mass, which was then reprecipitated from hot ethyl acetate; 1.42 g. (44.8%), m. p. 125—130°C. A sample was reprecipitated from ethyl acetate for analyses; m. p. 129—134°C, $[\alpha]_D^{23}$ $-29.3\pm1°$ (*c* 2.053, methanol). Lit.[17] m. p. 115—125°C, $[\alpha]_D^{27}$ $-29.8\pm1°$ (*c* 2.1, methanol). A single spot was detected in thin-layer chromatography; $R_f=0.57$, methanol-ethyl acetate (15 : 85).

Found: C, 52.15; H, 6.88; N, 19.55; S, 5.38. Calcd. for $C_{26}H_{40}N_4O_{10}S$: C, 51.99; H, 6.71; N, 19.33; S, 5.34%.

***t*-Butyloxycarbonyl-seryl-tyrosyl-seryl-methionine Hydrazide (XIV).**—Compound XIII (0.78 g.) was dissolved in 5 ml. of dimethylformamide, and to this was added 0.3 ml. of hydrazine hydrate. The mixture was kept at 0—4°C for 40 hr. The tetrapeptide hydrazide XIV was then precipitated by the addition of ethyl acetate. The precipitates crystallized upon treatment with hot water; 0.76 g. (96.9%), m. p. 187—189°C (decomp.) (sintering at 175°C). A sample was recrystallized from water for analyses without any change in the melting point; $[\alpha]_D^{23.5}$ $-35.8°$ (*c* 1.966, 50% methanol). Lit.[17] m. p. 191—193°C, $[\alpha]_D^{25}$ $-36.7\pm1°$ (*c* 2.0, water-methanol 1 : 1).

Found: C, 49.09; H, 6.79; N, 13.99; S, 5.42. Calcd. for $C_{25}H_{40}N_6O_9S$: C, 49.99; H, 6.79; N, 13.99; S, 5.34%.

***t*-Butyloxycarbonyl-glycyl-tyrosyl-seryl-methionyl-γ-*t*-butyl-glutamyl-histidyl-phenylalanyl-arginyl-tryptophyl-glycine Dihydrate (IX).**—To a solution of compound VIII (0.348 g.., 0.6 mmol.) in 3.5 ml. of dimethyl-formamide 1.8 ml. of ice-cold N hydrochloric acid and 0.66 ml. of M sodium nitrite were added at an ice-salt-bath temperature. After 4 min. saturated sodium chloride (20 ml.) was introduced, and the separated azide was taken into ethyl acetate. The organic extracts were combined, washed with ice-cold M sodium bicarbonate and water, and dried over anhydrous sodium sulfate. To this was added a solution of 0.496 g. (0.5 mmol.) of γ-*t*-butyl-glutamyl-histidyl-phenylalanyl-arginyl-tryptophyl-glycine[13] and 0.21 ml. of triethylamine in 15 ml. of dimethylformamide, and the mixture was concentrated at 5—10°C in vacuo until it became clear. The reaction mixture was then allowed to stand at 0—4°C. The freshly prepared azide (derived from 0.232 g. (0.4 mmol.) of VIII as described above) was added after 20 hr. of reaction. After 40 hr. acetic acid (0.5 ml.) was added, and the mixture was poured into 200 ml. of cold ethyl acetate to separate the crude protected decapeptide, which were collected by filtration (0.607 g.). The crude product was twice reprecipitated from dimethylformamide-methanol (1 : 2); 0.461 g. (63.1%), m. p. 213—216°C (decomp.), $[\alpha]_D^{24}$ $-10.8\pm2°$ (*c* 1.077, dimethylformamide). A single spot was detected in thin-layer chromatography; $R_f=0.60$ (Silica-gel G, dimethylformamide - ethyl acetate - acetic acid (15 : 10 : 2).

Found: C, 55.04; H, 6.65; N, 15.30; S, 2.04. Calcd. for $C_{67}H_{92}N_{16}O_{17}S \cdot 2H_2O$: C, 55.05; H, 6.62; N, 15.33; S, 2.19%.

***t*-Butyloxycarbonyl-seryl-tyrosyl-seryl-methionyl-γ-*t*-butyl-glutamyl-histidyl-phenylalanyl-arginyl-tryptophyl-glycine Dihydrate (XV).**—The azide, which was derived from 0.685 g. (1.14mmol.) of compound XIV, and 0.750 g. (0.76 mmol.) of γ-*t*-butyl-glutamyl-histidyl-phenylalanyl-arginyl-tryptophyl glycine[13] were made to react in an ethyl acetate-dimethylformamide solution at 0—4°C for 44 hr. in almost the same manner as in the case of the synthesis of IX. After the addition of 0.75 ml. of acetic acid, the reaction mixture was introduced into cold ethyl acetate; the resultant precipitates of crude XV were filtered off to give 1.041 g. The crude product was reprecipitated from dimethylformamide-methanol to afford 0.910 g. (80.2%) of the pure material, which was found to be homogeneous in thin-layer chromatography, $R_f=0.47$ (Silica-gel G, dimethylformamide - ethyl acetate - acetic acid (15 : 10 : 2)).; m. p. 202°C (decomp.), $[\alpha]_D^{24}$ $-13.2\pm2°$ (*c* 1.045, dimethylformamide). Lit. m. p. 203°C decomp., $[\alpha]_D$ $-12.4\pm0.8°$ (*c* 1.328, dimethylformamide);[20] m. p. 201—204°C (decomp.), $[\alpha]_D^{22}$ $-13.0\pm1°$ (*c* 1, dimethylformamide).[21]

Found: C, 55.24; H, 7.25; N, 14.99; S, 2.56. Calcd. for $C_{68}H_{94}N_{16}O_{18}S \cdot 2H_2O$: C, 54.75; H, 6.62; N, 15.02; S, 2.15%.

Seryl-tyrosyl-seryl-methionyl-glutamyl-histidyl-phenylalanyl-arginyl-tryptophyl-glycine (I).—The protected decapeptide XV (50 mg.) was dissolved in 1 ml. of anhydrous trifluoroacetic acid, and the solution was ketp at room temperature for 60 min. The solvent was removed by evaporation at a bath temperature of 35—40°C in vacuo to give a sirupy residue, which was dried over sodium hydroxide in vacuo. The residue was then dissolved in water, and to this was added 2 ml. (wet volume) of Amberlite CG-4B (acetate form), and the mixture was stirred at room temperature for 40 min. After the resin had been removed by filtration, the filtrate was lyophilized to give quantitatively the decapeptide I as a colorless powder with a silky luster; it gave a single spot ($R_f=0.52$) reactive to ninhydrin, Pauly, Ehrlich, Sakaguchi and methionine (PtI_6'') reagents on paper in the solvent system of *n*-butanol - acetic acid - pyridine - water (30 : 6 : 20 : 24);[14] $\lambda_{max}^{N/10\ HCl}=280$ mμ (ε 6490), $\lambda_{shoulder}^{N/10\ HCl}=288.5$ mμ (ε 4870), $\lambda_{max}^{N/10\ NaOH}$ 281.5 mμ (ε 6810),

288.5 mμ (ε 6600), $[\alpha]_D^{24}$ −30.3±2° (*c* 0.551, N acetic acid). Amino acid ratios in acid hydrolysate:[15] Ser 1.83, Tyr 1.06, Met 1.03, Glu 1.00, His 0.99, Phe 1.02, Arg 0.94, Gly 0.92, Try 0.55,*3 NH_3 0.51.

Glycyl-tyrosyl-seryl-methionyl-glutamyl-histidyl-phenylalanyl-arginyl-tryptophyl-glycine (II).—The protected decapeptide IX (60 mg.) was treated with trifluoroacetic acid in exactly the same manner as has been described above for I, thus giving the free decapeptide II as a colorless fluffy powder, which gave a single spot (R_f=0.37) reactive to ninhydrin, Pauly, Ehrlich, Sakaguchi and methionine (PtI_6'') reagents in paper chromatography in *n*-butanol-acetic acid-pyridine-water (30 : 6 : 20 : 24);[14] $\lambda_{max}^{N/10\ HCl}$ =280 mμ (ε 6320), $\lambda_{shoulder}^{N/10\ HCl}$=288.5 mμ (ε 4820), $\lambda_{max}^{N/10\ NaOH}$=281.5 mμ (ε 7220), 288.5 mμ (ε 6950), $[\alpha]_D^{13.5}$ −32.2±2° (*c* 0.631, N acetic acid). Amino acid ratios in acid hydrolysate:[15] Gly 1.80, Tyr 1.04, Ser 0.87, Met 0.98, Glu 1.00, His 0.95, Phe 0.92, Arg >0.83, Try 0.57,*3 NH_3 0.37.

***N-t*-Butyloxycarbonyl-*O*-benzyl-serine Dicyclohexylamine Salt (XVI).**—*O*-Benzyl-serine[22,23] (4.88 g., 0.025 mol.) was acylated with 5.37 g. (0.0375 mol.) of *t*-butyl azidoformate and sodium bicarbonate in a water-dioxane (1 : 1) solution in almost the same manner as was used for compound III. The sirupy product (7.1 g.) was converted into the dicyclohexylamine salt as usual; 9.25 g. (77.6%), m. p. 135—136°C. Recrystallization from ethanol-ether gave a sample for analyses; m. p. 135.5—136°C, $[\alpha]_D^{24.5}$ +24.3±1° (*c* 2.494, methanol).

Found: C, 68.23; H, 9.34; N, 5.91. Calcd. for $C_{15}H_{21}NO_5 \cdot C_{12}H_{23}N$: C, 68.03; H, 9.03; N, 5.88%.

***N-t*-Butyloxycarbonyl-*O*-benzyl-seryl-tyrosine Hydrazide (XVII).**—A solution of 3.58 g. (7.5 mmol.) of compound XVI in 40 ml. of 50% ethanol was shaken in the presence of 10 ml. (wet volume) of Dowex-50W X8 (H^+ form) at room temperature for 30 min. After the resin had been removed by filtration, the filtrate was evaporated at 40—45°C in vacuo. The sirupy residue was dissolved in ether, and the solution was dried over sodium sulfate and evaporated in vacuo to give *N-t*-butyloxycarbonyl-*O*-benzyl-serine as a clear oil. To this were added a methylene chloride solution of 1.47 g. (7.5 mmol.) of the tyrosine methyl ester and then a methylene chloride solution of 1.55 g. (7.5 mmol.) of DCCI. The mixture was kept in a refrigerator overnight. Subsequent treatment was carried out in almost the same manner as for compound IV. The resulting dipeptide ester (3.60 g.) failed to crystallized, but it was found to be homogeneous in thin-layer chromatography; (R_f=0.53 (Silica-gel G, ethyl acetate)).

A 5.85 g.-sample of the dipeptide ester obtained as described above was dissolved in 40 ml. of anhydrous ethanol, and to this was added 1.45 ml. of hydrazine hydrate. The mixture was allowed to stand at room temperature for 40 hr. and then refrigerated. The crystalline product which separated was filtered off, washed with cold ethanol-ether and ether, and dried; 3.62 g., m. p. 178—181°C (decomp.) (sintering at 165°C). The concentration of the mother liquor afforded an additional 1.00 g. of the crystals with a m.p. of 168—170°C (decomp.). The total yield amounted to 4.62 g. (81.7%). Recrystallization from anhydrous ethanol gave, in a recovery of 93 per cent, crystals with a m. p. of 179—181°C decomp. (sintering at 168°C), $[\alpha]_D^{23.5}$ −12.2±1° (*c* 2.037, dimethylformamide).

Found: C, 61.02; H, 6.90; N, 11.88. Calcd. for $C_{24}H_{32}N_4O_6$: C, 61.00; H, 6.83; N, 11.86%.

***N-t*-Butyloxycarbonyl-*O*-benzyl-seryl-methionine Methyl Ester (XVIII).**—*N-t*-Butyloxy-carbonyl-*O*-benzyl-serine, which was derived from 4.76 g. (0.01 mol.) of the dicyclohexylamine salt (XVI) with the Dowex-50 treatment described above, and the methionine methyl ester (prepared from 2.40 g. (0.012 mol.) of the hydrochloride) were coupled in methylene chloride by the DCCI procedure, in almost the same manner as was used in the case of the synthesis of Compound IV, to give the protected dipeptide XVIII, which crystallized from ethyl acetate-petroleum ether; 4.11 g. (93.4%), m. p. 40—43°C. Recrystallization from the same solvent gave fine needles; m. p. 51—52°C, $[\alpha]_D^{25}$ −13.4±1° (*c* 2.169, methanol).

Found: C, 57.35; H, 7.51; N, 6.60; S, 7.52. Calcd. for $C_{21}H_{32}O_6N_2S$: C, 57.25; H, 7.32; N, 6.36; S, 7.28%.

***N-t*-Butyloxycarbonyl-*O*-benzyl-seryl-tyrosyl-*O*-benzyl-seryl-methionine Methyl Ester (XIX).**—Compound XVIII (2.20 g., 5.0 mmol.) was treated with hydrogen chloride in ethyl acetate to obtain *O*-benzyl-seryl-methionine methyl ester hydrochloride, which was then converted into the free base by treatment with 50% aqueous potassium carbonate in ether. Compound XVII (2.36 g., 5.0 mmol.) was dissolved in 8 ml. of dimethylformamide and chilled in an ice-salt bath. To this solution 20 ml. of ice-cold N hydrochloric acid and 2.75 ml. of ice-cold 2 M sodium nitrite were added. After 3 min. the azide which separated was taken into ether. The etheral solution was washed successively with ice-cold M potassium carbonate, water and saturated sodium chloride, and dried over sodium sulfate. This solution was then added to the oily dipeptide ester obtained above, and the reaction mixture was allowed to stand at 0—4°C for three days. The separated crystalline precipitates of the tetrapeptide XIX were filtered off, washed with cold ether, and dried; 1.41 g., m. p. 123.5—126°C. The mother liquor was washed with acid and bicarbonate as usual, and concentrated to a small volume to yield an additional quantity of XIX; 0.99 g., m. p. 124—127°C. The total yield amounted to 2.40 g. (61.3%). These crystals were recrystallized from ethyl acetate-petroleum ether in a recovery of 96.2 per cent; m. p. 127—129°C, $[\alpha]_D^{25.5}$ −11.1±0.7° (*c* 2.982, methanol).

Found: C, 61.67; H, 6.85; N, 7.26; S, 4.16. Calcd. for $C_{40}H_{52}N_4O_{10}S$: C, 61.52; H, 6.71; N, 7.17; S, 4.11%.

***O*-Benzyl-D-serine.**—*N*-Acetyl-*O*-benzyl-D-serine[23] (9.50 g., m. p. 110—111°C, $[\alpha]_D^{23}$ −46.7±1° (*c* 2.660, acetic acid); lit.[22] m. p. 103°C) was dissolved in 95 ml. of 80% hydrazine hydrate, and the mixture was heated under reflux at 100°C for 6 hr. Most of the hydrazine was removed by evaporation at 50—60°C in vacuo; the residue was dried over sulfuric acid in vacuo. The resultant crystalline solid was washed with cold water, ethanol and ether to give *O*-benzyl-D-serine; 5.69 g. (72.8%). A sample was recrystallized from water for analyses; $[\alpha]_D^{24.5}$ −7.2±0.3° (*c* 2.046, N hydrochloric acid).

*3 Tryptophan had been partially destroyed with acid.

Found: C, 61.55; H, 6.72; N, 7.18. Calcd. for $C_{10}H_{13}NO_3$: C, 61.45; H, 6.91; N, 6.81%.

***N*-*t*-Butyloxycarbonyl-*O*-benzyl-D-serine Dicyclohexylamine Salt.**—*O*-Benzyl-D-serine (0.98 g., 5.0 mmol.) and 1.375 g. (1.25 mmol.) of sodium carbonate were dissolved in 5 ml. of water, and to this was added 1.80 g. (7.5 mmol.) of *t*-butyl *p*-nitrophenyl carbonate[26] which had been dissolved in 7 ml. of *t*-butanol. The mixture was heated under reflux at 100°C for 30 min. and then evaporated to dryness in vacuo. The residue was extracted with cold water. The aqueous extract was neutralized to pH 5 by 4 N hydrochloric acid and washed with ether to remove the *p*-nitrophenol. The aqueous solution was then acidified to below pH 2 at 0°C and extracted with ether. The ether extract was dried over anhydrous sodium sulfate, and to this was added 1 ml. of dicyclohexylamine to afford the crystalline salt of *N*-*t*-butyloxycarbonyl-*O*-benzyl-D-serine; 1.22 g. (71.3%), m. p. 130—131°C, $[\alpha]_D^{24}$ $-23.6\pm1°$ (*c* 2.28, methanol).

Found: C, 68.54; H, 9.48; N, 5.96. Calcd. for $C_{15}H_{21}NO_5 \cdot C_{12}H_{23}N$: C, 68.03; H, 9.30; N, 5.88%.

The authors wish to express their deep thanks to Dr. Mitsuo Ebata and his staff for their amino acid analyses, to Dr. Kaoru Kuriyama and his staff for their optical rotation measurements, and to Dr. Satoshi Mizukami and his staff for their elemental microanalyses.

BULLETIN OF THE CHEMICAL SOCIETY OF JAPAN VOL. 39 1178—1182 (1966)

The Homogeneous Hydrogenation of Acetylenes by Dicyclopentadienyltitaniumdicarbonyl[1)]

By Kenkichi SONOGASHIRA and Nobue HAGIHARA

The Institute of Scientific and Industrial Research, Osaka University, Sakai, Osaka

(Received August 28, 1965)

The homogeneous hydrogenation of acetylenes and olefins in the presence of dicyclopentadienyltitaniumdicarbonyl (I) was studied. The results of the hydrogenation varied with the acetylene substituent. The relative activating effects of the substituents on the hydrogenation of such acetylenes as RC≡CH and R'C≡CR' are as follows: R: Ph>*t*-butyl>*n*-alkyl, R' : Ph>*n*-alkyl. The order is the reverse of that observed with the usual metal catalysts of the VIII group. In order to elucidate the mechanism of hydrogenation, the reaction of the dicarbonyl (I) with various acetylenes was studied, and the structures of the products were discussed.

Previous works in this laboratory have elucidated the catalytic behaviors of various metallocenes and their analogues, such as dibenzenechromium,[2)] nickelocene[3)] and vanadocene.[4)] During the course of an investigation of the catalytic actions of dicyclopentadienyltitaniumdicarbonyl (I) as a part of the above works, it was found that the compound I acts as a catalyst in a homogenous phase for the hydrogenation of 1-pentyne to 1-pentene under mild conditions.

The hydrogenations of other acetylenes and olefins by this catalyst have now been studied. The reductions were generally carried out in hydrocarbon solutions for 30 min. at 50—65°C under an initial hydrogen pressure of 50 atm. The results are summarized in Table I. The results of the catalytic reactions varied with the acetylene substituent. For example, 1-alkynes such as 1-pentyne and 1-hexyne were partially hydrogenated to 1-alkenes, while phenylacetylene was completely reduced to ethylbenzene and *t*-butylacetylene gave a mixture of partially and completely hydrogenated products. No hydrogenation was observed in the case of an alkyne without a terminal methylidyne group, 3-heptyne, although diphenylacetylene was completely hydrogenated to dibenzyl. On the basis of these results, the relative activating effects of the substituents of such acetylenes as RC≡CH and R'C≡CR' on the hydrogenation may be estimated as follows: R: Ph>*t*-butyl>*n*-alkyl, R': Ph>*n*-alkyl. It is interesting that the order is the reverse of that observed in the hydrogenations by the group VIII metal catalysts.

When the hydrogenation of phenylacetylene was carried out using a half quantity of hydrogen for complete reduction, 30% of ethylbenzene, 40% of styrene and 30% of recovered phenylacetylene were detected. The reduction must, therefore, involve a two-step process in which the phenylacetylene is first hydrogenated to styrene. In contrast with the complete hydrogenation of

1) Presented at the 18th Annual Meeting of the Chemical Society of Japan, Osaka, April, 1965.

2) H. Yamazaki, M. Yamaguchi and N. Hagihara, *J. Chem. Soc. Japan, Pure Chem. Sect.* (*Nippon Kagaku Zasshi*), **83**, 959 (1962); *Annual Reports of the Institute for Fibre Reserch*, **16**, 495 (1963).

3) H. Yamazaki, T. Nishido and N. Hagihara, Abstracts of the 18th Annual Meeting of the Chemical Society of Japan, Osaka, April (1965), p. 448.

4) R. Tsumura and N. Hagihara, This Bulletin, **37**, 1889 (1964).

Table I. Hydrogenation of olefins and acetylenes with dicyclopentadienyltitaniumdicarbonyl[a]

Substrate	Catalyst solution[b]	Reaction temp. °C	Reaction time min.	Product (yield, %)	Recovery %	Remarks
Styrene	A	50—60	30	Ethylbenzene (15)	85	c
Styrene	A	50—65	120	Ethylbenzene (70)	30	c
trans-Stilbene	A	50—60	30	—	100	d
Butadiene	B	50—65	30	—	—	d
1, 3-Cyclooctadiene	A	50—65	30	—	—	d
Acetylene	B	50—60	30	—	—	d
1-Pentyne	A or B	50—60	30	1-Pentene (95)	0	c, e
1-Hexyne	A	50—60	30	1-Hexene (90)	10	c
t-Butylacetylene	A	50—60	30	3, 3-Dimethyl-1-butene (40) 2, 2-Dimethylbutane (60)	0	c
3-Heptyne	A or C	50—65	30	—	100	c
Phenylacetylene	A or B	50—60	30	Ethylbenzene (95)	5	c, e
Diphenylacetylene	A	50—60	30	Dibenzyl (90)	0	e

a) Reactions were generally carried out with 20 mmol. of substrate, dissolved in 20 ml. of the catalyst solution, in a 100 ml. autoclave under an initial hydrogen pressure of 50 atm.
b) The catalyst solutions A, B and C were prepared as follows. Freshly sublimed dicyclopentadienyl titaniumdicarbonyl was dissolved in benzene (catalyst A), in *n*-heptane (B) or in xylene (C) (the concentration 25 mmol./l.) and stocked in a Schlenk tube under argon.
c) Yield was determined by gas chromatography.
d) No absorption of hydrogen was observed.
e) Yield was determined by isolation.

Table II. Nuclear magnetic resonance data

Compound	Position of peak (τ)[a]	Relative intensity[b]	Multiplicity	Assignment
$(\pi\text{-}C_5H_5)_2Ti(C_6H_5C{\equiv}CC_6H_5)_2$ in CCl_4	3.8	10	Singlet	C_5H_5
	3.3	20	Multiplet	C_6H_5
$(\pi\text{-}C_5H_5)_2Ti(C_6H_5C{\equiv}CH)_2$ in CCl_4	3.8	12	Singlet	C_5H_5 + ≡CH
	3.2	10	Multiplet	C_6H_5

a) Relative to $SiMe_4$ as internal standard.
b) Estimated to whole numbers by method of counting squares, relative to $C_5H_5=5$.

phenylacetylene, 1-alkynes were effectively subjected to partial hydrogenation to 1-alkenes. These facts also suggest that the kind of the substituent on acetylenes affects the type of hydrogenation.

In the hydrogenation of olefins and butadiene, only very slow absorption, or no absorption at all, of hydrogen was observed.

On the other hand, it was reported by Breslow and his collaborators[5] that the soluble Ziegler-type catalysts activated hydrogen for the homogeneous hydrogenation of olefins. It has been suggested that the study of the cited soluble catalysts should shed some light on the mechanism of the heterogeneous hydrogenat·on of olefins. However, in order to explain the mechanism of the hydrogenation in terms of organometallic chemistry, it is more useful to study the simple organometallic complex catalyst than to study a combined one, such as the Ziegler-type catalyst, because such a simple complex will make more convenient the isolation of an intermediate of the reaction.

Thus, in the present study the isolation of the intermediate was attempted. The dicarbonyl complex (I) was heated to 60°C for 20 min. with diphenylacetylene in a benzene solution under an inert atmosphere. From the reaction mixture, by chromatography on alumina and recrystallization from *n*-hexane, air-stable green crystals (II) were obtained in a 15% yield. On the other hand, Volpin and his collaborators[6] reported the synthesis of the same complex (II) by the reaction of diphenylacetylene, sodium cyclopentadienide and titanium tetrachloride. On the basis of the products of the reaction with hydrochloric acid or potassium hydroxide, they proposed the structures A and B. The present authors also investigated the structure of the complex II by means of studies of the NMR, infrared and electronic absorption spectra. The infrared spectrum of the complex II is in accord with either structure, A or B, because it shows π-bonded cyclopentadienyl

5) M. F. Sloan, A. S. Matlack and D. S. Breslow, *J. Am. Chem. Soc.*, **85**, 4014 (1963).

6) M. E. Volpin, V. A. Dubovitskii, O. V. Nogina and D. N. Kursanov, *Dokl. Akad. Nauk SSSR*, **151**, 1100 (1963); *Chem. Abstr.*, **59**, 14012 (1963).

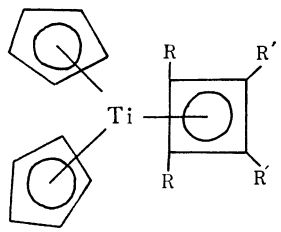

(A)

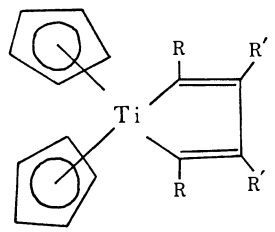

(B)

ligand absorptions and absorptions of sterically-hindered phenyl groups which are similar to that of π-cyclopentadienylcobalttetraphenylcyclobutadiene.[7] The data of NMR spectra are given in Table II, together with some assignments. The NMR spectrum of the complex II shows the aromatic multiplet at 3.2—3.65 τ and a sharp π-bonded cyclopentadienyl singlet at 3.8 τ. The phenyl/cyclopentadienyl proton ratio is 2.0 (calcd. 2.0).

The electronic absorption spectrum of the complex II is very similar to those of hexaphenylsilole, pentaphenylarsole and pentaphenylphosphole,[8] and it shows no characteristic absorption band of tetrasubstituted cyclobutadiene derivatives in the region of 320 mμ.[9,10] This fact supports the structure B, which has more sterrically-hindered phenyl groups than does the structure A.

The reaction of phenylacetylene with dicyclopentadienyltitaniumdicarbonyl was carried out under similar conditions. After the purification by chromatography on alumina, air-stable green needles (III) and a linear oligomer of phenylacetylene were obtained (yields, 7% and 25% respectively). The infrared spectrum of the complex III shows no acetylenic absorption bands, but it does show phenyl and π-bonded cyclopentadienyl absorptions. The NMR spectrum also shows phenyl and π-bonded cyclopentadienyl absorptions, where the ≡CH-proton band overlaps with the cyclopentadienyl band. The proton

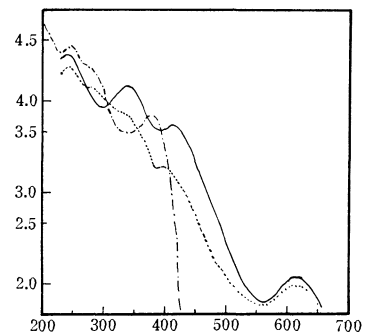

Fig. 1. The electronic absorption spectra of the complexes II and III and hexaphenylsilole.[8]
····· II in tetrahydrofuran
—— III in tetrahydrofuran
–·–· hexaphenylsilole in cyclohexane

ratio of cyclopentadienyl (including methylidyne protons)/phenyl is 1.2 (calcd. 1.2). The electronic absorption spectrum of the complex III is given in Fig. 1. From the above consideration, it may be concluded that the complex III should have either the structure A or B. Of these structures, B seems more probable for the complex III as in the case of the complex II, since the complex III is even more stable than the complex II. However, we failed in an attempt to obtain structural proof by the direct synthesis of the complex III from the dicyclopentadienyltitanium dichloride and 1, 4-dilithiotetraphenylbutadiene by analogy with the synthesis of 1, 1-bis(π-cyclopentadienyl)-2, 3, 4, 5-tetraphenylzirconacyclopentadiene.[8]

When acetylene or pentyne is employed in a similar reaction with the dicarbonyl I, unstable green oils are obtained. Further investigation of these oils has been given up, however, because of their instability. Olefins and butadiene do not react with the dicarbonyl I. This finding agrees with the fact that the hydrogenation of olefins and butadiene is very slow.

Neither complex, II or III, catalyzes the hydrogenation of acetylenes. Therefore, the exact mechanism of the catalytic hydrogenation of acetylenes is not yet clear. However, it is possible at present to speculate that the active intermediate in the hydrogenation is a precursor of

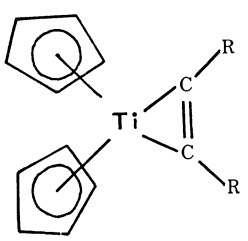

(IV)

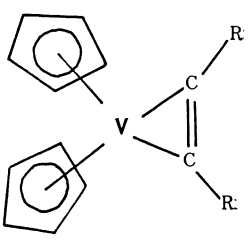

(V)

7) A. Nakamura and N. Hagihara, This Bulletin, **34**, 452 (1961).
8) E. H. Braye, W. Hübel and J. Caplier, *J. Am. Chem. Soc.*, **83**, 4406 (1961).
9) H. P. Fritz, *Z. Nautrforsch.*, **16b**, 415 (1961).
10) R. Huttel and H. J. Neugebauer, *Tetrahedron Letters*, **1964**, 3541.

the complex II or III, such as the complex IV, an analogue of the vanadium complex V which was reported on in a previous paper.[11]

Recently, the hydrogenation of olefins by dicyclopentadienyltitanium, which had been obtained by the decomposition of dicyclopentadienyldimethyltitanium with hydrogen,[12] was reported by Shikata and his collabolators.[13]

Experimental

The proton NMR data were obtained on a Varian A 60 spectrometer and a Japan Electron Optics Lab. JNM-4H-100 spectrometer, using tetramethylsilane as the internal standard. The infrared spectra were recorded on a Hitachi EPI-1 spectrometer. Gas chromatographic anaylses were carried out on Shimadzu GC-1 and GC-2B gas chromatographs. The melting and decomposition temperatures were observed by means of a hot-stage microscope and were not corrected.

The General Procedure of Hydrogenation.—The hydrogenation reactions were carried out in a 100-ml. autoclave. Since the catalyst was sensitive to air and moisture, all operations were carried out in an inert atmosphere. After the autoclave had been flushed with nitrogen, 20 ml. of the catalyst solution A, B or C (see below) was transferred from the stock tube by a syringe; then acetylene or olefin was charged in. The reduction was carried out under an initial hydrogen pressure of about 50 atm. and at 50—60°C for 30 min.. Although the hydrogenation of acetylenes did not proceed under 50°C, the rapid hydrogen uptake started at 50°C. In the case of olefins, no rapid reduction took place, even at 100°C. After the reaction, the hot solution was left standing in order to cool it. The products were analyzed and identified either by isolation or by gas chromatography. Several typical hydrogenation experiments are described below.

The Preparation of the Catalyst Solution.—Freshly-sublimed dicyclopentadienyltitaniumdicarbonyl was dissolved in benzene (catalyst A), in *n*-heptane (catalyst B) or in xylene (catalyst C), each concentration being 25 mmol./l., and stocked in a Schlenk tube under argon.

The Hydrogenation of 1-Pentyne.—A 100-ml. autoclave was charged with 2 ml. (20 mmol.) of 1-pentyne and 20 ml. of the catalyst solution A under nitrogen, and then with hydrogen up to a pressure of 50 atm. It was heated under shaking. A rapid hydrogen uptake started at 50°C, and the hydrogenation finished almost completely within 10 min. After it had been cooled with water, the reaction mixture was analyzed by gas chromatography. Found: 1-pentene 95%. Pentyne and pentane were not detected. (Dinonyl phthalate 3 m.; flow rate 32 ml./min. N_2; 55°C.) In a similar experiment, in which 5 g. of 1-pentyne, 0.5 g. of dicyclopentadienyltitaniumdicarbonyl and 20 ml. of benzene were used, 4.5 g. (90%) of 1-pentene was isolated by fractional distillation.

The Hydrogenation of Diphenylacetylene.—Into a 100-ml. autoclave, 3.4 g. of diphenylacetylene, 30 ml. of the catalyst solution A and 50 atm. of hydrogen were charged. The autoclave was shaken and heated. A rapid pressure drop took place at 50°C. After 30 min., the autocalve was cooled with water. The removal of the solvent yielded 3.6 g. of a pale yellow solid. It was purified by sublimation and recrystallization from methyl alcohol to give 3 g. of dibenzyl, m. p. 50—51°C (lit. 51.5—52.5°C). The infrared spectrum was identical with that of an authentic specimen.

The Partial Hydrogenation of Phenylacetylene. Into a 100-ml. autoclave, 2.7 g. (22 mmol.) of phenylacetylene, 20 ml. of the catalyst solution A and 6 atm. of hydrogen (22 mmol. of hydrogen) were charged. The autoclave was then shaken and heated. A rapid pressure drop took place at 50°C. After all the hydrogen had been absorbed, the autoclave was cooled with water. The reaction mixture was analyzed by gas chromatography, a study of its infrared spectrum, and the amount of the hydrogen absorption. Found: ethylbenzene 30%, styrene 40%, phenylacetylene 30%. (Thermol-2 3 m. and silicon-550 1.5 m.; flow rate 67 ml./min. N_2; 120°C; retention time: ethylbenzene 13 min.; styrene and phenylacetylene 16.5 min.) The styrene/phenylacetylene ratio was determined by the a amount of hydrogen absorption.

The Reaction of Diphenylacetylene with Dicyclopentadienyltitaniumdicarbonyl (I).—Dicylcopentadienyltitaniumdicarbonyl (I) (1.0 g., 4.3 mmol.) and diphenylacetylene (1.5 g., 8.6 mmol.) were heated in 20 ml. of benzene for 20 min. at 60°C. A violent evolution of gas took place, and the color of the reaction mixture changed to a greenish brown from red brown. After the mixture had cooled, the solvent was removed in vacuo and a green solid was obtained. Purification by chromatography on alumina and recrystallization from *n*-hexane yielded 0.3 g. of green crystals (II), m. p. 150°C in a sealed tube under nitrogen. A longer reaction time and a higher reaction temperature diminished the yield. Chromatographic purification must be carried out as quickly as possible because the green complex (II) slowly decomposes on alumina.

Found: C, 85.02; H, 5.59. Calcd. for $C_{38}H_{30}Ti$: C, 85.38; H, 5.66%.

An infrared spectrum in Nujol showed absorptions at 3080(w), 3040(w), 1590(m), 1495(sh), 1478(sh), 1442(m), 1362(w), 1257(s), 1175(w), 1152(w), 1145(w), 1095(sh), 1073(s), 1015(s), 940(vw), 905(vw), 835(w), 825(m), 803(vs), 796(vs), 772(m), 768(s), 750(m), 720(m), 697(vs), and 692(vs).

An electronic spectrum showed absorptions at 624 mμ (log ε, 1.90), 405 mμ (log ε, 3.16), 334 mμ (sh), 278 mμ(sh), and 240 mμ (logε, 4.24) in tetrahydrofuran.

The Reaction of Phenylacetylene with Dicyclopentadienyltitaniumdicarbonyl. — The dicarbonyl complex I (2.34 g., 10 mmol.) and phenylacetylene (2.0 g., 20 mmol.) were heated in 20 ml. of *n*-hexane for 20 min. at 60°C under nitrogen. A violent evolution of gas was observed, and the reaction mixture turned dark brown. The chromatography of the reaction mixture on alumina yielded 0.15 g. of an oxygenated product of the dicarbonyl complex I, 0.3 g. of a green solid (III), and 0.5 g. of a brown oligomer of phenylacetylene. After the recrystallization of the green solid (III) from *n*-hexane, 0.25 g. of green needles were obtained. M. p., 134—136°C in a sealed tube under nitrogen; yield, 7%.

11) R. Tsumura and N. Hagihara, This Bulletin, **38**, 861 (1965).
12) K. Caus and H. Bestian, *Ann.*, **654**, 8 (1962).
13) K. Shikata, K. Nishino and K. Azuma, *J. Chem. Soc. Japan, Ind. Chem. Sect.* (*Kogyo Kagaku Zasshi*), **68**, 358 (1965).

Found: C, 81.95; H, 5.84. Calcd. for $C_{26}H_{22}Ti$, C, 81.67; H, 5.82%.

An infrared spectrum in Nujol showed absorptions at 3080(w), 3055(w), 1590(s), 1568(w), 1482(s), 1443(m), 1437(m), 1300(vw), 1277(w), 1262(vw), 1200(vw), 1175(vw), 1150(vw), 1125(vw), 1070(m), 1020(s), 1010(s), 992(vw), 920(vw), 895(vw), 840(s), 820(vs) 810(vs), 802(sh), 750(vs), 745(sh), and 690(s).

An electronic absorption spectrum showed λ_{max} at 608 mμ (log ε, 2.14), 410 mμ (log ε, 3.55), 340 mμ (log ε, 4.16), and 238mμ (log ε, 4.32) in tetrahydrofuran.

The Attempted Reaction of Dicyclopentadienyltitanium Dichloride with 1, 4-Dilithiotetraphenylbutadiene.—A suspension of 1, 4-dilithiotetraphenylbutatriene, prepared from 2 g. of diphenylacetylene in 5 ml. of ether as described by Braye and his collaborators,[8] was added to a suspension of 2 g. of dicyclopentadienyltitanium dichloride in 100 ml. of ether. After the mixture had been refluxed for 3 hr., the formation of no product could be observed and the dichloride was recovered. A similar reaction was also attempted in tetrahydrofuran, but no reaction took place.

The authors wish to thank Mr. Toshiki Shibano for the elemental analyses and Dr. Akira Nakamura for the measurement of the NMR spectra.

BULLETIN OF THE CHEMICAL SOCIETY OF JAPAN VOL. 39 1182—1185 (1966)

The Polymerization of Acetonitrile in the Presence of Acidic and Basic Substances

By Eizo OIKAWA, Kyoichi MORI and Goro SAITO

Faculty of Engineering, Niigata University, Nagaoka, Niigata

(Received September 3, 1965)

Complexes of saturated nitriles with metal chlorides polymerize readily. In this paper, the polymerization of acetonitrile was carried out with more nitrile, than was needed to form the complex with metal chlorides. The conversion of the polymer increased in comparison with the case of the polymerization of the complex, indicating that the complex would partly dissociated in the reaction. The trimer of acetonitrile, 4-amino-2, 6-dimethylpyrimidine, was isolated, and ammonia was detected in addition to the brown polymer. The mechanism of the trimer formation in the presence of metal chlorides was illustrated through the removal of a proton from acetonitrile with the help of the chlorides, and through dimer formation. Hydrochloric acid and metaphosphoric acid were less active than metal chlorides. Ammonia itself was found to be inactive for the trimerization, bringing only acetamide. Water was also inactive in response to acetonitrile in the absence of acidic or basic substances. The derivation of ammonia was attributed to the decomposition of the pyrimidine compound and/or to the degradation of the polymer, but not to the hydrolysis of acetamide. The reaction of the polymer with propionaldehyde, the hydrolysis of the product, the carbylamine test, and a treatment of the trimer similar to that used for the complex suggested that the pyrimidine rings are involved in the polymer structure.

In previous papers[1,2] the polymerization of complexes of saturated nitriles with metal chlorides and the structure of the polymers have been reported. The composition of complex of the nitrile (RCN) with metal chloride (MCl_n) is definite (generally $2RCN:MCl_n$). If however, the metal chlorides behave as catalysts in the polymerization, the chlorides need not necessarily be added in amounts large enough to convert the whole nitrile into the complex. In the present investigation the polymerization was carried out with the excess nitrile; in other words, more nitrile than was needed to form the complex was added to the polymerization system in order to investigate if it is valid to say that only the nitrile that forms the complex is able to polymerize, while the free nitrile in the system is not.

In the polymerization, the trimer, 4-amino-2, 6-dimethylpyrimidine, and ammonia were obtained in addition to the polymer. The formation of the trimer has briefly been reported by Kabanov et al.[3] The mechanism of these formations in the presence of acidic substances was investigated, and it was suggested that the polymers include pyrimidine rings.

Experimental

Materials and Procedure.—The materials and the procedure were the same as those described in a previous paper.[2] The nitrile was added to the metal chlorides under a nitrogen atmosphere.

The sealed tube was heated in an autoclave under

1) E. Oikawa and S. Kambara, *J. Polymer Sci.*, **B2**, 649 (1964).

2) E. Oikawa and S. Kambara, This Bulletin, **37**, 1849 (1964).

3) V. A. Kabanov, V. P. Zubov, V. P. Kovaleva and V. A. Kargin, *J. Polymer Sci.*, **C** No. 4, 1009 (1963).

the pressure of isobutyl alcohol in order to prevent the tube from breaking. After they had been heated for the required time, the dark brown mass and liquid were transferred to a sublimation apparatus. The unconverted nitrile was distilled off, and sublimation followed. The white sublimate was submitted to elementary analyses. The ratio of acetamide and the pyrimidine in the sublimate was determined from the nitrogen concent by means of the Kjeldahl method using the following equation:

$$X = (N-23.7)/0.105$$

where X is the percentage of the pyrimidine compound (%) and N is the nitrogen content of the sublimate (%).

The Reaction of the Polymer with Propionaldehyde.—In a 100-ml. three-necked flask with a stirrer, a condenser and a thermometer, 25 ml. of propionaldehyde[4] and 0.3 g. of the pulverized polymer were placed. The reaction vessel was then heated in a water bath at 40°C, with stirring continued for 6 hr. After the propionaldehyde (b. p. 49°C) had been distilled off, the residue was washed with water and dried in a vacuum at 60°C. This specimen was subjected to infrared analysis. The hydrolysis of the reaction product was accomplished by refluxing it in a 0.1 N sodium hydroxide solution for 9 hr.

The Heat Treatment of 4-Amino-2, 6-dimethylpyrimidine with Metal Chlorides.—The pyrimidine compound was prepared by the trimerization of acetonitrile with sodium metal.[5] The procedure was the same as that described previously.[2] After the sublimation of the dark brown mass produced by heating, the residue was pulverized, washed with a diluted hydrochloric acid solution and water, and dried in a vacuum. For example, the heating of 1.03 g. of the pyrimidine compound with 2.38 g. of titanium tetrachloride ($[(CH_3CN)_3]/[TiCl_4]=2/3$) at 250°C for 4 hr. produced 0.50 g. of a brown solid (Found: N, 20.5%). The same treatment of 0.60 g. of the pyrimidine compound with 0.97 g. of zinc chloride for 8 hr. produced 0.24 g. of the product (Found: N, 16.6%). These products were insoluble or sparingly soluble in common organic solvents, but soluble in concentrated sulfuric acid.

Results and Discussion

The results of the polymerization with excess acetonitrile are shown in Table I.

In the same method as has been reported previously[1] the activation energy of the polymerization at a molar ratio of $r=13.8$ was found to be about 19 kcal./mol., which is equal to the value obtained from the polymerization of the acetonitrile complex with titanium tetrachloride. The conversions in Table I show that more nitrile than was needed to form the complex was converted to the polymer. These facts indicate that the following dissociation will occur at least partially under the polymerization conditions:

$$\begin{array}{l} 2RCN:MCl_n \rightleftharpoons 2RCN + MCl_n \\ \quad\downarrow \\ 2(RCN)_m:mMCl_n \rightleftharpoons 2(RCN)_m + mMCl_n \end{array}$$

The metal chlorides derived from dissociation can form a complex with free nitrile. Thus, the new complex and the undissociated complex will be converted to the polymer at the activation energy of 19 kcal./mol. The conversions in parentheses in Table I suggest that the chlorides do not have any remarkable catalytic effect.

The dark brown solutions of TA_32520 and ZA_22520 after polymerization were dried, and the residues were submitted to sublimation. A small amount of a white, crystalline substance was obtained; this was, for the most part, identified as 4-amino-2, 6-dimethylpyrimidine by a study of its melting point (179°C; 182°C[5]) and infrared spectrum and by elementary analyses (Found: C, 59.0; H, 7.4; N, 33.9. Calcd. for CH_3CN: C, 58.5; H, 7.3; N, 34.1%). This pyrimidine compound is usually prepared with basic catalysts, such as alkali metals and alkali metal alcoholates.[5]

In the polymerization of acetonitrile, there occurred the evolution of ammonia[2]; this might cause the trimerization of acetonitrile. The ammonia may be derived from the hydrolysis of acetamide with a trace of water included in the acetonitrile, or from the thermal degradation of the polymer.[2] The influence of ammonia on the trimerization, therefore, was investigated with and without water. The results are summarized in Table II. All the system changed dark brown and produced the polymer. Sublimation isolated a fine, opaque sublimate and transparent sublimate, which were identified by their melting points as 4-amino-2, 6-dimethylpyrimidine (179°C) and acetamide (81°C) respectively. The gradual decrease in the pyrimidine compound and the increase of acetamide with the increase in water content suggest that water was consumed only to form acetamide; the evolution of ammonia by the hydrolysis of acetamide was not confirmed.

In each experiment of Table II there was the odor of ammonia. Whether or not the ammonia exerts the catalytic action for trimerization was examined by adding concentrated ammonia (28%) to the nitrile. Table III shows the results. The sublimatoin of a white crystalline substance after distilling off the excess nitrile isolated almost only acetamide, which was also identified by a study of its infrared spectrum; there was no colored substance. Hence, ammonia does not behave as a catalyst for the formation of the pyrimidine.

It is considered that not only Lewis acid but also proton donating inorganic acids like hydrochloric acid will promote the polymerization of the nitrile if the reaction is initiated by the removal of a proton from the $H^+—{}^-CH_2{\equiv}C–N:{\rightarrow}MCl_n$ complex. The results of the experiments adding 35% hydrochloric acid and metaphosphoric acid

4) C. D. Hurd and R. N. Meinert, "Organic Syntheses," Coll. Vol. II, 541 (1948).

5) A. R. Ranzio and W. B. Cook, ibid., Coll. Vol. III, 71 (1951); T. L. Cairns, A. W. Larchar aad B. C. Mckusick, *J. Am. Chem. Soc.*, **74**, 5633 (1952).

are given in Table IV. Ammonia was detected, and there was a very small yield of a brown polymer. The infrared spectrum of the white sublimate revealed the formation of a small amount of the pyrimidine compound. Therefore, hydrochloric acid and metaphosphoric acid are less active in the trimerization and polymerization than are zinc chloride and titanium tetrachloride.

Table I. Polymerization of acetonitrile (excess nitrile)

No.	CH_3CN g.	Metal chloride MCl_n, g.	Molar ratio, r $[CH_3CN]/[MCl_n]$	Temp. °C	Time hr.	Yield g.	Conversion* %
TA_1 258	2.58	$TiCl_4$ 2.2	5.4	250	8	1.66	174(64)
TA_1 2520	2.58	2.2	5.4	250	20	1.78	186(69)
TA_2 233	2.58	0.86	13.8	230	3	0.24	63(9.1)
TA_2 236	2.58	0.86	13.8	230	6	0.34	92(13)
TA_2 258	2.58	0.86	13.8	250	8	0.87	233(34)
TA_2 2514	2.58	0.86	13.8	250	14	0.93	250(36)
TA_2 2520	2.58	0.86	13.8	250	20	0.93	250(36)
TA_2 270	2.58	0.86	13.8	270	0.5	0.36	97(14)
TA_2 271	2.58	0.86	13.8	270	1	0.42	112(16)
TA_3 2520	2.58	0.14	84.7	250	20	0.27	454(11)
ZA_1 2520	2.58	$ZnCl_2$ 0.10	85.6	250	20	0.06	93(2.2)
ZA_2 2520	3.35	0.81	13.8	250	20	0.42	88(13)

* The calculation is based on the amount of the nitrile which was needed to form the complex $2CH_3CN : MCl_n$; ( ): These are based on the whole nitrile added.

Table II. Sublimates in polymerizations[a]

No.	CH_3CN g.	$ZnCl_2$ g.	H_2O g.	Molar ratio $\frac{[CH_3CN]}{[ZnCl_2]}$	Molar ratio $\frac{[H_2O]}{[CH_3CN]}$	Sublimate g.	Conversion[b] %	Pyrimidine %	Acetamide %	Odor of NH_3
ZA	3.79	0.149	0	85.6	0	0.809	21.3	71.3	28.6	yes
ZA′	4.45	0.173	0	85.6	0	0.956	21.5	73.6	26.4	yes
ZB	1.95	0.162	0	40.0	0	0.589	30.2	91.1	8.9	yes
ZB′	1.65	0.138	0	40.0	0	0.583	35.3	87.5	12.5	yes
ZC	2.76	0.108	0.0013	85.6	0.0010	0.412	14.9	54.5	45.5	yes
ZD	3.80	0.147	0.0490	85.6	0.0294	1.098	28·9	33.3	66.7	yes

a) Reaction conditions; 250°C, 20 hr.
b) This is based on the whole nitrile added.

Table III. Reaction of acetonitrile in the presence of NH_3[a]

No.	CH_3CN g.	NH_3 g.	H_2O g.	Molar ratio $\frac{[CH_3CN]}{[NH_3]}$	Molar ratio $\frac{[H_2O]}{[CH_3CN]}$	Product[b] g.	Conversion, %	N[c] %	Formation of polymer
NE	2.18	0.011	0.029	8	0.33	0.420	19.3	24.0	no

a) Reaction conditions: 250°C, 20 hr.
b) M. p. 78°C
c) CH_3CONH_2; N 23.7%

Table IV. Reaction of acetonitrile in the presence of inorganic acid

No.	CH_3CN g.	Acid g.	H_2O g.	Molar ratio $\frac{[CH_3CN]}{[Acid]}$	Molar ratio $\frac{[H_2O]}{[CH_3CN]}$	Sublimate g.	Conversion, %	Odor of NH_3	Formation of polymer[b]
HF	1.58	HCl 0.009	0.016	151	0.073	0.125	7.9	yes	very little
HG	1.94	0.020	0.037	88.5	0.043	0.310	16.0	yes	very little
PH	1.57	HPO_3 0.041	0	81	0	0.015	1.0	—	very little

a) Reaction conditions: 250°C, 20 hr.
b) Conversion: <0.2%

The presence of water in the system in all the above results increased the yield of acetamide. The polymer formed during the reaction time has been found to cause autocatalysis.[3] Thus, an attempt was made to carry out the reaction under the same reaction conditions (250°C, 20 hr.), adding to the system separately a little water and the polymer prepared from the complex,[2] without any acidic and basic substances. In either case neither colored product nor sublimable substance was formed, and there was no odor of ammonia. Hence, the polymer does not behave as a catalyst for the trimerization, nor does it give the pyrimidine compound by the degradation of the polymer.

Since the evolution of ammonia was always accompanied with the formation of the trimer or the polymer, it may be concluded that ammonia would probably be given by the decomposition of the pyrimidine compound and/or the degradation of the polymer.

When the reaction conditions were changed from 250°C for 20 hr. to the refluxing condition for 20 hr. under an atmospheric pressure, the system of excess nitrile with zinc chloride did not give any colored product or sublimable substance. Therefore, the rise in pressure (about 30 atm. in the sealed tube at 250°C) and temperature seems always necessary. The application of high pressure (50000 atm.) and high temperature (200—400°C) to acetonitrile has brought about a similar formation of 4-amino-2, 6-dimethylpyrimidine.[6] However, the addition of metal chlorides does not need such drastic conditions, and it facilitates the trimerization and polymerization. The high conversion of the trimer with a strong basic catalyst is due to the easy removal of a proton from acetonitrile. The complex formation of the nitrile with metal chlorides may also help the removal of a proton from acetonitrile, which will in turn facilitate the following formation of a dimer and, finally, the trimer. The formation of the trimer through the dimer has been confirmed in a basic catalyst.[7]

1) Removal of a proton:

$$CH_3CN + MCl_n \rightarrow H^+ — {}^-CH_2\text{-}C{\equiv}N{:}{\rightarrow}MCl_n$$

$$H^+ + CH_3CN \rightarrow H_3C\text{-}C^+{=}NH$$

2) Formation of a dimer:

$$H_3C\text{-}C^+{=}NH + {}^-CH_2\text{-}C{\equiv}N{:}MCl_n \rightarrow H_3C\text{-}\underset{\underset{NH}{\|}}{C}\text{-}CH_2\text{-}C{\equiv}N{:}MCl_n \rightarrow H_3C\text{-}\underset{\underset{NH_2}{|}}{C}{=}CH\text{-}C{\equiv}N{:}MCl_n$$

3) Formation of a pyrimidine ring:

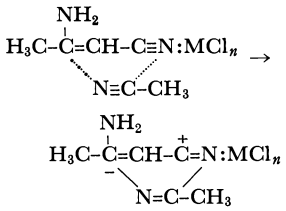

4) Rearrangement:

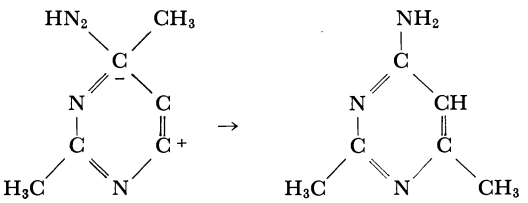

The polymer obtained in Tables I and II was similar in infrared spectra and nitrogen content to those obtained previously.[2] The polymer from the complex, when subjected to a carbylamine test, revealed positive results, while the sublimation of the polymer isolated nothing. Moreover, the infrared spectrum of a pulverized polymer suspended in propionaldehyde for 6 hr. at 40°C showed sharp new absorptions at 2850, 2920, and 2950 cm^{-1} which are probably due to C–H stretching vibrations, and a stronger absorption at 1620 cm^{-1} due to C=N. The former three absorptions disappeared upon alkaline hydrolysis. These facts support the idea that the polymer has an amino group.

The treatment of 4-amino-2, 6-dimethylpyrimidine with metal chlorides similar to that of the complex produced a dark brown solid whose infrared spectrum revealed absorptions similar to those of the polymer prepared from the complex (3400, 3000—2900 cm^{-1}: weak and broad; 1600 cm^{-1}: strong and broad). A strong odor of ammonia was found, and nothing was isolated by sublimation. The nitrogen contents of the products were comparable with those of the polymer obtained from the complex.[2]

Considering the formation of the pyrimidine compound in addition to the brown mass, it may be concluded that the pyrimidine compound takes part in the formation of the polymer as well as conjugated C–N groups.

The authors wish to acknowledge that these investigations have been undertaken with the aid of Yamaguchi funds. One of the authors (E. O.) is also indebted to Professor Shu Kambara of the Tokyo Institute of Technology for his generous help in carrying out a part of the experiments.

6) I. S. Bengelsdorf, *J. Org. Chem.*, **28**, 1369 (1963).
7) R. Holtzwart, *J. Prakt. Chem.*, (2) **39**, 230 (1889).

BULLETIN OF THE CHEMICAL SOCIETY OF JAPAN VOL. 39 1186—1192 (1966)

Osmotic Pressure Measurements for Poly-*p*-Chlorostyrene Solutions

By Kan'ichiro TAKAMIZAWA*

Department of Chemistry, Faculty of Science, Tokyo University of Education, Otsuka, Tokyo

(Received September 8, 1965)

Osmotic pressure measurements were made on poly-*p*-chlorostyrene fractions in toluene. Their intrinsic viscosities were measured in toluene, butanone, and chlorobenzene at 30°C. The intrinsic viscosity - molecular weight relationships of these systems were then evaluated for the monodisperse homologue by applying the proper correction for the heterogeneity in the sample. The unperturbed dimension of the polymer was estimated by the Kurata-Stockmayer method. A comparison of this estimate with that for polystyrene indicated that the chlorine atom at the para-position had no appreciable effect on the hindrance to the internal rotation of chain. The heat of the dilution of the polymer in toluene and chlorobenzene was also determined from measurements of the temperature coefficient of the osmotic pressure. It was endothermic in toluene and approximately zero in chlorobenzene. These results were then discussed in relation to the cohesive energy densities of the polymer and the solvents.

In the study of high polymers, the osmotic pressure is a primary source of information on the number average molecular weights of polymers and on the thermodynamic properties of polymer-solvent systems. In the measurement, however, we often encounter many technical difficulties which have not yet been completely solved. The main difficulty arises from solute permeation through semi-permeable membranes.[1,2] In practice, however, we may avoid this difficulty in the measurement of fractionated samples with molecular weights higher than 2×10^4 by making a suitable choice of the semi-permeable membrane.

A large number of experimental and theoretical work has been carried out in an effort to elucidate the solution properties of high polymers. It is interesting to examine how these properties are influenced by the structural units of the polymer molecule. In this connection, light-scattering measurements carried out in our laboratory have shown that, in comparison with a polystyrene chain, the chain extension of poly-*p*-chlorostyrene is modified in solution, possibly because of the polar character of its structural unit.[3]

The present investigation was undertaken in order to make a further study of the solution behavior of poly-*p*-chlorostyrene. As is well known, this behavior, for example, the relation between the intrinsic viscosity and the molecular weight, is affected by the heterogeneity in molecular weight. This difficulty can apparently be overcome by estimating the relation corresponding to a homogeneous homologue, using an appropriate molecular weight distribution function and the data for weight- and number-average molecular weights for each fraction of the fractionated sample. Furthermore, the temperature dependence of the osmotic pressure of the system was also measured in order to examine the way in which a polar group substituted in the polymer molecule affects the polymer-solvent interaction.

Experimental

Materials.—The poly-*p*-chlorostyrene fractions used were those described in a previous report.[3] The sample had been thermally polymerized at 100°C for 48 hr. and then fractionated by a successive precipitation procedure employing butanone as a solvent and methanol as a precipitant. The steps followed were to dissolve the fraction in butanone (about 2 per cent concentration) and then to pour the solution into excess methanol, which had previously been cooled by a dry ice - methanol mixture, before filtering and drying the sample in a vacuum (below 10^{-4} mmHg) for 10 hr. at 60°C.

Each solvent was purified in the usual manner.

Osmometry.—The osmotic pressure measurements were carried out with modified Zimm-Myerson osmometers. This type of osmometer was preferred because of its simple construction and operation.[4] Further, some investigators have developed refinements in the use of this instrument.[5-10] Our modification of the

* Present address: Department of Applied Science, Faculty of Engineering, Kyushu University, Hakozaki, Fukuoka.

1) A. V. Staverman, *Rec. trav. chim.*, **70**, 344 (1951); **71**, 623 (1952).

2) F. Alvang and O. Samuelson, *J. Polymer Sci.*, **24**, 353 (1957).

3) T. Saito, This Bulletin, **35**, 1580 (1962).

4) B. H. Zimm and I. Myerson, *J. Am. Chem. Soc.*, **68**, 911 (1946).

5) E. H. Immergut and H. Mark, *J. Polymer Sci.*, **7**, 345 (1951).

6) K. Ishikawa, T. Kawai and M. Tokunaga, *J. Chem. Soc. Japan, Ind. Chem. Sect.* (*Kogyo Kagaku Zasshi*), **55**, 736 (1952).

7) S. H. Pinner and J. V. Stabin, *J. Polymer Sci.*, **9**, 575 (1952).

8) E. H. Immergut and J. V. Stabin, ibid., **14**, 209 (1954).

9) H. Takenaka and T. Ikeda, The 5th Annual Meeting of the Society of Polymer Science, Japan, May, 1956.

10) T. Matsuo, *Chem. High Polymers Japan* (*Kobunshi Kagaku*), **15**, 640 (1958).

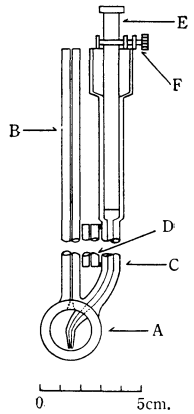

Fig. 1. Modified cell of Zimm-Myerson osmometer.
A, cell; B, measuring capillary; C, filling tube; D, reference capillary; E, positioning rod; F, screw cock

cell is presented in Fig. 1. The glass cell is 1.2 cm. deep and 2 cm. in inner diameter. The filling tube (in. diam. 2 mm.) extends from the side of the cell to within a few millimeters of the bottom, and the measuring capillary (int. diam. 0.8 mm.) extends to the top of the cell so that air bubbles in the cell may be easily eliminated. The filling tube is closed by a glass rod with a mercury seal, similar to that devised by Takenaka and Ikeda,[9] the rod being used to adjust the meniscus level of the solution. Membranes are clamped on by means of 18—8 stainless-steel plates with Teflon packings. The cell is filled and emptied with a hypodermic syringe fitted with a long needle. The osmometer cell is held in a large glass cylinder containing the solvent.

Gel-cellophane #300* was used as the semi-permeable membrane. After the membranes had been allowed to swell in water, they were clamped on the cell and then conditioned to a measuring solvent by a procedure similar to that proposed by Carter and Record.[11] Namely, they were transferred to toluene through 50/50 water-ethanol, absolute ethanol and 50/50 ethanol-toluene, being allowed to remain in each solvent for two days. Before measurements the membranes on the cell were immersed in toluene for at least two weeks.

The osmotic pressure measurements for the poly-*p*-chlorostyrene fractions were performed at 30.0 and 60.0°C by employing toluene and chlorobenzene as solvents. Though the osmometer was cotrolled in an thermostat within ±0.001°C at 30°C and ±0.005°C at 60°C, the results did not stabilize because of fluctrations of the room temperature; therefore, the thermostat was then placed in an air-bath, one controlled to within ±0.1°C of the measuring temperature.

In order to eliminate effects due to the absorption of the solute on the membranes,[2] new membranes were further conditioned with a solution at a higher concentration before use, and then the cell was rinsed three times with the solution to be measured. In the third rinsing it was immersed for a period of 0.5 to 1 hr. The osmotic pressure data were obtained by reading the height differences over 24 to 48 hr., since at least 5 hr. were required to attain equilibrium. No lowering of the height of the solution meniscus, which is possibly due to the permeation of the solute through the membranes, was observed during the measurement except in the case of the most concentrated solution (about 2.5 g./100 cc.). The dynamic osmotic procedure failed to give any reliable results because the relation between the rate of solvent permeation and the pressure difference was not linear. Membrane symmetries were assured within a range of ±0.01 cm. during each measurement.

Viscometry.—Viscosity was measured at 30±0.01°C with an Ubbelohde viscometer which had been modified to facilitate successive dilutions. Its flowing volume was about 2 cc., and the length of the capillary was 10 cm. The flow time of butanone was about 200 sec., permitting us to ignore the kinetic energy correction. The solvents used were toluene, butanone and chlorobenzene. The data obtained were treated according to Huggins' equation.

Results and Discussion

Extrapolation to Infinite Dilution.—Most of the fractions were osmotically measured in toluene at 30.0°C in a concentration range of 0.2 to 1×10^{-2} g./cm³. The values of the reduced osmotic pressure, π/c, are plotted against the concentration, c, in Fig. 2 (π in g./cm² and c in g./cm³). They are apparently represented by this equation:

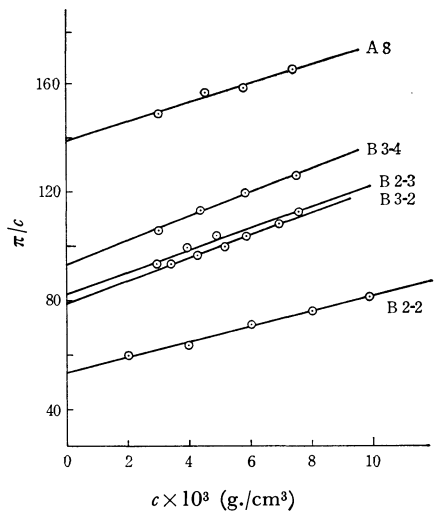

Fig. 2. Plots of π/c against c for fractions of poly-*p*-chlorostyrene in toluene at 30°C.

$$\pi/c = \boldsymbol{R}T[(1/M_n) + A_2c] \quad (1)$$

where $\boldsymbol{R}$ is the gas constant in g.cm./deg.mol.; M_n, the number-average molecular weight, and A_2, the second virial coefficient in cm³mol./g². The constants, M_n and A_2, were evaluated by the method of least squares, where Eq. 1 was rewritten

11) S. R. Carter and B. R. Record, *J. Chem. Soc.*, **1939**, 664.
* This was kindly supplied by the Tokyo Cellophane Co., Ltd.

in the form expressed as a c series, as recommended by Ducker et al.[12] Figure 2 apparently shows a good agreement between the experimental points and the rectilinear relation.

On the other hand, the osmotic pressures of toluene solutions of the fraction B 2-2 were measured over a larger concentration range, up to 2.5×10^{-2} g./cm^3, at two different temperatures, 30.0 and 60.0°C. Furthermore, the osmotic pressure of the fraction in chlorobenzene was measured at the same temperatures. A plot (Fig. 3) of the observed data, listed in Table I,

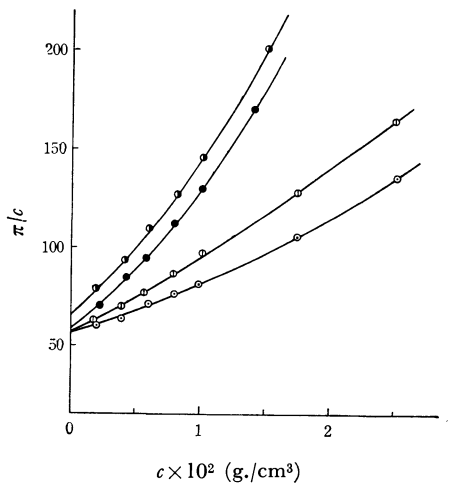

Fig. 3. Plots of π/c against c for fraction of B 2-2 in toluene (⊙ at 30°C, ⓘ at 60°C) and in chlorobenzene (● at 30°C, ◑ at 60°C).

shows that the values for both solvents fit curves with an upward curvature. Therefore, the relationship between π/c and c should be represented by an equation with larger virial coefficients:

$$\pi/c = \boldsymbol{R}T[(1/M_n) + A_2c + A_3c^2] \qquad (2)$$

where A_3 is the third virial coefficient in cm^{6}mol./g^3. In this case, there are two methods of analyzing the observed data; one is to determine the most possible curve for the experimental points by the least squares technique, as has been previously described, while the other is to fit the curve according to the equation derived from Flory's theory of dilute polymer solutions, i. e.,

$$\pi/c = (\boldsymbol{R}T/M_n)(1 + \Gamma_2c + g\Gamma_2^2c^2) \qquad (3)$$

where g is a factor whose value depends on the intermolecular potential energy.[13] As the theoretical work of Stockmayer and Casassa gave $g=1/4$, Eq. 3 may be written as:

$$(\pi/c)^{1/2} = (\boldsymbol{R}T/M_n)^{1/2}[1 + (\Gamma_2/2)c] \qquad (4)$$

12) E. Ducker, E. C. Fieller, H. T. Hookway and R. Townsend, *J. Chem. Soc.*, **1952**, 4390.

13) P. J. Flory, *J. Chem. Phys.*, **17**, 1347 (1949); P. J. Flory and W. R. Krigbaum, ibid., **18**, 1086 (1950).

TABLE I. OSMOTIC PRESSURE DATA FOR THE FRACTION B 2-2

Temp. °C	$c\times10^2$ g./cm^3	π g./cm^2	π/c
	Toluene solution		
30	0.200	0.120	60
	0.398	0.253	64
	0.601	0.428	71
	0.801	0.610	76
	0.989	0.804	81
	1.751	1.855	106
	2.513	3.418	136
60	0.178	0.112	63
	0.392	0.274	70
	0.570	0.436	77
	0.792	0.686	87
	1.016	0.988	97
	1.751	2.250	129
	2.504	4.129	165
	Chlorobenzene solution		
30	0.224	0.157	70
	0.426	0.360	85
	0.579	0.549	95
	0.799	0.900	113
	1.013	1.320	130
	1.408	2.402	171
60	0.196	0.154	79
	0.421	0.394	94
	0.605	0.666	110
	0.820	1.044	127
	1.010	1.474	146
	1.511	3.036	201

This equation gives a linear relation between $(\pi/c)^{1/2}$ and c.[14]

The data observed for the fraction B 2-2 were treated by both methods; the results, i. e., M_n, A_2, and A_3, are summarized in Table II. The plots of $(\pi/c)^{1/2}$ against c, also shown in Fig. 4, indicate that they apparently obey a linear relationship. From Table II, however, it appears that the values of M_n and A_2 are nearly the same for both treatments, while the agreement between those of A_3 is far from satisfactory. The standard deviations of the observed values of π from those calculated by Eq. 3 with $g=1/4$ are larger than those obtained from Eq. 2. However, because the osmotic pressures of the fractions in toluene, except that of B 2-2, were measured for only a few concentrations and over a smaller concentration range, it may be better if the data for the fractions are treated by Flory's equation with $g=1/4$. The results are summarized in Table III, which contains the weight average molecular weight, M_w, as determined by Saito from light-scattering measurements.[3]

The Dependence of Solution Properties on the Molecular Weight.—The plot of the

14) W. H. Stockmayer and E. F. Casassa, ibid., **20** 1560 (1952).

TABLE II. COMPARISON OF THE VALUES, FOR M_n, A_2, AND A_3, FOR THE FRACTION B 2-2, CALCULATED FROM THE METHOD OF LEAST SQUARES (Eq. 2) AND FROM THE FLORY EQUATION USING $g=1/4$ (Eq. 3)

Solvent	Temp. °C	Eq.	$M_n\times10^{-4}$	$A_2\times10^4$ cm³mol./g².	$A_3\times10^3$ cm⁶mol./g³.
Toluene	30	2	45.4	0.80	1.7
		3	48.3	0.98	1.2
Toluene	60	2	51.0	1.33	0.9
		3	47.3	1.12	1.2
Chlorobenzene	30	2	42.9	1.86	8.5
		3	50.3	2.16	5.9
Chlorobenzene	60	2	42.5	2.04	7.3
		3	45.5	2.32	6.2

TABLE III. EXPERIMENTAL RESULTS FOR THE POLY-*p*-CHLOROSTYRENE FRACTIONS

Fraction	$M_n\times10^{-4}$	$A_2\times10^4$ cm³mol./g.²	$M_w\times10^{-4}$	$[\eta]$ Toluene	$[\eta]$ Butanone	$[\eta]$ Chlorobenzene
A 2	50.7	—	115	—	1.11_4	1.39_6
B 2-2	47.2	0.96	99	0.85_0	0.91_5	1.24_7
B 2-3	30.9	1.47	75	0.65_8	0.73_5	0.92_2
B 3-2	31.9	1.42	66	0.65_2	0.71_2	0.91_8
B 3-4	27.2	1.54	47	0.55_6	0.59_4	0.75_3
A 8	19.2	1.69	31	0.39_5	0.43_5	0.53_7

Intrinsic viscosity is expressed in 100 ml./g.

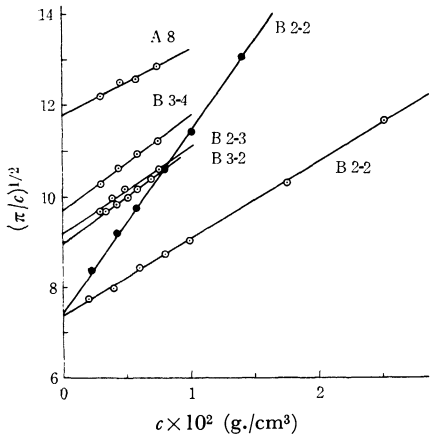

Fig. 4. Plots of $(\pi/c)^{1/2}$ against c according to Eq. 4 for fractions in toluene (open circles) and in chlorobenzene (filled circles) at 30°C.

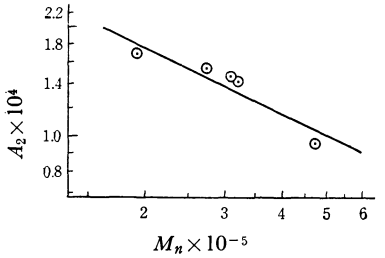

Fig. 5. Dependence of second virial coefficient on molecular weight for poly-*p*-chlorostyrene fractions in toluene at 30°C.

second virial coefficient against the molecular weight is shown in Fig. 5. It appears that A_2 decreases as M_n increases, as is generally recognized, and has a linear logarithmic relationship to M_n, corresponding to $A_2\propto M_n^{-0.6}$. The osmotic second virial coefficients have slightly higher values and a more marked dependence on the molecular weight than that determined by light-scattering measurements. This may be partly attributed to the molecular weight distribution of the fractions.

As a result of light-scattering measurements, it has been shown that the presence of a polar group in the molecule of poly-*p*-chlorostyrene has a marked influence on its solution behavior and increases its solubility in polar solvents. This tendency may be deduced from the fact that A_2 in a chlorobenzene solution is remarkably higher than that in toluene, as is shown in Table II, and also from the fact that the magnitude of the intrinsic viscosity of the fractions in toluene, butanone, and chlorobenzene increases as the polarity of the solvent is increased. The data for the intrinsic viscosity, $[\eta]$, are also summarized in Table III. The plot of $[\eta]$ against M_n for each solvent (Fig. 6) shows that the relation for each solution is apparently linear on a log-log scale. However, it is known that the degree of homogeneity with respect to the molecular weight has a much greater effect on the relation between $[\eta]$ and M_n than on that between $[\eta]$ and M_w. For comparison, the plot of $[\eta]$ against M_w is also shown in Fig. 6. These plots represents the effect of the heterogeneity on the Mark-Houwink equation:

$$[\eta] = KM^{\alpha} \tag{5}$$

It is desirable that the equation be established for a homogeneous homologue of the polymer

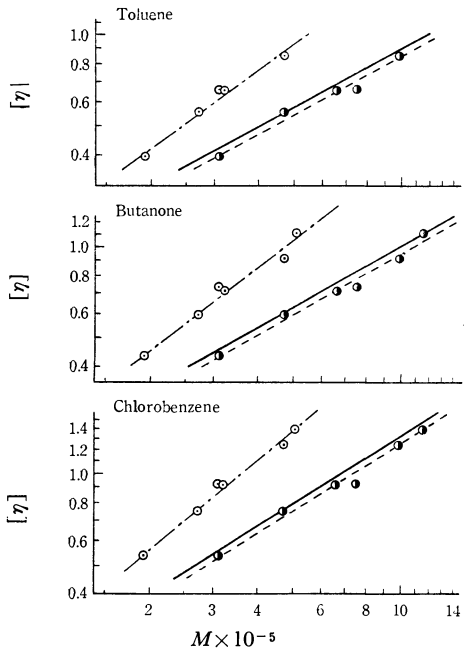

Fig. 6. Relation between intrinsic viscosity and molecular weights. Open circles, $[\eta]$-M_n; half-filled circles, $[\eta]$-M_w; full line, relation corresponding to homogeneous homologue.

before entering into a precise discussion. The K-value corresponding to homogeneous samples may be estimated from the experimental values, i. e., K_w in the $[\eta]$-M_w or K_n in the $[\eta]$-M_n relation, by assuming that the molecular weight distribution for each of the fractions is represented by the familiar Schulz-Zimm function:

$$w(M) = [y^{h+1}/\Gamma(h+1)]M^h \exp(-yM)$$

where

$$y = h/M_n = (h+1)/M_w$$

where Γ represents the gamma function, and where the value of the exponent, α, is approximately the same for the $[\eta]$-M_w relationship. The parameter, h, characterizing the heterogeneity of each fraction was experimentally determined. Therefore, the K value may be calculated by the equation:

$$K = K_w\Gamma(h+1)(h+1)^\alpha/\Gamma(\alpha+h+1)$$

or $$K = K_n\Gamma(h+1)h^\alpha/\Gamma(\alpha+h+1)$$

A detailed discussion will be given elsewhere. Thus, the relations were evaluated for the homogeneous homologue:

$$[\eta] = 1.29\times10^{-4}M^{0.64} \text{ (in toluene)}$$
$$[\eta] = 0.96\times10^{-4}M^{0.67} \text{ (in butanone)}$$
$$[\eta] = 0.48\times10^{-4}M^{0.74} \text{ (in chlorobenzene)}$$

They are shown by the full curves in Fig. 6. They show that the molecule of poly-*p*-chlorostyrene assumes the largest dimension in chlorobenzene and the smallest in toluene, and that the magnitude of the exponent increases with an increase in the polarity of the solvent.

Unperturbed Dimension.—According to the theory of the excluded volume effect, developed by Kurata, Stockmayer and Roig,[15] it may be possible to evaluate an unperturbed dimension of a polymer molecule from its $[\eta]$-M relationships. Recently a detailed review of the procedure has been presented.[16] Their theory results in the following equation:

$$[\eta]^{2/3}/M^{1/3} = K_\theta^{2/3} + Bg(\alpha_\eta)M^{2/3}/[\eta]^{1/3} \quad (6)$$

where K_θ is K in Eq. 5, corresponding to the theta condition; B, the constant which depends on the structure of the polymer molecule and the polymer-solvent interaction, and α_η, the hydrodynamic linear expansion factor, $([\eta]/[\eta]_\theta)^{1/3}$. The function of α_η, $g(\alpha_\eta)$, is given by the equation:

$$g(\alpha_\eta) = 8\alpha_\eta^3/(3\alpha_\eta^2+1)^{3/2} \quad (7)$$

From the first plot of $[\eta]^{2/3}/M^{1/3}$ against $M^{2/3}/[\eta]^{1/3}$, K_θ was approximately estimated by an extrapolation according to Eq. 6, and the α_η value for each fraction was evaluated. Then, $[\eta]^{2/3}/M^{1/3}$ was plotted against $g(\alpha_\eta)M^{2/3}/[\eta]^{1/3}$, using the estimated α_η value, thus affording an improved value for K_θ.

Our data were repeatedly analyzed with the least-square technique of Deming until K_θ converaged to a constant value. In this case the effect of the molecular weight distributions of each fraction was taken into account. That is, the observed value of $[\eta]$ for each fraction was corrected to that corresponding to a homogeneous sample by assuming the Schulz-Zimm distribution function. From the intercepts of the Kurata-Stockmayer plots for poly-*p*-chlorostyrene, which are shown in Fig. 7, the values of K_θ in toluene, butanone, and chlorobenzene are derived as

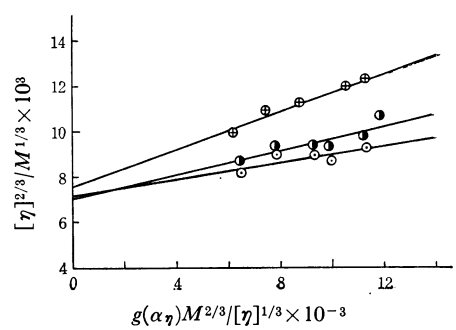

Fig. 7. Kurata-Stockmayer viscosity plots for poly-*p*-chlorostyrene fractions in toluene (open circles), butanone (half-filled circles), and chlorobenzene (crossed circles).

15) M. Kurata, W. H. Stockmayer and A. Roig, *J. Chem. Phys.*, **33**, 151 (1960).
16) M. Kurata and W. H. Stockmayer, *Fortschr. Hochpolymere Forsch.*, **3**, 196 (1963).

6.1, 5.9, and 6.6×10^{-4} respectively. These values are considered to be in excellent agreement and give $K_\theta=(6.1\pm0.4)\times10^{-4}$. The unperturbed end-to-end distance of a polymer chain, $\langle r^2\rangle_0^{1/2}$, in cm., may be calculated by the equation:

$$\langle r^2\rangle_0^{1/2}=(K_\theta/\Phi)^{1/3}M^{1/2} \quad (8)$$

where Φ is a universal constant, given as 2.87×10^{21} for monodispersed systems. The σ factor may be generally used as a measure of the hindrance to internal rotations about the single bonds of the chain; it is defined as the ratio of $\langle r^2\rangle_0^{1/2}$ to the dimension, $\langle r^2\rangle_{0f}^{1/2}$, which corresponds to the model with fixed valence angles and a completely free internal rotation. In the case of poly-*p*-chlorostyrene, this gives a value for σ of 2.30 ± 0.06, which is slightly higher than that, 2.18 ± 0.07, cited in the literature.[16] On the other hand, the σ value for polystyrene is 2.22 ± 0.05.[16] It appears that the chlorine atom at the para-position has only a small effect on the hindrance to the internal rotations, whereas the presence of this polar group remarkably modifies the solubility of the polymer in comparison with that of polystyrene.

Thermodynamic Properties. — In examining polymer-solvent interactions, the results are usually expressed in terms of a purely empirical parameter, χ_1, which is expressed according to the Flory-Huggins lattice theory of polymer solutions by the equation:

$$A_2=[(1/2)-\chi_1]/V_1d_2^2 \quad (9)$$

where V_1 is the molar volume of the solvent and d_2, the density of the polymer. The density of the polymer was calculated from the relation between the solution density and the weight fraction of the polymer, the additivity of the partial volumes being assumed. The χ_1 values for the fraction B 2-2 at 30°C are 0.483 in toluene and 0.462 in chlorobenzene. Ogino reported that the values of the parameter for polystyrene and poly-*p*-chlorostyrene in benzene, as determined by the measurement of initial stress-strain relations for gels in the solvent, were 0.47 for the former system and 0.49_5 for the latter.[17] From the osmotic pressure measurements, Bawn et al. obtained χ_1 values of 0.443 to 0.447 for polystyrene solutions in toluene and of 0.484 to 0.487 for butanone solutions.[18] These figures show that toluene, as well as benzene, is a poor solvent for poly-*p*-chlorostyrene, and that the better solvent has a structure similar to that of the monomer unit of the polymer, i. e., chlorobenzene for poly-*p*-chlorostyrene and toluene for polystyrene.

Further information can also be obtained from the measurement of the temperature dependence of the osmotic pressure. According to thermodynamic relationships, the excess molar heat of dilution, Δh_1^E, and the excess entropy of dilution, Δs_1^E, are given by the temperature coefficients of the second and third virial coefficients, i. e.,

$$\Delta\mu_1^E/c^2V_1=-RT(A_2+A_3c)$$
$$\Delta h_1^E/c^2V_1=RT^2\{(\partial A_2/\partial T)+(\partial A_3/\partial T)c\}$$
$$T\Delta s_1^E/c^2V_1=RT\{A_2+T(\partial A_2/\partial T)+A_3c+T(\partial A_3/\partial T)c$$

where $\Delta\mu_1^E$ represents the excess free energy of dilution. The results are summarized in Table IV, in which the values of A_2 and A_3, evaluated by means of the method of the least squares, were used. The heat of dilution in chlorobenzene could be taken to be zero within the limits of experimental error over the concentration range from zero to 2×10^{-2} g./cm³. With a toluene solution the values show an endothermic heat of dilution. Bawn and Wajid reported that the heat of dilution in a polystyrene-toluene system was zero at all concentrations.[19] Polystyrene has a cohesive energy density (C. E. D.) of 82 cal./cm³, as elucidated by swelling experiments.[20] On the other hand, the value of the Hildebrand solubility parameter for toluene is reported to be 8.90 $(\text{cal./cm}^3)^{1/2}$ at 25°C; i. e., the C. E. D. of toluene is 79 cal./cm³. The solubility behavior of the polystyrene-toluene system may be interpreted in terms of their C. E. D.'s and in terms of the resemblance of the solvent molecule to the structural unit of the polymer. If this situation also holds in the case of a poly-*p*-chlorostyrene - chlorobenzene system, the C. E. D. of poly-*p*-chlorostyrene may lie near the value of that of chlorobenzene, i. e., 91 cal./cm³.

Table IV. Excess thermodynamic functions of dilution for poly-*p*-chlorostyrene in toluene and chlorobenzene at 30°C (cal.cm³/g.²)

$c\times10^2$ g./cm³	$\Delta\mu_1^E/c^2V_1$	$\Delta h_1^E/c^2V_1$	$T\Delta s_1^E/c^2V_1$
	Toluene solution		
0	-0.048 ± 0.002	0.32 ± 0.04	0.37 ± 0.04
1	-0.058 ± 0.003	0.27 ± 0.04	0.33 ± 0.04
2	-0.069 ± 0.003	0.23 ± 0.04	0.30 ± 0.04
	Chlorobenzene solution		
0	-0.112 ± 0.007	0.11 ± 0.09	0.22 ± 0.09
1	-0.163 ± 0.007	0.04 ± 0.10	0.20 ± 0.10
2	-0.215 ± 0.008	-0.04 ± 0.10	0.18 ± 0.10

Summary

The osmotic pressure of poly-*p*-chlorostyrene fractions in toluene and the intrinsic viscosities at 30°C in toluene, in butanone, and in chlorobenzene have been measured. The relation

17) K. Ogino, This Bulletin, **32**, 553 (1959).
18) C. E. H. Bawn, R. J. F. Freeman and A. D. Kamaliddin, *Trans. Faraday Soc.*, **46**, 862 (1950).
19) C. E. H. Bawn and M. A. Wajid, *J. Polymer Sci.*, **12**, 109 (1954).
20) R. E. Boyer and R. S. Spencer, ibid., **3**, 97 (1948).

between the intrinsic viscosity and the molecular weight corresponding to a homogeneous homologue has been determined, taking into consideration the effect of the heterogeneity of each fraction on this relationship. The unperturbed dimension of the polymer, as evaluated by Kurata-Stockmayer's plots, showed that the polar group at the position of the benzene ring does not appreciably affect the hindrance to internal rotations about single bonds of its chain in comparison with the polystyrene chain. The heat of the dilution of poly-*p*-chlorostyrene in chlorobenzene and toluene has been determined from measurements of the temperature coefficients of the osmotic pressure. In the concentration range up to 2.5×10^{-2} g./cm^3, the $\Delta h_1^E/c^2V_1$ value, where V_1 is the molar volume of the solvent, was approximately zero in chlorobenzene and 0.3 cal. cm^3/g.^{2} in toluene. The results have been discussed in relation to the cohesive energy densities of the polymer and the solvents.

The author takes this opportunity to express his thanks to Professor Akira Kotera and Professor Keizo Suzuki for their continuing encouragement and helpful discussion. Thanks are also due to Dr. Takahide Saito for supplying the samples and permission to use his results and to Mr. Yasuo Hashino and Mr. Hiroshi Okamoto for their assistance in the experimental work.

BULLETIN OF THE CHEMICAL SOCIETY OF JAPAN VOL. 39 1192—1196 (1966)

The Solution Behavior of Polystyrene Derivatives: Poly-*p*-methoxystyrene

By Akira KOTERA, Keizo SUZUKI, Takahide SAITO, Hideomi MATSUDA, Toshio KAMATA and Yoshiko HASHINO

Department of Chemistry, Faculty of Science, Tokyo University of Education, Otsuka, Tokyo

(Received September 8, 1965)

The solution behavior of poly-*p*-methoxystyrene in toluene and butanone was measured by light-scattering and viscosity methods, and the results were compared with those of polystyrene and poly-*p*-chlorostyrene in order to discuss the mutual interactions between the solvent and the substituent on the phenyl group. The results show that toluene is a good solvent and butanone a poor one for poly-*p*-methoxystyrene; these relationships between poly-*p*-methoxystyrene and solvents are inverse to those for poly-*p*-chlorostyrene and similar to those for polystyrene, although the extensions of poly-*p*-chlorostyrene and poly-*p*-methoxystyrene are much larger than that of polystyrene at the same degree of polymerization because of the strong mutual interaction between the solvent and the substituent on the phenyl group. It is clear, from the application of Kurata-Stockmayer theory to the experimental results obtained for poly-*p*-methoxystyrene, that the unperturbed dimension of poly-*p*-methoxystyrene is larger than that of polystyrene; this result may be interpreted as being due to an increase in the volume of the chain element of the polymer molecule.

In a preceding paper,[1] the viscosity and light-scattering characteristics of poly-*p*-chlorostyrene in butanone and toluene were compared with those of polystyrene; it was concluded that the para substituent (chlorine atom) of the phenyl group affected the dependence of the viscosity, the extension, and the second virial coefficient on the molecular weight, and that the extension of poly-*p*-chlorostyrene, as compared with that of polystyrene, is markedly influenced by the polarity of the substituent.

In the present paper the viscosity and light-scattering characteristics of poly-*p*-methoxystyrene in butanone and toluene are compared with those of polystyrene and poly-*p*-chlorostyrene. This comparison provides information on the effect of the para methoxy substituent on the solution behavior of the polymer.

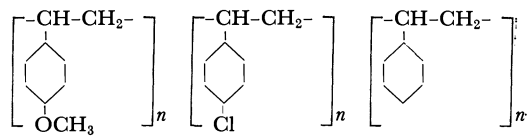

poly-*p*-methoxystyrene | poly-*p*-chlorostyrene | polystyrene

Experimental

Materials. — *p*-Methoxystyrene was polymerized without an initiator for 24 hr. at 100°C. The polymer was dissolved in benzene and was precipitated (from this solution) with methanol. Polymerization occurred to the extent of almost 100%.

Butanone and toluene were purified by the method used in the preceding paper.[1]

1) T. Saito, This Bulletin, **35**, 1580 (1962).

Fractionation.—About 14 g. of poly-*p*-methoxystyrene was dissolved in 500 ml. of butanone. Then fractions were obtained by the successive precipitation method with methanol as a precipitant at 37°C. Seven fractions were used for the measurements.

Viscosity and Light Scattering.—A conventional Ubbelohde viscometer was modified so that successive dilution could be performed. The intrinsic viscosity, $[\eta]$, and the Huggins constant, k', were obtained for the solution in toluene at 30°C and in butanone at 25°C.

An Aminco photometer was used for the measurement of the light scattering. The details of the measurement have been described in the preceding paper. The values of dn/dc, the increment of the refractive index of the solution with the concentration, were determined with a Zeiss interferometer; they were 0.219 ml./g. in butanone and 0.105 ml./g. in toluene at room temperature.

To remove dust, the solutions for light-scattering and viscosity studies were centrifuged for one hour at 20000 g. on a Phywe ultracentrifuge and were filtered into the light-scattering cell or the reservoir of the viscometer through a sintered glass filter (No. 6) just before the measurements.

Results and Discussions

Results.—Plots of the reduced viscosity, η_{sp}/C, vs. the concentration, C, for each fraction are shown in Figs. 1 and 2; the intrinsic viscosity, $[\eta]$, and the Huggins constant, k', were determined from these plots. The Zimm plot for Fraction 7, as an example of light-scattering measurements, is given in Fig. 3; the weight-average molecular weight, M_w, the second virial coefficient, A_2, and the z average root mean square end-to-end distance, $\langle D^2\rangle_z^{1/2}$,

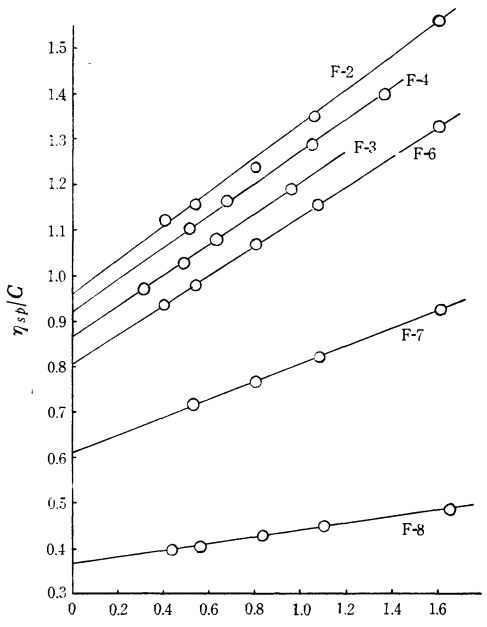

Fig. 1. Relation between reduced viscosity and concentration for poly-*p*-methoxystyrene in butanone at 25°C.

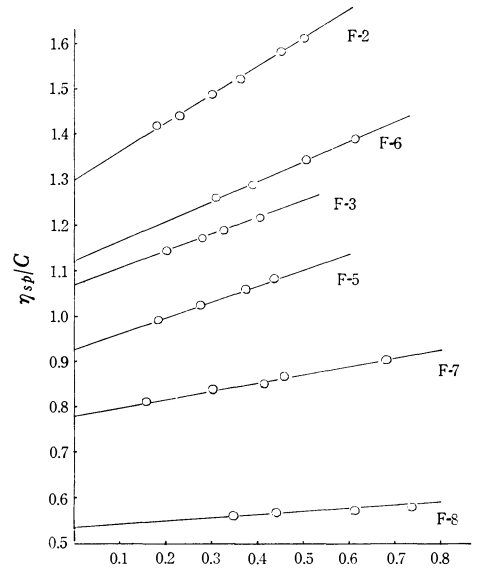

Fig. 2. Relation between reduced viscosity and concentration for poly-*p*-methoxystyrene in toluene at 30°C.

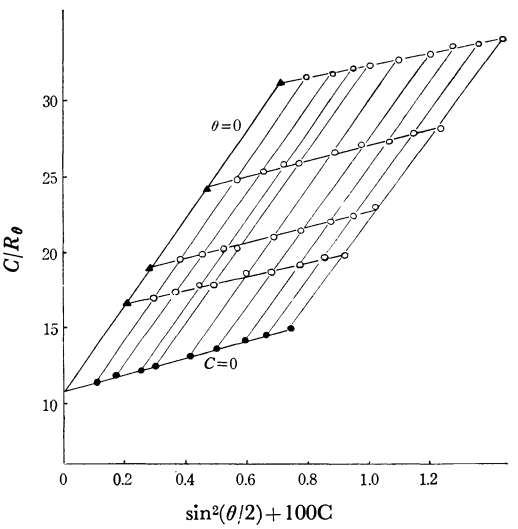

Fig. 3. Zimm plot of poly-*p*-methoxystyrene Fraction 7 in toluene for 436 mμ.

were determined for seven fractions from Zimm plots similar to those in Fig. 3.

The experimental results for seven fractions determined from the measurements of viscosity and light scattering are summarized in Tables I and II.

The log-log plot of the intrinsic viscosity vs. the weight-average molecular weight is shown in Fig. 4.

The relation between the intrinsic viscosity and the molecular weight is represented by the equation:

$$[\eta] = KM_w^{\alpha} \qquad (1)$$

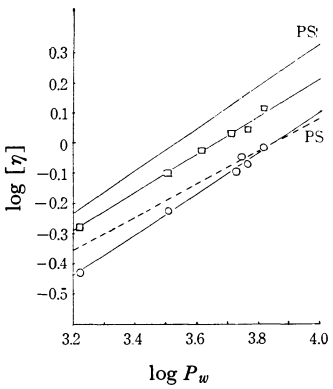

Fig. 4. Plots between intrinsic viscosity and degrees of polymerization.
—— PS: Polystyrene-toluene
---- PS: Polystyrene-butanone
-□-: Poly-*p*-methoxystyrene - toluene
-○-: Poly-*p*-methoxystyrene - butanone

TABLE I. THE EXPERIMENTAL RESULTS FOR POLY-*p*-METHOXYSTYRENE IN BUTANONE.

The values of M_w, A_2 and $\langle D^2\rangle_z^{1/2}$ are the averaged results for two wavelengths, 436 mμ and 546 mμ. Viscosity measurements were carried ou tat 25°C.

Fraction	$[\eta]$	k'	$M_w\times 10^{-4}$	$A_2\times 10^4$	$\langle D^2\rangle_z^{1/2}$ mμ	$\Phi\times 10^{-21}$
2	0.957	0.39	87	1.2_5	85	1.4
3	0.864	0.44	78	1.4_0	75	1.6
4	0.907	0.44	75	1.5_0	73	1.8
6	0.800	0.50	73	1.6_0	73	1.5
7	0.617	0.48	43	1.7_2	55	1.6
8	0.364	0.54	22	1.7_8	37	1.6

Notation: M_w: weight average molecular weight, A_2: second virial coefficient, $\langle D^2\rangle_z^{1/2}$: z average root mean square end-to-end distance, $[\eta]$: intrinsic viscosity, k': Huggins constant, Φ: Flory parameter.

TABLE II. THE EXPERIMENTAL RESULTS FOR POLY-*p*-METHOXYSTYRENE IN TOLUENE

The light scattering measurements were made at 436 mμ and the viscosity measurements were carried out at 30°C.

Fraction	$[\eta]$	k'	$M_w\times 10^{-4}$	$A_2\times 10^4$	$\langle D^2\rangle_z^{1/2}$ mμ	$\Phi\times 10^{-21}$
2	1.300	0.36	85	2.1_3	92	1.4
3	1.080	0.23	70	1.8_9	83	1.3
5	0.935	0.40	56	2.1_8	71	1.5
6	1.120	0.36	78	2.0_4	87	1.3
7	0.783	0.29	43	3.1_0	66	0.9
8	0.532	0.30	22		41	1.7

The notations used in this table are the same as those in Table I.

where M_w is a weight-average molecular weight and K and α are constants determined from a plot of $\log[\eta]$ against $\log M_w$. Equation 1 for poly-*p*-methoxystyrene is as follows:

$$[\eta]=0.80\times 10^{-4} M_w^{0.69} \text{ in butanone at 25°C,}$$

$$[\eta]=2.41\times 10^{-4} M_w^{0.62} \text{ in toluene at 30°C.}$$

The dependence of the root mean square end-to-end distance on the molecular weight is expressed by:

$$\langle D^2\rangle_z^{1/2} \sim M_w^{\beta} \tag{2}$$

where β is a constant as determined from a plot of $\log(\langle D^2\rangle_z^{1/2})$ against $\log M_w$, and the relations for poly-*p*-methoxystyrene are:

$$\langle D^2\rangle_z^{1/2} \sim M_w^{0.57} \text{ in butanone}$$

$$\langle D^2\rangle_z^{1/2} \sim M_w^{0.58} \text{ in toluene}$$

The second virial coefficient of a polymer solution depends on the molecular weight:

$$A_2 \sim M_w^{\gamma} \tag{3}$$

and the dependences of poly-*p*-methoxystyrene are:

$$A_2 \sim M_w^{-0.20} \text{ in butanone}$$

$$A_2 \sim M_w^{-0.40} \text{ in toluene}$$

Discussion.—The constants, K, α, β and γ, in Eqs. 1, 2 and 3 are summarized in Table III, where the constants for polystyrene and poly-*p*-chlorostyrene are also included for the sake of comparison. The values of the constants for poly-*p*-methoxystyrene are similar to those given in the literature for various vinyl polymers, and it seems likely that there is no abnormal tendency in the solution behavior of poly-*p*-methoxystyrene. However, a detailed comparison of the data for poly-*p*-methoxystyrene with those for polystyrene and poly-*p*-chlorostyrene brings to light some interesting facts with regard to the effects of the solvent on the extension of the polymer chain. The dimensions of poly-*p*-methoxystyrene in toluene are larger than those in butanone; this relationship between the solvent and the dimension is the same as in the case of polystyrene, but it is reversed in the case of poly-*p*-chlorostyrene.

In order to clarify the effects of solvents on the dimensions of polymer chains, the $\langle D^2\rangle_z^{1/2}/D_f$ values for polystyrene derivatives in toluene and butanone are compared with one another at $P_w=10^4$; these values are shown in Table IV, where D_f is the end-to-end distance of the chain, assuming a free rotation model, and where $\langle D^2\rangle_z^{1/2}$ is obtained from a plot of $\log(\langle D^2\rangle_z^{1/2})$ vs. $\log P_w$.

Of course, a comparison of the effect of a solvent on the dimensions of the chain must be based on a value of $\langle D^2\rangle_z^{1/2}/\langle D_0^2\rangle_z^{1/2}$, where $\langle D_0^2\rangle_z^{1/2}$ is a z-average root mean square unperturbed end-to-end distance, but when the basic structures of the polymers are similar to each other, the $\langle D^2\rangle_z^{1/2}/D_f$ ratio can be considered to be a relative measure of the solvent effect.

As is shown in Table III or IV, toluene is a better solvent for poly-*p*-methoxystyrene than butanone;

TABLE III. CONSTANTS FOR THE SOLUTION BEHAVIOR OF POLYSTYRENE DERIVATIVES IN TOLUENE AND BUTANONE

Solvent	Polymer	$K\times10^4$	α	β	γ
Butanone (25°)	Poly-*p*-chlorostyrene	2.9_4	0.59	0.55	−0.17
	Poly-*p*-methoxystyrene	0.8_0	0.69	0.57	−0.20
	Polystyrene	3.9_0	0.58	0.58	−0.23
Toluene (30°C)	Poly-*p*-chlorostyrene	1.2_3	0.64	0.60	−0.40
	Poly-*p*-methoxystyrene	2.4_1	0.62	0.58	−0.40
	Polystyrene	1.3_0	0.70	0.68	−0.33

this relationship is the same as that for polystyrene.[2-4] However, the values of $\langle D^2\rangle_z^{1/2}/D_f$ obtained for poly-*p*-methoxystyrene show that the *p*-methoxy-phenyl groups are involved in greater mutual interactions than are the phenyl groups.

The finding that the extension of poly-*p*-methoxystyrene in toluene is nearly the same as, or slightly larger than, that of poly-*p*-chlorostyrene may be explained as follows: the increased stability of the extended form of the chain in the case of poly-*p*-methoxystyrene in comparison with the case of poly-*p*-chlorostyrene is to be attributed to the mutual interaction between the C_6H_5–OCH_3 group being greater than that between the C_6H_5–Cl groups.

Kotera et al.[5,6] measured the dipole moments of poly-*p*-chlorostyrene and poly-*p*-methoxystyrene at different temperatures and concluded from their experimental results that the chain of poly-*p*-methoxystyrene is more extensive than that of poly-*p*-chlorostyrene. Their measurements were carried out in a non-polar solvent; hence, their results are substantially in accord with our data.

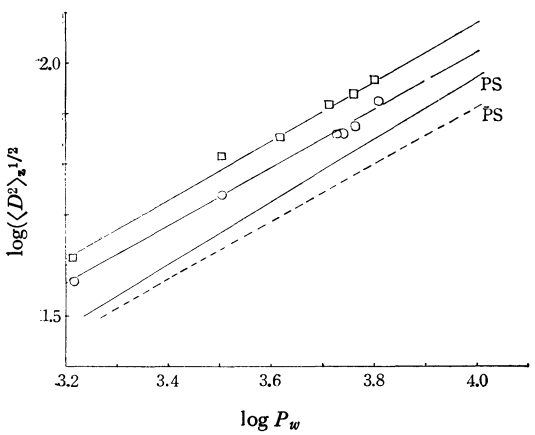

Fig. 5. Comparison of extension of chain of poly-*p*-methoxystyrene; the data for polystyrene is included.
—— PS: Polystyrene-toluene
---- PS: Polystyrene-butanone
-□-: Poly-*p*-methoxystyrene - toluene
-○-: Poly-*p*-methoxystyrene - butanone

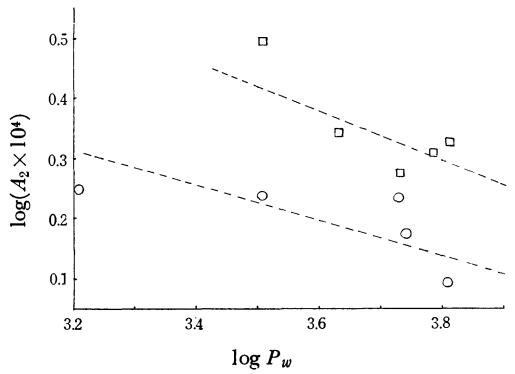

Fig. 6. Relation between second virial coefficient and degrees of polymerization of poly-*p*-methoxystyrene.
-□-: Poly-*p*-methoxystyrene - toluene
-○-: Poly-*p*-methoxystyrene - butanone

Kurata and Stockmayer have recently proposed new equations for deriving the unperturbed dimension of polymer molecule from the intrinsic viscosity data of the polymer molecule in a good solvent; they have also shown the wide applicability of their method to the correct estimation of short-range interactions of a polymer molecule.[7] The new equations proposed by them are as follows:

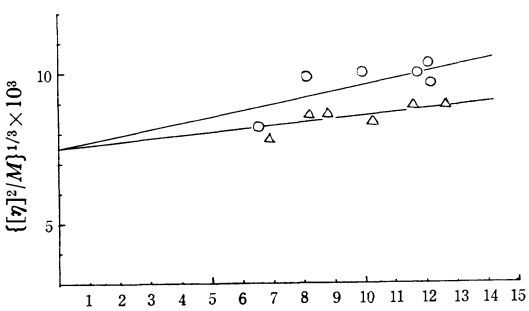

Fig. 7. The dependence of $([\eta]^2/M)^{1/3}$ on $g(\alpha\eta)\times(M^2/[\eta])^{1/3}$ for poly-*p*-methoxystyrene.
○ Butanone at 25°C
△ Toluene at 30°C

2) P. Outer, C. I. Carr and B. H. Zimm, *J. Chem. Phys.*, **18**, 30 (1950).
3) T. Oyama and K. Kawahara, *J. Chem. Soc. Japan, Pure Chem. Sect.* (*Nippon Kagaku Zassi*), **78**, 484 (1957).
4) C. E. H. Bawn and M. A. Wajid, *J. Polymer Sci.*, **12**, 109 (1953).
5) A. Kotera, Annual Meeting of the Chemical Society of Japan, April, 1943.
6) A. Kotera, K. Matsumura, K. Fujimori and H. Yamamoto, Annual Meeting of the Society of Polymer Science, Japan, May, 1952.
7) M. Kurata and W. H. Stockmayer, *Fortschr. Hochpolymer. Forsch.*, **3**, 196 (1963).

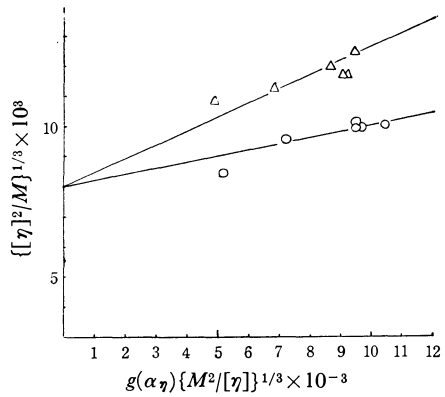

Fig. 8. The dependence of $([\eta]^2/M)^{1/3}$ on $g(\alpha_\eta)\times(M^2/[\eta])^{1/3}$ for poly-*p*-chlorostyrene.
△ Toluene at 30°C
○ Butanone at 25°C

TABLE IV. VALUES OF $\langle D^2\rangle_z^{1/2}/D_f$ FOR POLYSTYRENE DERIVATIVES IN TOLUENE AND BUTANONE AT $P_w=10^4$

The values for polystyrene were calculated from the data in Refs. 2 and 3.

Polymer	$\langle D^2\rangle_z^{1/2}/D_f$ Solvent	
	Butanone	Toluene
Poly-*p*-chlorostyrene	3.24	2.57
Poly-*p*-methoxystyrene	2.39	2.73
Polystyrene	1.86	2.14

TABLE V. THE RATIOS BETWEEN THE UNPERTURBED DIMENSIONS AND THE DIMENSION WHEN A FREE ROTATION MODEL IS ASSUMED FOR POLYSTYRENE, POLY-*p*-METHOXYSTYRENE AND POLY-*p*-CHLOROSTYRENE

Polymer	r
Poly-*p*-methoxystyrene	2.39
Poly-*p*-chlorostyrene	2.34
Polystyrene	2.30

$$([\eta]^2/M)^{1/3} = K^{2/3}+0.363B\Phi_0(g(\alpha_\eta)M^2/[\eta])^{1/3}$$
$$K^{1/3} = \Phi_0{}^{1/3}A$$
$$\alpha_\eta = [\eta]/[\eta]_\theta$$
$$g(\alpha_\eta) = 8\alpha_\eta{}^3/(3\alpha_\eta{}^2+1)^{2/3}$$

where α_η is an expansion parameter of the polymer molecule obtained from the intrinsic viscosity; M, the molecular weight; Φ_0, the Flory parameter (2.8×10^{21}); $g(\alpha_\eta)$, a function of the volume exclusion of the polymer, and a parameter, A, is related to the unperturbed dimension of the polymer. An approximate value of K, which permits us to obtain α_η or $g(\alpha_\eta)$, is obtained from plots of $([\eta]^2/M)^{1/3}$ against $(M^2/[\eta])^{1/3}$, ignoring $g(\alpha_\eta)$; then, using this result, an improved value of K is obtained from plots of $([\eta]^2/M)^{1/3}$ against $g(\alpha_\eta)(M^2/[\eta])^{1/3}$. The final value of K, K_θ, is obtained in the second trial.

The unperturbed dimension of the polymer molecule is calculated from the value of A and the ratio, r, between the unperturbed dimension of poly-*p*-methoxystyrene, or poly-*p*-chlorostyrene, obtained from this plot, and that obtained when a free rotation model for the polymer chain is assumed; these values of r, together with the one quoted for polystyrene in the literature, are shown in Table V. The values of r for both these para-substituted polymers (2.34 for poly-*p*-chlorostyrene and 2.39 for poly-*p*-methoxystyrene) are larger than that for polystyrene 2.30),* and the value of r for poly-*p*-methoxystyrene seems to be a little larger than that for poly-*p*-chlorostyrene; these results are in accord with that described above.

A detailed discussion of the values for the unperturbed dimension for the para-substituted polymer molecule obtained from the plots shown in Figs. 7 and 8, will be avoided here because some scatter exists in the plots of the dependences of $([\eta]^2/M)^{1/3}$ on $g(\alpha_\eta)(M^2/[\eta])^{1/3}$ and no experimental data for samples with small molecular weights are available.

Although there seems to be a little ambiguity in the values of K_θ obtained from our data for poly-*p*-methoxystyrene and poly-*p*-chlorostyrene, both r values for these polymers are larger than that for polystyrene; this result may be due to the larger molecular volumes of the monomer units for these polymers.**

The Flory parameter, Φ, is calculated by using the equation:

$$[\eta]=\Phi\langle D^2\rangle_z{}^{3/2}/M_w \qquad (4)$$

where $\langle D^2\rangle_z{}^{1/2}$ is the z-average root mean square end-to-end distance, M_w is the weight average molecular weight, and $[\eta]$ is the intrinsic viscosity. The values of Φ for poly-*p*-methoxystyrene are 1.5×10^{21} in toluene and 1.6×10^{21} in butanone; these results are similar to those for various vinyl polymers given in the literature.

Conclusion

The solution behavior of poly-*p*-methoxystyrene is similar to that of polystyrene; this may be ascribed to the comparatively similar basic structure of the two polymers. However, poly-*p*-methoxystyrene has the more extended chain, because the mutual interactions of *p*-methoxy-phenyl groups are larger than those of phenyl groups or *p*-chlorophenyl groups.

A part of the cost of this research has been defrayed from a Scientific Research Encouragement Grant from the Ministry of Education, to which the author's thanks are due.

* Obtained in our laboratory for polystyrene by measuring the light-scattering properties in cyclohexane at 35°C. The value of r for atactic polystyrene given by Kurata and Stockmayer is 2.20 ± 0.05.[7]

** The other approximation for the determination of the unperturbed dimension depending upon the same theoretical viewpoint as that by Kurata and Stockmayer was given by W. Stockmayer and M. Fixman (*J. Polymer Sci.*, **C1**, 137 (1963)). The results obtained from both approximations are the same.

BULLETIN OF THE CHEMICAL SOCIETY OF JAPAN VOL. 39 1197—1201 (1966)

Syntheses of Organic Phosphates. I. Pyridylmethyl Phosphates*,**

By Yukito MURAKAMI, Makoto TAKAGI and Hiroshi NISHI

Department of Organic Synthesis, Faculty of Engineering, Kyushu University, Hakozaki, Fukuoka

(Received September 8, 1965)

The reaction of pyrophosphoric acid with 2-, 3- and 4-pyridylmethanols resulted in the formation of the corresponding pyridylmethyl phosphates. The separation of each ester from the corresponding phosphorylation mixture was performed by passing the mixture through a column of Dowex 50W-X8 [H^+] resin. The 2-, 3-, and 4-isomers were recrystallized from ethanol-water as white crystals with melting points of 182—182.5°C (part. decomp.), 194.5—195.5°C (part. decopm.), and 201.5—202.5°C (decomp.) respectively. An attempt to separate each of these esters from an artificial mixture of them consisting of an equal amount of each was performed by using an ion-exchange resin, Dowex 50W-X8 [H^+]. The acid dissociation constants were determined by a potentiometric method at 25.0°C and $\mu=0.10$ M (KNO_3); this gave three pK's for each phosphate, pK_{H_3A}, pK_{H_2A}, and pK_{HA}: 2-pyridylmethyl phosphate, 1.8, 4.42, 6.29; 3-pyridylmethyl phosphate, 1.9, 4.86, 6.23; 4-pyridylmethyl phosphate, 1.7, 5.14, 6.25. Of these pK's, pK_{HA} refers to the dissociation of a pyridinium proton, while the other pK's refer to those of phosphate protons.

In connection with the studies of nucleotides, various organic phosphates have been synthesized extensively, and many useful phosphorylating reagents have been developed as reviewed in the literature.[1-4] However, since the existing reagents have evident limitations, an appropriate phosphorylating reagent needs to be selected for a specified synthesis depending upon the structure and properties of the alcohol which is to undergo reaction.

In the present work, pyridylmethyl phosphates (I), the simplest analogs of vitamin B_6 phosphate, were prepared. The phosphorylation of 2-, 3-, and 4-pyridylmethanol by the use of pyrophosphoric acid, prepared from 85% orthophosphoric acid and phosphorus pentoxide, was performed with some modification, according to the procedures employed for the syntheses of the substituted 3-pyridylmethyl phosphates.[5] 3-Pyridylmethyl phosphate was also synthesized by the reaction of 3-chloromethylpyridine hydrochloride with trisilver phosphate in ether. The yield was not, however, satisfactory because of the heterogeneous nature of the reaction. Among the phosphates synthesized in this study, 3-pyridylmethyl phosphate had been prepared before and the vasodilating effect of its salts described.[6]

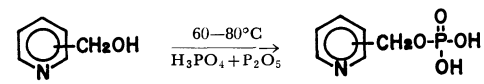

I

The Isolation of Phosphate Esters from Phosphorylation Mixtures.—The main problem in the present preparation was how to achieve the separation of the desired phosphates from phosphorylation mixtures which contain a large excess (about 6 to 12 times mol.) of inorganic phosphoric acid. A chromatographic method using cation-exchange resin, Dowex 50W-X8, was found most effective and simple for the separation of phosphate esters.

Some other methods of separation were also tried, however, for the sake of comparison. For 3- and 4-pyridylmethyl phosphates, the phosphates were separated as precipitates from coexisting inorganic phosphates when the reaction mixtures were treated with ethanol-ether. On the other hand, in the case of 2-pyridylmethyl phosphate, such a precipitation procedure failed to have any advantage. Only a small amount of the precipitate, which contains a fairly large amount of inorganic phosphate, was obtained from the reaction mixture. This precipitate was then dissolved in a small amount of water, and saturated aqueous barium hydroxide was added to adjust the final pH of the solution to about 11. Then the mixture was filtered to remove the white precipitate formed. The addition of two

* Contribution No. 94 from the Department of Organic Synthesis, Faculty of Engineering, Kyushu University.

** Presented at the 18th Annual Meeting of the Chemical Society of Japan, Osaka, April, 1965.

1) G. M. Kosolapoff, "Organophosphorus Compounds," John Wiley & Sons, New York (1950).

2) D. M. Brown, "Advances in Organic Chemistry," Vol. 3, Interscience Publishers, New York (1963), p. 75.

3) H. G. Khorana, "Some Recent Developments in the Chemistry of Phosphate Esters of Biological Interest," John Wiley & Sons, New York (1961).

4) F. Cramer, *Angew. Chem.*, **72**, 236 (1960).

5) E. A. Peterson and H. A. Sober, *J. Am. Chem. Soc.*, **76**, 169 (1954).

6) R. F. Long and A. L. Morrison, U. S. Pat. 2777851 (1957); *Chem. Abstr.*, **51**, 12984 (1957).

volumes of ethanol to the filtrate brought down the white precipitate of barium salt. The barium salt was purified by re-precipitation with ethanol from its aqueous solution. Although the phosphorus analysis showed this white solid to be nearly pure as barium 2-pyridylmethyl phosphate, $C_6H_6NO_4PBa$, the yield was poor not exceeding a few per cent. Two major factors may be responsible for this low yield: first, the precipitation of phosphate ester from the reaction mixture was not effected by the combination of ethanol and ether at the initial step; and second, the inorganic phosphate precipitated upon the addition of saturated barium hydroxide contained a fairly large fraction of an organic substance. An attempt has been made to separate 3-pyridylmethyl phosphate as its barium salt through a procedure similar to that mentioned above, but it resulted in a poor yield. The barium salt of an ester was converted into the corresponding free form, either by precipitating barium sulfate with sulfuric acid or by passing its water suspension through a column of Dowex 50W-X8 [H^+] resin.

On the other hand, for the isolation of 3-pyridylmethyl phosphate from the phosphorylation mixture, repeated precipitation with ethanol was proved to be effective, though less so than the chromatographic method using cation-exchange resin.

The Separation of Phosphate Esters from an Artificial Mixture.—The experimental conditions which were required for the isolation of each isomeric phosphate ester from the coexisting orthophosphoric acid were somewhat different from each other. Therefore, the separation procedure used for 2-pyridylmethyl phosphate was not applicable to the other isomers. In order to obtain some additional information about these separation procedures, an artificial mixture which contained equal amounts of the three esters in an aqueous solution was run onto an ion exchange column of Dowex 50W-X8 resin, both in the acid and in the ammonium forms. The eluting behavior is illustrated in Fig. 1. It may be seen that a satisfactory separation of 2-pyridylmethyl phosphate was achieved with the acid-form resin, while 3- and 4-isomers were not separated from each other even though the initial fractions of the mixed effluent were largely composed of the 3-isomer and the final fractions were composed of the 4-isomer, judging from their ultraviolet absorption spectra (Fig. 1-A). With the ammonium-form resin used, 2-pyridylmethyl phosphate failed to be recovered from the ion exchange column in this experiment (Fig. 1-B). It should be noted that the eluting behavior of 3- and 4-pyridylmethyl phosphate were considerably different from those in the presence of inorganic phosphoric acid, where these phosphates exhibited a retention time as short as that of inorganic phosphate and failed to be separated from the latter as a result.

Acid Dissociation Constants.—The three

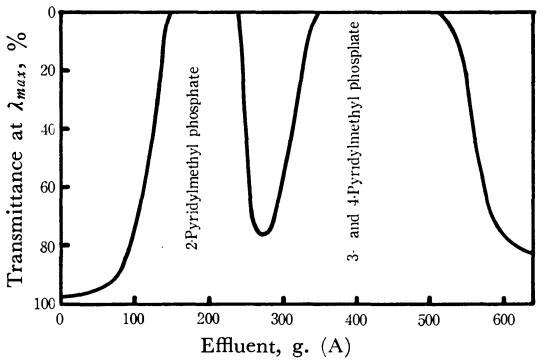

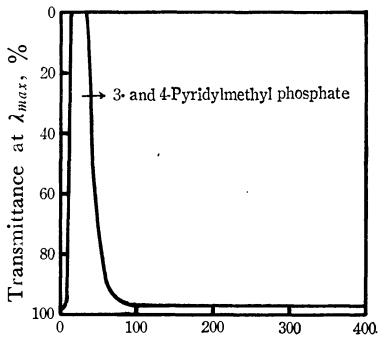

Fig. 1. Separation of phosphate esters from an artificial mixture by ion exchange chromatography.
Mixture: 20 mg. each of the three isomeric esters in 4 ml. aqueous solution.
Column: (A) Dowex 50W-X8 [H^+] (40 meq.), 1.5×15 cm.
(B) Dowex 50W-X8 [NH_4^+](40 meq.), 1.5×15 cm.
Eluent: mineral-free water.
Elution rate: 10 g./hr.

TABLE I. ACID DISSOCIATION CONSTANTS OF PYRIDYLMETHYL PHOSPHATES

25.0±0.1°C, μ=0.10 M (KNO_3)

Acid	pK_{H_3A}	pK_{H_2A}	pK_{HA}
2-Pyridylmethyl phosphate	1.8	4.42	6.29
3-Pyridylmethyl phosphate	1.9	4.86	6.23
4-Pyridylmethyl phosphate	1.7	5.14	6.25

isomeric pyridylmethyl phosphates prepared in this work were proved to be tribasic acids, as illustrated by the three kinds of acid dissociation constants in Table I. The value of $K_{H\ A}$ and that of K_{HA} do not vary significantly among the three isomers, while the K_{H_2A} value changes from one to the other. In addition, these pK_{H_3A} and pK_{HA} values are within a range of magnitude of the acid dissociation constants for ordinary dibasic phosphate monoesters.[7] Therefore, those protons dissociating in the first and third processes are most likely to be attributed to the phosphate-protons, while

the second dissociation step seems to involve a pyridinium proton, as is shown in Chart 1.* The

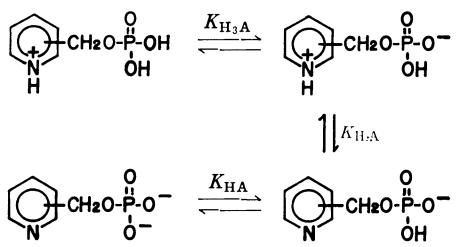

Chart. 1 Acid dissociation processes for pyridylmethyl phosphates.

pK_{H_2A} value is seen to be smallest with the methylphosphate group at the 2-position, and it increases as the substituent is placed further from the 1-position, the largest value being obtained with the 4-isomer. The electron-withdrawing effect of the substituent may provide a reasonable basis for the variation in the acidity of a pyridinium proton. An additional effect would be generated through the participation of the phosphate group in the formation of hydrogen bonding with pyridine-nitrogen in the case of 2-pyridylmethyl phosphate. In other words, such a tendency of hydrogen bond formation would facilitate the liberation of a pyridinium proton.

Experimental

2-Pyridylmethanol.—This material was synthesized from 2-picoline through the rearrangement of 2-picoline *N*-oxide to the acetate of 2-pyridylmethanol, which was subsequently hydrolyzed by acid to the methanol according to the method of Boekelheide and Linn;[8] b. p. 114—116°C/16—17 mmHg (reported[8] b. p. 110—112°C/15 mmHg); the picrate, m. p. 160.5—162.0°C (reported[8] m. p. 160.5—161.0°C).

3-Pyridylmethanol.—This alcohol was prepared by the reduction of ethylnicotinate (purchased from the Tokyo Kasei Kogyo Co. Ltd., Tokyo) with lithium aluminum hydride;[9-11] b. p. 117.5—118°C/3 mmHg (reported b. p. 144—145°C/20 mmHg,[9] 144°C/10 mmHg[10]); the picrate, m. p. 162.2—162.7°C (reported m. p. 159°C,[10] 158—160°C[11]).

4-Pyridylmethanol.—This methanol was synthesized from 4-picoline through a preparative route similar to that used for 2-pyridylmethanol, though the procedures were slightly modified from those mentioned in the literature.[8,12] 4-Picoline *N*-oxide was allowed to react with acetic anhydride at approximately 45°C for 2 hr., and then the reaction temperature was gradually raised to 90°C in 4 hr. After the mixture had been refluxed for a few minutes, the acetate of 4-pyridylmethanol containing an appreciable amount of acetic anhydride was distilled off. This acetate fraction with a boiling range of 99—107°C at 6 mmHg was hydrolyzed with 5 N hydrochloric acid, and then concentrated to dryness in vacuo. The residue was neutralized with aqueous potassium carbonate, made strongly alkaline with 20% sodium hydroxide, and then extracted with chloroform and ether. The combined extracts dried over anhydrous potassium carbonate were distilled to give the product; b. p. 124—128°C at 6 mmHg (reported b. p. 107—110°C/1 mmHg,[13] 152—154°C/15 mmHg[14]); m. p. 51—55°C (reported m. p. 57—60°C,[8] 57.8—58.8°C[12]); the picrate, m. p. 156.5—158°C in a sealed tube (reported m. p. 157—161°C[13]); yield 13 g. (14% from *N*-oxide).

2-Pyridylmethyl Phosphate.—A clear viscous liquid was obtained by the brief heating of 85% orthophosphoric acid and of phosphorus pentoxide at a 1 : 1 weight ratio.[15] A 20.2 g. sample of this mixture was mixed with 3.7 g. of 2-pyridylmethanol at room temperature in a 50-ml. flask protected from moisture. This reaction mixture, after having been heated on a water-bath at 77°C for 10 hr. with frequent shaking, was diluted with 10 ml. of water and then heated at 90°C for 30 min. in order to hydrolyze any polyphosphoric compounds. Approximately an equal volume of water was added to the hydrolysate, which was then divided into two portions, each applied to the top of a column (2×28 cm.) of Dowex 50W-X8 [H^+] resin (130 meq.) and eluted with water at 30 g. per hour. After the front effluent, which was strongly acidic (pH≈0.4), came off, the acidity of the effluent gradually lowered, reaching pH 4.0 at a total effluent of 100 ml. The collection of the fractions of the next 100-ml. portion resulted in the further pH elevation at the end to 4.8, which is nearly the same as that of the eluent (water). The ultraviolet measurements of the eluted fractions collected up to this stage showed the presence of no, or only trace amounts of, aromatic species. Then, an effluent turned acidic, accompanied by a strong increase in the optical density. After 450 ml. of the subsequent effluent had been collected, the pH came back to 4.8—5.0 and the ultraviolet absorption at 261 mμ disappeared. These latter fractions (450 ml.), which contained the phosphate ester, were concentrated to about 10 ml. under reduced pressure below 40°C. Tiny, white, pillar-like crystals were precipitated by adding 100 ml. of ethanol and by leaving the solution in a refrigerator overnight. After filtration, the precipitate was washed with ethanol; yield 5.5 g. (85%); m. p. 181—181.5°C (part. decomp.); upon recrystallization from ethanol-water (4 : 1), m. p. 182—182.5°C (part. decomp); extremely soluble in water and insoluble in ethanol; neutralization equivalence 94.8 (calcd.

7) J. R. Van Wazer, "Phosphorus and Its Compounds," Vol. I, Interscience Publishers, New York (1958), p. 583.

* These dissociation processes do not exclude the possibillity of equilibria existing within each ionic species illustrated in Chart 1; i. e., for the monoionic species:

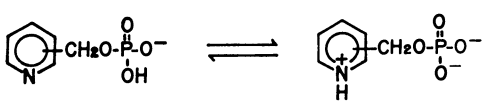

8) V. Boekelheide and W. J. Linn, *J. Am. Chem. Soc.*, **76**, 1286 (1954).

9) R. G. Jones and E. C. Kornfeld, ibid., **73**, 107 (1951).

10) K. W. Rosenmund and F. Zymalkoski, *Chem. Ber.*, **85**, 152 (1952).

11) F. Bohlmann and M. Bohlmann, ibid., **86**, 1419 (1953).

12) J. A. Berson and T. Cohen, *J. Am. Chem. Soc.*, **77**, 1281 (1955).

13) H. S. Mosher and J. E. Tessieri, ibid., **73**, 4925 (1951).

14) M. Protiva, *Chem. Listy*, **45**, 20 (1951); *Chem. Abstr.*, **45**, 8997 (1951).

15) J. E. Malowan, "Inorganic Syntheses," Vol. III, 96 (1950).

94.6); λ_{max} 261 mμ (10^{-4} M aqueous solution), ε 6200.

Found: C, 38.22; H, 4.42; N, 7.54; P, 16.0. Calcd. for $C_6H_8NO_4P$: C, 38.11; N, 4.26; H, 7.41; P, 16.4%.

A satisfactory separation was also attained by neutralizing the partially-hydrolyzed phosphorylation mixture with concentrated aqueous ammonia, followed by chromatographic separation with a column of Dowex 50W-X8 [H^+] resin. In this case, a larger amount of the ion exchanger was needed to convert the ammonium salt to the corresponding free acid, but the elution was carried out in the same manner, as is shown in Fig. 2.

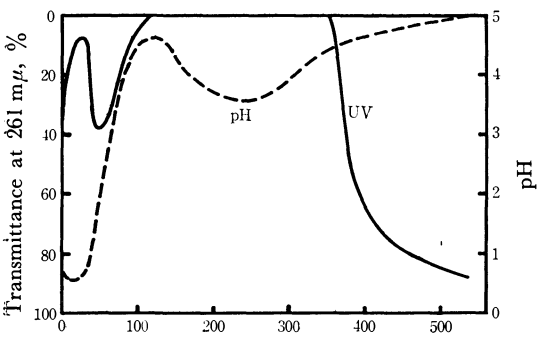

Fig. 2. Chromatographic separation of 2-pyridylmethyl phosphate from the phosphorylation mixture.

Mixture: partially-hydrolyzed phosphorylation mixture (with 0.4 g. of the alcohol as a starting material) neutralized to pH 8 with concentrated aqueous ammonia

Column: Dowex 50W-X8 [H^+] (130 meq.), 2×28 cm.

Eluent: mineral-free water

Elution rate: 30 g./hr.

3-Pyridylmethyl Phosphate.—The phosphorylation mixture, which was obtained by the reaction of 4 g. of 3-pyridylmethanol and 40 g. of pyrophosphoric acid in accordance with the method of Long and Morrison,[6] was poured into ethanol, and then ether was added. After the mixture had been kept in a refrigerator overnight, the clear supernatant liquid decanted. The residue dissolved in 70 ml. of 1 N hydrochloric acid and heated at 75°C for 30 min. To this acidic solution, after it had been concentrated to about 20 ml. on a water-bath (45°C) in vacuo, 100 ml. of hot acetone was added with vigorous shaking. After the mixture had then been cooled to room temperature, 100 ml. of ether was poured into it. The oily material which separated from the supernatant liquid was dissolved in a small volume of water and reprecipitated with ethanol. Three quarters* of the precipitate were neutralized to pH 8 with aqueous ammonia, then evaporated to dryness in vacuo. The residue, crystalline ammonium salt, was again dissolved in a minimum amount of water and charged to the top of a column (1.4×30 cm.) of Dowex 50W-X8 [H^+] resin (about 80 meq.). The elution was conducted with water at the rate of 20 g. per hour. As the pH of the effluent rose rather steadily throughout the elution, from strongly acidic to neutral without any distinctive features for separation, the effluent fractions were divided into two parts according to the optical density around 260 mμ. The second part consisted of fractions which came off beyond pH 2.0; its total volume (about 500 ml.) was concentrated to about 5 ml. in vacuo below 40°C. A white crystalline precipitate was recovered from the concentrated solution by adding 50 ml. of ethanol; it was recrystallized from ethanol-water (4 : 1) as tiny white pillars; yield 2.4 g. (50%); m. p. 194.5—195.5°C (part. decomp.) (reported m. p. 195—196°C[6]); extremely soluble in water and insoluble in ethanol; neutralization equivalence 94.3 (calcd. 94.6); λ_{max} 260 mμ (10^{-4} M aqueous solution), ε 5100.

Found: C, 38.17; H, 4.64; N, 7.34; P, 17.1. Calcd. for $C_6H_8NO_4P$: C, 38.11; H, 4.26; N, 7.41; P, 16.4%.

4-Pyridylmethyl Phosphate.—The phosphorylation of 4-pyridylmethanol (4 g.) with pyrophosphoric acid[15] (20 g.) was conducted at 80°C in a manner similar to that mentioned for 3-pyridylmethyl phosphate. After the addition of ethanol and ether to the reaction mixture, the oily material was separated from the clear supernatant liquid, dissolved in 15 ml. of water, and heated at 80°C for 45 min. Concentrated aqueous ammonia enough to convert the acid to the corresponding ammonium salt was added, and the salt was precipitated as white crystals by adding 200 ml. each of acetone and ether. The ammonium salt dissolved in a minimal volume of water was run onto a column of Dowex 50W-X8 [H^+] resin and eluted with water. The eluting behavior was found to be similar to that in 2-pyridylmethyl phosphate, as is shown in Fig. 2, and the product was recovered in a similar manner; recrystallization from ethanol-water (4 : 1); 3.8 g. of white rhombic prisms; extremely soluble in water and insoluble in ethanol; neutralization equivalence 94.6 (calcd. 94.6); λ_{max} 254 mμ (10^{-4} M aqueous solution), ε 4500.

Found: C, 38.06; H, 4.40; N, 7.28; P,* 15.2. Calcd. for $C_6H_8NO_4P$: C, 38.11; H, 4.26; N, 7.41; P, 16.4%.

The Separation of Phosphate Esters from an Artificial Mixture.—An aqueous solution containing 20 mg. each of the three isomeric esters in 4 ml. was applied to the top of a column (1.5×15 cm.) of Dowex 50W-X8 resin in the acid type (Fig. 1-A) and in the ammonium type (Fig. 1-B). The elution was conducted with water at the rate of 10 g. per hour. The effluents were classified according to their behavior in ultraviolet absorption, and each assembled portion was concentrated to dryness in vacuo. The measurements of the infrared and ultraviolet spectra as well as of the melting point were performed in order to identify such recovered material. With the ammonium-type resin, no 2-pyridylmethyl phosphate came off from the column, at least not while 400 g. of the effluent was being collected.

* One-quarter of the precipitate was purified by repeated precipitation with ethanol. The precipitate was dissolved in a small volume of water and reprecipitated with hot ethanol, the initial crop being removed. On repetition, the precipitate became somewhat crystalline; it was then suspended in boiling ethanol for an hour to remove the last traces of inorganic phosphoric acid, and finally recrystallized from ethanol-water.

* A sample for analysis was decomposed by heating it with concentrated nitric acid in a test tube. The amount of orthophosphoric acid thus formed was determined colorimetrically by the method of Allen (*Biochem. J.* (*London*), **34**, 858 (1940)). This method was applied to all the phosphates prepared in this work.

The Determination of Acid Dissociation Constants.—The acid dissociation constants of the three phosphate esters synthesized in this study were determined by potentiometric measurements. The apparatus and procedures have been described elsewhere.[16] The measurements were carried out at 25.0±0.1°C and at the ionic strength of 0.10 M in potassium nitrate for two different concentrations of the esters, i. e., 1.00×10^{-3} M and 2.00×10^{-3} M, by ensuring that no hydrolysis occurred during the measurements. In accordance with the tribasic nature of the esters, three acid dissociation constants were defined in the usual way:

$$K_{H_3A}=\frac{[H_2A][H^+]}{[H_3A^+]};\quad K_{H_3A}=\frac{[HA^-][H^+]}{[H_2A]};\quad K_{HA}=\frac{[A^{2-}][H^+]}{[HA^-]}$$

where H_2A stands for the neutral ester species, and the brackets indicate the concentration. For the first approximation, K_{H_2A} and K_{HA} were calculated from the data obtained in a moderate pH range, where K_{H_3A} did not play any important role, in accordance with a usual algebraic method described previously.[17] These calculated values then permitted to evaluate the K_{H_3A} value from the data in the more acidic region. The three kinds of acid dissociation constants obtained in the above manner were then re-investigated to give the more satisfactory values listed in Table I.

16) Y. Murakami, This Bulletin, **35**, 52 (1962).
17) Y. Murakami, K. Nakamura and M. Tokunaga, ibid., **36**, 669 (1963).

BULLETIN OF THE CHEMICAL SOCIETY OF JAPAN VOL. 39 1201—1207 (1966)

The Vicinal Orientation. I. The Pivaloylation of Polymethylbenzenes[1)]

By Hitomi SUZUKI, Hisayuki WADA, Kazuhiro MARUYAMA and Ryozo GOTO

Department of Chemistry, Faculty of Science, Kyoto University, Sakyo-ku, Kyoto

(Received September 9, 1965)

The direct introduction of a pivaloyl group by Friedel-Crafts acylation has been carried out with the following polymethylbenzenes: *o*-xylene, *m*-xylene, hemimellitene, pseudocumene, mesitylene, prehnitene and durene. The decarbonylation was not very significant, and seven new polymethylpivalophenones were prepared in fairly high yields. The hydrocarbon mixtures obtained simultaneously in these reactions usually consisted of at least four or five substances. In the pivaloylation of durene, the Jacobsen-type migration (vicinal orientation) of a methyl group was observed.

The introduction of a bulky group into the nucleus of polyalkylbenzenes often brings about the migration of alkyl groups, and results in the formation of unexpected products in which all the alkyl groups occupy the vicinal positions. The most typical of these anomalous reactions is the Jacobsen reaction.

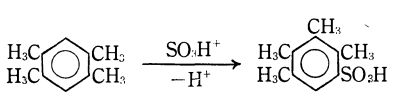

This reaction has long been the object of many investigators' interest, but in spite of several recent proposals,[2)] its mechanism still remains uncertain. In order to get more precise knowledge about the puzzling features of this reaction, it seems pertinent to investigate some other reactions in which similar phenomena (vicinal orientation) are observed.

In the Friedel-Crafts acylation of polymethylbenzenes, one can sometimes observe unusual reactions in which the alkyl group migrates to the position meta to the entering acyl group, thus yielding the vicinal compounds[3,4)]:

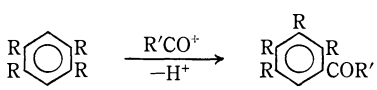

This anomaly is generally attributed to steric stress and may be interpreted as follows: the migration of the alkyl group occurs in order to reduce the overcrowding caused by the introduction of the bulky acylium ion, while the entering acyl group, strongly electron-attracting in its nature, directs the migrating methyl group to the position meta to its original position.

1) The Reaction of Polysubstituted Aromatics. Part IX; Part VIII: This Bulletin, **39**, 128 (1966).

* For the numbering by Roman numerals, refer to the Experimental section.

2) M. Kilpatrick and M. W. Meyer, *J. Phys. Chem.*, **65**, 1312 (1961); H. Suzuki, This Bulletin, **36**, 1642 (1963); F. Bohlmann and J. Riemann, *Chem. Ber.*, **97**, 1515 (1964).

3) G. Baddeley and A. G. Pendleton, *J. Chem. Soc.*, **1952**, 807.

4) W. L. Mosby, *J. Am. Chem. Soc.*, **74**, 2564 (1952); *J. Org. Chem.*, **18**, 483 (1953); G. M. Badger, W. Carruthers and J. W. Cook, *J. Chem. Soc.*, **1949**, 2044; R. R. Aitken, G. M. Badger and J. W. Cook, ibid., **1950**, 331; B. J. Abadir, J. W. Cook and D. T. Gibson, ibid., **1953**, 8.

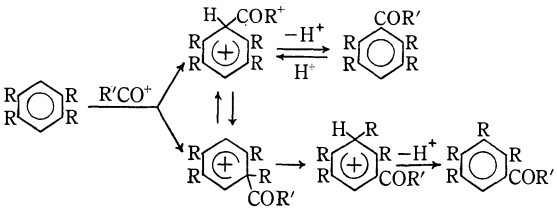

If the reaction occurs for such a sterical reason, the bulky tertiary acylium ion would be more effective in inducing these phenomena. In the literature, however, reactions are limited only to those with the primary acyl group; the direct introduction of the tertiary acyl group into the nucleus of polymethylbenzenes seems never to have been attempted. The use of a tertiary acyl halide as the acylating agent, however, creates some complications. Tertiary acyl halides, such as pivaloyl chloride, often decarbonylate in the presence of the Friedel-Crafts catalysts and act as an alkylating agent.[5] With such highly-reactive substrates as anisole or phenol, the acylation takes place almost exclusively. If the aromatic nucleus is more weakly activated, as in benzene and in toluene, both processes occur simultaneously, yielding the corresponding acylation and alkylation products. An increase in the number of the methyl groups attached to the ring would activate the nucleus and so favor the attack of the tertiary acylium ion upon it. This advantage would, however, be in part counterbalanced by the opposite effect — an increased resistance to the entrance of the bulky tertiary acyl group into the crowded nucleus. Furthermore, the tertiary alkyl cation formed by the decomposition of the tertiary acylium ion is also bulky, and in some cases brings about the alkyl migration.[6] Thus, in the Friedel-Crafts acylation of polyalkylbenzenes with tertiary acyl halides, one might expect the possibility of an alkyl migration analogous to the Jacobsen reaction, regardless of whether the reaction proceeds mainly through the acylation or through the alkylation.

Results

In the present work, we used pivaloyl chloride as the acylating agent; the non-vicinal polyalkylbenzenes used were pseudocumene, mesitylene and durene. *o*- and *m*-Xylene hemimellitene and prehnitene were also acylated for the sake of comparison. Aluminum chloride, titanium chloride and stannic chloride were employed as the catalysts, and carbon disulfide or nitromethane as the solvents. Preliminary experiments proved aluminum chloride to be the most effective catalyst; the other two brought about the decomposition of pivaloyl chloride to a great extent. Carbon disulfide was preferred to nitromethane, because the latter also favored the decarbonylation of the acid chloride.

On treatment with pivaloyl chloride in carbon disulfide at a low temperature, all the polymethylbenzenes used underwent acylation without any remarkable decarbonylation, although with less activated *o*- and *m*-xylene, or with mesitylene and durene, in which only the hindered positions were available, decarbonylation leading to the formation of a complex mixture of polymethylbenzenes was observed to a certain extent. The hydrocarbon mixtures simultaneously obtained in the reactions were found by gas chromatography to contain at least four or five, and in some cases even seven or eight, substances. Most of them, however, could not be identified. As the original hydrocarbons had little tendency toward disproportionation under the experimental conditions employed, the formation of various polyalkylbenzenes is probably to be attributed both to the alkyl migration caused by the introduction of the bulky pivaloyl group into the ring, and to the alkylation of polymethylbenzenes with isobutylene or its condensate products, formed by the decomposition of pivaloyl chloride.

Contrary to our expectations, most of the acylation, except in the case of durene, proceeded without any rearrangement. Only durene underwent an anomalous acylation to yield the vicinal product, 2, 3, 4, 5-tetramethylpivalophenone (VI).* A prolonged reaction time or an elevated temperatures resulted in an increased formation of the hydrocarbon parts and resinous matter, with a consequent decrease in the yield of the ketonic products.

The hindered ketones are generally known, in the presence of aluminum chloride, to isomerize

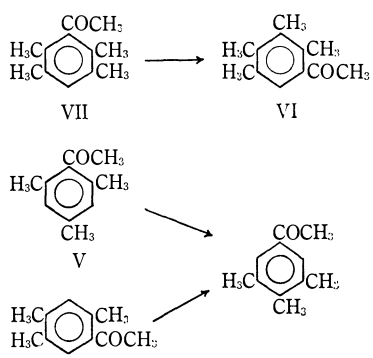

5) E. Rothstein and R. W. Saville, ibid., **1949**, 1946, 1950, 1954, 1959, 1961; E. Rothstein and M. A. Saboor, ibid., **1943**, 425; E. Rothstein, ibid., **1951**, 1459; M. E. Grundy, W. H. Hsü and E. Rothstein, ibid., **1952**, 4136; M. E. Grundy, E. Rothstein and W. H. Hsü, ibid., **1956**, 4558, 4561; M. E. Grundy, W. H. Hsü and E. Rothstein, ibid., **1958**, 581; D. E. Pearson, *J. Am. Chem. Soc.*, **72**, 4169 (1950).

6) L. R. C. Barclay and E. E. Betts, *J. Am. Chem. Soc.*, **77**, 5735 (1955); L. R. C. Barclay and J. W. Hilchie, *J. Org. Chem.*, **22**, 633 (1957); P. C. Myhre and W. M. Schubert, ibid., **25**, 708 (1960). Also cf. R. M. Roberts and D. Schienthong, *J. Am. Chem. Soc.*, **86**, 2851 (1964).

gradually to the isomers of the less hindered structures. Thus acetodurene isomerizes to acetoprehnitene,[3,7] and acetomesitylene or acetopseudocumene, to acetohemimellitene.[8]

In expectation of such isomerization to the vicinal structure, 2, 3, 5, 6-tetramethylpivalophenone (VII) and 2, 4, 6-trimethylpivalophenone (V) were subjected to the action of an excess of aluminum chloride at room temperature. VII readily underwent a Jacobsen-type isomerization to give the vicinal isomer (VI). Such an easy transformation of VII into VI in comparison with that of the corresponding acetyl derivative[3,7] is no doubt due to the greater steric repulsion between the pivaloyl group and the adjacent ortho methyl group. In contrast to the tetramethyl compound, V was comparatively stable towards the action of aluminum chloride, and no alkyl migration was observed under ordinary condition even with a prolonged reaction time. The only reaction that took place was deacylation, followed by complicated side reactions involving alkylation by isobutylene or its condensates. This difference of ease between V and VII towards the vicinal orientation may be attributed to the buttressing effect of the methyl groups at the meta positions to the pivaloyl group.

In the hydrocarbon mixtures obtained by the rearrangement of VII, no noticeable amount of isodurene was found. This suggests that the Jaccobsen-type isomerization occurs via a direct rearrangement of the hindered ketone VII. If the vicinal product VI were formed through the step-by-step 1, 2-alkyl migration, as has been explained by Dewar,[9] with the intermediary formation of 2, 3, 4, 6-tetramethylpivalophenone, much isodurene would be detected in the hydrocarbon fraction, because the pivaloyl group in the highly-hindered position would readily be removed from the ring in the presence of a large excess of aluminum chloride. This however, did not happen. Durene was the only main tetramethylbenzene isolated.

Experimental

Materials. — Pivalic acid, prepared from *t*-butyl chloride by the Grignard reaction,[10] was carefully fractionated twice; the product had a b. p. of 159.5—161.5°C and an m. p. of 31—33°C. Freshly-distilled thionyl chloride was used for preparing the pivaloyl chloride, which, after careful distillation, had a b. p. of 104—106°C. Durene (m. p. 79—80°C) and prehnitene (b. p. 80—82°C/18 mmHg) were prepared as has been described by Smith and his co-workers.[11,12] Pseudocumene (b. p. 166—167°C) was prepared by the lithium hydride reduction[13] of 2, 5-dimethylbenzyl chloride (b. p. 99—102°C/15 mmHg), which in turn was obtained by the chloromethylation of *p*-xylene[14]. The *o*-xylene, *m*-xylene, mesitylene and hemimellitene were commercial products.

Measurements.—The infrared spectra were determined on liquid films or on potassium bromide disks, with a Perkin-Elmer Model 021 spectrophotometer. The ultraviolet absorption spectra (above 220 mμ) were measured in methanol solutions with a Hitachi EPS-30 automatic recording spectrophotometer. The NMR spectra were obtained in carbon tetrachloride solutions, with tetramethylsilane as the internal reference, using a JNM-3H 60 spectrometer manufactured by the Japan Electron Optics Laboratory Co., Ltd. The chemical shifts are expressed in τ-units. The NMR spectrum was very helpful in the structure assignment of each isomer obtained; in most cases it permitted an unequivocal choice (Fig. 1).

The General Procedure for Pivaloyl Chloride Acylations.—In a three-necked flask fitted with a thermometer, a reflux condenser and a dropping funnel, finely-powdered aluminum chloride was covered with small amounts of carbon disulfide and then cooled to the temperature of ice-water. The mixture was magnetically-stirred and a solution of pivaloyl chloride and a polymethylbenzene dissolved in carbon disulfide was added drop-by-drop over a period of 20—30 min. As the pivaloyl chloride entered the aluminum chloride suspension, gas evolved immediately. The gas was a mixture of hydrogen chloride, carbon monoxide and isobutylene, the proportions varying markedly with the structure of the aromatic hydrocarbon and the experimental conditions used. After the addition of the pivaloyl chloride, the mixture was stirred for half an hour at room temperature and then decomposed with dilute hydrochloric acid mixed with crushed ice. The organic layer was separated, carbon disulfide was removed by passing a current of air through it, and the residual dark oil was subjected to steam distillation. The oily layer of the steam-distillate was extracted with ether and dried over anhydrous calcium chloride. The ether extract was concentrated, and the residue was fractionated at reduced pressure.

In the distillation of VII, however, so much foaming was encountered that this compound was first chromatographed on a short alumina column, using petroleum ether as an eluant, and then repeatedly crystallized from light-boiling ligroin.

Compounds I, II and V have already been synthesized by Nightingale and his co-workers[15] through quite the same procedure, but the precise physical constants of them have not been described. Compounds III, IV and VII were first synthesized by the present authors.

2, 4-Dimethylpivalophenone (I).—To the stirred suspension of aluminum chloride (30 g.) in carbon disulfide (40 ml.), pivaloyl chloride (10 g.) and *m*-xylene (13.0 g.) dissolved in carbon disulfide (30 ml.) were added at 0—5°C over a 30-min. period. After

7) M. Lukin and B. B. Carson, *J. Org. Chem.*, **23**, 1007 (1958).
8) G. Baddeley and S. Varma, *J. Chem. Soc.*, **1957**, 2727.
9) M. J. S. Dewar, "The Electronic Theory of Organic Chemistry," Oxford Press, London (1956).
10) "Organic Syntheses," Coll. Vol. 1, 524. 2nd ed. (1956).
11) "Organic Syntheses," Coll. Vol. 2 (1948), p. 248.
12) "Organic Reactions," Vol. 1, John Wiley & Sons, Inc., New York, N. Y. (1942), p. 382.
13) J. E. Johnson, R. H. Blizzard and H. W. Carhart, *J. Am. Chem. Soc.*, **70**, 3664 (1948).
14) J. Von Braun and J. Nelles, *Ber.*, **67**, 1096 (1934); D. A. Shirley, "Preparation of Organic Intermediates," John Wiley & Sons, Inc., New York, N. Y. (1951), p. 129.
15) D. V. Nitingale, R. L. Sablett, R. A. Capenter and H. D. Radford., *J. Org. Chem.*, **16**, 655 (1951).

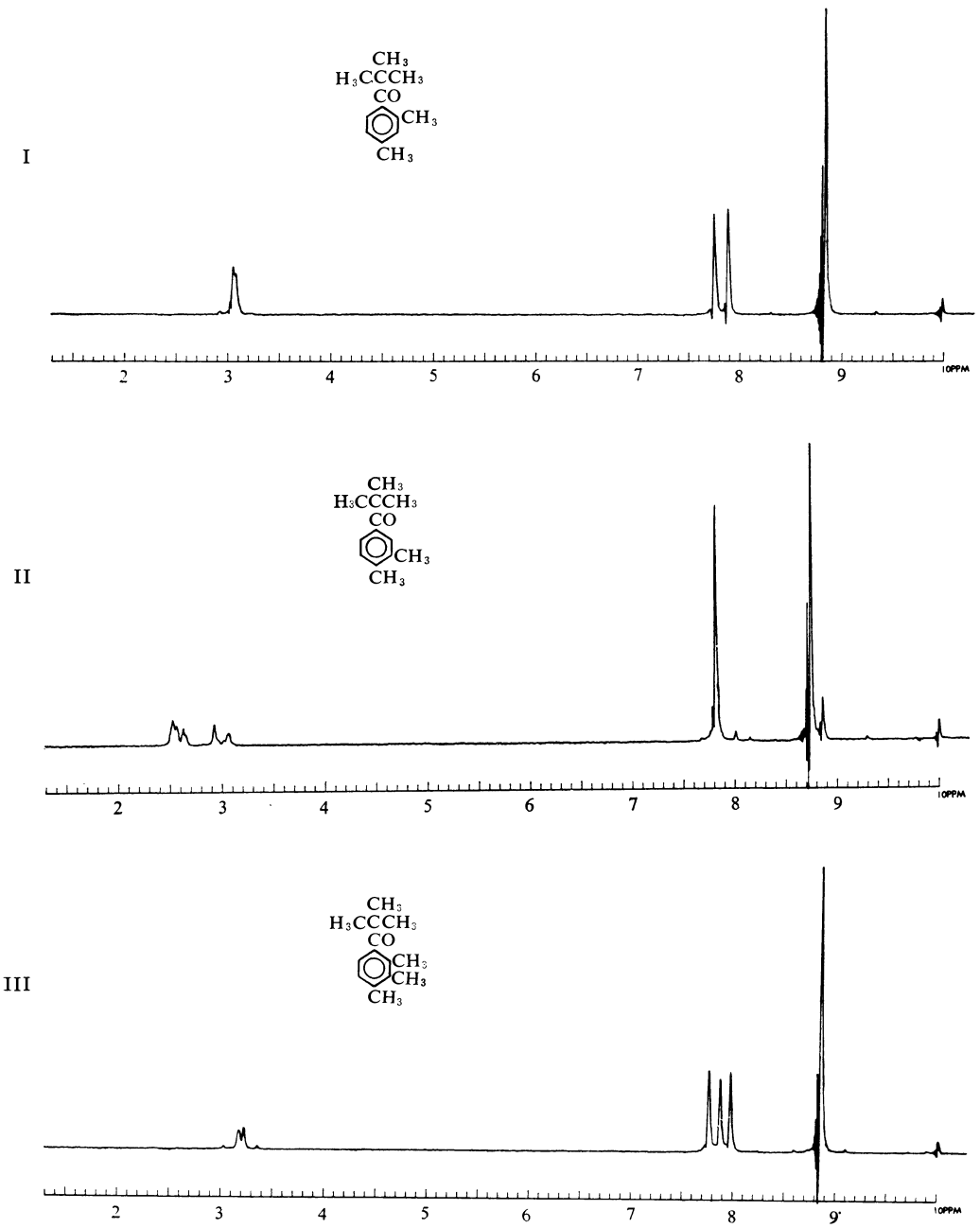

Fig. 1. NMR spectra of polymethylpivalophenones.

1 hr., the mixture was worked up as described above. The distillation of the oily product gave three hydrocarbon fractions: b. p. —90°C/22 mmHg, 1.5 g.; b. p. 93—95°C/22 mmHg, 7.7 g. (5-*t*-butyl-*m*-xylene); b. p. 121—122°C/22 mmHg, 1.5 g., and a ketonic fraction (b. p. 132—133°C/22 mmHg, 6.6 g.). The redistillation of the ketonic fraction yielded 5.6 g. of I, boiling at 131—132°C/21 mmHg.

Found: C, 82.18; H, 9.80. Calcd. for $C_{13}H_{18}O$: C, 82.06; H, 9.54%.

Its infrared bands were at 867 (isolated ring hydrogen), 827 (two adjacent ring hydrogen) and 1664 cm^{-1} (carbonyl). The ultraviolet absorption bands were at 244.5, 271—272 (*infl*)** and 310 mμ (*s*)**. The NMR methyl peaks at were 7.91 (*o*-methyl), 7.76 (*p*-methyl) and 8.85 (*t*-butyl).

3, 4-Dimethylpivalophenone (II).—II was prepared in the manner described above. B. p. 141—143°C/20—21 mmHg. The yield of steam-distilled ketone was a little lower than that of I. The hydrocarbon

** *infl* denotes inflection; *s*, shoulder.

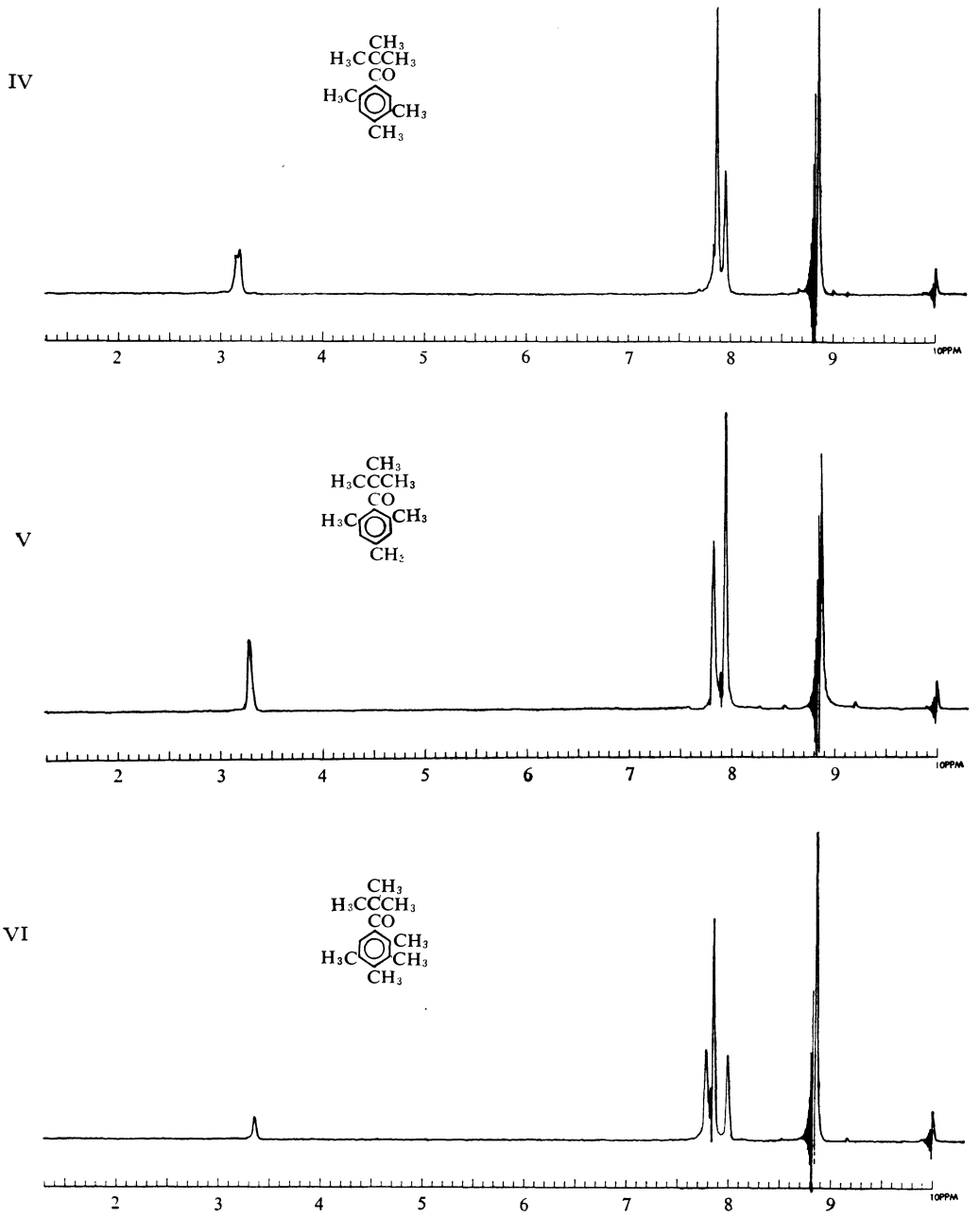

Fig. 1. Continued

fraction was mainly composed of 4-*t*-butyl-*o*-xylene, b. p. 102—103°C/22 mmHg.

Found: C, 82.33; H, 9.65. Calcd. for $C_{13}H_{18}O$: C, 82.06; H, 9.54%.

Strong infrared bands were found at 867 (isolated ring hydrogen), 827 (two adjacent ring hydrogens) and 1665 cm^{-1} (carbonyl). The ultraviolet absorption bands were at 252, 276—277 (*infl*) and 317—318 mμ (*s*). The NMR methyl peaks were at 7.81 (*m*- and *p*-methyl) and 8.74 (*t*-butyl).

2, 3, 4-Trimethylpivalophenone (III).—Hemimellitene (10 g.) was acylated with a mixture of pivaloyl chloride (6.6 g.) and aluminum chloride (20 g.) at 0—3°C by the procedure used above. An ordinary work-up followed by the distillation of the residual oil, gave two hydrocarbon fractions (b. p. 78—79°C/31 mmHg, 2.0 g.; b. p. 125—127°C/31 mmHg, 3.5 g.), a ketonic fraction (b. p. 149—151°C/21 mmHg, 9.5 g.), and a residue (ca. 1.0 g.). After redistillation, the ketone (b. p. 151—152°C/20—21 mmHg, 8.5 g.) solidified to white prisms melting at 39—40°C.

Found: C, 82.47; H, 10.11. Calcd. for $C_{14}H_{20}O$:

VII

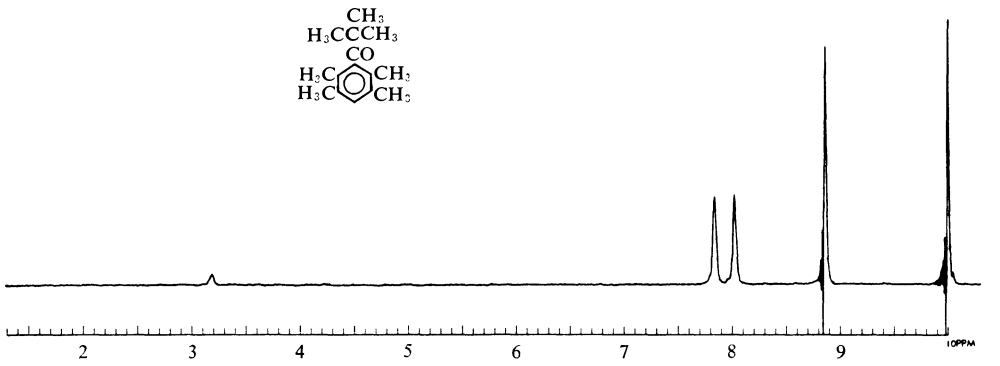

Fig. 1. Continued

C, 82.30; H, 9.87%.

The infrared bands were at 832 (two adjacent hydrogens) and 1685 cm^{-1} (carbonyl). The ultraviolet absorption bands were at 238—242 (broad) and 301—303 mμ (s). The NMR methyl peaks were at 7.76 (*p*-methyl), 7.87 (*m*-methyl), 7.97 (*o*-methyl) and 8.84 (*t*-butyl).

2, 4, 5-Trimethylpivalophenone (IV).—IV was prepared from pseudocumene (15 g.), pivaloyl chloride (10 g.) and aluminum chloride (30 g.). The fractionation of the oily product gave the hydrocarbon mixture (b. p. chiefly 66—68°C/22 mmHg. 2.0 g.) and the ketone (b. p. 152—154°C/30—31 mmHg, 13.7 g.). On standing, the ketone solidified to white prisms melting at 32—33°C.

Found: C, 82.17; H, 9.87. Calcd. for $C_{14}H_{20}O$: C, 82.30; H, 9.87%.

Its infrared bands were at 874 (isolated ring hydrogen) and 1691 cm^{-1} (carbonyl). The ultraviolet absorption bands were at 250, 278 (*s*) and 307 mμ (*infl*). The NMR peaks were at 7.86 (*m*- and *p*-methyl), 7.95 (*o*-methyl) and 8.85 (*t*-butyl).

2, 4, 6-Trimethylpivalophenone (V).—Mesitylene (15.0 g.) was acylated using pivaloyl chloride (10.0 g.) and aluminum chloride (30.0 g.) at 0—5°C. The distillation of the oily product gave two hydrocarbon fractions (b. p. 61—63°C/22 mmHg, 4.5 g.; b. p. chiefly 91—92°C/22 mmHg, 0.5 g.), a ketonic fraction (b. p. 141—143°C/22 mmHg, 10.2 g.) and a residue (ca. 1.0 g.). The redistillation of the ketonic fraction gave 9.5 g. of V, boiling at 142—143°C/22 mmHg, which, on standing in the refrigerator, solidified to white crystals, m. p. 19—21°C.

Found: C, 82.50; H, 10.08. Calcd. for $C_{14}H_{20}O$: C, 82.30; H, 9.87%.

The infrared bands were at 875 (isolated ring hydrogen) and 1682 cm^{-1} (carbonyl). The ultraviolet absorption bands were at 274—276 (*infl*) and 305—306 mμ. The disappearance of the K-band indicates the steric inhibition of the conjugation due to the *o*, *o'*-disubstitution. The NMR methyl peaks were at 7.82 (*p*-methyl), 7.94 (*o*-methyl) and 8.86 (*t*-butyl).

2, 3, 4, 5-Tetramethylpivalophenone (VI).—Prehnitene (15.0 g.) was acylated with pivaloyl chloride (9.0 g.) and aluminum chloride (30 g.) at 0—5°C. The liberation of carbon monoxide was not significant. A similar work-up, followed by the distillation of the product, afforded hydrocarbon fractions (b. p. 85—89°C/25 mmHg, 1.6 g.; b. p. 90—130°C/25 mmHg, 1.0 g.), a ketone (b. p. 161—165°C/21 mmHg, 11.2 g.) and a residue (1.3 g.). The redistillation of the ketonic fraction gave 10.5 g. of pure VI, b. p. 162—163°C/21 mmHg, which readily solidified to prisms and melted at 37—39°C.

Found: C, 82.25; H, 10.45. Calcd. for $C_{15}H_{22}O$: C, 82.51; H, 10.16%.

There were strong infrared bands at 867 (isolated ring hydrogen) and 1691 cm^{-1} (carbonyl). The ultraviolet absorption bands were at around 240—250 (*s*), 275—280 (*infl*) and 310—314 mμ (*infl*). The NMR methyl peaks were at 7.79 (*p*-methyl), 7.86 (*m*-methyl), 7.99 (*o*-methyl) and 8.85 (*t*-butyl).

2, 3, 5, 6-Tetramethylpivalophenone (VII).—Durene (14.0 g.) was acylated with pivaloyl chloride (8.9 g.) and aluminum chloride (30 g.) at 5—10°C. A usual work-up followed by distillation under reduced pressure, was difficult because of the remarkable foaming; thus the oily product was subjected to chromatographic separation on an alumina column (1.8×30 cm.). Elution with petroleum ether afforded a hydrocarbon fraction (b. p. chiefly 98°C/37 mmHg, 2.5 g.), an oily mixture of VI and VII (11.0 g.), and small amounts of yellow needles of an unidentified ketonic substance. After the ketonic mixture had stood in the refrigerator, about 4.0 g. of white crystals separated out; on several recrystallizations from petroleum ether, these gave white needles melting at 104—105°C.

Found: C, 82.66; H, 10.25. Calcd. for $C_{15}H_{22}O$: C, 82.51; H, 10.16%.

The infrared bands were at 868 (isolated ring hydrogen) and 1685 cm^{-1} (carbonyl). The ultaviolet absorption bands were at 272—273 (*s*), 280 and 311 mμ (*s*). Its NMR methyl peaks were at 7.85 (*m*-methyl), 8.03 (*o*-methyl) and 8.86 (*t*-butyl).

The remaining oily part (b.p. 165—167°C/36 mmHg) was found by spectroscopic inspection to be mainly composed of the vicinal product VI.

The yellow needles, after recrystallization from boiling petroleum ether, melted at 183—185°C. They showed a strong absorption at 1685 cm^{-1} (carbonyl).

Found: C, 86.19; H, 8.92%.

The Isomerization of the Ketones.—A mixture of a ketone (3.3 or 4.0 g.), aluminum chloride (10 g.) and carbon disulfide (20 ml.) was agitated for 3—4 hr. at room temperatures and subsequently worked up in the manner described above. VII (4.0 g.) gave about 0.5 g. of a hydrocarbon fraction and 1.7 g. of a ketonic fraction. The spectral data of the latter nearly coincide

with those of the vicinal isomer VI. On the other hand, V (3.3 g.) gave 0.8 g. of the hydrocarbon fraction and 2.0 g. of the ketonic fraction (b. p. 144—146°C/22 mmHg, 2.0 g.). The spectral inspection of the latter disclosed that V was recovered unchanged. On the gas chromatograms of these hydrocarbon fractions simultaneously obtained there were found four or six peaks. In both cases some polymeric by-products were formed.

BULLETIN OF THE CHEMICAL SOCIETY OF JAPAN VOL. 39 1207—1211 (1966)

The Alkaline Sulfide Reduction of Aromatic Nitro Compounds. VIII. The Correlation between Sodium Monosulfide and Hydrosulfide in the Reduction of Sodium *m*-Nitrobenzene Sulfonate

By Shizunobu HASHIMOTO and Junzo SUNAMOTO

Department of Applied Chemistry, Doshisha University, Karasuma-imadegawa, Kamikyo-ku, Kyoto

(Received September 14, 1965)

In order to examine the correlation between sodium hydrosulfide and sodium monosulfide, the reduction of sodium *m*-nitrobenzene sulfonate by these aqueous sulfides has been studied kinetically. The rates of the hydrosulfide reduction and the main reaction of the monosulfide reduction were found to be proportional to the concentration of the nitro compound and the square of the concentration of the reducing agent. In the hydrosulfide reduction, the hydroxide ion concentration has a negative effect on the initial state and a positive effect on the final state. The polarographic study on the hydrosulfide reduction confirmed the presence of disulfide ions. From the available data, the correlation among the alkaline sulfides in the reduction was discussed.

The alkaline sulfides may be classified into alkaline hydrosulfide, monosulfide, and polysulfide. In studying the significance of the method of preparation, each stoichiometric equation has been employed for the reduction of aromatic nitro compounds by them, for example:[1]

$$4\,\text{Ar-NO}_2 + 6\,\text{NaSH} + \text{H}_2\text{O} \rightarrow 4\,\text{Ar-NH}_2 + \text{Na}_2\text{S}_2\text{O}_3 \quad (1)$$

$$4\,\text{Ar-NO}_2 + 6\,\text{Na}_2\text{S} + 7\,\text{H}_2\text{O} \rightarrow 4\,\text{Ar-NH}_2 + 3\,\text{Na}_2\text{S}_2\text{O}_3 + 6\,\text{NaOH} \quad (2)$$

$$\text{Ar-NO}_2 + \text{Na}_2\text{S}_2 + \text{H}_2\text{O} \rightarrow \text{Ar-NH}_2 + \text{Na}_2\text{S}_2\text{O}_3 \quad (3)$$

However, it seems reasonable to assume that sodium monosulfide is nothing but sodium hydrosulfide in an aqueous solution, because sodium monosulfide is almost completely hydrolyzed into sodium hydrosulfide and sodium hydroxide in an aqueous solution, as in Eq. 4.[2]

$$\text{Na}_2\text{S} + \text{H}_2\text{O} \rightleftarrows \text{NaSH} + \text{NaOH} \quad (4)$$

In an earlier paper dealing with the polarographic oxidation of sodium sulfides, the relation of their reducing power has discussed.[3] In the present paper the correlation among the sodium sulfides in the reduction of sodium *m*-nitrobenzene sulfonate will be investigated.

Experimental

Materials.—Sodium monosulfide and disulfide were prepared and purified by the method used in the preceding experiment.[3] Sodium hydrosulfide was prepared and purified according to the method given in the literature.[4] Sodium *m*-nitrobenzene sulfonate was the same as that used in the previous report.[5]

Product Study.—The reduction of sodlum *m*-nitrobenzene sulfonate was carried out under the same conditions as those used in the kinetic experiments, after a reaction of a sufficient duration, the resulting solution was acidified with concentrated hydrochloric acid, boiled on a water bath for about 20 min., and filtered. After it had been washed, the filtrate and the washings were combined and diluted with water to the appropriate voulme. From this solution a sample was taken and submitted to the diazometry according to the usual method. At the same time a part of this solution was submitted to paper chromatography. The reaction gave the corresponding amine in a 92.5% yield by the disulfide reduction, in a 95.5% yield by the monosulfide reduction, and in a 97.3% yield by the hydrosulfide reduction.

The paper chromatography of the resulting solution with several solvents, such as 2% hydrochloric acid,

1) For example, P. H. Groggins, "Unit Processes in Organic Synthesis," John Wiley & Sons, New York (1952), p. 100.

2) For example, "Gmelins Handbuch der Anorganischen Chemie," Bd. 21 (1928), pp. 481—494.

3) S. Hashimoto and J. Sunamoto, *J. Chem. Soc. Japan, Ind. Chem. Sect.* (*Kogyo Kagaka Zasshi*), **68**, 669 (1965).

4) G. Brauer, "Handbuch der Präparativen Anorganischen Chemie," Ferdinand Enke Verlag, Stuttgart (1954), p. 278; Ed. by Chem. Soc. Japan, "Zikken Kagaku Koza," Vol. 9, Maruzen, Tokyo (1958), p. 56.

5) S. Hashimoto and J. Sunamoto, This Bulletin, **39**, 100 (1966).

n-butanol - concentrated hydrochloric acid (4 : 1), 2% aqueous ammonia, and pure water, confirmed only the presence of metanilic acid; the insoluble residue in hydrochloric acid was only sulfur.

Procedure for Rate Measurement.—The procedure for the rate measurement and analysis was the same as the method described earlier.[5] The probable error for the determination of the produced amines was ±0.23%.

Procedure for pH Measurement.—A glass electrode and a caromel elelctrode were placed in a reaction flask for the rate measurements; the pH was then followed during the reduction on a Horiba-Hitachi M4-type pH meter.

Polarography on Hydrosulfide Reduction.—Using the same method as in the rate measurements, at appropriate time intervals an aliquot was taken and subjected to a.c. polarography on a Yanagimoto PA-102-type polarography. As the supporting electrolyte, the buffer solution, 0.01 M sodium borate and 0.04 M sodium hydroxide, was used (pH=12.15, as measured by a glass electrode).

Results and Discussion

The differences in the rates of reduction in the initial stage were unexpectedly large when sodium *m*-nitrobenzene sulfonate was reduced by aqueous sodium hydrosulfide, monosulfide, and disulfide. Therefore, these rates could not all be measured under the same reduction conditions; the rates of reduction by monosulfide and hydrosulfide were therefore measured under one set of conditions, while those of reduction by disulfide and hydrosulfide were measured under another set of conditions. These data are compared each other in Fig. 1.

The initial rate of the disulfide reduction was very large and the reaction reached an apparent equilibrium rather early, while in the monosulfide reduction there was an induction period,[5] after which the main reaction proceeded at much the same rate as the disulfide reduction. The hydrosulfide reduction showed a medium reaction rate between the rates of the monosulfide and the disulfide reduction. The order of the apparent rates in the initial stage was $S_2^{2-}>SH^->S^{2-}$, and that at corresponding times after the induction period of the monosulfide reduction was $S^{2-}>SH^->S_2^{2-}$.

Sodium hydrosulfide undergoes ionic dissociation, but it hardly hydrolyzes at all in an aqueous solution.[2] On the other hand, sodium monosulfide undergoes hydrolysis, as has been described above. It may, therefore, be supposed that the difference in the reaction conditions between the monosulfide and the hydrosulfide reductions depends upon the pH of the medium.

A more direct basis for comparison between them is found in the pH dependence of the reaction.

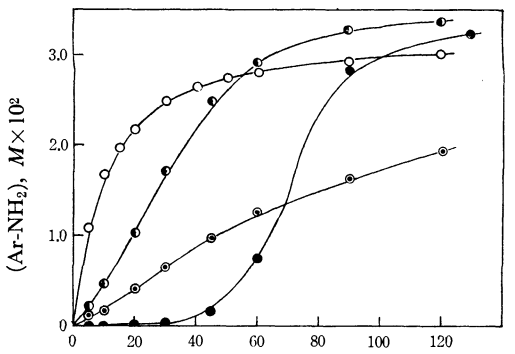

Fig. 1. Reductions of sodium *m*-nitrobenzenesulfonate by sodium hydrosulfide, monosulfide, and disulfide (30°C).
Initial concentrations: (Ar-NO_2)=3.50×10^{-2} M
○ (Na_2S_2)=7.19×10^{-2} M
⊙ (NaSH)=7.19×10^{-2} M
◐ (NaSH)=10.9×10^{-2} M
● (Na_2S)=10.9×10^{-2} M

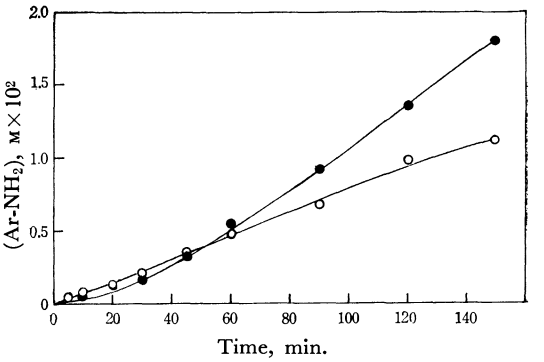

Fig. 2. The effect of sodium hydroxide on the sodium hydrosulfide reduction (30°C).
Initial concentrations: (Ar-NO_2)=3.49×10^{-2} M
(NaSH)=6.99×10^{-2} M
● (NaOH)=8.10×10^{-3} M ○ None

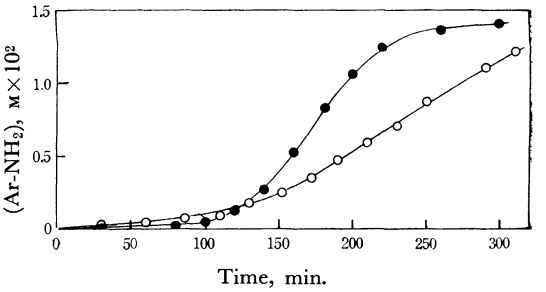

Fig. 3. The effect of hydrogen sulfide in the sodium monosulfide reduction (35°C).
Initial concentrations: (Ar-NO_2)=1.56×10^{-2} M
● (Na_2S)=5.63×10^{-2} M
○ (Na_2S)*=2.81×10^{-2} M

* Gaseous hydrogen sulfide was introduced into the aqueous sodium monosulfide solution till the color of phenolphthalein disappears and excess hydrogen sulfide was removed by nitrogen till the removed gas shows negativity on a lead acetate paper.

The addition of sodium hydroxide in the hydrosulfide reduction made the initial rate slower, while it accelerated the rate of the subsequent reaction. In the reduction by the aqueous monosulfide solution, which absorbed hydrogen sulfide, the induction period disappeared and the rate of the overall reaction became slower, approaching that of the hydrosulfide reduction. The correlation between them is shown in Figs. 2 and 3.

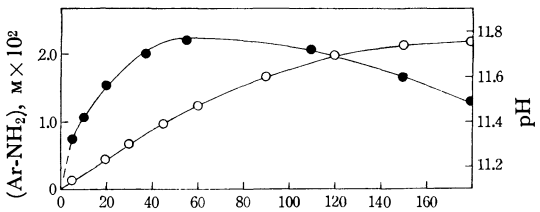

Fig. 4. pH change during the course of the hydrosulfide reduction (30°C).
Initial concentrations: $(Ar\text{-}NO_2)=3.49\times10^{-2}$ M
$(NaSH)=7.19\times10^{-2}$ M
● pH ○ Yield of amine

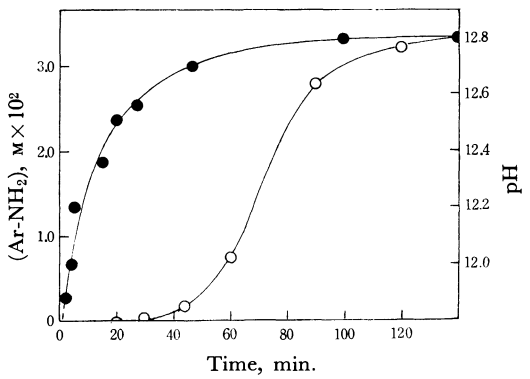

Fig. 5. pH change during the course of the monosulfide reduction (30°C).
Initial concentrations: $(Ar\text{-}NO_2)=3.49\times10^{-2}$ M
$(Na_2S)=7.19\times10^{-2}$ M
● pH ○ Yield of amine

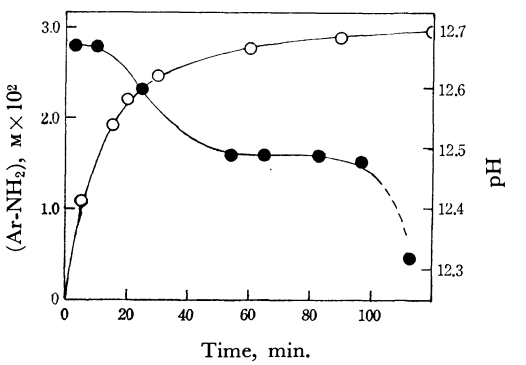

Fig. 6. pH change during the course of the disulfide reduction (30°C).
Initial concentrations: $(Ar\text{-}NO_2)=3.49\times10^{-2}$ M
$(Na_2S_2)=7.19\times10^{-2}$ M
● pH ○ Yield of amine

pH Change During Reduction.—In the alkaline sulfide reduction, the pH changes during the course of the reduction. On the hydrosulfide reduction, the monosulfide reduction, and the disulfide reduction, therefore, the pH values were followed under the conditions indicated in Figs. 4, 5, and 6 respectively.

In the hydrosulfide reduction the pH first increased with the progress of the reduction, but after a while it decreased a little. In the monosulfide reduction the pH continuously increased with the progress of the reaction; indeed, the pH in the induction-period intervals of the reduction increased remarkably. In the disulfide reduction, unlike the monosulfide reduction, the pH only decreased during the course of the reduction.

The rate of the main step in the monosulfide reduction of sodium *m*-nitrobenzene sulfonate depends upon the pH, as we previously reported.[5] Hojyo et al. also presented evidence that the rate of the disulfide reduction of nitrobenzene in an aqueous methanolic solution shows a first-order dependence on the hydroxide ion concentration.[6] On the basis of these data, it is clear that the alkaline-sulfide reductions are always closely connected with the pH of the medium.

In spite of the foregoing results, which show the pH dependence of the rate of alkaline-sulfide reductions, there remains the interesting question of why no induction period appears in the reduction by a hydrosulfide that shows a lower pH value than the monosulfide in an aqueous solution.

The Rate of the Hydrosulfide Reduction.—Since the hydrosulfide hardly hydrolyzes at all in an aqueous solution, it may be assumed that its stoichiometric concentration is almost equal to the kinetically-available concentration. The rate of the hydrosulfide reduction is given by runs in

Table I. The effect of the initial concentration of the nitro compound and sodium hydrosulfide on the apparent third order rate constants (30°C)

Initial concn. $(Ar\text{-}NO_2)$ M×10²	Initial concn. $(NaSH)$ M×10²	Apparent rate const. k, $l^2mol^{-2}min^{-1}$
2.00	4.12	1.74±0.12
2.55	7.19	1.32±0.09
2.79	5.73	2.13±0.08
2.86	7.19	1.59±0.08
3.50	3.60	1.20±0.08
3.50	7.19	1.62±0.08
3.50	10.8	2.95±0.33
6.99	7.19	2.59±0.23

6) M. Hojyo, Y. Takagi, and Y. Ogata, *J. Am. Chem. Soc.*, **82**, 2459 (1960).

which the initial concentrations of the nitro compound and of sodium hydrosulfide have been interchanged. The rate of the reduction is found to be proportional to the concentration of the nitro compound and to the square of the concentration of sodium hydrosulfide:

$$\frac{d(\text{Ar-NH}_2)}{dt} = k(\text{Ar-NO}_2)(\text{NaSH})^2 \qquad (5)$$

The apparent third-order rate constants as calculated by Eq. 5 and the initial concentrations of both reactants are shown in Table I.

The temperature effect obeys the Arrhenius equation, as is shown in Fig. 7; the activation energy was thereby estimated graphically to be $E=$ 9.38 kcal. mol^{-1}.

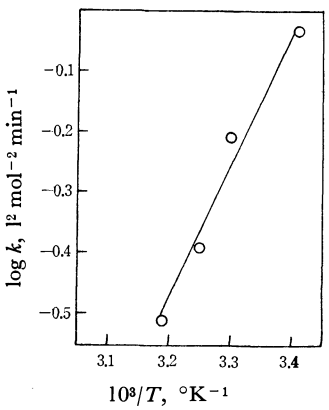

Fig. 7. The temperature dependence of the apparent third order rate constants.

Sodium monosulfide and sodium hydrosulfide are in a hydrolytic equilibrium, as has been described above. If these reducing agents, therefore, are used in the same stoichiometric concentration and compared with each other, the difference in their reduction conditions will be due to the pH in their medium; if the pH change which occurs during the course of the reduction is not considered, the two reactions must be essentially identical in their kinetics. The rate equation in the main step of the monosulfide reduction[5] is, in fact, the same as that given for the hydrosulfide reduction:

$$\frac{d(\text{Ar-NH}_2)}{dt} = k(\text{Ar-NO}_2)(\text{Na}_2\text{S})^2 \qquad (6)$$

A comparison of the apparent third-order rate constants of the hydrosulfide reduction with those of the main step of the monosulfide reduction is shown in Table II. It seems most reasonable to assume that the differences in the rate constants on the two sulfide reductions are due to the hydroxide ion concentration in the medium.

It was previously suggested that the induction period observed in the monosulfide reduction was due to the formation of the sulfide ion radical and its dimerization, as follows:[5]

$$(\text{S}^{2-}\text{-H}_2\text{O}) \xrightarrow[\text{Fe}^{3+}, \text{ or } \text{S}_2\text{O}_3^{2-}, \text{ etc.}]{h\nu,\ O_2} \text{S}^{-}\cdot + \text{H}\cdot + \text{OH}^- \qquad (7)$$

$$\text{S}^{-}\cdot + \text{S}^{-}\cdot \rightarrow (\text{S-S})^{2-} \qquad (8)$$

In view of the above correlation between monosulfide and hydrosulfide, it may similarly be reasonable to assume that the following processes are also involved in the initial stage of the hydrosulfide reduction:

$$\text{SH}^- \xrightarrow{h\nu,\ O_2,\ \text{etc.}} \text{S}^{-}\cdot + \text{H}\cdot \qquad (9)$$

$$\text{S}^{-}\cdot + \text{H}_2 \rightarrow \text{SH}^- + \cdot\text{OH} \qquad (10)$$

$$\text{H}\cdot + \cdot\text{OH} \rightarrow \text{H}_2\text{O} \qquad (11)$$

$$\text{H}\cdot + \cdot\text{H} \rightarrow \text{H}_2 \qquad (12)$$

It appears that the hydrosulfide ion readily gives a sulfide ion radical and a hydrogen radical in the presence of light or oxygen, and that the sulfide ion radical produced immediately dimerizes to give the disulfide ion, as in Eq. 8. The hydrogen radical may couple with the hydroxide radical produced according to Eq. 10 to give water, or dimerize to hydrogen gas. It may be supposed that the hydrogen radical or hydrogen gas produced here is not directly concerned with the reduction of the nitro compound, but further work is in progress on this point and will be reported on at a later date.

On the basis of the results which show that the initial stages in the hydrosulfide reduction and in the monosulfide reduction depend upon the pH of the medium, it may be supposed that this auto-oxidation process of the hydrosulfide ion to the disulfide ion is also affected by the pH and that the rate of the auto-oxidation becomes in accordance with the pH increment.* That is to say, the rate of the formation of the disulfide ion in the aqueous hydrosulfide solution is rapid, but that in the aqueous

TABLE II. THE COMPARISON OF THE APPARENT THIRD ORDER RATE CONSTANTS OF THE HYDROSULFIDE REDUCTION WITH THOSE OF THE MAIN REACTION OF THE MONOSULFIDE REDUCTION

Initial concn. (Ar-NO$_2$) M×10^2	Initial concn. (Reducing agent) M×10^2	Apparent rate const. k l^{2}mol^{-2} min^{-1}	Temp. °C
3.50	7.19*	2.47	35
1.56	5.63**	2.79	
3.50	7.19*	1.62	30
2.18	6.51**	2.11	

* Sodium hydrosulfide ** Sodium monosulfide

* When an aqueous monosulfide solution was irradiated with ultraviolet light, the rate of the formation of the disulfide ion became lower with an increase in the hydroxide ion concentration in the medium.[7]

7) S. Hashimoto and J. Sunamoto and K. Sato, Presented at the Local Meeting of the Chemical Society of Japan, Fukuoka, July 17th, 1965.

Table III. A. c. polarography on the hydrosulfide reduction of sodium *m*-nitrobenzenesulfonate in aqueous solution (30°C)
Initial concn.: $(Ar\text{-}NO_2)=5.8\times10^{-2}$ M
$(NaSH)=6.8\times10^{-2}$ M

Reaction time min.	Peak potentials (V. vs. SCE) and wave heights ($\mu\mho$)							
	E_1	h_1	E_2	h_2	E_4	h_4	E_5	h_5
0		—	−0.44	160	−0.72	160	−0.80	115
10		—	−0.43	180	−0.70	180	−0.79	120
40	−0.15	120	−0.43	180	−0.70	180	−0.80	180
60	−0.18	140	−0.43	190	−0.70	190	−0.81	190
90	−0.20	190	−0.44	180	−0.70	200	−0.80	190
180	−0.17	195	−0.43	160	−0.70	190	−0.79	200
1620	−0.20	325		—	−0.70	200		—
$Ar\text{-}NO_2$		—		—	−0.70	130		—
NaSH		—		—	−0.68	130	−0.80	140

monosulfide solution is very slow, because of the high concentration of hydroxide ions. An induction period, therefore, appears only in the monosulfide reduction.

The Polarographic Study of the Hydrosulfide Reduction.—In order to examine the above hypothesis that the disulfide ion will be formed in the hydrosulfide reduction, a. c. polarography was applied to the hydrosulfide reduction of sodium *m*-nitrobenzene sulfonate. As is shown in Table III, the heights of the first, the fourth, and the fifth waves all increased as the reduction proceeded. The increase in the height of the first wave shows the formation of the oxide of sulfide, that is, thiosulfate.[3] The fourth wave was overlapped with the wave of the nitro compound. However, the increase in the height of this wave clearly shows the formation of the polysulfide ions, as is true also with the fifth wave.[3] The polarography of the hydrosulfide reduction confirmed the formation of the disulfide ion and supported the above hypothesis.

Conclusion

Sodium monosulfide and sodium hydrosulfide are in a hydrolytic equilibrium. The reductions by both sulfides, therefore, must be essentially identical in their kinetics. The rate equation in the main reaction of the monosulfide reduction was, in fact, identical with that of the hydrosulfide reduction (cf. Eqs. 5 and 6).

It may be reasonable to assume that the reduction of aromatic nitro compounds by the aqueous monosulfide or the aqueous hydrosulfide proceeds as follows. First, the hydrosulfide ion, as well as the one produced by the hydrolysis of the monosulfide ion in an aqueous solution, gives the sulfide ion radical with light or oxygen and dimerized to the disulfide ion. Secondly, the disulfide ion produced attacks the positively-charged nitrogen atom of the nitro group, because the reducing power of the monosulfide ion or of the hydrosulfide ion is very small in itself.

The hydroxide ion has a negative effect on the first process, involving the formation of the sulfide ion radical and its dimerization, and a positive effect on the second process, which involves the reduction of the nitro group. From these relationships, it is clear that no induction period appears in the hydrosulfide reduction as a result of its low concentration of hydroxide ions at the initial stage.

Hojyo et al. presented evidence that the disulfide reduction of nitrobenzene in an aqueous methanolic solution is given by Eq. 13, in conjunction with the hydrolytic equilibrium of the disulfide ion:[6]

$$-\frac{d(Ar\text{-}NO_2)}{dt}=k(Ar\text{-}NO_2)(S_2^{2-}) \qquad (13)$$

On the basis of the assumptions that the rate of the auto-oxidation of the hydrosulfide ion is rather rapid compared with the rate of the reduction of the nitro group, and that the reduction of the nitro group takes place not by the way of the action of the hydrosulfide ion or the monosulfide ion, but by way of that of the disulfide ion,

i) the auto-oxidation of the sulfide ion;

$$S^{2-}\xrightarrow{H_2O}SH^-\xrightarrow[\text{oxygen, etc.}]{\text{light or}}S_2^{2-}$$

(rather rapidly)

ii) the reduction of the nitro group;

$$S_2^{2-}\xrightarrow{Ar\text{-}NO_2}S_2O_3^{2-} \qquad \text{(slowly)}$$

it is clear that the rate can be expressed by a third-order equation, second order with respect to the hydrosulfide or the monosulfide, and first order with respect to the nitro compound. In this way the relationship between the disulfide reduction and the hydrosulfide (or the monosulfide) reduction can also be explained.

Thanks are due to Mr. Miyoshi Oshima for his assistance in some of the experimental work. The authors are also indebted to the Daiwa Dyestuff Co., Ltd., for its gift of materials.

BULLETIN OF THE CHEMICAL SOCIETY OF JAPAN VOL. 39 1212—1216 (1966)

The Mechanism of the Alkaline Fusion of Benzenesulfonic Acid.[1,2]

By Shigeru OAE, Naomichi FURUKAWA, Masahiro KISE and Mitsuyoshi KAWANISHI

Department of Applied Chemistry, Faculty of Engineering, Osaka City University, Sumiyoshi-ku, Osaka

(Received September 16, 1965)

Benzenesulfonic acid-1-^{14}C was fused with potassium hydroxide at 320—350°C for five minutes. The phenol obtained was then degraded as usual, and the distribution of carbon-14 in the phenol was determined. Practically all the ^{14}C activity was found at the 1 position of the phenol, which means that there is no migration of the ^{14}C originally labeled at the position 1 or the benzenesulfonic acid. Benzenesulfonic acid was also treated with potassium hydroxide enriched with ^{18}O. The resulting phenol was found to be incorporated, with the same concentration of ^{18}O as that of the ^{18}O enriched water used. The results show that the mechanism of the reaction is of a simple S_N2 type and not of the elimination-addition type involving the benzyne intermediate, while there was no oxygen migration in the reaction.

The alkaline fusion of benzenesulfonic acid was first effected by Wurtz[3] or Kekulé[4] more than a hundred years ago. Since then, the method has been used as a conventional technique for the manufacture of phenol and related hydroxy compounds. Recently, however, the alkaline fusion process has been giving way to other, more simple methods for the production of phenol, and its use is quite limited nowadays. Yet the alkaline fusion is still considered to be one of the best methods to introduce the hydroxyl group into the aromatic ring. As for the reaction mechanism, the alkaline fusion of aromatic sulfonic acids has been classified only as a simple S_N2-type nucleophilic aromatic substitution,[5] without any concrete evidence. However, under strong alkaline conditions such as those employed in this reaction, one can postulate another mechanism involving the formation of a benzyne-type intermediate. It is interesting, in this respect, to compare the alkaline fusion of benzenesulfonic acid with that of halobenzene in a strong alkaline medium such as sodiumamide in liquid ammonia,[6] where the reaction is known to proceed via the initial abstraction of an ortho proton by the strong base, followed by the formation of an unstable intermediate benzyne which reacts very rapidly with a nucleophile to give the final product. In fact, a few previous works have not accepted the simple S_N2-type mechanism for the alkaline fusion reaction.[7] For instance, *p*-benzenedisulfonic acid or *p*-chlorobenzenesulfonic acid have been reported to produce resorsinol to some extent, and hence it has been suggested[8-10] that the alkaline fusion might not be a simple S_N2-type mechanism, but an elimination-addition type process which involves the participation of a benzyne-type intermediate to some extent. Meanwhile, another alternative pathway is also conceivable, the one involving the initial attack of the hydroxide anion on the sulfur atom, followed by the intramolecular migration of the oxygen atom to the benzene ring, thus giving phenol. This mechanism is not unlikely in view

I. Simple aromatic S_N-type mechanism

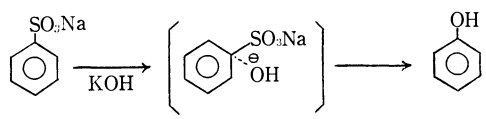

II. Elimination-addition mechanism

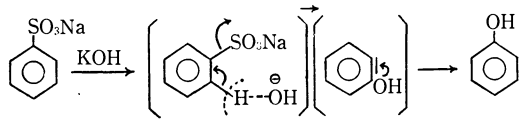

III. Oxygen migration mechanism

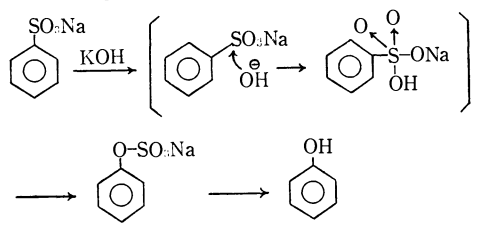

Fig. 1.

1) Phenols and Phenolic Esters. XI.

2) This work was supported in part by the Petroleum Research Fund, administered by the American Chemical Society. Grateful acknowledgment is hereby made to the donors of this Fund.

3) C. Wurtz, *Ann.*, **144**, 121 (1867).

4) A. Kekulé, *Compt. rend.*, **64**, 753 (1866).

5) C. K. Ingold, "Structure and Mechanism in Organic Chemistry," Cornell Univ. Press, Ithaca (1953), p. 814.

6) J. D. Roberts, H. E. Simmons, Jr., L. A. Carlsmith and C. W. Vaughan, *J. Am. Chem. Soc.*, **75**, 3290 (1953).

7) H. E. Fierz-David and G. Stamm, *Helv. Chim. Acta*, **25**, 364 (1942).

8) R. Huisgen, *Angew. Chem.*, **72**, 91 (1960).

9) D. J. Cram and G. S. Hammond, "Organic Chemistry," McGraw-Hill, New York (1964), p. 396.

10) J. D. Roberts and M. Casserio, "Basic Principles in Organic Chemistry," W. A. Benjamin, New York (1964), p. 901.

of the fact that the sulfur atom is known to be attacked readily by a strong nucleophile because of its ability to expand the valence shell from an octet to a decet by using its d-orbitals.[11] In fact, in the alkaline fusion of diphenyl sulfone, the sulfur atom is the primary site of the nucleophilic attack by the hydroxide anion.[12] These three postulated mechanisms may be summarized as follows.

One of the most powerful ways to get a clear understanding of the mechanistic information of the alkaline fusion is the isotopic tracer technique. If one uses sodium benzenesulfonate specifically labeled with ^{14}C at its 1 position for the alkaline fusion and traces the ^{14}C radioactivity distribution in the resulting phenol, one can readily discriminate undesirable from desirable mechanistic schemes. If the reaction follows the mechanism I, all the ^{14}C activity originally labeled at benzenesulfonic acid-1-^{14}C will remain at the position 1 in the resulting phenol, whereas if the reaction proceeds through the benzyne-type intermediate, the distribution of the ^{14}C will be completely different from that to be expected from the mechanism I, and exactly a half of the ^{14}C will be found at the position 1 in the phenol, whereas the remaining half will be distributed equally at the 2 and 6 positions. In the meantime, the mechanism III can be tested by the use of $K^{18}OH$. If the reaction follows the path indicated by the mechanism III, the concentration of ^{18}O in the resulting phenol will be considerably lower than that of the potassium hydroxide employed, since the four oxygen atoms attached to the sulfur will be substantially equilibrated before collapsing to form the rearranged phenyl sodium sulfate. If the proton transfer among four oxygen atoms is very fast in the intermediate addition complex, the oxygen-18 content in the resulting phenol will become one-quarter that of the $K^{18}OH$ originally employed.

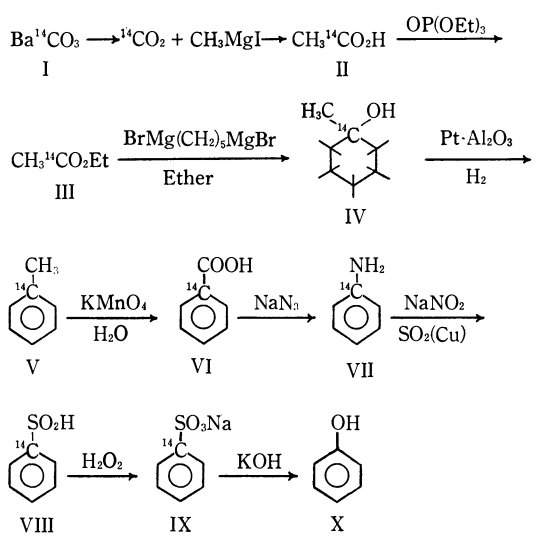

Scheme 1.

11) C. C. Price and S. Oae, "Sulfur Bonding," Ronald Press, New York (1962).

12) D. R. Christman and S. Oae, *Chem & Ind.*, **1959**, 1251.

Results and Discussion

Benzensulfonic acid-1-^{14}C was synthesized as is shown in Scheme 1.

The degradative method is shown in Scheme 2.

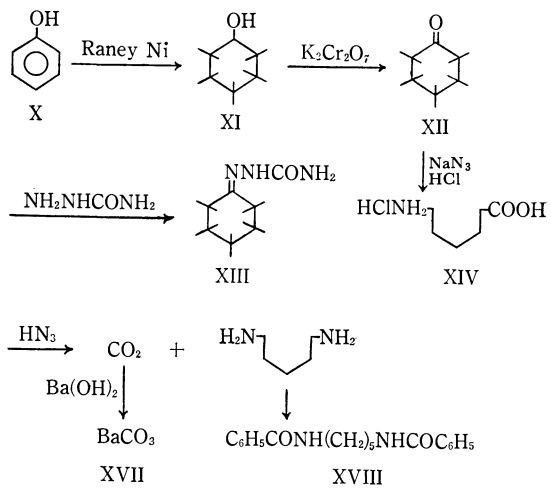

Scheme 2.

The results derived from the runs are shown in Table I. Cyclohexanonesemicarbazone was chosen as the standard sample for evaluating the activities of all the other products.

The degradation study indicates that practically all the ^{14}C activity of the phenol was found at position 1 where ^{14}C was originally labeled and the

Table I. The ^{14}C counting obtained in Scheme 2

	NNHCONH2 (XIII)	CO2 (XVII)	NH2-C6H4-NH2 (dibenzoyl) (XVIII)
c.p.m.	1726[a]	11714[a]	11[a]
	(2013)	(1952)	(42)
%	100	97.6	2.1
c.p.m.	912	6205	—
	(1064)	(1030)	
%	100	97.2	—

a) The activities are given after correction for background. The observed values are standardized to phenol, i. e., the corrected values are shown in brackets.

TABLE II. THE ALKALINE FUSION WITH $K^{18}OH$

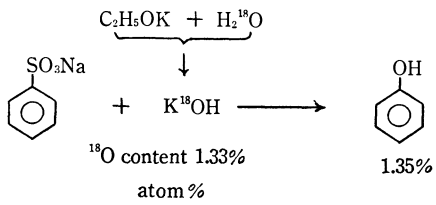

sulfonic acid group was originally attached. This observation clearly excludes the elimination-addition mechanism involving a benzyne-type intermediate, for it requires a half of the ^{14}C activity to be divided equally at the two ortho positions, and the remaining half to be at the position 1.

When the alkaline fusion of benzenesulfonic acid was carried out with ^{18}O-enriched potassium hydroxide (atom % of ^{18}O: 1.33), the resulting phenol was found to be incorporated with exactly the same concentration of ^{18}O (atom % of ^{18}O: 1.35). This observation does not favor the other alternative mechanism, which involves the initial nucleophilic attack of the hydroxide ion on the sulfur atom of the sulfonic acid, followed by the migration of the phenyl group from the sulfur atom to oxygen, since it is utterly inconceivable that he migration of the phenyl group takes place only at the entering oxygen atom. This fact is consistent with the findings of Makolkin.[13] According to this mechanism, the oxygen-18 concentration in the hydroxyl group of the resulting phenol should be between natural and a one-quarter excess of what was incorporated in the potassium hydroxide used, depending on the amount of proton-transfer during the reaction. The actual finding is not in accord with this prediction, but it is quite consistent with the mechanism of the simple aromatic S_N-reaction. In fact, this simple mechanism is only compatible with the data on the ^{14}C experiments. Therefore, both ^{14}C and ^{18}O tracer experiments unequivocally suggest that the alkaline fusion of benzenesulfonic acid proceeds through the path involving the direct nucleophilic attack of hydroxide on carbon 1, in a simple aromatic S_N-reaction as is shown by eq. I.

Another piece of evidence in support of the aromatic S_N-type mechanism for this reaction may be found in the fact that the alkaline fusion of *p*-toluenesulfonic acid did not give a mixture of *p*- and *m*-cresols, but only the isomer. Thus, the only product of the alkaline fusion of *p*-toluenesulfonic acid was, in all respects, identical to *p*-cresol. The cresol obtained from the alkaline fusion of *p*-toluidine via *p*-toluenesulfinic acid and *p*-toluenesulfonic acid (shown in Scheme 3) was also completely identical with that of an authentic sample prepared from the direct hydrolysis of the diazotized-*p*-toluidine.

13) I. A. Makolkin, *Acta Physicochim.*, **16**, 88 (1942).

In order to obtain further supporting evidence for the direct aromatic S_N mechanism, mesitylenesulfonic acid was subjected to alkaline fusion.[14] Since this compound has no ortho hydrogen available for the elimination of the hydrogen and sulfonic acid groups to form a benzyne-like intermediate, the formation of mesitylenol through the benzyne intermediate is not possible. Yet a substantial amount of mesitylenol was obtained in the ordinary alkaline fusion of mesitylenesulfonic acid. The rather low yield of the phenol, 30%, is probably due to the large steric compression of the transition complex of the reaction. All these observations clearly suggest that the alkaline fusion of these sulfonic acids proceeds through the path involving the nucleophilic replacement the SO_3H group by the hydroxide ion at position 1, much the same as in the usual aromatic S_N reaction of aromatic halides.

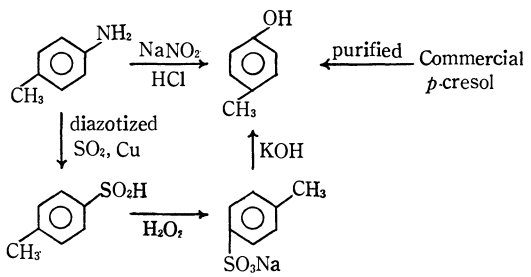

Scheme 3.

Characteristic infrared absorption band (cm^{-1}), *p*-cresol 815 (very strong) 1105 (strong) *m*-cresol 855, 875 (strong) 115 (strong) 1080 (doublets).

Experimental

The preparation of Benzenesulfonic Acid-1-^{14}C. —*Acetic Acid-1-^{14}C.*—Acetic acid-1-^{14}C was prepared following the usual method.[15] A typical example is as follows. A Grignard solution prepared from 1.89 g. of methyl iodide and 291 mg. of magnesium in 50 ml. of dry ether was carboxylated with dried $^{14}CO_2$ generated from 0.655 g. of barium carbonate, which has 1.0 mc. of ^{14}C activity in a vacuum system. Acetic acid-1-^{14}C was converted to sodium acetate. The yield was 0.200 g. (quantitative).

Ethyl Acetate-1-^{14}C.[16]—Sodium acetate-1-^{14}C (0.40 g.) was esterified with 1.5 ml. of freshly-prepared ethyl phosphate. The yield was 0.395 g. (90%).

1-Methyl Cyclohexanol-1-^{14}C.[16]—To the Grignard solution prepared from 32.5 g. of pentamethylenedibromide and 5.22 g. of magnesium, 2.96 g. of ethyl acetate-1-^{14}C in 150 ml. of absolute ether added. After the decomposition of the above Grignard solution with an ammonium chloride solution, 1-methyl cyclohexanol-1-^{14}C was obtained. The yield was 2.82 g., a 97% yield.

14) R. Biedermann and A. R. Ledoux, *Ber.*, **8**, 250 (1875).
15) A. Murray and D. L. Williams, "Organic Synthesis with Isotopes," Part I, Interscience, New York (1958), p. 34.
16) A. Murray and D. L. Williams, ibid., p. 102.

Toluene-1-^{14}C.[17]—The conversion of 1-methyl-cyclohexanol-1-^{14}C to toluene-1-^{14}C was carried out following the method employed by Sixma et al., using platinum chloride on alumina as the dehydration and dehydrogenation catalyst. From 5.00 g. of 1-methyl cyclohexanol-1-^{14}C, 2.60 g. of toluene-1-^{14}C was obtained (a 65% yield).

Benzoic Acid-1-^{14}C.[16]—Toluene-1-^{14}C (1.53 g.) was oxidized with 7.0 g. of potassium permanganate in an aqueous solution. Benzoic acid (1.47 g.) was thus obtained (a 79% yield). Recrystallization from water gave colorless crystals with a m. p. of 122°C.

Aniline-1-^{14}C.[18]—Benzoic acid-1-^{14}C (6.1 g.) was treated with 5.0 g. of sodium azide in a mixture of 40 ml. of chloroform and 20 ml. of concentrated sulfuric acid; aniline-1-^{14}C (3.9 g.) was thus obtained (a 84% yield). The b. p. was 181—182°C.

Benzenesulfinic Acid-1-^{14}C.[19]—Aniline (3.9 g.) was diazotized with 3.2 g. of sodium nitrite and 5 ml. of concentrated sulfuric acid in 60 ml. of water. The diazonium solution was saturated with sulfur dioxide gas which had been generated from sodium bisulfite and sulfuric acid until the weight of the gas reached to 20 g. Then to this solution was added 25 g. of copper metal which had been freshly prepared from cupric salfate and zinc powder, with the temperature maintained below 5°C. After the gas evolution had ceased, the precipitated copper was filtered and washed with ether several times. The filtrate was then extracted three times with 50 ml. of ether. The combined ether solution was dried over anhydrous magnesium sulfate overnight. Then the ether was evaporated, and benzenesulfinic acid-1-^{14}C was obtained as slightly yellow-colored crystals. The yield was 4.7 g.; 78.3%; m. p. 84°C.

Benzenesulfonic Acid-1-^{14}C.—Benzenesulfinic acid-1-^{14}C (4.7 g.) was suspended in 90 ml. of a 2% hydrogen peroxide solution at room temperature. The mixture was then stirred with a magnetic stirrer at room temperature until the suspended sulfinic acid had been completely dissolved. The solution was kept standing overnight. Then the solution was titrated with a standard sodium hydroxide solution and dried over a water bath. Colorless hair-like crystals of sodium benzenesulfonate-1-^{14}C were thus obtained. The yield was 5.7 g. (100%).

The Alkaline Fusion of Sodium Benzenesulfonate-1-^{14}C.—A typical run was as follows. In a 50-ml. nickel muffle was fused 10 g. of potassium hydroxide. Into this molten potassium hydroxide 3.0 g. of sodium benzenesulfonate-1-^{14}C was stirred with a steel rod equipped with a thermometer. The reaction was carried out at temperatures between 300 and 340°C for 5 min. After that the vessel was rapidly cooled with water. The solidified reactants were dissolved with a concentrated hydrochloric acid solution until the solution had strongly acidified. The aqueous solution was then steam-distilled until the precipitate with bromine did not appear. The distillate was saturated with sodium chloride and then extracted three times with 60 ml. of ether. The ether solution was distilled. The yield of phenol-*x*-^{14}C was 1.1 g. (68%); b. p. 73°C/10 mmHg. Since no detectable change was observed when the experiment was performed under a nitrogen gas stream, the fusion was carried out in the open air.

The Degradation of Phenol-*x*-^{14}C.—The degradation method for phenol-*x*-^{14}C is shown in Scheme 2. A typical run was as follows:

Cyclohexanol-x-^{14}C.[20]—Phenol-*x*-^{14}C was reduced as usual using Raney's nickel as a hydrogenation catalyst in a 100-ml. autoclave. The solvent used was methanol. From 5.0 g. of phenol-*x*-^{14}C, 4.2 g. of cyclohexanol-*x*-^{14}C was obtained (a 78% yield). B. p. 159—162°C.

Cyclohexanone-x-^{14}C.[20]—Cyclohexanol-*x*-^{14}C was oxidized to cyclohexanone-x-^{14}C using with potassium bichromate as the oxidizing agent. From 4.2 g. of cyclohexanol-*x*-^{14}C, 3.5 g. of cyclohexanone-*x*-^{14}C was obtained (81.6%; b. p. 155—159°C). A part of the cyclohexanone was converted to its semicarbazone, which was then used as the standard sample for original ^{14}C activities. M. p. 167—167.5°C.

6-Aminohexanoic Acid-x-^{14}C.[19]—Cyclohexanone-x-^{14}C was converted to 6-aminohexanoic acid according to the Schmidt reaction. Cyclohexanone (2.1 g.) in 30 ml. of water was treated with 7.4 g. of sodium azide; the ε-aminocaprolactum-x-^{14}C obtained was then hydrolyzed to afford 6-aminohexanoic acid-*x*-^{14}C hydrochloride. The hydrochloride was recrystallized from absolute-alcohol-anhydrous ether. The yield was 3.4 g. (90% yield).

The Decarboxylation of 6-Aminohexanoic Acid-*x*-^{14}C.[20]—6-Aminohexanoic acid-*x*-^{14}C hydrochloride (10.7 g.) was treated with 3.7 ml. of concentrated sulfuric acid, the resulting hydrochloride gas was removed by heating the solution up to 70°C under reduced pressure. The residue was placed in 100-ml. three-necked flask and connected to a Schmidt decarboxylation apparatus. To this mixture 20 ml. of 1.17 N hydrazoic acid was added drop wise over a 40-min. period at 40°C, and the $^{14}CO_2$ generated was trapped with 0.25 N barium hydroxide. After the reaction had been completed (the time needed for this was 15 hr.), the apparatus was swept with CO_2-free nitrogen gas. The $Ba^{14}CO_3$ thus precipitated was collected in a dry box and washed with hot water and then with acetone. The yield of barium carbonate was 1.5 g. (84% yield). The residual 1,5-pentanediamine was changed to a dibenzoyl derivative, which was recrystallized four times from ethyl acetate-benzene. M. p. 133—133.5°C.

The Measurement of the Activities.—The activities of the samples were measured using a JRC Aloka-2π-gas flow G. M. counter using Q-gas. Known amounts of the samples were completely oxidized to carbon dioxide following the Van-Slyke wet-combustion method. The carbon dioxide generated was collected as barium carbonate; it was made into pellets and the activity were measured. The samples measured were cyclohexanone semicarbazone (XIII) as a standard total activity, barium carbonate (XV) generated by a Schmidt decarboxylation, and 1, 5-dibenzoyl pentanediamine (XVII). The amounts of pellets of barium carbonate obtained were 124 mg. (95%) from cyclohexanone semicarbazone, 173 mg. from barium carbonate and 151 mg. (97%) from 1, 5-dibenzoylaminopentane. The counting data are shown in Table I.

The Alkaline Fusion of Benzenesulfonic Acid

17) H. Steinberg and F. L. J. Sixma., *Rec. Trav. Chim.*, **79**, 679 (1960).

18) E. F. Jenny and J. D. Roberts, *Helv. Chim. Acta*, **38**, 1248 (1955).

19) J. D. Roberts, D. A. Semenow, H. E. Simmons, Jr., and L. A. Carlsmith, *J. Am. Chem. Soc.*, **78**, 601 (1956).

20) R. B. Loftfield, *J. Am. Chem. Soc.*, **73**, 4707 (1951).

with $K^{18}OH$.—*The Preparation of Potassium Hydroxide-^{18}O.*—To a solution of 3 g. of potassium in 30 ml. of absolute ethanol, 1.5 ml. of water-^{18}O was added (^{18}O 1.645 atom %; Yeda Research and Development Co., Ltd., Israel). The ethanol and excess water were removed by distillation under reduced pressure, and the residue was dried over phosphorus pentoxide in vacuo. Thus, about 4.0 g. of potassium hydroxide-^{18}O (^{18}O 1.33 atom%) was obtained.

The Potassium Hydroxide-^{18}O Fusion of Sodium Benzenesulfonate.—A mixture of 1 g. of sodium benzenesulfonate and 2 g. of potassium hydroxide-^{18}O was heated at 320—330°C for 5 min. in a steel vessel, and cooled rapidly with tap water. The reaction mixture was then extracted with 50 ml. of hot water and acidified with concentrated hydrochloric acid. After the steam distillation of the mixture, a slight excess of bromine was added to the distillate, resulting in the formation of crude 2, 4, 6-tribromophenol; this was separated by filtration, washed, and dried. Repeated recrystallizations from aqueous ethanol and *n*-hexane afforded about 1.4 g. of colorless needles of a silky luster needles which melted at 92—94°C with sublimation. (Reported[21] m. p. 94—96°C). The atom percentage of ^{18}O was found to be 1.35%.

Attempts to Find Rearranged Products during the Alkaline Fusion of *p*-Toluene Sulfonic Acid.—Samples of *p*-cresols obtained by the following methods were checked by means of an Infrared Spectrum study to see if any rearrangement takes place during the alkaline fusion.

a) Commercially-available p-Cresol was purified by repeated distillation under reduced pressure; a fraction with a b. p. of 105°C/28 mmHg was collected.

b) p-Cresol from p-Toluidine.—*p*-Toludine was converted into its diazonium chloride, which was subsequently warmed on a water bath. Repeated distillation gave a fraction with a b. p. of 102°C/31 mmHg. The *p*-cresol thus obtained was used as a standard smaple for the infrared study.

c) p-Cresol from p-Toluenesulfonic Acid.—Potassium *p*-toluenesulfonate was fused with molten potassium hydroxide in a steel reaction vessel. Cresol was isolated and distilled under reduced pressure to give the main fraction (b. p. 104—105°C/28 mmHg).

d) p-Cresol from p-Toluenesulfonic Acid which had been Synthesized from p-Toluidine.—*p*-Toluidine was diazotized with sodium nitrite, and then converted into *p*-toluenesulfinic acid. *p*-Toluenesulfonic acid was prepared by oxidizing the above sulfinic acid with hydrogen peroxide. The method of alkaline fusion was the same as that described for the sodium benzene sulfonate. The infrared spectra of all these *p*-cresols, prepared by different methods, were consistent in all respects with that of the standard sample. In no case was there found any rearranged isomers or any other product than the starting material.

The Alkaline Fusion of Mesitylenesulfonic Acid.—Mesitylenesulfonic acid was synthesized from mesitylene and concentrated sulfuric acid following the usual procedure[14] (m. p. 76—78°C). To 30 g. of fused potassium hydroxide 12.5 g. of mesitylenesulfonic acid was added at 300—310°C for 5 min. After rapid cooling, the mixture was acidified with hydrochloric acid. Mesitylenol (3.5 g.) was obtained in a relatively low yield (29%); m. p. 70°C (sublimed).

21) N. D. Cheronis and J. B. Entrikin, "Semimicro Qualitative Organic Analysis," Crowell, New York (1957), p. 517.

BULLETIN OF THE CHEMICAL SOCIETY OF JAPAN VOL. 39 1216—1220 (1966)

The Intermolecular Hydrogen Bonding between Methanol and Triethylamine in Various States

By Etsuko HIRANO and Kunio KOZIMA

Laboratory of Chemical Spectroscopy, Tokyo Institute of Technology, Ookayama, Meguro-ku, Tokyo

(Received September 18, 1965)

The intermolecular hydrogen bond energy between methanol and triethylamine was determined by infrared studies in the vapor state and in solutions. It was also found that, with an increase in the dielectric constant, ε, of the solvents, the free O–H stretching band of methanol shifts to a lower frequency, the molar absorptivity of this band increases, and the hydrogen bond energy of this system decreases. As is well known, the hydrogen-bonded system is mainly stabilized by the contribution of two resonating structures, the non-bonded structure and the charge-transfer structure. It seems probable that the weight of the latter for a relatively weak hydrogen-bonded complex is small. Therefore, if the energies for both resonating structures are assumed to be mainly determined by the electrostatic interaction, the hydrogen bond energy may be expected to be reciprocal to the dielectric constant of the environment. This is actually true within the limits of experimental error in a few solutions. It was also found, however, that the relation cannot be extrapolated to the case of $\varepsilon=1$, i. e., to the case of vapor.

While a considerable number of infrared studies of hydrogen bonding in solutions have been reported, little attention has been paid to the vapor state. It seems that it would be interesting to

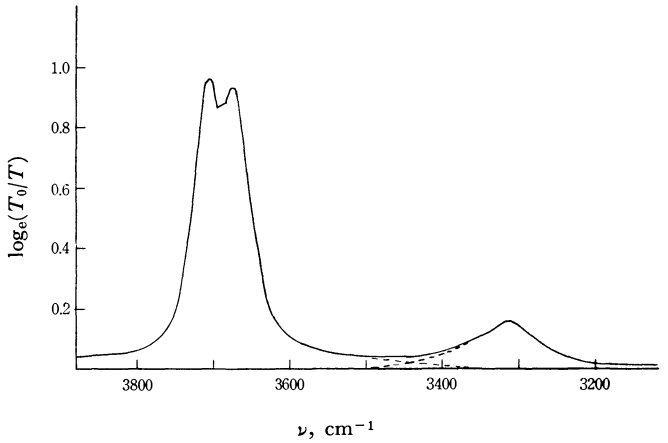

Fig. 1. The infrared spectrum of the O-H stretching band for methanol and the complex in the vapor.

Table I. Hydrogen bond energy in the vapor

Molar fraction of methanol	Total pressure mmHg at 0°C	Temp., °C	I_h, cm^{-1}	$-\Delta E$, kcal./mol.
0.324	30	19.0 33.6	21.1 10.6	8.4
0.318	28	22.2 34.8	20.5 12.4	7.1
0.322	25	20.0 34.4	17.1 9.43	7.4
				mean : 7.6

Spectral slit width : $S=4.46$ cm^{-1} at 3313 cm^{-1}

study the hydrogen bonding in the vapor state as well as in solutions for the same substances in order to obtain information about the effect of environment on the hydrogen bonding.

For this study methanol and triethylamine have been chosen as the proton donor and the proton acceptor respectively, and the intermolecular hydrogen bond energy will be measured spectroscopically in the vapor state and in solutions.

Experimental

Materials.—Methanol, triethylamine, carbon tetrachloride, chlorobenzene, dichloromethane, and chloroform were purified by the usual methods[1]; for each substance only that fraction was used which distilled at a constant temperature.

Infrared Spectra.—For the measurements in the vapor state, two thin glass ampules, in which methanol and triethylamine had been sealed separately, were broken in a three-liter spherical, vacuumed flask; the two vapors were thus mixed. The quantity of each substance should be adequately adjusted so as to make each vapor pressure less than its own saturated vapor pressure in the flask. After prolonged mixing, the mixture was expanded into a one-meter vacuumed gas cell for infrared studies.

For the measurements in solutions, a 3.0 mm. fixed cell was used throughout this study.

The spectra were measured over the range from 3000 to 3900 cm^{-1} with a Perkin-Elmer Model 112 Infrared Spectrometer equipped with a lithium fluoride prism for both states.

The temperature of the samples was measured by a copper-constantan thermocouple.

Measurements of the Integrated Intensities.—An infrared spectrum of a mixed vapor of methanol and triethylamine is shown in Fig. 1. The band near 3683 cm^{-1} is due to the hydroxyl stretching vibration of the free methanol molecules, while the band near 3313 cm^{-1} can be assigned to that of the hydrogen-bonded complex of methanol and triethylamine, for this band disappears in the spectrum of pure methanol vapor.

The change in the relative intensities of these bands with the temperature was measured. As the two bands overlap near 3500 cm^{-1}, the observed curve of absorbances was divided into two smooth curves so that their sum was equal to the observed value, as is shown in Fig. 1. The ambiguity in dividing these bands does not seem to have any noticeable influence on the results. The area intensities were obtained by the graphical integration of the absorbances by using a planimeter, since the contours of the bands were not so simple for the vapor. The integrations were carried out from 3150 to 3480 cm^{-1} and from 3500 to 3865 cm^{-1} for the two bands respectively. This sufficiently covers a range of about four times the half-intensity width for each band. The integration outside this

1) J. A. Riddick and E. E. Toops, Jr., "Organic Solvents," Interscience Publishers, New York (1955), p. 445, p. 413 (by the method of Günther et al.), p. 408 (by the method of McAlpine and Smyth), p. 409 (by the method of Maryott et al.), and p. 411 (by the method of Morgan and Lowry).

interval may be neglected without noticeable influence on the evaluation of the relative intensities, because their absorbances at these limits are smaller than one-fifteenth of those at the peaks. The correction for finite slit widths can be neglected for the vapor, because of the breadth of the bands. The results obtained for the vapor are shown in Table I.

For the studies of solutions it did not seem that it would be accurate to determine the concentration of the complex by measuring the intensity of the hydrogen-bonded O-H stretching band, because both O-H stretching bands shift to lower frequencies in solutions than in the vapor and the hydrogen-bonded O-H band overlaps with the C-H stretching bands at the wing. Therefore, the concentration of the complex was estimated by measuring the decrease in the intensity of the free O-H stretching band. For this the intensity of the free O-H stretching band in solutions should be studied first. The methanol solutions used for this purpose were so dilute that the spectra showed no evidence of the band characteristic of the hydrogen bonding. In the solvent of carbon tetrachloride or dichloromethane, the free O-H band was represented by Lorentz's equation. Although in the solvent of chlorobenzene the shape of the band was asymmetric, each side of the band could be represented by the equation. Therefore, the true integrated absorption intensity per mole (the true molar absorptivity), a, corrected for finite slit widths, was calculated by the equation:

$$a = K(1/CL)\log_e(T_0/T)_{max}\Delta\nu^a{}_{1/2}$$

where the letters have their usual meanings.[2] The values of K were obtained from Ramsay's table.[2] For the non-polar solvent of carbon tetrachloride, the area intensity of this band is independent of the temperature. However, for the polar solvent of chlorobenzene or dichloromethane the intensity decreases slightly with an increase in the temperature. The results obtained are shown in Table II and should be used for the evaluation of the concentration of the complex shown in Table III.

The infrared spectra of the mixture of methanol and triethylamine in carbon tetrachloride or dichloromethane also have these bands, of which one is due to the free molecule and the other to the hydrogen-bonded complex. In chlorobenzene, however, the band due to the hydrogen-bonded complex cannot be detected because the band is masked by an absorption of the solvent.

Results and Discussion

The change in the internal energy, ΔE, which is equal to the hydrogen bond energy in its absolute magnitude, can be evaluated by the van't Hoff equation:

$$\mathrm{d}\log_e K_c/\mathrm{d}T = \Delta E/\boldsymbol{R}T^2$$

The equilibrium constant, K_c, is given by:

$$K_c = C_X/(C_D - C_X)(C_A - C_X),$$

where C_D is the initial concentration of methanol, C_A that of triethylamine, and C_X the concentration of the hydrogen-bonded complex.

In the vapor, the area intensity, I_f, of the free O-H stretching band at 20°C and that of that at 35°C were almost the same, within the limits of experimental error. Therefore, it may be a good approximation to take $(C_D - C_X)$ and $(C_A - C_X)$ as constant over this temperature range, since the values of C_X were shown to be very small compared with those of C_D and C_X. On the other hand, the area intensity, I_h, of the O-H stretching band of the complex markedly decreases with a rise in the temperature, as is shown in Table I. Therefore, by measuring this change with the temperature, the ratio of C_X's at two temperatures could be obtained. The fact that the intensity of the band is very sensitive to small variations in the concentration of the complex is due to the marked increase in the molar absorptivity of the O-H stretching band when hydrogen bonding occurs. The evidence for this may be seen in Table IV for the case of the dilute carbon tetrachloride solution. The suffixes f and h refer to the values of the free molecule and of the complex respectively.

The hydrogen bond energy in the vapor can then be evaluated by:

$$\log_e\frac{(K_c)_1}{(K_c)_2} = \log_e\frac{(C_X)_1}{(C_X)_2} = \log_e\frac{(I_h/a_h)_1}{(I_h/a_h)_2} = \frac{-\Delta E}{\boldsymbol{R}}\left(\frac{1}{T_1} - \frac{1}{T_2}\right)$$

The suffixes 1 and 2 refer to the values at the temperatures T_1°K and T_2°K respectively. The values of molar absorptivity, a_h, were cancelled in this equation, because of its independence of the temperature.

The values thus obtained are shown in the last column of Table I. The values of $|\Delta E|$ is larger by about 2.9 kcal./mol. than that for the methanol-ethyl ether complex in the vapor reported by Inskeep et al.[3] This result agrees with the expectation in that the frequency shift of the O-H stretching band, $\Delta\nu_{OH} = (\nu_{OH})_f - (\nu_{OH})_h$, is larger for the former than the latter.

In solutions the C_D and C_A concentrations were obtained by weighing. The C_X concentration could be evaluated by:

$$C_X = C_D - (I_f/a_f L)$$

where I_f is the area intensity of the free O-H stretching band. The equilibrium constants at various temperatures thus obtained are listed in Table III. From these data the hydrogen bond energy* can be calculated; the results are shown in Table V, together with the changes in the free energy and the entropy.

2) D. A. Ramsay, *J. Am. Chem. Soc.*, **74**, 72 (1952).

3) R. G. Inskeep, F. E. Dickson and J. M. Kelliher, *J. Mol. Spectroscopy*, **4**, 477 (1960).

* For solutions the difference between ΔE and the change in the enthalpy can be neglected.

TABLE II. MOLAR ABSORPTIVITY OF THE O-H STRETCHING BAND OF METHANOL IN SOLUTIONS

Solvent : CCl_4
Spectral slit width : $S=4.75\,cm^{-1}$ at $3642\,cm^{-1}$

Temp. °C	Concn. 10^{-2} mol./l.	$\log_e(T_0/T)_{max}$	$\Delta\nu^a{}_{1/2}$ cm^{-1}	K	a_f 10^3 darks
	2.50	0.867	27.5	1.56	5.01
31.0	1.98	0.715	25.6	1.56	4.83
				mean :	4.9
	2.22	0.795	26.8	1.56	4.99
10.5	2.04	0.805	23.6	1.56	4.81
				mean :	4.9

Solvent : C_6H_5Cl
Spectral slit width : $S=6.39\,cm^{-1}$ at $3633\,cm^{-1}$

Temp. °C	Concn. 10^{-2} mol./l.	$\log_e(T_0/T)_{max}$	$\Delta\nu^a{}_{1/2}$ cm^{-1}	K	a_f 10^3 darks
	2.01	1.20	14.1 and 12.7	1.56	8.30
24.0	2.22	1.23	17.0 and 12.5	1.56	8.47
				mean :	8.4
	2.05	1.30	13.2 and 14.1	1.56	9.01
6.0	2.26	1.48	13.2 and 15.2	1.56	9.88
				mean :	9.5

Solvent : CH_2Cl_2
Spectral slit width : $S=7.92\,cm^{-1}$ at $3628\,cm^{-1}$

Temp. °C	Concn. 10^{-2} mol./l.	$\log_e(T_0/T)_{max}$	$\Delta\nu^a{}_{1/2}$ cm^{-1}	K	a_f 10^3 darks
	2.15	1.29	29.5	1.56	9.20
20.0	2.26	1.46	27.5	1.56	9.23
				mean :	9.2
	2.23	1.43	29.1	1.56	9.70
0.0	2.34	1.46	31.5	1.56	10.2
				mean :	10

TABLE III. EQUILIBRIUM CONSTANTS FOR THE METHANOL-TRIETHYLAMINE COMPLEX IN SOLUTIONS

Solvent : CCl_4

Temp. °C	C_D 10^{-2} mol./l.	C_A 10^{-2} mol./l.	I_f/L $10^2\,cm^{-2}$	C_D-C_X 10^{-2} mol./l.	K_c l./mol.
	2.05	4.71	0.780	1.59	6.9
31.0	1.42	4.49	0.557	1.14	5.9
	1.97	4.95	0.721	1.47	7.6
				mean :	6.8
	2.03	4.74	0.620	1.27	15
10.5	2.19	4.76	0.690	1.41	14
	2.03	5.08	0.626	1.28	14
				maen :	14

Solvent : C_6H_5Cl

Temp. °C	C_D 10^{-2} mol./l.	C_A 10^{-2} mol./l.	I_f/L $10^2\,cm^{-2}$	C_D-C_X 10^{-2} mol./l.	K_c l./mol.
	2.21	4.96	1.47	1.76	5.8
24.0	1.80	4.92	1.20	1.42	5.9
	2.01	4.90	1.32	1.57	6.3
				mean :	6.0
	2.25	5.06	1.45	1.53	10.8
6.0	1.84	5.02	1.23	1.30	9.3
	2.05	5.00	1.40	1.47	8.9
				mean :	9.7

Solvent : CH_2Cl_2

Temp. °C	C_D 10^{-2} mol./l.	C_A 10^{-2} mol./l.	I_f/L $10^2\,cm^{-2}$	C_D-C_X 10^{-2} mol./l.	K_c l./mol.
	2.26	4.88	1.58	1.72	7.2
24.0	2.19	4.96	1.57	1.71	6.3
				mean :	6.8
	2.34	5.06	1.56	1.56	11
−1.0	2.27	5.14	1.55	1.55	11
				mean :	11

TABLE IV. MOLAR ABSORPTIVITY OF THE HYDROGEN BONDED O-H STRETCHING BAND IN THE CCl_4 SOLUTION

C_D 10^{-2} mol./l.	C_A 10^{-2} mol./l.	I_h/L 10^2 cm^{-2}	I_f/L 10 cm^{-2}	C_X 10^{-3} mol./l.	a_h 10^4 darks
2.01	4.77	4.13	6.23	7.4	5.6
2.16	4.76	3.77	6.90	7.6	5.0
				mean :	5.3

By using the value of a_f shown in Table II, $a_h/a_f = 11$.

TABLE V. THE PROPERTIES OF THE INTERMOLECULAR HYDROGEN BONDING BETWEEN METHANOL AND TRIETHYLAMINE

State	Solvent	ε	$(\nu_{OH})_f$ cm^{-1}	$\Delta\nu_{OH}$ cm^{-1}	a_f 10^3 darks	$-\Delta E$ kcal./mol.	$-\Delta F$ kcal./mol.	$-\Delta S$ ca.l/mol.·deg.
Vapor		1	3683	370	—	7.6	—	—
Soln.	CCl_4	2.24	3642	430	4.9	6.0	1.2(31°C)	15 (31°C)
	C_6H_5Cl	5.71	3633	—	8.3	4.3	1.1(24°C)	10 (24°C)
	CH_2Cl_2	9.08	3628	328	9.2	3.0	1.1(24°C)	6.4(24°C)

It can be seen from Table V that the free O–H stretching band shifts to a lower frequency and that the molar absorptivity, a_f, of the band increases with an increase in the dielectric constant of the solvents. This fact indicates that the ionic character of the free O–H bond increases with an increase in the dielectric constant of the solvents.

As is well known, the hydrogen-bonded system is mainly stabilized by the contribution of two resonating structures, the non-bonded structure, –O–H···N$\lessgtr$, and the charge-transfer structure, $-O^-\cdots H-{}^+N\lessgtr$. Because the energy of the non-bonded structure is mainly due to the electrostatic interaction, the energy may be reciprocal to the dielectric constant, ε, of environment. As for the charge-transfer structure, it seems to be hard to estimate the effects of a solvent on its energy. However, it seems probable that the weight of the charge-transfer structure for such a relatively weak hydrogen-bonded complex is small[4] and that even for this structure the main part of energy is due to the electrostatic interaction. Therefore, if the energies for both resonating structures are considered to be mainly determined by the electrostatic interaction, the hydrogen bond energy may be expected to be a linear function of $1/\varepsilon$.

It is well known that, with an increase in the strength of hydrogen bonding, the O–H stretching bands in linear hydrogen bonds are progressively lowered in frequency.[5] Therefore, the $\Delta\nu_{OH}$ shift may be considered to be a measure of the strength of the hydrogen bonding.

The data of $\Delta\nu_{OH}$ shown in Table V and the value of $\Delta\nu_{OH}$, 360 cm^{-1}, obtained in the chloroform solution ($\varepsilon = 4.81$) are plotted against $1/\varepsilon$ in Fig. 2-(a). The values for the solutions are represented by a straight line, which is in agreement with the expectation mentioned above.

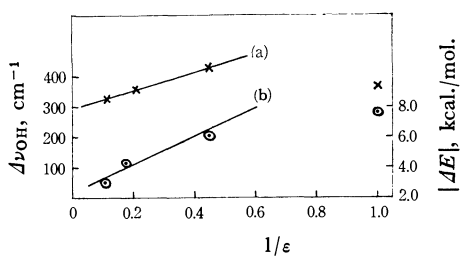

Fig. 2. (a) $\Delta\nu_{OH}$ vs. $1/\varepsilon$
(b) $|\Delta E|$ vs. $1/\varepsilon$

Furthermore, since a direct measure of the strength of the hydrogen bonding is the value of $|\Delta E|$, the values of $|\Delta E|$ are also plotted against $1/\varepsilon$ in Fig. 2-(b). Because of the possibility of experimental error in the evaluation of $|\Delta E|$, it is not conclusive; nevertheless it is very probable that the values of $|\Delta E|$ for the solutions can also be represented by a straight line.

The values of $\Delta\nu_{OH}$ or $|\Delta E|$ for the vapor phase do not fall on the straight line extrapolated from those obtained in the solutions. This fact may be taken as showing that the mechanism of the hydrogen bonding is somewhat different in the vapor from that in the solutions.

4) C. A. Coulson, "Hydrogen Bonding," Ed. by D. Hadži, Pergamon Press, London (1959), p. 67.
5) See, e. g., N. Sheppard, ibid., p. 87.

BULLETIN OF THE CHEMICAL SOCIETY OF JAPAN VOL. 39 1221—1227 (1966)

Studies of the Photoreduction of Acridine in Ethanol by the Flash Technique

By Akira KIRA, Shunji KATO*1 and Masao KOIZUMI

Department of Chemistry, Faculty of Science, Tohoku University, Katahira-cho, Sendai

(Received October 6, 1965)

With the flash technique, the absorption spectra of the triplet state and of the semireduced form of acridine were observed, and the kinetics of the reactions involving these transient species was investigated. It was established that the photoreduction of acridine in the deaerated ethanol solution proceeds via two paths. One is a path via semireduced acridine; this path is strongly inhibited by the presence of oxygen, which efficiently oxidizes semireduced acridine. In the other path, the final product, acridan, is produced immediately after flashing, with no appreciable transient species being formed. The photoreduction by this path is not affected by the presence of oxygen. It may be presumed that this process is a molecular one between singlet acridine and alcohol. The reactive species in the former path also seems to be the singlet excited state instead of the lowest triplet state.

The photoreduction of acridine in alcohol has recently been studied by several workers,[1-5] but no attempt to elucidate the detailed mechanism seems to have been made except by Kellmann and Dubois[6]. They proposed the possibility of the n-π^* triplet being a reactive species. Here, however, we have paid attention only to the problem of whether the reactive species is the singlet excited state or the lowest triplet state. Our results, particularly those concerning the effect of oxygen on the reaction, have nevertheless revealed another important feature of the reaction mechanism which Kellmann and Dubois did not mention. Hence the authors would like to stress this point in the present stage, postponing a decision whether our "singlet excited state" is a true singlet excited state or an n-π^* triplet state or whether it consists of both these states.

In previous papers[4,5] the steady light photoreduction of acridine in ethanol, methanol and isopropanol was studied in both aerated and deaerated solutions. The quantum yields of the photoreduction for the degassed solutions are 0.13 (ethanol), 0.13 (methanol) and 0.09 (isopropanol), while for the air-saturated solutions, they are 0.043 (ethanol), 0.032 (methanol) and 0.032 (isopropanol). When the concentration of dissolved oxygen is low, the reaction first proceeds at a rate approximately equal to that in the air-saturated solution, but a sharp break becomes apparent at a certain timepoint in the decay curve, after which the rate becomes approximately equal to that of the degassed solution.

On the basis of the above results, a scheme was tentatively proposed in which half-hydrogenated acridine is attacked by oxygen and the resultant $AH\cdots O_2$ reacts bimolecularly in the following two, alternative ways:

$$2AH\cdots O_2 \rightarrow AH_2 + A + 2O_2$$

$$2AH\cdots O_2 \rightarrow 2A + H_2O_2 + O_2$$

The above scheme, however, had no definite experimental evidence; moreover, it was not decided whether the reactive species is the singlet excited state or the triplet state. The purpose of the present paper is to identify the transient species produced during the reaction and to study the kinetics of the elementary reactions which are related with the overall reaction. No transient absorption due to $AH\cdots O$ was observed; indeed, the analysis of the data led to quite a different scheme in which singlet excited acridine reacts with alcohol in two alternative ways. One produces acridan or its derivatives,*2 presumably by a molecular mechanism, while the other produces semireduced acridine as a transient intermediate which, in the presence of oxygen, is easily reoxidized to acridine.

Experimental

Our flash photolysis apparatus is the same as that

*1 Present address: Osaka University, Shibahara, Toyonaka, Osaka.

1) V. Zanker and P. Schmid, *Z. physik. Chem., N. F.*, **17**, 11 (1958).

2) A. Kellmann, *J. Chim. Phys.*, **57**, 1 (1960).

3) M. Giurgea, G. Mihai, V. Topa and M. Musa, ibid., **61**, 619 (1964).

4) S. Kato, S. Minagawa and M. Koizumi, This Bulletin, **34**, 1026 (1961).

5) S. Niizuma and M. Koizumi, ibid., **36**, 1629 (1963).

6) A. Kellmann and J. T. Dubois, *J. Chem. Phys.*, **42**, 2518 (1965).

*2 As to the final product, it is not certain whether it is acridan or its derivative with a fragment of an alcohol molecule attached to the 9-position. Cf. Ref. 3. Since our main interest is in elucidating the primary processes, we tentatively assume that the product is acridan.

previously described.[7,8] The cells used are 10 cm. long. The procedure for degassing is the same as that described in a previous paper.[4] The samples were illuminated by a 90—125 Joule flash through a ultaviolet filter, which transmits the light from 320 mμ to 400 mμ. The concentration range of acridine examined was from 1×10^{-5} to 1×10^{-4} M, but in most experiments a 3×10^{-5} M solution was used. Under the above conditions, 4—7% of acridine undergoes a permanent change after one flash.

The acridine was recrystallized three times from the water-ethanol mixture. The ethanol was fractionally distilled.

Results

The Quantity of Acridan Produced as a Function of the Oxygen Concentration.— Acridan has a prominent peak at 286 mμ[4]; therefore, the optical density at 290 mμ after flashing was used as a measure of the quantity of acridan produced. This is plotted against the oxygen concentration in Fig. 1. It is evident that above ca. 5×10^{-6} M of oxygen, the yield of acridan is about 1/2.8 of that in the degassed solution, independent of the oxygen concentration. This result agrees quite well with that for the steady-light experiment.[4] The concentrations of acridan in the two cases are 2.2×10^{-6} M and 0.8×10^{-6} M respectively, corresponding to 7 and 2.5% of the original acridine. These refer to the case of the 125 J. flash illumination with the ultraviolet filter.

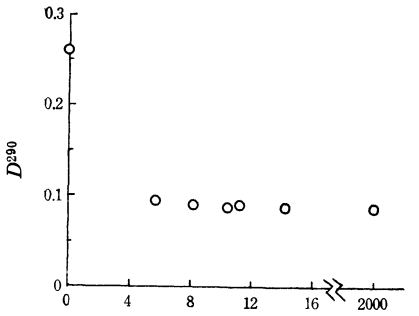

Fig. 1. Effect of oxygen concentration on the quantity of acridan produced by a flash illumination.

The Absorption Spectra of the Transient Intermediates.—The absorption spectra of the transient intermediates are shown in Figs. 2a and 2b. They are assigned as follows.

The band at 440 mμ, with a rather short life time, is attributed to the triplet state A^T, as was done by Jackson and Porter.[9] The molar extinction coefficient of the triplet state, $\varepsilon_A T$, could not be determined since semireduced acridine has an appreciable absorption in the region of the acridine absorption band, as plate 1 shows. $\varepsilon_A T$ in a benzene solution is ca. 7×10^4 M^{-1} cm^{-1}, as will be reported later; this value will be used tentatively when necessary.

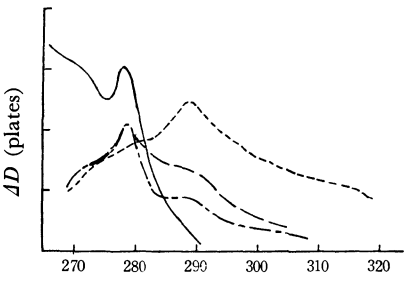

Fig. 2a. Transient absorption spectra in UV region.
ΔD(plates) is the difference in the density of two plates, one of which was measured at a given time after flashing and the other, before flashing.
—— 80 μsec — — — 1.42 msec
— — 3.5 msec - - - - 3 min

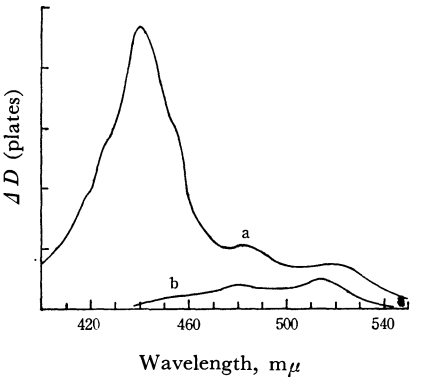

Fig. 2b. Transient absorption spectra in the visible region.
a, 80 μsec. b, 360 μsec.

Jackson and Porter attributed the band at 520 mμ to the triplet state. However, this band, which clearly has a longer life time than that at 440 mμ, must be attributed to a species different from A^T.

The sharp peak at 278 mμ has a rather long life, and as it declines, the abosrption near 290 mμ due to acridan rises. Hence, it can safely be concluded that this is semireduced acridine. A superposing broad absorption band from aronud 290 mμ extending to a shorter wavelength region is assigned to A^T, since its duration is about the

7) S. Kato, M. Morita and M. Koizumi, This Bulletin, **37**, 117 (1964).
8) S. Kato, T. Ohno and M. Koizumi, ibid., **38**, 1023 (1965).
9) G. Jackson and G. Porter, *Proc. Roy. Soc.*, **A260**, 13 (1961).

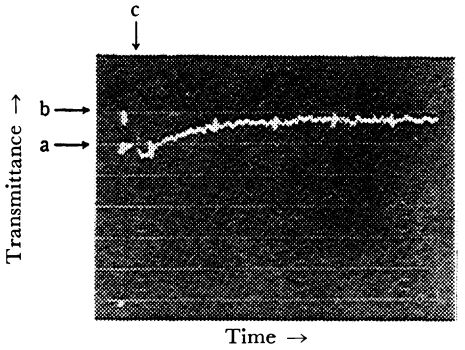

Plate 1. Change in the transmittance at 360 mμ, where the molar extinction coefficient of acridine is 6×10^{3} M^{-1} cm^{-1}.
Time marker; 1 msec.
(a) Signal before flashing. This refers to the absorption of acridine.
(b) Signal at a long time after flashing. The decrease in the acridine absorption is due to the formation of acridan.
(c) The time when a flash was fired, The increase in transmittance is due to a flash, and immediately after the flash absorption exceeds that of the original acridine, This is due to the formation of semireduced acridine as described in the text.

same magnitude as that of 440 mμ.

The air-saturated solution (the oxygen concentration is 2.0×10^{-3} M) does not give any transient absorption spectrum. The solutions containing 10^{-6} M—10^{-5} M of oxygen give an absorption band quite similar to that in the degassed solution, but only to a small extent. No new absorption band appeared. Thus no evidence could be obtained for the formation of such intermediates as $A^{T}\cdots O_2$ and $AH\cdots O_2$.

The Decay of the Triplet State.—The decay of the triplet state was examined by measuring the optical density change at 440 mμ under vairous illuminating conditions. The results are shown in Fig. 3. Evidently the decay curves do not obey a first-order law. The decay at the initial stage becomes faster when the initial concentration of A^{T} is higher. Further, it is seen that the decay curves cross one another. The former finding may imply that a first-order process and a second-order process are superposed. If one plots the apparent first-order rate constant at the initial stage against the optical density, a fairly satisfactory linear relation is obtained. From the slope and the intercept, one gets for the first-order rate constant, $k_1\cong10^{2}$—10^{3} sec^{-3}, and for the second-order rate constant, $2k_2\cong1\times10^{10}$ M^{-1}·sec^{-1}. These are, of course, very rough values, since it is thought that other decay processes are also taking place. Other molecular species which may attack the triplet state of acridine are the ground state acridine, acridan, and semi-

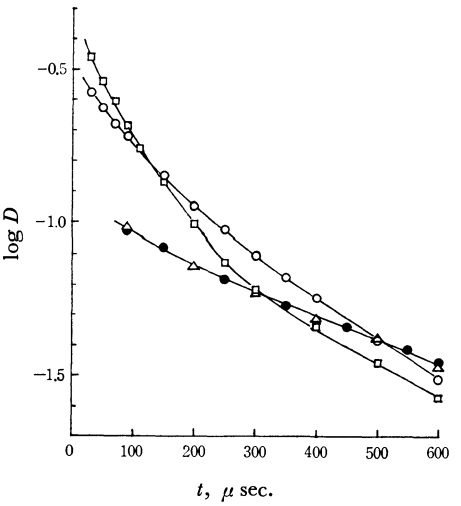

Fig. 3. Decay curves of the absorption at 440 mμ.
The order of the flash intensity is
□ > ○ > △, ●.

reduced acridine. If $A^{T}+A\rightarrow$ occurs with about the equal rate constant as that of $A^{T}+A^{T}\rightarrow$, then the first-order decay curve should be obtained, but this is not the case. $A^{T}+AH_2\rightarrow$ is judged not to contribute so much, because of the following check. In Fig. 3, □, ○ and △ refer to the plots for similar samples illuminated with different intensities, the first with strong, the second with medium, and the third with weak intensities. Plot ● is the one obtained when the sample for ○ was again flashed with the same intensity as that used for △. It may be seen that the ● plot agrees quite well with the △ plot; this rules out the contribution of $A^{T}+AH_2\rightarrow$. Thus, it seems that acridan and the ground-state acridine do not deactivate triplet acridine very much. It may be inferred, however, that $A^{T}+AH\rightarrow$ occurs to some extent, because this process is now the only one left that gives rise to the crossing of the curves. At any rate, the exact analysis of the plots at the present stage of study is very difficult, and no further attempt was undertaken. The above values of k_1 and k_2 are tentative, but it is thought that they are correct in the order of magnitude.

When oxygen is added, the decay of triplet acridine becomes faster with an increase of the oxygen concentration. In the air-saturated solution the absorption at 440 mμ is not observed, even immediately after flashing. When the concentration of oxygen is $\geq1\times10^{-5}$ M, the decay satisfactorily obeys the first-order rate law. In Fig. 4, the first-order rate constants are plotted against the oxygen concentration. The data for 5.7×10^{-6} M of oxygen is somewhat doubtful. From the inclination of the line, the rate constant for $A^{T}+O_2\rightarrow$ can be calculated as $k=2.2\times10^{9}$ M^{-1}·sec^{-1}.

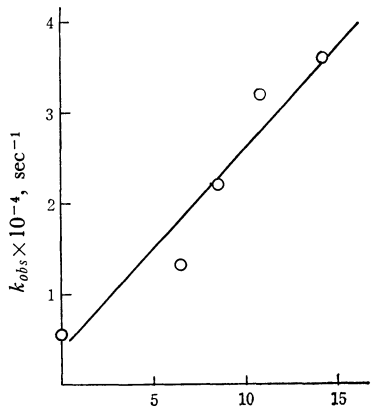

Fig. 4. Effect of oxygen concentration on the first-order rate constant of the triplet state, measured at 440 mμ.

The Decay of Semireduced Acridine and the Rate of the Formation of Acridan.—As Fig. 5 shows, the decline in the optical density at 278 mμ and the rise at 290 mμ proceed in parallel, supporting the view that the $2AH \rightarrow AH_2+A$ reaction is taking place. These curves will be analyzed later, since such an analysis requires some information concerning the reaction mechanism.

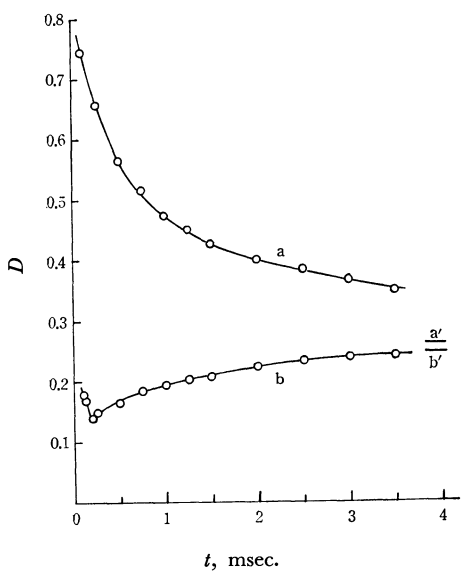

Fig. 5. Change in optical density at (a) 278 mμ and (b) 290 mμ. (a') and (b') refer to a long time after flashing.

When the concentration of oxygen is about 10^{-5} M, the disappearance of the 278 mμ peak is much faster, but this is not accompanied by the production of acridan. In other words, the optical density at 290 mμ remains constant, with

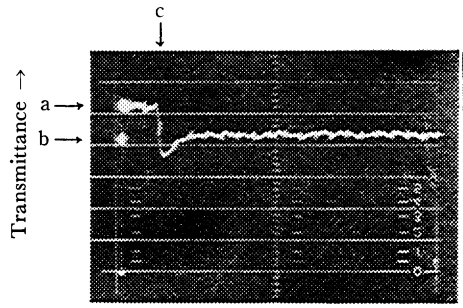

Plate 2. Change in the transmittance at 290 mμ in the presence of oxygen. $[O_2]=8.6\times10^{-6}$ M. Time marker 100 μsec.
(a) Signal before flashing.
(b) Signal at a long time after flashing.
(c) The time when a flash was fired. The increase in the absorption immediately after a flash is due to the formation of the triplet state and semireduced acridine.

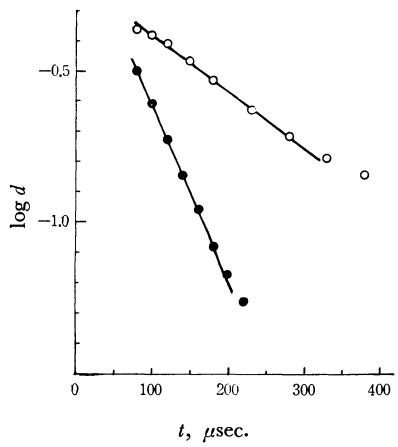

Fig. 6. Examples of decay curves of semireduced acridine in the presence of oxygen.
$[O_2]$ ○ 5.7×10^{-6} M, ● 1.1×10^{-5} M

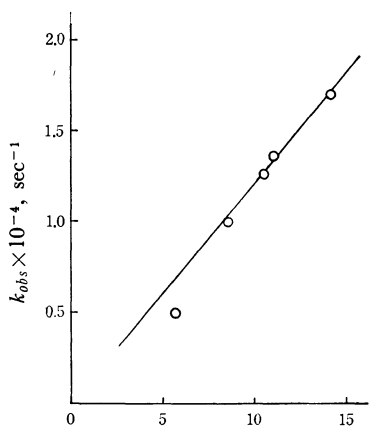

Fig. 7. Effect of oxygen concentration on the decay rate constant of semireduced acridine, measured at 278 mμ.

the same value as that for $\gtrsim 5\times10^{-6}$ M oxygen in Fig. 1 (see plate 2). The reaction is a first-order one. Some examples are shown in Fig. 6, where d is $D^{278}_{AH}-D^{278}_{AH_2\cdot\infty}$. In these experiments the concentration of acridine was 3×10^{-5} M and the input for the flash was 125 J.; an ultraviolet filter was used. In Fig. 7, the first-order rate constants are plotted against the oxygen concentration. From the slope one gets $k=1.2\times10^{9}$ M^{-1} sec^{-1}.

Discussion

In connection with the mechanism for the photoreduction in the presence of oxygen assumed in the previous paper, the following two findings are most important: 1) The deactivation of the triplet state by oxygen occurs very fast, with a rate constant of $k=2.2\times10^{9}$ M^{-1} sec^{-1}, and no transient absorption spectrum is observed in the air-saturated solution. 2) In the presence of about 10^{-5} M of oxygen, the reaction between semireduced acridine and oxygen is very rapid, with a rate constant of 1.2×10^{9} M^{-1} sec^{-1}, and there is no formation of acridan. The first finding strongly supports the view that the reactive species in the air-saturated solution is the singlet excited state. Because practically all the triplet state is annihilated by oxygen, there is no room to consider the occurrence of the $A^T+RH_2\rightarrow AH+RH$, $AH+O_2\rightarrow AH\cdots O_2$ reaction. A conceivable different mechanism which can be reconciled with the present kinetic data is the one involving the formation of $A^T\cdots O_2$ (a loose molecular complex which Schenck[10] proposed), which abstracts the hydrogen atom from alcohol. However, this mechanism is also improbable because, according to our unpublished results, triplet acridine in the presence of oxygen at a high concentration does not react with acridan, which is a more powerful hydrogen donor.

Next, judging from the second finding, the singlet state of acridine cannot yield semireduced acridine, and so the only possible mechanism for the air-saturated solution is:

$$A^* + RH_2 \rightarrow A\cdots H_2R \rightarrow AH_2 + R$$

$$(A\cdots H_2R)$$

In the absence of oxygen, an additional reaction involving the formation of semireduced acridine occurs. Thus, the reaction occurs via the two paths.

The remainning problem is now to decide:

1) whether $A\cdots H_2R$, if it is formed, is partially attacked by oxygen or not;

2) whether $A\cdots H_2R$ partially produces half-hydrogenated acridine or not;

$$A\cdots H_2R \rightarrow AH + RH$$

and in addition,

3) whether semireduced acridine is formed via the singlet or the triplet state, or both.

First, the results presented in Fig. 5 will be analyzed. Of all the acridan produced,*3 a 1.8/2.8 part is considered to result from the $2AH\rightarrow AH_2+A$ reaction; it is convenient to discuss only this part. Since the absorption due to the triplet state (T-T absorption) is negligible during the time interval in question, one can write:

$$\overline{D}^{278} = l\{\varepsilon^{278}_{AH}[AH] + \varepsilon^{278}_{AH_2}[AH_2]\} \quad (1)$$

$$\overline{D}^{290} = l\{\varepsilon^{290}_{AH}[AH] + \varepsilon^{290}_{AH_2}[AH_2]\} \quad (2)$$

where l is the length of a cell and $[AH_2]$ is the concentration of acridan produced only via semireduced acridine; accordingly, both $\overline{D}$'s are the differences between the observed optical density and 1/2.8 of the optical density of acridan at a sufficiently long time after flashing, $D_{AH_2\cdot\infty}$. If one assumes the $2AH\rightarrow AH_2+A$ disproportionation reaction, the following relation:

$$[AH]_i = 2[AH_2]_\infty$$

holds, where $[AH]_i$ is the initial concentration of semireduced acridine after flashing and $[AH_2]_\infty$ is the concentration of acridan a long time after flashing. This relation and the values of $D^{278}_\infty \equiv (D^{278}_{AH_2\cdot\infty})$, D^{290}_∞ and $\varepsilon^{290}_{AH_2}=1.2\times10^{4}$ M^{-1} cm^{-1}, combined with Eqs. 1 and 2, enable us to estimate the values of ε^{278}_{AH} and ε^{290}_{AH} to be as follows:

$$\varepsilon^{278}_{AH} = 2.4\times10^{4}\ \text{M}^{-1}\,\text{cm}^{-1}$$

$$\varepsilon^{290}_{AH} = 6\times10^{2}\ \text{M}^{-1}\,\text{cm}^{-1}$$

$$[AH]_i = 2.0\times10^{-6}\ \text{M}$$

Since ε^{290}_{AH} is only 1/20 of $\varepsilon^{290}_{AH_2}$, the optical density in the region of 290 mμ is a measure of the quantity of acridan. The following table gives D_i and D_∞ at three wavelengths for a typical case.

λ, mμ	290	295	300
D_i	0.07	0.07	0.05—0.06
D_∞	0.21	0.19	0.16

Thus $[AH_2]_i$ is about one-third of $[AH_2]_\infty$. This agrees with the ratio of the quantity of acridan produced in the evacuated and in the aerated solutions, leading to the conclusion that one-third of the acridan is produced by the $A^*+RH_2\rightarrow AH_2+R$ reaction and not via semireduced acridine. One can, therefore, safely rule out the possibility of this process:

$$A\cdots H_2R + O_2 \rightarrow A + R + H_2O_2$$

10) G. O. Schenck, *Naturwissenschaften*, **40**, 212 (1953).

*3 In the flash experiment where a large quantity of semireduced acridine is formed, some of the product may be diacridan. However, to make the description simple, we assume that all the product is acridan. Some of the data must be modified if the above situations really hold.

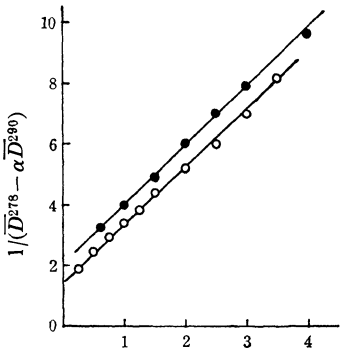

Fig. 8. Second-order decay of semireduced acridine calculated from the decrease of semireduced acridine.
$[A]_0$: ● 2×10^{-5} M, ○ 3×10^{-5} M

Now from Eqs. 1 and 2, one obtains:

$$\overline{D}^{278} - \alpha\overline{D}^{290} = l(\varepsilon_{AH}^{278} - \alpha\varepsilon_{AH}^{290})[AH]$$

where $\alpha \equiv \varepsilon_{AH_2}^{278}/\varepsilon_{AH_2}^{290}$ and where the value of α is approximately one. Hence, $1/(\overline{D}^{278}-\alpha\overline{D}^{290})$ should be linear with time. As Fig. 8 shows, this relation really holds, and the slope gives $2k/l(\varepsilon_{AH}^{278}-\alpha\varepsilon_{AH}^{290})$, where k is the true second-order rate constant for $2AH \rightarrow AH_2+A$. The rate constant, k, obtained is 2.5×10^8 M^{-1} sec^{-1}. This rate constant can also be evaluated by the following independent method. From 1 and 2 one obtains:

$$\overline{D}^{278}\varepsilon_{AH}^{290} - \overline{D}^{290}\varepsilon_{AH}^{278} = l[AH_2]\{\alpha\varepsilon_{AH}^{290} - \varepsilon_{AH}^{278}\}\varepsilon_{AH_2}^{290}$$

By the $[AH]=2\{[AH_2]_\infty-[AH_2]\}$ relation and by taking into account that $\varepsilon_{AH}^{290} \simeq (1/40)\varepsilon_{AH}^{278}$, one can write:

$$[AH] = \frac{2}{l\varepsilon_{AH_2}^{290}}\left\{\overline{D}_\infty^{290} - \overline{D}^{290} + \overline{D}^{278}\frac{\varepsilon_{AH}^{290}}{\varepsilon_{AH}^{278}}\right\}$$

Hence, the rate constant is evaluated from the plot of $1/(\overline{D}_\infty^{290} - \overline{D}^{290} + \overline{D}^{278}\cdot\varepsilon_{AH}^{290}/\varepsilon_{AH}^{278})$ against time.

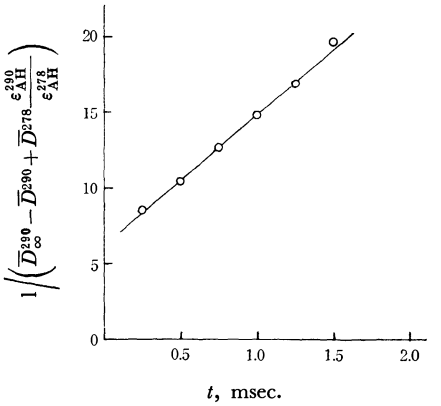

Fig. 9. Second-order decay of semireduced acridine calculated from the increase of acridan.

An example of the plot is given in Fig. 9; from the slope one gets $k=2.5\times10^8$ M^{-1} sec^{-1}, which is in good agreement with the above value.

The success of the above analysis eliminates the participation of the $AH+RH \rightarrow AH_2+R$ reaction, for the following reason. According to Taub and Dorfman,[11] the rate constant, $2k$, for $RH+RH \rightarrow$ is larger than 8×10^8 M^{-1} sec^{-1}; thus, if the above reaction occurs, the second-order rate formula should not hold.

The question whether semireduced acridine is produced in the singlet excited state or in the triplet state of acridine can not be answered clearly in the present stage of study, but the former seems to be more probable. The reason for this is as follows.

First, the value of $[AH]_1$ obtained above (2.0×10^{-6} M) is much larger than the value of $[A^T]_1$ obtained under similar conditions ($\sim9\times10^{-7}$ M). Moreover, it must be taken into account that most of the triplet acridine disappears, at least in the initial stage, according to the $A^T+A^T \rightarrow$ reaction. In agreement with this, the plot in Fig. 8 remains linear, even in the $t<1$ msec. region. Figure 6 also supports this view because, since triplet acridine is deactivated by oxygen very efficiently ($k=2.2\times10^9$ M^{-1} sec^{-1}), the initial concentration of semireduced acridine should largely decrease with the concentration of oxygen if semireduced acridine is really produced via the triplet state.

Concluding Remarks.—The elementary reactions substantiated by the present flash photolysis experiment may be summarized as follows:

$$A \xrightarrow{h\nu} A^*$$

$$A^* + RH_2 \rightarrow \left(A\!:\!\overset{H}{\underset{H}{\cdots}}\!:R\right) \rightarrow AH_2 + R \qquad (1)$$

$$\left(A\!:\!\overset{H}{\underset{H}{\cdots}}\!:R\right) \xrightarrow{O_2} A + R + H_2O_2 \qquad (2)$$

$$A^* + RH_2 \rightarrow AH + RH \qquad (3)$$

$$A^* \rightarrow A^T \qquad (4)$$

$$A^T \xrightarrow{k_5} A \qquad (5)$$

$$A^T + A^T \xrightarrow{k_6} (A + A) \qquad (6)$$

$$A^T + RH_2 \not\rightarrow AH + RH \qquad (7)$$

$$A^T + O_2 \xrightarrow{k_8} A + O_2 \qquad (8)$$

$$2AH \xrightarrow{k_9} AH_2 + A \qquad (9)$$

$$AH + O_2 \xrightarrow{k_{10}} A + HO_2 \qquad (10)$$

$$AH + RH \not\rightarrow AH_2 + R \qquad (11)$$

× denotes the non-occurrence of the reaction. The rate constants obtained are:

11) I. A. Taub and L. M. Dorfman, *J. Am. Chem. Soc.*, **84**, 4053 (1962).

$k_5 \cong 10^2 - 10^3$ sec^{-1}

$k_6 \cong 5 \times 10^9$ M^{-1} sec^{-1}

$k_8 = 2.2 \times 10^9$ M^{-1} sec^{-1}

$k_9 = 2.5 \times 10^8$ M^{-1} sec^{-1}

$k_{10} = 1.2 \times 10^9$ M^{-1} sec^{-1}

The scheme for the reaction in the presence of oxygen is 1, this may be a one-step molecular process, with A$\cdots$H$_2$R or the like being its transition state. In the absence of oxygen, the scheme consists of 3 and 9 in addition to 1. However, it can not yet be said certainly that 7 does not occur. It remains to be solved, as was mentioned at the beginning, whether our "singlet excited state" is really a true singlet excited state or an n-π^* triplet state, as Kellmann and Dubois[6] proposed; in any case, however, there is no doubt that the photoreduction of acridine in ethanol occurs via two different paths.

BULLETIN OF THE CHEMICAL SOCIETY OF JAPAN VOL. 39 1227—1229 (1966)

Aldehydes in Lake and Sea Waters

By Eijiro KAMATA

Laboratory of Analytical Chemistry, Faculty of Science, Nagoya University, Chikusa-ku, Nagoya

(Received October 20, 1965)

The vertical distribution of aldehydes in Lake Kizaki during summer stagnation is described. Aldehydes are found only in the hypolimnion, not in the upper aerobic water layers. The highest aldehyde content in three series of vertical samples is 0.11 mg./l. in terms of formaldehyde equivalents. It was shown by laboratory experiments that formaldehyde is rapidly decomposed in aerobic lake water, but very slowly in anaerobic lake water. In sea waters, aldehydes are not found in the surface water layer, and no systematic variation is noticed in the verticall distribution.

The decomposition of organic substances to carbon dioxide is an important process in the carbon cycle in natural waters. In order to investigate this process thoroughly, it is first necessary to elucidate the distribution of the organic substances produced and preserved in a water body and its deposits. In this connection we have previously reported on carbohydrates and organic acids in lake waters.[1,2]

In the present paper some results will be given on aldehydes in lake and sea waters and in an interstitial water of a lake mud.

Results and Discussion

Lake Waters and Interstitial Water of Lake Mud.—Three series of the vertical distribution of aldehydes in Lake Kizaki during summer stagnation are given in Table I. Aldehydes are found only in water layers below a depth of 20 m., not in the upper aerobic water layers. The highest aldehyde content is 0.11 mg./l. in terms of formaldehyde equivalents; this is observed in anaerobic water layers near the bottom. The aldehyde content in an interstitial water of the bottom mud is 0.044 mg./l. in terms of formaldehyde equivalents (Table II).

In order to make it clear why aldehydes are found only in the hypolimnion, the decomposition rates of formaldehyde under aerobic or anaerobic conditions at 20°C and 8°C in lake water were assertained.*1 The anaerobic conditions at 8°C refer approximately to the conditions at a depth of 25 m. in the lake. The results are shown in Fig. 1. As is shown in Fig. 1-A, under aerobic conditions at 20°C, 50 μg./l. of formaldehyde is completely decomposed in 30 hr., but under anaerobic conditions at 8°C, 50 μg./l. of formaldehyde invariably remains for 3 days, and then is gradually decomposed and so completely lost over the next 3 days. Even at 20°C the lifetime of formaldehyde under anaerobic conditions is twice that under aerobic conditions. It is clearly demonstrated that formaldehyde is decomposed through microbiological processes by the fact that no decrease in formaldehyde is observed in sterilized lake water*2 over an 8 day period. From these experimental results it may be concluded that aldehydes can not be found in aerobic water layers because of their rapid decomposition rate, while in anaerobic hypolimnion their slow rate of decomposition allows them to be preserved in a detectable concentration. Thus

1) K. Sugawara and E. Kamata, *J. Chem. Soc. Japan, Pure Chem. Sect.* (*Nippon Kagaku Zasshi*), **86**, 1275 (1965).
2) E. Kamata, ibid., **87**, 244 (1966).

*1 Surface water from Lake Kizaki was used for these experiments.
*2 The water was intermittently heated in a boiling water bath 8 times for 30 min. a day.

TABLE I. THE VERTICAL DISTRIBUTION OF ALDEHYDES IN LAKE KIZAKI

Depth m.	Temp. °C	O_2 ml./l.	pH	Fe^{2+} mg./l.	HCHO mg./l.
		Aug. 7, 1961			
0	25.9	7.3	7.0		<0.01
5	19.5	12.5	9.5		<0.01
10	10.5	6.8	6.5		<0.01
15	8.2	5.8	6.5		<0.01
20	7.7	5.6	6.3		<0.01
25	7.1	3.2	6.1		0.01
26	—	—	—		0.01
28	—	0.4	—		0.01
28.5	—	—	—		0.02
29 (bottom)	7.0	—	—		0.02
		Nov. 2, 1961			
0	15.1	6.54	6.9		<0.01
5	15.0	6.41	6.8		<0.01
10	13.6	5.35	6.5		<0.01
15	8.6	2.93	6.3		<0.01
20	7.7	1.57	6.3		<0.01
25	7.1	0.00	6.3	0.8	0.02
28	7.05	0.00	6.6	5.6	0.07
28.5 (bottom)	—	0.00	6.5	8.4	0.11
		Oct. 30, 1962			
0	13.0	6.82	7.0		<0.01
5	13.7	6.71	7.0		<0.01
10	13.8	5.80	6.8		<0.01
15	13.7	1.85	6.3		<0.01
20	8.70	0.17	6.2		<0.01
25	6.60	0.10	6.4	0.5	0.01
27.5	—	0.00	6.2	5.4	0.02
28.5 (bottom)	6.53	0.00	6.6	6.0	0.01

TABLE II. THE ALDEHYDE CONTENT IN AN INTERSTITIAL WATER OF THE BOTTOM MUD FROM LAKE KIZAKI

Date of sampling: Sept. 21, 1963.
Water content: 78 g./100 g. of fresh mud.
Fe^{2+}: 20 mg./l.
Aldehydes as HCHO: 0.044 mg./l.

aldehydes liberated from organic matters are decomposed to carbon dioxide and can be found in anaerobic hypolimnion as a result of dynamic equilibrium, production-decomposition.

Sea Water.—Sea waters were obtained during the cruise of the Ryofu Maru belonging to the Japan Meteorological Agency made as the JEDS-4 (The Fourth Japanese Deep Sea Expedition). After being frozen, the samples were transported to our laboratory. Table III gives three series of the vertical distribution of aldehydes down to a depth of about 4000 m. The degree of the aldehyde content is expressed by a + sign. A + unit is approximately equivalent to 0.01 mg./l. in terms of formaldehyde equivalents. Aldehydes are not found in the surface water layer. This is caused by the higher temperature and the aerobic conditions. No systematic variation in aldehydes is

TABLE III. THE VERTICAL DISTRIBUTION OF ALDEHYDES IN SEA WATERS

Depth m.	Temp.* °C	Cl* o/oo	O_2* ml./l.	Aldehyde
St. JEDS-4-E_{4-1}(Ry 1508) 38°01'N, 146°00'E Jun. 20, 1961				
0	18.3	19.05	5.50	0
50	13.61	19.10	5.11	++++
100	10.09	18.96	4.66	+++
197	7.19	18.79	5.23	+++
395	4.28	18.74	3.43	++++
593	4.05	18.91	1.60	+++
791	3.46	18.99	1.13	+++
988	2.94	19.03	0.94	++++
1483	2.30	19.10	1.15	+
2188	1.78	19.16	2.12	+++
2733	1.62	19.19	2.65	++
3278	1.52	19.19	3.08	+
St. JEDS-4-E_5 (Ry 1510) 38°00'N, 146°57'E Jun. 22, 1961				
0	18.7	19.04	5.40	0
20	16.72	19.04	5.95	0
50	12.96	19.08	5.27	+++
100	9.76	18.93	4.72	+
199	6.72	18.79	5.07	0
398	4.39	18.79	2.91	0
596	3.94	18.94	1.46	+++
787	3.28	19.00	1.04	+
989	2.91	19.03	0.97	++
1474	2.29	19.10	1.15	+++
1990	1.89	19.14	1.83	0
2488	1.67	19.18	2.52	++
2988	1.54	19.19	2.96	+++
3409	1.51	19.20	3.31	0
3907	1.41	—	—	+
St. JEDS-4-E_6 (Ry 1511) 38°01'N, 148°00'E Jun. 23—24, 1961				
0	18.9	19.06	5.30	0
50	14.60	19.05	5.72	+++
100	10.78	18.97	4.81	+++
391	4.69	18.81	2.77	+++
588	4.09	18.92	1.55	+++
783	3.41	18.98	1.11	+++
980	2.98	19.04	0.99	+++
1226	2.50	19.08	0.96	++
1472	2.28	19.12	1.16	+++
2143	1.81	19.16	2.05	++
2643	1.62	19.19	2.71	++
3140	1.53	19.19	3.01	++
3235	1.52	19.19	3.09	+
3735	1.48	19.19	3.27	0
4108	1.49	19.20	3.29	+++

* J. Masuzawa and H. Akamatu, *Oceanogr. Magazine* (Tokyo), **13**, 122 (1962).

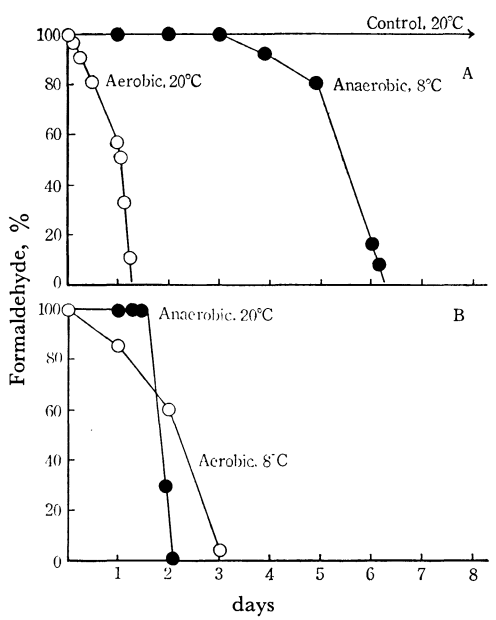

Fig. 1. Decomposition of formaldehyde in lake water under the aerobic or anaerobic condition. The concentration of formaldehyde added, 50 μg./l.

noticed. The lower temperature of the water layers below the surface layer should explain the preservation of a detectable amount of aldehydes.

Experimental

Reagents.—*A Standard Solution of Formaldehyde.*—A stock solution of formaldehyde is standardized by the dimedone method.[3] The aliquot of the stock solution is then used as the standard solution (1 μg./ml.).

3-Methyl-2-benzothiazolone Hydrazone Hydrochloride (MBTH) Reagents.—1) 0.4% aqueous solution. 2) 0.4% (1+1000) hydrochloric acid solution.

1% *Ferric Chloride Solution.*

Saturated Sodium Chloride Solution.

Crystals of Anhydrous Sodium Sulfate.

Organic Solvents.—1) Acetone. 2) A mixed solvent, (1+1) acetone-chloroform.

Apparatus.—Coleman model 14 spectrophotometer. Tokyo Photo-electric Laboratory filter photometer, model 7A (for field work). Sharp TE-10 automatically temperature-controlled water bath.

Procedure 1 (for lake water).—To 10 ml. of a test solution 2 ml. of a 0.4% MBTH aqueous solution is added. After the mixture has stood for 20 min., 0.5 ml. of 1% ferric chloride solution is added. After an additional 10 min., 12.5 ml. of acetone is added. The absorbance is read at the wavelength of 670 mμ within 30 min.

Procedure 2*[3] (for the interstitial water and sea water).—To 9 ml. of a test solution 1 ml. of a saturated sodium chloride solution is added; then 2 ml. of a 0.4% MBTH (1+1000) hydrochloric acid solution is added. After the mixture has stood for 20 min., 0.5 ml. of 1% ferric chloride solution is added. After an additional 10 min., the mixture is transferred into a separatory funnel with 12 ml. of a (1+1) acetone-chloroform solvent and shaken twenty times. The extract is poured into a 10 ml. measuring flask, and the flask is filled up to the mark with the solvent. Then the extract is quickly dehydrated in a stoppered test tube with 6 g. of anhydrous sodium sulfate. The suspended particles in the extract are filtered off through dry filter paper. The absorbance is read at the wavelength of 670 mμ. The color is stable for at least two hours.

For the determination of aldehydes in sea water, 10 ml. of a test solution is used without the addition of the sodium chloride solution.

The Separation of the Interstitial Water from Lake Mud.—A lump of frozen lake mud (~200 g.) is melted and filtered through a Millipore Filter (type HA) under a nitrogen atmosphere.

The author wishes to express his gratitude to Dr. Ken Sugawara, Professor Emeritus of Nagoya University, and to Dr. Yoshio Sugiura and the crew of the Ryofu Maru, the Japan Meteorological Agency, for kindly supplying sea water samples.

*[3] A modified procedure[4] of the original method by Sawicki et al.[5]

3) J. H. Yoe and L. C. Reid, *Ind. Eng. Chem., Anal. Ed.*, **13**, 238 (1941).
4) E. Kamata, This Bulletin, **38**, 2005 (1965).
5) E. Sawicki, T. R. Hauser, T. W. Stanley and W. Elbert, *Anal. Chem.*, **33**, 93 (1961).

BULLETIN OF THE CHEMICAL SOCIETY OF JAPAN VOL. 39 1230—1235 (1966)

The Solvation of Ions in Liquid Sulfur Dioxide

By Yasuhiko KONDO, Tsutomu GOTO, Isamu SUO and Niichiro TOKURA

The Chemical Research Institute of Non-Aqueous Solutions, Tohoku University, Katahiracho, Sendai; Department of Applied Chemistry, Faculty of Engineering, Osaka University, Miyakojima-ku, Osaka

(Received October 20, 1965)

The variation in the density and in the sound velocity with the concentration was measured in a liquid sulfur dioxide solution of electrolytes. The amounts of solvations and the volume changes which accompany the dissolving of the electrolytes were estimated. In liquid sulfur dioxide they were found to be considerably greater than those in water. The relations between the volume changes and the solvations were also discussed.

It has been generally accepted that solvents play an important role in synthetic organic chemistry; in this connection, various attempts have been made to specify the type of effects exerted by solvents on the reaction rates. Liquid sulfur dioxide is a good ionizing aprotic solvent, and various specific phenomena have been found in this solvent.[1-4]

In order to elucidate the effect of this solvent on a chemical reaction and the relation between a chemical reaction and a solvation phenomenon, an attempt has now been made to measure the solvations of ions in liquid sulfur dioxide. In this report, the volume changes and the amounts of solvation will be measured by means of density[5] and compressibility[6] measurements in liquid sulfur dioxide, and the data for various solutes will be compared.

Experimental

Materials.—Liquid sulfur dioxide was dried with phosphorus pentoxide and distilled twice. The electrolytes used were synthesized and dried in vacuo at 60°C and recrystallized three times from solvents indicated by known methods.[7-9]

The Method of Density Measurement.[5]—The volume change, ΔV, which accompanies the dissolving of one mole of a substance may be shown as follows:

$$\begin{aligned}\Delta V &= (\text{Volume of the solution}) \\ &\quad - \{(\text{Volume of the solute}) \\ &\quad + (\text{Volume of the solvent})\} \\ &= \frac{1}{n}\left[\frac{W+w}{D} - \left\{\frac{w}{d_0} + \frac{W}{D_0}\right\}\right] \qquad (1)\end{aligned}$$

where W, w, D_0, d_0, D, n are the weights of a pure solvent and of a solute, the densities of a pure solvent, of a solute and of a solution, and moles of the substance respectively. In the case of solid substances, from the view point of thermodynamics, the volume of a fused substance which is supercooled must be used as the volume of the solute. As for the salt used in this experiment, since it was impossible to measure these densities in a fused state, the densities of the solid states were used in the following calculations. For those which could not be compared with previous results in the literature, the densities were measured by using a pycnometer.

The densities of the solids used in the calculation are: KI: 3.121, $(CH_3)_4NI$: 1.819, $(C_2H_5)_4NI$: 1.552, MePyrI: 1.827, $(C_2H_5)_4NBr$: 1.388, $(C_2H_5)_4NClO_4$: 1.259, $(C_2H_5)_4NCl$: 1.112, $(C_2H_5)_4NPic.$: 1.356, $(CH_3)_4NClO_4$: 1.346, MePyr ClO_4: 1.423.

MePyr=Methylpyridinium Pic.=Picrate

The Measurement of the Densities of Liquid Sulfur Dioxide Solutions of Electrolytes.—A glass float was calibrated to a standard state of pure water using a mixed solution of sulfuric acid and water. The densities of solutions of electrolytes in liquid sulfur dioxide were measured by means of the glass float in a sealed pressure vessel.

The value of the density of liquid sulfur dioxide (d=1.3700 at 25°C) obtained by the present authors differs by 0.1 percent from the value (1.3718) which was obtained by the extrapolation to 25°C of the values quoted from the International Critical Tables.[11a]

Since, however, only a correlation between the densities of solutions and the concentrations of the solutes is needed in this experiment, the values obtained by the present authors were used throughout the calculations in spite of the slight discrepancy mentioned above. The values for densities in aqueous salt solutions used

1) G. Jander, "Die Chemie in Wasserähnlichen Lösungsmitteln," Springer-Verlag, Berlin (1949), pp. 209—306.
2) L. F. Audrieth and J. Kleinberg, "Non-Aqueous Solvents," Wiley, New York (1953), pp. 210-233.
3) N. Tokura, *Kagaku-to-Kogyo* (*Chem. & Chem. Ind.*), **15**, 212 (1962).
4) N. N. Lichtin, "Progress of Phys. Org. Chemistry," Vol. I, Wiley-Interscience, New York (1963), p. 75.
5) a) E. Darmois, *J. Phys. Radium*, **2**, 2 (1941). b) T. Sasaki and T. Yasunaga, *J. Chem. Soc. Japan, Pure Chem. Sect.* (*Nippon Kagaku Zassi*), **72**, 89 (1951).
6) a) A. Passinski, *Acta Physicochim U. S. S. R.*, **8**, 385 (1938). b) T. Sasaki and T. Yasunaga, *J. Chem. Soc. Japan, Pure Chem. Sect.* (*Nippon Kagaku Zassi*) **72**, 87 (1951). c) Y. Wada, *Oyo Butsuri*, **17**, 257 (1948). d) Y. Miyahara, This Bulletin, **25**, 326 (1952). e) T. Miyahara, ibid., **26**, 390 (1953).
7) A. W. Hofmann, *Ann.*, **78**, 263 (1851).
8) L. Ebert and J. Lange, *Zeit. für Phys. Chemie*, **A139**, 591 (1928).
9) I. M. Kolthoff, *J. Am. Chem. Soc.*, **79**, 871 (1957).
10) F. J. Gucker, *Chem. Revs.*, **13**, 111 (1933).
11) N. R. C. of U. S. A., "The International Critical Tables," McGraw-Hill, New York (1933). a) Vol. III, p. 22. b) Vol. III, p. 88. c) Vol. III, p. 62.

Table I. Typical run for the calculation of the ΔV value and the v value

Sample : Pyridinium methyl perchlorate

$D_0=1.3700$ $\lambda_0=2\times4.4808\times10^{-1}$ mm., $M=197.627$ (25°C)

W	w	n	D	ΔV	C	$C^{1/2}$	$(\lambda/2)\times10$	v
258.435	3.7150	0.018798	1.3792	62.54	0.09890	0.3145	—	—
281.025	7.4243	0.037567	1.3848	54.53	0.1803	0.4247	4.6038	263.8
267.570	13.0954	0.066263	1.3948	49.61	0.3293	0.5738	4.7060	243.2
257.935	16.3023	0.082490	1.4000	46.63	0.4211	0.6489	4.7775	238.3
198.596	19.7794	0.100085	1.4127	42.34	0.6475	0.8046	4.9238	208.0
242.937	41.9086	0.212059	1.4314	36.68	1.0656	1.032	5.2290	186.6
283.685	2.7797	0.014065	1.3763	62.7	0.06757	0.2599	—	—

unit. W: gram, V: ml. mol^{-1} C: mol. l^{-1}, λ: mm.

in the calculations are quoted from the International Critical Tables.[11b,c]

The Method of Compressibility Measurement.[6] —The following equation was used to calculate the amount of solvation from compressibility measurements. If a part of the solvent, v, changes to v' as a result of solvation, the volume of the solution, V, may be expressed as follows,[6] where V_0, V_1, v are the volumes of the solvent before mixing, the solute and the solvent molecules which solvate on the solute respectively:

$$V = V_0 + V_1 - v + v' \tag{2}$$

By using β, an adiabatic compressibility which is determined experimentally by measuring the sound velocity, u, and the density, d, Eq. 4 is obtained from the relation:[6]

$$\beta = \frac{1}{u^2 d} \tag{3}$$

$$V\beta = V_0\beta_0 + V_1\beta_1 - v\beta_0 + v'\beta_0' \tag{4}$$

If it can be assumed that $\beta_1=\beta_0'=0$, Eq. 5 is obtained from Eq. 4.[6] Also, v, the amount of solvation per mole of solute, can be calculated from Eq. 6, where D_0, D, λ_0, λ, C, M, are the densities of pure solvent and of solution, the wavelengths in a pure solvent and in a solution, the concentration of the solute [mol.l^{-1}] and the molecular weight of the solute respectively.[6]

$$V\beta = V_0\beta_0 - v\beta_0 \tag{5}$$

The number of solvation, n, was calculated from Eq. 7,[6] where v_0 is the molar volume of liquid sulfur dioxide at 25°C.

$$v = \frac{1000}{C}\left(\frac{D}{D_0} - \frac{D_0\lambda_0^2}{D\lambda^2}\right) - \frac{M}{D_0} \quad \text{[ml. mol}^{-1}\text{]} \tag{6}$$

$$v = nv_0 \ (v_0 = 46.7 \text{ ml.mol}^{-1} \text{ at } 25°C) \tag{7}$$

The sound velocities in liquid sulfur dioxide and in an electrolyte solution were measured with an ultrasonic interferrometer at a frequency of 1 Mc./sec.

Apparatus.—The interferrometer cell shown in Fig. 1 was made of stainless steel and made it possible to measure the velocity under an equilibrium vapor pressure of liquid sulfur dioxide [ca. 3.5 atom at 25°C].

The reflector was also made of stainless steel; it moves vertically without rotation, and its position was determined by a micrometer with a traveling range of 25 mm. The pressure bottle was attached to the cell in order to keep the pressure equal on both sides of the crystal during the measurement. The sample solution was introduced through the lead pipe after the cell had been evacuated, and the measurements were conducted in a thermostat bath held at 25°C. A typical run is presented in Table I.

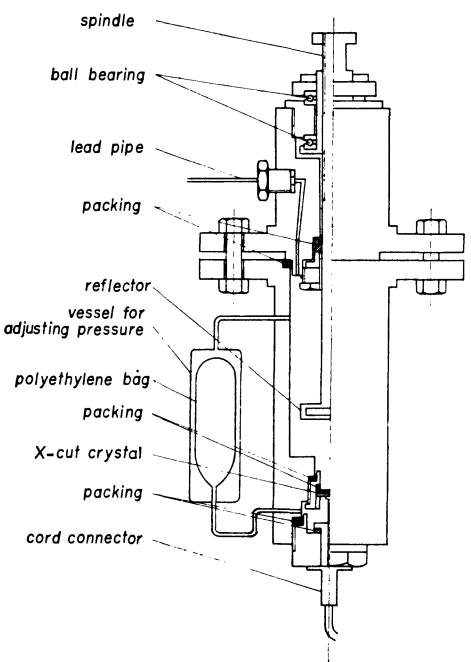

Fig. 1. Ultrasonic interferrometer for use under pressure.

Results and Discussion

Figures 2 and 3 give the results of the measurements of the densities and sound velocities (wavelengths) in liquid sulfur dioxide solutions of electrolytes.

The volume change, ΔV, and the amount of solvation, calculated from Eq. 1 and Eq. 6 respectively, are plotted against the square root of the concentration of the solute in Figs. 4, 5 and 6. It has been said that ΔV and v are linear functions of $C^{1/2}$ in water;[5b,6b,7] it is apparent from Figs. 4, 5 and 6 that a similar relation holds for the results in liquid sulfur dioxide.[4]

Generally, the behavior of an electrolyte in a

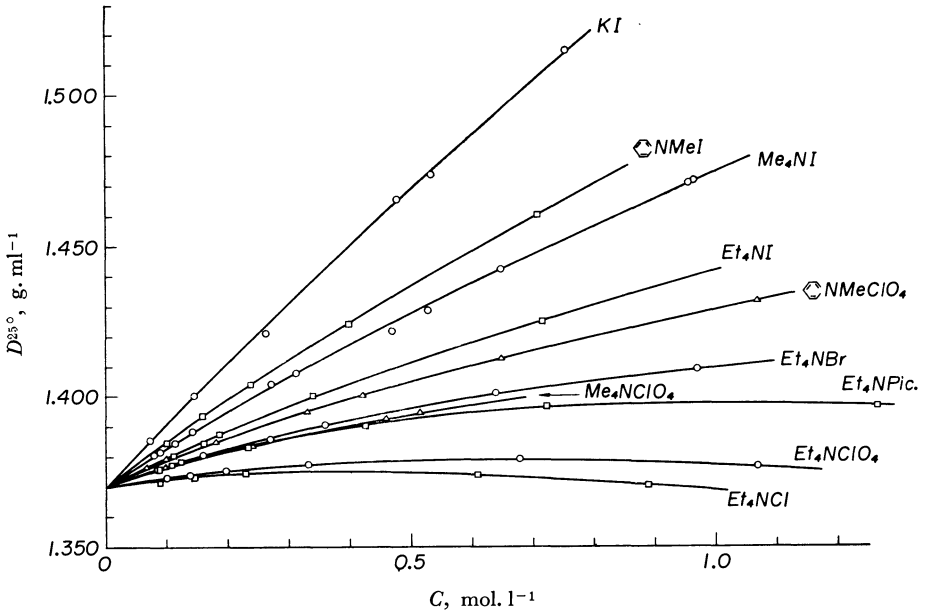

Fig. 2. Variation of the density of electrolyte solution in liq·SO_2 with the concentration of the solute.

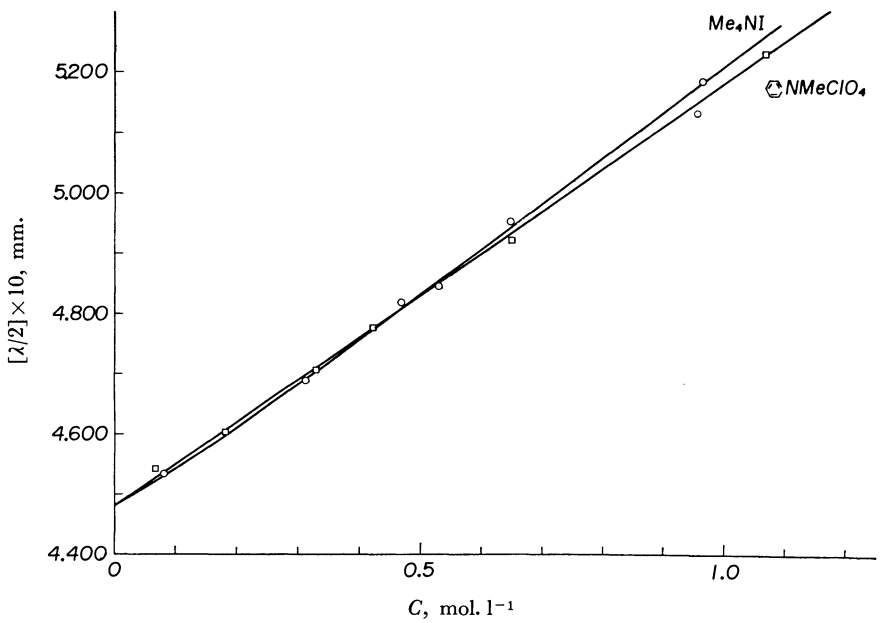

Fig. 3. Variation of wavelength with the concentration of the solute.

non-aqueous solvent is quite different from that in water. It has often been discussed also on the behavior in liquid sulfur dioxide. It was impossible to conduct measurements over the entire range where data are required for a detailed discussion and formulation of an electrolyte, since in this experiment the measurements were limited to the region where ΔV is a linear function of $C^{1/2}$, we did not consider the detailed nature of the electrolyte. The results obtained by extrapolating to a zero concentration of the solute are summarized in Table II.

From the view point of thermodynamics, the standard state of the electrolyte must be a state of fused salt in a supercooled state, and the volume changes which were calculated using the data for the solid state must include those which accompany the fusion of the solid substance.

The differences in the $[-\Delta Ve]$ value between iodides and perchlorates are presented in Table

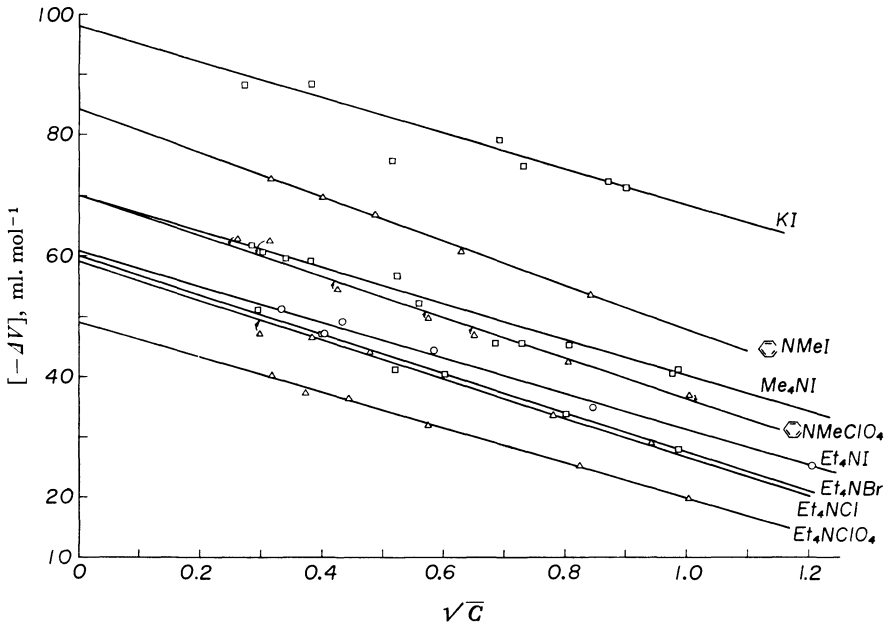

Fig. 4. Plots of the $[-\Delta V]$ value vs. $C^{1/2}$ of the solute.

Table II. Data obtained in this experiment (25°C)

Electrolyte	$[-\Delta Ve]$ ml. mol^{-1}	v ml. mol^{-1}	Number of solvation
KI	98		
MePyrI	84		
Me_4NI	70	375	8
Et_4NI	61		
Et_4NBr	60		
Et_4NCl	59		
$Et_4NPic.$	65		
Et_4NClO_4	49		
$MePyrClO_4$	70	320	6.8
Me_4NClO_4	60		
KI in H_2O	8		
Et_4NCl in H_2O	−13		

Table III. The stoichiometric additivity of the $[-\Delta Ve]$ values

Counter cation	$[-\Delta Ve]_{Iodide}-[-\Delta Ve]_{Perchlorate}$
$MePyr^+$	14 ml. mol^{-1}
Me_4N^+	10 ml. mol^{-1}
Et_4N^+	12 ml. mol^{-1}
Av.	12 ml. mol^{-1}

III. From the table, it is apparent that these differences are constant within the range of ±2 ml. mol^{-1}, which would be within the limit of experimental errors for the measurement in liquid sulfur dioxide. Since the ΔVe value is stoichiometrically additive, as is shown above, it would be possible to use the ΔVe value as a measure of the solvation of the constituent ion. The ΔVe values for the salts which have the same counter ion are compared in Table IV. From Table IV, it may be seen that the important factors influencing the ΔVe values, that is, effecting the solvation of the ion, are the bulkiness and the shape of the ion, which controls the approach of a solvent molecule to the ion.

Table IV. A comparison of the $[-\Delta Ve]$ value for the ion

For iodide

$$\underset{98}{K^+} > \underset{84}{MePyr^+} > \underset{70}{Me_4N^+} > \underset{61}{Et_4N^+}$$

For tetraethyl ammonium

$$\underset{65}{Picrate^-} > \underset{61}{I^-} \geqq \underset{60}{Br^-} \geqq \underset{59}{Cl^-} > \underset{49}{ClO_4^-}$$

As may be seen from Table II, the ΔVe value for potassium iodide in liquid sulfur dioxide is −98, much smaller than that in water, −8. The same relation holds for the value of Et_4NCl (−59 in liquid sulfur dioxide, +15 in water). This suggests that there exists a considerable interaction between the solute and solvent molecules for such a large solute as Et_4NI in liquid sulfur dioxide.

The small $[\Delta Ve]$ value in a sulfur dioxide solution may be explained by the following two points:

1) Sulfur dioxide is slightly associated in the liquid state, as is shown in its low boiling temperature and small vaporizing heat, and it may be easily compressed in the vicinity of the ionic charge.

2) The sulfur dioxide molecule is larger than the water molecule, and the interaction of sulfur dioxide with a large ion such as the tetraethyl ammonium ion may be predominant. The solvation

TABLE V. THE ΔVe VALUE AND THE DISSOCIATION CONST. OF THE SALTS

Salt	Picrate	Iodide	Bromide	Chloride	Perchlorate
$K_d \times 10^4$ for Me_4N^+ ion[4]	19.5	13.9	11.8	10.3	8.4
$[-\Delta Ve]$ for Et_4N^+ ion	65	61	60	59	49

Salt	$MePyr^+$	$Me_4\overset{+}{N}$
$K_d \times 10^4$ for Picrate[4]	29	19.5
$[-\Delta Ve]$ for Perchlorate	70	60

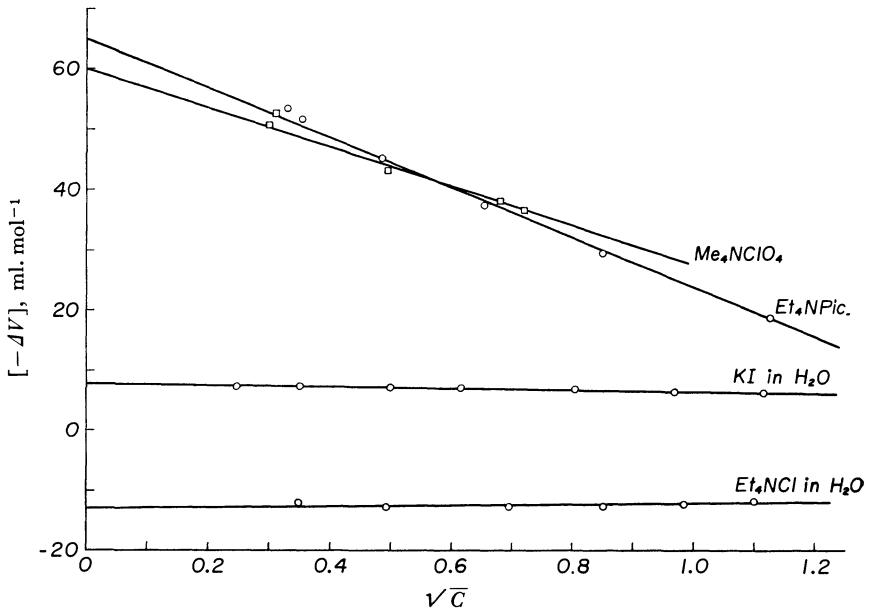

Fig. 5. Plots of the $[-\Delta V]$ value vs. $C^{1/2}$ of the solute.

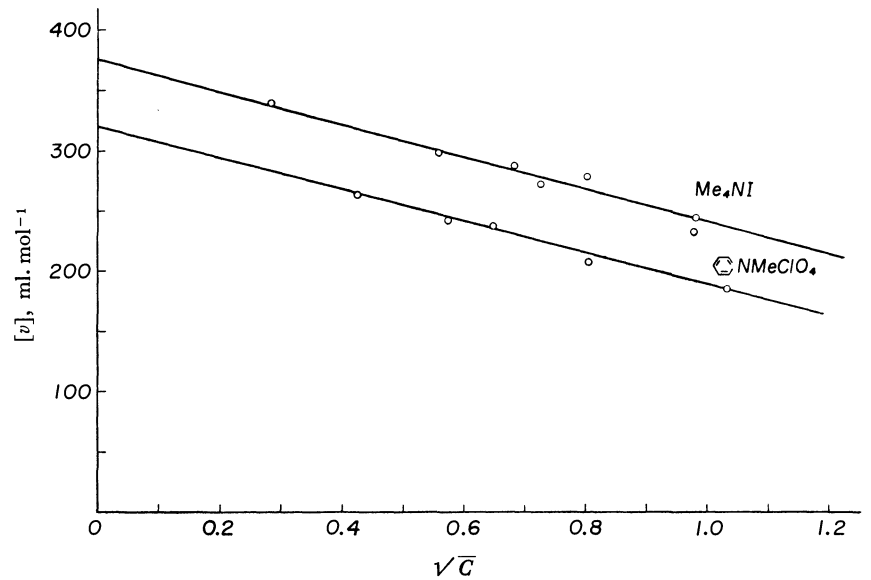

Fig. 6. Plots of the v value vs. $C^{1/2}$ of the solute.

number in a sulfur dioxide solution as calculated from Eq. 6 is eight for Me_4NI and about seven for $MePyr \cdot ClO_4$. Judging from these values it is again likely that such large solutes are considerably solvated in liquid sulfur dioxide.

It is generally accepted that the volume change is a measure of solvent-solute interactions, but this does not necessarily indicate the thermodynamic stability of the solute in the solution. However, as is shown in Table V, in liquid sulfur dioxide the order of the increase in the $[-\Delta Ve]$ value is in accord with that in the K_d value.[4]

It would be reasonable to assume that the $[-\Delta Ve]$ values thus obtained express the thermodynamic behavior of the ion in liquid sulfur dioxide.

BULLETIN OF THE CHEMICAL SOCIETY OF JAPAN VOL. 39 1235—1243 (1966)

Studies of Aminosugars. XI. Configurational Studies of Aminosugar Glycosides and Aminocyclitols by a Copper Complex Method*1

By Sumio UMEZAWA, Tsutomu TSUCHIYA and Kuniaki TATSUTA

Department of Applied Chemistry, Faculty of Engineering, Keio University, Koganei-shi, Tokyo

(Received October 23, 1965)

An extensive study has been made of the determination of the rotational shift of aminosugars in three kinds of cuprammonium solutions, i. e., in solutions of tetramminecopper(II) sulfate, ammoniacal cuprous chloride and Cupra B, with special consideration of the spacial relationships between adjacent amino and hydroxyl groups in six-membered chair molecules. This paper is an extension of the work of Reeves which provided a tool for the determination of the spacial relationships between adjacent two-hydroxyl groups. Some significant generalizations have been obtained. About ten derivatives of glucosamine have been prepared, and their structures, as indicated by their rotational shifts, have been discussed. The absolute configurations of *d*- and *l-trans*-2-aminocyclohexanol have been successfully determined.

The optical rotatory behavior of glucopyranosides in a cuprammonium solution was first explained by Reeves[1a] by means of conformational considerations, and his experimental evidence confirmed the predicted favored conformational structures.

The findings of Reeves are concerned with the structural relationship between hydroxyl groups on adjacent carbon atoms. It has been concluded that, in the case of a substance with a six-membered chair form, a pair of adjacent hydroxyl groups in the molecule can form a copper complex when dissolved in "Cupra B,"[1b] and if the pair is located sterically so as to give near the $\pm 60°$ projected angle,[2a] the difference in the molecular rotations of the substance in Cupra B and in water, $\Delta[M]_{\text{Cupra B}}$,[3] is approximately ± 2000.

The present investigation was undertaken to see if a practical method could be worked out for the determination of a configurational relationship between amino and hydroxyl groups on adjacent carbon atoms in a six-membered chair molecule. The need for such a method is keenly felt for the elucidation of the absolute structures of a variety of aminosugar glycosides recently found in the field of antibiotics.

Optical rotatory studies have been carried out with a series of aminosugar derivatives and aminocyclitols in a tetramminecopper(II) sulfate[4] solution (TACu), a solution of cuprous chloride in concentrated aqueous ammonia (CuAm), and a

*1 This constitutes Part XXIV of a series entitled "Studies of Antibiotics and Related Substances," by Sumio Umezawa. A portion of this paper was presented at the 18th Annual Meeting of the Chemical Society of Japan, Osaka, April, 1965. Previous reports on aminosugars: S. Umezawa and Y. Ito, This Bulletin, **34**, 69 (1961); Y. Ito, S. Koto and S. Umezawa, ibid., **35**, 1618 (1962); S. Umezawa, S. Koto and Y. Ito, ibid., **36**, 183 (1963); T. Suami, S. Ogawa and S. Umezawa, ibid., **36**, 459 (1963); T. Tsuchiya and S. Umezawa, ibid., **38**, 1181 (1965); S. Fukatsu and S. Umezawa, ibid., **38**, 1443 (1965); S. Koto, Y. Ito and S. Umezawa, ibid., **38**, 1447 (1965); S. Umezawa and T. Tsuchiya, *J. Antibiotics*, **A15**, 51 (1962); T. Tsuchiya, H. Fujita and S. Umezawa, ibid., **A17**, 181 (1964); S. Umezawa and S. Koto, ibid., **A17**, 186 (1964).

1) a) R. E. Reeves, "Advances in Carbohydrate Chemistry," Vol. 6, Academic Press, New York (1951), p. 107; b) Cupra B is a standard cuprammonium solution containing 15 g. of copper, 240 g. of ammonia and 1 g. of glycerol per liter: R. E. Reeves, *J. Am. Chem. Soc.*, **71**, 2116 (1949).

2) a) Reeves called the projection of the angle made by the two valence bonds onto a plane perpendicular to the carbon-carbon bond the projected angle between the groups under consideration. By convention this angle is negative if measured in a clockwise direction from the nearer group, and positive if measured counterclockwise, (Ref. 1a, p. 110). b) Ref. 1a, p. 127.

3) $\Delta[M]_{\text{Cupra B}} = ([\alpha]_{436}\ \text{Cupra B} - [\alpha]_{436}\ \text{water}) \times \frac{\text{Mol. wt.}}{100}$

4) Tetramminecopper(II) sulfate can easily be prepared from cupric sulfate pentahydrate dissolved in concentrated aqueous ammonia by adding ethanol and drying the resulting precipitate (D. W. Horn and E. E. Taylor, *Am. Chem. J.*, **32**, 253 (1904)).

TABLE. I.

		$[\alpha]_{589}^{15}$	$[\alpha]_{436}^{15}$	$\Delta[M]_{TACu}$	$\Delta[M]_{CuAm}$	$\Delta[M]_{Cupra\ B}$
I	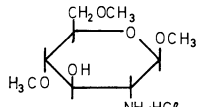	− 2	− 18	− 930	− 850	− 980
II	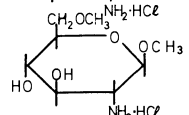	− 4	− 8	− 1010	+ 1580	+ 1570
III	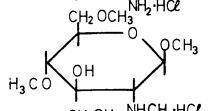	− 1	− 15	− 980	− 880	—
IV	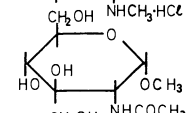	+ 103	+ 180	+ 52	+ 2210	+ 1930
V	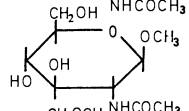	− 48	− 86	+ 50	+ 2180	+ 2040
VI	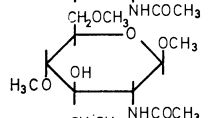	− 23	− 51	− 20	+ 50	+ 43
VII	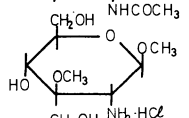	+ 10	+ 17	− 60	− 80	− 40
VIII	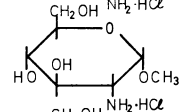	+ 153	+ 242	− 840	+ 1710	+ 1710
IX	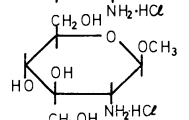	− 20	− 34	− 820	+ 1830	+ 1820
X	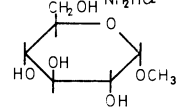	+ 161	+ 309	+ 30	+ 430	+ 260
XI	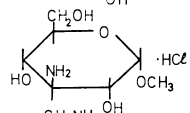	+ 110	+ 193	− 70	+ 460	+ 270
XII	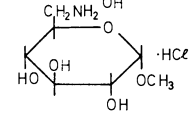	+ 135	+ 249	+ 80	+ 570	+ 390
XIII	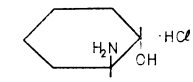	+ 42	+ 71	− 920	− 960	− 950
XIV	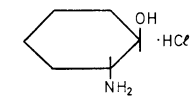	− 40	− 67	+ 930	+ 970	+ 920

Cupra B solution. The results obtained by experiments on a number of substances of known configurations have led to some general conclusions, by which the absolute configurations of *d*- and *l*-*trans*-2-aminocyclohexanol[5] have been successfully determined.

As an example of a configurationally-known substance with a pair of adjacent amino and hydroxyl groups, methyl 2-amino-2-deoxy-4, 6-di-*O*-methyl-β-D-glucopyranoside (I) has been measured for the Δ[M] values in the above-mentioned three kinds of copper solutions; it gave $\Delta[M]_{TACu}$ −930, $\Delta[M]_{CuAm}$ −850 and $\Delta[M]_{Cupra\ B}$ −980 respectively. The projected angle between the adjacent amino and hydroxyl groups of the substance is about −60°.

An *N*-methyl derivative (III) of I, methyl 2-deoxy-4, 6-di-*O*-methyl-2-methylamino-β-D-glucopyranoside, showed nearly the same Δ[M] values as did I (Table I).

Methyl 2-acetamido-2-deoxy-α- and -β-D-glucopyranosides (IV, V), which have a pair of adjacent hydorxyl groups, showed the values of $\Delta[M]_{TACu}\sim 0$, $\Delta[M]_{CuAm}\sim+2200$ and $\Delta[M]_{Cupra\ B}\sim+2200$ respectively. The projected angles between the adjacent hydroxyl groups of both substances are about +60°.

Methyl 2-acetamido-2-deoxy-4, 6-di-*O*-methyl-β-D-glucopyranoside (VI), in which no hydroxyl or amino groups are free except for a hydroxyl group of C-3, showed nearly zero Δ[M] values in the above-mentioned three kinds of copper solutions. Methyl 2-amino-2-deoxy-3-*O*-methyl-β-D-glucopyranoside (VII), which has isolated hydroxyl and amino groups, also showed nearly zero Δ[M] values.

It has been further found that none of the compounds mentioned above showed any change in optical rotations when determined in an aqueous solution of cupric sulfate.

Methyl 2-amino-2-deoxy-α- and -β-D-glucopyranoside (VIII, IX) were also examined. These glucosides contain two kinds of pairs of adjacent groups, a pair of adjacent amino and hydroxyl groups and a pair of adjacent hydroxyl groups; they correspond to the case in which a competitive formation of a copper complex is to be expected between a pair of amino and hydroxyl groups and a pair of hydroxyl groups because these glucosides contain the $-C(OH)-C(OH)-C(NH_2)-$ grouping. It has been found that the corresponding Δ[M] values of VIII and IX are essentially equal, being $\Delta[M]_{TACu}\sim-830$, $\Delta[M]_{CuAm}\sim+1770$ and $\Delta[M]_{Cupra\ B}\sim+1770$ respectively. The negative sign and the magnitude of $\Delta[M]_{TACu}$ indicate that a formation of copper complex occurs with a pair of adjacent amino and hydroxyl groups at C-2 and C-3, not with a pair of hydroxyl groups at C-3 and C-4, and that the projected angle between the amino and hydroxyl groups is −60°. On the contrary, the positive sign and the magnitude of $\Delta[M]_{CuAm}$ and $\Delta[M]_{Cupra\ B}$ indicate that a complex formation occurs with a pair of adjacent hydroxyl groups at C-3 and C-4, and that the projected angle between them is +60° (Chart 1).

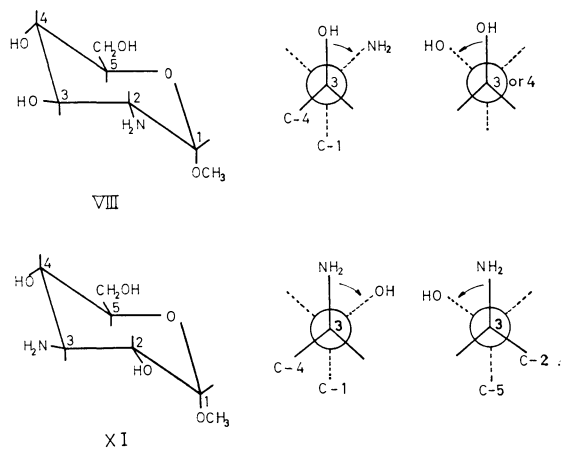

Chart 1.

Methyl α-D-glucopyranoside (X), methyl 3-amino-3-deoxy-α-D-glucopyranoside[6] (XI) and methyl 6-amino-6-deoxy-α-D-glucopyranoside[6] (XII) were further measured for Δ[M]. These glucosides correspond to the cases in which we can pick up two pairs of adjacent hydroxyl groups or adjacent amino and hydroxyl groups, and the projected angles of the two pairs are equal, though opposite in sign. For example, in XI, the projected angular relationship between the amino group at C-3 and the hydroxyl group at C-2 is clockwise and that between the amino group at C-3 and the hydroxyl group at C-4 is counterclockwise. As expected, the experimental values of Δ[M] were all small (Table I); however, $\Delta[M]_{CuAm}$ and $\Delta[M]_{Cupra\ B}$ showed values which, though slight, could not be deemed nearly zero or negligible, suggesting that the complex formation is slightly one-sided. A similar tendency had been observed by Reeves.[2b]

The above observation led to the following generalizations:

(1) TACu shows a significant $\Delta[M]_{TACu}$ value in compounds which have a pair of adjacent amino (or methylamino) and hydroxyl groups in a six-membered chair molecule, but in compounds which have a pair of adjacent hydroxyl groups or isolated hydroxyl or amino groups, $\Delta[M]_{TACu}$ is nearly zero. The sign of $\Delta[M]_{TACu}$ is in accord with the sign conventionally expected from the projected angle

5) R. M. Godchot and M. Mousseron, *Compt. rend.*, **194**, 981 (1932). The separation of the optical antipodes was improved by T. Suami, S. Ogawa and S. Umezawa, This Bulletin, **36**, 459 (1963).

6) H. Ogawa, T. Ito and S. Kondo, *J. Antibiotics*, **11A**, 70, 72 (1958).

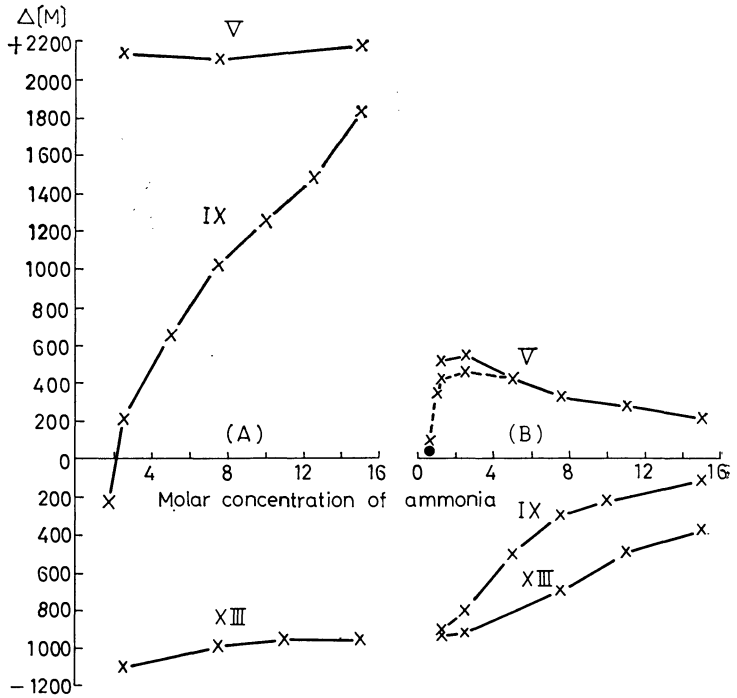

Fig. 1. Effect of the concentration of ammonia on Δ[M] of compounds V, IX and XIII (0.02 mmol.) in solutions (2 ml.) containing cuprous chloride (0.32 mmol.) (A), and cupric chloride (0.32 mmol.) (B). Since the cupric chloride solutions of low concentration of ammonia (<1.5 M ammonia) were not clear, cupric sulfate (0.32 mmol.) was used instead of cupric chloride; this range is represented by a dotted line.
● in B designates $\Delta[M]_{TACu}$ value of V.

made by adjacent hydroxyl groups.[2a] However, the magnitude of the $\Delta[M]_{TACu}$ value of the compounds with a pair of adjacent amino (or methylamino) and hydroxyl groups is about a half of the $\Delta[M]_{CuAm}$ or $\Delta[M]]_{Cupra\ B}$ value of the compounds with a pair of adjacent hydroxyl groups.

(2) Both CuAm and Cupra B show significant $\Delta[M]_{CuAm}$ and $\Delta[M]_{Cupra\ B}$ values in both cases, i. e., in cases of compounds which have a pair of adjacent amino (or methylamino) and hydroxyl groups and in cases of compounds which have a pair of adjacent hydroxyl groups. The sign of these Δ[M] values is again in accord with that conventionally expected from the projected angle. However, the magnitudes of the Δ[M] values in the former cases are about a half of those in the latter cases.

(3) In compounds with pairs both of adjacent amino and hydroxyl groups and of adjacent hydroxyl groups, TACu shows Δ[M] values exclusively corresponding to the pair of the former groups, while CuAm and Cupra B show Δ[M] values exclusively corresponding to the pair of the latter groups.

The above-mentioned generalizations were then successfully applied to an elucidation of the absolute configurations of *d*- and *l-trans*-amino-cyclohexanol.[5] The high negative increment ($\Delta[M]_{TACu}-920$) observed with the former was similar to that observed with I ($\Delta[M]_{TACu}-930$), but of a sign opposite to that of the latter ($\Delta[M]_{TACu}$ +930). Thus, (1s : 2s)-2-aminocyclohexanol (XIII) and (1R : 2R)-2-aminocyclohexanol (XIV) have been assigned to *d*- and *l-trans*-2-aminocyclohexanol respectively.

Discussion

As can be seen from the Table I, TACu has a significant effect in Δ[M], one quite different from that of CuAm and Cupra B, which are essentially similar. It may be considered that the significant difference is due to the formation of a copper(II) complex in the case of TACu and of a Copper(I) complex in the case of CuAm. On the other hand, however, it became of special interest to investigate how the concentration of ammonia affects the Δ[M] value, because either CuAm or Cupra B contains a far larger amount of ammonia than TACu.

Three compounds (V, IX and XIII) were chosen for the investigation. Each of them was dissolved in mixtures of aqueous ammonia of a series of concentrations, and of cuprous or cupric chloride. The Δ[M] values of the resulting solutions are

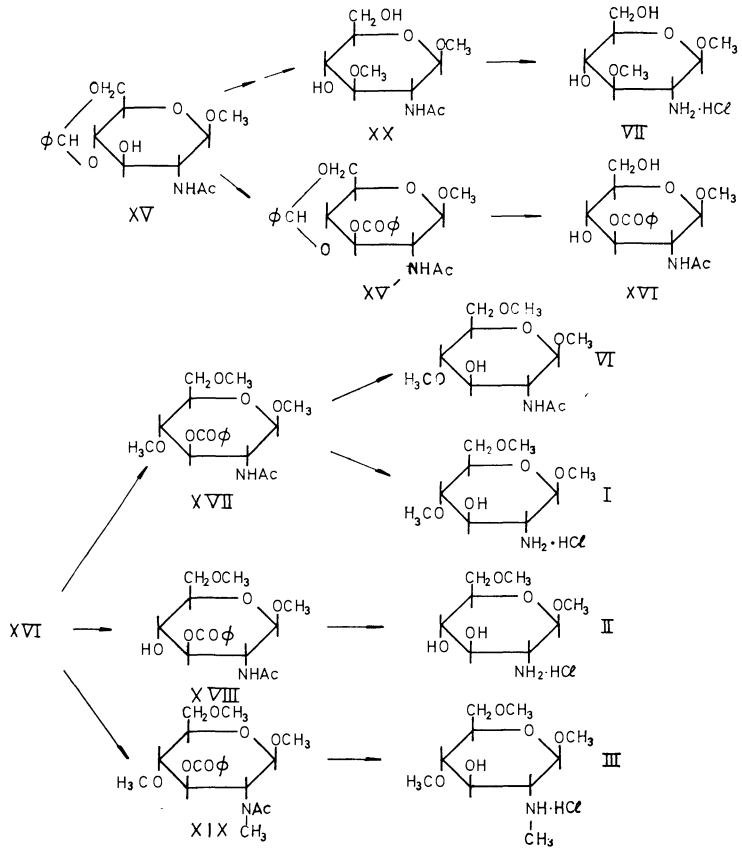

Chart 2. Scheme for the syntheses of derivatives of glucosamine.
Φ: C_6H_5 Ac: $COCH_3$

plotted against the molar concentrations of ammonia in Fig. 1.

As can be seen there, the Δ[M] values of cupric solutions of compounds with a pair of adjacent amino and hydroxyl groups are closely related to the concentration of ammonia. In the cupric chloride - ammonia solutions, the Δ[M] values for IX and XIII are significantly dependent on the concentration of ammonia. The absolute values of IX and XIII increase with the decrease in the concentration of ammonia, reaching a maximum where the concentration of ammonia is nearly equivalent to that in TACu. This indicates that TACu is an excellent reagent for the determination of Δ[M]. The Δ[M] value for V in the cupric solutions showed low values at various concentrations of ammonia.

In the cuprous chloride - ammonia solution, the Δ[M] values for both V and XIII are nearly independent of the concentrations of ammonia between two and fifteen moles, whereas the values for IX increase with the concentration of ammonia, reaching a point where the concentration of ammonia is nearly equivalent to that (14 mol.) in Cupra B. This suggests that, in a region of high concentration of ammonia, a preferential complex-formation occurs with adjacent hydroxyl groups and, as the concentration of ammonia becomes lower, adjacent amino and hydroxyl groups competitively participate in the complex-formation.

Synthesis.—Chart 2 outlines the synthetic steps for the derivatives of glucosamine. Excepting XV and XX, all the derivatives have never been prepared to the authors' knowledge. Methyl 2-amino-2-deoxy-4, 6-di-*O*-methyl-β-D-glucopyranoside (I) has been prepared by starting with methyl 2-acetamido-4, 6-*O*-benzylidene-2-deoxy-β-D-glucopyranoside[7] (XV). The 3-*O*-benzoyl derivative (XV') of XV was debenzylidenated to give methyl 2-acetamido-3-*O*-benzoyl-2-deoxy-β-D-glucopyranoside (XVI). The Purdie methylation of XVI by a general procedure gave methyl 2-acetamido-3-*O*-benzoyl-2-deoxyl-4, 6-di-*O*-methyl-β-D-glucopyranoside (XVII) in a low yield. However, it has been found that the use of a "flash mixer" equipped with an eccentrically-rotating stirrer gave a high yield of XVII, as will be described in the "Experimental" section. The

7) W. Roth and W. Pigman, *J. Am. Chem. Soc.*, **82**, 4608 (1960).

hydrolysis of XVII to I was performed by treatment with hydrazine, a method which was first introduced by Fujinaga and Matsushima[8] for the deacetylation of *N*-acetylated aminosugar glucosides.

In the above methylation, if the reaction period was curtailed, a partially-methylated product, methyl 2-acetamido-3-*O*-benzoyl-2-deoxy-6-*O*-methyl-β-D-glucopyranoside (XVIII), was obtained in addition to XVII, indicating that 6-*O*-methylation occurs easier than 4-*O*-methylation. The evidence for the structure of XVIII was obtained by a study of the infrared and NMR spectra (Fig. 2) and by the determination of three Δ[M] values of the deacetylated product (II) of XVIII (Table I).

Furthermore, it has been found that, if more hours were used in the above methylation, the *N*-methyl derivative of XVII, i. e., methyl 3-*O*-benzoyl-2-deoxy-4,6-di-*O*-methyl-2-*N*-methylacetamido-β-D-glucopyranoside (XIX), was obtained in a low yield. This was then converted to methyl 2-deoxy-4, 6-di-*O*-methyl-2-methylamino-β-D-glucopyranoside (III) by the action of hydrazine.

Methyl 2-acetamido-2-deoxy-4, 6-di-*O*-methyl-β-D-glucopyranoside (VI) was obtained by curtailing the reaction period of XVII with hydrazine for the preparation of I.

Methyl 2-amino-2-deoxy-3-*O*-methyl-β-D-glucopyranoside (VII) was prepared by starting with XV. Methyl 2-acetamido-2-deoxy-3-*O*-methyl-β-D-glucopyranoside (XX) obtained from XV by the method of Roth et al.[7] was treated with hydrazine to give VII. Fujinaga and Matsushima[9] have recently reported that XX can be converted to VII with hydrazine in a low yield; it has been found that the yield of VII can be successfully increased by raising the reaction temperature to about 130°C.

The mixture of α- and β-anomers (VIII and IX) of methyl 2-amino-2-deoxy-D-glucopyranoside was prepared by the route of Irvine et al.[10] However, as an alternative synthesis, the above mixture has been successfully prepared by a direct Fischer method, only raising the reaction temperature to about 150°C. The anomers could be separated by the method of Austin et al.[11] with resin column chromatography using Dowex 1×2. The separation patterns of anomers in the resin chromatography of the two mixtures were nearly the same, giving two clear-cut peaks. The anomers obtained from the both mixtures were proved to be identical in their physical properties.[12]

8) M. Fujinaga and Y. Matsushima, This Bulletin, **37**, 468 (1964).

9) M. Fujinaga and Y. Matsushima, at the 18th Annual Meeting of the Chemical Society of Japan, Osaka, April, 1965.

10) J. C. Irvine, D. McNicoll and A. Hynd, *J. Chem. Soc.*, **99**, 250 (1911).

11) P. W. Austin, F. E. Hardy, J. G. Buchanan and J. Baddiley, ibid., **1963**, 5350.

12) Recently we learned of another method for the preparation of VIII and IX using Amberlite IR-120 (Y. Matsushima and T. Miyazaki, This Bulletin, **38**, 1325 (1965)).

Experimental

The Preparation of Copper Solutions.—Cupra B: This was prepared by the method of Reeves.[1b] CuAm (cuprous chloride in aqueous ammonia): Cuprous chloride (1.60 g.) was dissolved in 15 N ammonia (100 ml.) at 15°C. TACu (tetramminecopper-(II) sulfate solution): Tetramminecopper(II) sulfate ($[Cu(NH_3)_4]SO_4 \cdot H_2O$) (3.95 g.) was dissolved in fresh distilled water (100 ml.).

The Determination of Optical Rotations.—A sample (0.1 mmol.) was dissolved in each of the above-mentioned three copper solutions (10 ml.), placed in a usual optical cell (10 cm. in length, 1—2 ml.), and the optical rotation at 436 mμ was measured at 15°C by the method of symmetrical angles using a Hitachi EPU-2 spectrophotometer coupled with a Hitachi A-2 polarimeter. An aqueous solution of the same sample was prepared, and the optical rotations at 436 and 589 mμ were also measured.

Thin Layer Chromatography and Silica Gel Column Chromatography.—Thin layer chromatography was conducted by the use of silica gel (Daiichi Pure Chemicals Co.); the prepared plate was activated at 110°C and then stored in a desiccator. Coloration was performed with concentrated sulfuric acid or 0.25% ninhydrin in pyridine. Solvent systems used: benzene-ethyl acetate-acetone (1 : 1 : 1) (Solvent I) and benzene-methanol-acetone (1 : 1 : 8) (Solvent II). Silica gel column chromatography was carried out by the use of silica gel (Kanto Chemical Co.) and was activated at 110°C before use.

Methyl 2-Acetamido-4, 6-*O*-benzylidene-3-*O*-benzoyl-2-deoxy-β-D-glucopyranoside (XV′).—According to the procedure used for the preparation of the corresponding α-anomer by Jeanloz,[13] XV′ was prepared from XV in a 60% yield; m. p. 292—294°C, $[\alpha]_{589}^{15}$ −97° (*c* 0.5, chloroform).

Found: C, 64.66; H, 5.89; N, 3.14. Cacld. for $C_{23}H_{25}O_7N$: C, 64.62; H, 5.90; N, 3.28%.

Methyl 2-Acetamido-3-*O*-benzoyl-2-deoxy-β-D-glucopyranoside (XVI).—A mixture of XV′ (380 mg.) and glacial acetic acid (14 ml.) was heated to 80°C, and to this mixture water (9.7 ml.) was added portion by portion. After 30 min. of heating at the same temperature, the mixture was cooled and evaporated to dryness under reduced pressure. To the residue water was again added, and it was again evaporated to dryness; this treatment was thrice repeated. To the residue toluene (3 ml.) was then added and the mixture was evaporated; this treatment was thrice repeated. Finally, the toluene solution was filtered and, after the removal of the solvent, petroleum ether was added to afford crystals of XVI; m. p. 100—102°C (decomp.), $[\alpha]_{589}^{15}$ −47° (*c* 0.5, chloroform).

Found: C, 56.30; H, 6.39. Calcd. for $C_{16}H_{21}O_7N$: C, 56.63; H, 6.24%.

Methyl 2-Acetamido-3-*O*-benzoyl-2-deoxy-4, 6-di-*O*-methyl-β-D-glucopyranoside (XVII), Methyl 2-Acetamido-3-*O*-benzoyl-2-deoxy-6-*O*-methyl-β-D-glucopyranoside (XVIII) and Methyl 3-*O*-Benzoyl-2-

13) The derivative XV′ had been isolated as a minor product from a reaction mixture obtained from methyl 2-acetamido-4, 6-*O*-benzylidene-2-deoxy-α-D-glucopyranoside (R. W. Jeanloz, *J. Am. Chem. Soc.*, **76**, 555 (1954)); reported m. p. 293—295°C, $[\alpha]_D$ −102±2° (*c* 0.73, chloroform).

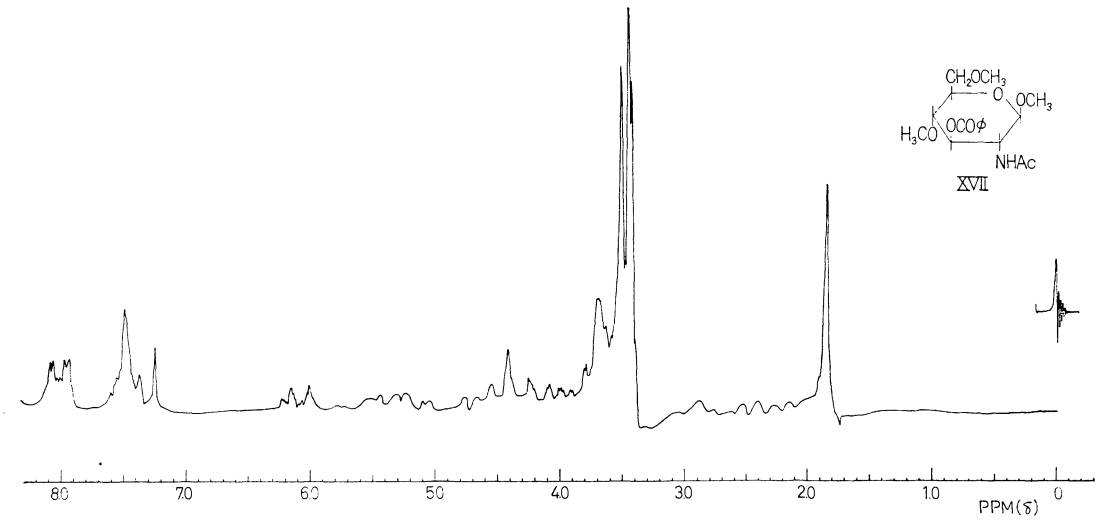

Fig. 2-A. The NMR spectrum at 60 Mc.p.s. of methyl 2-acetamido-3-*O*-benzoyl-2-deoxy-4, 6-di-*O*-methyl-β-D-glucopyranoside (XVII) in deuteriochloroform.

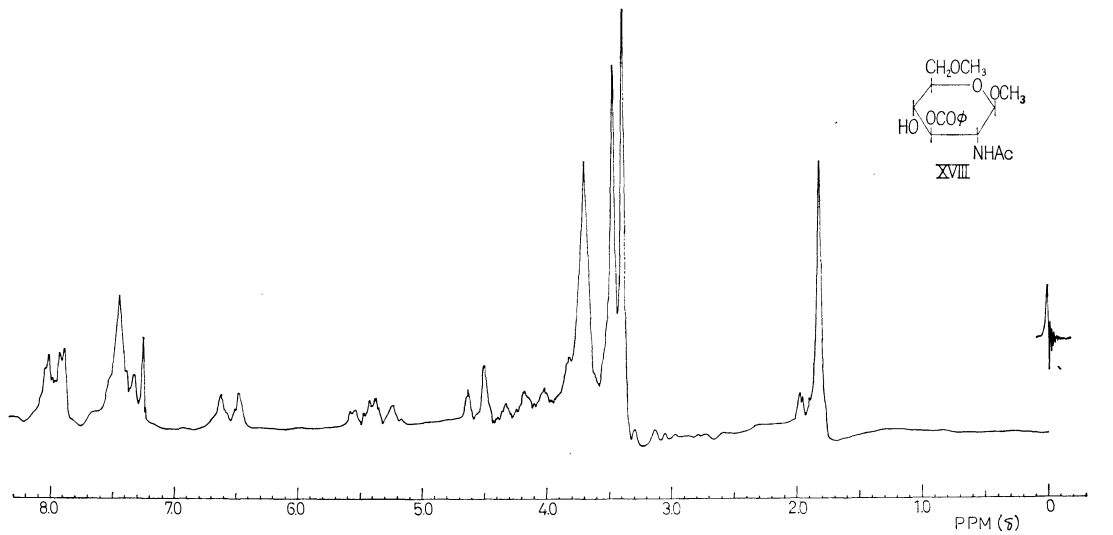

Fig. 2-B. The NMR spectrum at 60 Mc.p.s. of methyl 2-acetamido-3-*O*-benzoyl-2-deoxy-6-*O*-methyl-β-D-glucopyranoside (XVIII) in deuteriochloroform.

deoxy-4, 6-di-*O*-methyl-2-(*N*-methylacetamido)-β-D-glucopyranoside (XIX).—A mixture of methyl 2-acetamido-3-*O*-benzoyl-2-deoxy-β-D-glucopyranoside (XVI) (300 mg.), silver oxide (1.2 g.), methyl iodide (0.9 g.), Drierite (anhydrous calcium sulfate) (0.9 g.) and dry acetone (3 ml.) was placed in a thick, tightly-capped glass tube and agitated vigorously for 6 hr. at room temperature with an eccentrically-rotating stirrer.*2 After filtration, the precipitate was washed with acetone, and the combination of the filtrate and the washings was evaporated to dryness, giving 330 mg. of a solid. In thin layer chromatography with solvent I, the solid was proved to be composed of three components with R_f values of 0.42, 0.58 and 0.90 (minor spot). The solid was dissolved in a solvent mixture of benzene-ethyl acetate-acetone (1 : 1 : 1) and chromatographed on a silica gel column (48×130 mm.) with the same solvent. Every fraction (11 g.) was tested by thin layer chromatography. Substances with R_f values of 0.58 and 0.42 appeared in the fractions of tubes Nos. 16—19 and 22—27 respectively. The former fractions were collected and evaporated to give a residue which crystallized from chloroform, thus affording XVII, 130 mg.; m. p. 167—169°C, $[\alpha]_{589}^{15}$ −11.1° (*c* 0.9, methanol); IR spectrum (KBr disk): 3305 (νNH, sharp), 2940, 2850, 1735 (ester), 1665 (Amide I), 1565 (Amide II), 1455, 1378 cm^{-1}.

Found: C, 58.92; H, 6.85; N, 3.82. Calcd. for $C_{18}H_{25}O_7N$: C, 58.84; H, 6.86; N, 3.81%.

*2 A "Flash Mixer" (Mitamura Riken Kogyo Co.) with an eccentric radius of 1 mm. was used at 2000 r. p. m.

From the latter fractions, XVIII was obtained in the way described above; yield, 115 mg. (hygroscopic); m. p. 179—181°C (sintered once at 75—85°C), $[\alpha]_{589}^{15}$ +17.7° (*c* 1.2, methanol); IR spectrum (KBr disk): 3340, 2920, 2830, 1725, 1660, 1550, 1450, 1375 cm^{-1}.

Found: C, 54.89; H, 6.72; N, 3.74. Calcd. for $C_{17}H_{23}O_7N \cdot H_2O$: C, 54.98; H, 6.79; N, 3.77%.

When the above agitaion with an eccentrically-rotating stirrer was continued for 20 hr., the resulting crude product was composed of two components, R_f 0.59 and 0.90 (minor component). On a silica gel chromatography on the scale described above, the eluted fractions of tubes Nos. 16—21 and 10—12 gave 180 mg. of XVII and 30 mg. of XIX respectively.

When the above agitation was continued for 45 hr., the yield of XIX was increased to 67 mg., ($[\alpha]_{585}^{15}$ −10.5° (*c* 1, methanol); IR spectrum (KBr disk): 2930, 2900, 2830, 1730 (ester), 1690 (Amide I), 1455, 1380 cm^{-1}). No absorption bands corresponding to νNH (~3300) and δNH (~1550, Amide II) were observed, indicating that XIX is a *N*-methylated product.

Found: C, 59.60; H, 6.88; N, 3.54. Calcd. for $C_{19}H_{27}O_7N$: C, 59.83; H, 7.13; N, 3.67%.

The NMR spectra of compounds XVII and XVIII were determined in deuteriochloroform at a frequency of 60 Mc. p. s. with a Varian A60 spectrometer (Fig. 2). Tetramethylsilane was used as an internal reference. The comparison of the relative strength of the peaks at ~6.5 τ (methyl protons of methoxyl groups) with the other peaks [acetoxyl protons at ~8.2 τ, anomeric protons (3.91 τ for XVII and 3.45 τ for XVIII), and aromatic protons] revealed that XVII and XVIII have three and two methoxyl groups respectively.

Methyl 2-Amino-2-deoxy-4, 6-di-*O*-methyl-β-D-glucopyranoside Hydrochloride (I).—A mixture of XVII (60 mg.) and hydrazine hydrate*3 (0.9 ml.) in a sealed tube was heated in a boiling water bath for 17 hr. After the hydrazine had been removed in vacuo, the residue was dissolved in a mixture of benzene-methanol-acetone (1 : 1 : 8) and chromatographed on a silica gel column (27×70 mm.) with the same solvent. A ninhydrin active product was eluted between 40—120 ml. This fraction was evaporated to dryness; the aqueous solution of the residue was passed through a small column of Dowex 1×2 (OH form), and the ninhydrin-active portion was again collected and evaporated to dryness. The residue was dissolved in chloroform and dried over sodium sulfate, and, after filtration, the filtrate was evaporated to dryness. The residue was again dissolved in water, neutralized with hydrochloric acid, treated with active charcoal, and evaporated to give a solid which was crystallized from methanol by adding acetone; yield, 23 mg.; m. p. 203—204°C (decomp.), $[\alpha]_{589}^{15}$ −2.0° (*c* 0.3, water); IR spectrum (KBr disk): 3320, 2900, 1600 ($\delta_{as}NH_3^+$), 1500 (δ_s NH_3^+), 1450, 1400—1370 (3 bands) cm^{-1}.

Found: C, 41.71; H, 7.61; N, 5.41. Calcd. for $C_9H_{19}O_5N \cdot HCl$: C, 41.94; H, 7.81; N, 5.44%.

On thin layer chromatography with solvent II, I showed an R_f of 0.54. To an aqueous solution (2.6 ml.) of the hydrochloride (I) (2.6 mg.) periodic acid (9.1 mg.), was added, and the mixture was allowed to stand at room temperature for 20 hr. A drop of the solution was then subjected to thin layer chromatography. No spot corresponding to I was discerned.

Methyl 2-Amino-2-deoxy-6-*O*-methyl-β-D-glucopyranoside Hydrochloride (II).—A mixture of XVIII (110 mg.) and hydrazine hydrate (1.6 ml.) was treated for 60 hr. as above. The thin layer chromatography of the crude product showed an R_f value of 0.32 with solvent II. Isolation and purification was carried out in the same way as described in the above synthesis of I; yield, 39 mg. (hygroscopic), $[\alpha]_{589}^{15}$ −4.0° (*c* 0.5, water); IR spectrum (KBr disk): ~3300, 2900, 1600, 1510, 1450, 1400—1380 (2 bands) cm^{-1}.

Found: C, 39.62; H, 7.41. Calcd. for $C_8H_{17}O_5N \cdot HCl$: C, 39.43; H, 7.45%.

Methyl 2-Acetamido-2-deoxy-4, 6-di-*O*-methyl-β-D-glucopyranoside (VI).—A mixture of XVII (150 mg.) and hydrazine hydrate (2.3 ml.) in a sealed tube was heated in a boiling water bath for 1.5 hr. The removal of the solvent in vacuo left a solid which, on thin layer chromatography with solvent II, showed a single spot (R_f 0.7). The solid was then dissolved in the same solvent system and chromatographed on a silica gel column (27×200 mm.) with the same solvent. An eluate between 50—80 ml. was evaporated to dryness, and the residue was dissolved in ethanol. The solution was treated with active charcoal and concentrated to a small volume, from which crystals of VI was obtained by the addition of ether; yield, 75 mg.; m. p. 177—179°C (decomp.), $[\alpha]_{589}^{15}$ −23.3° (*c* 0.9, water); IR spectrum (KBr disk): 3500—3400, 3270, 2920, 2820, 1650 (Amide I), 1565 (Amide II), 1450, 1375 cm^{-1}.

Found: C, 50.44; H, 7.74; N, 5.20. Calcd. for $C_{11}H_{21}O_6N$: C, 50.18; H, 8.04; N, 5.32%.

Methyl 2-Deoxy-4, 6-di-*O*-methyl-2-methylamino-β-D-glucopyranoside Hydrochloride (III).—A mixture of XIX (90 mg.) and hydrazine hydrate (1.4 ml.) in a sealed tube was heated in a boiling water bath for 22 hr. The removal of the solvent in vacuo left a solid which, on thin layer chromatography with solvent II, showed a single spot (R_f 0.52).

The solid was then dissolved in the same solvent system and chromatographed on a silica gel column (27×90 mm.) with the same solvent. An eluate between 50—110 ml. was evaporated, and the residue was treated in the way described in the synthesis of I; yield, 39 mg. (hygroscopic); $[\alpha]_{589}^{15}$ −1.1° (*c* 0.5, water); IR spectrum (KBr disk): 3350, 2900, 1600 (δ_{as} NH_3^+), 1505 (δ_s NH_3^+), 1455, 1405 cm^{-1}.

Found: C, 43.81; H, 8.03. Calcd. for $C_{10}H_{21}O_5N \cdot HCl$: C, 44.19; H, 8.16%.

Methyl 2-Amino-2-deoxy-3-*O*-methyl-β-D-glucopyranoside Hydrochloride (VII).—A mixture of methyl 2-acetamido-2-deoxy-3-*O*-methyl-β-D-glucopyranoside*4 (XX) (83 mg.) and hydrazine hydrate (2 ml.) in a sealed tube was heated at 130°C for 40 hr. The removal of the solvent in vacuo left an solid which, on thin layer chromatography with solvent II, showed a single spot (R_f 0.38). (XX showed an R_f of 0.54 with solvent II.) The solid was then dissolved in a mixture of benzene, methanol and acetone (1 : 1 : 8); the mixture was chromatographed on a sillica gel column (27×88 mm.) with the same solvent. An eluate (between 40—100 ml.) was evaporated, and the residue was treated

*3 Commercial hydrazine hydrate (80%) was fractionally distilled; the fraction constant at 119°C was taken for use.

*4 M. p. 221—222°C (decomp.) (lit.[7] m. p. 229°C); $[\alpha]_{589}^{15}$ −46.2°, $[\alpha]_{436}^{15}$ −85.3° (*c* 0.6, water) (lit.,[7] $[\alpha]_D$ −45.9°); Found: C, 48.04; H, 7.57. Calcd. for $C_{10}H_{19}O_6N$: C, 48.17; H, 7.70%.

in the way described in the synthesis of I; yield, 55 mg. (70%). A sample (11 mg.) was recrystallized from ethanol to yield 9 mg. of an analytically-pure sample of VII; m. p. 139—140°C (decomp.). $[\alpha]_{589}^{15}$ +10.3° (*c* 0.3, water); IR spectrum (KBr disk): 3370, 2920, 1600 (δ_{as} NH_3^+), 1500 (δ_s NH_3^+), 1450, 1395 cm^{-1}.

Found: C, 39.54; H, 7.39; N, 5.68. Calcd. for $C_8H_{17}O_5N \cdot HCl$: C, 39.43; H, 7.45; N, 5.75%.

Methyl 2-Amino-2-deoxy-α- and -β-D-glucopyranoside Hydrochloride (VIII and IX).—A mixture of 2-amino-2-deoxy-D-glucose hydrochloride (215 mg.) and 2 N hydrochloric acid in methanol (5 ml.) was placed in a sealed glass tube and heated at 150°C for 4 hr. The resulting solution was evaporated to give a brown syrup, which was then dissolved in water and passed through a small column of Dowex 1×2 (OH form). This solution, after having been treated with active charcoal, was then evaporated to give a syrup; this syrup was then applied to a column (18×270 mm.) of Dowex 1×2 (OH form), and elution was carried out with water. Methyl 2-amino-2-deoxy-α-D-glucopyranoside and methyl 2-amino-2-deoxy-β-D-glucopyranoside emerged in the eluates between 63—69 ml. and between 75—84 ml. respectively. The former fraction was collected, concentrated to a small volume, and neutralized with hydrochloric acid. After evaporation to dryness, the solid obtained was recrystallized from ethanol to give 34 mg. of VIII, m. p. 189°C (decomp.)*5 $[\alpha]_{589}^{15}$ +153° (*c* 0.23, water)*5.

Found: C, 36.78; H, 7.23; N, 5.95. Calcd. for $C_7H_{15}O_5N \cdot HCl$: C, 36.61; H, 7.02; N, 6.10%.

From the latter fraction, by the same procedure as above, IX was obtained, 36 mg., m. p. 188°C (decomp.)*6 $[\alpha]_{589}^{15}$ −20° (*c* 0.23, water)*6.

Found: C, 36.72; H, 7.01; N, 6.14. Calcd. for $C_7H_{15}O_5N \cdot HCl$: C, 36.61; H, 7.02; N, 6.10%.

Methyl 2-Acetamido-2-deoxy-α- and -β-D-glucopyranoside (IV and V).—To an aqueous ethanol (7 : 3) solution of the hydrochloride VIII (1.0 g.), acetic anhydride and powdered barium hydroxide octahydrate were added alternately until the solution became negative to a ninhydrin test; then a little excess of sulfuric acid was added and the mixture was filtered. The filtrate was treated with Dowex 2×8 (OH form) and, after the solvent had been removed, the residue was recrystallized from ethanol to give 680 mg. of IV, m. p. 187—188°C*7 $[\alpha]_{589}^{15}$ +103° (*c* 0.3, water); IR spectrum (KBr disk): 3370, 3300, 2920, 2860, 1655 (Amide I), 1550 (Amide II), 1445, 1375, 900 (Type 1 of pyranose ring), 853 (Type 2a) cm^{-1}.

Found: C, 46.18; H, 7.23; N, 5.87. Calcd. for $C_9H_{17}O_6N$: C, 45.95; H, 7.28; N, 5.95%.

The β-anomer (V) was also prepared from IX (1.0 g.) in the same way as above; yield, 610 mg.; m. p. 199—200°C,*8 $[\alpha]_{589}^{15}$ −48° (*c* 0.3, water);*8 IR spectrum (KBr disk): 3400, 3300, 2930, 2880, 1650 (Amide I), 1555 (Amide II), 1450, 1380, 940 (Type 1 of pyranose ring), 859 (Type 2b) cm^{-1}.

Found: C, 45.94; H, 7.24; N, 5.90. Calcd. for $C_9H_{17}O_6N$: C, 45.95; H, 7.28; N, 5.95%.

***d*- and *l*-*trans*-2-Aminocyclohexanol Hydrochloride (XIII and XIV).**—To an aqueous solution of *d*-*trans*-2-aminocyclohexanol L-(+)-tartrate (200 mg.), 10 ml. of Amberlite IRA-400 (OH form) was added. After filtration, the filtrate was concentrated to a small volume and neutralized with hydrochloric acid. The addition of acetone gave crystals of XIII; yield, 80 mg.; m. p. 157.5—158°C, $[\alpha]_{589}^{15}$ +41.7° (*c* 0.5 water); IR spectrum (KBr disk): 3435, 3330, 2990, 2920, 2840, 1975 (νNH_3^+), 1595 (δ_{as} NH_3^+), 1505 (δ_s NH_3^+), 1465, 1385, 1358 cm^{-1}.

Found: C, 47.63; H, 9.02; N, 9.08. Calcd. for $C_6H_{13}ON \cdot HCl$: C, 47.52; H, 9.31; N, 9.24%.

The hydrochloride (XIV) of the *l*-isomer was prepared from *l*-*trans*-2-aminocyclohexanol L-(+)-tartrate (200 mg.); yield, 77 mg.; m. p. 157.5 −158°C, $[\alpha]_{589}^{15}$ −40.3° (*c* 0.5, water).

Found: C, 47.67; H, 9.17; N, 9.10. Calcd. for $C_6H_{13}ON \cdot HCl$: C, 47.52; H, 9.31; N, 9.24%.

Part of the expenses for this work were defrayed by a grant-in-aid for Scientific Research from the Ministry of Education, which grant is gratefully acknowledged. We are also indebted to Mr. Saburo Nakada of this Laboratory for his microanalysis. The authors also wish to thank Professor Tetsuo Suami of our Department for providing the sample of *d*- and *l*-*trans*-2-aminocyclohexanol.

*5 Reported m. p. 190—192°C, $[\alpha]_D$ +145° (Ref. 11).
*6 Reported m. p. 191—192°C, $[\alpha]_D$ −26° (Ref. 11).
*7 Reported m. p. 187—188°C (R. Kuhn, F. Zilliken and A. Gauhe, *Ber.*, **86**, 466 (1953)).
*8 Reported m. p. 190—191°C, $[\alpha]_D$ −42° (Ref. 7).

BULLETIN OF THE CHEMICAL SOCIETY OF JAPAN VOL. 39 1244—1248 (1966)

Studies of Aminosugars. XII. The Absolute Structure of Kanamycin as Determined by a Copper Complex Method*1

By Sumio UMEZAWA, Kuniaki TATSUTA and Tsutomu TSUCHIYA

Department of Applied Chemistry, Faculty of Engineering, Keio University, Koganei-shi, Tokyo

(Received October 23, 1965)

N, *N'*-Dimethyl-di-*O*-methyldeoxystreptamine has been prepared from kanamycin through the hydrolysis of the totally-methylated product of *O*-(3-acetamido-3-deoxy-α-D-glucopyranosyl)-*N*, *N'*-diacetyldeoxystreptamine. On the other hand, *N*, *N'*-dimethyl-4, 5, 6-tri-*O*-methyldeoxystreptamine has been prepared by hydrolysis of the totally-methylated product of *N*, *N'*-diacetyldeoxystreptamine. The shifts in molecular rotations of the both products have then been determined, with solutions of tetramminecopper(II) sulfate, ammoniacal cuprous chloride and Cupra B being substituted for water as the solvent. By the application of the generalizations described in the foregoing paper, it has been found that the former product includes a pair of adjacent methylamino and hydroxyl groups and that the projected angle between them is about +60°. These findings led to the conclusion that the free hydroxyl group in the former product is attached to the C-6 of deoxystreptamine, indicating that, in kanamycin, 6-amino-6-deoxy-α-D-glucosyl and 3-amino-3-deoxy-α-D-glucosyl moieties are attached to the C-4 and C-6 of deoxystreptamine respectively.

In earlier papers, we reported the results of the methylation[1] and partial hydrolysis studies[2] of kanamycin; thus the structure[1a] of kanamycin was deduced, with the reservation that the absolute sequence of the substitution of 3-amino-3-deoxy-D-glucose and 6-amino-6-deoxy-D-glucose at the C-4 and C-6 of deoxystreptamine remained undetermined.

Recently, Hichens and Rinehart[3] successfully applied the cuprammonium method of Reeves[4] to the investigation of the absolute structure of neomycins, paromomycins and kanamycins, by measuring the shift of the molecular rotation, $\Delta[M]_{\text{Cupra B}}$, of *N*, *N'*-diacetyl-6-*O*-methyldeoxystreptamine obtained from neomycin B and C and from paromomycin. Tatsuoka et al.[5] used the same method to elucidate the absolute configuration of kanamycin, measuring the $\Delta[M]_{\text{Cupra B}}$ of tri-*N*-acetyl-kanosaminyl-deoxystreptamine.

The work of Reeves, using "Cupra B," provides a tool for the determination of the stereochemical relationship between adjacent hydroxyl groups. In the preceding paper[6], the determination of $\Delta[M]_{\text{TACu}}$*2 has been introduced as a method for the revelation of the stereochemical relationship between adjacent amino and hydroxyl groups in a molecule of a six-membered chair form; this method involves measuring the shift in the opticalrotation when a tetramminecopper(II) sulfate solution (TACu) is substituted for water as the solvent.

The present report will describe the determination of the absolute structure of kanamycin by the use of TACu in addition to an ammoniacal cuprous chloride solution and "Cupra B." For this purpose, *N*, *N'*-dimethyl-di-*O*-methyldeoxystreptamine (IV) has been prepared, starting from kanamycin, by the route shown in Scheme I(1). Additionally, *N*, *N'*-dimethyl-tri-*O*-methyldeoxystreptamine (VII) has been prepared from deoxystreptamine as a reference substance (Scheme I (2)).

(1) Kanamycin → 6-*O*-(3-amino-3-deoxy-α-D-glucopyranosyl)-deoxystreptamine (I) → 6-*O*-(3-acetamido-3-deoxy-α-D-glucopyranosyl)-*N*, *N'*-diacetyl-deoxystreptamine (II) → 6-*O*-[3-deoxy-2, 4, 6-tri-*O*-methyl-3-(*N*-methylacetamido)-α-D-glucopyranosyl]-*N*,*N'*-diacetyl-*N*, *N'*-dimethyl-4, 5-di-*O*-methyl-deoxystreptamine (III) → *N*, *N'*-dimethyl-4, 5-di-*O*-methyl-deoxystreptamine (IV).

(2) Deoxystreptamine → *N*, *N'*-diacetyl-deoxystreptamine (V) → *N*,*N'*-diacetyl-*N*,*N'*-dimethyl-4, 5, 6-tri-*O*-methyldeoxystreptamine (VI) → *N*, *N'*-dimethyl-4, 5, 6-tri-*O*-methyl-deoxystreptamine (VII).

Scheme 1

*1 This constitutes Part XXV of a series entitled "Studies of Antibiotics and Related Substances," by Sumio Umezawa. A portion of this paper was presented at the 18th Annual Meeting of the Chemical Society of Japan, Osaka, April, 1965.

1) a) S. Umezawa, Y. Ito and S. Fukatsu, *J. Antibiotics*, **A11**, 120, 162 (1958); This Bulletin, **32**, 81 (1959); b) *J. Antibiotics*, **A12**, 187 (1959); S. Umezawa and Y. Ito, This Bulletin, **34**, 69 (1961).

2) S. Umezawa and T. Tsuchiya, *J. Antibiotics*, **A15**, 51 (1962).

3) M. Hichens and K. L. Rinehart, Jr., *J. Am. Chem. Soc.*, **85**, 1547 (1963).

4) R. E. Reeves, "Advances in Carbohydrate Chem.," Vol. 6, Academic Press, New York (1951), pp. 107—134.

5) S. Tatsuoka, S. Horii, K. L. Rinehart, Jr., and T. Nakabayashi, *J. Antibiotics*, **A17**, 88 (1964).

6) S. Umezawa, T. Tsuchiya and K. Tatsuta, This Bulletin, **39**, 1235 (1966).

*2 $\Delta[M]_{\text{TACu}} = ([\alpha]_{436}\ \text{TACu} - [\alpha]_{436}\ \text{water}) \times \frac{\text{Mol. wt.}}{100}$

TABLE I.

	$[\alpha]_{589}^{15}$	$[\alpha]_{438}^{15}$	$\Delta[M]_{TACu}$	$\Delta[M]_{CuAm}$	$\Delta[M]_{Cupra\ B}$
IV·2HCl	+14	+30	+1100	+1090	+1110
VII·2HCl	+3	+6	+1	+10	−9
II	+80	+154	+40	+1590	+1420*

* Reported $\Delta[M]_{Cupra\ B}$ +1380 by Tatsuoka et al. (Ref. 5).

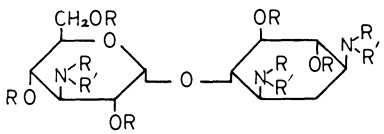

I : R=R'=H
II : R=H; R'=COCH$_3$
III : R=CH$_3$; R'=COCH$_3$

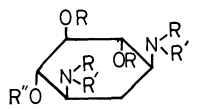

IV : R=CH$_3$; R'=R''=H
V : R=R''=H ; R'=COCH$_3$
VI : R=R''=CH$_3$; R'=COCH$_3$
VII R=R''=CH$_3$; R'=H

The three kinds of $\Delta[M]$ values for IV measured in TACu, CuAm and Cupra B were all approximately +1100, while those for VII were approximately zero, indicating that no complexing occurs between two methylamino groups of the deoxystreptamine moiety VII (Table I). These results, when subjected to the generalizations described in the preceding paper[6], led to the conclusion that the projected angle*3 between adjacent methylamino and hydroxyl groups is about +60° in the molecule of IV, that is, that IV is *N*, *N'*-dimethyl-4, 5-di-*O*-methyldeoxystreptamine; thus, kanamycin is deduced to be 4-*O*-(6-amino-6-deoxy-α-D-glucopyranosyl)-6-*O*-(3-amino-3-deoxy-α-D-glucopyranosyl)-deoxystreptamine. This accords with the results obtained by the above-mentioned authors.[3,5] If IV were 5, 6-di-*O*-methyl isomer instead of the substance mentioned above, the $\Delta[M]_{TACu}$ value would be about −1000.

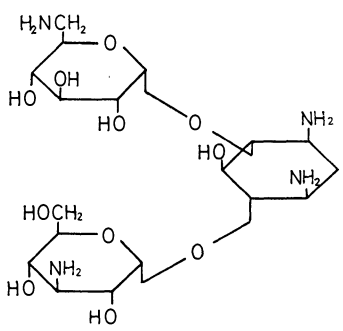

Kanamycin

The three $\Delta[M]$ values for II have also been measured to give an additional proof of the above structure assignment of kanamycin (Table I).

6-*O*-(3-Amino-3-deoxy-α-D-glucopyranosyl)-deoxystreptamine (I), which was first isolated by Maeda et al.,[7] was prepared by the hydrolysis of kanamycin with 3 N hydrochloric acid, heating them at about 100°C for one hour, followed by column chromatography using active carbon and Dowex 1×2; this procedure gave a high yield of I.

The acetylation of I has been effected by the use of acetic anhydride and barium hydroxide, thus giving II. The acetylation of deoxystreptamine briefly run in methanolic acetic anhydride gave V.

As to the methylation of II and V, a modified Purdie method was used; the methylation was effected in a sealed tube at 75—80°C. It has been found that the methylation of acetamino groups was performed as well as that of hydroxyl groups, affording III and VI respectively. This was proved by the determination of the infrared and NMR spectra; after the methylation, the absorption band at 1550 cm^{-1} (Amide II) observed in the infrared spectra of II and V disappeared in those of IV and VII respectively, while, in the NMR spectra of IV and VII, signals for *N*-methyl groups (~7.5τ) were clearly discerned (Fig. 1).

The hydrolysis of III and VI has been carried out in dilute hydrochloric acid, with the application of heat, giving IV and VII respectively.

Experimental

The preparation of a tetramminecopper(II) sulfate solution (TACu) and of cuprous chloride in 15 N aqueous ammonia (CuAm), and the determination of optical rotation were carried out as described in the preceding paper.[6] Paper chromatography was conducted by the descending technique on Toyo filter paper No. 50, and the locations of the substances on the papergrams were established by 0.25% ninhydrin in pyridine. Thin layer chromatography was carried out as described in the preceding paper, and the coloration of substances bearing amino groups was performed with concentrated sulfuric acid or 0.25% ninhydrin in pyridine.

6-*O*-(3-Amino-3-deoxy-α-D-glucopyranosyl)-deoxystreptamine (I).—A solution of a kanamycin base (10 g.) in 3 N hydrochloric acid (150 ml.) was heated in a boiling water bath for 1 hr. and then evaporated under reduced pressure. The resulting syrup was refluxed for 30 min. with dry methanol (500 ml.)

*3 See footnote of Ref. 6.

7) K. Maeda, M. Murase, H. Mawatari and H. Umezawa, *J. Antibiotics*, **A11**, 163 (1958).

containing dry hydrogen chloride (10 g.). By this procedure, aminosugars were converted to their glucosides; this was confirmed by paper chromatography. After the solution had been cooled, dry hydrogen chloride (100 g.) was gradually introduced, with the temperature kept at about −10°C, to precipitate a white solid. This solid was collected, washed with cold methanol and dried (8.5 g.). This was proved by paper chromatography to be composed of approximately equal amounts of I and deoxystreptamine, accompanied by 4-*O*-(6-amino-6-deoxy-α-D-glucopyranosyl)-deoxystreptamine (6AD) (minor product) and unchanged kanamycin. The filtrate contained deoxystreptamine, methyl 3-amino-3-deoxy-D-glucoside[8] and methyl 6-amino-6-deoxy-D-glucoside.[8] The solid (8.5 g.) was dissolved in a small quantity of water, placed on a column containing 100 g. of carbon (Wako Pure Chemical Industries, 70—150 mesh, activated at 120°C before use), and developed with water. After an initial portion (600 ml., ninhydrin negative) had been removed, the eluate was cut into 10 g. fractions; deoxystreptamine, 1, 6AD and kanamycin were then eluted in the fractions Nos. 4—18, 16—28, 27—50 and 45—63 respectively. The eluate of Nos. 16—28 was evaporated and dried (3.5 g.). An aqueous solution of the residue was passed through a column of Dowex 1×2 (OH form, 29×500 mm.) and eluted with water. After a small amount of deoxystreptamine had been eluted, the free base of I emerged in a 110—300 ml. portion. This was concentrated to a small volume and neutralized with hydrochloric acid; from the resulting solution, trihydrochloride of I was crystallized by adding methanol and ethanol. Yield, 2.8 g. (31%), m. p. 235—236°C (decomp.) (lit.,[7] 219—219.5°C (decomp.)), $[\alpha]_{589}^{13}$ +75.1°, $[\alpha]_{438}^{13}$ +140.6° (*c* 1.3, water) (lit.,[7] $[\alpha]_{D}^{28}$ +76.1°).

Found: C, 33.43; H, 6.66. Calcd. for $C_{12}H_{25}N_3O_7 \cdot 3HCl$: C, 33.31; H, 6.51%.

6-*O*-(3-Acetamido-3-deoxy-α-D-glucopyranosyl)-*N*, *N*'-diacetyl-deoxystreptamine (II). — Trihydrochloride (500 mg.) of I suspended in aqueous ethanol (7 : 3) was acetylated with acetic anhydride and barium hydroxide. After the solvent had been removed in vacuo, the residue was extracted with ethanol and then evaporated. An aqueous solution of the residue (708 mg.) was treated with Amberlite IRA-400 (OH form) and Amberlite IR-120 (H form) successively. After the solvent had been removed, the residue was crystallized from its methanol solution (1.5 ml.) by adding acetone (5 ml.); it gave 450 mg. of II, which was proved to be pure on thin layer chromatography (R_f, 0.29)*4 with a solvent system of *n*-butanol - pyridine - water - acetic acid (6 : 4 : 3 : 1). A pure sample of II had a m. p. of 238—242°C (decomp.) (lit., m. p. 235—242°C,[5] 176—181°C[9] (decomp.)), $[\alpha]_{589}^{12}$ +80° (*c* 0.45, water) (lit.,[5] $[\alpha]_{D}^{27}$ +72°); IR spectrum (KBr disk): ~3400, 1645 (Amide I), 1557 (Amide II), 1415, 1375 cm^{-1}.

Found: C, 47.16; H, 6.71; N, 8.72. Calcd. for $C_{18}H_{31}N_3O_{10} \cdot 1/2H_2O$: C, 47.16; H, 7.04; N, 9.16%.

6-*O*-(3-Deoxy-2,4,6-tri-*O*-methyl-3-*N*-methylacetamido-α-D-glucopyranosyl)-*N*, *N*'-diacetyl-*N*, *N*'-dimethyl-4, 5-di-*O*-methyl-deoxystreptamine (III). —In a 10 ml.-glass-pressure tube coupled with a pressure gauge there were placed methyl iodide (2.5 g.) and a thoroughly-ground mixture of II (200 mg.) and silver oxide (2.0 g.); the mixture was then heated at 75°C for 3 hr. At the end of this period, the inner pressure reached to 3 atm. After cooling, the whole content was extracted twice with methanol, and the extract was evaporated to dryness. The methylation was repeated several times. During the course of the reaction, in the infrared absorption spectra of the resulting products, the absorption bands at ~3400 cm^{-1} (OH) and ~1550 cm^{-1} (Amide II) gradually faded and those at ~2920 cm^{-1} and 1450 cm^{-1} became clearer, while the absorption at ~1640 cm^{-1} (Amide I) remained unchanged. The final product thus obtained was dissolved in chloroform, and, after filtration, the solution was evaporated to dryness. An aqueous solution of the residue was treated with active charcoal and then evaporated to give a white solid, 187 mg.; m. p. 98—100°C, $[\alpha]_{D}^{18}$ +94° (*c* 1, water). On thin layer chromatography with dioxane, the product showed a single spot with an R_f of 0.2. IR spectrum (KBr disk): 2920, 2815, 1640, 1450, 1410, 1375 cm^{-1}.

Found: C, 55.42; H, 8.47; N, 7.51. Calcd. for $C_{26}H_{47}O_{10}N_3$: C, 55.59; H, 8.43; N, 7.48%.

***N*, *N*'-Dimethyl-4, 5-di-*O*-methyldeoxystreptamine (IV).** — A sample of III (400 mg.) was dissolved in 3 N hydrochloric acid (20 ml.) in a sealed tube and then heated in a boiling water bath for 6 hr. After evaporation in vacuo, the syrup was deacidified by co-evaporation with water. A solution of the residue in a solvent system of *n*-butanol - pyridine - water - acetic acid (6 : 4 : 3 : 1) was chromatographed on a cellulose powder column (45×165 mm.) and eluted with the same solvent. Ninhydrin-active substances emerged in 100—120, 180—240 and 260—380 ml. portions. The last portion, which had no reducing property, was concentrated to a small volume and then again chromatographed through a Dowex 1×2 column (OH form, 8×320 mm.) with water. Ninhydrin-active fractions were collected and evaporated to dryness. The residue was dissolved in chloroform, and, after filtration, the solution was evaporated to dryness (140 mg.). The residue was dissolved in water, neutralized with hydrochloric acid, and evaporated to dryness to give a solid, which was then recrystallized from ethanol to give dihydrochloride of IV; yield, 120 mg.; m. p. 228—231°C (decomp.), $[\alpha]_{589}^{15}$ +13.6° (*c* 0.3 water); IR spectrum (KBr disk): 3360, 2940, 2825, 2740, 2440, 1585 (δNH_2^+), 1465, 1385, 1340 cm^{-1}.

Found: C, 41.00; H, 8.12; N, 9.37. Calcd. for $C_{10}H_{22}O_3N_2 \cdot 2HCl$: C, 41.24; H, 8.31; N, 9.62%.

The NMR spectrum of the base IV was determined at a frequency of 60 Mc.p.s. with a Varian A 60 spectrometer in deuteriochloroform, and also in the same solvent including a few drops of deuteroxide (Fig. 1). Tetramethylsilane was used as the internal reference.

***N*, *N*'-Diacetyldeoxystreptamine (V).**—A deoxystreptamine base (500 mg.) suspended in dry methanol (5 ml.) was vigorously stirred into acetic anhydride (1.3 ml.); the reaction was then continued for 3 hr.

8) H. Ogawa, T. Ito, S. Inoue and S. Kondo, ibid., **A11**, 70, 72 (1958).

*4 The free base I has an R_f value of 0.15 with the same solvent.

9) H. Ogawa, T. Ito, S. Kondo and S. Inoue, *J. Antibiotics*, **A11**, 169 (1958).

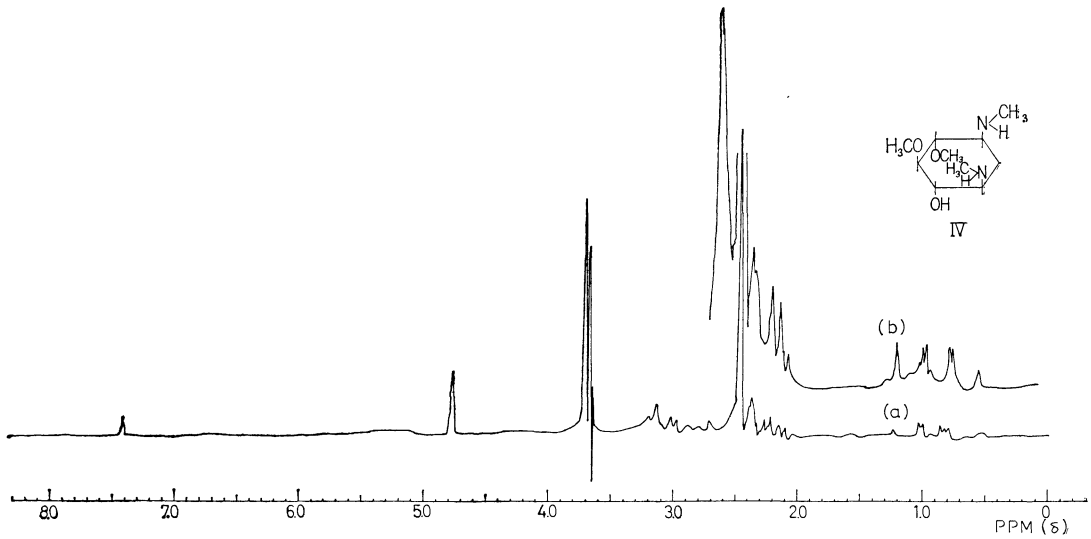

Fig. 1-A. The NMR spectra of *N*, *N'*-dimethyl-4, 5-di-*O*-methyldeoxystreptamine (IV); (a): in the mixture of $CDCl_3$ and a few drops of D_2O, (b): in $CDCl_3$.

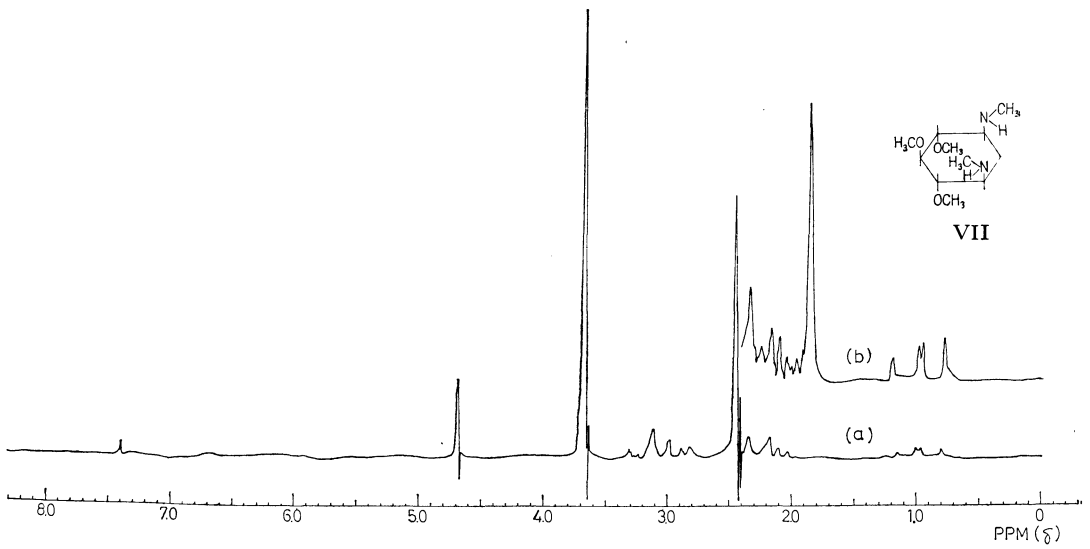

Fig. 1-B. The NMR spectra of *N*, *N'*-dimethyl-4, 5, 6-tri-*O*-methyldeoxystreptamine (VII); (a): in the mixture of $CDCl_3$ and a few drops of D_2O, (b): in $CDCl_3$.

The precipitate was filtered, washed with methanol, and then dissolved in water. To the solution, a small quantity of Amberlite IR-120 (H form) was added to remove the unchanged material; after filtration, the solution was concentrated to a small volume, and ethanol was added to cause crystallization. Yield, 570 mg.; m. p. 250°C (lit.,[10] 292—293°C); IR spectrum (KBr disk): 3450, 3340, 3300, 3120, 2900, 1650 (Amide I), 1580 (Amide II), 1445, 1417, 1385 cm^{-1}.

Found: C, 48.55; H, 7.28; N, 11.08. Calcd. for $C_{10}H_{18}O_5N_2$: C, 48.77; H, 7.37; N, 11.38%.

10) H. A. Luts, R. H. Sprague, M. Dickerson and L. C. Cheney, *J. Pharmaceutical Sciences*, **50**, 328 (1961).

N, N'-Diacetyl-N,N'-dimethyl-4, 5, 6-tri-O-methyldeoxystreptamine (VI).—In a 20 ml.-glass-pressure tube there were placed methyl iodide (7.0 g.) and a thoroughly-ground mixture of V (200 mg.) and silver oxide (7.0 g.); the mixture was then heated at 85°C for 5 hr. After cooling, the reaction mixture was evaporated. The residue was extracted thrice with water, and the combined extracts were evaporated to dryness. The methylation was repeated thrice more. The change in infrared spectra during the repeated methylation was substantially the same as that concerning III. The product was dissolved in chloroform, and, after filtration, the solution was evaporated to give a white solid, 209 mg.; m. p. 207—208°C (decomp.); IR spectrum (KBr disk): 2920,

2820, 1640 (Amide I), 1445, 1410, 1380 cm^{-1}.

Found: C, 56.94; H, 8.92; N, 8.85. Calcd. for $C_{15}H_{28}O_5N_2$: C, 56.73; H, 8.71; N, 8.70%.

***N*, *N'*-Dimethyl-4, 5, 6-tri-*O*-methyl-deoxystreptamine (VII).**—A solution of VI (400 mg.) in 2 N hydrochloric acid (20 ml.) was heated in a boiling water bath for 5 hr. and then concentrated under reduced pressure. The residual syrup was deacidified by co-evaporation with water. A solution of the residue in a small quantity of a solvent mixture of *n*-butanol - pyridine - water - acetic acid (6 : 4 : 3 : 1) was chromatographed on a cellulose powder column (45×250 mm.) with the same solvent, and each fraction (15 ml.) was tested by ninhydrin-coloration. Ninhydrin-active substances were eluted in Tubes Nos. 37—42 and Nos. 47—49. The former fractions were collected, evaporated, and dried. The residue (220 mg.) was dissolved in a small quantity of water and passed through a column of Dowex 1×2 (OH form, 8× 370 mm.) with water. The ninhydrin-active fractions were again collected and evaporated to dryness. The residue was dissolved in chloroform, and, after filtration, the solution was again evaporated to dryness. An aqueous solution of the residue was treated with active charcoal, neutralized with hydrochloric acid, and evaporated. Recrystallization from its methanol solution by adding acetone gave crystalline dihydrochloride of VII; yield, 155 mg.; m. p. 215—216°C (decomp.), $[\alpha]_{589}^{15}$ +3° (*c* 0.3, water). This has an R_{fIV}*5 value of 1.5 on paper chromatography with a solvent system of *t*-amylalcohol - pyridine - water - acetic acid (6 : 4 : 3 : 1). IR spectrum (KBr disk); 3380, 2940, 2820, 2720, 2450, 1610 (δNH_2^+), 1470, 1390 cm^{-1}.

Found: C, 43.19; H, 8.40; N, 8.97. Calcd. for $C_{11}H_{24}O_3N_2 \cdot 2HCl$: C, 43.28; H, 8.58; N, 9.18%.

The NMR spectrum of the base VII was determined as described in the procedure for IV (Fig. 1).

The authors are indebted to Mr. Saburo Nakada of this Laboratory for the microanalysis. This research was supported in part by a grant from the Microbial Chemistry Foundation, to which the authors' thanks are due.

*5 R_{fIV} is an R_f value relative to the R_f value of *N*, *N'*-dimethyl-4, 5-di-*O*-methyldeoxystreptamine (IV), the latter taken as 1.0.

BULLETIN OF THE CHEMICAL SOCIETY OF JAPAN VOL. 39 1248—1253 (1966)

A New Mode of the Formation of the Meso-ionic Pyrido[2, 1-b]-3, 4-dihydro-4-oxothiazole: An Attempted Preparation of Pyrido[2, 1-b]-3, 5-dihydro-5-oxothiazole[1-3]

By Hiroshi KATO, Kazuo TANAKA and Masaki OHTA

Laboratory of Organic Chemistry, Tokyo Institute of Technology, Ookayama, Meguro-ku, Tokyo

(Received October 27, 1965)

The acylation of 2-mercaptopyridine gives *S*-acyl derivatives, which, on treatment with chloroacetic acid, give the title compound.

The structure of the reaction product of (2-pyridylthio)acetic acid (I) and acetic anhydride was reinvestigated by Duffin and Kendall[4] and was shown to have a pyrido [2, 1-b]thiazole skeleton (II). This type of ring formation has since then been extended to many aza-heterocyclic systems with a mercapto group *ortho* to the ring nitrogen atom.[6-8]

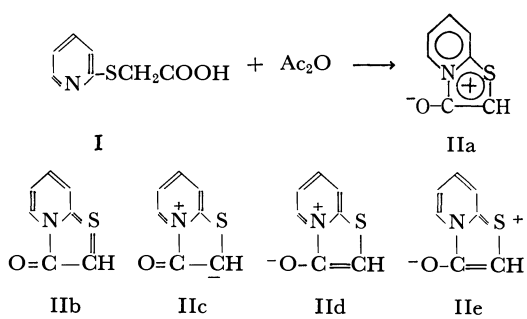

I IIa

IIb IIc IId IIe

Duffin and Kendall first[5] classified this type of compound as meso-ionic, but later[6] they abandoned this idea in favor of the structure IIb, in which the participation of the sulfur d-orbitals gives rise to a wholly covalently-bonded structure. In our opinion, however, though the structure

1) Studies on Meso-ionic Compounds. Part XXIV. Part XXIII: M. Ohta and C. Shin, This Bulletin, **38**, 1816 (1965).

2) For a preliminary communication, see H. Kato, K. Tanaka and M. Ohta, This Bulletin, **35**, 1901 (1962).

3) In this communication, we will use the symbol which was officially adopted by The Chemical Society (London) for meso-ionic compounds.[4] This, however, does not necessarily mean that we consider these compounds to exist in strongly polarized forms, as is suggested by the symbol. For a more detailed discussion, see M. Ohta and H. Kato, *J. Chem. Soc. Japan, Pure Chem. Sect.* (*Nippon Kagaku Zasshi*), **86**, 661 (1965).

4) W. Baker, *Proc. Chem. Soc.*, **1959**, 75.

5) G. F. Duffin and J. D. Kendall, *J. Chem. Soc.*, **1951**, 734.

6) G. F. Duffin and J. D. Kendall, ibid., **1956**, 361.

7) M. Hashimoto and M. Ohta, This Bulletin, **33**, 1394 (1960).

8) M. Ohta and K. Kishimoto, ibid., **34**, 1403 (1961).

IIb certainly would contribute to some degree to the resonance of this compound, other cannonical structures, such as IIc-e, would also be important participants in the resonance; therefore, we feel it more reasonable to assume the meso-ionic structure for this type of compound.

The present investigation was initiated with the idea of preparing a condensed ring system III, in which the positions of the CH and CO groups in the ring are reversed relative to the structure II. The preparation of such a ring system may be interesting because, for this ring system, no single satisfactory covalently-bonded structure can be devised, even if the sulfur d-orbitals are considered for the bonding. The preparation of such a ring system and comparison of its properties with those of the compound II would give a wealth of information concerning the evaluation of the degree of the contribution of the sulfur d-orbitals to the ring. Uncondensed ring system with the same arrangement of the atoms in the meso-ionic part of the ring as in III has been prepared by Lawson and others,[9] and has been found to be quite stable.

Results and Discussion

As a possible route toward a synthesis of III, we first tried the reaction of 2-mercaptopyridine with chloroacetyl chloride, anticipating the formation of an intermediate, IV. When this reaction was carried out in a dilute aqueous solution of sodium hydroxide, the reaction product was (2-pyridylthio)acetic acid (I). In order to avoid hydrolytic conditions, the same reaction in dry benzene was attempted; the crude reaction product was then treated immediately with acetic anhydride and sodium acetate. The reaction product isolated was compound II. From this result, it seems likely that the reaction first gave an *N*-acylated product (V), which then went through ring closure to give compound II.

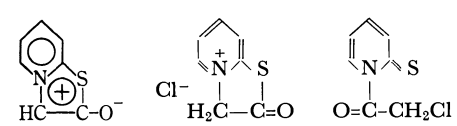

III IV V

VI

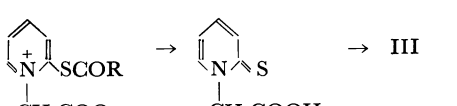

A similar reaction is reported by Goerdeler et al.,[10] who report that the acylation of thioamides with acyl chlorides gives *N*-acyl derivatives, or that the *S*-acyl derivatives first formed rearrange to give the *N*-acyl derivatives.

In order to secure the pyridine nitrogen atom as the only available position to an attack of chloroacetyl group, we tried to prepare III by the above-described series of reactions. 2-Acylthiopyridines (VI) were prepared by heating 2-mercaptopyridine with acetic anhydride, or by the treatment of sodium 2-pyridylmercaptide with acetyl or benzoyl chloride. Infrared absorptions of the acetylated compound at 1050, 652 and 768 cm^{-1} which have been assigned to a (C=O)S group,[11] the lack of absorptions of a non-aromatic double-bond system between 1600 and 1700 cm^{-1} (1620 and 1623 cm^{-1} have been reported for 2-thiopyridone and *N*-methyl-2-thiopyridone[12]); and a similar absorption pattern of the acetyl derivative to that of 2-methylthiopyridine[13] support the *S*-acetyl structure against the *N*-acetyl structure. Further, they are soluble in dilute hydrochloric acid, from which they can be recovered by rapid and careful neutralization. From this fact, it may be deduced that *S*-acylated 2-mercaptopyridines are not very sensitive to hydrolysis, but they are readily attacked by nucleophilic reagents; 2-acetylthiopyridine, for example, reacts rapidly at room temperature with aniline to form 2-mercaptopyridine and acetanilide. When 2-acetylthiopyridine was warmed with chloroacetic acid in benzene, an exothermic reaction took place to give a resinous product, the treatment of which with water or ethanol created a new precipitate which was identical with II. The same product, II, was formed by a similar reaction of 2-benzoylthiopyridine with chloroacetic acid. In this case, benzoic acid was also formed.

These results suggest a rapid reaction of 2-acylthiopyridines with chloroacetic acid to give (2-pyridylthio)acetyl acylates VIIa or chloride VIIb. To check this possibility, 2-acetylthiopyridine was warmed in benzene with ethyl chloroacetate. The reaction products were ethyl (2-pyridylthio)acetate (VIII) and acetyl chloride, the former being identified by conversion to (2-pyridylthio)acetic acid, and the latter, by conversion to acetanilide.

Of special interest would be the reaction of 2-acylthiopyridines with chloroacetamide, because,

9) A. Lawson and C. E. Searle, *J. Chem. Soc.*, **1957**, 1556; M. Ohta and C. Shin, This Bulletin, **38**, 704 (1965).

10) J. Goerdeler and K. Stadelbauer, *Chem. Ber.*, **98**, 1556 (1965), and the references cited therein.

11) R. Sasin, W. F. Aschley, J. W. Manning, Jr., A. Paolini, Jr., and G. S. Sasin, *J. Am. Oil Chemists Soc.*, **35**, 192 (1958).

12) A. R. Katritzky, "Physical Methods in Heterocyclic Chemistry," Vol. II, Academic Press, New York (1963), p. 259.

13) E. Spinner, *J. Chem. Soc.*, **1960**, 1237; Compare the strongest infrared absorptions of 2-methylthiopyridine at 1584, 1456, 1415, 1126 and 753 cm^{-1} with 1578, 1450, 1420, 1110 and 768 cm^{-1} of 2-acetylthiopyridine.

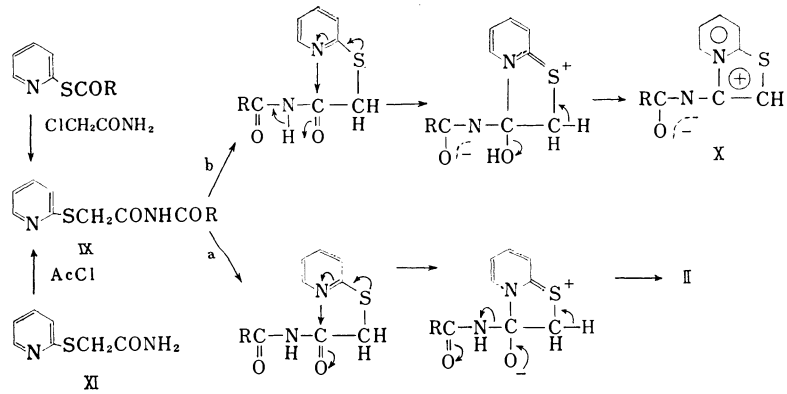

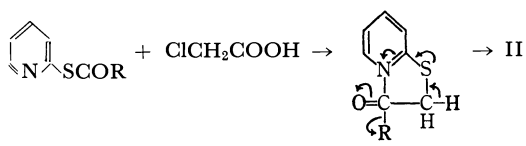

VIIa, R=$OCOCH_3$
VIIb, R=Cl

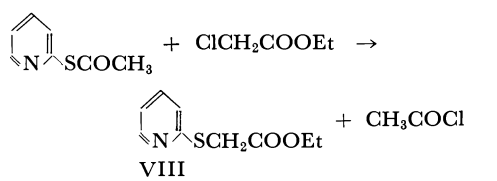

VIII

if a similar type of reaction takes place, it would give an *N*-acyl derivative IX, which would give either compound II by the removal of the acylimino group (route a) or a new meso-ionic compound, X, by dehydration (route b).[14] When 2-acetylthiopyridine was warmed in benzene with chloroacetamide, compound II was formed. The same compound, II, was formed from 2-benzoylthiopyridine. When (2-pyridylthio)acetamide (XI), prepared from 2-mercaptopyridine and chloroacetamide, was treated with acetyl chloride, the same compound, II, was again formed. It has been reported[5] that no reaction occurs upon the treatment of (2-quinolylthio)acetamide with acetic anhydride, though the corresponding anhydro base was formed when (2-quinolylthio)acetic acid was heated with acetic anhydride. This is probably due to an insufficient acylating power of an acid anhydride to give an *N*-acyl derivative, IX.

The foregoing reactions would, in principle, be the same as the reaction of (2-pyridylthio)-acetic acid with an equimolar amount of acyl chloride. This type of reaction was applied to 4-phenyl-2-mercaptothiazole and to 2-mercaptobenzothiazole. With the (thiazolylthio)acetic acids derived from these compounds, it has been reported[7] that the reaction with acetic anhydride always gives intractable red pigments of unknown structures instead of the corresponding meso-ionic rings. The treatment of 4-phenyl-2-mercaptothiazole with acetic anhydride gave the acetyl derivative (XIIa); this derivative, on being warmed with chloroacetic acid in benzene, gave the same pigment as that reported earlier[7] and a compound with the formula $C_{11}H_{11}ON_3S_2$ after recrystallization from ethanol. The latter compound gave a hydrazide with hydrazine hydrate and, on hydrolysis, gave (4-phenylthiazolyl-2-thio)acetic acid. The compound was identified as ethyl (4-phenylthiazolyl-2-thio)acetate (XIII) by comparison with a specimen which was prepared from 4-phenyl-2-mercaptothiazole and ethyl chloroacetate. The same amorphous pigment and benzoic acid were formed by the reaction of chloroacetic acid and 2-benzoylthio-4-phenylthiazole

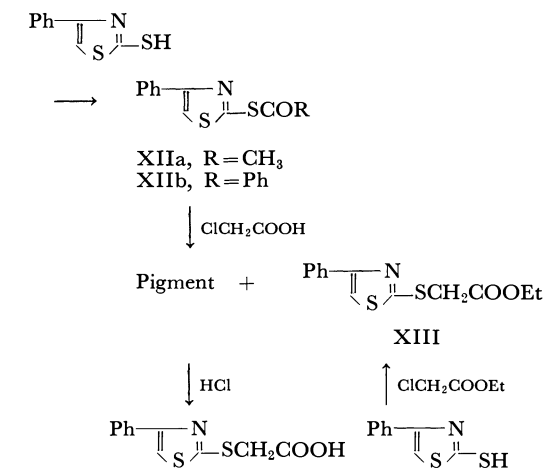

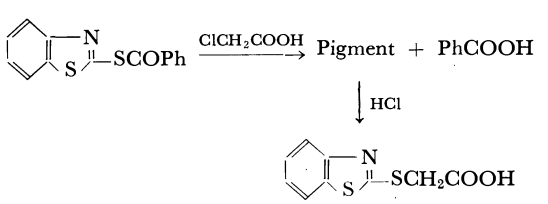

14) The preparation of this ring system will be the subject of the following paper.

(XIIb), which had been prepared from 4-phenyl-2-mercaptothiazole and benzoyl chloride. The pigment gave (4-phenylthiazolyl-2-thio)acetic acid (XIV) by acid hydrolysis. The fact that an identical substance was formed from both the *S*-acetyl and *S*-benzoyl derivatives shows that these acyl groups are absent in the reaction product; the actual structure of this product, however, still remains to be elucidated. When 2-benzoylthiobenzothiazole was treated with chloroacetic acid in benzene, a red pigment, with a quantitative amount of benzoic acid, and a small amount of 2-mercaptobenzothiazole were formed. The pigment was identical with the reaction product of (2-benzothiazolylthio)acetic acid and acetic anhydride.[7] The red pigment gave a small amount of (2-benzothiazolylthio)acetic acid by acid hydrolysis.

Experimental

All melting points were determined on a micro hot stage and are corrected. All boiling points are uncorrected. The infrared spectra were taken on a Nippon Bunko Spectrophotometer, Model S, equipped with an NaCl prism on KBr tablets, unless otherwise stated.

The Reaction of 2-Mercaptopyridine and Chloroacetyl Chloride.—a) To a solution of 2 g. of 2-mercaptopyridine and 1.4 g. of sodium hydroxide in 50 ml. of water, 4 g. of chloroacetyl chloride was added in one portion with cooling and vigorous stirring. The stirring was continued until the excess chloroacetyl chloride had been decomposed. The crystals which separated out were collected and were recrystallized from ethanol to give 2.3 g. of yellow crystals with a green fluorescence, m. p. 130°C. Recrystallization from ethanol raised the m. p. to 136—137°C. This substance is soluble in 5% aqueous sodium bicarbonate. The melting point of this substance was undepressed on admixture with an authentic specimen of (2-pyridylthio)acetic acid (I).

b) An aqueous solution of 2 g. of 2-mercaptopyridine and 0.8 g. of sodium hydroxide was concentrated to dryness under reduced pressure. Benzene was added to the residue, and to this suspension was added 2.2 g. of chloroacetyl chloride in one portion with cooling and stirring. After thirty minutes, the dark green precipitate was collected and then warmed on a water bath for thirty minutes with a mixture of acetic acid, acetic anhydride and anhydrous sodium acetate. The mixture was concentrated under reduced pressure, the residue was treated with ice water, and the greenish yellow precipitate was collected and recrystallized from ethanol to give 0.5 g. of yellow silky needles, m. p. 189°C, undepressed on admixture with an authentic specimen of pyrido[2,1-b]-3,4-dihydro-4-oxothiazole (II).

Found: C, 55.24; H, 3.60; N, 9.23. Calcd. for C_7H_5ONS (II): C, 55.63; H, 3.34; N, 9.27%.

2-Acetylthiopyridine (VI, R=CH_3).—a) A mixture of 14 g. of 2-mercaptopyridine and 26 ml. of acetic anhydride was refluxed for one hour. The excess acetic anhydride and acetic acid were then distilled off under reduced pressure, and the residual oil was distilled to give 13 g. of a yellow liquid, boiling at 96—99°C/3.5 mmHg.

Found: C, 54.56; H, 4.86; N, 9.30. Calcd. for C_7H_7ONS: C, 54.90; H, 4.61; N, 9.15%.

This substance is soluble in dilute hydrochloric acid. IR (liquid film); strong absorptions at 1708, 1578, 1450, 1420, 1350, 1110, 1050, 991, 952 and 768 cm^{-1}.

b) An aqueous solution of 0.8 g. of sodium hydroxide and 2.2 g. of 2-mercaptopyridine was concentrated to dryness under reduced pressure. The residue was suspended on benzene, and to this suspension was added 2 ml. of acetyl chloride under stirring and cooling. After an hour, water was added to this suspension, and the solution was neutralized with sodium bicarbonate. The benzene layer was separated, and the aqueous layer was extracted with ether. The combined extracts were dried over sodium sulfate and distilled under reduced pressure to give 2 g. of the same substance as that prepared by the preceding procedure.

2-Benzoylthiopyridine (VI, R=C_6H_5).—An aqueous solution of 4.1 g. of sodium hydroxide and 11.6 g. of 2-mercaptopyridine was concentrated to dryness under reduced pressure. The residue was suspended on dry benzene, and 15 g. of benzoyl chloride was stirred into this suspension with cooling. The newly-formed precipitate was filtered off, and the filtrate was distilled under reduced pressure to give 7.3 g. of a colorless liquid boiling at 171.6—172°C/3 mmHg; this liquid soon solidified to white needles, m. p. 44—45°C. This substance is soluble in dilute hydrochloric acid.

Found: C, 66.67; H, 4.39; N, 6.48. Calcd. for $C_{12}H_9ONS$: C, 66.97; H, 4.22; N, 6.51%.

The Reaction of 2-Acetylthiopyridine with Aniline.—To a solution of 1 g. of 2-acetylthiopyridine in 10 ml. of benzene, 1 ml. of aniline was added with cooling by an ice bath. After thirty minutes, benzene was removed by distillation under reduced pressure. The residual oil solidified upon the addition of petroleum ether. It was then washed with 5% hydrochloric acid, and the residue (0.7 g., m. p. 115°C) was recrystallized from water to give 0.4 g. of colorless leaflets, m. p. 116°C, undepressed on admixture with an authentic specimen of acetanilide.

The hydrochloric acid washings were neutralized with sodium bicarbonate and were extracted with chloroform. The chloroform extracts were dried over magnesium sulfate and concentrated, and the residue was recrystallized from benzene to give 0.2 g. of yellow prisms, melting at 129—130°C, undepressed on admixture with an authentic specimen of 2-mercaptopyridine.

The Reaction of 2-Acetylthiopyridine and Chloroacetic Acid.—To a solution of 0.5 g. of 2-acetylthiopyridine in dry benzene, 0.31 g. of chloroacetic acid was added; then the mixture was slightly warmed on a water bath. An exothermic reaction took place, and an oily substance separated out. After five minutes, the benzene layer was decanted and, on the addition of ethanol, the oily substance solidified to give a yellowish-green powder. This powder was collected by filtration, suspended on water, and neutralized with sodium bicarbonate. The yellow suspension which resulted was collected and recrystallized from ethanol to give 0.3 g. of yellow silky needles, melting at 181—183°C,

undepressed on admixture with an authentic specimen of pyrido[2, 1-b]-3, 4-dihydro-4-oxothiazole.

Found: C, 55.24; H, 3.60; N, 9.23. Calcd. for C_7H_5ONS (II): C, 55.63; H, 3.34; N, 9.27%.

The Reaction of 2-Benzoylthiopyridine and Chloroacetic Acid.—To a solution of 0.5g. of 2-benzoylthiopyridine in 2 ml. of dry benzene, 0.22 g. of chloroacetic acid was added. The mixture was then warmed on a water bath for five minutes. When the oily substance which separated out was worked up by essentially the same procedure as that described above, 0.1 g. of yellow silky needles were obtained; the m. p. and mixed m. p. with II was 178—179°C.

The benzene mother liquor of the above experiment was extracted wtih an aqueous solution of sodium bicarbonate, and the aqueous extract was acidified with hydrochloric acid to give 0.1 g. of benzoic acid.

The Reaction of 2-Acetylthiopyridine and Ethyl Chloroacetate.—A solution of 1.53 g. of 2-benzoylthiopyridine and 1.23 g. of ethyl chloroacetate in 10 ml. of benzene was gently boiled on a water bath and the heating was so adjusted that a small but steady amount of a distillate came out through a short air condenser. The distillate, with a peculiar odor of acetyl chloride, was poured into a solution of 1 g. of aniline in 2 ml. of benzene. The crystals which separated out were collected and washed with a small amount of water to afford 0.75 g. of white crystals, m. p. 108—110°C. One crystallization from hot water gave pure acetanilide as colorless leaflets, m. p. 114°C, undepressed on admixture with an authentic specimen.

The reaction mixture of the above experiment was concentrated under reduced pressure, and the viscous oily residue which could not be crystallized was washed with 5% aqueous sodium bicarbonate and warmed with 10 ml. of 10% hydrochloric acid on a water bath for thirty minutes. The mixture was then concentrated under reduced pressure, and the residue was extracted with aqueous sodium bicarbonate. The extract was washed with benzene and was neutralized with hydrochloric acid to give 1.0 g. of yellow crystals melting at 133—134°C. One recrystallization from ethanol gave a pure sample of (2-pyridylthio)acetic acid, melting at 136°C, undepressed on admixture with an authentic specimen.

The Reaction of 2-Acetylthiopyridine with Chloroacetamide.—A solution of 1.5 g. of 2-acetylthiopyridine and 0.94 g. of chloroacetamide in 10 ml. of dry benzene was refluxed for thirty minutes on a water bath. The residue which separated out was collected, washed with ethanol and water, and neutralized with sodium bicarbonate. The green precipitate was recrystallized from benzene to give 0.35 g. of orange silky needles, melting at 181—183°C. The melting point of this substance was undepressed on admixture with an authentic specimen of II.

Found: N, 9.13. Calcd. for C_7H_5ONS: N, 9.27%.

The Reaction of 2-Benzoylthiopyridine with Chloroacetamide.—A solution of 2.15 g. of 2-benzoylthiopyridine and 0.94 g. of chloroacetamide in 5 ml. of benzene was refluxed on a water bath for one hour. The green precipitate which separated out was worked up by the procedure described in the above experiment, to give 0.1 g. of greenish yellow needles of II, m. p. 181—183°C, undepressed on admixture with an authentic specimen.

Found: N, 8.96. Calcd. for C_7H_5ONS: N, 9.27%.

(2-Pyridylthio)acetamide (XI).—To a solution of 1 g. of 2-mercaptopyridine and 0.36 g. of sodium hydroxide in 4 ml. of ethanol, 0.48 g. of chloroacetamide was added with cooling and stirring. The precipitate which separated out was filtered off, the filtrate was concentrated under reduced pressure, and the residue was recrystallized from benzene to give 1.5 g. of white leaflets, m. p. 80°C.

Found: C, 49.88; H, 4.88; N, 16.88. Calcd. for $C_7H_8ON_2S$: C, 50.00; H, 4.80; N, 16.66%.

The Reaction of (2-Pyridylthio)acetamide and Acetyl Chloride.—A solution of 0.9 g. of (2-pyridylthio)acetamide and 0.5 g. of acetyl chloride in 5 ml. of benzene was refluxed for one hour. The precipitate which separated out was collected, washed with aqueous sodium bicarbonate, and recrystallized from benzene to give 0.36 g. of greenish yellow needles, m. p. 181—183°C undepressed on admixture with an authentic specimen of II.

4-Phenyl-2-acetylthiothiazole (XIIa).—A mixture of 2 g. of 4-phenyl-2-mercaptothiazole and 4 ml. of acetic anhydride was refluxed for one hour, the resultant solution was concentrated under reduced pressure, and the residue was recrystallized from benzene to give 1.8 g. of white plates melting at 89°C (yield, 77%).

Found: C, 55.94; H, 4.06; N, 5.94. Calcd. for $C_{11}H_9ONS_2$: C, 56.17; H, 3.86; N, 5.96%.

The Reaction of 4-Phenyl-2-acetylthiothiazole with Chloroacetic Acid.—A mixture of 10 g. of 4-phenyl-2-acetylthiothiazole and 4.7 g. of chloroacetic acid in 20 ml. of benzene was warmed on a water bath for one hour. Ethanol was added to the mixture, and the red amorphous powder which separated out was collected and recrystallized from pyridine to give 5 g. of a red amorphous powder, m. p. 185°C.

Found: C, 56.37; H, 3.64; N, 6.16%.

The infrared spectrum of this substance was identical with that of the reaction product between (4-phenylthiazolyl-2-thio)acetic acid and acetic anhydride.[7]

The filtrate of the above experiment was concentrated under reduced pressure, and the residue was purified by column chromatography (alumina-benzene) and recrystallized from ethanol to give 3.6 g. of colorless prisms, m. p. 62°C, undepressed on admixture with ethyl (4-phenylthiazolyl-2-thio)acetate (XIII) prepared by the method described below.

Found: C, 55.74; H, 4.91; N, 4.91. Calcd. for $C_{13}H_{13}O_2NS$: C, 55.91; H, 4.70; N, 5.02%.

Hydrazide: white needles, m. p. 105—106°C, undepressed on admixture with a sample prepared by another route (see below).

Found: N, 15.97. Calcd. for $C_{11}H_{11}ON_3S_2$: N, 15.84%.

Ethyl (4-Phenylthiazolyl-2-thio)acetate (XIII).—To a solution of 5 g. of 4-phenyl-2-mercaptothiazole and 1.5 g. of potassium hydroxide in 50 ml. of ethanol, there was added 3.2 g. of ethyl chloroacetate with stirring and cooling. The precipitate was removed by filtration, the filtrate was concentrated, and the residue was recrystallized from ethanol to give 5.5 g. of white needles, m. p. 62—63°C.

Found: N, 15.97. Calcd. for $C_{13}H_{13}O_2NS_2$: N, 5.02%.

Hydrazide: white needles, m. p. 105—106°C.

4-Phenyl-2-benzoylthiothiazole (XIIb).—A mixture of 2 g. of 4-phenyl-2-mercaptothiazole and 3 ml. of benzoyl chloride was gently refluxed for one hour. After cooling, the crystals which separated out were collected and recrystallized from benzene to give 2.3 g. of pale yellow crystals, m. p. 95—96°C (yield, 81%).

Found: C, 64.89; H, 3.72; N, 4.48. Calcd. for $C_{16}H_{11}ONS_2$: C, 64.64; H, 3.72; N, 4.71%.

The Reaction of 4-Phenyl-2-benzoylthiothiazole with Chloroacetic Acid.—When 4-phenyl-2-benzoylthiothiazole was treated with chloroacetic acid under conditions similar to those in the case of 2-acetylthio derivative, the same red pigment (identical in infrared spectrum with that from 2-acetylthio derivative) was isolated. From the mother liquor of the reaction medium, a quantitative amount of benzoic acid was isolated.

The Acid Hydrolysis of the Red Pigment.—The red substance isolated from the preceding experiment (0.5 g.) was refluxed for one hour in 20 ml. of concentrated hydrochloric acid, and then the reaction mixture was concentrated under reduced pressure. The residue was extracted with aqueous sodium bicarbonate, and the extracts were acidified by the addition of hydrochloric acid. The crystals (0.2 g.) which separated out were recrystallized from ethanol to give white needles, m. p. 91—92°C, undepressed on admixture with an authentic specimen of (4-phenylthiazolyl-2-thio)acetic acid.[7]

The Reaction of 2-Benzoylthiobenzothiazole with Chloroacetic Acid.—A mixture of 10 g. of 2-benzoylthiobenzothiazole and 3.5 g. of chloroacetic acid in 20 ml. of benzene was warmed at 60°C for one and a half hours, and then the benzene was removed under reduced pressure. The red residue was washed with ether and ethanol, and then recrystallized from ethanol to give 4.6 g. of fine red needles, m. p. 234°C. The infrared spectrum of this substance was identical with that of the reaction product between (benzothiazolyl-2-thio)acetic acid and acetic anhydride.[7]

Found: C, 53.05; H, 2.56; N, 6.34%.

The ether washings of the above experiment were extracted with aqueous sodium bicarbonate, the extract was acidified with hydrochloric acid, and the crystals which separated out were collected and recrystallized from water to give 1.5 g. of benzoic acid as white leaflets melting at 122°C, undepressed on admixture with an authentic specimen of benzoic acid.

The ether layer separated from sodium bicarbonate washing was concentrated, and the residue was extracted with ethanol to give a small amount of an amorphous yellow powder melting at 179—180°C, undepressed on admixture with an authentic specimen of 2-mecrapto-benzothiazole.

Found: N, 8.70. Calcd. for $C_7H_5NS_2$: N, 8.38%.

The Acid Hydrolysis of the Red Pigment.—The red pigment obtained by the above-described experiment (0.5 g.) was refluxed in 10 ml. of concentrated hydrochloric acid for one hour, and then the mixture was concentrated under reduced pressure. The residue was extracted with aqueous sodium bicarbonate, the extract was acidified with hydrochloric acid, and the precipitate which separated out was recrystallized from ethanol to give 0.1 g. of (benzothiazolyl-2-thio)acetic acid, melting at 156°C, undepressed on admixture with an authentic specimen.

We wish to thank to The Kawakami Foundation for its partial financial support of this work.

BULLETIN OF THE CHEMICAL SOCIETY OF JAPAN VOL. 39 1253—1257 (1966)

The Synthesis of Pyrido[2, 1-b]-3, 4-dihydro-4-iminothiazole Derivatives. A New Meso-ionic Heterocyclic System[1,2]

By Hiroshi KATO and Masaki OHTA

Laboratory of Organic Chemistry, Tokyo Institute of Technology, Ookayama, Meguro-ku, Tokyo

(Received October 27, 1965)

The action of acyl chlorides on 2-pyridylthioacetonitrile and related compounds gives the corresponding *N*-acylated pyrido[2, 1-b]-3, 4-dihydro-4-iminothiazoles and related compounds.

In the preceding paper of this series,[1] the formation of pyrido[2, 1-b]-3, 4-dihydro-4-oxothiazole (I) by a new mode of formation was reported. Although a considerable amount of work has been reported on this ring system, the corresponding imino derivatives (e. g., II) were not known when this investigation was completed.[3] An attempt to prepare this compound by the reaction of (2-pyridylthio)acetamide and acetyl chloride gave the oxo derivative I, as we have reported.[1] In the present communication, we will report the successful preparation of *N*-acyl-pyrido[2, 1-b]-3, 4-dihydro-4-iminothiazoles (II) and related compounds.

1) Studies on Meso-ionic Compounds. Part XXV. Part XXIV: H. Kato, K. Tanaka and M. Ohta, This Bulletin, **39**, 1248 (1966).

2) For a preliminary communication, see H. Kato, K. Tanaka and M. Ohta, ibid., **35**, 1901 (1962).

3) As a result of our preliminary communication,[2] a number of condensed and uncondensed compounds of this type have been prepared in this laboratory: H. Chosho, K. Ichimura and M. Ohta, This Bulletin, **37**, 1670 (1964); K. Ichimura and M. Ohta, ibid., **38**, 707 (1965).

Results and Discussion

The reaction of 1-mercaptoisoquinoline and chloroacetonitrile gave 1-isoquinolylthioacetonitrile

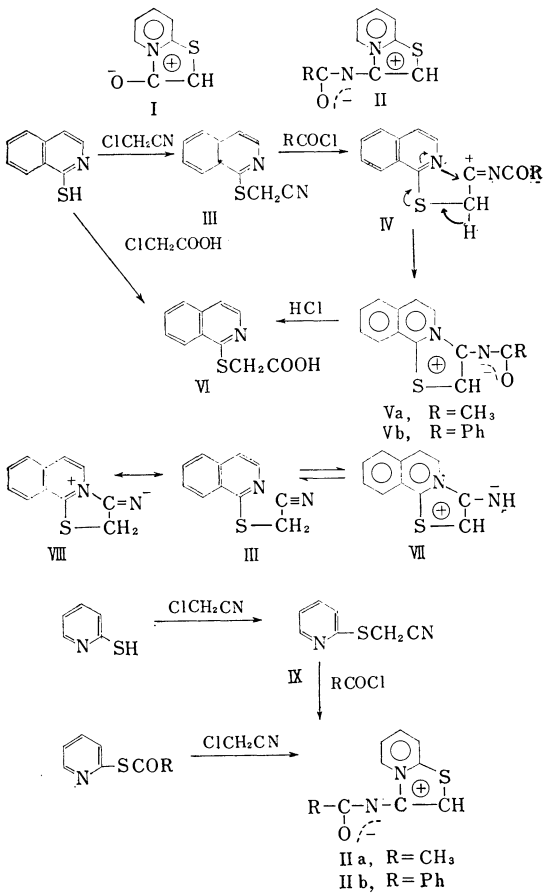

(III). The presence of a nitrile group was revealed by an infrared absorption at 2240 cm^{-1}. No ring closure took place when it was treated with hydrogen chloride[4] or acetic anhydride. Successful ring closures with these reagents to give meso-ionic compounds have been reported in the case of *N*-nitroso-*N*-phenylglycinonitrile (with hydrogen chloride)[5] and *N*-benzyl-2-pyridylaminoacetonitrile (with acetic anhydride).[6] On heating a benzene solution of 1-isoquinolylthioacetonitrile with acetyl chloride, a hydrochloride was formed, which gave a free base with the empirical formula $C_{13}H_{12}ON_2S$ on treatment with alkali. A similar reaction occurred with benzoyl chloride to give a free base, $C_{18}H_{12}ON_2S$. The infrared absorption at 2240 cm^{-1} has disappeared in these compounds, suggesting that the nitrile group has participated in the reaction. From the above results and known analogous ring formation reactions, it may safely be deduced that the reaction products are *N*-acetyl and *N*-benzoyl-isoquinolo[1, 2-b]-3, 4-dihydro-4-iminothiazole (Va and Vb). The formation of this compound can reasonably be explained by considering the attack of an acyl cation on the nitrile group to give the intermediate cation IV, followed by ring formation and a proton removal to give the products V shown in the above chart. Since the ring nitrogen atom is by far the more basic than the nitrile nitrogen atom, a strong acid such as hydrogen chloride preferably would add to the ring nitrogen atom rather than to the nitrile nitrogen atom to facilitate the polarization, thus resulting in the loss of the nucleophilic aptitude of the ring nitrogen atom. Such is evidently not the case with *N*-nitroso-*N*-substituted glycinonitrile, which gives a sydnone-imine derivative when treated with hydrogen chloride. The failure of ring formation with acetic anhydride is probably due to its poor acylating power in forming the intermediate IV. The fact that it does not give the product with acetic anhydride and the presence of the infrared absorption of III at 2240 cm^{-1} further show the absence of an equilibrium between the open-chain (III) and cyclic (VII) isomers, and even the absence of an intramolecular interaction such as III↔VIII, which is sometimes to be found in structurally similar systems.[7]

This meso-ionic system seems rather stable, and when the *N*-benzoyl derivative Vb was treated with phenylhydrazine, aniline, chromic acid or zinc powder in acetic or hydrochloric acid, or when heated in acetic acid, no reaction took place and the starting material was recovered unchanged. Sydnone-imines which are structurally similar to compound V are quite stable to strong acidic conditions, but the hydrolysis of the *N*-benzoyl derivative Vb by hydrochloric acid caused a cleavage of the ring to give benzoic acid and (1-isoquinolylthio)acetic acid (VI). The structure of the reaction product was established by preparing the compound independently from 1-mercaptoisoquinoline and chloroacetic acid.

The treatment of 2-mercaptopyridine with chloroacetonitrile gave 2-pyridylthioacetonitrile (IX), which, by the action of acetyl and benzoyl chloride, gave *N*-acetyl- and *N*-benzoyl-pyrido-[2, 1-b]-3, 4-dihydro-4-iminothiazole (IIa and IIb) respectively. The same compounds, IIa and IIb, were obtained by the action of 2-acetylthio- and 2-benzoylthio-pyridine and chloroacetonitrile, albeit in lower yields. The mode of formation

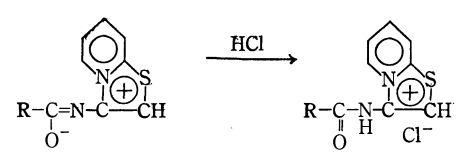

4) It was later found[3] that an uncondensed ring system could be prepared by the action of hydrogen chloride.

5) H. Kato, M. Hashimoto and M. Ohta, *J. Chem. Soc. Japan, Pure Chem. Sect.* (*Nippon Kagaku Zassi*), **78**, 707 (1957).

6) N. W. Bristow, P. T. Charlton, D. A. Peak and W. F. Short, *J. Chem. Soc.*, **1954**, 616.

7) See, e.g., M. Ohta and H. Kato, *J. Chem. Soc. Japan, Pure Chem. Sect.* (*Nippon Kagaku Zasshi*), **86**, 661 (1965).

in the latter case would be essentially the same as that of the formation of the corresponding oxo compound I from 2-acylthiopyridine and chloroacetic acid.

Mention should be made of the infrared spectra of these compounds. Neither of the *N*-acetyl free bases, IIa or Va, shows any absorption in the normal amide carbonyl region. This is in marked contrast to the corresponding oxo ring system (e. g., I), which shows an alsmost normal carbonyl absorption at 1675 cm^{-1}, suggesting that the carbonyl groups of II and V are very strongly polarized; it supports further the rather superficial similarity of the oxo and imino-type meso-ionic compounds, as has been discussed elsewhere in the case of sydnones and sydnone-imines.[7,8] In contrast to the common idea, these "amides," II and V, are soluble in dilute hydrochloric acid and form stable hydrochlorides. The infrared absorption of IIa hydrochloride shows a strong absorption due to an amide group at 1702 cm^{-1}. This fact, and the absorption centered at 3180 cm^{-1} show that the proton is attached neither to the ring nitrogen atom nor to the polarized carbonyl oxygen, but to the exocyclic "amide" nitrogen atom, to give a tropylium salt-like structure, X.

A similar treatment of 2-mercapto-4-lepidine with chloroacetonitrile gave 4-lepidly-2-thioacetonitrile (XI), this, however, did not give the expected corresponding imino derivative by the action of acyl chlorides. Since the basicity of this compound is considered to lie between, or to be nearly equal to, those of the pyridyl and isoquinolyl derivatives, this anomalous behavior is certainly not related to the basicity of this compound. (The pK_a's of 2-methylthiopyridine, 2-methylthioquinoline and 1-methylthioisoquinoline are reported to be 3.62, 3.71 and 3.93 respectively.[9]) This result may most reasonably be explained by considering a steric hindrance between the *N*-acyl group and the hydrogen atom of the 8-position of the quinoline nucleus. A similar effect has been observed in an attempted synthesis of the oxo analogue; though (2-quinolylthio)-acetic acid gave the corresponding oxo-compound, when the 8-position of the quinoline ring was substituted, no ring formation took place.[10] In the present case, a study of a model indicates that even a small atom like hydrogen at that position is bulky enough to interact with relatively bulky acyl groups.

It was found that the chlorine atoms of 1-chloroisoquinoline and 2-chloro-4-lepidine are active enough to give, on brief heating with mercaptoacetic acid, almost a quantitative yield of the corresponding mercapto derivatives which are required as the starting materials in this study. This phenomenon can reasonably be explained by considering an attack of the acetothioxy anion on protonated azines XII to give XIII, followed by the removal of a molecule of hydrogen chloride to give XIV, which later gives the mercapto derivatives by hydrolysis or thioacetolysis. This fact led us to try to prepare a new meso-ionic compound, XV, by the following sequence of reactions. When 1-chloroisoquinoline and chloroacetic acid were heated in benzene, the reaction product was isocarbostyril, showing that the attack of chloroacetic acid at the 1-position of the isoquinoline ring precedes the formation of the quaternary salt formation.

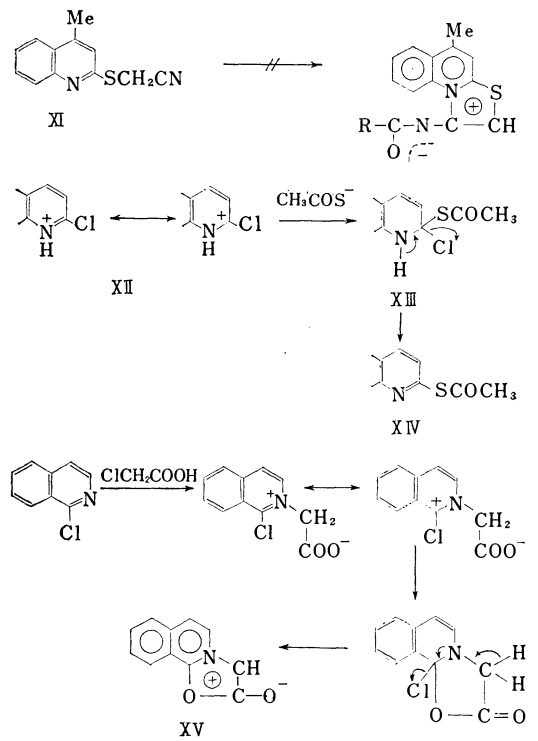

Experimental

All melting points were determined on a micro hot stage and are corrected. Boiling points are uncorrected. The infrared spectra were taken on a Nippon Bunko Infrared Spectrometer, Model S, equipped with an NaCl prism on KBr tablets.

1-Isoquinolylthioacetonitrile (III).—To a solution of 1.24 g. of sodium hydroxide and 5 g. of 1-mercaptoisoquinoline in 50 ml. of ethanol, a solution of 2.35 g. of chloroacetonitrile in 10 ml. of ethanol was added; the mixture was then warmed on a water bath for twenty minutes. The precipitate which separated out was filtered off, the filtrate was concentrated under reduced pressure, and the pale yellow plates which separated out on cooling were collected (4 g., m. p. 95.0—95.5°C) and recrystallized from ethanol to give white plates, m. p. 95.5°C. IR, 2240 cm^{-1}.

8) F. H. C. Stewart, *Chem. Revs.*, **64**, 129 (1964).
9) A. Albert and G. B. Barlin, *J. Chem. Soc.*, **1959**, 2384.
10) G. F. Duffin and J. D. Kendall, ibid., **1951**, 734.

Found: C, 65.91; H, 3.84; N, 14.27. Calcd. for $C_{11}H_8NS_2$: C, 65.99; H, 4.03; N, 13.99%.

***N*-Acetyl-isoquinolo[1, 2-b]-3, 4-dihydro-4-iminothiazole (Va).**—To a solution of 1 g. of 1-isoquinolylthioacetonitrile in 6 ml. of benzene, a solution of 0.4 g. of acetyl chloride in 4 ml. of benzene was added; the mixture was then refluxed on a water bath for one hour. The pale yellow precipitate was collected (1.2 g., m. p. 255—256°C) and dissolved in water. The aqueous solution was made alkaline with sodium bicarbonate and was extracted with chloroform. The chloroform extract was dried over sodium sulfate and concentrated, and the yellow fine needles which separated out were collected (0.4 g., m. p. 210—212°C). Recrystallization from benzene afforded 0.2 g. of yellow prisms, melting at 215°C. This substance is soluble in dilute hydrochloric acid. IR: no absorption around 2240 cm^{-1}.

Found: C, 64.25; H, 4.40; N, 11.59. Calcd. for $C_{13}H_{10}ON_2S$: C, 64.46; H, 4.16; N, 11.59%.

***N*-Benzoyl-isoquinolo[1,2-b]-4,3-dihydro-4-iminothiazole (Vb).**—To a solution of 1 g. of 1-isoquinolylthioacetonitrile in 10 ml. of benzene 0.7 g. of benzoyl chloride was added. The mixture was then refluxed on a water bath for ten minutes. The benzene was evaporated, and the residue was warmed on the water bath for another two hours. The dark mass which formed was tritulated with 5 ml. of ethanol, and the solid was collected by filtration to afford 1.25 g. of a brown powder (m. p. 255—260°C). This was dissolved in water, the solution was made alkaline with sodium bicarbonate, and the precipitate which formed was collected to give 1.13 g. of a yellow powder, melting at 271°C. One recrystallization from *n*-butanol gave 0.88 g. of yellow leaflets melting at 273°C. This substance is soluble in 10% hydrochloric acid.

Found: C, 71.30; H, 3.81; N, 9.49. Calcd. for $C_{18}H_{12}ON_2S$: C, 71.04; H, 3.98; N, 9.21%.

The Acid Hydrolysis of the *N*-Benzoyl Compound Vb.—A solution of 1 g. of *N*-benzoyl-isoquinolo[1, 2-b]-3, 4-dihydro-4-iminothiazole in 50 ml. of 10% hydrochloric acid was heated on a water bath for one hour. After cooling, the crystals (portion A) which separated out were collected, and the filtrate was concentrated under reduced pressure. The residue was washed with aqueous sodium bicarbonate and recrystallized from ethanol-ligroin to give 0.25 g. of silky white needles melting at 96°C. The melting point of this substance was not depressed on admixture with a sample of (1-isoquinolylthio)acetic acid prepared by the method to be described below.

Found: N, 6.62. Calcd. for $C_{11}H_9O_2NS$: N, 6.39%.

The sodium bicarbonate washings were acidified with hydrochloric acid, and the crystals which separated out were added to portion A and recrystallized from water to give 0.35 g. of colorless needles; these needles were identified as benzoic acid by their melting point (122°C) and mixed melting point with an authentic sample of benzoic acid.

(1-Isoquinolylthio)acetic Acid (VI).—Into a solution of 0.8 g. of 1-mercaptoisoquinoline and 0.4 g. of sodium hydroxide in a mixture of 20 ml. of ethanol and 2 ml. of water, 0.5 g. of chloroacetic acid was stirred. After two hours, the precipitate of sodium chloride was filtered off; the new crystals which separated out on cooling were collected and dissolved in water, and the aqueous solution was acidified with acetic acid. The crystals which separated out were recrystallized from ethanol-ligroin to give 0.5 g. of silky white needles melting at 98°C.

Found: N, 6.53. Calcd. for $C_{11}H_9O_2NS$: N, 6.39%.

2-Pyridylthio acetonitrile (IX).—Into a solution of 9.3 g. of 2-mercaptopyridine and 5.3 g. of sodium hydroxide in 50 ml. of ethanol, 6.3 g. of chloroacetonitrile was stirred while the solution was being cooled. The precipitate of sodium chloride was removed by filtration, and the filtrate was concentrated and distilled under reduced pressure to give 9.5 g. of a yellow liquid boiling at 118—120°C/3 mmHg.

Found: C, 55.03; H, 3.90; N, 18.26. Calcd. for $C_7H_6N_2S$: C, 56.00; H, 4.03; N, 18.66%.

This substance darkened quite rapidly, and no good analytical agreement was obtained on several repeated analyses.

***N*-Acetyl-pyrido[2, 1-b]-3, 4-dihydro-4-iminothiazole (IIa).**—a) A solution of 2 g. of 2-pyridylthioacetonitrile and 0.95 ml. of acetyl chloride in 10 ml. of benzene was refluxed on a water bath for one hour. The precipitate which formed was then collected to give 3.0 g. of a yellow powder. Recrystallization from ethanol afforded 2.1 g. of yellow prisms melting at 250°C. IR: 1702 cm^{-1}.

Found: N, 12.04. Calcd. for $C_9H_9ON_2SCl$: N, 12.25%.

This substance was dissolved in water, made alkaline with potassium carbonate, and extracted with chloroform. The chloroform extracts were concentrated, and the residue was recrystallized from benzene to give 1.3 g. of yellow needles, melting at 73—74°C.

Found: C, 51.52; H, 5.06; N, 13.58. Calcd. for $C_9H_8ON_2S+H_2O$: C, 51.42; H, 4.80; N, 13.33%.

After being dried at 60°C under a vacuum for a day:

Found: N, 14.02. Calcd. for $C_9H_8ON_2S$: N, 14.58%. This substance is soluble in dilute hydrochloric acid. IR: no strong absorption between 1700—1600 cm^{-1}.

b) A solution of 1 g. of 2-acetylthiopyridine and 0.5 g. of chloroacetonitrile in 3 ml. of benzene was refluxed on a water bath for one hour. The crystals which separated out were collected to give 0.9 g. of a dark yellow powder, which was then recrystallized from ethanol to give 0.45 g. of orange needles, m. p. 252—254°C (decomp.).

Found: N, 12.03. Calcd. for $C_9H_9ON_2SCl$: N, 12.25%.

***N*-Benzoyl-pyrido[2, 1-b]-3, 4-dihydro-4-iminothiazole (IIb).**—a) A solution of 2 g. of 2-pyridylthioacetonitrile and 1.54 ml. of benzoyl chloride in 10 ml. of benzene was refluxed for one hour on a water bath. The benzene was then evaporated, and the residue was warmed on a water bath for another thirty minutes. The crystals which separated out on cooling were collected to give 3 g. of a pale yellow powder. This substance was suspended in water and made basic with sodium bicarbonate. The resultant solid was collected to give 2.35 g. of a brown powder, which was recrystallized from ethanol to give 1.75 g. of yellow needles with a green fluorescence, m. p. 206°C.

Found: C, 66.14; H, 3.75; N, 10.76. Calcd. for $C_{14}H_{10}ON_2S$: C, 66.13; H, 3.96; N, 11.02%.

b) A solution of 2 g. of 2-benzoylthiopyridine and 0.7 g. of chloroacetonitrile was refluxed on a water

bath for twelve hours. After cooling, the yellow precipitate was collected to give 0.25 g. of yellow crystals, which were basified with sodium bicarbonate and recrystallized from ethanol to give 0.1 g. of yellow needles, m. p. 206°C, undepressed on admixture with a sample prepared by Method a).

4-Lepidyl-2-thioacetonitrile (XI).—Into a solution of 3.2 g. of 2-mercapto-4-lepidine and 0.74 g. of sodium hydroxide in 30 ml. of ethanol, 1.4 g. of chloroacetonitrile was added dropwise with cooling and stirring. The precipitate of sodium chloride was filtered off, and the filtrate was concentrated to give 4.1 g. of pale yellow needles melting at 64—65°C. Recrystallization from ethanol afforded colorless needles melting at 65°C.

Found: C, 67.28; H, 4.71; N, 13.09. Calcd. for $C_{12}H_{10}ON_2S$: C, 67.28; H, 4.71; N, 13.08%.

The Attempted Preparation of *N*-Acyl-4-lepido-[2, 1-b]-3, 4-dihydro-4-iminothiazole.—A solution of 1.3 g. of 4-lepidyl-2-thioacetonitrile and 0.58 g. of acetyl chloride in 5 ml. of benzene was refluxed for one hour on a water bath. The precipitate which separated out was collected (0.8 g.) and recrystallized from ethanol to give yellow needles. It was suspended on water, made alkaline with potassium carbonate, and extracted with chloroform. The chloroform extract was then concentrated under reduced pressure, and the residue was recrystallized from ligroin to give colorless needles melting at 65—66°C, undepressed on admixture with 4-lepidyl-2-thioacetonitrile.

When 4-lepidyl-2-thioacetonitrile was treated with benzoyl chloride in benzene, the starting material was recovered unchanged after it had been heated on a water bath for five hours.

1-Mercaptoisoquinoline.—a) To a suspension of 2 g. of isoquinoline in 5 ml. of water, 0.94 g. of thioacetic acid was added, and the mixture was warmed for thirty minutes on a water bath. The crystals which separated out were collected to give 1.75 g. of yellow prisms melting at 171°C. One recrystallization from ethanol gave yellow prisms, m. p. 171°C.

b) An exothermic reaction occurred when 2 g. of 1-chloroisoquinoline was mixed with 2 ml. of thioacetic acid. After it had been warmed on a water bath for ten minutes, the mixture was cooled and the pale yellow prisms which separated out were collected (1.8 g., m. p. 166°C) and recrystallized from ethanol to give 1.65 g. of yellow prisms, m. p. 170°C.

2-Mercapto-4-lepidine.—a) To a suspension of 0.5 g. of 2-chloro-4-lepidine in 10 ml. of water, 0.22 g. of thioacetic acid was added and the mixture was warmed on a water bath for thirty minutes. The crystals which separated out were collected to give 0.45 g. of yellow needles, melting at 260°C.

b) A mixture of 0.5 g. of 2-chloro-4-lepidine and 1 ml. of thioacetic acid was warmed on a water bath for thirty minutes. The mixture was concentrated under reduced pressure, and the residue was washed with water to give 0.5 g. of yellow needles, melting at 261°C.

The Reaction of 1-Chloroisoquinoline and Chloroacetic Acid.—A solution of 1 g. of 1-chloroisoquinoline and 0.6 g. of chloroacetic acid in 10 ml. of benzene was refluxed on a water bath for two hours. Benzene was distilled off under reduced pressure, and the residue which solidified was recrystallized from ethanol to afford 0.3 g. of pale yellow needles, m. p. 210—211°C, undepressed on admixture with an authentic specimen of isocarbostyrile.

We warmly appreciate the technical assistance of Mr. Kazuo Tanaka in a part of the experiment reported here. This work was supported in part by The Kawakami Foundation, to which our thanks are due.

BULLETIN OF THE CHEMICAL SOCIETY OF JAPAN VOL. 39 1257—1261 (1966)

Studies of the Mixed Amino-acid Complexes of Cobalt(III). I. The Geometrical Isomers of the [Co en gly (chelate)] Series

By Nobuko MATSUOKA, Jinsai HIDAKA and Yoichi SHIMURA

Department of Chemistry, Faculty of Science, Osaka University, Toyonaka, Osaka

(Received October 28, 1965)

Five new complexes of the [Co en gly (chelate)] type, i. e., *mer(N)*- and *fac(N)*-[Co en gly CO_3], *mer(N)*- and *fac(N)*-[Co en gly ox] and *mer(N)*-[Co en gly malo], have been derived from a new dinitro complex, *cis*-[Co en gly $(NO_2)_2$], through an intermediate complex, [Co en gly Cl (OH_2)]Cl. The geometrical structures of these complexes have been determined on the basis of the processes of their derivation and their absorption spectra. Two new bisglycinato complexes, *trans(O)*- and *cis(O)*-[Co en gly_2]I·H_2O, have been prepared from *mer(N)*- and *fac(N)*-[Co en gly CO_3] respectively.

Recently the mixed amino-acid complexes of cobalt(III) have been recognized as interesting in relation to the optical rotatory dispersion or the circular dichroism studies of metal complexes,

and several reports have appeared.[1-6] However, only a few mixed amino-acid complexes have been known; they belong to the [Co^{III} N_4O_2]- or the [Co^{III} N_3O_3]-type. In particular, we know of extremely few examples of pairs of geometrical isomers, for example, the *trans(O)*- and *cis(O)*-isomers of a [Co N_4O_2] complex or the *mer(N)*- and *fac(N)*-isomers of a [Co N_3O_3] complex.

In the present paper, five new complexes of the [Co en gly (chelate)] type, including two pairs of geometrical isomers, and a pair of the *trans(O)*- and *cis(O)*-isomers of [Co en gly_2]X, will be reported on. All of these new complexes will be derived from a new starting material, [Co en gly $(NO_2)_2$]. The absorption spectra of these complexes will then be discussed in the same way as in a previous paper.[7]

Experimental

Preparation.—*1) Dinitroglycinatoethylenediaminecobalt(III):* [$Co(NO_2)_2$ gly en].—A solution containing 25 g. of potassium nitrite in 30 ml. of water was added to a solution containing 20 g. of cobalt(II) chloride hexahydrate in 20 ml. of water, and then 7 g. of glycine in 40 ml. of water and 6 g. of 93% aqueous ethylenediamine were added to the solution in this order. The dark brown solution was oxidized by bubbling air in for about ten hours, whereupon the desired complex separated as yellow precipitates. The crude complex was filtered and washed with a small quantity of water, and then with ethanol, and dried in air. This complex is sparingly soluble in water at room temperature, moderately soluble in hot water, and insoluble in methanol, ethanol, acetone and benzene. The pure crystals were obtained by recrystallization from hot water. Yield, 18 g.

Found: C, 17.33; H, 4.44; N, 24.30. Calcd. for [$Co(NO_2)_2(C_2H_4NO_2)(C_2H_8N_2)$]: C, 16.85; H, 4.24; N, 24.57%.

The following three complexes, 2—4), were prepared by the same method as above using racemic alanine and racemic propylenediamine.

2) Dinitroalaninatoethylenediaminecobalt(III): [$Co(NO_2)_2$ ala en].—Found: C, 20.21; H, 4.64; N, 23.26. Calcd. for [$Co(NO_2)_2(C_3H_6NO_2)(C_2H_8N_2)$]: C, 20.08; H, 4.72; N, 23.41%.

3) Dinitroglycinatopropylenediaminecobalt(III): [$Co(NO_2)_2$ gly pn].—Found: C, 20.29; H, 4.66; N, 23.39. Calcd. for [$Co(NO_2)_2(C_2H_4NO_2)(C_3H_{10}N_2)$]: C, 20.08; H, 4.72; N, 23.41%.

4) Dinitroalaninatopropylenediaminecobalt(III): [$Co(NO_2)_2$ ala pn].—Found: C, 23.06; H, 5.06; N, 22.26. Calcd. for [$Co(NO_2)_2(C_3H_6NO_2)(C_3H_{10}N_2)$]: C, 23.01; H, 5.15; N, 22.36%.

5) Potassium Dinitrobisglycinatocobaltate(III): K[Co $(NO_2)_2$ gly_2]. Potassium nitrite (50 g.) in 70 ml. of water and glycine (26 g.) in 150 ml. of water were added in this order to a solution containing 40 g. of cobalt(II) chloride hexahydrate in 50 ml. of water. The dark brown solution was then oxidized by bubbling air in for about three hours. After the addition of 200 ml. of ethanol, the solution was kept in a refrigerator overnight. The yellow brown crystals were filtered and recrystallized from hot water. They were dried by heating at 105°C. Yield, 30 g.

Found: C, 13.99; H, 2.85; N, 17.13. Calcd. for K[$Co(NO_2)_2(C_2H_4NO_2)_2$]: C, 14.21; H, 2.38; N, 16.57%.

6) Chloroglycinatoaquoethylenediaminecobalt(III) Chloride: [Co Cl gly (OH_2) en]Cl.—The ground sample of the [Co $(NO_2)_2$ gly en] complex (20 g.) was suspended in 50 ml. of concentrated hydrochloric acid and warmed on a water bath. The yellowish suspension began to dissolve with the bubbling of nitrogen dioxide, and the mixture became violet. After the bubbling of gas had ceased, the violet solution was cooled to room temperature. The violet crystalline complex deposited was then filtered and washed with diluted hydrochloric acid (1 : 1) and dried in air. This complex is soluble in water, with an accompanying aquation but insoluble in ethanol and methanol. Yield, 14 g.

Found: C, 16.86; H, 5.06; N, 14.79. Calcd. for [Co Cl $(C_2H_4NO_2)OH_2(C_2H_8N_2)$]Cl: C, 17.03; H, 5.00; N, 14.90%.

7) Diisothiocyanatoglycinatoethylenediaminecobalt(III): [Co $(NCS)_2$ gly en].—To a solution of 2 g. of potassium thiocyanate in 20 ml. of water, 2 g. of [Co Cl gly (OH_2) en]Cl was added, and the mixture was warmed on a water bath. The color of the solution changed from violet to dark red, and the red crystals began to deposit. After the solution had been cooled to room temperature, the crystals were separated and washed with a little water, and then with ethanol, and dried in air. This complex is insoluble in water, ethanol and methanol. Yield, 2 g.

Found: C, 23.54; H, 3.97; N, 22.22. Calcd. for [$Co(NCS)_2(C_2H_4NO_2)(C_2H_8N_2)$]: C, 23.30; H, 3.91; N, 22.65%.

8) The mer(N) or Violet Form of Carbonatoglycinatoethylenediaminecobalt(III) Monohydrate: mer(N)-[Co CO_3 gly en]·H_2O. — In 100 ml. of water 10 g. of [Co Cl gly (OH_2) en]Cl and 10 g. of potassium hydrogen carbonate were dissolved; the mixture was then heated on a water bath for an hour. The solution was cooled to room temperature, and 50 ml. of ethanol was added to it. Some violet crystals began to separate in this step. After the solution had been kept in a refrigerator overnight, a large amount of the violet crystals, which were contaminated with a little amount of the reddish violet *fac(N)*-form, was obtained. The pure violet needles were obtained by recrystallization from hot water, washed with ethanol, and dried in air. This complex is insoluble in methanol and ethanol. Yield, 6.8 g.

Found: C, 22.14; H, 5.24; N, 15.23. Calcd. for [$Co\ CO_3(C_2H_4NO_2)(C_2H_8N_2)$]·$H_2O$: C, 22.15; H, 5.20; N, 15.50%.

9) The fac(N) or Red Form of Carbonatoglycinatoethylenediaminecobalt(III): *fac(N)*-[Co CO_3 gly en]. — Five grams of [Co Cl gly (OH_2) en]Cl were dissolved in a solution of 5 g. of potassium hydrogen carbonate

1) Y. Shimura, This Bulletin, **31**, 173, 315 (1958).
2) M. Ogawa, Y. Shimura and R. Tsuchida, *J. Chem. Soc. Japan, Pure Chem. Sect.* (*Nippon Kagaku Zasshi*), **81**, 72 (1960).
3) M. Murakami, S. Senoh, N. Matsusato, H. Itatani and J. W. Kang, ibid., **83**, 734 (1962).
4) C. T. Liu and B. Douglas, *Inorg. Chem.*, **3**, 1356 (1964).
5) J. H. Dunlop and R. D. Gillard, *J. Chem. Soc.*, **1964**, 2822.
6) J. Fujita, T. Yasui and Y. Shimura, This Bulletin, **38**, 654 (1965).
7) N. Matsuoka, Y. Shimura and R. Tsuchida, *J. Chem. Soc. Japan, Pure Chem. Sect.* (*Nippon Kagaku Zasshi*), **82**, 1637 (1961).

in 100 ml. of water. The solution was heated on a water bath for an hour and then cooled to room temperature. After about 20 ml. of methanol had been added to the solution, it was allowed to stand for about ten hours. The crude complex deposited as reddish violet crystals. This was recrystallized from water by the usual procedure. Yield, 0.2 g.

Found: C, 23.62; H, 4.98; N, 16.71. Calcd. for $[Co\,CO_3(C_2H_4NO_2)(C_2H_8N_2)]$: C, 23.73; H, 4.78; N, 16.60%.

10) The mer(N) or Violet Form of Oxalatoglycinato-ethylenediaminecobalt(III): mer(N)-[Co ox gly en].—In 20 ml. of warm water 4 g. of potassium oxalate and 5 g. of [Co Cl gly (OH_2) en]Cl were dissolved, and the mixture was heated on a water bath. After about 5 min. the desired complex gradually separated as reddish-violet needle crystals. This was recrystallized from hot water. Yield, 4 g.

Found: C, 25.66; H, 4.33; N, 14.98. Calcd. for $[Co\,(C_2O_4)(C_2H_4NO_2)(C_2H_8N_2)]$: C, 25.63; H, 4.30; N, 14.95%.

This complex was also prepared from *mer(N)*-[Co CO_3 gly en] and oxalic acid.

11) The fac(N) or Red Form of Oxalatoglycinato-ethylenediaminecobalt(III): fac(N)-[Co ox gly en].—This complex was prepared from *fac(N)*-[Co CO_3 gly en] and oxalic acid by the same method as that used for *mer(N)*-[Co ox gly en]. The pure complex was obtained as a pink powder. Yield, 0.1 g. from 0.5 g. of the carbonato complex.

Found: C, 25.54; H, 4.29; N, 14.89. Calcd. for $[Co\,(C_2O_4)(C_2H_4NO_2)(C_2H_8N_2)]$: C, 25.63; H, 4.30; N, 14.95%.

12) mer(N)-Malonatoglycinatoethylenediaminecobalt(III): mer(N)-[Co malo gly en].—To a solution of 2.5 g. of malonic acid in 50 ml. of water, 5 g. of *mer(N)*-[Co CO_3 gly en] was added and heated on a water bath. After the bubbling of carbon dioxide had finished, the solution was heated for more about one hour. It was then cooled and allowed to stand overnight. Reddish-violet crystals were recrystallized from water. Yield, 3.8 g. The same product was also obtained from the *fac(N)* carbonato complex.

Found: C, 28.42; H, 4.80; N, 14.18. Calcd. for $[Co(C_3H_2O_4)(C_2H_4NO_2)(C_2H_8N_2)]$: C, 28.49; H, 4.78; N, 14.24%.

13) trans(O)-Bisglycinatoethylenediaminecobalt (III) Iodide Monohydrate: trans(O)-[Co gly_2 en]$I\cdot H_2O$.—Two grams of *mer(N)*-[Co CO_3 gly en] was added to a solution containing 1.2 g. of glycine in 20 ml. of water. The solution was evaporated to 5 ml. on a water bath at about 70°C and filtered in hot. The filtrate was cooled to room temperature. After a calculated amount of potassium iodide had been added to the solution, dark red crystals began to separate. The mixture was kept in a refrigerator overnight. The recrystallization was made from water by the usual procedure.

Found: C, 17.78; H, 4.51; N, 13.61. Calcd. for $[Co\,(C_2H_4NO_2)_2(C_2H_8N_2)]I\cdot H_2O$: C, 17.48; H, 4.40; N, 13.62%.

14) cis(O)-Bisglycinatoethylenediaminecobalt(III) Iodide Monohydrate: cis(O)-[Co gly_2 en]$I\cdot H_2O$.—This complex was obtained by the same method as that used for the *trans(O)*-isomer, using *fac(N)*-[Co CO_3 gly en] instead of the *mer(N)*-isomer. After a little red precipitate produced by the addition of a calculated amount of potassium iodide had been filtered off, a small quantity of ethanol was added to the filtrate; the solution was then kept in a refrigerator overnight. The pinkish red powder deposited was recrystallized from water.

Found: C, 17.46; H, 4.34; N, 13.80. Calcd. for $[Co(C_2H_4NO_2)_2(C_2H_8N_2)]I\cdot H_2O$: C, 17.48; H, 4.40; N, 13.62%.

Measurements.—The absorption spectra were measured by a Beckman DU spectrophotometer at room temperature. The concentrations of the solutions varied from 1.0×10^{-2} to 0.5×10^{-4} F.

Results and Discussion

As a representative absorption spectrum of the complexes of the dinitro(amino-acidato)diamine type, the curve of [Co en gly$(NO_2)_2$], which was used as the starting compound in the preparations of the [Co en gly (chelate)] series, is shown in Fig. 1,

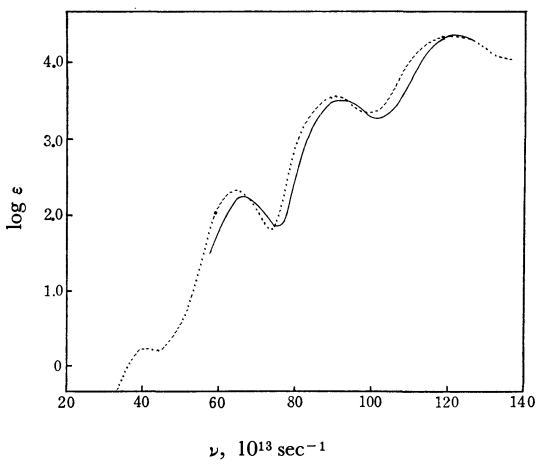

Fig. 1. Absorption curves of ——[Co en gly $(NO_2)_2$] and ·····K[Co $gly_2(NO_2)_2$].

in which the curve of a new bisglycinato complex, K[Co gly_2 $(NO_2)_2$], is also plotted. Previously one of the present authors[8] showed that the so-called nitro specific band of a *trans*-dinitrocobalt(III) complex was located at about 350—335 mμ, while, on the other hand, the band of the corresponding *cis*-dinitro complex was located at about 335—320 mμ. Judging from the positions of the nitro specific band of the present complexes, which are at 325 and 332 mμ for [Co en gly $(NO_2)_2$] and K[Co gly_2 $(NO_2)_2$] respectively, it may be considered that the two coordinated NO_2^- ligands of both the complexes are in the *cis* positions.

By warming up the starting complex, [Co en gly $(NO_2)_2$], with concentrated hydrochloric acid, the two coordinated NO_2^- ligands are easily freed from the cobalt(III) ion without the decomposition of the two chelate rings, while the two glycine

8) Y. Shimura, *J. Am. Chem. Soc.*, **73**, 5079 (1951).

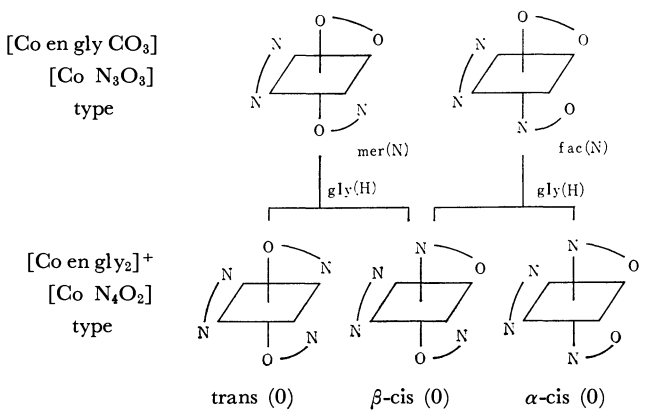

Fig. 2. Geometrical isomers of [Co en gly CO_3] and [Co en gly_2]$^+$.

Table I. Absorption data of the complexes of the [Co N_3O_3] type

Complex	A-band ν_{max} (log ε_{max})	I-band ν_{max} (log ε_{max})	II-band ν_{max} (log ε_{max})
mer(N)-[Co en gly CO_3]	{31.0 (0.04) {34.9 (0.01)	56.6 (2.07)	81.1 (2.17)
fac(N)-[Co en gly CO_3]	33.0 (0.17)	56.6 (2.17)	80.4 (2.13)
mer(N)-[Co en gly ox]	ca. 35 (0.15)	57.7 (1.96)	81.1 (2.23)
fac(N)-[Co en gly ox]		57.7 (2.13)	81.1 (2.24)
mer(N)-[Co en gly malo]		58.3 (1.95)	80.6 (2.13)
mer(N)-[Co gly_3][9]	29.8 ($\bar{1}$.82)	55.7 (2.00)	80.6 (2.18)
fac(N)-[Co gly_3][9]	33.0 (0.02)	57.7 (2.20)	80.2 (2.15)

The frequencies are given in 10^{13} sec^{-1}.

rings of K[Co gly_2 $(NO_2)_2$] are decomposed by such treatment. The complex salt resulting from the treatment of [Co en gly $(NO_2)_2$] is quantitatively obtained as a violet crystalline powder. The analytical data show that this complex has one water molecule which is not removed even by heating at 105°C for a few days. It may be assumed that this water molecule is coordinated to the cobalt(III) ion.

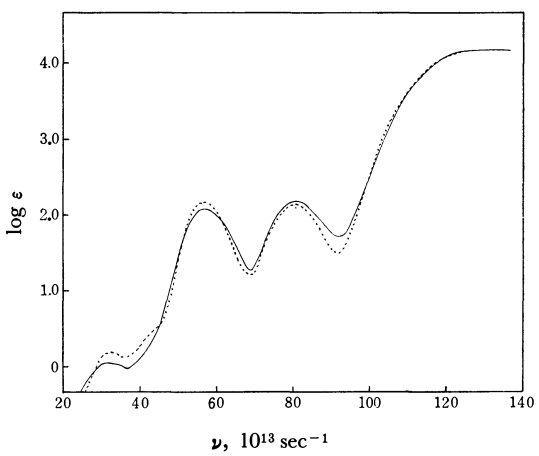

Fig. 3. Absorption curves of —— *mer(N)*- and ····· *fac(N)*-[Co en gly CO_3].

From the reaction of [Co en gly Cl (OH_2)]Cl with potassium hydrogen carbonate, two kinds of the carbonato complex, the violet form and the red form, are obtained. Now, the [Co en gly (CO_3)] complex may be expected to have two geometrical isomers, *mer(N)* and *fac(N)*, as is seen in Fig. 2. The absorption curves and the numerical data of both the isomers are shown in Fig. 3 and Table I. The first absorption band of the violet isomer is broader in shape and lower in intensity than that of the red isomer. It has been well established that the first band of a *mer(N)*-isomer of the complex of the [Co N_3O_3] type is broadened by the overlap of the split three absorption components and that the degenerate first band of a *fac(N)*-isomer is higher in intensity than that of the *mer(N)*-isomer.[7] Consequently, it may be concluded that the violet isomer of [Co en gly CO_3] is a *mer(N)*-form, and the red one, a *fac(N)*-form.

As is shown in Fig. 4 and Table I, the absorption curves of the two isomers of [Co en gly ox] show the same trends in the first bands as those of the *mer(N)*- and *fac(N)*-isomers of [Co en gly CO_3]. Furthermore, the violet oxalato isomer is derived from *mer(N)*-[Co en gly CO_3], and the red one, from *fac(N)*-[Co en gly CO_3]. These facts confirm

9) J. Fujita and Y. Shimura, This Bulletin, **36**, 1281 (1963).

TABLE II. ABSORPTION DATA OF BIS(AMINO-ACIDATO) SERIES

Complex ion	A-band ν_{max} (log ε_{max})	I-band ε_{max} (log ε_{max})	II-band ν_{max} (log ε_{max})
trans(O)-[Co en gly_2]$^+$	31.6 ($\bar{1}$.90)	56.6 (1.94) 66.0 (1.64)	83.3 (2.12)
cis(O)-[Co en gly_2]$^+$	37.0 ($\bar{1}$.90)	59.8 (2.09)	83.3 (2.13)
trans(O)-[Co en (β-ala)$_2$]$^+$ [2]		55.2 (2.00) 65.8 (1.61)	82.8 (1.94)

The frequencies are given in 10^{13} sec^{-1}.

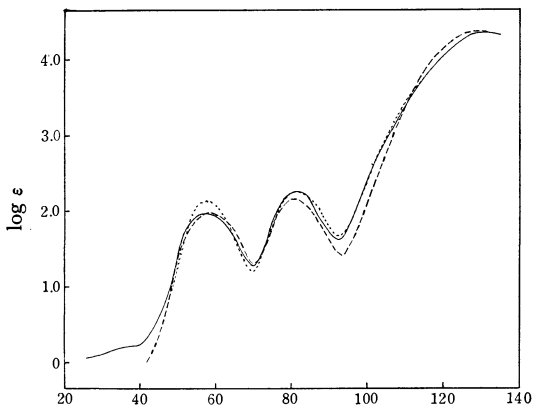

Fig. 4. Absorption curves of —— *mer(N)*- and ····· *fac(N)*-[Co en gly ox] and ---- *mer(N)*-[Co en gly malo].

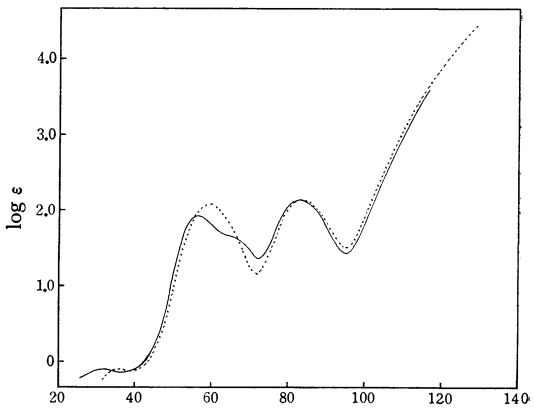

Fig. 5. Absorption curves of —— *trans(O)*- and ····· *cis(O)*-[Co en gly_2]I·H_2O.

that the violet [Co en gly ox] is of the *mer(N)* - form, and the red one, of the *fac(N)*-form.

The complexes which are derived from *mer(N)*- and *fac(N)*-[Co en gly CO_3] by the reaction with malonic acid are identical. From the fact that the first band of this complex agrees with that of *mer(N)*-[Co en gly ox], as is seen in Fig. 4, the *mer(N)* structure is assigned to this complex.

Three geometrical isomers, *trans(O)*-, *β-cis(O)*- and *β-cis(O)*-forms,* are expected for the [Co en gly_2]$^+$ ion. The *trans(O)*- and *α-cis(O)*-[Co en gly_2]$^+$ ions will be derived from *mer(N)*-[Co en gly CO_3] if the substitution reaction of the CO_3^{2-} ligand by the gly^- ion proceeds with the retention of the geometrical configuration of the [Co en gly —] part, while the *α-cis(O)*- and the *β-cis(O)*-[Co en gly_2]$^+$ ions are derived from *fac(N)*-[Co en gly CO_3], as is shown in Fig. 2.

In fact, the dark red complex is derived from *mer(N)*-[Co en gly CO_3], accompanied by a small quantity of a pinkish red complex, while from *fac(N)*-[Co en gly CO_3] the pinkish red complex, which is more soluble than the dark red one, is derived. The first absorption band of the dark red complex splits into two distinct components (Fig. 5 and Table II). This splitting pattern agrees well with the data[2,10] of the other *trans(O)*-[Co N_4O_2] complexes and with the pattern which is to be expected for the *trans* form from the semi-empirical molecular orbital calculations.[11] The first absorption band of the pinkish red complex is normal in shape; it may reasonably be considered that the pinkish red complex is *cis(O)*-[Co en gly_2]$^+$. It is difficult, however, on the basis of only the absorption spectrum, to discriminate between *α-cis(O)*- and *β-cis(O)*-structures.

* The prefix *α* denote that the two nitrogen atoms of the coordinated amino-acid ions occupy the *trans*-positions, and prefix *β* the *cis*-positions.

10) M. Linhard and M. Weigel, *Z. anorg. Chem.*, **264**, 321 (1951).

11) H. Yamatera, This Bulletin, **31**, 95 (1958).

BULLETIN OF THE CHEMICAL SOCIETY OF JAPAN VOL. 39 1262—1269 (1966)

Electronic Spectra and Electronic Structures of α- and β-Nitronaphthalenes and 1, 8-Dinitronaphthalene

By Maomi KOJIMA and Saburo NAGAKURA

The Institute of Physical and Chemical Research, Komagome, Bunkyo-ku, Tokyo

(Received October 29, 1965)

The absorption spectra of α-, β-nitronaphthalenes and 1, 8-dinitronaphthalene were measured in the near and vacuum ultraviolet regions. The peak wavelengths are as follows: α-nitronaphthalene, 213, 243 and 326.5 mμ; β-nitronaphthalene, 210.5, 259.5, 303 and 342 mμ; 1, 8-dinitronaphthalene, 199.5, 229.5 and 303 mμ. The transition energies and oscillator strengths were calculated with these three molecules by considering the configurational interaction among the ground, locally-excited and charge-transfer configurations. By combining the theoretical results with the observed peak wavelengths and the oscillator strengths, the nature of the electronic excitations corresponding to the observed absorption bands was clarified. Concerning 1, 8-dinitro-naphthalene, the twisting angle between the nitro groups and the naphthalene ring was estimated to be 60—70° by comparing the observed peak wavelengths and intensities with the calculated values. The effect of solvents on the absorption spectrum of 1, 8-dinitronaphthalene was found to be explained by the energy change in the charge-transfer configurations caused by the polarity of solvents. By considering the contribution of the charge-transfer configurations in the ground state, the increment in the dipole moment due to the delocalization of π-electrons was estimated for α- and β-nitronaphthalenes and 1, 8-dinitronaphthalene. The estimated dipole moment could explain the fact that the observed dipole moment of β-nitronaphthalene is greater than that of α-nitronaphthalene.

In previous papers,[1,2] we studied the electronic spectra and the electronic structures of nitrobenzene, nitromesitylene and 1, 5-dinitronaphthalene from both experimental and theoretical points of view. Concerning nitrobenzene,[1] a new band characteristic of the charge-transfer interaction between the benzene ring as an electron donor and the nitro group as an electron acceptor was observed at 240 mμ. This band almost completely disappeared in nitromesitylene, in which the nitro group is twisted from the benzene ring plane and in which, therefore, the resonance interaction is largely prohibited. In addition to this, the theoretical consideration based on the configurational interaction calculation and the direction of the transition moment measured by Labhart[3] lead to the conclusion that the 240 mμ band of nitrobenzene is an intramolecular charge-transfer absorption. A similar study has also been made with 1, 5-dinitronaphthalene.[2]

In the present study, we have undertaken to study the electronic spectra and electronic structures of α- and β-nitronaphthalenes and 1, 8-dinitronaphthalene by measuring the absorption spectra in the near and vacuum ultraviolet regions. Particularly, concerning 1, 8-dinitronaphthalene, the relation between the electronic spectra and the twisting angle of the nitro groups from the naphthalene ring plane was investigated, with the result that the twisting angle is 60—70° in solution.

Experimental

Materials.—Commercial 1, 8-dinitronaphthalene was purified by repeating recrystallizations from methanol and ethanol (m. p. 167°C).

Purified samples of α- and β-nitronaphthalenes were kindly presented by Mr. Akira Ishitani.* The *n*-heptane and methanol used as solvents were purified by the method described in the literature.[4,5] Commercial acetonitrile (OK type Special Grade, manufactured by the Asahi Chemical Industry, Ltd.) was first refluxed over calcium hydride for ten hours and then roughly distilled. The distillate was refluxed again over phosphorus pentoxide for half an hour and distilled. Finally it was distilled again from calcium hydride.

Measurements.—The absorption spectra of mononitro- and dinitronaphthalenes in the wavelength region of 190—500 mμ were measured with a Cary recording spectrophotometer, model 14. The absorption measurements of the acetonitrile solutions in the 180—200 mμ region were made with a vacuum ultraviolet spectrophotometer constructed in our

1) S. Nagakura, M. Kojima and Y. Maruyama, *J. Mol. Spect.*, **13**, 174 (1964).
2) M. Kojima and S. Nagakura, *Theoret. Chim. Acta*, **3**, 432 (1965).
3) H. Labhart, *Tetrahedron*, **19**, Suppl., 2, 223 (1963).

* We should like to express our hearty thanks to Mr. Ishitani for his kindness in providing us with the purified samples.

4) H. Yada, J. Tanaka and S. Nagakura, This Bulletin, **33**, 1660 (1960).
5) S. Nagakura, *Mol. Phys.*, **3**, 152 (1960).

TABLE I. THE ABSORPTION PEAK WAVELENGTHS AND INTENSITIES OF α-NITRONAPHTHALENE

Absorption peak wavelength, mμ	Molar extinction coefficient	Transition energy eV. Obs.	Transition energy eV. Calcd.	Oscillator strength Obs.	Oscillator strength Calcd.	Transition
326.5	4200	3.79	3.99	0.17	0.01	$W_0 \rightarrow W_1$
			4.14		0.17	$W_0 \rightarrow W_2$
243	10600	5.10	4.96	~0.22	0.01	$W_0 \rightarrow W_3$
			5.37		0.21	$W_0 \rightarrow W_4$
213 (long tail at the shorter wavelength side)	52900	5.83	5.67	~1.41	0.01	$W_0 \rightarrow W_5$
			5.86		0.45	$W_0 \rightarrow W_6$
			6.14		0.16	$W_0 \rightarrow W_7$
			6.19		0.06	$W_0 \rightarrow W_8$
			6.51		0.79	$W_0 \rightarrow W_9$

The experimental values were observed in the *n*-heptane solution.

TABLE II. THE ABSORPTION PEAK WAVELENGTH AND INTENSITIES OF β-NITRONAPHTHALENE

Absorption peak wavelength, mμ	Molar extinction coefficient	Transition energy eV. Obs.	Transition energy eV. Calcd.	Oscillator strength Obs.	Oscillator strength Calcd.	Transition
342	2500	3.62	3.95	0.04	0.03	$W_0' \rightarrow W_1'$
303	8100	4.09	4.45	0.13	0.12	$W_0' \rightarrow W_2'$
259.5	33400	4.78	5.23	0.59	0.48	$W_0' \rightarrow W_3'$
210.5 (long tail at the shorter wavelength side)	41400	5.89	5.77	~1.14	0.08	$W_0' \rightarrow W_4'$
			5.77		0.46	$W_0' \rightarrow W_5'$
			6.17		0.29	$W_0' \rightarrow W_6'$
			6.33		0.07	$W_0' \rightarrow W_7'$
			6.45		0.01	$W_0' \rightarrow W_8'$
			6.64		0.50	$W_0' \rightarrow W_9'$

The experimental values were observed in the *n*-heptane solution.

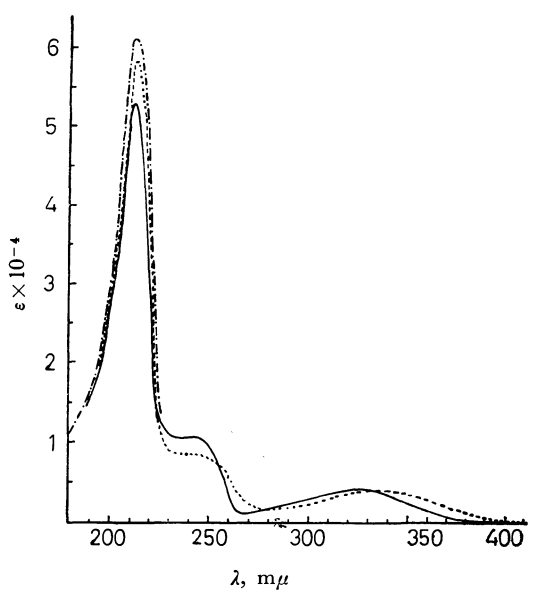

Fig. 1. The absorption spectrum of α-nitronaphthalene in several solvents.
—— *n*-heptane, ····· methanol,
-·-· acetonitrile

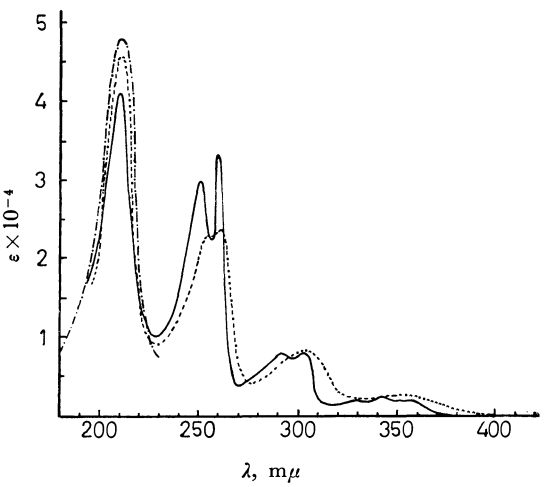

Fig. 2. The absorption spectrum of β-nitronaphthalene in several solvents.
—— *n*-heptane, ····· methanol,
-·-· acetonitrile

laboratory,**,6) an absorption cell with a path length of 0.1 mm. and with quartz windows being used.

Results.—The absorption spectra of mononitro- and dinitronaphthalenes are shown in Figs. 1—3. Furthermore, the peak wavelengths and molar extinction coefficients in their spectra are given in Tables I—III. In these tables the observed oscillator strength

** Our thanks are due to Mr. Koji Kaya and Mr. Masashi Tanaka for their kindness in measuring the vacuum ultraviolet absorption spectra.

6) H. Tsubomura, K. Kimura, K. Kaya, J. Tanaka and S. Nagakura, This Bulletin, **37**, 417 (1964).

Table III. The absoprtion peak wavelengths and intensities of 1, 8-dinitronaphthalene

Absorption peak wavelength, mμ	Molar extinction coefficient*1	Transition energy eV. Obs.	Transition energy eV. Calcd.*2	Oscillator strength Obs.	Oscillator strength Calcd.*2	Transition*3
303	6600	4.09	4.15	0.19	0.19	$W_0'' \rightarrow W_2''$
			4.46		0.02	$W_0'' \rightarrow W_3''$
229.5	35800	5.40	5.49	0.60	0.40	$W_0'' \rightarrow W_6''$
			5.69		0.02	$W_0'' \rightarrow W_7''$
199.5	38400	6.21	6.16	0.91	0.62	$W_0'' \rightarrow W_{10}''$
			6.18		0.09	$W_0'' \rightarrow W_{11}''$
			6.85		0.73	$W_0'' \rightarrow W_{12}''$

The experimental values were observed in the *n*-heptane solution.

*1 Since 1, 8-dinitronaphthalene is hardly soluble in *n*-heptane and the concentration of the *n*-heptane solution could not be determined accurately, all the molar extinction coefficient values are adjusted on the assumption that the values of the peak molar extinction coefficient of the longest wavelength band in the *n*-heptane solution coincides with that observed with the methanol solution. This may cause the errors of the order of 10%.

*2 Values calculated with $\theta=60°$.

*3 The other transitions are all forbidden.

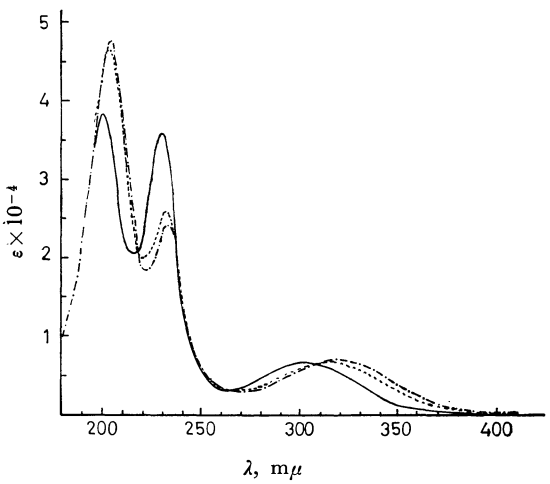

Fig. 3. The absorption spectrum of 1,8-dinitronaphthalene in several solvents.
—— *n*-heptane, ····· methanol,
–·–· acetonitrile

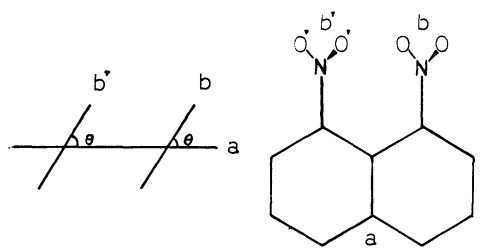

Fig. 4. 1,8-dinitronaphthalene with a hypothetical molecular symmetry C_2.
a: naphthalene ring plane
b, b': nitro group plane
θ: twisting angle

(*f*) values are also tabulated. In some cases, several bands overlap with each other and so we can not determine the oscillator strength value separately for each band. In these cases, the sums of the oscillator strengths for the overlapped bands are shown.

Theoretical

The π-electron structures of α- and β-nitronaphthalene and 1, 8-dinitronaphthalene were studied theoretically by the method used in the cases of 1, 5-dinitronaphthalene,[2] nitrobenzene and nitromesitylene.[1] That is to say, the respective nitronaphthalene molecules were separated into the naphthalene ring and the nitro groups, and the molecular orbitals of the components were evaluated by combining the results of the MO calculations with the experimental data of the electronic spectra. Thereafter, the interaction between the components was considered in terms of the configurational interaction among the ground, locally excited and charge-transfer configurations.

Concerning the geometrical configurations of the three molecules under consideration, no experimental data were found, so we assumed them to be follows: in β-nitronaphthalene, the nitro group is coplanar with the naphthalene ring plane; on the other hand, in α-nitronaphthalene, the nitro group is twisted from the aromatic ring plane by 49°, as in the case of 1, 5-dinitronaphthalene[7]; in 1, 8-dinitronaphthalene, the angle between the nitro group and the naphthalene ring plane may be assumed to change from 90° to 49° with a molecular symmetry (C_2) (see Fig. 4) and the calculation of the electronic structure was made with four values of the angle (49°, 60°, 70°, 80°). The other data necessary for the calculations were taken to be equal to the experimental data observed with 1, 5-dinitronaphthalene.[7] The C–N, N–O and C–C bond lengths were taken to be equal to 1.486 Å, 1.207 Å and 1.405 Å respectively, the C–C bond length being an averaged value for the ring

7) J. Trotter, *Acta Cryst.*, **13**, 95 (1960).

Table IV. The diagonal matrix elements used for the calculation of α-, β-nitronaphthalene and 1, 8-dinitronaphthalene

Configuration (No.)	Energy, eV.	Wave function	Wavelenghth of corresponding band, mμ[b]
Ground (I)[c,d]	0	Ψ_G	—
Locally excited (II)[c,d]	4.45	$\Psi_{B^+_{2u}}$	278.5[i]
Locally excited (III)[c,d]	5.73	$\Psi_{A^-_{1g}}$	—
Locally excited (IV)[c,d]	5.99	$\Psi_{B^-_{1g}}$	—
Locally excited (V)[c,d]	5.51	$\Psi_{B^+_{1g}}$	—
Locally excited (VI)[c,d]	3.97	$\Psi_{B^-_{3u}}$	312[i]
Locally excited (VII)[c,d]	5.89	$\Psi_{B^+_{3u}}$	210.5
Locally excited (VIII)[c]	6.62	Ψ_{NO_2}	198[j]
Charge-transfer (IX)[c]	4.56[e], 4.79[f]	Ψ_{CT_5}	
Charge-transfer (X)[c]	5.52[e], 5.76[f]	Ψ_{CT_4}	
Locally-excited (XI)[d]	6.32[g], 5.22[h]	$(\Psi_{NO_2}-\Psi_{NO_2'})/\sqrt{2}$	198[j]
Charge transfer (XII)[d]	4.56[g], 4.41[h]	$(\Psi_{CT_5}+\Psi_{CT_5'})/\sqrt{2}$	—
Charge-transfer (XIII)[d]	5.52[g], 5.57[h]	$(\Psi_{CT_4}-\Psi_{CT_4'})/\sqrt{2}$	—
Locally excited (XIV)[d]	6.20[g], 7.30[h]	$(\Psi_{NO_2}+\Psi_{NO_2'})/\sqrt{2}$	198[j]
Charge-transfer (XV)[d]	4.56[g], 4.41[h]	$(\Psi_{CT_5}-\Psi_{CT_5'})/\sqrt{2}$	—
Charge-transfer (XVI)[d]	5.52[g], 5.57[h]	$(\Psi_{CT_4}+\Psi_{CT_4'})/\sqrt{2}$	—

a) The exact forms of the locally excited configurations are given in Refs. 11 and 12.
b) Data from the spectra observed in the gaseous states.
c) Used for the calculation of α- and β-nitronaphthalenes.
d) Used for the calculation of 1, 8-dinitronaphthalene.
e) Values for α-nitronaphthalene.
f) Values for β-nitronaphthalene.
g) Values at $\theta=49°$.
h) Values at $\theta=90°$.
i) Taken from Ref. 13.
j) Taken from Ref. 5.

Table V. The off-diagonal matrix elements used for the calculation of α-nitronaphthalene

$H_{I\cdot IX}=-0.4214\beta'_{CN}$	$H_{V\cdot VIII}=0.1109$ eV.
$H_{I\cdot X}=0.0120\beta'_{CN}$	$H_{V\cdot IX}=-0.1978\beta'_{CN}$
$H_{II\cdot VIII}=0.1051$ eV.	$H_{V\cdot X}=0.0060\beta'_{CN}$
$H_{II\cdot IX}=0.2882\beta'_{CN}$	$H_{VI\cdot IX}=-0.0179\alpha'_{CN}$
$H_{II\cdot X}=0.0064\beta'_{CN}$	$H_{VI\cdot X}=0.2055\beta'_{CN}$
$H_{III\cdot IX}=0.0910\beta'_{CN}$	$H_{VII\cdot VIII}=-0.2288$ eV.
$H_{III\cdot X}=0.1660\beta'_{CN}$	$H_{VII\cdot IX}=0.0309\beta'_{CN}$
$H_{IV\cdot IX}=-0.1969\beta'_{CN}$	$H_{VII\cdot X}=0.2010\beta'_{CN}$
$H_{IV\cdot X}=0.0097\beta'_{CN}$	$H_{IX\cdot X}=0.0997$ eV.

($\beta'_{CN}=-1.57$ eV.)

The other off-diagonal matrix elements are zero.

Table VI. The off-diagonal matrix elements used for the calculation of β-nitronaphthalene

$H_{I\cdot IX}=-0.2595\beta_{CN}$	$H_{V\cdot VIII}=-0.1080$ eV.
$H_{I\cdot X}=0.3988\beta_{CN}$	$H_{V\cdot IX}=0.0859\beta_{CN}$
$H_{II\cdot VIII}=0.1190$eV.	$H_{V\cdot X}=-0.0097\beta_{CN}$
$H_{II\cdot IX}=-0.1782\beta_{CN}$	$H_{VI\cdot IX}=-0.1836\beta_{CN}$
$H_{II\cdot X}=0.0705\beta_{CN}$	$H_{VI\cdot X}=-0.1270\beta_{CN}$
$H_{III\cdot IX}=-0.1017\beta_{CN}$	$H_{VII\cdot VIII}=-0.1334$ eV.
$H_{III\cdot X}=-0.0921\beta_{CN}$	$H_{VII\cdot IX}=0.1693\beta_{CN}$
$H_{IV\cdot IX}=0.0855\beta_{CN}$	$H_{VII\cdot X}=-0.1243\beta_{CN}$
$H_{IV\cdot X}=-0.0158\beta_{CN}$	$H_{IX\cdot X}=0.2211$ eV.

($\beta_{CN}=-2.4$ eV.)

The other off-diagonal matrix elements are zero.

C–C bonds.

We took the energy of the ground configuration as the standard. Beside this, several locally excited configurations and the two types of charge-transfer configurations were taken into account.

The diagonal and off-diagonal matrix elements of the total electronic Hamiltonian were evaluated according to the methods presented by Pariser and Parr,[8] by Longuet-Higgins and Murrell[9] and by Pople[10]. They are shown in Tables IV—VII. The secular equations were solved by the aid of an electronic computer, FACOM 202, located at the Institute for Solid State Physics.

The finally-obtained energy levels and wave functions are shown in Tables VIII—X.

Discussion

α-Nitronaphthalene.—It is seen from Fig. 1 that the absorption spectrum of α-nitronaphthalene consists of three bands in the observed wavelength region. They appear at 213, 243 and 326.5,

8) R. Pariser and R. G. Parr, *J. Chem. Phys.*, **21**, 466, 767 (1953).
9) H. C. Longuet-Higgins and J. N. Murrell, *Proc. Phys. Soc.*, **A68**, 601 (1955).
10) J. A. Pople, ibid., **A68**, 81 (1955).

Table VII. The off-diagonal matrix elements used for the calculation of 1, 8-dinitronaphthalene

$H_{I\cdot XII}=-0.5959\beta''_{CN}$ $H_{II\cdot XIII}=0.0090\beta''_{CN}$ $H_{IV\cdot XV}=-0.2785\beta''_{CN}$ $H_{V\cdot XVI}=0.0085\beta''_{CN}$ $H_{VII\cdot XV}=0.0436''_{CN}$

$H_{I\cdot XIII}=0.0170\beta''_{CN}$ $H_{III\cdot XII}=0.1287\beta''_{CN}$ $H_{IV\cdot XVI}=0.0138\beta''_{CN}$ $H_{VI\cdot XV}=-0.0253\beta''_{CN}$ $H_{VII\cdot XVI}=0.2843\beta''_{CN}$

$H_{II\cdot XI}=0.1486(49°)$—0 eV.(90°) $H_{III\cdot XIII}=0.2348\beta''_{CN}$ $H_{V\cdot XIV}=0.1568(49°)$—0 eV.(90°) $H_{VI\cdot XVI}=0.2906\beta''_{CN}$ $H_{XV\cdot XVI}=0.0996$ eV.

$H_{II\cdot XII}=0.4076\beta''_{CN}$ $H_{XII\cdot XIII}=0.0996$ eV. $H_{V\cdot XV}=-0.2797\beta''_{CN}$ $H_{VII\cdot XIV}=-0.3236(49°)$—0 eV.(90°)

$\beta''_{CN}(\theta)=\beta_{CN}(0°)\cos\theta$ (θ: 49°—90°); $\beta_{CN}(0°)=-2.4$eV.

The other off-diagonal matrix elements are zero.

Table VIII. Calculated energy levels and wave functions of α-nitronaphthalene

Energy, eV.		Wave function									
		Ψ_G	$\Psi_{A_{1g}^-}$	$\Psi_{B_{1g}^-}$	$\Psi_{B_{1g}^+}$	$\Psi_{B_{3u}^-}$	$\Psi_{B_{2u}^+}$	$\Psi_{B_{3u}^+}$	Ψ_{CT_5}	Ψ_{CT_4}	Ψ_{NO_2}
$W_9=$ 6.42	$\Psi_9=$	0.0044	−0.0920	0.0274	0.1154	−0.0278	0.0319	−0.4922	0.0487	0.2149	0.8274
$W_8=$ 6.09	$\Psi_8=$	0.0269	−0.3626	0.6927	0.0685	−0.0518	−0.0946	−0.2527	0.2578	0.3627	−0.3309
$W_7=$ 6.04	$\Psi_7=$	0.0121	0.3208	0.6480	0.1333	0.0697	−0.0033	0.3779	0.0981	−0.4384	0.3309
$W_6=$ 5.77	$\Psi_6=$	0.0110	−0.7187	−0.1348	0.2145	−0.0070	−0.0156	0.5947	0.0977	0.0478	0.2305
$W_5=$ 5.58	$\Psi_5=$	0.0310	0.2016	−0.1988	0.8937	0.0097	−0.1196	−0.1051	0.2600	−0.0258	−0.1621
$W_4=$ 5.27	$\Psi_4=$	−0.0047	0.4334	0.0235	0.0061	−0.1895	0.0121	0.4286	−0.0163	0.7628	0.0974
$W_3=$ 4.86	$\Psi_3=$	0.0857	0.0912	−0.1734	−0.3169	0.0345	−0.6708	0.0352	0.6268	−0.0408	0.0813
$W_2=$ 4.04	$\Psi_2=$	0.1050	0.0566	−0.1019	−0.1339	0.1850	0.7155	0.0162	0.6403	0.0150	−0.0255
$W_1=$ 3.90	$\Psi_1=$	−0.0253	0.0184	0.0227	0.0283	0.9592	−0.1142	0.0302	−0.1428	0.2076	0.0066
$W_0=$ −0.10	$\Psi_0=$	0.9894	−0.0032	0.0073	0.0079	0.0014	−0.0143	−0.0008	−0.1437	0.0057	0.0000

Table IX. Calculated energy levels and wave functions of β-nitronaphthalene

Energy, eV.		Wave function									
		Ψ_G	$\Psi_{A_{1g}^-}$	$\Psi_{B_{1g}^-}$	$\Psi_{B_{1g}^+}$	$\Psi_{B_{3u}^-}$	$\Psi_{B_{2u}^+}$	$\Psi_{B_{3u}^+}$	Ψ_{CT_5}	Ψ_{CT_4}	Ψ_{NO_2}
$W_9'=$ 6.40	$\Psi_9'=$	0.0705	−0.0629	−0.1112	−0.1321	−0.0183	0.1099	−0.5278	0.1550	−0.3705	0.7133
$W_8'=$ 6.21	$\Psi_8'=$	−0.0940	0.3544	0.0300	−0.0902	0.1087	−0.0044	0.2718	0.0904	0.6691	0.5611
$W_7'=$ 6.09	$\Psi_7'=$	−0.0133	−0.3681	0.6901	0.0670	−0.1014	−0.0584	0.3109	−0.3722	−0.1599	0.3242
$W_6'=$ 5.93	$\Psi_6'=$	−0.0037	−0.3898	−0.6951	0.0375	−0.0642	−0.0291	0.5016	−0.2079	−0.1122	0.2254
$W_5'=$ 5.53	$\Psi_5'=$	0.0857	0.7129	0.0112	−0.0885	−0.1277	0.0605	0.3888	−0.0759	−0.5450	0.0482
$W_4'=$ 5.53	$\Psi_4'=$	−0.0211	0.1888	−0.0741	0.9431	−0.0423	−0.0535	−0.1526	−0.1617	0.0171	0.1202
$W_3'=$ 4.98	$\Psi_3'=$	0.1011	−0.1829	0.1334	0.2553	0.2406	0.5479	0.3215	0.6319	−0.1155	0.0039
$W_2'=$ 4.21	$\Psi_2'=$	−0.0949	0.0339	−0.0453	−0.0649	−0.4309	0.7851	−0.1239	−0.3591	0.1838	−0.0569
$W_1'=$ 3.71	$\Psi_1'=$	−0.0559	0.0659	−0.0394	−0.0517	0.8436	0.2449	−0.0747	−0.4524	−0.0773	−0.0175
$W_0'=$ −0,24	$\Psi_0'=$	0.9776	−0,0003	−0.0053	−0.0053	0.0020	0.0178	−0.0166	−0.1314	0.1620	−0.0007

TABLE X. CALCULATED ENERGY LEVELS AND WAVE FUNCTIONS OF 1, 8-DINITRONAPHTHALENE ($\theta=60°$)

Energy, eV.		Symmetric wave function					
		Ψ_G	$\Psi_{A_{1g}^-}$	$\Psi_{B_{2u}^+}$	$\frac{(\Psi_{CT_5}-\Psi_{CT_5'})}{\sqrt{2}}$	$\frac{(\Psi_{CT_4}+\Psi_{CT_4'})}{\sqrt{2}}$	$\frac{(\Psi_{NO_2}-\Psi_{NO_2'})}{\sqrt{2}}$
$W_9''=$ 5.96	$\Psi_9''=$	−0.0164	0.8009	0.0591	−0.1535	−0.5707	0.0728
$W_8''=$ 5.88	$\Psi_8''=$	−0.0025	−0.0669	0.0818	−0.0197	0.0467	0.9930
$W_5''=$ 5.34	$\Psi_5''=$	−0.0047	0.5787	−0.0030	−0.0123	0.8153	0.0006
$W_4''=$ 5.00	$\Psi_4''=$	0.1064	0.1268	−0.6388	0.7426	−0.0807	0.0800
$W_2''=$ 4.04	$\Psi_2''=$	0.1121	0.0536	0.7624	0.6328	−0.0249	−0.0451
$W_0''=-0.11$	$\Psi_0''=$	0.9878	−0.0037	−0.0165	−0.1545	0.0060	0.0003

Energy, eV.		Antisymmetric wave function						
		$\Psi_{B_{1g}^-}$	$\Psi_{B_{1g}^+}$	$\Psi_{B_{3u}^-}$	$\Psi_{B_{3u}^+}$	$\frac{(\Psi_{CT_5}+\Psi_{CT_5'})}{\sqrt{2}}$	$\frac{(\Psi_{CT_4}-CT_4')}{\sqrt{2}}$	$\frac{(\Psi_{NO_2}+\Psi_{NO_2'})}{\sqrt{2}}$
$W_{12}''=6.74$	$\Psi_{12}''=$	0.0098	0.0939	−0.0113	−0.3107	0.0269	0.0925	0.9407
$W_{11}''=6.07$	$\Psi_{11}''=$	0.8848	0.1082	−0.0327	−0.2838	0.2368	0.2175	−0.1424
$W_{10}''=6.05$	$\Psi_{10}''=$	0.3763	0.0954	0.0894	0.6973	0.0465	−0.5296	0.2687
$W_7''=5.58$	$\Psi_7''=$	−0.1955	0.9420	−0.0119	0.0539	0.2401	0.0759	−0.0886
$W_6''=5.37$	$\Psi_6''=$	0.0112	−0.0893	−0.1932	0.5760	0.0180	0.7798	0.1194
$W_3''=4.35$	$\Psi_3''=$	−0.1914	−0.2729	0.1138	0.0249	0.9344	−0.0427	0.0162
$W_1''=3.89$	$\Psi_1''=$	0.0175	0.0217	0.9697	0.0349	−0.0991	0.2186	0.0022

TABLE XI. THE SOLVENT EFFECT ON THE ABSORPTION BANDS OF 1, 8-DINITRONAPHTHALENE

Solvent	Absorption maxima and molar extinction coefficients		
n-Heptane	303.0 mμ (6600)	229.4 mμ (35800)	199.6 mμ (38400)
Methanol	313.5 mμ (6600)	231.2 mμ (25800)	201.9 mμ (46600)
Acetonitrile	318.8 mμ (7000)	232.9 mμ (24000)	203.5 mμ (47800)

TABLE XII. DEPENDENCE OF TRANSITION ENERGIES AND OSCILLATOR STRENGTHS UPON THE CHARGE-TRANSFER CONFIGURATIONS (Calculated for $\theta=60°$)

Case	1	2	3	4	5
H_{CT_5}	4.52 eV.	4.32 eV.	4.12 eV.	3.92 eV.	3.72 eV.
H_{CT_4}	5.54 eV.	5.34 eV.	5.14 eV.	4.94 eV.	4.74 eV.
Energy(I)*	4.18 eV.	4.09 eV.	3.98 eV.	3.84 eV.	3.70 eV.
f(I)**	0.21	0.21	0.20	0.19	0.21
Energy(II)*	5.50 eV.	5.36 eV.	5.21 eV.	5.15 eV.	4.99 eV.
f(II)**	0.42	0.28	0.19	0.15	0.10
Energy(III)*	6.51 eV.	6.45 eV.	6.41 eV.	6.40 eV.	6.38 eV.
f(III)**	1.44	1.58	1.66	1.71	1.75

* Mean values weighted by calculated oscillator strengths for all the transitions assigned to a band.
** Sum of the calculated oscillator strength values classified to the same observed band.
(The numbers in bracket correspond to the 303.0 mμ band 229.4 mμ band and 199.6 mμ band (observed with the *n*-heptane solution), respectively.)

mμ. From a comparison of the observed absorption spectrum with the theoretical results, the broad 326.5 mμ band may be considered to include the two overlapped bands corresponding to the $W_0\rightarrow W_1$ and $W_0\rightarrow W_2$ transitions. The wave functions, Ψ_1 and Ψ_2, given in Table VIII show that the former corresponds to the $A_{1g}^-\rightarrow B_{3u}^-$ transition of naphthalene, while the latter contains the $A_{1g}^-\rightarrow B_{2u}^-$ transition of naphthalene and the CT_5-type charge-transfer transition in almost equal proportions. As is revealed by the calculated oscillator strengths given in Table I, the $W_0\rightarrow W_1$ transition is weaker than the $W_0\rightarrow W_2$ transition.

The 243 mμ band may be ascribed to the $W_0\rightarrow W_3$ and $W_0\rightarrow W_4$ transitions. In view of the calculated oscillator strength values given in Table I, this band may be assigned substantially to the W_0—W_4 transition, which results mainly from the CT_4-type charge-transfer transition.

The strong band at 213 mμ seems to include various transitions, transitions from the ground state, W_0, to the W_5, W_6, W_7, W_8 and W_9 states. An inspection of the calculated oscillator strengths given in Table I reveals that the $W_0\rightarrow W_5$ and $W_0\rightarrow$

W_8 transition bands are weak and may be covered by the other transition bands. The $W_0 \rightarrow W_6$ transition is mainly composed of the $A_{1g}^- \rightarrow B_{3u}^+$ and $A_{1g}^- \rightarrow A_{1g}^+$ transitions. The $W_0 \rightarrow W_7$ transition has a complicated character and comes from the $A_{1g}^- \rightarrow B_{1g}^-$, $A_{1g}^- \rightarrow B_{3u}^+$ and $A_{1g}^- \rightarrow A_{1g}^-$ transitions, besides the local transition within the nitro group and CT_4-type charge-transfer transitions. The $W_0 \rightarrow W_9$ transition results largely from the local excitation within the nitro group. The tail at the shorter wavelength side of the 213 mμ band might be due to this transition.

β-Nitronaphthalene.—The absorption spectrum of β-nitronaphthalene shown in Fig. 2 consists of four bands in near and vacuum ultraviolet regions down to 180 mμ. They appear at 210.5, 259.5, 303 and 342 mμ.

The 342 mμ band may safely be assigned to the $W_0' \rightarrow W_1'$ transition. The wave function, Ψ_1', given in Table IX shows that the band may be regarded as the shifted band of the $A_{1g}^- \rightarrow B_{3u}^-$ transition band of naphthalene.

The 303 mμ band can be assigned to the $W_0' \rightarrow W_2'$ transition. Its character is, for the most part, that of the shifted band of the $A_{1g}^- \rightarrow B_{2u}^+$ transition of naphthalene, though it also includes, to some extent, the $A_{1g}^- \rightarrow B_{3u}^-$ and CT_5-type charge-transfer transitions.

The $W_0' \rightarrow W_1'$ and $W_0' \rightarrow W_2'$ transitions of β-nitronaphthalene are similar to, respectively, the $W_0 \rightarrow W_1$ and $W_0 \rightarrow W_2$ transitions of α-nitronaphthalene in their nature. Therefore, it may be said that the overlapping bands at 326.5 mμ in α-nitronaphthalene appear separately at 342 and 303 mμ in β-nitronaphthalene. This difference can be explained satisfactorily by the present theoretical treatment. That is to say, the B_{2u}^+ locally excited configuration is stabilized by the contribution of the charge-transfer configurations to a greater extent in the W_1' state of β-nitronaphthalene than in the W_1 state of α-nitronaphthalene; the reverse is the case for the W_2 and W_2' states.

The 259.5 mμ band is undoubtedly due to the $W_0' \rightarrow W_3'$ transition. From the wave function, Ψ_3', given in Table IX, this transition is known to result mainly from the $A_{1g}^- \rightarrow B_{2u}^+$ and CT_5-type transitions. This transition corresponds to the $W_0 \rightarrow W_3$ transition of α-nitronaphthalene, whose transition probability is very small.

The 210.5 mμ band may be regarded as overlapping bands corresponding to the $W_0' \rightarrow W_4'$, $W_0' \rightarrow W_5'$, $W_0' \rightarrow W_6'$, $W_0' \rightarrow W_7'$ and $W_0' \rightarrow W_8'$ transitions. An inspection of the calculated oscillator strength values given in Table IX shows that this band consists substantially of the $W_0' \rightarrow W_5'$ and $W_0' \rightarrow W_6'$ transitions. The $W_0' \rightarrow W_4'$, $W_0' \rightarrow W_7'$ and $W_0' \rightarrow W_8'$ transitions are very weak in intensity. Roughly speaking, the $W_0' \rightarrow W_5'$ and $W_0' \rightarrow W_6'$ transitions of β-nitronaphthalene correspond to the $A_{1g}^- \rightarrow A_{1g}^-$ and $A_{1g}^- \rightarrow B_{1g}^-$ transitions of naphthalene respectively, though the $A_{1g}^- \rightarrow B_{3u}^+$ transition of naphthalene also contributes considerably to these two transitions. The tail at the shorter wavelength side of the 210.5 mμ band might be due to the $W_0' \rightarrow W_9'$ transition. Table IX shows that the upper state of this transition is mainly composed of the local excitation within the nitro group (50%) and of the local excitation ($A_{1g}^- \rightarrow B_{3u}^+$) within the naphthalene ring (25%).

1, 8-Dinitronaphthalene. — As is shown in Fig. 3, the absorption spectrum of 1, 8-dinitronaphthalene consists of three bands in the observed wavelength region. They appear at 199.5, 229.5 and 303 mμ.

The Determination of the Angle between the Naphthalene Ring and the Nitro Groups.—In order to evaluate the twisting angle between the nitro groups and the naphthalene ring, we calculated the transition energies and oscillator strengths for the four angles of 49°, 60°, 70° and 80°. Each of the observed bands consists of multiple transitions. Therefore, the mean value of the calculated transition energies, weighted by the calculated oscillator strengths, was evaluated for each observed band. Consequently, the deviation, δw_i, between the observed and calculated transition energies could be obtained for each band. The minimum sum of the $|\delta w_i|$ values for the three observed bands was found to be that for the angle of 70°. From the comparison between the calculated and observed oscillator strengths, the most suitable value of the angle was determined to be 60°. Therefore, it is most probable that the angle between the naphthalene ring plane and the nitro groups in 1, 8-dinitronaphthalene is 60°—70° in solution. This value seems reasonable in view of the fact that the nitro groups are twisted by 49° from the naphthalene ring in 1, 5-dinitronaphthalene.[7]

The Assignment of the Absorption Bands.—The 303 mμ band may safely be assigned to the $W_0'' \rightarrow W_2''$ and $W_0'' \rightarrow W_3''$ transitions. Judging from the calculated oscillator strengths, the latter transition band may be considered to be hidden under the former. The latter mainly consists of the CT_5-type charge-transfer transition. An inspection of Ψ_2'' given in Table X shows that the $W_0'' \rightarrow W_2''$ transition is a mixture of the $A_{1g}^- \rightarrow B_{2u}^+$ transition of naphthalene and the charge-transfer (CT_5-type) transition.

In view of the oscillator strength values of the $W_0'' \rightarrow W_6''$ and $W_0'' \rightarrow W_7''$ transitions, the character of the 229.5 mμ band comes mostly from the former. The latter is composed of the shifted $A_{1g}^- \rightarrow B_{1g}^-$ transition. The $W_0'' \rightarrow W_6''$ transition consists mainly of the CT_4-type charge-transfer

11) J. Tanaka, *J. Chem. Soc. Japan, Pure Chem. Sect.* (*Nippon Kagaku Zassi*), **78**, 1643 (1957).
12) R. Pariser, *J. Chem. Phys.*, **24**, 250 (1956).
13) G. D. Nordheim and H. S. Sponer, *Discussions Faraday Soc.*, **9**, 19 (1950).

band, although it also includes the $A_{1g}^{-} \rightarrow B_{3u}^{+}$ transition to some extent. The 199.5 mμ band may owe its character chiefly to the $W_0'' \rightarrow W_{10}''$, $W_0'' \rightarrow W_{11}''$ and $W_0'' \rightarrow W_{12}''$ transitions. The $W_0'' \rightarrow W_{11}''$ transition is very weak in comparison with the other two. The $W_0'' \rightarrow W_{10}''$ transition may be regarded as a mixture of the $A_{1g}^{-} \rightarrow B_{3u}^{+}$ and CT_4-type transitions. The $W_0'' \rightarrow W_{12}''$ transition corresponds to the local excitation of the NO_2 groups.

The Solvent Effect on the Absorption Bands.—Figure 3 shows that the 199.5 mμ and 229.5 mμ bands of 1, 8-dinitronaphthalene are sensitive to the polarity of the solvent; these bands change not only in the peak wavelength but also in the intensity with the polarity of the solvent. These tendencies are tabulated in Table XI. In order to explain the solvent effect, we calculated the energy levels and wave functions, changing the energy values of the two types of charge-transfer configurations, H_{CT_5} and H_{CT_4}. The results are shown in Table XII. It is seen that the decrease in the energies of the two types of charge-transfer configurations brings about a decrease in the transition energies (mean values) corresponding to the three absorption bands at 199.5, 229.5 and 303 mμ, and that it causes a decrease and an increase in the oscillator strength values of the 229.5 mμ and 199.5 mμ bands respectively. On the other hand, the oscillator strength of the 303 mμ band is insensitive to the solvent. These theoretical results satisfactorily explain the observed solvent effects shown in Table XI. Thus the absorption spectrum of 1, 8-dinitronaphthalene may be regarded as a typical example showing conspicuous solvent effects through the energy change of the charge-transfer configurations.

Dipole Moments of α- and β- Nitronaphthalenes.—According to the present theoretical consideration, the contributions of the charge-transfer configurations in the ground state are 2.1% and 4.4% for α- and β- nitronaphthalenes respectively. From this it may be expected that the dipole moments due to π-electrons would be greater in β-nitronaphthalene than in α-nitronaphthalene. In fact, the dipole moments of α- and β-nitronaphthalenes were observed to be 3.62—3.88D and 4.36—4.4D respectively.[14] In order to treat the problem more quantitatively, we calculated the dipole moments of these compounds by considering the additional moment due to the contribution of the charge-transfer configurations.[15] Consequently, the dipole moments of α- and β-nitronaphthalenes were calculated to be 3.52 and 4.10D respectively. Therefore, it may be said that the present theoretical treatment can explain quantitatively, or at least semi-quantitatively, the difference in the dipole moment between α- and β-nitronaphthalenes. A similar calculation was made for the dipole moment of 1, 8-dinitronaphthalene, with the result of 6.77D. This value also coincides well with the observed value, 7.1—7.87D.[14]

14) L. G. Wesson, "Tables of Electric Dipole Moments," The Technology Press, Massachusetts Institute of Technology, Cambridge, Massachusetts (1948), pp. 13, 45.

15) The dipole moments of the charge-transfer configurations were evaluated to be as follows from the π-electron distribution of each CT configuration:

α-Nitronaphthalene CT_4, CT_5; 16.40D

β-Nitronaphthalene CT_4, CT_5; 20.74D

From these values and the contribution of each charge-transfer configuration in the ground state, the additional dipole moments due to resonance interaction are evaluated to be 0.36 and 0.92 D for α- and β-nitronaphthalenes respectively. By combining these additional dipole moments with the observed dipole moment of nitromethane, 3.2D, the dipole moments of α- and β-nitronaphthalenes were evaluated to be 3.52 and 4.10D respectively.

BULLETIN OF THE CHEMICAL SOCIETY OF JAPAN VOL. 39 1269—1273 (1966)

The Reaction of the Exo-cyclic Imino Group of "4-Thiazone Imine"[1)]

By Masaki OHTA, Kei YOSHIDA and Shigeru SATO

Laboratory of Organic Chemistry, Tokyo Institute of Technology, Ookayama, Meguro-ku, Tokyo

(Received November 1, 1965)

In order to accumulate further information about the properties of meso-ionic compounds with an exo-cyclic imino group, the reactivity of an exo-cyclic imino group of thiazone imine as compared with that of sydnone imine was investigated. Moreover, for the purpose of the pharmacological test, 2, 3-disubstituted thiazone imine hydrochlorides and their *N*-acetyl derivatives were prepared.

Meso-ionic compounds of various ring systems with an exo-cyclic imino group have been reported in the literatures; of these, sydnone imine has been most extensively investigated. The stabilities of the free bases of these meso-ionic compounds differ markedly, depending on the ring systems. In some

1) This paper is the Part XXVI of studies on meso-ionic compounds.

TABLE I. 2, 3-DISUBSTITUTED-4-THIAZONE IMINE HYDROCHLORIDES

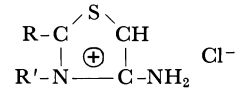

No.	R	R′	M. p., °C (decomp.)	Yield %	N, % Found	N, % Calcd.
1	C_6H_5	p-Cl-C_6H_4	200—201	86	8.84	8.66
2	C_6H_5	o-Cl-C_6H_4	245—247	75	8.74	8.66
3	C_6H_5	p-$CH_3OC_6H_4$	213—215	82	8.73	8.81
4	C_6H_5	o-$CH_3OC_6H_4$	207—208	65	8.89	8.81
5	p-CH_3O-C_6H_4	C_6H_5	220—223	75	8.92	8.81
6	C_6H_5	2-C_5H_4N	147—148	30	14.53	14.47

cases, as in "nitron", free bases can be obtained in a stable form, but sydnone imine or "thiazone imine", which we reported on previously,[2] is unstable and can not be obtained as a free base; it exists only in the form of a salt or an *N*-acyl derivative. Furthermore, the reactivity of the exo-cyclic imino group varies according to the ring system and appreciably differs from that of a usual imino group, which suggests the presence of intrinsic characteristics of the meso-ionic ring. The structure of meso-ionic compounds other than sydnone imine has scarcely been investigated; there remain many points for discussion concerning the representation of these compounds. In some cases, the representation of one specific polar structure might be satisfactory, although as a common feature the compounds can be regarded as resonance hybrids consisting of many polar structures. The structure of the hydrochloride of thiazone imine, which we considered as a meso-ionic compound, may be represented not only by formulae I and II, but also by the quaternary salt structure III, as will be shown below. The hydrochloride of an *N*-acyl derivative of thiazone imine may similarly be represented by IV, V, VI, etc.

The present investigation of the reactivity of the exo-cyclic imino group of thiazone imine, as compared with that of sydnone imine, was undertaken in order to accumulate further information about the structure of thiazone imine. Moreover, stimulated by the recent interest in pharmacological activities,[3] we synthesized 2, 3-disubstituted thiazone imine derivatives for the pharmacological test and also for the purpose of testing the applicability of the methods reported in a previous paper.[2]

Two procedures for the synthesis of thiazone imine derivatives are available: the ring closure of intermediate nitriles prepared by refluxing a benzene solution of chloroacetonitrile and *N*-monosubstituted thioamides by treatment with hydrogen chloride (method A), and a one-step condensation of thioamides and chloroacetonitrile by heating, with or without diphenyl as a diluent (method B).

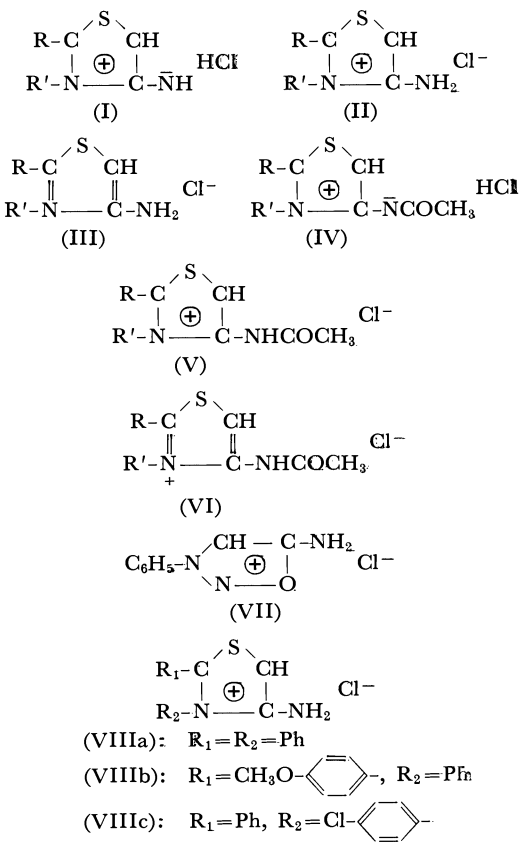

Fig. 1.

The data on the newly-synthesized thiazone imine hydrochlorides are summarized in Table I. Compounds No. 1 and No. 2 were prepared by both methods A and B, and the others, by only method B; an attempt to isolate the intermediates was in vain to give the starting materials. The reaction of thioformanilide and chloroacetonitrile to prepare 3-phenyl-thiazone imine hydrochloride could not be accomplished by method B. The reaction of thiocaprolactam with chloroacetonitrile by

2) H. Chosho, K. Ichimura and M. Ohta, This Bulletin, **37**, 1670 (1964).

3) H. V. Daeniker and J. Druey, *Helv. Chim. Acta*, **45**, 2426 (1962); L. B. Kier and D. Dhawan, *J. Pharm. Sci.*, **51**, 1058 (1962); V. G. Yashunskii and V. G. Ermolaeva, *J. Gen. Chem. U. S. S. R.*, **32**, 182 (1962).

TABLE II. *N*-ACETYL-4-THIAZONE IMINE HYDROCHLORIDES

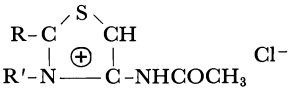

R	R′	M. p., °C (decomp.)	Yield %	N, % Found	N, % Calcd.	Reaction time hr.
C_6H_5	*p*-Cl-C_6H_4	215—216	85	7.72	7.67	2
C_6H_5	*o*-Cl-C_6H_4	>300	82	7.76	7.67	12
C_6H_5	*p*-CH_3O-C_6H_4	194—195	87	7.80	7.78	2
C_6H_5	*o*-CH_3O-C_6H_4	248—250	85	7.96	7.78	2
p-CH_3O-C_6H_4	C_6H_5	232—233	75	7.50	7.78	1.5
C_6H_5	2-C_5H_4N	232—234	55	12.85	12.69	1

method B to prepare 2, 3-cyclopentamethylene thiazone imine salt gave *S*-acetoamido-isothiocaprolactam hydrochloride. These facts suggest that, in thiazone imine salt, the ring is stabilized by conjugation with aromatic substituents.

As a preliminary work for the subsequent experiments, the stability of the salt and bases of 2, 3-diphenyl thiazone imine was examined. Concerning the stability of sydnone imine, we[4] and Daeniker[3] have reported that its hydrochloride VII is quite stable when heated with water or dilute hydrochloric acid, while its free base can not be obtained by neutralization, which resulted only in decomposition yielding the nitrosoacetonitrile derivative. When an aqueous solution of sydnone imine hydrochloride is neutralized with sodium bicarbonate, a solution of bicarbonate of sydnone imine is formed; this solution, although it is decomposed on heating and carbon dioxide is evolved, can be used immediately for further experiments such as the preparation of *N*-acyl-derivatives. On the other hand, 2, 3-diphenyl-4-thiazone imine hydrochloride (VIIIa) is converted to the acid amide derivative by heating it in 10% hydrochloric acid at 100°C. When an aqueous solution of VIIIa was allowed to stand for a long period, heated at 100°C or neutralized with sodium bicarbonate, a tarry substance was separated out; from this substance nothing could be isolated in a pure state. However, an intermediate nitrile, *S*-cyanomethyl-isothiobenzoyl-*p*-chloroanilide, was isolated from the neutralization products of 2-phenyl-3-(*p*-chlorophenyl)-4-thiazone imine hydrochloride (VIIIc). The above facts indicate that the decomposition of VIIIa does not proceed through a simple reversed process of its formation and that VII is more sensitive to hydrolytic attack than is sydnone imine hydrochloride.

In the studies of reactions at the exo-cyclic imino group of thiazone imine hydrochloride, manipulations in an aqueous or alkaline media seem undesirable. Therefore, taking the results obtained here into consideration, several reactions of VIII under special conditions were examined.

VII can be acetylated with acetic anhydride or acyl chloride by usual methods. In contrast to sydnone imine, VIIIa can not be benzoylated with benzoyl chloride in pyridine, and VIII is recovered unchanged. The acetylation of VIIIa by heating it with acetic anhydride at 100°C for many hours in either the absence or the presence of pyridine gave an acetyl derivative, but the yield was not satisfactory. The use of boron trifluoride as a condensing agent shortened the reaction time considerably and gave a better yield. The data on newly synthesized *N*-acetyl-derivatives of 2, 3-disubstituted-4-thiazone imine hydrochlorides are summarized in Table II. However, the applicability of the method to the synthesis of various acyl-derivatives is extremely limited due to the necessity of using an acid anhydride. We have now found that acylation can be easily accomplished by the simple heating of VIIIa with acid chloride without a solvent or in an inert solvent; by this method various acyl derivatives are obtained in good yields. In a similar way, VII is easily acylated with aliphatic acid chloride, but not with aromatic acid chloride, presumably because of the high reaction temperature, which causes the decomposition of VII.

The carbamoylation and thiocarbamoylation of VII were also attempted. Phenylcarbamoyl and thiocarbamoyl derivatives are unknown. When VII was treated with potassium cyanate in water at room temperature overnight, the *N*-carbamoyl derivative (IX) of VII was obtained, along with a small quantity of *N*-nitroso-*N*-phenyl-glycinonitrile. Under similar conditions, VII and sodium thiocyanate gave only thiocyanate salts of sydnone imine X. All attempts to convert this into the thiocarbamoyl derivative (XI) were unsuccessful. In the case of VIIIa and VIIIb, the reaction with potassium cyanate in a chloroform solution under reflux produced the *N*-carbamoyl derivative, XIIa and XIIb. The reaction of VIIIa with sodium thiocyanate in water gave thiocyanate salts of thiazone imine XIII, which forms the same picrate

4) H. Kato, M. Hashimoto and M. Ohta, *J. Chem. Soc. Japan, Pure Chem. Sect.* (*Nippon kagaku Zassi*), **78**, 707 (1957).

as that obtained from VIII. Attempts to isomerize the thiocyanate of thiazone imine into a thiocarbamoyl derivative XIV were unsuccessful.

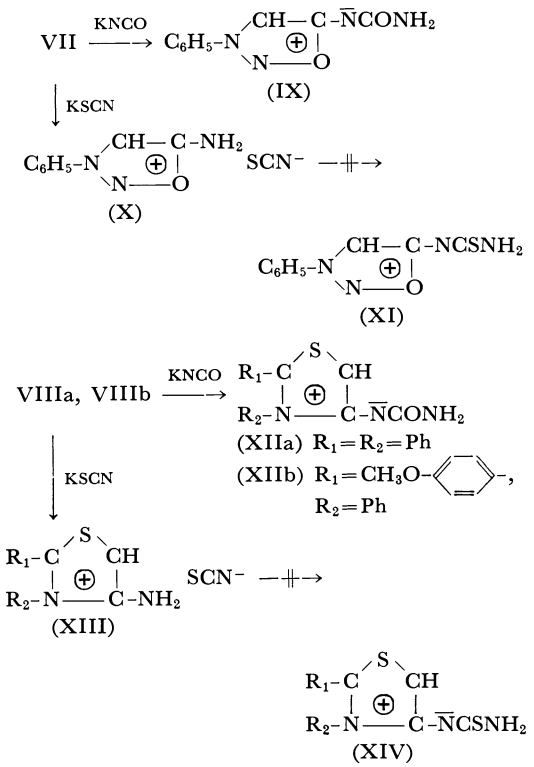

Fig. 2.

Experimental

The Preparation of 2-Phenyl-3-*p*-chlorophenyl-4-thiazone Imine Hydrochloride (VIIIc) by Method A.—A solution of 45 g. of thiobenzoyl-*p*-chloroanilide, 14 g. of chloroacetonitrile and 23 g. of triethylamine in 300 ml. of benzene was refluxed for 3 hr. After the solution had cooled, the precipitated triethylamine hydrochloride was filtered off, and benzene was removed by evaporating it under reduced pressure. The oily residue crystallized after the solution had then stood overnight. The recrystallization from methanol gave *S*-cyanomethyl-isothiobenzoyl-*p*-chloroanilide as white prisms; m. p. 118°C. The yield was 55 g.

Found: C, 62.82; H, 4.01; N, 9.82. Calcd. for $C_{15}H_{11}ClN_2S$: C, 62.94; H, 3.85; N, 9.79%.

Into the solution of 55 g. of *S*-cyanomethyl-isothiobenzoyl-*p*-chloroanilide in 300 ml. of dry acetone, 30 ml. of 30% alcoholic hydrogen chloride was added under cooling in an ice-water bath. The yellow crystals of VIIIc which precipitated were recrystallized from ethanol. *S*-Cyanomethyl-isothiobenzoyl-*o*-chloroanilide (m. p. 80°C) and 2-phenyl-3-*o*-chlorophenylthizaone imine hydrochloride were prepared in the same way.

The Preparation of 2, 3-Disubstituted-4-thiazone Imine Hydrochloride by Method B.—In order to avoid needless repetition, the experimental conditions for carrying out these reactions have been generalized. A mixture of *N*-substituted thioamides, a slight excess over the calculated amount of chloroacetonitrile and an equal amount of diphenyl was heated at 100—120°C in an oil bath. First the reaction mixture melted to a clear solution, and then, as the reaction proceeded, the hydrochloride began to crystallize out. Usually, the reaction is accompanied by a considerable temperature elevation which must be controlled by cooling. After ten to twenty minutes heating, acetone was added to the cooled mixture, and the insoluble crystals were collected by filtration and washed with an acetone-ether mixture. The products can be recrystallized from an ethanolic solution by gradually adding ether.

The Preparation of *N*-Acetyl-2, 3-disubstituted-4-thiazone Imine Hydrochloride.—The experimental conditions for carrying out these reactions have been generalized.

A suspension of 2, 3-disubstituted-4-thiazone imine hydrochloride in about ten times as much acetic anhydride by weight containing a small amount of boron trifluoride etherate was heated at 100°C while being stirred. The reaction times are shown in Table I.

Into the cooled solution, ether was added and the precipitates were collected by filtration and recrystallized from ethanol.

The Reaction of VIIIc and Sodium Bicarbonate.—Into the solution of 1 g. of VIIIc in 10 ml. of water, 5 ml. of 5% sodium bicarbonate solution was added. The solution was allowed to stand overnight. During this time a brown solid was separated out; it was then recrystallized from methanol. 0.3 g. of *S*-cyanomethyl-isothiobenzoyl-*p*-chloroanilide (m. p. 118°C) was thus obtained.

The Acylation of Sydnone- and Thiazone Imine Hydrochlorides with Acyl Chloride.—*General Procedure.* Sydnone- or thiazone imine hydrochloride was heated with an excess of acyl chloride without a solvent or in an inert solvent such as toluene, and the hydrochloride of the acyl derivative was collected by filtration, washed with benzene, and recrystallized from an appropriate solvent.

The following acyl derivatives were prepared by this method: Acetyl-: m. p. 290°C (decomp.). Free base: m. p. 198°C (decomp.). Propionyl-: m. p. 220°C (decomp.).

Found: N, 7.60; Calcd. for $C_{18}H_{17}ClN_2OS$: N, 8.10%.

Benzoyl-: m. p. 223°C (decomp.). Free base: m. p. 212°C (decomp.). Cinnamoyl-: m. p. 272°C (decomp.). Found: N, 6.70; Calcd. for $C_{23}H_{19}ClN_2OS$: N, 6.72%.

The Reaction of Thiocaprolactam with Chloroacetonitrile.—Two grams of thiocaprolactam with 1.2 g. of chloroacetonitrile was heated at 100°C on a water bath. The reaction was completed in several minutes, yielding a viscous oil which solidified when left standing at room temperature. Acetone was added, and the insoluble products were collected by filtration. Recrystallization from benzene-ethanol gave *S*-carbamoylmethyl-isothiocaprolactam hydrochloride as colorless prisms. Yield, 1.6 g; m. p. 158—159°C.

Found: C, 43.54; H, 6.52; N, 12.57. Calcd. for $C_{18}H_{13}ClN_2S$: C, 43.14; H. 6.74; N, 12.48%.

***N*-Carbamoyl-3-phenyl-sydnone Imine (IX).**—One gram of VII was dissolved in water, and then an aqueous solution of 0.4 g. of potassium cyanate was added. After the solution had been allowed to stand

overnight, the pale yellow precipitates were collected by filtration and recrystallized from ethanol to give IX as yellow crystals, m. p. 153°C (decomp.).

Found: C, 52.91; H, 4.17; N, 27.38. Calcd. for $C_8H_8N_4O_2$: C, 52.94; H, 3.95; N, 27.44.%

3-Phenylsydnone Imine Thiocyanate (X).—Into an aqueous solution of 1 g. of VII, a solution of 0.42 g. of sodium thiocyanate was added. The precipitate was immediately separated out and recrystallized from ethanol to give pale yellow needles, m. p. 155°C (decomp.).

Found: C, 49.57; H, 3.66; N, 25.30. Calcd. for $C_8H_8N_4OS$: C, 49.09; H, 3.66; N, 25.45%.

This was not converted into *N*-thiocarbamoyl-3-phenylsydnone imine when heated.

***N*-Carbamoyl-2, 3-diphenylthiazone Imine (XIIa).**—One gram of VIIIa and 0.9 g. of pulverized potassium cyanate were refluxed in 80 ml. of chloroform for 5 hr. After the solvent had been removed under reduced pressure, the residue was recrystallized from ethanol to give XIIa as yellow crystals, m. p. 275°C (decomp.).

Found: C, 65.02; H, 4.48; N, 14.38. Calcd. for $C_{16}H_{13}N_3OS$: C, 65.08; H, 4.44; N, 14.23%.

2, 3-Diphenylthiazone Imine Thiocyanate (XIIIa).—To an aqueous solution of 1 g. of VIIIa, a solution of 0.3 g. of sodium thiocyanate was added. The yellow precipitate which was immediately separated out was collected and recrystallized from 70% aqueous ethanol to give yellow needles, m. p. 113°C (decomp.).

Found: C, 65.02; H, 4.48; N, 14.38. Calcd. for $C_{16}H_{13}N_3S_2$: C, 65.08; H, 4.34; N, 13.49%.

This thiocyanate could not be converted into *N*-thiocarbamoyl-2, 3-diphenylthiazone imine by heating it.

***N*-Carbamoyl-2-(*o*-methoxyphenyl)-3-phenylthiazone Imine (XIIb).**—One gram of VIIIb was dissolved in chloroform, and then 0.75 g. of powdered potassium cyanate was added. After the mixture had been allowed to stand overnight at room temperature, it was evaporated under reduced pressure to yield a crystalline residue. The residue was recrystallized from ethanol to give yellow scales, m.p. 287°C (decomp.).

Found: N, 14.41. Calcd. for $C_{17}H_{15}N_3O_2S$: N, 13.59%.

2-(*p*-Methoxyphenyl)-3-phenylthiazone Imine Thiocyanate (XIIIb).—When an aqueous solution of 1 g. of VIIIb, a solution of 0.3 g. of sodium thiocyanate was added, yellow crystals were crystallized out immediately. Recrystallization from ethanol gave yellow needles, m. p. 163°C (decomp.).

Found: N, 12.39. Calcd. for $C_{17}H_{15}N_3OS_2$: N, 12.30%.

BULLETIN OF THE CHEMICAL SOCIETY OF JAPAN VOL. 39 1273—1279 (1966)

Amino Acid-Carbohydrate Coordinated Compounds.* II. The Synthesis and the Stability of 3-*O*-Aminoacyl-D-glucoses**

By Nobutoshi MURAMATSU

Central Research Laboratory, Ajinomoto Co., Kawasaki

(Received November 2, 1965)

3-*O*-Aminoacyl-D-glucoses (amino acids; Gly, L-Ala, L-Lys, L-Asp (α and β) and L-Glu (α and γ)) have been prepared by the condensation of 1, 2; 5, 6-di-*O*-isopropylidene-D-glucose with suitably protected amino acid derivatives in the presence of *N*, *N'*-dicyclohexylcarbodiimide, followed by the removal of the protected groups. The effect of free amino and carboxyl groups on the stability of these compounds has been clarified.

In the investigations of the mode of the linkage of amino acids to carbohydrates in glycoproteins, a few reports[1,2] on the synthesis of 6-*O*-aminoacyl-D-glucoses have been presented, with it taken as a low molecular model compound for the examination of the stability of the glycopeptide linkage. Suzuki et al.[1] synthesized 6-*O*-(*N*-benzyloxycarbonyl=Cbz)aminoacyl-D-glucoses by the condensation of 1, 2 ; 3, 5-di-*O*-benzylidene-D-glucose with *N*-Cbz-amino acids (Gly, L-Lys, L-Asp-α-benzyl and L-Asp-β-benzyl) in the presence of *N*, *N'*-dicyclohexylcarbodiimide (the DCC method), followed by the hydrolytic removal of benzylidene groups. Kochetkov et al.[2] developed the direct synthesis of the compounds by the condensation of unprotected glucose with *N*-Cbz-amino acids (Gly, DL-Ala, DL-Val, DL-Norleu, β-Ala and ε-amino caproic acid) by the DCC method. The removal of the Cbz-group from these compounds by catalytic hydrogenolysis in neutral media causes the ester bond to break; only in acidic media it is successfully accomplished. Kochetkov et al.[3] clarified the effect of the amino group in the aminoacyl group on the stability of these compounds.

* Part I: N. Muramatsu, *J. Chem. Soc. Japan, Pure Chem. Sect.* (*Nippon Kagaku Zasshi*), **84**, 861 (1963).

** Presented at the 17th annual Meeting of the Chemical Society of Japan, Tokyo, April, 1964.

1) T. Ukita and S. Suzuki, *J. Pharm. Soc. Japan*, **81**, 222 (1961).

2) N. K. Kochetkov, V. A. Derevitskaya, L. M. Likhosherston, N. V. Moldtsov and S. G. Kara-Murza, *Tetrahedron*, **18**, 273 (1962).

3) N. K. Kochetkov, B. A. Dereviskaya and L. M. Likhosherston, *Izvest, Akad, Nauk SSSR*, **33**, 688 (1963).

TABLE I

Compd.	Mol. Formula	Yield %	M. p.	α_D	Analysis N, % Found	N, % Calcd.	C, % Found	C, % Calcd.	H, % Found	H, % Calcd.	Remarks
I-a	$C_{22}H_{29}O_9N$	53	82—83	−16.5 MeOH $c=1$, 23°	3.18	3.10	58.06	58.53	6.50	6.47	
I-b	$C_{23}H_{31}O_9N$	60	89—90	−29.9 MeOH $c=1$, 22°	3.29	3.01	59.44	59.34	6.97	6.71	
I-c	$C_{34}H_{44}O_{11}N_2$	80	79—80		4.57	4.29	62.38	62.56	7.08	6.79	
I-d	$C_{31}H_{37}O_{11}N$	71	syrup	−22.84 MeOH $c=1$, 19°	2.27	2.33	62.18	62.09	6.42	6.22	
I-e	$C_{31}H_{37}O_{11}N$	43	68—71	−17.3 MeOH $c=1$, 19°	2.51	2.33	61.85	62.09	6.36	6.22	
I-f	$C_{32}H_{39}O_{11}N$	73	83—85	−35.2 MeOH $c=0.2$, 20°	2.45	2.28	62.76	62.62	6.71	6.40	
I-g	$C_{32}H_{39}O_{11}N$	66	80—81	+6.0 MeOH $c=0.8$, 23°	2.45	2.28	62.93	62.62	6.47	6.40	
II-b	$C_{17}H_{23}O_9N$	51	79—80	28.7 MeOH $c=0.4$, 26°	3.30	3.04	52.65	52.98	6.20	6.02	
II-c	$C_{23}H_{36}O_{11}N_2$	48	89—90	50.7 H_2O $c=0.2$, 26°	4.57	4.86	58.45	58.32	6.32	6.29	
III-a	$C_9H_{16}O_9N$	74	90—92	41.6 H_2O $c=0.6$, 25°	4.54	4.72	40.33	40.54	6.81	6.72	1/2 Oxalate
III-b	$C_{10}H_{18}O_9N_1$ 1/2 H_2O			23.1 H_2O $c=0.5$, 26°	4.15	4.58	39.17	39.34	6.29	6.27	1/2 Oxalate 1/2 Hydrate
III-c	$C_{14}H_{28}O_{12}N_2$	54	101—105	71.9 H_2O $c=0.1$, 26°	6.64	7.03	42.05	42.20	6.64	6.58	1 Oxalate
III-d	$C_{10}H_{21}O_{11}N$	60	108—111	28.1 H_2O $c=0.2$, 22°	4.48	4.47	38.68	38.33	5.80	6.11	1 Hydrate
III-e	$C_{10}H_{21}O_{11}N$	66	105	28.1 H_2O $c=0.2$, 22°	4.60	4.47	38.68	38.33	5.80	6.11	1 Hydrate
III-f	$C_{11}H_{23}O_{11}N$	52	amorph.	15.8 H_2O $c=0.2$, 26°	4.27	4.28	40.72	40.36	6.13	6.46	1 Hydrate
III-g	$C_{11}H_{23}O_{11}N$	84	amorph.	34.7 H_2O $c=0.7$, 22°	4.13	4.28	39.90	40.36	6.15	6.46	1 Hydrate
IV-a	$C_{14}H_{26}O_9N$	82	180—181°	−26.3 MeOH $c=1$, 22°	4.02	3.43	47.25	47.19	6.31	6.18	1 Oxalate
IV-b	$C_{17}H_{27}O_{11}N$	85	185—188	−24.9 MeOH $c=1$, 20°	3.31	3.32	48.12	48.45	6.52	6.45	1 Oxalate
IV-c	$C_{22}H_{36}O_{15}N_2$	66	193—195	−17.1 H_2O $c=1$, 22°	4.88	4.93	45.96	46.47	6.55	6.38	2 Oxalate

This paper will deal with the preparation and the stability of 3-*O*-aminoacyl-D-glucoses (amino acids; Gly, L-Ala, L-Lys, L-Asp-α-benzyl, L-Asp-β-benzyl, L-Glu-α-benzyl and L-Glu-γ-benzyl). According to Kochetkov's report[2] 3-*O*-*N*-Cbz aminoacyl-D-glucose was formed as a minor product of these condensations. It was identified with the authentic sample by a synthesis using the condensation of 1, 2 ; 5, 6-di-*O*-isopropylidene-D-glucose with *N*-Cbz-glycine, followed by the removal of the isopropylidene groups. The procedure employed in one of the author's reports[4] was used here. Equal moles of 1, 2 ; 5, 6-di-*O*-isopropylidene-D-glucose[5] and suitably protected *N*-Cbz-amino acid derivatives were condensed in the presence of DCC in absolute pyridine.

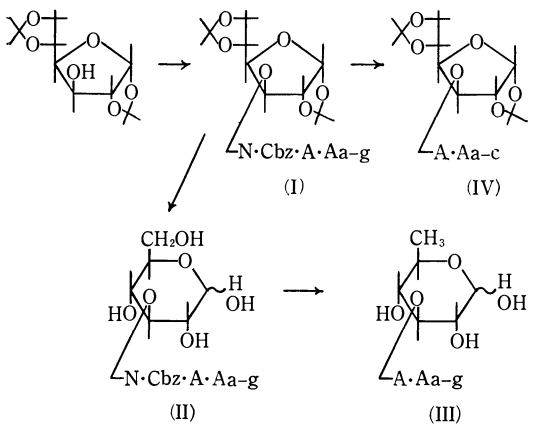

–A·A.

a, $-OCCH_2NH_2$

b, $-OCCHCH_3$ (NH$_2$)

c, $-OCCH(CH_2)_4NH_2$ (NH$_2$)

d, $-OCCHCH_2COOH$ (NH$_2$)

e, $-OCCH_2CHCOOH$ (NH$_2$)

f, $-OCCHCH_2CH_2COOH$ (NH$_2$)

g, $-OCCH_2CH_2CHCOOH$ (NH$_2$)

After the filtration, the precipitated *N*, *N'*-dicylohexylurea was washed with excess benzene. The combined mixture of the filtrate and the washings was washed with dilute hydrochloric acid, aqueous sodium bicarbonate and water, and then dried over sodium sulfate. The benzene layer was evaporated under reduced pressure to a thick syrup, and crystallized by trituation with petroleum ether. The 1, 2 ; 5, 6-di-*O*-isopropylidene-3 - *O* - *N* -Cbz-aminoacyl-D-glucoses (I) thus obtained gave negative silver ammonia and ninhydrin reactions, and exhibited absorption bands characteristic of ester carbonyl at 1740—1755 cm^{-1} and the bands characteristic of urethane carbonyl at 1675—1710cm^{-1} in the infrared spectra. The hydrolysis of isopropylidene groups of I in 75% acetic acid at 80°C for two or three hours gave 3-*O*-*N*-Cbz-aminoacyl-D-glucoses (II). Although II was purified by cellulose powder chromatography, only a few compounds could be obtained as crystals. These compounds gave positive silver ammonia and negative ninhydrin reactions. The compound II was converted to 3-*O*-aminoacyl-D-glucoses (III) by hydrogenolysis in aqueous methanol in the presence of Pd-C. In the case of neutral and basic aminoacyl-derivatives, III was obtained as oxalate. The compound III gave positive silver ammonia and ninhydrin reactions. The structure of III was confirmed by periodate oxidation, in which the consumption of the periodate was three moles per mole of III. 1, 2 : 5, 6-di-*O*-isopropylidene - 3 - *O* - aminoacyl-D-glucose (IV) was obtained from I by the procedure described above. The physical properties of I, II, III and IV are summarized in Table I.

The stability of these compounds was investigated at various pH values under the experimental conditions shown in Table II.

Table II. Conditions on hydrolysis for the investigation on the stability of ester bond

Temperature: 40°C
Concentration: 0.02 mol.
PH: 1, 2.2, 3, 4, 5, 6, 8.
Buffer: McIlvain's Buffer.
Separation of the degradation products:
Paper chromatography: Solv. *n*-BuOH sat. with H_2O
Paper electrophoresis: Solv. Pyridine : HOAc : H_2O (2 ml. : 4 ml. : 1000 ml.)
Determination of the degradation products:
D-Glucose: Anthrone method
Amino acids: Bioassay

The hydrolysis was carried out in the concentration of 0.02 mmol. in order to obtain the half-life periods and rate constants as the first order reaction.[3] As an example, diagrams of reaction time-liberated glucose in the hydrolysis of 3-*O*-L-alanyl-D-glucose at pH 6 and 1 are shown in Fig. 1. In the case of pH 1, the half-life period was calculated by the extrapolation of the data. The half-life periods of various compounds at pH 6 and 1 are listed in Table III.

In order to compare the stability of the neutral and basic amino acid esters, the half-life periods of 3-*O*-L-alanyl-D-glucose and of 3-*O*-L-lysyl-D-glucose are plotted against the individual pH values in Fig. 2. Figure 3 shows the half-life period of the acidic amino acid esters; 3-*O*-α-L-aspartyl-D-glucose and 3-*O*-β-L-aspartyl-D-glucose.

4) N. Muramatsu, *J. Chem. Soc. Japan, Pure Chem. Sect.* (*Nippon Kagaku Zasshi*), **84**, 861 (1963).
5) O. Schmidt, "Method in Carbohyd.," Vol. II, Academic Press Inc., New York. (1963), p. 320.

TABLE III

Compd.	Structure	$\tau_{1/2}$ (pH, 1)	$\tau_{1/2}$ (pH, 6)	$k\times10^3$ (pH, 6)
III-b	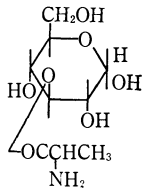	107	33/4	2.1
III-c	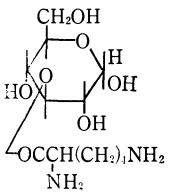	192	33/4	2.2
III-d	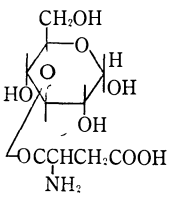	∞	31/2	2.1
III-e	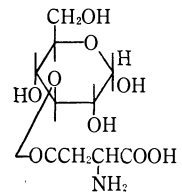	∞	57	0.08
II-b	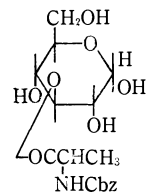	100	101/3	0.83
IV-b	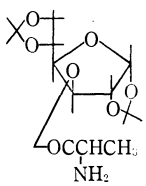	—	31/4	1.1

Discussion

The neutral and the basic 3-*O*-aminoacyl-D-glucoses gave similar curves, as is shown in Fig. 2. In the region of pH 4—7, their stabilities are almost identical. This reflects the effect of the α-amino group mainly, while the ε-amino group in the L-lysyl ester has almost no effect. In the region of pH 1—3, however, 3-*O*-L-lysyl-D-glucose is more stable than 3-*O*-L-alanyl-D-glucose. This may be understood in terms of Kochetkov's interpretation[3] that the protonation on the free amino

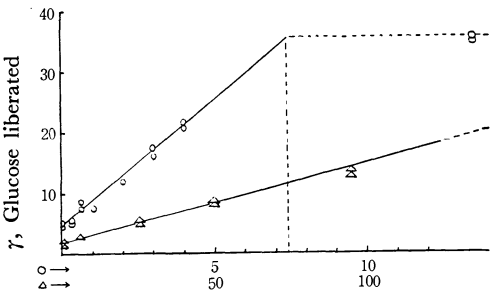

Fig. 1. The diagram of reaction time-liberated D-glucose of 3-*O*-L-alanyl-D-glucose at pH 6 and 1.
○: at pH 6 △: at pH 1

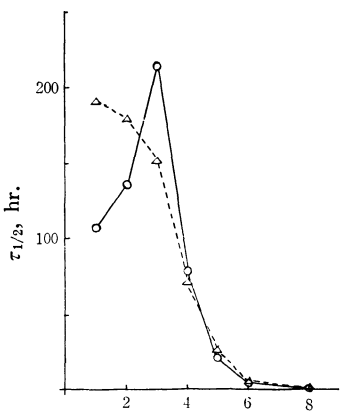

Fig. 2. The half life periods of 3-*O*-L-alanyl-D-glucose (○) and 3-*O*-L-lysyl-D-glucose (△) at pH 1—8.

TABLE IV. R_f VALUES (PPC) AND MOBILITY OF PAPER ELECTROPHORESIS

Compd.	D-Glucose	L-Ala	II-b	IV-b	III-b	L-Lys	II-c	III-c	IV-c	L-Aps	II-d	II-e
R_f values	0.08	0.08	0.29	0.04	0.68	0.03	0.33	0.67	0.02	0.01	0.31	0.25
Mobl. of PEP*	−1.5	−2.5	−7.5	−7.6	−1.6	−11.5			−15.8	5.5		
Compd.	III-d	III-e	IV-d	IV-e	L-Glu	II-f	II-g	III-f	III-g	IV-f	IV-g	
R_f values	0.72	0.73	0.01	0.01	0.02	0.31	0.34	0.75	0.75	0.01	0.02	
Mobl. of PEP*			−0.8	−0.8	2.7	−2.0	−3.5	−1.5		−1.0	−1.2	

* cm./2 hr.

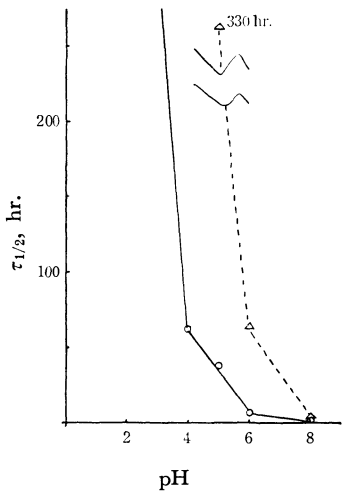

Fig. 3. The half life periods of 3-*O*-α-L-aspartyl-D-glucose (△) and 3-*O*-β-L-aspartyl-D-glucose (○) at pH 1—8.

group prevents the attack of the proton on the ester bond. This tendency is more prominent in the case of the L-lysyl ester because it has two amino groups.

The acidic amino acid esters, as described in Fig. 3, show almost the same stability as the neutral and the basic amino acid esters in the region of pH 5—7. The difference in stability between 3-*O*-β-L-aspartyl-D-glucose and 3-*O*-α-L-aspartyl-D-glucose in the region of pH 4—6 is caused by the interrelation of distance between the ester bond and the amino group. In more acidic media below pH 4, these acidic amino acid esters are extremely stable. This may be explained by the hydride ion formation of the intramolecular carbonyl group with the amino group, which reduces the effect of the amino group. The effects of both the stability and the instability of the free amino group on these compounds are unambiguous in view of the fact that the half-life periods of 3-*O*-L-alanyl-D-glucose and 3-*O*-*N*-Cbz-L-alanyl-D-glucose at pH 1 and 6 (shown in Table III) are interchanged alternately.

On the other hand, the interaction of the amino and the carbonyl groups in these aminoacyl sugars must be considered to be one of the factors causing instability, in addition to the effect of the amino group mentioned above. The half-life period of 1, 2 ; 5, 6-di-*O*-isopropylidene-3-*O*-L-alanyl-D-glucose at pH 6 listed in Table III is almost the same value as that of 3-*O*-L-alanyl-D-glucose, this seems to be negative evidence for the deduction above. However, such an estimation should be based upon a comparison of the corresponding derivatives with the same conformations. This aspect is now under examination.

Experimental

For paper chromatography and paper electrophoresis "Toyo Roshi filter paper No. 51A" was used. The paper chromatography technique used was the ascending procedure using the buffer cited in Table II. Paper electrophoresis was carried out using the buffer of pH 4 cited in Table II, the condition selected was 26.7 V./cm. The R_f values for paper chromatography and the mobilities for electrophoresis may be summarized as follows: These spots were detected with silver ammonia[3] (free carbonyl), ninhydrin (amino) and Rydn reactions[6] (imino). The melting points are not corrected.

1, 2 ; 5, 6-Di-*O*-isopropylidene-3-*O*-*N*-benzyloxycarbonyl-aminoacyl-D-glucoses (I).—DCC (0.011 mol.) was added to a solution of *N*-Cbz-amino acid derivatives (0.01 mol.) in dry pyridine (100 ml.) which had been cooled to 0°C, 1, 2 ; 5, 6-di-*O*-isopropylidene-D-glucose (0.01 mol.) was added to the mixture a few minutes later, and then the solution was kept at room temperature overnight. The precipitated *N, N'*-dicyclohexylurea was filtered and washed with benzene (150 ml.). The mixture of the filtrate and the washings was washed several times with 5% hydrochloric acid, 2% sodium bicarbonate solution and water, then dried over anhydrous sodium sulfate, and evaporated to a syrup under reduced pressure. The syrup thus obtained was dissolved in ether and treated with petroleum ether until it became turbid; then it was left in a refrigerator. The crude crystals were recrystallized from ethyl acetate and water. The physical constants of 1, 2 ; 5, 6-di-*O*-isopropylidene-3-*O*-*N*-Cbz-aminoacyl-D-glucoses (I) prepared by this method are presented in Table I.

3-*O*-*N*-Benzyloxycarbonyl-aminoacyl-D-glucoses (II).—A solution of 1, 2 ; 5, 6-di-*O*-isopropylidene-3-*O*-*N*-Cbz-aminoacyl-D-glucose (I) (0.01 mol.) in 75% acetic acid (40 ml.) was refluxed for three hours, and then the solution was evaporated to a syrup under reduced pressure. In this syrup, 3-*O*-*N*-Cbz-aminoacyl-D-glucose, D-glucose resulting from the hydrolysis of the ester bond, and an unknown substance which is perhaps the partial-hydrolysed product "1, 2-*O*-isopropylidene-3-*O*-*N*-Cbz-aminoacyl-D-glucose" were detected by paper chromatography. The purification of 3-*O*-*N*-Cbz-aminoacyl-D-glucose was attempted by partition chromatography over cellulose powder (Tokyo Roshi: Grade B) as an adsorbent and *n*-butyl alcohol saturated with water as the effluent. Each fraction was detected by paper chromatography. The elution pattern is shown in Fig. 4. The fractions of the peak of A were collected and evaporated under reduced pressure, and a syrup of 3-*O*-*N*-Cbz-aminoacyl-D-glucose was obtained. Among these a few compounds were crystallized from ethyl acetate. The physical constants of 3-*O*-*N*-Cbz-aminoacyl-D-glucoses are presented in Table I.

3-*O*-Aminoacyl-D-glucoses (III).—*a) The Case of Neutral and Basic Amino Esters.*—To a solution of 3-*O*-*N*-Cbz-aminoacyl-D-glucose (0.005 mol.) in methanol (50 ml.), oxalic acid (0.01 mol.) and 10% Pd-C (2 g.) suspended in water were added; the mixture was then subjected to hydrogenolysis. Hydrogen gas was bubbled into the stirred mixture at room temperature until no carbondioxide was detected in the exhaust. This

6) H. N. Rydon and P. W. G. Smith, *Nature*, **169**, 922 (1952).

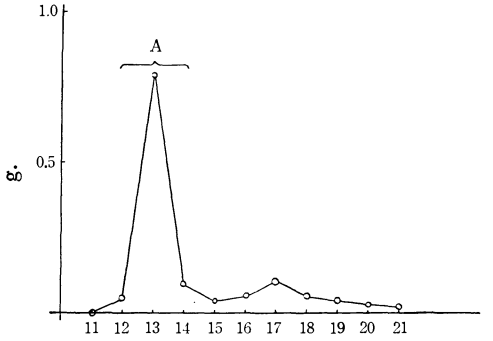

Elution pattern of 3-*O*-*N*-Cbs-L-alanyl-D-glucose.
Column: cellulose powder "Toyo Roshi: Grade B" ϕ4 cm. × 55 cm.
Effluent: *n*-BuOH saturated with H_2O

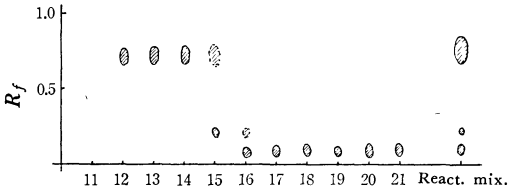

Paper chromatography of each fractions.

Fig. 4.

took about 4—5 hr. The catalyst was removed by filtration and washed with water. The filtrate and the washings were combined and evaporated to a syrup under reduced pressure below 40°C. The syrup was dissolved in methanol and crystallized with the addition of acetone. Recrystallization was then repeated with the same procedure. The yields of these products were about 60—70%.

b) The Case of Acidic Amino Acid Esters.—In this case oxalic acid is not necessary. The other procedures were conducted with the method described above. The yields were 55—85%. The physical constants of 3-*O*-aminoacyl-D-glucoses are presented in Table I.

1, 2 ; 5, 6-Di-*O*-isopropylidene-3-*O*-aminoacyl-D-glucoses (IV).—Compounds I were hydrogenolysed with the procedure mentioned above and so transformed to 1, 2 ; 5, 6-di-*O*-isopropylidene-3-*O*-aminoacyl-D-glucose (IV). In these cases, after the filtration of the catalyst, the filtrate was concentrated and crystallized from methanol or methanol and ether. The physical constants of 1, 2 ; 5, 6-di-*O*-isopropylidene-3-*O*-aminoacyl-D-glucoses are presented in Table I.

General Procedure for the Investigation of Hydrolysis.—A 0.02 mol. solution of 3-*O*-aminoacyl-D-glucoses in an appropriate buffer was soaked into a thermostat controlled at 40°C; 0.05 ml. portions of the solution were sampled intermittently; they are spotted along Line A in Fig. 5. At the same time, the standard solution of D-glucose or amino acid was spotted on the paper at Point B. The spots were developed on paper electrophoresis. The part containing the degradation product was excised along Line A and eluted with 10 ml. of water as shown in Fig. 6.[7] D-

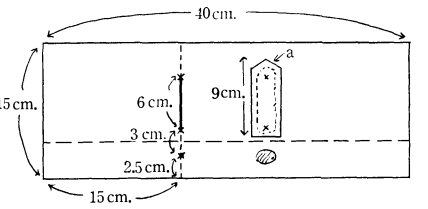

Fig. 5.

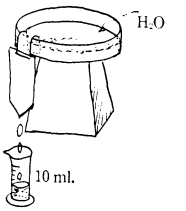

Fig. 6.

Glucose was estimated by the Anthron method[8] and amino acid by bioassay[9] using the eluted solution.[10] The recovery of the method was 100±6%, and the reference sample was made by the procedure described above using non-spotted paper.

a) Neutral and Basic Amino Acid Esters.—In these cases the hydrolysis was pursued by the estimation of D-glucose, as the mobility of D-glucose was different from that of 3-*O*-aminoacyl-D-glucoses. For example, in Table IV and Fig. 1 the progress of the hydrolysis of 3-*O*-L-alanyl-D-glucose at pH 6 and 1 is shown. In this case 3-*O*-L-alanyl-D-glucose was weighed (6.0 mg.) and dissolved in 1 ml. of a buffer. The final value of the D-glucose liberated should be 36 γ in 0.01 ml. of the solution. Figure 2 was the result of plotting the half-life period against the pH values.

b) Acidic Amino Acid Esters.—In this case the hydrolysis could not be pursued by the estimation of D-glucose, for the mobility of 3-*O*-aminoacyl-D-glucose was similar to that of D-glucose. Therefore, it was pursued by the estimation of amino acid by the bioassay method, as the mobility of the amino acid was different from that of 3-*O*-aminoacyl-D-glucose. The half-life periods at all the pH values are shown in Fig. 3.

c) The Hydrolysis of 3-O-N-Benzyloxycarbonyl-L-alanyl-D-glucose.—In this case the hydrolysis was pursued by the estimation of D-glucose after the development of the spot by paper chromatography.

d) The Hydrolysis of 1, 2 ; 5, 6-*Di-O-isopropylidene-3-O-L-alanyl-D-glucose.*—In this case the hydrolysis was

7) Dipping of the filter paper into water is practically effective for the estimation of amino acids.

8) T. A. Scott. Jr., and E. H. Melvin, *Anal. Chem.*, **25**, 1656 (1953).

9) T. Tsunoda, "Tanpakushitsu kagaku," Vol. I, Kyoritsu Shuppan Co., Ltd., Tokyo (1954), p. 232. The assay was essentially the same as described on it, and Microorganisms used were as follows: Lactobacillus Arabinocus 17-5 (ATCC 8014) for the assay of L-Glu. Leuconostoc Mesentaroides p-60 (ATCC 8042) for that of L-Asp. Leuconostoc Citrovoum ATCC 8081 for that of L-Ala.

10) Direct densitometry using the filter paper could not be accepted on both case of D-glucose and amino acids by its great error. And ninhydrin method for amino acids also could not be accepted.

pursued by the estimation of L-alanine after the development of the spot by paper chromatography.

The author wishes to express his sincere thanks to Dr. Juji Yoshimura of the Tokyo Institute of Technology for many helpful discussions and valuable suggestions made during the work, and also to Dr. Haruomi Oeda of the Ajinomoto Co., Inc., for his kind encouragement. He is also thankful to Miss Michiko Shibayama for her assistance in the experimental work and to Miss Kikuko Narui for the bioassay analysis.

BULLETIN OF THE CHEMICAL SOCIETY OF JAPAN VOL. 39 1279—1282 (1966)

Vinyl-substituted Polysilanes

By Hideki SAKURAI, Kenji TOMINAGA and Makoto KUMADA

Department of Synthetic Chemistry, Faculty of Engineering, Kyoto University, Sakyo-ku, Kyoto

(Received November 4, 1965)

1-Vinylheptamethyltrisilane, 2-vinylheptamethyltrisilane and vinylpentamethyldisilane have been prepared from the corresponding chlorosilanes and vinylmagnesium chloride. In these compounds, intense absorption maxima were observed in the ultraviolet region, and both the λ_{max} and ε increased with an increase in the chain length. Nuclear magnetic resonance and infrared data are also recorded here. Free radical copolymerizations were carried out with styrene and with acrylonitrile, and the monomer reactivity ratios of vinylpentamethyldisilane and 2-vinylheptamethyltrisilane were determined. It has been concluded that the 3d orbital resonance is not important for the stabilization of an odd electron adjacent to the silicon atom in the free radical intermediate in copolymerization in spite of spectral and chemical evidence of enhanced conjugation between the vinyl group and the polysilanyl group.

In their studies of the copolymerization of vinyltriethoxysilane and vinyltrimethylsilane, Scott and Price reported a very low resonance stabilization factor, Q.[1] The low values of Q for both monomers (0.03—0.035) were further supported by the ultraviolet spectra of these compounds, which disclosed only a little conjugation between the vinyl group and the silicon atom. On the other hand, for vinyl sulfides[2] it was concluded, from the large Q values and the relatively intense ultraviolet absorption band, that a sulfide sulfur atom could conjugate with a p electron, either in the free radical intermediate or in the excited state, possibly through 2p-3p conjugation but *not through 2p-3d conjugation.*[1]

Recently, Hague and Prince[3] described an absorption at 246.5 mμ for hexaphenyldisilane and explained this absorption as due to an interaction between phenyl groups through the silicon-silicon bond. Subsequently, it was reported from this laboratory[4,4a] that polysilanes with phenyl or vinyl groups, unlike monosilanes, have a very intense absorption in the ultraviolet region, and it was proposed that the silicon-silicon bond itself is a chromophore, making an enhanced conjugation with pi-electron systems. This interesting ultraviolet property of polysilanes has also been studied independently by Gilman et al.[5,6] In relation to these findings our primary interest was to investigate if the enhanced conjugation of the disilanyl group with the ethylenic double bond influences the copolymerization characteristics and other properties of these vinylpolysilanes.

In the present paper we wish to describe the results of the preparation, spectral study and copolymerization study of vinyl-substituted polysilanes.

Results and Discussion

Vinylpentamethyldisilane (I), 1-vinylheptamethyltrisilane (II), and 2-vinylheptamethyltrisilane (III) were prepared from vinylmagnesium chloride and the corresponding chloropolysilanes in tetrahydrofuran. These three compounds were all colorless liquids and showed no tendency to spontaneous polymerization. Chernyshev et al.[7] reported on the preparation of vinylpentamethyldisilane, together with related disilanyl compounds.

1) C. E. Scott and C. C. Price, *J. Am. Chem. Soc.*, **81**, 2670 (1959).
2) T. Alfrey and C. C. Price, *J. Polymr Sci.*, **2**, 101 (1947).
3) D. N. Hague and R. H. Prince, *Proc. Chem. Soc.*, 300 (1962).
4) H. Sakurai and M. Kumada, This Bulletin, **37**, 1894 (1964).
4) a) H. Sakurai, H. Yamamori and M. Kumada, This Bulletin, **38**, 2024 (1965).
5) H. Gilman, W. H. Atwell and G. L. Schwebke, *Chem. & Ind.*, **1964**, 1063.
6) H. Gilman, W. H. Atwell and G. L. Schwebke. *J. Organometal. Chem.*, **2**, 369 (1964).
7) E. A. Chernyshev, N. G. Tolstikova, A. A. Ivashenko, A. A. Zelenetskoya and L. A. Leites, *Izv. Akad. Nauk, S.S.S.R., Otd. Khim. Nauk*, 660 (1963).

TABLE I. ULTRAVIOLET SPECTRA OF SOME VINYL SUBSTITUTED SILANES

Compound	Solvent	λ_{max}, mμ	ε_{max}	Ref.
CH_2=CH-$SiMe_3$ (IV)	Isooctane	202	1470	1
CH_2=CH-$Si(OEt)_3$ (V)	Isooctane	210	300	1
CH_2=CH-$SiMe_2SiMe_3$ (I)	*n*-Hexane	223.2	5200	4
$(CH_2$=CH-$SiMe_2-)_2$ (VI)	*n*-Hexane	227.0	9790	4
CH_2=CH-$SiMe_2SiMe_2SiMe_3$ (II)	*n*-Hexane	218.0 (sh)		This work
		237.0	6760	
CH_2=CH-$SiMe(SiMe_3)_2$ (III)	*n*-Hexane	221.0 (sh)		This work
		238.0	6090	
$(CH_2$=CH-$SiMe_2SiMe_2-)_2$ (VII)	Cyclohexane	243.5	14000	6

TABLE II. INFRARED ABSORPTION ASSOCIATED WITH VINYL GROUP (cm^{-1})

Mode of vibration	Compound I	Compound II	Compound III
CH stretching	3055 (m)	3040 (m)	3060 (m)
	3010 (w)	2998 (w)	3005 (w)
C=C stretching	1587 (w)	1585 (w)	1580 (vw)
CH out-of-plane deformation	1009 (m)	1005 (m)	1003 (m)
CH_2 out-of-plane deformation	945 (s)	942 (s)	934 (s)

TABLE III. NUCLEAR MAGNETIC RESONANCE DATA[a)]

Band	Compound (chemical shifts in τ) IV	I	II	III	VI
$Si(CH_3)_3$	9.95	9.94	9.95	9.91	
$Si(CH_3)_2$		9.87	9.87		9.87
$Si(CH_3)$				9.87	
Vinyl group, multiplet centered at	4.14	4.09	4.02	4.01	4.05

a) Chemical shifts are expressed as τ values in p.p.m. relative to tetramethylsilane. When cyclohexane was used as internal standard, we have taken 1.43 p. p. m. as the signal difference between cyclohexane and tetramethylsilane to obtain τ values.

TABLE IV. COPOLYMERIZATION CHARACTERISTICS OF I AND III

M_2	M_1	r_1	r_2	Q_2	e_2
I	Styrene	50±10	0	0.02	−0.6
	Acrylonitrile	3±1	0		
III	Styrene	38±5	0	0.02	−0.7
	Acrylonitrile	2±1	0		

They gave 120—121°C as the boiling point of vinylpentamethyldisilane, but our repeated preparation of this compound disclosed its boiling point to be 131°C.

Table I lists the ultraviolet spectral properties observed for I, II and III, together with vinyltrimethylsilane (IV), vinyltriethoxysilane (V), 1, 2-divinyltetramethyldisilane (VI) and 1, 4-divinyloctamethyltetrasilane (VII). With an increase in the number of silicon atoms, the position of the absorption maximum shifted to a longer wavelength and the molar extinction coefficient increased regularly. This is a tendency which was also observed with phenylsubstituted polysilanes[3,6)] and with permethylated polysilanes.[6)]

Recently West[8)] illustrated the effect of metalloid substitution on the electronic spectra of simple chromophores using a qualitative molecular orbital theory. Since the electronic absorption of a simple olefin must be associated with only a transition from bonding pi-orbitals to antibonding pi-orbitals (π-π^* transitions) and since the resonant interaction of a vacant silicon d_π orbital is expected to be stronger with the antibonding orbital than with the bonding orbital,[8)] the increasing bathochromic shift with an increase in the chain length of vinylpolysilanes may be a reflection of the lowering of the d_π level by the catenation of the silicon atom. As has been observed for 1-phenylheptamethyltrisilane,[3)] it is interesting to note that vinylheptamethyltrisilanes possess two absorption maxima (or shoulders). All permethylated straight-chain polysilanes except hexamethyldisilane have been reported[6)] to possess a characteristic absorption in

8) R. West, *J. Organometal. Chem.*, **3**, 314 (1965).

the normal ultraviolet region. Since octamethyltrisilane was found to have an absorption maximum at 215.0 mμ, the broad shoulder observed at 216—218 mμ for II and III may be attributed to the absorption of the trisilane chain itself, which originates in a different sort of transition, independent of the π-π^* transition.

The infrared absorption bands associated with the vinyl group are given in Table II. Significant shifts in CH_2 deformation and C=C stretching frequencies from normal positions in analogous carbon compounds were observed. Potts and Nyquist[9] pointed out that the out-of-plane CH_2 deformation frequencies in substituted ethylenes of the Y–CH=CH_2 type are sensitive to the nature of the substituent, Y. Thus, the CH_2 deformation band shifts to a higher frequency when the pi-electron-attracting power of Y becomes greater. As can be seen from Table II, the out-of-plane CH_2 deformation frequencies of the vinyl group for I, II and III shift from the normal frequency of the CH_2 deformation band to a frequency higher by 35 cm^{-1}. This abnormally high frequency of the CH_2 deformation may be explained by the interaction of silicon with an unsaturated system through a dative p_π-d_π overlap.[10] In a series of vinylsilanes of the $R_3SiCH=CH_2$ type, Eisch and Trainor[10] also found a correlation between the position of the CH_2 deformation frequency and the electron-withdrawing power of R as measured by σ_p or σ.* Although this interesting correlation may not be directly applicable to the vinylpolysilane system, it is likely that the electron-releasing inductive character of the pentamethyldisilanyl group is slightly greater than that of the trimethylsilyl group.

Table III lists the proton magnetic resonance data for carbon tetrachloride solutions of some vinyl-substituted silanes. The deshielding effect of the vinyl group on the proton of the methyl groups bound to silicon was observed to be transmitted along the polysilane chain. As the same trend was also observed for phenyl-substituted polysilanes,[11] these results suggest some d_π-d_π double-bond character of the polysilane chain. As one can see from Table III, only two kinds of methyl peaks were observed for II. It had been found[11] that internal Si-CH_3 groups were more shielded than terminal Si-CH_3 groups* in octamethyltrisilane, although inner Si-CH_3 groups were generally more deshielded than outer Si-CH_3 groups in homologous permethylated straight polysilanes.[11,12] Therefore, the peak of the internal $Si(CH_3)_2$, rather than of the $Si(CH_3)_2$ attached to the vinyl group, was supposed to fall at the position for the terminal $Si(CH_3)_3$.

The copolymerizations of both I (M_2) and III (M'_2) with styrene (M_1) and with acrylonitrile (M'_1) were carried out at 60°C. From the composition analyses of the resulting copolymers, the monomer reactivity ratios were determined. These copolymerization characteristics are summarized in Table IV.

The values of Q for both monomers are low and in the same range of magnitude as for many other vinyl-substituted monosilanes.[13] This fact suggests that the 3d orbital resonance is not important for the stabilization of an odd electron adjacent to the silicon atom in the free radical intermediate in the copolymerization in spite of spectral and chemical evidence of enhanced conjugation between the vinyl group and the polysilanyl group. The more negative e values of both monomers than the value for trimethylvinylsilane could be ascribed to a slightly greater electron-releasing character of the disilanyl group and of the 2-trisilanyl group. This observation is compatible with the infrared spectral evidence.

Experimental

Boiling points are uncorrected. NMR spectra were obtained in carbon tetrachloride solution with a Varian A-60 spectrometer. Tetramethylsliane or cyclohexane was used as an internal standard. The infrared spectra were obtained with a Nippon Bunko DS-402G Grating Infrared Spectrophotometer. The ultraviolet spectra were obtained with a Shimadzu SV-50A Automatic Recording Spectrophotometer.

1-Chloroheptamethyltrisilane,[14] 2-chloroheptamethyltrisilane[14] and chloropentamethyldisilane[15] were prepared as reported previously. Styrene was distilled under reduced pressure in a stream of nitrogen after steam distillation. Acrylonitrile was redistilled through a 30-cm. column packed with glass helicoils under nitrogen.

Vinylpentamethyldisilane. — In a 2-l. flask equipped with a stirrer, a reflux condenser filled with dry-ice and a gas inlet tube, 32 g. (1.32 g.-atoms) of magnesium turnings and 700 ml. of tetrahydrofuran freshly distilled from lithium aluminum hydride were placed. A few drops of ethyl iodide, together with a crystal of iodine, was added to initiate the reaction. To the stirred solution there was then added through a gas inlet vinyl chloride, which had been previously passed through a saturated solution of sodium hydroxide, a Drielite tube and a phosphorus pentoxide tube. When the Grignard preparation was complete, the condenser was replaced with a water condenser and chloropentamethyldisilane (171.5 g., 1.03 mol.), dissolved in an equal volume of tetrahydrofuran, was added at such a rate that a gentle reflux was maintained. After this addition was complete (after one hour), the reaction

9) W. J. Potts and R. A. Nyquist, *Spectrochim. Acta*, **15**, 679 (1959).
10) J. J. Eisch and J. T. Trainor, *J. Org. Chem.*, **28**, 487 (1963).
11) Unpublished results in this Laboratory.
* The τ values of terminal Si-CH_3 and internal Si-CH_3 are 9.93 and 9.95 respectively.[11]
12) U. G. Stolberg, *Angew. Chem.*, **75**, 206 (1963).
13) L. J. Young, *J. Polymer Sci.*, **54**, 411 (1961).
14) M. Kumada, M. Ishikawa and S. Maeda, *J. Organometal. Chem.*, **2**, 478 (1964).
15) M. Kumada, M. Yamaguchi, Y. Yamamoto, J. Nakajima and K. Shiina *J. Org. Chem.*, **21**, 1264 (1956).

mixture was refluxed for further 20 hr. It was subsequently cooled and hydrolyzed by the addition of a saturated aqueous solution of ammonium chloride. The organic layer was separated, washed, and distilled to remove the solvent. The residue was then fractionally distilled through a 30-cm. column packed with glass helices to give 99 g. (60.8%) of vinylpentamethyldisilane, b. p. 131—132°C, n_D^{20} 1.4497, d_4^{20} 0.7673 (lit.,[7] b, p. 120—121°C, n_D^{20}, 1.4441, d_4^{20} 0.7621).

1-Vinylheptamethyltrisilane.—To a stirred solution of vinylmagnesium chloride prepared from 5 g. (0.2 g.-atom) of magnesium and vinyl chloride in 200 ml. of tetrahydrofuran in the same manner as described above there was added, drop by drop, 31 g. (0.14 mol.) of 1-chloroheptamethyltrisilane over a 40-min. period. After the addition was complete, the reaction mixture was refluxed for 5 hr.; then the solvent was distilled off through a short column to ensure a complete reaction and the residual mass was hydrolyzed with an aqueous solution of ammonium chloride. After the usual treatment simple distillation gave 26 g. of a practically pure liquid (on v. p. c.) boiling over the range of 70—79°C (16 mmHg). Fractional distillation gave 18 g. (59%) of 1-vinylheptamethyltrisilane, b. p. 79°C (16 mmHg), n_D^{20} 1.4741, d_4^{20} 0.7972. (Found: C, 49.32; H, 10.83; MR_D, 76.35. Calcd. for $C_9H_{24}Si_3$: C, 49.92; H, 11.17%; MR_D, 76.32.)

2 - Vinylheptamethyltrisilane. — Vinylmagnesium chloride was prepared from 15 g. (0.62 g.-atom) of magnesium and vinyl chloride in 300 ml. of tetrahydrofuran. 2-Chloroheptamethyltrisilane (37 g., 0.16 mol.) was added drop by drop to the Grignard reagent over a period of 40 min. After the treatment in virtually the same manner as with 1-vinylheptamethyltrisilane, 21 g. (61%) of 2-vinylheptamethyltrisilane was obtained as a colorless liquid, b. p. 75°C (17 mmHg), n_D^{20}, 1.4761, d_4^{20}, 0.7945. (Found: C, 50.04; H, 10.99; MR_D, 76.89. Calcd. for $C_9H_{24}Si_3$: C, 49.92; H, 11.17%; MR_D, 76.32.)

Copolymerization Procedure. — The copolymerizations of pairs of monomers were carried out at 60±0.1°C in sealed glass tubes which had been degassed three times on a vacuum line. Benzene and dimethylformamide were used as the solvent for the copolymerization with styrene and with acrylonitrile respectively, while azobisisobutyronitrile (0.5 mol. per cent to the total of monomers) was used as the initiator. Polymerization was interrupted when it was estimated that 5—10% of the copolymer had been formed. The copolymers were then precipitated by pouring the reaction mixture into 200 ml. of cold methanol. The resultant copolymers were further purified by repeated reprecipitations and were subjected analysis; the results are listed in Tables V, VI, VII and VIII.

TABLE V. COPOLYMERIZATION OF STYRENE (M_1) WITH VINYLPENTAMETHYLDISILANE (M_2)

M_2	Reaction time, hr.	Conversion, %	C, %	m_2
0.400	4.5	4.89	91.12	0.0194
0.500	7	5.25	91.04	0.0207
0.600	12	5.84	90.64	0.0276
0.800	24	2.72	88.27	0.0694
0.850	35	2.16	86.51	0.101

TABLE VI. COPOLYMERIZATION OF ACRYLONITRILE (M'_1) WITH VINYLPENTAMETHYLDISILANE (M_2)

M_2	Reaction time, hr.	Conversion, %	N, %	m_2
0.200	2	7.36	21.07	0.078
0.400	5	5.81	18.53	0.125
0.500	8	6.21	17.65	0.143
0.600	15	5.84	17.13	0.154

TABLE VII. COPOLYMERIZATION OF STYRENE (M_1) WITH 2-VINYLHEPTAMETHYLTRISILANE (M'_2)

M'_2	Reaction time, hr.	Conversion, %	C, %	m'_2
0.400	3	1.20	89.84	0.0283
0.500	7	4.22	90.31	0.0227
0.600	22	6.54	89.33	0.0345
0.800	29	2.09	87.43	0.0583

TABLE VIII. COPOLYMERIZATION OF ACRYLONITRILE (M'_1) WITH 2-VINYLHEPTAMETHYLTRISILANE (M'_2)

M'_2	Reaction time, hr.	Conversion, %	N, %	m'_2
0.200	2	5.21	19.41	0.081
0.400	4	1.51	16.94	0.120
0.500	13	5.56	15.77	0.135
0.600	22	3.31	14.57	0.166

From the data of analysis the monomer reactivity ratios, r_1 and r_2, were estimated by the intersection method using Eq. 1. The r_2 values in each case were virtually zero, so the Q and e values were calculated by solving Eqs. 2 and 3:

$$r_2 = \frac{M_1}{M_2}\left[\frac{dM_2}{dM_1}\left(1+\frac{M_1}{M_2}\,r_1\right)-1\right] \quad (1)$$

$$r_1 = \frac{Q_1}{Q_2}\exp\left[-e_1(e_1-e_2)\right] \quad (2)$$

$$r'_1 = \frac{Q'_1}{Q_2}\exp\left[-e'_1(e'_1-e_2)\right] \quad (3)$$

The authors are indebted to Dr. Kazuo Tori of The Shionogi Research Laboratory for NMR to Mr. Tadao Kobatake and Mr. Katsuhiko Sato for their microanalyses, and to the Tokyo Shibaura Electric Co., Ltd., for its gifts of chlorosilanes and a methylchlorosilane residue.

This research was supported in part by a grant-in-aid of the Ministry of Education and by the Kawakami Memorial Foundation, to which the authors' thanks are due.

BULLETIN OF THE CHEMICAL SOCIETY OF JAPAN VOL. 39 1283—1287 (1966)

Organic Sulfur Compounds. IV. The Reactions of Arylsulfonic Acids with Alkyl Chlorocarbonates

By Asami YAMAMOTO* and Michio KOBAYASHI**

Department of Chemistry, Yokohama City University, Matsuura-machi, Kanazawa-ku, Yokohama

(Received November 15, 1965)

The reactions of *p*-toluenesulfonic acid salt with alkyl chlorocarbonates have been investigated and their mechanism discussed. The reactions were slow at low temperature, and the intermediates, sulfonic carbonic anhydrides, could be isolated. When heated, these mixed anhydrides decomposed to alkyl sulfonates and carbon dioxide. *p*-Toluenesulfonic acid-^{18}O was prepared and its reaction with ethyl chlorocarbonate examined. All three oxygen atoms of the sulfonic acid were retained in the ethyl sulfonate formed. The reaction of isobutyl chlorocarbonate with silver *p*-toluenesulfonate gave a mixture of isobutyl- and *s*-butyl sulfonate. On the basis of these experiments, the mechanism involving the free alkyl cation has been proposed for the decomposition of the sulfonic-carbonic anhydrides.

Alkyl and aryl chlorocarbonates have been known to react with the carboxylic acid salts to form the carboxylic-carbonic anhydrides, which have drawn much attention recently.[1-6] The chlorocarbonates also give the nitric-carbonic anhydrides with silver nitrate; the decomposition of the anhydrides to nitric esters and carbon dioxide has been the subject of several recent publications.[7-9] Although many other reactions of the chlorocarbonates have been reported,[10] little is known about their reaction with sulfonic acid. In this paper, studies of the reaction of *p*-toluenesulfonic acid salt with alkyl chlorocarbonates will be described.

Results and Discussion

When ethyl chlorocarbonate (Ib) was added to a solution of silver *p*-toluenesulfonate (II) in acetonitrile at room temperature, the reaction proceeded very slowly with the precipitation of silver chloride. When this solution was warmed, a copious formation of carbon dioxide was observed and ethyl *p*-toluenesulfonate (IIIb) was isolated from the reaction mixture in 35% yield.

At room temperature this reaction was very slow; it was only one-third completed after 17 days, as estimated by the yield of silver chloride precipitated. The reaction mixture was concentrated under reduced pressure, the residue was extracted with methylene chloride, and its infrared spectrum (Fig. 1) was measured to show the presence of a strong carbonyl band in the 1786 cm^{-1} region which could not be attributed to the unchanged ethyl chlorocarbonate. By the evaporation of the solvent in a vacuum, a colorless oil was obtained. The similarity of its infrared spectrum to that of the corresponding methyl ester (IVa) described below suggested that this oil was carboethoxy *p*-toluenesulfonate (IVb). When this oil was heated on a water-bath, carbon dioxide was evolved and the infrared spectrum of the residue showed no C=O absorption. By the elution chromatography, pure IIIb was isolated.

$$RSO_3Ag + \underset{\underset{\text{I}}{\overset{\|}{O}}}{Cl\text{-}C\text{-}OR'} \rightarrow \underset{\text{IV}}{R\text{-}\overset{\uparrow}{\underset{\downarrow}{S}}(=O)\text{-}O\text{-}\underset{\underset{O}{\|}}{C}\text{-}OR'} + AgCl \qquad (1)$$

$$\underset{\text{IV}}{R\text{-}\overset{\uparrow}{\underset{\downarrow}{S}}(=O)\text{-}O\text{-}\underset{\underset{O}{\|}}{C}\text{-}OR'} \rightarrow \underset{\text{III}}{R\text{-}\overset{\uparrow}{\underset{\downarrow}{S}}(=O)\text{-}O\text{-}R'} + CO_2 \qquad (2)$$

Ia, IIIa, IVa R′ = methyl
Ib, IIIb, IVb R′ = ethyl
Ic, IIIc, IVc R′ = isobutyl

* Present address: Department of Chemistry, Faculty of Science, The University of Tokyo, Hongo, Tokyo.

** To whom correspondence should be sent; present address: Department of Chemistry, Faculty of Science, Tokyo Metropolitan University, Setagaya-ku, Tokyo.

1) D. S. Tarbell and N. A. Leister, *J. Org. Chem.*, **23**, 1149 (1958).
2) T. B. Windholz, ibid., **23**, 2044 (1958).
3) D. S. Tarbell and E. J. Longosz, ibid., **24**, 774 (1959).
4) T. B. Windholz, ibid., **25**, 1703 (1960).
5) E. J. Longosz and D. S. Tarbell, ibid., **26**, 2161 (1961).
6) C. J. Michejda, D. S. Tarbell and W. H. Saunders, Jr., *J. Am. Chem. Soc.*, **84**, 4113 (1962).
7) R. Boschan, ibid., **81**, 3341 (1959).
8) G. A. Mortimer, *J. Org. Chem.*, **27**, 1876 (1962).
9) D. N. Kevill and G. H. Johnson, *J. Am. Chem. Soc.*, **87**, 928 (1965).
10) M. Matzner, R. P. Kurkjy and R. J. Cotter, *Chem. Revs.*, **64**, 645 (1964).

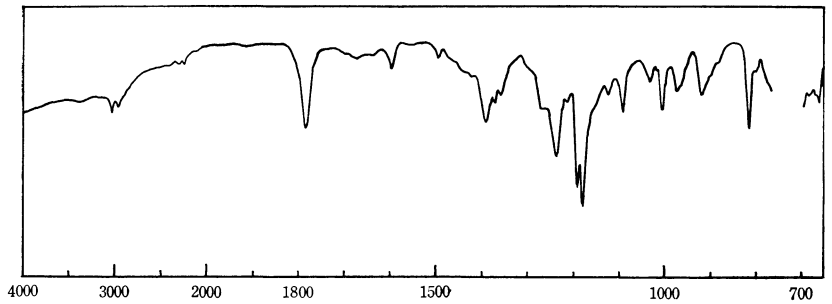

Fig. 1. Infrared spectrum of $CH_3C_6H_4SO_2$-O-C(=O)-OC_2H_5 in CH_2Cl_2.

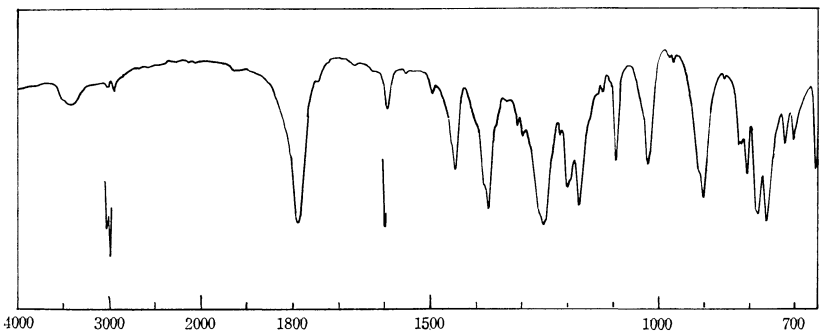

Fig. 2. Infrared spectrum of $CH_3C_6H_4SO_2$-O-C(=O)-OCH_3 in KBr disk.

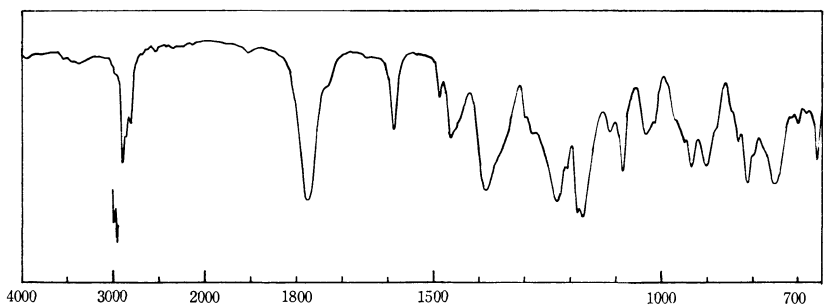

Fig. 3. Infrared spectrum of $CH_3C_6H_4SO_2$-O-C(=O)-O-Bu^i capillary film.

A similar treatment of methyl chlorocarbonate (Ia) with II in acetonitrile gave carbomethoxy *p*-toluenesulfonate (IVa) as colorless crystals in 10% yield. This compound has been prepared recently in a completely different way.[11] The infrared spectrum of our sample is shown in Fig. 2. Unexpectedly, this compound was rather stable in a pure state, but it decomposed to methyl *p*-toluenesulfonate (IIIa) when heated at 120—140°C for 5 hr. When warmed with water, it was hydrolyzed to form a clear solution of the sulfonic acid.

The reaction of silver nitrate with alkyl chlorocarbonate has been reported to be catalyzed by pyridine.[8] The reaction of Ib with II in the presence of pyridine was carried out in the hope of accelerating the rate of an otherwise very slow formation of the mixed anhydride (IVb), but it was found that in the presence of pyridine merely the decomposition of Ib occurred, while the sulfonic acid remained unchanged, indicating the absence of any catalytic effect of the tertiary base.

The same mixed anhydride (IVa) was expected to be formed by the reaction of *p*-toluenesulfonyl chloride with sodium methyl carbonate (V) as is shown below:

11) R. J. Crawford and R. Raap, *J. Org. Chem.*, **28**, 2419 (1963).

$$RSO_2Cl + NaO\text{-}C(=O)\text{-}OCH_3 \rightarrow$$

V

$$RSO_2\text{-}O\text{-}C(=O)\text{-}OCH_3 + NaCl \quad (3)$$

(R=*p*-tolyl)

Equimolecular amounts of tosyl chloride and V were treated in acetonitrile for one week, and the insoluble powder was filtered off. The solvent was removed by vacuum distillation and the residue was dissolved in methylene chloride. The infrared spectrum of this solution showed strong absorption bands at 1830 and 1790 cm^{-1} which were attributed to dimethyl pyrocarbonate (VI). Upon evaporation, a mixture of methyl *p*-toluenesulfonate and this pyrocarbonate, but no mixed anhydride (IVa), was obtained. Probably, once formed, IVa reacted with the unchanged V to give VI according to the reaction 4:

$$RSO_2\text{-}O\text{-}C(=O)\text{-}OCH_3 + NaO\text{-}C(=O)\text{-}OCH_3 \rightarrow$$

IVa V

$$RSO_3Na + CH_3O\text{-}C(=O)\text{-}O\text{-}C(=O)\text{-}OCH_3 \quad (4)$$

VI

The preparation of diethyl pyrocarbonate from 2 mol. of sodium ethyl carbonate and one mole of tosyl chloride, reported in a recent publication,[12] may be based on the formation of IVb as an intermediate.

There are two possibilities in the decomposition of the sulfonic carboxylic anhydride (IV) to alkyl sulfonate, namely path a and path b, as is shown below:

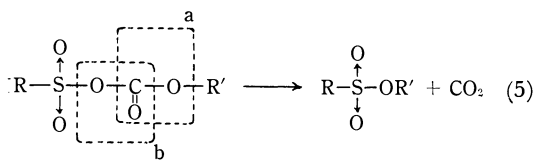

(5)

Path a is alkyl-oxygen splitting, while path b alkoxycarbonyl splitting. This problem has been solved by the isotope labeling. If the sulfonic acid containing the heavy oxygen is used, path a should give the sulfonic ester which retains all three oxygen atoms. On the other hand, path b would lead to the sulfonic ester, which should have 2 out of the 3 oxygen atoms which originally exist in the sulfonic acid.

p-Toluenesulfonic acid-^{18}O was prepared from tosyl chloride and $H_2{}^{18}O$. The reaction of its silver salt with Ib gave ethyl *p*-toluenesulfonate-^{18}O, which ^{18}O atom% was the same as that of the ethyl ester prepared by the direct alkylation of the same silver salt with ethyl bromide.[13] This finding definitely shows that the path a is the only way of cleavage.

However, there remained another question to solve concerning the mechanism of the decomposition of the mixed anhydride IV. The alkyl-oxygen splitting of IV could occur by either the intramolecular four-center cyclic mechanism (reaction 6) or the free alkyl carbonium ion mechanism (reaction 7):

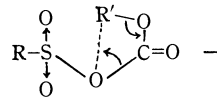

(6)

$$RSO_2\text{-}O\text{-}C(=O)\text{-}OR' \rightarrow RSO_3^- + CO_2 + R'^+ \quad (7)$$

To solve this question, the reaction of isobutyl chlorocarbonate (Ic) and II was investigated. If the free alkyl cation, isobutyl carbonium ion in this case, was formed, the rearrangement to *s*-butyl and *t*-butyl carbonium ion would be expected, finally resulting in the formation of *s*-butyl *p*-toluenesulfonate. *t*-Butyl *p*-toluenesulfonate is unstable and is not expected to survive under the reaction conditions.

When an equimolecular amounts of Ic and II were treated at room temperature in acetonitrile, a slow reaction started, forming a compound which was believed to be carboisobutoxy *p*-toluenesulfonate (IVc). Its decomposition gave a mixture of isobutyl *p*-toluenesulfonate and *s*-butyl *p*-toluenesulfonate in a 0.8 : 1.0 mol. ratio, with a quantity of isobutene and free *p*-toluenesulfonic acid. Isobutene was considered to be derived from the *t*-butyl cation.

Therefore, the following mechanism is proposed to the decomposition of the mixed anhydride IVc:

$$RSO_3Ag + ClC\text{-}OBu\text{-}i \rightarrow$$

$$RSO_2\text{-}O\text{-}C(=O)\text{-}OBu\text{-}i + AgCl \quad (8)$$

IVc

$$IVc \rightarrow [RSO_3^-][O \equiv C \cdots OBu\text{-}i]^+ \quad (9)$$

$$[O \equiv C \cdots OBu\text{-}i] \rightarrow CO_2 + i\text{-}Bu^+ \quad (10)$$

$$i\text{-}Bu^+ \rightleftarrows s\text{-}Bu^+ \rightleftarrows t\text{-}Bu^+ \quad (11)$$

$$RSO_3^- + i\text{-}Bu^+ \rightarrow RSO_3Bu\text{-}i \quad (12)$$

$$RSO_3^- + s\text{-}Bu^+ \rightarrow RSO_3Bu\text{-}s \quad (13)$$

12) L. Rosnati, *Chem. Ber.*, **96**, 3098 (1963).

13) W. D. Emmons and A. F. Ferris, *J. Am. Chem. Soc.*, **75**, 2257 (1953).

$$RSO_3^- + t\text{-}Bu^+ \rightarrow RSO_3H + (CH_3)_2C{=}CH_2 \quad (14)$$

When the reaction temperature was raised, a reaction giving the sulfonic anhydride (VII) occurred, along with the decomposition to the alkyl sulfonate. The most probable reaction to form VII would be the disproportionation of the mixed anhydride IV (reaction 15), but no detailed discussion of this reaction will be given at the present stage since only a slight amount of diisobutyl carbonate was detected among the products.

$$RSO_2\text{-}O\text{-}\underset{\underset{O}{\|}}{C}\text{-}OBu\text{-}i \rightarrow$$

IVc

$$^1/_2(RSO_2)_2O + ^1/_2(i\text{-}BuO)_2CO + ^1/_2CO_2 \quad (15)$$

VII

Experimental

Materials. — Silver *p*-toluenesulfonate (II) was prepared from silver oxide and *p*-toluenesulfonic acid, recrystallized from distillled water, and dried in a vacuum. Methyl chlorocarbonate (Ia) and ethyl chlorocarbonate (Ib) were commercial products and purified by distillation. Isobutyl chlorocarbonate (Ic) was prepared from phosgen and isobutyl alcohol in chloroform, b. p. 126—128°C. $\nu_{C=O}$ absorption band in 1780 cm^{-1} (neat). Isobutyl *p*-toluenesulfonate was prepared from tosyl chloride and isobutyl alcohol in the presence of pyridine, b. p. 161—165°C/3—4 mmHg. IR 1372 (antisymm. s-o), 1192, 1180 (symm. s-o), 982, 944, 818 cm^{-1} (in CCl_4 or CH_2Cl_2). *s*-Butyl *p*-toluenesulfonate was prepared from *s*-butyl alcohol in a similar way and purified by rapid elution chromatography over silica gel with petroleum ether - benzene mixture, since the repeated attempts to purify it by vacuum distillation resulted in a partial decomposition. IR 1370, 1192, 1180, 910, 819 cm^{-1} (in CH_2Cl_2).

The Reaction of Silver *p*-Toluenesulfonate with Ethyl Chlorocarbonate.—*Reaction at the Boiling Point.*—To a solution of 11.5 g. of II in 40 ml. of warm acetonitrile 4.0 g. of Ib diluted with 3 ml. of the same solvent was added. The precipitation of silver chloride proceeded slowly, along with a slow evolution of carbon dioxide (50 ml. in one night; calculated volume, 870 ml.). This mixture was refluxed until the evolution of gas ceased. The total gas volume was 800 ml., and the weight of silver chloride was 5.1 g. (90% of the theoretical yield). Acetonitrile was expelled from the filtrate by vacuum distillation, and the residue was taken up in benzene to remove the unchanged II, washed with aqueous sodium carbonate, and dried over magnesium sulfate. The evaporation of the solvent from this solution and the recrystallization of the residue gave 2.0 g. of IIIb, m. p. 32—34°C, in a 30% yield of the theoretical.

Reaction at Room Temperature.—To a solution of 7.0 g. of II in 35 ml. of acetonitrile 2.7 g. of Ib in 10 ml. of acetonitrile was added drop by drop; the mixture was then left at room temperature for 17 days. The solvent and all other volatile materials were removed by vacuum distillation at room temperature, and the residue was dissolved in 50 ml. of methylene chloride and filtered. Its infrared spectrum is shown in Fig. 1. From the yield of silver chloride, 1.2 g., the reaction was estimated to have been 1/3 completed. The evaporation of this solution under reduced pressure gave a sirup which showed the same infrared spectrum as in Fig. 1, suggesting the presence of carboethoxy *p*-toluenesulfonate (IVb)[11] contaminated with some ethyl *p*-toluenesulfonate. When heated, this sirup formed carbon dioxide, and the residue gave pure IIIb by column chromatography over alumina with benzene.

The Reaction of II with Methyl Chlorocarbonate.—The reaction of II (7.0 g.) with Ia (2.3 g.) was carried out in a way similar to that described above for the ethyl ester. After 17 days at room temperature, silver chloride was filtered off and the volatile matter was expelled from the filtrated by vacuum distillation at room temperature. To the residue 50 ml. of methylene chloride was added and the infrared spectrum was measured; we thus found a strong C=O band at 1790 cm^{-1}. From the yield of silver chloride, 1.2 g., and also from the intensity of the above C=O band, a 35% conversion was estimated. Upon the evaporation of the solvent in a vacuum and the recrystallization of the residue from a mixture of *n*-hexane: benzene (2 : 1), 0.65 g. of IVa was obtained as a colorless prism, m. p. 57—59°C (lit.[11] 60—61°C). Heating at 120°C for 20 min. produced no change in the infrared spectrum of IVa, while heating at 120—140°C for 5 hr. resulted in a complete decomposition to methyl *p*-toluenesulfonate.

The Reaction of *p*-Toluenesulfonyl Chloride with Sodium Methyl Carbonate (V).—When 9 g. of tosyl chloride was mixed with 4.0 g. of V, prepared by passing carbon dioxide into a solution of sodium methoxide in methanol and by the evaporation of the reaction mixture in a vacuum to complete dryness, an exothermic reaction started at once. The mixture was cooled immediately, diluted with 30 ml. of acetonitrile, and kept at room temperature for one week. The insoluble powder was filtered off, and the solvent was removed in vacuo. The residue was dissolved in methylene chloride and its infrared spectrum examined; this spectrum exhibited strong absorptions at 1830 and 1790 cm^{-1}, corresponding to those of methyl pyrocarbonate. The work-up of this solution gave methyl *p*-toluenesulfonate too, but no IVa.

The Preparation of Silver *p*-Toluenesulfonate-^{18}O.—A mixture of 20 g. of tosyl chloride and 5 ml. of $H_2{}^{18}O$ (^{18}O: 1.5 atom%) was heated in a water bath for 2 days; the contents of the flask were thereby solidified. Another few milliliters of $H_2{}^{18}O$ and 10 ml. of anhydrous dioxane were added to this solid, and the homogeneous mixture was heated for sevaral hours. The volatile matter was expelled by vacuum evaporation, and distilled water was added to the residue. The water was then distilled off in vacuo to ensure the removal of the hydrogen chloride formed. Finally the residue was dissolved in 100 ml. of distilled water and warmed with 13 g. of silver oxide. This solution was filtered while hot, and the filtrate was cooled in ice water to deposit the desired salt. The concentration of the mother liquid gave a second croup. Recrystallized silver salt was dried in a vacuum, powdered, and dried again in vacuo.

The Preparation of Ethyl *p*-Toluenesulfonate-^{18}O.—To a solution of 5.0 g. of silver *p*-toluenesulfonate-^{18}O in 20 ml. of warm acetonitrile, 4.0 g. of ethyl bromide was added; the reaction mixture was then refluxed for one hour and cooled. After another hour at room temperature, the mixture was filtered and the solvent was distilled off from the filtrate. The crystalline residue was recrystallized from petroleum ether to give 2.4 g. of ethyl *p*-toluenesulfonate-^{18}O. The ^{18}O atom% of this ester was 0.61%.

The Reaction of Silver *p*-Toluenesulfonate-^{18}O with Ib.—A solution of 5.5 g. of Ib (1.4 mol. equivalent) in 5 ml. of acetonitrile was added to a solution of 10.0 g. of silver salt-^{18}O in 40 ml. of acetonitrile at 95°C. The precipitation of silver chloride started at once. The total volume of the evolved gas was 950 ml.; it thus exceeded the calculated volume, 860 ml. The infrared spectrum of the filtrate indicated the presence of some diethyl carbonate ($\nu_{C=O}$, 1740 cm^{-1}). Acetonitrile was removed from the filtrate by vacuum distillation, and the residue was taken up in methylene chloride to free it from unchanged silver sulfonate. The evaporation of this solution, the repeated extraction of the residue with petrolum ether, and finally filtration chromatography through alumina gave 0.4 g. of ethyl *p*-toluenesulfonate-^{18}O, m. p. 31°C. The ^{18}O atom% of this ester was 0.62%.

The Reaction of II with Isobutyl Chlorocarbonate.—*i) Reaction at Room Temperature.*—To a solution of 7.0 g. of II in 30 ml. of acetonitrile, 3.4 g. of Ic in 10 ml. of the same solvent was added. No change was observed. The mixture was then kept at room temperature for 8 days, and the precipitated silver chloride (1.0 g., 1/3 of the calculated) was filtered off. Acetonitrile was removed in a vacuum, and the residue was dissolved in methylene chloride and filtered from the unchanged II. The solvent was distilled off in vacuo, and the residue was warmed with a mixture of benzene-petroleum ether (1 : 2). Upon cooling, some colorless crystals separated; they were identified as *p*-toluenesulfonic acid. The filtrate and the insoluble matter in the solvent mixture were combined, diluted with ether, washed with a sodium carbonate solution and water, and dried over magnesium sulfate. Upon the evaporation of the solvent in vacuo, a colorless sirup was obtained which exhibited a strong C=O absorption in the infrared spectrum (Fig. 3), suggesting the presence of carboisobutoxy *p*-toluenesulfonate (IVc), probably contaminated with some butyl *p*-toluenesulfonate. All attempts to isolate the mixed anhydride (IVc) in the crystalline form were unsuccessful. After one week at room temperature, the sirup was dissolved in ether, treated with an excess of *p*-phenylenediamine to decompose the unchanged IVc to *N*-carboisobutoxy *p*-phenylenediamine and the sulfonic acid, washed with diluted sulfuric acid, filtered through decolorizing carbon, and finally evaporated. The oil thus obtained in a small yield was a mixture of isobutyl and *s*-butyl *p*-toluenesulfonate, plus a slight amount of diisobutyl carbonate. The ratio of isobutyl sulfonate to *s*-butyl sulfonate was estimated by infrared spectroscopy to be 0.79: 1.00. The low yield of butyl *p*-toluenesulfonates was attributed to the too mild decomposition conditions (one week at room temperature).

ii) Reaction at Boiling Point.—A solution of 7.0 g. of II and 3.7 g. of Ic in 40 ml. of acetonitrile was refluxed until the evolution of gas (total 565 ml., nearly 1 mol.) ceased. The presence of isobutene in gas was confirmed by converting it into dibromide (identified by boiling point and infrared spectrum). Acetonitrile was removed under reduced pressure, and the residue was taken up in methylene chloride, filtered, washed with dilute sodium carbonate solution, and dried over magnesium sulfate. Upon the evaporation of the solvent, a mixture of *p*-toluenesulfonic anhydride (VII) and its free acid was crystallized. The infrared spectrum of the filtrate indicated that the yield of butyl *p*-toluenesulfonates was very low, if there was any at all. An attempt to isolate them from the filtrate by column chromatography was unsuccessful.

iii) Reaction at a Moderate Temperature.—A solution of 7.0 g. of II and 3.4 g. of Ic in 30 ml. of acetonitrile was warmed at 40—60°C for several hours; a gaseous mixture of carbon dioxide and isobutene (identified as dibromide) evolved. Treatment similar to that in i) gave an oil which again exhibited a strong C=O band at 1788 cm^{-1}. Excess aniline was added to this oil to form a semisolid mixture, which left the white crystals undissolved upon the addition of diluted nitric acid. The recrystallization of these crystals from petroleum ether gave carboisobutoxyaniline, m. p. 82—84°C; melting point upon admixture with authentic specimen, 82—83°C. The acidic aqueous filtrate gave only a trace of silver chloride with a silver nitrate solution. Therefore, the presence of the C=O absorption band and the formation of urethan could not be attributed to the presence of the unchanged Ic in the oil. The concentration of the petroleum ether mother filtrate from urethan and treatment with active carbon gave a mixture of isobutyl and *s*-butyl *p*-toluenesulfonate. The mole ratio of *iso* : *sec.* was estimated by infrared spectroscopy to be 0.86 : 1.00. By elution chromatography over silica gel with petroleum ether-benzene, these two esters could be separated (the isobutyl ester was eluted first), from each other, and the formation of *s*-butyl ester was confirmed. From the yield of carboisobutoxyaniline and butyl sulfonates, about half of the mixed anhydride IVc was considered to have decomposed to butyl sulfonates.

The Preparation of Carboisobutoxyaniline.—When an excess of aniline was added to 0.3 g. of Ic, the reaction occurred immediately, giving a solid mass. The addition of diluted nitric acid to this mass left undissolved crystals; they were recrystallized from 10 ml. of petroleum ether to give the desired product, m. p. 85—86°C (lit. 80 or 86°C). Its high yield indicated the absence of any appreciable *s*-butyl chlorocarbonate as an impurity in the sample used for the present study.

The authors are grateful to Professor Shigeru Oae of Osaka City University for his donation of heavy oxygen water, and to Dr. Reiko Kiritani of the Radiation Center of Osaka Prefecture for her ^{18}O analysis.

BULLETIN OF THE CHEMICAL SOCIETY OF JAPAN VOL. 39 1288—1292 (1966)

Organic Sulfur Compounds. V. Reactions of Arylsulfonic Acids with Alkyl and Aryl Chlorosulfites

By Asami YAMAMOTO* and Michio KOBAYASHI**

Department of Chemistry, Yokohama City University, Mutsuura-machi, Kanazawa-ku, Yokohama

(Received December 14, 1965)

Silver *p*-toluenesulfonate has been found to react with alkyl and aryl chlorosulfite to give *p*-toluenesulfonic esters. Mixed anhydrides of the sulfonic acid and monoalkyl or monoaryl sulfite were postulated as the intermediates. No rearrangement of the alkyl group was observed during the reaction. The reaction mechanism was studied by means of the ^{18}O tracer technique.

The reaction of arylsulfonic acid with alkyl chlorocarbonates was described in a previous paper.[1] Studies of the reactions of *p*-toluenesulfonic acid with alkyl and aryl chlorosulfites will be reported in this paper.

Results and Discussion

The Reaction of Alkyl Chlorosulfites.—Ethyl chlorosulfite (Ia) reacted with silver *p*-toluenesulfonate (II) in acetonitrile at room temperature to precipitate silver chloride quantitatively. Upon the warming of the filtrate, sulfur dioxide evolved and ethyl *p*-toluenesulfonate (IIIa) was obtained in a 30% yield. *p*-Toluenesulfonic anhydride (IV) and *p*-toluenesulfonic acid were by-products.

A mixed anhydride (Va) of the sulfonic acid and monoalkyl sulfite, namely, ethoxysulfinyl *p*-toluenesulfonate, may be postulated as a probable intermediate:

$$RSO_3Ag + Cl\text{-}S\text{-}OC_2H_5 \rightarrow \underset{\underset{\text{Ia}}{\downarrow O}}{} \quad RSO_2\text{-}O\text{-}S\text{-}OC_2H_5 + AgCl \qquad (1)$$
$$\underset{\underset{\text{Va}}{\downarrow O}}{}$$

(R = *p*-tolyl)

Although the formation of Va could not be verified, the presence of analogous mixed anhydrides in the case of isobutyl and phenyl derivatives was supported by infrared spectra, as will be described below.

There seem to be two reactions, one to lead to the formation of the alkyl sulfonate and another to produce the sulfonic anhydride. These two reactions will be considered separately in the following discussion.

Alkyl Sulfonate Formation.—i) The Mode of the Cleavage of the Mixed Anhydride.—There are two possible modes of cleavage by which Va can give ethyl sulfonate IIIa, namely, alkyl-oxygen splitting (path a) and alkoxy-sulfonyl splitting (path b):

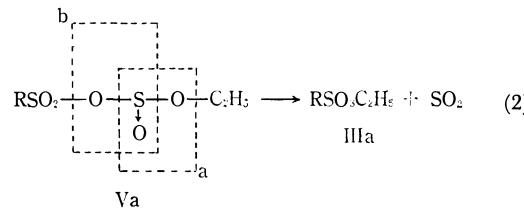

(2)

In a similar decomposition of the mixed anhydride of *p*-toluenesulfonic acid and monoalkyl carbonate[1] alkyl-oxygen splitting has been established, while alkoxy-acyl splitting has been established as taking place in the cases of the mixed anhydride of *p*-toluenesulfinic acid and monoalkyl sulfite[2] and of the carbonic-carboxylic anhydride.[3] On the other hand, 75% alkoxy-acyl splitting and 25% alkyl-oxygen splitting were observed in the nitric-carbonic anhydride.[4]

When the reaction of silver *p*-toluenesulfonate-^{18}O and ethyl chlorosulfite was carried out, the resultant ethyl *p*-toluenesulfonate-^{18}O was found to retain all three oxygen atoms originally present in silver sulfonate. Therefore, alkyl-oxygen cleavage (path a) is definitely established for the reaction 2.

ii) Mechanism.—Several mechanisms may be formulated for the reaction 2, every one of them consistent with the alkyl-oxygen splitting. At first, the mechanism shown below involving a free alkyl cation was considered to be the most plausible:

* Present address: Department of Chemistry, Faculty of Science, The University of Tokyo, Hongo, Tokyo.

** To whom correspondence should be sent: Department of Chemistry, Faculty of Science, Tokyo Metropolitan University, Setagaya-ku, Tokyo.

1) Part IV of this series. This Bulletin, **39**, 1283 (1966).

2) Part I of this series. M. Kobayashi, M. Terao and A. Yamamoto, ibid., **39**, 802 (1966).

3) C. J. Michejda, D. S. Tarbell and W. H. Saunders, Jr., *J. Am. Chem. Soc.*, **84**, 4113 (1962).

4) R. Boschan, ibid., **81**, 3341 (1959).

$$RSO_2\text{-}O\text{-}\underset{\underset{O}{\downarrow}}{S}\text{-}O\text{-}R' \longrightarrow [RSO_3^-][O{=}S^{+}{-}O{-}R']^+ \quad (3)$$

VI

$$[R'{-}O{=}S{\equiv}O]^+ \longrightarrow SO_2 + R'^+ \quad (4)$$

$$RSO_3^- + R'^+ \longrightarrow RSO_3R' \quad (5)$$

(R = *p*-tolyl, R' = alkyl)

In hope of confirming this assumption, the reaction of II with isobutyl chlorosulfite (Ib) was investigated. If a free isobutyl cation was formed over the intermediate Vb (V: R'=isobutyl) as is shown in the reactions 3 and 4, its facile rearrangement to *s*-butyl and *t*-butyl carbonium ion would lead to the formation of *s*-butyl *p*-toluenesulfonate, as is found in the decomposition of carboisobutoxy *p*-toluenesulfonate.[1]

In repeated attempts, however, the isolation of *s*-butyl *p*-toluenesulfonate was always unsuccessful. In the ester fraction, isobutyl sulfite and isobutyl *p*-toluenesulfonate (IIb) were detected, in yields varying according to the reaction conditions.

Thus, a free alkyl cation mechanism (reactions 3, 4 and 5) can find no experimental support for the decomposition of alkoxysulfinyl arylsulfonate V. This contrasts clearly with the decomposition of the formally analogous sulfonic-carbonic anhydride.[1]

The following three mechanisms, involving no free alkyl cation formation, could be presumed:

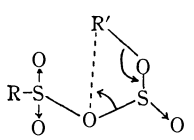

$$\longrightarrow RSO_3R' + SO_2 \quad (6)$$

$$RSO_3^- + [R'{-}O{=}S{\equiv}O]^+ \longrightarrow$$

VI

$$RSO_3R' + SO_2 \quad (7)$$

and finally:

$$RSO_3^- + R'\text{-}O\text{-}\underset{\underset{O}{\downarrow}}{\overset{\overset{O}{\uparrow}}{S}}\text{-}O\text{-}\underset{\underset{O}{\downarrow}}{\overset{\overset{O}{\uparrow}}{S}}\text{-}R \rightarrow$$

V

$$RSO_3R' + [RSO_2\text{-}O\text{-}SO_2]^- \quad (8)$$

VII

$$VII \rightarrow RSO_3^- + SO_2 \quad (9)$$

Of these three mechanisms, the second (reaction 7) and third (reaction sequence 8 and 9) belong to the S_N2 type, whereas the first one (reaction 6) is a S_Ni type four center cyclic mechanism. The study of the reaction of an optically active chlorosulfite with II would help to decide which mechanism should be chosen.

The mechanism of the Formation of the Sulfonic Anhydride.—The formation of IV and isobutyl sulfite suggests the occurrence of the disproportionation reaction (10) in the decomposition of the mixed anhydride V:

$$RSO_2\text{-}O\text{-}\underset{\underset{O}{\downarrow}}{S}\text{-}OR' \rightarrow$$

$$1/2(RSO_2)_2O + 1/2(R'O)_2SO + 1/2SO_2 \quad (10)$$

For the mechanism of this reaction, the following ionic chain reaction sequence seems to be plausible:

$$V \longrightarrow RSO_3^- + [O{=}S^{+}{-}OR']^+ \quad (3)$$

VI

$$RSO_3^- + V \longrightarrow (RSO_2)_2O + \left[R'O\text{-}S\begin{matrix}O\\O\end{matrix}\right]^- \quad (11)$$

$$[R'O\text{-}SO_2^-] \longrightarrow R'O^- + SO_2 \quad (12)$$

$$R'O^- + V \longrightarrow RSO_3^- + (R'O)_2SO \quad (13)$$

The attack on V by $R'O^-$ anion might occur on the sulfone group, not on the sulfinyl group, as is shown below:

$$R'O^- + V \rightarrow RSO_3R' + [R'O\text{-}SO_2^-] \quad (14)$$

However, if this is the case, the resultant sulfonic ester should retain only two out of the three oxygen atoms of the sulfonic acid; this is contrary to the experimental evidence obtained with ^{18}O, at least for alkyl chlorosulfite.

Another mechanism, which postulates the intermediate formation of a sulfonyl cation (VIII), could be formulated for the disproportionation reaction 10:

$$RSO_2^+ + V \longrightarrow (RSO_2)_2O + [R'O{=}S{\equiv}O]^+ \quad (15)$$

VIII VI

$$VI + V \longrightarrow (R'O)_2SO + [RSO_2{-}O{=}S{\equiv}O]^+ \quad (16)$$

IX

$$IX \longrightarrow RSO_2^+ + SO_2 \quad (17)$$

Although the sulfonyl cation VIII has been postulated in the Friedel-Crafts' sulfonylation[5] and in the reaction of tosyl chloride with Lewis acids[6], its formation as a free molecular species seems rather doubtful.[7]

While the anionoid attack of $R'O^-$ on V (reaction 13) is considered to occur on the sulfinyl group, as has been stated above, the other anionoid attack by RSO_3^- on V seems to occur only on the sulfonyl group (reaction 11). Probably the attack

5) F. R. Jensen and H. C. Brown, ibid., **80**, 4042 (1958).
6) F. Klages and K. Hoheisel, *Chem. Ber.*, **96**, 2057 (1963).
7) Studies on the sulfonylation will be described in the following paper.

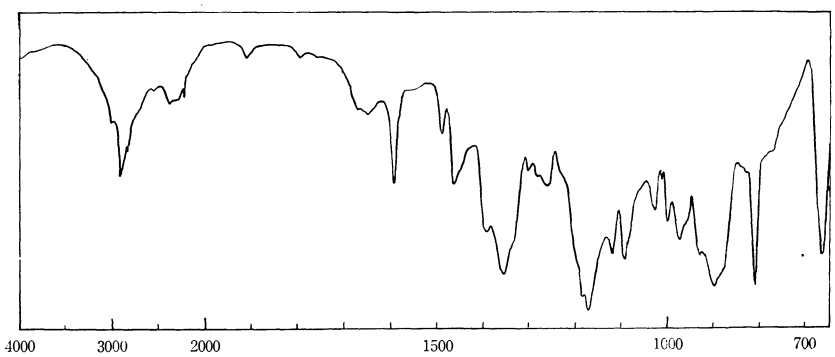

Fig. 1. Infrared spectrum of $CH_3C_6H_4SO_2$-O-S-OBu^i (Vb) in CH_2Cl_2.
O

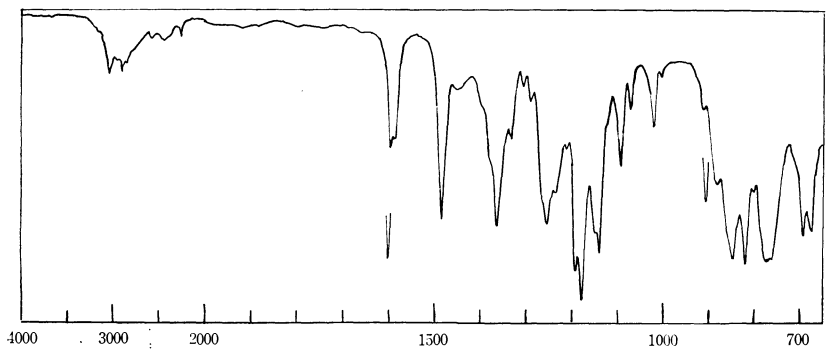

Fig. 2. Infrared spectrum of $CH_3C_6H_4SO_2$-O-S-OC_6H_5 (Vc) in acetonitrile.
O

by RSO_3^- could take place on sulfinyl sulfur too, but with the net result of a simple exchange of RSO_3^- (18):

$$RSO_3^- \cdots\rightarrow \underset{\underset{OR'}{\downarrow}}{\overset{\overset{O}{\uparrow}}{S}}\text{-O-}O_2SR \rightarrow \underset{\underset{OR'}{\downarrow}}{\overset{\overset{O}{\downarrow}}{RSO_2\text{-O-S}}} + RSO_3^- \qquad (18)$$

A Question about the Existence of the Mixed Anhydride V.—For the formation of the alkyl sulfonate in the reaction of II with alkyl chlorosulfite, the following mechanism, which could take place without the formation of the intermediate V, can be postulated:

$$\underset{\underset{O}{\downarrow}}{Cl\text{-S-}OR'} + Ag^+ \longrightarrow AgCl + \underset{VI}{\left[O{=}S{=}OR'\right]^+} \qquad (19)$$

$$RSO_3^- + VI \longrightarrow RSO_3R' + SO_2 \qquad (7)$$

The reaction sequence 19 and 7 is analogous to the one, which has been proposed[4] and later denied on the basis of kinetic evidence for the formation of the nitric ester from silver nitrate and alkyl chlorocarbonate.[8]

In order to verify the formation of an intermediate Vb and to support our postulation against the above mechanism (19 and 7), the reaction between II and Ib was carried out at 0°C and the solvent was distilled off in a vacuum at 0°C. The infrared spectrum of the residue in methylene chloride (Fig. 1) was rather close to that of *s*-butyl *p*-toluenesulfonate, but upon the treatment of this solution with ice water, isobutyl sulfite and a small amount of isobutyl *p*-toluenesulfonate were obtained without any trace of *s*-butyl *p*-toluenesulfonate. This experiment was repeated three times. Since a similar spectrum was recorded in every case, this spectrum is now believed to be attributable to Vb. The evaporation of the methylene chloride solution in a vacuum resulted in an oily residue containing crystals of the sulfonic anhydride IV. The work-up of this residue gave isobutyl sulfite in a good yield and isobutyl *p*-toluenesulfonate as a minor product. These products were considered to have been produced from Vb during the evaporation and/or the subsequent work-up.

8) D. N. Kevill and G. H. Johnson, *J. Am. Chem. Soc.*, **87**, 928 (1965).

The Reaction of Phenyl Chlorosulfite.—As has been described above, the decomposition of the sulfonic-monoalkylsulfurous anhydride V and sulfonic-carbonic anhydride proceeds by alkyl-oxygen cleavage, while the decomposition of the carbonic-carboxylic anhydride and of the sulfinic-monoalkylsulfurous anhydride proceeds by alkoxy-acyl cleavage. These facts correspond to the other facts that the alkyl sulfonate was hydrolyzed by alkyl-oxygen splitting,[9] while alkyl sulfinate[10] and carboxylic ester[11] were hydrolyzed by alkoxy-acyl splitting. Therefore, it seems that it would be interesting to examine the mode of the decomposition of phenoxysulfinyl *p*-toluenesulfonate Vc, since aryl sulfonate has been known to undergo aryloxy-sulfonyl splitting[12] upon hydrolysis.

The reaction of silver *p*-toluenesulfonate-^{18}O with phenyl chlorosulfite was carried out in order to answer this question. Although the yield of the expected phenyl *p*-toluenesulfonate-^{18}O was low, its ^{18}O atom% was exactly 2/3 of that of the starting silver sulfonate. Consequently, phenoxy-acyl cleavage is operative in the decomposition of Vc; this again corresponds to the mode of the hydrolysis.

$$RS^{18}O_2\text{-}^{18}O\text{-}S\text{-}OC_6H_5 \rightarrow \underset{\underset{O}{\downarrow}}{} \quad RS^{18}O_2OC_6H_5 + SO^{18}O \qquad (20)$$

The infrared spectrum of an intermediate, believed to be Vc, was observed in acetonitrile (Fig. 2). After boiling for 9 hr., this solution was evaporated under reduced pressure. From the residue, *p*-toluenesulfonic acid and a lot of a resinous material were obtained, besides phenyl *p*-toluenesulfonate.

The mechanism of the decomposition of Vc has not yet been determined. Mechanism 14 could be applied to reaction 20, but the formation of the phenoxy anion would lead to the formation of diphenyl sulfite, at least as a by-product. Actually, however, none of this compound was detected. Instead, a large amount of a resinous material with an unknown structure was produced, as has been described above.

Experimental

Materials.—Ethyl chlorosulfite (Ia), b. p. 59°C/85 mmHg, was prepared from ethyl alcohol and thionyl chloride. Isobutyl chlorosulfite, b. p. 61°C/25 mmHg, was obtained in a similar way. Phenyl chlorosulfite, b. p. 105—107°C/10 mmHg, was synthesized from phenol and 4 mol. of thionyl chloride.[13] *p*-Toluenesulfonic acid-^{18}O was the same sample as was used in a previous paper.[1] The ^{18}O atom% was 0.61%. The preparation of isobutyl- and *s*-butyl *p*-toluenesulfonates was also described in the same report.[1]

The Reaction of Silver p-Toluenesulfonate (II) and Ethyl Chlorosulfite (Ia).—To a solution of 13.5 g. of II in 50 ml. of acetonitrile, there was added, drop by drop, 7.0 g. of Ia in 10 ml. of acetonitrile; the precipitate of silver chloride appeared at once. The mixture was then left for 35 min., and silver chloride was filtered off. Its weight was 6.7 g. (97%). After the filtrate had been warmed on a water bath for several hours and left overnight, the solvent was distilled off in vacuo. The residue was dissolved in ether, washed with water, and evaporated to give 3.45 g. of IIIa, m. p. 32—34°C, in a 36% yield.

Reaction of Silver p-Toluenesulfonate-^{18}O with Ia.—The reaction of 4.5 g. of Ia with 9.2 g. of silver *p*-toluenesulfonate-^{18}O in 40 ml. of acetonitrile was carried out in a way similar to that described above. The solvent was expelled in a vacuum, the residue was dissolved in benzene, and silver chloride (4.5 g.; 100%) was filtered off. The filtrate was washed with a sodium carbonate solution, dried, and evaporated. The oily residue was then extracted with petroleum ether to give 4.2 g. of ethyl *p*-toluenesulfonate-^{18}O, m. p. 32—33°C. Upon recrystallization, 3.0 g. (46%) of the pure ester was obtained. The ^{18}O atom% of this sample was 0.62%. From the insoluble part in petroleum ether, 1.6 g. of *p*-toluenesulfonic anhydride-^{18}O was obtained as colorless crystals, (m. p. 122—124°C; lit. 122—125°C) in a yield 30% of the theoretical yield.

The Reaction of II with Isobutyl Chlorosulfite Ib.—i) Reaction at 0°C.—A solution of 3.5 g. of Ib in a few milliliters of acetonitrile was added, drop by drop, to an ice-cooled solution of 7.0 g. of II in 30 ml. of the same solvent. After the reaction mixture has been cooled in ice water for a few hours, acetonitrile was distilled off in vacuo at 0°C to leave the colorless oil; it turned purple overnight. This oil was dissolved in methylene chloride, filtered, and evaporated in vacuo to give a mixture of crystals and oil. The crystals were separated by filtration and identified as IV. Oil was extracted with petroleum ether, and 0.5 g. of *p*-toluenesulfonic acid was obtained from the insoluble part. The soluble part was chromatographed over alumina with petroleum ether, (b. p. under 40°C) to afford 0.9 g. of diisobutyl sulfite (40% of the theoretical yield) from the early eluent and 0.3 g. of isobutyl *p*-toluenesulfonate (IIIb) (6%). Although every fraction in elution chromatography was examined by infrared spectroscopy, there was no indication of the presence of *s*-butyl *p*-toluenesulfonate.

ii) The Identification of the Intermediate.—The reaction was carried out with the same amounts of the reactants and in a manner similar to that described above. After the solvent had been removed in vacuo, the residue was taken up in methylene chloride and filtered. The infrared spectrum of the filtrate is shown in Fig. 1. This solution was poured into ice water; the organic layer was washed with 5% sodium carbonate and water successively, and dried over potassium carbonate, and then its infrared spectrum was measured again. Although the infrared spectrum in Fig. 1 was similar to that of *s*-butyl *p*-toluenesulfonate, the second infrared spectrum, taken after the hydrolysis with ice water,

9) Ader, Thesis, London, 1949, quoted in Ref. 12.
10) C. A. Bunton and B. N. Hend, *J. Chem. Soc.*, **1962**, 2562; **1963**, 627.
11) J. Hine, "Physical Organic Chemistry," second ed., McGraw-Hill, New York, N. Y. (1962), p. 275.
12) C. A. Bunton and Y. F. Frei, *J. Chem. Soc.*, **1951**, 1872.
13) W. E. Bissinger and F. E. Kung, *J. Am. Chem. Soc.*, **70**, 2664 (1948).

showed only a very weak absorption of the sulfonic ester in the 1380 cm^{-1} region. The main product was identified as diisobutyl sulfite. In a separate experiment, a specimen of *s*-butyl *p*-toluenesulfonate was treated with a sodium carbonate solution and potassium carbonate, as described above; no appreciable decomposition was found to be effected by such purification procedure.

iii) The Hydrolysis of the Intermediate.—A reaction with the same amounts of the reactants as in i) was carried out, and then the reaction mixture was decomposed with ice water after 20 min. at 0°C. The organic matter was extracted with 200 ml. of methylene chloride, washed with water and 5% sodium carbonate, and dried over magnesium sulfate; the solvent was then removed in vacuo to give a colorless oil, which was shown by infrared spectrum to be pure diisobutyl sulfite. Upon distillation, 1.7 g. of sulfite was isolated at 100°C/20 mmHg in a 78% yield. Since no *p*-toluenesulfonic anhydride was detected among the products, this sulfite was considered to be produced by the interaction of Vb with isobutyl alcohol, one of the products of the hydrolysis of Vb, not by the disproportionation reaction (11).

The Reaction of Phenyl Chlorosulfite (Ic) with II.—i) The Identification of an Intermediate.—A solution of 4.0 g. of Ic in a few milliliters of acetonitrile was added, drop by drop, to a solution of 6.0 g. of II in 30 ml. of the same solvent at room temperature; thereupon silver chloride began to precipitate immediately. The mixture was filtered through a fritted glass funnel, and the infrared spectrum of the filtrate was recorded (Fig. 2). This solution was then refluxed in an oil bath for 9 hr., and the solvent was removed in vacuo. The viscous residue was extracted repeatedly with carbon tetrachloride to leave a mixture of *p*-toluenesulfonic acid and a resinous matter. The extract was evaporated, and the residue (2.2 g.) was chromatographed over alumina with benzene to give 1.1 g. of phenyl *p*-toluenesulfonate (identified by melting point and infrared), in 21% yield.

ii) Reaction at the Boiling Point.—To a solution of 2.2 g. of II in 10 ml. of acetonitrile, 1.5 g. of Ic in a few milliliters of the same solvent was added at room temperature. The reaction mixture was refluxed without the filtration of the precipitated silver chloride for 2 hr. The next day, then, the solution was filtered and the solvent was distilled off from the filtrate in a vacuum. The crystalline residue was dissolved in ether to remove some insoluble matter and again evaporated. There was a strong smell of sulfur dioxide. The residue was extracted with benzene, and the soluble part was chromatographed to afford 0.5 g. of phenyl *p*-toluenesulfonate (25%). From the insoluble part in benzene, 0.5 g. of *p*-toluenesulfonic acid was isolated (35%).

The Reaction of Silver p-Toluenesulfonate-^{18}O with Ic.—A solution of 1.5 g. of Ic in a few milliliters of acetonitrile was added to a solution of 2.2 g. of silver sulfonate ^{18}O in 10 ml. of the same solvent over a 1.5 hr. period; then the mixture was refluxed for a few hours. Silver chloride was filtered off, and the solvent was removed from the filtrate by distillation. The residue was taken up in 70 ml. of benzene, washed with a sodium carbonate solution and water successively, and dried over magnesium sulfate. Upon elution chromatography over alumina with benzene, 0.2 g. of phenyl *p*-toluenesulfonate-^{18}O was obtained. The ^{18}O atom% of this ester was 0.49%. (The calculated atom% based on 2/3 retention was 0.48%).

Thanks are due to Dr. Reiko Kiritani of the Radiation Center of Osaka Prefecture for the analysis of ^{18}O, and to Professor Shigeru Oae of Osaka City University for the donation of the heavy oxygen water.

BULLETIN OF THE CHEMICAL SOCIETY OF JAPAN VOL. 39 1292—1296 (1966)

Organic Sulfur Compounds. VI. The Reactions of Arylsulfinic Acids with Alkyl Chlorocarbonates

By Michio KOBAYASHI* and Miki TERAO

Department of Chemistry, Yokohama City University, Matsuura-machi, Kanazawa-ku, Yokohama

(Received November 8, 1965)

The reactions of the arylsulfinic acid salts with alkyl chlorocarbonates in various alcohols as solvents gave the alkyl sulfinates, in which the alkoxyl groups originated from the solvent alcohols, not from the chlorocarbonates. Sodium *p*-toluenesulfinate-^{18}O and ethyl chlorocarbonate in a large excess of methanol gave methyl *p*-toluenesulfinate-^{18}O, which was shown to contain about half of the ^{18}O atoms of the starting salt. The mixed anhydride of sulfinic acid and monoalkyl carbonate is postulated as an intermediate, the alcoholysis of which would give the sulfinate ester. Reactions have been studied also in the nonhydroxylic solvents.

The formation of sulfinic esters by the reaction of sodium sulfinates with alkyl chlorocarbonates in alcohols has long been known.[1,2] In solvents other than alcohol, the reaction was reported to

* To whom correspondence should be sent: Department of Chemistry, Faculty of Science, Tokyo Metropolitan University, Setagaya-ku, Tokyo.

1) R. Otto and A. Rössing, *Ber.*, **18**, 2493 (1885).
2) R. Otto, ibid., **26**, 308 (1893).

be low and to stop in an early stage.[1] The reaction proceeded also without any solvent, but the yield and the purity of the resultant sulfinate ester were low.[3]

$$RSO_2Na + ClCO_2R' = \underset{\underset{O}{\downarrow}}{RS\text{-}OR'} + CO_2 + NaCl \quad (1)$$

In this paper, studies of the reactions of sodium arylsulfinates with alkyl chlorocarbonates in various solvents will be described.

Results

Sodium *p*-toluenesulfinate (I) reacted with ethyl chlorocarbonate (II) without solvent at room temperature very slowly. The reaction was accompanied by the evolution of carbon dioxide in a 40—60 mol. % yield, but the yield of ethyl *p*-toluenesulfinate (III) was only 10—18%, with the by-production of sulfinyl sulfone (IV) in a low yield. When dioxane was the solvent, hardly any sulfinate ester formation was observed and thiolsulfonate (V) was the chief product. Warming the reaction mixture at 70°C did not improve the result, although carbon dioxide evolution could reach a peak of 30 mol. % under some conditions.

In acetonitrile, the yields of the sulfinic ester depended on the reaction period; it was nearly 0% in 1—15 hr., 22% in 2 days. 13% in 5 days, and 39% in 8 days (with carbon dioxide in 35%) at room temperature. In pyridine, which dissolved sodium sulfinate partly, the reaction was rapid and the yield of the sulfinic ester was increased to 30% of the theoretical yield. When ethyl chlorocarbonate was added to a solution of free *p*-toluenesulfinic acid in anhydrous pyridine, carbon dioxide evolved immediately and ethyl sulfinate was obtained in a 42% yield. In a similar way, ethyl *p*-nitrobenzenesulfinate was prepared in a 43% yield.

Reactions between sodium sulfinate and chlorocarbonates in a large excess of alcohols were very rapid, and the yields of the sulfinic esters were usually satisfactory. For instance, the reaction of I with ethyl chlorocarbonate in ethanol gave ethyl *p*-toluenesulfinate in yields 36—62% of the theoretical yield. In a large excess of methanol, the reaction between ethyl chlorocarbonate and sodium *p*-toluenesulfinate was also very rapid, but in this case the ester formed was methyl *p*-toluenesulfinate, not the ethyl ester. The yield was 69—73%.

When I was treated with ethyl chlorocarbonate in *n*-butyl alcohol, *n*-butyl *p*-toluenesulfinate was obtained in 57 mol. %. The use of isopropyl alcohol as the solvent gave isopropyl *p*-toluenesulfinate in 20 mol. %. No sulfinic ester, neither ethyl nor *t*-butyl, was formed in *t*-butyl alcohol. Allyl alcohol gave allyl *p*-toluenesulfinate in a 55% yield. In carbitol, the reaction proceeded rapidly at room temperature, but no ethyl sulfinate formation was observed and carbitol sulfinate decomposed during the vacuum distillation.

From the above results, the reaction of sulfinate salts with ethyl chlorocarbonate in the primary or secondary alcohols was shown to form, not ethyl sulfinate, but alkyl sulfinates containing the alkyl group of the solvent alcohols.

These alkyl sulfinates might be the result of the ester exchange between ethyl sulfinate, a possible primary product, and the solvent alcohols. However, the reaction of sodium *p*-toluenesulfinate and ethyl chlorocarbonate in a mixture of ethyl *p*-toluenesulfinate of a 1/2 mol. equivalent of the sodium salt and a large excess of methanol gave a sulfinate ester mixture, which contained the same amount of ethyl *p*-toluenesulfinate as in the beginning and methyl *p*-toluenesulfinate in 42 mol. %. Under similar conditions without added ethyl sulfinate, the yield of methyl sulfinate from methyl chlorocarbonate and I in methanol was 42% of the theoretical yield. Therefore, it can be concluded that almost no ester exchange occurred under these reaction conditions, and the various alkyl sulfinates mentioned above may safely be regarded as the primary reaction products.

To confirm this point, the reaction of sodium *p*-toluenesulfinate with ethyl chlorocarbonate in dioxane containing 1 mol. of methanol was carried out; the sulfinate ester mixture, consisting of 82 mol. % of the methyl ester and 18 mol. % of the ethyl ester was thus found to be formed in 60% combined yield. On the other hand, the reaction of sodium *p*-toluenesulfinate and methyl chlorocarbonate in a mixture of 1 mol. of ethanol and a large volume of dioxane gave a mixture of methyl sulfinate and ethyl sulfinate in nearly the same molar ratio. In order to compare the relative reactivities of methanol and ethanol, the reaction of ethyl chlorocarbonate with I in a large excess of an equimolecular mixture of methanol and ethanol was carried out, resulting in the formation of a mixture of methyl- and ethyl-sulfinate in a 2 : 1 molar ratio.

These findings clearly indicate that the alkyl group of the alcohol used as a solvent entered into the resultant sulfinate ester, as is shown below:

$$RSO_2Na + ClCO_2C_2H_5 + R'OH = \underset{\underset{O}{\downarrow}}{RS\text{-}OR'} + CO_2 + NaCl + C_2H_5OH \quad (2)$$

Whether this alkyl group entered into the ester in company with the oxygen atom should be clarified by the isotope labeling method. Sodium *p*-toluenesulfinate-^{18}O was prepared by the reaction of $H_2{}^{18}O$ with *p*-toluenesulfinyl chloride or by the hydrolysis of ethyl *p*-toluenesulfinate with sodium hydroxide in $H_2{}^{18}O$.

3) A. J. H. Houssa and H. Phillips, *J. Chem. Soc.*, **1929**, 2510.

$$\begin{matrix} CH_3C_6H_5S\text{-}Cl + H_2{}^{18}O \\ \quad\quad\downarrow \\ \quad\quad O \end{matrix} = CH_3C_6H_5S{}^{18}OOH + HCl = \quad (3)$$

$$\begin{matrix} CH_3C_6H_5S\text{-}OC_2H_5 + H_2{}^{18}O \\ \quad\quad\downarrow \\ \quad\quad O \end{matrix} CH_3C_6H_5S{}^{18}OOH + C_2H_5OH \quad (4)$$

Bunton and his collaborator[4] established that the hydrolysis of alkyl sulfinate proceeded with an alkoxy-sulfinyl splitting; this was indicated by the absence of heavy oxygen atom in the alcohol formed in the reaction 4. We have confirmed this point by detecting the presence of ^{18}O in nearly the calculated amount in the sulfinic acid formed.

The reaction of sodium *p*-toluenesulfinate-^{18}O containing 0.65 atom % of ^{18}O with ethyl chlorocarbonate in a large excess of methanol gave methyl *p*-toluenesulfinate-^{18}O, the ^{18}O atom % of which was found to be 0.41%. This finding clearly indicated that the methoxyl group of the sulfinate ester came from methanol used as a solvent. (The calculated ^{18}O atom % based on the reaction shown below is 0.427%.)

$$\begin{matrix} RS{}^{18}O_2Na + ClCO_2C_2H_5 + CH_3OH = \\ RS\text{-}OCH_3 + CO{}^{18}O + NaCl + C_2H_5OH \\ \quad\downarrow \\ \quad {}^{18}O \end{matrix} \quad (5)$$

This alkoxy-acyl binding in the sulfinate ester formation corresponds well to the alkoxy-acyl splitting in the hydrolysis mentioned above.

Discussion

From the experimental results, the differences between the reaction in the alcoholic solvents and that in the non-hydroxylic solvents are clearly indicated. In primary or secondary alcohols, the reaction is fast, the yields of the sulfinate esters are high, and the alkoxy group of the solvent is introduced into the ester. On the other hand, the reaction is slow, the yield of the ester is very low, sometimes almost zero, and the sulfinate ester produced contains an alkyl radical of chlorocarbonates in a non-hydroxylic solvent other than pyridine. Pyridine is exceptional; in it the reaction proceeds rapidly and the ester yields are high.

Since no ester formation was observed when the sodium sulfinate was treated with alcohols, there should be some intermediates which react with alcohols to give the sulfinate esters. Sulfinic carbonic anhydride VI, which has been suggested[3] in the reaction without alcohol, is considered to be the most probable such intermediate:

$$RSO_2Na + ClCO_2R' = \underset{\substack{\downarrow \\ O}}{\overset{\substack{\downarrow \\ O}}{R\text{-}S\text{-}O\text{-}C\text{-}OR'}} + NaCl \quad (6)$$

VI

Among similar mixed anhydrides, several carboxylic sulfurous anhydrides VII have been known,[5] and the probable existence of the sulfinic carboxylic anhydrides VIII has been pointed out.[6]

$$\underset{\substack{\downarrow \\ O}}{\overset{\substack{\downarrow \\ O}}{R\text{-}O\text{-}S\text{-}O\text{-}C\text{-}R'}} \quad \underset{\substack{\downarrow \\ O}}{\overset{\substack{\downarrow \\ O}}{R\text{-}S\text{-}O\text{-}C\text{-}R'}} \quad \underset{\substack{\downarrow \\ O}}{\overset{\substack{\uparrow \\ O}}{R\text{-}S\text{-}S\text{-}R}}$$

VII VIII IV

The decomposition of VI would give the sulfinic ester thus:

$$\underset{\substack{\downarrow \\ O}}{\overset{\substack{\downarrow \\ O}}{R\text{-}S\text{-}O\text{-}C\text{-}OR'}} = \underset{\substack{\downarrow \\ O}}{R\text{-}S\text{-}OR'} + CO_2 \quad (7)$$

This decomposition seems to be base-catalyzed, since in pyridine the formation of carbon dioxide is very rapid. In other non-hydroxylic solvents, the reaction 7 is slow compared to such side reactions as 8, where the primary product, sulfinic anhydride (X), takes well-known, complicated courses to give the sulfinyl sulfone or thiolsulfonate[6]:

$$\begin{matrix} R\text{-}S\text{-}O\text{-}C\text{-}OR' + RSO_2{}^- = \\ \quad\downarrow\quad\downarrow \\ \quad O\quad O \end{matrix}$$

$$\underset{\substack{\downarrow \quad \downarrow \\ O \quad O}}{R\text{-}S\text{-}O\text{-}S\text{-}R} + [{}^-O_2C\text{-}OR'] \quad (8)$$

X

In the hydroxylic solvents, the intermediate VI suffers attack by the solvent molecules, ahead of the decomposition 7, as follows:

$$VI + R''OH \longrightarrow \underset{\substack{\downarrow \quad \downarrow \\ O \quad O}}{R\text{-}S\text{-}O\text{-}C\text{-}OR'} \longrightarrow R\text{-}S\text{-}OR'' + HO_2C\text{-}OR' \quad (9)$$

$$[HO_2C\text{-}OR'] \rightarrow CO_2 + R'OH \quad (10)$$

This alcoholysis may also be base-catalyzed. The alcohol liberated in the reaction 10 could participate in the alcoholysis too; this evidently explains why the ester mixture is always afforded in the reaction in dioxane containing an equimolecular amount of alcohol. If the reactivity of two alcohols, one added and one liberated, are equal, an ester mixture containing 75 mol. % of the ester of the added alcohol and 25 mol. % of that of the liberated alcohol may be expected. Actually, methanol has a greater reactivity than ethanol, as is

4) C. A. Bunton and B. N. Hendy, *J. Chem. Soc.*, **1962**, 2562.
5) Part II of this series. M. Kobayashi and A. Yamamoto, This Bulletin, **39**, 961 (1966).
6) Part III of this series. M. Kobayashi, ibid., **39**, 967 (1966).

indicated by the competitive alcoholysis; this causes the formation of an ester mixture richer in methyl ester than had been calculated.

In the reaction of sodium *p*-toluenesulfinate-^{18}O, the labeled, mixed anhydride (XI) is alcoholized to give the alkyl sulfinate-[sulfinyl ^{18}O], which should retain half of the heavy oxygen atom in the original sodium sulfinate:

$$\underset{\underset{^{18}O}{\downarrow}}{R\text{-}S\text{-}^{18}O\text{-}\overset{\overset{O}{\|}}{C}\text{-}OR'} + R''OH$$

XI

$$\rightarrow R\text{-}\underset{\underset{^{18}O}{\downarrow}}{S}\text{-}OR'' + CO^{18}O + R'OH \qquad (11)$$

Experimental

Materials.—Dioxane was purified as usual[7] and dried over sodium. Acetonitrile was refluxed over phosphorus pentoxide until a colorless product was obtained and then rectified. The alcohols were dehydrated by distillation from lithium hydride.

The Reaction of Sodium *p*-Toluenesulfinate (I) with Ethyl Chlorocarbonate (II). Without a Solvent.—To 4.0 g. of finely-powdered, anhydrous sodium salt (I) 2.4 g. of II was added at room temperature. About 330 ml. of carbon dioxide (60 mol. %) evolved slowly over 3 hr. The reaction mixture was then extracted with petroleum ether, and the extract concentrated and vacuum distilled to give 0.66 g. of ethyl *p*-toluenesulfinate (III) in a 18% yield. Most of the insoluble white powder in petroleum ether was soluble in water, but 0.2 g. of *p*-tolylsulfinyl *p*-tolylsulfone (IV: R=*p*-tolyl) remained. This was identified by melting point and mixture melting point determinations (87—90°C).

The General Procedure of the Reactions in Solvents Other Than Alcohols or Pyridine.—An equimolecular amount of II was stirred into a suspension of I; then the mixture was kept for an appropriate reaction period, from a few hours to several days, at room temperature. Water and petroleum ether were added to the resulting jelly, and the organic layer was separated, dried over magnesium sulfate, and subjected to vacuum distillation to give III. It was identified by its infrared spectrum and b. p. (102—106°C/5 mmHg, 98—102°C/3 mmHg).

Reaction in Pyridine.—A suspension of 4.0 g. of I in 30 ml. of pyridine was boiled once to effect the partial solution and then cooled to room temperature. To this mixture 3.2 g. of II was added, drop by drop, during which process the evolution of slight heat and 450 ml. of carbon dioxide was observed. After dilution with water, the product was extracted with petroleum ether, washed with dilute hydrochloric acid and water, dried, and distilled in vacuo to give 1.3 g. of III (30%).

Reactions in Alcohols.—i) In 30 ml. of methanol 5.0 g. of I was shaken to effect the partial solution. When 3.1 g. of II was added, drop by drop, to this solution, cooled with ice water, carbon dioxide formed immediately. After a few hours the reaction mixture was then diluted with water and extracted with petroleum ether. Vacuum distillation gave 3.3 g. of methyl *p*-toluenesulfinate at 90°C/3 mmHg in 69% yield.

ii) To a suspension of 17.5 g. of I in 100 ml. of ethanol 10.8 g. of II was added. Treatment similar to that above gave 6.7 g. of III at 98—102°C/3 mmHg in 36% yield.

iii) A suspension of 5.0 g. of I in 30 ml. of *n*-butanol was treated with 3.0 g. of III as described in i). After 15 hr. at room temperature, 4.3 g. of *n*-butyl *p*-toluenesulfinate was isolated; b. p. 118—120°C/3 mmHg in 57% yield.

iv) From 5.0 g. of I in 30 ml. of allyl alcohol and 3.0 g. of II, 3.0 g. of allyl *p*-toluenesulfinate, b. p. 98—102°C/3 mmHg, was obtained in 55% yield after one day's reaction.

v) A suspension of 5.0 g. of I in a mixture of 0.9 g. of methanol and 30 ml. of dioxane was treated with 3.0 g. of II at room temperature. After 10 min., the reaction started, accompanied by the evolution of carbon dioxide. The yield of the sulfinate ester mixture was 2.8 g. after 40 hr. Using the 970 cm^{-1} absorption band for methyl *p*-toluenesulfinate and the 884 cm^{-1} band for the ethyl ester, the composition of this ester mixture was estimated as 82 mol.% the methyl ester and 18 mol.% the ethyl ester by infrared spectrum, the total yield being 60% of the theoretical.

vi) When 2.8 g. of methyl chlorocarbonate was added to 5.0 g. of I in a mixture of 1.8 ml. of ethanol and 30 ml. of dioxane, 200 ml. of carbon dioxide (30%) evolved in 5 min. The reaction mixture afforded the sulfinate ester mixture, the composition of which was found by its infrared spectrum to be 48 mol.% the methyl ester and 52 mol.% the ethyl ester in a total yield 30% of the theoretical.

vii) The reaction of 5.0 g. of I and 3.0 g. of II in a mixture of 2.0 g. of III and 30 ml. of methanol gave 4.0 g. of the sulfinate ester mixture, b. p. 92—104°C/3 mmHg. Its infrared spectrum revealed the presence of 2.1 g. of III and 1.9 g. of methyl sulfinate (43% of the theoretical yield) in this mixture.

viii) Reaction in an equimolecular mixture of methanol and ethanol: To 7.0 g. of I in a mixture of 16 g. of methanol and 23 g. of ethanol, 4.5 g. of II was added with cooling in ice water. After one hour, the reaction mixtue was diluted with an excess of water and extracted with 60 ml. of carbon tetrachloride. The extract was found by infrared spectroscopy to contain 2.25 g. of methyl *p*-toluenesulfinate and 1.25 g. of III. The relative reactivity of methanol and ethanol for this reaction was calculated to be 2 : 1 from this competitive reaction.

Reaction in Pyridine.—i) When 2.5 g. of II was added, drop by drop, to a solution of 3.0 g. of *p*-toluenesulfinic acid in 20 ml. of anhydrous pyridine, the reaction occurred immediately, with the evolution of carbon dioxide and with the precipitation of pyridine hydrochloride. From the reaction mixture, 1.5 g. of III was obtained in 42% yield.

ii) When 2.0 g. of *p*-nitrobenzenesulfinic acid (10.7 mmol.) was added to 15 ml. of pyridine, a red suspension was obtained. The addition of 5.5 g. (50.7 mmol.) of II to this suspension over 40 min. caused the formation of 320 ml. (13.3 mml.) of carbon dioxide. The pale brown reaction mixture was then

7) A. Weissberger and E. S. Proskauer, "Organic Solvents," 2nd Ed. (1955).

diluted with water and extracted by petroleum ether; the extract was washed with diluted hydrochloric acid and water, dried over magnesium sulfate, and evaporated. The recrystallization of the residue from petroleum ether gave 1.0 g. of ethyl *p*-nitrobenzenesulfinate, m. p. 48.5—50.5°C, in 34% yield.

Sodium *p*-Toluenesulfinate-^{18}O.—i) To 11.5 g. of *p*-toluenesulfinyl chloride[8] 2.5 g. of $H_2{}^{18}O$ (^{18}O= 1.5 atom %) was slowly added with ice cooling. After 2 hr., the white reaction product mass was neutralized with 5 g. of sodium hydroxide in a few milliliters of light water; the crystals thus formed were recrystallized from distilled water to give 7.6 g. of sodium *p*-toluenesulfinate dihydrate, which was dehydrated in vacuo. The ^{18}O atom % of this salt was 0.86%. (The calculated value is 0.86%.)

ii) A mixture of 6.7 g. of III and 1.44 g. of sodium hydroxide in 6.00 ml. of $H_2{}^{18}O$ (1.5 atom % ^{18}O) was stirred with a magnetic stirrer for 2 hr., and cooled in an ice bath; the resultant crystals were filtered through a fritted-glass funnel to give 7.0 g. of the labeled dihydrate of I, which was then dehydrated in vacuo at 110°C for one hour. The ^{18}O atom % of this anhydrous salt was 0.65%, lower than the calculated value, 0.71%.

Ethyl *p*-Toluenesulfinate - [sulfinyl ^{18}O]. — A suspension of 5.0 g. of the labeled sodium sulfinate prepared as above ii) in 30 ml. of methanol was treated with 3.0 g. of II; after 3 hr., the reaction mixture was extracted by petroleum ether. The vacuum distillation of the extract after drying over magnesium sulfate gave 3.5 g. of methyl *p*-toluenesulfinate-[sulfinyl ^{18}O] in 74% yield. The ^{18}O atom % of this specimen was 0.41%. (The caluclated value, based on the reaction 5, was 0.43%).

Thanks are due to Dr. Teijiro Kitao and Miss Reiko Kiritani of the Radiation Center of Osaka Prefecture for their analyses of ^{18}O, and also to Professor Shigeru Oae of Osaka City University for his donation of the heavy oxygen water.

8) "Organic Syntheses," Vol. 34, 93 (1954).

BULLETIN OF THE CHEMICAL SOCIETY OF JAPAN VOL. 39 1296—1297 (1966)

Organic Sulfur Compounds. VIII. The Formation of Sulfinate Esters by the Alkylation of Sulfinic Acid Salts

By Michio KOBAYASHI*

Department of Chemistry, Yokohama City University, Mutsuura-machi, Kanazawa-ku, Yokohama

(Received December 3, 1965)

The alkylation of the sulfinic acid salts with triethyloxonium fluoroborate results in the formation of the ethyl sulfinates, not in the usual sulfone formation.

Sulfinic acid salts are known to react with many alkylating reagents to give the sulfones; indeed, this reaction is one of the established methods for the preparation of sulfones.[1]

Although the fact that the electronegativity of an oxygen atom is higher than that of sulfur suggests the localization of the negative charge mainly on the oxygen atoms in a sulfinate anion, every reported alkylation of the sulfinic acid salts has taken place on the sulfur atom, thus resulting in the formation of the sulfones; this mode of *S*-alkylation has been believed to be the general one for the sulfinate anion.

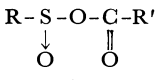

(I)

In the course of our study of the reaction of the sulfinic acid salt with carboxylic chloride, the formation of a sulfinic carboxylic anhydride (I) as an intermediate has been deduced.[2] This means an *O*-alkylation in the sulfinate anion. Since the above reaction is a very rapid one (completed in a few minutes even at −70°C) compared to the usual slow alkylation of the sulfinic acid salts to form the sulfones, it occurred to the author that a highly-reactive alkylating reagent may attack the sulfinate anion on oxygen atom to give a sulfinic ester.

Triethyloxonium fluoroborate is known to be a very efficient ethylating reagent.[3] When the reaction of sodium *p*-toluenesulfinate with this oxonium salt was attempted, the formation of ethyl *p*-toluenesulfinate in an almost quantitative yield was observed. The ethylation of a pyridinium *p*-nitrobenzenesulfinate with the same reagent also gave ethyl sulfinate. No sulfone formation was detected. Therefore, it may be concluded that,

* To whom correspondence should be sent: Department of Chemistry, Faculty of Science, Tokyo Metropolitan University, Setagaya-ku, Tokyo.

1) Houben-Weyl, "Methoden der Organischen Chemie," 4th ed., Vol. IX, Georg Thieme, Stuttgart (1955), p. 231.

2) Part III of this series: M. Kobayashi, This Bulletin, **39**, 967 (1966).

3) N. Kornblum and R. A. Brown, *J. Am. Chem. Soc.*, **86**, 2681 (1964).

with a highly-reactive alkylating reagent, the attack on the sulfinate anion proceeds in a kinetically controlled manner to give a relatively unstable sulfinate ester, while in the reaction with weak alkylating reagents a thermodynamically controlled attack gives more stable isomeric sulfones. A similar idea concerning the dual nature of the electrophilic attack on the ambident anions has been well established by Kornblum and his coworhers in the cases of active methylene compounds.[4]

Experimental

Ethyl *p*-Toluenesulfinate.—Into a solution of 3.5 g. of triethyloxonium fluoroborate[5] in 20 ml. of methylene chloride, 3.0 g. of finely-powdered anhydrous sodium *p*-toluenesulfinate in several portions was vigorously stirred over a 5 minute period. The reaction proceeded quickly, with a slight evolution of heat. After 30 ml., the reaction mixture was repeatedly shaken with a large volume of water and the organic layer was dried over magnesium sulfate. The infrared spectrum of an aliquot of this solution indicated the formation of 2.92 g. of ethyl *p*-toluenesulfinate in 95% yield. The vacuum distillation of the remaining part of the solution gave the pure ethyl ester, b. p. 100°C/1 mmHg.

Ethyl *p*-Nitrobenzenesulfinate.—When 0.45 g. of dry pyridine in 20 ml. of methylene chloride was added to a suspension of 0.92 g. of *p*-nitrobenzenesulfinic acid in 50 ml. of the same solvent, a yellow solution was obtained. The addition of 2 g. (excess) of triethyloxonium fluoroborate in 20 ml. of methylene chloride to the above solution with the stirring over a 2 minute period resulted in the decolorization of the solution and the precipitation of white crystals. After 5 min., the reaction mixture was poured into a lot of water, and the methylene chloride layer was separated, dried, and evaporated. The pale yellow residue was recrystallized from petroleum ether to give 0.39 g. of ethyl *p*-nitrobenzenesulfinate, m. p. 48—50°C (lit.[6] 49—51°C) in 37% yield. Its identity was confirmed by its infrared spectrum.

4) N. Kornblum, P. J. Berrigan and W. J. Le Noble, ibid., **82**, 1257 (1960); **85**, 1141 (1963); N. Kornblum, P. Pink and K. V. Yorka, ibid., **83**, 2780 (1961); N. Kornblum, R. Seltzer and P. Haberfield, ibid., **85**, 1148 (1963).

5) H. Meerwein, E. Battenberg, H. Gold, E. Pfeil and G. Willfang, *J. Prakt. Chem.*, **154**, 83 (1939).

6) T. Dewing, W. H. Gray, B. C. Platt and D. Stephenson, *J. Chem. Soc.*, **1942**, 239.

BULLETIN OF THE CHEMICAL SOCIETY OF JAPAN VOL. 39 1297—1301 (1966)

The Preparation of 2-Alkoxy-1, 3, 2-oxazaphospholidines and Some Reactions

By Teruaki MUKAIYAMA and Yasuto KODAIRA

Laboratory of Organic Chemistry, Tokyo Institute of Technology, Ookayama, Meguro-ku, Tokyo

(Received November 16, 1965)

The preparation of 2-alkoxy-1, 3, 2-oxazaphospholidines and some reactions will be described. 2-Alkoxy-1, 3, 2-oxazaphospholidines were prepared either from ethyl phosphorodichloridite and aminoethanols or, more conveniently, from tris[diethylamino]phosphite, aminoethanols and alcohols. 2-Alkoxy-1, 3, 2-oxazaphospholidines reacted easily with alcohols or *p*-toluenesulfonic acid monohydrate to give dialkyl aminoethyl phosphites or alkyl aminoethyl phosphite by the ring-opening at the P–N linkage of the phospholidines. It was oxidized by means of sulfur or nitrogen tetroxide to give 2-thione or 2-one in high yields. Further, it was found that it reacted with ethyl isocyanate to form 1 : 1 adducts. The structure of the adducts was confirmed, by a study of its chemical transformations, to be a seven-membered cyclic compound. It also reacted with carbon dioxide at about 120°C to yield the phosphorous-containing polyamide.

It has been reported in a previous paper[1] that 2, 3-diphenyl-1, 3, 2-oxazaphospholidine can be prepared by treating phenyl phosphinous dichloride with 2-phenylaminoethanol in the presence of two molecular equivalents of triethylamine.

It was also found by the present work that 2-alkoxy-3-methyl-1, 3, 2-oxazaphospholidine (IIb) can be prepared in a 69% yield from ethyl phosphorodichloridite and 2-methylaminoethanol. However, 2-alkoxy-1, 3, 2-oxazaphospholidine (IIa) could not be obtained by the use of 2-aminoethanol, which has a primary amino group, whereas 2-(2-aminoethyl)-1, 3, 2-oxazaphospholidine (IIc)[2] resulted in a 25% yield. It was further established that the phospholidines can be conveniently prepared from aminoethanols and tris[diethylamino]-phosphite. Various 2-alkoxy-1, 3, 2-oxazaphospholidines (II) were synthesized by the reaction

1) T. Mukaiyama and Y. Yokota, This Bulletin, **38**, 858 (1965).

2) R. Burgada, *Ann. Chim.*, **8**, 348 (1963).

of alcohols with 2-diethylamino-1, 3, 2-oxazaphospholidine (I), which had been prepared from tris-[diethylamino]phosphite and aminoethanols, as is shown in the following scheme. These results

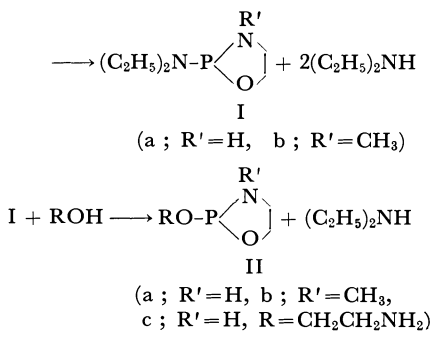

are summarized in Table I.

TABLE I. PREPARATION OF 2-ALKOXY-1, 3, 2-OXAZAPHOSPHOLIDINES

Alcohol	B. p. °C/mmHg	Yield %	Anal. N, % Calcd.	Found
C_2H_5OH	62—67/17	80	9.40	9.16
n-C_3H_7OH	83—85/20	79	8.59	8.70
i-C_3H_7OH	57—60/10	66	8.59	8.38
n-C_4H_9OH	98—100/21	77	7.91	8.16
t-C_4H_9OH	75—86/15	80	7.91	8.05
CH_2=$CHCH_2OH$	75—77/13	76	8.69	8.75
$CH_3NHCH_2CH_2OH$	105—107/0.14	80	15.73	15.91

The phospholidines react with alcohols in refluxing benzene to give dialkyl 2-aminoethyl phosphites (III) in excellent yields by ring opening at the P–N linkage of the phospholidine. These results are summarized in Table II.

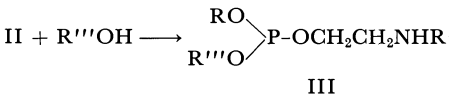

The phospholidines were oxidized easily by means of sulfur in benzene at room temperature or by means of nitrogen tetroxide in dichloromethane at −78°C, thus forming 2-alkoxy-1, 3, 2-oxazaphospholidine-2-thione (IVa) or 2-one (IVb) in 86% or 61% yields respectively.

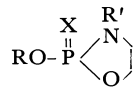

When the phospholidines were treated with an equimolecular amount of p-toluenesulfonic acid monohydrate in benzene at room temperature, a ring-opening reaction took place exclusively at the P–N linkage of the phospholidine, giving the p-toluenesulfonium salt of ethyl 2-methylaminoethyl phosphite (V) in a quantitative yield. In a similar way, the p-toluenesulfonium salt of ethyl 2-methylaminoethyl phosphate (VI) was obtained in an excellent yield from IVb. It was then converted to the ethyl 2-methylaminoethyl phosphate (VII), which was identified as a barium salt, by treating it with barium hydroxide in an ethanol solution.

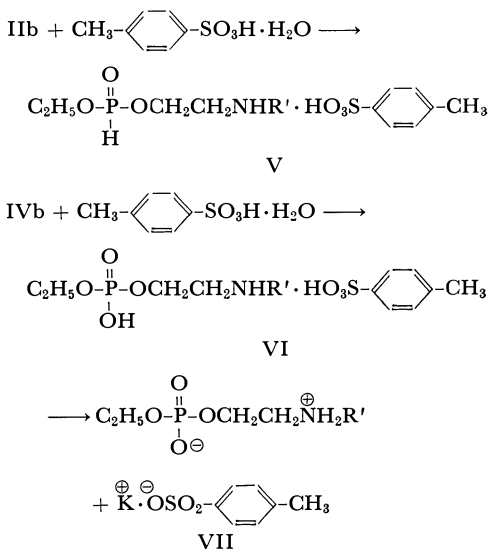

The phospholidines react with an equimolecular amount of ethyl isocyanate at about 110—120°C, resulting in the formation of 1 : 1 adducts (VIII).

TABLE II. REACTION OF 2-ETHOXY-1, 3, 2-OXAZAPHOSPHOLIDINES WITH ALCOHOLS

R′	R‴OH	B. p. °C/mmHg	Yield %	Anal. N, % Calcd.	Found
CH_3	C_2H_5OH	50—51/1	67	7.18	7.25
CH_3	n-C_3H_7OH	52—53/1	68	6.70	6.76
CH_3	i-C_3H_7OH	79—83/7	73	6.70	6.74
CH_3	t-C_4H_9OH	44—47/6	46	6.28	6.29
CH_3	CH_2=$CHCH_2OH$	72—84/2	84	6.76	6.59
H	C_2H_5OH	50—52/2	56	7.73	7.76
H	n-C_3H_7OH	60—63/1	75	7.18	7.37
CH_3	$CH_3NHCH_2CH_2OH$	77—83/4	58	12.50	13.32

The structures of these adducts VIII were confirmed to be seven-membered cyclic ureid derivatives (XI) by the following spectral data and their chemical transformations. The infrared spectra of these adducts (VIII) showed an absorption at 1660 cm^{-1} due to the ureid carbonyl group. VIII was oxidized exothermally by means of sulfur in a benzene solution at room temperature to yield IX in a 89% yield. This was in turn hydrolyzed to the *p*-toluenesulfonium salt (X) by ring opening when treated with *p*-toluenesulfonic acid monohydrate in refluxing benzene.

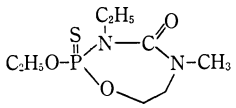

IX

X

When heated at about 180°C, the adducts decomposed to give ethyl isonitrile (XIII) and oxazaphospholidine-2-one (IVb) by way of an internal nucleophilic displacement, as is shown below.

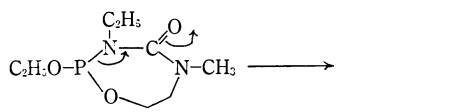

XI

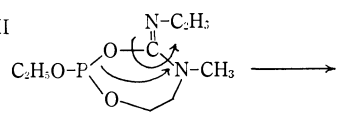

XII

IVb + $C_2H_5N{=}C$

XIII

On the other hand, the reaction of phenyl isocyanate and the phospholidine at 110—120°C gave an undistillable oily substance, which decomposed to give a small amount of phenyl isonitrile and oxazaphospholidine-2-one (IVb) along with a glassy, hygroscopic resinous substance.

Similarly, isonitriles and oxazaphospholidine-2-thione were prepared when ethyl isothiocyanate or phenyl isothiocyanate was heated with II, as is shown in the following scheme.

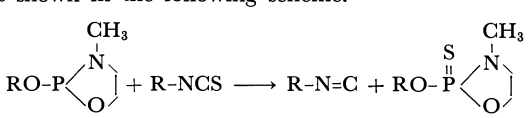

2-Ethoxy-1, 3, 2-oxazaphospholidine (IIa) absorbed carbon dioxide at 0°C, giving a viscous oily adduct (XIV) with infrared absorptions at 1650 and 1565 cm^{-1} due to the amide carbonyl group. When XIV was heated under reduced pressure, 35% of the IIa was recovered, whereas when it was heated at 110—120°C in a sealed tube or under a carbon dioxide atmosphere, a glassy, hygroscopic polymer (XV), m. p. 186—188°C, was produced.

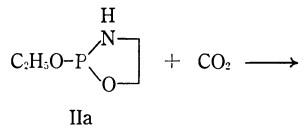

IIa

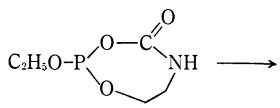

XIV

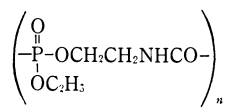

XV

Experimental

All melting points and boiling points are uncorrected.

Solvents and Reagents.—The solvents and alcohols were dried and purified by ordinary procedures.

The Preparation of 2-Alkoxy-3-methyl-1, 3, 2-oxazaphospholidine (IIb).—A mixture of 2-methylaminoethanol (3.75 g., 0.05 mol.) and triethylamine (15.45 g., 0.125 mol.) was added, drop by drop, into a solution of ethyl dichloro phosphite (7.35 g., 0.05 mol.) in 100 ml. of ether at 0°C with stirring. After the solution had been stirred for 2 hr. at room temperature, the precipitate of triethylammonium hydrochloride was filtered and washed twice with ether (10 ml.). After the ether had been removed under reduced pressure, 2-ethoxy-3-methyl-1, 3, 2-oxazaphospholidine (IIb) (b. p. 62—67°C/17 mmHg, 3.1 g., 69%) was obtained.

Found : N, 9.16. Calcd. for $C_5H_{12}O_2NP$: N, 9.40%.

The Reaction of Ethyl Dichloro Phosphite with 2-Aminoethanol. — A mixture of 2-aminoethanol (3.05 g., 0.05 mol.) and triethylamine (10.1 g., 0.10 mol.) was added, drop by drop, into a solution of ethyl dichloro phosphite (7.35 g., 0.05 mol.) in 70 ml. of ether at 0°C with stirring. After the mixture had been stirred for 2 hr. at room temperature, the precipitate of triethylammonium hydrochloride was removed from the reaction mixture. The removal of the solvent from the filtrate under reduced pressure gave an oily product which crystallized after it had been allowed to stand overnight. The needle crystalline of 2-(2-aminoethyl)-1, 3, 2-oxazaphospholidine (IIc) (m. p. 106—120°C, 3.7 g., 25%) was collected. Recrystallization from benzene gave an analytical sample (m. p. 116°C).

Found : N, 9.45. Calcd. for $C_4H_{11}O_2N_2P$: N, 9.33%.

The vaccum distillation of the filtrate gave an unidentified oil (b. p. 80—86°C/0.05 mmHg, 0.82 g.).

The Preparation of 2-Diethylamino-3-methyl-1, 3, 2-oxazaphospholidine (Ib).—A solution of tris[diethylamino]phosphite (4.94 g., 0.02 mol.) and 2-methylaminoethanol (1.50 g., 0.02 mol.) in 30 ml. of benzene was refluxed for 3 hr. After the benzene and diethylamine had been removed under reduced pressure, 2-diethylamino-3-methyl-1, 3, 2-oxazaphospholidine (b. p. 88—90°C/3 mmHg, 2.1 g., 60%) was obtained by vacuum distillation.

Found: N, 15.91. Calcd. for $C_7H_{17}ON_2P$: N, 15.91%.

The Preparation of 2-Diethylamino-1, 3, 2-oxazaphospholidine (Ia).—By a procedure analogous to that mentioned above, 2-diethylamino-1, 3, 2-oxazaphospholidine (b. p. 91—97°C/5 mmHg, 1.52 g., 47%) was obtained from the reaction of tris[diethylamino]-phosphite (4.94 g., 0.02 mol.) and 2-aminoethanol (1.42 g., 0.02 mol.). A small amount of the needle crystalline of 2-(2-aminoethyl)-1, 3, 2-oxazaphospholidine was also obtained as a by-product.

Found: N, 17.29. Calcd. for $C_6H_{15}ON_2P$: N, 16.95%.

The Preparation of 2-Alkoxy-1, 3, 2-oxazaphospholidines.—A solution of 2-diethylamino-2-methyl-1, 3, 2-oxazaphospholidine (1.76 g., 0.01 mol.) and ethanol (0.46 g., 0.01 mol.) in 20 ml. of benzene was refluxed for 2 hr. After the benzene and diethylamine had been removed under reduced pressure, 2-ethoxy-3-methyl-1, 3, 2-oxazaphospholidine (b. p. 62—67°C/17 mmHg, 1.19 g., 80%) was obtained by vacuum distillation.

In a similar fashion, the reaction of various alcohols and 2-diethylamino-1, 3, 2-oxazaphospholidine gave the corresponding 2-alkoxy-1, 3, 2-oxazaphospholidines. The results are summarized in Table I.

The Reaction of 2-Ethoxy-1, 3, 2-oxazaphospholidine with Alcohols.— A solution of 2-ethoxy-3-methyl-1, 3, 2-oxazaphospholidine (1.49 g., 0.01 mol.) and ethanol (0.46 g., 0.01 mol.) in 15 ml. of benzene was refluxed for 2 hr. After the solvent had been removed under reduced pressure, 2-methylaminoethyl diethyl phosphite (b. p. 49—51°C/1 mmHg, 1.3 g., 67%) was obtained by vacuum distillation.

In a similar fashion, the reaction of various alcohols and 2-ethoxy-1, 3, 2-oxazaphospholidines gave the corresponding dialkyl 2-aminoethyl phosphites, as is shown in Table II.

The Oxidation of 2-Ethoxy-3-methyl-1, 3, 2-oxazaphospholidine by Means of Sulfur.—Into a solution of 2-ethoxy-3-methyl-1, 3, 2-oxazaphospholidine (1.49 g., 0.01 mol.) in 20 ml. of benzene was added sulfur in small portions with stirring at room temperature. After the stirring had been continued for an additional hour, the unreacted sulfur was removed by filtration. Benzene was removed from the filtrate under reduced pressure and the residue was distilled in a vaccum, giving 2-ethoxy-3-methyl-1, 3, 2-oxazaphospholidine-2-thione (b. p. 76—78°C/0.12 mmHg, 1.56 g., 86%).

Found: N, 7.53. Calcd. for $C_5H_{12}O_2SNP$: N, 7.73%.

The Oxidation of 2-Ethoxy-3-methyl-1, 3, 2-oxazaphospholidine by Means of Nitrogen Tetroxide.—Into a solution of 2-ethoxy-3-methyl-1, 3, 2-oxazaphospholidine (1.49 g., 0.01 mol.) in 15 ml. of dichloromethane there was added, drop by drop, a solution of nitrogen tetroxide in dichloromethane at −78°C with stirring; this was continued until the solution turned blue. After the solvent had been removed under reduced pressure, 2-ethoxy-3-methyl-1, 3, 2-oxazaphospholidine-2-one (b. p. 90—91°C/0.2 mmHg, 1.0 g., 61%) was obtained.

Found: N, 8.52. Calcd. for $C_5H_{12}O_3NP$: N, 8.48%.

The Reaction of 2-Ethoxy-3-methyl-1, 3, 2-oxazaphospholidine with *p*-Toluenesulfonic Acid Monohydrate.—A solution of 2-ethoxy-3-methyl-1, 3, 2-oxazaphospholidine (1.49 g., 0.01 mol.) and *p*-toluenesulfonic acid monohydrate (1.90 g., 0.01 mol.) in 15 ml. of benzene was refluxed for an hour. A transparent viscous oil separated from the reaction mixture. After the mixture had been kept standing overnight at room temperature, the benzene was removed by decantation. The oil was then rinsed three times with benzene (10 ml.) in order to remove the by-products; this gave the *p*-toluenesulfonium salt of ethyl 2-methylamino phosphite (3.30 g., 97%).

Found: N, 4.37. Calcd. for $C_{12}H_{22}O_6NP$: N, 4.31%.

The Reaction of 2-Ethoxy-3-methyl-1, 3, 2-oxazaphospholidine-2-one with *p*-Toluenesulfonic Acid Monohydrate.—Into a solution of 2-ethoxy-3-methyl-1, 3, 2-oxazaphospholidine-2-one (6.60 g., 0.04 mol.) in 50 ml. of benzene was added *p*-toluenesulfonic acid monohydrate (7.60 g., 0.04 mol.) in small portions with stirring at room temperature. After stirring had been continued for an additional 2 hr., the reaction mixture was kept standing overnight at room temperature. A transparent viscous oil thereupon separated from the reaction mixture. The benzene was removed by decantation and the oil was rinsed three times with benzene (10 ml.), thus giving *p*-toluenesulfonium salt of ethyl 2-methylaminoethyl phosphate (14.0 g., 98%).

Into a solution of the salt in 50 ml. of ethanol, a solution of potassium hydroxide (2.24 g., 0.04 mol.) in 50 ml. of ethanol was added, drop by drop, with stirring. A white precipitate, the potassium salt of *p*-toluenesulfonic acid (8.40 g., 74%), was then collected by filtration. To the filtrate there was added an aqueous solution of barium hydroxide; this gave a white precipitate of the barium salt of ethyl 2-methylaminoethyl phosphate (9.2 g., 52%).

Found: C, 22.33; H, 5.59; N, 4.73. Calcd. for $C_{10}H_{30}O_{10}N_2P_2Ba$: C, 22.07; H, 5.61; N, 5.21%.

The Reaction of 2-Ethoxy-3-methyl-1, 3, 2-oxazaphospholidine with Ethyl Isocyanate.—A mixture of 2-ethoxy-3-methyl-1, 3, 2-oxazaphospholidine (1.49 g., 0.01 mol.) and ethyl isocyanate (0.71 g., 0.01 mol.) was heated at 110—120°C for 4 hr. in a sealed tube. The reaction mixture was then distilled under reduced pressure, thus obtaining a 1 : 1 adduct (b. p. 80—83°C/0.11 mmHg, 1.57 g., 68%). Its infrared spectrum showed absorptions at 1700 and 1660 cm^{-1}.

Found: N, 12.69. Calcd. for $C_8H_{17}O_3N_2P$: N, 12.71%.

The Oxidation of the Adduct by Means of Sulfur.—Into a solution of the adduct (2.20 g.) in 20 ml. of benzene was added sulfur in small portions with stirring at room temperature. After it had been stirred for additional 30 min., the reaction mixture was kept standing overnight. After the solvent had been removed under reduced pressure, IX (b. p. 111—126°C/

0.09 mmHg, 2.24 g., 89%) was obtained by vacuum distillation.

Found: N, 11.40. Calcd. for $C_8H_{17}O_2SN_2P$: N, 11.11%.

The Hydrolysis of IX by Means of *p*-Toluenesulfonic Acid Monohydrate.—Into a solution of IX (1.09 g.) in 10 ml. of benzene was added *p*-toluenesulfonic acid monohydrate (0.95 g.) with stirring at room temperature. The reaction soon started, with a liberation of heat. After stirring had been continued for 30 min., the reaction mixture was further refluxed for 2 hr., whereupon a transparent viscous oil was separated from the reaction mixture. After the solvent had been removed by decantation, the oil was rinsed twice with benzene (10 ml.). The *p*-toluenesulfonium salt of the thiophosphate X (2.04 g., 100%) was obtained.

Found: N, 6.89. Calcd. for $C_{15}H_{27}O_7N_2SP$: N, 6.83%.

The Thermal Decomposition of the Adduct.—The adduct (2.20 g.) was heated at 180°C for 2 hr. under nitrogen. The vacuum distillation of the adduct gave 2-ethoxy-3-methyl-1, 3, 2-oxazaphospholidine-2-one (b. p. 85—93°C/0.2 mmHg, 0.2 g.) and ethyl isonitrile (about 0.5 g.) which was trapped in dry-ice acetone bath, a resinous solid remained in a Claisen flask.

The Reaction of 2-Ethoxy-1, 3, 2-oxazaphospholidine with Ethyl Isocyanate.—A solution of 2-ethoxy-1, 3, 2-oxazaphospholidine (1.35 g., 0.01 mol.) and ethyl isocyanate (0.71 g., 0.01 mol.) in 15 ml. of benzene was refluxed for 2 hr. After the benzene had been removed under reduced pressure, an adduct (b. p. 107—110°C/0.15 mmHg, 1.32 g., 64%) was obtained by vacuum distillation. Its infrared spectrum showed absorptions at 1700 and 1650 cm^{-1}.

Found: N, 13.51. Calcd. for $C_7H_{15}O_3N_2P$: N, 13.59%.

The Reaction of 2-Ethoxy-3-methyl-1, 3, 2-oxazaphospholidine with Phenyl Isocyanate.—A mixture of 2-ethoxy-3-methyl-1, 3, 2-oxzaphospholidine (1.49 g., 0.01 mol.) and phenyl isocyanate (1.19 g., 0.01 mol.) was heated at 110—120°C for 4 hr. in a sealed tube. The fractional distillation of the mixture gave phenyl isonitrile (0.3 g.) and 2-ethoxy-3-methyl-1, 3, 2-oxazaphospholidine-2-one (0.2 g.), along with a large amount of a transparent, hygroscopic resinous solid.

The Reaction of 2-Ethoxy-3-methyl-1, 3, 2-oxazaphospholidine with Phenyl Isothiocyanate and Ethyl Isothiocyanate.—A mixture of 2-ethoxy-3-methyl-1, 3, 2-oxazaphospholidine (1.49 g., 0.01 mol.) and phenyl isothiocyanate (1.35 g., 0.01 mol.) was heated at 110—120°C for 4 hr. in a sealed tube. The fractional distillation of the mixture gave phenyl isonitrile (b. p. 65—72°C/28 mmHg, 0.45 g., 45%) and 2-ethoxy-3-methyl-1, 3, 2-oxazaphospholidine-2-thione (b. p. 77—78°C/0.16 mmHg, 1.12 g., 62%). Similarly, the reaction of ethyl isothiocyanate (0.87 g., 0.01 mol.) and 2-ethoxy-3-methyl-1, 3, 2-oxazaphospholidine (1.49 g., 0.01 mol.) gave ethyl isonitrile and 2-ethoxy-3-methyl-1, 3, 2-oxazaphospholidine-2-thione (1.40 g., 77%).

The Reaction of 2-Ethoxy-1, 3, 2-oxazaphospholidine with Carbon Dioxide.—A) 2-Ethoxy-1, 3, 2-oxazaphospholidine (2.31 g., 0.018 mol.) absorbed 0.24 g. of carbon dioxide under atmospheric pressure at 0°C, giving a transparent viscous oil. Its infrared spectrum showed absorptions at 1650 and 1565 cm^{-1}. The fractional distillation of the oily adduct recovered 2-ethoxy-1, 3, 2-oxazaphospholidine (0.8 g., 35%). A white glassy hygroscopic solid was obtained when the oily adduct was heated at 110—120°C for 6 hr. in a sealed tube. The resultant polymer was crushed, refluxed in 15 ml. of benzene, and collected (m. p. 186—188°C, 1.15 g.). Its infrared spectrum showed absorptions at 1650 and 1560 (CONH), 1220 (P=O), 1050 (POC) cm^{-1}. It did not dissolve in water, dichloromethane, benzene, acetonitrile or *o*-dichlorobenzene.

From the benzene extract, 0.9 g. of 2-ethoxy-1, 3, 2-oxazaphospholidine (b. p. 75—83°C/21 mmHg) was recovered.

B) 2-Ethoxy-1, 3, 2-oxazaphospholidine (3.0 g.) was heated at 110—120°C for 3 hr. under a carbon dioxide atmosphere of 55 kg./cm^2 in an autoclave. After the mixture had been kept standing overnight, a white glassy, hygroscopic solid was obtained. The polymer was crushed, refluxed in 20 ml. of benzene, and collected by filtration (m. p. 179—183°C, 3.7 g.). Its infrared spectrum showed absorptions at 1650 and 1540 (CONH), 1220 (P=O), and 1050 (POC) cm^{-1}.

The authors wish to express their hearty thanks to Dr. Oyo Mitsunobu for his helpful suggestion and Miss Keiko Nakamura for her microanalyses.

BULLETIN OF THE CHEMICAL SOCIETY OF JAPAN VOL. 39 1302—1306 (1966)

The Sensitive Gas Chromatography of Para-, Orthohydrogen, Hydrogen Deuteride and Deuterium[1)]

By Iwao YASUMORI and Seigo OHNO

Department of Chemistry, Tokyo Institute of Technology, Ookayama, Meguro-ku, Tokyo

(Received November 17, 1965)

A sensitive gas chromatograph of the reduced-pressure type was devised to analyze hydrogen nuclear spin isomers and isotopes, and its characteristics were studied in order to obtain the optimum conditions for analysis. It was shown that the para and ortho composition of 0.01 ml. S. T. P. of normal hydrogen could be determined within an accuracy of 1% by employing an alumina column cooled at −196°C, while the composition of 0.02 ml. S. T. P. of the equilibrated mixture of hydrogen, hydrogen deuteride and deuterium at 25°C could be determined within the same accuracy by employing an alumina column coated with manganese chloride. The alumina column was no longer capable of separating the spin isomers when it was treated above 350°C. Kinetic studies of the hydrogen-deuterium equilibration (21°C) and of the orthohydrogen conversion (−196°C), using the alumina as a catalyst, revealed that this strong activation creates active sites for the equilibration and the magnetic conversion which makes the peak separation obscure. The nature of these active centers was briefly discussed.

Since the nuclear spin isomers of hydrogen, para- and orthohydrogen, and isotopic molecules, including deuterium and tritium, were found, the method of measuring the thermal conductivity, originally developed by Farkas, has long been used for the analysis of their mixture, while mass spectrometry has been used for the analysis of the isotopes. These methods of analysis, however, are somewhat unsatisfactory, apart from their lack of convenience, the applicability of the thermal conductivity method is practically limited to the binary mixtures, while the mass spectroscopy can not be used for the analysis of the spin isomers.

Recently Kwan et al. and a number of other investigators have reported that it is possible to separate these isomers or isotopic molecules by gas chromatography when a column packing such as alumina is operated at a low temperature of liquid nitrogen.[2-11)] Moreover, the simultaneous separation of these four modifications, para-, orthohydrogen, hydrogen deuteride and deuterium molecules, has been successful.[12,13)] This method, therefore, may be a useful alternative to the current ones for the analysis if the present ambiguity in accuracy and the low sensitivity are improved, all the results reported hitherto, except for those in Venugopalan and Kutschke's work,[11)] indicate that it is necessary, for the quantitative determination of the composition, to use a gaseous sample of more than one milliliter at a standard temperature and pressure. In order to follow the change in composition at low pressure, it is desirable to develop a highly-sensitive apparatus which can work with a sample of several hundredths of a milliliter. For this purpose, a gas chromatograph of the reduced-pressure type was adopted, and the optimum conditions for the analysis were examined using the equilibrium mixture of hydrogen modifications.

The present paper will present the details of this method and also some information about the catalytic activities of gamma-alumina in the ortho-parahydrogen conversion and in the hydrogen-deuterium equilibration reactions which were studied by its application.

Experimental

Apparatus and Procedure.—A gas chromatograph of the reduced-pressure type was used in this study; a schematic diagram of it is shown in Fig. 1. The helium employed as the carrier gas was adjusted to atmospheric pressure by a bubbler (A) and was then purified over a Linde molecular sieve 13X trap (C) at −196°C. Gas sampling was performed by a gas pipette (D). In most experiments, an alumina column

1) Presented at the 18th Annual Meeting of the Chemical Society of Japan, Osaka, April, 1965.
2) S. Ohkoshi, Y. Fujita and T. Kwan, This Bulltin, **31**, 771 (1958).
3) W. R. Moore and H. R. Ward, *J. Am. Chem. Soc.*, **80**, 2909 (1958).
4) T. Kwan, *J. Res. Inst. Catalysis*, Hokkaido Univ., **8**, 18 (1960).
5) H. A. Smith and P. P. Hunt, *J. Phys. Chem.*, **64**, 383 (1960).
6) W. van Hook and P. H. Emmett, ibid., **64**, 673 (1960).
7) W. R. Moore and H. R. Ward, ibid., **64**, 832 (1960).
8) P. P. Hunt and H. A. Smith, ibid., **65**, 87 (1961).
9) L. Bachmann, E. Bechtold and E. Cremer, *J. Catalysis*, **1**, 113 (1962).
10) G. F. Shipman, *Anal. Chem.*, **34**, 877 (1962).
11) M. Venugopalan and K. O. Kutschke, *Can. J. Chem.*, **41**, 548 (1963).
12) S. Furuyama and T. Kwan, *J. Phys. Chem.*, **65**, 190 (1961).
13) K. Fujita and T. Kwan, *Japan Analyst (Bunseki Kagaku)*, **12**, 15 (1963).

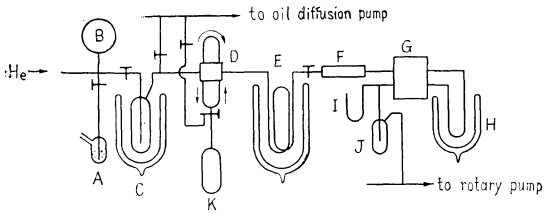

Fig. 1. Schematic diagram of the gas chromatograph.

A bubbler	G katharometer
B buffer	H U-tube trap
C moleculer sieve trap	I manometer
D gas sampling system	J pressure drop
E column	K reaction vessel or gas reservoir
F combustion furnace	

was used for the separation of isomers, and an alumina column coated with manganese chloride, for that of isotopes at −196°C. A Linde molecular sieve 13X column was also examined in order to compare it with the characteristics of these column packings. The eluted hydrogen samples were converted into water vapor on a cupric oxide column (F) heated at 750°C and were detected by a katharometer (G) made of stainless steel block with paths for the gas flow (5 mm. in diameter) and coiled tungsten filaments (30 ohms) in it. In order to avoid the condensation of water vapor, the katharometer was kept at 45°C, and the path between the combustion column and the katharometer, at 110°C. In order to maximize the sensitivity, the pressure in the katharometer was adjusted by a pressure drop (J) to 55—60 mmHg, which is the lowest value where the drifts of base lines are negligible.

Kinetic studies of the orthohydrogen conversion at −196°C and the hydrogen-deuterium equilibration at 21°C were made using column packings as catalysts. A reaction vessel of about 950 ml. with a circulator was connected with the gas pipette (D). The gases were left in contact with the catalyst for a suitable time and then led to the gas chromatograph for analysis. Prior to each experiment, the catalyst was degassed for 5 hr. at a definite temperature in vacuo better than 10^{-6} mmHg.

Materials.—Hydrogen was purified by diffusing it through a heated palladium thimble, while high purity deuterium purchased from the Takachiho Chemical Co. which contained hydrogen deuteride 0.7%, was used without further purification. Tank helium was passed through a trap filled with a Linde molecular sieve 13X immersed in liquid nitrogen in order to remove oxygen and other condensables; it was then used as the carrier gas.

Preparation of Columns.—Aluminum hydroxide prepared by the hydrolysis of distilled aluminum isopropoxide was dried at 500°C for 10 hr. in a current of dried air and was then left in contact with water vapor overnight. The alumina (80—100 mesh) thus obtained was packed into a glass tube (1.7 m. long and 2 mm. in inside diameter) and was treated in a current of helium under various conditions. The spectroscopic analysis of the alumina indicated that it contained iron 0.019%, manganese 0.002% and chromium 0.005% by weight. An X-ray diffraction study showed that this alumina had gamma structure.

The column for the separation of isotopes was prepared in the following way. Five grams of the alumina were immersed in 100 ml. of a 0.075 mol./l. manganese chloride solution overnight. The alumina was quickly washed with distilled water, dried at 200°C for 10 hr., packed into a glass tube (2.2 m. × 2 mm.), and then treated in a current of helium at 200°C for 25 hr. A Linde molecular sieve 13X (30—60 mesh) was also used as a column; it was packed into a glass tube (1.7 m. × 3 mm.) and treated in a current of helium at 100°C for 20 hr. The spectroscipic analysis of the molecular sieve indicated that it contained iron 0.12%, manganese 0.005% and chromium 0.005% by weight.

Results and Discussion

The Determination of Para- and Orthohydrogen.—As is shown in Fig. 2, chromatograms with two well-separated peaks were obtained by using an alumina column which was activated at 100—150°C. It was observed that the shape of the peaks at the beginning of activation was appreciably asymmetrical, but after activation for more than 20 hr. it became almost symmetrical. This treatment made it possible to evaluate the peak area by a rather simple method—by multiplying the height by the half-width of the peak. A column which was strongly activated at higher temperatures (350°C) no longer had the function

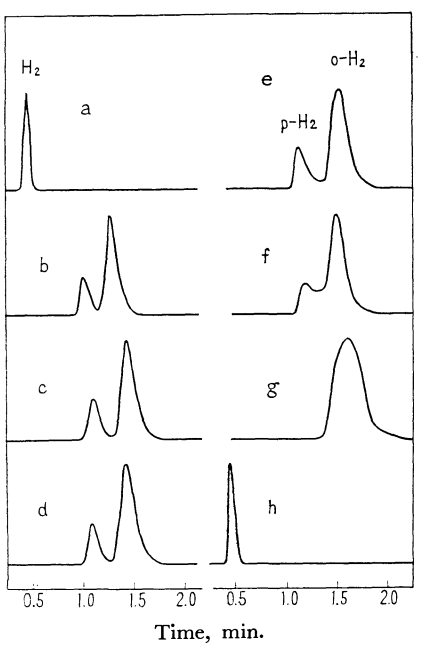

Fig. 2. Chromatograms of normal hydrogen on an alumina column activated at various temperatures.
Column: alumina (80—100 mesh, 1.7 m. × 2 mm.; −196°C) activated at a, 20°C, b, 100°C, c, 120°C; d, 150°C; e, 200°C, f, 270°C; g, 350°C; for 9 hr. and h, kept in contact with water vapor after activating at 350°C. Flow rate of carrier: 100 ml./min.

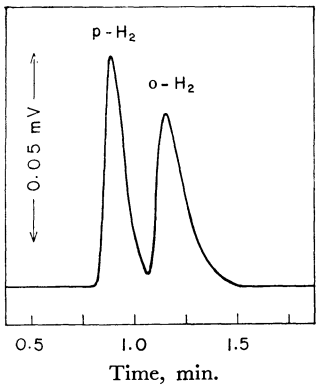

Fig. 3. Chromatogram of para-riched hydrogen equilibrated at −196°C.
Column: alumina (80—100 mesh, 1.7 m × 2 mm; −196°C) activated at 100°C for 45 hr.
Flow rate of carrier: 100 ml./min.
Sample: 0.015 ml.

of separation. However, it was easily recovered by the adsorption of water vapor. Figure 3 shows a chromatogram of the para-riched hydrogen obtained by the use of an alumina column. From a comparison of peak areas, it was established that the first-eluted peak corresponds to parahydrogen and the second peak, to orthohydrogen.

Figure 4 shows the calibration lines for these isomers. There was a good linear relationship between the peak area and the volume for each isomer; this relationship held up to 0.2 ml. of the sample. It was also shown that, for the analysis of normal hydrogen (para: ortho=1 : 3), it is sufficient to use more than 0.01 ml. of the sample,

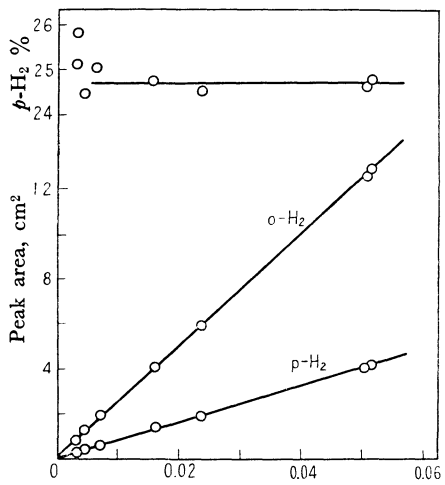

Fig. 4. Calibration lines for para- and ortho-hydrogen.
Column: alumina (80—100 mesh, 1.7 m. × 2 mm.; −196°C) activated at 100°C for 45 hr.
Flow rate of carrier: 100 ml./min.

and that the estimated mole fraction of the isomers agreed with the expected value within an accuracy of 1%.

The Linde molecular sieve 13X column has some unsatisfactory points. It gives not only longer retention times, but also a lower sensitivity than alumina. Moreover, the observed ratio of ortho to para in normal hydrogen becomes 2.88±0.03, which is lower than the expected value, 3.00. This is, as will be seen later, a result of the fact that the interconversion catalyzed by some paramagnetic impurities, mainly iron (0.12%), proceeds within the column. Therefore, it is advisable to employ highly-purified alumina as the column packing for the quantitative separation of para- and orthohydrogen.

The Determination of Hydrogen, Hydrogen Deuteride and Deuterium.—Analogous to the case of para- and orthohydrogen, well-separated chromatograms for isotopes were also obtained by using an alumina column coated with manganese chloride; they are shown in Fig. 5. The specific peak area which is defined as that for a unit volume of the sample, had the same value for both hydrogen and deuterium within the range of experimental error. Therefore, the ratio of the peak area for hydrogen isotopes corresponded practically to their mole ratios.

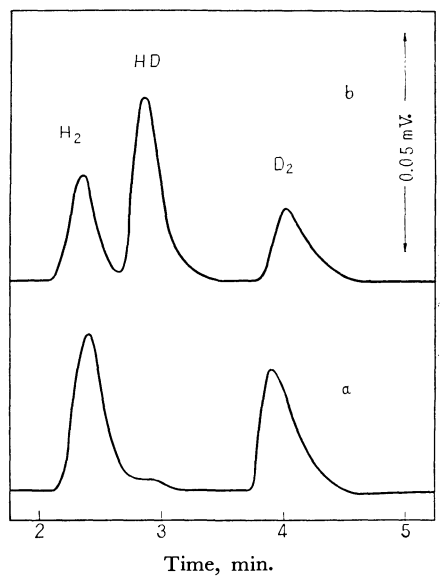

Fig. 5. Chromatograms of mixture of hydrogen, hydrogen deuteride and deuterium.
Column: alumina coated with manganese chloride and activated at 200°C for 25 hr. (80—100 mesh, 2.2 m. × 2 mm.; −196°C)
Flow rate of carrier: 90 ml./min.
a, mixture of hydrogen and deuterium (0.02 ml.) ($H_2/D_2=1.076$)
b, equilibrated mixture of hydrogen, hydrogen deuteride and deuterium at 25°C (0.022 ml.)

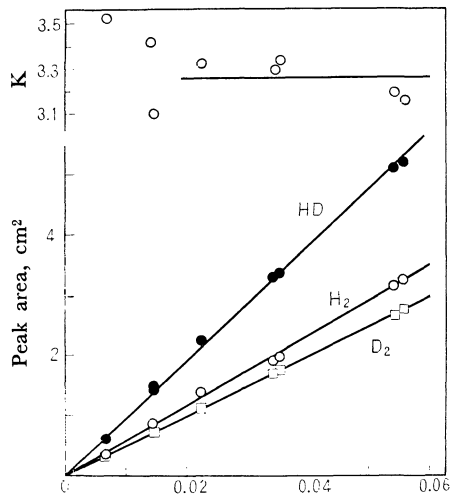

Fig. 6. Calibration lines for mixture of hydrogen, hydrogen deuteride and deuterium equilibrated at 25°C.
Column: alumina coated with manganese chloride and activated at 200°C for 25 hr.
(80—100 mesh, 2.2 m. × 2 mm.; −196°C)
Flow rate of carrier: 90 ml./min.

Figure 6 includes the calibration lines for these isotopes, which also held a good linear relationship between the peak area and the volume for each species. In this case of an isotopic mixture, it was verified, using an equilibrated mixture of hydrogen, hydrogen deuteride and deuterium at 25°C as the sample, that 0.02 ml. of a gaseous sample is sufficient for the quantitative determination of the composition within an accuracy of 1%. The observed value of the equilibrium constant, 3.26± 0.1, agreed with the calculated value, 3.268, within an accuracy of 3%. This improvement in sensitivity is mainly due to the lowering of the pressure of the carrier gas at which the katharomeer and to the conversion of eluted hydrogen into water, which amplifies the difference in thermal conductivity between the sample and the carrier gas.

Since a microthermal conductivity method can analyze 0.01—0.03 ml. of a sample,[14] the present method may be a useful alternative.

Orthohydrogen Conversion and Hydrogen-Deuterium Equilibration on Column Packings.—As is shown in Fig. 2, the separating power of alumina varied greatly according to the temperature at which alumina was activated. It has been reported that on separation occurs on a strongly-activated column; this is due to rapid interconversion between the isomers within the column.[7] In order to get further proof of this, kinetic studies of orthohydrogen conversion and also of hydrogen-deuterium equilibration were performed, using column packings as the catalysts.

The time course in all cases of constant pressure followed the first-order law; therefore, the rate constant may be expressed as:

$$k_e = (1/t) \ln (C_0/C_t) \text{ min}^{-1}$$

where C_0 or C_t is the excess concentration of species at time zero, or t, over the equilibrium value at the experimental temperature. The absolute rate constant was calculated to be:

$$k_m = k_e pV/60AkT \text{ molecules} \cdot \text{cm}^{-2} \text{ sec}^{-1}$$

where p is the gas pressure; V, the reaction volume at the temperature, T; A, the surface area of the catalyst, and k, Bolzmann's constant.

Figure 7 shows the specific activities for the conversion (−196°C) and for the equilibration (21°C) of catalysts which were subjected to the evacuation at various temperatures. Not all catalysts showed activity for the equilibration at −196°C. Therefore, the conversion proceeding at that temperature is of a physical nature.

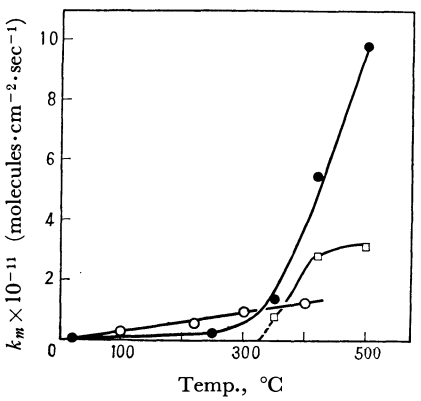

Fig. 7. Effect of evacuating temperature on the specific activities of catalysts.
● conversion on alumina at −196°C
○ conversion on molecular sieve 13X at −196°C
□ equilibration on alumina at 21°C

When the alumina was evacuated at temperatures higher than 350°C, the conversion activity increased abruptly; the equilibration activity also became appreciable at 21°C. On the contrary, the conversion activity of the molecular sieve 13X gradually increased with the evacuating temperatures, and the equilibration did not occur at temperatures up to 100°C.

As may be seen in Fig. 7, the activity of the physical conversion increases in two stages with the evacuating temperatures. The transition point between these stages nearly corresponds to the temperature at which the separated peaks begin to merge with each other, as is shown in Fig. 2. It may, therefore, be suggested that this phenomenon

14) H. Melville and B. G. Gowenlock, "Experimental Methods in Gas Reaction," Macmillan and Co., London (1964), p. 239.

results from the rapid interconversion within the column.

In order to get insight into this phenomenon, the effect of paramagnetic impurities was roughly examined by applying Wigner's theory. The activity of neodymium oxide in the parahydrogen conversion[15] was taken as a reference, and it was assumed that the conversion proceeds over the ferric ions on the surface of alumina the concentration of which is the same as that in bulk, and that the accessible distances between hydrogen molecules and active centers for γ-alumina and neodymium oxide are similar. The concentration of ferric ions is, therefore, given by the expression:

$$[Fe_2O_3]/[Nd_2O_3] = \{\mu(Nd^{3+})/\mu(Fe^{3+})\}^2 k_m(Fe^{3+})/k_m(Nd^{3+})$$

where $\mu(Fe^{3+})$ and $\mu(Nd^{3+})$ represent the magnetic monents of the cations. Thus the value of the concentration was estimated to be 0.04% by the evacuation at 250°C and 1.7% by that at 500°C. The former value agrees approximately with the observed iron content (0.019%), while the latter can not be explained from only its existence, even if all the ferric ions are exposed on the surface. Moreover, highly-purified alumina (Fe, Cu, Mg, and Mn$<$1 p. p. m.) which had been carefully prepared by three distillations of aluminum isopropoxide showed no activity in the evacuation at 250°C, but a high activity at 500°C, corresponding to a ferric ion content of 9.5%. Therefore, the first, gradual increase in activity is due to the exposure of paramagnetic impurities caused by dehydration, while the second, aburpt increase implies that "paramagnetic" sites of a different origin are created on the surface of γ-alumina.

Eley et al. have reported that α-alumina evacuated at 550°C has active sites for the H_2–D_2 equilibration and for the magnetic conversion, and also that new thermolabile paramagnetic sites are created by γ-ray irradiation.[16] Therefore, it is conceivable that α- and γ-alumina behave similarly in the catalysis of these reactions.

Further studies of the nature of these sites on γ-alumina are in progress; details will be reported later.

The authors wish to express their thanks to Professor Takao Kwan of the University of Tokyo for his helpful discussions and also to Professor Tadao Shiba of Tokyo Institute of Technology for the generous gift of alumina which made this work possible.

15) D. R. Ashmead, D. D. Eley and R. Rudham, *Trans. Faraday Soc.*, **59**, 207 (1963).

16) G. J. K. Acres, D. D. Eley and J. M. Trillo, *J. Catalysis*, **4**, 12 (1965).

BULLETIN OF THE CHEMICAL SOCIETY OF JAPAN VOL. 39 1306—1310 (1966)

Rearrangements of Tertiary Amine Oxide. XV.[1] The Reaction of Heterocyclic *N*-Oxides with *p*-Nitrobenzenesulfinyl Chloride

By Shigeru OAE and Katuyata IKURA

Department of Applied Chemistry, Faculty of Engineering, Osaka City University, Sumiyoshi-ku, Osaka

(Received November 24, 1965)

In the reaction of pyridine and α-picoline *N*-oxide with *p*-nitrobenzenesulfinyl chloride, the N–O bond of the intermediate salt appears to cleave homolytically, as in the case of *N*-oxide with *p*-nitrobenzenesulfenyl chloride, and the *p*-nitrosulfonyl radical which arises from the homolytic cleavage of the N–O bond is considered to be so stable that only the secondary reaction products from the sulfonyl radical, and no heteroring-substituted products, are obtained. It is the same in the case of unsubstituted benzenesulfinyl chloride.

We have reported earlier that, in the reaction of *p*-nitrobenzenesulfenyl chloride with pyridine and α-picoline *N*-oxides, the N-O bond of the incipient salt I was homoliticaly cleaved, giving only reduced pyridine bases, while neither ring-substituted rearrangement products nor unreacted *N*-oxides were obtained.[2]

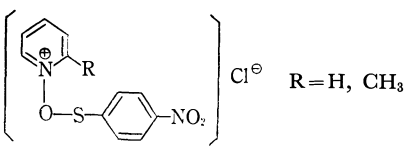

I

On the other hand, the reactions of pyridine and isoquinoline *N*-oxide with tosyl chloride gave ring-substituted rearrangement products, apparently

1) Part XIV: S. Oae and S. Kozuka, *Tetrahedron*, **21**, 1971 (1965).
2) S. Oae and K. Ikura, This Bulletin, **38**, 58 (1965).

formed through the heterolytic cleavage of the N–O linkage of the intermediate IIA, formed by the nuclear addition of Cl ion to the II salt.[3]

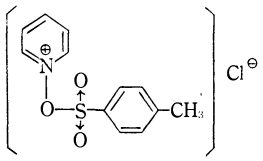

II

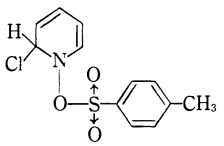

IIA

The marked difference between these two reactions may lie in the difference in the reacting organic sulfur chlorides. Namely, the former, *p*-nitrobenzenesulfenyl chloride, is electronically neutral, while the latter has the positive character of the sulfur atom, which would cause a facile heterolytic cleavage of the N–O bond. This may lead to the idea that sulfinyl chlorides, which has a more positive sulfur atom than sulfenyl chlorides and a less positive sulfur atom than sulfonyl chlorides, would give rise to a reaction between the two above reactions.

Thus we have investigated the reaction of *p*-nitrobenzenesulfinylchloride with pyridine and α-picoline *N*-oxides, a reaction which involves the incipient formation of the III salt.

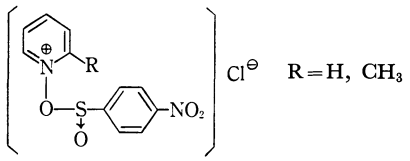

III

Results and Discussion

p-Nitrobenzenesulfinyl chloride was prepared by chlorinating *p*, *p*'-dinitrodiphenyldisulfide in glacial acetic acid with chlorine gas, and it was identified by means of the reaction product with acetone, which has the analytical composition of the α-sulfinylacetone. When equivalent amounts of pyridine *N*-oxide and *p*-nitrobenzenesulfinyl chloride were mixed in a benzene solution, colorless crystalline precipitates were formed immediately, with an evolution of heat. The crystals, which are very hygroscopic, have the analytical composition of the salt IV, as is shown below:

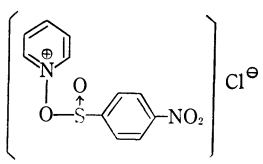

IV

The IV salt was obtained after the thorough removal of the solvent benzene under the vaccum; the salt was then heated at 180—200°C for two hours under a nitrogen stream. It began to melt at around 80°C, but no color change was observed until around 180°C; at around 180°C the salt started to melt, giving a dark, oily mass, and sulfur dioxide was evolved.

Among the reaction products isolated were pyridine, *p*-nitrochlorobenzene, *p*-nitrobenzenesulfonic acid, and *p*, *p*'-dinitrodiphenyldisulfide.

Neither a ring-substituted rearrangement product nor unreacted pyridine *N*-oxide was isolated among the products. These reaction products and their distributions seem to indicate that this reaction is also initiated by the cleavage of the N–O bond of the IV salt, just as in the case of *N*-oxide with *p*-nitrobenzenesulfenyl chloride, and not like the case of *N*-oxide with tosyl chloride. Here again the sulfonyl radical, V, which was presumed to be formed at first by the cleavage of the N–O bond of the IV salt, is apparently stable.

The existence of this radical was reported previously by Kice[4] and Overberger[5]. Namely, Kice has reported that the thermal decomposition of aromatic sulfinyl sulfonate gives the tolyl sulfonyl radical, which can be trapped with gulvinoxyl. He has also shown that the radical can add to an olefine to give a stable addition product, as is shown below:

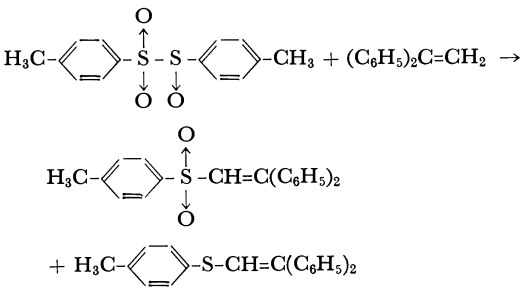

This radical stability may be due to the 3d-orbital resonance of the sulfur atom as follows.

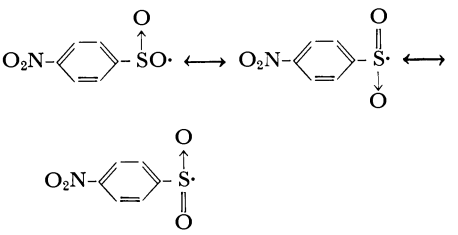

If the reaction would follow a path similar to that of pyridine *N*-oxide with tosyl chloride, one

3) S. Oae, T. Kitao and Y. Kitaoka, *Tetrahedron*, **19**, 827 (1963).
4) J. L. Kice and N. E. Pawlowski, *J. Am. Chem. Soc.*, **86**, 4898 (1964).
5) C. G. Overberger and A. J. Rosenthal, ibid., **82**, 117 (1960).

would expect some pyridine ring-substituted compound among the product mixture, for the heterolytically-cleaved species, presumably the nitrobenzene sulfonium ion, is considered to react with the other cleaved partner to give perhaps a very stable sulfonyl product.

In this reaction, however, there was apparently no formation of any heteroring-substituted product, and the yield of the pyridine recovered was nearly quantitative. The entire reaction is quite similar to the reaction with *p*-nitrobenzenesulfenyl chloride. These findings, and the results of the previous work on the thermal decomposition of aromatic sulfinyl sulfonate, seems to favor the homolytic cleavage of the N–O bond of the IV salt. Thus, the overall reaction scheme may be formulated nicely as below:

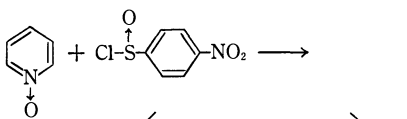

(1)

IV

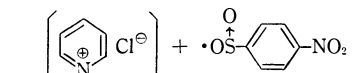

(2)

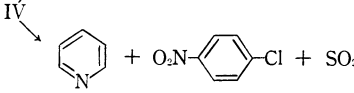

(3)

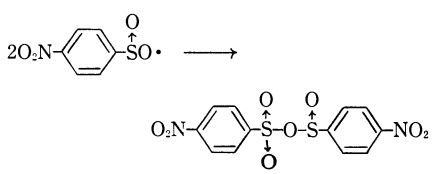

(4)

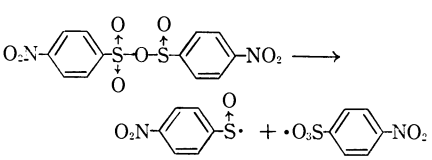

(5)

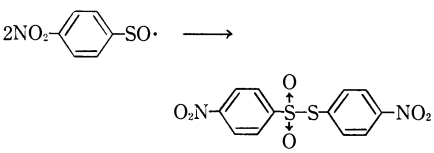

(6)

p-Nitrochlorobenzene was probably formed by step 3. Here again the *p*-nitrochlorobenzene was

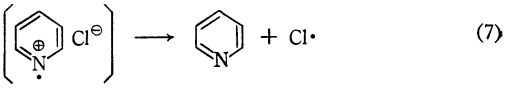

(7)

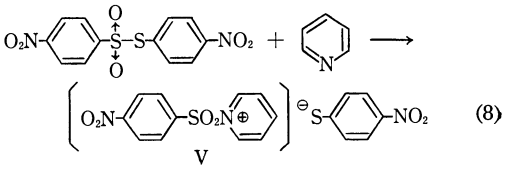

(8)

V

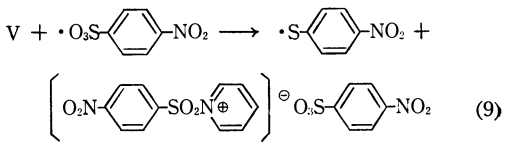

(9)

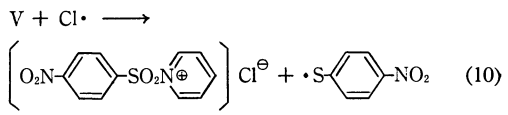

(10)

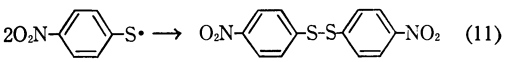

(11)

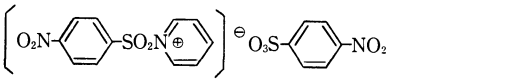

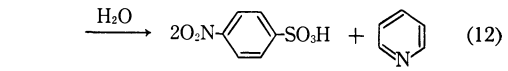

(12)

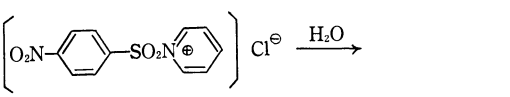

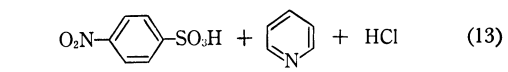

(13)

obtained as in the case of the reaction of *p*-nitrobenzenesulfenyl chloride with α-picoline *N*-oxide, where the formation of *p*-nitrochlorobenzene was considered to proceed through the following pathway:[2]

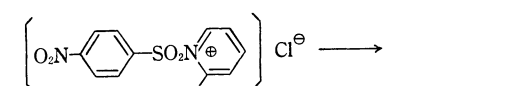

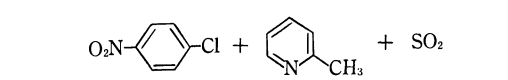

In this reaction the amount of this compound actually isolated was rather large as compared to those of the disulfide and *p*-nitrobenzenesulfonic acid.

About the formation of the radical, (O_2N– 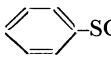 –$SO_3\cdot$) is now yet questionable, but if step

5 is assumed, the reaction products are cleverly explained, and this radical might be occur with the charge transfer with V, as is shown by step 9.

The same reaction was applied to α-picoline N-oxide. In this case, too, equimolar amounts of α-picoline N-oxide and p-nitrobenzenesulfinyl-chloride were mixed in a benzene solution. White crystalline precipitates gradually formed, with an evolution of heat; these precipitates changed to a dark oil during the removal of the solvent. The dark oil was found by analysis to have the composition derived from the VI salt.

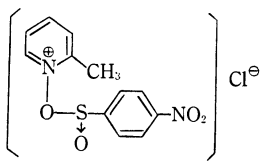

VI

This salt was heated at 140—150°C for two hours under a nitrogen stream. The evolution of hydrogen chloride began at around 140°C, and sulfur dioxide gas was also observed during the heating, although the amounts of both gases were small. The reaction products isolated were α-picoline, p,p'-dinitrodiphenyl disulfide, and p-nitrobenzenesulfonic acid. Here again an undetectable amount of any hetero ring-substituted products was obtained among the reaction products in spite of the noticeable amounts of hydrogen chloride evolved. Here, p-nitrochlorobenzene was not obtained. However, the amount of disulfide was larger than in the case of pyridine N-oxide. Judging from these reaction products, therefore, the reaction also seems to proceed via a similar homolytic cleavage of the N–O bond of the VI salt, and the overall reaction scheme may be considered to be quite analogous to the one previously postulated for that with pyridine N-oxide except for step 3.

We have also extended the reaction to unsubstituted benzenesulfinyl chloride with α-picoline N-oxide. When equimolar amounts of α-picoline N-oxide and benzenesulfinyl chloride were mixed in a benzene solution, heat evolved and a dark red oil was gradually precipitated. Apparently the decomposition of the conceivable incipient salt was very facile, and the resultant dark oil was a reacted mixture. However, in this case, it is considered that the reaction proceeds through the formation of the VII salt. The reaction products isolated were α-picoline, diphenyl disulfide, and benzenesulfonic acid.

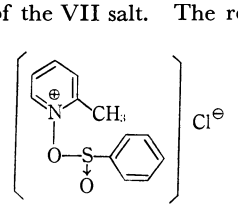

VII

This reaction was also considered to proceed like the other two reactions.

Experimental

The Preparation of p-Nitrobenzenesulfinyl Chloride.—p,p'-Dinitrodiphenyl disulfide was mixed with exactly twice as much glacial acetic acid in chloroform, and chlorine gas was introduced at −5——10°C until no hydrogen chloride evolution was recognized. Then the chloroform and acetyl chloride formed were thoroughly removed in vacuo at room temperature.

The residue formed cubic crystals. This was used for the succeeding reaction without further purification; m. p. 58—60°C.

Found: N, 7.12. Calcd. for $C_6H_4NO_3SCl$: N, 6.81%.

This chloride was identified by reacting it with acetone at room temperature until its derivatives were produced. The product has the correct analytical composition of the α-sulfinylacetone, O_2N-C$_6$H$_3$(-SO-)-SCH_2COCH_3; m.p. 66—67°C.

Found: C, 47.56; H, 4.02; N, 6.64; S, 14.90. Calcd. for α-sulfinylacetone: C , 47.56; H, 3.99; N, 6.16; S, 14.11%.

The Reaction of Pyridine N-Oxide with p-Nitrobenzenesulfinyl Chloride.—When both a benzenes solution of pyridine N-oxide (1.00 g.) and p-nitrobenzenesulfinyl chloride (2.00 g.) were mixed at room temperature, the white salt, IV, precipitated at once. Then the solvent was removed in vacuo at room temperature, and the residue was heated at around 180—200°C for two hours under a nitrogen stream. The reaction mixture became a dark, oily mass, and sulfur dioxide was evolved. After the reaction, dilute hydrochloric acid was added, and the mixture was extracted with chloroform.

The removal of the solvent chloroform gave p-nitrochlorobenzene (1.10 g.) and p,p'-dinitrodiphenyl disulfide (0.05 g.).

The aqueous layer was made neutral with sodium carbonate and extracted with chloroform. The removal of the solvent gave pyridine (0.6 g.). Then, a 10% ethanol solution of benzylisothiourea hydrochloride salt was added to the aqueous mother solution, from which pyridine had already been recovered, and the crystals thus precipitated was collected and recrystallized from a water-ethanol mixture. These crystals were thiuronium salt of p-nitrobenzenesulfonic acid (0.78 g.).

The sulfur dioxide was trapped by passing it through a solution of barium hydroxide; the quantity of SO_2 was 0.36 g.

The Isolation of 1-p-Nitrobenzenesulfinylpyridinium Salt IV.—The hygroscopic crystalline precipitate obtained by reacting p-nitrobenzenesulfinyl chloride and pyridine N-oxide was washed with ethanol, dried, and analyzed; m. p. 98—100°C.

Found: C, N, 9.62. Calcd. for $C_{11}H_9N_2O_4SCl$: N, 9.32%.

The Reaction of α-Picoline N-Oxide with p-Nitrobenzenesulfinyl Chloride. — α-Picoline N-

oxide (2.0 g.) and *p*-nitrobenzenesulfinyl chloride (4.0 g.) were used. The colorless salt which was gradually precipitated changed to a dark oil during the removal of the solvent. After the solvent had been removed, the dark oil was heated at 140—150°C for two hours under a nitrogen stream. The treatment of the reaction products was exactly the same as in the case of pyridine *N*-oxide.

The product from the chloroform layer was *p*, *p*'-dinitrodiphenyl disulfide (2.1 g.). From the aqueous layer α-picoline (1.3 g.) and *p*-nitrobenzenesulfonic acid (1.6 g.) were obtained.

The Isolation of 1-*p*-Nitrobenzenesulfinyl-2-picolinium Salt VI.—The dark oil precipitate obtained by reacting *p*-nitrobenzenesulfinyl chloride and α-picoline *N*-oxide was washed well with water and recrystallized from a water-ethanol mixture; m. p. 174—177°C.

Found: N, 9.09. Calcd. for $C_{12}H_{11}N_2O_4SCl$: N, 8.90%.

The Reaction of α-Picoline *N*-Oxide with Phenylsulfinyl Chloride.—α-Picoline *N*-oxide (1.5 g.) and phenylsulfinyl chloride (2.1 g.) were reacted as usual in a benzene solution. Apparently the reaction got started immediately, forming no precipitated salt, but a dark red oil was gradually precipitated while the solvent was bing removed with a vigorous reaction. Then the dark oil was heated an additional hour at around 160°C. The treatment of the reaction products was exactly the same as in the above two cases.

The product from the chloroform layer was diphenyl disulfide (1.1 g.). From the aqueous layer, α-picoline (1.0 g.) and benzenesulfonic acid (0.8 g.) were obtained.

All the compounds were identified by mixed melting point, infrared spectra, and elemental analyses.

BULLETIN OF THE CHEMICAL SOCIETY OF JAPAN VOL. 39 1310—1316 (1966)

The Synthesis and Reactions of 2-Chloro-5-hydroxytropone*[1]

By Tetsuo NOZOE, Toyonobu ASAO, Eijiro TAKAHASHI*[2] and Kazuko TAKAHASHI

Department of Chemistry, Faculty of Science, Tohoku University, Katahira-cho, Sendai

(Received November 24, 1965)

The acid hydrolysis of some polyhalotropones and some reactions of the products were investigated. The treatment of 2, 5-dichlorotropone with hydrochloric or sulfuric acid afforded 2-chloro-5-hydroxytropone (I) and a small amount of 5-chlorotropolone. The compound I gives only one kind of the methyl ether and one kind of the acetyl or benzoyl derivative. From the methyl ether, 5-amino- and 5-methylamino-2-chlorotropone were derived. The methoxyl and the amino groups of these compounds are reactive to alkaline hydrolysis, giving I without any of the skeletal rearrangement usually observed in the alkaline treatment of similar 2-halotropones. The hydrolysis of 2, 4, 7-tribromotropone with hydrochloric acid gave 3, 6-dichlorotropolone and 7-chloro-4-hydroxytropolone.

It is known[1] that 2-halotropones react with alkalis to give benzoic acid derivatives mainly, besides a small amount of tropolones, and that polyhalotropones, under similar treatment, afford benzoic acid and salicylaldehyde derivatives, in addition to considerable amounts of tropolones in some cases.

However, on being heated with strong acids, halotropones, (for example, I; X=halogen), are converted into a conjugated acid cation (III), whose hydrolysis yields hydroxytropone (II; Y=OH) without any rearrangement to benzenoid compounds. When hydrogen halides are used

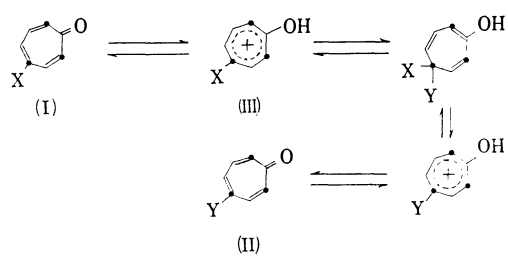

in this reaction, the exchange of the halogen atom often occurs and a different halotropone (II; Y=halogen) may be obtained besides the products of hydrolysis.[1] Apparently, in the acid treatment of halotropones, halogen atoms located at the 3- or 4-position undergo such reactions easier than those at the 2-position. This is probably due not only to steric interference but also to facile anionoid attack at positions β or δ to the conjugated unsaturated ketone.

*1 Presented at the 14th Annual Meeting of the Chemical Society of Japan, Tokyo, April, 1961.

*2 Present address: Dai-Nippon Ink Co., Ltd., Itabashi-ku, Tokyo.

1) T. Nozoe, "Non-Benzenoid Aromatic Compounds," Ed. by D. Ginsburg, Interscience Publishers, New York (1959), p. 410; T. Nozoe et al., "Dai Yuki Kagaku (Comprehensive Organic Chemistry)," Vol. 13, Asakura-Shoten, Tokyo (1960), pp. 181, 217.

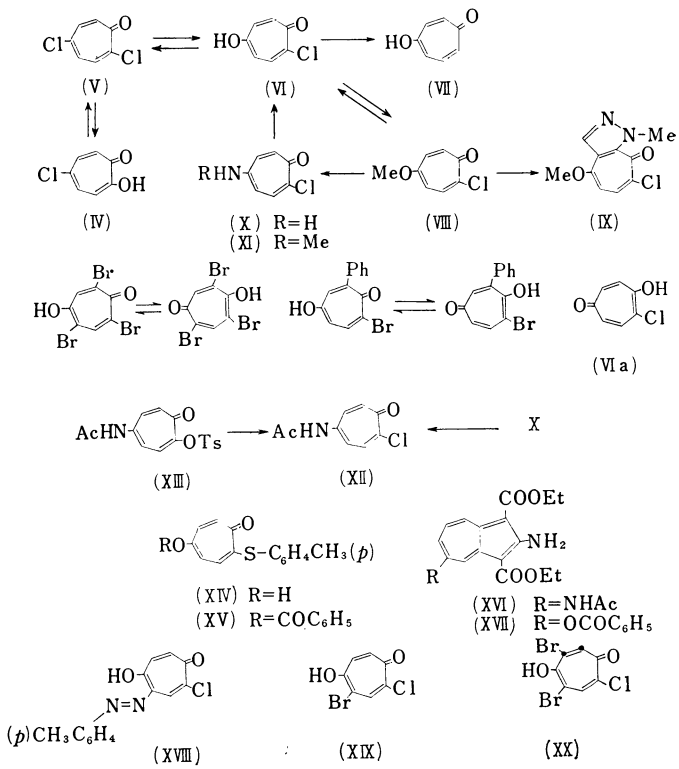

For instance, the conversion[2] of 4-bromotropone into 4-hydroxy- or 4-chlorotropone, when it was heated with hydrochloric acid in acetic acid, occured more easily than the conversion of 2-bromotropone into 2-chloro- or 2-hydroxytropone under the same conditions. 3-Bromo-2-chlorotropone gave 2-chloro-3-hydroxytropone and 2, 3-dichlorotropone by a similar treatment, but it did not afford any 3-chlorotropolone.[3] On being heated with concentrated sulfuric acid, 2, 4, 7-tribromotropone[4] and 2-phenyl-4, 5, 7-tribromotropone[5] yielded 4-hydroxy-2, 5, 7-tribromotropone and 5, 7-dibromo-4-hydroxy-2-phenyltropone respectively. The former compound must have been produced by the bromination of 2, 7-dibromo-4-hydroxytropone with bromine that had been generated from the sulfuric acid oxidation of the hydrobromic acid liberated by the initial hydrolysis of 2, 4, 7-tribromotropone.*3

This paper is one of a series devoted to an investigation of the order of relative ease with which halotropones undergo hydrolysis or halogen exchange, and to the utilization of such results in the preparation of 3- or 4-hydroxytropones, whose syntheses have otherwise been difficult. For the present paper, the acid hydrolysis of 2, 5-dichlorotropone and 2, 4, 7-tribromotropone has been investigated, and some reactions of the products have been studied.

2, 5-Dichlorotropone (V),[6] obtained by the reaction of 5-chlorotropolone (IV) and thionyl chloride, on being heated with concentrated hydrochloric acid or concentrated sulfuric acid in acetic acid afforded a considerable amount of pale yellow crystals (VI), m. p. 218°C, and a small amount of 5-chlorotropolone (IV).

The compound VI is acidic and shows a pale green coloration with ferric chloride, but with ferric or cupric ion it does not form a chelate complex which is soluble in chloroform, as is the case with tropolone.

The infrared absorption spectrum of VI in KBr shows OH bands at 3020, 2660 and 2550 cm^{-1} which are assumed to be due to intermolecular hydrogen bonding similar to that found with 4-hydroxytropone.[7,8] The ultraviolet absorption spectrum (Fig. 1) of VI exhibits maxima.

2) a) T. Nozoe, T. Mukai, Y. Ikegami and T. Toda, *Chem. & Ind.*, **1955**, 66; b) T. Nozoe, T. Mukai and Y. Ikegami unpublished work.

3) S. Seto, *Sci. Repts. Tohoku Univ., I*, **37**, 275 (1953).

4) T. Nozoe, Y. Kitahara and H. Abe, *Proc. Japan Acad.*, **29**, 347 (1953).

5) T. Muroi, This Bulletin, **33**, 1166 (1960).

*3 In the early stage of the investigation, it had been explained that the formation of 4-hydroxy-2, 5, 7-tribromotropone proceeded by the direct oxidation of the tropone ring with sulfuric acid. Cf. Ref. 4.

6) T. Sato, *J. Chem. Soc. Japan, Pure Chem. Sect.* (*Nippon Kagaku Zasshi*) **80**, 1771 (1959).

7) R. S. Coffey and A. W. Johnson, *J. Chem. Soc.*, **1958**, 1741.

8) Y. Ikegami, *Kagaku-no-Ryoiki, Extra*, **38**, 46 (1959).

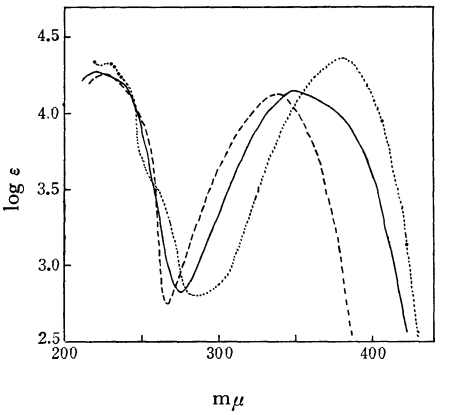

Fig. 1. Ultraviolet absorption spectra.
—— VI in methanol, ····· VI in 0.1 N NaOH,
---- VIII in methanol.

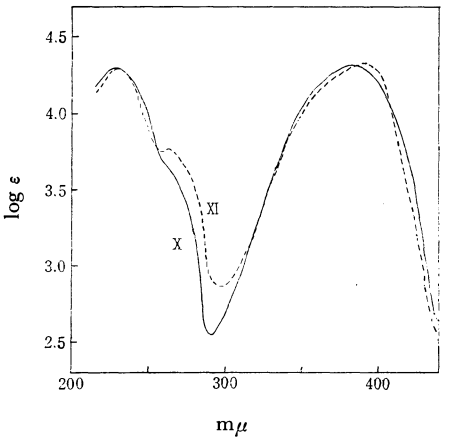

Fig. 2. Ultraviolet absorption spectra of X and XI in methanol.

at wavelengths similar to those observed in the spectrum of 2-bromo-5-hydroxytropone.[7] In addition to the abvoe spectroscopic evidence, VI affords 4-hydroxytropone (VII)[2a,7] on catalytic hydrogenation; therefore, it must be 2-chloro-5-hydroxytropone.

Nozoe et al.[9] and Muroi[10] have reported that a tautomeric relationship exists between 4-hydroxy-2, 5, 7-tribromotropone and 5-hydroxy-2, 4, 6-tribromotropone, and between 5, 7-dibromo-4-hydroxy-2-phenyltropone and 2, 4-dibromo-5-hydroxy-6-phenyltropone, and that in each case the tautomers gave different methyl ethers when allowed to react with diazomethane.

It was thought that VI might also exist as an equilibrium mixture of 2-chloro-5-hydroxytropone and 4-chloro-5-hydroxytropone (VIa); however, the treatment of VI with thionyl chloride afforded only 2, 5-dichlorotropone, and no isomeric 4, 5-dichlorotropone was obtained. Furthermore, compound VI yielded only one acetate, one benzoate and one tosylate, and with diazomethane it afforded only one methyl ether (VIII), besides a nitrogen-containing compound (IX).

Since Nozoe et al.[11] have found that the reaction of halotropones or 4-hydroxytropone with diazomethane gives pyrazolotropone (1-methyl-8-oxocyclohepta[d]pyrazole) derivatives, and since IX was also obtained by the action of diazomethane on the methyl ether (VIII), IX must be the pyrazolotropone derivative, as is shown in the scheme.

The methoxy compound (VIII) was easily hydrolyzed by alkali to give VI. VIII reacts with ammonia and methylamine to afford amino and methylamino compounds (X and XI) respectively; these compounds, on alkaline hydrolysis, yield VI, a reaction similar to the hydrolysis of 2-aminotropone. The ultraviolet absorption spectrum of amino compounds (Fig. 2) are quite different from that of 2-aminotropone,[12] but they are similar to that of 4-aminotropone.[13] The Acetylation of X afforded 5-acetamido-2-chloro tropone (XII), which was also obtained by the action[14] of hydrochloric acid on 5-acetamido-2-tosyloxytropone (XIII); therefore, it is clear that VIII and X are 2-chloro-5-methoxy- and 5-amino-2-chlorotropone respectively.

It is known that 5-methoxy-2, 4, 7-tribromotropone,[4] 2, 4-dibromo-5-methoxytropone[15] and 7-bromo-4-methoxy-2-phenyltropone[10] give only the corresponding rearranged compounds, i. e., anisic acid derivatives, upon treatment with alkali or alkoxide, but not the products of a simple hydrolysis, i. e., 4-hydroxytropone derivatives. In contrast to the above, it is noteworthy that the alkaline treatment of the methoxy compound (VIII) afforded only hydroxytropone (VI).

As has been mentioned above, the methoxyl group of VIII underwent anionoid substitution reaction; however, the reaction of *p*-tolylthiophenol with 2-chloro-5-hydroxytropone (VI) or its benzoyl derivative yielded 2-(*p*-tolylthio)tropone derivatives (XIV or XV respectively). 5-Acetamido-2-chlorotropone (XII) and the benzoyl derivative of VI reacted with ethyl cyanoacetate, in the same way as do 2-chlorotropones, to give 5-acetamido-[16] and 5-benzoyloxyazulene derivatives (XVI and XVII respectively).

9) T. Nozoe, Y. Kitahara, J. Shin and T. Toda, to be published.
10) T. Muroi, This Bulletin, **34**, 178 (1961).
11) T. Nozoe, T. Mukai and T. Asao, to be published.
12) T. Nozoe, S. Seto, H. Takeda, S. Morosawa and K. Matsumoto, *Proc. Japan Acad*, **27**, 556 (1951); *Sci. Repts. Tohoku Univ., I*, **36**, 126 (1952).
13) K. Doi, This Bulletin, **33**, 887 (1960).
14) H. Matsumura, *J. Chem. Soc. Japan, Pure Chem. Sect.* (*Nippon Kagaku Zasshi*), **82**, 623 (1961).
15) T. Mukai, unpublished results.
16) T. Nozoe, K. Takase and M. Tada, This Bulletin, **36**, 1006 (1963).

With diazotized *p*-toluidine, 2-chloro-5-hydroxytropone (VI) reacted, similarly to 4-hydroxytropone, to give the azo compound (XVIII), The bromination of VI yielded 4-bromo-2-chloro-5-hydroxytropone (XIX) and 4, 6(or 4, 7)-dibromo-2-chloro-5-hydroxytropone (XX). The structures of these compounds were assumed to be as above from the reactivity of 4-hydroxytropone[2a]; however, the position of the second bromine atom in XX was not clarified.

When 2, 4, 7-tribromotropone (XXI) was heated with hydrochloric acid in acetic acid at 100°C for one hour, it gave dichloromonobromotropone (XXII), whereas the same solution, on being heated at 135°C for 10 hr., afforded 70% of chlorodihydroxytropone (XXIII) and 10% of dichlorohydroxytropone (XXIV). The compounds XXIII and XXIV were also obtained by a similar acid treatment of XXII. The dihydroxytropone (XXIII) was identified as 7-chloro-4-hydroxytropolone since, on hydrogenolysis, it

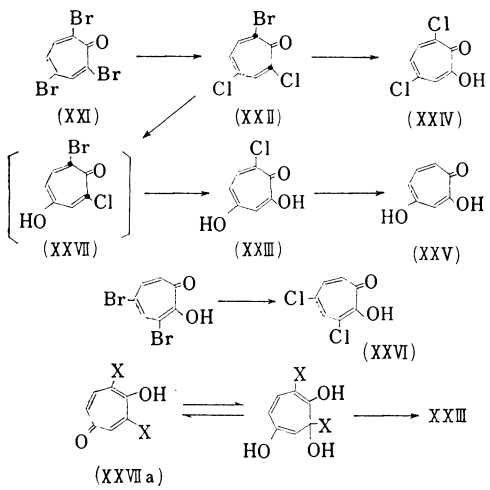

gave 4-hydroxytropolone (XXV).[17] Compound XXIV was not identical with 3, 5-dichlorotropolone (XXVI), obtained by the anionoid substitution of 3, 5-dibromotropolone[18] with hydrochloric acid; therefore, it must be 3, 6-dichlorotropolone.

During the treatment of polyhalotropones with acids, the halogen at the γ-position (C_4) undergoes anionoid substitution more easily than that at the α-position (C_2 or C_7); therefore, XXII is assumed to be 7-bromo-2, 4-dichloro- or 2-bromo-4, 7-dichlorotropone.

As has been shown above, the vigorous treatment of XXI or XXII with hydrochloric acid caused the hydrolysis of the halogens at the 2- and 4-positions, but not at the 7-position. This may indicate that the 2- and 4-positions, in both XXI and XXII, are more reactive than the 7-position.

It is considered that XXII undergoes a competitive hydrolysis of the halogen at the 2- and 4-positions to give XXIV and XXVII, and that there is no further hydrolysis of XXIV under these reaction conditions, whereas the further hydrolysis of XXVII proceeds through its tautomeric form (XXXVIIa) to yield XXIII.

Further investigations are being undertaken to clarify the above reaction path, and to study the reactivity of the 4-hydroxy- and 2, 4-dihydroxytropones which were obtained in this work.

Experimental*4

The Treatment of 2, 5-Dichlorotropone (V) with Hydrochloric Acid.—a) A solution of 2, 5-dichlorotropone (2 g.) in acetic acid (15 ml.) containing water (0.1 ml.) was saturated with hydrogen chloride gas; the solution was then kept at 110°C for 10 hr. in a sealed tube. The solvent was removed, and the residue was extracted with benzene. The insoluble part (1.65 g.) was recrystallized from ethanol to give 2-chloro-5-hydroxytropone (VI) as yellow needles, m. p. 217—218°C.

Found: C, 53.69; H, 3.16. Calcd. for $C_7H_5O_2Cl$: C, 53.69; H, 3.20%.

λ_{max}^{MeOH} mμ (log ε): 220(4.27), 350(4.14).

$\lambda_{max}^{0.1N\ NaOH}$ mμ (log ε): 228(4.33), 260^{sh} (3.52), 381-(4.37).

From the benzene-soluble part, 5-chlorotropolone (IV) (200 mg.) was obtained after being recrystallized from methanol.

b) After a solution of 2, 5-dichlorotropone (3 g.) in acetic acid (27 ml.) and concentrated hydrochloric acid (15 ml.) in a sealed tube had been allowed to stand at 100°C for 10 hr., the solvent was evaporated. By treating the residue described above, 2.2 g. of VI and 300 mg. of IV were obtained.

The Treatment of 2, 4, 7-Tribromotropone (XXI) with Hydrochloric Acid.—a) A solution of 2, 4, 7-tribromotropone (500 mg.) in acetic acid (10 ml.) saturated with hydrochloric acid gas was kept in a sealed tube at 100°C for 10 hr. The colorless needles precipitated out by cooling the solution in an ice box were recrystallized from cyclohexane, yielding colorless needles (XXII), m. p. 149—150°C.

Found: C, 32.70; H, 1.25. Calcd. for $C_7H_3OBrCl_2$: C, 32.12; H, 1.91%.

b) A solution of XXI (500 mg.) in a mixture of acetic acid (4 ml.) and concentrated hydrochloric acid (3 ml.) was kept in a sealed tube at 135—140°C for 10 hr. The residue which was obtained by removing the solvent was dissolved in water and extracted with benzene and then with ethyl acetate. The yellow powder obtained from the extract with ethyl acetate was washed with benzene, and the insoluble part (130 mg.) was recrystallized from dilute ethanol giving yellow long prisms, 3-chloro-6-hydroxytropolone

17) T. Nozoe and Y. Kitahara, *Proc. Japan Acad.*, **30**, 214 (1954); Y. Kitahara, *Sci. Repts. Tohoku Univ., I*, **39**, 258 (1956).
18) T. Nozoe, Y. Kitahara, K. Yamane and A. Yoshikoshi, *Proc. Japan Acad.*, **27**, 18 (1951).

*4 All melting points are uncorrected.

(XXIII), m. p. 242°C.

Found: C, 48.71; H, 3.13. Calcd. for $C_7H_5O_3Cl$: C, 48.72; H, 2.92%.

λ_{max}^{MeOH} mμ (log ε): 255(4.47), 340(3.81), 367(3.93).

The residue obtained by removing the solvent from the benzene extract was recrystallized from cyclohexane affording crystals of 3, 6-dichlorotropolone (XXIV), m. p. 129—130°C.

Found: C, 44.26; H, 2.36. Calcd. for $C_7H_4O_2Cl_2$: C, 44.02; H, 2.11%.

λ_{max}^{MeOH} mμ (log ε): 252(4.39), 336(3.98), 377(3.75), 388(3.75), 397^{sh}(3.68), 428(3.31).

The Treatment of XXII with Hydrochloric Acid.—A solution of XXII (500 mg.) in acetic acid (5 ml.) and concentrated hydrochloric acid (3 ml.) was heated around 140°C for 10 hr. in a sealed tube. The solvents were removed under reduced pressure, and the residue was separated into a soluble part (260 mg.) and an insoluble part in benzene. The former was sublimed under reduced pressure to give 114 mg. of sublimate, which was then recrystallized from dilute ethanol to give XXIII, m. p. 240—242°C. The insoluble part in benzene was sublimed in vacuo to afford 30 mg. of the sublimate, which was then recrystallized from methanol, giving XXIV, m. p. 129—130°C. The infrared spectra of both of the compounds were superimposable upon those of XXIII and XXIV respectively, which had been obtained before.

The Reduction of 7-Chloro-4-hydroxytropolone (XXIII).—A solution of XXIII (50 mg.) and sodium acetate (25 mg.) in ethanol (6 ml.) was submitted to catalytic hydrogenation in the presence of 5% Pd-C (20 mg.); 9 ml. of hydrogen was thus absorbed. The residue obtained by removing the solvent was sublimed in vacuo, yielding yellow crystals, m. p. 191—194°C. Recrystallization from acetic acid gave yellow crystals (10 mg.), m. p. 221—223°C, these crystals showed no depression of melting point on admixture with 4-hydroxytropolone (XXV), m. p. 225—226°C, obtained by the alkaline hydrolysis of 3-bromotropolone.[9]

3, 5-Dichlorotropolone. — A solution of 3, 5-dibromotropolone (100 mg.) in acetic acid (4 ml.) and concentrated hydrochloric acid (3 ml.) was refluxed for 10 hr. The solvent was removed, and the residue was recrystallized from benzene-cyclohexane, affording micro needles of 3, 5-dichlorotropolone (XXVI), m. p. 138—139°C.

Found: C, 44.00; H, 2.50. Calcd. for $C_7H_4O_2Cl_2$: C, 44.02; H, 2.11%.

The Reduction of 2-Chloro-5-hydroxytropone (VI).—A solution of VI (100 mg.) and sodium acetate (55 mg.) in methanol (9 ml.) was submitted to catalytic hydrogenation using 5% Pd-C (40 mg.) as a catalyst; 13 ml. of hydrogen was thus absorbed. The removal of the solvent left yellow crystals, which were then sublimed under reduced pressure. The recrystallization of the sublimate from methanol afforded yellow needles (50 mg.), m. p. 210°C (decomp.), which showed no depression of melting point on admixture with authentic 4-hydroxytropone (VII).

5-Acetoxy-2-chlorotropone.—After a solution of 2-chloro-5-hydroxytropone (100 mg.) and acetic anhydride (3 ml.) had been heated at 110°C for one hour, the solution was poured onto ice and extracted with benzene; the extract was dried over sodium sulfate, and the solvent was removed. The residue was recrystallized from cyclohexane, giving 5-acetoxy-2-chlorotropone (80 mg.) as colorless needles, m. p. 101.5—102°C.

Found: C, 54.81; H, 3.34. Calcd. for $C_9H_7O_3Cl$: C, 54.42; H, 3.55%.

5-Benzoyloxy-2-chlorotropone.—To a solution of 2-chloro-5-hydroxytropone (500 mg.) in pyridine (4 ml.), benzoyl chloride (450 mg.) was added, the mixture was then poured onto ice. The crystals (800 mg.) which precipitated out were recrystallized from ethanol to afford 5-benzoyloxy-2-chlorotropone (650 mg.) as colorless needles, m. p. 153—154°C.

Found: C, 64.48; H, 3.31. Calcd. for $C_{14}H_9O_3Cl$: C, 64.50; H, 3.48%.

2-Chloro-5-tosyloxytropone.—To a solution of 2-chloro-5-hydroxytropone (600 mg.) in pyridine (6 ml.), *p*-toluenesulfonyl chloride (740 mg.) was added. After having been allowed to stand at room temperature for 20 min., the solution was poured onto ice to give colorless crystals (680 mg.), m. p. 110—115°C. Recrystallization from ethanol afforded 2-chloro-5-tosyloxytropone (600 mg.) as colorless needles, m. p. 119—120°C.

Found: C, 54.46; H, 3.30. Calcd. for $C_{14}H_{11}O_4SCl$: C, 54.11; H, 3.57%.

The Reaction of VI with Thionyl Chloride.—By gentle refluxing the suspended mixture of VI (100 mg.) in thionyl chloride (2 ml.), VI was gradually dissolved. After 30 min., the excess thionyl chloride was removed in vacuo; the residue was extracted with benzene, and the extract was washed with water and dried. The crystals which were obtained after passing the benzene solution through an alumina column were sublimed and then recrystallized from cyclohexane, yielding pale yellow needles (65 mg.). This crystals showed no depression of melting point on admixture with 2, 5-dichlorotropone.

The Methylation of VI with Diazomethane.—To a suspension of VI (2 g.) in ether (30 ml.), an ethereal solution of diazomethane prepared from *N*-nitrosomethylurea (2 g.) was added; the mixture was then allowed to stand in an ice box for 50 hr. The starting material (700 mg.) was recovered as an insoluble part by filtration, the solvent was removed from the filtrate in vacuo, and the residue was dissolved in ether and passed through an alumina column. From the rapidly-eluted fraction by ether, crystals (1.1 g.), m. p. 85—90°C, were obtained, and recrystallization from cyclohexane afforded colorless plates, m. p. 91—92°C, of 2-chloro-5-methoxytropone (VIII).

Found: C, 56.42; H, 3.99. Calcd. for $C_8H_7O_2Cl$: C, 56.34; H, 4.04%.

λ_{max}^{MeOH} mμ (log ε): 225(4.25), 338(4.13).

From the latter fraction of elution, crystals (50 mg.), m. p. 190—193°C, were obtained. Recrystallization from ethanol gave colorless needles (IX), m. p. 195—196°C.

Found: C, 53.80; H, 3.84; N, 12.24. Calcd. for $C_{10}H_9O_2N_2Cl$: C, 53.47; H, 4.04; N, 12.48%.

5-Hydroxy-2-(*p*-tolylthio)tropone (XIV).—A solution of VI (156 mg.), *p*-thiocresol (152 mg.) and sodium hydroxide (45 mg.) in ethanol (20 ml.) was refluxed for 30 min. A small amount of the precipitate was removed, and the filtrate was evaporated, leaving a yellow solid, which was then washed with water and

recrystallized from methanol, yielding 95 mg. of yellow micro prisms (XIV), m. p. 231—232°C (decomp.).

Found: C, 68.76; H, 4.72. Calcd. for $C_{14}H_{12}O_2S$: C, 68.84; H, 4.95%.

5-Benzoyloxy-2-(*p*-tolylthio)tropone (XV). — A solution of 5-benzoyloxy-2-chlorotropone (245 mg.), *p*-thiocresol (152 mg.) and sodium hydroxide (45 mg.) in ethanol (20 ml.) was refluxed for 10 hr. The solvent was removed, and the residue was dissolved in water, extracted with benzene, and dried. The crystals obtained by removing the benzene were recrystallized from methanol; 150 mg. of greenish yellow plates (XV), m. p. 159—160°C, were thus obtained.

Found: C, 72.59; H, 4.57. Calcd. for $C_{21}H_{16}O_3S$: C, 72.40; H, 4.63%.

5-Amino-2-chlorotropone (X).—a) A solution of 2-chloro-5-methoxytropone (VIII) (100 mg.) in ethanol (20 ml.) saturated with ammonia was allowed to stand at room temperature for 3 days. The removal of the solvent afforded crystals (90 mg.), m. p. 187—190°C, which were then recrystallized from methanol, giving 5-amino-2-chlorotropone (X) as yellow needles, m. p. 204—205°C.

Found: C, 53.75; H, 3.85; N, 9.21. Calcd. for C_7H_6ONCl: C, 54.04; H, 3.89; N, 9.00%.

λ_{max}^{MeOH} mμ (log ε): 230(4.28), 260^{sh}(3.67), 383(4.32).

b) After a mixture of VIII (200 mg.) and liquid ammonia (5 ml.) had been kept at room temperature overnight, the excess ammonia was removed. The residue was dissolved in chloroform, passed through an alumina column, and recrystallization from methanol gave yellow needles (80 mg), m. p. 203—204°C, which showed no depression of melting point on admixture with 5-amino-2-chlorotropone obtained in procedure a).

2-Chloro-5-methylaminotropone (XI). — A solution of VIII (130 mg.) and a 28% aqueous solution of methylamine (0.2 ml.) in methanol (3 ml.) was kept at room temperature for 4 days. The solvent was removed, and the residue was recrystallized from ethanol-ether, giving 2-chloro-5-methylaminotropone (80 mg.) as yellow plates, m. p. 148—149°C.

Found: C, 56.98; H, 4.79; N, 8.20. Calcd. for C_8H_8ONCl: C, 56.65; H, 4.77; N, 8.26%.

λ_{max}^{MeOH} mμ (log ε): 230(4.29), 365(3.75), 390(4.32).

5-Acetamido-2-chlorotropone (XII).—a) After a solution of X (50 mg.) in acetic anhydride (0.5 ml.) had been refluxed for 10 min., the acetic anhydride was removed; the recrystallization of the residue from ethanol afforded XII (50 mg.) as colorless needles, m. p. 210—212°C.

Found: C, 54.56; H, 4.03; N, 7.09. Calcd. for $C_9H_8O_2NCl$: C, 54.70; H, 4.03; N, 7.09%.

λ_{max}^{MeOH} mμ (log ε): 223(4.23); 248(4.15), 269^{sh}(3.91), 350(4.17), 370^{sh}(4.06).

b) After a suspension of 5-acetamido-2-tosyloxytropone (220 mg.) in dioxane (10 ml.) had been saturated with dry hydrogen chloride gas, it was warmed at 80°C for 5 min. The tosyloxytropone had disappeared; it was replaced by colorless crystals. After the reaction mixture had been cooled in an ice box for 2 hr., the precipitate was filtered, affording colorless crystals (120 mg.), which were then recrystallized from ethanol to gave colorless needles, m. p. 210—212°C; these needles showed no depression of melting point on admixture with the sample obtained in procedure a).

5-Acetamido-2-tosyloxytropone (XIII).—To a solution of 5-acetamidotropolone (550 mg.) in pyridine (2.5 ml.), *p*-toluenesulfonyl chloride (1 g.) was added, and the mixture was heated at 80°C for one hour. Water (50 ml.) was added, and the precipitate was filtered, washed with water, and recrystallized from ethanol to give 1.1 g. of XIII as pale yellow micro plates, m. p. 177—178°C.

Found: C, 57.26; H, 4.65; N, 3.90. Calcd. for $C_{16}H_{15}O_5NS$: C, 57.66; H, 4.54; N, 4.20.

λ_{max}^{MeOH} mμ (log ε): 228(4.42), 262^{sh}(4.03), 344(4.16).

Diethyl 2-Amino-5-acetamidoazulene-1, 3-dicarboxylate (XVI).—To a solution of ethyl cyanoacetate (180 mg.) in a sodium ethoxide solution prepared from ethanol (10 ml.) and sodium (20 mg.), XII (140 mg.) was added; the mixture was then kept at room temperature for 3 days. The solvent was removed in vacuo, water was added, and the insoluble part was recrystallized from ethanol, giving yellow crystals (110 mg.), m. p. 178—180°C. This was identified as diethyl 2-amino-5-acetamidoazulene-1, 3-dicarboxylate[16] by a mixed melting point determination and by a comparison of their infrared spectra.

Diethyl 2-Amino-5-benzoyloxyazulene-1, 3-dicarboxylate (XVII).—To a solution of sodium ethoxide prepared from 70 mg. of sodium in anhydrous ethanol (20 ml.), ethyl cyanoacetate (560 mg.) and 5-benzoyloxy-2-chlorotropone (520 mg.) were added. After the mixture had been kept at room temperature for a day, the solvent was removed, water was added, and the solution was extracted with chloroform and then dried. The extract was passed through an alumina column, and 100 mg. of yellow crystals, m. p. 124—127°C, were obtained. Recrystallization from ether gave yellow crystals (XVII), m. p. 129—130°C.

Found: C, 67.65; H, 5.19; N, 2.91. Calcd. for $C_{23}H_{21}O_6N$: C, 67.80; H, 5.20; N, 3.44%.

λ_{max}^{MeOH} mμ (log ε): 245(4.66), 317(4.78), 327(4.88), 370(3.94), 390(3.96), 450(3.44).

When the original water layer was acidified with 2 N sulfuric acid, 180 mg. of a precipitate was obtained. This precipitate was dissolved in methanol and treated with charcoal; yellow crystals, m. p. over 300°C, were thus obtained. The structure of these crystals was not determined.

2-Chloro-5-hydroxy-4-(*p*-tolylazo)tropone (XVIII). — To a stirred solution of VI (156 mg.) and potassium hydroxide (80 mg.) in water (3 ml.), diazotized *p*-toluidine prepared from 118 mg. of *p*-toluidine was added drop by drop. The precipitate was filtered and washed with water, giving 250 mg. of a reddish solid. Recrystallization from benzene-cyclohexane afforded deep red micro needles (XVIII), m. p. 176—177°C.

Found: C, 61.56; H, 3.65; N, 10.45. Calcd. for $C_{14}H_{11}O_2N_2Cl$: C, 61.20; H, 4.04; N, 10.21%.

The Bromination of 2-Chloro-5-hydroxytropone. —To a stirred solution of VI (312 mg.) in acetic acid (8 ml.), bromine (700 mg.) in acetic acid (1 ml.) was added drop by drop at room temperature. The reaction mixture was then allowed to stand overnight, giving 320 mg. of a precipitate. The recrystallization of the precipitate from dilute ethanol afforded pale yellow needles of 2-bromo-4-chloro-5-hydroxytropone (XIX), m. p. 178—179°C.

Found: C, 35.27; H, 2.20; Calcd. for $C_7H_4O_2ClBr$: C, 35.70; H, 1.64%.

The filtrate obtained from the original reaction mixture was evaporated, and the residue was extracted with ethyl acetate. Crystals obtained from the extract were recrystallized from dilute ethanol, affording pale yellow crystals (XX), m. p. 211—212°C.

Found: C, 28.07; H, 1.63. Calcd. for $C_7H_3O_2ClBr_2$: C, 26.72; H, 0.96%.

BULLETIN OF THE CHEMICAL SOCIETY OF JAPAN VOL. 39 1316—1322 (1966)

The Crystal and Molecular Structure of the Dehydrated Tetramer of 1, 2-Dimethyldisilanetetraol, $(CH_3)_8Si_8O_8$

By Taiichi HIGUCHI and Akira SHIMADA

Department of Chemistry, Faculty of Science, Osaka City University, Sumiyoshi-ku, Osaka

(Received November 30, 1965)

The crystal and molecular structure of $(CH_3)_8Si_8O_8$ has been determined by means of the Patterson projections and refined by the two-dimensional Fourier technique and the least-squares method. The space group is $P4/nnc$, with four molecules per unit cell. The unit cell constants are $a=11.73\pm0.02$ Å, and $c=17.17\pm0.02$ Å. The skeleton of a molecule consists of two "crown-shaped" $(-Si-O-)_4$ rings which are crystallographically independent of each other and are connected by four Si–Si bonds along the c axis. The four six-membered $(-Si-Si-O-)_2$ rings thus formed have boat forms. Hence, a molecule forms a cage-like conformation with an approximate symmetry of $4/mmm$. Each molecule in the unit cell is surrounded by four adjacent molecules related with centers of symmetry; these molecules form, in a sense, a layer perpendicular to the c axis.

In structural investigations of cyclic organosilicon compounds, some interesting characteristics have been elucidated.[1-8] Thus, several types of rings have been reported to exist in those compounds containing Si–O, Si–Si, or Si–N bonds. Planar conformations are found in $(-Si-O-)_3$ and $(-Si-N-)_2$ skeletons,[3,7] and the $(-Si-Si-O-)_2$ ring has a chair form close to a plane.[6] As for an eight-membered ring system, the $(Si-O-)_4$ skeleton exists either in a puckered ring of a $\bar{1}$ symmetry[4] or in a "crown-shaped" ring,[5] while $(-Si-N-)_4$ skeletons have "chair" and "cradle" forms.[8] In view of the strain associated with these ring conformations, the valence angle of the oxygen or nitrogen atom with two silicon atoms shows a wide range of variation; the former bond angle especially is reported to be larger than the corresponding angle in common organic compounds.

The dehydrated tetramer of 1, 2-dimethyldisilanetetraol, $(CH_3)_8Si_8O_8$ (I), herein reported on, was isolated by Kumada[9] from acid hydrolyzates of 1, 1, 2, 2-tetraethoxydimethyldisilane, $(C_2H_5O)_2$-$CH_3SiSiCH_3(OC_2H_5)_2$. Purely chemical studies had suggested that this new compound has a cage-like configuration, as is shown in Fig. 1. This

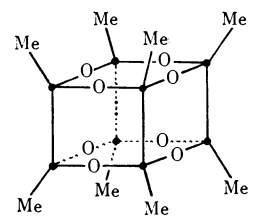

Fig. 1. Dehydrated tetramer of 1,2-dimethyldisilanetetraol, $(CH_3)_8Si_8O_8$.
Me: CH_3, ●: Si.

configuration may be considered to consist of two eight-membered $(-Si-O-)_4$ rings and four six-membered $(-Si-Si-O-)_2$ rings. In this respect, this molecule may be closely related to bistetramethyldisilanylenedioxide, $((CH_3)_4Si_2O)_2$,[6] and octa-(methylsilsesquioxane), $(CH_3SiO_{1.5})_8$ (III),[5] the molecular structures of which have already been established, by X-ray analyses, to be shown in Figs. 2(a) and (b).

The present X-ray work was undertaken to confirm this molecular configuration, with the

1) L. K. Frevel and M. J. Hunter, *J. Am. Chem. Soc.*, **67**, 2275 (1945).
2) W. L. Roth and D. Harker, *Acta Cryst.*, **1**, 34 (1948).
3) G. Peyronel, *Chim. Industr.*, **36**, 441 (1954).
4) H. Steinfink, B. Post and I. Fankuchen, *Acta Cryst.*, **8**, 430 (1956).
5) K. Larrson, *Ark. Kemi*, **16**, 203 (1960).
6) T. Takano, N. Kasai and M. Kakudo, This Bulletin, **36**, 585 (1963).
7) P. J. Wheatley, *J. Chem. Soc.*, **1962**, 1721.
8) G. S. Smith and L. E. Alexander, *Acta Cryst.*, **16**, 1015 (1963).
9) M. Kumada, M. Ishikawa and B. Murai, *J. Chem. Soc. Japan, Ind. Chem. Sect. (Kogyo Kagaku Zasshi)*, **66**, 37 (1963).

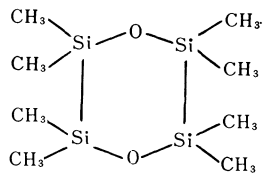

Fig. 2 (a). Bistetramethyldisilanilene-dioxide, $((CH_3)_4Si_2O)_2$.

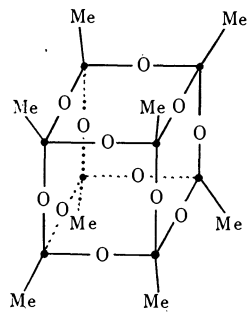

Fig. 2 (b). Octa-(methylsilsesquioxane), $(CH_3SiO_{1.5})_8$.
Me: CH_3, ●: Si.

hope that such information will contribute to the structural chemistry of organosilicon compounds in connection with the various problems mentioned above. The structural information regarding the silicon-oxygen configuration obtained by this work will also be useful in discussing the course of polymerization reactions and the conditions under which linear polymers can be terminated by ring formation.[10]

Experimental

The specimens were kindly prepared and supplied by Professor Makoto Kumada of Kyoto University.[9] They are soluble in most organic solvents and are recrystallized several times from the solution in chloroform. The crystals thus obtained were colorless cubes. They were decomposed so quickly because of the moisture that they were sealed into thin-walled glass capillary tubes.

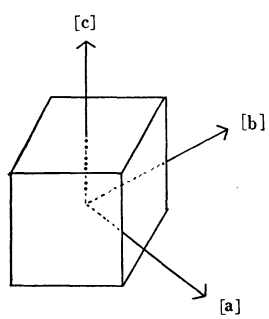

Fig. 3. The relation of principal axes to the crystal form.

Oscillation and Weissenberg photographs were taken with Cu$K\alpha$ radiation. These photographs indicate that the crystal has the Laue symmetry, $4/mmm$, and that the unit cell dimensions are $a=11.73\pm0.02$ Å and $c=17.17\pm0.02$ Å. The relation of principal axes to the crystal form is shown in Fig. 3.

There are four molecules per unit cell. The physical constants are found to be as follows: m. p. 320°C, mol. wt.=473.0, $D_{obs}=1.30$ g. cm^{-3}, and $D_{calcd}=1.33$g. cm^{-3}. The following types of reflections were systematically absent: $(hk0)$ with $h+k$ odd, $(h0l)$ with $h+l$ odd, and (hhl) with l odd. The corresponding space group is $P4/nnc$. The time of exposure was limited because of the decomposition of crystals, and it was very difficult to obtain three-dimensional intensity data. The equatorial and 1st-layer Weissenberg photographs around the b- and c-axes were taken by the multiple-film technique. The relative intensities of the reflections were measured by a visual comparison with calibrated intensity strips. The usual Lorentz and polarization corrections were applied to the measured intensities. No correction was made for absorption (the linear absorption coefficient for Cu$K\alpha$ radiation, $\mu=46.5$ cm^{-1}). The observed structure factors were brought to an absolute scale, primarily by means of Wilson's method.[11]

Structure Determination

Since the unit cell contains four molecules, the centers of the four molecules in each unit cell are located at fourfold positions; three sets of these positions are listed for the $P4/nnc$ space group, with reference to the origin at $\bar{1}$, in the *International Tables for X-ray Crystallography*. Positions $4(c)$ and $4(d)$ seem to be unwise choices, since they require that the centers of adjacent molecules be separated by half a length of the c axis, but no trains of peaks perpendicular to the c axis exist near at $U=0$ and $W=1/2$ of the Patterson map $P(UW)$. The $4(e)$ position, on the other hand, is suitable for the packing of molecules and it seems to explain the Patterson peaks; therefore, it was chosen for the center of a molecule. In this position the center of a molecule lies at the fourfold axis. The asymmetric unit consists of a quarter of one molecule, namely, two silicon atoms, two oxygen atoms and two methyl groups. Hence, eighteen parameters must be determined in this analysis, hydrogen atoms not being considered.

The first clue to the structure determination was obtained from the Patterson function, $P(UV)$, onto the (001) plane, which showed interatomic vectors between oxygen and silicon atoms as well as between silicon atoms. These vector peaks were easily interpreted with the aid of the fact that the molecule has a fourfold symmetry with conventional bond distances. These approximate positions of the $(-Si-O-)_8$ skeleton gave a fairly

10) E. J. Lawton, W. T. Grubb and J. S. Balwit, *J. Polymer Sci.*, **19**, 455 (1956).

11) A. J. C. Wilson, *Nature*, **150**, 152 (1942).

good agreement between calculated and observed structure factors.

The electron-density projection along c axis was then synthesized. It revealed the positions of four sets of silicon and oxygen atoms which are related by a fourfold axis and form squares respectively. Two methyl groups could also be found in the second electron-density projection. However, the heavy overlapping of all silicon and oxygen atoms prevented us from proceeding with a further refinement of this projection. A Patterson projection along the b axis gave some information about the z parameters of silicon and oxygen atoms, and the electron-density projection along the b axis was computed. This electron-density map along the b axis, together with the aid of the projection along the c axis, was sufficient to give all of the atomic positions except those of hydrogen atoms. The coordinates of the atoms were then refined by trial and error method, and later by successive Fourier syntheses. After these procedures, the (F_o-F_c) syntheses were applied in order to refine the coordinates and temperature factors further. At this stage of the structure determination, the reliability factors for $(hk0)$

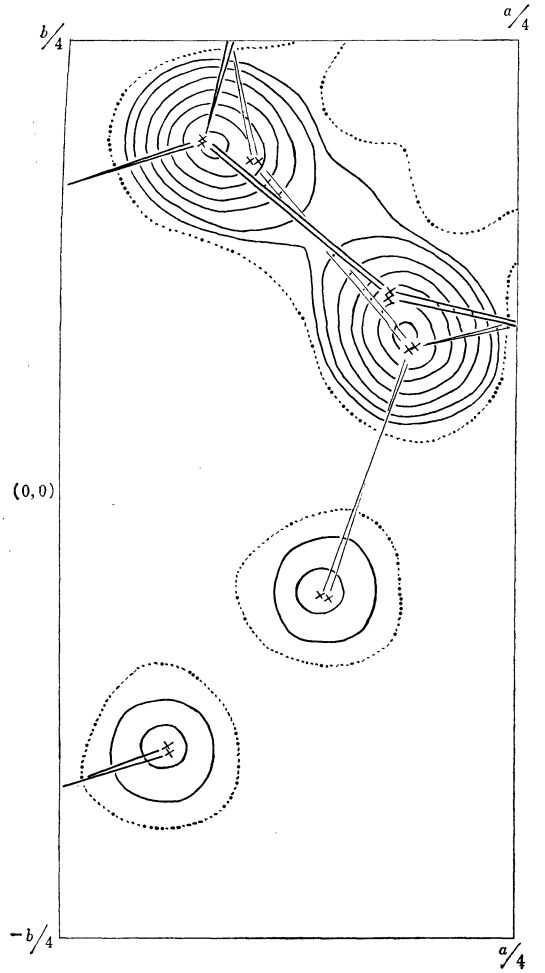

Fig. 4. Electron density projected on the (001). Contours at intervals of 4e. Å^{-2} start with 2e. Å^{-2} contour (broken line), the interval being 10e. Å^{-2} after 10e. Å^{-2}.

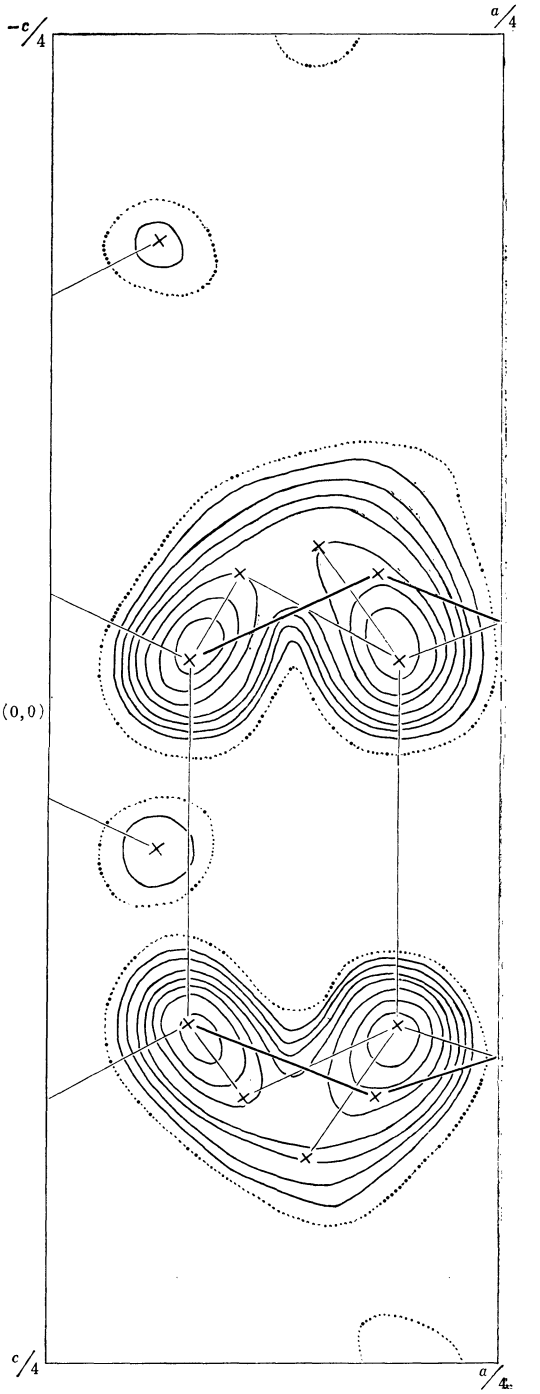

Fig. 5. Electron density projected on the (010). Contours at intervals of 2e. Å^{-2} start with 2e. Å^{-2} contour (broken line), the interval being 4e. Å^{-2} after 10e. Å^{-2}.

TABLE I. ATOMIC PARAMETERS.

σ value in parenthesis.

	x	y	z	B (Å^2)
Si(1)	0.1914 (0.0009)	0.0767 (0.0010)	−0.0132 (0.0006)	2.54 (0.34)
Si(2)	0.1930 (0.0009)	0.0778 (0.0009)	0.1242 (0.0006)	2.60 (0.35)
O(1)	0.3202 (0.0023)	0.1039 (0.0027)	−0.0432 (0.0013)	2.83 (0.54)
O(2)	0.3196 (0.0019)	0.1083 (0.0022)	0.1509 (0.0012)	2.16 (0.48)
C(1)	0.1470 (0.0048)	−0.0596 (0.0041)	−0.0568 (0.0018)	3.97 (1.13)
C(2)	0.1438 (0.0049)	−0.0598 (0.0041)	0.1740 (0.0021)	4.05 (1.00)

TABLE II. OBSERVED AND CALCULATED STRUCTURE FACTORS

h	k	l	F_o	F_c	h	k	l	F_o	F_c	h	k	l	F_o	F_c	h	k	l	F_o	F_c
0	2	0	67	43	12	6	0	25	26	* 3	0	11	6	18	8	0	4	13	2
	4		202	180		8		18	15			13	42	40			6	60	66
	6		33	32	13	1		25	26	*		15	6	15			8	101	106
	8		197	187		3		21	15	*		17	6	2			10	28	30
	10		73	83		5		11	10	*		19	6	4			12	22	23
	12		31	33	*	7		4	1		4	0 2	39	45	*		14	6	12
	14		6	1	14	2		25	21			4	12	19			16	28	40
1	1	0	276	268		4		16	18			6	34	50	9	0	1	53	52
2	2		212	210	0	0	2	267	291	*		8	5	5			3	31	39
3	1		126	131	*		4	3	60			10	54	45			5	92	94
	3		225	212			6	196	220	*		12	6	10			7	95	99
4	2		64	58			8	173	136	*		14	6	1	*		9	6	3
*	4		5	7			10	84	54	*		16	6	2	*		11	6	13
* 5	1		4	8			12	34	55	*		18	6	5			13	57	77
	3		92	79	*		14	6	17	*		20	6	6			15	48	52
	5		45	31			16	54	59		5	0 1	18	25	10	0	2	34	40
6	2		194	182			18	16	22			3	69	64	*		4	6	9
	4		64	50			20	19	19			5	91	81			6	26	34
	6		164	161	1	0	1	132	155			7	36	29			8	58	66
7	1		21	11			3	77	9	*		9	6	3	*		10	6	4
	3		148	138			5	303	292	*		11	6	11			12	15	20
	5		82	75			7	145	153			13	42	50	*		14	6	10
	7		92	90			9	26	6			15	36	38	*11	0	1	6	7
8	2		16	10			11	19	38	*		17	6	5	*		3	6	3
	4		75	64			13	98	80	*		19	5	3	*		5	6	14
	6		61	55			15	34	44		6	0 2	17	19	*		7	6	4
	8		64	48			17	6	6	*		4	5	0	*		9	6	5
9	1		146	137	*		19	6	7			6	13	11	*		11	6	6
	3		80	73			21	18	26			8	35	35	*		13	5	6
	5		42	36	2	0	2	7	24			10	15	20	12	0	2	14	19
	7		36	26			4	33	8	*		12	6	7	*		4	6	2
	9		97	95	*		6	3	18	*		14	6	2	*		6	6	12
*10	2		7	7			8	40	33	*		16	6	15			8	20	20
	4		20	22			10	13	7	*		18	5	1	*		10	5	4
	6		38	30	*		12	6	11		7	0 1	20	13	*		12	5	6
	8		49	42	*		14	6	6			3	11	16	*13	0	1	6	7
	10		20	25	*		16	6	2			5	17	22	*		3	6	7
*11	1		7	1	*		18	6	3			7	39	35			5	19	24
	3		71	61	*		20	5	1	*		9	6	1	*		7	5	7
	5		26	20	3	0	1	41	37	*		11	6	3	*		9	5	1
	7		21	18			3	34	21			13	18	30	*14	0	2	5	4
	9		14	3			5	77	72			15	16	24	*		4	5	4
12	2		43	39			7	58	59	*		17	6	5	*		6	4	2
*	4		7	5	*		9	5	3		8	0 2	94	88					

The value of index followed by an asterisk indicates reflection below the observable limit. The value of F_o in this case is minimumum observed value.

and ($h0l$) reflections were found to be 12.9% and 22.8% respectively, the isotropic temperature factors being $B_C=3.5$, $B_O=3.5$ and $B_{Si}=3.0$ for carbon, oxygen and silicon atoms.

The least-squares method was applied in the next stage of the refinement. After nine cycles of the refinement of the positional and isotropic temperature factor parameters, the reliability factors for the final parameters dropped to 14.0%, with only observed reflections. The value of F_o listed for the unobserved reflections (marked with an asterisk in Table II) is $F_{min}/2$; this value was used in the least-squares refinements. The calculations of the structure factors were made with an IBM 1401 computer. The least-squares refinements were carried out with the program written by Mr. Noritake Yasuoka[12] for an OKITAC-5090D electronic computer. In these calculations, the Hartree-Fock atomic scattering curves were used for carbon and oxygen atoms, and Slater's curve for silicon atoms, the contribution of hydrogen atoms being disregarded. The final atomic coordinates and isotropic temperature factors are listed in Table I. The final electron-density maps along the c and b axes are shown in Figs. 4 and 5, where the final positions of atoms are marked with crosses. The observed and calculated structure factors are given in Table II.

Results and Discussion

Some intersesting results were revealed in this structural work, although the poor experimental data resulting from the decomposition of crystals and the exclusion of many hydrogen atoms in the calculation of structure factors might not permit us to discuss the details of structural features. The conformation of a molecule and the molecular arrangement in the crystal, together with intermolecular distances, may be seen in Figs. 6 and 7, which represent the c and b axes projections for this crystal. Table III lists the independent bond lengths, the bond angles and the non-bonded interatomic distances in a molecule. Table IV compares the bond lengths and angles found in this analysis with those found in the related compounds.

TABLE III. BOND LENGTHS, BOND ANGLES AND NON-BONDED INTERATOMIC DISTANCES IN A MOLECULE

Bond lengths, Å

Si(1)	Si(2)	2.36	Si(2)	O(2‴)	1.63
Si(1)	O(1)	1.63	Si(1)	C(1)	1.84
Si(1)	O(1‴)	1.67	Si(2)	C(2)	1.92
Si(2)	O(2)	1.60			

Non-bonded interatomic distances, Å

Si(1)	Si(1′)	3.04	O(2)	O(2′)	2.62
Si(2)	Si(2′)	3.01	O(1)	O(1″)	3.80
Si(1)	Si(1″)	4.29	O(2)	O(2″)	3.70
Si(2)	Si(2″)	4.26	O(1)	O(2′)	3.33
O(1)	O(1′)	2.69			

Bond angles (°)

Si(2)	Si(1)	O(1)	107.9	O(2)	Si(2)	O(2‴)	108.8
Si(2)	Si(1)	O(1‴)	108.0	C(1)	Si(1)	Si(2)	114.4
Si(1)	Si(2)	O(2)	107.2	C(2)	Si(2)	Si(1)	116.1
Si(1)	Si(2)	O(2‴)	106.3	C(1)	Si(1)	O(1)	107.7
Si(1)	O(1)	Si(1′)	134.1	C(1)	Si(1)	O(1‴)	109.3
Si(2)	O(2)	Si(2′)	138.2	C(2)	Si(2)	O(2)	110.0
O(1)	Si(1)	O(1‴)	109.4	C(2)	Si(2)	O(2‴)	108.3

The skeleton of a molecule consists of two eight-membered $(-Si-O-)_4$ rings which are crystallographically independent of each other and which are connected by four Si-Si bonds along the c axis. Hence, the molecule forms a cage-like conformation with the approximate symmetry of $4/mmm$ predicted by chemical grounds. Two sets of four silicon atoms which are related by a fourfold axis form two square planes (3.04 Å × 3.04 Å, 3.01 Å × 3.01 Å) perpendicular to the c axis. Similarly, two sets of four oxygen atoms form two square planes, the sides of which are 2.69 Å and 2.62 Å. All of these planes are parallel to one another. The distance between two "silicon-square planes" is 2.36Å, while that between two "oxygen-square planes" is 3.33Å. The distances between the silicon-square plane and the oxygen-square plane are 0.52Å and 0.46Å respectively. Consequently, each of two $(-Si-O-)_4$ rings form a "crown-shaped" eight-membered ring. In this respect, the conformation of these rings is similar to that in octa-(methylsilsesquioxane) (III),[5] although the corresponding interplanar distance is 0.34Å in the latter. However, it differs from that in octamethylcyclotetrasiloxane (IV),[4] the puckered ring of $\bar{1}$ symmetry with a dihedral angle of 150° between the silicon- and oxygen-planes.

On the other hand, a set of the other four silicon atoms, Si(1), Si(1′), Si(2′) and Si(2), forms a plane approximately parallel to the c axis, and the best least-squares plane A, calculated by the program of Mr. Tsunehiro Takano for a NEAC 2101 computer, has the following equation:

$$0.4986x - y + 0.0061z - 0.2237 = 0$$

Table V shows the deviation of atoms from this plane, the individual atoms lying out of the plane by only insignificant amounts. The equation of a plane B through the Si(1), O(1), and Si(1′) atoms is:

$$0.4946x - y + 0.8315z - 0.0224 = 0$$

while that of a plane C through the Si(2), O(2), and Si(2′) atoms is:

12) N. Yasuoka and T. Mitsui, *Bull. Osaka Ind. Research Inst.*, **16**, 37 (1960).

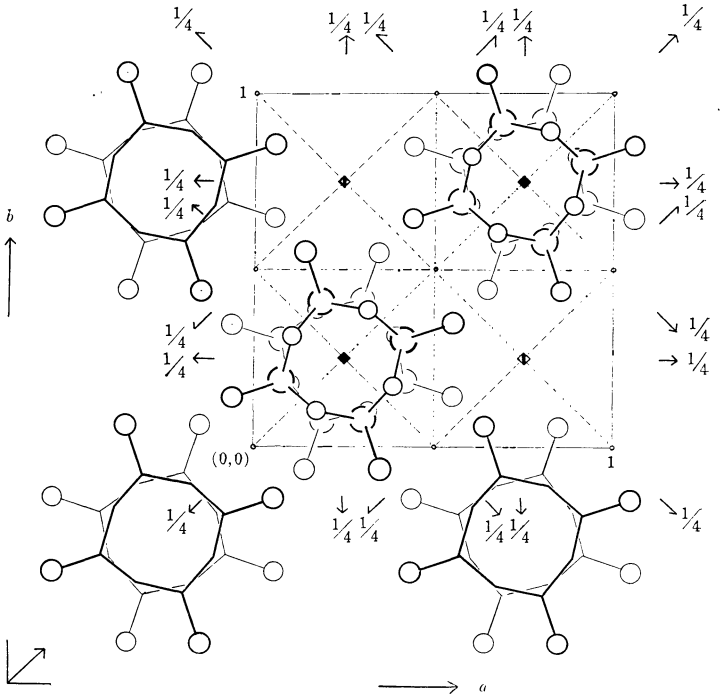

Fig. 6. Arrangement of the molecules projected on the (001).

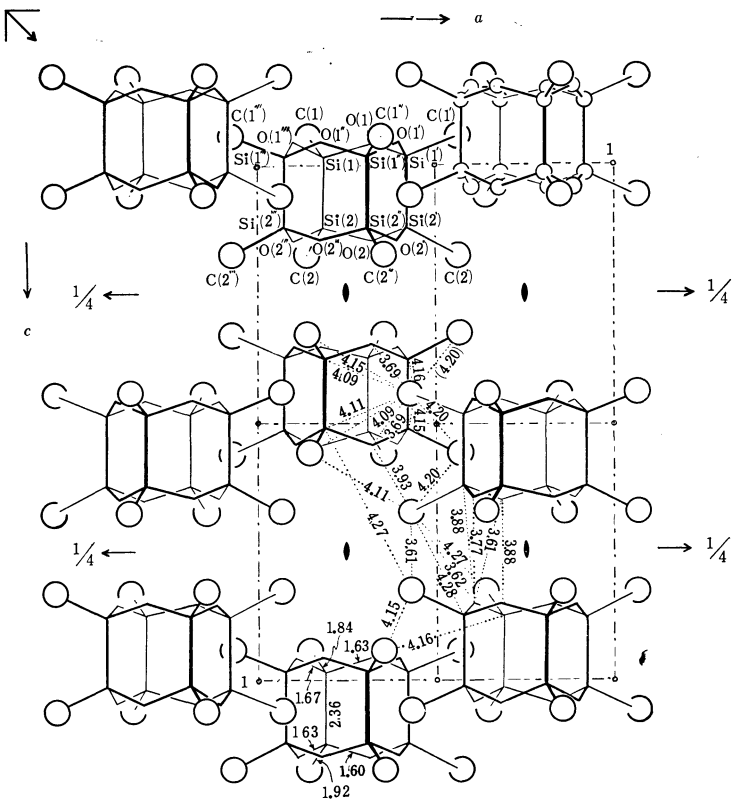

Fig. 7. Arrangement of the molecules projected on the (010).

TABLE IV. BOND LENGTHS AND ANGLES

Molecule		Si-Si	Si-O	Si-C	Si-O-Si	O-Si-O	C-Si-C	O-Si-Si
$(CH_3)_8Si_8O_8$	Dehydrated tetramer of 1,2-dimethyldisilanetetraol	2.36	1.63	1.88	136	109	—	107
$(CH_3)_8Si_5O_6$	Spirosiloxane	—	1.64	1.88	130	106	106	—
$[(CH_3)_2SiO]_3$	Hexamethylcyclotrisiloxane	—	1.614	1.929	136	104	106	—
$[(CH_3]_2SiO]_4$	Octamethylcyclotetrasiloxane	—	1.65	1.92	142.5	109	106	—
$(CH_3SiO_{1.5})_8$	Octa-(methylsilsesquioxane)	—	1.61	1.90	145	111	—	—
$[(CH_3)_4Si_2O]_2$	Bistetramethyldi-silanylenedioxide	2.35	1.61	1.88	143	—	108	109
$[(CH_3)_3NSi(CH_3)_2]_2$	Tetramethyl-*N*,*N'*-bistri-methylsilylcyclodisilazane	—	—	1.876	—	—	107	—
$[(CH_3)_2SiNH]_4$	Octamethylcyclotetrasilazane	—	—	1.88	—	—	111	—

TABLE V. DEVIATION OF ATOMS FROM THE BEST PLANE (Si(1), Si(1'), Si(2'), Si(2))

Atom	Deviation, Å	Atom	Deviation, Å
Si(1)	−0.005	Si(2')	−0.005
Si(1')	0.005	O(1)	0.381
Si(2)	0.005	O(2)	0.350

$$0.5026x - y - 0.8479z + 1.5828 = 0$$

The dihedral angle between the two planes, A and B, is 144°, while that between the two planes, A and C, is 143°. Thus, the skeleton of the ring, Si(1), O(1), Si(1'), Si(2'), O(2) and Si(2), has a boat form, whereas the ring in compound II has a chair form, with a dihedral angle of 170°. The adoption of a crown-shaped conformation by eight-membered rings would necessitate these four six-membered rings having boat forms.

The Si-Si bond distance, 2.36Å, in the molecule is almost the same as the 2.34Å and 2.35Å distances found in metallic silicon and II. The differences in non-equivalent Si-O distances, Si-C distances and Si-O-Si bond angle would probably not be significant, the mean values being 1.63Å, 1.88Å and 136°. The mean Si-O bond lengths agree well with those reported by other investigators.[1-6] The mean Si-C distance agrees with those found for II and spirosiloxane.[2] The bond distances calculated from the sum of covalent radii with electronegativity[13] corrections are Si-O=1.76Å and Si-C=1.88Å; the latter value is in good agreement with those found here, although the deviations of the Si-C bond lengths from the everage bond length are not small. The Si-O-Si bond angles are significantly smaller than those of II, III and IV, but they are the same as that in hexamethylcyclotrisiloxane. The corresponding angle in the spirosiloxane is 130°. The Si-N-Si angle of octamethylcyclotetrasilazane is 132°.[8] These shorter bond lengths and the larger bond angles around the oxygen atoms might confirm that the Si-O-Si configuration is more flexible than the corresponding one in carbon compounds, probably due to the existence of an ionic character and the contribution of the *d*-orbital to Si-O bonds. The bond angles around the silicon atoms are almost tetrahedral.

Each molecule in the unit cell is surrounded by four adjacent molecules related by centers of symmetry; these molecules form, in a sense, a layer perpendicular to the *c* axis. They are held together in such a way that a methyl group on one silicon atom is located just upon the six-membered ring of an adjacent molecule. This molecular arrangement in a layer might suggest polar interaction between the methyl group and the oxygen atom. Each layer seems to be held together along the *c* axis by only van der Waals forces; this mode of molecular packing in the crystal is in good agreement with the fact that this crystal has a cleavage perpendicular to the *c* axis.

The authors wish to express their gratitude to Professor Makoto Kumada and Dr. Mitsuo Ishikawa of Kyoto University for kindly supplying the samples for this study, to Mr. Noritake Yasuoka of the Osaka Industrial Research Institute and Dr. Tsunehiro Takano of Osaka University for their programs of electronic computer calculation, and to the Oki Electric Industry Co., Ltd., for the use of their electronic computer. The present study was partly supported by a scientific research grant from the Ministry of Education.

13) V. Schomaker and D. P. Stevenson, *J. Am. Chem. Soc.*, **63**, 37 (1941).

BULLETIN OF THE CHEMICAL SOCIETY OF JAPAN VOL. 39 1323—1326 (1966)

The Studies of the Cage Effect of Solvents. VI. The Photolysis of Methylazoethane in *n*-Heptane

By Shin'ichi FUJITA, Sukeya KODAMA and Osamu TOYAMA

Department of Applied Chemistry, College of Engineering, University of Osaka Prefecture, Sakai, Osaka

(Received December 8, 1965)

Methylazoethane was photolyzed in *n*-heptane in order to study the effect of a solvent cage quantitatively; the results obtained were then compared with those for azomethane and azoethane previously studied. By using styrene as a scavenger for radicals, it was demonstrated that a large fraction (90% at −75°C and 58% at 100°C) of a pair of methyl and ethyl radicals formed by the decomposition of a molecule of methylazoethane combines to form propane or disproportionates to form methane and ethylene in an original solvent cage. The ratio of the rate constant for the disproportionation to that for the combination is small, and it decreases with a rise in the temperature, as was previously found for azoethane. The effect of the temperature on the yields of the products of cage reactions in the present work and in the previous work with azomethane and azoethane shows that the combination of ethyl radicals and the cross-combination of methyl and ethyl radicals in a solution require appreciable activation energies, even if that for the combination of methyl radicals is zero.

The photolysis of methylazoethane in a solution yields a pair of methyl and ethyl radicals in a solvent cage. The ratios of their subsequent combination and disproportionation have recently been investigated by Szwarc and his co-workers.[1] In the present work, the photolysis of the same substrate in *n*-heptane has been studied in order to elucidate the general kinetics, including the cage reactions mentioned above, and in order to compare the results with those previously obtained for azomethane[2] and azoethane[3].

Experimental

Materials.—Methylazoethane was prepared by the thermal decomposition of the methylazoethane-cuprous chloride which had been obtained by the ethylation and oxidation of methylhydrazine sulfate,[4] in a way similar to that used for azomethane.[5] Since the prepared gas was about 2% azomethane, it was purified by a gas chromatographycal method with a column of dimethylformamide on activated alumina and was stored in a dark-colored reservoir. It was further purified before each use by condensation and evacuation at −140°C.

There has to date been no report on the properties of methylazoethane. We have now determined a few of them. The plot of the logarithmic vapor pressure vs. $1/T$ gives a good linear relation in the range from −48 to 20°C and is represented by $\log P = 7.78 - 1487/T$ The normal boiling point is calculated as 30.3°C from the equation. The molecular extinction coefficient,

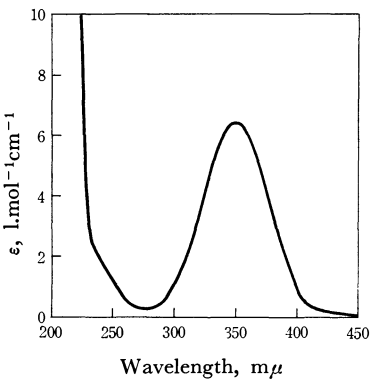

Fig. 1. Absorption spectrum of methylazoethane vapor at 29°C.

calculated from $\log(I/I_0) = -\varepsilon cd$ and with the optical densities determined in the gas phase, is illustrated in Fig. 1. The value for the absorption maximum situated at 352 mμ is 6.44 l. mol^{-1} cm^{-1}.

In this work *n*-heptane was used as the solvent for the reasons described in a previous paper[3] for azoethane, and styrene was used as the scavenger for radicals. They were taken from commercial samples which had been found to be gas chromatographically pure, and were subjected before use to thrice-repeated bulb-to-bulb distillation using a dry ice - acetone bath.

Procedure.—The apparatus was similar to that used for azomethane and previously described.[2] The reaction cells were glass cylinders about 3.6 cm. in diameter, 1.0 cm. long and about 10 cc. in volume. The full arc from a high-pressure mercury lamp, Mazda

1) P. S. Dixon, A. P. Stefani and M. Szwarc, *J. Am. Chem. Soc.*, **85**, 3344 (1963).
2) S. Kodama, This Bulletin, **35**, 652, 658, 824, 827 (1962).
3) S. Kodama, S. Fujita, J. Takeishi and O. Toyama, ibid., **39**, 1009 (1966).
4) H. H. Hatt, "Organic Syntheses," Coll. Vol. II, 395 (1943).
5) Ibid., Coll. Vol. II, 208 (1943); O. Diels and W. Koll, *Ann.*, **443** 262 (1925); F. P. Jahn, *J. Am. Chem. Soc.*, **59**, 1761 (1937).

TABLE I. PHOTOLYSIS IN THE ABSENCE OF STYRENE AT 0°C

Time min.	Rate of formation $\times 10^{11}$ mol. cc^{-1} sec^{-1}					CH_4/N_2 %	C_2H_6/N_2 %	C_2H_4/N_2 %	C_3H_8/N_2 %	$(C_2H_4+C_3H_8)/N_2$ %	$(CH_4+C_3H_8)/N_2$ %	$(C_2H_6+C_2H_4+C_3H_8)/N_2$ %
	N_2	CH_4	C_2H_6	C_2H_4	C_3H_8							
75[a]	22.2	5.21	2.68	0.855	15.85	23.6	12.1	3.9	71.7	75.6	95.3	87.7
195[a]	8.45	2.23	1.19	0.350	6.00	26.4	14.1	4.2	71.0	75.2	97.4	89.3
240[b]	15.50	3.94	2.04	0.610	10.80	24.6	13.2	3.9	69.4	78.3	93.5	86.5
280[b]	6.05	1.52	0.80	0.253	4.30	25.1	13.3	4.2	71.2	75.4	96.3	88.7

a) Without filter b) With filter

TABLE II. PHOTOLYSIS IN THE PRESENCE OF STYRENE

Temp. °C	CH_4/N_2 %	C_2H_4/N_2 %	C_3H_8/N_2 %	$(C_2H_4+C_3H_8)/N_2$ %	C_2H_4/C_3H_8 %
−75	5.55±0.30	6.00	83.5	89.5	7.2
−50	4.77±0.24	5.20±0.14	80.70±0.34	85.90	6.5
−25	4.40±0.27	4.5	76.70±0.34	81.20	5.9
0	3.67±0.12	4.03±0.09	72.90±0.20	76.93	5.5
25	3.65±0.24	3.70±0	68.9	72.60	5.4
50	3.87±0.19	—	—	—	—
75	4.15±0.10	2.70±0.14	60.5 ±1.0	63.2	4.5
100	4.55±0.24	2.50±0	55.30±0.41	57.80	4.5

TABLE III. COMPARISON OF THE THREE AZO-COMPOUNDS

Radical source	A_6/A_4	A_6/A_5	A_5/A_4	E_6-E_4	E_6-E_5	E_5-E_4
				cal./mol.		
Azomethane	4.32			1520		
Methylazoethane	3.86	134	0.026	1360	1760	−400
Azoethane	3.40	39.0	0.087	1050	1420	−370

SHL-100UV, was used for the photolysis in most experiments. The effective wavelength range seems to be restricted to 300—400 mμ, judging from the light absorption by methylazoethane and the transmission through the cell. In order to check the effect of the wavelength, a few experiments were carried out with a UV-Dl filter which transmits only the 366 mμ line. The extent of photolytic conversion in each run was usually about 5%. After the required time of irradiation, the reaction cell was opened to the analytical system, which consisted of traps set at −145°C and −210°C. The products of the photolysis were nitrogen, methane, ethane, ethylene and propane. After the gaseous components had been separated from the solution by thrice-repeated bulb-to-bulb distillation and by an autodistillation vessel[6] at the dry ice - acetone temperature, methylazoethane was condensed at −145°C and ethane, ethylene and propane were trapped at −210°C. Noncondensable products, nitrogen and methane, were introduced into a Toepler guage and the volume of the mixture was determined. Each component was further analyzed by a gas chromatograph with a 2 m. silica gel column. The fraction trapped at −210°C was dealt with similarly. The column used for it was a series consisting of 2 m. of activated alumina with 2% squalane and 2 m. of ethylene glycol saturated with silver nitrate on celite at room temperature.

Results

Table I shows the results of photolysis in the absence of styrene at 0°C. As will be shown below, $(C_2H_4+C_3H_8)/N_2$ is a measure of the cage effect, and $(CH_4+C_3H_8)/N_2$ and $(C_2H_6+C_2H_4+C_3H_8)/N_2$ represent the material balances with reference to methyl and ethyl radicals respectively. It may be seen in the table that the irradiation of filtered light (366 mμ) produces little change in the yields of gaseous products, as would be expected from the effective wavelength range for the unfiltered light mentioned above. Table I further shows that the variation in light intensity or in the rate of nitrogen formation is almost without effect on the relative yields of gaseous products.

Table II shows the effect of the temperature in

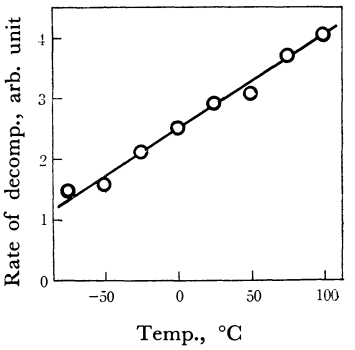

Fig. 2. Dependence of the decomposition rate on temperature.

6) J. Smid, A. Rembaum and M. Szwarc, *J. Am. Chem. Soc.*, **78**, 3315 (1956).

the presence of styrene. The ethane yields were found to be negligible in this case; in the two runs carried out at −75 and 100°C, they were 0.21 and 0.48% respectively. The formation of butane was negligible even in the absence of styrene. Figure 2 shows the effect of the temperature on the rate of photolysis; this effect may be taken as reflecting the dependence of the quantum yield on the temperature, although the latter quantity was not measured in this work.

Discussion

Mechanism.—A comparison of the results obtained in this work with those previously obtained for azomethane[2] and azoethane[3] suggests that the following reaction scheme is probable for the present photolysis:

$$CH_3N_2C_2H_5 + h\nu \rightarrow CH_3N_2C_2H_5^* \quad (1)$$

$$CH_3N_2C_2H_5^* + M \rightarrow CH_3N_2C_2H_5 + M \quad (2)$$

$$CH_3N_2C_2H_5^* \rightarrow [CH_3 + N_2 + C_2H_5] \quad (3)$$

$$[CH_3 + N_2 + C_2H_5] \rightarrow C_3H_8 + N_2 \quad (4)$$

$$\rightarrow CH_4 + C_2H_4 + N_2 \quad (5)$$

$$\rightarrow CH_3 + N_2 + C_2H_5 \quad (6)$$

$$CH_3 + RH \rightarrow CH_4 + R \quad (7)$$

$$C_2H_5 + RH \rightarrow C_2H_6 + R \quad (8)$$

$$CH_3 \text{ (or } C_2H_5) + CH_3N_2C_2H_5 \rightarrow \text{addition products} \quad (9)$$

$$CH_3 \text{ (or } C_2H_5) + R \rightarrow CH_3R \text{ or } (C_2H_5R) \quad (10)$$

Reaction 1 represents the formation of excited molecules of the substrate by light absorption; reaction 2, their deactivation by solvent molecules, and reaction 3, the formation of a pair of methyl and ethyl radicals in a solvent cage by the decomposition of the excited molecule. Reactions 4 and 5 are, respectively, the combination and disproportionation of such a pair of radicals in the original solvent cage, while reaction 6 represents the separation of these radicals by diffusion prior to their combination or disproportionation. The remaining reactions are those for the methyl and ethyl radicals thus separated.

Figure 2 shows that the quantum yield of the photolysis falls off with a lowering of the temperature. Such a behavior is similar to that found for azoethane[3] and may be accounted for by reactions 2 and 3, provided that the latter reaction requires an appreciable activation energy.

A comparison between Tables I and II shows that the yields of propane and ethylene are not affected by the presence of styrene, and that, consequently, these gaseous products are formed only by cage reactions 4 and 5. The sum of relative yields, $(C_3H_8+C_2H_4)/N_2$, thus gives the fraction of the radicals that react in the solvent cage in reactions 4 and 5. Table II shows that this fraction is nearly 90% at −75°C, but that it falls to about 60% at 100°C, indicating that the escape of radicals from the solvent cage by diffusion is favored at elevated temperatures.

In the presence of a sufficient concentration of styrene, the reaction scheme given above requires that methane be formed solely by reaction 5, and that, consequently, the yield of methane equal that of ethylene. Table II shows that these yields are in fact nearly equal to each other at low temperatures, while above room temperature there is a substantial difference between them. This presumably indicates that, at high temperatures, a part of the methane comes from the hydrogen atom abstraction by the methyl radical from the solvent molecule constituting the cage.

A comparison between Tables I and II further shows that the yield of methane was reduced by the addition of from 25% to 4% of styrene at 0°C. Similarly, the yield of ethane was reduced from 13% to a negligibly small value at 0°C. These observations may be explained by reactions 7 and 8. As may be seen from the figures given above, the yield of methane in reaction 7 is higher than that of ethane in reaction 8. Consequently, the material balance for methyl radicals as represented by $(CH_4+C_3H_8)/N_2$ is higher than that for ethyl radicals, $(C_2H_6+C_2H_4+C_3H_8)/N_2$ (Table I). These findings probably reflect the lesser ability of ethyl radicals to abstract hydrogen atoms from solvent molecules; this fact was previously inferred from the results of the photolysis of azoethane in solution.

The losses in the material balances for methyl and ethyl radicals may be accounted for by reactions 9 and 10. Their relative weights in importance are however not clear from this work.

Rate Constant Ratios of Cage Reactions.—When reactions 4—6 are regarded as ordinary elementary steps, it follows that:

$$k_5/k_4 = (C_2H_4)_s/(C_3H_8)_s$$

$$k_6/k_4 = [(N_2)_s - (C_2H_4)_s - (C_3H_8)_s]/(C_3H_8)_s$$

$$k_6/k_5 = [(N_2)_s - (C_2H_4)_s - (C_3H_8)_s]/(C_2H_4)_s$$

where the suffix s denotes the presence of styrene. On applying these equations to the experimental results, we obtain the Arrhenius plots shown in Figs. 3 and 4. The plot for k_5/k_4 is linear, but those for k_6/k_4 and k_6/k_5 show deviations above room temperature, as was the case with azoethane. These deviations presumably arise from the inadequacy of the crude representation given in reaction 6 for the escape of radicals from a solvent cage at high temperatures.

Table III shows the Arrhenius parameters determined from Figs. 3 and 4; for the latter figure these quantities refer to the linear portions of the plots. The table also contains the corresponding

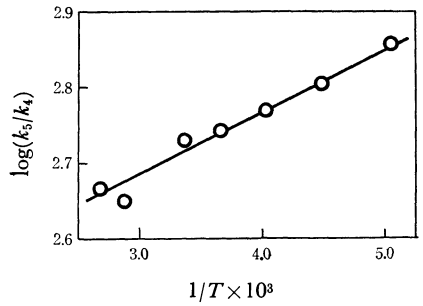

Fig. 3. Arrhenius plot for k_5/k_4.

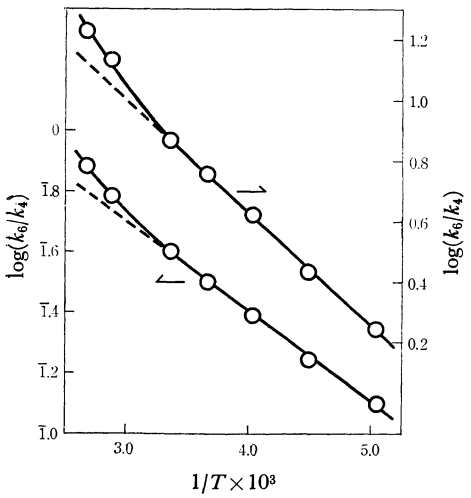

Fig. 4. Arrhenius plots for k_6/k_4 and k_6/k_5.

values for azomethane[7] and azoethane[3]. It may be seen in the table that E_5-E_4 is slightly negative for methylazoethane as well as for azoethane. These results are in agreement with those obtained and discussed in detail by Szwarc and his co-workers.[1,8]

The energy differences, E_6-E_4 and E_6-E_5, on the other hand, are definitely positive, indicating that the effect of the temperature on the cage reactions is largely controlled by the energy of activation for the diffusion of radicals.

Table III shows that E_6-E_4 decreases in the order of azomethane, methylazoethane, and azoethane. If the value of E_4 were zero for all of the methyl-methyl, methyl-ethyl and ethyl-ethyl combination, the trend in the values of E_6-E_4 would mean a greater activation energy for the diffusion of methyl radicals than that for ethyl radicals, contrary to what would be expected. Table III, therefore, leads to the conclusion that the combination of ethyl radicals and the cross-combination of methyl and ethyl radicals require activation energies greater than about 0.5 and 0.2 kcal./mol. respectively at least. This conclusion is compatible with previously-reported values. The activation energy for the combination of ethyl radicals has been reported as 2 kcal./mol. in the gas phase[9] and as 0.8 kcal./mol. in solution,[10] while that for methyl radicals is regarded as approximately zero in the gas phase.[11]

7) In the previous work with azomethane no experiment was carried out in *n*-heptane. The values for azomethane listed in the table are those determined in this work by photolyzing azomethane in *n*-heptane.

8) M. Matsuoka, P. S. Dixon, A. P. Stefani and M. Szwarc, *Proc. Chem. Soc.*, 304 (1962); P. S. Dixon, A. P. Stefani and M. Szwarc, *J. Am. Chem. Soc.*, **85**, 2551 (1963).

9) A. Shepp and O. K. Kutschke, *J. Chem. Phys.*, **26**, 1020 (1957).

10) R. W. Fessenden and R. H.Schuler, ibid., **39**, 2147 (1963).

11) R. Gomer and G. B. Kistiakowsky, ibid., **19**, 85 (1951); G. B. Kistiakowsky and E. K. Roberts, ibid., **21**, 1637 (1953); A. Shepp, ibid., **24**, 939 (1956).

NOTES

Reactions of Coordinated Organic Ligands with Cupric Bromide

By Robert H. BARKER, Michinobu KATO,* G. W. MCLAUGHLIN and Hans B. JONASSEN

Department of Chemistry, Tulane University, New Orleans, Louisiana, U. S. A.

(Received June 5, 1965)

Metal halides, such as cupric bromide, are known to act as halogenating agents for ketones and reactive aromatics. We have now been able to extend these reactions to include the halogenation of some coordinated organic nuclei.

The treatment of the copper(II) chelate of 8-hydroxyquinoline with cupric bromide in absolute alcohol produces a mixture of products. Hydrolysis with hydrochloric acid yields 5, 7-dibromo-8-hydroxyquinoline,[1] plus some monobrominated material.

The copper(II) chelate of salicylaldehyde is brominated in a similar fashion to yield 5-bromosalicylaldehyde upon acid hydrolysis.

Several metal acetylacetonates also undergo this type of reaction. The treatment of bis(2, 4-pentanedionato)copper(II) with cupric bromide produced bis(3-bromo-2, 4-pentanedionato)copper-(II) very rapidly. The cobalt(III) and chromium-(III) chelates of acetylacetone were brominated in the same manner as the copper(II) complex, except that the reaction proceeded somewhat more slowly. Substitution occurred only on the number 3 carbon of the ligands. No detectable amounts of bis(3-bromo-2, 4-pentanedionato)copper(II) were found to result from these reactions which might be formed through ligand exchange in a solution.[2] We have found that the copper(II) complexes readily form from the free ligand and cupric bromide under the conditions of the bromination, whereas the cobalt(III) and chromium(III) complexes do not. In agreement with a variety of such brominations reported by Collman et al.,[3] the bromination of these trivalent metal chelates may involve direct electrophilic substitution on the chelate ring.

* Present address: Aichi Prefectural Women's College, Mizuho-ku, Nagoya, Japan.

1) K. D. Maguire and M. M. Jones, *J. Am. Chem. Soc.*, **84**, 2316 (1962).

2) R. W. Kluiber, ibid., **82**, 4839 (1960).

3) J. P. Collman, R. A. Moss, H. Maltz and C. C. Heindel, ibid., **83**, 531 (1961); J. P. Collman, *Angew. Chem., Intern. Ed.*, **4**, 132 (1965) and the references quoted therein.

Experimental

The Bromination of Bis(8-hydroxyquinolinato)-copper(II) and Bis(salicylaldehydato)copper(II).—A mixture of one of the metal chelates (0.01 mol.) of 8-hydroxyquinoline (A) or salicylaldehyde (B) and cupric bromide (0.02 mol.) in 100 ml. of absolute ethanol was stirred for 1 hr. at 50—60°C. (A): The reaction mixture was collected on a filter and dissolved in 6 N hydrochloric acid by being warmed. The resulting solution was saturated with hydrogen sulfide to precipitate cupric sulfide and then filtered. The free base of 5, 7-dibromo-8-hydroxyquinoline was recovered from the aqueous filtrate and recrystallized from *N*, *N*-dimethylformamide. It was identified by comparing its infrared spectrum with that of standard spectra shown in the Sadtler catalog (No. 7168); yield, 30%. (B): The reaction mixture was collected on a filter. The evaporation of the filtrate left some residue. These materials were put together and dissolved in 6 N hydrochloric acid to give a precipitate. An alcoholic extract of the precipitate gave needles of 5-bromosalicylaldehyde (yield, 35%), identified by a comparison of its m. p. (105°C) (Beilstein's Handbook) and infrared spectrum (Sadtler No. 5769) with those of a standard sample.

The Bromination of the Metal Acetylacetonates.—A mixture of one of the complexes (0.0075 mol.) and well-dried cupric bromide (0.018 mol.) in 100 ml. of absolute ethanol was stirred for 30 min. at room temperature. After filtration to remove the cuprous bromide formed during the reaction, the filtrate was evaporated to dryness under reduced pressure. Recrystallization from chloroform and heptane produced the pure product in the copper(II) series (yield, ca. 20%), but cobalt-(III) and chromium(III) products required further purification by chromatography on alumina in order to remove small amounts of mono- and dibrominated materials from them. Each compound was identified by a comparison of its melting point and infrared spectra with those in the literature[3]; yields after chromatography: 10% for the chromium(III) complex and 17% for the cobalt(III) complex.

Partial financial support by the Office of Naval Research, United States Navy, is hereby gratefully acknowledged.

The Infrared Absorption Spectrum of the Vinyl Chloride - Vinyl Acetate Copolymer and Its Tacticity

By Tsugio TAKEUCHI and Sadao MORI

Department of Synthetic Chemistry, Faculty of Engineering, Nagoya University, Chikusa-ku, Nagoya

(Received June 9, 1965)

We have already reported a method for the infrared analysis of the vinyl chloride - vinyl acetate copolymer.[1] In that paper we suggested the possibility of discriminating between the copolymer and a mixture of the homopolymer of vinyl chloride and that of vinyl acetate (henceforth referred to as PVC and PVAc respectively); no difference in the frequencies of the absorption bands was observed, but the absorption intensities of some bands of the copolymer were markedly different from those of a mixture with the same composition. In this paper the infrared spectra in the 400—700 cm^{-1} range of the same samples will be measured. We will also study the relation between the vinyl acetate content of the copolymer and the tacticity of its vinyl chloride part. The crystallinity of the copolymer will also be discussed.

Experimental

The infrared spectra of the polymers were observed by means of a Nihon-Bunko double-beam infrared spectrophotometer, Model DS-402G. The samples of PVC, PVAc and the copolymers were the same as those used in a previous experiment.[1] The polymer films were obtained from the tetrahydrofuran solutions of the polymers by evaporating the solvent on mercury under reduced pressure.

Results and Discussion

The Infrared Absorption Spectra and Relative Absorption Intensities.—Shimanouchi et al.[2,3] have assigned the bands of PVC at 638 cm^{-1} and 615 cm^{-1} to the C–Cl stretching frequencies associated with the syndiotactic structure, an extended chain, and the band at 690 cm^{-1} to the isotactic structure, a three-fold helix. They have also concluded that the bands at 690 cm^{-1} and 615 cm^{-1} are due to the amorphous region of the polymer, and the band at 638 cm^{-1} to the crystalline region.

Three bands, at 690 cm^{-1}, 637 cm^{-1} and 615 cm^{-1}, were observed in the spectra of the copolymers and the mixtures. They were inferred to arise as follows: the 690 cm^{-1} band from the C–Cl vibration, and the 637 cm^{-1} band and the 615 cm^{-1} band from the vibrations of C–Cl and the acetyl group.[2,4] In Fig. 1 the ratios of the absorbance at 690 cm^{-1} to that at 637 cm^{-1}, of that at 637 cm^{-1} to that at 615 cm^{-1}, and of that at 690 cm^{-1} to that at 615 cm are plotted against the vinyl acetate content. It may be seen that there are great differences in the absorbance ratios between the copolymer and the mixture, the difference in the absorbance ratio of the 690 cm^{-1} and 637 cm^{-1} bands being the most noticeable.

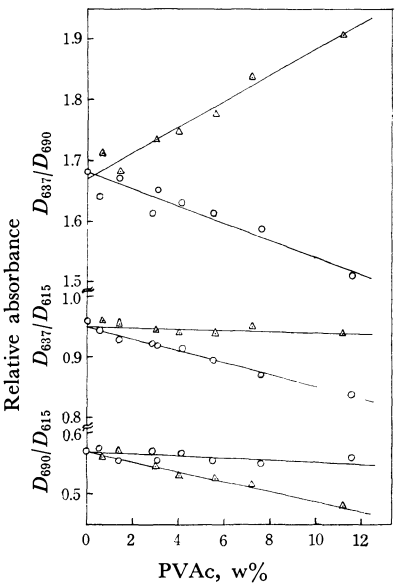

Fig. 1. Relative absorbances of the 690, 637 and 615 cm^{-1} bands.
○—○: Copoymers
△—△: Mixtures

The Tacticity of the Copolymer.—On the basis of the differences in absorbance ratio between the copolymer and the mixture, the tendency of the crystallinity and the tacticity of the copolymer to change with an increase in the vinyl acetate content of the copolymer was considered.

Figure 2 shows that the absorption intensity of the band at 690 cm^{-1} of the copolymers decreases less than that of the mixtures as the vinyl acetate content increases. If the intensity of the 690 cm^{-1}

1) T. Takeuchi and S. Mori, *J. Chem. Soc. Japan, Ind. Chem. Sect.* (*Kogyo Kagaku Zasshi*), **68**, 643 (1965).
2) T. Shimanouchi, S. Tsuchiya and S. Mizushima, *Kobunshi*, **8**, 202 (1959).
3) T. Shimanouchi, S. Tsuchiya and S. Mizushima, *J. Chem. Phys.*, **30**, 1365 (1959).
4) H. W. Thompson and P. Torkington, *J. Chem. Soc.*, **1945**, 640.

band is not subjected to the influence of the copolymerization of PVAc, it might be possible to explain this result qualitatively in terms of the fact that the amorphous content of the isotactic region of the vinyl chloride part increases as the vinyl acetate content increases. As the bands at 637 cm^{-1} and 615 cm^{-1} were assigned to the bands due to the vibrations of both the acetyl group of PVAc and the C–Cl of PVC, it might not be appropriate to discuss the tacticity of the copolymer quantitatively. However, the relative absorbance of the 637 cm^{-1} band to the 615 cm^{-1} band of the copolymer was smaller than that of the mixture; this means that the absorption intensity at 637 cm^{-1} of the copolymer decreased, or that at 615 cm^{-1} increased, more than those of the mixture. If the influence

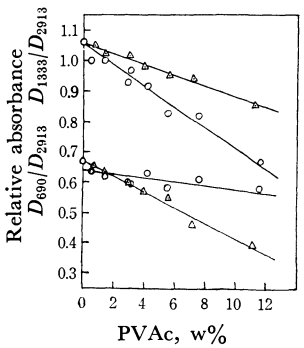

Fig. 2. Relative absorbances of 1333 and 690 cm^{-1} bands to the 2913 cm^{-1} band.[1)]

○—○: Copolymers △—△: Mixtures

of the copolymerization of PVAc is disregarded, it should be possible to explain these results by concluding that the crystalline content of the syndiotactic region of vinyl chloride decreases, or that the amorphous content of the syndiotactic region of the vinyl chloride part increases, as the copolymerization degree of vinyl acetate increases.

The band at 1333 cm^{-1} of PVC was considered to be the crystalline band[1)]; its absorbance of the copolymer decreased much more than that of the mixture as the vinyl acetate content increased (see Fig. 2). It was clear that the degree of crystallinity of the copolymer was smaller than that of a mixture of two homopolymers of the same composition. This fact was confirmed by the finding that the densities of the copolymers were smaller than those of the mixtures calculated from the densities of PVC and PVAc.

Grisenthwaite and Hunter[5)] have pointed out that the degree of crystallinity and the content of the syndiotactic region of the amorphous part of PVC increase as the polymerization temperature is lowered; basides, its isotactic region decreases. The results presented above lead to the following, differing conclusions: the degree of the crystallinity of the copolymer decreases as the vinyl acetate content increases, while the isotactic region of the amorphous vinyl chloride part increases.

5) R. J. Grisenthwaite and R. F. Hunter, *Chem. & Ind.*, **1958**, 719.

The Mechanism of the Oxidative Decarboxylation of Benzoic Acid*

By Shigeru OAE, Takao WATANABE and Naomichi FURUKAWA

Department of Applied Chemistry, Faculty of Engineering, Osaka City University, Sumiyoshi-ku, Osaka

(Received July 12, 1965)

The oxidative decarboxylation of benzoic acids with copper has been known as a method to produce phenols.[1] Although its precise mechanism is not clear, it has been suggested that the reaction involves the initial formation of cupric benzoate between two molecules of benzoic acid and cupric oxide, followed by the intramolecular attack of the carboxyl oxygen at the ortho-position of the other benzene ring, producing, via the equilibrium formation of a six-membered cyclic intermediate, phenyl benzoate, which is presumed to be the precursor of phenol.[2] In this case the oxygen atom of the phenol formed is expected to come from the carboxyl group. Meanwhile, if salicylic acid is formed by the pyrolysis of basic cupric benzoate,[3] the oxygen atom of the resulting phenol is likely to come from the water used. Another possibility is that the oxygen atom in the resulting phenol originates in the air. Thus, we have undertaken the pyrolysis of ^{18}O-labeled benzoic acid and traced the origin of the oxygen atom in the resulting phenol.

Experimental

Benzoic Acid Labeled with ^{18}O.—A mixture of 3.5 g. of benzoyl chloride and 2 ml. of $H_2{}^{18}O$ was refluxed until no hydrogen chloride gas evolved. After the mixture had then cooled, colorless crystalline

* Phenols and Phenolic Esters. Paper X.

1) W. W. Kaeding, R. O. Lindblom and R. G. Temple, *Ind. End. Chem.*, **53**, 805 (1961).

2) W. G. Toland, *J. Am. Chem. Soc.*, **83**, 2507 (1961).

3) W. W. Kaeding and A. T. Schulgin, *J. Org. Chem.*, **27**, 3551 (1962).

precipitates were filtered, washed with a small amount of water, and then recrystallized from water. The yield was 2.6 g. (84.9%); m. p. 123°C.

The Decarboxylation of ^{18}O-Labeled Benzoic Acid.—The apparatus used for the reaction is shown in Fig. 1. In a generator an air-steam mixture was prepared by bubbling air into hot water. The air-steam mixture was thus generated at the rate of 0.5—0.6 l./hr., the temperature of the water being kept at 80—90°C. As a reaction vessel, it is convenient to use a three-necked flask equipped with an air-steam-mixture-inlet tube, a thermometer, and a reflux condenser packed with glass beads and heated by an electric furnace, the temperature being kept at 130—140°C. The upper end of the reflux condenser was connected to a receiver. Phenol, water and other volatile products were collected in a receiver, and the carbon dioxide generated was entrapped by passing it through a barium hydroxide solution. A typical run for decarboxylation was as follows. In a reaction vessel, a mixture of 2.0 g. of ^{18}O-labeled benzoic acid, 40 mg. of cupric oxide and 68 mg. of magnesium oxide was charged and heated to 230—240°C by stirring it with a magnetic stirrer. The air-steam mixture was then introduced. After treatment for 5 hr., an excess of bromine water was added to the receiver flask. By this method, 1.5 g. of tribromophenol was obtained, in a 29% yield, when mixed with an authentic sample, its melting point did not drop. A brownish residue in a reaction vessel was washed with water and ether. Crude benzoic acid (0.95 g.) was thus recovered, while phenyl benzoate was obtained as a by-product. The overall yield was 53%.

^{18}O-Analysis.—^{18}O analyses of phenol, the recovered benzoic acid and carbon dioxide were carried out as usual by changing each sample into carbon dioxide gas, which was then subjected to mass spectrometry.

The Reaction of Phenol with Water.—Control experiments were carried out in order to test the oxygen exchange between phenol and $H_2{}^{18}O$ under the same reaction conditions. After phenol had been recovered as its 2, 4, 6-tribromide, the ^{18}O-content of the phenol was analyzed by the same procedure. The ^{18}O-concentration was found to be 0.20 atom%, which is that of the natural abundance of ^{18}O. The results showed no ^{18}O exchange between phenol and water.

Discussion

The analytical data on the ^{18}O content of the resulting phenols and benzoic acids, both those initially-employed and those recovered, are summarized in Table I.

Most of the ^{18}O initially-labeled in the carboxyl group was found in the phenol produced, except when the reaction was carried out with the extensive introduction of a steam. However, in every run, a small decrease in the ^{18}O content of the products was observed, especially in the recovered benzoic acid. This is presumably because of an oxygen exchange between ^{18}O-labeled benzoic acid and water during the reaction. These observations are clearly in accord with the mechanism involving the formation of phenol via the cyclic intermediate. As is shown by the run 3 in Table I, the intervention of another possible reaction, i e., that of the basic salt of benzoic acid, is conceivable in this case, since the basic salt is presumably formed quite readily in the presence of an excess of water. Accordingly, it seems that only a minor portion of the reaction proceeds through a path involving the basic salt, while the major part of the reaction proceeds through an ordinary process with cupric salt of benzoic acid, with the ^{18}O concentration gradually reduced during the reaction.

Table I. ^{18}O Contents of benzoic acid and phenol in the decarboxylation of ^{18}O-labeled benzoic acid (^{18}O-atom%)

Run	Benzoic acid		CO_2	Phenol
	Initial	Recovered		
1a)	1.05	0.93	0.81	1.02
2a)	1.25	0.99	—	1.01
3b)	0.87	0.46	0.33	0.42

a) The reaction was carried out at 230—240°C for 5 hr.

b) A large excess of steam was passed through the vessel, and the reaction was performed at 230—240°C for 10 hr.

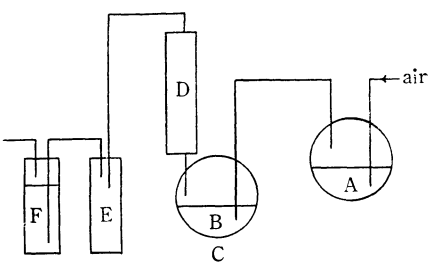

Fig. 1. Apparatus.

A Hot water
B Reacter
C Hotting stirrer
D Reflux condenser
E Product receiver
F CO_2 trap

The Sheet Scintillation Counting of Tritium in Surface Films*

By Mitsuo MURAMATSU and Noboru TOKUNAGA

Department of Chemistry, Faculty of Science, Tokyo Metropolitan University, Setagaya-ku, Tokyo
Japan Radiation and Medical Electronics, Inc., Mitaka, Tokyo

(Received August 10, 1965)

Because of the extremely soft nature of β-rays, tritium is expected to be the most effective radioactive tracer for elucidating the mechanism of such surface-chemical processes as the adsorption of detergents at the solution/gas interface, as well as for studying the nature of solid surfaces. Thus, the adsorbed amount of tritiated sodium dodecyl sulfate was determined with a 2π proportional counter, with humidified hydrocarbon gas flowing over the detergent solution.[1] The surface roughness of solid samples was determined by measuring the radioactivity of a tritiated specimen.[2] Similar techniques have been employed in studying the behavior of tritiated lauric acid in thin layers on metal[3] and that of hydrocarbons on metallic[4] and aqueous[5] hypophases.

All these experiments have been carried out with a windowless flow counter of a limited size. In these experiments, therefore, the experimental devices had to be small enough to fit into the counter; they can not include, for example, a trough for insoluble monolayers. In addition, the surface is inevitably exposed to the hydrocarbon gas, which in some cases dissolves in the hypophase.[6] To avoid these difficulties, an attempt has been made to develop a method of scintillation counting which does not require a flowing gas and where the space for the sample is not limited.

Experimental

The counting probe consisted mainly of a sheet of plastic scintillator and a photomultiplier tube (EMI 9536s). To minimize the optical loss due to total reflection, coupling of the sheet to the tube window was achieved with silicone oil of the same refractive index, 1.60, as that of the scintillator sheet. The assembled probe was placed, at a distance of 1 mm., face to face with a thin film (0.17—0.85 μg./cm^2) of an extremely pure sample of stearic-9, 10-^{3}H, ^{3}H acid (9.5 c./mol.)[7] spread over the circular range (1.13 cm^2) of a concentric aluminum disk. The whole assembly was thermostated to $\pm$0.5°C throughout the measured temperature range of —5 to 10°C.

The output pulses led to a linear amplifier (Aloka LA-10; maximum amplification, 30000), then to a pulse height analyzer (Aloka PA-22, 2 channel) for counting.

Two types of plastic scintillator sheets were used in the experiments. The sheets of the Pilot Scintillator B, which contained *p*, *p'*-diphenylstilbene as a scintillator, were obtained from the Pilot Chemicals, Inc., Watertown, Mass., U. S. A. The other type, containing terphenyl, was kindly supplied by the Matsushita Denko K. K., Osaka.

Results and Discussion

The background values were generally high, because of the low discrimination levels which we inevitably chose for counting the pulses of tritium β-rays. Therefore, attempts were made to overcome the difficulty by the aid of optical coupling

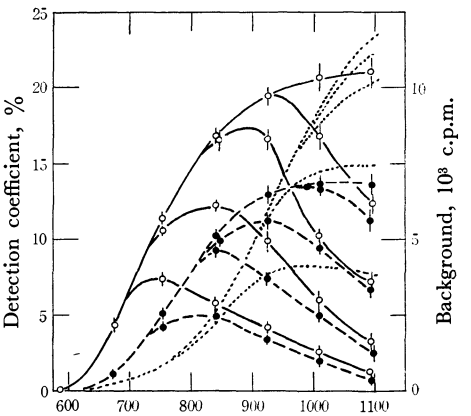

Fig. 1. Voltage dependences of background (dotted lines) and of detection coefficient with terphenyl sheet with (full) or without (chained) optical coupling.
Temperature, 10°C; window width, down to up, 5—12.5, 5—25, 5—50, 5—100 and 5—∞ V.
Each point expresses the average from 5—10 independent experiments.

* Paper presented at the 17th National Colloid Symposium, Tokyo University, Tokyo, 1965.

1) G. Nilsson, *J. Phys. Chem.*, **61**, 1135 (1957); M. Muramatsu, K. Tajima and T. Sasaki, Proc. 6th Japan Conference on Radioisotopes, Japan Atomic Ind. Forum, Tokyo (1964), pp. 105, 108.

2) O. Sepall and S. G. Mason, *Tappi*, **44**, 899 (1962).

3) K. Tajima, T. Sasaki and M. Muramatsu, This Bulletin, **36**, 700 (1963).

4) M. Muramatsu and T. Sasaki, *Science*, **131**, 302 (1960).

5) K. Tajima, T. Sasaki and M. Muramatsu, Paper presented at the 15th National Colloid Symposium, Okayama University, Okayama, 1962.

6) M. Muramatsu and T. Sasaki, Proc. 3rd Japan Conference on Radioisotopes, Japan Atomic Ind. Forum, Tokyo (1959), p. 453.

7) M. Muramatsu, O. Fujii and T. Sasaki, *Radioisotopes*, **10**, 100 (1961).

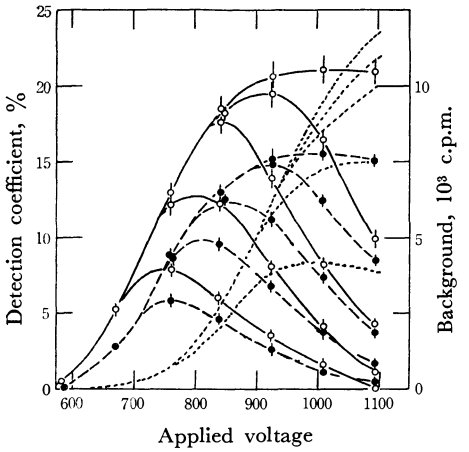

Fig. 2. Voltage dependences of background (dotted lines) and of detection coefficient with the Pilot Scintillator B sheet with (full) or without (chained) optical coupling.

Temperature, 10°C; window width, down to up, 5—12.5, 5—25, 5—50, 5—100 and 5—∞ Volts.

Each point expresses the average from 5—10 independent experiments.

for the efficient transformation of the optical scintillae into electronic pulses. Figures 1 and 2 show the counting characteristics for terphenyl and the Pilot Scintillator B sheets, respectively, with and without an optical coupling at 10°C. It can be seen in the figures that the coupling has caused a shift of the curve to lower voltage and has increased the detection coefficient. Accordingly, the background value at a 10% detection coefficient, for example, was decreased by the coupling from 2600 to 650 c.p.m. with the terphenyl sheet (Fig.1) and 1000 to 330 c. p. m. with the Pilot Scintillator B sheet (Fig. 2).

Precise experiments using 0.01—0.25 mm.-thick scintillator sheets have shown that the counting characteristics do not depend on the thickness.

The lowering of the temperature causes a remarkable decrease in the background, especially in the high voltage region, but it has little influence upon the detection coefficient. For obtaining a 10% detection coefficient, for instance, the background values were 90 c.p.m. at −5°C and 700 c.p.m. at 10°C. Similar or more exaggerated difference was found for obtaining another value of the detection coefficient. Very low temperature, however, could not be used, especially for adsorption experiments with an aqueous system.

Figure 3 shows the effect of sample thickness on the count rate, obtained at the applied voltage in order to give the maximum detection coefficient for each window width using a Pilot Scintillator B at 10°C. The linearity is fairly good, regardless of the counting conditions. If we assume the 20 Å²/molecule to be the cross-sectional area of

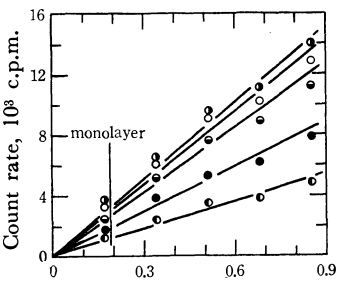

Fig. 3. Effect of sample thickness on count rate. Temperature, 10°C; scintillator, optically coupled Pilot Scintillator B.

Window width and applied voltage; ◐, 5—12.5 V. and 755 V.; ●, 5—25 V. and 800 V.; ◒, 5—50 V. and 840 V.; ○, 5—100 V. and9 25V.; and ◑, 5—∞ V. and 1010 V.

stearic acid, 1200 c.p.m. for a 5—12.5 V. window width would, for example, be obtained as the net count rate of a monolayer of tritiated stearic acid spread over a circle of 1.13 cm.² in area. Therefore, if we would have a monolayer of the same substance with the same specific activity spread on a surfac wider than the tube window, we could expect ca. 21600 c.p.m. as the net count rate, A, due to the tritium in the monolayer,* the value being much more than the background, B, 490 c.p.m. in this case. Figure 4 illustrates the values of A and B/A as a function of B under counting conditions which give a maximum detection coefficient for each window width. The

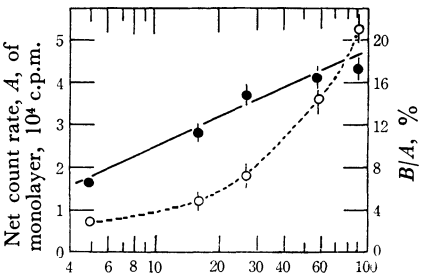

Fig. 4. Net count rate, A, (●) of stearic acid monolayer and the B/A ratio (○) as a function of background, B, at 10°C. Scintillator, optically coupled Pilot Scintillator B; window width, left to right, 5—12.5, 5—25, 5—50, 5—100 and 5—∞ V.

Each point expresses the average from 5 independent experiments.

* It was confirmed that the geometric factor for a point source does not depend on its radial position, almost up to the edge of the scintillator sheet. The constancy of the factor is due to the short distance (1mm.) between the sheet and the sample and, possibly, to the structure of the Venetian-blind-type phototube to which our photomultiplier belongs.

figure shows that the value of B/A increases remarkably with an increase in the background, showing the better conditions obtainable with a narrower window width and, correspondingly, with a lower voltage. It must also be mentioned that the temperature dependence of the background is decreased markedly by a decrease in the applied voltage and by a narrowing of the window width.

The sheet scintillation, which was first reported for counting tritiated hydrogen[8] and for the low-background counting of hard β-rays[9] will thus be of great use in determining the amount of a tritiated substance present in very thin layers at the air/water interface of any size available. It will enable us to determine simultaneously the radioactivity and such other properties as surface pressure and potential.

The authors wish to thank Mr. Nobuo Motida, President of JRME, for his interest in this work.

8) I. S. Boyce, J. F. Cameron and K. J. Taylor, *Int. J. Appl. Rad. Isotopes*, **9**, 122 (1960).

9) J. H. Harley, N. A. Hallden and I. M. Fisenne, *Nucleonics*, **20**, No. 1, 59 (1962).

Syntheses and Structures of Acetylformoin and Related Compounds. V. *p-t*-Butylbenzoylformoin and *t*-Toluylformoin

By Sadao KIMURA, Yo MIYAGI and Ryozo GOTO

Department of Chemistry, Faculty of Science, Kyoto University, Sakyo-ku, Kyoto

(Received August 19, 1965)

In our earlier investigations[1] it has been reported that α-ketoaldehydes undergo a self-condensation similar to benzoin condensation to give formoins, for which several structures are possible. The results may be summarized as follow: structure I is preferred in solutions in alcohols and ethers; structure II is preferred in solutions in chloroform and carbon tetrachloride; the structure in the solid state is dependent on the substituent R. The two struc tures have been found to have quite different spectral characteristics. Compound

$$2\ \mathrm{RCOCHO} \xrightarrow{\mathrm{CN^-}} \mathrm{RCOCH(OH)COCOR}$$

I shows $\nu_{C=C}$ at ca. 1605, $\nu_{C=O}$ a ca. 1685, and two bands of ν_{OH} between 3000and 4000 cm^{-1} in the solid state, and $\nu_{C=C}$ at ca. 1615, $\nu_{C=O}$ at ca. 1705 and one band of ν_{OH} between 3500 and 3800 cm^{-1} in a solution. Compound II shows $\nu_{C=C}$ at ca. 1620 cm^{-1} and no discernible bands of ν_{OH} and $\nu_{C=C}$ in either state. λ_{max} is located ca. 360 and 240 mμ in compound I and ca. 400 and 300 mμ in compound II when R is the phenyl group.

In this paper the authors will report on the condensation products of *p-t*-butylphenylglyoxal and *t*-tolylglyoxal, namely, *p-t*-butylbenzoylformoin (BBF) and *t*-toluylformoin (TF).[2] The glyoxals prepared by the selenium oxide oxidation of the *p*-substituted acetophenones were subjected to condensation in an aqueous alcoholic solution containing sodium cyanide.

It has been established by elementary analysis and molecular weight determination that the product is composed of two molecules of the glyoxal.

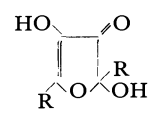

I

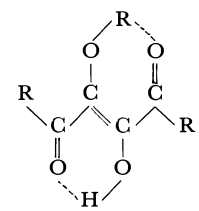

II

The infrared spectrum of BBF has the spectral characteristics of structure I in the solid state: $\nu_{C=C}$ 1593, $\nu_{C=O}$ 1680 and ν_{OH} 3100 and 3300 cm^{-1}. In THF or ethanol it also shows the spectral properties of structure I: $\nu_{C=C}$ 1625, $\nu_{C=O}$ 1700 and ν_{OH} 3260 cm^{-1}; λ_{max}^{EtOH} 358 (ε, 13700) and 245 (ε, 12500) mμ.

When BBF is dissolved in chloroform in air, it is rapidly oxidized to give a red solution as benzoylformoin.[1d] For this reason, the ultraviolet spectrum in this solvent was measured in a cell sealed in vacuc. The situation is rather complicated, as in the case cf benzoylformoin. In ethanol-free chloroform, λ_{max}'s are located at 400 and 300 mμ, indicating structure II. The solution in ethanol-containing (ca. 1%) chloroform shows λ_{max} 371 and 245 mμ. However, it can not be thereby concluded that this spectrum indicates structure II, for benzoylformoin may react with ethanol in chloroform to give *O*-ethyl

1) a) R. Goto, Y. Miyagi and H. Inokawa, This Bulletin, **36**, 147 (1963); b) Y. Miyagi and R. Goto, ibid., **36**, 650; c) Ibid., **36**, 921; d) Y. Miyagi, ibid., **37**, 12 (1964).

2) TF was first synthesized by Abenius and Söderbaum (*Ber.*, **25**, 3473 (1892)), but its structure needs to be investigated further.

benzoylformoin II (R=OH, R'=Et).[3]

When the ultraviolet spectrum is quickly recorded in the 340—420 mμ range, it is found that the absorption arises around 370 mμ immediately after dissolving in ethanol-free chloroform and that it shifts to 405 mμ in about five minutes. This fact indicates that the structure of BBF, which is I soon after dissolving, turns to II by a quick shift of the equilibrium between I and II.

TF also has the spectral properties of structure I in the solid state and in solution in THF and ethanol: $\nu_{C=C}$ 1598, $\nu_{C=O}$ 1693, and ν_{OH} 3240 and 3520 cm^{-1} in the solid state; $\nu_{C=C}$ 1630, $\nu_{C=O}$ 1705 and ν_{OH} 3280 and 3540 cm^{-1} in THF; λ_{max}^{EtOH} 355 (ε, 11100) and 245 (ε, 11100) mμ.

The ultraviolet spectrum of TF in chloroform is also complicated. In ethanol-free chloroform, λ_{max} is located at 400 mμ. In ethanol-containing chloroform it shifts to 380 mμ, a position a little longer in wavelength than the band of BBF in this solvent, 371 mμ. Moreover, a shoulder is observed on the longer wavelength side of the 380 mμ band. This spectrum indicates the presence of a mixture of two components. One of these may be established as II with certainty. However, the other component can not be concluded unequivocally to be I for the same reason as has held in the case of BBF.

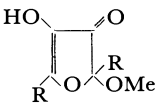

III

As does benzoylformoin,[1b-c,4] BBF and TF undergo methanolysis by methanolic hydrogen chloride to give *O*-methyl dericatives with spectral properties similar to those of structure I. Since etherification by alcoholic hydrogen chloride is characteristic of glycosidic linkage, the structure of these *O*-methyl derivatives may be established as III.

The situation is now being investigated in more detail.

3) B. Eistert, private communcation; see also Ref. 1d.
4) A. H. Blatt, *J. Am. Chem. Soc.*, **58**, 1894 (1936).

Experimental

Glyoxals.—*p-t*-Butylacetophenone[5] and *p*-methylacetophenone[6] were oxidized with selenium oxide by the general procedure[7] to *p-t*-butylphenylglyoxal and *p*-tolylglyoxal respectively. The latter was isolated as a hydrate, m. p. 105.5—106.5°C. The former, however, failed to give a hydrate.

***p-t*-Butylbenzoylformoin (BBF).**—Crude *p-t*-butylphenylglyoxal was redistilled to give a yellow liquid boiling at 99—104°C/4 mmHg. After 10 g. of this had been dissolved in 80% aqueous ethanol (65 ml.), to this solution an aqueous solution (5 ml.) containing 0.2 g. of sodium cyanide was added. The color of the solution turned a reddish yellow, and yellow crystals were deposited. After 2 hr., the crystals were filtered off, which were dissolved in warm ethanol and recrystallized by adding water: yield, 7 g.; m. p. 168.5—169.0°C.

Found: C, 75.43; H, 7.44; mol. wt. (Rast), 400. Calcd. for $C_{24}H_{28}O_4$: C, 75.76; H, 7.42%; mol. wt., 380.

***p*-Toluylformoin (TF).**—The procedure was the same as above except that glyoxal hydrate was used instead of the glyoxal monomer. Yellow needles: recrystallized from 50% aqueous ethanol; m. p. 154—159°C (lit. 161°C[2]). Found: C, 72.98; H, 5.15; mol. wt. (Rast), 298. Calcd. for $C_{18}H_{16}O_4$: C, 72.96; H, 5.44%; mol. wt., 296.

***O*-Methyl *p-t*-Butylbenzoylformoin.**—BBF (3 g.) was dissolved in 10% methanolic hydrogen chloride (50 ml). Immediately pale yellow crystals were deposited. The whole mixture was allowed to stand overnight in a refrigerator. Crystals were collected and recrystallized from methanol; yield, 2.5 g.; m. p. 206—207°C; ν_{max}^{Nujol} 1615, 1690 and 3360 cm^{-1}; λ_{max}^{EtOH} 358 (ε, 12900) and 245 (ε, 12000) mμ.

Found: C, 75.95; H, 7.81; CH_3O, 7.73. Calcd. for $C_{25}H_{30}O_4$: C, 76.11; H, 7.67; CH_3O, 7.68%.

***O*-Methyl *p*-Toluylformoin.**—The procedure was the same as above. Pale yellow needles, recrystallized from methanol; m. p. 195—196°.2C; ν_{max}^{Nujol} 1615, 1690 and 3400 cm^{-1}; ν_{max}^{EtOH} 358 (ε, 12400) and 245 (ε, 11300) mμ.

Found: C, 73.38; H, 5.81; CH_3O, 10.18. Calcd. for $C_{19}H_{18}O_4$: C, 73.53; H, 5.85; CH_3O, 10.00%.

5) H. C. Brown, J. P. Brady, M. Grayson and W. H. Bonner, *J. Am. Chem. Soc.*, **79**, 1897 (1957).
6) R. Adams and C. R. Noller, "Organic Syntheses," Coll. Vol. I, 111.
7) H. A. Riley and A. R. Gray, ibid., Coll. Vol. II, 513.

The Synthesis of Linalool

By Kyoichi SUGA, Shoji WATANABE and Imako OKOSHI

Department of Applied Chemistry, Faculty of Engineering, Chiba University, Yayoicho, Chiba

(Received August 20, 1965)

Linalool is widely used in perfumery. Various methods have been used successfully for the synthesis of linalool. The authors will now describe a new method of preparing linalool from α-acetyl-γ-butyrolactone (I), which is an intermediate of vitamin B_1[1]. This new method is shown in the following scheme:

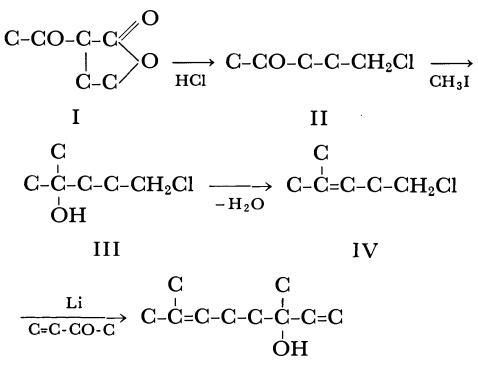

5-Chloro-2-pentanone (II) was prepared by the action of aquous hydrochloric acid[2] on I in a good yield. The ketone (II) with methylmagnesium iodide gave the alcohol 1-chloro-4-methyl-4-hydroxy-pentane (III) in a 60% yield. The alcohol (III) was then dehydrated easily by potassium bisulfate to 1-chloro-4-methyl-3-pentene (IV). The alkenyl lithium from the chloride (IV) reacted with methylvinyl ketone to give linalool (V). The identity of V was confirmed by comparing its infrared absorption spectrum and its gas liquid chromatography with those of authentic linalool.

Similarly, dihydrolinalool was prepared from the alkenyl lithium of the chloride (IV) and ethyl methyl ketone.

Experimental

α-Acetyl-γ-butyrolactone (I). — It was obtained from the Sankyo Co., Ltd., and from the Takasago Perfumery Co., Ltd.

5-Chloro-2-pentanone (II).—A mixture of 45 ml. of concentrated hydrochloric acid, 53 ml. of water, and 38.4 g. (0.3 mol.) of I was placed in a 200 cc. distilling flask fitted with a condenser and a receiver immersed in an ice-water bath. The reaction mixture was heated for 10 min., and then distilled as rapidly as possible. After 90 ml. of distillate had been collected, 50 ml. of water was added to the distilling flask and another 30 ml. of distillate was collected. The yellow organic layer was extracted with ether. The ether extracts were dried over calcium chloride. Fractional distillation gave a crude II (28 g., yield 78%). It was redistilled for characterization, b. p. 70—72°C/12 mmHg; n_D^{25} 1.4371 (reported[2] 70—72°C/12 mmHg, n_D^{25} 1.4371).

1-Chloro-4-methyl-4-hydroxypentane (III).—Methylmagnesium iodide, obtained from magnesium (4 g.) and methyl iodide (22 g.) in ether (200 ml.), was cooled to 0°C and stirred during the addition (10 min.) of II (20 g.) in ether (100 ml.). After a further 60 min., acetic acid (25 ml.) in ether (50 ml.) was added. The mixture was then stirred with water (200 ml.), and the aqueous layer was extracted with ether. The ether extracts were washed with aqueous sodium hydrogen carbonate, dried over anhydrous sodium sulfate, and distilled to give 1-chloro-4-methyl-4-hydroxypentane (III) (8 g.), b. p. 80—83°C/16 mmHg; d_4^{20} 1.1091; n_D^{20} 1.4522; IR: ν_{max} 3380 cm^{-1} (OH), ν_{max} 1120 cm^{-1} (a tertiary OH), the gas chromatogram showed a single peak.

1-Chloro-4-methyl-3-pentene (IV). — The above chloride (III) (8 g.) was heated at 160°C with fine-powdered potassium bisulfate (2 g.). After an hour 10 ml. of water was added, and the mixture was extracted with ether. The ether extracts were dried over anhydrous sodium sulfate. Fractional distillation gave 1-chloro-4-methyl-3-pentene (IV) (4.5 g.), b. p. 125—130°C; d_4^{20} 0.9721; n_D^{20} 1.4414; IR: ν_{max} 890 cm^{-1} (-C=CH); gas chromatography showed a single peak.

Linalool (IV).—Lithium (0.47 g.; thin strips freshly cut) and ether (50 cc.) under nitrogen were stirred during the slow addition of 1-chloro-4-methyl-3-pentene (IV) (4 g.) in ether (60 cc.). When reaction began, a cooling bath (−20°C) was applied. Stirring was then continued at −15°C until nearly all the lithium had reacted (2 hr.). To the solution at −70°C, methyl vinyl ketone (2.3 g.) in ether (10 cc.) was added (5 min.). Twelve hours later a 50% alcoholic solution (10 cc.) in ether was added, and the mixture was treated as usual. Fractional distillation gave 3 g. of linalool (V), b. p. 78—80°C/6 mmHg; d_4^{15} 0.8702; n_D^{0} 1.4681; IR: 3400 cm^{-1} (OH), 1120 cm^{-1} (a tertiary OH), 890 cm^{-1} (-C=CH-), 910 and 990 cm^{-1} ($-CH=CH_2$).

Its nature was confirmed by comparing its infrared absorption spectrum and gas chromatography with those of an authentic sample. (Found: C, 77.80; H, 11.73%).

Dihydrolinalool (VI).—Much as has been described above, dihydrolinalool was prepared from 1-chloro-4-methyl-3-pentene (IV) and ethyl methyl ketone. The dihydrolinalool so prepared had the following

1) E. R. Buchman, *J. Am. Chem. Soc.*, **58**, 1803 (1936).
2) G. W. Cannon, R. C. Ellis and J. R. Leal, "Organic Syntheses," Vol. 31, 74 (1951).

properties: b. p. 92.5—93°C/13 mmHg; n_D^{17} 1.4568; d_4^{17} 0.8573 (reported[3]) b. p. 94—94.5°C/14 mmHg; n_D^{15} 1.4569; d_4^{15} 0.8695; d_4^{17} 0.8572); IR: 3400 cm^{-1} (OH), 1150 cm^{-1} (OH), 890 cm^{-1} (–$\overset{|}{C}$=CH–). The infrared absorption spectrum and gas chromatography of VI agreed with those of an authentic sample (VI). (Found: C, 76.83; H, 12.81%)

3) H. Wienhaus and W. Treibs, *Ber.*, **56**, 1651 (1923); Beilstein **I**, 452.

The authors are indebted to the Takasago Perfumery Co., Ltd., and the Sankyo Co., Ltd., for providing materials.

Studies of Some Radical Transfer Reactions. II.† Electron Transfer Reactions Involving Halide and Oxalate Ions with OH Radicals during the Aqueous Polymerization of Methylmethacrylate

By Mihir K. SAHA, Premamoy GHOSH* and Santi R. PALIT

Indian Association for the Cultivation of Science, Jadavpur, Calcutta 32, India

(Received September 28, 1965)

Hydroxyl radicals (OH·) in solution may possible participate in electron transfer reactions with some anions (X^-) present in the same medium, thereby losing their radical nature and being replaced by new radicals (X·) derived from the anions in question:

$$OH\cdot + X^- \rightarrow OH^- + X\cdot$$

In polymerization experiments in such systems, the occurrence of the above type of radical transfer reactions may easily be traced by the analysis of the polymer endgroups. The present paper will report the results of our investigation of such reactions involving halide (F^-, Cl^- and Br^-) and oxalate ions with OH· radicals in aqueous media, based on the analysis of the endgroup of the polymethylmethacrylate prepared in such systems.

Experimental

The aqueous polymerization of purified methylmethacrylate (MMA) was carried out in Pyrex flasks under a nitrogen atmosphere at room temperature; it was initiated by OH radicals derived either by the photolysis of H_2O_2 in ultraviolet light or by redox reaction with Fe^{2+} ions in the dark. Sodium fluoride, potassium chloride and potassium bromide were separately added at varied concentrations in the polymerization media. The PMMA samples obtained after the completion of polymerization were filtered, washed, and then dried in an air oven at 45°C.

The polymers were then heated with pyridine in sealed tubes in order to transform any halogen atom endgroups presumably incorporated in them to quaternary pyridinium halide endgroups. The quaternised polymers were then properly purified of pyridine and dried. Tests for halogen in the polymers were then carried out by the dye-partition technique, using an aqueous disulfine blue reagent. Quantitative analysis was carried out spectrophotometrically.[1] The determination of the carboxyl endgroup in polymers obtained in the presence of oxalate ions was carried out by the dye interaction test using a Rhodamine reagent.[2]

Results and Discussion

The hydrogen peroxide-initiated polymerization of MMA in the presence of the halide salts in aqueous media proceeds with certain characteristics, the polymers being obtained in a coarse precipitated form. The increase in the salt concentration results in an increase in the induction period, probably due to some replacement of the active OH· radicals by the less active halogen atoms according to the above reaction. The increase in salt concentration also leads to an appreciable decrease in the yield of the polymer. No polymerization occurs in the presence of potassium iodide, probably because of the fast oxidation of the iodide ion by the active OH· radicals with the liberation of iodine, which acts as a strong inhibitor. The general features of polymerization in the presence of oxalate ion in aqueous media are more or less the same as in presence of F^-, Cl^- or Br^- ions.

The polymers obtained with the use of H_2O_2 as the initiator in aqueous media have been found, by the application of the sensitive dye technique,[3] to bear an OH endgroup only to the extent of about 1 per chain. However, when prepared in the presence of the halide ions (F^- Cl^- and Br^-), they also give a positive response to the dye partition

† Part I of the seriss Published in *J. Polymer. Sci.*, **A4**, 901 (1966).

* Present address: Department of Applied Chemistry, University College of Science & Technology, 92, Acharyya P. C. Road, Calcutta 9, India

1) M. N. Saha, P. Ghosh and S. R. Palit, *J. Polymer Sci.*, **A2**, 1365 (1964).

2) S. R. Palit and P. Ghosh, ibid., **58**, 1225 (1962).

3) P. Ghosh, A. R. Mukherjee and S. R. Palit, ibid., **A2**, 2807 (1964).

TABLE I.* ENDGROUP RESULTS OF PMMA OBTAINED BY AQUEOUS PHOTOINITIATION WITH H_2O_2 IN PRESENCE OF HALIDE IONS

[MMA] = 0.094 mol./l.

Concn. of H_2O_2 mol./l.	Concn. of halide ion mol./l.	$[\eta]$[a] of the polymer	OH/ chain	Halogen chain	Total endgroup/ chain	$\frac{[Hal]}{[OH]+[Hal]}$ %
	[NaF]			[Fluorine]		
0.05	0.0	0.81	1.05	0.0	1.05	0.0
0.05	0.012	0.75	1.20	0.15	1.35	11.1
0.05	0.024	0.70	1.13	0.10	1.23	8.1
0.05	0.047	0.65	1.20	0.15	1.35	11.1
0.05	0.119	0.53	1.14	0.16	1.30	12.3
0.05	0.238	0.40	1.00	0.07	1.07	6.5
0.05	1.190	0.35	1.08	0.05	1.13	4.6
	[KCl]			[Chlorine]		
0.05	0.134	0.38	1.21	0.06	1.27	5.3
0.05	0.402	0.36	1.13	0.07	1.20	6.0
0.05	0.938	0.30	1.00	0.03	1.03	3.7
	[KBr]			[Bromine]		
0.02	0.0	1.09	1.20	0.0	1.20	0.0
0.02	0.42	1.02	1.29	0.090	1.38	6.5
0.02	0.89	0.90	1.30	0.098	1.39	7.0
0.02	1.26	0.82	1.26	0.060	1.32	4.5
0.02	1.68	0.64	1.31	0.056	1.36	4.1
0.05	4.20	0.35	1.22	0.12	1.34	8.9
0.05	5.88	0.28	1.04	0.07	1.11	6.7
0.05	7.56	0.24	0.96	0.053	1.01	5.2

* Similar trend of result was also obtained using Fe^{2+}/H_2O_2 system as the source of hydroxyl radicals.

a) The intrinsic viscosity $[\eta]$ of the polymers, obtained by the usual extrapolation method was transformed to the number average molecular weight ($\overline{M}_n$) by the application of the following equation.

$$\overline{M}_n = 2.81 \times 10^5 \times [\eta]^{1.32} \quad \text{(PMMA in benzene)}$$

TABLE II. ENDGROUP RESULTS OF PMMA OBTAINED BY AQUEOUS PHOTOINITIATION WITH H_2O_2 IN PRESENCE OF OXALATE IONS

[MMA] = 0.094 mol./l.

Concn. of H_2O_2 mol./l.	Concn. of Na-oxalate mol./l.	$[\eta]$ of the polymer	OH/ chain	Carboxyl/ chain	Total endgroup/ chain	$\frac{[COOH]}{[OH]+[COOH]}$ %
0.0176	0.00074	1.06	1.18	0	1.18	0.0
0.0176	0.0037	1.04	1.23	0	1.23	0.0
0.0176	0.0074	1.01	1.26	0.06	1.32	4.5
0·0176	0.0370	0.95	1.11	0.11	1.22	9.0
0.0176	0.0740	0.881	1.15	0.20	1.35	14.8

test with aqueous disulfine blue reagents for halogen atom endgroups (transformed to quaternary halide groups) (Table I). For quantitative purposes, it is assumed that the different pyridinium halides (fluoride, chloride and bromide) groups are all equally responsive to the appropriate dye test; the spectrophotometric determinations are based on a comparison of the experimental optical density values with the same calibration curve of a particular model compound. There is, of course, some uncertainty about the quantitative values for halogen contents in the polymers, as these are highly contingent upon the very slow and sluggish process of quaternisation,[4,5] which is slower and more sluggish than usual in the present case as the concentration of halogens, (appearing only at chain ends) in the polymer is extermely low. The process of quaternisation may be completed to varying extents in different samples. Due to these limitations, a proper order in halogen content in the polymers as determined from any consideration is probably far from expectation; in fact, none is realised by our experiments. However, qualitatively the dye techniques employed for the endgroup characterisation of the polymers obtained

4) R. M. Fuoss and U. P. Strauss, ibid., **3**, 246 (1948).
5) R. M. Fuoss and M. Watanabe, ibid., **48**, 5 (1960).

in the present set of experiments give a simple and sound demonstration of the radical transfer reaction between OH· radicals and F^-, Cl^- and Br^- ions in aqueous media.

It is known that chloride ions inhibit the reactions of OH· radicals, and this can be explained on the basis of radical ion transfer reaction under discussion.[6-9] Expectedly, the effect is greater with bromide ion. However, with fluoride ions with a very high affinity for electrons, a similar effect appears to be much less favoured,[10] if not improbable. A fairly positive test for fluorine-atom endgroups in polymers prepared in the presence of fluoride ions indicates, however, the occurrence of the electron transfer reaction between the OH· radical and the F^- ion.

Much as hadide ions, oxalate ions also take part in electron transfer reaction with OH· radicals; this is clearly indicated by the presence of carboxyl endgroups in the respective polymers (Table II). The generation of carboxyl radicals probably occurs by means of the following mechanism:

$$\mathrm{OH\cdot} + \begin{matrix}\mathrm{COO^-}\\ |\\ \mathrm{COO^-}\end{matrix} \rightarrow \begin{matrix}\mathrm{COO\cdot}\\ |\\ \mathrm{COO^-}\end{matrix} + \mathrm{OH^-}$$

$$\downarrow$$

$$\mathrm{CO_2} + \mathrm{\dot{C}OO^-}$$

Thanks are due to CSIR (Government of India) for its financial assistance.

6) H. Taube and W. C. Bray, *J. Am. Chem. Soc.*, **62**, 3357 (1940).
7) A. O. Allen, *J. Phys and Colloid Chem.*, **52**, 479 (1948).
8) I. M. Kolthoff and A. I. Medalia, *J. Am. Chem. Soc.*, **71**, 3777, 3784 (1949).
9) W. G. Barb, J. H. Baxendale, P. George and K. R. Hargrave, *Trans. Faraday Soc.*, **47**, 462, 591 (1951).
10) N. Uri, *Chem Revs.*, **50**, 375 (1952).
11) J. H. Baxendale, S. Bywater and M. G. Evans, *J. Polymer Sci.*, **1**, 237 (1946).

The Copolymerization of Trimethylethylene and Tetramethylethylene with Maleic Anhydride*

By Shunsuke MURAHASHI, and Shun'ichi NOZAKURA

Department of Polymer Science, Faculty of Science, Osaka University, Toyonaka, Osaka

and Katsutoshi YASUFUKU

Institute of Physical & Chemical Research, Bunkyo-ku, Tokyo

(Received October 11, 1965)

In a previous paper,[1] it was reported that *cis*-butene-2 was more reactive than the *trans*-isomer in the copolymerization with maleic anhydride (MAn). We wish now to report the copolymerization behavior of trimethylethylene and tetramethylethylene with MAn in comparison with that of butene-2. Trimethylethylene was readily copolymerized with MAn to give a copolymer with a relatively high molecular weight, whereas tetramethylethylene gave practically no copolymer with MAn.

Momoners were copolymerized at 60°C in benzene in the presence of 2, 2'-azobisisobutyronitrile as an initiator. Conversions were less than 5% in all cases. Copolymers were purified by repeated reprecipitation from an acetone solution with dry ether. The copolymer compositions were calculated from the analysis with correction for absorbed water. Specific viscosities were measured in acetone at 30°C, using an Ostwald viscometer. The results are shown in Fig. 1.

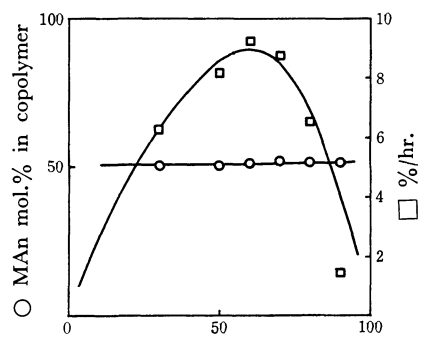

Fig. 1. Copolymerization of trimethylethylene (M_2) with MAn (M_1). $[M_1+M_2]=2.0$ mol./l., [AIBN]=0.01 mol./l. in benzene at 60°C.

The resulting copolymers of trimethylethylene with MAn were found to have a 1 : 1 molar composition and almost identical specific viscosities (0.14—0.18, $c=0.3$ g./dl.), independent of the monomer compositions. It was observed that

* Paper VIII in a series on "The Polymerization of Internal Olefins." For the preceding paper, see S. Murahashi, S. Nozakura, T. Okamoto and Y. Kotake, *Chem. High Polymer (Kobunshi Kagaku)*, in press.

1) S. Murahashi, S. Nozakura and K. Yasufuku, This Bulletin, **38**, 2082 (1965).

Table I. Comparison of the reactivities of butene-2, trimethylethylene (M_2) and tetramethylethylene in the copolymerization with MAn (M_1)
$[M_1]=[M_2]=1.0$ mol./l., [AIBN]=0.01 mol./l. in C_6H_6, 60°C

M_2	Rate %/hr.	$\eta_{sp/c}$	Soft p. °C	r_1
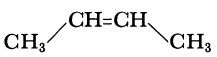	0.8	0.08	185—190	0.016±0.005
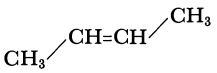	0.6	0.07	175—185	0.030±0.009
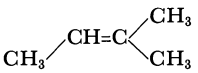	10.0	0.18	245—250	0.005±0.002
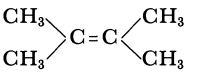	0	—	~150	—

* $c=0.3$ g./dl.

the rate of copolymerization reached a maximum value at the monomer composition of about 60 mol.% of MAn. A distinct yellow coloration was observed on mixing tetramethylethylene with MAn, suggesting the formation of a charge transfer complex between monomers. However, this system did not give an appreciable amount of copolymer by the usual procedure. A very slow polymerization was recognized from the facts that a slight volume contraction was observed in a dilatometric measurement and that a trace of colored noncrystalline powder (soft. p. ~150°C) was obtained by the careful treatment of the contents of the dilatometer.

Table I gives a comparison of the copolymerization behavior of trimethylethylene, tetramethylethylene, *cis*- and *trans*-butene-2[1] with MAn under similar conditions. Trimethylethylene, in comparison with butenes, copolymerized with a higher rate and with a greater tendency to alternation with MAn, yielding copolymers of higher specific viscosities. This result was rather unexpected, but it was rationalized as follows. The higher reactivity of trimethylethylene compared with butene-2 may be due to the increase in the electron density of the C=C double bond by the substitution of one more methyl group, since the MAn radical is partially positive in character. Also, the increase in the resonance stability of the resulting radical might have contributed to the reactivity. The increase in steric hindrance due to the additional methyl group might not play a significant role in this case.

The introduction of the fourth methyl group resulted in a further increase in the electron density, as is shown in the yellow coloration of a charge transfer complex. The low reactivity of tetramethylethylene, however, suggests the overwhelming effect of the steric inhibition of four methyl groups. Similar behavior of the multi-substituted ethylenes had been found in the copolymerizations of chlorinated ethylenes with various monomers.[2]

2) K. W. Doak, *J. Am. Chem. Soc.*, **70**, 1525 (1948).

T-E_γ Charts of Short-Lived Nuclides Formed by Neutron Activation

By Minoru OKADA*

Government Chemical Industrial Research Institute, Tokyo, Shibuya-ku, Tokyo

(Received October 11, 1965)

Whenever γ-active radionuclides formed by nuclear-reactor exposure are dealt with, it is useful to identify the nuclides by using a chart in which the half-life, T, is plotted against the γ-ray energy, E_γ. For the half-life range from 36 sec. to 10^4 hr., T-E_γ charts have been made by Westermark and Sjöstrand.[1] Recently, however, nuclides with shorter half-lives have become familiar in rapid radioactivation analysis. Therefore, a T-E_γ chart for shorter half-lives is needed. Since neutrons in nuclear reactors exhibit an extremely broad energy range, from zero to at least 15 MeV.,[2] various types of neutron reactions are likely to occur simultaneously. The charts presented here include the nuclides formed by these reactions.

The data have been taken from the table of the "Short-Lived Nuclides"[3]. The reactions considered are: (n, γ), (n, n'), (γ, γ'), (n, p), (n, α), $(n, 2n)$, (γ, n), $(n, n'\alpha)$, (n, pn), (n, t), $(n, {}^3\mathrm{He})$ and $(n, 2p)$. The charts show nuclides formed from naturally-occurring elements; they do not include the following:

(a) Nuclides formed by secondary nuclear reactions, e. g., $^{28}\mathrm{Al}(t, p)^{28}\mathrm{Mg}$ with lithium present.

(b) Nuclides formed by multiple neutron capture.

(c) Fission products.

Annihilation radiations are included in the charts unless they are very weak. X-rays are omitted. Whenever possible, the most intense γ-ray has been especially labeled in the charts.

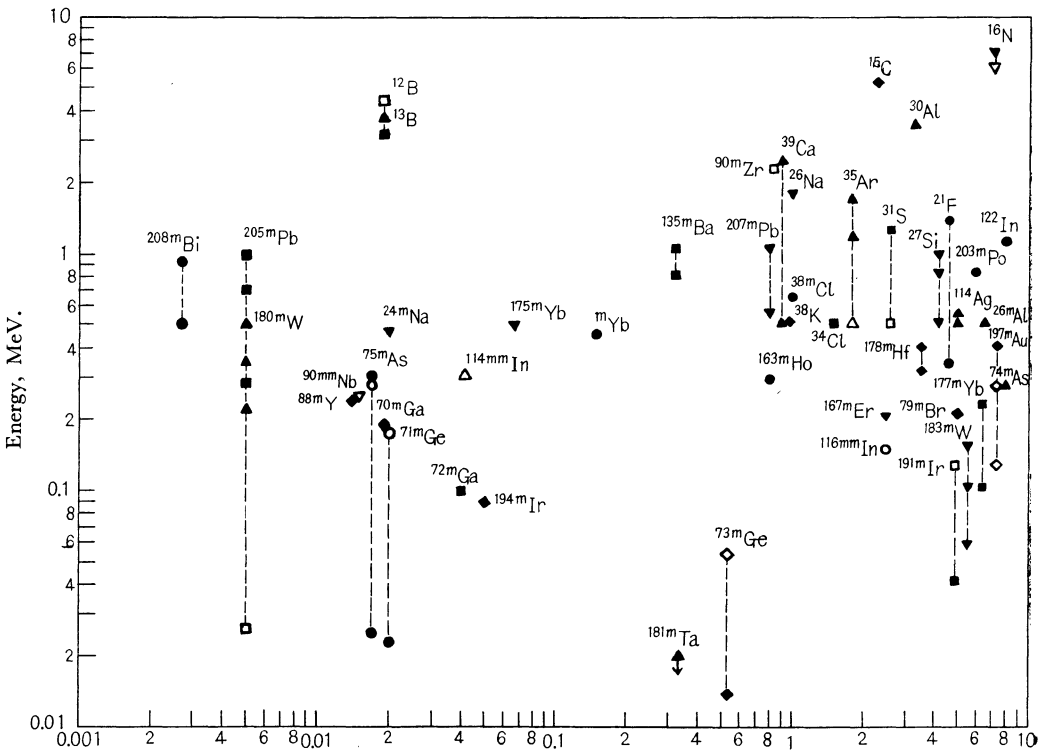

Fig. 1. T-E_γ chart No. I covering half-lives of 0.001—10 sec. The most intense γ-rays are labeled with open circles, open triangles, etc. If several γ-rays are emitted from the same nuclide, dots connect the corresponding points. Arrow in the charts shows that the true value should appear on the direction but only a limit is known.

* Present address: Japan Atomic Energy Research Institute, Takasaki, Gumma.

1) T. Westermark and B. Sjöstrand, *Intern. J. Appl. Radiation and Isotopes*, **9**, 63 (1960).
2) D. J. Hughes, *Nucleonics*, **11**, No. 1, 30 (1953).
3) M. Okada, ibid., **22**, No. 8, 110 (1964).

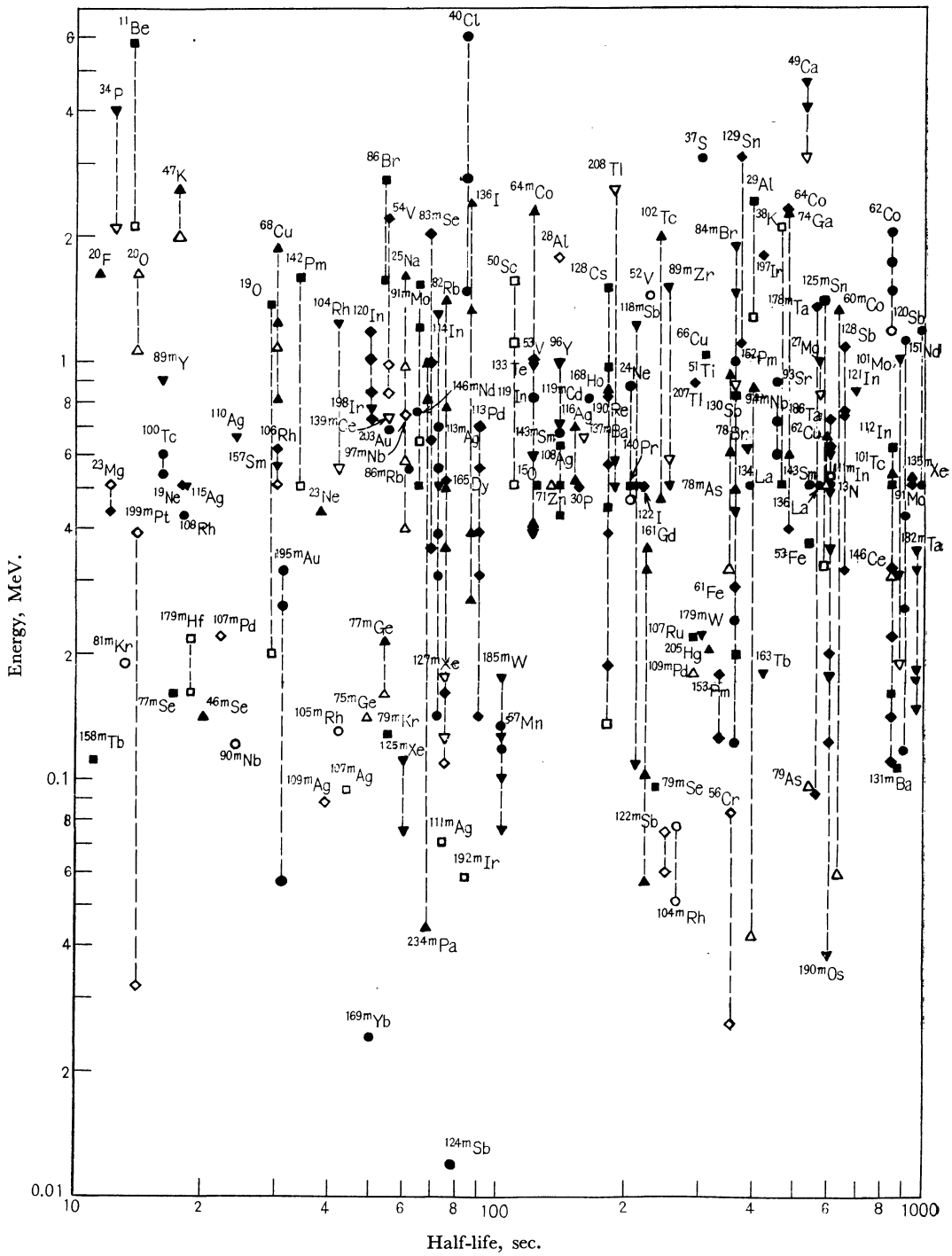

Fig. 2. T-E_γ chart No. II covering 10—1000 sec. For notes on use, see Fig. 1.

The Reaction of Benzenediazonium-2-carboxylate with Acrylonitrile and Ethyl Acrylate

By Tsutomu MATSUDA and Tetsuo MITSUYASU

Department of Organic Synthesis, Faculty of Engineering, Kyushu University, Hakozaki, Fukuoka

(Received October 23, 1965)

Stiles et al.[1] have reported a new route for obtaining the benzyne intermediate (I) by the thermal decomposition of benzenediazonium-2-carboxylate (II); they confirmed its formation by studying a Diels-Alder reaction with furan and anthracene. This procedure to obtain I has several advantages over the method usually adopted, in which aryl halides are reacted with strong bases, alkali metals or organometallic compounds in the presence of appropriate substrates. First, I can be allowed to react in situ with the compounds which have functional groups that are sensitive to strong bases or organometallic reagents. Second, the reaction may be carried out in various solvent.

In the course of our study of the chemical behavior of I in this route, we found that 1, 2-cycloaddition of I, with acrylonitrile and ethyl acrylate, proceeded to give benzocyclobutene derivatives under some conditions.

Stiles et al. carried out their experiment on I in non-polar solvents, such as benzene or furan. However, the reaction of II with either acrylonitrile or ethyl acrylate at 50—60°C for 6 hr. resulted in excessive polymerization, and no other isolable product was obtained. In view of the salt-like nature of II, we felt that the use of some polar solvent in place of a non-polar solvent would give rise to a better result. Although dimethylformamide and II, when treated at 55—60°C for 6 hr., afforded salicylaldehyde in a 18% yield[2] (as identified by a study of its infrared spectrum and that of its semicarbazone), dioxane was found to be a favorable solvent. Thus, the reaction of II and furan in dioxane at 50—55°C for 13 hr. gave a 65% yield of 1, 4-dihydronaphthalene-1, 4-endoxide, m. p. 55.5—56.1°C (lit.[1] 55.2—56.2°C). A comparable yield was, therefore, attained in a much shorter reaction time than that reported by Stiles et al. The following experiments were, then, all carried out in dioxane.

A suspension of 10.9 g. of freshly-prepared II in a mixture of 5.74 g. of acrylonitrile and 150 ml. of dioxane was stirred under nitrogen at 50—55°C

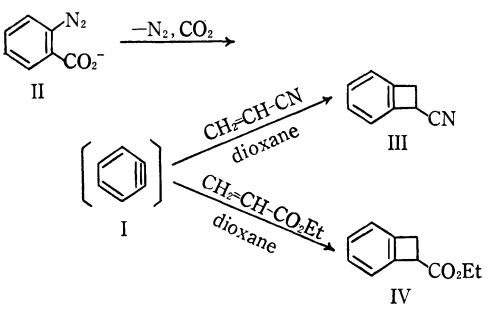

for 6 hr. After the dioxane and acrylonitrile had been distilled off under a vacuum, the flash distillation of the residue gave a yellow liquid, b. p. 48—86°C/0.6 mmHg; 1.92 g. (20%). The redistilled product, b. p. 54—55°C/0.3 mmHg; n_D^{26} 1.5442, which was found to be pure by gas chromatographic analysis, showed a C=N stretching band at 2250 cm^{-1}, and both its ultraviolet absorption and its NMR spectrum [(p. p. m. from TMS and relative areas), 7.14 (4.3), 4.09 (1.0): quartet, and 3.45 (1.9): triplet], were found to be consistent with the structure of 1-cyano benzocyclobutene (III). Further proof of the structure was obtained by the hydrolysis of the nitrile to the carboxyamide, m. p. 155.1—155.6°C (lit.[3] 155—156°C) and to the carboxylic acid, m. p. 74.8—75.4°C (lit.[3] 74.0—75.5°C).

In nearly the same procedure, the reaction of II, 2.09 g., and freshly-distilled ethyl acrylate, 2.0 g., in 50 ml. of dioxane at 50—55°C for 6 hr. gave a raw product, b. p. 82—108°C/3.5 mmHg; 0.25 g. (8%), and a considerable amount of a residue. The separation of the main constituent (90%) of the product by the gas chromatographic method gave nearly pure ethyl benzocyclobutene-1-carboxylate (IV); its identity was confirmed by a comparison of its infrared specturm with that of the authentic ester, prepared by the esterification of benzocyclobutene-1-carboxylic acid.

The reaction of II with maleic anhydride in dioxane was examined, but phenol was the only product identified.

1) M. Stiles and R. G. Miller, *J. Am. Chem. Soc.*, **82**, 3802 (1960); M. Stiles, R. G. Miller and U. Burckhardt, ibid., **85**, 1792 (1963).

2) S. Yaroslavsky (*Tetrahedron Letters*, **1965**, 1503) has recently reported the formation of salicylaldehyde in a 32% yield.

3) J. F. Bunnett and J. A. Skorcz, *J. Org. Chem.*, **27**, 3836 (1962).

Organic Sulfur Compounds. VII. The Reaction of Methyl *p*-Toluenesulfinate-[sulfinyl-^{18}O] with Phenylmagnesium Bromide

By Michio KOBAYASHI* and Miki TERAO

Department of Chemistry, Yokohama City University, Mutsuura-machi, Kanazawa-ku, Yokohama

(Received November 1, 1965)

The formation of sulfoxides from the sulfinic esters and Grignard reagents has been long known.[1] Recently this method has been utilized for the preparation of the optically active sulfoxides from *l*-menthyl sulfinates and Grignard reagents.[2] Since the configuration of the resulted sulfoxide is opposite to that of the starting sulfinate ester, this reaction has been considered to proceed by a S_N2 type nucleophilic attack on the sulfur atom, with an inversion and displacement of the alkoxide anion[3]:

$$R\text{-}\underset{\underset{O}{\downarrow}}{S}\text{-}OR' + R''MgBr \rightarrow R\text{-}\underset{\underset{O}{\downarrow}}{\overset{\overset{R''}{|}}{S}} + R'OMgBr \quad (1)$$

However, it has not yet been experimentally established which oxygen atom of the sulfinate ester is replaced. This point should be clarified by an examination of the reaction of a Grignard reagent with sulfinate ester-[sulfinyl-^{18}O].

Methyl *p*-toluenesulfinate-[sulfinyl-^{18}O], prepared by the reaction of sodium *p*-toluenesulfinate-^{18}O and ethyl chlorocarbonate in methanol,[4] was therefore treated with phenylmagnesium bromide to give phenyl *p*-tolyl sulfoxide. The excess atom percentage of ^{18}O of this sulfoxide was found to be exactly twice that of the starting methyl sulfinate. This fact can best be explained by postulating the retention of the sulfinyl oxygen atom of the methyl ester in the sulfoxide formed.

The above result is consistent with the currently accepted S_N2 mechanism which may be depicted thus:

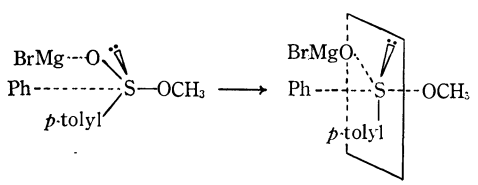

(transition state)

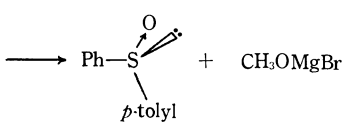

(2)

On the other hand, the coordination of the bromomagnesium cation with the sulfinyl oxygen atom of the ester could result in the formation of the sulfonium cation, in which a lone pair electron may enter the 3s orbital and in which three 3p orbitals are available for the formation of three single bonds. The attack of the anionoid phenyl group on the sulfur atom of this cation may occur from the unhindered open side, to give a tetrahedral intermediate (I) using a 3d orbital:

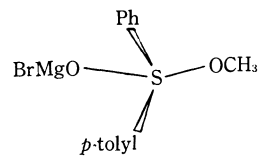

(I)

Similar tetrahedral intermediates with a lone pair in a 3s orbital have been postulated in the reaction of triphenylsulfonium bromide with phenyllithium or *n*-butyllithium.[5]

The elimination of a methoxide anion from I would lead to the sulfoxide with an inverted configuration. Therefore, both the above experimental results and the asymmetric syntheses in the literature can be explained by either the S_N2 mechanism or the tetrahedral intermediate mechanism. The S_N2 mechanism seems to be most plausible in the analogous ester exchange reaction of the sulfinate esters,[6] but in those cases the formation of the sulfonium cation, in which the positive charge on the sulfur atom could cause the $3p^3$ electronic structure discussed above, is impossible.

Experimental

Methyl *p*-Toluenesulfinate-[sulfinyl-^{18}O]. — Prepared from sodium *p*-toluenesulfinate-^{18}O and ethyl

* To whom correspondence should be sent: Department of Dhemistry, Faculty of Science, Tokyo Metropolitan University, Setagaya-ku, Tokyo.

1) H. Gilman, J. Robinson and N. H. Beaber, *J. Am. Chem. Soc.*, **48**, 2715 (1926); H. Gilman and J. Robinson, *Bull. soc. chim. France*, [4] **45**, 636 (1929).
2) K. K. Anderson, *Tetrahedron Letters*, No. 3, 93 (1962).
3) K. K. Anderson, *J. Org. Chem.*, **29**, 1953 (1964); K. Mislow, M. M. Green, P. Laur, J. J. Melillo, T. Simmons and A. L. Ternay, Jr., *J. Am. Chem. Soc.*, **87**, 1958 (1965).
4) Part VI of this series: M. Kobayashi and M. Terao, This Bulletin, **39**, 1292 (1966).
5) V. Franzen and C. Mertz, *Angew. Chem.*, **72**, 416 (1960).
6) H. Phillips, *J. Chem., Soc.*, **127**, 2552 (1925).

chlorocarbonate in methanol.[4] The ^{18}O atom percentage of this ester was 0.41%.

Phenyl *p*-Tolyl Sulfoxide-^{18}O.—A Grignard reagent prepared from 5.0 g. of bromobenzene and 0.8 g. of magnesium in 20 ml. of ether was added, drop by drop to 2.0 g. of methyl *p*-toluenesulfinate-^{18}O in 30 ml. of benzene. An excess of 3 N hydrochloric acid was then added to the reaction mixture to dissolve the white precipitate, and the organic layer was separated, washed with alkali and water, and dried over magnesium sulfate. The solvent was evaporated, and the oily residue was dissolved in warm petroleum ether and kept overnight. The colorless crystals of sulfoxide which separated were purified by elution chromatography over alumina with benzene to give an analytical sample. The atom percentage of ^{18}O in this product was 0.62%. The calculated ^{18}O atom%, based on the assumption of a reaction of the sulfinyl oxygen of the ester, is 0.61%.

The authors are indebted to Dr. Reiko Kiritani of the Radiation Center of Osaka Prefecture for the analyses of ^{18}O and to Professor Shigeru Oae for the donation of heavy oxygen water.

The Electrical Conduction of Organic Dye Complex Salt between Cationic and Anionic Dyes*

By Shigekazu KUSABAYASHI,** Akimasa TANIGUCHI and Hiroshi MIKAWA**

The Institute of Scientific and Industrial Research, Osaka University, Sakai, Osaka

(Received November 8, 1965)

Many investigations have been made into the semiconducting properties of organic dyes. All classes of the dyes—cationic, anionic or non-ionic—exhibit a small conductivity in the dark. In all these ionic dyes but oxalate, the anion of the cationic dye and the cation of the anionic dye consist of inorganic ions. Concerning the cationic dyes with the triphenylmethane structure, Nelson reports that the dark conductivity is greatly changed by a change of anion.[1]

It is supposed that cationic and anionic dyes together make a salt which is composed of organic cations and organic anions, many combinations of the two dye ions being possible. The present paper will deal with the dark conductivity of some organic dye complex salts.

Experimental

Material.—Malachite green, crystal violet and methylene blue were selected as the cationic dyes, and eosine Y, erythrosine, rose bengal and acid rhodamine were selected as the anionic dyes. All the dyes except erythrosine were recrystallized three times; erythrosine was purified by repeated precipitations.

Organic dye complex salts were prepared by dissolving both component dyes in water at room temperature. To take the dye complex salt between malachite green and eosine as an example, it was prepared as follows. A 2/100 molar aqueous solution of malachite green and a 1/100 molar aqueous solution of eosine are stirred together, and then stirring is continued for another hour. The crystalline product thus obtained is washed with water until the washed water is almost colorless, and recrystallized twice from alcohol. Organic dye complex salts obtained in the same way are tabulated in Table I.

Measurement. — The electrical resistivity was measured on a compressed disk made under 5 t/cm^2 in a vacuum, with silver electrodes by the DC method.

Results and Discussion

The mole ratio between the components of the dye complex salts, as calculated from the carbon percentage, does not always agree with the theoretical composition anticipated from the chemical structures of the component dyes. However, the composition of the dye complex salts is supposed to be as shown in the first column of Table I. Seyewetz[2] and Pelet-Jolivet[3] have reported that a 2 mol. portion of fuchsine combines with 1 mol. of eosine or erythrosine, and also that methylene blue makes a product of a definite composition with eosine.

The absorption sepctra of complex salts were measured in an alcohol solution. Generally, the wavelengths of the absorption peaks were nearly identical with those of the components.

Some absorption spectra of the solid film were also measured. Of these, the absorption spectrum of $(MB)_2(RB)$ is shown in Fig. 1; it is quite different from that of a solution. Its longest-wavelength absorption band is split into two bands in spite of the fact that no splitting is found in the solid absorptions of the two component dyes.

Electrical Property.—The relation between the current and the applied voltage obeyed Ohm's

* Presented at the 18th Annual Meeting of the Chemical Society of Japan, Osaka, April, 1965.

** Present address: Department of Chemical Technology, Faculty of Engineering, Osaka University, Miyakojima-ku, Osaka.

1) R. C. Nelson, *J. Chem. Phys.*, **20**, 1327 (1952).

2) M. A. Seyewetz, *Bull. Soc. Chim. France* [3], **23**, 618 (1900); *Compt. rend.*, **130**, 1770 (1900).

3) M. L. Pelet-Jolivet, ibid., **145**, 1182 (1907).

TABLE I. PROPERTIES OF ORGANIC DYE COMPLEX SALTS

Composition*	Color of powder	Decomp. p. (approx.) °C	C %		Elec. properties	
			Found	Calcd.	ρ_{20}, Ω cm.	ε, eV.
$(MG)_2(EO)$	dark purple	160	62.24	60.75	5.8×10^{13}	2.35
$(MG)_2(ER)$	dark brown	240	53.78	53.10	2.4×10^{12}	1.73
$(MG)_2(RB)$	purple	155	50.48	48.62	3.1×10^{14}	1.42
(MG)(AR)	dark green	220	64.00	67.70	1.1×10^{10}	1.24
$(CV)_2(EO)$	dark green	190	58.68	60.44	2.3×10^{13}	1.41
$(CV)_2(ER)$	dark purple	195	52.95	53.25	1.7×10^{13}	1.31
$(CV)_2(RB)$	greenish brown	175	51.50	48.98	1.7×10^{11}	2.33
(CV)(AR)	dark green	120	62.85	67.14	3.5×10^{11}	1.98
$(MB)_2(EO)$	dark green	190	49.04	51.42	2.5×10^{9}	1.32
$(MB)_2(ER)$	dark green	185	42.75	44.53	3.0×10^{9}	1.10
$(MB)_2(RB)$	brown	200	42.05	40.54	1.3×10^{10}	1.32
(MB)(AR)	green	210	57.85	61.33	2.5×10^{12}	1.17

* Cationic part of malachite green, crystal violet and methylene blue are abbreviated as MG, CV and MB, respectively. Anionic part of eosine, erythrosine, rose bengal and acid rhodamine are abbreviated as EO, ER, RB and AR, respectively.

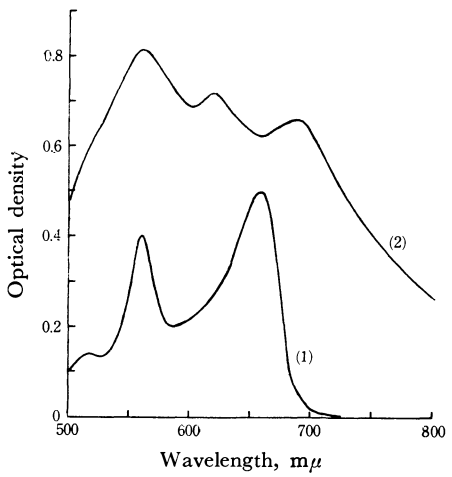

Fig. 1. Absorption spectra of dye complex salt between methylene blue and rose bengal.
(1) alcohol solution (2) solid film

law. In $(CV)_2(RB)$, for example, the relation obeyed Ohm's law up to 3460 V./cm. at least. In (MG)(AR), however, the current is proportional to the voltage to the power of 1.5. The resistivity at 20°C (ρ_{20}) and the band gap energy (ε), as calculated from the temperature dependence of the resistivity by the equation $\rho=\rho_0\exp(\varepsilon/2kT)$, are tabulated in Table I. The values of the resistivity and the band gap energy for dye complex salts fall in the 10^9—10^{15} Ωcm. and 1.1—2.3 eV. ranges respectively. The values of ρ_{20} and ε change with the change in the partner ion in dye complex salt. Generally the complex salts of methylene blue have low values in ρ_{20} and ε.

The authors wish to express their thanks to Mr. Tsuneyo Shishido for his elementary analyses.

SHORT COMMUNICATIONS

Lithium Aluminum Oxyfluoride Spinel

By Hiroaki YANAGIDA, Goro YAMAGUCHI and Yuzo ONO

Department of Industrial Chemistry, Faculty of Engineering, The University of Tokyo, Hongo, Tokyo

(Received March 7, 1966)

Kordes[1] obtained a spinel-like mineral from a mixture of lithium fluoride and aluminum oxide by heating it to 1300°C. He supposed that a $LiF\text{-}Al_2O_3$ spinel form exists. However, he determined the mineral obtained at 1300°C to be $Li_2O\text{-}5Al_2O_3$, which did not contain fluorine; he did not mention the composition of the products at lower temperatures further. All of the spinel structures previously investigated contain only oxygen or sulfur as an anion, except for the aluminum oxynitride spinel, $AlN\text{-}Al_2O_3$, investigated by Yamaguchi and Yanagida[2] and by Adams, AuCoin and Wolff.[3] It may be supposed, from a consideration of the ionic radii, that there exists a spinel form, $LiF\text{-}Al_2O_3$, which contains fluorine as an anion, in comparison with $MgO\text{-}Al_2O_3$ or $AlN\text{-}Al_2O_3$.

TABLE I. DIFFERENCES BETWEEN THE TWO SPINELS

	I $Li_2O\cdot 5Al_2O_3$	II The spinel obtained from $LiF\text{-}Al_2O_3$
Starting materials	Li_2CO_3 + $\gamma\text{-}Al_2O_3\cdot 3H_2O$	LiF 40 mol.%-$\gamma\text{-}Al_2O_3\cdot 3H_2O$
Temp.	>900°C	800—900°C
Lattice dimention	$a=7.906$ Å	$a=7.922$Å
Super lattice peaks		
(2,1,1)	12.7	—
(2,1,0)	16.5	4.4
(1,1,0)	11.6	4.0
F content by NMR	none	present at least 11%

Mixtures of fine-grained $\gamma\text{-}Al_2O_3\text{-}3H_2O$ or $\alpha\text{-}Al_2O_3$ and chemically pure lithium fluoride or lithium carbonate were heated at 600—1200°C for 0.5—3 hr. in an electric furnace in air. The products were then washed with hydrochloric acid to eliminate a trace of contamination by lithium fluoride and were analyzed by powder X-ray diffraction.

The single spinel phase was formed from the mixtures of lithium fluoride (35—40 mol. percent) and $\gamma\text{-}Al_2O_3\text{-}3H_2O$ (60—65 mol. percent) heated at 800—900°C for more than an hour. This spinel phase was then compared with the lithium aluminum oxide spinel, $Li_2O\text{-}5Al_2O_3$ (denoted as I in Table I). The cubic lattice dimensions, the intensity ratios of such super lattice lines[4] as (2, 1, 1), (2, 1, 0), (1, 1, 0) to a normal line (3, 1, 1), are distinctly different in the two spinels. This shows that the II spinel in Table I is to be distinguished from the I spinel.

The semi-quantitative analysis of fluorine was carried out by broad-line NMR using a mixture of AlF_3 and $\alpha\text{-}Al_2O_3$ as a reference. It was ascertained that the II spinel contained more than 11 percent fluorine, which corresponded to about 70 percent of the value calculated from the $LiF\text{-}Al_2O_3$ formula.

Thus, it is suggested that the II spinel obtained in the present work may either be in a spinel formula, $LiF\text{-}(1+x)Al_2O_3$, or in a solid solution of $LiF\text{-}Al_2O_3$ and $Li_2O\text{-}5Al_2O_3$. The true formula will be determined after an exact quantitative analysis of fluorine, which is now being attempted by the present authors using different methods.

1) E. Kordes, *Z. Krist.*, **A91**, 193 (1935).
2) G. Yamaguchi and H. Yanagida, This Bulletin, **32**, 1264 (1959).
3) I. Adams, T. R. AuCoin and G. A. Wolff, *J. Electrochem. Soc.*, **109**, 1050 (1962).
4) P. B. Braun, *Nature*, **27**, 1123 (1952).

Molecular and Intramolecular Relaxation in Several Biphenyls

By N. K. MEHROTRA and M. C. SAXENA

Physics Department, Lucknow University, Lucknow, India

(Received February 7, 1966)

The relaxation times of some biphenyls have been determined in the 3 cm. microwave region at a temperature of 20°C, using benzene as the solvent. It has been concluded from the smaller values of the relaxation time that the molecules are relaxed by both molecular and intramolecular rotations.

DiCarlo and Smyth[1] have determined the relaxation times of diphenyl sulphide, diphenyl methane and triphenyl amine. Kalman and Smyth[2] have investigated 4-bromobiphenyl in making a study of its dielectric dispersion. However, apparently no attempt has yet been made to study the mechanism of intramolecular rotation in the many biphenyls with different dipole-bearing groups. The aim of the present investigation is to get an idea about the nature of the molecular unit responsible for group rotation in *o*-aminobiphenyl, *p*-aminobiphenyl and 3, 5-dinitro-2-hydroxybiphenyl.

The free energies of the activation for dipole orientation and viscous flow have been calculated at the same temperature, using Eyring's[3] relations and estimated values of the constants A and B.

The relaxation times are determined by means of the fixed frequency method of Gopala Krishna.[4] The standing-wave technique of Von Hippel and Roberts[5] has been used for the measurements of the dielectric constant, ε', and the loss factor, ε''.

All the substances used were of pure quality L. R. grade and were obtained from the British Drug House. The purest-quality benzene obtained from the British Drug House was distilled before use.

The observed values of the relaxation time, along with the values of the activation energy, are given in Table I.

It may be seen from Table I that the relaxation time of *o*-aminobiphenyl is greater than that of *p*-aminobiphenyl, although the size of the two molecules is the same. This difference in the relaxation time can be explained by considering intramolecular group rotation. The polar $-NH_2$ group, which is capable of rotation round its bond with the ring, experiences a greater steric hindrance to rotation at the ortho position than at the para position. Further, however, while the molar volumes of the two molecules may be approximately same, the volumes swept out for dipole orientation by the two molecules must be different.

The relaxation time of 3, 5-dinitro-2-hydroxybiphenyl is found to be greater than those of *o*-amino- and *p*-aminobiphenyls. This may be due to the fact that there is a greater steric hindrance to the rotation of the –OH group at the position 2 due to the presence of a $-NO_2$ group at the position 3. Further, the observed larger value of relaxation time is in accordance with the bigger size of the molecule due to the presence of two nitro groups.

It may, therefore, be concluded from the rotations of the $-NH_2$ and –OH groups that the molecules are relaxed predominantly by the process of intramolecular rotations, resulting in a decrease in the observed relaxation time.

The value of the free energy of activation for *o*-aminobiphenyl has been found to be greater than that of *p*-aminobiphenyl, suggesting that the inner friction experienced by the former molecule is greater than that of the latter.

The free energies of activation for a viscous flow (H_η) are always found to be greater than those for the dielectric relaxation (H_τ). This is in conformity with the finding of Franklin and his coworkers[6] that H_τ and H_η are nearly equal only in the case of low viscosity solvents. A similar result was also obtained by Ahmad and Sharma[7] in the case of solutions of nitrotoluenes and *o*-chlorotoluene in cyclohexane.

TABLE I. VALUES OF THE RELAXATION TIME (τ) AND THE FREE ENERGIES OF ACTIVATION FOR DIPOLE ORIENTATION AND VISCOUS FLOW

Compound	$\tau \times 10^{12}$ sec.	H_τ kcal./mol.	H_η kcal./mol.	H_η/H_τ
(1) *o*-Amino-biphenyl	7.47	2.23	2.90	1.30
(2) *p*-Amino-biphenyl	6.64	2.16	2.90	1.34
(3) 3, 5-dinitro-2-hydroxy-biphenyl	9.96	2.39	2.90	1.21

1) E. N. DiCarlo and C. P. Smyth, *J. Am. Chem. Soc.*, **84**, 3638 (1962).
2) O. F. Kalman and C. P. Smyth, ibid., **82**, 783 (1960).
3) H. Eyring, S. Glasstone and K. J. Laider, "The Theory of the Rate Process," McGraw Hill Co, New York (1941), p. 548.
4) K. V. Gopala Krishna, *Trans. Faraday Soc.*, **53**, 767 (1957).
5) S. Roberts and A. Von Hippel, *J. Appl. Phys.*, **17**, 610 (1946).
6) A. D. Franklin, W. H. Heston, E. J. Hennelly and C. P. Smyth, *J. Am. Chem. Soc.*, **72**, 3447 (1950).
7) S. I. Ahmad and M. N. Sharma, *Indian, J. Phys.* **39**, 149 (1965).

The Temperature Dependence of the Absorption Spectra of Wurster's Blue-type Ion Radicals

By Ko UEMURA, Shigeki NAKAYAMA, Yukiko SEO, Keisuke SUZUKI and Yuzuru OOSHIKA

Faculty of Science, Kwansei Gakuin University, Nishinomiya

(Received March 12, 1966)

Hausser and Murrell[1] suggested dimer formation in Wurster's Blue solution and assigned the 12000 cm^{-1} band appearing at the temperature of liquid nitrogen to a charge-transfer absorption. We ourselves have previously studied the absorption spectra of *p*-phenylenediamine bromide (I), *N*, *N*-dimethyl-*p*-phenylenediamine (Wurster's Red) perchlorate (II), and *N*, *N*, *N'*, *N'*-tetramethyl-*p*-phenylenediamine (Wurster's Blue) perchlorate solutions (III).[2,3]

The spectra of solutions and solids of I and III are shown in Figs. 1 and 2, respectively. The

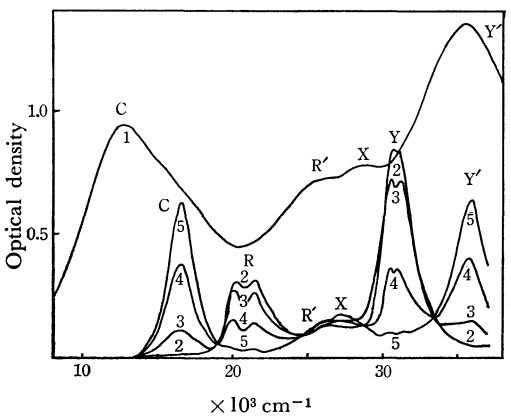

Fig. 1. Spectra of *p*-phenylenediamine radicals. Curve 1: solid (22°C), 2: solution (22°C), 3: solution (−78°C), 4: solution (−99°C), 5; solution (−129°C). Stoichiometric concentration ca. 4×10^{-5} mol./l. Optical path length 1.00 cm. Volume changes of the cell and the solution by cooling were calibrated.

spectra of II are very similar to those of I except for a slight red shift. The concentration dependence of the intensities of the above three compounds can be interpreted as due to the $2R^{+}+X^{-}\rightleftarrows(R_2X)^{+}$ equilibrium, assuming that the R and Y bands are to be attributed to the monomer, and R', Y', and C, to the dimer. The heats of dimerization are approximately 8, 10, and 5 kcal./mol. for I, II, and III, respectively. The weak binding in III is probably due to the increased steric repulsion between the methyl groups. The similarity of the solid

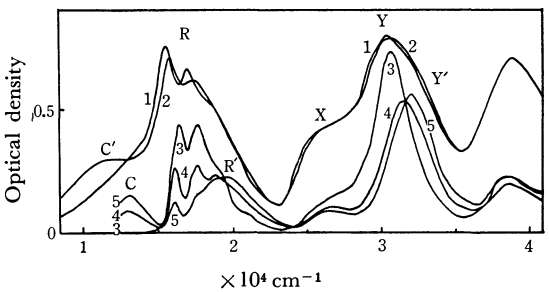

Fig. 2. Spectra of Wurster's Blue. Curve 1: solid (22°C), 2: solid (−196°C), 3: solution (22°C), 4: solution (−149°C), 5: solution (−160°C). Stoichiometric concentration of the solution: 7.58×10^{-5} mol./l. Solvent: ether-alcohol (1 : 2). Optical path length: 0.50 cm. Volume changes of the cell and the solution by cooling were calibrated.

spectra of I and II to those of the dimer suggests that the radicals exist as dimers in the solids; this is in accordance with ESR studies in this laboratory. The spectra of the solid of III at room temperature resemble those of the monomer, but this does not necessarily mean that the spectra are to be attributed to the monomer, for the main features of the spectra are preserved at low temperatures, where a weak charge-transfer band, C', is observed. Two types of models have been proposed for the low temperature solid of III, i. e., the doublet$\rightleftarrows$singlet[1] and singlet$\rightleftarrows$triplet[4] models. The concentration of the singlet dimer at the nitrogen temperature estimated from the magnetic susceptibility[5] is larger than 85%. The contradiction between the spectroscopic and magnetic data may be eliminated by assuming that the dimers are so loosely bound that the electronic states of the radicals are only slightly perturbed by the dimerization. This "loosely bound" model explains that the low temperature solid spectra are similar to the monomer spectra accompanied by a weak charge-transfer band.[6]

A detailed report will be published later elsewhere.

1) K. H. Hausser and J. N. Murrell, *J. Chem. Phys.*, **27**, 5000 (1957).

2) A part of this work was presented at the 18th Annual Meeting of the Chemical Society of Japan, April, 1965.

3) S. Nagakura, J. Tanaka and T. Sakata have also obtained the spectra of Wurster's Blue in alcoholic solution. It was presented at the 18th Annual Meeting of the Chemical Society of Japan, April, 1965.

4) D. D. Thoams, H. Keller and H. M. McConnell, *J. Chem. Phys.* **39**, 2321 (1963).

5) Data of K. Okumura (*J. Phys. Soc. Japan*, **18**, 69 (1963)) was used.

6) Boyd and Phillips recently obtained solution spectra of TCNQ anion radical and analyzed their results by assuming the simple dimerization equilibrium. Their heat of dimerization is of the same order of magnitude with those of II and III (*J. Chem. Phys.*, **43**, 2927 (1965)).

Hydrazine Formation in the γ-Radiolysis of an Aqueous Solution of Ammonia

By Akihisa SAKUMOTO

Tokai Research Establishment, Japan Atomic Energy Research Institute, Tokai, Ibaraki-ken

(Received March 15, 1966)

The effect of additives on the γ-radiolysis of liquid ammonia has been studied by only a few investigators.[1,2] In the present work, the hydrazine formation in the γ-radiolysis of a mixture of liquid ammonia and water at a high-dose irradiation was studied. Hydrazine was determined by the Watt and Chrisp method.[3] Figure 1 shows the relationships between the yield of hydrazine and the concentration of ammonia at room temperature and at -50°C. At the irradiation temperature of -50°C, the yield of hydrazine increases gradually to a maximum value at about 85 mol. %, and then decreases with an increase in the concentration of ammonia. On the other hand, the maximum yield of hydrazine is obtained at about 50 mol. % of ammonia when irradiation is performed at room temperature. The yield of hydrazine at -50°C is larger than that at room temperature at 100 mol. % of ammonia. The dashed lines represent the yield of hydrazine which may be expected if the formation of hydrazine is unaffected by the presence of water.

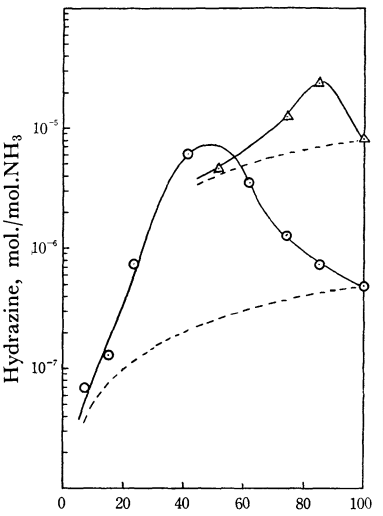

Fig. 1. Yield of hydrazine as a function of ammonia concentration at room temperature and at -50 ± 2°C when irradiated to a total dose of 9.15×10^6 r. at a dose rate of 4.5×10^4 r./hr.
○ Room temperature
△ -50 ± 2°C

As is shown in Fig. 1, the observed yields of hydrazine are larger than those to be expected from the molar fraction of ammonia and water. This indicates that the formation of hydrazine is influenced in some way by the interaction of ammonia with water. From the ionization potential[4] and the proton affinity[5] for ammonia, the proton transfer to ammonia may be expected to occur:

$$NH_3 + H_2O^+ \rightarrow NH_4^+ + OH \qquad (1)$$

though another possibility cannot be excluded:

$$NH_3 + H_3O^+ \rightarrow NH_4^+ + H_2O$$

The enhancement in the yield of hydrazine can be explained if the neutralization of NH_4^+ were to produce amino radicals as follows:

$$NH_4^+ + e^-_{amm}(\text{or } e^-_{aq}) \rightarrow \cdot NH_2 + H_2 \qquad (2)$$

$$\cdot NH_2 + \cdot NH_2 \rightarrow N_2H_4 \qquad (3)$$

On the basis of the above mechanism, we may say that the addition of ammonium ion would also contribute to the increment in the formation of hydrazine.

The details of this will be described elsewhere.

1) D. Cleaver, E. Collinson and F. S. Dainton, *Trans. Faraday Soc.*, **56**, 164 (1960); F. S. Dainton, T. Skwarski, D. Smithies and E. Wezranowski, ibid., **59**, 1063 (1963).
2) J. R. Puig and E. Schwarz, *Industrial Uses of Large Radiation Sources*, **1**, 57 (1963).
3) D. W. Watt and J. D. Chrisp, *Anal. Chem.*, **24**, 2006 (1952).
4) K. Watanabe and J. R. Mottl, *J. Chem. Phys.*, **26**, 1773 (1957).
5) A. P. Altshuller, *J. Am. Chem. Soc.*, **77**, 3480 (1955).

The Base-catalyzed Dimerization of 1, 4-Cyclohexadienes[1]

By Ken-ichi MORITA and Zennosuke SUZUKI

The Basic Research Laboratories, Toyo Rayon Company, Ltd., Kamakura

(Received March 15, 1966)

Hoffmann et al.[2] have reported that the treatment of 1, 4-cyclohexadiene (I) with *t*-butoxide in dimethylsulfoxide at 55°C gave a mixture of benzene and cyclohexene in a quantitative yield, while an analogous reaction in *t*-butyl alcohol as a solvent has afforded a mixture of I and 1,3-cyclohexadiene.[3] We now wish to report a base-catalyzed dimerization of 1, 4-cyclohexadinene derivatives in alcoholic solvents at an elevated temperature.

The reaction of 1, 4-cyclohexadiene (I) in alcoholic solvents such as methanol, ethylene glycol or *t*-amyl alcohol in the presence of a base such as potassium alkoxide, sodium alkoxide, potassium hydroxide or sodium hydroxide (10^{-1} to 10^{-3} mol.) at 200—230°C for 15 to 20 hr. afforded dicyclohexadiene (II),[4,8] b. p. 60—61°C/2 mmHg; n_D^{20} 1.5263, in 20 to 30% yields, and a mixture (60—70%) of benzene, cyclohexene and cyclohexadienes.

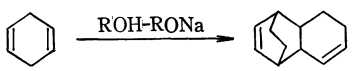

I II

An analogous base-catalyzed dimerization of dihydrotoluene[9] at 250—255°C for 17 hr. furnished a dimeric mixture of dihydrotoluene, b. p. 75—77°C/4 mmHg, in 20 to 25% yields. The treatment of 2-methoxy-1, 4-cyclohexadiene[9] (III) (7 g.) with 1 ml. of 10% potassium *t*-amyloxide (in *t*-amyl alcohol) in a glass ampoule[10] at 220°C for 24 hr. furnished a dimer V, $C_{14}H_{20}O_2$, (24%); b. p. 110—115°C/2 mmHg; $\nu_{C=C}^{film}$ 1669 cm^{-1}, 1-methoxy-1, 3-cyclohexadiene (IV) (19%), and a mixture (14%) of anisol, III, 1-methoxycyclohexene and benzene. Compound V was identical with a sample prepared in a 16% yield[12] (conversion) by the thermal dimerization of IV[11] at 200—220°C for 32 hr. An acid hydrolysis of V gave the keto ether VI, $C_{13}H_{18}O_2$, $\nu_{C=O}^{film}$ 1715, ν_{OMe}^{film} 1109 cm^{-1}; semicarbazone, m. p. 220—220.5°C decomp. The hydrogenation of VI over a palladium catalyst afforded VII, $C_{13}H_{20}O_2$; b. p. 135—137°C/2 mmHg, $\nu_{C=O}^{film}$ 1714 cm^{-1}, ν_{OMe}^{film} 1109 cm^{-1}. The reaction of pyrrolidyl enamine of 4-methoxybicyclo[2.2.2]octan-2-one (VIII)[14] with methyl vinyl ketone afforded IX., b. p. 145—147°C/1.4 mmHg; τ 6.85 (OMe); 4.37 (doublet, J= 2.5 c. p. s; a vinyl proton); $\nu_{C=O}^{film}$ 1665, $\nu_{C=C}^{film}$ 1632, ν_{OMe}^{film} 1102 cm^{-1}; semicarbazone, m. p. 204—205°C. The hydrogenation of IX over a palladium catalyst gave X, b. p. 135—136°C/2 mmHg, $\nu_{C=O}^{film}$ 1714 cm^{-1}, ν_{OMe}^{film} 1109 cm^{-1}; semicarbazone, m. p. 206—207°C (decomp.).[15] The infrared spectra of VII and X were similar, but some difference was noted in the fingerprint region.

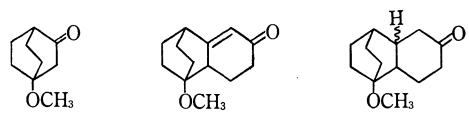

VIII IX X

1) Bridged Ring Compounds. VII. Paper VI: K. Morita and T. Kobayashi, *J. Org. Chem.*, in press.

2) J. E. Hoffmann, P. A. Argabright and A. Schriesheim, *Tetrahedron Letters*, **1964**, 1005.

3) Cf. R. B. Bates, R. H. Carnigham and C. E. Staples, *J. Am. Chem. Soc.*, **85**, 3032 (1963).

4) The identity was established by a comparison of the infrared spectra and the retention time of v. p. c. with those of a sample prepared according to the method of Kazanskii and Svirskaya,[5] who obtained dicyclohexadiene (II), b. p. 110—111°C/14mmHg; n_D^{20} 1.5269 in a 50% yield by the Diels-Alder dimerization of 1,3-cyclohexadiene. Since 1,4-cyclohexadiene (I) can readily be prepared from benzene,[6,7] the method described in this paper provides a convenient way to prepare II. It should be noted that a large amount of polymers have been obtained as by-products in the case of the thermal dimerization of 1,3-cyclohexadiene, whereas only a small amount of polymers were formed in the base-catalyzed dimerization of 1,4-cyclohexadiene.

5) B. A. Kazanskii and P. I. Svirskaya, *J. Gen. Chem., USSR*, **29**, 2550 (1959). See also K. Alder and G. Stein, *Ann.*, **496**, 197 (1932).

6) J. P. Wibaut and F. A. Haak, *Rec. trav. chim.*, **67**, 85 (1948).

7) R. A. Benkeser, E. M. Kaiser and R. F. Lambert, *J. Am. Chem. Soc.*, **86**, 5272 (1964).

8) The reaction of I with phenyllithium in tetrahydrofuran as a solvent afforded no II, but a moderate yield of biphenyl.

9) A. L. Wilds and N. A. Nelson, *J. Am. Chem. Soc.*, **75**, 5360 (1953).

10) An analogous reaction in a stainless steel autoclave gave a trace of V.

11) J. A. Birch, E. M. A. Shoukry and F. Stansfield, *J. Chem. Soc.*, **1961**, 5376.

12) It should be noted that the base-catalyzed reaction proceeded somewhat faster than the thermal dimerization. We have found that the Diels-Alder dimerization of 2-methoxy-1,3-butadiene afforded 1-methoxy-4-(1-methoxyvinyl)-1-cyclohexene in a 32% yield when a catalytic amount of potassium *t*-butoxide was added to a reaction mixture, whereas the same reaction proceeded in only a 20% yield without a base.[13]

13) I. N. Nazarov, G. P. Verkholetova and L. D. Bergel'son, *Izv. Akad. Nauk*, 511 (1948); *Chem. Abstr.*, **43**, 2576i (1949).

14) K. Morita and T. Kobayashi, *J. Org. Chem.*, **31**, 229 (1966).

15) All the novel compounds described here gave satisfactory analyses.

Reaction of Tropone with Cyclopentadiene

By Shô Itô,*1 Yutaka Fujise, Tomoko Okuda and Yoshiko Inoue

Department of Chemistry, Tohoku Uaiversity, Katahira-cho, Sendai

(Received March 30, 1966)

The Diels-Alder reaction of tropone was reported by Nozoe et al.[1] and the structure of the adduct with maleic anhydride was established. However, the nature of the product which results from the reaction of tropone as a dienophile has not been clarified, although a few reactions have been carried out.[2,3] We wish to present evidence for the structure of the adduct obtained from the reaction of tropone and cyclopentadiene; the reaction comprising the first example of a concerted 6+4 cycloaddition.[4]

Heating of tropone and cyclopentadiene at 80°C in benzene for 5 hr. yielded the 1 : 1 adduct I, m. p. 70—71.5°C (Found: C, 83.78; H, 6.98. Calcd. for $C_{12}H_{12}O$: C, 83.68; H, 7.02%. UV λ_{max}^{MeOH} 238 ($\varepsilon=2840$), 248 (3370), 257 (4520), 266 (4630), 300 mμ (480), IR ν_{max}^{KBr} 1715 cm^{-1}, MS *m/e*: 172 (M^+), 107 (base peak), 78, 66, 39. 2, 4-DNP., 185°C (decomp.) (Found: C, 61.32; H, 4.75. Calcd. for $C_{18}H_{16}O_4N_4$: C, 61.36; H, 4.58%. UV λ_{max}^{MeOH} 365 mμ ($\varepsilon=19100$)). These spectral observations confirm the molecular formula and indicate the presence of an isolated carbonyl group and a conjugated diene system. The NMR spectrum of I in benzene exhibited signals at 1.22 (1H, sextet, $J=11.3$, 4.8), 2.12 (1H, d. $J=11.0$), 2.54 (2H, br.s.), 3.03 (2H, m.), and 5.03—5.88 p. p. m. (6H, m.) supporting structure Ib or Ic rather than Ia.

Ia Ib Ic

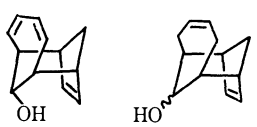

II III

Although the reduction of I with sodium borohydride or sodium in ethanol failed to take place, reduction with lithium aluminum hydride in tetrahydrofuran yielded an alcohol II, m. p. 32.5—34.5°C (Found: C, 82.88; H, 7.99, Calcd. for $C_{12}H_{14}O$: C, 82.72; H, 8.10%. UV λ_{max}^{MeOH} 243 ($\varepsilon=4552$, sh.), 252(5720), 262(5668), 273 mμ (3173), IR ν^{KBr} 3490 cm^{-1}. NMR δ^{CDCl_3} 1.49 (1H, m.), 2.21 (1H, d. $J=10.4$), 2.74 (5H, br.m.), 3.90 (1H, br.), 5.83 (4H, m.), 6.21 p. p. m. (2H, br.s.)). From a comparison of the NMR spectra of I and II in deuterochloroform, it is apparent that the methylene protons in I are practically unaffected by the anisotropy of the carbonyl group, a finding in accord with structure Ib but not Ic; an appreciable shift of these protons would be expected in the latter. The fact that the protons on the isolated double bond absorb at appreciably higher field in the case of I (5.99 p. p. m.) than in the case of II (6.27 p.p.m.) is also in accord with structure Ib. Thus the structure Ib was concluded as the correct representation of the structure of I.

Reduction of I with sodium in *n*-butanol yielded the corresponding dihydroalcohol 3, m. p. 95—97°C (Found: C, 81.89; H, 9.10. Calcd. for $C_{12}H_{16}O$: C, 81.77; H, 9.15%) which showed only end absorption in its ultraviolet spectrum. NMR δ^{CDCl_3} 1.1—2.6 (11H, br. m.), 3.97 (1H, br.), 5.53 (2H, br.s.), 5.97 (2H, s.). The stereochemistry of the hydroxyl group in II is tentatively assigned by analogy with the cases of norbornyl derivatives.[5] The structure Ib assigned for the adduct is in agreement with the prediction[4] of Hoffmann and Woodward for concerted cycloaddition.*2

*1 To whom all correspondences should be addressed.

1) T. Nozoe, T. Mukai, T. Nagase and Y. Toyooka This Bulletin, **33**, 1147 (1960).

2) T. Nozoe, T. Mukai, K. Takase and T. Nagase, *Proc. Japan Acad.*, **28**, 447 (1952).

3) Reaction of 3,4-benzotropone and tetrachlorocyclopentadiene gives an adduct similar to that obtained here. The structure of the adduct, however, has not been fully established (private communication from Professor Y. Kitahara, Tohoku University).

4) R. Hoffmann and R. B. Woodward, *J. Am. Chem. Soc.*, **87**, 2046, 4388 (1965).

5) E. I. Snyder and B. Franzus, ibid., **86**, 1166 (1964); P. Laszlo and P. von Ragué Schleyer, ibid., **86**, 1171 (1964).

*2 After completion of this work, we became aware of a paper recently published by Cookson et al. (*Chem. Comm.*, 15 (1966)), in which the authors assigned the same structure for the adduct.

Magnetic Properties of Bis(imidazolato)copper(II)

By Motomichi INOUE, Michihiko KISHITA and Masaji KUBO

Department of Chemistry, Nagoya University, Chikusa, Nagoya

(Received April 7, 1966)

In a preceding paper,[1] we have reported that bis(imidazolato)copper(II) forms three modifications differing in their magnetic moments: a blue modification (1.57 Bohr magnetons), a green modification (1.62 B. M.), and a brown modification (1.46 B. M.). The subnormal magnetic moments suggest the existence of spin interaction between copper atoms in these modifications. In order to obtain further information, we have determined the temperature dependence of magnetic susceptibilities of these compounds.

The magnetic susceptibilities and the moments are shown in Figs. 1 and 2, respectively, as functions of temperature. The susceptibility of the blue modification obeys the Curie-Weiss law over a temperature range of 80—300°K. The Curie constant is 0.491 e. m. u. °K/mol. and the Weiss constant is −171°K. The magnetic behavior of the green modification conforms to the Curie-Weiss law above 170°K with a Curie constant of 0.460 and a Weiss constant of −118°K, but shows an appreciable deviation below 170°K. The broken curve in Fig. 1 was calculated assuming the validity of the Curie-Weiss law with the aforementioned parameters. The large Weiss constants indicate the existence of strong interaction between copper atoms through imidazole rings.

The brown modification definitely differs from other modifications in the magnetic behavior. Its magnetic susceptibility curve resembles the theoretical curve of isolated clusters,[2] but does not agree with Bleaney-Bowers' expression.[3] This fact suggests that in this modification a polymeric structure is involved rather than a binuclear structure.

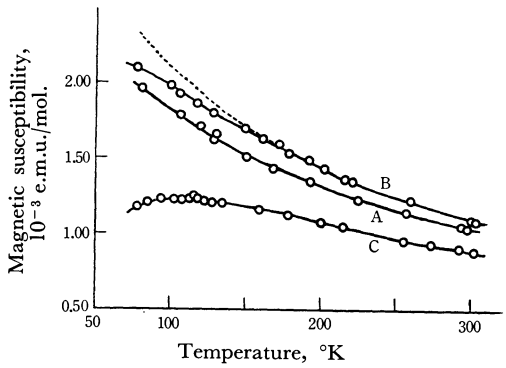

Fig. 1. Temperature dependence of the magnetic susceptibilities of bis(imidazolato)copper(II).
A: Blue modification. B: Green modification.
C: Brown modification.

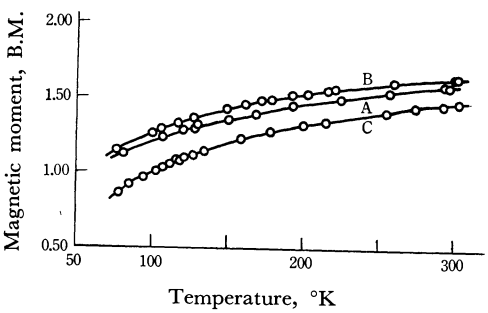

Fig. 2. Magnetic moments of bis(imidazolato)-copper(II).
A: Blue modification. B: Green modification.
C: Brown modification.

1) M. Inoue, M. Kishita and M. Kubo, *Inorg. Chem.*, **4**, 626 (1965).
2) J. S. Smart, "Magnetism III," Ed. by G. T. Rado and H. Shul, Academic Press, New York (1963); V. L. Ginsburg and V. M. Fain, *Soviet Phys.-JETP*, **15**, 131 (1962).
3) B. Bleaney and K. D. Bowers, *Proc. Roy. Soc.*, **A214**, 451 (1952); B. N. Figgis and R. L. Martin, *J. Chem. Soc.*, **1956**, 3837.

The Indirect Gas Chromatographic Determination of Palladium in an Aqueous Solution

By Tadashi KOGA and Tadashi HARA

Department of Chemical Engineering, Faculty of Engineering, Doshisha University, Kyoto

(Received April 11, 1966)

In conventional gas chromatographic determinations of non-volatile substances, the constituents have always been converted into their volatile forms; therefore, metal ions have been converted into their β-diketone chelates.[1] Practical analyses of metal ions, however, require operations of several steps and involve serious problems, such as the interference of an excess chelating agent or solvent and decompositions of the metal chelates.

The present paper will offer a simple and indirect method for the determination of palladium ion in an aqueous solution. In this method a mixture of propylene and propane in a definite volume ratio is placed in contact with a perchloric acid solution containing palladium ions, and the resultant gas is analyzed by a gas chromatograph, using propane as an internal standard. Since the reaction between propylene and palladium ions proceeds quantitatively and very fast to form metallic palladium, a linear relationship is held in an acidic solution between the amounts of propylene and the palladium ions.

A mixture of propylene and propane in a 1 : 1 vol. ratio is stored in a balloon, and an aliquot of it is used for each experiment. In order to determine the amount of palladium, 1 ml. of the mixed gas is placed in the gas sampler A, and then A is connected, as is shown in Fig. 1, with the tube, B, in which a palladium solution has previously been charged. After the different ingredients have been in contact with one another at room temperature for some time, the gas is collected in A. The tube is removed and the gas is analyzed under the following conditions: 30 ml./min. of H_2 as the carrier gas; activated alumina as the stationary phase; a 0.4×225 cm. column (70°C), and a thermal coductivity cell as the detector. The relative retention volumes of propane and propylene are 162 and 300 ml. respectively. Up to 480 p. p. m. of palladium gives a straight line against the ratio of the peak area of propylene/propane (Fig. 2).

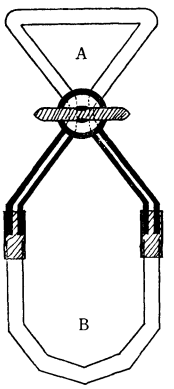

Fig. 1. Gas sampler and tube.
A: Gas sampler B: Tube

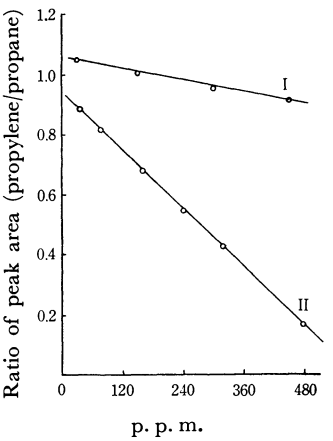

Fig. 2. Calibration curves.
I: Ag^+, II: Pd^{2+}.

The present method is not interfered with by platinum(II) copper(I) mercury(II), or nickel(II) ions which have d^8 or d^{10} electrons and which more or less show affinities for olefins, but it is slightly interfered with by a large amount of silver ions.

An analysis can be made in about 15 min.

1) For example, R. E. Sievers, B. W. Ponder, M. L. Morris and R. W. Moshier, *Inorg. Chem.*, **2**, 693 (1963); K. J. Eisentraut and R. E. Sievers, *J. Am. Chem. Soc.*, **87**, 5254 (1965).

A Novel Synthesis of 1, 4-Diketone

By Akira TAKEDA, Hiroyuki HOSISIMA, and Sigeru TORII

Department of Industrial Chemistry, School of Engineering, Okayama University, Tsushima, Okayama

(Received April 11, 1966)

Recently some new ways of preparing dihydrojasmone (I) have been reported in the literature.[1-4] One of the key routes to I is the cyclization of 2, 5-undecadione (II)[2,5,6] or its homologue[7], and so much attention has been paid to the preparation of this diketone (II). In this paper we will describe a synthesis of II via the ω-methylsulfinylmethyl ketone derivative (IV), which is obtainable by the reaction of ethyl γ-ethyleneketaldecanoate (III) with methylsulfinyl carbanion.[8]

The conversion of γ-ketodecanoic acid[9] to the ethyleneketal ester (III), b. p. 117°C/2 mmHg, n_D^{20} 1.4450. Found: C, 65.15; H, 9.99. Calcd. for $C_{14}H_{26}O_4$: C, 65.09; H, 10.14%, IR: 1730 (ester C=O), and 1180, 1140, 1095, and 1045 cm^{-1} (ketal), was carried out by boiling it with ethyl γ-ketodecanoate and ethylene glycol in the presence of *p*-toluenesulfonic acid.[4] The ketal ester (III) was treated with a solution of the methylsulfinyl carbanion (two equivalents) in dimethylsulfoxide-tetrahydrofuran at 0°C under nitrogen.[8] The β-ketosulfoxide (IV) thus produced boiled at 110—120°C/0.08 mmHg (partly isomerized) and gradually solidified, IR: 1705 (C=O) and 1040 cm^{-1} (S=O). The reduction of the crude IV with aluminum amalgam[8] in 90% tetrahydrofuran-10% water gave 5-ethyleneketal-2-undecanone (V), 40% (based on III); b. p. 110°C/2 mmHg, n_D^{20} 1.4648, IR: 1713 (C=O), 1170, 1145, 1100, and 1060 cm^{-1} (ketal). Found: C, 68.29; H, 10.32. Calcd. for $C_{13}H_{24}O_3$: C, 68.38; H, 10.59%. The ketal ketone (V), when heated with dilute acid for 2 hr., was converted into the diketone (II) in a good yield, b. p. 118—120°C/10 mmHg (lit.[5] b. p. 141°C/14 mmHg); IR: 1710 cm^{-1} (C=O). Further evidence for II was obtained by its cyclization to dihydrojasmone (I), whose structure was identified by means of the infrared and mixed-melting-point determination of the 2, 4-dinitrophenylhydrazone of I.[1]

During the course of reaction, the ketonic compounds were purified by using a Girard P reagent. The retention times of the intermediates were as follows (Hitachi F6-D, Chromosorb W (NAW), Silicone SE-30 column, 1 m. long, 0.7 atm. N_2, at 160°C): ethyl γ-ketodecanoate, 14 min.; the ketal ester (III), 38 min.; the ketal ketone (V), 19 min., and the diketone (II), 8 min.

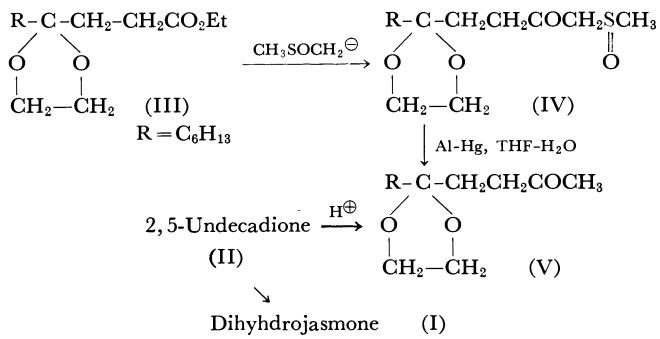

1) K. Sisido, S. Torii and M. Kawanisi, *J. Org. Chem.*, **29**, 904 (1964).
2) G. Stork and J. Borch, *J. Am. Chem. Soc.*, **86**, 935 (1964).
3) J. L. E. Erickson and F. E. Collins, *J. Org. Chem.*, **30**, 1050 (1965).
4) E. Gordon, F. Martens and H. Gault, *Compt. rend.*, **261**, 4129 (1965).
5) H. Hunsdiecker, *Ber.*, **75**, 455 (1942).
6) J. H. Amin, R. K. Razden and S. C. Bhattacharyya, *Perfumery Essent. Oil Record*, **49**, 502 (1958).
7) L. Crombie, J. B. Edgar, S. H. Harper, M. W. Lowe and D. Thompson, *J. Chem. Soc.*, **1950**, 3552.
8) E. J. Corey and M. Chaykovsky, *J. Am. Chem. Soc.*, **84**, 866 (1962); ibid., **86**, 1639 (1964); ibid., **87**, 1345 (1965).
9) A. Takeda, K. Takahasi, S. Torii and T. Moriwake, *J. Org. Chem.*, **31**, 616 (1966).

The Photoinduced Isomerization of Anthrone to Anthranol

By Nobuaki KANAMARU and Saburo NAGAKURA

The Institute for Solid State Physics, The University of Tokyo, Azabu, Tokyo

(Received May 12, 1966)

The photoinduced isomerization reaction from anthrone to anthranol was observed in several solvents, such as ethanol, ether, *n*-heptane and acetonitrile; the yield was large in the former two solvents, and very small in the latter two. Detailed experiments were done only in the case of the ether solution, on which we will report here.

By the irradiation of the degassed ether solution of anthrone by a light flash, anthrone was isomerized to anthranol. This may be clearly seen from Fig. 1, where the absorption spectrum (curve 1) of anthrone (~300 mμ) changes into that (curve 3) of anthranol (~370 mμ) after the irradiation.

The absorption spectrum immediately (~25 μ sec.) after the irradiation by the flash was photographed by the aid of the flash-spectroscopy technique; a new absorption band thus appeared at 340 mμ. This band may be expected to be due to the reaction intermediate from the facts that the 300 mμ band of anthrone disappears with the appearance of the new 340 mμ band and that, furthermore, the 370 mμ band of anthranol appears as the 340 mμ band disappears.

The 340 mμ band of the intermediate was found to be similar in position and shape to the spectrum of the benzophenone ketyl radical observed by Porter et al.[1,2] (curve 4 in Fig. 1). Therefore, the 340 mμ band may safely be assigned to the anthrone ketyl radical, whose π electron structure is very similar to that of the benzophenone ketyl radical. This shows that the abstraction of the hydrogen by the anthrone from solvent molecules occurs as the first step of the reaction. This conclusion seems to be supported also by the experimental fact that the yield of anthranol is large in ethanol and ether, solvents whose hydrogen is rather easily abstracted.

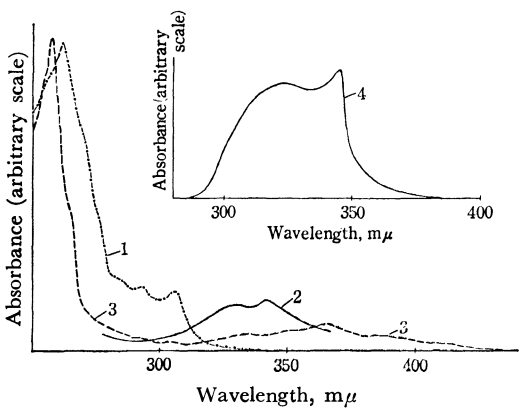

Fig. 1. Absorption spectra (curves 1—3) of the ether solution of anthrone under various conditions and the absorption spectrum (curve 4) of the benzophenone ketyl radical.
1. before irradiation
2. immediately (25 μsec.) after irradiation
3. (a few minutes) after irradiation
4. benzophenone ketyl radical[1,2]

The second step of the isomerization reaction, namely, the change of the ketyl radical to anthranol, was detected photoelectrically by measuring the absorption intensity of the 340 mμ band of the intermediate. The results show that the intermediate decays at the initial stage, following the second-order reaction formula, with the rate constant of about 10^7 mol^{-1} sec^{-1}, and at the next stage, following the first-order reaction formula.

The formation of the intermediate ketyl radical and its decay curve observed by the present authors can be explained satisfactorily in terms of the following reaction scheme:

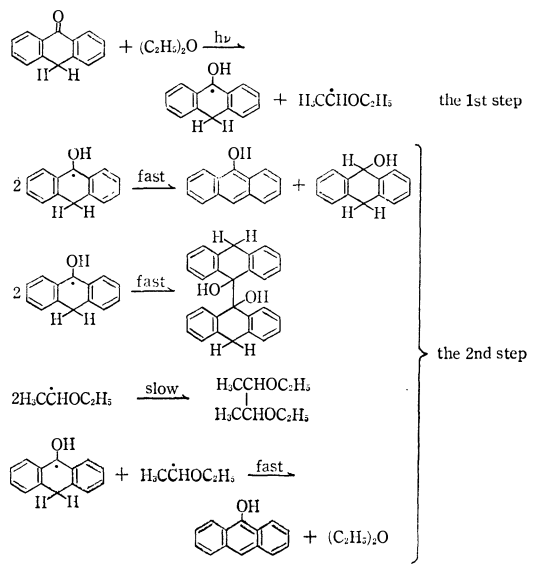

The details of the present study will be published in the future.

1) G. Porter and M. W. Windsor, *Proc. Roy. Soc.*, **A245** 238 (1958).
2) G. Porter and F. Wilkinson, *Trans. Faraday Soc.*, **57** 1686 (1961).

Reply to Torkar and Krishner's Comment on "A New Alumina Hydrate, Tohdite"

By Goro YAMAGUCHI, Hiroshi YANAGIDA and Shuichiro ONO

Department of Industrial Chemistry, Faculty of Engineering, The University of Tokyo, Hongo, Tokyo

(Received March 1, 1966)

In reply to Torkar and Krishner's comment on our article "A New Alumina Hydrate, Tohdite," we would like to mention as follows.[1]

In our article we gave the chemical composition $5Al_2O_3 \cdot H_2O$ as well as the atomic arrangement of the alumina hydrate. We now realize that at least two articles appeared on the alumina hydrate in question before the publication of our article.[2,3] In these articles, however, the chemical composition and the structure are not explicitly stated. Because of the fact that the alumina hydrate has a spinel structure of low symmetry, a further investigation will be of value.[4]

1) G. Yamaguchi, H. Yanagida and S. Ono, This Bulletin, **37**, 752 (1964).

2) K. Torkar and H. Krishner, *Ber. deut. keram. Ges.*, **39**, 13 (1961).

3) S. Aramaki and R. Roy, *Am. Mineralogist*, **48**, 1322 (1963). The X-ray data of AS(H)-1 in this article correspond to those of Tohdite.

4) G. Yamaguchi, H. Yanagida and S. Ono, This Bulletin, **37**, 1556 (1964); ibid., **38**, 1226 (1965).

BULLETIN OF THE CHEMICAL SOCIETY OF JAPAN VOL. 39 1357—1364 (1966)

The Oligomerization of Butadiene with Iron Complex Catalysts. II. The Effects of Additives

By Masanobu HIDAI, Katsumi TAMAI, Yasuzo UCHIDA and Akira MISONO

Department of Industrial Chemistry, Faculty of Engineering, The University of Tokyo, Hongo, Tokyo

(Received October 2, 1964)

In the oligomerization of butadiene with the catalyst composed of iron(III) acetylacetonate and triethylaluminum, the degree of digomerization and the structures of the oligomers were strongly affected by the addition of an electron donor as a catalyst component. When triphenylphosphine was added, linear dimers composed of 3-methylhepta-1, 4, 6-triene and *n*-octa-1, 3, 6-triene were formed, while the addition of 2, 2'-dipyridyl produced cyclic dimers composed of cycloocta-1, 5-diene and 4-vinylcyclohex-1-ene. Besides the above donors, triphenylphosphite, tri(*o*-tolyl)-phosphite, tri(*p*-tolyl)phosphite, phosphorus trichloride, triethylamine and pyridine as monodentate, and *o*-phenanthroline, 2(2'-pyridyl)imidazoline and oxine as bidentate ligands, were tried, and the effects of those donors upon the reaction were studied. The transition states in these catalyst systems were also considered by means of studies of the effects of the molar ratio of catalyst components and by the measurements of infrared, ESR and visible light absorption spectra or magnetic susceptibilities of the reaction solutions.

Introduction

In a previous report[1] the authors mentioned that butadiene trimerized to *n*-dodeca-1, 3, 6, 10-tetraene with the catalyst prepared from the reaction of iron(III) acetylacetonate and triethylaluminum in the presence of butadiene. The formation of the *n*-dodecatetraene was considered to proceed through an intermediate complex in which three molecules of butadiene are coordinated to a low valent iron atom. It may, then, be expected that if a proper electron donor is added to the system, the donor will occupy one or more coordination sites around the low valent iron atom corresponding to the available coordinating sites of the electron donor and its amount, and that, hence, the degree of oligomerization and the structure of the oligomers will be changed. During the course of our study, it was found that butadiene dimerizes selectively to 3-methylhepta-1, 4, 6-triene with a catalyst combining iron(III) acetylacetonate, triethylaluminum and triphenylphosphine; on the other hand, butadiene dimerized selectively to cycloocta-1, 5-diene and 4-vinylcyclohex-1-ene with the catalyst prepared from the reaction of iron(III) acetylacetonate, triethylaluminum and 2, 2'-dipyridyl. In this report, besides the above donors, phosphorus trichloride, triphenylphosphite, tri(*o*-tolyl)phosphite, tri(*p*-tolyl)phosphite, triethylamine and pyridine as monodentate and *o*-phenanthroline, 2(2'-pyridyl)-imidazoline and oxine as bidentate ligands were used, and the effects of these donors upon the products were studied. The nature of the catalyst systems was also discussed by measuring the infrared spectra, the visible light absorption spectra, the ESR spectra and the magnetic susceptibilities of the reaction solutions.

1) M. Hidai, Y. Uchida and A. Misono, This Bulletin, **38**, 1243 (1965).

Experimental

Reagents.—The methods of preparing or purifying butadiene, benzene, triethylaluminum and iron(III) acetylacetonate were the same as those mentioned in the previous paper.[1] The electron donors, such as triethylamine, phosphorus trichloride, triphenylphosphine, 2, 2'-dipyridyl, *o*-phenanthroline and oxine, were those of commercial reagents. Triphenylphosphite, tri(*o*-tolyl)phosphite, tri(*p*-tolyl)phosphite and 2(2'-pyridyl)imidazoline were prepared by usual methods.

Procedure.—The reaction was usually carried out with a 30-ml.glass tube. In a typical reaction, benzene (9.2 g.), butadiene (3.0 g.), and triethylaluminum (0.1 g.) were added in this order to the tube which had been charged with iron(III) acetylacetonate (0.10 g.) and a calculated amount of an electron donor. Butadiene, benzene and triethylaluminum were added in a dry nitrogen atomosphere. The tube was cooled during the operations to prevent the evaporation of butadiene. The tube was then closed by fusing and kept at 50°C during the reaction. The reaction products were then analyzed by gas chromatography. The columns and the conditions employed were the same as those described in the previous paper.[1]

For the isolation and confirmation of the reaction products, the reaction was carried out in a 200-ml. glass autoclave. The reaction solution was first washed with dilute hydrochloric acid and then with water. After the solution had been dried with anhydrous sodium sulfate, it was distilled under a nitrogen atmosphere. Products of a high purity were obtained

by preparative gas chromatography. The infrared spectra, visible light absorption spectra, ESR spectra and magnetic susceptibilities of the reaction solutions were measured in order to study the reaction intermediates in these catalyst systems. These measurements were carried out in the same way as has been described in the previous paper.[1)]

Results

In order to examine the effects of electron donors on the reaction, a series of reactions with various catalyst systems were carried out. The main products formed by the catalysts with various electron donors are listed in Table I.

The Addition of Monodentate Ligands.—*The Addition of Triethylamine.*—The addition of triethylamine did not affect the composition of the products. The conversion of butadiene was slightly decreased by the addition of triethylamine, but the selectivity of the formation of *n*-dodecatetraene was the same as in the case of an iron(III) acetylacetonate and triethylaluminum system.

The Addition of Triphenylphosphine.—When more than one mole of triphenylphosphine was added to one mole of iron(III) acetylacetonate, butadiene dimerized selectively. The dimers were identified as 3-methylhepta-1, 4, 6-triene and *n*-octa-1, 3, 6-triene by the measurements of the retention times by means of gas chromatography and a study of the infrared spectra. The relationship between the conversion of butadiene or the yield of the dimers and the molar ratio of triphenylphosphine to iron(III) acetylacetonate is shown in Fig. 1. When one mole of triphenylphosphine was added to one mole of iron(III) acetylacetonate (the molar ratio of triethylaluminum to iron(III) acetylacetonate was 3 to 1), the products lower than the trimer were methylheptatriene and *n*-octatriene, and no linear trimers formed by the catalyst without triphenylphosphine could be observed. The conversion of butadiene and the dimer formation increased until the molar ratio of the donor to iron(III) acetylacetonate reached 4—5, although the selectivity of dimer formation decreased slightly. When more than 5 times as much triphenylphosphine as iron(III) acetylacetonate was added, the formation of

Table I. Effect of electron donors

Donor	D/Fe	Reaction temp., °C	Reaction time, hr.	Conv. %	Yield, % MHT	NOT	VCH	COD	NDTe & a trimer
None	0	46	3	90	t	t	t	t	16
NEt_3	1—20	46	3	80	t			t	16
PPh_3	5.4	50	6	60	37	7			
$P(OPh)_3$	1	50	3	100	t				Polybutadiene
$P\left(O\text{-}C_6H_4\text{-}CH_3\right)_3$ a)	3	50	5	25	t				
$P\left(O\text{-}C_6H_4\text{-}CH_3\right)_3$	1	50	3	100					High polybutadiene
PCl_3	1	50	25	5					
a)	7.3	50	3.5	20					
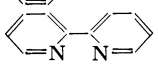	1	50	4	73			12	33	
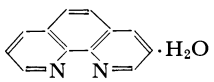	1	50	4	100			3	13	Polybutadiene
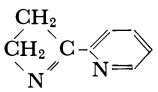	1	50	4	100					Polybutadiene
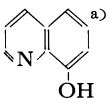 a)	1	50	7	100	t			t	14

Unless noted, 3.0 g. of butadiene was reacted with the catalyst composed of 0.100 g. of $Fe(acac)_3$, 0.100 g. of $AlEt_3$, and calculated amout of a donor in 9.2 g. of benzene.

a) In these cases 2.4 g. of butadiene was reacted with the catalyst composed of 0.100 g. of $Fe(acac)_3$, 0.100 g. of $AlEt_3$, and calculated amount of a donor in 14 g. of benzene.

b) Abbreviation
MHT: 3-methylhepta-1,4,6-triene, VCH: 4-vinylcyclohex-1-ene, NOT: *n*-octa-1,3,6-triene
COD: cycloocta-1,5-diene, NDTe: *n*-dodeca-1,3,6,10-tetraene, t: yield below 5%
D/Fe: mol. ratio of a donor to iron(III) acetylacetonate

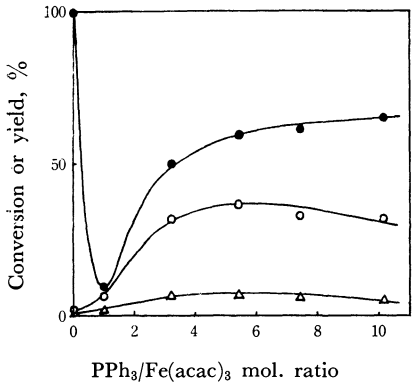

Fig. 1. Effect of molar ratio of triphenylphosphine to iron(III) acetylacetonate.
Reaction temp.: 50°C, Reaction time: 6 hr.
$AlEt_3/Fe(acac)_3$ mol. ratio: 3.1
●: Conversion of butadiene, %
○: Yield of 3-methylhepta-1,4,6-triene, %
△: Yield of *n*-octa-1,3,6-triene, %

dimers was rather depressed, although the conversion of butadiene was increased. In this case liquid polybutadiene was formed as a by-product. On the other hand, both the conversion of butadiene and the dimer formation were also affected by the amount of triethylaluminum added, as is shown in Fig. 2. In the case of the catalyst composition in which 3 times as much triphenylphosphine as iron(III) acetylacetonate was added, both the conversion of butadiene and the yield of dimers reached maxima at the point in which the ratio of triethylaluminum to iron(III) acetylacetonate was three. When more than 3 times as much triethylaluminum as iron(III) acetylacetonate was used, the conversion of butadiene and the dimer formation were rather depressed. It is remarkable that in the catalyst system in which more than 3 times as much triphenylphosphine as iron(III) acetylacetonate was added, the effect of triethylaluminum in depressing the methylheptatriene formation became smaller as the amount of triphenylphosphine added was increased.

The Addition of Phosphites.—By the addition of triphenylphosphite, tri(*o*-tolyl)phosphite, and tri(*p*-tolyl)phosphite, polybutadiene was formed as a main product. In the case of tri(*o*-tolyl)phosphite, the reaction was vigorous as compared with other phosphites, and the polybutadiene formed was solid, although in the case of triphenylphosphite and tri(*p*-tolyl)phosphite the polybutadiene formed was liquid.

Addition of Other Donors.—When one mole of phosphorus trichloride was added to one mole of iron(III) acetylacetonate, the reaction was strongly inhibited. The addition of pyridine also stopped the reaction.

The Addition of Bidentate Ligands. — *The Addition of 2, 2'-Dipyridyl.*—When more than one mole of 2, 2'-dipyridyl was added to one mole of iron(III) acetylacetonate, butadiene dimerized selectively. The dimers were identified as cycloocta-1, 5-diene and 4-vinylcyclohex-1-ene (in the ratio 3 : 1) by the measurements of the retention times by means of gas chromatography and a study of the infrared spectra. The relationship between the conversion of butadiene or the yields of the dimers and the molar ratio of 2, 2'-dipyridyl to iron(III) acetylacetonate is given in Fig. 3. When the molar ratio of 2, 2'-dipyridyl to iron(III) acetylacetonate was 1, for example, after 4-hrs.' reaction at 50°C, 73% of the butadiene reacted, of which 45% was changed to cycloocta-1, 5-diene and 15% to 4-vinylcyclohex-1-ene. All the products except the dimers were polybutadiene, and no *n*-dodecatetraene formed by the catalyst without

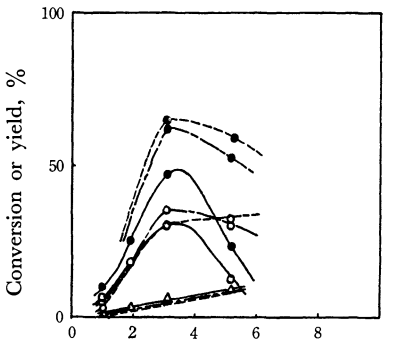

Fig. 2. Effect of composition of catalyst components.
——: $PPh_3/Fe(acac)_3$ mol. ratio: 3.0
– – –: $PPh_3/Fe(acac)_3$ mol. ratio: 7.0
– – – –: $PPh_3/Fe(acac)_3$ mol. ratio: 10.0

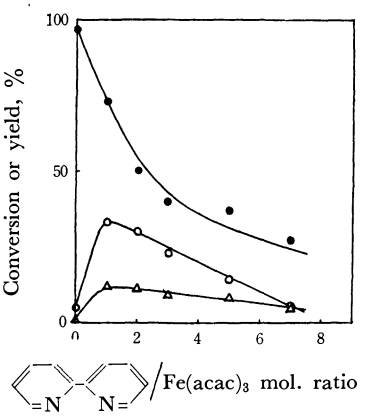

Fig. 3. Effect of molar ratio of 2,2'-dipyridyl to iron(III) acetylacetonate.
Reaction temp.: 50°C, Reaction time: 4 hr.
$AlEt_3/Fe(acac)_3$ mol. ratio: 3
●: Conversion of butadiene, %
○: Yield of cycloocta-1,5-diene, %
△: Yield of 4-vinylcyclohex-1-ene, %

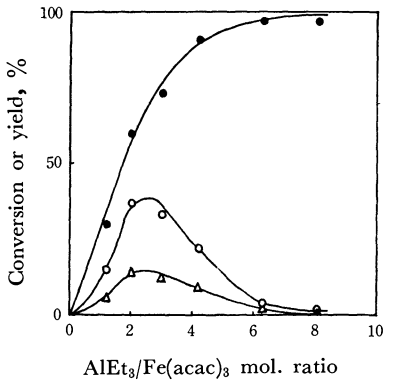

Fig. 4. Effect of molar ratio of triethylaluminum to iron(III) acetylacetonate.
Reaction temp.: 50°C, Reaction time: 4 hr.
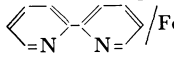
/Fe(acac)$_3$ mol. ratio: 1

2, 2'-dipyridyl was observed. When the molar ratio of 2, 2'-dipyridyl to iron(III) acetylacetonate became more than 1, both the conversion of butadiene and the yield of the dimers were decreased. In Fig. 4 is shown the effect of triethylaluminum added. When more than 3 times as much triethylaluminum as iron(III) acetylacetonate was added, the conversion of butadiene increased, but the polymerization became dominant and the yield of dimers was decreased. The same phenomenon had been observed in the case of the linear trimerization of butadiene with a catalyst composed of triethylaluminum and iron(III) acetylacetonate.

The Addition of o-Phenanthroline. — The addition of *o*-phenanthroline also gave the cyclic dimers as in the case of 2, 2'-dipyridyl, but the selectivity of dimer formation was lower than in the case of the catalyst system with 2, 2'-dipyridyl.

The Addition of 2(2'-Pyridyl)imidazoline or Oxine.— Upon the addition of 2(2'-pyridyl)imidazoline, only polymerization took place. On the other hand, when oxine was added as a catalyst component, the reaction almost the same as in the system without oxine.

Discussion

In the series of reactions described above, not only the dimerization or trimerization of butadiene took place; polymerization also occurred as a result of the change of catalyst components. As was reported in a previous paper,[2] the essential reaction of catalyst components to form active species is the reduction of iron(III) acetylacetonate with triethylaluminum to a low valent state, estimated as zero valent. We consider that the coordination of a donor as a catalyst component to the reduced iron atom changes the active complex form. If some kinds of complex formation are realized among butadiene, an electron donor, and iron atom, then the magnetic properties of the resultant system must differ from those of the system without the electron donor. With this in mind, the magnetic susceptibilities of the reaction solutions were measured. The results are listed in Table II. As was mentioned in the previous papers,[1,2] when triethylaluminum was added to a benzene solution of iron(III) acetylacetonate, Fe^{3+} was reduced to Fe^{2+} and then to a zero valent state. The resultant solution was unstable, and immediately a black precipitate appeared. The system showed the ferromagnetism of an effective magnetic moment of 11—18 B. M., probably caused by the metallic iron. In the presence of butadiene, the solution became reddish brown and showed the paramagnetism of an effective magnetic moment of 4—5 B. M. A shoulder absorption was found at about 400—450 mμ in the visible light absorption spectrum; this absorption has been observed in bis-butadiene dicobalt tetracarbonyl and butadiene iron tricarbonyl.[3] From these results, a paramagnetic intermediate complex in which butadiene is coordinate to the zero valent iron atom may be expected.

A Reaction Solution with a Catalyst Composed of Iron(III) Acetylacetonate, Triethylaluminum and Triphenylphosphine.—In this case, when triphenylphosphine was added, even if in the absence of butadiene, the value of the magnetic susceptibility of the solution decreased, as is shown in Table II-3. When butadiene was present before the addition of triethylaluminum, the reaction solution was bright brown and showed an effective magnetic moment of about 1 B. M.; this finding supported the coordination of both butadiene and triphenylphosphine to the reduced iron atom. In this case a shoulder absorption at 400—420 mμ was also observed. From the observation of the infrared spectra in the potassium bromide region of the reaction solution with various contents of triphenylphosphine, it was observed that, when the ratio of triphenylphosphine to iron(III) acetylacetonate was equal to 0.6 and 1, the absorption at near 500 cm^{-1} characteristic of triphenylphosphine did not appear and that, when the ratio was larger than 1, this absorption appeared and increased with an increase in the ratio of triphenylphosphine to iron(III) acetylacetonate (shown in Figs. 5-1 and 5-2). On the other hand, when the ratio was 0.6, new absorptions at 512 and 538 cm^{-1} appeared. These absorptions became strong when the ratio approached 1. However, the absorptions almost did not change at all when the ratio increased above 1. These new absorptions at 512 and 538 cm^{-1} were also observed in a triphenylphosphine iron complex

2) K. Tamai, T. Saito, Y. Uchida and A. Misono, This Bulletin, **38**, 1575 (1965).

Table II-1. Effective magnetic moment of $Fe(acac)_3$-$AlEt_3$ system

Al/Fe	Weight fraction			$\chi_g \times 10^6$ for solution	$\chi_m \times 10^6$	μ_{eff}(B.M.)
	C_6H_6	$Fe(acac)_3$	$AlEt_3$			
1.3	0.980	0.0147	0.0061	+4.55	126000	16.7
2.4	0.972	0.0155	0.0122	+5.07	131000	17.6
4.8	0.962	0.0149	0.0228	+1.932	62500	10.9

χ_g : gram susceptibility of sample solution
χ_m : molar susceptibility based on iron atom
μ_{eff} : effective magetic moment

Table II-2. Effective magnetic moment of $Fe(acac)_3$-C_4H_6-$AlEt_3$ system

Al/Fe	Weight fraction				$\chi_g \times 10^6$ for solution	$\chi_m \times 10^6$	μ_{eff}(B.M.)
	C_6H_6	D_4H_6	$Fe(acac)_3$	$AlEt_3$			
2.2	0.915	0.0562	0.0171	0.0121	−0.318	7660	4.2
2.8	0.908	0.0529	0.0207	0.0188	+0.065	12840	5.4
5.1	0.907	0.0512	0.0157	0.0258	−0.222	10600	4.9

Table II-3. Effective magnetic moment of $Fe(acac)_3$-PPh_3-AlEt system

Al/Fe	P/Fe	Weight fraction				$\chi_g \times 10^6$ for solution	$\chi_m \times 10^6$	μ_{eff}(B.M.)
		C_6H_6	PPh_3	$Fe(acac)_3$	$AlEt_3$			
2.1	2.0	0.969	0.0144	0.0098	0.0066	+1.935	95500	15.1
2.2	6.1	0.933	0.0490	0.0108	0.0073	+0.945	53700	11.1
4.8	6.2	0.902	0.0630	0.0138	0.0213	−0.389	7950	4.3

Table II-4. Effective magnetic moment of $Fe(acac)_3$-C_4H_6-PPh_3-$AlEt_3$ system

Al/Fe	P/Fe	Weight fraction					$\chi_g \times 10^6$ for solution	$\chi_m \times 10^6$	μ_{eff}(B.M.)
		C_6H_6	PPh_3	C_4H_6	$Fe(acac)_3$	$AlEt_3$			
2.0	4.0	0.893	0.0325	0.0564	0.0109	0.0071	−0.695	diamag	
2.1	4.0	0.875	0.0456	0.0542	0.0154	0.0103	−0.671	482	1.1
2.1	4.0	0.889	0.0354	0.0599	0.0120	0.0080	−0.642	1450	1.8
5.2	1.0	0.887	0.0113	0.0510	0.0152	0.0255	−0.568	2920	2.6
5.1	3.9	0.869	0.0424	0.0495	0.0148	0.0244	−0.650	1050	1.5
4.3	6.1	0.850	0.0638	0.0524	0.0142	0.0196	−0.664	745	1.3

Table II-5. Effective magnetic moment of $Fe(acac)_3$-C_4H_6-Donor-$AlEt_3$ system

Donor	Al/Fe	D/Fe	Weight fraction					$\chi_g \times 10^6$ for solution	$\chi_m \times 10^6$	μ_{eff}(B.M.)
			C_6H_6	Donor	C_4H_6	$Fe(acac)_3$	$AlEt_3$			
a	3.1	1.1	0.963	0.0070		0.0149	0.0149	+0.490	28000	8.0
a	3.2	1.0	0.904	0.0068	0.0579	0.0151	0.0158	−0.555	3060	2.6
a	4.7	6.8	0.869	0.0422	0.0531	0.0140	0.0212	−0.648	908	1.4
b	2.9	6.6	0.872	0.0362	0.0546	0.0192	0.0179	−0.246	8230	4.3
c	3.0	3.2	0.851	0.0594	0.0531	0.0185	0.0180	−0.622	1220	1.7
d	2.8	3.3	0.857	0.0536	0.0540	0.0186	0.0167	−0.626	1081	1.6

a: 2, 2'-Dipyridyl b: Triethylamine c: Tri(*o*-tolyl)phosphite d: Triphenylphosphite

Table III. Valency orbitals of some ligands stabilizing low oxidation states of transition metals

Ligand	Donor orbital	Acceptor orbital	Effectiveness as a σ donor	Effectiveness as a π acceptor
PCl_3	sp^3 on P	$d\pi$ on P	poor	good
$P(OPh)_3$	sp^3 on P	$d\pi$ on P	poor	good
PPh_3	sp^3 on P	$d\pi$ on P	moderate	moderate
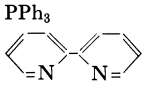	sp^2 on N	$p\pi$ delocalized	good	moderate
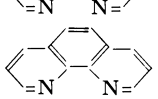	sp^2 on N	$p\pi$ delocalized	good	moderate

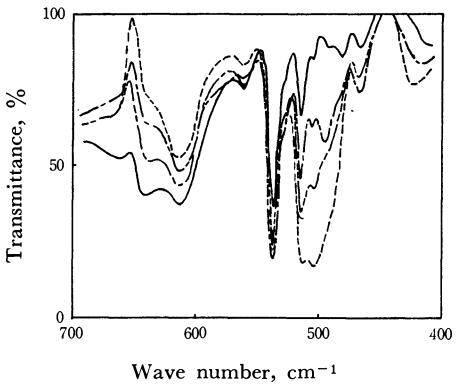

Fig. 5-1. Infrared spectra of reaction solution in KBr region.
——: $PPh_3/Fe(acac)_3=0.6$
– – –: $PPh_3/Fe(acac)_3=1.0$
——–: $PPh_3/Fe(acac)_3=3.2$
– – – –: $PPh_3/Fe(acac)_3=7.0$
$Fe(acac)_3 : C_4H_6 : AlEt_3 : C_6H_6=1.0 : 4.5 : 3.1 : 56$ (mol. ratio)

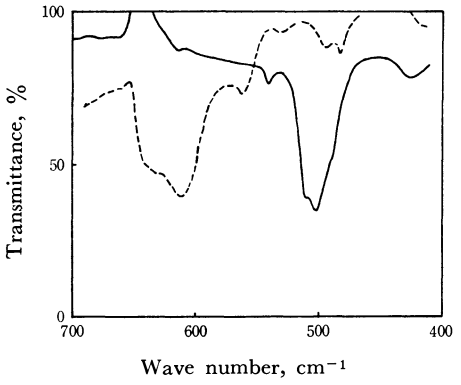

Fig. 5-2. Infrared spectra of reaction solution in KBr region.
——: $PPh_3 : C_6H_6=1 : 24$
– – – –: $Fe(acac)_3 : C_4H_6 : AlEt_3 : C_6H_6=$ $1.0 : 4.5 : 3.1 : 56$ (mol. ratio)

isolated from the solution containing diethylmonoethoxyaluminum, iron(III) acetylacetonate and triphenylphosphine. Therefore, these absorptions were supposed to be characteristic of triphenylphosphine coordinated to an iron atom. From these results it was considered that one molecule of triphenylphosphine is coordinate to the reduced iron atom in the reaction solution, even if an excess of triphenylphosphine is present in the solution.

The effect of amounts of triphenylphosphine on the reaction can be explained by the following consideration. In the reaction system composed of iron(III) acetylacetonate, triethylaluminum and triphenylphosphine, the iron atom coordinated by triphenylphosphine and butadiene is solvated by a solvent or by an aluminum compound such as diethylaluminum acetylacetonate and stabilized as a homogeneous solution. When more than one mole of triphenylphosphine to one mole of iron(III) acetylacetonate is present in the solution, the excess of triphenylphosphine which is not coordinate to the iron atom interacts with the aluminum compound surrounding the iron-butadiene-triphenylphosphine intermediate. This causes a change in solvation and a resultant change in the oligomerization reaction. The phenomena that an excess of triethylaluminum depresses the reaction may also be explained as the solvation of the aluminum compound to the reaction intermediate complex. In the case of a large excess of triphenylphosphine in the solution, the excess of triethylaluminum does not affect the reaction course. It may be supposed that the excess triphenylphosphine reacts with triethylaluminum and that the resultant compound is probably not so active as to affect the solvation conditions surrounding the intermediate. Therefore, the reaction was almost the same as the one catalyzed by the system which did not contain an excess of triethylaluminum.

These solvation effects will also affect the magnetic properties of the solution. However, the

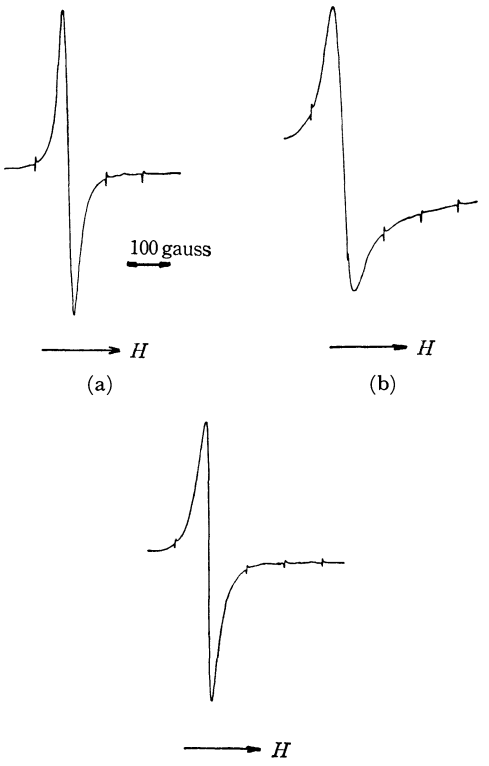

Fig. 6. ESR spectra of reaction solution.

	$Fe(acac)_3$	$AlEt_3$	PPh_3	C_4H_6	C_6H_6
(a)	1.0	3.3	4.0	10	145
(b)	1.0	7.9	3.9	10	137
(c)	1.0	7.9	9.5	10	137

(mol. ratio)

accuracy of the measurement of the magnetic susceptibility does not allow any further discussion. The ESR observation of the reaction solution with various ratios of catalyst components is shown in Fig. 6. When triphenylphosphine : iron(III) acetylacetonate : triethylaluminum was 1 : 1 : 3, a broad signal due to the iron atom was observed at the *g*-value of 2.08. This signal was sharpened by the further addition of triphenylphosphine. When the amount of triethylaluminum increased, the absorption became broad again, and upon the further addition of excess triphenylphosphine, the absorption became sharp again. These phenomena may be supposed to be due to the change in coordination or solvation conditions around the iron atom and to be consistent with the above explanation.

The Reaction Solutions with Other Monodentate Ligands.—The addition of triethylamine did not affect the reaction. The effective magnetic moment of the solution was about 4, which is almost the same as that of the reaction solution containing iron(III) acetylacetonate, butadiene and triethylaluminum. From this result, it may be supposed that triethylamine does not coordinate to a low valent iron atom in the system.

When phosphite compounds were added to the catalyst system, the main product was a polymer. In these cases, the reaction solutions were almost diamagnetic and the coordination of phosphites to iron atom may be supposed.

The Reaction Solution with 2, 2'-Dipyridyl.—The magnetic susceptibility of the reaction solution became smaller than the case without a donor, and the difference was greater as the amount of 2, 2'-dipyridyl increased. This suggests that 2, 2'-dipyridyl coordinates to the iron atom in the reaction system. Actually, in the reaction between iron(III) acetylacetonate, 2, 2'-dipyridyl and diethylmonoethoxyaluminum in ether, the diethyl bis-2, 2'-dipyridyl iron complex was isolated. This complex showed catalytic activity in the cyclic dimerization of butadiene.[4] When butadiene was reacted with the complex, 2, 2'-dipyridyl was isolated from the reaction solution. On the other hand, the best ratio of 2, 2'-dipyridyl to iron(III) acetylacetonate was 1 for the cyclooctadiene formation. From these results, a paramagnetic complex in which butadiene and one molecule of 2, 2'-dipyridyl coordinated to the iron atom may be supposed to be an intermediate of this reaction.

The Elucidation of the Transition State and the Effect of Electron Donors.—From the above-mentioned experimental results and discussions, it was concluded that, by the addition of an adequate electron donor as a catalyst component, the oligomerization of butadiene with an iron complex catalyst was strongly affected. It was also found that, for the formation of the linear dimers, the addition of a monodentate ligand such as triphenylphosphine was effective, while for the formation of the cyclic dimers, such bidentate ligands as 2, 2'-dipyridyl or *o*-phenanthroline were effective.

During the course of his study of the oligomerization of butadiene, Dr. Wilke[5] isolated a complex, $NiC_{12}H_{18}$, in which three molecules of butadiene were changed to a C_{12} chain by the formation of one trans double bond and two terminal π-allyl groups. He also isolated a complex, $Ni(PR_3)C_8H_{12}$, in which two molecules of butadiene were changed to a C_8 chain by the formation of two terminal π-allyl groups. It was suggested that the former complex was the intermediate complex for the all-trans-cyclododecatriene formation in the reaction of butadiene with the catalyst composed of nickel acetylacetonate and triethylaluminum, while the latter complex was the intermediate complex for the cyclic dimerization of butadiene with the catalyst composed of nickel acetylacetonate, triphenylphosphine and triethylaluminum. According to his view, three molecules of butadiene approach the nickel atom to form the cyclic trimer through the $NiC_{12}H_{18}$ complex. In the case of the catalyst composed of nickel acetylacetonate, triphenylphosphine and triethylaluminum, one of the coordination sites of nickel is occupied by triphenylphosphine; therefore, only two molecules of butadiene can approach the reaction field, so the dimers are formed through the $Ni(PPh_3)C_8H_{12}$ complex. The degree of the oligomerization of products by the iron complex catalyst can be similarly explained. The formation of the cyclic dimers with the combined catalyst of iron(III) acetylacetonate, 2, 2'-dipyridyl and triethylaluminum can be explained by considering that the donor occupies two coordination sites of the low valent iron atom and that two molecules of butadiene approach the iron atom to form the cyclic dimers through a $Fe(dipy)C_8H_{12}$ complex. The formation of methylheptatriene can also be explained in the same way. Two molecules of butadiene approach the iron atom to which one molecule of triphenylphosphine is coordinated.

Besides the above-mentioned discussions about the number of coordination sites of metal, the sort or the nature of donor must be considered. The polymerization proceeds by some electron donors, while by the other donors the reaction was inhibited or specific oligomerization occurred. These are considered to be due to the difference in the strength of the coordination of a donor to metal and the resultant change in bond strength between the butadiene and the metal. The ligands which are

3) S. Ohtsuka, Kagaku-Zokan, No. 13, 87 (1964).
4) A. Yamamoto, K. Morifuji, S. Ikeda, T. Saito, Y. Uchida and A. Misono, *J. Am. Chem. Soc.*, **87**, 4652 (1965).
5) G. Wilke, *Angew. Chem.*, **73**, 755 (1961); G. Wilke, ibid., **75**, 10 (1963).

found experimentally to stabilize the lower valency states of the transition metals are collected in Table III.[6] It will be noted that each of these ligands has available acceptor orbitals for π electrons and that other ligands, which do not have these acceptor orbitals, are much less effective stabilizers of low valencies, though they have similar properties in every other way. Thus, it may readily be understood that the reaction of butadiene by the combined catalyst of iron(III) acetylacetonate and triethylaluminum was not affected by the addition of triethylamine, which does not have available acceptor orbitals for π electrons, but it was affected by the addition of an electron donor, such as 2, 2'-dipyridyl, triphenylphosphine, phosphorus trichloride, or triphenylphosphite, which has acceptor orbitals. Moreover, it will be noted that such ligands as 2, 2'-dipyridyl or triphenylphosphine, by the addition of which an active complex for dimerization is formed, are moderate as acceptors for π electrons, while triphenylphosphite, by which an active complex for polymerization is formed, is strong as an acceptor, and phosphorus trichloride, by the addition of which the reaction of butadiene is stopped, is a very strong acceptor for π electrons. Thus, a ligand which is coordinated to the low valent iron atom and forms an active complex for the dimerization of butadiene, must have available acceptor orbitals for π electrons of adequate energy levels.

6) L. E. Orgel, "An Introduction to Transition-Metal Chemistry," Methuen, London (1961).

BULLETIN OF THE CHEMICAL SOCIETY OF JAPAN VOL. 39 1364—1368 (1966)

A Comparison of Equations for Powder Compression

By Kimio KAWAKITA and Yuhbun TSUTSUMI

Department of Chemistry, Faculty of Engineering, Hosei University, Koganei-shi, Tokyo

(Received December 21, 1964)

Several equations representing the relation between the pressure and the apparent volume of a powdered mass under compression, as proposed by various authors, sometimes have essentially the same form as one other, and sometimes have contradictory characters. Various equations can be modified so as to be a function of the porosity and thus compared with each other. As a result, they can be classified into two types by means of the gradient of the porosity with the pressure ($-dn/dP$, n=porosity). One is $-dn/dP=kn^x$ (Athy: $x=1$, Kawakita: $x=2$), and the other is $-dn/dP=k(1-n)^y/P^z$ (Smith: $y=0$, $z=2/3$, Nutting: $y=1$, $z\fallingdotseq 1$, Balshin: $y=2$, $z\sim 1$, Terzaghi: $y=2$, $z\sim 1$, Jones: $y=3$, $z=1$), where k is a constant and x, y and z are parameters. In Kawakita's equation the rate of the decrease of the porosity is considerably larger in an early period of compaction than in Athy's equation. The second type of equation indicates that a major part of the porosity disappears at lower pressures.

The compacting behavior of a powdered mass was previously analyzed by Kawakita,[1-2] one of the present authors. He proposed an empirical Eq. 1:

$$C=\frac{V_0-V}{V_0}=\frac{abP}{1+bP} \qquad (1)$$

where C=the relative reduction of the volume by compression; V_0=the initial apparent volume; V=the volume under the applied pressure P, and a and b=constants.

The constant a corresponds to the limiting value of the relative reduction of the volume by compression: it should be equal to the initial porosity of a powdered mass, as expressed by Eq. 2:

$$a=C_\infty=\frac{V_0-V_\infty}{V_0} \qquad (2)$$

where V_∞ is the net volume of the powder. The b constant should be equal to the reciprocal of the pressure when the value, C, reaches one-half of the limiting value ($C=C_\infty/2$).

Several equations of other types have also been proposed for the powder compression by various

1) K. Kawakita, *Science, Japan*, **26**, 149 (1956).
2) K. Kawakita, *Ann. Report Takamine Lab. (Sankyo Co., Tokyo)*, **8**, 83 (1956).
3) K. Kawakita, ibid., **8**, 87 (1956).
4) K. Kawakita, ibid., **8**, 92 (1956).
5) K. Kawakita, ibid., **10**, 93 (1958).
6) K. Kawakita, *J. Japan Soc. Powder Metallurgy*, **10**, 71 (1963).
7) K. Kawakita, *J. Soc. Materials Science, Japan*, **13**, 421 (1964).
8) R. E. Collins, *Transactions American Geophysical Union*, **45**, 161 (1964).
9) K. Kawakita and Y. Tsutsumi, *Japan. J. Appl. Phys.*, **4**, 56 (1965).

Table I. Powder compression equations

Author	Equation	Remarks
Balshin	$\ln P = -L \cdot V_r + C$	P=applied pressure, V_r=specific volume, L, C=constants
Smith	$\rho - \rho_0 = C_f \cdot P^{1/3}$	ρ=apparent density, ρ_0=initial apparent density, C_f=compressibility factor
Murray	$\ln\left(\frac{1}{1-D_E}\right) = \frac{\sqrt{2\gamma}\, n^{1/3}}{\sigma_0}\left(\frac{D_E}{1-D_E}\right)^{1/3} 4\pi^{1/3} + \frac{P}{\sqrt{2\sigma_0}}$	D_E=relative density at pressure P, γ=surface tension, n=number of pores in unit volume, σ_0=yield strength at compressing temperature
Ballhausen	$\ln\left(\frac{D}{1-D}\right) \propto P$	D=relative density at pressure P
Konopicky	$\ln\left(\frac{1}{1-D}\right) = kP + \ln\left(\frac{1}{1-D_0}\right)$	D=relative density at pressure P, D_0=relative density at zero pressure, k=constant
Jones	$\frac{dP}{dW} = -kPW$	P=applied pressure, W=relative apparent volume, k=constant
Burr	$D = f_1(P) + f_2(P) + f_3(P) + A$	D=relative apparent density, f_1, f_2, f_3=functions of pressure P, A=constant
Athy	$n = n_0 \cdot \exp(-bx)$	n=porosity, n_0=average porosity of surface clays, b=constant, x=depth of burial
Nutting	$\varepsilon = \psi^{-1} t^{\kappa} f^{\beta}$	ε=volumetric strain, f=compressive stress, t=time, ψ, β, κ=constants
Tanimoto	$\delta = \frac{1-\mu}{E}\sigma + \frac{\sigma \varepsilon_m + A\varepsilon_0}{\sigma + A}$	δ=change of volume, E=elastic factor, σ=compressive stress, ε_m=initial void, ε_0=strain at initial state, μ, A=constants
Terzaghi	$\varepsilon = -\alpha \ln(P+P_c) - \beta(P+P_c) - \gamma P + C$	ε=ratio of porosity, P=applied pressure, $\alpha, \beta, \gamma, P_c, C$=constants
Cooper	$\overset{*}{V} = a_1 \cdot \exp(-k_1/P) + a_2 \cdot \exp(-k_2/P)$	$\overset{*}{V}$=fractional compaction, P=applied pressure, a_1, a_2=fractional coefficients, k_1, k_2=constants
Kawakita	$C = \frac{abP}{1+bP}$	P=applied pressure, C=relative reduction of volume, a, b=constants

Equations from Balshin's to Konopicky's are from Ref. 11, Jones' and Burr's are from Ref. 12, Athy's, Nutting's, Tanimoto's, Terzaghi's and Cooper's are from Refs. 13, 14, 15, 16 and 18 respectively.

investigators, and some of them have been used in practice, though only in a few cases. This paper will deal with our attempt to compare these equations.

Powder Compression Equations.—So far as we are aware, the following equations have been reported (Table I[11-18]).

In order to make a comparison of these equations, each of them should be rewritten by the same notations (Table II).

Burr's equation was not evaluated since no representation was given for the pressure functions. As for Nutting's equation, which includes a time-dependent factor, the measuring time was taken as a constant. In Athy's equation we substituted the depth of burial, x, with a pressure term, P.

Murray's, Konopicky's and Tanimoto's Equations.—Murray's equation is rather complicated:

$$\ln\left(\frac{V}{V-V_\infty}\right) = c_4\left(\frac{V_\infty}{V-V_\infty}\right)^{1/3} + c_5 P$$

However, if the first term of the right side is the constant (k), we find:

$$\frac{V-V_\infty}{V} = k \cdot e^{-c_5 P}$$

which is the same in form as Athy's equation. It is possible, therefore, to say that Murray's equation is a sort of modification of Athy's.

The equations of Balshin, Smith, Murray, Ballhausen and Konopicky were evaluated in the light of experimental data provided by Heckel.[11] He concluded that Konopicky's equation agreed best with the data. We have previously stated[9] that Konopicky's equation could be regarded as the same as that of Athy.

Tanimoto's equation may be rewritten as follows:

$$\frac{V_0 - V}{V_0} = \frac{\beta P + \gamma P^2}{1 + \alpha P}$$

10) K. Kawakita, Y. Tsutsumi, C. Ikeda and H. Yagi, *Oyo Buturi (Japan)*, **35**, 360 (1965).
11) R. W. Heckel, *Trans. AIME Met.*, **221**, 1001 (1961).
12) M. J. Donachie and M. F. Burr, *J. Metals*, **15**, 849 (1963).
13) L. F. Athy, *Bull. Am. Assoc. Petrol. Geologists*, **14**, 1 (1949).
14) G. W. Scott Blair and F. M. Valda Coppen, *Nature*, **146**, 840 (1940).
15) K. Tanimoto, *Transactions Japan Soc. Civil Engineers*, **43**, 53 (1957); T. Wakabayashi, *J. Japan Soc. Powder Metallurgy*, **10**, 83 (1963).
16) K. Terzaghi, "Erdbaumechanik," Franz Deuticke Publ. Co., Leipzig and Wien (1925), p. 91.
17) B. S. Neumann, "Flow Properties of Disperse Systems," North-Holland Publ. Co., Amsterdam (1953), p. 397.
18) A. R. Cooper and L. E. Eaton, *J. Am. Ceramic Soc.*, **45**, 97 (1962).

TABLE II. VARIOUS EQUATIONS REPRESENTED BY THE SAME NOTATIONS

Balshin	$\ln P = -c_1 \frac{V}{V_\infty} + c_2$
Smith	$\frac{1}{V} - \frac{1}{V_0} = c_3 \cdot P^{1/3}$
Murray	$\ln\left(\frac{V}{V-V_\infty}\right) = c_4\left(\frac{V_\infty}{V-V_\infty}\right)^{1/3} + c_5 P$
Ballhausen	$\ln\left(\frac{V_\infty}{V-V_\infty}\right) = c_6 P + \ln c_7$
Konopicky	$\ln\left(\frac{V}{V-V_\infty}\right) = c_8 P + \ln\left(\frac{V_0}{V_0-V_\infty}\right)$
Jones	$\ln P = -c_9\left(\frac{V}{V_\infty}\right)^2 + c_{10}$
Athy	$\frac{V-V_\infty}{V} = \frac{V_0-V_\infty}{V_0} \cdot e^{-c_{11}P}$
Nutting	$\ln\left(\frac{V_0}{V}\right) = c_{12}P^{c_{13}}$
Tanimoto	$\frac{V_0-V}{V_0} = \frac{c_{14}P}{V_0} + \frac{c_{16}P}{P+c_{15}}$
Terzaghi	$\frac{V-V_\infty}{V_\infty} = -c_{17}\ln(P+c_{18}) - c_{19}(P+c_{18}) - c_{20}P + c_{21}$
Cooper	$\frac{V_0-V}{V_0-V_\infty} = c_{22} \cdot e^{-c_{23}/P} + c_{24} \cdot {}^{-c_{25}/P}$
Kawakita	$\frac{V_0-V}{V_0} = \frac{c_{25}c_{26}P}{1+c_{26}P}$

V_0=initial apparent volume of powder
V=volume of powder under the applied pressure P
V_∞=net volume of powder
c_1—c_{26} are the constants.

where α, β and γ are the constants. This equation contains the self-contradiction that the volume of powder, V, should approach $-\infty$ at the region of large pressure as a result of the γP^2 term. Our experimental data[10] of the tablet compression of many kinds of powder were applied to this equation, and the coefficients, α, β and γ, were calculated by the method of least squares. As a result, the value of γ was smaller than one several thousandth of the value of either α or β on every occasion. Practically, then, the value of γ can be regarded as zero. If the constant γ is zero, Tanimoto's equation should be the same in form as Kawakita's equation.

A Comparison of Equations Expressed in Terms of Porosity.—Excepting the equations of Murray, Konopicky and Tanimoto, each equation shown in Table II was modified so as to include the same porosity term as a scale.

The apparent compacting volume, V, can be derived from each equation; this volume is used to express the porosity term, $(V-V_\infty)/V$. The results obtained are given in Table III. In Cooper's equation, we considered only the first term in the right side.

As is demonstrated in Table III, Balshin's and Jones' equations can only be applied in some limited ranges of pressure, because the degree of porosity must assume an unreasonable value, 100%, if the compacting pressure is either very low or very high. Similarly, Smith's, Nutting's, Terzaghi's and Cooper's equations cannot be applied to the higher pressure range. Thus, concerning the change in porosity, it is shown that only Ballhausen's, Athy's and Kawakita's equations are applicable over the entire range of pressure.

Porosity Gradient with Applied Pressure.—With regard to the rate of porosity change as a function of the pressure, some differences exist among the equations in question, as is shown below.

TABLE III. COMPARISON OF POROSITIES DERIVED FROM VARIOUS EQUATIONS

Author	Porosity (n=)	$P \to 0$	$P \to \infty$	Necessary condition
Balshin	$1-\frac{c_1}{c_2-\ln P}$	1	1	$c_1 \neq 0$
Smith	$n_0 - c_3 V_\infty P^{1/3}$	n_0	$-\infty$ ($c_3>0$) $+\infty$ ($c_3<0$)	$c_3 \neq 0$
Ballhausen	$\frac{1}{1+c_7 \cdot \exp(c_6 P)}$	$\frac{1}{1+c_7}$	0	$c_6 \neq 0$ $c_7 \neq 0$
Jones	$1-\left(\frac{c_9}{c_{10}-\ln P}\right)^{1/2}$	1	1	$c_9 \neq 0$
Athy	$n_0 \cdot e^{-c_{11}P}$	n_0	0	$c_{11} \neq 0$
Nutting	$1-\left(\frac{V_\infty}{V_0}\right)e^{c_{12}P^{c_{13}}}$	n_0	n_0 ($c_{13}<0$) $-\infty$ ($c_{12}>0, c_{13}>0$) 1 ($c_{12}<0, c_{13}>0$)	$c_{12} \neq 0$ $c_{13} \neq 0$
Terzaghi	$1-\frac{1}{1-c_{17}\ln(P+c_{18})-c'_{19}(P+c_{18})+c'_{21}}$	$1-\frac{1}{1-c_{17}\ln c_{18}-c'_{19}c_{18}+c'_{21}}$	1	
Cooper	$1-\frac{(V_\infty/V_0)}{1-n_0 c_{22} \cdot \exp(-c_{23}/P)}$	n_0	$\frac{1-c_{22}}{(1/n_0)-c_{22}}$	$c_{22} \neq 0$ $c_{23} \neq 0$
Kawakita	$\frac{n_0}{1+(V_\infty/V_0)c_{26}P}$	n_0	0	$c_{26} \neq 0$

n=porosity, n_0=initial porosity

$$\text{Balshin} : -\frac{dn}{dP} = a\cdot(1-n)^2P^{-1}$$

$$\text{Smith} : -\frac{dn}{dP} = b\cdot P^{-2/3}$$

$$\text{Ballhausen}: -\frac{dn}{dP} = c\cdot(1-n)\cdot n$$

$$\text{Jones} : -\frac{dn}{dP} = d\cdot(1-n)^3\cdot P^{-1}$$

$$\text{Athy} : -\frac{dn}{dP} = e\cdot n$$

$$\text{Nutting} : -\frac{dn}{dP} = f\cdot(1-n)\cdot P^{c_{13}-1}$$

$$\text{Terzaghi} : -\frac{dn}{dP} = (1-n)^2\cdot\left(\frac{c_{17}}{P+c_{18}}+c_{19}\right)$$

$$\text{Cooper} : -\frac{dn}{dP} = g\cdot\frac{(1-n)}{P^2}\cdot(n_0-n)$$

$$\text{Kawakita} : -\frac{dn}{dP} = h\cdot n^2$$

where n is the porosity at the applied pressure, P; n_0, the initial porosity, and a, b, c, d, e, f, g and h are the constants. According to Neumann,[17] the c_{13} value in Nutting's equation is very small, that is, the order of 0.1. Furthermore, Terzaghi's equation becomes identical with Balshin's if the c_{18} and c_{19} constants are very small.

Thus, these equations may be represented by two different types of equations:

$$\text{(I)}: -\frac{dn}{dP} = k\cdot n^x : \text{Athy } (x=1),\ \text{Kawakita } (x=2)$$

$$\text{(II)}: -\frac{dn}{dP} = k\cdot\frac{(1-n)^y}{P^z}: \text{Smith } (y=0,\ z=2/3),\ \text{Nutting } (y=1,\ z\fallingdotseq 1),\ \text{Balshin } (y=2,\ z=1),\ \text{Terzaghi } (y=2,\ z\sim 1),\ \text{Jones } (y=3,\ z=1)$$

where k is a proportional constant. Ballhausen's equation is a multiplication of the types I and II ($x=1$, $y=1$, $z=0$). Cooper's equation is the sum of the type II and the type I×II.

From these equations we note that the rate of the change in porosity due to the pressure is related to the ratio of the void to the volume of powder in Athy's and Kawakita's equations, while it is related to the applied pressure and the ratio of the net volume in the other equations.

Figures 1(A) and (B) illustrate the porosity change as a function of the pressure. In these figures we picked out Athy's ($x=1$) and Kawakita's ($x=2$) equations from the type I, Smith's ($y=0$), Nutting's ($y=1$), Balshin's ($y=2$) and Jones' ($y=3$) equations from the type II, and Ballhausen's from the type I×II.

The initial porosity was taken to be 80 and 40% for A and B respectively, while at 3000 kg./cm² it was taken to be 10% in both cases. Even if these percentages are taken otherwise, the general trend of the curves should be the same.

When we made Fig. 1, we used the value of 0.1 for c_{13} in Nutting's equation. In the case of Balshin's and Jones' equations, we constructed the curves for the pressure higher than 0.001 kg./cm², because in both equations the porosity become 100% when the pressure was zero.

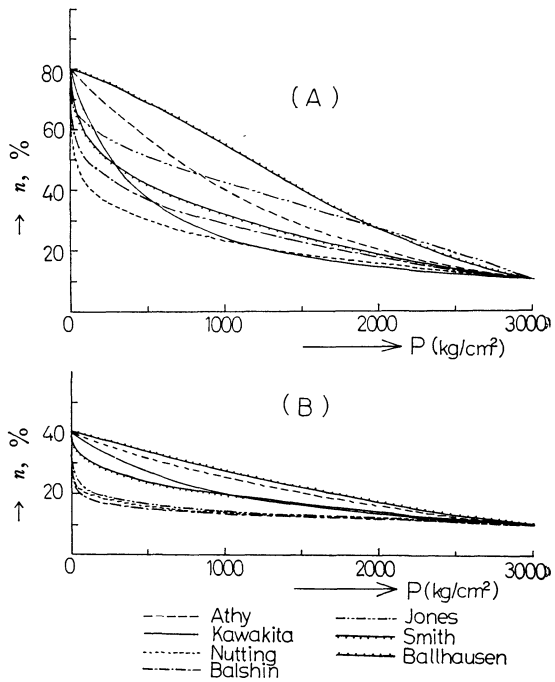

Fig. 1 (A), (B). Comparison of various equations using the term of porosity.

It may, thus, be concluded from Fig. 1 that Ballhausen's equation predicts the most gradual decrease in porosity as the pressure increases, and that the next most gradual decrease is in Athy's equation. Kawakita's equation indicates a considerable decrease in porosity in an early period of compaction. The other equations show that a major portion of the porosity disappears at lower pressures.

According to our experiments on tablet compression,[10] powder of common nonspherical particles changed its porosity largely in an early period of compaction; its compacting behavior was in good agreement with Kawakita's equation. On the other hand, powder of spherical glass or metal particles did not change its porosity appreciably as a result of the pressure; therefore, Athy's equation became applicable.

Finally, the compacting behavior of powder depends remarkably on the experimental conditions and on the physical properties of particles;

therefore, it is difficult to find a single equation which is in exact accord with the experimental data on different kinds of powder and different experimental conditions.

The authors wish to thank Dr. R. E. Collins (University of Houston), who visited Japan in 1964, for his valuable discussions.

BULLETIN OF THE CHEMICAL SOCIETY OF JAPAN VOL. 39 1368—1372 (1966)

The Non-Newtonian Flow of Poly(Dimethyl Siloxane)

By Yoshio Ito

Department of Chemistry, Faculty of Science, Niigata University, Niigata

(Received February 22, 1965)

The non-Newtonian flow of poly(dimethyl siloxanes) with a wide variety of degrees of polymerization (Z), 31.6 to 6.02×10^3, was studied by using short capillary viscosimeters. Measurements were performed in the range of rate of shear from 10^{-1} to 3×10^6 sec^{-1}. It was found that the flow behavior was markedly affected by the value Z of the test materials. That is, the flow was practically Newtonian over the entire range of shear rates when Z was less than 1.55×10^2. For higher values of Z, however, typical non-Newtonian behavior was observed in the range of moderate shear rates. At extremely high shear rates, the materials with $Z=3.23\times10^2$ to 2.63×10^3 exhibit the upper (or second) Newtonian flow, but the materials with still higher values of Z exhibit the spiral flow. It was also found that the Shishido equation (*J. Chem. Soc. Japan, Pure Chem. Sect. (Nippon Kagaku Zasshi)*, **84**, 889 (1963)) was applicable to this polymer in describing the observed viscosity vs. shear rate dependence. Finally, an empirical method was proposed for estimating the upper Newtonian viscosity value from the viscosities at zero shear stress and at the inflection point of the flow curve.

Recently, the flow behavior of molten polymers or polymer solutions in short capillaries has attracted the attention of many investigators. This is because: (a) the flow data at a very high shear stress or shear rate are obtainable by this means if an adequate end correction is made to the capillary length, and (b) the data obtained can be used to evaluate the various rheological properties of polymer systems.

Shishido[1-4] proposed a semi-empirical theory for the non-Newtonian flow on the assumption that the viscosity of the fluid is closely related to the deformation of the polymer molecules caused by shear stress; he applied this theory to dilute and concentrated solutions of high polymers.

This paper will present the results of the application of his theory to poly(dimethyl siloxanes) of various molecular weights in the molten state. The measurements cover a wide range of shear stress, from the lower (or first) Newtonian region up to the upper (or second) Newtonian region.

Experimental

The poly(dimethyl siloxanes) used in this study were obtained from the Shin-Etsu Chemical Industry Co., Ltd. The degree of polymerization (Z) were calculated from the zero shear viscosities (η_0) by using the relationship given in Refs. 5 and 6. These values of η_0 and Z are given in Table I.

The viscosity measurements were performed with extrusion capillary viscosimeters[1] driven by nitrogen pressure. The lengths (l) and radii (r) and the ratios between them (l/r) of the capillaries used are listed in Table II. The temperature was kept at 35°C throughout the measurements. The extruding pressure was adjustable up to 150 kg./cm^2.

Results and Discussion

The End Correction of Capillary.—For the flow of a Newtonian fluid in a long capillary, the maximum shear rate (D_N) and shear stress (τ') (at the wall of the capillary) are given by:

$$D_N = 4Q/\pi r^3 \quad (1)$$

$$\tau' = Pr/2l \quad (2)$$

where r and l are the radius and the length of the capillary respectively, Q is the output rate of the fluid, and P is the applied pressure corrected by the kinetic energy effect.

1) S. Shishido and Y. Ito, *J. Chem. Soc. Japan, Pure Chem. Sect. (Nippon Kagaku Zasshi)*, **84**, 889 (1963).
2) S. Shishido and Y. Ito, ibid., **85**, 13 (1964).
3) S. Shishido and Y. Ito, ibid., **85**, 191 (1964).
4) S. Shishido and Y. Ito, ibid., **85**, 195 (1964).
5) M. J. Hunter, E. L. Warrick, J. F. Hyde and C. C. Currie, *J. Am. Chem. Soc.*, **68**, 2284 (1946).
6) T. G. Fox, S. Gratch and S. Loshaek, "Rheology, Theory and Application," Vol. 1, Academic Press Iac., New York (1956), p. 431.

Table I. Viscosities at zero shear stress and degrees of polymerization for poly(dimethyl siloxanes)

Name of sample		Viscosity η_0 (poise)	Degree of polymerization Z *4	
KF96	(10)	9.4×10^{-2}	3.16×10	*1
	(30)	2.9×10^{-1}	7.07×10	
	(50)	4.35×10^{-1}	9.55×10	
	(100)	8.7×10^{-1}	1.55×10^{2}	
	(300)	2.45	3.23×10^{2}	*2
	(500)	4.4	5.00×10^{2}	
	(1000)	9.7	8.70×10^{2}	
	(3000)	2.45×10	1.15×10^{3}	
KF96H	(6000)	4.9×10	1.41×10^{3}	
	(10000)	8.0×10	1.66×10^{3}	
	(50000)	4.2×10^{2}	2.63×10^{3}	
	(100000)	8.5×10^{2}	3.31×10^{3}	*3
	(500000)	4.3×10^{3}	5.25×10^{3}	
	(1000000)	7.2×10^{3}	6.02×10^{3}	

Footnotes, *1—3, show the flow behaviors.
*1: Newtonian flow throughout the whole range of shear stress measured.
*2: Non-Newtonian flow at moderate shear stress and upper Newtonian flow at high shear streess.
*3: Non-Newtonian flow at moderate shear stress and spiral flow at high shear stress.
*4: The degree of polymerization (Z) was calculated by the equations in Refs. 5 and 6 from the viscosities at zero shear stress.

Table II. Dimensions of capillaries

Capillary No.	Radius r, cm.	Length l, cm.	l/r
I	0.0526_9	0.994_0	18.9
II	0.0527_5	0.636_5	12.0
III	0.0680_0	0.275_0	4.05
IV	0.0682_5	0.114_5	1.68
E	0.202_6	4.48_0	22.1
H	0.0134_9	1.95_5	145
K	0.0135_0	0.687_0	50.9
W	0.0135_0	0.149_5	11.0
X	0.0112_5	0.0785	6.98
Y	0.0135_0	0.0762	5.64
Z	0.0265_0	0.0818	3.09

Considering the entrance effect (Couette correction) ($c=0.65$)[1-3] and the elastic effect (e), we may obtain, instead of Eq. 2, the following relationship for a non-Newtonian fluid passing through a comparatively short capillary:

$$\tau = P/2(l/r+c+e) \qquad (3)$$

where $(c+e)$ is the total end correction and τ is the corrected shear stress. The total end correction can be determined by extrapolating the plot of P versus l/r to the zero value of P at a constant shear rate (D_N). This is the usual method for determining the end correction. Figure 1 shows such plots obtained for Shin-Etsu Silicone KF96H-(10000).

An approximate method for obtaining the end correction, e, has been proposed by Shishido on the basis of his empirical theory of the non-Newtonian flow of polymer solutions.[1-4] This method has been applied to our molten polymers. The results are shown in Fig. 2, where the approximate estimates of e obtained by the Shishido method (open circles) are compared with the ordinary estimates obtained by the above extrapolation method (solid curve). The agreement between the

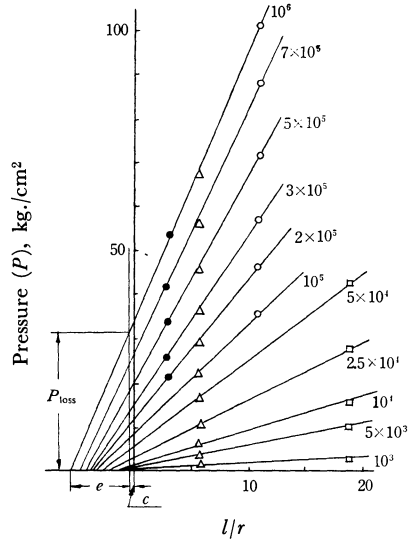

Fig. 1. Relations between pressure and capillary dimension (l/r) at a constant shear rate (D_N) for Shin-Etsu Silicone KF96H (10000).
The numerals in the figure represent the shear rates in sec^{-1}.
Symbols of capillaries in Table II.
●: Z, △: Y, ○: W, □: I

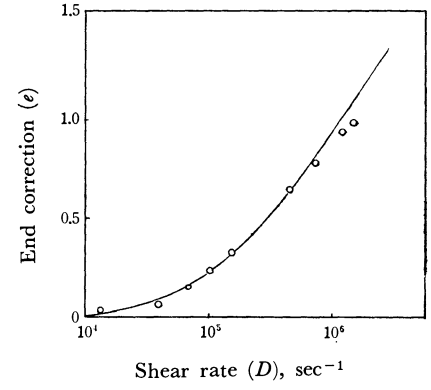

Fig. 2. Comparison between a usual end-correcting method (solid curve) and results (open symbols) calculated by Shishido's method[1] for Shin-Etsu Silicone KF96 (1000).

two estimates was satisfactory over a wide range of shear rate, D.

Flow Curve.—After the end correction is established, it is possible to calculate the corrected flow curve, i. e., the τ vs. D relationship, which should be independent of the l/r values of the capillaries used. The results obtained for the present samples are shown in Fig. 3, where the non-Newtonian shear rate (D) was calculated by:

$$D=(D_N/4)(3+\mathrm{d}\log D_N/\mathrm{d}\log\tau) \qquad (4)^{7)}$$

From Fig. 3, it may be seen that the siloxanes with degrees of polymerization less than 1.55×10^2 exhibit Newtonian behavior. For the materials with a higher degree of polymerization, i. e., from 3.23×10^2 to 8.7×10^2, typical non-Newtonian behavior is observed at moderate shear rates. These materials exhibit the upper (or second) Newtonian flow at extremely high shear rates. The materials of still higher degrees of polymerization, i. e., 1.15×10^3 to 2.63×10^3, do not exhibit the upper Newtonian flow, probably because of the disturbance by the spiral flow. The dotted parts of the flow curves for the materials with $Z=3.31\times10^3$, 5.25×10^3, and 6.02×10^3 indicate this range of spiral flow. When the spiral flow occurs instead of the upper Newtonian flow, the apparent viscosity becomes smaller for the materials with higher degrees of polymerization than for those with lower degrees of polymerization, as is shown in Fig. 3. Such inversion must be physically nonsensical; accordingly, we shall omit these parts of the flow curves from the following discussions.

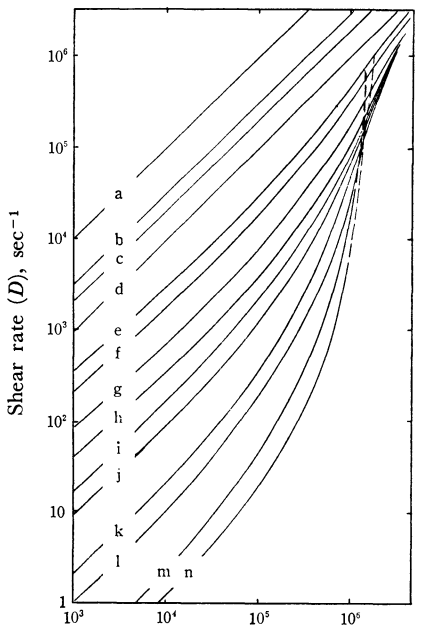

Fig. 3. Flow curves for poly(dimethyl siloxanes) of different molecular weights.
The dotted part in the curve indicates the region of spiral flow.
Degree of polymerization
a : 3.16×10 b : 7.07×10 c : 9.55×10
d : 1.55×10^2 e : 3.23×10^2 f : 5.00×10^2
g : 8.70×10^2 h : 1.15×10^3 i : 1.41×10^3
j : 1.66×10^3 k : 2.63×10^3 l : 3.31×10^3
m : 5.25×10^3 n : 6.02×10^3

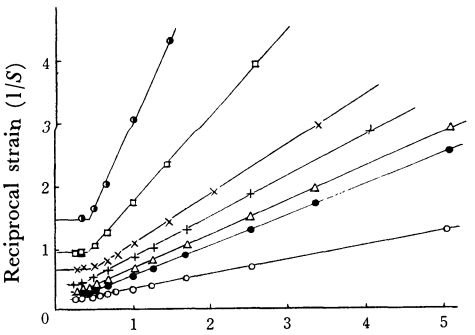

Fig. 4. Relations between $1/S$ and $1/\tau$ for different poly(dimethyl siloxanes).
Degree of polymerization
◑: 3.23×10^2 □: 5.00×10^2 ×: 8.70×10^2
+: 1.15×10^3 △: 1.41×10^3 ●: 1.66×10^3
○: 2.63×10^3

Flow Equation.—Shishido's proposed equations for the non-Newtonian flow of a polymer solution are:[1)]

$$(\eta_{app}-\eta^*)/(\eta_0-\eta^*)=\exp(-S) \qquad (5)$$

$$1/S=1/S_\infty+(1/\tau-1/\tau_c)/S_\infty\beta \qquad (6)$$

where τ is the shear stress; η_{app}, the apparent viscosity; η^*, the viscosity of the solvent, and η_0, the viscosity at zero shear stress. The symbol S represents the strain exerted on each polymer molecule; S_∞, the value of S in the flow of the upper Newtonian range; β, the flexibility parameter of the polymer molecule, and τ_c, the critical shear stress above which S attains its saturated value (S_∞). These equations may also be applicable to molten polymers. In this case, η^* is zero, Eq. 5 is then reduced to:

$$\eta_{app}/\eta_0=\exp(-S) \qquad (7)$$

Figure 4 shows the plots of $1/S$ versus $1/\tau$ for the present samples under the conditions of normal flow. It may be seen that Eqs. 6 and 7 are approximately valid for these molten polymers. The rheological values obtained from the relation between $1/S$ and $1/\tau$ are listed in Table III, where S_∞^{cal} and η_∞^{cal} are estimated to be as follows. Denote by S_{inf}^{exp} the value of S at the inflection point on the curve of $\log\tau$ versus $\log D$. The

7) O. H. Clark and M. L. Deutsch, *J. Appl. Phys.*, **21**, 713 (1950).

TABLE III. RHEOLOGICAL VALUES FOR DIFFERENT POLY(DIMETHYL SILOXANES)

Degree of polymerization of samples (Z)	S_∞^{exp}	S_∞^{cal}	η_∞^{exp} poise	η_∞^{cal} poise	β cm²/dyn.	βS_∞ (cm²/dyn.) from $1/\tau \sim 1/S$	from Eq. 10	from Eq. 11
3.23×10^2	0.703	0.86	1.1	1.02	5.2×10^{-7}	3.7×10^{-7}	3.1×10^{-7}	4.1×10^{-7}
5.00×10^2	1.14	1.56	1.3	1.07	6.6×10^{-7}	7.5×10^{-7}	4.1×10^{-7}	4.1×10^{-7}
8.70×10^2	1.77	1.89	1.5	1.46	7.2×10^{-7}	1.28×10^{-6}	6.9×10^{-7}	5.8×10^{-7}
1.15×10^3		2.45		2.11	6.7×10^{-7}	1.65×10^{-6}	7.7×10^{-7}	1.3×10^{-6}
1.41×10^3		2.80		2.95	6.4×10^{-7}	1.80×10^{-6}	1.9×10^{-6}	1.3×10^{-6}
1.66×10^3		3.30		2.97	6.5×10^{-7}	2.15×10^{-6}	2.3×10^{-6}	1.2×10^{-6}
2.63×10^3		5.13		2.47	1.0×10^{-6}	5.15×10^{-6}	6.0×10^{-6}	2.4×10^{-6}

ratios of S_∞ to S_{inf}^{exp} may then be determined for our samples, e, f and g, the upper Newtonian region of which has been experimentally established (see Fig. 3). Thus, we find that $S_\infty/S_{inf}^{exp} \doteqdot 1.7$ independent of the degree of polymerization. The relations between S_∞ and S_{inf}^{exp} of other polymer systems are available from the literature; they are shown in Fig. 5. This figure clearly suggests that the S_∞/S_{inf}^{exp} ratio is practically a constant, 1.7, independent of the polymer and solvent species. Accordingly, if the curve of $\log \tau$ versus $\log D$ is available up to its inflection point, S_∞ can be determined to be $1.7S_{inf}^{exp}$. The values of S_∞ thus

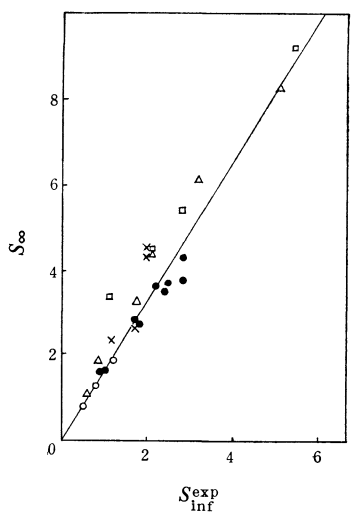

Fig. 5. Relations between S_∞ and S_{inf}^{exp} for various polymer systems.
Molten polymer
○: poly (dimethyl siloxane)
Polymer solutions
●: polystyrene in diethyl phthalate at 20°C[1]
△: polyisobutylene in dicaline at 25°C[8]
□: cellulose nitrate in *n*-butyl acetate at 25°C[9]
×: cellulose triacetate in ethylene chlorohydrine at 25°C[10].

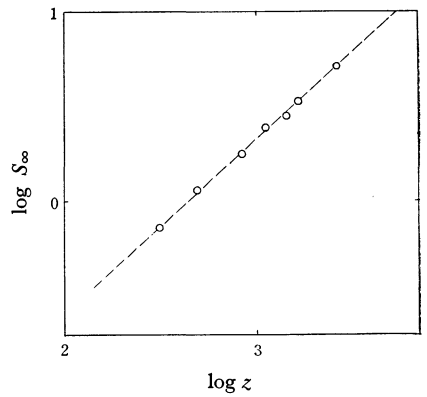

Fig. 6. Dependence of S_∞ on the degree of polymerization for poly(dimethyl siloxane).

obtained for the present samples are plotted in Fig. 6 against the degree of polymerization (Z). From the figure, we find that:

$$S_\infty = 3.62\times10^{-3}\times Z^{0.92} \quad (8)$$

Accordingly, by using Eq. 7 or Eq. 8 and the relations of η_0 and Z in Refs. 5 and 6, the η_∞ (upper Newtonian viscosity) value can be estimated from η_0 and S_∞, or directly from Z. The values of β are calculated from $S_\infty\beta$ by using S_{inf}^{exp} for the siloxanes with degrees of polymerization from 3.23×10^2 to 8.70×10^2, and by using S_∞^{cal} for the siloxanes with degrees of polymerization from 1.15×10^3 to 2.63×10^3.

Shearing Strain, Pressure Loss and End Correction in the Capillary Flow.—From the theory[1-3] previously proposed, the relations among strain (S), end correction (e), shear stress (τ), and pressure loss (P_{loss}) are:

$$2e = \sqrt{2}S/[1-(1-1/\beta\tau_c)S/S_\infty] \quad (9)$$

$$P_{loss} = \sqrt{2}\beta S_\infty \tau^2 \quad (10)$$

$$= (2\sqrt{2}e^2)/(\beta S_\infty) = (2e)^2/(\sqrt{2}\beta S_\infty) \quad (11)$$

Equations 9, 10, and 11 were examined for the present cases. The solid curves in Fig. 7 indicate the results calculated from Eq. 9 by using the β, τ_c, and S_∞ values obtained experimentally. The experimental results (various point marks) and the theoretical results (solid curve) are substantially in accordance with each other. Two kinds of

8) J. G. Brodnyan, F. H. Gaskins and W. Philippoff, *Trans. Soc. Rheo.*, **1**, 109 (1957).
9) W. Philippoff, F. H. Gaskins and J. G. Brodnyan, *J. Appl. Phys.*, **28**, 1118 (1957).
10) J. Schurz and K. Windisch, *Kolloid-Z.*, **177**, 149 (1961).

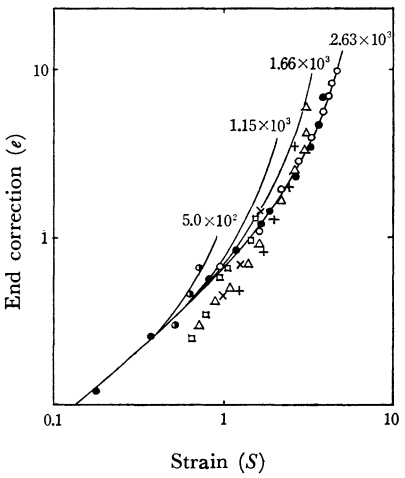

Fig. 7. Relations between e and S for poly(dimethyl siloxanes).
The solid curves indicate the results calculated from Eq. 9 by using β, τ_c, and S_∞ obtained. The numerals on the curves indicate the degrees of polymerization. The symbols represent the experimental values for the degree of polymerization as follows.
◑: 3.23×10^2 □: 5.00×10^2 ×: 8.70×10^2
+: 1.15×10^3 △: 1.41×10^3 ●: 1.66×10^3
○: 2.63×10^3

βS_∞ values, obtained graphically by using Eqs. 10 and 11, are given in Table III, together with the βS_∞ value obtained from the slope of the plot of $1/S$ versus $1/\tau$. These three kinds of βS_∞ values are in agreement with one another. These results show that the above relations proposed[3] for polymer solutions are also applicable to the molten state of poly(dimethyl siloxanes).

Summary

The non-Newtonian flow of poly(dimethyl siloxanes) of various mol. wts. has been studied with a short capillary viscosimeter. The experiment has covered a wide range of shear rate, from 10^{-1} to 3×10^6 sec^{-1}. The results are as follows:

1) The flow behavior of the sample changes with the degree of polymerization. For the siloxanes with degrees of polymerization less than 1.55×10^2, the flow of the fluid is Newtonian throughout the whole range of shear rates; in the cases of the siloxanes with degrees of polymerization from 3.23×10^2 to 2.63×10^3, however, the flow is non-Newtonian at moderate shear rates; it again becomes Newtonian at high shear rates. With degrees of polymerization of more than 3.31×10^3, the spiral flow rises to a high shear rate.

2) The flow behavior of the sample is expressed by modifying Shishido's equation proposed for non-Newtonian polymer solutions.

3) When the flow curve observed contains its inflection point, the upper Newtonian viscosity can be estimated by a new method proposed here.

4) The relations among the end correction of capillary, the pressure loss and the shear stress proposed by Shishido for polymer solutions are applicable to poly(dimethyl siloxane) also.

The author wishes to express his deep appreciation to Professor Dr. Shunsuke Shishido for many helpful discussions and suggestion made during this work. He also wishes to thank Mr. Hiroshi Kondo for his assistance in the experimental work. Finally, this research was supported in part by a grant-in-aid for Fundamental Scientific Research, for which the author is grateful.

BULLETIN OF THE CHEMICAL SOCIETY OF JAPAN VOL. 39 1372—1377 (1966)

A Spectroscopic Study of Alkylnitrobenzene Anion Radicals

By Yasuto NAKAI

Central Research Laboratory, Sumitomo Chemical Co., Ltd., Takatsuki, Osaka

(Received August 30, 1965)

A series of alkylnitrobenzene anion radicals has been studied by both electron spin resonance and infrared spectroscopy. It has been shown that there is a relationship between the magnitude of the nitrogen hyperfine splitting constant and the steric effect of the bulky alkyl group adjacent to the nitro group. In addition to the physical deformation factors, the effects of solvents, counter-ions, and temperature variation have been discussed. In the infrared spectra, the differences between anion radicals and neutral molecules have been found to be small, except for the change in the absorption intensity of the nitro-group stretching vibration.

The facility with which aromatic nitro compounds can accept an electron and the stability of the resulting radical anions have been reported on in a number of recent studies. A previous study

has also been made of nitrobiphenyl anion radicals in the presence of alkali metal cations by means of electron spin resonance spectroscopy.[1] In this study the unique behavior of the nitro group in conjugate hydrocarbon systems with single-ring structures will be investigated.

The steric influences of substituents, chiefly alkyl groups, on such properties of aromatic nitro compounds as the ultraviolet spectrum, the infrared spectrum, the dipole moment, the molecular refraction, the basicity, and the reaction rate have been reported. In connection with these investigations, the question naturally arises whether the steric influence can also be detected for anion radicals, because there is an expected tendency towards coplanarity due to the additional pi-electron in the case of anion radical systems.

The structural nature of the negatively-charged molecules has been discussed mostly in electron spin resonance studies, whereas little information gained from other spectroscopic studies, particularly from infrared spectroscopy, has so far been made available.

Experimental

Solvents were dehydrated thoroughly and then redistilled in vacuo to remove the molecular oxygen. Each alkali metal was purified by repeated distillations in vacuo. Since the same procedure could not be applied to alkaline earth metals, each granular alkaline earth metal was cut or ground in order to obtain fresh surfaces; each metal was washed with carbon tetrachloride, dried in vacuo, and then amalgamated in order to facilitate the reducing activity.

For the study of the anion radicals by infrared spectroscopy, a special vacuum-tight rock-salt cell 0.1 mm. thick was connected to a glass system in which the anion radicals were produced (a detailed account of the latter has been given elesewhere[2]). The connection was made with polyethylene tubing which could withstand atmospheric pressure and was yet soft enough so that the sample solution could be forced into the optical cell by simply pressing the tubing. When the maximum resolution was required, a Model 521 Perkin-Elmer grating spectrophotometer at the Institute for Chemical Research of Kyoto University was used.

The ESR spectrometer employed was a high-resolution apparatus (JES-3B type) of the Japan Electron Optics Lab. Co., Ltd. The magnetic field was modulated at a frequency of 100 kc./sec. and at a modulation width of 0.1 gauss.

Results and Discussion

Analysis of Infrared Spectra.—The infrared spectra in the range from 800 to 2000 cm^{-1} contain distinct absorption bands corresponding to the symmetric stretching vibration and the asymmetric vibration of the nitro group, with frequencies at about 1350 and 1530 cm^{-1} respectively.[3] The frequencies at the maxima of these bands were carefully determined for each neutral compound, using nitrobenzene as a standard. The frequency of the asymmetric stretching vibration is practically the same for all the compounds investigated, as Table I shows. In other words, the variation in the values observed seems to be independent of the size of the alkyl groups adjacent to the nitro group. On the other hand, the frequencies of the symmetric stretching vibrations of the nitro group vary appreciably.

The spectra for the anion radical solution in dioxane in the presence of the potassium cation were measured for *o*-isopropyl-, *o*-*t*-butyl-, 2, 4, 6-trimethyl-, and 2, 4, 6-tri-*t*-butylnitrobenzenes. In each case the same solution was remeasured after the anion radical had been oxidized, by exposure to air, in order to reform the original neutral species.

Differences between the reduced and unreduced states were evidenced in the infrared spectra by the enhanced absoprtion associated with the asymmetric vibrations, but there was no shift in the frequency within the resolution of the instrument. If the decrease in the frequency of the symmetric stretching vibration is directly related to the coplanarity of the nitro group with the aromatic ring, as has been suggested by Wepster et al.,[4] the present results might predict that the configurations of the neutral molecule and its anion radical are similar. This matter will be discussed in the next section.

The Steric Effect of Alkyl Groups.—The sterically induced decoupling of the nitro group

Table I. The stretching frequency of nitro group in the IR spectra

Compoud (in CCl_4)	Asymmetric frequency cm^{-1}	(Difference from nitrobenzene)	Symmetric frequency cm^{-1}	(Difference from nitrobenzene)
Nitrobenzene	1529	0	1346	0
Nitromesitylene	1524	−5	1363	17
2,4,6-Triethylnitrobenzene	1524	−5	1366	20
2,4,6-Triisopropylnitrobenzene	1524	−5	1372	26
2,4,6-Tri-*t*-butylnitrobenzene	1530	1	1375	29

1) Y. Nakai, K. Kawamura, K. Ishizu, Y. Deguchi and H. Takaki, This Bulletin, to be published.
2) Y. Deguchi, *J. Chem. Phys.*, **32**, 1584 (1960).
3) J. F. Brown, *J. Am. Chem. Soc.*, **77**, 6341 (1955).
4) A. Van Veen, P. E. Verkade and B. M. Wepster, *Rec. Trav. Chem.*, **76**, 801 (1957).

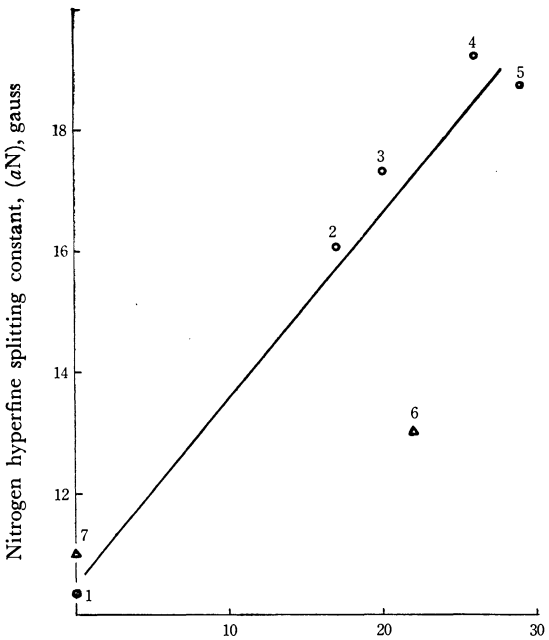

Difference in symmetric stretching vibration frequency between nitrobenzene and alkylnitrobenzene, cm^{-1}

Fig. 1. A relation between the observables for the nitro group as measured by ESR and IR.
1) Nitrobenzene
2) Nitromesitylene
3) 2,4,6-Triethylnitrobenzene
4) 2,4,6-Triisopropylnitrobenzene
5) 2,4,6-Tri-*t*-butylnitrobenzene
6) *o*-*t*-Butylnitobenzene
7) *o*-Methylnitrobenzene

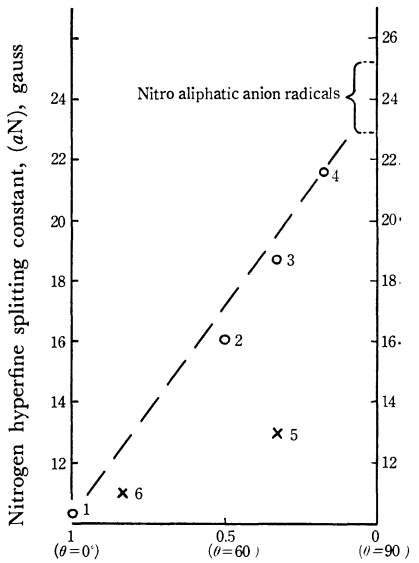

$\varepsilon/\varepsilon_0 = \cos^2\theta$

Ratio of extinction coefficients for the ultraviolet absorption between alkylnitrobenzenes and nitrobenzene at 250 mμ.*

Fig. 2. A relation between the observables for the nitro group as measured by ESR and UV.
1) Nitrobenzene
2) Nitromesitylene
3) 2,4,6-tri-*t*-Butylnitrobenzene
4) 2,3,5,6-Tetramethylnitrobenzene**
5) *o*-*t*-Butylnitrobenzene
6) *o*-Methylnitrobenzene
* Data from Ref. 14.
** Data from Ref. 15.

pi-electron system from the aromatic pi-electron system has been postulated solely on the basis of an interpretation of the electron spin resonance spectra.[5] On the basis of the observed changes in the nitrogen hyperfine splitting constants, a simple model involving hindered rotation in nitro aromatic anion radicals may be suggested. In this model the nitro group is twisted around the C–N bond.

Since the amount of twisting is likely to be similar in the anion radicals and in the neutral molecules, we have anticipated and found a linear relation between the nitrogen hyperfine splitting constants, a_N, and the shift of the symmetric stretching vibration frequency, as is shown in Fig. 1.

The decrease in the C–N bond order was also deduced from the ultraviolet absorption at 250 mμ by the equation of Braude[6] :

$$\varepsilon/\varepsilon_0 = \cos^2\theta \qquad (1)$$

where ε and ε_0 are the molar extinction coefficients for alkylnitrobenzene and nitrobenzene respectively, and where θ is the angle of twist of the nitrogroup out of the plane of the benzene ring. The ratio versus a_N is again plotted in Fig. 2.

The fact that the value of a_N extrapolated to $\theta = 90°$ falls in the range of a_N values characteristic of aliphatic nitro anion radicals confirms the expectation of the absence of conjugation between the nitro group and any groups to which it is bonded. In other words, the unpaired electron appears to be completely localized on the nitro group in this case.

For monoalkylnitrobenzenes, however, neither the infrared nor the ultraviolet spectroscopic data conform to the proportionality behavior shown in Figs. 1 and 2. For example, the nitrogen hyperfine splitting constant for *o*-*t*-butylnitrobenzene anion is 13.0 gauss, while the steric deformation predicted by Eq. 1 is 65 degrees, a value which cannot be predicted from Fig. 2. The cause of this deviation may be as follows. The resonance interaction of the nitro group with the benzene

5) D. H. Geske, J. L. Ragle, M. A. Bambenek and A. L. Balch, *J. Am. Chem. Soc.*, **86**, 987 (1964).
6) E. A. Braude and F. Sondheimer, *J. Chem. Soc.*, **1955**, 3754.

Table II. Calculated nitrogen hyperfine splitting constants

	o-*t*-Butylnitrobenzene	Nitromesitylene	2,4,6-Triethylnitrobenzene	2,4,6-Tri-*t*-butylnitrobenzene
$\beta_{C-N}=1$ ($\theta=0°$)				
ρ_N	0.3121	0.2519	0.2249	0.3121
ρ_O	0.1846	0.1028	0.1085	0.1846
a_N (Eq. 3)	13.1	17.4	14.5	17.7
a_N (Eq. 4)	15.3	12.3	11.0	15.2
$\beta_{C-N}=0.7$ ($\theta=45°34'$)				
ρ_N	0.3769	0.3501	0.3607	
ρ_O	0.2081	0.1934	0.2026	
a_N (Eq. 3)	22.4	20.8	21.2	
a_N (Eq. 4)	18.5	17.2	17.7	
$\beta_{C-N}=0.5$ ($\theta=60°$)				
ρ_N		0.405		0.3817
ρ_O		0.214		0.2087
a_N (Eq. 3)		24.8		22.8
a_N (Eq. 4)		19.8		18.7
a_B(Experimental)	13.0	16.1	17.3	18.7

ring is believed to be such as to constrain the nitrogen and the two oxygens to lie on the same plane, or such as to minimize the out-of-plane deflection, even in the presence of an alkyl group on one side, by bending the two groups away from each other, particularly in the case of the anion radicals. In those cases where the nitro group has alkyl groups on both sides, such bending is prevented, regardless of whether it is the neutral molecule or the radical anion. Thus, the changes in the observables in optical spectroscopy may be directly related to the extent of twisting. Any shift in the nitro-group absorption bands in the infrared spectra would reflect the twisting in the case of the monoalkylnitrobenzenes, but in the case of anion radicals, the shift may reflect both twisting and bending. Since the infrared spectra have not shed light on structural differences between the neutral molecule and the radical anion, as has been described in the last section, electron spin resonance spectra still seem to be a valuable source of infromation on the extent of intramolecular rotation for radical anions.[7]

The Computation of Hyperfine Splitting Constants.—Spin density (ρ) calculations based on the simple Hückel LCAO approximations have been carried out for a variety of parameters in the C–N bond integral expressed in the equation:

$$\beta_{NC} = \beta^0_{NC} \cos\theta \qquad (2)$$

The nitrogen hyperfine splitting constants computed

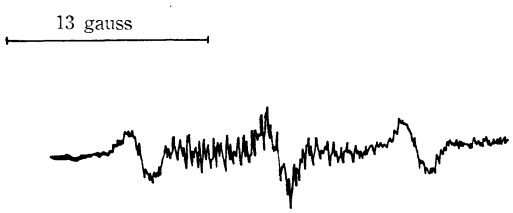

Fig. 3. The ESR spectrum of 2,4,6-triethylnitrobenzene anion radical.

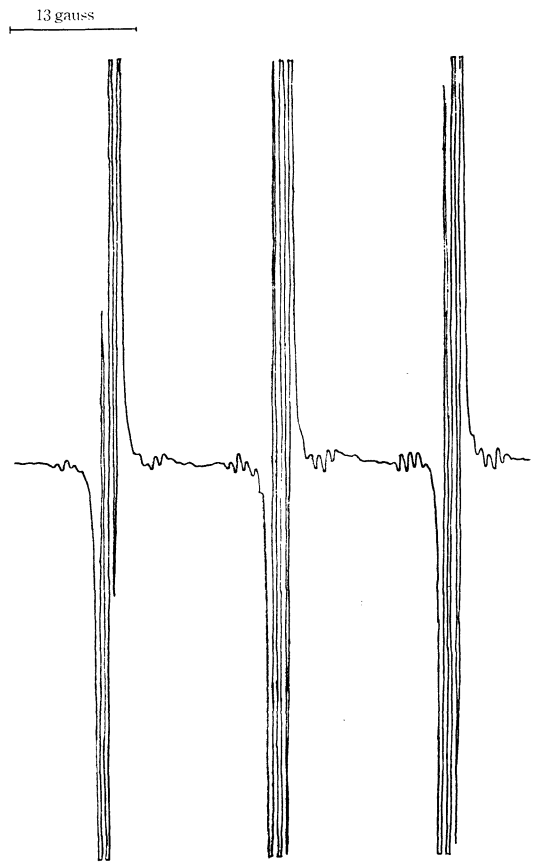

Fig. 4(a). The ESR spectrum of 2,4,6-tri-*t*-butylnitrobenzene anion radical.

7) K. Ishizu, This Bulletin, **37**, 1093 (1964).

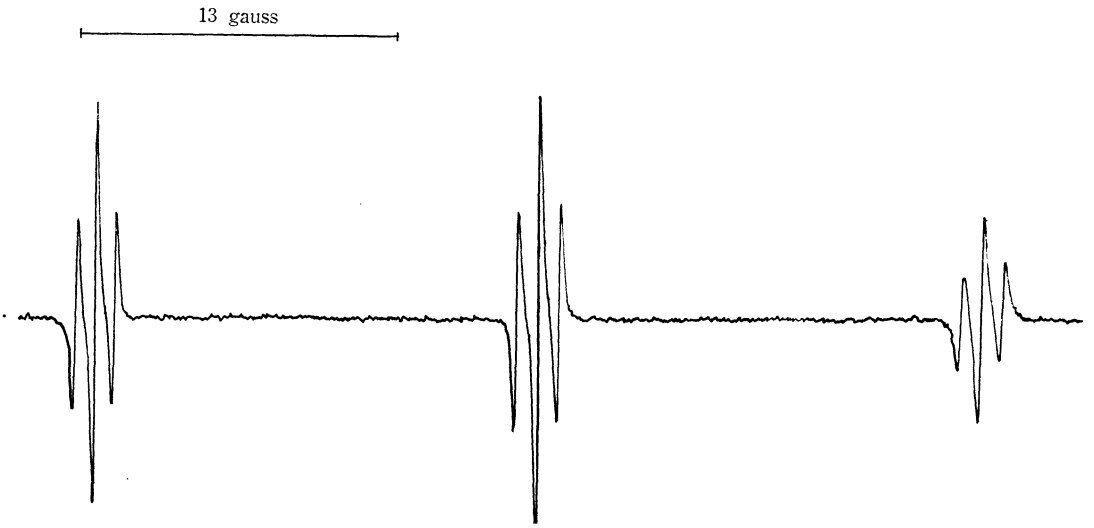

Fig. 4(b). The ESR spectrum of 2,4,6-tri-*t*-butylnitrobenzene anion radical.

by the equations[8,9]:

$$a_N = 99.0\,\rho_N - 71.6\,\rho_O \quad (3)$$

$$a_N = Q_N\rho_N = 49\,\rho_N \quad (4)$$

are compared with the experimental values in Table II.

Analysis of the ESR Spectra.—An electron spin resonance spectrum always consists of three well-defined groups of lines corresponding to the interaction with a ^{14}N nucleus if a proper radical concentration is maintained, as is illustrated in Fig. 3. Without deuterium substitutions, the alkyl-proton splittings cannot be distinguished from the ring-proton splittings. The reliable computation of hyperfine components is prevented by linewidth alternations, and by the overlap of the spectral lines due to the presence of cation-paired and isolated radical anions.[10] Efforts to observe the hyperfine splitting of the tertiary-butyl group which has been observed for those derivatives of phenoxyl[11] have been fruitless. The hyperfine splitting of ^{13}C and ^{17}O nuclei are shown in Fig. 4.

The Effect of Metal Cations on the Spectra.—The nitrogen hyperfine splitting constant (a_N) increases with the reciprocal of the cationic radius (r) or with the electronic charge of the cation (z) in solution. A tight ion-pair formation may be directly predicted by a comparison with meta-substituted nitrobenzenes which follows the equation:[12]

$$a_N = \text{constant} \times z/(r + 0.6) \quad (5)$$

Equation 5 is consistent with the presence of a rather loose ion-pair (a solvent shared to a limited extent), in contrast to the results of the present investigation.

TABLE III VARIATION OF THE NITROGEN HYPERFINE SPLITTING CONSTANT OF 2,4,6-TRI-*t*-BUTYLNITROBENZENE

(A)*

Solvent	a_N
p-Dioxane	18.45
Tetrahydrofuran	18.44
1,2-Dimethoxyethane	18.66
Tetrahydropyran	18.74
N,*N'*-Dimethylformamide	18.76

(B)**

Cation	a_N
Lithium	19.11
Sodium	18.80
Potassium	18.66
Calcium	18.34
Strontium	18.95
Barium	18.44

* The cation was K^+ in all cases.
** The solvent was 1,2-dimethoxyethane in all cases.

Effect of Solvents.—The decrease in the hyperfine splitting constant with an increase in the dipole moments of the solvents (shown in Table III) suggests that an oriented ionic atmosphere

8) P. H. Rieger and G. K. Fraenkel, *J. Chem. Phys.*, **39**, 609 (1963).
9) A. Ishitani, K. Kuwata, H. Tsubomura and S. Nagakura, This Bulletin, **36**, 1357 (1963).
10) H. Nishiguchi, Y. Nakai, K. Nakamura, K. Ishizu, Y. Deguchi and H. Takaki, *Mol. Phys.*, **9**, 153 (1965); *J. Chem. Phys.*, **40**, 241 (1964).
11) K. Mukai, private communication.
12) K. Nakamura, private communication.

of the solvent molecule may release the ion-pair, pulling the metal cation away from the anion radical as well as inducing a more unpaired electron spin on the bulky aromatic ring so as to decrease that on the nitro group. This result is to be contrasted with those with phenoxyls[11] or diphenyl nitric oxide,[13] which are supposed not to be present as ion-pairs in the solution.

The Effect of Temperature Variation.— The nitrogen hyperfine splitting constant increases once below room temperature to a maximum in the temperature range from 0 to −10°C, and then it decreases at a rate of about a hundredth of a gauss per degree.

13) J. Pannell, *Mol. Phys.*, **7**, 317 (1964).

The author wishes to thank Professors Hideo Takaki, Ryozo Goto and Rempei Goto for making ESR and IR spectrometer available for this study. He is also much obliged to Dr. Yasuo Deguchi and Dr. Yoshio Kubota for their helpful discussions and to Dr. Kazuhiko Ishizu and Dr. Naobumi Oi for the synthesis and measurement of samples. The author wishes to thank the Sumitomo Chemical Co., Ltd., for making this study possible.

14) B. M. Wepster, "Progress in Stereochemistry," Vol. 2, Butterworths Scientific Publications, London (1958), p. 100.

15) D. H. Geske and J. L. Ragle, *J. Am. Chem. Soc.*, **83**, 3532 (1961).

BULLETIN OF THE CHEMICAL SOCIETY OF JAPAN VOL. 39 1377—1382 (1966)

The Electronic Structures of Hydrides, Halides and Alkyl Compounds of Boron and Aluminum. II. Dimers

By Hiroshi KATO, Kaichiro YAMAGUCHI and Teijiro YONEZAWA

Faculty of Engineering, Kyoto University, Sakyo-ku, Kyoto

(Received September 20, 1965)

The electronic structures of dimers containing boron and aluminum atoms, i. e., B_2H_6, $B_2H_2(CH_3)_4$, Al_2Cl_6, $Al_2Cl_2(CH_3)_4$ and $Al_2(CH_3)_6$, are investigated by an extended Hückel method. The calculations show that the central linkages are weak and that their bonding natures are very different from those of the bonds between the metals and terminal atoms. Judging from the orbital energies and populations, these dimers still hold a strong acidity, like that in the monomers, an acidity which depends mainly on the existence of the almost unfilled $p\pi$ orbitals of the metal atoms, where the electrons occupying the lower vacant orbitals in these dimers are almost localized. The results are compared with other calculations and experimental results. It is, further, shown by examining the electronic structures of two hypothetical compounds that these dimers can be easily formed by using the vacant valence orbitals of the metal atoms, and that the metal-metal bonds in some dimers are considerably strong.

The structures of dimers containing boron or aluminum atoms have attracted the interest of many researchers. The bridged model has been applied to the structures of these dimers, and several interpretations have been attempted.[1]

In the present paper, we will treat these dimers by the extended Hückel method proposed by Hoffmann.[2] In our previous paper, Part I,[3] the electronic structures of monomers and ions, including boron or aluminum atoms, were considered by the same method. These dimer compounds are the so-called "electron-deficient compounds," and the usual concept of the electron-pair bond fails as a basis for an interpretation of their electronic structures. Hoffmann's method represents the molecular orbitals (MO) in terms of the linear combinations of the atomic orbitals (AO) of all the valence electrons of the atoms in the compounds; therefore, it is not necessary to predetermine the hybridizations or the orientations of the base orbitals. For this reason, this approximate method is suitable for the treatment of those compounds which have unusual valencies or configurations.

The dimer compounds to be studied in the present paper are B_2H_6, $B_2H_2(CH_3)_4$, Al_2Cl_6, $Al_2(CH_3)_4Cl_2$, $Al_2(CH_3)_6$, and some related compounds. Their electronic structures will be calculated, and,

1) E. g., C. A. Coulson, "Valence," Oxford Univ. Press, Oxford (1952), 2nd edition (1961); H. Zeiss, ed., "Organometallic Chemistry," Reinhold Pub. Co., New York (1960).

2) R. Hoffmann, *J. Chem. Phys.*, **39**, 1397 (1963); ibid., **40**, 2474 (1964).

3) H. Kato, K. Yamaguchi, T. Yonezawa and K. Fukui, This Bulletin, **38**, 2144 (1965).

TABLE I. THE GEOMETRY OF DIMERS

Compound	Bond distance, Å			Bond angle, deg.	
	M-X	M-Y	M-M	∠XMX	∠YMY
B_2H_6	1.187	1.334	1.77	120	(83)*
$B_2H_2(CH_3)_4$	1.59	1.34	1.86	120	(83)*
Al_2Cl_6	2.06	2.21	3.410580	120	79
$Al_2Cl_2(CH_3)_4$	1.90	2.31	3.266834	120	90
$Al_2(CH_3)_6$	2.00	2.23	2.558150	120	110

* Approximate values calculated from bond distances.

TABLE II. THE M(A) and M(A-B) VALUES OF VARIOUS MONOMERS AND DIMERS

Compound	M(M)	M(X)	M(Y)	M(M-X)	M(M-Y)*
BH_3	2.562	1.146	—	0.852	—
B_2H_6	2.697	1.163	0.976	0.865	0.463
$BH(CH_3)_2$	2.143	4.726	1.238**	0.730	0.800**
$B_2H_2(CH_3)_4$	2.249	4.762	1.030	0.672	0.492
$AlCl_3$	1.029	7.657	—	0.488	—
Al_2Cl_6	1.084	7.681	7.553	0.472	0.328
$AlCl(CH_3)_2$	1.005	5.050	7.651**	0.384	0.496**
$Al_2Cl_2(CH_3)_4$	0.964	5.099	7.574	0.344	0.319
$Al(CH_3)_3$	0.985	5.049	—	0.382	—
$Al_2(CH_3)_6$	0.985	5.090	5.011	0.384	0.188

* The notations, M, X and Y refer to those given in Fig. 1.

** The values correspond to the hydrogen atom and the chlorine atom in $BH(CH_3)_2$ and in $AlCl(CH_3)_2$ respectively.

especially, the nature of the bonds and some physico-chemical properties will be discussed.

The values of the parameters used in this paper (the Coulomb and resonance integrals) were given in Part I of this series.[3] The coordinates of the above compounds are shown in Fig. 1, where the notation M denotes the boron or aluminum atom; Y, the bridge atom or group, and X, the terminal atom or group. The two M and four X atoms are on the XY plane, and the two Y atoms are on the Z-axis (one in the + region and the other in the − region). The px, py and pz orbitals of each atom have their positive parts in the X, Y and Z directions, respectively, of the coordinates in Fig. 1. The bond distances and bond angles are estimated with reference to the values given in Ref. 4. For the sake of simplicity in the calculation, however, the values listed in Ref. 4 have been modified slightly; for all the methyl groups, the valence angle is assumed to be tetrahedral, and the C–H bond distance is set equal to 1.09 Å throughout the calculations. The adopted values are summarized in Table I.

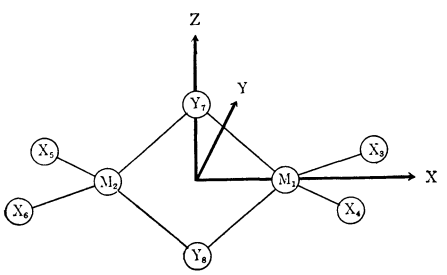

Fig. 1. The coordinates of dimers.

The Electronic Structures of the Dimers

Population Analysis. — The calculated values of the atomic populations of the atom A, M(A), and those of the atom bond populations between A and B atoms, M(A-B),[5] are listed in Fig. 2, where the M(A) values are represented by the numbers on the atom A, and the M(A-B) values, by those between the A–B bond (the values of the hydrogen atoms in the methyl groups are omitted for the sake of simplicity). The results given in Fig. 2 show that the M(A) and M(A-B) values in these dimers are similar to those in their monomers as given in Table II (the values of which are taken from our previous paper),[3] except for the quantities related to the bridge atoms or groups.

They also show that two types of bonds exist in these dimeric compounds; one is the M–X bond (corresponding to M and X in

4) A. D. Mitchell and L. C. Cross, eds., "Table of Interatomic Distances and Configurations in Molecules and Ions," The Chemical Society, London (1958).

5) K. Morokuma, H. Kato, T. Yonezawa and K. Fukui, This Bulletin, **38**, 1263 (1965).

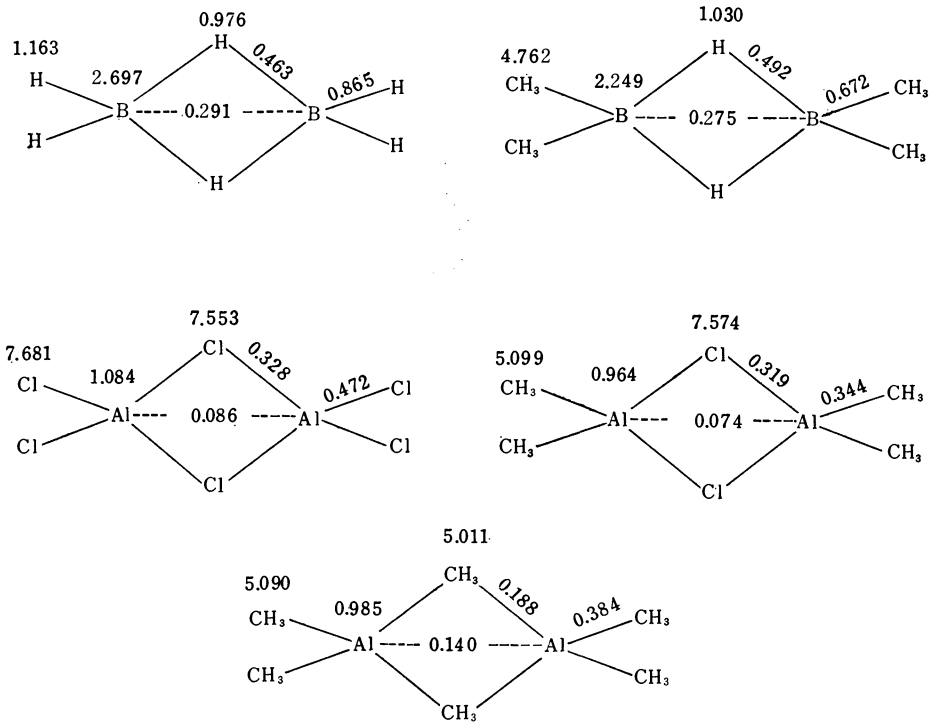

Fig. 2. The M(A) and M(A–B) values of dimers.

Fig. 1), which is nearly the same as the normal electron-pair bond, and the other is the M–Y bond (Y in Fig. 1), which is weak and which may be called a "semi-bond." For example, the calculated values of M(B–H_T) (where H_T indicates the terminal hydrogen) are 0.852 in BH_3 and 0.865 in B_2H_6, while that of M(B–H_B) (H_B denotes the bridge hydrogen) is 0.463. For $Al(CH_3)_3$, the values of M(Al–C_T) are 0.382 in the monomer and 0.384 in the dimer, while the M(Al–C_B) value is 0.188.

As to the M(A) values in M_2A_6-type compounds, those of the atoms in the bridge are slightly smaller than those of the terminal atoms. However, this result is partly in conflict with other results, as is mentioned below. For B_2H_6, our result leads to the $M(H_T) > M(H_B)$ relation, whereas the results of an LCAO SCF calculation by Yamazaki indicate $M(H_T) < M(H_B)$;[6] Yamazaki's findings agree with the experimental findings. On the other hand, it was reported, for Al_2Br_6, on the basis of a PQR measurement,[7] that the charges in the bridge bromine atoms are smaller than those in the terminal atoms; in this case, accordingly, this tendency may agree with our finding for Al_2Cl_6.

Our M(A) and M(A–B) values and some orbital energies for B_2H_6 are listed in Table III, together with the results obtained by Yamazaki. Except for the $M(H_B)$ and some MO energy values, the agreement between them is satisfactory.

Table III. Comparison of the calculated results for B_2H_6

		Present	Yazaki's SCF
M(A)	M(B)	2.697	2.78
	$M(H_T)$	1.163	0.99
	$M(H_B)$	0.976	1.24
M(A–B)	M(B–H_T)	0.865	0.85
	M(B–H_B)	0.463	0.39
	M(B–B)	0.291	0.34
Orbital energy, eV.		$-21.58(a_g)$	$-23.57(a_g)$
		$-18.00(b_{2u})$	$-19.27(b_{2u})$
		$-14.39(b_{3u})$	$-17.96(b_{1u})$
		$-14.20(b_{1u})$	$-16.58(b_{3u})$
		$-13.29(b_{1g})$	$-15.40(b_{1g})$
		$-13.20(a_g)$*	$-13.83(a_g)$*
		$-6.53(b_{3g})$**	$+2.62(b_{1u})$**

* The highest-occupied orbitals.
** The lowest-vacant orbitals.

Energy Levels.—The calculated energy values (in eV.) of the highest occupied (HO) orbitals and the lowest vacant (LV) orbitals of some monomers, dimers and ions are collected in Table IV (those of the monomers and ions were given in Part I). Through the monomers, dimers and ions, the energies of the HO orbital of these compounds do not change significantly, although the LV levels become higher, and those of the dimers lie close

6) M. Yamazaki, *J. Chem. Phys.*, **27**, 1401 (1957).
7) P. A. Casabella, P. J. Bray and R. G. Parnes, *J. Chem. Phys.*, **30**, 1393 (1959).

TABLE IV. THE HO AND LV ORBITAL ENERGIES OF SOME MONOMERS, DIMERS AND IONS

Compound	Orbital energy, eV.	
	HO	LV
BH_3	−13.91	−8.53
B_2H_6	−13.20	−6.53
BH_4^-	−13.71	+10.02
$AlCl_3$	−14.94	−4.73
Al_2Cl_6	−13.86	+1.28
$AlCl_4^-$	−14.81	+13.21
$BH(CH_3)_2$*	−12.50	−6.97
$B_2H_2(CH_3)_4$	−12.28	−5.23
$AlCl(CH_3)_2$*	−12.12	−4.91
$Al_2Cl_2(CH_3)_4$	−12.00	+1.04
$Al(CH_3)_3$*	−12.14	−5.01
$Al_2(CH_3)_6$	−12.03	−0.78

* The MO energies of these ions have not been calculated.

TABLE V. THE LV ORBITALS IN SOME DIMERS*

B_2H_6: $0.810(Z_{B1}-Z_{B2})$

$B_2H_2(CH_3)_4$**: $0.826(Z_{B1}-Z_{B2})-0.095(Z_{C3}+Z_{C4}-Z_{C5}-Z_{C6})$

Al_2Cl_6: $0.879(Z_{A11}-Z_{A12})-0.193(Z_{C13}+Z_{C14}-Z_{C15}-Z_{C16})-0.483(X_{C17}-XC_{18})$

$Al_2Cl_2(CH_3)_4$**: $0.900(Z_{A11}-Z_{A12})-0.153(Z_{C3}+Z_{C4}-Z_{C5}-Z_{C6})-0.459(X_{C17}-X_{C18})$

* The numbers in the suffices are given in Fig. 1 and the notations Z_{B1} and Z_{B2} denote the pz orbitals of the boron 1 and 2 atoms respectively, and so on.

** For the sake of simplicity, the values of the hydrogen atoms in the methyl groups and the smaller ones ($<10^{-2}$) are neglected.

to the monomers. This rising trend of the LV levels indicates that the dimeric compounds have an appreciable nucleophilic character, like that in the monomers pointed out in Part I.[3] Furthermore, the nucleophilic character of these dimers depends mainly on the existence of the almost unfilled $p\pi$ orbital of the metal atom, as may be seen in Table V, in which the values of the AO coefficients of the LV orbitals in some dimers are presented. It is there shown that the electrons in these orbitals are largely localized on the $p\pi$ orbitals of the metal atom, and that the anti-bonding character is strongest in the metal-metal bonds. Accordingly, the nucleophilic reagents or electron donors may coordinate with the metal atoms in the dimers, and the transfered electrons may primarily cause the metal-metal bonds to weaken or break. This result agrees with experience.[1]

Some Physico-chemical Properties. — The force constants of various Al-dimers have been evaluated;[8] the magnitudes have been shown to be parallel with those of the bond populations.[9]

TABLE VI. THE M(A-B) VALUES AND THE FORCE CONSTANTS OF Al-DIMERS

(a) Al-Al Bond

	M*	K**
Al_2Cl_6	−0.086	0
$Al_2Cl_2(CH_3)_4$	−0.074	0
$Al_2(CH_3)_6$	0.140	0.50

(b) Al-Cl Bond

	Terminal		Bridge	
	M	K	M	K
Al_2Cl_6	0.472	2.35	0.328	1.05
$Al_2Cl_2(CH_3)_4$	—	—	0.319	1.05

(c) Al-C Bond

	Terminal		Bridge	
	M	K	M	K
$Al_2Cl_2(CH_3)_4$	0.344	2.05	—	—
$Al_2(CH_3)_6$	0.384	2.05	0.188	0.83

* The atom bond population, M(A-B).

** The force constant (in the units of md./Å) taken from Ref. 8.

Those values are summarized in Table VI. It has been pointed out recently that the observed ^{13}C–H spin-spin coupling constants are proportional to the values of the square of the bond order, p, between the ls AO of the hydrogen and the 2s AO of the carbon atom.[10] For B_2H_6, the ^{11}B–H_T and ^{11}B–H_B coupling constants have been measured as 137 c.p.s. and 48 c.p.s. respectively.[11] The calculated p^2 values, 0.149 and 0.029 respectively, are in accordance with the above experimental values. For $Al_2(CH_3)_6$, the NMR signals of the bridge methyl protons are observed in the lower field, and those of the terminal methyl protons in the higher field, at a low temperature.[12] The values for the charges of the bridge and the terminal hydrogens are similar to each other. Thus, the experimental results can not be explained by our calculated charges of hydrogens.*

The Nature of the Bonds in Dimers

The above discussions point out that the M(A–B) values of the metal-terminal atom bond are very different from those of the metal-bridge atom bonds.

8) T. Onishi and T. Shimanouchi, *Spectro. chim. Acta*, **20**, 325 (1964).
9) C. A. Coulson and H. C. Longuet-Higgins, *Proc. Roy. Soc.*, **A193**, 456 (1948).
10) T. Yonezawa, I. Morishima, M. Fujii and K. Fukui, This Bulletin, **38**, 1224 (1965).
11) W. D. Phillips, H. C. Miller and E. L. Mutterlies, *J. Am. Chem. Soc.*, **81**, 4496 (1959).
12) N. Muller and D. E. Pritchard, ibid., **82**, 248 (1960).

* The proton chemical shift is influenced by other factors, such as the magnetic anisotropy of the adjacent carbon atom. Hence, it is impossible at the present stage to determine whether or not our result is valid.

The difference between these bonds will be examined further in this section by means of the values of the AO bond population, N(r–s). For instance, the N(s–s)/M(A–B) ratio, where N(s–s) denotes the AO bond population between the valence s AO's belonging to the A and B atoms, may be used as a measure of this difference. In other words, these values represent the s-nature of the bond X–Y. For B_2H_6, the values obtained are 0.27 for the $B–H_B$ bond and 0.37 for the $B–H_T$ bond. For Al_2Cl_6, the values are 0.20 for the $Al–Cl_B$ bond and 0.29 for the $Al–Cl_T$ bond. For $Al_2(CH_3)_6$, the values are 0.14 for the $Al–C_B$ bond and 0.20 for the $Al–C_T$ bond. Thus, the s-natures of these two bonds in the dimers are clearly different from each other; therefore, if one wants to use the hybrids of the metal atoms to explain the electronic structures of these dimers, at least two kinds of hybrids should be used. A similar point has already been made in Ref. 6.

For a further discussion of these points, two hypothetical compounds are considered. One is the compound which is produced by the symmetrical cleavage of the dimer without changing other conditions; it is named the "deformed monomer." The other is the compound which is produced by omitting the two bridge atoms or groups from the dimers; it is named the "omitted dimer." The shapes of these two compounds and the calculated M(A) and M(A–B) values are given in Fig. 3, in which the deformed monomer is indicated by MX_2Y, and the omitted dimer, by M_2X_4 (the notations M, X and Y are given in Fig. 1).

Some information can be drawn from the results in Fig. 3. For the deformed monomers, the M(M–Y) values (where Y is situated at the same position as the bridge atom in the dimer) are not appreciably different from the M(M–X) values (where X is the terminal atom in the dimer);

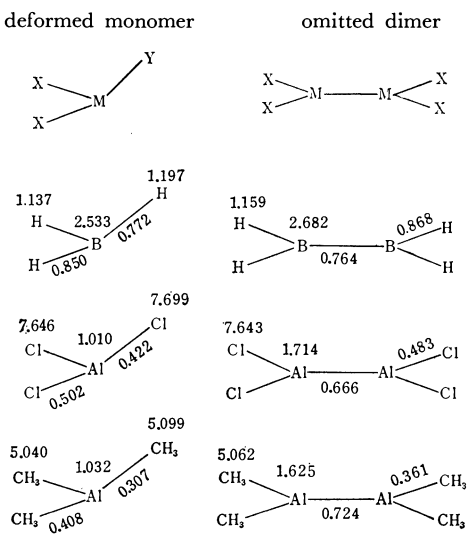

Fig. 3. The M(A) and M(A–B) values of the deformed monomers and omitted dimers.

upon dimerization, though, the M(M–Y) values decrease largely, while the M(M–X) values remain almost constant. For instance, the M(M–Y) values are 0.772 in the deformed BH_3 monomer and 0.463 in the dimer, while the M(M–X) values are 0.850 in the deformed monomer and 0.865 in the dimer. In the deformed monomers, the M(Y) values are slightly larger than the M(X) values; this tendency is reversed in the dimers, as has already been shown. Thus, as a result of the dimer formation the metal-bridge atom bonds become very weak, and a small amount of charge transfer may occur from the "bridge" atom to the other deformed monomer. As to the result for the omitted dimers, the M(M–M) values are quite large, showing that the metal-metal bonds are normal covalent bonds, such as those in B_2Cl_4.[3] The M(A) and M(A–B) values of the other parts are mostly comparable to the corresponding values in the normal dimers. For B_2H_4, the M(B–B) value is 0.764; this value decreases to 0.291 in B_2H_6. For Al_2Cl_4, the M(Al–Al) value is 0.666, and for Al_2Cl_6, –0.086, showing that the Al–Al bond becomes anti-bonding. Thus, as a result of the addition of the two bridge atoms to the omitted dimers, the metal-metal bonds become very weak.

Table VII presents the calculated values of the AO population, N(r). Those of the AO bond population, N(r–s), are given in Table VIII for various compounds including the boron atoms. The results in these tables indicate that the py orbital of the boron atom takes part in the boron-terminal hydrogen bonding, and that the pz and px orbitals take part in the boron-bridge hydrogen and the boron-boron bondings respectively.* In addition, the N(r) values of the px and pz orbitals of the boron atoms vary considerably, while the M(B) values do not change significantly, with the change in the structure from monomer to dimer. The changes in the configuration seem to take place easily by means of the rearrangement of valence electrons in an atom, since the valence orbital (in

Table VII. The N(r) values of the boron atoms in various compounds

	$N(S_B)$	$N(X_B)$	$N(Y_B)$	$N(Z_B)$	M(B)*
B_2H_4	0.979	0.893	0.811	0	2.683
B_2H_6	0.833	0.588	0.811	0.464	2.696
deformed BH_3	0.911	0.554	0.825	0.242	2.532
BH_3	0.912	0.825	0.825	0	2.562

* The notations $N(S_B)$ and $N(X_B)$ denote the atomic orbital populations of the 2s AO and the 2px AO of the boron atom respectively, and so on.

* From the results in Table VIII, it may be seen that the B–B bond in B_2H_6 has some π character; the same tendency is observed for the other M–M bonds in dimeric forms.

TABLE VIII. THE N(r–s) VALUES OF VARIOUS B-COMPOUNDS

a) B_2H_6

s \ r	S_{B1}	X_{B1}	Y_{B1}	Z_{B1}*
S_{B2}	−0.012	0.034	—	—
X_{B2}	0.034	0.166	—	—
Y_{B2}	—	—	−0.028	—
Z_{B2}	—	—	—	0.096
h_T	0.320	0.128	0.416	
h_B	0.126	0.124	—	0.228

b) B_2H_4

s \ r	S_{B1}	X_{B1}	Y_{B1}	Z_{B1}
S_{B2}	0.094	0.176	—	—
X_{B2}	0.176	0.346	—	—
Y_{B2}	—	—	−0.028	—
Z_{B2}	—	—	—	—
h_T	0.332	0.120	0.416	—

c) Deformed BH_3

s \ r	S_{B1}	X_{B1}	Y_{B1}	Z_{B1}
h_T	0.332	0.108	0.410	—
h_B	0.334	0.310	0	0.228

* The notations, S_{B1}, X_{B1}···Z_{B1} denote the 2s, 2px···2pz orbitals of the boron atom 1, and h_T and h_B are the 1s orbital of the terminal and bridge hydrogen atoms respectively.

this case, the pz orbital of the boron atom)** remains unoccupied.

Figure 4 lists the correlations between the orbitals in the omitted and normal BH_3 dimers. In B_2H_4, the HO orbital is mainly the σ-type bonding orbital between the boron atoms, while the LV orbital is the π-type bonding orbital between the boron atoms. When hydrogens are added to the bridge, these HO and LV orbitals are stabilized remarkably,

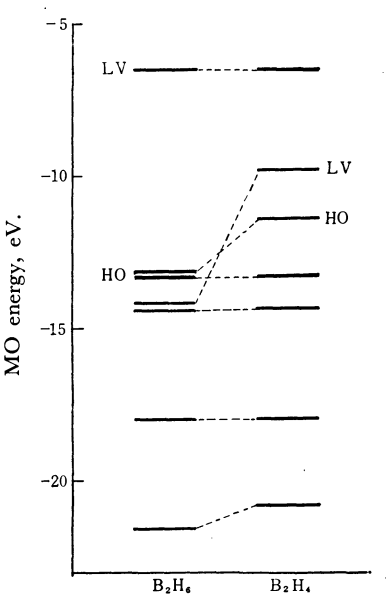

Fig. 4. The MO energies of B_2H_6 and B_2H_4.

and the LV orbital turns out to be the occupied orbital of the BH_3 dimer. These results agree with the tendency of the N(r) values; further, this change in the LV orbital may indicate that the bridge hydrogens are caught by the vacant pπ orbitals of the boron atoms.

Accordingly, our results may be summarized as follows:

1) In a dimer such as the M_2X_6 type, at least two kinds of M–X bonds exist.

2) The metal-terminal atom bonds are almost unchanged upon changes in the structure.

3) The metal-bridge atom bonds become quite weaker.

4) The metal-metal bonds are strong in some dimers.

5) The unfilled p orbitals of the metal atoms play an improtant role in the structural changes.

The calculations were carried out on the IBM 7090 computer of the Japan IBM Co., by the permission of the UNICON Committee, whose kindness we acknowledge.

* For the compounds with boron and hydrogen atoms, these results appear more clearly, since the electronegativities of the B and H atoms are almost equal to each other, and the effect of the migration of the electron between the atoms is negligible.

BULLETIN OF THE CHEMICAL SOCIETY OF JAPAN VOL. 39 1383—1387 (1966)

The Refined Calculation of the Band-gap Energy of Tetramethylammonium Pentaiodide

By Shigekazu KUSABAYASHI,†,* Hiroshi MIKAWA,†,*
Misako KONDA†† and Masano HAYASHI†,*

† *The Institute of Scientific and Industrial Research, Osaka University, Sakai, Osaka*
†† *Japan Atomic Energy Research Institute, Tokai, Ibaraki*

(Received October 18, 1965)

The band-gap energy has been calculated by a tight-binding approximation in a previous report. Although the value thus calculated coincided rather well with the experimental value, it might yet be possible that the band-gap energy will change appreciably when the interactions of all the energy levels are considered at one time. It was, therefore, calculated by the following method, which considers in principle all the level interactions. A repeating unit is composed of 30 atomic orbitals. Each atomic wave function makes three-dimensional Bloch functions. The crystal wave function is set up in the form of a linear combination of these 30 Bloch functions. The energy is then calculated by applying the variation principle and by using the Hückel approximation. The band-gap energy thus calculated is 1.20 eV. This value is near the experimental value, 1.36 eV.; it was also close to the previous result, 1.26 eV., thus confirming the previous calculations. The consideration of the band-widths and the density of the state may interpret the experimental results on the sign of the carrier. The results offer additional support for our previous conclusion regarding the conduction mechanism.

In a previous paper,[1] the band-gap energy of tetramethylammonium pentaiodide was calculated by a tight-binding approximation. The value thus calculated was 1.26 eV., which was satisfactorily near the experimental value, 1.36 eV., obtained from the conductivity measurements.[2] The method used was, briefly, as follows: The iodine framework in the crystal was looked upon as being constructed by repeated translations of a group of two pentaiodide ions (the repeating unit). The wave function of a repeating unit was calculated by Hückel approximation, the resonance integrals between iodine 5 p orbitals being estimated empirically from the data for the gaseous iodine molecule. The wave functions of the crystal were set up in the form of a Bloch function from the wave functions of the repeating unit. No mutual interactions of the Bloch functions of different energies were taken into consideration; thus, interactions between the levels with different energies were neglected.

Although the value thus calculated coincided rather well with the experimental value, it might yet be possible the band-gap energy will change appreciably when the interactions of all the energy levels are taken into consideration at one time.

We have, therefore, attempted in the present paper to calculate the band-gap energy of tetramethylammonium pentaiodide by another method, one which, in principle, takes all the level interactions into consideration (see Appendix).

Method

To solve the problem of the one-electron energy of a three-dimensional crystal from a general point of view, we have modified and extended the method which has previously been used to calculate the energy gap of one-dimensional macromolecules with conjugated double bonds[3] and which has also been used in calculating the band structure of a one-dimensional polynucleotide model.[4]

Primitive translations are denoted by $\boldsymbol{a}$, $\boldsymbol{b}$ and $\boldsymbol{c}$, and the numbering of the elementary cells, by N. It is assumed that one molecule composed of n atomic orbitals is contained in each elementary cell. The n atomic orbitals of a molecule are denoted by $\varphi_1, \varphi_2, \cdots, \varphi_l, \cdots, \varphi_n$, which make three-dimensional Bloch functions extending over the whole crystal.

$$\psi_{l\boldsymbol{k}}(\boldsymbol{r}) = \sum_{j=1}^{N} \exp(i\boldsymbol{k}\boldsymbol{R}_j)\varphi_l(\boldsymbol{r}-\boldsymbol{R}_j) \quad (l=1,2,\cdots,n)$$

where j is the numbering of the molecules and l, the numbering of the atomic orbitals in a molecule.

* Present address: Department of Chemical Technology, Faculty of Engineering, Osaka University, Miyakojima-ku, Osaka.

1) S. Kusabayashi and H. Mikawa, This Bulletin, **39**, 736 (1966).

2) S. Kusabayashi, H. Mikawa, S. Kawai, M. Uchida and R. Kiriyama, ibid., **37**, 811 (1964); S. Kawai, R. Kiriyama, M. Uchida, S. Kusabayashi and H. Mikawa, ibid., **38**, 799 (1965).

3) J. Koutecký and R. Zahradník, *Collection Czech. Chem. Commun.*, **25**, 811 (1960).

4) J. Ladik and K. Appel, *J. Chem. Phys.*, **40**, 2470 (1964).

The crystal wave function is then set up in the form of a linear combination of these n Bloch functions;

$$\Psi_{\boldsymbol{k}}(\boldsymbol{r}) = \sum_{l=1}^{n} C_l \phi_{l\boldsymbol{k}}$$

By applying the variation principle and using the Hückel approximation, one arrives at a system of secular equations as usual. The following matrix eigenvalue problem for the determination of the possible energies of the electrons is obtained:

$$\boldsymbol{\gamma C} = \lambda \boldsymbol{C}$$

where an element of the matrix, $\boldsymbol{\gamma}$, is:

$$\begin{aligned}\gamma_{lm} = \beta_{lm} &+ \{\bar{\beta}^{a}_{lm} \exp(-i\boldsymbol{ka}) + \overset{+}{\beta}{}^{a}_{lm} \exp(i\boldsymbol{ka})\} \\ &+ \{\bar{\beta}^{b}_{lm} \exp(-i\boldsymbol{kb}) + \overset{+}{\beta}{}^{b}_{lm} \exp(i\boldsymbol{kb})\} \\ &+ \{\bar{\beta}^{c}_{lm} \exp(-i\boldsymbol{kc}) + \overset{+}{\beta}{}^{c}_{lm} \exp(i\boldsymbol{kc})\}\end{aligned}$$

Here, β_{lm} is a resonance integral between atomic orbitals, l and m, in the same molecule, and β_{ll} in the diagonal element of the matrix, $\boldsymbol{\gamma}$, is the Coulomb integral of the atomic orbital, l; $\bar{\beta}^{a}_{lm}$ is a resonance integral between the l atomic orbital of the $\boldsymbol{R}_j$ molecule and the m atomic orbital of the $\boldsymbol{R}_j - \boldsymbol{a}$ molecule; $\overset{+}{\beta}{}^{a}_{lm}$ is a resonance integral between the l atomic orbital of the $\boldsymbol{R}_j$ molecule and the m atomic orbital of the $\boldsymbol{R}_j + \boldsymbol{a}$ molecule, and $\bar{\beta}^{b}_{lm} \cdots \overset{+}{\beta}{}^{c}_{lm}$ have similar meanings. The nearest neighboring molecules of a molecule $\boldsymbol{R}_j$ are assumed to be $\boldsymbol{R}_j \pm \boldsymbol{a}$, $\boldsymbol{R}_j \pm \boldsymbol{b}$, and $\boldsymbol{R}_j \pm \boldsymbol{c}$.

The matrix, $\boldsymbol{\gamma}$, is shown to be Hermitian. Column vector $\boldsymbol{C}$ is set equal to $\boldsymbol{u} + i\boldsymbol{v}$. Then, the $\gamma_{lm}C_m$ term of the secular equations is:

$$\gamma_{lm}C_m = (A_{lm}u_m - B_{lm}v_m) + i(B_{lm}u_m + A_{lm}v_m)$$

where:

$$\begin{aligned}A_{lm} &= \beta_{lm} + (\overset{+}{\beta}{}^{a}_{lm} + \bar{\beta}^{a}_{lm}) \cos \boldsymbol{ka} \\ &\quad + (\overset{+}{\beta}{}^{b}_{lm} + \bar{\beta}^{b}_{lm}) \cos \boldsymbol{kb} + (\overset{+}{\beta}{}^{c}_{lm} + \bar{\beta}^{c}_{lm}) \cos \boldsymbol{kc} \\ B_{lm} &= (\overset{+}{\beta}{}^{a}_{lm} - \bar{\beta}^{a}_{lm}) \sin \boldsymbol{ka} + (\overset{+}{\beta}{}^{b}_{lm} - \bar{\beta}^{b}_{lm}) \sin \boldsymbol{kb} \\ &\quad + (\overset{+}{\beta}{}^{c}_{lm} - \bar{\beta}^{c}_{lm}) \sin \boldsymbol{kc}\end{aligned}$$

By separating further the secular equation into the real part and the imaginary part, and by equating both to zero, one obtains secular equations of the $2n$ order.

The equations can be considered as the partitioned forms of a real eigenvalue problem of twice the original size:

$$\begin{pmatrix} \boldsymbol{A} & -\boldsymbol{B} \\ \boldsymbol{B} & \boldsymbol{A} \end{pmatrix} \begin{pmatrix} \boldsymbol{u} \\ \boldsymbol{v} \end{pmatrix} = \lambda \begin{pmatrix} \boldsymbol{u} \\ \boldsymbol{v} \end{pmatrix}$$

This matrix is also Hermitian. In solving this problem, each eigenvalue appears twice.

In the actual calculation of tetramethylammonium pentaiodide, the same parameter values as in the previous paper were used. Each resonance integral was estimated on the basis of the relation:

$$\beta' = \beta \frac{S'/(1+S')}{S/(1+S)}$$

where β' and S' are resonance and overlap integrals respectively between the interesting orbitals, and β and S are the resonance and overlap integrals respectively for a standard. The values of β and S are those for $(5p\sigma, 5p\sigma)$ at the interatomic distance, 2.68 Å, of an iodine molecule. The appropriate overlap integrals between the interesting orbitals were calculated by Mulliken's formulas[5] for Slater-AO overlap integrals for $t=0$, taking the geometry of the atomic orbitals in crystal into consideration.

As has been stated before, the iodine framework in the crystal can be looked upon as being constructed simply by repeated translations of a group of two pentaiodide ions; this repeating unit is looked upon as a molecule. There are 30 Slater-type 5p atomic orbitals belonging to the 10 iodine atoms in a repeating unit. The nearest neighboring repeating units are located in the five directions, $\boldsymbol{a}$, $\boldsymbol{b}$, $\boldsymbol{c}$, $\boldsymbol{a}-\boldsymbol{b}$ and $\boldsymbol{b}+\boldsymbol{c}$.

Therefore, in our case, a 60-order matrix must be set up for each parametric $\boldsymbol{k}$ value, and then solved for eigenvalues.

Results and Discussion

A special computer program was set up, and the calculations of the eigenvalues for nearly one hundred different $\boldsymbol{k}$ values were performed with an IBM 7044 electronic computer. The maximum

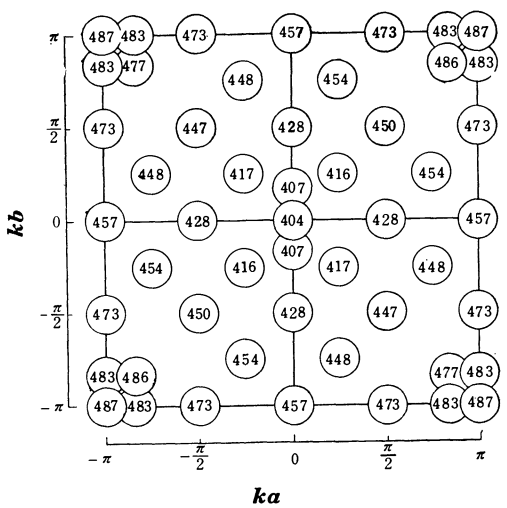

Fig. 1. Maximum energy value of filled band at $\boldsymbol{kc}=0$. $(-10^{-3}\beta$ unit).

5) R. S. Mulliken, C. A. Rieke, D. Orloff and H. Orloff, *J. Chem. Phys.*, **17**, 1248 (1949).

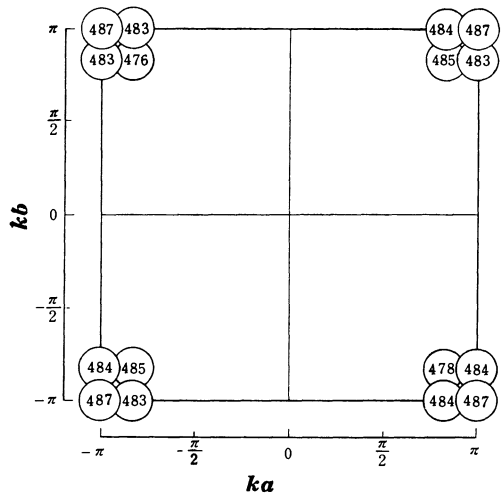

Fig. 2. Maximum energy value of filled band at $kc=\pi/6$. ($-10^{-3}\beta$ unit)

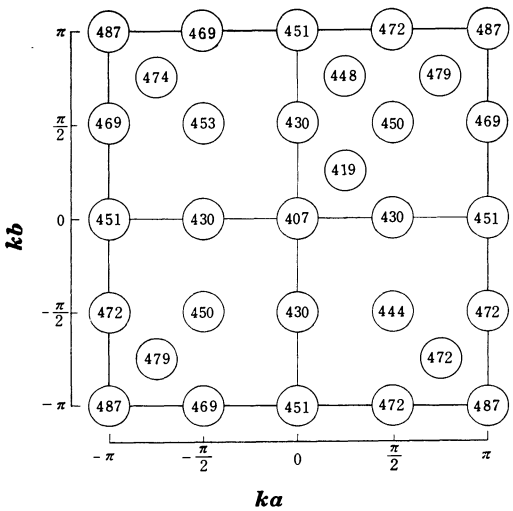

Fig. 3. Maximum energy value of filled band at $kc=\pi/2$. ($-10^{-3}\beta$ unit).

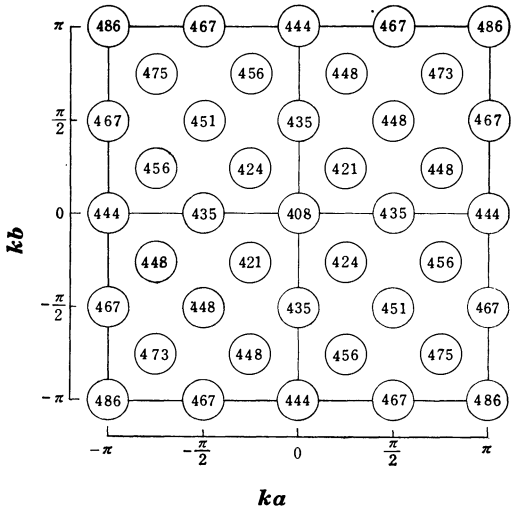

Fig. 4. Maximum energy value of filled band at $kc=\pi$. ($-10^{-3}\beta$ unit)

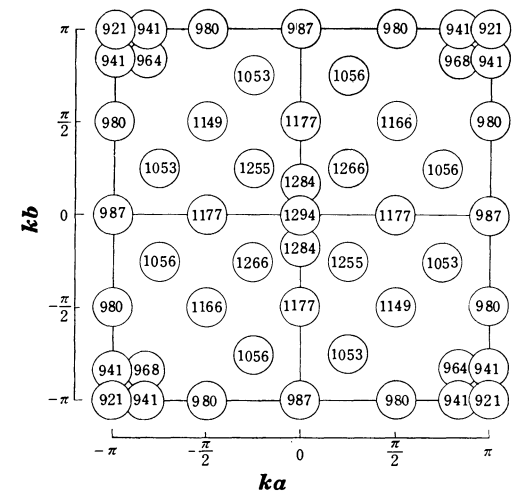

Fig. 5. Minimum energy value of unfilled band at $kc=0$. ($-10^{-3}\beta$ unit)

energy values of the filled bands are shown in Figs. 1—4, while the minimum energy values of the unfilled band are shown in Figs. 5—8. It seems that the energy values do not change much with the variation in kc value, and that the point of ($ka=\pi$, $kb=\pi$, $kc=0$) or some points closed to (π, π, 0) give the lower limit of the unfilled band and the upper limit of the filled band.

The band-gap energy is found to be 0.434β by using the value of (π, π, 0). The substitution of the $\beta=-2.76$ eV. from a previous assumption[1] into 0.434β gives 1.20 eV. This value is near the experimental value of 1.36 eV., and it is also close to 1.26 eV., the value obtained in the previous calculation.

The present method gives information about the band-gap energy, but the characteristics of each level are still not clear, as it is not possible to know $E(k)$ in an analytical form nor the functional forms of wave functions. As is shown in Fig. 9, 22 levels are filled by electrons and as a whole form a hole band, while the upper 4 levels are all vacant and form an electron band. It is found that the width of the electron band is nearly the same as that obtained in the previous report, but the width of the hole band is about 5 times as large as the previous result. (In the previous paper, it was thought tentatively that the hole band was constructed by an overlap of the upper 8 filled bands.) After all, the width of the hole band is about 3 times as large as the width of the electron band.

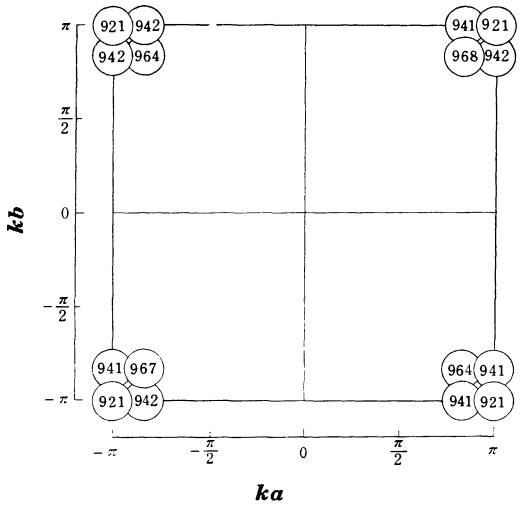

Fig. 6. Minimum energy value of unfilled band at $kc=\pi/6$. ($-10^{-3}\beta$ unit)

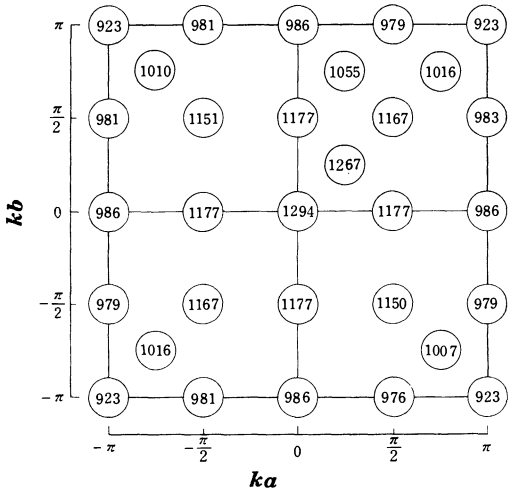

Fig. 7. Minimum energy value of unfilled band at $kc=\pi/2$. ($-10^{-3}\beta$ unit)

As for mobility, no experimental data has yet been obtained. Preliminary thermoelectric power measurements showed that the sign of the carrier was positive.[2] The fact that the width and the density of states in the hole band are much larger than those in the electron band might explain the experimental finding on the sign of the carrier.

Although the method used in the present calculations is more reliable than the previous method, the results are very near the previous results. This tends to confirm the prevoius calculation. Moreover, the results presented here are in agreement with the experimental results. They support our previous conclusion that the iodine framework in the crystal structure is of primary importance in determining the conductivity. They also offer additional support for the idea that the band

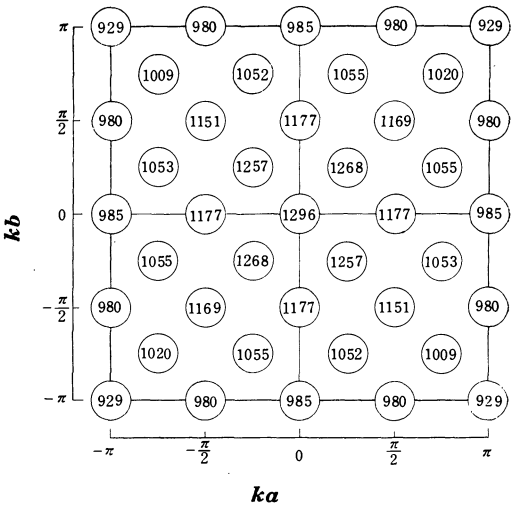

Fig. 8. Minimum energy value of unfilled band at $kc=\pi$. ($-10^{-3}\beta$ unit)

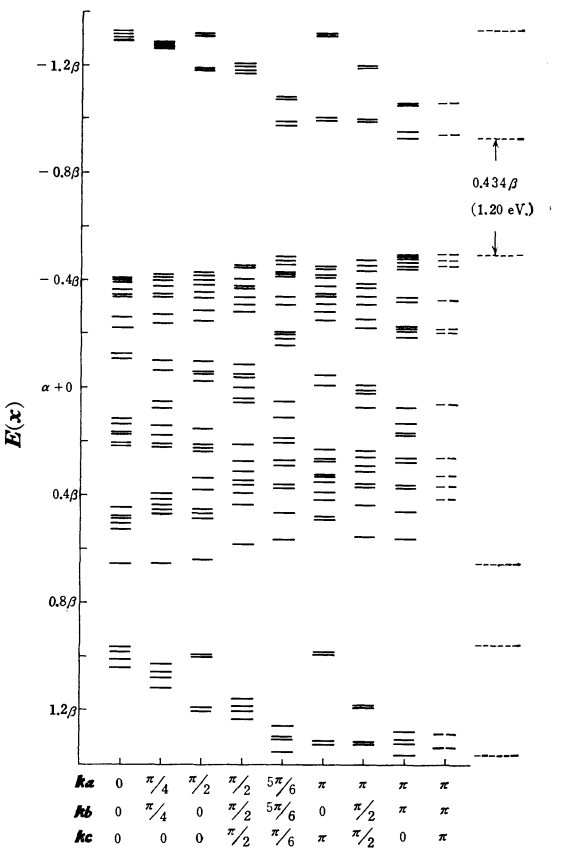

Fig. 9. Energy bands of pentaiodide. (α is the coulomb energy of the iodine 5p atomic orbital.)

model is applicable to the conduction mechanism of tetramethylammonium pentaiodide.

Appendix

The molecular orbital function, Φ^t, is approximated with a linear combination of atomic orbitals, φ_l;

$$\Phi^t = \sum_{l=1}^{n} a_l^t \varphi_l \tag{1}$$

where a_l^t is the coefficient of the lth atomic orbital of the tth level in the jth molecule. By multiplying both sides of (1) with $\exp(i\boldsymbol{k}\boldsymbol{R}_j)$, and by summing them up with respect to j,

$$\sum_{j=1}^{N} \Phi_{j\boldsymbol{k}}^t = \sum_{l=1}^{n} a_l^t \left(\sum_{j=1}^{N} \varphi_{l\boldsymbol{k}}\right) \tag{2}$$

where $\sum_{j=1}^{N} \Phi_{j\boldsymbol{k}}^t$ and $\sum_{j=1}^{N} \varphi_{l\boldsymbol{k}}$ are Bloch functions derived from the tth molecular orbital and from the atomic orbital respectively. In order to take all the level interactions into consideration, both sides of (2) are multiplied with an arbitrary coefficient, c^t, and the values from 1 to n are summed up with respect to t; hence,

$$\sum_{t=1}^{n} c^t \left(\sum_{j=1}^{N} \Phi_{j\boldsymbol{k}}^t\right) = \sum_{t=1}^{n} \sum_{l=1}^{n} c^t a_l^t \left(\sum_{j=1}^{N} \varphi_{l\boldsymbol{k}}\right)$$

As $\sum_{t=1}^{n} c^t a_l^t$ is an arbitrary parameter, one obtains:

$$\sum_{t=1}^{n} c^t \left(\sum_{j=1}^{N} \Phi_{j\boldsymbol{k}}^t\right) = \sum_{l=1}^{n} c_l' \left(\sum_{j=1}^{N} \varphi_{l\boldsymbol{k}}\right)$$

This formula indicates that the linear combination of the Bloch functions derived from each atomic orbital is equivalent to the case of the linear combination of the Bloch functions derived from each molecular orbital (level), i.e., to the case where all level interactions are taken into consideration.

The authors wish to express their thanks to Professor Junjiro Kanamori of Osaka University for his kind discussion.

BULLETIN OF THE CHEMICAL SOCIETY OF JAPAN VOL. 39 1387—1391 (1966)

The Rotatory Dispersion and Stereochemistry of Organic Compounds. X.[1] Nitrates of α-Hydroxy-carboxylic Acids

By Yojiro TSUZUKI, Koko TANABE, Kikuhiko OKAMOTO and Michiyo FUKUBAYASHI

Department of Chemistry, Tokyo College of Science, Kagurazaka, Shinjuku-ku, Tokyo

(Received October 19, 1965)

The rotatory dispersion (RD) and ultraviolet absorption of some α-hydroxy-carboxylic acids and their nitrates have been measured and analyzed. A distinct relation has been found between the configuration and the sign of the Cotton effect; namely, nitrates of α-D-hydroxy-carboxylic acids (R-configuration) show positive Cotton effects, while those of α-L-hydroxy-carboxylic acids (S-configuration) show negative Cotton effects. Thus a rotatory contribution by the nitrates of the α-hydroxyl group has been suggested, though it is opposite in sign to the xanthates of the α-hydroxy-carboxylic acids.

In previous papers[1,2] it has been reported, with various nitrates of glucose, that a regular relation exists between the configuration of the carbon atom carrying a nitrate chromophore and the sign of the Cotton effect; namely, α-glucosides with a nitrate chromophore in the D-configuration show negative Cotton effects, while the sign of the Cotton effects of the corresponding β-glucosides is positive. On the contrary, α-glucosides with a nitrate chromophore in the L-configuration show positive Cotton effects, while the sign of the Cotton effects of the corresponding β-glucosides is negative.

This paper will report similar studies made on the nitrate esters of some aliphatic α-hydroxy-carboxylic acids (compounds II—IV, VI, VII, IX—X, XII), namely, tartaric, malic and lactic acids and their alkyl esters, in order to find the sign of the rotatory contribution of the hydroxyl group and, at the same time, to learn that of the carboxyl group, and thus to confirm the view already expressed in earlier papers[3] that the OH group of α-hydroxy-carboxylic acids of the D-configuration contributes to a positive rotation and the COOH group to a negative rotation.

Results and Discussion

Figure 1 collects the RD curves of the derivatives of D(+)-tartaric acid observed in methanol as well

1) Part IX: Y. Tsuzuki, K. Tanabe and K. Okamoto, This Bulletin, **39**, 761 (1966).

2) Y. Tsuzuki, K. Tanabe and K. Okamoto, ibid., **38**, 274 (1965).

3) a) Y. Tsuzuki, *Sci. Pap. Inst. Phys. Chem. Res. (Tokyo)*, No. 890, Vol. **35**, 432 (1939); b) *J. Chem. Soc. Japan (Nippon Kwagaku Kwaisi)*, **64**, 282 (1943); c) ibid., **64**, 290 (1943) (in Japanese).

Table I. Hydroxy-carboxylic acids and their Nitrates

Compound		
I	Diethyl D(+)-tartrate	$COOC_2H_5$ $H-C-OH$ $HO-C-H$ $COOC_2H_5$
II	Diethyl D(+)-tartrate mononitrate	$COOC_2H_5$ $H-C-ONO_2$ $HO-C-H$ $COOC_2H_5$
III	Diethyl D(+)-tartrate dinitrate	$COOC_2H_5$ $H-C-ONO_2$ $O_2NO-C-H$ $COOC_2H_5$
IV	D(+)-Tartaric acid dinitrate	$COOH$ $H-C-ONO_2$ $O_2NO-C-H$ $COOH$
V	Dimethyl D(+)-tartrate	$COOCH_3$ $H-C-OH$ $HO-C-H$ $COOCH_3$
VI	Dimethyl D(+)-tartrate mononitrate	$COOCH_3$ $H-C-ONO_2$ $HO-C-H$ $COOCH_3$
VII	Dimethyl D(+)-tartrate dinitrate	$COOCH_3$ $H-C-ONO_2$ $O_2NO-C-H$ $COOCH_3$
VIII	Diethyl L(−)-malate	$COOC_2H_5$ $HO-C-H$ $CH_2COOC_2H_5$
IX	Diethyl L(−)-malate nitrate	$COOC_2H_5$ $O_2NO-C-H$ $CH_2COOC_2H_5$
X	L(−)-Malic acid nitrate	$COOH$ $O_2NO-C-H$ CH_2COOH
XI	Ethyl D(−)-lactate	$COOC_2H_5$ $H-C-OH$ CH_3
XII	Ethyl D(−)-lactate nitrate	$COOC_2H_5$ $H-C-ONO_2$ CH_3

as in dioxane. The mononitrate (compound II) exhibits a positive Cotton effect with a peak at

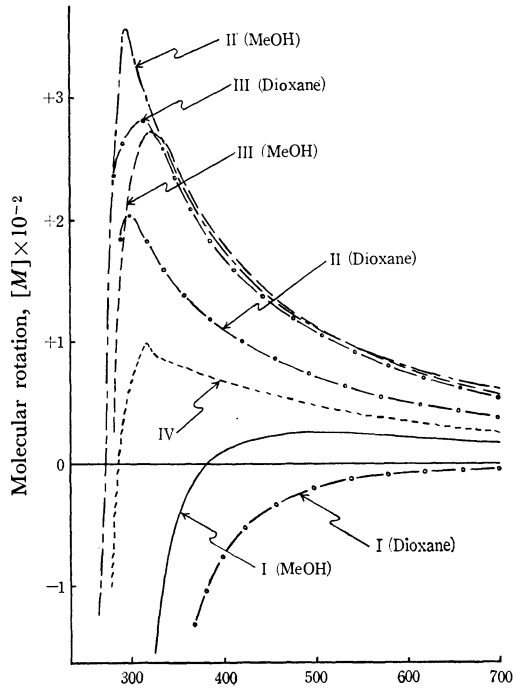

Fig. 1. RD of I—IV.

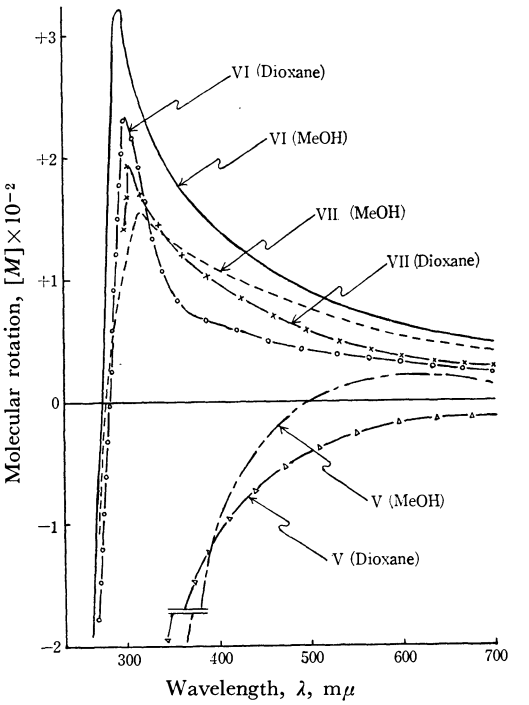

Fig. 2. RD of V—VII.

294 mμ, and the dinitrates (compounds III and IV) also show positive Cotton effects, the peaks of which both appear at 315 mμ. It should, however, be remarked that some anomalies are visible on

the RD curves of these two dinitrates in the region from 330 to 430 mμ, anomalies which can apparently be related to the ultraviolet multiple absorption curves (III and IV) shown in Fig. 4, but the region of the absorption (320—380 mμ) is considerably red-shifted as compared with the peak of the Cotton effect.

In contrast to the dinitrates, a larger decrease in rotation is observed in dioxane than in methanol with the mononitrate (Fig. 1); this decrease is likely to be due to intramolecular hydrogen bond formation in non-polar solvents, as has already been suggested.[3a] Here the intramolecular hydrogen bond may be formed between the OH group and either the carbalkoxy or the nitrate group, whereby the rotatory contribution of the OH group is reduced to a more or less large extent. At any rate, the positive sign of the Cotton effect of the three nitrates agrees with the R-configuration assigned according to the rule of Cahn et al.[4]

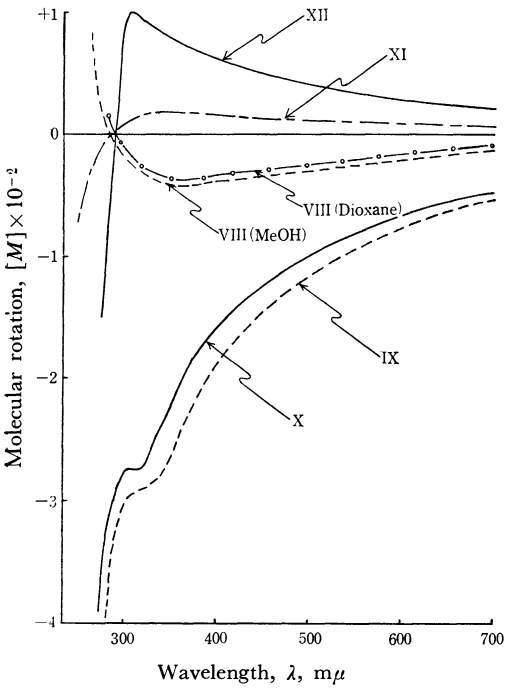

Fig. 3. RD of VIII—XII.

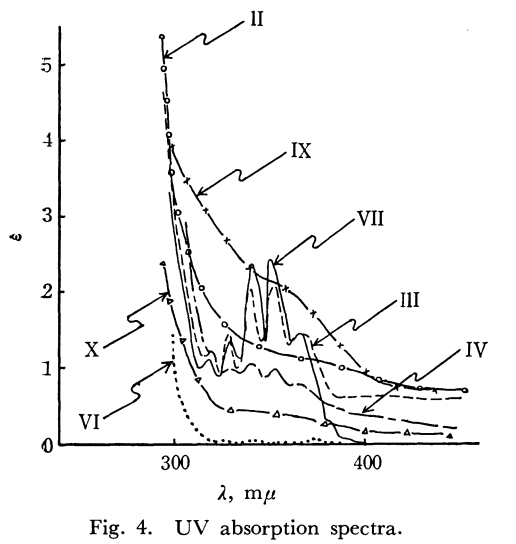

Fig. 4. UV absorption spectra.

In Fig. 2 are shown the RD curves of the mono- and dinitrates of dimethyl D(+)-tartrates (V—VI), observed both in methanol and dioxane. They are not essentially different in their main features from those of Fig. 1. However, the rotation increases in the positive direction in the order:

$$COOH < COOCH_3 < COOC_2H_5$$

Figure 3 gives the RD curves of the three derivatives of L(−)-malic acid (VIII—X), as well as those of D(−)-lactic acid (XI—XII). The nitrate of diethyl L(−)-malate (IX) has a feeble negative Cotton effect, with a shoulder in the region from 300 to 320 mμ, the peak being at 303 mμ and the trough at 310 mμ, while the RD curve (IX) can be expressed by the following Drude equation:

$$[M] = \frac{-0.723}{\lambda^2-(0.313)^2} + \frac{-23.82}{\lambda^2-(0.169)^2} \qquad (1)$$

The negative sign of the Cotton effect can also be confirmed by the negative dispersion constant ($A=-0.723$) of the first term of Eq. 1 as well as by the S-configuration of the asymmetric center. The ultraviolet absorption spectrum does not show a fine structure, as do those of the nitrates of tartaric acid, and it has a slight shoulder at 325—380 mμ (IX in Fig. 4).

Thus, it may be concluded that the nitrates of α-hydroxy-carboxylic acids of the D-type (R-configuration) show positive Cotton effects, whereas the nitrates of the L-type (S-configuration) exhibit negative Cotton effects.

It is noteworthy that this conclusion is just the opposite of the observations[5] that all the xanthates of L-hydroxy-carboxylic acids show positive Cotton effects, while those of D-acids exhibit negative Cotton effects. A similar "inversion" of the sign of rotation has been observed in the xanthates of various derivatives of monosaccharides.[6]

As to the correlation between the RD curve and the configuration, lactic acid is expected to provide

4) R. S. Cahn, C. K. Ingold and V. Prelog, *Experientia*, **12**, 81 (1956).

5) A. Fredga, *Svensk. Kem. Tidskr.*, **53**, 221 (1941); **54**, 26 (1942); S. Sjöberg, A. Fredga and C. Djerassi, *J. Am. Chem. Soc.*, **81**, 5002 (1959); C. Djerassi, H. Wolf and E. Bunnenberg, ibid., **84**, 4552 (1962).

6) Y. Tsuzuki, K. Tanaka and K. Tanabe, This Bulletin, **35**, 1614 (1962); Y. Tsuzuki, K. Tanabe, M. Akagi and S. Tejima, ibid., **37**, 162 (1964); Y. Tsuzuki, K. Tanaka, K. Tanabe, M. Akagi and S. Tejima, ibid., **37**, 730 (1964).

Table II. Dispersion data and Constants

$$[M]=\frac{A_1}{\lambda^2-\lambda_1^2}+\frac{A_2}{\lambda^2-\lambda_2^2}$$

Compound	Drude's equation				$\lambda_{RD}(\mu)$	Sign of Cotton effect	Configuration[4]
	A_1	A_2	$\lambda_1(\mu)$	$\lambda_2(\mu)$			
I	−34.20	+44.68	0.237	0.173			
II	+ 1.29	+27.03	0.312	0.076	0.294	+	R
III	+ 0.815	+29.37	0.303	0.160	0.315	+	R
IV	+ 0.440	+10.3	0.310	0.150	0.315	+	R
V	−36.98	+42.28	0.237	0.173			
VI	+ 0.10	+25.10	0.305	0.207	0.296	+	R
VII	+ 1.58	+15.21	0.300	0.159	0.315	+	R
VIII	+ 2.24	−11.13	0.255	0.000		+	R
XI	− 0.723	−23.82	0.313	0.169		−	S
X	− 1.36	−23.20	0.288	0.000		−	S
XI	− 0.733	+ 3.186	0.255	0.099			
XII	+ 0.496	+ 8.50	0.309	0.158	0.310	+	R

an interesting problem. As may be seen in Fig. 3, ethyl D(−)-lactate really shows a RD curve (XI) quite similar in shape to those of alkyl D(+)-tartrates (I in Fig. 1 and V in Fig. 2); this fact may easily be understood since the lactate coincides with the tartrates in configuration, so that a positive Cotton effect may be expected of the nitrate of D(−)-lactic acid; really, this has already been confirmed with the nitrate of ethyl D(−)-lactate (XII).

Dispersion Constants

The data of the RD measurements were calculated according to a two-term expression of the Drude equation:

$$[M]=\frac{A}{\lambda^2-\lambda_1^2}+\frac{B}{\lambda^2-\lambda_2^2} \qquad (2)$$

They have been found to conform to the equation tolerably well, with two exceptions (compounds VIII and X), which can rather better be expressed by an abbreviated form ($\lambda_2=0$).

The dispersion constants of these compounds thus computed are given in Table II, together with some other data on the Cotton effect and on the configuration of the chromophore-bearing asymmetric center.

Experimental

The nitrates of the hydroxy-carboxylic acids and their esters were prepared according to the methods of the literature. The rotatory dispersion was measured with a Rudolph spectropolarimeter over the region from 250 to 700 mμ. The ultraviolet absorption was measured with a Hitachi EPU-II self-recording spectrophotometer. The dispersion constants of the Drude equations were calculated from the data by means of the least-square method with a Fuji FACOM 201 electronic computer.

Diethyl D(+)-Tartrate (Compound I)[7].—Colorless syrup, b. p. 157—158°C/11 mmHg. The RD was measured at 17°C in methanol (*c*, 1.3758). $[\alpha]_{700}^{17}$ +8.31°, $[\alpha]_{600}$ +10.7°, $[\alpha]_{589}$ +10.9°, $[\alpha]_{500}$ +14.3°, $[\alpha]_{400}$ +7.12°, $[\alpha]_{350}$ −21.5°, $[\alpha]_{320}$ −75.0°.

Diethyl D(+)-Tartrate Mononitrate (Compound II)[8].—Colorless needles, m. p. 46—47°C. The RD was measured at 21°C in methanol (*c*, 0.9970). $[\alpha]_{700}^{21}$ +22.2°, $[\alpha]_{650}$ +27.8°, $[\alpha]_{589}$ +31.6°, $[\alpha]_{500}$ +44.1°, $[\alpha]_{400}$ +69.9°, $[\alpha]_{300}$ +131°, $[\alpha]_{294}$ +142° (peak), $[\alpha]_{280}$ +66.0°, $[\alpha]_{270}$ −39.6°.

Diethyl D(+)-Tartrate Dinitrate (Compound III)[7].—Colorless prisms, m. p. 26—27°C. The RD was measured at 20°C in methanol (*c*, 1.1603). $[\alpha]_{700}^{20}$ +20.1°, $[\alpha]_{600}$ +25.9°, $[\alpha]_{589}$ +27.8°, $[\alpha]_{500}$ +35.9°, $[\alpha]_{400}$ +56.8°, $[\alpha]_{315}$ +92.9° (peak), $[\alpha]_{300}$ +74.1°, $[\alpha]_{280}$ +38.6°.

D(+)-Tartaric Acid Dinitrate (Compound IV)[9].—White needles, melt with decomp. The RD was measured at 21°C in methanol (*c*, 1.9923). $[\alpha]_{700}^{21}$ +10.4°, $[\alpha]_{600}$ +13.6°, $[\alpha]_{589}$ +14.4°, $[\alpha]_{500}$ +19.6°, $[\alpha]_{400}$ +27.5°, $[\alpha]_{315}$ +41.2° (peak), $[\alpha]_{300}$ +26.1°, $[\alpha]_{280}$ −38.7°.

Dimethyl D(+)-Tartrate (Compound V)[7].—Colorless syrup, b. p. 158—158.5°C/12 mmHg. The RD was measured at 18°C in methanol (*c*, 1.2445). $[\alpha]_{700}^{18}$ +2.33°, $[\alpha]_{650}$ +3.70°, $[\alpha]_{589}$ +3.86°, $[\alpha]_{500}$ +0.321°, $[\alpha]_{400}$ −16.6°, $[\alpha]_{330}$ −74.5°.

Dimethyl D(+)-Tartrate Mononitrate (Compound VI)[10].—Colorless prisms, m. p. 96—97°C. The RD was measured at 18°C in methanol (*c*, 0.9552). $[\alpha]_{700}^{18}$ +22.0°, $[\alpha]_{600}$ +26.7°, $[\alpha]_{589}$ +27.3°, $[\alpha]_{500}$ +38.4°, $[\alpha]_{400}$ +60.1°, $[\alpha]_{350}$ +79.5°, $[\alpha]_{300}$ +15.3°, $[\alpha]_{290}$ +172° (peak), $[\alpha]_{280}$ +81.8°, $[\alpha]_{270}$ −79.5°, $[\alpha]_{255}$ −706°.

Dimethyl D(+)-Tartrate Dinitrate (Compound VII)[10].—Colorless prisms, m. p. 75°C. The RD was measured at 20°C in methanol (*c*, 0.5028). $[\alpha]_{700}^{20}$ +15.6°, $[\alpha]_{600}$ +20.3°, $[\alpha]_{589}$ +21.0°, $[\alpha]_{500}$ +29.6°, $[\alpha]_{400}$ +40.8°, $[\alpha]_{350}$ +47.4°, $[\alpha]_{315}$ +57.4° (peak), $[\alpha]_{295}$ +33.0°, $[\alpha]_{280}$ −9.00°, $[\alpha]_{270}$ −39.8°.

Diethyl L(−)-Malate (Compound VIII)[7].—Colorless syrup, b. p. 128°C/10 mmHg. The RD was

7) E. Fischer and A. Speyer, *Ber.*, **28**, 3255 (1895).
8) P. Frankland, H. L. Heathcote and F. Hartle, *J. Chem. Soc.*, **83**, 157 (1903).
9) A. Lachman, *J. Am. Chem. Soc.*, **43**, 577 (1921).
10) P. Walden, *Ber.*, **35**, 4366 (1902); **36**, 778 (1903).

measured at 19°C in methanol (*c*, 2.6240). $[\alpha]_{700}^{19}$ −7.67°, $[\alpha]_{600}$ −10.6°, $[\alpha]_{589}$ −11.1°, $[\alpha]_{500}$ −14.8°, $[\alpha]_{400}$ −20.7°, $[\alpha]_{355}$ −22.4°, $[\alpha]_{300}$ −11.5°, $[\alpha]_{280}$ +10.3°, $[\alpha]_{270}$ +34.0°.

Diethyl L(−)-Malate Nitrate (Compound IX).[11] —Colorless syrup, b. p. 148°C/25 mmHg. The RD was measured at 21°C in methanol (*c*, 0.6321). $[\alpha]_{700}^{21}$ −22.3°, $[\alpha]_{600}$ −32.3°, $[\alpha]_{589}$ −33.8°, $[\alpha]_{500}$ −48.2°, $[\alpha]_{400}$ −79.1°, $[\alpha]_{350}$ −110°, $[\alpha]_{320}$ −123°, $[\alpha]_{300}$ −127°, $[\alpha]_{290}$ −146°, $[\alpha]_{275}$ −235°.

L(−)-Malic Acid Nitrate (Compound X).[12]— White needles, m. p. 111°C at 112°C with decomp. The RD was measured at 21°C in methanol (*c*, 1.1822). $[\alpha]_{700}^{21}$ −27.1°, $[\alpha]_{600}$ −36.4°, $[\alpha]_{589}$ −38.0°, $[\alpha]_{500}$ −53.8°, $[\alpha]_{400}$ −87.5°, $[\alpha]_{350}$ −124°, $[\alpha]_{310}$ −154° (trough), $[\alpha]_{303}$ −152° (peak), $[\alpha]_{300}$ −154°, $[\alpha]_{275}$ −231°.

11) G. E. Holm and R. Berg, ibid., **61**, 1888 (1928).
12) A. Lachman, *J. Am. Chem. Soc.*, **43**, 2084 (1921).

Ethyl D(−)-Lactate (Compound XI).[13]—Colorless syrup, b. p. 65—66°C/27 mmHg. A sample of D(−)-lactic acid of 50% optical purity furnished by the Kyowa Hakko Kogyo Co. was esterified with *p*-toluenesulfonic acid.[13] The RD was measured at 20°C in the liquid state. $[\alpha]_{700}^{20}$ +4.86°, $[\alpha]_{589}$ +6.25°, $[\alpha]_{500}$ +8.42°, $[\alpha]_{400}$ +11.9°, $[\alpha]_{350}$ +12.8°, $[\alpha]_{300}$ +7.17°, $[\alpha]_{280}$ −4.20°, $[\alpha]_{265}$ −23.7°.

Ethyl D(−)-Lactate Nitrate (Compound XII).[14] —Colorless syrup, b. p. 58.0°C/31 mmHg. Optical purity 50%. The RD was measured at 22°C in methanol (*c*, 3.3890). $[\alpha]_{700}^{22}$ +20.6°, $[\alpha]_{589}$ +28.6°, $[\alpha]_{500}$ +39.6°, $[\alpha]_{400}$ +62.5°, $[\alpha]_{350}$ +80.4°, $[\alpha]_{310}$ +99.9° (peak), $[\alpha]_{300}$ +92.5°, $[\alpha]_{290}$ −1.66°, $[\alpha]_{275}$ −97.8°.

13) Y. Tsuzuki, *J. Chem. Soc. Japan (Nippon Kwagaku Kwaisi)* **64**, 297 (1943) (in Japanese).
14) L. Henry, *Ber.*, **3**, 529 (1870).

BULLETIN OF THE CHEMICAL SOCIETY OF JAPAN VOL. 39 1391—1397 (1966)

The Rotatory Dispersion and Stereochemistry of Organic Compounds. XI.[1] The Nitrates of Some Hexoses

By Yojiro TSUZUKI, Koko TANABE, Kikuhiko OKAMOTO and Noriko YAMADA

Department of Chemistry, Tokyo College of Science, Kagurazaka, Shinjuku-ku, Tokyo

(Received December 18, 1965)

The rotatory dispersions (RD) and the ultraviolet absorptions of eight nitrates of galactopyranoside, altropyranosides, glucofuranoside, mannopyranosides and of glucopyranosides, and also of five hexosepyranosides, have been measured. Studies have also been made of the correlation between the configuration and the Cotton effect, the sign of which has been determined by the RD curve as well as by the dispersion constant computed from the dispersion data, and in some cases by means of the circular dichroism (CD). All the findings and conclusions are consistent with the generalized rule originally found with glucose derivatives (Y. Tsuzuki, K. Tanabe and K. Okamoto, This Bulletin, **39**, 761 (1966)). The rule has been shown to be extensively applicable to several hexoses; namely, α-glycosides with a C–ONO_2 chromophore of an α(or D)-configuration show negative Cotton effects, and those with a C–ONO_2 group of a β(or L)-configuration exhibit positive Cotton effects, while with nitrates of β-glycosides the signs of the Cotton effects are exactly reversed (ref. Conclusion).

As has already been reported,[2] the nitrates of glucopyranoside show curves of a rotatory dispersion (RD) with a Cotton effect, and a distinct, regular relationship was observed between the sign of the Cotton effect and the configuration of the nitrates.

In this paper it will be reported that the same regular relation can be observed between the configuration and the rotatory dispersion of eight nitrates of altropyranosides, mannopyranosides, glucopyranosides and a glucofuranoside (Table I); moreover, the RD curves of five other hexose derivatives (Table II) will be described and discussed with reference to the background rotations of the nitrates, and, further the RD curves, of five other nitrates already reported on will be referred to, namely, those of pentaacetyl-α-D-glucopyranose[2] (compound XIV), 2, 3, 4, 6-tetra-*O*-acetyl-1-*O*-nitro-α-D-glucopyranose (compound XV), methyl 4 : 6-*O*-benzylidene-α-D-glucopyranoside 3-nitrate[2] (compound XVI), 1, 2 : 5, 6-*O*-diisopropylidene-D-glucofuranose[3] (compound XVII) and of methyl

1) Part X: Y. Tsuzuki, K. Tanabe, K. Okamoto and M. Fukubayashi, This Bulletin, **39**, 1387 (1966).

2) Y. Tsuzuki, K. Tanabe and K. Okamoto, ibid., **39**, 761 (1966).

3) Y. Tsuzuki, K. Tanaka, K. Tanabe, M. Akagi and S. Tejima, ibid., **37**, 730 (1964).

Table I. Nitrates of Hexoses

Number	Name	Structure
I	2,3,4,6-Tetra-*O*-acetyl-1-*O*-nitro-α-D-galactopyranose	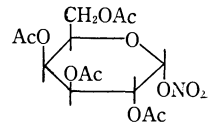
II	Methyl 4 : 6-*O*-benzylidene-α-D-altropyranoside 3-nitrate	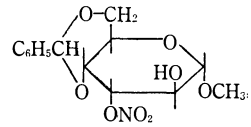
III	1,2 : 5,6-Diisopropylidene-3-*O*-nitro-α-D-glucofuranose	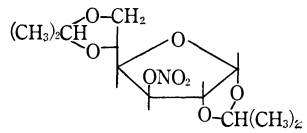
IV	Methyl 4 : 6-*O*-ethylidene-α-D-mannopyranoside 2 : 3-dinitrate	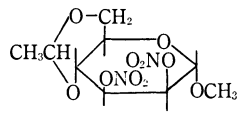
V	Methyl 4 : 6-*O*-benzylidene-α-D-altropyranoside 2 : 3-dinitrate	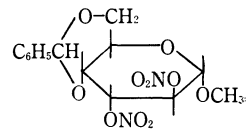
VI	Methyl 6-*O*-acetyl-2,3,4-tri-*O*-nitro-β-D-glucopyranoside	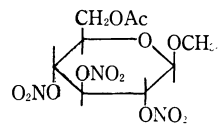
VII	Methyl 2,3,4,6-tetra-*O*-nitro-β-D-glucopyranoside	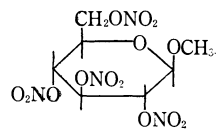
VIII	Methyl 2,3,4,6-tetra-*O*-nitro-α-D-glucopyranoside	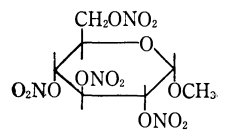

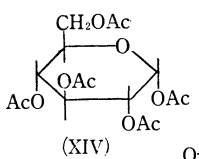
(XIV)

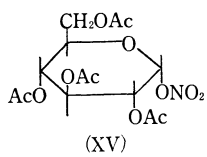
(XV)

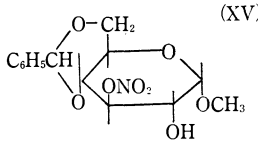
(XVI)

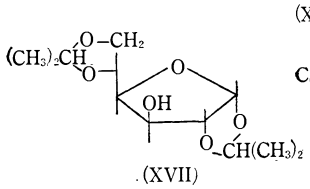
(XVII)

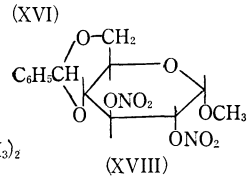
(XVIII)

4 : 6-*O*-benzylidene-α-D-glucopyranoside 2 : 3-dinitrate[2] (compound XVIII).

Results and Discussion

Figure 1 gives the RD curve of 2, 3, 4, 6-tetra-*O*-acetyl-α-D-galactopyranoside-1-nitrate (compound I), whose inflection below 280 mμ indicates no clear sign of the Cotton effect. However, from the positive curve of the circular dichroism (CD) of I (Fig. 1), the weak Cotton effect can be concluded to be positive in sign. This is in harmony with the convention of Cahn et al.,[4] for the C_1-configuration of I is of an R-conformation.

The RD curve (I) above the absorption region

4) R. S. Cahn, C. K. Ingold and V. Prelog, *Experientia*, **12**, 81 (1956).

TABLE II. BACKGROUND'S COMPOUNDS

Number	Name	Structure
IX	Pentaacetyl-α-D-galactopyranose	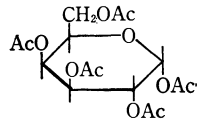
X	Methyl α-D-mannopyranoside	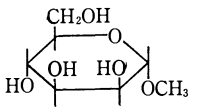
XI	Methyl 4 : 6-*O*-benzylidene-α-D-altropyranoside	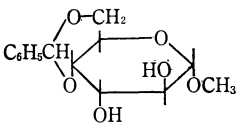
XII	Methyl 4 : 6-*O*-ethylidene-α-D-glucopyranoside	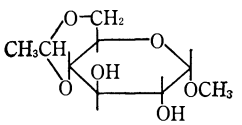
XIII	Methyl β-D-glucopyranoside	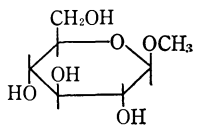

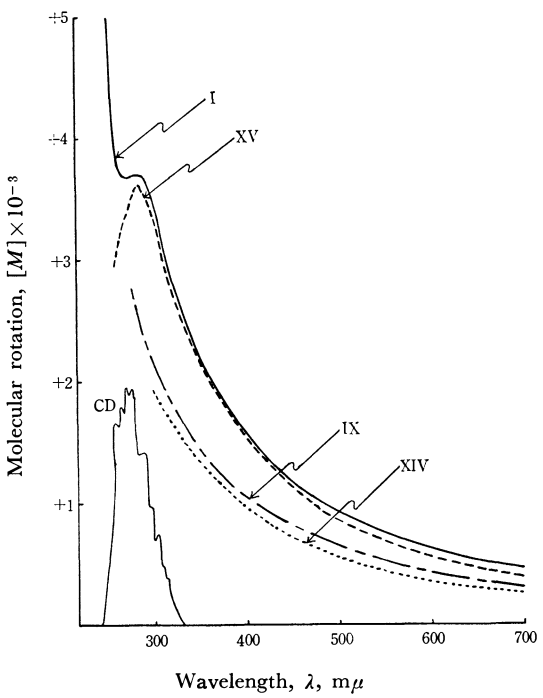

Fig. 1. RD of C_1-nitrates of hexoses (I, IV) and CD of I.

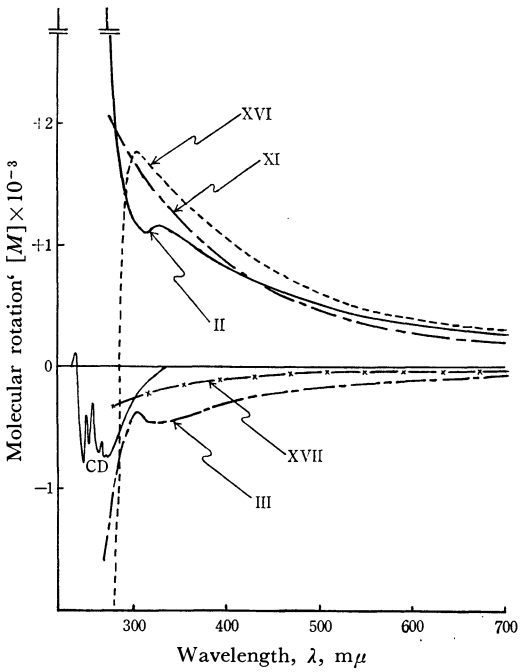

Fig. 2. RD of C_3-nitrates of hexoses (II, III, XVI) and CD of II.

(265—300 mμ) approximates that of 2, 3, 4, 6-tetra-*O*-acetyl-1-*O*-nitro-α-D-glucopyranose (compound XV), which has been reported to show a positive Cotton effect in nearly the same region, the peak of which lies at 285 mμ.[2] These two pyranosides differ only in C_4-OAc configuration; namely, the acetoxyl group is axial in the galactopyranoside (I) and equatorial in the glucopyranoside (XV). They conform to the isorotation

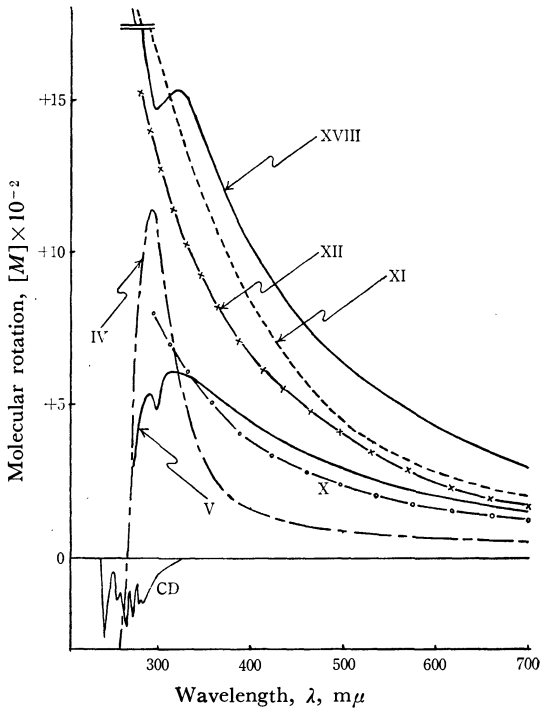

Fig. 3. RD of 2,3-dinitrates of hexoses and CD of V.

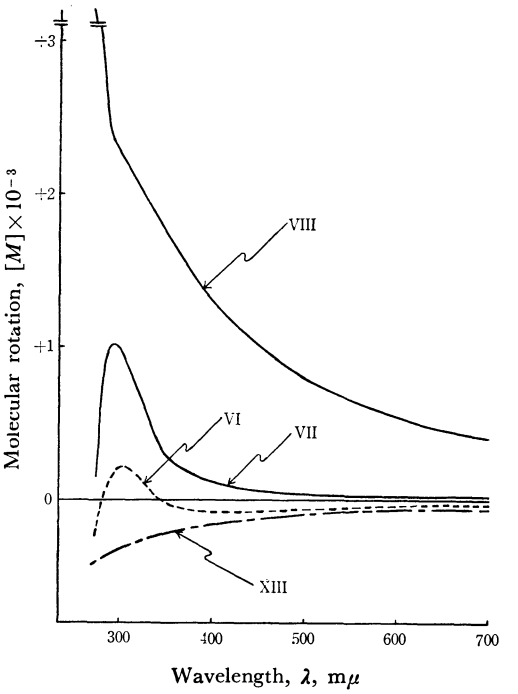

Fig. 4. RD of tri- (VI) and tetranitrates (VII, VIII) of methyl glucopyranosides.

rule of Hudson. The ultraviolet absorption of compound I (Fig. 5) due to the $n\rightarrow\pi^*$ transition of the nitrate group coincides in position with the Cotton effect.

The background optical rotations of compounds I and XV are given, respectively, as the plain curves IX and XIV in Fig. 1; from these it may be seen that the α-C_1-ONO_2 group makes a greater positive rotatory contribution than the α-C_1-OAc.

Figure 2 shows the RD curves of three C_3-ONO_2 derivatives (II, III and XVI). In contrast to methyl 4 : 6-*O*-benzylidene-α-D-glucopyranoside-3-nitrate (XVI),[2] which exhibits a sharp positive Cotton effect with a peak at 300 mμ, methyl 4 : 6-*O*-benzylidene-α-D-altropyranoside 3-nitrate (compound II), which is the C_3-ONO_2, C_2-OH diastereomer of XVI, shows a very weak Cotton effect around 315—320 mμ, the sign of which was determined to be negative by observing the CD curve (Fig. 2), which proved to be negative in sign. That the negative Cotton effect is located at a longer wavelength (315 mμ) is considered to be due to some steric interaction between the C_3–ONO_2 and α-C_1-OMe groups, for the ultraviolet absorption (II) is observed at nearly the same position as the other nitrates (Fig. 6).

The RD curve of the compound III with a furanose ring shows a positive Cotton effect, as may be seen in the negative domain of Fig. 2, with a peak, at 295 mμ, the sign of which coincides with that of the C_3-nitrate of glucose (XVI). Their C_3-ONO_2 configurations are both in the β-position, although their ring structures are different; the sign of the Cotton effect (due to the nitrate group) seems to be independent of the ring structure.

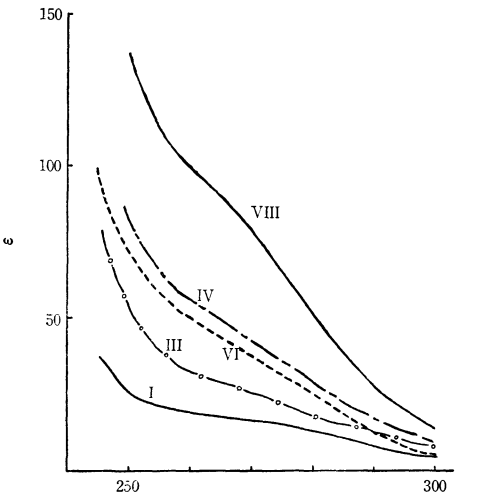

Fig. 5. UV absorption spectra of nitrates.

Mention should also be made that the corresponding xanthate[3] exhibits a positive Cotton effect, just as the nitrate (III) does, although their effects are quite different in strength.

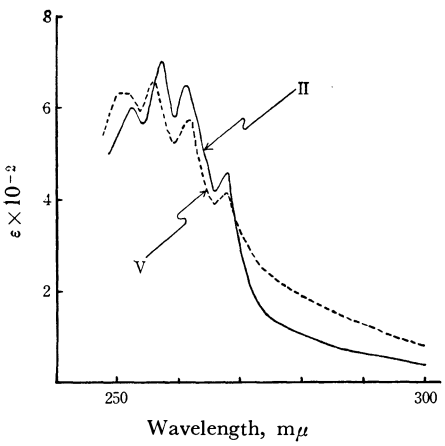

Fig. 6. UV absorption spectra of II and V.

Figure 3 gives the RD curves of some 2, 3-dinitrates. A distinct positive Cotton effect, with a peak at 293 mμ, is seen in methyl 4 : 6-*O*-ethylidene-α-D-mannopyranoside 2 : 3-dinitrate (IV), since the C_2-ONO_2 and C_3-ONO_2, both of the L-configuration, contribute to the positive Cotton effect; this is in conformity with the principle established in an earlier paper[2] (see Table IV of this paper).

The compound XVIII (Fig. 3), which is the C_2-epimer of compound IV, shows, as has been reported,[2] a higher dextrorotation, one due to the contribution of the C_2-group of the D-configuration, but it also exhibits a negative Cotton effect, with a trough at 300 mμ due to the predominating vicinal effect of the C_2-ONO_2 group over that of the C_3-ONO_2 group.

The complex Cotton effect seen in Fig. 3 is exhibited by the RD curve of methyl 4 : 6-*O*-benzylidene-α-D-altropyranoside 2 : 3-dinitrate (V), whose C_2-ONO_2, being of the L-type, contributes to a positive Cotton effect, while the C_3-ONO_2 of the D-type causes a negative Cotton effect. It is most likely that the peak at 290 mμ is responsible for the C_2-ONO_2 group, and that the somewhat wide trough extending from 300 to 310 mμ is an expression of a Cotton effect due to the C_3-ONO_2 chromophore. The sign of this chromophore is probably negative, for the CD curve (Fig. 3) seems to be negative in sign, but the complicated nature of the curve permits no hasty conclusion. Figure 3 also gives the RD curves of the compounds X—XII in order that information on the background rotations of the three 2, 3-dinitrates (IV, V and XVIII) can be obtained by comparing their RD curves.

The RD curve of IV is lower than the background curve of X above the absorption region; because both of the C_2- and C_3-nitrate groups are of the L-type, they contribute to a greater negative rotation than do the corresponding C_2- and C_3-hydroxy groups. The background rotation of XI is also more enhanced than the RD curve of the corresponding 2, 3-dinitrate (V) of the L-type, since the C_2-nitrate group of the L-type is a dominant contributor to a negative rotation as compared to the C_3-nitrate group of the D-type, which might contribute to a positive rotation.

On the contrary, the dinitrate (XVIII),[2] with a C_2-nitrate of the D-type, exhibits in the transparent region a higher positive rotation than does the corresponding background compound (XII) in spite of the presence of the levorotatory C_3-nitrate group.

Figure 4 gives the RD curves of the tri- and tetranitrates of methyl glucopyranosides. Methyl 6-*O*-acetyl-2, 3, 4-tri-*O*-nitro-β-D-glucopyranoside (VI) shows a weak positive Cotton effect, with a broad peak around 295 mμ. This feature is in good harmony with the fact that methyl 4 : 6-*O*-ethylidene-β-D-glucopyranoside 2 : 3-dinitrate, as has already been reported,[2] shows a similar RD curve, with a weak positive Cotton effect.

As may be seen from Fig. 4, a distinct positive Cotton effect is exhibited by the tetranitrate (VII) (methyl 2, 3, 4, 6-tetra-*O*-nitro-β-D-glucopyranoside), whose RD curve has a peak at 290 mμ, whereas its α-anomer (VIII) shows no clear Cotton effect, but only a shoulder around 285—325 mμ. From the regularity already stated, it may be expected that the C_2-ONO_2 and C_4-ONO_2 chromophores, both of the D-configuration (VIII), would give rise to negative Cotton effects; in reality, however, they appear to have been suppressed by the overwhelming, dextrorotatory contribution of the α-C_1-OMe group. The negative plain curve of XIX shows that the β-C_1-OMe group, as a powerful levorotatory contributor, even predominates over the α-C_2-OH group, which would contribute to a strong dextrorotation.

As to the effect of the C_6-ONO_2-chromophore, it can safely be concluded, by comparing several glucopyranose nitrates (compounds VI and VII in this paper, compounds XIV and XV in Part IX[2]), that the C_6-ONO_2 group contributes more or less to positive rotation.

Figures 5 and 6 give the ultraviolet spectra of the eight nitrates described in this paper. As has arleady been reported,[2,5] sugar nitrates usually exhibit weak shoulders ($\varepsilon < 100$) in the region from 250 to 280 mμ of the ultraviolet absorption spectra; this region nearly coincide with the regions of absorption found by a study of their RD curves. However, a somewhat anomalous behavior appears in the ultrariolet absorptions of the compounds II and V (Fig. 6), which occur in the region from 270 to 290 mμ, presumably as a result of the absorption of the phenyl group superposed upon the absorption of the nitrate chromophore around 250—280 mμ.

5) Y. Tsuzuki, K. Tanabe and K. Okamoto, This Bulletin, **38**, 274 (1965).

Table III. Dispersion data and constants

Nitrate	Drude's equation			$\lambda_{RD}(\mu)$	Sign of Cotton effect	Configuration of C_1
	A	B	$\lambda_0(\mu)$			
I	+35.8	+179	0.244	0.280	+	α
II	− 1.58	+130	0.276	0.315	−	α
III	+ 4.21	− 47.0	0.296	0.295	+	α
IV	+ 8.80	+ 11.7	0.275	0.293	+	α
VI	+ 5.51	− 22.0	0.285	0.295	+	β
VII	+ 8.91	− 2.27	0.296	0.290	+	β
VIII	− 3.21	+201	0.299	0.290—0.310 (shoulder)	−	α

Dispersion Constants

It has been found that the data obtained by the RD measurements conform well to the simplified two-term equation of Drude:

$$[M] = \frac{A}{\lambda^2-\lambda_0^2} + \frac{B}{\lambda^2} \qquad (1)$$

The results of calculation, the signs of the Cotton effect and the C_1-configurations are collected in Table III. As may be seen in Table III, the sign of the A-value agrees with that of the Cotton effect in every case, while the absolute value of A well expresses the intensity of the Cotton effect, in harmony with the RD curve.

Here it is worthy of remark that the compound VIII has only a small A value, but its negative sign (−3.21) undoubtedly shows that the Cotton effect is also negative. In reality, however, the sign of its Cotton effect cannot readily be determined by the RD curve, which shows only a shoulder in the absorption region. This slight negative Cotton effect supports the view that the C_2-ONO_2 chromophore of the D-configuration in α-glucosides is a dominant contributor to a negative Cotton effect; this is in conformity with the general rule previously proposed by the present authors.[1]

The B-value in general represents the background rotation, the positive sign of which corresponds to the α-C_1-configuration, and the negative sign, to the β-C_1-configuration. Apparently this regularity does not hold with the compound III, but even so it is not necessarily an exception, for this furanoside 3-nitrate (III) is bridged, between C_1 and C_2, by an isopropylidene radical.

The value of λ_{RD} in Table III represents the position of the peak or the trough of the RD curve; the real absorption center is presumed to be located in a region of a somewhat shorter wavelength. This may be seen from the ultraviolet absorption curve, and the results of calculation really support this reasoning.

Conclusion

As has been stated above, the regular rule established in a previous paper,[2] a rule as to the correlation between the sign of the Cotton effect and the configuration, holds true with the nitrates shown in Table I. The conclusions are summarized in Table IV.

Table IV. The configurations and the signs of the Cotton effect of nitrates of glucosides

C_1-Configuration of glucosides	Configuration of C-ONO_2	Sign of the Cotton effect	Contribution of the rotation
α-Anomer	D or α	−	+
α-Anomer	L or β	+	−
β-Anomer	D or α	+	+
β-Anomer	L or β	−	−

In conclusion, it should also be pointed out that the regular relation observed between the sign of the Cotton effect and the configuration with the nitrates of some α-hydroxy-carboxylic acids[1] corresponds to the case of the β-anomer shown in Table III, and that, conversely, the similar rule found with sugar xanthates[3,6] corresponds to the case of the α-anomer.

Experimental

The derivatives of sugars were prepared according to the methods of the literature. The rotatory dispersion was measured with a Rudolph spectropolarimeter over the wavelength region from about 260 mμ to 700 mμ. The circular dichroism curves were obtained using a JASCO optical rotatory dispersion recorder of the ORD/UV-5 type. The ultraviolet absorption was measured with a self-recording spectrophotometer of the Hitachi EPU-II type. The dispersion constants of the Drude equation were computed from the data by means of the least-square method with an electronic computer of the Fuji FACOM 201 type.

2, 3, 4, 6-Tetra-*O*-acetyl-1-*O*-nitro-α-D-galactopyranoside (Compound I).[7]—White prisms; m. p. 94°C. The RD was measured at 20°C in chloroform (c, 1.0148). $[\alpha]_{700}^{20}$ +114°, $[\alpha]_{589}$ +160°, $[\alpha]_{500}$ +228°,

6) Y. Tsuzuki, K. Tanaka and K. Tanabe, This Bulletin, **35**, 1614 (1962); Y. Tsuzuki, K. Tanabe, M. Akagi and S. Tejima, ibid., **37**, 162 (1964); Y. Tsuzuki, K. Tanabe, M. Akagi and S. Tejima, ibid., **38**, 270 (1965).

7) W. Koenigs and E. L. Knorr, *Ber.*, **34**, 978 (1901).

$[\alpha]_{400}$ +386°, $[\alpha]_{350}$ +547°, $[\alpha]_{300}$ +878°, $[\alpha]_{280-265}$ +942° (shoulder), $[\alpha]_{260}$ +1436°.

Methyl 4 : 6-*O*-Benzylidene-*α*-D-altropyranoside 3-Nitrate (Compound II).[8]—Colorless prisms; m. p. 157—157.5°C. The RD was measured at 22°C in chloroform (*c*, 0.9768). $[\alpha]^{22}_{700}$ +79.9°, $[\alpha]_{589}$ +112°, $[\alpha]_{500}$ +157°, $[\alpha]_{400}$ +250°, $[\alpha]_{340}$ +340°, $[\alpha]_{325}$ +354°, $[\alpha]_{315}$ +338° (trough), $[\alpha]_{280}$ +572°, $[\alpha]_{270}$ +1050°.

1, 2 : 5, 6-Diisopropylidene-3-*O*-nitro-*α*-D-glucofuranose (Compound III).[9]—Colorless syrup. The RD was measured at 20°C in chloroform (*c*, 1.3788). $[\alpha]^{20}_{700}$ −25.9°, $[\alpha]_{589}$ −37.7°, $[\alpha]_{500}$ −54.2°, $[\alpha]_{400}$ −95.8°, $[\alpha]_{320}$ −145° (broad extreme), $[\alpha]_{300}$ −115° (positive peak), $[\alpha]_{280}$ −224°, $[\alpha]_{265}$ −499°.

Methyl 4 : 6-*O*-Ethylidene-*α*-D-mannopyranoside 2 : 3-Dinitrate (Compound IV).[10]—White crystals, m. p. 72—73°C. The RD was measured at 22°C in chloroform (*c*, 0.7858). $[\alpha]^{22}_{700}$ +15.1°, $[\alpha]_{589}$ +20.3°, $[\alpha]_{500}$ +30.0°, $[\alpha]_{400}$ +55.3°, $[\alpha]_{300}$ +345°, $[\alpha]_{293}$ +366° (peak), $[\alpha]_{280}$ +244°, $[\alpha]_{260}$ −604°.

Methyl 4 : 6-*O*-Benzylidene-*α*-D-altropyranoside 2 : 3-Dinitrate (Compound V).[8]—Colorless syrup. The RD was measured at 20°C in chloroform (*c*, 0.3580). $[\alpha]^{20}_{700}$ +45.1°, $[\alpha]_{589}$ +59.5°, $[\alpha]_{500}$ +81.2°, $[\alpha]_{400}$ +124°, $[\alpha]_{350}$ +141°, $[\alpha]_{310}$ +162° (broad extreme), $[\alpha]_{290}$ +143° (peak), $[\alpha]_{280}$ +121°.

Methyl 6-*O*-Acetyl-2, 3, 4-tri-*O*-nitro-*α*-D-glucopyranoside (Compound VI).[11]—White plates, m. p. 104.5—105.5°C. The RD was measured at 22°C in chloroform (*c*, 1.4430). $[\alpha]^{22}_{700}$ −8.32°, $[\alpha]_{589}$ −12.2°, $[\alpha]_{500}$ −15.1°, $[\alpha]_{400}$ −18.0°, $[\alpha]_{340}$ −5.34°, $[\alpha]_{310}$ +41.3°, $[\alpha]_{295}$ +57.2° (peak), $[\alpha]_{280}$ +21.9°, $[\alpha]_{279}$ −50.9°.

Methyl 2, 3, 4, 6-Tetra-*O*-nitro-*β*-D-glucopyranoside (Compound VII).[12]—White prisms, m. p. 115.5—117.5°C. The RD was measured at 22°C in chloroform (*c*, 0.9850). $[\alpha]^{22}_{700}$ +3.66°, $[\alpha]_{589}$ +6.29°, $[\alpha]_{500}$ +11.5°, $[\alpha]_{400}$ +29.5°, $[\alpha]_{300}$ +259°, $[\alpha]_{290}$ +270° (peak), $[\alpha]_{280}$ +213°, $[\alpha]_{270}$ +111°.

Methyl 2, 3, 4, 6-Tetra-*O*-nitro-*α*-D-glucopyranoside (Compound VIII).[13]—Colorless syrup. The RD was measured at 20°C in chloroform (*c*, 1.1449). $[\alpha]^{20}_{700}$ +107°, $[\alpha]_{589}$ +148°, $[\alpha]_{500}$ +208°, $[\alpha]_{400}$ +345°, $[\alpha]_{350}$ +466°, $[\alpha]_{300}$ +610°, $[\alpha]_{290}$ +641°, $[\alpha]_{275}$ +857°.

Pentaacetyl-*α*-D-galactopyranose (Compound IX).[14]—White amorphous solid, m. p. 95°C. The RD was measured at 20°C in chloroform (*c*, 0.6046). $[\alpha]^{20}_{700}$ +81.8°, $[\alpha]_{589}$ +115°, $[\alpha]_{500}$ +163°, $[\alpha]_{400}$ +269°, $[\alpha]_{300}$ +547°, $[\alpha]_{280}$ +662°.

Methyl *α*-D-Mannopyranoside (Compound X).[15]—White crystals, m. p. 190°C. The RD was measured at 19°C in water (*c*, 0.6700). $[\alpha]^{19}_{700}$ +63.1°, $[\alpha]_{589}$ 88.0°, $[\alpha]_{500}$ +122°, $[\alpha]_{400}$ +199°, $[\alpha]_{315}$ +349°.

Methyl 4 : 6-*O*-Benzylidene-*α*-D-altropyranoside (Compound XI).[16]—Colorless prisms, m. p. 165°C. The RD was measured at 19°C in chloroform (*c*, 0.297). $[\alpha]^{19}_{700}$ +67.3°, $[\alpha]_{589}$ +99.7°, $[\alpha]_{500}$ +155°, $[\alpha]_{400}$ 292°, $[\alpha]_{300}$ +579°, $[\alpha]_{280}$ +710°.

Methyl 4 : 6-*O*-Ethylidene-*α*-D-glucopyranoside (Compound XII).[17]—White needles, m. p. 75.5—76.5°C. The RD was measured at 20.5°C in chloroform (*c*, 1.2420). $[\alpha]^{20.5}_{700}$ +85.9°, $[\alpha]_{589}$ +125°, $[\alpha]_{500}$ +177°, $[\alpha]_{400}$ +293°, $[\alpha]_{300}$ +581°, $[\alpha]_{280}$ +691°.

Methyl *β*-D-Glucopyranoside (Compound XIII).[18]—White needles, m.p. 107—108°C. The RD was measured at 20.8°C in water (*c*, 1.3456). $[\alpha]^{20.8}_{700}$ −23.3°, $[\alpha]_{589}$ −33.2°, $[\alpha]_{500}$ −47.3°, $[\alpha]_{400}$ −78.0°, $[\alpha]_{300}$ −158°, $[\alpha]_{280}$ −191°.

The authors wish to express their sincere gratitude to the Japan Spectroscopic Co., Ltd. for the CD measurement.

8) K. S. Ennor, J. Honeyman, C. A. G. Shaw and T. C. Stening, *J. Chem. Soc.*, **1958**, 2921.
9) J. Honeyman and T. C. Stening, *J. Chem. Soc.*, **1958**, 537.
10) J. Honeyman and J. W. W. Morgan, ibid., **1954**, 744.
11) D. J. Bell and R. L. M. Synge, ibid., **1937**, 1715.
12) J. Dewar and G. Fort, ibid., **1944**, 500.
13) W. Will and F. Lenze, *Ber.*, **31**, 80 (1898).
14) C. S. Hudson and J. M. Johnson, *J. Am. Chem. Soc.*, **37**, 1276 (1915).
15) This material was obtained commercially.
16) G. J. Robertson and W. Whitehead, *J. Chem. Soc.*, **1935**, 1193.
17) E. G. Amsell and J. Honeyman, ibid., **1952**, 2778.
18) E. Fischer, *Ber.*, **28**, 1151 (1895).

BULLETIN OF THE CHEMICAL SOCIETY OF JAPAN VOL. 39 1398—1401 (1966)

On the Carbon-13 Chemical Shifts of Saturated Hydrocarbons

By Teijiro YONEZAWA, Isao MORISHIMA and Hiroshi KATO

Faculty of Engineering, Kyoto University, Sakyo-ku, Kyoto

(Received October 23, 1965)

A molecular orbital interpretation of the carbon-13 chemical shifts of saturated hydrocarbons is presented. The shielding constant of the carbon atom is shown to be roughly proportional to the excess charge densities of 2p electrons, which is in accordance with experiments. The so-called β- and γ-effects in the carbon-13 chemical shifts are explained on the basis of an MO theory.

Recently carbon-13 nuclear magnetic resonance studies of various compounds have been carried out systematically.[1] In a series of aromatic compounds, many workers have observed a direct relationship between the cabron-13 chemical shift and the π-electron charge density; a theoretical basis for this relation has been given by Karplus and Pople.[2] However, there have been few theoretical interpretations[3] of carbon-13 chemical shifts of saturated hydrocarbons. Carbon-13 chemical shifts of linear and some branched alkanes with a range of about 40 p.p.m. have been found to conform with a simple additivity law.[4] This empirical linear expression, of the type given by Eq. 1

$$\delta^{13}\mathrm{C}(j) = \delta^{13}\mathrm{C}(\mathrm{CH_4}) + \sum_i N_{ij}\delta_i \qquad (1)$$

has yet to be interpreted theoretically. The chemical shift for methane is $\delta^{13}\mathrm{C}(\mathrm{CH_4})$, and the substituent parameters, δ_i, reflect the effect of a carbon atom in the ith position upon the carbon-13 being investigated, where i denotes the α, β, γ, δ and ε carbon atoms. N_{ij} is the number of ith carbon atoms relative to the jth carbon. In the present paper, an attempt is made to give a molecular orbital interpretation of the carbon-13 chemical shift of these compounds.

Theoretical

The nuclear magnetic shielding constant, σ, may be conveniently expressed as a sum of diamagnetic and paramagnetic terms:[5]

$$\sigma = \sigma_\mathrm{d} + \sigma_\mathrm{p} \qquad (2)$$

where:

$$\sigma_\mathrm{d} = (e^2/3mc^2)\sum_i \langle\psi_0|r_i^{-1}|\psi_0\rangle$$

$$\sigma_\mathrm{p} = (\sigma_\mathrm{pxx} + \sigma_\mathrm{pyy} + \sigma_\mathrm{pzz})/3 \qquad (3)$$

$$\sigma_\mathrm{pzz} = -(e^2/2m^2c^2)\sum_{n\neq 0}(E_n - E_0)^{-1} \times [\langle\psi_0|\sum_i l_z^{(i)}|\psi_n\rangle\langle\psi_n|\sum_j l_z^{(j)} r_j^{-3}|\psi_0\rangle + \langle\psi_0|\sum_j l_z^{(j)} r_j^{-3}|\psi_n\rangle\langle\psi_n|\sum_i l_z^{(i)}|\psi_0\rangle] \qquad (4)$$

where $l_z^{(i)}$ is the Z-component of the orbital angular momentum of the ith electron, r_i distant from the nucleus in question, and where ψ_0 and ψ_n are the wave functions of the ground and the n-th excited states, with the energies E_0 and E_n respectively. The approximate values of σ_d can be calculated with the Slater atomic orbitals for the carbon sp^3 hybridized atomic orbital. The diamagnetic shielding constant, σ'_d, per 2s or 2p electron becomes:

$$\sigma'_\mathrm{d}(\text{2s or 2p electron}) = 4.45\,Z^* \text{ (p.p.m.)} \qquad (5)$$

where Z^* is the "effective nuclear charge" estimated according to Slater's rules. Since these yield a Z^* value of 3.25 for a neutral carbon atom, by taking into account a screening per 2s or 2p electron of 0.35 we can write Z^* for a carbon atom, A, in a molecule as:

$$Z^* = 3.25 - 0.35(q^\mathrm{A} - 4) \qquad (6)$$

where q^A is the σ-electron density on the atom. Since σ_d is due to four valence electrons of a carbon atom, we obtain

$$\sigma'_\mathrm{d} = 4.45\,Z^* q^\mathrm{A} \qquad (7)\dagger$$

where q^A is the electron density around the carbon atom A and where, for a neutral carbon ($q^\mathrm{A}=4$), σ'_d is 57.2. The increase in σ'_d if a 2s or a 2p electron is added is 16 p. p. m., about 50% of

1) Cf., e. g., J. B. Stothers, *Quart. Rev.*, **19**, 144 (1965).
2) M. Karplus and J. A. Pople, *J. Chem. Phys.*, **38**, 2803 (1963); J. A. Pople, *Mol. Phys.*, **7**, 301 (1964).
3) Recently, a valence bond interpretation of $^{13}\mathrm{C}$ chemical shifts of saturated hydrocarbons was presented by D. M. Grant at the Interantional Symposium on NMR, Tokyo (1965).
4) E. G. Paul and D. M. Grant, *J. Am. Chem. Soc.*, **85**, 1701 (1963).
5) N. F. Ramsey, *Phys. Rev.*, **78**, 699 (1950); A. Saika and C. P. Slichter, *J. Chem. Phys.*, **22**, 26 (1954).

† σ_d is associated with all electrons, whereas σ'_d is associated only with valence electrons.

the observed effect. However, the change in the calculated σ-electron density in this study is at most 0.3, while the effect due to the diamagnetic term is calculated to be about 4.8 p. p. m. Thus, the diamagnetic shielding, σ'_d, cannot make a principal contribution in the σ-frame carbon compounds. An approximate formula for σ_p may be obtained[2,3,6] by treating $E_n - E_0$ as a constant ΔE in Eq. 4 and by using the LCAO molecular orbital, where each molecular orbital is expressed as a linear combination of valence-shell atomic orbitals:

$$\sigma_p^A = -[2e^2h^2/3m^2c^2(\Delta E)]\langle r^{-3}\rangle_{2p}(P_1 - P_2 - P_3) \quad (8)$$

where:

$$P_1 = (P_{xx} + P_{yy} + P_{zz})_{AA}$$
$$P_2 = (P_{xx}P_{yy} + P_{yy}P_{zz} + P_{zz}P_{xx})_{AA}/2$$
$$P_3 = \sum_{B(\neq)A} (P_{xx}P_{yy} + P_{yy}P_{zz} + P_{zz}P_{xx})_{AB}/2$$

In this formulation, $(P_{xx})_{AB}$, for example, designates:

$$(P_{xx})_{AB} = 2\sum_i^{occ} C_{xA}{}^i C_{xB}{}^i \quad (9)$$

where $C_{xA}{}^i$ is the coefficient of the $2P_x$ atomic orbital of the carbon, A, in the ith molecular orbitals. It corresponds to the electron desnity (A=B of the $2P_x$ AO or bond order matrix (A$\neq$B) between two $2P_x$ orbitals of the A and B atoms. P_1 is the 2P electron density on the carbon A and has a value of 3 in the neutral carbon. The $\langle r^{-3}\rangle_{2P}$ factor, which is the mean inverse cube radius for carbon 2P orbitals, depends on the local electron desity on the carbon atom.[2] For a Slater 2P orbital, $\langle r^{-3}\rangle_{2P}$ is found to be:

$$\langle r^{-3}\rangle_{2P} = \frac{1}{24a_0{}^3}[3.25 - 0.35(P_1 - 3)]^3 \quad (10)$$

where a_0 is the Bohr radius and $(P_1 - 3)$ is the excess charge density of the 2P electron.

For the calculation of P_1 and P_2, we use a simple LCAO MO theory for the σ-electron developed by Fukui, Kato and Yonezawa.[7] A molecular orbital, φ, is expressed as a linear combination of the sp^3 hybridized orbital of the carbon atom, $\chi_{C,i}$ and the ls orbital of the hydrogen atom, $\chi_{H,l}$, as is shown by the expression:

$$\varphi = \sum_i^n C_i\chi_{C,i} + \sum_l^n C_l\chi_{H,l}$$

The coulomb and resonance integrals are given by the following:

$$\langle\chi_{C,i}|H|\chi_{C,i}\rangle = \alpha$$
$$\langle\chi_{H,l}|H|\chi_{H,l}\rangle = \alpha + a\beta$$
$$\langle\chi_{C,i}|H|\chi_{C,i+1}\rangle = \beta$$

between two sp^3 orbitals of two adjacent carbon atoms:

$$\langle\chi_{C,i}|H|\chi_{C,i} + 1\rangle = m\beta$$

between two sp^3 orbitals to one and the same carbon atom:

$$\langle\chi_{C,j}|H|\chi_{H,j+1}\rangle = b\beta$$

where a is taken as -0.2; m, as 0.34, and b, as 1.1[7]. In solving the secular equation, we neglected the overlap integrals. Then the electron density, q_r, of the rth atomic orbital is defined by:

$$q_r = 2\sum_i^{ooc} C_{ir}{}^2$$

The x, y, z, components of the charge density and the bond order matrix (Eq. 9) can be represented in terms of electron densities, q_r, as follows if we take x, y and z axes to be as shown in Fig. 1:

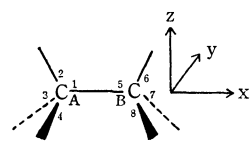

Fig 1.

$$P_{xx} = (3/4)q_1 + (1/12)(q_2 + q_3 + q_4)$$
$$P_{yy} = (1/6)(q_2 + q_4) + (2/3)q_3$$
$$P_{zz} = (1/2)(q_2 + q_4)$$
$$(P_{yy})_{AB} = 2\sum_i^{occ}[-1/\sqrt{6}\,(C_{i2} + C_{i3}) + \sqrt{2/3}C_{i4}]$$
$$\times[-1/\sqrt{6}\,(C_{i6} + C_{i7}) + \sqrt{2/3}C_{i8}]$$

The calculated values of P_1, P_2, P_3, $\langle r^{-3}\rangle_{2p}$ and σ_p, together with the observed[3] δ ^{13}C and calculated $\delta^{13}C$ values, are summarized in Table I for several compounds.

When we take ΔE as 10 eV. for Eq. 8, we have:

$$\sigma_p = (44.8Q_{2p\sigma} - 138.1)(P_1 - P_2 - P_3) \quad (11)$$

where $Q_{2p\sigma}$ designates $(P_1 - 3)$. The values of $(P_1 - P_2 - P_3)$ is almost constnat $(P_1 - P_2 - P_3 = 1.498)$. Therefore, if we take $(P_1 - P_2 - P_3)$ as 1.498 for Eq. 11, the total shielding constant, $\sigma(= \sigma'_d + \sigma_p)$, due to the valence electrons of the carbon atom A in a saturated hydrocarbon is, from Eq. 7 and Eq. 11:

$$\sigma = 87.8Q_{2p\sigma} - 1.6Q_{2p\sigma}{}^2 - 207.2 \text{ (p.p.m.)} \quad (12)$$

In order to test the validity of Eq. 12, which was derived theoretically, we plot in Fig. 3 the observed carbon-13 chemical shift against the excess charge density of 2p electrons for several compounds. We thus find an approximate proportionality between $Q_{2p\sigma}$ and $\delta^{13}C$.

6) J. A. Pople, *Proc. Roy. Soc.*, **A239**, 550 (1957); M. Karplus and T. P. Das, *J. Chem. Phys.*, **34**, 1683 (1961).

7) K. Fukui, H. Kato and T. Yonezawa, This Bulletin, **34**, 442, 1111 (1961).

TABLE I. THE CALCULATED VALUES OF ^{13}C CHEMICAL SHIFT FOR SOME SATURATED HYDROCARBONS

Molecule	P_1	P_2	P_3	$(P_1-P_2-P_3)$	$\langle r^{-3}\rangle_{2p}$ a.u.	$-\sigma_p$(calcd.) p.p.m.	$\delta^{13}C$(calcd.) p.p.m.	$\delta^{13}C$(obs.)[a] p.p.m.
CH_4	3.2241	1.7295	0	1.4946	1.326	191.4	—	—
C*-C	3.1707	1.6752	0	1.4955	1.351	195.4	−4.0	−8.0
C*-C-C	3.1691	1.6734	0	1.4957	1.352	195.5	−4.1	−17.0
C-C*-C	3.1209	1.6231	0	1.4978	1.374	198.8	−7.4	−18.0
C(C)-C*-C	3.0706	1.5713	0	1.4993	1.397	202.3	−10.9	−27.3
C*-C(C)-C	3.1689	1.6731	0	1.4958	1.352	196.0	−4.6	−26.4

a) Chemical shift is referred to methane. (Ref. 4.)

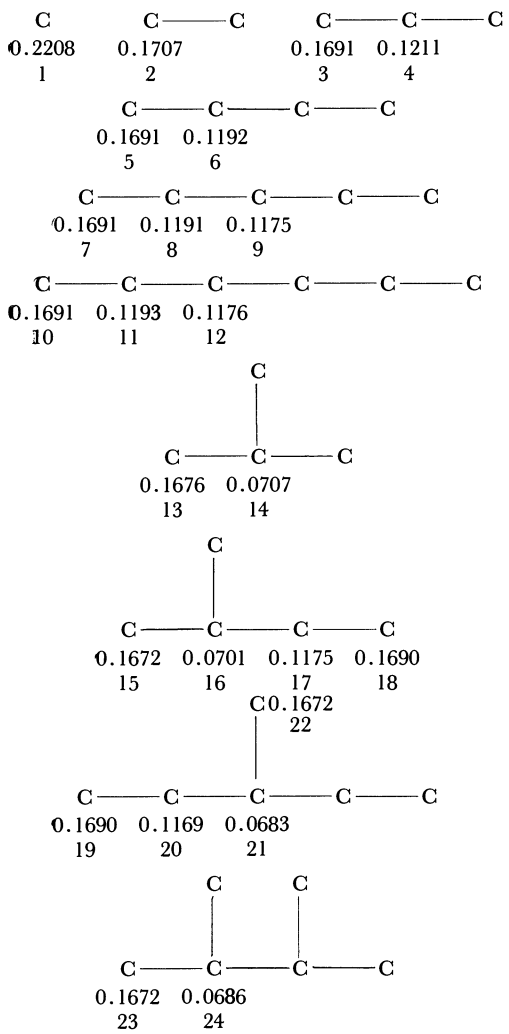

Fig. 2. Excess charge density of 2P electrons ($Q_{2p\sigma}$) of carbon atoms for linear and branched hydrocarbons.

Discussion

Theoretical considerations predict the same simple linear relationship between the excess charge density and the carbon-13 chemical shifts for saturated hydrocarbons as has been exhibited in the aromatic compounds. However, Fig. 3 shows a fairly large scattering.

This is mainly due to the failure of the theoretical interpretation of the anomalous β-effect suggested by Paul and Grant,[4] which gives an unexpectedly large down-field contribution than the α-effect. The β-effect may be interpreted in terms of the change in the mean excitation energy, ΔE, or the change of the effective nuclear charge, Z^*, due to the influence of the β-methyl group on the radial part of the 2p atomic orbital.[8] In

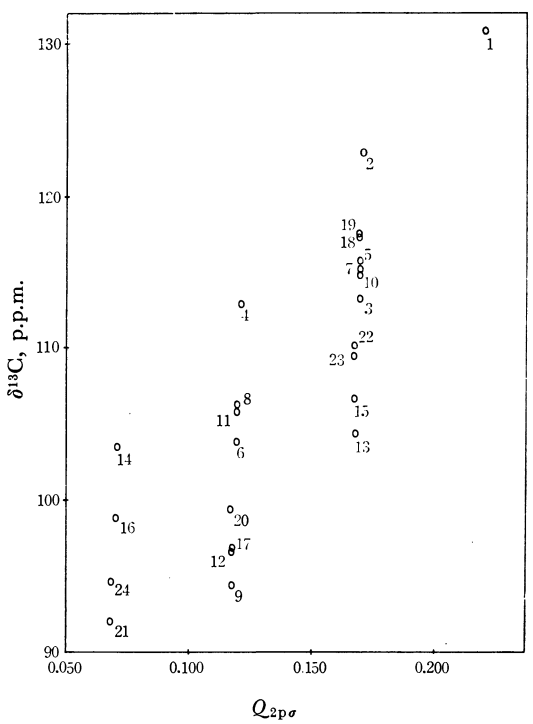

Fig. 3. A plot of the excess charge density of 2P electron ($Q_{2p\sigma}$) versus observed ^{13}C chemical shift ($\delta^{13}C$). The values of $Q_{2p\sigma}$ are summarized in Fig. 2 and the values of ^{13}C chemical shift ($\delta^{13}C$) are given in p.p.m. from CS_2 (Ref. 4).

8) This was suggested by D. M. Grant at the International Symposium on NMR, Tokyo (1965).

fact, the diminution of ΔE may be expected in a branched alkane with reference to the value of the ionization potential.[9] The increase in Z^* and the decrease in ΔE may be considered to cause the paramagnetic shift. Another anomalous γ-effect which makes a positive contribution to the carbon-13 chemical shifts can be partly interpreted in terms the electronic effects. The γ-carbon relative to the carbon atom can occupy both a gauche and a trans position relative to the carbon atom under study. For example, consider a trans butane (I) and a gauche butane (II):

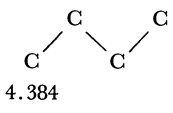

trans
(I)

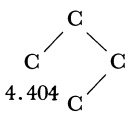

gauche
(II)

We calculated the atom population of the terminal carbon atom by an extended Hückel molecular orbital theory,[10] which is useful in discussing the conformational change of the electronic sturcture by taking account of the resonance integral between non-bonded atoms. The terminal carbon for the gauche form with a larger charge density is more shielded than that for the trans form. Using Eq. 12 this effect was evaluated to be about 1.5 p. p. m. Hence the contribution of the gauche form causes a diamagnetic shift to the terminal carbon of normal butane. Recently, Grant presented[8] a theoretical interpretation of this effect by the valence bond method and also showed experimentally that *trans*-1, 4-carbon-carbon interactions should have a negative effect, while *cis*-1, 4-carbon-carbon interactions has a positive effect. Table I and Fig. 3 also show that the calculated values of $\delta^{13}C$ are fairly small, this may be attributed to a small difference in the calculated excess charge densities. This difficulty may be overcome by the improvement of the parametrization of the coulomb and resonance integrals. However, it may be stressed that the general trends of the carbon-13 chemical shifts of saturated compounds, with the exception of a large βth carbon effect, can be qualitatively interpreted by simple molecular orbital calculations. Our treatment is also applicable to other saturated systems, haloalkanes, for example, but the anomalous upfield tendency of the ^{13}C chemical shifts of the multisubstituted bromo and iodo methane cannot be interpreted by the electronic effect only.

The calculations were carried out partly on the digital compouter KDC-I of Kyoto University and partly on the IBM 7090 at the Japan IBM CO. with the permission of the UNICON Committee, whose help we hereby acknowledge.

9) The ionization potential (Ip) might be a measure of the mean excitation energy, ΔE. The Ip values of ethane, propane, *n*-butane and isobutane are 11.76, 11.21, 10.86 and 10.40 eV. respectively.

10) R. Hoffmann, *J. Chem. Phys.*, **39**, 1397 (1963).

BULLETIN OF THE CHEMICAL SOCIETY OF JAPAN VOL. 39 1401—1406 (1966)

A Thermodynamic Approach to Thixotropy

By Manabu SENŌ

The Institute of Industrial Science, The University of Tokyo, Azabu, Tokyo

(Received October 29, 1965)

The thixotropic behavior is discussed on the basis of the thermodynamics of irreversible processes. The fundamental equations are given for the thixotropic fluids by accepting the concept that the internal structure of the system is destroyed by the applied forces, and the general phenomenological equations are written for all the processes occurring in this system. The process by which the thixotropic recovery takes place is non-stationary. A method of specifying this process is proposed by introducing the concept of a fictitious pressure tensor; the data on a rubber latex suspension given by Mooney is analyzed by this method.

The isothermal process by which a system is softened by the disturbance of external forces and is hardened to the original state on settling is called thixotropy. This process is observed under appropriate conditions in the mechanical behavior of bodies showing the so-called structural viscosity. The thixotropy and the structural viscosity have been treated by many researchers since Freundlich[1]; it has been revealed that they are caused as a result of the breakdown and recovery of the internal structure of the system.

1) H. Freundlich and H. L. Löder, *Trans. Faraday Soc.*, **34**, 308 (1938).

In special cases, such as a suspension of rod-like particles, a detailed mechanism has been proposed for the behavior of anomalous viscosity under advanced treatment.[2] However, no general theoretical work is yet available, probably because the varieties and complexity are involved in terms of the internal structure.

Recently, a fundamental approach to the rheological behavior has been undertaken by Meixner[3] and by Kluitenberg[4] on the basis of the thermodynamics of irreversible processes. This treatment is phenomenological; for this reason, it is excellent, for it does not require detailed information on the internal structure. The latter author considered the thixotropic behavior to be a higher-order effect, introducing an internal degree of freedom, in his general theory of rheological processes. The purpose of this paper is to extend this approach and to interpret the thixotropy in terms of the general principles of thermodynamics.

General Equations of Thixotropic Fluids.— The viscous processes of isotropic fluids are described, on the basis of the thermodynamics of irreversible processes,[6] as follows. The Gibbs' equation reads;

$$T\frac{ds}{dt}=\frac{du}{dt}+v\sum_{\alpha,\beta=1}^{3}P_{\alpha\beta}^{eq}\frac{d\varepsilon_{\alpha\beta}}{dt} \tag{1}$$

where s is the specific entropy; u, the specific internal energy; v, the specific volume; T, the absolute temperature; t, the time; $P_{\alpha\beta}^{eq}$, the equilibrium stress tensor, and $\varepsilon_{\alpha\beta}$, the total strain tensor. This is the equation that is applied to the Voigt model, i. e., the bodies having a parallel viscoelasticity; the fluid is one of special cases, as Kluitenberg has pointed out.[4]

It is assumed that the total pressure causes both the flow of the fluids and the destruction of the internal structure; that is,

$$P_{\alpha\beta}=P_{\alpha\beta}^{def}+P_{\alpha\beta}^{des} \tag{2}$$

Then, the balance equation for the total energy reads;

$$\rho\frac{du}{dt}= -\mathrm{div}\boldsymbol{J}^{q}-\sum_{\alpha,\beta=1}^{3}P_{\alpha\beta}^{def}\frac{d\varepsilon_{\alpha\beta}}{dt}-\sum_{\alpha,\beta=1}^{3}P_{\alpha\beta}^{des}\frac{d\xi}{dt} \tag{3}$$

where ρ is the density (the reciprocal of the specific volume); $\boldsymbol{J}^{q}$, the heat flow, and ξ, the degree of internal structure (a measure of the internal structure). The last term on the right-hand side of the equation represents the change in the internal structure of the fluid caused by the forces; it may be omitted in the case of the simple fluid with no structural viscosity, as Kluitenberg did.

The stress tensor for deformation, $P_{\alpha\beta}^{def}$, is divided into two parts, the equilibrium stress tensor and the viscous stress tensor,

$$P_{\alpha\beta}^{def}=P_{\alpha\beta}^{eq}+P_{\alpha\beta}^{v} \tag{4}$$

The equation for the entropy balance is derived from Eqs. 1, 3 and 4 as follows:

$$\rho\frac{ds}{dt}=-\mathrm{div}J^{s}+\sigma^{s} \tag{5}$$

where:

$$J^{s}=J^{q}/T \tag{6}$$

$$\sigma^{s}=\frac{1}{T}\left(-\frac{J^{q}}{T}\cdot\mathrm{grad}\,T-\sum P_{\alpha\beta}^{v}\frac{d\varepsilon_{\alpha\beta}}{dt}-\sum P_{\alpha\beta}^{des}\frac{d\xi}{dt}\right) \tag{7}$$

The former is the entropy flow, and the latter is the irreversible production of entropy, which consists of three terms, the heat flow, the viscous flow and the rate of the breakdown of the internal structure.

The stress and the strain tensors are divided into a tangential part and a normal part as:

$$P_{\alpha\beta}=\tilde{P}_{\alpha\beta}+P\delta_{\alpha\beta} \tag{8}$$

$$P_{\alpha\beta}^{v}=\tilde{P}_{\alpha\beta}^{v}+P^{v}\delta_{\alpha\beta} \tag{9}$$

$$\varepsilon_{\alpha\beta}=\tilde{\varepsilon}_{\alpha\beta}+\varepsilon\delta_{\alpha\beta} \tag{10}$$

where $\delta_{\alpha\beta}$ is Kronecker's symbol and P, P^{v} and ε are traces of the corresponding tensors. It must be noticed that the tensors, $P_{\alpha\beta}$, $P_{\alpha\beta}^{v}$ and $\varepsilon_{\alpha\beta}$, and also $\tilde{P}_{\alpha\beta}$, $\tilde{P}_{\alpha\beta}^{v}$ and $\tilde{\varepsilon}_{\alpha\beta}$ are all symmetrical. The same division is applied to the stress tensor for destruction. We set the trace of this tensor, P^{des}, as equal to zero. This implies that only the tangential force breaks down the internal structure of the system.

Under these procedures, Eq. 7 is rewritten as:

$$\sigma^{s}=\frac{1}{T}\left(-\frac{J^{q}}{T}\cdot\mathrm{grad}\,T-\sum\tilde{P}_{\alpha\beta}^{v}\frac{d\tilde{\varepsilon}_{\alpha\beta}}{dt}-3P^{v}\frac{d\varepsilon}{dt}-\sum\tilde{P}_{\alpha\beta}^{des}\frac{d\xi}{dt}\right) \tag{11}$$

In this equation, the viscous flow term of Eq. 7 is separated into the shearing viscous and the volumetric viscous term. From this formulation of the entropy production, the following phenomenological equations are derived:

$$J^{q}=-\lambda\,\mathrm{grad}\,T \tag{12}$$

$$\tilde{P}_{\alpha\beta}^{v}=-\eta\,d\tilde{\varepsilon}_{\alpha\beta}/dt \tag{13}$$

2) N. A. Scheraga, *J. Chem. Phys.*, **23**, 1526 (1955).
3) J. Meixner, *Z. Naturforschg.*, **4a**, 594 (1949); **9a**, 654 (1954).
4) G. A. Kluitenberg, *Physica*, **28**, 217, 561, 1173 (1962); **29**, 633 (1963).
5) S. R. de Groot and P. Mazur, "Non-equilibrium Thermodynamics," North-Holland Publ. Co., Amsterdam (1962).

$$P^{v} = -\eta^{v}\mathrm{d}\varepsilon/\mathrm{d}t \tag{14}$$

$$\tilde{P}_{\alpha\beta}^{\mathrm{des}} = -\zeta\,\mathrm{d}\xi/\mathrm{d}t \tag{15}$$

The first is the equation of the heat conduction, and the last, that of the breakdown and recovery of the internal structure.

When the fluid is not elastic on the shearing deformation, the equilibrium pressure tensor does not have non-diagonal components and the trace of this tensor, P^{eq}, is dependent on the volume (therefore, the trace of the total strain tensor, ε) and the temperature. Therefore, the linearized equation is assumed:

$$P^{\mathrm{eq}} = b\varepsilon + c(T-T_0) \tag{16}$$

where b and c are phenomenological constants and T_0 is the reference temperature. Using these relations, the phenomenological equations, 13 and 14, may be rewritten as:

$$\tilde{P}_{\alpha\beta} = -\eta\,\mathrm{d}\tilde{\varepsilon}_{\alpha\beta}/\mathrm{d}t \tag{17}$$

$$P = b\varepsilon - \eta^{v}\frac{\mathrm{d}\varepsilon}{\mathrm{d}t} + c(T-T_0) \tag{18}$$

The equation of entropy production is, by the use of these linearized phenomenological equations:

$$\sigma^{s} = \frac{1}{T}\left\{\frac{\lambda}{T}(\mathrm{grad}\ T)^2 + \eta\sum\left(\frac{\mathrm{d}\tilde{\varepsilon}_{\alpha\beta}}{\mathrm{d}t}\right)^2 + 3\eta^{v}\left(\frac{\mathrm{d}\varepsilon}{\mathrm{d}t}\right)^2 + \zeta\sum\left(\frac{\mathrm{d}\xi}{\mathrm{d}t}\right)^2\right\} \tag{19}$$

The phenomenological coefficients defined in the phenomenological equations are positive, as the second principle of thermodynamics requires. λ is the coefficient of thermal conduction, η is the shearing viscosity, b is the volumetric elasticity and η^{v} is the volumetric viscosity; all are conventional terms. These coefficients depend on the state variables, $\tilde{P}_{\alpha\beta}$, T and ξ.

The structural viscosity and the thixotropy may be understood on the basis of the above formulation. In the first place, the apparent viscosity, η', which is measured experimentally, is defined as:

$$\tilde{P}_{\alpha\beta} = \tilde{P}_{\alpha\beta}^{\mathrm{def}} + \tilde{P}_{\alpha\beta}^{\mathrm{des}} = -\eta'\frac{\mathrm{d}\tilde{\varepsilon}_{\alpha\beta}}{\mathrm{d}t} \tag{20}$$

This quantity is expressed from Eqs. 15, 17 and 20 as:

$$\eta' = \eta + \zeta\left(\frac{\mathrm{d}\xi}{\mathrm{d}t}\right)\Big/\left(\frac{\mathrm{d}\tilde{\varepsilon}_{\alpha\beta}}{\mathrm{d}t}\right) \tag{21}$$

It should be noted that the ordinary viscosity, η, is not dependent on the rate of shear, $\mathrm{d}\tilde{\varepsilon}_{\alpha\beta}/\mathrm{d}t$, but is dependent on T and ξ. These formulations explain most of the viscous behavior of the fluids with internal structures.

When the internal structure is built up by deformation, i. e., $(\mathrm{d}\xi/\mathrm{d}\tilde{\varepsilon}_{\alpha\beta})>0$, the fluid exhibits the non-Newtonian viscosity of shear-rate hardening, i. e., $\eta'>\eta$. On the contrary, when the internal structure is broken down by deformation, i. e., $(\mathrm{d}\xi/\mathrm{d}\tilde{\varepsilon}_{\alpha\beta})<0$, the fluid exhibits the non-Newtonian viscosity of shear-rate softening, i. e., $\eta'<\eta$. When $\tilde{P}_{\alpha\beta}$, therefore $\tilde{\varepsilon}_{\alpha\beta}$, is very high, the internal structure of the fluids is broken down completely; then

$$(\mathrm{d}\xi/\mathrm{d}\tilde{\varepsilon}_{\alpha\beta})\tilde{P}_{\alpha\beta}\to\infty \to 0, \quad \eta'=\eta \tag{22}$$

and the apparent viscosity becomes identical with the ordinary viscosity.

It should be noted that we have been considering the case in which the time-scale of the rate of change in the internal structure is sufficiently small compared to that of observation.

When the rate of change in the internal structure is comparable to or higher than the time-scale of observation, we observe a time-dependent behavior. This is the case when the thixotropic behavior takes place.

The Characterization of Thixotropic Fluids. —The simplest behavior of thixotropy is observed when the internal structure is destroyed instantaneously when force is applied, followed by stationary deformation and recovery, but the recovery of the structure into the stationary state is so slow sufficiently as not to be detected experimentally. This behavior is represented schematically in Fig. 1.

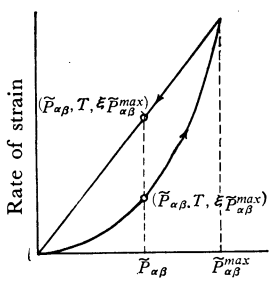

Fig. 1. A schematic plot of a simplest thixotropic behavior.

The up-curve of this figure is in the stationary state. The state variables of this fluid are $\tilde{P}_{\alpha\beta}$, T and ξ, and the following condition is required for the affinity of the change in the internal structure in the stationary thixotropic state from the theorem of minimum entropy production;[6]

$$\frac{\mathrm{d}}{\mathrm{d}t}\tilde{P}_{\alpha\beta}^{\mathrm{des}}(\tilde{P}_{\alpha\beta}, T, \xi) = 0 \tag{23}$$

By this equation the degree of internal freedom, ξ, is determined uniquely by $\tilde{P}_{\alpha\beta}$ and T.

From this consideration, it is clear that the state

6) I. Prigogine, "Introduction to Thermodynamics of Irreversible Processes," 2nd. Ed., Interscience Publishers, New York (1961).

of the up-curve in Fig. 1 is stationary and that it is specified with the two variables of the three state variables, $\tilde{P}_{\alpha\beta}$, T and ξ. On the other hand, the state of the down-curve of Fig. 1 is not stationary. Since Eq. 23 does not hold in a non-stationary state, this state is specified by all three variables. That is, in the above case, the up-curve state is in $(P_{\alpha\beta}, T, \xi_{\tilde{P}_{\alpha\beta}})$ and the down-curve state is in $(\tilde{P}_{\alpha\beta}, T, \xi_{\tilde{P}_{\alpha\beta}^{max}})$, where $\tilde{P}_{\alpha\beta}^{max}$ is the maximum stress applied to the system.

However, no information is available on the degree of internal freedom in general. In order to overcome this difficulties, let us introduce the fictitious pressure tensor, $\tilde{P}_{\alpha\beta}^{f}$; the fictitious pressure tensor is defined as the pressure tensor at which the non-stationary state of interest becomes the corresponding stationary one; i. e.,

$$\frac{d}{dt}\tilde{P}_{\alpha\beta}^{des}(\tilde{P}_{\alpha\beta}^{f}, T, \xi_{\tilde{P}_{\alpha\beta}^{f}}) = 0 \tag{24}$$

By this relation the fictitious pressure is a function of T and ξ, and the non-stationary state is specified by the two variables, $\tilde{P}_{\alpha\beta}$ and $\tilde{P}_{\alpha\beta}^{f}$. In the above case, the fictitious pressure is $\tilde{P}_{\alpha\beta}^{max}$.

The non-stationary state approaches the stationary one with the lapse of time. At the stationary state, only the flow conjugated with the forces fixed externally remains at a constant value; the other flows vanish, resulting their conjugated forces attaining constant values.[6] If the total force is fixed and the stationary viscous flow is established instantaneously, the system is non-stationary, as with the change in the internal structure. The entropy production of this non-stationary irreversible process is expressed as;

$$\sigma_{\xi}^{s} = \tilde{P}_{\alpha\beta}^{des}\frac{d\xi}{dt} \tag{25}$$

When the system is near to the stationary state, the following linear equation is assumed;

$$\tilde{P}_{\alpha\beta}^{des}(\tilde{P}_{\alpha\beta}, T, \xi) = (\xi - \xi^{f})\left(\frac{\partial \tilde{P}_{\alpha\beta}^{des}}{\partial \xi}\right)_{P_{\alpha\beta}, T}$$

$$= (\tilde{P}_{\alpha\beta} - \tilde{P}_{\alpha\beta}^{f})\left(\frac{\partial \tilde{P}_{\alpha\beta}^{des}}{\partial \tilde{P}_{\alpha\beta}}\right)_{T,\xi} \tag{26}$$

where ξ^{f} is the fictitious degree of internal structure, which is defined by the same consideration as the fictitious pressure tensor. Moreover, the signs of the quantities, $(\partial \tilde{P}_{\alpha\beta}^{des}/\partial\xi)_{\tilde{P}_{\alpha\beta}, T}$ and $(\partial \tilde{P}_{\alpha\beta}^{des}/\partial \tilde{P}_{\alpha\beta})_{T,\xi}$, may be determined by simple consideration as follows:

$$\left(\frac{\partial \tilde{P}_{\alpha\beta}^{des}}{\partial \xi}\right)_{\tilde{P}_{\alpha\beta}, T} < 0, \quad \left(\frac{\partial \tilde{P}_{\alpha\beta}^{des}}{\partial \tilde{P}_{\alpha\beta}}\right)_{T,\xi} < 0 \tag{27}$$

From Eqs. 25 and 26;

$$(\tilde{P}_{\alpha\beta} - \tilde{P}_{\alpha\beta}^{f})\left(\frac{\partial \tilde{P}_{\alpha\beta}^{des}}{\partial \tilde{P}_{\alpha\beta}}\right)_{T,\xi} = \zeta\left(\frac{d\xi}{dt}\right) \tag{28}$$

and, using the equation of total differential;

$$\frac{\partial \tilde{P}_{\alpha\beta}^{des}}{\partial t} =$$

$$\left(\frac{\partial \tilde{P}_{\alpha\beta}^{des}}{\partial \tilde{P}_{\alpha\beta}}\right)_{T,\xi}\frac{d\tilde{P}_{\alpha\beta}^{f}}{dt} + \left(\frac{\partial \tilde{P}_{\alpha\beta}^{des}}{\partial \xi}\right)_{\tilde{P}_{\alpha\beta}, T}\frac{d\xi}{dt} = 0 \tag{29}$$

the equation

$$\frac{d\xi}{dt} = -\left\{\left(\frac{\partial \tilde{P}_{\alpha\beta}^{des}}{\partial \tilde{P}_{\alpha\beta}}\right)_{T,\xi}\Big/\left(\frac{\partial \tilde{P}_{\alpha\beta}^{des}}{\partial \xi}\right)_{\tilde{P}_{\alpha\beta}, T}\right\}\frac{d\tilde{P}_{\alpha\beta}^{f}}{dt} \tag{30}$$

is derived. Equation 28 then becomes

$$\tilde{P}_{\alpha\beta} - \tilde{P}_{\alpha\beta}^{f} = -\left\{\zeta\Big/\left(\frac{\partial \tilde{P}_{\alpha\beta}^{des}}{\partial \xi}\right)_{\tilde{P}_{\alpha\beta}, T}\right\}\frac{d\tilde{P}_{\alpha\beta}^{f}}{dt} \tag{31}$$

By the integration of this equation, the final expression is obtained; that is;

$$\tilde{P}_{\alpha\beta} - \tilde{P}_{\alpha\beta}^{f} = (\tilde{P}_{\alpha\beta} - \tilde{P}_{\alpha\beta}^{fo})\exp(-t/\tau) \tag{32}$$

where the positive coefficient, τ, is defined as;

$$\tau = -\zeta\Big/\left(\frac{\partial \tilde{P}_{\alpha\beta}^{des}}{\partial \xi}\right)_{\tilde{P}_{\alpha\beta}, T} \tag{33}$$

and $\tilde{P}_{\alpha\beta}^{fo}$ is the initial value of the fictitious pressure tensor. As Eq. 32 predicts, the fictitious pressure, $\tilde{P}_{\alpha\beta}^{f}$, approaches the real pressure, $\tilde{P}_{\alpha\beta}$, with the lapse of time. This is a process of the thixotropic recovery.

When the thixotropic recovery takes place and its relaxation time is larger than the time-scale of observation, a complicated behavior is observed, as we see in most of the colloidal suspensions. The above-described treatment can be applied to the interpretation of this behavior. For instance, if the stationary up-curve is obtained with the slow observation and if the measurement at the point A of Fig. 2 is made over the time-interval, Δt, in order to obtain the down-curve, the fictitious pressure changes from the initial value, $\tilde{P}_{\alpha\beta}^{max}$, to:

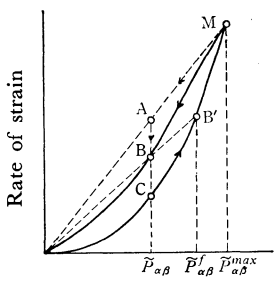

Fig. 2. Analysis of a flow curve of the thixotropic fluid.

$$\tilde{P}^{f}_{\alpha\beta}=\tilde{P}_{\alpha\beta}-(\tilde{P}_{\alpha\beta}-\tilde{P}^{max}_{\alpha\beta})\exp(-\Delta t/\tau) \quad (34)$$

after the lapse of time Δt. Points A, B, B' and C of this figure are specified by:

Point A, $\frac{d}{dt}\tilde{P}^{des}_{\alpha\beta}(\tilde{P}_{\alpha\beta}, T, \xi_{\tilde{P}^{max}_{\alpha\beta}})\neq 0$,

Point B, $\frac{d}{dt}\tilde{P}^{des}_{\alpha\beta}(\tilde{P}_{\alpha\beta}, T, \xi_{\tilde{P}^{f}_{\alpha\beta}})\neq 0$,

Point B', $\frac{d}{dt}\tilde{P}^{des}_{\alpha\beta}(\tilde{P}^{f}_{\alpha\beta}, T, \xi_{\tilde{P}^{f}_{\alpha\beta}})=0$, and

Point C, $\frac{d}{dt}\tilde{P}^{des}_{\alpha\beta}(\tilde{P}_{\alpha\beta}, T, \xi_{\tilde{P}_{\alpha\beta}})=0$

That is to say, Point B, which is measured by the experimental procedure, can be predicted by the fact that Point B' is at the fictitious pressure, $\tilde{P}^{f}_{\alpha\beta}$, on the stationary up-curve and that Point B is at the pressure, $\tilde{P}_{\alpha\beta}$, on the straight line, OB'.

If the recovery of the thixotropic structure is very fast and if the pressure is lower than $\tilde{P}_{\alpha\beta}$ before the measurement at $\tilde{P}_{\alpha\beta}$, the apparent negative thixotropy may be observed. The real negative thixotropy can, however, be observed only when $(\partial\xi/\partial\tilde{P}^{des}_{\alpha\beta})_T>0$. To this case the above treatment can be applied also. More generally, there may happen this behavior in case where the rate process occurs by the procedure of the up-curve measurement. The above treatment may easily be extended for such a case.

An Analysis of the Experimental Results and Discussion—Many efforts have been made by many researchers to elucidate thixotropic behavior. Although concrete discussions have been given for the mechanism of the thixotropic breakdown and recovery in some cases, a full quantitative description has not yet been successful. Of the researchers, Green and Weltmann made the most extensive study.[7,8] They proposed the hysteresis curve method for the characterization of thixotropic behaviors. However their experimental parameter is selected arbitrarily, and the comparison of the thixotropic behaviors of various samples is possible only under limited conditions; that is, their work is principally practical. In order to get a better description, Mooney,[9] Alfrey and Rodewald,[10] and Rehbinder[11] undertook to record the time-dependent shear-rate at a fixed shearing stress in order to characterize the thixotropic behaviors. By these studies, the thixotropic behavior is described by well-defined parameters, but their work has not had a general basis for the refined treatment.

The theoretical work described above provides a plausible basis for these studies. For example,

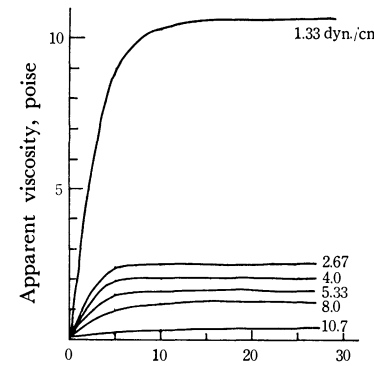

Fig. 3. Recovery curves of a suspension of a compounded rubber latex by Mooney.[9]

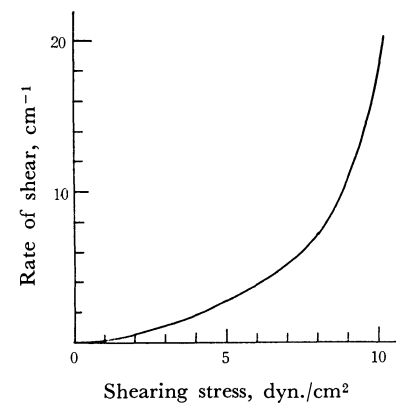

Fig. 4. The stationary curve of the rate of shear against the shearing stress of the latex suspension.

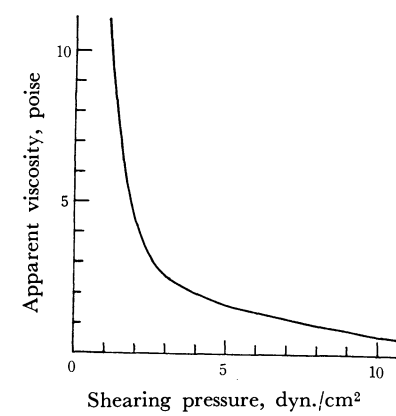

Fig. 5. Apparent viscosity vs. shearing pressure curve at the stationary flow.

7) R. N. Weltmann, *J. Appl. Phys.*, **14**, 343 (1943); H. Green and R. N. Weltmann, ibid., **15**, 414 (1944); *Ind. Eng. Chem., Anal. Ed.*, **15**, 201 (1943); **18**, 167 (1946).
8) H. Green, "Industrial Rheology and Rheological Structures," John Wiley & Sons, New York (1949).
9) M. Mooney, *J. Colloid Sci.*, **1**, 195 (1946).
10) T. Alfrey, Jr., and C. W. Rodewald, ibid., **4**, 283 (1949).
11) P. Rehbinder, *Discussions Faraday Soc.*, **18**, 151 (1954).

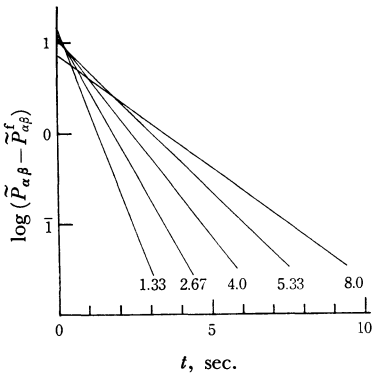

Fig. 6. Verification of the prediction of Eq. 32 using Mooney's data.

Mooney's work may be analyzed by this treatment as follows. Mooney measured the apparent viscosity of a suspension of a compounded rubber latex, the internal structure of which had been broken down completely beforehand, as a function of settling time at fixed shearing stresses; he thus obtained the results reproduced in Fig. 3. From this data the stationary shearing stress is drawn against the rate of shear in Fig. 4, while the apparent viscosity is replotted in Fig. 5.

When the fluid, the internal structure of which has been broken down completely, is fixed at a fixed shearing stress lower than that necessary for the complete destruction, the system is initially in the non-stationary state and approaches the stationary state. This non-stationary state is specified by the real and the fictitious shearing stress described in the preceding sections. The fictitious shearing stress is a function of the time at a constant shearing stress and becomes the real shearing stress as the time becomes infinite. The fictitious shearing stress is determined from the stationary stress vs. rate of shear curve as a value of the shearing stress at the corresponding value of the apparent viscosity or the rate of shear. The values calculated by this procedure are shown on the logarithmic scale against the time. This curve obeys to the prediction of Eq. 32, with the parameter, τ, varying with the stress; this is reasonable considering its definition given by Eq. 33.

From this treatment, all the stress vs. rate of shear curves may be constructed from the stationary curve and the parameter of the rate process of the thixotropic recovery. Green and Weltmann's hysteresis curve is also included in these curves.

In this treatment the fluids are assumed to be ideally viscous. Actually, the thixotropic fluids have yield values in most cases, as Freundlich first noted. This fluid may be treated by introducing the principle of relaxability in small proposed by Eckart[12] and by Kluitenberg[4]. However, this treatment is omitted here, for the extension of the present treatment to such a substances results in complicated expressions.

Lastly, it should be noted that the effect of the temperature on the thixotropic behavior is significant in most cases, as Lower, Walker and Zettlemoyer have already pointed out.[13] This effect is considered precisely in such fundamental equations as Eq. 19. However, no detailed discussions can be made here because of the lack of experimental data.

12) C. Eckart, *Phys. Rev.*, **73**, 373 (1948).
13) G. Lower, W. C. Walker and A. C. Zettlemoyer, *J. Colloid Sci.*, **8**, 116 (1953).

BULLETIN OF THE CHEMICAL SOCIETY OF JAPAN VOL. 39 1406—1409 (1966)

The Application of the Molecular Orbital Theory to the Bond Scission of Aliphatic Amines*

By Kozo HIROTA

Faculty of Science, Osaka University, Toyonaka, Osaka and Institute for Protein Research, Osaka University, Joan-cho, Kita-ku, Osaka

and Michiyasu ITOH

Institute for Protein Research, Osaka University, Joan-cho, Kitaku, Osaka

(Received November 8, 1965)

The relative scission-probabilities of C–C bonds of *n*-propyl, *n*-butyl and isobutyl amines being formed by electron impact (90 V.) were determined by the use of mass spectrometers of the usual type and of the high-resolution type. They were in good accordance with the theoretical values calculated by the LCBO-MO theory which had been proposed and found successful in explaining the mass spectra of *n*-paraffins and methyl alkyl ketones.

It was proposed by Thompson,[1] with regard to the mass spectrum of normal octane, that the relative amount of the abundant ions could be given theoretically if the "scission probability" of each C–C bond in the parent ion were assumed to be proportional to the electron density at the bond on the highest occupied molecular orbital (MO) of a starting molecule, and if the MO were expressed by the linear combination of the bond-orbitals (LCBO). Such a molecular orbital theory could be applied successfully to the relative abundance of the ions produced by several normal paraffins[2] (C_4H_{10}—$C_{10}H_{22}$) and by several methyl alkyl ketones[3]. Nevertheless, the application of this LCBO theory to the other paraffins higher than decane has not proved satisfactorily. This is the reason why there are some objections[4] to this theory, though its application to the evaluation of ionization potentials is generally admitted. The above discordance can, however, be explained by introducing the multiple scission of bonds in the parent ions of large carbon numbers.

The point of criticism on the theory may lie, rather, in a new assumption, one which is quite different from that of the statistical theory of Rosenstock et al.[5] According to this assumption, even the good coincidence may seem to be fortuitous, especially in the cases of ketones which contain lone-pair and π-bonding electrons as well as σ-bonding electrons in the molecules. On the other hand, the scission of the bonds determined by comparing the spectra of ketones labeled with deuterium may arouse some doubt about using them as the experimental data to be compared, because the transposition of deuterium is possible during the process of fragmentation. If it occured markedly, the above comparison would be of little meaning.

It is the object of the present paper to extend the applicability of the theory to the calculation of the relative abundance of ions produced from *n*-propyl (*n*-PA), *n*-butyl (*n*-BA) and isobutyl amines (*i*-BA), using mass spectrometers of the high-resolution type as well as of the usual type, in order to clarify the ambiguity of the assignment of the ion produced.

Experimental

Mass spectra with usual resolutions were obtained with a Hitachi RMU-5B apparatus (magnetic scanning type), with a bombarding electron beam of 90 V. These data, shown in Table I, indicate that the peaks resulting from the scission of the C–N bond are negligible. However, some of the peaks (indicated by asterisks in Table I) (m/e=15, 27, 28, 29, 41, 42, 43) could not be assigned in the cases of *n*-BA and *i*-BA by these spectra alone; e. g., each of the seven peaks corresponding to different fragmentations is described in the third and the fourth columns of Table II. Therefore, for the sake of determining the probability of bond-scission, their ratios (A/B) were determined by their relative peak height in the spectra of the high-resolution type. They were obtained with a Hitachi PMU-7Hr apparatus. Its resolution is at least 5000 at m/e=28. However, it was found unnecessary to make such an allocation in the case of propylamine, so the spectrum of this amine was not measured. The results for the two butylamines are shown in Table II; they were obtained also with a bombarding electron beam of 90 V. The ratio was determined by opening the collector slit so that both tops of the peak to be compared become flat; the mean value for three runs was used.

Assuming the peak-ratio thus obtained to be the same as that in the usual spectra (shown in Table I),

Table I. Relative intensity of main peaks in the mass spectra of the amines[a]

m/e	Assignment	*n*-$C_3H_7NH_2$	*n*-$C_4H_9NH_2$	*i*-$C_4H_9NH_2$
15	*	3.7	2.4	3.1
27	*	8.1	6.0	5.9
28	*	16.5	8.2	11.2
29	*	4.6	3.8	4.9
30	CNH_4	100	100	100
31	CNH_5	11.3	7.4	17.5
41	*	5.9	4.3	7.3
42	*	3.9	2.4	2.7
43	*	2.8	1.8	2.8
44	C_2NH_6	1.7	2.6	3.7
45	C_2NH_7	0.6	0.7	1.1
58	C_3NH_8	2.1	1.9	4.3
59	C_3NH_9	9.5	0.3	0.9
72	C_4NH_{10}	—	0.9	1.5
73	C_4NH_{11}	—	6.8	8.4

a) Measured by H. Otouma, K. Fueki and M. Hatada.

Table II. The ratio of the peak heights of the ions whose m/e ratios are the same

C_i	m/e	Possible ions A	Possible ions B	A/B *n*-$C_4H_9NH_2$	A/B *i*-$C_4H_9NH_2$
C_1	15	CH_3	NH_2	∞	∞
C_2	27	C_2H_3	CNH	17.7	14.0
	28	C_2H_4	CNH_2	0.13	0.56
	29	C_2H_5	CNH_3	1.09	1.63
C_3	41	C_3H_5	C_2NH_3	5.55	31.8
	42	C_3H_6	C_2NH_4	0.042	0.18
	43	C_3H_7	C_2NH_5	0.26	1.11

* Part V of a series on the molecular orbital theory of mass spectra. Parts II, III and IV are listed in Ref. 3.

1) R. Thompson, "Applied Mass Spectrometry," Inst. of Petroleum, London (1953), p. 154.
2) K. Fueki and K. Hirota, *J. Chem. Soc. Japan, Pure Chem. Sect.*, (*Nippon Kagaku Zasshi*), **81**, 212 (1960).
3) M. Hatada and K. Hirota, This Bulletin, **38**, 599 (1965); *Z. physik. Chem. N. F.*, **44**, 328 (1965); *J. Chem. Soc. Japan, Pure Chem. Sect.*, (*Nippon Kagaku Zasshi*), **86**, 307 (1965).
4) N. D. Coggeshall, *J. Chem. Phys.*, **33**, 1247 (1960); S. Meyerson, ibid., *J. Chem. Phys.*, **42**, 2181 (1965).
5) H. M. Rosenstock, M. B. Wallenstein, A. L. Wahrhaftig, and H. Eyring, *Proc. Natl. Acad. Sci.*, **38**, 667 (1952).

the percentages of all the ions concerned are allotted in Table II.

It is noteworthy that the ions produced by the scission of the C–N bond could not be found in both butyl amines; e. g., the ions containing nitrogen (N, NH, NH_2) and those corresponding to C_4H_9, C_4H_8 and C_4H_7 were not observed actually in the case of *n*-butylamine. This is the reason why propyl amine was not subjected to mass spectrometry of the high-resolution type. By combining the other data in Table I with Table II, the relative abundance of all the ions can be obtained to be as shown in Table III.

The relative probabilities of the scission of bonds can be determined from the data in Tables I and III, so a comparison of the theoretical values with the experimental ones becomes possible.

Table III. Relative intensities of ions produced from the amines

m/e	Ions	*n*-$C_3H_7NH_2$	*n*-$C_4H_9NH_2$	*i*-$C_4H_9NH_2$
15	CH_3	3.7	2.4	3.1
	NH	0	0	0
27	C_2H_3	8.1[a]	5.7	5.5
	CNH		0.3	0.4
28	C_2H_4	16.5[a]	1.0	0.6
	CNH_2		7.2	10.6
29	C_2H_5	4.6[a]	2.0	1.9
	CNH_3		1.8	3.0
41	C_3H_5	—	3.7	7.1
	C_2NH_3	5.9	0.6	0.2
42	C_3H_6	—	0.1	0.4
	C_2NH_4	3.9	2.3	2.3
43	C_3H_7	—	0.4	1.5
	C_2NH_5	2.8	1.4	1.3

a) The sums of both ions are listed, but they can be estimated to belong mainly to hydrocarbon ions, as is explained in the text.

LCBO-MO Theory

In the case of ethyl alkyl ketone,[3] the bond orbitals of C–C and C=O bonds were calculated under the assumption that CH_2 and CH_3 were united atoms, because the electron density of the C–C bond was practically the same in the case of paraffins whether it was calculated with the united atom approximation[6] or with a more rigorous treatment[7]. Besides, a mutual interaction between only the neighboring bond-orbitals was taken into consideration in both the above papers, as is usually done generally in simple LCAO-MO theory.

These approximations were also adopted in the present paper, regarding NH_2 as a united atom as well as CH, CH_2, and CH_3; e. g.,

n-Propyl amine (*n*-PA): $CH_3\overset{2}{-}CH_2\overset{1}{-}CH_2\overset{0}{-}NH_2$

n-Butyl amine (*n*-BA): $CH_3\overset{3}{-}CH_2\overset{2}{-}CH_2\overset{1}{-}CH_2\overset{0}{-}NH_2$

Isobutyl amine (*i*-BA): $\begin{matrix}CH_3\overset{3}{}\\ CH_3\overset{3}{}\end{matrix}\!\!>\!\overset{2}{CH}\overset{1}{-}CH_2\overset{0}{-}NH_2$

The numbering of each bond-orbital, i, will be indicated by the numerals attached to the bond shown above.

Table IV shows the Coulomb (α) and exchange (β) integrals necessary to solve the secular equation for each molecule: $[e_{ij}-\delta_{ij}E]=0$, where e_{ij} equals α or β, according as $i=j$ or $i\neq j$, the suffix N denotes the integrals concerning the nitrogen atom.

Table IV. Explanation of integrals.

	$\overset{i}{C-C}$	$\overset{i+1}{C-C}$	$\overset{0}{C-N}$
$\overset{i}{C-C}$	α	β	β_N
$\overset{i+1}{C-C}$	β	α	0
C—N	β_N	0	α_N

Among these integrals, α and β were taken to be -13.75 V., and -1.80 V. respectively from Fueki's values,[8] which were determined in the evaluation of the ionization potential of saturated hydrocarbons. The values of α_N and β_N were determined by solving the secular equations for *n*-ethylamine and *n*-butylamine, so that they satisfy their observed ionization potentials, 9.26 and 9.19 V. respectively. The values thus obtained were $\alpha_N=-9.60$ V. and $\beta_N=-1.24$ V.

The necessary electron density can be calculated by the squares of the coefficient, C_i, in the wave function of the highest-occupied orbital, $\Psi=\sum_i c_i\phi_i$.

Results

For the sake of comparison, the calculated ionization potentials for *n*-PA and *i*-BA are shown in Table V, along with the observed values. Though the accuracy of the observed values is not very good, the tendency for the ionization potential to decrease with a decrease in the carbon number is shown by the calculated values in Table V.

Table V. Calculated and observed I.P. values of the amines

	Observed		Calculated
$C_2H_5NH_2$	9.32[9]	9.19[10]	(9.26)
n-$C_3H_7NH_2$	9.17[9]		9.20
n-C_4H_9NH	9.19[9]		(9.19)
i-$C_4H_9NH_2$	9.00[9]		9.17

N.B. The values in parentheses are used for the calculation.

The squares of the coefficient, C_i, of the *i*th bond orbital in the highest occupied MO concerned are shown in Table VI. In Table VI, case I or II

6) G. R. Lester, "Advanc. Mass Spectrometry", Proc. Conf. Univ. London, (1958) **1**, 287 (1959).
7) G. G. Hall, *Proc. Roy. Soc.*, **A205**, 541 (1951); *Trans. Faraday Soc.*, **49**, 113 (1953).
8) K. Fueki, *J. Phys. Chem.*, **68**, 2656 (1964).
9) J. D. Morrison and A. J. Nicholson, *J. Chem. Phys.*, **20**, 1021 (1952).
10) J. Collin, *Can. J. Chem.*, **37**, 1053 (1059).

represents, respectively when the coefficient of the C–N bond is taken into calculation or when it is not. The values are normalized, in both cases. Since the scission of the C–N bond can be neglected because of the small peaks resulting from its scission, as has been mentioned already, it is unnecessary to consider the electron density at the C–N bond; however, some discussion is desirable and will, therefore, be given. Thus, the case II was used in the comparison of the observed probability with the calculated probability.

Table VI. Square of the C_i's

Bond number		0	1	2	3
n-$C_3H_7NH_2$	obs.	—	88.3	11.7	—
	I	89.26	9.29	1.45	—
	II	—	86.5	13.5	—
n-$C_4H_9NH_2$	obs.	—	85.3	12.5	3.2
	I	87.95	9.62	2.10	0.33
	II	—	79.8	17.4	2.7
i-$C_4H_9NH_2$	obs.[a]	—	87.7	6.15	6.15
	I	87.77	10.55	0.84	0.84
	II	—	86.5	6.75	6.75

a) The contributions of peaks produced by two bond-scissions are not included.

In previous papers[3] the experimental probability of each bond-scission was discussed by comparing the spectrum of ketones with that of the corresponding deuterated species. Similarly, three amines were compared, as is shown in Fig. 1; the degree of coincidence is the same as that in the case of ketones. This result supports the method of research adopted for ketones.

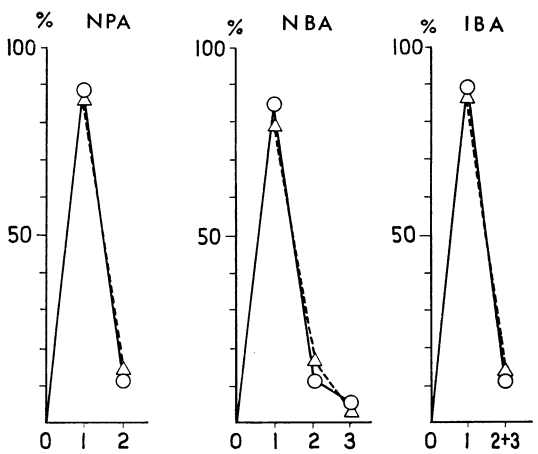

Fig. 1. Bond-scission probability and positive charge distribution.
○——○ : Experimental
△----△ : Theoretical

Discussion

We may now discuss why the adoption of the case II is more justified than that of the case I; i. e., this choice means that only the scission probability of the C–C bond can be considered, with no regard to that of the C–N bond. The same criticism may be given concerning the stability of the C=O bond in the case of alkyl-methyl ketones.

From the standpoint of the rate theory, the scission probability would be proportional to the specific rate, k, which is expressed by the Arrhenius formula:

$$k = X\exp(-E_a/\boldsymbol{R}T) \qquad (2)$$

In the cases of comparisons between the same bonds, e. g., C–C, the activation energy, E_a, will be the same. The difference in the scission probability in the case of paraffins is, therefore, determined only by the pre-exponential factor, X. On the other hand, the difference may depend also on E_a in the comparison of scission probabilities between different bonds. This is the reason why fragment ions produced by the scission of C–H and C–N bonds are, respectively smaller and very much smaller, than those produced by the scission of the C–C bond.

Now, as has often been done, the bond energy may be assumed to be proportional to the E_a value, if the potential curves of the bonds have the same shape. This first approximation seems successful as far as C–C (ca. 80 kcal.), C–H (ca. 100 kcal.) and C=O (>127 kcal.) are concerned, because the scission probability decreases in this order: C–C>C–H>C=O.

However, this approximation does not hold well if the C–N bond is considered, because its bond energy is nearly equal to or even smaller than that of the C–C bond. Considering this, the shape of the potential curve of the C–N bond may be quite different from that of the other bonds.

In conclusion, it seems promising to apply the present LCBO-MO theory on mass spectra to substances of kinds other than paraffins, though the theory is completely different in standpoint from the usual statistical theory of Rosenstock et al.[5] However, some assumptions will be necessary in using the theory so as to be able to predict which fragment will be charged after the scission of a bond.

We wish to express our deep thanks to Dr. M. Hatada for his help in this research.

This paper is dedicated to Professor Masao Kotani, the University of Tokyo, in celebration of his 60th birthday.

BULLETIN OF THE CHEMICAL SOCIETY OF JAPAN VOL. 39 1410—1414 (1966)

Vibrational Frequencies and Normal Coordinates: Their Relationship to Force Constants and Inertial Coefficients

By Tatsuo MIYAZAWA

Institute for Protein Research, Osaka University, Kita-ku, Osaka

and John OVEREND

Molecular Spectroscopy Laboratory, Department of Chemistry, University of Minnesota, Minneapolis, Minnesota 55455, U. S. A.

(Received November 11, 1965)

Small variations in the $\boldsymbol{G}$ and $\boldsymbol{F}$ matrices can be related linearly to variations in the calculated frequencies and normal coordinates through a transformation matrix, $\boldsymbol{J}$. Explicit expressions are given for the elements of $\boldsymbol{J}$ and $\boldsymbol{J}^{-1}$. Isotope effects on normal-coordinate coefficients are also treated.

In the harmonic-oscillator theory of molecular vibrations, the molecular variables (the frequency parameters, $\lambda_a = 4\pi^2c^2\nu_a^2$, and the normal-coordinate coefficients, L_{ia}) are determined completely by the parameters of the model (the elements of the $\boldsymbol{G}$ and $\boldsymbol{F}$ matrices in Wilson's notation[1]) and vice versa, through the equations:

$$\boldsymbol{G} = \boldsymbol{L}\tilde{\boldsymbol{L}} \tag{1}$$

and

$$\boldsymbol{\Lambda} = \tilde{\boldsymbol{L}}\boldsymbol{F}\boldsymbol{L} \tag{2a}$$

or

$$\boldsymbol{F} = \tilde{\boldsymbol{L}}^{-1}\boldsymbol{\Lambda}\boldsymbol{L}^{-1} \tag{2b}$$

In the general case, in which the molecule has n vibrational degrees of freedom, there are n frequency parameters and n^2 normal-coordinate coefficients, making a total of $n(n+1)$. Since $\boldsymbol{G}$ and $\boldsymbol{F}$ are symmetric, each has $n(n+1)/2$ independent elements— a total of $n(n+1)$. Thus there should be, in general, $n(n+1)$ relationships between the $[\boldsymbol{G}, \boldsymbol{F}]$ and $[\boldsymbol{\Lambda}, \boldsymbol{L}]$ elements present in Eqs. 1 and 2. Although these relationships are nonlinear, small variations in $\boldsymbol{\Lambda}$ and $\boldsymbol{L}$ can be interpreted in terms of small changes in $\boldsymbol{G}$ and $\boldsymbol{F}$ through a linear transformation:

$$[\Delta\boldsymbol{\Lambda}, \Delta\boldsymbol{L}] = \boldsymbol{J}[\Delta\boldsymbol{G}, \Delta\boldsymbol{F}]$$

Similarly, small changes in $\boldsymbol{G}$ and $\boldsymbol{F}$ can be related to small changes in $\boldsymbol{\Lambda}$ and $\boldsymbol{L}$ through the reverse transformation:

$$[\Delta\boldsymbol{G}, \Delta\boldsymbol{F}] = \boldsymbol{J}^{-1}[\Delta\boldsymbol{\Lambda}, \Delta\boldsymbol{L}]$$

These transformations, $\boldsymbol{J}$ and $\boldsymbol{J}^{-1}$, can be written as square matrices, the elements of which are the partial derivatives $\partial[\boldsymbol{\Lambda}, \boldsymbol{L}]/\partial[\boldsymbol{G}, \boldsymbol{F}]$ and $\partial[\boldsymbol{G}, \boldsymbol{F}]/\partial[\boldsymbol{\Lambda}, \boldsymbol{L}]$ respectively. The purpose of this paper is to present the algebraic form of these two transformations and to show that each is, in fact, the inverse of the other.

Parts of the $\boldsymbol{J}$ matrix are well known, and their utility has been well established.[2,3] However, the $\boldsymbol{J}$ transformation from $\Delta\boldsymbol{G}$ to $\Delta\boldsymbol{L}$ or the $\boldsymbol{J}^{-1}$ transformation have not previously been described and, as far as we know, the existence of the inverse relationship has not been pointed out.

We will follow current practice and cast the problem in the form of the first-order perturbation theory. Consider the small perturbations $\boldsymbol{G}_1$ and $\boldsymbol{F}_1$ such that:

$$\boldsymbol{G} = \boldsymbol{G}_0 + \boldsymbol{G}_1 \tag{3}$$

and

$$\boldsymbol{F} = \boldsymbol{F}_0 + \boldsymbol{F}_1 \tag{4}$$

These will result in corresponding perturbations in $\boldsymbol{\Lambda}$ and $\boldsymbol{L}$:

$$\boldsymbol{\Lambda} = \boldsymbol{\Lambda}_0 + \boldsymbol{\Lambda}_1 \tag{5}$$

$$\boldsymbol{L} = \boldsymbol{L}_0 + \boldsymbol{L}_1 = \boldsymbol{L}_0(\boldsymbol{E} - \boldsymbol{P}) \tag{6}$$

where $\boldsymbol{E}$ is the unit matrix.[3] It then follows that

$$\boldsymbol{L}^{-1} = \boldsymbol{L}_0^{-1} + \boldsymbol{L}_1^{-1} = (\boldsymbol{E} + \boldsymbol{P})\boldsymbol{L}_0^{-1} \tag{7}$$

From Eqs. 1 and 6, neglecting higher order terms;

$$\boldsymbol{G}_0 + \boldsymbol{G}_1 = \boldsymbol{L}_0(\boldsymbol{E} - \boldsymbol{P})(\boldsymbol{E} - \tilde{\boldsymbol{P}})\tilde{\boldsymbol{L}}_0 \tag{8}$$

whence:

$$\boldsymbol{G}_1 = -\boldsymbol{L}_0(\boldsymbol{P} + \tilde{\boldsymbol{P}})\tilde{\boldsymbol{L}}_0 \tag{9}$$

1) E. B. Wilson, Jr., J. C. Decius and P. C. Cross, "Molecular Vibrations," McGraw Hill Book Company, New York (1955).

2) T. Miyazawa, *J. Chem. Soc. Japan, Pure Chem. Sect.* (*Nippon Kagaku Zasshi*), **76**, 1132 (1955); W. T. King, I. M. Mills and B. L. Crawford, Jr., *J. Chem. Phys.*, **27**, 455 (1957).

3) I. Nakagawa and T. Shimanouchi, *J. Chem. Soc. Japan, Pure Chem. Sect.* (*Nippon Kagaku Zasshi*), **80**, 128 (1959). The notation in Eqs. 6 and 7 follows theirs.

or, by rearranging:

$$\boldsymbol{L}_0^{-1}\boldsymbol{G}_1\tilde{\boldsymbol{L}}_0^{-1} = -(\boldsymbol{P}+\tilde{\boldsymbol{P}}) \tag{10}$$

Similarly, from Eqs. 2a and 6:

$$\boldsymbol{\Lambda}_0 + \boldsymbol{\Lambda}_1 = (\tilde{\boldsymbol{L}}_0 - \tilde{\boldsymbol{P}}\tilde{\boldsymbol{L}}_0)(\boldsymbol{F}_0+\boldsymbol{F}_1)(\boldsymbol{L}_0 - \boldsymbol{L}_0\boldsymbol{P}) \tag{11}$$

whence:

$$\boldsymbol{\Lambda}_1 = \tilde{\boldsymbol{L}}_0\boldsymbol{F}_1\boldsymbol{L}_0 - (\tilde{\boldsymbol{P}}\boldsymbol{\Lambda}_0 + \boldsymbol{\Lambda}_0\boldsymbol{P}) \tag{12}$$

or

$$\boldsymbol{F}_1 = \tilde{\boldsymbol{L}}_0^{-1}\boldsymbol{\Lambda}_1\boldsymbol{L}_0^{-1} + \tilde{\boldsymbol{L}}_0^{-1}(\tilde{\boldsymbol{P}}\boldsymbol{\Lambda}_0 + \boldsymbol{\Lambda}_0\boldsymbol{P})\boldsymbol{L}_0^{-1} \tag{13}$$

As has been suggested by Nakagawa and Shimanouchi,[3] the transformation is more usefully expressed with respect to $\boldsymbol{P}$ rather than to $\boldsymbol{L}$; therefore, the transformations have been redefined accordingly:

$$[\Delta\boldsymbol{\Lambda},\ \boldsymbol{P}] = \boldsymbol{J}[\Delta\boldsymbol{G},\ \Delta\boldsymbol{F}]$$

and

$$[\Delta\boldsymbol{G},\ \Delta\boldsymbol{F}] = \boldsymbol{J}^{-1}[\Delta\boldsymbol{\Lambda},\ \boldsymbol{P}]$$

The elements of $\boldsymbol{J}^{-1}$ are then obtained from Eqs. 9 and 13. In designating matrix elements by a double subscript, we follow convention and write the row index first and the column index second. The $i, j, k, \cdots$ indices refer to internal coordinates, while the $a, b, c, \cdots$ indices refer to normal coordinates.

$$\partial G_{ij}/\partial\lambda_a = 0 \tag{14}$$

$$\partial G_{ij}/\partial P_{ab} = \partial G_{ij}/\partial P_{ba} = -(L_{ia}L_{jb} + L_{ib}L_{ja}) \tag{15}$$

$$\partial F_{ij}/\partial\lambda_a = L_{ai}^{-1}L_{aj}^{-1} \tag{16}$$

$$\partial F_{ij}/\partial P_{ab} = \lambda_a(L_{ai}^{-1}L_{bj}^{-1} + L_{bi}^{-1}L_{aj}^{-1}) \tag{17}$$

$$(\partial F_{ij}/\partial P_{ba})/\lambda_b = (\partial F_{ij}/\partial P_{ab})/\lambda_a \tag{18}$$

Equations 14—18 complete the elements of $\boldsymbol{J}^{-1}$.

To determine the elements of $\boldsymbol{J}$, we require $\boldsymbol{\Lambda}$ and $\boldsymbol{P}$ to be explicit functions of $\boldsymbol{G}$ and $\boldsymbol{F}$. It is important to recognize that $\boldsymbol{P}$ is, through Eqs. 10 and 12, a function of $\boldsymbol{G}_1$ and $\boldsymbol{F}_1$. From the diagonal elements of Eq. 12:

$$(\boldsymbol{\Lambda}_1)_{aa} = (\tilde{\boldsymbol{L}}_0\boldsymbol{F}_1\boldsymbol{L}_0)_{aa} - (P_{aa}\Lambda_{aa} + \Lambda_{aa}P_{aa}) \tag{19}$$

From Eq. 10:

$$(\boldsymbol{L}_0^{-1}\boldsymbol{G}_1\tilde{\boldsymbol{L}}_0^{-1})_{aa} = -2\boldsymbol{P}_{aa} \tag{20}$$

and, by combining Eqs. 19 and 20:

$$(\boldsymbol{\Lambda}_1)_{aa} = (\tilde{\boldsymbol{L}}_0\boldsymbol{F}_1\boldsymbol{L}_0)_{aa} + \lambda_a(\boldsymbol{L}_0^{-1}\boldsymbol{G}_1\tilde{\boldsymbol{L}}_0^{-1})_{aa} \tag{21}$$

from which:

$$\partial\lambda_a/\partial G_{ij} = 2\lambda_a L_{ai}^{-1}L_{aj}^{-1} \tag{22}$$

$$\partial\lambda_a/\partial G_{ii} = \lambda_a(L_{ai}^{-1})^2 \tag{23}$$

$$\partial\lambda_a/\partial F_{ij} = 2L_{ia}L_{ja} \tag{24}$$

and

$$\partial\lambda_a/\partial F_{ii} = (L_{ia})^2 \tag{25}$$

The expression for P_{ab} as an explicit function of $\boldsymbol{G}$ and $\boldsymbol{F}$ follows from the off-diagonal elements of Eqs. 10 and 12:

$$-(P_{ab} + P_{ba}) = (\boldsymbol{L}_0^{-1}\boldsymbol{G}_1\tilde{\boldsymbol{L}}_0^{-1})_{ab} \tag{26}$$

and

$$P_{ba}\lambda_b + \lambda_a P_{ab} = (\tilde{\boldsymbol{L}}_0\boldsymbol{F}_1\boldsymbol{L}_0)_{ab} \tag{27}$$

By multiplying Eq. 26 by λ_b and by adding Eq. 27:

$$P_{ab}(\lambda_a - \lambda_b) = (\tilde{\boldsymbol{L}}_0\boldsymbol{F}_1\boldsymbol{L}_0)_{ab} + \lambda_b(\boldsymbol{L}_0^{-1}\boldsymbol{G}_1\tilde{\boldsymbol{L}}_0^{-1})_{ab} \tag{28}$$

Similarly:

$$P_{ba}(\lambda_b - \lambda_a) = (\tilde{\boldsymbol{L}}_0\boldsymbol{F}_1\boldsymbol{L}_0)_{ab} + \lambda_a(\boldsymbol{L}_0^{-1}\boldsymbol{G}_1\tilde{\boldsymbol{L}}_0^{-1})_{ab} \tag{29}$$

From Eqs. 28 and 29:

$$\partial P_{ab}/\partial F_{ij} = -\partial P_{ba}/\partial F_{ij} = (\lambda_a - \lambda_b)^{-1}(L_{ia}L_{jb} + L_{ib}L_{ja}) \tag{30}$$

$$\partial P_{ab}/\partial F_{ii} = -\partial P_{ba}/\partial F_{ii} = (\lambda_a - \lambda_b)^{-1}L_{ia}L_{ib} \tag{31}$$

$$\partial P_{ab}/\partial G_{ij} = [\lambda_b/(\lambda_a - \lambda_b)](L_{ai}^{-1}L_{bj}^{-1} + L_{aj}^{-1}L_{bi}^{-1}) \tag{32}$$

$$\partial P_{ab}/\partial G_{ii} = [\lambda_b/(\lambda_a - \lambda_b)]L_{ai}^{-1}L_{bi}^{-1} \tag{33}$$

$$(\partial P_{ba}/\partial G_{ij})/\lambda_a = -(\partial P_{ab}/\partial G_{ij})/\lambda_b \tag{34}$$

$$(\partial P_{ba}/\partial G_{ii})/\lambda_a = -(\partial P_{ab}/\partial G_{ii})/\lambda_b \tag{35}$$

Finally, from the diagonal elements of Eq. 9:

$$\partial P_{aa}/\partial G_{ij} = -L_{ai}^{-1}L_{aj}^{-1} \tag{36}$$

and

$$\partial P_{aa}/\partial G_{ii} = -\frac{1}{2}(L_{ai}^{-1})^2 \tag{37}$$

and from Eq. 20:

$$\partial P_{aa}/\partial F_{ii} = \partial P_{aa}/\partial F_{ij} = 0 \tag{38}$$

Eqs. 22—25, 30—33, and 36—38 complete the elements of $\boldsymbol{J}$.

The complete transformations, $\boldsymbol{J}$ and $\boldsymbol{J}^{-1}$, for the particular case of $n=2$ are given in Tables I and II. The product matrices, $\boldsymbol{J}\boldsymbol{J}^{-1}$ and $\boldsymbol{J}^{-1}\boldsymbol{J}$, for the general case have also been constructed. As is shown in Tables III and IV, these matrices are indeed equal to the unit matrix [order of $n(n+1)$]. Accordingly, $\boldsymbol{J}^{-1}$ is now confirmed to be both the left and the right inverse of $\boldsymbol{J}$.

Similar transformations relate $[\Delta\boldsymbol{\Lambda},\ \Delta\boldsymbol{L}]$ and also $[\Delta\boldsymbol{\Lambda},\ \Delta\boldsymbol{L}^{-1}]$ to $[\Delta\boldsymbol{G},\ \Delta\boldsymbol{F}]$. From Eqs. 6 and 7.

$$\boldsymbol{P} = \boldsymbol{L}_1^{-1}\boldsymbol{L}_0 = -\boldsymbol{L}_0^{-1}\boldsymbol{L}_1 \tag{39}$$

whence:

$$\partial P_{ab}/\partial L_{ai}^{-1} = L_{ib} \tag{40}$$

and

$$\partial P_{ba}/\partial L_{ia} = -L_{bi}^{-1} \tag{41}$$

Table I. The J matrix

	ΔG_{11}	ΔG_{22}	ΔG_{12}	ΔF_{11}	ΔF_{22}	ΔF_{12}
$\Delta\lambda_1$	$\lambda_1(L_{11}^{-1})^2$	$\lambda_1(L_{12}^{-1})^2$	$2\lambda_1 L_{11}^{-1}L_{12}^{-1}$	L_{11}^2	L_{21}^2	$2L_{11}L_{21}$
$\Delta\lambda_2$	$\lambda_2(L_{21}^{-1})^2$	$\lambda_2(L_{22}^{-1})^2$	$2\lambda_2 L_{21}^{-1}L_{22}^{-1}$	L_{12}^2	L_{22}^2	$2L_{12}L_{22}$
ΔP_{11}	$-\frac{1}{2}(L_{11}^{-1})^2$	$-\frac{1}{2}(L_{12}^{-1})^2$	$-L_{11}^{-1}L_{12}^{-1}$	0	0	0
ΔP_{22}	$-\frac{1}{2}(L_{21}^{-1})^2$	$-\frac{1}{2}(L_{22}^{-1})^2$	$-L_{21}^{-1}L_{22}^{-1}$	0	0	0
ΔP_{12}	$\frac{\lambda_2}{\lambda_1-\lambda_2}L_{11}^{-1}L_{21}^{-1}$	$\frac{\lambda_2}{\lambda_1-\lambda_2}L_{12}^{-1}L_{22}^{-1}$	$\frac{\lambda_2}{\lambda_1-\lambda_2}(L_{11}^{-1}L_{22}^{-1}+L_{12}^{-1}L_{21}^{-1})$	$\frac{1}{\lambda_1-\lambda_2}L_{11}L_{12}$	$\frac{1}{\lambda_1-\lambda_2}L_{21}L_{22}$	$\frac{1}{\lambda_1-\lambda_2}(L_{11}L_{22}+L_{12}L_{21})$
ΔP_{21}	$\frac{\lambda_1}{\lambda_2-\lambda_1}L_{21}^{-1}L_{11}^{-1}$	$\frac{\lambda_1}{\lambda_2-\lambda_1}L_{22}^{-1}L_{12}^{-1}$	$\frac{\lambda_1}{\lambda_2-\lambda_1}(L_{21}^{-1}L_{12}^{-1}+L_{22}^{-1}L_{11}^{-1})$	$\frac{1}{\lambda_2-\lambda_1}L_{12}L_{11}$	$\frac{1}{\lambda_2-\lambda_1}L_{22}L_{21}$	$\frac{1}{\lambda_2-\lambda_1}(L_{12}L_{21}+L_{11}L_{22})$

Table II. The J^{-1} matrix

	$\Delta\lambda_1$	$\Delta\lambda_2$	ΔP_{11}	ΔP_{22}	ΔP_{12}	ΔP_{21}
ΔG_{11}	0	0	$-2L_{11}^2$	$-2L_{12}^2$	$-2L_{11}L_{12}$	$-2L_{12}L_{11}$
ΔG_{22}	0	0	$-2L_{21}^2$	$-2L_{22}^2$	$-2L_{21}L_{22}$	$-2L_{22}L_{21}$
ΔG_{12}	0	0	$-2L_{11}L_{21}$	$-2L_{12}L_{22}$	$-(L_{11}L_{22}+L_{12}L_{21})$	$-(L_{12}L_{21}+L_{11}L_{22})$
ΔF_{11}	$(L_{11}^{-1})^2$	$(L_{21}^{-1})^2$	$2\lambda_1(L_{11}^{-1})^2$	$2\lambda_2(L_{21}^{-1})^2$	$2\lambda_1 L_{11}^{-1}L_{21}^{-1}$	$2\lambda_2 L_{21}^{-1}L_{11}^{-1}$
ΔF_{22}	$(L_{12}^{-1})^2$	$(L_{22}^{-1})^2$	$2\lambda_1(L_{12}^{-1})^2$	$2\lambda_2(L_{22}^{-1})^2$	$2\lambda_1 L_{12}^{-1}L_{22}^{-1}$	$2\lambda_2 L_{22}^{-1}L_{12}^{-1}$
ΔF_{12}	$L_{11}^{-1}L_{12}^{-1}$	$L_{21}^{-1}L_{22}^{-1}$	$2\lambda_1 L_{11}^{-1}L_{12}^{-1}$	$2\lambda_2 L_{21}^{-1}L_{22}^{-1}$	$\lambda_1(L_{11}^{-1}L_{22}^{-1}+L_{21}^{-1}L_{12}^{-1})$	$\lambda_2(L_{21}^{-1}L_{12}^{-1}+L_{11}^{-1}L_{22}^{-1})$

Table III. The elements of the JJ^{-1} matrix

Row	Column	Elements*
$\Delta\lambda_a$	$\Delta\lambda_c$	E_{ca}^2 $\begin{cases}=1 \text{ only if } a=c\\=0 \text{ otherwise}\end{cases}$
$\Delta\lambda_a$	ΔP_{cd}	$2\lambda_c E_{ca}E_{da}-2\lambda_a E_{ac}E_{ad}=0$
ΔP_{aa}	$\Delta\lambda_c$	0
ΔP_{aa}	ΔP_{cd}	$E_{ac}E_{ad}\begin{cases}=1 \text{ only if } a=c=d\\=0 \text{ otherwise}\end{cases}$
ΔP_{ab} $(a\neq b)$	$\Delta\lambda_i$	$E_{ca}E_{cb}/(\lambda_a-\lambda_b)=0$
ΔP_{ab} $(a\neq b)$	ΔP_{cd}	$[\lambda_c(E_{ca}E_{db}+E_{cb}E_{da})-\lambda_b(E_{ac}E_{bd}+E_{ad}E_{bc})]/(\lambda_a-\lambda_b)$ $=(E_{ac}E_{bd}+E_{ad}E_{bc})(\lambda_c-\lambda_b)/(\lambda_a-\lambda_b)\begin{cases}=1 \text{ only if } a=c \text{ and } b=d\\=0 \text{ otherwise}\end{cases}$

* The unit matrix $\boldsymbol{E}$ was derived from the product of $\boldsymbol{L}^{-1}\cdot\boldsymbol{L}$.

Table IV. The elements of the $J^{-1}J$ matrix

Row $(i\leq j)$	Column $(k\leq l)$	Elements*
ΔG_{ij}	ΔG_{kk}	$E_{ik}E_{jk}\begin{cases}=1 \text{ only if } i=j=k\\=0 \text{ otherwise}\end{cases}$
ΔG_{ij}	ΔG_{kl} $(k\neq 1)$	$E_{ik}E_{jl}+E_{il}E_{jk}\begin{cases}=1 \text{ only if } i=k \text{ and } j=l\\=0 \text{ otherwise}\end{cases}$
ΔG_{ij}	ΔF_{kl}	0
ΔF_{ij}	ΔG_{kl}	0
ΔF_{ij}	ΔF_{kk}	$E_{ki}E_{kj}\begin{cases}=1 \text{ only if } i=j=k\\=0 \text{ otherwise}\end{cases}$
ΔF_{ij}	ΔF_{kl} $(k\neq l)$	$E_{ki}E_{lj}+E_{kj}E_{li}\begin{cases}=1 \text{ only if } i=k \text{ and } j=l\\=0 \text{ otherwise}\end{cases}$

* The unit matrix $\boldsymbol{E}$ was derived from the product of $\boldsymbol{L}\cdot\boldsymbol{L}^{-1}$.

Then:

$$\frac{\partial}{\partial L_{ia}}=\sum_b\frac{\partial P_{ba}}{\partial L_{ia}}\cdot\frac{\partial}{\partial P_{ba}}=\sum_b(-L_b^{-1}{}_i)\frac{\partial}{\partial P_{ba}} \tag{42}$$

and

$$\frac{\partial}{\partial L_a^{-1}{}_i}=\sum_b\frac{\partial P_{ab}}{\partial L_a^{-1}{}_i}\cdot\frac{\partial}{\partial P_{ab}}=\sum_b L_{ib}\frac{\partial}{\partial P_{ab}} \tag{43}$$

Simple expressions may be derived for example, by substituting Eq. 39 into Eq. 9:

$$\boldsymbol{G}_1=\boldsymbol{L}_0(\boldsymbol{L}_0^{-1}\boldsymbol{L}_1+\tilde{\boldsymbol{L}}_1\tilde{\boldsymbol{L}}_0^{-1})\tilde{\boldsymbol{L}}_0=\boldsymbol{L}_1\tilde{\boldsymbol{L}}_0+\boldsymbol{L}_0\tilde{\boldsymbol{L}}_1 \tag{44}$$

whence:

$$\partial G_{ii}/\partial L_{ia}=2L_{ia} \tag{45}$$

$$\partial G_{ij}/\partial L_{ja}=L_{ia} \tag{46}$$

$$\partial G_{ij}/\partial L_{ka}=0 \qquad (k\neq i,\ j) \tag{47}$$

Expressions for the $\boldsymbol{F}$ matrix may be derived by substituting Eq. 39 into Eq. 13:

$$\begin{aligned}\boldsymbol{F}_1=\tilde{\boldsymbol{L}}_0^{-1}\boldsymbol{\Lambda}_1\boldsymbol{L}_0^{-1}&-\tilde{\boldsymbol{L}}_0^{-1}(\boldsymbol{\Lambda}_0\boldsymbol{L}_0^{-1}\boldsymbol{L}_1\\&+\tilde{\boldsymbol{L}}_1\tilde{\boldsymbol{L}}_0^{-1}\boldsymbol{\Lambda}_0)\tilde{\boldsymbol{L}}_0^{-1}=\tilde{\boldsymbol{L}}_0^{-1}\boldsymbol{\Lambda}_1\boldsymbol{L}_0^{-1}\\&-(\boldsymbol{F}_0\boldsymbol{L}_1\boldsymbol{L}_0^{-1}+\tilde{\boldsymbol{L}}_0^{-1}\tilde{\boldsymbol{L}}_1\boldsymbol{F}_0)\end{aligned} \tag{48}$$

whence:

$$\partial F_{ij}/\partial L_{ka}=-(F_{ik}L_a^{-1}{}_j+F_{jk}L_a^{-1}{}_i) \tag{49}$$

We have found the $\boldsymbol{J}$ and $\boldsymbol{J}^{-1}$ transformations to be particularly useful in the propagation of uncertainties in the force constants and geometrical parameter to obtain estimates of the uncertainties in derived quantities; these derived quantities may include, for example, calculated frequencies, normal coordinate coefficients, Coriolis coefficients, and dipole-moment derivatives with respect to internal coordinates. They may also be useful in the more chemical group-frequency problems which are usually handled by perturbation formalism.

Appendix

Isotope Effects on Normal Coordinate Coefficients.—Small variations in atomic masses Δm_t have been previously[4] related with variations in frequency parameters λ_a. The present results may also be used to treat the isotope effects on normal-coordinate coefficients.

The $\boldsymbol{G}$ matrix is given by[1]

$$\boldsymbol{G}=\boldsymbol{B}\boldsymbol{M}^{-1}\tilde{\boldsymbol{B}} \tag{A-1}$$

where $\boldsymbol{M}^{-1}$ is the inverse mass matrix and the matrix $\boldsymbol{B}$ is the transformation from the Cartesian coordinates to the internal coordinates. Consider small variations[5] $\boldsymbol{M}_1$ such that

4) T. Miyazawa, *J. Mol. Spectry.*, **13**, 321 (1964).
5) The requirement is that the relative changes in masses, i. e. the elements of $\boldsymbol{M}_1\boldsymbol{M}_0^{-1}$, are small.

$$\boldsymbol{M} = \boldsymbol{M}_0 + \boldsymbol{M}_1 \tag{A-2}$$

The corresponding perturbation in $\boldsymbol{M}^{-1}$ is

$$\boldsymbol{M}^{-1} = \boldsymbol{M}_0^{-1} + \boldsymbol{M}_1^{-1} \tag{A-3}$$

where

$$\boldsymbol{M}_1^{-1} = -\boldsymbol{M}_0^{-1}\boldsymbol{M}_1\boldsymbol{M}_0^{-1} \tag{A-4}$$

This results in a small perturbation in $\boldsymbol{G}$, given by

$$\boldsymbol{G}_1 = \boldsymbol{B}\boldsymbol{M}_1^{-1}\tilde{\boldsymbol{B}} = -\boldsymbol{B}\boldsymbol{M}_0^{-1}\boldsymbol{M}_1\boldsymbol{M}_0^{-1}\tilde{\boldsymbol{B}} \tag{A-5}$$

whence

$$\boldsymbol{L}_0^{-1}\boldsymbol{G}_1\tilde{\boldsymbol{L}}_0^{-1} = -\boldsymbol{L}_0^{-1}\boldsymbol{B}\boldsymbol{M}_0^{-1}\boldsymbol{M}_1\boldsymbol{M}_0^{-1}\tilde{\boldsymbol{B}}\tilde{\boldsymbol{L}}_0^{-1} \tag{A-6}$$

Since the normal-coordinate coefficients $\boldsymbol{L}^{\mathrm{X}}$ for Cartesian displacement coordinates are given[6] as

$$\boldsymbol{L}^{\mathrm{X}} = \boldsymbol{M}^{-1}\tilde{\boldsymbol{B}}\tilde{\boldsymbol{L}}^{-1} \tag{A-7}$$

it follows that

$$\boldsymbol{L}_0^{-1}\boldsymbol{G}_1\tilde{\boldsymbol{L}}_0^{-1} = -\tilde{\boldsymbol{L}}_0^{\mathrm{X}}\boldsymbol{M}_1\boldsymbol{L}_0^{\mathrm{X}} \tag{A-8}$$

Small corresponding variations in the frequency parameters may be derived by substituting Eq. A-8 into Eq. 19,

$$\Delta\lambda_a = (\tilde{\boldsymbol{L}}_0\boldsymbol{F}_1\boldsymbol{L}_0)_{aa} - \lambda_a(\tilde{\boldsymbol{L}}_0^{\mathrm{X}}\boldsymbol{M}_1\boldsymbol{L}_0^{\mathrm{X}})_{aa} \tag{A-9}$$

giving, as derived previously,[4]

$$\partial\lambda_a/\partial m_t = -\lambda_a[(L_{t\,a}^x)^2 + (L_{t\,a}^y)^2 + (L_{t\,a}^z)^2] \tag{A-10}$$

where m_t is the mass of the t-th atom.

Similarly, by substituting Eq. A-8 into Eqs. 20 and 28,

$$P_{aa} = \frac{1}{2}(\tilde{\boldsymbol{L}}_0^{\mathrm{X}}\boldsymbol{M}_1\boldsymbol{L}_0^{\mathrm{X}})_{aa} \tag{A-11}$$

and

$$P_{ab}(\lambda_a - \lambda_b) = (\tilde{\boldsymbol{L}}_0\boldsymbol{F}_1\boldsymbol{L}_0)_{ab} - \lambda_b(\tilde{\boldsymbol{L}}_0^{\mathrm{X}}\boldsymbol{M}_1\boldsymbol{L}_0^{\mathrm{X}})_{ab} \tag{A-12}$$

Accordingly,

$$\partial P_{aa}/\partial m_t = \frac{1}{2}[(L_{t\,a}^x)^2 + (L_{t\,a}^y)^2 + (L_{t\,a}^z)^2] \tag{A-13}$$

and

$$\partial P_{ab}/\partial m_t = -[\lambda_b/(\lambda_a - \lambda_b)] \times [L_{t\,a}^x L_{t\,b}^x + L_{t\,a}^y L_{t\,b}^y + L_{t\,a}^z L_{t\,b}^z] \tag{A-14}$$

This $\boldsymbol{P}$ matrix may also be used in expressing small variations in the $\boldsymbol{L}^{\mathrm{X}}$ matrix as shown below,

$$\boldsymbol{L}^{\mathrm{X}} = \boldsymbol{L}_0^{\mathrm{X}} + \boldsymbol{L}_1^{\mathrm{X}} \tag{A-15}$$

where

$$\begin{aligned}\boldsymbol{L}_1^{\mathrm{X}} &= (\boldsymbol{M}_0^{-1} - \boldsymbol{M}_0^{-1}\boldsymbol{M}_1\boldsymbol{M}_0^{-1}) \\ &\quad \times \tilde{\boldsymbol{B}}\tilde{\boldsymbol{L}}_0^{-1}(\boldsymbol{E} + \tilde{\boldsymbol{P}}) - \boldsymbol{L}_0^{\mathrm{X}} \\ &= \boldsymbol{L}_0^{\mathrm{X}}\tilde{\boldsymbol{P}} - \boldsymbol{M}_0^{-1}\boldsymbol{M}_1\boldsymbol{L}_0^{\mathrm{X}}\end{aligned} \tag{A-16}$$

6) B. L. Crawford, Jr., and W. H. Fletcher, *J. Chem. Phys.*, **19**, 141 (1951).

BULLETIN OF THE CHEMICAL SOCIETY OF JAPAN VOL. 39 1414—1418 (1966)

The Basicities of Tropone and Tropolone

By Haruo Hosoya and Saburo Nagakura

The Institute for Solid State Physics, The University of Tokyo, Azabu, Minato-ku, Tokyo (S. N.)
The Institute of Physical and Chemical Research, Komagome, Bunkyo-ku, Tokyo (H. H. & S. N.)

(Received November 19, 1965)

The ultraviolet absorption spectra of tropone (I) and tropolone (II) were measured with sulfuric acid solutions of various acidities. The accurate pK_a values, as determined by the proposed method, were -1.02 and -0.86 for I and II respectively. The Raman spectra of II were measured with sulfuric acid solutions of various acid concentrations. The bands in the 6 and 15 μ regions change sharply when the solvent acidity changes from 5 to 25%, corresponding well to the ultraviolet absorption change. The infrared absorption spectra of II were measured with the concentrated deuterosulfuric acid solution in the 6 μ region. The vibrationals mode of the protonated tropolone were discussed.

As evidenced by the facile production of their hydrochlorides, tropone and tropolone are known to be relatively stronger bases than most other unsaturated ketones.[1,2] We have shown theoretically in a previous paper[3] that this anomalously large basic character of tropone derivatives is attributable to the large (16%) contribution of the polar structure to the ground state. The

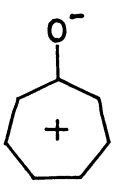

1) T. Nozoe, T. Mukai and K. Takase, *Sci. Rep. Tohoku Univ. Ser. I*, **39**, 164 (1956).
2) T. Nozoe, "Non-benzenoid Aromatic Compounds," Interscience Publishers, New York (1959), p. 339.
3) H. Hosoya, J. Tanaka and S. Nagakura, *Tetrahedron*, **18**, 859 (1962).

stabilities of tropone and tropolone hydrochlorides are also related to the stability of a unipositively charged seven-membered ring (the tropylium ion $C_7H_7^+$) system.

Recently Raman spectra have come to be used to study the structural change of organic bases in strong acidic media,[4,5] while ultraviolet absorption measurements have been shown to be suitable for the critical analyses of equilibria, even in strong acidic media.[4] Therefore, both methods were applied to the study of the protonations of tropone and tropolone.[6]

Experimental

Materials.—Tropone and tropolone were purified by the methods described in previous papers.[3,7] Concentrated sulfuric acid of a G. R. grade (95%) was used without further purification. Deuterosulfuric acid (97% acid concentration and 99% deuterium concentration) was purchased from the Showa Denko K. K.

Measurements.—A Cary recording spectrophotometer, model 14 M, was used for the ultraviolet absorption measurements. The ultraviolet absorption spectra of tropone and tropolone (ca. 10^{-4} M) were measured with sulfuric acid solutions of various acidities (H_0), fused quartz cells with a path length of 1 cm. being used. Because of its unstability, tropone was purified by distillation just before the solution was prepared. The numerical values for the acidity function (H_0) of the solvent sulfuric acid were taken from the table of Paul and Long (at 25°C).[8] The measurements were carried out in a temperature-controlled room adjusted at 20°C (±1°C). Since the temperature dependency of acidity functions is small, no temperature corrections to them were made.

The Raman spectra of tropolone (5—10 wt. %) in various acidities of sulfuric acid solutions were measured with the Cary model 81 recording Raman spectrophotometer located at the Government Chemical Industrial Research Institute, Tokyo.[9] The solution in the cell was warmed as high as about 40°C during the Raman spectral measurements.

The infrared absorption spectrum of tropolone in a concentrated deuterosulfuric acid solution was measured with a Hitachi EPI-2 infrared spectrophotometer, with a rock salt prism attached. Polyethylene bag cells were used for this purpose; the details have been described elsewhere.[10]

Results and Discussion

The Basicities of Tropone and Tropolone.—The ultraviolet absoprtion spectrum of tropolone consists of two parts. We have assigned that the longer wavelength bands (250—400 mμ, A and B bands in Ref. 3) are due to the tropone excitation (perpendicular to the C=O axis) perturbed by the hydroxyl group. The spectrum changes with the sulfuric acid concentration of the solvent, the change at about 360 mμ being the most prominent (Fig. 1). For solutions with sulfuric acid concentrations higher than 60% the absorption curve gradually shifts to shorter wavelengths, but its shape remains unchanged. The former change unequivocally corresponds to the following equilibrium (X=OH) between tropolone and its conjugated acid,[11] while the latter change is probably due to the solvent effects. We have shown that the latter effects can be eliminated from the pK determination by applying the least

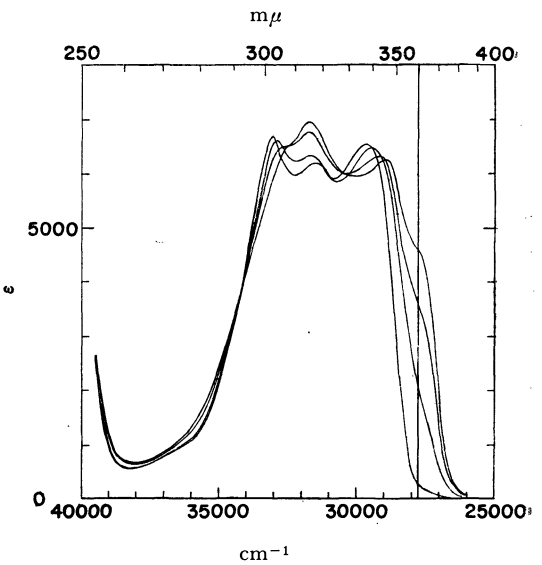

Fig. 1. Ultraviolet absorption spectra of tropolone in sulfuric acid of various concentrations.
The acidity constants H_0's of the solvents are −0.02, −0.48, −1.24, and −3.38 (from the top to the bottom at 360 mμ).

4) H. Hosoya and S. Nagakura, *Spectrochim. Acta*, **17**, 324 (1961).
5) N. C. Deno and M. J. Wisotsky, *J. Am. Chem. Soc.*, **85**, 1735 (1963).
6) In the course of preparing this paper, we found that Kende and his collaborators measured the pK_a value of tropone to be −0.6±0.3 with the change in ultraviolet absorption spectra. Since Kende did not report the temperature and the detailed method of the pK_a determination, no discussion was made for the discrepancy between his and our pK_a values. A. Kende, "Advances in Chemical Physics," Vol. 8, Interscience Publishers, London (1965), p. 133.
7) We thank Professor Yoshio Kitahara and Professor Kozo Doi, Tohoku University, for their kindness in giving us the samples of tropolone and cycloheptatriene.
8) M. A. Paul and F. A. Long, *Chem. Revs.*, **57**, 1 (1957).
9) We thank Mrs. Michiko Fukuyama for measuring the Raman spectra.
10) H. Hosoya and S. Nagakura, This Bulletin, **37**, 249 (1964).
11) The X-ray analysis of tropolone hydrochloride showed that protonation occurs at the carbonyl oxygen atom. Y. Sasada, K. Osaki and I. Nitta, *Acta Cryst.*, **7**, 113 (1954).

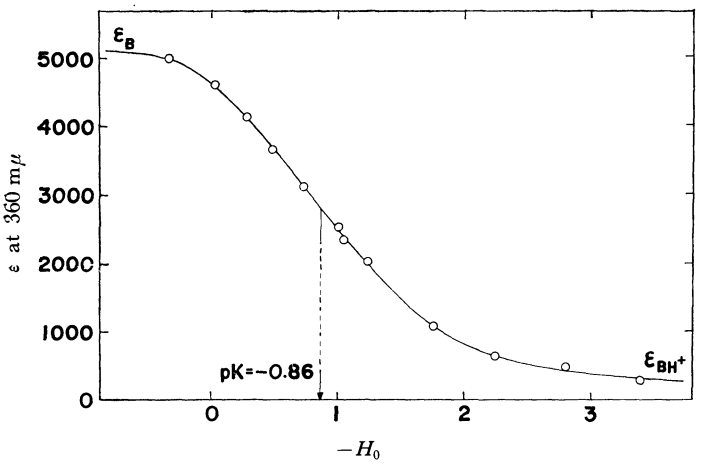

Fig. 2. Acidity dependency of the molar extinction coefficients at 360 mμ of tropolone in sulfuric acid. The vertical line and dots represent the inflection point of the sigmoid curve giving the pK_a value.

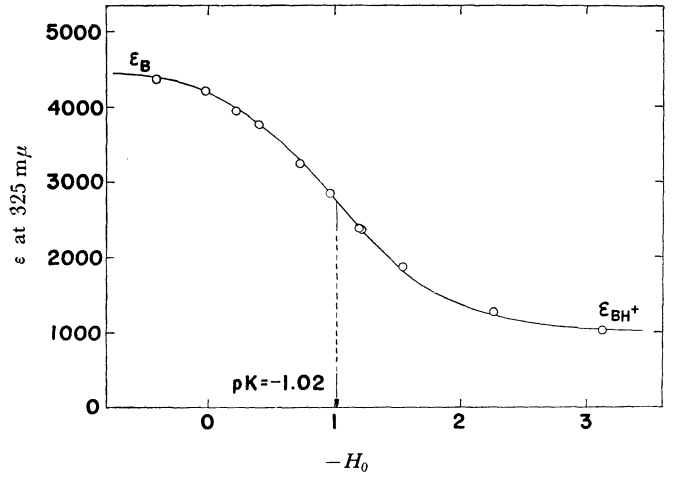

Fig. 3. Acidity dependency of the molar extinction coefficients at 325 mμ of tropone in sulfuric acid.

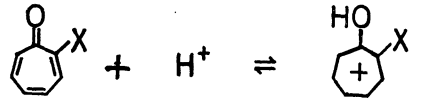

(1)

(X=H, OH)

squares calculation.[4,12] Namely, the H_0 value for the inflection point of the ε_λ—H_0 curve is just the pK value wanted, where ε_λ is the extinction coefficient subjected to the correction of solvent effects at the wavelentgh λ.

As is shown in Fig. 2, the observed ε values, at 360 mμ, for instance, change with the sulfuric acid concentration (H_0). The iterative calculation for determining simultaneously the pK_a, ε_B, and ε_{BH^+} values was executed following the method previously described.[4,12]

$$pK_a = -\log([B][H^+]/[BH^+]) \quad (2)$$

After repeating the least squares calculations for twelve pairs of data, we found the pK_a value of tropolone to be −0.86.

The same method was applied to the tropone-sulfuric acid system, ε's at 325 mμ being used. The pK_a value was thus found to be −1.20 (see Fig. 3); namely, tropone is less basic than tropolone. The existence of the equilibrium 1 was confirmed by the H_0—log $[(\varepsilon-\varepsilon_{BH^+})/(\varepsilon_B-\varepsilon)]$ plots, with slopes of 0.96 and 0.89 for tropolone and tropone respectively (Fig. 4).[4]

The pK_a value of −1 means that the concentrations of a base, B, and its conjugated acid, BH^+

12) The quantity in the summation of the last term in each of the three Eqs. 14 in Ref. 4 should be multiplied by ε.

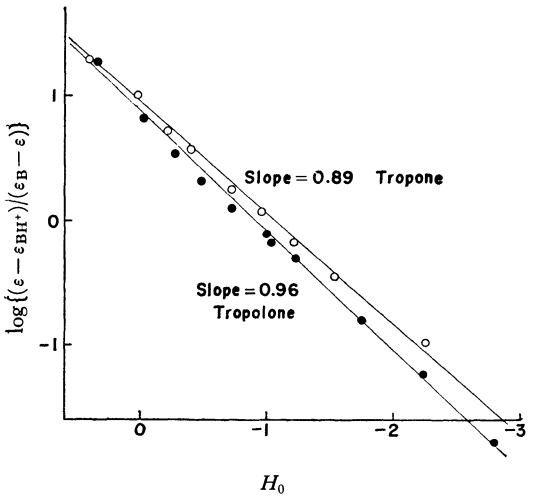

Fig. 4. Check of the existence of the equilibria 1. Open and filled circles stand, respectively, for tropone and tropolone.

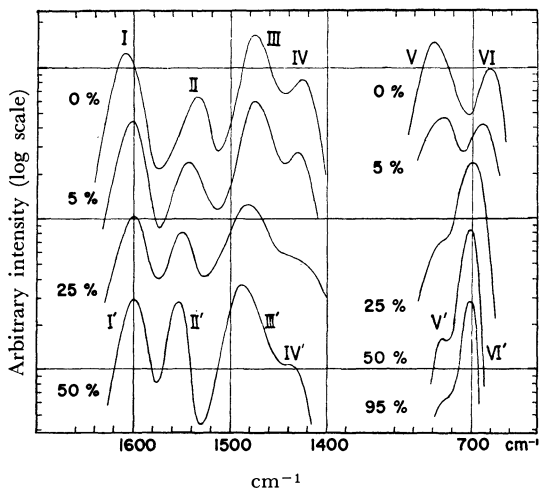

Fig. 5. Raman spectra of tropolone in sulfuric acid of various concentrations. The peak wave numbers of the characteristic bands of the neutral and protonated tropolone are, respectively, 1608 (I) and 1539 (II), and 1598 (I') and 1553 (II') cm^{-1}.

are almost equal in a 20% sulfuric acid solution (4.7 N), while the sigmoid ε - H_0 curve observed shows that in sulfuric acid solutions more concentrated than 40% (the same acid concentration as the concentrated hydrochloric acid), these compounds are completely protonated. However, a host of carbonyl compounds, such as aromatic and aliphatic ketones, aldehydes and carboxylic acids, have their pK_a values in the -6——7 range (in 70—80% sulfuric acid half-protonated).[13] This anomalously basic character of the carbonyl groups of troponoid compounds is due to the stability of the tropylium cation, as derivatives of which the protonated tropone or tropolone have been described. This is also the case for the anomalously basic cyclopropenone derivative.[6,14]

The dilution of the sulfuric acid solutions of these compounds with water gives almost the same spectra for their respective aqueous solutions, within an accuracy of about five per cent. This fact suggests the fair stabilities of these two compounds in concentrated sulfuric acid and the reversivility of the protonation processes.

Changes in Vibrational Spectra.—The infrared and Raman spectra of tropolone and its conjugated acid have characteristic but complicated features in the 1400—1650 cm^{-1} region, making a plausible assignment difficult.[15] Although the absolute intensities of the Raman spectra were not obtained accurately, therefore, a good reproducibility was obtained in each run. Thus, we have reproduced the spectra in various concentrations of sulfuric acid solutions on a logarithmic scale. Figure 5 shows the acicity dependency of the Raman spectra of this system in the 14 and 6—7 μ regions. It may be noticed that the relative intensities of several bands within each run greatly change in the concentration range of sulfuric acid between 5 and 25 per cent. Namely, the 1539 cm^{-1} band (II) has the weakest intensity in the 6—7 μ region spectra of tropolone in sulfuric acid with a concentration lower than 5 per cent, while the 1553 cm^{-1} band (II'), the shifted band of the 1539 cm^{-1} band, has an intensity comparable to the strongest 1490 cm^{-1} band (III') in the spectra of the solutions with concentrations of sulfuric acid higher than 25 per cent. The same tendency is also seen for the two bands in the 14 μ region. It should be remembered that the ultraviolet absorption data shows that the sharpest transference of the equlibrium 1 occurs at about a 20 per cent sulfuric acid solution. Thus, it may be concluded that the changes in the Raman spectra shown in Fig. 5, namely, the shifts of the bands to the respective bands, are caused by the protonation of tropolone.

The Assignments of the Vibrational Spectra of Tropolone and the Protonated Tropolone in the 6—7 μ Region.—As has been mentioned above, the vibrational spectrum of tropolone has several bands in the 6—7 μ region which have not yet been given conclusive assignments. Among these, the two bands near 1610 cm^{-1} (Band I) and 1540 cm^{-1} (Band II) have been recognized as having a mixed character C=C and C=O stretching vibrational modes. Recently Ikegami[16] showed

13) E. M. Arnett, "Progress in Physical Organic Chemistry," Vol. 1, Interscience Publishers, New York (1963), p. 223.
14) Y. Amako, private communication.
15) See the references cited in L. J. Bellamy, "The Infrared Spectra of Complex Molecules," Methuen and Co., London (1958), p. 151.
16) Y. Ikegami, This Bulletin, **35**, 972 (1962).

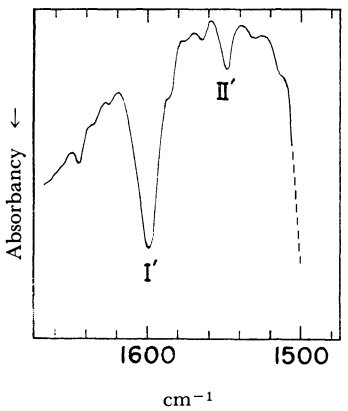

Fig. 6. Infrared absorption spectra of tropolone in a concentrated deuterosulfuric acid solution. The peak wave numbers are 1598 and 1547 cm^{-1} for I′ and II′, respectively.

that the infrared absorption band, II, is more liable to be influenced by the solvent change than Band I. As is evident in Fig. 5, the acidity dependency of the Raman Band II is the most prominent among the four in the 6—7 μ region. The intensity of the Raman Band II′ (1553 cm^{-1}) is increased to almost the same value as that of Band I′ (1598 cm^{-1}) for the protonated tropolone spectrum. Contrary to this, the infrared Band II′ (1547 cm^{-1}) of tropolone in a deuterosulfuric acid solution is much weaker than Band I′ (see Fig. 6). They have almost equal intensities in the spectrum of neutral tropolone.

Since the band pertinent to the C=O stretching vibration is expected to be sensitive to the protonation, Band II of tropolone may be assigned as largely due to the C=O stretching, and partly due also to the ring C=C stretching. The reverse is the case for Band I.

The protonated tropolone was shown by the X-ray crystal analysis technique to have two nearly equal C–OH bonds.[11] Therefore, it may be expected that absorption bands corresponding to the symmetrical and antisymmetric C–O stretching vibrations will appear. Band II′ may be assigned as due to symmetrical C–O stretching, because the intensity of Band II′ relative to that of Band I′ is stronger in the Raman spectrum than in the infrared spectrum.

BULLETIN OF THE CHEMICAL SOCIETY OF JAPAN VOL. 39 1418—1422 (1966)

The Effect of Oxygen on the Semiconductivity of Quaterrylene

By Yusei MARUYAMA and Hiroo INOKUCHI

The Institute for Solid State Physics, The University of Tokyo, Azabu, Tokyo

(Received November 30, 1965)

The electrical conductivity of an evaporated film of quaterrylene varied with the pressure of the ambient oxygen. The resistivity was 1.1×10^{12} Ωcm. in a vacuum of 4×10^{-8} mmHg; this was very large compared with the previously-reported value, $\sim 10^{6}$ Ωcm., which was obtained after exposing the film to the air of an atmospheric pressure. The temperature dependence of the resistance of the film was also affected by the ambient oxygen. The intrinsic semiconductor model could be applied only in the case of a high vacuum ($\sim 10^{-8}$ mmHg); the band gap, $\Delta\varepsilon$, was 1.7 eV. in this case. From the resistance-temperature relations at the various oxygen pressures, it seems that two acceptor levels, 0.03 eV. and 0.6 eV. above the valence band respectively, exist.

The effect of an impurity on the semiconduction of organic molecular crystals is very important and has been studied by several workers. Adsorbed oxygen, as one kind of impurity, is known to modify the semiconductivity and the photoconductivity of organic semiconductors. Anthracene, one of the most frequently-investigated organic semiconductors, is also rather sensitive to oxygen[1]; this fact is partly responsible for the difficulty of interpreting experimental results reliably.

Recently, Heilmeier and Harrison observed the Hall effect in copper phthalocyanine single crystals and explained their results in terms of an extrinsic band model, in which the oxygen impurity formed a donor or an acceptor level.[2] Kuroda and Flood also reported on the effect of ambient oxygen on the semiconductivities of the evaporated films of mesonaphthodianthrene and mesonaphthodianthrone.[3]

1) H. Pick and W. Wissman, *Z. Physik*, **138**, 436 (1954); A. Bree and L. E. Lyons, *J. Chem. Soc.*, **1960**, 5179.

2) G. H. Heilmeier and S. E. Harrison, *Phys. Rev.*, **132**, 2010 (1963).

3) H. Kuroda and E. A. Flood, *Canad. J. Chem.*, **39**, 1475, 1981 (1961).

In this experiment, we will report how a high vacuum of the order of 10^{-8} mmHg has been employed to ascertain the dark conductivity of the evaporated films of quaterrylene; the conductivity and also the band gap, $\Delta\varepsilon$, have thus been found to be strongly sensitive to ambient oxygen.

The applied hydrocarbon, quaterrylene $C_{40}H_{20}$, is a very stable organic substance, unlike anthracene or mesonaphthodianthrene;* it is, therefore, hard to subject it to ordinary chemical oxidation. The electronic properties of quaterrylene were reported by the present authors some years ago.[4] As will be described below, the oxygen effect on the semiconduction of quaterrylene is so large and so decided that the interpretation in terms of the extrinsic band model is rather reasonable quantitatively.

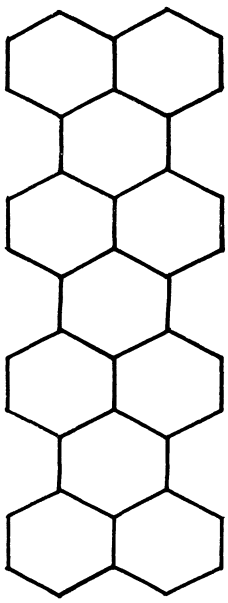

Fig. 1. The molecular structure of quaterrylene.

Only a little of the absorbed oxygen can be removed by evacuation without heating, and its adsorption energy may be expected to be fairly large compared with the usual van der Waals' energy. Therefore, careful treatment is needed in order to measure the intrinsic properties after the substance has been exposed to air.

Experimental Procedures

The high-vacuum evaporation apparatus was designed to obtain a clean vacuum of the order of 10^{-8} mmHg. As the main pumping system, a NEC 40 l./sec. ion pump (1) was employed, while a usual rotary pump was applied as the fore-line. An oil trap (2) containing a molecular sieve was used in the fore-line system. An ultra-high-vacuum cut-off valve (3) between the fore-line and the high-vacuum chamber separated the latter from the atmospheric pressure during the operation. A Bayard-Alpert gauge (5) on the top of the chamber recorded the degree of vacuum.

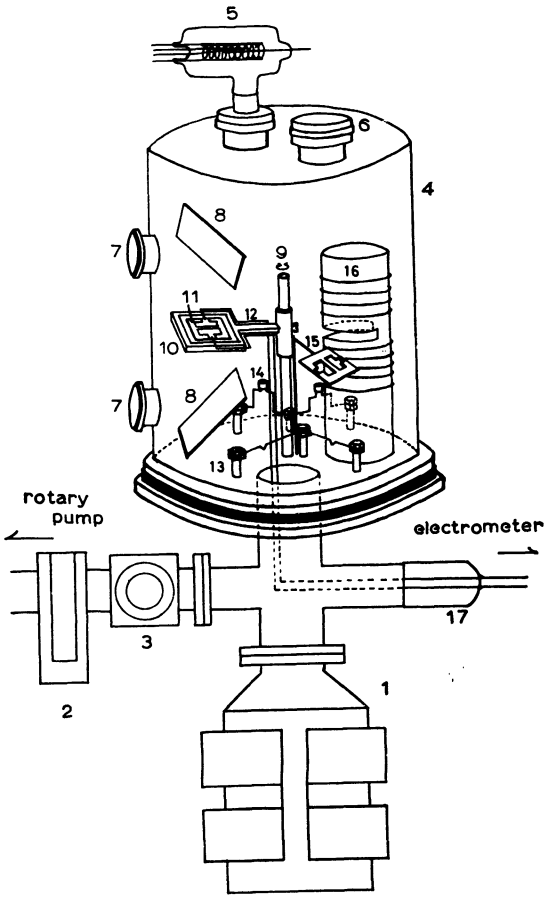

Fig. 2. The high-vacuum evaporation apparatus.
1. NEC 40 l./sec. ion pump
2. molecular sieve
3. ultra-high-vacuum cut-off valve
4. stainless-steel bell-jar
5. Bayard-Alpert gauge
6. viewing port
7. window
8. mirror
9. rotary axis
10. sample holder
11. glass plate cell
12. silver lead wire
13. electrodes for evaporation
14. gun
15. mask
16. electric heater for temperature control
17. high-resistance glass seal

Figure 2 illustrates the whole system schematically.

The sample holder (10) was supported by the rotary axis in the center of the base plate. Four pairs of electrodes (13) were placed on the base plate; two of them

* A farily strong oxidation of these two aromatic hydrocarbons is found under atmospheric circumstances.

4) Y. Maruyama, H. Inokuchi and Y. Harada, This Bulletin, **36**, 1193 (1963).

served for the metal evaporation, and the other two, for the evaporation of organic substances. Above the electrodes the appropriate masks for evaporation (15) were applied. Metals for the cell electrodes and the samples of organic compounds were successively evaporated on the clean glass plate fitted on the sample holder by rotating it magnetically from the outside around the center axis (9).

The glass plate mentioned above had been thoroughly cleaned with a chromic acid mixture in advance. The surface conductivity of the plate was lower than 10^{-16} Ω^{-1}. No difference in electrical resistance between the two surface-type cells, arranged as glass plate - electordes - organic film and also as glass - organic film-electrodes, could be found.

The stainless-steel bell-jar (4) was heated to about 200°C under evacuation for a few days in order to remove the adsorbed gases, mainly water vapor; the inside of the jar also warmed to about 120°C. The evaporation sources (14), the gun and the sample, were also degassed by preheating in order to make them capable of maintaining a vacuum in the order of 10^{-8} mmHg during the evaporation.

In order to measure the conductivity of the cell which had been kept in a high-vacuum evaporation vessel, silver lead wires (12) were attached to the edges of the glass plate cell by silver paste before evacuation; these wires were connected at the other ends to a Cary-31 vibration-reed electrometer through a high-resistance glass seal (17). The evaporation velocity of the organic substances was about 10—50 Å in thickness per second; the value was calculated from the increase in the electrical conduction of the film specimen during evaporation.

Either side, the top or the bottom, of the cell could be irradiated by appropriate light sources through the two windows (7) and the mirrors (8).

It took five hours to evacuate the cell from an atmospheric pressure up to about 10^{-7} mmHg, and then a few days to obtain a high vacuum of 2×10^{-8} mmHg; during this time the vessel was kept at a fairly high temperature (120°C) to facilitate degassing.

After these treatments, the metal to be used for electrodes, aluminum or gold, was evaporated to bring it in contact with the silver paste which was stuck to the silver lead wire, and then an organic substance was evaporated to form a surface-type conductivity cell. The sample dimensions were 15 mm. $\times$ 3 mm. $\times$ a few microns (thickness). Dried oxygen passed through active charcoal, itself cooled by liquid nitrogen, was then introduced into the vessel, and its effect on the conductivity was examined.

Results

Some previous results of measurements of the resistivity of quaterrylene are listed in Table I.

TABLE I.

Sample	Resistivity, Ωcm.	$\Delta\varepsilon$, eV.
Powder	10^{10}	0.6
Single crystal	10^{6}	
Sandwich-type cell	10^{13}	0.6
Surface-type cell	10^{6}	0.6

The present results show a large discrepancy from the previous ones; particularly, the effect of oxygen is rather extraordinary. The resistivity, however, fluctuated according to the conditions of the preparation of the conductivity cell. One of the typical results for the quaterrylene films was as follows: The resistivity of the film, when it was kept in a high vacuum of 4×10^{-8} mmHg, reached 1.1×10^{12} Ωcm.; this was very large compared with the previously-obtained value, $\sim10^{6}$ Ωcm.

When the evaporated film was brought in contact with a trace of oxygen at room temperature, the resistance gradually decreased with the time. When the increase in oxygen pressure was large, the decrease in resistance was also large during a short initial period; after this period, however, the rate of decrease fell off, and the resistance approached a constant value. The resistance of the quaterrylene film varied with the pressure of the ambient oxygen, as is shown in Fig. 3.

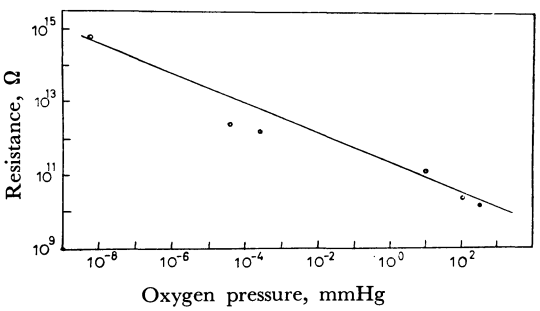

Fig. 3. The resistance of the quaterrylene film as a function of the pressure of the ambient oxygen.

When the pressure of the oxygen was lower than about 10^{-4} mmHg, the change in the resistance was reversible at room temperature. However, when the oxygen pressure increased to a point higher than this value, the process of recovering the sharply-decreased resistance was a very slow one at room temperature. Particularly when the film was exposed to oxygen in the air of an atmospheric pressure, the reduced resistance hardly increased at all after more than 1×10^{3} hrs' evacuation at room temperature; that is to say, the adsorption of oxygen on the organic crystal was practically irreversible. During this evacuation, however, when the cell was heated at about 100°C, the recovery of the resistivity was nearly attained after about 30 hr.

In Table II the resistivities of a quaterrylene surface-type film are summarized according to the ambient pressure of oxygen, P_{O_2}. No change in the resistance of the films was found when herium gas was introduced. Further, only a small effect of hydrogen gas in increasing the resistivity, or

Table II. The resistivity of the quaterrylene film as a function of the pressure of oxygen (P_{O_2})

Pressure, mmHg	Resistivity (15°C, Ωcm.)
$P_{O_2}=8\times10^{-9}$	1.1×10^{12}
$P_{O_2}\sim2\times10^{-5}$	3.5×10^{9}
$P_{O_2}\sim2\times10^{-4}$	2.7×10^{9}
$P_{O_2}=10$	2.1×10^{8}
$P_{O_2}=100$	5.0×10^{7}
$P_{O_2}=152$	3.3×10^{7}

the $\Delta\varepsilon$ value, of the oxygen-exposed film was observed.

Figure 4 shows the temperature dependence of the resistance of the quaterrylene film. The resistance was observed at temperatures from 23°C to about 120°C. With an film prepared under a vacuum of the order of 10^{-8} mmHg (Curve 1 of Fig. 4: $P_{O_2}=8\times10^{-9}$ mmHg), a linear relation was obtained between $\log R$ and $1/T$. The temperature dependence of Curve 1 can be expressed by an exponential function such as is usually found with intrinsic semiconductors:

$$R = R_0\exp(\Delta\varepsilon/2kT) \quad (1)$$

where $\Delta\varepsilon$ is the band gap for the semiconductivity. The value of $\Delta\varepsilon$ determined from the experimental results was 1.7 eV. After the ion pump had been switched off, the pressure in the vessel gradually increased to about 10^{-3} mmHg after five days. For this pressure ($P_O\sim2\times10^{-4}$ mmHg), the resistance-temperature relation curve, Curve 2, was obtained; it showed a large departure from Curve 1 in the low temperature region, which seemed to be the saturation region, but in the high temperature region it coincided exactly with Curve 1. When dried oxygen gas was introduced into the jar, linear relations, Curve 3 and Curve 4, were again obtained over the temperature range measured. However, their inclinations and resistance values were much smaller than those of Curve 1. Curve 3 was found to hold for $P_{O_2}=10$ mmHg, and Curve 4, for $P_O=100$ mmHg. Curve 5 was obtained in 10^{-3} mmHg after exposure to air under an atmospheric pressure; it corresponded to $P_{O_2}=152$ mmHg.

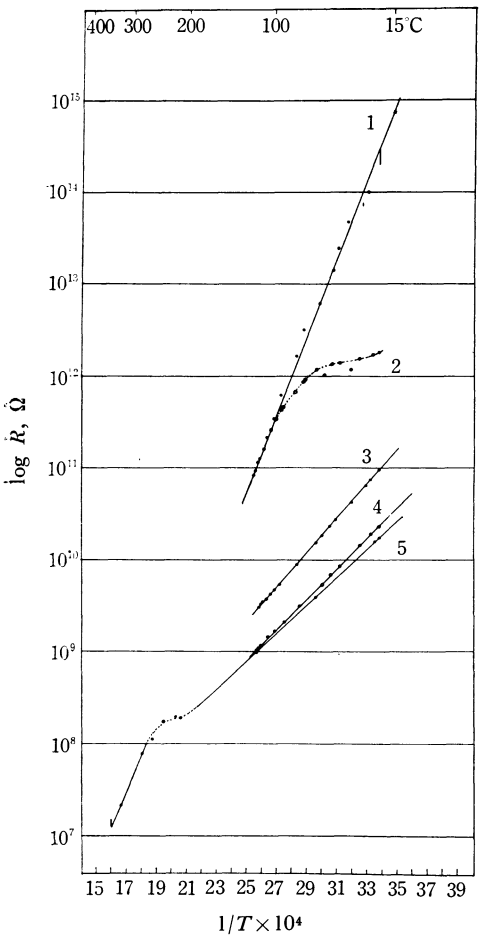

Fig. 4. The temperature dependence of the resistance of the quaterrylene film.
Curve 1 : $P_{O_2}=8\times10^{-9}$ mmHg, $\Delta\varepsilon=1.7$ eV.
Curve 2 : $P_{O_2}\sim2\times10^{-4}$ mmHg, $\varepsilon_A\sim0.03$ eV.
Curve 3 : $P_{O_2}=10$ mmHg, $\varepsilon_A=0.74$ eV.
Curve 4 : $P_{O_2}=100$ mmHg, $\varepsilon_A=0.66$ eV.
Curve 5 : $P_{O_2}=152$ mmHg, $\varepsilon_A=0.6$ eV.

This behaviour seems to be due to the adsorption of oxygen; it may be analysed by the method for extrinsic semiconductors:

$$R = R_0'\exp(\varepsilon_A/2kT) \quad (2)$$

where ε_A is the depth of the acceptor or donor levels from the valence or conduction band. The values of ε_A calculated from the slope for each curve (Curves 3, 4 and 5) are also shown in Fig. 4.
When we extended Curve 5 to the high temperature region (up to 350°C), a sharp kink in the curve was found at around 250°C; the curve at high temperatures lay exactly on the line extraporated from Curve 1.

Other organic compounds, circumanthracene,[5] tetrathiotetracene,[6] and violanthrene,[7] were also investigated briefly. The effects of oxygen were not as evident as for quaterrylene, but a decrease in the resistivities caused by the ambient oxygen was found in all compounds.

The time-response curves of the current when the electric field was applied to the specimen film were also affected by the ambient oxygen pressure. In a high-vacuum region the response curve was of a rather square type, but above 10^{-3} mmHg it was an exponential-decay curve which corresponded to the establishment of the polarization field by trapping the carriers. The photoconduction response curves against the time were also of the

5) H. Inokuchi, N. Matsubara, Y. Maruyama and E. Clar, *Nature*, **205**, 64 (1965).
6) H. Inokuchi and M. Kochi, unpublished results.
7) N. Imatake, private communication.

decay type above 10^{-3} mmHg, in contrast to the clear-cut square-type response in a high vacuum.

Discussion

The experimental results described above suggest that the semiconduction of quaterrylene films may be identified as of the extrinsic type except for the case of a high vacuum. In this case it may be classified as an intrinsic type from the linear relation between log$R$ and $1/T$; its energy gap is about 1.7 eV.

As was described in presenting the results, at high temperatures the experimental points for different specimens lie on a single line, a line which coincides with Curve 1. This is a reason to assume that the energy gap, $\Delta\varepsilon = 1.7$ eV., is an intrinsic one. Further, in the optical absorption spectrum of quaterrylene film, Fig. 5, the long-wavelength-side shoulder at 710—760 mμ seems to correspond to this fundamental absorption threshold. These peaks may correspond to the 564—668 mμ peaks in the solution state spectrum of quaterrylene. The 668 mμ peaks (1.86 eV.) may be assigned to the lowest singlet excitation of the quaterrylene molecule. We obtained -0.3691 β (β: resonance integral) as this excitation energy by means of the Simple Molecular Orbital (SMO) calculation

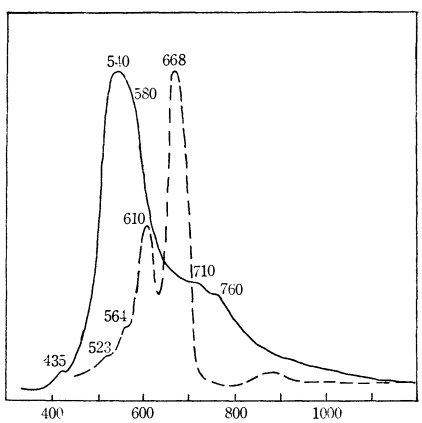

Fig. 5. The absorption spectra of the evaporated film (full line) and the solution (dashed line) of quaterrylene.

of the quaterrylene molecule. In order to fit this calculated value to the 668 mμ observed peaks, one must assume the value of -5.01 eV. for β. For the case of perylene, β is estimated as -4.11 eV. to obtain the agreement between the observed spectrum and the SMO calculation; therefore, this large value of β for quaterrylene is not unreasonable. Thus, the value of 1.7 eV., which corresponds to the lowest singlet excitation energy for the quaterrylene molecule in the solid state, can be considered to be the intrinsic band gap.

For the extrinsic semiconduction, it is not clear whether the oxygen impurity forms an acceptor or a donor level, but the former may be more likely in view of the fact that the electronegativity of oxygen is larger than that of the hydrocarbon. Therefore, as has been well established for the p-type semiconductor, the carrier density, n, may be given by the formula:

$$\frac{n(n+N_D)}{N_A-N_D-n} = \frac{N_C}{2}\exp(-\varepsilon_A/\boldsymbol{k}T) \qquad (3)$$

where N_A or N_D is the density of the acceptors or donors, ε_A is the energy depth of the acceptor level measured from the top of the valence band, and N_C is the effective state density. When $N_A \gg n \gg N_D$, Eq. 3 is reduced to the form:

$$n = \left(\frac{N_C N_A}{2}\right)^{1/2}\exp\left(-\frac{\varepsilon_A}{2\boldsymbol{k}T}\right) \qquad (4)$$

This corresponds to Eq. 2.

The adsorption of oxygen may occur not only on the surface of the film, but also in its bulk. This was verified by the measurement of the oxygen effect on a cell which had a guard ring electrode* applied to its surface.

The electrode effect is also important in this experiment.[8] The details of the study of this effect will be presented in due time.

One of the present authors, Y. M., would like to express his thanks to financial support of Sakkokai Fundation in performing study.

8) H. Inokuchi, Y. Maruyama and H. Akamatu, This Bulletin, **34**, 1093 (1961).

* The electrodes and guard ring were evaporated onto the organic film. The guard ring was located in the center line portion between two electrods; it was grounded to prevent any surface current.

BULLETIN OF THE CHEMICAL SOCIETY OF JAPAN VOL. 39 1423—1426 (1966)

The Benzene-photosensitized Isomerization of Butene-2 and Pentene-2

By Masahiro TANAKA, Masaaki KATO and Shin SATO

Department of Applied Physics, Tokyo Institute of Technology, Ookayama, Tokyo

(Received December 8, 1965)

The benzene-photosensitized *cis-trans* isomerization of butene-2 has been reinvestigated, using 2537 Å as the light source. A comparative study with pentene-2 has also been carried out. In all experiments, pentene-2 behaved very similarly to butene-2. The quantum yield of the isomerization was estimated to be 0.27 ± 0.03, irrespective of the olefin used. The following photostationary ratios of the *cis* to the *trans* isomer were obtained: $1.0_5\pm0.1$ for butene-2, and $0.9_9\pm0.1$ for pentene-2. The ratio of the initial rates of isomerization was, for both olefins, $1.1_5\pm0.1_5$, in favor of the isomerization from the *cis* to the *trans* isomer. Both ratios are very close to unity; this finding is in agreement with our previous results (M. Tanaka, T. Terao and S. Sato, *Bull. Chem. Soc. Japan*, **38**, 1645 (1965)).

The benzene-photosensitized *cis-trans* isomerization of butene-2, first observed by Cundall and Palmer,[1] provides one of the simplest examples of intermolecular energy transfer in the gas phase. Cundall et al. recently carried out[2] a more detailed study of this reaction, using pyridine as well as benzene as the sensitizer; they concluded that the isomerization takes place through a triplet-triplet interchange. We have also studied this reaction[3,4] and have obtained similar results except for the *cis-trans* photostationary ratio, ours is about unity, while Cundall et al. reported it to be 1.37 in favor of *trans*-butene-2.

Some complications may arise in this system because the fate of the photoexcited benzene[5,6] depends on the experimental conditions, such as the wavelength of the irradiating light, the pressure of the reactants, the temperature, and so on.

In the present work, we have re-examined the butene-2 reaction in order to confirm the data previously obtained; we also attempted to find the reason for the discrepancy with the results of Cundall et al. At the same time, we have also carried out a comparative study with pentene-2.

Experimental

Materials.—The benzene and *cis-* and *trans*-butene-2 used were the same as those previously reported.[4] *Cis-* and *trans-* pentene-2 supplied by the Takachiho Shoji Co., which contained 3% of various pentene isomers, were purified gas chromatographically on a 30 m. column of dimethylsulfolane on celite. After the separation on this column, no impurities could be detected.

Apparatus.—The apparatus[4] was freshly reconstructed, with special attention paid to avoiding contamination by mercury. Since neither isomerization nor decomposition could be detected on prolonged irradiation in the absence of benzene, it was evident that competitive mercury photosensitization did not occur.

The pressure was measured roughly with an oil manometer (Silicone DC 704) which absorbed the reactants to some extent. More accurate values were calculated indirectly from the chromatographic peak areas of samples of the reacting mixture. The gas chromatograph was composed of two columns; one, packed with 30 to 50 mesh celite with Silicone DC 550 as the liquid phase (3 m. long; 80°C), was used for the separation of benzene and olefins, while the other, packed with 30 to 50 mesh celite with dimethylsulfolane (20 m. long; room temperature), was used for the separation of the *cis* and *trans* isomers.

The vacuum was checked with a Pirani gauge (supplied by The Japan Vacuum Engineering Co.), its filament being always kept below 200°C in order to avoid thermal reactions. The cylindrical quartz reaction vessel was 5 cm. in diameter and of nearly the same length. Metal valves were used in a few required places to prevent the reactants from being absorbed in the stopcock grease. The vessel was illuminated with a low-pressure mercury arc through a UV 25 filter (supplied by the Toshiba Denki Co.) which cut off the light of wavelengths shorter than 2000 Å. In order to determine the incident light intensity (I_0), the previously-described mercury-photosensitized decomposition of ethylene was employed.[7,8] The fraction of the light transmitted (I_t/I_0) at various benzene pressures (p) was found to be given by the empirical expression:

$$\log_{10}(I_0/I_t) = 0.0245\,p - 0.00014\,p^2$$

where I_t is the intensity of the transmitted light. The incident intensity, I_0, was occasionally redetermined

1) R. B. Cundall and T. F. Palmer, *Trans. Faraday Soc.*, **56**, 1211 (1960).
2) R. B. Cundall, F. J. Fletcher and D. G. Milne, ibid., **60**, 1146 (1964).
3) S. Sato, K. Kikuchi and M. Tanaka, *J. Chem. Phys.*, **39**, 239 (1963).
4) M. Tanaka, T. Terao and S. Sato, This Bulletin, **38**, 1645 (1965).
5) P. Sigal, *J. Chem. Phys.*, **42**, 1953 (1965).
6) G. B. Kistiakowsky and C. S. Parmenter, ibid., **42**, 2942 (1965).
7) D. J. LeRoy and E. W. R. Steacie, ibid., **9**, 829 (1941).
8) Kang Yang, *J. Am. Chem. Soc.*, **86**, 3941 (1964).

TABLE I. ISOMERIZATION RATES AT VARIOUS PRESSURES OF OLEFINS
(Benzene pressure: 47.0 mmHg. Light intensity has not been measured.)

Starting compound							
cis-Butene-2		*trans*-Butene-2		*cis*-Pentene-2		*trans*-Pentene-2	
P	R_{isom}	P	R_{isom}	P	R_{isom}	P	R_{isom}
1.6	0.43	1.6	0.36	2.0	0.44	1.6	0.37
2.1	0.41	1.9	0.44	2.3	0.49	1.9	0.35
2.3	0.50	2.4	0.48	3.1	0.48	2.4	0.38
3.1	0.45	3.2	0.37	4.7	0.47	3.1	0.47
4.7	0.39	4.7	0.38	7.8	0.43	4.7	0.40
7.8	0.51	7.9	0.34	15.8	0.47	7.8	0.44
15.7	0.51	15.7	0.39	31.2	0.50	15.7	0.40
31.3	0.49	31.2	0.51	62.4	0.48	31.2	0.47
62.4	0.48						
Ave.	0.46	Ave.	0.41	Ave.	0.47	Ave.	0.41

P=mmHg $R_{isom}=\mu$ mol./min.

in order to check the stability of the low-pressure mercury arc.

Results

As expected, the behavior of pentene-2 was found to be very similar to that of butene-2. Table I summarizes the initial rates of isomerization at a constant benzene pressure and at varying olefin pressures. The conversion was always kept below 5%. There is a tendency for the rate to increase slightly with an increase in the pressure. Another trend observed is that $R(cis\rightarrow trans)$, the rate of isomerization from *cis* to *trans*, seems to be slightly larger than $R(trans\rightarrow cis)$ in both olefins. The ratio is $1.1_5\pm0.1_5$.

TABLE II. EFFECT OF BENZENE PRESSURE ON THE ISOMERIZATION RATE
(Olefin pressure: 7.8 mmHg, $I_0=2.6\times10^{-6}$ Einstein/min.)

Benzene pressure mmHg	I_a/I_0	R_{isom} μ mol./min.	Quantum yield
		cis-Butene-2	
2.0	0.097	0.07	0.28
3.9	0.191	0.12	0.24
7.1	0.298	0.23	0.30
7.1	0.298	0.22	0.29
11.7	0.467	0.28	0.23
15.0	0.541	0.35	0.25
24.6	0.698	0.41	0.23
31.3	0.776	0.53	0.26
40.5	0.831	0.55	0.25
			Ave. 0.26
		cis-Pentene-2	
2.0	0.097	0.10	(0.40)*
3.7	0.182	0.21	(0.45)*
7.6	0.338	0.24	0.27
11.9	0.469	0.34	0.28
15.5	0.552	0.48	0.33
15.7	0.554	0.44	0.31
19.0	0.616	0.36	0.23
23.4	0.681	0.43	0.24
24.2	0.692	0.48	0.27
31.5	0.722	0.57	0.30
39.0	0.823	0.59	0.28
			Ave. 0.28

* The values in parentheses are not used for averaging.

The effect of the variation in benzene pressure on the isomerization has also been examined, using the *cis* isomers of the two olefins as the starting compounds. The results are shown in Table II. Here I_a/I_0 is the ratio of the absorbed light intensity to the incident light intensity as calculated from the empirical relation quoted in the preceding section. The data are consistent with those of the previous paper.

Figure. 1 shows the time dependence of the *cis-trans* ratio, with olefin and benzene pressures of 3.9 and 39 mmHg respectively. It is evident that butene-2 and pentene-2 behave very similarly, except that the photostationary ratios differ. Table III summarizes the photostationary ratios.

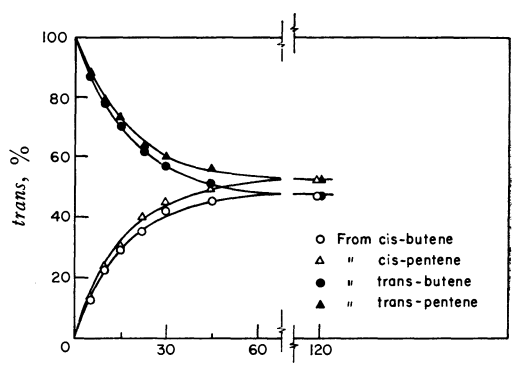

Fig. 1. The time dependence of the *cis-trans* ratio.
Olefin pressure: 3.9 mmHg, Benzene pressure: 39 mmHg.

Table III. Photostationary *cis-trans* ratios at various pressures

Benzene pressure mmHg	Olefin pressure mmHg	Stationary ratio (*trans* %)* Butene-2	Pentene-2
39.2	0.20	47	58
39.2	0.39	50	52
39.2	0.78	50	53 (53)
39.2	3.92	48 (48)	52 (53)
39.2	7.83	48	53 (52)
7.8	1.57	(48)	(53)

* The values were obtained with the *cis* isomer as the starting compound, except for the values in parentheses, which were obtained with the *trans* isomer as the starting compound.

thus obtained at various pressures of benzene and olefins. In the case of butene-2, the *cis* compound is favored, while in the case of pentene-2 the reverse is true, although the difference is not very pronounced.

Discussion

As may be seen in Table I, all the isomerization rates are nearly the same, irrespective of the pressure of the olefins, if the benzene pressure is kept constant. In other words, the fractions of the excited benzene molecules which sensitize the isomerization are almost constant over the pressure range investigated. At considerably lower pressures, however, the isomerization rate has been observed to decrease.[5]

As a basis for discussion, we will employ the same reaction mechanism as that assumed in a previous paper.[4]

$$B + h\nu \rightarrow {}^1B_n \quad (1)$$

$${}^1B_n + M \rightarrow {}^1B_0 \quad (2)$$

$${}^1B_0 \nearrow B + h\nu \quad (3)$$

$${}^1B_0 \searrow {}^3B_n \quad (4)$$

$${}^1B_0 + B \rightarrow B + B \quad (5)$$

$${}^3B_n + M \rightarrow {}^3B_0 + M \quad (6)$$

$${}^3B_0 \rightarrow B \quad (7)$$

$${}^3B_0 + B \rightarrow B + B \quad (8)$$

$${}^1B_0 + C \rightarrow B + {}^1A \quad (9)$$

$${}^3B_0 + C \rightarrow B + {}^3A \quad (10)$$

$${}^1A \xrightarrow{1-\alpha} C \quad (11)$$
$${}^1A \xrightarrow{\alpha} T$$

$${}^3A \xrightarrow{1-\beta} C \quad (12)$$
$${}^3A \xrightarrow{\beta} T$$

where B, C and T refer to benzene, *cis* and *trans*-olefins respectively, and where A refers to the excited olefin.

In this paper, we are concerned only with the *cis-trans* isomerizations. These reactions are believed to occur through the triplet-triplet[2,9] energy transfer, at least in the pressure range investigated.*1 Consequently, we will neglect reactions 9 and 11 in the following discussion.

A steady-state treatment gives the following relation:[4]

$$\frac{\beta I_a}{R_{\mathrm{isom}}} = \frac{k_3+k_4+k_5[B]}{k_4}\,\frac{k_7+k_8[B]+k_{10}[C]}{k_{10}[C]} \quad (I)$$

Equation I indicates that a plot of the reciprocal of the isomerization rate, R_{isom}, against that of the olefin pressure should give a straight line when the pressure of benzene is kept constant. These plots are shown in Fig. 2. The ratio of slope to intercept in Fig. 2 should give $(k_7+k_8[B])/k_{10}$, which is calculated to be 0.3 ± 0.1 mmHg^{-1} irrespective of the olefin used.*2 Therefore, with more than 3 mmHg of the olefin and at benzene pressures below 50 mmHg, more than 90% of the triplet-excited benzene is utilized for the *cis-trans* isomerization.

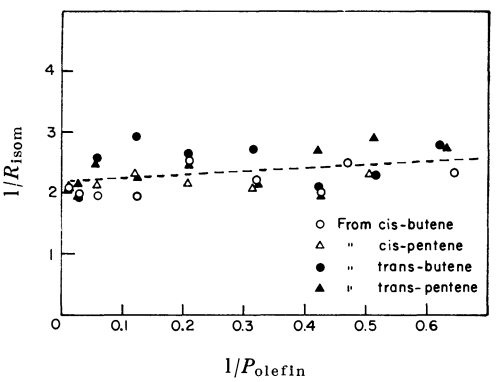

Fig. 2. The relationship between the reciprocals of the isomerization rate and of olefin pressure.

The quantum yields of isomerization are also shown in Table II. The values range from 0.25 to 0.30, again irrespective of the olefin used. Cundall et al. give 0.36 ± 0.02 for this value with butene-2.[2]

In order to discuss the photostationary ratio, it is necessary to consider also the reverse reactions:

$${}^1B_0 + T \rightarrow B + {}^1A \quad (13)$$

$${}^3B_0 + T \rightarrow B + {}^3A \quad (14)$$

9) H. Ishikawa and W. A. Noyes, Jr., *J. Chem. Phys.*, **37**, 583 (1962).

*1 The absence of products of decomposition and the pressure independence of the isomerization rates shown in Table I also support this assumption.

*2 If $k_7 \ll k_8[B]$, the value of k_{10}/k_8 can be calculated for the two olefins. The value thus calculated, $(1.5\pm0.2)\times10^2$, is about 10 times larger than that obtained in a previous paper.[4] The reason for this discrepancy is not certain, but it could be due to the very small magnitude of the slope of the plot in Fig. 2.

Here, however, reaction 13 can be disregarded for the same reason for which reactions 9 and 11 were previously neglected. From the proposed mechanism, the following relation is, then, readily obtained:

$$\frac{[C]_\infty}{[T]_\infty} = \frac{(1-\beta)k_{14}}{\beta k_{10}} \qquad \text{(II)}$$

where $[C]_\infty/[T]_\infty$ is the photostationary ratio of *cis* to *trans*. The observed values are $1.0_5\pm0.1$ for butene-2 and $0.9_5\pm0.1$ for pentene-2. On the other hand, in view of Eq. I, the ratio of the initial rates of isomerization at identical benzene pressures is:

$$\frac{R(trans\rightarrow cis)}{R(cis\rightarrow trans)} = \frac{(k_7+k_8[B])/k_{10}[C]+1}{(k_7+k_8[B])/k_{14}[T]+1}\frac{1-\beta}{\beta} \simeq \frac{1-\beta}{\beta} \qquad \text{(III)}$$

The experimental values are $1.1_5\pm0.1_5$, irrespective of the olefin used. Cundall et al. reported 1.37 ± 0.01 for both the photostationary ratio and the ratio of the initial rates of isomerization with butene-2. This would require that k_{10} be exactly equal to k_{14}. In the mercury photosensitization, quenching cross-sections of *cis*- and *trans*-butene-2 have indeed been found to be the same within the limits of experimental error.[10] Although the reason for the discrepancy in the value of the photostationary ratios as found by Cundall et al. and by us remains unknown, it seems worth mentioning that the photostationary ratio is not necessarily equal to the ratio of the initial rates of isomerization, since k_{10} need not necessarily be equal to k_{14}.

Recently, Noyes has pointed out[11] that the quantum yields of fluorescence and intersystem crossing from $^1B_{1u}$ to $^3B_{1u}$ in benzene strongly depend on the wavelength of the irradiating light in the region from 2400 to 2600 Å. This presents another potential complication in the investigated reaction.

10) S. Tsunashima and S. Sato, to be published.
11) W. A. Noyes, Jr., W. A. Mulac and D. A. Harter, *J. Chem. Phys.*, **44**, 2100 (1966).

BULLETIN OF THE CHEMICAL SOCIETY OF JAPAN VOL. 39 1426—1431 (1966)

Nuclear Magnetic Resonance Spectra of Polyethylene*

By Yoshinori KATO and Atsuo NISHIOKA

The Electrical Communication Laboratory, Musashino, Tokyo

(Received December 11, 1965)

A quantitative study of some structural irregularities of polyethylenes by an improved proton magnetic resonance method is reported. The background noise of a nuclear magnetic resonance spectrometer can be remarkably eliminated with the aid of the Mnemotron Computer of Average Transients. The total numbers of methyl groups in polyethylenes were estimated by this method using 5% solutions of the polymer in tetrachloroethylene. Spectra were obtained at about 110°C in order to suppress the thermal degradation of the polymer. The results agree well with those estimated by an infrared compensating method. Information about the species of branches and, in some cases, the number-average molecular weight of the polymer can be obtained by examining the resonance shape of methyl groups. The chemical shift difference between the triplet due to ethyl branches and that due to the other longer branches was found to be less than 0.05 p.p.m. This method can also be applied to the detection of unsaturations in polyethylene. In this case, however, the signal-to-noise ratio has to be increased to a factor of at least 20. Thus, the purification of the solvent is very important in the experiment.

It is well known that the various solid state properties of polyethylene (PE) are strongly affected by the degree of chain branching. Therefore, many papers[1-6] have been published on the determination of the number of methyl groups in PE. Most of them were based on the measurements of the infrared absorption (IR) at 1378 cm^{-1}. Of course, the lengths of the branches as well as

1) J. J. Fox and A. E. Martin, *Proc. Roy. Soc.*, **A175**, 208 (1940).
2) A. Elliott, E. J. Ambrose and R. B. Temple, *J. Chem. Phys.*, **16**, 877 (1948).
3) L. H. Cross, R. B. Richard and H. A. Willis, *Discussions Faraday Soc.*, No. 9, 235 (1950).
4) F. M. Rugg, J. J. Smith and L. H. Waterman, *J. Polymer Sci.*, **11**, 1 (1953).
5) F. P. Redding and C. M. Lovell, ibid., **21**, 157 (1956).
6) A. H. Willbourn, ibid., **34**, 569 (1959).

* This paper was read at the International Symposium on Nuclear Magnetic Resonance, Tokyo, September, 1965.

their numbers will be very important in characterizing this polymer.

Recently, an infrared absorption method, a double-beam compensation method,[6] has proved to be very effective in the quantitative analysis of chain branching in PE. However, in making an "absolute" measurement of the methyl group content, the IR method appears to present a serious complication because a series of samples containing known different numbers of branches are necessary for the calibration work.

On the contrary, the "absolute" concentration of methyl groups can be directly determined by the nuclear magnetic resonance (NMR) technique. We have already briefly reported that the degree of chain branching in a commercial low-density PE can be estimated by measuring the relative area of the methyl proton signal.[7] Though our results are in fairly good agreement with those obtained by the conventional IR method, the accuracy of the ordinary NMR method is not satisfactory because of some difficulties in applying it to commercial PE. Since the methyl proton signal is very weak and appears at 9.1 τ, near the strong methylene peak at 8.7 τ, an overlap occurs between them. Moreover, there is considerable background noise in some cases. Thus, an accurate evaluation of the methyl concentration is difficult. Fortunately, however, if we use a new accessory like the Mnemotron Computer of Average Transients (CAT), we can obtain an improved signal. By repetitively adding the signal under investigation, the signal-to-noise ratio (S/N) can usually be increased by a factor of the square root of the number of scans. With this technique, the exact evaluation of the methyl concentration will be possible by the NMR method.

The work to be described in the present paper was undertaken in an effort to study some structural irregularities of polyethylenes quantitatively. A preliminary experiment of the same kind was first reported by Porter et al.,[8] with respect to low-molecular-weight PE.

Experimental

Most of our works were carried out with an NMR spectrometer, Mullard SL44 Mk. II, at 40 Mc./s., together with a variable temperature probe and the CAT 400B. Each spectrum was obtained at about 110°C in order to suppress the thermal degradation of the polymer.

The samples examined were commercially-available polyethylenes, manufactured by E. I. du Pont de Nemours & Co. (Alathon 5BNC-10), the Allied Chemical Corporation (AC-617), and the Phillips Chemical Company (Marlex 6009), and some laboratory grades made by the Furukawa Chemical Ind. Co. (Staflen E570L) and the Mitsui Petrochemical Ind. Co. (Hizex E, I and K).

All the samples were reprecipitated from a xylene solution into a large amount of methanol; they were then dried in vacuo at about 60°C. Each sample was put into a specimen tube, together with tetrachloroethylene containing 2% tetramethylsilane (TMS). Then the tube was sealed and heated at 130°C for a few minutes in order to dissolve the PE completely. The concentration of the polymer solution suitable for our experiment was found to be 5% (w/w).

The CAT-averaging technique in the methyl resonance region was accomplished by using the TMS peak itself as a reference point from which a sweep of the decreasing magnetic field started. In the other cases, a sideband technique was employed to place the TMS sideband just before the region of interest in the spectrum, and an increasing magnetic field sweep was adopted. In order to complete each analysis as quickly as possible, a sweep rate of about 1.7 milligauss/sec. was chosen. A little slower sweep rate is needed, however, to avoid the relaxation wiggles which distort the line shape. The averaged spectra were read out in analog form onto an ordinary stripchart recorder. In our experiment, each division of 0.25 c. p. s. or less was stored in each memory address of the CAT.

Results and Discussion

Linearity.—The accuracy of the CAT-averaging technique depends upon the linearity of the modulator incorporated in it. This is shown in Fig. 1.

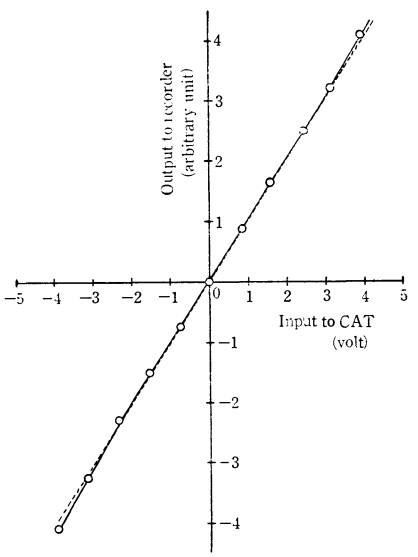

Fig. 1. Modulator linearity.

The linear relationship between the area under the averaged resonance curve and the number of runs is also shown in Fig. 2. If the magnitude of the input signal to the CAT is chosen to be less than ± 3 V., and if we take care to avoid the saturation phenomenon, the area under the resultant

7) Y. Kato and A. Nishioka, Lecture at the Annual Meeting of the Physical Society of Japan, Nagoya, October, 1964.

8) R. S. Porter, S. W. Nicksic and J. F. Johnson, *Anal. Chem.*, **35**, 1948 (1963).

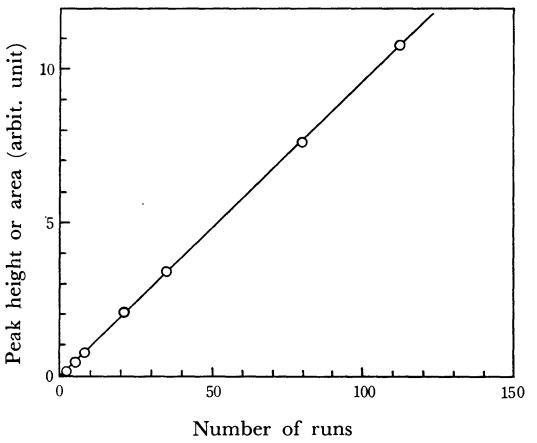

Fig. 2. Linearity check of CAT averaging technique.

peaks can be expected to be closely proportional to the number of protons involved.

Total Number of Branches.—A typical NMR spectrum of low-density PE, Alathon 5BNC-10, obtained in an ordinary way is illustrated in Fig. 3. A small signal of methyl protons can be seen

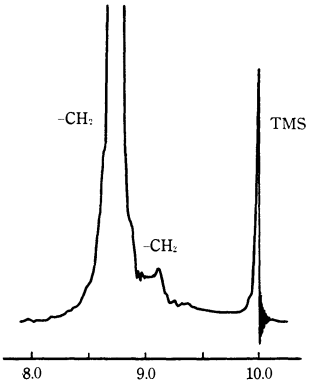

Fig. 3. NMR spectrum of polyethylene (Alathon 5BNC-10, Original pellet).

TABLE I. ESTIMATED NUMBER OF METHYL GROUPS PER 100 CARBON ATOMS IN LOW DENSITY POLYETHYLENE, ALATHON 5BNC-10

Sample	NMR	IR
Original pellet	3.0	—
Reprecipitated sample	2.3	2.8
Lower molecular weight fraction	2.2	—
Higher molecular weight fraction	1.7	—

near the very strong peak due to methylene protons. We measured the relative areas of these two peaks separately in order to estimate the number of methyl groups in the various states of this PE, which are treated differently. The results are shown in Table I. Since this sample is a low-density PE, it contains as many as 30 methyl branches for every thousand carbon atoms. As has been mentioned above, however, these results are not as accurate as those obtained by a conventional IR method.

Figure 4 illustrates the NMR spectrum of PE with CAT. In this case, a slow sweep rate of 25 milligauss per min. was adopted in order to get rid of the relaxation wiggles completely. The lower spectrum b was recorded after 19 runs, while the upper spectrum a was obtained after 30 runs. In practice the a spectrum is equivalent to that recorded after 300 runs except for the S/N, because the magnification of the ordinate is exactly ten times as large as that of the spectrum b.

Two examples of the methyl resonance patterns obtained at 40 Mc./s. are shown in Fig. 5. The methylene peak is not shown in these spectra. The methyl resonance at about 9.1 τ is located in the tail of the methylene peak. With a spectrometer operating at 100 Mc./s., this trouble can be eliminated to a great extent. In this case, however, it should be noticed that a spinning sideband of the TMS signal may appear in this region frequently. Therefore, we have to examine the spectrum very carefully. In the case of a spectrometer operating at 40 Mc./s., we can easily remove the spinning sideband, even to the low field side of the methylene signal, by increasing the rate of spinning. Shoolery[9] obtained the spectra of some *n*-hydrocarbons by a spectrometer operating at 200 Mc./s. with a superconducting electromagnet; they observed a clear-cut separation between the methyl and the methylene resonances.

The total number of runs necessary for the averaging-out of noises depends on the intensity of the signal under investigation. The spectra shown in

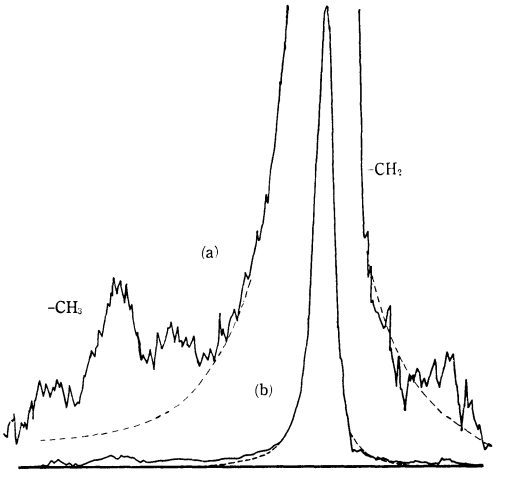

Fig. 4. NMR spectrum of polyethylene with CAT using a slow sweep.
Sample: AC-617, Sweep rate: 25 milligauss/min.

Spectrum	No. of runs	Magnification
(a)	30	×10
(b)	19	× 1

9) J. N. Shoolery, Paper presented at the International Symposium on NMR, Tokyo, September, 1965.

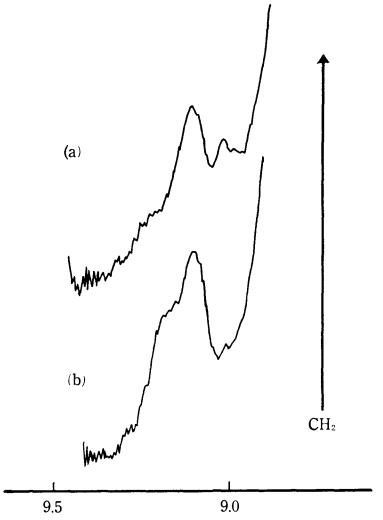

τ, p.p.m.

Fig. 5. CH_3 NMR patterns with CAT for polyethylenes.
(a) AC-617 (30 runs), (b) Hizex K (180 runs)

TABLE. II. TOTAL NUMBERS OF BRANCHES IN POLYETHYLENES

Polyethylene	Total numbers of branches per 1000 C atoms: IR method	NMR[a] method	NMR-CAT method	No. of runs	Observed resonance pattern
AC-617	49	(4±1)×10	40±1	70	t
Alathon 5BNC-10	28	(2±1)×10	22±1	180	t
Staflen E570L	—	—	14±1	200	d
Hizex-I	4.0	—	3±1	120	d+t (?)
Hizex-E	4.5	—	5±1	60	d
Hizex-K	24	—	20±1	40	d
Marlex 6009	—	—	<2[b]	400	t

a) NMR Spectrometer in its ordinary operation.
b) The upper limit was determined with the fractionated sample ($M_n=2.0\times10^4$).
t: triplet, d: doublet

Fig. 5 were obtained after 30 and 180 runs. For a linear PE, such as Marlex 6009, it was necessary to scan more than four hundred times; this corresponds to an increase in the S/N by a factor of more than 20. Since exactly the same resonance pattern as that shown in Fig. 5 can easily be obtained by the normal NMR method without CAT when the sample of AC-617 is melted at 130°C, we are confident that this new method can be safely used in estimating the minute concentrations of several types of double bonds, such as terminal vinyl, internal vinylene and vinylidene, in PE.

On the basis of the above-mentioned linearity, we compared the intensities of the two signals including the methyl resonance in a spectrum by taking account of the number of runs. All the results are summarized in Table II. The determination of the total number of branches, i. e. CH_3/1000C, by the double-beam infrared compensating method was carried out by Mr. Kobayashi of our laboratory.

Although the results shown in the second and the fourth columns of Table II agree with each other fairly well, a small discrepancy can still be found between them, mainly in low-density PE. This is perhaps due to a distribution of methyl groups among different species of branches; that is, an ethyl branch may have quite a different absorption coefficient from that of a butyl branch. From this point of view, we would suggest that the total number of branches evaluated by the NMR-CAT method might be the most reliable one at present.

Resonance Patterns of the Methyl Groups.— The methyl proton resonance would be expected to show either a doublet or a triplet, because methyl groups in PE can form either methyl branches, or ends of the main chain and of such branches as ethyl, propyl, butyl and other long-chain branches. This consideration can be easily substantiated by an examination of some model compounds and polymers containing methyl groups such as is shown in

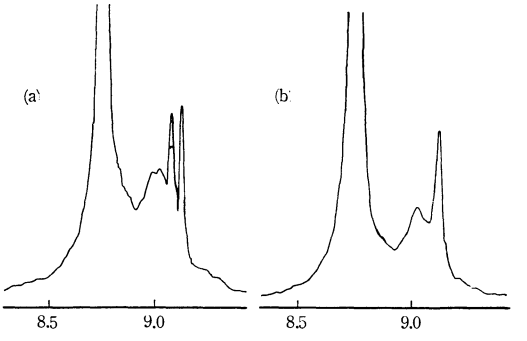

τ, p.p.m. τ, p.p.m.

Fig. 6. NMR spectra of (a) 5, 8-diethyl-*n*-dodecane and (b) *n*-hexadecane.

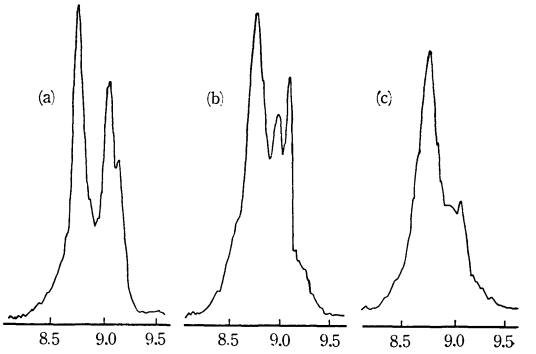

τ, p.p.m. τ, p.p.m. τ, p.p.m.

Fig. 7. NMR spectra of (a) ethylene-propylene copolymer, (b) polybutene-1 and (c) polyhexene-1.

Fig. 6. The chemical shifts of methyl protons in these compounds are summarized in Table III. The chemical shift difference between the triplets due to the ethyl branch and those due to other, longer branches is found to be less than 2 c. p. s. at 40 Mc./s. Some kinds of polymers with methyl, ethyl and butyl branches were also examined (see Fig. 7). These results concerning the chemical shifts of the triplets in ethyl, butyl and other longer branches are in accordance with the suggestion that the shape of the triplet seems to be almost independent of the length of chain branches, except for a slight shift.[10] Therefore, it is difficult to discriminate between ethyl and butyl branches by examining the resonance shapes.

TABLE III. CHEMICAL SHIFT (τ) OF METHYL PROTONS IN SOME MODEL COMPOUNDS AND POLYMERS

Compounds and polymers	Types of branches			
	Methyl	Ethyl	Butyl	Longer chain
5, 8-Diethyl-*n*-dodecane	—	9.09	9.13	—
n-Hexadecane	—	—	—	9.12
Ethylene-propylene copolymer	d {9.07, 9.17}	—	—	—
Poly-butene-1	—	t {9.00, 9.12, 9.24?}	—	—
Poly-hexene-1	—	—	9.11	—

The methyl signal of the AC-617 sample can be recognized as a distorted triplet. However, the intensity ratios of the three peaks are remarkably different from those of a typical triplet, i. e., 1 : 2 : 1. A simple illustration of the theoretical spectrum for the A_3 part of the A_3B_2 spin system is given in Fig. 8, where J and δ represent, respectively, the spin coupling constant and the chemical shift difference between the A and B nuclei. The characteristic feature is that the two outer peaks are much broader than the central one. By assuming a Lorentzian line shape with the half-height line-width of 2 c. p. s., the discrete spectrum can be synthesized into a continuous spectrum, as is shown in the middle pattern. However, the observed spectrum cannot be fully explained by the A_3B_2 spin system. For instance, the downfield peak of the theoretical spectrum seems a little higher than that of the one observed for AC-617. A part of this discrepancy can probably be removed by analyzing a more complicated spin system. The observed patterns of the methyl resonance of various kinds of polyethylenes were identified as being given in the 6th column of Table II.

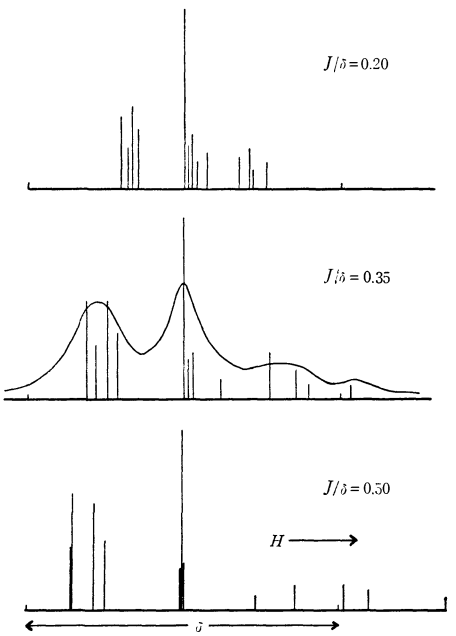

Fig. 8. Theoretical spectra for A_3 part of A_3B_2 spin system.

Figure 9 shows an example of the analysis. The

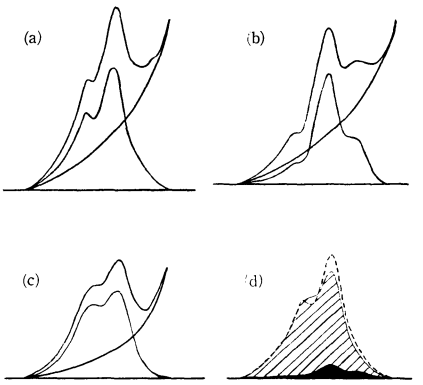

Fig. 9. Line shapes of CH_3 resonance signals of polyethylenes.
(a) Staflen E570L
(b) AC-617, Alathon 5BNC-10
(c) Hizex K and
(d) (Staflen E570L)

methyl resonance pattern obtained by the NMR-CAT method will give us fruitful information as to the structure of PE. For instance, the spectral pattern of the methyl groups in Staflen E570L, which is a ethylene-propylene copolymer containing a small amount of propylene, appears to be a doublet mixed with a small triplet. This finding is in good accordance with the suggested molecular structure of this copolymer. From the simple graphical treatment illustrated at the bottom right, we find that their areas are in the ratio of about ten to one, where it is assumed that the methyl NMR patterns of AC-617 and Hizex K give a typical triplet and a doublet respectively. If only the terminal methyl groups give rise to the triplet, the number-average molecular weight (M_n) of this polymer is

10) K. W. Bartz and N. F. Chamberlain, *Anal. Chem.*, **36**, 2151 (1964).

about 22000. On the other hand, an osmotic measurement of the M_n for the polymer gave a higher value of 36000. The difference may be explained by the permeation of low-molecular-weight polymers through the osmotic membrane, because it is estimated that the limit of permeation of the membrane is about 11000.

The Determination of Unsaturation.—The problem of determining the degree of bond unsaturation in PE has also been discussed mainly in the field of IR.[3,11-14] We have now also applied the NMR-CAT method to this problem. There are three types of unsaturations in PE, i. e., vinyl, vinylidene, and vinylene. Typical NMR spectra of these groups are shown in Fig. 10, using three kinds of model compounds, that is, hexadecene-1, 2-ethyl-hexene-1 and methyl linolenate, which correspond respectively to the above unsaturation groups.

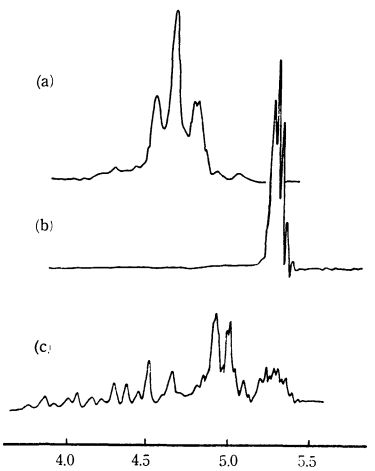

τ, p.p.m.

Fig. 10. NMR patterns of unsaturations in (a) methyl linolenate, (b) 2 ethyl-hexene-1 and (c) hexadecene-1.

In Fig. 11 several results obtained by the NMR-CAT method are shown. These three spectra were recorded after 420 runs. The characteristic signals appear between 4.5 and 5.2 in the τ-scale. For instance, the NMR resonance due to vinylene unsaturation can be found at about 4.7 τ; this seems quite reasonable when compared with the chemical shift of vinylene protons in the model compounds. In these experiments the S/N has to be increased to a factor of at least 20. Having done so, the spectrum must be examined vey carefully because a small quantity of impurities in the solvent, or even in TMS, may disturb it. Thus most of the peaks at about 6.5 τ are perhaps due to the impurity in the solvent itself.

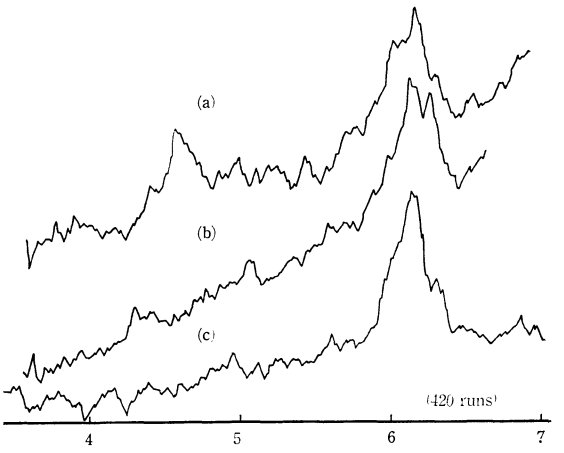

τ, p.p.m.

Fig. 11. NMR spectra due to unsaturations in polyethylene.
(a) Staflen E570L, (b) AC-617, (c) Solvent

Summary

In the past decade the number and the length of branches in PE have been estimated mainly by IR methods. We have realized that, with the aid of the CAT, the NMR method is also very useful in studying them. In order to suppress the thermal degradation of the polymer, we obtained the NMR spectrum of PE in solution at about 110°C. In spite of a little uncertainty in our case in separating the NMR signal of methyl protons from that of methylene protons, the total numbers of methyl groups obtained by our NMR-CAT method agree well with those estimated by an infrared compensating method. The small discrepancy between them may be attributed to the IR method's ambiguous treatment of the absorption coefficient for the branch of each length.

From the resonance shape we can obtain information about the species of branches and, in some cases, the molecular weight of PE. With the NMR spectrometer operating at 40 Mc./s., however, the chemical shift difference between the triplet due to ethyl branches and that due to the other longer branches is so small that we cannot discriminate between them.

We have also applied the NMR-CAT method to the detection of the unsaturations in PE.

The authors are indebted to Mr. Kamiya of the Furukawa Chemical Industrial Co., Ltd., for his courtesy in supplying us with the sample of Staflen, to Mr. Kobayashi of our laboratory for his kind permission to quote his results using the IR method, and to Mr. Sekikawa for the osmometry.

11) J. N. Lomonte, ibid., **34**, 129 (1962).
12) E. C. Cemia, C. Mancini and G. Montando, *Polymer Letters*, **1**, 371 (1963).
13) J. C. Woodbrey and P. Ehrlich, *J. Am. Chem. Soc.*, **85**, 1580 (1963).
14) R. J. de Kock and P. A. H. M. Hol, *Polymer Letters*, **2**, 339 (1964).

BULLETIN OF THE CHEMICAL SOCIETY OF JAPAN VOL. 39 1432—1436 (1966)

The Electron Spin Resonance of γ-Irradiated Sodium Polyphosphate. I. The Glass and the Single Crystal

By Masaji MIURA and Akinori HASEGAWA

Department of Chemistry, Faculty of Science, Hiroshima University, Hiroshima

and Tokinori FUKUI*

Research Reactor Institute, Kyoto University, Kumatori, Osaka

(Received December 13, 1965)

Under irradiation with γ-rays at room temperature, the glass of sodium polyphosphate or its single crystal doped with sodium sulfate becomes red, whereas the pure single crystal remains colorless. The glass and the doped single crystal exhibit ESR spectra which can be attributed to the hole trapped in the non-bonding orbital on the oxygen atom. The pure single crystal, of course, exhibits no ESR spectra. The determination of the degree of polymerization in the aqueous solution of the glass showed a decrease in the length of the main chain caused by the γ-ray irradiation. It may be concluded from these facts that the P–O–P bond is ruptured under the irradiation and that the effect of γ-rays on sodium polyphosphate is closely correlated with the local strain of the P–O–P bond.

A number of works have shown that a glass develops a color under exposure to ionizing radiation. The electron spin resonance (ESR), which has been remarkably developed, has become a most important means for the study of the coloration induced by such irradiation. ESR studies have already been made of irradiated silicate,[1] borate,[2] and phosphate glasses.[3] As to the γ-irradiated phosphate glass, Krapetyan and Yudin,[3a] observing the ESR spectrum consisting of a two-line hyperfine structure, have concluded that the spectrum is caused by an electron trapped on the phosphorus atom. By taking g values and coupling constants into account, however, it has recently been pointed out that the spectrum is to be attributed to the hole trapped by the oxygen atom rather than to the electron trapped by the phosphorus atom.[3b,c]

In ESR investigations, powder and glassy samples have hitherto been used. It is, however, more valuable to deal with a single crystal, since the data from the single crystal give directly not only three g values and coupling constants, but also the orientation of the radical. Therefore, the present investigation has been undertaken in order to obtain the ESR signals from the γ-irradiated single crystal of sodium polyphosphate, to analyze them, and then to compare them with those from the γ-irradiated glass. A mechanism for the coloration caused by the irradiation will also be discussed in this paper.

Experimental

The melt of sodium polyphosphate $(NaPO_3)_n$ was prepared by heating sodium dihydrogen phosphate dihydrate ($NaH_2PO_4 \cdot 2H_2O$) at 800°C for 6 hr. The glass of sodium polyphosphate was obtained by quenching the melt rapidly on dry ice; the single crystal was grown in the melt by slowly cooling and seeding it.[4] The single crystal of sodium polyphosphate doped with a small amount of sodium sulfate (the atomic ratio of sulfur to phosphorus: 1/100) was prepared by the same procedure as was used in the case of the pure single crystal. By X-ray diffractions, both of these crystals were identified as Type A of Kurrol's sodium salt,[5] which is a monoclinic crystal with the space group of $P2_1/n$ and the following crystallographic constants:

$a=12.12$ Å; $b=6.20$ Å; $c=6.99$ Å; $\beta=92°$.

These crystals have definite faces of cleavage (101) and plane ($\bar{3}01$).

These samples were exposed to γ-rays of 5×10^6 r. from a ^{60}Co source at room temperature. The ESR measurements were carried out at room temperature.

In an irradiated single crystal doped with sulfate, a rectangular co-ordination system, a'b'c', was selected for convenience; the a' axis is perpendicular to the plane of ($\bar{3}01$), the b' axis is identical with the crystallographic b axis, and c' axis is perpendicular to a' and b' axes. The crystal was rotated upon each of these axes in turn, and the ESR spectra were recorded at intervals of 15°.

The ESR spectra were obtained by using a T.D.S. (Tokyo Denki Seiki) Model T-5000 ESR spectrometer at a microwave frequency of 9225 Mc./sec. for the X-band and at one of 23000 Mc./sec. for the K-band

* On leave from Tokyo Denki Seiki Laboratory.

1) S. Lee and P. J. Bray, *Phys. Chem. Glass*, **3**, 37 (1962); C. M. Nelson and R. A. Weeks, *J. Am. Ceram. Soc.*, **43**, 399 (1960).

2) a) S. Lee and P. J. Bray, *J. Chem. Phys.*, **39**, 2863 (1963); b) S. Lee and P. J. Bray, ibid., **40**, 2982 (1964).

3) a) G. O. Krapetyan and D. M. Yudin, *Fiz. Tverd. tela*, **3**, 2827 (1961); b) Y. Nakai, This Bulletin, **38**, 1308 (1965); c) T. Feldmann, A. Treinin and V. Volterra, *J. Chem. Phys.*, **42**, 3366 (1965).

4) E. Thilo, G. Schulz and E. M. Wichmann, *Z. anorg. u. allgem. Chem.*, **272**, 182 (1953).

5) K. H. Jost, *Acta Cryst.*, **14**, 844 (1961).

operating with a 100 kc./sec. field modulation. The g values were determined by comparing them with the value for DPPH, by using DPPH and a gaussmeter by means of nuclear magnetic resonance.

The viscosities of aqueous solutions of non-irradiated and γ-irradiated (7.8×10^7 r.) glasses were measured[6] at the concentration of 0.80 g./100 ml. and at 25°C (Fig. 2). The degrees of the polymerization of non-irradiated and irradiated glasses were determined by the pH titration of end groups[7] after the hydrolysis at the branching points had been completed (Fig. 3).

Results and Discussion

Sodium Polyphosphate Glass.—When sodium polyphosphate glass was irradiated with γ-rays, it turned dark red and exhibited two asymmetric ESR absorption lines (Fig. 1). The width of these

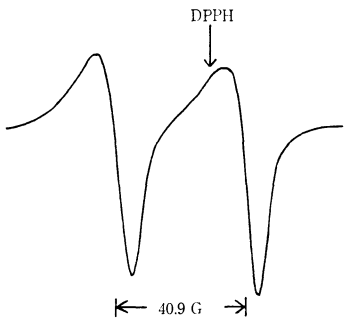

Fig. 1. The ESR spectrum of the γ-irradiated sodium polyphosphate glass at room temperature.

absorption lines at the temperature of liquid nitrogen is a little narrower than that at room temperature. These ESR spectra, as reported by some authors,[3] seem to be a doublet arising from the hyperfine structure due to the ^{31}P nucleus. The following facts are also known: they are not affected by the kind of cation and they are closely correlated with the visible absorption band with a maximum absorption at ca. 500 mμ. By taking account of the ESR spectrum consisting of the repetition of an asymmetric absorption line, this doublet is expected to have a practically isotropic coupling constant and three different g values; two of them resemble each other, and the other is the largest.

Sodium polyphosphate glass has branching points which are unstable and are easily hydrolyzed in the aqueous solution. The degradation at branching points can be detected by the decrease in the viscosity of the aqueous solution;[6] it is completed after about 8 hr. at 25°C, as may be seen in Fig. 2. This figure also shows that the γ-irradiation reduces the viscosity of the aqueous

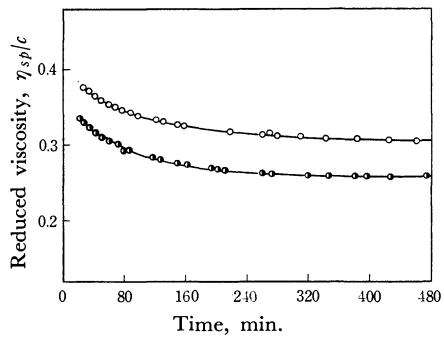

Fig. 2. Time dependence of the viscosity of the aqueous solutions of non-irradiated (○) and γ-irradiated (◑) glasses. $c=0.80$ g./100 ml. 25°C

solution of the glass without having an appreciable effect on the degradation at branching points. Further, the degree of polymerization, $\bar{n}$, decrease with the increase in irradiation dose, as is shown in Fig. 3, where $\bar{n}$ of non-irradiated glass is also

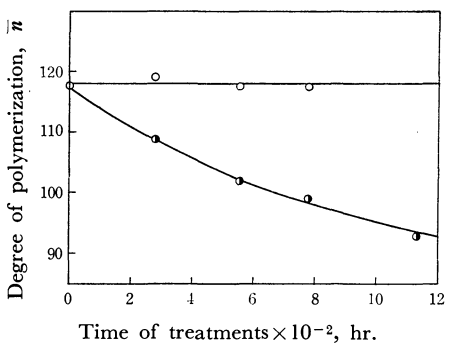

Fig. 3. The decrease in the degree of polymerization of polyphosphate glass with the irradiation dose.
○ stored in the room
◑ irradiated with γ-rays at 1×10^5 r/hr.

plotted against its storage period. These results show that the main chain of polyphosphate is ruptured by γ-irradiation.

The Pure Single Crystal of Type A of Kurrol's Sodium Salt.—The single crystsl of Type A of Kurrol's sodium salt irradiated with γ-rays at room temperature gave neither color nor any ESR absorption, even at the temperature of liquid nitrogen. When the single crystal, a part of which was covered with the glass, was irradiated, the glassy part turned dark red, but the part of the single crystal underneath acquired no color. Irradiation with γ-rays at room temperature seems to have no lasting effect on the pure single crystal of Kurrol's sodium salt.

The Single Crystal of Type A of Kurrol's Sodium Salt Doped with a Small Amount of Sodium Sulfate.—According to the facts described above, the effect of γ-rays on sodium polyphosphate seems to depend remarkably on its state, whether

6) U. P. Strauss, E. H. Smith and P. L. Wineman, *J. Am. Chem. Soc.*, **75**, 3935 (1953).
7) J. R. van Wazer, ibid., **72**, 647 (1950).

it is glassy or crystalline. In order to investigate the primary factor for this phenomenon and to speculate on the mechanism of the coloration, we attempted to inquire into the single crystal incorporating an impurity. Sodium sulfate was selected as the impurity because its structure is similar to PO_4. The single crystal of Kurrol's sodium salt doped with sodium sulfate was colorless and gave no ESR absorption before exposure to γ-rays, but it turned red and gave five ESR absorption lines after such exposure. Four of these lines show almost the same intensity, while the fifth one, which will be discussed below, shows a very weak intensity. The g values of these ESR absorption lines depend upon the orientation of the single crystal with relation to the direction of the magnetic field. The ESR spectra obtained when c' axis of the single crystal is parallel to the direction of the magnetic field are illustrated in Fig. 4, where

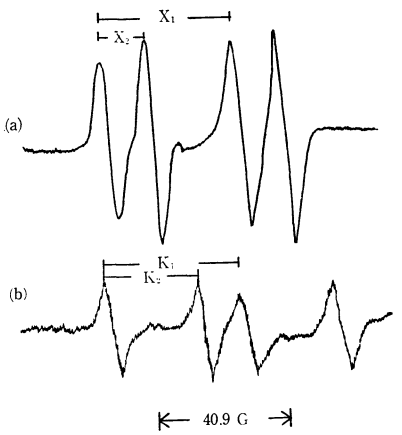

Fig. 4. The ESR spectra for the single crystal doped with sodium sulfate with (a) X-band and (b) K-band.

Fig. 4(a) shows the result with an X-band and Fig. 4(b) that with a K-band. The X_1 spacing shown in Fig. 4(a) is equal to the K_1 spacing in Fig. 4(b), and X_2 is about 1/2.5 times K_2; the frequency of the microwave has an influence not on the spacings X_1 and K_1, but on X_2 and K_2. These four absorption lines, therefore, are due to two doublets originating from two magnetically nonequivalent sites in the single crystal. These doublets are hyperfine structures arising from the interaction between an unpaired electron and a ^{31}P nucleus. The values of their coupling constants are equal to each other and are the same as that from the irradiated glass.

Figure 5 shows the variation in the four ESR absorption lines with the orientation of the single crystal in relation to the magnetic field. From these calculated components, the principal values of g and the direction cosines of the principal axes were evaluated as is shown in Table I. These principal values are different from one another;

TABLE I. PRINCIPAL VALUES AND THEIR DIRECTIONS.

Principal values	Direction cosines in a'b'c' axis system			
$g_1=2.006_4$	−0.496	−0.024	0.868	(I)
	0.995	−0.078	0.045	(II)
$g_2=2.008_2$	−0.123	0.314	0.945	(I)
	0.983	−0.157	0.024	(II)
$g_3=2.016_1$	0.912	0.111	0.395	(I)
	−0.330	0.009	−0.944	(II)

* (I) and (II) arise from two different nonequivalent sites.

g_1 is close to g_2, g_3, is largest, and all of them are larger than the value of the free spin, $g=2.0023$.

The isotropic coupling constant, A_{iso}, was determined from the spacing of the hyperfine structure, while the anisotropic coupling constant, B_{aniso}, was estimated from the anisotropic coupling components (<1 Gauss) in each plane.

$$A_{iso} = 50.9 \text{ Gauss}$$

$$B_{aniso} = 3—5 \text{ Gauss}$$

Here, this hyperfine structure is due to the interaction of an unpaired electron with a ^{31}P nucleus; the contributions to the hyperfine coupling constant from 3s and 3p electrons of the ^{31}P atom have already been calculated:[8]

$$A_{3s} = 3630 \text{ Gauss}$$

$$B_{3p} = 204.8 \text{ Gauss}$$

From the values of A_{iso}, B_{aniso}, A_{3s} and B_{3p}, the spin densities on the ^{31}P atom were calculated to be as follows:

$$\rho_{3s} = 1.1\%$$

$$\rho_{3p} \simeq 2\%$$

where ρ_{3s} and ρ_{3p} are the spin densities in the 3s and 3p orbitals of the phosphorus atom respectively. The phosphorus atom of polyphosphate, however, seems to combine with the oxygen atom by using its sp^3 hybridization.[9] Accordingly, the estimated spin density for the 3p orbital is smaller than the value expected from the 3s spin density.

The rest of the spin density, ca. 97%, may exist in the non-bonding orbital of the oxygen atom. Since the ESR spectrum of this single crystal, as will be described below, is equivalent to that of the glass which is independent of the kind of cation, the color in this single crystal seems to be due to the hole trapped in the non-bonding orbital of an oxygen atom shared by two phosphorus atoms before irradiation.

These spectra are also equivalent to that observed by Nakai.[3b] He has attributed the spectrum to

8) M. C. R. Symons, *Advances Phys. Org. Chem.*, 1, 332 (1963).
9) J. R. van Wazer, "Phosphorus and its Compounds. I," Interscience Pub. Inc., New York (1958).

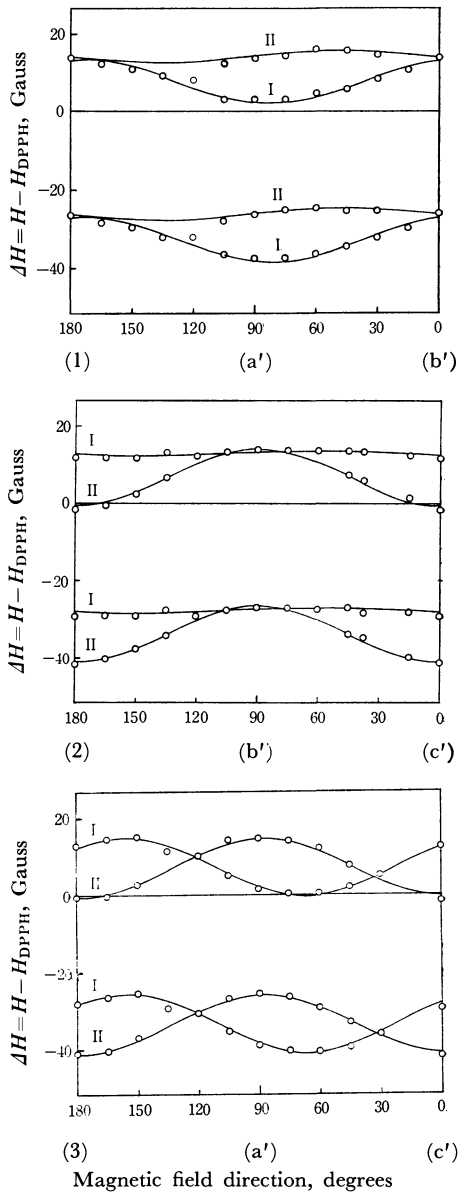

Fig. 5. Observed values and calculated curves for the hyperfine structure in the single crystal doped with sodium sulfate relative to the resonance of DPPH; the magnetic field being parallel to (1) a′b′, (2) b′c′ and (3) c′a′ planes. I and II are resonance lines arising from two nonequivalent sites respectively.

the hole trapped on the oxygen atom of the polyphosphate chain (P–O–P). Lee and Bray,[2a] from their study of the borate glass, have suggested that the hole giving rise to the ESR spectrum is trapped on an oxygen atom shared by two boron atoms, one three-coordinated and the other four-coordinated, and that it diffuses one-sidely to the latter atom. In polyphosphate glass, two phosphorus atoms at the branching point probably have somewhat different electronic configurations; therefore, it may be supposed that the hole is trapped on the oxygen shared by these two phosphorus atoms, as in the case of borate glass. However, as may be seen in Fig. 2, the branching point has an unappreciable effect upon γ-ray irradiation, though the degree of polymerization is reduced. Therefore, such a supposition as that described above seems to be unreasonable for the present case.

The crystal structure of Kurrol's sodium salt,[5] with its principal axes, is shown in Fig. 6. There

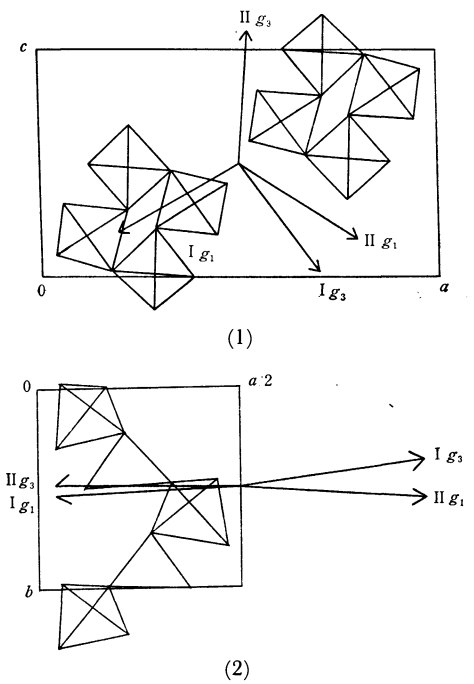

Fig. 6. The orientation of the principal axes against the crystal structure of type A of Kurrol's sodium salt; (1) and (2) are projections to ca and ab planes, where phosphorus atoms exist at the centers and oxygen atoms at the corners of these tetrahedrons.

is a considerable discrepancy between the principal axes and the non-bonding orbitals of oxygen in the main chain to be expected from the crystal structure. The following two explanations for this discrepancy are possible. One is that the center giving rise to the ESR spectrum is near the SO_4^{2-} group, which may exist at the interstice between polyphosphate chains where the chain may experience a local strain. The other is that the P–O–P bond strained by the SO_4^{2-} group is ruptured under the irradiation and that the resultant polyphosphate radicals occupy the stable orientation in the crystal. The latter interpretation is supported by the following facts: the absorption lines of the quartet, which must be expected from two equivalent phosphorus

atoms if the P–Ô–P bond is not ruptured, are not found, and the calculated principal values of g, which are different from one another and are larger than the value of the free spin, suggest that the two bonds in P–Ô–P are not equivalent to each other, but that one of these two bonds is rather ruptured.[10]

The principal values obtained from the irradiated single crystal doped with the sulfate are compared with the ESR spectrum from the irradiated glass in Fig. 7. This comparison obviously shows that

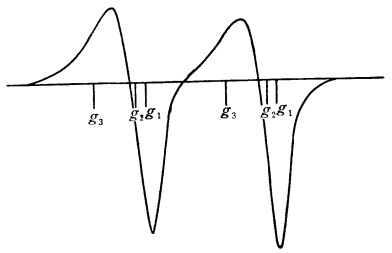

Fig. 7. The comparison between the principal values of g for the doped single crystal and the ESR spectrum of the glass.
$g_1=2.006_4$ $g_2=2.008_2$ $g_3=2.016_1$

the center produced in this single crystal is just the same as that produced in the glass.

On the other hand, the degrees of the polymerization of non-irradiated and irradiated glasses were measured after thermal treatment at 250°C for 6 min. The red color of the irradiated glass was bleached by this treatment. Although the $\bar{n}$ values of both glasses decreased upon this treatment, the value of irradiated glass was distinctly smaller than that of non-irradiated glass (Fig. 8). This indicates that the degree of polymerization, which is reduced by irradiation with γ-rays, is not restored by thermal treatment, though the color is bleached.

In addition to these results, account must be taken of the facts that the ESR absorption lines with a large coupling constant expected from ·P–O–P do not appear, while an additional absorption band, probably due to the scattered electrons, appears in the ultraviolet region. Therefore, the following speculation may be given regarding the mechanism of the coloration by γ-ray irradiation. The P–O–P bond in the glass or the single crystal doped with the sulfate is ruptured under the irradiation, resulting in the production of a radical, a positive ion, and a scattered electron:

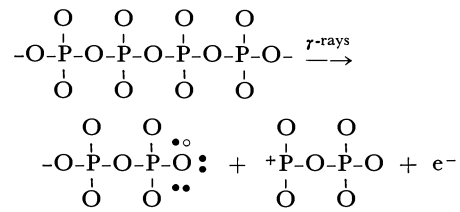

The radical thus produced gives rise to the red color.

A weak ESR absorption line in the irradiated single crystal doped with the sulfate was found at $g=2.007$; this absorption line is different from that due to a radical of the sulfate, for the latter was found at $g=2.003$ when the content of the sulfate in the glass increased. The ESR spectrum of irradiated glass has a weak shoulder at $g=2.007$ which becomes more noticeable as the degree of the polymerization of the glass decreases. These observations lead us to the conclusion that the center producing the weak absorption line at $g=2.007$ arises from the hole trapped by oxygen atoms of the end group.[11]

Thus, under irradiation with γ-rays, the single crystal doped with the sulfate acquires the same color center as in the case of the glass, whereas the pure single crystal shows no effect. These phenomena may be interpreted in the following way. The P-O-P bond in the pure single crystal is too stable to be ruptured under the irradiation with γ-rays, whereas the bond near the sulfate in the single crystal is weakened by the local strain caused by the foreign element. The bond in the glass may also be strained, as the glass was prepared by quenching the melt. Such strained bonds are easily ruptured, and the red color results from irradiation with γ-rays.

In conclusion, the effect of γ-rays on sodium polyphosphate seems to be closely correlated with the local strain of the P–O–P bond.

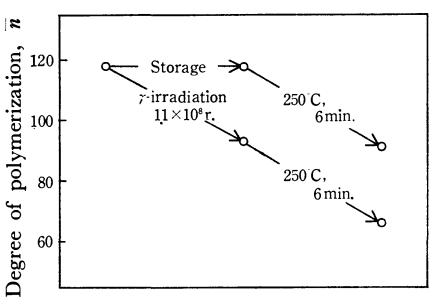

Fig. 8. The variation in the degree of polymerization of the glass with several treatments.

The authors wish to express their hearty thanks to Assistant Professor Takenobu Higashimura of Kyoto University and Assistant Professor Keiji Kuwata of Osaka University for their valuable discussions. Special thanks are also extended to Professor Satoru Tsuda and Mr. Akira Yokohata of Hiroshima University for kindly offering facilities for the γ-irradiation.

10) M. C. M. O'Brien, *Proc. Roy. Soc.*, **A231**, 404 (1955).

11) M. Miura and A. Hasegawa, This Bulletin, **39**, 196 (1966).

BULLETIN OF THE CHEMICAL SOCIETY OF JAPAN VOL. 39 1437—1439 (1966)

A Study of the Pyrolysis of Toluene Using ^{14}C as a Tracer

By Toyosaburo TAKEUCHI, Masakazu SAKAGUCHI* and Yoshio TOGASHI

Faculty of Literature and Science, Toyama University, Gofuku, Toyama

(Received December 13, 1965)

The pyrolysis of toluene-1-^{14}C was carried out by means of the semi-flow method at 800 and at 1000°C in the presence of the registers of porcelain, and the distributions of the radioactive carbon in gaseous products and that of the deposited carbon were determined. The molar c.p.m. of methane and that of a mixture of C_2-compounds were about 1/20 of and twice the molar c.p.m. of the original toluene respectively, while the c.p.m. per gram-atom of the deposited carbon was about twice that of toluene, when the temperature of reaction was 800°C. In the case of the reaction at 1000°C, the c.p.m. per gram-atom of carbon of each product was found to be practically equal to that of the original toluene. It was proposed that methane is formed by the removal of the methyl group of toluene, and that the main source of the carbon of C_2-compounds and the deposited carbon is the 1-carbon of toluene. The equalization of the radioactive carbon in every product at a high temperature was interpreted by assuming that the tropyl radical is formed as an intermediate after the formation of the phenyl radical in the initial stage of the reaction.

The decomposition of toluene by heat, γ-ray irradiation or electron impact has been studied by many investigators.[1-8] These studies have concentrated on measurements of the reaction products, the reaction velocity and the behavior of hydrogen atoms using deuterium as a tracer; the behavior of carbon atoms in the reaction and the influence of the reaction temperature upon the mechanism remain unexplored. It is evident, however, that tracer study using ^{14}C would make the mechanism clearer. This paper is concerned with the pyrolysis of toluene by using toluene-1-^{14}C. The change in the distribution of ^{14}C in the reaction products by the change in reaction temperature from 800 to 1000°C was investigated in order to clarify the mechanism.

Experimental

The toluene-1-^{14}C used was provided by the New England Nuclear Co. Its specific activity was 1.23 mc./mmol. It was diluted to 2.63 mc./mol. with extra pure toluene before use. No impurity was detected in the sample by gas chromatography. The apparatus for the reaction is shown in Fig. 1, where A is a sample reservoir and B is the reaction tube of quartz, whose diameter and length were 2.0 cm. and 50cm. respectively. The tube was fixed in the furnace together with a thermo-junction of Pt-Pt·Rh. The registers of porcelain were packed in the tube in order to decompose the reactant readily. U_1 and U_2 are traps for the gaseous products, such as acetylene, ethylene and benzene, and U_3 is for carbon dioxide converted by the combustion of the deposited carbon to assay the ^{14}C. These traps were cooled by liquid nitrogen baths. C is a combustion tube filled with copper oxide. N and M_1 are a McLeod gauge and the manometers respectively. G is a gas-counting tube (about 50cc.), which is connected with an amplifier and a scaler. D is a safety bottle which contains mercury and is used for the admission of oxygen.

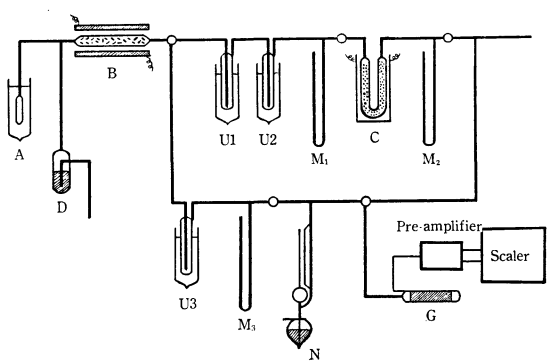

Fig. 1. Apparatus for reaction and assay of ^{14}C.

For each run of experiments, 0.2 cc. of toluene was taken in the sample reservoir. After the air dissolved in the sample had been removed by repeatedly freezing and evacuating the sample, the reaction tube was evacuated up to the pressure of 10^{-3} mmHg, keeping the reservoir at the temperature of liquid nitrogen; then the temperature of the reaction tube was raised to

* Present address: Faculty of Technology, Niigata University, Nagaoka.

1) O. M. Szwarc, *J. Chem. Phys.*, **16**, 128 (1948).
2) A. T. Brade and E. W. R. Steacie, *Can. J. Chem.*, **32**, 1142 (1954).
3) M. Takahashi, This Bulletin, **33**, 801 (1960).
4) J. B. Farmer, I. H. S. Henderson, C. A. McDowell and F. P. Lossing, *J. Chem. Phys.*, **22**, 1948 (1954).
5) F. H. Field and J. L. Franklin, ibid., **22**, 1895 (1954).
6) P. N. Rylander, S. Meyerson and H. M. Grubb, *J. Am. Chem. Soc.*, **79**, 842 (1957).
7) L. H. Gale, B. E. Gordon, G. Steinberg and G. D. Wagner, *J. Phys. Chem.*, **66**, 1537 (1962).
8) R. A. Meyer and J. G. Burr, *J. Am. Chem. Soc.*, **85**, 478 (1963).

1000°C. The reaction was started by replacing the bath of the sample reservoir with a water bath kept at 45°C. The vapor pressure of toluene at this temperature is 75 mmHg. When the sample in the reservoir had run out, the uncondensable gas produced, a mixture of hydrogen and methane, was passed over copper oxide in order to convert the hydrogen into water; then this water was condensed in trap U_3. The amounts of hydrogen and methane were determined by the measurement of pressures before and after the combustion by oxygen. Acetylene and ethylene were separated from benzene and toluene by replacing the liquid nitrogen baths of traps U_1 and U_2 with dry ice baths; they were collected in U_3 by cooling the trap with liquid nitrogen. The combined amount of ethylene and acetylene was determined from the pressure difference produced when the liquid nitrogen baths were replaced with the dry ice baths. The gas was then drawn off until the pressure in the reaction tube showed less than 1 mmHg; the dry ice baths were then replaced by ice baths in order to measure the amount of the mixture of benzene and toluene remaining in the traps. The deposited carbon on porcelain was oxidized to carbon dioxide by passing oxygen through the reaction tube at the temperature of 800°C.

The applied potential of the cathode of the counting tube was 2200V. PR gas, a mixture of argon and methane, was used for a filling gas. The details of the procedure of the assay of ^{14}C were the same as that adopted for tritium, which has been described elsewhere.[9]

Results and Discussion

A large amount of nonvolatile tar was found at the outlet of the reaction tube. The assay of ^{14}C in the substances was not attempted, however, because of the difficulty of collecting them completely. The amounts of gaseous products and the respective counting values are summarized in Tables I and II. The 4th column in each table indicates the molar c. p. m. of the products, while the 5th column indicates the c. p. m. per gram-atom of carbon in each molecule. In order to confirm the reliability of the results of analysis by the method mentioned above, the results were compared with those obtained by a mass spectrometer on the same sample. Nonradioactive toluene was used for this purpose. It was found that the results agree approximately with each other.

The molar c. p. m. of C_2-compounds was about twice, while that of methane was only 1/20 of, the molar c. p. m. of the original toluene in the reaction at 800°C. The small counting value of methane suggests that the carbon comes mainly from the methyl group of toluene. The conspicuously great counting value of C_2-compounds can not be explained in terms of reaction kinetics or mass effect. This point must be left for future investigation. The fact, however, would suggest that the carbon atoms of the C_2-compound come mainly from the 1-carbon atom of toluene. A similar result was reported recently by White et al.[10] Their study of the oxidation of propylene-1-^{14}C indicated that some of the reaction products must be formed from the combination of two or more radioactive fragments.

The c. p. m. per gram-atom of carbon of graphite was about twice that of toluene. This suggests that the graphite might be produced mainly from the carbon atoms of C_2-compounds.

In the case of 1000°C, the c. p. m. per gram-atom of carbon in each product was practically equal to that of toluene. This fact would suggest that each carbon atom of toluene, including that of methyl group, became equivalene in relation to each hydrogen atom at the elevated temperature. Consequently, the seven-membered ring structure of the tropyl radical can be considered, at a high temperature, as an intermediate which is produced by the rearrangement of the benzyl radical first formed. A plausible mechanism of the reaction in the initial stage may be represented as follows:

TABLE I. RESULT OF THE REACTION AT 800°C

Exp. No.	Product	Amount mol.	c.p.m./mol $\times 10^{-7}$	c.p.m./g. atom of C $\times 10^{-7}$
1	Hydrogen	0.486		
2		0.363		
1	Methane	0.224	1.51	1.51
2		0.164	2.20	2.20
1	C_2 compds.	0.011	90.0	45.0
2		0.015	88.1	44.1
1	*Mixture of	0.998	32.1	4.87
2	benzene and toluene	0.591	39.2	5.94
1	Carbon	0.331	13.7	13.7
2	(as CO_2)	0.342	13.2	13.2

The c.p.m. of the original toluene was 46.0/mol. $\times 10^{-7}$.

* The mol. ratio, (benzene)/(toluene), obtained by mass spectrometer after the reaction was 0.63.

TABLE II. RESULT OF THE REACTION AT 1000°C

Exp. No.	Product	Amount mol.	c.p.m./mol. $\times 10^{-7}$	c.p.m./g. atom of C $\times 10^{-7}$
1	Hydrogen	2.21		
2		1.11		
1	Methane	0.52	6.0	6.0
2		0.26	6.1	6.1
1	C_2 compds.	0.30	11.0	5.5
2		0.26	12.6	6.3
1	*Mixture of	0.33	38.4	6.4
2	benzene and toluene	0.19	34.1	5.7
1	Carbon	0.11	5.4	5.4
2	(as CO_2)	0.67	5.5	5.5

The c.p.m. of the original toluene was 45.0/mol. $\times 10^{-7}$.

* The mole ratio, (benzene)/(toluene), obtained by mass spectrometer after the reaction was 80.

9) T. Takeuchi, M. Sakaguchi and M. Tatsushima, *Radioisotopes*, **10**, 106 (1961).

10) E. R. White, H. C. Davis and E. S. Hammack, *J. Am. Chem. Soc.*, **87**, 1175 (1965).

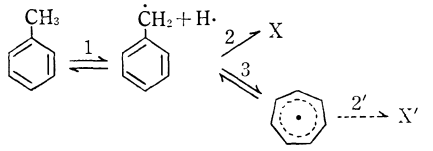

where X and X′ denote the products produced successively from the benzyl radical and the tropyl radical respectively. If the velocity of step 2 is greater than that of step 3, it will be difficult for the redistribution of ^{14}C to occur. If step 2′ is included in the reaction paths of the decomposition, it seems, from a study of the configuration of carbon atoms, that benzene is not formed as the product. The experimental results suggests that the velocity of step 2 would be greater than that of step 3 at 800°C, but would be smaller at 1000°C, as is diagrammatically represented in Fig. 2. The velocity of the reverse reaction of step 3 would predominate if the reaction temperature were raised to 1000°C. If the velocity of the reverse reaction of step 3 is fairly great even at 800°C, ^{14}C should be detected more or less in methane. In addition to this, the c. p. m. per mol. of benzene would be smaller than that of the original toluene. The results of the reaction at 800°C (Table I) can be interpreted in such a way.

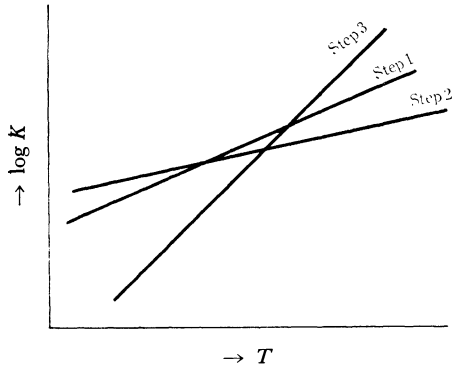

Fig. 2. Approximate representation of dependency of rate constant K in each reaction path on temperature.

Rylander et al.[6], who had found the mass number corresponding to C_7H_7 in the decomposition reaction of deuterated toluene by electron impact, proposed that the principal intermediate of the reaction is the tropylium ion. Recently, however, Gale et al.[7] have proposed, from a study by electron impact using toluene-α-^{14}C, that the tropylium ion should be excluded from the paths of the reaction. Our results would indicate that the reaction mechanisms in electron impact and thermal decomposition are substantially different from one another.

Summary

The pyrolysis of toluene at 800 and 1000°C has been made using toluene-1-^{14}C, and the ^{14}C in the reaction products of the gaseous state, such as methane, acetylene, ethylene and benzene, and the deposited carbon has been assayed.

The molar c. p. m. of methane and that of the mixture of C_2-compounds were about 1/20 of and twice that of the original toluene respectively, when the reaction was carried out at 800°C. The c. p. m. per gram-atom of the carbon in each product was practically equal to that of the original toluene when the reaction was carried out at 1000°C. It has been proposed that methane is formed by the removal of the methyl group and that the deposited carbon is formed mainly by the decomposition of C_2-compounds produced by the reaction. The formation of the tropyl radical has also been proposed as an intermediate in the reaction at a high temperature, through the formation of the benzyl radical.

The authors are grateful to Mr. Yoshisato Tezuka and Mr. Senji Watanabe for their assistance with much of the experimental work.

BULLETIN OF THE CHEMICAL SOCIETY OF JAPAN VOL. 39 1440—1442 (1966)

On the Asymmetric Interaction of the Optical Antipodes with Amylose

By Masaaki OHARA, Chau-Yang CHEN and Takao KWAN

Division of Physicochemical Technology, Faculty of Pharmaceutical Sciences, The University of Tokyo, Hongo, Tokyo

(Received December 20, 1965)

The asymmetric adsorption of D, L-mandelic acid and its homologues has been demonstrated on amylose by means of the column chromatographic and static techniques. The D-(−)-isomer of mandelic acid has been found to be adsorbed more weakly than the L-(+)-isomer; the separation factor of the two antipodes has been estimated to be 1.09 at 0°C. This value is greater than that on starch, suggesting that amylose may have a somewhat higher selectivity for the asymmetric adsorption of the optical antipodes than amylopectin. The anomalous interaction of D, L-atrolactic acid has been observed on the amylose much as in the case with starch reported previously.

It has been demonstrated,[1,2] that the optical antipodes of mandelic acid and its homologues are selectively adsorbed on starch. Since starch is composed of amylose and amylopectin, one question of interest would be which constituent is responsible for the asymmetric interaction. Another point of interest is what modes of selectivity are found in the interaction of the optical antipodes with these starch constituents.

In the present report, the authors will describe the asymmetric adsorption of D, L-mandelic acid and its homologues on amylose. The distinct difference in the adsorption affinity will be revealed between the two optical antipodes by means of the column chromatographic and static techniques. Some information concerning the asymmetric adsorption on starch will then be deduced from the results obtained.

Experimental

The Preparation of the Adsorbent.—The following route of pretreatment was taken in order to obtain the water-insoluble amylose. Commercially-available amylose was immersed in distilled water at room temperature for 24 hr. The precipitates were filtered and repeatedly washed with distilled water until the optical rotation due to water-soluble fractions of the adsorbent completely disappeared from the mother liquor. Water-insoluble precipitates were obtained and then dried in air at room temperature. The amylose sample thus obtained was 20.1% moisture. This sample was characterized in an anhydrous state by measuring the limiting viscosity number, $[\eta]$, in a dimethyl sulfoxide solution at 25°C using an Ubbelohde-type viscometer.[3] The $[\eta]=0.257\ \overline{P}_w^{0.82}$,[4] relation, was employed to calculate the mean degree of polymerization, $\overline{P}_w$, from which the viscosity-average molecular weight was estimated to be about 210000.

Chromatographic Procedure.—The compounds subjected to the chromatographic separation were as follows; DL-mandelic acid, DL-methyl mandelate, DL-ethyl mandelate and DL-atrolactic acid.

Each racemate (1—2 g.) in 50% aqueous methanol was put on an amylose column (1.6×42 cm.) at room temperature and then eluted with the same solvent. The flow rate was 4.0 ml./min. The optical rotation of each fraction (1.6 ml.) was determined by a Zeiss-Kreis polarimeter, and the concentration of mandelic acid was determined by the optical absorption at 257 mμ. In the case of DL-atrolactic acid, the optical rotation in each fraction was too small to affirm the asymmetric interaction. Therefore, some enriched L-(+)- or D-(−)-isomer samples were subjected separately to chromatographic separation.

The Determination of Adsorption Equilibrium.—3.5 g. of the pretreated amylose was immersed in 30 ml. of a DL-mandelic acid solution. The system was allowed to stand at 0°C for 48 hr., by which time equilibrium had been attained. The supernatant liquid drawn off was then analyzed. The optical rotation of the solution was measured by a Yanagimoto Model OR-20-type photomagnetic polarimeter, and the concentration of the acid was determined by the optical absorption, as has been mentioned already.

Results

The asymmetric adsorption on amylose has been distinctly revealed by the column chromatography. Figures 1 and 2 show the specific rotation, $[\alpha]_D$, of mandelic acid and its homologues with respect to each fraction of the effluent. The observed angle of rotation, α_D, and the concentration of the adsorbates, c, in g. per 100 ml. of an aqueous methanol solution are given for some of the fractions.

It is apparent that (−)-isomers of mandelic acid and its esters were eluted first, followed by (+)-isomers. On the other hand, the order of elution was reversed with DL-atrolactic acid. The same situation was observed when starch was used as

1) M. Ohara, K. Ohta and T. Kwan, This Bulletin, **37**, 76 (1964).
2) M. Ohara, C.-Y. Chen and T. Kwan, ibid., **39**, 137 (1966).
3) W. W. Everett and J. F. Foster, *J. Am. Chem. Soc.*, **81**, 3464 (1959).
4) W. Burchard, *Makromol. Chem.*, **64**, 110 (1963).

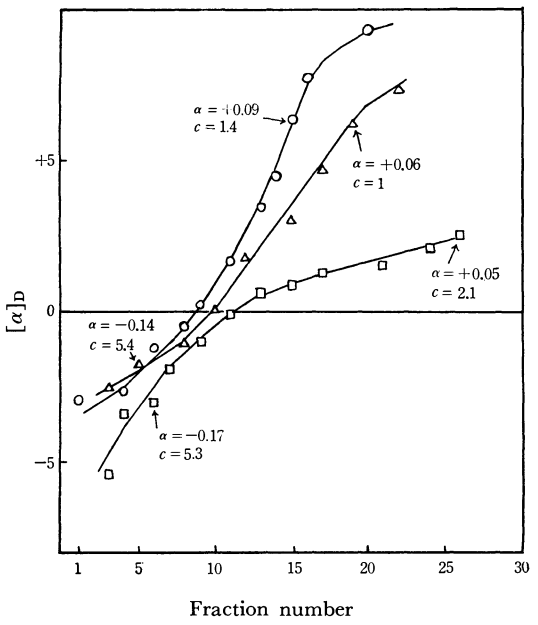

Fig. 1. The specific rotation $[\alpha]_D$ of mandelic acid and its esters against fraction numbers.
□ Mandelic acid 2.0 g.
○ Methyl mandelate 1.0 g.
△ Ethyl mandelate 1.0 g.

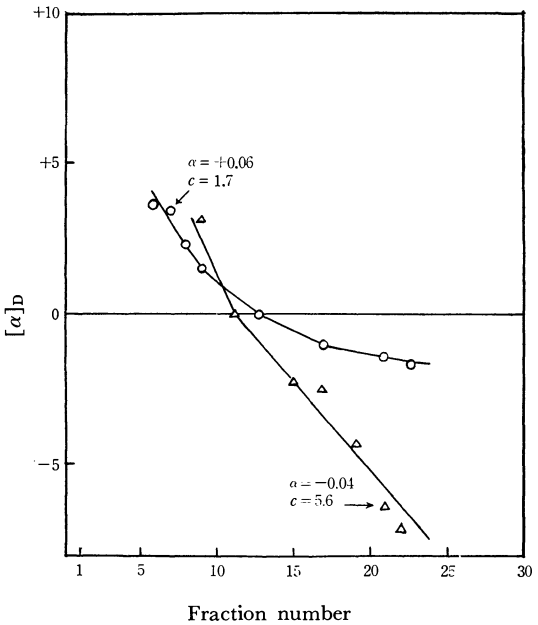

Fig. 2. The specific rotation $[\alpha]_D$ of atrolactic acid against fraction numbers.
○ (+)-enriched sample
△ (−)-enriched sample

the adsorbent.[1] This behavior of the enantiomers on amylose indicates that there is a parallel relationship between adsorption affinity and configuration, since optical isomers with the same sign can be assigned the same configuration for mandelic acid and its esters.[1] The adsorption affinity of D, L-atrolactic acid may be considered to be reversed on the basis of the generally-established theory that optical isomers of mandelic acid and atrolactic acid with the same sign can be assigned to the same configuration.[5]

Table I lists typical adsorption equilibrium data obtained by a static method. The adsorption data on starch[2] are also shown for the sake of comparison.

Table I. Adsorption equilibrium data of D, L-mandelic acid on amylose and starch (T=0°C)

Absorbent	Amylose	Starch
Amount of adsorbent, g.	3.5	9.0
Initial concentration of D, L-mandelic acid, C_i, mg./ml.	100.0	100.3
Equilibrium concentration of D, L-mandelic acid, C_e, mg./ml.	95.9	91.8
Amount of D, L-mandelic acid adsorbed, W, mg./g.	64	57
Optical rotation of the solution α_D	−0.036	−0.060
Specific rotation of the solution $[\alpha]_D$	−0.375	−0.66
$\Delta W/W$ %	3.8	2.6
Separation factor f	1.09	1.06

The values of the optical rotation described here were ascribed to the net rotation values of mandelic acid in the solution, which were determined by using a glycolic acid solution (concentration: 143 mg./ml.), as has been reported previously.[2] From these negative values, it may be inferred that the D-(−)-isomer is less adsorbable than the L-(+)-isomer. This finding is consistent with those revealed by the column chromatography. The amount of D, L-mandelic acid adsorbed per gram of amylose, W, was calculated much as that absorbed on starch[2] by assuming that the amounts of water bound to the two adsorbents were of the same magnitude. ΔW is the excess amount of the (+)- over the (−)-isomer adsorbed, so that $\Delta W/W$ may indicate the degree of the asymmetric adsorption of the optical antipodes. The separation factor, f, is defined by the ratio of the adsorption equilibrium constants of the two enantiomers and is expressed as:

$$f = \frac{W_d/C_{ed}}{W_l/C_{el}}$$

where W_d and W_l are, respectively, the amounts of the L- or D-isomer adsorbed, while C_{ed} and C_{el} are the concentrations of the L- and D-isomers,

5) See Footnotes 3—6 in a previous article by Ohara et al.[1]

respectively, in the liquid phase at equilibrium. It was found to be greater on amylose than on starch.

Discussion

It is interesting to note that amylose possesses the same mode of selectivity as starch for the asymmetric adsorption of the optical antipodes.

Separate static experiments[6] similar to that on amylose have been made using potato amylopectin and starch as the adsorbents in the methanol phases. In these cases, the asymmetric adsorption of D, L-mandelic acid has also been revealed on both adsorbents, and the orders of the adsorption affinity for the enantiomers have been shown to be as follows:

$$\text{L-}(+)\text{-isomer} > \text{D-}(-)\text{-isomer}$$

Accordingly, for the enantiomers of mandelic acid, it can be concluded that the modes of selectivity on amylose and amylopectin are identical with that on starch.

Now, let us consider which constituent of the starch is more responsible for the asymmetric adsorption of D, L-mandelic acid. It is generally accepted that amylose and amylopectin constitute 20—25% and 75—80% portions of the starch granule respectively.[7] By considering that the degree of the asymmetric adsorption, $\Delta W/W$, on amylose and on starch are 3.8% and 2.6% respectively, and by assuming that the amylose portion in the granular starch possesses the same $\Delta W/W$ value as the amylose employed in this experiment, the $\Delta W/W$ value ascribed to the amylopectin portion may be estimated as 2.2—2.3%. It is suggested, therefore, that amylose may have a somewhat higher selectivity for the asymmetric adsorption of D, L-mandelic acid than amylopectin. However, no large difference in selectivity can be seen between that on amylose and that on amylopectin. These facts may be explained from the fact that there is not essentially a large difference in structure between amylose and amylopectin, although amylose (with a linear-chain structure) has a somewhat more regular structure than amylopectin (with a branched-chain structure).

Finally, we want to refer to the anomalous interaction of amylose with atrolactic acid. This phenomena cannot be found in β-cyclodextrin, which is known to be a cycloheptaose connected with α-1, 4 glucosidic linkage. It was found[8] that β-cyclodextrin builds inclusion compounds stereospecifically with a series of mandelic acid homologues. Both in the case of ethyl mandelate and in the cases of atrolactic acid and ethyl atrolactate, (−)-isomers were proved to be more strongly interacting than (+)-isomers. Cramer and Dietsche elucidated the parallelism between the affinities of the two enantiomers to β-cyclodextrin and their configurations in terms of the generally-established theory,[5] as has been mentioned already.

However, this is not the case with amylose. This may be explained from the fact that the structure of β-cyclodextrin is fixed, while that of amylose is flexible.[9]

Consequently, it may be inferred that, in the case of β-cyclodextrin, the normal interaction of D, L-mandelic acid homologues can be observed. On the other hand, in the case of amylose, the adsorption structures of the optical isomers of mandelic acid are probably different from those of atrolactic acid.

The authors wish to make a special acknowledgement of the gift of an amylose sample by the Chugai Pharm. Co. The authors also wish to express their thanks to Professor Shun-ichi Yamada of The University of Tokyo for allowing them to use the photomagnetic polarimeter. This research was supported in part by a grant-in-aid from the Ministry of Education, to which the authors' thanks are due.

6) M. Ohara and T. Kwan, unpublished data.

7) J. Nikuni, "Starch Handbook" (Denpun Handbook), Ed. by J. Nikuni, Asakura Pub. Co., Tokyo (1960), Chapter 1, p. 54.

8) F. Cramer and W. Dietsche, *Chem. Ber.*, **92**, 378 (1959).

9) V. S. R. Rao and J. F. Foster, *Biopolymers*, **1**, 527 (1963); T. Kuge and S. Ono, This Bulletin, **34**, 1264 (1961); J. M. G. Cowie, *Makromol. Chem.*, **42**, 230 (1961).

BULLETIN OF THE CHEMICAL SOCIETY OF JAPAN VOL. 39 1443—1448 (1966)

Photoemission from Polycyclic Aromatic Crystals in the Vacuum Ultraviolet Region

By Yoshiya HARADA and Hiroo INOKUCHI

The Institute for Solid State Physics, The University of Tokyo, Azabu, Tokyo

(Received December 20, 1965)

The external photoelectric effect of thin films of tetracene, pentacene, violanthrene, quaterrylene and tetrathiotetracene was studied in the vacuum ultraviolet region. The contact potential differences between the emitters, organic crystals, and the collector (Aquadaq) were determined from the saturation points of the current-voltage characteristics. It was observed that the quantum yields of photoemission increase markedly with an increase in the photon energy, reaching the order of 10^{-2} electrons/quantum at $h\nu=10$ eV. The threshold energies were lower by 1—2 eV. than the molecular ionization potentials. An energy diagram for the external photoelectric process of organic molecular crystals was introduced on the basis of the intrinsic band model. With the aid of this diagram, the band gap energies, $\Delta\varepsilon$, were obtained from the observed values of photoemission. The values of $\Delta\varepsilon$ thus obtained were in fairly good agreement with those based on the results of the temperature dependence of semiconduction.

The external photoelectric effect is valuable in investigating the electrical properties of organic molecular crystals, because the current-voltage characteristics and the spectral distribution of the yield offer knowledge concerning the electronic structure of the crystal.

At the beginning of this century the external photoelectric effect of a polycyclic aromatic hydrocarbon, anthracene, was observed by Pochettino.[1] Subsequently Hughes[2] and Volmer[3] measured the threshold of photoemission from anthracene and reported the values of 5.6—6.2 eV. and 5.5 eV. respectively. After these works, there was no observation of photoemission from polycyclic aromatic hydrocarbons until the 1950's. In 1953, Carswell and Iredale[4] investigated the photoelectric emission from anthracene and phenanthrene. Later the external photoelectric effect of aromatic hydrocarbons was studied by Kearns and Calvin,[5] Lyons and Morris,[6] and Vilessov, Sagrubsky, and Grabusov.[7] In the latter two articles observations of the emission extending to the vacuum ultraviolet region were reported.

In this paper, we will present the external photoelectric effect of some polycyclic aromatic hydrocarbons and tetrathiotetracene in the vacuum ultraviolet region. Further, an energy diagram for the photoelectric process will be introduced in order to correlate the observed values of photoemission with the activation energy of the electrical conduction.

Experimental

The materials used in the present study are shown in Fig. 1. Violanthrene (III) and tetrathiotetracene (V) were kindly furnished by Junji Aoki and Yoshio Matsunaga respectively. The other compounds were

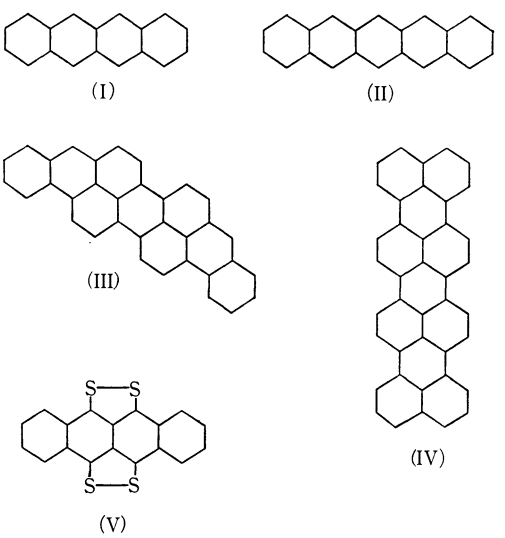

Fig. 1. Structural formulae of materials.
(I) Tetracene
(II) Pentacene
(III) Violanthrene
(IV) Quaterrylene
(V) Tetrathiotetracene

1) A Pochettino, *Atti reale Accad. Lincei*, **1**, 355 (1906); **2**, 17 (1906).
2) A. L. Hughes, *Phil. Mag.*, **24**, 380 (1912).
3) M. Volmer, *Ann. Phys.*, **40**, 775 (1913).
4) Carswell and Iredale, *Aust. J. Appl. Sci.*, **4**, 329 (1953).
5) D. R. Kearns and M. Calvin, *J. Chem. Phys.*, **34**, 2026 (1961).
6) L. E. Lyons and G. C. Morris, *J. Chem. Soc.*, **1960**, 5192.
7) F. I. Vilessov, A. A. Sagrubsky and D. S. Garbusov, *Physika Tverdogo Tela*, **5**, 2000 (1963).

provided by the Rütgeswerke-Aktiengeselshaft A. G., Germany. All of the materials were carefully purified by the recrystallization and vacuum sublimation method.

The photoemission was measured with a 0.5 meter Seya-Namioka-type[8] vacuum ultraviolet monochromator.* The monochromator, with its associated equipment, is shown schematically in Fig. 2. The grating was made by Bausch and Lomb Optical Company and had 1200 lines per mm. The wavelength calibration was made using the central image of the grating (0 Å) and also the line spectra of mercury (3650.2, 3654.8 and 3663.3 Å). Further, in the vicinity of the 1800 Å peak the wavelengths of the Schumann-Runge absorption band system of oxygen were compared with those described in the literature.[9]

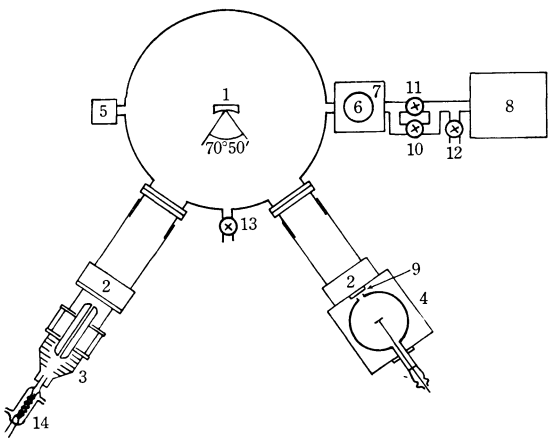

Fig. 2. Vacuum spectrometer.
1 Grating, 2 slit, 3 light source, 4 photoemission attachment, 5 Phillipps gauge, 6 oil diffusion pump, 7 cold trap, 8 rotary pump, 9 lithium fluoride window, 10 reducing valve, gate valve, 12 loak valve, 13 chamber leak valve and 14 palladium tube.

As a light source a Hinteregger-type hydrogen discharge lamp[10] was used. With the lamp turned on, pure hydrogen, prepared by passing commercial hydrogen from a cylinder through a palladium thimble (14 in Fig. 2), was introduced into the instrument. In order to control the velocity of the passage through the thimble, the Pd thimble was heated electrically by a coil wound on a Pyrex envelope. The temperature of the palladium tube and also of the opening of the reducing valve (10 in Fig. 2) were adjusted so that pure hydrogen flowed continuously through the monochromator chamber at an appropriate pressure. The normal operating pressure of hydrogen was around 4 mmHg.

In order to measure the photoemission the attachment illustrated in Fig. 3 was mounted onto the exit slit of the monochromator by iron fittings (6) and sealed vacuum-tight by means of an 0-ring (4). A photoemission cell (1) was mounted in a cylindrical chamber made of brass. A collector lead of the cell was taken out of the chamber through a glass-fused seal (3). When the vacuum spectrometer was used in the near-ultraviolet or visible region, the use of a set of filters became necessary in order to separate the higher-order spectra. From 2100 Å to 3500 Å, a potassium bromide plate was provided as a filter. Further, a glass filter was used in the wavelength region longer than 3500 Å. The filters (5) were mounted on a holder and were made exchangeable by sliding the holder shaft from the outside of the chamber.

In Fig. 4 the photocell is shown in detail. It is basically similar to that designed by Apker et al.[11] The collector is a glass sphere about 13 cm. in diameter. On the inside it is coated with a conducting layer of Aquadag (3), which was baked at 500°C in an electric furnace. After the heat treatment the work function

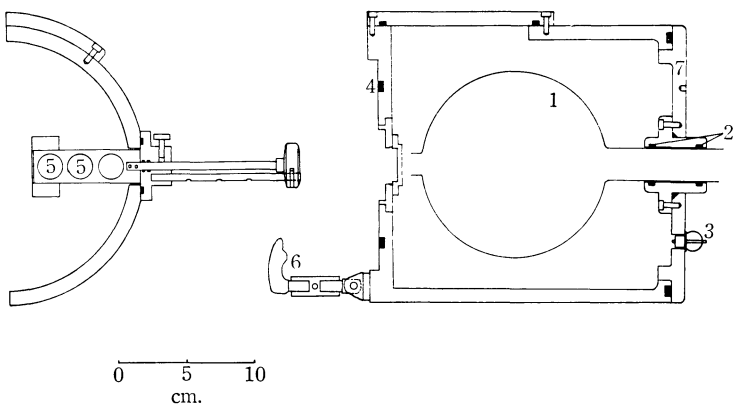

Fig. 3. Photoemission attachment.
1 Photoemission cell, 2 0-ring, 3 glass fused seal, 4 0-ring, 5 filter, 6 iron fitting, 7 flange.

* The monochromator used in this experiment was a considerable improvement over the instrument produced by Jarrell-Ash Co.

8) M. Seya, *Science of Light*, **2**, 8 (1952); T. Namioka, *J. Otp. Soc. Am.*, **49**, 951 (1959).

9) K. Watanabe, E. Edward, C. Y. Inn and M. Zelikoff, *J. Chem. Phys.*, **21**, 1026 (1953); R. W. Ditschburn and D. W. O. Heddle, *Proc. Roy. Soc.*, **A226**, 509 (1954); A. M. Bass and H. P. Broida, *J. Mol. Spect.*, **12**, 221 (1964).

10) R. G. Newburgh, L. Heroux and H. E. Hinteregger, *App. Optics*, **1**, 733 (1962).

11) L. Apker, E. Taft and J. Dickey, *Phys. Rev.*, **74**, 1462 (1948).

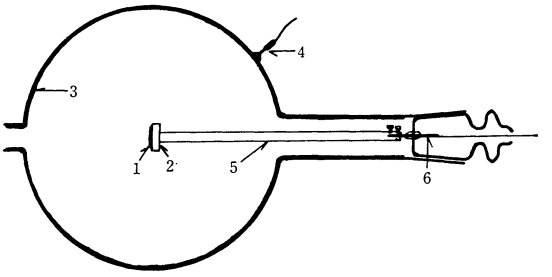

Fig. 4. Photocell.
1 Sample, 2 copper substrate, 3 graphite coating, 4 collector lead (tungsten rod), 5 brass rod, 6 tungsten rod.

of the Aquadag layer was practically always 4.74± 0.05 eV.[11] A polycyclic organic compound (1) deposited onto a copper disk (2) (12 mm. in diameter) was fixed at the centre of the glass bulb as an emitter. The sublimation of the compound was carried out in vacuo (10^{-6} mmHg), the thickness of a film being several microns. Since the cell had no window, the pressure in it was equal to that in the attachment chamber (10^{-6} mmHg).

The absolute measurement of the light intensity was made by means of an Eppley circular thermopile, the sensitivity of which was 0.30 μV./μW. in vacuo. The output potential was amplified by a Keithley model 149 milli-micro voltmeter. The relative light intensity was obtained by measuring the fluorescence intensity from a coronene film evaporated onto a glass plate.[12] In this case the flange of the attachment chamber (7 in Fig. 3) is changed for another one which can be fitted with an end-on-type photomultiplier tube, RCA 5819. The intensity of the light source was examined in relative units after each series of photoemission measurements.

The emission current was amplified by a Cary 31 vibrating-reed electrometer.

Results

Current - voltage Characteristics. — Monochromatic lights were used to observe the current-voltage characteristics of photoemission. The experimental results for tetracene and quaterrylene films are given in Figs. 5 and 6, where the ordinates

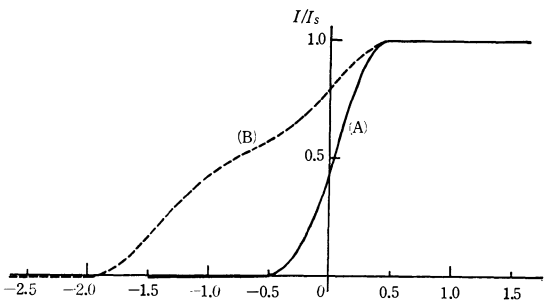

Applied potential, V.

Fig. 5. Current-voltage relation of tetracene.
hν: (A) 6.20, (B) 7.75 eV.

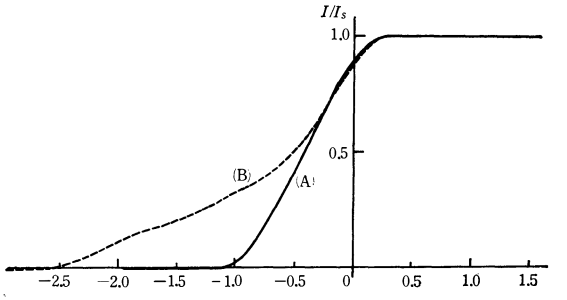

Applied potential, V.

Fig. 6. Current-voltage relation of quaterrylene.
hν: (A) 6.20, (B) 7.75 eV.

are normalized with the saturation current, I_s= 1.0. The values of the saturation voltage, V_s, of the current-voltage curves (the contact-potential differences between the emitters and the collector) are given in Table I for all of the compounds studied.*

Table I. Saturation voltages of the current-voltage characteristic

Compound	V_s, volt
Tetracene	0.44
Pentacene	0.41
Violanthrene	0.21
Quaterrylene	0.28
Tetrathiotetracene	0.42

In order to determine the saturation point, the data of the current-voltage relation are plotted in the form:

$$1 - (1 - I/I_s)^{1/2} \text{ vs. } V. \qquad (1)$$

The intersection of two straight lines, one in the retarding potential region, and the other in the saturation region, obtained by the plot gives the value V_s.[13]

In the case of tetracene, since the value of the electrical resistivity is high enough ($\rho_{15} = 10^{15}\Omega$cm.), the potential drop within a thick film becomes comparable to that between its surface and the collector. Hence, a thin film ($<1\ \mu$) should be examined if we are to observe the correct current-voltage characteristics. The current-voltage relations of the other compounds were successfully obtained for films with thicknesses of several microns.

Spectral Distributions of the Yield.—The spectral responses of photoemissive currents were

12) H. Inokuchi, Y. Harada and T. Kondow, *J. Opt. Soc. Am.*, **54**, 849 (1964).

* The V_s values obtained from I-V curves observed at different photon energies were in good agreement with each other.

13) L. Apker, E. Taft and J. Dickey, *Phys. Rev.*, **73**, 46 (1948).

observed under an applied potential of 10 V. In Figs. 7—9 the results for tetracene, pentacene and violanthrene are given. In each figure the ordinate shows the quantum yield, Y, derived from the ratio between the number of the incident photons and that of the emissive electrons.

The threshold values of the photon energies required for photoemission are compared in Table II with those obtained by other investigators. The table also includes the molecular ionization potentials. Since no appropriate extraporation formula has yet been found, the numerical value of the threshold was determined by extraporation to a quantum yield of 10^{-8} electrons per incident quantum.

Discussion

As may be seen from Table I, photocurrents saturate at low applied potentials (potentials of less than one volt). This phenomenon shows that the photocell used in the present study has a good

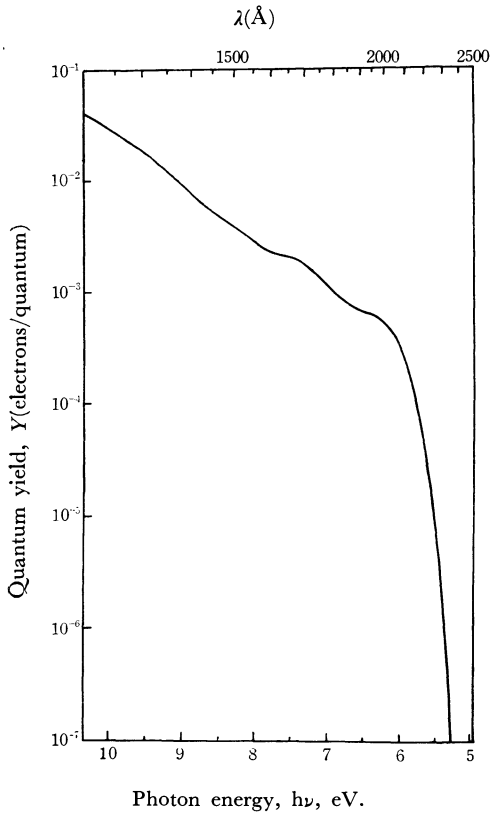

Fig. 7. Spectral distribution of the photoemission yield for tetracene.

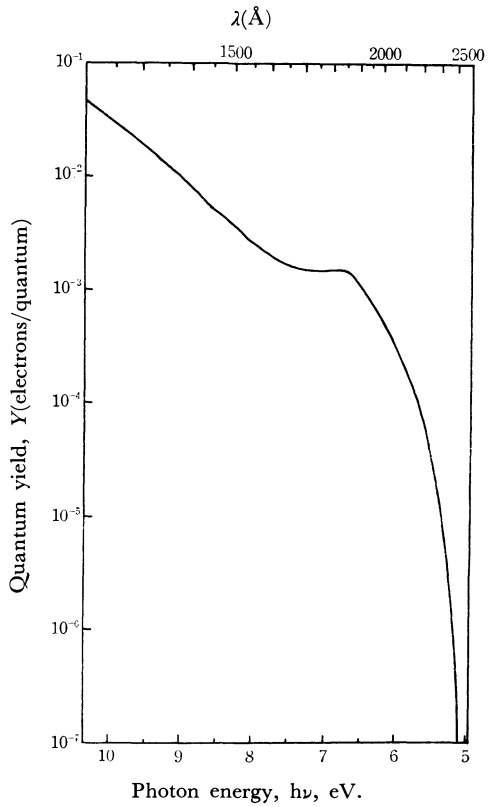

Fig. 8. Spectral distribution of the photoemission yield for pentacene.

TABLE II. THRESHOLD VALUES OF PHOTOEMISSION, E_{th} IN ADDITION TO MOLECULAR IONIZATION POTENTIALS, I_g

Compound	I_g, eV.	E_{th}, eV.			
		Present work			
Tetracene	6.88[a]	5.24	5.26[e]	5.38[f]	5.25[g]
Pentacene	6.73[b]	5.07	5.08[f]	5.1[g]	
Violanthrene	6.55[c]	4.96	5.20[f]		
Quaterrylene	5.98[d]	4.76	—		
Tetrathiotetracene	—	4.56	—		

a) F. I. Vilessov, *Dokl. Akad. Nauk SSSR*, **132**, 632 (1960).
b) R. M. Hedges and F. A. Matsen, *J. Chem. Phys.*, **28**, 950 (1958).
c) F. A. Matsen, *J. Chem. Phys.*, **24**, 602 (1955).
d) Estimated from the energy of the longest absorption band (cf. Ref. c).
e) Ref. 6.
f) Ref. 5.
g) Ref. 7.

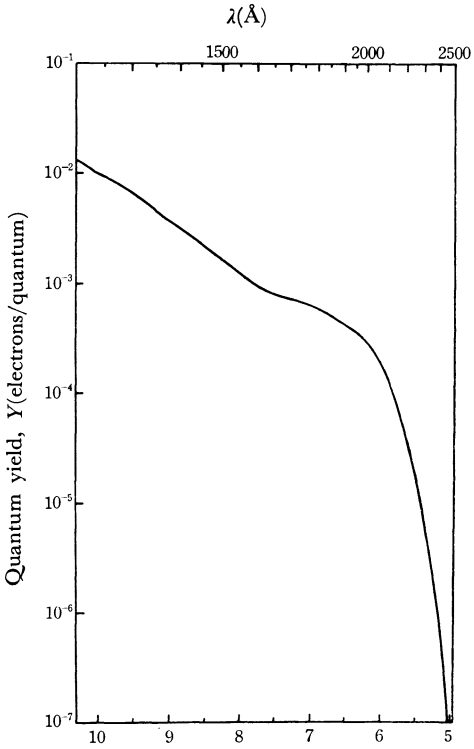

Fig. 9. Spectral distribution of the photoemission yield for violanthrene.

spherical geometry.

In the region of low applied potentials, the current-voltage curves are not parabolic (Figs. 5 and 6); especially, the curves for the incident light of 7.75 eV. have inflections. Hence, it can be pointed out that the kinetic energy distributions of the emitted electrons have several maxima. This behaviour of the emitted electrons will be discussed in a subsequent article.

Figures 7—9 show that the quantum yields of photoemission from tetracene, pentacene and violanthrene increase with an increase in the photon energy and reach the order of 10^{-2} electrons/quantum at $h\nu = 10$ eV. The other compounds give similar results. Thus, at large photon energies the yield of aromatic hydrocarbons is relatively large, comparable to those observed in such metals as palladium, tungsten and molybdenum.[14]

Table II shows that the threshold of photoemission (solid state ionization potential) occurs at an energy lower than by 1—2 eV. than the molecular ionization potential. As was suggested by Lyons,[15] this difference may be due to the polarization energy of the crystals by a positive centre.

14) W. C. Walker, N. Wainfan and G. L. Weisser, *J. Appl. Phys.*, **24**, 1318 (1953); **26**, 1366 (1955).
15) L. E. Lyons, *J. Chem. Soc.*, **1957**, 5001; L. E. Lyons and J. C. Mackie, *Proc. Chem. Soc.*, **1962**, 71.

Finally, let us consider the external photoelectric process of the organic molecular crystal quantitatively using the observed threshold values of the photoemission and the saturation potential of the current-voltage curve. In the case of the intrinsic semiconductor, the energy difference, δ, between the top of the valence band and the Fermi level is a half of the band gap energy, $\Delta\varepsilon/2$, based on the results of the temperature dependence of the semiconduction. Generally, in the external photoelectric process, the Fermi level of the emitter coincides with that of the collector in thermal equilibrium. Thus, if we assume that the organic molecular crystals studied are intrinsic semiconductors, the schematic diagram in Fig. 10 can be introduced. In the diagram, the threshold energy, E_{th}, is determined by the energy difference between the

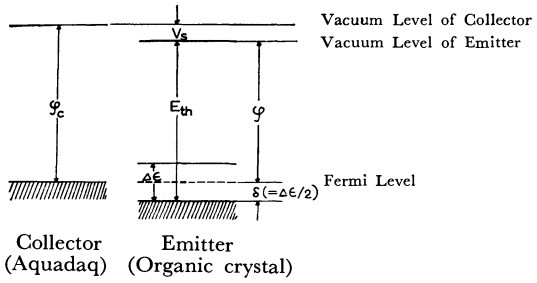

Fig. 10. Shematic diagram for the external photoelectric process of the organic molecular crystal.

vacuum level and the top of the valence band. On the other hand, the work function, φ, is the energy difference between the vacuum level and the Fermi level. Hence;

$$E_{th} = \varphi + \delta = \varphi_c - eV_s + \Delta\varepsilon/2 \qquad (2)$$

Table III. Comparison of band gap energies

Componud	$\Delta\varepsilon$, eV.[a]	$\Delta\varepsilon$, eV.[b]
Tetracene	1.88	1.70[c]
Pentacene	1.48	1.50[d]
Violanthrene	0.86	0.85[e]
Quaterrylene	0.60	0.60[f]
Tetrathiotetracene	0.48	0.41—0.57[g]

a) Present work; obtained from Eq. 3.
b) Obtained from the results of the temperature dependence of semiconduction.
c) D. C. Northrop and O. Simpson, *Proc. Roy. Soc.*, **A234**, 124 (1956). This value of $\Delta\varepsilon$ seems to be too low as compared with those of other hydrocarbons of polyacene series (anthracene, $\Delta\varepsilon = 2.7$ eV.; pentacene, $\Delta\varepsilon = 1.50$ eV.). The correct value may be near 2 eV.
d) Ref. c.
e) H. Inokuchi, This Bulletin, **24**, 222 (1951).
f) Y. Maruyama, H. Inokuchi and Y. Harada, ibid, **36**, 1193 (1963).
g) M. Kochi, private communication.

where φ_c is the work function of a colloidal graphite, Aquadag. Setting $\varphi_c=4.74$ eV.,[11] we can obtain the band gap energy from the observed values of V_s and E_{th}:

$$\Delta\varepsilon = 2(E_{th} + eV_s) - 9.48\,\text{eV}. \qquad (3)$$

In Table III the $\Delta\varepsilon$ values obtained from Eq. 3 are compared with those found from the temperature dependence of the semiconduction. The table indicates that the two values of the band gap energy are in fairly good agreement. It has thus been established that the present diagram can explain the external photoelectric process of the organic molecular crystals studied.*

Future experiments on the photoemission of these crystals will be devoted to a study of the spectral dependence of the quantum yield at low temperatures and also to a detailed analysis of the current-voltage relation.

It is a great honour to dedicate this paper to Professor Masao Kotani in celebration of his sixtieth birthday.

* Recently, Maruyama and Inokuchi (This Bulletin, **39**, 1418 (1966)) studied the effect of oxygen on the semiconductivity of a quaterrylene film and found that the intrinsic semiconductor model is applicable only when there is a high vacuum ($\sim 10^{-8}$mmHg), the band gap being 1.7 eV. in this case. According to their results, the band gap of 0.6 eV. which is observed for a film exposed to air is due to an acceptor level formed by an oxygen impurity. Thus, the present results for quaterrylene should be interpreted in terms of the extrinsic band model. Since, in this case, the Fermi level is located halfway between the acceptor level and the top of the valence band, and since also, the emitted electrons from the acceptor level can be neglected, the energy diagram shown in Fig. A (instead of Fig. 10) may be considered to hold for photoemission from quaterrlene.

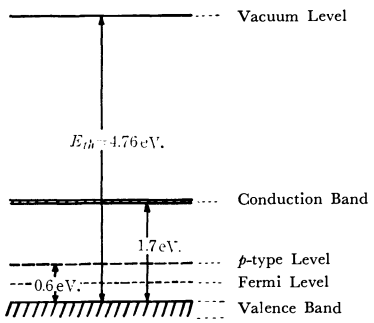

Fig. A

BULLETIN OF THE CHEMICAL SOCIETY OF JAPAN VOL. 39 1448—1452 (1966)

The Determination of Oxygen in Metals with High Melting Points by the Inert Gas Fusion Method: A Silicon Fusion Technique

By Jiro KASHIMA and Takuo YAMAZAKI

The Castings Research Laboratory, Waseda University, Shinjuku-ku, Tokyo

(Received April 12, 1965)

The determination of oxygen in metals with high melting points is important for the development of metallurgy. This paper will describe a very simplified apparatus and a procedure which gives precise results almost without a blank test. A silicon fusion technique developed by the present authors is used instead of the platinum bath method for the purpose of decomposing oxides in metals. It enables us to determine oxygen in a small quantity of a sample by the use of a highly-sensitive gas chromatograph. The amount of oxygen in the purified tantalum and niobium was determined within a standard deviation of 0.0038%. The precision established in tests of titanium samples containing 0.074% of oxygen was 0.0018%; this observed value is in good agreement with that obtained by the vacuum fusion method.

The precise determination of the oxygen content in metals with high melting points is important for the development of metallurgy. Many authors[1-5] have described complicated high-vacuum equipment and have obtained precise results by means of the platinum bath method, but for practical use some points may be improved at small expense.

Recently, various attempts, such as that using

1) R. S. McDonald, J. E. Fagel and E. W. Jr. Balis, *Anal. Chem.*, **27**, 1632 (1955).
2) S. J. Bennett and L. C. Covington, *Anal. Chem.*, **30**, 363 (1958).
3) N. A. Gokcen, *Trans. Am. Inst. Mining Met. Petrol. Engineers*, **212**, 93 (1958).
4) CH. Venkateswarlu and M. W. Mallett, *Anal. Chem.*, **32**, 1888 (1960).
5) T. Somiya, S. Hirano, H. Kamada and I. Ogahara, *Talanta*, **11**, 581 (1962).

the inert gas fusion method[9-12] without vacuum equipment and that using the neutron activation analysis method,[6-8] have been made to simplify the determination. Concerning the coulometric determination of oxygen in zirconium and zircaloy, Elbling and Goward[10] showed that Smiley's[9] platinum bath technique in a vacuum fusion method was applicable in the case of an inert gas fusion method. In other recent investigations, Holt and Goodspeed[12] have reported the simultaneous manometrical determination of oxygen and nitrogen in metals, while Evens and Fassel[13] have described a d.c. carbon-arc fusion method using gas chromatography for the determination of oxygen and nitrogen in steels.

This paper will describe a very simplified apparatus, a silicon fusion technique and a highly-sensitive method of gas chromatographic analysis. This method enables us to carry out the determination of oxygen in metals with high melting points almost entirely without a blank test; the agreement of this result with that obtained by the platinum bath method is satisfactory.

Experimental

Apparatus.—The apparatus was similar in principle to that already described[14] by the present authors. It consisted of gas extraction, collection, and measurement apparatus. The fusion products were transferred from the extraction system by means of an argon stream, and the concentration of this carbon monoxide was measured by the gas chromatograph.

A schematic diagram of the apparatus is given in Fig. 1. A high frequency induction furnace, Kokusai Denki combustion unit, Model HFT-7a, was used for the analyses of carbon and sulfur. The furnace assembly is shown in Fig. 2. A graphite crucible in the thimble was placed in a transparent silica tube, A, by controling the screw, G, attached to the pedestal, E. As the furnace was small, a special thimble was used instead of the silica thimble and graphite powder conventionally used; this new method has been found to be convenient and practical. The tube, D, was connected with a ground joint (a ball-shaped joint; 18 mm. in spherical diameter and with a 9 mm. bore) to the upper side of the silica tube, A, using a little Daifloil 50 grease and a spring clamp, I. The lower side was sealed by a metal cup, H, and a ring packing of silicone rubber. Purified argon, containing 0.0001% oxygen, 0.0005% nitrogen and 0.01 ml./l. water, was fed from a gas cylinder through a reducing valve, a needle valve, and a reference tube of the thermal conductivity cell, N. The gas was dried by passing it through columns of activated alumina, I, and phosphorus pentoxide, J. The fusion products were then transferred through a hard vinylon tube (3 mm. in diameter) to the concentration column.

Gas Chromatography. — The chromatographic column was built in a copper tube 1.5 m. long and 4 mm. in diameter. It was packed with Molecular Sieve 5A of 30—60 mesh. The column was maintained at 75°C, and the argon flow rate was 50 ml./min. The recorder had a sensitivity of 1.5 mV. at the full scale, as was determined by using a pre-amplifier; for a thermal conductivity cell of the gas chromatograph, the bridge current was adjusted to 150 mamp.

The concentration column, F, was a copper tube 50 cm. long and 4 mm. in diameter; it was packed with activated charcoal of 30—60 mesh. This column was capable of concentrating carbon monoxide in about 7 min. under ordinary conditions, with a flow rate of the argon carrier gas of 50 ml./min. at about −10°C. The concentrated gas was eluted from this column within one minute by warming it to 130°C.

Fusion Technique.—In the silicon fusion technique developed by the present authors, the platinum bath was not used. This technique was, however, found

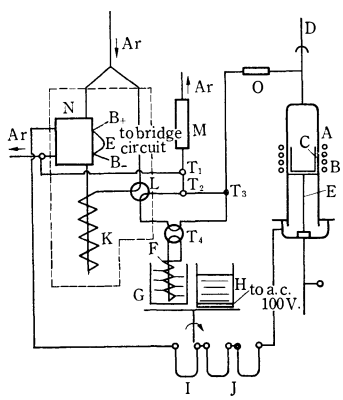

Fig. 1. Schematic diagram of apparatus.
A Transparent silica tube
B H-F coil
C Thimble and graphite crucible
D Entrance
E Pedestal
F Precolumn for collection of carbon monoxide
G Saline-ice solution
H Hot potash bath
I Activated alumina
J Phosphorus pen-oxide
K G. C. column
L Gas sampling cock
M Flow meter
N Thermal conductivity cell
O Silica gel tube
T_1 T_2 T_3, Greased cocks, T_3 By-pass cock

6) E. L. Steele and W. W. Meinke, *Anal. Chem.*, **32**, 185 (1962).
7) D. J. Veal and C. F. Cook, ibid., **34**, 178 (1962).
8) I. Fujii, H. Muto and K. Miyoshi, *Japan Analyst*, **13**, 249 (1963).
9) W. G. Smiley, *Anal. Chem.*, **27**, 1098 (1955).
10) P. Elbling and G. W. Goward, ibid., **32**, 1610 (1960).
11) T. A. Sullivan, B. J. Boyle, A. J. Mackie and R. A. Plott, *U. S. Bur. Mines. Rept. Invest.*, **No. 5834**, 30 (1961).
12) B. D. Holt and H. T. Goodspeed, *Anal. Chem.*, **35**, 1510 (1963).
13) F. M. Evens and V. A. Fassel, ibid., **35**, 1444 (1963).
14) J. Kashima and T. Yamazaki, *Rept. of the Castings Research Lab., Waseda Univ. (Tokyo)*, **13**, 15 (1962).

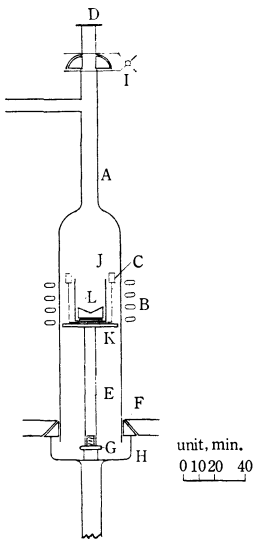

Fig. 2. Furnace assembly.
A Transparent silica tube
B H-F working coil
C Leco crucible No. 528-30 and sleeve
D Window of flat clear silica plate
E Silica pedestal
F Silicon ring packing
G Screw
H Metal cup
I Spring clump
J Degussit AL23 crucible
K Sintered alumina disk
L Graphite crucible

to give just as good results as those obtained with the platinum bath technique.

Procedure.—The concentration column was pretreated at about 130°C. by passing the argon carrier gas through it at a flow rate of 50 ml./min. for about 30 min.

The sample (approximately 20 mg.), after the surface contamination had been removed, was weighed into a capsule (10—20 mg.) made of tin foil. The capsule was then introduced into a degassed graphite crucible, together with a piece of silicon (100—150 mg.), via the entrance, D. After air had been expelled from the extraction system by an argon flow for 30 sec., the concentration column was connected to the silica tube. This concentration column was dipped into a Dewar flask filled with a saline-ice solution. The inert gas fusion was started, and the fusion products were transferred into the column. A fusion time of about 3 min. was needed in order to decompose the oxides in the sample perfectly. The flow was then continued for about 5 more min., when only a trace of the gas remained. After the column had been separated from the extraction system by turning the cocks, T_2, T_3 and T_4, the column was warmed by dipping it into the boiling bath, H. It was then connected to the chromatographic column, K, by turning the gas sampling cock, L, and the concentrated gas was measured chromatographically. Typical chromatograms are shown in Fig. 3.

The carbon monoxide content was obtained from a

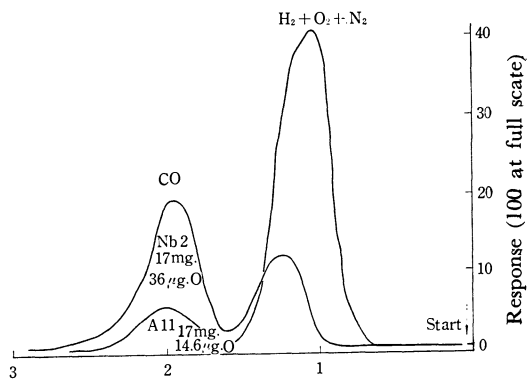

Fig. 3. Typical chromatograms of the gases collected.

peak area measured either by a planimeter or by the conventional approximate method. The oxygen content was obtained by means of the following equation;

$$\text{Oxygen, } \% = (a_t - a_b)/w \cdot K$$

where a_t: the area of the chromatogram of carbon monoxide (in sq. mm.) for the sample; a_b: the area of the chromatogram of carbon monoxide (in sq. mm.) for the blank test; w: the sample weight (in mg.); and K: the constant (0.014 μg. oxygen per sq. mm.). K was determined by using standard carbon monoxide. The standard gas is of a special grade (99.999%) which may be used for the calibration of gas chromatography or mass spectrometry. The calibration was carried out with gas samples containing 3.0—50.0 μg. of oxygen, which was introduced into the sampling cell (1.0 ml.) manometrically by the use of a silicone oil gauge (sp. gr. 0.987, at the temperature of 15°C). For simple calibration, it is also possible to use known steel samples as a secondary standard.

Results and Discussion

The accuracy of this method was tested with titanium samples. The results are compared with those obtained by other authors in Tables I and II. It was found that this method gives a good reproducibility. The determined values are in good agreement with the AED values of 0.085(A7) and of 0.103(B7) respectively for the samples of A11 and B21. The average value of the sample, B, which was obtained by ten co-operating laboratories using the vacuum fusion method was 0.098.

This method can be used for the determination of the amounts of oxygen in tantalum, niobium, molybdenum and tungsten. The results are summarized in Table III.

In order to degas the graphite crucible used in the experiment, it was necessary to heat it above 1800°C for about 10 min. In the case of the silicon fusion technique using 100—150 mg. of the metallic silicon, the time of heating was reduced (3—5 min.). The graphite-SiC crucible obtained by the above

treatment was heated at about 2000°C for 30 sec. before the experiment. If the fusion of the sample is completed within 3 min., the value obtained by the blank test is only about 0.3 μg. oxygen; this value is negligible.

Table I. Comparison of oxygen values found by vacuum fusion, argon fusion and neutron activation analysis methods

Methods	Co-operating laboratory*	Titanium sample designation	Oxygen wt.%
Vacuum fusion	D.I.C.	A5	0.078_5
		B11	0.103
		2-1-2-(1)	0.067_7
Argon fusion	R.I.I.	A9	0.070
		B15	0.091
		2-1-4-(2)	0.055
Neutron activation analysis	A.E.D.	A7	0.085
		B7	0.103
		2-1-1-(1)	0.066

* D.I.C.=Department of Industrial Chemistry, Faculty of Engineering, University of Tokyo.
R.I.I.=Research Institute of Iron, Steel and Other Metals, Tohoku University.
A.E.D.=Atomic Energy Department, Central Research Laboratory, Tokyo Shibaura Electric Co., Ltd.

The silicon fusion technique is effective in decomposing oxides in metals in the following ways; (1) metals with high melting points (tungsten,

Table II. Precision of simplified method (titanium)

Sample designation	Oxygen wt.%		Standard deviation. %
A11 (Sheet)	0.0864		
	0.0883		
	0.0871		
	0.0805		
	0.0880		
	0.0882		
	0.0852		
	0.0867		
	Mean 0.086_3	0.087*	0.002_2
B21 (Sheet)	0.106		
	0.096		
	0.092		
	0.091		
	0.103		
	Mean 0.097_9	0.0109*	0.006_6
2-1-5-(2) (Rod)	0.0728		
	0.0741		
	0.0736		
	0.0756		
	0.0774		
	Mean 0.074_9	0.077*	0.001_8

* Values obtained by platinum bath technique.

Table III. Oxygen content in high-melting-point metals

Material	No. of determinations	Oxygen, wt.% simplified method		Vacuum fusion method	Std. Dev.. %	Figulation of sample
		Si bath	Pt bath			
Tantalum-1	5		0.15_3	0.20	0.02_0	Powder
Tantalum-2	4	0.067_1		0.075	0.002_4	Powder
Tantalum-3	6	0.036_2		0.030	0.004_5	Powder
Niobium-1	5		0.095_5		0.004_5	Powder
Niobium-2	5		0.21_5		0.02_3	Powder
Niobium-3	4		0.33_8		0.03_6	Powder
Molybdenum	8	0.11_5			0.01_5	Wire
Tungsten	6	0.069_0			0.01_7	Wire

Table IV. X-ray analyses of metal residue in crucible used at silicon bath*1 technique

Material	Weight, mg.	Peak height (at chart responce)*3			
		SiK_α	2θ*4	Metals K_α	2θ*4
Titanium (sheet)	30	1.5	108°-15′	0.2	30°-15′
Molybdenum (wire)	20	0.6		0.4	20-15
Zircalloy (rod)	65	2.0		6.0 (Zr)	22-30
Tungsten (wire)	16	0.3		trace (W$L_{\alpha 1}$)	42-15
Zircalloy (rod)*2	40	—		3.9 (Zr)	22-30
Titanium (sheet)*2	40	—		0.05	36-15
Niobium (powder)	30	0.3		0.8	21-20
Tantalum (powder)	40	0.7		trace	

*1 Approximately 100 mg. of pure silicon was added.
*2 Without silicon
*3 Recorders indication is ten at full scale
*4 Goniometer position
Instrumental conditions: crystal topaz LiF or EDDT; 50 kV. 50 mamp., base line 2.5 V., counter high voltage S. C. 890 V.; rate meter 2×10^5; time constant 0.5 sec.; Norelco

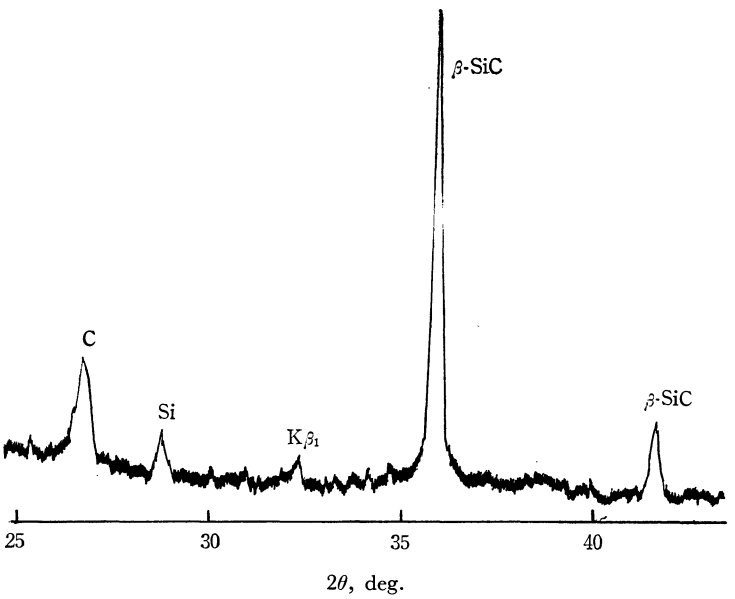

Fig. 4. Fluorescent X-ray spectroscopic observation of crucible wall used silicon bath technique.

molybdenum, tantalum, etc.) are very fusible at high temperatures in a large quantity of liquid silicon, because the Si-MSi_2 eutectics which are formed in the 78—95 wt.% range of silicon have melting points of 1300—1400°C (2) at very high temperatures (>1800°C), silicon and silicon-rich alloys penetrate into the crucible within one minute to form carbides. Six-hundred milligram of liquid silicon or 400 mg. of liquid silicon alloys (containing 50—100 mg. of metals) can be penetrate into a graphite crucible (about 2.5 g.) (3) semiconductor grade silicon or pure silicon (99.8—99.9 wt.% silicon containing 0.0005 wt.% of oxygen) can be used, because metals with high melting points contain large amounts of oxygen.

In the graphite-SiC crucible, the free silicon was found by a chemical method to be 1.24 wt.%. A fluorescent X-ray diffraction diagram of this crucible is given in Fig. 4. The metals contained in the crucible could be detected by studying the intensity of the sharp peak of the X-ray diagram; the intensity readings are summarized in Table IV. It was found that all of the metals combined to form carbides. By this fusion technique the oxide contained in the sample was almost decomposed when the sample was in the form of a filament, wire, powder, or a thin sheet.

The reactive metals, such as titanium, tantalum and niobium powders, fuse quickly and scatter from the crucible upon the addition of silicon; this produces erratic results. These metals must be treated with tin foil; when they are so treated, the duration of fusion increases from 20 sec. to about 50 sec. without scattering.

In the case of tantalum and niobium powder which contain more than 0.1 wt.% oxygen, the value of deviation increases slightly, as is shown in Table III. When the quantity of the sample is small, the analytical results will also be affected by the segregation of oxygen.

BULLETIN OF THE CHEMICAL SOCIETY OF JAPAN VOL. 39 1453—1456 (1966)

The Routine Determination of Nitrogen in Cast Iron by the Chemical Distillation and Inert Gas Fusion Methods

By Jiro KASHIMA and Takuo YAMAZAKI

The Castings Research Laboratory, Waseda University, Shinjuku-ku, Tokyo

(Received July 3, 1965)

Although the chemical distillation method is generally employed for the determination of nitrogen in metals, it has been found that this method involves some difficulties in cast iron and pig iron samples. This paper will, therefore, describe new, repreoducible methods for the determination of nitrogen in chilled cast iron. They are the inert gas fusion and the chemical distillation methods. The most suitable sample for obtaining almost the same results with regard to ordinary cast iron by both methods was found to be a thin plate chilled by a copper mold. The accuracy of both methods was ±0.0004% when thin-plate samples containing from 0.0030 to 0.010% nitrogen were used.

The determination of nitrogen in cast iron and pig iron has acquired increasing importance in recent metallurgy. Nitrogen—one of the slightly-alloying elements in these metals—affects their mechanical properties. Therefore, it is necessary that the nitrogen contents of 0.001 to 0.01% in commercial cast irons be determined accurately by using the adequate analytical methods.

The standard method for the determination of nitrogen in metals is the chemical distillation method. This method is described in JIS G 1228 for the determination of nitrogen in steels and cast irons. The vacuum fusion method may also be used in the determination of hydrogen, oxygen and nitrogen in metals. However, in this method, the residual gas is assumed to be all the nitrogen contained in the metals, and it cannot be utilized as a standard method, for the nitrogen is not completely evolved. Therefore, the vacuum fusion and chemical distillation methods of obtaining the nitrogen contents have previously been described[1-2]; these methods involve the simultaneous determination of hydrogen, oxygen and nitrogen, as well as the determination of nitrogen alone.

Recently, in order to measure the evolved nitrogen in the vacuum fusion and the inert gas fusion methods, gas chromatography was attempted,[3-5] and some authors have described[6-8] how colorimetry can be used to find a trace of nitrogen in metals.

With regard to low carbon steels and alloy steels (with the exception of chromium and manganese steels), investigators have different opinions; one of them[9,10] considers that lower nitrogen value would be obtained in the vacuum fusion method, while others[1,2] consider that the same results would be obtained in both methods. In order to determine accurately the amount of nitrogen, the stable nitrides (e. g., CrN, Si_3N_4 and TiN) must be decomposed before analysis by suitable methods (for instance, solidifying the liquid metals quickly).

With regard to stainless steels, carbon steels and some cast irons, the results obtained by these methods have been discussed in a recent paper.[5] The nitrogen in cast iron is determined accurately in two ways. One of them is the use of a thin plate chilled from liquid metal by a copper mold in the inert gas fusion method; the other is the use of a powder prepared by crushing the chilled sample in the chemical distillation method.

Experimental

Materials.—All the cast iron samples, whose chemical compositions are shown in Table I, were prepared by means of several kinds of molds (shown in Table II). The samples were prepared as follows: (1) preparing a specimen 100 mm. in height from a chilled ingot 120 mm. in height, (2) abrasing its surface, (3) washing it in carbon tetrachloride, (4) crushing it in 9—64 mesh (until each sample is about 0.3—1.0 g.) for the inert gas fusion method, and crushing it in 100—200 mesh for the chemical distillation method, by using a mortar and a pestle of high-manganese cast steel.

Standard Sodium Hydroxide Solution.—Granular sodium

1) Third Report of the Oxygen Sub-Committee, *J. Iron and Steel Inst.*, **143**, 295 (1941).
2) Fourth Report of the Oxygen Sub-Committee, ibid., **148**. 302 (1943).
3) A. Fuchs, H. Reinhard, J. Niebuhr and R. Beck, *Arch Eisenhuttenw.*, **34**, 361 (1963).
4) F. M. Evens and V. A. Fassel, *Anal. Chem.*, **35**, 1444 (1963).
5) J. Kashima and T. Yamazaki, *Rept. Castings Research Lab., Waseda Univ. (Tokyo)*, **14**, 33 (1963).
6) H. F. Beeghly, *Ind. Eng. Chem., Anal. Ed.*, **14**, 137 (1962).
7) J. Epotein, *Anal. Chem.*, **19**, 272 (1947).
8) J. P. Riley, *Anal. Chim. Acta.*, **9**, 575 (1953).
9) M. Ihida, *Japan Analyst*, **8**, 786 (1959).
10) K. Furuya and H. Kamada, ibid., **14**, 336 (1965).

TABLE I. CHEMICAL COMPOSITION OF WHITE CAST IRON

Designation	Element, %						
	C	Si	Mn	P	S	Al	Cr
A01, 02, 05, 08, 10	3.04—3.64	1.60—1.94	0.41—0.95	0.045—0.052	0.025—0.090	0.03—0.04	0.03—0.04
A03, 04, 06, 09	2.94—3.24	2.20—3.52	0.27—1.20	0.041—0.048	0.041—0.080	0.03—0.05	0.01—0.15
A07	0.66	13.72	0.43	0.029	0.034		0.15

TABLE II. PREPARATION OF CHILLED SAMPLE

Sample designation	Form	Size	Mold
A01, 02	bar	0.7 cm. in dia. × 12 cm. length	cast iron
A05	bar	1.0 cm. in dia. × 12 cm. length	cast iron
A06	bar	0.6 sq. cm. × 60 cm. length	CO_2-process
A09	plate	1.0 cm. thick. × 5 cm. width × 10 cm. length	cast iron
A08	plate	0.2 cm. thick. × 2+3 cm. wid. × 10 cm. length	copper
A03, 04, 07, 10	sheet	0.14 cm. thick. × 4 cm. wid. × 10 cm. length	direct rolling

hydroxide of analytical grade was dissolved in pure water obtained by passing water through an ion-exchange resin column; it was diluted to a concentration of 1/400 N. This solution was stored in a 1000-ml. polyethylene vessel connected to a Metrohm piston burette, Model E 274. The concentration of this solution was accurately determined by titrating it with benzoic acid. To reduce the nitrogen blank value, sulfuric acid and potassium sulfate of analytical grade were used; the other reagents, of the first grade, were used without purification.

Apparatus.—A Shimadzu high-frequency titrator, Model HF-1, was employed to determine the end-point. For the determination of the amount of nitrogen gas, a Yanagimoto Model GCG-100 gas chromatograph, an Ohkura Model AM 101 d. c. amplifier, and a Minneapolis-Honeywell (U. S. A.) Model SY-153 recorder were used. As the furnace used in the inert gas fusion, a Kokusai Denki Model HFT-7a high-frequency combustion furnace was adopted.

Procedure.—*The Chemical Distillation Method.*—The apparatus was that of JIS G 1228, the measurements were carried out conductometrically by means of a commercially-available H-F titrator.

The sample, approximately 5.0 g., was slowly dissolved in 100 ml. of dilute hydrochloric acid (1 : 1) in a 500 ml. round-bottom flask with a condenser, while the solution was being heated by an electric heater for at least 60 min. To determine the acid-soluble nitrogen, the solution was separated from the residue by means of a centrifuger (at 2500 r.p.m.).

The solution was then transferred to a distillating flask containing 75 ml. of a 12 N sodium hydroxide solution and 200 ml. of pure water; steam distillation was then carried out. The distillate was collected in a 100 ml. receiving flask containing 10 ml. of 1/10 N sulfuric acid. The distillation was continued until the distillate reached about 95 ml.; this process took about 20 min. The distillate was then transferred to a 100 ml. measuring flask and diluted to the mark with pure water. The amount of acid-soluble nitrogen was obtained by titrating the excess sulfuric acid with a 1/400 N standard sodium hydroxide solution; the total nitrogen content was also calculated. Actually, a 20 ml. portion of this solution was transferred to the cell of a commercially-available high-frequency titrator and was titrated with the standard sodium hydroxide solution. The residue separated by a centrifuger was treated with a mixture of 10 ml. of concentrated sulfuric acid and 5 g. of potassium sulfate at 350°C for about 2 hr., in order to decompose the acid-insoluble nitrides completely. In this way, the acid-soluble and the acid-insoluble nitrogen contents were determined.

The Inert Gas Fusion Method.—This method has been described in recent papers.[5,12] It is capable of measuring immediately the nitrogen content from the chromatogram obtained by the gas chromatographic separation in the gases evolved by the inert gas fusion. The experiments were carried out in the following ways: (1) the argon gas flow was at a rate of 50 ml./min.; (2) in the gas chromatograph experiment, the bridge current of the thermal conductivity cell was 150 mamp., the potential at the full scale of the recorder was 0.5 mV., and the temperature of the thermostat chamber was 115°C; (3) the gas chromatographic column was a copper tube (1.5 m. long and 4 mm. in dia) packed with Molecular Sieve 5A, and (4) the capacity of the gas sampling cell was 1.0 ml.

Many data concerning nitrogen were obtained from the observations based on the time-concentration curve described in a previous paper.[5] This curve was obtained by introducing 1.0 ml. portions of the argon stream into the gas chromatograph at intervals of 0.6 to 1.0 min.

Results and Discussion

The nitrogen contents of many chilled cast iron samples were determined. The plate samples prepared by the copper-chilled method, shown in Fig. 1, are suitable for the nitrogen analysis of ordinary cast iron; when they are used, the results obtained by the fusion method are almost exactly

11) J. Kashima and M. Kubota, *J. Spectro. Soc. Japan (Bunko Kenkyu)*, **13**, 83 (1965).
12) J. Kashima and T. Yamazaki, *Japan Analyst*, **12**, 347 (1962).

Table III. Nitrogen contents in cast iron

Designation	Inert gas fusion method: No. of determinations	Nitrogen %	Deviation from mean %	Chemical distillation method: No. of determinations	Nitrogen, % sol.	insol.	total	Deviation from mean %	Sample size
A01	5	0.0081	±0.0006	3	0.0086		0.0088	±0.0002	
A02	4	0.0042	0.0005	3	0.0070	0.0002	0.0072	0.0004	bar
A05	4	0.0058	0.0005	3	0.0073	0.0003	0.0076	0.0003	
A06	3	0.0016	0.0001	3	0.0018		0.0020	0.0003	
A03	4	0.0030	0.0003	3	0.0033		0.0035	0.0002	
A04	4	0.0030	0.0004	4	0.0034		0.0036	0.0001	
A07	2	0.0086	0.0004	2	0.0075	0.0010	0.0085	0.0002	
A08*	4	0.0100	0.0003	3	0.0100		0.0102	0.0005	plate
A09	4	0.0085	0.0003	3	0.0083	0.0002 0.0003	0.0085	0.0002	
A10	4	0.0051	0.0003	3	0.0056		0.0059	0.0003	

* The portion of plate chill sample obtained by split copper mold.

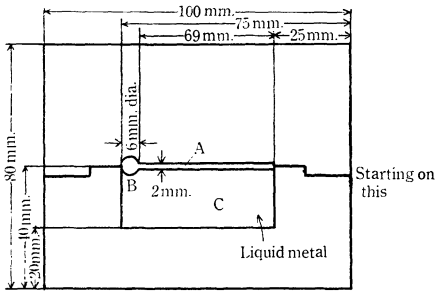

A plane figure

Fig. 1. Copper chill for sampling liquid metal.
A Plate sample with 2 mm. thickness × 44 mm. width × 10 cm. length
B Bar sample
C Pouring basin with 20 mm. curvature

Table IV. Nitrogen content obtained by the concentration—injection method*

Designation	No. of determinations	Nitrogen %	Deviation from mean %
A02	6	0.0043	0.0006
A08	5	0.0102	0.0003
A09	3	0.0087	0.0001

* Application of this method does pricisely proved on the analytical method for oxygen in metals.

the same as those obtained by the solution method. The data are shown in Tables III and IV. The nitrogen contents obtained by the inert gas fusion method are somewhat lower, as is also shown in the tables. The plate samples, which show a deviation from the average value of below ±0.0004%, were preferable to the bar samples, which show a deviation from the average value of ±0.0004% in the chemical distillation method and a deviation from the average value of ±0.0006% in the inert gas fusion method. Therefore, the sample which can be used for both the methods is the plate form of the A08 sample, which is prepared by the split copper mold shown in Fig. 1.

The cast iron samples generally used for the chemical distillation method were of gray cast iron with a matrix of eutectic graphite cells growing about a cluster of kish graphite, for this sample can easily be treated by the machinery and dissolved in acid. The nitride contents in a sample are determined separately, an acid-soluble nitrogen and an acid-insoluble nitrogen. Some remarks on the determination of the acid-insoluble nitrogen demonstrated in a recent paper[5] are given below:

1) The blank value for nitrogen found in the decomposition of insoluble nitride is very high, about 50 μg., while the nitrogen contained in the sample is 50—200 μg.

2) The nitrogen contents of the sample containing insoluble nitrides show a deviation from the average value of ±0.0009%; this value is 2—9 times that found in the case of soluble nitrides obtained by the chemical distillation method.

3) It is necessary to separate graphite from the solution before steam distillation, because the graphite residue prevents the evolution of ammonia to some extent.

4) Some investigators[13,14] have had the opinion that the amount of acid-insoluble nitrogen is

13) Y. Ueda, *J. Japan Foundrymens Soc. (Imono)*, **33**, 776 (1961).
14) B. B. Bach, J. V. Dawson and I. W. L. Smith, *J. Iron and Steel Inst.*, **176**, 257 (1954).

changed by the sampling methods or by the annealing treatment.

This must be taken into account before executing the conventional chemical distillation. However, if the total nitrogen content of the cast iron can be established by the simple chemical distillation procedure, without treating the acid-insoluble residue, this procedure may be most desirable. For this reason, the authors have studied this problem, particularly in connection with white cast irons.

The acid-soluble powdered samples were prepared by crushing solid white cast iron (acid-proof), but their acid-dissolution-time was not short, even though the nitrides included were almost acid-soluble compared with those of the gray cast iron. However, the deviation of the nitrogen content of each sample is small in white cast iron, as Table III shows.

In this experiment, the calibration for the nitrogen content was performed by the following procedure: the relation between the concentration and the chromatogram area was obtained by introducing into the 1.0-ml. samping cell of the gas chromatograph manometrically-measured standard nitrogen in liter glass container.

The sample chilled by the copper mold is suitable for nitrogen analysis or for spectroscopic analysis.[11] This may be due to the fact that nitrogen is dissolved in cast iron. If refractory nitrides are included in the sample, it seems impossible to decompose the nitrides perfectly by the inert gas fusion method, by which the sample is quickly heated to 2000°C. Although it may be difficult to decompose the refractory nitrides formed in some cast iron by ordinary methods, they may be decomposed by the inert gas fusion method using a platinum bath.

BULLETIN OF THE CHEMICAL SOCIETY OF JAPAN VOL. 39 1456—1462 (1966)

Hydrothermal Synthesis of Fluor-Hydroxyl Muscovite

By Tokiti Noda, Yasuhiko Endo and Masumi Ushio

Department of Applied Chemistry, Faculty of Engineering, Nagoya University, Chikusa-ku, Nagoya

(Received September 8, 1965)

Fluor-hydroxyl muscovite was synthesized from a mixture of gels and chemicals of the $KAl_3Si_3O_{10}F_x(OH)_{2-x}$ composition, where $x=0$, 0.5, 1.0, 1.5 and 2.0, in the temperature range of 500—600°C under pressures ranging from 500 to 900 atm. The fluorine content of the synthetic muscovite increased with the increase in x, but the distribution coefficient of fluorine [(the fluorine content of the crystal)/(the fluorine concentration of the solution)] decreased with the increase in x, increased with the increase in the temperature of synthesis, and decreased with the increase in the pressure of synthesis. The synthetic fluor-hydroxyl muscovite crystallized mainly in 1M polymorph, and very little in 2M polymorph, at 500°C in 20 hr. The fraction of 2M muscovite increased with the increasing temperature of synthesis. The d_{005} and d_{060} lattice spacings of the mica were observed to decrease linearly with the increase in the fluorine content of the mica.

Noda and Roy[1] carried out the hydrothermal treatment of fluor-phlogopite with a dilute alkali solution, intending to replace F^- ions partially by $(OH)^-$ ions; they found that hydroxyl-phlogopite formed in a separated phase and that no appreciable ion exchange between $(OH)^-$ ions in the solution and F^- ions in the mica occurred. Noda and Ushio[2] reported the dependence of the fluorine content of fluor-hydroxyl phlogopite on the conditions of hydrothermal synthesis, such as the fluorine content of the starting material of phlogopite composition and the temperature and pressure of the synthesis. They also found a good linearity between c_0 spacing and the fluorine content of the mica.

In this paper, the results of similar experiments on fluor-hydroxyl muscovite will be reported. The syntheses of muscovite have been reported by various investigators and reviewed briefly by Yoder and Eugster.[3] Yoder and Eugster determined the pressure-temperature equilibrium in the decomposition of hydroxyl muscovite. They obtained 1 M and 2 M polymorphs of muscovite and reported that 1 M muscovite transformed to 2 M muscovite at higher temperatures, the transition temperature being in the 200—350°C range at 1000 kg./cm^2. Crowley and Roy[4] re-examined

1) T. Noda and R. Roy, *Am. Mineral.*, **41**, 929 (1956).
2) T. Noda and M. Ushio, *J. Chem. Soc. Japan, Ind. Chem. Sect.* (*Kogyo Kagaku Zasshi*), **67**, 292 (1964); *Geochem. Internatl.*, **1964** (1), 96.
3) H. S. Yoder and H. R. Eugster, *Geochim. et Cosmochim. Acta*, **8**, 225 (1955).
4) M. S. Crowley and R. Roy, *Am. Mineral.*, **49**, 348 (1964).

the temperature-pressure equilibrium of hydroxyl-muscovite and determined the limits of the substitution of Mg^{2+} and Fe^{3+} ions in the muscovite structure. They also obtained muscovite by the hydrothermal treatment of a mixture of calcined gels and $KF \cdot 2H_2O$ with the requisite composition. Eitel[5] prepared fluor-muscovite from a mixture of calcined kaoline and K_2SiF_6 in a solid state reaction. According to Yoder and Eugster,[3] fluor-muscovite was obtained hydrothermally from a mixture of silica glass, γ-Al_2O_3 and K_2SiF_6 in only two runs, of one hour's duration, at 500 and 600°C. In longer runs and at higher temperatures, sanidine and topaz were usually obtained. They reported that the average fluorine content of some 60 specimens of natural muscovite was 0.58% (0.124 mol./2 mol. [F+(OH)]) and that the largest fluorine content of natural muscovite was 1.28%. The presence of fluorine ions in muscovite in place of hydroxyle ions may affect the stability range of the muscovite.

Experimental

Apparatus.—A cold-sealed test tube-type bomb[6] 12 mm. in inner diameter, 50 mm. in outer diameter and 280 mm. long and made of Stellite D6-K was used for the hydrothermal experiments. Mixtures of gels, potassium hydrogen fluoride and potassium carbonate with the requisite compositions were placed in sealed platinum tubes, 10 mm. in diameter, 90 mm. long and 0.03 mm. thick, and treated hydrothermally in the bomb. The bomb was pressurized by a pump. It was kept at a fixed temperature and pressure for 20-hr. After the treatment, the bomb was taken out of the furnace and cooled by a forced draft.

Materials.—$SiO_2 \cdot nH_2O$ gel was prepared by the hydrolysis of pure silicon tetrachloride and dried at 110°C. The dry gel was amorphous, and its water content was 5.0%. $Al_2O_3 \cdot nH_2O$ gel was precipitated by ammonia from a aluminum chloride solution which had been prepared by dissolving pure metallic aluminum (99.99%) in hydrochloric acid. The gel was washed with water and dried at 110°C. The dry gel was identified as gibbsite by the X-ray diffraction method. Its water content was 33.4%. The potassium hydrogen fluoride and potassium carbonate used were both pure chemicals. The calculated amounts of the gels and the chemicals were well mixed in an agate mortar. The water contents of the gels were determined before every mixing. The mixture contained about 18% water.

For experiments in which the fluorine distribution between crystal and solution was investigated, two parts of water was added to one part of the original mixture of the gels and the chemicals. The resulting mixture will be called the A-mix. Because the original mixture contained ca. 18% water, the ratio of solid substance to water in the A-mix was 0.38/1.00, or the ratio of the mica composition to water was 0.39/1.00, i. e., 0.97 mol./kg. water. In order to prepare specimens for the determination of lattice spacings, the original mixture moistened with a little water was used. This mix will becalled the B-mix. For both mixes, the chemical compositions given in Table I were used.

Table I. The chemical composition of the starting mixture in $KAl_2AlSi_3O_{10}(OH)_{2-x}F_x$

x	0,	0.5,	1.0,	1.5,	2.0
Abbreviations for the designation of the composition	F_0,	$F_{0.5}$,	$F_{1.0}$,	$F_{1.5}$,	$F_{2.0}$

After the hydrothermal treatment, the pH value of the coexisting solution was measured, and then the solution was separated from the solid substance. The solid substance was suspended in Thoule's solution (mercury(II) iodide - potassium iodide solution) with a density of ca. 3.0 in order to separate the heavier impurities by a centrifuge, and then the solution was diluted to a density of ca. 2.7 in order to separate the lighter impurities. For the determination of the fluorine content of the mica, the purified mica was fused with sodium carbonate and zinc oxide, the fused mass was dissolved in water, perchloric acid was added to the solution, the fluoride in the solution was distilled as fluosilicic acid, and the distillate was titrated with a thorium nitrate ($Th(NO_3)_4$) solution.[7] The fluorine in the coexisting solution was distilled from the solution and titrated with a thorium nitrate ($Th(NO_3)_4$) solution.

Results

The Distribution of Fluorine between Crystal and Solution.—The plot of the fluorine content of the muscovite crystal vs. the fluorine content of the starting mixture (dry basis) is give in Fig. 1. The fluorine content of the muscovite increases with the increase in the fluorine content of the starting mixture, x, with some variation with the temperature and pressure of syntheses.

The plot of the mean value of the fluorine content of muscovite, C_m, vs. the mean value of the fluorine concentration of the coexisting solution, C_s, is given in Fig. 2. In general, for the same starting mixture, F_x, C_m increases and C_s decreases with an increase in the temperature at a constant pressure, while C_m decreases and C_s increases with an increase in the pressure at a constant temperature. The dependences of C_m on the temperature at a constant pressure and of C_m on the pressure at a constant temperature are more clearly shown in Figs. 4a and 4b.

The plot of C_s vs. x in F_x is given in Fig. 3. The dependences of C_s on the temperature at a constant pressure and of C_s on the pressure at a constant temperature are given in Figs. 5a and 5b. C_s

5) W. Eitel, *Proc. Internatl. Symposium on the Reactivity of Solids, Gothenburg*, 335 (1952).
6) O. F. Tuttle, *Bull. Geol. Soc. Am.*, **60**, 1727 (1949).
7) H. R. Shell and R. L. Craig, *Anal. Chem.*, **26**, 996 (1954).

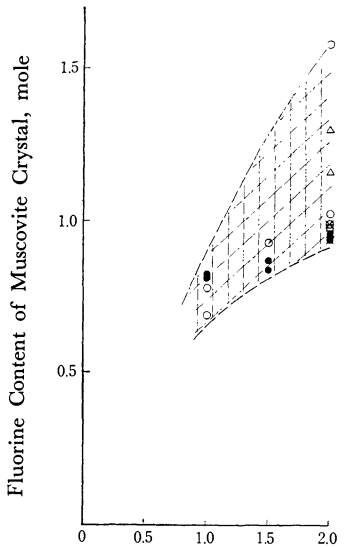

x(Fluorine content of the starting mixture $KAl_2AlSi_3O_{10}F_x(OH)_{2-x}$), mole

Fig. 1. Dependence of fluorine content of muscovite crystal on the fluorine content of the starting mixture.

○ 600°C 700 atm.
● 500°C 700 atm.
□ 550°C 900 atm.
× 550°C 700 atm.
△ 550°C 500 atm.

decreases with an increase in temperature and increases with an increase in pressure. The dependences of C_s on the temperature and pressure are thus just the reverse of those of C_m. Because a definite amount of the starting mixture was used in a sealed platinum tube, thus making a closed system, the increase in C_m results in the decrease in C_s. The amount of C_m relative to C_s is determined by the distribution coefficient of fluorine between crystal and solution.

The distribution coefficient (C_m/C_s) is given in Table II.

Table II. The distribution coefficient of fluorine between crystal and solution

Starting mixture	Pressure atm.	Temperature, °C 500	550	600	(B-mix)
$F_{2.0}$	500	—	2.0	—	
	700	1.0	1.2	1.6—1.9	(1.7)
	900	—	1.1	—	
$F_{1.5}$	700	1.2	—	2.2	(1.9)
$F_{1.0}$	700	6.5	—	6.1	(5.8)

The distribution coefficient increases with the increase in temperature for $F_{2.0}$ and $F_{1.5}$, but it does not change much for $F_{1.0}$. The coefficient decreases with the increase in pressure. It decreases with the increase in x.

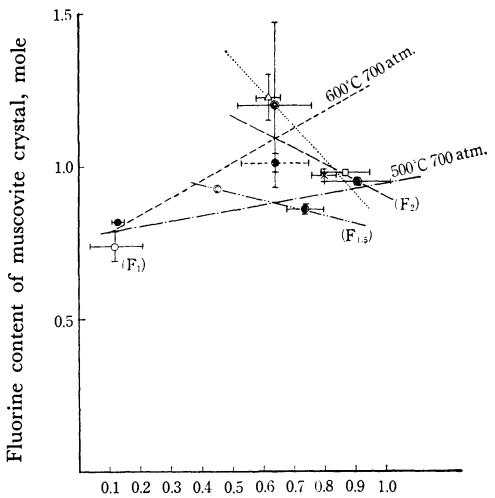

Fluorine concn. of solution, mol./l.

Fig. 2. Dependence of fluorine content of muscovite crystal on the fluorine concentration of solution.

○ 600°C 700 atm. (F_1)
◎ 600°C 700 atm. ($F_{1.5}$)
◎ 600°C 700 atm. ($F_{2.0}$)
● 500°C 700 atm. (F_1)
⊙ 500°C 700 atm. ($F_{1.5}$)
◎ 500°C 700 atm. ($F_{2.0}$)
□ 550°C 900 atm. ($F_{2.0}$)
× 550°C 700 atm. ($F_{2.0}$)
△ 550°C 500 atm. ($F_{2.0}$)
◍ 600°C 700 atm. ($F_{2.0}$)[a)]

(a) Indicate the mean value excluding a value deviating greatly.

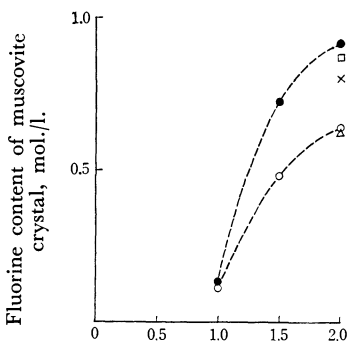

x(Fluorine content of starting mixture $KAl_2AlSi_3O_{10}F_x(OH)_{2-x}$), mole

Fig. 3. Dependence of fluorine concentration of solution on the fluorine content of the starting mixture.

○ 600°C 700 atm.
● 500°C 700 atm.
□ 550°C 900 atm.
× 550°C 700 atm.
△ 550°C 500 atm.

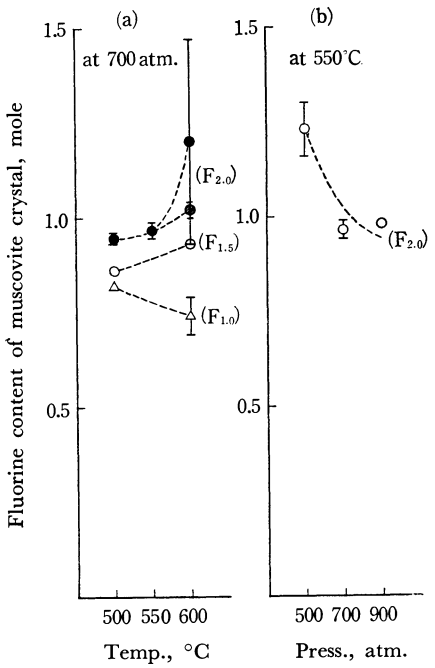

Fig. 4. Dependence of fluorine content of muscovite crystal on (a) temperature and (b) pressure of synthesis.

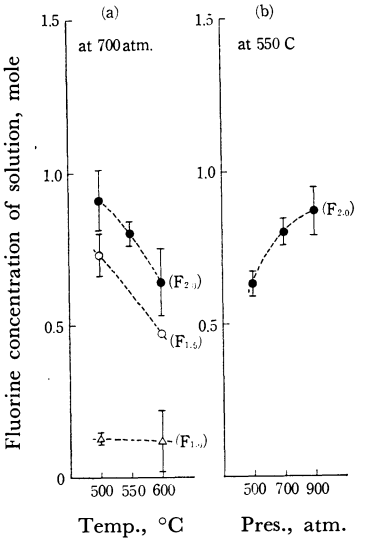

Fig. 5. Dependence of fluorine concentration of solution on (a) temperature and (b) pressure of synthesis.

Almost the same results were obtained in the experiments using the B-mix. The series experiments were carried out at 600°C under 700 atm. The dependence of C_m on x given in Fig. 6 is almost identical with that found in the A-series experiments carried out at 600°C under 700 atm. One could estimate the C_s values of B-series experiments from the C_s vs. x curve of the A-series experiments

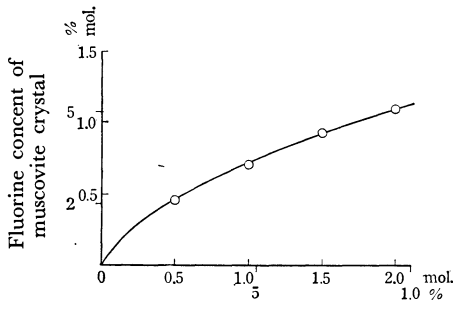

Fig. 6. Dependence of fluorine content of muscovite crystal on fluorine content of starting mixture (B-Series).

at the same temperature and pressure. The C_m/x vs. x ratio of the B-mix is shown in Fig. 7. One can see that the ratio decreases with the increase in x. Using the C_s values of Fig. 3 and the C_m values of Fig. 6, the distribution coefficients were obtained; they are given in parentheses in Table II.

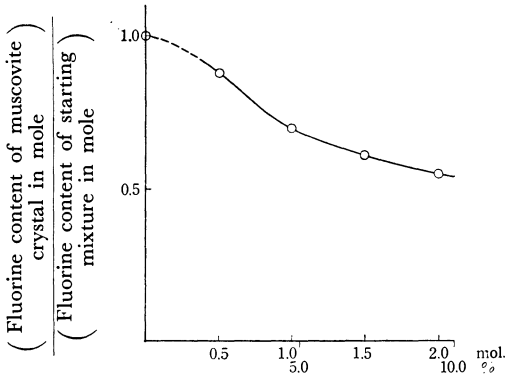

Fig. 7. Dependence of the ratio [(Fluorine content of muscovite crystal)/(Fluorine content of starting mixture)] on fluorine content of starting mixture.

The pH values of the coexisting solution increase with the increase in C_s, although there is a considerable scattering of points, as is shown in Fig. 8. There are approximate proportionalities of pH with C_s among the experiments made at 500, 550 and 600°C under 700 atm., and among the experiments made at 500, 700 and 900 atm. at 550°C for the F_2 composition. There is also an approximate proportionality of pH with x among the experiments using $F_{2.0}$, $F_{1.5}$, $F_{1.0}$ at 500°C under 700 atm. However, there are too few points to establish a definite relationship for each set of experimental conditions.

The Polymorphism and Lattice Spacing of Fluor-Hydroxyl Muscovite.—The muscovite crystals hydrothermally synthesized from the mixture

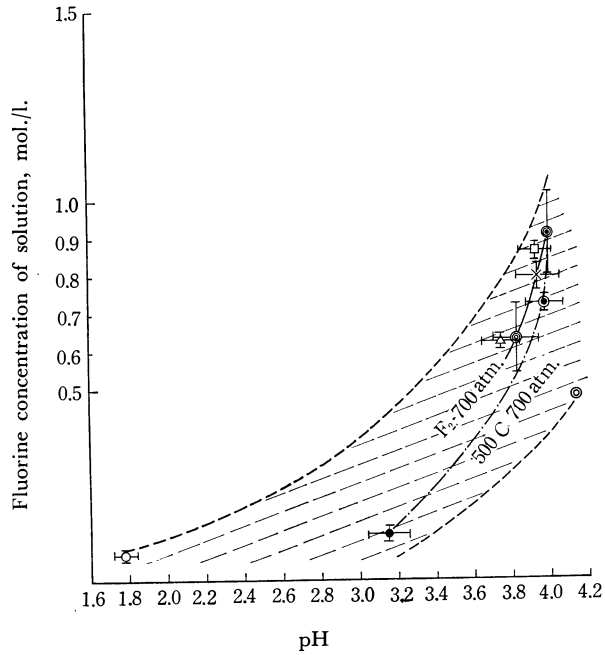

Fig. 8. Plot of fluorine concentration of solution vs. pH of solution.

○ 600°C 700 atm.($F_{1.0}$) ◎ 600°C 700 atm.($F_{1.5}$) ◎ 600°C 700 atm.($F_{2.0}$)
● 500°C 700 atm.($F_{1.0}$) ⊙ 500°C 700 atm.($F_{1.5}$) ◉ 500°C 700 atm.($F_{2.0}$)
□ 550°C 900 atm.($F_{2.0}$) × 550°C 700 atm.($F_{2.0}$) △ 550°C 500 atm.($F_{2.0}$)

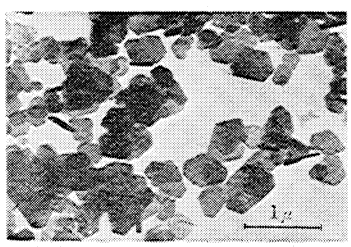

Plate I. Fluor-hydroxyl muscovite synthesized from $F_{2.0}$-composition at 600°C, 700 atm.

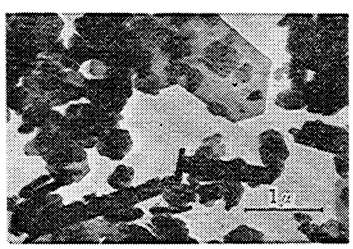

Plate II. Heavy fraction of synthetic product from $F_{2.0}$-composition at 600°C, 700 atm.

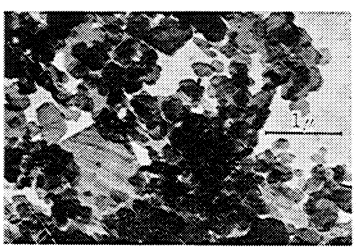

Plate III. Fluor-hydroxyl muscovite synthesized from $F_{1.0}$-composition at 600°C, 700 atm.

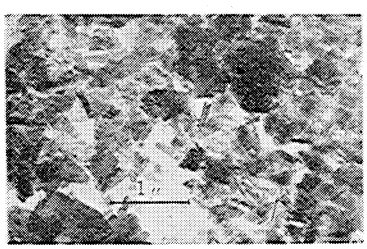

Plate IV. Hydroxyl muscovite synthesized from $F_{0.0}$-composition at 600°C, 700 atm.

of gels of silica and alumina and potassium fluoride in muscovite composition were accompanied by small amounts of topaz and feldspar. Topaz was concentrated in the heavier fraction separated by centrifuging the mixture in Thoule's solution. Topaz crystals are seen as columnar crystals in the electron micrographs shown in Plates I and II.

Fluor-hydroxyl muscovite crystallized from fluorine-containing compositions mainly in 1 M or 1 Md polymorph, and very little in 2 M polymorph, at 500°C in 20 hr. (cf. the X-ray diffraction patterns shown in Fig. 9, Nos. 1, 4 and 7). The fraction of 2 M muscovite gradually increased with the increase in the temperature of synthesis (Fig.

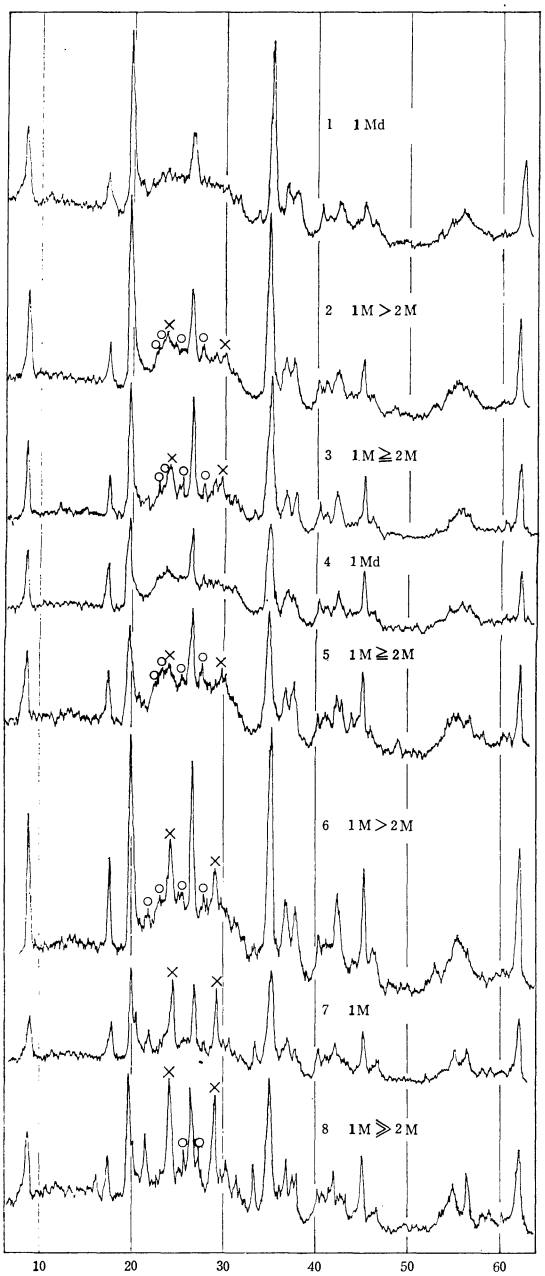

Fig. 9. X-ray powder patterns of fluor-hydroxyl muscovites prepaperd from
1. $F_{2.0}$-composition at 500°C 700 atm.
2. $F_{2.0}$-composition at 550°C 700 atm.
3. $F_{2.0}$-composition at 600°C 500 atm.
4. $F_{1.5}$-composition at 500°C 500 atm.
5. $F_{1.5}$-composition at 600°C 500 atm.
6. $F_{1.0}$-composition at 600°C 500 atm.
7. $F_{0.5}$-composition at 500°C 500 atm.
8. $F_{0.5}$-composition at 600°C 500 atm.

○ 2 M × 1 M

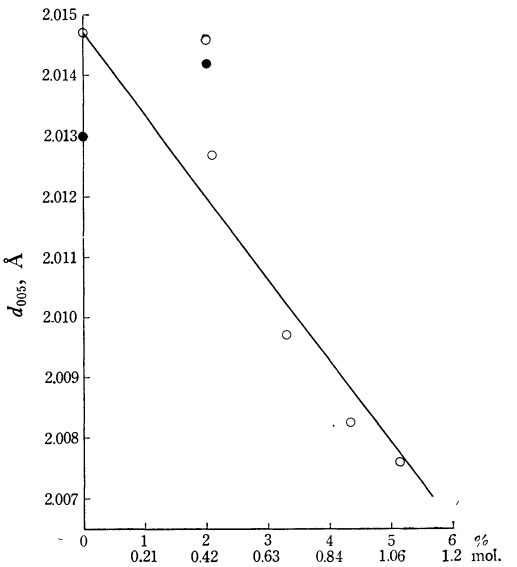

Fig. 10. Dependence of lattice spacing d_{005} on fluorine content of muscovite.
○ Experimental value
● Yoder and Eugster (1955)

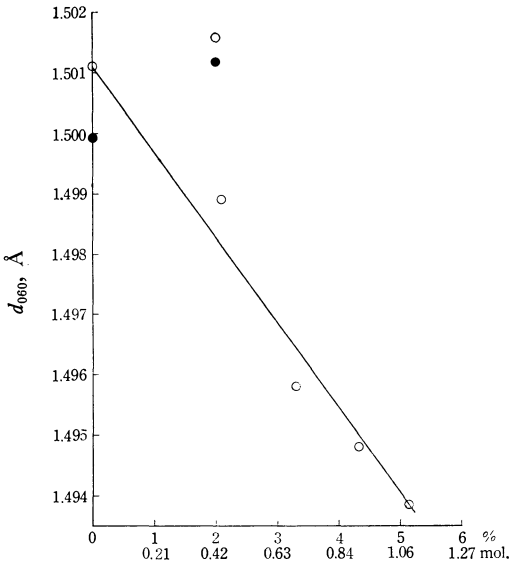

Fig. 11. Dependence of lattice spacing d_{060} on fluorine content of muscovite.
○ Experimental value
● Yoder and Eugster (1955)

9, Nos. 1, 2 and 3 for $F_{2.0}$, Nos. 4 and 5 for $F_{1.5}$, and Nos. 7 and 8 for $F_{0.5}$). The X-ray diffraction patterns of some of the muscovite specimens synthesized at 500°C from $F_{2.0}$ and $F_{1.5}$ compositions were found to be that of the 1 Md structure (Fig. 9, Nos. 1 and 4), while that of muscovite synthesized at 500°C from a $F_{0.5}$ composition was found to be of the 1 M structure (Fig. 9, No. 7). The muscovite synthesized at 600°C from $F_{2.0}$ and $F_{1.5}$ compositions was composed of almost equal amounts of 1 M and 2 M polymorphs (Fig. 9, Nos. 3 and 5), while

muscovite synthesized at 600°C from $F_{1.0}$ and $F_{0.5}$ compositions (Fig. 9, Nos. 6 and 8) contained a smaller fraction of 2 M polymorph than those obtained from $F_{2.0}$ and $F_{1.5}$ compositions. It seems that muscovite containing a larger amount of fluorine tends to crystallize more in 2 M polymorph than those containing a smaller amount of fluorine at higher temperatures. Hydroxyl-muscovite which had crystallized at 600°C in 20 hr., was 1 M polymorph. Well-developed hexagonal crystals with the prism faces on the basal plate were observed in muscovite specimens synthesized from $F_{2.0}$ and $F_{1.0}$ compositions by an electron microscope (Plates I and III). Hydroxyl-muscovite crystals had less well-developed plates (Plate IV). Also, in the case of synthetic fluor-hydroxyl phlogopite,[8] fluorine-containing mica crystallized in a better-developed form than did hydroxyl-phlogopite.

The lattice spacings of synthetic muscovite were determined by an X-ray diffractometer with copper radiation and a nickel filter, using extra pure silcon powder as an inner standard.

The plots of d_{005} and d_{060} vs. C_m are given in Figs. 10 and 11. The spacings change linearly with the change in the fluorine content of muscovite, and both plots have the same slope. The deviation of a point from the straight line may mostly be caused by an error in the determination of the fluorine content in the mica. The linear dependence of the spacings on the fluorine content in muscovite is very obvious, although Crowley and Roy[4] observed a very slight increase in the spacings of "F" mica as compared with those of "OH" mica.

8) T. Noda and N. Yamanishi, *J. Chem. Soc. Japan, Ind. Chem. Sect.* (*Kogyo Kagaku Zasshi*), **67**, 289 (1964); *Geochem. Internatl.*, **1964** (1), 90.

BULLETIN OF THE CHEMICAL SOCIETY OF JAPAN VOL. 39 1462—1468 (1966)

The Chlorine and Fluorine Contents of Tertiary Sediments on the Miura Peninsula

By Bunji IWASAKI, Kenzo KITAYAMA and Takashi KATSURA

Department of Chemistry, Tokyo Institute of Technology, Ookayama, Tokyo

(Received September 15, 1965)

Tertiary sediments were collected from the Miura group on the Miura Peninsula, and the total chlorine and fluorine in these sediments were determined colorimetrically, together with the water-soluble chlorine and fluorine. There was little correlation of the contents of insoluble chlorine and fluorine in the sediments to their locations and ages. The insoluble chlorine contents of the psammitic rocks were higher than those of the pelitic rocks, whereas the insoluble fluorine contents of the former were lower than those of the latter. There seemed to be a moderately negative correlation between the contents of insoluble chlorine and fluorine in the sediments. All the sediments analyzed contained very small amounts of water-soluble fluorine (0.001 to 0.002% F). The frequency distributions of the insoluble chlorine contents in both the psammitic and pelitic rocks were lognormal.

Studies of the chlorine content of sedimentary rocks have been published by Behne,[1] Akaiwa and Nishimura,[2] and Gulyaeva.[3] On the other hand, the fluorine content of sedimentary rocks has been studied by Koritnig,[4] Kokubu,[5] and Itkina.[6] These studies have chiefly been made in order to see whether or not the two halogens are useful as geochemical indicators of marine and fresh water sediments, and to obtain the average contents of the two halogens in sediments in order to estimate their geochemical balance. For the most part, the data described above were obtained from a very few samples, without considering the distribution of the two halogens in sedimentary rocks throughout a member, a smaller unit of stratigraphy, of a region. Among these studies, however, Akaiwa

1) W. Behne, *Geochim. et Cosmochim. Acta,* **3**, 186 (1953).

2) H. Akaiwa and M. Nishimura, *J. Chem. Soc. Japan, Pure Chem. Sect.* (*Nippon Kagaku Zasshi*), **84**, 721 (1963); **85**, 363 (1964).

3) L. A. Gulyaeva, *Doklady Akad. Nauk S. S. S. R.,* **86**, 911 (1951); L. A. Gulyaeva and E. S. Itkina, *Geokhimiya,* 524 (1962); L. A. Gulyaeva and I. F. Lositskaya, *Geokhim. i Gidrokhim. Neft. Mestorozhd., Akad. Nauk S. S. S. R., Inst. Geol. i Razrabetki Goryuch. Iskop.,* 40 (1963).

4) S. Koritnig, *Geochim. et Cosmochim. Acta,* **1**, 89 (1951).

5) N. Kokubu, *Memoirs Fac. Sci., Kyushu Univ. Ser. C, Chem.,* **2**, 95 (1956).

6) E. S. Itkina, *Geokhim. i Gidrokhim. Neft. Mestorozhd., Akad. Nauk S. S. S. R., Inst. Geol. i Razrabetki Goryuch. Iskop.,* 57 (1963).

and Nishimura[2] have made clear the vertical distribution of chlorine in two regions, i. e., the Yubari district, Hokkaido, and the Niigata district.

In this paper, an attempt will be made to see how the two halogens, chlorine and fluorine, in sediments vary vertically and horizontally throughout a member of a region, and to gain some information on the behavior of the two halogens in the sedimentary and diagenetic processes.

The tertiary sediments of the Miura group on the Miura Peninsula have been well studied in detail by many geologists[7] from the geological standpoint, and it has been said that no metamorphic process has affected these sediments. This is the reason why we chose this area for determining the chlorine and fluroine contents in sediments. After having collected the samples from this area, we determined colorimetrically the content of total and two water-soluble halogens in these samples. From the basis of the results obtained, we will discuss the following: 1) the horizontal and vertical distributions of the two halogens throughout a member; 2) their distributions among the various members formed in different geological ages; 3) the effect of the particle size of the sediments on their distributions, and 4) the correlation between the chlorine and fluorine contents in these sediments.

Experimental

Sample.—The Miura group is usually divided into three formations consisting of fourteen members. All members except the Tomioka member are composed of marine sediments, e. g., siltstone, silt, sandstone, sand, pebble conglomerate, breccia, and pyroclastic sediment. The number of the samples collected from each member is shown in Table I.

TABLE I. THE NUMBER OF THE SAMPLES COLLECTED FROM THE VARIOUS MEMBERS

Misaki formation	
Misakimachi member	10
Aburatsubo member	5
Kamakura formation	
Shimoyamaguchi member	2
Zushi member	35
Ikego member	6
Kanazawa formation	
Hukazawa member	2
Nojima member	5
Hayashi member	2
Ohuna member	12
Koshiba member	1
Nakazato member	7
Tomioka member	4
Total	91

The members are presented in the order of the stratigraphical sequence. Only a few specimens were collected from most of the members, while thirty-five samples were collected from the Zushi member in order to ascertain the horizontal and vertical distributions of its two elements. The locations of the samples are shown in Fig. 1.

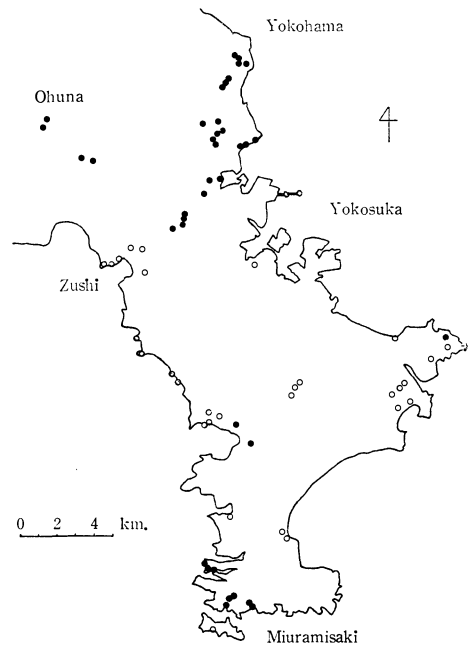

Fig. 1. The location of samples.
○ The samples from the Zushi member
● The samples from the other member

About 1 kg. of a sample was collected from each point and dried in the sunshine. Then about 100 g. of each 1 kg. was split away from the central part of the sample and crushed with a steel mortar. After about 100 g. of the sample had been quartered, about 25 g. of the sample was ground to fineness with an agate mortar in order to make a chemical analysis.

Analytical Methods.—The total chlorine was determined by the method of Iwasaki et al.[8] with some improvements. The water-soluble chlorine was determined by the thiocyanate method[9] after extraction as described in a previous paper.[10] The total fluorine was determined as follows: After about 1.00 g. of the sample had been fused with sodium peroxide in a nickel crucible, the melt was leached with a small amount of water and treated with an excess of sulfuric acid, and the fluorine was steam-distilled as fluosilicic acid. The total fluorine in distillate was colorimetrically determined by the method of Kamada et al.[11] The water-soluble

7) H. Akamine, S. Iwai, Y. Naruse, S. Ogose, M. Omori, Y. Seki, K. Suzuki and K. Watanabe, *Geoscience* (*Chikyukagaku*), No. 30, 1 (1956); T. Mitsunashi and K. Yazaki, *J. Japanese Association of Petroleum Technologist* (*Sekiyu Gizyutsu Kyokaishi*), **23**, 16 (1958), etc.

8) I. Iwasaki, T. Katsura and N. Sakato, *J. Chem. Soc. Japan, Pure Chem. Sect.* (*Nippon Kagaku Zassi*), **76**, 1116 (1955).

9) A. Tomonari, ibid., **83**, 693 (1962).

10) B. Iwasaki and T. Katsura, This Bulletin, **37**, 1827 (1964).

11) M. Kamada and T. Onishi, *J. Chem. Soc. Japan, Pure Chem. Sect.* (*Nippon Kagaku Zasshi*), **80**, 275 (1959).

fluorine was determined by the same method after the same extraction and separation processes as were for water-soluble chlorine.

Duplicated analyses were made for all of the samples, and it may safely be said that the precision of the present determination of chlorine is within ±5%, while that of fluorine is within ±10%, over the whole range obtained here. The fluorine contents of the standard rock samples, W-1 and G-1, and the basaltic rock samples of O-sima Volcano, A-15 and H-13, were determined in order to confirm the accuracy of our present results. The results are shown in Table II, together with the results of other authors. As is shown in Table II, our values are fairly well consistent with the data of Yoshida.

Table II. Analytical data of the standard rocks (fluorine content %)

	Yoshida[a]	Ingamells[b]	Jeffery[c]	The present authors
G-1	0.066	0.069—0.074	0.0629	0.059
W-1	0.024	0.030—0.031	0.0290	0.021
H-3[d]	0.012			0.009
A-15[d]	0.012			0.009

a) M. Yoshida, Doctral Thesis, Tokyo Institute of Technology (1962).
b) C. O. Ingamells, *Talanta*, **9**, 507 (1962).
c) P. G. Jeffery, *Geochim. et Cosmochim. Acta*, **26**, 1335 (1962).
d) The basaltic rock in 1950—1951 from O-sima volcano.

Results

Tables III-a and III-b give the insoluble chlorine and fluorine contents of the tertiary sediments on the Miura Peninsula, together with the water-soluble chlorine and fluorine contents.

Table III-b shows the findings on pairs of the sediments, e. g., siltstone and sandstone, and silt and sand, which were contiguous to one another.

Table III-a. The chlorine and fluorine contents of the tertiary sediments in the Miura peninsula

Sample No.	W-Cl %	I-Cl %	W-F %	I-F %	Remarks
Shimoyamaguchi member					
2807	0.005	0.028			P
0404-1	0.003	0.004			P
Zushi member					
2801	0.008	0.009	0.002	0.024	S
3106	0.006	0.009			S
3107	0.002	0.010	0.001	0.032	S
0301	0.002	0.010	0.002	0.033	S
0302	0.004	0.011	0.001	0.026	S
0303	0.004	0.033	0.002	0.031	S
0401	0.17	0.01	0.001	0.013	B
0402	0.008	0.021	0.001	0.015	S
0403	0.003	0.060	0.001	0.015	B
0404-2	0.45	0.00	0.001	0.021	P
0405	0.20	0.01	0.001	0.029	S
0406	0.009	0.022	0.001	0.009	S
0407	0.004	0.010	0.002	0.033	S
0501	0.003	0.061	0.001	0.009	B
0501-1	0.003	0.030	0.001	0.017	Ss
0502	0.034	0.007	0.001	0.011	B
0503	0.006	0.009	0.002	0.021	S
0504	0.066	0.016			S
0505	0.15	0.00	0.001	0.017	S
0601	0.002	0.011	0.001	0.032	S
0603	0.010	0.018	0.001	0.028	S
0604	0.004	0.012	0.001	0.028	S
0605	0.009	0.019	0.001	0.018	S
0607	0.011	0.024	0.001	0.031	S
0701	0.021	0.003	0.001	0.024	S
0702	0.019	0.003	0.001	0.031	S
Ikego member					
2916	0.006	0.023			Py P
2917	0.008	0.013			S
2918	0.003	0.017	0.002	0.027	S
2918-1	0.012	0.020			S
0606	0.005	0.046			P
0606-1	0.25	0.00			Py Ss
Hukazawa member					
0204	0.92	0.00	0.001	0.009	Ss
0204-1	1.49	0.00			Ss
Nojima member					
0203	0.004	0.017			S
2913	0.35	0.00			Ss
2915	0.15	0.01			Ss
Hayashi member					
3112	0.002	0.038			P
3113	0.002	0.010			Sand
Ohuna member					
2908	0.002	0.016			Ss
2909	0.20	0.00			S
2911	0.004	0.007			S
2912	0.001	0.007			S
0201	0.003	0.007			S
0201-1	0.002	0.008			S
0202	0.007	0.010	0.001	0.025	S
0703	0.003	0.012			S
0705	0.004	0·008	0.001	0.042	S
0706	0.004	0.022	0.001	0.018	S
Koshiba member					
0.704	0.082	0.001			Sand
Nakazato member					
0704-1	0.39	0.00			Silt
Tomioka member					
2901	0.003	0.008			Silt
2902	0.014	0.005			Silt
2903	0.003	0.008	0.000	0.024	Silt
2904	0.005	0.005	0.001	0.030	Silt

Table III-b. The chlorine and fluorine contents of the tertiary sediments in the Miura Peninsula

Sample No.	W-Cl %	I-Cl %	W-F %	I-F %	Remarks
Misakimachi member					
0102	0.006	0.050	0.001	0.001	Py Ss
0102-1	0.41	0.00	0.001	0.021	S
0103	0.029	0.011			S
0103-1	0.003	0.022			Ss
0104	0.027	0.018	0.000	0.023	S
0104-1	0.005	0.037	0.001	0.007	Ss
0105	0.12	0.00			S
0105-1	0.008	0.030			Ss
0106	0.024	0.015			S
0106-1	0.006	0.029			Ss
Aburatsubo member					
0107	0.38	0.00	0.001	0.010	S
0107-1	0.055	0.05			Py P
0107-2	0.019	0.033			Py Ss
0108	0.082	0.03			Ss
0108-1	0.006	0.042			S
Zushi member					
3108	0.003	0.070	0.002	0.028	S
3108-1	0.002	0.025	0.002	0.018	Ss
3108-2	0.002	0.012			S
0101	0.019	0.008	0.002	0.030	S
0101-1	0.006	0.021			Ss
0506	0.018	0.002	0.001	0.026	S
0506-1	0.004	0.016	0.002	0.017	Ss
0602	0.004	0.013	0.000	0.027	S
0602-1	0.004	0.016	0.002	0.021	Ss
Nojima member					
2914	0.003	0.027	0.002	0.009	P
2914-1	0.012	0.020	0.001	0.018	S
Ohuna member					
2910	0.007	0.010	0.002	0.028	S
2910-1	0.009	0.09	0.001	0.033	Ss
Nakazato member					
2905	0.001	0.008			Sand
2905-1	0.003	0.003			Silt
2906	0.001	0.007	0.001	0.018	Silt
2906-1	0.001	0.007	0.001	0.014	Sand
2907	0.002	0.005			Silt
2907-1	0.002	0.006			Sand

Abbreviation used in Tables III-a and III-b has the following meaning:
W-Cl, water-soluble chlorine content; I-Cl, insoluble chlorine content; W-F, water-soluble fluorine content. I-F; insoluble fluorine content.
B, breccia; P, pebble conglomerate; Py P, pyroclastic pebble conglomerate; Py Ss, pyroclastic sandstone; S, siltstone; Ss, sandstone.

Discussion

Water-soluble Chlorine. — As is shown in Tables III-a and III-b, the water-soluble chlorine contents range from 0.001 to 1.5%. The samples containing a large amount of water-soluble chlorine seem to be contaminated with sea-water; they were collected on or near the coast. Therefore, we will omit the data which can be suspected of being contaminated with sea-water.

The frequency diagrams of the water-soluble chlorine contents of psammitic and pelitic rocks are shown in Fig. 2.

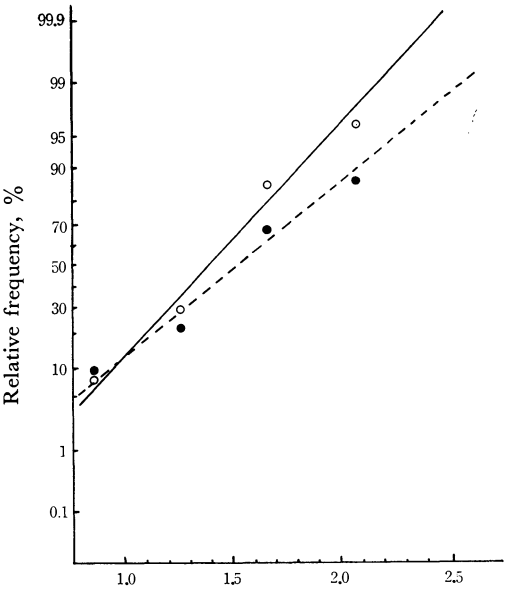

Fig. 2. Cumulative frequency distribution of water-soluble chlorine content of sediments.
○ Psammitic rocks
● Pelitic rocks

In this paper, we will divide all the sediments into two rock types. One is the psammitic rock type, in which sandstone, sand, pebble conglomerate, breccia, and pyroclastic sediment are included, and the other is the pelitic rock type, in which siltstone and silt are included. As is shown in Fig. 2, these two types of sediments show approximate lognormalities, rather than normalities. Provided that the frequency diagrams of the water-soluble chlorine contents of both psammitic and pelitic rocks obey the lognormal distribution, we obtain the geometrical means of the water-soluble chlorine contents of the two types of rock as 0.002 and 0.003 per cent respectively. From these values, it is clear that the samples which are not likely to be contaminated with sea-water contain very small amounts of water-soluble chlorine. Judging from their geometrical means, no significant effect caused by particle size was found on the distribution of water-soluble chlorine in these rock types. However, the water-soluble chlorine contents of the pelitic rocks are frequently higher than those of the psammitic rocks, as Table III-b shows. The tendency may be explained by saying that the

pelitic rocks are much more retentive of chlorine than the psammitic rocks because of the larger adsorption surface and the lower permeability of the pelitic rocks.

Insoluble Chlorine.—The insoluble chlorine contents range from 0.00 to 0.09%. Figure 3 gives the frequency diagrams of the insoluble chlorine contents of the psammitic and pelitic rocks.

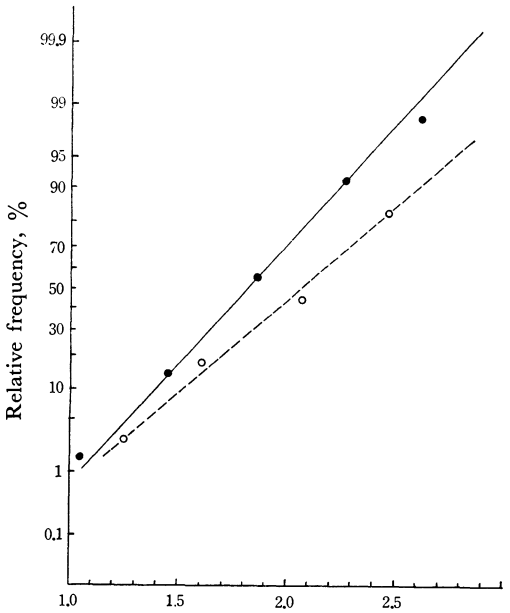

Fig. 3. Cumulative frequency distribution of insoluble chlorine content of sediments.
○ Psammitic rocks
● Pelitic rocks

They also show the lognormal distributions. We obtain the geometrical means of the insoluble chlorine contents of both psammitic and pelitic rocks as 0.011 and 0.006% respectively.

Figure 4 gives the horizontal and vertical distributions of the insoluble chlorine contents of the pelitic rocks in the Zushi member.

As Tables III-a and III-b show, the insoluble chlorine contents range from 0.00 to 0.070%. The terms "coast" and "deep sea" imply coastal and deep sea conditions during the age when the sediments were formed. The alphabetical letters on the right hand side of Fig. 4 indicate the names of the pyroclastic key beds. The thickness of the sediments among each key bed is arbitrarily drawn. We cannot find any regularity in the distribution of insoluble chlorine in the Zushi member from Fig. 4; this means that one specimen, or even a few specimens, collected from a member may not be truly indicative of the insoluble chlorine content. Also, it may be seen that the insoluble chlorine contents of the sediments can not be related to their sedimentary ages.

Water-soluble Fluorine.—As is shown in Tables III-a and III-b, the water-soluble fluorine contents range from 0.001 to 0.002%. Such small amounts of the water-soluble fluorine in the sediments are in striking contrast to the larger amounts of the water-soluble chlorine in the sediments previously shown. It is, however, clear that the water-soluble fluorine content may only slightly be influenced by the contamination of sea-water, because sea-water contains only 1.4 p.p.m. fluorine.

Assuming the extreme case that fluorite is a main carrier of fluorine in sediments and that the solution extracted is an aqueous solution saturated with

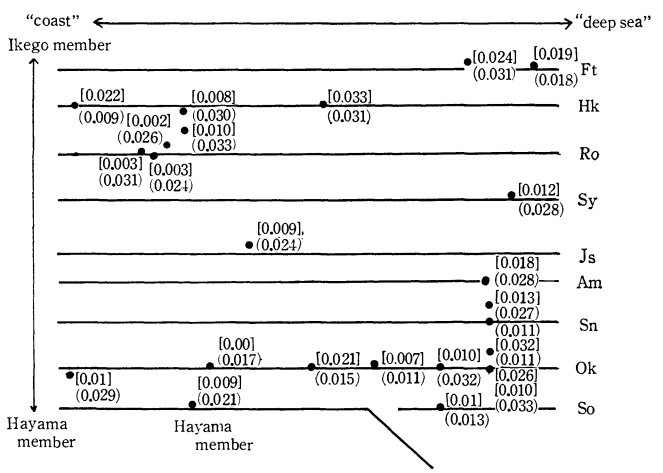

Fig. 4. Vertical and horizontal distributions of insoluble chlorine and fluorine in the Zushi member.
[ ] Insoluble chlorine content
( ) Insoluble fluorine content

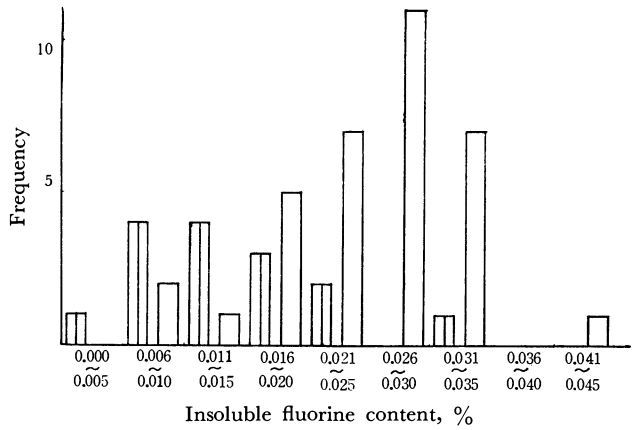

Fig. 5. Frequency distribution of insoluble fluorine contents of the psammitic and pelitic rocks.
Psammitic rocks
Pelitic rocks

fluorite (13.1 mg. fluorite per liter at 0°C[12]) in the case of water-soluble fluorine from 1 g. of a sample with 20 ml. of water, the fluorine content of the solution may be expected to become 0.013%. Actually, the water-soluble fluorine contents of samples were about ten times smaller than that calculated above. Therefore, it is thought that fluorine in these sediments does not exist as fluorite but as other forms.

Insoluble Fluorine.—As Tables III-a and III-b show, the insoluble fluorine contents of the sediments range from 0.001 to 0.042%. Figure 5 gives the frequency diagrams of the insoluble fluorine contents of both psammitic and pelitic rocks.

They seem to have neither normal nor lognormal distributions. Provided that they show normalities, we obtain the arithmetical means of psammitic and pelitic rocks as 0.025 and 0.014% respectively. The mean insoluble fluorine content of the former is twice as much as that of the latter. As may be seen in Fig. 5 and Table III-b, it is evident that the insoluble fluorine contents of the pelitic rocks are higher than those of the psammitic rocks, as has already been pointed out by Koritnig.[4] It is generally believed that the amounts of OH-bearing minerals in pelitic rocks are higher than those of psammitic rocks; thus, assuming that hydroxide ions in these minerals are replaced by fluoride ion in an aqueous solution, it may be reasonable to say that fluorine is concentrated in pelitic rocks.

Figure 4 gives the horizontal and vertical distributions of the insoluble fluorine in the Zushi member. As is shown in Tables III-a and III-b, the insoluble fluorine contents range from 0.009 to 0.033%. Figure 4 does not, however, show any trend in the distribution of insoluble fluorine in the Zushi member horizontally or vertically.

The Correlation between the Content of Insoluble Chlorine and of Fluorine in the Sediments.—Figure 6 shows the correlation between the contents of insoluble chlorine and fluorine in the sediments.

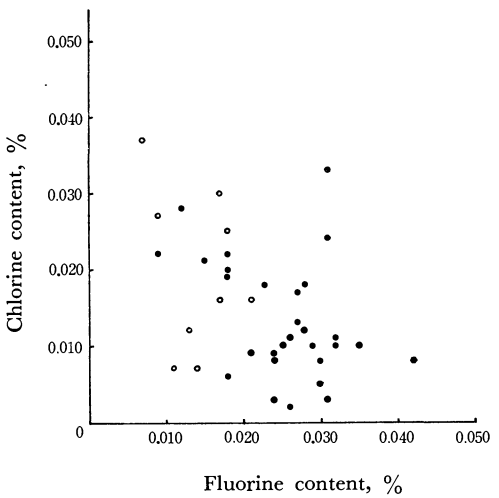

Fig. 6. Relationship between the contents of insoluble chlorine and fluorine of sediments.
○ Psammitic rocks
● Pelitic rocks

This shows a moderately negative correlation. Indeed, we have very little knowledge of the properties of OH-bearing minerals in sedimentary rocks, by which property some sort of replacement reaction might be expected to occur between halide and hydroxide ions. However, if we simply assume that the effective amount of hydroxide ions in the

12) F. Kohlrausch, *Z. physik. Chem.*, **50**, 355 (1904-5); **64**, 121 (1908).

sediments is constant and that the hydroxide ions are completely replaced by fluoride and chloride ions, there will be a negative correlation between the contents of fluorine and chlorine. As has been seen in Fig. 6, fluorine is more concentrated in pelitic rocks than in psammitic rocks, and concentrations above 0.02% fluorine are found exclusively in pelitic rocks. This may be attributed to the larger electronegativity and the smaller ionic radius of the fluoride ion than those of the chloride ion.

Conclusion

We may conclude from the above discussions that; 1) there is little correlation between the contents of insoluble chlorine and fluorine in the sediments and their sedimentary locations and ages; 2) it is almost impossible to estimate the contents of both insoluble chlorine and fluorine in a given member of sediments by using only one specimen geologically regarded as representative of the sediment in the member; 3) the insoluble chlorine contents of the psammitic rocks are higher than those of the pelitic rocks, whereas the insoluble fluorine contents of the former are lower than those of the latter; 4) there seems to be a moderately negaitve correlation between the contents of insoluble chlorine and fluorine; 5) all the sediments analyzed contain very small amounts of water-soluble fluorine (0.001 to 0.002% F), and 6) the frequency distributions of the insoluble chlorine contents in both psammitic and pelitic rocks are approximately lognormal.

The authors wish to express their thanks to Dr. Takashi Mitunashi, Geological Survey of Japan, for his valuable advice and criticism in the field observations. They are also much obliged to Dr. Sunao Ogose, the University of Tokyo, for his advice in the collection of the samples. They wish also to express their thanks to Professor Iwaji Iwasaki, Tokyo Institute of Technology, for his encouragement throughout this study. The expenses of this reseach were defrayed by a Scientific Reseach Encouragement Grant from the Ministry of Education, to which the authors' thanks are due.

BULLETIN OF THE CHEMICAL SOCIETY OF JAPAN VOL. 39 1468—1471 (1966)

The Crystal Structure of Succinonitrilo-disilver Nitrate, $2AgNO_3 \cdot NC(CH_2)_2CN$

By Teruo NOMURA and Yoshihiko SAITO

The Institute for Solid State Physics, The University of Tokyo, Azabu, Tokyo

(Received December 2, 1965)

The structure of $2AgNO_3 \cdot NC(CH_2)_2CN$ has been determined by X-ray analysis. It is monoclinic; $a=5.87$, $b=17.79$, $c=4.61$ Å, $\beta=118.2°$, space group $P2_1/a$, two formula units in the cell. The structure is essentially ionic and consists of the complex cations, $[AgNC(CH_2)_2CNAg]^{2+}$ (Ag–N, 1.97 Å), and the nitrate anions. All the bond lengths are normal. The molecule of succinonitrile was found to take the trans configuration; this is in conformity with the conclusion drawn from the infrared study.

In a series of investigations of the structures of the complexes with the general formula $[Cu\{NC(CH_2)_nCN\}_2]NO_3$,[1-3] Kinoshita and one of the present authors have found that succinonitrile molecules coordinate to central metal atoms, taking a "gauche" configuration. In the case of succinonitrile silver nitrate complexes, however, Shimanouchi et al. concluded, by infrared study, that succinonitrile molecules take a trans configuration in the crystals of $2AgNO_3 \cdot NC(CH_2)_2CN$.[4] In cooperation with their study, this crystal has now been subjected to X-ray analysis in order to establish the coordination about the silver atoms and the configuration of the succinonitrile molecules.

Crystallographic Data

White needle-like crystals of $2AgNO_3 \cdot NC(CH_2)_2CN$ were kindly supplied by Prof. Shimanouchi. From oscillation and Weissenberg photographs taken using Cu$K\alpha$ radiation ($\lambda=1.542$ Å), the unit cell was found to be monoclinic and to have the

1) Y. Kinoshita, I. Matsubara and Y. Saito, This Bulletin, **32**, 741 (1959).
2) Y. Kinoshita, I. Matsubara and Y. Saito, ibid., **32**, 1216 (1959).
3) Y. Kinoshita, I. Matsubara, T. Higuchi and Y. Saito, ibid., **32**, 1221 (1959).
4) M. Ohara, T. Fujiyama and T. Shimanouchi, presented at the 17th Annual Meeting of the Chemical Society of Japan, Tokyo, April, 1964.

following cell dimensions:

$$a = 5.87 \pm 0.04 \text{ Å}$$
$$b = 17.79 \pm 0.05 \text{ Å}$$
$$c = 4.61 \pm 0.03 \text{ Å}$$
and $$\beta = 118.2 \pm 0.2°.$$

On the basis of this unit cell, the needle axis of the crystals was determined to be [$\bar{2}$01]. The space group was found to be $P2_1/a$—C_{2h}^5 from systematic absences. The cell contains two formula units of $2AgNO_3 \cdot NC(CH_2)_2CN$ (density; calculated, 3.30 g./cm^3; found, 3.34 g./cm^3).

The crystals are fragile and decompose gradually on exposure to daylight as well as to X-rays. The intensity data for the *hk*0, 0*kl* and *h*0*l* reflections were recorded about each principal axis on zero-level Weissenberg films by the multiple film technique, in each case using 0.05 mm. × 0.05 mm. × 1mm. crystals. Since we are merely interested in the establishment of the coordination about the silver atom and the configuration of the ligand molecule, and not in attaining high precision in the structural parameters, no special pains have been taken with the intensity estimates; they were carried out visually and were uncorrected for absorption errors. The estimated intensities were corrected for Lorentz and polarization factors. The observed structure amplitudes were brought to an absolute scale by scaling them against the calculated values at a later stage.

The Determination of the Structure

Since there are two molecules of succinonitrile in the unit cell, their center of gravity must lie on a set of twofold special positions. Thus, the succinonitrile molecule must have a center of symmetry and must assume a trans configuration.

The structure determination is based mainly on the analysis of the *hk*0 and 0*kl* reflections, which can be carried out in quite a straightforward fashion. Because of the occurrence of the heavy silver atoms, the Patterson functions are extremely simple and can be solved without difficulty, thus yielding the approximate positions of silver atoms. The signs for all but weak reflections can be derived on the basis of the positions of the silver atoms. Fourier syntheses of the electron density projected along [001] and [100] were evaluated without the weak reflections of uncertain signs. On both projections, all the atoms appeared. The maxima of some light atoms deformed under the influence of heavy silver atoms. In the refined two-dimensional Fourier syntheses, including all the terms, all the peaks of the light atoms were found in the expected positions. The atomic parameters thus obtained were refined by performing cycles of least-squares refinement of the positional and isotropic thermal parameters of the atoms: the programme employed was devised by Iitaka. The value of the discrepancy factor was 0.15 for all *hk*0, 0*kl* and *h*0*l* reflections.

The final projection of the electron density, together with that of the structure, is shown in Fig. 1.

Table I contains the final parameters of all the atoms. The observed and calculated structure amplitudes are compared in Table II.

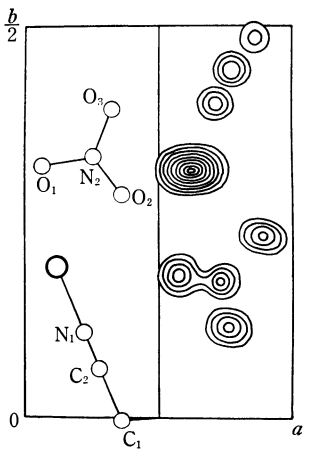

Fig. 1. The electron density and the structure projected along [001].

Table I. Final atomic coordinates and temperature factors

Atom	*x*/*a*	*y*/*b*	*z*/*c*	*B*, Å^2
Ag	0.1103	0.1921	0.1623	3.3
C1	0.354	−0.004	0.896	4.3
C2	0.274	0.061	0.660	3.2
N1	0.209	0.109	0.483	3.0
N2	0.240	0.333	0.653	3.1
O1	0.052	0.324	0.635	3.8
O2	0.312	0.395	0.646	4.3
O3	0.356	0.282	0.673	4.7

The calculations of the structure amplitudes, Fourier syntheses and least-squares refinement were carried out on the PC 2 computer of this Institute.

Description of the Structure and Discussion

The interatomic distances and bond angles are given in Table III.

The structure is essentially ionic and consists of the complex ion, $[AgNC(CH_2)_2CNAg]^{2+}$, and nitrate ions. The structure is most easily understood with the aid of Fig. 2, in which the arrangement of the complex ions and nitrate ions projected upon the crystallographic plane ($\bar{2}$01) is illustrated. The complex ion has a center of symmetry. A succinonitrile molecule takes a trans configuration; this is in conformity with the conclusion drawn from the infrared study. It is coordinated to two silver

TABLE II. OBSERVED AND CALCULATED STRUCTURE AMPLITUDES

h	k	l	$F_o/4$	$F_c/4$	h	k	l	$F_o/4$	$F_c/4$	h	k	l	$F_o/4$	$F_c/4$	h	k	l	$F_o/4$	$F_c/4$
2	0	0	6.4	− 6.7	1	7	0	18.6	−17.6	4	1	0	7.4	− 8.0	0	14	1	2.8	0.4
4	0	0	15.4	−14.0	1	8	0	3.9	4.0	4	2	0	13.5	11.7	0	15	1	10.5	7.2
6	0	0	3.8	− 4.0	1	9	0	3.0	3.3	4	3	0	4.6	2.7	0	16	1	10.0	6.5
0	0	1	8.7	2.0	1	10	0	9.3	6.8	4	4	0	6.7	− 4.8	0	17	1	11.0	−11.0
0	0	2	16.1	−14.6	1	11	0	10.4	8.9	4	6	0	9.6	− 7.6	0	18	1	6.6	− 6.9
0	0	3	11.2	−11.9	1	12	0	12.8	−10.3	4	7	0	7.1	− 5.2	0	19	1	7.5	7.5
0	0	4	10.7	− 9.2	1	13	0	14.2	−14.0	4	8	0	11.5	10.1	0	1	2	35.6	−34.7
2	0	1	18.2	−18.5	1	14	0	12.6	12.4	4	9	0	3.8	5.5	0	2	2	11.6	12.2
2	0	2	18.6	−16.0	1	15	0	9.1	7.5	4	10	0	11.0	−10.9	0	3	2	9.3	9.4
2	0	3	4.9	− 4.3	1	16	0	6.7	− 4.3	4	12	0	3.8	3.9	0	4	2	2.5	− 3.3
2	0	4	4.0	4.1	1	18	0	2.5	− 2.2	4	15	0	3.3	2.1	0	5	2	4.9	6.6
2	0	5	3.4	3.7	1	19	0	4.3	− 3.3	4	16	0	5.9	− 5.4	0	6	2	5.4	− 6.6
4	0	1	9.2	− 9.2	1	20	0	5.2	4.1	4	17	0	3.0	− 2.1	0	7	2	17.0	−19.4
4	0	2	1.2	− 0.6	1	21	0	5.6	4.8	4	18	0	5.9	5.5	0	8	2	9.3	11.8
4	0	3	4.0	5.5	1	22	0	5.2	− 4.7	5	1	0	3.6	− 3.0	0	9	2	18.7	19.2
2	0	−1	47.3	48.5	2	1	0	29.2	−27.7	5	2	0	4.4	2.6	0	10	2	6.3	− 5.6
2	0	−2	25.4	21.6	2	2	0	9.7	− 8.2	5	3	0	10.5	8.6	0	11	2	8.9	− 8.7
2	0	−3	4.2	− 3.1	2	3	0	10.5	13.1	5	4	0	5.2	− 5.4	0	12	2	6.1	2.1
2	0	−4	10.2	−10.4	2	4	0	7.5	5.4	5	5	0	11.2	−11.0	0	14	2	2.1	1.1
2	0	−5	4.7	− 6.2	2	5	0	14.1	11.5	5	7	0	6.2	5.5	0	15	2	8.7	7.4
4	0	−1	8.2	−11.8	2	6	0	8.3	7.0	5	9	0	6.2	2.9	0	16	2	5.4	− 3.7
4	0	−2	18.4	19.8	2	7	0	21.3	−24.0	5	10	0	2.7	− 2.8	0	17	2	5.4	− 6.8
4	0	−3	14.2	14.7	2	8	0	5.6	− 6.1	5	11	0	4.8	− 4.7	0	18	2	3.9	3.4
4	0	−4	1.2	1.7	2	9	0	23.6	20.5	5	12	0	4.6	2.7	0	19	2	4.5	3.2
4	0	−5	5.9	− 4.3	2	11	0	9.5	−10.2	5	13	0	6.5	5.1	0	20	2	1.9	− 1.0
4	0	−6	3.8	− 4.2	2	13	0	3.5	− 2.4	5	14	0	1.6	− 1.1	0	21	2	1.9	− 1.0
6	0	−1	8.6	− 8.8	2	15	0	10.9	9.4	5	15	0	4.6	− 4.3	0	2	3	10.9	10.4
6	0	−2	4.2	− 5.1	2	17	0	10.0	−10.3	6	1	0	5.1	4.7	0	6	3	8.8	− 8.1
6	0	−3	2.4	3.5	2	18	0	3.8	− 3.8	6	2	0	4.0	3.1	0	8	3	11.6	10.2
6	0	−4	7.0	7.8	2	19	0	7.7	5.9	6	3	0	3.0	− 2.3	0	10	3	10.1	−11.6
6	0	−5	3.8	3.7	2	20	0	2.1	0.0	6	6	0	3.0	− 2.5	0	12	3	3.2	4.4
0	2	0	32.2	−35.6	3	1	0	4.1	− 6.2	6	7	0	4.8	4.2	0	14	3	5.7	3.0
0	4	0	1.2	− 1.8	3	2	0	13.3	−11.5	6	8	0	4.2	4.0	0	16	3	7.1	− 6.5
0	6	0	21.7	23.2	3	3	0	12.5	16.1	6	9	0	5.2	− 4.5	0	18	3	7.5	6.4
0	8	0	34.0	−30.2	3	4	0	17.2	20.1	6	11	0	3.0	2.3	0	1	4	10.6	10.3
0	10	0	27.5	27.4	3	5	0	8.1	− 7.9	0	1	1	13.6	−13.6	0	2	4	4.3	5.0
0	12	0	5.8	− 4.3	3	6	0	10.1	−12.6	0	2	1	8.4	− 8.9	0	3	4	2.2	− 3.3
0	14	0	9.7	− 8.4	3	7	0	9.5	7.7	0	3	1	16.0	16.6	0	6	4	6.0	− 4.7
0	16	0	12.0	11.8	3	8	0	3.2	2.3	0	4	1	12.9	12.9	0	7	4	5.9	6.2
0	18	0	8.4	− 5.3	3	9	0	2.3	− 1.8	0	5	1	6.8	5.8	0	8	4	6.9	6.2
0	20	0	5.9	4.3	3	10	0	6.1	6.6	0	6	1	11.4	12.6	0	9	4	6.2	− 7.2
0	22	0	1.9	0.5	3	11	0	5.6	− 5.4	0	7	1	17.6	−17.5	0	10	4	7.5	− 3.9
1	1	0	5.7	8.8	3	12	0	12.7	−11.0	0	8	1	8.4	−11.0	0	11	4	4.1	3.7
1	2	0	8.2	−11.3	3	13	0	6.8	7.7	0	9	1	17.1	17.5	0	14	4	4.1	1.2
1	3	0	24.4	−27.4	3	14	0	7.9	7.7	0	10	1	9.7	8.9	0	15	4	3.3	− 3.1
1	4	0	10.0	11.0	3	15	0	3.6	− 1.5	0	11	1	10.7	−12.4	0	7	5	3.8	3.6
1	5	0	20.2	20.1	3	16	0	3.9	− 3.8	0	12	1	5.0	− 3.0	0	9	5	3.7	− 3.7
1	6	0	18.9	−15.3	3	20	0	4.3	4.3	0	13	1	4.4	0.8					

atoms belonging to two adjacent unit cells and with a Ag–N distance of 1.97 Å. The complex ion, $[AgCN(CH_2)_2CNAg]^{2+}$, may be compared with $[AgCNAg]^+$, the existence of which has been fairly well established in cyanide solutions containing an excess of silver ions.[5-7]

The observed C–N distance of 1.12 Å is close to the value expected for the triple C–N bond length. The Ag–N–C–C bond is nearly linear. These features are similar to those found in the crystals of $[Cu\{NC(CH_2)_2CN\}_2]NO_3$. In the case of the

5) S. Glasstone, *J. Chem. Soc.*, **1930**, 1237.

6) K. Hellwig, *Z. anorg. Chem.*, **25**, 157 (1900).

7) T. Erdey-Gruz, *Z. Physk. Chem.*, **172**, 157 (1935).

Table III. Interatomic distances and bond angles

Ag···Ag	9.69 Å		
Ag—N1	1.97	∠AgN1C1	179°
N1—C2	1.12	∠N1C2C1	178
C2—C1	1.50	∠N1C1C1′	105
C1—C1′	1.52	∠O1N2O2	120
N2—O1	1.10	∠O2N2O3	123
N2—O2	1.19	∠O1N2O3	117
N2—O3	1.11		

latter, however, there exist polymeric chains of the composition,

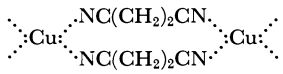

and a succinonitrile molecule in the complex takes a gauche configuration with respect to the central C–C bond.

As is shown in Fig. 2, the complex ions and the nitrate ions are arranged approximately in one layer parallel to the ($\bar{2}01$) plane. In each layer nitrate ions are arranged with their planes nearly perpendicular to it.

A silver atom at the end of the complex ion is surrounded by four oxygen atoms of the nitrate ions, with interatomic distances ranging from 2.49 Å to 3.36 Å. Two of them belong to the nitrate ions in the same layer as the silver atom, while the others belong to those in the adjacent layers. All the interatomic distances are in good agreement with those obtained for other crystals.

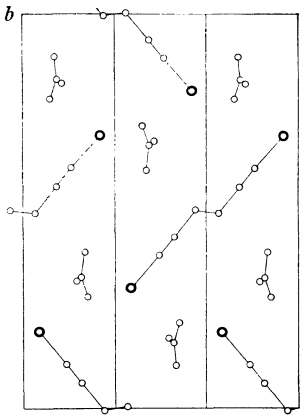

Fig. 2. The arrangement of the complex ions and nitrate ions projected on the plane ($\bar{2}01$).

Part of the cost of this investigation has been defrayed by a Scientific Research Grant of the Ministry of Education, to which the authors' thanks are due.

BULLETIN OF THE CHEMICAL SOCIETY OF JAPAN VOL. 39 1471—1476 (1966)

The Stability of Fused Rings in Metal Chelates. III. The Relative Stability of Copper(II) Complexes of Aldehyde- and Ketone-Schiff Bases[1]

By Yasuo NAKAO, Ken-ichi SAKURAI and Akitsugu NAKAHARA

Institute of Chemistry, College of General Education, Osaka University, Toyonaka, Osaka

(Received December 4, 1965)

The relationship between the structure of fused-ring systems and the relative stability of copper(II) Schiff base chelates has been discussed, on the basis of the properties of six copper(II) complexes, in connection with the transamination reaction. As the conclusion it has been suggested that the transamination reaction in fused-ring systems containing copper(II)-glyoxylate- or -pyruvate-Schiff bases may be expected only in such appropriately unstable systems as have two five-membered rings and that it is generally accompanied by a stabilization of the system. The preparation and properties of the two new copper(II) chelates, glyoxylidene-β-alaninatoaquocopper(II) and pyruvidene-α-alaninatoaquocopper(II), have been described.

The previous effort in this laboratory has been directed toward the investigation of the properties of fused-ring systems in copper(II) complexes of Schiff bases derived from salicylaldehyde[2] or pyruvic acid[3] and amino acids or other amino compounds. In order to extend our previous interpretation concerning the relationship between the relative stability of metal chelates and the

1) A part of this work has already been published as a "Short Communication": Y. Nakao, K. Sakurai and A. Nakahara, This Bulletin, **38**, 687 (1965).

2) A. Nakahara, H. Yamamoto, and H. Matsumoto, *Sci. Rep.* (*College of General Education, Osaka University*), **12**, 11 (1963).

3) A. Nakahara, H. Yamamoto and H. Matsumoto, This Bulletin, **37**, 1137 (1964).

structure of fused-ring systems, we have recently undertaken the syntheses of some copper(II) chelates of Schiff bases derived from glyoxylic acid and amino acids.

In the meantime we have found that there is a delicate correlation between the structure of fused-ring systems and the transamination reaction. For example, the complex isolated in the crystalline state from the copper(II)-glyoxylate-alaninate system has been proved to be pyruvideneglycinato-aquocopper(II) instead of glyoxylidenealaninato-aquocopper(II). This finding is apparently related to a transamination reaction occurring in the fused-ring system of the metal complex. It seems noteworthy that only a chelate of glycine with pyruvate and copper(II), not of one alanine with glyoxylate and copper(II), is isolated. In such a way we can describe the relative stability of fused ring systems containing aldehyde- or ketone-Schiff bases in connection with the transamination reaction.

The preparation and some properties of two new complexes, glyoxylidene-β-alaninatoaquocopper(II) and pyruvidene-α-alaninatoaquocopper(II), will also be described.

The Transamination Reaction of the Copper-(II)-glyoxylate-α-alaninate System.—We prepared a pair of copper(II) Schiff base complexes which could be discriminated from each other only through the relative location of the >C=N- double bond in the fused-ring system, as is indicated by the structures I and II. The two complexes isolated

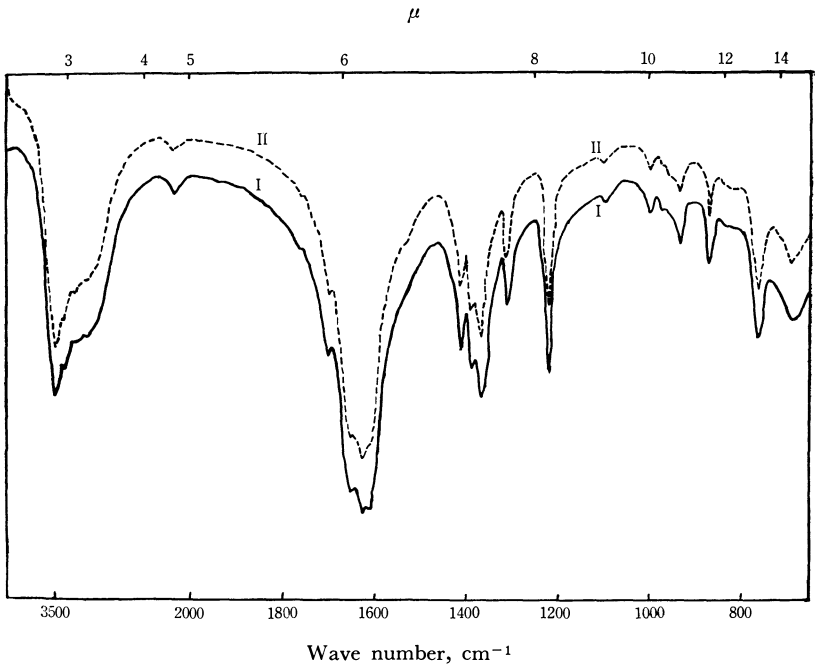

Fig. 1. Infrared spectra of [Cu pyv=gly(H_2O)]·$2H_2O$, I, and the complex derived from copper(II), α-alanine and glyoxylic acid, II.

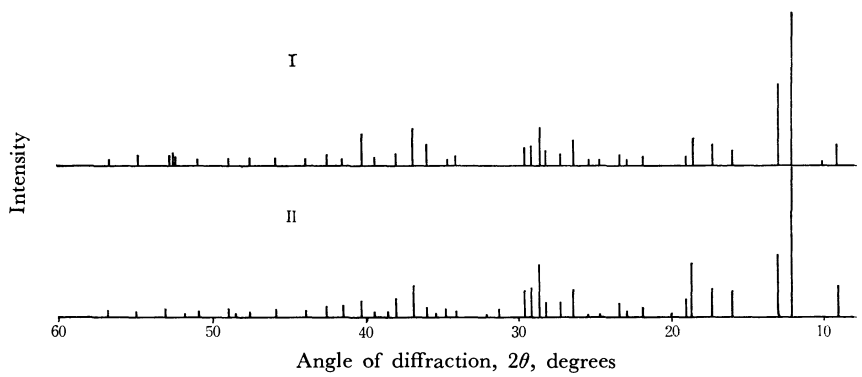

Fig. 2. X-Ray diffraction patterns of [Cu pyv=gly(H_2O)]·$2H_2O$, I, and the complex derived from copper(II), α-alanine and glyoxylic acid, II.

in the crystalline state, however, revealed that there was no difference in their colors, shapes and habits; both the compounds displayed the same decomposition temperature (192°C). No difference was observed either in their solubilities in water, ethanol and dimethylsulfoxide. The infrared study and the X-ray powder measurements of the two crystals also verified their identity, as is shown in Figs. 1 and 2 respectively, although there were some apparently meaningless small differences in relative intensity of the X-ray diffraction pattern. These differences can probably be supposed to be due to inevitable errors in the preparation of the powder. However, an additional decisive proof for the identity of the two compounds and the elimination of the possibility for the structure II was given by a cleavage reaction of the Schiff base >C=N- double bond of the respective complex. The two solutions obtained by precipitating copper(II) as cupric sulfide exhibited only one spot corresponding to glycine in the presence of pyruvic acid in their paper chromatographic examination. An amino acid analyzer was also employed to ascertain the above result. While the existence of glycine was confirmed for both the solutions, no sign for alanine was recorded in either case. If the real structure of the complex produced from the copper(II)-glyoxylate-alaninate system were II, α-alanine would have been detected instead of glycine.

Although this kind transamination and of the glyoxylate-pyridoxamine system in the presence of metal ions have already been reported, the previous conclusions were drawn only from equilibrium studies of solutions[4]; the intermediate complexes were not isolated. Furthermore, it should be emphasized that the present transamination proceeds almost quantitatively. This may be one of the most clear-cut examples of an effective transamination catalyzed by a metal ion.

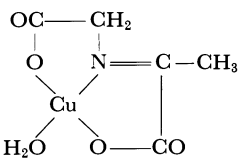
(I)
[Cu pyv=gly(H_2O)]

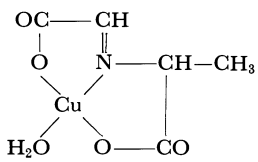
(II)
[Cu glyox=α-ala(H_2O)]

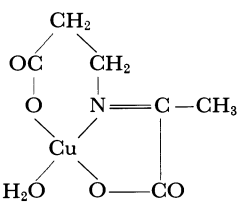
(III)
[Cu pyv=β-ala(H_2O)]

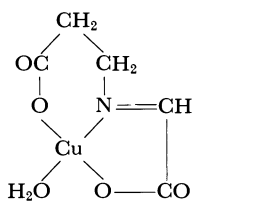
(IV)
[Cu glyox=β-ala(H_2O)]

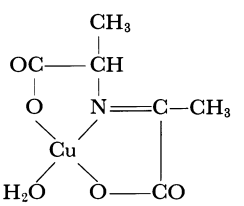
(V)
[Cu pyv=α-ala(H_2O)]

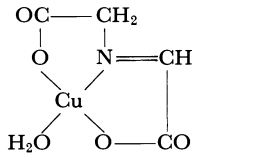
(VI)
[Cu glyox=gly(H_2O)]

Thus it can be concluded that the complex I is more stable than the complex II (I>II).

Copper(II) Complexes of Schiff Bases with β-Alaninate.—The copper(II) complex of the Schiff base derived from β-alanine and pyruvic acid, III, was introduced in a previous paper.[3] In order to obtain knowledge concerning the delicate difference between aldehyde- and ketone-Schiff base complexes, the copper(II) complex of the Schiff base derived from glyoxylic acid and β-alanine, IV, has now been prepared.

First of all, no transamination reaction was observed in the cases of III and IV. This was recognized by means of the paper chromatographic examination of the solutions obtained from III and IV using the same procedure as was used for I and II. The decisive factor was the failure to find the spot for α-alanine or for glycine; only β-alanine was detected for both the solutions. It seems, however, rather reasonable that the transamination reaction in the β-alaninate-Schiff base complexes does not occur, since the electronic arrangement in the transaminated structure is supposed to be quite unfavorable for the stabilization of the fused-ring system. Apart from the transamination reaction, one may conclude, on the basis of the experimental data indicated in Table I, that the complex III is probably more stable than the complex IV. An inspection of Table I reveals that the decomposition temperature of the complex III is distinctly higher than that of IV, and that the polarographic half-wave potential for the reduction of copper(II) is more negative in III than in IV. In addition to those numerical data, their behavior in an aqueous solution shows that the complex III is more stable than IV. For instance, it is considerably difficult to recover the complex IV from its aqueous solution without decompsotion, while it is not so difficult to recover the complex III.

Although it is not the authentic way of discussing the stability of complexes, the above described view may aid in the consideration of the qualitative relative stabilities of the two compounds. Hence, we may conclude that pyruvidene-β-alaninato-aquocopper(II), III, is more stable than glyoxylidene-β-alaninatoaquocopper(II), IV (III>IV).

Copper(II) Complexes of Schiff Bases with α-Alaninate.—The complex produced from copper(II), α-alanine and glyoxylic acid has already

4) D. E. Metzler, J. Olivard and E. E. Snell, *J. Am. Chem. Soc.*, **76**, 644 (1954); H. Mix, *Z. physiol. Chem.*, **325**, 106 (1961).

TABLE I. PROPERTIES OF COPPER(II) SCHIFF BASE COMPLEXES

	Schiff base (ligand)	Decomp. temp. °C	Absorp. max. (ν_{max} in 10^{13} sec^{-1} and log ε_{max})	Half-wave potential vs. SCE at 25°C	Transamination reaction
I	Pyruvic acid and glycine	192—206	ν, 40.5 log ε, 1.85	$E_{1/2}^{(1)}$ −0.09 V. $E_{1/2}^{(2)}$ −0.42 V.	No
II	Glyoxylic acid and α-alanine	—	—	—	↑ Yes
III	Pyruvic acid and β-alanine	205—215	ν, 42.9 log ε, 1.82	$E_{1/2}^{(1)}$ −0.15 V. $E_{1/2}^{(2)}$ −0.28 V.	No
IV	Glyoxylic acid and β-alanine	188—193	ν, 42.9 log ε, 1.84	$E_{1/2}^{(1)}$ −0.05 V. $E_{1/2}^{(2)}$ −0.28 V.	No
V	Pyruvic acid and α-alanine	181—190	ν, 42.9* log ε, 1.62*	$E_{1/2}^{(1)}$ −0.09 V. $E_{1/2}^{(2)}$ −0.27 V.	No
VI	Glyoxylic acid and glycine	—	—	—	Probably yes

* These values for ν_{max} and log ε_{max} are considered as inappropriate to be the data for a fused ring system having two five-membered rings compared with those of other same type chelates.[3] This is perhaps because of a coexistence of a small amount of bis(alaninato)-copper(II) on which we described in the section of the Experimental.

TABLE II. SPECIFIC ROTATION OF A STANDARD AND THE RECOVERED L-α-ALANINE
Solvent: 1 N HCl, Cell: 5 cm.

Sample	$[\alpha]_D^{15}$	$[\alpha]_{500}^{15}$	$[\alpha]_{450}^{15}$	$[\alpha]_{460}^{15}$
L-α-Alanine (standard)	+14.3°	+20.9°	+27.8°	+40.4°
α-Alanine (recovered from the complex V)	+13.0°	+19.5°	+26.2°	+37.6°

been described above. The complex II is not isolated as crystals since it spontaneously transforms itself into the I structure. On the other hand, the complex derived from copper(II), α-alanine and pyruvic acid, V, is comparatively easy to prepare. In this particular case, however, the paper chromatographic test is not suitable for investigating the transamination reaction in the fused-ring system, since the solution obtained from V is always expected to give the spot for α-alanine, regardless of the transamination reaction, as may be understood from the V structure. We have, therefore, measured the loss of the optical rotatory power of the L-α-alanine recovered from the complex V. If the transamination reaction occurs freely in the fused-ring system, the alaninate moiety will transform into pyruvate, and, conversely, the original pyruvate moiety will transform into alaninate. In the course of that intramolecular rearrangement, L-α-alanine will entirely be racemized. However, we have observed just a slight loss of the rotatory power for the recovered alanine, even after the complex had been allowed to stand in water for more than three days at 30 to 40°C. It may, therefore, be concluded that no remarkable transamination reaction proceeds in the copper(II)-α-alaninate-pyruvate system. However, this finding doees not eliminate all possibility of transamination in the complex V, since our experiment has been confined to the neutral region.

As a matter of course, it can be asserted that the complex V is more stable than the complex II (V>II). This is because the complex II undergoes the transamination, while the complex V does not.

Attempts to Isolate the Copper(II) Complex of the Schiff Base Derived from Glyoxylic Acid and Glycine.—It has been disclosed above that the copper(II) complexes of glyoxylate-Schiff bases are always less stable than the corresponding complexes of pyruvate-Schiff bases. If this conclusion is valid, the fused-ring in the copper(II)-glyoxylate-glycinate system may be expected to be quite unstable, since the complex is obliged to have a glyoxylate moiety regardless of the transamination reaction, as may be understood from the VI structure. Indeed, all our efforts to isolate the complex VI have been in vain, though we could observe, for several minutes, a bluish green color which was probably due to the formation of the complex VI. It may be speculated that the instability of this particular complex originates from the violent transamination reaction occurring to-and-fro in the fused-ring system. Though we do not have a proper way of verifying this, an investigation using ^{18}O is now under way.

At all events, the complex VI is apparently less stable than the complex I or V (I>VI; V>VI).

The Structure of Fused-rings and the Transamination Reaction.—On the basis of the properties of the six copper(II) complexes, we have discussed the relationship between the structure of fused-rings and the relative stability of copper(II) Schiff base chelates in connection

with the transamination reaction. All the findings concerning the relative stability of copper(II) complexes of aldehyde- and ketone-Schiff bases may be summarized as follows:

$$I>II;\ III>IV;\ V>II;\ V>VI;\ I>IV.$$

All these relations indicate that the fused-rings of aldehyde-Schiff bases are generally less stable than those of ketone-Schiff bases. Therefore, the transamination from the aldehyde- to the ketone-type structure corresponding to a stabilization of the fused-ring system in the metal chelate. On the other hand, it has already been pointed out that the copper(II) complexes of Schiff bases with β-alaninate do not undergo transamination, even in the case of the less stable aldehyde-type structure. This was elucidated in terms of the unfavorable electronic arrangement of the fused-ring system in the transaminated structure. However, it may also be supposed to be important to take into account that the β-alaninate Schiff base chelates are too stable to undergo transamination.

This is because of the previous conclusion that the fused-ring system with one five- and one six-membered ring is more stable than that with two five-membered rings.

By combining all this knowledge, we may suggest that *the non-enzymatic transamination reaction of the present kind can be expected only in such appropriately unstable fused-ring system as one with two five-membered rings and that it is generally accompanied by a stabilization of the system.* A different catalytic effect may be expected for a different metal ion; investigations of this are now in progress in this laboratory.

Experimental

Pyruvideneglycinatoaquocopper(II), I, [Cu pyv=gly(H_2O)].—The compound was prepared by the reaction of cupric acetate with a mixture of pyruvic acid and glycine according to the directions presented in a previous paper.[3]

The Copper(II) Complex of the Schiff Base Derived from Glyoxylic Acid and α-Alanine.—To a mixture of 7.1 g. of D, L-α-alanine and 9.1 g. of sodium glyoxylate monohydrate in 25 ml. of aqueous ethanol (two-to-one by volume mixture) was added 4.8 g. of glacial acetic acid. Into this was added 16 g. of copper(II) acetate monohydrate with constant stirring at room temperature. The reaction was completed within one hour to give a dark blue solution, with the precipitation of pale blue microscopic crystals. After it had been filtered, the solution yielded more of the same product. The precipitate was recrystallized from a small amount of water. The final pure product appears as thin pale blue plates which begin to decompose at 192°C. The compound is soluble in water and dimethylsulfoxide and slightly soluble in ethanol, but it is insoluble in acetone and chloroform.

Found: C, 23.03; H, 4.27; N, 5.29; H_2O, 20.31. Calcd. for dihydrate of I or II: C, 23.00; H. 4.27; N, 5.36; H_2O, 20.65%.

All the experiment to discriminate the present complex from I were in vain. In other words, the complex was proved to be pyruvideneglycinatoaquocopper(II), I, and not glyoxylidene-α-alaninatoaquocopper(II), II.

Pyruvidene-β-alaninatoaquocopper(II), III, [Cu pyv=β-ala(H_2O)].—Although the method of preparing this compound has already been reported in a previous paper,[3] the procedure used here was a little simplified by using cupric acetate and aqueous ethanol instead of freshly preciptated cupric oxide and water respectively.

Glyoxylidene-β-alaninatoaquocopper(II), IV, [Cu glyox=β-ala(H_2O)].—To a mixture of 5.1 g. of β-alanine and 6.5 g. of sodium glyoxylate monohydrate in 20 ml. of aqueous ethanol (two-to-one by volume mixture) 3.4 g. of glacial acetic acid was added. Into this 11.4 g. of copper(II) acetate monohydrate was added with constant stirring at room temperature. The reaction was completed within one hour, giving a dark blue solution. After it had been fiiltered, the solution was cooled at about 5°C. To this ethanol was added until the solution became turbid.

The reaction mixture was then allowed to stand for a few hours in a refrigerator. Hereupon a sky blue crystalline product was deposited.

The product was filtered and recrystallized from a small amount of water. M. p. 188—193°C(decomp.).

Found: C, 23.09; H, 4.20; N, 5.35. Calcd. for dihydrate of IV: C, 23.00; H, 4.21; N, 5.36%.

Pyruvidene-α-alaninatoaquocopper(II), V, [Cu pyv=α-ala(H_2O)].—Into a solution of 8.9 g. of D, L-α-alanine and 9 g. of pyruvic acid in 30 ml. of water 20 g. of copper(II) acetate monohydrate was added at 40°C with constant by stirring. The reaction was completed within one hour to give a dark blue solution. After it had been filtered, the solution was cooled at about 5°C. To this a large amount of ethanol was then added. Hereupon a large amount of a precipitate was obtained. This was recrystallized repeatedly from water by adding a large amount of ethanol. Finally the crystalline powder was washed by acetone and dried over silica gel. M. p. 181—189°C (decomp.). Found: C, 29.00; H, 4.55; N, 6.37; Cu, 25.5; H_2O, 10.2. Calcd. for hemihydrate of V: C, 29.03; H, 4.03; N, 5.65; Cu, 25.6; H_2O, 10.9%. As is clear from these values, the experimental values for nitrogen and hydrogen did not agree well with the corresponding calculated values on account of the difficulty in purifying the complex. However, this was not so serious as to negate the proposed structure, V, since there had to be taken into consideration the possibility of the co-precipitation of bis(alaninato)-copper(II) in such a recrystallization process as has been described above. The properties of the complex V are listed in Table I.

The Copper(II) Complex of the Schiff Base Derived from Glyoxylic Acid and Glycine.—Although the same method of preparation as was used for V was employed, only a dark brown solid, which was believed to be a decomposition product, was obtained. By the use of a nitrogen atmosphere, the reaction was improved to some extent, but no complex was isolated. In the midst of the reaction, however, a greenish blue solution, probably based on the formation of the complex VI, could be observed for a few minutes.

Other Chemicals Used.—Sodium glyoxylate was

prepared from tartaric acid according to the method in the literature.[5] Unless otherwise specified, all the chemicals used in the measurements were of analytical reagent grade.

Transamination Study.—The following procedure was employed to estimate the transamination reactions in the fused-ring systems of chelates.

Through an aqueous solution of the chelate concerned, the hydrogen sulfide was bubbled until the bluish color characteristic of copper(II) complexes vanished. To this an appropriate amount of charcoal was added for the convenience of rapid filtration. After it had been filtered, the brown solution was concentrated to a small volume in vacuo at 30 to 40°C. The intact solution was used as a sample solution for the paper chromatographic test, which employed the solvent system of *n*-butanol : acetic acid : water (4 : 2 : 1) and Toyo filter paper No. 50. The same solution had to be appropriately diluted as a sample solution for an amino-acid analyzer. A Hitachi Amino-Acid Analyzer Model KLA-3 was used.

Optical Rotation Study.—The purpose of the experiment was to determine the loss of the optical rotatory power of L-α-alanine by the formation of the Schiff base chelate. Therefore, the specific rotation of a standard L-α-alanine was compared with that of a recovered α-alanine using several wave-lengths. The results are tabulated in Table II. In order to recover α-alanine from the pyruvidene-α-alaninatoaquo-copper(II), V, principally the same procedure as that described above (Transamination Study) was employed. In this particular case, however, the complex solution had been allowed to stand at 30 to 40°C for about 75 hr. before the hydrogen sulfide was bubbled in; the solution which had been separated from cupric sulfide was evaporated to dryness in vacuo at about 50°C in order to remove the pyruvic acid. The white crystalline residue was dissolved in water and freed centrifugally from the insoluble residue. The solution was then concentrated again to a small volume. To this an appropriate amount of ethanol was added until the solution became turbid. When the solution was allowed to stand in a refrigerator, white crystals of α-alanine were deposited. These were used for the optical rotation study. The measurements were made by the use of a Yanagimoto Spectropolarimeter OR-100 at 15°C. The concentrations of α-alanine used were 4.77 and 4.79% in 1 N hydrochloric acid for the standard L-α-alanine and the recovered α-alanine respectively. The details are shown in Table II.

X-Ray Powder Measurements.—The X-ray powder patterns were recorded by the use of a Toshiba ADX-103 X-ray diffractometer at room temperature, with the Cu-$K\alpha$ line filtered through nickel. The diffraction patterns are depicted diagrammatically in Fig. 2.

Spectroscopic Measurements.—The visible and ultraviolet absorption spectra were determined with a Shimadzu Spectrophotometer QR-50 at room temperature. The solvent used in this work was water in all cases, while the concentration of the solutions varied from 10^{-2} to 10^{-3} M. Only the numerical data for the absorption band in the visible region are listed in Table I. The infrared spectra were recorded by the use of a Hitachi EPI-2 Infrared spectrophotometer. The measurements were made at room temperature using the pressed potassium bromide disk technique in the wave number range from 700 to 4000 cm^{-1} and using a rock salt prism.

The spectra obtained are shown in Fig. 1.

Polarographic Measurements.—The measurements were made with a Yanagimoto Recording Polarograph PA-102. An "H" cell was used, the reference electrode being a saturated calomel electrode and the whole cell being thermostated at 25±0.5°C. Pure distilled mercury was used throughout. Tank nitrogen was, without any further purification, bubbled through the sample to remove the dissolved oxygen. The concentration of the copper(II) chelates varied from 10^{-4} to 10^{-3} M. The supporting electrolyte used was 0.1 M potassium nitrate in all cases. The plot of log $i/(i_d-i)$ against the voltage revealed that the reduction wave for copper(II) was irreversible in all cases except in the complex I and the complex III. In addition, the half-wave potentials determined in this work for the complex I and the complex III did not agree well with the corresponding values reported previously.[3] This was, however, clarified as being due to the different concentration of the maximum suppressor, methyl red. As far as the present work was concerned, a constant concentration of methyl red was used throughout (0.03%).

The authors hereby gratefully acknowledge the helpful assistance in this study of Mr. Hisao Imayasu. Grateful acknowledgment is also made to Professor Tokunosuke Watanabe of this College of General Education for many valuable suggestions and discussions, particularly concerning the interpretation of the results of the X-ray powder measurements.

A part of the expenses for this work was defrayed by a grant from the Ministry of Education, to which the authors' thanks are due.

5) D. E. Metzler, J. Olivard and E. E. Snell, *J. Am. Chem. Soc.*, **76**, 647 (1954).

BULLETIN OF THE CHEMICAL SOCIETY OF JAPAN VOL. 39 1477—1482 (1966)

The Effect of Acetates on the Synthesis of Acetic Acid from Methanol and Carbon Monoxide in the Presence of Cobalt(II) Iodide as a Catalyst

By Tsutomu MIZOROKI and Mikitake NAKAYAMA

Government Chemical Industrial Research Institute, Tokyo, Meguro-ku, Tokyo

(Recived July 23, 1965)

In the synthesis of acetic acid from methanol and carbon monoxide in the presence of cobalt(II) iodide as a catalyst, the addition of an acetate has been shown to have a great influence upon the methanol conversion into total acetic acid. When the added amounts of potassium acetate are from one to two times as much as that of cobalt(II) ion, both methanol conversion and its reaction rate reach a maximum, and methanol is prevented from forming dimethyl ether. On the other hand, the reaction nearly stops when the amount of potassium acetate becomes more than four times as large. The variation in the absorption spectrum of cobalt(II) ion in course of the reaction shows that the increase in the added amount of an acetate is favorable for the formation of cobalt carbonyls and that most cobalt(II) ions are tetrahedral species of the $[Co(AcO)_{4-n}I_n]^{2-}$ type so long as the reaction is promoted with the catalyst. From these experimental results, the course of the reaction has been discussed.

The reaction rate of the synthesis of acetic acid from methanol and carbon monoxide is promoted by the use of cobalt(II) iodide as a catalyst, a method which originated in Reppe's work.[1] The present authors have previously reported that, when a mixture of cobalt(II) acetate and an iodide*1 was used as the catalyst, both the conversion of methanol into acetic acid and the absorption rate of carbon monoxide were always larger than in the case where only cobalt(II) iodide was used as the catalyst.[2] There is no difference in their components between cobalt(II) iodide and a mixture of cobalt(II) acetate and an iodide except that the latter contains acetates. In our last paper,[3] dealing with the variation in the absorption spectrum of cobalt(II) ion catalysts during the course of the reaction of methanol with carbon monoxide-hydrogen mixtures, it was shown that, when iodide ions were also present, most of the cobalt(II) ions did not form cobalt carbonyls, but tetrahedral species of the $[Co(AcO^{*2})_{4-n}I_n]^{2-}$ type. These facts suggest that an acetate should have some influence upon the methanol conversions into C_2-oxygenated organic compounds as well as on the absorption spectrum of cobalt(II) during the course of the reaction.

This work was undertaken in order to make clear the effect of an acetate, especially on the acetic acid synthesis reaction, and in order to study the behavior of cobalt(II) ion through recording its absorption spectrum.

Experiments

Apparatus for Carrying Out the Reaction.—The apparatus for carrying out the reaction was nearly the same as that described in previous papers.[2] The reaction vessels used were 180 ml. and 230 ml. vessels lined with a titanium manganese alloy. After a mixture of methanol, acetic acid and water containing a given amount*3 of the catalyst had been placed in the vessel, carbon monoxide was introduced up to 50 kg./cm^2 at room temperautre. The mixture was then heated up to 210—215°C (the pressure became about 120 kg./cm^2) by a shaking type of electric furnace (60 r.p.m.) within 2 hr. After the temperature had been kept constant for about one hour., carbon monoxide of a higher pressure was introduced up to a definite reaction pressure (200—400 kg./cm^2) from a pressure accumulator. During the reaction, the pressure was kept constant by supplying carbon monoxide; the amount of it was measured in order to ascertain its absorption rate. The heating and additiob of gas were stopped after a predetermined time of the reaction, and then the vessel was allowed to cool to room temperature.

Apparatus for Taking the Absorption Spectra in the Course of the Reaction.—The special autoclave used for taking the absorption spectrum of the cobalt(II) ion catalyst during the course of the reaction was essentially the same as that described in the last paper, except that it was improved so as to endure pressures of 250—350 kg./cm^2 at 210°C. A solution of 2.5 ml. was placed in the special autoclave (6.0 ml. in vol.) with a couple of thick quartz windows, and then carbon

1) W. Reppe, *Ann. Chem. Jutus Liebigs*, **582**, 74 (1953).

*1 LiI, NaI, KI, CaI^2 etc.

2) T. Mizoroki, M. Nakayama, Y. Andō and M. Furumi, *J. Chem. Soc. Japan, Ind. Chem. Sect. (Kogyo Kagaku Zasshi)*, **65**, 1049, 1054 (1962).

3) T. Mizoroki and M. Nakayama, This Bulletin, **38**, 1876 (1965).

*3 AcO=CH_3COO.

*2 This is represented by the percentage composition in moles of the solution.

monoxide was introduced up to the pressure of 70—80 kg./cm^2 at room temperature. The autoclave was heated up to 21°C within one hour. After the temperature had been kept constant (±0.5°C) for about 20 min. by an electronic thermo-controller, carbon monoxide was introduced up to 300 kg./cm^2 and the absorption spectra were recorded by an automatic spectrophotometer from 340 mμ to 1000 mμ.

Materials.—The carbon monoxide and hydrogen were obtained from the decomposition of formic acid and the electrolysis of water respectively; they were compressed into the pressure accumulator. All of the other materials used were obtained from commercial sources.

Analytical Procedures.—The main components in the liquid products were determined by a gas chromatographic procedure. A 4.0 meter glass column or a 6.0 meter copper one with PEG-400 on a Diabase-A*4 was used at the temperature of 80°C, with the hydrogen carrier at the gas flow rate of 50 ml. per min. In this way, the amounts of methanol, methyl acetate and water in the liquid products obtained from the acetic acid synthesis were determined quantitatively,*5 using diethyl ketone as an internal standard substance. On the other hand, the amounts of dimethyl ether, acetaldehyde, methyl acetate, ethyl acetate, methanol, ethanol and water in the liquid products, obtained from the reaction of methanol with carbon monoxide and hydrogen mixtures, were determined by using pyridine as an internal standard, because it was difficult to separate diethyl ketone from ethanol by this gas chromatography. The amount of free acetic acid was determined by titration with an aqueous potassium hydroxide solution. The other analytical procedures were exactly the same as those used in previous papers.

Results and Discussion

The Effect of Acetates on the Methanol Conversion.—When a mixture of cobalt(II) acetate and an iodide is used as the catalyst in the reaction of methanol with carbon monoxide to form acetic acid, the presence of a relatively large amount of an iodide favors an increase in its rate.[2] When cobalt(II) iodide is used, however, neither the methanol conversion into total acetic acid (free acid and its ester) nor its rate increases, even if an iodide is added in considerable amounts. It was very difficult, therefore, to obtaine the most favorable mole ratio of iodide ions to cobalt(II) ions for this reaction. In all experiments, the I^-/Co^{2+} ratios present in the solutions used were always adjusted to be four by using proper amounts of cobalt(II) iodide and sodium iodide. Lithium acetate, sodium acetate, magnesium acetate or manganese(II) acetate was added as an acetate*6 to the solutions, although there were no differences in their effects. The effects of potassium propionate, sodium benzoate, sodium succinate, potassium isobutyrate and borax were examined at the same time in order to compare them with that of potassium acetate. The results are summarized in Fig. 1 and Table I. Both the absorption rate*7 of carbon monoxide and the methanol conversion into acetic

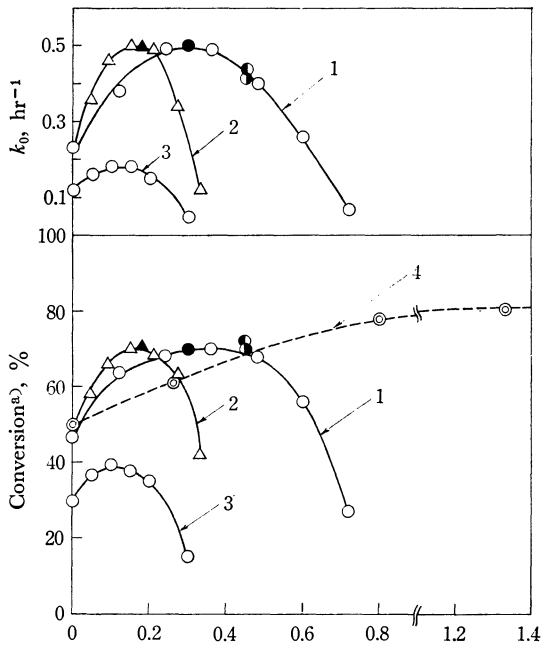

Fig. 1. The effect of an acetate on the acetic acid synthesis.

Curves 1 and 2: CH_3OH 1.80 mol. (54 mol.%), AcOH 0.20 mol. (6.0 mol.%), H_2O 1.33 mol. (40 mol.%), CoI_2 8.0 mmol. (0.24 mol.%), NaI 16 mmol. (0.48 mol.%); temp. 210—215°C, press. 350 kg./cm^2, time 2.5 hr.; ○ AcOK ◑ $(CH_3)_2$-CHCOOK, ◐ C_6H_5COONa, ● C_2H_5COONa, △ $Na_2B_4O_7 \cdot 10H_2O$, ▲ $C_2H_4(COONa)_2 \cdot 6H_2O$

Curve 3: CH_3OH 1.80 mol. (54 mol.%), AcOH 0.20 mol. (6.0 mol.%), H_2O 1.33 mol. (40 mol.%), CoI_2 3.3 mmol. (0.10 mol.%), NaI 6.7 mmol. (0.20 mol.%); temp. 210—215°C, press. 300 kg./cm^2, time 2.5 hr.

Curve 4: $AcOCH_3$ 0.85 mol. (31 mol.%), AcOH 0.10 mol. (3.7 mol.%), H_2O 1.75 mol. (65 mol.%), CoI_2 7.2 mmol. (0.27 mol.%), NaI 14.4 mmol. (0.53 mol.%); temp. 210—215°C, press. 350 kg./cm^2, time 2.5 hr.

a) The acid acetic previously added to the solutions was excluded.

*4 Prepared by The Kotaki Seisakusho Co., Ltd., Tokyo.

*5 Their errors were less than 3%.

*6 Nickel(II) acetate had no effect. Its dissociation is probably small.

*7 It is nearly in proportion to the total amounts of methanol and methyl acetate present in the autoclave. k_0 (hr.$^{-1}$) is the absorption rate constant of carbon monoxide at a constant temperature and pressure.[2] $dC/dt = k_1(1-C)$, where C is the methanol conversion into total acetic acid.

TABLE I. THE EFFECT OF POTASSIUM ACETATE AND BORAX ON THE ACETIC ACID SYNTHESIS AT VARIOUS PRESSURES

CH_3OH 1.35 mol. (43.2 g.), AcOH 0.15 mol. (9.0 g.), H_2O 1.00 mol. (18.0 g.), Purity of CO. 98%. Temp. 215°C, Time 2.5 hr. The added amount of catalyst (mmol.): (1) CoI_2 6.0, NaI 12.0. (2) CoI_2 6.0, NaI 12.0, AcOK 9.0. (3) CoI_2 6.0, NaI 12.0, $Na_2B_4O_7 \cdot 10H_2O$ 4.5. (4) $Co(AcO)_2 \cdot 4H_2O$ 6.0, NaI 24.0.

Press. kg./cm²	Cat.	The amounts of liq. prod., g.	Compositions of liq. prod., wt.%					Mass balance of CH_3OH,[a] %		
			$(CH_3)_2O$	$AcOCH_3$	CH_3OH	H_2O	AcOH	Total AcOH	CH_3OH	Others[b]
250	1	73.2	7.5	19.0	10.1	33.0	22.2	22.9	35.6	41.5
	2	88.5	1.6	29.6	11.6	26.3	23.6	40.8	50.9	8.3
	3	89.8	2.6	30.9	10.2	27.4	23.6	42.8	50.2	7.0
	4	89.9	—	29.1	11.4	26.5	23.9	41.6	50.8	7.6
300	1	83.1	8.4	21.8	7.0	30.4	30.6	38.5	34.5	27.0
	2	93.9	1.5	25.7	6.0	25.4	36.9	55.8	37.9	6.3
	3	96.0	1.4	26.3	6.7	25.1	36.4	57.3	40.4	2.3
	4	94.7	—	24.8	5.5	25.2	36.1	54.6	36.5	8.9
350	1	89.6	6.1	21.6	4.3	28.3	37.7	50.0	30.5	19.5
	2	97.7	0.8	20.1	2.9	22.0	47.7	66.2	26.8	7.0
	3	97.6	1.2	20.1	2.9	23.2	48.9	67.5	26.8	5.7
	4	98.3	—	17.7	2.4	21.8	50.0	67.0	23.9	9.1
420	1	97.3	2.6	16.8	2.0	22.1	50.8	66.4	22.2	11.4
	2	101.2	0.5	12.3	1.4	21.1	58.6	74.5	16.7	8.8
	3	99.3	0.4	14.2	1.5	20.3	57.6	73.5	18.5	8.0
	4	101.7	—	12.5	1.2	22.3	57.4	73.5	16.7	9.8

a) The acetic acid previously added to the solutions was excluded.
b) Most of them are dimethyl ether, methane and acetaldehyde.

TABLE II. THE EFFECT OF POTASSIUM ACETATE ON THE REACTION OF METHANOL WITH CARBON MONOXIDE - HYDROGEN MIXTURES

CH_3OH 1.35 mol. (43.2 g.), AcOH 0.15 mol. (9.0 g.), CoI_2 6.0 mmol., NaI 12.0 mmol., CO/H_2= 1.0, Temp. 200°C, Press. 400 kg./cm², Time 120 min.

The added amount of AcOK mmol.	The amount of liq. prod. g.	Mass balance of CH_3OH[a] %						Conversion into C_2 %
		$(CH_3)_2O$	AcH	Total C_2H_5OH	Total AcOH	Total CH_3OH	Others[b]	
0.0	75.0	9.9	4.5	4.5	10.4	25.8	44.9	19.4
3.0	77.3	5.8	3.6	3.7	10.3	33.0	43.6	17.6
6.0	82.6	1.0	5.0	13.8	13.7	26.7	39.7	32.5
9.0	86.2	0.9	4.5	19.3	15.6	33.5	26.2	39.4
12.0	86.8	0.9	3.7	24.0	15.6	37.7	18.1	43.3
15.0	78.5	0.3	10.4	14.7	13.7	46.2	15.0	38.5
18.0	60.5	—	—	—	8.5	88.5	3.0	8.5

Total C_2H_5OH = C_2H_5OH + $AcOC_2H_5$
Total AcOH = AcOH + $AcOCH_3$ + $AcOC_2H_5$
Total CH_3OH = CH_3OH + $AcOCH_3$
a) The acetic acid previously added to the solutions are excluded.
b) Most of them are crotonaldehyde, butylaldehyde, butanol, dimethyl acetal and methane and dimethy ether of the purged gases.

acid reach a maximum when the amount of potassium acetate added is from 1.0 to 2.0 times as much as that of cobalt(II) ions. However, the reaction nearly stops when it becomes more than four times as large. Nearly the same results are obtained by using other salts of carboxylic acid or borax in place of the acetates. The curve 4 in Fig. 1 is the result obtained from the reaction of methyl acetate with carbon monoxide, in which case methyl acetate was placed into the autoclave instead of methanol. It is different from the curves 1 and 2 in that the conversion of methyl acetate into acetic acid ($AcOCH_3 + CO + H_2O \rightarrow 2AcOH$) does not decrease with an increase in the amount of potassium acetate added. These salts also have a great influence on the reaction of methanol with

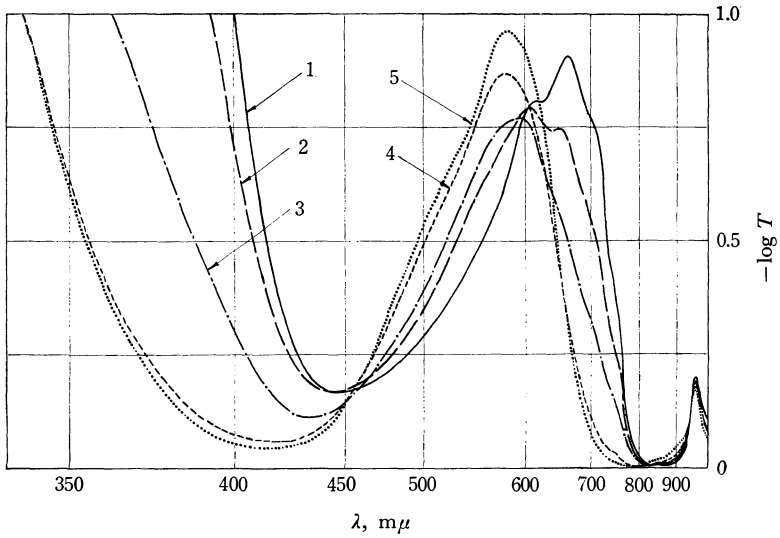

Fig. 2. The effect of potassium acetate on the absorption spectrum of cobalt(II) ion at 210°C.
The solution used are mixtures of CH_3OH (54 mol.%), AcOH (6.0 mol.%) and wates (40 mol.%) containing CoI_2 (0.10 mol.%), NaI (0.20 mol.%) and potassium acetate (0.0—0.30 mol.%). The added amounts of potassium acetate are (1) 0 mol.%, (2) 0.05 mol.%, (3) 0.10 mol.%, (4) 0.20 mol.%, (5) 0.30 mol.%

carbon monoxide - hydrogen*8 to form acetaldehyde, ethanol and acetic esters. As is shown in Table II, the addition of potassium acetate surely increase the methanol conversions into C_2-oxygenated compounds, especially into ethanol, but the reaction nearly stops when the amount of potassium acetate added becomes about three times as much as that of cobalt(II) ions.

These salts of carboxylic acids dissolve well in aqueous solutions and dissociate nearly completely, although the dissociation constants of their acid forms are small.*9 It is to be expected, therefore, that the addition of these salts results in a decrease in the concentration of hydrogen ions in the solutions, especially in the early period of the reactions mentioned above. This expectation is supported by the results obtained using borax, which is well known to make a good buffer solution. Hydrogen ions are considered to increase the reaction rates of dimethyl ether formation and the polymerizations of the acetaldehyde produced. The addition of suitable amounts of these salts, therefore, results in a decrease in the amount of dimethyl ether formed and an increase in the methanol conversions into C_2-oxygenated compounds, as is shown in Table I and II. However, it was very difficult to obtain more direct information regarding the behavior of hydrogen ions during the course of the reactions.*10

The Absorption Spectrum of Cobalt(II) Ions.—The cobalt(II) ion species is octahedral in aqueous solutions, while at an elevated temperature it is tetrahedral. The tetrahedral species of the $[CoX_4]^{2-}$ type, where X represents Cl^-, Br^-, I^-, AcO^-, NCS^-, etc., shows only one main absorption band in the visible region of the spectrum due to d'd electronic transitions. In glacial acetic acid, $[Co(AcO)_4]^{2-}$ has an absorption from 450 to 650 mμ, the maximum wavelength of which is 565 mμ, and the extinction coefficient of which is 1700 mol^{-1}. cm^{-1}; $[CoI_4]^{2-}$ has an absorption from 620 to 810 mμ, the maximum wavelength of which is 755 mμ, and the extinction coefficient of which is 1050 $mol.^{-1}$ cm^{-1}. When the temperature of the solution containing cobalt(II) ions, acetate ions and iodide ions is raised to 210°C, cobalt(II) ions form tetrahedral species of the $[Co(AcO)_{4-n}I_n]^{2-}$ (n= 0—4) type and the addition of acetate shifts the visible absorption to shorter wavelength. Figure 2 shows the effect of potassium acetate on the absorption of cobalt(II) ions at 210°C in the absence of the reaction of methanol with carbon monoxide. On the other hand, cobalt carbonyls as $Co_2(CO)_8$ and $HCo(CO)_4$ have no absorption in the visible region because of their electronic configurations of

*8 In this reaction, it is unnecessary to add water to methanol (See This Bulletin, **37**, 236 (1964)).

*9 10^{-4}—10^{-5} at 25°C. For example, the dissociation constants of acetic acid are 1.75×10^{-5} (25°C) and 1.54×10^{-5} (60°C); these constants are nearly independent of the concentrations.

*10 A preliminary experiment indicated that the amount of dimethyl ether formed increased upon an increase in the amount of sodium iodide added, while it decreased upon an increase in the amount of potassium acetate.

d^{10}, although they have very strong absorptions in the near ultraviolet region. Therefore, the visible absorption of cobalt(II) ions would disappear if most of cobalt(II) ions formed cobalt carbonyls in the course of the reaction. Figure 3 shows the absorption spectra in the course of the reaction of the acetic acid synthesis under the same conditions as those used in the experimental run of the curve 3 in Fig. 1, except that the special autoclave for taking absorption spectra could not be shaken so much. When small amounts of potassium acetate are present in the solution, the absorption from 500 to 650 mμ decreases and that in the longer wavelengths increases as soon as carbon monoxide has been introduced up to 300 kg./cm^2 at 210°C. However, the absorption from 500 to 600 mμ gradually increases as the reaction time goes on. This shows that the reaction is accompanied by an increase in the amount of tetrahedral iodo-cobalt(II) complex ions. However, all the absorptions from 500 to 700 mμ decrease when the amount of acetate added becomes large until they disappear nearly completely when 0.30 mol.% is added. In the near ultraviolet region, the strong absorptions always take place. These are considered to be partly due to the charge transfer from iodide ions to cobalt(II) ions and partly due to cobalt carbonyls, although it was very difficult to distinguish them from each other. The variation in the absorption spectra of Fig. 3 and the curve 3 in Fig. 1 shows that the amount of cobalt(II) ions present in the solution during the course of the reaction of methanol with carbon monoxide decreases with an increase in the amount of acetate added and that, when the reaction rate is promoted with this catalyst, most of the cobalt(II) ions do not form cobalt carbonyls, but tetrahedral complex ions of the $[Co(AcO)_{4-n}I_n]^{2-}$ type.

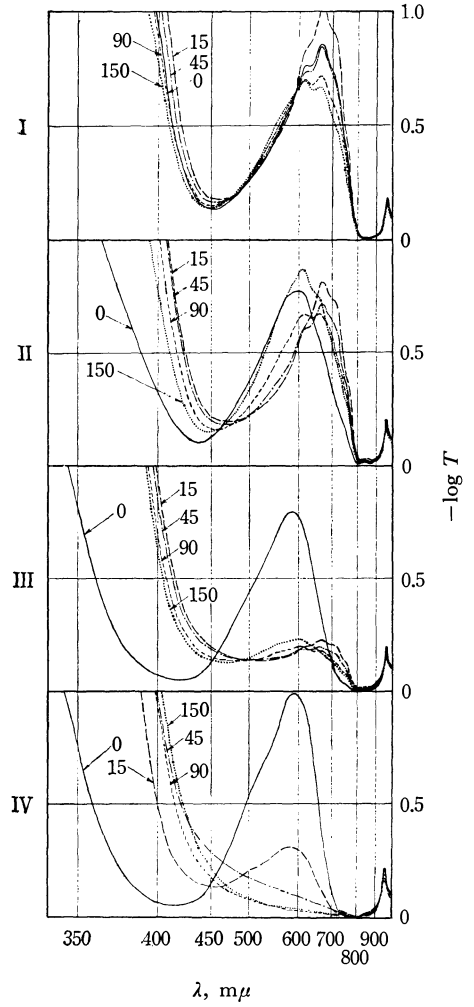

Fig. 3. The variation in the absorption spectrum of cobalt(II) ion in course of the reaction of the acetic acid synthesis under the constant pressure of 300 kg./cm^2 at 210°C.

The solution used are the same as these used in Fig. 2. and the added amounts of potassium acetate are I 0 mol.%, II 0.10 mol.%, III 0.20 mol.% and IV 0.30 mol.%. Numbers in the figure are the times (min.) since carbon monoxide has been introduced up to 300 kg./cm^2 at 210°C.

On the Reaction Mechanism.—Reppe estimated the course of the reaction to be as follows[1,5]:

$$3\,CoI_2 + 2\,H_2O + 10\,CO \rightarrow Co_2(CO)_8 + 4HI + 2\,CO_2$$

$$Co_2(CO)_8 + H_2O + CO \rightarrow 2\,HCo(CO)_4 + CO_2$$

$$CH_3OH + HI \rightarrow CH_3I + H_2O$$

$$CH_3I + HCo(CO)_4 \rightarrow CH_3Co(CO)_4 + HI$$

$$CH_3Co(CO)_4 \rightleftarrows CH_3COCo(CO)_3$$

$$CH_3COCo(CO)_3 + CO \rightarrow CH_3COCo(CO)_4$$

$$CH_3COCo(CO)_4 + H_2O \rightarrow HCo(CO)_4 + AcOH$$

The effect of acetate on methanol conversion into C_2-oxygenated compounds may be correlated with the concentration of hydrogen ions in the solution. The following explanation on the basis of Reppe's mechanism seems possible. The increase in the amount of acetate added will be favorable to the formation of cobalt carbonyls and will prevent the formation of dimethyl ether from methanol, however, it will be unfavorable to the formation of methyl iodide from methanol and hydroionic acid because of the decrease in the concentration of hydrogen ions in the solution. The reaction rate, therefore, reaches its maximum only when a suitable amount of acetate is added to the solution. However, his mechanism is obviously inconsistent

5) The abstract of Reppe's lecture given in Japan, April, 1965, or N. von Kutepow, W. Himmele and H. Hohenschutz, *Chem. Ingr.-Tech.*, **37**, 383 (1965).

with the fact that most of the cobalt(II) ions are tetrahedral species during the course of the reaction so long as the reaction rate is promoted by this catalyst. From the experimental results, it may be postulated that both the conversion of methanol into acetic acid and its rate decrease with the increase in the amount of cobalt carbonyls formed in the early period of the reaction. This suggests that the main course of the reaction may be represented as follows:

$$I^- + H^+ \rightleftarrows HI, \quad AcOH \rightleftarrows AcO^- + H^+$$

$$CH_3OH + HI \rightleftarrows CH_3I + H_2O$$

$$[Co(AcO)_{4-n}I_n]^{2-} + CO \rightarrow [(OC)Co(AcO)_{4-n}I_n]^{2-}$$

$$[(OC)Co(AcO)_{4-n}I_n]^{2-} + CH_3I \rightarrow [CH_3COCo(AcO)_{4-n}I_{n+1}]^{2-}$$

$$[CH_3COCo(AcO)_{4-n}I_{n+1}]^{2-} + HR \rightarrow [Co(AcO)_{3-n}I_{n+1}]^{2-} + CH_3COR + AcOH$$

(R: OCH_3, OH or H)

$$[Co(AcO)_{3-n}I_{n+1}]^{2-} + AcO^- \rightarrow [Co(AcO)_{4-n}I_n]^{2-} + I^-$$

Summary

We have examined the effects of the salts of carboxylic acids, especially acetates, on the reaction of methanol with carbon monoxide in the presence of a mixture of cobalt(II) ion and iodide ion ($I^-/Co^{2+}=4$) as a catalyst, and on the visible absorption spectra of cobalt(II) ions during the course of the reaction. Both the methanol conversions into C_2-oxygenated compounds and their reaction rates reach a maximum when the amounts of potassium acetate added are from one to two times as much as that of cobalt(II) ions. However, these reactions stop nearly completely when they become more than four times. The variation in the absorption spectrum of cobalt(II) ion in the course of the reaction shows that most of the cobalt(II) ions are tetrahedral species of the $[Co(AcO)_{4-n}I_n]^{2-}$ type so long as the reaction is promoted by the catalyst. From the experimental results and our discussion, it has been postulated that the increase in the amount of an acetate added is favorable to the formation of cobalt carbonyls and helps prevent methanol from forming dimethyl ether, while the reaction rate of methanol with carbon monoxide to form C^2-oxygenated compounds decreases with an increase in the amount of carbonyls formed in the early period of the reaction.

BULLETIN OF THE CHEMICAL SOCIETY OF JAPAN VOL. 39 1482—1486 (1966)

The Preparation of Ethylenes with Polyfluorocyclobutenyl and Polyfluorocyclopentenyl Groups

By Hiroshige MURAMATSU,† Soyao MORIGUCHI†† and Kan INUKAI†

† *Government Industrial Research Institute, Nagoya, Kita-ku, Nagoya*

†† *Central Research Laboratory, Showa Denko Co., Ota-ku, Tokyo*

(Received August 30, 1965)

The new ethylenes, with a 2-hydroperfluorocyclobutyl, 2-chlorotetrafluoro-1-cyclobutenyl or 2-chlorohexafluoro-1-cyclopentenyl group, were synthesized in good yields by the dehydration of the 1 : 1 adducts prepared by the addition of the alcohols to perfluorocyclobutene, 1, 2-dichlorotetrafluorocyclobutene or 1, 2-dichlorohexafluorocyclopentene respectively. The dehydrofluorination of 2-hydroperfluorocyclobutylalkylethylenes gave a mixture of perfluoro-1-cyclobutenyl- and perfluoro-2-cyclobutenylethylene. In the mixture, the former was predominant over the latter. Some polyfluorocycloalkenylethylenes prepared polymerized in the presence of peroxide to yield transparent polymers.

Several ethylenes containing polyfluorocyclobutenyl groups have been synthesized, mainly by the cycloaddition of fluoroolefin with conjugated enyne[1] or diene[2], followed by dehydrohalogenation. No papers have, however, been published on the syntheses of polyfluorocyclopentenyl ethylenes.

In a previous report,[3] the radiation-induced addition reactions of alcohols to perfluorocyclobutene were found to produce the corresponding

1) D. D. Coffman, P. L. Barrick, R. D. Cramer and M. S. Raasch, *J. Am. Chem. Soc.*, **71**, 490 (1949).

2) J. D. Park and W. C. Frank, *J. Org. Chem.*, **29**, 1445 (1964).

3) H. Muramatsu, S. Moriguchi and K. Inukai, ibid., **31**, 1306 (1966).

TABLE I. THE DEHYDRATION OF 2-HYDROPERFLUOROCYCLOBUTYLALKYLCARBINOLS (I)

Carbinol				P_2O_5	Ethylene		
R	R'	g.	*trans*/*cis*[a]	g.	g.	Yield, %	*trans*/*cis*[a]
H	H	215.9	2.7	225	140	71	2.3
H	CH_3	315.0	1.6	312	183.9	63	1.8
CH_3	H	81.0		78	58.5	79	5.0

a) *Trans* and *cis* forms in the halocyclobutyl group.

TABLE II. (2-HYDROPERFLUOROCYCLOBUTYL)ETHYLENES,

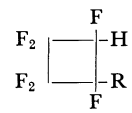

R	B. p. °C	n_D^{20}	d_4^{20}	F, % Found	F, % Calcd.	$\nu_{C=C}$ μ
			Trans form[a]			
-CH=CH_2[3]	63.5	1.3303	1.358	59.7	60.0	6.06
-C(CH_3)=CH_2	91	1.3460	1.340	56.2	55.9	6.05
-CH=CHCH_3 *trans*	92	1.3454	1.324	55.8	55.9	5.98
cis	93.5	1.3458	1.321	56.0	55.9	5.98
-CH_2CH=CH_2	89.5	1.3429	1.320	55.9	55.9	6.07
			Cis form[a]			
-CH=CH_2[3]	86.5	1.3348	1.378	59.8	60.0	6.00
-C(CH_3)=CH_2	105.5	1.3500	1.319	56.0	55.9	6.03
-CH=CHCH_3 *trans*	116.5	1.3514	1.332	55.5	55.9	5.98
cis	118	1.3530	1.337	55.0	55.9	5.98
-CH_2CH=CH_2	110	1.3482	1.325	55.8	55.9	6.08

a) In the halocyclobutyl group.

TABLE III. (2-CHLOROTETRAFLUORO-1-CYCLOBUTENYL)ETHYLENES,

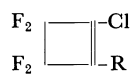

R	B. p. °C	n_D^{20}	d_4^{20}	F, % Found	F, % Calcd.	Cl, % Found	Cl, % Calcd.	$\nu_{C=C}$,[a] μ
-CH=CH_2	104	1.4030	1.350	41.0	40.7	20.3	19.0	6.03, 6.19
-C(CH_3)=CH_2	126	1.4155	1.321	37.7	37.9	18.3	17.7	6.10, 6.18
-CH=CHCH_3[b]	131	1.4249	1.316	37.9	37.9	17.6	17.7	6.00, 6.21,[c] 6.27[d]

a) The first absorption bands are due to the C=C of the cyclobutenyl groups and second bands due to the C=C of the ethylenes.
b) A mixture of *trans* and *cis* form.
c) *Trans*.
d) *Cis*.

TABLE IV. (2-CHLOROHEXAFLUORO-1-CYCLOPENTENYL)ETHYLENES,

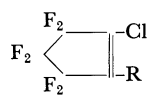

R	B. p. °C	n_D^{20}	d_4^{20}	F, % Found	F, % Calcd.	Cl, % Found	Cl, % Calcd.	$\nu_{C=C}$,[a] μ
-CH=CH_2	121	1.3983	1.490	48.7	48.2	15.2	15.0	6.09, 6.26
-C(CH_3)=CH_2	132	1.3968	1.428	44.3	45.5	14.3	14.2	6.14, 6.25
-CH=CHCH_3 *trans*	152	1.4185	1.438	46.0	45.5	14.2	14.2	6.05, 6.23
cis	138	1.3986	1.418	45.8	45.5	13.7	14.2	6.09, 6.30
-CH_2CH=CH_2	134	1.3872	1.414	46.5	45.5	14.2	14.2	6.04, 6.09

a) The first absorption bands are due to the C=C of the cyclopentenyl groups and the second bands due to the C=C of the ethylenes.

TABLE V. THE DEHYDROFLUORINATION OF 2-HYDROPERFLUOROCYCLOBUTYLETHYLENES (IV)

Ethylene			KOH	Products			
R	R'	g.	g.	V, g.	VI, g.	V/VI	Total yield, %
H	H	90	87	17.8	5.8	3.1	29
H	CH_3	31	34	12.6	3.7	3.4	58
CH_3	H	81.5	40.5	21.7	3.0	7.2	49

TABLE VI. (PERFLUOROCYCLOBUTENYL)ETHYLENES

R	B. p. °C	n_D^{20}	d_4^{20}	F, % Found	F, % Calcd.	$\nu_{C=C}$,[a] μ
			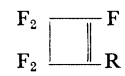			
$-CH=CH_2$	68	1.3558	1.304	55.7	55.9	5.84, 6.20
$-C(CH_3)=CH_2$	92	1.3698	1.260	51.4	51.6	5.87, 6.16
$-CH=CHCH_3$	105	1.3820	1.262	50.5	51.6	5.83, 6.11
			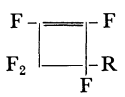			
$-CH=CH_2$	58	1.3382	1.311	56.4	55.9	5.60
$-C(CH_3)=CH_2$	76	1.3554	1.242	51.2	51.6	5.60, 5.81
$-CH=CHCH_3$	89	1.3579	1.265	51.0	51.6	5.59, 5.78

a) The first absorption bands are due to the C=C of the cyclobutenyl groups and the second bands due to the C=C of the ethylenes.

1 : 1 adducts, the carbinols with a 2-hydroperfluorocyclobutyl group (I). Similar additions of alcohols to 1, 2-dichlorotetrafluorocyclobutene or 1, 2-dichlorohexafluorocyclopentene[4] gave mainly the dehydrochlorinated 1 : 1 adducts, 2-chloro-3,3,4,4-tetrafluoro-1-cyclobutenylcarbinol (II) and 2-chloro-3,3,4,4,5,5-hexafluoro-1-cyclopentenylcarbinol (III) respectively.

By the dehydration of these 1 : 1 adducts with phosphorus pentoxide, new ethylenes, with polyfluorocyclobutyl (IV), polyfluorocyclobutenyl (VII), or polyfluorocyclopentenyl (VIII) groups, were prepared in good yields.

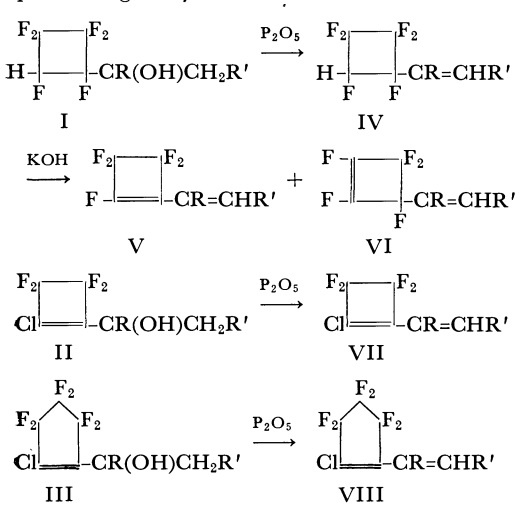

Since the (2-hydroperfluorocyclobutyl)alkylcarbinol (I) two stereoisomers[5] (the *trans* and *cis* forms in the halocyclobutyl group), the product, (2-hydroperfluorocyclobutyl)ethylene (IV), was a mixture of the *trans* and *cis* forms. In the dehydration of the *cis* or *trans* form of (2-hydroperfluorocyclobutyl)ethylcarbinol, the proton rearrangement was observed, yielding a mixture of three isomers in each case. The proton rearrangement occured also in the dehydration of (2-chlorotetrafluoro-1-cyclobutenyl)- or (2-chlorohexafluoro-1-cyclopentenyl)ethylcarbinol.

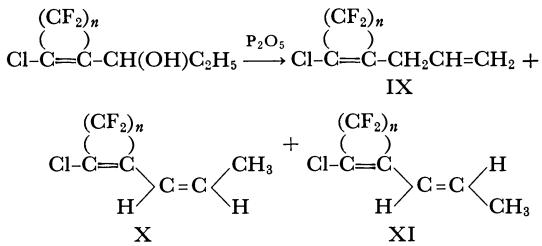

The compositions of the isomers, IX, X, and XI, were calculated from the areas under each peak of the gas chromatograms of the products; they

4) H. Muramatsu, K. Inukai and T. Ueda, ibid., **30**, 2546 (1965).

5) The stereoisomers were assigned to the *trans* and *cis* form from the dipole moment of the isomers of 2-hydroperfluorocyclobutylethylene, which were derived from 2-hydroperfluorocyclobutylmethylcarbinol. See Ref. 3.

were found to be 6%, 5%, and 89% in the case of the chlorotetrafluorocyclobutenylcarbinol and 9%, 13%, and 78% in the case of the chlorohexafluorocyclopentenylcarbinol respectively. The structures of the isomers were determined from their infrared spectra.

The conditions and yields for the dehydration of I are summarized in Table I. Each stereoisomer was isolated by a Shimadzu 10A preparative gas chromatograph. The physical properties of the (2-hydroperfluorocyclobutyl)ethylene (IV), (2-chlorotetrafluoro-1-cyclobutenyl)ethylene (VII), and (2-chlorohexafluoro-1-cyclopentenyl)ethylene (VIII) are shown in Tables II, III, and IV respectively. The *cis* form of 2-hydroperfluorocyclobutylethylene has a boiling point higher by about 20°C than the *trans* form.

The dehydrofluorination of (2-hydroperfluorocyclobutyl)ethylenes was accomplished using powdered potassium hydroxide; this gave two isomers, (perfluoro-1-cyclobutenyl)ethylene (V) and (perfluoro-2-cyclobutenyl)ethylene (VI). The isomer V, which has the conjugated double bonds, was predominant over the isomer VI. The conditions for dehydrofluorination and the physical properties of the (perfluorocyclobutenyl)ethylenes prepared are summarized in Tables V and VI respectively.

The peroxide-induced polymerization was attempted on these ethylenes. Only the ethylenes which have a $-CH=CH_2$ group conjugated with the double bond in the halocycloalkenyl group were found to be polymerized to give the transparent polymers.

Experimental[6]

The Dehydration of the (2-Hydroperfluorocyclobutyl)alkylcarbinols. — To 312 g. (2.18 mol.) of phosphorus pentoxide in a flask with a reflux condenser there was added, drop by drop, 315 g. (1.42 mol.) of (2-hydroperfluorocyclobutyl)ethylcarbinol (a mixture of the *trans* and *cis* in a molar ratio of 1.6 : 1.0) over a 2 hr. period. The reaction mixture was then heated to reflux for 3 hr. and distilled. Since a gas chromatogram[7] of the distillate has six peaks, the compounds of each peak were isolated using preparative gas chromatography. The stereoisomer was assigned on the basis of the products obtained in the dehydration of the clean *trans* or *cis* form of the carbinol. During dehydration, no conversion between the *trans* and *cis* forms was observed. The structures of the isomers were determined from elemental analyses and from a study of their infrared spectra. Thus, the products were 35.5 g. of the *trans* form of 3-(2-hydroperfluorocyclobutyl)-1-propene (retention time, 3.0 min.), 83.7 g. of the *trans* form of 1-(2-hydroperfluorocyclobutyl)-1-propene (a mixture of the *trans* and *cis* forms in a double bond; retention times, 3.6 and 3.8 min. respectively), 19.4 g. of the *cis* form of 3-(2-hydroperfluorocyclobutyl)-1-propene (retention time, 5.3 min.), and 45.5 g. of the *cis* form of 1-(2-hydroperfluorocyclobutyl)-1-propene (a mixture of the *trans* and *cis* forms in a double bond; retention times, 6.8 and 8.1 min. respectively). Upon standing at room temperature, the isolated *cis* forms (in a double bond) gradually changed to the *trans* forms.

Other (2-hydroperfluorocyclobutyl)alkylcarbinols were dehydrated under similar conditions; they are shown in Table I.

The Dehydration of the (2-Chloro-3, 3, 4, 4-tetrafluoro-1-cyclobutenyl)carbinols. — To 24.7 g. (0.17 mol.) of phosphorus pentoxide there was added, drop by drop, 23.1 g. (0.11 mol.) of the halocyclobutenylmethylcarbinol. A reaction mixture was then heated in an oil bath at about 130°C for 20 min. and distilled. The distillation of the product gave 13.8 g. (0.074 mol., 65% yield) of 2-chloro-3, 3, 4, 4-tetrafluoro-1-cyclobutenylethylene, b. p. 103—104°C.

Under similar conditions, the reaction of 29.2 g. (0.21 mol.) of phosphorus pentoxide and 30.0 g. (0.14 mol.) of the halocyclobutenyldimethylcarbinol yielded 16.6 g. (0.083 mol., 60% yield) of 2-(2-chloro-3, 3, 4, 4-tetrafluoro-1-cyclobutenyl)-1-propene. In the dehydration of the halocyclobutenylethylcarbinol (12.8 g., 0.059 mol.) with phosphorus pentoxide (12.5 g., 0.088 mol.), 8.9 g. (0.048 mol.; 82% yield) of the products were obtained. The products were found from gas chromatogram[8] to be a mixture of three isomers, 3-(2-chloro-3, 3, 4, 4-tetrafluoro-1-cyclobutenyl)-1-propene (retention time, 3.5 min.), the *cis* form (4.3 min.), and the *trans* form (6.3 min.) of 1-(2-chloro-3, 3, 4, 4-tetrafluoro-1-cyclobutenyl)-1-propene. The products were fractionated in order to separate a mixture of the *cis* and *trans* isomers. Though not each isomer was isolated, their structures were determined from the infrared spectra.

The physical properties and analyses of the ethylenes containing 2-chlorotetrafluoro-1-cyclobutenyl group are listed in Table III.

The Dehydration of the (2-Chloro-3, 3, 4, 4, 5, 5-hexafluoro-1-cyclopentenyl)carbinols.—A mixture of 52 g. (0.20 mol.) of the halocyclopentenylmethylcarbinol and 43.5 g. (0.31 mol.) of phosphorus pentoxide was heated at about 135°C for 35 min. and then distilled to give 42.5 g. (0.18 mol.; 88% yield) of 2-chloro-3, 3, 4, 4, 5, 5-hexafluoro-1-cyclopentenylethylene, b. p. 119—121°C. Using the same procedure, 32.5 g. (0.12 mol.) of the halocyclopentenyldimethylcarbinol was reacted with 25.8 g. (0.18 mol.) of phosphorus pentoxide to yield 26.6 g. (0.11 mol.; 88% yield) of 2-(2-chloro-3, 3, 4, 4, 5, 5-hexafluoro-1-cyclopentenyl)-1-propene.

The dehydration of 31.0 g. (0.12 mol.) of the halocyclopentenylethylcarbinol with 24.6 g. (0.17 mol.) of phosphorus pentoxide gave 25.5 g. (0.10 mol.; 83% yield) of the products, which were found to consist of three isomers, 3-(2-chloro-3, 3, 4, 4, 5, 5-hexafluoro-1-cyclopentenyl)-1-propene (retention time,[9] 3.0 min.),

6) All temperature readings are uncorrected.

7) A Hitachi-KGL-2 was employed using helium carrier gas at flow rate of 60 ml./min. and column temperature of 64°C; 2 m. of column packed with 25% Silicone DC-550 was used.

8) The same conditions as Ref. 7 except a helium flow rate 55 ml./min.; column temperature, 93°C.

9) A helium flow rate 50 ml./min.; column temperature 98°C.

the *cis* form (3.9 min.), and the *trans* form (5.9 min.) of 1-(2-chloro-3, 3, 4, 4, 5, 5-hexafluoro-1-cyclopentenyl)-1-propene. The isomers were separated by preparative gas chromatography, and their structures were determined from their infrared spectra.

The physical properties and analyses of the ethylenes containing 2 - chloro-3, 3, 4, 4, 5, 5-hexafluoro-1-cyclopentenyl group are shown in Table IV.

The Dehydrofluorination of (2-Hydroperfluorocyclobutyl)ethylenes.—To 87 g. (1.55 mol.) of powdered potassium hydroxide there was added 90 g. (0.47 mol.) of (2-hydroperfluorocyclobutyl)ethylene. The reaction mixture was then heated under reflux for 1 hr. and distilled. The gas chromatogram of the distillate (23.6 g., 0.14 mol., 29% yield) had two peaks, showing the existence of two isomers. They were isolated by preparative gas chromatography and found to be perfluoro-1-cyclobutenylethylene and perfluoro-2-cyclobutenylethylene from their elemental analyses and from a study of their infrared spectra. The perfluoro-1-cyclobutenylethylene was readily polymerized upon standing in the air.

Other (2-hydroperfluorocyclobutyl)ethylenes, dehydrofluorinated under similar conditions, are summarized in Table V.

The Peroxide-Induced Polymerization of the Halocyclobutenylethylene and Halocyclopentenylethylene.—2-Chloro-3,3,4,4-tetrafluoro-1-cyclobutenylethylene (2 g.) and benzoyl peroxide (0.1 g.) were placed in a glass tube. The tube was then sealed and kept at 100°C for 3 hr. The ethylene polymerized to give a transparent solid. Upon heating, the polymer (0.8 g.) was dissolved in *o*-chlorobenzotrifluoride (7 ml.), and the solution was poured into methanol (80 ml.). The polymer thus precipitated (0.6 g.) was washed with methanol and dried. In its infrared spectrum, the absorption bands of 3.23 ($=CH_2$), 3.30 (=CH–), and 6.19 μ (C=C) in the ethylene disappeared, and a band due to the C=C stretching in the halocyclobutenyl group shifted from 6.03 μ to 6.07 μ.

In a similar procedure, 2-chloro-3, 3, 4, 4, 5, 5-hexafluorocyclopentenylethylene was polymerized in the presence of benzoyl peroxide to give a transparent solid. The polymer was dissolved in trifluorotrichloroethane and precipitated in methanol. The absorption bands of 3.205 ($=CH_2$), 3.29 (=CH–), and 6.26 μ (C=C) in the ethylene disappeared, and a band due to C=C stretching in the halocyclopentenyl group shifted from 6.09 μ to 6.11 μ.

In a similar way, (perfluoro-1-cyclopentenyl)ethylene was polymerized to give a pale brown solid. The polymer was dissolved in acetone and precipitated in methanol. The absorption bands of 3.205 ($=CH_2$) and 6.20 μ (C=C) in the ethylene disappeared, and a band due to C=C stretching in the perfluorocyclobutenyl group shifted from 5.84 μ to 5.81 μ.

BULLETIN OF THE CHEMICAL SOCIETY OF JAPAN VOL. 39 1486—1490 (1966)

The Reaction of Amino Alcohols with Acrylates

By Naoya OGATA* and Tomohiko ASAHARA

Basic Research Laboratories, Toyo Rayon Co., Ltd., Tebiro, Kamakura

(Received August 31, 1965)

The addition reaction of amino alcohols with acrylates were studied. The addition takes place at the amino group of amino alcohol, producing *N*-(hydroxyalkyl)-β-alanine in a good yield. The reaction rate becomes slower as the ester group of acrylate becomes larger, and phenyl acrylate gives a polymer as soon as it is mixed with ethanolamine. The rates of the addition reaction with acrylate are in the following order: $NH_2CH_2CH_2OH > CH_3NHCH_2CH_2OH \gg RNH_2 > NH(CH_2CH_2OH)_2$.

It is well known (the Michael reaction) that a conjugated system of the C=C–C=O type, such as an α, β-unsaturated carbonyl compound, adds a compound with an active hydrogen group in the presence of the base.

When a compound with two active hydrogen groups reacts with acrylates, the product could be a new monomer for polymer materials, since a further polycondensation between the remaining group and carboxylate group is possible:

$$H\text{-}X\text{-}H + CH_2{=}CHCOOR \rightarrow H\text{-}X\text{-}CH_2CH_2COOR \rightarrow -(X\text{-}CH_2CH_2CO)- + ROH$$

It is reported[1] that β-aminoethyl mercaptane reacts with acrylates as is shown bleow to give a thialactam:

$$H_2NCH_2CH_2SH + CH_2{=}CHCOOR \rightarrow \begin{array}{c} CONH \\ | \quad | \\ S \end{array} + ROH$$

If an amino alcohol is used in place of β-aminoethyl mercaptane, the following products would be formed in the system:

* Present address: Dept. of Chem., Sophia Univ., Chiyoda-ku, Tokyo.

1) F. Jacob and P. Schlack, *Chem. Ber.*, **96**, 88 (1963).

$$HOCH_2CH_2NH_2 + CH_2{=}CHCOOR \rightarrow \begin{array}{c} CONH \\ | \quad | \\ O \end{array}$$

$$H_2NCH_2CH_2OCH_2CH_2COOR$$

$$HOCH_2CH_2NHCH_2CH_2COOR$$

Therefore, kinetic studies on the Michael-type reaction between amino alcohols and acrylates have been carried out. They will be described below.

Experimental

Reagents.—Commercial amino alcohols and acrylates were dried in the presence of calcium hydride and distilled by means of a Shibata fractional distillation column.

Reaction.—Amino alcohols and acrylates were dissolved in solvents at given concentrations, and the solutions were mixed at a given temperature, with or without an alkali alkoxide. The reaction rates were followed by the gas chromatographic method, using a polyethyleneglycol 6000 column. After the evaporation of the solvents, the products were distilled under a high vacuum and the products were characterized by an elementary analysis and by a study of their infrared and 100 Mc. NMR spectra.

Results and Discussion

Reaction with Amino Alcohols.—The reaction rates of amino alcohols with acrylates were measured in tetrahydrofuran in the absence of an alkali alkoxide at 0, 20 and 50°C. In each case, the reactions were completed within 10 hr. at 20°C and unchanged acrylates were found in the system only in amounts of 1 to 2% .

The rates apparently followed a second-order reaction; the rate constants are summarized in Table I. In the case of methyl acrylate, the rate constant decreased at the initial stage of the reaction and an auto-catalytic effect was apparently observed. The rate constants in Table I for methyl acrylate are extrapolated values at $t=0$ for the linear part.

It may be seen from Table I that the rate constants decreased with the size of ester groups in the following order: $-CH_3 > -C_2H_5 > nC_4H_9$. The effect of alkyl groups on the addition reaction may be ascribed to the increasing –I effect, which may reduce the carbonium ion character of the β-carbon atom and, hence, may prevent a neucleophilic attack of the amino group.

$$CH_2{=}CH{-}\overset{\overset{O}{\|}}{C}{-}O{-}R \rightleftarrows C^+H_2{-}CH{=}\overset{\overset{|}{O^-}}{C}{-}O{-}R$$

When phenyl acrylate and ethanolamine were mixed in tetrahydrofuran at a concentration of 0.1 mol./l., the reaction rate was too rapid to measure and a polymer was precipitated as soon as they were mixed. A theoretical amount of phenol was found, and neither phenyl acrylate nor ethanolamine remained in the system. The

Table I. Rate constants* of the reaction of amino alcohols and acrylates

Amino alcohol	Acrylate	0°C	20°C	50°C
Ethanolamine	$-CH_3$	3.9×10^{-2}	9.0×10^{-2}	4.7×10^{-2}
	$-C_2H_5$	1.3×10^{-2}	2.4×10^{-2}	4.3×10^{-2}
	$-nC_4H$	0.8×10^{-2}	1.8×10^{-2}	2.6×10^{-2}
	$-C_6H_5$		(reacted immediately)	
N-Methyl ethanolamine	$-CH_3$	—	5.0×10^{-2}	—
Diethanolamine	$-C_2H_5$	—	9.0×10^{-2}	—
Propanolamine	$-CH_3$	—	4.0×10^{-2}	—
	$-C_2H_5$	—	2.0×10^{-2}	—

* Concentration is 1 mol./l. of tetrahydrofuran, unit; min^{-1}

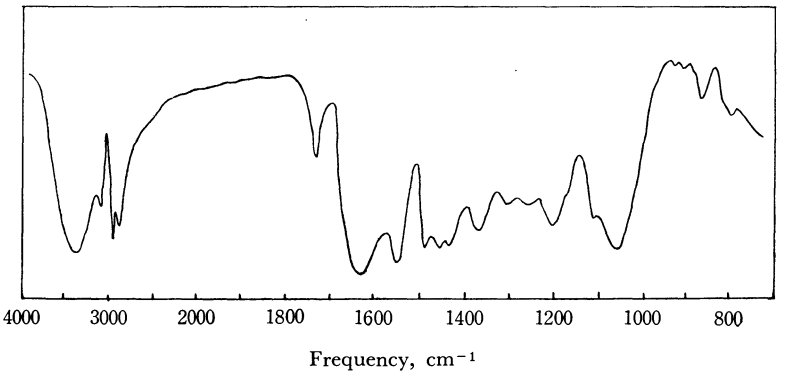

Fig. 1. Infrared spectrum of the polymer from phenyl acrylate and ethanolamine.

analytical data of this polymer were as follows: C=49.0%, H=8.5%, N=7.9%, M. W.=500. The infrared spectrum of the polymer, shown in Fig. 1, suggests a polyamide structure.

When an amine hydrogen of ethanolamine is replaced by an alkyl group, the rate becomes slower, especially for diethanolamine, the rate constant being one-thousandth that of ethanolamine.

The solvent effect on the addition reaction of ethanolamine and methyl acrylate was measured to be as shown in Table II. Generally speaking, the reaction is faster in a solvent with a higher dielectric constant. This finding suggests that the reaction might proceed through an ionic mechanism.

TABLE II. RATE CONSTANTS* OF THE REACTION OF ETHANOLAMINE AND METHYL ACRYLATE IN VARIOUS SOLVENTS AT 20°C

Solvent	Dielectric constant (20°C)	k_1, min^{-1}
Methanol	3.26	9×10^{-2}
Tetrahydrofurane	—	7×10^{-2}
Acetonitrile	38.8	4×10^{-2}
Dimethylformamide	36.6	4×10^{-2}
Pyridine	12.3	3×10^{-2}
Dioxane	2.2	2×10^{-2}

* Concentration is 1 mol./l.

Reactions with Amines or Alcohol.—When an amino alcohol is added to an acrylate, there are two reaction sites, namely, an amino and a hydroxy group. Therefore, the rates of the addition reaction of simple amine or alcohol to ethyl acrylate were compared; they are summarized in Table III.

TABLE III. RATE CONSTANTS* OF THE REACTION OF AMINE OR ALCOHOL WITH ETHYL ACRYLATE IN TETRAHYDROFURANE AT 20°C

Reactant	pK_a	k_1, min^{-1}
Aniline	4.62	0
Benzylamine	9.34	5.0×10^{-5}
Diethanolamine	8.80	9.0×10^{-5}
Allylamine	9.49	1.6×10^{-4}
n-Buthylamine	10.59	2.1×10^{-3}
Ethanolamine	9.50	2.4×10^{-2}
Ethanol**	—	1.2×10^{-1}

* Concentration is 1 mol./l.

** In the presence of 5 mol.% of potassium metal.

Aniline does not react at all, even in the presence of 5 mol.% CH_3OK, and, generally, amines with higher pK values react faster. However, ethanolamine, which has almost the same pK value as allylamine, reacts about 150 times as fast as allylamine. The greatac cerelating effect of the hydroxyethyl group on the reactivity of the amino group is very interesting; it needs a further investigation. On the other hand, when an amine hydrogen of ethanolamine is further replaced by the hydroxyethyl group, the rate of the addition reaction decreases:

$$NH_2CH_2CH_2OH > CH_3NHCH_2OH \gg RNH_2 > NH(CH_2CH_2OH)_2$$

This peculiar behavior of ethanolamine suggests that the reaction involves not only a simple nucleophilic mechanism, but also a more complicated mechanism.

Alcohol does not react at all with ethyl acrylate, while in the presence of 5 mol.% of potassium ethoxide it reacts 5 times as fast as ethanolamine.

The Structure and Properties of the Reaction Products.—*Amine or Alcohol.*—The analytical results of the reaction product on *n*-butyl amine or ethanol with ethyl acrylate are as follows:

	B. p.	M.W.	C,%	H,%	N,%	Yield
n-Butyl amine						
Obs.	70/3 mmHg	173	62.3	6.9	8.1	87
Calcd.	—	173	62.4	7.5	8.1	—
Ethanol						
Obs.	54/8 mmHg	146	58.3	9.59	—	60
Calcd.	—	146	58.1	9.62	—	—

The analytical data and infrared spectra of the products support the following reactions:

$$C_2H_5OH + CH_2{=}CHCOOC_2H_5 \rightarrow C_2H_5OCH_2CH_2COOC_2H_5$$

$$n\text{-}C_4H_9NH_2 + CH_2{=}CHCOOC_2H_5 \rightarrow n\text{-}C_4H_9NHCH_2CH_2COOC_2H_5$$

Amino Alcohol.—The reaction products were polymerized into a sticky polymer by letting them stand at room temperature for several days, though it was necessary to keep them below 0°C. Their analytical results are shown in Table IV.

The infrared spectra of the products showed strong absorptions at 1720, 1200 and 1100 cm^{-1}; these absorptions were easily assigned to an ester group, as can be seen in Fig. 2. The absorption peak at 3400 cm^{-1} is assigned to a hydroxy group, since no absorption at 1600 cm^{-1} resulting from an amine deformation was found; the strong absorption observed at 1050 cm^{-1} was assigned to a hydroxy deformation band. The infrared spectrum of the reaction product of *N*-methyl ethanolamine also showed the existence of a hydroxy group.

The qualitative analysis of the reaction products gave strong support for the existence of a secondary amine. The NMR spectra of the products are shown in Fig. 3. In the case of the methyl ester, a sharp peak at 6.2 τ and a broad peak at 6.53 τ can be assigned to $-OCH_3$ and OH or $-NH_2$ respectively. As the absorption strengths of 6.31, 7.03, 7.24 and 7.43 τ are almost identical, there

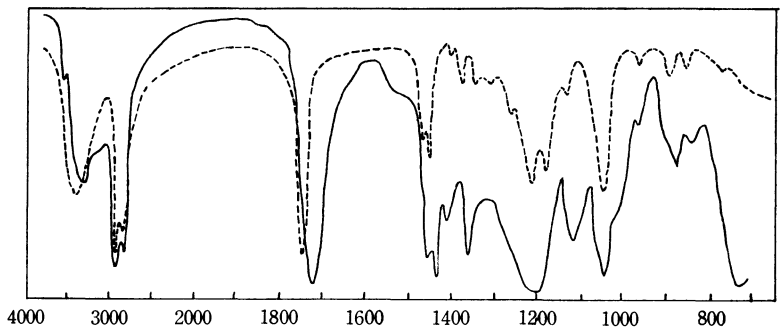

Fig. 2. Infrared spectra of the reaction products.
—— Ethanolamine and methyl acrylate
---- *N*-Methyl ethanolamine and ethyl acrylate

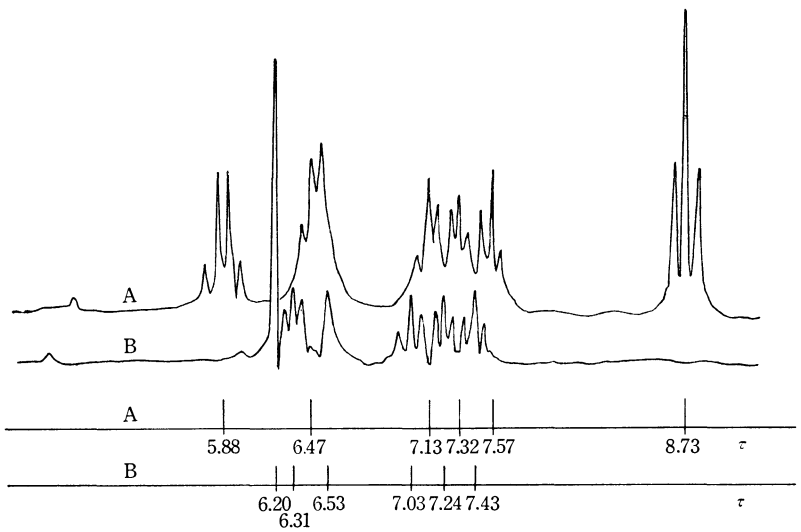

Fig. 3. NMR Spectra of the reaction products.

Table IV. Analytical results of the reaction products of amino alcohol and acrylates

Amino alcohol	Acrylate	B.p. °C/mmHg	M.p. °C	M. W. Calcd.	M. W. Obs.	Base, mol./g. Calcd.	Base, mol./g. Obs.	N, % Calcd.	N, % Obs.
Ethanolamine	$-CH_3$	107/3	40	148	148	6.8×10^{-3}	6.8×10^{-3}	8.7	10.0
	$-C_2H_5$	135/3	28	161	165	6.2×10^{-3}	6.0×10^{-3}	8.7	8.9
	$-nC_4H_9$	116/1	—	189	188	5.3×10^{-3}	5.1×10^{-3}	7.4	7.6
N-Methyl ethanolamine	$-CH_5$	95/4	—	161	162	6.2×10^{-3}	6.2×10^{-3}	8.7	8.8
Propanolamine	$-CH_3$	102/2	—	161	227	—	—	8.7	9.8
	$-C_2H_5$	137/3	—	175	180	—	—	8.0	8.5

are four methylene groups. The chemical shift of $-OCH_2$ is generally in the range from 5.5 to 6.7 τ,[2] and the peak at 6.31 τ may be assigned to $-OCH_2-$. The peak at 7.43 τ is assigned to $-N-CH_2$, which was split into two peaks by the influence of a functional group at the β-position.

It is known[3] that ethanolamine adds to acrylonitrile and the structure of the product is *N*-(β-cyanoethyl)-ethanolamine. The NMR spectrum of this product reconfirms that ethanolamine adds to an acrylate at the amino group as is shown below:

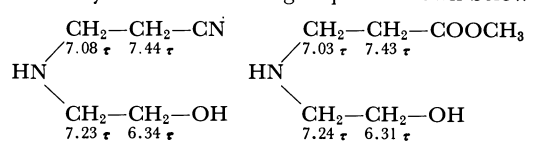

2) K. Nukada, O. Yamamoto, T. Suzuki, M. Takeuchi and M. Ohnishi, *Anal. Chem.*, **35**, 1892 (1963).
3) Y. Ogata, *J. Am. Chem. Soc.*, **78**, 5426 (1956).

Hydroxylamine reacts with acryamide[4] at the amino group;

$$HONH_2 + CH_2{=}CHCONH_2 \rightarrow HONHCH_2CH_2CONH_2$$

From these results, it may be said that the reaction of amino alcohols with acrylates in the absence of a basic catalyst takes place at the amino group, yielding *N*-(hydroxyalkyl)-β-alanine:

$$NH_2{-}R{-}OH + CH_2{=}CHCOOR' \rightarrow HO{-}R{-}NHCH_2CH_2COOR'$$

(Yield=95—99%)

As has been stated above, the reaction rate of alcohol with ethyl acrylate in the presence of a potassium catalyst is about 600 times as fast as that of amine itself, and it is much faster than ethanolamine. The reaction of ethanolamine in the presence of an alkali alkoxide is expected to take place at the hydroxy group of ethanolamine. However, the reaction in the presence of an alkali alkoxide caused a polymerization, yielding a theoretical amount of alcohol; a low-molecular-weight polymer was also precipitated, the analytical data of which showed the same results as in the case of phenyl acrylate, and the polymer was not a homo-polyacrylate. This peculiar reaction, as well as the reaction of phenyl acrylate, will be elucidated in the near future.

The authors wish to express their thanks to Dr. Toshio Hoshino for permission to publish this paper and also to Dr. Kenkichi Nukada for his helpful discussion of the NMR spectra.

4) A. R. Sayigh, *J. Org. Chem.*, **29**, 2042 (1964).

BULLETIN OF THE CHEMICAL SOCIETY OF JAPAN VOL. 39 1490—1495 (1966)

Intramolecular Hydrogen Bonds. VII.[1] Methyl Mandelates and Related Compounds

By Nobuo MORI, Yoshiteru TANAKA and Yojiro TSUZUKI

Department of Chemistry, Tokyo College of Science, Kagurazaka, Shinjuku-ku, Tokyo

(Received September 21, 1965)

The infrared OH spectra of an $ArCH(OH)(CH_2)_nCOOMe$ series ($n=0$ and 1) in dilute carbon tetrachloride solutions have been measured at 25°C with a Perkin-Elmer 21 spectrometer. A comparison of the data with those of other related compounds shows that the OH group forms a hydrogen bond predominantly with the carbonyl-oxygen atom and also with the ether-oxygen atom and/or the π-electrons of the phenyl group, while, practically speaking, no free OH group is present. Further, the NMR chemical shifts of the methine- and the methyl-protons when $n=0$, as measured with a Varian A-60 spectrometer, have been correlated with the Hammett substituent constants; the shift of the methine-proton, when the ring-substituent is a halogen, does not fall on the correlation line, but falls on a separate line.

The infrared spectrum of ethyl mandelate in a dilute carbon tetrachloride solution exhibits, in the OH-stretching region, a very strong band at 3534 cm^{-1} and a weak shoulder at 3602 cm^{-1}.[2] Flett[2] assigned the former to the OH group bonded to the carbonyl-oxygen atom of the ester group and the latter to the free OH group, mainly on the basis of a comparison of the frequencies and the half-band widths; he also suggested that the lowering of the free OH frequency from that of ca. 3625 cm^{-1} characteristic of secondary alcohols is to be attributed to the electrostatic influence of the adjacent ester group. However, the assignment of the shoulder seems doubtful because the frequency is very close to that of the OH group internally bonded to the ether-oxygen atom of an alkoxycarbonyl group in aliphatic α-hydroxycarboxylates[3] and to that of the OH group bonded to the π-electrons of a phenyl group in α-phenylalkanols.[4]

This paper will report on an investigation which has solved this problem by measuring the infrared spectra of a variety of methyl mandelates in dilute carbon tetrachloride solutions. Further, this paper will deal with their characteristics in nuclear magnetic resonance, and also with the intramolecular hydrogen bonding in two methyl β-phenyl-β-hydroxypropionates.

1) Part VI: N. Mori, S. Ōmura and Y. Tsuzuki, This Bulletin, **38**, 2199 (1965).
2) M. St. C. Flett, *Spectrochimica Acta*, **10**, 21 (1957).
3) N. Mori, S. Ōmura, N. Kobayashi and Y. Tsuzuki, This Bulletin, **38**, 2149 (1965).
4) M. Ōki and H. Iwamura, ibid., **32**, 950 (1959).

Experimental

Samples.—All the esters investigated, some of which have hitherto been unknown, are listed in Table I. The mandelates, except for Nos. 4 and 6, were prepared in the usual way[5-7] by the conversion of the corresponding benzaldehyde-cyanohydrins into the iminomethylether hydrochlorides, followed by hydrolysis. The cyanohydrins were synthesized by treating a suspension of the corresponding substituted benzaldehyde in glacial acetic acid with potassium cyanide[5,6] (in the case of Nos. 1 and 2) or by treating a mixture of the corresponding benzaldehyde and potassium cyanide with concentrated hydrochloric acid[7] (in the case of Nos. 3, 5, 7 and 8); they were used without further purification for the preparation of the esters. The ester of No. 4 was derived from *p*-bromoacetophenone by way of *p*-bromomandelic acid,[8] while the ester of No. 6 was prepared by the conversion of the benzaldehyde into mandelic acid,[9] followed by esterification. Methyl β-phenyl-β-hydroxypropionates 9 and 10 were prepared by the Reformatsky reaction[10] from benzaldehydes and methyl bromoacetate. All the esters were purified by recrystallization from a mixture of benzene and ligroin or by fractional distillation; their physical constants and the data of analysis are summarized in the table. The constants of the known esters agree closely with those reported in the literature.

Infrared and NMR Measurements.—The infrared measurements in the OH-stretching region were carried out, by the method previously described,[3] at 25°C with a Perkin-Elmer 21 spectrometer equipped with a lithium fluoride prism and a cell 3 cm. long. The concentrations were about 0.004 mol./l. in carbon tetrachloride, at which concentration no intermolecularly hydrogen-bonded OH band was observed; however, a very weak absorption, due to the overtone of a carbonyl-stretching vibration, appeared at ca. 3460 cm^{-1}.

The NMR spectra were measured at ca. 25°C using a Varian A-60 spectrometer on pre-calibrated chart paper, in which TMS was used as the internal standard. The concentration was 5 w./v. % in carbon tetrachloride and in chloroform. Preliminary measurements with solutions from 0.5 to 40% in both solvents showed that the resonance positions of the methine- and the methyl-protons were constant*1 within the limits of experimental accuracy (±0.5 c. p. s.). The NMR data listed in Table III are the average of two measurements.

Results and Discussion

The infrared OH spectra of the mandelates apparently consist of two resolved bands, whose frequencies are in the range from 3601 to 3611 cm^{-1} and from 3526 to 3536 cm^{-1} respectively; the higher frequency band is much weaker than the lower frequency band, as Fig. 1 shows, and the separation between the two peaks is constant to 77 cm^{-1}. It should be noted that the stronger band is located at ca. 3526 cm^{-1} and that it is somewhat broadened

Table I. The physical constants and analysis of methyl mandelates (Nos. 1—8) and methyl β-phenyl-β-hydroxypropionates (Nos. 9 and 10)

No.	Substituent	M.p., °C (B.p., °C/mmHg)	Anal., % Calcd. C	Calcd. H	Found C	Found H
1	*p*-NO_2	86.5—87[6,11]				
2	*m*-NO_2	63[12]				
3	*m*-Cl	83—84[13]				
4	*p*-Br	61	For $C_9H_9O_3Br$ (245.09) 44.11	3.70	44.24	3.89
5	*p*-Cl	55[13] (131/5)				
6	H	57[14]				
7	*p*-Me	49 (130/6)	For $C_{10}H_{12}O_3$ (180.20) 66.65	6.71	66.60	6.57
8	*p*-MeO	36 (152/5.5)	For $C_{10}H_{12}O_4$ (196.20) 61.21	6.17	61.12	6.27
9	H	(150/10)[15]				
10	*p*-MeO	(159—162/3.5)	For $C_{11}H_{14}O_4$ (210.22) 62.84	6.71	62.91	6.45

5) G. Heller, *Ber.*, **46**, 280 (1913).
6) L. S. Fosdick and G. D. Wessinger, *J. Am. Chem. Soc.*, **60**, 1465 (1938).
7) E. Knorr, *Ber.*, **37**, 3172 (1904).
8) T. L. Cairns, Editor-in-Chief, "Organic Syntheses," **35**, 11 (1955).
9) H. Gilman, Editor-in-Chief, ibid., Coll. Vol. I, 336 (1941).
10) E. C. Horning, Editor-in-Chief, ibid., Coll. Vol. III, 408 (1955).
11) C. Engler and O. Zielke, *Ber.*, **22**, 207 (1889).
12) L. S. Fosdick and J. C. Calandra, *J. Am. Chem. Soc.*, **63**, 1101 (1941).
13) S. S. Jenkins, ibid., **53**, 2341 (1931).
14) S. F. Acree, *Ber.*, **37**, 2767 (1904).
15) A. McKenzie and C. Martin, *J. Chem. Soc.*, **103**, 112 (1913).

*1 It is noteworthy that the methine-proton resonance of aliphatic α- and β-hydroxycarboxylates depends on the concentration in carbon tetrachloride.[16]

16) N. Mori, S. Omura, O. Yamamoto, T. Suzuki and Y. Tsuzuki, This Bulletin, **36**, 1401 (1963).

Table II. The infrared data of methyl substituted mandelates (Nos. 1—8) and methyl β-substituted phenyl-β-hydroxypropionates (Nos. 9 and 10) as well as some related compounds (Nos. 11—16)

No.	Substituent	Band*	ν_{OH}, cm^{-1}	$\Delta\nu_{1/2}$, cm^{-1}	D**
1	*p*-NO_2	I	3526	37	0.58
		II, III	3602	ca. 18	0.10
2	*m*-NO_2	I	3525	40	1.03
		II, III	3601	ca. 18	0.13
3	*m*-Cl	I	3526	42	0.86
		II, III	3603	ca. 25	0.14
4	*p*-Br	I	3526	35	1.17
		II, III	3606	ca. 25	0.19
5	*p*-Cl	I	3532	41	0.92
		II, III	3611	ca. 22	0.16
6	H	I	3536	44	0.89
		II, III	3610	ca. 25	0.16
7	*p*-Me	I	3532	44	0.79
		II, III	3610	ca. 24	0.15
8	*p*-MeO	I	3536	40	0.61
		II, III	3611	ca. 26	0.09
9	H	I	3537	102	0.47
		II	3588	38	0.06
		III	3618	23	0.28
10	*p*-MeO	I	3545	100	0.37
		II	3587	31	0.04
		III	3618	22	0.23
11	CH_2COOEt[3]	I	3550	46	0.68
	OH	II	3618	25	0.13
12	$(CH_3)_2CCOOEt$[3]	I	3544	48	0.43
	OH	II	3606	21	0.09
13	CH_3CHCH_2COOMe[3]	I	3559	82	0.49
	OH	II	3592	32	0.08
		IV	3622	30	0.16
14	$(CH_3)_2CCH_2COOMe$[3]	I	3537	54	0.59
	OH	II	3588	20	0.04
		IV	3613	22	0.06
15	$C_6H_5CH_2OH$[4]	III	3617		
		IV	3636		
16	$C_6H_5C(CH_3)_2OH$[4]	III	3607		
		IV	3620		

* Bands I, II and III denote those due to the OH groups bonded to the proton-acceptors, =O, -O- and π-electrons, respectively, and band IV means the free OH band.

** $D=\log I_0/I$, for the apparent OH band in the case of Nos. 1—8 and for the separated OH band-component in the case of Nos. 9—14.

on the higher frequency side (the most broadened position being at ca. 3535 cm^{-1}) when the ring-substituent is of an electron-attracting nature (Nos. 1—4), while it appears at ca. 3534 cm^{-1} and is substantially symmetric in respect to the ordinate at the maximum when the substituent is a *p*-chlorine or hydrogen atom or an electron-repelling group (Nos. 5—8). The reason for this is not clear at the present time. The β-hydroxy-esters 9 and 10 show a strong, broad band around 3540 cm^{-1} and a sharp band at 3618 cm^{-1}, the former being highly broadened on the higher frequency side; each of the observed spectra can be graphically separated into three symmetric components,*2 as is shown in Fig. 2.

*2 Although it is not clear whether or not the individual band-components are intrinsically symmetric, their symmetry is, at any rate, assumed to simplify the graphical separation. This separation was thus made by reflecting the major component about the ordinate at the apparent maximum and by subtracting the mirror image from the observed spectrum. The residual minor part, which had a shoulder at ca. 3590 cm^{-1}, was then similarly separated into two. Alternatively, by reflecting the minor component and subtracting the mirror image, the major part remained; this was highly broadened around 3590 cm^{-1}. It is unlikely that either the major or the minor component is intrinsically unsymmetric with the broadening or the shoulder at 3590 cm^{-1}. Rather, the part at 3590 cm^{-1} may reasonably be attributed to an absorption of another bonded OH group, as will be discussed in detail later.

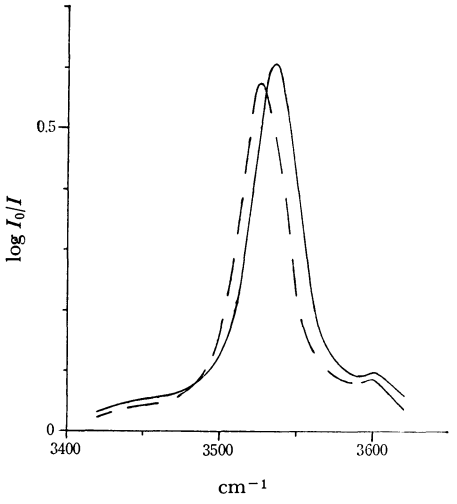

Fig. 1. IR spectra of methyl *p*-nitromandelate (— —) and *p*-methoxymandelate (——).

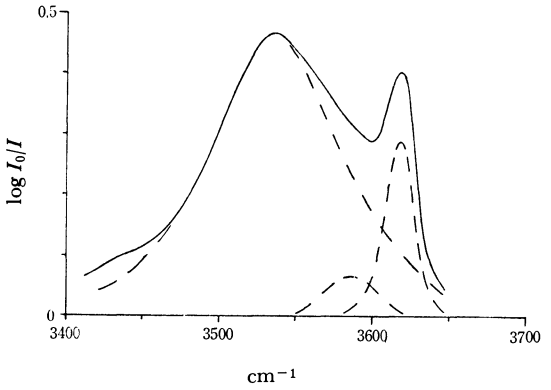

Fig. 2. IR spectrum of methyl β-phenyl-β-hydroxypropionate.

Table II includes the IR data of the apparent OH bands of the mandelates and the OH band-components separated from the observed spectra of the β-phenyl-β-hydroxypropionates, together with those of some related compounds for the purpose of comparison.

In order to assign the bands, it is convenient to take account of the six hydrogen-bonded conformations possible by rotation around the C–O axis; these conformations are shown in Fig. 3. Further, there must be considered the electrostatic and the steric influence on the OH frequency of the phenyl group and the methoxycarbonyl group, both skew

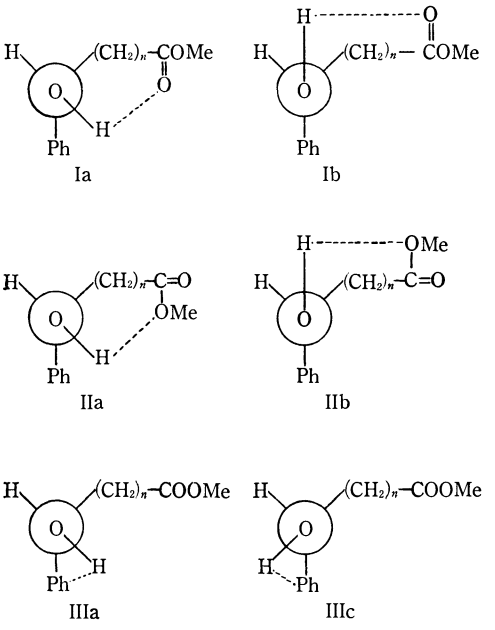

Fig. 3. Hydrogen-bonded conformations possible around the C–O axis.

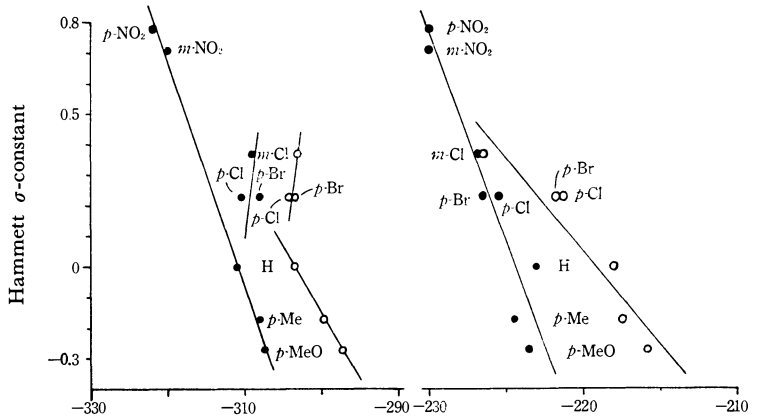

Fig. 4. Chemical shifts vs. Hammett σ-constants for: (left) the methine- and (right) the methyl-protons in chloroform (-●-) and carbon tetrachloride (-○-).

to the OH group. Fortunately, it is known that the influences both of an unsubstituted and a substituted phenyl group are substantially of the same degree as those of a methyl group,[4,17] while the electron-attracting nature of the methoxycarbonyl group lessens the OH frequency by 10 cm^{-1} at most.[3]

In the mandelates ($n=0$ in Fig. 3), the lower frequency band is undoubtedly due to the OH group bonded to the carbonyl-oxygen atom in form Ia and to the bonded OH group in form Ib, since its frequency agrees with that of band I of the comparative α-hydroxycarboxylates. The higher frequency band should not be attributed to a free OH group, since it is considerably lower than the frequency of 3620 cm^{-1} or more which is to be expected for the OH group in form Ib, IIb or IIIc, if it is not hydrogen-bonded. The frequency is also lower than the 3618 cm^{-1} of band II of ethyl glycolate 11 in a form corresponding to form IIb, but it is rather close to the 3606 cm^{-1} of band II of ethyl α-hydroxyisobutyrate 12 in a form corresponding to form IIa. On the other hand, the bonded OH frequencies of forms IIIa and IIIc may fall within the frequency range from 3601 to 3611 cm^{-1}, if the lowering of frequency due to the electron-attracting nature of the methoxycarbonyl group is 7 cm^{-1} and this is then subtracted from the bonded OH frequencies of 3607 and 3617 cm^{-1} of phenyldimethylcarbinol 16 and benzylalcohol 15. Consequently, the band is due to the bonded OH group in at least one of the forms, IIa, IIb, IIIa and IIIc. For a more detailed discussion, it is necessary to investigate the electronic effect of a ring-substituent influencing on the band-intensity. Unfortunately, however, the observed absorbance is too low and inexact to make such an investigation possible.

In the β-phenyl-β-hydroxypropionates ($n=1$ in Fig. 3), the three bands can easily be assigned by comparing their frequencies with those of aliphatic β-hydroxycarboxylates and α-phenylalkanols, as, practically speaking, it is not necessary to take account of the frequency-lowering effect of the methoxycarbonyl group.[3] The band at around 3540 cm^{-1} can undoubtedly be assigned to the OH group bonded to the carbonyl-oxygen atom in form Ia and the bonded OH group in form Ib, while the band at ca. 3590 cm^{-1} may be assigned to the OH group bonded to the ether-oxygen atom in forms IIa and IIb for two reasons: (1) such forms should be present to some extent, though less stable than forms Ia and Ib, and (2) the frequency closely agrees with the ν_{OH} of 3590—3600 cm^{-1} of some 1, 3-diol monoacetates[18] in a similar six-membered ring formed through the intramolecular hydrogen bonding. On the other hand, the highest frequency band may be due to the OH group bonded to the π-electrons of the phenyl group in forms IIIa and IIIc, rather than due to a free OH group. This assignment may be further supported by the fact that the relative intensity of band III to II is higher than those of the free OH band, IV, to band II in β-hydroxycarboxylates 13 and 14; this heightening may result from the hydrogen bonding of the OH group with the π-electrons. As can be seen from a comparison of the data of esters 9 and 10, the p-methoxy substituent appears to raise the relative intensity of band III to II; this is in agreement with the effect of an electron-repelling substituent in strengthening the bonded OH band in series of α- and β-phenylalkanols.[17,19] Thus, no free OH group is present in these esters, since there is no absorption in the frequency region around 3627 cm^{-1} characteristic of the free secondary OH group of α-phenylalkanols.[4]

The above assignments are reasonable also in view of the half-band widths. Thus, the $\Delta\nu_{1/2}$ values of bands I and II (or III) of the mandelates are essentially equal to those of the α-hydroxycarboxylates 11 and 12. The same relationship can be found between the two series of β-hydroxycarboxylates (9 and 10) and (13 and 14).

The Correlation of the Chemical Shift with the Hammett σ-Constant.—Table III includes the NMR data of the methine- and the methyl-protons of the mandelates.

The chemical shifts of protons not directly bonded to the aromatic ring in some aryl compounds have recently been correlated with the Hammett σ-constants.[20] In Fig. 4 the chemical shifts of the methine- and methyl-protons in the mandelates are plotted vs. the Hammett σ-constants.*3 When the substituent is a halogen, the methine-proton point in both solvents does not fall on the correlation line, but falls on a separate line. A similar deviation of the halogens from the correlation line has been obtained when they are plotted vs. the σ^0-values reported by Taft.[21] This at present admits of no explanation. However, it is noteworthy that the falling of the halogens on a separate line is

17) M. Ōki and H. Iwamura, This Bulletin, **35**, 1552 (1962).

18) H. B. Henbest and B. J. Lovell, *J. Chem. Soc.*, **1957**, 1965; R. West, J. J. Korst and W. S. Johnson, *J. Org. Chem.*, **25**, 1976 (1960).

19) M. Ōki and H. Iwamura, This Bulletin, **32**, 1135 (1959).

20) Y. Yukawa, M. Sakai and K. Kabazawa, *Memoirs of Sci. & Ind. Research Osaka Univ.*, **17**, 185 (1960); Y. Yukawa and H. Yamada, *J. Chem. Soc. Japan, Pure Chem. Sect.* (*Nippon Kagaku Zasshi*), **85**, 501 (1964); R. E. Klinick and J. B. Stothers, *Can. J. Chem.*, **40**, 1071 (1962); W. G. Paterson and N. R. Tipman, ibid., **40**, 2122 (1962); C. Heathcock, ibid., **40**, 1865 (1962); C. D. Cook and S. S. Danyluk, *Tetrahedron*, **19**, 177 (1963).

*3 The constants are those based on the ionization of substituted benzoic acids, as reported by D. H. McDaniel and H. C. Brown, *J. Org. Chem.*, **23**, 420 (1958).

21) R. W. Taft, Jr., *J. Phys. Chem.*, **64**, 1805 (1960).

TABLE III. THE NMR DATA ($-\delta$, IN c.p.s. FROM TMS)

No.*	in $CHCl_3$		in CCl_4	
	-CH-	$-COOCH_3$	-CH-	$-COOCH_3$
1	322.0	229.8	Insoluble	
2	320.0	229.8	Insoluble	
3	309.0	226.8	303.1	226.6
4	307.9	226.5	303.5	221.8
5	310.5	225.5	304.1	221.3
6	311.0	223.0	303.5	218.0
7	308.0	224.5	299.5	217.5
8	307.5	223.5	297.0	215.8

* The number refers to that used for the ester described in Tables I and II.

found for the α-protons in *p*-substituted ethylbenzenes[22] and in the plotting of NMR substituent constants vs. Hammett σ_p-constants for a series of *p*-disubstituted benzenes.[23]

The authors wish to thank Mr. Teruo Kajiura and Mr. Tadao Tamura of the Government Chemical Industrial Research Institute, Tokyo, for their infrared measurements.

22) K. L. Williamson, N. C. Jacobus and K. T. Soucy, *J. Am. Chem. Soc.*, **86**, 4021 (1964).
23) G. W. Smith, *J. Mol. Spectroscopy*, **12**, 146 (1964).

BULLETIN OF THE CHEMICAL SOCIETY OF JAPAN VOL. 39 1495—1498 (1966)

Studies of the Organic Reaction of Metal Carbonyl. VIII.* The Isomerization of Aliphatic C_5- and C_6-Acylcobalt Carbonyls

By Yoshinobu TAKEGAMI, Yoshihisa WATANABE, Hiromitsu MASADA
Yasukazu OKUDA, Keiji KUBO and Chikao YOKOKAWA

Department of Fuel Chemistry, Faculty of Engineering, Kyoto University, Sakyo-ku, Kyoto

(Received September 24, 1965)

The isomerization of C_5-acyl(*n*-valeryl- and α-methylbutyryl-) and C_6-acyl(*n*-caproyl-, α-methylvaleryl- and α-ethylbutyryl-)cobalt carbonyls has been studied and compared with that of C_4- acyl(*n*- and isobutyryl-)cobalt carbonyls previously reported. It has been observed that solvents have great effects on the isomerization (the rate and equilibrium) of the C_5-acylcobalt carbonyls. The equilibrium proportion of the isomers (iso/normal) is almost 1 in diethyl ether and tetrahydrofuran. In solvents such as dioxane, ethyl acetate and benzene it seems difficult for this isomerization to occur. α-Ethylbutyrylcobalt carbonyl appears to isomerize directly to *n*-caproylcobalt carbonyl. However, *n*-caproylcobalt carbonyl isomerizes only to α-methylvaleryl-cobalt carbonyl; the reverse isomerization also occurs, but it seems very difficult for any other isomerization between the two of them to occur.

The previous studies of this series have shown that acylcobalt carbonyls readily isomerize and that this isomerization is remarkably affected by the various reaction conditions; with the isomerization of *n*- and isobutyrylcobalt carbonyl (C_4-acylcobalt carbonyls), such solvents as diethyl ether and ethyl acetate have a great effect on the rate and the equilibrium.[1-3]

In the present investigation, the isomerization of C_5- and C_6-acylcobalt carbonyls has been studied in detail by examining the effects of solvents on this reaction. In addition, the possible course of the isomerization of α-ethylbutyrylcobalt carbonyl to *n*-caproylcobalt carbonyl has been investigated.

Experimental

The General Procedures.—The reactions were carried out in the way described in previous papers.[1,2]

The Analytical Procedures.—The reaction products were analyzed by means of a study of their infrared spectra, which were measured on a Shimadzu model IR-27 spectrophotometer, and by gas chromatography; a column 4.5 m. long and 3 mm. in diameter, filled with dilauryl phthalate or silicon DC 550 on cerite, was used. The column temperature was 80 to 110°C, and the flow rate was 50 to 75 ml. per minute.

Materials.—Cobalt hydrocarbonyl was prepared

* Part VII: Y. Takegami, C. Yokokawa, Y. Watanabe and H. Masada, This Bulletin, **38**, 1649 (1965). Presented at the 18th Annual Meeting of the Chemical Society of Japan, Osaka, April, 1965.

1) Y. Takegami, C. Yokokawa, Y. Watanabe, H. Masada and Y. Okuda, This Bulletin, **38**, 787 (1965).

2) Y. Takegami, C. Yokokawa, Y. Watanabe and Y. Okuda, ibid., **37**, 181 (1964).

3) Y. Takegami, C. Yokokawa, Y. Watanabe, H. Masada and Y. Okuda, ibid., **37**, 1190 (1964).

according to the method described in a previous paper.[2] Valeryl chloride, α-methylbutyryl chloride, and *n*-caproyl chloride were commercial products. α-Ethylbutyryl chloride and α-methylvaleryl chloride were prepared by the chlorination of α-ethylbutyric acid and α-methylvaleric acid respectively with thionyl chloride. As the authentic samples, methyl, ethyl, and propyl esters of these acids, prepared by the alcoholysis of the acid halides, were used. The solvents used were dried by the usual methods.

Results and Discussion

The Reaction of *n*-Valeryl and α-Methylbutyryl Chloride with Potassium Cobalt Carbonylate.—The results of the reactions of *n*-valeryl chloride and α-methylbutyryl chloride are summarized in Tables I and II.

In the isomerization of *n*- and isobutyrylcobalt carbonyls, equilibrium between the two isomers has been observed to exist and to be remarkably affected by the solvents; the equilibrium proportion of the isomers (iso/normal) is almost zero in dioxane and tetrahydrofuran, 1/3 in ethyl acetate, and about 1 in diethyl ether, but in a nonpolar solvent such as benzene this isomerization does not occur at all.[1,2]

In this program, the isomerization of C_5-acylcobalt carbonyls was carried out in various solvents in order to study the effect of solvents in detail. The percentages in the last columns of the tables indicate the degree of the isomerization, the proportion of isomerized *n*-valeryl- or α-methylbutyrylcobalt carbonyls. As the reaction products, about 0.7 to 0.3 mol. of valerate and methylbutyrate per mole of potassium cobalt carbonylate was obtained. The yield of the esters decreased with an increase in the reaction time. This may be partly attributed to a thermal instability of the acylcobalt carbonyls.

In diethyl ether under carbon monoxide or nitrogen, *n*-valerylcobalt carbonyl isomerized readily to α-methylbutyrylcobalt carbonyl (Exps. 1—3). The degree of the isomerization amounted to 43% after 9 hr. On the other hand, α-methylbutyrylcobalt carbonyl also isomerized, to give 30% of *n*-valerate, after 9 hr. (Exp. 13). In these

TABLE I. THE REACTION OF *n*-VALERYL CHLORIDE WITH POTASSIUM COBALT CARBONYLATE

Exp. No.	Reaction conditions*1			Yield of esters*2 mol./mol.-$KCo(CO)_4$	The degree of isomerization*3 %
	Atmosphere	Solvent	Time, hr.		
1	CO	Diethyl ether	4	0.63	32
2	CO	Diethyl ether	9	0.35	43
3	N_2	Diethyl ether	4	0.53	35
4	CO	THF	4	0.40	12
5	CO	THF	8	0.36	20
6	CO	THF	16	0.30	30
7	N_2	THF	4	0.37	22
8	N_2	THF	8	0.35	30
9	CO	Dioxane	4	0.42	2
10	CO	Ethyl acetate	4	0.42	2
11	CO	Benzene	4	0.30	1

*1 At 30°C. THF = tetrahydrofuran
*2 The reaction products were identified as *n*-propyl valerate and *n*-propyl α-methylbutyrate.
*3 (α-Methylbutyrate/(α-Methylbutyrate+Valerate))×100

TABLE II. THE REACTION OF α-METHYLBUTYRYL CHLORIDE WITH POTASSIUM COBALT CARBONYLATE

Exp. No.	Reaction condition*1			Yield of esters*2 mol./mol.-$KCo(CO)_4$	The degree of isomerization*3 %
	Atmosphere	Solvent	Time, hr.		
12	CO	Diethyl ether	4	0.41	25
13	CO	Diethyl ether	9	0.30	30
14	N_2	Diethyl ether	4	0.40	25
15	CO	THF	4	0.35	18
16	CO	THF	8	0.27	28
17	CO	THF	16	0.20	35
18	N_2	THF	4	0.46	33
19	N_2	THF	8	0.41	42
20	CO	Dioxane	4	0.50	2
21	CO	Ethyl acetate	4	0.32	6
22	CO	Benzene	4	0.30	7

*1 At 30°C
*2 *n*-Propyl valerate and *n*-propyl α-methylbutyrate
*3 (Valerate/(Valerate+α-Methylbutyrate))×100

Table III. The reaction of α-methylvaleryl and *n*-caproyl chloride with potassium cobalt carbonylate (at 30°C and CO atmosphere)

Exp. No.	Substance	Reaction condition		Yield of esters*1 mol./mol.-$KCo(CO)_4$	The percentage of the isomerized products*2		
		Solvent	Time, hr.		*n*-Caproate %	α-Methyl-valerate %	α-Ethyl-butyrate %
33	α-Methylvaleryl chloride	Diethyl ether	14	0.30	10	—	0 (trace)
34	α-Methylvaleryl chloride	Ethyl acetate	13	0.37	0	—	0
35	α-Methylvaleryl chloride	Dioxane	13	0.50	2	—	0
36	*n*-Caproyl chloride	Diethyl ether	4	0.45	—	23	0
37	*n*-Caproyl chloride	Diethyl ether	9	0.52	—	26	0
38	*n*-Caproyl chloride	Diethyl ether	14	0.47	—	28	0
39	*n*-Caproyl chloride	Ethyl acetate	9	0.67	—	6	0
40	*n*-Caproyl chloride	Ethyl acetate	14	0.56	—	10	0
41	*n*-Caproyl chloride	Ethyl acetate	23	0.55	—	17	0
42	*n*-Caproyl chloride	Dioxane	20	0.50	—	0	0

*1 Ethyl *n*-caproate, ethyl α-methylvalerate and ethyl α-ethylbutyrate
*2 (*n*-Caproate, α-Methylvalerate or α-Ethylbutyrate/Total esters)×100

Table IV. The reaction of α-ethylbutyryl chloride with potassium cobalt carbonylate (at 30°C and CO atmosphere)

Exp. No.	Reaction condition		Yield of esters*1 mol./mol.-$KCo(CO)_4$	The percentage of the isomerized products*2	
	Solvent	Time, hr.		*n*-Caproate %	α-Methylvalerate %
23	Diethyl ether	4	0.66	6	0
24	Diethyl ether	9	0.54	10	~0
25	Diethyl ether	22	0.56	25	~0 (<2)
26	Ethyl acetate	9	0.52	11	~0
27	Ethyl acetate	20	0.30	14	~0
28	Benzene	8	0.41	2	0
29	Toluene	3	0.50	5	0
30	Toluene	10	0.35	24	0
31	Dioxane	10	0.46	0	~0
32	Dioxane	20	0.38	0	0

*1 Ethyl *n*-caproate, ethyl α-methylvalerate and ethyl α-ethylbutyrate
*2 (*n*-Caproate or α-Methylvalerate/Total esters)×100

two cases, the degree of isomerization seemed to increase with an increase in the reaction time. These facts seem to suggest that there is an isomerization equilibrium between the isomers:

$$\text{C-C-C-C-COCo(CO)}_{3\text{ or }4} \rightleftharpoons \begin{array}{c} \text{C} \\ | \\ \text{C-C-C-COCo(CO)}_{3\text{ or }4} \end{array}$$

The equilibrium proportion (iso/normal) may be about 1 under the conditions used. Similarly, in tetrahydrofuran the equilibrium proportion (iso/normal) of the same reaction seemed to be about 1. However, with butyrylcobalt carbonyls the equilibrium is almost completely favorable to *n*-butyrylcobalt carbonyl in tetrahydrofuran.[1] Therefore, the behavior of tetrahydrofuran in the isomerization of the C_5-acylcobalt carbonyls appears to be different from that in the isomerization of the C_4-acylcobalt carbonyls.

In dioxane, ethyl acetate and benzene *n*-valerylcobalt carbonyl isomerized, but they gave only about 2% of α-methylbutyrate after 4 hr. (Exps. 9—11), while α-methylbutyrylcobalt carbonyl gave 2 to 7% of *n*-valerate after 4 hr. (Exps. 20—22), suggesting that the C_5-acylcobalt carbonyls isomerize with much difficulty in these solvents. On the other hand, it has been observed that, in dioxane, isobutyrylcobalt carbonyl readily isomerized to give almost 100% of *n*-butyrylcobalt carbonyl after 2.5 hr. at 25°C, whereas the C_4-acylcobalt carbonyls seem very difficult to isomerize in benzene.[1] Thus, dioxane and benzene also seem to have effects on the isomerization of the C_5-acylcobalt carbonyls apparently different from those

on the isomerization of the C_4-acylcobalt carbonyls.

The Reaction of α-Ethylbutyryl Chloride, α-Methylvaleryl Chloride, and n-Caproyl Chloride with Potassium Cobalt Carbonylate. —The isomerization of C_6-acylcobalt carbonyls was also investigated. The results of these reactions are summarized in Tables III and IV.

As is shown in Table III, α-methylvalerylcobalt carbonyl (II) isomerized to give some *n*-caproate, but only a trace of α-ethylbutyrate (Exps. 33, 35).

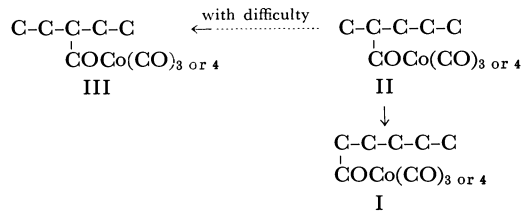

The reverse isomerization of I to II was also observed (Exps. 36—41); in diethyl ether, 23, 26 and 28% of α-methylvalerate was obtained after 4, 9, and 14 hr. respectively, and in ethyl acetate 17% of α-methylvalerate was formed after 23 hr., these facts suggest that the proportion of the isomerized product increases with an increase in the reaction time. However, in ether or ethyl acetate I gave only a trace of α-ethylbutyrate, even after 14 to 23 hr. From this fact, I appears to isomerize to II rather easily, but only with much difficulty to III:

$$\text{II} \longleftarrow \text{I} \dashrightarrow \text{III}$$

On the other hand, III isomerized to give I in a relatively good yield (Exps. 23—30); in diethyl ether, III gave 6, 10, and 25% of I after 4, 9, and 22 hr. respectively; similarly, in ethyl acetate, benzene or toluene, *n*-caproate was also obtained as the isomerization product. However, α-methylvalerate, which was expected to be one of the isomerization products, was obtained in only a low yield in all of these cases; in these solvents, only a trace or less than 2% of α-methylvalerate was obtained after 4 to 22 hr. These facts seem to indicate that III isomerizes relatively readily to I but only with difficulty to II:

$$\text{III} \begin{cases} \longrightarrow \text{I} \\ \dashrightarrow \text{II} \end{cases}$$

As the course of this isomerization (III to I), two ways are possible: in the first course, III directly isomerizes to I, while in the second course III isomerizes to I via II.

In the present case, the isomerization of III to I seems to proceed through the first course, This conclusion is drawn from the following facts: a) The isomerization of II to I occurred relatively slowly; in diethyl ether, II gave 10% of *n*-caproate, even after 14 hr. but III gave 10% of *n*-caproate after 9 hr. These facts have a strong suggest that the isomerization of II to I occurs more slowly than that of III to I. It is, however, reasonable to consider that the isomerization of III to I via II can not proceed more rapidly than that of II to I. Thus, the isomerization of III to I seems not to take the second course. b) In the isomerization of III, α-methylvalerate, i. e., II, was obtained in only a very low yield. This fact could be explained by the second course as follows: the isomerization of III to II was slower than that of II to I, the isomerization of III to II being the rate-determining step. However, the actual isomerization of III to I proceeds more readily than that of II to I, as has been described in a). Accordingly, in the isomerization of III, II seems to be formed by the successive isomerizations, III to I and then I to II.

On the base of facts mentioned above, the isomerization relation among the C_6-acylcobalt carbonyls (I, II and III) may be summarized as follows:

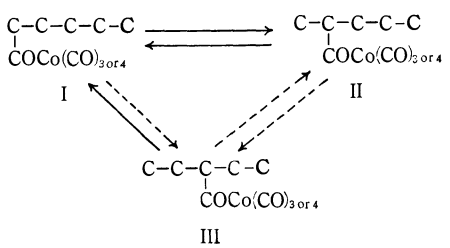

That is, such isomerizations as I to II, II to I and III to I occur relatively readily, but it appears difficult for the other isomerizations to occur.

The isomerization equilibrium among the three isomers could not be determined since the C_6-acylcobalt carbonyls generally isomerize more slowly than the C_5-acylcobalt carbonyls (for example, cf. Exps. 1 and 36).

As Exps. 32, 35, and 42 show, in dioxane it seems difficult for C_6-acylcobalt carbonyls to isomerize, suggesting that the behavior of a solvent may be different in the isomerization of the C_6-acylcobalt carbonyls and in that of the C_4-acylcobalt carbonyls.[10]

BULLETIN OF THE CHEMICAL SOCIETY OF JAPAN VOL. 39 1499—1501 (1966)

Studies of the Organic Reaction of Metal Carbonyl. IX.*[1] The Formation of *o*-Toluylcobalt Carbonyl in the Reaction of Benzyl Chloride with Potassium Cobalt Carbonylate

By Yoshinobu TAKEGAMI, Yoshihisa WATANABE, Hiromitsu MASADA and Chikao YOKOKAWA

Department of Fuel Chemistry, Faculty of Engineering, Kyoto University, Kyoto

(Received October 1, 1965)

The reaction between benzyl halide and potassium cobalt carbonylate has been studied. *o*-Toluylcobalt carbonyl is found among the reaction products. This carbonyl seems to be formed by the isomerization of benzyl cobalt carbonyl via phenylacetylcobalt tricarbonyl or *o*-tolylcobalt carbonyl. This isomerization occurs only at relatively high temperatures (30—50°C). At 0°C, only phenylacetyl cobalt carbonyl is formed in a good yield. The isomerization is highly promoted by the addition of cobalt hydrocarbonyl. The reaction atmosphere (carbon monoxide and nitrogen) also has a great effect on the isomerization. Such additives as oxalic acid, *p*-toluenesulfonic acid, trichloroacetic acid, and ethyl alcohol-hydrogen chloride have no promoting effect on the isomerization.

The previous works of this series have shown that α-ethylbutyrylcobalt carbonyl directly isomerizes to *n*-caproylcobalt carbonyl as follows:[1,2]

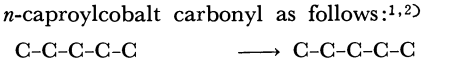

Namely, the acylcobalt carbonyl group bonded to the middle carbon atom of the *n*-C_5 structure appears to rearrange to the terminal carbon atom by leaping one carbon atom at the 2-position.

In this connection, it seems of considerable interest to study whether phenylacetylcobalt carbonyl may analogously isomerize to *o*-toluylcobalt carbonyl:

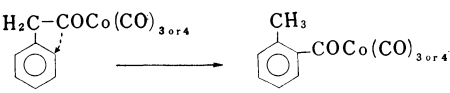

In the present paper, the reaction between benzyl halide and potassium cobalt carbonylate has been investigated in order to examine the possibility of this isomerization.

Experimental

The Reaction Procedures.—A 100-ml. four-necked flask, equipped with a 50-ml. dropping funnel, a stirrer and a rubber stopple, was connected with a gas buret, and the air in the system was replaced with carbon monoxide or nitrogen. By the use of a syringe, 50-ml. of a 0.09 M cobalt hydrocarbonyl solution in *n*-hexane was put into the flask; then the solution was titrated with a 1/2 N ethyl alcohol solution of potassium hydroxide, using phenolphthalein as indicator. To the potassium cobalt carbonylate thus formed, 4.5 mmol. of benzyl halide and an appropriate amount of a cobalt hydrocarbonyl solution in *n*-hexane or various organic acids were introduced; then the mixture was stirred at various temperature for 2 to 15 hr.

Analytical Procedure.—After a certain reaction time, about 30 ml. of a saturated solution of iodine in toluene and about 4 ml. of alcohol (methyl, ethyl or propyl alcohol) were stirred into the reaction mixture. By this treatment acylcobalt carbonyl was converted into the corresponding ester of carboxylic acid. The solution of the ester was concentrated to about 5 ml. and then analyzed by means of a study of the infrared spectra, which were measured on a Shimadzu model IR-27 spectrophotometer, and by gas chromatography. A column (3 m. long and 3 mm. in diameter), filled with dilauryl phthalate on cerite, was used; the column temperature was 170°C, and the flow rate of the carrier gas (hydrogen) was 70 ml./min.

Materials.—Cobalt hydrocarbonyl was prepared according to the method described in a previous paper.[3] The benzyl chloride, the bromide and the various organic acid were commercial products.

Results and Discussion

The results of the reactions of benzyl halide with potassium cobalt carbonylate are summarized in Table I.

*1 Part VIII: Y. Takegami, Y. Watanabe, H. Masada, Y. Okuda, K. Kobo and C. Yokokawa, This Bulletin, **39**, 1495 (1966). Presented a the 18th Annual Meeting of the Chemical Society of Japan, April, Osaka, 1965.

1) Y. Takegami, C. Yokokawa, Y. Watanabe, H. Masada and Y. Okuda, This Bulltin, **38**, 787 (1965).

2) Y. Takegami, Y. Watanabe, H. Masada, Y. Okuda, K. Kubo and C. Yokokawa, ibid., **39**, 1495 (1966).

3) Y. Takegami, C. Yokokawa, Y, Watanabe and Y. Okuda, ibid., **37**, 181 (1964).

TABLE I. THE REACTION OF BENZYL CHLORIDE WITH POTASSIUM COBALT CARBONYLATE

Exp. No.	Reaction condition: Atmosphere	Temp. °C	Time hr.	Additive*1 0.5 mol./mol.-$KCo(CO)_4$	Gas absorbed*2 mol./mol.-$KCo(CO)_4$	Yield of esters*3 mol./mol.-$KCo(CO)_4$	The percentage of *o*-toluate*4 %
1	CO	40	11	None	−0.45	0.30	~0
2	N_2	40	3	None	−1.28	0.35	~0
3	N_2	40	15	None	−1.32	0.32	~0
4	CO	20	13	$HCo(CO)_4$	0.70	0.40	0
5	CO	40	5	$HCo(CO)_4$	−1.70	0.46	11
6	CO	40	7	$HCo(CO)_4$	−2.06	0.24	12
7	CO	40	8	$HCo(CO)_4$	−2.68	0.24	17
8	CO	40	11	$HCo(CO)_4$	−3.06	0.1	55
9	N_2	30	8	$HCo(CO)_4$	−1.40	0.55	10
10	N_2	40	2	$HCo(CO)_4$	−1.28	0.59	7
11	N_2	40	4	$HCo(CO)_4$	−1.40	0.51	24
12	N_2	40	5	$HCo(CO)_4$	−1.53	0.25	36
13	N_2	40	7	$HCo(CO)_4$	−2.13	0.1	>95
14	N_2	50	2	$HCo(CO)_4$	−2.15	0.15	40
15*5	CO	0, 40	3, 4	$HCo(CO)_4$	0.91—2.03	0.42	0
16*5	CO	0, 40	3, 6	$HCo(CO)_4$	0.90—2.33	0.37	3
17	N_2	40	4	Oxalic acid	−0.95	0.51	~0
18	N_2	40	4	*p*-Toluene-sulfonic acid	−1.00	0.51	~0
19	N_2	40	4	Trichloro-acetic acid	−1.00	0.55	~0
20	N_2	40	4	EtOH-HCl	−0.83	0.30	~0

*1 Solution in *n*-hexane.
*2 The negative sign shows the gas evolution.
*3 The reaction products were identified as ethyl phenylacetate and ethyl *o*-toluate.
*4 (*o*-Toluate/(*o*-Toluate + Phenylacetate))×100
*5 Benzyl bromide was used. The reaction was carried out in two stages: at first at 0°C for 3 hr. (0.91 mol. of carbon monoxid was absorbed.) and then at 40°C for 4 hr. (2.03 mol. of gas was evolved.).

As Exp. 1 shows, without additives the reaction of benzyl chloride at 40°C under carbon monoxide proceeded with the evolution of gas*2 to give ethyl phenylacetate as the main product. Besides this ester, only a small amount of ethyl *o*-toluate was obtained as an isomerization product. Under nitrogen, a larger amount of gas was evolved, but *o*-toluate was also obtained in a low yield (Exps. 2 and 3):

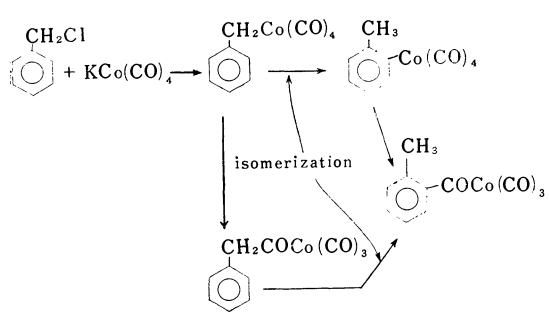

The formation of *o*-toluylcobalt carbonyl seemed to proceed by the isomerization of benzylcobalt carbonyl and/or phenylacetylcobalt carbonyl, as has been shown above. However, it is considered difficult for such an isomerization to occur under these conditions. At a lower reaction temperature (20 to 0°C) under carbon monoxide, the reaction proceeded with the absorption of gas*3, to give ethyl phenylacetate in a relatively good yield, but no ethyl *o*-toluate, indicating that under milder conditions the isomerization occurs with much difficulty.

However, this type of isomerization was remarkably promoted by the addition of cobalt hydrocarbonyl. When 0.5 mol. of cobalt hydrocarbonyl per mole of potassium cobalt carbonylate was present, a tolerable amount of *o*-toluate*4 was

*2 The evolution of gas seemed to be partly attributable to the decomposition of the alkyl- and acylcobalt carbonyls formed.
*3 The gas absorption seemed to be attributable to the formation of phenylacetylcobalt tetracarbonyl.
*4 (*o*-Toluate/(*o*-Toluate+Phenylacetate))×100 Indentified by gas chromatography and by a study of the infrared spectrum of the solution of the products in toluene, which showed absorption bands at 1729 and 1740 cm^{-1}: The retention time of the esters in gas chromatography increased with the molecular weight of the alcohol used in the cleavage of the crude products;

$$RCOCo(CO)_{3\text{ or }4} \xrightarrow{I_2 + R'OH} RCOOR'$$

obtained (Exps. 4—14). Under carbon monoxide at 40°C, the percentage of *o*-toluate amounted to 55% after 11 hr. (Exp. 8). The total yield of esters, i. e., phenylacetate and *o*-toluate, decreased with an increase in the reaction time. Under these conditions, large gas evolution gradually occurred; this amounted to about 3 mole*[5] after 11 hr. On the other hand, at 20°C gas absorption occurred, but no isomerized product was obtained, even after 13 hr. (Exp. 4). These facts indicate that a relatively high temperature, which seems to cause the acyl- and alkylcobalt carbonyls to decompose, may be effective in the isomerization.

Under nitrogen, *o*-toluate was also formed in the presence of cobalt hydrocarbonyl. At 40°C about 7% of *o*-toluate was obtained after only 2 hr. (Exp. 10); this percentage became 36 and more than 95% after 5 and 7 hr. respectively. Thus, the isomerization, the formation of *o*-toluylcobalt carbonyl, occurred under nitrogen more readily than under carbon monoxide, as in the isomerization of aliphatic acylcobalt carbonyls.[1-4] At 50°C, 40% of *o*-toluate was formed after only 2 hr., but at 30°C only 10% of *o*-toluate was obtained, even after 8 hr. Therefore, higher temperatures seem to promote the isomerization. In these cases, a large gas evolution was also observed. The total yield of the esters appeared to decrease with an increase in the amount of gas evolved; when about 2 to 3 mol. of gas were evolved, the yield of the esters amounted to only 0.1—0.2 mol.

As for the course of the isomerization, two ways are possible; in the first course, benzylcobalt carbonyl, which is derived by the reaction of benzyl halide with potassium cobalt carbonylate, isomerizes to *o*-toluylcobalt carbonyl via phenylacetylcobalt carbonyl, while in the second course this isomerization occurs via *o*-tolylcobalt carbonyl. In the present study, it can not be decided which course should be chosen for this type of isomerization. From the fact that a nitrogen atmosphere remarkably promotes the isomerization, however, *o-tolylcobalt carbonyl and phenylacetylcobalt* tricarbonyl, i. e., carbon monoxide-lacking states, appear to be very important as isomerization species, as in the isomerization of aliphatic acylcobalt carbonyls.[1-4] This consideration is supported by the results of Exps. 15 and 16, in which the reaction was carried out in two stages under carbon monoxide, first at 0°C and then at 40°C. At 0°C, about 0.9 mol. of carbon monoxide was absorbed over 3 hr. period, indicating that benzylcobalt carbonyl might be converted into phenylacetylcobalt tetracarbonyl in a good yield; then the reaction temperature was changed to 40°C, which is effective for the isomerization, but only a small amount of the isomerized product was obtained after 6 hr., even in the presence of cobalt hydrocarbonyl. From this fact, it seems that phenylacetylcobalt tetracarbonyl is difficult to isomerize.

It has been known that cobalt hydrocarbonyl is a strong acid.[5] In relation to this character of cobalt hydrocarbonyl, the effects of the addition of various organic acids on the reaction have been examined. Oxalic acid, *p*-toluenesulfonic acid, trichloroacetic acid and ethyl alcohol - hydrogen chloride were used, 0.5 mol. portions of these acids were added to the reaction system instead of cobalt hydrocarbonyl. However, these acids seemed to have no promoting effect on the isomerization, even at 40°C, as Exps. 17—20 show. Thus, the promoting effect of cobalt hydrocarbonyl seems not to be attributable to only its acidic character. The reason why cobalt hydrocarbonyl has this effect could not be determined in the present investigation.

*5 "Mole" means mole per mole of potassium cobalt carbonylate in this description.

4) Y. Takegami, C. Yokokawa, Y. Watanabe and H. Masada, This Bulletin, **37**, 1190 (1964).

5) W. Hieber and E. Lindner, *Chem. Ber.*, **94**, 1417 (1961); W. Hieber and G. Wagner, *Z. Naturforschung*, **13b**, 339 (1958).

BULLETIN OF THE CHEMICAL SOCIETY OF JAPAN VOL. 39 1502—1507 (1966)

Ferrocene-containing Polymers. VIII. Polycondensation of *N*, *N*-Dimethylaminomethylferrocene with Ferrocene

By Eberhard W. NEUSE and Kazuko KODA

Polymer Laboratory, Missile & Space Systems Division, Douglas Aircraft Company, Inc. Santa Monica, California, 90406, U. S. A.

(Received September 25, 1965)

Based on previous investigations involving the self-condensation of the ferrocenyl Mannich base, *N*, *N*-dimethylaminomethylferrocene (I), the present paper describes the co-condensation of this Mannich base with ferrocene. The reactions are conducted in the melt phase in the presence of a $ZnCl_2$/HCl catalyst system. The resulting polymeric products are soluble and partially fusible and have number-average molecular weights in the 500—4000 range (unfractionated). The polymers, exhibiting the idealized structure III, are closely related to the products of self-condensation (II), with recurring units composed of ferrocenylene and methylene groups and homoannular substitution predominating along the chain. Due to the presence of ferrocene, however, an additional termination step is introduced into the overall reaction, leading to a reduced degree of polymerization. The considerable excess over the stoichiometric amount of ferrocene required to achieve this competitive termination and concomitant decrease in M_n suggests that pronounced inductive and hyperconjugative effects are operative in the ferrocenylene-methylene system, resulting in activation of the methylene-substituted ring. The isolation of the lowest homolog possible, diferrocenylmethane, lends further support to the proposed structure of the recurring unit. Spectroscopic evidence obtained on subfractionated material suggests the substitution pattern along the chain to be essentially the same as in the earlier described homocondensation polymers, which is consistent with the assumption of essentially like propagation mechanisms in both cases. A small degree of branching is also inferred from spectroscopic data.

In a previous publication,[1] the $ZnCl_2$/HCl-catalyzed formation of ferrocene-containing polymers from the ferrocenyl Mannich base, *N*, *N*-dimethylaminomethylferrocene (I), was described. The products of condensation were shown essentially to be composed of ferrocenylene-methylene recurring units, and the overall polymer structure was depicted, somewhat idealized, by the novolac-type formula II. Each polymer molecule was believed to contain a double-bridged segment resulting from termination steps through self-substitution on the penultimate ferrocenylene group of the growing chain, much as proposed[2] for the identical polycondensation product of hydroxymethylferrocene. In continuation of these earlier efforts, the present paper describes work on the polycondensation of the Mannich base in the presence of ferrocene, in which case essentially the same propagation sequence, but a different termination step, may be expected, leading to polymer III rather than II.

Results and Discussion

As in the case of homocondensation of I, the co-condensation of this Mannich base with ferrocene, summarized in Eq. 1, will proceed in several steps, the first of these[1] being the formation of adduct IV. By stepwise ionization, with V occurring as successor species,[3] complex IV will generate the metallocarbonium ion VIa (or VIb from polyhomologs of IV and V in an advanced stage of the condensation). For ions VI, the same three reaction steps can be visualized as in the homocondensation of I. These steps involve: (1) nuclear substitution of monomeric and polymeric complexes of the types IV and V (growth

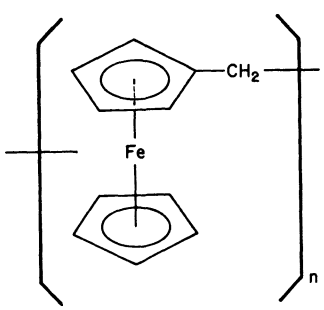

II

1) E. W. Neuse and E. Quo, *J. Polymer Sci.*, **A3**, 1499 (1965).

2) E. W. Neuse and D. S. Trifan, *J. Am. Chem. Soc.*, **85**, 1952 (1963).

3) E. W. Neuse and E. Quo, *Nature*, **205**, 494 (1965).

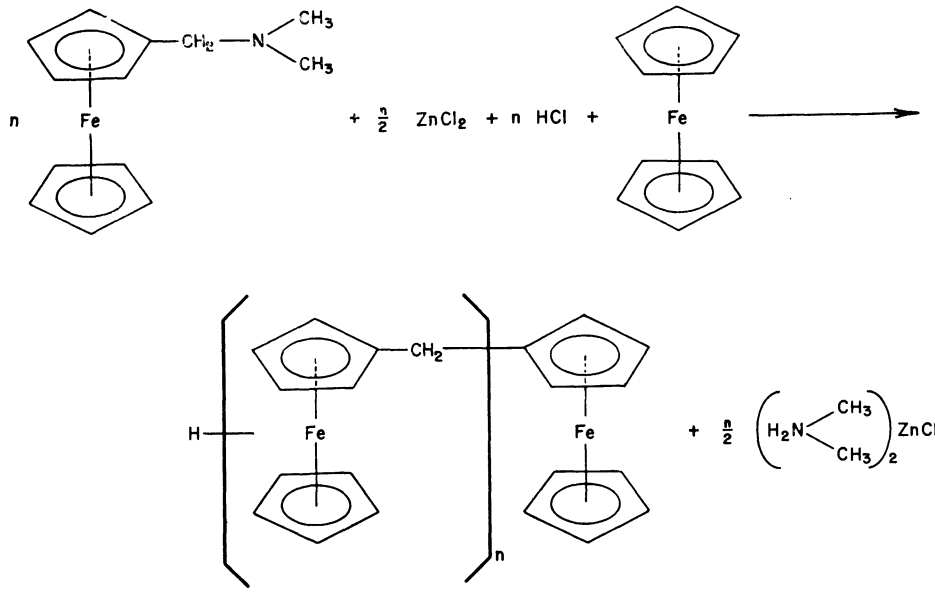

III

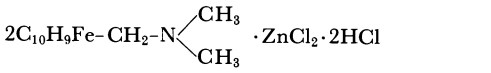

IV

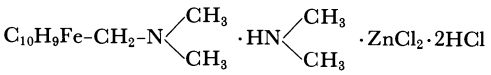

V

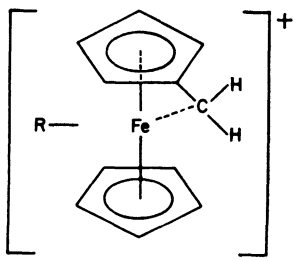

VIa, R=H
VIb, R=Residual polymer chain

step); (2) self-substitution on penultimate ferrocene nucleus with resulting formation of a double-bridged segment as part of a nitrogen-free polymer chain (termination step); (3) nuclear substitution of nitrogen-free polymer (growth step). In addition to these three reaction steps involved in the homocondensation of the Mannich base, nuclear substitution of ferrocene may now occur as an alternate termination step (4) competing with the self-substitution reaction (2). To what extent the self-substitution step in this largely diffusion-controlled process can be suppressed as a terminating reaction in favor of (4) will largely depend on both the ferrocene concentration in the melt and the difference in reactivity between the ferrocene molecule and the substituted ferrocenyl or ferrocenylene units. Prevalence of steps (1) through (3) over (4) may be predicted as a result of inductive and hyperconjugative[4-8] activation of the substituted ferrocene rings. Therefore, in order to enforce a reaction course according to Eq. 1 by suppressing the other three reaction steps in favor of (4), it would appear necessary to employ the ferrocene co-reactant in concentrations considerably higher than required by the stoichiometry of Eq. 1.

The experimental results of a series of co-condensations confirmed these expectations. When heated with various amounts of ferrocene in the presence of zinc chloride and hydrogen chloride (or zinc chloride and water, thus generating hydrogen chloride by hydrolysis) under conditions similar to those applied in homocondensations,[1] the Mannich base readily underwent condensation to give polymers in 75—85% yield. By combining extraction, precipitation and sublimation steps, the polymer was separated in each case from unreacted ferrocene, zinc salts and traces of crosslinked polymer, to be finally collected in two crude fractions of different average molecular weights. The first fraction consisted of polymeric material, whereas the second fraction, usually somewhat

4) K. Rinehart, Jr., K. L. Motz and S. Moon, *J. Am. Chem. Soc.*, **79**, 2749 (1957).
5) M. Rosenblum and R. B. Woodward, ibid., **80**, 5443 (1958).
6) M. Rosenblum, ibid., **81**, 4530 (1959).
7) M. Rosenblum and W. G. Howells, ibid., **84**, 1167 (1962).
8) K. L. Rinehart, Jr., D. E. Bublitz and D. H. Gustafson, ibid., **85**, 970 (1963).

TABLE I

Expt. No.	Concentrations of reactants, mol. I	Hydrochloride of I	Ferrocene	$ZnCl_2$	HCl	H_2O	Temp. °C	Time hr.	Total yield of crude polymer,[a] %	HCl introduced as
1	1.0	—	0.2	0.5	1.0	3.305	165	7.5	82.6	Hydrochloric acid
2	1.0	—	0.33	0.55	1.0	3.305	170	7	82.9	Hydrochloric acid
3	1.0	—	0.5	0.5	1.0	3.305	170	8	85.8	Hydrochloric acid
4	—	1.0	0.5	0.5	—	—	170	6	78.8	Hydrochloride of I
5	1.0	—	1.0	0.55	1.0	3.305	165	12	77.5	Hydrochloric acid
6[b]	1.0	—	2.0	0.5	1.0	3.305	170	7	80.6	Hydrochloric acid
7	1.0	—	0.25	1.0	—	1.0	170	6	87.2	$ZnCl_2$ (hydrolysis)
8	1.0	—	0.5	1.0	—	1.0	160	8	78.8	$ZnCl_2$ (hydrolysis)
9	1.0	—	1.0	1.1	—	1.1	170	11	80.9	$ZnCl_2$ (hydrolysis)
10[b]	1.0	—	2.5	1.0	—	1.0	155	9	88.5	$ZnCl_2$ (hydrolysis)

a) Combined yield of 1st and 2nd fraction, in % of theory.
b) Dioxane used as solvent.

TABLE II

Expt. No.	Fraction[a]	M_n	M. p. °C[b]	Yield %	Anal. Calcd. for III C, %	H, %	Fe, %	Anal. Found C, %	H, %	Fe,[c] %
1	1st	3650	155	69.6	66.60	5.10	28.30	67.01	5.13	27.34
	2nd	850	85	13.0	66.24	5.16	28.60	66.34	5.31	28.38
2	1st	2970	140	67.5	66.58	5.11	28.31	66.51	5.20	27.58
	2nd	790	95	15.4	66.21	5.17	28.62	66.41	5.39	28.29
3	1st	2590	125	74.6	66.56	5.11	28.33	66.69	5.32	27.82
	2nd	660	90	11.2	66.10	5.18	28.72	66.30	5.24	29.10
4	1st	2790	135	68.0	66.57	5.11	28.32	66.84	5.19	27.97
	2nd	740	80	10.8	65.17	5.17	28.66	66.09	5.29	28.83
5	1st	2310	120	61.2	66.54	5.12	28.34	66.80	5.25	27.76
	2nd	620	110	16.3	66.06	5.19	28.75	65.96	5.26	28.66
6	1st	2440	125	24.7	66.55	5.12	28.33	66.39	5.37	27.49
	2nd	560	100	55.9	66.02	5.19	28.79	66.10	5.32	28.49
7	1st	3700	135	77.3	66.60	5.10	28.30	66.79	5.26	27.83
	2nd	820	80	9.9	66.22	5.17	28.61	66.39	5.14	28.23
8	1st	2330	130	65.4	66.54	5.12	28.34	66.59	5.45	27.84
	2nd	720	90	13.4	66.15	5.18	28.67	65.83	5.24	28.53
9	1st	2550	125	52.2	66.56	5.11	28.33	66.07	5.13	28.02
	2nd	550	95	28.7	65.97	5.20	28.83	65.75	5.40	29.17
10	1st	1980	115	22.9	66.51	5.12	28.37	66.45	5.24	28.11
	2nd	490	100	65.9	65.89	5.22	28.89	65.58	5.31	29.10

a) First and second fractions; see text.
b) Upper limiting value of melting range.
c) Up to 0.8% low for higher-molecular compounds.

smaller, contained essentially oligomeric constituents. The reactions are illustrated by 10 examples[9] summarized in Table I, and the pertaining analytical data are compiled in Table II.

The analytical results recorded confirm the anticipated structure III.[10] Furthermore, the effect of the ferrocene co-reactant on the average degree of polymerization is demonstrated by a

9) For comparison, several polycondensations were conducted with aluminum chloride as catalyst, applying experimental conditions similar to those summarized in Table I for zinc chloride. In a typical run employing Mannich base and $AlCl_3$ in a 2 : 1 molar ratio, polycondensation occurred even in the absence of additional catalyst components such as HCl or H_2O. However, due to unusually strong crosslinking and decomposition effects even at the comparatively low temperature applied (150°C), the reaction had to be terminated at an incomplete stage, and the yield in linear polymer barely approached 40%. These discouraging results prompted the abandonment of $AlCl_3$ as the Lewis acid component in these condensations.

10) Undoubtedly, the first fractions from experiments employing a high Mannich base/ferrocene ratio contain some polymer II formed via the self-substitution step (2). However, this cannot be borne out by chemical analysis since in the molecular weight ranges concerned the differences in elemental composition are too small to be analytically discernible, as becomes evident from a comparison of the calculated analytical data in Table II with those for the homocondensation product II recorded earlier[1] (Calcd. for II: C, 66.71; H, 5.09; Fe, 28.20%).

comparison of the M_n and yield values, lowest molecular weights being obtained at highest ferrocene concentrations. The data also show the enhanced susceptibility of the substituted, as compared to the unsubstituted, ferrocene moiety toward electrophilic attack. This can readily be seen in such experiments as Nos. 5, 6, 9 and 10, in which the yields in oligomeric III ($n \approx 2$) were markedly lower than would have been expected for comparable ring activation of substituted and unsubstituted ferrocene units.

Employing standard fractionation procedures, several typical polymer batches were separated into subfractions of enhanced monodispersity. These subfractions had molecular weights (M_n) ranging from about 400 to 11000 and showed elemental analyses in the same good agreement with structure III as noted above for the unsubfractionated products. An X-ray diffraction study revealed crystallinity only for fractions with $M_n <$ 700. This lack of crystallinity in fractions with constituents containing four or more ferrocene nuclei is not surprising in view of assumed branching (see below) and random distribution of the 1, 2-, 1, 3- and 1, 1'-disubstituted recurring units. The lowest subfraction isolated, after chromatographic purification, proved to be identical in m. p., M_n and elemental composition with the known[11,12] diferrocenylmethane (III, $n=1$), whose structure was confirmed by percent homoannularity value[2] (96.9) and NMR spectrum, the latter showing singlets due to ferrocene (18 protons) and methylene (two protons) resonances at τ 6.09 and 6.70, respectively.[13] This unambiguous identification of the lowest homolog as diferrocenylmethane is well in support of the structural assignment III to the presently discussed polymer.

The infrared spectra (KBr pellet) of polymer III showed the bands characteristic of the ferrocenylene-methylene unit as discussed elsewhere.[2] The spectra of high-molecular fractions were practically superimposable with those of polymer II prepared either from *N*, *N*-dimethylaminomethylferrocene[1] or from hydroxymethylferrocene.[2] This spectroscopic identity is predictable, since the effect, if any, of a double-bridged segment in homopolymer II on the absorption pattern of the ferrocenylene-methylene units is probably too small to be detectable, with interfering absorption of other origin appearing in all characteristic regions, notably in that at 10.6—11.0μ. The occurrence of the typical medium-intensity band near 7.8 μ not only in higher molecular fractions, but even in the lowest, solely monosubstituted member (diferrocenylmethane), prohibits utilization of this peak in distinguishing 1, 3- from 1, 2-disubstituted ferrocene derivatives as suggested by Nesmeyanov.[18] (Cf., in this connection, Rosenblum and Howells.[7]) By the same reasoning, the band in the 10.8—10.9μ range exhibited by diferrocenylmethane and all higher molecular fractions cannot be utilized for this distinction.[4,6,8,19] In going from low- to high-molecular fractions, the two bands near 9 and 10μ indicative of the presence of unsubstituted ferrocene rings[19] were attenuated in intensity. At the same time, an intensity decrease of the ring-breathing absorption near 7.1μ became apparent; while observed with other homoannularly substituted ferrocene derivatives made available for this comparison, this band failed to occur, or at best appeared very weakly, in a great number of heteroannular compounds investigated and may, therefore, be utilized in suitable cases as corroborative evidence for the presence of unsubstituted rings. The weak band at 10.60μ originally ascribed to a CH_2 rocking mode[2] was found to be exhibited in nearly unchanged intensity by all fractions except the lowest member, thus indicating a different origin; possibly, the band is associated with a 1, 3-disubstitution scheme[4,6] on ferrocene.

The majority of subfractions of III with $M_n <$ 5000 showed a defined melting behavior. This is in contrast to the predominantly infusible (when fractionated) polymer II; various degrees of monodispersity and branching possibly acount for this inconsistency. The m. p.-M_n relationship depicted in Fig. 1 may, within the molecular weight range from about 1000 to 4000, be employed for useful characterization purposes, as was done

11) K. Schlögl and A. Mohar, *Monatsh. Chem.*, **92**, 219 (1961).
12) P. L. Pauson and W. E. Watts, *J. Chem. Soc.*, **1962**, 3880.
13) The compound was converted by selenium dioxide treatment to the known[11,14-17] diferrocenylketone, for which additional structural proof resulted from its weak-coupling A_2X_2-type NMR spectrum exhibiting, in the expected area ratio, a singlet at τ 5.83 (unsubstituted ring protons) and two apparent triplet signals centered at 5.02 and 5.51 (strongly deshielded $\alpha-\beta$ protons) with practically identical "ortho" and cross-ring coupling constants ($J_{\alpha\beta} \approx J_{\alpha\beta'} \approx 2.0$ c.p.s.). These detailed analytical efforts on diferrocenylmethane appeared to be in order in view of some disagreement in the literature as to the identity of this compound. While both Schlögl's[11] and Pauson's[12] groups reported melting points in the 143—149°C range, Rinehart and co-workers, in an earlier communication,[14] assigned the diferrocenylmethane structure to a compound with m. p. 124—125°C. The analytical and spectroscopic data presented above, coupled with the oxidation to the ketone, substantiate the present assignment in accord with Schlögl's and Pauson's findings.
14) K. L. Rinehart, Jr., A. F. Ellis, C. J. Michejda and P. A. Kittle, *J. Am. Chem. Soc.*, **82**, 4112 (1960).
15) S. I. Goldberg, *J. Org. Chem.*, **25**, 482 (1960).
16) M. D. Rausch, E. O. Fischer and H. Grubert, *J. Am. Chem. Soc.*, **82**, 76 (1960).
17) K. L. Rinehart, Jr., P. A. Kittle and A. F. Ellise, ibid., **82**, 2082 (1960).
18) A. N. Nesmeyanov, L. A. Kasitsyna, B. V. Lokshin and V. D. Vilchevskaya, *Dokl. Akad. Nauk SSSR*, **125**, 1037 (1959).
19) M. Rosenblum, Ph. D. Thesis, Harvard University, 1953.

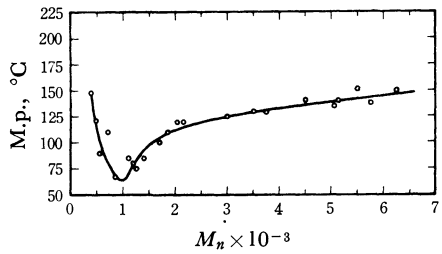

Fig. 1. Melting point, m. p., vs. number-average molecular weight, M_n, for polymer III.

earlier in related cases.[2,20] For further characterization, again using subfractionated samples, the correlation

$$[\eta] = 1.1 \times 10^{-3} M^{0.38}$$

between intrinsic viscosity, $[\eta]$, and molecular weight was determined by standard procedures. The low value of the exponent points to more globular than rod-like shape of the polymer molecules, as was similarly inferred[1] for polymer II. This behavior suggests a slightly branched structure, for which corroborative spectroscopic evidence results from the downward trend[1] of the percent homoannularity-molecular weight curve plotted in Fig. 2 for 15 subfractions. This curve, furthermore, demonstrates a slight prevalence of homoannular over heteroannular bonding along the polymer backbone, as is predictable on electronic grounds.[1,2,4-8,21] It is of interest to note the complete coincidence of the curve in Fig. 2 with the corresponding plot[1] for polymer II reproduced here for comparison, supporting the earlier assumption in this paper of an identical propagation sequence (with resulting identical substitution orientation) for both polymers II and III.

In order to arrive at a quantitative value of the degree of intralinear homoannular bonding, i. e., that proportion of homoannular bonding which is restricted to links of the backbone, a monodisperse, trinuclear fraction composed of the isomeric bis(ferrocenylmethyl)ferrocenes (III, $n=2$) was isolated by chromatography from the hexane-soluble portions of the polymer, thus offering the possibility to study the substitution orientation in III unaffected by the occurrence of side-chains. Monodispersity of this fraction and absence of components other than isomers III, $n=2$, was demonstrated[22] by molecular weight determinations, elemental analyses and NMR spectra (ferrocene/methylene proton signals in the expected 26 : 4 area ratio) on subfractions obtained by repeated crystallization.[23] Determination of the percent-homoannularity of this trinuclear fraction gave a value of 86.5 (average of results from three parallel chromatographic runs). From this figure, one may calculate a 59.6% content of homoannular compounds (combined 1, 2- and 1, 3-bis(ferrocenylmethyl)ferrocene) in the trinuclear isomer mixture and, hence, approximately so, of ferrocenylene units bonded homoannularly into the polymer backbone.

Work on the separation of the trinuclear mixture into its components (the heteroannular compound was recently described[12]) is in progress and will be reported elsewhere.[24]

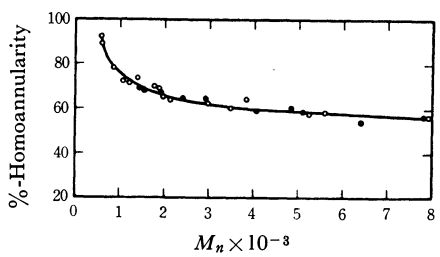

Fig. 2. Percent-homoannularity vs. number-average molecular weight, M_n, for:
Poloymer III (open circles)
Polymer II (filled-in circles)

Experimental

Materials and Analytical Procedures. — Solvents were reagent grade; for chromatographic purposes, they were fractionated on a spinning-band column. Starting materials and other chemicals were obtained commercially or prepared and purified as described.[1,2] Elemental and instrumental analyses were performed as in the earlier work.[1] The solvents used for NMR and M_n determinations were, respectively, carbon

20) E. W. Neuse and D. S. Trifan, Abstr. Papers presented at 148th National Meeting, Am. Chem. Soc., September, 1964, p. 5S.

21) R. A. Benkeser, Y. Nagai and J. Hooz, *J. Am. Chem. Soc.*, **86**, 3742 (1964). Among the two possible homoannular dispositions, steric effects are likely to lead predominantly to 1,3-substituted units.

22) In addition, similar analyses of the preceding and subsequent chromatographic bands showed these to be devoid of isomers III, $n=2$, thus attesting to the quantitative collection of these isomers in the trinuclear fraction under consideration.

23) The conventional process of fractional precipitation and crystallization, resting on the different solubility behavior of the components, could obviously not be utilized for this separation of a monodisperse fraction, since strict dependence of the solubility on the chain-length would be expected only for those polyhomologous series in which all members are composed of identical recurring units. In contrast, with polymers composed, as in the present case, of isomeric recurring units differing in the relative position of the two substituting methylene groups, a different fractionation behavior is predictable in the low-molecular range insofar as the different solubility of isomeric oligomers possessing equal molecular weight would invariably result in the distribution of such isomers over several fractions, which hence would no longer be strictly monodisperse.

24) This effort has since been reported: E. W. Neuse, E. Quo, and W. G. Howells, *J. Org. Chem.*, **30**, 4071 (1965).

tetrachloride (deuteriochloroform for diferrocenylketone) and benzene; viscosities were measured in benzene.

Polycondensation Reactions: Formation of III.—Employing the equipment and general technique described in an earlier paper,[2] the mixtures of Mannich base I and ferrocene with the catalyst system were heated in the molar ratios and under the experimental conditions summarized in Table I. While the catalyst system in runs No. 1—3, 5 and 6 was anhydrous zinc chloride and concentrated aqueous hydrochloric acid, zinc chloride and water were used in Nos. 7—10, thus generating hydrochloric acid by hydrolysis.[1] In run No. 4, hydrochloric acid was introduced as the hydrochloride of I, with no water added to the system. From the reaction products, extraction with warm water removed catalyst residues and dimethylammonium tetrachlorozincate, as well as unreacted complexes IV and V. The crude polymer III was then reprecipitated from benzene[25] solution by excess 2-propanol. The solid precipitate, designated as first fraction, was washed with methanol and was dried for 10 days at 50°C in vacuo. The mother-liquor, combined with the alcoholic washings, was concentrated on a rotating evaporator to remove the major portion of benzene and was poured into excess water. The resinous precipitate was taken up in benzene, filtered and the solution evaporated to dryness. The orange-brown solid remaining after removal of admixed ferrocene by vacuum sublimation, composed of oligomeric material, was designated as second fraction. The analytical data for both fractions are collected in Table II. The first (higher-molecular) fractions dissolved readily in benzene, dioxane and chloroform; the second (oligomeric) fractions, in addition, showed enhanced solubility in aliphatic alcohols, ketones and hydrocarbons.

Subfractionation of polydisperse polymer (combined first and second fractions) by conventional precipitation procedures at 25±1°C, using benzene as solvent, resulted in separation of fractions possessing enhanced monodispersity. The precipitant was 2-propanol which was diluted increasingly with water as the fractionation proceeded. The total number of subfractions obtained in each series was 15—20; the last 8 of these, with molecular weights below 1000, were collected by stepwise concentrating the mother-liquor at 30°C in a rotating evaporator for benzene removal and allowing the solution to stand for 12 hr. at 25±1°C. The products gave analytical results comparable to those for the unsubfractionated polymers. For example, the highest subfraction isolated analyzed as follows: C, 66.83; H, 5.17; Fe, 27.49%; M_n, 11200 (Calcd. for III: C, 66.68; H, 5.09; Fe, 28.23%), while for a typical oligomeric subfraction the findings were: C, 65.77; H, 5.20; Fe, 29.02%; M_n, 690 (Calcd. for III: C, 66.12; H, 5.18; Fe, 28.70%).

Chromatographic Oligomer Separation.—For the chromatographic separation of dinuclear and trinuclear III, low-molecular fractions were extracted with cyclohexane, thus taking up only compounds with M_n essentially below 1000—1100. In a typical run, employing 2.0 g. of the second fraction from experiment No. 5 (Table II), a cyclohexane solution (20 ml.) was prepared, from which 0.19 g. of higher-molecular III (Found: C, 66.70; H, 5.23; Fe, 28.10%; M_n, 1840) was separated by filtration. The filtrate was chromatographed under light protection on Alcoa grade F-20 alumina partially deactivated by 12 hr. exposure to air of 40% r.h., using hexane as eluent. After elution of traces of ferrocene not previously removed by sublimation, there was eluted a second band containing 0.63 g. of diferrocenylmethane, m. p. 147—149°C (from 2-propanol). X-Ray diffractogram, Å: 5.05, 5.69, 4.88, 6.13, 4.21, 4.27. Upon fusing at 160°C and re-cooling, the compound crystallized in a different system (X-ray diffractogram, Å: 5.18, 5.88, 5.66, 4.81, 4.58, 4.45); this modification was occasionally found intermixed with the stable form crystallizing from 2-propanol. A third modification crystallized from hexane (X-ray diffractogram, Å: 4.80, 5.09, 9.60, 4.20). All modifications showed the same melting point and analytical data (Found: C, 65.67; H, 5.27; Fe, 28.86%; mol. wt. 370. Calcd. for $C_{21}H_{20}Fe_2$: C, 65.67; H, 5.25; Fe, 29.08%; mol. wt. 384). By treatment with selenium(IV) oxide in refluxing benzene (10 hr.), the compound was oxidized in 48% yield to diferrocenylketone, reddish needles, m. p. 206—210°C (sealed; lit.[16,17]: 204°C, 210—211°C).

Elution of a third orange band gave 0.53 g. of the crude trinuclear isomer mixture (III, $n=2$), melting range 100—145°C. Found: C, 66.20; H, 5.08; Fe, 28.66%; mol. wt. 550. Calcd. for $C_{32}H_{30}Fe_3$: C, 66.02; H, 5.19; Fe, 28.78%; mol. wt. 582; percent-homoannularity, 88.1 (the average of three values on fractions obtained in parallel chromatographic runs was 86.5). All subfractions obtained from this fraction by extended fractional crystallization, while varying in melting points, showed analytical and molecular weight data in the same ranges.

Two higher bands of the chromatogram gave only brittle, X-ray amorphous resins, from which no subfractions with $M_n<750$ were isolable by reprecipitation or crystallization.

25) In several parallel runs, peroxide-free dioxane was employed in lieu of benzene as solvent in the precipitation operation. Owing to the excellent water compatibility of this solvent, the second fractions could in these cases be isolated as tack-free solids, thus facilitating their work-up. This modification offered advantages in those reactions that gave predominantly oligomeric compounds and was, therefore, employed in condensations Nos. 6 and 10 (Table I). In general, however, use of benzene was preferred because of enhanced purity of the polymer fractions collected.

This investigation was conducted by the Douglas Aircraft Company under company-sponsored research and development funds. The authors gratefully acknowledge the assistance of Mr. E. Quo in the experimental work, and of Messrs. H. N. Holland and C. F. Wissman in conducting some of the elemental and instrumental analyses.

BULLETIN OF THE CHEMICAL SOCIETY OF JAPAN VOL. 39 1508—1514 (1966)

Ferrocene-containing Polymers. IX. Polycondensation of Ferrocene with Formaldehyde[1]

By Eberhard W. NEUSE and Edward QUO

Polymer Laboratory, Missile & Space Systems Division, Douglas Aircraft Company, Inc. Santa Monica, California, 90406, U. S. A.

(Received December 15, 1965)

The Lewis acid-catalyzed polycondensation of ferrocene with formaldehyde or its dimethylacetal gives rise to the formation of soluble, novolac-type polymers comprising ferrocenylene units interlinked by methylene bridges. In contrast to earlier work performed by other investigators in liquid hydrogen fluoride or sulfuric acid media, where only non-polymeric products were described, propagation is accomplished in the present case by condensing the reactants in a closed system in bulk at temperatures up to 170°C. The resulting polymers, with M_n values up to 4000 (unfractionated), are shown by elemental and spectroscopic analyses and viscometric data to be essentially identical with the previously reported polycondensation products of *N*, *N*-dimethylaminomethylferrocene with ferrocene. Infrared spectroscopy shows the intralinear substitution to be predominantly homoannular, which is expected as a result of the electronic effects exercised by the methylene substituent. Under appropriate conditions, additional methylene groups can be incorporated into the polymer, giving rise to double-bridged segments and inter-chain bridging. Strongly crosslinked polymers are obtained if excess aldehydic reactant is employed at temperatures in the 170—185°C range.

It has been shown in a recent paper[2] that ferrocene can be polycondensed with benzaldehyde in the melt phase to give polymers essentially conforming to structure I. This smooth generation of I from ferrocene and benzaldehyde suggested utilization of the same synthetic procedure for the preparation of the analogous, novolac-type polymer II obtained earlier[3] by polycondensation of *N*, *N*-dimethylaminomethylferrocene with ferrocene. However, all attempts in the previous work[2] to prepare this polymer by the direct condensation of ferrocene with formaldehyde (*s*-trioxane, paraformaldehyde, dimethoxymethane) failed. Neither in bulk nor in solution, employing various aliphatic or aromatic hydrocarbon solvents, could defined polymeric products be isolated.

It has now been found that under appropriate conditions, using a closed system, polycondensation of ferrocene with formaldehyde in its various forms can be enforced. This reaction, which is described in the present paper, leads to polymeric reaction products and is, thus, in contrast to ferrocene-formaldehyde condensations performed by other workers[4-8] in liquid hydrogen fluoride or sulfuric acid media, where only monomeric reaction products were reported.[8a]

Results

The polycondensation of ferrocene with formaldehyde leading to polymer II may be expressed by the summarizing Eq. 1.

When ferrocene was heated in sealed tubes with *s*-trioxane or paraformaldehyde in the presence of Lewis acids, polycondensation according to Eq. 1 was indeed observed. However, under all conditions of temperature, time, and catalyst type and concentration employed, polymer yields were generally low (25—50%) owing to side-reactions involving self-polymerization of the aldehyde and crosslinking. In contrast, good results were obtained by using the dimethyl acetal of formaldehyde, dimethoxymethane (formal). This

1) The work presented herein, briefly summarized in a recent note (*Nature*, **204**, 179 (1964)), was conducted by the Douglas Aircraft Company under company-sponsored research and development funds. The assistance of Messrs. R. C. Baird and R. J. Dimarzo in performing the iron analyses and scanning the infrared spectra is gratefully acknowledged. The authors are also indebted to Mr. C. A. Seil for many stimulating discussions on this subject.

2) E. W. Neuse and D. S. Trifan, Abstr. of papers presented at 148th National Meeting, Am. Chem. Soc., 1964, p. 5S.

3) E. W. Neuse and K. Koda, This Bulletin, **39**, 1502 (1966).

4) V. Weimayr, *J. Am. Chem. Soc.*, **77**, 3009 (1955).

5) A. N. Nesmeyanov and I. Kritskaya, *Izv. Akad. Nauk SSSR, Otd. Khim. Nauk*, **1956**, 253.

6) R. Riemschneider and D. Helm, *Chem. Ber.*, **89**, 155 (1956).

7) K. L. Rinehart, Jr., C. J. Michejda and P. A. Kittle, *J. Am. Chem. Soc.*, **81**, 3162 (1959).

8) P. L. Pauson and W. E. Watts, *J. Chem. Soc.*, **1962**, 3880.

8a) While this manuscript was in print, we became aware of a note by H. Valot, *Compt. rend.*, **258**, 5870 (1964), describing the isolation of polymers under conditions of sulfuric acid condensation.

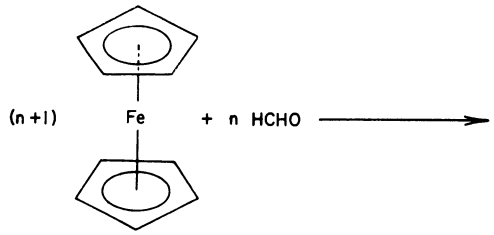

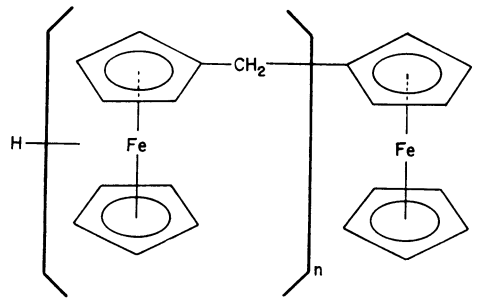

+ n H_2O (1)

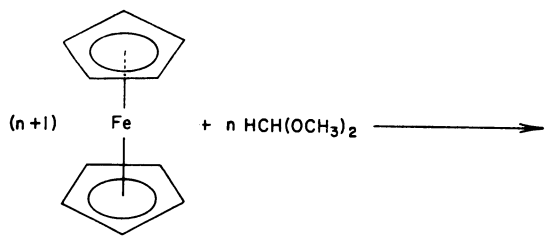

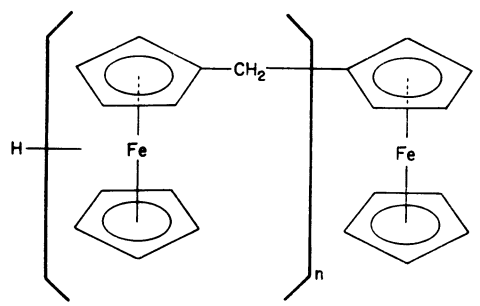

+ 2n CH_3OH (2)

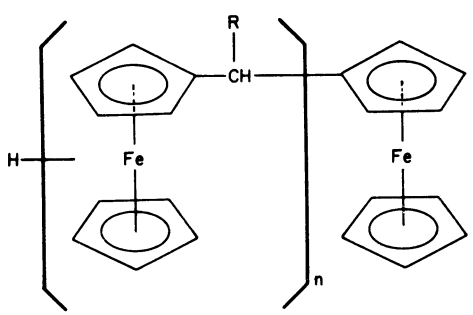

I, R=C_6H_5
II, R=H

compound was therefore employed as the aldehyde-furnishing reactant throughout the present work, and the summarized polycondensation course may accordingly be depicted by Eq. 2.

The reactions (8—12 hr., 150—170°C) were carried out in sealed tubes or high-pressure autoclaves, using zinc chloride as catalyst in concentrations ranging from 3 to 20% by wt. of ferrocene. Under such conditions, and at equimolar or near-equimolar ratios of the reactants, overall conversions were generally in the 55—70% range. At temperatures substantially lower than 150°C, only oligomers were isolable in low yields, whereas temperatures markedly higher than 170°C led to

Table I

Expt. No.	Molar ratio Ferrocene/Acetal	Catalyst type and concentration,[a] % $ZnCl_2$	% $AlCl_3$	Temp. °C	Time hr.	Total crude yield of soluble condensation products,[b] %	Yield of insoluble matter[a] %
1	1 : 0.8	5	—	170	10	53.7	< 1
2	1 : 1.0	5	—	170	9	59.5	< 1
3	1 : 1.0	10	—	170	6	64.4	< 1
4	1 : 1.2	5	—	170	9	60.9	< 1
5	1 : 1.4	5	—	165	10	66.2	< 2
6	1 : 1.7	10	—	130	5	46.9	10.4
7	1 : 1.0	5	—	180	12	72.9	< 2
8	1 : 1.0	—	10	170	3	27.0	68.3
9[c]	1 : 2.0[d]	10	—	170	6	80.4	6.1
10[c]	1 : 0.64[e]	10	—	170	10	84.8	2.2

a) By wt. of ferrocene (of starting material in Nos. 9, 10).
b) Combined yields of first and second fractions.
c) Post-condensation of oligomer.
d) Molar ration oligomeric II (M_n 780)/acetal.
e) Molar ration oligomeric II (M_n 260)/acetal.

Table II

Expt. No.	Fraction[a]	M_n	M.p.[b] °C	Yield %	Calcd. for II C, %	Calcd. for II H, %	Calcd. for II Fe, %	Found C, %	Found H, %	Found Fe, %
1	1st	860	70	19.8	66.24	5.16	28.60	66.27	5.10	28.51
	2nd	590	95	33.9	66.02	5.19	28.79	65.86	5.07	28.69
2	1st	1320	110	20.3	66.41	5.13	28.46	66.63	5.30	28.14
	2nd	650	90	39.2	66.10	5.18	28.72	66.23	5.25	28.47
3	1st	1570	110	29.0	66.45	5.13	28.42	66.19	5.23	28.37
	2nd	590	85	35.4	66.02	5.19	28.79	66.49	5.42	28.19
4	1st	2190	130	40.5	66.52	5.12	28.36	66.33	5.19	28.06
	2nd	500	105	20.4	65.90	5.21	28.89	66.43	5.42	28.52
5	1st	2250	125	42.7	66.53	5.12	28.35	66.63	5.16	28.08
	2nd	630	85	23.5	66.07	5.18	28.75	66.14	5.46	28.10
6	1st	2140	120	27.9	66.52	5.12	28.36	66.28	5.18	28.29
	2nd	670	90	19.0	66.10	5.18	28.72	66.22	5.19	28.60
7	1st	2370	120	51.7	67.25[c]	5.01[c]	27.74[c]	67.46	5.29	27.58
	2nd	510	100	21.2	65.92	5.21	28.87	66.50	5.50	28.63
8	1st	3900	155[d]	20.9	66.61	5.10	28.29	66.50	5.38	26.88
	2nd	980	60	6.1	66.30	5.15	28.55	66.06	5.38	27.70
9	1st	1870	140[e]	61.6	66.49	5.12	—	66.33	5.11	—
	2nd	810	65	18.8	66.22	5.17	28.61	66.41	5.36	28.21
10	1st	1130	90	58.1	66.35	5.14	28.51	66.08	5.25	—
	2nd	540	90	26.7	66.96	5.21	28.83	66.58	5.37	28.53

a) First and second fractions; see text.
b) Upper limiting value of melting range.
c) Calculated for polymer with four additional methylene groups per molecule (see text).
d) Sintering only.
e) Very large range, indicating wide molecular weight distribution.

polymers with compositions deviating from the desired structure II.

Table I summarizes the reaction conditions and resulting polymer yields for a number of typical experiments. The reactions listed were performed in an autoclave to establish conditions more suitable for large-scale preparations. For small-scale condensations conducted in ampoules, correspondingly shortened reaction times sufficed. The reaction products were worked up by earlier described procedures[3] and were collected as two fractions: a first fraction composed of higher-molecular polymer and a second fraction containing oligomeric condensation products. All pertinent analytical data for the two fractions are compiled in Table II.

An inspection of the first three experiments listed, in which no excess aldehyde was employed, clearly shows the agreement in elemental composition of

the condensation products with the anticipated structure II. Due to the presence of unreacted starting materials in the equilibrium ultimately attained, this agreement is evident even for the reaction products of such condensations (Nos. 4, 5, and especially 6) in which the acetal was employed in excess over the equimolar amount at temperatures low enough to prevent entire utilization of this reactant.

With temperatures in these reactions further increased, however, the products of polycondensation showed changes in composition distinctly detectable by elemental analysis. This is demonstrated, for instance, in experiment No. 7, in which the temperature was raised to 180°C; after 12 hr. of total heating time, the resulting polymer was found to contain as many as four $-CH_2-$ bridges[9] per molecule (M_n 2370) in excess over the number required for structure II.

For comparison, a reaction employing aluminum chloride as catalyst is included in the tables as No. 8; again, the ratio of the reactants was equimolar. The drastic increase in insoluble matter at the expense of soluble polymer resulting from crosslinking and partial destruction of the ferrocene molecule is clearly demonstrated by the analytical and yield data presented. In view of earlier communications[10-15] describing the reaction of ferrocene with aluminum chloride in chlorohydrocarbon solution, the observed effects of this Lewis acid under the presently applied conditions are not unexpected. Both Rosenberg[10,11] and Nesmeyanov[12-14] with their co-workers have shown such ferrocene derivatives to contain cyclopentyl and cyclopentenyl groups stemming from partial ferrocene cleavage. If a similar cleavage and ensuing cyclopentenyl substitution is assumed in the present case,[16] the observed crosslinking reactions might in part be explicable in terms of a polymerization mechanism involving double bonds of the cyclopentenyl rings. The major portion of crosslinks, however, was probably formed by inter-chain bridging through methylene groups as will be discussed below in detail.

On a combined polymer batch composed of fractions consistent in elemental composition with structure II, a subfractionation by precipitation and crystallization was performed as described loc. cit.[3] for the Mannich base-ferrocene polycondensation product. The 16 subfractions collected showed M_n values up to 10000 and corresponded in composition to II much as did the parent material. Chromatography of the final, lowest-molecular subfraction gave a compound shown to be identical in melting point and X-ray diffractogram with diferrocenylmethane (II, $n=1$).[3,8,17] These findings confirm the compositional identity of the present polymer with the earlier product[3] derived from *N*, *N*-dimethylaminomethylferrocene. Corroborative evidence for this identity arose from spectroscopic data, the infrared spectra recorded on comparable subfractions of both products being strictly superimposable. In addition, the viscosity-molecular weight correlation[3,18] for both products was found to be the same within experimental error, as was the relationship between intensity of the 9 μ infrared band (in terms of percent-homoannularity[2,3,19]) and number-average molecular weight depicted by the curve in Fig. 1. The coincidence of the plots in the latter case attests to the essentially identical branching pattern and substitution orientation along the polymer backbone. The trend of the graph in Fig. 1, predominantly homoannular in the oligomeric range and gradually approaching a minimum value of the percent-homoannularity, suggests[2,19] an increase in the degree of branching with rising molecular weight, this branching preferentially occurring on those ferrocene rings that are not part of the chain proper.

Figure 2 represents a plot of melting point (upper limit of melting range) against M_n, determined again

9) Incorporation of additional methylene bridges was accompanied by competing crosslink formation if, under heating conditions similar to those above, acetal concentrations substantially higher than equimolar were applied. Thus, at an acetal/ferrocene molar ratio of 1.4 and a heating time of 14 hr. at 185°C, crosslinked polymer amounted to a total of 53.7% (by wt. of ferrocene), with soluble polymer simultaneously collected in 33.2% yield. With 100% molar excess of the acetal (acetal/ferrocene ratio=2), even at only three hours heating time at 170°C, the yield in soluble polymer decreased to 17%, while the major portion of condensation product was isolated as crosslinked matter. In each of these cases, both the crosslinked product and the corresponding soluble polymer portion were of practically the same elemental composition. Also their infrared spectra were practically identical except that slightly enhanced methylene bands were exhibited by the crosslinked compound. From this observation, a close structural relationship between the soluble polymers and their crosslinked counterparts must be inferred, with the latter types differing in their structural build-up from the former merely by the existence of inter-chain methylene bridges.

10) S. G. Cottis and H. Rosenberg, *Chem. & Ind.*, **1963**, 860.

11) S. G. Cottis and H. Rosenberg, *J. Polymer Sci.*, **2B**, 295 (1964).

12) A. N. Nesmeyanov and N. S. Kochetkova, *Dokl. Akad. Nauk SSSR*, **126**, 307 (1959).

13) A. N. Nesmeyanov, N. S. Kochetkova and R. B. Materikova, ibid., **136**, 1096 (1960).

14) A. N. Nesmeyanov, N. S. Kochetkova, P. V. Petrovsky and E. I. Fedin, ibid., **152**, 875 (1963).

15) S. I. Goldberg, *J. Am. Chem. Soc.*, **84**, 3022 (1962).

16) Evidence for such reaction coures not only in $AlCl_3$-catalyzed condensations, but even in the conventional cases employing $ZnCl_2$, rests on the broad, albeit weak proton signals occasionally observed near τ 8 in the NMR spectra of oligomeric fractions.

17) K. Schlögl and A. Mohar, *Monatsh. Chem.*, **92**, 219 (1961).

18) E. W. Neuse and E. Quo, *J. Polymer Sci.*, **A3**, 1499 (1965).

19) E. W. Neuse and D. S. Trifan, *J. Am. Chem. Soc.*, **85**, 1952 (1963).

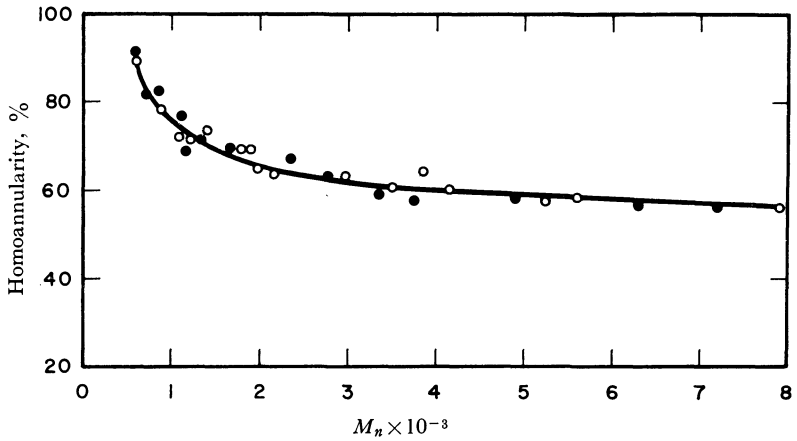

Fig. 1. Percent-homoannularity vs. number-average molecular weight for polymer II prepared by co-condensation of ferrocene with:
Formaldehyde (filled-in circles);
N, *N*-Dimethylaminomethylferrocene (open circles).

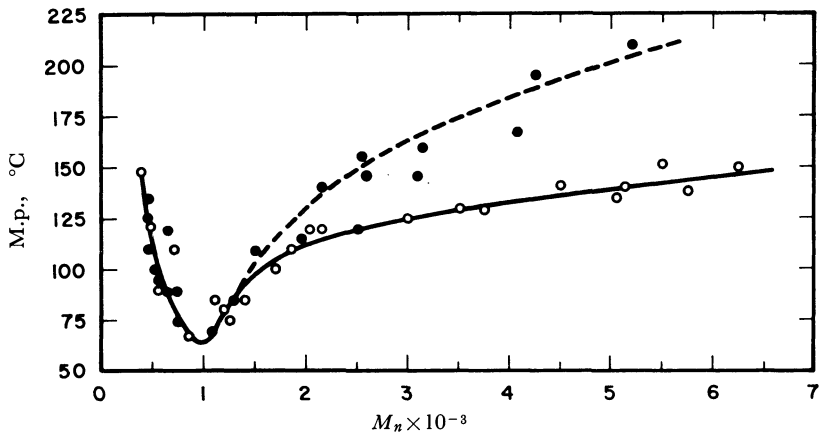

Fig. 2. Melting point vs. number-average molecular weight for polymer II prepared by co-condensation of ferrocene with:
Formaldehyde (dashed line, filled-in circles);
N, *N*-Dimethylaminomethylferrocene (solid line, open circles).

on subfractionated samples. As expected, the curve passes through a minimum in the oligomer range. In the M_n range above ~1500, it ascends more steeply than does the corresponding curve replotted for the Mannich base-ferrocene polycondensation product,[3] pointing to some structural differences to be discussed below.

Discussion

If, in the reaction of ferrocene with formaldehyde or its dimethyl acetal, one assumes the intermediary occurrence of hydroxymethylferrocene or its methyl ether, methoxymethylferrocene, much as in the analogous case of ferrocene-benzaldehyde condensation,[2] the various propagation and termination steps comprised by the summarizing Eqs. 1 and 2 may be visualized as follows:

The primary step is the Lewis acid-catalyzed generation of ferrocenylcarbinyl cations from hydroxymethyl- or methoxymethylferrocene. For these cations, in principle, the same four reaction steps are available as in the self-condensation of ferrocenyl carbinols discussed at greater length elsewhere.[19] However, because of the low instantaneous concentrations of the hydroxymethyl- or methoxymethylferrocene intermediate expected under the experimental conditions (their further reaction proceeding at a rate considerably higher than their rate of formation[2]), the first two of these reaction steps, interaction with oxygen-containing species, will be irrelevant as compared to the third step, nuclear substitution of oxygen-free species. The latter step comprises the primary

reaction of the cation with free ferrocene present initially in large excess over carbinol, ether or polynuclear species. The arising dinuclear derivative, diferrocenylmethane (II, $n=1$), will now compete with ferrocene for further nuclear attack by the carbinyl cation, thus resulting in trinuclear and, as propagation proceeds, in polynuclear II. In this propagation step, the effects of the methylene group on the position of the entering ferrocenylmethyl substituent will be much the same as those operative in the analogous Mannich base - ferrocene polycondensation,[3] an assumption which is borne out by the coinciding percent-homoannularity - M_n plots for the two polymer series (Fig. 1). In addition to the prevalent propagation step involving electrophilic attack by the ferrocenylcarbinyl cation on ferrocene and the oligomeric and polymeric homologs of II, primary reaction of aldehyde or acetal with ferrocene units of II to give methylol- or methoxymethyl-substituted II must be expected in an advanced stage of the condensation. The cations generated therefrom may react intramolecularly, i. e., in a terminating self-substitution reaction (step 4 in the earlier quoted paper[19]; cf. restrictions discussed therein), resulting in double-bridged segments.[18] Competing with this self-substitution, they may also react intermolecularly, i. e., by attack on a different polymer molecule. If both the cationic site and the ferrocene unit attacked are in terminal position, as expected to be the predominant case during an early stage of the reaction, the result will be linear chain extension. In an advanced stage, with increasing probability of cationic site and/or attacked ferrocene unit being in an internal position, side-chain or crosslink formation will result. The occurrence of side-chain and inter-chain methylene bridging as a result of the latter reaction course must be expected accordingly in all higher-molecular fractions and is manifested experimentally in both the aforementioned trend of the curve in Fig. 1 and the higher ordinate values (in the M_n range beyond $\sim$1500) of the curve in Fig. 2 (filled-in circles) as compared to the corresponding plot (open circles) for the Mannich base-derived polymer. Such side-chain and inter-chain methylene bridge formation will become progressively important as excess aldehydic reactant is employed at elevated temperatures. The increased amounts of crosslinked polymer isolated in such typical experiments mentioned initially in which molar acetal/ferrocene ratios of 1.4—2.0 were employed at temperatures ranging from 170 to 180°C bear out this expectation.[20]

Considering the low average molecular weight range, notably of the second fractions, attained under the conditions of our closed-system experiments, it was of interest to investigate the possibility of post-condensing these low-molecular-weight products with aldehydic reactant. Such post-condensation would be expected to proceed as pointed out above, viz. through formation of methylol- or methoxymethyl-substituted II, followed by nuclear attack of the cations arising therefrom on a different polymer chain, thus resulting in distinctly increased molecular weights. In a series of experiments employing fractions of polymer II with M_n in the low 300—800 range the feasibility of such post-condensation could indeed be demonstrated. Again, the zinc chloride-catalyzed reactions were conducted in a closed-system under conditions similar to those applied in the primary condensations, formaldehyde being employed as its dimethyl acetal in concentrations ranging from 0.5 to 2 mol. per mol. of oligomer employed. A typical experiment is summarized as No. 9 in Table I. The analytical data collected for the reaction product in Table II show that the starting material, a fairly monodisperse fraction with M_n 780, was largely converted to higher-molecular polymer still exhibiting the elemental composition of II. These results suggested the direct utilization, without prior removal of the unreacted ferrocene, of the very low-molecular, crude second fractions obtained in experiments of the types listed as Nos. 1 through 7 in Table I. The post-condensation of such fractions, with concomitant partial consumption of the admixed ferrocene, is demonstrated by experiment No. 10. By circumventing the time-consuming removal of ferrocene by sublimation from the remainder of oligomers in the second fractions, the possibility of such post-condensations of ferrocene-containing oligomer batches may add to the economy of the closed-system condensations here described.

Experimental

Materials and Analytical Procedures.—*s*-Trioxane, paraformaldehyde and formal (dimethoxymethane) were used as received from commercial sources. Zinc chloride, ferrocene and solvents, all commercial products, were purified as described.[18,19] Procedures for elemental and instrumental analyses have also been presented earlier.[3,18]

Polycondensation Reactions.—The experiment described below, summarized as No. 4 in Tables I and II, exemplifies the conventional syntheses in which

20) While the products arising from branching and single-bridge crosslinking reactions cannot be distinguished by elemental analysis from linear II, the self-substitution products (and also those structures arising from multiple inter-chain bridging), possessing additional methylene groups, deviate in composition from II and thus lend themselves to analytical characterization, provided the number of such methylene groups additionally incorporated is large enough to exceed the experimental error limits of analysis. As a typical example of products which elemental analyses show to contain double-bridged segments, i. e., CH_2 bridges in excess over the number required for structure II, the experiment listed as No. 7 in Table I was mentioned above.

the aldehydic component was employed as the acetal.[21] The reactor was a stainless steel-lined, high-pressure autoclave of 1 l. capacity, equipped with mechanical stirrer, thermometer well and thermocouple, bleeding valve, and a special safety head (rupture disc tested to 3500 psi). The vessel was flushed with dry nitrogen and was charged with the mixture of 372.1g. (2.0 mol.) of ferrocene and 18.6 g. of anhydrous zinc chloride previously ground together in a dry-box. Upon the addition of 183.0 g. (2.4 mol.) of dimethoxymethane pre-cooled to 0°C, the sealed autoclave was heated with stirring for 9 hr. at 170±2°C. The reaction product was thoroughly digested and washed with water and, after drying, was reprecipitated from benzene solution (280 ml.) by 2-propanol (4 l.). Reprecipitation in the same manner gave a yellow solid which was washed with 2-propanol and vacuum-dried for 10 days at 60°C. This portion of polymer II, 159.6 g. (40.5% yield), is listed as lst fraction in Table II. From the combined and concentrated mother-liquors and washings, a mixture of oligomeric II and ferrocene was precipitated by excess water. From the dried product, ferrocene was removed by vacuum sublimation (81.7 g. recovered). The orange-yellow residual solid, 79.0 g. (20.4% yield), is listed in Table II as 2nd fraction. In a parallel experiment, 65.0 g. of the crude second precipitate still containing the admixed ferrocene was chromatographed in the manner described in detail loc. cit.[3] to give 32.40 g. of ferrocene, m. p. 173—176°C; 14.65 g. of diferrocenylmethane, m. p. 143—146°C; and 5.86 g. of crude trinuclear isomer mixture, melting range 95—145°C.

Subfractionation of II was accomplished by fractional precipitation and crystallization as discussed previously,[3] employing a polymer batch containing portions of the first and second fractions stemming from runs No. 4 and 5. The 16 subfractions collected, with M_n values ranging from 410 to 9850, gave elemental analyses consistent with II and showed the same infrared spectroscopic and solubility behavior as did the analogous fractions of the Mannich base - ferrocene polymer.[3] Some of these fractions were used for the viscometric measurements and the plots in Figs. 1 and 2.

For analytical rather than preparative purposes, several condensations were conducted using glass ampoules or stainless steel tubes in lieu of the high-capacity autoclave. Batch sizes for glass-tube reactions ranged from 5 to 30 g., whereas the steel tubes allowed for 50—200 g. batches. The solid components were well ground together in a dry-box and were placed in the tubes inserted into a dry ice - acetone bath. Upon addition of the liquid acetal (when using the solid paraformaldehyde or trioxane, all components were directly mixed and charged into the tube), the tube contents were frozen and degassed in the conventional manner. The re-cooled tubes were then flushed with dry nitrogen, sealed and heated in a thermo-regulated aluminum block, and the reaction products were worked up as described. These products showed no essential deviations in elemental composition from the corresponding polymers prepared in autoclave reactions.

Post-condensation of Oligomeric II with Formaldehyde.—The experiment described here, listed as No. 10 in Table I, may illustrate the post-condensations of low-molecular II. The well-ground mixture of 40.0 g. of anhydrous zinc chloride and 400.0 g. (1.563 mol.) of oligomeric II still containing ferrocene (M_n 260) was placed in the nitrogen-flushed autoclave. Upon the addition of 76.09 g. (1.0 mol.). of pre-cooled dimethoxymethane, the vessel was closed and heated at 170±2°C for 10 hr. with stirring as described. The reaction product was worked up in the conventional manner. The first and second fractions obtained in yields of 240.6 g. (58.1%) and 109.3 g. (26.7%) respectively, showed the melting point and analytical data collected in Table II.

21) Experiments employing formaldehyde in its solid, polymeric form (paraformaldehyde, *s*-trioxane) rather than as its acetal were conducted in the same manner as described above, except that the pulverized aldehyde was immediately ground together with ferrocene and catalyst. In these reactions, large amounts of insolubles were formed, and the polymers, obtained in yields up to 50%, showed elemental compositions less satisfactory than in the ferrocene-formal condensations tabulated. A typical reaction product (6 hr., 170°C, 10% $ZnCl_2$, equimolar ratio ferrocene/trioxane) analyzed as follows: C, 67.50; H, 5.23, Fe, 25.99%; M_n, 1960 (calcd. for II: C, 66.51; H, 5.12; Fe, 28.37%).

BULLETIN OF THE CHEMICAL SOCIETY OF JAPAN VOL. 39 1515—1519 (1966)

Specific Effects in Acid Catalysis by Polymeric Sulfonic Acids in the Hydrolysis of Some Carboxylic Esters[1)]

By Sadao YOSHIKAWA and Oh-Kil KIM

Department of Synthetic Chemistry, Faculty of Engineering, The University of Tokyo, Hongo, Tokyo

(Received October 5, 1965)

The catalytic effects of polymeric sulfonic acids in ester hydrolysis in aqueous acetone were inferior to that of hydrochloric acid. However, the hydrolysis rate was accelerated by increasing the water content of acetone-water mixtures, and, in a water solution, polymeric sulfonic acids were much more effective catalysts. Furthermore, the catalytic efficiency of polymeric sulfonic acid in ester hydrolysis in water increased with the length of the ester molecule. The polymeric sulfonic acid with a strong hydrophobic character was more effective; 69% sulfonated polystyrenesulfonic acid, for example, hydrolyzed methyl hydrogen azelate in water over five times more rapidly than hydrochloric acid. The specificity thus obtained suggests that, in the hydrolysis of electrically-neutral esters in water, ester molecules are concentrated in the neighborhood of the polymer by the hydrophobic interaction between catalyst and substrate. Besides, in the hydrolysis of aliphatic esters catalyzed by polyvinylsulfonic acid in 50% aqueous acetone, there was a linear relationship between the reciprocal of the rate constant and the intrinsic viscosity of the polymer, while in the case of polystyrenesulfonic acid hardly such any relationship was found. These remarkably different behaviors of the two kinds of polymer catalysts should be attributed to the difference in the expansion of the polymer chain in solutions.

The acid-catalyzed hydrolysis of esters by polymeric sulfonic acids, as previously reported by others,[2)] has been carried out mostly in heterogeneous systems with cross-linked sulfonated polystyrene resins. Therefore, there is some difficulty in estimating and discussing precisely the catalytic activity relating to the molecular structure of the polymer in solutions.

It is the aim of the present paper to report on the specific behavior of water-soluble polymeric sulfonic acids in the hydrolysis of esters in various medium compositions of the homogeneous solution. The sulfonic acids were prepared by different polymerizing processes from their respective monomers, except sulfonated polystyrene sulfonic acid. Polymeric sulfonic acid is a strong polybasic acid comparable to sulfuric acid and protons are considered to be localized along the polymer chain. Hence, the proton density in solutions may be locally concentrated, unlike as in mineral acid. It may, therefore, be expected that if an interaction between the polymer catalyst and a substrate occurs, this interaction can be specifically changed according to the characteristics of the substrate and the outer solution used.

Experimental

Monomers.—Sodium vinylsulfonate was prepared from sodium β-bromoethanesulfonate and sodium hydroxide by modifying the patent directions.[3)] To 60 g. of sodium β-bromoethanesulfonate 29 g. of 40% sodium hydroxide was vigorously stirred drop by drop. During the addition the temperature was kept below 50°C. Further stirring was continued until the temperature fell to room temperature, and then the reaction mixture was neutralized with concentrated hydrochloric acid at 0—5°C. After large portions of sodium bromide had been filtered, an equal volume of alcohol was added to the filtrate at 0°C. Sodium vinylsulfonate was thus precipitated and filtered off. The yield was 24 g. (65% of the theoretical amount).

Potassium *p*-styrenesulfonate was prepared by the method of Wiley and Reed.[4)] To 65 ml. of chlorosulfonic acid at 0—5°C, there was added, drop by drop, 27.5 ml. (0.2 mol.) of β-bromoethylbenzene, which had been prepared according to the directions of Whitmore.[5)] After 30 min. the reaction mixture was poured onto ice with stirring in order to precipitate the sulfonyl chloride, which was then washed with ice water and taken up in ether. The ether solution was washed with dilute sodium bicarbonate and dried. The residue remaining on the evaporation of the ether was dissolved in 70 ml. of cold 95% ethanol. To this solution there

1) Dissertation submitted by Oh-Kil Kim in partial fulfillment of the requirement for the Ph. D. degree in the Graduate School of The University of Tokyo.

2) a) V. C. Haskell and L. P. Hammett, *J. Am. Chem. Soc.*, **71**, 1284 (1949); b) C. W. Davies and G. G. Thomas, *J. Chem. Soc.*, **1952**, 1607; c) P. Riesz and L. P. Hammett, *J. Am. Chem. Soc.*, **76**, 992 (1954); d) C. H. Chen and L. P. Hammett, ibid., **80**, 1329 (1958).

3) D. B. P. 836491, Farbwerker Hoechst, *Chem. Abstr.*, **47**, 2766 (1953).

4) R. H. Wiley and S. F. Reed, Jr., *J. Am. Chem. Soc.*, **78**, 2171 (1956).

5) F. C. Whitmore, C. H. Herr, D. G. Clarke, C. S. Rowland and R. W. Schiessler, ibid., **67**, 2059 (1945).

was slowly added a solution of 45 g. of potassium hydroxide in 200 ml. of 95% ethanol. This reaction mixture was refluxed for one hour and filtered. The solid thus collected was washed with an additional 100 ml. of hot ethanol and filtered. The combined filtrates were cooled to −20°C to precipitate the crude product. This crude product was dissolved in a minimum quantity of hot water and filtered. The filtrate was extracted with benzene and cooled to precipitate the product. A final recrystallization from 95% ethanol gave 13 g. (30% yield) of potassium *p*-styrenesulfonate.

The polymerizations of sodium vinylsulfonate and potassium *p*-styrenesulfonate were carried out with three different methods.

Poly(sodium vinylsulfonate) was obtained as follows:

a) PVSH(A): Five grams of sodium vinylsulfonate in 4.9 ml. of water was poured into an ampoule, chilled in ice, and evacuated to about 2 mmHg; the evacuation and pressuring with nitrogen were repeated, and then the ampoule was sealed. The polymerization was carried out by exposing the mixture to a ^{60}Co source yielding about 2×10^5 r./hr. for 72 hr. at 0°C. The resulting stickey solid was dissolved in 30 ml. of water and precipitated by adding 45 ml. of methanol. Treating the gummy precipitate with methanol yielded 3.5 g. (70% conversion) of a straw-colored polymer after it had been dried in vacuo over phosphorus pentoxide. The intrinsic viscosity*1 of the polymer was 12.8, and the molecular weight*1 was 20000.

b) PVSH(R)[6]: Twelve grams of a 50% sodium vinylsulfonate solution (6 g. of sodium vinylsulfonate) containing 0.075 g. of potassium persulfate and 0.023 g. of sodium bisulfite was poured into an ampoule; the ampoule was evacuated and pressured repeatedly with nitrogen, and then sealed. The ampoule was tumbled in a bath at 18°C for 72 hr. The resulting viscous oil was dissolved in 30 ml. of water and precipitated with 45 ml. of methanol; 4.08 g. of a polymer was obtained after drying in vacuo over phosphorus pentoxide. The intrinsic viscosity was 7.20, and molecular weight was 12000.

c) PVSH(S): Five grams of the finely-powdered and dried crystalline sodium vinylsulfonate was sealed in an ampoule and exposed to a ^{60}Co source yielding about 2.5×10^5 r./hr. for 72 hr. at room temperature. The irradiated crystals, after precipitation with 70% aqueous methanol in the usual fashion to remove the monomer, gave 2.5 g. of a polymer. The intrinsic viscosity and the molecular weight of the polymer were 1.70 and 3000 respectively.

Poly(potassium *p*-styrenesulfonate) was obtained as follows:

a) PSSH(A): Four grams of potassium *p*-styrenesulfonate in 16 ml. of water was poured into an ampoule. Polymerization was carried out in the same manner as in PVSH(A). After exposure to γ-radiation for 72 hr. at room temperature, the polymer formed was precipitated from 70% aqueous dioxane. Drying the precipitates in vacuo over phosphorus pentoxide, yielded 2.5 g. of a polymer. The intrinsic viscosity*2 of the polymer was 42.0.

b) PSSH(R)[7]: Five grams of potassium *p*-styrenesulfonate in 15 ml. of water was taken into an ampoule, and then a solution of 1.35 g. of potassium persulfate (2.66% based on the monomer) and 0.66 g. of sodium bisufite (1.34% on the monomer) in 2 ml. of water was added as an initiator. The ampoule was then evacuated and sealed in the usual fashion. The polymerization was carried out under tumbling in a bath at 18°C for 72 hr. The resulting viscous oil was precipitated from 70% aqueous dioxane; 3.2 g. of polymer was obtained after drying in vacuo over phosphorus pentoxide. The intrinsic viscosity was 30.7.

c) PSSH(S): Five grams of finely-powdered and dried crystalline potassium *p*-styrenesulfonate was sealed in an ampoule and exposed to a ^{60}Co source yielding about 2.5×10^5 r./hr. for 72 hr. at room temperature. The irradiated crystals yielded 2.3 g. of polymer after it had been precipitated with 75% aqueous methanol and dried according to the usual manner. The intrinsic viscosity was 18.09. All the sodium and potassium polymer sulfonates were completely converted into free acids by passing them through a column of cation exchange resin in hydrogen form, such as Amberlite IR-120.

The sulfonation of polystyrene was carried out using the addition-compound of sulfur trioxide and dioxane by the method described by Signer and his co-workers.[8] The addition-compound was easily formed by the addition of one mole of sulfur trioxide to one mole of dry dioxane. To the finely-divided suspension of the adduct, consisting of 20 g. of sulfur trioxide and 26 ml. of dioxane in 140 ml. of dichloroethane, a solution of polystyrene ($\overline{M}_w=15\times10^4$) in 140 ml. of dichloroethane was added in one portion; then the mixture was agitated for several minutes. The sulfonation proceeded to 69% after the mixture had stood at 20°C for 24 hr. The reaction was stopped by the addition of water. The polymer was dissolved easily in water and neutralized with sodium hydroxide. The sulfonated polymer salt was dialysed to remove sulfuric acid through a semipermeable membrane by keeping it in distilled water. The specific conductivity of the outer solution dropped below $3\times10^{-5}\cdot ohm^{-1}\cdot cm^{-1}$ after a period of one month. The dialysed sulfonated polymer salt was converted into free acid through the ion exchange resin in hydrogen form in the usual method. The degree of the sulfonation of polystyrene was determined by both gravimetric and elementary analyses of the sulfur atom. The two results corresponded satisfactorily.

Other Reagents.—The esters and acetone were obtained commercially (except methyl hydrogen succinate, methyl hydrogen glutarate and ethyl hydrogen adipate) and were further fractionated in a thirty-inch column of glass helices. Methyl hydrogen succinate was prepared according to the procedure of Cason,[9] by

*1 The value of intrinsic viscosity of poly(sodium vinylsulfonate) was determined in 0.5 N sodium chloride solution at 20°C and the molecular weight was calculated by K. Dialer and R. Kerber, *Makromol. Chem.*, **17**, 56 (1956).

*2 The value of intrinsic viscosity of poly (potassium *p*-styrenesulfonate) was determined in 2 N sodium hydroxide solution at 20°C.

6) D. S. Breslow and A. Kutner, *J. Polymer Sci.*, **27**, 295 (1958).
7) R. H. Wiley, N. R. Smith and C. C. Ketterer, *J. Am. Chem. Soc.*, **76** 720 (1954).
8) R. Signer, A. Demagistri and C. Müller, *Makromol. Chem.*, **18/19**, 139 (1956).
9) J. Cason, "Organic Syntheses," Coll. Vol. 3, 169 (1945).

the reaction of succinic anhydride and methanol (m. p. 57—58°C). Methyl hydrogen glutarate was prepared by the reaction of glutaric anhydride and methanol using the method described by Harris[10] (b. p. 158—165°C/23 mmHg). Methyl hydrogen adipate was prepared from adipic acid and methanol according to the procedure of Morgan and Walton[11] (b. p. 128°C/30 mmHg). The methyl hydrogen azelate was a gift of the Soda-Perfumery Co., Ltd.

Procedures.—The initial concentrations of esters and acid catalysts were adjusted to 0.2 mol./l. in acetone (or 0.05 mol./l. in water) and 0.08 N in water respectively. Three or four samples were used in each run, and each reaction mixture was made up of 4 ml. of the initially-adjusted ester in acetone (or water) and an equal volume of aqueous acid. The reaction mixtures were placed in 10 ml. glass-stoppered bottles suspended in a thermostat controlled to 45±0.01°C. The reaction was followed by withdrawing samples from the bath at suitable intervals, and by titrating the acid present with 0.05 N standard sodium hydroxide, using a phenolphthalein indicator. The first-order rate constants were calculated using the expression:

$$k=\frac{2.303\log a/(a-x)}{(\text{Catalyst})\,t}$$

where a is the initial ester concentration; x is the concentration of acid formed after time t, and (Catalyst) is the concentration of added polymeric sulfonic acid or hydrochloric acid. The catalytic efficiency, q, was defined as the ratio of the specific rate of hydrolysis catalyzed by polymeric sulfonic acid to that catalyzed by hydrochloric acid.

Results and Discussion

The catalytic effects of cross-linked sulfonated polystyrene resins are supposed to be appreciably different from those of water-soluble polymeric sulfonic acids because of cross-linking and particle size. The effects of particle size and cross-linking reported by Haskell and Hammett[2a] and Davies and Thomas[2b] suggested that the outer layers of the resin particles are responsible for much of the catalytic effect, the diffusion of non-electrolytes towards or away from the center of the particles being a slow process.

The results obtained in the present hydrolysis showed several new aspects by eliminating the complicating factors. The catalytic effects of polyvinylsulfonic acid (PVSH) and polystyrenesulfonic acid (PSSH) (polymerized by different methods) on the hydrolysis in 50% (v./v.) aqueous acetone were inferior to that of hydrochloric acid, especially PVSH, as is illustrated in Table I. The hydrolysis rate was, however, found to be accelerated by the increasing of volume % water in acetone-water mixtures. The hydrolysis rates

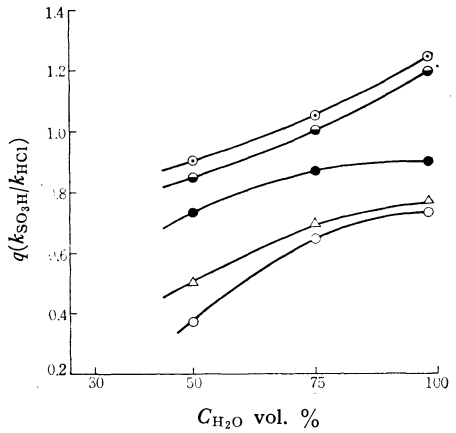

Fig. 1. Catalytic efficiencies of polymeric sulfonic acids for ethyl acetate in various mixtures of water and acetone at 45°C:
●, PVSH(S); △, PVSH(R); ○, PVSH(A); ⊙, PSSH(S); ◓, PSSH(A).

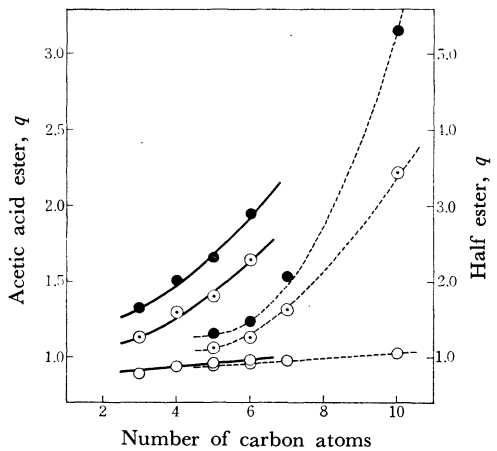

Fig. 2. Catalytic efficiencies of polymeric sulfonic aicds as a function of the chain length of acetic acid ester (solid line) and half ester (dotted line) hydrolyzed in water at 45°C (acid and ester concentrations are fixed at 0.04 and 0.025 mol./l., except 0.015 for phenyl acetate and 0.012 for methyl hydrogen azelate, respectively). Points on solid line are for methyl-, ethyl-, *n*-propyl-, *n*-butyl- and phenyl acetate and on dotted line are methyl hydrogen succinate, glutarate, adipate and azelate in increasing order:
●, (PS)SH (69%); ⊙, PSSH(S); ○, PVSH(S).

measured in the presence of varying acetone concentrations are plotted in Fig. 1. In a water solution polymeric sulfonic acids were much more efficient than hydrochloric acid. This tendency is apparent in polystyrenesulfonic acid. The catalytic efficiency, q, of polymeric sulfonic acids, especially partially-sulfonated polystyrene ((PS)SH), in ester hydrolysis in water increased with the

10) S. A. Harris, D. E. Wolf, R. Mozingo, G. E. Arth, R. C. Anderson, N. R. Easton and K. Folkers, *J. Am. Chem. Soc.*, **67**, 2098 (1945).
11) G. T. Morgan and E. Walton, *J. Chem. Soc.*, **1933**, 91.

Table I. The rates of hydrolysis of esters catalyzed by hydrochloric acid, polyvinylsulfonic acids and polystyrenesulfonic acid having different molecular weight in 50% (v./v.) aqueous acetone at 45°C

$k \times 10^3$ (l. mol^{-1} min^{-1})

Acid	$[\eta]$	Et. Ac.	Et. *n*-Bu.	Et. *n*-Capro.	Et. Ph. Ac.
PVSH(S)	1.7	14.62	7.23	5.10	5.06
PVSH(R)	7.2	9.51	5.12	2.61	3.29
PVSH(A)	12.8	7.30	3.79	1.84	2.03
PSSH(S)	15.3	18.09	8.01	5.22	6.26
PSSH(R)	30.7	—	7.21	5.27	5.96
PSSH(A)	42.0	16.80	7.16	5.12	5.92
(PS)SH (69%)	—	18.32	9.03	7.39	7.36
HCl		19.84	9.28	7.31	7.30

Table II. The rate difference in the hydrolysis of esters differing only in ester concentration in aqueous solution

$k \times 10^3$ (l. mol^{-1} min^{-1})

Ester	Me. Ac.		Et. Ac.		Me. H. Adip.		Me. H. Azel.
Acid	0.1	0.025	0.1	0.025	0.1	0.025	0.012 (mol./l.)
(PS)SH	42.59	46.85	49.02	51.01	44.58	50.87	128.02
PSSH(S)	39.04	40.10	44.66	44.63	32.44	37.52	77.53
PVSH(S)	30.38	31.94	32.67	32.22	20.53	22.10	25.60
PVSH(A)	27.68	29.10	26.14	26.85	15.45	16.57	16.27
HCl	35.49	33.02	36.31	33.56	22.07	23.02	23.93

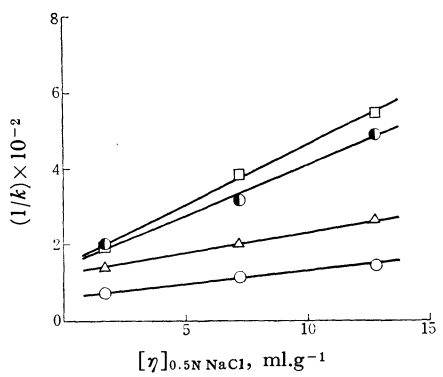

Fig. 3. Relation between hydrolysis rate of esters with PVSH and its intrinsic viscosity in 50% aq. acetone at 45°C:
○, ethyl acetate; △, ethyl *n*-butyrate;
◐, ethyl phenylacetate, □, ethyl *n*-caproate.

number of carbon atoms in the ester, as is shown in Fig. 2. The catalytic efficiency, q, of PVSH is closest to unity for every ester, while that of (PS)SH (69%), for example, is more than five for methyl hydrogen azelate. This contrasts remarkably with the reaction in aqueous acetone. The specificity thus obtained suggests that in aqueous acetone, because of the preferential solvation of the organic solvent with the polymer, hardly any interaction between the polymer and the ester occurs, while in water the hydrophobic interaction between the polymer catalyst and the substrate may become predominant and increase apparently with an increase in the hydrophobic character of the ester and the polymer molecule, such as (PS)SH (69%). Accordingly, it may result in an increase of the ester concentration in the neighborhood of the polymer chain by the hydrophobic interaction. Thus, the rate difference in PVSH and PSSH under these conditions should be attributed mainly to the hydrophobic character of the molecule.

The above interpretation is supported by the facts that cross-linked sulfonated polystyrene resin absorb organic solvents preferentially rather than esters in the mixed solvents, while esters or organic acids in a water solution are positively adsorbed on the resin in proportion to the length of the carbon atoms.[12]

Furthermore, the catalytic activity of PVSH in the hydrolysis of several aliphatic esters depends on the molecular weight of the polymer catalyst in 50% aqueous acetone more distinctly than it does in water. There was a linear relationship between the reciprocal of the rate constant and the intrinsic viscosity of the polymer, while hardly any such relationship was detectable in the presence of PSSH and (PS)SH (69%). A plot of $1/k$ against $[\eta]$ is shown in Fig. 3.

It is believed that the remarkably different catalytic behaviors of these two kinds of polymers are due to the difference in the expansion of polymer chains in solutions and to the hydrophobic interaction between catalyst and substrate. The molecules of PVSH in solutions, especially in aqueous acetone, are not appreciably expanded as compared to those of PSSH. Since the expansion is subject to steric

12) C. W. Davies and G. G. Thomas, *J. Chem. Soc.*, **1951**, 2624.

restraints as the molecular weight of PVSH increases, the localized protons along the polymer chain result in confinement within an extremely limited region in the reaction system, thereby making the molecular weight of PVSH responsible for the reduction of the catalytic activity. This interpretation is supported by the observation that the catalytic effects of PVSH, in cases where the molecular weight was below 2000, were much the same as those of hydrochloric acid.

Although there is another view that the distance between sulfonic acid groups on the polymer chain may also be responsible for the catalytic activity, this is contradicted by the fact that the catalytic behavior of sulfonated isotactic polystyrene sulfonic acid (70% sulfonation) was nearly the same as that of the atactic one ((PS)SH (69%)). The hydrolysis rate constants with the former under the conditions shown in Table I were 17.12×10^{-3} for ethyl acetate and 6.08×10^{-3} for ethyl *n*-caproate. Moreover, the hydrolysis rates of esters with polymeric sulfonic acid in water were affected, to some extent, by the ester concentration. The results of some experiments are shown in Table II. The decrease in catalytic activity occurring when the concentration ratio of the ester to the polymer catalyst increased may be related to the reduction of the overall hydrolysis of esters as a result of a lack of an active site on the polymer. The above results suggest the presence of hydrophobic interaction between the polymer catalyst and the ester.

BULLETIN OF THE CHEMICAL SOCIETY OF JAPAN VOL. 39 1519—1521 (1966)

Synthetic Studies starting from β-Cyanopropionaldehyde. III.* The Synthesis of β-Cyanoacrolein

By Shinichi MOTOKI, Sadayoshi SATSUMABAYASHI and Takashi MASUDA

Department of Chemistry, Faculty of Science, Tokyo College of Science, Shinjuku-ku, Tokyo

(Received October 19, 1965)

β-Cyanopropionaldehyde dimethyl acetal was brominated in the presence of calcium carbonate to give α-bromo-β-cyanopropionaldehyde dimethyl acetal. This was then dehydrobrominated with 10% alcoholic potash at −5 to 0°C, β-cyanoacrolein dimethyl acetal was thus obtained in a high yield. Free aldehyde of a light green liquid was given by the hydrolysis of the acetal. A similar procedure using α-chloro-β-cyanopropionaldehyde dimethyl acetal was also examined. On the other hand, β-cyanoacrolein was prepared by the direct dehydrogenation of β-cyanopropionaldehyde with selenium dioxide.

In the present paper, we wish to report the synthesis of β-cyanoacrolein (VI) starting from β-cyanopropionaldehyde (β-CPA) (I) through the process illustrated in Fig. 1.

The synthesis of VI by the oxidation of β-methyl acrylonitrile with selenium dioxide has been reported by Rambaud and others.[1] However, β-cyanoacrolein was not isolated by them, and the 2, 4-dinitrophenylhydrazone and semicarbazone of VI gave low *N*-analytical values.

In the present study, two methods of the synthesis of VI will be described. First, β-cyanopropionaldehyde dimethyl acetal (II) was brominated in carbon tetrachloride. Calcium carbonate had previously been added to the solution in order to remove any hydrogen bromide produced in this

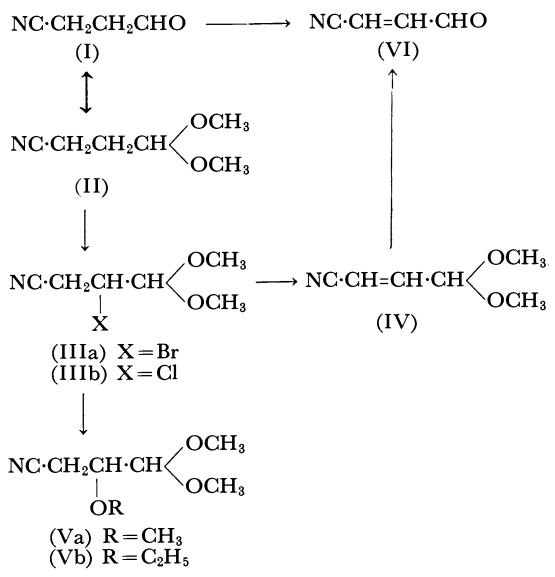

Fig. 1.

* Part II: S. Motoki, S. Satsumabayashi and H. Kusano, This Bulletin, **38**, 922 (1965).

1) R. Rambaud and M. Vessiere, *Bull. soc. chim. France*, **1961**, 1567.

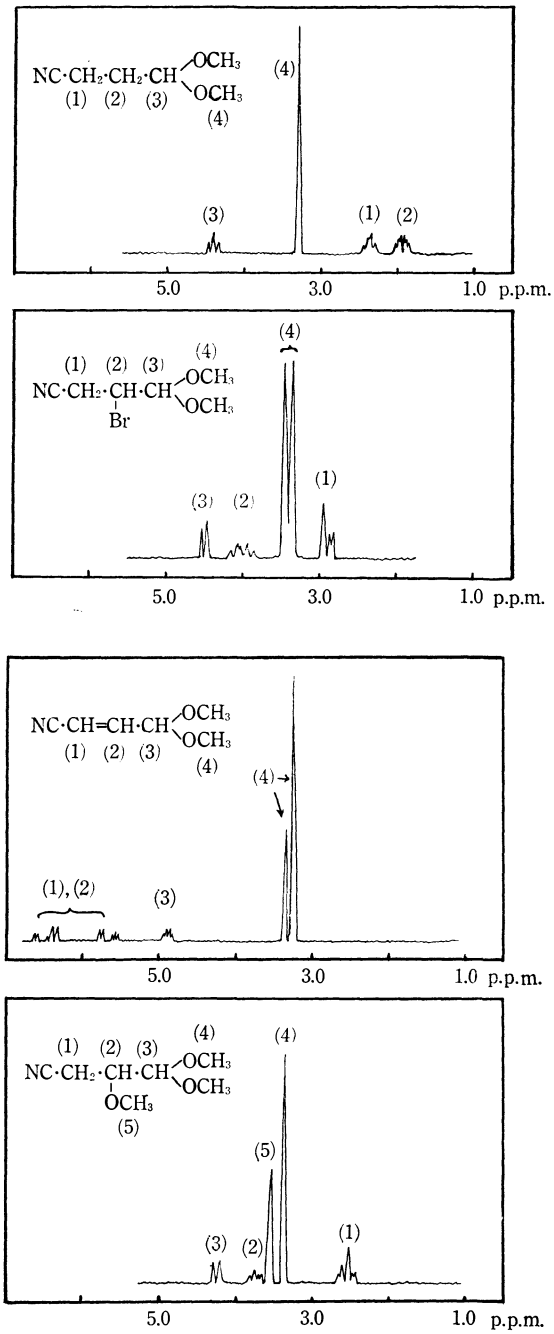

Fig. 2. A varian A-60 NMR spectrometer operating at 60 Mc./sec. was employed for all measurements.

reaction.[2] It was found, by means of a study of the NMR spectra (Fig. 2), that the bromine was introduced into the α-position of the aldehyde group; that is, the absorption of the protons of α-methylene group disappeared and the triplet of the aldehyde group changed to a doublet. Thus, the product was presumed to be α-bromo-β-cyanopropionaldehyde dimethyl acetal (IIIa). When IIIa was dehydrobrominated with 10% methanolic potash at -5 to 0°C, β-cyanoacrolein dimethyl acetal (IV) was obtained in high yield. The analytical values of the product were in accord with the calculated values of IV, and the infrared spectra showed the characteristic absorptions of methine at 3070 cm^{-1} and 3000 cm^{-1} and of carbon-carbon double bond at 1639 cm^{-1}. Moreover, in the NMR spectrum, all the absorptions of methylene groups disappeared, while new absorptions of methine groups appeared.

In the dehydrobromination, the main product was α-methoxy-β-cyanopropionaldehyde dimethyl acetal (Va in Table I) when the temperature was elevated or when the concentration of alkali was increased. Under the same reaction conditions, the corresponding ethoxy derivative (Vb in Table I) was obtained in an ethanol solvent.

The dimethyl acetal (IV) was easily hydrolyzed by dilute hydrochloric acid to β-cyanoacrolein (VI) in a nearly quantitative yield. Though VI is a light green liquid which is a comparatively stable compound, it gradually becomes brown upon standing at room temperature for several days.

Halogenation was also carried out with chlorine instead of bromine. Chlorine gas was blown into the chloroform solution of β-cyanopropionaldehyde dimethyl acetal (II) in the presence of calcium carbonate. However, in this case, the chlorinated product did not show a definite boiling point. Therefore, the fraction (which had a b. p. of 88—93°C/5 mmHg) was collected; dehydrochlorination by alcoholic potash carried out in a similar manner gave a product, boiling at 65—66°C/6 mmHg, which was identified as IV. However, the yield was much less than with bromine.

Chlorination by sulfuryl chloride gave nearly the same results as when chlorine was used, and no single product could be obtained.

In the second method of the synthesis of VI, the direct dehydrogenation of β-CPA was examined. When β-CPA was allowed to react with selenium dioxide in a mixed solvent of water and dioxane, β-cyanoacrolein (VI) was obtained

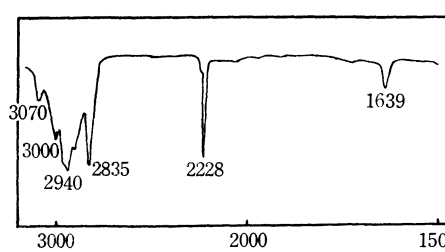

Fig. 3. The IR spectrum of β-cyanoacrolein dimethyl acetal.

2) W. H. Hartung and H. Adkins, *J. Am. Chem. Soc.*, **49**, 2517 (1927).

in a relatively good yield. As may be seen in Table II, the yield was highest when the proportion of dioxane to water was 100 : 20; the yield decreased as the amount of dioxane or of water increased.

Table I

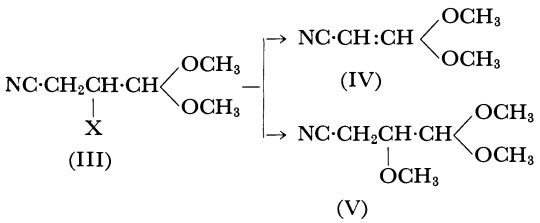

(III) (IV) (V)

Concn. of alkali, %	Temp., °C	Product	Yield, %
20	25—30	V	66.2
20	−5— 0	V	63.8
10	25—30	IV	68.0
10	−5— 0	IV	78.5
15	25—30	IV+V	29.1+40.9
15	−5— 0	IV+V	55.3+19.4

Table II

$$2NC{\cdot}CH_2CH_2CHO + SeO_2 \xrightarrow[70°C]{} 2NC{\cdot}CH{:}CH{\cdot}CHO + Se + 2H_2O$$

(I) (VI)

Solvent Dioxane : Water	Molar ratio I : SeO_2	Yield %
100 : 10	2 : 1	15.3
100 : 20	2 : 1	29.1
100 : 50	2 : 1	19.1
0 : 50	2 : 1	5.1
100 : 20	2 : 1.5	49.4

Experimental

α-Bromo-β-cyanopropionaldehyde Dimethyl Acetal (IIIa). — In a three-necked 1000 ml. flask, 65.5 g. (0.5 mol.) of II was dissolved in 300 g. of carbon tetrachloride, and then 30 g. (0.3 mol.) of powdered calcium carbonate was added. After the solution had been heated to boiling, vigorous stirring was started and 80 g. of bromine in 100 g. of carbon tetrachloride was added drop by drop, to the refluxing solution over approximately a two-hour period. After another one hour's stirring, the mixture was filtered and the filtrate was washed with water several times. The fractional distillation of the carbon tetrachloride solution gave 52.5 g. of pure IIIa; b. p. 87°C/2 mmHg; yield, 50.5%.

Found: C, 34.44; H, 4.97; N, 6.70; Br, 38.90. Calcd. for $C_6H_{10}O_2NBr$: C, 34.63; H, 4.87; N, 6.73; Br, 38.40%.

Care must be taken to stop the distillation when the contents of the flask become viscous and the temperature of the distillate begins to rise; otherwise, a vigorous decomposition of the contents will occur. The bromo-acetal thus obtained turned yellow or dark brown after standing at room temperature for several days.

β-Cyanoacrolein Dimethyl Acetal (IV).—The dehydrobromination of α-bromo-β-cyanopropionaldehyde dimethyl acetal was carried out with alcoholic potash in the usual manner. β-Cyanoacrolein dimethyl acetal, b. p. 62°C/4 mmHg.

Found: C, 56.40; H, 7.28; N, 11.14. Calcd. for $C_6H_9O_2N$: C, 56.68; H, 7.14; N, 11.02%.

α-Alkoxy-β-cyanopropionaldehyde dimethyl acetal was formed as a by-product. α-Methoxy-β-cyanopropionaldehyde dimethyl acetal (Va), b. p. 92°C/5 mmHg.

Found: C, 52.57; H, 8.37; N, 8.94. Calcd. for $C_7H_{13}O_3N$: C, 52.81; H, 8.23; N, 8.80%.

α-Ethoxy-β-cyanopropionaldehyde dimethyl acetal (Vb), b. p. 98°C/5 mmHg.

Found: C, 55.25; H, 8.89; N, 8.21. Calcd. for $C_8H_{15}O_3N$: C, 55.47; H, 8.73; N, 8.09%.

The results are summarized in Table I.

The hydrolysis of the acetal (IV) with dilute hydrochloric acid gave β-cyanoacrolein (VI), b. p. 52°C/5 mmHg; yiled ca. 90%.

Found: C, 58.99; H, 3.92; N, 17.50. Calcd. for C_4H_3ON: C, 59.26; H, 3.73; N, 17.28%.

2, 4-Dinitrophenylhydrazone: m. p. 176°C.

β-Cyanoacrolein (VI) (The Dehydrogenation of β-CPA).—Into a solution of 16.6 g. (0.2 mol.) of β-CPA in 30 ml. of dioxane there was stirred a solution of 11.1 g. (0.1 mol.) of selenium dioxide in 20 ml. of water and 70 ml. of dioxane over a two-hour period, with the temperature maintained at about 70°C. After the solution had been refluxed for another three hours, the reaction mixture was extracted with ether, washed with water, and dried over anhydrous sodium sulfate. By fractional distillation, 8.0 g. of VI was obtained, b. p. 52—53°C/5 mmHg; yield 29.1%.

Found: C, 59.17; H, 3.91; N, 17.21. Calcd. for C_4H_3ON: C, 59.26; H, 3.73; N, 17.28%.

The yield of VI was raised to 49.4% when an excess of selenium dioxide was used.

The authors wish the thank Professor Yojiro Tsuzuki for his helpful advice and encouragement. Acknowledgement is also made to the Ajinomoto Co., Ltd. for a grant and for a supply of raw materials.

BULLETIN OF THE CHEMICAL SOCIETY OF JAPAN VOL. 39 1522—1524 (1966)

The Catalytic Dehyrochlorination of 1, 2-Dichloroethane on Active Carbon in the Presence of Some Hydrocarbons

By Kunio OKAMOTO, Noboru TANAKA, Kiyoshi ADACHI and Haruo SHINGU

Department of Fuel Chemistry, Faculty of Engineering, Kyoto University, Sakyo-ku, Kyoto

(Received October 19, 1965)

The catalytic pyrolysis of 1, 2-dichloroethane on active carbon, carried out at 300 and 400°C in the presence of toluene, benzene and *n*-hexane, resulted predominantly in ethylene instead of vinyl chloride, which is known in the literature as the major pyrolysis product of the titled compound; the pyrolysis rates were suppressed by these hydrocarbons. These results have been explained by assuming a radical-chain mechanism similar to that suggested for the "homogeneous" pyrolysis of this compound. The chain length derived from the proposed mechanism has been estimated to be 20 to 50.

A number of studies concerned with the mechanism of the homogeneous pyrolysis of 1, 2-dichloroethane have been reported in recent years.[1] In contrast, little work has been done with the catalytic mechanism of the pyrolysis on active carbon, although the use of active carbon for the pyrolytic manufacture of vinyl chloride from 1, 2-dichloroethane has been extensively investigated.[2] During the course of our study of the active carbon catalyst for the preparation of vinyl chloride from 1, 2-dichloroethane,[2g,h] we felt it desirable to carry out several experiments in order to clarify the mechanistic nature of this catalytic reaction; in this paper we will report on some of the results, which support unambiguously the mechanism including radicals as the intermediates of the reaction on the surface of the active carbon catalyst.

The dehydrochlorination was carried out by means of a flow method at 300 and 400°C in the presence of hydrocarbons, such as *n*-hexane, toluene and benzene. 1, 2-Dichloroethane or a mixture of it with the hydrocarbons was fed to an integral reactor filled with the active carbon catalyst[2h] in a fixed bed. At the exit of the reactor the gaseous effluent entered a water-cooling condenser and ice-water trap; then hydrogen chloride was trapped by an absorption bottle containing aqueous sodium hydroxide, and finally the non-condensables were collected in a gas holder. The composition of the condensates and gases were analyzed by gas-liquid chromatography. The results are shown in Table I.

In the absence of hydrocarbons, 1, 2-dichloroethane decomposed almost completely under the reaction conditions employed. At the reaction temperatures of 300 and 400°C, the percentage conversion amounted, respectively, to 94.5 and 99% at the flow rate of 0.22 cc. of liquid 1, 2-dichloroethane per 1 cc. of active carbon per hour (Runs 1 and 2).

By the addition of hydrocarbons, the decomposition of 1, 2-dichloroethane was considerably inhibited. The addition of 4 mol. of toluene reduced the conversion percentage of 1, 2-dichloroethane from 94.5 to 8.5% at 300°C (Run 4). 1, 2-Dichloroethane mixed with 3 mol. of *n*-hexane gave a 50% conversion at 402°C (Run 7), whereas pure 1, 2-dichloroethane gave a 98% conversion at 380°C at a comparable flow rate (Run 3).

Furthermore, we found that the nature of the pyrolysis products was dramatically changed by the addition of these hydrocarbons. In the absence

---

* Presented at the 17th Annual Meeting of the Chemical Society of Japan, Tokyo, April, 1964. *Abstracts*, p. 336.

1) a) D. H. R. Barton, *J. Chem. Soc.*, **1949**, 148; b) D. H. R. Barton and K. E. Howlett, ibid., **1949**, 155; c) K. E. Howlett, *Trans. Faraday Soc.*, **48**, 25 (1952); d) M. Kitabatake and T. Onoda, *J. Chem. Soc. Japan, Ind. Chem. Sect. (Kogyo Kagaku Zasshi)*, **65**, 931 (1962); e) M. Kitabatake, ibid., **65**, 935 (1962); f) G.A. Kapralova. See N.N. Semenov, "Some Problems of Chemical Kinetics and Reactivity," (translated by J. E. S. Bradley), Vol. I, Pergamon Press, London (1958), p. 242; g) G. A. Kapralova and N. N. Semenov, *Zh. Fiz. Khim.*, **37**, 73 (1963); *Chem. Abstr.*, **59**, 2612 (1963); h) G. A. Kapralova and N. N. Semenov, ibid., **37**, 301 (1963); *Chem. Abstr.*, **59**, 4995 (1963); i) S. Inokawa, R. Goto, H. Arioka and M. Kuze, *J. Chem. Soc. Japan, Ind. Chem. Sect. (Kogyo Kagaku Zasshi)*, **67**, 1540 (1964).

2) a) I. G. Farbenind. A.-G., German Pat. 585793 (Oct. 9, 1933); b) S. S. Bobkov and P. P. Shepeneva, U. S. S. R. Pat. 66688 (July 31, 1946); c) J. C. Vlugter, W. L. J. de Nie and R. H. M. Meyer (to N. V. de Bataafsche Petroleum Maatschappij), Dutch Pat. 59461 (June 16, 1947); d) Société belge de l'azote et des produits chimiques du Marly, S. A., Belg. Pat. 563247 (June 14, 1958); Japanese Pat. 35-13909 (Sept. 22, 1960); e) L. K. Doraiswamy and M. U. Pai, *J. Sci. Ind. Research*, **158**, 87 (1956); *Chem. Abstr.*, **52**, 12749 (1958); f) T. Enkvist, *Finska Kemistsamfundetes Medd.*, **67**, 45 (1958), *Chem. Abstr.*, **53**, 13451 (1959); g) H. Shingu, K. Okamoto, K. Adachi, H. Ichikawa and N. Tanaka, Abstracts of the 5th Symposium of Japan Petroleum Institute, Tokyo, Sept., 1962, Supplement, p. 10; h) K. Okamoto, T. Oda, N. Ninomiya, H. Ichikawa and H. Shingu, Japanese Pat. 39-24870 (Nov. 5, 1964).

TABLE I. CATALYTIC DEHYDROCHLORINATION OF 1,2-DICHLOROETHANE ON ACTIVE CARBON

Run No.	Feed: 1,2-Dichloroethane mole	Feed: Hydrocarbon mole	Temp. °C	Vol. of act. carbon cc.	Liquid space velocity of 1,2-dichloroethane hr^{-1}	HCl% based on 1,2-dichloroethane	Conversion%[a] of 1,2-dichloroethane	Distribution, %: Ethylene	Distribution, %: Vinyl chloride	k[b] sec^{-1}
1	0.162	none	300	30	0.22	98.0	94.5	1.7[c]	98.3	0.154
4	0.200	Toluene 0.800	300	30	0.22	14.1	8.5	94.8[c]	4.7	0.0034
2	0.318	none	400	30	0.22	101	99.0	1.0[c]	99.0	0.293
5	0.200	Benzene 0.910	400	30	0.22	102	82.3	16.9[d]	81.7	0.109
6	0.200	*n*-Hexane 0.800	400	30	0.22	188	98.3	95.7[e]	3.1	0.348
3	0.317	none	380	40	1.25	98.0	98.0	0.5[c]	99.0	1.37
7	0.095	*n*-Hexane 0.300	402	10	1.00	98.0	50.0	90.5[c]	6.0	0.200

a) Calculated from the amount of the recovered 1,2-dichloroethane.
b) Total rate constant, calculated from the conversion % of 1,2-dichloroethane and the composition of the products by using the equation similar to that cited by Barton.[1a]
c) For the other minor products see text.
d) Acetylene 0.05%; benzene, recovered, 98.5%.
e) Acetylene 0.3%; ethane, 0.8%; ethyl chloride, 0.1%; hexane, recovered, 94.0%.

of the hydrocarbons, pure 1, 2-dichloroethane gave vinyl chloride exclusively (more than 98% of the composition of the product); at most 2% of ethylene was found as a minor product (Runs 1, 2 and 3). A gas chromatographical examination of the other minor components reveales the presence of small amounts of ethyl chloride (about 0.1% in composition), *cis*-1, 2-dichloroethylene (0.05%), 1, 1-dichloroethane (0.02%), *trans*-1, 2-dichloroethylene (0.02%) and vinylidene chloride (0.01%). In the presence of the hydrocarbons, however, the major product was not vinyl chloride, but, rather, ethylene (more than 90% of the composition of the product). For instance, in the decomposition of 1, 2-dichloroethane mixed with 4 mol. of toluene, a mixture consisting of 94.8% ethylene, 4.7% vinyl chloride, and a small amount of other, minor products, such as ethyl chloride (about 0.04%) and acetylene (at most 0.01%), was obtained at 300°C (Run 4). More than 97.4% of the toluene was recovered; about 0.2% of it was then converted to *trans*-stilbene. In another example at 400°C (Run 7), a mixture of *n*-hexane and 1, 2-dichloroethane (3 : 1 by mole) gave a gaseous product containing 90% ethylene as a major product, 6% vinyl chloride, 0.04% acetylene, 0.54% ethane, and, at most, 0.01% ethyl chloride; more than 90% of the added *n*-hexane was recovered.

On the basis of the above results, we may suggest that the pyrolysis of 1, 2-dichloroethane on the active carbon catalyst proceeds by a radical chain mechanism similar to that suggested for the "homogeneous" dehydrochlorination.[1a,b] Namely, the homogeneous pyrolysis is also inhibited in the presence of these hydrocarbons,[1a] and the chain propagation can be initiated mainly at the treated, i. e., carbon-coated, walls.[1f,g]

Thus, for this catalytic dehydrochlorination, the initiation step may be formulated as:

$$ClCH_2CH_2Cl + \text{Active carbon} \xrightarrow{k_1} Cl + \cdot CH_2CH_2Cl$$

or $$\cdot CH_2CH_2Cl + \text{Active carbon} \xrightarrow{k_2} Cl + CH_2{=}CH_2$$

In the absence of the hydrocarbons, the chain propagation would proceed in the same manner as in the homogeneous pyrolysis, as is indicated below:

$$Cl + ClCH_2CH_2Cl \xrightarrow{k_3} HCl + Cl\dot{C}HCH_2Cl$$
$$Cl\dot{C}HCH_2Cl \xrightarrow{k_4} Cl + ClCH{=}CH_2 \quad \text{Chain}$$
$$Cl + Cl\dot{C}HCH_2Cl \xrightarrow{k_5} ClCH_2CHCl_2 \quad \text{Termination}$$

The further pyrolytic decomposition of 1, 1, 2-trichloroethane would form 1, 1-dichloroethane, *cis*- and *trans*-1, 2-dichloroethylene; these compounds have been identified in the minor reaction products.

In the presence of the hydrocarbons, the chain-carrying chlorine atom would be destroyed by the hydrogen donation from these hydrocarbons. As a result, the formation of vinyl chloride would be suppressed; accordingly, the decomposition of a 2-chloroethyl radical to ethylene would become preponderant:

$$Cl + RH \xrightarrow{k_6} HCl + \cdot R\downarrow \quad \text{Termination}$$

This termination of the radical-chain by the

hydrocarbons cansequently causes a decrease in the total rate of the conversion of 1, 2-dichloroethane. This is illustrated by a comparison of the following total rate expressions for 1, 2-dichloroethane alone and for its mixture with the hydrocarbons.

In the absence of the hydrocarbons:

$$-\frac{d(EDC)}{dt}=\left(\frac{2k_1k_3k_4}{k_5}\right)^{1/2}(EDC)+k_1(EDC) \quad (1)$$

In the presence of the hydrocarbons:

$$-\frac{d(EDC)}{dt}=\left\{\left(\frac{k_6k_4}{2k_5}\right)^2(RH)^2+\frac{2k_1k_3k_4}{k_5}(EDC)^2\right\}^{1/2}-\frac{k_4k_6}{2k_5}(RH)+k_1(EDC) \quad (2)$$

where (EDC) and (RH) are, respectively, the effective concentrations of 1, 2-dichloroethane and of the hydrocarbon on the surface of the active carbon; it is assumed that the reaction proceeds in the adsorbed layer and that the rate of adsorption and desorption are rapid as compared to the reaction rates.

If the above reaction sequence is accepted and the second term of Eq. 1 is neglected compared to the first, it is possible to compute the chain length in the propagation stage for this catalytic dehydrochlorination:

$$\text{Chain length}=\frac{k_3(EDC)}{k_5(ClCHCH_2Cl)}=\frac{1}{2}\cdot\left(\frac{2k_1k_3k_4}{k_5}\right)^{1/2}\cdot\frac{1}{k_1}=\frac{1}{2}\cdot\frac{d(\text{Vinyl Chloride})}{d(\text{Ethylene})}=\frac{1}{2}\cdot\frac{(\text{Vinyl Chloride }\%)}{(\text{Ethylene }\%)} \quad (3)$$

Therefore, the chain length at temperatures ranging from 300 to 400°C is estimated to be 20 to 50 from the data in Runs 1 and 2.

Experimental

Apparatus. — All the reactions were studied by streaming the vapor of 1, 2-dichloroethane* or its mixture with hydrocarbons at a constant rate through a catalyst bed in a hard-glass tube, 1.9 cm. in internal diameter. The tube was 70 cm. in length of which 50 cm. were heated in an electric furnace inclined at a slight angle to the horizon. An active carbon catalyst[2h] (manufactured by the Takeda Chemical Ind. Co., Ltd., Osaka; 15 g.; 40 cc. bulk volume; 8 to 12 mesh) was supported by a plug of glass wool. A glass thermocouple well (7 mm. o. d.) ran through the center of the catalyst bed, which was 20 cm. long for 40 cc. of the catalyst, and was situated in the center portion of the furnace. The bed temperature was uniform along its length to ±2°C (300 to 400°C). The 10 cm. portion of the tube immediately in front of the catalyst served as an evaporator and a preheater. 1, 2-Dichloroethane, placed in a graduated liquid feed tube with a capillary outlet tubing fitted at the top, was forced into a reaction vessel by feeding mercury from a dropping funnel into the tube at a constant rate. The delivery rates (liquid space velocity) of 1, 2-dichloroethane were 0.22 and 1.25 (cc. per cc. of the catalyst per hr.). In the case of the latter liquid space velocity, the bed temperature and the temperature at the preheater portion were kept about 10°C higher than the reaction temperature just before the feeding in of 1, 2-dichloroethane, because the endothermicity of this pyrolysis causes a temperature depression at such a high feeding rate. The temperature of the inlet of the bed was 5 to 10°C lower than that of the outlet. Thus, the reaction temperature was measured at the midpoint of the bed. At the exit of the reactor the gas flow entered a series of tared product traps, i. e., a water-cooling condenser fitted with a graduated cylinder, a graduated trap at 0°C (ice water), and a graduated gas-holder filled with saturated aqueous sodium chloride. In the case of the run for analysis of the minor reaction products, the gas-holder was replaced with another trap at −70°C (solid carbon dioxide - methanol). Except in this analysis run, hydrogen chloride was caught by means of an absorption bottle filled with 2—5 N sodium hydroxide provided between the gas-holder and the other traps. Before each run, the air in the free space was replaced by nitrogen, and after the run the gaseous products in the free space were transfered to the condensers or traps by a nitrogen stream.

Product Analysis.—The reaction products were analyzed gas chromatographically with a Perkin-Elmer model 154B Vapor Fractometer. The column for chlorine compounds was a Perkin-Elmer column A (2 m. long with diisodecyl phthalate as the liquid). The retention times for ethyl chloride, 1, 1-dichloroethane, 1, 2-dichloroethane, 1, 1, 1-trichloroethane, 1, 1, 2-trichloroethane, 1, 1, 2, 2-tetrachloroethane, vinyl chloride, vinylidene chloride, *trans*-1, 2-dichloroethylene, *cis*-1, 2-dichloroethylene and 1, 2-dichloropropane were, respectively, 1.7, 6.1, 13.0, 9.4, 54, 217, 1.2, 3.0, 4.7, 8.8, and 18.5 min., as determined at 64°C with hydrogen as a carrier gas and at a flow rate of 55 cc. per min. The column for hydrocarbon gases was a Perkin-Elmer column J (2 m. long, with silica gel as the solid). The retention times for ethane, ethylene, acetylene and vinyl chloride were, respectively, 3.6, 5.5, 13.6, and 51 min., as determined at 84°C with helium as the carrier gas and at a flow rate of 50 cc. per min.

After the run the aqueous sodium hydroxide in the absorption bottle was neutralized with nitric acid and the chlorine content was determined by the Mohr method. The condensates in the water-cooling condenser were distilled, and most of the hydrocarbons were recovered (Runs 4—7). In the run with toluene (Run 4), a small amount of the distillation residue (a solid) gave 0.20 g. of *trans*-stilbene, m. p. 120—122°C, after the recrystallization from ethanol. The identity of this with authentic *trans*-stilbene was established by comparing the infrared spectra taken with a Shimadzu model IR-27.

* The material contained as impurities 0.029% 1, 1-dichloroethane, 0.023% 1, 2-dichloropropane, and 0.058% 1, 1, 2-trichloroethane (analysis by gas chromatography).

BULLETIN OF THE CHEMICAL SOCIETY OF JAPAN VOL. 39 1525—1529 (1966)

Sophorol[1]

By Hiroshi SUGINOME

Department of Chemistry, Faculty of Science, Hokkaido University, Sapporo

(Received October 20, 1965)

The structure of sophorol was confirmed to be 2′: 7-dihydroxy-4′: 5′-methylenedioxyisoflavanone by the synthesis of dehydro-*O*-dimethylsophorol, 2′: 7-dimethoxy-4′: 5′-methylenedioxyisoflavone.

This paper will describe the synthesis of 2′:7-dimethoxy-4′: 5′-methylenedioxyisoflavone (VII), which is one of the possible formulas of the dehydro-*O*-dimethylsophorol derived from *O*-dimethylsophorol[2] by palladium dehydrogenation. The paper will, therefore, complete the elucidation of the structure of sophorol (VIII).

The starting material, 2-hydroxy-4:5-methylenedioxybenzaldehyde (III) (R=H), was synthesized by Campbell et al.[3] through nitration and amination, followed by hydroxylation from piperonal. The repetition of this procedure did not, however, lead to satisfactory results; the reduction of 6-nitropiperonal with ferrous sulfate does not give good yields and leads to unreproducible results because of the quality of the ferrous sulfate, as the previous workers found. As the compound is a useful building stone for the syntheses of some naturally occurring oxygen heterocyclics with a 2-hydroxy-4:5-methylenedioxy oxygenation pattern, ayapin,[4] pachyrrhizon,[5] pachyrrhizin,[6] and jamaicin,[7] a new method of preparation was developed. Piperonal, a readily-available natural product, was submitted to Baeyer and Villiger's oxidation in order to form sesamol,[8] using performic acid. In the present experiments it was observed that the use of diluted peracids gave rather poor yields. However, for the preparation of sesamol in quantity, Beroza's modified procedure[8] was useful. The application of Gattermann aldehyde synthesis to sesamol,[9] in the presence of anhydrous zinc chloride as a catalyst, yielded almost quantitatively 2-hydroxy-4:5-methylenedioxybenzaldehyde (III) (R=H). No isomeric 6-hydroxyaldehyde was obtained.

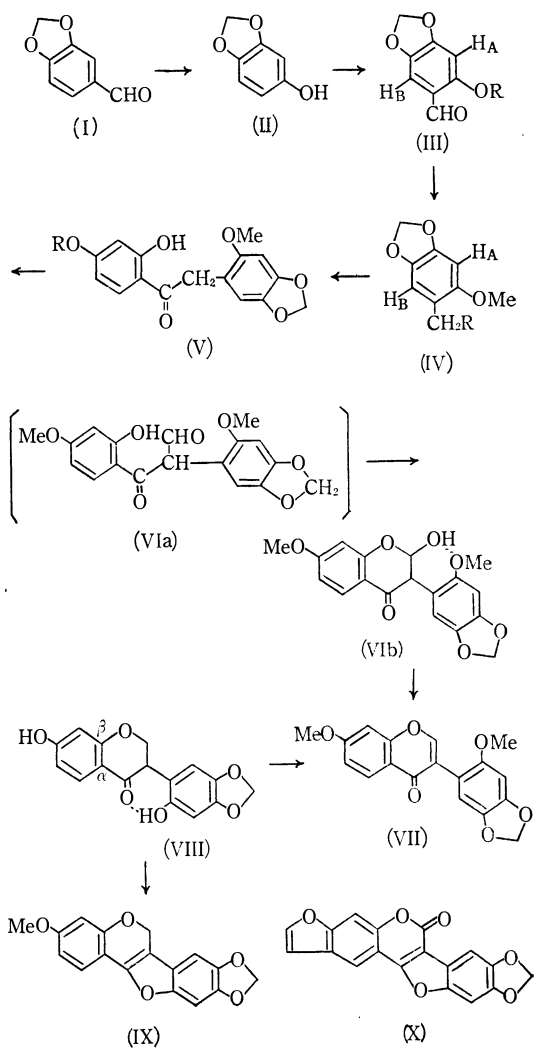

1) Oxygen Heterocycles, VI. Read before the Local Meeting of the Chemical Society of Japan, Sapporo, July, 1960. Brief account of this work was already published. H. Suginome, *Tetrahedron Letters*, **1960**, 16.

2) H. Suginome, *J. Org. Chem.*, **24**, 1655 (1959).

3) K. N. Campbell, P. F. Hopper and B. K. Cambell, ibid., **16**, 1746 (1951).

4) E. Späth, P. K. Bose and J. Schläger, *Ber.*, **70**, 702 (1937).

5) H. Bickel and H. Schmid, *Helv. Chim. Acta*, **36**, 664 (1953).

6) E. Simonitsch, H. Forei and H. Schmid, *Monat.*, **88**, 541 (1957). P. Rajagopalan and A. I. Kosak, *Tetrahedron Letters*, **1959**, 5.

7) O. A. Stamm, H. Schmid and J. Büchi, *Helv. Chim. Acta*, **41**, 2006 (1958).

8) J. Boeseken, W. D. Cohen and C. J. Kip, *Rec. Trav. Chim.*, **55**, 815 (1936). M. Beroza, *J. Agr. Food Chem.*, **4**, 49 (1956). Also cf. Y. Takata and T. Matsuda, *J. Pharm. Soc. Japan* (*Yakugaku Zassi*), **74**, 693 (1954).

9) Sesamol used in the present experiments was provided by custom synthesis of Aldrich Chemical Company, Inc., Milwaukee, Wis., U. S. A.

The condensation of methylated aldehyde with hippuric acid in the presence of acetic anhydride readily afforded the corresponding azlactone, which was then hydrolysed to the corresponding phenylpyruvic acid by the usual method. 2-Methoxy-4 : 5-methylenedioxyphenylpyruvic acid was converted into the corresponding oxime. The treatment of the oxime with acetic anhydride yielded 2 - methoxy - 4 : 5 - methylenedioxyphenylacetonitrile (IV) (R=CN), which exhibited a weak characteristic band at 2241 cm^{-1} attributable to C≡N.[10]

This nitrile was condensed with resorcinol to give a desoxybenzoin derivative in a poor yield; the condensation was effected by Hoesch procedure, using a mixed solvent of chloroform and ether. Hoesch condensation in ether did not proceed smoothly, and when the reaction mixture was saturated with hydrogen chloride, a crystalline precipitation which was different from ketimine hydrochloride was obtained. This compound was found to be the corresponding amide (IV) (R=$CONH_2$) by a study of its infrared and ultraviolet spectra.

Attempts to synthesize the desoxybenzoin by the condensation of phenylacetic acid (IV) (R=COOH) with resorcinol in the presence of BF_3[11] failed.

This desoxybenzoin, on partial methylation with ethereal diazomethane, gave 2-hydroxy-4:2'-dimethoxy-4':5'-methylenedioxydesoxybenzoin, (V) (R=CH_3), m. p. 131—132°C, which was identical with the ketone, $C_{17}H_{16}O_6$,[2] obtained by the mild alkaline hydrolysis of *O*-dimethyl ether of sophorol.

The cyclization of 2-hydroxy-4:2'-dimethoxy-4':5'-methylenedioxydesoxybenzoin with sodium and ethyl formate[12] furnished a product, $C_{18}H_{16}O_7$, which melted at 185°C, in a good yield. The presence of an alcoholic hydroxyl band in its infrared spectrum and its ultraviolet spectrum indicated that this compound was a 2-hydroxyisoflavanone derivative (VIb).

The cyclization of *O* - hydroxyphenylbenzyl ketones to isoflavones with sodium and alkyl formates has frequently been postulated as proceeding through intermediates of the VIb type or through the direct dehydration of an intermediate (VIa).[13a] In only a very small number of instances, however, namely, the conversions of 2-methoxydesoxybenzoins into the corresponding isoflavones, have crystalline products of 2-hydroxyisoflavanone been isolated and characterized.[13b] Whalley[13a] has postulated that the stability of the products may be attributed, in part at least, to the possibility of hydrogen bonding between 2-hydroxyl and 2'-methoxyl groups of the type shown in VIb. The infrared spectrum of 2-hydroxy-2' : 7-dimethoxy-4' : 5'-methylenedioxyisoflavanone in a dilute chloroform solution shows two hydroxyl bands, at 3413 and 3563 cm^{-1}. The former (broad) is attributable to an internal hydrogen bonding between 2-hydroxyl and 2'-methoxyl groups.

When boiled in acetic acid, this intermediary isoflavanone was readily dehydrated to 2':7-dimethoxy-4':5'-methylenedioxyisoflavone, which melted at 209—210°C. The selenium dioxide oxidation product (m. p. 203—205°C)[2] derived from the natural substance was identical with this synthetic isoflavone.

Thus, the correctness of the assumed structure (VIII)[2] for sophorol was fully proved.

On the basis of this formula, some comments on the compound derived from sophorol should be added.

When sophorol was methylated with dimethyl sulfate containing a trace of acid, a new compound, $C_{17}H_{12}O_5$, was obtained in a poor yield. The absence of carbonyl and hydroxyl bands in the infrared spectrum of this substance, as well as the close similarity of its ultraviolet spectrum (Fig. 1) to that of anhydrosophorol (IX) (R=H), confirmed the formula IX (R=CH_3) as holding for this compound. Attention should also be directed to the structural similarity of anhydrosophorol and erosnin (X).[14]

The possible half-chair conformation of chromanone and chroman has been discussed, notably by Whalley.[15] Philbin and Wheeler[16] pointed out that the chromanone system may occupy a plane, except for carbon 2, which can be the only cyclic atom out of that plane because the infrared spectra of a series of flavanones show the carbonyl frequency to be in the range of 1695—1661 cm^{-1}, showing the conjugation of the carbonyl group

10) R. E. Kitson and N. E. Griffith, *Anal. Chem.*, **24**, 334 (1952).
11) K. Venkataraman et al., *Proc. Ind. Acad. Sci.*, **51**, 192 (1955).
12) W. H. Perkin and R. Robinson, *J. Chem. Soc.*, **1908**, 489.
13) a) W. B. Whalley, *J. Am. Chem. Soc.*, **75**, 1059 (1953); W. B. Whalley, *J. Chem. Soc.*, **1953**, 3366; **1955**, 105; W. B. Whalley and A. Robertson, ibid., **1954**, 1440; W. B. Whalley and G. Lloyd, ibid., **1956**, 3213,
b) M. L. Wolfrom and R. L. Brown, *J. Am. Chem. Soc.*, **63**, 1246 (1941); S. H. Harper, *J. Chem. Soc.*, **1942**, 595; N. Narasimhachari, O. Rajagopalan and T. R. Seshadri, *J. Sci. Ind. Research*, (India), **11B**, 347 (1952); ibid., **12**, 287 (1953); S. Varadarajan and T. R. Seshadri, *Proc. Indian Acad. Sci.*, **38A**, 381 (1953).
14) J. Eisenbeiss and H. Schmid, *Helv. Chim. Acta*, **42**, 61 (1959).
15) W. B. Whalley, J. Soc. Leather Trades' Chemists, "Cambridge Symposium on Vegetable Tannins," (1956), p. 151; W. B. Whalley, in "The Chemistry of Flavonoid Compounds," Ed. by T. A. Geissman, Pergamon Press, (1962), p. 441. Also cf. E. A. H. Roberts, *Chem. & Ind.*, **1955**, 631, 1551; ibid., **1956**, 737; J. W. Clark-Lewis, ibid., **1955**, 1218.
16) E. M. Philbin and T. S. Wheeler, *Proc. Chem. Soc.*, **1958**, 167. Also cf. H. Hart and C. R. Wagner, ibid., **1958**, 284.

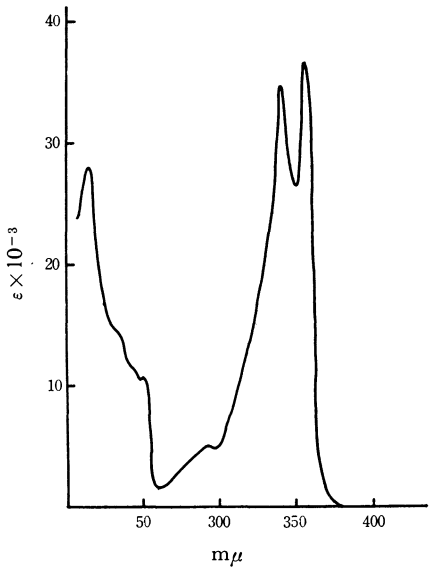

Fig. 1. UV spectrum.

with the fused benzene ring. Furthermore, a substituted phenyl group on the number 3 carbon of isoflavanone can occupy either an equatorial or an axial position, because the isoflavanone system would have a tendency toward conformational inversion by diminishing the repulsion of nonbonded atoms through the lack of hydrogen atoms at positions 1 and α.

An examination of the model of sophorol showed that when the phenyl group was in the 3-equatorial position, the 2'-phenolic hydroxyl group on the phenyl group was located near enough to the dihydropyrone carbonyl group to form an intramolecular hydrogen bond, but when it was in the 3-axial position, the distances were too great to allow the formation of this bond.

Table I shows the carbonyl and hydroxyl frequencies in the infrared spectra of sophorol and *O*-dimethylsophorol, together with those of the model compounds.

From Table I it can be seen that isoflavanones with 2'-methoxyl groupings have a carbonyl band in the 1677—1681 cm^{-1} range, almost identical with the location of the parent flavanone (1680 cm^{-1}). However, this band, is shifted to 1658 cm^{-1} in compounds with 2'-hydroxyl groupings, giving evidence of an intramolecular hydrogen bond. It is also clear that a dilute solution of isoflavone or isoflavanone with 2'-hydroxyl groupings exhibits a broad hydrogen-bonded hydroxyl band in the hydroxyl stretching region, showing intramolecular hydrogen bonding. The above observation indicates that the 3-phenyl group of sophorol is in an energetically favorable equatorial orientation, and it shows the presence of a hydrogen bond between the dihydropyrone carbonyl and the 2'-hydroxyl groups.

Table I

Compound	OH(cm^{-1})	C=O(cm^{-1})	
2'-Hydroxyisoflavone[17]	3187[a]	1621[a]	Δ21 cm^{-1}
2'-Methoxyisoflavone[17]		1642[a]	
2'-Hydroxyisoflavanone[17]	3576, 3307[b]	1658[b]	Δ23 cm^{-1}
2'-Methoxyisoflavanone[17]		1681[b]	
Sophorol[2]	3333, 3195[c]	1661[c]	Δ11 cm^{-1}
O-Dimethylsophorol[2]		1672[c]	
2-Hydroxy-7:2'-dimethoxy-4':5'-methylenedioxy-isoflavanone	3563, 3413[b]	1677[b]	
7:4'-Dimethoxy-2-methylisoflavanone[18]		1680	
7:4'-Dimethoxyisoflavanone[18]		1678[b]	
Flavanone[19]		1680[c]	
7:2':4'-Trimethoxyisoflavanone[2]		1677[c]	

a) KBr tablet. b) Chloroform solution.
c) Nujol mull.

Experimental[20]

2 - Hydroxy - 4 : 5 - methylenedioxybenzaldehyde (III) (R=H).—Dry hydrogen chloride was bubbled through a solution of 713 mg. of sesamol and 1.5 ml. of hydrogen cyanide in absolute ether (5 ml.) containing anhydrous zinc chloride (300 mg.) under ice cooling. After 30 min., the solution showed a blue color, and violet precipitates of ketimine hydrochloride were deposited. The product was then separated and washed with ether (3 ml.). This ketimine hydrochloride was recrystallized from water (4 ml.), forming fine green-colored crystals (825 mg.). The product was stable in air and was not hygroscopic. When this ketimine hydrochloride was boiled with water (7 ml.) for 1 min., crude 2-hydroxy-4 : 5-methylenedioxybenzaldehyde (620 mg.) separated from the solution. After purification, this was found to be identical with an authentic specimen.

The Azlactone of 2-Methoxy-4 : 5-methylenedioxybenzaldehyde. — 2-Methoxy-4 : 5-methylenedioxybenzaldehyde (15.7 g.), hippuric acid (15.7 g.), and fused sodium acetate (7.9 g.) were powdered to an intimate mixture and heated with 30 ml. of acetic anhydride for 2 hr. on a bath to give an orange crystalline mass. After evaporation and washing with small volumes of alcohol and water successively, crude azlactone (20.6 g.) was obtained. This porduct was recrystallized from alcohol, forming fine orange-colored

17) H. Suginome and T. Iwadare, This Bulletin, **33**, 568 (1960).
18) R. B. Bradbury and D. E. White, *J. Chem. Soc.*, **1953**, 874.
19) H. L. Hergert and E. F. Kurth, *J. Am. Chem. Soc.*, **75**, 1662 (1953).

20) Melting points are uncorrected. The ultraviolet absorption spectra were measured on a Beckman Model D. U. spectrophotometer in ethanol. The infrared spectra were measured in Nujol, unless otherwise stated. NMR spectra were taken in deuteriochloroform by Japan Electron Optics 3H 60 high resolution spectrometer (60 Mc.). Tetramethylsilane was used as an internal standard.

crystals, m. p. 266—267°C.[21]

Found: C, 66.95; H, 4.27. Calcd. for $C_{18}H_{13}O_5N$: C, 66.87; H, 4.05%.

2-Methoxy-4 : 5-methylenedioxyphenylpyruvic Acid.—The azlactone (5.0 g.) obtained above was suspended in 25 ml. of a 10% sodium hydroxide solution and then refluxed for 2 hr. on an oil bath in a nitrogen stream. The dark brown solution, after cooling, was extracted with ether and then saturated with sulfur dioxide. After the evaporation of the solvent from the ethereal solution, crude 2-methoxy-4 : 5-methylenedioxybenzaldehyde (0.28 g.) was obtained. After the benzoic acid had been removed by filtration, the filtrate was extracted with ether. The ethereal solution contained 0.7 g. of benzoic acid. The aqueous solution was then concentrated under reduced pressure to about 7 ml. and set aside overnight under ice cooling. The bisulfite-addition compound of 2-methoxy-4 : 5-methylenedioxyphenylpyruvic acid (6.0 g.) which separated was collected by filtration. When this bisulfite-addition compound (1.0 g.) was heated with 6 ml. of 2 N hydrochloric acid for a few min., colorless 2-methoxy-4 : 5-methylenedioxyphenylpyruvic acid (0.3 g.) separated. This was recrystallized from water, m. p. 220—221°C.

Found: C, 55.77; H, 4.36. Calcd. for $C_{11}H_{10}O_6$: C, 55.46; H, 4.23%.

The bisulfite-addition compound was used conveniently in the next oxime formation.

The Oxime. — The bisulfite-addition compound obtained above (20 g.), hydroxylamine hydrochloride (7.8 g.), and an 8% caustic soda solution (95 ml.) were warmed for a few minutes at 50°C and then set aside overnight. On acidification with hydrochloric acid, the crude oxime (9.6 g.) separated. This was recrystallized from water, m. p. 162—163°C (decomp.).

Found: C, 52.32; N, 4.50. Calcd. for $C_{11}H_{11}O_6N$: C, 52.17; H, 4.38%.

2-Methoxy-4 : 5-methylenedioxyphenylacetonitrile (IV) (R=CN).—The oxime (5.0 g.) was heated with acetic anhydride (3 ml.) on a water bath and, after the vigorous reaction had subsided (after 2—3 min.), a large volume of water added. The nitrile (3.3 g.) then separated and solidified. On repeated washings with water and recrystallization from alcohol, the nitrile was obtained as needles, m. p. 123—124°C. The crystals dissolved with difficulty in ether, but they were readily soluble in chloroform and acetone.

Found: C, 63.10; H, 5.00; N, 7.18; OCH_3, 16.5. Calcd. for $C_{10}H_9O_3N$: C, 62.82; H, 4.75; N, 7.33; OCH_3, 16.2%.

UV λ_{max} (ε_{max}): 213 (4741), 239 (5540) and 301 (6945) IR: 2241 cm^{-1} (w) (C≡N).

2'-Methoxy-2 : 4-dihydroxy-4' : 5'-methylenedioxydesoxybenzoin (V) (R=H).—a) For 2 hr. at room temperature, dry hydrogen chloride was passed through a solution of resorcinol (0.8 g.) and 2-methoxy-4 : 5-methylenedioxyphenylacetonitrile (0.5 g.) in a mixture of dry ether (6 ml.) and chloroform (10 ml.) containing fused anhydrous zinc chloride (0.5 g.). After this mixture had been kept overnight, orange ketimine hydrochloride separated; this was washed with ether and heated for about 40 min. with 5 ml. of water. On cooling, the crystalline solid separated; after it had been washed with 5% aqueous sodium hydrogen carbonate and water successively, it was crystallized from aqueous alcohol (0.28 g.), m. p. 160—162°C. After recrystallization, it formed needles, melting at 164—165°C.

Found: C, 63.29; H, 4.50. Calcd. for $C_{16}H_{14}O_6$: C, 63.57; H, 4.67%.

IR: 3537—3747 cm^{-1} (m), (OH) 1618 cm^{-1} (s) (chelated conjugated C=O).

b) A solution of resorcinol (0.63 g.) and 2-methoxy-4 : 5-methylenedioxyphenylacetonitrile (0.5 g.) in dry ether (80 ml.) containing zinc chloride (0.3 g.) was saturated with dry hydrogen chloride for 2 hr. under ice-cooling. After a few days, feeble brown crystals separated from the solution. This material was very hygroscopic and dissolved readily in water. When the aqueous solution was heated for a few min. on a bath, colorless 2-methoxy-4 : 5-methylenedioxyphenyl acetamide (IV) ($R=CONH_2$) separated in a poor yield. After recrystallization from water, it had a m. p. of 156—157°C.

Found: C, 57.29; H, 5.54. Calcd. for $C_{10}H_{11}O_4N$: C, 57.41; H, 5.30%.

IR: 3396, 3221 cm^{-1} (NH_2), 1654 cm^{-1} (s), (amide 1) 1621 cm^{-1} (m), (amide 2) 1501 cm^{-1} (m) (aromatic C=C).

2-Methoxy-4 : 5-methylenedioxyphenylacetic Acid (IV) (R=COOH).—2-Methoxy-4 : 5-methylenedioxyphenyl acetonitrile (0.5 g.), a 4 N potassium hydroxide solution (10 ml.), and methanol (10 ml.) were refluxed for 12.5 hr. After the evaporation of the methanol under reduced pressure and the acidification of the aqueous solution, colorless crystals separated, they were collected by filtration (0.5 g.). These crystals were then recrystallized from water, forming 0.45 g. of 2-methoxy-4 : 5-methylenedioxyphenylacetic acid (IV) (R=COOH). This solid acid melted at 155—157°C.[6,22] IR: 1690 cm^{-1} (s) (C=O).

Found: C, 57.38; H, 4.92. Calcd. for $C_{10}H_{10}O_5$: C, 57.14; H, 4.80%.

Methyl Ester (IV) (R=COOMe).—The above acid (0.1 g.) in acetone (2 ml.) was treated with ethereal diazomethane obtained from nitrosomethylurea (0.2 g.). After the evaporation of the solvent, the residual crude ester (IV) ($R=COOCH_3$) was recrystallized from aqueous acetone. Plates, m. p. 69—70°C.

Found: C, 59.02; H, 5.60. Calcd. for $C_{11}H_{12}O_5$: C, 58.92; H, 5.40%.

2-Hydroxy-4 : 2'-dimethoxy-4' : 5'-methylenedioxydesoxybenzoin (V) (R=Me).—The above ketone (0.23 g.) in acetone (3 ml.) was treated with an ethereal solution of diazomethane and then set aside overnight. The evaporation of the solvent under diminished pressure and the recrystallization of the residue from aqueous alcohol yielded 2-hydroxy-4:2'-dimethoxy-4':5'-methylenedioxydesoxybenzoin. Needles, m. p. 131—132°C.

Found: C, 64.50; H, 5.07. Calcd. for $C_{17}H_{16}O_6$: C, 64.55; H, 5.10%.

IR: 1632 cm^{-1} (s) (chelated conjugated C=O) 1616 (s), 1590 (m) and 1506 cm^{-1} (m) (aromatic C=C) 1039, 931 cm^{-1} (m) (-C-O-C-O-C-). A mixed melting point determination with a specimen of the hydrolysed product (m. p. 120—123°C)[2] of *O*-dimethylsophorol was undepressed.

21) Reported m. p. 273—274°C.

22) Reported m. p. 97—98°C.[6]

2-Hydroxy-7 : 2′-dimethoxy-4′ : 5′-methylenedioxyisoflavanone (VIb).—A solution of 2-hydroxy-4 : 2′-dimethoxy-4′ : 5′-methylenedioxydesoxybenzoin (100 mg.) in ethylformate (4 ml.) was added to powdered sodium (200 mg.) at 0°C. After it had been kept for 66 hr. at −5°C, the reaction mixture was decomposed by the addition of ice water. The aqueous solution was then acidified and freed from ethylformate under reduced pressure. The separated solid was extracted with ether (30 ml.×2). The evaporation of the solvent left a brown crystalline residue, m. p. 181—183°C. This residue was washed with a small amount of alcohol, resulting in the formation of 2-hydroxy-7 : 2′-dimethoxy-4′ : 5′-methylenedioxyisoflavanone (85 mg.). The material purified from aqueous alcohol formed colorless crystals (m. p. 185°C).

Found: C, 62.60; H, 4.80. Calcd. for $C_{18}H_{16}O_7$: C, 62.79; H, 4.68%.

IR spectrum (chloroform) 1677 cm^{-1} (s) (C=O) 3413, 3563 cm^{-1} (m) (OH) UV λ_{max} (ε_{max}) 230 (19200), 274 (17700) and 303 (16400).

7 : 2′-Dimethoxy-4′ : 5′-methylenedioxyisoflavone (VII). — When a solution of the above 2-hydroxyisoflavanone (50 mg.) in acetic acid (0.5 ml.) was boiled for 30 min. and was then diluted with water, a pale pink-colored material separated. Purification from aqueous ethanol gave rise to 2′ : 7-dimethoxy-4′ : 5′-methylenedioxyisoflavone in fine, colorless needles, m. p. 208—209°C.

Found: C, 65.98; H, 4.20. Calcd. for $C_{18}H_{14}O_6$: C, 66.25; H, 4.32%.

IR 1642 cm^{-1} (s) (γ-pyrone C=O) 1028 and 940 cm^{-1} (m) (methylenedioxyl). UV λ_{max} (ε_{max}): 247 (22200), 264 (13460), 304 (19570). $\lambda_{min}(\varepsilon)$: 245 (21650), 260 (13400) 280 (11020). A mixed melting point determination with dehydro-*O*-dimethylsophorol derived from a natural substance (m. p. 203—205°C)[2] showed no depression.

***O*-Methylanhydrosophorol (IX) (R=H).**—A mixture of sophorol (20 g.) and dimethylsulfate (20 ml.) containing a trace of acid in methanol (40 ml.) was set aside overnight. The next day, 30% aqueous sodium hydroxide was added, drop by drop, to this solution. After the reaction had subsided, the solution was diluted with water.

The resultant precipitation was washed and then recrystallized five times from aqueous acetone, thus forming silky needles (m. p. 187—188°C) of *O*-methylanhydrosophorol (ca. 80 mg.). The material recovered from the filtrate had a wide range of melting points (ca. 120—180°C), but it was not examined in detail.

Found: C, 68.96; H, 4.12; OCH_3, 10.48. Calcd. for $C_{17}H_{12}O_5$: C, 68.91; H, 4.08; OCH_3, 10.5%.

The PMR spectra of the synthetic sesamol derivatives. (τ)

		-O-CH_2-O-	OMe	A	B	CH_2
(III)	R=Me	4.00	6.14	3.46	2.75	—
(IV)	R=CN	4.10	6.24	3.50	3.21	6.46
(IV)	R=CO_2H	4.08	6.25	3.46	3.30	6.45
(III)	R=H	4.00	—	3.57	3.17	—
(IV)	R=$CONH_2$	4.11	6.24	3.48	3.31	6.57

The author is grateful to Professors Tōshi Irie, Takeshi Matsumoto and Tadashi Masamune for their kind interest in this work and to Mr. Mitsuru Kusama for assistance in the preparation of starting materials and to Mr. Hanzo Shimokawa for the measurements of the NMR spectra. The author thanks Mrs. Noriko Etoh for the elemental analyses.

BULLETIN OF THE CHEMICAL SOCIETY OF JAPAN VOL. 39 1529—1534 (1966)

Maackiain[1),*]

By Hiroshi SUGINOME

Department of Chemistry, Faculty of Science, Hokkaido University, Sapporo

(Received October 20, 1965)

This isolation and determination of the structure of a new, naturally-occurring chromanocoumaran, maackiain (I) R=H, are described. On the basis of these results, the structure of pterocarpin is revised to (I) R=CH_3.

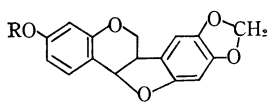

(I)

In preceding papers[2,3)] the isolation and the structure of a new isoflavanone, sophorol $C_{16}H_{12}O_6$, were discussed. Biogenetical considerations[2)] suggest the probable coexistence of pterocarpinoids

1) Oxygen Heterocycles. VII. Read before the 14th Annual Meeting of the Chemical Society of Japan, Tokyo, April, 1961. A brief account of this work has been published. H. Suginome, *Experientia,* **18**, 161 (1962).

* It was suggested to call this class of naturally occurring substances pterocarpinoids.

2) H. Suginome, *Tetrahedron Letters,* **1960**, 16; and preceding paper.

3) H. Suginome, *J. Org. Chem.,* **24**, 1655 (1959).

or rotenoids in the same plant. Therefore, we decided to examine this problem. A previous paper[3] described the isolation of an unknown phenolic substance, which was accompanied by sophorol and which had the molecular formula $C_{16}H_{12}O_5$. In reference to the source of this new compound, the name "maackiain" is suggested. The following proof of the structure of the compound as a chromanocoumaran gives support to the earlier biogenetical suggestions.[2]

Maackiain formed leaflets containing a half-equivalent molecule of water from aqueous methanol. The analytical data of dried maackiain crystals (m. p. 180—181°C) are in excellent agreement with the molecular formula of $C_{16}H_{12}O_5$ as has already been reported.[3] The compound is optically active, giving a value of $[\alpha]_D^{20}$ 251.7° in a chloroform solution. The optical rotatory dispersion curve of maackiain exhibits a negative Cotton effect curve. This was phenolic. A Zeizel determination showed no methoxyl group to be present. The presence of a methylenedioxyl group in the maackiain molecule was, however, suggested by the positive color tests. Maackiain showed the following maxima in infrared absorption, confirming all of the chemical evidence for the functional groups in the maackiain molecule: (3472: phenolic hydroxyl) (1617, 1600, 1507: aromatic C=C) (1496, 1379, 1347, 1315, 1292, 1267, 1234, 1204, 1180) (1161: C–O in dihydropyran) (1150, 1125, 1112, 1078, 1064, 1016, 978). (1035, 929: –C–O–CH_2–O–C–) (888, 861, 844, 813, 781, 758, 740 cm^{-1}).

On the basis of the above evidence, the functional groups of maackiain may be summarized as follows:

$$C_{15}H_9 \begin{cases} -O- \\ -O- \\ -O-CH_2-O- \\ -OH \text{ (phenolic)} \end{cases}$$

In accordance with the above results, maackiain readily formed mono-*O*-methyl ether, $C_{17}H_{14}O_5$, with ethereal diazomethane or with methyliodide and potassium carbonate in dry acetone. The *O*-methyl ether showed no band attributable to a hydroxyl stretching frequency in the infrared region.

In connection with a possible biogenetic linking of pterocarpin and homopterocarpin to naturally-occurring 2'-hydroxyisoflavonoids, the reduction of a carbonyl in the functional pattern (I) of sophorol, followed by dehydration to ether linkage, should give rise to a functional pattern (II) of maackiain.

$$C_{14}H_8 \begin{cases} C=O \\ OH \text{ phenolic} \\ OH \text{ phenolic} \\ -O-CH_2-O- \\ -O- \end{cases} \xrightarrow[-H_2O]{+H_2} C_{15}H_9 \begin{cases} -O- \\ \text{——} \\ OH \text{ phenolic} \\ -O-CH_2-O- \\ -O- \end{cases}$$

(I) (II)

Furthermore, *O*-methylmaackiain has the same functional groups as pterocarpin. These considerations lead to the assumption that the two arylic systems in the maackiain molecule may be the A and B groupings, which are chromophores of sophorol:[2]

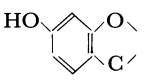

(A)

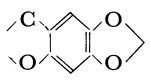

(B)

The ultraviolet spectra of maackiain and *O*-methylmaackiain in alcohol gave valuable information on the structure. Maackiain exhibits characteristic absorption peaks in two main regions, one of high intensity at 311 mμ (ε, 8510), and the other of a lower intensity at 286 mμ (ε, 5120). The medium intensities of these absorption maxima showed that the aromatic nucleus is in no conjugation with any other chromophore, e. g., ethylenic linkage.

Curves a, b, c, and d, in Fig. 1 show the ultraviolet absorption curves of 2:4-dimethoxyphenylacetonitrile, 2-methyl-4:5-methylenedioxyphenol, *O*-methylmaackiain and the summation of curves a and b respectively. As may be expected from the above discussion, curves c and d are very similar in shape.

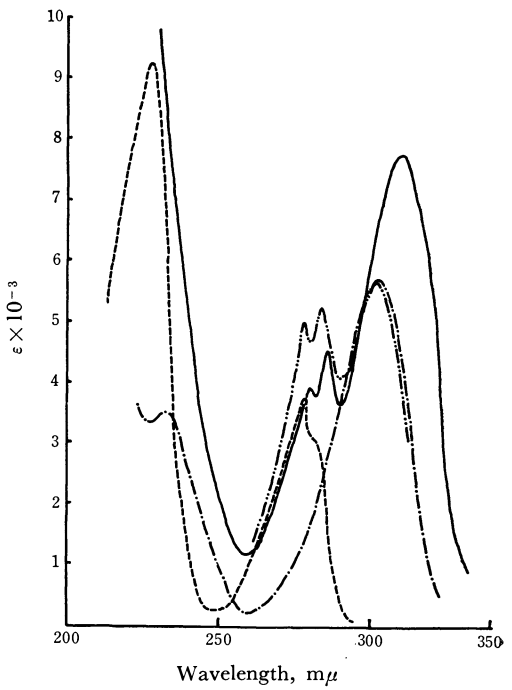

Fig. 1. UV spectra.
------ 2, 4-Dimethoxyphenylacetonitrile (curve a)
—·—· 2-Methyl-4: 5-methylenedioxyphenol (curve b)
——— *O*-Methylmaackiain (curve c)
—··— Curve a + b (curve d)

On the other hand, the ultraviolet absorption spectrum of *O*-methylmaackiain and that of pterocarpin** were also superimposable, and a mixed melting point determination of the two substances showed no depression.

Therefore, the structure of *O*-methylmaackiain was thought to be either III ($R=CH_3$) or IV ($R=CH_3$).

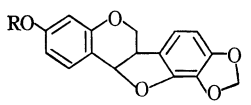

(III)

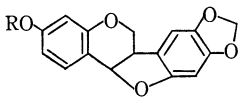

(IV)

Formula IV ($R=H$) for maackiain was proved as follows: the catalytic reduction of *O*-methylmaackiain gives rise to a new phenolic substance, $C_{17}H_{14}O_5$, melting at 146—148°C. The same substance was also produced in a good yield by the Birch reduction[4] of *O*-methylmaackiain. This phenol gave mono-*O*-methyl ether.

On the basis of formula IV, the structure of this phenolic compound should be explained by the isoflavan structure (V) formed by the hydrogenolysis of the benzilic-type ether linkage.

The structure of the *O*-methyl ether of dihydro-*O*-methylmaackiain was confirmed by the synthesis

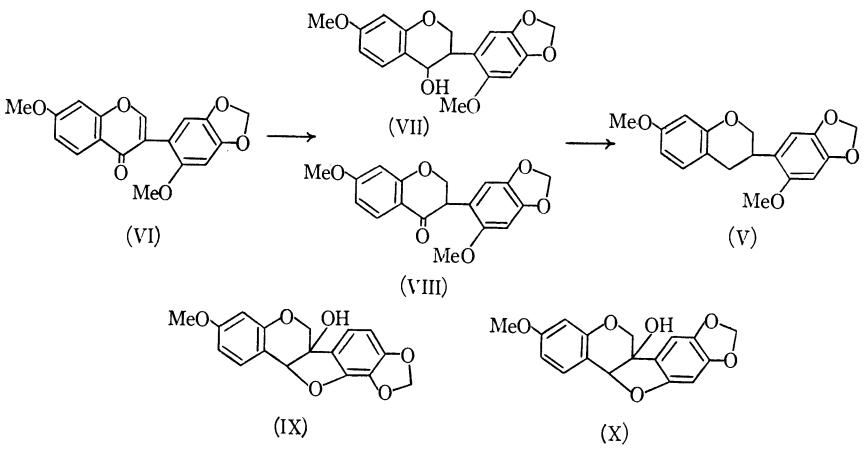

(VI) (VII) (VIII) (V)

(IX)

(X)

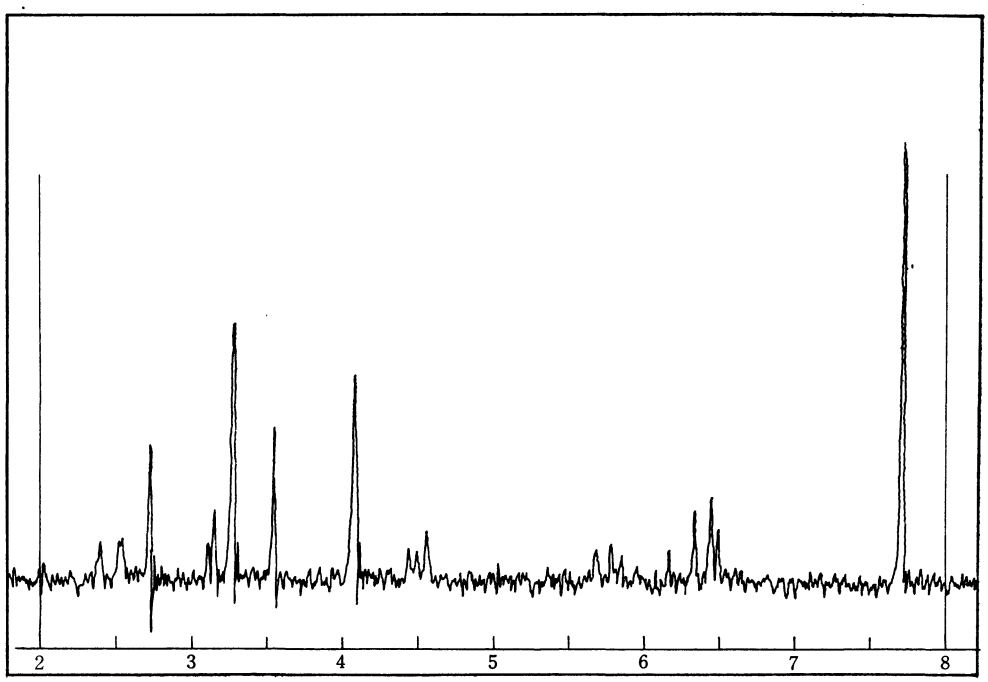

Fig. 2. NMR spectrum.

** Kindly provided by Dr. J. W. W. Morgan from the collection of Dr. F. E. King.

4) A. J. Birch, *Quart. Rev.*, **4**, 69 (1950).

of racemic 2': 7-dimethoxy-4': 5'-methylenedioxy-isoflavan (V, R=CH_3). The catalytic reduction of 2' :7-dimethoxy 4': 5'-methylene-dioxyisoflavone (VI)[3] gave an oily mixture of the corresponding isoflavan-4-ol (VII) and isoflavanone (VIII). The Clemmensen reduction of this gave racemic 2':7-dimethoxy - 4':5' - methylenedioxy - isoflavan (V), which had a m. p. of 111—113°C (V, R=CH_3).*** The latter and *O*-methyldihydro-*O*-methylmaackiain gave identical infrared-spectra in a chloroform solution, thus establishing the structure IV (R=H) for maackiain.[5] Since a comparison of the infrared spectra of *O*-methylmaackiain and pterocarpin in a chloroform solution disclosed that the two substances are identical, the structure of pterocarpin should be corrected to IV (R=CH_3). This finding is complementary to the conclusion, from the NMR spectrum, on the structure of pterocarpin.[6] Moreover, this conclusive evidence for the structure of pterocarpin and biogenetical considerations suggest that the structure of pisatin,[7] for which the structure IX has been given, should be X.

On the basis of a direct comparison with *O*-methylanhydrosophorol[3] and some spectral properties, the structure of pisatin was recently revised[8] to X. The NMR spectrum of *O*-acetylmaackiain (Fig. 2) further confirms the above conclusion.

The sharp single peak at $\tau=7.72$ which has the relative area of three hydrogens is due to the acetoxy group at the position 7. The value is in good agreement with the value of the acetoxy group attached to the aromatic ring. The peaks between $\tau=2.0$ and $\tau=3.6$ are attributed to aromatic protons. Ring A in *O*-acetylmaackiain has a pair of hydrogen atoms at the positions 5 and 6 and a hydrogen atom at the position 8. As expected, a hydrogen at the position 5 which is coupled with only one hydrogen on C6 appeared as a doublet centered at $\tau=2.44$. The coupling constant ($J=8.9$ c. p. s.) is an expected value for the ortho coupling of hydrogens on a benzene ring. Of the rest of the signals of this ABX system of the ring A, only one doublet, at $\tau=3.13$ and $\tau=3.16$, was observable. This doublet is considered to be a part of the quartet arising from a hydrogen on the position 6 which is coupled with a proton on the position 8 (meta coupling) and with a proton on the position 5 (ortho coupling). Other protons on the benzene ring B, will give two singlet peaks attributable to a proton on the position 3' and to a proton on the position 6' (para coupling). The lines at $\tau=3.56$ (1 proton) and $\tau=3.29$ (2.5 protons) are assigned to these protons. The observed broadening and the area of the former suggested that this had to include another proton. A proton on the position 8 will give rise to a doublet by meta coupling with a proton on the position 6. However, no isolated doublet was observed in the expected position. The peaks which are due to a hydrogen on the position 8 apparently formed a broad single peak at $\tau=3.29$, together with the signal of a hydrogen of the position 6'. It should be noted that, due to the *O*-acetyl substituent on the position 7, the position of the signal of a proton on the position 8 is shifted to a lower magnetic field than that to be expected for a proton adjacent to two oxygens. The peak at $\tau=3.29$ also includes the rest of the quartet of a proton on the position 6. The methylenedioxy peak appeared at 4.09 τ as a singlet. The triplets with center of 4.51 τ are assigned to a hydrogen on the position 4, which is coupled with only a proton of the position 3.

Since the interaction with a proton on the position 3 should give rise to doublets with the lines of a proton on the position 4, the following can explain the situation. The shape of the peaks indicates that they may be an unresolved quartet. *O*-Acetylmaackiain in deuteriochloroform could exist in an equilibrium of the two possible cis conformations, which will have somewhat different coupling constants for a proton on the position 4. The molecular model of the strainless configuration of *O*-acetylmaackiain, in which the two hydrogens on carbons 3 and 4 are cis, suggests that two conformations are possible. The conformational inversion between these two forms could be favorable in a chromanocoumaran system due to the lack of some 1, 3-hydrogen interaction. The two hydrogens on the position 2 which consititute the AB part of the ABX system and a hydrogen on the position 3 appeared in the range from $\tau=5.5$ to $\tau=6.6$. The two hydrogens on the position 2 should give rise to eight lines; these hydrogens appeared as a triplet centered at $\tau=6.42$. The rest of this ABX system, i. e., a hydrogen at the position 3, formed the multiplets $\tau=5.69$ to $\tau=6.17$.

*** A communication from the University of Manchester recorded m. p. 110—111°C for the same compound which was derived from pterocarpin.
C. W. L. Bevan, A. J. Birch, B. Moore and S. K. Mukerjee, *Tetrahedron Letters*, **1962**, 673.

5) After this work was completed, Professor Shibata of The University of Tokyo informed us that he and his colleague had isolated several chromanocoumarans from *Sophora subprostrata chun et T. Chen* and *Sophora japonica* L. By direct comparison, one of the chromanocoumarans was proved to be identical with maackiain. S. Shibata and Y. Nishikawa, *Chem. and Pharm. Bull.*, **11**, 167 (1963).
Furthermore, inermin isolated from *Andira inermis* H. B. K. by Cocker et al. is identical with maackiain. W. Cocker, T. Dahl, C. Dempsey and T. B. H. McMurry, *Chem. & Ind.*, **1962**, 216.

6) J. B. Bredenberg and J. N. Shoolery, *Tetrahedron Letters*, **1961**, 285.

7) D. R. Perrin and W. Bottomley, *Nature*, **191**, 76 (1961).

8) D. R. Perrin and W. Bottomley, *J. Am. Chem. Soc.*, **84**, 1919 (1962); D. D. Perrin and D. R. Perrin, ibid., **84**, 1922 (1962).

In view of the observed antifungicidal activity of this group of compounds, it is of interest to compare the variation in biological activity with the variation in structure. The results of tests on the antimicrobial activity[7] of maackiain and related compounds, kindly performed by Professor Yuji Sasaki and his colleagues, are recorded in the Experimental section.

Experimental[9]

The isolation and purification were described, with the isolation of sophorol, in the Experimental section of the previous paper.[3] Maackiain formed leaflets from aqueous methanol. After it had been dried under a vacuum, the melting point of this compound (178.5—179°C) rose to 180—181°C.

Found: C, 65.68; H. 4.69; 1/2H_2O, 3.7, 3.6. Calcd. for $C_{16}H_{12}O_5 \cdot 1/2H_2O$: C, 65.53; H, 4.46; 1/2$H_2O$; 3.6%. Found: (in a sample dried at 100—110°C in vacuo) C, 67.67; 67.33; H, 4.41; 4.58. Calcd. for $C_{16}H_{12}O_5$: C, 67.60; H, 4.26%.

$[\alpha]_D^{22}$ −251.7° (*c* 0.46, chloroform). RD[10] (*c* 0.074, methanol). 26°: [α]700 −175.8, [α]589 −227.0, [α]400 −559.0, [α]360 −684.0.

Maackiain was soluble in aqueous 2 N sodium hydroxide but insoluble in aqueous sodium hydrogen carbonate. Maackiain dissolved readily in acetone, ethylacetate, dioxane, chloroform and benzene. It gave no ferric reaction. The solution of maackiain in concentrated sulfuric acid became green when a drop of a 5% alcoholic gallic acid solution was added.

Maackiain-*O*-methyl Ether (Pterocarpin).—*a*) *With Diazomethane.*—Maackiain (150 mg.) in acetone (6 ml.) was treated with an ethereal solution of diazomethane (from nitrosomethylurea. 1.5 g.) and then set aside overnight. Evaporation under diminished pressure and the recrystallization of the crystalline residue from absolute ethanol yielded *O*-methylmaackiain, m. p. 168—169°C.

Found: C, 67.92; H. 4.74; OCH_3, 10.35. Calcd. for $C_{17}H_{14}O_5$: C, 68.45; H, 4.37; OCH_3, 10.40%. RD[6] (*c* 0.077, chloroform), 16°:[α] 700 −119.4, [α]589 −223.5, [α]400 −530.1, [α]340 −481.0.

UV *max.*: 310 mμ (ε, 10156), 386 mμ (ε 5687), 280 mμ (ε, 4813).

This was insoluble in a 2 N sodium hydroxide solution. The solution of the compound in concentrated sulfuric acid became green when one drop of a 5% alcoholic gallic acid solution was added.

b) *With Methyl iodide.*—A mixture of maackiain (670-mg.), potassium carbonate (2 g.), methyl iodide (15-ml.), and acetone (14 ml.) was heated under reflux for 4 hr. The filtered solution was then evaporated, and the residue was washed with water and recrystallized from alcohol.

Colorless leaflets; m. p. 168—169°C (560 mg.).

Dihydro-*O*-methylmaackiain Obtained by the Hydrogenolysis of *O*-Methylmaackiain.—*a*) *By Catalytic Hydrogenation.*—*O*-Methylmaackiain (200 mg.), dissolved in glacial acetic acid (24 ml.) containing a pre-reduced platinum catalyst (platinum oxide, 40 mg.), was hydrogenated for 2 hr. at room temperature. After the catalyst had then been removed, the filtrate was evaporated to dryness. The residue was treated with aqueous 2 N sodium hydroxide. Upon the acidification of the sodium hydroxide solution, crude dihydro-*O*-methylmaackiain separated. This was recrystallized from aqueous ethanol, forming colorless leaflets (m. p. 146—148°C) (8 mg.). Crude *O*-methylmaackiain (158 mg.) was recovered unchanged.

Found: C, 68.10; H, 5.12. Calcd. for $C_{17}H_{16}O_5$: C, 67.99; H, 5.37%.

IR spectrum: 3285 cm^{-1} (phenolic OH); 1618, 1591 and 1499 cm^{1-} (aromatic C=C).

UV max.: 290 and 302 mμ (ε, 6729 and 6467).

b) *With Sodium and Liquid Ammonia.*—Sodium (50 mg.) in small pieces was stirred into *O*-methylmaackiain (150 mg.) in toluene (8 ml.) and liquid ammonia (28 ml.) within a five-minute period. After the reaction mixture had been set aside overnight, 10 ml. of water was added. After the extraction of the mixture with ether (40 ml.), the ethereal solution was extracted with 4 N aqueous sodium hydroxide (20 ml.×2). The alkaline layer was acidified with 6 N hydrochloric acid and extracted with ether (40 ml.+20 ml.+20 ml.), washed with water, and dried. The solution was evaporated to dryness to yield an intractable residue (120 mg.). The neutral fraction, after it had been washed and dried, yielded a crystalline residue of 155 mg. This was recrystallized from dilute ethanol, yielding dihydro-*O*-methylmaackiain (m. p. 146—148°C, 67 mg.) which was identical with the specimen obtained from procedure a) above.

***O*-Methyl Ether of Dihydro-*O*-methylmaackiain.**—Dihydro-*O*-methylmaackiain (20 mg.), methyliodide (0.02 ml.), anhydrous potassium carbonate (60 mg.), and dry acetone (1 ml.) were refluxed for 4 hr. After the potassium carbonate had been removed, the filtrate was evaporated to dryness and the residue was washed with a small volume of water and then recrystallized from aqueous ethanol, yielding *O*-methyl ether as short needles, m. p. 109—110°C.

Found: C, 68.66; H, 5.70. Calcd. for $C_{18}H_{18}O_5$: C, 68.78; H, 5.77%.

***O*-Acetylmaackiain.**—Maackiain (85 mg.) was dissolved in 0.5 ml. of pyridine and 0.5 ml. of acetic anhydride and then set aside. A work-up by the standard procedure gave crude *O*-acetylmaackiain (93 mg.). This was recrystallized from aqueous ethanol. M. p. 177—178°C; leaflets; 60 mg.

Found: C, 66.37; H, 4.29. Calcd. for $C_{18}H_{14}O_6$: C, 66.25; H, 4.32%.

The Hydrogenation of 2′ : 7-Dimethoxy-4′ : 5′-methylenedioxyisoflavone.—When isoflavone (84 mg.) in acetic acid (20 ml.) was hydrogenated in the presence of a pre-reduced platinum catalyst (PtO_2, 20 mg.) for 26 min., it absorbed 1.1 mol. of hydrogen. The solvent was then removed under reduced pressure to yield 77 mg. of a residue, which showed hydroxyl and γ-pyranone carbonyl in its infrared spectrum and

9) Melting points are uncorrected. Ultraviolet spectra were taken in ethanol unless otherwise stated. Analyses were made by Mrs. Noriko Etoh in this laboratory and Mr. Kusuo Narita, Department of Pharmacy, Faculty of Medicine, Hokkaido University. The NMR spectrum was taken by Japan electron optics 3H 60 high resolution NMR spectrometer (60 Mc.). Tetramethylsilane was used as internal standard.

10) Measurements by Dr. Masao Maruyama of Tohoku University.

which was immediately submitted to the next reduction.

The Clemmensen Reduction of the Mixture of 7 : 2'-Dimethoxy 4' : 5'-methylenedioxyisoflavan-4-ol and 7 : 2'-Dimethoxy-4' : 5'-methylenedioxyisoflavanone.—The mixture (77 mg.) of isoflavan-4-ol and isoflavanone obtained above was dissolved in 2 ml. of toluene. To this solution was then added mercury amalgam, which had been prepared from zinc (0.79 g.), mercuric chloride (0.087 g.), concentrated hydrochloric acid (3 ml.), and water (1.5 ml.). The solution was refluxed for 14 hr. and 20 min. To the solution further amounts of hydrochloric acid (0.12 ml. × 3) were then added after 2 hr. 40 min., 6 hr. 5 min., and 9 hr. 15 min. The zinc amalgam was filtered and washed with toluene-ether. To the combined filtrate and washings, there was added a further volume of ether. The ethereal solution was washed with water, a 2 N sodium hydroxide solution (5 ml.) and twice again with water (5 ml. × 2) successively. The solution was then dried over sodium sulfate. On evaporation, the residual yellow oil crystallized. M. p. 96—107°C; 50 mg. This was recrystallized from ethanol to yield d, *l*-7: 2'-dimethoxy-4': 5'-methylenedioxyisoflavan, m. p. 111—113°C.

Found: C, 68.66; H, 5.86. Calcd. for $C_{18}H_{18}O_5$: C, 68.78; H, 5.77%.

2-Methyl-4 : 5-methylenedioxyphenol.—A mixture of zinc dust (5 g.), 0.5 g. of mercuric chloride, 0.25 ml. of concentrated hydrochloric acid, and 7.5 ml. of water was stirred for 15 min. The aqueous solution was decanted, and the zinc amalgam was covered with 5 ml. of water and 5 ml. of concentrated hydrochloric acid. To this refluxed solution, there was then added 0.5 g. of sesamol in 2.5 ml. of concentrated hydrochloric acid and 2.5 ml. of water over the course of 1 hr. and twenty minutes. After a further 2 ml. of concentrated hydrochloric acid had been added, the solution was refluxed for 2 hr. The solution was then cooled to room temperature. The aqueous layer was separated from the zinc amalgam, and sodium chloride was added to the solution. This was extracted with ether. The ethereal solution was combined with the ethereal washings of the zinc amalgam and washed with an aqueous sodium chloride solution, decolorized with activated charcoal, and dried. After the ether had been removed, the residue (0.36 g.) was distilled under reduced pressure (2.5 mmHg) (bath temp. 132—142°C) (0.172 g.). This distillate was recrystallized from petroleum benzine. 96 mg. M. p. 58—59°C. IR: 3573 cm^{-1} (OH) (chloroform) UV λ_{max} (ε_{max}): 232 (3525) 302 (5720).

Antimicrobial Tests (Performed by Professor Yuji Sasaki and his colleagues, Laboratory of Applied Microbiology, Department of Agricultural Chemistry, Faculty of Agriculture, by courtesy of Professor Tōshi Irie).—The inhibition of the growth of bacteria, fungi or yeast was assayed according to the agar-plate method. The compounds were introduced in the form of acetone dilutions or in the form of crystals on agar. The strains of bacteria, fungi or yeasts used are described in Table I. These were incubated on the agar medium at the optimum temperature.

TABLE I.

		Staphylococcus aureus	*Escherichia coli*	*Bacillus subtilis*	*Saccharomyces cerevisiae*	*Candida albicans*	*Aspergillus niger*	*Aspergillus fumigatus*	*Penicilium roqueforti*
a)	2'-Hydroxyisoflavanone	−	−	−	−	−	−	−	−
b)		−	−	−	−	−	−	−	−
a)	Sophorol	−	−	−	−	−	−	−	−
b)		−	−	−	−	±	−	−	−
a)	Maackiain	−	−	−	++	++	++	++	++
b)		−	−	−	−	−	−	−	−
a)	Pseudobaptigenin	−	−	−	−	−	−	−	−
b)		−	−	−	−	−	−	−	−

a) acetone solution b) crystals

When the compounds were introduced in the form of crystals, no antimicrobial activity was observed in any of the specimens. However, in an acetone solution, maackiain exhibited antimicrobial action in reaction to yeast and fungi.

The author is grateful to Professors Tōshi Irie, Takeshi Matsumoto and Tadashi Masamune for their kind interest in this work, and Drs. F. E. King and J. W. W. Morgan, for providing the sample of pterocarpin. The author wishes to thank Mr. Toshiro Kio for help in experiment and Mr. Hanzo Shimokawa for the measurements of NMR spectra.

BULLETIN OF THE CHEMICAL SOCIETY OF JAPAN VOL. 39 1535—1541 (1966)

The Synthesis of *d, l*-Homopterocarpin[1]

By Hiroshi SUGINOME and Tsukasa IWADARE

Department of Chemistry, Faculty of Science, Hokkaido University, Sapporo

(Received October 20, 1965)

The synthesis of chromanocoumaran (I) ($R^1=R^2=H$), the skeleton of pterocarpinoids, is described. This method, which follows a plausible biogenetic pathway, is then extended to the synthesis of *d, l*-homopterocarpin (I) ($R^1=R^2=OMe$). The synthesis and NMR studies allow us to assign a cis B/C ring junction to the compounds of this class.

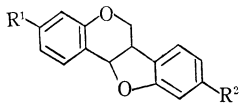

(I)

Pterocarpin and homopterocarpin were first isolated by Cazeneuve in 1874.[2] The structure of homopterocarpin was elucidated in 1940 by Späth and Schläger[3] and by Robertson et al.[4] as III ($R^1=R^3=OMe$, $R^2=H$). The structure of pterocarpin was also elucidated by Robertson et al.[4] and, more recently, by Bredenberg and Shoolery[5] spectroscopically, and also by one of the present authors synthetically,[6] as III ($R^3=OMe$, R^1, $R^2=-O-CH_2-O-$). However, the syntheses of these natural products, even their simple cores, have not been completed. This paper is an account of the syntheses of their skeleton and the racemic homopterocarpin.

In view of an apparent biogenetic link of these naturally-occurring chromanocoumarans to 2'-hydroxyisoflavonoids,[7] the synthetic sequence was chosen in order to trace a plausible biogenetic path.

In explorative studies, the skeleton III ($R^1=R^2=R^3=H$) of pterocarpin was synthesized for the first time.

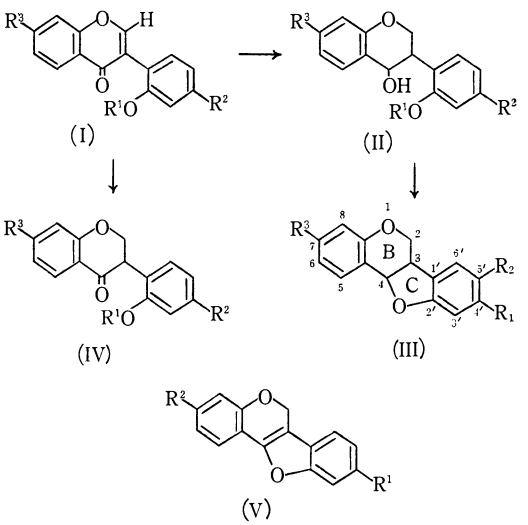

(I) (II) (IV) (III) (V)

It was found that the mild acid hydrolysis of liquid 2 : 2'-bismethoxymethoxybenzoin[8] which had been purified by distillation yielded 2 : 2'-dihydroxybenzoin, together with a second product. This was identified as the corresponding benzil. It showed a doublet carbonyl absorption in its infrared spectrum (1614 cm^{-1} and 1631 cm^{-1}) and an absorption maxima at 256 mμ (ε, 14930) and 330 mμ (ε, 6300) in its ultraviolet spectrum. It was apparent that the original, protected benzoin was contaminated by the corresponding benzil, which could be isolated as crystals from liquid 2 : 2'-bismethoxymethoxybenzoin. This benzil may be produced by autooxidation during distillation, and La Forge's liquid bismethoxymethoxybenzoin could be a mixture of benzoin and the

1) Oxygen Heterocycles. VIII. Read before the 15th Annual Meeting of the Chemical Society of Japan, Tokyo, April, 1962. A brief account of this work has already been published. H. Suginome and T. Iwadare, This Bulletin, **33**, 568 (1960); *Experientia*, **18**, 163 (1962).

2) a) P. Cazeneuve, *Ber.*, **7**, 1798 (1874); P. Cazeneuve, *Bull. Soc. Chim. France.*, **23**, 97 (1875); P. Cazeneuve, and L. Hugouneng, *Compt. Rend.*, **104**, 1722 (1887). b) P. L. Sawhney and T. R. Seshadri, *J. Sci. and Ind. Res.*, **13B**, 5 (1954). c) F. E. King, C. B. Cotterill, D. H. Godson, L. Jurd and T. J. King, *J. Chem. Soc.*, **1953**, 3693. d) A. Akisanya, C. W. L. Bevan and J. Hirst, ibid., **1959**, 2679.

3) E. Späth and J. Schläger, *Ber.*, **73**, 1 (1940).

4) A. McGookin, A. Robertson and W. B. Whalley, *J. Chem. Soc.*, **1940**, 787.

5) J. B. Bredenberg and J. N. Shoolery, *Tetrahedron Letters*, **1961**, 285.

6) H. Suginome, *Experientia*, **18**, 161 (1962); and preceding paper.

7) H. Suginome, *J. Org. Chem.*, **24**, 1655 (1959); H. Suginome, *Tetrahedron Letters*, **1960**, 16.

8) F. B. LaForge, *J. Am. Chem. Soc.*, **55**, 3040 (1933).

corresponding benzil. The mixture of 2 : 2'-dihydroxybenzoin and benzil thus obtained was reduced with zinc and sodium hydroxide to yield 2 : 2'-dihydroxydesoxybenzoin (m. p. 102—103°C), together with a small amount of 2'-(*O*-hydroxyphenyl)-coumarone. This desoxybenzoin was then transformed to the corresponding 2'-hydroxyisoflavone with sodium and ethyl formate.[9] No isomeric 3-benzoylcoumarone and intermediary 2-hydroxyisoflavanone could be isolated. It has already been suggested by Whalley[10] that a 2'-methoxy subsituent is necessary to isolate an intermediary 2-hydroxyisoflavanone in the reaction of desoxybenzoin with sodium and alkyl formates, since a weak hydrogen bonding between the 2-hydroxyl group and the 2'-methoxy group will be a major contributing factor to the stability of the 2-hydroxyisoflavanone system. In the present investigation, obviously the hydrogen bond between the 2'-hydroxyl group and the carbonyl group is stronger than that between the 2' and 2-hydroxyl functions. This must be the reason for the failure to isolate an intermediate 2-hydroxyisoflavanone. The 2'-hydroxyisoflavone thus obtained was reduced to the corresponding isoflavanone in the presence of Adams' platinum catalyst. This isoflavanone was very easily converted to chromenocoumarone (V) ($R^1=R^2=H$) (m. p. 87—89°C) with 50% acetic acid, thus confirming the conversion of sophorol to anhydrosophorol.[7] The ultraviolet spectrum of chromenocumarone is shown in Fig. 1. The tetrasubstituted double bond in chromenocoumarone (V) ($R^1=R^2=H$) resists catalytic hydrogenation in the presence of the platinum catalyst. 2'-Hydroxyisoflavone was reduced to a liquid stereoisomeric mixture of 2'-hydroxyisoflavan-4-ol with either sodium borohydride[11] or lithium aluminum hydride. In the case of dehydrorotenone, reduction with lithium aluminum hydride leads to the corresponding isoflavan-4-ol, whereas reduction with sodium borohydride results in the formation of the corresponding isoflav-2-en-4-ol.[11] It is of interest to note that, in the present case, reduction with both these metal hydrides resulted in the isolation of the same product, which is probably due to the 1, 4-addition of hydride reagents to the γ-pyrone system followed by further reduction. This crude isoflavan-4-ol was successfully converted into the pterocarpin ring system. III ($R^1=R^2=R^3=H$) in a 70% yield by mild treatment with 50% acetic acid. No appreciable formation of isoflav-(3)-ene was observed.

The NMR spectrum (Fig. 2) in deuteriochloroform of the synthetic chromanocoumaran shows 8 aromatic protons as the multiplet ranging $\tau=2.34$ to $\tau=3.18$. The doublet centering at $\tau=4.47$, $J=5.7$ c. p. s. (1 proton) is assigned to a proton on position 4, which is coupled only to a proton on the position 3. The Karplus equation[12] has

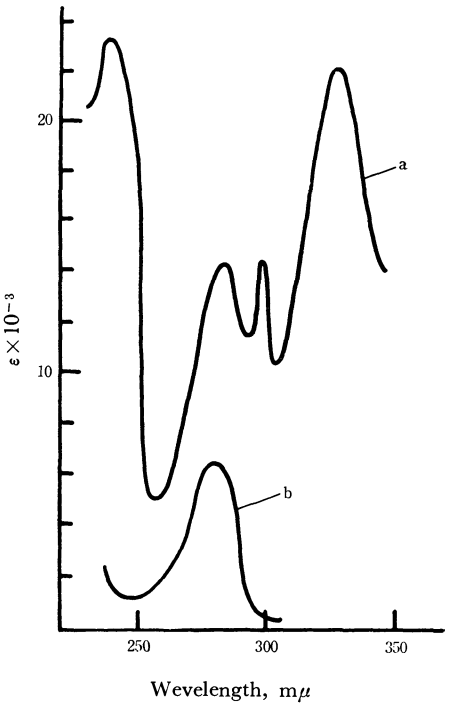

Fig. 1. UV spectra.
a, Chromanocoumarone
b, Chromanocoumaran

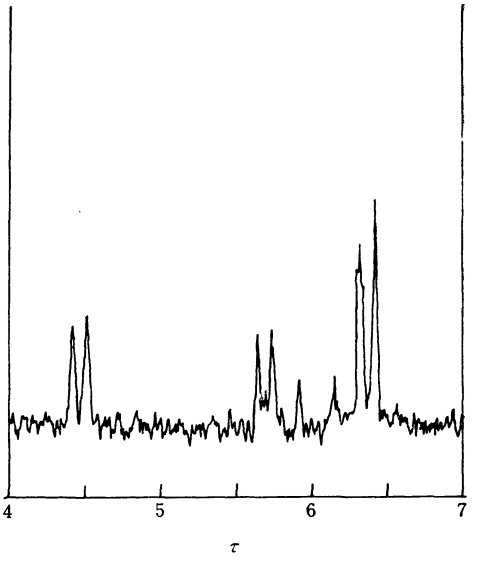

Fig. 2. NMR spectrum of chromanocoumaran.

9) W. H. Perkin and R. Robinson, *J. Chem. Soc.*, **1908**, 489.
10) W. B. Whalley, *J. Am. Chem. Soc.*, **75**, 1059 (1953).
11) M. Miyano and M. Matsui, *Chem. Ber.*, **91**, 2044 (1958).
12) M. Karplus, *J. Chem. Phys.*, **30**, 11 (1959); R. J. Abraham and K. A. MacLauchlan, *Mol. Phy.*, **5**, 513 (1962); R. J. Abraham and J. S. E. Holker, *J. Chem. Soc.*, **1963**, 806.

been shown experimentally to apply to a wide variety of compounds.

The equation gives $\phi = 33°$ for the dihedral angle $-HC^3-C^4H-$. The model inspection obviously favored a B/C ring junction of cis for chromanocoumaran. Although the calculated angle seems to give a higher value than that to be expected from the model, the deviation is perhaps attributable to the electronegativity[13] of the substituent adjacent to the coupling protons. The two hydrogens on the position 2 which constitute the AB part of the ABX system appeared as the triplet centered at $\tau = 6.28$. A proton on the position 3 gives rise to the multiplet ranging from $\tau = 5.65$ to $\tau = 5.92$.

In view of the above described results, the same sequence of reaction was applied to the 2′: 4′: 7-trihydroxyisoflavone (I) ($R^1=H$, $R^2=R^3=OH$) series. The starting material, 2′: 4′: 7-trimethoxyisoflavone, had been synthesized by Späth and Schläger[3] by the reaction of 2-hydroxy-2′ : 4′-trimethoxydesoxybenzoin with methylformate in the presence of sodium. Although they did not isolate any intermediary 2-hydroxyisoflavanone from this reaction, one repetition of this work by using ethylformate led to the isolation of 2-hydroxy-7 : 2′ : 4′-trimethoxyisoflavanone in a 94% yield. The result is in accord with the experienced facts and the previous assumption.[10] The isoflavanone obtained above was dehydrated with acetic acid to yield 2′: 4′: 7-trimethoxyisoflavone in a 69% yield. The demethylation of 2′: 4′: 7-trimethoxyisoflavone[3,7] to 2′: 4′: 7-trihydroxyisoflavone was achieved in a 98% yield by using anhydrous aluminum chloride.[14] Since it was found that the relatively strong acidic character of the 7′-hydroxyl group prevented the use of complex metal hydride, the 7′-phenolic function of 2′: 4′: 7-trihydroxyisoflavone had to be methylated before reduction. This selective methylation of the 7′-phenolic function was accomplished in a 73% yield at 30 to 40°C using methyl iodide and potassium carbonate in acetone. The same substance was also obtained by partial methylation with diazomethane. The structure of monomethoxyisoflavone was confirmed by studying its ultraviolet spectra in neutral and alkaline solutions. Thus, as expected, the ultraviolet spectrum of 7-methoxy-2′: 4′-dihydroxyisoflavone does not reveal any appreciable bathochromic shift in an alkaline solution (Fig. 3). However, the ultraviolet spectrum of the corresponding 7-hydroxyisoflavone in an alkaline solution exhibits batho- and hypochromic shifts when compared with that in a neutral solution (Fig. 4). When the 7-methoxy-2′: 4′-dihydroxyisoflavone thus obtained was submitted to sodium borohydride reduction, it gave rise to an oily stereoisomeric mixture of 7-methoxy-2′: 4′-dihydroxyisoflavan-(4)-ols. The final step of the synthesis was accomplished as follows. The oil obtained above was refluxed with 50% acetic acid for one hour.

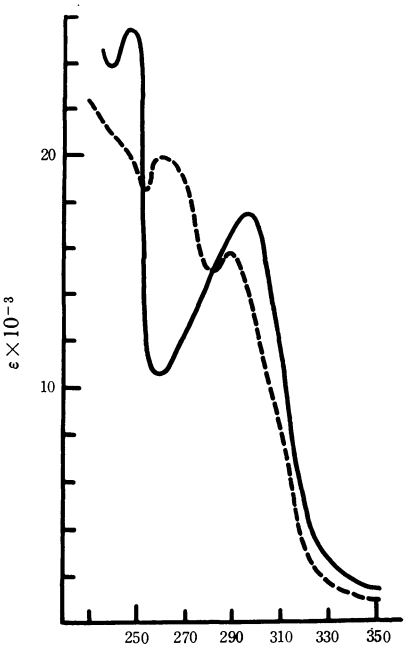

Fig. 3. Ultraviolet spectra of 7-methoxy-2′: 4′-dihydroxyisoflavone.
—— Neutral
---- In 0.1 N aq. NaOH solution

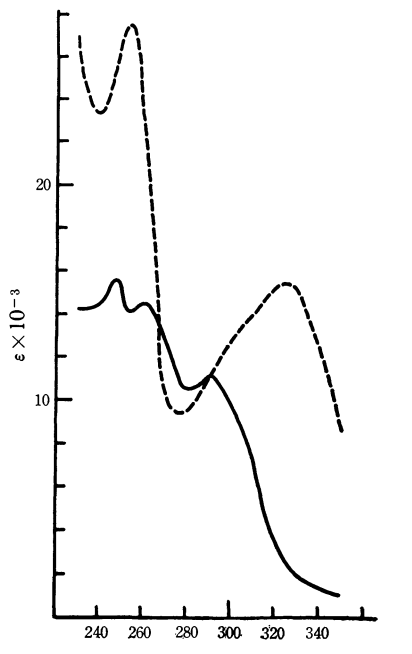

Fig. 4. Ultraviolet spectra of 7-hydroxyisoflavone.
---- 0.1 N aq. NaOH solution
—— Neutral

13) K. L. Williamson, *J. Am. Chem. Soc.*, **85**, 516 (1963).
14) W. B. Whalley, *J. Chem. Soc.*, **1953**, 3366.

The product was then treated with methyl iodide and potassium carbonate in acetone for 3 hr. When the product was treated with aqueous ethanol, short needles of *d, l*-homopterocarpin, m. p. 123—125°C, was obtained in a rather poor yield. When compared with the natural specimen, m. p. 87—88°C, synthetic *d, l*-homopterocarpin showed NMR, infrared and ultraviolet spectra identical with those of natural homopterocarpin.

The aryl group in the carbon 3 of isoflavan-4-ol obtained from the reduction of the isoflavone with sodium borohydride should be almost entirely in an equatorial position. However, the hydroxyl group in the carbon 4 of diol II can be either in the quasi equatorial or quasi axial position,[15] because of the easy conformational inversion of intermediary isoflavanone during metal hydride reduction. That is, the isoflavan-4-ol obtained is a mixture of cis 3(eq.): 4(ax.) and trans 3(eq.): 4(eq.) with respect to 3 and 4-substituents. Although the SN2 mechanism of the ring formation can not be entirely excluded, the smooth formation of chromanocoumaran (III) ($R^1=R^2=R^3=H$) from isoflavan-4-ol (II) ($R^1=R^2=R^3=H$) in a high yield (70%) can perhaps be better explained by assuming the SNl character of the reaction in which the common carbonium ion is produced from the protonated form VI of cis and trans isomers, and by also assuming a simultaneous attack by the phenolic hydroxyl.

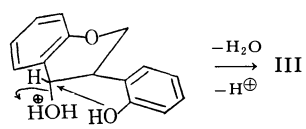

(VI)

From these considerations, it may be concluded that the reaction should produce a stable cis B/C ring junction and that, therefore, the B/C ring junction of natural homopterocarpin and the related compounds are cis.

The NMR spectrum of the synthetic *d, l*-homopterocarpin in deuteriochloroform showed a proton on position 4 as a doublet centered at $\tau=4.54$ ($J=6.0$ c. p. s.). The Karplus equation gives $\phi=55°$ for the dihedral angle HC^3–C^4H–. Assignment of other protons: $\tau=6.27$ and 6.30 (4′ and 7 methoxyls), the multiplet, $\tau=5.75$ to $\tau=6.54$ (two hydrogens on position 2 and one hydrogen on position 3), a doublet centered at $\tau=2.91$ ($J=8.6$) (a hydrogen on the position 6′) and the multiplet $\tau=3.32$—3.66 (protons on the positions 3′, 5′, 6′ and 8).

Experimental[16]

2 : 2′-Bismethoxymethoxybenzoin and 2 : 2′-Bismethoxymethoxybenzil.—Potassium cyanide (1 g.) and 2-methoxymethoxybenzaldehyde[8,17] (b. p. 112.5—115.5°C/5 mmHg, 6 g.) in 7.2 ml. of ethanol were refluxed on a water bath for 2 hr. The solvent was then removed under reduced pressure, and the oily residue was extracted with ether. The ethereal solution was washed with water and dried. After the ether had been removed, and the starting material (b. p. 103°C/3 mmHg) had been distilled, the viscous, reddish residue yielded 2 g. of a viscous, pale yellow oil boiling at 176—186°C/0.05 mmHg.[18] On standing, this oil partially crystallized. It was recrystallized from 80% ethanol, giving 2 : 2′-bismethoxybenzil; m. p. 107—107.5°C. IR: 1665 cm^{-1} and 1675 cm^{-1} (–CO-CO–).

Found: C, 64.79; H, 5.59. Calcd. for $C_{18}H_{18}O_6$: C, 65.4; H, 5.5%.

2 : 2′-Dihydroxybenzoin and 2 : 2′-Dihydroxybenzil.—The oily mixture of benzoin and benzil (1.7 g.) obtained above, in 50% acetic acid (12 ml.) containing 0.05 g. of sulfuric acid, was refluxed for 15 min. The solution was then cooled and poured into ice water containing 6 g. of sodium carbonate. The solid which separated was extracted with ether. The ethereal extract was washed with water and dried over sodium sulfate. After the solvent had been removed, the residual yellowish brown substance was recrystallized from benzene to yield 0.6 g. (m. p. 161—163°C) of benzoin.[19] IR: 1643 cm^{-1} (C=O) 3305 and 3507 cm^{-1} (OH). The filtrate from the isolation of benzoin was concentrated to yield crude benzil, which was then recrystallized from 80% ethanol. Yellow needles, m. p. 156—157°C.[20] IR: 1631 and 1614 cm^{-1} (COCO) 1635 cm^{-1} (–CO–CO–, chloroform) 3180 cm^{-1} broad, (OH). UV λ_{max} (ε_{max}): 256 (14930), 330 (6300); λ_{min} (ε_{min}): 292 (1850). This benzil (0.5 g.) in acetone (20 ml.) was refluxed with dimethylsulfate (0.5 g.) and sodium carbonate (1.5 g.) for 20 hr. After the solvent had been removed, the residue was extracted with ether, washed with water, 2 N sodium hydroxide, and water successively, and dried. The residue was then recrystallized from 80% ethanol to yield 2 : 2′-dimethoxybenzil. Colorless needles, m. p. 127—128°C.[21] IR: 1653 and 1673 cm^{-1} (–CO–CO–) 1663 cm^{-1} (–CO–CO–, chloroform). This benzil formed a quinoxaline derivative; m. p. 181.5—182.0°C.

2 : 2′-Dihydroxydesoxybenzoin and 2-(*O*-Hydroxyphenyl)-coumarone. — 2 : 2′-Dihydroxybenzoin (14 g.) in 50% ethanol (90 ml.) and 15% aqueous potassium hydroxide (150 ml.) were refluxed with powdered zinc (40 g.) for 8 hr. After the zinc had been removed and the solution had been neutralized with 2 N

15) E. M. Philbin and T. S. Wheeler, *Proc. Chem. Soc.*, **1958**, 167.

16) Melting points are uncorrected. Infrared spectra were taken in Nujol, and ultraviolet spectra were taken in ethanol unless otherwise stated. Analyses by Mr. Kusuo Narita in the Department of Pharmacy, Faculty of Medicine, Hokkaido University. NMR spectra were taken in deuteriochloroform by Japan electron optics 3H 60 high resolution NMR spectrometer. (60 Mc.) Tetramethylsilane was used as internal standard.

17) Reported b. p. 128—130°C/11 mmHg.[8]

18) Reported b. p. 200—210°C/1 mmHg.[8]

19) Reported m. p. 142—149°C.[5]

20) Reported m. p. 154—155°C. R. Kuhn, L. Birkofer and E. F. Möller, *Ber.*, **76**, 900 (1943).

21) Reported m. p. 130°C, A. Schönberg and O. Kraemer, *Ber.*, **55**, 1174 (1922).

hydrochloric acid, ethanol was evaporated under reduced pressure. The solution was extracted with ether, washed with water, and dried. The residue was then recrystallized from benzene to yield desoxybenzoin. Colorless needles; m. p. 102—103°C.[22] Yield 9.3 g. (71%). IR (KBr): 1629 cm^{-1} (–CO–CO–) 3465 cm^{-1} (OH). UV λ_{max} (ε_{max}): 327 (3060), 253 (8310); λ_{min} 293 (1360).

The filtrate was concentrated to yield crude 2-(*O*-hydroxyphenyl)-coumarone, which was then recrystallized from 80% ethanol. Feeble pink colored needles; m. p. 95—95.5°C.[23] A ferric chloride color reaction was negative. IR (KBr): 3213 cm^{-1} (broad, OH). UV λ_{max} (ε_{max}): 328 (16750), 314 (17650), 289 (12410); λ_{min} (ε_{min}): 323 (14880), 293 (10740), 249 (2320).

2' - Hydroxyisoflavone (I) ($R^1=R^2=R^3=H$).—2 : 2'-Dihydroxydesoxybenzoin (8 g.) in ethylformate (280 ml.) was added, dropwise to powdered sodium (11 g.) under ice-cooled conditions. After the solution had been set aside for three days at −5°C, the reaction mixture was slowly poured into 100 g. of ice water. The aqueous solution was neutralized with 2 N hydrochloric acid and freed from ethylformate under reduced pressure, and the solution was extracted with chloroform. The chloroform solution was washed with water and dried. After the solvent had been removed, the residue was recrystallized from methanol. Yield 6.3 g. (75.5%). Colorless plates; m. p. 153—154°C.

Found: C, 75.67; H, 4.45. Calcd. for $C_{15}H_{10}O_3$: C, 75.62; H, 4.23%. UV λ_{max} (ε_{max}): 285 (10100), 240 (24320); λ_{min} (ε_{min}): 271 (7720). IR: 1633 cm^{-1} (–CO–), 3185 cm^{-1} (OH) (broad).

2'-Hydroxyisoflavanone (IV) ($R^1=R^2=R^3=H$).—2'-Hydroxyisoflavone (2 g.) in acetic acid (110 ml.) was hydrogenated in the presence of a platinum catalyst. 220 ml. of hydrogen was thus absorbed. After the catalyst had been removed, the solvent was evaporated to dryness. The residue was thus extracted with chloroform, washed with water, and dried. After the solvent had been removed, the residue was recrystallized from 80% ethanol; m. p. 118—122°C.

Found: N, 13.27. Calcd. for $C_{21}H_{16}O_6N_4$: N, 13.33%. UV λ_{max} (ε_{max}): 318 (3400), 276 (3310), 250 (9700). IR: 1660 cm^{-1} (–CO–) 3297 cm^{-1} (broad, OH).

2, 4-Dinitrophenylhydrazone was prepared in the usual way; m. p. 223°C (decomp.); red needles.

2'-Methoxyisoflavone[24] (I) ($R^1=CH_3$, $R^2=R^3=$ OMe).—2'-Hydroxyisoflavone (0.2 g.) in a mixed solvent of ether and acetone (20.3 g.) was treated with ethereal diazomethane (from nitrosomethylurea, 1.5 g.) and then set aside for 24 hr. The solution was washed with 2 N sodium hydroxide solution, and with water, and dried. After the solvent had been removed, the residue was recrystallized from methanol; m. p. 174—178°C. Yield 0.05 g. (23.6%). IR (KBr): 1642 cm^{-1} (CO). UV λ_{max} (ε_{max}): 299 (6440), 282 (6560), 240 (18850, inflection); λ_{min} (ε_{min}): 290 (5980), 270 (5280). (Found: C, 16.53; H, 5.14%.)

Chromenocoumarone (V) ($R^1=R^2=H$).—2'-Hydroxyisoflavanone (1 g.) and sulfuric acid (0.5 g.) in 50% acetic acid (100 ml.) were refluxed for 1 hr. on a heating mantle. The solvent was then removed under reduced pressure, and the residue was extracted with ether. The ethereal solution was washed with a 2 N sodium hydroxide solution, and with water, and dried over sodium sulfate. After the solvent had been removed, the residue was recrystallized from ethanol (2 ml.). Colorless needles, m. p. 87—89°C. Yield (0.55 g.) (59.4%).

Found: C, 81.21; H, 4.73. Calcd. for $C_{15}H_{10}O_2$: C, 81.06; H, 4.54%.

2'-Hydroxyisoflavan-(4)-ol (II) ($R^1=R^2=R^3=H$).—Into 2'-hydroxyisoflavone (1 g.) in dry dioxane (100 ml.), there was stirred sodium borohydride (200 mg.) in 95% ethanol (7.5 ml.) at 60 to 65°C. The solution was kept at 60 to 65°C for 1 hr. and then it was set aside overnight. After acetone (75 ml.) had been added, the solution was stirred for 15 ml. in order to destroy any excess sodium borohydride. The precipitation yielded was removed by filtration. After the solvent had been removed, the residue was extracted with chloroform, washed with water, and dried. After the chloroform had been removed, a light brown oil (0.8 g). was obtained. This oil was used for the next step without further purification.

IR (liquid film). No carbonyl absorption; a broad band around 3327 cm^{-1} (OH). UV λ_{max} (ε_{max}): 275 (3110); λ_{min} (ε_{min}) 252 (1390).

Chromanocoumaran (III) ($R^1=R^2=R^3=H$).—2'-Hydroxyisoflavan-(4)-ol (0.2 g.) in 50% acetic acid (20 ml.) was refluxed for 1 hr. After the solvent had been removed, the residue was extracted with ether (15 ml.). The ethereal solution was then washed with water (5 ml.), and dried. After the solvent had been removed, the residue was recrystallized from ethanol. Colorless needles; m. p. 126—127°C (125 mg.).

Found: C, 79.83; H, 5.49. Calcd. for $C_{15}H_{12}O_2$: C, 80.33; H, 5.39%. UV λ_{max} (ε_{max}): 278 (3260); λ_{min} (ε_{min}): 247 (590).

2 : 4-Dihydroxy-2' : 4'-dimethoxydesoxybenzoin.[25]—This was prepared by the Hoesch reaction in the usual manner. 25 g. of 2 : 4-dimethoxyphenylacetonitrile[26] (by the procedure of Mitter and Mitra[27]) and resorcinol (35.5 g.) in the presence of zinc chloride (249 g.) in dry ether (630 ml.) yielded 25.2 g. of the desired desoxybenzoin, m. p. 152—153°C.[25]

2 - Hydroxy-2' : 4 : 4'-trimethoxydesoxybenzoin.[3]—2 : 4-Dihydroxy-2' : 4'-dimethoxydesoxybenzoin (23.8 g.) and methyliodide (7.7 ml.) in acetone (450 ml.) were refluxed for 70 min. in the presence of potassium carbonate (30 g.) After the acetone and potassium carbonate had then been removed, the residue was recrystallized from 70% ethanol to yield 12.7 g. (51%) of the desired material, m. p. 109—113°C. The residue from the filtrates yield the corresponding tetramethoxydesoxybenzoin as colorless needles, m. p. 73.5—74.0°C (0.9 g.). A ferric chloride color reaction was negative.

2-Hydroxy-7 : 2' : 4'-trimethoxyisoflavanone.—2-Hydroxy-7 : 2' : 4'-trimethoxydesoxybenzoin (6.6 g.) in 178 ml. of ethylformate was added, dropwise to

22) Reported m. p. 104°C.[8]
23) Reported m. p. 95—98°C.[8]
24) W. B. Whalley and G. Lloyd, *J. Chem. Soc.*, **1956**, 3213. Reported m. p. 184°C.
25) J. M. Sehal and T. R. Seshadri, *Proc. Ind. Acad. Science*, **42A**, 36 (1955). Reported m. p. 158—159°C.
26) B. Reichert and W. Koch, *Arch. Pharm.*, **273**, 265 (1935).
27) P. C. Mitter and S. S. Mitra, *J. Ind. Chem. Soc.*, **13**, 236 (1936).

powdered sodium (6 g.), which had been cooled to −5°C, in the course of 30 min. After the reaction mixture had been set aside at 0°C for 55 hr., the deep reddish solution was poured onto ice (100 g.) and the solution was acidified with 30 ml. of 2 N hydrochloric acid. The ethyl formate layer was separated, washed with 50 ml. of water, and concentrated under reduced pressure. The crystals which separated were collected by filtration to yield 12.8 g. of nearly pure isoflavanone (m. p. 130—141°C). The concentration of the filtrate yielded a further 0.88 g. of the isoflavanone. Recrystallization from aqueous ethanol; m. p. 149—150°C.

Found: C, 65.40; H, 5.48. Calcd. for $C_{18}H_{18}O_6$: C, 65.44; H, 5.49%. IR: 1665 cm^{-1} (pyranone C=O) 3392 cm^{-1} (OH).

2′: 4′: 7-Trimethoxyisoflavone (I) (R^1=CH_3, R^2=R^3=OMe). — 2 - Hydroxy - 2′ : 4′ : 7 - trimethoxyisoflavone (11.8 g.) in acetic acid (100 ml.) was refluxed for half an hour. To the filtered solution there was then added water (170 ml.). The crystals which separated were collected by filtration; m. p. 138—142°C, 9.9 g. They were then recrystallized from 70% ethanol to yield a pure material (7.8 g.), m. p. 146—148°C.[28] IR: 1635 cm^{-1} (C=O).

2′: 4′: 7-Trihydroxyisoflavone (I) (R^1=H, R^2=R^3=OH).—2′: 4′: 7-Trimethoxyisoflavone (0.5 g.) dissolved in benzene (60 ml.) was refluxed with anhydrous aluminum chloride (5.5 g.) for two hours on a water bath. The supernatant benzene was removed by decantation and then under reduced pressure. The residual benzene-free complex was decomposed with ice-cooled water. The precipitation was collected by filtration and dissolved in methanol (40 ml.). Upon the concentration of the above solution to approximately 5 ml., 2′: 4′: 7-trihydroxyisoflavone (0.42 g.) was separated; m. p. 272°C (decomp.). IR: 1617 cm^{-1} (C=O), associated OH 3400 cm^{-1}. UV λ_{max} (ε_{max}): 248 (15600), 262 (14500), 292 (11110). UV 0.1 N sodium hydroxide solution λ_{max} (ε_{max}): 254 (27400), 325 (15390).

Found: C, 63.64; H, 4.01. Calcd. for $C_{15}H_{10}O_5$: C, 66.67; H, 3.73%.

2′: 4′: 7-Triacetoxyisoflavone (I) (R^1=$COCH_3$, R^2=R^3=$OCOCH_3$).—This was prepared in the usual way; m. p. 148—150°C. (from 80% ethanol). Yield 70%.

Found: C, 63.50; H, 4.30. Calcd. for $C_{21}H_{16}O_8$: C, 63.63; H, 4.07%.

7-Methoxy-2′: 4′-dihydroxyisoflavone (I) (R^1=H, R^2=OH, R^3=OCH_3).—a) 2′ : 4′ : 7-Trihydroxyisoflavone (1 g.) and methyl iodide (1 g.) in acetone (100 ml.) were treated with potassium carbonate (2 g.) at 30—40°C for 10 hr. while being stirred. After the potassium carbonate and acetone had been removed, the residue was recrystallized from 80% alcohol (25 ml.), thus yielding 7-methoxy-2′: 4′-dihydroxyisoflavone (767 mg.) m. p. 207—208°C.

Found: 63.92; H, 4.83. Calcd. for $C_{16}H_{12}O_5 \cdot H_2O$: C, 63.57; H, 4.67%. Water of crystallization. Found: 5.93. Calcd.: 5.96%.

IR: 1625 cm^{-1} (C=O), 3490, 3420 and 3135 cm^{-1} (associated OH).

UV λ_{max} (ε_{max}): 260 (19800), 290 (15650).

UV 0.1 N sodium hydroxide λ_{max} (ε_{max}) solution: 250 (25400), 297 (17400).

28) Reported m. p. 148—149°C.[8]

b) To 2′ : 4′ : 7-Trihydroxyisoflavone (49 mg.) in acetone (10 ml.) there was added ethereal diazomethane (from 80 mg. of nitrosomethylurea) (15 ml.). The solution was then set aside for 24 hr. and 40 min. After the solvent and diazomethane, had been removed, the residue (46 mg.) was recrystallized from 80% ethanol (1 ml.), thus yielding 27 mg. of yellow needles, m. p. 206—207°C. This material was identical with the 7-methoxy-2′: 4′-dihydroxyisoflavone obtained by procedure a).

7-Methoxy-2′: 4′-dihydroxyisoflavan-(4)-ol, (II) (R^1=H, R^2=OH, R^3=OCH_3).—Sodium borohydride (200 mg.) in 95% alcohol (25 ml.) was added, dropwise to a solution of 7-methoxy-2′: 4′-dihydroxyisoflavone (680 mg.) in dioxane (45 ml.) at 60—65°C. The reaction mixture was kept for 1 hr. at 60—65°C and then set aside overnight at room temperature. After acetone (5 ml.) had been added to decompose the excess reducing reagent, the solvents were removed under reduced pressure, and the residue was extracted with ether (25 ml.) and water (20 ml.). The ethereal layer was washed with water and dried. After the solvent had been removed, the light-brown, oily isoflavan-4-ol (457 mg., 67%) was obtained.

UV λ_{max} (ε_{max}): 280 (5500); λ_{min} (ε_{min}): 248 (248).

IR (liquid film), no carbonyl absorption. Broad band around 3300 cm^{-1} (OH).

***d, l*-Homopterocarpin (III) (R^1=R^3=OCH_3, R^2=H).**—The oil obtained above was refluxed with 50% acetic acid (11 ml.) for one hour, and then the solvents were removed under reduced pressure. The ultraviolet spectrum (Fig. 5) of the residue (438 mg.) exhibited two maxima, at 286 mμ (ε, 6900) and at 325 mμ (ε, 3130). The latter is due to the presence of isoflav-3-ene in the product. The residue was refluxed with

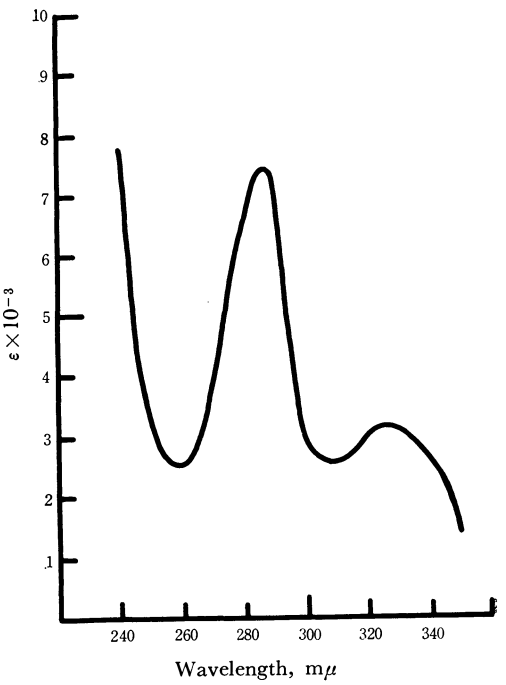

Fig. 5.

methyl iodide (4 g.) and potassium carbonate (2 g.) in acetone (20 ml.) for three hours. After the potassium carbonate and acetone had been removed, the residue was extracted with ether (25 ml.) and with water (20 ml.); after extraction with a 2 N aqueous sodium hydroxide solution (10 ml.), the dried ethereal solution yielded a light yellow oil (219 mg.). This oil in acetone (50 ml.) was refluxed with Norit (100 mg.) for 1 hr. The removal of Norit and acetone left the residue (84 mg.). This was chromatographed on Merck acid-washed alumina (5 g.). The first elution (27 mg.), with benzene (20 ml.), yielded 27 mg. of *d, l*-homopterocarpin (121—124.5°C). A further 9 mg. of the substance was obtained by the elution of Norit with acetone (30 ml.). On recrystallization from ethanol, colorless short needles of *d, l*-homopterocarpin (m. p. 123—125°C) were obtained. Its infrared spectrum in chloroform and its ultraviolet spectrum were superimposable upon those of a natural specimen. UV λ_{max} (ε_{max}): 286 (9200).

Found: C, 71.72; H, 5.59. Calcd. for $C_{17}H_{16}O_4$: C, 71.82; H, 5.67%.

The authors are grateful to Professors Tōshi Irie, Takeshi Matsumoto and Tadashi Masamune for their kind interest in this work, and to Drs. F. E. King and J. W. W. Morgan for providing the sample of homopterocarpin. The authors thank Mr. Hanzo Shimokawa for the measurements of NMR spectra. The work was supported in part by a Grant in Aid of Scientific Research from the Ministry of Education.

BULLETIN OF THE CHEMICAL SOCIETY OF JAPAN VOL. 39 1541—1543 (1966)

The Co-occurrence of Isoflavonoids at Different Oxidation Levels[1]

By Hiroshi SUGINOME and Toshiro KIO

Department of Chemistry, Faculty of Science, Hokkaido University, Sapporo

(Received October 20, 1965)

Some biogenetic aspects of the co-occurrence of pseudobaptigenin, maackiain and sophorol are discussed.

In previous papers[2] the isolation from the same plant of two new oxygen heterocycles, which are designated sophorol (V) and maackiain (VI), has been described, and their structures have been elucidated.

Biogenetical interests led the author to examine the other components in this plant. Ethanol extracts contained considerable amounts of a product which was relatively insoluble to polar solvents and exhibited strong infrared absorption bands at 935 cm^{-1} and 1630 cm^{-1}, attributable to aromatic methylenedioxyl and γ-pyrone carbonyl groups respectively. The purification of this fraction afforded the colorless component, $C_{16}H_{10}O_5$.

Ultraviolet, infrared, NMR spectra and some chemical evidences proved that this compound is identical with ψ-baptigenin (III). This was confirmed by a direct comparison of it with synthetic ψ-baptigenin *O*-acetate.

Although ψ-baptigenin is known to occur at the 7-*O*-rhamnoglucoside,[3,4] pseudobaptisin, in *Baptisia tinctoria,* and as 7-*O*-3-methylbut-2-enylyl ether, Maxima substance B, in *Tephrosia maxima,*[5] the present finding is the first example of the occurrence of its aglycone in nature.

In view of the wide problem of aromatic biogenesis, the co-occurrence of ψ-baptigenin, sophorol and maackiain is of interest; it may have some implication regarding the biogenesis of this class of natural products.

It was in 1921 that Robinson first put forward his ideas on the phytosynthetic process of flavonoids[6] (the condensation of the C_6–C_3 unit with the C_6 of ring A).

The biogenesis of isoflavones has recently been investigated with the aid of ^{14}C tracer techniques, by Grisebach,[7] and it has been the subject of an

1) Oxygen Heterocycles. IX. Part of this paper was read before the 14th Annual Meeting of the Chemical Society of Japan, April, 1961. The work has been interrupted since September, 1961 but is published now.

2) Preceding papers.

3) K. Gorter, *Arch. Pharm.,* **235**, 494 (1897).

4) E. Späth and O. Schmidt, *Monatsh,* **53**, 454 (1929); E. Späth and E. Lederer, *Ber.,* **63**, 743 (1930).

4) See for further syntheses.
a) H. S. Mahal, H. S. Rai and K. Venkataraman, *J. Chem. Soc.,* **1934**, 1120, 1769. b) W. Baker, J. Chadderton, J. B. Harborne and W. D. Ollis, ibid., **1953**, 1852. c) L. Farkas, A. Major, L. Pallos and J. Varady, *Ber.,* **91**, 2858 (1958). d) W. B aker, R. Robinson, and N. M. Simpson, *J. Chem. Soc.,* **1937**, 805. e) L. Farkas and V. Szántho, *Acta. Chim. Acad. Sci.* (Hugnary), **19**, 217 (1959).

5) S. Rangaswami and B. U. R. Sastry, *Current Sci.* (India), **24**, 13, 337 (1955).

6) R. Robinson, *Nature,* **137**, 172 (1936).

extensive review article.[8] It has been shown that ring B of formononetin in *Triforlium pratense* can be derived from phenylalanine,[8a] while ring A is derived from acetate.[9] This pathway of the formation of isoflavones seems to be generally acceptable. Although the formation of an intermediary chalcone also seems generally accepted, however, the mechanism of the formation of the isoflavones from intermediary chalcones (accompanied by aryl rearrangement) is still ambiguous.[10]

In the present investigation, the common oxygenation pattern in ring A of the three compounds involves the reductive loss of the 5-oxygen function (perhaps in an open-chain forerunner[9]).

As has previously been emphasized,[11] 2'-oxygenation in ring B of sophorol raises an interesting problem. Regarding the introduction of the 2'-oxygen function for isoflavonoids, a process involving the participation of an intermediary coumarin has been suggested by Ollis and Grisebach.[8] However, a recent investigation has shown that the ortho-hydroxylation of *trans-p*-methoxy cinnamic acid could occur; this may be generally true for the *ortho*-oxidation of cinnamic acids.[12]

Considering these speculations and experimental facts, the following tentative scheme of biogenesis to account for the co-occurrence of ψ-baptigenin, sophorol and maackiain can be drawn.

In the chart, the formation of an ether ring by an attack of the benzylic hydroxyl group on the 2' position (e. g., IV)[12a] would be improbable, because of the possibility of the easy formation of the benzylic cation.

2-Oxygenated isoflavanone and simple isoflavone may be derived from the common intermediate, either cinnamic acid (I) or chalcone (II). In this connection, it is noteworthy that in *Ferreirea spectabilis* a relationship parallel to the present example, i. e., the co-occurrence of isoflavone, biochanin-A and a 2'-oxygenated isoflavanone, ferreirin, has been reported.[13]

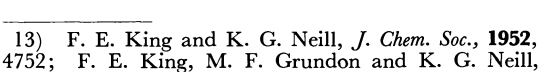

A possible interrelationship between 2'-oxygenated isoflavanones and coumaranochromans was originally suggested by King.[14] Although the possibility of maackiain being a forerunner of sophorol

7) H. Grisebach and N. Doerr, *Naturwissenschaften*, **17**, 514 (1959); H. Grisebach, *Z. Natur.*, **14b**, 802 (1959); H. Grisebach and N. Doerr, *Z. Natur.*, **15b**, 284 (1960).

8) H. Grisebach and W. D. Ollis, *Experientia*, **17**, 4 (1961).

8a) Regarding shikimic acid→aromatic amino acids pathways see D. B. Sprinson, *Adv. Carbohyd. Chem.*, **15**, 235, (1960). B. D. Davis, in "Biochemist's Handbook," Ed. by C. Long, E & F. N. John S. Pon Ltd., London (1961), p. 595. J. M. Edwards and L. M. Jackman, *Aust. J. Chem.*, **18**, 1227 (1965).

9) A. J. Birch, *Fortschr. Chem. Org. Naturst.*, **14**, 186 (1957); A. J. Birch "Perspectives in Organic Chemistry," Ed. by A. R. Todd, Interscience Publishers Inc., New York (1956), p. 134; A. J. Birch and H. Smith "Chemical Society Symposia, Bristol 1958," Chemical Society Special Publication, No. 13, The Chemical Society, London (1958), p. 1.

10) H. O. House, D. J. Reif and R. L. Wasson, *J. Am. Chem. Soc.*, **79**, 2490 (1957); H. Grisebach and W. Barz, "Biogenesi Delle Sostanze Naturali," Milano, (1964), p. 102.

11) H. Suginome, *Tetrahedron Letters*, **1960**, 16.

12) S. A. Brown, *Phytochem.*, **2**, 137 (1963); D. J. Austin and M. B. Meyers, *Tetrahedron Letters*, **1964**, 765.

12a) S. Shibata and M. Yamazaki, "Shokubutsu-seibun no Seigosei," Tokyo Kagaku dojin, Tokyo (1965), p. 182.

13) F. E. King and K. G. Neill, *J. Chem. Soc.*, **1952**, 4752; F. E. King, M. F. Grundon and K. G. Neill, ibid., **1952**, 4580.

14) F. E. King and W. Bottomley, ibid., **1954**, 1399.

can not be entirely excluded, the co-occurrence of maackiain and sophorol can perhaps be better understood by assuming the presence of a reductive process (isoflavanone → chromanocoumaran) in nature. Furthermore, a close laboratory analogy to this process involving mild experimental procedures has recently been achieved by the authors.[15]

The corresponding reduction sequence was already noted by King[14] in the flavonol→catechin series, as is illustrated by structures A→D, beginning with flavonol and ending with catechins.

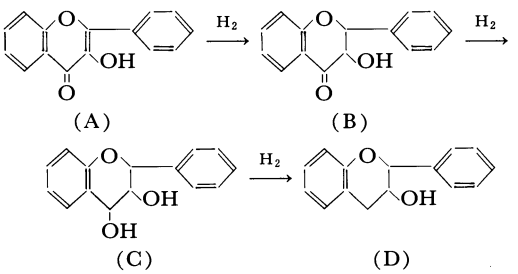

It has previously been noted[11] that sophorol has the essential core and the oxygenation pattern of rotenoids. Speculative pathways on the biogenesis of rotenoids have been proposed by Robinson,[16] by Schmid et al.,[17] and by Grisebach and Ollis.[8] The problem has also recently been reviewed.[18]

Experimental[19]

The Isolation and Purification of ϕ-Baptigenin. —A light brown solid obtained from the ethanol extracts of *Maackia amurensis Rupr. et Maxim. var. Buergeri (Maxim). C. K. Schneid* (3 kg.) was digested with boiling dilute methanol. (Methanol/water 1 : 1). An insoluble material (0.9 g.) was thus collected. Four grams of this material were dissolved in aqueous 2 N sodium hydroxide (20 ml.), and the solution was filtered from a small amount of an insoluble material. After acidification, the material was collected by filtration and then recrystallized from a large volume of ethanol, yielding crystals of ϕ-baptigenin. (M. p. 294°C (decomp.)),[20] 200 mg. UV λ_{max} (ε_{max}): 223 (16820), 251 (16350), 294 (11730).

IR: 3150 (w) (phenolic OH); 1630 (s) (γ-pyrone C=O), 1621 (s), 1598 (s), 1574 (s) and 1490 (s) (aromatic C=C); 1032 (s) and 935 (s) (C–O–C–O–C–). *O*-Methyl ether[21] with dimethylsulfate and potassium carbonate in dry acetone (m. p. 182°C, short needles from ethanol.)

UV λ_{max} (ε_{max}): 223 (25040), 249 (20580), 263 (20880) and 293 (16830). IR: 1636 (γ-pyrone carbonyl); 1625, 1607, 1573 and 1487 (aromatic C=C); 1037 and 906 cm^{-1} (C–O–C–O–C). *O*-Acetate[22] (m. p. 178°C, short needles from ethanol), 1641 cm^{-1} (C=O), 1656 cm^{-1} (acetate C=O).

The author is grateful to Professors Tōshi Irie, Takeshi Matsumoto and Tadashi Masamune for their kind interest in this work, and to Professor Naoto Inoue, Tohoku University, for providing the sample of synthetic ϕ-baptigenin acetate.

15) H. Suginome and T. Iwadare, *Experientia,* **18**, 163, (1962).
16) Sir R. Robinson, "The Structural Relations of Natural Products," Oxford University Press, Oxford (1955), p. 43.
17) O. A. Stamm, H. Schmid and J. Büchi, *Helv. Chim. Acta,* **41**, 2006 (1958).
18) L. Crombie, *Fortschr. Chem. Org. Naturstoffe,* **21**, 275 (1963).
19) Melting points are uncorrected. Ultraviolet spectra were taken in ethanol, and infrared spectra were taken in Nujol unless otherwise stated. Elemental analyses by Mr. Kusuo Narita, Department of Pharmacy, Faculty of Medicine, Hokkaido University.
20) Reported m. p. 292°C,[4b] m. p. 292—293°C.[4a]
21) Reported m. p. 179—180°C.[4a]
22) Reported m. p. 173°C,[3] m. p. 176°C,[4a] m. p. 165°C.[4b]

BULLETIN OF THE CHEMICAL SOCIETY OF JAPAN VOL. 39 1544—1547 (1966)

The Absolute and Relative Stereochemical Correlation of Isoflavanone, Sophorol and Naturally-occurring Isoflavan Derivatives[1]

By Hiroshi SUGINOME

Department of Chemistry, Faculty of Science, Hokkaido University, Sapporo

(Received December 9, 1965)

By rotatory-dispersion studies, it was confirmed that sophorol, (−) maackiain, pterocarpin, equol and homopterocarpin have the same absolute configuration at position 3. The results of the O. R. D. examination of (−) halostachine and pterocarpinoids allow us to assign the 3R, 4R configuration to pterocarpin and to the related compounds.

A number of natural isoflavanones have been discovered,[2] although sophorol[2a] is the only member of the group which has been isolated in an optically active state. In recent years, the existence of various chromanocoumarans*, which are closely related biogenetically to isoflavanones, has been disclosed. It is of interest to determine the stereochemical relationship between these compounds and their absolute configurations.

At present, nine chromanocoumarans, their glycosides (I—VIII)[3] and isoflavan equol (IX) are known; they have all been isolated in an optically active form.

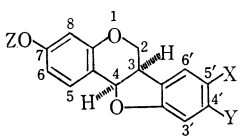

(A)

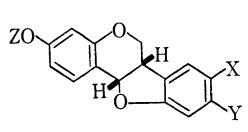

(B)

(I—V)

I (−) Homopterocarpin,[4] X=H; Y=OMe; Z=Me

II (−) Pterocarpin,[5] X and Y=methylenedioxy; Z=Me

III (±) Maackiain,[6] X and Y=methylenedioxy; Z=H

(−) Maackiain[7] (Inermin), X and Y=methylenedioxy; Z=H

IV (−) Triforlirhizin,[8] X and Y=methylenedioxy; Z=-D-glucose

V (+) Sophojaponicin,[6] X and Y=methylenedioxy; Z=-D-glucose

VI (−) Neodulin[9]

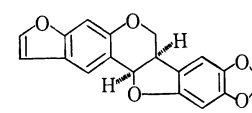

VII (−) Phaseolin[10]

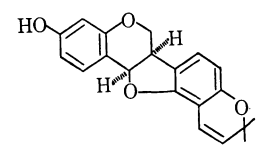

VIII (+) Pisatin[11]

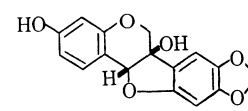

1) Oxygen Heterocycles. X. The work has been interrupted since September, 1961 but is published now. A brief account of this paper has already been published. This Bulletin, **39**, 409 (1966).

2) a) H. Suginome, *J. Org. Chem.*, **24**, 1655 (1959) and examples cited therein. b) L. Crombie and D. A. Whiting, *J. Chem. Soc.*, **1963**, 1569; S. Balakrishna, J. D. Ramanathan, T. R. Seshadri and B. Venkataramani, *J. Sci. Ind. Res.* (India), **20B**, 134 (1961).

* Group name "Pterocarpinoids" was suggested for the compounds.

3) The numbering system of chromanocoumaran was chosen arbitrarily as derivative of isoflavones. However, an alternative numbering would be analogous

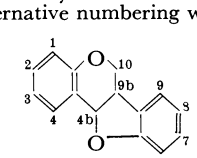

to the numbering of 6,12-dioxachrysene. The ring index, p. 708 (1960), American Chemical Society.

4) E. Späth and J. Schläger, *Chem. Ber.*, **73**, 1 (1940).

5) A. McGookin, A. Robertson and W. B. Whalley, *J. Chem. Soc.*, **1940**, 787; J. B. Bredenberg and J. N. Shoolery, *Tetrahedron Letters*, **1961**, 285.

6) S. Shibata and Y. Nishikawa, *Chem. and Pharm. Bull.*, **11**, 167 (1963).

7) S. Shibata and Y. Nishikawa, ibid., **11**, 167 (1963); W. Cocker, T. Dahl, C. Dempsey and T. B. H. McMurry, *Chem. & Ind.*, **1962**, 216; H. Suginome, *Experientia*, **18**, 161 (1962).

8) J. B. Brendenberg and P. K. Hietala, *Acta Chem. Scand.*, **15**, 936, (1961).

9) B. L. Van Duuren, *J. Org. Chem.*, **26**, 5013 (1961).

10) D. R. Perrin, *Tetrahedron Letters*, **1964**, 29.

11) D. R. Perrin and W. Bottomley, *Nature*, **191**, 76 (1961).

IX (−) Equol[12]

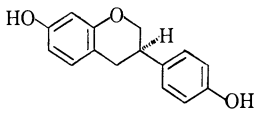

X (+) Sophorol

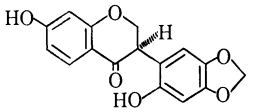

The absolute and relative stereochemical correlations between corresponding asymmetric centers of sophorol and those chromanocoumarans have not yet been defined, however. Therefore, the relative stereochemistry of these compounds has now been examined by rotatory-dispersion studies. The rotatory dispersion curves are recorded in Figs. 1 and 2.

Figure 1 shows the rotatory-dispersion curves of sophorol,[2a] the oxidation product of *O*-methyldihydropterocarpin obtained from pterocarpin by hydrogenolysis, followed by methylation and oxidation with potassium permanganate,[5] and *O*-dimethylsophorol.[2a] These three substances

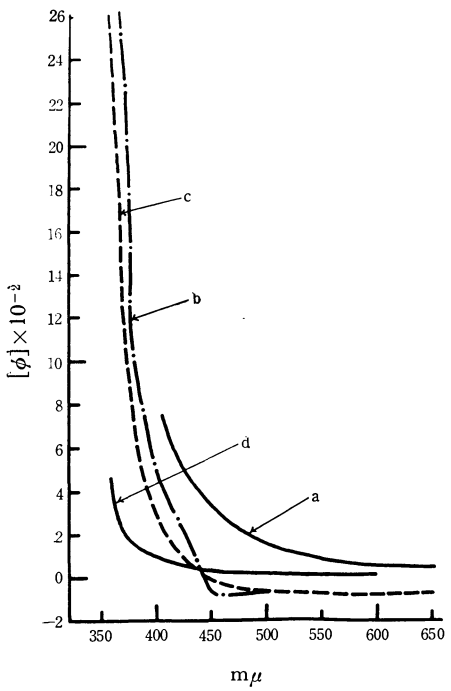

Fig. 1

a Sophorol in dioxane
b Potassium permanganate oxidation product
c Sophorol in ethanol
d *O*-Dimethylsophorol

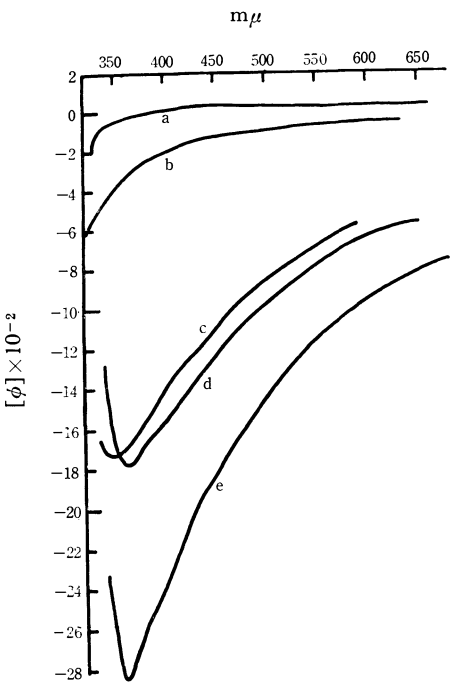

Fig. 2

a Dihydro-*O*-methylmaackiain-*O*-methylether
b Equol diacetate
c Homopterocarpin
d Pterocarpin
e Maackiain

exhibit virtually identical plain positive dispersion curves throughout the spectral range under examination. This result can be taken as conclusive evidence of an identical absolute configuration at C^3 in sophorol and the corresponding asymmetric center of pterocarpin and related compounds; it confirms previous assumptions.[13]

In Fig. 2 are collected the rotatory-dispersion curves of homopterocarpin, pterocarpin, maackiain, equol diacetate and dihydro-*O*-methylmaackiain-*O*-methylether. Homopterocarpin, pterocarpin and maackiain all exhibit negative Cotton-effect curves. It is apparent from the figure that in these cases C^3 asymmetric carbon in the chromanocoumaran molecule makes a very weak negative contribution,[14] as is shown in the dispersion curves of dihydro-*O*-methylmaackiain-*O*-methylether. Therefore, the relatively strong negative rotation accompanying the Cotton effects in these compounds is probably produced by the C^4 asymmetric center with an aromatic ring and an ether linkage.

12) G. F. Marrian and D. Beall, *Biochem. J.*, **29**, 1586 (1935); R. Suemitsu, M. Hiura and M. Nakajima, *J. Agr. Chem. Soc. Japan*, **29**, 591 (1955).

13) W. B. Whalley, "The Chemistry of Flavonoid Compounds," T. A. Geissman ed., Pergamon Press, London, (1962), p. 441.

14) The formation of ring compounds from open chains is accompanied by an increase in optical rotation.[16] Needless to say, no Cotton effect will be produced by C3 center after ring formation to chromanocoumaran.

Lyle reported that the compounds of the XI, XII, XIII, (−) ephedrine and (−)-ψ-ephedrine types showed negative Cotton effects of a similar

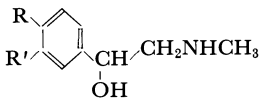

(XI) R=R′=H
(XII) R=H, R′=OH
(XIII) R=R′=OH

shape; he also identified the absolute configuration of (−) halostachine (XI) as R on the basis of an unequivocal chemical correlation.[15]

Attention must be paid to the structural similarity between the asymmetric center of halostachine (XI) and the environment of the corresponding asymmetric center of pterocarpin.

Although in the present series of compounds, the aromatic ring is not free to rotate, and the enhancement of optical activity can be observed,[16] the negative Cotton effects of the asymmetric center of the R configuration in halostachine (XI) and the C^4 environment of pterocarpin are strong evidence for assuming that the asymmetric centers of these compounds have the same absolute configuration R.

Since the B/C ring junction in pterocarpin is cis,[17] pterocarpin is represented as having the C^4R, C^3R, configuration IIA. Consequently, all the other chromanocoumarans which have been reported to exhibit a negative rotation can be identified as having the C^4R, C^3R configuration, IA, IIA, IVA, VIA, VIIA. Since it is apparent from Fig. 2 that C^3 in equol and the corresponding asymmetric center of dihydro-*O*-methylmaackiain-*O*-methylether have the same absolute configuration, the R configuration is assigned to be the C^3 center of equol. Then sophojaponicin[8] must have the C^4S, C^3S configuration (VB). Pisatin is of particular interest in that there is an extra hydroxyl function in the angular position.

This situation leads to two benzyl alcoholic functions in a molecule which would cause a stronger rotation than in pterocarpin. The reported $[\alpha]_D$ of pisatin is +280° (pterocarpin, −230°). It is considered that an asymmetric center with an angular hydroxyl group is much less effective in causing a negative rotation because of the free rotation of the hydroxyl group. Since C^3 hydroxyl and C^4 hydrogen have cis interrelationship,[17a] the C^4S, C^3S configuration (VIII) is also assigned to pisatin.

Furthermore, it follows that the absolute configuration of C^3 of sophorol is (R) (X). It is perhaps surprising that sophorol has an opposite absolute configuration in the corresponding asymmetric center of rotenone and the rotenoids, which was assigned the 4b(s) 9b(s) configuration (XIV).[18]

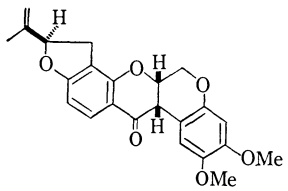

(XIV)

Although no isoflavanone of the s-configuration has yet been found in nature, apparently two enzymatic reactions which lead to a pair of enantiomers of the isoflavanone, as shown by the coexistence of *d*-maackiain and *l*-maackiain,[6] operate in plants.

The present assignment of the absolute configuration should be examined further by unequivocal chemical correlation.*

Experimental

All measurements of rotation were made on a Rudolph Model 200S, 80, photoelectricspectropolarimeter with an oscillating polarizer prism, using zirconium arc.

Sophorol.—R. D. (Fig. 1) in ethanol (*c* 0.22) 22.5°: $(\phi)_{589}$ −70°: $(\phi)_{500}$ −56°: $(\phi)_{450}$ −10°: $(\phi)_{430}$ +79°: $(\phi)_{410}$ +194°: $(\phi)_{400}$ +301°: $(\phi)_{390}$ +464°: $(\phi)_{380}$ +752°: $(\phi)_{355}$ +2726°: R. D. (Fig. 1) in dioxane (*c* 0.29) 24.5°: $(\phi)_{700}$ +41°: $(\phi)_{650}$ +54°: $(\phi)_{589}$ +65°: $(\phi)_{500}$ +161°: $(\phi)_{450}$ +332°: $(\phi)_{408}$ +710°.

Pottasium Permanganate Oxidation Product of *O*-Methyldihydropterocarpin.—R. D. (Fig. 1) in dioxane (0.024) 4.5°: $(\phi)_{665-475}$ −63°: $(\phi)_{450}$ −74°: $(\phi)_{425}$ +243°: $(\phi)_{400}$ +506°: $(\phi)_{375}$ +1212°: $(\phi)_{360}$ +4175°: $(\phi)_{350}$ +5672°.

***O*-Dimethylsophorol.**—R. D. (Fig. 1) in dioxane (*c* 0.11) 24.5°: $(\phi)_{587-475}$ +33°: $(\phi)_{450}$ +38°: $(\phi)_{400}$ +101°: $(\phi)_{368}$ +254°: $(\phi)_{359}$ +467°.

Dihydro-*O*-methylmaackiain-*O*-methylether.—R. D. (Fig. 2) in dioxane (*c* 0.15) 24.5°: $(\phi)_{650-450}$ +31°: $(\phi)_{415}$ +14°: $(\phi)_{385}$ −4.1°: $(\phi)_{355}$ −40°: $(\phi)_{340}$ −71°: $(\phi)_{330}$ −167°.

Pterocarpin.—R. D. (Fig. 2) in dioxane (*c* 0.055) 24.5°: $(\phi)_{700}$ −400°: $(\phi)_{589}$ −662°: $(\phi)_{500}$ −976°: $(\phi)_{425}$ −1396°: $(\phi)_{375}$ −1702°: $(\phi)_{365}$ −1786°: $(\phi)_{360}$ −1789°: $(\phi)_{355}$ −1786°: $(\phi)_{350}$ −1666°: $(\phi)_{340}$ −1276°.

Maackiain.—R. D. (Fig. 2) in dioxane (*c* 0.044) 24.5°: $(\phi)_{680}$ −757°: $(\phi)_{589}$ −983°: $(\phi)_{500}$ −1431°: $(\phi)_{425}$ −2030°: $(\phi)_{375}$ −2628°: $(\phi)_{365}$ −2695°: $(\phi)_{360}$ −2852°: $(\phi)_{355}$ −2771°: $(\phi)_{350}$ −2632°: $(\phi)_{345}$ −2472°: $(\phi)_{340}$ −2290°.

15) G. G. Lyle, *J. Org. Chem.*, **25**, 1779 (1960).
16) W. J. Kauzmann, J. E. Walter and H. Eyring, *Chem. Revs.*, **26**, 339 (1940).
17) H. Suginome, *Experientia*, **18**, 163 (1962).
17a) C. W. L. Bevan, A. J. Birch, B. Moore and S. K. Mukerjee, *Tetrahedron Letters*, **1962**, 673.
18) G. Büchi, L. Crombie, P. J. Godin, J. S. Kalternbronn, K. S. Siddalingaiah and D. A. Whiting, *J. Chem. Soc.*, **1961**, 2843; C. Dierassi, W. D. Ollis and R. C. Russell, ibid., **1961**, 1448.

* After this paper was prepared, Professor S. Ito informed us that he and his colleagues had assigned C^4R, C^3R as the absolute configuration of trifolirhizin on the basis of the chemical correlation.

Homopterocarpin.—R. D. (Fig. 2) in dioxane (*c* 0.16) 24.5°: $(\phi)_{700}$ −403°: $(\phi)_{589}$ −579°: $(\phi)_{500}$ −856°: $(\phi)_{425}$ −1240°: $(\phi)_{360}$ −1699°: $(\phi)_{350}$ −1735°: $(\phi)_{340}$ −1701°: $(\phi)_{355}$ −1650°.

Equol Diacetate.—R. D. (Fig. 2) in dioxane (*c* 0.16) 24.5°: $(\phi)_{693}$ −23°: $(\phi)_{589}$ −65°: $(\phi)_{500}$ −108°: $(\phi)_{425}$ −163°: $(\phi)_{375}$ −274°: $(\phi)_{330}$ −548°: $(\phi)_{320}$ −649°.

The author is grateful to Professors Tōshi Irie, Takeshi Matsumoto and Tadashi Masamune for their kind interest in this work.

The author is also grateful to the following for kindly supplying samples. Dr. J. W. W. Morgan (Pterocarpin and homopterocarpin), Professor W. B. Whalley (an oxidation product of dihydropterocarpin *O*-methyl ether), and Professor Rikisaku Suemitsu (equol diacetate). Rotatory dispersions were measured through the courtesy of Professor Yuji Tonomura of the Research Institute of Catalysis Hokkaido University, in the summer of 1961.

BULLETIN OF THE CHEMICAL SOCIETY OF JAPAN VOL. 39 1547—1551 (1966)

Plastic Scintillators. II. The Synthesis of Some Distyrylbenzene Derivatives as Wavelength Shifters in Plastic Scintillators

By Tadao NAKAYA and Minoru IMOTO

Department of Applied Chemistry, Faculty of Engineering, Osaka City University, Sumiyoshi-ku, Osaka

(Received October 25, 1965)

The synthesis and the absorption and fluorescence spectra of 2, 5-dimethoxy-1, 4-distyrylbenzene derivatives and the related compounds are reported on. Their absorption and their fluorescence spectra, are then discussed. According to the spectra, some of the compounds synthesized here are better wavelength shifters in plastic scintillators that the compounds described in the literature.

The use of some anthracene derivatives as efficient wavelength shifters in plastic scintillators were described in our previous paper.[1] In 1954, Pichat and Pesteil[2] showed that distyrylbenzene acts as a scintillation solute in plastic scintillators. Recently, Heller[3] suggested that substituted distyrylbenzenes would be highly efficient wavelength shifters in organic liquid scintillators. In the present paper, in order to increase the fluorescent intensity, the solubility in alkylbenzene solution, and the separation of the nearest maxima of the absorption and fluorescence spectra, two methoxy groups were introduced into the central benzene nucleus of the substituted distrylbenzenes. Ten derivatives of 2, 5-dimethoxy-1, 4-distyrylbenzene were synthesized by Wittig reaction.[4]

In order to ascertain the effect of substituents in the *meta* position on the absorption and fluorescence spectra, we also prepared some derivatives of *meta*-distyrylbenzene. The compounds synthesized here may be summarized as follows:

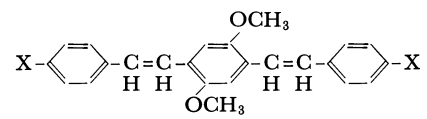

(I)

X=H(1), CH_3(2), OCH_3(3), NO_2(4), $N(CH_3)_2$(5), Cl(6), $CH(CH_3)_2$(7)

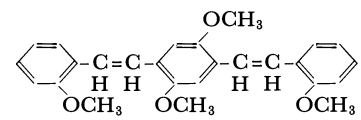

(II)

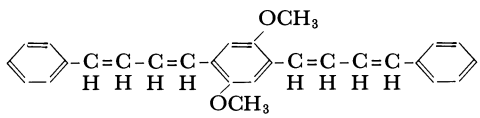

(III)

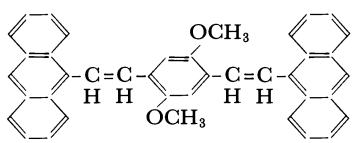

(IV)

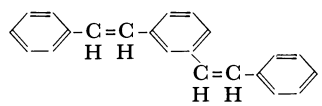

(V)

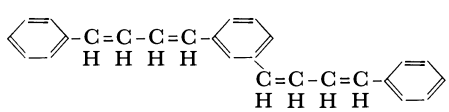

(VI)

1) Part I of this series: M. Imoto and T. Nakaya, This Bulletin, **36**, 785 (1963).
2) L. Pichat and P. Pesteil, French Pat. 1071794 (1954); *Chem. Abstr.*, **53**, 3904 (1959).
3) A. Heller, *J. Chem. Phys.*, **36**, 2858 (1962); **40**, 2839 (1964).
4) T. W. Campbell and R. W. McDonald, *J. Org. Chem.*, **24**, 1246 (1959).

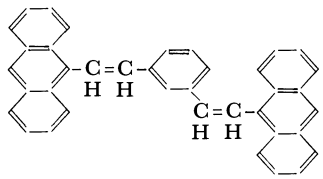

(VII)

These compounds all have *trans*-forms with the exception of 1, 4-bis(*p*-dimethylaminostyryl)-2, 5-dimethoxybenzene; they have been little described in the literature, as far as we have been able to determine. Some of the compounds synthesized here have been proved by Osio and his co-workers[5] to be equal to the wavelength shifters reported in the literature.[6-7]

Experimental

1, 4-Dichloromethyl - 2, 5 - dimethoxybenzene. — Thirty-five grams of *p*-dimethoxybenzene was added at 0°C to a mixture of 230 ml. of a 37% formaldehyde solution and 600 ml. of concentrated hydrochloric acid. The temperature was kept below 35°C while the mixture was stirred for 4 hr. The solid was then collected, washed twice with water, and dried in vacuo. It was recrystallized from carbon tetrachloride to give 23 g. of 1, 4 - dichloromethyl - 2, 5 - dimethoxybenzene (43% yield), melting at 164—165°C.[8]

Found: C, 51.20; H, 5.36; Cl, 30.0. Calcd. for $C_8H_{10}Cl_2O_2$: C, 51.06; H, 5.11; Cl, 30.2%.

2, 5 - Dimethoxy - *p* - xylylene-bis(triphenylphosphonium chloride).—A solution of 2.3 g. of 1, 4-dichloromethyl-2, 5-dimethoxybenzene and 7.4 g. of triphenylphosphine in 350 ml. of dry xylene was refluxed at the boiling point of the solvent while being stirred for 11 hr. A crystalline solid began to separate after 10 min. The reaction products were collected, washed with dry xylene, and then dried in a vacuum desiccator at 10—20 mmHg and 60—70°C. Yield, 6.5 g. (85%); m. p. 271—275°C.

Found: Cl, 9.1. Calcd. for $C_{46}H_{42}O_2Cl_2P_2$: Cl, 9.4%.

The Derivatives of 2, 5-Dimethoxy-1, 4-distyrylbenzene (I_1—I_7).—To a solution of 0.01 mol. of the 2, 5 - dimethoxy - *p* - xylylene-bis(triphenylphosphonium chloride) and 0.028 mol. of the corresponding *p*-substituted benzaldehyde in 100 ml. of absolute ethanol, 150 ml. of a 0.3 M lithium ethoxide solution was added. After 10 hr., the excess ethanol was removed by distillation under reduced pressure. The crystalline solid which separated was collected and dried in vacuo. The solid was crystallized from cyclohexane. The *cis-trans*-mixture was changed to a *trans*-compound by refluxing it in cyclohexane which contained a trace of iodine. However, 1, 4-bis(*p*-dimethylaminostyryl)-2, 5-dimethoxybenzene (I_3) could not be isomerized, because of the formation of a complex between the compound and iodine in cyclohexane or benzene. The melting points, yields, and analysis of the compounds are shown in Table I.

1, 4 - Bis(*o* - methoxystyryl) - 2, 5 - dimethoxybenzene (II). — To a solution of 3.2 g. of 2, 5-dimethoxy-*p*-xylylene-bis(triphenylphosphonium chloride) and 2.0 g. of *o*-methoxybenzaldehyde in 100 ml. of absolute ethanol, 100 ml. of a 0.3 M lithium ethoxide solution was added. After a while, yellow crystals began to separate from the solution. After 15 hr., the yellow crystalline solid was collected and dried in vacuo. Recrystallization from cyclohexane containing a trace of iodine gave II with a m. p. of 178—179°C in a yield of 80%.

Found: C, 77.72; H, 6.82. Calcd. for $C_{26}H_{26}O_2$: C, 77.49; H, 6.44%.

1, 4 - Bis(4-phenylbutadienyl)-2, 5- dimethoxybenzene (III).—250 ml. of a 0.25 M lithium ethoxide solution was added to a solution of 5.5 g. of 2, 5-dimethoxy-*p*-xylylene-bis(triphenylphosphonium chloride) and 5 g. of cinnamaldehyde in 150 ml. of absolute ethanol. After a while, deep yellow crystals began to separate from the solution. The crystals were collected, washed with ethanol, and dried in vacuo. Recrystallization from benzene containing a trace of iodine gave III as a deep yellow powder with a m. p. of 229—231°C in a yield of 75%.

Found: C, 85.14; H, 6.68. Calcd. for $C_{28}H_{26}O_2$: C, 85.28; H, 6.60%.

1, 4-Bis (9-anthrylvinyl) - 2, 4 - dimethoxybenzene (IV).—To a solution of 6 g. of 2, 5-dimethoxy-*p*-xylylene-bis(triphenylphosphonium chloride) and 5.5 g. of 9-anthraldehyde in 380 ml. of absolute ethanol, 200 ml. of a 0.25 M lithium ethoxide solution was added. After a while, a deep yellow crystalline solid began to separate from the solution. After 10 hr., the mixture

TABLE I. DERIVATIVES OF 2, 5-DIMETHOXY-1, 4-DISTYRYLBENZENE

Compound	Substitute X	M.p. °C	Yield %	Molecular formula	Analysis, % Found	Calcd.
I_1	H	177—178	72	$C_{24}H_{22}O_2$	C: 84.11 H: 6.74	C: 84.21 H: 6.44
I_2	CH_3	176—178	70	$C_{26}H_{26}O_2$	C: 84.14 H: 7.40	C: 84.32 H: 7.03
I_3	OCH_3	209—210	73	$C_{26}H_{26}O_4$	C: 77.38 H: 6.82	C: 77.49 H: 6.47
I_4	NO_2	274—278	80	$C_{24}H_{20}N_2O_6$	C: 66.25 H: 4.98 N: 6.51	C: 66.67 H: 4.63 N: 6.45
I_5	$N(CH_3)_2$	238—248	75	$C_{28}H_{32}N_2O_2$	C: 78.29 H: 7.55 N: 6.49	C: 78.50 H: 7.45 N: 6.54
I_6	Cl	214—216	48	$C_{24}H_{20}Cl_2O_2$	C: 70.27 H: 5.35	C: 70.08 H: 4.87
I_7	$CH(CH_3)_2$	181—183	68	$C_{30}H_{34}O_2$	C: 84.14 H: 7.40	C: 84.32 H: 7.03

5) T. Osio, private communication.
6) R. C. Sangster and J. W. Irvine, *J. Chem. Phys.*, **24**, 670 (1956).
7) A. Heller and D. Katz, ibid., **35**, 1987 (1961).
8) S. E. Hunt and A. S. Lindseg, *J. Chem. Soc.*, **1962**, 4550.

was filtered, washed with ethanol, and dried in vacuo. The solid product was recrystallized several times from benzene in the presence of a trace of iodine to give IV as deep yellow prisms with a m. p. of 298—299°C in a yield of 78%.

Found: C, 88.11; H, 5.76. Calcd. for $C_{40}H_{30}O_2$: C, 88.56; H, 5.53%.

***m*-Xylylene-bis(triphenylphosphonium bromide).**—A solution of 25 g. of *m*-xylylene dibromide and 58 g. of triphenylphosphine in dry xylene was heated under reflux for 10 hr. After a while, white crystals began to separate from the solution. The solid product was collected, washed with dry xylene, and dried in a vacuum desiccator at 10 mmHg and 60°C for 15 hr. The white crystals, melting at 275—278°C were obtained The white crystals, melting at 275—278°C, were obtained in a yield of 83%.

Found: Br, 6.3. Calcd. for $C_{42}H_{34}Br_2P_2$: Br, 6.6%.

1, 3-Distyrylbenzene (V).—To a solution of 2.1 g. of *m*-xylylene-bis(triphenylphosphonium bromide) and 2.9 g. of benzaldehyde in 50 ml. of absolute ethanol, 50 ml. of a 0.2 M lithium ethoxide solution was added. After 15 hr., 110 ml. of water was added to the reaction mixture. The crystals then began to separate from the solution. The separated crystals were dried in vacuo and recrystallized from *n*-hexane in the presence of a trace of iodine to give V as white prisms, with a m. p. of 167—168°C and in a yield of 55%.

Found: C, 93.81; H, 6.18. Calcd. for $C_{22}H_{18}$: C, 93.62; H, 6.38%.

1, 3-Bis(4-phenylbutadienyl)benzene (VI).—To a solution of 2.0 g. of *m*-xylylene-bis(triphenylphosphonium bromide) and 2.9 g. of cinnamaldehyde in 50 ml. of absolute ethanol, 50 ml. of a 0.2 M lithium ethoxide solution was added. After 10 hr., a solid product was collected and recrystallized from benzene in the presence of a trace of iodine to give VI as white prisms, with a m. p. of 189—190°C and in a yield of 60%.

Found: C, 92.86; H, 6.73. Calcd. for $C_{26}H_{22}$: C, 93.41; H, 6.51%.

1, 3-Bis(9-anthrylvinyl)benzene (VII).—To a solution of 2.4 g. of *m*-xylylene-bis(triphenylphosphonium bromide) and 2.8 g. of anthraldehyde in 150 ml. of absolute ethanol, 100 ml. of a 0.2 M lithium ethoxide solution was added. After 8 hr., the yellow crystals were collected and recrystallized from benzene containing a trace of iodine to give VII, melting at 229—231°C, in a yield of 40%.

Found: C, 94.17; H, 5.59. Calcd. for $C_{38}H_{26}$: C, 94.60; H, 5.40%.

Spectra and Discussion

Absorption Spectra.—The absorption spectrum of 2, 5-dimethoxy-1, 4-distyrylbenzene (I_1) is given in Fig. 1. This compound exhibits, in the ultraviolet and visible region, three absorption maxima, at 233 mμ ($\varepsilon=27900$), 324 mμ ($\varepsilon=33100$) and 390 mμ ($\varepsilon=48600$).

The absorption spectra of the derivatives of 2, 5-dimethoxy-1, 4-distyrylbenzene (I_2—I_7), are similar in shape to that of I_1.

The wavelengths and molar extinction coefficients of the longest-wavelength absorption maxima of compounds I_1—IV and 1, 4-distyrylbenzene are summarized in Table II.

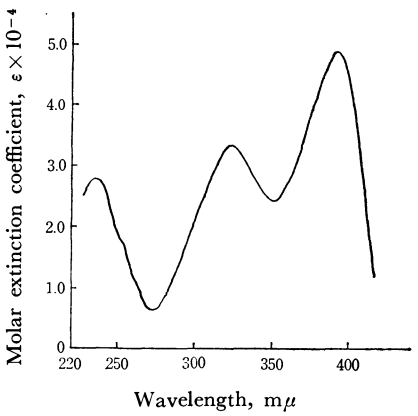

Fig. 1. The absorption spectrum of 2, 5-dimethoxy-1, 4-distyrylbenzene (I_1). (in dioxane)

Table II. The wavelengths and molar extinction coefficients of the longest-wavelength absorption maxima of 2, 5-dimethoxy-1, 4-distyrylbenzene and the related compounds (I_1—IV) (in dioxane)

Compound	Color	λ_{max}, mμ	$\varepsilon\times10^{-4}$
I_1	yellow	390	4.86
I_2	yellow	392	3.70
I_3	yellow	396	3.60
I_4	pink yellow	431	3.51
I_5	pink yellow	420	4.20
I_6	deep yellow	395	4.62
I_7	yellow	390	6.45
II	yellow	396	4.49
III	deep yellow	419	3.21
IV	deep yellow	413	4.36
1, 4-Distyryl-benzene[3]	colorless	357	5.70

The absorption maximum of 2, 5-dimethoxy-1, 4-distyrylbenzene shifts toward a longer wavelength than that of 1, 4-distyrylbenzene, as is shown in Table II. As the cause of this red shift, the full participation of lone pair electrons on the oxygen atoms of the methoxy groups in the π electron system of the benzene rings may be considered. Furthermore, this red shift may be due to the effect of hydrogen bonds between the oxygen atoms of the methoxy groups and the hydrogen atoms on the near β-carbon atoms:

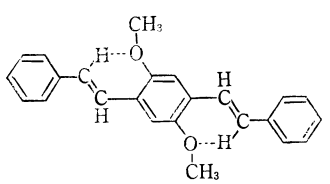

The maximum wavelength of compound III shifted to a wavelength longer than that of compound IV. The longest-wavelength bands of III and IV may be both associated with the *p*-band.

According to a method developed by Dewar,[9] if the methoxy groups are disregarded, the π electron systems of III and IV can be considered to be formed by joining up two odd-AH radicals as follows:

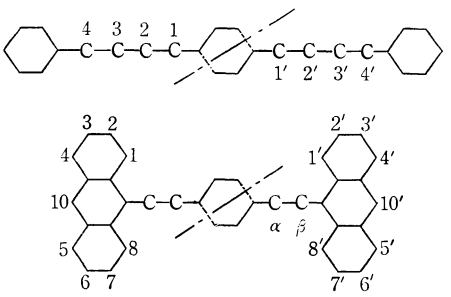

The magnitude of the splitting of the NBMO's of the two odd-AH radicals corresponds to the energy of the *p*-band. The splitting values for III and IV were 16/19 and 16/22, in units of β-(resonance integral), respectively. From the results of the calculation, the longest-wavelength band of III is expected to be at a shorter wavelength than that of IV.

However, the calculated values seem to be inconsistent with the experimental finding that the longest-wavelength band of III is observed in a longer-wavelength region than that of IV. Regarding the cause of this phenomenon, it may be considered that IV has a less planar structure than III, because of the repulsive forces of steric hindrance between the hydrogen atoms on the β-carbon atoms and the hydrogen atoms at the 1, 1′, 8 and 8′ positions of the terminal anthracene rings. The longest-wavelength absorption maxima and the molar extinction coefficients of compounds V—VII and *trans*- and *cis*-stilbene are shown in Table III. In the case of *meta*-substituted compounds, the conjugation between two terminal substituents is unimportant because it involves a structure with long, or ineffective, bonds, as in the following figure:

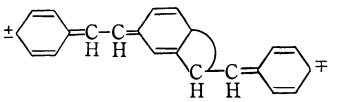

For example, 1, 3-distyrylbenzene and *trans*-stilbene absorbed at nearly the same wavelength, as is shown in Table III.

Fluorescence Spectra. — The fluorescence spectra of compounds I_1 and I_7 are shown in Figs. 2 and 3. The fluorescence spectra of the other compounds of the I series are similar in shape to those of I_1 and I_7. The shortest-wavelength fluorescence maxima and the difference in wavelength between the nearest maxima of fluorescence

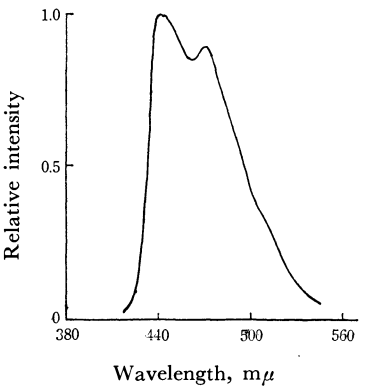

Fig. 2. Fluorescence spectrum of 2,5-dimethoxy-1,4-distyrylbenzene (I_1). (1.0×10^{-5} mol./l. in dioxane)

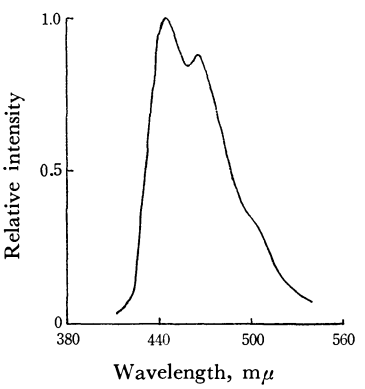

Fig. 3. Fluorescence spectrum of 1,4-bis(*p*-isopropylstyryl)-2,5-dimethoxybenzene (I_7). (1.1×10^{-5} mol./l. in dioxane)

TABLE III. THE WAVELENGTHS AND MOLAR EXTINCTION COEFFICIENT OF THE ABSORPTION MAXIMA OF THE COMPOUNDS (V—VII)

Compound	Color	λ_{max} mμ	$\varepsilon\times10^{-4}$	Solvent
V	colorless	325	2.33	dioxane
VI	colorless	356	4.53	dioxane
VII	yellow	390	2.46	dioxane
trans-Stilbene[α]	colorless	320.5	1.60	heptane
cis-Stilbene[β]	colorless	280	1.05	ethanol

α: H. Suzuki, This Bulletin, **33**, 381 (1960).
β: R. N. Beale and E. M. F. Roe, *J. Chem. Soc.*, **1953**, 2755.

9) M. J. S. Dewar, *J. Chem. Soc.*, **1950**, 329; **1952**, 3529.

Table IV. The shortest-wavelength fluorescence maxima and difference in nearest maxima of spectra between fluorescence and absorption (in dioxane)

Compound	Shortest-wavelength fluorescence maximum mμ	Difference in nearest maxima between fluorescence and absorption mμ
I_1	440	50
I_2	445	53
I_3	460	64
I_4	(525)	—
I_5	477	57
I_6	442	47
I_7	444	49
II	439	43
III	(444)	—
IV	466	53
V	370	45
VI	395	39
VII	478	88
Distyrylbenzene[3)]	394	37

and the absorption of the compounds synthesized here are tabulated in Table IV.

The separation of the maxima of absorption and fluorescence spectra for I_1 is larger than that of 1, 4-distyrylbenzene. Since it is desirable that there be little probability of the reabsorption of the photons emitted, the separation of the maxima of absorption and fluorescence is required. This requirement is fully satisfied in I_1 and in the other compounds synthesized here, as is seen in Table IV. The compounds are of practical use because of their high solubilities. Furthermore, the derivatives of 2, 5-dimethoxy-*p*-distyrylbenzene are better wavelength shifters in plastic scintillators, because the strongest-fluorescence maxima of these compounds match the most sensitive region of a phototube. Except for VII, the difference in wavelength between the nearest maxima of fluorescence and the absorption of the derivatives of *meta*-distyrylbenzene is nearly equal to those in *para*-distyrylbenzene derivatives.[3)]

The authors wish to express their hearty thanks to Professor Takahumi Osio and his co-workers for their helpful advice.

BULLETIN OF THE CHEMICAL SOCIETY OF JAPAN VOL. 39 1551—1556 (1966)

Plastic Scintillators. III. The Synthesis of Some Anthracene Derivatives as Wavelength Shifters in Plastic Scintillators

By Tadao NAKAYA, Takanori TOMOMOTO and Minoru IMOTO

Department of Applied Chemistry, Faculty of Engineering, Osaka City University, Sumiyoshi-ku, Osaka

(Received October 25, 1965)

Fifteen anthracene derivatives have been synthesized, and their absorption and fluorescence spectra have been measured. The spectra will be discussed in this paper. According to the spectra, some of anthracene derivatives synthesized here are better wavelength shifters than the compounds previously described in the literature.

In the first paper of this series,[1] we described the synthesis of some anthracene derivatives and their absorption and fluorescence spectra.

We have now synthesized fifteen more derivatives of anthracene; they are listed below.

9, 10-Bis(4-methoxybenzyl)anthracene (I) was obtained by the reaction of anthracene with 4-methoxybenzylalcohol. 9, 10-Bis(α-bromobenzyl)-anthracene (II_1), 9, 10-bis(α-*o*-toluidinobenzyl)-anthracene (II_2) and 9, 10-bis(α-acetoxybenzyl)-anthracene (II_3) were, respectively, obtained with the successive bromination, amination and acetoxylation of 9, 10-dibenzylanthracene. The derivatives of 9, 10-*trans*, *trans*-distyrylanthracene (III_1—III_2) were synthesized by the Wittig reaction of 9, 10-anthracenedimethyl-bis(triphenylphosphonium chloride) with the corresponding aldehydes. 9, 10-Anthracene-dimethanol diacetate (IV_1) and 9, 10-anthracene-dimethanol (IV_2) were prepared by the procedure described by Miller and his co-workers.[2]

9-Anthraldehyde tosylhydrazone (V) was synthesized by the reaction of 9-anthraldehyde with tosylhydrazine. The derivatives of 9, 10-dihydro-9, 10-*cis*-di(phenylcarbamoyl)anthracene (VI_1—VI_7) were obtained by the treatment of

1) M. Imoto and T. Nakaya, This Bulletin, **36**, 785 (1963).

2) M. W. Miller, R. W. Amison and P. O. Tawney, *J. Am. Chem. Soc.*, **77**, 2845 (1955).

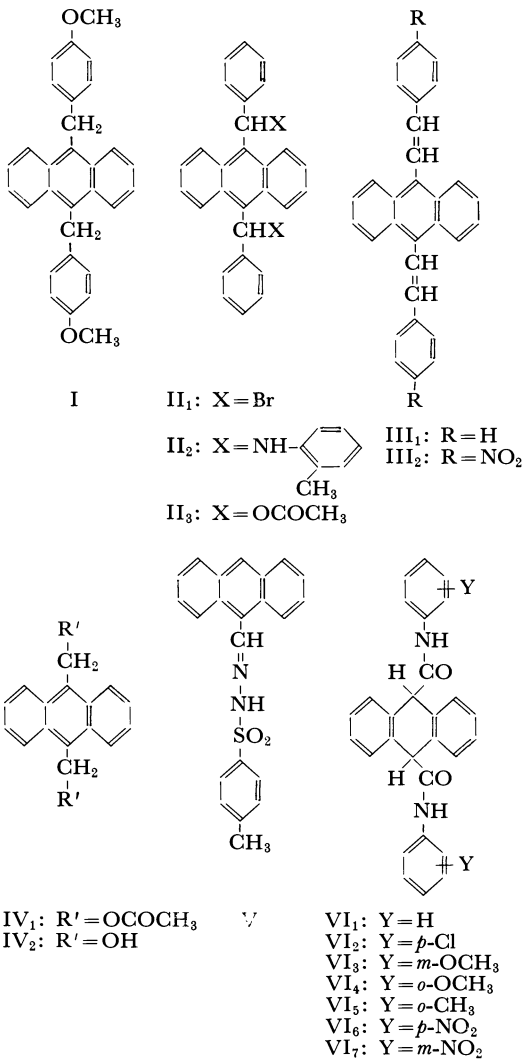

9, 10-dihydro-9, 10-*cis*-dicaroxylic chloride with substituted anilines.

This paper is concerned also with the absorption and fluorescence spectra of the compounds synthesized here. Some of them have been proved by Osio and his co-workers[3] to be superior to the wavelength shifters described in the literature.[4-6]

Experimental

9, 10-Bis(4-methoxybenzyl)anthracene (I).—1.7 g. of anthracene and 2.5 g. of 4-methoxybenzylalcohol were added to 50 ml. of acetic acid, and then the mixture was heated under reflux with a current of nitrogen gas for 4.5 hr. After the reaction mixture had been concentrated to removed the excess acetic acid, pale yellow crystals began to separate from the solution. The crystals were recrystallized several times from benzene to give I, with a m. p. of 223—224.5°C, in a 65% yield.

Found: C, 86.28; H, 6.33. Calcd. for $C_{30}H_{26}O_2$: C, 86.12; H, 6.22%.

9, 10-Bis(α-bromobenzyl)anthracene (II_1).—9, 10-Dibenzylanthracene was obtained by a method similar to that described in the previous paper.[1] A mixture of 9, 10-dibenzylanthracene (3.8 g.) and *N*-bromosuccinimide (4.0 g.) was heated in 250 ml. of oxygen-free carbon tetrachloride. To take off the *N*-bromosuccinimide, the mixture was filtered. The mixture was then concentrated by distillation under reduced pressure to give yellow crystals. The separated crystals were washed twice with diethylether, dried in vacuo, and crystallized from carbon tetrachloride to give II_1, melting at 193—195°C, in a 60% yield.

Found: Br, 30.8. Calcd. for $C_{28}H_{20}Br_2$: Br, 31.0%.

9, 10-Bis(α-*o*-toluidinobenzyl)anthracene (II_2).—Three grams of 9, 10-bis(bromobenzyl)anthracene and 3 g. of *o*-toluidine were added to 80 ml. of benzene, and then the mixture was heated for 9 hr. at the boiling point of the solvent. The reaction mixture was then chilled. The crystals which separated were collected and washed with cold benzene. The pale yellow crystalline solid was recrystallized from benzene to give II_2, with a m. p. of 261—262°C, in a 39% yield.

Found: C, 89.08; H, 6.01; N, 4.91. Calcd. for $C_{42}H_{36}N_2$: C, 88.93; H, 6.34; N, 4.93%.

9, 10-Bis(α-acetoxybenzyl)anthracene (II_3).—Two grams of 9, 10-bis(bromobenzyl)anthracene and 1.5 g. of silver acetate were added to 30 ml. of benzene, and then the mixture was heated under reflux for 1.5 hr. The reaction mixture was filtered at about 50°C. The mother liquor was concentrated to separate white crystals. The separated crystals were recrystallized several times from benzene to give II_3, with a m. p. of 227—229°C, a 52% yield. This compound showed the infrared absorption of the carbonyl group at 1735 cm^{-1}.

Found: C, 80.74; H, 5.94. Calcd. for $C_{32}H_{26}O_4$: C, 81.01; H, 5.48%.

9, 10-Anthracenedimethyl-bis(triphenylphosphonium chloride).—A solution of 2.7 g. of 9, 10-dichloromethylanthracene and 7.0 g. of triphenylphosphine in 350 ml. of dry xylene was heated at the boiling point of the solvent with stirring for 9 hr. The yellow crystals began to separate after 15 min. The mixture was then cooled to room temperature. The crystals were filtered, washed several times with excess dry xylene, and then dried in a vacuum desiccator at 10 mmHg and 60°C. The solid product, melting at 298—300°C, was obtained in a yield of 85%.

Found: Cl, 9.1. Calcd. for $C_{52}H_{42}Cl_2P_2$: Cl, 8.9%.

9, 10-*trans*, *trans*-Distyrylanthracene (III_1).—To a solution of 2.0 g. of 9, 10-anthracenedimethyl-bis(triphenylphosphonium chloride) and 0.8 g. of benzaldehyde in 30 ml. of absolute ethanol, 70 ml. of a 0.2 M lithium ethoxide solution was added. A yellow crystalline solid began to separate from the solution after 7 hr. After the solution had stood for 15 hr., the solid was collected on a filter glass and dried in vacuo. The

3) T. Osio, private communication.
4) R. C. Sangster and J. W. Irvine, *J. Chem. Phys.*, **24**, 670 (1956).
5) V. N. Kerr, F. N. Hayes, D. G. Ott and E. Hansbury, *J. Org. Chem.*, **24**, 1861 (1959); **24**, 1864 (1959).
6) A. Heller and D. Katz, *J. Chem. Phys.*, **35**, 1987 (1961).

solid product was crystallized from benzene. The solid, which was a mixture of cis and trans isomers, was recrystallized several times from boiling benzene containing a trace of iodine to give III_1 as yellow crystals, m. p.>310°C in a 24% yield.

Found: C, 93.19; H, 6.81. Calcd. for $C_{30}H_{22}$: C, 92.79; H, 7.21%.

9, 10-*trans*, *trans* - Bis(*p*-nitrostyryl)anthracene (III_2).—To a solution of 4.4 g. of 9, 10-anthracenedimethyl-bis(triphenylphosphonium chloride) and 2.0 g. of 4-nitrobenzaldehyde in 80 ml. of absolute ethanol, 110 ml. of a 0.2 M lithium ethoxide solution was added. A yellow red crystalline solid began to separate from the solution after a while. After the solution had stood for 10 hr, the solid was collected on a filter glass and dried in vacuo. The solid was then treated as above. The solid product was recrystallized several times from benzene in the presence of a trace of iodine to give III_2 as yellow red crystals, with a m. p. of >320°C, in a 28% yield.

Found: N, 5.90. Calcd. for $C_{30}H_{20}N_2O_4$: N, 5.93%.

9, 10-Anthracene-dimethanol Diacetate (IV_1).—This compound was prepared by the procedure reported by Miller and his co-workers.[2] A solution of 20 g. of 9, 10-dichloromethylanthracene and 25 g. of anhydrous sodium acetate in 400 ml. of glacial acetic acid was heated at reflux for 5 hr. The mixture was then allowed to cool to room temperature; yellow crystals were filtered out and dried in vacuo. The solid product was recrystallized from benzene to give IV_1 as yellow needles, melting at 220—222°C, in a 70% yield.

Found: C, 74.75; H, 6.07. Calcd. for $C_{20}H_{18}O_4$: C, 74.31; H, 5.66%.

9, 10-Anthracene-dimethanol (IV_2).—This compound was also prepared by the procedure reported by Miller and his co-workers.[2] To 4.9 g. of IV_1 in 400 ml. of methanol, 15 g. of 85% potassium hydroxide was added. After the mixture had been stirred under reflux for 2 hr., it was poured into 500 ml. of cold water. The solid products were collected, dried in vacuo, and recrystallized from benzene to give IV_2 as yellow prisms, melting at 280—282°C, in a 75% yield.

Found: C, 80.23; H, 6.10. Calcd. for $C_{16}H_{14}O_2$: C, 80.07; H, 5.88%.

9-Anthraldehyde Tosylhydrazone (V).—Anthraldehyde (2 g.) was added to a solution of 2g. of *p*-toluenesulfonylhydrazine in ethanol by an adaptation of the method described by Depuy and Froemsdolf.[7] The reaction mixture was kept at 70—80°C for 3 hr. and then chilled to room temperature. The solid product was collected and crystallized from ethanol. Recrystallization from ethanol gave V as yellowish prisms, melting at 183—184°C, in a 75% yield.

Found: C, 70.59; H, 5.13; N, 7.55. Calcd. for $C_{22}H_{18}N_2O_2S$: C, 70.67; H, 4.81; N, 7.49%.

9, 10-Dihydroanthracene-9, 10-*cis*-dicarboxylic Chloride.[8]—Two grams of 9, 10-dihydroanthracene-9, 10-*cis*-dicarboxylic acid[9] in thionyl chloride was heated under a nitrogen atmosphere for 2 hr. The reaction mixture was concentrated to remove the thionyl chloride. The yellow crystals, with a melting point of 169—170°C, were obtained in a 80% yield.

Found: Cl, 23.2. Calcd. for $C_{16}H_{10}O_2Cl_2$: Cl, 22.9%.

Derivatives of 9, 10-Dihydro-9, 10-*cis*-di(phenylcarbamoyl)anthracene (VI_1—VI_7).—To a solution of 0.01 mol. (3.1 g.) of the dicarboxylic chloride in benzene was 0.05 mol. of the corresponding substituted aniline at room temperature. An immediate precipitate formed. The mixture was then stirred at room temperature. The crystalline solid was collected, washed with benzene and water, and dried in vacuo. The solid was recrystallized from ethanol. The melting points and analysis of the compounds VI_1—VI_7 are tabulated in Table I. The yields of the compounds were quantitative.

Spectra and Discussion

Absorption Spectra.—The absorption spectrum of compound I closely resembles that of 9, 10-dibenzylanthracene, as is shown in Fig. 1. The shapes of the absorption spectra of II_1, II_2 and II_3, in which the hydrogen atoms of the methylene

Table I. Derivatives of 9, 10-dihydro-9, 10-*cis*-di(phenylcarbamoyl)anthracene (VI_1—VI_7)

Sample No.	Substitute Y	M.p. °C	Molecular formula		Analysis, % C	H	N	Cl
VI_1	H	297—298	$C_{28}H_{22}N_2O_2$	Calcd.	80.36	5.30	6.98	
				Found	80.02	5.36	6.93	
VI_2	*p*-Cl	>360 (decomp.)	$C_{28}H_{20}Cl_2N_2O_2$	Calcd.	68.99	4.11	5.75	14.8
				Found	68.62	4.50	5.83	14.1
VI_3	*m*-OCH_3	283—284	$C_{30}H_{26}N_2O_4$	Calcd.	75.31	5.44	5.85	
				Found	74.98	5.91	5.99	
VI_4	*o*-OCH_3	303—304	$C_{30}H_{26}N_2O_4$	Calcd.	75.31	5.44	5.85	
				Found	75.74	5.52	6.23	
VI_5	*o*-CH_3	336—337	$C_{30}H_{26}N_2O_2$	Calcd.	81.44	5.88	6.27	
				Found	80.89	6.06	6.27	
VI_6	*p*-NO_2	>360 (decomp.)	$C_{28}H_{20}N_4O_6$	Calcd.	66.14	3.94	11.02	
				Found	66.04	3.77	10.81	
VI_7	*m*-NO_2	280—282	$C_{28}H_{20}N_4O_6$	Calcd.	66.14	3.94	11.02	
				Found	65.82	4.28	10.91	

7) C. H. Depuy and D. H. Froemsdolf, *J. Am. Chem. Soc.*, **82**, 634 (1960).
8) P. J. Mathien, *Ann. Chim.*, **20**, 215 (1945).
9) A. H. Beckett, R. G. Ligard and B. A. Mulley, *J. Chem. Soc.*, **1953**, 3328.

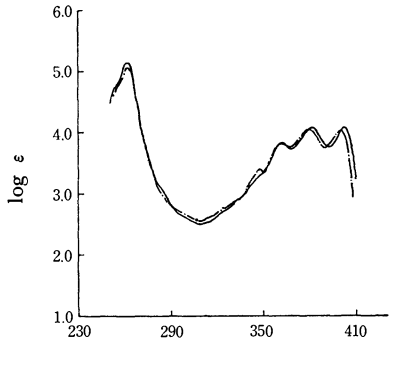

Fig. 1. Absorption spectra of 9,10-bis(4-methoxybenzyl)anthracene (I): —— and 9,10-dibenzylanthracene: —·— (in dioxane).

TABLE II. THE WAVELENGTHS AND MOLAR EXTINCTION COEFFICIENTS OF THE LONGEST-WAVELENGTH ABSORPTION MAXIMA OF COMPOUNDS I—IV_2 (IN DIOXANE)

Compound	Appearance	λ_{max} mμ	log ε
I	colorless	403	4.09
II_1	yellow	415	4.00
II_2	pale yellow	406	4.01
II_3	colorless	397	4.03
III_1	yellow	417	—a)
III_2	yellow red	428	—a)
IV_1	yellow	394	4.06
IV_2	yellow	393	3.98
9,10-Dibenzylanthracene	colorless	400	4.03

a) The molar extinction coefficient could not be determined because of the low solubility.

groups of 9, 10-dibenzylanthracene are replaced by bromine, *o*-toluidino and acetoxy groups respectively, are also similar to that of 9, 10-dibenzylanthracene. The wavelengths and molar extinction coefficients of the longest-wavelength absorption maxima of II_1, II_2 and II_3 are shown in Table II. The spectra of III_1 and III_2 indicate some resemblance to that of the parent anthracene, except for the considerable red shift, although the molar extinction coefficients could not be determined because of the low solubilities in organic solvents. The spectra of IV_1 and IV_2 are very similar to that of 9, 10-dimethylanthracene.[10] The wavelengths and molar extinction coefficients of the longest-wavelength absorption maxima of IV_1 and IV_2 are shown in Table II. When the longest-wavelength absorption maximum of II_3 are compared with those of II_1, II_2 and 9, 10-dibenzylanthracene, it is obvious that the introduction of acetoxy groups shifts the absorption band toward a shorter wavelength. As the reason for this blue shift, two interpretations are possible. One is that the acetoxy groups withdraw the π electron in the anthracene ring, since we would expect that the introduction of an electron-attracting group such as an acetoxy group increases the energy difference between the highest occupied and lowest vacant orbitals of the molecule; the other is the deformation of conjugation by the steric hindrance between the acetoxy groups and the hydrogen atoms at the 1, 4, 5 and 8 positions of the anthracene nucleus. Probably, both the effects play important roles. The spectrum of V is given in Fig. 2. The spectra of VI_2 and VI_5 are shown in Fig. 3. The wavelengths and molar extinction coefficients of the longest-wavelength absorption maxima of compounds V—VI_7 are tabulated in Table III.

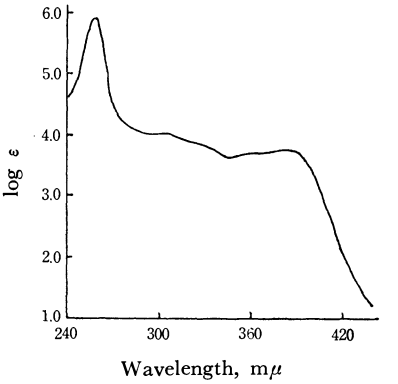

Fig. 2. Absorption spectrum of 9-anthraldehyde tosylhydrazone (V). (in dioxane)

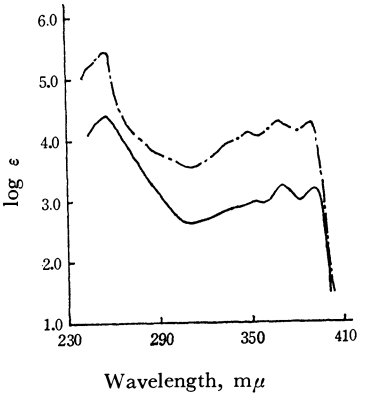

Fig. 3. Absorption spectra of 9,10-dihydro-9,10-*cis*-di(*p*-chlorophenylcarbamoyl)anthracene (VI_2): —— and 9,10-dihydro-9,10-*cis*-di(*o*-toylcarbamoyl)anthracene (VI_5): —·—. (in dioxane)

Within compounds VI_1—VI_7, the absorption intensities of VI_3, VI_4 and VI_5 are higher than those of the other compounds. It is apparent

10) H. H. Jaffé and M. Orchin, "Theory and Application of Ultraviolet Spectroscopy," John Wiley & Sons, New York (1962), p. 323.

Table III. The wavelengths and molar extinction coefficients of the longest-wavelength absorption maxima of compounds V—VI_7 (in dioxane)

Compound	Appearance	λ_{max} mμ	log ε
V	yellow	388	4.08
VI_1	colorless	392	—a)
VI_2	colorless	385	3.28
VI_3	colorless	393	4.22
VI_4	colorless	393	4.32
VI_5	colorless	390	4.08
VI_6	yellow	392	3.80
VI_7	yellow	390	3.81

a) The molar extinction coefficient could not be determined because of the low solubility.

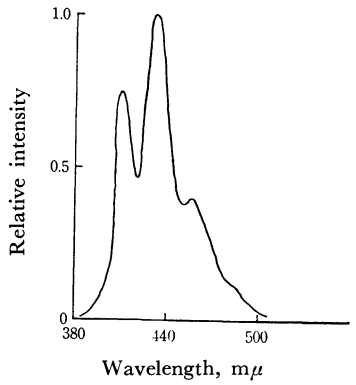

Fig. 4. Fluorescence spectrum of 9,10-bis(4-methoxybenzyl)anthracene (I). (2.5×10^{-5} mol./l. in dioxane)

Table IV. Fluorescence spectra (in dioxane)

Compound	Maxima of fluorescence spectra mμ	Relative intensity	Separation of nearest maxima of absorption and fluorescence mμ
I	411	0.75	8
	431	1.00	
	456	0.46	
II_3	405	0.77	8
	424	1.00	
	445	0.55	
IV_1	404	0.75	10
	424	1.00	
	448	0.53	
IV_2	405	0.63	12
	424	1.00	
	448	0.49	
V	(460)	(1.00)	—

that the methoxy or methyl groups increase the intensities of those compounds, because the methoxy or methyl groups exert electron-donating and conjugative effects on the anthracene nucleus.

Fluorescence Spectra. — The fluorescence spectrum of I are shown in Fig. 4. The shortest-wavelength fluorescence maxima and the difference in wavelength between the nearest maxima of the absorption and the fluorescence are given in Table IV.

The differences are 8—12 mμ, as is shown in Table IV. This may be ascribed to the fact that the conjugation of the molecules occurs more easily in the excited state than in the ground state, because the molecules are somewhat less strained in the excited state.

The fluorescence intensity of II_1 was very weak. This may be due to the effect of the heavy atoms of bromine in the molecule.[11] The fluorescence intensity of II_2 was also weak, as the substituents of the bulky *o*-toluidino groups prevent the conjugation between anthracene and benzene rings. The intensity of the fluorescence spectrum of II_3 was strong, because the acetoxy groups in the molecule should increase the intensity of the fluorescence in spite of the introduction of the bulky acetoxy groups.

The fluorescence intensities of III_1, III_2 and VI_1—VI_7 were also too weak to be observed.

The fluorescence spectrum of IV_2 is given in Fig. 5. The fluorescence spectrum of IV_1 closely resembles that of IV_2. The strongest fluorescence maximum of I is near the maximum sensitivity region of the widely-used photoelectron amplifier. In addition, the separation of the nearest maxima of the spectra of absorption and of fluorescence is sufficient. Therefore, there is a small probability of the reabsorption of photons, and a good scintillation property is predicted for it. This compound attains practical importance because of its high solubility in an alkylbenzene solution.

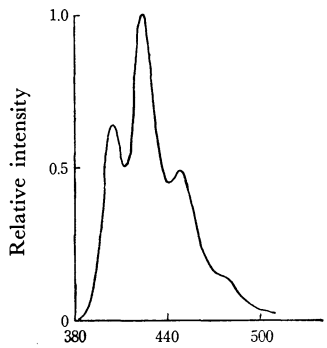

Fig. 5. Fluorescence spectrum of 9,10-anthracenedimethanol (IV_2). (2.3×10^{-5} mol./l. in dioxane)

The scintillation properties of II_3, IV_1 and IV_2 are also good in undergoing conformational changes in the excited states and in high solubilities in an alkylbenzene solution. In the case of V, the broad peak of fluorescence covers the maximum

11) J. Ferguson, *J. Mol. Spectroscopy*, **3**, 177 (1959).

sensitivity region of the phototube. The compound shows a greenish fluorescence in the crystals. Furthermore, it has a very good solubility in an alkylbenzene solution.

The authors are indebted to Professor Takahumi Osio and his coworkers for measuring the absorption and fluorescence spectra and the helpful discussion.

BULLETIN OF THE CHEMICAL SOCIETY OF JAPAN VOL. 39 1556—1559 (1966)

The Synthesis of Bicyclic Lactam Ether

By Naoya OGATA* and Shyunroku TOHOYAMA

Basic Research Laboratories, Toyo Rayon Co. Ltd. Tebiro, Kamakura

(Received October 28, 1965)

The bicyclic lactam ether, 3-aza-10-oxabicyclic[4.3.1]decane-4-one has been attempted to synthesize by the Beckmann rearrangement of the oxime of 9-oxabicyclo[3.3.1]nonane-3-one; this rearrangement caused polymerization through the cleavage of the ether group in acidic media. Therefore, it may be presumed that the cationic polymerization of lactam ethers in the presence of Lewis acid proceeds through the opening of the ether linkage.

The polymerization of lactam ethers gave[1] polyamide ethers in the presence of Lewis acid catalysts at relatively low temperatures. It was assumed that the polymerization proceeds through the coordination of Lewis acid to the ether group, followed by the cleavage at the ether group, since lactams do not polymerize under the same reaction conditions. However, lactam ethers give the same kind of polyamide ethers by means of the cleavage of either ether or amide linkages, and the reaction scheme is not clear.

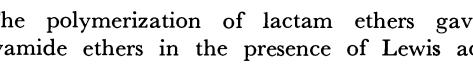

The ring-opening polymerization of the following bicyclic lactam ether gives different kinds of polymers according to whether the ring-cleavage occurs at the amide or ether linkages: hence, the structural analysis of the resultant polymer should show where the ring-opening occurs.

Therefore, the synthesis of 3-aza-10-oxabicyclo-[4.3.1]decane-4-one has been attempted for the first time.

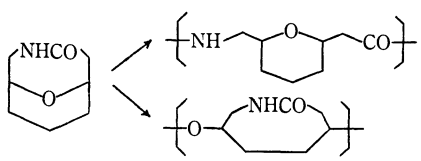

Experimental

The synthetic route of 3-aza-10-oxabicyclo[4. 3. 1]-decane-4-one is shown as follows:

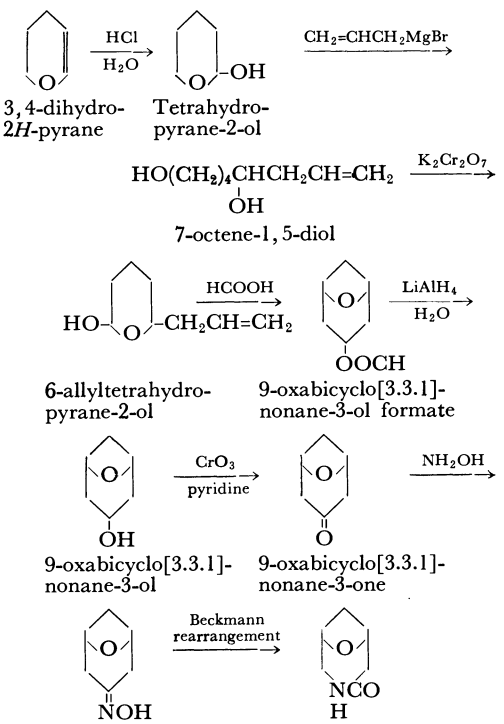

Tetrahydropyrane-2-ol.—A solution of 94 g. of purified dihydropyrane in 400 ml. of 0.2 N hydrochloric acid was heated under reflux for 1 hr. After the solution had been neutralyzed by sodium hydroxide, the product was extracted with ether and distilled. B. p. 60.7—65.0°C/9 mmHg; yield, 88.3 g. (74%).

Found: C, 58.65 (58.80); H, 9.83% (9.87).

7-Octene-1, 5-diol.—A solution of 61 g. (0.5 mol.) of allylbromide in 200 ml. of ether was dropped, with stirring, into 300 ml. of ether in the presence of 72 g.

* Present address: Chemistry Department, Sophia University, Tokyo.

1) N. Ogata, T. Asahara and S. Tohoyama, *J. Polymer Sci.*, to be published.

(3.2 mol.) of magnesium. The mixture was heated for a period of 4 hr. at such a rate that the ether refluxed gently; then the solution was heated at a gentle reflux for an additional 30 min. The Grignard solution was transferred into a 1l. three-necked flask, and then a solution of 15 g. of tetrahydropyrane-2-ol in 150 ml. of ether was added, drop by drop. The solution was heated under reflux for an additional 40 min. and then decomposed with a saturated aqueous solution of ammonium chloride. The product was extracted with ether and distilled. B. p. 114—127°C/5 mmHg; yield, 11.4 g. (53%).

Found: C, 66.42 (66.43): H, 11.18 (11.24); mol. wt., 148 (144).

6-Allyltetrahydropyrane-2-ol.—A portion of 15 g. (0.1 mol.) of 7-octene-1, 5-diol was dissolved in 30 ml. of benzene, and then 65 ml. of a Beckmann solution (12 g. $K_2Cr_2O_7$, 10 g. H_2SO_4 and 120 ml. of water) was

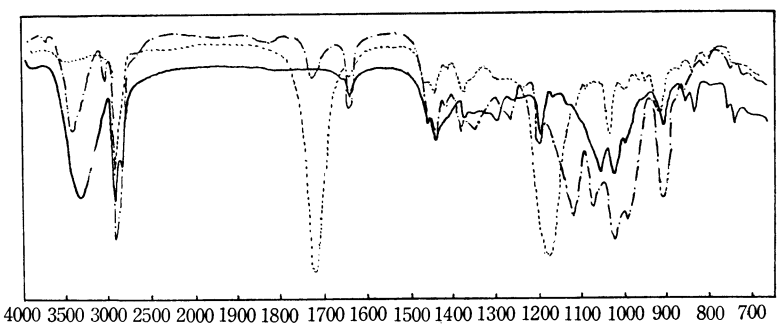

Fig. 1. Infrared spectra of products (KBr)
——— 6-Allyltetrahydropyrane-2-one
------ 9-Oxabicyclo[3.3.1]nonane-3-ol formate
——— 9-Oxabicyclo[3.3.1]nonane-3-ol

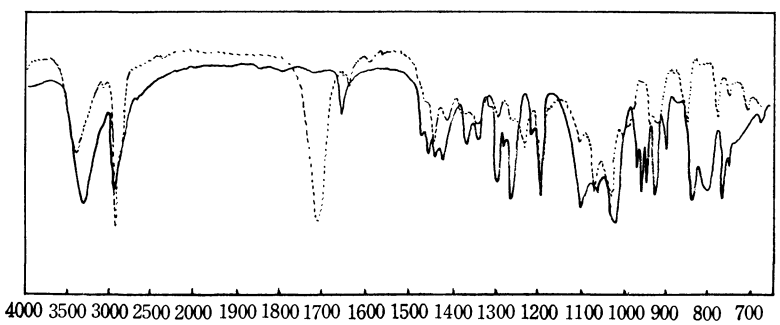

Fig. 2. Infrared spectra of products.
---- 9-Oxabicyclo[3.3.1]nonane-3-one
—— 9-Oxabicyclo[3.3.1]nonane-3-one oxime

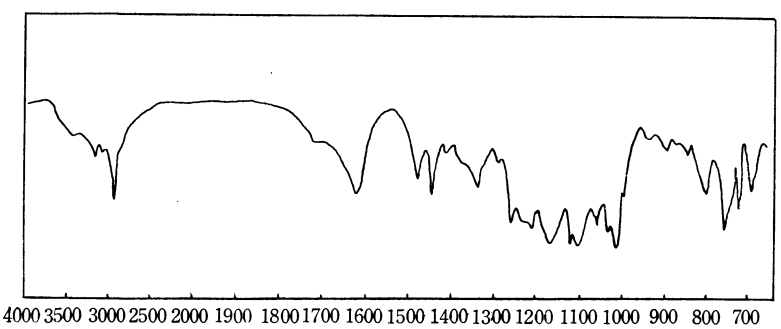

Fig. 3. Infrared spectrum of polymer (Film).

dropped, with stirring, into the solution over a period of 2 hr., with the temperature maintained at 35°C. The stirring was then continued for an additional hour at 35°C. The benzene layer was separated, and the aqueous solution was extracted twice with 100 ml. of dichloroethane. Benzene and dichloroethane solutions were combined, washed with water, and dried in the presence of magnesium sulphate. The distillation of the solution gave a fraction (7.2 g. (48%)) of 120—128°C/0.5 mmHg. The infrared spectrum of the product is shown in Fig. 1.

Found: C, 66.57 (66.77); H, 9.93% (9.78).

9-Oxabicyclio[3. 3. 1]nonane-3-ol formate. — A solution of 7.45 g. (0.05 mol.) of 6-allyltetrahydropyrane-2-ol in 50 ml. of 92% formic acid was heated while being stirred for 1 hr. at 40°C and then distilled. The gaschromatographic analysis of the distillate showed two peaks in almost equivalent amounts; separation could not be effected either by distillation or by column chromatography. The analytical data as well as the infrared spectrum showed that the distillate was the aimed-for product and it might include stereoisomers. B. p. 96—102°C/3 mmHg; yield, 4.83 g.

Found: C, 62.97 (63.51); H, 8.25 (8.29); mol. wt., 170 (170).

9-Oxabicyclo[3. 3. 1]nonane-3-ol.—A solution of 4.8 g. of 9-oxabicyclo[3. 3. 1]nonane-3-ol formate in 50 ml. of ether was added, drop by drop, into a solution of 4.8 g. of lithium aluminum hydride in 200 ml. of ether, with the temperature maintained at 0°C. The solution was allowed to stand, while being stirred for an additional 2 hr. at 0°C, then it was decomposed with a saturated aqueous solution of ammonium chloride. A continuous extraction with ether, followed by distillation, yielded 8 g. (80%) of the product. B. p. 132—134°C/0.5 mmHg.

Found: C, 66.90 (67.6); H, 9.00 (9.20).

9-Oxabicyclo[3. 3. 1]nonane-3-one.—A solution of 1.5 g. (0.01 mol.) of 9-oxabicyclo[3. 3. 1]nonane-3-one in 20 ml. of pyridine was added, drop by drop, into a solution of 4.2 g. (0.042 mol.) of chromic acid in 42 ml. of pyridine, with the reaction temperature at 0°C. kept by the use of an ice bath. Stirring was then concontinued at room temperature for an additional 4 hr., after which the solution was neutralized by the addition of concentrated hydrochloric acid. Continuous extraction, followed by the removal of the ether, yielded 0.78 g. of the product.

Oximation. — 9-Oxabicyclo[3. 3. 1]nonane-3-one (2 g.(0.014 mol.)), hydroxylamine hydrochloride (2 g.) and sodium carbonate (2 g.) were dissolved in a mixture of 20 ml. of ethanol and ether; the solution was then heated under reflux for 20 hr. After the solution had been extracted with ether and the ether removed, white crystals were obtained. The recrystallization of these from ethanol yielded 1.2 g. (56%) of needle crystals, m. p. 124—125°C.

Found: C, 60.40 (61.9); H, 8.30 (8.4); N, 8.5% (9.0) mol. wt., 160 (155).

Beckmann Rearrangement.—A strong reagent for the Beckmann rearrangement, such as sulfuric acid, decomposed oximes with an ether group, and mild reaction conditions, using thionyl chloride at a low temperature, have been recommended[1] for the synthesis of lactam ethers.

In this case, however, not even thionyl chloride could give the aimed-for product; only a sticky polymer was obtained. Neither phosphorus pentachloride nor benzene sulfonyl chloride could give the aimed-for bicyclic lactam ether, even at such a low temperature as below 0°C., and the product was a polymer with molecular weight of about 580 to 650. The polymer was a soft solid, and its melting point was not clear. The infrared spectrum of the polymer is shown in Fig. 3.

Found: C, 61.5 (61.9); H, 8.5 (8.4); N, 8.6% (9.0).

Discussion

Bohlmann[2] synthesized 9-oxabicyclo[3.3.1]-nonane-3-ol through the alkaline hydrolysis of the formate of the alcohol. However, the yield was poor by this method; the reduction of the formate, followed by hydrolysis, gave a better yield of the alcohol. The oxidation of the alcohol into ketone in the presence of the chromic acid-pyridine complex gave a better yield than in the Beckmann solution ($K_2Cr_2O_7/H_2SO_4$) since a ring cleavage was observed in an acidic medium. Pure bicyclic lactam ether was not able to isolate by means of the Beckmann rearrangement of the oxime, but a polymer was easily obtained. The infrared spectrum of the polymer showed absorption resulting from the amide group at 3250, 3100 and 1625 cm^{-1}. The strong absorption at 1625 cm^{-1} is supposed to be due to an amide carbony group; no absorption was observed in the range from 1550 to 1600 cm^{-1}.

The chain trans amide group shows a strong absorption, the so-called amide II band, in the region from 1550 to 1600 cm^{-1}. Therefore, the ring cleavage may be presumed to have occured at the ether linkage, because no absorption resulting from a chain trans amide group was observed, as would be expected if the amide group was cleaved.

The derivatives of bicyclic ether show an absorption band resulting from the ether group in the region from 1030 to 1020 cm^{-1}, while the cleaved product of the bicyclic lactam ether shows an ether band at 1010 cm^{-1}. A monocyclic oxime ether, tetrahydro-γ-pyrone oxime and its isoxime, gave an absorption band resulting from the ether group at 1100 cm^{-1}, a band which was shifted to 1070 cm^{-1} in the polymer from a monocyclic lactam ether, tetrahydro-1, 4-oxazepine-5(4*H*)-one. The tetrahydropyrane derivatives show an ether band around 1100 cm^{-1}. Therefore, the shift of the ether band toward a lower frequency also support the above presumption.

The protonation of the ether group, followed by the cleavage, caused the polymerization of bicyclic lactam ether at a low temperature. Therefore, the cationic polymerization of lactam ethers proceeds

2) F. Bohlmann, H. T. Schulz and J. Poamann, *Tetrahedron Letters*, **1964**, 1705.

through the opening of the ether group. Further evidence on the structure of the polymer will provide for the elucidation of the reaction scheme.

The authors wish to thank Dr. Toshio Hoshino for his permission to publish this paper. Thanks are also due to Dr. Bohlmann, who sent us detailed informations on the synthesis of the bicyclic ketone ether.

BULLETIN OF THE CHEMICAL SOCIETY OF JAPAN VOL. 39 1559—1562 (1966)

Methylene-hydantoin and Related Compounds. I. On the Reaction of Pyruvic Acid and Urea: The Synthesis of 5-Methylene-hydantoin

By Shunsuke MURAHASHI,† Heimei YUKI,†† Koichi KOSAI†† and Fumihiro DOURA†

† *Department of Polymer Science, Faculty of Science, Osaka University, Toyonaka, Osaka*

†† *Department of Chemistry, Faculty of Engineering Science, Osaka University, Toyonaka, Osaka*

(Received November 10, 1965)

Various condensation products were obtained by the reaction between pyruvic acid and urea. They are 5-hydroxy-5-methyl-hydantoin, homoallantoin, homoallantoic acid, and dipyruvic triureide. 5-Methylene-hydantoin was prepared from some of these compounds, or directly from pyruvic acid and urea, by reactions in organic acid. The most convenient method was the dehydration of 5-hydroxy-5-methyl-hydantoin, which is a new compound melting at 166°C. 5-Methylene-hydantoin, m. p. 214°C, is a new monomer of the vinylidene type which polymerizes easily by means of a free radical mechanism. 3-Methyl-5-methylene-hydantoin was also prepared from 5-hydroxy-5-methyl-hydantoin through its 3-methyl derivative.

The derivatives of 5-methylene-hydantoin may be vinylidene-type monomers of some interest because they give polymers containing hydantoin groups along the hydrocarbon main chains. However, 5-methylene-hydantoin (I) itself has not been prepared, although the preparation of substituted 5-methylene-hydantoins, such as 1-phenyl-5-methylene-hydantoin[1] and 3-phenyl-5-methylene-hydantoin,[2] has been reported in the literature.

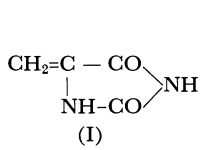

(I)

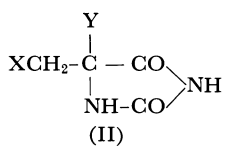

(II)

Various attempts to derive I from the compounds represented by formula II, such as 5-bromo-5-methyl-hydantoin (X=H, Y=Br),[3] 5-bromomethyl-hydantoin (X=Br, Y=H),[4] 5-hydroxymethyl-hydantoin (X=OH, Y=H),[5] and 5-carboxymethylene-hydantoin,[6] by the elimination of XY or by decarboxylation in the case of 5-carboxymethylene-hydantoin were not successful because of the difficulty of the elimination reaction and/or the polymerization of the product during the reaction.

5-Methylene-hydantoin is considered to be the condensation product of equimolar amounts of pyruvic acid and urea; this suggests the possibility of its formation from these compounds. It was found that 5-methylene-hydantoin could be prepared from pyruvic acid and urea directly or through their reaction products as intermediates. In this paper, the synthesis of 5-methylene-hydantoin and, in connection with this, the results of the investigation of the reaction of pyruvic acid and urea will be described.

Results and Discussion

The prolonged reaction of equimolar amounts of pyruvic acid and urea in water at room temperature gave 5-hydroxy-5-methyl-hydantoin (III) in a fairly good yield. If the reaction was carried out with higher concentrations of the reagents, homoallantoic acid (α, α-diureidopropionic acid) (IV) was produced predominantly, and at higher temperatures mainly homoallantoin (5-methyl-5-ureido-hydantoin) (V) and dipyruvic triureide (VI) were obtained. The reaction probably proceeded by the course shown in Fig. 1. The condensation product (VII) of pyruvic acid and urea is converted into 5-hydroxy-5-methyl-hydantoin by cyclization in a dilute solution, but at

1) R. K. Ralph, G. Shaw and R. N. Naylor, *J. Chem. Soc.*, **1959**, 1169.
2) M. Bergmann and D. Delis, *Ann.*, **458**, 82 (1927).
3) S. Gabriel, ibid., **348**, 50 (1906).
4) G. Nadeau and R. Gaudry, *Can. J. Research*, **27B**, 421 (1949).
5) D. Billet, *Bull. soc. chim. France*, **1954**, 815.
6) J. E. Nyc and H. K. Mitchell, *J. Am. Chem. Soc.*, **69**, 1382 (1947).

higher concentrations of the reagents urea may attack VII and give homoallantoic acid. This acid is slightly soluble in water and is precipitated from a cold solution. At higher temperatures, homoallantoic acid is converted into homoallantoin by dehydration or into dipyruvic triureide through condensation with VII.

5-Hydroxy-5-methyl-hydantoin is a new compound whose melting point is 166°C. The reduction of 5-hydroxy-5-methyl-hydantoin with hydroiodic acid gave 5-methyl-hydantoin. It has been known that homoallantoic acid itself can be prepared from one mole of pyruvic acid and two of urea.[7] When heated at 100°C in 80% formic

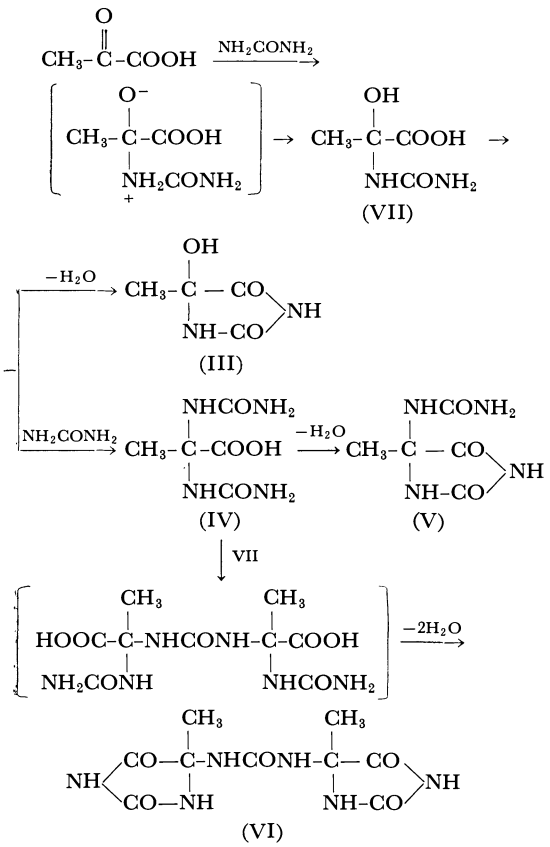

Fig. 1. Reaction of pyruvic acid and urea.

TABLE I. THE REACTION OF PYRUVIC ACID AND UREA
Pyruvic acid, 5.0 g.; Urea, 3.4 g. (1 : 1 molar ratio)

Solvent	ml.	Temp. °C	Time	Product (% Yield) III	IV	V	VI
H_2O	5	20	2 days	—	40	—	—
H_2O	25	20	14 days	69	—	10	—
H_2O	5	90	2 hr.	—	—	10	22
H_2O	20	90	2 hr.	30	—	10	11
1/100 N HCl	20	20	3 days	21	—	—	—
1 N NaOH	15	20	3 days	48	—	7	—

7) I. J. Simon, *Compt. rend.*, **133**, 587 (1901).

acid, 5-hydroxy-5-methyl-hydantoin easily gave 5-methylene-hydantoin in a 60% yield. The prolonged reaction did not improve the yield, but by the addition of acetic anhydride to the reaction mixture as a dehydrating agent, 5-methylene-hydantoin was obtained almost quantitatively, even in several minutes. The reaction carried out in acetic acid or in 1 N hydrochloric acid gave 5-methylene-hydantoin in only low yield. However, 5-methylene-hydantoin was obtained in a high yield when a mixture of glacial acetic acid and a small amount of concentrated hydrochloric acid was used as the solvent. 5-Methylene-hydantoin gave 5-methyl-hydantoin by reduction with hydroiodic acid.

3, 5-Dimethyl-5-hydroxy-hydantoin (VIII) was prepared by the methylation of 5-hydroxy-5-methyl-hydantoin with dimethyl sulfate. The dehydration of this compound gave 3-methyl-5-methylene-hydantoin (IX) under the same conditions as produced 5-hydroxy-5-methyl-hydantoin.

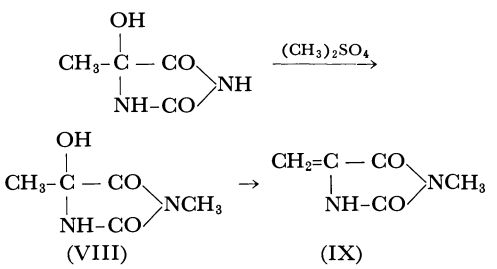

Dipyruvic triureide has been known to be easily obtainable by a reaction of 2 moles of pyruvic acid and 3 of urea in concentrated hydrochloric acid.[8] Dipyruvic triureide was hydrolyzed to give 5-hydroxy-5-methyl-hydantoin and homoallantoin almost quantitatively by boiling it in water for several hours. By a prolonged reaction at a much slower rate, homoallantoin could be hydrolyzed to 5-hydroxy-5-methyl-hydantoin and urea.

5-Methylene-hydantoin could also be obtained from dipyruvic triureide and from homoallantoin by hydrolysis in organic acid under conditions similar as those in the dehydration of 5-hydroxy-5-methyl-hydantoin. In these cases, however, some difficulties were encountered in isolating 5-methylene-hydantoin from the other hydrolysis products, urea and homoallantoin, while 5-methylene-hydantoin might polymerize during the isolation if it requires too long a time.

Davidson[8] has reported that dipyruvic triureide was converted by concentrated sulfuric acid into dipyruvic ureide (X), the dimer of 5-methylene-hydantoin, which is stable and almost insoluble in cold water. In this reaction the initial product must be 5-methylene-hydantoin, which dimerizes in sulfuric acid by the cationic mechanism.

8) D. Davidson, *J. Am. Chem. Soc.*, **47**, 255 (1925).

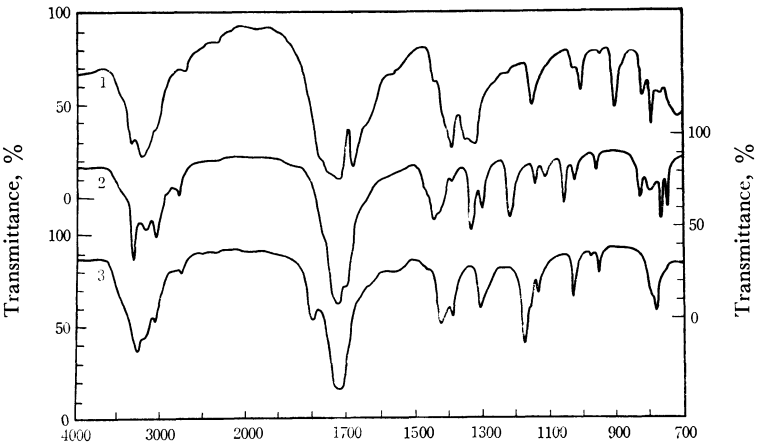

Fig. 2. Absorption spectra of: 1, 5-methylene-hydantoin; 2, 5-methyl-hydantoin; 3, 5-hydroxy-5-methyl-hydantoin (in KBr disks).

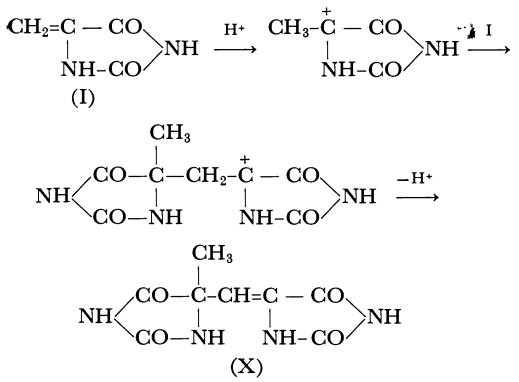

Directly from pyruvic acid and urea, 5-methylene-hydantoin could be prepared in a low yield by heating it in acetic acid containing a small amount of hydrochloric acid. However, the slow rate of reaction left the reagents unreacted, or resulted in the polymerization of the hydantoin produced during the long period of reaction.

As has been described above, there are various routes possible in the synthesis of 5-methylene-hydantoin from pyruvic acid and urea as starting materials. However, the most convenient route among these is that via 5-hydroxy-5-methyl-hydantoin because of its high yield and the simple procedure.

The infrared spectra of 5-methylene-hydantoin, 5-methyl-hydantoin and 5-hydroxy-5-methyl-hydantoin are shown in Fig. 2.

Experimental

5-Hydroxy-5-methyl-hydantoin.—A solution of pyruvic acid (50 g., 0.57 mol.) and urea (34 g., 0.57 mol.) in water (250 ml.) was allowed to stand at room temperature for 14 days and then evaporated under reduced pressure. Methanol (350 ml.) was added to the residue, and the insoluble materials were filtered off. Then the unreacted urea was removed by precipitation by adding dry ether to the filtrate. When the solution was evaporated, crude crystals of 5-hydroxy-5-methyl-hydantoin were obtained. Recrystallization from acetic acid gave colorless crystals; yield, 51 g. (69%); m. p. 166°C. This compound was soluble in water, alcohol, acetone, and tetrahydrofuran, sparingly soluble in ethyl ether, and insoluble in petroleum ether.

Found: C, 36.82; H, 4.61; N, 21.62. Calcd. for $C_4H_6N_2O_3$: C, 36.93; H, 4.65; N, 21.53%.

The reaction carried out at a higher concentration of the reagents, at a higher temperature or in the presence of an acid or a base did not improve the yield of 5-hydroxy-5-methyl-hydantoin. The results of the reaction under varying conditions are shown in Table I.

Homoallantoic Acid.—This compound was prepared according to Simon.[7] It was converted into homoallantoin in hot water in a 50% yield.

5-Methylene-hydantoin from 5-Hydroxy-5-methyl-hydantoin.—5-Hydroxy-5-methyl-hydantoin (10 g., 0.077 mol.) was dissolved in a mixture of 80% formic acid (100 ml.) and acetic anhydride (120 ml.), and then heated at 100°C for 5 min. in the presence of a small amount of hydroquinone. The solution was then cooled and evaporated under reduced nitrogen pressure. The residue was recrystallized from acetic acid. 5-Methylene-hydantoin (8 g.) was thus obtained almost quantitatively; m. p. 214°C.

Found: C, 42.80; H, 3.62; N, 25.13. Calcd. for $C_4H_4N_2O_2$: C, 42.86; H, 3.60; N, 25.00%.

5-Methylene-hydantoin was soluble in water, alcohol, and acetone, sparingly soluble in ethyl ether, and insoluble in hexane and benzene. It polymerized easily when heated in the presence of a radical initiator. The polymerization and the properties of the polymer will be described in a following paper.[9]

To a solution of 5-methylene-hydantoin (0.05 g.) in acetic acid (2 ml.), hydroiodic acid (2 ml., d=1.6)

9) S. Murahashi, H. Yuki, K. Kosai and F. Doura, This Bulletin, **39**, 1563 (1966).

was added. Immediately the brown color of iodine appeared. The solution was heated at 100°C for 10 min. and then concentrated under reduced pressure. Water was added to the residue, and the solution was evaporated. This procedure was repeated five times in order to remove the iodine. Colorless crystals of 5-methyl-hydantoin were thus obtained; m. p. 142°C. They showed the same infrared spectrum as an authentic sample, and their melting points were undepressed on admixture.

The reaction of 5-hydroxy-5-methyl-hydantoin and hydroiodic acid gave the same product as that described above.

3, 5-Dimethyl-5-hydroxy-hydantoin. — 5-Hydroxy-5-methyl-hydantoin (20 g., 0.15 mol.) was dissolved in 1 N sodium hydroxide, after which dimethyl sulfate (21 g., 0.17 mol.) was stirred in drop by drop. The temperature was then kept at 35°C for about one hour. The evaporation of the solvent left a syrupy residue, which was extracted with absolute alcohol. Dry ether was added to the solution, and the precipitates produced were filtered off. When the filtrate was evaporated, a white solid (18 g.) was obtained. Recrystallization from acetone-petroleum ether gave pure 3, 5-dimethyl-5-hydroxy-hydantoin; yield, 17 g. (77%); m. p. 104°C. The compound was soluble in water, alcohol and acetone, slightly soluble in ether, and insoluble in petroleum ether.

Found: C, 44.66; H, 5.66; N, 19.27. Calcd. for $C_5H_8N_2O_3$: C, 44.66; H, 5.59; N, 19.44%.

3-Methyl-5-methylene-hydantoin. — This compound was obtained quantitatively from 3, 5-dimethyl-5-hydroxy-hydantoin by the same procedure as that described in the synthesis of 5-methylene-hydantoin from 5-hydroxy-5-methyl-hydantoin. 3-Methyl-5-methylene-hydantoin, m. p. 142°C, was soluble in water, alcohol and acetone, slightly soluble in ether, and insoluble in petroleum ether.

Found: C, 47.52; H, 4.89; N, 22.33. Calcd. for $C_5H_6N_2O_2$: C, 47.62; H, 4.80; N, 22.22%.

Dipyruvic Triureide.—Dipyruvic triureide was prepared according to Davidson[8] as follows. To a solution of urea (75 g., 1.3 mol.) in concentrated hydrochloric acid (85 ml.), pyruvic acid (50 g., 0.57 mol.) was added. After the solution had been allowed to stand for 3 days, it solidified completely. Recrystallization from dilute aqueous ammonia and acetic acid gave long needles; yield, 73 g. (72%); m. p. above 300°C (decomp.).

Found: C, 33.88; H, 5.13; N, 26.41. Calcd. for $C_9H_{12}N_6O_5 \cdot 2H_2O$: C, 33.74; H, 5.04; N, 26.25%.

The Hydrolysis of Dipyruvic Triureide.—A suspension of dipyruvic triureide (50 g., 0.15 mol.) in water (1.2 l.) was refluxed for 5 hr. The resultant solution was evaporated to dryness. The residue was then triturated with dry methanol (130 ml.) and filtered. Homoallantoin was thus obtained as colorless crystals; yield, 24 g. (91%); m. p. 260°C (decomp.) (lit.,[7] m. p. 260°C (decomp.)).

Found: C, 34.79; H, 4.78; N, 32.69. Calcd. for $C_5H_8N_4O_4$: C, 34.88; H, 4.88; N, 32.55%.

The filtrate was concentrated after urea had been removed by adding dry ether. The crude crystals of 5-hydroxy-5-methyl-hydantoin were recrystallized from acetic acid; yield, 19 g. (91%).

The Hydrolysis of Homoallantoin.—Homoallantoin (10 g., 0.058 mol.) was dissolved in hot water (100 ml.), and the solution was refluxed for 10 hr. By the same procedure as has been described above, unreacted homoallantoin (5.5 g.) was recovered and 5-hydroxy-5-methyl-hydantoin (3.2 g.) was obtained from the mother liquor in a 94% yield (based on the consumed homoallantoin).

5-Methylene-hydantoin from Dipyruvic Triureide.—A suspension of dipyruvic triureide (5 g., 0.016 mol.) in 80% formic acid (100 ml.) or in a mixture of acetic acid (100 ml.) and concentrated hydrochloric acid (1 ml.) was heated at 100°C for 20 min. in the presence of hydroquinone. The concentration of the resultant solution under a reduced nitrogen pressure left a syrupy residue, which was dissolved in water (80 ml.) and filtered to remove homoallantoin and the polymer produced during the reaction. After the filtrate had been freeze-dried, the residual crystals were extracted with tetrahydrofuran (100 ml.) to remove the urea. When the extracted solution was evaporated, crude crystals of 5-methylene-hydantoin were obtained. Recrystallization from acetonitrile yielded 2.1 g. (60%). From the water-insoluble fraction, homoallantoin (0.5 g.) was obtained.

5-Methylene-hydantoin from Homoallantoin.—By a procedure similar to that described above, 5-methylene-hydantoin was obtained from homoallantoin in a 60% yield.

5-Methylene-hydantoin from Pyruvic Acid and Urea.—A solution of pyruvic acid (5.0 g., 0.06 mol.) and urea (3.4 g., 0.06 mol.) in acetic acid (20 mol.) containing a small amount of hydrochloric acid was heated at 100°C for 2 hr. 5-Methylene-hydantoin (1.5 g.) was thus obtained in a 24% yield.

BULLETIN OF THE CHEMICAL SOCIETY OF JAPAN VOL. 39 1563—1567 (1966)

Methylene-hydantoin and Related Compounds. II. Poly-5-methylene-hydantoin and Poly-α-aminoacrylic Acid

By Shunsuke MURAHASHI,† Heimei YUKI,†† Koichi KOSAI†† and Fumihiro DOURA†

† *Department of Polymer Science, Faculty of Science, Osaka University, Toyonaka, Osaka*

†† *Department of Chemistry, Faculty of Engineering Science, Osaka University, Toyonaka, Osaka*

(Received November 10, 1965)

5-Methylene-hydantoin was polymerized easily by free radical initiators, and showed a higher reactivity in copolymerization with styrene. From the copolymerization of styrene (M_1) and 5-methylene-hydantoin (M_2), the monomer reactivity ratios, r_1 and r_2, were found to be 0.03 and 24, while the Q and e values in Alfrey-Price's Q-e scheme were found to be 21 and -0.23, respectively. As is shown by the large Q value, the high reactivity of 5-methylene-hydantoin is based on the high resonance stabilization of its radical, a stabilization which results from the conjugation system. This was also confirmed by a study of the ultraviolet spectrum. Poly-5-methylene-hydantoin showed electrolytic behavior in its solubility and solution viscosity. This property is due to the dissociation of NH at the 3 position of the hydantoin group. The polymers of 3-methyl-5-methylene-hydantoin and 3-phenyl-5-methylene-hydantoin were observed to show very weak acidities, resulting from the NH at the 1 position. Poly-α-aminoacrylic acid was obtained by the alkaline hydrolysis of poly-5-methylene-hydantoin. This polymer was soluble in water, and showed an unusual amphoteric behavior in solution viscosity.

In a previous paper,[1] the synthesis of 5-methylene-hydantoin (I) from pyruvic acid and urea was reported. This material is an exo-methylene compound, one which polymerizes easily in spite of having a bulky group at the double bond. In this paper, the investigations of the polymerization of 5-methylene-hydantoin, the properties of its polymer (II) and of a poly-ampholyte, poly-α-aminoacrylic acid (III), prepared by the hydrolysis of poly-5-methylene-hydantoin, will be reported on.

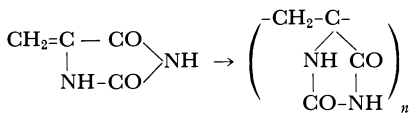

(I)

(II)

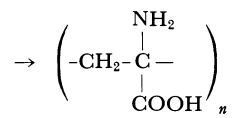

(III)

Results and Discussion

5-Methylene-hydantoin was polymerized in water and in acetic acid with free radical initiators. The polymerization was also carried out in situ with the monomer produced by the decomposition of dipyruvic triureide or by the reaction between pyruvic acid and urea without isolation. 3-Methyl- and 3-phenyl-5-methylene-hydantoin were polymerized in organic solvents with azobisisobutyronitrile. The results are shown in Table I.

The rate of the polymerization of 5-methylene-hydantoin was very fast. The precipitation of the polymer began immediately and was almost complete within one hour. The differences between the molecular weights of these polymers were shown by their solution viscosities. The smaller molecular weight of the polymer produced in water may be caused by the smaller solubility of the polymer in this solvent. It was found that the viscosities of polymers produced from the monomer in situ were almost the same as that obtained from the purified monomer.

The polymers were proved to be formed by the addition polymerization at the double bond in 5-methylene-hydantoin; there was a remarkable similarity between the infrared spectra of the polymer and of fused 5, 5-dimethyl-hydantoin, as is shown in Fig. 1.

It was found that 5-methylene-hydantoin did not copolymerize with vinyl acetate, but that it did copolymerize with styrene, methyl methacrylate and acrylonitrile when treated by a free radical initiator. Copoly-(acrylonitrile - 5 - methylene-hydantoin), containing a small amount of the latter monomer unit, showed good dyeing properties against a basic dyestuff such as Rhodamine 6G.

The copolymerization of styrene (M_1) and 5-methylene-hydantoin (M_2) was investigated in order

1) S. Murahashi, H. Yuki, K. Kosai and F. Doura, This Bulletin, **39**, 1559 (1966).

Table I. Polymerization of 5-methylene-hydantoin and its analogues

Monomer or starting material	g.	Solv.,	ml.	Init.,	mg.	Temp. °C	Yield %	$\eta_{sp/c}$*1 (c=1)
5-Methylene-hydantoin	1.0	H_2O	15	$K_2S_2O_8$	20	60	100	0.51
5-Methylene-hydantoin	1.0	AcOH	25	AIBN	10	60	100	1.16
Pyruvic acid, urea	5.0, 3.4	AcOH	25	AIBN	100	80	37	1.12
Dipyruvic triureide	5.0	HCOOH	100	AIBN	50	60	72	1.19
3-Me-5-methylene-hyd.	1.0	MeOH	20	AIBN	10	60	100	0.45*2
3-Ph-5-methylene-hyd.	2.0	Me_2CO	35	AIBN	60	53	85	0.49*3

1* Solvent, 0.09 N NaOHaq; c=1 g./100 ml.; temp., 30.0°C.
2* Solvent, 0.04 N NaOHaq.
3* Solvent, THF.

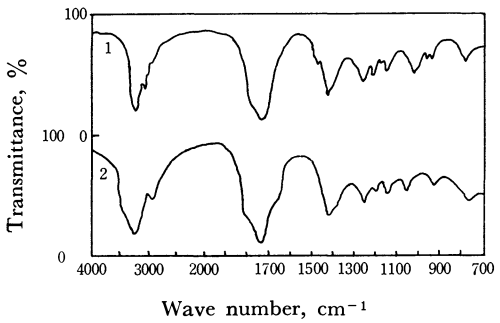

Fig. 1. Absorption spectra of: 1, fused 5,5-dimethyl-hydantoin; 2, poly-5-methylene-hydantoin in KBr disk.

Table II. Copolymerization of 5-methylene-hydantoin (M_2) and styrene (M_1)

Total monomer 10^{-2} mol.	M_2*1	Time min.	Conv. %	Anal. N%	m_2*2
4.19	0.098	150	4.9	18.55	0.727
4.95	0.160	120	3.1	21.36	0.845
4.71	0.251	60	3.6	22.34	0.886
4.68	0.507	40	4.0	23.81	0.949
4.72	0.771	20	4.4	24.16	0.964
4.52	0.910	12	2.3	24.35	0.972

*1 M_2: Mole fraction of 5-methylene-hydantoin in monomer mixture.
*2 m_2: Mole fraction of 5-methylene-hydantoin in copolymer.

to obtain the monomer reactivity ratios of these two monomers. The copolymerization reaction was carried out in methanol at 70°C using azobisisobutyronitrile as the initiator. The results are shown in Table II. It was found that 5-methylene-hydantoin was incorporated predominantly in all the copolymers. The composition curve derived from the results in Table II is shown in Fig. 2. The curve shows a higher reactivity of 5-methylene-hydantoin than that of styrene; the monomer reactivity ratios, r_1 and r_2, were calculated to be 0.03±0.02 and 24±1 respectively. The Q and e values calculated from these r_1 and r_2 were 21 and −0.23 respectively.

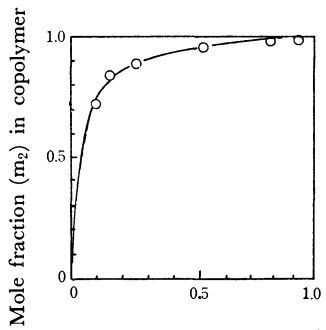

Fig. 2. Copolymer composition curve in the copolymerization of styrene (M_1) and 5-methylene-hydantoin (M_2).
Open circle: observed value
Full line: theoretical curve for r_1=0.03, r_2=24

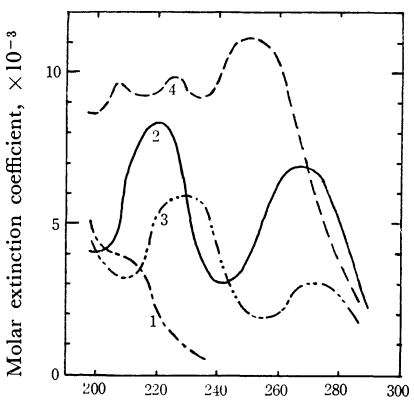

Fig. 3. Absorption spectra of: 1, 5-methyl-hydantoin in H_2O; 2, 5-methylene-hydantoin in H_2O; 3, 3-methyl-5-methylene-hydantoin in H_2O; 4, 3-phenly-5-methylene-hydantoin in EtOH.

The ultraviolet spectra of 5-methylene-hydantoin, 5-methyl-hydantoin, 3-methyl-5-methylene-hydantoin and 3-phenyl-5-methylene-hydantoin are shown in Fig. 3. 5-Methyl-hydantoin showed only an absorption band at 215 mμ, but the three methylene-hydantoins gave strong absorption bands at 240—280 mμ, resulting from the π—π* transition,

besides the bands in the 200—240 mμ region. The high reactivity of 5-methylene-hydantoin represented by the Q value is apparently correlated with this spectroscopic observation, which shows a strongly conjugated structure in this monomer.

Poly-5-methylene-hydantoin was a colorless solid which was insoluble in water and in common organic solvents, but soluble in dilute aqueous solutions of bases such as sodium hydroxide, ammonia, pyridine, triethylamine and ethanolamine. The dissolution of the polymer in a basic aqueous solution suggests the ionization of hydrogen at the 3 position of the hydantoin group. The hydrogen is made considerably acidic by the inductive effect of two neighboring carbonyl groups, contrary to the very weak acidity of the hydrogen at the 1 position. The mono-sodium salt of poly-5-methylene-hydantoin was obtained by pouring a solution of polymer and a large excess of sodium hydroxide into methanol. The polymers of 3-methyl- and 3-phenyl-5-methylene-hydantoin, which have no hydrogen at the 3 position, were also soluble in a basic aqueous solution, but higher concentrations of the base were required for their dissolution. Poly-5-methylene-hydantoin was soluble in a 0.02 N sodium hydroxide solution, and 0.5 N was needed to dissolve poly-3-phenyl-5-methylene-hydantoin with a bulky hydrophobic phenyl group.

The electrolytic properties of the polymers were observed by means of their viscosities. These are shown in Figs. 4 and 5. The reduced viscosities of a solution of poly-5-methylene-hydantoin in aqueous sodium hydroxide were measured at a constant concentration of the polymer but with varying concentrations of the base (Fig. 5), and vice versa (Fig. 4). Each viscosity curve showed a maximum at the equivalent concentrations of the polymer and the base. On the other hand, the reduced viscosity of the polymer in a 0.045 mol. aqueous triethylamine solution increased with a decrease in the concentration of the polymer (Fig. 4, Curve 2). The higher viscosity at a lower concentration of the polymer, even in the presence of an excess of triethylamine, is probably due to the small ionization of this weak base.

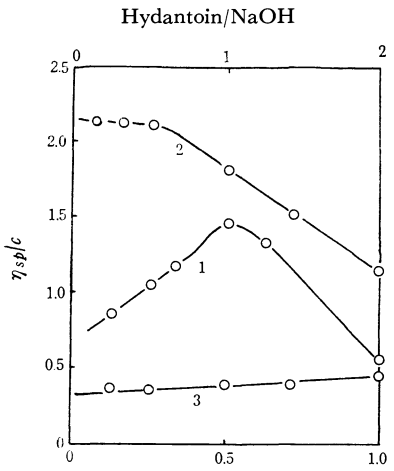

Fig. 4. Viscosities of poly-5-methylene-hydantoin and poly-3-methyl-5-methylene-hydantoin.
1 Poly-5-methylene-hydantoin in 0.179% aqueous NaOH solution
2 Poly-5-methylene-hydantoin in 0.460% aqueous Et_3N solution
3 Poly-3-methyl-5-methylene-hydantoin in 0.159 % aqueous NaOH solution
Temp., 30.0°C

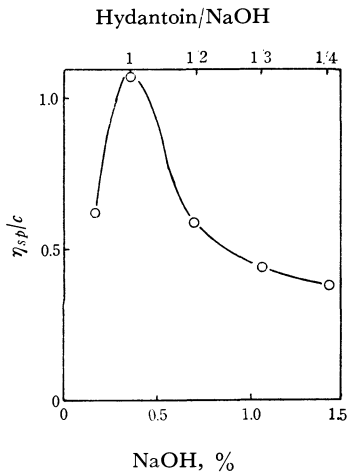

Fig. 5. Viscositiy of poly-5-methylene-hydantoin. Temp., 30.0°C; solvent, aq. NaOH; $c=1$ (g./100 ml.)

The solubility of poly-3-methyl-5-methylene-hydantoin in an alkaline solution suggests the electrolytic nature of this polymer. However, probably as a very weak poly-electrolyte, it gave only a linear relationship between the reduced viscosity and the polymer concentration in a 0.04 N aqueous sodium hydroxide solution.

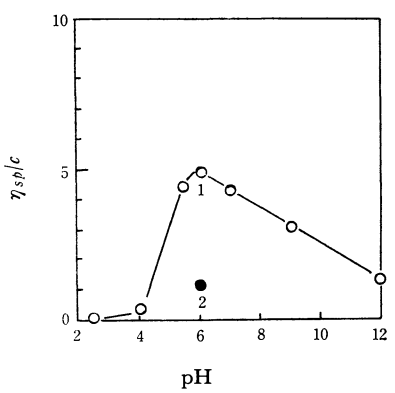

Fig. 6. Viscosity of poly-α-aminoacrylic acid.
1 Poly-α-aminoacrylic acid
2 Poly-5-methylene-hydantoin Na salt
Temp., 30.0°C; solvent, H_2O; $c=1$ (g./100 ml.)

Poly-5-methylene-hydantoin apparently behaved as a poly-acid upon the dissociation of the NH group at the 3 position. However, the changes in its viscosity with the variation in the circumstances were small in comparison with those of a typical poly-electrolyte, such as poly-acrylic acid or poly-methacrylic acid. This is probably due to the small degree of polymerization of the poly-5-methylene-hydantoin obtained. Furthermore, the bulky hydantoin group directly attached to the main chain may so largely prevent the internal rotation that the transformation of the polymer chain is restricted.

Poly-α-aminoacrylic acid is one of the most simple poly-ampholytes; several attempts to prepare it have been reported.[2-4] However, poly-α-aminoacrylic acid with quantitative amounts of free amino and acid groups has not been obtained. It has been found, though, that the neighboring amino and carboxyl groups easily reacted to form a lactam ring in strongly acidic media.

The hydrolysis of poly-5-methylene-hydantoin was carried out in aqueous sodium hydroxide at the boiling point. About fourteen days were necessary to complete the reaction. The careful neutralization of the reaction mixture gave a colorless polymer, which was soluble in water and dimethylformamide. The solubility in water was preserved not only in the alkaline region but also in the acidic region above pH 3. At pH 3 the polymer began to precipitate, but it was dissolved reversibly by the addition of aqueous alkali.

The elemental analysis showed the polymer to be poly-α-aminoacrylic acid and that it did not have a lactam ring in any appreciable amount. The number of free amino groups in the polymer was determined spectroscopically with the dinitrophenylated polymer. The amino-nitrogen content as calculated from the data was consistent with that of poly-α-aminoacrylic acid.

The amphoteric nature of the polymer was observed by means of a study of its solution viscosity. The effects of acid and base on the reduced viscosity are shown in Fig. 6. The viscosity of natural protein usually shows a minimum at the isoelectric point. Contrary to the usual poly-ampholyte, however, the viscosity of this polymer showed a maximum at pH 6, and decreased on both sides of that point almost symmetrically. This peculiar behavior of this polymer may be considered to be due to its intermolecular association in the neutral region and to its dissociation on the acidic and basic sides. The crowded amino and carboxyl groups along the main chain of this polymer seem to form zwitter-ions not only intramolecularly but also between the polymer molecules. This is also suggested by the viscosity of poly-α-aminoacrylic acid, which is very much higher than that of its parent polymer, poly-5-methylene-hydantoin.

Experimental

The Preparation of Poly-5-methylene-hydantoin.—a) The solution of 5-methylene-hydantoin (1.0 g.) and azobisisobutyronitrile (0.01 g.) in acetic acid (25 ml.) was sealed in an ampoule under nitrogen, and then left to stand at 60°C for 20 hr. The polymer thus precipitated was filtered, washed with methanol, and dried in vacuo at 100°C for one day. Poly-5-methylene-hydantoin (1.0 g.) was obtained. It was a colorless solid which decomposed above 300°C and was soluble in aqueous alkali, and was insoluble in water and in common organic solvents.

Found: C, 42.80; H, 3.74; N, 24.74. Calcd. for $C_4H_4N_2O_2$: C, 42.86; H, 3.60; N, 25.00%.

Its infrared spectrum is shown in Fig. 1.

b) Pyruvic acid (5.0 g.) and urea (3.4 g.) were dissolved in acetic acid (25 ml.) containing a small amount of hydrochloric acid, and the solution was heated at 100°C for 20 min. Then azobisisobutyronitrile (0.1 g.) was added to the cooled solution, and the solution was left to stand at 80°C for 20 hr. Poly-5-methylene-hydantoin (2.3 g., 37%) was obtained by the treatment described above.

c) A suspension of dipyruvic triureide (5.0 g.) in 80% formic acid (100 ml.) was heated at 100°C for 20 min.; after it had then cooled, the resultant clear solution was left to stand at 60°C for 20 hr. with azobisisobutyronitrile (0.05 g.). Poly-5-methylene-hydantoin (2.5 g., 72%) was obtained such as in the above-described treatment.

The Polymerization of 3-Phenyl-5-methylene-hydantoin.—The monomer was prepared according to Bergmann.[5] It melted at 200°C and polymerized immediately. (Lit.[5] 270°C (decomp.)).

A solution of 3-phenyl-5-methylene-hydantoin (2.0 g.) and azobisisobutyronitrile (0.06 g.) in acetone (35 ml.) was heated at 53°C for 20 hr. and then poured into methanol. The precipitates were washed with methanol and dried. The colorless polymer thus obtained (1.9 g.) was reprecipitated from tetrahydrofuran and methanol, and then dried. Poly-3-phenyl-5-methylene-hydantoin (1.7 g.) was thus obtained; yield, 85%. It was decomposed above 300°C; it was soluble in tetrahydrofuran, pyridine, dimethylformamide and dimethyl sulfoxide, and insoluble in water, alcohol, benzene and ether.

Found: C, 63.83; H, 4.54; N, 14.22. Calcd. for $C_{10}H_8N_2O_2$: C, 63.82; H, 4.29; N, 14.89%.

The Polymerization of 3-Methyl-5-methylene-hydantoin.—The monomer was prepared as has been described in the previous paper.[1] The polymerization was carried out in the same manner as that of 3-phenyl-5-methylene-hydantoin. Poly-3-methyl-5-methylene-hydantoin was thus obtained in a 78% yield. It was decomposed above 270°C; it was soluble in tetrahydrofuran, pyridine, dimethylformamide and

2) R. Adams, J. L. Johnson and B. Englund, *J. Am. Chem. Soc.*, **72**, 5080 (1950).

3) E. Katchalski, I. Grossfeld and M. Frankel, ibid., **70**, 2094 (1948); M. Frankel and M. E. Reichmann, *J. Chem. Soc.*, **1952**, 289.

4) S. Sakakibara, This Bulletin, **32**, 13 (1959); **33**, 814 (1960); **34**, 171, 205 (1961).

5) M. Bergmann and D. Delis, *Ann.*, **458**, 82 (1929).

dimethyl sulfoxide, and insoluble in alcohol and benzene.

Found: C, 45.70; H, 5.07; N, 21.17. Calcd. for $C_5H_6N_2O_2$: C, 47.62; H, 4.80; N, 22.21%.

Sodium Salt of Poly-5-methylene-hydantoin.—A solution of poly-5-methylene-hydantoin (0.1 g., 0.89 mmol.) in 1 N sodium hydroxide (5 ml., 5.0 mmol.) was left to stand at room temperature for 30 min. Colorless precipitates were then produced by pouring the solution into methanol, filtering it, washing it with methanol, and drying it. Mono-sodium salt of poly-5-methylene-hydantoin (0.12 g.) was thus obtained. The salt was dissolved in water, and the original polymer was recovered by the addition of dilute hydrochloric acid.

Found: N, 20.2; Na, 16.0. Calcd. for $C_4H_3N_2O_2Na$: N, 20.9; Na 17.2%.

The Copolymerization of 5-Methylene-hydantoin with Styrene.—5-Methylene-hydantoin, freshly distilled styrene and azobisisobutyronitrile (about 5 mol% against the total of monomers) were dissolved in purified methanol (8 ml.). The copolymerization was carried out in a sealed glass tube under nitrogen at 70°C. The polymer composition was calculated from the results of a nitrogen analysis (Table II).

The Hydrolysis of Poly-5-methylene-hydantoin.—The solution of poly-5-methylene-hydantoin (1.5 g.) in 15% sodium hydroxide (100 ml.) was refluxed under a nitrogen stream. The evolution of ammonia ceased after 14 days. Hydrochloric acid was then added to the cold solution, and the pH was adjusted to about 6. The silicic acid produced from the glass vessel was precipitated, filtered off, and washed with water. The filtrate and washings were combined and concentrated in vacuo. To the residual solution (50 ml.), dilute hydrochloric acid was added, the pH of the solution was adjusted to 3, and the polymer was precipitated. The polymer was filtered, washed with 0.001 N hydrochloric acid and methanol, and dried in vacuo at 100°C for one day. A Beilstein test showed no chloride ion to be present. Poly-α-aminoacrylic acid (0.8 g.) was obtained; yield, 60%; colored above 250°C; soluble in water and dimethylformamide, and insoluble in common organic solvents.

Found: C, 40.7; H, 5.5; N, 16.0. Calcd. for $C_3H_5NO_2$: C, 41.4; H, 5.8; N, 16.1%.

The Determination of the Free Amino Group in Poly-α-aminoacrylic Acid.—The dinitrophenylation of the polymer was carried out according to Levy.[6] Poly-α-aminoacrylic acid (20.00 mg.) was dissolved in a solution of sodium carbonate (84.4 mg.) in water (30.0 ml.). 2, 4-Dinitrofluorobenzene (200 mg.) was then added to the solution, and it was stirred vigorously at 40°C for 2 hr. The excess reagent and the phenol thus produced were extracted off with ether from the acidified reaction mixture. The solution was neutralized with sodium bicarbonate. The ultraviolet spectrum of the solution of poly-α-(*N*-2, 4-dinitrophenyl)-aminoacrylic acid was measured with a Hitachi Perkin-Elmer type S 12-B spectrophotometer. The solution showed a λ_{max} at 360 mμ; the content of the dinitrophenyl group in the polymer was estimated using *N*-2, 4-dinitrophenyl glycine ($\lambda_{max}=360$ mμ, $\varepsilon_{max}=16.5\times10^3$; Lit.[7] $\lambda_{max}=360$ mμ, $\varepsilon_{max}=16.6\times10^3$) as the standard substance. The calculated amount of the free amino group for poly-α-aminoacrylic acid was 98 per cent of the theoretical amount.

We wish to express our deepest thanks to Mr. Heihachiro Kawaguchi for his active collaboration in the experiments.

6) A. L. Levy and D. Chung, *J. Am. Chem. Soc.*, **77**, 2899 (1955).

7) C. Hashimoto, This Bulletin, **28**, 385 (1955).

BULLETIN OF THE CHEMICAL SOCIETY OF JAPAN VOL. 39 1567—1572 (1966)

The Trifluoroacetate Method of Peptide Synthesis. II. An Improved Synthesis of Bradykinin

By Shumpei SAKAKIBARA and Noriyoshi INUKAI*

Institute for Protein Research, Osaka University, Kita-ku, Osaka

(Received November 11, 1965)

When *p*-nitrophenyl trifluoroacetate (I), 2, 4, 5-trichlorophenyl trifluoroacetate (II) and *N*-hydroxysuccinimide trifluoroacetate (III) were subjected to Anderson's racemization test, only reagent III showed resistance against racemization. However, reagents I and II were also found to be useful for fragment-condensation with acylpeptides possessing glycine or proline at the *C*-terminus. Bradykinin was prepared using these reagents. During the synthesis, a combination of the *t*-amyloxycarbonyl *N*-protecting group and the benzyl ester was mainly used, and the alkaline hydrolysis procedure of the ester group was eliminated. Thus, colorless bradykinin with full activity was obtained in a satisfactory yield without any purification procedure.

In the first paper of this series,[1] the syntheses of various esters of trifluoroacetic acid were presented, and it was confirmed that *p*-nitrophenyl

* Present address: Yamanouchi Pharmaceutical Co., Ltd., Azusawa-cho, Itabashi-ku, Tokyo.

1) S. Sakakibara and N. Inukai, This Bulletin, **38**, 1979(1965); **37**, 1231 (1964).

trifluoroacetate (I), 2, 4, 5-trichlorophenyl trifluoroacetate (II) and *N*-hydroxysuccinimide trifluoroacetate (III) are the best reagents for preparing the respective active esters of urethan-type acyl-L-amino acids by ester-exchange reactions in pyridine. Further, it was suggested that the method should be valuable for the stepwise elongation of peptides by the active ester method without the isolation of the intermediates.

The present paper is concerned with a study of the use of reagents I, II and III not only for the stepwise synthesis, but also for so called fragment-condensation of peptides. First, reagents I, II and III were subjected to Anderson's racemization test,[2] i. e., carbobenzoxyglycyl-L-phenylalanine was treated with each reagent in pyridine until the ester-exchange reaction was complete, and then, the mixture was directly subjected to the coupling reaction with glycine ethyl ester. It was found that the ester-exchange reaction of the acylpeptide with reagent I or II was comparatively slow at room temperature, and a completely racemized product was obtained. With reagent III, however, the ester-exchange reaction was completed smoothly within one hour at room temperature, and only about 2.5% of the entire product, which was obtained in a 80% yield, was found to be racemate. Therefore, the use of reagents I and II for the fragment-condensation of peptides must be limited to the condensation of acylpeptides with glycine at their *C*-terminus. As will be described later in this paper, the *C*-terminal L-proline residue in an acylpeptide was found to be stable against racemization with reagent I, II or III. Furthermore, it has been mentioned previously[1] that amino acid residues with active hydrogen (such as histidine, serine, threonine and tyrosine) and *C*-terminal glutamine or asparagine are susceptible to these trifluoroacetate reagents in pyridine. Therefore, unless they are protected with suitable groups, acylpeptides with amino acid residues such as these should not be treated by this method. However, when these amino acid residues are in the amine components (i. e., peptide esters), this method, of course, can be used freely.

Second, the synthesis of bradykinin was carried out as an example of the application of the trifluoroacetate method using reagents I, II and III. The *t*-amyloxycarbonyl (AOC) group was mainly used as an *N*-protecting group; it had already been confirmed in this laboratory that the AOC group is useful in peptide synthesis.[3,4] The use of a methyl or ethyl ester group for protecting the carboxylic acid, the method adopted by Nicolaides and De Wald[5,6] for bradykinin synthesis, was replaced by the use of a benzyl ester group in this study, except for the preparation of hydrazide, because the removal of benzyl group by catalytic hydrogenolysis is much safer than the saponification of alkyl esters at the end of the synthesis. It was also confirmed that the AOC-group can be removed safely using trifluoroacetic acid, without any effect on the benzyl ester.[4] Moreover, it may be recalled that, although the removal of the carbobenzoxy group with anhydrous hydrogen bromide in acetic acid is accompanied by the partial *O*-acetylation of the serine residue during the procedure,[6] treatment with trifluoroacetic acid does not result in any modification of the serine residue. Boissonnas et al.[7] first prepared bradykinin using a combination of carbobenzoxy and *p*-nitrobenzyl ester groups. However, the hydrogenolysis of the *p*-nitrobenzyl group yield *p*-toluidine, and the separation of *p*-toluidine from the main product was a problem. Then, Guttmann et al.[8] improved the synthetic method by using tosylarginine as a material. The tosyl group, however, can only be removed by sodium reduction in liquid ammonia, and, after the reduction, the product had to be purified by column chromatography and/or counter current distribution.

The best route of bradykinin synthesis found so far in this study is shown in Fig. 1. The nitro-L-arginine benzyl ester was prepared from nitro-L-arginine in a good yield, using two moles of *p*-toluenesulfonic acid and excess benzyl alcohol, by the azeotropic dehydration procedure with chloroform.[9] Compound VII, AOC-L-prolyl-L-phenylalanyl-nitro-L-arginine benzyl ester, was synthesized step by step from the nitroarginine benzyl ester by the trifluoroacetate method using reagent I. In this case, it should be considered that AOC-L-phenylalanine and the AOC-L-proline *p*-nitrophenyl ester are both oily materials, while the AOC-L-phenylalanine *p*-nitrophenyl ester (V) and AOC-L-proline are easily crystallizable substances.[3] Therefore, compound V was isolated as crystals and then subjected to the reaction with the nitroarginine benzyl ester, while AOC-L-proline was coupled directly to the dipeptide ester without isolating the *p*-nitrophenyl ester. The linking of serine to the tripeptide ester was a problem, as has been mentioned above. Since the

2) G. W. Anderson and R. W. Young, *J. Am. Chem. Soc.*, **74**, 5307 (1952); G. W. Anderson, J. Blodinger and A. D. Welcher, ibid., **74**, 5409 (1952); G. W. Anderson and F. M. Callahan, ibid., **80**, 2902 (1958); G. W. Anderson and R. Paul, ibid., **82**, 4596 (1960).

3) S. Sakakibara, M. Shin, M. Fujino, Y. Shimonishi, S. Inouye and N. Inukai, This Bulletin, **38**, 1522 (1965).

4) S. Sakakibara and M. Fujino, ibid., **39**, 947 (1966).

5) E. D. Nicolaides and H. A. De Wald, *J. Org. Chem.*, **26**, 3872 (1961).

6) E. D. Nicolaides and H. A. De Wald, ibid., **28**, 1926 (1963).

7) R. A. Boissonnas, S. Guttmann and P. A. Jaquenoud, *Helv. Chim. Acta*, **43**, 1349 (1960).

8) S. Guttmann, J. Pless and R. A. Boissonnas, ibid., **45**, 170 (1962).

9) S. Akabori, S. Sakakibara and S. Shiina, This Bulletin, **31**, 784 (1958).

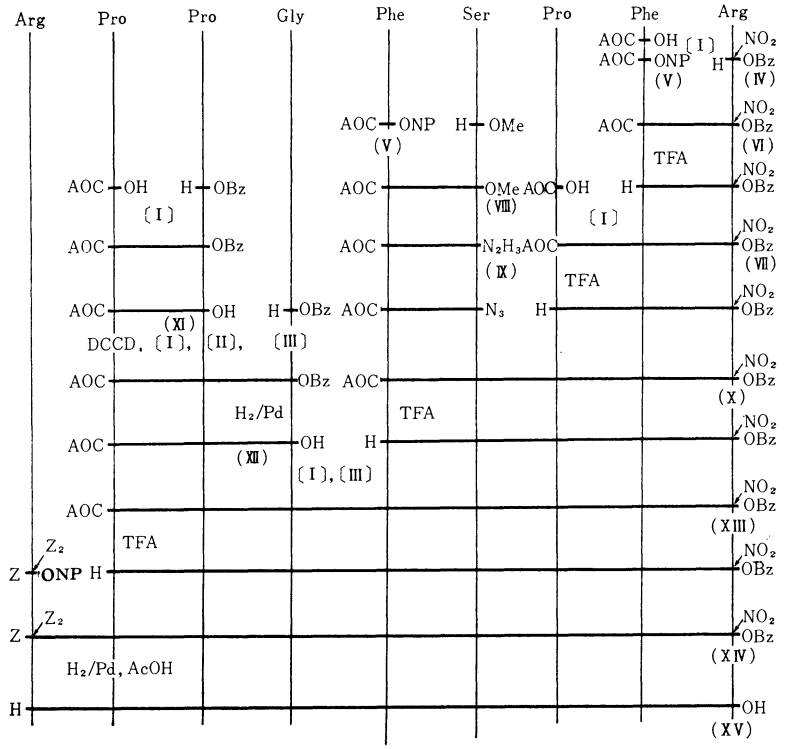

Fig. 1. Schematic diagram of the synthesis of bradykinin.

Bz=benzyl; NP=*p*-nitrophenyl; AOC=*t*-amyloxycarbonyl; TFA=trifluoroacetic acid; DCCD=dicyclohexylcarbodiimide; Z=carbobenzoxy.

application of the trifluoroacetate method for *N*, *O*-protected serine was not practical, the azide method was adopted in this case. After various attempts, it was found that the coupling of AOC-L-phenylalanyl-L-serine azide to the *C*-terminal tripeptide ester gave a much better result than that of AOC-L-serine azide. Next, AOC-L-prolyl-L-prolylglycine (XII) was prepared by coupling AOC-L-prolyl-L-proline (XI) with the glycine benzyl ester, followed by catalytic hydrogenation. A comparison was made using the reagents I, II and III in this condensation reaction; also, the dicyclohexylcarbodiimide method for preparing the same compound XII was tested. It was found that there was no difference in the optical purity of the respective products with these reagents; this result shows that the prolyl residue at the *C*-terminus of an acylpeptide is stable against racemization with the trifluoroacetate reagents I, II and III. The AOC-L-prolyl-L-prolylglycine thus formed was then satisfactorily coupled with the previously-prepared pentapeptide benzyl ester by the direct condensation method using reagent I. Finally, the tricarbobenzoxy-L-arginine *p*-nitrophenyl ester, which had been prepared by the reported method,[10] was coupled with the octapeptide,[11] and then all the protecting groups were removed simultaneously from the final product (XIV) by a single catalytic hydrogenation. The bradykinin thus obtained was completely colorless, and its biological activity was found to be slightly greater than that of a bradykinin sample prepared in the laboratory according to the method described by Nicolaides et al.[5,6]

Thus, the method of the condensation of peptides with trifluoroacetate reagents was demonstrated to be useful for the synthesis of complicated peptides.

Experimental*

Anderson's Racemization Test with Reagent III. A solution of carbobenzoxyglycyl-L-phenylalanine (0.8 g., 0.0025 mol.) in pyridine (5 ml.) was cooled to 0°C; a solution of reagent III (0.7 g., 0.0033 mol.) in pyridine (2 ml.) was then slowly added to the above solution. After the mixture had been allowed to stand at room temperature for one hour, water (0.02 ml.) was added to the reaction mixture to destroy any excess reagent. A solution of glycine ethyl ester hydrochloride (0.47 g.,

10) E. D. Nicolaides, H. A. De Wald, P. G. Shorley and H. O. J. Collier, *Nature*, **187**, 773 (1960).

11) Since one carbobenzoxy group in tricarbobenzoxyarginine was found to be susceptible to reagent I in pyridine, the use of the trifluoroacetate method in this case was disadvantageous.

* All melting points given are uncorrected. Each reaction process was checked by thin-layer chromatography.[1]

0.0034 mol.) and triethylamine (0.47 ml., 0.0034 mol.) in chloroform (5 ml.) was then stirred into the reaction mixture, and the mixture was allowed to react for 3 hr. at room temperature. The solvent was removed in vacuo, and a small volume of water was added to the residue to obtain the product as crystals; wt. 0.775 g. (78.3%); m. p. 115—117°C. The whole product was dissolved in absolute ethanol (38 ml.), and the solution was seeded with a small amount of the carbobenzoxyglycyl-DL-phenylalanylglycine ethyl ester and stored in a refrigerator. The crystals which appeared in the solution were collected by filtration at intervals and weighed. The data obtained are given below:

	Time after seeding	Crystals obtained
1)	6.5 hr.	No crystal appeared
2)	25 hr.	0.01 g., m. p. 132—133°C (DL-form)
3)	49 hr.	0.005 g., m. p. 130—133°C (DL-form)

Then the solution was concentrated to 25 ml., and stored in a refrigerator after having been seeded with L-form crystals.

4)	4.5 hr	0.315 g., m. p. 118—121°C
5)	24 hr.	0.15 g., m. p. 118—119.5°C
6)	54 hr.	0.13 g., m. p. 118—119.5°C

The optical rotation of the last three portions was $[\alpha]_D^{22}$ −12.6° (*c* 2, ethanol); lit. m. p. 118—119°C, $[\alpha]_D^{24}$ −12.3° (*c* 2, ethanol).[2] The recovery of the recrystallized whole product was 0.61 g. (79%), which includes 0.015 g. of racemate. When reagent I or II was applied in the same test, three or more hours were necessary for the completion of the ester-exchange reaction in pyridine at room temperature, and the final product was found to be entirely in the DL-form; the yield with reagent I was 81%, while the yield with reagent II was 70%.

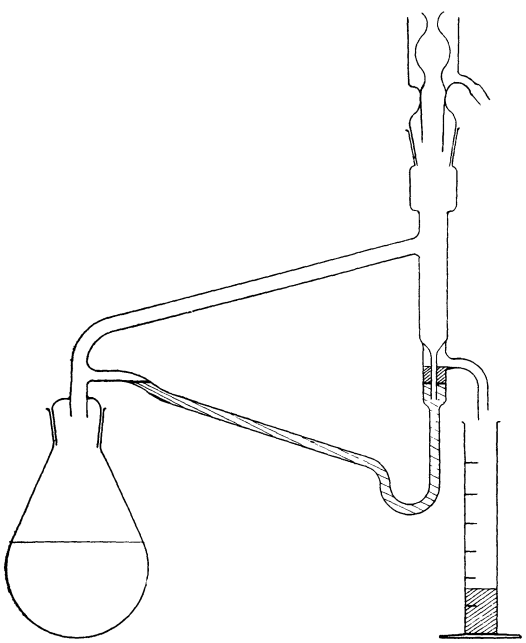

Fig. 2. An apparatus for the azeotropic dehydration with chloroform.

***g*-Nitro-L-arginine Benzyl Ester Ditosylate (IV).**—A mixture of *g*-nitro-L-arginine (11 g., 0.05 mol.), *p*-toluene sulfonic acid mono-hydrate (20 g., 0.1 mol.) and benzyl alcohol (40 ml.) in chloroform (100 ml.) was refluxed for 7—10 hr. in a dehydrating apparatus, as is illustrated in Fig. 2. After concentration to a small volume, the reaction mixture was extracted several times with petroleum ether, and the residue was crystallized by adding ether. The crude product was recrystallized from methanol-ether; wt. 29 g. (88.7%), m. p. 132—134°C, $[\alpha]_D^{24}$ +11.7° (*c* 3, pyridine).

Found: C, 49.40; H, 5.34; N, 10.61. Calcd. for $C_{27}H_{35}O_{10}N_5S_2$: C, 49.60; H, 5.41; N, 10.72%.

***t*-Amyloxycarboxyl-L-phenylalanine *p*-Nitrophenyl Ester (V).**—A solution of *t*-amyloxycarbonyl-L-phenylalanine (2.8 g., 0.01 mol.) in pyridine (5 ml.) was treated with *p*-nitrophenyl trifluoroacetate (2.7 g., 0.012 mol.) for about 2 hr. at room temperature; then water was added to the reaction mixture in order to precipitate the product as crude crystals (3.1 g., 77.5%). It was recrystallized from ethyl acetate and petroleum ether; wt. 2.6 g., yield 65%, m. p. 127—127.5°C, $[\alpha]_D^{24}$ −14.8° (*c* 1.4, ethanol); lit.[3] m. p. 128—129°C, $[\alpha]_D^{21}$ −14.4° (*c* 1.3, ethanol).

***t*-Amyloxycarbonyl-L-phenylalanyl-*g*-nitro-L-arginine Benzyl Ester (VI).**—Compound V (4 g., 0.01 mol.) was added to a solution of IV (6.5 g., 0.01 mol.) and triethylamine (2.8 ml., 0.02 mol.) in dimethylformamide (30 ml.), and the mixture was allowed to react for 60 hr. at room temperature. Then the mixture was diluted with ethyl acetate (about 200 ml.), and the solution was washed successively with water, N ammonia, 0.75 N hydrochloric acid and water, and dried over anhydrous sodium sulfate. The evaporation of the solvent left a crude product, which was recrystallized from ethyl acetate and petroleum ether; wt. 5.1 g. (ca. 90%), m. p. 120—124°C, $[\alpha]_D^{23}$ −15.8° (*c* 3, ethanol).

Found: C, 59.05; H, 6.44; N, 14.39. Calcd. for $C_{28}H_{38}O_7N_6$: C, 58.93; H, 6.71; N, 14.73%.

***t*-Amyloxycarbonyl-L-prolyl-L-phenylalanyl-*g*-nitro-L-arginine Benzyl Ester (VII).**—Compound VI (2.5 g., 0.0044 mol.) was treated with trifluoroacetic acid (5 ml.) for 30 min. at room temperature, and then the product was precipitated by adding dry ether. It was collected by filtration, washed with ether, and dried over sodium hydroxide in vacuo. *t*-Amyloxycarbonyl-L-proline (1.01 g., 0.0044 mol.) was treated with I (1.25 g., 0.0053 mol.) in pyridine (5 ml.) for about 2 hr. at room temperature, and then a solution of L-phenylalanyl-L-nitroarginine benzyl ester trifluoroacetate (2.5 g., 0.0044 mol.), prepared as described above, and triethylamine (1.36 ml., 0.0097 mol.) in dimethylformamide (55 ml.) was added to the reaction mixture. After it had stood for 2 days at room temperature, the reaction mixture was diluted with ethyl acetate. The diluted solution was washed successively with water, N ammonia, 0.75 N hydrochloric acid and water, and dried over anhydrous sodium sulfate. The dried solution was concentrated to a syrup which was solidified by trituration with ether. The product was reprecipitated from ethyl acetate and ether; wt. 2.64 g. (90.5%), m. p. 80—86°C, $[\alpha]_D^{21}$ −39.6° (*c* 1, ethanol).

Found: C, 59.86; H, 6.79; N, 14.24. Calcd. for $C_{33}H_{45}O_8N_7$: C, 59.35; H, 6.79; N, 14.68%.

***t*-Amyloxycarbonyl-L-phenylalanyl-L-serine**

Methyl Ester (VIII).—Compound V (4 g., 0.01 mol.) and L-serine methyl ester hydrochloride (1.6 g., 0.01 mol.) were dissolved in dimethylformamide (35 ml.), and then triethylamine (1.4 ml., 0.01 mol.) was added to the mixture. After 20 hr. at room temperature, the reaction mixture was diluted with ethyl acetate (300 ml.), and the solution was washed successively with water, N ammonia, 0.75 N hydrochloric acid and water, and dried over sodium sulfate. The dried solution was concentrated to a syrup, which was then solidified with petroleum ether. The product was reprecipitated as an amorphous powder from ethyl acetate-petroleum ether; wt. 3.7 g., (97.5%), m. p. 60—90°C, $[\alpha]_D^{25}$ −3.2° (*c* 1, dimethylformamide).

Found: C, 59.82; H, 7.46; N, 7.34. Calcd. for $C_{19}H_{28}O_6N_2$: C, 59.98; H, 7.42; N, 7.36%.

***t*-Amyloxycarbonyl-L-phenylalanyl-L-serine Hydrazide (IX).**—Compound VIII (4.2 g., 0.011 mol.) was dissolved in ethanol (9 ml.), and then 90% hydrazine hydrate (1.7 ml.) was added to the solution. After about 2 hr. at room temperature, the crystals (needles) which appeared were collected by filtration and recrystallized from ethanol; wt. 3.35 g. (88%), m. p. 175—177°C, $[\alpha]_D^{25}$ −4.0° (*c* 1, dimethylformamide).

Found: C, 56.44; H, 7.27; N, 14.66. Calcd. for $C_{18}H_{28}O_5N_4$: C, 56.82; H, 7.42; N, 14.73%.

***t*-Amyloxycarbonyl-L-phenylalanyl-L-seryl-L-prolyl-L-phenylalanyl-*g*-nitro-L-arginine Benzyl Ester (X).**—Compound VII (2 g., 0.003 mol.) was treated with trifluoroacetic acid (4 ml.) for 30 min. at room temperature, and then the product was precipitated by adding dry ether. The precipitate was collected by filtration, washed well with ether, and dried over sodium hydroxide in vacuo; wt. 2.06 g. A solution of compound IX (1.03 g., 0.0027 mol.) in dimethylformamide (10 ml.) was cooled to −10°C; 2 N hydrochloric acid (2.73 ml., 0.0055 mol.) was stirred into the chilled solution and then a solution of sodium nitrite (0.207 g., 0.003 mol.) in water (1.5 ml.) was carefully added to the mixture at −10—−15°C. After about 15 min., a solution of previously-prepared tripeptide benzyl ester trifluoroacetate, dissolved in a mixture of dimethylformamide (3 ml.) and chloroform (8 ml.), was added to the reaction mixture, and then the pH was adjusted to 8 with triethylamine (about 0.84 ml.). Stirring was continued for 3 hr. at −10°C, and subsequently for 2 hr. at 0°C. During this period, the pH of the solution was maintained at 8 by adding triethylamine. The mixture was then stored in a refrigerator for 20 hr., after which the product was extracted thoroughly with ethyl acetate. The extracts were combined and washed well with N sodium bicarbonate, 0.75 N hydrochloric acid and water, and dried over sodium sulfate. The dried solution was concentrated to a syrup, and this was reprecipitated twice from methanol and ether as an amorphous powder; wt. 1.7 g. (70%), m. p. 100—115°C, $[\alpha]_D^{22}$ −38.2° (*c* 0.5, dimethylformamide).

Found: C, 59.85; H, 6.76; N, 14.17. Calcd. for $C_{45}H_{59}O_{11}N_9$: C, 59.92; H, 6.60; N, 13.98%.

***t*-Amyloxycarbonyl-L-prolyl-L-proline (XI).**—Reagent I (0.71 g., 0.003 mol.) was added to a solution of *t*-amyloxycarbonyl-L-proline (0.57 g., 0.0025 mol.) in dry pyridine (1.5 ml.) at room temperature. After about 2.5 hr., the excess reagent was destroyed with one small drop of water, and then a solution of L-proline benzyl ester hydrochloride (0.67 g., 0.0028 mol.) and triethylamine (0.385 ml., 0.0028 mol.) in chloroform (2.5 ml.) was added to the above reaction mixture. One more equivalent of triethylamine (0.4 ml.) was added to the mixture, which was then allowed to react for 3 days at room temperature. Then it was concentrated to a residue, which was dissolved in ethyl acetate (about 100 ml.); the solution was washed successively with N ammonia, 0.75 N hydrochloric acid and water, and dried over sodium sulfate. The dried solution was concentrated to a syrup, which was dissolved in methanol (20 ml.), and a small amount of palladium black was added to the solution. Hydrogen was bubbled through the solution for about 2 hr. with stirring, and then the catalyst was removed by filtration. The filtrate was concentrated to a syrup, and the material was crystallized by adding ether. The recrystallization of the product from ethyl acetate - petroleum ether gave prisms; wt. 0.66 g. (81%), m. p. 155—158°C, $[\alpha]_D^{21}$ −112.8° (*c* 1, ethanol).

Found: C, 58.97; H, 8.00; N, 8.53. Calcd. for $C_{16}H_{26}O_5N_2$: C, 58.88; H, 8.03; N, 8.58%.

***t*-Amyloxycarbonyl-L-prolyl-L-prolylglycine (XII).**—a) Compound XI (6.5 g., 0.02 mol.) and glycine benzyl ester tosylate (6.75 g., 0.02 mol.) were dissolved in chloroform (100 ml.), and triethylamine (2.8 ml., 0.02 mol.) was added to the mixture. After dicyclohexylcarbodiimide (4.12 g., 0.02 mol.) had been slowly added to the mixture, it was allowed to react for one day at room temperature. The urea formed was removed by filtration, and the filtrate was concentrated to a residue, which was then redissolved in ethyl acetate (about 100 ml.). This solution was washed successively with N sodium bicarbonate, N hydrochloric acid and water, and dried over anhydrous sodium sulfate. The dried solution was subjected to the hydrogenation procedure described above, and the final product was obtained as fine prisms which were dried over sulfuric acid in vacuo at room temperature; wt. 6.15 g. (80.5%), m. p. 109—112°C, $[\alpha]_D^{21}$ −132.8° (*c* 1, ethanol).[12]

Found: C, 53.70; H, 7.81; N, 10.49. Calcd. for $C_{18}H_{29}O_6N_3 \cdot H_2O$: C, 53.85; H, 7.78; N, 10.48%. The same sample was dried over phosphorous pentoxide in vacuo at 110°C for 3 hr. to remove the water of crystallization.

Found: C, 56.14; H, 7.56; N, 11.15. Calcd. for $C_{18}H_{29}O_6N_3$: C, 56.38; H, 7.62; N, 10.96%.

b) A solution of XI (0.815 g., 0.0025 mol.) in dry pyridine (1.8 ml.) was treated with reagent I, II or III at room temperature for 1—5 hr. until the ester-exchange reaction was complete; this was checked by thin-layer chromatography. Then a solution of glycine benzylester tosylate (0.93 g., 0.0028 mol.) and triethylamine (0.39 ml., 0.0028 mol.) in dimethylformamide (1.5 ml.) was added to the reaction mixture, and in the cases of reagents I and II, one more equivalent of triethylamine (0.4 ml.) was also added to the reaction mixture. After about 3 or 4 days, ethyl acetate (100 ml.) was added to the reaction mixture, and the solution was washed successively with N ammonia, 0.75 N hydrochloric acid and water, and dried over sodium sulfate. After the dried solution had been concentrated to a residue, it was dissolved in methanol (about 30 ml.), and then a small amount of palladium black was added to the

solution. Hydrogen was bubbled through the solution for about 3 hr., and then the catalyst was removed by filtration. The filtrate was concentrated to a syrup, and the material was crystallized from ethyl acetate and petroleum ether. The results are listed below.

Reagent	Weight	m. p.	$[\alpha]_D^{23}$ (c 1, ethanol)[12]
I	0.84 g. (88%)	110—113°C,	−132.8°
II	0.59 g. (62%)	109—112°C,	−132.5°
III	0.82 g. (86%)	110—112°C,	−132.2°

***t*-Amyloxycarbonyl-L-prolyl-L-prolylglycyl-L-phenylalanyl-L-seryl-L-prolyl-L-phenylalanyl-*g*-nitro-L-arginine Benzyl Ester (XIII).**—Compound X (0.72 g., 0.8 mmol.) was dissolved in trifluoroacetic acid (2 ml.), and after about 30 min. at room temperature, the product was precipitated by adding dry ether, collected by filtration, and dried over sodium hydroxide in vacuo; wt. 0.7 g. A solution of the dried compound, XII (0.33 g., 0.86 mmol.), in pyridine (0.8 ml.) was treated with reagent I (0.3 g., 1.3 mmol.) for 2—3 hr. at room temperature. Then one small drop of water was added to the reaction mixture in order to destroy any excess reagent, and a solution of the previously-prepared pentapeptide benzylester trifluoroacetate (0.7 g.) and triethylamine (0.33 ml., 2.36 mmol.) in dimethylformamide (6 ml.) was added to the mixture. After about 24 hr. at room temperature, the reaction mixture was diluted with ethyl acetate (about 200 ml.) and the solution was washed successively with N ammonia, 0.75 N hydrochloric acid and water, and dried over anhydrous sodium sulfate. The dried solution was concentrated to a residue, which was triturated well with ether to obtain an amorphous powder. The product was reprecipitated from ethyl acetate and ether; wt. 0.69 g. (77%), m. p. 125—130°C, $[\alpha]_D^{22}$ −46.8° (c 0.5, dimethylformamide).

Found: C, 58.87; H, 6.61; N, 14.52. Calcd. for $C_{57}H_{76}O_{14}N_{12}$: C, 59.36; H, 6.64; N, 14.58%.

When reagent III was used instead of I, the yield of the product was 76%.

Tricarbobenzoxy-L-arginyl-L-prolyl-L-prolylglycyl-L-phenylalanyl-L-seryl-L-prolyl-L-phenylalanyl-*g*-nitro-L-arginine Benzyl Ester (XIV).—Compound XIII (0.2 g., 0.17 mmol.) was dissolved in trifluoroacetic acid (0.4 ml.), and after 40 min. the product was precipitated by adding dry ether. The precipitate was collected by filtration, washed well with ether, and dried over sodium hydroxide in vacuo; wt. 0.2 g. After the dried material had been dissolved in dimethylformamide (3.5 ml.), the tricarbobenzoxy-L-arginine *p*-nitrophenyl ester[10] (0.121 g., 0.175 mmol.) and triethylamine (0.0243 ml., 0.17 mmol.) were added to the solution. After one day at room temperature dry ether was added to the reaction mixture, and the precipitate which formed was washed well with ether by means of decantation. The residue was triturated with ethyl acetate, and then dissolved in chloroform. The solution was washed with water, N hydrochloric acid and water, and dried over anhydrous sodium sulfate. The dried solution was concentrated to a syrup under reduced pressure, and the remaining syrup was crystallized from ethyl acetate and ether. For purification the precipitation procedure from ethyl acetate and ether was repeated; wt. 0.17 g. (61%); m. p. 115—118°C, $[\alpha]_D^{22}$ −44.5° (c 0.5, dimethylformamide).

Found: C, 60.73; H, 6.23; N, 13.93. Calcd. for $C_{81}H_{96}O_{19}N_{16}$: C, 60.89; H, 6.06; N, 14.03%.

Bradykinin Triacetate.—Compound XIV (25 mg.) was dissolved in a mixture of acetic acid (3 ml.) and methanol (2 ml.), and a small amount of freshly-prepared palladium black was added to the solution. Hydrogen was bubbled through it for about 10 hr., until the absorption band of the solution at 267 mμ disappeared. This was measured at a concentration of 0.1 mg./5 ml. Then the catalyst was removed by filtration, and the filtrate was concentrated to a syrup under reduced pressure at room temperature. The residue was dissolved in water (15 ml.) and lyophilized. The product was completely colorless (wt. 16.7 mg.), and it was found to be homogeneous without any further purification. The homogeneity was tested by paper electrophoresis (pH 4.75, pH 3.5, pH 8.8) and by paper chromatography (BuOH : AcOH : H_2O=4 : 1 : 1, 80% pyridine, *t*-BuOH : AcOH : H_2O=2 : 1 : 1), using ninhydrin and Sakaguchi reagents respectively. The amino acid ratio in a hydrolyzate prepared with 6 N hydrochloric acid was as follows: Arg, 1.98; Pro, 2.89; Gly, 1.04; Phe, 1.96; Ser, 1.00. For analysis this material was dried at 110°C in vacuo over phosphorous pentoxide for 18 hr. About 13% of the weight was reduced during the procedure.

Found: C, 54.30; H, 7.01; N, 17.10. Calcd. for $C_{50}H_{73}O_{11}N_{15}\cdot 3CH_3COOH$: C, 54.22; H, 6.91; N, 16.94%.

The biological activity of this material was determined by the guinea-pig ileum contraction test;[13] it was thus found to be 1.4 times more than that of a sample prepared in this laboratory by the procedure of Nicolaides et al.[5,6]

The authors wish to express their thanks to Professor Tomoji Suzuki for determining the biological activity of the synthetic material.

12) The concentration was calculated in a dry base.

13) T. Suzuki, Y. Mizushima, T. Sato and S. Iwanaga, *J. Biochem.* (Japan), **57**, 14 (1965).

BULLETIN OF THE CHEMICAL SOCIETY OF JAPAN VOL. 39 1573—1577 (1966)

Altenin. I. The Isolation of Altenin from *Alternaria Kikuchiana* Tanaka

By Noboru SUGIYAMA, Choji KASHIMA, Makoto YAMAMOTO and Toki SUGAYA

Department of Chemistry, Tokyo Kyoiku University, Otsuka, Tokyo

and Ryotaro MOHRI

The Liberal Arts Department, Tottori University, Tachikawa-cho, Tottori

(Received December 4, 1965)

Alternaria Kikuchiana Tanaka is a fungus which produces a black spot disease in pears. The metabolite of this fungus contains a phytopathogenic substance for which the name "Altenin" has been proposed. A drop of an aqueous solution of altenin (2×10^{-5} mg./ml.) produces a black spot on pear leaves. The stability of altenin at 80, 60, and 40°C, and the behavior of altenin in relation to some adsorbents and solvents, were studied. Its isolation from the culture filtrate was found to be properly accomplished by adsorption with active charcoal, elution with acetone, and chromatography with silica gel and alumina columns. By these procedures, besides altenin, six metabolites, diheptyl phthalate, myristic acid, succinic acid, and the ester of C_{15}-carboxylic acid, C_{19}-steroid and trihydroxy anthraquinone, were obtained.

Alternaria Kikuchiana Tanaka is a fungus which is phytopathogenic to pears especially to the improved sort of *Pyrus Ussuriensis var. Aromatica* Rehder (Japanese name *Nijusseiki*).[1] On the leaves and fruits of the pears, it produces a black spot disease.[2] When the culture broth of this fungus, or ethyl ether or an ethyl acetate extract of the culture, is put on the plucked leaves of the pear, a similar black spot grows along the veins of the leaf. These phenomena suggest that there is some pathogenic substance in the metabolite of this fungus.[3] This substance was called "Altenin."[4] This paper will deal with the isolation of altenin and with some of its chemical properties.

Results and Discussion

As the first step, the stability of altenin was examined.[3] Its aqueous solution (pH 7.5) lost its pathogenic activity in 10 min. at 80°C, and in an hour at 60°C, but kept it for several hours at 40°C, as is shown in Table I. When the acetone solution with silica gel or alumina was left standing at room temperature, no change in activity was observed over a period of several hours. Further, the activities of the solutions in organic solvents, such as benzene, acetone, ethyl ether, methanol, ethanol or ethyl acetate, did not change at room temperature over a period of several hours.

TABLE I. THE STABILITY OF ALTENIN IN AQUEOUS SOLUTION (pH 7.5)

Time min.	40°C	60°C	80°C
0	18.6	18.6	7.4 (mm²)
5	17.8	19.8	2.3
10	19.2	21.2	0.5
20	9.1	11.0	0
40	12.7	4.8	0
80	17.9	3.2	0

The isolation and purification of altenin was attemped by two routes. In the first, it was extracted with ethyl acetate from the culture filtrate and then purified through silica gel-column chromatography. By this procedure, besides the active substance, five inactive metabolites, diheptyl phthalate, myristic acid, the ester of C_{15}-carboxylic acid, C_{19}-steroid and trihydroxy anthraquinone were obtained.

In the second route, the adsoption, extraction and chromatography were employed. Several adsorbents and eluting solvents were tested. The

TABLE II. ADSORPTION POWER OF ADSORBENTS

Adsorbent (g./l.)	Time hr.	Activity, % Remained in solution	Adsorbed on adsorbent
Calcium carbonate (40)	1	55	45
Animal charcoal (10)	1	22	78
Hyflosupercel (20)	1	23	77
Active charcoal (10)	1	20	80
Active charcoal (20)	1	1	99
Active charcoal (20)	5	0	100

1) K. Toyama, N. Takase and R. Sakai, *Ann. Phytopathol. Soc. Japane (Nihon Shokubutsu Byorigaku Kaiho)*, **20**, 106 (1955).
2) R. Mohri, *The Liberal Arts Journal of Natural Science of Tottori University (Tottori Daigaku Gakugei Gakubu Kenkyu Hokoku)*, **13**, 55 (1962).
3) I. Hiroe, S. Nishimura and M. Sato, *Transactions of Tottori Society of Agriculture Science (Tottori Nogaku Kaiho)*, **11**, 291 (1958).
4) N. Sugiyama, C. Kashima, M. Yamamoto and R. Mohri, This Bulletin, **38**, 2028 (1965).

TABLE III. ELUTION POWER OF SOLVENTS

Adsorbent (g./l.)		Elution (%) by solvent				
		Methanol	Ethanol	Acetone	Ethyl ether	Benzene
Calcium carbonate	40	2	1.6	2.5	1	0.1
Animal charcoal	10	0.4	0.4	0.2	0.1	0.2
Hyflosupercel	20	17	16	22	2	6
Lead acetate	40	1.2	1.6	6.2	1.6	2.8
Active charcoal	10	23	40	40	28	6

The yield of pathogenic substance through the adsorption for 1 hr. and elution for 1 hr.

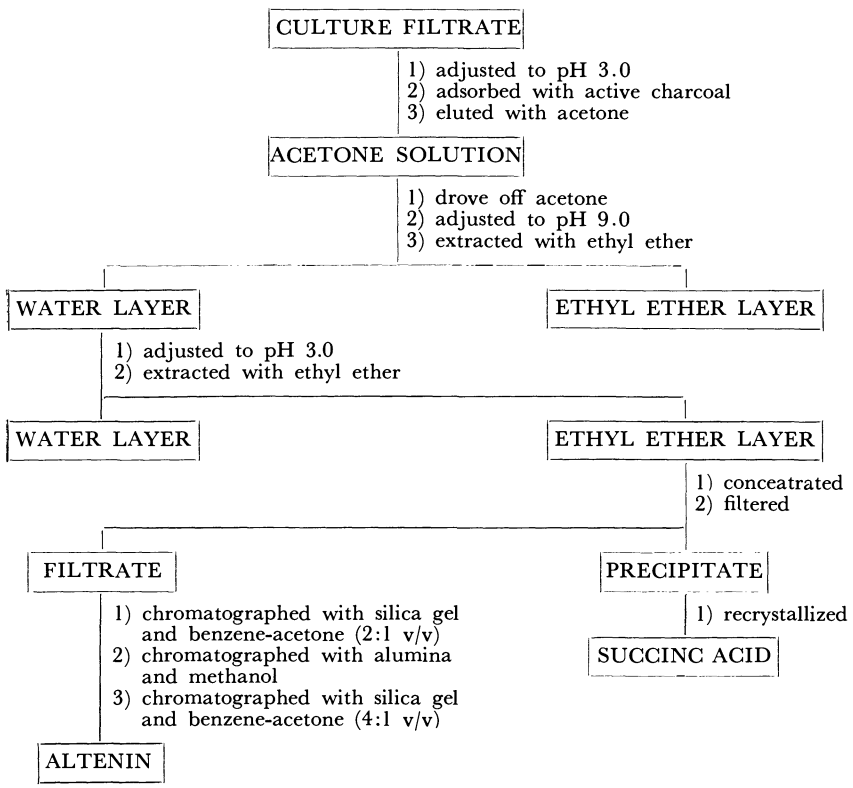

Fig. 1. Isolation of altenin.

results of these experiments are shown in Tables II and III. It was found that the most effective adsorbent was the active charcoal; from it acetone could elute altenin most effectively. By this procedure, besides altenin, succinic acid was obtained.

Altenin was also extracted with ethyl ether from the culture filtrate, which had been adjusted to pH 3 with hydrochloric acid. The distribution coefficients, K, of altenin at 20°C between ethyl ether and water were measured by the counter-current distribution method; they were found to be as follows: >10 (pH 3.5), 5 (pH 5.0), 2 (pH 5.5), 1 (pH 6.0) and <0.1 (pH 9.0).

By applying these results, altenin was isolated by the process illutsrated schematically in Fig. 1. One milligram of altenin was obtained from about 4 l. of the culture filtrate. One drop of an aquoeus solution of altenin (2×10^{-5} mg./ml.) exhibited a distinct phytopathogenic effect.

TABLE IV. THE DISTRIBUTION COEFFICIENT, K, OF ALTENIN AT 20°C

pH	3.5	5.0	5.5	6.0	9.0
Tube No.*	10	9	7	5	1
K	10	5	2	1	0.1

* The tube number of maximum activity.

Altenin is a yellow liquid which gives only one spot on silica-gel thin-layer chromatography with a benzene-acetone (1 : 1 v/v) mixture; its R_f value was 0.76, while that of methyl red, a pilot dye, was 0.37. On alumina thin-layer chromatography with a methanol-water (5 : 1 v/v) mixture, its R_f value was 0.87, while that of methyl red was 0.41. The spot of the thin-layer chromatogram was developed by heating it after it had been

sprayed with concentrated sulfuric acid or with a *o*-dianisidine solution. By this method, it was demonstrated that altenin was the unique phytopathologically active substance in the metabolites of the fungus *Alternaria Kikuchiana* Tanaka.

The details of the cultivation of this fungus and the chemical studies of altenin will be reported on in the near future.

Experimental

The Cultivation of *Alternaria Kikuchiana* Tanaka (No. 5).—Though this fungus had previously been cultivated in stationary cultivation,[5] altenin enough for chemical study could not be obtained by this method. After many trial experiments, the following method was found to be effective.

A 200-l. tank fermenter was employed; it was charged with 120 l. of an aqueous solution of 4% sucrose, 0.2% dibasic ammonium phosphate, 1.1% monobasic potassium phosphate, 0.05% magnesium sulfate and 0.05% potassium chloride.

During cultivation, rotary stirring was effected, the temperature was maintained at 30°C, and air (20 l./min.) was bubbled in continuously. On the third day, a small quantity of silicon oil was added as an antifoam agent. On the ninth day, the culture broth exhibited a pH value of 3.0 and the maximum altenin activity. At this point the cultivation was stopped.

The Black-spots Test.—Fresh, young leaves of *Pyrus Ussuriensis var. Aromatica* Rehder (Japanes name *Nijusseiki*) were employed for this test. When an ethyl ether extract of the culture filtrate (270 ml.) was concentrated under a diminished pressure, a residue (85 mg.) was obtained. This residue was dissolved in an ammonium acetate-buffered (pH 8.0) solution, the concentrations of which were 85, 17, 3.4 and 0.7 mg./ml. A drop of each of these four solutions was put on the pear leaf. After 17 hr. at 23°C, the areas of the black spots were measured (Fig. 2).

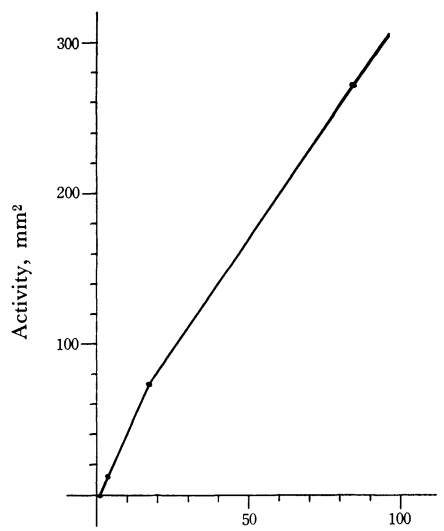

Fig. 2.

The Stability of Altenin.—The culture filtrate was heated to 40, 60, and 80°C for 80 min. and then the change in altenin activity was measured by the black spots test. At 40°C, the activity was observed for several hours. At 60°C, however the activity was lost in 40 min. and at 80°C in 10 min. The results are listed in Table I. However, altenin was stable for 2 days at room temperature, even when air was passed through the altenin aqueous solution.

The Isolation of Altenin (Route 1.)—The culture filtrate (130 l.) was extracted with ethyl acetate (13 l.). After the ethyl acetate had been removed under reduced pressure, the residue (40 g.) was passed through the silica gel (Wakogel C-2) column with benzene (fraction A) and with acetone (fraction B). After the evaporation of the benzene, the residue of fraction A (12.3 g.) was passed through the silica gel (Wakogel C-2) column with a benzene-acetone (20 : 1 v/v) mixture (fraction C) and with acetone (fraction D). The evaporation residue from the fraction C was chromatographed with silica gel (Merck 7729) and with a benzene-acetone (2 : 1 v/v) mixture; a yellow fluorescent elution contained 7 mg. of crude altenin, which showed spots with R_f values of 0.60, 0.70 and 0.78 on silica-gel (Wakogel B-5) thin-layer chromatography with a benzene-acetone (1 : 1 v/v) mixture.

During the above mentioned procedures, the following five metabolites were isolated.

Diheptyl Phthalate.—The residue from the fraction D was chromatographed with silica gel (Wakogel C-2) and with a benzene-acetone (1 : 1 v/v) mixture. A colorless liquid was thus obtained, b. p. 332—337°C.

Found: C, 72.89; H, 9.45; mol. wt. (Rast), 360. Calcd. for $C_{22}H_{34}O_4$: C, 73.23; H, 8.95%; mol. wt., 362.5.

From the infrared absorption spectrum, this substance was presumed to be an ester of some aromatic carboxylic acid. Liquid-gas chromatography suggested that the hydrolysate of this substance consisted of one alcohol and one aromatic acid. This acid was sublimed to a crystalline substance, m. p. 129°C, which was identified with phthalic anhydride. From these results alcohol was proved to be a heptanol. Therefore, the original substance was diheptyl phthalate.

Myristic Acid.—The fraction C was chromatographed through the silica gel (Merck 7729) column with a benzene-acetone (2 : 1 v/v) mixture. The solid substance which remained after the solvent had been removed from the first elution was recrystallized from aqueous acetone, m. p. 51.5°C; its infrared absorption spectrum showed absorptions at 1700 ($\nu_{C=O}$), 1290 (δ_{C-O}) and 940 cm^{-1} (δ_{C-O}). This substance with myristic acid.

An Ester of C_{15}-Carboxylic Acid.—By the chromatography of the fraction C with silica gel (Merck 7729) and chloroform, a liquid metabolite was isolated. Its infrared absorption spectrum showed the ester carbonyl group at 1740 cm^{-1}. By hydrolysis, a free carboxylic acid, m. p. 50.5°C, was obtained. The reaction of this substance with benzyl amine produced the *N*-benzyl amide, m. p. 88.5°C.

Found: C, 79.64; H, 11.17; N, 3.83; mol. wt.

5) R. Mohri and S. Ikeda, *The Liberal Arts Journal of Natural Science of Tottori University (Tottori Daigaku Gakugei Gakubu Kenkyu Hokoku)*, **10**, 38 (1960).

(Rast), 330. Calcd. for $C_{22}H_{37}NO$: C, 79.70; H, 11.25; N, 4.23%; mol. wt., 331.5.

It was suggested that this metabolite was an ester of C_{15}-saturated carboxylic acid.

C_{19}-Steroid.—After chromatography with silica gel (Wakogel C-2) and with a benzene-acetone (20 : 1 v/v) mixture, fraction A gave a solid material, which was then recrystallized from aqueous methanol. Colorless needles (11 mg.; m. p. 180°C) were obtained from 1.2 l. of the culture filtrate.

Found: C, 78.64; H, 10.35; mol. wt. (Rast), 301. Calcd. for $C_{19}H_{30}O_2$: C, 78.57; H, 10.41%; mol. wt., 290.4.

Its infrared absorption spectrum showed absorptions at 3450 (νOH), 1630 ($\nu_{C=C}$), 2950 and 2850 cm^{-1} (νCH), while the ultraviolet absorption spectrum showed a maximum at 230 mμ (ε 690) in ethanol, and at 257 (ε 20000), 253 (ε 18000), 262 (ε 14000), 375 (ε 2000) and 522 mμ (ε 9600) in concentrated sulfuric acid.[6] The color reactions of this substance were as follows: Liebermann-Burchard's reaction,[7] green; Salkowski's reaction,[8] red; Rosenheim's reaction,[9] green; Kägi-Miescher's reaction,[10] violet. These color reactions suggested the presence of an unsaturated steroid. By acetylation with acetic anhydride and pyridine, a mono acetate, m. p. 201°C, was obtained.

Found: C, 75.70; H, 9.66. Calcd. for $C_{21}H_{32}O_3$: C, 75.86; H, 9.70%.

2, 8-Dihydroxy-1-hydroxymethyl-9, 10-anthraquinone.—The solvent of the blue fluorescent elution from the silica gel (Wakogel C-2) chromatography of the fraction A with a benzene-acetone (20 : 1 v/v) mixture was removed. When the residue was then sublimed, pale yellow needles, m. p. 269°C (decomp.), were obtained.

Found: C, 64.78; H, 4.60; mol. wt. (Rast), 230. Calcd. for $C_{15}H_{10}O_5$: C, 66.67; H, 3.73%; mol. wt., 270.2.

The infrared absorption spectrum showed absorptions at 3420, 3350, 1665, 1620, 1590, 980, 850, 830 and 740 cm^{-1},[11] while the ultraviolet absorption spectrum showed its maxima at 257 (ε 49700), 289 (ε 10400), 300 (ε 10200) and 340 mμ (ε 11500) in ethanol,[3,12,13] these values shifted in an alkaline solution to 265 (ε 37600), 314 (ε 11300) and 370 mμ (ε 16600), and a pK_a value of 9.6 was obtained by a spectrometric method. This substance showed a negative color reaction with zirconium nitrate. This substance was methylated with diazomethane to a methylated substance, m. p. 177°C. These data suggested that this substance was possibly 2, 8-dihydroxy-1-hydroxymethyl-9, 10-anthraquinone.

The Test of an Adsorbent and an Eluting Solvent.—To each 1 l. of the culture filtrate, adsorbents, calcium carbonate, animal charcoal, hyflosupercel and active charcoal, in the amounts shown in Table II, were added; they were then stirred for one hour at room temperature. After the adsorbent had been filtered off with a suction pump, the altenin activity of the filtrate was examined. The activity was then compared with that of the original culture filtrate. The results are listed in Table II. Each filtered adsorbent in the preceding experiments was air dried and divided into ten equal parts. Each of these parts was added to a test solvent (10 ml.) and stirred for one hour at room temperature. After the adsorbent had been filtered off, the solvent was evaporated off under reduced pressure. To each residue there was added 100 ml. of a buffer solution of ammonium acetate adjusted to pH 7.8. The altenin activity of each solution was tested on the leaves of the pear, and it was compared with the altenin activity of the original culture filtrate. The results are expressed in percentages in Table III. Because of its greater volatility and greater eluting power, acetone was the most suitable eluting solvent.

The Distribution Coefficient of Altenin.—The ethyl ether extract of the culture filtrate was subjected to the counter-current distribution at 20°C with ethyl ether and aqueous solutions of various pH values. For the sake of simplicity, only ten tubes were used. From the altenin activity of each layer, the distribution coefficient, K, was calculated to be as shown in Table IV.

The Isolation of Altenin (Route 2).—A process for the isolation of altenin from the culture filtrate is schematically showed in Fig. 1. The culture filtate (101.) was adjusted to pH 3.0; then active charcoal (100 g.) was added, and the mixture was stirred for five hours. The active charcoal was filtered, and on it the pathogenic substance was adsorbed. After it had been dried in the air, the active charcoal was eluted with acetone (1 l.), and the acetone solution was concentrated to ca. 200 ml. under reduced pressure at 35—40°C in a nitrogen atomsphere. The residual solution was adjusted to pH 9.0 with aqueous ammonia, and the dusty substance was filtered off. This alkaline solution was extracted with ethyl ether (100 ml.). The aqueous layer was adjusted to pH 3.0 with dilute hydrochloric acid, and extracted with three 70 ml. portions of ethyl ether. The combined ethyl ether extracts were then dried over anhydrous sodium sulfate. On the removal of the solvent under reduced pressure at 35—40°C, the residue (170 mg.) was obtained. It was dissolved in a cold mixture of benzene and acetone (2 : 1 v/v) and filtered. The precipitate was recrystallized from ethyl ether, m. p. 183°C, which was identified with succinic acid. The filtrate was passed through a silica-gel (Merck 7729) column with a benzene-acetone (2 : 1 v/v) mixture. The blue fluorescent elution which was obtained was again passed through an alumina (Wako alumina) column with methanol. (The alumina had been deactivated with 6.7 per cent of water before use.) The methanol elution was then again passed through a silica-gel (Merck 7729) column with a benzene-actone (4 : 1 v/v) mixture. Altenin (2.5 mg.) was thus obtained as a yellow liquid.

6) S. Bernstein and R. H. Lenhard, *J. Org. Chem.*, **18**, 1153 (1953).
7) H. Burchard, *Chem. Zentr.*, [I] **61**, 25 (1890).
8) E. Salkowski, *Z. Physiol. Chem.*, **57**, 523 (1908).
9) O. Rosenheim, *Biochem. J.*, **23**, 47 (1929).
10) K. Miescher, *Helv. Chim. Acta*, **29**, 743 (1946).
11) H. Bloom, L. H. Briggs and B. Cleverley, *J. Chem. Soc.*, **1959**, 178.
12) T. Ikeda, Y. Yamamoto, K. Tsukida and S. Kanatomo, *J. Pharm. Soc. Japan (Yakugaku Zasshi)*, **76**, 217 (1956).
13) K. Lauer and M. Horio, *J. Prakt. Chem.*, **145**, 273 (1936).
14) R. Wasicky and O. Frehden, *Mikrochim. Acta*, **1**, 55 (1937).

Altenin showed a spot on silica-gel (Wakogel B-5) thin-layer chromatography with a benzene-acetone (1 : 1 v/v) mixture; the R_f value was 0.76, while that of methyl red, a pilot dye, was 0.37. On alumina (Merck 1090) thin-layer chromatography with a methanol-water (5 : 1 v/v) mixture, the R_f value was 0.87, while that of methyl red was 0.41. Altenin was developed on thin-layer chromatography by heating it over 80°C for one hour after it had been sprayed with concentrated sulfuric acid. Altenin was developed to yellow by heating it after it had been sprayed with an *o*-dianisidine solution.[14]

The Activity of Altenin.—The phytopathogenic activity of aqueous solutions of altenin with concentrations of 1×10^{-4}, 2×10^{-5}, 5×10^{-6} mg./ml. were examined by the black-spots test; it was found that the lower limit of the pathogenic activity was about 2×10^{-5} mg./ml.

The Test of the Pathogenic Activity of Other Metabolites.—The ethyl ether extract of the culture filtrate was developed by silica-gel (Wakogel B-5) thin-layer chromatography with a benzene-acetone (1 : 1 v/v) mixture; the chromatogram was divided into ten parts: R_f value, 0—0.1; 0.1—0.2; ··· ; 0.8—0.9; 0.9—1.0. Each part of the silica gel was eluted with acetone (5 ml.), and the elution was concentrated under reduced pressure. The residues obtained were each diluted to 0.1 ml. with an aqueous buffer solution of ammonium acetate (pH 7.4). The pathogenic activity of these solutions were then examined by the black-spots test. Only the solution from the R_f 0.5—0.6 division, which contained altenin, exhibited the black spot on a pear leaf.

The authors wish to express their thanks to Professor Tatsukichi Kobayashi and Dr. Isei Nakamura, Department of Agriculture, Tokyo Kyoiku University, for their kind advice and for their generous permission to use the 200 l. fermenter there. The authors also wish to thank Mr. Kazutoshi Koyama for a generous supply of the fresh young pear leaves.

BULLETIN OF THE CHEMICAL SOCIETY OF JAPAN VOL. 39 1577—1582 (1966)

The Photochemical Reactions of Ethylene Glycol and Its Ethers in the Presence of Ferric Chloride

By Hiroo INOUE, Kentaro TAMAKI, Nobuyuki KOMAKINE and Eiji IMOTO

Department of Applied Chemistry, College of Engineering, The University of Osaka Prefecture, Sakai, Osaka

(Received December 8, 1965)

The photochemical reactions of ethylene glycol, ethylene glycol monomethyl ether and ethylene glycol dimethyl ether with ferric chloride have been carried out under a nitrogen atmosphere and with irradiation by ultraviolet light. These reactions have involved the cleavage of the carbon-carbon bond to give formaldehyde and chloromethyl methyl ether; of the carbon($-CH_2-$)-oxygen bond to give acetaldehyde, methanol and water, or of the carbon(CH_3-)-oxygen and hydrogen-oxygen bonds to give methane, ethane, hydrogen chloride and methyl chloride. Furthermore, they have been accompanied by the photo-reduction of ferric chloride to ferrous chloride. From these results, it has been assumed that ferric chloride acts as an oxidizing reagent and Lewis acid in the photochemical reactions.

It has well been known that a transition metal ion can serve as an oxidation-reduction or Lewis acid reagent in some thermal reactions. Recently, an interest in the behavior of a transition metal ion in the photochemical reactions has been taken by several investigators. The catalysis of the photo-oxidation of ethanol by copper ions,[1] and the photochemical reactions of peresters in the presence of copper ions, have been reported on.[2] The properties of a transition metal ion in the excited state would be different from those in the normal state, and an excited transition metal ion may have a characteristic effect on a substrate through the formation of a transition metal ion-substrate complex. In this paper, we will describe our studies of the photochemical reactions of ethylene glycol and its ethers with ferric chloride under a nitrogen atomosphere. Ethylene glycol and its ethers were chosen in this study because their photo-oxidation by oxygen has well been studied in our previous paper.[3]

Experimental

Meterials.—Anhydrous ferric chloride, ethylene glycol and ethylene glycol monomethyl ether were of a commercial grade. Ethylene glycol dimethyl ether

1) H. R. Cooper and B. M. Talbot, *Trans. Faraday Soc.*, **61**, 506 (1965).
2) G. Sonsnovsky, *J. Org. Chem.*, **28**, 2934 (1963).
3) H. Inoue, K. Tamaki and E. Imoto, *J. Chem. Soc. Japan, Ind. Chem. Sect.* (*Kogyo Kagaku Zasshi*), **69**, 654 (1966).

was prepared according to the methods described in the literature.[4] These materials were purified by the manner described in a previous paper.[3]

The Procedure of the Photo-reaction.—A weighed amount of ferric chloride was dissolved into an appropriate amount of ethylene glycol or its ethers. This solution was then introduced into a cylindrical reaction vessel with a capacity of about 250 ml., and a 100 W. mercury lamp with a water-cooling jacket was placed in this vessel. After nitrogen gas had been bubbled in for about 5 min., the vessel was connected with a gas burette, the air space of which had previously been filled with nitrogen gas. The solution was then irradiated for 24 hr.

The Analysis of the Products.—The analysis of the products was mainly accomplished by means of gas chromatography (g. c.), using a Hitachi KGL-2 gas chromatograph. The irradiated solution was analyzed by immediately withdrawing 5 to 10 μl. of the solution into a syringe. A column containing polyethylene glycol-1600 and/or high vacuum silicon grease was used in the g. c. analyses. The major product peaks in the gas chromatogram were identified by a comparison of their retention times with those of authentic materials, if possible. Acetaldehyde, acetaldehyde ethylene acetal and methanol were identified by the methods described in the previous paper.[3] Chloromethyl methyl ether and ethylene glycol dimethyl ether were identified by trapping the materials from the column, and by then comparing the infrared spectra of the trapped materials with those of authentic materials. Besides the analyses by g. c., the total amounts of the compounds containing carbonyl groups were determined as their 2, 4-dinitrophenylhydrazones (2, 4-D.). The components of 2, 4-D.'s were identified by paper chromatography according to Horner's method.[5] Here, the 2, 4-D.'s of acetaldehyde and formaldehyde were confirmed to be the main components.

The Spectrophotometric Study of the Photo-reaction.—Solutions of 0.05 mol. of ferric chloride in 20 ml. of ethylene glycol, ethylene glycol monomethyl ether or ethylene glycol dimethyl ether were introduced into a spherical ampule (2 cm. radius). The sample solutions were cooled with a dry ice - acetone bath; the air was removed under the reduced pressure of 1—2 mmHg, and then the ampule was filled with nitrogen gas. After the procedure of the replacement by nitrogen gas had been repeated 4—5 times, the sample solution was poured into a reaction cell, which consisted of a spectrophotmeter cell (1 × 1 × 4 cm.) and the upper part of which was connected to the above ampule. The apparatus used is shown in Fig. 1. The cell was irradiated at a distance of 4 cm. from a light source, a 100 W. mercury lamp, at room temperature. At various time intervals, the sample cell was taken out and the absorption spectra were measured with a Hitachi spectrophotometer.

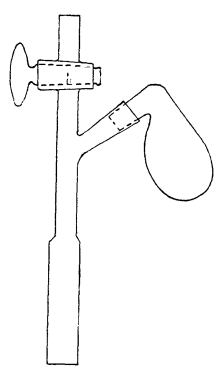

Fig. 1. Spectrophotometer cell.

Results and Discussion

Spectrophotometric Studies. — The visible absorption spectra of ferric chloride in ethylene glycol, ethylene glycol monomethyl ether and ethylene glycol dimethyl ether showed large absorption bands lower than 550 mμ and absorption peaks at 600, 620 and 685 mμ in all cases, as is shown in Figs. 2, 3 and 4. The visible spectra of these solutions varied with the irradiation of light.

In the case of ethylene glycol monomethyl ether and ethylene glycol dimethyl ether, the large band lower than 550 mμ and the peaks at 600, 620 and 685 mμ decreased with the irradiation time and two new peaks appeared, at 532 and 1000 mμ, as is shown in Figs. 3 and 4. The former new peak, at 532 mμ, corresponds to that of H^+FeCl_4 in diisopropyl ether reported by Metzler.[6] We also observed absorption peaks at 532, 600, 620 and 685 mμ in a ferric chloride - ethylene glycol monomethyl or ethylene glycol dimethyl ether - hydrochloric acid or methyl chloride system, as is shown in Fig. 5.

On the basis of these results, we are now able to suggest that in the course of the photo-reaction hydrochloric acid or methyl chloride is produced and that this forms a complex with ferric chloride according to the following scheme:

$$FeCl_3(\text{solvent}) \xrightarrow{RCl} RFeCl_4(\text{solvent})$$

This new peak, at 532 mμ, also decreased with the irradiation time. On the other hand, the latter new peak, at 1000 mμ, corresponded to the peak in a ferrous chloride - ethylene glycol system. This peak increased with the irradiation time. These results indicate that ferric chloride is photo-reduced by ether to ferrous chloride.

In the case of ethylene glycol, the peaks at 600, 620 and 685 mμ decreased with the irradiation. However, the decrease in the large band lower than 550 mμ could not be observed. This may result from the fact that the large band in the ferric chloride - ethylene glycol system does not vary even upon the addition of hydrochloric acid. A new peak appeared at 1000 mμ. The intensity

4) A. L. Kanzfelder and R. R. Vogt, *J. Am. Chem. Soc.*, **60**, 1714 (1938).
5) L. Horner and W. Kirmse, *Ann.*, **597**, 48 (1955).
6) D. E. Metzler and R. J. Myers, *J. Am. Chem. Soc.*, **72**, 3777 (1950).

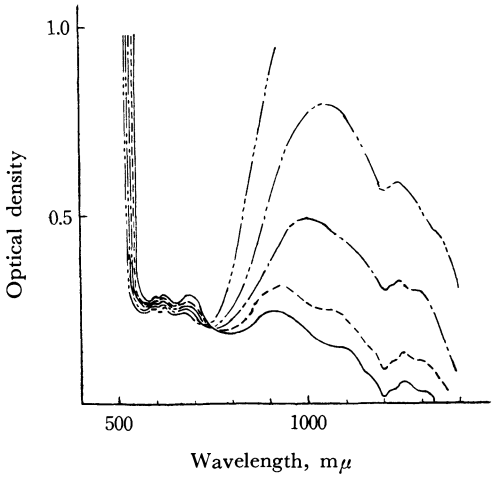

Fig. 2. The variation of visible spectrum to irradiated time (ethylene glycol - $FeCl_3$ system). Concn. of $FeCl_3$: 0.90 mol./l.
——— 0.0 hr. ------ 2.5 hr.
— — — 6.0 hr. — — — 9.0 hr.
—·—·— 24.0 hr.

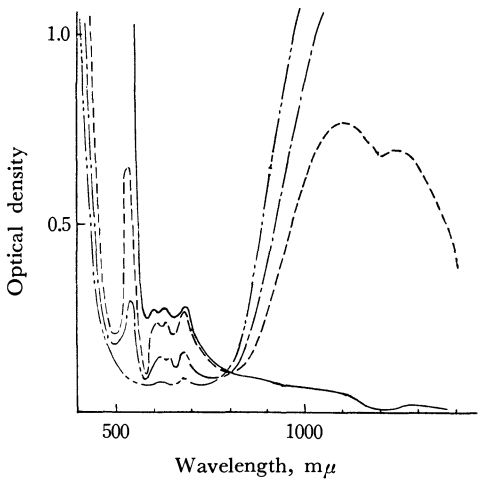

Fig. 3. The variation of visible spectrum to irradiated time (ethylene glycol monomethyl ether - $FeCl_3$ system). Concn. of $FeCl_3$: 0.64mol./l.
——— 0.0 hr. ------ 2.5 hr.
— — — 8.5 hr. — — — 24.0 hr.

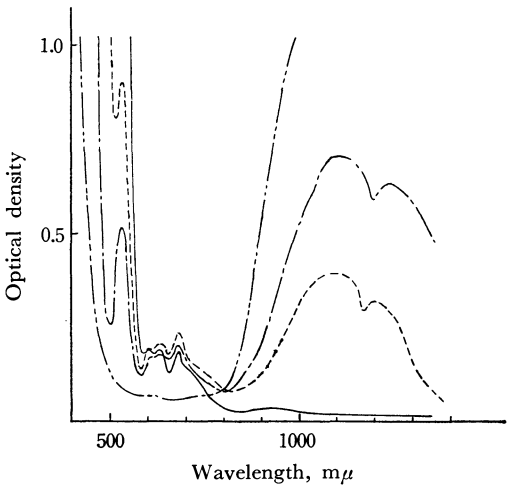

Fig. 4. The variation of visible spectrum to irradiated time (ethylene glycol dimethyl ether - $FeCl_3$ system). Concn. of $FeCl_3$: 0.47 mol./l.
——— 0.0 hr. ------ 1.5 hr.
— — — 3.0 hr. — — — 18.0 hr.

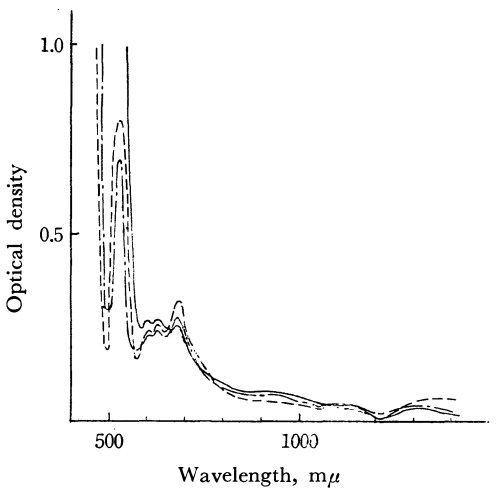

Fig. 5. The effect of hydrochloric acid or methyl chloride on visible spectrum of ferric chloride - ethylene glycol monomethyl ether system.
Concn. of $FeCl_3$: 0.64 mol./l.
——— Ferric chloride - ethylene glycol monomethyl ether
------ Addition of 0.60 mol./l. of hydrochloric acid
— — — Addition of methyl chloride

of this peak increased at an extremely slower rate than that in the case of ethers.

We may, therefore, assume that the photoreduction of ferric chloride by ethylene glycol proceeds very slowly.

A Comparison between the Photochemical and Thermal Reactions of Ethylene Glycol in the Presence of Ferric Chloride. — *Thermal Reaction.* — The thermal reaction of ethylene glycol in the presence of ferric chloride was investigated. A solution of 1.44 g. of anhydrous ferric chloride in 10 ml. of ethylene glycol was placed into a reaction vessel equipped with a condenser which had been connected to a trap cooled with a dry ice - acetone bath; the solution was then heated at 130°C for 5 hr. During this period no products were obtained in the trap. Although the reaction mixture was analyzed by g. c. and 2, 4-D. methods, no reaction products were observed. When 6.0 g. of the reaction mixture was distilled at 83—85°C/8 mmHg, most

TABLE I. THE AMOUNTS OF THE MAIN PRODUCTS IN THE PHOTOCHEMICAL REACTIONS*

Starting material	Amount mol.	$FeCl_3$ mol.	Amount of products obtained mol. $\times 10^2$				Total amount of gas mol. $\times 10^2$	Recovery %
			H_2CO	CH_3CHO	CH_3OCH_2Cl	CH_3OH		
$HOCH_2CH_2OH$	3.56	0.18	0	13.3	0	0	0.4	81
$CH_3OCH_2CH_2OH$	2.84	0.14	4.9	2.1	Trace	3.9	1.4	90
$CH_3OCH_2CH_2OCH_3$	1.64	0.08	2.1	0	1.2	0.8	0.2	91

* Reaction time: 24 hr.

of the ethylene glycol was recovered, and 1.2 g. of the polymeric material was obtained as the distilled residue.

Photochemical Reaction. — A solution of 28.8 g. of anhydrous ferric chloride in 200 ml. of ethylene glycol was irradiated with a 100 W. mercury lamp according to the method described above. In the course of the photo-reaction, the evolution of 0.4×10^{-2} mol. (at S. T. P.) of gas was observed. An analysis of the gas by g. c. showed that its gas mainly consisted of hydrogen, methane and carbon monoxide.

The reaction mixture was then fractionated through a Vigreux column to give (1) a fraction of b. p. 25—80°C/8 mmHg (trapped by a dry ice - acetone bath; approximately 26 g.), (2) a fraction containing mainly unchanged ethylene glycol (approximately 180 g.), and (3) a distilled residue (approximately 40 g.). From fraction 1, acetaldehyde ethylene acetal, acetaldehyde and water were confirmed and determined by g. c. The amounts of these products are shown in Table I. The distilled residue was a dark brown oily material; this material was not, however, analyzed in detai. Besides these products, a small amount of glyoxal was isolated as the 2, 4-D.

As has been described above, apparent differences between the photochemical and thermal reactions were observed. The photochemical reaction of ethylene glycol in the presence of ferric chloride proceeds via the dehydration of ethylene glycol to give acetaldehyde, followed by the reaction 1 with ethylene glycol to produce acetaldehyde ethylene acetal. The reaction mechanism will be discussed later.

$$\begin{array}{l} CH_2{-}CH_2 \\ | \quad | \\ OH \quad OH \end{array} \xrightarrow[FeCl_3]{h\nu} CH_3CHO + H_2O \xrightarrow{\begin{array}{l} CH_2{-}CH_2 \\ | \quad | \\ OH \quad OH \end{array}} CH_3CH\begin{array}{l} O{-}CH_2 \\ \quad | \\ O{-}CH_2 \end{array} + H_2O \qquad (1)$$

Photochemical and Thermal Reactions of Ethylene Glycol Monomethyl Ether with Ferric Chloride.—*Thermal Reaction.*—A solution of 2.08 g. of anhydrous ferric chloride in 20 ml. of ethylene glycol monomethyl ether was refluxed for 5 hr. The reaction mixture was then fractionated through a Vigreux column to give (1) a fraction of b. p. 80—90°C (approximately 3 g.), (2) a fraction containing mainly unchanged ethylene glycol monomethyl ether (approximately 15 g.), and (3) the distilled residue (approximately 3 g.). Ethylene glycol dimethyl ether was obtained from the fraction 1. The distilled residue was a black-brown clay-like solid containing ferric ions and chlorine ions.

As has been described above, the thermal reaction of ethylene glycol monomethyl ether with ferric chloride gave mainly ethylene glycol dimethyl ether. The reaction probably proceeds by a disproportionation 2. Although ethylene glycol was not confirmed in this investigation, it may be present in the distilled residue in the form of a complex with ferric chloride, or in the form of the polymeric material.

$$2\,CH_3OCH_2CH_2OH \xrightarrow{FeCl_3} CH_3OCH_2CH_2OCH_3 + HOCH_2CH_2OH \qquad (2)$$

Photochemical Reaction. — The irradiation of ethylene glycol monomethyl ether with ferric chloride was made by the same procedure as in the case of ethylene glycol. In the course of irradiation, methane, ethane, hydrogen and carbon monoxide evolved. Among the products present in the reaction mixture, acetaldehyde, chloromethyl methyl ether, methanol, methoxymethyl methoxyethyl ether, methyl chloride and water were determined by g. c. In addition to these products, formaldehyde was determined by the 2, 4-D. method. The results are shown in Table I.

These results show that the mechanism of the photochemical reaction is different from that of the thermal reaction. Ferric chloride and ethylene glycol monomethyl ether form a complex, though the structure of the complex is not certain. (The formation of a complex was observed by spectrophotometric studies.) Ferric ions in a complex are reduced by ethylene glycol monomethyl ether to ferrous ions under ultraviolet irradiation. This means that the transfer of a lone-pair electron on an oxygen atom of a hydroxy or methoxy group to the excited ferric chloride occurs. This step is the primary process in the photochemical reaction. The formation and the amount of formaldehyde and chloromethyl methyl ether show the cleavage of the carbon-carbon bond (reaction 4), while those of acetaldehyde and methanol or water show the cleavage of the carbon-oxygen bond ($-CH_2-O-$) (reaction 5). From the results of the spectrophotometric studies, it may also be supposed that the

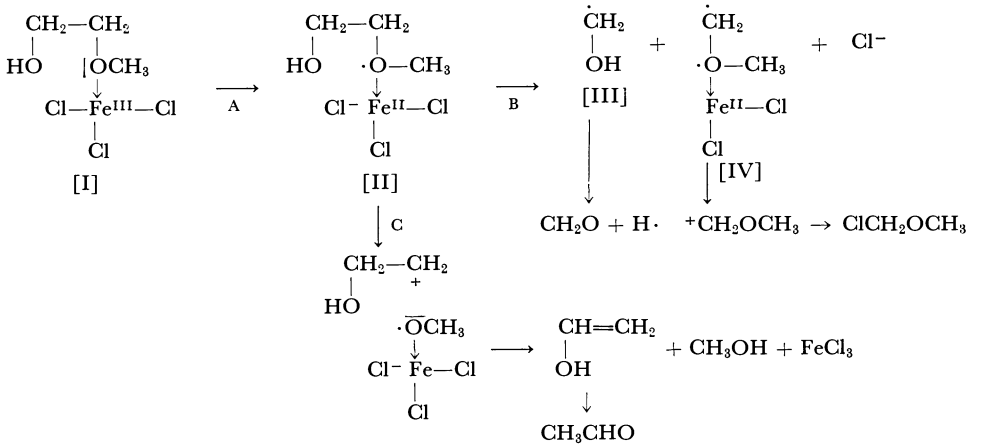

Scheme 1

reactions 4 and 5 are accompanied with the reaction 3, that is, the cleavage reaction of the R–O– bond to R^+ and ^-O–, because in the course of the reaction the formation of methyl chloride or hydrogen chloride was observed.

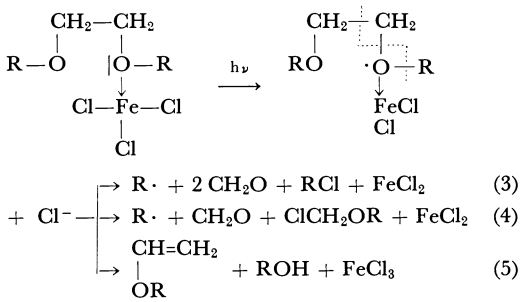

The cleavage of the carbon-carbon or carbon-oxygen bond is caused by the electron transfer in the primary process. It is not clear whether the cleavage of the carbon-carbon bond is ionic or homolytic. If the structure of a complex is I, and if the cleavage of the carbon-carbon bond is homolytic, the reaction proceeds via Paths A and B; that is, I is converted to II by the electron transfer, and then the cleavage reaction of II gives formaldehyde and chloromethyl methyl ether via the intermediate, III and IV. On the other hand, acetaldehyde and methanol are produced by the reaction paths A and C, in which the oxidative cleavage of the carbon-oxygen bond occurs, as is shown in Scheme 1. The fact that the amount of chloromethyl methyl ether is small (Table I) seems to show that chloromethyl methyl ether is converted into methanol, formaldehyde and methoxymethyl methoxyethyl ether by the following thermal reactions:

$$CH_3OCH_2Cl + H_2O \rightarrow CH_3OH + CH_2O + HCl$$

$$CH_3OCH_2Cl + CH_3OCH_2CH_2OH \rightarrow CH_3OCH_2OCH_2CH_2OCH_3 + HCl$$

Methyl vinyl ether, which can be produced by the dehydration of ethylene glycol monomethyl ether, and its polymer were not confirmed. The polymer may be present in the distilled residue.

Photochemical and Thermal Reactions of Ethylene Glycol Dimethyl Ether in the Presence of Ferric Chloride. — The photochemical and thermal reactions and the identification of the products were carried out by the same methods as in the cases of ethylene glycol and ethylene glycol monomethyl ether.

Thermal Reaction.—No reaction products were confirmed by g. c. and 2, 4-D. methods.

Photochemical Reaction. — In the course of irradiation, methane, ethane, hydrogen and carbon monoxide evolved, and crystals in the form of colorless prisms appeared on the walls of the lamp. These crystals were collected by filtration, washed with dry ether, and dried on phosphorus(V) oxide overnight. Attempts to measure the infrared spectrum and to make an elemental analysis of those crystals failed, since they were very unstable in relation to air or moisture. However, the results of the combustion test, Beilstein's test, and the other qualitative tests showed the presence of ferrous or ferric ions, chlorine ions and an organic compound in the crystals. When the crystals were allowed to stand under an air atmosphere they turned yellow, and the form of the crystals changed from colorless prisms to a semi-crystalline mush, the infrared spectrum of which showed large absorption bands at 3400, 1630 and 1600 cm^{-1} and other broad absorption bands at 1780, 1450, 1365, 1240, 1190, 1090 and 1045 cm^{-1}. The large absorption bands at 3400, 1630 and 1600 cm^{-1} corresponded to those of $FeCl_2 \cdot 4H_2O$.[7] Although the components of the colorless crystals are not clear, they seem to be a complex of ferrous chloride and an organic compound. The method of formation and the amounts of chloromethyl methyl ether and

7) I. Gamo, This Bulletin, **34**, 1495 (1961).

formaldehyde seem to support the assumption of the oxidative cleavage mechanism described above. However, an inbalance in the amounts of the products was observed, as is shown in Table I. This may be caused by the formation of colorless crystals under ultraviolet irradiation. A reaction would proceed by steps analogous to the steps of the reactions 3, 4 and 5, that is, an oxidative cleavage of a carbon-carbon bond to $\cdot CH_2OCH_3$ and $^+CH_2$-OCH_3.

Summary

The photochemical reactions of ethylene glycol, ethylene glycol monomethyl ether and ethylene glycol dimethyl ether in the presence of ferric chloride involve the cleavage process of the carbon-carbon bond to give formaldehyde and chloromethyl methyl ether; of the carbon($-CH_2-$)-oxygen bond to give acetaldehyde, methanol and water, or of the carbon(CH_3-), hydrogen-oxygen bond to give methane, ethane, hydrogen chloride and methyl chloride. These reactions are accompanied by the photoreduction of ferric chloride to ferrous chloride.

BULLETIN OF THE CHEMICAL SOCIETY OF JAPAN VOL. 39 1582—1584 (1966)

Organoboron Compounds. X. On the Reaction of *o*-Hydroxybenzeneboronic Acid Anhydride with Some Sulfonamides

By Seiji KATO,* Keiko KIMURA, Katsuhisa NAGATA and Yojiro TSUZUKI

Department of Chemistry, Tokyo College of Science, Kagurazaka, Shinjuku-ku, Tokyo

(Received December 20, 1965)

Several new azo compounds containing boron atoms have been synthesized by the use of sulfonamides; these compounds have an excellent effect on bacilli. It was expected that the antibiotic effect would be very remarkable, since it had been reported that boron-containing azo dyes are useful for therapy on brain tumors. A mixed solvent of ethanol-water (1 : 1) and acetone was found useful for recrystallizing this class of compounds. The infrared spectra of these compounds show absorption bands at the 1090—1100 cm^{-1}, 1375—1380 cm^{-1} and 1600—1610 cm^{-1} regions these bands may be assigned to the carbon-boron, boron-oxygen and nitrogen-nitrogen bonds respectively.

Some azo compounds containing boron atoms were found to be effective in the medical treatment of brain tumors by Kruger[1] and by Zall et al.[2] It had been known that a number of azo compounds containing negative atoms or groups such as halogens, as well as hydroxyl, nitro and trifluoro groups, are also effective, if irradiated, even without boron atoms; however, the azo compounds containing boron atoms are more effective with respect to the absorption by tumors than the compounds without boron atoms. Gilman et al.[3] obtained a number of azo compounds containing boron atoms by coupling *o*-hydroxybenzeneboronic acid anhydride with the diazonium chlorides of benzene, *p*-bromobenzene and nitrobenzene. It was expected that if boron atoms were introduced into sulfonamides by coupling them with boronic acid, the antibiotic effect would be even more remarkable. This paper will deal with some studies of the reactions of *o*-hydroxybenzeneboronic acid anhydride with certain sulfonamides which contain at least one amino group capable of being diazotized, namely, sulfanilamide, N^1-2-thiazolylsulfanilamide, N^1-(2, 6-dimethoxy-4-pyrimidinyl)sulfanilamide and N^1-(6-methoxy-3-pyridazinyl)sulfanilamide. This coupling could occur at the position either ortho or para to the hydroxy group, but primarily at the para position.

Figure 1 illustrates the compounds of this class thus obtained.

The solubility of these products was tested with a solvent such as that used by Gilman[3] for the azo dyes from *o*-hydroxybenzeneboronic acid anhydride (Table I).

A solvent system including ethanol-water (1 : 1) was always found to be a better solvent for recrystallization than acetone.

Although melting point determination has been profitably employed as a criterion of purity for most organic compounds, it does not seem to hold generally true for azo boron compounds. The-

* Died April 9, 1965.

1) P. G. Kruger, *Radiation Research*, **3**, 1 (1955).

2) P. A. Zall and F. S. Cooper, *Science*, **93**, 64 (1941).

3) H. Gilman, L. Santucci, D. R. Swayampati and R. O. Ranck, *J. Am. Chem. Soc.*, **79**, 2889 (1957).

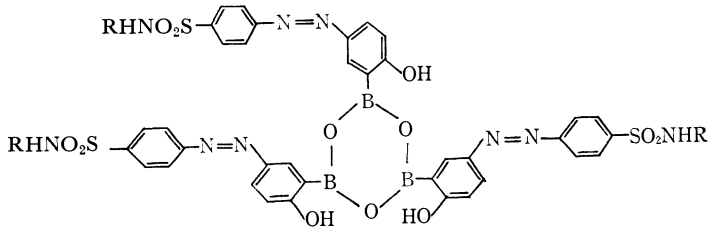

Fig. 1. Azo compound of *o*-hydroxybenzeneboronic acid anhydride.

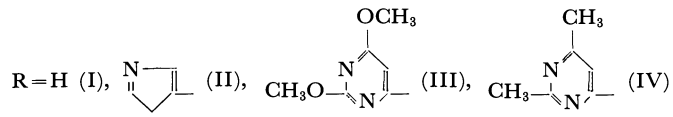

TABLE I. THE SOLUBILITY OF PRODUCTS

Solvent	R			
	I[a]	II[b]	III[c]	IV[d]
Chloroform - Carbon tetrachloride (1 : 1)	i	i	i	i
Acetone	s	hs	hs	hs
Benzene - Petroleum ether (1 : 1)	i	i	i	i
Ethanol-Water (1 : 1)	hs	hs	hs	hs
Benzene	i	i	i	i
Ethylene chloride	i	i	ls	i

i : insoluble, s : soluble, hs : soluble by heating, ls : a little soluble

a) 2-Hydroxy-5-(sulfonamidophenylazo)benzeneboronic acid anhydride

b) 2-Hydroxy-5-(N^1-2-thiazolylsulfonamidophenylazo)benzeneboronic acid anhydride

c) 2-Hydroxy-5-(N^1-(2,6-dimethoxy-4-pyrimidinyl)-sulfonamidophenylazo)benzeneboronic acid anhydride

d) 2-Hydroxy-5-(N^1-(6-methoxy-3-pyridazinylsulfonamidophenylazo))benzeneboronic acid anhydride

materials obtained also decomposed over 200°C before melting.

The infrared spectra of these azo boronic acids showed absorption bands at two regions, from 1090 to 1100 cm^{-1} and from 1375 to 1380 cm^{-1}, as have many of the boronic acids already reported; these bands may be assigned to the carbon-boron and the boron-oxygen bonds respectively. A band of a weak intensity appeared at 1600 to 1610 cm^{-1} in all the azo derivatives of boronic acid; this band may be due to the azo group.

Experimental

o-Hydroxybenzeneboronic Acid Anhydride.—*o*-Hydroxybenzeneboronic acid anhydride was prepared from 35.0 g. (0.2 mol.) of *o*-bromophenol and an equivalent quantity of tri-*n*-butyl borate (98.6 g.) in an atmosphere of nitrogen, almost exactly according to Gilman's method.[4] The ethereal solution of lithium *o*-lithiophenoxide was sucked up through a glass tube into a graduated dropping funnel which had previously been flushed with nitrogen. The crude material was then recrystallized three times from toluene using activated charcoal. This represents ca. a 44% yield of a nearly pure material with a melting point range of 176—179°C.

Diazotization and Coupling.—*With Sulfanilamide* (R=I).—The diazotization of sulfanilamide (1.7 g., 0.01 mol.) was carried out according to Datta's method.[5] The diazotized sulfanilamide solution was then slowly added to a stirred solution composed of 0.9 g. (0.0225 mol.) of sodium hydroxide, 1.4 g. (0.01 mol.) of *o*-hydroxybenzeneboronic acid anhydride, and 10 ml. of water, and cooled to 5°C by means of an ice-salt bath. Agitation was continued for two hours at 0—5°C following the completion of the addition. The reaction mass was then filtered, and the filter cake was suspended in 100 ml. of water at 40°C and acidified by adding 10% hydrochloric acid. After it had been cooled to room temperature, the precipitated solid was removed by filtration and dried in a vacuum oven; yield, 2.9 g. (96%). This solid does not change until 300°C. The crude product was recrystallized twice from an ethanol-water (1 : 1) mixture.

Found: C, 47.88; H, 3.79; B, 3.37; N, 13.90. Calcd. for $C_{12}H_{10}BN_3O_4S$: C, 47.52; H, 3.33; B, 3.58; N, 13.87%.

With N^1-2-Thiazolylsulfanilamide (R=II). — N^1-2-Thiazolylsulfanilamide (2.5 g., 0.01 ml.) was diazotized according to the method of Datta.[5] This diazonium chloride solution was then stirred over a 15-min. period into a solution composed of 1.1 g. (0.0275 mol.) of sodium hydroxide, 1.4 g. (0.01 mol.) of *o*-hydroxybenzeneboronic acid anhydride, and 10 ml. of water; then the solution was cooled in an ice-salt bath. Agitation was continued for 2 hr. following the completion of the addition, with the temperature maintained at 0—5°C. The reaction mixture was then filtered, and the filter cake was suspended in 100 ml. of water at 40°C and then acidified with 10% hydrochloric acid. The solid thus precipitated was removed by filtration after it had been cooled to room temperature;

4) H. Gilman, L. Santucci, D. R. Swayampati and R. O. Ranck, ibid., **79**, 3077 (1957).

5) S. K. Datta and S. N. Saha, *Z. anal. Chem.*, **174**, 38 (1960).

it was then dried in a vacuum oven. The brown crude material was recrystallized twice from an ethanol-water (1 : 1) mixture to give 2.5 g. of a pure, bitter, orange product decomposing at 220°C. Yield, 66%.

Found: C, 46.27; H, 2.62; B, 2.64; N, 14.77. Calcd. for $C_{15}H_{11}BN_4O_4S_2$: C, 46.62; H. 2.88; B, 2.80. N, 14.52%.

With N^1-(2, 6-Dimethoxy-4-pyrimidinyl)sulfanilamide (R =III). — N^1-(2, 6-Dimethoxy - 4 - pyrimidinyl)sulfanil - amide (4.3 g., 0.01 mol.) was dissolved in 3 ml. of 30% hydrochloric acid and diazotized with 0.7 g. of sodium nitrite and 25 ml. of water at −1 to −3°C. The diazonium chloride solution was added to a stirred solution composed of 1.4 g. of *o*-hydroxybenzeneboronic acid anhydride, 1.1 g. (0.01 mol.) of sodium hydroxide, and 10 ml. of water cooled to 0—5°C by means of an ice-salt bath. Agitation was continued for 2 hr. following the completion of the addition, with the temperature maintained below 5°C. The reaction mass was then filtered, and the residue was suspended in 100 ml. of water and acidified by adding 10% hydrochloric acid. The product was filtered, washed, and recrystallized from an ethanol-water (1 : 1) mixture. The yield was 3.8 g. (86%). This product decomposes at 210°C.

Found: C, 49.60; H, 3.69; B, 2.62; N, 16.09. Calcd. for $C_{18}H_{15}BN_5O_6S$: C, 49.08; H, 3.44; B, 2.46; N, 15.92%.

With N^1-(6-Methoxy-3-pyridazinyl)sulfanilamide (R=IV). —To a stirred solution of 1.4 g. (0.01 mol.) of *o*-hydroxybenzeneboronic acid anhydride and 1.2 g. (0.03 mol.) of sodium hydroxide in 10 ml. of water, cooled to 0—5°C in an ice-salt bath, there was slowly added a solution containing 2.8 g. of N^1-(6-methoxy-3-pyridazinyl)-sulfanilamide, 4.8 ml. of 30% hydrochloric acid, 0.7 g. sodium nitrite, and 25 ml. of water. The alkaline reaction mixture was stirred for 2 hr. at 0—5°C and was then filtered. The filter cake was suspended in 100 ml. of water and acidified with 10% hydrochloric acid. A product with a decomposition point of 210°C was thus obtained in a 70% yield. The crude product was recrystallized twice from an ethanol-water (1 : 1) mixture.

Found: C, 49.26; H, 3.12; B, 2.80; N, 16.93. Calcd. for $C_{17}H_{14}BN_5O_5S$: C, 49.62; H, 3.44; B, 2.63; N, 17.04%.

BULLETIN OF THE CHEMICAL SOCIETY OF JAPAN VOL. 39 1584—1588 (1966)

The Effects of Some Antioxidants on a Polyurethane Fuel Binder

By Kiroku YAMAZAKI

Institute of Space and Aeronautical Science, The University of Tokyo, Komaba, Meguro-ku, Tokyo

and Harusuke TOKUI

Daicel Ltd., Yuraku-cho, Chiyoda-ku, Tokyo

(Received August 27, 1965)

The antioxidation effect of *N*, *N*'-diphenyl-*p*-phenylene diamine and *N*, *N*'-di-(2-naphthyl)-*p*-phenylene diamine was studied with polyol-cured polyurethane containing an organo-ferric compound as a curing catalyst. These antioxidants, after weathering for one year, were found to be very effective. The same polymer without the antioxidants was degraded and flowed after only three weeks exposure (during the month of May). Although most of the inhibited polymers showed no depression in tensile properties after being exposed for one year, it was noted that the reddish transparent polymers turned dark brown and became opaque. Polyurethane is, in general, strong and resistant to weathering and aging. The degradation mentioned in this study, however, should be attributed to the degradative action of sunlight and the atmospheric conditions. The characteristics of the specimens for tensile strength and elongation at the breaking point have generally been improved without any remarkable change in the tensile modulus, the effect of the "after cure" should be taken into account in addition to the degradative action of sunlight and air.

It is well known that elastomeric polyurethanes are quite resistant to the degradative action of oxygen, ozone and ultraviolet light and more durable in the face of aging and weathering than natural or synthetic diene-type rubbers. Generally, the products catalyzed or cured by amine display excellent resistance. This may be attributed to the fact that polyurethanes have no double bonds in their molecular structure although they are apt to hydrolyse. There are some cases in which a retarder of hydrolysis plays an effective role as a stabilizer.

It has been frequently observed, however, that the polyurethanes produced from toluene diisocyanate, trimethylol propane and diols (such as polyoxybutylene-polyoxypropylene glycol or polyoxypropylene glycol) containing a ferric compound as a catalyst deteriorate and gradually flow

from the edge of the surface when exposed to sunlight in a conventional atmosphere. This observation has been restricted only to the case of the polyurethane obtained by the catalytic action of the ferric compound. Direct exposure to sunlight seems to accelerate the deterioration process remarkably.

An amine-catalyzed polyurethane and those elastomers obtained from polyoxypropylene glycol, trimethylol propane and naphthylene diisocyanate using no catalyst are quite stable.

As the deterioration is due to the hydrolysis or to the depolymerization of urethane linkage, it should not be restricted to polymers produced by means of a ferric catalyst.

The following scheme is presumed for the deterioration of polymers[1]:

Activation

$$RH + h\nu \text{ (or thermal energy)} \rightarrow R\cdot + H\cdot$$

$$RH \xrightarrow{O_2} R\cdot + HOO\cdot$$

where RH : polymer molecule

Propagation

$$R\cdot + O_2 \rightarrow ROO\cdot$$

$$RH + ROO\cdot \rightarrow R\cdot + ROOH$$

$$ROOH \rightarrow RO\cdot + HO\cdot$$

$$2ROOH \rightarrow RO\cdot + ROO\cdot + H_2O$$

$$RH + RO\cdot \rightarrow R\cdot + ROH$$

$$RH + ROO\cdot \rightarrow R\cdot + ROOH$$

Termination

$$2R\cdot \rightarrow R\text{–}R$$

$$R\cdot + RO\cdot \rightarrow R\text{–}O\text{–}R$$

$$2RO\cdot \rightarrow R\text{–}O\text{–}O\text{–}R$$

$$2ROO\cdot \rightarrow R\text{–}O\text{–}O\text{–}R + O_2$$

Since ferric and ferrous ions would serve as catalysts to promote the decomposition reactions of the hydroperoxides, the weathering and aging of the polymer might then be accelerated:

$$Fe^{3+} + ROOH \rightarrow Fe^{2+} + H^+ + ROO\cdot$$

$$Fe^{2+} + ROOH \rightarrow Fe^{3+} + OH^- + RO\cdot$$

Tobolsky and his co-workers[2-4] pointed out that the weak bonds in polyurethane elastomers are those of the biuret, disubstituted urea, and allophanate linkages. The urethane linkage is relatively strong, although weaker than that of the polyesters or polyethers which constitute the main chains of the elastomer. Biuret and disubstituted urea are formed by means of the following reactions:

$$\sim NCO + H_2O + OCN\sim \rightarrow \sim N(H)\text{-}C(=O)\text{-}N(H)\sim + CO_2$$

$$\sim NCO + H_2N\sim \rightarrow \sim N(H)\text{-}C(=O)\text{-}N(H)\sim$$

$$\sim N(H)\text{-}C(=O)\text{-}N(H)\sim + \sim NCO \rightarrow \sim N(H)\text{-}C(=O)\text{-}N(\text{-}C(=O)\text{-}N(H)\sim)\sim$$

While aging, amine-catalyzed and cured polymers were quite stable. Deterioration, however, occurred with polyol-cured products. Accordingly, it may be reasonable to assume that the mechanism for aging (described above) in conjunction with the accelerating effect of ferric ions.

Schollenberger and his co-workers[5] studied the aging of the polyurethane, produced from the diphenylmethane diisocyanate and polyester derived from adipic acid and butanediol-1, 4. According to their theory, the incident radiant energy initiates free radical chains in the elastomer; the surface radicals in contact with air form hydroperoxides, which then decompose and produce an extensively cross-linked surface and cause hardened deterioration. This is in accordance with the mechanism mentioned above. Consequently, an ultraviolet light accepter and conventional antioxidants would be effective, since they improved the resistance against weathering of the polyurethane by the addition of carbon blacks, *N*, *N'*-diphenyl-*p*-phenylene diamine or *N*, *N'*-di-(2-naphthyl)-*p*-phenylene diamine.

The effect of the last two diamines as antioxidants was studied in order to improve the resistivity of the polyurethane against weathering or aging. In this work, however, the hardening as a result of cross-linking reaction did not occur, but the flowing due to the chain scission of the polymer was observed.

Polyoxybutylene-polyoxypropylene glycol was used as one of the starting materials for the polyurethane. Madorsky and Straus[6] reported, however, that introduction of oxygen in the skeleton of an aliphatic hydrocarbon lowered the stability of the chain, and that the C–C bond strength in the skeleton decreased with the substitution of alkyl groups for hydrogen atoms. Therefore, the polyurethanes employed in this work might be unstable against aging as compared with hydrocarbon polymers having C–C bond skeleton or polyethers containing no side alkyl groups (such as polyoxybutylene glycol or polyoxyethylene glycol).

1) T. Matsuda et. al., "Degradation of High Molecular Materials (Kobunshi-Zairyo no Rekka)," Corona Pub., Tokyo (1958).
2) J. A. Offenbach and A. V. Tobolsky, *J. Colloid Sci.*, **11**, 39 (1956).
3) P. C. Colodny and A. V. Tobolsky, *J. Am. Chem. Soc.*, **79**, 4320 (1957).
4) A. V. Tobolsky, V. Johnson and W. J. MacKnight, *J. Phy. Chem.*, **69**, 476 (1965).
5) C. S. Schollenberger, H. Scott and G. R. Moore, *Rubber World*, **137**, 547 (1958).
6) S. L. Madorsky and S. Straus, *J. Polymer Sci.*, **36**, 183 (1959).

Raw Materials

Polyoxybutylene-polyoxypropylene Glycol (*Sanyo Chem. Co.*).—A random copolymer of oxybutylene and oxypropylene units containing 25 mol. % of the latter. The hydroxyl number was 58.7.

Toluene Diisocyanate (*Mitsui Chem. Co.*).—A 80/20 mixture of 2, 4- and 2, 6- isomers.

Antioxidants (*Ouchi Shinko Co.*).—*N*, *N'*-Diphenyl-*p*-phenylene diamine and *N*, *N'*-di(2-naphthyl)-*p*-phenylene diamine sold under the trade names Nocrac DP and Nocrac White respectively.

Commercial materials were used without any further treatment.

Curing Catalyst.—An organo-ferric compound was synthesized.

Experimental

Polyurethane was synthesized by means of the one-shot method. A round flask is equipped with a gas outlet and a mechanical stirrer. Polyether, trimethylol propane, the curing catalyst and the antioxidant were mixed together in the flask; the mixture was heated to 80°C in an oil bath for one hour under a vacuum of 3—4 mmHg. In the course of the heating, the catalyst and trimethylol propane were dissolved, and the impregnated water was removed. After the mixture had then been cooled to 20°C, toluene diisocyanate

TABLE I. CHANGES IN PHYSICAL PROPERTIES OF POLYURETHANE ELASTOMERS ON WEATHERING

No.	Anti-oxidant added*	Before or after exposure	Tensile strength kg./cm²	Elongation at break point %	Stress at 100% elongation kg./cm²	Stress at 300% elongation kg./cm²	Hardness	Appearances after exposure
1	Nocrac DP 0.25	Before	11.9	1490	—	3.4	20.6	Turned dark brown, lozenge patterned crack
		After	22.3	1930	2.3	3.6	22.6	
2	Nocrac DP 0.50	Before	14.2	1710	—	3.6	20.2	Turned dark brown, no appreciable change
		After	17.4	1530	2.7	4.2	24.1	
3	Nocrac DP 0.75	Before	12.2	720	—	6.1	21.8	Turned dark brown
		After	14.5	810	3.6	6.2	28.8	
4	Nocrac DP 1.00	Before	14.8	1750	—	3.5	16.6	Turned dark brown
		After	18.5	1730	2.2	3.7	22.3	
5	Nocrac DP 1.50	Before	16.9	1630	—	3.6	20.0	Turned dark brown
		After	16.6	1500	2.3	3.8	22.6	
6	Nocrac DP 2.00	Before	17.5	2580	—	2.3	16.8	Turned dark brown
		After	—	>2000	1.9	2.7	15.7	
7	Nocrac DP 3.00	Before	—	>2500	—	—	11.2	Turned dark brown
		After	—	>2000	1.2	1.6	11.3	
8	NONE	Before	15.0	1390	3.0	5.1	24.4	Deteriorated, flown on exposure of only three weeks
		After	—	—	—	—	—	
9	Nocrac White 0.25	Before	19.4	1540	—	4.6	19.0	Turned dark brown, lozenge patterned crack
		After	22.9	1950	2.3	3.7	25.5	
10	Nocrac White 0.50	Before	13.6	980	3.1	5.1	18.1	Turned dark brown, lozenge patterned crack
		After	17.4	1230	2.9	5.0	26.6	
11	Nocrac White 0.75	Before	13.4	1220	2.6	4.3	20.0	Turned dark brown
		After	19.8	1610	2.8	4.6	24.8	
12	Nocrac White 1.00	Before	13.6	1080	—	4.9	23.2	Turned dark brown
		After	20.5	1500	3.2	5.1	26.2	
13	Nocrac White 1.50	Before	17.1	1340	—	4.5	25.2	Turned dark brown
		After	15.3	1370	2.8	4.5	24.8	
14	Nocrac White 2.00	Before	18.5	1570	—	4.3	19.0	Turned dark brown
		After	21.1	1810	2.8	4.3	25.0	
15	Nocrac White 3.00	Before	12.0	830	3.2	5.5	22.6	Turned dark brown
		After	15.8	1180	3.5	5.5	28.3	

* Parts per hundred parts of polyether.

was added, and stirred again for 15 min. While the stirring, the pressure in the flask was held in vacuum. The reaction mixture was then poured into a cavity (2—3 mm. thick) formed by two parallel surface-lubricated glass plates, and cured at 50°C in an electric oven for 48 hr.

The ratio of the equivalents of isocyanates to hydroxyl groups, $R=1.10$, and the fraction of –OH from triol, $\rho_t=0.25$ were set as the composition of the polyurethane.[7] While R and ρ_t were kept constant, the amount of the antioxidants added were varied from 0 to 3%.

The tensile properties of the elastomers were determined on the basis of the JIS-K-6301 (Physical Testing Methods for Vulcanized Rubber); No. 3 dumbbell-shaped specimens were used, and the strain rate was 500 mm./min. The hardness was measured using an Asker Durometer J.

The weathering process was carried out as follows: Dumbbell-shaped specimens were fixed on the plates of the polyethylene-lined plywood and exposed on the roof of the Central Research Laboratory of the Daicel Ltd. (171 Ohi-mura Tsuruoka, Iruma-gun, Saitama Pref., Japan; longitude 139°30′ E; latitude 35°53′ N). The plates stood at a 30° angle to the floor and faced south. The exposure test was carried out from May 4, 1964 to May 6, 1965.

Results and Discussion

The results of the weathering test are tabulated in Table I.

Figures 1 and 2 show the changes in the tensile properties with the amounts of the antioxidants before and after exposure.

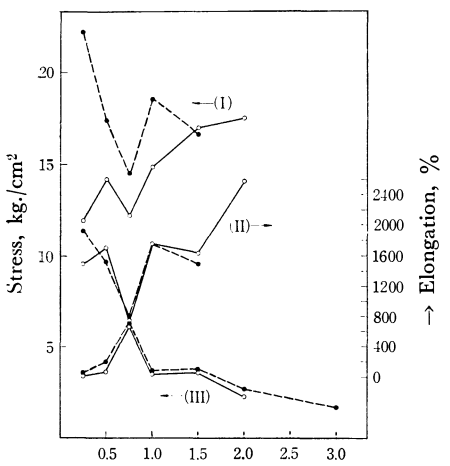

Nocrac DP added, (g./100 g. polyether)

Fig. 1. Tensile properties of polyurethane containing Nocrac DP.
(I) Tensile strength
(II) Elongation at break point
(III) Stress at 300% elongation
—— before exposure ---- after exposure

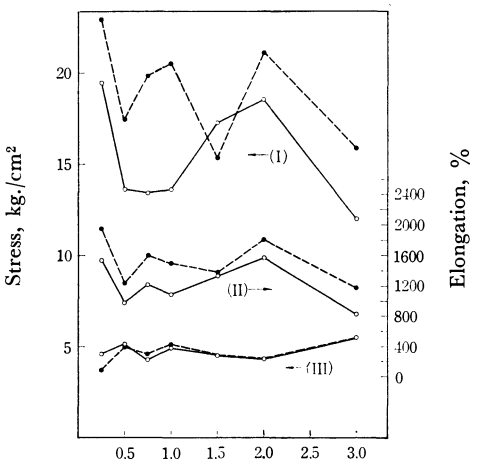

Nocrac White added, (g./100 g. polyether)

Fig. 2. Tensile properties of polyurethane containing Nocrac White.
(I) Tensile strength
(II) Elongation at break point
(III) Stress at 300% elongation
—— before exposure ---- after exposure

Since Nocrac DP was soluble to the reaction mixture, the produced elastomers were transparent, while Nocrac White was insoluble and the produced elastomers were less clear. After being exposed for one year, the reddish transparent elastomers turned dark brown and became opaque.

Die-cut specimens containing small amounts of the antioxidants (Nos. 1, 9 and 10) were attacked on exposure, and lozenge-patterned cracks developed on the surfaces from the edge. Figure 3 shows the appearance of the exposed surface of Specimen No. 9. (The back surface remained unchanged.)

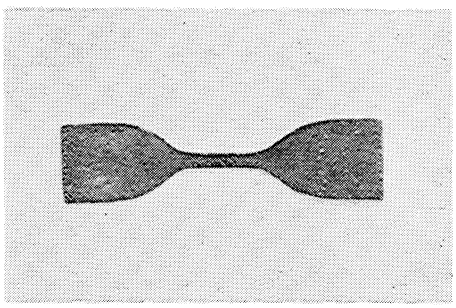

Fig. 3. View of the deteriorated surface of a specimen.
(No. 9, after exposure for one year)

Apparently, the tested antioxidants were very effective, for the uninhibited polymer deteriorated and showed a flow upon exposure for only three weeks in May. The quantities of the antioxidants, 0.5—1.0 parts per hundred parts of polyether, would be sufficient to inhibit the flow of the elastomer for at least one year.

7) H. E. Marsh, Jr., *Ind. Eng. Chem.*, **52**, 768 (1960).

Since amino groups would react faster than hydroxyl groups do with isocyanate, the R values and the degree of cross-linking changed from the predetermined values; then the physical properties of the elastomers changed irregularly with the amounts of the antioxidants. For this reason, the lines in Figs. 1 and 2 have little meaning; they make it easy, however, to look over the figures.

After being exposed, the stress at 300% elongation was slightly increased; the tensile strength, however, was increased remarkably. In the case of the specimens containing Nocrac White, moreover, the values of elongation at the breaking point also increased. Some polybutadiene rubbers were tested similarly. In this case, the tensile modulus was increased, while the tensile strength and elongation at the breaking point decreased and became very brittle. Since the polyurethanes did not show any decrease in tensile properties, these changes may be attributed to be the effect of the "after cure." The change in physical properties would be partly due to the aging by the mechanism mentioned above, and the slight increase in stress at 300% elongation might be the result of the cross-linking reaction caused by sunlight and air. The degrees of augmentation in tensile strength and elongation, however, were too large to attribute to the action of sunlight and air alone. In addition, the exposed specimens did not become brittle.

An effort was made to explain the effect of the "after cure" of polyurethane in connection with the residual quantity of isocyanate groups in the elastomer.[8] In the case of polyurethane containing Nocrac DP, the degree of augmentation in tensile strength after exposure decreased as the quantity of the antioxidant increased. Since, in all cases, toluene diisocyanate was used in excess; the more the quantity of the antioxidant, the less the quantity of unreacted isocyanate, and then the possibility of the succeeding reaction would be decreased. Nocrac White was insoluble to the reaction mixture; therefore, the reaction rate of isocyanate with an amino group could not be so fast as to influence the degree of the "after cure". Therefore, the amount of augmentation in tensile strength was almost the same as far as the data in Fig. 2 was concerned.

All of the specimens except Nos. 1, 8, 9 and 10 showed no depression in physical properties or any remarkable change in their appearance.

There still remain problems to solve for practical processing; for example, the unaimed side reactions as well as the reduction of pot life as a result of the catalytic effect of the antioxidants should be controlled, since these compounds may serve as a kind of amino compounds. The polyurethane used in this study was developed as a fuel binder for composite propellants; since ammonium perchlorate is widely used as an oxidizer for solid fuel, however, it may liberate ammonia and react with isocyanate.[9]

$$RNH_2 + NH_4^+ \rightarrow RNH_3^+ + NH_3$$

Phenolic antioxidants seems to be preferable to use in solving the problems cited above; it has been shown, however, that the propellant grain containing such a compound as an antioxidant is generally inferior to amino derivatives against aging.[10]

The authors wish to express their thanks to Mr. Toshimitsu Iwase for his assistance for the experiment.

8) Y. Komaki, K. Murai and Y. Fukuda, *Synthesized Resin (Gosei Jushi)*, **10**, 36 (1964).

9) B. Siegel and L. Schieler, "Energetics of Propellant Chemistry," Wiley, New York (1964).

10) K. Yamazaki and K. Kishi, unpublished.

NOTES

Formation Constants of Malonato- and Succinatochromium(III) Complexes*1

By Hiroko MURO (née ISEKI) and Ryokichi TSUCHIYA

Department of Chemistry, Faculty of Science, Kanazawa University, Marunouchi Kanazawa

(Received April 1, 1965)

In comparison with several reports[1,2] on formation constants in bivalent metal complexes with malonic and succinic acids, there have been no papers on those in tervalent metal complexes excepting for some rare earth metal complexes[3] with these ligands.

The formation constants of chromium(III) complexes with the oxalate ion have been reported in an earlier paper[4] by one of the present authors. In continuation of the above work, the formation constants of chromium(III) complexes containing the malonate and succinate anions as a ligand have been determined; the relationship between the stability and stereostructure among these complexes, including the oxalate complexes, will be discussed in the present work.

Experimental

In a manner similar to that described in a previous paper,[4] the formation constants were determined by means of pH measurements in solutions containing the hexaaquochromium(III) perchlorate and either malonic or succinic acid at the ionic strength, μ, of 0.1 at 25°C.

The preparation and analysis of the hexaaquochromium(III) perchlorate were also carried out according to procedures similar to those in the previous paper.[4] The malonic and succinic acids used were of an analytical reagent grade and were from Nakarai Chemicals, Ltd., and Wako Pure Chemical Industries, Ltd., respectively.

Results

The values of the acid dissociation constants of malonic and succinic acids required for the determination of formation constants of their complexes were taken from the literature.*2 The method of calculating the average number of corrdinated carboxylate anions as ligand per gram-ion of the chromium(III) ion, $\bar{n}$, and the method of calculating the concentration of non-coordinated one, $[A^{2-}]$, in solutions, are the same as those described in the previous paper.[4] The plots of $\bar{n}$ vs. $p[A^{2-}]$ for both malonato- and succinatochromium(III) systems are shown in Fig. 1.

By applying the successive approximation method to the tentative values of the formation constants obtained from the formation curve shown in Fig. 1, the stepwise formation constants of both

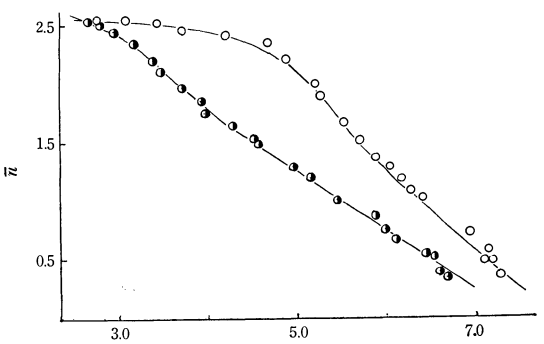

Fig. 1. The formation curve, $\bar{n}\sim p[A^{2-}]$.
—○— Malonatochromium(III) complex
—◑— Succinatochromium(III) complex

TABLE I. THE FORMATION CONSTANTS OF OXALATO-, MALONATO- AND SUCCINATOCHROMIUM(III) COMPLEXES, AT $\mu=0.1$ AND 25°C

	$\log k_1$	$\log k_2$	$\log k_3$	$\log k_1k_2k_3$
Oxalato complex	5.34	5.17	4.93	15.44
Malonato complex	7.06	5.79	3.30	16.15
Succinato complex	6.42	4.57	2.86	13.85

*1 Presented at the 17 th Annual Meeting of the Chemical Society of Japan, Tokyo, April, 1964.

1) M. Bobtelsky and J. Bar-Gadda, *Bull. Soc. Chim. France*, **1953**, 276.

2) J. Schubert and A. Lindenbaum, *J. Am. Chem. Soc.*, **74**, 3529 (1952).

3) E. Gelles and G. H. Nancollas, *Trans. Faraday Soc.*, **52**, 680 (1956).

4) K. Nagata, A. Umayahara and R. Tsuchiya, This Bulletin, **38**, 1059 (1965).

*2 The first and second acid dissociation constants of malonic acid, $pK_1=2.76$ and $pK_2=5.29$, and those of succinic acid, $pK_1=4.00$ and $pK_2=5.21$, are cited from M. Yasuda, K. Yamasaki and H. Ohtaki, This Bulletin, **33**, 1067 (1960).

malonato- and succinatochromium(III) complexes were obtained; they are listed in Table I, together with those of the oxalatochromium(III) complexes reported previously[4] by one of the present authors.

Discussion

It may be seen from Table I that the stepwise formation constants, log k_1 and log k_1k_2, of the chromium(III) complexes decrease in the order: malonato<succinato<oxalato. This phenomenon will be discussed below.

First, one of the main factors controlling the difference in stability among these complexes may be a bond angle, like O–Cr–O, in its own chelate ring. The oxalate ion can usually form a five-membered chelate ring with a central chromium(III) ion, whereas the malonate and succinate ions can form six- and seven-membered rings with the same metal ion. Thus a O–Cr–O bond angle in a chelate ring may be expected to become larger as the size of the ring increases. Despite the above intuitive prediction, however, if the structure of the oxalatochromium(III) complex appearing in the literature[5] is compared with schematic structure of malonato- or succinatochromium(III) complex which is depicted by the aid of the bond angles and bond lengths reported for the former, it may be presumed that the bond angle, O–Cr–O, in these complexes does not deviate so greatly from rectangular as to have a vital effect on the difference in stability among these complexes.

Consequently, the most important factors determining the stability of these complexes seem to be the entropy and enthalpy changes brought about by the formation of these complexes.

The first factor is the entropy change in the complex formation. The degree of freedom of a molecule or ion becomes larger as the carbon chain in the acids becomes longer. Therefore, when the dicarboxylate anions coordinate to metal ions, the degree of the freedom of the anions decreases, depending upon the length of the carbon chain in the ligand. Thus, closely related to the above effect on the entropy change, the stability of complexes may be expected to decrease in the order: oxalato> malonato>succinato.

The results obtained in this study show that the stepwise formation, and also the overall formation constants of malonato complexes are larger than those of succinato complexes; such a stability sequence may, therefore, be reasonably explained in terms of the entropy change mentioned above. However, as this entropy factor alone may not give a complete answer to the stability order measured in the case of the oxalato complex, another factor must also be taken into account.

Since the overall acid dissociation constants of oxalic, malonic and succinic acids, pK_1+pK_2, are 4.98,[4] 8.05*[2] and 9.21*[2] respectively, the basicity of the oxygen atoms in carboxylate groups which can coordinate to a metal ion seems to be the smallest in oxalic acid, a little larger in malonic acid, and the largest in succinic acid. Although the basicity of the donor atoms is not the only factor in deciding the enthalpy change upon the coordination of these dicarboxylic acids with chromium(III) ion, it seems to be one of the most effective factors. Thus, the enthalpy change may be presumed to decrease in the order: succinato> malonato>oxalato. In the light of the enthappy change, only the stabilities of these complexes should range in the same order.

However, so far as log k_1 and log k_1k_2 are concerned, the stability order obtained here is: malonato>succinato>oxalato. This finding will be explained below.

Since the difference in the acid dissociation constants between the malonic and succinic acids is really smaller than that between the oxalic and malonic or succinic acid, the stability order in the malonato and succinato complexes seems to be not very much affected by the enthalpy change, but to depend mainly upon the entropy change, as has been assumed above, whereas the smaller stability of the oxalato complex than that of the malonato or the succinato complex is thought to be mainly due to the differences in the enthalpy effect among these complexes. In evaluating the above two main factors which may control the first and second stepwise stability constants of the complexes treated in this paper, it should perhaps be emphasized that an extra stability of the malonato complex over the succinato one is assumed to be responsible for the larger loss of entropy in the complex formation of the latter than in that of the former; the fact that the stability of the succinato complex is a little larger than that of the oxalato complex can be explained on the assumption that the enthalpy decrease accompanying the formation of the former is larger than that accompanying the latter's formation.

On the other hand, the third stepwise formation constant is largest in the oxalato complex and then descreases in the order: malonato>succinato complexes. This shows that the stepwise formation constants of the oxalato complex do not decrease so markedly as those of malonato or succinato complexes, as is shown in Table I. When the overall formation constants are arranged, the stability order is given as: malonato>oxalato> succinato. The trend in stepwise formation constants among the complexes involved in this work may be explained in terms of the concept of steric interaction existing among ligand molecules coordinated to a metal ion; the nearly planar structure of the oxalate ion is still held in the complex formation, whereas in the cases of both the malonate

5) J. N. Van Niekerk and F. R. L. Schoening, *Acta Cryst.*, **4**, 35 (1951).

and succinate anions it is possible for the mutual steric hindrance to occur among coordinated ligands as a result of their larger chelate rings.

The partial support received for this investigation from the Ministry of Education is gratefully acknowledged.

The Application of the Additivity Principle to the Ionization of 2, 3- and 2, 4-Dimethoxybenzoic Acids

By K. C. SRIVASTAVA

Department of Engineering Chemistry, Birla Institute of Technology & Science, Pilani (Rajasthan), India

(Received September 3, 1965)

The overall effect of multiple substitution in a molecule is generally the sum of the individual contributions of the substituents, and, according to Jaffé,[1] the Hammett equation can be applied to most of the cases. Exceptions to this rule have, however, been recorded,[2,3] especially when a methoxyl group is present in the system. Our findings on the ionization of 4-hydroxy 3, 5-dimethoxybenzoic acid,[4] however, strictly conform to the additivity principle. In view of the relatively few investigations reported on substituted benzoic acids, the author has determined the apparent dissociation constants of 2, 3- and 2, 4-dimethoxybenzoic acids at different temperatures. From the data obtained, it then appeared of interest to examine the applicability of the additivity principle to dimethoxybenzoic acids. The results of these investigations will be reported in the present communication.

Experimental

The 2, 3- and 2, 4-dimethoxybenzoic acids used were of E. Merck C. P. grade (m. p. 122°C and 110°C; lit.[5] 120—122°C and 109°C). The caustic soda used was of a B. D. H. AnalaR quality.

The pK values of the acid at different temperatures were determined pH-metrically with a Beckman pH meter (Model G), using an extension electrode assembly. The temperature of the titration cell was maintained at the desired value of ± 0.1°C by employing an oil thermostat operated by a micro relay.

Results and Discussion

In Table I are recorded the pK_a values of the acids at different temperatures as obtained from the pH-metric titration curves of the acid. These values were computed essentially by the method discussed by Britton[6]; the average values were obtained by the graphical procedure discussed earlier.[1] From these data the thermodynamic ionization constants of the acid corresponding to different temperatures were calculated; the data are given in column 3, Table I.

The values for methoxy-substituted benzoic acids, along with the contributions of the substituents to the pK_a of benzoic acid,[7] are recorded

Table I. The ionization constant of dimethoxybenzoic acids at different temperatures

Temp., °C	pK_a	pK_a (Thermodynamic)
2, 3-Dimethoxybenzoic acid:		
25	3.98	3.98
30	3.96	3.94
40	3.94	3.90
50	3.90	3.86
60	3.88	3.86
2, 4-Dimethoxybenzoic acid:		
25	4.36	4.36
30	4.34	4.32
40	4.30	4.28
50	4.28	4.26
60	4.25	4.24

Table II. pK_a Values of methoxy-substituted benzoic acids

Acid	pK	Contribution of substituents
Benzoic acid	4.21	—
2-Methoxy benzoic acid	4.09	−0.12
3-Methoxy benzoic acid	4.09	−0.12
4-Methoxy benzoic acid	4.47	+0.26
2, 3-Dimethoxy benzoic acid	3.98	−0.23
	(3.97)*	(−0.24)
2, 4-Dimethoxy benzoic acid	4.36	+0.15
	(4.35)*	(+0.14)

* The theoretical values are given in parentheses.

1) H. H. Jaffé, *Chem. Revs.*, **53**, 243 (1953).
2) R. M. Keefer and L. J. Andrews, *J. Am. Chem. Soc.*, **78**, 5623 (1956).
3) P. J. McNulty and D. E. Pearson, ibid., **81**, 612 (1959).
4) K. C. Srivastava, *Bull. L'Academie Polonaise Des Sciences*, to be published.
5) S. I. Heilbron and H. M. Bunbury, "Dictionary of Organic Compounds," Vol. I, Eyre & Spottiswoode, London (1946), p. 881.
6) H. T. S. Britton, "Hydrogen Ions," Macmillan, London (1942).
7) J. F. J. Dippy, *Chem. Revs.*, **25**, 151 (1939).

in Table II. These data indicate that the substitution of a methoxy group in the meta position lowers the pK_a value by 0.12 unit, while that in the para position enhances the same by 0.26 unit. These considerations lead, by the application of the additivity principle, to an unexpected contribution of −0.24 for methoxy substituents in 2 and 3 positions, and to a contribution of 0.14 for methoxy substituents in 2 and 4 positions, thus giving a value of 3.97 and 4.35 for pK of the acid (Table II).

This theoretical value is in close agreement with the values of 3.98 and 4.36 for the pK_a values of 2, 3- and 2, 4-dimethoxybenzoic acids obtained in the present investigation.

The author wishes to thank Professor V. Lakshmi Narayanan, Director, B. I. T. S., Pilani, for providing the facilities to carry out this work.

The Anodic Behavior of Lead-Platinum and Lead-Palladium Bielectrodes in Chloride and Sulfate Solutions

By Eiichi SATO

Industrial Research Institute of Kanagawa Prefecture, Tomioka-cho, Kanazawa-ku, Yokohama

(Received September 18, 1965)

In recent years the electrolytic anodes with platinum coating on the metallic bases, such as tantalum, titanium and tungsten, have attracted extensive attention in the fields of sodium chloride electrolysis and cathodic protection against corrosion.

Shreir[1] found that the lead anodes in chloride electrolytes were prevented from corroding when a platinum, indium or graphite microelectrode was introduced.

While tentative explanations have been made of the effects of platinum, it is considered, in view of the complications involved, that further experimental studies are necessary in order to get a clearer understanding of the reaction mechanisms.

Experimental

Lead anodes with an area of 1 cm^2 were prepared at a purity of 99.99%. Test specimens of platinum and palladium, as well as the lead anodes, were then immersed into the surfaces of resinous blocks.

The potential was determined by means of a saturated calomel electrode in a sodium chloride solution or in laboratory sea water and by means of a 1 N mercurous sulfate electrode in a sodium sulfate solution.

Results and Discussion

Lead Electrode in 0.5 N Sodium Chloride. —The anodic current of the lead electrode in the passive region was smaller than that in the active region, though the latter came below the anodic current of the other two electrodes. Figure 1 shows the anodic polarization curve for lead in 0.5 N sodium chloride.

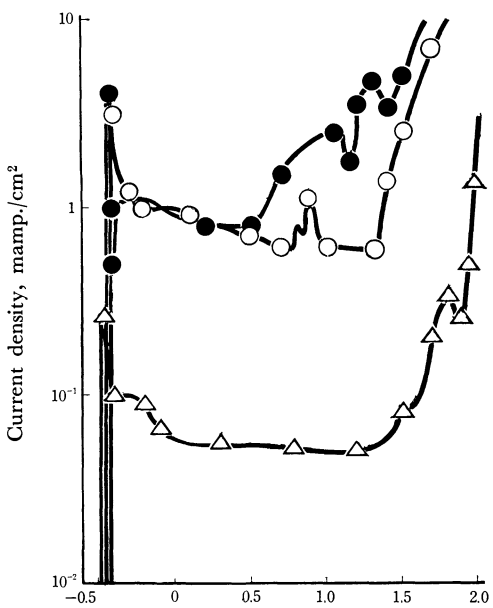

Fig. 1. Anodic polarization curve of lead electrode, lead-platinum bielectrode and lead-palladium.
△ Pb, ○ Pb-Pt bielectrode
● Pb-Pd bielectrode
Electrolyte: 0.5 N NaCl 100 cc.
Rate of potential change: 0.005 V./min.

This result suggests that lead chloride, formed and then dissolved in the active region, deposits on the electrode surface as illustrated in the following formulae:

$$Pb \rightarrow Pb^{2+} + 2e$$

$$E = -0.368 + 0.0295 \log A_{Pb^{2+}} \qquad (1)$$

1) L. L. Shreir, *Corrosion*, **17**, 118t (1961).

$$Pb^{2+} + 2Cl^- \rightarrow PbCl_2$$
$$E = -0.510 + 0.0295 \log A_{Cl^-} \quad (2)$$
$$K = 1.6 \times 10^{-5}$$

The palladium anode in a 0.5 N sodium chloride solution gave an incipient current in the potential region from 1.1 to 1.2 V., this was 500 mV. higher than the current for platinum. As has been decribed above, this means that the chloride ions are absorbed on the firmly-formed lead chloride layer, which is thus changed into lead dioxide. As the potential region from 1.4 to 1.9 V. is transpassive, the isolated lead present in the porous lead chloride layer will be dissolved as quadri-valent lead ions, according to the following reactions:

$$Pb \rightarrow Pb^{4+} + 4e$$
$$Pb^{4+} + 4OH^- \rightarrow PbO_2 + 2H_2O$$

The quadrivalent lead ions which are hydrated in the vicinity of the electrode are discharged and then deposited on it in this potential region. The lead dioxide formed still displays a fine appearance at first, but the film immediately decomposes as a result of the discharge of chloride ions.

It is considered that, in the passive region, the formation of metallic lead and chloride in the defective anode layer are involved in the absorption reaction of hydroxide ions. Fleischmann and Liler[2] established, using a lead acetate electrolyte, that lead dioxide easily neucleated and grew up on the platinum anode. They suggested the following reaction processes:

$$OH^- - e = OH_{ads} \quad (3)$$
$$Pb^{2+} + OH_{ads} + OH^- - e = Pb(OH)_2^{2+} \quad (4)$$
$$Pb(OH)_2^{2+} = PbO_2 + 2H^+ \quad (5)$$

Reaction 4 presumably controls the reaction rate. Feitknecht and Gäumann[3] proposed the following reactions:

$$OH^- = OH + e \quad (6)$$
$$PbO^+ + 2OH = Pb(OH)_2^{2+} + O^- \quad (7)$$
$$Pb(OH)_2^{2+} = PbO_2 + 2H^+ \quad (8)$$

For the anodic reaction of the Pb electrode in the presence of chloride ions, the authors inferred, instead of formulae 4 and 8, that:

$$Pb^{2+} \text{ (in layer)} + OH_{ads} + OH^- - e \rightarrow Pb(OH)_2^{2+},\ Pb(OH)_2^{2+} + 4Cl^- \rightarrow [PbCl_4(OH)_2]^{2-} \rightarrow PbO_2 + 4Cl^- + 2H^+ \quad (9)$$

and

$$PbCl_4 + 2OH^- - 2e \rightarrow [PbCl_4(OH_{ads})_2]^{2-} - 2e \rightarrow PbO_2 + 2Cl^- + 2H^+ + Cl_2 \quad (10)$$

Platinum and Palladium in Solutions of Sodium Chloride, Sodium Sulfate and Artificial Sea Water.—If palladium does not dissolve as well as platinum, the evolution potential of chlorine gas for palladium will be about 1.02 V., that is, 0.03 V. less than that for platinum. The evolution potential of oxygen on palladium is 0.075 V., and on platinum, 0.80 V. (referred to the mercurous sulfate electrode). It was found that the incipient anodic current for palladium appeared at 0.9 V., while that for platinum appeared at 0.9 V., too. Heumann and Schürmann[4] reported that the current-potential curves for the palladium anode in electrolytes containing chloride ions exhibited an active region, a primary passive region, and a secondary passive region; these correspond, respectively to the dissolution of palladium into the divalent state, the chlorine evolution from the passive electrode, and the oxygen evolution. They stated the experimental results as follows: For the palladium anode in 0.5 N hydrochloric acid, the anodic current begins at the potential of 0.62 V. and passes through a

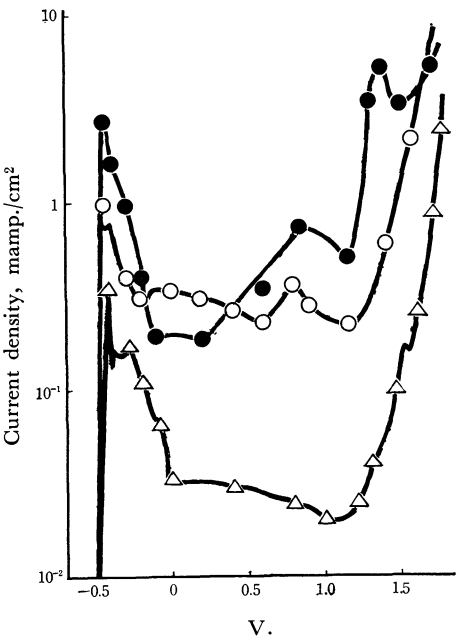

Fig. 2. Anodic polarization curve of Pb, Pb-Pt bielectrode and Pb-Pd bielectrode in artificial sea water.
△ Pb, ○ Pb-Pt, ● Pb-Pd
Electrolyte: artificial sea water: 100 cc., 30°C
Rate of potential change: 0.005 V./min.

2) M. Fleischmann and H. R. Liler, *Trans. Faraday Soc.*, **54**, 1370 (1958).
3) W. Feitknecht and A. Gäumann, *J. Chim. Physique, Physicochim. Biol.*, **49**, 135 (1956).
4) Th. Heumann and R. Schürmann, *Ber. Bensen Ges. Phys. Chem.*, **67**, 601 (1963).

maximum current density of about 0.04 amp./cm² at 1.4 V. in the active region; then it decreases towards the minimum value of 0.01 amp./cm² at 1.6 V. Another maximum in current density (0.06 amp./cm²) comes at the anodic potential of 1.75 V., after which the current again descends to 0.04 amp./cm². A further rise in the potential results in a monotonous increase in the anodic current.

Figure 2 depicts the anodic polarization curves for all the electrodes in aritificial sea water. On account of the dissolved oxygen, the current for the lead electrode becomes negative in the potential region from −0.8 to −0.55 V. The reaction mechanism was discussed in a previous report.[5] In our present experiments, the transpassivity region ranged between 0.6 and 0.9 V. when oxygen gas evolved on the electrode. The behavior of the lead platinum bielectrode is very like that of the lead electrode, but lead-palladium is so different that the anodic current begins to rapidly increase at −0.23 V. and the polarization curve is reflected at 0 V., above which point the transpassive region ranges from 0.8 to 1.1 V. Vetter[6] considered that the anodic current on the lead-palladium bielectrode indicated palladium dissolution but not lead dissolution in the potential region from −0.2 to 0 V., since the active region of palladium is in the potential region around −0.2 V.

The Influence of the Current Density on the Corrosion Rate of Palladium in Artificial Sea Water.—If palladium dissolves in the bivalent form, the dissolved ion amounts, according to Faraday's law, to 1.9903 g. at the current of 1 amp. for 1 hr. and 7.6416 g. at the current of 1 amp./dm² (32 mamp./3.2 cm²) for 5 days. The practical corrosion, however, weighed 0.00064 g., about 8/1000000 of the theoretical dissolved quantity. The difference in amount of electric charge between the calculation and the practical corrosion is caused by the gas evolution.

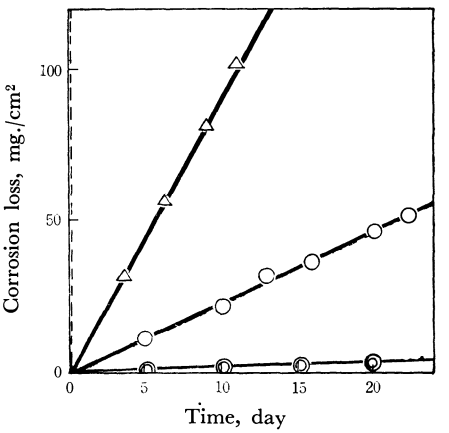

Fig. 3. Corrosion rates of Pd in artificial sea water.
◎ 1 amp./dm², ○ 5 amp./dm²
△ 10 amp./dm²
---- theoretical deposit amount of Pd^{2+} at 1 amp./dm²
Electrolyte: artificial sea water 500 cc., room temp.

Summary

A potentiostatic method was used to investigate the behavior of lead electrodes and lead-platinum and lead-palladium bielectrodes in sodium chloride and sodium sulfate solutions and in sea water. The experimental results showed lead-palladium bielectrode to be of practical use in the electrolysis of sea water.

5) E. Sato and T. Shiina, *J. Electrochem. Soc. Japan*, **32**, 148 (1964).
6) K. J. Vetter and D. Berndt, *Z. Elektrochem.*, **62**, 378 (1958).

A Preliminary Study of the Determination of Hydrogen Content in Heavy Water by Means of Neutron Transmission

By Masayoshi ONO and Yoshiyuki KISO

Research Reactor Institute, Kyoto University, Kumatori-cho, Sennan-gun, Osaka

(Received September 22, 1965)

The aim of this work is to examine the applicability of a neutron transmission procedure to the determination of the hydrogen content in heavy water, although the mass spectrometric and infrared absorption spectrophotometric methods[1,2] are most commonly used for this purpose.

The principle suggested here is based on the difference in total cross sections of thermal neutrons between light and heavy water.[3]

1) I. Kirshenbaum, "Physical Properties and Analysis of Heavy Water," McGraw Hill, New York (1951), p. 201.
2) G. Gordon and H. Yamatera, *Anal. Chem.*, **36**, 1866 (1964).
3) ANL-5800, Reactor Physics Constants.

The following formula is derived to give the sensitivity as a function of the amount of light water in heavy water, while the relation is shown in Fig. 1.;

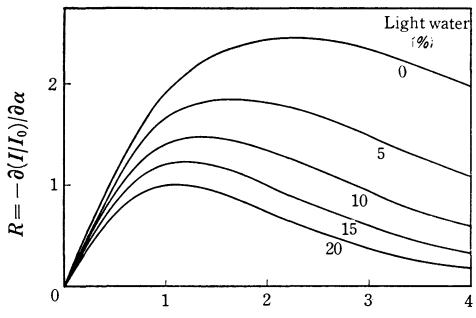

Fig. 1. Relation of R to thickness d of cell.

$$R = -\frac{\partial(I/I_0)}{\partial\alpha} = a.d.\exp\{-(a\alpha + b)d\} \quad (1)$$

where I_0 is the number of well-collimated incident neutrons falling on a small area; I, the number of neutrons which succeed in passing through the thickness, d, of the target over the same area; a, the difference between the macroscopic total cross sections for light and heavy waters; b, the macroscopic total cross section of heavy water, and α, the fractional molar concentration of light water.

From each maximum of the curves in Fig. 1 one can predict the optimum thickness, d, which will give the highest sensitivity of measurement for any arbitrary concentration of light water.

A preliminary experiment was performed by the arrangement shown in Fig. 2.

A series of samples were prepared by diluting pure heavy water (99.94 mol.%). The samples were poured into a dried cell by nitrogen-gas pressure. A cell 2 cm. thick was used, since this thickness, according to the curves in Fig. 1, seemed to give the maximum sensitivity for a 95—100 percent concentration of heavy water.

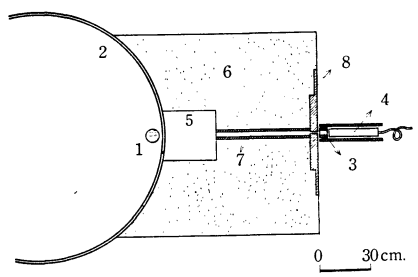

Fig. 2. Experimental arrangement.

(1): Neutron source (Am-Be, 6 curies)
(2): H_2O tank
(3): Cell (Al, 10×70 mm$^2\times20$ mm.)
(4): BF_3 counter (25 mm$\phi\times30$ cm.)
(5): Paraffin
(6): Boron paraffin
(7): Coarse collimeter
(8): Cadmium plate.

The counting rate of incident thermal neutrons through the cadmium slit (1.5×30 mm.) was 5.92 ± 0.01 c.p.m. during 12 hr. of measurement, and the background was 1.02 ± 0.025 c. p. m. during a 24 hr. period.

Figure 3 shows the curves obtained by the experiments and by calculations based on the neutron linear attenuation formula. This formula gives the highest sensitivity which can be expected by this method.

The fairly large disagreement between the two curves seems to be caused by more complicated phenomena than are taken into account by a simplified consideration like the linear attenuation formula. However, the results obtained experimentally show that this measurement procedure can be established as a method of chemical chemical analysis.

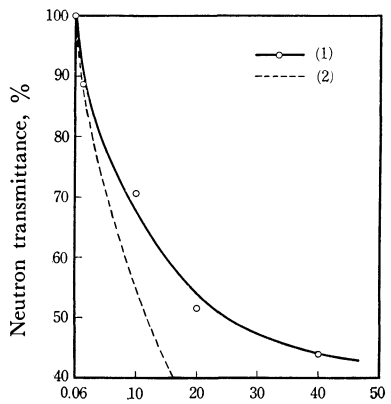

Fig. 3. Relation between neutron transmittance and concentration of light water (normalized to D_2O 99.94 mol. percent concentration).

(1): Experimental
(2): Calculated for linear attenuation formula $I/I_0 = \exp\{-(a\alpha+b)d\}$

The transmittance of the arbitrary sample to the standard (99.94 mol.%) at high concentrations of heavy water (98—100%) decreased to 11.1 percent for the concentration of light water shown in Fig. 3.

If a higher neutron flux, such as that from a nuclear reactor were used, this procedure could be established as a method for hydrogen determination of an even higher accuracy and an even greater rapidity.

The Japp-Klingemann Reaction of Diethyl Benzoylsuccinate

By Heinosuke YASUDA and Hiroshi MIDORIKAWA

The Institute of the Physical and Chemical Research, Bunkyo-ku, Tokyo

(Received September 28, 1965)

An extensive review of the Japp-Klingemann reaction has been made by Phillips.[1] It is well known that the coupling reaction of a diazotized aniline with a methinyl carbon gives an unstable azo compound, which then decomposes to give a hydrazone, whereas the coupling product between the same diazotized aniline and a methylene carbon is not an azo compound, but a hydrazone.

A previous paper[2] has presented a formation of 2-pyrazoline-5-one dye in an attempt to prepare the diethyl α-ketosuccinate phenylhydrazone by coupling diazotized aniline to diethyl acetylsuccinate in an alkaline medium.

This paper will describe the results obtained from the coupling reaction of diazotized anilines with diethyl benzoylsuccinate (I). The succinate I was prepared from ethyl sodiobenzoylacetate and ethyl monochloroacetate in boiling ethanol.

When benzenediazonium chloride reacted with I in ethanol containing sodium hydroxide, a product melting at 151—152°C was obtained; this product showed different behavior from expected diethyl α-ketosuccinate phenylhydrazone in melting point (76—78°C) or in debenzoylation. The analysis has suggested that this coupling product is 1-phenyl - 3 - ethoxycarbonyl - 4 - phenylhydrzaono-2-pyrazolin-5-one (IIa). The structure of the coupling product was further established by independent synthesis from the coupling reaction of benzenediazonium chloride with 1-phenyl-3-ethoxycarbonyl-2-pyrazolin-5-one.

Similarly, the reaction of I with two equivalents

TABLE I. 1-ARYL-3-ETHOXYCARBONYL-4-ARYLHYDRAZONO-2-PYRAZOLIN-5-ONES OBTAINED

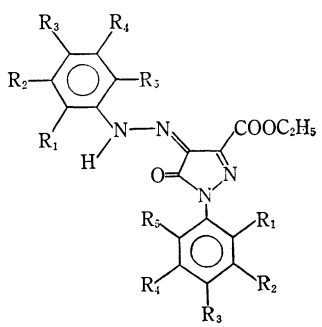

Compound	R_1	R_2	R_3	R_4	R_5	Yield %	M.p. °C[c]	Lit. m.p. °C	Formula	Carbon, % Calcd.	Carbon, % Found	Hydrogen, % Calcd.	Hydrogen, % Found	Nitrogen, % Calcd.	Nitrogen, % Found
IIa	H	H	H	H	H	42	151—2	152[a]	$C_{18}H_{16}O_3N_4$	64.27	64.84	4.80	4.55	16.67	16.85
IIb	Me	H	H	H	H	45	112—3	145[b]	$C_{20}H_{20}O_3N_4$	65.92	65.98	5.53	5.36	15.38	15.41
IIc	H	Me	H	H	H	38	141—2	146—7[b]	$C_{20}H_{20}O_3N_4$	65.92	66.17	5.53	5.37	15.38	15.28
IId	H	H	Me	H	H	38	142—3	143[b]	$C_{20}H_{20}O_3N_4$	65.92	65.91	5.53	5.24	15.38	15.59
IIe	H	OMe	H	H	H	39	124—5		$C_{20}H_{20}O_5N_4$	60.60	60.64	5.09	5.01	14.14	14.39
IIf	H	H	OMe	H	H	39	163—4		$C_{20}H_{20}O_5N_4$	60.60	60.80	5.09	5.06	14.14	14.21
IIg	H	Br	H	H	H	42	166—7		$C_{18}H_{14}O_3N_4Br_2$	43.73	43.58	2.83	2.67	11.34	11.29
IIh	Me	Me	H	H	H	36	163—4		$C_{22}H_{24}O_3N_4$	67.33	67.51	6.16	6.05	14.28	14.43
IIi	Me	H	Me	H	H	25	158—9		$C_{22}H_{24}O_3N_4$	67.33	67.38	6.16	5.86	14.28	14.43
IIj	Me	H	H	Me	H	36	137—8		$C_{22}H_{24}O_3N_4$	67.33	67.37	6.16	5.91	14.28	14.42
IIk	Me	H	H	H	Me	36	130—1		$C_{22}H_{24}O_3N_4$	67.33	67.24	6.16	6.02	14.28	14.49

a) S. Astin and H. L. Riley, *J. Chem. Soc.*, **1934**, 844.
b) V. V. Feofilaktov and T. N. Ivanova, *J. Gen. Chem.* (*U. S. S. R.*), **25**, 111 (1955).
c) All melting points are uncorrected.

1) R. R. Phillips, "Organic Reaction," Vol. 10, John Wiley & Sons, New York, N. Y. (1959), Chapter 2.

2) H. Yasuda, *J. Sci. Res. Inst. (Tokyo)*, **30**, 199 (1954).

of the respective diazotized anilines gave the corresponding dyes (II) in varying yields, ranging from 25 and 46% respectively. In each case, the remainder of the reaction mixture was a non-distillable, resinous material which could not be identified further. The relatively low yields may be due to the formation of appreciable amounts of the resinous material during the coupling reaction. This reaction is illustrated in the following equations.

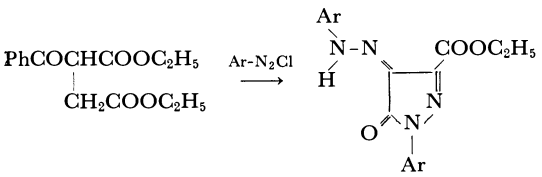

I II

Very recently,[3] the actual structures of 2-pyrazolin-5-one dyes, in which 4-positions are coupled with various diazotized anilines, have been shown to be the hydrazone-keto form and not an azo-keto or an azo-enol form. Table I summarizes the yield and other data obtained in the Japp-Klingemann reaction of I with eleven diazotized anilines.

The mechanism of the formation of the pyrazolinone dyes (II) from I and diazotized anilines apparently involves azo coupling on the α-methinyl carbon, thus forming an intermediate diethyl α-ketosuccinate arylhydrazones (III) via debenzoylation. This intermediate is expected to undergo an intramolecular cyclization by the elimination of one molecule of ethanol, thus giving 1-aryl-3-ethoxycarbonyl-2-pyrazoline-5-ones (IV). Compound IV, once formed, reacts with another molecule of diazotized aniline to give the pyrazolinone dyes (II). The probable scheme is illustrated as follows.

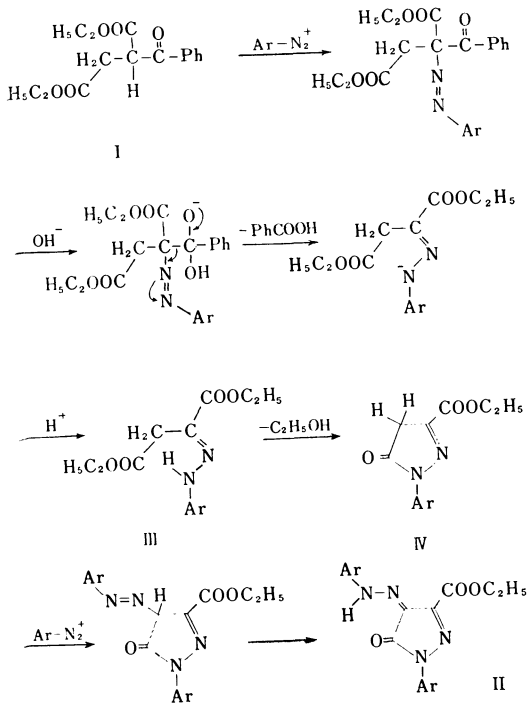

I

III IV II

Experimental

General Procedure for the Japp-Klingemann Reaction.—To a mechanically-stirred solution of 1 g. of sodium hydroxide in 50 ml. of 90% ethanol, 2 g. (0.00719 mol.) of diethyl benzoylsuccinate was added; the mixture was then cooled to 0°C. A diazonium solution (prepared by dissolving 0.0719 mol. of the appropriate aniline in 15 ml. of 2 N hydrochloric acid, cooling it to 0°C, and adding a saturated aqueous solution of 1.1 g. of sodium nitrite) was slowly stirred in mechanically. During the addition, a colored, oily, resinous matter separated. This matter was collected in a suitable manner and poured into a stirred mixture of 30 ml. of acetone and 30 ml. of ethanol. After the stirring had continued for 30 min., the mixture was diluted with water until clouding persisted. The colored solid which separated was collected, washed with methanol-water, and recrystallized from dioxane-water. The results are listed in Table I.

The authors wish to express their deep appreciation to Professor Taro Hayashi and Professor Tatsuo Takeshima for their invaluable discussions. All analyses were performed by Dr. Haruo Homma and the stuff of the Micro Analytical Laboratory in this Institute.

3) H. Yasuda and H. Midorikawa, *J. Org. Chem.*, in printing.

The Synthesis of 3, 6-Bis(α-hydroxyethyl)-2, 5-diketopiperazine

By Tadashiro FUJII and Kenji OKAWA

Department of Chemistry, Faculty of Science, Kwansei Gakuin University, Nishinomiya

(Recieved October 6, 1965)

It is well known that diketopiperazine derivatives of the usual amino acids are readily obtained from the methyl or ethyl ester of the corresponding amino acid.[1] However, there has been no report concerning the synthesis of 3, 6-bis(α-hydroxyethyl)-2, 5-diketopiperazine, although other diketopiperazine derivatives of many hydroxy amino acids have already been synthesized.[2]

The authors obtained 3, 6-bis(α-hydroxyethyl)-2, 5-diketopiperazine from the product of the reaction, and then the catalytic hydrogenation, of carbobenzoxy-L-threonine and dicyclohexylcarbodiimide, it could also be obtained by the thermal condensation of the crystalline L-threonine methyl ester.* The infrared spectra of the products prepared by the two methods were identical, and both exhibited characteristic peaks at 3390 cm^{-1} (OH), 1680 cm^{-1} (amide I) and 1470 cm^{-1} (amide II).

The structure of the product was confirmed by the elemental analysis and molecular weight measurements by the cryosocopic method of Schwyzer.[3]

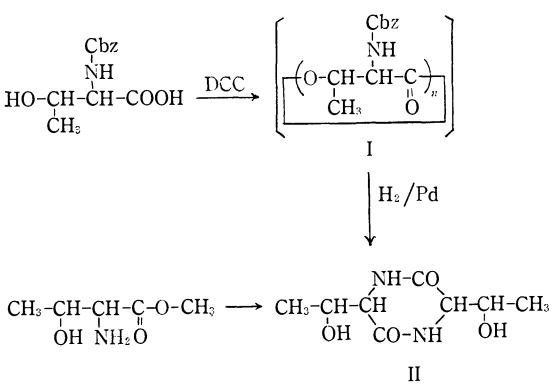

Fig. 1.

Experimental

The Synthesis of the Lacton Derivative (I).—A solution of 10.5 g. (0.054 mol.) of dicyclohexylcarbodiimide in 50 ml. of methylene chloride was added, drop by drop, into a solution of 13 g. of carbobenzoxy-L-threonine in 100 ml. of methylene chloride at room temperature.

After the addition had been completed, the stirring was continued for 1 hr. at room temperature. The reaction mixture was then allowed to stand overnight, the urea produced was filtered off (11.3 g., 100%), and the filtrate was washed with a N sodium bicarbonate solution and water and finally dried over anhydrous sodium sulfate. The filtrate was then concentrated in vacuo to give an oily product (12 g.) (I).

3, 6-Bis(α-hydroxyethyl)-2, 5-diketopiperazine (II).—To a 180 ml. methanol solution of 8 g. of I, 5 g. of palladium-charcoal was added, the mixture was then hydrogenated at room temperature for 5 hr. After the catalyst and the solvent had been removed, the product was dissolved in methanol.

Crystals were gradually separated. The yield was 625 mg. M. p. 254—256°C (decomp.). $[\alpha]_D^{23.5}$ −87.0° (*c* 1.01, water).

Found. C, 47.51; H, 7.09; N, 13.53; Mol. wt., 208.** Calcd. for $C_8H_{14}N_2O_4$: C, 47.56; H, 6.99; N, 13.87%; Mol. wt., 202.

The L-Threonine Methyl Ester.—Into a suspension of 5.95 g. (0.05 mol.) of L-threonine in 60 ml. of absolute methanol, 6.5 g. of thionyl chloride was added, drop by drop, under cooling at about −5°C, the stirring was then continued for 1.5 hr. at room temperature. After the reaction product had been allowed to stand at room temperature for 24 hr., the solvent was removed under reduced pressure at 30°C, an oily product (L-threonine methylester hydrochloride) was thus obtained (8.4 g. (99%)).

Three grams of triethylamine were added, drop by drop, into a solution of 5 g. of the above ester hydrochloride under cooling. After the addition was over, 150 ml. of ether was added to the resulting mixture, and it was stored in a refrigerator for 1 hr. The triethylamine hydrochloride was then filtered off, the solvent was removed, the resulting partly-crystallized oily material was dissolved in a small amount of ether, and the insoluble material was filtered off. The filtrate was then concentrated under reduced pressure until crystals appeared.

From the mother solution, other crops of crystals were obtained. The total yield was 2 g. (32%).

Recrystallization from ether gave 1 g. of fine crystals. M. p. 63—65°C $[\alpha]_D^{23.5}$ −21.0° (*c* 0.999, N HCl).

Found. C, 45.08; H, 8.22; N, 10.75. Calcd. for $C_5H_{11}NO_3$. C, 45.15; H, 8.34; N, 10.53%.

The Synthesis of 3, 6-Bis(α-hydroxyethyl)-2, 5-diketopiperazine (III) from the L-threonine Methyl Ester.—In a small vessel connected with a vacuum system there was placed 316 mg. of a free ester, after

1) J. P. Greenstein, "Chemistry of the Amino Acids," John Wiley & Sons, New York (1961), p. 797.

2) T. Sherdsky, Y. Knobler and Max Franknel, *J. Org. Chem.*, **26**, 1482 (1961).

* No attempts to crystalize this free ester have been made previously.

3) R. Schwyzer and P. Sieber, *Helv. Chim. Acta*, **41**, 2190 (1958).

** The molecular weight was determined by the cryoscopic method of Schwyzer.[3]

the bath temperature had then been gradually raised until the crystals melted (about 75°C), the temperature was kept at 75°C for 3 hr. After cooling, the reaction mixture was dissolved in 3 ml. of methanol and allowed to stand in a refrigerator until crystals appeared. The crystals were then filtered and dried (30 mg.). Recrystallization from methanol gave 21 mg. (12%) of material. M. p. 254—256°C (decomp.). No depression in melting point was observed upon the admixture of II and III.

Found. C, 47.41; H, 7.33; N, 13.64. Calcd: for $C_8H_{14}N_2O_4$. C, 47.56; H, 6.99; N, 13.87%.

The Partial Specific Compressibility of Polyvinylpyrrolidone

By Hiroyasu NOMURA and Yutaka MIYAHARA

Department of Chemical Engineering, Faculty of Engineering, Nagoya University, Chikusa-ku, Nagoya

(Recieved October 18, 1965)

In our previous papers[1-4] it has been shown that, in the study on the solution properties of high polymers, the compressibility of the solution can be used as a valuable parameter. In our treatment, the data of the compressibility of a dilute solution were extrapolated to an infinite dilution to give a quantity which limits the partial specific compressiblity (LC). So far the LC values of such polymers as polyvinyl acetate,[1,2] polystyrene,[3] and dextran[4] have been determined under various conditions. In the organic solvents, the LC was intimately related to the intrinsic viscosity. The LC of dextran in the aqueous solution was negative as a result of the hydration, and the amount of hydration water was estimated from the LC value.

In the present note, the LC of polyvinylpyrrolidone (PVP) was determined at various temperatures by ultrasonic velocity measurements. The details of the experimental procedure have been reported previously.[1,3] The PVP used was a commercial product, PVP K-30, supplied by the Tokyo Kasei (Chemical) Industrial Co., Ltd., the noted molecular weight was 40000. The sample was used without further purification.

TABLE I.

$t°$	$\kappa_1 \times 10^{12}$ cm²/dyn.	$\bar{v}_{20}$ cc./g.	$\bar{\kappa}_{20} \times 10^{12}$ cm²/dyne	ω cc./g.	$[\eta]$ cc./g.
5	49.14	0.783	−18.2	0.458	24.5
15	46.53	0.793	−8.2	0.230	24.5
25	44.84	0.794	−1.1	0.033	24.5
35	43.57	0.806	8.1		21.8
45	42.81	0.808	20.7		23.5
55	42.40	0.821	24.0		25.5

The experimental results are summarized in Table I, where κ_1 is the compressibility of the solvent; $\bar{v}_{20}$, the partial specific volume of the solute at infinite dilution; $\bar{\kappa}_{20}$, the LC; ω, the amount of hydration, and $[\eta]$, the intrinsic viscosity. The methods of the determination of these quantities were given in the previous papers. In the table, it should be noted that the LC increases from a negative value to a positive with the rise in temperature. As was discussed in the previous paper,[4] the negative value of LC can be ascribed to the hydration in the present case. The amount of hydration decreases with the increase in temperature, as in the cases of sucrose[5] and dextran,[4] as a result of the exothermic nature of the hydration process.

It is interesting to see that the value of LC becomes positive above 30°C. The temperature rise breaks the structure of water to some extent, and at the same time it reduces the amount of hydration. Then the behavior of dehydrated bare molecules of PVP becomes similar to that of a synthetic chain polymer, such as polystyrene in an organic solvent, and the LC becomes positive.

The intrinsic viscosities at various temperatures are also listed in the table. It may be seen that the variation in the intrinsic viscosity with the temperature is not so remarkable. This result is in contrast to the linear relationship between the intrinsic viscosity and the LC for the such synthetic chain polymers as polystyrene and polyvinyl acetate in the organic solvents.

1) Y. Miyahara and Y. Masuda, *J. Chem. Soc. Japan, Pure Chem. Sect. (Nippon Kagaku Zasshi)*, **81**, 692 (1960).
2) Y. Masuda, T. Hasegawa and Y. Miyahara, ibid., **82**, 1131 (1961).
3) H. Nomura and Y. Miyahara, *J. Appl. Polymer Sci.*, **8**, 1643 (1964).
4) H. Nomura, S. Yamaguchi and Y. Miyahara, ibid., **8**, 2731 (1964).
5) H. Shiio, *J. Am. Chem. Soc.*, **80**, 70 (1958).

The Calculation of the State Energies of *cis*- and *trans*-Terephthalaldehyde

By Kōzō Inuzuka

Department of Applied Science, Tokyo Electrical Engineering College, Chiyoda-ku, Tokyo

and Toshio Yokota

Tokyo University of Foreign Studies, Nishigahara, Kita-ku, Tokyo

(Received October 20, 1965)

Terephthalaldehyde is a carbonyl derivative of benzaldehyde and its *cis*- and *trans*-forms in solution have been found by Maki[1] by means of ESR experiments.

Since *cis*-terephthalaldehyde has the C_{2v} symmetry, its π-electronic state belongs to the A_1 or B_1 of the C_{2v} symmetry group. Electronic transitions of A_1 and B_1 types have transition moments parallel to the z and x axes respectively.

On the other, *trans*-terephthalaldehyde has the C_{2h} symmetry and its π-electronic state belongs to the irreducible representation, A_g or B_u, of the symmetry group. Electronic transitions from the A_g ground state to the A_g excited states are impossible, but transitions to the B_u excited state are possible. Their transition moments are localized in the molecular plane.

We calculated the state energies for the two isomers by the semiempirical SCF-MO-CI method. The calculated procedure was the same as that used in a previous paper,[2] in which the state energies of benzaldehyde were calculated. The molecular models of *cis*- and *trans*-terephthalaldehydes are shown in Fig. 1, in which the bond angle of C–C=O is assumed to be 120°.

Results and Discussion

The SCF-MOs and MO energies are listed in Table I. In large molecules multiply-excited configurations should make a negligibly small contribution to the lower excitation energies. Therefore, we take account of single excitations only in the present calculation. The configuration

Table I. SCF-MOs and their energies of *cis*-terephthaladehyde (I) and *trans*-terephthalaldehyde (II)

(I)	MO	Sym	$(\chi_1 \pm \chi_{10}$*)	$(\chi_2 \pm \chi_9)$	$(\chi_3 \pm \chi_6)$	$(\chi_4 \pm \chi_5)$	$(\chi_7 \pm \chi_8)$	ε_i, eV.
	1	b_2	0.23522	0.22994	0.39085	0.36480	0.32551	−16.1377
	2	a_2	−0.53149	−0.39424	−0.22251	−0.08270	0.07577	−15.1986
	3	b_2	−0.53837	−0.32042	0.14416	0.21913	0.19670	−14.5752
	4	b_2	−0.00759	0.00637	0.03124	−0.48815	0.51053	−12.4567
	5	a_2	0.27285	0.03923	−0.53202	−0.27160	0.25923	−12.3713
	6	b_2	0.28375	−0.33686	−0.42022	0.24236	0.26587	− 2.1367
	7	a_2	−0.06492	0.09752	0.02813	−0.53373	−0.44789	− 1.0182
	8	a_2	−0.36143	0.54141	0.02278	−0.07749	0.26405	− 0.4924
	9	b_2	0.27250	−0.48057	0.38587	−0.14792	−0.15500	0.6996
	10	a_2	0.09068	−0.20100	0.40760	−0.35849	0.39588	2.4959

(II)	MO	Sym	$(\chi_1 \pm \chi_{10}$**)	$(\chi_2 \pm \chi_9)$	$(\chi_3 \pm \chi_6)$	$(\chi_4 \pm \chi_7)$	$(\chi_5 \pm \chi_8)$	ε_i, eV.
	1	a_u	0.23700	0.23089	0.39093	0.35030	0.33910	−16.1380
	2	b_g	−0.53195	−0.39376	−0.22194	−0.08932	0.06883	−15.2072
	3	a_u	−0.53803	−0.31909	0.14595	0.21053	0.20755	−14.5834
	4	b_g	−0.12466	−0.02692	0.22092	0.56903	0.33338	−12.4904
	5	b_g	0.24247	0.02981	−0.48449	−0.02269	0.45285	−12.3486
	6	a_u	0.28233	−0.33625	−0.41978	0.29191	0.21401	− 2.1527
	7	a_u	−0.02610	0.02992	0.02374	0.47582	−0.52102	− 0.9905
	8	b_g	−0.36664	0.55020	0.02765	−0.17113	0.18110	− 0.5149
	9	a_u	0.27196	−0.48054	0.38613	−0.14613	−0.15708	0.6953
	10	b_g	0.09091	−0.20152	0.40798	−0.37206	0.38243	0.4890

* Double signs ± mean $\chi_1+\chi_{10}$ for symmetry b_2 and $\chi_1-\chi_{10}$ for a_2.
** $\chi_1+\chi_{10}$ for symmetry a_u and $\chi_1-\chi_{10}$ for b_g.

1) A. H. Maki, *J. Chem. Phys.*, **35**, 761 (1961).

2) K. Inuzuka and T. Yokota, This Bulletin, **38**, 1055 (1965).

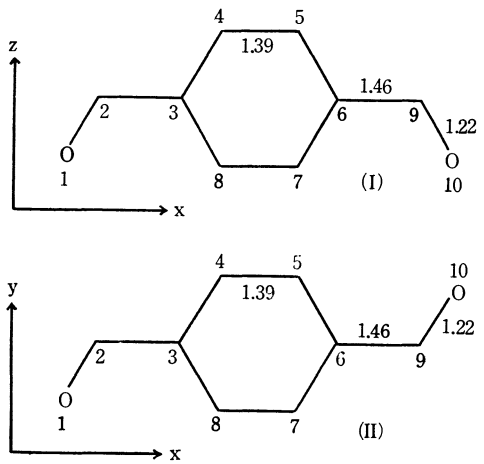

Fig. 1. Molecular models of *cis*- and *trans*-terephthalaldehydes (I and II).

mixing for *cis*-terephthalaldehyde leads to two 12th-order secular equations for the $^1A_1$ and $^3A_1$ states, and to two 13th-order secular equations for the $^1B_1$ and $^3B_1$ states. For *trans*-terephthalaldehyde, configuration mixing leads to two 12th-order secular equations for ^1A_g and ^3A_g states and to two 13th-order secular equations for ^1B_u and ^3B_u states. The state energies and wave functions are obtained from the solutions of these secular equations. The lower-lying state energies and oscillator strengths are listed in Table II.

Table II. Calculated energy levels of terephthalaldehyde

	cis			*trans*			Obs.
	State	E, eV.	f	State	E, eV.	f	eV.
G	$^1A_1$	0		^1A_g	0		0
1	$^1A_1$	4.657	0.017	^1B_u	4.645	0.040	4.05
2	$^1B_1$	4.859	0.165	^1B_u	4.868	0.164	4.68
3	$^1B_1$	6.269	1.15	^1B_u	6.250	0.963	6.13
4	$^1A_1$	6.429	0.033	^1A_g	6.540	0	
5	$^1A_1$	6.823	0.704	^1B_u	6.736	0.962	
1	$^3B_1$	3.145		^3B_u	3.143		
2	$^3A_1$	3.845		^3A_g	3.856		
3	$^3B_1$	3.948		^3B_u	3.928		
4	$^3A_1$	4.029		^3B_u	4.042		

We observed terephthalaldehyde to have three π-π^* absorption bands, at about 300, 260 and 200 mμ, in an *n*-hexane solution. The energy values corresponding to these absorption bands are also listed in Table II. The calculated values are in agreement with the observed values. From Table II we can not find any significant difference in state energies between the *cis*-isomer and the *trans*-isomer, but the 1st excited energy of the *trans*-isomer is lower than that of the *cis*-isomer. The values of the Coulomb integral are almost invariant over a great atomic distance. The change in the position of the carbonyl group from the *trans*-form to the *cis*-form does not have any appreciable effect on the molecular integral, because the distance between carbonyl groups is large. The similarity in electronic structure of *cis*- and *trans*-terephthalaldehydes is attributed to the above fact. The absorption spectrum of terephthalaldehyde resembles that of benzaldehyde. The spectrum of the former shifts to a longer wavelength side than that of the latter. The similarity in absorption spectra can be seen in the transition energies and oscillator strengths obtained for benzaldehyde[2,3] and for terephthalaldehyde. The charge densities and the free valences of both isomers for the ground and lower excited states are listed in Table III. These values of the excited states are calculated by assuming the same molecular structures as in the ground state. The charge densities of the position 4 of *cis*- and *trans*-terephthalaldehydes indicate a high reactivity to electrophilic reagents.

The present study was partially financed by the Scientific Research Fund of the Ministry of Education.

Table III. Charge densities (q_i) and free valences (f_i) of *cis*-terephthalaldehyde (I) and *trans*-terephthalaldehyde (II) in the ground and lower excited states

	State		q_1	q_2	q_3	q_4	q_7	f_2	f_3	f_4	f_7
(I)	$^1A_1$	G	1.404	0.625	1.101	1.000	0.957	0.617	0.214	0.411	0.415
	$^1A_1$	1	1.431	0.707	1.036	0.951	0.875	0.605	0.360	0.710	0.711
	$^1B_1$	2	1.405	0.716	0.939	0.997	0.943	0.598	0.463	0.627	0.618
	$^1B_1$	3	1.381	0.684	0.989	1.019	0.926	0.677	0.339	0.759	0.733
(II)	State		q_1	q_2	q_3	q_4	q_7	f_2	f_3	f_4	f_7
	^1A_g	G	1.406	0.624	1.014	0.999	0.958	0.618	0.215	0.412	0.413
	^1B_u	1	1.420	0.705	0.991	0.969	0.915	0.601	0.407	0.677	0.674
	^1B_u	2	1.415	0.706	0.979	0.995	0.905	0.599	0.418	0.649	0.678
	^1B_u	3	1.372	0.676	0.978	0.960	1.014	0.680	0.347	0.768	0.707

3) K. Inuzuka and T. Yokota, ibid., **37**, 1224 (1964).

Some Rheological Properties of Sodium Polyacrylate Solutions

By Shiro KUROIWA and Matao NAKAMURA

Institute of Industrial Science, The University of Tokyo, Azabu, Tokyo

(Received October 20, 1965)

The viscoelastic properties of aqueous solutions of sodium polyacrylate (degree of polymerization= 45000) were studied. It seems that the results described below reveal some characteristics of the polyelectrolyte studied.

The dynamic rigidity and viscosity (G', η') and the steady flow viscosity (η_a) were measured by a coaxial double cylinder rheometer,*1 in which the outer cylinder was driven to oscillate or revolve. G' and η' were calculated by the method described by Markovitz.[1] η_a is the apparent viscosity, assuming the Newtonian flow.

For a comparison of G' with the rigidity G, calculated from the elastic recovery following a steady flow,*2 the data reported in a previous paper were used.[2]

The experimental results are illustrated in Figs. 1 and 2. In Fig. 1, the vertical shifts along the log G' axis for the superposition of log G' — log ω curves of varied concentrations were not proportional to (C_0/C), but to $(C_0/C)^{1.2}$, as may be seen in Fig. 3. C is the concentration, and the subscript refers to the reference concentration. Therefore, Ferry's reduced variables,[3] G_r', η_r'

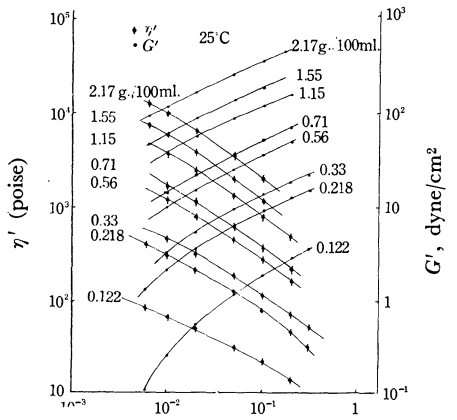

Fig. 1. Dependence of η' and G' on ω and concentration.

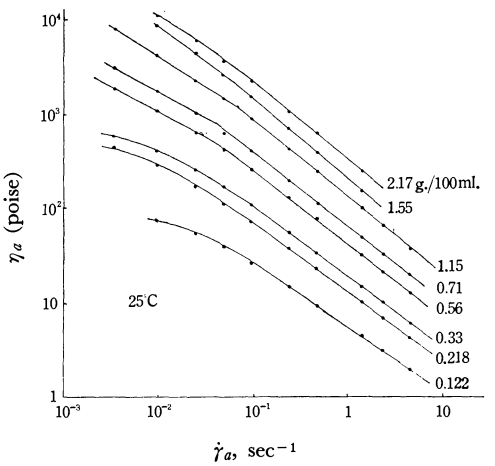

Fig. 2. Dependence of η_a on $\dot{\gamma}_a$ and concentration.

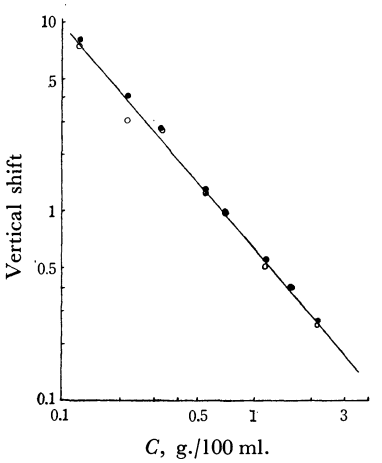

Fig. 3. Relation between vertical shift and concentration for the superposition of log G' vs. ω plotts.
○ Graphical procedure
● $(C_0/C)^{1.2}$ (calc. value)

and ω_r, for the concentration were modified as follows at a costant temperature:

$$G'_r = G'(C_0/C)^{1.2} \quad (1)$$

$$\eta'_r = \eta'(\eta_0/\eta) \quad (2)$$

$$\omega_r = \omega(\eta/\eta_0)(C_0/C)^{1.2} \quad (3)$$

η indicates the zero shear viscosity. η/η_0 as a

*1 Rheometer Almighty, manufactured by the Iwamoto Seisakusho Co. Ltd.

*2 Appendix

1) H. Markovitz, *J. Appl. Phys.*, **23**, 1070 (1952).
2) S. Kuroiwa and M. Nakamura, *Chem. High Polymer*, **22**, 385 (1965).
3) J. D. Ferry, *J. Am. Chem. Soc.*, **72**, 1102 (1950).

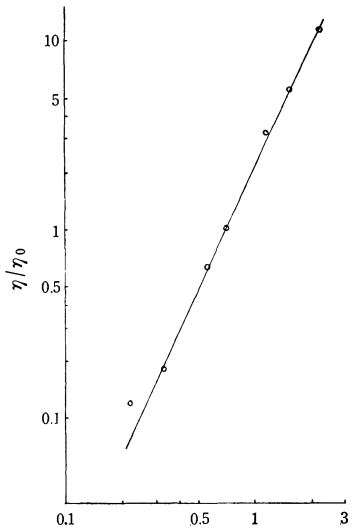

Fig. 4. Relation between η/η_0 and concentration.

function of C was determined from $(C_0/C)^{1.2}$ and the horizontal shifts along the log ω axis by means of Eq. 3. A linear relation between log η/η_0 and log C was obtained, as is illustrated in Fig. 4.

Reduced variables for η_a and $\dot{\gamma}_a$ (the average shearing rate) were defined as:

$$\eta_{ar} = \eta_a(\eta/\eta_0) \tag{4}$$

$$\dot{\gamma}_{ar} = \dot{\gamma}_a(\eta/\eta_0)(C_0/C)^{1.2} \tag{5}$$

Master curves reduced to 0.71 g./100 ml. are represented by Figs. 5 and 6. In Fig. 6, η_{ar} shows a small fluctuation, but it seems to be within the range of experimental error. It may be observed in Fig. 6 the difference between η_{ar} and η'_r becomes obvious with an increase in $\dot{\gamma}_{ar}$ or ω_r, as have been described by several authors for various polymer systems.[4-8] However, the concentration dependence of the zero shear viscosity seems to be very small compared with that of usual polymers, i e. $\eta/\eta_0 \propto C^2$. In the concentration range (0.25—1.5 g./100 ml.) studied, products of the chain length, Z, and the volume fraction of the solute, v, were calculated as 230—1400. The critical value of Zv, i. e., $Z_c v_c$, is known to be about 200—1400 in usual polymers.[9] The $Z_c v_c$ value for aqueous solutions of polyacrylic acid had been reported as 130.[10] Further, the η of the sample may be expected from Fig. 2 to be larger than 10^2 poise. Usually, under such conditions, the η values of many polymer solutions depend on C^{5-6}.[7,11-14] For example, Fukada reported that the η/η_0 values of aqueous collagen solutions in a concentration range similar to that of this study depend on C^6,

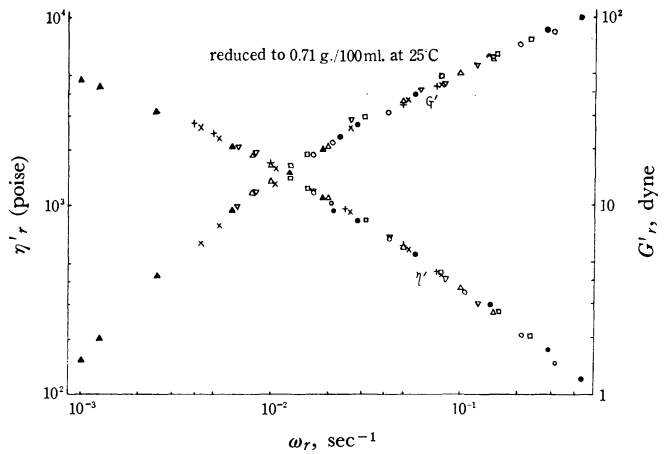

Fig. 5. Results of superposition, using modified shift factors.

●	2.17 g./100 ml.	○	1.55 g./100 ml.
□	1.15 g./100 ml.	△	0.71 g./100 ml.
▽	0.56 g./100 ml.	×	0.33 g./100 ml.
+	0.218 g./100 ml.	▲	0.122 g./100 ml.

4) T. W. Dewitt, H. Markovitz, E. D. Padden and J. Zapas, *J. Colloid Sci.*, **10**, 174 (1955).
5) H. Markovitz and B. Williamson, *Trans. Soc. Rheol.*, **1**, 25 (1965).
6) W. Philippoff, *J. Appl. Phys.*, **25**, 1102 (1954).
7) S. Onogi, I. Hamana and H. Hirai, ibid., **29**, 1503 (1958).
8) T. Arai, *Chem. High Polymer*, **18**, 292 (1961).
9) T. G. Fox and S. Gratch S. Loshaek, "Rheology, 1," Ed. by Eirich, Acad. Press, New York (1965).
10) J. G. Brodnyan and E. L. Kelly, *Trans. Soc. Rheol.*, **7**, 125 (1963).
11) R. F. Landel, J. W. Berg and J. D. Ferry, *J. Colloid Sci.*, **12**, 400 (1957).
12) J. D. Ferry, ibid., **7**, 498 (1951).
13) D. J. Plazek and J. D. Ferry, ibid., **8**, 592 (1953).
14) E. Fukada and M. Data, *Kobunshi*, **11**, 1284 (1964).

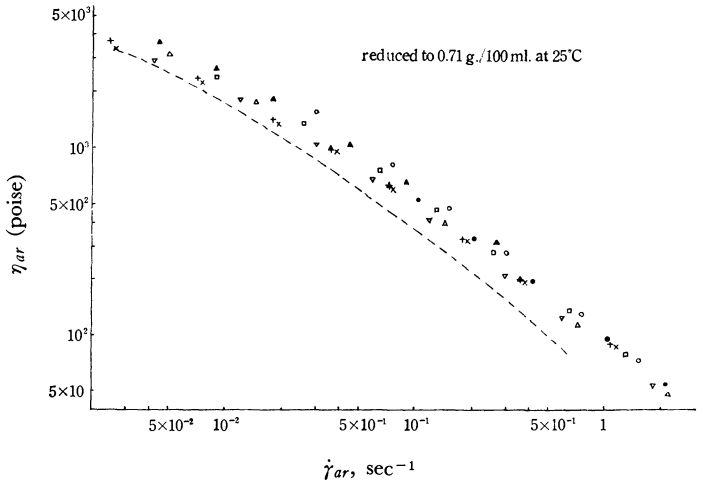

Fig. 6. Result of superposition, using modified shift factors.
● 2.17 g./100 ml. ○ 1.55 g./100 ml.
□ 1.15 g./100 ml. △ 0.71 g./100 ml.
▽ 0.56 g./100 ml. × 0.33 g./100 ml.
+ 0.218 g./100 ml. ▼ 0.122 g./100 ml.
---- η'

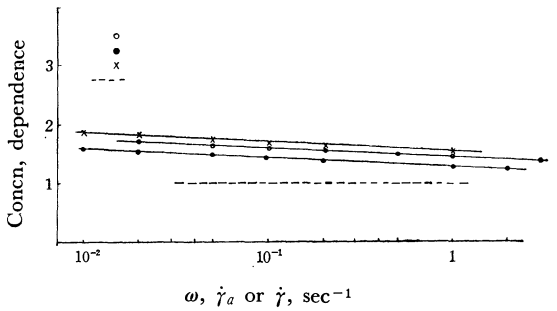

Fig. 7. Variation of concentration dependencies of η', G', η_a and G with ω, $\dot{\gamma}_a$ and $\dot{\gamma}$, respectively.
○ $\eta_a \sim \dot{\gamma}_a$ ● $\eta' \sim \omega$
× $G' \sim \omega$ ---- $G \sim \dot{\gamma}$

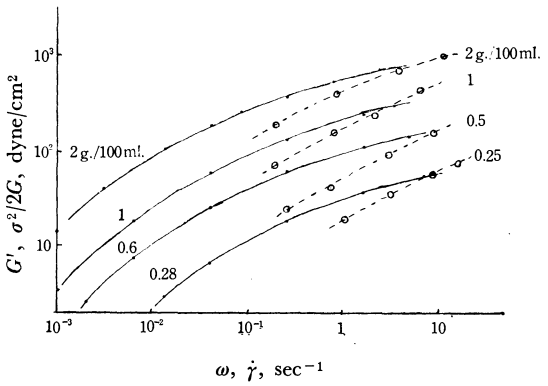

Fig. 8. Comparison of $\sigma^2/2G$ with G'.
● G' ○ $\sigma^2/2G$

where a procedure analogous to that used in this study was employed for evaluating η/η_0.[14]

Accordingly, it may be said that the nature of the molecular interactions of the polyelectrolyte studied here is remarkably different from that of other polymers. In other words, some mechanisms other than the so-called Bueche entanglements[12,15] may dominate the viscosity of the solutions, in spite of their high Zv and η values. The extraordinarily anomalous non-linearity of flow and the very large recoverable strain of the sample[2] can probably be interpreted by means of this abnormal intermolecular mechanism.

When $\log G'$, $\log \eta'$, $\log \eta_a$ and $\log G$ were plotted against $\log C$ at fixed ω, $\dot{\gamma}_a$ and $\dot{\gamma}$ (true shearing rate) values respectively, straight lines were obtained. The slopes of these lines were estimated; they are plotted against ω, $\dot{\gamma}_a$ and $\dot{\gamma}$ respectively in Fig. 7. In this figure the concentration dependence of η_a seems to be extrapolated to about 2, whereupon $\dot{\gamma}_a$ becomes small. This is in agreement with the relation, $\eta/\eta_0 \propto C^2$, described above.

In Fig. 8, $\log G'$ is compared with $\log(\sigma^2/2G)$, where ω and $\dot{\gamma}$ are assumed to be equivalent. σ is the shearing stress. $\sigma^2/2G$ may be equal to $(P_{11}-P_{22})/2$, in which $P_{11}-P_{22}$ is the normal stress in rheogoniometry. According to the theory of Coleman et al.,[16] $(P_{11}-P_{22})/2$ as a function of the shearing rate must approach G' as a function of ω, when shearing rate of ω becomes small. This theory was confirmed by Kotaka et al. to hold for polystyrene solutions.[17] In Fig. 8, however, there

15) F. Bueche, *J. Chem. Phys.*, **22**, 603 (1954).
16) B. D. Coleman and H. Markovitz, *J. Appl. Phys.*, **35**, 1 (1954).
17) T. Kotaka and K. Osaki, *Bull. Insi. Chem. Res. Kyoto Univ.*, **39**, 331 (1962).

seems to be no tendency for G' and $\sigma^2/2G$ to approach each other when ω or $\dot{\gamma}$ becomes small. The reason for this is not clear. However, it is not inconceivable that the discrepancy between the theoretical and the experimental results comes from some thixotropic characteristic of the substance.

Appendix

$$G = \sigma_i S_i = \sigma_i \Big/ \left\{ \frac{2n\theta_e}{1+(R_i/R_0)^{2n}} \right\}$$

S_i; Recoverable strain at the inner cylinder surface
θ_e; Angular displacement of the inner cylinder following steady flow
σ_i; Shearing stress at the inner cylinder surface
R_i; Inner cylinder radius
R_0; Outer cylinder radius
n; Slope of the $\log \theta_e$ - $\log \sigma_i$ plot

The Bromination of 1, 1, 3, 3-Tetracyanopropane*

By Akimasa TANIGUCHI, Kojiro SUZUKI and Hiroshi MIKAWA

Institute of Scientific and Industrial Research, Osaka University, Sakai, Osaka

(Received November 1, 1965)

Two compounds were obtained by the bromination of 1,1,3,3-tetracyanopropane[1] (I) in the presence of pyridine.

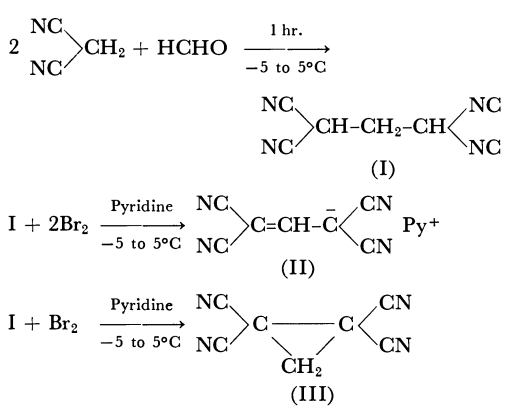

When I was brought into reaction with two moles of bromine, a white crystalline solid (II) melting at 157—159°C was obtained. II was pyridinium-1, 1, 3, 3-tetracyanopropenide. The sodium salt of the same compound has been reported by Urushibara.[2]

When I was brought into reaction with one mole of bromine, a white crystalline solid (III) was obtained, it melted at 224°C and sublimed at 150—180°C under diminished pressure. Its properties and melting point agree with those for 1, 1, 2, 2-tetracyanocyclopropane reported by Scribner et al.[3]

Thus, the reaction gave quite different products when the mole numbers of bromine were changed.

The mechanism of the reaction may be supposed to be as follows:

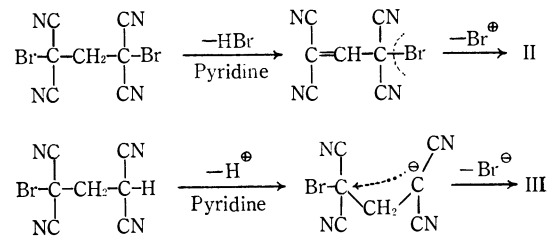

It is known that the active methylene is readily brominated by bromine in the presence of pyridine. In the case of the reaction using two moles of bromine, both active hydrogens are replaced by bromine and bromotetracyanopropene is formed by the elimination of hydrogen bromide. A cation of bromine is liberated from the propane to give tetracyanopropenide anion (II). It was recoginized by Trofimenko et al.[4] that the bromocation was produced from bromotricyanomethane.

On the other hand, when one mole of bromine is used, the first step is the replacement o one of the active hydrogens of I by bromine, and then the another active hydrogen is eliminated by pyridine. The cyclopropane ring is formed by an intramolecular condensation.

This reaction provides an excellent route for the preparation of III.

Experimental

Pyridinium-1, 1, 3, 3-tetracyanopropenide (II).— Four grams (0.028 mol.) of 1, 1, 3, 3-tetracyanopropane, 10 g. (0.0625 mol.) of bromine and 38 ml. of acetonitrile

* Presented at the 18 th Annual Meeting of the Chemical Society of Japan, Osaka, April, 1965.

1) O. Diels, H. Gartner and R. Kaack, *Ber.*, **45**, 3445 (1912).

2) Y. Urushibara, This Bulletin, **2**, 2798 (1927).

3) R. M. Scribner, G. N. Sausen and W. W. Princhard, *J. Org. Chem.*, **25**, 1440 (1960).

4) S. Trofimenko, E. L. Little and H. F. Mower, ibid., **27**, 433 (1962).

were mixed at −5°C and then 9.0 g. (0.114 mol.) of pyridine was added over a period of 10 min. The mixture was stirred at 0°C for two hours until the red-orange solution became colorless; then the solution was poured into a mixture of 20 ml. of concentrated hydrochloric acid and 40 g. of crushed ice. The solution was concentrated at low temperature in vacuo and the white solid which was precipitated out from the solution was collected and washed with a mixture of cold water, alcohol and petroleum ether, and dried in a vacuum desiccator. It was then recrystallized from tetrahydrofurane to give 1.2 g. (34.3%) of white crystalls, m. p. 157—159°C.

Found: C, 64.98; H, 3.76; N, 31.76. Calcd. for $C_{11}H_7N_5$: C, 65.1; H, 5.78; N, 31.70%.

IR: 4.55 (CN), 6.14, 6.24, 6.38, 6.55, 6.75, 7.45, 8.10, 9.55, 10.6, 11.2, 12.3, 13.5 μ.

1,1,2,2-Tetracyanocyclopropane (III).—Ten grams (0.07 mol.) of 1, 1, 2, 2-tetracyanopropane, 12.5 g. (0.78 mol.) of bromine and 100 ml. of acetonitrile were mixed at 0.°C and then 11.3 g. (0.143 mol.) of pyridine was added over a period of 15 min. When the mixture was stirred at 0°C for an hour, it lost its red-orange color. The solution was then poured into a mixture of 30 ml. of concentrated hydrochloric acid and 60 g. of crushed ice. After an hour, a white solid separated from the solution. The product was collected and washed with a mixture of cold water, alcohol and petroleum ether, and dried in a vacuum desiccator. It was crystallized from ethyl acetate to give 7.5 g. (76.0%) of white crystals, m. p. 220—224°C. It sublimed at about 150°C (1 mmHg).

Found: C, 59.16; H, 1.42; N, 39.42. Calcd. for $C_7H_2N_4$: C, 58.62; H, 1.78; N, 39.42%.

IR: 3.23, 3.32, 4.43(CN), 6.90, 7.01, 8.25, 9.07, 9.88, 13.8 μ.

The authors wish to thank Mr. Takuzo Fujino and Mr. Tsuneyo Shishido for their elementary analyses.

Fluorescence Spectra of Acridine-Mercuric Halide Complexes

By Michio KONDO and Harumitsu KUWANO

Central Research Laboratories, Sankyo Co., Ltd, Shinagawa-ku, Tokyo

(Received November 13, 1965)

It has been reported that acridine is non-fluorescent in the solid state and in nonpolar solvents such as hexane and benzene.[1] In polar solvents such as alcohol and water capable of forming hydrogen bonds, acridine emits a blue fluorescence.[1,2] The radiationless deactivation of an excited molecule of acridine has been ascribed to interaction between n- and π-electrons.[2] In polar solvents, an excited molecule of acridine combines rapidly with the nearest OH group of a solvent molecule. Such a hydrogen-bonded molecule may be considered to be a fluorescent species, since the formation of hydrogen bonds in the excited state results in a decrease in the n—π interaction.[1,2] Acridinium ions emit a green fluorescence in various solvents[1] as well as in the solid state. This fact also supports the interpretation that the non-radiative degradation of acridine in the excited state is due to the n—π interaction.

Matsushita[3] examined the emission spectra of a number of benzylideneamine and salicylideneamine derivatives. He showed that the formation of intramolecular hydrogen bonds intensifies the emissivity of fluorescence because of the diminution of the n-electron contributions to the non-radiative degradation of the excited state.

Acridine forms crystalline molecular complexes with some inorganic compounds.[4] If the n-electrons at the nitrogen atom of acridine are involved in the formation of these molecular complexes, it is to be expected that the n—π interaction in the excited state will be reduced to a great extent and that the fluorescence emission will be enhanced.

Experimental

Materials.—Acridine and mercuric halides were purified by sublimation or recrystallization. An acetone solution of acridine was added to an acetone solution of an appropriate mercuric halide in order to prepare the molecular complexes.

Fluorescence Measurements.—The fluorescence spectra of the molecular complexes were recorded with a Shimadzu model SV-50 AL spectrophotometer equipped with an accessory for measuring the fluorescence spectra of solid samples.

Results and Discussion

Acridine-mercuric halide (1 : 1) complexes emit a green fluorescence in the solid state. Table I shows the results obtained under illumination with

1) E. J. Bowen, N. J. Holder and G. B. Woodger, *J. Phys. Chem.*, **66**, 2491 (1962).
2) N. Mataga and S. Tsuno, This Bulletin, **30**, 368 (1957).
3) S. Matsushita, *J. Chem. Soc. Japan, Pure Chem. Sect. (Nippon Kagaku Zasshi)*, **84**, 373 (1963).
4) a) H. Buss, H. W. Kohlschuetter and D. Maulbecker, *Z. Naturforsch.*, **18b**, 417 (1963); b) W. Ludwig and G. Wittmann, *Helv. Chim. Acta*, **47**, 1265 (1964).

Table I. Fluorescence spectra and photoconductivities of acridine-mercuric halide complexes

Compound	Emission max., mμ*	Relative intensity	Photo-conductivity	Analysis N Calcd.	Analysis N Obsd.
Acridine·HCl	491, 512(s)	100, 86	—	—	—
Acridine·$HgCl_2$	505	50	—	3.11	3.27
Acridine·$HgBr_2$	492	20	—	2.60	2.59
Acridine·HgI_2	500	2	—	2.21	2.35

* Corrections due to photomultiplier sensitivity were not carried out. (s) means a "shoulder."

a light of $\lambda=350$ mμ. It should be noted that the intensity of emission depends markedly on the kind of halogen ions, while fluorescence maxima are located at nearly the same wavelengths. The small variation in the peak position is probably due to a small change in the interaction between acridine and mercuric halides. The decrease in the fluorescence intensity of complexes with the increase in the atomic weight of the halogen ions may be attributed to the spin-orbit coupling which is generally considered to be a mechanism promoting the radiationless deactivation of excited molecules.

It is of interest, in this connection, to note that mercury atoms, in spite of their heavy atomic weight, do not strongly promote the spin-orbit coupling in diminishing the emission. This fact suggests that the mercury atoms may be located in the molecular plane of acridine, because the π-orbitals have their nodal planes on the molecular plane of acridine and, therefore, the spin-orbit interaction might be small. As judged from the efficiency of the spin-orbit coupling of the halogen ions, the mercuric halide molecules may be oriented perpendicular to the molecular plane of acridine, and the spin-orbit coupling between the nearest neighbor complex molecules may contribute to the diminution of emission. The square planar configuration about the metal atom was pointed out for NiI_2-(Acridine)$_2$ in the solid state.[4b]

The present authors examined the absorption spectra of two kinds of films of acridine-mercuric halides, one of which was prepared by the sublimation of an appropriate mercuric halide onto a presublimated film of acridine, while the other was prepared by the sublimation of acridine-mercuric halide complexes. The latter gave better results except for the case of acridine-mercuric iodide. Acridine hydrochloride yielded no good results, probably because it decomposes by losing hydrogen chloride. These complexes show broad absorption bands very similar to those of acridinium cations in solution with structures over the range of 350—440 mμ. From the similarity observed in the absorption and the fluorescence spectra, it may be considered that the electronic structure of the acridine part in the complexes is essentially the same as that of the acridinium cation. Thus, it may be concluded that the *n*-electrons at the nitrogen atom of acridine are partially transferred to the mercury atom, affording an intermolecular binding force.

Good photoconductive materials can be found among luminescent species.[5] In fact, anthracene is a representative photoconductive material in organic compounds, whereas acridine shows no good photoconductive property. From this point of view, the photoconductivity of these complexes was measured in a surface cell consisting of a polycrystalline pellet pressed under 1 kbar and two gold electrodes spattered onto the same surface of the pellet with a narrow gap of 1 mm. No positive results were obtained. In aromatic hydrocarbons, the photocarrier generation process in the crystal absorption region has been discussed in terms of the dissociation of singlet excitons on the crystal surface, but the idea that the photocarrier generation originates in exciton-exciton annihilation can not be eliminated.[6] In any case, the energy transfer of excitons produced by light absorption is essentially required for generating carriers. In the present case, acridine molecules seem to be separated from one another by intervening mercuric halide molecules. This weakens the overlap between the π-orbitals of the nearest neighbor acridine molecules to the extent that the exciton transfer is impossible. Therefore, no photocurrents were observed.

5) M. Kleinerman, L. Azarraga and S. P. McGlnny, *J. Chem. Phys.*, **37**, 1825 (1962).

6) P. J. Reucroft, O. N. Rudyj, R. E. Salomon and M. M. Labes, ibid., **43**, 767 (1965), and references therein.

The Preparation and Properties of Dipotassium Bis(glycylglycinato)cuprate(II)

By Yasuo NAKAO, Ken-ichi SAKURAI and Akitsugu NAKAHARA

Institute of Chemistry, College of General Education, Osaka University, Toyonaka, Osaka

(Received November 18, 1965)

In a previous communication[1] we reported the preparation of dipotassium bis(diketopiperazinato)-cuprate(II). The investigation was, there after, continued in an attempt to obtain more detailed information on the structure of that novel compound; contrary to our expectations, we reached the conclusion that the complex we had isolated before was bis(glycylglycinato)cuprate(II) instead of bis(diketopiperazinato)cuprate(II). Our results do, however, seem worth reporting because the isolation of dipotassium bis(glycylglycinato)cuprate(II) is still new, and it does contribute to the knowledge in this field. In fact, all the papers previously published dealing with the bis(glycylglycinato)cuprate(II) complex were concerned only with the complex formation in solution.[2] The purpose of the present paper is not only to rectify the erroneous conclusion in the previous communication, but also to describe the preparation and properties of the dipotassium bis(glycylglycinato)cuprate(II).

Experimental

Dipotassium Bis(glycylglycinato)cuprate(II).—A mixture of 11.4 g. (0.1 mol.) of diketopiperazine and 8.4 g. (0.15 mol.) of potassium hydroxide was dissolved in 150 ml. of water. To the solution there was added about 4 g. of freshly precipitated cupric oxide with a rapid agitation at about 25°C. Though the solution had been red-purple at the beginning of the reaction, it gradually became blue-purple. The reaction was completed within a few hours. After it had been filtered, the solution was evaporated to dryness in vacuo to give a red-purple, crystalline product. The product was repeatedly recrystallized from water by adding a large amount of acetone. The same compound was also prepared, employing the same procedure, from glycylglycine instead of diketopiperazine.

Although the thoroughly-purified crystal is fairly stable in a dry atmosphere, it is quite unstable to moisture; hence, it is impossible to obtain a red-purple aqueous solution without the coexistence of a large quantity of glycylglycinate ions. M. p. 113—120°C (decomp.). The results of the elemental analysis of the non-dehydrated crystal were as follows:

Found: K, 15.66; Cu, 12.75; C, 19.08; H, 5.00; N, 10.96; H_2O, 22.6. Calcd. for $K_2[Cu(C_4H_6N_2O_3)_2]\cdot 6H_2O$: K, 15.31; Cu, 12.43; C, 18.83; H, 4.71; N, 10.98; H_2O, 21.2%.

On the other hand, the results of the analysis of a completely dehydrated crystal were as follows:

Found: C, 24.12; H, 3.22; N, 13.15. Calcd. for $K_2[Cu(C_4H_6N_2O_3)_2]$: C, 23.88; H, 2.94; N, 13.90%.

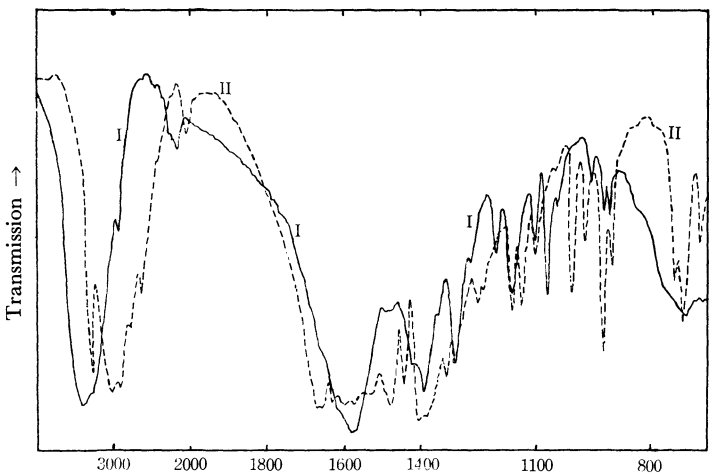

Fig. 1. Infrared absorption spectra of: I, dipotassium bis(glycylglycinato)cuprate(II); II, glycylglycine.

1) A. Nakahara, K. Sakurai, K. Suzuki and Y. Nakao, This Bulletin, **38**, 1051 (1965).

2) H. Dobbie and W. O. Kermack, *Biochem. J.*, **59**, 246 (1955); S. P. Datta and B. R. Rabin, *Trans. Faraday Soc.*, **52**, 1117 (1956); F. R. N. Gurd and P. E. Wilcox, "Advances in Protein Chemistry," Academic Press, New York (1956), p. 311; W. L. Koltun, R. H. Roth and F. R. N. Gurd, *J. Biol. Chem.*, **238**, 124 (1963).

Diketopiperazine (2, 5-Piperazinedione) was prepared according to the directions of Sannié,[3] while in preparing glycylglycine we applied the method of Fischer et al.[4]

Measurements.—The infrared spectra were obtained by a Hitachi EPI-2 Infrared Spectrophotometer. The measurements were made at room temperature using the pressed potassium bromide disk technique in the wave number range from 700 to 4000 cm^{-1} with a rock-salt prism. The spectra are shown in Fig. 1.

The visible and ultraviolet spectra were obtained with a Shimadzu Spectrophotometer, Type QB-50. Since the bis(glycylglycinato)cuprate(II) complex was readily dissociated in an aqueous solution, a solution containing 1F of potassium glycylglycinate was employed as the solvent.

The concentration of the complex used varied from 10^{-2} to 10^{-3}F. The spectra are shown in Fig. 2.

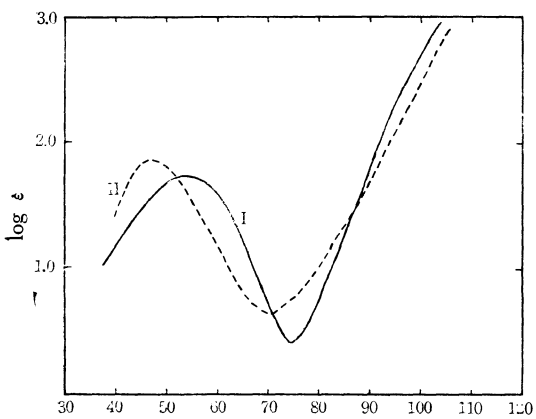

Fig. 2. Visible and ultraviolet absorption spectra of I, dipotassium bis-(glycylglycinato)cuprate(II) in water solution containing 1F of glycylglycine and 2F of potassium hydroxide; II, the same complex in water.

Results and Discussion

It will, first of all, be necessary to correct our previous communication, which reported the successful preparation of bis(diketopiperazinato)-cuprate(II). The diketopiperazinatocuprate(II) structure was finally negated by the following two facts. First, it has been disclosed that the complex derived from glycylglycine is identical with that derived from diketopiperazine. Second, it has also been found that the results of the elemental analysis of the perfectly dehydrated complex eliminate the possibility of diketopiperazinato-cuprate(II) structure. The second fact may be supposed to be particularly important because the analytical values of the constituent elements in the non-dehydrated complex are expected to be same (except for the value of the water of crystallization) in the case of either the octahydrate of diketopiperazinatocuprate(II) or the hexahydrate of bis(glycylglycinato)cuprate(II). Thus, we may conclude that the complex prepared from the reaction between a mixture of potassium hydroxide and diketopiperazine and cupric oxide is not diketopiperazinatocuprate(II) but the bis(glycylglycinato)cuprate(II) complex.

The formation of this complex in solution has been investigated by several chemists.[2] They have presented a structure in which copper(II) links to the glycylglycinate anion only through the terminal amino group and the nitrogen of the peptide linkage. In other words, the carboxylate group is not involved in the coordination. The present work strongly supports the above proposal, giving more evidence for the structure I.

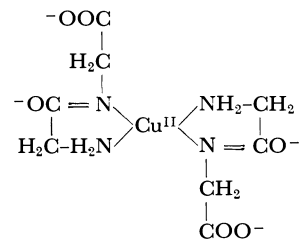

Structure I. The Bis(glycylglycinato)cuprate(II) Ion.

For example, all the four donor atoms (apart from the further coordination sites of copper(II)) are apparently nitrogen, judging from the color of the crystal and the location of the ligand field absorption band of the complex in solution, as is clear from Fig. 2. Indeed, the absorption maximum of the complex in the presence of an excess of glycylglycinate ions, 54×10^{13} sec^{-1}, nearly coincides with that of bis(ethylenediamine)copper(II), suggesting its $Cu(N)_4$-type structure.

The proposal that the carboxylate group is not involved in the coordination can also reasonably be accepted, since there is estimated to be a considerable strain in the structure which contains the additional links of the carboxylate oxygens to the $Cu(N)_4$-type planar complex. As to the geometrical isomerism, the trans configuration, which has been suggested by Gurd and Wilcox,[2] is positively supported, because X-ray study* has recently shown that there is a center of symmetry in the complex.

The complex is readily dissociated in water, without the aid of a large quantity of glycylglycinate ions, to give a blue solution which may be considered to correspond to a $Cu(N)_3(O)_1$- or $Cu(N)_2(O)_2$-type structure.[5] This may be seen as the result of a displacement of peptide nitrogen in the coordination by water molecules. Indeed, the absorption

3) C. Sannié, *Bull. Soc. Chim. France*, **9**, 487 (1942).
4) E. Fischer and E. Fourneau, *Ber.*, **34**, 2868 (1901).

* Private communication from Dr. Yoshio Sasada of the Institute for Protein Research, Osaka University.
5) A. Nakahara, This Bulletin, **32**, 1195 (1959).

maximum of the complex alone in water appears in the region of considerably longer wavelengths, as is shown in Fig. 2, suggesting the validity of the above consideration.

Thus, the hygroscopic nature of this particular complex crystal does not imply the simple dissolution of the complex in the absorbed water, but it does imply the partial dissociation of the complex in the absorbed water. On the other hand, the water molecules which displaced the peptide nitrogen from the coordination sites can be expelled by a large amount of acetone to give the $Cu(N)_4$-type structure again. The recrystallization of the present complex using water and acetone may proceed by means of such a mechanism.

Summary

The previous conclusion has been corrected as follows. The complex prepared from the reaction of cupric oxide with a mixture of potassium hydroxide and diketopiperazine is not diketopiperazinatocuprate(II) but bis(glycylglycinato)-cuprate(II).

The preparation and some properties of dipotassium bis(glycylglycinato)cuprate(II) have been described. As to the structure of the complex, it has been concluded, from powerful evidence, that two glycylglycinate anions are coordinated around copper(II) in the trans configuration only through the terminal amino group and the nitrogen in the peptide linkage.

The authors wish to thank Dr. Shigeo Kida of Wakayama University for his analysis of potassium and the Ministry of Education for a grant-in-aid.

The Reaction of Friedelin with *N*-Bromosuccinimide

By Takahiko TSUYUKI, Yoshiaki TANAHASHI, Yoshiro SUDO
Sigeki NAKAMATA and Takeyoshi TAKAHASHI

Department of Chemistry, Faculty of Science, The University of Tokyo, Hongo, Tokyo

(Received November 19, 1965)

Kane and Stevenson[1,2] have reported the reactions of *N*-bromosuccinimide (NBS) with friedelin (I) and with friedelane (II). Friedelin is brominated with 1 mol. of NBS to give 4α-bromofriedelin (III), which in turn yields, after purification, 4α-bromofriedel-18-en-3-one (IV) upon further treatment with 1 mol. of NBS.

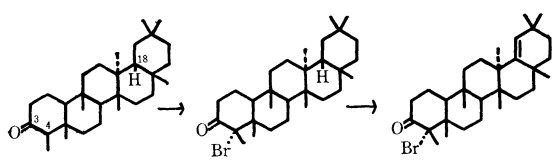

I III IV

Fig. 1

In the case of the hydrocarbon, friedelane, it is oxidized by NBS to the olefin, friedel-18-ene (V); furthermore, Stevenson et al. have more recently shown[3] that when a solution of bromine in carbon tetrachloride is added to friedelane, it is decolorized, and that the reaction mixture yields friedel-18-ene (V) in a yield comparable to that in the NBS reaction. This indicates that, in this highly selective oxidation, the intermediacy of the succinimidyl radical is not essential.[4-9]

They also isolated an unstable 18-bromofriedelane, which readily afforded friedel-18-ene (V), and they inferred that in the case of friedelin (I), particularly in the formation of di- and tri-bromo-derivatives at C-2 and/or C-4, a bromination at 18-position took place concurrently.

We first examined the bromination products of

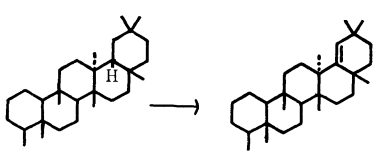

II V

Fig. 2

1) V. V. Kane and R. Stevenson, *Chem. & Ind.*, **1960**, 1243.
2) V. V. Kane and R. Stevenson, *Tetrahedron*, **15**, 223 (1961).
3) F. Kohen and R. Stevenson, *J. Org. Chem.*, **30**, 2479 (1965).
4) P. Goldfinger, P. A. Gosselain and R. H. Martin, *Nature*, **168**, 30 (1951).
5) F. L. J. Sixma and R. H. Riem, *Koninkl. Ned. Akad. Wetenschap. Proc.*, **61B**, 183 (1958).
6) B. P. McGrath and J. M. Tedder, *Proc. Chem. Soc.*, **1961**, 80.
7) P. S. Skell, D. L. Tuleen and P. D. Readio, *J. Am. Chem. Soc.*, **85**, 2850 (1963).
8) R. E. Pearson and J. C. Martin, ibid., **85**, 354 (1963).
9) G. A. Russell, C. DeBoer and K. M. Desmond, ibid., **85**, 365 (1963).

friedelin (I). According to the method of Kane and Stevenson,[2] friedelin was brominated with 1 mol. of NBS. The reaction mixture, showing two spots on the thin-layer chromatogram, was separated into bromo derivatives and bromine free derivatives. The latter was shown by gas chromatography to be a mixture of friedelin (I) and friedel-18-en-3-one (VI). The former was reduced with zinc in a boiling solution of benzene and ethanol, and examined by gas chromatography. Its retention time showed the presence of friedelin and friedel-18-en-3-one. It followed that the bromo-derivatives had contained 4α-bromofriedelin (III) and 4α-bromofriedel-18-en-3-one (IV).

It now appears likely that in the reaction of friedelin with 1 mol. of NBS, a competitive reaction occurs; namely, the bromine atoms independently attack the 4α- and 18-hydrogens of friedelin, giving rise to III and VI respectively, and then further attack the 18-position of III and /or the 4α-position of VI to afford 4α-bromofriedel-18-en-3-one (IV).

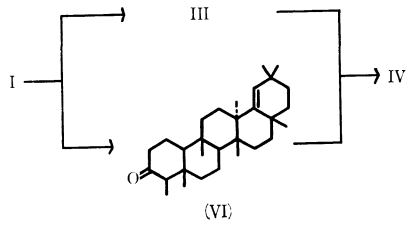

Fig. 3

The reaction products are shown in Table I, from which it is obvious that the main reaction pathway is I→III and that the I→VI pathway is minor.

In order to determine the catalytic action of 2, 2'-azo-bis-isobutyronitrile (AIBN) toward the reaction of friedelin with NBS, we treated friedelin in a carbon tetrachloride solution with 1 mol. of NBS and a catalytic amount of AIBN under irradiation with an infrared lamp. The reaction products were nearly the same as in the case without AIBN, as is shown in Table I.

Table I

Product (in mol.%)	III	IV	I	VI	Lost product
NBS(1.1 mol.), AIBN(0.01 mol.) in CCl_4	63	12	22	2	1
NBS(1.4 mol.) in CCl_4	61	13	10	0.4	16

Experimental

The Reaction of Friedelin with NBS (Method described by Kane and Stevenson[2]).—*N*-Bromosuccinimide (150 mg.) was added to a solution of friedelin (250 mg.) in carbon tetrachloride (70 ml.); the mixture was then heated under reflux for 37 min. by means of an infrared lamp. After 8 min. irradiation a yellow color appeared and the bromine color persisted for 3 min. The mixture was cooled and filtered, and the solvent was removed under reduced pressure. The yellow residue, which weighed 307 mg., was dissolved in petroleum ether - benzene (9 : 1, 70 ml.) and chromatographed on silica gel (Davison, 200 mesh, 7.5 g.). Elution with this solvent (ca. 1 l.) gave the bromofriedelin mixture (221 mg.). After elution with petroleum ether-benzene (4 : 1, 100 ml.), petroleum ether - benzene (1 : 1, 300 ml.) yielded 26 mg. of bromine-free materials, which were shown by gas chromatography* to be a mixture of friedelin (25.1 mg., retention time 8.0 min.) and friedel-18-en-3-one (0.9 mg., retention time 6.5 min.).

The Reduction of the Bromofriedelin Mixture.—Zinc dust (4.3 g.) was added, portion by portion and over 1-hr. period, to a boiling solution of the above bromofriedelin mixture (122 mg.) in benzene-ethanol (1 : 1, 150 ml.). After an additional 2 hrs.' boiling, the hot solution was filtered. The evaporation of the solvent under reduced pressure gave a solid. Gas chromatography showed that it was a mixture of friedelin and friedel-18-en-3-one in the ratio of 4.5 to 1, which indicated that the original bromofriedelin mixture (221 mg.) contained 181 mg. of 4α-bromofriedelin and 40 mg. of 4α-bromofriedel-18-en-3-one.

The Action of AIBN on the Reaction of Friedelin with NBS.—To a solution of friedelin (100 mg.) in carbon tetrachloride (28 ml.), NBS (49 mg.) and AIBN (0.4 mg.) were added. The solution was heated by means of an infrared lamp. After 13 min. a yellow color appeared, but it faded instantly. Heating at reflux was continued for 45 min. until the yellow color completely disappeared; the reaction mixture was then treated as before. The residue was chromatographed on silica gel (Davison, 200 mesh, 3.0 g.). Elution with petroleum ether - benzene (9 : 1) gave a solid (89.2mg.), and continued elution with petroleum ether - benzene (1 : 1) also afforded a solid (23.6 mg.). The former was reduced with zinc (3.2 g.), and the product was shown by gas chromatography to be a mixture of friedelin (67.2 mg.) and friedel-18-en-3-one (8.0 mg.), which corresponded to 79.7 mg. of 4α-bromofriedelin and 9.5 mg. of 4α-bromofriedel-18-en-3-one respectively. The latter was found by gas chromatography to be a mixture of friedelin (21.9 mg.) and friedel-18-en-3-one (1.7 mg.).

* Column; 3/4% SE-30 on Chromosorb-W.

Analytical Approximations for Coherent and Incoherent Atomic Scattering Factors

By Shuzo SHIBATA

Department of Chemistry, Faculty of Science, Shizuoka University, Oiwa, Shizuoka

(Received November 29, 1965)

For the analysis of gas electron-diffraction data by the use of an electronic computer, analytical approximations[1] for coherent and incoherent atomic scattering factors are useful in order to decrease the amount of input data and to obtain their values for arbitrary scattering angles by smooth interpolation. A simple analytical function, $\exp(\sum a_n q^n)$, was found to be a good approximation for the coherent and incoherent atomic scattering factors. Here q is the scattering variable defined by $40\sin(\theta/2)/\lambda$, where θ is the scattering angle and λ is the wavelength of the incident X-rays or electrons. Such an expression was used by Silverman and Simonsen[2] for atomic scattering factors for an X-ray analysis. In their work, however, the values of the scattering variable, q, were limited to within 50. The q values usually convered by the experimental data of gas electron diffraction, however, range from 10 to 100. The present calculation of the analytical constants has, therefore, been carried out to cover this range of the scattering variable. The scattering factors given by Viervoll and Ögrim[3] were adopted in the present calculation, because no other scattering factors[4] calculated thus far extend to sufficiently large scattering angles.*1

The parameters of the polynomials were determined by a least-square method by minimizing $\sum_i(\ln f_{0i}-\ln f_i)^2$, where f_0 is the theoretical value and f is the calculated value. The evaluation was straightforward because the parameters were taken as linear. The function was tested mainly with polynomials of the fifth, sixth and seventh degrees. The standard deviation, σ, given by $[\sum_i(f_{0i}-f_i)^2/N]^{1/2}$, was calculated in each case. Here N is the number of the values fitted. The sixth-degree polynomial exponent gave a σ value smaller than that for the fifth-degree, whereas the polynomial exponent of a degree higher than the sixth did not give a much better fit. A typical case is presented in Table I. The parameters obtained are tabulated in Table II, with their standard deviations for twenty-three atoms from hydrogen to copper. Theoretical values below 9.55 in q were not used for the fitting, since the values in this range are not needed for usual analyses of gas electron diffraction.*2 Therefore, another set of parameters should be used if coherent scattering factors for smaller q values are required. This latter set was obtained by fitting thirty theoretical values of Viervoll and Ögrim*3, beginning with 3.18 in q, by a sixth-degree polynomial exponent. The standard deviation was somewhat larger. Table III shows several different sets of analytical constants for the coherent atomic scattering factor of carbon with varying minimum q values and varying numbers of the theoretical values fitted.

The incoherent scattering factor, $S(v)$, calculated by Bewilogua[7] was approximated by an analytical function, $1-\exp(\sum b_n v^n)$, where $v=0.0553\cdot Z^{-2/3}\cdot q$ and Z is the atomic number. The exponent of a fifth-degree polynomial was found to be sufficient to reproduce the theoretical values with a good accuracy over the entire range of v. The sets of parameters are tabulated in Table IV for various degrees of polynomial exponents. The incoherent scattering factors approximated by the fifth-degree polynomial exponent are compared in Table V with those calculated by Bewilogua.

1) For example, R. A. Bonham and L. S. Bartell, *J. Chem. Phys.*, **31**, 702 (1959).

2) J. N. Silverman and S. H. Simonsen, *Acta Cryst.*, **13**, 50 (1960).

3) H. Viervoll and O. Ögrim, ibid., **2**, 277 (1949).

4) "International Tables for X-Ray Crystallography," Vol. III, The Kynoch Press, Birmingham (1962), p. 201.

*1 One exception is the atomic scattering factor calculated by Hanson et al.[5] from the Hartree-Fock-Slater wave function, but Viervoll and Ögrim's factors agree better with the absolute values of complex atomic scattering factors,[4] $|f|$, than Hanson's factors.

*2 Another reason for this was that the scattering factors in this region may be uncertain because of the exchange effect of electrons.

*3 It is desirable, however, to use other theoretical scattering factors obtained with reference to the exchange effect. For example, by the use of the scattering factor of carbon by Berghuis et al.,[6] the fit with a sixth-degree polynomial exponent resulted in the standard deviation of 0.013. Silverman and Simonsen, however, obtained 0.095 for the standard deviation from the same fit with a fixed coefficient, a_0.

5) H. P. Hanson, F. Herman, J. D. Lea and S. Skillman, *Acta Cryst.*, **17**, 1040 (1964).

6) J. Berghuis, I. M. Haanappel, M. Potters, B. O. Loopstra, C. H. MacGillavry and A. L. Veenendaal, ibid., **8**, 478 (1955).

7) L. Bewilogua, *Physik. Z.*, **32**, 740 (1931); R. F. Pohler and H. P. Hanson, *J. Chem. Phys.*, **42**, 2347 (1965).

TABLE I. COEFFICIENTS OF nTH-DEGREE POLYNOMIALS FOR THE COHERENT ATOMIC SCATTERING FACTOR OF CARBON ($N=28$)

n	a_0	a_1	a_2	a_3	a_4	a_5	a_6	a_7	σ
5	1.8433−00*	−1.3932−01	5.4999−03	−1.1420−04	1.0676−06	−3.7104−09			0.021
6	2.1970−00	−2.0823−01	1.0283−02	−2.7020−04	3.6524−06	−2.4757−08	6.6793−11		0.011
7	2.4910−00	−2.7565−01	1.6082−02	−5.1739−04	9.4019−06	−9.8896−08	5.6394−10	−1.3512−12	0.007

* The last number repnesents a negative exponent of ten.

TABLE II. COEFFICIENTS OF SIXTH-DEGREE POLYNOMIALS FOR COHERENT ATOMIC SCATTERING FACTORS ($N=28$)

	a_0	a_1	a_2	a_3	a_4	a_5	a_6	σ
H*	−3.2611−01	5.4004−02	−1.9266−02	7.8699−04	−1.4974−05	1.3675−07	4.7794−10	0.001
Li	8.4174−01	−3.3521−02	4.9715−04	−6.8484−05	1.7129−06	−1.6384−08	5.4439−08	0.005
Be	7.3021−01	−5.0064−03	−1.0412−03	1.6923−05	−2.2814−07	2.0500−09	−7.0528−12	0.007
B	1.6535−00	−1.6119−01	9.1676−03	−2.8670−04	4.4760−06	−3.4297−08	1.0272−10	0.005
C	2.1970−00	−2.0823−01	1.0283−02	−2.7020−04	3.6524−06	−2.4757−08	6.6793−11	0.011
N	2.8661−00	−2.5134−01	1.0868−02	−2.5204−04	3.1174−06	−1.9902−08	5.1786−11	0.010
O	2.9909−00	−2.0115−01	6.4790−03	−1.1203−04	1.0062−06	−4.4423−09	7.2910−12	0.014
F	2.9959−00	−1.6678−01	3.8705−03	−3.2369−05	−1.7407−07	4.1810−09	−1.7718−11	0.023
Na	2.3403−00	7.0460−03	−5.7283−03	2.0797−04	−3.3038−06	2.4970−08	−7.3365−11	0.017
Mg	2.0420−00	6.0336−02	−7.9086−03	2.4955−04	−3.7272−06	2.7255−08	−7.8583−11	0.008
Al	2.0656−00	5.2360−02	−6.2717−03	1.7894−04	−2.4310−06	1.6253−08	−4.3016−11	0.026
Si	2.1408−00	3.4000−02	−4.1630−03	9.9729−05	−1.0707−06	5.1857−09	−8.3662−12	0.021
P	2.3697−00	−1.0998−02	−5.7333−04	−1.7808−05	7.9342−07	−9.1204−09	3.4265−11	0.031
S	2.7052−00	−6.8324−02	3.2356−03	−1.2704−04	2.3420−06	−1.9856−08	6.3385−11	0.033
Cl	3.0847−00	−1.3010−01	7.0695−03	−2.3133−04	3.7560−06	−2.9283−08	8.8069−11	0.032
K	3.4737−00	−1.5181−01	6.5707−03	−1.6360−04	2.0654−06	−1.2648−08	2.9892−11	0.020
Ca	3.4323−00	−1.2669−01	4.5825−03	−9.8072−05	1.0585−06	−5.4341−09	1.0398−11	0.029
Cr	3.4279−00	−8.4891−02	1.4187−03	2.6254−06	−4.4222−07	5.1776−09	1.8620−11	0.027
Mn	3.3939−00	−6.9591−02	4.9198−04	2.6688−05	−7.4449−07	7.0212−09	−2.3053−11	0.028
Fe	3.3823−00	−5.4476−02	−5.2283−04	5.5036−05	−1.1352−06	9.7154−09	−3.0558−11	0.021
Co	3.3874−00	−4.2935−02	−1.2734−03	7.4851−05	−1.3906−06	1.1348−08	−3.4753−11	0.025
Ni	3.3937−00	−3.3398−02	−1.7302−03	8.1794−05	−1.4025−06	1.0862−08	−3.1949−11	0.014
Cu	3.4643−00	−3.0981−02	−1.7937−03	7.7501−05	−1.2464−06	9.1136−09	−2.5368−11	0.022

* $N=23$

TABLE III. COEFFICIENTS OF POLYNOMIALS FITTED WITH N THEORETICAL VALUES FOR THE COHERENT ATOMIC SCATTERING FACTOR OF CARBON ($n=6$)

N	a_0	a_1	a_2	a_3	a_4	a_5	a_6	σ	Min. of q
31	1.8724−00	−1.2645−01	3.9282−03	−5.1303−05	−7.7045−08	6.0468−09	−3.1649−11	0.143	0.000
30	2.1996−00	−2.0492−01	9.9091−03	−2.5529−04	3.3787−06	−2.2393−08	5.9015−11	0.030	3.183
29	2.3437−00	−2.3317−01	1.1830−02	−3.1624−04	4.3608−06	−3.0185−08	8.3172−11	0.012	6.366
28	2.1970−00	−2.0823−01	1.0283−02	−2.7020−04	3.6524−06	−2.4757−08	6.6793−11	0.011	9.549
27	1.8072−00	−1.4880−01	6.8739−03	−1.7434−04	2.2395−06	−1.4286−08	3.6023−11	0.006	12.732

TABLE IV. COEFFICIENTS OF nTH-DEGREE POLYNOMIALS FOR INCOHERENT SCATTERING FACTORS

n	b_0	b_1	b_2	b_3	b_4	b_5	b_6	b_7	σ
2	−1.2400−1	−4.9727−0	1.8619−0						0.036
3	−5.5375−2	−6.1628−0	5.0333−0	−2.1275−0					0.018
4	−2.4933−2	−7.1168−0	9.7444−0	−9.6371−0	3.7490−0				0.009
5	−7.5548−3	−8.0228−0	1.7051+1	−3.0220+1	2.7384+1	−9.4823−0			0.003
6	−4.1362−3	−8.3308−0	2.0873+1	−4.7045+1	6.0497+1	−3.9346+1	1.0060+1		0.002
7	−9.2425−4	−8.8929−0	3.0952+1	−1.1073+2	2.4845+2	−3.2171+2	2.1938+2	−6.0752+1	0.001

TABLE V. COMPARISON BETWEEN BEWILOGUA'S INCOHERENT SCATTERING FACTORS S_0 AND LEAST-SQUARES VALUES S CALCULATED WITH FIFTH-DEGREE POLYNOMIAL EXPONENT

v	S_0	S	v	S_0	S	v	S_0	S
0.00	0.000	0.007	0.3	0.776	0.776	0.7	0.929	0.929
0.05	0.319	0.310	0.4	0.839	0.838	0.8	0.944	0.944
0.10	0.486	0.487	0.5	0.880	0.880	0.9	0.954	0.954
0.20	0.674	0.677	0.6	0.909	0.909	1.0	0.963	0.963

The Crystal and Molecular Structure of 10-Halo-5, 10-dihydrophenarsazine*

By Makoto FUKUYO, Kazumi NAKATSU and Akira SHIMADA

Department of Chemistry, Faculty of Science, Osaka City University, Sumiyoshi-ku, Osaka

(Received January 5, 1966)

The 10-halo-5, 10-dihydrophenarsazine (phenarsazine halide) might be regarded as a tricyclic ring in which two benzene rings are connected by the arsenic and the nitrogen atoms. The present work was undertaken in order to elucidate the influence of the arsenic and the nitrogen atoms upon the configuration of this tricyclic ring. The disposition of halogen atoms around the arsenic atom would also be of interest in connection with the valence state of the arsenic atom. In the course of the present investigation, a paper on the structure of the chloride has already been published.[1] It would be interesting to compare this result with ours, although ours is still in the stage of refinement.

Preliminary powder photographs seem to indicate that the crystals of the chloride, the bromide, and the iodide belong to the same crystal system, while the fluoride crystal belongs to a different system. Among these halides, the chloride, the bromide and the iodide gave needle crystals suitable for X-ray work. These crystals were found to be elongated along the *c* axes. Oscillation and Weissenberg photographs were prepared with Cu$K\alpha$ radiation. The crystal data are listed in Table I. The intensities were estimated visually with a calibrated scale by making use of the multiple-film technique. The corrections for polarization and Lorentz factors were applied in the usual way, and that for absorption was neglected.

The chloride was first studied. Since the *c* axis is shorter, the Patterson projection onto the (001) plane was computed, and it clearly revealed the interatomic vectors between arsenic and chlorine atoms as well as between arsenic atoms.

TABLE I. CRYSTAL DATA

Phenarsazine chloride	Phenarsazine bromide
$C_{12}H_9AsClN$	$C_{12}H_9AsBrN$
Orthorhombic	Orthorhombic
$a=13.82$Å	$a=15.06$Å
$b=14.12$Å	$b=15.09$Å
$c=5.40$Å	$c=5.22$Å
$D_x=1.749$ g. cm^{-3} ($Z=4$)	$D_x=1.803$ g. cm^{-3} ($Z=4$)
$P2_12_12_1$	$P2_12_12_1$

The electron-density projection was then synthesized with the signs determined by the arsenic and chlorine atoms alone. Subsequent Fourier refinements made clear the positions of the lighter atoms. Electron-density projections along the other axes, obtained by means of the same procedure, gave the *z* coordinate of each atom. The reliability indices, *R*, were found to be 14.3, 17.7 and 22.4% for the *hk*0, *h*0*l* and 0*kl* spectra respectively. The isotropic temperature factors for all the atoms were estimated to be 3.2 Å^{-2} for the *hk*0 and 3.0 Å^{-2} for the *h*0*l* and 0*kl* spectra. Almost the same procedure of structure analysis was then applied to the bromide, the crystal structure of which was isomorphous with that of the chloride. The reliability index, *R*, was found to be 24.2, 22.1 and 36.3% for the *hk*0, *h*0*l* and 0*kl* spectra, the isotropic temperature factor being 5.0 Å^{-2} for the arsenic atom, 3.5 Å^{-2} for the bromine atom, and 5.0 Å^{-2} for the other atoms. The atomic coordinates in each crystal structure are listed in Table II.

Although the accuracy of analyses at this stage of refinement is not sufficient for us to discuss the results in detail, some interesting features of the molecular and crystal structure have been revealed. It may be remarked that the present results concerning the structure of the chloride agree approximately with those given by Camerman and Trotter,[1] although our work was done independently with two-dimensional data. The general scheme of the crystal structure may be seen in Fig. 1, which shows the crystal structure of the bromide isomorphous with the chloride. The interatomic distances within a molecule as well as between nearest molecules were found to be plausible in comparison with conventional values. A molecule consists of two nearly equivalent halves related by a plane of symmetry through nitrogen, arsenic and bromine atoms. The tricyclic ring can be regarded as a plane, from which only the halogen atom deviates significantly. Thus, the nitrogen atom may be in the sp^2 state of hybridization, while the arsenic atom may be in the p^3 state, probably with a slight *d* character. This situation indicates the delocalization of the lone-pair electrons in these two atoms to the benzene rings; this is in conformity with the ultraviolet spectra results shown in Fig. 2. There may be no intermolecular forces other than those of the van der Waals type, which are seen in all the intermolecular distances.

*) The major part of this paper was read at the symposium on Organometallic Compound, Nagoya, October, 1963, and also at the 17th Annual Meeting of the Chemical Society of Japan, Tokyo, March, 1964.

1) A. Camerman and J. Trotter, *J. Chem. Soc.*, **1965**, 730.

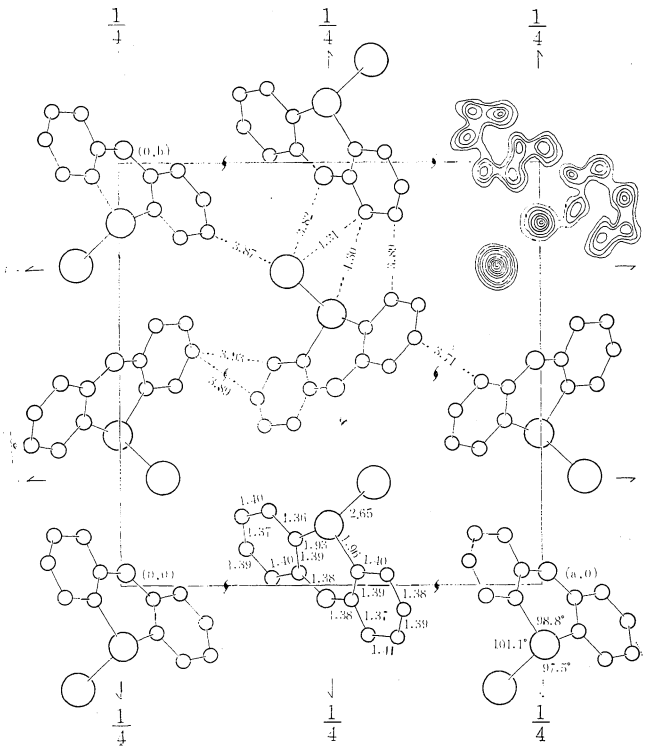

Fig. 1. Crystal structure and electron density projection of the bromide onto (001) plane, contours being at arbitrary scale.

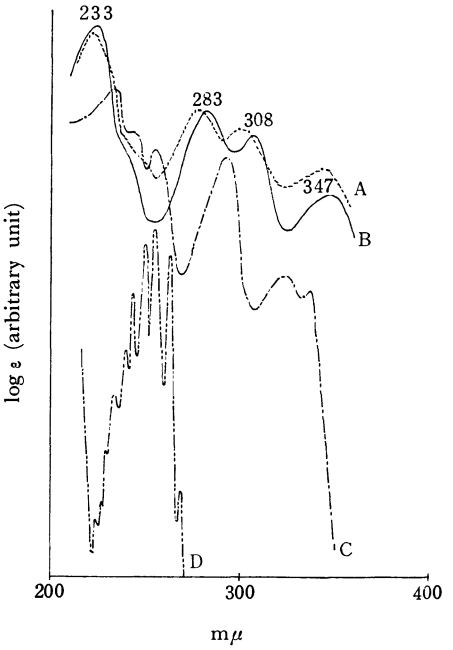

Fig. 2. Ultraviolet absorption spectra.
(A) Phenarsazine bromide
(B) Phenarsazine chloride
(C) Carbazole
(D) Benzene

Table II. Atomic parameters

Phenarsazine chloride				Phenarsazine bromide			
Atom	x/a	y/b	z/c	Atom	x/a	y/b	z/c
C_1	0.549	0.049	0.142	C_1	0.563	0.032	0.193
C_2	0.619	0.038	0.300	C_2	0.633	0.025	0.367
C_3	0.687	−0.044	0.343	C_3	0.673	−0.057	0.361
C_4	0.653	−0.118	0.158	C_4	0.658	−0.123	0.180
C_5	0.604	−0.100	−0.008	C_5	0.587	−0.117	0.004
C_6	0.525	−0.017	−0.050	C_6	0.548	−0.035	0.012
C_7	0.407	0.053	−0.290	C_7	0.424	0.031	−0.238
C_8	0.350	0.037	−0.468	C_8	0.359	0.018	−0.425
C_9	0.269	0.098	−0.495	C_9	0.298	0.086	−0.468
C_{10}	0.271	0.177	−0.358	C_{10}	0.289	0.163	−0.333
C_{11}	0.325	0.187	−0.189	C_{11}	0.354	0.176	−0.146
C_{12}	0.401	0.133	−0.142	C_{12}	0.415	0.110	−0.103
N	0.477	−0.015	−0.233	N	0.488	−0.032	−0.188
Cl	0.583	0.249	−0.118	Br	0.603	0.243	−0.100
As	0.481	0.166	0.130	As	0.495	0.142	0.172

The authors are indebted to Dr. Ikuzo Kageyama of the Central Research Laboratory, Daikin Kogyo Co., Ltd., for supplying the specimens.

SHORT COMMUNICATIONS

The Sintering of Colloidal Titanium

By Akira OKA

Department of Chemical Technology, Faculty of Engineering, Tokai University, Shibuya-ku, Tokyo

(Received March 24, 1966)

It is said that, in powder metallurgy, the finer the particle size of metallic powder, the more simplified conditions can be used in sintering it. So far as we can determine, however, nothing has been reported about the sintering of any metallic powder as colloidal as pyrophoric.

Recently, pure colloidal titanium was obtained through the dehydrogenation of titanium hydride, the composition of which was exactly stoichiometric ($TiH_{2.00}$). This dehydrogenated titanium was compacted at a pressure of 5 ton/cm^2, and then sintered for two hours at 1400°C. By this process a non-porous product was obtained; the density was found to be 4.54 g./cm^3, which corresponds to the full density of metallic titanium.

First of all, a mass of sponge titanium (purity 99.9% by ASTM standard) was subjected to reaction with pure hydrogen gas in a vessel at a red hot temperature; the hydrogen was carefully kept in the vessel, and prevented from being degraded lower than 99.999% in purity by passing it through a membrane of palladium alloy. A titanium hydride material with a composition exactly equal to $TiH_{2.00}$ was obtained by this process.

The titanium hydride obtained above was then milled for 40 hr. with a rotary mill made of sintered alumina. When the hydride powder thus pulverized was observed by electronmicroscopy, it was seen that the particles are of sizes between 60 Å and 300 Å, plus aggregated thereof. The hydride was then thremally dehydrogenated at 450°C in a tube furnace evacuated at 2×10^{-5} mmHg. A colloidal titanium was obtained, the specific surface of which was found to be 16 m^2/g. by the B.E.T. method; its mean particle size was therefrom calculated to be 0.08μ. The residual hydrogen of 27.7 p. p. m. was found by the fusion method. The colloidal titanium was kept in an air-tight jar filled with bomb nitrogen, as it is considerably pyrophoric in air.

The colloidal titanium obtained was then compacted in nitrogen atmosphere, by applying a pressure of 5 ton/cm^2, into a disk, with a diameter of 11.3 mm., a thickness of approximately 2 to 3 mm., and a green density of 3.1 g./cm^3. The disk thus obtained, after impregnation with liquid paraffin in order to protect it from air, was sintered at 1400°C for two hours in a vacuum furnace kept at 5×10^{-5} mmHg. The density of this product was 4.54 g./cm^3, as measured by a picnometer, while a nonporous structure was observed by means of microscopy (Mag. ×400).

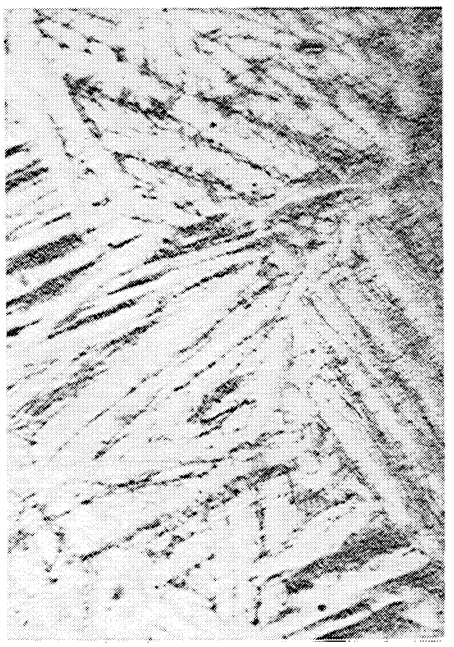

Structure of non-porous titanium sintered at 1400°C for two hours. (Mag. ×400)

In contrast to the common idea that some porosity is unavoidable in a product obtained through the sintering of metallic powder, it may be seen that, if a colloidal particle of titanium is taken as the starting meterial, a substantially-full density of metallic titanium can be obtained by means of sintering alone, using a powder compacted at a sufficiently high pressure and kept away from air.

A Twinning Structure in Crystals of Potassium Terephthalate, p-$C_6H_4(COOK)_2$

By Shozo FURUYAMA and Nozomu EBARA

Department of Chemistry, College of General Education, The University of Tokyo, Meguro-ku, Tokyo

(Received April 14, 1966)

An unusual twinning structure of potassium terephthalate, p-$C_6H_4(COOK)_2$, has been found by means of an X-ray study using Cu$K\alpha$ radiation (λ=1.542 Å). The rotation, oscillation and the Weissenberg photographs on three principal axes displayed an orthorhombic symmetry, together with extinctions of $h0l$ when h=odd and $0k0$ when k=odd. No space group conformed to such diffraction patterns; it was, therefore, concluded that the crystal had the space group of $P2_1/a$ and that it twinned on the (100) plane by reflection. The crystal data are:

$a = 19.4$ Å

$b = 5.76$ Å

$c = 3.94$ Å

$\beta = 90°$

and $Z = 2$

β could not be measured directly, but it must be very near to 90°, so that the reciprocal lattice of one individual may fall by twinning on the lattice of the other individual, simulating a reciprocal lattice of an orthorhombic symmetry and preserving its original extinction.

The approximate positions of potassium cations, as projected on the (001) plane, were determined from the Patterson synthesis; a fairly good projection of the electron density (R=0.205), as is indicated in Fig. 1, was obtained after several trials. Figure 1 clearly demonstrates the very reasonable packing of molecules. Assuming a regular benzene ring with a C–C distance of 1.4 Å, the molecular axis tilts to the c-axis by about 70 −76°.

Further refinements are now being carried out.

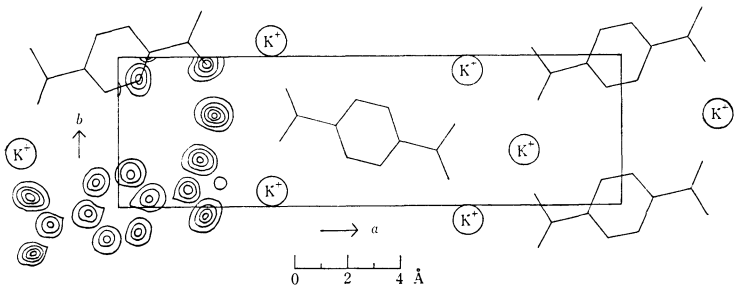

Fig. 1. Electron density projection and the schematic representation on (001) plane of potassium terephthalate crystals.

Azetidine Enamines

By Teng-Yueh CHEN, Hiroshi KATO[1] and Masaki OHTA

Laboratory of Organic Chemistry, Tokyo Institute of Technology, Ookayama, Meguro-ku, Tokyo

(Received May 9, 1966)

The increasing interest in the chemistry of azetidines and recent reports[2a-d] on the addition reactions of aziridines to dimethyl acetylenedicarboxylate prompt us to report some similar results with azetidines.

Azetidine was added exothermally to dimethyl acetylenedicarboxylate and to methyl propiolate in ether to give dimethyl 1-azetidinylmaleate and methyl β-(1-azetidinyl)-*trans*-acrylate respectively. Similar enamine-type azetidinyl derivatives were readily prepared by the concondensation of azetidine with suitable ketones at room temperature; ethyl acetoacetate gave β-(1-azetidinyl)-crotonate, while cyclopentanone and cyclohexanone gave 1-(1-azetidinyl)cyclopentene and 1-(1-azetidinyl)cyclohexene respectively. With the more acidic ketones, such as ethyl benzoylacetate, dibenzoylmethane and acetylacetone, however, the rapid separation of a precipitate (presumably the azetidinium salts) was observed, while the expected condensation products could not be isolated. The results, as well as the characteristic spectral data, are summarized in Table I.

All the compounds show a strong infrared absorption of the enamine double bond in the 1500—1660 cm^{-1} region while a typical triplet-quintet NMR pattern of an azetidinyl group is present at 6.20—6.70 and 7.75—7.81 τ. An NMR peak of a vinylic hydrogen at quite a high resonance field is relevant to the cis addition of azetidine to the triple bond; this idea is further supported by the large coupling constant ($J=15$ c.p.s.) of the two trans vinylic protons of azetidinylacrylate. This is in contrast to the behavior of aziridine, where the trans addition competes to some degree with the cis addition.

The appearence of the vinylic proton chemical shifts in such a high field is remarkable. Indeed, it is probably the highest among all the chemical shifts of this type so far reported.

The exclusive formation of (*cis*)-crotonate by the reaction with acetoacetate may be explained by the initial attack of azetidine from the less crowded site.

TABLE I

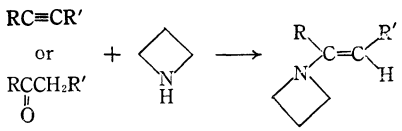

R	R′	Constants	IR (cm^{-1})[c]	NMR (τ)[d]	Anal. Found/Calcd. C	H	N
COOMe	COOMe	66.5—67[a]	1740, 1680 1570	5.90 (singlet)	54.35 54.27	6.85 6.53	7.04 7.03
H	COOMe	46.5—47[a]	1680 1590	2.93 (doublet) 5.91 (doublet)	59.95 59.55	8.06 7.85	10.33 9.92
Me	COOEt	110—113/2 mmHg[b] n_D^{25} 1.5068	1680 1585	6.05 (singlet)	63.58 63.88	9.23 8.94	8.59 8.28
$(CH_2)_3$		60—66/15 mmHg[b] n_D^{25} 1.4835	1630	Not measured	76.00 77.99	10.62 10.64	11.12[e] 11.37
$(CH_2)_4$		51—53/4 mmHg[b] n_D^{25} 1.4840	1660	6.08 (triplet)	78.67 78.77	11.35 11.02	10.63 10.21

a) M.p.; b) B.p.; c) Ester carbonyl and double bond; d) Vinylic proton only; e) Unstable

1) To whom inquiries should be addressed.

2) a) E. Winterfelt and H. Preuss, *Angew. Chem.*, **77,** 679 (1965); b) J. E. Dolfini, *J. Org. Chem.*, **30,** 1298 (1965); c) H. W. Heine and R. Peavy, *Teirahedron Letters*, **1965,** 3123; d) A. Padwa and L. Hamilton, ibid., **1965,** 4363.

Evidence for Nonplanarity in an Oxalamide*

By T. H. SIDDALL, III, and M. L. GOOD

Savannah River Laboratory, E. I. du Pont de Nemours and Co., Aiken, South Carolina

(Received May 13, 1966)

Mizushima[1] concluded that steric repulsion is the most important force determining the stable configuration of rotational isomers. We wish to report an interesting demonstration of the correctness of this conclusion.

Tetraisopropyl oxalamide (I) was obtained by the reaction of diisopropyl amine with oxalyl chloride, followed by repeated crystallization from a variety of solvents. Proton magnetic resonance (PMR) spectra were obtained with a Varian A-60 spectrometer equipped with a variable temperature insert.

The spectra of I in CD_3COCD_3 show two sets of methyl proton signals at 10°C and higher temperatures as would be expected from analogy with simple amides.[2] At −15°C these signals broaden and finally emerge as four sets at −40°C. The two isopropyl radicals on a nitrogen atom are nonequivalent as also are the two methyl groups within a radical. There can be nonequivalent methyl groups only if there is no molecular symmetry plane between the groups.[3] Since there must be such a plane if the whole molecule is planar, it must be that the halves of the molecule are not coplanar and, further, that rotation around the

rotation axis (–C—C–) is slow on the PMR time scale below about −15°C. Double bond character[1] in the rotation axis favors coplanarity. In spite of this, steric factors, that arise from the bulky amide groups, stabilize the nonplanar structure.

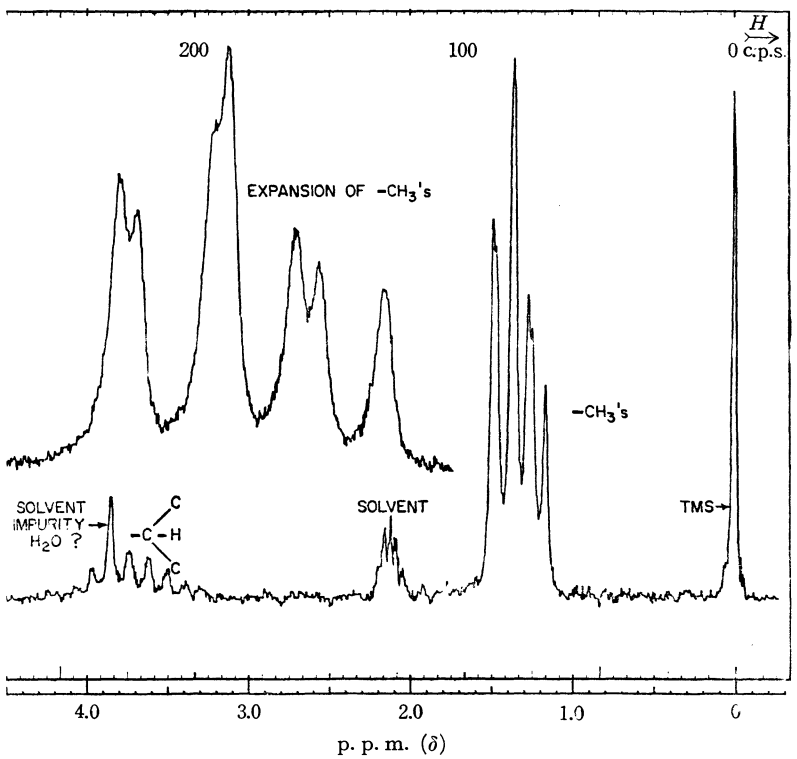

Fig. 1. PMR spectrum of I at −40°C 50 mg./ml.

* The information contained in he short communication was developed during the course of work under countract AT(07-2)-1 with the U. S. Atomic Energy Commission.

1) S. Mizushima, "Structure of Molecules and Internal Rotation," Academic Press, New York (1954).
2) H. S. Gutowsky and C. S. Holm, *J. Chem. Phys.*, **25**, 1228 (1956).
3) T. H. Siddall, accepted for publication in *J. Phys. Chem.*

Intramolecular Hydrogen Bonding Between the Carboxyl O-H Group and Nitrogen

By Michinori Ōki, Minoru Hirota and Yutaka Morimoto

Department of Chemistry, Faculty of Science, The University of Tokyo, Hongo, Tokyo
Department of Applied Chemistry, Faculty of Engineering, Yokohama National University, Minato-ku, Yokohama

(Received May 18, 1966)

A series of previous investigations in the laboratories of the present authors[1] confirmed the existence of the intramolecular COOH···O hydrogen bond. The rather rare occurence of the hydrogen bond was explained in terms of the stability of the *cis* conformer.

The investigation is now extended to the hydrogen bond including nitrogen as a hydrogen acceptor. The infrared ν_{OH} and the $\nu_{C=O}$ absorptions of pyridine-2-carboxylic (I) and quinoline-2-carboxylic (II) acids were determined as examples of the five-membered hydrogen chelates, and the existence of the intramolecular hydrogen bond was indicated by the appearance of the ν_{OH} bands at lower frequencies (as are listed in the table). The higher $\nu_{C=O}$ frequencies of the acids, I and II, than the acids without intramolecular hydrogen bonds may be attributable to the trans conformation, which is a natural consequence of the formation of the hydrogen bonds, as has been discussed earlier in connection with the oxygen analogs.

The enthalpies of hydrogen bond formation were obtained from the temperature dependence of the relative intensities of the two ν_{OH} absorptions. From a comparison of the data with those for α-alkoxy- and α-keto-carboxylic acids, it has been shown that the COOH···N hydrogen bonds in I and II are by far more favorable in spite of the smaller ΔH values. These results may be explained as follows. The hydrogen bonded conformer should have a planar *s-trans* conformation such as 1, which is one of the stable conformations from the viewpoint of the maximal conjugation between the aromatic heterocycles and the carboxyl group. In other words, the carboxyl groups of the molecules are so arranged as to be likely to form hydrogen bonds. Consequently, it is not the enthalpy but the entropy factor which controls the formation of the hydrogen bonds. The absence of the COOH···N hydrogen bond in *N*-methylanilinoacetic acid lends support to this conclusion; the COOH—N system is not planar in this molecule.

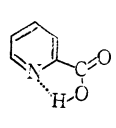

1

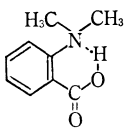

2

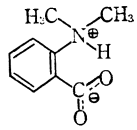

2_a

The hydrogen bond shifts of the ν_{OH} frequencies for *o*-dimethylaminobenzoic (III) and quinoline-8-carboxylic acids are extraordinarily large. The only ν_{OH} absorption observed is a broad band, distributed at from 2200 to 2750 cm^{-1}; it can be assigned to a hydrogen-bonded form such as 2. Intramolecular salt (2_a) formation seems to be improbable, since the carboxylic $\nu_{C=O}$ absorption appears at 1711 cm^{-1}* in both III and IV; this is too high for the antisymmetric stretching absorptions of the carboxylate anion. Ebullioscopic measurement also provides evidence for the strong hydrogen bond. Thus, no dimerization is observed over the concentration range in which benzoic acid dimerizes considerably; it can be explained that the strong intramolecular hydrogen bond prevents these acids from dimerization. Though no comparison of their thermodynamic quantities has been carried out, the larger $\Delta\nu$ value and the disappearance of the free ν_{OH} absoprtion in III and IV implies that a stronger hydrogen chelate is formed when a six-membered ring is to be made.

Table I. Infrared spectra and heat of hydrogen bond formationin dilute CCl_4 solution

Acid	ν_{OH} Absorption, cm^{-1} (Molar extinction coefficient)			$\nu_{C=O}$ Absorption, cm^{-1} (Molar extinction coefficient)	ΔH of H-bond formation (kcal./mol.)
	cis	trans	A_t/A_c		
Pyridine-2-carboxylic	3535 (9.1)	3328 (73.4)	17.8	1783 (657), 1772 (688)	0.2
Quinoline-2-carboxylic	3535 (13.0)	3333 (73.8)	12.8	1776 (1002)	0.8
N-Methylanilinoacetic	3535 (143)	—	—	1768 (822)	—

1) M. Ōki and M. Hirota, *J. Chem. Soc. Japan, Pure Chem. Sect.* (*Nippon Kagaku Zasshi*), **86**, 115 (1965).

* This absorption lies at abnormally low wave numbers, compared with the ordinary *s-trans* carboxylic acid (ca. 1750 cm^{-1}). This may imply that there is some contribution of 2_a.

BULLETIN OF THE CHEMICAL SOCIETY OF JAPAN VOL. 39 1621—1627 (1966)

The Viscosity and Conductivity of Aqueous Solutions of Electrolytes Mixed with Glycine and Urea

By Tokuzo TONOMURA and Katsunobu OKAMOTO

Department of Chemistry, Faculty of Science, Kanazawa University, Kanazawa

(Received July 2, 1965)

The viscosities, the densities, and the conductivities of aqueous solutions of electrolytes mixed with glycine or with urea have been measured at 15, 25 and 35°C. The relative viscosities and the relative conductivities of the mixed solutions have been expressed by the empirical formulae, $\eta=\eta'+\eta_0\beta C$ and $\Lambda=\Lambda_0(1-\gamma C)$, respectively. The retarding effect of glycine on the conductivity of the strong electrolytes has been found to be greater than that of urea in the mixed solutions. The states of the hydration of glycine, urea and the strong electrolytes have been discussed on the basis of the relations between B-values in the viscosity formula of Jones and Dole and the effective volumes in aqueous solutions.

Some studies of the electrochemical properties of aqueous solutions of strong electrolytes using several methods have been reported,[1-4] but only a few data are available in the literature[5-8] for aqueous solutions of mixed electrolytes. The purpose of the present study is to obtain some information concerning hydration and related problems, and to determine the behavior of weak electrolytes from measurements of the viscosity, density and conductivity of various electrolyte solutions in which weak electrolytes are mixed with strong electrolytes. In the present studies, glycine and urea[9] were used as weak electrolytes, and potassium chloride and lithium chloride, as strong ones. An aqueous solution of potassium chloride has a negative viscosity coefficient, while that of lithium chloride is well known to have an abnormal concentration dependence of the viscosity. The viscosity coefficients and densities of aqueous solutions of electrolytes were measured over and appropriate concentration range. Their conductivities were also measured in order to compare the retarding effects of glycine on the mobility of ions with those of urea. The viscosity formula of Jones and Dole is:

$$\eta = \eta_0(1 + AC^{1/2} + BC) \qquad (12)$$

where η is the viscosity of the solution; η_0, that of the medium, and C, the concentration of the solute, A and B being constants characteristic of the solute. The A coefficient in the above formula is considered to be chiefly due to the contribution of interionic forces, electrostatic in nature, and the B coefficient to the interaction between solute and solvent in the solution. As the second term, AC, in Eq. 1 is usually so small that it can be neglected,[10] Eq. 1 becomes:

$$\eta = \eta_0(1 + BC) \qquad (2)$$

According to Stokes and Mills,[11] the B coefficient in Eq. 2 may be expressed as follows:

$$\eta^E + \eta^A + \eta^D = \eta_0 BC \qquad (3)$$

where η^E is the viscosity increment arising from the size and shape of an ion; it normally increases with an increase in the ion size. η^A is the increment due to the alignment or orientation of polar molecules by the ionic field. η^D is the viscosity change associated with the distortion of the solvent structure; this effect can be interpreted as being due to competing forces from the solvent structure in the bulk and from the ionic field. It will cause the viscosity to decrease.

One gram of solution, whose specific volume is v at concentration of C mol./l., contains x g. of solute of the molecular weight M and $(1-x)$g. of solvent. Then,

$$x = MC/1000\rho \qquad (4)$$

where ρ is the density of the solution. We assume that the partial specific volume of the solute in

1) H. S. Harnd and B. B. Owen, "Physical Chemistry of Electrolytic Solutions," Reinhold Publ. Corp., 3rd. Ed., New York (1957).
2) R. W. Gurney, "Ionic Processes in Solution", McGraw-Hill Book Co., New York (1953).
3) M. Kaminsky, *Discussions Faraday Soc.*, **24**, 171 (1957).
4) E. R. Nightingale, Jr., *J. Phys. Chem.*, **63**, 1381 (1959).
5) R. M. Roberts and J. G. Kirkwood, *J. Am. Chem. Soc.*, **63**, 1373 (1941).
6) E. J. King, ibid., **73**, 155 (1951).
7) J. M. Stokes and R. H. Stokes, *J. Phys. Chem.*, **60**, 217 (1956).
8) R. A. Robinson and R. H. Stokes, "Electrolyte Solutions," Butterworths Scientific Publ., London (1955).
9) V. K. Venkatesan and C. V. Suryanarayana, *J. Phys. Chem.*, **60**, 775 (1956).
10) R. H. Stokes and R. Mills, "Viscosity of Electrolytes and Related Properties," Int. Encyclopedia of Phys. and Chem., Pergamon Press, New York (1965), p. 30.
11) R. H. Stokes and R. Mills, Ioc. cit., p. 40.

solution is v' at the concentration C; then:

$$v = (1 - x)v_0 + xv' \quad (5)$$

where $v_0(\fallingdotseq 1/\rho_0)$ is the partial specific volume of the solvent in a solution. From Eqs. 4 and 5,

$$\rho/\rho_0 = 1 + (M \cdot C \cdot 10^{-3})(v_0 - v') \quad (6)$$

The effective volume, V, of the ions in solution is equal to $M \cdot v' \cdot 10^{-3}$ l./mol.

Experimental

All of substances used here were of an analytical reagent grade. Glycine was purified by recrystallization from an ethanol-water solution, and potassium chloride and urea, by recrystallization from conductivity water, but lithium chloride was used without further purification. Solutions from 0.05 to 0.25 molality were prepared. The systems of aqueous solutions were as follows:

System 1. Strong electrolytes: KCl and LiCl.

System 2. Weak electrolytes: Glycine and Urea.

System 3. Mixed electrolytes:

KCl + Glycine, KCl + Urea,

LiCl + Glycine, LiCl + Urea,

The viscosities of the solutions were measured at 15, 25 and 35±0.05°C by an Ostwald viscometer with a flow time of about 260 sec. for water at 25°C. The reproducibility of the flow times was within ±0.2 sec. Two viscometers were always used for a given system, and each measurement was repeated six to ten times and then the average was taken to get the desired result. By the measurement of the viscosity of water, dioxane and benzene, the correction term for kinetic energy was found to be so small that it was ignored. The relative viscosity was calculated by the usual formula:

$$\eta/\eta_0 = \frac{t(\text{flow time of solns.})\rho(\text{density of solns.})}{t_0(\text{flow time of water})\rho_0(\text{density of water})} \quad (7)$$

The densities of the solutions were measured by an Ostwald pycnometer of about 4 ml. The resistance of the solutions was measured with a universal bridge, Yokogawa BV-Z-13A. Three cells with platinized electrodes were used, their cell constants being 7.379, 1.445 and 0.8541, respectively; the electrodes were checked frequently with the 0.01 N or 0.1 N potassium chloride solutions. The data were reproducible within ±0.5%.

Results and Discussion

The relative and absolute viscosities of aqueous solutions of glycine and urea are given in Table I. Also, the relative viscosities of the mixed solutions are given in Figs. 1, 2 and 3.

Plotting $(\eta/\eta_0 - 1)/C^{1/2}$ versus $C^{1/2}$, the A coefficient is the ordinate intercept, while the B coefficient is given by the slope. The A and B coefficients thus obtained are summarized in Table II. Figures 1, 2 and 3 show that the relationship between the relative viscosities of the solution of mixed electrolytes and the concentration of the weak electrolytes is linear. The empirical formula of the relative viscosities (System 3) was obtained by the method of least squares; namely:

$$\eta = \eta' + \eta_0 \beta C \quad (8)$$

Table I. Relative and absolute viscosities of aqueous solutions of glycine and urea at 15, 25 and 35°C

Glycine (m)	15°C		25°C		35°C	
	η/η_0	η (poise)	η/η_0	η (poise)	η/η_0	η (poise)
0	1.000	0.01144*	1.000	0.008949*	1.000	0.007208*
0.050	1.007	0.01152	1.007	0.009012	1.007	0.007258
0.100	1.013	0.01159	1.013	0.009065	1.014	0.007309
0.175	1.023	0.01171	1.024	0.009164	1.025	0.007388
0.250	1.034	0.01183	1.035	0.009262	1.036	0.007467
Urea (m)						
0.050	1.002	0.01147	1.002	0.008967	1.002	0.007222
0.100	1.004	0.01149	1.004	0.008985	1.004	0.007237
0.175	1.007	0.01152	1.007	0.009012	1.007	0.009012
0.250	1.009	0.01155	1.009	0.009030	1.010	0.00728

* Quoted from data of the International Critical Tables at each temp. (absolute viscosity of water)

Table II. Coefficients A and B of the viscosity Eq. 1

	15°C		25°C		35°C	
	A	B	A	B	A	B
LiCl	0.001	0.143	0.002	0.140	0.002	0.140
KCl	0.003	−0.037	0.003	−0.014	0.003	0.013
Glycine	0	0.136	0	0.140	0	0.143
Urea	0	0.037	0	0.037	0	0.040

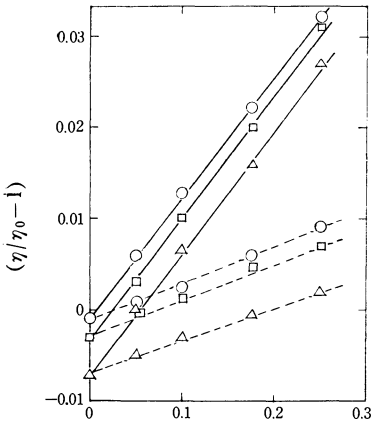

Concn. (m) of weak electrlytes

—○— KCl 0.05 m + Glycine
--○-- KCl 0.05 m + Urea
—□— KCl 0.10 m + Glycine
--□-- KCl 0.10 m + Urea
—△— KCl 0.25 m + Glycine
--△-- KCl 0.25 m + Urea

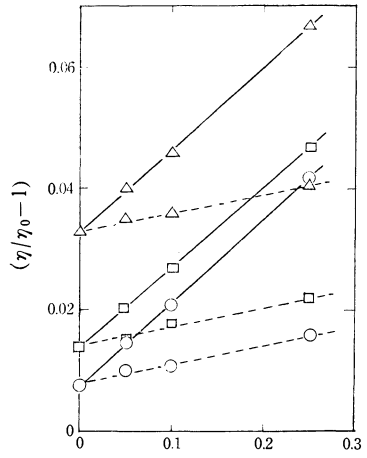

Concn. (m) of weak electrolytes

—○— LiCl 0.048 m + Glycine
--○-- LiCl 0.048 m + Urea
—□— LiCl 0.095 m + Glycine
--□-- LiCl 0.095 m + Urea
—△— LiCl 0.22 m + Glycine
--△-- LiCl 0.22 m + Urea

Fig. 1. Relative viscosities of mixed electrolyte solutions as a function of the concentration of added weak electrolyte, at 15°C.

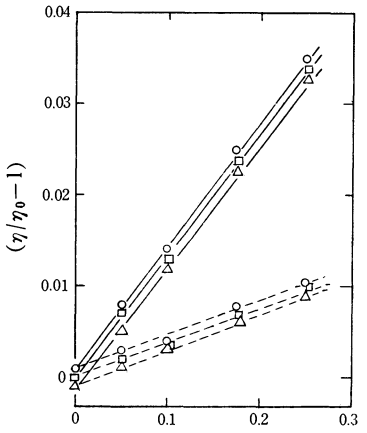

Concn. (m) of weak electrolytes

—○— KCl 0.05 m + Glycine
--○-- KCl 0.05 m + Urea
—□— KCl 0.10 m + Glycine
--□-- KCl 0.10 m + Urea
—△— KCl 0.25 m + Glycine
--△-- KCl 0.25 m + Urea

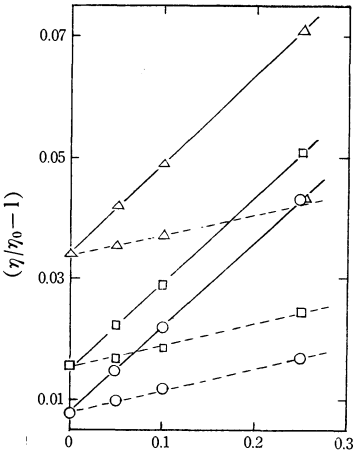

Concn. (m) of weak electrolytes

—○— LiCl 0.05 m + Glycine
--○-- LiCl 0.05 m + Urea
—□— LiCl 0.10 m + Glycine
--□-- LiCl 0.10 m + Urea
—△— LiCl 0.24 m + Glycine
--△-- LiCl 0.25 m + Urea

Fig. 2. Relative viscosities of mixed electrolyte solutions as a function of the concentration of added weak electrolyte, at 25°C.

where η' is the viscosity of the strong electrolyte at a given concentration, β is a constant characteristic of the weak electrolyte, and C is the molal concentration of the weak electrolyte. From the fact that the values of β thus found are nearly constant for a given weak electrolyte, as is shown in Figs. 1, and 2 and 3, the viscosity of weak electrolytes when mixed with strong electrolytes seems not to be influenced by the strong ones.

The specific gravities and the partial specific volumes of an aqueous solution of the weak electrolytes are given in Table III. In Fig. 4, a plot

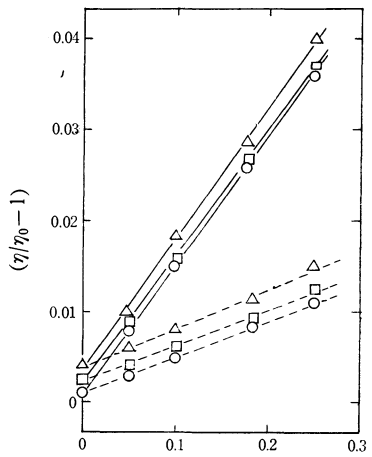

Concn. (m) of weak electrolytes

—○— KCl 0.06 m + Glycine
--○-- KCl 0.06 m + Urea
—□— KCl 0.10 m + Glycine
--□-- KCl 0.11 m + Urea
—△— KCl 0.25 m + Glycine
--△-- KCl 0.25 m + Urea

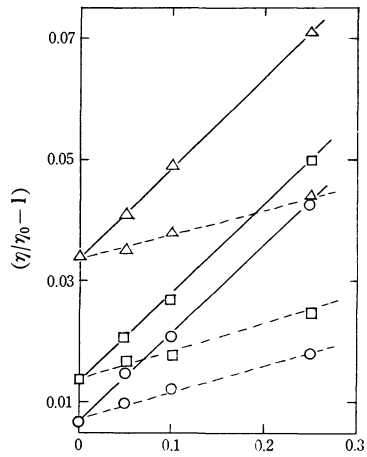

Concn. (m) of weak electrolytes

—○— LiCl 0.05 m + Glycine
--○-- LiCl 0.06 m + Urea
—□— LiCl 0.10 m + Glycine
--□-- LiCl 0.10 m + Urea
—△— LiCl 0.26 m + Glycine
--△-- LiCl 0.26 m + Urea

Fig. 3. Relative viscosities of mixed electrolyte solutions as a function of the concentration of added weak electrolyte, at 35°C.

of the ratio of the densities (ρ_3/ρ_1)* versus the concentration of the weak electrolyte gives a linear relation and is in accord with that of pure weak electrolyte solutions given in Table III. It is shown that the curves are independent of the temperature and species of the strong electrolyte used. From this fact, there seems to be little influence on the effective volume due to the electrostatic interaction between the ions and solutes of weak electrolytes, even though the solute is glycine, which has a comparatively large dipole moment,[5] in a polar solvent. Undoubtedly, the interaction between water molecules and all solutes in solution is more dominant than that between ions of the strong electrolyte and solutes of the weak one. It seems that the ions and the solutes in the mixed solution retain much the state of hydration they have in pure water, at least at the concentration considered.

The partial specific volumes of the electrolyte in solution are calculated from Eq. 5. The effective volumes(V) of ions in those solutions were estimated from the partial specific volume and are given in the third column of Table IV; other electrolytes quoted from the literature are given in the same column.

Let us assume that, for all the species thus obtained, the effective volume is a measure of the static volume occupied by the species in solution. Thus the B-values in the viscosity formula are considered to be the kinetic volumes of the solvated species in solution, and the values of the (B/V) ratio are considered to be closely related to the hydration. From Table IV it is apparent that the B/V values of alkaline halides, with the exception of lithium and sodium halides, are considerably different from

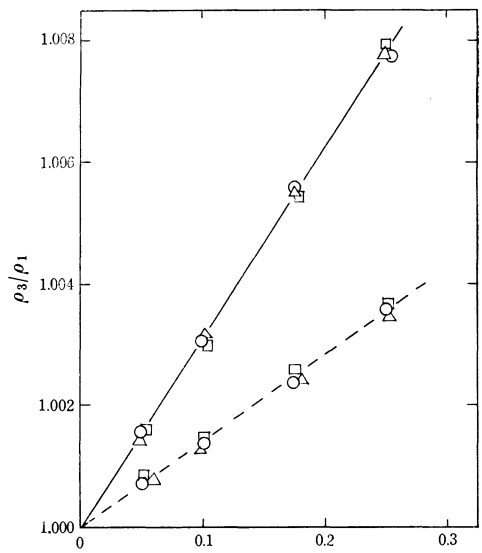

Concn. (mol./l.) of weak electrolyte (Glycine, Urea)

Fig. 4. Ratio of relative density as a function of the concentration of added weak electrolyte at 25°C.

(Coded as in Fig. 2. Full line: LiCl + Glycine
Broken line: LiCl + Urea

* ρ_3 is the density of the mixed solution and ρ_1 is that of the strong electrolyte solution, the concentration of the strong electrolyte in both solutions being kept constant.

TABLE III. SPECIFIC GRAVITIES AND PARTIAL SPECIFIC VOLUMES OF AQUEOUS SOLUTIONS OF GLYCINE AND UREA AT 15, 25 AND 35°C

Glycine mol./l.	ρ/ρ_0	v'	Urea mol./l.	ρ/ρ_0	v'	Temp. °C
0.0498	1.0016	0.572	0.0498	1.0007	0.767	15
0.0995	1.0031	0.585	0.0995	1.0015	0.750	15
0.1735	1.0055	0.578	0.1735	1.0025	0.761	15
0.2471	1.0079	0.575	0.2469	1.0037	0.751	15
0.0497	1.0016	0.574	0.0497	1.0007	0.768	25
0.0993	1.0032	0.573	0.0992	1.0014	0.767	25
0.1731	1.0053	0.594	0.1731	1.0026	0.753	25
0.2466	1.0078	0.581	0.2465	1.0036	0.759	25
0.0496	1.0016	0.575	0.0496	1.0007	0.771	35
0.0990	1.0031	0.589	0.0990	1.0014	0.770	35
0.1726	1.0054	0.587	0.1726	1.0025	0.765	35
0.2459	1.0079	0.578	0.2457	1.0036	0.762	35

The values of ρ_0 were quoted from data of the International Critical Tables at each temperature.

TABLE IV. CONSTANTS OF DENSITY AND VISCOSTIY EQUATIONS AND HYDRATION NUMBER AT 25°C

Solute	V_c**	$V=Mv'10^{-3}$ l./mol.	B	B/V	Hydration number (a)	(b)	(c)	(d)
LiCl	0.0206	0.0175	0.140	8.00	7.0	6	2.9—6.3	3.7—4.2
LiBr	0.0249	0.0249*	0.108[3]	4.34	7.6	5—6	2.9—5.6	—
LiI	0.0325	0.0363*	0.081[3]	2.23	2.0	—	—	—
NaCl	0.0268	0.0181*	0.079[3]	4.34	3.5	7	1.1—3.5	4.5—5.2
NaBr	0.0315	0.0245*	0.044[3]	1.80	4.2	6—7	1.2—2.8	—
NaI	0.0406	0.0358*	0.018[3]	0.50	5.5	—	2.2—3.0	—
KCl	0.0375	0.0278	−0.017	−0.61	1.9	7	0.6—0.8	3.6—4.3
KBr	0.0429	0.0349*	−0.048[3]	−1.38	2.1	6—7	0.3—1.2	—
KI	0.0528	0.0470*	−0.076[3]	−1.62	2.5	6—7	−0.3—1.5	—
RbCl	0.0438	0.0332*	−0.037[3]	−1.11	1.2	—	—	4.3—5.0
RbBr	0.0488	0.0402*	−0.072[3]	−1.79	0.9	—	—	—
RbI	0.0592	0.0516*	−0.099[3]	−1.92	0.6	—	—	—
CsCl	0.0424	0.0420*	−0.052[3]	−1.29	—	—	—	2.9—3.5
CsBr	0.0480	0.0472*	−0.087[3]	−1.84	—	—	—	—
CsI	0.0578	0.0580*	−0.113[3]	−1.93	—	—	—	—
$MgCl_2$	0.0410	0.0193*	0.371[3]	19.2	13.7	16—17	—	9.5—10.5
$CaCl_2$	0.0511	0.0218*	0.271[3]	12.4	12.0	10	—	9.2—10.3
$SrCl_2$	0.0519	0.0203*	0.251[3]	12.3	10.7	—	—	11.4—12.9
Glycine	0.0469	0.0435	0.140	3.22	—	—	—	2.7—3.4
Urea	0.0450	0.0457	0.036	0.79	—	—	—	—
Acetic acid	—	0.0514*	0.117[2]	2.28	—	—	—	—
Sucrose	—	0.2153*	0.879[1]	4.08	—	3.8	—	—

* The V-values were calculated by Eq. 6 from the data of densities in the International Critical Tables, their molal concentrations were from 0.05 to 0.25 m.

** The V_c values for inorganic salts were quoted from the International Critical Tables and the Kagaku Binran. For orgagnic compounds were quoted from the literature.[14]
(a) Ref. 1, (b) Ref. 12, (c) Ref. 8, (d) Ref. 13

those of alkaline earth metal chlorides, glycine and urea. Potassium, rubidium and cesium halides have negative B/V values. This will be discussed below. It is generally believed that the degree of hydration in aqueous electrolyte solutions decreases with an increase in the radius of the univalent cation.[2] Moreover, anions have the effect of breaking the structure of water.[3,4] As has been described previously, the ions with large crystal radii, such as Cs^+ or I^-, have a weak orienting effect in the first layer because of their small surface charge densities. Thus η^A would be small. However,

12) H. Shiio, *J. Am. Chem. Soc.*, **80**, 70 (1958).
13) S. Goto and T. Isemura, This Bulletin, **37**, 1693 (1964).
14) A. N. Winchell, "The Optical Properties of Organic Compounds," Academic Press Inc., Publishers, New York, N. Y. (1954).

a considerable distortion of the solvent structure may occur in the vicinity of the ion, and accordingly, η^D will become predominant. In this class of ions $\eta^A < \eta^D$ and the B/V value is negative. According to Samoilov,[15] the negative hydration was taken for the above case, and the molecules of water near the ion become more mobile than in pure water. On the other hand, as may be seen in Table IV, lithium chloride and alkaline earth metal chlorides produce a viscosity increment[16] greater than that corresponding to their effective volume in solution. The small size of cations with large surface charge densities, such as Li^+ and Mg^{2+}, cause a strong orientation of water molecules and they are believed to have a primary hydration. The η^E value will be large because of its primary sheath. The sum, $\eta^E + \eta^A$, will be larger than the decrement due to η^D. In this class, $\eta^A \gg \eta^D$ and the B/V value is fairly large and positive. Molecular ions such as glycine may be expected to have large η^E values because of their large size. As is shown in Table IV, the volume (V_c) of glycine in the crystal state is 0.0469 (l./mol.) and the effective volume (V) in solution is 0.0435 (l./mol.). This suggests that the behavior of glycine in hydration may resemble that of the strong electrolytes, such as lithium chloride, whose volume in a solution is apparently smaller than the volume in the crystal state due to the contraction of the solvent by electrostriction.[2] In addition, large η^A values may be expected from their large dipole moments, as has been pointed out already. However, the distortion effects would be the same as that of large ions mentioned above.

From the results obtained, it is evident that $\eta^A > \eta^D$ and that the B/V value for glycine is still positive. Isemura and Goto[17] have suggested, as a result of studies by the ultrasonic method, that glycine and strong electrolytes resemble each other in the mechanism of hydration; their suggestion is supported by the present results. The B/V values of urea is smaller than that of glycine, though the effective volume of urea, as may be seen in Table IV, is nearly equal to that of glycine. Again, we found that the V of urea in solution, as determined from the densities, is nearly equal to the volume(V_c) in the crystal state: V, 0.0457 (l./mol.); V_c, 0.0450 (l./mol.). It is well known that water molecules are attracted to the urea molecule, as urea has hydrophilic groups. From these findings, the hydration of urea can be interpreted as the result of competition between the breaking and the formation of the hydrogen bonding.

By means of measurements[13] of the NMR, the relative shifts of the proton resonances of aqueous solutions containing various electrolytes or organic compounds may be discussed with regard to their state of hydration. The results indicate that the degree of relative shifts of anions increase with an increase in the ionic radius. The differences in the B/V values in the lithium halides, therefore, seem to correspond with that of the relative shifts of anions, as they have a common cation in solution. Several methods,[8,12,13,16] from different standpoints and different assumptions, have been reported for determining the degree of hydration of electrolytes in an aqueous solution; these values are given in Table IV. The B/V values obtained may be compared with their hydration numbers, which are shown in the same table.

The relative conductivities of the mixed solutions are given in Figs. 5, 6 and 7. By plotting Λ/Λ_0 versus C, the γ coefficient is given by the slope. These figures show that the relative conductivities, Λ/Λ_0, are dependent on the concentration of the added weak electrolyte. Then, an empirical formula was obtained at each temperature, as follows:

$$\Lambda = \Lambda_0(1 - \gamma C) \qquad (9)$$

Table V. γ-Coefficient of the conductivity Eq. 9 at each temperature

	15°C	25°C	35°C
System 3.			
KCl + Glycine	0.127	0.130	0.128
LiCl + Glycine	0.120	0.129	0.130
KCl + Urea	0.068	0.075	0.076
LiCl + Urea	0.071	0.076	0.073

$\Lambda = \Lambda_0(1-0.127 \cdot C)$ for glycine,
$\Lambda = \Lambda_0(1-0.073 \cdot C)$ for urea.

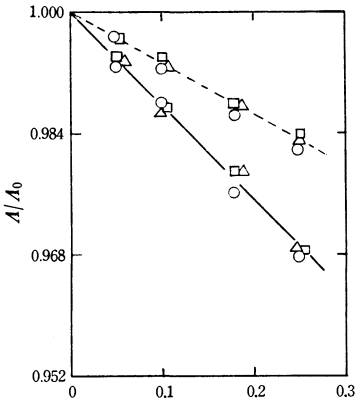

Fig. 5. Relative conductivities of mixed electrolyte solutions as a function of the concentration of added weak electrolyte, at 15°C.
Concn. of strong electrolyte:
○, 0.05 mol.; □, 0.10 mol.; △, 0.25 mol.
Full line: KCl + Glycine
Broken line: KCl + Urea
(Systems of lithium chloride are not given here, but their figures are nearly identical with the above systems.)

15) O. Ya. Samoilov, *Discussions Faraday Soc.*, **24**, 141 (1957).
16) H. S. Frank and W. Y. Wen, ibid., **24**, 133 (1957).
17) T. Isemura and S. Goto, This Bulletin, **37**, 1697 (1964).

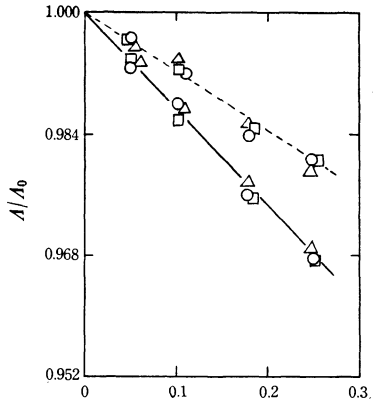

Concn. (mol./l.) of weak electrolytes

Fig. 6. Relative conductivities of mixed electrolyte solutions as a function of the concentration of added weak electrolyte, at 25°C.
(Coded as in Fig. 5)

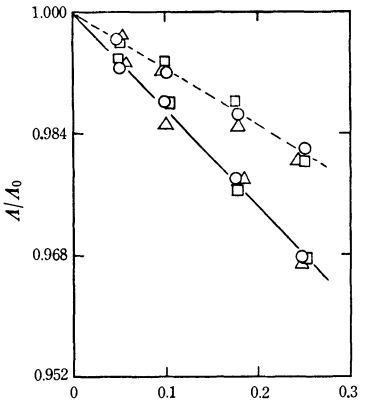

Concn. (mol./l.) of weak electrolytes

Fig. 7. Relative conductivities of mixed electrolyte solutions as a function of the concentration of added weak electrolyte, at 35°C.
(Coded as in Fig. 5)

where Λ is the equivalent conductivity of the mixed solution; Λ_0 is that of a strong electrolyte in the pure solution, and γ is a constant characteristic of the added weak electrolyte. The γ coefficients thus obtained are summarized in Table V. From these results, it was found that the retarding effect of glycine on the ionic mobility of the strong electrolyte is greater than that of urea and that it is independent of the species of strong electrolyte used here. The ions of strong electrolytes, for example, are retarded to approximately the same extent when glycine is added to the solution at a given concentration. However, the viscosities of electrolytes are considerably different from each other. It seems that the retardation is independent of the frictional property of mixed solutions.

BULLETIN OF THE CHEMICAL SOCIETY OF JAPAN VOL. 39 1627—1632 (1966)

Monolayer Adsorption with Nearest Neighbor Interactions

By Ralph J. TYKODI

Department of Chemistry, Southeastern Massachusetts Technological Institute
North Dartmouth, Massachusetts 02747, U. S. A.

(Received July 23, 1965)

A sequence of approximate combinatorial treatments of the localized monolayer adsorption of a gas on a lattice of uniform sites with only nearest neighbor interactions allowed generates a one parameter family of isotherm equations. For each of those cases where the general lattice problem has been solved exactly, it is possible to find a value of the adjustable parameter such that critical behavior on the lattice in question is reproduced exactly.

In 1939 Fowler and Guggenheim[1] analyzed the treatment of localized monolayer adsorption of a gas on a lattice of uniform sites with only nearest neighbor (n. n.) interactions allowed in an elegant manner and discussed in detail two isotherm relations (*crude* and *refined*) showing first order phase change behavior under suitable conditions. Since the 1939 formulation of Fowler and Guggenheim, the parallel problem of the Ising model for ferromagnetism has received a great deal of attention.

1) R. H. Fowler and E. A. Guggenheim, "Statistical Thermodynamics," Ch. X, Cambridge University Press (1939).

The many advances made toward a complete solution of the general problem of nearest neighbor (n. n.) lattice statistics and the powerful and sophisticated mathematical methods employed by recent workers in the field have been reviewed by (e. g.) Temperley,[2] Hill,[3] and Domb.[4] The known exact solutions for two-dimensional lattices[4] show that it is not enough to consider only the coordination number of a lattice (as in the work of Fowler and Guggenheim[1])—more specific properties of the lattice must also be taken into account. In this paper, however, we shall consider a sequence of approximate combinatorial treatments of the adsorption problem based on coordination number arguments alone. Our results will generate a one parameter family of isotherm equations with the rather unexpected property of *exactly* reproducing critical behavior on the lattice in question for a suitable choice of the adjustable parameter. The effect of the more detailed features of the lattice that are neglected in the approximate treatments is merely to shift the value of the parameter in the basic family of equations. The combinatorial arguments, then, establish a set of "calibration points," with an easily comprehended physical basis, across the spectrum of possible values of the adjustable parameter.

In what follows we shall deal in a simple combinatorial manner with the problem of N identical gas molecules adsorbed on N_s identical sites, trying to take into account the n. n. (nearest neighbor) interactions among the adsorbed molecules.

The Combinatorial Problem

In many respects we shall follow the notation of Fowler and Guggenheim[1] closely; however, we shall feel free to vary that notation wherever it proves convenient to do so. We express the Helmholtz free energy for the macro state of a localized monolayer with N identical gas molecules adsorbed on N_s identical sites by

$$F^{ads}/\boldsymbol{k}T = -\ln \Omega\,(n_i) - N(n_i) \ln a^\circ(T) + \varepsilon(n_i)/\boldsymbol{k}T \quad (1)$$

where the n_i are parameters of a geometric nature (bonds, triangles, etc.) by means of which we shall take into account n. n. interactions among the adsorbed molecules, A is the *extra* potential energy (relative to the gas state at infinite separation) due to n. n. interactions, $a^\circ(T)$ is the partition function of an isolated adsorbed molecule,* and Ω is a combinatorial expression for the number of micro states corresponding to the set of parameters n_i.[5]

We shall minimize $F^{ads}/\boldsymbol{k}T$ with respect to the parameters n_i, subject to the restriction $N=N(n_i)$ = constant:

$$\delta\left(\frac{F^{ads}}{\boldsymbol{k}T}\right) = -\sum_i\left[\frac{\partial \ln \Omega}{\partial n_i} + \frac{\partial N}{\partial n_i}\ln a^\circ(T) - \frac{1}{\boldsymbol{k}T}\frac{\partial A}{\partial n_i}\right]\delta n_i = 0$$

$$\delta N = \sum_i (\partial N/\partial n_i)\delta n_i = 0 \quad (2)$$

Introducing the Lagrange multiplier α, we obtain i equations of the form

$$\frac{\partial \ln \Omega}{\partial n_i} + \frac{\partial N}{\partial n_i}(\ln a^\circ(T) - \alpha) - \frac{1}{\boldsymbol{k}T}\frac{\partial A}{\partial n_i} = 0 \qquad i=1,2,\cdots \quad (3)$$

Solution of the set of simultaneous equations given by Eq. 3 leads to the isotherm relation.

Our chief problem is the finding of adequate expressions for $\Omega=\Omega(n_i)$. We shall examine special cases, starting with simple ones and gradually proceeding to those more complex. Our ultimate goal is to find the appropriate form of the isotherm relation for the general case where adsorption takes place on a plane lattice for which each site is surrounded by z nearest neighbor (n. n.) sites.

Isolated Clusters

Turning now to the basic combinatorial problem, let us consider a set of N_s adsorption sites. If we were actually to draw in bonds between n. n. sites, we could divide those bonds into classes on the basis of the state—occupied (O) or unoccupied (U) by an adsorbed molecule—of the sites connected by a n. n. bond. Allowing the n. n. bonds to have a directional character (for proper multiplicity) we could distinguish four classes of bonds OO, OU, UO, and UU. We shall often find it convenient to discuss the combinatorial problem on a given lattice in terms of these classes of n. n. bonds.

Let us first turn to the case where the sites of a given set are treated as isolated clusters of sites. We consider the N_s sites as divided up into N_s/i clusters such that the clusters are relatively far apart but within any cluster each site has i-1 *equivalent* n. n. sites. If we denote a cluster containing i sites, everyone of which can be connected to each of the other i-1 sites by a n. n. bond, as an (i)-cluster, then in a (2)-cluster we have a pair of sites connected (connectable) by a n. n. bond,

2) H. V. N. Temperley, "Changes of State," Ch. VI, Cleaver-Hume Press Ltd., London (1956).
3) T. L. Hill, "Statistical Mechanics," Ch. 7, McGraw-Hill Book Company, Inc., New York (1956).
4) C. Domb, *Advances in Physics*, **9**, 149 (1960).
* See Ref. 1, p. 429.
5) J. Hijmans and J. de Boer, *Physica*, **21**, 471 (1955).

and in a (3)-cluster the triplet of sites may be regarded as forming an equilateral triangle with n. n. bonds for sides. For clusters of higher order it is not possible to arrange the sites in a plane configuration so that all the sites of a cluster are equivalent, i. e. each site of the cluster connected to the other i-1 sites of the cluster by n. n. bonds.

In distributing N molecules over the N_s sites grouped into isolated clusters we need a scheme for counting the number of n. n. bonds of the type OO and for keeping track of configurational permutations. We could set up a scheme in terms of the n. n. bond classes mentioned at the beginning of this section, but in this particular case we choose to proceed differently.

Let us first turn to the case of isolated (2)-clusters. Suppose we place our N molecules on the N_s sites in such a way that the number of clusters containing *at least* one molecule is n_1 and the number of clusters containing *at least* two molecules is n_2. The number of clusters containing *at least* zero molecules is equal to the total number of clusters, i. e. $n_0=N_s/2$, and (included for convenience in notation) the number of clusters containing *at least* three molecules (n_3) is zero. Similarly the number of clusters containing *exactly* i molecules ($i=0$, 1, 2) is just n_i-n_{i+1}; here, and in the remainder of the paper, the symbol n_i denotes the number of clusters (of a given type) containing *at least* i molecules.

With due allowance for the possible permutations within a cluster, the number of micro states corresponding to the above specification (in terms of the n_i) is

$$\Omega = \frac{2^{n_1-n_2}\, n_0!}{(n_0-n_1)!\,(n_1-n_2)!\,n_2!} \tag{4}$$

If $-\varepsilon$ is the interaction potential energy (relative to the gas state at infinite separation) of a pair of adsorbed molecules a n. n. distance apart, then the total extra potential energy due to n. n. interactions among the adsorbed molecules is just $-\varepsilon$ times the number of n. n. bonds of type OO. Thus, for isolated (2)-clusters

$$A = -\varepsilon n_2 \tag{5}$$

and

$$N = n_1 + n_2 \tag{6}$$

Setting $n_i/n_0=f_i$, where f_i is the fraction of the total number of clusters containing *at least* i molecules, and making use of Stirling's approximation for the logarithm of a factorial, we obtain from Eqs. 3, 4—6 the relations

$$\frac{f_1-f_2}{1-f_1} = 2x \qquad \frac{f_2}{f_1-f_2} = \frac{\zeta x}{2} \tag{7}$$

where $\zeta=\exp(\varepsilon/\boldsymbol{k}T)$ and $x=a^\circ(T)e^{-\alpha}=\lambda_g a^\circ(T)=p/p^\circ$ (λ_g being the absolute activity of the gas molecules*). Our ζ corresponds to the quantity $\exp(-2\omega/z\boldsymbol{k}T)$ in the notation of Fowler and Guggenheim.[1] Equation 7 yields the relation

$$4f_2(1-f_1)/(f_1-f_2)^2 = \zeta \tag{8}$$

Equation 8 is a slightly disguised version of the equation of quasichemical equilibrium discussed by Fowler and Guggenheim[1]; it is an exact equation for the case of isolated (2)-clusters and is often invoked as an approximation in the case of more complex lattice situations.

From Eq. 7 and the relation $f_1+f_2=2\theta$ we obtain

$$\frac{\theta}{1-\theta} = \frac{x(1+\zeta x)}{1+x} \tag{9}$$

Solving Eq. 9 for x we get

$$x = \frac{\theta}{1-\theta}\cdot\frac{1}{\zeta}\cdot\left[\frac{\beta-1+2\theta}{2\theta}\right] \tag{10}$$

where

$$\beta = [1-4\theta(1-\theta)(1-\zeta)]^{1/2}$$

If there are no interactions among the adsorbed molecules, then $\varepsilon=0$, $\zeta=1$, and Eqs. 9 and 10 reduce to the simple Langmuir equation $x=\theta/(1-\theta)$. If there are attractive interactions among the adsorbed molecules, then $\varepsilon>0$, $\zeta>0$, and the coverage θ is greater for a given temperature and pressure than that predicted by the Langmuir equation.

The treatment of isolated clusters is useful because it allows us to examine the effect of n. n. interactions on the adsorption isotherm for a simple case for which the combinatorial expression $\Omega(n_i)$ can be evaluated exactly. The formalism that we have set up for treating isolated clusters then serves as a starting point for the treatment of connected lattices where the exact evaluation of the combinatorial expression $\Omega(n_i)$ is an extremely difficult problem.

Rule of Thumb Approximation

We now wish to consider a plane connected lattice* for which each site has z n. n. sites and wish to treat the adsorption problem on such a lattice according to an approximate method which is modeled after the treatment of isolated clusters. The connectivity of the lattice is a great source of trouble in setting up an appropriate combinatorial expression. While in the isolated cluster treatment it was possible to change the parametric specification n_i in unitary steps by the addition of

* See Ref. 1, p. 431, for details.

* A lattice is called *connected* if the sites are all equivalent and it is possible to pass from an arbitrary site to any other site of the set by traveling along n. n. bonds only.

single molecules, on a connected lattice the parameters more often change by z units upon the addition of single molecules to the lattice; thus, if we place one molecule on an otherwise empty connected lattice we immediately form z n. n. bonds of type OU (or UO).

Now it is reasonably evident that to the first molecule placed on a uniform lattice (connected or otherwise) all the N_s sites are equivalent, and the connectivity of the lattice is a dormant feature which becomes important when more molecules are added. Thus there are just N_s ways of placing one molecule on N_s uniform sites, regardless of the connectivity of the lattice. We now adopt the following rule of thumb condition:

In any approximate treatment of adsorption on a connected lattice the combinatorial expression when evaluated for the case of one molecule on N_s sites must be at least approximately equal to N_s for all values of z.

If we let $\Omega(1)$ represent the value of the combinatorial expression Ω for the case of one molecule on the N_s sites of a plane connected lattice, then the mathematical form of the rule of thumb requirement is that

$$\lim_{N_s\to\infty} \{\ln \Omega(1)/\ln N_s\} = 1$$

for all values of z.

A plane connected lattice, each site having z n. n. sites, has $zN_s/2$ n. n. bonds between the sites. We should now like to treat these $zN_s/2$ n. n. bonds in a manner similar to the treatment of n. n. bonds in isolated (2)-clusters. In the case of isolated (2)-clusters we had a 1 - 1 correspondence between the number of clusters and the number of n. n. bonds, and we were at liberty to set up the combinatorial expression in terms of cluster parameters or bond parameters; in fact we chose cluster parameters. In this section we wish to deal with the n. n. bonds themselves, carrying the development through in terms of n. n. bond parameters.

In a familiar fashion we set m_i ($i=0, 1, 2$) equal to the number of n. n. bonds whose terminal sites are occupied by *at least* i adsorbed molecules. We shall assume that our directional convention for n. n. bonds is such that for any distribution of N molecules on the N_s sites the number of n. n. bonds of type OU is approximately equal to the number of type UO. Letting the symbol itself (OO e.g.) stand for the number of n. n. bonds of that type, we have, in terms of our more familiar parameters,

$$\left.\begin{aligned} zN_s/2 &= m_0 \\ \mathrm{UU} &= m_0 - m_1 \\ \mathrm{UO} = \mathrm{OU} &= (m_1 - m_2)/2 \\ \mathrm{OO} &= m_2 \end{aligned}\right\} \qquad (11)$$

If we were to treat the $zN_s/2$ n. n. bonds as *permutable things*, the number of distinguishable bond configurations corresponding to a definite set m_i would be

$$\Omega = \frac{m_0!}{(m_0-m_1)!\,[(1/2)(m_1-m_2)]!^2\,m_2!} \qquad (12)$$

Within the limits of Stirling's approximation for factorials Eq. 12 is the same as

$$\Omega = \frac{m_0!\,2^{m_1-m_2}}{(m_0-m_1)!\,(m_1-m_2)!\,m_2!} \qquad (13)$$

which bears out what we were saying previously about the treatment of isolated (2)-clusters.

In dealing with n. n. bond configurations (with $m_0=zN_s/2$) we are (for $z>1$) counting many more configurations than can be physically realized by distributing N molecules on N_s sites; we find, in fact, that

$$\lim_{N_s\to\infty} \{\ln \Omega(1)/\ln N_s\} = z$$

for Eq. 13. We note, however, that if we set

$$\Omega = \left\{\frac{m_0!}{(m_0-m_1)!\,[(1/2)(m_1-m_2)]!^2\,m_2!}\right\}^{1/z} \qquad (14)$$

the rule of thumb condition is satisfied.

Equations 3 and 14 together with the conditions

$$\left.\begin{aligned} A &= -\varepsilon m_2 \\ N &= (m_1 + m_2)/z \\ m_0 &= zN_s/2 \\ g_i &= m_i/m_0 \\ 2\theta &= g_1 + g_2 \end{aligned}\right\} \qquad (15)$$

lead to the isotherm equation

$$x = \frac{\theta}{1-\theta}\cdot\frac{1}{\zeta^z}\cdot\left[\frac{\beta^{(1)}-1+2\theta}{2\theta}\right] \qquad (16)$$

where $\beta^{(\nu)}=[1-4\theta(1-\theta)(1-\zeta^{z/\nu})]^{1/2}$. According to this convention our previous β (Eq. 10) is to be written as $\beta=\beta^{(z)}$.

In establishing Eq. 12 we assumed that all the n. n. bonds were freely permutable; for a connected lattice such is not the case, e. g. it is not physically meaningful to *singly* permute a bond of type OO with one of type UU. In the following we shall try to obtain a better treatment of the combinatorial problem.

For convenience we shall consider only connected lattices for which z is even. Let us adopt some convention whereby the z n. n. bonds connecting a given site with its z n. n. sites can be specified as pointing to the *left* or to the *right*, $z/2$ bonds belonging to each category. We now demand that all the n. n. bonds be considered as pointing to the *right*, say; this uniquely fixes the site of origin of each n. n. bond. We identify a given n. n. bond by giving the name of the site of origin and the name of the site of termination. There are

N_s sites which can serve as origin; and, for any of those sites, there are $z/2$ additional sites which can serve as terminus (lie to the *right*) for a n. n. bond—$zN_s/2$ possibilities in all, which is as it should be.

We now freely permute only n. n. bonds of similar origin; i. e. we permute bonds of type OV among themselves and those of type UV among themselves (V=O, U). The number of distinguishable n. n. bond configuarations corresponding to the above restriction is

$$\Omega = \frac{[(1/2)zN]!\,[(1/2)z(N_s-N)]!}{(m_0-m_1)!\,[(1/2)(m_1-m_2)]!\,[(1/2)(m_1-m_2)]!\,m_2!} \tag{17}$$

Within the limits of Stirling's approximation, Eq. 17 is the same as

$$\Omega = \frac{m_0!\,2^{m_1-m_2}}{(m_0-m_1)!\,(m_1-m_2)!\,m_2!} \times \frac{[(1/2)zN]!\,[(1/2)z(N_s-N)]!}{[(1/2)\,zN_s]!} \tag{18}$$

Once again we find that if we set

$$\Omega = \left\{\frac{[(1/2)zN]!\,[(1/2)z(N_s-N)]!}{(m_0-m_1)!\,[(1/2)(m_1-m_2)]!^2\,m_2!}\right\}^{2/z} \tag{19}$$

the rule of thumb condition is satisfied.

Equations 3, 15, and 19 lead to the isotherm equation

$$x = \frac{\theta}{1-\theta}\cdot\frac{1}{\zeta^z}\cdot\left[\frac{\beta^{(2)}-1+2\theta}{2\theta}\right]^2 \tag{20}$$

Finally, after a little casting about, we find that the expression

$$\Omega = \frac{m_0!\,2^{m_1-m_2}}{(m_0-m_1)!\,(m_1-m_2)!\,m_2!} \times \frac{[(z-1)N]!\,[(z-1)(N_s-N)]!}{[(z-1)N_s]!} \tag{21}$$

satisfies the rule of thumb condition and together with Eqs. 3 and 15 leads to the isotherm equation

$$x = \frac{\theta}{1-\theta}\cdot\frac{1}{\zeta^z}\cdot\left[\frac{\beta^{(z)}-1+2\theta}{2\theta}\right]^z \tag{22}$$

which (remembering that $\beta^{(z)}=\beta$) is just the *refined* isotherm relation of Fowler and Guggenheim.[1]

In order to solve the problem of adsorption with n. n. interactions by the methods of this section what is needed is a way of counting the number of *coherent* bond configurations corresponding to the set of parameters m_i. A bond configuration is called *coherent* if for each lattice site the bonds originating and terminating at that site are physically compatible; i. e., for a site occupied by an adsorbed molecule the bonds originating and terminating at that site must be of type O- and -O, respectively. In Eqs. 12 and 17 we counted the number of *incoherent* and *semi-coherent* bond configurations, respectively, corresponding to the set of parameters m_i; these numbers being considerably larger than the number sought, we reduced them to approximately the right order by raising them to fractional powers (Eqs. 14 and 19). In Eq. 21 we took the number of incoherent bond configurations and multiplied it by a (variable) reduction factor.

The sequence *incoherent, semicoherent, coherent* brings to mind a geometric progression, and we ask ourselves if perhaps it may not be the case (approximately) that

$$\Omega_{\text{coh}}/\Omega_{\text{semicoh}} = \Omega_{\text{semicoh}}/\Omega_{\text{incoh}}$$

Carrying out the implications of this assumption (Eqs. 14 and 19) we produce the isotherm equation

$$x = \frac{\theta}{1-\theta}\cdot\frac{1}{\zeta^z}\cdot\left[\frac{\beta^{(3)}-1+2\theta}{2\theta}\right]^3 \tag{23}$$

It is of interest to note that the various approximate isotherm relations of this section all have the common form

$$x = \frac{\theta}{1-\theta}\cdot\frac{1}{\zeta^z}\cdot\left[\frac{\beta^{(\nu)}-1+2\theta}{2\theta}\right]^\nu \qquad \nu = 1, 2, 3, z \tag{24}$$

The family of isotherms represented by Eq. 24 contains members that show first order phase change behavior. The critical condition is found by setting $\partial x/\partial\theta=0$ for $\theta=1/2$;* this operation leads to the relation

$$\zeta_c^{1/2} = [\nu/(\nu-2)]^{\nu/z} \tag{25}$$

We see that the class of isotherm equations with $\nu\leqq 2$ does not show first order phase change behavior, whereas the class of equations with $\nu>2$ does show such behavior. Now it is our conjecture that in deriving those equations with $\nu\leqq 2$ (in the context of the present series of approximations) we consistently *overcount* the number of distinguishable configurations Ω corresponding to a *given* amount of energy A and that in deriving the equation with $\nu=z$ we consistently *undercount* the requisite number of configurations. If our conjecture is valid, then Ω_{correct} should lie somewhere between the Ω values of Eqs. 19 and 21.

The foregoing considerations suggest that by suitable averaging of pairs of combinatorial expressions, one of which overcounts while the other undercounts, new approximations can be made to Ω_{correct}. By way of example, using the notation $\Omega_{(y)}$ to stand for the combinatorial expression stated in Eq. y, let us investigate the combinations

* See Ref. 1. All the members of the family of Eq. 24 have the same symmetry properties as the *refined* isotherm relation discussed by Fowler and Guggenheim.

$$\Omega_{\varphi} = \Omega_{(14)}{}^{1-\varphi}\Omega_{(21)}{}^{\varphi} \qquad (26\varphi)$$

$$\Omega_{\chi} = \Omega_{(19)}{}^{1-\chi}\Omega_{(21)}{}^{\chi} \qquad (26\chi)$$

$$\Omega_{\psi} = \left[\frac{N_s!}{N!\,(N_s-N)!}\right]^{1-\psi}\Omega_{(21)}{}^{\psi} \qquad (26\psi)$$

These combinatorial expressions together with Eqs. 3 and 15 lead to isotherm relations of the form 24 with $\nu=2+\varphi(z-2)$, $1+\chi(z-1)$, ψz respectively.

Conclusion

It is now clear that combinatorial arguments of the present type will preserve the form of Eq. 24 and will merely change the numerical value of the parameter ν. We have, then, as the end result of our combinatorial considerations the family of Eq. 24 containing the adjustable parameter ν. The individual values of ν thus far produced cannot be entirely satisfactory since the derivations took no explicit notice of lattice properties other than coordination number. The surprising thing about Eq. 24 is that it can reproduce *exactly* critical behavior on any given lattice by suitable adjustment of the parameter ν; this result should be of some importance in the general problem of lattice statistics.

In order to display the properties of Eq. 24 we have tabulated some exact results for two-dimensional lattices, as well as some "best" results for three-dimensional ones, as given in the article by Domb.[4] In Table I we display the quantity $(\ln \zeta_c{}^{z/4})^{-1}$, which corresponds to the quantity $\boldsymbol{k}T_c/qJ$ in Domb's notation,[4] together with the corresponding z and ν values for a number of lattice situations:

$$(\ln \zeta_c{}^{z/4})^{-1} = 2[\nu \ln (\nu/(\nu-2))]^{-1} \qquad (27)$$

TABLE I. EXACT OR "BEST" VALUES OF $(\ln \zeta_c{}^{z/4})^{-1}$ AND ν FOR VARIOUS LATTICE SITUATIONS

Lattice	z	$(\ln \zeta_c{}^{z/4})^{-1}$	ν
Linear chain	2	0	2
Honeycomb	3	0.506	2.54
Kagomé	4	0.536	2.65
Simple quadratic	4	0.567	2.79
Triangular	6	0.607	3.00
Simple cubic	6	0.752	4.42
Body centered cubic	8	0.794	5.25
Face centered cubic	12	0.816	5.78

BULLETIN OF THE CHEMICAL SOCIETY OF JAPAN VOL. 39 1632—1635 (1966)

The Behavior of Free Radicals Produced by Ultraviolet Irradiation in the Frozen Propargyl Alcohol - Hydrogen Peroxide System

By Keiji TAKEDA, Hiroshi YOSHIDA,* Koichiro HAYASHI and Seizo OKAMURA

Department of Polymer Chemistry, Faculty of Engineering, Kyoto University, Sakyo-ku, Kyoto

(Received August 27, 1965)

In order to assertain the polymerization mechanism in the solid state, a solid mixture of propargyl alcohol (monomer), hydrogen peroxide and water was irradiated at −196°C by an ultraviolet light. The structure of the free radicals so formed in the solid medium was then studied by the electron-spin-resonance method. The trapped free radical was a monomer radical, $CH{\equiv}C{-}\dot{C}HOH$. This shows that the HO· radicals produced by the photolysis of hydrogen peroxide abstracted the methylenic hydrogen atoms from the alcohol. An examination of the kinetic behavior of free radicals revealed that HO· radicals migrated freely and reacted with monomers at −196°C. The reaction between the monomer radical and HO· radicals is more important than the recombination between monomer radicals.

Several studies have revealed that the radiation-induced solid state polymerization proceeds by means of a free radical mechanism.[1-7] In the solid state, the usual steady-state condition of the radical concentration does not hold because of a suppressed recombination between propagation

* Research Reactor Institute, Kyoto University.

1) G. Adler, D. Ballantine and B. Baysal, *J. Polymer Sci.*, **48**, 195 (1960).

2) T. A. Fadner, I. Rubin and H. Morawetz, ibid., **37**, 549 (1959).

3) H. Ueda and Z. Kuri, ibid., **61**, 333 (1962).

4) T. A. Fadner and H. Morawetz, ibid., **45**, 475 (1960).

5) H. Morawetz and T. A. Fadner, *Makromol. Chem.*, **34**, 162 (1959).

6) H. Morawetz and I. D. Rubin, *J. Polymer Sci.*, **57**, 669 (1962).

7) C. H. Bamford and A. D. Jenkins, ibid., **48**, 37 (1960).

radicals. Therefore, the kinetic behavior of the polymerizations is more complex than that of usual liquid state polymerizations.

In order to assertain the mechanism of radiation-induced solid state polymerizations, it may be helpful to know the behavior of free radicals in the solid state, where they are formed by a simple photolysis. So far, several electron-spin-resonance (ESR) studies have been published on photo-irradiated frozen systems of hydrogen peroxide-alcohols or vinyl monomers.[8-11] In many of the saturated and unsaturated alcohols studied, HO· radicals formed by the photolysis of hydrogen peroxide abstract α-hydrogen atoms from the alcohols.[8,9] Alcohols with triple bonds have not yet been studied in the frozen state. The reactions of a few vinyl monomers with HO· have been studied kinetically by Kuwata et al.[11] And they also studied the polymerization kinetics in detail at a temperature at which the steady state was held for the concentration of propagating radicals. However, no kinetic study has yet been made of the radical behavior at such a low temperature that the ends of the propagating radical cannot move around. In the present work, the structure of free radicals formed in the solid state of propargyl alcohol-hydrogen peroxide by photolysis at −196°C was first assigned on the basis of its ESR spectra, and then the kinetic behavior of free radicals at −196°C was examined quantitatively by varying the concentration of the monomer or of the initiator.

Experimental

Materials.—Commercial propargyl alcohol was purified by vacuum distillation. A 30% aqueous solution of hydrogen peroxide was distilled in a vacuum, and the concentrated peroxide was used for the experiment. Purified water was used as the solvent.

The Ultraviolet Irradiation of Samples.—The monomer (propargyl alcohol), hydrogen peroxide, and water were pipetted into a qualtz tube, sealed in a vacuum, and irradiated with a high pressure mercury arc (Toshiba SHL-100UV, 75Watt) for a certain length of time in a liquid nitrogen bath. The distance between the sample and the arc was about 10 cm. The irradiation conditions were the same throughout this investigation. The emission spectra of the mercury arc spread widely from 3000 Å to the visible region. The solid mixture of propargyl alcohol and a concentrated aqueous solution of hydrogen peroxide formed a transparent glass at −196°C. It could be irradiated uniformly, except for a high concentration of water, when the sample is opaque.

ESR Measurements.—The microwave frequency was 9400Mc., and the field modulation frequency was 80C. After irradiation, the sample was quickly inserted into the cavity resonator and the ESR measurements were carried out at −196°C. The concentration of free radicals was determined in comparison with that of a standard sample of a DPPH (α, α'-diphenyl-β-picryl hydrazyl) solid solution in polystyrene, the radical concentration of which had already been determined.

Results and Discussion

ESR Spectra and Their Assignment.—The ESR spectra in Fig. 1(a) were obtained with samples immediately after irradiation at −196°C. The spectra were independent of the irradiation time and the concentration of the monomer or hydrogen peroxide. Since the free radical concentration was unchanged over a long period of time at −196°C, they were completely frozen and no recombination reaction could have occurred. No ESR signal was observed when the pure hydrogen peroxide was irradiated under the same conditions. Therefore, the spectra shown in Fig. 1(a) are due to monomer radicals formed from the reaction of the monomer with the HO· radical which was produced by the photolysis of hydrogen peroxide.

The observed spectrum is a poorly-resolved triplet. It is assigned to the structure of the free radical;

$$CH{\equiv}C\text{-}\dot{C}HOH \longleftrightarrow \dot{C}H{=}C{=}CHOH$$

formed by the abstraction of one of the methylenic hydrogen atoms of a monomer molecule by HO·

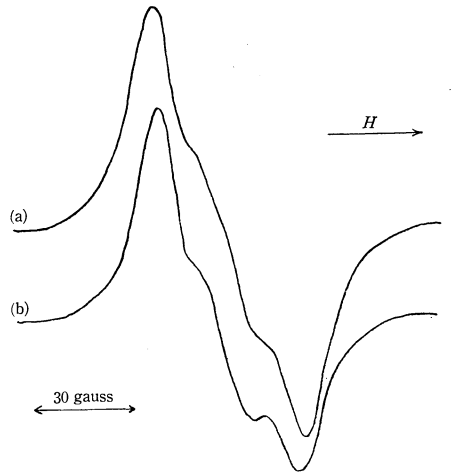

Fig. 1. ESR spectra of ultraviolet-irradiated propargyl alcohol-hydrogen peroxide glass and the effect of temperature on the spectra. (a) observed at −196°C immediately after irradiation for 4 hr. at −196°C. (b) observed at −196°C after warming at −150°C for 15 min.

8) J. F. Gibson, D. J. E. Ingram, M. G. R. Symons and M. G. Townsend, *Trans. Faraday Soc.*, **53**, 914 (1957).
9) K. Kuwata, T. Ichikawa and K. Hirota, *J. Chem. Soc. Japan, Pure Chem. Sect. (Nippon Kagaku Zasshi)*, **83**, 652 (1962).
10) D. J. E. Ingram, M. C. R. Symons and M. G. Townsend, *Trans. Faraday Soc.*, **54**, 409 (1958).
11) K. Kuwata, K. Nishikida, H. Kawazura and K. Hirota, This Bulletin, **36**, 925 (1963).

radicals. Dixon et al.[12] observed the ESR spectra of the above radicals formed in the reaction between propargyl alcohol and HO· using a flow method. They reported the coupling constants due to each proton as $a_H(CHOH)=18.5$ gauss and $a_H(CH)=10.2$ gauss. Fessenden et al.[13] also found similar radicals by the electron-irradiation of allene:

$$CH{\equiv}C\text{-}\dot{C}H_2 \longleftrightarrow \dot{C}H{=}C{=}CH_2$$

These authors reported the following coupling constants: $a_H(CH)=12.6$ gauss and $a_H(CH_2)=18.9$ gauss. These spectra of the free radicals in the liquid phase showed a well-resolved hyperfine structure. However, the same type of free radicals showed poorly-resolved triplet spectra, as is shown in Fig. 1(a), since they were trapped in a rigid medium. Other possible radicals which may be formed by the reaction between the monomer and HO· are addition-type radicals, i.e. $H(OH)C{=}\dot{C}\text{-}CH_2OH$ or $\dot{C}H{=}C(OH)CH_2OH$. These σ-type radicals, however, may show large coupling constants.[13] Therefore, the observed spectra cannot be attributed to them.

When the temperature of the irradiated sample was raised, the concentration of free radicals decreased and the spectrum changed to that shown in Fig. 1(b). This change is caused by a new overlapping spectrum with a different g-value. The new spectrum is probably due to the growing polymer radicals.

The Kinetics of Free Radical Reactions.—*Experimental Results.*—The kinetic behavior of free radical reactions was studied by examining the dependence of the monomer radical ($CH{\equiv}C\text{-}\dot{C}HOH$) formation rate on the monomer and hydrogen peroxide concentrations at −196°C. When the hydrogen peroxide concentration, $[H_2O_2]$, was varied (the maximum $[H_2O_2]$ value was about 6 mol./l.) and the monomer concentration, [M], was kept constant, the concentration of the trapped monomer radicals, [M·], increased with an increase in the irradiation time, as shown in Fig. 2. (The maximum [M·] value was about 10^{-3} mol./l.) Figure 3 shows the initial rate of monomer radical formation, $[d[M\cdot]/dt]_{t=0}$, against $[H_2O_2]$. Apparently the rate is proportional to $[H_2O_2]$. When, in turn, $[H_2O_2]$ was kept constant and [M] was varied, (the maximum [M] was about 14 mol./l.), the $[d[M\cdot]/dt]_{t=0}$ value remained the same for all [M] values. With an increase in the irradiation time, the $d[M\cdot]/dt$ value decreased. This phenomenon cannot be ascribed to a decrease of $[H_2O_2]$ because the concentration of the trapped radicals and, consequently, the consumption of hydrogen peroxide was smaller than the initial $[H_2O_2]$.

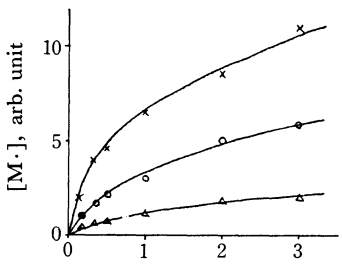

Fig. 2. The effect of irradiation time on the concentration of monomer radicals trapped in ultraviolet irradiated propargyl alcohol-H_2O_2 glass at −196°C.
[M] is kept constant.
$[H_2O_2]$: the ratio of × : ○ : △ is 5 : 3 : 1.

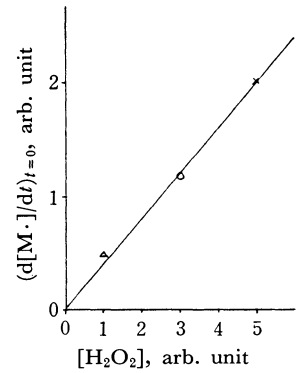

Fig. 3. The effect of hydrogen peroxide concentration on the initial rate of monomer radical formation in ultraviolet-irradiated propargyl alcohol-H_2O_2 glass at −196°C.

The Derivation of Kinetic Equations.—No ESR spectrum from HO· is observed after irradiation. Consequently, the HO· radicals formed from hydrogen peroxide during irradiation at −196°C are believed to migrate and to react readily, so that they disappear immediately after their formation. It is, therefore, reasonable to assume a steady-state HO· concentration in the solid state during irradiation. The experimental results indicate that monomer radicals are immobilized and that recombination between monomer radicals need not be considered. On the other hand, the concentration of monomer radicals increases to a considerable extent. This fact implies that recombination between trapped monomer radicals and the initiating HO· radicals should be considered as an elementary reaction, which is usually neglected in kinetic treatments of radical polymerizations in the liquid state. Consequently, the elementary reactions are as follows:

$$H_2O_2 \xrightarrow{k_1} 2HO\cdot \qquad (1)$$

12) W. T. Dixon and R. O. C. Norman, *J. Chem. Soc.*, **1963**, 3119.
13) R. W. Fessenden and R. Schuler, *J. Chem. Phys.*, **39**, 2147 (1963).

$$HO\cdot + HO\cdot \xrightarrow{k_2} H_2O_2 \quad (2)$$

$$HO\cdot + M \xrightarrow{k_3} M\cdot \quad (3)$$

$$HO\cdot + M\cdot \xrightarrow{k_4} \text{molecule} \quad (4)$$

From the assumption of a steady-state concentration of [HO·],

$$k_1[H_2O_2] - k_2[HO\cdot]^2 - k_3[HO\cdot][M] - k_4[HO\cdot][M\cdot] = 0$$

As [HO·] is small enough, one can neglect the second term. Thus, the following equation is obtained for the steady-state concentration of HO· radicals:

$$HO\cdot = \frac{k_1[H_2O_2]}{k_3[M]+k_4[M\cdot]} \quad (5)$$

From Eq. 5, the rate of monomer radical formation can be expressed as follows:

$$\frac{d[M\cdot]}{dt} = k_3[HO\cdot][M] - k_4[HO\cdot][M\cdot] = \frac{1 - k_4[M\cdot]/k_3[M]}{1 + k_4[M\cdot]/k_3[M]} k_1[H_2O_2] \quad (6)$$

Since $[M] \gg [M\cdot]$,

$$d[M\cdot]/dt \simeq \{1 - 2k_4[M\cdot]/k_3[M]\}k_1[H_2O_2] \quad (7)$$

By assuming that the consumption of monomer molecules and hydrogen peroxide is very small and that [M] and $[H_2O_2]$ are unchanged, the integration of Eq. 7 yields:

$$[M\cdot] = k_3[M]/2k_4\left\{1 - \exp\left[-\frac{2k_1k_4[H_2O_2]}{k_3[M]}t\right]\right\} \quad (8)$$

Comparison of Experimental Results with Kinetic Equations.—The experimental results shown in Figs. 3 and 4 indicate that $d[M\cdot]/dt \propto [H_2O_2]^1[M]^0$

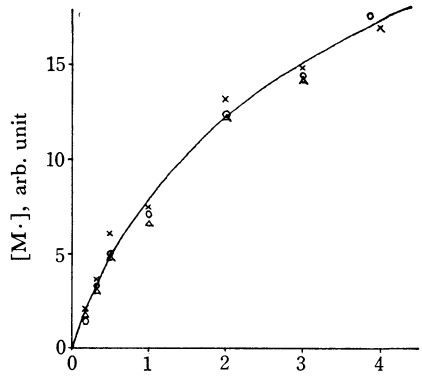

Fig. 4. The effect of irradiation time on the concentration of monomer radicals trapped in ultraviolet irradiated propargyl alcohol-H_2O_2 glass at −196°C.
$[H_2O_2]$ is kept constant.
[M]: the ratio of × : ○ : △ is 20 : 17 : 14.

for $t=0$. They are in good agreement with Eq.7, which shows that $d[M\cdot]/dt=k_1[H_2O_2]$ for $t=0$. From Eq. 8, [M·] is expected to show a saturating tendency with an increase in the irradiation time. In fact, this is obvious from the results shown in Figs. 2 and 4. Therefore, the two assumptions, i. e., the existence of a steady state of [HO·] and of recombination between HO· and M·, which have been made in deriving the kinetic equations, are found to be reasonable.

From the above discussion, it may be concluded that HO· radicals migrate in the irradiated solid mixture and react readily with monomers. The reaction between the monomer radical and HO· radical is much more important than the recombination reaction between monomer radicals. This is a significant feature of the behavior of free radicals in solid state polymerization.

BULLETIN OF THE CHEMICAL SOCIETY OF JAPAN VOL. 39 1636—1640 (1966)

Silent Discharge Reactions in Aqueous Solutions. III. Acidic Aqueous Solutions of Ferrous Sulfate and Ceric Sulfate in a Hydrogen Atmosphere*

By Akira YOKOHATA and Satoru TSUDA

Department of Chemistry, Faculty of Engineering, Hiroshima University, Senda-machi, Hiroshima

(Received September 10, 1965)

A study has been made of silent discharge reactions in aqueous solutions of ferrous sulfate and ceric sulfate acidified with sulfuric acid in a hydrogen atmosphere. The present study has confirmed that silent discharge leads to the formation of hydrogen peroxide from water molecules in a dilute sulfuric acid solution, the oxidation of ferrous ions to ferric ions, and the reduction of ceric ions to cerous ions. The same reactions were previously studied in inert gases. A satisfactory interpretation can be made of their mechanisms by taking into consideration the action on the solvent of slow electrons produced in the gaseous phase. In a hydrogen atmosphere, the yields of the foregoing reactions were very small when compared with those in the case of inert gases; however, a good linear correlation was observed between the yield and the duration time of discharge. From these results it has been concluded that the yields can be well interpreted by taking into consideration the action of active species of hydrogen generated in the gaseous phase on the radicals formed from liquid water, besides the action of slow electrons; moreover, the action of active species on the solute cannot be serious. The absorbed dose in the solution was estimated to be approximately 1.9×10^7 r./hr. from the relation of the dissipated energy calculated electrically to the absorbed dose.

In previous reports[1] it has been pointed out that (1) in a helium or argon atmosphere the chemical reactions in an aqueous solution of ferrous sulfate or ceric sulfate by silient discharge can be well interpreted by taking into consideration the actions on the solvent of slow electrons produced in the gaseous phase, and that (2) neither the effect of the metastable excited state of helium and argon nor that of luminescence can be serious, while the silent discharge reaction apparently corresponds to the radiolysis caused by a particle of high LET (linear energy transfer).

The foregoing conclusions were drawn from a study of silent discharge in helium and argon atmospheres. However, in the case of gases other than inert gases, the reaction mechanisms may become complicated, for the effect of active species,[2-7] besides that of slow electrons, should also be taken into consideration.

In the current study, hydrogen gas was used as an atmosphere: the effect of active species of hydrogen generated in the gaseous phase was investigated, and the results were compared with those obtained with inert gases.

In acidic aqueous solutions, the experimental results showed the formation of hydrogen peroxide, the oxidation of ferrous ions to ferric ions, and the reduction of ceric ions to cerous ions. The reaction mechanisms were complicated by the formation of active species of hydrogen in the gaseous phase. However, the results could be well interpreted in terms of the radiolysis of an aqueous solution under the active species of hydrogen.

Experimental

The discharge tube and the electrical circuit were identical to those previously reported. All the experiments were performed at a constant solution volume of 10 ml. The surface of the solution vibrated gently during the discharge. This may be useful in renewing the surface of the solution. All the experiments were conducted at about 20°C after the oxygen dissolved in the solution had been completely removed by bubbling hydrogen gas into the solution. A constant discharge current of 1 mamp. was employed in most of the experiments, letting hydrogen gas flow at a velocity of about 120 ml./min. through the gas space of the discharge tube. The water used was purified by the multiple distillation procedure described by Johnson and Allen.[8] The Merck guaranteed reagents ferrous sulfate and ceric sulfate were used without further treatment. As pure hydrogen gas (99.95%) provided the same results

* Presented in part at the 17th Annual Meeting of the Chemical Society of Japan, Tokyo, April, 1964.

1) Parts I and II of this series: A. Yokohata and S. Tsuda, This Bulletin, **39**, 46, 53 (1966).

2) S. Miyamoto, *J. Chem. Soc. Japan (Nippon Kagaku Kaishi)*, **55**, 611 (1934).

3) T. Davis, S. Gordon and E. J. Hart, *J. Am. Chem. Soc.*, **80**, 4487 (1958).

4) G. Czapski and G. Stein, *J. Phys. Chem.*, **63**, 850 (1959).

5) M. Schiavello and G. G. Volpi, *J, Chem. Phys.*, **37**, 1510 (1962).

6) G. Czapski and G. Stein, *Israel J. Chem.*, **2**, 15 (1964).

7) H. A. Kazmi and L. D. J. Roy, *Can. J. Chem.*, **42**, 1145 (1964).

8) E. R. Johnson and A. O. Allen, *J. Am. Chem. Soc.*, **74**, 4147 (1952).

as purified hydrogen gas, it was used without further purification in later experiments. The concentrations of sulfuric acid, ferrous sulfate and ceric sulfate solutions varied from 1.5 to 0.1 N, from 1×10^{-2} to 1×10^{-3} M and from 2×10^{-3} to 5×10^{-4} M respectively.

Results

In the gaseous phases, hardly any ozone or hydrogen peroxide was formed. Moreover, hardly any hydrogen sulfide was formed from the dilute aqueous solution of sulfuric acid.

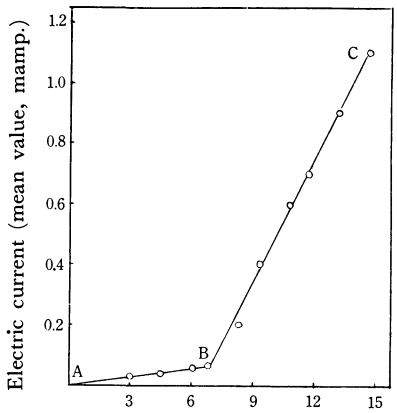

Fig. 1. Relation between applied voltage and electric current.

Figure 1 shows the relationship between the applied voltage and the electric current as measured by the method described in the previous report, where B is the firing voltage.

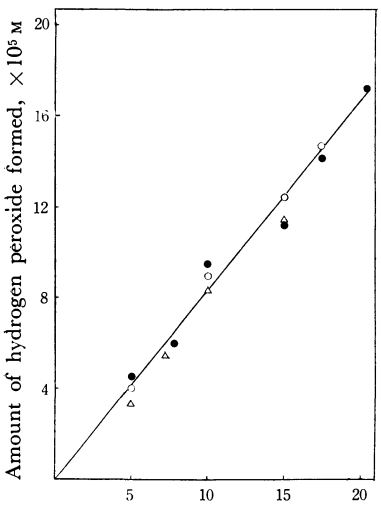

Fig. 2. Relationship between amount of hydrogen peroxide formed and duration time of discharge.
● 1.5 N H_2SO_4 ○ 0.8 N H_2SO_4
△ 0.1 N H_2SO_4

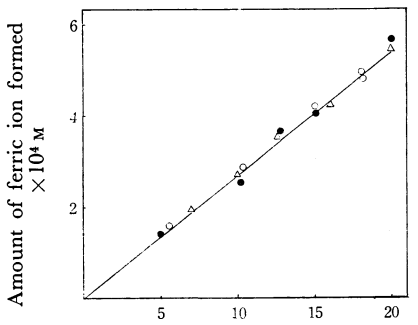

Fig. 3. Relationship between amount of ferric ion formed and duration time of discharge.
Initial concentration of ferric ion;
○ 1×10^{-3} M △ 5×10^{-3} M ● 1×10^{-2} M
H_2SO_4: 0.8 N

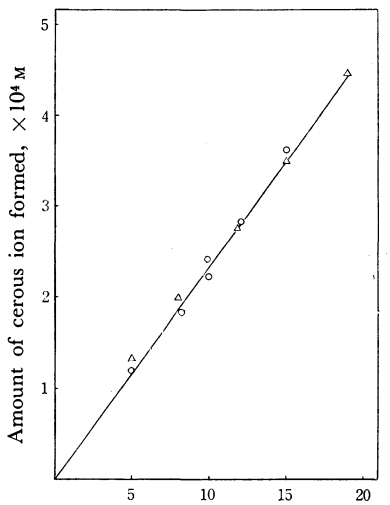

Fig. 4. Relationship between amount of cerous ion formed and duration time of discharge.
Initial concentration of ceric ion;
○ 5×10^{-4} M △ 2×10^{-3} M
0.8 N H_2SO_4

In a dilute aqueous solution of sulfuric acid, hydrogen peroxide appeared following the discharge. Also, in acidic solutions of ferrous sulfate and ceric sulfate, the oxidation of ferrous ions to ferric ions and the reduction of ceric ions to cerous ions were noted respectively. Figures 2, 3 and 4 show, respectively, the relationship between the amounts of hydrogen peroxide, ferric ion and cerous ion formed and the duration of the discharge. The results produced a good linear curve.

In the range from 0.1 N to 1.5 N of sulfuric acid, the yield of hydrogen peroxide was independent of the concentration of sulfuric acid. An independence of the solute concentration with relation to the yield was also found when the

ferrous ion concentration ranged from 1×10^{-2} M to 1×10^{-3} M, and when that of ceric ions ranged from 2×10^{-3} M to 5×10^{-4} M.

The yield of each product was obtained as follows:

$$Y(H_2O_2) = 8.3\times10^{-5}\text{ M},\ Y(Fe^{3+}) = 2.7\times10^{-4}\text{ M},$$
$$Y(Ce^{3+}) = 2.3\times10^{-4}\text{ M}$$

where Y shows the yield with the discharge current at 1 mamp. and with the duration of discharge at 10 min. These yields were very small when compared with those in helium and argon.

These points will be discussed in detail later.

Discussion

The Estimation of the Absorbed Dose in the Aqueous Solution.—It is very important to determine the absorbed dose in silent discharge chemistry. However, the estimation of the absorbed dose has been little studied. In our previous reports, we pointed out that, in an inert gas atmosphere, it is possible to estimate the absorbed dose in silent discharge by chemical dosimetry. Furthermore, it was shown that Eq. 1 holds good:

$$A(\text{He})/A(\text{Ar}) = E(\text{He})/E(\text{Ar}) \qquad (1)$$

where A is the value calculated by Eq. 3 from the standpoint of electrical engineering and gives the total energy dissipated per second by silent discharge. E gives the absorbed dose in the solution per second. Equation 1 shows that E is proportional to A and that the proportional constant is independent of the kind of gas, at least in the cases of helium and argon.

At the present stage, no adequate method is available to check experimentally whether Eq. 1 applies to other gases or not. However, in view of the fact that Eq. 1 holds good in helium and argon, despite the difference in such properties as the ionization potential, the mean free path, the firing voltage, and the absolute value of A, it may be said that Eq. 1 applies to other gases. If so, Eq. 2 can be obtained:

$$A(H_2)/A(X) \simeq E(H_2)/E(X) \qquad (2)$$

where X is helium or argon. Since $A(H_2)$ and $A(X)$ can be calculated by Eq. 3 and since $E(X)$ is known, $E(H_2)$ can be determined from 2. In Eq. 3,[9] C_{die} and C_a depend on the shape of the discharge tube, while V_i and V_d depend on the kind of gas used under given experimental conditions.

$$A=\frac{f(C_{die}+C_a)(V_i+V_d)\{2E_m-(V_i+V_d)(1+C_a/C_{die})\}}{1+C_a/C_{die}} \qquad (3)$$

where

f : the frequency of the electric source used
C_{die} : the total capacitance of the insulator
C_a : the capacitance due to the gap space in the tube
V_i : the voltage across the gap space at the firing voltage
V_d : the stopping voltage
E_m : the maximum value of the applied voltage

The relation between V_d and V_i is not well known, but the value of V_d/V_i is said to be approximately 0.4—0.2.[10]

Under our experimental conditions, $C_{die}=180$pF, $C_a=36$pF, $V_i=1.3$ kV. and $E_m=15.4$ kV. in helium, while $V_i=6.9$ kV. and $E_m=19$ kV. in hydrogen. By applying these values to Eq. 3, the ratio of the dissipated energy in helium and hydrogen may be estimated. Table I shows the

Table I. Calculated ratio of $A(H_2)$ to A(He)

V_d/V_i	$A(H_2)/A$(He)
0.2	5.2
0.4	4.9

calculated results when $V_d/V_i=0.2$ and 0.4. In this study the mean value for $A(H_2)/A$(He) was assumed to be 5. As E(He) is equal to 3.8×10^6 r./hr., $E(H_2)$ is estimated to be about 1.9×10^7 r./hr. This value, of course, varies with the value of the electric discharge current. Shown here are the values in the case of 1 mamp. This also gives the average integral dose absorbed by the aqueous solution in the apparatus used by the authors, where the volume of the solution is 10 ml.

An Estimation of the Apparent LET.—In order to estimate theoretically the radical or molecular yield from the absorbed dose, it is necessary to ascertain the LET values of electrons produced in a hydrogen atmosphere by silent discharge.[11]

Generally speaking, in silent discharge at one atmospheric pressure, electrons have an energy distribution from just above zero to somewhat above the ionization potential of the gas in which the discharge occurs.[12]

In view of the fact[13] that the ionization potential of the hydrogen molecule is equal to 15.4 eV., that of argon, to 15.7 eV., and that of helium, to 24.5 eV., the LET values of electrons in a hydrogen atmosphere may closely resemble that in argon. Therefore, a value of about 8(eV./Å) was

9) S. Fuji and N. Takimura, *Bulletin of the Electrotechnical Laboratory (Denki Shikensho Hokoku)*, **16**, 837 (1952).

10) M. Suzuki, *J. Electrochem. Soc. Japan (Denki Kagaku)*, **24**, 354 (1956).

11) The G value depends on the LET value.

12) N. R. Dibelius, J. C. Fraser, M. Kawahata and C. D. Doyle, *Chem. Eng. Progress*, **60**, 41 (1964).

13) K. Watanabe, T. Nakayama and J. Mottl, *J. Quant. Spectry. Radiation Transfer*, **2**, 369 (1962).

assumed for the LET value of electrons in hydrogen.[14]

The Formation of Hydrogen Peroxide.—The silent discharge reaction in a hydrogen atmosphere showed the formation of hydrogen peroxide from dilute aqueous solutions of sulfuric acid. As precursor of hydrogen peroxide, the hydroxyl radical has heretofore been proposed, but recent studies have also suggested contribution of the excited state of water.[15] Inasmuch as details of this new mechanism are yet to be elucidated, this remains a problem for future study. In this study an attempt will be made to explain the mechanism involved from the previously-proposed theory of the recombination reaction of hydroxyl radicals.

Two processes can be considered for the formation of hydroxyl radical, that is, the interaction of (a) water vapor and (b) liquid water, with slow electrons. As has been pointed out by Hart et al.,[3] however, the process a cannot be great in the presence of a large excess of molecular hydrogen. Therefore, the process b should be considered:

$$\text{lig.}H_2O \xrightarrow[\text{slow electron}]{\sim\!\!\wedge\!\!\vee\!\!\sim} OH,\ H \qquad (4)$$

$$OH + OH \rightarrow H_2O_2 \qquad (5)$$

The estimated yield of hydrogen peroxide calculated on the basis of the absorbed dose and the $G(H_2O_2)$ value, $Y_{cal}(H_2O_2)$, should be about 4.4×10^{-3} M. In the experiment, however, the value of $Y(H_2O_2)$ was only 8.3×10^{-5} M. This discrepancy might be ascribed to the radiolysis of an aqueous solution under the active species of hydrogen. In silent discharge, the radicals from liquid water are formed mainly just below the surface, because the energy of the electrons is very small. Therefore, a scavenging action of active species of hydrogen on these radicals may be expected:

$$H_{at} + OH \rightarrow R \qquad (6)$$

$$H_{at} + H \rightarrow S \qquad (7)$$

where H_{at} is the active species of hydrogen (H, H^+, etc.) generated in the atmosphere. R and S are the reaction products (H_2O or H_2 is mainly expected respectively). Therefore, this scavenging reaction 6 should lead to a decreased yield of hydrogen peroxide. In fact, as will be shown later, the estimated yield of hydroxyl radicals and hydrogen atoms were both very small. This is suggestive evidence that reactions 6 and 7 should be considered.

Other cases can also be mentioned. First, the action of the hydroxyl radical on hydrogen molecules dissolved in the solution-reaction 8; second, the action of hydrogen atoms on hydrogen peroxide in the solution-reaction 9, and third, the action of active species of hydrogen in the gaseous phase on hydrogen peroxide-reaction 10.[16]

$$OH + H_2 \rightarrow H + H_2O \qquad (8)$$

$$H + H_2O_2 \rightarrow H_2O + OH \qquad (9)$$

$$H_{at} + H_2O_2 \rightarrow H_2O + OH \qquad (10)$$

These reactions lead to the formation of another radical, in company with the disappearance of one radical. As will be shown later, however, the Y(H) and Y(OH) estimated from the experiments on ferrous sulfate and ceric sulfate being very small, reactions 8, 9 and 10 may not be serious.

The Formation of Ferric Ions.—The estimated yield of ferric ions, calculated on the basis of the absorbed dose and the $G(Fe^{3+})$ value, $Y_{cal}(Fe^{3+})$ should be about 1.3×10^{-2} M. However, the experiment gave the value of $Y(Fe^{3+})$ to be only 2.7×10^{-4} M, with the solute concentration ranging from 1×10^{-2} M to 1×10^{-3} M.

In silent discharge, the mechanism of oxidizing ferrous ions to ferric ions in an acidic solution might be shown as follows:

$$OH + Fe^{2+} \rightarrow Fe^{3+} + OH^- \qquad (11)$$

$$H + H^+ + Fe^{2+} \rightarrow Fe^{3+} + H_2 \qquad (12)$$

$$H_2O_2 + Fe^{2+} \rightarrow Fe^{3+} + OH + OH^- \qquad (13)$$

The yield of ferric ions, $Y(Fe^{3+})$, should, then, be expressed by Eq. 14:

$$Y(Fe^{3+}) = 2Y(H_2O_2) + Y(H) + Y(OH) \qquad (14)$$

Even if reaction 8 is caused by dissolved hydrogen molecules, the yield of ferric ions would be independent of 8, because one hydrogen atom and one hydroxyl radical oxidize one ferrous ion, and also one hydrogen atom obtained via 8 oxidizes one ferrous ion via 12. Therefore, with regard to the discrepancy between the observed yield and the calculated ferric ion yield, we must assign the reactions to reasons other than 8. Also, the value of Y(H+OH) estimated by 14, about 1×10^{-4} M, was very small when compared with the calculated value of about 4.4×10^{-3} M. This suggests that only a small part of the yield of hydrogen atoms and hydroxyl radicals expected theoretically from the radiolysis of water by slow electrons contributes to the oxidation of ferrous ions to ferric ions. The above facts are suggestive evidence which support reactions 6 and 7.

In addition, ferric ions produced via reactions 11—13 may be reduced by the active species generated in the gaseous phase:

$$H_{at} + Fe^{3+} \rightarrow Fe^{2+} + H^+ \qquad (15)$$

This reaction, however, may be not important in

14) Accordingly, the G value can be assigned as follows:
G(H)=0.7, G(OH)=0.7, $G(H_2O_2)$=1.4, $G(Fe^{3+})$=4.2, $G(Ce^{3+})$=2.8.

15) M. Anbar, S. Guttmann and G. Stein, *J. Chem. Phys.*, **34**, 703 (1961).

16) C. J. Hochanadel, *J. Phys. Chem.*, **56**, 587 (1952).

the range of a good linear correlation between the yield and the duration of discharge.

The Formation of Cerous Ions.—The estimated yield of cerous ions, calculated on the basis of the absorbed dose and the $G(Ce^{3+})$ value, should be about 8.9×10^{-3} M. However, the experiment gave a yield of only 2.3×10^{-4} M within the range from 2×10^{-3} M to 5×10^{-4} M in a solute concentration in a 0.8 N sulfuric acid solution. With regard to the discrepancy between the observed and calculated values, the following reasons might be mentioned.

In the case of gamma-ray irradiation and also silent discharge in an inert gas atmosphere, $Y(Ce^{3+})$ can be expressed by Eq. 16.[1b]

$$Y(Ce^{3+}) = 2Y(H_2O_2) + Y(H) - Y(OH) \qquad (16)$$

In a hydrogen atmosphere, if the active species of hydrogen act directly on the solute, a comparatively large increment in $Y(Ce^{3+})$ may be expected when compared with the case of inert gas. The experimental value of $Y(Ce^{3+})$, however, was very small, contrary to expectation. This suggests that the action of active species on the solute cannot be serious. Also, for the same reason, it might be said that the reaction of the hydrogen molecule on the hydroxyl radical (8) cannot be serious. Next, by combining Eq. 16 with 14, the values of $Y(H)$ and $Y(OH)$ can be separately estimated; that is, $Y(H)=8\times10^{-5}$ M and $Y(OH)=2\times10^{-5}$ M. Both values are very small when compared with the calculated values, $Y_{cal}(H)=2.2\times10^{-3}$ M and $Y_{cal}(OH)=2.2\times10^{-3}$ M. The above is also suggestive evidence for the adequacy of reactions 6 and 7.

It is our conclusion that the scavenging action of the active species of hydrogen on the hydroxyl radical and the hydrogen atom formed from liquid water by slow electrons plays an important role.

BULLETIN OF THE CHEMICAL SOCIETY OF JAPAN VOL. 39 1640—1643 (1966)

The Radiolysis of a Binary Mixture of Tetrahydrofuran with Furan

By Masao MATSUI

The Institute of Physical and Chemical Research, Bunkyo-ku, Tokyo

(Received September 27, 1965)

The radiolysis of a tetrahydrofuran(THF) and furan system was studied at a dose of about 2×10^{19} eV. ml^{-1} of ^{60}Co-γ-rays, and the hydrogen which may be formed by the no-ring opening and the carbon monoxide which should be formed by the ring scission were determined. The decrease in the hydrogen yield with an increase fraction of furan was found to be greater than had been expected, while $G(CO)$ fit the expected value. The charge transfer mechanism was presumed for the decrease in the hydrogen yield in the γ-radiolysis of this mixture. Suggestions were made on the probable mechanism of the ring opening of the excited molecule for the formation of carbon monoxide, and on the ionic reaction for hydrogen formation. Furthermore, the probability of the ring scission of the THF molecule was roughly estimated by using the assumed decomposition reaction and the determined G values.

We have as yet very little information on the γ-radiolysis of liquid cyclic ethers, such as dioxane, tetrahydrofuran(THF) and furan. Granzow et al[1] have discussed the relevancy between the stability for ionizing radiation and the aromaticity of the compound by comparing the radiolysis of furan, thiophen and benzene. Llabador et al.[2] have determined the G values of the gas and liquid products in the γ-radiolysis of cyclic ethers and have discussed the reaction mechanism, especially that of the radiolysis of dioxane.

The present work was carried out in order to examine the existence of the protection in the radiolysis of the binary system of THF and furan system which has the lowest aromaticity among the heterocyclic compounds, and, furthermore, to establish the mechanism of the radiolysis of THF which is a typical heterocyclic compound.

Experimental

Materials. — The G. R.-grade furan was further purified by bulb-to-bulb distillation, the middle fraction was used for the run. The impurities in the furan were found to be negligible by gas chromatography. The G. R.-grade THF, stored with sodium hydroxide, was distilled through an about 50 cm., glass-helix-packed column at a reflux ratio of 10 : 1 after it had been refluxed with metallic potassium for about 24 hr.

1) A. Granzow, J. Wedenburg and A. Henglein, *Z. Naturforsch.*, **19b**, 1015 (1964).
2) Y. Llabador and J. P. Adloff, *J. chim. phys.*, **61**, 681, 1467 (1964).

The fraction collected at 66.0—67.0°C was retained in storage vessel placed in the vaucum line in the dark. The remaining impurities were in the C_6 region and were found by gas chromatographic determination to total about 0.05%. These impurities were unchanged by γ-irradiation.

Sample Preparation, Irradiation and Analysis. —THF was distilled into a calibrated bulb from the storage vessel, and the middle fraction (about 10 ml.) was condensed into an irradiation cell. The furan for irradiation was prepared in a similar way.

These samples were subjected to ^{60}Co-γ-irradiation at 25.0±1.0°C and at a dose rate of $(1.22—1.30)\times10^{17}$ eV. ml^{-1} min^{-1}. The dose rate was determined by the Fricke method, assuming $G(Fe^{3+})=15.6$, and $\varepsilon_{Fe^{3+}}=2150$ at 20.0°C and 304 mμ.

The gas fraction volatile at −196°C was determined on a conventional calibrated gas burette and a Toepler pump. The hydrogen content of the −196°C fraction was determined by means of a heated palladium thimble, while carbon monoxide was analyzed by the method using copper(II) oxide containing 1.3% iron(III) oxide, prepared by the method of Brücker and Schick.[3]

The fraction volatile at −80°C, consisting of C_2–C_4 hydrocarbons, and liquid products such as furan and butanol, was analyzed gas-chromatographically by using a 6 m. column of squalane at 30°C, and a 2.25 m. column of P. E. G.-1000 at 100°C.

Result and Discussion

If the radiolysis products of THF in a binary solution are unaffected by the presence of furan, the expected G value, G_{ex}, for a product, P, from the solution should be given approximately by the expression:

$$G_{ex}(P) = G_T^0(P)\varepsilon_T + G_F^0(P)\varepsilon_F$$

where $G_T^0(P)$ and $G_F^0(P)$ refer to the yields of P from pure THF and furan respectively, and where ε_T and ε_F refer to the electron fraction in the solution radiolyzed. The G_{ex} values in Fig. 2 are represented by a linear dashed line.

The hydrogen which may be formed by the no-ring opening, and the carbon monoxide which should be formed by the ring opening were determined in this binary system. Llabador and Adloff have shown that $G(H_2)$ and $G(CO)$ are independent of the total dose up to about 10^{20} eV. ml^{-1} in the radiolysis of liquid furan. Since a similar result was also obtained for THF in the region of low dosage, as is shown in Fig. 1, the binary system was irradiated at a dose of about 2×10^{19} eV. ml^{-1}.

The G value of the hydrogen and carbon monoxide from the purified liquid sample were 2.95± 0.22 and 0.13±0.02 for THF, and 0.12 and 0.31 for furan. Those of the binary system of THF and furan are given in Table I and Fig. 2.

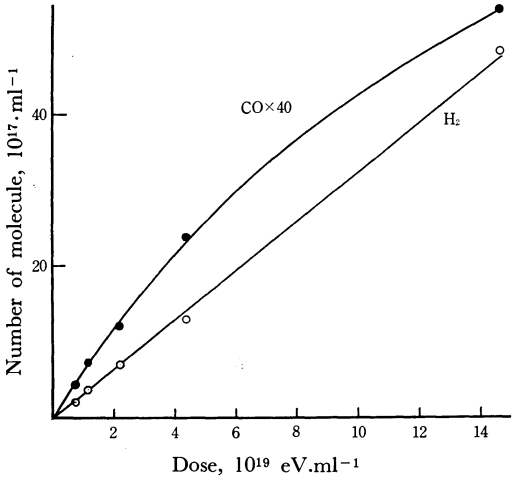

Fig. 1. The variation of $G(H_2)$ and $G(CO)$ with dose.

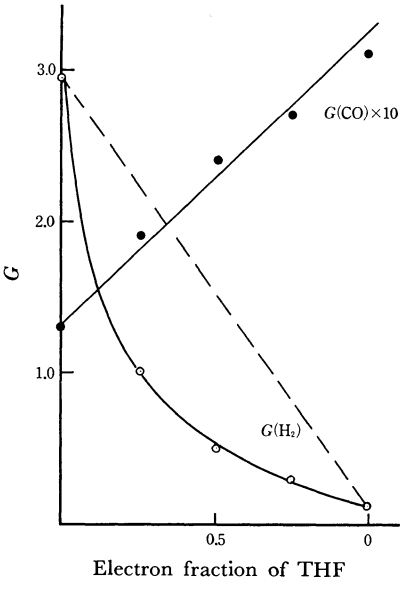

Fig. 2. Yields of H_2 and CO from the system THF-furan

Table I. Yields of hydrogen and carbon monoxide from mixture of THF and furan irradiated at ca. 25.0°C and 10^{19} eV. ml^{-1}

ε_T	$G(H_2)$ Obsvd.	$G(H_2)$ Calcd.	ΔG	$G(CO)$ Obsvd.	$G(CO)$ Calcd.	ΔG
1.00	2.95	2.95	0	0.13	0.13	0
0.74	1.01	2.21	−1.20	0.19	0.18	+0.01
0.49	0.50	1.51	−1.01	0.24	0.22	+0.02
0.25	0.29	0.83	−0.54	0.27	0.26	+0.01
0	0.12	0.12	0	0.31	0.31	0

The decrease in the hydrogen yield is shown to be greater than that to be expected from the above equation, whereas the yields of carbon monoxide fit the expected values. According to the current

3) H. Brückner and R. Schick, *Gas u. Wasserfach.*, **82**, 189 (1939).

theories of radiation chemistry, radiolysis begins with the production of molecules of vibrationally- and electronically-excited state, in addition to that of ionic species. The different mechanisms may be possible for the formation of hydrogen and carbon monoxide in the radiolysis of liquid THF.

The decrease in hydrogen yield might be due to the protection of THF from reaction by an activation transfer mechanism which reduces the amount of the initial decomposition of the THF itself; it might be due to a scavenging process that removes precursors of hydrogen, or it might be due to a combination of the two.

The yields of hydrogen and carbon monoxide from neither THF nor furan are affected by adding I_2 and hydroquinone respectively as radical scavengers. Their constant G values were also observed by adding ethylene (0.56—3.55 mol.) in the γ-radiolysis of THF. Moreover, if furan acts as the scavenger for the H-atom, the amount of residual hydrogen should be constant at a high concentration of added furan. However, this is not the case, as is shown in Fig. 2. Consequently, there should be no hydrogen atoms scavenged by the added furan, and the decrease in $G(H_2)$ in the radiolysis of the THF-furan system might be due to the "sponge-type" protection[4] action of furan with relation to THF.

Since $G(CO)$ and the amount of constructional units containing oxygen atoms in the THF molecule are both half of those of dioxane, the mechanism of the formation of the carbon monoxide in the γ-radiolysis of THF may be similar to that of dioxane. Llabador and Adloff have suggested that the decomposition of the excited dioxane molecule gives rise to the formation of carbon monoxide. Furthermore, in the photolysis of ethyleneoxide, the ring opening was the main reaction, and in the mercury-sensitized photolysis of de-aerated THF, the ratio of carbon monoxide to hydrogen was about 10 times that in the γ-radiolysis. Therefore, it may be concluded that the excited molecule of THF is the most important precursor of the formation of carbon monoxide, though its energy state is not yet clear. However, the excitation transfer which is related to the reaction can not be assumed in this binary system, since $G(CO)$ fits the expected values, as has been seen in Fig. 2.

The mode of the ring opening in the THF molecule is supposed to be as follows:

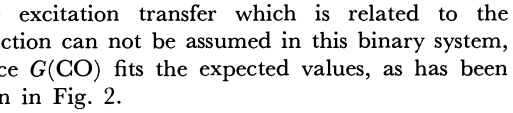

The carbon monoxide should be formed by the decomposition of the active species, such as I, II and III, when those species have excess energy after the ring opening. If the C–O bond rupture also occurs preferentially in these active species, as has been suggested by Newton[5] and, Ng and Freeman[6] in the α-and γ-radiolysis of linear ethers respectively, the formation of carbon monoxide may be explained by the following scheme:

$$\mathrm{I} \longrightarrow (\mathrm{CH_2CH_2}\cdot)^* + (\mathrm{OCH_2CH_2}\cdot)^* \quad (1)$$

$$(\mathrm{CH_2CH_2}\cdot)^* \longrightarrow \mathrm{C_2H_4} \text{ or } \mathrm{C_2H_5}\cdot \quad (2)$$

$$(\mathrm{OCH_2CH_2}\cdot)^* \xrightarrow{\mathrm{C_4H_7O}\cdot} \mathrm{CO} + \mathrm{CH_3}\cdot + \mathrm{C_4H_8O} \quad (3)$$

$$\mathrm{CH_3}\cdot + \mathrm{C_4H_8O} \longrightarrow \mathrm{CH_4} + \mathrm{C_4H_7O}\cdot \quad (4)$$

According to Llabador's data, since the yields of ethylene and carbon monoxide indicate the "molecular" yield and since 90% methane was scavenged by the radical scavenger, the reactions 1, 2 and 3 may be taking place in the spur region. Carbon monoxide is considered to be formed also by the following scheme:

$$\mathrm{II} \longrightarrow (\mathrm{CH_2CH_2CH_2}\cdot)^* + (\mathrm{OCH_2}\cdot)^* \quad (5)$$

$$(\mathrm{OCH_2}\cdot)^* \longrightarrow \mathrm{CO} + \mathrm{H_2} \quad (6)$$

$$(\mathrm{CH_2CH_2CH_2}\cdot)^* \longrightarrow \mathrm{CH_3\text{-}CH{=}CH_2} \text{ or } (\mathrm{CH_2})_3 \text{ or } \mathrm{C_3H_7}\cdot \quad (7)$$

As the yields of propylene, cyclopropane, CO and H_2 indicate the "molecular" yield in Llabador's data at a high dosage, while no cyclopropane and only a trace of propylene were determined in the low-dosage experiment of this report, reactions 5, 6 and 7 may occur in spur region anyhow. A similar process may be presumed for the III species as follows:

$$\mathrm{III} \longrightarrow \mathrm{CH_3CH_2CH_2CH_2OH} \quad (8)$$

$$\mathrm{III} \xrightarrow{\mathrm{C_4H_7O}\cdot} \mathrm{CO} + \mathrm{C_3H_7}\cdot + \mathrm{C_4H_8O} \quad (9)$$

$$\mathrm{C_3H_7}\cdot + \mathrm{C_4H_8O} \longrightarrow \mathrm{C_3H_8} + \mathrm{C_4H_7O}\cdot \quad (10)$$

The decrease in $G(C_3H_8)$ caused by the added radical scavenger in Llabador's data at high dosage may be explained qualitatively by assuming the reactions 7 and 9 in the spur. Since $G(C_3H_8)$ is negligible in the low-dosage experiments of this report, reaction 8 may be more dominant than 9.

The probability of the formation of active species I, II and III by ring opening can roughly be estimated as I : II : III = 1.0 : ~0 : 1.3, by using the above scheme, and the results determined at a total does of 4.39×10^{19} eV. ml^{-1}. These results are $G(C_4H_9OH) = 0.40$, $G(CH_4) = 0.01$, $G(C_2H_4) = 0.30$, $G(C_2H_6) = 0$, $G(c\text{-}C_3H_6) = 0$, $G(C_3H_6) =$ trace and $G(C_3H_8) =$ trace. It may be presumed, by taking its estimated value, that the probability of the C–O bond rupture is a little greater than

4) M. Burton and S. Lipsky, *J. Phys. Chem.*, **61**, 1461 (1957).

5) A. S. Newton, *J. Phys. Chem.*, **61**, 1485, 1490 (1957).

6) M. K. M. Ng and G. R. Freeman, *J. Am. Chem. Soc.*, **87**, 1635, 1639 (1965).

the rupture of the C(β)–C(β') bond. The actual ratio of ring opening might be greater than these estimated values, depending upon the identity of the dimeric and polymeric products.

As for the formation of the hydrogen in this binary system, a charge transfer is probable. A positive ion of THF may easily be formed by ejecting, by means of ionizing radiation, one of the lone-pair electrons located at the oxygen atom. Since the ionization potentials of THF and furan are 10.3 and 9.06 eV. respectively, the charge transfer from the ground state of the THF ion to a furan molecule is probable, because the process is exothermic. Therefore, an ionic reaction, such as an ion-molecule reaction or an ion recombination reaction, is most probable for the formation of the hydrogen.

Dainton et al.[7] have suggested that the dominant primary species formed in the γ-radiolysis of methyltetrahydrofuran (MTHF) in the glassy state are an electron and a free radical (corresponding to the solvent molecule minus a hydrogen atom), followed by the ion-molecule reaction between MTHF and its ion. The experimental finding that the hydrogen yield was unaffected by an added radical scavenger could also be explained by the process of the ion-molecule reaction, because the "molecular" hydrogen is produced by this reaction. As the formation of "molecular" hydrogen may also be considered in the ion-recombination reaction, which is another process of the parent ion, it is convenient to conclude that the hydrogen is formed mainly by the ionic reaction, and that the precursor of the carbon monoxide is the directly-excited THF molecule.

7) F. S. Dainton, J. P. Keene, T. J. Kemp, G. A. Salmon and J. Teply, *Proc. Chem. Soc.*, **1964**, 265; F. S. Dainton, F. R. S., and G. A. Salmon, *Proc. Roy. Soc.*, **A285**, 319 (1965).

Summary

The charge transfer is presumed for the formation of hydrogen in the γ-radiolysis of liquid THF-furan mixtures. The ring opening of the excited molecule has been suggested to be the main process in the formation of carbon monoxide. It has also been suggested that hydrogen might be formed mainly by an ionic reaction including the parent positive ion of THF. The probability of the ring opening has been roughly estimated.

The author's thanks are due to Dr. Kenichi Shinohara, Masashi Imamura and Ko Taki for their stimulating discussions of the problems, and to Miss Noriko Tsunoo for her analysis by gas chromatography.

BULLETIN OF THE CHEMICAL SOCIETY OF JAPAN VOL. 39 1643—1650 (1966)

The Reaction of Oxygen Atoms with Dimethyl Ether*

By Yoshimasa TAKEZAKI, Sadayuki MORI and Hironobu KAWASAKI

Institute for Chemical Research, Kyoto University, Sakyo-ku, Kyoto

(Received November 6, 1965)

The gas-phase reaction of dimethyl ether with oxygen atoms produced by the mercury photosensitized decomposition of nitrous oxide has been studied by means of quantitative determinations of the reaction products. Characteristic products are water, methanol, formaldehyde, carbon monoxide, methoxy ethanol and methyl formate. The possible mechanisms of the oxygen attack on the substrate have been considered, and the following steps postulated on the basis of the relative importance of these products and their time variations:

$O + CH_3OCH_3 \xrightarrow{k_E} OH + CH_3OCH_2$, $OH + CH_3OCH_3 \longrightarrow H_2O + CH_3OCH_2$
and $CH_3OCH_2 + OH \longrightarrow CH_3O + CH_2OH$.

The rate constant, k_E, of the first step has been determined in the competitive reaction with *n*-butane as:

$$k_E = 6.3 \times 10^{10}\exp(-4700/\boldsymbol{R}T)\ 1.\ \mathrm{mol}^{-1}\,\mathrm{sec}^{-1}.$$

Rate data have been increasingly accumulated in recent years on the reactions of oxygen atoms with such saturated molecules as hydrogen and paraf-

* This paper was read at the International Conference on Photochemistry, Tokyo, 1965.

fins.[1-4] However, papers dealing with oxygen-containing compounds are still scant (Ref. 1f and Ref. 5), and the mode of the initial attack by oxygen seems still not to be conclusively known.

The mechanisms proposed hitherto may be classified into the following four types: hydrogen abstraction, a common type of reaction in atomic or monoradical reactions (ex., $CH_3CHO+O\rightarrow CH_3CO+OH$),[5] direct insertion into a C–H bond (ex., $CH_4+O\rightarrow CH_3OH$),[2] the displacement of one or two group(s) by O (ex., $n\text{-}C_4H_{10}+O\rightarrow CH_2O+H_2+:CHC_2H_5$ or $H_2+CH_3CHO+:CHCH_3$,[3] $(CH_3)_3CH+O\rightarrow(CH_3)_2CO+CH_4$ or $(CH_3)_2CO+H+CH_3$),[6] and the combination of an oxygen atom with two hydrogen atoms to form water (ex., $CH_4+O\rightarrow:CH_2+H_2O$).[7]

In all these instances, however, the methods of producing oxygen atoms vary; in the discharge in oxygen or water vapor, the formation of oxygen atoms of a single electronic energy state seems hardly to be expected, and the co-existence of oxygen molecules must obscure the proper reactions of oxygen atoms. Moreover, in high-temperature oxidation the features of the reaction may differ markedly from those prevailing in normal temperatures, further, in microwave discharge where the oxygen atom concentration is very high, the reactions of oxygen atoms with the produced radicals may complicate the discrimination of the primary action of oxygen atoms on the substrate.

In view of these facts, with the intention of determining the features of the oxygen attack on the oxygen-containing *saturated* compounds, dimethyl ether (referred to as DME hereafter) has been taken as an example, while as a source of oxygen atoms the mercury-photosensitized decomposition of nitrous oxide was used, since it has been established by Cvetanović[8] that the oxygen atoms in the ground ^3P state are produced in this reaction:

$$Hg(^1S_0)+h\nu(2537\ Å)\rightarrow Hg^*(^3P_1)$$
$$Hg^*+N_2O\rightarrow Hg(^1S_0)+N_2+O(^3P_2).$$

The qualitative aspects of this reaction have already been reported by the present authors,[9] but in this paper a more detailed discussion based on the quantitative results will be given.

Experimental

The reaction was carried out in a static system of the usual type. A Vycor glass reactor ($28\phi\times400$ mm.,

TABLE I. G.L.C. CONDITIONS AND OTHER ANALYTICAL METHODS

Figures in the table denote the operation temperatures, °C, of g.l.c.

Column	A	B	C
H_2	35	24	
N_2, O_2			24
CO	70	24	
CO_2		107	
CH_4, C_2H_6, C_2H_4	70	107	
N_2O		107	
Column	**D**	**E**	**F**
N_2O	108	0	
$n\text{-}C_4H_{10}$		0	
DME	108	0	
H_2O	108/99		
CH_3OH	47		
Dimer	108		114
GTME	108		114
BMEE	108		114
$CH_3OC_2H_4OH$	99	119	82
$HCOOCH_3$	108		
$CH_3OC_2H_5$	47		
$CH_3OCH_2OCH_3$	108/47		
CH_3OOCH_3	108/47		
Ethylene oxide	108/47		
1,4-Dioxane	108		114
$(CH_2OH)_2$			114
CH_3CHO	108		

Column A: Al_2O_3 2 m.
B: Active carbon 2.5 m.
C: Molecular sieve 5A 2 m.
D: D.O.P.+Polyethylene glycol 4000 2 m.
E: Dibenzyl ether 2 m.
F: Silicone oil 550 3 m.

Other determinations or detections:

HCHO	Colorimetry with Schiff's reagent in acid condition
H_2O_2	Coloration with KI solution
Higher *N*-oxides	Griess' test[10]
$HCOOCH_3$	Hg_2Cl_2 precipitation when boiling with $HgCl_2$ solution.

1) a) E. L. Wong and A. E. Potter, Jr., *J. Chem. Phys.*, **39**, 2211 (1963) for H_2 and CH_4. b) V. V. Azatyan, A. B. Nalbandyan and Meng-Yuan Ts'ui, *Kinetika i Kataliz.*, **5**, (2) 201 (1964) for CH_4; *Dokl. Akad. Nauk SSSR*, **147**, 361 (1962) for C_2H_6; ibid., **36**, (1) 23 (1963) for C_2H_6 and C_4H_{10}. c) V. V. Azatyan, V. V. Voedodskii and A. B. Nalbandyan, *Kinetica i Kataliz.*, **2**, 340 (1961) for H_2. d) H. W. Ford and N. Endow, *J. Chem. Phys.*, **27**, 1277 (1957) for $n\text{-}C_4H_{10}$ and 3-Meheptane. e) M. A. A. Clyne, "9th Symp. on Combustion," Academic Press, New York (1963), p. 211 for H_2. f) L. I. Avramenko, "Advances in Photochemistry, II," Interscience Publishers, New York (1963), p. 57 for CH_4, C_2H_6 and $n\text{-}C_4H_{10}$.

2) L. I. Avramenko and R. V. Kolesnikova, *Dokl. Akad. Nauk SSSR*, **91**, 107 (1953).

3) L. I. Avramenko, R. V. Kolesnikova and G. I. Savinova, *Izv. Akad. Nauk SSSR, Otd. Khim. Nauk*, **1963**, 976.

4) L. Elias and H. I. Schiff, *Can. J. Chem.*, **38**, 1657 (1960).

5) R. J. Cvetanovic, ibid., **34**, 775 (1956).

6) F. J. Wright, *J. Chem. Phys.*, **38**, 950 (1963).

7) E. W. R. Steacie and N. A. D. Parlee, *Can. J. Research*, **B16**, 203 (1938).

8) R. J. Cvetanović, *J. Chem. Phys.*, **23**, 1203 (1955); ibid., **30**, 19 (1959); S. Sato and R. J. Cvetanović, *Can. J. Chem.*, **36**, 970 (1958).

9) H. Kawasaki and Y. Takezaki, *Bull. Inst. Chem. Res., Kyoto Univ.*, **42**, 378 (1964).

10) F. D. Treadwell, "Lehrbuch der Anal. Chem. I," Fr. Deuticke, Leipzig (1935), p. 337.

210 cc.) was placed parallel to a low-pressure mercury lamp (25ϕ × 436 mm., Toshiba Electric Co. germicidal lamp GL-15, dc-operated, 15 W.) in an air bath furnished with heating elements in the wall and a fan at the bottom. The Vycor glass cuts off the light wavelength shorter than 2200 Å; the temperature variation in the reactor was kept within 2°C during the reaction by means of forced air circulation. The reactant mixture was saturated with mercury vapor at room temperature prior to the reaction.

At the end of the irradiation, the reactor was warmed up to 70°C in order to vaporize the heavy liquid products; almost all the products, except for a trace of the heaviest ones, were then drawn out through a liquid nitrogen trap by means of a Töpler pump; then the permanent gases and vapors, and liquids condensing at room temperature were separately analyzed, mainly by gas chromatography, as is shown in Table I, where the products were identified with the authentic samples in 2 or 3 different coulmns (the methods of preparations of some of the samples have been given in the previous paper).[9]

The impurities of the reactants as measured by g.l.c. are: $O_2<0.00\%$, $N_2=0.15\%$, $CH_4=0.13\%$ in N_2O purified by the evacuation of the solid in a liquid nitrogen trap; $CH_3OH<0.01\%$, $H_2O<0.00\%$ in DME purified by repeated bulb-to-bulb distillation; the guaranteed purity of *n*-butane obtained from Takachiho Co.=99.8%.

Results

The Mercury-photosensitized Decomposition of DME.—In order to distinguish the reaction products of oxygen-atom reactions from those of the mercury-photosensitized decomposition of DME which takes place concomitantly, we have to know about the products of the latter reaction alone. This reaction has already been studied by Marcus et al.[11] in a flow system, but in order to make comparison easier, product analyses have now been performed in a static system under the conditions of the present investigation. Typical results are given in the columns 2 and 4 of Table II; the main products are H_2 and $(CH_3OCH_2)_2$ (ethylene glycol dimethyl ether; abbr. Dimer), together with small quantities of $CH_3OCH_2CH_2OCH_2CH_2OCH_3$ (bis-(β-methoxy ethyl) ether; abbr. BMEE or Trimer) and $CH_3OCH_2(OCH_3)CHCH_2OCH_3$ (glycerol trimethyl ether; abbr. GTME or Trimer). In column 4 are given those products which might exist but could not be detected, or which existed as only trace amounts.

Table II. Products of Hg photosensitized reactions

Initial			
DME, mmHg	100	100	
N_2O, mmHg	0	300	
Temp., °C	30	30	Compds. not detected or <0.0% in both cases
Irradiation	15 min.	1 hr.	
Product mol. % to charged DME			
DME	−20.3	−58.2	CO_2
N_2	—	30.0	O_2
H_2	13.4	3.1	CH_4
CO	0.0	2.0	C_2H_6
H_2O	0.0	27.6	C_2H_4
CH_3OH	0.0	3.8	H_2O_2
HCHO	0.0	0.7	$CH_3OC_2H_5$
Dimer*	4.8	4.6	$CH_3OCH_2OCH_3$
GTME} Trimer*	0.8	1.9	CH_3OOCH_3
BMEE}	0.3	0.5	Ethylene oxide
$CH_3OCH_2CH_2OH$	0.0	0.4	1, 4-Dioxane
$HCOOCH_3$	0.0	0.2	CH_2OHCH_2OH
Unidentified high boil. compds.		4 kinds each ca. 0.2%	CH_3CHO
			Oxides of N

* For abbreviations see the text.

The present results generally agree with those of Marcus[11] obtained at room temperature except for the additional observation of trimers; these products may be explained by:

$$\left.\begin{aligned} &CH_3OCH_3 + Hg^* \rightarrow CH_3OCH_2 + H + Hg \\ &CH_3OCH_3 + R \rightarrow CH_3OCH_2 + RH \\ &2CH_3OCH_2 \rightarrow (CH_3OCH_2)_2 \text{ Dimer} \end{aligned}\right\} \text{(Marcus)}^{11)}\ R=H \text{ or any radical}$$

$$(CH_3OCH_2)_2 + R \begin{cases} \rightarrow CH_3OCH_2CH_2OCH_2\cdot \\ \xrightarrow{+CH_3OCH_2} CH_3OCH_2CH_2OCH_2CH_2OCH_3 \text{ (BMEE)} \\ \rightarrow CH_3OCH_2\dot{C}HOCH_3 \\ \xrightarrow{+CH_3OCH_2} CH_3OCH_2CH(OCH_3)CH_2OCH_3 \text{ (GTME)}\cdot \end{cases}$$

One point to be noticed in connection with the following discussion is the absence of carbon monoxide, methane, ethane, methanol, formaldehyde, 1, 4-dioxane and ethylene oxide, which would rule out the possibilities of the $CH_3OCH_2 \rightarrow CH_3 + CH_2O$ and $CH_3OCH_2 + R \rightarrow \cdot CH_2OCH_2\cdot + RH$ reactions at room temperature.

In this study it is necessary to know the ratio of the decomposition of DME by the excited mercury to that of N_2O; the effective quenching cross-section of N_2O decomposition (Reaction 2 in the next scheme) has been given by Cvetanović[12] as 12.6 Å^2, but concerning DME the only available value is for the total quenching (7 Å^2 for (1)+(1′)[13]). Therefore, a rough estimation was made, according

11) R. A. Marcus, B. deB. Darwent and E. W. R. Steacie, *J. Chem. Phys.*, **16**, 987 (1948).
12) R. J. Cvetanović, ibid., **23**, 1208 (1955).
13) B. deB. Darwent and M. K. Phibbs, ibid., **22**, 110 (1954).

to the following scheme, of the effective cross section for DME decomposition, (1), from the rate measurements of the hydrogen formation in DME alone and of the nitrogen formation in the mixture of DME and nitrous oxide. The results are represented in Fig. 1.

			Rate const.
$Hg(^1S_0)+h\nu$	$\rightarrow Hg^*(^3P_1)$		
Hg^*	$\rightarrow Hg+h\nu$		(k_0)
Hg^*+DME	$\rightarrow Hg+CH_3OCH_2+H$	(1)	(k_1)
	$\rightarrow Hg'(^3P_0)+DME$	(1')	(k_1')
Hg^*+N_2O	$\rightarrow Hg+N_2+O(^3P_2)$	(2)	(k_2)
	$\rightarrow Hg'+N_2O$	(2')	(k_2')

We then have, in DME alone:

$$1/(\text{rate } H_2) = (1/I_{abs})(1 + k_1'/k_1) + (k_0/k_1I_{abs})/(DME) \quad \text{(Fig. 1-A)}$$

and in the mixture of DME and N_2O:

$$1/(\text{rate } N_2) = (1/I_{abs})(1 + k_1'/k_1)(k_1/k_2)\times\{(k_2+k_2')/(k_1+k_1') + (DME)/(N_2O)\} \quad \text{(Fig. 1-B)}$$

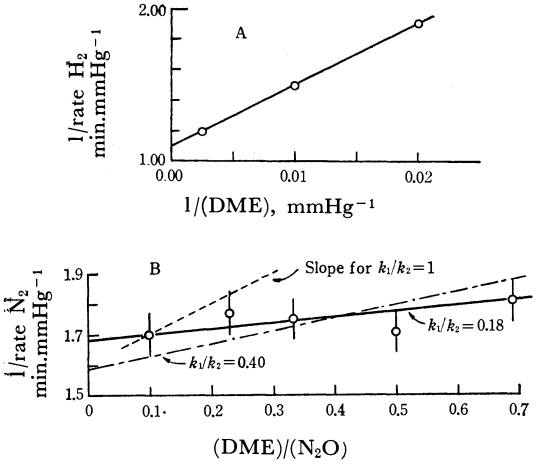

Fig. 1. Determination of cross section of DME.

	k_1/k_2	$(k_2+k_2')/(k_1+k_1')$	$k_0/(k_1+k_1')$
mean	0.18	9.55	3.83 mmHg
max.	0.40	3.92	

In this treatment we have omitted the further reactions of Hg', $Hg'+N_2O\rightarrow Hg+N_2+O$ and $Hg'+DME\rightarrow Hg+CH_3OCH_2+H$, following the argument of Cvetanović;[12] though the apparatus used here was not adequate for the exact determination, we have the cross section of $\sigma_{DME} \doteqdot 2$ Å^2 with the upper limit of 5 Å^2 for (1).

The Reaction of Oxygen Atoms with DME. —In the photo-reaction of a mixture of DME, nitrous oxide and mercury, an effort has been made to determine as many reaction products as possible in a large reactor ($88\phi\times612$ mm., 2941 cc.; lamp coaxially enclosed in a Vycor sheath) and with prolonged irradiation. The results are given in Table II, columns 3 and 4, together with the conditions.

Characteristic products are water, methanol, formaldehyde, carbon monoxide, methoxy ethanol and methyl formate; moreover, though in quite small quantities, at least four kinds of peaks were observed in the gas chromatogram after the elution of the trimers. As may be seen in the last column of Table II, no lower hydrocarbons and carbon dioxide were present, and no molecular oxygen could be found, even after a long irradiation, if DME was present in an amount 1/80 of nitrous oxide at the beginning.

In Fig. 2 the variation of products with the irradiation time in a standard reactor is represented; the N_2O/DME ratio was kept high so as to reduce the mercury-photosensitized decomposition of DME (these conditions will be referred to as the standard conditions hereafter). Most of the oxygen atoms produced seem to appear as water, and from the features of the curves we see that the formation of the dimer is followed by subsequent reactions leading to trimers and other unknowns, and that carbon monoxide is produced by a sequence of steps.

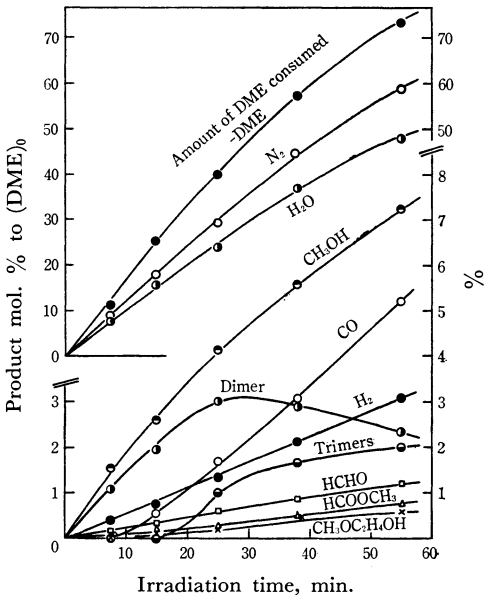

Fig. 2. Time dependence of products.
Standard condition: $(DME)_0=50$ mmHg, $(N_2O)_0=500$ mmHg, 30°C

The material balances on C, H and O in terms of the identified products are:

$$N_2 = H_2O + HCOOCH_3 + 1/2(CH_3OH + CH_3OC_2H_4OH + HCHO + CO)$$

Obs. $N_2 = 30.0\%$ to $(DME)_0$

Calc. $= 31.1\%$,

$$\text{Consumed DME} = 2H_2O + 3/2CH_3OH + 1/2CH_3OC_2H_4OH + 2H_2 - (\text{Trimers} + 1/2HCHO + 5/2CO + HCOOCH_3)$$

Obs. consumed DME=58.2%

Calc. =61.0%,

$$H_2O = \text{Dimer} + 2\text{Trimers} + 1/2CH_3OC_2H_4OH + 1/2HCHO + 3/2CO - (H_2 + HCOOCH_3 + 1/2CH_3OH)$$

Obs. H_2O=27.6%

Calc. 10.5% .

In these equations the balances not involving dimer are fairly good, but the last one is far from sufficient, probably due to a number of missing higher products small in quantity.

Discussion of the Mechanism

The Mode of the O Attack on DME.—Following elementary steps may be conceivable in the initial attack of oxygen atoms according to the classification given in the introduction:

$O + DME \rightarrow$:

1. $\rightarrow OH + CH_3OCH_2$,
   $OH + CH_3OCH_3 \rightarrow H_2O + CH_3OCH_2$,
2. $\left.\begin{array}{l}\longrightarrow \\ \rightarrow CH_3OOCH_3 \rightarrow\end{array}\right\} 2CH_3O$, (a)
   $\rightarrow CH_3OCH_2OH \rightarrow \begin{cases} CH_3O + CH_2OH & \text{(b)} \\ CH_3OCH_2 + OH, & \text{(c)} \end{cases}$
3. $\rightarrow HCOOCH_3 + H_2$ or 2H, (a)
   $\rightarrow CH_3O + CH_2O + H$, (b)
4. $\rightarrow CH_3OCH{:} + H_2O$,
   $\rightarrow \cdot CH_2OCH_2\cdot + H_2O$.

Case 1 is quite attractive to account for the production of a large amount of water, an amount which is close to that of the oxygen atoms produced, which in turn corresponds to about a half of the DME consumed. However, other possibilities leading to the water formation should be considered here; in the present study the following three processes can conceivably account for the origins of OH:

$$H + O + M \rightarrow OH + M, \quad H + N_2O \rightarrow OH + N_2 \text{ and } H_2 + O \rightarrow OH + H.$$

However, since these hydrogens can all originate from the photosensitized decomposition of DME, calculation has been made on the rate of hydrogen atom formation in the competitive quenching of Hg* in the mixture of DME and nitrous oxide under the standard experimental conditions ($(N_2O)_0$= 500 mmHg, $(DME)_0$=50 mmHg, 30°C) using the effective cross section, σ_{DME}, obtained in the preceding section. Then, by comparing the calculated rate of hydrogen atom production (0.023 mmHg/min.) with the observed rate of water formation (0.47 mmHg/min. in Fig. 2), it could be concluded that the photosensitized decomposition of DME contributes at most 5% to the total water formation. (It is of interest to note that the observed rate of hydrogen production (0.027 mmHg/min.) is close to the calculated rate of hydrogen atom production.)

Case 2 involves direct double decomposition into two radicals or insertion into a C–H or O–C bond; but since the insertion reactions are highly exothermic, since the O–O bond energy is only 36.9 kcal. in dimethyl peroxide,[14] and since the hemiacetal is known to be too unstable to exist in a free state, the inserted molecules will eventually decompose into the radicals shown in the scheme. We could not prove the presence of dimethyl peroxide.

The two steps, 2 (a) and 2 (b), cannot be the main courses of the oxygen attack, however, since they fail to explain the formation of a large amount of water, and the sum of methanol (resulting from $RH+CH_3O$ or $RH+CH_2OH$) and its decomposition products, formaldehyde and carbon monoxide and methoxy ethanol (assuming the reaction $CH_2OH+CH_2OCH_3$), is much less than the amount of oxygen produced. Further, ethylene glycol (by $2CH_2OH$) and formal (by $CH_2OCH_3+CH_3O$) could not be detected; they may be supposed to be produced if these mechanisms are predominantly operative. Case 2 (c) is not distinguished from Case 1. However, in any case, it should be admitted that for these insertion reactions to take place, spin conservation rule has to be violated, because the oxygen atom participating here is in the triplet state.

In Case 3, (a) would contribute at most a small portion of the total oxygen attack, as judged from the minuteness of methyl formate which, according to the result of Thynne's experiments,[15] has the usual reactivity towards the subsequent radical attack. Further, as will be shown later, there is evidence that methyl formate can be produced by the reaction of OH+DME in the absence of oxygen atoms. The fact that the total amount of $1/2H_2O+H_2$ is by far greater than that of $CH_3OH+HCHO+CO+CH_3OC_2H_4OH$ excludes 3-(b) as the main course of oxygen atom reaction.

As for Case 4, none of the recombination products expected from this mechanism (ethylene oxide, 1, 4-dioxane and $(CH_3OCH{:})_2$) were found. Although this does not lead to the complete exclusion of this mechanism, the elementary reactions involving biradical formation in one process do not seem to proceed so easily as to compete with monoradical formation steps, even for the

14) Y. Takezaki and C. Takeuchi, ibid., **22**, 1527 (1954).

15) C. J. Thynne and P. Gray, *Trans. Faraday Soc.*, **59**, 1140 (1963); C. J. Thynne, ibid., **58**, 676 (1962).

exothermic reaction, at least to an extent enough to account for a large amount of water.

Thus the abstraction of the hydrogen atom (Case 1) may be concluded to be the most predominant process, although the minor contributions of other modes cannot be entirely ruled out.

Another oxygen atom reaction to be considered is $CH_3OCH_2+O \rightarrow CH_3OCH_2O$ or $CH_3O+HCHO$; the former must have a large rate constant and has been taken into account in the argument of Wright on the reaction of oxygen atoms with isobutane.[6] However, both these reactions can be shown to be negligible under the present experimental conditions by the following considerations.

Consider the following scheme which is simplified but sufficient to get the upper limit values necessary for the present discussion:

$$Hg+h\nu \rightarrow Hg^*$$

		Rate const.
$N_2O+Hg^* \rightarrow N_2+O+Hg$		
$O+DME \rightarrow CH_3OCH_2+OH$	(E)	k_E
$OH+DME \rightarrow CH_3OCH_2+H_2O$	(E')	k_E'
$2CH_3OCH_2 \rightarrow (CH_3OCH_2)_2$	(3)	k_3
$O+CH_3OCH_2 \rightarrow CH_3OCH_2O \rightarrow \cdots$	(4)	k_4
$\rightarrow CH_3O + CH_2O\cdot$	(4')	k_4' .

The steady concentration of the O atom is:

$$(O) = \frac{I_{abs}}{k_E(DME) + k_4'(CH_3OCH_2) + \cdots} \leq \frac{d(N_2)/dt}{k_E(DME)} .$$

Therefore, under the standard conditions (rate N_2(obs.) = 0.65 mmHg/min. $= 5.8\times10^{-7}$ mol./l. sec. at 30°C, (DME) = 50 mmHg $= 2.68\times10^{-3}$ mol./l.), we have $(O)\leq 7.7\times10^{-12}$ g.-atom/l. and $\beta\equiv(DME)/(O)\geq 3.5\times10^{8}$.

Now, k_3 and k_4 should be close to the collision numbers, i. e., $k_4'<k_3\fallingdotseq k_4\fallingdotseq 10^{11}$ l./mol.sec. and $k_E=2.8\times10^{7}$ l./mol.sec. at 30°C, as will be established later; then, dropping unimportant terms in numerical calculation, we have $(CH_3OCH_2)\fallingdotseq\{(O)(DME)k_E/k_3\}^{1/2}$ within an accuracy of 0.2%; finally the following expressions are obtained:

$$\frac{\text{rate (4')}}{\text{rate (3)}} < \frac{\text{rate (4)}}{\text{rate (3)}} \fallingdotseq \left(\frac{k_3}{2k_E\beta}\right)^{1/2} \leq 1.6\times10^{-3} \text{ and}$$

$$\frac{\text{rate (4')}}{\text{rate (E)}} < \frac{\text{rate (4)}}{\text{rate (E)}} \fallingdotseq \left(\frac{k_4}{k_E\beta}\right)^{1/2} \leq 3.2\times10^{-3}.$$

Thus the reactions between the oxygen atom and CH_3OCH_2 can well be ignored with respect to both reactants.

The Origin of Methanol and Methoxy Ethanol.—Since the $CH_3OCH_2\rightarrow CH_3+CH_2O$ decomposition has been proved to be unlikely in the preceding section, combination of CH_3 and OH cannot be the source of methanol. Hence, the steps responsible for the formation of methanol are probably the C–O bond fission of DME or derived radicals to produce CH_3O or CH_2OH; however, $CH_3OCH_2\rightarrow CH_3O+:CH_2$ is too endothermic to occur at normal temperatures, and the elementary steps, $O+DME\rightarrow 2CH_3O$, CH_3O+CH_2OH, or CH_3O+CH_2O+H and $O+CH_3OCH_2\rightarrow CH_3O+CH_2O$, have already been ruled out. Therefore, we would like to propose here:

$$CH_3OCH_2 + OH \rightarrow (CH_3OCH_2\cdots OH) \rightarrow CH_3O+CH_2OH+21 \text{ kcal./mol.} \quad (5)^*$$

The assumption that the transient complex of the hemiacetal type decomposes instantly at the weakest methyl C–O bond would be reasonable because of the extreme instability of hemiacetal just mentioned. Moreover, since OH and $CH_3\cdot OCH_2$ are the most abundant radicals during the reaction, this inter-radical process may explain the medium amount of methanol and also the minute amount of methoxy ethanol* which have resulted from

$$CH_2OH \text{ or } CH_3O + RH \rightarrow CH_3OH + R$$
$$CH_3OH + R \rightarrow CH_2OH + RH$$
$$CH_2OH + CH_3OCH_2 \rightarrow CH_3OCH_2CH_2OH.$$

However, no positive evidence was obtained on the presence of the products to be expected from the following equations when CH_3O and CH_2OH were present:

$$2CH_2OH \rightarrow (CH_2OH)_2 \quad \text{(trace?)}$$
$$CH_3O + CH_2OCH_3 \rightarrow CH_3OCH_2OCH_3 \quad \text{(rather unstable?)}$$

Further, the possibility of the $OH+CH_3OCH_2\rightarrow CH_3OH+HCHO$ reaction cannot be entirely ruled out, though this cannot be the main source of methanol since the observed methanol /(HCHO + CO) ratio is less than unity.

In order to test above-mentioned postulate—methanol formation without the participation of the oxygen atom, a supplementary study was made on the reaction of DME with the OH radicals produced by the photolysis of hydrogen peroxide. It has been well established that H_2O_2 produces

* The heat of reaction is calculated using the data given by Gray[16] and Field[17]. The approximate calculation as before has given the lower limit of rate(5)/rate(E') or rate(5)/rate(3) as ca. 0.02 when kE' $= 10^{11}\exp(-6000/RT)$ l./mol.sec., which is assumed, by referring to other OH reactions[18], to be the highest value for this reaction.

16) P. Gray, *Chem. Revs.*, **59**, 239 (1959).

17) F. H. Field and J. L. Franklin, "Electron Impact Phenomena," Academic Press, New York (1957), p. 137.

18) Ref. lf, p. 32.

2OH by 2537 Å light,[19] and the decomposition into $O+H_2O$ has been stated to be implausible at least in the gas phase.[19] The results are as follows:

DME 93 mmHg, H_2O_2 (87% concn.), 70°C, 2537 Å, 1 hr.;

CH_3OH 3.7%, HCHO 0.3%, $CH_3OC_2H_4OH$ 0.2%, Dimer 4.0%, GTME 1.0%, BMEE 0.2%, CO 1.2%, $HCOOCH_3$ 0.7%, relative to $(DME)_0$ respectively.

Of course, no methanol, formaldehyde or carbon monoxide could be found, either when the mixture of DME and hydrogen peroxide was merely kept at 70°C, or when the mixture of DME and oxygen, the latter being a product on the heating of hydrogen peroxide, were irradiated by a 2537 Å light. The presence of the expected products supports the proposed mechanism strongly; furthermore, the methyl formate found here suggests that the presence of this compound in the reaction of the oxygen atom cannot be evidence for Case 3-(a) in the preceding section.

The Rate Constant of $O+CH_3OCH_3 \rightarrow OH+CH_3OCH_2$.—With the aim of determining the absolute rate constant of the first attack of oxygen on DME, the rate of the consumption of each substrate has been measured in the competetive reaction of oxygen atoms with DME and *n*-butane; the rate for the latter had been determined to be $k_B=(3.01\pm0.96)\times10^{10}\exp(-4200\mp200)/RT$ l./mol.sec. by Elias and Schiff.[4]

According to the discussion above, we take:

	Rate const.
$O + CH_3OCH_3 \rightarrow OH + CH_3OCH_2$	k_E
$OH + CH_3OCH_3 \rightarrow H_2O + CH_3OCH_2$	k_E'
$O + n\text{-}C_4H_{10} \rightarrow OH + C_4H_9$	k_B
$OH + n\text{-}C_4H_{10} \rightarrow H_2O + C_4H_9$	k_B'

as the sole substrate-consuming steps. This scheme should hold only for the early stage of the reaction; further, it implies the neglect of the following cross reaction:

$C_4H_9 + CH_3OCH_3 \rightleftarrows C_4H_{10} + CH_3OCH_2 - 0.6$ kcal.** k_E'' and k_B'',

that is, we are to assume *tentatively* that the net extent of this reaction (second term) is negligible as compared with the main substrate-consuming reactions (first term) in

$$\frac{-d(DME)}{dt} = \{k_E(O) + k_E'(OH)\}(DME) + \{k_E''(C_4H_9)(DME) - k_B''(C_4H_{10})(CH_3OCH_2)\},$$

$$\frac{-d(C_4H_{10})}{dt} = \{k_B(O) + k_B'(OH)\}(C_4H_{10}) - \{k_E''(C_4H_9)(DME) - k_B''(C_4H_{10})(CH_3OCH_2)\}.$$

Therefore, we have

$$\alpha \equiv \frac{\ln[(DME)_0/(DME)_t]}{\ln[(C_4H_{10})_0/(C_4H_{10})_t]} = \frac{\int_o^t(O)dt + (k_E'/k_E)\int_o^t(OH)dt}{\int_o^t(O)dt + (k_B'/k_B)\int_o^t(OH)dt} \cdot \frac{k_E}{k_B}.$$

In solving this, a further assumption is made that the ratios of the reaction rates between O and OH are the same for both substrates, i. e., $k_E'/k_E=k_B'/k_B$; then we get a simple relation $\alpha=k_E/k_B$. In order for this assumption to hold over the entire range of temperature, however, the next two conditions must be satisfied:

$$\frac{Z_E'/Z_E}{Z_B'/Z_B} \cdot \frac{P_E'/P_E}{P_B'/P_B} = 1$$

and $E_E - E_E' = E_B - E_B'$.

(Z, P and E have the usual meanings.)

As to the collision numbers, this ratio has been shown to be unity by calculation, but, strictly speaking, there is no such intrinsic necessity for the remaining two factors. However, the thermodynamical situations are almost the same in these two sets of exothermic reactions,

$\Delta H_E = -8.4$ kcal./mol. $\Delta H_B = -7.8$**

$\Delta H_E' = -25.2$ $\Delta H_B' = -24.6$,

and the reaction center in the configuration of the activated complex is, in all these cases, thought to be the same, $-O\cdots H\cdots C\equiv$. Such being the case, the approximation of the equality of the ratios of steric factors and of the differences in activation heats may be accepted as being fairly reasonable.

Moreover, the correction factor by which the observed α should be multiplied to obtain k_E/k_B when the above-mentioned ratio deviates from unity is only 2 or so against a tenfold deviation of that ratio in both directions, as is seen in the next table calculated using the values obtained with the present approximation.

19) D. H. Volman, "Advances in Photochemistry, I," Interscience Publishers, New York (1963), p. 69.

** Calculated from
$OH + H \rightarrow H_2O + 119.2$ kcal./mol.
$O + H \rightarrow HO + 102.4$
$n\text{-}C_4H_{10} \rightarrow H + C_4H_9 - 94.6$[20]
$CH_3OCH_3 \rightarrow H + CH_3OCH_2 - 94$[21]

20) G. C. Fettis and A. F. Trotman-Dickenson, *J. Chem. Soc.*, **1961**, 3037.

21) S. W. Benson and D. V. S. Jain, *J. Chem. Phys.*, **31**, 1008 (1959).

$\frac{k_E'/k_E}{k_B'/k_B}$	0.1	0.2	0.5	1	2	5	0
C for $\frac{k_E}{k_B} = C\alpha$	2.4	2.0	1.4	1.0	0.71	0.50	0.46

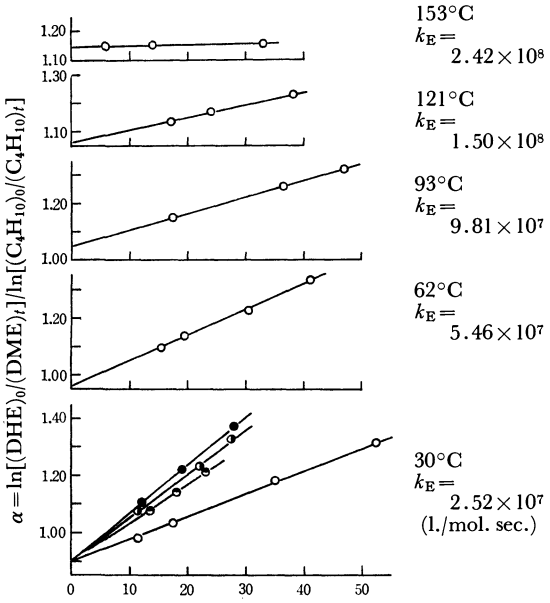

Fig. 3. Determination of α at various temperatures.

Initial pressures of reactants (mmHg)

	DME	n-C_4H_{10}	N_2O
○	24	24	405
●	43	22	419
◑	24	45	415
◓	42	44	395

As may be seen in Fig. 3, the α's lie near unity in the temperature range examined, but tend to increase as the decomposition proceeds, probably as a result of the accumulation of the primary products which would produce other radicals which replace the rôle of oxygen atom. Though the slopes differ according to the amounts of the reactants, the curves converge to one point at zero conversion, so the extrapolated values at zero conversion have been adopted. From the Arrhenius plot (Fig. 4), we find the activation heat to be

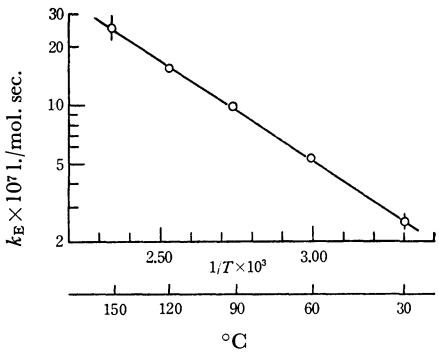

Fig. 4. Arrhenius plot of k_E.

4.7 kcal./mol.; finally, the rate expression is given as:

$$k_E = (6.3\pm3.5)\times10^{10}\exp(-4710\mp400)/\boldsymbol{RT}$$ l./mol.sec.

Although the experimental error is less than about 5%, the combined allowance is rather large, and if the afore-mentioned two assumptions do not hold, the error in k_E will become still larger. However, the frequency factor found here seems to be of the usual order of magnitude for the abstraction reactions of atoms.

BULLETIN OF THE CHEMICAL SOCIETY OF JAPAN VOL. 39 1651—1659 (1966)

The Quenching Action of Benzoic Acid and Methyl Benzoate on the Fluorescene of Naphthalene Derivatives. II

By Takuji MIWA and Masao KOIZUMI

Department of Chemistry, Faculty of Science, Tohoku University, Sendai

(Received November 8, 1965)

The quenching action of benzoic acid on the fluorescence of naphthalene derivatives, for instance, *N*, *N*-dimethyl-2-naphthylamine, is phenomenologically ascribed to its dimer. In order to examine its molecular mechanism, absorption and fluorescence spectra have been measured on solutions of *N*, *N*-dimethyl-2-naphthylamine with and without benzoic acid, using as a solvent cyclohexane to which various amounts of dioxane or ethyl ether has been added. The quenching action of benzoic acid has also been measured in similar solvents. A good parallelism has been found between the change in the absorption spectra of benzoic acid and the change in the quenching action of benzoic acid when both are examined as functions of the concentration of dioxane or ether. From this finding, and from the more precise analysis of the data described in a previous paper (This Bulletin, **38**, 529 (1965)), it has been concluded that the quenching action of benzoic acid may be ascribed to the direct interaction between the fluorescer and the benzoic acid dimer. Further, similar quenching actions have been observed in *o*-, *m*- and *p*-toluic acids, and *p*-methoxybonzoic acid.

In a previous paper,[1] the authors investigated the quenching action of benzoic acid and methyl benzoate on the fluorescence of naphthalene derivatives from the standpoint of the charge-transfer mechanism of quenching. It was shown that benzoic acid has a rather large quenching action on *N*, *N*-dimethyl-2-naphthylamine and 2-naphthyl methyl ether compared with that of methyl benzoate; this quenching action was phenomenologically attributed to the benzoic acid dimer. As for the molecular mechanism, the charge transfer interaction between the fluorescer and the benzoic acid dimer seemed plausible. However, it was not yet quite clear whether the benzoic acid ring dimer itself really has a quenching action or whethere the ring dimer dissociates partially (this produces the linear dimer) and gives rise to quenching by forming a hydrogen bond with an excited fluorescer molecule. The present paper deals with: i) the effect of the addition of ether-type compounds on the quenching action of benzoic acid and methyl benzoate on the fluorescence of *N*, *N*-dimethyl-2-naphthylamine, and ii) the quenching action of benzoic acid derivatives on the fluorescence of *N*, *N*-dimethyl-2-naphthylamine. The results lead to the conclusion that the dimer itself has the quenching action.

Experimental

p-Dioxane was purified by the method of Eigenberger.[2] Benzoic acid from the Natural Resources Institute (standard sample for calorimetry) was zone-refined ten times, and then recrystallized from benzene. *o*-Toluic acid of Wako Junyaku (G. R. grade) was recrystallized four times from a benzene - *n*-hexane mixture. *m*-Toluic acid of Wako Junyaku (G. R. grade) was recrystallized once from benzene, twice from *n*-hexane, and once from a water-methanol mixture. *p*-Toluic acid of Tokyo Kasei (G. R. grade) was recrystallized three times from benzene. *o*-Methoxy- and *p*-methoxybenzoic acid of Tokyo Kasei (G. R. grade) were recrystallized twice from benzene, and twice from a ligroin-benzene mixture. Naphthalene of Kanto Kagaku (G. R. grade) was recrystallized three times from ethanol, and then zone-refined ten times. Benzene and cyclohexane were purified in the manner described in the previous paper. The *N*, *N*-dimethyl-2-naphthylamine was the same sample as in the earlier work. The absorption spectra were measured with a Hitachi EPS spectrophotometer. The fluorescence and action spectra were measured with an Aminco-Bowman spectrofluorimeter. Measurements were made for both degassed and non-degassed solutions at room temperature.

Results and Discussion

I) The Effect of the Addition of Ether-type Compounds on the Quenching Action of Benzoic Acid.—This effect was studied in a cyclohexane solution of *N*, *N*-dimethyl-2-naphthylamine. Before investigating the quenching action, the hydrogen bonding equilibrium in the ground state was studied by analyzing the absorption spectra. In nonpolar solvents, benzoic acid exists mainly

1) T. Miwa and M. Koizumi, This Bulletin, **38**, 529 (1965).

2) E. Eigenberger, "Technique of Organic Chemistry," Ed. by A. Weissberger et al., Vol. VII, Interscience Pub., New York (1955), p. 372.

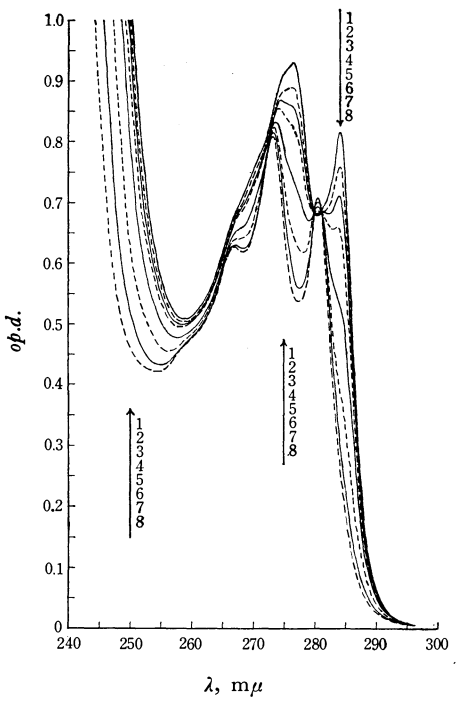

Fig. 1a. Absorption spectra of benzoic acid 1.50 $\times 10^{-2}$ M in cyclohexane plus dioxane (0—1.17 M). The molar concentrations of dioxane: 1) 0, 2) 3.50×10^{-2}, 3) 7.02×10^{-2}, 4) 1.17×10^{-1}, 5) 2.34×10^{-1}, 6) 4.68×10^{-1}, 7) 7.02×10^{-1}, 8) 1.17

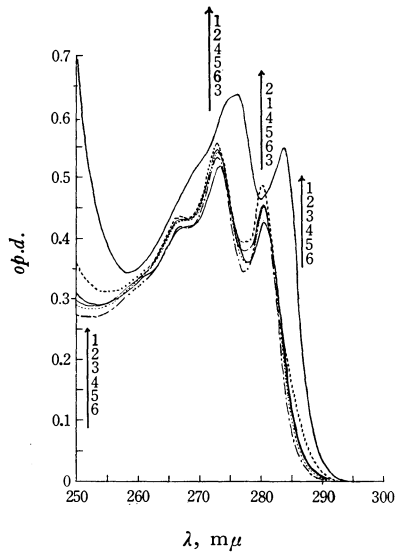

Fig. 1b. Absorptioon spectra of benzoic acid 1.00 $\times 10^{-2}$ M in dioxane-cyclohexane mixed solvent. The molar concentrations of dioxane: 1) 0, 2) 0.583, 3) 11.7 (dioxane only), 4) 8.74, 5) 5.83, 6) 2.91

as a ring dimer formed by intermolecular hydrogen bonding.* When dioxane or ethyl ether, either

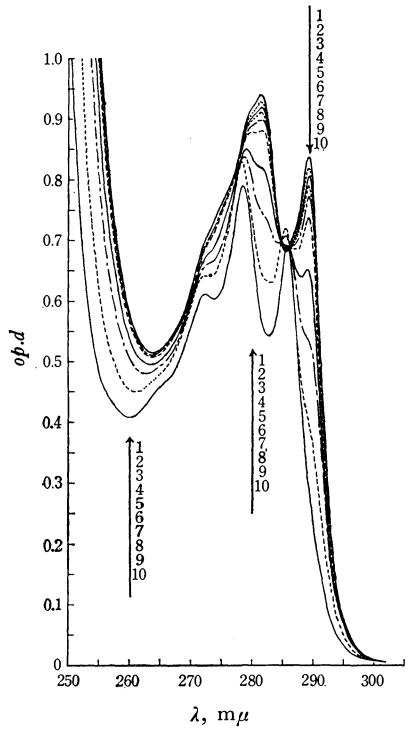

Fig. 2. Absorption spectra of benzoic acid 1.50×10^{-2} M in cyclohexane plus ethyl ether (0—1.55 M).
The concentrations (M) of ether: 1) 0, 2) 9.70×10^{-3}, 3) 1.94×10^{-2}, 4) 3.88×10^{-2}, 5) 5.82×10^{-2}, 6) 9.72×10^{-2}, 7) 1.94×10^{-1}, 8) 3.88×10^{-1}, 9) 7.76×10^{-1}, 10) 1.55

of which is capable of forming a hydrogen bond with benzoic acid, is added, a newly-established equlibrium of hydrogen bonding causes a considerable change in the absorption spectra as the concentration of the added substance is increased. The results are shown in Figs. 1a, 1b and 2.

The spectral behavior is very regular, and we can evaluate the equilibrium constant of hydrogen bond ing between benzoic acid and dioxane or ethyl ether in the following way. The optical density at a fixed wavelength is given by:

$$op.\,d. = (\varepsilon_{A_2}[A_2] + \varepsilon_A[A] + \varepsilon_{AB}[AB])d \qquad (1)$$

where A_2, A, AB, ε and d are, respectively, the benzoic acid dimer, its monomer, the hydrogen-bonded complex between benzoic acid and an added substance, the molar extinction coefficient, and the depth of the optical path. If one makes the plausible assumption that $\varepsilon_{AB}\approx\varepsilon_A$,[3-5] Eq. 1

* Hereafter, "the dimer" means the benzoic acid ring dimer and not the linear dimer.

3) H. Hosoya, J. Tanaka and S. Nagakura, *J. Mol. Spectry*, **8**, 257 (1962).
4) M. Ito, H. Tsukioka and S. Imanishi, *J. Am. Chem. Soc.*, **82**, 1559 (1960).
5) M. Ito, *J. Mol. Spectry*, **4**, 144 (1960).

Table I. Evaluation of hydrogen bond formation constant between benzoic acid and dioxane

Benzoic acid (1.50×10^{-2} M) - dioxane (0—1.17 M) in cyclohexane

[dioxane], M	*op.d.*	R	$[A_2]$	[A]	[B]	[AB]	K_2
0.00	0.840	0.616	7.03×10^{-3}	9.40×10^{-4}	0.00	0.00	—
5.83×10^{-3}	0.840	0.615	7.03	9.40	5.83×10^{-3}	0.00	0.00
1.17×10^{-2}	0.817	0.592	6.77	9.23	1.12×10^{-2}	0.543×10^{-3}	52.8
3.51×10^{-2}	0.779	0.554	6.33	8.93	3.37×10^{-2}	1.44	48.0
7.02×10^{-2}	0.730	0.505	5.77	8.52	6.76×10^{-2}	2.60	45.2
1.17×10^{-1}	0.675	0.450	5.14	8.04	1.13×10^{-1}	3.91	43.0
2.34×10^{-1}	0.556	0.331	3.78	6.90	2.27×10^{-1}	6.74	43.0
4.68×10^{-1}	0.414	0.189	2.16	5.21	4.58×10^{-1}	10.2	42.6
7.02×10^{-1}	0.294	0.069	0.789	3.15	6.89×10^{-1}	13.1	60.5
1.17	0.249	0.024	0.274	1.86	1.16	14.3	66.6

$R=op.d.-\varepsilon_A[A]_0d=op.d.-0.225$, *op.d.* : *op.d.* at 284.1 mμ.

Table II. Evaluation of hydrogen bond formation constant between benzoic acid and ethyl ether

Benzoic acid (1.50×10^{-2} M) - ethyl ether (0—1.55 M) in cyclohexane

$[Et_2O]$, M	*op.d.*	R	$[A_2]$	[A]	[B]	[AB]	K_2
0.00	0.840	0.615	7.03×10^{-3}	9.40×10^{-4}	0.00	0.00	—
0.970×10^{-2}	0.823	0.598	6.84	9.27	0.930×10^{-2}	0.401×10^{-3}	46.5
1.94×10^{-2}	0.809	0.584	6.68	9.16	1.87	0.732	42.8
3.88×10^{-2}	0.792	0.567	6.48	9.03	3.77	1.14	33.4
5.82×10^{-2}	0.775	0.550	6.29	8.89	5.67	1.54	30.5
0.970×10^{-1}	0.741	0.516	5.90	8.61	9.47	2.34	28.7
1.94×10^{-1}	0.653	0.428	4.89	7.85	19.0	4.43	29.8
3.88×10^{-1}	0.530	0.305	3.49	6.62	38.1	7.36	29.2
7.76×10^{-1}	0.400	0.175	2.00	5.02	76.6	10.5	27.3
1.55	0.290	0.065	0.743	3.06	154	13.2	28.1

od.d.: *op.d.* at 284.1 mμ, $R\equiv op.d.-\varepsilon_A[A]_0d$.

can be rewritten as:

$$op.\ d.=[A_2](\varepsilon_{A_2}-2\varepsilon_A)d+\varepsilon_A[A]_0d$$

where $[A]_0$ is the added concentration of benzoic acid. Hence:

$$[A_2]=(op.d.-\varepsilon_A[A]_0d)/(\varepsilon_{A_2}-2\varepsilon_A)d \qquad (2)$$

Since ε_{A_2} and ε_A can be estimated from the extreme cases, $[A_2]$ can be calculated with the above formula. In the actual calculation, the optical densities of the dimer peak at 284.1 mμ, and the value of $K_1=7950$ reported by Hosoya et al.[3] for the solution of benzoic acid in *n*-heptane at 30°C, were used. Then, from the following relations:

$$\left.\begin{aligned}[A] &= \sqrt{[A_2]/K_1}\\ [AB] &= P-[A]=P-\sqrt{[A_2]/K_1}\\ [B] &= [B]_0-[A]\\ P &= [A]_0-2[A_2]\end{aligned}\right\} \qquad (3)$$

[A], [AB] and [B] were evaluated, and the formation constant of the hydrogen bond between benzoic acid and the added compound, $K_2=[AB]/([A]\cdot[B])$, could be obtained. The results obtained are given in Tables I and II. The K_2 values between benzoic acid and dioxane or ether are about 40 and 30 respectively.

The next item was to investigate how the quenching effect of benzoic acid depends on the amount of added dioxane or ether. First, the effect of the addition of benzoic acid on the absorption spectra of *N*, *N*-dimethyl-2-naphthylamine in cyclohexane containing various amounts of dioxane or ethyl ether was examined; it was confirmed that there

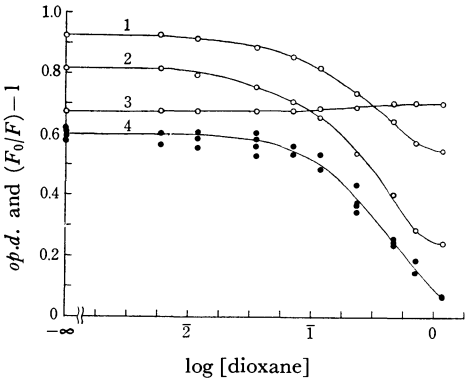

Fig. 3. Fluorescence intensity ratio $(F_0/F)^{-1}$ of *N*, *N*-dimethyl-2-naphthylamine (1.00×10^{-4} M) in the absence (F_0) and in the presence (F) of benzoic acid (1.50×10^{-2} M) and optical densities of benzoic acid (1.50×10^{-2} M) as functions of the added amount (M) of dioxane.
1) *op.d.* at 276.5 mμ, 2) *op.d.* at 284.1 mμ, 3) *op.d.* at 280.6 mμ, 4) $(F_0/F)-1$

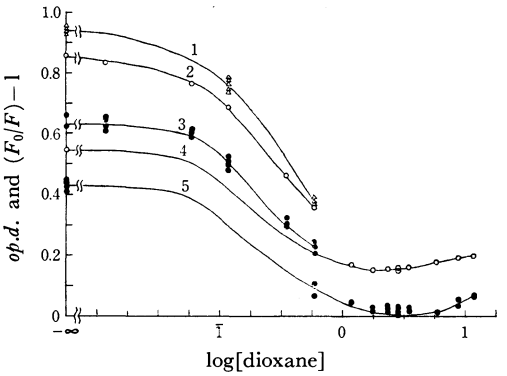

Fig. 4. Fluorescence intensity ratio $(F_0/F)-1$ of *N*, *N*-dimethyl-2-naphthylamine (1.00×10^{-4} M) in the presence (F) and in the absence (F_0) of benzoic acid (A) and optical densities of benzoic acid as functions of the added amount (M) of dioxane.
1) $(F_0/F)-1$, [A]: 1.50×10^{-2} M, degassed soln.
2) *op.d.*, [A]: 1.50×10^{-2} M, aerated soln.
3) $(F_0/F)-1$, [A]: 1.50×10^{-2} M, aerated soln.
4) *op.d.*, [A]: 1.00×10^{-2} M, aerated soln.
5) $(F_0/F)-1$, [A]: 1.00×10^{-2} M, aerated soln.

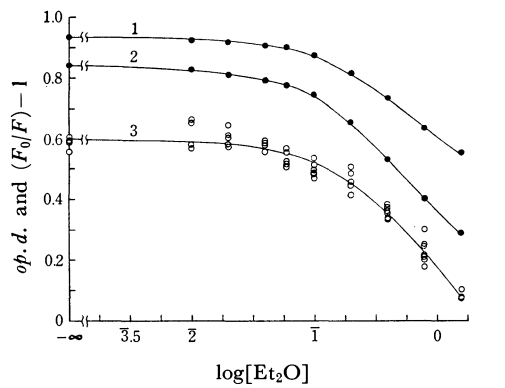

Fig. 5. Fluorescence intensity ratio $(F_0/F)-1$ of *N*, *N*-dimethyl-2-naphthylamine (1.00×10^{-4} M) in the presence (F) and in the absence (F_0) of benzoic acid (1.50×10^{-2} M) and optical densities of benzoic acid (1.50×10^{-2} M) as functions of the added amount (M) of ethyl ether.
1) *op. d.* at 277.0 mμ, 2) *op. d.* at 284.2 mμ,
3) $(F_0/F)-1$.

is not essential effect. This means that there is no appreciable interaction between the ground-state fluorescer and the benzoic acid dimer or monomer (hydrogen-bonded with ether or dioxane). Next, the fluorescence intensity, F_0, of *N*, *N*-dimethyl-2-naphthylamine 10^{-4} M in the above solvent system and that, F, of a similar solution containing 1.5×10^{-2} M or 1.0×10^{-2} M benzoic acid were measured in order to evaluate the quenching effect of benzoic acid. In Figs. 3, 4 and 5, the values of of $(F_0/F)-1$ and the optical densities of benzoic acid at several wavelengths are plotted against the concentration of dioxane or ether. In Fig. 4, the filled circles and triangles show the results for non-degassed and degassed solutions respectively. The quenching action of benzoic acid on the fluorescence is greater in the degassed solutions than in the non-degassed solutions, but no anomaly due to the dissolved oxygen was observed. Figures 3, 4 and 5 show a very good correlation between the spectral change in benzoic acid and the change in the quenching action of benzoic acid. Since the optical densities at 277 and 284 mμ, which are the absorption maxima of the dimer, give the measure for the dimer concentration, this correlation enables us to rule out a quenching mechanism in which the benzoic acid dimer dissociates partially or completely and forms a hydrogen bond with the excited fluorescer. If such were the case, the benzoic acid monomer hydrogen-bonded with dioxane or ether, the formation constant of which is much smaller than that of the dimer, would have a larger quenching action than the dimer. This expectation does not fit the results obtained; one can, therefore, safely conclude that if the dimer does act as a quencher, it really remains as the dimer throughout the quenching process.

II) The Effect of the Addition of an Ether-type Compound on the Quenching Action of Methyl Benzoate.—Similar experiments have been made using methyl benzoate as a quencher and *N*, *N*-dimethyl-2-naphthylamine as a fluorescer, in order to get a better understanding of the quenching action of benzoic acid. First, the absorption and fluorescence spectra of the solutions of methyl benzoate and *N*, *N*-dimethyl-2-naphthylamine were measured using dioxane-cyclohexane mixtures of various compositions as solvents. The absorption spectra of methyl benzoate in cyclohexane do not change when a small amount of dioxane is added. With the increase in dioxane concentration, the spectra of methyl benzoate gradually become broad as a result of the so-called solvent effect, but there is no marked effect. Next, the absorption and fluorescence spectra and the fluorescence intensity of *N*, *N*-dimethyl-2-naphthylamine were measured with and without 0.800 M methyl benzoate, using the above-mentioned solvents. The addition of methyl benzoate intensifies the absorption spectra of *N*, *N*-dimethyl-2-naphthylamine and causes a shift to longer wavelengths; the fluorescence spectra also shift to red and become broad. These shifts are more marked than the shifts observed in absorption spectra. On the further addition of methyl benzoate, a new emission band appears near 480 mμ.* The quenching action of methyl benzoate increases with the increase in the dioxane concentration. The fluorescence intensity (F) of the solution with the quencher and that of the solution without it (F_0) were determined at the maxima of the

* The details will be described elsewhere.

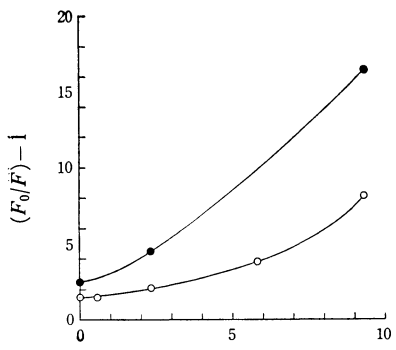

Fig. 6. The change of the quenching action of methyl benzoate due to the variation of the composition of solvent.
The concentration of methyl benzoate: 8.800 M, solvent: cyclohexane-dioxane mixture.
●: degassed soln., ○: non-degassed soln.

fluorescence spectra. No correction was made for the spectral sensitivity distribution of the fluorimeter. The calculated values are summarized in Fig. 6.

In this figure, the open circles show the values for the aerated solutions, while the filled circles show the values for the deaerated solutions. It is evident that there is no extraordinary effect of the dissolved oxygen. It is worthwhile to note here that a similar effect was also found in the case of benzoic acid systems. Thus, as may be seen from Fig. 4, the quenching action of benzoic acid at an extremely high concentration region of dioxane, begins to increase to some extent after having passed through a minimum, at which point the absorption spectra of the benzoic acid dimer must have completely turned to monomer-type ones (hydrogen-bonded with dioxane). At the same time, the absorption spectra of the hydrogen-bonded complex with dioxane begin to suffer the so-called solvent effect and the spectra become broad, as in the case of methyl benzoate (see Fig. 1b). These results strongly suggest the same quenching mechanism in both cases and favors the C. T. quenching mechanism which was assumed for the quenching action of the methyl benzoate in a previous paper.[1]

III) The Quenching Action of the Benzoic Acid Derivatives on the Fluorescence of *N*, *N*-Dimethyl-2-naphthylamine.—In order to find other examples of quenching action similar to that of benzoic acid and to examine the relation between the quenching constants and the formation constants of the ring dimer, we have examined the quenching action of the benzoic acid derivatives on the fluorescence of *N*, *N*-dimethyl-2-naphthylamine. This was investigated only with aerated solutions, because it had already been confirmed that there is no extraordinary effect due to dissolved oxygen. The benzoic acid derivatives used as quenchers were *o*-, *m*-, *p*-toluic acid, and *o*-, *p*-methoxybenzoic acid.

Cyclohexane Solution.—The absorption spectra of these substituents of benzoic acid show a concentration effect analogous to that of benzoic acid. The dimerizations of benzoic acid and its derivatives have been extensively investigated on the basis of the concentration dependence of their absorption spectra. Especially, Forbes et al.[6,7] measured the absorption spectra of benzoic acid and its derivatives systematically, and also examined the relationship between the molecular structure and the tendency toward dimerization. They expressed the ability to dimerize by "critical maximal concentration," which is the concentration above which the values of ε_{max} become approximately independent of the concentration, and below which the acid appreciably exists in the monomeric form. The values in Table III are quoted from their paper, thus facilitating an examination of the correlation between the ability to dimerize and the ability to quench. When benzoic acid derivatives are added to a solution of *N*, *N*-dimethyl-2-naphthylamine, the absorption and fluorescence spectra

Table III. The quenching action of benzoic acid derivatives on the fluorescence of *N*, *N*-dimethyl-2-naphthylamine

N, *N*-Dimethyl-2-naphthylamine: 1.00×10^{-4} M Solvent: cyclohexane

Quencher	The concn. range of quencher, M	Excitation wavelength mμ	Quenching constant	Critical max*,7,8) concn., M
Benzoic acid	$0—1.75\times10^{-2}$	350	36	8.0×10^{-4}
o-Toluic acid	$0—4.00\times10^{-2}$	355	37	11×10^{-4}
m-Toluic acid	$0—4.00\times10^{-2}$	370	38	1.6×10^{-4}
p-Toluic acid	$<5.00\times10^{-3}$	can not be obtained		4.7×10^{-4}
o-Methoxybenzoic acid	$<1.00\times10^{-2}$	can not be obtained		—a)
p-Methoxybenzoic acid	$<5.00\times10^{-3}$	can not be obtained		0.34×10^{-4}

* Values for cyclohexane solutions or cyclohexane solutions containing small amount of ethyl ether, e. g. 5%.
a) Not within range

6) W. F. Forbes and A. R. Knight, *Can. J. Chem.*, **37**, 334 (1959).

7) W. F. Forbes, A. R. Knight and D. L. Loffen, ibid., **38**, 728 (1959).

Table IV. The quenching action of benzoic acid derivatives on the fluorescence of *N*, *N*-dimethyl-2-naphthylamine

N,*N*-Dimethyl-2-naphthylamine 1.00×10^{-4} M Solvent: benzene

Quencher	The concn. range of quencher, M	Excitation wavelength mμ	Quenching constant	Critical max. concn.,* M
Benzoic acid	$0—4.00\times10^{-1}$	350	48	8.0×10^{-4}
o-Toluic acid	$0—4.00\times10^{-1}$	355	40	11×10^{-4}
m-Toluic acid	$0—3.00\times10^{-1}$	370	47	1.6×10^{-4}
p-Toluic acid	$0—4.00\times10^{-2}$	370	37	4.7×10^{-4}
o-Methoxybenzoic acid	$0—9.00\times10^{-2}$	370	71	—a)
p-Methoxybenzoic acid	0 and 5.00×10^{-3}	370	38	0.34×10^{-4}

* Same as in Table III.

of the fluorescer do not change, but the fluorescence intensity decreases considerably. The phenomena are quite similar to those observed with benzoic acid. The fluorescence intensities of the solutions of *N*,*N*-dimethyl-2-naphthylamine with the quenchers (F) and without them (F_0) were measured, and the quenching constants were determined from the slope of the $(F_0/F)-1$ vs. $[A]_0$ plot. This treatment is approximately correct, since, in the concentration range of the present experiments, the quenchers examined exist almost entirely in the dimeric form, as judged from the values of the critical maximal concentration and from the linearity of the $(F_0/F)-1$ vs. $[A]_0$ plot. The quenching constants obtained are summarized in Table III. By comparing the quenching constants with the critical maximal concentration, it may be observed that although the critical maximal concentrations are distinctly different from compound to compound, the quenching constants are almost the same, and there is no correlation between the two quantities.

Benzene Solutions.—Since benzene absorbs the light at wavelengths shorter than 280 mμ, one can not measure the absorption spectra of benzoic acid and its derivatives. It may be assumed, however, that the behavior of benzoic acid and its derivatives in benzene is essentially the same as that in cyclohexane. The absorption spectra and the fluorescence spectra of *N*,*N*-dimethyl-2-naphthylamine are scarcely affected, but its fluorescence intensity is considerably quenched by the addition of benzoic acid and its derivatives. The results are quite similar to those for cyclohexane solutions. In the lower concentration range of quenchers, the plots of $(F_0/F)-1$ against the quencher concentrations are nearly linear, but in the higher concentration range, the plots deviate upwards. The quenching constants obtained from the slope of the $(F_0/F)-1$ vs. $[A]_0$ plot at the low concentration range are summarized in Table IV.

The critical maximal concentration of those derivatives obtained with cyclohexane solutions or with a cyclohexane-ether mixture are also listed. From this table, it may be seen that there are appreciable differences among the quenching constants of benzoic acid, *o*- and *m*-toluic acid. This finding is different from that in the case of a cyclohexane solution.

It is remarkable that *o*-methoxybenzoic acid has a very large quenching constant. As has been pointed out by Forbes et al.,[6,7] this substance scarcely exists as a dimer, but it exists in the form of a monomer with an intramolecular hydrogen bond between methoxy and carbonyl groups. It is interesting that such an intramolecularly hydrogen-bonded monomer has a large quenching action. It should be noted, however, that the apparent quenching constants for the other compounds forming a ring dimer are refered to the monomer unit and that the quenching constant of the dimer is about twice the apparent one. Therefore, it can be said that the quenching power of the intramolecularly hydrogen-bonded monomer of *o*-methoxybenzoic acid is almost the same as that of the intermolecularly hydrogen-bonded dimer of other benzoic acid derivatives. Another notable result is that *p*-substituted compounds with a rather large tendency toward dimerization are less powerful quenchers than other compounds. In summary, there is no correlation between the dimerization tendency and the quenching efficiency.

IV) A More Rigorous Analysis of the Quenching Data.—Although all the results described in I), II) and III) favor the view that the dimer and not the monomer of benzoic acid or its derivatives acts as a quencher, still this is not conclusive. Hence, it is desirable to examine further whether only the dimer or only the free monomer, which exists in a small quantity, or both, act as quenchers; this examination is to be done by a more rigorous analysis of the quenching data. As has been stated in the previous paper, the $(F_0/F)-1$ vs. $[A]_0$ plot is linear, but this treatment is approximate in nature if only the dimer is a quencher. It is only when the dimer acts as twice as efficient a quencher as the monomer that this relation strictly holds. However, the mechanism for quenching by the monomer, if it exists, is considered to be quite different from that of the dimer, and this possibility seems improbable. Therefore, an analysis will be given below for the case when only the dimer or only the monomer acts as a quencher.

i) The Quenching Action of Benzoic Acid on N, N-Dimethyl-2-naphthylamine, 2-Naphthyl Methyl Ether or 2-Naphthol.—In these cases the addition of benzoic acid does not affect the absorption spectra nor the fluorescence spectra in spite of a large quenching effect.

a) If the dimer acts as a quencher and the monomer does not, the following scheme holds:

$$D + h\nu \rightarrow D^*$$

$$D^* \xrightarrow{k_d} D$$

$$D^* \xrightarrow{k_f} D + h\nu$$

$$D^* + A_2 \xrightarrow{k_q} D + A_2$$

$$A + A \underset{K_1}{\rightleftarrows} A_2$$

and the steady-state method leads to the following formula:

$$F_0/F = 1 + \{k_q/(k_f+k_d)\}[A_2] \qquad (4)$$

It should be noted that, in this case, the formation of a molecular complex between the fluorescer and a free monomer of benzoic acid need not be taken into account, because it scarcely affects the concentration of the dimer as long as the equilibrium constant of this reaction is not very large.

b) When only the monomer acts as a quencher, the scheme may be written as follows (in this case the possibility of the fluorescer being hydrogen-bonded with the quencher is taken into account because the monomer has a free carboxyl group):

$$\begin{array}{ccc} D^* + A & \xrightarrow{k_q} & D^*A \\ {\scriptstyle k_d+k_f}\downarrow\uparrow & & \downarrow\uparrow \\ D + A & \underset{K_3}{\rightleftarrows} & DA \end{array}$$

From this scheme the following relation is derived:

$$\frac{F_0}{F} = 1 + \left\{\frac{k_q}{k_d+k_f} + K_3\right\}[A] + K_3\frac{k_q}{k_d+k_f}[A]^2 \qquad (5)$$

The concentrations of the benzoic acid monomer and the dimer are calculated from the analytical concentration of benzoic acid, using the value of $K_1=7950$.[3] When the solvent is cyclohexane, the results of analyses are as follows. The linear relationship is slightly better in the $(F_0/F)-1$ vs. $[A_2]$ plot than in the $(F_0/F)-1$ vs. $[A]_0$ plot. The slopes of these plots are given in Tables V and VI. The $(F_0/F)-1$ vs. $[A]$ plot is concave upwards, while the $\{(F_0/F)-1\}/[A]$ vs. $[A]$ plot is nearly linear. The values of the slopes and intercepts are also given in Tables V and VI. For benzene solutions, the results are quite similar to those for cyclohexane solutions as long as the quencher concentration is $0—5\times10^{-2}$ M. At higher concentrations of the quencher, however, both the $(F_0/F)-1$ vs. $[A_2]$ plot and the $\{(F_0/F)-1\}/[A]$ vs. $[A]$ plot deviate upward from linearity. Some examples of these analyses are shown in Figs. 7, 8, 9 and 10, and the results are summarized in Table VI.

From the above results one can rule out the mechanism in which only the free monomer acts as a quencher (case b). As may be seen in Tables

Table V. The values of the slope of $(F_0/F)-1$ vs. $[A]_0$ and $(F_0/F)-1$ vs. $[A_2]$ plots, and the values of the slope and the intercept of $\{(F_0/F)-1\}/[A]$ vs. $[A]$ plot

Solvent: cyclohexane, quencher: benzoic acid, A: the slope of $(F_0/F)-1$ vs. $[A]_0$ plot, B: the slope of $(F_0/F)-1$ vs. $[A_2]$ plot, C: the slope of $\{(F_0/F)-1\}/[A]$ vs. $[A]$ plot, D: the intercept of $\{(F_0/F)-1\}/[A]$ vs. $[A]$ plot

Fluorescer	Excitation wavelength mμ	A	B	C	D
N, N-Dimethyl-2-naphthylamine	350	36	79	6.8×10^5	−40
2-Naphthylamine	330	55	114	9.8×10^5	−50
2-Naphthyl methyl ether	320	17	36	3.1×10^5	−40
2-Naphthol	320	43	92	9.0×10^5	−130

Table VI. The values of the slope of $(F_0/F)-1$ vs. $[A]_0$ and $(F_0/F)-1$ vs. $[A_2]$ plots, and the values of the slope and the intercept of $\{(F_0/F)-1\}/[A]$ vs. $[A]$ plot

Solvent: benzene, quencher: benzoic acid. A: the slope of $(F_0/F)-1$ vs. $[A]_0$ plot, B: the slope of $(F_0/F)/1$ vs. $[A_2]$ plot, C: the slope of $\{(F_0/F)-1\}/[A]$ vs. $[A]$ plot, D: the intercept of $\{(F_0/F)-1\}/[A]$ vs. $[A]$ plot

Fluorescer	Excitation wavelength mμ	A	B	C	D
N, N-Dimethyl-2-naphthylamine	350	50	104	8.9×10^5	−100
2-Naphthylamine	330	48	101	9.1×10^5	−100
2-Naphthyl methyl ether	328	22	48	4.8×10^5	−50
2-Naphthol	330	35	71	5.7×10^5	~ 0

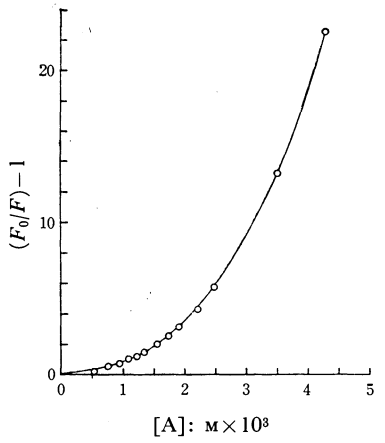

Fig. 9. $(F_0/F)-1$ vs. [A] plot in the system of *N*, *N*-dimethyl-2-naphthylamine (1.00×10^{-4} M)-benzoic acid (0—4.00×10^{-1} M) in benzene. Excitation wavelength: 350 mμ.

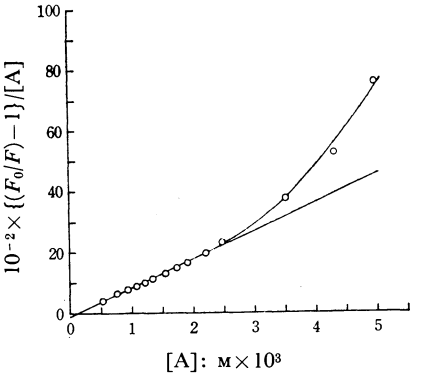

Fig. 10. $\{(F_0/F)-1\}/[A]$ vs. [A] plot in the system of *N*, *N*-dimethyl-2-naphthylamine (1.00×10^{-4} M)-benzoic acid (0—4.00×10^{-1} M) in benzene. Excitation wavelength: 350 mμ.

V and VI, each $\{(F_0/F)-1/\}[A]$ vs. [A] plot has an intercept that is nearly zero or that has a small negative value. However, this is not conceivable, because the intercept which corresponds to $K_3+k_q/(k_d+k_f)$ can never be negative. Furthermore, all the values of the slopes, which are K_3 multiplied by the quenching constant, $k_q/(k_d+k_f)$, are larger than 3×10^5; these figures cannot be reconciled with the b) mechanism for the following reason. The value of K_3 is estimated to be 100* at most, and so the quenching constant is estimated to be larger than 3×10^3; this is far too large for a value expected from the diffusion controlled process.[8] Such a large value can only be interpreted on the basis of static quenching mechanism, which would contradict the present situation. Thus, it seems impossible that only the benzoic acid monomer is responsible for the quenching action.

It should be added that the above discussion is scarcely affected even when the values of K_1 are

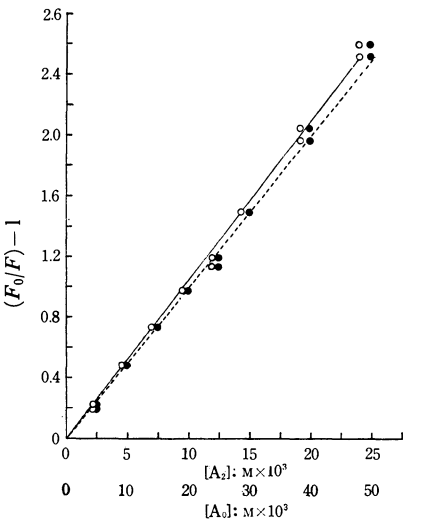

Fig. 7. $(F_0/F)-1$ vs. $[A]_0$ and $[A_2]$ plots in the system of *N*, *N*-dimethyl-2-naphthylamine (1.00×10^{-4} M)-benzoic acid (0—5.00×10^{-2} M) in benzene. Excitation wavelength: 350 mμ.
○; $(F_0/F)-1$ vs. $[A_2]$, ●; $(F_0/F)-1$ vs. $[A]_0$

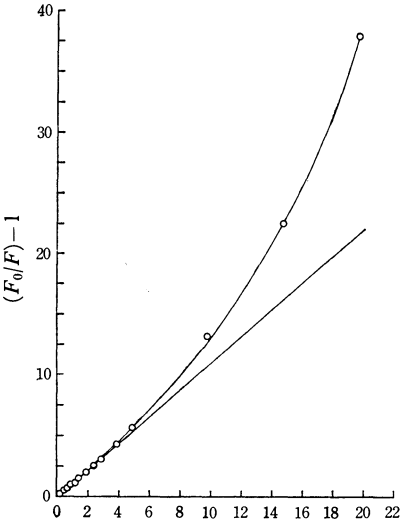

Fig. 8. $(F_0/F)-1$ vs. $[A_2]$ plot in the system of *N*, *N*-dimethyl-2-naphthylamine (1.00×10^{-4} M)-benzoic acid (0—4.00×10^{-1} M) in benzene. Excitation wavelength: 350 mμ.

8) T. Miwa and M. Koizumi, This Bulletin, **36**, 1619 (1963).

* In the system consisting of 2-naphthylamine (fluorescer) and benzoic acid (quencher), which will be described later, the hydrogen bond is formed between the fluorescer and the quencher, to an extent observable by means of a study of the ultraviolet absorption spectra. From the spectral change the hydrogen bond formation constant is evaluated as 110.

changed over a wide range. The result that the $\{(F_0/F)-1\}/[A]$ vs. [A] plot deviates from linearity is also not affected by changing K_1 over a wide range. Thus, the above analysis leads to the conclusion that only the a) mechanism is reasonable. The deviation from linearity shown by the $(F_0/F)-1$ vs. $[A_2]$ plot in benzene solutions may be ascribed to static quenching by A_2; in this case the $(F_0/F)-1$ vs. $[A_2]$ plot is not essentially affected by the value of K_1, since K_1 is large enough for most of the benzoic acid molecules to exist in the dimeric form.

ii) The Quenching Action of Benzoic Acid on 2-Naphthylamine.—The solutions of 2-naphthylamine in cyclohexane show no spectral change with the addition of benzoic acid up to the limit of solubility. The solutions of 2-naphthylamine in benzene show a remarkable change in absorption spectra due to hydrogen bonding (Fig. 11), but they do

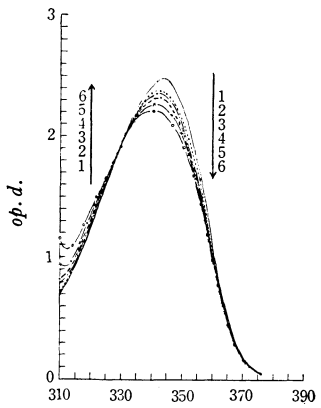

Fig. 11. Absorption spectra of the solutions containing 2-naphthylamine (1.00×10^{-4} M) and benzoic acid (0—4.00×10^{-1} M). Solvent: cyclohexane.
The concentrations (M) of benzoic acid are as follows.
1) 0, 2) 2.00×10^{-2}, 3) 6.00×10^{-2}, 4) 1.00×10^{-1}, 5) 2.00×10^{-1}, 6) 4.00×10^{-1}

not show any change in fluorescence spectra. Therefore, the hydrogen-bonded complex in this case is also nonfluorescent. In the previous paper, the equilibrium constant of hydrogen bonding was calculated from the spectral data, using an analytical concentration of benzoic acid. However, this procedure was not rigorous, and so first a more exact value was calculated, using 7950 as K_1[3]:

$$A + D \rightleftarrows AD: K_3$$

$$K_3=\frac{[AD]}{([A]_0-2[A_2]-[AD])([D]_0-[AD])}$$

$$\approx\frac{[AD]}{([A]_0-2[A_2])([D]_0-[AD])} \quad (6)$$

$[D]_0$: 1.00×10^{-4} M

At 5.00×10^{-4} M of benzoic acid, the lowest concentration used in this experiment, [A] is equal to 1.49×10^{-4} M when [D] is zero. Therefore, K_3 may be approximated as above by neglecting [AD], so long as the equilibrium constant, K_3, is of the order of a few hundred. By combining Eq. 6 and $op.d.=(\varepsilon_{AD}[AD]+\varepsilon_D[D])d$ at a suitable wavelength, one at which there is no absorption of benzoic acid or of its dimer, the following formula is obtained:

$$\frac{1}{P}K_3(\varepsilon_{AD}-\varepsilon_D)[D]_0\frac{1}{op.d.-\varepsilon_D[D]_0d}-K_3 \quad (7)$$

$$P\equiv[A]_0-2[A_2]=[A]+[AD]\approx[A]$$

As Fig. 12 shows, the $1/P$ vs. $[D]_0/(op.d.-\varepsilon_D[D]_0d)$ plot is linear. From the intercept and the slope

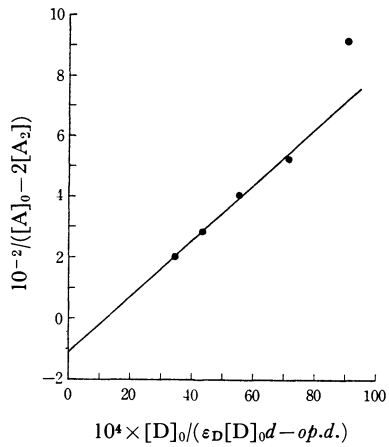

Fig. 12. The evaluation of the hydrogen-bond formation constant between 2-naphthylamine (1.00×10^{-4} M) and benzoic acid (0—4.00×10^{-1} M), using the formula (4) and the *op.d.* at 350 mμ. Solvent: benzene, temperature: 20°C.

of this plot, $K_3=110$ and $\varepsilon_{AD}\doteqdot1400$ are obtained respectively. The fluorescence intensity is analyzed as in the case of *N, N*-dimethyl-2-methylamine under the assumption that the formation of the hydrogen-bonded complex, AD, causes scarcely any change in the concentration of A. The results obtained are very similar to those obtained for *N, N*-dimethyl-2-naphthylamine, etc. At higher concentrations of benzoic acid, the $\{(F_0/F)-1\}/[A]$ vs. [A] curve deviates from linearity, while the curve has a very large slope, 8.90×10^5, at lower concentrations of benzoic acid. When 110 is used as K_3, the quenching constant becomes 8.01×10^3, which is ridiculous as a dynamical quenching constant. Thus, in this case also, it can be concluded that the quenching of the fluorescence is not due to the direct action of the monomer.

BULLETIN OF THE CHEMICAL SOCIETY OF JAPAN VOL. 39 1660—1670 (1966)

Sensitization in the Photoconductance of Poly-*N*-vinylcarbazole

By Yoshiki HAYASHI, Makoto KURODA and Akira INAMI

Research Laboratory, Wireless Division, Matsushita Electric Industrial Co., Ltd., Kadoma, Osaka

(Received November 8, 1965)

The sensitization in photoconductive poly-*N*-vinylcarbazole was studied systematically. The sensitizers were conveniently divided into two types, *optical* and *chemical*. The optical sensitization occurs with a smaller content of a dye, which extends the photoconductivity spectrum to its absorption band. Effective optical (or dye) sensitizers are found to be themselves photoconductive and *n*-type cationic and to have a slow photoresponse. The chemical sensitization occurs through the formation of a charge transfer complex with a considerable amount of a Lewis acid. The simultaneous addition of optical and chemical sensitizers induces amplified or additive effects; an amplified effect is observed when a strong acid is employed as a chemical sensitizer. A sensitized system with a strong acid shows a very slow photoresponse and may have fairly deep traps which act as a cause of the memory effect.

In a previous paper,[1] the authors reported that *poly-N-vinylcarbazole* (PVCZ) film has a small peak of its action spectrum for photoconduction and that the threshold of its optical absorption is in the near-ultraviolet region. Because of its transparency, it is expected that this film is applicable to a transparent, sensitive, electrophotographic layer which prints by a conventional technique. However, pure PVCZ has a low potentiality as a material for electrophotographic purposes since it has only a slight sensitivity in the visible spectrum.

According to a patent by Kalle & Co.,[2] it is possible to sensitize the photoconduction of PVCZ film by the addition of a small amount of certain dyes or by the addition of Lewis acid-type organic compounds. The cause or mechanism of the sensitization is not clear in the patent. The present authors conjecture that the dye sensitization or optical sensitization in this case is analogous to that of cadmium sulfide or glass, which have been investigated by Nelson,[3-6] and that the chemical sensitization occurs by means of the formation of charge transfer complexes between PVCZ and the sensitizers. The terms "optical sensitization" and "chemical sensitization" are empirically proposed by the authors for the sake of convenience in the classification of sensitizers after the model of silver halide photography.

From this point of view, we have investigated the electrophotographic behavior of PVCZ thin films sensitized with commercial dyes or electron acceptor compounds, and have examined the combined effects on sensitization when two different types of sensitizers are added to the PVCZ matrix. Recently, Hoegl[7] presented a paper in which the photosensitometries of doped PVCZ with miscellaneous acceptors were studied. In view of his results, our view of charge transfer in chemical sensitization seems to be pertinent.

In this paper, the authors will describe the results obtained from systems to which about forty dyes and fifty chemical sensitizers have been added, from the standpoint of improving the practical electrophotographic sensitivity.

Experimental

Materials.—PVCZ powder (Luvican M-170, Badische A. G.) was purified by the reprecipitation method described in the previous paper.[1] The dyestuffs and chemical sensitizers used were the GR-grade reagents listed in Tables I and III.

The Addition of Dyestuffs.—To a 10% solution of PVCZ dissolved in purified methylene chloride, a 1% dye solution in methanol was dropped; then the solution was stirred until it was homogeneously colored by the dye.

The solubilities of dyes in such organic solutions were so small that the micro crystals of dyes were deposited if added in excess. By preliminary tests, the optimum concentrations of dyes were found to lie between 0.02 and 0.06%, where the sensitization data of the same dye showed no remarkable difference. To compare dye sensitizers, all the concentrations were fixed at 0.05% by weight.

The Addition of Chemical Sensitizers.—Lewis acid-type sensitizers, such as acids, acid anhydrides, aldehydes, ketones, quinones, and polynitrated derivatives, were used. Their solubilities in PVCZ varied. For example, 2-methylanthraquinone was soluble to 25%, whereas monochloroacetic acid was soluble to 3% and the polymer solution showed a co-

1) Y. Hayashi, M. Kuroda, K. Imura and A. Inami, *Chem. High Polymer (Japan)*, **21**, No. 234, 557 (1964).
2) German Pat. 1068115.
3) R. C. Nelson, *J. Opt. Soc. Am.*, **46**, 13 (1956).
4) R. C. Nelson, ibid., **48**, 948 (1958).
5) R. C. Nelson, ibid., **51**, 1182 (1961).
6) R. C. Nelson, ibid., **50**, 1029 (1960).
7) H. Hoegl, *J. Phys. Chem.*, **69**, 755 (1965).

agulation tendency at this concentration. As a whole, except for the quinone compounds, they have low solubilities.

As it was troublesome to find the optimum concentration of each sensitizer, the addition quantities of the less soluble compounds were fixed at 1%, and those of the quinone groups, at 10%. For only a few good sensitizers (see Table II) were the optimum concentrations examined.

When sensitization with a dye - Lewis acid system was investigated, the Lewis acid was added to the above dye-polymer solution. The final solution was stirred until it became transparent. The process of film formation from the final solution was carried out by a method similar to that described in the previous paper.[1]

Electrophotographic Sensitivities.—To compare the sensitivities of the specimens, the electrophotographic charge-decay method was used. In another paper[8] the present authors have explained the physical aspects of the method, the principle of which is almost analogous to that of the ordinary method for measuring photoconduction. The experimental set-up is presented schematically in Fig. 1. The sample was mounted on a

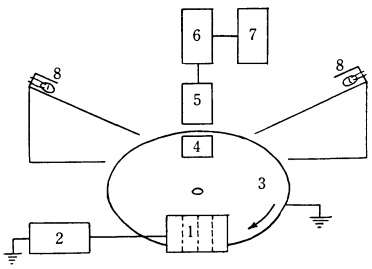

Fig. 1. Schematic representation of experimental set up for charge and light decay recording: 1, corona discharge device; 2, high voltage source; 3, turntable; 4, a sample; 5, 6, electrometer probe and amplifier; 7, recorder; 8, light sources.

grounded aluminum turntable rotating at 78 r. p. m. Above the periphery of the disc, a corona wire unit, an exposure unit, and a probe of a sector-type electrometer were fixed. A specimen which had been stored in the dark for at least 48 hr. was positively charged at 7 kV. by the corona to a saturation potential. Then the corona discharge and the turntable were simultaneously stopped, and the dark decay due to the dark resistance was measured under the probe. Several seconds later, an incandescent light was applied to the specimen and the light decay was measured. An example of the recorded data is shown in Fig. 2. As a representation of sensitivity, the authors adopted the half-decay exposure, $E_{1/2}$, obtained from the diagram, which corresponds to the half-decay time, $t_{1/2}$.

In order to study the spectral sensitivity, a charged specimen was put into a grating spectrograph (Narumi & Co., investigated by J. Koana).[9] The surface exposed to the continuous spectrum generated a latent static image. A negatively-charged xerographic toner was then dispersed onto the surface, and the visible image was printed. All the processes mentioned above were carried out in the dark.

Photoconductivity.—The photoconductivity was measured by using the same types of cells and apparatus as have been described in a previous paper.[1]

Optical Absorption.—A photometer (Hitachi EPS-II) was used for the determination of the optical absorption. The samples used were of a dilute solution in a certain medium or of a solid, thin film laminated onto a quartz plate by the same method as used with the conductivity cell.

Results and Discussion

Spectral Responses of Sensitized Systems by a Conventional Electrophotographic Technique.—We classified the sensitizers into two types, the optical sensitizers and the chemical sensitizers.

From the spectral responses obtained by a grating spectrograph, we found that the dye sensitization was similar to the optical sensitization with dyes used in silver-halide photographic techniques. For instance, a spectral response of the PVCZ-crystal violet system is shown in Fig. 3B. In addition to the original small response at 356 mμ, a large peak is found at 592 mμ which corresponds to the optical absorption or photoconduction peak of crystal violet.

As an example of chemical sensitization, a spectral response of the PVCZ - trichloroacetic acid system is presented in Fig. 3C, where the exposure time was 5 min. The behavior in a longer exposure is shown in Fig. 3D. Here, in addition to the amplified original response of PVCZ, the series of peaks between 400 mμ and 600 mμ is found. This fact seems to be contrary to our assumed definition of chemical sensitization. However, when the single system of PVCZ has been exposed for 2 hr., a similar series of peaks was found (see Fig. 3E).

This series of peaks appears to be due to sensitization by unknown original impurities; this impurity sensitization effect seems to be so small that no response can be found by the ordinary method of photoconductivity measurement described in our previous paper.

With other chemical sensitizers, the peaks are amplified as well as with trichloroacetic acid, and the impurity effect is also observed. Upon the addition of only a chemical sensitizer, the PVCZ film becomes a little more sensitive in tungsten light, and its sensitization is of the order of a bad dye sensitizer.

As is shown in Fig. 3F, picric acid behaves as another type of chemical sensitizer. As a whole, acid, acid anhydrides, aldehydes, and ketones which were colorless behave as chemical sensitizers.

Next, an example of the photoresponse of a

8) A. Inami, K. Morimoto and Y. Hayashi, This Bulletin, **37**, 842 (1964).

9) Z. Koana and Z. Wakimoto, *Electrophotography (Japan)*, **2**, No. 1, 8 (1960).

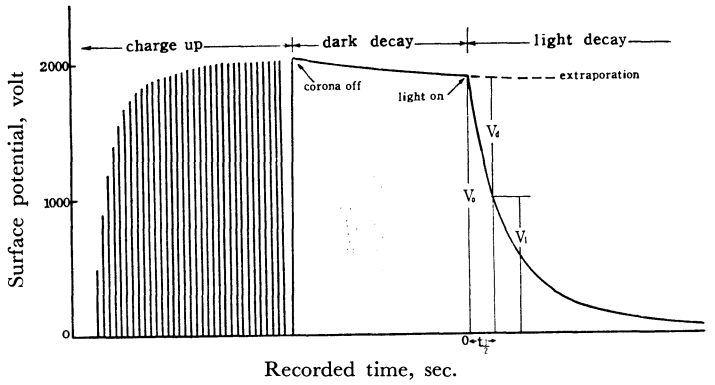

Fig. 2. A recorded example of charge build up and decay curve obtained by the apparatus in Fig. 1. V_0 means an initial potential. The time when V_l/V_d reduces to a half is arranged as $t_{1/2}$.

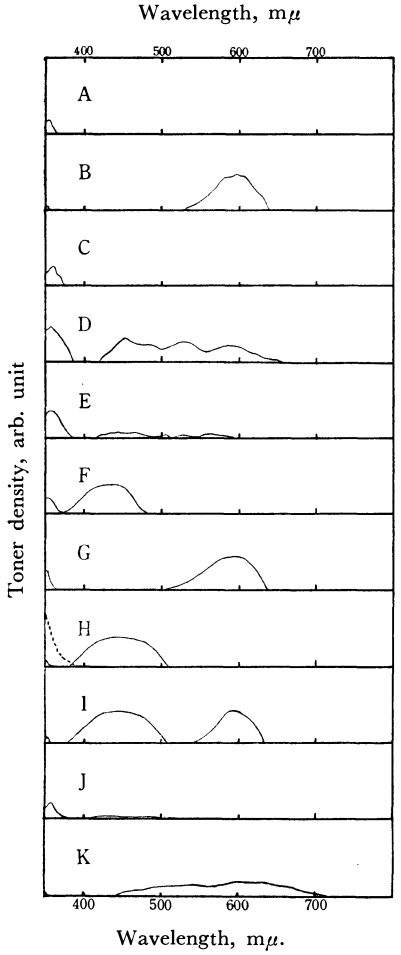

	Exposure period sec.	Sensitizer
A	1200	None
B	60	Crystal violet: 0.05%
C	300	Trichloroacetic acid: 1%
D	1200	Trichloroacetic acid: 1%
E	7200	None
F	1200	Picric acid: 1%
G	5	Crystal violet: 0.05% Trichloroacetic acid: 1%
H	30	2-Methylanthraquinone: 10%
I	30	2-Methylanthraquinone: 10% Crystal violet: 0.05%
J	1200	Pinacyanole: 0.05%
K	60	*p*-Chloranil, 10%

Fig. 3. Spectral responses of some sensitized or unsensitized samples by grating spectrographic measurements.

system formed of three components (PVCZ-crystal violet - trichloroacetic acid) is presented in Fig. 3G. Upon the addition of trichloroacetic acid, the spectral response of crystal violet at 600 mμ becomes very high after only five seconds' exposure (cf. Fig. 3B).

On the other hand, sensitized systems with a quinone compound behave differently than with

the five kinds of Lewis acids mentioned above. As may be seen in Fig. 3H, the spectral response of the PVCZ-2-methylanthraquinone system has a peak in 440 mμ, while its optical absorption spectrum rises at 400 mμ and shows a strong and broad absorption to the short wavelength side (dotted line in Fig. 3H). The peak wavelength at 440 mμ obtained by the electrophotographic process has been found by our preliminary experiment*[1] to correspond with the wavelength of the photoconduction peak of 2-methylanthraquinone itself.

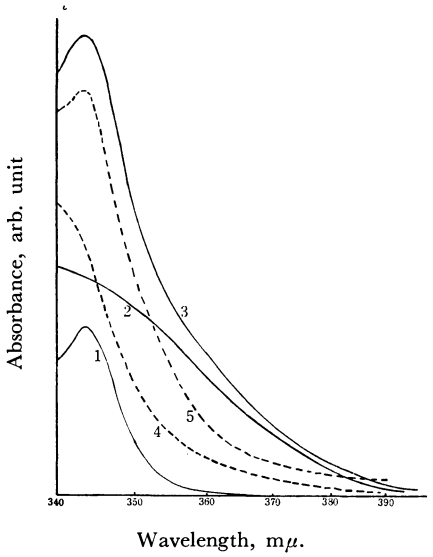

Fig. 4. Absorption spectra of picric acid and 2-methylanthraquinone (dotted line) doped samples: 1, pure PVCZ; 2, pure picric acid; 3, equivalent mixture of 1 and 2 ; 4 pure 2-methylanthraquinone; 5, equivalent mixture of 1 and 4. All samples are diluted with *sym*-dichloroethane.

Almost all the quinone compounds investigated here show the same sensitization as 2-methylanthraquinone. From these results the members of the quinone group which are classified as "chemical sensitizers" might rather be called "optical sensitizers." The quinones are as photoconductive themselves as such optical dye sensitizers as triphenylmethane or cyanine dyes. However, we dare to regard them as chemical sensitizers because the difference in effective amount is found to be appreciable between quinones and dyes.

Absorption Spectra in Sensitized Systems. —It is assumed that a new peak absorption spectrum which belongs to neither PVCZ nor a sensitizers may be realized if a chemical reaction or a charge transfer occurs between them. A part of the dye sensitizers are considered to be adsorbed in the amorphous regions of the polymer in the dried glassy state. However, no new absorption spectrum was found in the PVCZ-dye system.

No chemical sensitizers (except *p*-chloranil) which are regarded as usual electron acceptors afford any new absorption band when mixed with PVCZ. When a chemical sensitizer is added, the intensity of the absorption of PVCZ increases considerably in comparison with that of the parent polymer. Upon the addition of some quinones or polynitrated derivatives, such as 2-methylanthraquinone or picric acid, a slight red shift of the long wavelength edge of the spectrum

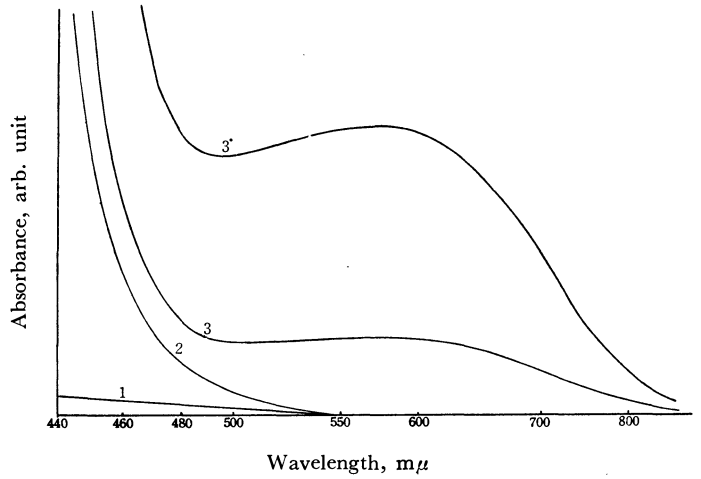

Fig. 5. Charge transfer band of *p*-chloranil doped sample: 1, pure PVCZ; 2; pure *p*-chloranil; 3, equivalent mixture of 1 and 2; 3', twice of 3 in conc. All samples are diluted with benzene.

*[1] From a spectral response measurement on 2-methylanthraquinone film evaporated on NESA glass (for a sandwich cell), we found a weak response peak at 440 mμ.

occurs. Figure 4 presents curves showing the red shifts produced by the addition of picric acid or 2-methylanthraquinone.

Chloroanil, which is well known as a strong acceptor, produces a new peak at 574 mμ as a result of forming a charge transfer complex with the polymer (Fig. 5). The shape of the broad charge transfer band (between 500 and 800 mμ) coincides with the electrophotographic spectral image in Fig. 3K, indicating that the chloranil sensitization is due to the formation of a new absorption band in the visible spectral region.

Optical (Dye) Sensitizations.—From Table I, crystal violet, methyl violet, and malachite green (triphenylmethane derivatives) rhodamine 6G, rhodamine B (xanthene derivatives), and methylene blue (thiazine derivative) may be seen to be good sensitizers. All of them have $=N^+<$ and are called basic dyes (or cationics).

Acid violet 6B and naphthalene green from triphenylmethane, and acid rhodamine G, eosine A, eosine S, fluorescein, rose bengale, and phloxine from xanthene are all acidic dyes (or anionics). From Table I, an interesting tendency is found: the effective dyes for PVCZ sensitization are not acidic dyes but cationics. As in rhodamine homologues, a sulfonated derivative, namely, sulforhodamine B (acidic), shows a considerably weak sensitizability compared to rhodamine B (basic). The oil-soluble nonionic dyes show no effect.

Nelson suggested that there is a general tendency for cationic dyes to be *n*-type and anionic *p*-type conductors.[10] In Table II, some dyes which have already been classified experimentally into the *p*- or *n*-type by other authors are summarized. From this table it may be seen that most *n*-type dyes seem to be effective for PVCZ except pinacyanole. This result contrasts with a considerable effect of acidic *p*-type dyes in the zinc oxide (*n*-type) photosensitive layer of the Electrofax*[2] process. In the previous paper, the present authors specified that the sign of charge carriers in PVCZ might be positive. Judging from this fact, there seems to be an empirical tendency for an organic *p*-type photoconductor to become more sensitive when doped with an *n*-type dye.

Pinacyanole, which is a good sensitizer for cadmium sulfide crystal, shows no effect. In Fig. 3J, no peak is found at the wavelength of 640 mμ, which is an absorption peak of the dye in the visible region. According to the works of Terenin[11] and Nelson,[3] a dye sensitization may occur by the following processes: electron-hole pairs (they might better be called "excitons") are produced by light; then they are separated

Table I. Sensitizations with dyes

Dye	Sensitivity, $E_{1/2}$, lux.sec.
Triphenyl Methanes	
Victoria pure blue	1137
Victoria blue	612
Crystal violet	350
Brilliant green	420
Methyl violet	1015
Acid violet 6B	10850
Fuchsine	none
Basic cyanine BX	612
Basic cyanine 6G	4550
Malachite green	490
Auramine	13300
Naphthalene green	none
Xanthenes	
Rhodamine 6G	657
Acid rhodamine G	none
Rhodamine B extra	725
Fluorescein	none
Rose bengale	none
Sulforhodamine B	4290
Eosine A	6300
Eosine S	5250
Phloxine	15750
Azines	
Phenosaflanine	6650
Pinacryptol green	13300
Selestine blue	none
Acridines	
Pinacryptol yellow	2800
Acridine orange	3355
Tripafravine	5900
Triazines	
Methylene blue	1750
New methylene blue	402
Cyanines	
Chinoline blue	42000
Pinacyanole	none
1, 1'-Diethyl-4, 4'-quinocarbocyanine iodide	40000
1, 1'-Diethyl-4, 4'-quinocyanine iodide	22000
3, 3'-Diethyl-thiacarbocyanine iodide	8250
3, 3'-Diethyl-2, 2'-thiacyanine iodide	15500
2-(*p*-Dimethylaminostyryl)-benzothiazole-ethiodide	4650
1, 1'-Diethyl-2, 4'-quino cyanine iodide	16000
Azo dyes	
Oil red B	14000
Chrom blue black RC	none
Butter yellow	14000
Fast light yellow G	none
Neutral red	8205
Anthraquinones	
Quinizarin	1260
Alizarin	9800

10) R. C. Nelson, *J. Mol. Spectroscopy*, **7**, 439 (1961).

*2 A trade mark of the Radio Corporation of America.

TABLE II. COMPARISON OF SENSITIZABILITIES OF SOME DYES WHICH HAVE BEEN DECIDED ON *p*- OR *n*- BY OTHER AUTHOURS

Dye	Chemical formula	$E_{1/2}$ lux. sec.	Type of *p*- or *n*-	Reference
Crystal violet	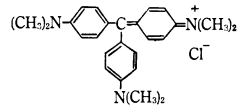	350	*n*	Terenin et al.[12]
Malachite green	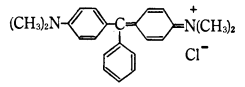	490	*n*	Terenin et al.[12]
Auramine	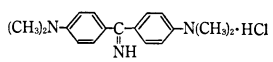	13300	*p*	Terenin et al.[12]
Rhodamine B extra	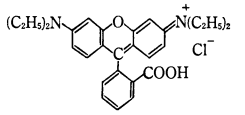	725	*n*	Terenin et al.[12] Takahashi et al.[13] Hauffe et al.[14]
Phloxine	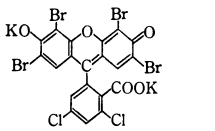	15750	*p*	Takahashi et al.[13]
Phenosafranine	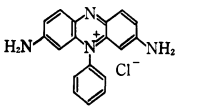	6650	*p*	Terenin et al.[12]
Tripaflavine	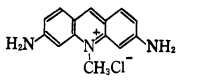	5900	*p*	Terenin et al.[12] Terenin et al.[13]
Chinoline blue	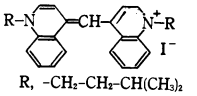	42000	*p*	Terenin et al.[12]
Pinacyanole	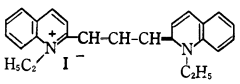	none	*n*	Terenin et al.[12]
3, 3′-Diethylthiacarbocyanine iodide	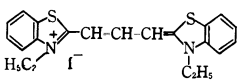	8250	*p*	Terenin et al.[12]

into charge carriers, which are injected into *N*-vinylcarbazole unit molecules.*3 If all dye sensitization were caused by this process, pinacyanole in cyanines should be just as effective as crystal violet in triphenylmethanes.

It may, therefore, be assumed that the difference in sensitization ability between pinacyanole and crystal violet may be casued by a difference in their photoconductive characteristics in their pure, solid states. There are many triphenylmethane dyes with slow responses of rise and decay, while pinacyanole has a very rapid response.[11] Moreover, the former has many trapping centers, while the latter is considered to have fewer.[10] From these facts, the electron-hole pairs produced by irradiation may not separate easily and are likely to have a longer life in the case of crystal violet than in that of pinacyanole.*4 As the distance between dye molecules in the polymer is considered to be rather longer than

*3 We substitute the inorganic photoconductive substrates (e. g., cadmium sulfide, zinc oxide, silver halide, etc.) for a vitreus polymeric photoconductor.

11) A. Terenin, "Electrical Conductivity in Organic Solids," Interscience Publ., New York (1961), p. 39.

*4 Although this assumption should be employed in the pure solid, we dare to make a deduction by applying it to a diluted state of a dye in the polymer.

12) A. Terenin, *Proc. Chem. Soc.*, 321, Sep. (1961).

13) T. Takahashi, C. Shishido, H. Hori and M. Wada, *Electrophotography (Japan)*, **3**, No. 3, 9 (1961).

14) K. Hauffe and J. Kaufhold, *Z. Electrochem.*, **66**, 316 (1962).

TABLE III. SENSITIZATIONS WITH A DYE AND/OR LEWIS ACIDS

	Without dye $E_{1/2}$, lux.sec.	With crystal violet $E_{1/2}$, lux.sec.
Acids and acid anhydrides		
Acetic acid	none	217
Monochloroacetic acid	10500	49
Dichloroacetic acid	5880	46
Trichloroacetic acid	3745	26
Monobromoacetic acid	11900	75
Tribromoacetic acid	13850	553
Benzoic acid	none	196
Tetrachlorophthalic acid	1595	112
Tetrachlorophthalic anhydride	3910	110
Succinic anhydride	39200	142
Maleic acid	7175	84
Maleic anhydride	11270	166
Telephthalic acid	none	350
Cinnamic acid	5250	143
Phthalic acid	4100	73
Phthalic anhydride	4230	85
Acetanilide	none	80
Benzenesulfonic acid	none	78
p-Toluenesulfonic acid	none	85
Phenol	none	2170
p-Nitrophenol	5950	85
Picric acid	650	36
Ketones		
Acetophenone	none	287
Benzoine	11600	245
Benzil	6800	270
Aldehydes		
p-Nitrobenzaldehyde	1030	287
o-Nitrobenzaldehyde	1350	325
2, 4-Dichlorobenzaldehyde	none	441
p-Dimethylaminobenzaldehyde	none	280
p-Hydroxybenzaldehyde	none	860
Furfural	none	175
Bromal	900	77
Quinones		
p-Quinone	2850	1103
p-Chloranil	1100	560
α-Naphthoquinone	1295	297
Anthraquinone	577	175
1-Aminoanthraquinone	1190	332
2-Aminoanthraquinone	490	280
1, 4-Diaminoanthraquinone	9325	9975
1-Nitroanthraquinone	297	140
1, 5-Dichloroanthraquinone	402	241
2-Chloroanthraquinone	595	260
2-Methylanthraquinone	621	186
2, 6-Dichloro-*p*-benzoquinone	665	224
1, 2-Benzanthraquinone	297	200
Anthraquinone-2-carboxylic acid	630	149
Anthraquinone-2-sulfonic acid	none	190
Polynitrate		
Trinitrobenzene	435	252

that in the pure, solid state, the longer the life of the electron-hole pair, the higher the injection probability for the polymer will be.

From Table I, crystal violet may be found to be the best optical sensitizer. Therefore, we adopted it as the dye component for tertiary systems (PVCZ, dye and Lewis acid). In the next section, the sensitivities of binary systems (PVCZ and Lewis acids) and of tertiary systems will be compared (see Table III).

Chemical (Lewis Acid) Sensitization.—Under the practical incandescent light used for electrophotography, usual acid and ketone derivatives are almost ineffective. On the other hand, picric acid in the acid group, *p*-nitroaldehyde, bromal in aldehydes, and most quinones are effective. It can be said that all of these effective chemical sensitizers are slightly colored themselves, and even after being doped into PVCZ solutions, they maintain their original color fairly well. (As a special case, chloranil changed from its original color (pale yellow) to dark green.)

From Table III, we can deduce the following information: with a small amount of crystal violet, an acid shows a tendency to sensitize more in conformity with an increase in the halogenation or nitration degree in its homologue; i. e.,

$$Cl_3CCOOH,\ Cl_2CHCOOH$$
$$> ClCH_2COOH \gg CH_3COOH$$

or

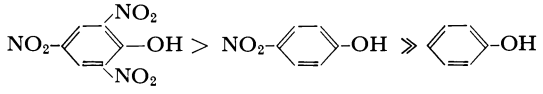

It is known that trichloroacetic acid is a stronger acid than di, mono, or unsubstituted acetic acid because of the inductive effect by Cl, the key atom. The same behavior exists in the latter case of the phenol homologue. Next, free acids are stronger sensitizers than anhydrides; i. e.,

maleic acid > maleic anhydride

phthalic acid > phthalic anhydride

These results suggest that the acidity seems to be a key point in the sensitization ability in white incandescent light when an effective dye is used. Colorless aldehydes also behave in the same way as colorless acids.

As has been mentioned above, these colorless acids, aldehydes, or ketones have a small effect in the visual spectral region when the smaples have been exposed for long periods. However, in the practical exposure of the electrophotographic process, these samples show no response.

Each quinone investigated here has a fair sensitization ability without a dye except for anthraquinone-2-sulfonic acid, which is less soluble to the polymer than the other quinones. As a dye is added, anthaquinone-2-sulfonic acid becomes sensitive. Thus, the acidic group ($-SO_3H$)

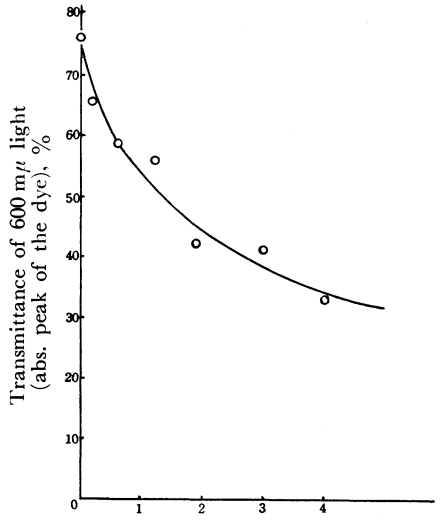

Weight ratio: $\frac{\text{wt. of dichloroacetic acid}}{\text{wt. of crystal violet}}$ in constant volume of benzene, arb. unit.

Fig. 6. Variation of solubility of crystal violet to benzene with increase of dichloroacetic acid concn.

seems to play a subsidiary role in the dye sensitization.

Some quinones were found to be organic photoconductors similar to many dyestuffs. Some anthraquinone and naphthoquinone derivatives are themselves dyestuffs or the intermediate products of dyestuffs.

These facts suggest that the members of the quinone group may be classified as optical sensitizers. However, their effective quantities are considerably larger (1—10%) than those of the dyes (10^{-3}—10^{-2}%); that is, as has been stated in the foregoing section, 2-methylanthraquinone is soluble into PVCZ to 20% by weight. The difference in effective concentration between quinones and dyes suggests some discrepancies between their sensitizing mechanisms.

Regarding the quinone group, the following empirical tendency is obtained from Table III:

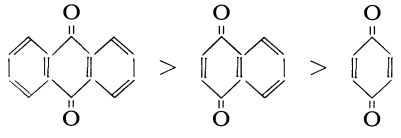

Thus the numbers of aromatic π electrons may contribute to the sensitization ability.

Polynitrated aromatic compounds, such as trinitrobenzene and picric acid, are good sensitizers under an incandescent light. Each of them has a slight yellowish color initially; the original slight yellow deepens bathochromatically when joined in a PVCZ solution. With 2-methylanthraquinone this tendency is also observed. This phenomenon is related clearly to a slight red shift in Fig. 4 (dotted line); it can be explained in terms of the formation of a weak charge transfer complex between 2-methylanthraquinone or picric acid and PVCZ. Picric acid seems to have two sensitizing functions, as acid and as nitro compound.

A chloroanil-added sample had a low sensitivity in spite of forming a stable charge transfer complex. Its optimum exposure in the electrophotographic process was 1500 lux. sec., about twice

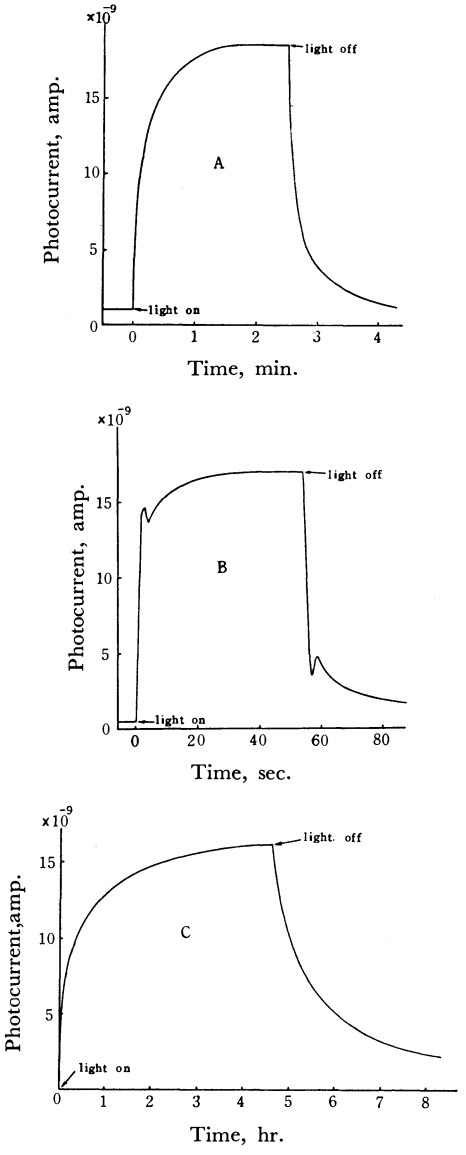

Fig. 7. Photoconduction responses on sandwich cells of PVCZ and the sensitized systems: A, PVCZ, 2μ (thickness), 5V. (applied voltage), 1000 lux. (illuminance); B, PVCZ with crystal violet 0.05%, 2μ, 5V., 20 lux.; C, PVCZ with 0.05% of crystal violet and 1% of trichloroacetic acid, 57μ, 10V., 100 lux., the illuminated electrodes positive, 3.1 cm^2 in area.

that in the foregoing two. One reason for this result may be the considerable decrease in dark resistivity with the formation of a charge transfer complex.

The Combined Effect of a Dye-acid System. —As has been mentioned in the foregoing section, an acid is an effective chemical sensitizer when used with a dye. It was observed that all the cationic dyes investigated dissolve slightly in benzene, and that their solubilities increase upon the slight addition of an acid. Figure 6 shows an example of the use of crystal violet and dichloroacetic acid. It is there shown that the solubility of crystal violet in benzene increases with an increase in the amount of dichloroacetic acid added. Consequently, the dye dispersion is converted into a solution and the chain unit of the polymer seems to be dyed smoothly.

Figure 3G indicates that an amplified sensitization is achieved by the PVCZ-dye-acid system in comparison with a system containing only a dye (Fig. 3B). On the contrary, the PVCZ - crystal violet - 2-methylanthraquinone system shows only an additional sensitization (Figs. 3H and I). An ordinary photoconduction measurement clearly shows that the response rate of the PVCZ-trichloroacetic acid system is much lower than that of the PVCZ - 2-methylanthraquinone system or the PVCZ - crystal violet system (Figs. 7A, B, and C). A chemical sensitizer with an amplification ability with a dye seems to show a slow rise and then a decay in its photoconduction response. Such a chemical sensitizer may increase the number of carrier-trapping centers as well as the number of photo-induced carriers.

Fatigue in the Photoresponse upon Repeated Use.—It is well known that a vitreus selenium layer loses its electrophotographic sensitivity upon the repetition of the charge-light decay cycle within a short period because of the space charge generation by trapped holes. To examine such memory effects in the organic photoconductors, a few higher sensitive systems were investigated. An example of the effect of repetition on a PVCZ-crystal violet - trichloacetic acid system is shown in Fig. 8. In one cycle, the sample was charged up by a positive corona discharge of 7000 V. for 1 min.; after it had then been put in the dark for 10 sec., it was exposed with an incandescent light of 500 lux. for 30 sec. The initial voltage, V_0, decreases and $E_{1/2}$ increased with the repetition of the cycle. Only at the tenth cycle was the exposure period extended to 10 min.; the conditions after the eleventh cycle was similar to the starting conditions. The dark voltage and $E_{1/2}$ at the eleventh cycle were very low and high respectively;

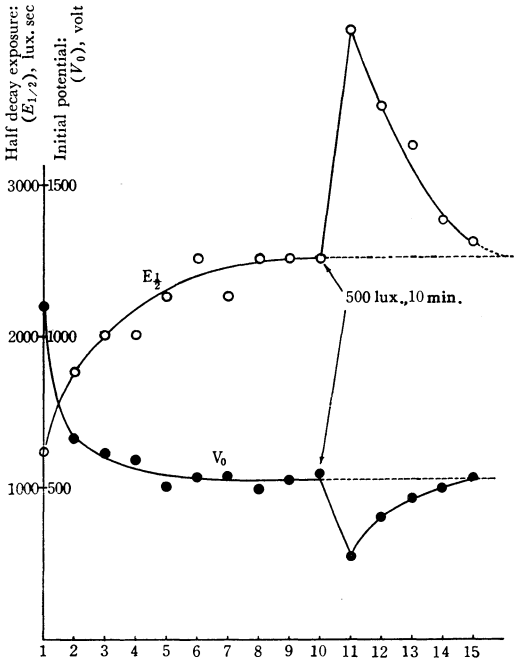

No. of repetition of charge-light decay cycle

Fig. 8. Variation of V_0 or $E_{1/2}$ with incease of number of repetition, ●, V_0; ○, $E_{1/2}$. The sample is same as 6 in Fig 9.

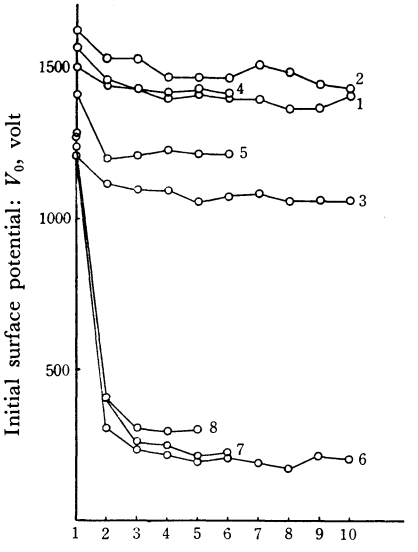

No. of repetition of charge-light decay cycle

Fig. 9. Variations of V_0 with increase of repetition cycles.
1, PVCZ with 0.05% of crystal violet; 2,PVCZ with 0.05% of crystal violet and 10% of 2-methylanthraquinone; 3, PVCZ with 10% of chloranil; 4, PVCZ with 0.05% of crystal violet and 1% of acetophenone; 5, PVCZ with 0.05% of crystal violet and 1% of *p*-dimethylamino benzaldehyde; 6, PVCZ with 0.05% of crystal violet and 1% of trichloroacetic acid; 7, PVCZ with 0.05% of crystal violet and 1% of picric acid; 8, PVCZ with 0.05% of crystal violet and 1% of bromal.

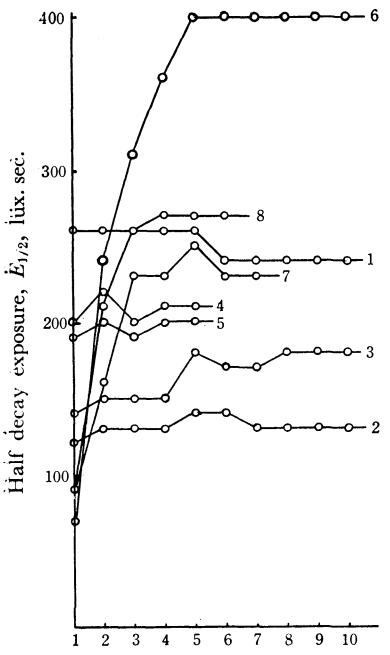

Fig. 10. Variations of $E_{1/2}$ with increase of repetition cycles on the same samples listed in Fig. 9.

then they approached the dotted saturation lines with repetition cycles. After the eleventh exposure, the values should have lain on the extrapolated constant line if a longer exposure had not been applied at the tenth cycle. The constant line may result from the balance between the fatigue by irradiation and the recovery by the high tension given in the dark. The fatigue is to be attributed to irradiation and not to charging.

In Figs. 9 and 10, the variations in V_0 and $E_{1/2}$ are shown. The dye-added sample (1) and the quinone-added sample (2) show few memory effects. Weak acid-added samples (4, 5) show the same. On the other hand, the samples with strong acids or strong acceptors (6, 7, 8) have large variations. These characteristics are parallel to the results from the photoconduction measurements described in the foregoing section. As is shown in Fig. 7B, a sample sensitized with crystal violet alone quickly loses its resistivity to a certain value upon irradiation, and then it turns back to the original value after the light is switched off. In the case of strong acids or strong acceptors, these responses are very slow. From these results, the fatigue (in other words, the hysteresis) is assumed to occur through the traps of carriers.

Some Aspects in Charge Porality.—Hoegl reported that a system of PVCZ doped with a Lewis acid-type acceptor (e. g., chloranil, anthraquinone and TCNE) acts as a *p*-type photoconductor because it has a higher discharge rate when positively

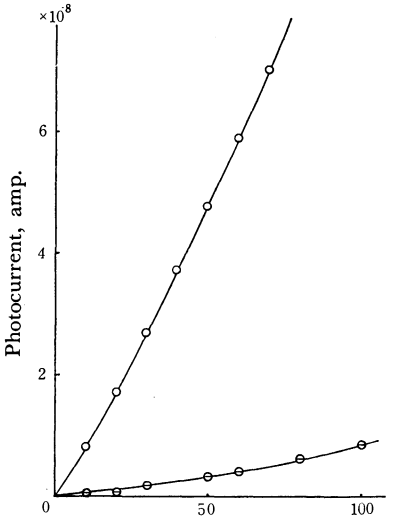

Fig. 11. V-I relations of sandwich cell as the illuminated electrode is positive (○) or negative (⊖) respectively: 20 lux. (illuminance), the same sample as used in Fig 7C.

charged than when negatively charged. In this case the dopants are assumed to be traps for electrons. Our data from the photoconduction measurements show similar results. In Fig. 11, a large photocurrent value is observed for the PVCZ-crystal violet - trichloroacetic acid system when the illuminated electrode is positive. On the other hand, the data from the charge decay method showed little difference between the two sign-charged samples. Actually in a practical process in electrophotography, the optimum printing exposure of a positively-charged sample is equivalent to that of negatively-charged one.

Conclusions

From the studies of sensitization in photoconductive poly-*N*-vinylcarbazole, some conclusions can be deduced: (1) It is convenient to divide the sensitization into two types, "optical sensitization" and "chemical sensitization." The former occurs at a smaller dye content, which extends the photoconduction spectrum of the polymer to the dye's absorption bands, while the latter is induced by the formation of a charge transfer complex in the presence of a considerable amount of a Lewis acid; (2) The most effective dyes are *n*-type cationics with slow photoresponses in their pure, solid states; (3) In the sensitization with two different types of components (dye and Lewis acid), an amplified effect or an additive effect is obtained. The former case occurs frequently when a strong acid is employed as a chemical sensitizer; (4) A sensitized system with a strong

acid shows very slow rates of rise and decay in the photoconduction measurements.

Although the systems containing strong acids show high sensitivities ($E_{1/2}<100$), they are not always of practical use for electrophotography because of their rapid dark decays and their intense memory effects.

The most useful photoconductive systems are those containing quinones, in spite of their showing only additive effects with crystal violet. 2-Methylanthraquinone is especially useful: (1) its solubility with PVCZ is large, (2) its charge transfer color is pale, and (3) its memory effect is very small. The xerographic characteristics of the practical sample were as follows. The maximum and minimum image densities were 3.0 and 0.1 respectively; the exposure was about 300 lux. sec. at the optimum range, and the γ value was 1.5 when a commercial xerographic toner was used.

The authors wish to express their thanks to Dr. Shunkichi Kisaka, Manager of their Laboratory, for his kind guidance and encouragement throughout the work, and to Mr. Tetsuro Ohtsuka for his helpful suggestions in the physical field.

BULLETIN OF THE CHEMICAL SOCIETY OF JAPAN VOL. 39 1670—1673 (1966)

Sensitization in the Photoconductance of Polyacenaphthylene

By Yoshiki HAYASHI, Makoto KURODA and Akira INAMI

Research Laboratory, Wireless Division, Matsushita Electric Industrial Co., Ltd., Kadoma, Osaka

(Received November 8, 1965)

The sensitization of the photoconductivity in polyacenaphthylene by a dye and/or a Lewis acid was investigated. The most effective materials are methylene blue ($E_{1/2}$= 1500 lux. sec.), rhodamine 6G (6000 lux. sec.), and victoria pure blue (6500 lux. sec.) in the dye sensitization, and 1-nitroanthraquinone (1200 lux. sec.), 2, 3-dichloronaphthoquinone (1400 lux. sec.), 1, 5-dichloroanthraquinone (1500 lux. sec.), chloranil (1800 lux. sec.), and 2-chloroanthraquinone (1900 lux. sec.) in the Lewis-acid sensitization. The combined effects of a dye and a strong acid were determined in the case of polyacenaphthylene as well as poly-*N*-vinylcarbazole.

In a previous paper,[1] the authors reported that polyacenaphthylene showed only a low photoconductivity, while the nitrated polymer obtained by the partial nitration of polyacenaphthylene showed a considerable photoconductivity. The effect of the nitration on photoconductivity may be interpreted by means of a charged transfer mechanism. The nitrated acenaphthylene group is considered to be an electron acceptor. This process may be called the intramolecular chemical sensitization.

Slough studied the semiconductivity of charge transfer complexes of polyacenaphthylene with Lewis acids in the dark,[2] and Hoegl reported in a recent paper that a charge transfer complex of polyacenaphthylene doped with hexabromonaphthalic anhydride could be made to show photoconductive behavior with the aid of the electrophotographic printing process.[3] The present authors found the same behavior: polyacenaphthylene, which is regarded as a polymeric donor, is sensitized by doping miscellaneous dyes and/or Lewis acids, just as poly-*N*-vinylcarbazole can be sensitized with them.[4]

This paper will report the experimental results obtained by adding dyes and Lewis acids to polyacenaphthylene in order to determine a useful composition of photosensitive material for the electrophotographic process.

Experimental

The Polymerization of Acenaphthylene.[5]—Ten grams of acenaphthylene was dissolved in 10 ml. of ethyl benzene and emulsified with 100 ml. of a sodium stearate solution.*1 As an initiator, 0.4 g. of potassium persulfate was added to the emulsion; then the mixture was agitated in a closed container for 10 hr. at 45°C. The resultant polymer was coagulated from the solution by dropping it slowly into dilute hydrochloric acid. The coagulated polymer was then filtered off, dissolved in benzene, and precipitated into methyl alcohol. Yield, 74%; $[\eta]$=0.53 (at 25°C in benzene).

1) A. Inami, K. Morimoto and Y. Hayashi, This Bulletin, **37**, 842 (1964).
2) W. Slough, *Trans. Faraday Soc.*, **58**, 2360 (1962).
3) H. Hoegl, *J. Phys. Chem.*, **69**, 755 (1965).
4) Y. Hayashi, M. Kuroda and A. Inami, This Bulletin, **39**, 1660 (1966).
5) U. S. Pat. 2563524 (1951).
*1 This emulsion consisted of 600 ml. of water, 14 g. of stearic acid, and 6 g. of potassium hydroxide.

The Preparation of a Photosensitive Specimen.—The method of preparation was substantially the same as to that used for poly-*N*-vinylcarbazole and reported previously.[4] Here, toluene was used as the solvent, and the dye concentration was fixed at 0.05% by weight for the solid polymer powder. The Lewis acids (chemical sensitizer) concentrations were fixed at 1% by weight in the case of acids, acid anhydrides, aldehydes, and ketones. In the case of the quinone group, however, all the addition amounts were fixed at 10%.

The final polymer solutions were coated onto aluminum plates 0.1 mm. thick with the aid of a Baker-type applicator; then the solvent was thoroughly evaporated in the drying oven. After the solvent had been evaporated, the specimen films were about 15 μ thick. The parent polymer was so brittle in the thin film form that, after the solvent had been evaporated, numerous cracks generated if the drying speed was too high. Therefore, the drying temperature was kept below 50°C at atmospheric pressure.

Sensitometry.—The photoconductive sensitivities of the doped samples were measured by the electrophotographic charge-decay method described in previous papers.[1,4] The sensitivities were represented as the half decay exposure, $E_{1/2}$, which serves as an index of the photoconduction. In this experiment, two light intensities were applied, i. e., 1000 lux. in less sensitive materials ($E_{1/2}>1000$ lux. sec.), and 100 lux. in highly sensitive materials ($E_{1/2}<1000$ lux. sec.). In order to indicate the dark decay due to the dark resistivity of a sample, the initial voltage, V_0, at the starting point of the light decay is listed along with $E_{1/2}$. These data were obtained at a constant temperature (20°C) and humidity (50%).

Results

Dye Sensitization.—It can be seen from Table I that the most effective dye is methylene blue ($E_{1/2}=1500$ lux. sec.), and the next is rhodamine 6G ($E_{1/2}=6000$ lux. sec.). Crystal violet, rhodamine B, and malachite green, which were very effective on poly-*N*-vinylcarbazole, show a lower sensitizability than the foregoing.

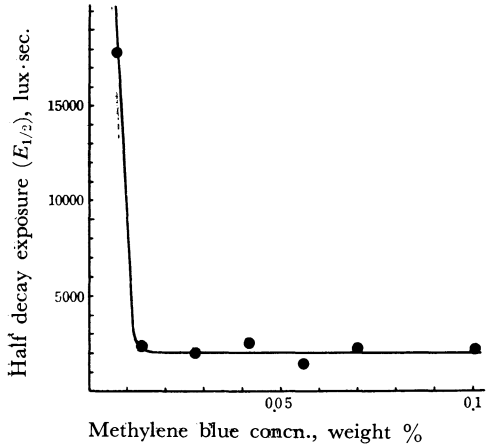

Fig. 1. Relation between sensitivity of dyed polyacenaphthylene and methylene blue concn.

Table I. Sensitizations by dyes

	V_0, V.	$E_{1/2}$ lux.sec.
Phenylmethanes		
Victoria pure blue	1660	6500
Victoria blue	1540	>100000
Crystal violet	1520	>100000
Brilliant green	1050	20000
Acid violet 6G	1720	73000
Fuchsin	2280	27000
Basic cyanine BX	1760	11000
Malachite green	1720	9000
Auramine	1520	75000
Naphthalene green	1520	93000
Xanthenes		
Rhodamine 6G	940	6000
Rhodamine B extra	1250	22000
Fluorescein	2140	40000
Sulforhodamine B	1590	73000
Eosine A	2330	61000
Eosine S	1950	49000
Phloxine	1840	64000
Rose bengale	1080	>100000
Azines		
Neutral red	1400	46000
Phenosafranine	2200	88000
Pinacryptol green	1900	62000
Selestine blue	1720	>100000
Acridines		
Acridine yellow	1840	76000
Acridine orange	1680	81000
Pinacryptol yellow	2080	>100000
Thiazines		
Methylene blue	1400	1500
New methylene blue	1340	14000
Cyanines		
Garocyanine	1800	>100000
Chinolin blue	1920	67000
Pinacyanole	450	>100000
Azo dyes		
Oill red B	1640	>100000
Chrom blue black RC	2080	54000
Butter yellow	1840	41000
Fast light yellow G	1680	74000

In the case of sensitization on poly-*N*-vinylcarbazole, methylene blue is a little less sensitive than crystal violet. It is not evident why a large difference occurs between methylene blue and new methylene blue, because the two chemical formulas are very similar to each other. Methylene blue, rhodamine 6G, and victoria pure blue are all cationic dyes. The empirical tendency for the effective dyes to be cationics in the dye sensitization of poly-*N*-vinylcarbazole may also be applied in the case of polyacenaphthylene. Methylene blue, a thiazine dye, is known as a desensitizer in the silver

Table II. Sensitizations by Lewis acids

	V_0, V.	$E_{1/2}$ lux.sec.
Acids and acid anhydrides		
Acetic acid	1535	>100000
Monochloroacetic acid	1550	>100000
Dichloroacetic acid	1040	>100000
Trichloroacetic acid	1340	11000
Monobromoacetic acid	1020	>100000
Tribromoacetic acid	1360	21000
Phenol	1245	>100000
p-Nitrophenol	1000	6000
Picric acid	1320	6000
Hydroquinone	1380	27000
Tetrachlorophthalic acid	960	7000
Tetrachlorophthalic anhydride	1310	7000
Benzoic acid	1500	82000
2,4,6-Trinitrobenzoic acid	1350	4000
Telephthalic chloride	1070	82000
Phthalic anhydride	1500	75000
Cinnamic acid	1630	80000
Acetanilide	1520	>100000
Oxalic acid	1120	92000
Succinic anhydride	1350	>100000
Maleic acid	1190	60000
Maleic anhydride	830	56000
Fumalic acid	1110	>100000
o-Toluic acid	1535	>100000
p-Aminobenzoic acid	1400	>100000
Aldehydes and Ketones		
p-Hydroxybenzaldehde	1480	>100000
2,4-Dichlorobenzaldehyde	1480	>100000
p-Nitrobenzaldehyde	1560	98000
p-Dimethylaminobenzaldehyde	1510	>100000
Bromal	1400	>100000
o-Nitrobenzaldehyde	1535	>100000
Acetophenone	1680	>100000
Benzophenone	1550	>100000
Benzil	1480	>100000
Benzoin	1610	>100000
Quinones		
α-Naphthoquinone	850	18500
2,3-Dichloronaphthoquinone	1090	1400
1-Nitoroanthraquinone	1420	1200
2,6-Dichloro-*p*-benzoquinone	1390	4000
2-Chloroanthraquinone	1390	1900
2-Methylanthraquinone	1110	11000
p-Benzoquinone	1320	36000
p-Chloranil	1520	1800
Anthraquinone	1210	8800
1,5-Dichloroanthraquinone	1100	1500
Anthraquinone-2-carboxilic acid	970	4000
Benzanthron	1470	>100000
α-Benzanthraquinone	1600	5000
1-Aminoanthraquinone	1330	>100000
2-Aminoanthraquinone	350	>100000
1,4-Diaminoanthraquinone	950	>100000
Alizarine	1350	>100000
Quinizarine	1670	4100
Others		
5-Nitroacenaphthylene	1535	>100000
Trinitrobenzene	1170	2400

halide emulsions. This dye has positive effects, and cyanine dyes which are good sensitizers for the silver halides have no effect on the polymeric donor-type photoconductors.

Effective Dye Concentration.—In Fig. 1, a relation between the photosensitivity and the doping concentration of methylene blue is presented. In view of the accuracy of measuring, it can be said that the optimum dye concentration range is 0.03—0.1%. As the dye concentration increases, the dark decay rate increases as a result of a decrease in the dark resistivity.

Lewis Acid Sensitization.—The pure polyacenaphthylene showed an $E_{1/2}$ value of 1.6×10^5—1.8×10^5 lux. sec. and a V_0 value of 1400—1600 V. The dark decay rate was about 5 times that of poly-*N*-vinylcarbazole. These results imply that polyacenaphthylene has a lower value in the dark resistivity and a higher value in the light resistivity.*2

From Table II, it can be said that quinone derivatives are effective. 1-Nitroanthraquinone, 2, 3-dichloronaphthoquinone, 1, 5-dichloroanthraquinone, chloranil, and 2-chloroanthraquinone, which are strongly electron-attractive, show high sensitizabilities in white light without dye. This shows that the clear formation of a charge transfer complex is a favorable method for the sensitization when an effective dye is not used. The $E_{1/2}$ values of 1-nitroanthraquinone (1.2×10^3 lux. sec.) and 2, 3-dichloroanthraquinone (1.4×10^3 lux. sec.) are comparable with that of methylene blue (1.5×10^3 lux. sec.).

The Combined Effect of a Dye and a Strong Acid.—It has already been found that poly-*N*-vinylcarbazole was sensitized very highly with a cationic dye and a strong acid. Such a combined effect with a dye and acid might also be expected in the case of polyacenaphthylene. A compounded system of methylene blue (0.05%)+2, 4, 6-trinitrobenzoic acid (1%) shows 250 lux. sec., while a system of methylene blue (0.05%)+1-nitroanthraquinone (10%) or methylene blue (0.05%) + chloranil (10%) shows 1.3×10^3 or 2.5×10^3 lux.sec. respectively (see Fig. 2). Thus, an amplified

*2 The $E_{1/2}$ value of pure poly-*N*-vinylcarbazole was found to be about 4000 lux.sec.

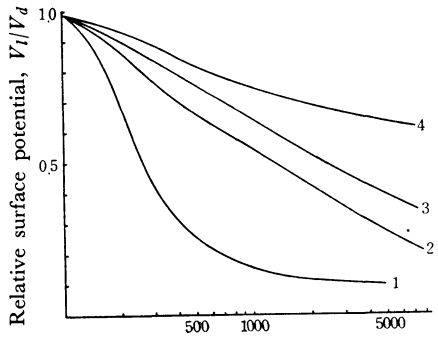

Fig. 2. Electrophotographic characteristic curves of some sensitized polyacenaphthylene: 1, doped with 0.05% of methylene blue and 1% of 2,4,6-trinitrobenzoic acid; 2, doped with 0.05% of methylene blue and 10% of 1-nitroanthraquinone; 3, doped with 0.05% of methylene blue and 10% of chloranil; 4, doped with 0.05% of methylene blue and 10% of 2,3-dichloronaphthoquinone.

effect by using a dye and an acid is also to be seen in the sensitization of polyacenaphthylene.

From the view point of practical use in electrophotography, only methylene blue is found to be a significant dye.

Conclusion

The sensitized polyacenaphthylene with 0.05% of methylene blue and 1% of 2, 4, 6-trinitrobenzoic acid shows 250 lux. sec. in sensitometry with a half decay exposure. Nitrated polyacenaphthylene, which has an optimum degree of nitration (20—40 mol. %),[6] shows about 2×10^3 lux.sec. The methylene blue-sensitized sample of the nitrated derivative was found to be 550 lux. sec., which is about twice the foregoing system of polyacenaphthylene. From these results, the nitration is not likely to be a practical method for preparing elctrophotographic-sensitive material.

The authors express their hearty thanks to Dr. Shunkichi Kisaka, the manager of the laboratory for his kind guidance and encouragement through the work.

6) K. Morimoto and A. Inami, *J. Chem. Soc. Japan, Ind. Chem. Sect.* (*Kogyo Kagaku Zasshi*), **67**, 232 (1964).

BULLETIN OF THE CHEMICAL SOCIETY OF JAPAN VOL. 39 1673—1678 (1966)

Reactive Species in the Photochemical Hydrogenation of Acridine in Ethanol

By Akira KIRA, Yoshinori IKEDA and Masao KOIZUMI

(Department of Chemistry, Faculty of Science, Tohoku University, Katahira-cho, Sendai

(Received November 24, 1965)

In order to determine the reactive state of acridine when it is photoreduced by ethanol, two types of experiments were undertaken. The first was to study the concentration effect of ethanol on the quantum yield in a benzene solution. These results, however, could not give any unequivocal answer. The second type of experiment was, therefore, made from the standpoint of the triplet energy transfer, using eosine as an energy acceptor for the photoreduction of acridine in an ethanol solution. It was found that, in a deaerated solution, the quantum yield of acridine photoreduction is not affected by the addition of eosine, whereas it was established by the flash technique that, under similar conditions, the energy transfer from the acridine triplet state to eosine occurs at approximately the diffusion-controlled rate. These results lead to the conclusion that the reactive state is not the lowest triplet state.

In a previous paper[1] two paths have been presented for the photochemical reduction of acridine in ethanol. One was:

$$\left.\begin{array}{l} A + h\nu \rightarrow A^* \\ A^* + RH_2 \rightarrow \left(A\begin{array}{c}H\\H\end{array}R\right) - AH_2 + R \end{array}\right\} \quad (1)$$

where A* is the singlet excited state of acridine and RH_2 is ethanol. The other was:

$$\left.\begin{array}{ll} & A^* + RH_2 \rightarrow AH + RH \quad (a) \\ \text{or} & A^T + RH_2 \rightarrow AH + RH \quad (b) \\ & (2AH \rightarrow A + AH_2) \end{array}\right\} \quad (2)$$

where A^T is the triplet state of acridine. When oxygen is present, only (1) occurs, since the half hydrogenated acridine produced by (2a) or (2b)

1) A. Kira, S. Kato and M. Koizumi, This Bulletin, **39**, 1221 (1966).

reverts to acridine by means of:

$$AH + O_2 \rightarrow A + HO_2$$

The question whether A* or A^T is involved in path 2, however, has not yet been decided. In the present paper attempts will be made to give an unequivocal answer to this question.

Results and Discussion

The Reaction between Acridine and Ethanol in a Benzene Solution.—It is expected that if AH is to be produced by (2a), then a rather high concentration of ethanol would be required for the reaction to occur because the lifetime of A* is 7.2×10^{-10} sec.[2] On the other hand, if AH is produced via the triplet state, it is possible that a rather low concentration of ethanol is enough for the reaction rate to become measurable, although it all depends upon the magnitude of the rate constant of $A^T+RH_2\rightarrow AH+RH$. Since, for the aerated solution, it has already been determined that the reaction really occurs at A*, there is a possibility that the problem can be answered by comparing the concentration effect of ethanol on the rate in aerated and deaerated benzene solutions.

The concentration of acridine was chosen as 5×10^{-5} M, while the concentration of ethanol was varied from 1×10^{-2} M to 17.3 M (pure ethanol). Changes in the absorption spectra in the course of the reaction were quite similar to those in the pure ethanol solution. The $\ln(e^{acd}-1)$ vs. t plots were satisfactorily linear, and the value of the quantum yield was determined from the slope of the plot. The results are shown in Table I.

It is notable that the ratio of Φ_{dea} to Φ_{aer} is almost constant, independent of the concentration of ethanol. When the reaction occurs at the singlet excited state, the quantum yield, Φ, for the simplest case is given as follows:

$$\Phi = \frac{k_r[RH_2]}{k_d + k_r^s[RH_2]} \quad (1)^{*1}$$

where k_r, k_r^s and k_d are the rate constants for, respectively, the genuine reaction with ethanol, the total reaction with ethanol (including simple deactivation), and the first-order decay constant in benzene. From Eq. 1 one gets:

$$\frac{\Phi}{1-\Phi}\times\left\{1+\frac{(k_r^s-k_r)}{k_d}[RH_2]\right\}=\frac{k_r}{k_d}[RH_2] \quad (2)$$

On the other hand, when the triplet state is a reactive species:

$$\Phi = \varphi_{S-T}^{A}\frac{k_r'[RH_2]}{k_d'+k_r^s'[RH_2]} \quad (3)$$

where φ_{S-T}^{A} is the probability of the intersystem crossing[3] and where k_r', k_r^s' and k_d' are the analogous rate constants for the triplet state, just as k_r, k_r^s and k_d are for A*. From Eq. 3:

$$\frac{\Phi}{\varphi_{S-T}^{A}-\Phi}\times\left\{1+\frac{(k_r^s'-k_r')[RH_2]}{k_d}\right\}=\frac{k_r'}{k_d'}[RH_2] \quad (4)$$

As may be expected from Eq. 2, the plot of $\log[\Phi_{aer}/(1-\Phi_{aer})]$ against $\log[RH_2]$ for the aerated solution does not give the slope of unity; rather, it gives approximately 0.8. In the same way, when both $\log[\Delta\Phi/(1-\Delta\Phi)]$ and $\log[\Delta\Phi/(\varphi_{S-T}^{A}-\Delta\Phi)]$ ($\Delta\Phi=\Phi_{dea}-\Phi_{aer}$) are plotted against $\log[RH_2]$ for the dearated solution, the slopes of the curves also have similar values. This deviation from unity might be due partly to the dependence of k_r's and k_d's on the composition of the solution, but it is more plausible to attribute this deviation mainly to the assumption that $k_r^s=k_r$, especially in the lower concentration region of ethanol. If one takes proper $(k_r^s-k_r)/k_d$ values, which are ca.

TABLE I. QUANTUM YIELDS* OF THE PHOTOREDUCTION OF ACRIDINE BY ETHANOL IN BENZENE
[acridine]: 5×10^{-6} M, Temperature: 25°C

Concn. of ethanol M	Φ_{dea}**	Φ_{aer}**	$\Delta\Phi(=\Phi_{dea}-\Phi_{aer})$	$\frac{\Phi_{dea}}{\Phi_{aer}}$
0	$3.0_6\times10^{-4}$	$4.4_6\times10^{-5}$		(6.9)
1×10^{-2}	8.2×10^{-4}	2.0×10^{-4}	6.2×10^{-4}	4.1
5×10^{-2}	$2.5_3\times10^{-3}$	$6.9_6\times10^{-4}$	$1.8_3\times10^{-3}$	3.6
1×10^{-1}	$6.1_3\times10^{-3}$	$1.6_4\times10^{-3}$	$4.4_9\times10^{-3}$	3.7
5×10^{-1}	$1.7_7\times10^{-2}$	$4.5_3\times10^{-3}$	$1.3_2\times10^{-2}$	3.9
1	$3.2_9\times10^{-2}$	$7.4_4\times10^{-3}$	$2.5_5\times10^{-2}$	4.4
				av. 4.0
8.6 (50% Vol.)	$9.0_0\times10^{-2}$	$1.9_7\times10^{-2}$	$7.0_2\times10^{-2}$	4.6
17.3 (100%)	$1.2_3\times10^{-1}$	$4.3_8\times10^{-2}$	$7.9_7\times10^{-2}$	2.8

* Correction is made for the quantum yield in pure benzene.
** Φ_{dea} and Φ_{aer} are respectively the quantum yield for the deaerated and aerated solutions.

2) H. Kokubum, Symposium of Photochemistry, Sendai, 1963.

*1 In general a factor depending on the succeeding steps should be multiplied.

3) According to our unpublished findings, the value of φ_{S-T}^{A} in a benzene solution is about 0.24.

1 in all cases, then the plot of the logarithm of the left side of Eqs. 2 and 4 against log[RH_2] can be made to have a slope of 1. The results are shown in Fig. 1.

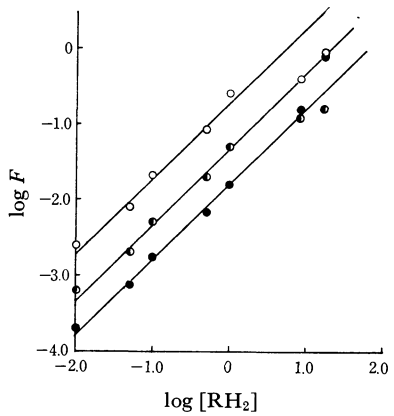

Fig. 1. Plots of log F vs. log [RH_2].
$F = \Delta\Phi \cdot K/(\varphi^{A}_{ST} - \Delta\Phi)$ for ○,
$\Delta\Phi \cdot K/(1-\Delta\Phi)$ for ◐ and
$\Phi_{aer} \cdot K/(1-\Phi_{aer})$ for ●,
where $K = \left\{1+\frac{(k_r^s - k_r)}{k_d}[RH_2]\right\}$ etc.
and where the coefficients of [RH_2] are put unity.

The values of k_r/k_d's are evaluted from the point at log[RH_2]=0. For the deaerated solution, the values of k_r and k_r^s are:

$$\begin{cases} k_r' = 2.0\times10^{-1}k_d' \\ k_r^s' = 1.2k_d' \end{cases} \qquad \begin{cases} k_r = 4.6\times10^{-2}k_d \\ k_r^s = 1.05k_d \end{cases}$$

and for the aerated solution:

$$\begin{cases} k_r = 1.6\times10^{-2}k_d \\ k_r^s = 1.02k_d \end{cases}$$

If one assumes $k_d \simeq 10^{10}$ sec^{-1} and $k_d' \approx 2\times10^3$ sec^{-1},[4] then for the reaction 2a:

$$k_r = 4.6\times10^8 \text{ M}^{-1}\text{ sec}^{-1}, \quad k_r^s = 10^{10} \text{ M}^{-1}\text{ sec}^{-1}$$

and for (2b):

$$k_r' = 4\times10^2 \text{ M}^{-1}\text{ sec}^{-1}, \quad k_r^s' = 2.4\times10^3 \text{ M}^{-1}\text{ sec}^{-1}.$$

Thus, the above values of the rate constants can make both the reactions, 2a and 2b, consistent with the experimental results, and so no definite answer can be given. However, the results in Table I, particularly the constancy of Φ_{dea}/Φ_{aer}, seem to favor the view that a reactive state is S* and not T. Even if A^T reacts with ethanol, there is no doubt that its reactivity is exceedingly small.

The Effect of the Addition of Eosine on the Photoreduction of Acridine in Ethanol.— In principle, the present problem can be solved if an effective quencher of A^T is added and if its effect on the rate of photoreduction is examined. Thus, if a reactive species is triplet acridine, then the rate may be expected to decrease to about one-third of the original value, whereas the rate should be scarcely affected if the reactive species is A*. However, we do not know what substance is a suitable triplet quencher. We have tried eosine as a test substance, since this dye has a triplet level definitely lower than that of acridine[5] and since its absorbance at 365 mμ is very small. It was found that the addition of eosine (5×10^{-6} M or 1×10^{-5} M) did not affect the rate beyond the limits of experimental error, and yet the optical density of eosine was found to decrease beyond the limit of experimental error, though to a small extent. The results are shown in Table II, where ΔD is the difference in the optical density of eosine before and after 5 minutes' irradition.

It should be noted that, according to our preliminary experiments, eosine is rapidly photoreduced by a 365 mμ light in the presence of 10^{-4} M acridan. In spite of this fact, it is believed that the ΔD value in Table II is not due to the produced acridan, though the bad reproducibility of the data might partially be due to it.

From the above results, there is scarcely any doubt that the addition of eosine does not affect the rate of the photoreduction of acridine. However, there still seems to be some doubt as to whether eosine is really acting as an efficient quencher under the present experimental conditions, since the decrease in the optical density of eosine is quite small. The order of the magnitude of ΔD to be expected can be estimated in the following way. If the above results are to be explained by the following scheme:

$$A + h\nu \rightarrow A^*$$
$$A^* + RH_2 \rightarrow AH_2 + R \qquad (1)$$
$$\quad \rightarrow AH + RH \qquad (2a)$$
$$A^* \rightarrow A^T \qquad (3)$$
$$A^T + E \rightarrow A + E^T \qquad (4)$$
$$E^T + RH_2 \rightarrow (EH + RH) \rightarrow EH_2 + R \qquad (5)$$

where E is eosine, then the decrease in the eosine concentration, −d[E], should be given by:

$$-\text{d[E]} = I^{A}_{ab} \cdot \varphi^{A}_{S-T} \cdot \alpha \cdot \beta \, dt$$

where I^{A}_{ab} is the quantity of light absorbed by acridine, where φ^{A}_{S-T} is the probability of the intersystem crossing of acridine, and where α and β are, respectively, a parameter for the efficiency of the energy transfer (process 4) and the probability that the triplet eosine reacts with ethanol.

4) To be published.

5) According to G. N. Lewis and M. Kasha (*J. Am. Chem. Soc.*, **66**, 2100 (1944)), the triplet level of eosine is 14900 cm^{-1}, while D. F. Evans (*J. Chem. Soc.*, **1957**, 1351) reported that the triplet level of acridine is 15840 cm^{-1}. See also Hammond et. al., *J. Am. Chem. Soc.*, **86**, 3197 (1964).

TABLE II. THE EFFECT OF ADDITION OF EOSINE ON THE QUANTUM YIELD OF PHOTOREDUCTION OF ACRIDINE
Temperature 25°C

Concn. of acridine M	Concn. of eosine M	Φ	ΔD
Deaerated solution			
5×10^{-5}	0	$1.2_5\times10^{-1}$	—
5×10^{-5}	0	$1.2_3\times10^{-1}$	—
5×10^{-5}	5×10^{-6}	$1.1_8\times10^{-1}$	0.015
5×10^{-5}	1×10^{-5}	$1.1_9\times10^{-1}$	0.22
1×10^{-4}	0	$1.2_9\times10^{-1}$	—
1×10^{-4}	5×10^{-6}	$1.1_8\times10^{-1}$	0.08
1×10^{-4}	7.5×10^{-6}	$1.2_1\times10^{-1}$	0.02
1×10^{-4}	7.5×10^{-6}	$1.2_3\times10^{-1}$	0.01
1×10^{-4}	9×10^{-6}	$1.2_5\times10^{-1}$	0.56
1×10^{-4}	1×10^{-5}	$1.2_0\times10^{-1}$	0.31
1×10^{-4}	1×10^{-5}	$1.2_7\times10^{-1}$	0.02 (after 3 min.) 0.04
Aerated solution			
5×10^{-5}	0	$4.3_8\times10^{-2}$	
5×10^{-5}	5×10^{-6}	$4.3_8\times10^{-2}$	−0.03 (after 10 min.)
1×10^{-4}	0	$4.3_5\times10^{-2}$	—
1×10^{-4}	1×10^{-5}	$4.6_5\times10^{-2}$	0
Controle (deaerated)			
0	1×10^{-5}		0.005 (after 3 min.) 0.08 (after 30 min.)
0	1×10^{-5}		0.025 (after 3 min.) 0.04 (after 30 min.)

Since

$$-\mathrm{d[A]} = I^{\mathrm{A}}_{ab}\cdot\Phi^{\mathrm{A}}_{dea}\,\mathrm{d}t$$

one gets:

$$-\mathrm{d[E]} = -\mathrm{d[A]}\times\frac{\varphi^{\mathrm{A}}_{\mathrm{S}-\mathrm{T}}\cdot\alpha\cdot\beta}{\Phi^{\mathrm{A}}_{dea}}$$

Integration gives:

$$\Delta[\mathrm{E}] = \Delta[\mathrm{A}]\times\frac{\varphi^{\mathrm{A}}_{\mathrm{S}-\mathrm{T}}\cdot\alpha\cdot\beta}{\Phi^{\mathrm{A}}_{dea}}$$

Φ^{A}_{dea} is $\simeq0.1$; if one tentatively puts $\varphi^{\mathrm{A}}_{\mathrm{S}-\mathrm{T}}\approx0.1$,[3] $\alpha\approx1$, and $\beta\approx0.01$,[6] then:

$$\Delta[\mathrm{E}] = \Delta[\mathrm{A}]\times\frac{1}{100}$$

When the concentration of acridine is 5×10^{-5} M and 1×10^{-4} M, the ΔD values should be 0.05 and 0.10 respectively after 5 minutes' illumination, by which time acridine disappears almost quantitatively. These values are perhaps the upper limit which can be expected, and the experimental values are quite reasonable, at least in the order of magnitude.

Thus, it seems quite plausible that the reactive species of acridine is the singlet excited state and not the triplet state. It is worthwhile to add here that the above results obviate any appreciable occurence of such a process as $\mathrm{AH}+\mathrm{E}\rightarrow\mathrm{A}+\mathrm{EH}$, i. e., the transfer of the hydrogen atom from semi reduced acridine to eosine. If this reaction were to occur, then the reduction of the acridine concentration should be caused by the addition of eosine.

Direct Proof of the $\mathrm{A^T}+\mathrm{E}\rightarrow\mathrm{A}+\mathrm{E^T}$ Process by Flash Photolytic Experiments. — In order to establish the $\mathrm{A^T}+\mathrm{E}\rightarrow\mathrm{A}+\mathrm{E^T}$ process more conclusively, flash photolytic studies were made of a solution of acridine and eosine in ethanol. The experimental conditions, such as the concentration of acridine, the flash intensity, and the filter system, are similar to those used for the acridine solution in ethanol.[1] The concentration of eosine was changed from 3×10^{-6} to 2×10^{-5} M. The filter transmits only the light in the absorption region of acridine.

An example of the transient absorption spectra is shown in Fig. 2.
The concentration of acridine in this case is 1×10^{-5} M. At 93 μ sec. after the flash, the absorption spectra are quite similar to those of the acridine triplet state.[1] At 360 μ sec., the shape of the spectra becomes quite different and resembles rather those of eosine intermediates,[7] although it is not exactly identical.

Judging from the decay of the triplet acridine,

6) According to M. Imamura and M. Koizumi (This Bulletin, **29**, 899 (1956)), the quantum yield of the photoreduction of eosine in ethanol is $\sim5\times10^{-4}$. The value of $\varphi^{\mathrm{E}}_{\mathrm{S}-\mathrm{T}}$ is 0.023 according to C. A. Parker (*Trans. Faraday Soc.*, **57**, 1894 (1961)), while in our unpublished results it is >0.05. The molar extinction coefficient of eosine in ethanol is $\sim10^5$.

7) A. Kira and S. Kato, *Science Rep. Tohoku Univ., Ser. 1*, **48**, 232 (1965).

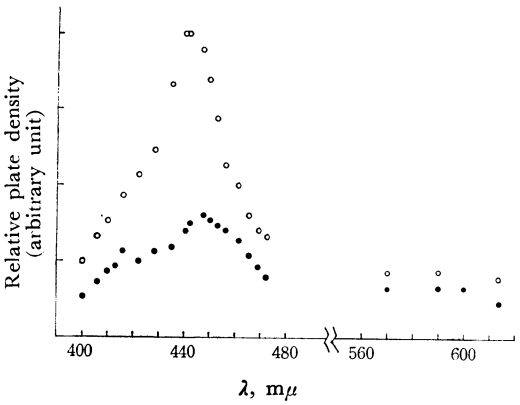

Fig. 2. Transient spectra of acridine in degassed ethanol solution containing eosine.
Acridine 1×10^{-4} M Eosine 1×10^{-5} M
○ 93 μ sec. and ● 360 μ sec. after the flash irradiation

its quantity at this stage is expected to be practically nil, so that there is no doubt that the absorption spectra at this stage are due to the transient intermediates originating from eosine. However, since the lifetime of the singlet excited state of acridine A* is of the order of 10^{-10} sec., there is no possibility for 10^{-5} M of eosine to react with A*. Besides, when a degassed solution of eosine in ethanol is irradiated under conditions similar to those above, no transient absorption is observable at 440 mμ. Therefore, it can be colculded that the transient species in question is produced by the reaction of the triplet state acridine, A^T, and eosine.

The decay curves of the optical density at 440 mμ for several eosine concentrations are shown in Fig. 3. The following features are to be noted; 1) The later stage of the decay curves, after ~300 μ sec., is exponential and has the same rate

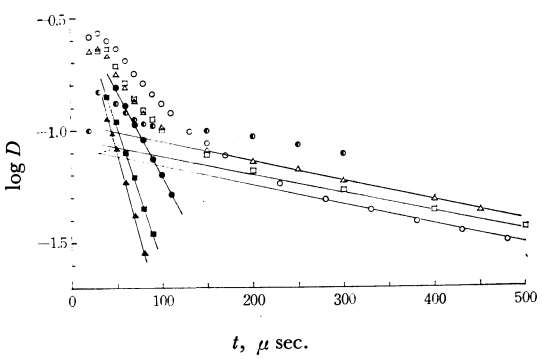

Fig. 3. Decay curves of the absorption at 440 mμ.
White symbols refer to observed data and black symbols, to the decay of the triplet state evaluted from them.
Acridine 3×10^{-5} M
Eosine concentrations: ○ and ● 3×10^{-6} M, □ and ■ 6×10^{-6} M, △ and ▲ 8×10^{-6} M and ◐ 2×10^{-5} M

constant, $k=2\times10^3$ sec^{-1}, irrespective of the eosine concentration. 2) The first stage decays much faster, but the effect of the eosine concentration on the decay rate is not appreciable. 3) At the initial stage, the optical density becomes smaller with the increase in the eosine concentration, whereas 4) in the later stage, it becomes higher with the increase in the eosine concentration.

Findings 1 and 4 lead to the view that the later stage involves a certain intermediate produced from eosine. Furthermore, the value of k and the spectral feature support the view that this is mainly the triplet state of eosine, E^T. Findings 2 and 3 can then be interpreted in terms of the superposition of the decay of A^T and the rise in E^T.

The above interpretation is further supported by the finding that the solution of acridine and eosine in ethanol ([A]: 5×10^{-5} M, [E]: 8×10^{-6} M), when irradiated by the light absorbed only by eosine, displays the transient absorption spectra the decay constant of which is $k=2.4\times10^3$ sec^{-7}, i. e., just the same as that above. This value also agrees with the decay constant of E^T in ethanol.[7]

Thus, the present results naturally lead to the following scheme:

$$A^T \xrightarrow{k_d^A} A \qquad A^T + E \xrightarrow{k_4} A + E^T$$

$$E^T \xrightarrow{k^E} E^X \text{ or } E \text{ (the yield of } E^X \text{ being } \beta)$$

where E^X is a secondary intermediate of eosine (probably semiquinone) but with a longer life. Since the initial concentration of A^T is 10^{-6} M at most, the following equations can easily be derived on the basis of the above scheme:

$$\begin{cases} [A^T] = [A^T]_0 e^{-(k_d^A + k_4[E]_0)t} = [A^T]_0 e^{-\kappa t} \\ [E^T] = \dfrac{k_4[E]_0[A^T]_0}{\kappa - E}(-e^{-\kappa t} + e^{-k^E t}) \\ \dfrac{1}{\beta}[E^X] = \dfrac{k_4[E]_0[A^T]_0}{\kappa} + \dfrac{k^E k_4[E]_0[A^T]_0}{\kappa - k^E} \\ \qquad \times\left(\dfrac{1}{\kappa}e^{-\kappa t} - \dfrac{1}{k^E}e^{-k^E t}\right) \end{cases}$$

However, since β is very small, as has been estimated above, the optical density at 440 mμ is given by:

$$D = (\varepsilon[A^T] + \varepsilon'[E^T])d \qquad (5)$$

with a good approximation, where ε and ε' are, respectively, the molar extinction coefficients of A^T and E^T.

The decay at the later stage is then given by:

$$\frac{k_4[E]_0[A^T]_0 d\varepsilon'}{\kappa - k^E} e^{-k^E t} \qquad (6)$$

This interprets quantitatively the increase in the optical density with the eosine concentration. In the initial stage, two terms containing $e^{-\kappa t}$ and $e^{-k^E t}$ superpose, and the contribution of the second

term increases with $[E]_0$, this is the reason why the apparent decay is not so much affected by the eosine concentration.

In order to evaluate κ, one has to subtract Eq. 6 from Eq. 5 and has to plot the logarithm of the residue against the time. The results are shown in Fig. 3 with black symbols. The observed κ-values thus obtained are plotted against the eosine concentrations in Fig. 4.

The value of k_4 obtained is 3.4×10^9 M^{-1}sec^{-1}. Although the above analysis is approximate in nature on account of the neglect of the second-order decay of A^T, yet it seems quite satisfactory, even quantitatively. Thus it may be concluded that the $A^T+E\rightarrow A+E^T$ process can occur very quickly, perhaps with a diffusion-controlled rate constant.

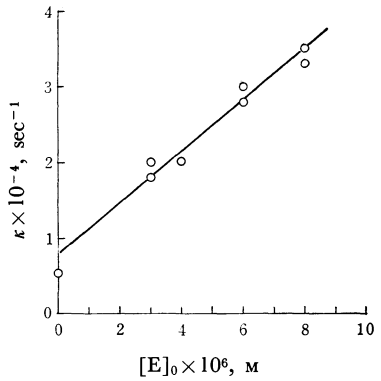

Fig. 4. The relation between the observed first order rate constant of triplet acridine and the eosine concentration.

Conclusion

The present study has shown that: 1) The energy transfer between the acridine triplet state and the ground state eosine occurs very efficiently, and that 2) in spite of this triplet energy transfer, the photoreduction of acridine is scarcely affected at all by the presence of eosine.

It may, therefore, be concluded that the reactive state of acridine is not the triplet state. As Kellmann and Dubois have proposed,[8] however, there is a possiblity of the $n-\pi^*$ T state being the reactive one. This state, according to them, has a lifetime of the order of 10^{-8} sec., so the presence of 10^{-5} M of eosine will scarcely affect this state. It is a problem for the future to decide how much of the reaction occurs at the S* and at the $n-\pi^*$ T states and, further, to decide the fraction of molecular and radical mechanisms in each reactive state.

8) A. Kellmann and J. T. Dubois, *J. Chem. Phys.*, **42**, 2518 (1965).

BULLETIN OF THE CHEMICAL SOCIETY OF JAPAN VOL. 39 1678—1681 (1966)

Ammoniak-Synthese an einigen legierten Katalysatoren

Von Rudolf BRILL und Yoshio OHSUMI*

Fritz-Haber-Institut der Max-Planck-Gesellschaft, Berlin Dahlem

(Eingegangen am 25 November, 1965)

Es wird versucht, Eisenkatalysatoren für die Ammoniak-Synthese herzustellen, bei denen dem Eisen Fremdmetalle (Chrom, Nickel, Kupfer) zulegiert sind. Um Katalysatoren mit einer Struktur zu erhalten, die der Struktur der aus reinem Eisen hergestellten vergleichbar ist, wurden die Fremdmetalle als solche oder als Oxide dem Carbonyleisen beigemischt, das dann in üblicher Weise durch Schmelzen im Sauerstoffstrom in Magnetit übergeführt wurde. Eine Mischkristallbildung in der Magnetitphase wurde nur bei Nickel und Chrom gefunden. Durch Reduktion der Spinelle wurde nur bei Nickel eine Legierungsbildung festgestellt. Cr_2FeO_4 war unter unseren Bedingungen (Reduktion bei 400°C mit Wassersoff-Stickstoff-Gemisch) nicht reduzierbar. Alle mit Kupfer hergestellten Katalysatoren zeigten im reduzierten Zustand Kupfer neben Eisen. Die Legierungskatalysatoren mit Nickel zeigten bei Gehalten bis zu 5% Nickel innerhalb der Fehlergrenze dieselbe Aktivierungsenergie wie reines Eisen, während Katalysatoren mit 10—30% Nickel eine merklich geringere Aktivierungsenergie aufweisen, jedoch tritt dabei ein Kompensationseffekt auf.

Einleitung

Die vorliegenden Untersuchungen befassen sich mit dem Problem der Beeinflussung der katalytischen Eigenschaften des Eisens für die Ammoniak-Synthese durch Legierungsbildung. Als Legierungspartner wurden zunächst Chrom, Nickel und

* Die jetzige Adresse: Zentrale Forschungsinstitut der Mitsubishi Chem. Ind., Kawasaki, Japan.

Kupfer herangezogen. Um mit reinem Eisen vergleichbare Werte zu erhalten, wurden auch die Legierungen durch Reduktion von Oxiden hergestellt. Die in der Technik gebräuchliche Methode besteht in der oxidativen Verbrennung reinen Eisens (mit geeigneten Zusätzen), wobei sich in weitaus überwiegender Menge der Spinell Fe_3O_4, der gegebenenfalls einige "Promotoren" unter Bildung eines Mischspinells in Lösung enthält, bildet. Um übersichtlichere Verhältnisse zu haben, wurde auf den Zusatz von Promotoren verzichtet und durch Verbrennung von Carbonyleisen erhaltenes Fe_3O_4 nach der Reduktion zu Eisen als Vergleichskatalysator benützt.

Experimentelle Methode

Die oxidischen Legierungskatalysatoren wurden durch Mischung von Carbonyleisen mit Carbonyl-Nickel, Chromtrioxid oder Kupfer(II)-oxid und Verbrennen der Mischung im Sauerstoffstrom erhalten. Auf diesem Wege könnten Mischspinelle erhalten werden ($Fe_3O_4+NiFe_2O_4$: $Fe_3O_4+FeCr_2O_4$; $Fe_3O_4+CuFe_2O_4$), die bei der Reduktion die Legierungen ergeben können.

Die Ammoniak-Synthese an den erwähnten Katalysatoren wurde teils nach der bei Brill und Tauster[1] angegebenen Methode (I), teils in einer Apparatur ausgeführt, die der von Ozaki, Taylor und Boudart[2] angegebenen (II) entspricht.

Experimentelle Ergebnisse und Diskussion

(1) Röntgenprüfung. — Die röntgenographische Untersuchung zeigte indessen, dass die Legierungsbildung auf diesem Wege unvollständig ist. Die Gitterkonstanten von so hergestellten Legierungen waren zwar, z. B. bei Zusatz von 10% oder 30% Nickel, gegenüber der des reinen Eisens vergrössert. Wegen der äusserst geringen Unterschiede zwischen dem metallischen Atomradius des Eisens (1.241 Å) und dem des Nickels (1.246 Å) konnte jedoch die röntgenographische Methode zur genauen Bestimmung des Nickelgehaltes nicht herangezogen werden.

Die Ergebnisse der röntgenographischen Analyse der untersuchten Katalysatoren sind in Tablle I zusammengefasst.

Der bete Literaturwert für reines Eisen ist 2.8664 Å bei 20°. Die Abweichung der in Tabelle I für reines Eisen gegebenen Zahl 2.865 von diesem Wert kennzeichnet etwa die Genauigkeit unserer Messungen, d. h. bei den Legierungen mit 5 und 10% Nickel ist eine Gitteraufweitung nicht zu konstatieren, während die nach dem Sintern der Legierung mit 10% sowie die bei den höherprozentigen Legierungen gefundenen Werte auf eine

Tabelle I. Gitterkonstanten von Eisen-Nickel-Katalysatoren (in Å)

%, Ni	Gitterkonstante der innenzentrierten Phase	Gitterkonstante der flächenzentrierten Phase	Bemerkungen
0	2.865	—	—
1	2.867	—	—
5	2.867	—	—
10	2.867	—	—
10	2.869	3.587	gesintert
20	2.870	3.587	—
30	2.868	3.578	—
30	2.869	3.587	gesintert

Aufweitung des Eisengitters durch eingebautes Nickel hinweisen. Die Probe mit 10% zeigte nach der Reduktion bei 350° im Röntgenogramm keinerlei Linie von Nickel. Nach dem Sintern bei 450° treten jedoch Nickel-Linien sehr schwach hervor.

Die Probe mit 30% Nickel zeigt diese Effekte nicht. Das Sintern ändert das Intensitätsverhältnis zwischen Eisen- und Nickel-Linien nicht. Eisen sollte in der Lage sein, Nickel bis zu 30% in sein Gitter aufzunehmen unter Erhaltung des kubisch-innenzentrierten Gitters des Alpha-Eisens. Diese Phase soll jedoch metastabil sein und sich in die kubisch-flächenzentrierte Struktur umwandeln.[3] Die neben den Eisenlinien in den Röntgenogrammen gefundenen Nickel-Linien zeigen nun interessanterweise eine Gitterkonstante, die erheblich von der des reinen Nickels abweicht. Sie ergibt sich bei allen Diagrammen zu 3.587 Å (bzw. in unbeträchtlicher Abweichung zu 3.587 Å) gegen 3.525 Å für reines Nickel. Für Gamma-Eisen bei Zimmertemperatur wird als Gitterkonstante 3.567 Å angegeben, woraus folgt, dass das Eisen in dieser Phase mehr Raum beansprucht als Nickel. Die gefundene Aufweitung deutet also darauf hin, dass ein Teil des Eisens auch in flächenzentrierter Phase vorliegt. Damit erklärt sich das Erscheinen von Nickel-Linien nach dem Sintern des 10% Nickel enthaltenden Katalysators als eine Ausscheidung der kubisch-flächenzentrierten Eisen-Nickel-Phase beim Sintern. Die beobachtete zusätzliche Aufweitung des Eisen-Gitters beim Sintern ist dann allerdings nicht erklärlich. Jedoch liegt diese Aufweitung innerhalb der Fehlergrenze.

Machen die vorliegenden Befunde bereits wahrscheinlich, dass in der oxidischen Phase Mischkristalle zwischen $NiFe_3O_4$ und Fe_3O_4 vorlagen, so wird dies durch die Röntgenogramme der oxidischen Katalysatoren bestätigt. Die Literaturwerte für $NiFe_2O_4$ und Fe_3O_4 sind 8.377 bzw. 8.407 Å. Unsere Messungen ergaben für den 10% Nickel enthaltenden oxidischen Katalysator 8.384 Å, für den mit 20% Nickel 8.382 und 8.386 Å (aus zwei verschiedenen Diagrammen) und für den mit

1) R. Brill und S. Tauster, *Ber. d. Bunsen Ges. f. phys. Chemie,* **67**, 390 (1963).
2) A. Ozaki, H. S. Taylor und M. Boudart, *Proc. Roy. Soc.,* **258**, 47 (1960).
3) R. E. Cech, *J. Metals, N. Y.,* **8**, 585 (1956).

30% Nickel 8.373 Å. Der letztere kommt der Zusammensetzung des reinen Spinells $NiFe_2O_4$ mit 34.4% Nickel sehr nahe.

Die röntgenographischen Untersuchungen zeigen also, dass im Falle des Nickels zwar die Verteilung dieses Elements im Eisen durch Mischkristallbildung in der Oxidphase bewirkt wird, dass jedoch eine Entmischung im festen Zustand stattfindet, wobei sich ein Teil des Nickel in Form der wahrscheinlich mit Eisen gesättigten Gamma-Phase ausscheidet. Die Vergleichsaufnahme einer mechanischen Mischung von Carbonyleisenpulver mit Carbonylnickelpulver im Verhältnis 70 : 30 zeigt, dass der grösste Teil des Nickels mit Eisen legiert ist und (im Falle des 30% Nickel enthaltenden Katalysators) nur ein kleiner Teil (höchstens 10%) in Form der Gamma-Phase vorliegt.

Der Versuch, Chrom in gleicher Weise in Eisen einzubauen wie Nickel scheitert an der Tatsache, dass der Spinell Cr_2FeO_4 unter unseren Versuchsbedingungen nicht reduziert wird. Dementsprechend treten in den Diagrammen reduzierter Katalysatoren die Linien dieses Spinells auf. Desgleichen besitzen die mit Chrom-Zusatz hergestellten Katalysatoren eine etwa 10 mal so grosse Oberfläche wie die aus reinem Eisen oder Eisen-Nickel-Legierungen bestehenden. Der Grund dafür liegt darin, dass sich der unreduzierte Spinell in sehr feinverteilter Form während der Reduktion zwischen den Eisenkristalliten ausscheidet und so die Bildung grosser Kriställchen hindert. Genau der gleiche Effekt wird bekanntlich durch den Zusatz von Al_2O_3 bewirkt. Ein kleiner Teil des Chroms könnte indessen im Eisen nach der Reduktion vorhanden sein, weil die Gitterkonstante des Eisens bei einem mit 5% hergestellten Katalysator ein wenig vergrössert ist (2,869 Å).

In gleicher Weise war der Einbau von Kupfer in Eisen in Form einer Legierung röntgenographisch nicht nachweisbar. In oxidischer Form zeigte der Katalysator die Linien des Fe_3O_4 und neben diesen noch andere, die vermutlich von $CuFe_2O_4$ herrühren. Im reduzierten Zustand erschienen bei Zumischung von 20% Kupfer die Linien des Eisens mit normaler Gitterkonstanten und daneben die des Kupfer gleichfalls mit normaler Gitterkonstanten. Da im System Eisen-Kupfer eine Mischungslücke existiert und nur bis etwa 6% Kupfer vom Eisen aufgenommen werden, könnte die durch Bildung dieser Legierung verursachte Vergrösserung der Gitterkonstanten noch gerade im Bereich unserer Fehlergrenze liegen. Jodoch treten bei einem 5% Kupfer enthaltenden Katalysator immer noch die Linien des Kupfer mit normaler Gitterkonstanten auf, so dass im Höchstfalle nur ein sehr geringer Teil des Kupfer mit Eisen legiert vorliegen könnte.

(2) Kinetik.—Die Geschwindigkeitskonstanten der Ammoniak-Synthese wurden mittels der Gleichung:

$$k = \frac{1}{t} \cdot \frac{p_{NH_3,gl}}{p_{N_2}} \times \left\{ \frac{1+a^2}{2} \ln \frac{1+x}{1-x} - a \ln(1-x^2) - a^2 x \right\}$$

ermittelt.[4] Hier ist $p_{NH_3,gl}$, der Gleichgewichtspartialdruck des NH_3, $x = p_{NH_3}/p_{NH_3,gl}$ und a eine temperaturabhängige Konstante, die ausserdem vom Gleichgewichtsdruck des Ammoniaks und vom Partialdruck des Wasserstoffes abhängt. Der letztere kann aber hier, ebenso wie der Stickstoffpartialdruck p_{N_2}, als konstant angesehen werden, weil die Ammoniak-Ausbeuten immer sehr klein waren.

Die Versuchstemperaturen lagen zwischen 225 und 350°C. Die aus der Temperaturabhängigkeit der Geschwindigkeitskonstanten gefundenen Aktivierungsenergien sind in der nachstehenden Tabelle II angeführt.

Tabelle II. Aktivierungsenergien der untersuchten Legierungskatalysatoren

Zusammensetzung des Katalysators	Aktivierungsenergie kcal		Oberfläche m^2/g des Katalysators
	Methode I	Methode II	
Reines Eisen	24.6	23.0	1.55
Eisen + 4% Al_2O_3	22.3 23.2	— —	— 28.2
Fe + 0.1% Ni	—	23.9	—
Fe + 1% Ni	23.9	26.3	—
Fe + 5% Ni	23.5	20.5	1.38
Fe + 10% Ni	17.1	—	—
Fe + 30% Ni	17.5	—	2.3
Fe + 0.1% Cr	—	22.3	—
Fe + 1% Cr	—	18.0	13.5
Fe + 5% Cr	23.4 24.2	21.1	13.5
Fe + 0.1% Cu	—	24.3	—
Fe + 1% Cu	—	19.9	—

Die Messwerte nach Methode I sind die zuverlässigeren. Eine Beeinflussung der Aktivierungsenergie ist nur beim Zusatz von Nickel mit hinreichender Sicherheit zu beobachten und dort auch nur bei den höheren Konzentrationen. Man könnte denken, dass die gefundene Erniedrigung mit dem Auftreten der Gamma-Phase bei diesen Zusammensetzungen verknüpft ist, weil der Frequenzfaktor der Arrhenius-Gleichung bei diesen Katalysatoren um einen Faktor von fast 10^3 kleiner ist. Die Ausbeuten, die mit diesen Katalysatoren erreicht werden, waren daher nicht grösser, als die von niedriger legierten oder unlegierten Kontakten (S. Tabelle III).

4) R. Brill und S. Tauster (1. c.), sowie R. Krabetz und Cl. Peters, *Ber. Bunsen Ges.*, **67**, 381 (1963).

Tablle III Verhältnis der Bildungsgeschwindigkeiten von Ammoniak an dem 30% Nickel enthaltenden zu dem 5% Nickel enthaltenden Katalysator pro Oberflächeneinheit unter gleichen Bedingungen für verschiedene Temperaturen

Temp., °C	Verhältnis der Bildungsgeschwindigkeit
200	1.02
300	0.38
400	0.18

Jedoch müsste dann zusätzlich angenommen werden, dass die Alpha-Phase in diesem Falle inaktiv ist. Einen gewissen Hinweis auf die zunehmende Desaktivierung der Alpha-Phase mit zunehmendem Nickel-Gehalt zeigen allerdings die Frequenzfaktoren der Arrhenius-Gleichung, die mit zunehmendem Nickel-Gehalt abnehmen, wie Tabelle IV zeigt:

Tabelle IV. Aktivierungsenergie und Frequenzfaktor von Eisen-Nickel-Katalysatoren im Vergeich zum Eisen

Katalysator	Aktivierungsenergie	Frequenzfaktor
Fe	24.6	2.4×10^{8}
Fe Ni (1%)	23.9	7.8×10^{7}
Fe Ni (5%)	23.5	3.8×10^{7}
Fe Ni (10%)	17.1	0.9×10^{5}
Fe Ni (30%)	17.5	1.3×10^{5}

Die Tabelle zeigt weiterhin, dass der Frequenzfaktor bei den hohen Nickel-Gehalten (10 und 30%) mit zunehmender Menge der Gamma-Phase wieder zunimmt. Eine endgültige Entscheidung können erst weitere Versuche ergeben.

BULLETIN OF THE CHEMICAL SOCIETY OF JAPAN VOL. 39 1681—1683 (1966)

The Dipole Moments of the Oligomer of Ethylenediamine

By Ko KIMURA, Yoshio TOSHIYASU and Ryoichi FUJISHIRO

Department of Chemistry, Faculty of Science, Osaka City University, Sumiyoshi-ku, Osaka

(Received November 29, 1965)

The dipole moments of ethylenediamine ($N=1$), diethylenetriamine ($N=2$), triethylenetetramine ($N=3$), and tetraethylenepentamine ($N=4$) were measured in a benzene solution at 25°C and 45°C. The observed dipole moments of $N=1$, $N=2$, $N=3$, and $N=4$ are 1.89 D, 2.22 D, 2.37 D, and 2.56 D respectively at 25°C, and 1.84 D, 2.22 D, 2.36 D, and 2.58 D respectively at 45°C. The dipole moments were theoretically calculated on the assumptions that; (i) the dipole moments of these chain molecules are given by the vector sum of the dipole moments of the polar groups of amine, and (ii) all internal rotations about single bonds are free. The calculated values of $N=1$, $N=2$, $N=3$, and $N=4$ are 1.84 D, 2.15 D, 2.43 D, and 2.68 D respectively. The agreement between the observed values and the calculated values is satisfactory. It may, therefore, be expected that the molecular chains will be in the random coil state. The intramolecular hydrogen-bonding is very weak, as there is no temperature dependence of the observed dipole moments.

The study of the electric dipole moments of the oligomer of ethylenediamine in solutions is important from the point of view of thermodynamic property of solutions as well as from that of the molecular structure. The dipole moments of oligomers such as those of ethylene glycol and oxymethylene have been measured and discussed by some authors[1] in terms of their molecular structures. This paper will present a similar study of the dipole moments of ethylenediamine, diethylenetriamine, triethylenetetramine, and tetraethylenepentamine in a benzene solution, and will give some information about the molecular configurations in solutions. Unfortunately, this oligomer is not dissolved in any nonpolar solvent other than benzene. The temperature dependence of dipole moments will be discussed in connection with the intramolecular hydrogen bond.

Experimental

The oligomer (a product of the Tokyo Kasei Chemicals Co., Ltd.) was dried over fresh sodium and distilled several times under a nitrogen atmosphere. The benzene was purified by shaking it with concentrated sulfuric acid, dried over phosphorus pentoxide, and distilled through a 100-cm. column packed with stainless steel helices.

1) T. Uchida, Y. Kurita and M. Kubo, *J. Polymer Sci.*, **19**, 365 (1956); T. Uchida, Y. Kurita, N. Koizumi and M. Kubo, ibid., **21**, 313 (1956); J. Marchal and H. Benoit, ibid., **23**, 223 (1957); K. Kimura and R. Fujishiro, This Bulletin, **39**, 608 (1966).

The measurements of the dielectric constants, ε, and the specific volumes, v, were carried out with an apparatus devised by Le Fevre and his collaborators.[2]

Results

The observed values of ε and v are expressed by equations linear in solute concentrations; they and the w values (the weight fraction of solutes) are summarized in Table I. The range of w values used in the present measurements ranged up to about 0.025. Measurements were carried out at 25°C and 45°C. The calculation of the molecular polarizations, P, from these experimental data was performed according to the standard method.[3] Molecular refractions, R_D, for the sodium D line were calculated on the assumption of the additivity of bond refractions, and distortion polarizations were assumed to be equal to $1.05\times R_D$. The polarization values and the observed dipole moments, μ, are tabulated in Table II, together with the theoretically-calculated dipole moments, which will be discussed in the next section.

Discussion

The dipole moment of a chain molecule (N-mer), consisting of $(n+1)$ polar units, is given by:

$$\vec{\mu} = \sum_{i=0}^{n}\vec{\mu}_{3i} = \vec{\mu}_0 + \sum_{k=1}^{n-1}\vec{\mu}_{3k} + \vec{\mu}_{3n} \qquad (1)$$

where $\vec{\mu}_{3i}$ is the dipole moment of amine, and the suffix "$3i$" indicates the location of a dipole in the chain schematically shown in Fig. 1. The

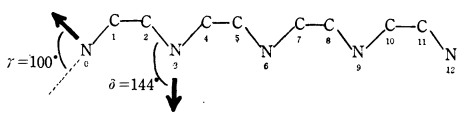

Fig. 1. Numbering of a chain of tetraethylenepentamine.

end groups of $\vec{\mu}_0$ and $\vec{\mu}_{3n}$ are primary amine. Its group moment is assumed to be 1.30 D.[4] This moment lies in the bisecting plane of the H–N–H valence angle, and it is directed along an arrow which makes an obtuse angle, $\gamma=100°$, with the $\vec{CN}$ bond, as is shown in Fig. 1. In the middle part of a chain, there is secondary amine. Its group moment is assumed to be 1.10 D.[4] This moment lies in the bisecting plane of the C–N–C valence angle, and it is directed along an arrow which makes obtuse angles, $\delta=144°$ with the $\vec{NC}$ bond and $\delta=146°$ with the $\vec{NH}$ bond of secondary amine, as is also shown in Fig. 1. The average value of μ^2 over all the angles of internal rotation is given by:

$$\overline{\mu^2} = \mu_0^2 + \sum_{k=1}^{n-1}\mu_{3k}^2 + \mu_{3n}^2 + 2(\overline{\vec{\mu}_0\cdot\vec{\mu}_{3n}}) + 2\sum_{k=1}^{n-1}(\overline{\vec{\mu}_0\cdot\vec{\mu}_{3k}}) + 2\sum_{k=1}^{n-1}(\overline{\vec{\mu}_{3k}\cdot\vec{\mu}_{3n}}) + 2\sum_{\substack{k,k'=1\\k<k'}}^{n-1}(\overline{\vec{\mu}_{3k}\cdot\vec{\mu}_{3k'}}). \qquad (2)$$

In order to calculate the fourth term in the right hand side of Eq. 2, two vectors, $\vec{\mu}_0$ and $\vec{\mu}_{3n}$ must be expressed with reference to the same coordinate system. This procedure has been used by many authors.[5] The x axis is chosen in the direction of each bond axis of a chain. For example, the coordinate system (x_2, y_2, z_2) of the C_2 origin is fixed as follows: the x_2 axis is taken in the direction of the $\vec{C_2N_3}$ vector, the z_2 axis is directed along the

Table I. Observed values of ε and v expressed by linear equations of w

	25°C	45°C
$N=1$	$\varepsilon=2.2725+6.33\,w$	$\varepsilon=2.2331+5.64\,w$
	$v=1.14490+0.014\,w$	$v=1.17302+0.004\,w$
$N=2$	$\varepsilon=2.2725+5.16\,w$	$\varepsilon=2.2331+4.67\,w$
	$v=1.14490-0.068\,w$	$v=1.17293-0.088\,w$
$N=3$	$\varepsilon=2.2725+4.24\,w$	$\varepsilon=2.2331+3.76\,w$
	$v=1.14502-0.119\,w$	$v=1.17275-0.126\,w$
$N=4$	$\varepsilon=2.2725+3.84\,w$	$\varepsilon=2.2331+3.55\,w$
	$v=1.14500-0.133\,w$	$v=1.17295-0.147\,w$

Table II. Polarization values and dipole moments

		25°C	45°C	The theoretically calculated dipole moment
$N=1$	p_∞*	1.536 cc.	1.392	
	P	92.31 cc.	83.67	
	$1.05\times R_D$	19.10 cc.		
	μ	1.89 D	1.84	1.84
$N=2$	p_∞	1.291	1.234	
	P	133.19	127.29	
	$1.05\times R_D$	32.66		
	μ	2.22	2.22	2.15
$N=3$	p_∞	1.103	1.044	
	P	161.28	152.62	
	$1.05\times R_D$	46.22		
	μ	2.37	2.36	2.43
$N=4$	p_∞	1.024	0.996	
	P	193.82	188.46	
	$1.05\times R_D$	59.77		
	μ	2.56	2.58	2.68

* p stands for the specific polarization.

2) R. J. W. Le Fevre, I. G. Ross and B. M. Smythe, *J. Chem. Soc.*, **1950**, 276.
3) I. F. Halverstadt and W. D. Kumler, *J. Am. Chem. Soc.*, **64**, 2988 (1942).
4) C. P. Smythe, "Dielectric Behavior and Structure," McGraw Hill, New York (1955), pp. 253, 311.
5) S. Oka, *Proc. Phys. Math. Soc. Japan*, **24**, 657 (1942); J. Marchal and H. Benoit, *J. Chim. Phys.*, **52**, 818 (1955); M. V. Volkenstein, "Configurational Statistics of Polymer Chains," Interscience Publishers, New York (1963).

vector product of $\overrightarrow{C_2N_3}$ and $\overrightarrow{C_1C_2}$, and the y_2 axis is determined by the x_2 axis and z_2 axis in order that the three axes may constitute a right-handed coordinate system. The same procedure is taken for the coordinate system (x_1, y_1, z_1) of the C_1 origin. The transformation of (x_2, y_2, z_2) to (x_1, y_1, z_1) is easily carried out by the help of the following transformation matrix, $\boldsymbol{T}_{12}$:

$$\boldsymbol{T}_{12} = \begin{pmatrix} \cos\omega & \sin\omega & 0 \\ -\sin\omega\cos\varphi_1 & \cos\omega\cos\varphi_1 & -\sin\varphi_1 \\ -\sin\omega\sin\varphi_1 & \cos\omega\sin\varphi_1 & \cos\varphi_1 \end{pmatrix}$$

where the valence angles $(\pi-\omega)$ are assumed to be tetrahedral about nitrogen atoms of amine as well as carbon atoms, and where φ_1 is an angle of the internal rotation about the C_1—C_2 bond (or an angle between the z_1 axis and the z_2 axis). Then the transformation of (x_2, y_2, z_2) to (x_0, y_0, z_0) is performed by the successive operation of $\boldsymbol{T}_{01}$ on $\boldsymbol{T}_{12}$. For example, the two vectors of $\vec{\mu}_0$ and $\vec{\mu}_3$ for $N=1$ are thus represented by the (x_0, y_0, z_0) coordinate system. If all the internal rotations are free, the average value of the scalar product $(\vec{\mu}_0\cdot\vec{\mu}_3)$ becomes independent of both φ_0 and φ_1, and is given by:

$$\cos^2\omega\cos^2\gamma\,\mu_0\mu_3 \qquad (4)$$

for $N=1$. The same procedure is applied to $N\geqq 2$. The calculated result may be summarized as follows:

$$\overline{\mu^2} = 2\mu^2_p(1-\xi^2\lambda^2) \quad \text{for} \quad N=1,$$

$$\overline{\mu^2} = 2\mu^2_p(1-\xi^2\lambda^5)+\mu^2_s+2\mu_p\mu_s\xi\eta(\lambda^2-\lambda^3) \quad \text{for} \quad N=2,$$

$$\overline{\mu^2} = 2\mu^2_p(1-\xi^2\lambda^{3N-1}) + \mu^2_s\left[N-1+\frac{2\eta^2\lambda^3}{1-\lambda^3}\left\{N-2-\frac{\lambda^3(1-\lambda^{3N-6})}{1-\lambda^3}\right\}\right] + 2\mu_p\mu_s\xi\eta(\lambda^2-\lambda^3)\frac{1-\lambda^{3N-3}}{1-\lambda^3} \quad \text{for} \quad N\geqq 3, \qquad (5)$$

where μ_p and μ_s are 1.30 D and 1.10 D respectively, and λ, ξ, and η are $\cos\omega$, $\cos\gamma$, and $\cos\delta$ respectively. The calculated dipole moments for $N=1$, $N=2$, $N=3$, and $N=4$ are 1.84 D, 2.15 D, 2.43 D, and 2.68 D respectively. The agreement between the calculated dipole moments and the observed ones is satisfactory in view of the model used in the above calculation. Strictly speaking, the effect of the excluded volume on dipole moments must be taken into consideration, but this effect may make only a minor contribution to dipole moments for such short chains as those considered here. It may, therefore, be inferred that the oligomer of ethylenediamine in a benzene solution is in the random coil state. This is also supported by the fact that the observed dipole moments do not show any temperature dependence. This suggests that the intramolecular hydrogen-bonding is very weak or that it does not occur at all in this case.

BULLETIN OF THE CHEMICAL SOCIETY OF JAPAN VOL. 39 1683—1689 (1966)

The Catalytic Hydrogen Exchange of Aniline on Supported Metal Catalysts[1)]

By Hiroshi HAGIWARA* and Etsuro ECHIGOYA

Research Laboratory of Resources Utilization, Tokyo Institute of Technology, Ookayama, Meguro-ku, Tokyo

(Received December 7, 1965)

The hydrogen exchange reaction of aniline with deuterium was investigated on supported nickel, cobalt and platinum. The following results were obtained: 1) At 150°C, the hydrogen of the amino group of aniline exchanges at a higher velocity than the hydrogen attached to the benzene ring. At temperatures as high as 300°C, the hydrogen exchange in the benzene ring increases further. 2) The suggested hydrogenation mechanism obtained from the results of the exchange reaction can not be correlated with that obtained from the kinetic study. 3) The catalytic activity for the exchange reaction in the benzene ring is in the order Pt>Co>Ni. 4) The basic oxide support seems to suppress the adsorption of the amino group. 5) The relationship between the adsorption state of the aniline on the catalyst surface and the various reaction products, such as cyclohexylamine, benzene and dicyclohexylamine, has been well established.

*1 Present address: Yoshitomi Pharmaceutical Co. Ltd., Yoshitomi, Fukuoka

1) Presented in part at the 17th Discussion Meeting on Catalysis of the Catalysis Society of Japan, Tokyo, October, 1965.

In experiments previously reported by the present authors,[2] it was observed that the hydrogenation of aniline to cyclohexylamine and to the secondary amines occurred in the temperature range from 150 to 250°C while the fission of the carbon-nitrogen bond (the hydrogenolysis) of aniline took place at temperatures above 250°C.

In order to understand this change in reactivity, it would be useful to know the adsorption state of the aniline molecule on the metal catalysts. Many reports have been published with respect to the metal-catalyzed exchange between aniline and deuterium oxide,[3-5] but few regarding the relationship between reactivities and the adsorption state. The aim of the present experiments was to investigate the catalytic activity of various kinds of catalyst in the hydrogen exchange reaction of aniline with deuterium, and then to deduce the relationship between reactivities and the adsorption state.

Experimental

Material.—Deuterium oxide obtained from the Showa Denko Co. (99.75% D_2O) was used without any additional purification. Deuterium was obtained from the electrolysis of deuterium oxide containing 20% sodium deuteroxide. The electrode was a nickel plate (see Fig. 1). Aniline (technical grade) was shaken with zinc powder and then purified by fractional distillation. The catalysts were prepared by the impregnation method.[6] Powdered support was added to a solution of metal nitrate. The slurry was stirred for some time, and then to it there was slowly added, at 20°C, a water solution of ammonium carbonate in a slight excess. After the precipitate had been filtered and washed, it was dried at 100°C and then calcined at 450°C for 2 hr.

Procedure.—*The Experimental Method of the Hydrogenation of Aniline and Benzene.*—The hydrogenation experiments were perforemed in a fixed-bed apparatus of the flow type. The products were analyzed by gas chromatography.

The Experimental Method of the Hydrogen Exchange of Aniline with Deuterium Oxide.—The metal catalyst was reduced by hydrogen inside the reaction tube, into which aniline and deuterium oxide were then introduced by distillation from their respective vessels.[7] The tube was kept at the reaction temperature in a thermostatic bath. After the reaction, both aniline and deuterium oxide were separated from the catalyst by distillation, and condensed in a cold trap. The aniline layer was treated with an amount of water about 20 times its volume in order to transform all the N-D bonds to N-H bonds. The aniline layer was then extracted with benzene, and the mixture of benzene and aniline was dehydrated by anhydrous sodium sulfate and separated by the gas chromatographic technique.

The Experimental Method of the Hydrogen Exchange of Aniline with Deuterium.—Figure 1 shows the flow diagram.[8] A mixture of aniline vapor and deuterium was introduced into a fixed-bed reactor. The reaction temperature was maintained by external electric heating. The gaseous products leaving the reaction zone were caught in a dry ice-and-methanol-cooled trap, from which condensates were drawn for the gas chromatographic analysis. The oxide catalysts were placed in the same fixed-bed apparatus used for the reaction, and reduced to the metal by a flow of hydrogen at the rate of 50 cc./min.* After the reduction procedure, the catalyst was cooled in a deuterium stream to the reaction temperature, and then a run of the hydrogenation of aniline with deuterium was carried out.

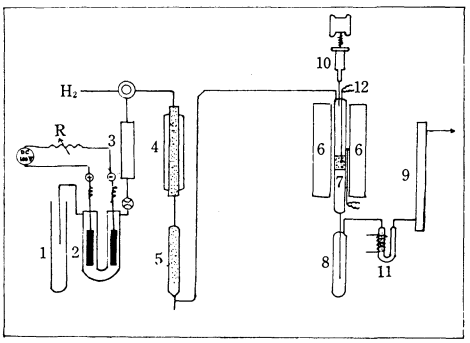

Fig. 1. Flow diagram.

1 Water head vessel for gas pressure regulation
2 Apparatus for electrolysis of deuterium oxide
3 Calcium chloride drying tube for D_2
4 Oxygen eliminator
5 Silica gel drying tube for D_2
6 Heater
7 Catalyst bed
8 Cold trap for gaseous products
9 Soap film meter for gas flow measuring
10 Aniline feeder
11 Nickel-kieselguhr catalyst
12 Thermometer

The Analysis of the Products.—The infrared, mass-spectroscopic and NMR methods were used. In addition, in order to determine the distribution of the deuterium in the aromatic nucleus, the aniline hydrobromide and the brominated derivatives of aniline (*p*-bromoacetanilide and 2, 4, 6-tribromoaniline) were prepared, and the percent-distribution of deuterium in the ring was determined by the calculation of the

2) H. Hagiwara and E. Echigoya, *Shokubai (Catalyst)*, **6**, 35 (1964).
3) W. A. Sollich and J. L. Garnett, *Aus. J. Chem.*, **14**, 56 (1961).
4) R. A. Ashby and J. L. Garnett, ibid., **16**, 549 (1963).
5) C. G. MacDonald and J. S. Shannon, *Tetrahedron Letters*, **45**, 3351 (1964).
6) H. Hagiwara, E. Kojima and E. Echigoya, This Bulletin, **39**, 1800 (1966).
7) K. Hirota, K. Kuwata and T. Ueda. *J. Chem. Soc. Japan, Pure Chem. Sect. (Nippon Kagaku Zasshi)*, **81**, 362 (1960).
8) A. Ozaki, F. Nozaki, Y. Kawasaki and K. Morikawa, *Shokubai (Catalyst)*, **3**, 138 (1961).

* Nickel and cobalt catalysts were reduced at 450°C for 2 hr.; the platinum catalyst was reduced at 300°C for 3 hr.

peak height at 2260 cm^{-1}** in the infrared spectra for each derivative. The estimation method was as follows:

$$D_{meta} = \frac{\text{peak height of the 2, 4, 6-tribromoaniline}}{\text{peak height of the aniline hydrobromide}} \times 100$$

$$D_{para} = \frac{\left(\text{peak height of the } p\text{-bromoacetanilide} - \text{peak height of 2, 4, 6-tribromoaniline}\right)}{\text{peak height of the aniline hydrobromide}} \times 100$$

Results

The Catalyst Activity in the Hydrogenation of Aniline and Benzene.—The results of the activity test for the hydrogenation reaction are presented in Figs. 2, 3 and 4.

From these data, it can be concluded that:

1) For the nickel-magnesia catalyst, the hydrogenation reaction occurred above 120°C. for aniline, while benzene was hydrogenated at lower temperatures.

2) The platinum catalyst showed the same tendency in acting in the hydrogenation of aniline and benzene. With both catalysts, under the same reaction conditions, the rate of the hydrogenation of benzene was higher than that of the hydrogenation of aniline.

3) The hydrogenation of benzene on nickel or on the platinum catalyst was inhibited by the presence of aniline or cyclohexylamine.

4) The hydrogenolysis of cyclohexylamine on the platinum catalyst yielded benzene rather than cyclohexane at 170—200°C.

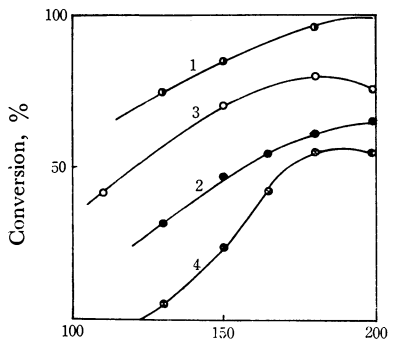

Fig. 2. The activity of Pt-Al_2O_3 and Ni-MgO for the hydrogenation of aniline and benzene.
1% Pt-Al_2O_3: 1, Benzene → Cyclohexane
2, Aniline → Cyclohexylamine
30% Ni-MgO: 3, Benzene → Cyclohexane
4, Aniline → Cyclohexylamine
Reaction conditions:
H_2/aniline feed mole ratio=10
$SV \approx 1100\ hr^{-1}$ (N. T. P.)

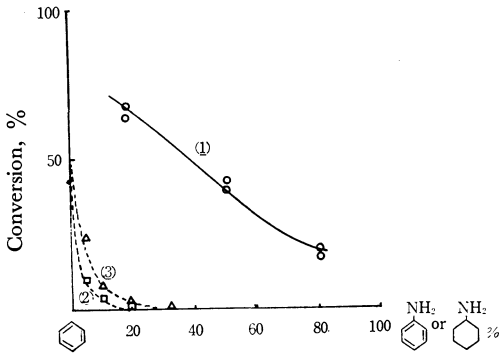

Mol % of aniline or cyclohexylamine

Fig. 3. The effect of aniline and cyclohexylamine on the hydrogenation of benzene over nickel-magnesia.
1 Aniline → Cyclohexylamine (Reactants: aniline+benzene)
2 Benzene → Cyclohexane (Reactants: aniline +benzene)
3 Benzene → Cyclohexane (Reactants: cyclohexylamine+benzene)
Reaction conditions:
180°C H_2/liquid mole ratio≈5
$SV \approx 1000\ hr^{-1}$ (N. T. P.)

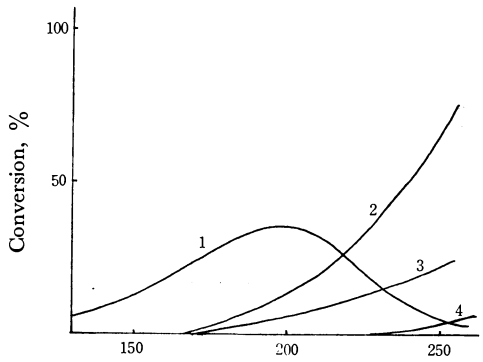

→ Reaction temp., °C

Fig. 4. The activity of Pt-Al_2O_3 for the decomposition of cyclohexylamine.
1 Yield of dicyclohexylamine
2 Yield of benzene
3 Yield of cyclohexane
4 Yield of aniline
Reaction conditions: H_2/Cyclohexylamine feed mole ratio=10
$S_v \approx 1000\ hr^{-1}$ (N. T. P.)

The Exchange Reaction of Aniline with Deuterium Oxide.—The results are shown in Table I. Examples of the NMR spectra and of the infrared spectra of the reaction products are shown in Figs. 5, 6 and 7. The data show that a little hydrogen-deuterium exchange occurs without the catalysts. It will be also evident

** With deuterium, a new band appeared at 2260 cm^{-1} due to the C–D stretching vibration in the ring.

Table I. Exchange reaction of aniline with deuterium oxide

Reaction conditions: Temp., 110—100°C; Residence time, 15 hr.;
Vessel volume, 20 cc.; Catalyst weight, 8 g.; Reactants (aniline 1 cc., D_2O 2 cc.)

Exp. No.	Catalyst	$\frac{D}{D+H}$ for the reacted sample	Number of Deuterium atoms per aromatic nucleus	Percent distribution of deuterium		
				ortho	meta	para
D_2O-6	20-Ni-Al_2O_3	0.39	2.73	70	=0	30
D_2O-7	20-Co-Al_2O_3	0.46	3.22	55	20	25
D_2O-9	1-Pt-Al_2O_3	0.62	4.4	45	20	35
D_2O-4	Without catalyst	0.075	0.5			

Table II. Exchange reaction of aniline with deuterium

Reaction condition: Catalyst weight 0.4 g. (1—0.5 cc.)
Feed: Molar ratio of D_2/aniline≈5
Space velocity: 1200—500 (N. T. P.) hr^{-1}

Exp. No.	React. temp. °C	Catalyst	Conversion of aniline				Deuterium distribution into the reacted aniline								$\frac{D_{amino}}{D_{total}}$**	Φ_D%*
			Aniline conver.	Yield of cyclohexyl-amine	Yield of dicyclo-hexylamine	Yield of benzene	d_0	d_1	d_2	d_3	d_4	d_5	d_6	d_7		
D-3	150	20-Ni-Al_2O_3	17	8	3.5		58	32.2	8.6	1.2					0.94	7.6
D-9	150	30-Ni-MgO	21	18	1.0		46.2	40.3	10.4	2.6	0.5				0.90	10.1
D-11	150	20-Co-Al_2O_3	15	12	0.8		50.0	37.2	10.1	2.4	0.3				0.83	9.4
D-5	150	1-Pt-Al_2O_3	45	15	12		67.9	20.9	9.5	2.1	0.5				0.77	6.75
D-14	150	Alumina	0	0	0											
D-21	300	20-Ni-Al_2O_3	7	—		6	36.0	42.1	17.5	3.6	0.8				0.79	13.0
D-23	300	30-Ni-MgO	21	—		17	22.3	38.4	27.0	9.4	2.5	0.4			0.73	19.0
D-27	300	20-Co-Al_2O_3	15	—		12	26.9	35.6	27.1	7.5	2.4	0.5			0.66	17.8
D-15	300	1-Pt-Al_2O_3	32	2		26	44.8	34.0	14.1	6.0	1.1				0.50	12.1
D-19	300	Alumina	0.5	≈0		0	98	2								0.3

* $\Phi_D = \frac{1}{7}\sum_{i=1}^{7} i d_i$ (Average deuterium content %)

** Both fractions of N-D and C-D were determined by the IR absorption height compared to that of standard samples and by the mass spectrum analysis.

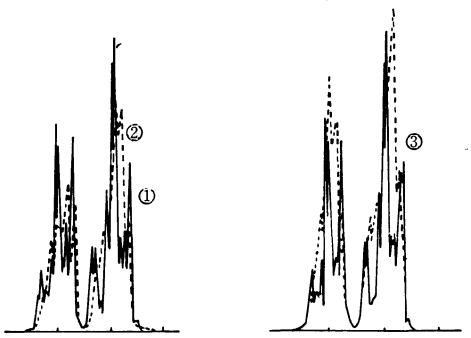

Fig. 5. NMR spectra for the reacted aniline.
1 Normal aniline (full line)
2 Deuterated aniline on Ni catalyst (No. D_2O-6) (dotted line)
3 Deuterated aniline on Pt catalyst (No. D_2O-9) (dotted line)

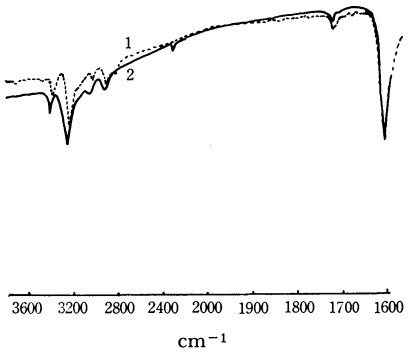

Fig. 6. IR spectra for 2,4,6-Tribromoaniline.
1 Normal aniline (dotted line)
2 Deuterated aniline on Ni-catalyst (No. D_2O-6) (full line)
KBr disc: NaCl prism

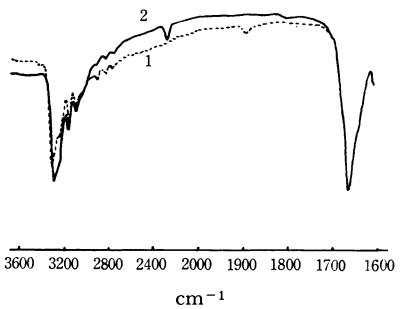

Fig. 7. IR-spectra for 4-bromoacetanilid.
1 Normal aniline (dotted line)
2 Deuterated aniline by Pt-catalyst (No. D_2O-9) (full line)

from an examination of Table I that the hydrogen atoms at the ortho and para positions of the benzene ring of aniline are catalytically exchanged by nickel, while over platinum, the exchange occurs in the ortho, para and meta positions. The existence

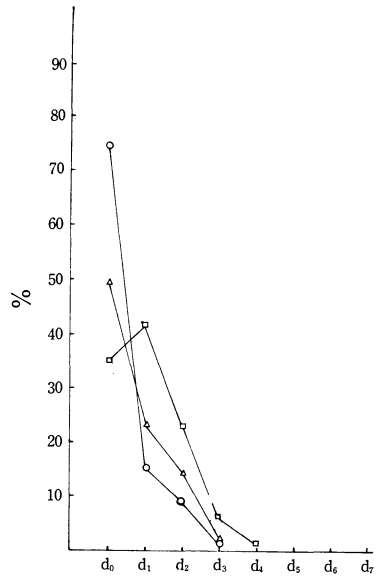

Fig. 8. Deuterium distribution in the exchange reaction of aniline with the deuterium at 300°C on $Ni\text{-}Al_2O_3$ at different space velocities.
D_2/aniline feed mole ratio≈5
○ SV 15000 hr^{-1} △ SV 7000 hr^{-1}
□ 700

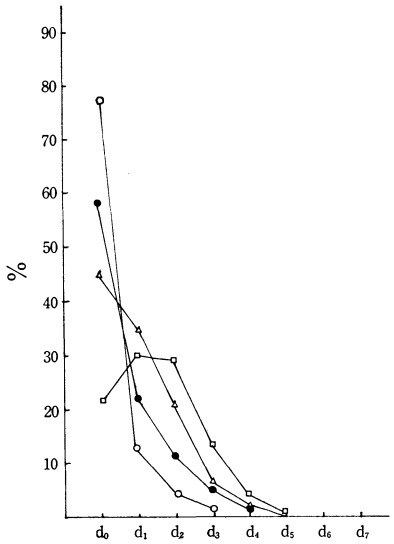

Fig. 9. Deuterium distribution in the exchange reaction of aniline with deuterium at 300°C on $Pt\text{-}Al_2O_3$ at different space velocities.
D_2/aniline feed mole ratio≈5
○ SV 20000 hr^{-1} ● SV 10000 hr^{-1}
△ 1800 □ 600

of highly-deuterated aniline in the case of the platinum catalyst indicates that all the hydrogen molecules in aniline are exchangable.

The Exchange Reaction of Aniline with Deuterium.—The data on the activities of all the catalysts used are summarized in Table II. From Table II, the following conclusions may be drawn:

1) At 150°C, the exchange in the amino group predomoninated in the deuteration of aniline. These results can perhaps be accounted for by assuming that the aniline molecule is anchored to the catalyst through the electron pair of the nitrogen.

2) At 300°C, the amount of the exchange of hydrogen-deuterium had further progressed, and the d_3- and d_4- species increased in proportion. At temperatures as high at 300°C, the exchange in the benzene ring of aniline was found to occur at the ortho, para and meta positions.

3) The difference in the catalytic activities of nickel, cobalt and platinum were shown by the amounts of d_3- and d_4-species produced. The order of d_3- and d_4-species production capacity was platinum>cobalt>nickel (see also Figs. 8 and 9).

4) No definite difference in activity between nickel-magnesia and nickel-alumina catalysts was observed. However, the proportion of the d_3- and d_4-species increased when nickel-magnesia was used.

Discussion

In order to discuss the adsorption state of aniline on the surface of the catalyst on the basis of the experimental results, it is neccessary to check the partial pressure of deuterium in the reaction atmosphere. An evaluation of the fraction of deuterium in the reactant gases shows that the pressure of deuterium is predominant compared with that of hydrogen; thus it may be reasonable to assume that all the exchange occurring takes place through the adsorption of aniline on the surface of the catalyst with deuterium under the adsorption equilibrium conditions. The results show that, at 150°C the amino group strongly interacts with the metal surface. The formation of the strong nitrogen-metal bond may be considered to play an important role in the production of secondary amines (dicyclohexylamine and phenylcyclohexylamine). The experimental results of the hydrogen exchange reaction at 150°C cannot, however, account for the ring hydrogenation of aniline established by the kinetic study: a) judging from the results obtained by the hydrogen exchange reaction, it seems that the ring-hydrogenation of aniline proceeds via a step-by-step addition of adsorbed hydrogen atoms to the benzene nucleus of the adsorbed aniline but, b) judging from the kinetic study of the hydrogenation reaction, the ring hydrogenation proceeds via the addition of adsorbed hydrogen molecules to the benzene nucleus of the adsorbed aniline. This apparent contradiction seems to indicate that the hydrogenation reaction and the hydrogen exchange reaction proceed via different courses.

At temperatures as high as 300°C, the formation of the ring-metal bond or the formation of some dehydrogenated complex such as $C_6H_xNH_y$ on the surface (for instance, $C_6H_{11}NH_2 \rightarrow C_6H_xNH_y + (13\text{-}x\text{-}y)H$) was thought to take place.

The stronger the adsorption, the smaller the $(x+y)$ value will be. Hence the fission of the C–N bond will result. According to our experiments, the basic oxide support brought about a weak adsorption of amine, this effect will probably lead to the efficient hydrogenation of the ring, as was the case in the hydrogenation of ethylene on nickel.[9] Reference should be made here to the work by Morikawa et al.,[10] who found, studying the hydrogenolysis of ethane on nickel with or without added alkali oxides, that the addition of an alkali oxide to nickel causes the suppression of the stripping of hydrogen from the hydrocarbon. In the hydrogenolysis of cyclohexylamine over platinum-alumina between 170 and 200°C, the hydrocarbon product was mostly benzene, plus a little cyclohexane. It is thought that, before decomposing, some of the adsorbed cyclohexylamine loses hydrogen atoms from the ring. Hydrogenolysis then leads to benzene. This mechanism seems reasonable from the standpoint of chemical thermodynamic calculation. That is, in the following equations, the course of Eq. 2 is important.

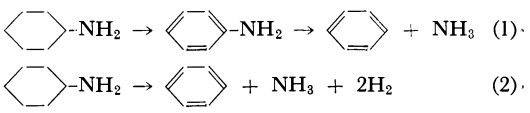

(1)

(2)

Summary

The hydrogen exchange reaction of aniline with deuterium has been investigated on the supported nickel, cobalt and platinum. The following results have been obtained:

1) At 150°C, the hydrogen of the amino group of aniline exchanges more easily than the hydrogen in the benzene ring. At temperatures as high as 300°C, the exchange in the benzene ring progresses further.

2) The suggested hydrogenation mechanism obtained from the results of the exchange reaction could not be correlated with that of the kinetic study.

3) The catalytic activity for the exchange reaction in the benzene ring was in the order platinum>cobalt>nickel.

9) S. T. Thomson and J. L. Wishlade, *Trans. Faraday Soc.*, **58**, 1170 (1962).

10) K. Morikawa, A. Ozaki and F. Nozaki, *Shokubai (Catalyst)*, **4**, 8 (1962).

4) The effect of basic oxide support seems to suppress the adsorption of the amino group.

5) The adsorption state of aniline on the catalyst surface is correlated with the variety in reactivity.

The authors wish to thank Professor Kiyoshi Morikawa for his useful discussion and guidance. Thanks are also due to Mr. Haruyoshi Sakurai for his kind assistance in the mass spectrum analyses.

BULLETIN OF THE CHEMICAL SOCIETY OF JAPAN VOL. 39 1689—1694 (1966)

Theoretical Studies of the Use of the Double Extrapolation Method to Determine the Forward Scattering of Light by Spherical Colloidal Particles

By Masayuki NAKAGAKI

Faculty of Pharmaceutical Sciences, Kyoto University, Sakyo-ku, Kyoto

(Received December 16, 1965)

An application of the double extrapolation method (the Zimm-plot method) for the reduced intensity of light scattered by colloidal dispersions, instead of polymer solutions, is discussed theoretically on the basis of the Mie theory. The correction factor, F, required to recalculate the experimental value of the molecular weight, M_R, to the true value, M ($M=FM_R$), is equal to unity in the case of the Rayleigh scattering ($\alpha\to 0$) and the Rayleigh-Gans-Debye (R-G-D) scattering ($|m-1|\to 0$, where m is the relative refractive index of the sphere to the medium). Usually, however, the value of F is not equal to unity, but is found to be given by an empirical equation, $F=1-0.155\ Q+bQ^{1.5}$, where Q is a quantity proportional to the reduced specific scattering intensity at $\theta\to 0$. For the determination of the radius of gyration from the "initial slope," the R-G-D equation is applicable even in cases where $|m-1|$ is not small. In order to determine the true molecular weight from the molecular weight, M_τ, obtained from the specific turbidity at the infinite dilution, the factor Φ is needed ($M=\Phi M_\tau$). The factor Φ is considered to be a product; that is, $\Phi=F\varphi$, where the factor φ seems to be independent of the m value. The empirical equation obtained was $\varphi=1+0.537\ \alpha^{2.08}$

In the studies of the light scattering of polymer solutions, a double extrapolation method, the so-called Zimm-plot method, is used extensively in order to determine the molecular weight, the radius of gyration, and so forth, according to the Debye theory. The method gives the molecular weight from the scattered light intensity doubly extrapolated to the forward direction ($\theta\to 0$) and to an infinite dilution ($c\to 0$). However, the application of the double extrapolation method to colloidal dispersions is justified only when the light scattering of the systems can be treated according to either the Rayleigh theory ($\alpha\to 0$) or the Rayleigh-Gans-Debye (to be abbreviated as R-G-D) theory ($|m-1|\to 0$). The method must not be applied, without corrections, to the colloidal systems for which neither $\alpha\to 0$ nor $|m-1|\to 0$ holds.

In the present paper,[1] the values of the correction factors to be used for colorless colloidal spheres are calculated according to the Mie theory, since the author believes that the application of the double extrapolation method in the studies of colloidal dispersions is useful because, first, the use of the scattered light intensity in the forward direction ($\theta\to 0$) has the theoretical advantage that maxima and minima on the curve of the scattered light intensity vs. the particle radius occur less frequently in the forward direction than in any other direction,[2] and because, second, it is convenient to use the experimental technique which is used so extensively in the studies of the polymer solutions.

Double Extrapolation Method.—The double extrapolation method is usually based on the following equation, derived by Debye[3] and modified by Zimm[4]:

$$Kc/R_u(\theta) = 1/MP(x) + 2A_2c \qquad (1)$$

where c is the concentration; $P(x)$ is the interference factor; M is the molecular weight of the polymer

1) Presented at the 18 th Annual Meeting of the Chemical Society of Japan, Kansai University, Osaka, April, 1965.

2) W. Heller, M. Nakagaki and M. L. Wallach, *J. Chem. Phys.*, **30**, 444 (1959).

3) P. Debye, *J. Appl. Phys.*, **15**, 338 (1944).

4) B. H. Zimm, *J. Chem. Phys.*, **16**, 1093 (1948).

or the colloid particle; A_2 is the second virial coefficient, and $R_u(\theta)$ is the reduced scattering intensity for unpolarized incident light;

$$R_u(\theta) = (r^2 I_u/I_0)/(1 + \cos^2\theta) \quad (2)$$

and K is a constant defined by:

$$K = (2\pi^2/N_A\lambda^4\mu_1^2)(\mathrm{d}\mu_{12}/\mathrm{d}c)^2 \quad (3)$$

Here $(r^2 I_u/I_0)$ is the Rayleigh ratio, r is the photometric distance; I_0 is the intensity of the incident light; I_u is the intensity of the scattered light at the scattering angle, θ; N_A is the Avogadro number; μ_{12} is the refractive index of the solution or dispersion, and λ is the wavelength of light in the medium, which is related to the wavelength in the vacuum, λ_0, and the refractive index of the medium, μ_1, according to the relation:

$$\lambda = \lambda_0/\mu_1 \quad (4)$$

In the double extrapolation method named the Zimm-plot method, the value of $Kc/R_u(\theta)$ is taken on the ordinate and the value of $\sin^2(\theta/2)+kc$ is taken on the abscissa, where k is an arbitrary constant. The data are extrapolated to an infinite dilution, and a curve for $c\to 0$ is drawn. This curve corresponds to the equation:

$$Kc/R_u(\theta) = 1/MP(x) \quad (5)$$

where x is defined by the equations:

$$x = 2\alpha \sin(\theta/2) \quad (6)$$

and

$$\alpha = 2\pi a/\lambda \quad (7)$$

Here, a is the radius of a spherical colloidal particle. A further extrapolation to $\theta\to 0$ yields an apparent value of molecular weight, M_R, according to the equation:

$$Kc/R_u(0) = 1/M_R \quad (8)$$

The value of M_R is, in general, not equal to the molecular weight, M. The factor F is, therefore, required in order to obtain the value of M from the value of M_R:

$$M = F \cdot M_R \quad (9)$$

If Eq. 5 is used,

$$F = 1/P(0) = MKc/R_u(0) \quad (10)$$

where $P(0)$ is the value of $P(x)$ at $x\to 0$ or $\theta\to 0$.

Theoretical Value of the Factor F.—The reduced scattering intensity for unpolarized incident light is given theoretically by the following equation:

$$R_u(\theta) = (\lambda^2/8\pi^2)Ni_T(\theta)/(1 + \cos^2\theta) \quad (11)$$

where N is the number of particles per unit of volume and where:

$$i_T(\theta) = 2i_u(\theta) = 2(4\pi^2/\lambda^2)(r^2 I_u/I_0)/N \quad (12)$$

The numerical value of $i_T(\theta)$ calculated according to the Mie theory[5] has been given by Pangonis and Heller[6] for colorless spherical particles. In order to calculate the value of K according to Eq. 3, the value of $(\mathrm{d}\mu_{12}/\mathrm{d}c)$ is required. The latter can be expressed by the equation:

$$\mathrm{d}\mu_{12}/\mathrm{d}c = (m' - 1)\mu_1/\rho_2 \quad (13)$$

where ρ_2 is the density of the particles and m' is the apparent relative refractive index. The theoretical values of m' calculated for colorless spherical particles according to the Mie theory have been given by Nakagaki and Heller.[7] Using these values, together with the equations:

$$c = (\lambda^3/6\pi^2)\rho_2 N\alpha^3 \quad (14)$$

$$M = (\lambda^3/6\pi^2)\rho_2 N_A\alpha^3 \quad (15)$$

Eq. 10 can be rewritten as:

$$F = (8/9)(m' - 1)^2\alpha^6/i_T(0) \quad (16)$$

In the case of the Rayleigh scattering,

$$F = 1 \quad (\alpha\to 0) \quad (17a)$$

is obtained from Eq. 16, because

$$i_T(0) = 2i_u(0) = 2[(m^2-1)/(m^2+2)]^2\alpha^6 \quad (17b)$$

and[7]

$$m' - 1 = (3/2)(m^2 - 1)/(m^2 + 2) \quad (17c)$$

where m is the relative refractive index of the sphere to the medium.

In the case of the R-G-D scattering, the intensity of the scattered light is equal to the Rayleigh value multiplied by $P(x)$, where:

$$P(x) = 9(\sin x - x\cos x)^2/x^6 \quad \text{(R-G-D)} \quad (18)$$

Since $P(0)=1$, the value of F given by Eq. 10 is:

$$F = 1 \quad (|m - 1| \to 0) \quad (19)$$

Therefore, the apparent molecular weight, M_R, obtained by the double extrapolation method[8] is equal to the true molecular weight, M, if either $\alpha\to 0$ or $|m-1|\to 0$ holds.

The theoretically calculated values of F for general cases ($\alpha \neq 0$ and $m \neq 1$) are shown in Fig. 1, where the quantity, Q, taken on the abscissa is a quantity proportional to the reduced specific scattering, $R_u(\theta)/c$, at $\theta\to 0$; that is:

$$Q = (8\lambda\rho_2/3)R_u(0)/c \quad (20)$$

Here the proportionality factor $(8\lambda\rho_2/3)$ is a constant for a given particle and a given wavelength. Therefore, the value of Q can be obtained

5) G. Mie, *Ann. Phys.*, (4), **25**, 377 (1908).

6) W. J. Pangonis and W. Heller, "Angular Scattering Functions for Spherical Particles," Wayne State University Press, Detroit (1960).

7) M. Nakagaki and W. Heller, *J. Appl. Phys.*, **27**, 975 (1956).

8) In the case of the random coil of high polymer molecules, it may also be concluded that $F=1$ and $M_R=M$, because $P(0)=1$ if the segments are considered to be Rayleigh spheres, where $P(x)=(2/x^4)[\exp(-x^2)-(1-x^2)]$.

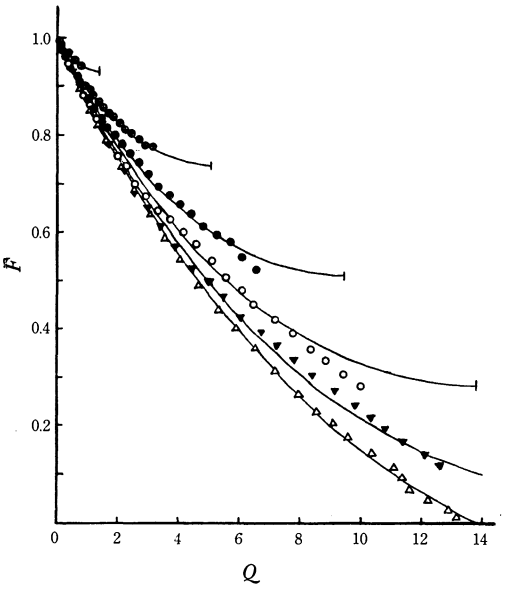

Fig. 1. Relation between F and Q.
$m=1.05$ (⊗), 1.10 (⊕), 1.15 (●), 1.20 (○), 1.25 (▼), and 1.30 (△)

experimentally. On the other hand, the theoretical value of Q is;

$$Q = i_T/\alpha^3 \tag{21}$$

It may be seen from Fig. 1 that an appreciable error will be introduced if the correction factor, F, is not used.

An empirical equation to find the value of F from the experimental value of Q was looked for. The equation obtained is:

$$F = 1 - 0.155\,Q + bQ^{1.5} \tag{22}$$

where;

$$b = 0.0115 + 0.00310(m - 1.01) \tag{23}$$

The solid lines of Fig. 1 show the values obtained from these empirical equations. The equations cannot be used, however, when Q is greater than Q^*;

$$Q^* = 0.01068/b^2 \tag{24}$$

The values of Q^* are shown in Fig. 1 by short vertical lines.

Initial Slope.—The double extrapolation method is used to determine the radius of gyration or the radius of the particles, besides the molecular weight or particle weight. In determining radius, the initial slope of the experimental curves drawn by taking $Kc/R_u(\theta)$ on the ordinate and $\sin^2(\theta/2)$ on the abscissa is used. It is, therefore, necessary to understand thoroughly what the theory will predict about the shape of the curves for spherical colloidal particles. For this purpose, a quantity, ξ, proportional to the $Kc/R_u(\theta)$ is used:

$$\xi = [Kc/R_u(\theta)]/[Kc/R_u(0)] \tag{25}$$

where $kc/R_u(0)$ is constant for a given colloidal system, as has been discussed above. On the other hand, the theoretical values of ξ can be calculated according to the relationship:

$$\xi = [i_T(0)/i_T(\theta)][(1 + \cos^2\theta)/2] \tag{26}$$

The results of the calculation are shown in Fig. 2 for $m=1.20$ and in Fig. 3 for $m=1.30$.

According to Eq. 5, it is obvious that the following equation holds:

$$\xi = P(0)/P(x) = 1/FP(x) \tag{27}$$

Therefore, in the case of the Rayleigh scattering, $\xi=1$, and in the case of the R–G–D scattering:

$$\xi = 1/P(x) = x^6/9(\sin x - x\cos x)^2 \tag{28}$$

In Figs. 2 and 3, the R-G-D values, too, are shown by the solid curves; the broken lines show the initial slope, and the dotted lines show the range of deviation from the R-G-D values. From these figures, it was concluded that the initial slope is

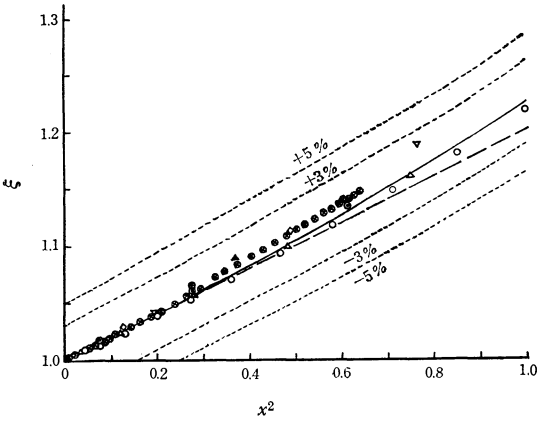

Fig. 2. Relation between ξ and x^2 for $m=1.20$.
$\alpha=0.4$ (⊗), 1.0 (○), 2.0 (△), 3.0 (⊙), 4.0 (◇), 5.0 (▽), 6.0 (⊕), and 7.0 (▲).

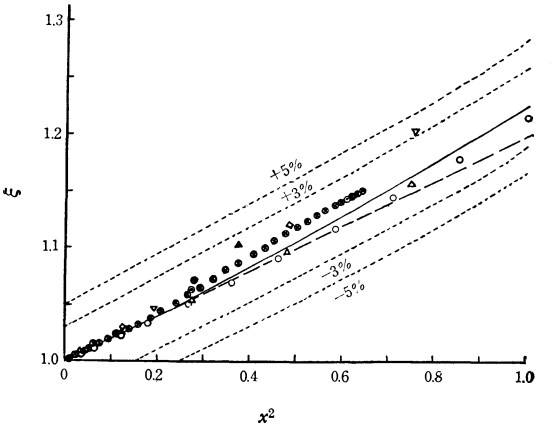

Fig. 3. Relation between ξ and x^2 for $m=1.30$.
$\alpha=0.4$ (⊗), 1.0 (○), 2.0 (△), 3.0 (⊙), 4.0 (◇), 5.0 (▽), 6.0 (⊕), and 7.0 (▲)

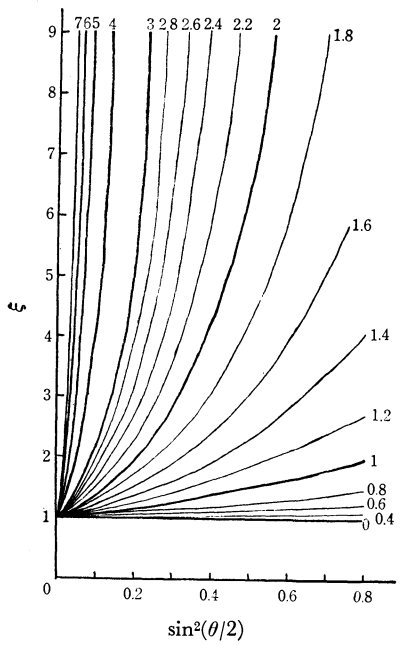

Fig. 4. Relation between ξ and $\sin^2(\theta/2)$ for various α-values.

approximated well enough by the R-G-D equation, irrespective of the values of m and α, if, at least, $m \leq 1.30$, $\alpha \leq 7.0$, and $x \leq 1.0$.

From the experimental point of view, however, it may be worthwhile to point out that the quantity to be taken on the abscissa is not x^2 but $\sin^2(\theta/2)$. This means that the scattering angle to make the value of x small enough is very small when the particle size or α is large, as may readily be understood from Eq. 6. The relation between ξ and $\sin^2(\theta/2)$, instead of x^2, is shown in Fig. 4 for the R-G-D scattering and for various α values. It may be seen that measurements in the range of very small θ values are required for the determination of the "initial" slope when α is large. The measurement of the scattering at such a small angle will be possible after the development of an apparatus which can provide a very narrow incident beam.

Extrapolated Values of Specific Turbidity. —In the studies of polymer solutions, Eq. 1 for the reduced scattering intensity, $R_u(\theta)$, is used exclusively. In the studies of colloidal dispersion, however, the turbidity, τ, may be used instead of the reduced scattering intensity, because the turbidity of the colloidal dispersions is not so small as that of polymer solutions, even in a fairly dilute concentration range.

It is well known historically that Debye's fluctuation theory was, at first, applied to the turbidity, τ, resulting in:

$$Hc/\tau = 1/M_\tau + 2A_2c \tag{29}$$

This equation was, then, rewritten to Eq. 1, by replacing the turbidity with the reduced scattering intensity and H with K, where:

$$H = (16\pi/3)K \tag{30}$$

The latter is an equation justifiable only in the case of the Rayleigh scattering ($\alpha \ll 1$).

If the particles are not so small that the Rayleigh theory does not hold, the molecular weight, M_τ, obtained by Eq. 29, or by the equation:

$$M_\tau = (1/H)(\tau/c)_0 \tag{31}$$

is not equal to the true molecular weight, M. Here, $(\tau/c)_0$ is the specifice turbidity at an infinite dilution. A factor Φ, just like the factor F in Eq. 9, is required to obtain M from M_τ:

$$M = \Phi M_\tau \tag{32}$$

The factor Φ may be considered to be a product of the above-mentioned factor, F, and another factor, φ:

$$\Phi = F\varphi \tag{33}$$

where:

$$\varphi = M_R/M_\tau \tag{34}$$

The theoretical expression of φ is given by:

$$\varphi = (16\pi/3)R_u(0)/\tau = (2/3)i_T(0)/\sum \tag{35}$$

where $\sum$ is a quantity related to the turbidity by the equation:

$$\tau = (\lambda^2/2\pi)N\sum \tag{36}$$

Numerical values of the factor φ can be calculated for colorless spherical particles according to Eq. 35 and by using the numerical values of $\sum$ given by Pangonis, Heller and Jacobson,[9] together with the numerical values of $i_T(0)$ already mentioned.[6] The numerical values of Φ, too, can be calculated according to Eq. 33 by using the values of F obtained above. The resulting Φ values are shown in Fig. 5 as a function of Q_τ. Here, the quantity Q_τ is defined as a quantity proportional to the specific turbidity at the infinite dilution $(\tau/c)_0$ by the following equation;

$$Q_\tau = (\lambda\rho_2/3\pi)(\tau/c)_0 \tag{37}$$

and the theoretical values of Q_τ can be obtained according to the following relation:

$$Q_\tau = \sum/\alpha^3 \tag{38}$$

In the case of the Rayleigh scattering ($\alpha \to 0$ or $Q_\tau \to 0$):

$$\varphi = 1, \quad \Phi = 1 \quad (\alpha \to 0) \tag{39a}$$

are obtained from Eq. 35, since the following equation:

$$\sum = (4/3)[(m^2-1)/(m^2+2)]^2\alpha^6 \tag{39b}$$

holds, besides Eqs. 17a and 17b.

9) W. J. Pangonis, W. Heller and A. Jacobson, "Tables of Light Scattering Functions for Spherical Particles," Wayne State University Press, Detroit (1957).

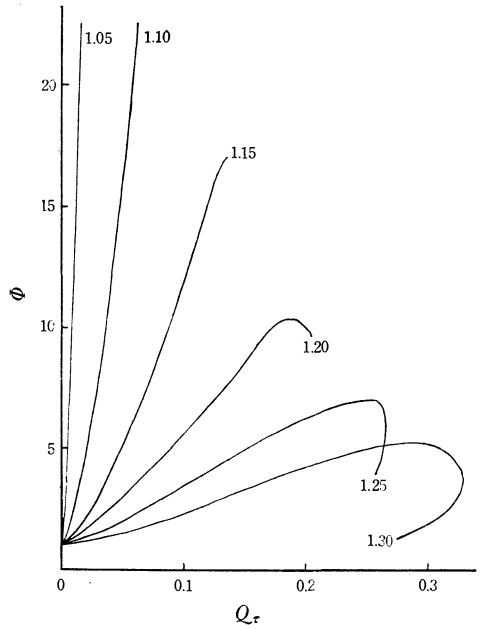

Fig. 5. Relation between Φ and Q_τ for various m-values.

On the other hand, a theoretical equation corresponding to Eq. 5 is also known:

$$Hc/\tau = 1/M\Pi \quad (c\to 0) \tag{40}$$

where Π is given by an integral containing $P(x)$:

$$\Pi = (3/4)\int_0^\pi [(1+\cos^2\theta)/2]P(x)\sin\theta\, d\theta \tag{41}$$

By reference to Eq. 32, it is obvious that:

$$\Pi = 1/\Phi \tag{42}$$

In the case of the Rayleigh scattering, Eq. 39a may be concluded from Eqs. 41 and 42, because $P(x)=1$ in this case.

In the case of the R-G-D scattering ($|m-1|\to 0$), Eq. 41 was solved, together with $P(x)$ of Eq. 18. The result:

$$\begin{aligned}\Pi = (27/64\alpha^4)\{&-7(1-\cos 4\alpha)/8\alpha^2\\ &-(\sin 4\alpha)/2\alpha+5+4\alpha^2\\ &+[(1/\alpha^2)-4][\gamma+\ln 4\alpha-\mathrm{Ci}(4\alpha)]\}\end{aligned} \tag{43}$$

was already known, and its numerical values, too, had been given.[10,11] Therefore, according to Eqs. 19 and 43, it may be concluded that:

$$\Phi = \varphi = 1/\Pi \quad (|m-1|\to 0) \tag{44}$$

When Eq. 44 is drawn on Fig. 5, the curve coincides with the ordinate, because $Q_\tau\to 0$ if $|m-1|\to 0$.

Usually the relation between Φ and Q_τ is expressed by the rather complicated curves shown in Fig. 5. The complication arises because the Φ quantity is a product of F and φ. Since F has already been discussed it is important now to study how simple the relations between φ vs. m and α will be. As the result of the numerical calculations, it is found that the value of φ scarcely depends at all on the m-value, at least in the range of $m\leq$ 1.30 and $\alpha=0.4$—7.0. This empirical conclusion is important, because it also states that the ratio between the reduced scattering intensity in the forward direction ($\theta\to 0$) and the turbidity is independent of the m-value (cf. Eq. 35), and that the forward scattering is, therefore, more important than the scattering at $\theta=90°$, although the latter has been used extensively in various experimental works.

Since the independence of φ from m holds even when $|m-1|\to 0$, the relation between φ and α should be given by:

$$\varphi = 1/\Pi \tag{45}$$

For Π, Eq. 43 is used as a fairly good approximation for various m values (at least for $m\leq$1.30, and very probably for higher m-values also), although this statement has not yet been justified theoretically. Equation 43 is, however, rather complicated. It is, therefore, of some interest to find a simple empirical relation between φ and α. According to Fig. 6, the following one seems to be acceptable:

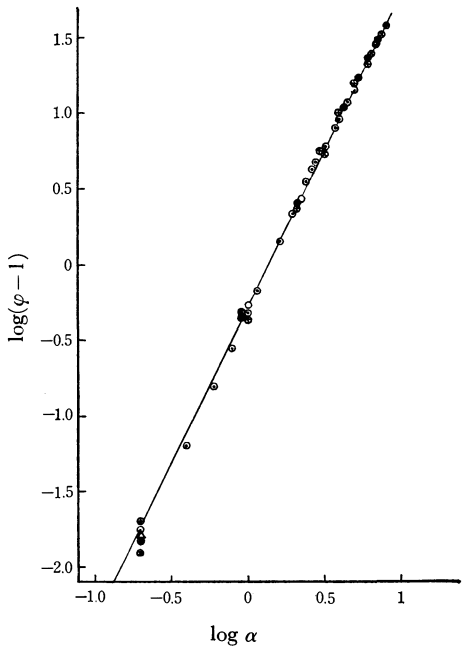

Fig. 6. Relation between $\log(\varphi-1)$ and $\log\alpha$. $m=1.05$ (⊗), 1.10 (⊕), 1.15 (●), 1.20 (○), 1.25 (▼), and 1.30 (△).

10) Lord Rayleigh, *Proc. Roy. Soc.*, **A84**, 25 (1911); **A90**, 219 (1914).
11) R. M. Tabibian, W. Heller and J. N. Epel, *J. Colloid Sci.*, **11**, 195 (1956); M. Nakagaki, *Kagaku no Ryoiki*, **12**, 287 (1958).

$$\varphi = 1+0.537\,\alpha^{2.08} \tag{46}$$

The independence of φ from m is a natural consequence if the relation between ξ and x^2 is independent of m, as has been stated above, although the latter statement might not hold for larger x-values.

BULLETIN OF THE CHEMICAL SOCIETY OF JAPAN VOL. 39 1694—1700 (1966)

On the Photochemical Behavior of Some Xanthenes and Xanthones and the Photochemical Formation of Dixanthenes, Mono-, and Dihydroxydixanthenes*

By V. ZANKER and E. EHRHARDT

Institute of Physical Chemistry, Technische Hochschule München

(Received December 20, 1965)

By ultraviolet spectrometric measurements we studied the photochemical behavior of xanthene, xanthone, 9, 9'-dihydroxydixanthene and dixanthene in aerated and deaerated ethanolic solutions in the range of concentration $5 \cdot 10^{-3}$ M to 10^{-4} M by Osram-HBO 200- and Hanau TQ 81- lamps. We found: Xanthenes are photostable similar to monoacridans in the absence of oxygen; in the presence of oxygen photooxidation to the corresponding xanthones takes place. The xanthones are photochemically unstable; in oxygen free solvents containing H-atoms, like methanol, ethanol, benzene, cyclohexane, dioxane, they are reduced to xanthenes. In cyclohexane we found a soluble xanthene, 9-cyclohexylxanthydrol. In hexane there is formed a precipitate with a yield above 80%; this is the dimeric xanthene 9, 9'-dihydroxydixanthene. The photoreaction presumably is going over a diradical, H-atom transfer from the solvent and formation of a xanthydrol monoradical in the primary step and dimerization to the 9, 9'-dihydroxydixanthene. Irradiation of solutions of xanthone and xanthene in benzene furnish 9-hydroxydixanthene. Solutions of equal molarity of xanthone and acridan yield under irradiation also a solid photoproduct; this is 9, 9'-diacridan. The first step of reaction is photoreduction, where xanthene tranfers a H-atom to xanthone and the hydroxyxanthyl radical dimerizes with the xanthyl radical or the acridanyl radical dimerizes with themselves and forms the diacridan.

In connection with studies about the spectroscopy and photochemistry of the acridines and acridine dyes,[1-6] we also began a few years ago, to investgate the photochemical and spectroscopic behavior of the cations and dianions of the fluorescein dyes.[7-11] Decisive and accurate investigations on this photochemical special field were especially carried out by the Japanese researchers Imamura, Koizumi, Kato and others;[12-16] Lindqvist[17] and Grossweiner[18] also contributed by their flash photolytic experiments to the elucidation of the mechanism of photo-reduction respectively oxidation of some substances of this class of dyes.

Our own investigations are still being fully ellaborated, and we hope that we can finish these studies in the next time. Similar to earlier experiments on the acridines,[19] we believe, that we

* Reported at the Informal Meeting on Photochemistry, Tohoku University, Sendai, September, 1965.

1) V. Zanker and P. Schmid, *Z. Phys. Chem., N. F.*, **17**, 11 (1958).
2) V. Zanker and F. Mader, *Chem. Ber.*, **93**, 850 (1960).
3) V. Zanker and J. Thies, *Z. Phys. Chem., N. F.*, **33**, 46 (1962).
4) V. Zanker and W. Flügel, *Z. f. Naturforschg.*, **19b**, 376 (1964).
5) F. Mader and V. Zanker, *Chem. Ber.*, **97**, 2418 (1964).
6) V. Zanker, E. Ehrhardt, F. Mader and J. Thies, *Z. Phys. Chem.*, in printing.
7) V. Zanker and E. Miethke, *Z. f. Naturforschg.*, **12a**, 385 (1957).
8) V. Zanker and W. Peter, *Chem. Ber.*, **91**, 572 (1958).
9) V. Zanker and H. Rammensee, *Z. Phys. Chem., N. F.*, **26**, 168 (1960).
10) V. Zanker and W. Peter, ibid., **26**, 160 (1960).
11) V. Zanker and W. Korber, *Z. Angewe. Physik.*, **14**, 43 (1962).
12) M. Imamura, *J. Inst. Polytechn.*, **5C**, 86 (1956).
13) M. Imamura, This Bulletin, **28**, 117 (1955).
14) M. Imamura and M. Koizumi, ibid., **29**, 899 (1956); **29**, 913 (1956).
15) M. Imamura, ibid., **30**, 249 (1957); **31**, 62 (1958).
16) M. Koizumi, M. Imamura and Cow., ibid., **31**, 962 (1958); **33**, 262 (1960); **33**, 169 (1960); **35**, 16 (1962); **35**, 185 (1962); **35**, 1875 (1962); **38**, 1022 (1965); **38**, 1015 (1965).
17) L. Lindqvist, *Arkiv Kemi*, **16**, 79 (1960). V. Kaoshe and L. Lindqvist, *J. Phys. Chem.*, **68**, 817 (1964).
18) E. F. Zwicker and L. I. Grossweiner, *J. Phys. Chem.*, **67**, 549 (1963).
19) V. Zanker, *Z. Phys. Chem. N. F.*, **52**, 2 (1954).

can analyze the absorption bands of di- and tetrahalide fluoresceins, starting from the parent substances of this dyestuff class and the monohydroxy derivatives. For this purpose we also have synthesized a series of xanthones, xanthenes, xanthydrols, and xanthylium cations and have carried out spectroscopic and photochemical experiments. The absorption spectroscopy and photochemistry of these compounds are very interesting for us, because so far we have had little knowledge about the parent substances of fluorescein and the other dyestuffs. On the other side the photochemical investigation of acridine and acridine cations lead us to the acridans and diacridans.[5,6] Analogously we could hope, to get similar results in the case of the xanthenes and xanthons. The results will be reported here in a short paper.

Experimental

The substances which we have used for our photochemical and spectroscopical investigations as xanthone, xanthene and the dixanthenes were prepared in optical purity by repeated crystallization out of hexane or ethanol. The solutions of a molarity of 10^{-3} to 10^{-4} were used and in most cases they were deoxygenized by repeated boiling and cooling under N_2-gassing. The last traces of oxygen were removed by aluminumtriethyl. The photolytical conversion was controlled spectrometrically by means of a Zeiss PM Q II and we also identified partly in this way the photochemical converted substances.

Results of the Photolytical Investigations and Discussion

As an example for the study of the photochemical behavior of the monoxanthenes we show at first a measurement of xanthene itself on Fig. 1. In the non-illuminated state this compound shows an electronic band with a vibrational structure at 34300 and 35500 cm^{-1}, classified in the terminology given by Platt[20] as a transition to the ^1L_b-state and at 40500 cm^{-1} it shows the transition to ^1L_a-state, mostly unstructured and of a higher intensity. Further to shorter wavelengths, we can see another very intensive band presumably due to the transition to the ^1B_b-state (^1B_b-band). Irradiating an air saturated ethanolic solution by a Mercury lamp HBO 200, an oxidation reaction quickly starts. In this case we see an increase but no decrease of the xanthene bands at 34000 to 35000 cm^{-1}. In the wavelength region longer than that of xanthene a new band appears and increases up to a yield of about 18%. Then this band decreases again and a second new band at 32000 to 33000 cm^{-1} arises. We suppose, that there is formed an intermediate out of xanthene and xanthone, but we have not yet identified this. In

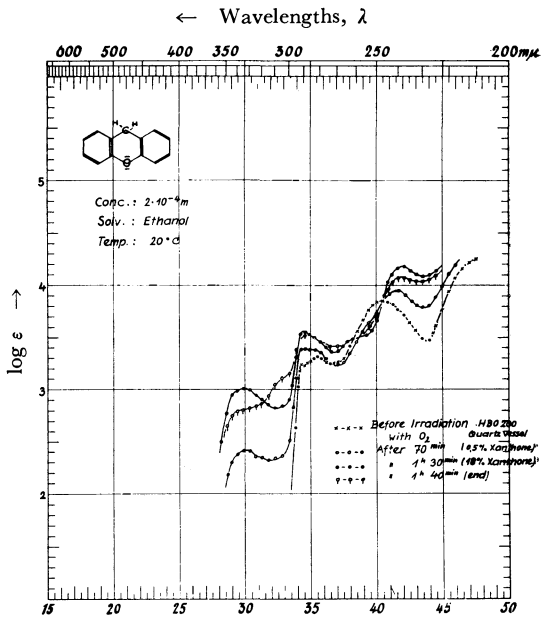

Fig. 1. Absorption spectra of xanthene during photolysis in oxygen containing solution.

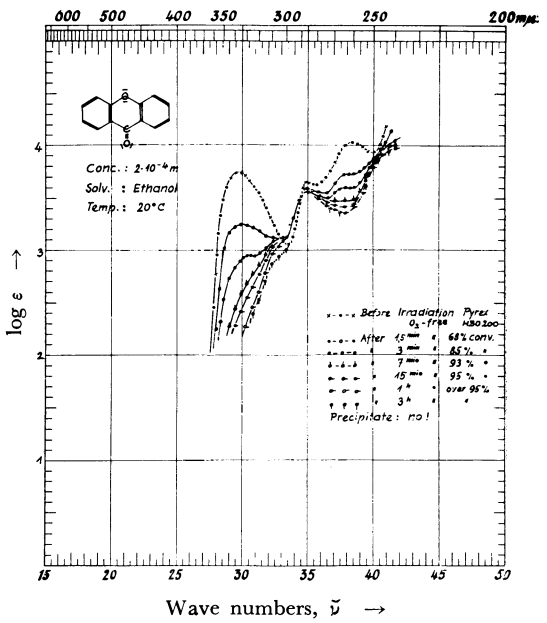

Fig. 2. Absorption spectra of xanthone during photolysis in oxygen free solution.

deoxygenized ethanolic and other polar and homopolar solutions the xanthenes, like the acridans, are photostable. Pure xanthone formed by photooxidation of the xanthene shows a spectrum as is shown on Fig. 2. Characteristic bands of it are an unstructured band at 29000 cm^{-1} and two bands

20) J. R. Platt, *J. Chem. Phys.*, **17**, 470, 484 (1949).

at 34700 and 38400 cm^{-1}. These intensive bands of the xanthone are responsible for the apparent rise of the xanthene bands under the photolysis in oxygen containing solutions. If a deoxygenized ethanolic solution of xanthone is illuminated in a pyrex vessel, xanthone undergoes quickly a photochemical reduction to xanthene, as is demonstrated by a very weak decrease of the band at 34500 cm^{-1}, the minimum at 38000 cm^{-1}, and the increase of the bands at 41000 to 42000 cm^{-1}. After an irradiation of 15 min. we reached a conversion of 95% out of 25 ml. solution and a concentration of 2×10^{-4} M: *we could not observe any formation of a solid photoproduct!*

In this case also, the band at 32000 to 33000 cm^{-1} is changed a little; this indicates again an intermediate between the generated xanthene and the xanthone.

If we irradiate an ethanolic solution of equal concentration in a quartz vessel, we get the same course of reaction; this is plotted on Fig. 3. Again we find that preferentially the formation of xanthene and an intermediate occurs. Under this condition we also find no precipitate or a solid product.

Proceeding from ethanol to dioxane as solvent and irradiating in a quartz vessel, no change in the reaction is detectable. This is shown on Fig. 4. The structure of the individual electronic transitions is indeed better resolved, but the photolysis itself is not influenced. We tried to separate the xanthene which was formed in these solvents. The crystallization from the oily residue was very

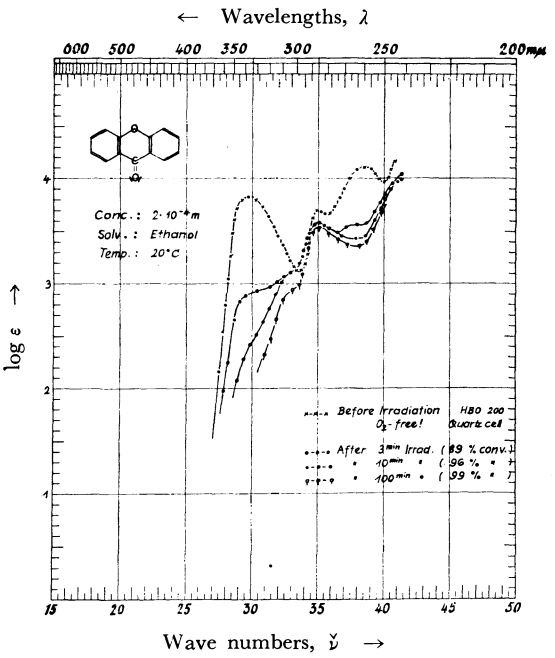

Fig. 3. Absorption spectra of xanthone during photolysis in oxygen free solution in a quartz cell.

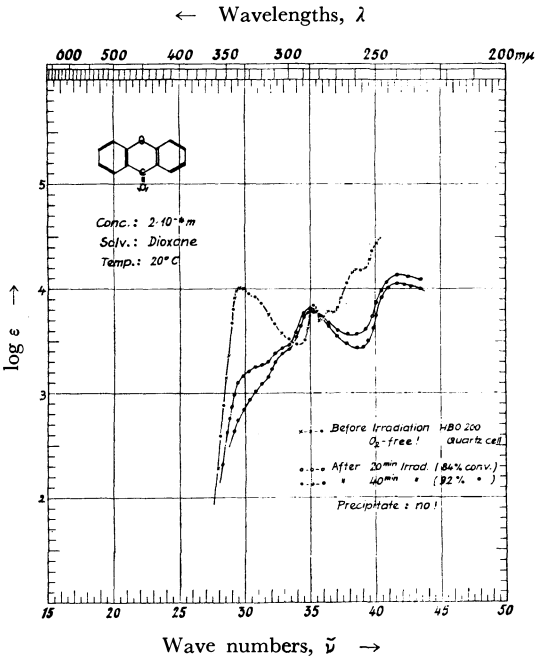

Fig. 4. Absorption spectra of xanthone during photolysis in oxygen free solution of dioxane.

bad and we were not successful. Always again we found bands at 32000 to 33000 cm^{-1}, indicating an unidentified intermediate.

Finally, our experiments to indentify the photolytical final product were successful. In this case we used a homopolar solvent, cyclohexane. We found the same course of reaction as for ethanol and dioxane, and again there was no formation of a solid product. If we remove here the greater part of cyclohexane out of the solution, we obtain a crystalline, colorless product. After repeated crystallization the constitution of the final product of the photolysis could be identified by elementary analysis, molecular weight and ultraviolet spectrum, as a 9-cyclohexylxanthydrol. This result is analogous to the behavior of acridine in deoxygenized cyclohexane or dioxane; we likewise have found for this compound a photochemical reduction to 9-cyclohexyl or 9-dihydroxanyl-substituted monoacridans. From this result we have to conclude, that the photoreactions of the xanthenes in ethanol, dioxane and other polar solvents also form similar soluble xanthydrols, with the corresponding solvent fragment in 9-C-position. But hitherto we could not isolate and identify these compounds.

If we use *n*-hexene as a solvent, we get the following somewhat surprising result. As plotted on Fig. 5, we observe a quick conversion from xanthone to xanthene. After 10 min. 95% are converted and we observe a precipitate of a solid photoproduct. After filtration and determination of the weight, we found over 80% of the substance which we had put in. The low solubility and the high melting

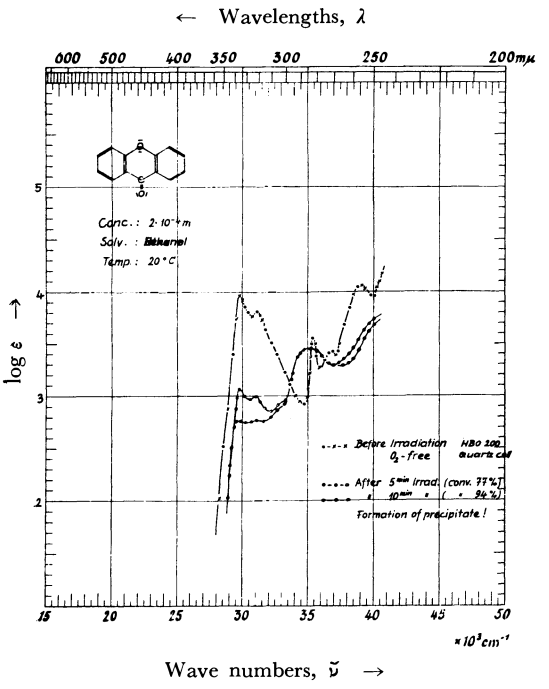

Fig. 5. Absorption spectra of xanthone during photolysis in oxygen free solution of hexane.

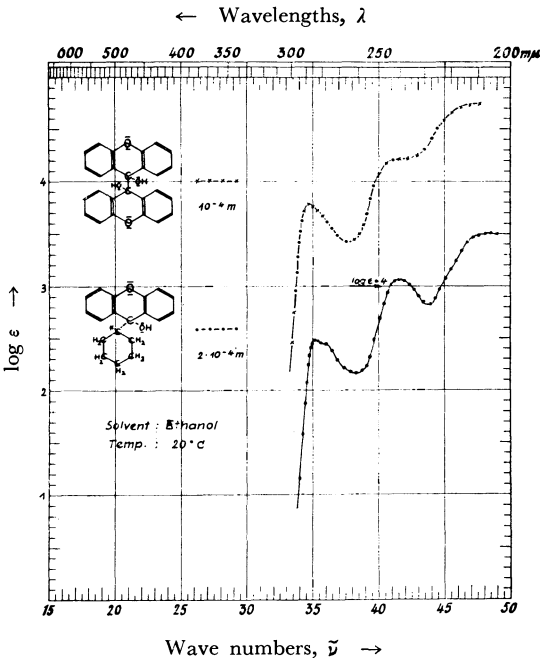

Fig. 6. Absorption spectra of 9, 9′-dihydroxydixanthene and 9-hydroxy-9-cyclohexylxanthene.

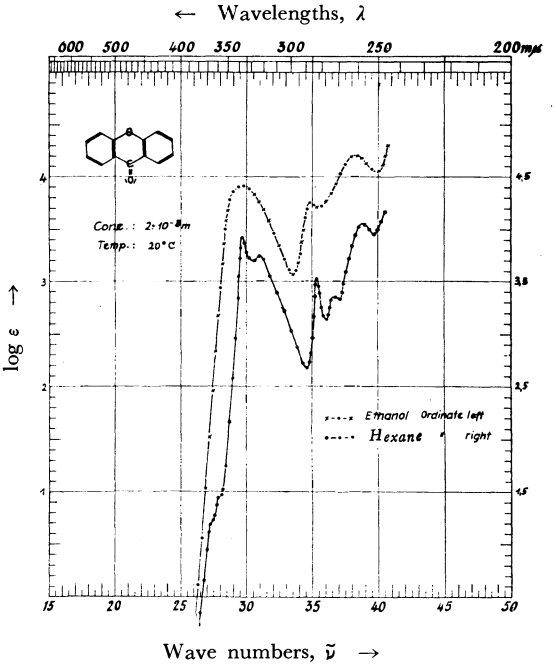

Fig. 7. Absorption spectra of xanthone in ethanol and hexane.

point of this substance gave us the first advice that in this case we had obtained a dimer. The elementary analysis and the determination of the molecular weight showed us, that we have here a double xanthydrol. By synthesis of a 9, 9′-dihydroxydixanthene according to literature[21] and by comparison with the photolytical substance, we found a complete agreement in ultraviolet and infrared spectrum, molecular weight and melting point. Thus we have proved, that this product is a 9, 9′-dihydroxydixanthene. From this we could show for the first time, that in the series of xanthones a photochemical dimerization out of equal building stones is also possible.

On Fig. 6 we demonstrate the ultraviolet spectra of 9-hydroxy-9-cyclohexylxanthene and 9, 9′-dihydroxy-9, 9′-dixanthene, which we have got in solutions of hexane and cyclohexane by photolysis. If we compare these spectra with the spectrum of xanthene, as plotted on Fig. 1, we see only a little difference in these two compounds against the parent substance. The dihydroxy derivative has the most intensive 0→0 transition of the ^1L_b-band, whereas the monohydroxy derivative shows 0→0 and 0→1 transitions of equal intensity; on the other hand, in the case of xanthene, the 0→1 transition is favored. In an opposite sequence, the intensity of this band increases from log $\varepsilon = 3.25$ over log $\varepsilon = 3.45$ to log $\varepsilon = 3.80$ of the dihydroxy derivative. From the appearance of their vibration structure, these three xanthenes are distinguishable. In the case of the dihydroxy derivative, also the minimum, following the ^1L_b-band, is most strongly marked.

21) M. Gomberg and W. E. Bachmann, *J. Am. Chem. Soc.*, **49**, 253 (1927).

To the Mechanism of Photochemical Formation of Mono- and Dihydroxyxanthenes out of Xanthone.—The first information about the course of the photolysis of the xanthone, can be got from the spectrum of the xanthone itself. Therefore, we give the enlarged plotting, down to log $\varepsilon=0$, for various solvents, on Fig. 7. The spectrum, measured in the polar ethanol, displays a striking little structure and especially the band at the longest wavelengths is strongly broadened and without vibrational structure. On the contrary, all electronic transitions in hexane show a very well marked structure and the band at the longest wavelengths from 29000 to 33000 cm^{-1}, especially responsible for the primary process of the photoreaction, shows a well marked $0\rightarrow0$ transition with two exponentially decreasing vibration bands. We doubtless have here a $\pi\rightarrow\pi^*$ transition, with all three rings coupling aromatically. For the spectrum in hexane, we find in the wavelength region longer than that of the xanthenes two weak attendants at 27500 and 28000 cm^{-1}; these we have interprete as members of a $n\rightarrow\pi^*$ transition of absorption band.

We can expect such transitions for the compounds with heteroatoms on which lone pair electrons appear. A $n\rightarrow\pi^*$ transition in ethanol is not observable; but this does not mean, that this transition is not present. We think, that this transition is shifted to shorter wavelengths due to the rising polarity of the solvent and it is superposed with the intensive $\pi\rightarrow\pi^*$ absorption band. This also is consistent to $n\rightarrow\pi^*$ transitions; they are usually shifted to shorter wavelengths with increasing polarity of the solvent.

Superposition of two bands goes mostly together with a loss of structure. Generally we can explain the big differences of the spectra measured in ethanol and *n*-hexane as due to the interaction with the solvent molecules. In ethanol, the solvent molecules interact distinctly with the solute xanthone molecule; this interaction is especially specific to the polar carbonyl group. The xanthone molecule in hexane is free and displays a spectrum, similar to that in gas phase. Therefore, the explanation for the various behavior, seems to be given by a strong or a weak interaction with the solvent.

On Figs. 8 and 9, we have pointed out reaction schedules, set up to elucidate the photochemical reduction of xanthone or generally of the xanthones. As to the formation of monohydroxy and dihydroxydixanthenes (xanthydrols) respectively we have the following conception: xanthone absorbs at the free electron pair of the CO-group a quantum ($n\rightarrow\pi^*$ transition) and passes over to a diradical. The high affinity of a O-radical position to H-atoms is responsible for the transfer of an H-atom from solvents with H-atoms resulting the reductive formation of a xanthydrol- or a hydroxyxanthyl-

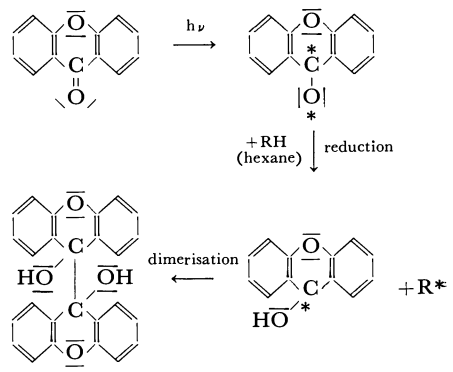

Fig. 8. Schedule of photoreaction of xanthone in solution of hexane.

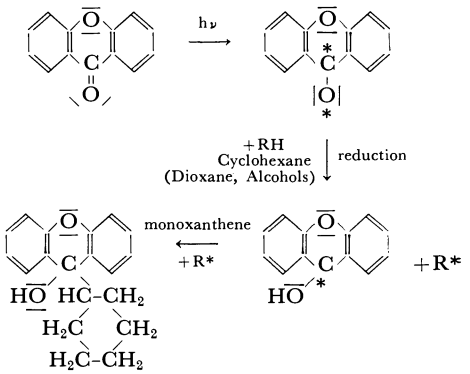

Fig. 9. Schedule of photoreaction of xanthone in solution of cyclohexane, dioxane and alcohols.

radical. Simultaneously the solvent ethanol is oxidized to aldehyde. This C-radical has the tendence to react with other C-radicals and to form stable hydroxyxanthene molecules. Therefore, we can realize two ways of reaction: On the one side the combination of two equal xanthyl radicals to dihydroxydixanthyl, and on the other side an association of the xanthyl radical with a solvent radical generated at the H-atom transfer. As is mentioned above, the latter seems to be especially favoured in the case of strong interaction of the solvent molecule with the CO-group, where only a small distance holds permanently between CO-group and solvent molecule. On the other side the probability of association with an equal xanthyl radical is similarly high, and according to low solubility of the dimer, this aggregation is in the foreground.

Photolytical Investigations on 9, 9'-Dihydroxy- and Dixanthenes.—In connection with the photochemical behavior of the diacridans, we were interested in the stability of the dixanthenes and in the question, if the dixanthenes, corresponding to the diacridans, decompose heterolytically to xanthylium cations and anions or to

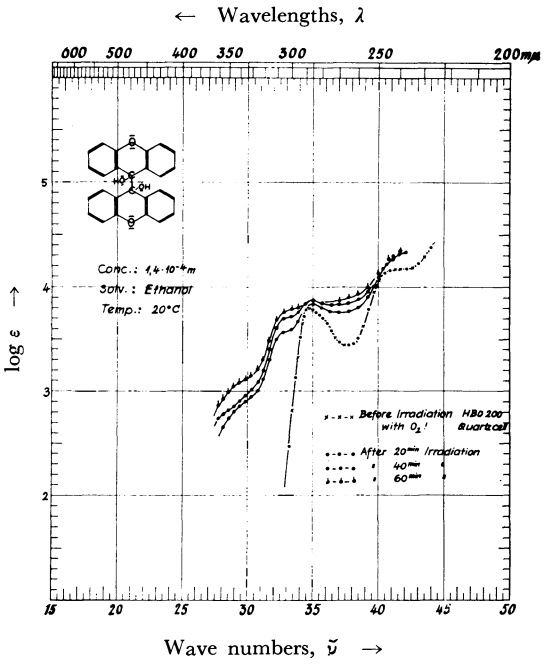

Fig. 10. Absorption spectra during photolysis of 9,9'-dihydroxydixanthene in oxygen containing solution.

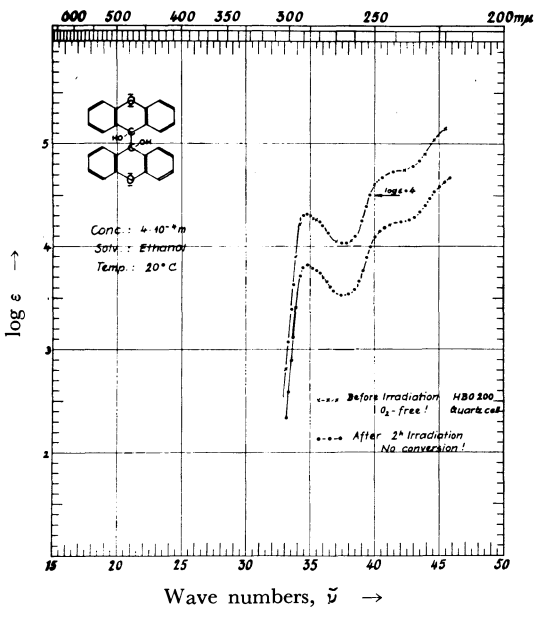

Fig. 11. Absorption spectra of 9,9'-dihydroxydixanthene before and after irradiation.

xanthydrols (hydroxyxanthenes). In order to investigate this, we have irradiated air saturated and deoxygenized ethanolic solutions of 9, 9'-dihydroxydixanthene. The results of this investigation are plotted on Figs. 10 and 11.

In the case of oxygen containing solutions, we

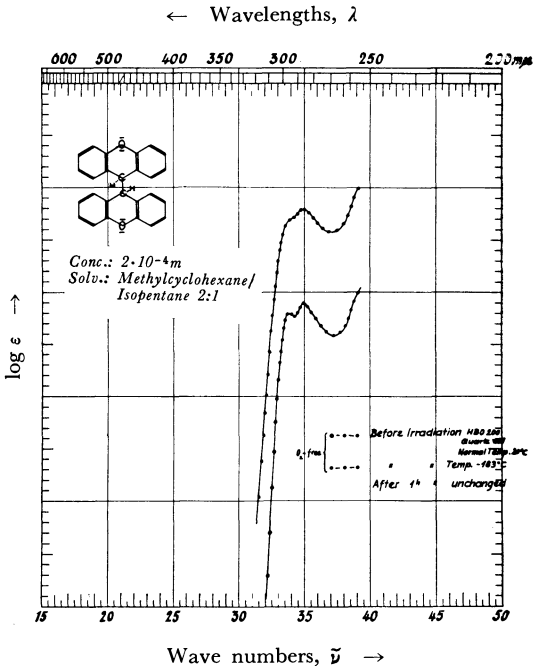

Fig. 12. Absorption spectra of dixanthene before and after irradiation.

have obtained an oxidation to xanthone; this result if it is compared to the reaction of the diacridans but here the oxidation leads to the acridine and partly to acridan, is not extraordinary. This is proved by the appearnce of a band at 30000 cm^{-1}. As in the case of the photoreduction of xanthone or the oxidation of xanthene, here also appears another product absorbing at 33000 cm^{-1} This is like before but not yet identified in its constitution.

In deoxygenized solutions the dixanthenes are photostable. This is shown by the experiments, carried out on 9, 9'-dihydroxydixanthene and 9, 9-'dixanthene. The results are pointed out on Figs. 11 and 12. After an illumination of two hours by a HBO 200 mercury lamp at a concentration of $4 \cdot 10^{-4}$ M, no change is observable. The same result we have got for chemically synthesized 9, 9'-dixanthene. In this case also no photolytical reaction is detectable. This substance is so far not yet synthesized by photolysis.

This behavior of the dixanthenes differs from that of the diacridans. There we find photoinstability, with an exception of 9, 9'-diphenyldiacridan. Now we have the problem to understand the properties of these compounds out of their spectroscopic data. As was demonstrated in a previous paper, the monoacridans differ essentially from the diacridans by an absorption band situated in the long wave absorption region. The intensity of this band is $\log \varepsilon = 3.4 - 3.5$. The appearance of this band is indicative of $\pi \rightarrow \pi^*$-interaction between the two acridan nuclei

of the diacridan, via the 9, 9'-bond. Light excitation especially affects this 9, 9'-bond and breaks it photochemically.

With the dixanthenes we miss completely such a band and they differ from the monoxanthene derivatives only little by intensity. This has been plotted on Figs. 11 and 12. The two chromophores are practically completely isolated from each other, and at the excitation no stressing of the 9, 9'-bond and no photosensibility is observable.

Photosynthesis of Further Dixanthenes.— Starting from the above mentioned results, which guided us to a reaction schedule shown before, we have supposed, that it may be possible to synthesize photolytically besides the symmetrical and unsymmetrical dixanthenes. Using a stronger H-donor than the solvent itself, we must get such products, if we would have the right conception. The stronger donor in the class of our compounds is the xanthene, respectively 9-alkyl- or 9-aryl-monoxanthenes.

If we add equimolar amounts of xanthone and xanthene in benzene solution and irradiate this mixture, we get indeed a solid photoproduct. We determined the melting point and the molecular weight and found this to be a 9-*hydroxydixanthene*. This compound was prepared already photochemically by Schönberg;[22] we now synthesized this substnace by another idea. Including the other H-donors for this synthesis, we also used acridan as an H-donor. If we irradiate equimolar solutions of xanthone and acridan in benzene, we can quickly observe the precipitate of a colorless solid substance. After repeated crystallization, we have found from molecular weight, elementary analysis, and ultraviolet and infrared spectra, that here is formed a *9, 9'-diacridan*.

In the last Fig. 13, we show a schedule to these dimerizations, which enlarges the mechanisms pointed out previously. Using suitable combination of filters, we irradiated only in the long wave absorption range of xanthone. This causes again the formation of a xanthone-diradical, fixed at the CO-group. This diradical takes over an H-atom from the stronger donor of xanthene and acridan and forms a 9-hydroxyxanthyl radical. The xanthene itself, which has the function as an H-donor, dismisses an H-atom and goes to a xanthyl radical. Combination of these two C-radicals yields the 9-hydroxydixanthene. In the second case, the xanthone diradical takes over an H-atom

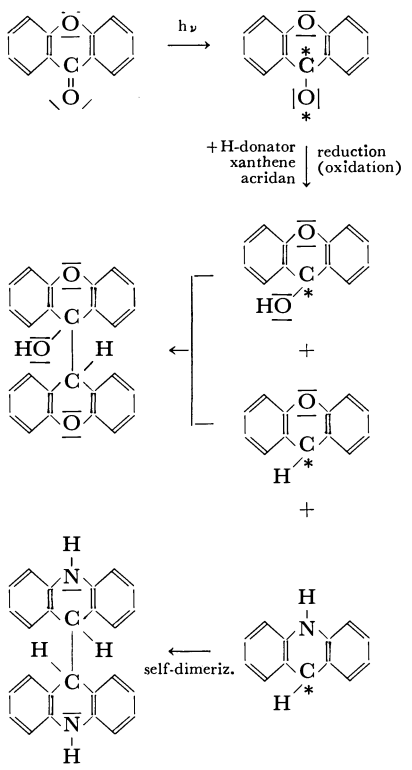

Fig. 13. Schedule of photoreaction of xanthone with xanthene resp. acridan.

from the acridan and passes over to a 9-hydroxydixanthyl-radical. Simultaneously the acridan is oxydized to acridanyl-radical furnishing H-atoms. We could expect here also the formation of a mixed xanthylacridanyl dimer. But this is not occurring or presumably occurring little. The extraordinary low solubility of this substance ($4 \cdot 10^{-5}$ molar against $5 \cdot 10^{-3}$ molar of the dixanthenes) prevents the formation of a mixed product or the likewise possible dihydroxydixanthene.

So we have settled a bridge to the photolytical formation of diacridans and have found a new way, to synthesize this dimer diacridan.

We wish to express our thanks to the Deutsche Forschungsgemeinschaft and the Verband der Chemischen Industrie, Federal Republic Germany, for personal help and especially to Professor Masao Koizumi for his invitation to the informal meeting on photochemistry at Sendai, Septmeber, 1965, on which we could discuss the present results.

22) A. Schönberg and A. Mustafa, *J. Chem. Soc.*, **1944**, 67.

BULLETIN OF THE CHEMICAL SOCIETY OF JAPAN VOL. 39 1701—1705 (1966)

A Molecular Compound between Glutamic Acid and Pyroglutamic Acid*

By Yoshihisa SUZUKI and Nobuya NAGASHIMA

Central Research Laboratories, Ajinomoto Co., Inc., Suzuki-cho, Kawasaki

(Received January 13, 1966)

A new molecular compound, which consists of L-glutamic acid, L-pyroglutamic acid and water of crystallization in a 1 : 1 : 1 mole ratio, has been discovered. In its crystal, the unit-cell is monoclinic with $a=5.10$, $b=7.20$, $c=18.38$ Å, and $\beta=96.6°$, and the space group has been determined to be $P2_1$. Equilibrium measurements in the system of L-glutamic acid, L-pyroglutamic acid and water at 20°C, 30°C, and 50°C, showed that the transition temperature from the molecular compound to L-pyroglutamic acid and α-form L-glutamic acid is 35.5°C, while that to L-pyroglutamic acid and β-form L-glutamic acid is 20.5°C. Thus, the molecular compound is stable only below this temperature. This molecular compound has an incongruent solubility. When it is placed in water, a crystallization of L-glutamic acid takes place as the molecular compound is dissolved. A similar molecular compound consisting of D-glutamic acid and D-pyroglutamic acid is also obtained, but no molecular compound of the L-glutamic acid and D-pyroglutamic acid, or vice versa, is obtainable. On the basis of these facts, an optical resolution is actually possible for glutamic acid. When this molecular compound is heated, it is converted into another molecular compound at about 70°C due to the loss of the water of crystallization; then it is decomposed to L-glutamic acid (β-form) and L-pyroglutamic acid at about 90°C.

A new molecular compound, which consists of L-glutamic acid, L-pyroglutamic acid and water of crystallization in a 1 : 1 : 1 mole ratio, was discovered, although complex of these two acids in solution had been assumed without any confirmation by Kergle.[1] It is prepared[2] in the following way: 10 g. of L-glutamic acid and 60 g. of L-pyroglutamic acid are dissolved in 100 g. of hot water, and then the solution is cooled to 20°C. After several hours, crystals with a shape of rhombic plate are obtained. The chemical analysis shows that these crystals are the 1 : 1 : 1 molecular compound.

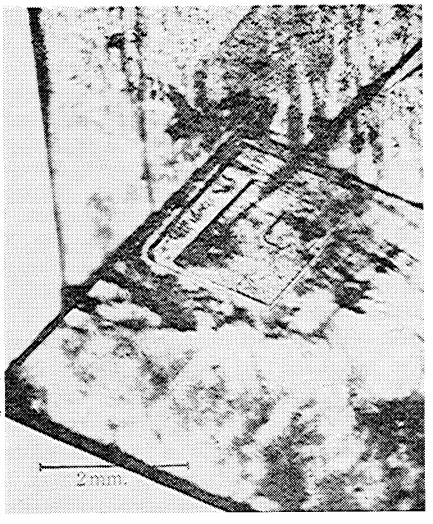

Fig. 1. A large spiral layer on the crystal surface of the molecular compound, which consists of L-glutamic acid, L-pyrroglutamic acid, and water of crystallization.

Found: C, 40.99; H, 6.30; N, 9.54; Amino-N, 4.81 (Van Slyke); L-glutamic acid, 50.8 (enzymatic analysis). Calcd. for L-glutamic acid - L-pyroglutamic acid - water: C, 40.81; H, 6.17; N, 9.52; Amino-N, 4.77; L-glutamic acid, 50.0%.

On the surface of one of these molecular compound crystals, a large spiral layer was found (Fig. 1).

Crystallographic Examination

X-Ray diffraction studies were carried out of the crystals obtained with CuK_α radiation. The oscillation and Weissenberg methods were used for single crystals, and diffractometer techniques, for powder specimens. The unit-cell is monoclinic with $a=5.10$, $b=7.20$, $c=18.38$ Å, and $\beta=96.6°$.

For reference, the cell dimensions of L-glutamic acid and L-pyroglutamic acid are shown below:

L-glutamic acid:

(α-form)[3] $a=7.06$, $b=10.3$, $c=8.75$kX

(β-form)[4] $a=5.17$, $b=17.34$, $c=6.95$Å

L-pyroglutamic acid:

* Presented in part at 14 th Annual Meeting of the Chemical Society of Japan, Tokyo, April, 1961.

1) E. Kergle, "Glutaminsäure," Wissenschaftliche Verlagsgesellschaft M. B. H., Stuttgart (1954), p. 12.

2) Japanese Pat. 414586 (Japanese Publ. 11140/1963).

3) J. D. Bernal, *Z. Krist.*, **78**, 363 (1931).

4) S. Hirokawa, *Acta Cryst.*, **8**, 637 (1955).

$a=14.6,\ b=8.99,\ c=13.5$Å

The Weissenberg pattern shows a systematic absence of $(0k0)$ reflections with $k \neq 2n$. This indicates that the space group is either $P2_1$ or $P2_1/m$. The density measurements ($d_0=1.454$, $d_c=1.456$ g. cm^{-3}) show that there are two molecular compounds (L-glutamic acid - L-pyroglutamic acid - water) in the unit cell. Accordingly, the possibility of $P2_1/m$ is eliminated, and the space group is determined to be $P2_1$. The X-ray powder diffraction data are shown in Table I. The intensities reported in Table I are peak heights above the background, so scaled that the most intense line is given a value of 100.

Table I. X-Ray powder diffraction data for molecular compounds

	L-Glutamic acid, L-pyroglutamic acid and water		L-Glutamic acid and L-Pyroglutamic acid	
hkl	*d*, Å	I/I_0	*d*, Å	I/I_0
001	18.4	60	16.8	15
002	9.2	5	7.02	15
011	6.7	15	5.52	10
003	6.15	25	5.43	5
012	5.68	10	5.12	5
100	5.11	10	4.67	5
013	4.69	10	4.38	5
004	4.60	10	4.21	100
110	4.15	100	4.13	20
112	3.98	60	4.07	10
014	3.88	10	3.93	10
005	3.68	20	3.74	3
104	3.60	50	3.59	40
020			3.41	5
021	3.53	10	3.34	5
022	3.36	15	3.27	10
015	3.28	15	3.15	5
105	3.16	3		
023	3.11	10		
120	2.94	30		

The Determination of the Conditions of the Molecular Compound Formation

In an attempt to determine the conditions under which the molecular compound is formed, solubility measurements of various saturated solutions of L-glutamic acid, L-pyroglutamic acid and water have been made. For each set of solubility measurements, an examination was also made of the constitution of the solid phase which is in equilibrium with the saturated solution in question.

Material.—*α-Form L-Glutamic Acid.*—The pH of a solution of 300 g. of commercial mono-sodium L-glutamate mono-hydrate dissolved in 10 l. of water was brought to about 3.2 by promptly adding 35% hydrochloric acid at room temperature. The crystals thus formed were filtered, washed with water, and dried in vacuo. The results of the analysis of this L-glutamic acid were as follows:

Found: N, 9.53%; $[\alpha]_D^{20}$ + 31.7 (*c* 8, 2N HCl).
Calcd.: N, 9.52%.

These crystals were found by the X-ray diffraction method[5] to be α-form, with a 98% purity.

β-Form L-Glutamic Acid.—First, a glutamate solution was prepared by dissolving 300 g. of mono-sodium L-glutamate monohydrate in 1.5 l. of water. Into this solution 35% hydrochloric acid was slowly stirred at 80°C. After 1 hour, the pH of the solution reached about 3.2; then the solution was cooled to room temperature. The crystals formed were filtered, washed with water, and dried in vacuo. The results of the analysis of this L-glutamic acid were as follows:

Found: N, 9.52%; $[\alpha]_D^{20}$ +31.8 (*c* 8, 2N HCl).

These crystals were found by the X-ray method to be 100% pure β-form L-glutamic acid.

L-Pyroglutamic Acid.—L-Glutamic acid was suspended in five times as much water and kept at 120°C for about 20 hr. The solution was then decolorized by active charcoal and passed through a column of the cation exchange resin (Diaion SK in H^+-form) in order to remove the unreacted glutamic acid. The effluent was concentrated in vacuo, the crystals first deposited were removed (DL-pyroglutamic acid), and then the resultant solution was cooled. The crystals formed in this stage were filtered, washed with cold water, and dried in vacuo. The results of the analysis of these crystals were as follows:

Found: N, 10.82%; $[\alpha]_D^{20}$, −11.3 (*c* 4, water).
Calcd.: N, 10.85%.

Procedure.—L-Glutamic acid, L-pyroglutamic acid and water were mixed in a glass tube with a spiral stirrer. The tube was placed for at least six hours in a water bath regulated at 20°C, 30°C, or 50°C. The temperature fluctuation of the bath was within ±0.1°C. An aliquot was taken with a cotton-stoppered pipet (warmed when necessary), and the concentration of L-glutamic acid in the filtrate was determined by the Warburg method with a decarboxylase from squash. The L-pyroglutamic acid content was determined as the difference between the total nitrogen determined by the Kjeldahl method and the amino nitrogen as calculated from the L-glutamic acid content. The solid-phase constitution was examined by the X-ray powder diffraction method. The equilibrium was sometimes reached from the under-saturation side, and sometimes from the supersaturation side.

Results.—The results of the solubility measurements are tabulated in Table II and are given graphically in Figs. 2, 3 and 4. The solubility of L-glutamic acid is somewhat different according to whether the solid phase is α-form glutamic acid or β-form glutamic acid.[6] It has been reported by Sakata[7] that L-glutamic acid in the α-form as a solid phase in a saturated aqueous solution gradually transforms into β-form, and that some amino acids have an inhibitory action on this transition. The present experiment showed

5) H. Takahashi, T. Takenishi and N. Nagashima, This Bulletin, **35**, 923 (1962).
6) Y. Sakata, *Agr. Biol. Chem.*, **25**, 835 (1961).
7) Y. Sakata, ibid., **25**, 829 (1961).

that L-glutamic acid tends to be crystallized in the α-form from the supersaturated solution in the presence of L-pyroglutamic acid, and that such an α-form crystal does not readily transform into the β-form in the solution.

As may be seen in Figs. 2, 3, and 4, the isotherm at 20°C shows a clear stable zone of the molecular compound, only a short stable zone at 30°C, and no stable zone, only a metastable zone, at 50°C. In the metastable zone, however, the molecular compound is easily crystallized by the cooling of the saturated solution at an elevated temperature.

The molecular compound was obtained only from the supersaturated side in the temperature range examined.

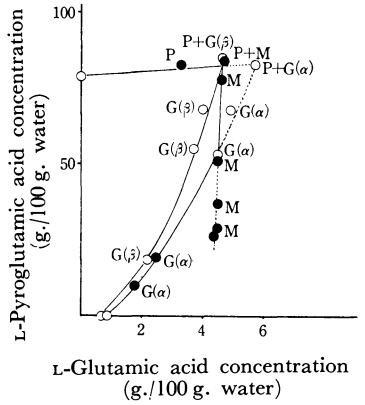

Fig. 2. Composition of the liquid phase in the system of L-glutamic acid, L-pyroglutamic acid and water at 20°C.
○ means the data from unsaturation side, and ● from supersaturation side. For each point observed, the constitution of the solid phase in equilibrium with the liquid phase in question is shown by P, M, G(α), and (β). The notations are the same as in Table II.

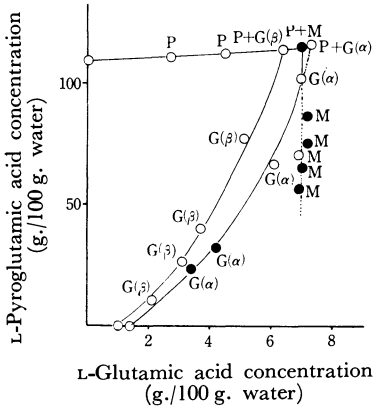

Fig. 3. Composition of the liquid phase and the constitution of the solid phase in the system of L-glutamic acid, L-pyroglutamic acid and water at 30°C. The notations are the same as in Table II.

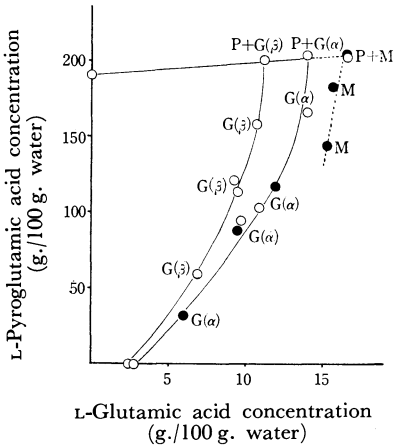

Fig. 4. Composition of the liquid phase and the constitution of the solid phase in the system of L-glutamic acid, L-pyroglutamic acid and water at 50°C. The notations are the same as in Table II.

Since this molecular compound has an incongruent solubility, it is decomposed by water, and at the same time a precipitation of L-glutamic acid takes place.

At each temperature three invariant points can be determined: at one of them, the solid phase is composed of both L-pyroglutamic acid and α-form L-glutamic acid; at the second point, the solid phase is composed of both L-pyroglutamic acid and β-form L-glutamic acid; and at the third point, the solid phase is composed of L-pyroglutamic acid and the molecular compound. The logarithm of the L-glutamic acid concentrations at the invariant points are plotted against the temperature in Fig. 5. Here three straight lines are obtained. The intersecting points of these lines give the transition temperatures from the molecular compound to the mixtures of the two acids. Thus the transition temperature from the molecular compound to L-glutamic acid in the α-form and L-pyroglutamic acid is about

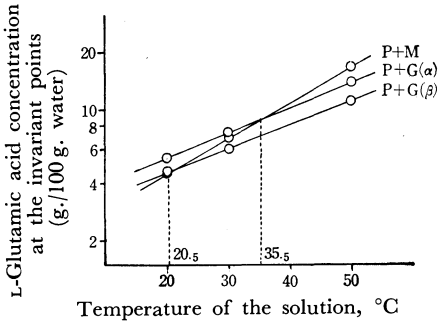

Fig. 5. Estimation of the transition points by three different invariant points.
The notations of the solid phase are the same as in Table II.

Table II. Equilibrium in the system of L-glutamic acid, L-pyroglutamic acid and water

U: from unsaturated side S: from supersaturated side
P: L-pyroglutamic acid M: the molecular compound
G(α): α-form L-glutamic acid G(β): β-form L-glutamic acid

Temp. °C	Method	Liquid phase composition (g. per 100 g. water) P	G	Solid phase composition
20	U	79	0	P
	U	82	2.8	P
	S	83	3.3	P
	S	84	4.7	P+M
	U	83	5.7	P+G(α), metastable
	S	78	4.6	M
	S	51	4.5	M, metastable
	S	37	4.5	M, metastable
	S	29	4.5	M, metastable
	S	26	4.4	M, metastable
	U	68	4.9	G(α), metastable
	U	53	4.5	G(α)
	S	19	2.5	G(α)
	S	10	1.8	G(α)
	U	0	0.94	G(α)
	U	85	4.6	P+G(β)
	U	68	4.0	G(β)
	U	55	3.7	G(β)
	U	18	2.2	G(β)
	U	0	0.71	G(β)
30	U	109	0	P
	U	111	2.7	P
	U	112	4.5	P
	S	115	7.0	P+M
	U	116	7.3	P+G(α), metastable
	S	86	7.2	M, metastable
	S	74	7.2	M, metastable
	U	70	6.9	M, metastable
	S	65	7.0	M, metastable
	S	56	6.9	M, metastable
	U	102	7.0	G(α), metastable
	U	66	6.1	G(α)
	S	32	4.2	G(α)
	S	23	3.4	G(α)
	U	0	1.4	G(α)
	U	114	6.4	P+G(β)
	U	77	5.1	G(β)
	U	40	3.7	G(β)
	U	26	3.1	G(β)
	U	9.9	2.1	G(β)
	U	0	1.0	G(β)
50	U	191	0	P
	U	204	14.0	P+G(α)
	S	203	16.5	P+M, metastable
	U	220	16.5	P+M, metastable
	S	183	15.7	M, metastable
	S	144	15.3	M, metastable
	U	165	14.0	G(α)
	S	117	11.9	G(α)
	U	103	10.9	G(α)
	U	94	9.7	G(α)
	S	88	9.5	G(α)
	S	31	6.0	G(α)
	U	0	2.8	G(α)
	U	201	11.2	P+G(β)
	U	159	10.7	G(β)
	U	121	9.3	G(β)
	U	113	9.5	G(β)
	U	59	6.9	G(β)
	U	0	2.4	G(β)

35.5°C, and the transition temperature from the molecular compound to L-glutamic acid in the β-form and L-pyroglutamic acid is about 20.5°C. The molecular compound is stable below this temperature.

The Optical Resolution of DL-Glutamic Acid by the Use of the Molecular Compound[8]

A similar molecular compound which consists of D-glutamic acid, D-pyroglutamic acid and water was also ascertained to be formed. It was found, however, that no molecular compound which consists of L-glutamic acid and D-pyroglutamic acid or vice versa can be obtained. It may be expected that, taking advantage of these facts, one can resolve the racemic form of glutamic acid or pyroglutamic acid. Such an optical resolution is actually possible for glutamic acid, but it is not for pyroglutamic acid.

Materials.—The racemic glutamic acid monohydrate and racemic pyroglutamic acid were presented by Dr. T. Akashi.* The results of the analysis of these two materials were as follows:

DL-glutamic acid monohydrate:
Found: N, 8.49%; $[\alpha]_D^{20}$, ±0.00 (*c* 8, 2 N HCl). Calcd.: N, 8.48%.

DL-pyroglutamic acid:
Found: N, 10.84%; $[\alpha]_D^{20}$, ±0.00 (*c* 4, water). Calcd.: N, 10.85%.

8) Japanese Pat. 412634 (Japanese Publ. 8311/1963).

* Chief Chemist in the Central Research Laboratories of Ajinomoto Co., Inc.

Procedure and Results.—I) A mixture of 13.6 g. of DL-glutamic acid mono-hydrate and 54.5 g. of L-pyroglutamic acid in 60 g. of water was heated until it dissolved at 80°C; then the solution was cooled at 20°C under stirring, with a slight seeding of the molecular compound between L-glutamic acid and L-pyroglutamic acid. After 4 hr. the precipitated crystals were filtered out. In the analysis of the crystals and the mother liquor, the method of amino-nitrogen determination in the ninhydrin method was adapted, as well as the two methods of analysis in the solubility measurements described above. The total concentration of optically active and inactive glutamic acid was determined by the amino-nitrogen measurements. The concentration of L-glutamic acid was determined by the enzymatic method.

The crystals were weighed (8.6 g.) and were found to be 68% the molecular compound (L-glutamic acid, L-pyroglutamic acid and water), 17% DL-glutamic acid monohydrate, and 10% L-pyroglutamic acid. The mother liquor was also weighed (103 g.); its concentration was as follows; DL-glutamic acid 4.0%, D-glutamic acid 2.6%, L-pyroglutamic acid 44%.

II) Into a mixture of 10.1 g. of DL-glutamic acid mono-hydrate and 24 g. of L-pyroglutamic acid in 31 g. of 5% hydrochloric acid, about 6 g. of 15% caustic soda, including 1.8 g. of L-pyroglutamic acid, was stirred. By cooling at 20°C with a slight seeding of the molecular compound (L-glutamic acid, L-pyroglutamic acid and water), 2 g. of the crystals were obtained after 1 hr. The crystals were 90% the molecular compound (L-glutamic acid, L-pyroglutamic acid and water) and 10% L-pyroglutamic acid. L-Glutamic acid was obtained from the decomposition of these crystals by water.

III) A mixture of 10 g. of DL-pyroglutamic acid and 2.5 g. of L-glutamic acid in 100 g. of water was cooled in an ice box. After 5 days the crystals precipitated were examined by the X-ray powder diffraction method; they were thus shown to be a mixture of the two acids, with none of the molecular compound present.

An Anhydrous Molecular Compound

A thermal analysis of the above-described molecular compound has been made. It was shwon that the compound is converted into another molecular compound of L-glutamic acid and L-pyroglutamic acid (1 : 1) at about 70°C; then it is decomposed to L-glutamic acid (β-form) and L-pyroglutamic acid at about 90°C. This transformation was shown in the differential thermal analysis curve, and in the X-ray diffraction patterns and the IR spectra of the specimens of all the stages. The results of the elementary analysis of the latter molecular compound were:

Found: C, 43.67; H, 5.95; N, 10.18. Calcd.: C, 43.4; H, 5.84; N, 10.14%.

This anhydrous molecular compound could not be obtained from the aqueous solution. The X-ray powder diffraction data are shown in Table I.

We wish to express our thanks to Professor Masamichi Tsuboi of the University of Tokyo for reading the manuscript of this paper, and also to Drs. Haruomi Oeda, Shinichi Motozaki, Mei Ohno and Tadao Takenishi in the Central Research Laboratories, Ajinomoto Co., Inc., for their encouragement.

BULLETIN OF THE CHEMICAL SOCIETY OF JAPAN VOL. 39 1705—1715 (1966)

The Chemistry of Protactinium. II. The Behavior of Pentavalent Protactinium in a Perchloric Acid Solution

By Shin SUZUKI and Yasushi INOUE

The Research Institute for Iron, Steel and Other Metals, Tohoku University, Katahira-cho, Sendai

(Received July 23, 1965)

Studies of the chemical behavior of protactinium(V) were carried out with the TTA-benzene extraction method, the ion exchange method and the filtration method. When the protactinium concentration is less than 10^{-6} M and the perchloric acid concentration is 0.3—2.0 N, the reaction of TTA extraction may proceed as:

$$PaO_m(OH)_n^{5-2m-n} + 4HT \rightleftarrows Pa(OH)T_4 + (m+n-1)H_2O + (5-2m-n)H^+$$

where $2m+n$ is 3 and 4, or as:

$$PaO_m(OH)_nT^{4-2m-n} + 4HT \rightleftarrows PaT_5 + (m+n)H_2O + (4-2m-n)H^+$$

where $2m+n$ is 2 and 3.

The cation exchange experiment gives results consistent with this conclusion. On the other hand, when the concentration of protactinium is higher than 10^{-6} M, the above relation does not hold, even in the 5 N perchloric acid solution, because protactinium forms the aggregates to a great extent. This has been confirmed by the filtration experiment.

It has been stated earlier that the results of investigations of the aqueous chemistry of protactinium are not always acceptable,[1] because the instability of the aqueous solution has resulted in some confusion on published works. This is true in investigations of the chemical behavior of pentavalent protactinium even in a perchloric acid solution, which is considered to be the most fundamental of the various aqueous systems. For example, Welch[2] assumed the existence of protactinyl ion in this medium from its behavior towards cation exchange resin, but Elson[3] concluded that, in weakly acid solutions, protactinium would be found in such hydrolyzed forms as $Pa_2(OH)_9^+$ and $Pa_2O_2(OH)_5^+$; in solutions of moderate acidity, in the form of PaO^{3+} or $Pa(OH)_2^{3+}$; and in a strong acid solution, perhaps in the hydrated form of Pa^{5+}. On the other hand, Bouiséres and his co-workers[4] assumed, from their TTA-benzene extraction experiments, that, in 0.9—3 M perchloric acid solutions, this element would be found in the form of $Pa(OH)_3^{2+}$ or $Pa(OH)_2A^{2+}$ (where A is the anion of TTA), and in 1.5×10^{-3}—2×10^{-5} M perchloric acid solutions, in the form of $Pa(OH)_2A_2^+$ or $PaO(OH)_2^+$. As to the stability of pentavalent protactinium, Guillaumont and his co-workers[5] reported that a weak absorption peak at 210 mμ which appeared in 2.4—11.8 M perchloric acid solutions containing about 10^{-5} M pentavalent protactinium disappeared in eight to ten days. Thus, the conclusions differ with the authors. For this reason, it is necessary to investigate more fully the chemical properties of pentavalent protactinium in a perchloric acid solution.

Thenoyl trifluoroacetone (TTA), as compared with the other organic complexing reagents, has a comparatively high acid dissociation constant; therefore, it is applicable even when the acidity of a solution is high. This is the reason why the TTA extraction method is frequently used for the separation of protactinium[6-11] as well as for fundamental research.

The purpose of this investigation is to elucidate the nature of pentavalent protactinium in a perchloric acid solution by the TTA-benzene extraction method, coupled with the ion exchange and filtration methods.

Experiments

Reagents and Apparatus.—*^{233}Pa and ^{231}Pa.*—Stock solutions of these isotopes were prepared by the methods reported previously.[1] Aliquots of these solutions were transferred into a platinum dish and evaporated almost to dryness, initially on a hot plate and finally on a water bath. The residue was then dissolved by heating it with concentrated perchloric acid, and again evaporated to dryness. This was cooled and diluted to the desired concentration with respect to protactinium with a perchloric acid solution of a suitable concentration.

Ion Exchange Resins.—Dowex-50×8 and Dowex-1×8, 200—400 mesh, were used for the cation and anion exchange experiments respectively. Before use, they were converted to the desired forms (Dowex-50 to the H^+ form; Dowex-1 to the ClO_4^- form), washed with distilled water, and dried in air.

Benzene was purified by distillation, and doubly-distilled water was used throughout this experiment. The other chemicals, such as thenoyl trifluoroacetone and perchloric acid, were of the highest-purity grade.

For the solvent extraction procedure, a Hiranuma-Seiki magnemixer, Model MMC-8, was used. All the vessels and radiation measurement instruments were those described in the foregoing report.[1]

Procedures.—Each value given was the average of the results of at least two determinations; care was taken to ascertain the material balance in each case.

TTA Extraction.—Ten milliliters of a perchloric acid solution of protactinium which had been adjusted to the desired condition and 10 ml. of a benzene solution of TTA in the desired concentration were mixed for 30 min. with a magnemixer in a thermostat at 30°C. After the two phases had completely separated, an aliquot of each phase was taken out and counted for γ radioactivity; the apparent distribution coefficient was calculated by means of the usual relationship:

$$K_d' = \frac{\dfrac{\text{Radioactivity in the org. phase}}{\text{Vol. of the org. phase (ml.)}}}{\dfrac{\text{Radioactivity in the aq. phase}}{\text{Vol. of the aq. phase (ml.)}}}$$

Ion Exchange.—The apparent distribution coefficient

1) S. Suzuki and Y. Inoue, This Bulletin, **39**, 490 (1966).
2) G. A. Welch, *Nature*, **172**, 458 (1953).
3) R. E. Elson, "The Chemistry of Protactinium," The Actinide Elements, Ed. by G. T. Seaborg and J. J. Katz, McGraw-Hill Book Co., New York (1954), p. 103.
4) G. Bouissières, M. C. Ferradini, M. Garcon, G. Guillaumont, M. Hussonois, R. Muxart, H. Pezerat, D. Robertson and T. Stchouzkoy, U. S. A. E. C., TID-4500, 160 (1963).
5) R. Guillaumont, R. Muxart, G. Bouissières and M. Haissinsky, *Compt. rend.*, **248**, 3298 (1959).
6) F. L. Moore, *Anal. Chem.*, **27**, 70 (1955).
7) D. Brown, A. J. Smith and R. G. Wilkins, *J. Chem. Soc.*, **1959**, 1463.
8) E. S. Pal'shin and B. F. Myasoedov, *J. Anal. Chem. U. S. S. R.*, **18**, 651 (1963).
9) J. Fudge and J. L. Wood, *Analyst*, **81**, 417 (1956).
10) B. F. Myasoedov and R. Mukhart, *J. Anal. Chem., U. S. S. R.*, **17**, 343 (1962).
11) W. W. Meinke, U. S. A. E. C., AECD-2738 and AECD-2750 (1949).

was determined by equilibrating 500 mg. of air-dried ion exchange resin with 20 ml. of a 10^{-8} M protactinium solution under the desired condition for 2 days with intermittent shaking. Then the slurry was centrifuged in order to accelerate the complete separation of the two phases. In centrifugation, care was taken not to exceed 2000 r. p. m. because such a high speed is in danger of producing the sedimentation of some protactinium. An aliquot of the supernatant liquid was taken for the measurement of the γ radioactivity. The apparent distribution coefficient was calculated from the following equation:

$$K_d' = \frac{\dfrac{\text{Radioactivity in resin}}{\text{Amount of resin (g.)}}}{\dfrac{\text{Radioactivity in soln.}}{\text{Vol. of soln. (ml.)}}}$$

The radioactivity in the resin after equilibration was estimated from the difference between the total activity and the final activity present in the solutions.

Filtration.—Toyo-Roshi No. 5C filter paper (fine filter for quantitative use) and a membrane filter (supplied by Membrane-Filter-Gesellschaft, Göttingen), with diameters of 26 mm. and 30 mm. respectively, were used in this investigation. Filtration was performed under suction with a glass filtration apparatus with a perforated filter disk, the diameter of which was 18 mm. One or two milliliters of a sample solution was filtered, and then the filter paper was washed with 4 or 3 ml. of distilled water respectively. The filtrate and washings were then put together in the same polyethylene test tube. The radioactivities of its contents and of the filter paper were measured under the same geometrical conditions. The percentage of protactinium retained on the filter paper was then calculated from these values.

Results

TTA-benzene Extraction.—*The Relation between the Apparent Distribution Coefficient and the TTA Concentration.*—The influence of the TTA concentration on the apparent distribution coefficient was investigated by means of the constant acidity of the solution. The concentrations of protactinium used were 10^{-7} M and 10^{-10} M. The logarithm of the apparent distribution coefficient was plotted as a function of the logarithm of the TTA activity in the benzene phase, as is shown in Fig. 1.

The activity of TTA in the benzene phase at equilibrium was calculated from its initial concentration by the following equations:

$$\frac{(\mathrm{HT})_i}{(\mathrm{HT})_B} = 1.02 + 10^{-8}/\mathrm{H}^+ \qquad (1)^{12)}$$

$$f_{\mathrm{HT}} = 1 - 0.25(\mathrm{HT})_B^{0.48} \qquad (2)^{13)}$$

where f_{HT} is the activity coefficient of TTA in benzene; $(\mathrm{HT})_B$, the final concentration in benzene when equilibrated with an equal volume of an aqueous phase, and $(\mathrm{HT})_i$, the initial concentration.

It is clear from Fig. 1 that, in the case of a directly-prepared solution, the log-log plot of the apparent distribution coefficient and the activity of TTA shows a good linearity, with a slope of about 4 over a wide range of reagent concentration, except in the case of an extremely low acidity, where exact linearity does not hold. The difference between solutions containing protactinium concentrations of 10^{-7} M and 10^{-10} M is not obvious. Furthermore, even when the solution is left to stand for a long time, these relationships do not change beyond the range of experimental error.

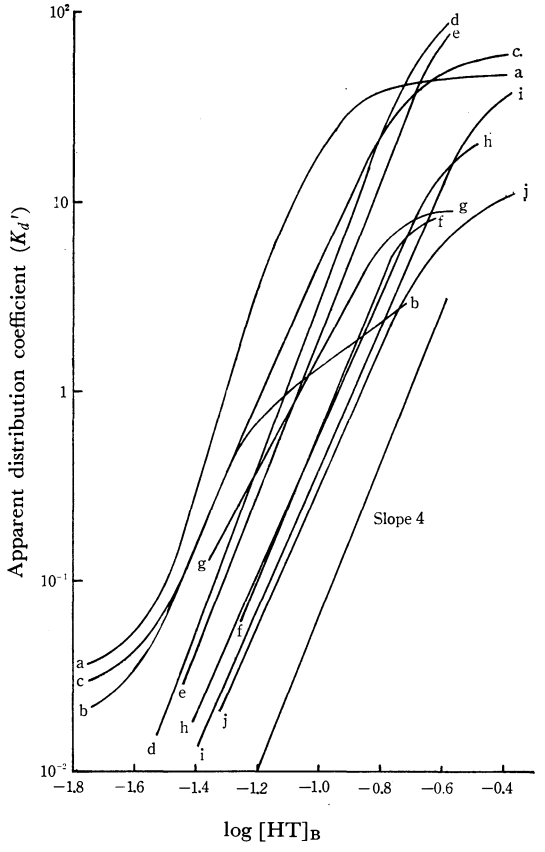

Fig. 1. Dependence of distribution coefficient on TTA activity.

a: 0.13 N $HClO_4$, 10^{-7} M Pa
b: 0.29 N $HClO_4$, 10^{-7} M Pa diluted from 10^{-5} M Pa solution in 5 N $HClO_4$
c: 0.37 N $HClO_4$, 10^{-10} M Pa
d: 0.40 N $HClO_4$, 10^{-7} M Pa
e: 0.58 N $HClO_4$, 10^{-7} M Pa
f: 1.00 N $HClO_4$, 10^{-7} M Pa
g: 0.53 N $HClO_4$, 10^{-7} M Pa diluted from 10^{-5} M Pa solution in 5 N $HClO_4$
h: 4.85 N $HClO_4$, 10^{-7} M Pa
i: 2.06 N $HClO_4$, 10^{-7} M Pa
j: 2.06 N $HClO_4$, 10^{-10} M Pa

12) A. M. Poskanzer and B. M. Foreman, *J. Inorg. Nucl. Chem.*, **16**, 323 (1961).
13) E. L. King and W. H. Reas, *J. Am. Chem. Soc.*, **73**, 1804 (1951).

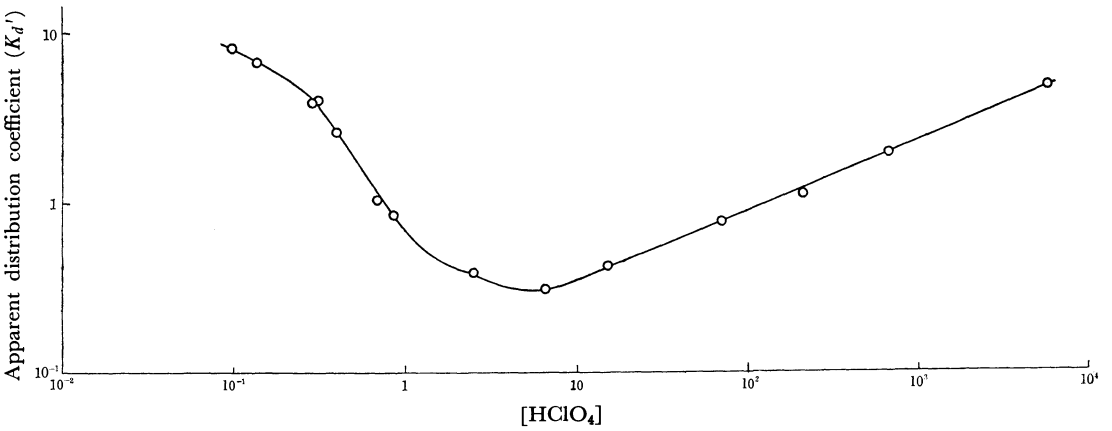

Fig. 2. Dependence of distribution coefficient of TTA extraction on perchloric acid activity.

On the contrary, when a sample solution is prepared indirectly from a 10^{-5} M stock solution, the range bearing a linear relation is narrower and the slope of the straight line is smaller than in the former case, decreasing as the aging time increases.

The Relation between the Apparent Distribution Coefficient and the Perchloric Acid Concentration.—Experiments were performed on the effect of perchloric acid concentration on the extraction of a 10^{-7} M solution of protactinium with 0.12 M TTA. The results are shown in Fig. 2. The activity of perchloric acid was calculated from the activity coefficient obtained by Robinson and Stokes.[14] As is shown in Fig. 2, the apparent distribution coefficient decreases with an increase in the concentration of perchloric acid, reaching a minimum at about 3 N acid, and then it increases with an increase in the acidity. In the range of acidity from 0.4 N to 1 N, the plot of the logarithm of the apparent distribution coefficient against the logarithm of the activity of perchloric acid shows a linear relationship with a slope of -1.45, whereas above 4 N it shows a straight line with a slope of 0.41.

The Relation between the Apparent Distribution Coefficient and the Hydrogen Ion Concentration in a Constant Ionic Srength Medium.—The effect of the acidity of the aqueous phase was studied at a constant ionic strength (2.03) by using various mixtures of perchloric acid and lithium perchlorate. Benzene solution of 0.07 M and 0.12 M TTA were used for the extraction. As is shown in Fig. 3, curves with a maximum were thus obtained, the position of the maximum differing with the difference in the TTA concentration used; with 0.12 M TTA the maximum is at 0.3 M acidity, while with 0.07 M TTA, it is at 0.1 M acidity. In a higher acidity range than the acidity that corresponds to the maximum point, the log-log plot of the apparent distribution coefficient and the hydrogen

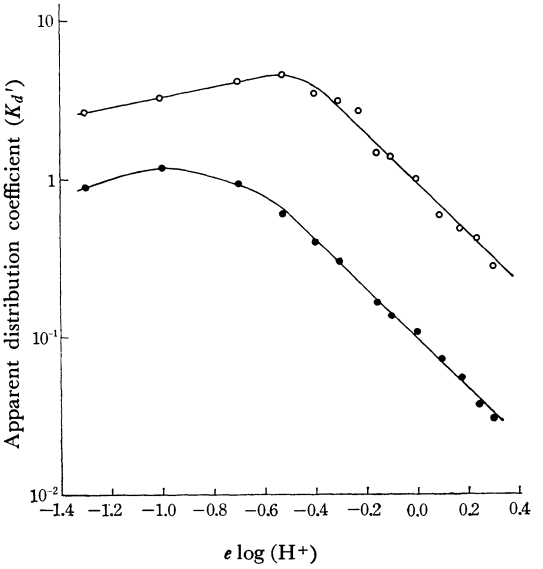

Fig. 3. Dependence of distribution coefficient of TTA extraction on hydrogen ion concentration in constant ionic strength medium.
Ionic strength, 2.03; Pa, 10^{-7} M; —○— 0.12 M TTA; —●— 0.07 M TTA.

ion concentration shows a linear relationship with a slope of -1.6. This observation is different from that of Bouissieres and his co-workers[4], who obtained a slope of -2.0 in the acidity range higher than 1 N.

The Variation in the Apparent Distribution Coefficient with the Concentration of Protactinium.—The relation between the apparent distribution coefficient and the protactinium concentration, from carrier-free to 10^{-6} M, was investigated at the constant acidities of 0.47, 1.0 and 5.0 N. The concentrations of TTA solution were 0.06, 0.10 and 0.12 M respectively. The results are shown in Fig. 4. Although at an acidity of 0.47 N the apparent distribution coefficient of carrier-free ^{233}Pa solutions is higher than that

14) R. A. Robinson and R. H. Stokes, *Trans. Faraday Soc.*, **45**, 612 (1949).

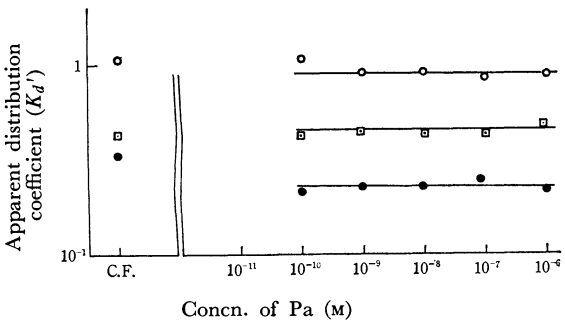

Fig. 4. Dependence of distribution coefficient of TTA extraction on protactinium concentration.
—●— 0.47 N $HClO_4$, 0.06 M TTA
—○— 1.0 N $HClO_4$, 0.12 M TTA
—⊡— 5.00 N $HClO_4$, 0.10 M TTA

of a more concentrated solution, this may be attributed to the ill reproducibility of the experiment in a trace concentration; therefore, it is considered that the apparent distribution coefficient is virtually constant in the concentration range below 10^{-6} M.

The Effect of Aging of the Solution on the Apparent Distribution Coefficient.—The relation between the apparent distribution coefficient and the aging time after the preparation of 10^{-7} M solutions of protactinium in various concentrations of perchloric acid was examined at a TTA concentration of 0.12 M. The results are presented in Fig. 5a. When the concentration of perchloric acid is low, the apparent distribution coefficient changes somewhat, but above an acidity of 0.6 N it does not change, at least not for 90 days. Then the solutions, 10^{-7} M in protactinium, were prepared just before use by the dilution of a 10^{-5} M solution which

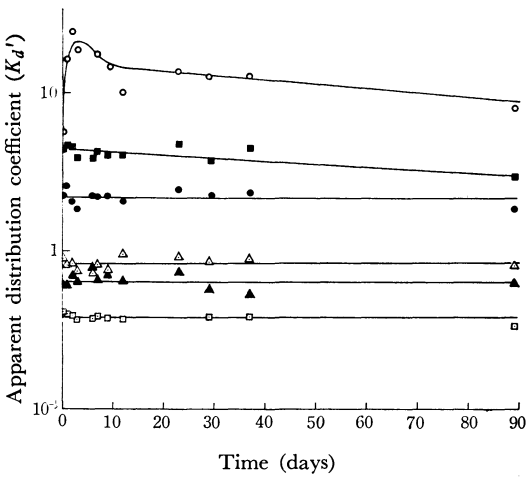

Fig. 5a. The effect of time of standing on the TTA extraction of Pa.
Pa, 10^{-7}M; TTA, 0.12M; —○— 0.087 N $HClO_4$; —■— 0.39 N $HClO_4$; —●— 0.58 N $HClO_4$; —△— 1.10 N $HClO_4$; —⊡— 2.05 N $HClO_4$; —▲— 4.91 N $HClO_4$.

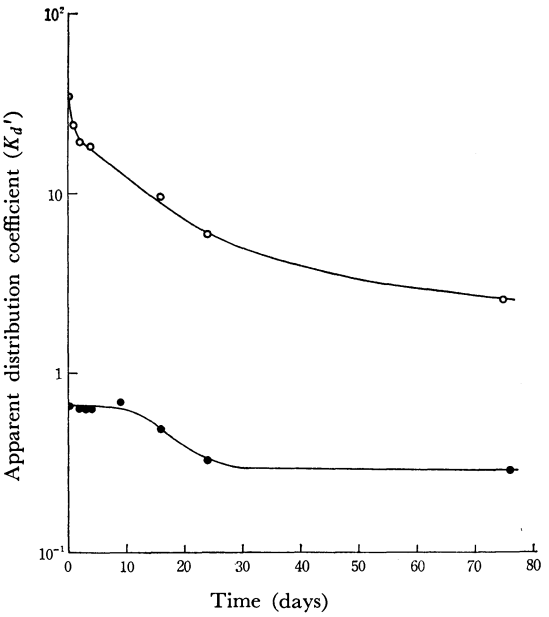

Fig. 5b. Thc effect of time of standing on the TTA extraction of Pa.
Pa, 10^{-7} M diluted from 10^{-5} M Pa solution of 5.62 N perchloric acid concentration; TTA, 0.12 M; —○— 0.056 N $HClO_4$; —●— 4.86 N $HClO_4$.

had an acidity of 5.165 N and which had been aged for a definite time. This was then extracted with a 0.12 M TTA-benzene solution in order to obtain the apparent distribution coefficients. The relations between the aging time and the distribution coefficients are shown in Fig. 5b. In contrast with the former case, the apparent distribution coefficient decreases appreciably with the time of standing.

Ion Exchange.—The apparent distribution coefficient of protactinium was determined for cation and anion exchange resins at various concentrations of perchloric acid. As is shown in Fig. 6, protactinium is adsorbed on cation exchange resin to a considerable extent, and the distribution coefficient decreases with an increase in the concentration of perchloric acid, reaching a minimum at about 3 N; then it increases with an increase in the acidity. In the ranges from 0.4 M to 1.0 N and over 3 N, plots of the logarithm of the apparent distribution coefficient against the logarithm of the activity of perchloric acid show linear relationships, with slope of −1.5 and 0.5 respectively. As to anion exchange, the apparent distribution coefficient is lower by one order than in the case of cation exchange over the entire range of acidity, but the relation between the apparent distribution coefficient and the acidity is similar to that in cation exchange.

In order to examine the adaptability of the mass action law to cation exchange, the distribution of

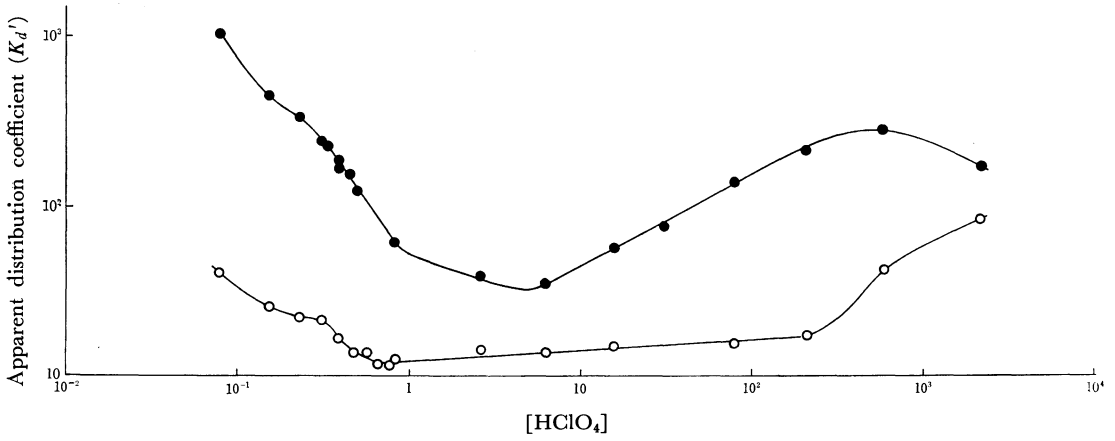

Fig. 6. Dependence of distribution coefficient of ion exchange on perchloric acid activity.
—●— Cation exchange; —○— Anion exchange

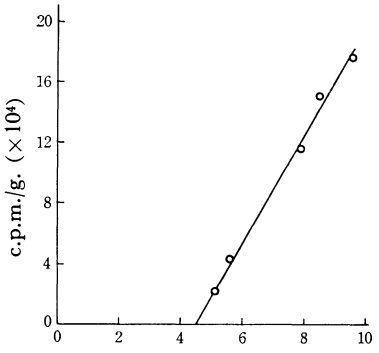

Fig. 7a. Determination of the proportion of protactinium which is not adsorbed on cation exchange resin.
Pa, 10^{-8} M; $HClO_4$, 0.50 N

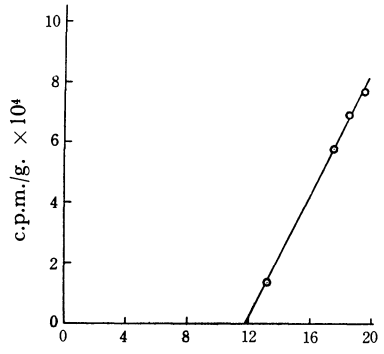

Fig. 7b. Determination of the proportion of protactinium which is not adsorbed on cation exchange resin.
Pa,10^{-8} M; $HClO_4$, 3.10 N

protactinium between two phases was measured, with varying ratios between the aqueous phase

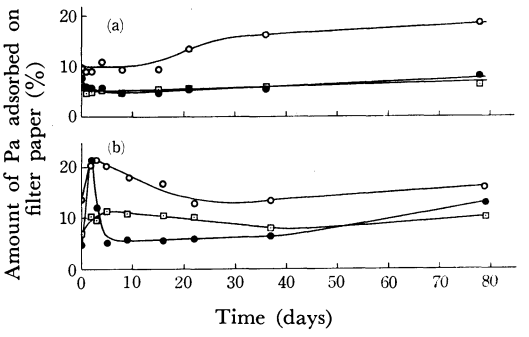

Fig. 8a. Filtration of protactinium solution.
Pa, 10^{-7} M; —●— 0.25 N $HClO_4$;
—⊡— 2.0 N $HClO_4$; —○— 5.61 N $HClO_4$

Fig. 8b. Filtration of protactinium solution.
Pa, Carrier-free ^{233}Pa; —●— 0.36 N $HClO_4$;
—⊡— 2.05 N $HClO_4$; —○— 5.00 N $HClO_4$.

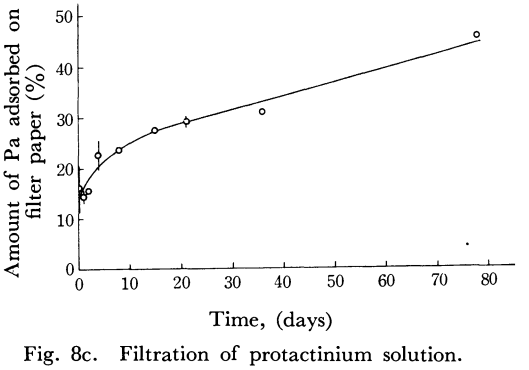

Fig. 8c. Filtration of protactinium solution.
Pa, 8.41×10^{-6} M; $HClO_4$, 5.45 N

volume and the amount of resin. The concentration of protactinium in the resin phase was plotted as an ordinate against the concentration of protactinium in the aqueous phase as abscissa, as is shown in Fig. 7. Experiments were undertaken at the acidities of 0.5 N and 3.10 N. In both cases,

linear relationships were observed which did not surpass the original.

Filtration.—*By Filter Paper.*—The effect of acidity on the removal of protactinium from a perchloric acid solution by filtration through filter paper is shown in Table I. In this case, 2 ml. of a sample solution was used. Furthermore, the effects of aging at various acidities and at various protactinium concentrations are presented in Fig. 8. The removal of protactinium decreases with an increase in the acidity, reaching a minimum at about 0.3 M; then it increases with an increase in the acidity. In the cases of carrier-free and 10^{-1} M solutions, the difference between the two cases is not obvious and virtually no effect of aging is recognized except for the drastic initial changes in carrier-free solutions. In contrast with this, in the case of a 10^{-1} M solution the removal is increased with the lapse of aging time, attaining a value of 45 per cent after 80 days.

Table I. The removal of protactinium from perchloric acid solution by filter paper

$HClO_4$ concn. N	Pa concn. M	% removal of Pa
0.072	C.F.	12.6
0.144	C.F.	5.52
0.216	C.F.	3.95
0.361	C.F.	4.79
2.05	C.F.	6.83
5.00	C.F.	13.5
0.248	10^{-7}	7.70
2.01	10^{-7}	5.90
5.61	10^{-7}	9.68
5.45	8.41×10^{-6}	16.3

Table II. The effect of pore size on the removal of protactinium from perchloric acid solution by filtration

Pa concn. M	$HClO_4$ concn. N	Filter	Pore size, mμ Max.	Mean	% removal of Pa
10^{-5}	4.65	Paper*			11.1
10^{-5}	4.65	Membrane**	300	200	9.98
10^{-5}	4.65	Membrane	275	175	10.3
10^{-5}	4.65	Membrane	250	150	20.0
10^{-5}	4.65	Membrane	<100		37.9
10^{-6}	4.90	Paper			5.88
10^{-6}	4.90	Membrane	250	150	11.7
10^{-6}	4.90	Membrane	<100		18.3
10^{-7}	4.07	Paper			7.16
10^{-7}	4.07	Membrane	250	150	9.71
10^{-7}	4.07	Membrane	<100		12.1
10^{-8}	5.46	Paper			9.38
10^{-8}	5.46	Membrane	250	150	11.6
10^{-8}	5.46	Membrane	<100		19.4
10^{-9}	4.97	Paper			10.3
10^{-9}	4.97	Membrane	250	150	15.9
10^{-9}	4.97	Membrane	<100		21.0
C.F.***	4.80	Paper			12.2
C.F.	4.80	Membrane	<100		9.84

* Paper is the abbreviation of Toyo-roshi No. filter paper.

** Membrane is the abbreviation of membrane filter supplied from Membrane-Filter-Gesellschaft, Göttingen.

*** C.F. is the carrier-free ^{233}Pa solution.

By a Membrane Filter.—The percentage of the removal of protactinium by membrane filters with various pore sizes was determined at a perchloric acid concentration of 5 N. In this experiment, 1 ml. of a sample solution was used. As is apparent in Table II, the percentage of removal increases with the decrease in pore size; this effect is especially noticeable when the protactinium concentration is 10^{-5} M.

Discussion

If the species extractable into the organic phase are considered not to have any charge, the general equation for the TTA extraction reaction can be written by modifying Connick and McVey's treatment[15] as:

$$\begin{aligned}PaO_m(OH)_nT_r^{5-2m-n-r}(aq.) &+ (5-2p-q-r)\\ &\times HT(org.) = PaO_p(OH)_qT_{5-2p-q}(org.)\\ &+ (m+n-p-q)H_2O(org.)\\ &+ (5-2m-n-r)H^+(aq.) \qquad (3)\end{aligned}$$

where HT represents the TTA molecule and T^-, the dissociated TTA anion. The equilibrium constants can then be defined as:

$$K_{m,n,p,q,r} = \frac{[PaO_p(OH)_qT_{5-2p-q}][H_2O]^{m+n-p-q}\times[H^+]^{5-2m-n-r}}{[PaO_m(OH)_nT_r^{5-2m-n-r}]\times[HT]^{5-2p-q-r}} \qquad (4)$$

where brackets have been used to represent the activities of the enclosed species. The designation of the phase in which each species exists has been omitted in order to simplify the writing of the equation. A distribution coefficient expressed in terms of activities is defined as the sum of the activities of protactinium species in the benzene phase divided by the sum of the activities of protactinium species in the aqueous phase;

$$K_d = \frac{\sum_{p,q}[PaO_p(OH)_qT_{5-2p-q}]}{\sum_{m,n,r}[PaO_m(OH)_nT_r^{5-2m-n-r}]} \qquad (5)$$

From Eq. 4, we obtain:

$$[PaO_m(OH)_nT_r^{5-2m-n-r}] = \frac{[PaO_p(OH)_qT_{5-2p-q}][H_2O]^{m+n-p-q}\times[H^+]^{5-2n-n-r}}{K_{m,n,p,q,r}[HT]^{5-2p-q-r}} \qquad (6)$$

15) R. E. Connick and W. H. McVey, *J. Am. Chem. Soc.*, **71**, 3182 (1949).

Since this equation holds for any set of values of p and q, we shall, for the sake of simplicity, choose $p=q=0$.

$$[PaO_m(OH)_nT_r^{5-2m-n-r}] = \frac{[PaT_5][H_2O]^{m+n}[H^+]^{5-2m-n-r}}{K_{m,n,o,o,r}[HT]^{5-r}} \quad (7)$$

From Eqs. 6 and 7, we obtain:

$$[PaO_p(OH)_qT_{5-2p-q}] = \frac{K_{m,n,p,q,r}[PaT_5][H_2O]^{p+q}}{K_{m,n,o,o,r}[HT]^{2p+q}} \quad (8)$$

Since Eq. 8 holds for any set of values of m, n and r, we shall choose these values to be zero.

$$[PaO_p(OH)_qT_{5-2p-q}] = \frac{K_{o,o,p,q,o}[PaT_5][H_2O]^{p+q}}{K_{o,o,o,o,o}[HT]^{2p+q}} \quad (9)$$

By substituting Eqs. 7 and 9 into Eq. 5, we obtain:

$$K_d = \frac{\sum_{p,q} \frac{K_{o,o,p,q,o}[H_2O]^{p+q}}{K_{o,o,o,o,o}[HT]^{2p+q}}}{\sum_{m,n,r} \frac{[H_2O]^{m+n}[H^+]^{5-2m-n-r}}{K_{m,n,o,o,r}[HT]^{5-r}}} \quad (10)$$

By taking the logarithm, we obtain:

$$\ln K_d = \ln \sum_{p,q} \frac{K_{o,o,p,q,o}[H_2O]^{p+q}}{K_{o,o,o,o,o}[HT]^{2p+q}} - \ln \sum_{m,n,r} \frac{[H_2O]^{m+n}[H^+]^{5-2m-n-r}}{K_{m,n,o,o,r}[HT]^{5-r}} \quad (11)$$

By taking the partial derivative of the logarithm of K_d with respect to the logarithm of the activity of HT and by substituting Eqs. 7 and 9, we obtain:

$$\frac{\partial \ln K_d}{\partial \ln [HT]} = \frac{-\sum_{p,q}(2p+q)[PaO_p(OH)_qT_{5-2p-q}]}{\sum_{p,q}[PaO_p(OH)_qT_{5-2p-q}]} + \frac{\sum_{m,n,r}(5-r)[PaO_m(OH)_nT_r^{5-2m-n-r}}{\sum_{m,n,r}[PaO_m(OH)_nT_r^{5-2m-n-r}]} = 5 - \sum_{p,q}(2p+q)f_{p,q} - \sum_{m,n,r} rf_{m,n,r} \quad (12)$$

where $f_{p,q}$ is the fraction of the total activity of the benzene phase contributed by the $PaO_p(OH)_qY_{5-2p-q}$ species, and where $f_{m,n,r}$ is that of the aqueous phase contributed by the $PaO_m(OH)_nT_r^{5-2m-n-r}$ species.

Hence:

$$\sum_{p,q} f_{p,q} = 1 \quad \text{and} \quad \sum_{m,n,r} f_{m,n,r} = 1 \quad (13)$$

Furthermore, as at least one molecule of TTA is co-ordinated to one atom of protactinium in the organic phase

$$2p + q \leqq 4 \quad (14)$$

holds.

If the activity coefficients of protactinium species are assumed to be constant, irrespective of the TTA concentration, the apparent distribution coefficient obtained empirically can be replaced for the thermodynamic distribution coefficient, K_d, expressed in terms of activity; no appreciable error should be introduced by this assumption. The curves in Fig. 1 show straight lines, with a slope of 4, in the range of TTA concentration, so that $\sum_{p,q}(2r+q)\cdot f_{p,q} + \sum_{m,n,r} rf_{m,n,r}$ should be unity. Suppose r is unity; that is, the average number of TTA molecules attached to protactinium in the aqueous phase is one; species extracted into the benzene phase should, then, have the PaT_5 form. If we can neglect the species having a TTA molecule in a perchloric acid solution, the $2p+q=1$ relation holds, so the average number of TTA attached to protactinium in the organic phase becomes 4 and then $Pa(OH)T_5$ predominates. It is clear that $r \geqq 2$ is impossible. The decrease in the slope in the higher concentration range of TTA can be explained by the increase in the average numbers of TTA attached to protactinium in the aqueous phase, and that in the range of lower concentration of TTA, by the decrease in the average number of TTA attached to protactinium in the benzene phase.

Taking the partial derivative of the logarithm of K_d with respect to the logarithm of the activity of hydrogen ion and by substituting Eq. 7, we can get:

$$\frac{\partial \ln K_d}{\partial \ln [H^+]} = -\frac{\sum_{m,n,r}(5-2m-n-r)PaO_m(OH)_n \times T_r^{5-2m-n-r}}{\sum_{m,n,r} PaO_m(OH)_nT_r^{5-2m-n-r}} = -5 + \sum_{m,n,r}(2m+n+r)f_{m,n,r} \quad (15)$$

If the activity coefficients of protactinium species and of hydrogen ion are assumed to be constant over the entire range of acidity when the ionic strength of a solution is held constant, the apparent distribution coefficient (K_d') obtained empirically can be replaced by the thermodynamic distribution coefficient(K_d) expressed in terms of activity; no appreciable error should be introduced by this assumption. As is clear from Fig. 3, the linear relationship with a slope of -1.6 holds between the logarithm of the apparent distribution coefficient and the logarithm of the hydrogen ion concentration with acidities of over 0.3 N and 0.1 N when the TTA concentrations are 0.12 M and 0.07 M respectively. Therefore,

$$-5 + \sum_{m,n,r}(2m+n+r)f_{m,n,r} = -1.6 \quad (16)$$

When $r=0$,

$$\sum_{m,n,o}(2m+n)f_{m,n,o} = 3.4 \quad (16')$$

Therefore, protactinium in a perchloric acid solution may be found in the forms $Pa(OH)_3^{2+}$ or $PaO(OH)^{2+}$ and $Pa(OH)_4^{+}$, $PaO(OH)_2^{+}$ or PaO_2^{+}. When $r=1$,

$$\sum_{m,n,1}(2m+n+1)f_{m,n,1}=3.4 \qquad (16'')$$

Species in perchloric acid may be in the forms $Pa(OH)_2T^{2+}$ or $PaOT^{2+}$ and $Pa(OH)_3T^{+}$ or $PaO(OH)T^{+}$.

From the above considerations, one can represent the reaction mechanism as:

$$PaO_m(OH)_n^{5-2m-n}+4HT \rightleftarrows Pa(OH)T_4 + (m+n-1)H_2O+(5-2m-n)H^+ \qquad (17)$$

where $2m+n$ is 3 and 4, or as:

$$PaO_m(OH)_nT^{4-2m-n}+4HT \rightleftarrows PaT_5 + (m+n)H_2O+(4-2m-n)H^+ \qquad (18)$$

where $2m+n$ is 2 and 3.

The reason for the phenomenon that the lower the perchloric acid concentration, the more remarkable the decrease in the slope of the curves in Fig. 1 at higher TTA concentrations, may be considered to be as follows. The solubility of TTA in the aqueous phase increases with the decrease in acidity, as is clear from Eq. 1, and the lower the acidity, the more easily TTA is dissociable. Therefore, TTA can form a complex with protactinium more easily in an aqueous solution with a low acidity. Similarly, in a weakly acidic solution, a high concentration of TTA facilitates the formation of anionic species, so that the maximum of the curves in Fig. 3 appears in the higher acidity region when the concentration of TTA is high. The curve in Fig. 2, the dependence of the apparent distribution coefficient on the perchloric acid concentration at a TTA concentration of 0.12 M, shows a straight line in the 0.3—1.0 N acidity range, with a slope of −1.5; this agrees with that in Fig. 3. The curve of an acidity below 0.3 N, however, is completely different from the results of Fig. 3. With an acidity of above 3 N, the apparent distribution coefficient increases with the increase in acidity, but this can not be understood in terms of the above-mentioned considerations, because the assumptions made in the preceding discussion are not applicable. In other words, the activity coefficients of protactinium species may change with the ionic strength; if so, in Eq. 15 the apparent distribution coefficient should not be used instead of the true distribution coefficient (K_d). Furthermore, it should be pointed out that, in performing the differentiation leading to Eq. 15, it was necessary that the activity of water remain constant, but this assumption may not hold in a case of a remarkable change in ionic strength.

For cation exchange reaction, we can write the general equation as:

$$PaO_m(OH)_n^{5-2m-n}+(5-2p-q)HR \rightleftarrows PaO_p(OH_qR_{5-2p-q}+(m+n-p-q)H_2O+(5-2m-n)H^+ \qquad (19)$$

where HR represents cation exchange resin. The equilibrium constant for this reaction can be defined as:

$$K_{m,n,p,q}=\frac{[PaO_p(OH)_qR_{5-2p-q}][H_2O]^{m+n-p-q}\times[H^+]^{5-2m-n}}{[PaO_m(OH)_n^{5-2m-n}][HR]^{5-2p-q}} \qquad (20)$$

and the distribution coefficient, as:

$$K_d=\frac{\sum_{p,q}[Pa(OH)_qR_{5-2p-q}]}{\sum_{m,n}[PaO_m(OH)_n^{5-2m-n}]} \qquad (21)$$

Proceeding as before gives:

$$\frac{\partial \ln K_d}{\partial \ln [H^+]}=-5+\sum_{m,n}(2m+n)f_{m,n} \qquad (22)$$

This equation is in the same form as (16''), so that the similarity between curves in Fig. 2 and Fig. 6 is not surprising. The difference between these curves may be due mainly to the following two reasons: first, the difference in the dependency of the activity coefficient on the perchloric acid concentration between the benzene phase and the resin phase, and second, the presence of non-adsorbable species on ion exchange resin.

Although no meaningful difference was observed between 10^{-7} M and 10^{-10} M protactinium solutions, a great difference in the stability of the solutions was observed between 10^{-5} M and 10^{-7} M solutions. This is probably due to the ease with which the 10^{-5} M solution polymerizes. It is interesting to note that this concentration is just below the limit of the solubility of protactinium in a 5 N perchloric acid solution.[6)]

To clarify this point, the effect of the protactinium concentration on the distribution coefficient for extraction was examined. It is apparent from Fig. 4, with a protactinium concentration of below 10^{-6} M, that the apparent distribution coefficient for TTA extraction is almost constant, regardless of the protactinium concentration, so this phenomenon may be characteristic of concentrated solutions such as 10^{-5} M. This is confirmed by the results of filtration experiments; that is, the amount uptaken on the filter from the solution of 10^{-5} M is extremely large. Above all, the results obtained by using a membrane filter may be an indication of the presence of colloidal aggregates of protactinium species. Furthermore, the remarkable dependence on the aging time encountered in the filtration of a 10^{-5} M solution through filter paper is consistent with the observation on the solvent extraction experiments.

16) R. Thompson, U. S. A. E. C., AECD-1897 (1948).

Even when the concentration of protactinium is lower than 10^{-6} M, a membrane filter with smaller pores removes radioactivity more effectively than one with larger pores. This is an indication of the presence of a small amount of colloidal aggregates. This assumption is also supported by the following consideration.

We suppose that one or more species, which are nonadsorbable on cation exchange resin and which do not reach equilibrium rapidly with adsorbable species, would be present in a solution and that the fraction of such species may be expressed by a. Under identical experimental conditions, one can assume that the activity coefficients of protactinium species are constant; therefore, the protactinium concentration, namely, the radioactivity in unit volume, might be proportional to the activity of protactinium species. For this reason, the radioactivity of protactinium, instead of its activity, will be used in the following discussion for the sake of simplicity. The distribution coefficient of the species adsorbable on the cation exchange resin can be defined as:

$$K_d = \frac{A_r/M}{A_{aq}/V} \tag{23}$$

where M represents the amount of cation exchange resin per gram; V, the volume of solution in ml. and A_r and A_{aq}, the radioactivity in each phase respectively. Let A, A'_r and A'_{aq} be the total radioactivity and the radioactivities in the resin phase and in the aqueous phase at equilibrium respectively; we can then write:

$$A'_r = A_r \tag{24}$$

$$A'_{aq} = A_{aq} - aA \tag{25}$$

By combining Eqs. 23, 24 and 25, we can get:

$$\frac{K_d}{V}(A'_{aq} - aA) = \frac{A'_r}{M} \tag{26}$$

From Eq. 26 we then obtain:

$$S_r = K_d S_{aq} - \frac{aA}{V} K_d \tag{27}$$

where:

$$A'_{aq}/V = S_{aq} \qquad A'_r/M = S_r \tag{28}$$

Equation 27 represents the relationship between S_{aq} and S_r to be linear and the slope to be K_d, namely, the distribution coefficient of the adsorbable species. If we represent the intercept of abscissa as $(S_{aq})_0$,

$$a = \frac{(S_{aq})_0}{A/V} \tag{29}$$

The ratio of the value of the intercept of abscissa to the initial activity in the unit volume of solution gives the fraction of nonadsorbable species. For a solution containing only adsorbable species in rapid equilibrium, we may obtain a straight line which passes through the point of origin. Figures 7a and b give the plot for solutions of about 10^{-8} M protactinium in 0.50 N and in 3.10 N perchloric acid respectively. These figures indicate that approximately 17% and 44% of nonadsorbable protactinium species are present in these media respectively. These results are compatible with the observations of the filtration experiment. No such phenomenon, however, can be observed in the solvent extraction. This difference between solvent extraction and ion exchange can be explained by the existence of a dynamic equilibrium in the solvent extraction, which in turn destroys the colloidal aggregates to some degree by means of the strong complexing action of TTA. This offers one reason for the small difference in behavior towards solvent extraction and cation exchange. The similarity between the effects of cation and anion exchange resins on the perchloric acid concentration seems curious, but in anion exchange experiments no such simple relation as Eq. 27 could be obtained and, therefore, further investigation is needed in order to illustrate the mechanism of anion exchange.

Summary

The chemical behavior of pentavalent protactinium in perchloric acid solutions has been investigated by TTA-benzene extraction, ion exchange and filtration methods. When the protactinium concentration is less than 10^{-6} M, the log-log plot of the apparent distribution coefficient and the activity of TTA in the benzene phase gives a straight line with a slope of 4, while the plot of the apparent distribution coefficient and the acidity in a constant ionic strength medium shows a linear relationship with a slope of -1.6 over the 0.3—2.0 N range of acidity. This relationship does not change with the aging of the solution.

Thus, under these conditions, the reaction of TTA extraction may proceed as:

$$PaO_m(OH)_n^{5-2m-n} + 4HT \rightleftarrows Pa(OH)T_4 + (m+n-1)H_2O + (5-2m-n)H^+$$

where $2m+n$ is 3 and 4, or as:

$$PaO_m(OH)_nT^{4-2m-n} + 4HT \rightleftarrows PaT_5 + (m+n)H_2O + (4-2m-n)H^+$$

where $2m+n$ is 2 and 3.

The cation exchange experiments give consistent results, leading to these conclusions. Contrary to this, when the concentration of protactinium is higher than 10^{-6} M, this relation does not hold and the apparent distribution coefficient decreases with the increase in aging time, even in a 5 N perchloric acid solution; therefore, it is considered that protactinium forms colloidal aggregates to a greater extent. This is also confirmed by the

filtration experiment; that is, the effect of the pore size of the filter and that of the aging time on the removal of protactinium from a solution by filtration are noticeable, especially when the concentration of protactinium is higher than 10^{-6} M. The behavior towards anion exchange resin can not be explained, however, and so further experiments are needed.

Part of the expenses for this investigation have been defrayed by a grant-in-aid by the Ministry of Education.

BULLETIN OF THE CHEMICAL SOCIETY OF JAPAN VOL. 39 1715—1720 (1966)

Studies of Mixed Cyano Cobalt(III) Complexes. II.[1] The Geometrical Isomers of $[CoX(CN)en_2]^+$

By Kuwako OHKAWA, Jinsai HIDAKA and Yoichi SHIMURA

Department of Chemistry, Faculty of Science, Osaka University, Toyonaka, Osaka

(Received November 30, 1965)

Two new mixed cyano complexes, *cis*-$[CoCl(CN)en_2]Cl$ (red) and *cis*-$[CoBr(CN)en_2]Br$ (deep rose), have been synthesized and resolved into their optical isomers. The splitting patterns of the ligand field absorption bands of the cis and the trans isomers of the halogenocyanobis(ethylenediamine)cobalt(III) ion have been discussed in relation to the geometrical configurations of the complexes and to the σ- and π-antibonding contribution of the cyanide or the halide ligands to the metal d-orbitals. These studies have been made successfully using the circular dichroism data of the optically active *cis*-$[CoX(CN)en_2]X$ (X=Cl, Br).

Recently several papers[1-4] have appeared dealing with the mixed cyano-ammine or the mixed cyano-diamine complexes of cobalt(III). A rather normal character of cyanide as a ligand for cobalt(III) has been well established, although the ligand has an exceptionally high position in the spectrochemical series. From a spectrochemical point of view, the mixed cyano cobalt(III) complexes which contain the halogeno ligands or both the halogeno and the ammine ligands are very interesting, since the position of a halogeno ligand in the spectrochemical series is well separated from the position of an ammine ligand in the direction opposite to that of the cyanide ligand. Chan and Tobe[5,6] prepared some such complexes, namely, the trans forms of $[CoX(CN)en_2]X$ (X=Cl, Br); however, the corresponding cis forms are yet unknown.

In the present paper, the syntheses of the missing cis forms of $[CoX(CN)en_2]X$ (X=Cl, Br) and their resolution into their optical isomers will be described. Besides proving the cis structure, the optical resolution will give a convenient tool for the assignment of the d-d absorption bands; the splitting patterns of the so-called first and second absorption bands are reflected profoundly in the circular dichroism spectra. The geometrical structures of the related mixed cyano cobalt(III) complexes will also be discussed.

Experimental

Materials.—*The Dark Yellow Form of* $Na_3[Co(CN)_2(SO_3)_2(NH_3)_2]\cdot 6H_2O$.—To a solution of 15 g. of sodium cyanide in 200 ml. of water, 36 g. of $NH_4[Co(SO_3)_2(NH_3)_4]\cdot 3H_2O$[7] was added. The desired complex precipitated gradually, and ammonia was evolved simultaneously. After about three hours, the resulting mixture was cooled in an ice bath and filtered. Another crop of the crude complex was obtained from the filtrate by cooling it in an ice bath and by adding alcohol. The yield was 37 g. This yellow complex was recrystallized from water below 35—40°C.

Found: C, 6.64; H, 1.61; N, 15.50. Calcd. for $C_2H_6N_4O_6S_2Na_3Co = Na_3[Co(CN)_2(SO_3)_2(NH_3)_2]$: C, 6.42; H, 1.62; N, 14.98%.

Found: H_2O, 22.28. Calcd. for $Na_3[Co(CN)_2(SO_3)_2(NH_3)_2]\cdot 6H_2O$: 22.41%.

The Orange-yellow form of $Na_3[Co(CN)_2(SO_3)_2(NH_3)_2]\cdot 5H_2O$.—To a solution of 10 g. of sodium cyanide in 150 ml. of water, 24 g. of $NH_4[Co(SO_3)_2(NH_3)_4]\cdot 3H_2O$[7] was added. The mixture was then warmed on a water bath and evaporated gently. When orange crystals began to appear, the reaction mixture was cooled in an ice bath. The complex was filtered and recrystallized from hot water by the addition of ethanol. Yield: 9 g.

1) Part I of this series: K. Ohkawa, J. Fujita and Y. Shimura, This Bulletin, **38**, 66 (1965).
2) N. R. S. Gupta, *Z. anorg. Chem.*, **325**, 108 (1963).
3) H. Siebert, ibid., **327**, 63 (1964).
4) M. Shibata, M. Mori and E. Kyuno, *Inorg. Chem.*, **3**, 1573 (1964).
5) S. C. Chan and M. L. Tobe, *J. Chem. Soc.*, **1963**, 966.
6) S. C. Chan, ibid., **1964**, 2716.
7) A. Werner and H. Grüger, *Z. anorg. Chem.*, **16**, 398 (1898).

Found: C, 6.82; H, 1.87; N, 14.45. Calcd. for $C_2H_6N_4O_6S_2Na_3Co = Na_3[Co(CN)_2(SO_3)_2(NH_3)_2]$: C, 6.42; H, 1.62; N, 14.98%.

Found: H_2O, 19.08. Calcd. for $Na_3[Co(CN)_2(SO_3)_2(NH_3)_2]\cdot 5H_2O$: 19.40%.

The Dark Yellow Form of $K_3[Co(CN)_2(SO_3)_2(NH_3)_2]\cdot H_2O$.—This was prepared by the same method as was the dark yellow form of $Na_3[Co(CN)_2(SO_3)_2(NH_3)_2]\cdot 6H_2O$. To a solution of 20 g. of potassium cyanide in 100 ml. of water, 28 g. of $NH_4[Co(SO_3)_2(NH_3)_4]\cdot 3H_2O$[7] was added. To complete the reaction the mixture was then stirred. After the solution had been cooled in an ice bath for one hour, the dark yellow complex which had deposited was filtered and washed with water-methanol (1 : 1) and methanol. Another crop of the complex was obtained from the filtrate by the addition of methanol. The crude complex was recrystallized from water by the addition of methanol. Yield: 25 g.

Found: C, 5.89; H, 1.75; N, 13.66. Calcd. for $C_2H_6N_4O_6S_2K_3Co = K_3[Co(CN)_2(SO_3)_2(NH_3)_2]$: C, 5.69; H, 1.43; N, 13.26%.

Found: H_2O, 4.14. Calcd. for $K_3[Co(CN)_2(SO_3)_2(NH_3)_2]\cdot H_2O$: 4.09%.

cis-$[Co(CN)(SO_3)en_2]$.—Thirty grams of the orange-yellow or the dark-yellow form of $M_3[Co(CN)_2(SO_3)_2(NH_3)_2]\cdot xH_2O$ (M=Na or K) was covered with 300 ml. of a 10% aqueous solution of ethylenediamine. When the mixture was heated on a water bath, it changed to a brown solution. After several minutes, a glittering complex began to crystallize. The mixture was kept on a water bath about three hours and then filtered. The crude complex was washed with a little of hot water about three times, with water, and finally with ethanol. Yield: 5.8 g.

The crystals which were recrystallized from hot water were pale brownish yellow and anhydrous.

Found: C, 20.22; H, 6.07; N, 23.47. Calcd. for $C_5H_{16}N_5O_3SCo = [Co(CN)(SO_3)en_2]$: C, 21.07; H, 5.65; N, 24.57%.

cis-$[CoCl(CN)en_2]Cl\cdot H_2O$.—In 135ml. of concentrated hydrochloric acid, 13 g. of *cis*-$[Co(CN)(SO_3)en_2]$ was suspended; this solution was then warmed on a water bath for about three hours. The color of the solution changed from yellow to red. After the solution had been evaporated to half of the original volume, it was filtered and 70 ml. of ethanol was added to the filtrate. The solution was then cooled in an ice bath; a red complex deposited gradually. The product was recrystallized from warm water by the addition of alcohol and washed with a water-ethanol mixture (1 : 2) and then with ethanol several times. Yield: 3.8 g.

Found: C, 21.71; H, 6.00; N, 24.97. Calcd. for $C_5H_{16}N_5Cl_2Co = [CoCl(CN)en_2]Cl$: C, 21.75; H, 5.84; N, 25.37%.

Found: H_2O, 6.56; Cl, 24.60. Calcd. for $[CoCl(CN)en_2]Cl\cdot H_2O$: H_2O, 6.12; Cl, 24.12%.

cis-$[CoBr(CN)en_2]Br\cdot H_2O$. — This complex was prepared by the same method as was the chloro complex, using 9.5 g. of *cis*-$[Co(CN)(SO_3)en_2]$ and 100 ml. of concentrated hydrobromic acid. Yield: 3 g.

Found: C, 16.46; H, 4.71; N, 19.00; Br, 43.63. Calcd. for $C_5H_{16}N_5Br_2Co = [CoBr(CN)en_2]Br$; C, 16.48; H, 4.42; N, 19.21; Br, 43.90%.

Found: H_2O, 4.73. Calcd. for $[CoBr(CN)en_2]Br\cdot H_2O$: 4.60%.

The Optical Resolution of cis-$[CoCl(CN)en]_2]^+$.—Racemic *cis*-$[CoCl(CN)en_2]Cl\cdot H_2O$ (9.06 g.) was dissolved in 90 ml. of water at about 35°C by rigorous shaking. To this solution, a solution of 5.31 g. of ammonium (+)-*d*-bromocamphor-π-sulfonate (NH_4-*d*-BCS) in 50 ml. of water was added at room temperature. After a few minutes, the diastereomer $(+)_{589}$-$[CoCl(CN)en_2]$-(*d*-BCS) began to separate as rosy crystals. To complete the reaction, the mixture was stirred, allowed to stand for about ten minutes, and then filtered. The diastereomer was washed with a little ice water five times and then with ethanol, and dried in air. The yield was 6.6 g. The recrystallization was made from a little water by the addition of alcohol. The diastereo mer is optically stable in water.

Found: C, 32.66; H, 5.54; N, 12.98. Calcd. for $C_{15}H_{30}N_5O_4SClBrCo = [CoCl(CN)en_2](C_{10}H_{14}O_4SBr)$: C, 32.74; H, 5.50; N, 12.73%.

For a 0.05% solution of the diastereomer in a 2 dm. tube:

$\alpha_{589} = (+)\ 0.14°$, $\alpha_{546} = (+)\ 0.11°$.

The recrystallized diastereomer (2.26 g.) and potassium iodide (7 g.) were ground in a mortar with a few drops of water. Ten milliliters of water was then added the mixture, and the resultant mixture was triturated for about half an hour. The complex thus deposited was separated by suction, and washed with a little ice water three times and then with alcohol. The complex was then recrystallized from warm water by the addition of alcohol in an ice bath.

Found: C, 16.57; H, 4.50; N, 19.32. Calcd. for $C_5H_{16}N_5ClICo = [CoCl(CN)en_2]I$: C, 16.34; H, 4.39; N, 19.06%.

For a 1/150 F solution of the complex in a 1/2 dm. tube:

$\alpha_{589} = (+)\ 0.02°$, $\alpha_{546} = (-)\ 0.10°$.

The Optical Resolution of cis-$[CoBr(CN)en_2]^+$—This complex was resolved by the same method as was the chloro complex. Racemic *cis*-$[CoBr(CN)en_2]Br\cdot H_2O$ (4.43 g.) was dissolved in 50 ml. of water at about 45°C by rigorous shaking. To this solution, a solution of 3.66 g. of ammonium (+)-*d*-bromocamphor-π-sulfonate in 20 ml. of water was added. After a few minutes, the precipitated diastereomer $(+)_{589}$-$[CoBr(CN)en_2]$-(*d*-BCS) was filtered, washed with a little ice water several times and then with ethanol, and dried in air. The yield was 2.9 g. The diastereomer is optically unstable in water.

For a 0.05% solution of the diastereomer in a 2 dm. tube:

$\alpha_{589} = (+)0.12°$, $\alpha_{546} = (-)0.10°$

The diastereomer (3.0 g.) was ground in a mortar with 6 ml. of concentrated hydrobromic acid; the complex thus deposited was filtered and washed with ethanol. The complwx recrystallized was anhydrous.

Found: C, 16.60; H, 4.52; N, 19.40. Calcd. for $C_5H_{16}N_5Br_2Co = [CoBr(CN)en_2]Br$: C, 16.48; H, 4.42; N, 19.21%.

For a 1/150 F solution of the complex;
in a 1/2 dm. tube, $\alpha_{589} = (+)\ 0.06°$;
in a 1/5 dm. tube, $\alpha_{546} = (-)\ 0.12°$.

trans-$[CoCl(CN)(NH_3)_4]Cl$.—The orange-colored complex[3] of $[Co(CN)(SO_3)(NH_3)_4]$ (10 g.) was suspended in 100 ml. of concentrated hydrochloric acid and warmed gently on a water bath. The color of the mixture became orange yellow, and sulfur dioxide gas was evolved. After about half an hour, the supernatant liquid was

decanted off; another 100 ml. of concentrated hydrochloric acid was added to the residue. The resulting mixture was warmed on a water bath for an hour, cooled to room temperature, and then allowed to stand overnight. The complex was separated from the liquid and washed several times by decantation using concentrated hydrochloric acid. This was washed with alcohol and dried in air. Yield: 9 g. This orange-yellow complex is rapidly aquated in water. No recystallization was made.

Found: C, 5.07; H, 5.59; N, 28.68; Cl, 31.58. Calcd. for $CH_{12}N_5Cl_2Co$ = [CoCl(CN)$(NH_3)_4$]Cl: C, 5.36; H, 5.40; N, 31.26; Cl, 31.68%.

trans-[CoBr(CN)$(NH_3)_4$]Br.—This complex was prepared by the same method as was the chloro complex, using 10 g. of [Co(CN)$(SO_3)(NH_3)_4$][3] and 100 ml. of concentrated hydrobromic acid. Yield: 10 g.

Found: C, 3.53; H, 3.93; N, 20.26; Br, 52.78. Calcd. for $CH_{12}N_5Br_2Co$ = [CoBr(CN)$(NH_3)_4$]Br: C, 3.84; H, 3.86; N, 22.40; Br, 51.10%.

The trans forms of [CoX(CN)en_2]X (X=Cl, Br) were prepared by the method of Chan.[5,6]

Measurements. — The absorption spectra were measured by a Beckman DU Spectrophotometer. The solvent employed for *cis*-[CoX(CN)en_2]X (X=Cl, Br) was water, and for *trans*-[CoX(CN)en_2]X, 70% perchloric acid. The circular dichroism spectra were recorded on a Spectropolarimeter, ORD/UV-5, of the Japan Spectroscopic Co. A Rudolph photoelectric spectropolarimeter, Model 200S-80, was used to check the optical rotation. All the measurements were made at room temperature.

Results and Discussion

The Geometrical Configurations of the Complexes.—Chan and Tobe[5] derived *trans*-[CoCl(CN)en_2]Cl from the orange-colored form of [Co(CN)$(SO_3)en_2$]. In the present study of the synthesis of the corresponding cis isomer, a new isomer of [Co(CN)$(SO_3)en_2$] was used as the parent compound; it was pale brownish-yellow in color and was derived from the brown form of $[Co(SO_3)_2(NH_3)_4]^-$ through an intermediate complex $[Co(CN)_2(SO_3)_2(NH_3)_2]^{3-}$. Two isomers of $M_3[Co(CN)_2(SO_3)_2(NH_3)_2]$, dark-yellow and orange-yellow, were obtained from the reaction between $[Co(SO_3)_2(NH_3)_4]^-$ and alkali cyanide. Babaeva and Baranovskii[8] had already obtained the yellow potassium salt as dihydrate and had assigned the cis(CN)-cis(SO_3)-trans(NH_3) structure to the complex. The structure of the new orange-yellow complex is unknown, At any rate, both the isomers produced the same yellow form of [C(CN)$(SO_3)en_2$]. This yellow-[Co(CN)(SO_3)·en_2] is less soluble in water than its orange-colored isomer, which has been prepared by Chan and Tobe. The cis configuration of the red-[CoCl·(CN)en_2]Cl, which was derived from the yellow-[Co(CN)$(SO_3)en_2$], was established by its optical

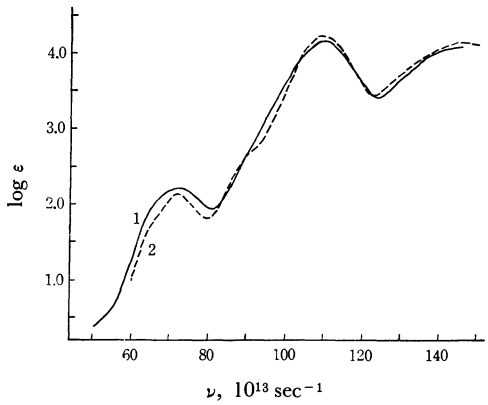

Fig. 1. Absorption spectra of [Co(CN)$(SO_3)en_2$].
1—— absorption curve of *cis*-[Co(CN)$(SO_3)en_2$] in 4% NH_3 aq.
2---- absorption curve of *trans*-[Co(CN)(SO_3)-en_2] in aqueous solution.

resolution; accordingly, it is certain that the yellow-[Co(CN)$(SO_3)en_2$] is the cis isomer, and the orange-[Co(CN)$(SO_3)en_2$], the trans isomer (see Fig. 1).

The corresponding tetrammin complex, [Co·(CN)$(SO_3)(NH_3)_4$], which is known only in one form (an orange colored form[3]), may be the trans isomer. The diffuse reflectance spectra of [CoX·(CN)$(NH_3)_4$]X (X=Cl, Br) support the theory that all these tetrammine complexes are trans isomers (see Table I).

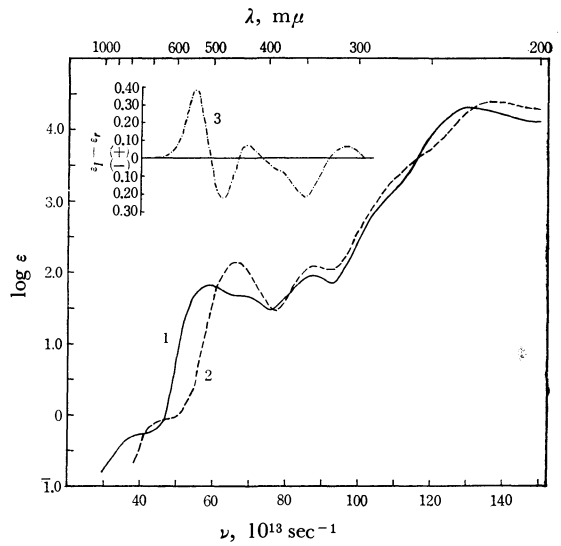

Fig. 2. Absorption and circular dichroism spectra of $[CoCl(CN)en_2]^+$.
1—— absorption curve of *cis*-[CoCl(CN)en_2]Cl·H_2O in aqueous solution.
2---- absorption curve of *trans*-[CoCl(CN)en_2]-Cl·H_2O in 70% $HClO_4$.
3-·-· CD curve of $(-)_{546}$-*cis*-[CoCl(CN)en_2]I in aqueous solution.

8) A. V. Babaeva and I. B. Baranovskii, *Zh. Neorgan. Khim.*, **7**, 783 (1962); *Chem. Abstr.*, **57**, 402 g.

Table I. Absorption data of *cis*- and *trans*-$[CoX(CN)N_4]X$ ν, $10^{13}sec^{-1}$, (log ε)

Complex	A Band	I Band	II Band	Charge transfer band	
				$p_\pi(X)\rightarrow d_{z^2}$	$p_\sigma(X)\rightarrow d_{z^2}$
cis-$[CoCl(CN)en_2]Cl$	ca. 40 ($\bar{1}$.74)	59.2 (1.82) ca. 69 sh	87.6 (1.95)	ca. 111 sh	130 (4.29)
trans-$[CoCl(CN)en_2]Cl$*	ca. 48 ($\bar{1}$.94)	66.2 (2.14)	88.6 (2.08)	ca. 106 sh	136 (4.37)
trans-$[CoCl(CN)(NH_3)_4]Cl$**	42	65.6	91.5	—	—
cis-$[CoBr(CN)en_2]Br$	37.6 (0.72)	58.5 (1.98) ca. 68 sh	—	ca. 97 sh	119 (4.29)
trans-$[CoBr(CN)en_2]Br$*	ca. 45 (0.74)	64.9 (2.11)	—	ca. 102 sh	124.5(4.44)
trans-$[CoBr(CN)(NH_3)_4]Br$**	42	64.5	—	—	—

* Measured in 70% $HClO_4$. ** Data of diffuse reflectance spectra.

Table II. CD data of $(-)_{546}$-*cis*-$[CoX(CN)en_2]^+$ (X=Cl, Br)

Complex	Absorption band region	ν_{max} $(10^{13}sec^{-1})$	$(\varepsilon_l-\varepsilon_r)_{max}$
$[CoCl(CN)en_2]I$	I	55.2	+0.38
		62.2	−0.22
		69.6	+0.07
	II	ca. 79.2	ca. −0.08
		85.0	+0.02
		96.2	+0.08
$[CoBr(CN)en_2]Br$	I	53.6	+0.38
		60.7	−0.25
		68.0	+0.10

Table III. Predicted shifts of the first and second bands due to the replacement of ligands*

Electronic transition	$[CoN_6]$	*trans*-$[CoX_2N_4]$ X(±*z*)		*cis*-$[CoX_2N_4]$ X(+*x*, +*y*)		*trans*-$[CoXYN_4]$ X(+*z*), Y(−*z*)		*cis*-$[CoXYN_4]$ X(+*x*), Y(+*y*)		$[CoX_6]$	
$d_{xy}\rightarrow d_{x^2-y^2}$	0	0	A_{2g}	$\frac{1}{2}\delta_\sigma(X)+\frac{1}{2}\delta_\pi(X)$	B_1	0	A_2	$\frac{1}{4}\delta_\sigma(X)+\frac{1}{4}\delta_\pi(X)+\frac{1}{4}\delta_\sigma(Y)+\frac{1}{4}\delta_\pi(Y)$	A′	$\delta_\sigma(X)+\delta_\pi(X)$	T_{1g}
$d_{yz}\rightarrow d_{y^2-z^2}$	0	$\frac{1}{2}\delta_\sigma(X)+\frac{1}{2}\delta_\pi(X)$	E_g	$\frac{1}{4}\delta_\sigma(X)+\frac{1}{4}\delta_\pi(X)$	A_2 & B_2	$\frac{1}{4}\delta_\sigma(X)+\frac{1}{4}\delta_\pi(X)+\frac{1}{4}\delta_\sigma(Y)+\frac{1}{4}\delta_\pi(Y)$	E	$\frac{1}{4}\delta_\sigma(Y)+\frac{1}{4}\delta_\pi(Y)$	A″	$\delta_\sigma(X)+\delta_\pi(X)$	
$d_{zx}\rightarrow d_{z^2-x^2}$	0	$\frac{1}{2}\delta_\sigma(X)+\frac{1}{2}\delta_\pi(X)$		$\frac{1}{4}\delta_\sigma(X)+\frac{1}{4}\delta_\pi(X)$		$\frac{1}{4}\delta_\sigma(X)+\frac{1}{4}\delta_\pi(X)+\frac{1}{4}\delta_\sigma(Y)+\frac{1}{4}\delta_\pi(Y)$		$\frac{1}{4}\delta_\sigma(X)+\frac{1}{4}\delta_\pi(X)$	A″	$\delta_\sigma(X)+\delta_\pi(X)$	
$d_{xy}\rightarrow d_{z^2}$	0	$\frac{2}{3}\delta_\sigma(X)$	B_{2g}	$\frac{1}{6}\delta_\sigma(X)+\frac{1}{2}\delta_\pi(X($	A_1	$\frac{1}{3}\delta_\sigma(X)+\frac{1}{3}\delta_\sigma(Y)$	B_2	$\frac{1}{12}\delta_\sigma(X)+\frac{1}{4}\delta_\pi(X)+\frac{1}{12}\delta_\sigma(Y)+\frac{1}{4}\delta_\pi(Y)$	A′	$\delta_\sigma(X)+\delta_\pi(X)$	T_{2g}
$d_{yz}\rightarrow d_{x^2}$	0	$\frac{1}{6}\delta_\sigma(X)+\frac{1}{2}\delta_\pi(X)$	E_g	$\frac{5}{12}\delta_\sigma(X)+\frac{1}{4}\delta_\pi(X)$	A_2 & B_2	$\frac{1}{12}\delta_\sigma(X)+\frac{1}{4}\delta_\pi(X)+\frac{1}{12}\delta_\sigma(Y)+\frac{1}{4}\delta_\pi(Y)$	E	$\frac{1}{3}\delta_\sigma(X)+\frac{1}{12}\delta_\sigma(Y)+\frac{1}{4}\delta_\pi(Y)$	A″	$\delta_\sigma(X)+\delta_\pi(X)$	
$d_{zx}\rightarrow d_{y^2}$	0	$\frac{1}{6}\delta_\sigma(X)+\frac{1}{2}\delta_\pi(X)$		$\frac{5}{12}\delta_\sigma(X)+\frac{1}{4}\delta_\pi(X)$		$\frac{1}{12}\delta_\sigma(X)+\frac{1}{4}\delta_\pi(X)+\frac{1}{12}\delta_\sigma(Y)+\frac{1}{4}\delta_\pi(Y)$		$\frac{1}{12}\delta_\sigma(X)+\frac{1}{3}\delta_\sigma(Y)+\frac{1}{4}\delta_\pi(X)$	A″	$\delta_\sigma(X)+\delta_\pi(X)$	

* The parameters δ_σ and δ_π are defined as Yamatera's.

TABLE IV. THE ABSORPTION AND CD DATA (CALCULATED AND OBSERVED) OF *cis*- AND *trans*-$[CoXYen_2]^+$

ν, $10^{13}sec^{-1}$

X·Y	Band region	*trans* Absorption max.	*trans* Calcd. value	*cis* Absorption max.	*cis* Circular dichroism max.	*cis* Calcd. value	Parameters**
Cl(CN)	I band	66.2	63.9(A_2) 64.0(E)	59.2 69 sh	55.2 62.2 69.6	55.8(A'') 64.0(A') 72.1(A'')	δ(CN)=32.9 δ(Cl)=−32.2
	II band	88.6	85.0(B_2) 90.4(E)	87.6	79.2* 85.0* 96.2*	79.2(A'') 85.0(A') 96.2(A'')	δ_σ(CN)=36.5 δ_σ(Cl)=−30.5 δ_π(CN)=−8.4 δ_π(Cl)=−7.4
Br(CN)	I band	64.9	62.5(E) 63.9(A_2)	58.5 68 sh	53.6 60.7 68.0	54.2(A'') 62.5(A') 72.1(A'')	δ(CN)=32.9 δ(Br)=−38.6
2(CN)	I band			74.4	68[b] 81[b]	72.2(A_2, B_2) 80.4(B_1)	δ(CN)=32.9
	II band			97.3	90[b] 99[b]	90.3(B_1) 101.5(A_2, B_2)	δ_σ(CN)=36.5 δ_π(CN)=−8.4
2Cl	I band	48.8*,[a] 64.9*,[a]	48.8(E_g) 64.9(A_{2g})	55.9	49.4[c] 52.9[c]	47.8(B_1) 55.8(A_2, B_2)	δ(Cl)=−32.2

* From these values the parameters were estimated.

** The zero line of the parameter δ is settled to the band positions of $[Co\,en_3]^{3+}$: 63.9($\times 10^{13}sec^{-1}$) for the first band and 88.4($\times 10^{13}sec^{-1}$) for the second band.

a) Y. Shimura and R. Tsuchida, This Bulletin, **28**, 572 (1955).

b) A. J. McCaffery, S. F. Mason and B. J. Norman, *Chem. Commun.*, **1965**, 133.

c) J.-P. Mathieu, *Bull. soc. chim. France*, [5] **3**, 476 (1936).

The Ligand Field Absorption Bands.— The absorption curves of *cis*- and *trans*-$[CoCl(CN)en_2]^+$ are shown in Fig. 2 with the circular dichroism (CD) curve of $(-)_{546}$-*cis*-$[CoCl(CN)en_2]^+$. The absorption data of this and related complexes are summarized in Table I. The main difference between the absorption curves of the two geometrical isomers occurs in the first band region. That is, the first band of the trans isomer does not show any split, while that of the cis isomer seems to split into two components. This behavior is considerably different from that of the first bands of *cis*- and *trans*-$[CoCl_2en_2]^+$.[9] Basolo et al. have already pointed out a similar fact about the absorption bands of *cis*- and *trans*-$[CoCl(NO_2)en_2]^+$.[10]

The absorption behavior in the first bands of *cis*- and *trans*-$[CoCl(CN)en_2]^+$ can reasonably be elucidated on the basis of Yamatera's theoretical treatment.[11] The expected patterns of the split and shift of the first and second bands can be seen in Table III, in which those of two geometrical isomers of the $[CoXYN_4]$ type are newly constructed. The *trans*-$[CoCl(CN)en_2]^+$ ion belongs to the approximate symmetry of C_{4v}, and the cis isomer, to the C_s symmetry. It may be expected that the first band of the trans isomer splits into two components, A' and E, and the cis siomer, into three components, A' and 2A''. Now, the expected components of the first bands of the two geometrical isomers can be calculated by using some parameters, δ, which can be estimated from the observed values of the first bands of $[Co\,en_3]^{3+}$, $[Co(CN)_6]^{3-}$ and *trans*-$[CoCl_2en_2]^+$. The calculation are based on the following definitions:

$$\delta(X) = \delta_\sigma(X) + \delta_\pi(X)$$

$$\delta(Y) = \delta_\sigma(Y) + \delta_\pi(Y)$$

The results are shown in Table IV, along with the observed data. When the observed bands are considered in connection with the calculated values, it may be understood that the two expected components for the trans isomer are located so close to each other that the observed band does not split. The three expected components of the cis isomer correspond with the three CD bands of $(-)_{546}$-*cis*-$[CoCl(CN)en_2]^+$ in their first band region, as is shown in Table IV.

Thus, it can easily be explained that the superposition of the expected absorption components which correspond to the three CD bands gives the two-maxima in the absorption curve measured. The parameter values, δ(Cl)=−32.2 and δ(CN)=32.9, which were used here are also fit for the first band region (the absorption and CD bands[12,13]) of *cis*-$[CoCl_2en_2]^+$ or *cis*-$[Co(CN)_2en_2]^+$.

As may be seen in Fig. 3 and Tables I, II and IV, the splitting patterns of the first band of the *cis*- and *trans*-$[CoBr(CN)en_2]^+$ closely resemble

9) M. Linhard and M. Weigel, *Z. anorg. Chem.*, **271**, 101 (1952).

10) F. Basolo, C. J. Ballhausen and J. Bjerrum, *Acta Chem. Scand.*, **9**, 810 (1955).

11) H. Yamatera, This Bulletin, **31**, 95 (1958).

12) J.-P. Mathieu, *Bull. soc. chim. France*, [5] **3**, 476 (1936).

13) A. J. McCaffery, S. F. Mason and B. J. Norman, *Chem. Commun.*, **1965**, 133.

those of the corresponding isomers of $[CoCl(CN)\cdot en_2]^+$, and the expected components of the cis isomer also match the observed CD bands of $(-)_{546}$-*cis*-$[CoBr(CN)en_2]^+$.

In general, no distinct splitting has been observed in the second absorption band of the cobalt(III) complexes. The second band of *cis*-$[CoCl(CN)\cdot en_2]^+$ is no exception, as may be seen in Fig. 2. According to the theoretical consideration, however, the second band of *trans*-$[CoCl(CN)en_2]^+$ may be expected to split into two components (B_2 and E), and that of the cis isomer, into three components (A′ and 2A″). In fact, the CD curve of $(-)_{546}$-*cis*-$[CoCl(CN)en_2]^+$ shows three CD bands in its second band region, that is, a negative band (at about $79.2\times10^{13}sec^{-1}$), another negative band ($85.0\times10^{13}sec^{-1}$) and a positive band, ($96.2\times10^{13}sec^{-1}$) listing from the longer to the shorter wavelengths.

In the same way as in the first band region, the parameters, δ_σ and δ_π, in the second band of *cis*-$[CoCl(CN)en_2]^+$ can be estimated by using the observed values; the following parameter values can thus be reasonably obtained:

$$\delta_\sigma(CN)=36.5 \qquad \delta_\pi(CN)=-8.4$$
$$\delta_\sigma(Cl)=-30.5 \qquad \delta_\pi(Cl)=-7.4.$$

The two expected components in the second band of the trans isomer are also derived from these four parameters (Table IV). Recently, the CD curve of $(+)_{546}$-*cis*-$[Co(CN)_2en_2]^+$ has been reported by McCaffery et al.[13] in the 515—260 mμ region. The observed CD bands agree well with the values calculated from the present parameter values (Table IV). The CD spectrum of $(-)_{546}$-*cis*-$[CoBr(CN)en_2]^+$ in the second band region is overlapped by the charge transfer absorption band due to the coordinated bromo ligand, and so the evaluation of the parameter values, $\delta_\sigma(Br)$ and $\delta_\pi(Br)$, was impracticable.

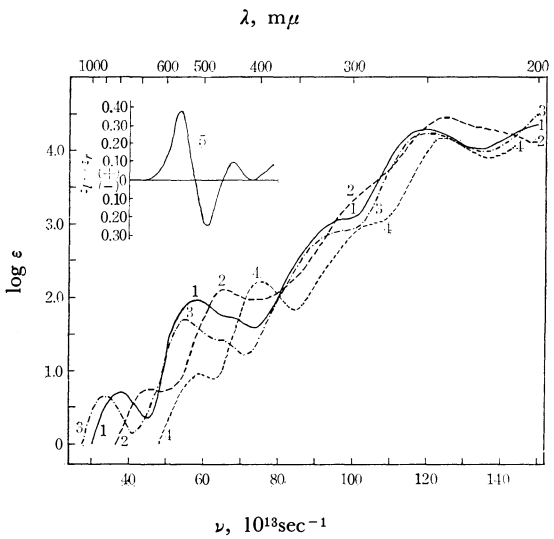

Fig. 3. Absorption and circular dichroism spectra of $[CoBr(CN)en_2]^+$ and the related complexes.
1—— absorption curve of *cis*-$[CoBr(CN)en_2]Br\cdot H_2O$ in aqueous solution.
2—— absorption curve of *trans*-$[CoBr)CN)en_2]Br\cdot H_2O$ in 70% $HClO_4$.
3-·-· absorption curve of *trans*-$[CoBr(NH_3)en_2]Br_2\cdot H_2O$ in aqueous solution.
4---- absorption curve of $K_3[CoBr(CN)_5]$ in aqueous solution.
5—— CD curve of $(-)_{546}$-*cis*-$[CoBr(CN)en_2]Br$ in aqueous solution.

The Charge Transfer Absorption Bands.— The present halogenocomplexes show two intense charge-transfer absorption bands due to the coordinated halogeno ligand X. The maxima of the shorter wavelength band, which was assigned to a $p_\sigma(X)$—d_{z^2} transfer,[14] are summarized in Table V, along with those of the related monohalogeno complexes.

From Figs. 2 and 3 and Table V, it may be seen that the bands of *cis*-$[CoX(CN)en_2]^+$ are located at longer wavelengths than those of the trans isomer. The band position of a cis isomer is about the same as that of the corresponding halogeno-pentammine complex; these are in the range from 130 to 133 ($\times10^{13}sec^{-1}$) for the chloro-complexes and from 117 to 120 ($\times10^{13}sec^{-1}$) for the bromo-complexes. On the other hand, the band position of *trans*-$[CoX(CN\ en_2]^+$ is about the same as that of the corresponding halogeno-pentacyano complexes. These facts suggest that the position of a charge transfer band depends on which kind of ligand occupies the trans position on the halogeno ligand, and that it does not depend on the kind of ligand in cis positions.

Table V. The charge transfer band maxima ($p_\sigma(X)\rightarrow d_{z^2}$) of monohalogeno complex ions

ν, $10^{13}sec^{-1}$

Complex ion	X=Cl	X=Br	Ref.
cis-$[CoX(CN)en_2]^+$	130	119	
$[CoX(NH_3)_5]^{2+}$	132.2	118.4	a
cis-$[CoX(NH_3)en_2]^{2+}$	131	117	b
trans-$[CoX(NH_3)en_2]^{2+}$	133	120	b
trans-$[CoX(CN)en_2]^+$	136	125	
$[CoX(CN)_5]^{3-}$	135	124.5	c

a) M. Linhard and M. Weigel, *Z. anorg. Chem.*, **266**, 49 (1951).
b) T. Yasui and Y. Shimura, This Bulletin, **36**, 1286 (1963).
c) J. Fujita, Private communication.

As far as the charge-transfer band is concerned, these complexes may be approximated as being a linear complex [X-Co-A], where A is NH_3, 1/2en or CN^-.

The authors wish to acknowledge the helpful suggestions made by Dr. Junnosuke Fujita of Tohoku University and Dr. Takaji Yasui of Osaka University.

14) H. Yamatera, *J. Inorg. Nucl. Chem.*, **15**, 50 (1960).

BULLETIN OF THE CHEMICAL SOCIETY OF JAPAN VOL. 39 1721—1724 (1966)

Studies of Calcichrome as a Spectrophotometric Reagent. IV. A New Spectrophotometric Method for the Determination of Aluminum with Calcichrome and Its Basic Study*

By Hajime Ishii and Hisahiko Einaga

Central Research Laboratory, Onoda Cement Co., Ltd., Koto-ku, Tokyo

(Received December 7, 1965)

It has been found that Calcichrome forms a stable complex with aluminum; the reaction has been studied spectrophotometrically in order to find the optimum conditions for the determination of aluminum. The aluminum-Calcichrome complex is formed gradually at about pH 6; its composition has been found to be 1 to 1. The complex has two absorption maxima, at approximately 312 and 560 mμ, when measured against water. On the other hand, two absorption maxima were found, at approximately 317 and 620 mμ, in the curve obtained as the difference between Calcichrome and its aluminum complex. A linear relationship was noticed between the concentration of aluminum and the absorbance under the conditions recommended. The molar extinction coefficients of the complex at 317 and 620 mμ were 11500 and 7200. and the sensitivities were 2.3×10^{-3} and 3.7×10^{-3} μg. Al/cm^2 respectively, which correspond to $\log(I_0/I)=0.001$. Some other metals, such as copper(II), iron(III), titanium(IV), vanadium(V), and zirconium(IV), interfere with the determination.

The present authors have found that Calcichrome, reported by Close and West[1] to be a reagent useful in the determination of calcium, forms stable complexes with copper(I and II) and iron(III); they have already reported new spectrophotometric methods for the determination of copper[2,3] and iron[4] on the basis of the formation of each complex. Furthermore, the present authors have recently discovered that this reagent also forms a stable complex with aluminum. The present paper will describe a direct spectrophotometric method for the determination of aluminum with Calcichrome and the results of its basic study.

Experimental

Reagents.—*Calcichrome Solution.* — A Calcichrome solution (2×10^{-4} M) was prepared by dissolving 0.1982 g. of Calcichrome in distilled water and by then diluting the mixture to 1 l. The Calcichrome used in this study was synthesized and purified by the method described in an earlier paper.[3]

Standard Aluminum(III) Solution.—A standard aluminum solution corresponding to 1×10^{-2} mol./l. of aluminum was prepared by dissolving 4.744 g. of aluminum potassium sulfate in distilled water, then adding small amounts of sulfuric acid to prevent any possible hydrolysis and diluting the mixture to 1 l. Working solutions of aluminum were prepared from this solution by dilution.

Buffer Solutions.—Buffer solutions were prepared by mixing 1 M acetic acid and 1 M sodium acetate in the ratios required.

Apparatus.—A Hitachi automatic recording spectrophotometer, model EPS-2, and a Hitachi spectrophotometer, model 139, were used, with 1 cm. matched cells, for obtaining absorption curves and for all the other absorbance measurements respectively. A Toa Dempa glass-electrode pH meter, model HM-5A, was used for all the pH measurements.

The Recommended Procedure for the Determination.—To a sample solution containing aluminum in a 25-ml. volumetric flask, 5 ml. of the Calcichrome solution and 5 ml. of a buffer solution (pH 6.0) are added. The solution is diluted with distilled water to the mark. After the solution has stood for 30 min., the absorbance of the solution is measured at 620 mμ against a reagent blank treated in a similar manner.

Results and Discussion

Absorption Curves.—From the results of preliminary experiments, it was found that Calcichrome forms a stable bluish-violet complex with aluminum in a neutral and/or a weak acidic medium. The ultraviolet and visible absorption curves of the complex at pH 6.0 are shown in Fig. 1, from which it will be found that the complex has two absorption maxima in the ultraviolet (λ_{max} 312 mμ) and visible (λ_{max} 560 mμ) regions, as may be seen from curve I obtained against water. On the other hand, in the curve III (the apparent absorption curve), which is obtained as the difference between Calcichrome and its aluminum complex,

*1 Presented at the 14th Annual Meeting of the Japan Society for Analytical Chemistry, Kyoto, November, 1965.

1) R. A. Close and T. S. West, *Talanta*, **5**, 221 (1960).

2) H. Ishii and H. Einaga, This Bulletin, **38**, 1416 (1965).

3) H. Ishii and H. Einaga, ibid., **39**, 1154 (1966).

4) H. Ishii and H. Einaga, *J. Chem. Soc. Japan, Pure Chem. Sect.* (*Nippon Kagaku Zasshi*), **87**, 440 (1966).

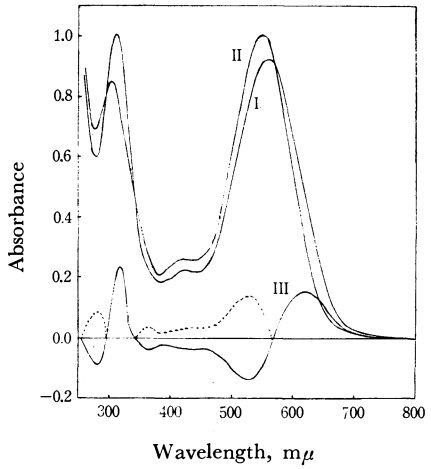

Fig. 1. Absorption spectra of Al(III)-Calcichrome complex.
Calcichrome: 4×10^{-5} mol./l.
Aluminum: 2.4×10^{-5} mol./l.
I: Al(III)-Calcichrome complex } Reference: water
II: Calcichrome alone
III: Difference between curves I and II (Parts under the abscissa were reversed to the positive side (as dotted line) for clearity.)

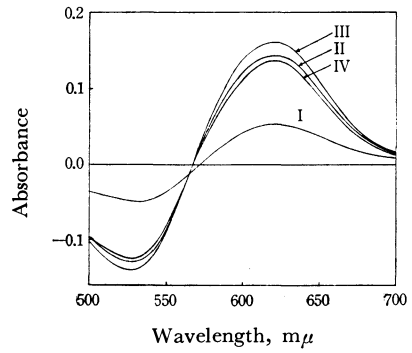

Fig. 2. Apparent absorption spectra of Al(III)-Calcichrome complex.
Calcichrome: 4×10^{-5} mol./l.
Aluminum: 2.4×10^{-5} mol./l.
Reference: Reagent blank
I: pH 4.3, II: pH 5.4, III: pH 6.0, IV: pH 6.3

two absorption maxima are found, at approximately 317 and 620 mμ. Figure 2 shows the apparent absorption curves of the complex at various pH values, from which it may be seen that the maximum absorption wavelength does not vary with the pH value. Taking account of this fact and of those described in the following paragraph, one species of the complex is considered to be formed under the conditions studied.

The Effect of pH on the Color Development.—The effect of pH on the color development of the aluminum-Calcichrome complex was examined at 620 mμ, with the concentrations of aluminum and Calcichrome made to 4×10^{-5} mol./l. The results are shown in Fig. 3, from which it can be seen that the maximum color can be obtained at approximately pH 6, and that the pH range in which nearly the same absorbance can be obtained is rather narrow. Therefore, the pH should be carefully controlled in the determination of aluminum.

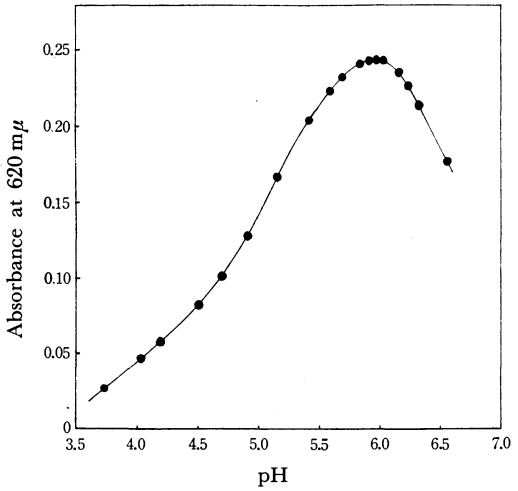

Fig. 3. Effect of pH on absorbance of the Al-(III)-Calcichrome complex.
Calcichrome: 4×10^{-5} mol./l.
Aluminum: 4×10^{-5} mol./l.

The Stability of the Color.—The color of the aluminum-Calcichrome complex develops gradually at room temperature; the full color is obtained 20 min. after the reagent is added. The time required to reach the full color can be, however, shortened remarkably by heating the solution to about 90°C. The color, once developed to the full, is very stable, and there is no change in absorbance over a period of 24 hr. Figure 4 shows the effect of the standing time on the absorbance.

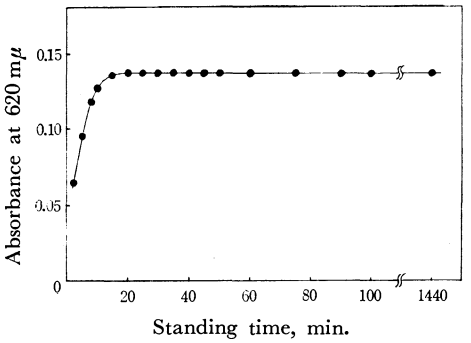

Fig. 4. Effect of standing time.
Calcichrome: 4×10^{-5} mol./l.
Aluminum: 2×10^{-5} mol./l.
pH: 6.0

The Effect of the Amount of Calcichrome.—The effect of the reagent concentration on color development was next examined, with the concentration of aluminum kept constant at 2×10^{-5} mol./l., with the pH values of the solutions at 6.0, and with the absorbance measurements carried out at 620 mμ. The results are shown in Fig. 5, from which it may be noticed that approximately a two-fold excess of the reagent over the aluminum concentration is necessary to obtain the maximum color intensity.

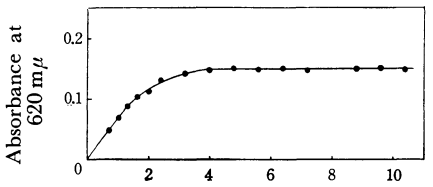

Concn. of Calcichrome, $\times10^5$ mol./l.

Fig. 5. Effect of amount of Calcichrome.
Aluminum: 2×10^{-5} mol./l.
pH: 6.0
Reference: Reagent blank

The Relationship between the Concentration of Aluminum and the Absorbance.—A linear relationship was found between the concentration of aluminum and the absorbance. The range of the aluminum concentration in which the linearity was noticed was, however, dependent upon the Calcichrome concentration; linearity was noticed up to the molar ratio of aluminum to Calcichrome of about 0.8. Figure 6 shows calibration curves for aluminum at 620 and 317 mμ. The molar extinction coefficient and the sensitivity which corresponds to $\log(I_0/I)=0.001$ are summarized in Table I. As may be seen from Fig. 6 and Table I, approximately 1.6 times as much sensitivity can be obtained when the

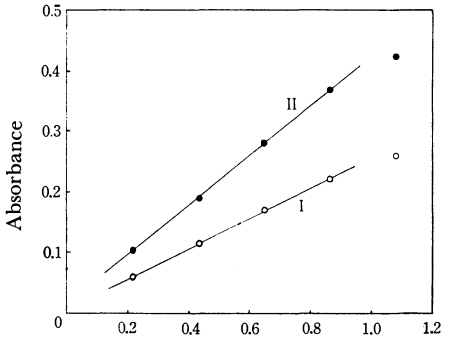

Al(III), p. p. m.

Fig. 6. Calibration curves.
Calcichrome: 4×10^{-5} mol./l.
pH: 6.0
Reference: Reagent blank
I: at 620 mμ, II: at 317 mμ

Table I. The molar extinction coefficient and the sensitivity

Wavelength mμ	Molar extinction coefficient	Sensitivity
620	7200	3.7×10^{-3} μg. Al/cm^2
317	11500	2.3×10^{-3} μg. Al/cm^2

Table II. Effect of diverse ions
Al taken: 0.62 p. p. m.

Diverse ion	p. p. m.	Al found p. p. m.	Relative error %
Ba(II)	5	0.62	± 0
Ca(II)	5	0.62	± 0
Cd(II)	5	0.62	± 0
Co(II)	1	0.63	+ 1.6
	4	0.65	+ 4.8
Cr(III)	0.1	0.59	− 4.8
	0.2	0.57	− 8.1
	0.4	0.52	−16.1
Cr(VI)	4	0.62	± 0
Cu(II)	0.1	0.62	± 0
	0.3	0.65	+ 4.8
	0.5	0.70	+12.9
Fe(III)	0.01	0.65	+ 4.8
	0.03	0.67	+ 8.1
	0.05	0.67	+ 8.1
	0.1	0.50	−19.4
Hg(II)	1	0.64	+ 3.2
	2	0.67	+ 8.1
	4	0.70	+12.9
Mg(II)	0.5	0.62	± 0
	1	0.57	− 8.1
Mn(II)	5	0.62	± 0
Ni(II)	0.1	0.64	+ 3.2
	0.3	0.65	+ 4.8
	0.5	0.67	+ 8.1
Pb(II)	5	0.62	± 0
Ti(IV)	0.3	0.67	+ 8.1
	0.5	0.69	+10.1
	1.0	0.72	+16.1
	2.0	0.62	± 0
	4.0	0.50	−19.4
V(V)	0.1	0.67	+ 8.1
	0.3	0.68	+ 9.7
	0.5	0.72	+16.1
Zn(II)	5	0.62	± 0
Zr(IV)	0.01	0.64	+ 3.2
	0.05	0.62	± 0
	0.1	0.61	− 1.6
	0.5	0.59	− 4.8
	1.0	0.57	− 8.1
Cl^-	100	0.62	± 0
$C_2O_4^{2-}$	0.2	0.61	− 1.6
	0.5	0.58	− 6.5
	1.0	0.55	−11.3
NO_3^-	100	0.62	± 0
SO_4^{2-}	100	0.62	± 0
$S_2O_3^{2-}$	100	0.61	− 1.6

absorbance of the solution is measured at 317 mμ as when it is measured at 620 mμ, however, the latter wavelength was employed in the recommended procedure because it seems to be more convenient than the former.

The Effect of Diverse Ions.—The effect of diverse ions on the determination of aluminum was examined at pH 6.0. The results are summarized in Table II. From this it can be concluded that cobalt(II), chromium(III), copper(II), iron(III), mercury(II), magnesium(II), nickel(II), titanium-(IV), vanadium(V), and zirconium(IV) interfere; this is considered to be due to the formation of their complexes with Calcichrome. The tendency for a negative error to be given with increasing amounts of such cations as iron(III), titanium(IV), and zirconium(IV) is probably to be attributed to the easier complex formation of Calcichrome with these cations than that with aluminum, and to the diminution of the effective amounts of Calcichrome for complexing with aluminum. The interference of oxalate is probably due to complex formation with aluminum.

The Composition of the Complex.—Attempts to determine the composition of the complex were carried out by two methods; the continuous variation method and the mole ratio method. These attempts were made at pH 6.0, and the absorbance measurements were made at three wavelengths, 520, 605, and 620 mμ. Both methods revealed that aluminum forms a 1 to 1 complex with Calcichrome. As an example, the results obtained by the continuous variation method are shown in Fig. 7. The results by the mole ratio method, which are omitted to avoid duplication, are clear from Fig. 5.

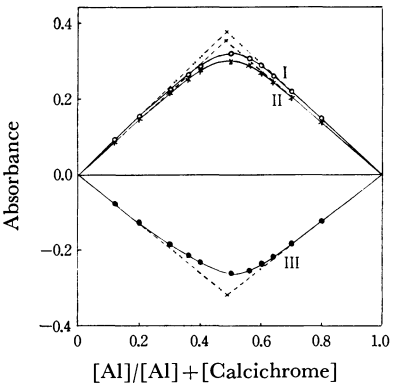

Fig. 7. Determination of mole ratio of Al(III)-Calcichrome complex.
[Al]+[Calcichrome]=1×10^{-4} mol./l.
pH: 6.0
I: 620 mμ, II: 605 mμ, III: 520 mμ

Conclusion

It has been found that Calcichrome forms a 1 to 1 complex with aluminum, and a new spectrophotometric method for the determination of traces of aluminum has been proposed.

BULLETIN OF THE CHEMICAL SOCIETY OF JAPAN VOL. 39 1724—1729 (1966)

Compounds Related to Imido-Substituted Ethylenes. I.* The Preparation of Diimido-Substituted Ethylenes

By Otohiko TSUGE, Kiyoshi YANAGI and Shōji FUKUHARA

The Research Institute of Science and Industry, Kyushu University, Hakozaki, Fukuoka

(Received August 31, 1965)

Methods for the preparation of *cis*-, *trans*-1, 2-diphthalimidoethylene, its nitro derivative, 1, 1-diphthalimido- and 1, 2-bis(*o*-sulfobenzimido)ethylene are described. In this connection, the thermal, irradiated and iodine-catalyzed isomerization of *cis*- and *trans*-1, 2-diphthalimidoethylene have also been studied in detail.

Unsaturated compounds I in which an unsaturated group is bonded with the nitrogen atom in an amino or imido group are expected to exhibit an interesting property under the influence of the unshared electron pair on the nitrogen atom.

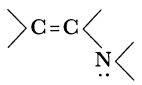

I

Particularly, it is presumed that the preparation of polyamino- or polyimido-substituted ethylenes becomes more difficult than that of mono-substituted ethylenes, and that the poly-substituted ethylenes exhibit an unusual reactivity under the influence both of the steric effect of the substituents and of the unshared electron pair on the nitrogen atom.

* Presented at the 18th Annual Meeting of the Chemical Society of Japan, Osaka, April, 1965.

Although monoimido-substituted ethylenes such as *N*-vinyl-phthalimide have been well studied,[1] no information has been available regarding polyimido-substituted ethylenes.

Therefore, in this work, the preparation of 1, 2-diphthalimidoethylenes (II—IV), 1, 1-diphthalimido- (V) and 1, 2-bis-(*o*-sulfobenzimido)ethylene (VI) has been attempted in the expectation that the diimido-substituted ethylenes would exhibit an unexpected reactivity.[2] In this connection, the present paper will describe the results of our experiments with the *cis-trans* isomerization of II under various conditions.

Results and Discussion

The Preparation of 1, 2-Diphthalimidoethylenes (II—IV).—1, 2-Diphthalimidoethylenes (II—IV) were synthesized by the pyrolytic elimination of acetic acid at about 250°C from the corresponding 1, 2-diphthalimido-1-acetoxyethane (IX), which had been prepared by the condensation of the potassium phthalimide (VII) and 1, 2-dibromo-1-acetoxyethane (VIII)[3] in dimethylformamide (DMF).

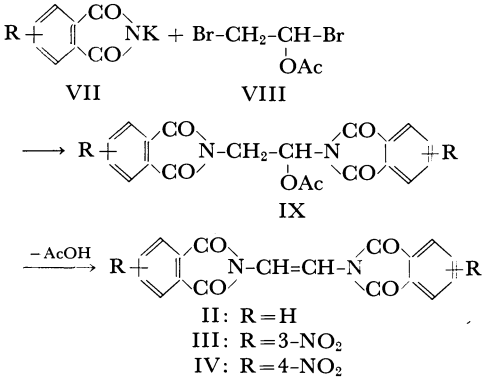

The crude II was recrystallized from DMF to give two compounds, whose solubilities in organic solvents were very small. The infrared spectrum of the more soluble, pale yellow needles (IIb) was in agreement with that of the crude II, but that of the less soluble, bright yellow grains or needles (IIa) was not.

As is shown in Fig. 1, the infrared spectra of IIa and IIb exhibit bands at 713 and 960 cm^{-1} which are to be ascribed to the -CH=CH- (*cis*) and -CH=CH- (*trans*) linkage respectively.[4] As

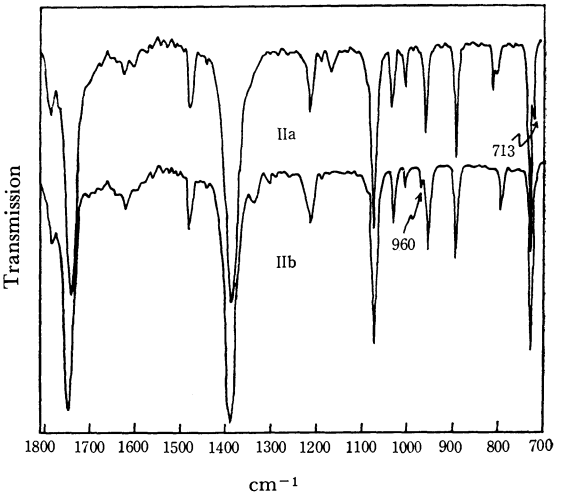

Fig. 1. Infrared spectra of IIa and IIb in KBr disks.

no suitable solvent of II could be found, the measurement of the NMR spectrum or of the dipole moment was not carried out.

On the basis of the infrared spectra as well as of elemental analyses, however, IIa and IIb were assumed to be *cis-* and *trans*-form respectively. In view of this fact, it may be suggested that *cis-trans* isomerization took place during recrystallization.

Furthermore, the ultraviolet spectra of IIa and IIb were almost the same (Fig. 2), and the two

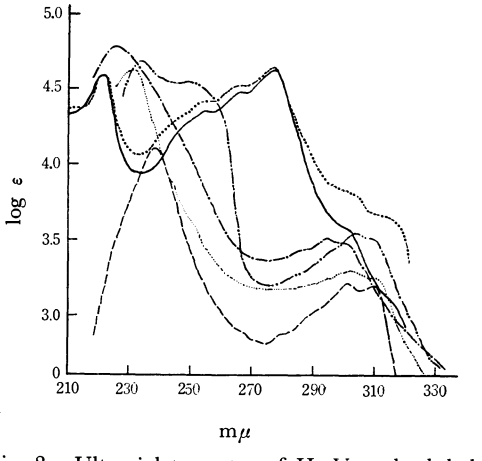

Fig. 2. Ultraviolet spectra of II, V and phthalimide derivatives.
---- IIa in tetrahydrofuran
—— IIb in tetrahydrofuran
—·— V in dioxane
— — Phthalimide in dioxane
····· *N*-Ethylphthalimide in dioxane
—··—·· Diphthalimidoethane in dioxane

1) M. Bachstez, *Ber.*, **46**, 3087 (1913); K. Yanagi et al., *J. Org. Chem.*, **24**, 428, 1121 (1959), and other publications.

2) For example, unusual phenomena were observed in addition reaction of bromine to II and V. (O. Tsuge, K. Yanagi and S. Fukuhara, *J. Chem. Soc. Japan, Ind. Chem. Sect.* (*Kogyo Kagaku Zasshi*), **69**, 932 (1966)).

3) H. O. L. Fischer and L. Feldmann, *Ber.*, **62**, 862 (1929).

4) L. J. Bellamy, "The Infra-red Spectra of Complex Molecules," John Wiley & Sons. Inc., New York (1954), p. 40.

isomers have the same melting point; however, IIa does not exhibit its own melting point, because IIa is easily isomerized to IIb by irradiation with light and by heating, as will be mentioned below. The geometric isomerism of III and of IV is not yet clear.

The Preparation of 1, 1-Diphthalimidoethylene (V).—1, 1-Diphthalimidoethylene (V) was synthesized by the pyrolytic elimination of acetic acid at 600°C from 1, 1-diphthalimido-2-acetoxyethane (XII) which had been prepared by the action of acetic anhydride on 1, 1-diphthalimido--2-bromoethane (XI), which had been obtained from VII and 1, 2-dibromo-1-phthalimidoethane (X)[1] in DMF.

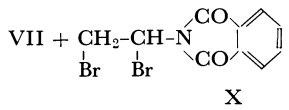

X

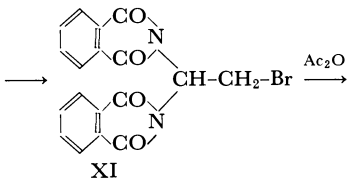

XI

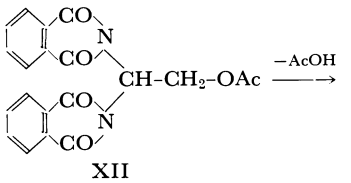

XII

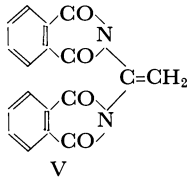

V

The formation of only XI in the reaction of VII with X suggests that VII attacked selectively at the α-carbon atom of X. The structure of XI was proved by the fact that XII was different from the IX isomer (R=H) as well as by elemental analyses.

The ultraviolet spectrum of V is also shown in Fig. 2. The ultraviolet spectrum of II is different from those of phthalimide derivatives, but the spectrum of V is very similar to those of the latter. These observations indicate that the electronic state of II is quite different from that of the phthalimide because of the interaction between the π-electron in the carbon-carbon double bond and unshared electron pairs on the nitrogen atoms, and that the interaction mentioned above does not exist in V, since the two phthalimido groups and the carbon-carbon double bond are not in the same plane because of the steric effect of the bulky phthalimido group.

The Preparation of 1, 2-Bis(*o*-sulfobenzimido)ethylene (VI). — The similar pyrolytic elimination of acetic acid from 1-acetoxy-1, 2-bis(*o*-sulfobenzimido)ethane (XIV) which had been prepared by the treatment of sodium salt of *o*-sulfobenzimide (XIII) with VIII in DMF, afforded 1, 2-bis(*o*-sulfobenzimido)ethylene (VI).

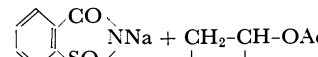

XIII VIII

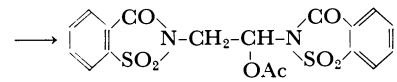

XIV

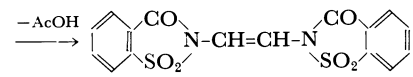

VI

The *cis-trans* Isomerization of IIa and IIb. —In order to obtain further information concerning the *cis-trans* isomerization of IIa and IIb, the isomerization reaction was carried out under various conditions.

The quantitative estimation of IIa and IIb in II was established by using the ratio method,[5] which was carried out by the measurement of the absorbances, A_1 and A_2, for the bands at 800 and 792 cm^{-1} respectively. Thus, samples of a mixture consisting of specified amounts of IIa and IIb in KBr were prepared and the absorbances, A_1 and A_2, were measured according to the respective baseline method. The calibration curves plotting

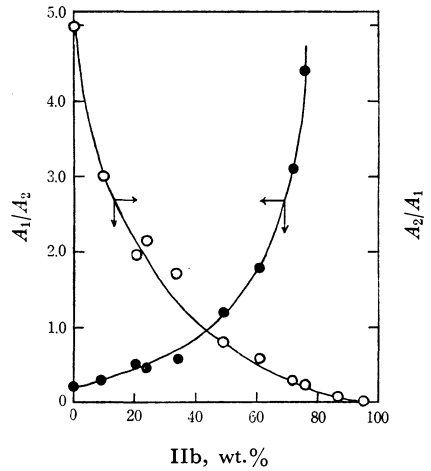

Fig. 3. Calibration curve.

5) S. Takagi, "Teiryō Bunseki no Jikken to Keisan (Experiment and Calculation of Quantitative Analyses)" (in Japanese), Vol. III, Kyoritsu, Tokyo (1961), p. 91.

the relationship between A_1/A_2 or A_2/A_1 and the concentration (wt. %) of IIb are shown in Fig. 3.

Thermal Isomerization.—The isomerization was observed on the recrystallization of II, as has been mentioned above; therefore, the thermal isomerization was examined in the solid state or in a solution.

The isomerization of IIa to IIb in the solid state was carried out in a sealed capillary tube under a nitrogen atmosphere. The results are shown in Table I.

Table I. The thermal isomerization of IIa to IIb

Temp. °C	Time min.	Degree of isomerization %	Temp. °C	Time min.	Degree of isomerization, %
100	60	0	200	5	12
100	180	4	250	5	100
150	30	0	300	5	100
150	60	4			

As is shown in Table I, the transition temperature from IIa to IIb in the solid state may be expected to be in the range from 200 to 250°C; hence, differential thermal analyses of IIa and IIb were carried out in order to establish the accurate transition temperature. The results are shown in Fig. 4. Although IIa showed a thermal abnormality at 220.5°C and melted at about 320°C, IIb showed no such anomalous curve and melted at about 320°C. Consequently, the transition temperature of IIa to IIb in the solid state may be concluded to be 220.5°C.

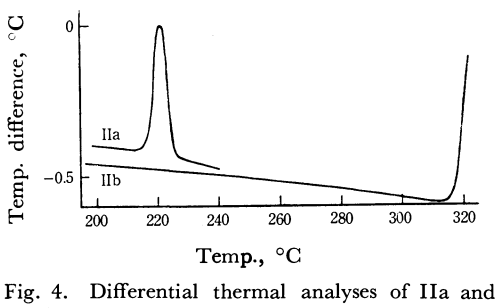

Fig. 4. Differential thermal analyses of IIa and IIb.

On the other hand, it was found that, in the isomerization in a solvent such as dioxane, tetrachloroethane, DMF or diethyleneglycol, IIb was isomerized to IIa in the range from 100 to 150°C, whereas IIa was isomerized to IIb above 150°C.

Iodine-Catalyzed Isomerization.—The isomerization under the influence of a catalytic amount of iodine was carried out in a tetrachloroethane solution at 20°C. The results are shown in Table II.

As Table II shows, the degree of isomerization of IIa to IIb in the presence of iodine increases with the increase in the reaction time, but in the absence of a catalyst neither form was isomerized.

While the recovered amount of IIb decreased as the iodine-catalyzed reaction time increased, the isomerization of IIb to IIa was not observed; the purple color of iodine and the yellow color of IIb disappeared after 24 hr., and an unidentified compound of colorless needles, m. p. 166—169°C, was formed. The same phenomenon was also observed in the treatment of IIa with iodine for a long while. The investigation of this side reaction is in progress and will be reported in the near future.

Table II. Iodine-catalyzed isomerization[a]

Reaction time, hr.	Yield, mg.	Degree of isomerization, %[b]
i) From IIa to IIb		
1	30	65
3	31	78
6	32	83
24	31	100
24[c]	31	0
ii) From IIb to IIa		
13	20	0
24	5	0
24[c]	32	0

a) A solution of 40 mg. of the starting material in 50 ml. of tetrachloroethane was treated with 1 mg. of iodine in 10 ml. of tetrachloroethane.
b) The wt.% of IIb or IIa in the product.
c) In the absence of iodine.

Isomerization by Irradiation with Light.—The isomerization by irradiation with light (3500—4000 Å) was carried out in a tetrachloroethane solution at 18—20°C. The isomerization of IIa to IIb was brought about, but that of IIb to IIa was not. As is shown in Fig. 2, the ultraviolet spectra of the two isomers are almost the same. This suggests either that both isomers are in nearly the same electronic state or that isomerization from one to another takes place during the measurement. In order to elucidate which of the alternatives is true, the isomerization was examined under the same conditions as when the spectrum was measured. As it was found that the *cis*-form was converted into the *trans*-form, the spectrum of IIa shown in Fig. 2 is that of the *trans*-form.

Experimental[6]

1, 2-Diphthalimido-1-acetoxyethane (IX, R=H).—To a suspension of 185 g. of potassium phthalimide (VII, R=H)[7] in DMF (450 ml.) 123 g. of 1, 2-dibromo-1-acetoxyethane (VIII)[3] was slowly added, drop by drop, while the temperature was kept below 55°C with cooling. After the addition had been completed, the reaction mixture was stirred at room temperature for 2hr., and then water (4 l.) was poured into it. After a white precipitate had been collected by filtration, washed with water, and dried, recrystallization from glacial acetic acid gave colorless prisms. Yield, about 200 g.; m. p. 232—233°C.

6) All melting points are uncorrected.
7) "Organic Syntheses," Coll. Vol. I, 119 (1948)

Found: C, 63.64; H, 3.73; N, 7.41. Calcd. for $C_{20}H_{14}O_6N_2$: C, 63.49; H, 3.73; N, 7.41%.

1, 2-Bis(3-nitrophthalimido)-1-acetoxyethane (IX, R=3-NO_2).—A mixture of 7.85 g. of potassium 3-nitrophthalimide (VII, R=3-NO_2)[8] and VIII (4.2 g.) in DMF (35 ml.) was heated at 100°C for 15 min., and then stirred at room temperature for another 5 hr. The reaction mixture was poured into ice water, and the precipitate was collected, washed with water, and dried. The acetic acid solution of the crude product was diluted with water, and the crystalline product was collected by filtration. Yield, 6.5 g. (81%); m. p. 115—116°C. The compound was not further refined.

1, 2-Bis(4-nitrophthalimido)-1-acetoxyethane (IX, R=4-NO_2).—A mixture of 4.6 g. of potassium 4-nitrophthalimide (VII, R=4-NO_2)[9] and VIII (2.46 g.) in DMF (30 ml.) was stirred at room temperature for 5 hr., and then the reaction mixture was poured into ice water (300 ml.). Recrystallization from glacial acetic acid gave IX (R=4-NO_2) as palely colored rods melting at 207—208.5°C; yield, 4.7 g. (48.5%).

Found: C, 51.45; H, 2.64; N, 12.15. Calcd. for $C_{20}H_{12}O_{10}N_4$: C, 51.29; H, 2.58; N, 11.96%.

1, 1-Diphthalimido-2-bromoethane (XI).—After a mixture of VII (11.12 g.) and 1, 2-dibromo-1-phthalimidoethane (X)[10] in DMF (70 ml.) had been stirred at room temperature for 9 hr., ice water (500 ml.) was added to the reaction mixture. The precipitate was collected by filtration; recrystallization from ethyl acetate gave XI as colorless grains melting at 206—207°C. Yield, 22.35 g. (93%).

Found: C, 54.14; H, 2.90; N, 7.19. Calcd. for $C_{18}H_{11}O_4N_2Br$: C, 54.16; H, 2.78; N, 7.02%.

1, 1-Diphthalimido-2-acetoxyethane (XII).—A mixture of XI (6.6 g.), fused potassium acetate (6.6 g.) and acetic anhydride (60 ml.) was heated under reflux for 9 hr. After it had then cooled, the mixture was poured into ice water (400 ml.) and allowed to stand overnight. The precipitate was collected and washed with water. Recrystallization from glacial acetic acid gave XII as colorless prismatic rods; m. p. 207—208°C. Yield, 4.0 g. (64%).

Found: C, 63.60; H, 3.74; N, 7.53. Calcd. for $C_{20}H_{14}O_6N_2$: C, 63.49; H, 3.73; N, 7.41%.

1-Acetoxy-1,2-bis(*o*-sulfobenzimido)ethane (XIV).—A mixture of 20.5 g. of sodium salt of commercial *o*-sulfobenzimide (XIII) and VIII (12.3 g.) in DMF (40 ml.) was heated for 1 hr. at 100°C, and then refluxed for another 2 hr. After the reaction mixture had cooled to room temperature, water (400 ml.) was added to it and the precipitate was collected and washed with water. Recrystallization from glacial acetic acid gave XIV as palely colored needles; yield, 15.03 g. (67%); m. p. 221.5—222.5°C.

Found: C, 47.97; H, 3.19; N, 6.24. Calcd. for $C_{18}H_{14}O_8N_2S_2$: C, 48.00; H, 3.13; N, 6.22%.

1, 2-Diphthalimidoethylene (II).—In a 500 ml. separable flask, 200 g. of IX (R=H) was heated at 250°C for 15 min. As acetic acid was eliminated, the reaction mixture was gradually solidified. The crude product was washed with alcohol and then with hot acetic acid to remove phthalimide and tarry material respectively. Recrystallization from DMF afforded yellow crystals, which were identified, by means of the infrared spectrum, as a mixture of *cis*- (IIa) and *trans*-form (IIb); yield, 118 g. (70%).

Pure *cis*-form (IIa), bright yellow grains or needles, was obtained quantitatively by heating the recrystallized product (10 g.) in dioxane (20 ml.) for 4—5 hr. at 100°C.

Found: C, 68.01; H, 3.26; N, 8.79. Calcd. for $C_{18}H_{10}O_4N_2$: C, 67.92; H, 3.17; N, 8.80%.

Pure *trans*-form (IIb) was prepared by heating a saturated DMF solution of the recrystallized product at 150°C, and by then rapidly cooling the solution to room temperature. Pale yellow needles; m. p. 318.5—319.5°C.

Found: C, 67.87; H, 3.23; N, 9.09. Calcd. for $C_{18}H_{10}O_4N_2$: C, 67.92; H, 3.17; N, 8.80%.

1, 2-Bis (3-nitrophthalimido) ethylene (III).—After 5 g. of IX (R=3-NO_2) had been heated by the procedure used to prepare II, recrystallization from DMF gave III as deep yellow needles melting at 344—344.5°C; yield, 1.3 g. (30%).

Found: C, 52.99; H, 2.02; N, 13.65. Calcd. for $C_{18}H_8O_8N_4$: C, 52.95; H, 1.98; N, 13.72%.

1, 2-Bis (4-nitrophthalimido)ethylene (IV).—After 1.7 g. of IX (R=4-NO_2) had been heated at 260°C for 15 min., recrystallization from DMF afforded 0.3 g. (20%) of IV as deep yellow needles; m. p. 334°C (decomp.).

Found: C, 53.21; H, 1.85; N, 13.80. Calcd. for $C_{18}H_8O_8N_4$: C, 52.95; H, 1.98; N, 13.72%.

From the filtrate, 1.17 g. (69%) of IX (R=4-NO_2) was recovered.

1, 1-Diphthalimidoethylene (V).—A solution of XII (30 g.) in acetone (700 ml.) was added, drop by drop, to a pyrolytic tube which had been placed in an electric furnace at 550°C. After about two-thirds of the acetone had been distilled out from the reaction mixture, which had been collected in the receiver, the residue was poured into water to separate the precipitate. The precipitate was collected by filtration and washed with water. Recrystallization from ethyl acetate gave V as palely-colored plates; m. p. 247—248°C. Yield, 5 g. (20%).

Found: C, 67.88; H, 3.17; N, 8.83. Calcd. for $C_{18}H_{10}O_4N_2$: C, 67.93; H, 3.17; N, 8.80%.

1, 2-Bis(*o* - sulfobenzimido)ethylene (VI).—After XIV (6.75 g.) had been heated at 250°C for 10 min. in a 10 ml. thin-walled flask, the reaction mixture was washed with 15 ml. of hot acetic acid. Recrystallization from DMF gave VI as pale brown grains; m. p. 283—284°C (decomp.). Yield, 5.3 g. (90%).

Found: C, 49.07; H, 2.54; N, 7.29. Calcd. for $C_{16}H_{10}O_6N_2S_2$: C, 49.23; H, 2.58; N, 7.18%.

Thermal Isomerization.—The thermal isomerization of *cis*- (IIa) and *trans*-form (IIb) in the solid state was carried out in a sealed tube under a nitrogen atmosphere. The effect of the reaction conditions on the isomerization is shown in Table I.

In this and in other isomerizations, the IIa and IIb in the reaction mixture were analyzed quantitatively by using the ratio method (Fig. 3).

Differential Thermal Analyses.—The differential thermal analyses were carried out by using the Rigaku Denki Type-V apparatus. Alumina was used as the reference compound, and the heating rate was kept

8) M. T. Bogert and V. J. Chambers, *J. Am. Chem. Soc.*, **27**, 652 (1905).
9) M. T. Bogert and L. Boroschek, ibid., **23**, 755 (1901).

constant at 0.7°C/min. The temperature of the sample was higher than that of alumina throughout the run (Fig. 4). Perhaps this is caused by the difference in specific heat between sample and alumina.

Iodine-Catalyzed Isomerization.—To a solution of 40 mg. of IIa or IIb in tetrachloroethane (50 ml.), a solution of iodine (1 mg.) in tetrachloroethane (10 ml.) was added. After the reaction mixture had been allowed to stand at 20°C for a certain time, it was poured into petroleum ether (500 ml.). The precipitate was filtered and analyzed. The results are shown in Table II.

In a reaction of IIb with iodine, the reaction mixture was allowed to stand for a week, and then tetrachloroethane was distilled out in vacuo. The residue was recrystallized from dichloroethane to give colorless needles; m. p. 166—169°C.

Found: C, 64.55; H, 3.70; N, 9.09%.

Beilstein's test of the compound was negative, and its infrared spectrum exhibits the bands at 1770 and 1710 cm^{-1} ascribed to the phthalimido group. The investigation of this side reaction is now in progress; the structure of the compound will be described elsewhere in the near future.

Isomerization by Irradiation with Light.—Irradiations were carried out employing a 150 W., high-pressure mercury lamp with a water-cooled, quartz immersion well (Taika Kogyo, HLV-B Type). A solution of 400 mg. of IIa or IIb in tetrachloroethane (500 ml.) was irradiated with light (3500—4000 Å) under nitrogen at 18—20°C for 6 hr. The reaction mixture was poured into petroleum ether, and the precipitate was collected by filtration and then analyzed.

BULLETIN OF THE CHEMICAL SOCIETY OF JAPAN VOL. 39 1729—1733 (1966)

Specific Effects in Acid Catalysis by Polymeric Sulfonic Acids in the Hydrolysis of the Amino Ester and Related Compounds

By Sadao YOSHIKAWA and Oh-Kil KIM[1]

Department of Synthetic Chemistry, Faculty of Engineering, The University of Tokyo, Hongo, Tokyo

(Received October 25, 1965)

The amino ester hydrolysis by polymeric sulfonic acids increased as the concentration ratio, C_{ester}/C_{acid}, was lowered, and a maximum in the plot of the rate constant, k, against the C_{ester}/C_{acid} ratio was attained near the ratio=0.4 in the case of the β-alanine methyl ester as well as in the case of γ-methyl L-glutamate. At this optimum concentration, the catalytic effect of polyvinylsulfonic acid (A), for example, in the hydrolysis of the β-alanine methyl ester was 16 times greater than that of hydrochloric acid, while the effect of polystyrenesulfonic acid was about 7 times greater. The catalytic effects of hydrochloric acid and ethanesulfonic acid were the same in all cases, and there was no such specific behavior as in the former. Furthermore, the catalytic efficiency of polyvinylsulfonic acid in amino ester hydrolysis increased with an increase in the polymer molecular weight, in contrast with the case of the carboxylic ester, while no such correlation was found in the polystyrenesulfonic acid. Besides, the catalytic effect of partially-neutralized polymeric sulfonic acid, polyvinylsulfonic acid especially, decreased remarkably with the degree of neutralization. These different kinds of behavior can be interpreted as being due to the difference in the expansion in solutions and in the geometrical distances between nearest-neighboring sulfonic acid groups on the polymer chain.

A number of studies[2] have been carried out in recent years on the charge interaction in the reactions using polyelectrolytes in order to reveal the mechanism of enzyme action. When organic reactions are carried out between a polymeric molecule and a simple substrate, functional interactions not only between neighboring groups, but also between polymer and substrate, especially when electrically-charged, are very often responsible for a change in the reaction path, consequently, they provide additional information regarding the mode of action of the enzyme. Since polymeric sulfonic acids with ionic groups along the polymer chain show properties of both electrolytes and polymers, one possible mechanism of enzyme specificity may be expected to be due to the electrostatic attraction of the poly-anion with the cationic reagent, when it is used as a catalyst in the reaction with a basic substrate. In a previous paper,[3] we have

1) Dissertation submitted by Oh-Kil Kim in partial fulfillment of the requirements for the Ph. D. degree in the Graduate School of the University of Tokyo.

2) a) H. Ladenheim, E. M. Loebl and H. Morawetz, *J. Am. Chem. Soc.*, **81**, 20 (1959); b) W. Kern and B. Scherhag, *Makromol. Chem.*, **28**, 209 (1958); c) R. L. Letsinger and T. J. Savereide, *J. Am. Chem. Soc.*, **84**, 114 (1962); d) C. G. Overberger, T. St. Pierre, N. Vorchheimer and S. Yaroslavsky, ibid., **85**, 3515 (1963).

3) S. Yoshikawa and O.-K. Kim, This Bulletin, **39**, 1515 (1966).

demonstrated that the acid-catalyzed hydrolysis of carboxylic esters by polymeric sulfonic acid was governed by the hydrophobic interaction between the polymer catalyst and the substrate and, moreover, influenced by the molecular weight of the polymer.

The present work was undertaken in an attempt to find how the charge interaction of the polymeric acid on amino esters is operative with the hydrolysis rate in a homogeneous solution and to explain the mechanism of hydrolysis upon the basis of the charge density of the polymer acid. In this study we selected the hydrolysis of amino ester and related compounds using polyvinylsulfonic acid (PVSH), polystyrenesulfonic acid (PSSH) and sulfonated polystyrene sulfonic acid ((PS)SH), in addition to the monomeric analogue, ethanesulfonic acid, and hydrochloric acid, in order to compare the hydrolysis with that of uncharged carboxylic esters. The sulfonic acids were prepared by different polymerizing processes from their respective monomers (except for sulfonated polystyrene sulfonic acid), and all were water-soluble.

Experimental

Amino Esters.—Glycine methyl ester hydrochloride was prepared by refluxing a solution of glycine in absolute methanol containing anhydrous hydrogen chloride. α- and β-Alanine methyl esters, the γ-aminobutyric acid methyl ester and γ-methyl L-glutamate were prepared by treating each amino acid with methanolic hydrogen chloride. All the esters were recrystallized from anhydrous methanol-ether and dried in vacuo over sodium hydroxide. Acetylcholine chloride was obtained commercially.

Polymeric Sulfonic Acid.—The monomers, sodium vinylsulfonate and potassium *p*-styrenesulfonate, were prepared from sodium β-bromoethanesulfonate and sodium hydroxide by modifying the patent directions,[4] and from β-bromoethylbenzenesulfonyl chloride and potassium hydroxide according to the method of Wiley and Reed.[5] The polymerizations of sodium vinylsulfonate and potassium *p*-styrenesulfonate were carried out by three different methods.

Poly-(sodium vinylsulfonate) was obtained as follows:

PVSH(A).—Five grams of sodium vinylsulfonate in 4.9 ml. of water was poured into an ampoule, chilled in ice, and evacuated to about 2 mmHg, the evacuation and pressuring with nitrogen was repeated, and then the ampoule was sealed. The polymerization was carried out by exposing it to a ^{60}Co source, yielding about 2×10^5 r./hr., for 72 hr. at 0°C. The resulting sticky solid was dissolved in 30 ml. of water and precipitated by adding 45 ml. of methanol. Treating the gummy precipitate with methanol yielded 3.5 g. of straw-colored polymer after it had been dried in vacuo over phosphorus pentoxide. The intrinsic viscosity[6] of the polymer was 12.8, and the molecular weight[6] was 20000.

PVSH(R).—Twelve grams of a 50% aqueous solution of sodium vinylsulfonate containing 0.057 g. of potassium persulfate and 0.023 g. of sodium bisulfite was poured into an ampoule; the ampoule was then evacuated, repeatedly filled with nitrogen, and then sealed. After the ampoule had been tumbled in a bath at 18°C for 72 hr., the resulting viscous oil was dissolved in 30 ml. of water and precipitated with 45 ml. of methanol; 4.08 g. of polymer was obtained after drying in vacuo over phosphorus pentoxide. The intrinsic viscosity was 7.20, and the molecular weight was 12000.

PVSH(S).—Five grams of finely-powdered and dried crystalline sodium vinylsulfonate was sealed in an ampoule and then exposed to a ^{60}Co source, yielding about 2.5×10^5 r./hr., for 72 hr. at room temperature. The irradiated crystals, after precipitation with 70% aqueous methanol in the usual fashion in order to remove monomers, gave 2.5 g. of the polymer. The intrinsic viscosity and the molecular weight of the polymer were 1.70 and 3000 respectively.

Poly-(potassium *p*-styrenesulfonate) was obtained as follows:

PSSH(A).—Four grams of potassium *p*-styrenesulfonate in 16 ml. of water was poured into an ampoule. Polymerization reactions were then carried out in the same manner, with γ-irradiation, as in the case of PVSH(A), except that this was done at room temperature. The polymer formed was precipitated from 70% aqueous dioxane. After drying in vacuo over phosphorus pentoxide, 2.5 g. of the polymer was yielded. The intrinsic viscosity[7] of the polymer was 42.0.

PSSH(R).—Five grams of potassium *p*-styrenesulfonate in 15 ml. of water was placed into an ampoule, and then a solution of 1.35 g. of potassium persulfate and 0.66 g. of sodium bisulfite in 2 ml. of water was added as an initiator. The polymerization was carried out in the same manner as has been described in the case of PVSH(R). The resulting viscous oil was precipitated from 70% aqueous dioxane; 3.2 g. of polymer was thus obtained after drying in vacuo over phosphorus pentoxide. The intrinsic viscosity was 30.7.

PSSH(S).—Five grams of finely-powdered and dried crystalline potassium *p*-styrenesulfonate was sealed in an ampoule and exposed to radiation under the same conditions as have been described in the case of PVSH(S). The irradiated crystals yielded 2.3 g. of the polymer after precipitation with 75% aqueous methanol; the polymer was dried according to the usual fashion. The intrinsic viscosity was 18.09. All the sodium and potassium polymer sulfonates were completely converted into free acids by passing them through a column of cation exchange resin in a hydrogen form such as Amberlite IR-120.

(PS)SH (69%).*—The sulfonation of polystyrene ($\overline{M}_w=15\times10^4$) was carried out, using the addition-compound of sulfur trioxide and dioxane, by the method

4) D. B. Pat. 836491, Farbwerker Hoechst, *Chem. Abstr.*, **47**, 2766 (1953).

5) R. H. Wiley and S. F. Reed, Jr., *J. Am. Chem. Soc.*, **78**, 2171 (1956).

6) The value of intrinsic viscosity of poly-(sodium vinyl sulfonate) was determined in 0.5 N NaCl solution at 20°C and the molecular weight was calculated by K. Dialer and R. Kerber, *Makromol. Chem.*, **17**, 56 (1956).

* The degree of sulfonation.

7) The value of initrnsic viscosity of poly-(potassium *p*-styrenesulfonate) was determined in 2 N NaOH solution at 20°C.

described by Signer and his co-workers.[8] To a finely-divided suspension of the adduct, consisting of 20 g. of sulfur trioxide and 26 ml. of dioxane in 140 ml. of dichloroethane, a solution of 26 g. of polystyrene in 140 ml. of dichloroethane was added in one portion, then the mixture was agitated for several minutes. The sulfonation proceeded to 69% after the mixture had stood at 20°C for 24 hr. The reaction was then stopped by the addition of water. The polymer was dissolved easily in water and neutralized with sodium hydroxide. The sulfonated polymer salt was dialyzed to remove sulfuric acid through a semipermeable membrane by keeping it in distilled water for one month. The dialyzed sulfonated polymer salt was converted into free acid through ion exchange resin in the hydrogen form by the usual method.

Ethanesulfonic acid (Et.-SO_3H) was prepared from ethyl bromide, sodium sulfite and water according to the directions of Houlton and Tartar.[9]

Hydrolysis Procedure.—All the kinetic studies reported here were carried out in aqueous solution at 45±0.01°C. The initial concentrations of amino acid ester hydrochlorides were adjusted to 0.20, 0.10, 0.05, 0.033, 0.025 and 0.020 mol./l., and the acid catalyst concentration, to 0.08 N. Three or four samples were used in each run, and each reaction mixture was made up by taking 4 ml. of the ester and an equal volume of the acid, both concentrations being initially adjusted. The reaction mixtures were contained in 10 ml. glass-stoppered bottles suspended in a thermostat controlled bath. The tubes were removed at suitable intervals and placed in an ice bath. After hydrolysis, the tubes were opened, and the contents were washed from the tube with water into a 100 ml. beaker; to this 10 ml. of the 37.5% formaldehyde solution, which had been neutralized with basic magnesium carbonate just before use, was added. A modified form of the Sörensen formol titration proposed by Dunn and Loshakoff[10] was used to determine the extent of hydrolysis. Titrations were made with 0.05 N sodium hydroxide, using an automatic titrator (Metrohm Co. potentiograph E336), in order to determine the end point. The titration of the known amino acid showed that this method gave satisfactory results, within ±0.2%. The hydrolysis rate constants were calculated using the first-order rate equation. The efficiency of the catalyst, q, was defined as the ratio of the specific rate of hydrolysis catalyzed by polymeric sulfonic acid to that catalyzed by hydrochloric acid.

Results and Discussion

Several series of experiments have been carried out, at a constant acid concentration (0.04 mol./l.), in order to examine the influence of the ester concentration on the order of the hydrolysis reaction. The experimental apparent first-order rate constant was evaluated from the slopes of the plots of the logarithm of the ester concentration against the time; it was found that the hydrolysis reaction proceeds through a first-order mechanism with respect to the ester concentration, as is shown in Fig. 1.

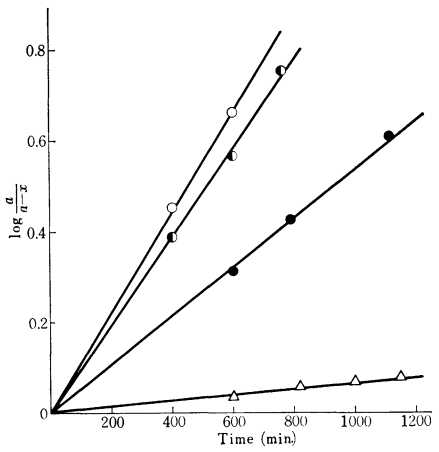

Fig. 1. Hydrolysis of β-alanine methyl ester catalyzed by 0.0405 N HCl and 0.0421 N PVSH-(A) in different ester concentrations (as indicated in the following parenthesis) at 45°C.
△ (0.0511 mol./l.) by HCl; ● (0.0511 mol./l.), ◐ (0.0255 mol./l.) and ○ (0.0170 mol./l.) by PVSH(A).

The effect of the structure of the amino ester on the rate of its hydrolysis can only be touched on here. One general point was that the α-amino ester tends to be less readily hydrolyzed than the β- or the γ-amino ester; this can be attributed to the fact that the former ester bond is nearer the positively-charged amino group in the amino ester. The results, given in Table I, indicate that all amino esters are hydrolyzed much more rapidly by polymeric sulfonic acids, especially PVSH(A), than by hydrochloric acid; the β-alanine methyl ester,

Table I. Hydrolysis rates of several amino acid methyl esters relating to the structure of amino acids

$10^3 k$ (l.mol^{-1}min^{-1})

Acid* \ Ester**	Gly.Me.	β-Ala.Me.	γ-Amino *n*-Bu.Me.
HCl	1.10	3.46	10.63
PVSH(S)	3.52	16.91	39.80
PVSH(R)	7.01	25.48	66.31
PVSH(A)	8.25	30.21	76.70
PSSH(R)	5.81	15.13	42.76
(PS)SH (69%)	6.60	19.37	44.37

* The concentrations of acids were: HCl, 0.0405 N; PVSH(S), 0.0428 N; PVSH(R), 0.0396 N; PVSH(A), 0.0421 N; PSSH(R), 0.0424 N; (PS)SH (69%), 0.0425 N.
** The concentrations of glycine-, β-alanine- and γ-aminobutyric acid methyl ester were 0.0500, 0.0511 and 0.0501 mol./l., respectively.

8) R. Signer, A. Demagistri and C. Müller, *Makromol. Chem.*, **18/19**, 139 (1956).
9) H. G. Houlton and H. V. Tartar, *J. Am. Chem. Soc.*, **60**, 544 (1938).
10) M. S. Dunn and A. Loshakoff, *J. Biol. Chem.*, **113**, 359 (1936).

Table II. Rate dependence as a function of the ratio of the concentration of the ester to the acid in the hydrolysis of several kinds of amino esters and related compounds

a) Glycine methyl

Acid* \ Ester	10^3k (l.mol^{-1}min^{-1}) 0.0500 (mol./l.)	0.025	0.0167
HCl	1.10	1.08	0.98
Et.-SO_3H	1.19	1.22	1.16
PVSH(S)	3.52	5.75	7.42
PVSH(R)	7.01	12.11	15.22
PVSH(A)	8.25	14.40	17.90
(PS)SH (69%)	6.60	10.56	14.47

b) β-Alanine methyl

Acid* \ Ester	10^3k (l.mol^{-1}min^{-1}) 0.0511 (mol./l.)	0.025	0.0170	0.0128
HCl	3.46	3.80	3.98	
Et.-SO_3H	3.69	3.94	3.67	
PVSH(S)	16.91	25.25	27.73	
PVSH(R)	25.48	46.03	54.27	46.06
PVSH(A)	30.20	50.51	60.47	45.52
PSSH(R)	15.13	22.78	25.82	
PSSH(A)	15.63	23.91	25.90	
(PS)SH (69%)	19.37	27.21	29.75	27.29

c) L-Glutamic acid γ-methyl

Acid* \ Ester	10^3k (l.mol^{-1}min^{-1}) 0.0384 (mol./l.)	0.0192	0.0128
HCl	2.84	3.50	3.76
Et.-SO_3H	2.75	3.21	3.50
PVSH(R)	35.10	52.84	46.12
PVSH(A)	38.74	60.60	55.55
PSSH(R)	19.83		
(PS)SH (69%)	20.27	35.10	42.86

d) Acetylcholine chloride

Acid* \ Ester	10^3k (l.mol^{-1}min^{-1}) 0.0501 (mol./l.)	0.0250
HCl	9.72	10.60
Et.-SO_3H	9.94	9.78
PVSH(R)	57.78	111.18
PVSH(A)	67.10	116.50
PSSH(R)	47.29	78.05
(PS)SH (69%)	48.96	76.15

* The concentrations of acids used in all runs were:
HCl, 0.0405 N; Et.-SO_3H, 0.0420 N; PVSH(S), 0.0428 N; PVSH(R), 0.0396 N; PVSH(A), 0.0421 N; PSSH(R), 0.0424 N; PSSH(A), 0.0413 N; (PS)SH (69)%, 0.0425 N.

for instance, was hydrolyzed 8.6 times faster by PVSH(A) than by hydrochloric acid.

Moreover, PVSH was a more effective catalyst than PSSH and (PS)SH (69%). A striking change was observed on varying the ester concentration in the hydrolysis of every amino ester with polymeric sulfonic acids, as is tabulated in Table II. The effect of the substrate concentration on the rates of hydrolysis with polymeric sulfonic acids at a constant acid concentration was determined. The hydrolysis rate constant increased with a decrease in the ester concentration (at a constant acid concentration), but subsequently rose to a maximum. It was reproduced in the plot of the ratio of the concentration of the ester-to-polymer catalyst, C_{ester}/C_{acid}, against the hydrolysis rate constant, k, with respect to the reaction of the β-alanine methyl ester, as is illustrated in Fig. 2. A maximum was attained near the concentration ratio of 0.4 in the case of the β-alanine methyl ester as well as in that of γ-methyl L-glutamate. No such specific behavior was, however, found in either the hydrolysis by hydrochloric acid or that by ethanesulfonic acid; the catalytic effects of these two acids were the same.

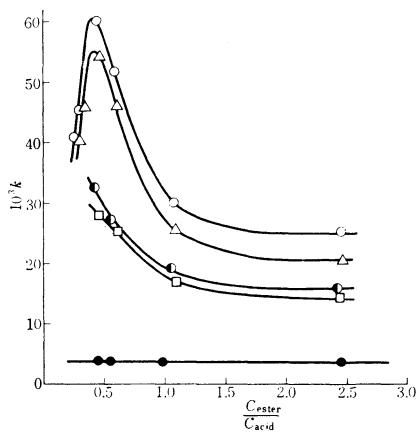

Fig. 2. Rate dependence as a function of the ratio of the concentration of the ester to the acid in the hydrolysis of β-alanine methyl ester:
●, HCl; □, PVSH(S); △, PVSH(R); ○, PVSH(A); ◐, (PS)SH (69%).

This accounts for the fact that hydrolysis takes place more easily at the optimum concentration of the ester within the domain of the polymer molecules. In other words, a larger value of the concentration ratio (over 0.4) leads to a shortage of the catalytically available neighboring free acid group towards the polymeric acid-substrate complex, while a smaller one (below 0.4) leads to a shortage of the complex available to attack by the nieghboring free acid group. This phenomenon is of interest in discussing the reaction mechanism in connection with the findings that the solvolytic rates of potassium 3-nitro-4-acetoxybenzenesulfonate catalyzed by 0.010 base molar poly-(4-vinylpyridine) increase as the pH is lowered and that a

maximum in the k - α plot (k is the rate constant, and α is the fraction of nitrogen present as the free base) is attained near $\alpha=0.6$ (pH 3.6), as has been reported by Letsinger and Savereide.[2c]

This specific effect in acid catalysis by polymeric sulfonic acids proves especially interesting when the catalytic activity relating to the structure of the polymer catalyst is discussed. The above data support the hypotheses that a free amino group must be present on the substrate if the anion of polymeric sulfonic acid is to be catalytically active, and that a complex is formed between the amino group of the substrate and the charged sulfonate group of the polymer catalyst before hydrolysis takes place.

Moreover, it was found that a methyl-substituted amino group of the substrate, such as acetylcholine chloride, also underwent the same specificity. This means that the reaction is governed only by the charged interaction between the polymer catalyst and the substrate insensitive to the steric factor of the substituents on the amino group. These observations are supported by the fact that the catalytic effects of polymeric sulfonic acids in the hydrolysis of the acetylglycine methyl ester were nearly the same as that of hydrochloric acid; the rate constants of HCl, PVSH(R) and PSSH(R), under the same conditions as is shown in Table II except for the ester concentration (0.021 mol./l.), were 9.08×10^{-3}, 9.45×10^{-3} and 9.81×10^{-3} respectively, which leads to the conclusion that there is no interaction between the substrate and polymeric sulfonic acid.

Furthermore, the difference in the catalytic effects between PVSH and PSSH can be attributed to the difference in the expansion in solutions and in the geometrical distances between sulfonic acid groups on the polymer chain, as has been described in a previous paper[3] with respect to the hydrolysis of carboxylic esters. The molecules of PVSH in solutions are possibly not greatly expanded as compared to that of PSSH; therefore, the localized protons along the polymer are confined within an extremely limited region in the reaction system in proportion to the magnitude of the molecular weight of PVSH. This interpretation is probably closely related to the fact that the catalytic efficiency, q, of PVSH increases gradually with the magnitude of its molecular weight, as is shown in Fig. 3, though no such correlation was found with PSSH-type catalysts. This observation can be explained by the fact that the complex formed by the preferential binding of the poly-anion to the positively-charged amino group of the substrate was surrounded by a high proton concentration in the polymer coil arising from the limited expansion of PVSH compared to that of PSSH.

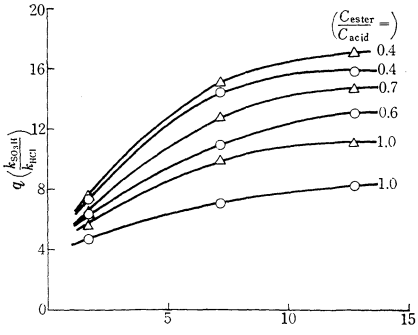

Fig. 3. Relation between the catalytic efficiency and the molecular weight of polyvinylsulfonic acid at constant C_{ester}/C_{acid} in the hydrolysis of β-alanine methyl ester (○) and L-glutamic acid γ-methyl ester (△).

Therefore, the local condensation of protons in the reaction system caused by the limited expansion of the polymer is largely responsible for the specific behavior of polymer catalysts, especially PVSH. The hydrolysis rate constants of the β-alanine methyl ester hydrolyzed by 30% neutralized PVSH(S) (0.0554 N) and by 30% neutralized (PS)SH (69%) (0.0620 N), both neutralized with barium hydroxide and where the ester concentration was 0.100 mol./l., were 6.84×10^{-3} and 12.57×10^{-3} (l. mol^{-1} min^{-1}) respectively, while the rate constants for the ester hydrolyzed by un-neutralized PVSH(S) and (PS)SH (69%) under the same conditions were 14.8×10^{-3} and 16.9×10^{-3} (l. mol^{-1} min^{-1}) respectively.

Such markedly different catalytic behavior of the two types of polymer catalysts can be attributed to the difference in the molecular expansion. The difference in the catalytic effects between sulfonated isotactic polystyrene sulfonic acid (70% sulfonation)[11] and the atactic one ((PS)SH(69%)) was, however, not very distinct for the series of amino esters; the hydrolysis rates with the former were 19.04×10^{-3} for the β-alanine methyl ester (0.0170 mol./l.), 35.16×10^{-3} for methyl γ-aminobutyrate (0.0501 mol./l.), and 44.10×10^{-3} for acetylcholine chloride (0.0501 mol./l.) at 45°C. These observations can be interpreted to mean that the difference in the geometrical distances between sulfonic acid groups on the polymer differing in configuration was not distinct enough in a solution to cause a difference in the catalytic activity.

11) Sulfonation of isotactic polystyrene ($\overline{M}_w>5\times 10^5$) was carried out in sulfuric acid for 6 hr. at 95°C using 10 g. of finely powdered isotactic polystyrene, 0.5 g. of silver sulfate and 100 ml. of concentrated sulfuric acid by modifying the directions by Takahashi and co-workers (*J. Chem. Soc. Japan, Ind. Chem. Sect. (Kogyo Kagaku Zassi)*, **61**, 1617 (1958)).

BULLETIN OF THE CHEMICAL SOCIETY OF JAPAN VOL. 39 1734—1738 (1966)

Methylene-hydantoin and Related Compounds. III. Synthesis of 5-Ethylidene-hydantoin: Attempts to Synthesize 5-Vinyl-hydantoin

By Shunsuke MURAHASHI,

Department of Polymer Science, Faculty of Science, Osaka University, Toyonaka, Osaka

and Heimei YUKI and Koichi KOSAI

Department of Chemistry, Faculty of Engineering Science, Osaka University, Toyonaka, Osaka

(Received November 10, 1965)

A number of methods of preparation were studied in an attempt to synthesize 5-vinyl-hydantoin using acrolein as a starting material. There were three possible routes: 1) the thermal decomposition of 5-(9, 10-dihydroanthracene-9, 10-*endo*-α, β-ethyl)-hydantoin at 400°C; 2) that of 5-(2-acetoxyethyl)-hydantoin and 3) the elimination reaction of dimethyl 2-(5-hydantoin)-ethyl sulfonium iodide in dimethyl sulfoxide by potassium *t*-butoxide. However, all the reactions gave 5-ethylidene-hydantoin as the product instead of 5-vinyl-hydantoin. An extreme ease of isomerization from 5-vinyl-hydantoin to 5-ethylidene-hydantoin was caused by the highly stable structure of the latter compound. The strong resonance stabilization of 5-ethylidene-hydantoin was observed in the ultraviolet spectrum. 5-Methyl-5-vinyl-hydantoin, which has no migrating hydrogen, could not be obtained from the 5-methyl derivatives of the above compounds.

In previous papers the present authors reported the synthesis of 5-methylene-hydantoin[1] (I) and its polymerization.[2] As an extension of these studies, the synthesis of 5-vinyl-hydantoin (II) was attempted. *C*-Vinyl-glycine and 5-vinyl-hydantoin are expected to form a new amino acid and new types of vinyl monomers, but these compounds have never been prepared, although their homologues, such as 5-allyl-hydantoin,[3] 5-(3-butenyl)-hydantoin,[4] and the corresponding amino acids derived from them, have been reported.

Among the several routes investigated, it seemed that three routes could give 5-vinyl-hydantoin. These are: (1) the retro Diels-Alder reaction of 5-(9, 10-dihydroanthracene-9, 10-*endo*-α, β-ethyl)-hydantoin (IV); (2) the elimination of acetic acid from 5-(2-acetoxyethyl)-hydantoin (V), and (3) the decomposition of dimethyl 2-(5-hydantoin)-ethyl sulfonium iodide (VI).

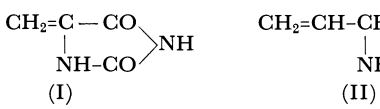

(I)

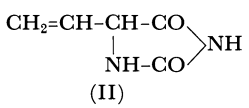

(II)

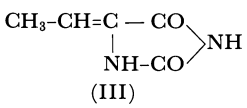

(III)

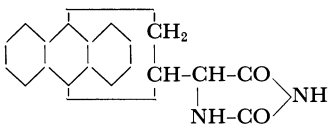

(IV)

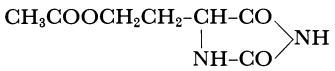

(V)

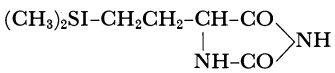

(VI)

In the present work, however, 5-vinyl-hydantoin could not be obtained; therefore, its isomer, 5-ethylidene-hydantoin (III) was taken as the product. 5-Ethylidene-hydantoin had been known since 1887,[5] and recently Guyot has prepared it by the decarboxylation of 5-carboxyethylidene-hydantoin.[6] This paper will give information on new methods of preparing 5-ethylidene-hydantoin.

Results and Discussion

The Decomposition of 5-(9, 10-Dihydroanthracene-9, 10-*endo*-α, β-ethyl)-hydantoin (IV). —5-Vinyl-hydantoin might seem to be easily prepared from acrolein in one step by Bucherer's

1) S. Murahashi, H. Yuki, K. Kosai and F. Doura, This Bulletin, **39**, 1559 (1966).
2) S. Murahashi, H. Yuki, K. Kosai and F. Doura, ibid., **39**, 1563 (1966).
3) R. Gaudry, L. Berlinguet, A, Langis and G. Paris, *Can. J. Chem.*, **34**, 502 (1956).
4) F. J. Marshall, *J. Am. Chem. Soc.*, **78**, 3696 (1956).
5) A. Pinner and J. Lifshutz, *Chem. Ber.*, **20**, 2345 (1887).
6) A. Guyot, J. Chopin and C. Mentzer, *Bull. soc. chim. France*, **1960**, 1596.

method[7] if the method could be applied to it. However, the addition of hydrogen cyanide to the C=C, instead of the C=O double bond, in acrolein takes place by Bucherer's reaction in a methanol-water mixture. Küchlin[8] has reported that the cyanohydrin could be obtained from acrolein and hydrogen cyanide in anhydrous ether, but in the presence of water the cyanohydrin dissociates to acrolein and hydrogen cyanide and gives an addition compound of hydrogen cyanide to the C=C double bond.

The difficulty in preparing 5-vinyl-hydantoin by a straightforward method from acrolein suggested to us that we employ an indirect route, including the Diels-Alder addition of acrolein and retro-reaction after the conversion of the adduct to its hydantoin derivative. In the present study anthracene was used as the diene because of the moderate stability of its acrolein adduct. 9, 10-Dihydroanthracene-9, 10-*endo*-α, β-propionaldehyde (VII) was obtained by heating a mixture of the components at 150°C.

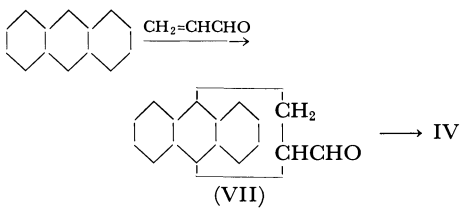

This was then converted to 5-(9, 10-dihydroanthracene-9, 10-*endo*-α, β-ethyl)-hydantoin (IV) by Bucherer's reaction in a methanol-water mixture. The decomposition of IV was carried out above 250°C in a stream of nitrogen by dropping a solution of IV in glacial acetic acid through a packed quartz tube (Table I). It was found that copper pellets have a good catalytic action in the retro-reaction. The efficiency was improved by using a copper gauze; the decomposition product was then obtained in a 85% yield at 400°C. However, as has been described above, the product was not 5-vinyl-hydantoin, but its isomer, 5-ethylidene-hydantoin. This was confirmed by the absorption band at 826 cm^{-1} due to $R_2C=CHR$ in its infrared spectrum (Fig. 1). The reaction was carried out at a lower temperature to avoid isomerization, but this resulted only in a lower yield of 5-ethylidene-hydantoin. The use of a silver gauze as a packing did not improve the reaction. When silica gel or alumina was used as the packing material, the decomposition occurred at the hydantoin group.

The decomposition of IV could not take place in a solution, in such a solvent as benzene, *o*-dichlorobenzene, nitrobenzene, decalin or acetic acid, at the boiling point. The dienophile exchange

Table I. Pyrolysis of 5-(9, 10-dihydroanthracene-9, 10-*endo*-α, β-ethyl)-hydantoin

Packing material	Starting material g.	Temp. °C	Press. mmHg	Products, g.* A	B	C
Glass	1.0	400	760	carbonized		
Glass	1.0	500	760	carbonized		
Silica gel	1.0	400	760	unknown**		
Alumina	1.0	425	760	unknown**		
Cu-pellet	1.0	250	760	0.01	0.89	
Cu-pellet	1.0	300	760	0.05	0.72	
Cu-pellet	1.0	400	760	0.10	0.70	
Cu-pellet	1.0	550	760	0.01	0.43	
Cu-gauze	2.0	250	760	0.32	0.76	0.41
Cu-gauze	2.0	250	100	0.45	0.85	0.18
Cu-gauze	4.0	400	760	1.42	0.40	1.56
Cu-gauze	4.0	400	100	1.28	1.24	0.57
Cu-gauze	2.0	500	100	0.38	0.18	0.86
Ag-gauze	1.0	300	760	0.30	0.13	0.36
Ag-gauze	1.0	400	760	0.33	0.07	0.38
Cu-gauze	1.0***	400	760	0		

* A: 5-Ethylidene-hydantoin, B: Unreacted, C: Anthracene.
** IR spectra showed no hydantoin group in the product.
*** Solvent: Benzene.

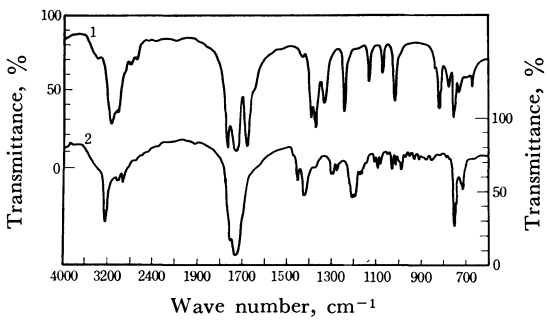

Fig. 1. Absorption spectra of: 1, 5-ethylidene-hydantoin; 2, 5-(9, 10-dihydroanthracene-9, 10-*endo*-α, β-ethyl)-hydantoin (in KBr disks).

reaction also did not proceed in these solvents. In the reaction, dimethyl acetylenedicarboxylate, maleic anhydride and dimethyl maleate were employed as dienophiles.

The Elimination of Acetic Acid from 5-(2-Acetoxyethyl)-hydantoin (V).—The next route investigated to approach 5-vinyl-hydantoin was the elimination of HX from the compounds of the type A:

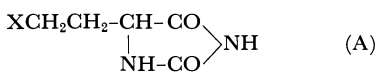

(A)

X: Br, I, OH or AcO

When 5-(2-halogenoethyl)-hydantoin was treated with strong bases, such as sodium methoxide and sodium hydroxide, in anhydrous alcohol, the decomposition took place at the hydantoin group.

7) H. Th. Bucherer, *J. prakt. Chem.*, **141**, 23 (1934).
8) A. T. Küchlin, Jr., *Rec. trav. chim.*, **49**, 705 (1930).

Silver oxide and morpholin did not react with the halogeno-compound. The compound gave only its pyridinium salt when heated in pyridine.

5-(2-Acetoxyethyl)-hydantoin was prepared from 5-(2-halogenoethyl)-hydantoin and potassium acetate. It was found that the elimination of acetic acid from 5-(2-acetoxyethyl)-hydantoin gave 5-ethylidene-hydantoin in a good yield. The elimination reaction was conducted with a procedure similar to that used in the retro-reaction of the anthracene adduct described above (Table II).

TABLE II. PYROLYSIS OF 5-(2-ACETOXYETHYL)-HYDANTOIN

Acetate g.	(Solvent)	ml.	Temp. °C	5-Et-Hyd. g.	Unreacted g.
1.0	AcOH	(100)	300	—	0.90
1.0	*t*-BuOH	(100)	300	0.40	0.37
1.0	*t*-BuOH	(100)	400	0.42	0.16
1.0	*t*-BuOH	(100)	500	0.39	0.07

The Decomposition of Dimethyl 2-(5-Hydantoin)-ethyl Sulfonium Iodide (VI).—The cause of the isomerization of 5-vinyl-hydantoin to 5-ethylidene-hydantoin during the reaction, described in the preceding sections, was supposed to be the high reaction temperature. As a third attempt, the decomposition of dimethyl 2-(5-hydantoin)-ethyl sulfonium iodide (VI) was investigated, as the reaction was expected to proceed under milder conditions. As the starting material, the sulfonium salt was prepared from *dl*-methionine:

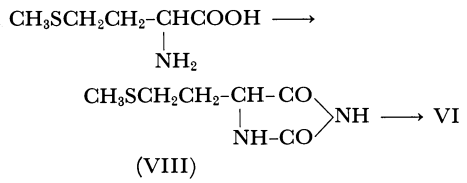

(VIII)

The salt was decomposed into dimethyl sulfide and 5-(2-iodoethyl)-hydantoin by heating it in *n*-butanol. By a reaction with sodium ethoxide in absolute ethanol, it gave a small quantity of 5-(2-ethoxyethyl)-hydantoin, and the residual part of the iodide was decomposed at the hydantoin group. In dimethyl sulfoxide, the hydantoin group was decomposed by potassium *t*-butoxide at 80°C, and 5-ethylidene-hydantoin was obtained from the sulfonium salt in a good yield at 20°C. In this case, also, no 5-vinyl-hydantoin was obtained, and the isomerization proceeded very easily and completely at such a low reaction temperature, even if the isomerization could be catalyzed by the base in the polar solvent.

The Stability of 5-Ethylidene-hydantoin.—Vinylacetic acid exists with sufficient stability, as does its isomer, crotonic acid. On the other hand, 5-vinyl-hydantoin, the derivative of vinylacetic acid, could not be obtained. The extreme ease of the isomerization of 5-vinyl-hydantoin to 5-ethylidene-hydantoin suggests that the high stability of 5-ethylidene-hydantoin is due to the resonance between the C=C double bond and the hydantoin group. This was proved by the strong absorption band of 5-ethylidene-hydantoin at 270 mμ, which was absent in the spectra of acrylic acid and 5-methyl-hydantoin (Fig. 2). The same band was observed in the spectrum of 5-methylene-hydantoin, which showed a large Q-value, a factor correlated with the resonance stabilization, in Alfrey-Price's Q-e scheme.[2]

5-Ethylidene-hydantoin not only polymerized by itself with a radical initiator, but even inhibited the polymerization of styrene in the copolymerization reaction with the latter monomer.

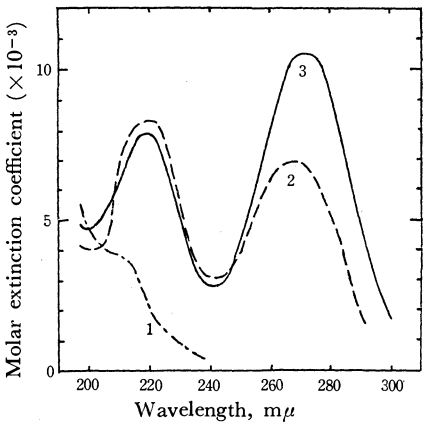

Fig. 2. Absorption spectra of: 1, 5-methyl-hydantoin in H_2O; 2, 5-methylene-hydantoin in H_2O (λ_{max} 268 mμ, ε_{max} 7×10^3); 3, 5-ethylidene-hydantoin in EtOH (λ_{max} 272 mμ, ε_{max} 10.5×10^3).

Furthermore, it was found that 5-vinyl-5-methyl-hydantoin (IX), which has no migrant hydrogen, could not be obtained from either 5-(9, 10-dihydroanthracene-9, 10-*endo*-α, β-ethyl)-5-methyl-hydantoin (X) or dimethyl 2-(5-(5-methyl)-hydantoin)-ethyl sulfonium iodide (XI) by the pro-

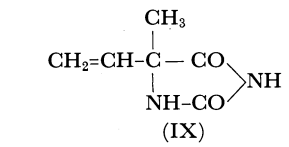

(IX)

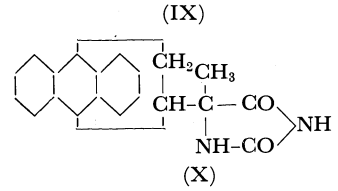

(X)

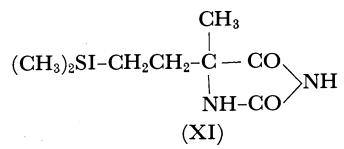

(XI)

cedures described previously. That is, these compounds not only gave 5-vinyl-5-methyl-hydantoin, but showed no decomposition reaction which did not destroy the hydantoin group in the course of the treatment.

These facts seem to explain the stable conjugate structure of 5-ethylidene-hydantoin and the ease of the isomerization of 5-vinyl-hydantoin to it.

Experimental

9, 10-Dihydroanthracene-9, 10-*endo*-α, β-propionaldehyde (VII).—A mixture of anthracene (40 g., 0.23 mol.), freshly-distilled acrolein (12 g., 0.21 mol.), benzene (90 ml.) and a small amount of hydroquinone was heated in an autoclave at 140—150°C for 12 hr. The reaction mixture was then concentrated under reduced pressure. The residual syrup was dissolved in methanol (250 ml.), and a small amount of the unreacted anthracene was removed by filtration. An equal amount of water was then added to the filtrate, and the mixture was left to stand overnight. Fine crystals of the adduct monohydrate were thus obtained almost quantitatively. The hydrate was recrystallized from acetone; m. p. 100°C.

Found: C, 81.15; H, 6.28. Calcd. for $C_{17}H_{14}O \cdot H_2O$: C, 80.92; H, 6.37%.

The hydrate was soluble in acetone and benzene, but insoluble in water and methanol. Its infrared spectrum showed no absorption band resulting from the carbonyl group of the aldehyde, but it did show the absorption band at 3300 cm^{-1} resulting from the hydroxy group of $-CH(OH)_2$. It gave anhydrous aldehyde when heated at 80°C under reduced pressure. The anhydrous aldehyde was a crystalline compound which melted at 95°C (lit.,[9] 95°C) and which was soluble in methanol. It was gradually converted into the monohydrate in moist air.

5-(9, 10-Dihydroanthracene-9, 10-*endo*-α, β-ethyl)-hydantoin (IV).—Into a solution of ammonium carbonate (92 g.) and sodium cyanide (20 g.) in water (200 ml.), a solution of the anhydrous aldehyde (VII) (50 g.) in methanol (250 ml.) was stirred at 60°C; the reaction was then continued for 10 hr. After the solution had cooled, the precipitates produced were filtered, washed with water, and then suspended in 6 N hydrochloric acid. The suspension was heated at 90°C for 2 hr., and the solid was filtered, washed with water, and dried. The raw product was then extracted with three portions of hot acetone (500 ml.). The concentration of the acetone solution gave the hydantoin (51 g.), which was recrystallized from acetic acid (800 ml.). Yield, 46 g. (71%); m. p. 225°C; colorless crystals sublimed at 220°C/30 mmHg; soluble in hot acetone and hot acetic acid, and insoluble in water, benzene and petroleum ether.

Found: C, 74.86; H, 5.24; N, 9.12. Calcd. for $C_{19}H_{16}N_2O_2$: C, 74.98; H, 5.30; N, 9.20%.

The Decomposition of 5-(9, 10-Dihydroanthracene-9, 10-*endo*-α, β-ethyl)-hydantoin.—A quartz tube (60 cm. long and 5.2 cm. in diameter) packed with the material described in Table I was placed vertically in an electric furnace and heated. The solution of IV in 100 parts of acetic acid was then introduced drop by drop into the tube under a nitrogen stream at atmospheric pressure or at a pressure of about 100 mmHg. The products were collected in two traps connected in a series, one cooled with ice water and the other with dry ice - acetone. After the solution had been added, the inside of the tube was washed with acetic acid (50 ml.) drop by drop. The products and the washings were then combined and evaporated to dryness under a reduced pressure of nitrogen. The residues were extracted with hot water, and the aqueous solution was concentrated under reduced pressure to give 5-ethylidene-hydantoin. The water-insoluble part was fractionated by extraction with hot acetic acid into anthracene and unreacted hydantoin. 5-Ethylidene-hydantoin was recrystallized from water. Colorless crystals subliming at 200°C; m. p. 265°C (lit.,[6] 265°C). The infrared spectrum is shown in Fig. 1.

Found: C, 47.69; H, 4.87; N, 21.50. Calcd. for $C_5H_6N_2O_2$: C, 47.62; H, 4.80; N, 22.21%.

5-(2-Acetoxyethyl)-hydantoin (V).—According to the method of Nyberg,[10] 5-(2-hydroxyethyl)-hydantoin and its brom- and iodo-derivatives were prepared from γ-butyrolactone. A solution of freshly-fused potassium acetate (9.8 g., 0.1 mol.) and 5-(2-iodoethyl)-hydantoin (25.4 g., 0.1 mol.) in ethyl methyl ketone (400 ml.) was refluxed for 10 hr. After the solution had then cooled, the precipitates were filtered off, and the filtrate was evaporated under reduced pressure. By the recrystallization of the residue from a mixture of equal amounts of chloroform and benzene, 5-(2-acetoxyethyl)-hydantoin (12 g.) was obtained in a 65% yield; m. p. 122°C; soluble in water, alcohol, acetone and chloroform, and slightly soluble in ethyl ether and benzene.

Found: C, 44.96; H, 5.45; N, 14.47. Calcd. for $C_7H_{10}N_2O_4$: C, 45.16; H, 5.42; N, 15.05%.

The same product was also obtained from 5-(2-bromoethyl)-hydantoin.

The Decomposition of 5-(2-Acetoxyethyl)-hydantoin.—The same apparatus and procedures described in the pyrolysis of IV were used, employing a copper gauze as a packing material. A solution of 5-(2-acetoxyethyl)-hydantoin in *t*-butyl alcohol was added, drop by drop and under a stream of nitrogen at atmospheric pressure, over a 2 hr. period. The products were fractionated into water-soluble and water-insoluble parts. 5-Ethylidene-hydantoin was obtained from the water-insoluble fraction. When acetic acid was used as a solvent for pyrolysis, the acetate was recovered almost unchanged. The results of the reaction are shown in Table II.

5-(2-Methylmercaptoethyl) - hydantoin (VIII).—This compound was synthesized from commercial *dl*-methionine according to the method of Livak.[11] Yield, 85.5%; m. p. 107°C (lit.[11] 105—106°C).

Dimethyl 2 - (5 - Hydantoin) - ethyl Sulfonium Iodide (VI).—VIII (10 g., 0.06 mol.) was dissolved in acetonitrile, and then methyl iodide (10 ml., 0.16 mol.) was added. Colorless crystals of the sulfonium salt were obtained from the solution after it had stood in

9) B. A. Arbuzov and E. Kh. Isklakov, *Chem. Abstr.*, **52**, 339 (1958).

10) D. D. Nyberg and B. E. Christenson, *J. Am. Chem. Soc.*, **79**, 1222 (1957).

11) J. E. Livak, E. C. Britton, J. C. VanderWeele and M. F. Murray, ibid., **67**, 2218 (1945).

a refrigerator for several hours. A recrystallization of the raw product (18 g.) from water (70 ml.) gave pure crystals (14 g.) (m. p. 168°C (decomp.); soluble in water and methanol, and sparingly soluble in ether and acetone).

Found: C, 26.59; H, 4.14. Calcd. for $C_7H_{13}N_2O_2IS$: C, 26.67; H, 4.12%.

The Decomposition of Dimethyl 2-(5-Hydantoin)-ethyl Sulfonium Iodide.—To a solution of VI (5.4 g., 0.017 mol.) in purified dimethyl sulfoxide (170 ml.), a solution of potassium *t*-butoxide (6.5 g., 0.033 mol.) in the same solvent (80 ml.) was added. The reaction mixture was then stirred at 20°C under a stream of dry nitrogen, and the dimethyl sulfide evolved was introduced into a 1% solution of mercuric chloride in water through a drying tube containing 4A molecular sieves. The progress of the reaction was observed by the precipitation of the dimethyl sulfide-mercuric chloride complex. After 48 hr. the reaction mixture was neutralized with acetic acid and concentrated to a syrup under reduced pressure. The syrup gave crystals when 5 ml. of water was added. By recrystallization from water, pure 5-ethylidene-hydantoin (1.7 g., 81%) was obtained.

When VI was heated in morpholin or in *N*-methyl morpholin at 100°C, a vigorous evolution of dimethyl sulfide was observed. After the evolution had ended, the reaction mixture was concentrated to dryness under reduced pressure. The obtained residue was, however, found to be 5-(2-iodoethyl)-hydantoin.

9, 10 - Dihydroanthracene-9, 10 - *endo*-α, β - ethyl Methyl Ketone.—This compound was prepared from anthracene and methyl vinyl ketone by a method which has been described for VII. The reaction mixture was then concentrated to dryness, and the residue was recrystallized from acetone. The adduct was thus obtained; yield, 72%; colorless crystals subliming at 100°C; m. p. 150°C.

Found: C, 87.29; H, 6.38. Calcd. for $C_{18}H_{16}O$: C, 87.06; H, 6.49%.

5-(9, 10-Dihydroanthracene-9, 10-*endo*-α, β-ethyl)-5-methyl-hydantoin (X).—This hydantoin was prepared, in a 78% yield, from the ketone by the method which has been described for IV. It did not melt below 300°C, it sublimed at 130°C/10 mmHg, and it was soluble in acetone, slightly soluble in acetic acid and benzene, and insoluble in water and methanol.

Found: C, 75.36; H, 5.72; N, 8.63. Calcd. for $C_{20}H_{18}N_2O_2$: C, 75.44; H, 5.69; N, 8.80%.

This compound could not be decomposed, even at 500°C, by the procedure used for IV, but its hydantoin group was decomposed at higher temperatures.

Dimethyl 2-(5-(5-Methyl)-hydantoin)-ethyl Sulfonium Iodide (XI).—A concentrated solution of 5-(2-methylmercaptoethyl)-5-methyl-hydantoin[12] (17 g.) in dry methanol was mixed with methyl iodide (20 g.). The precipitates thus produced were then filtered and dried. Recrystallization from methanol gave pure crystals; yield, 21 g.; m. p. 169°C (decomp.); soluble in water, methanol and dimethyl sulfoxide, slightly soluble in acetone and ether, and insoluble in benzene.

Found: C, 29.29; H, 4.53. Calcd. for $C_9H_{15}N_2O_2IS$: C, 29.10; H, 4.58%.

This compound was treated with potassium *t*-butoxide in dimethyl sulfoxide by the procedure described for VI. Dimethyl sulfide was observed to evolve at a very slow rate, but there was also a simultaneous decomposition of the hydantoin group. The expected compound was not obtained.

12) K. Pfister, W. J. Leanza, J. P. Conbere, H. J. Becker, A. R. Matzuk and E. F. Rogers, ibid., **77**, 697 (1955).

BULLETIN OF THE CHEMICAL SOCIETY OF JAPAN VOL. 39 1738—1747 (1966)

Studies of Peptide Antibiotics. IV. The Synthesis of Tyrocidine A*

By Motonori OHNO, Tetsuo KATO, Satoru MAKISUMI and Nobuo IZUMIYA

Laboratory of Biochemistry, Faculty of Science, Kyushu University, Fukuoka

(Received November 15, 1965)

The synthesis of a cyclic decapeptide, cyclo-L-phenylalanyl-D-phenylalanyl-L-asparaginyl-L-glutaminyl-L-tyrosyl-L-valyl-L-ornithyl-L-leucyl-D-phenylalanyl-L-prolyl, which has an amino acid sequence determined by Craig et al. for natural antibiotics, tyrocidine A, has been described. The chemical and biological properties of the synthetic product have been shown to be in agreement with those of the natural tyrocidine A.

Tyrocidine A is a basic polypeptide isolated as a hydrochloride by Battersby and Craig,[1] using a technique of countercurrent distribution, from the family of closely-related substances present in tyrocidine which is produced in autolyzed cultures of *Bacillus brevis*. Its structure has been determined by Craig and his colleagues[2,3] by means of a

* A part of this work has been briefly communicated: M. Ohno and N. Izumiya, *J. Am. Chem. Soc.*, **88**, 376 (1966).

1) A. R. Battersby and L. C. Craig, ibid., **74**, 4019 (1952).

2) A. R. Battersby and L. C. Craig, ibid., **74**, 4023 (1952).

3) A. Paladini and L. C. Craig, ibid., **76**, 688 (1954).

partial hydrolysis and by means of a study of the countercurrent distribution. Tyrocidine A is, like gramicidin S,[4,5] a cyclic decapeptide; it is constructed from three molecules of phenylalanine and one each of asparagine, glutamine, tyrosine, valine, ornithine, leucine and proline. All amino acid residues except two molecules of D-phenylalanine have a L-configuration. Figure 1 indicates

L-Phe-D-Phe-L-Asp(NH_2)-L-Glu(NH_2)-L-Tyr
↑ ↓
L - Pro - D - Phe - L - Leu - L - Orn - L - Val

Fig. 1. Constructional formula of tyrocidine A.

the constructional formula of tyrocidine A. The pentapeptide sequence, L-valyl-L-ornithyl-L-leucyl-D-phenylalanyl-L-prolyl, is also found in gramicidin S, tyrocidine B[6] and tyrocidine C.[7] The syntheses of the linear penta-[8] and decapeptide derivatives[9] related to tyrocidine A have been reported by Schwyzer et al., but the complete synthesis of tyrocidine A has not yet been accomplished. We, therefore, have here attempted to synthesize this cyclic decapeptide. This paper will describe the synthesis of the cyclic decapeptide hydrochloride (I_s) having the amino acid sequence of tyrocidine A (Fig. 1) and will attempt to establish the identity of the synthetic product (I_s) with natural tyrocidine A hydrochloride (I_n) in chemical and biological properties.

The cyclization of a linear decapeptide was carried out by a *p*-nitrophenyl ester method. Di-*p*-nitrophenyl sulfite was used as a reagent of the *p*-nitrophenyl esterification reaction.[10] It has been observed that, when *N*-protected peptide is treated with di-*p*-nitrophenyl sulfite in an attempt to obtain a corresponding *p*-nitrophenyl ester, the *C*-terminal amino acid residue is subjected to partial racemization, with the exception of glycine and proline residues.[10,11] For this reason, the proline residue was selected as the *C*-terminal amino acid in a linear decapeptide to be activated to the *p*-nitrophenyl ester (see the compound XXI in Fig. 5).[12]

p-Methoxybenzyloxycarbonyl[13] and benzyloxycarbonyl groups were employed for the selective blocking of the *N*-terminal amino group and the δ-amino group of ornithine residue respectively.

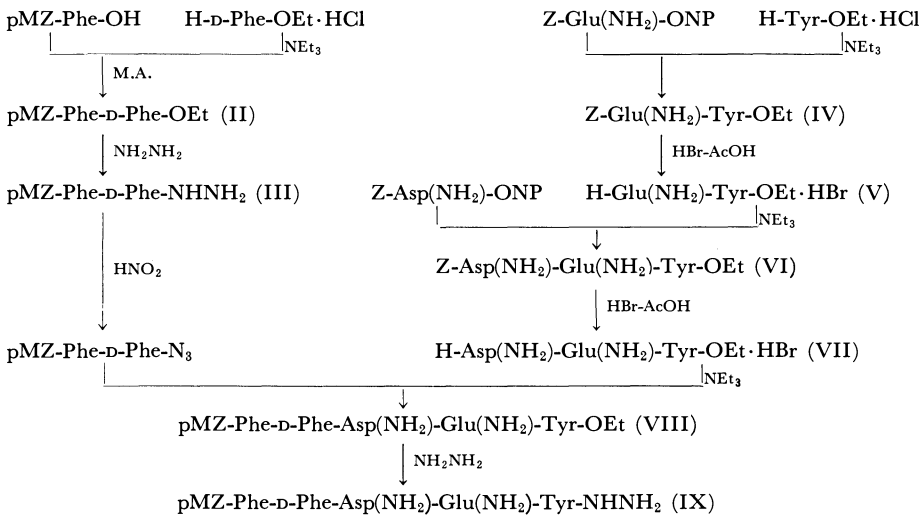

Fig. 2. Synthesis of pMZ-pentapeptide hydrazide (IX): prefix L for amino acids of L-configuration is omitted; pMZ, *p*-methoxybenzyloxycarbonyl; Z, benzyloxycarbonyl; Et, ethyl; NP, *p*-nitrophenyl; NEt_3, triethylamine; AcOH, acetic acid; M. A., mixed anhydride method.

4) R. Consden, A. H. Gordon, A. J. P. Martin and R. L. M. Synge, *Biochem. J.*, **41**, 596 (1947); A. R. Battersby and L. C. Craig, *J. Am. Chem. Soc.*, **73**, 1887 (1951).
5) R. Schwyzer and P. Sieber, *Helv. Chim. Acta*, **40**, 624 (1957).
6) T. P. King and L. C. Craig, *J. Am. Chem. Soc.*, **77**, 6627 (1955).
7) M. A. Ruttenberg, T. P. King and L. C. Craig, *Biochemistry*, **4**, 11 (1965).
8) R. Schwyzer and P. Sieber, *Helv. Chim. Acta*, **42**, 972 (1959).
9) R. Schwyzer, E. Surbeck-Wegmann and H. Dietrich, *Chimia*, **14**, 366 (1960).
10) B. Iselin and R. Schwyzer, *Helv. Chim. Acta*, **43**, 1760 (1960).
11) M. Ohno and N. Izumiya, This Bulletin, **38**, 1831 (1965).
12) In the synthesis of evolidin, natural cyclic heptapeptide, a leucine residue was selected as a *C*-terminal amino acid of a linear heptapeptide to be activated to the *p*-nitrophenyl ester by using di-*p*-nitrophenyl sulfite, in spite of the presence of a proline residue as a constituent. Nevertheless, the resulting cyclic heptapeptide was proved to be homogeneous with regard to the leucine residue; it was identical to the natural product in many properties (R. O. Studer and W. Lergier, *Helv. Chim. Acta*, **48**, 460 (1965)).
13) F. Weygand and H. Hunger, *Chem. Ber.*, **95**, 1 (1962).

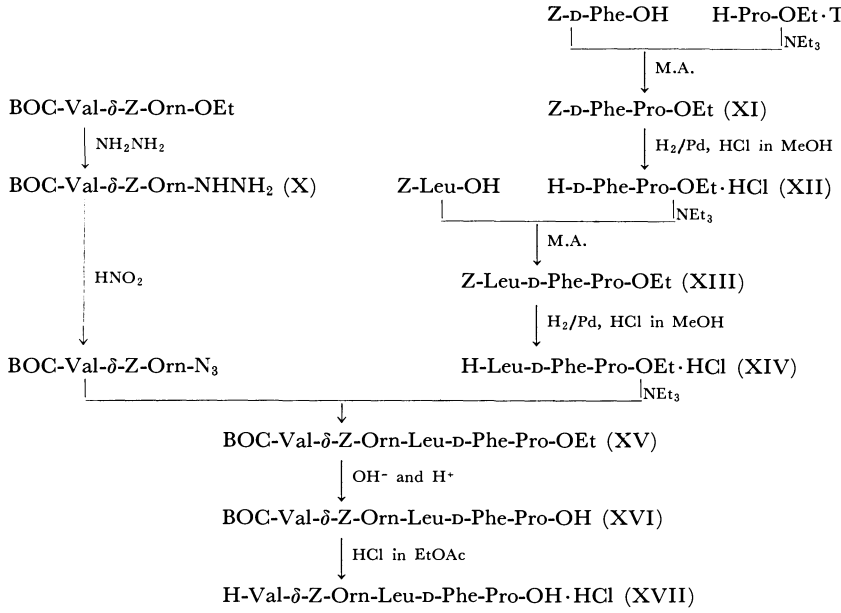

Fig. 3. Synthesis of pentapeptide hydrochloride (XVII): BOC, *t*-butyloxycarbonyl; TsOH, *p*-toluenesulfonic acid; MeOH, methanol; EtOAc, ethyl acetate.

As has been described in a previous paper, the *p*-methoxybenzyloxycarbonyl group is so available that it is released easily with the action of anhydrous trifluoroacetic acid, without hurt to the sensitive *p*-nitrophenyl ester group.[11]

The scheme for the synthesis of the *N*-terminal pentapeptide derivative, *p*-methoxybenzyloxycarbonyl-L-phenylalanyl-D-phenylalanyl-L-asparaginyl-L-glutaminyl-L-tyrosine hydrazide (IX), is presented in Fig. 2. *p*-Methoxybenzyloxycarbonyl-L-phenylalanyl-D-phenylalanine ethyl ester (II) was prepared by the reaction of *p*-methoxybenzyloxycarbonyl-L-phenylalanine[13] with D-phenylalanine ethyl ester by means of the mixed anhydride procedure. The subsequent treatment of II with twenty equivalents of hydrazine in dimethylformamide gave the hydrazide (III) in a 96% yield. The *C*-terminal tripeptide derivative (VI) was prepared by step-by-step elongation by means of the *p*-nitrophenyl ester method. The reaction of benzyloxycarbonyl-L-glutamine *p*-nitrophenyl ester with tyrosine ethyl ester gave the crystalline dipeptide derivative (IV). This was treated with hydrogen bromide in acetic acid and then allowed to react with benzyloxycarbonyl-L-asparagine *p*-nitrophenyl ester. VI was thus obtained in a crystalline form. The azide, which had been derived from III, was made to react with the tripeptide ester (VII) prepared from VI with the action of hydrogen bromide in acetic acid; the protected pentapeptide ester (VIII) was thus obtained in a 75% yield. VIII was converted to the hydrazide (IX) in a 86% yield by treatment with hydrazine.

Figure 3 indicates the scheme for the synthesis of the *C*-terminal pentapeptide derivative, L-valyl-δ-benzyloxycarbonyl-L-ornithyl-L-leucyl-D-phenylalanyl-L-proline hydrochloride (XVII). *t*-Butyloxycarbonyl-L-valyl-δ-benzyloxycarbonyl-L-ornithine hydrazide (X) was obtained in a 83% yeild by the treatment of the *t*-butyloxycarbonyl-L-valyl-δ-benzyloxycarbonyl-L-ornithine ethyl ester[14] with hydrazine. The tripeptide derivative (XIII) was synthesized by a step-by-step reaction by means of the mixed anhydride method. The reaction of the anhydride prepared from benzyloxycarbonyl-D-phenylalanine and isobutyl chloroformate with L-proline ethyl ester afforded the oily dipeptide derivative (XI) in a 86% yield. This was hydrogenolyzed in the presence of palladium black and then allowed to react with the anhydride derived from benzyloxycarbonyl-L-leucine. XIII was thus obtained in a 95% yield as an oily substance. The catalytic hydrogenolysis of XIII also gave the oily tripeptide ester hydrochloride (XIV), which was found to be homogeneous in paper chromatography. The azide, which had been derived from X, was made to react with XIV to give the pure crystalline, protected pentapeptide ester (XV) in a 69% yield. The saponification of XV afforded the crystals of the protected pentapeptide (XVI). The subsequent treatment of XVI with twenty equivalents of hydrogen chloride in ethyl acetate yielded the pentapeptide hydrochloride (XVII) in a crystalline form. On the other hand, the same treatment of XV afforded the crystalline pentapeptide ester hydrochloride (XVIII) (see Fig. 4).

Two approaches were applied to the synthesis

14) N. Izumiya, T. Kato, Y. Fujita, M. Ohno and M. Kondo, This Bulletin, **37**, 1809 (1964).

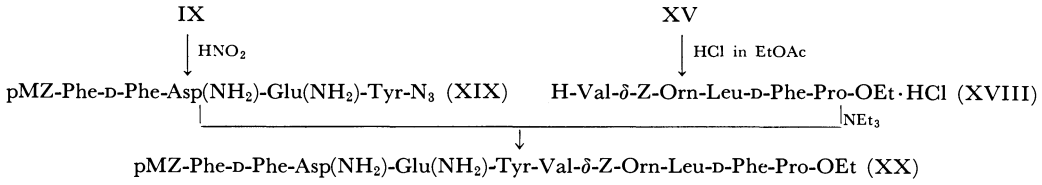

Fig. 4. Synthesis of pMZ - decapeptide ester (XX).

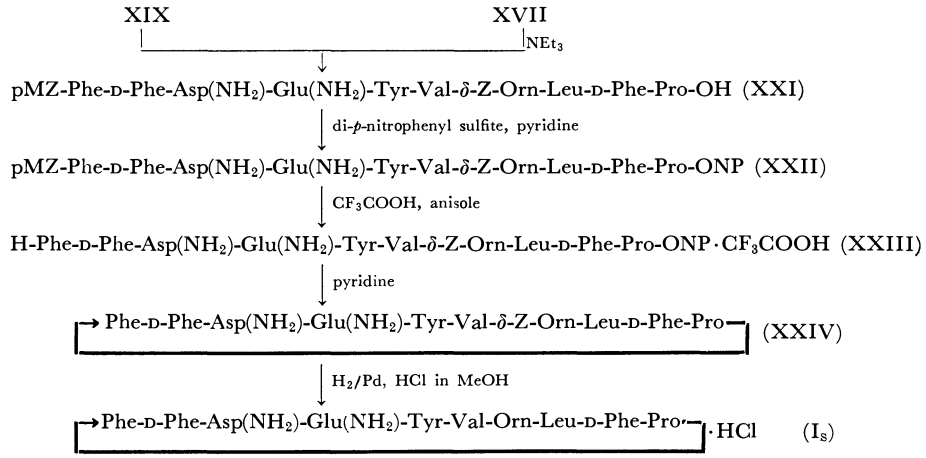

Fig. 5. Synthesis of cyclic decapeptide hydrochloride (I_s).

of the decapeptide derivative (XXI). The one route, via the synthesis of the protected decapeptide ester (XX), is presented in Fig. 4. The protected pentapeptide azide (XIX), which had been derived from IX, was allowed to react with XVIII in the presence of an equivalent amount of triethylamine. XX was thus obtained as an analytically-pure, crystalline product in a 70% yield. However, this approach was not feasible because the saponification of the ester (XX) by alkali was unsuccessful.

Figure 5 indicates another route for the synthesis of the protected decapeptide (XXI) and the subsequent synthesis of the cyclic decapeptides (XXIV and I_s). The reaction of the azide (XIX) with XVII in the presence of two equivalents of triethylamine gave the pure crystalline, protected decapeptide (XXI) in an yield of 75%. XXI was converted to the protected decapeptide *p*-nitrophenyl ester (XXII) with the action of ten equivalents of di-*p*-nitrophenyl sulfite in the presence of pyridine. The removal of the *p*-methoxybenzyloxycarbonyl group from XXII by treatment with trifluoroacetic acid yielded the amorphous decapeptide *p*-nitrophenyl ester trifluroacetate (XXIII) in an excellent yield. The cyclization reaction of XXIII in a large amount of pyridine gave the crude benzyloxycarbonyl-substituted cyclic peptide (XXIV), which was then purified by passing it through columns of strongly acidic and weakly basic ion exchangers. The yield of XXIV from XXI was excellent—60% after the recrystallization. The homogeneity of XXIV was established by the criteria of thin-layer and paper chromatographies and by elemental analysis. The molecular weight determination using the vapor pressure osmometer demonstrated that the molecular size of XXIV corresponded to that of cyclic decapeptide. The catalytic hydrogenolysis of XXIV in the presence of an equivalent amount of hydrogen chloride in methanol afforded the cyclic decapeptide hydrochloride (I_s) in a 74% yield. Although Battersby and Craig[2] found that the treatment of tyrocidine A hydrochloride (I_n) with excess hydrogen chloride in methanol formed its transformation product by the conversion of one primary amide group of asparagine or the glutamine residue to the methyl ester group, it has been shown, from the detection of two moles of ammonia in the amino acid analysis of the acid hydrolysate of I_s, that no such reaction occurred under the above conditions.

The synthetic cyclic decapeptide hydrochloride (I_s) was then compared with the natural product (I_n). In addition to having the same R_f values in paper and thin-layer chromatographies and having indistinguishable paper electrophoretic patterns (Fig. 6), I_s and I_n had superimposable infrared and well-agreeing ultraviolet spectra (Figs. 7 and 8), identical behaviors in the carboxymethylcellulose column (Fig. 9), and the same value in optical rotation. Furthermore, very close similarities were seen in the antibacterial activities

of the two compounds with regard to microorganisms (see Table I). These results show that the synthetic product is identical to natural tyrocidine A. The structure of tyrocidine A offered by Craig et al. has been further confirmed by the present synthesis.

Experimental

The melting points were not corrected. The optical rotations were measured on a Yanagimoto Photometric Polarimeter, OR-20 type. The paper chromatography was carried out on Toyo Roshi No. 52 chromatography paper. The thin-layer chromatography was carried out on Merck silica gel G. The developing solvents commonly used were *n*-butanol - acetic acid - pyridine - water (4 : 1 : 1 : 2 v/v) and *t*-butanol - formic acid - water (75 : 15 : 10 v/v). Spots of materials possessing a free amino group on a thin-layer plate were detected by spraying ninhydrin, and those of the amino group-blocked materials, by spraying 47% hydrobromic acid and then ninhydrin. Prior to analysis, the compounds were dried over phosphorus pentoxide at 100°C and 2 mmHg to a constant weight except for the compound I_S.

***p*-Methoxybenzyloxycarbonyl-L-phenylalanyl-D-phenylalanine Ethyl Ester (II).**—To a mixed anhydride prepared at −5°C from 6.58 g. (20 mmol.) of *p*-methoxybenzyloxycarbonyl-L-phenylalanine,[13] 2.60 ml. (20 mmol.) of isobutyl chloroformate and 2.80 ml. (20 mmol.) of triethylamine in 60 ml. of tetrahydrofuran, a chilled solution of 4.60 g. (20 mmol.) of D-phenylalanine ethyl ester hydrochloride dissolved in a mixture of 2.80 ml. (20 mmol.) of triethylamine and 60 ml. of chloroform was added. The reaction mixture was then allowed to stand overnight and then evaporated in vacuo. The oily residue was dissolved in 80 ml. of ethyl acetate, and the solution was washed successively with 0.5 M citric acid, a 3% sodium bicarbonate solution and water, dried over sodium sulfate, and then evaporated in vacuo. The oily residue was solidified by adding petroleum ether (8.68 g.). The product was recrystallized from ethanol - ether - petroleum ether. Yield, 8.0 g. (79%); m. p. 126—128°C; $[\alpha]_D^{20}$ −2.8° (*c* 4.4, dimethylformamide).

Found: C, 69.18; H, 6.13; N, 5.66. Calcd. for $C_{29}H_{32}O_6N_2$: C, 69.03; H, 6.39; N, 5.55%.

***p*-Methoxybenzyloxycarbonyl-L-phenylalanyl-D-phenylalanine Hydrazide (III).**—A solution of 6.06 g. (12 mmol.) of II and 12 ml. (240 mmol.) of hydrazine hydrate in 18 ml. of dimethylformamide was allowed to stand at room temperature for 2 days. The solution was then evaporated in vacuo in order to remove the excess hydrazine, after which 180 ml. of water was added to the residual solution; the resulting crystals were collected by filtration (5.80 g.). The crude hydrazide was purified by recrystallization from dimethylformamide - ether - petroleum ether. Yield, 5.64 g. (96%); m. p. 194—195°C; $[\alpha]_D^{20}$ −3.4° (*c* 5.0, dimethylformamide).

Found: C, 66.21; H, 6.03; N, 11.23. Calcd. for $C_{27}H_{30}O_5N_4$: C, 66.10; H, 6.16; N, 11.42%.

Benzyloxycarbonyl-L-glutaminyl-L-tyrosine Ethyl Ester (IV).—To a solution of 7.37 g. (30 mmol.) of L-tyrosine ethyl ester hydrochloride dissolved in a mixture of 8.40 ml. (60 mmol.) of triethylamine and 40 ml. of dimethylformamide, a solution of 12.0 g. (30 mmol.) of benzyloxycarbonyl-L-glutamine *p*-nitrophenyl ester in 40 ml. of dimethylformamide was added. After the solution had been allowed to stand for 4 hr. at room temperature, it was diluted with 1.5 l. of water. The crystalline precipitate was collected by filtration and washed successively with 2 N hydrochloric acid, a 3% sodium bicarbonate solution, and water (12.0 g.). It was recrystallized from ethanol-ether. Yield, 9.96 g. (70%); m. p. 197—199°C; $[\alpha]_D^{20}$ +1.8° (*c* 4.5, dimethylformamide).

Found: C, 61.18; H, 6.27; N, 8.81. Calcd. for $C_{24}H_{29}O_7N_3$: C, 61.13; H, 6.20; N, 8.91%.

L-Glutaminyl-L-tyrosine Ethyl Ester Hydrobromide (V).—To a suspension of 5.66 g. (12 mmol.) of IV in 24 ml. of acetic acid, 12 ml. of 6 N dry hydrogen bromide in acetic acid was added. After it had stood for one hour, the solution was evaporated to dryness in vacuo, and then ether was added. The oily residue was further washed with ether by decantation and dried over calcium chloride and sodium hydroxide. It weighed 4.61 g. (94%).

Benzyloxycarbonyl-L-asparaginyl-L-glutaminyl-L-tyrosine Ethyl Ester (VI).—To a solution of 4.61 g. (11.3 mmol.) of V in 20 ml. of dimethylformamide, 3 ml. of triethylamine was added, followed by a solution of 3.87 g. (10 mmol.) of the benzyloxycarbonyl-L-asparagine *p*-nitrophenyl ester in 10 ml. of dimethylformamide. After it had stood for 6 hr. at room temperature, the solution was diluted with 400 ml. of water. The crystalline product deposited was collected by filtration and washed successively with 2 N hydrochloric acid, a 3% sodium bicarbonate solution, and water (4.51 g.). It was then recrystallized from dimethylformamide-ether. Yield, 4.22 g. (72%); m. p. 224—225°C (decomp.), $[\alpha]_D^{20}$ −11.6° (*c* 2.45, dimethylformamide).

Found: C, 56.74; H, 6.33; N, 11.53. Calcd. for $C_{28}H_{35}O_9N_5 \cdot 1/2H_2O$: C, 56.56; H, 6.27; N, 11.78%.

L-Asparaginyl-L-glutaminyl-L-tyrosine Ethyl Ester Hydrobromide (VII).—To a suspension of 2.93 g. (5 mmol.) of VI in 12 ml. of acetic acid, 6.3 ml. of 6 N dry hydrogen bromide in acetic acid was added. After it had stood for one hour, the solution was evaporated to dryness in vacuo. The oily residue was then treated as has been described in the previous paragraph. The oil weighed 2.61 g. (98%).

***p*-Methoxybenzyloxycarbonyl-L-phenylalanyl-D-phenylalanyl-L-asparaginyl-L-glutaminyl-L-tyrosine Ethyl Ester (VIII).**—A solution of 1.96 g. (4 mmol.) of III dissolved in a mixture of 15 ml. of dimethylformamide and 24 ml. of acetic aicd was cooled to −5°C. To this, 8.8 ml. (8.8 mmol.) of N hydrochloric acid was added, followed by 2.2 ml. (4.4 mmol.) of 2 N sodium nitrite. After it had sood for 5 min. at this temperature, the solution was diluted with 200 ml. of cold water. The precipitated azide was collected by filtration, washed with a 3% sodium bicarbonate solution and water, and then dried in vacuo at 0°C. To a chilled (−5°) solution of 2.24 g. (4.2 mmol.) of VII dissolved in 15 ml. of dimethylformamide, 2 ml. of triethylamine was added, followed by the azide crystals prepared above. The solution was stirred for 2 days at 0°C and then diluted with 200

ml. of water. The precipitate was collected by filtration and washed successively with 0.5 M citric acid, a 3% sodium bicarbonate solution and water (3.05 g.). The product was recrystallized from dimethylformamide-ether. Yield, 2.73 g. (75%); m. p. 206—209°C (decomp.); $[\alpha]_D^{20}$ −10.4° (*c* 2.9, dimethylformamide).

Found: C, 62.58; H, 6.35; N, 11.00. Calcd. for $C_{47}H_{55}O_{12}N_7$: C, 62.03; H, 6.09; N, 10.78%.

***p*-Methoxybenzyloxycarbonyl-L-phenylalanyl-D-phenylalanyl-L-asparaginyl-L-glutaminyl-L-tyrosine Hydrazide (IX).**—This compound was prepared by the same procedure as has been described for the preparation of III. One and eighty-two hundredths grams (2 mmol.) of VIII and 2.0 ml. (40 mmol.) of hydrazine hydrate gave 1.64 g. of the crude product. It was recrystallized from dimethylformamide-ether. Yield, 1.54 g. (86%); m. p. 225—227°C (decomp.); $[\alpha]_D^{20}$ −26.0° (*c* 2.05, dimethylformamide).

Found: C, 59.44; H, 5.96; N, 13.62. Calcd. for $C_{45}H_{53}O_{11}N_9$: C, 60.32; H, 5.96; N, 14.07%.

***t*-Butyloxycarbonyl-L-valyl-δ-benzyloxycarbonyl-L-ornithine Hydrazide (X).**—This compound was also prepared by the same procedure as has been described for the preparation of III. Seven and forty hundredths grams (15 mmol.) of *t*-butyloxycarbonyl-L-valyl-δ-benzyloxycarbonyl-L-ornithine ethyl ester[14] and 15 ml. (300 mmol.) of hydrazine hydrate afforded 6.35 g. of the crude product. It was recrystallized from ethanol - ether - petroleum ether. Yield, 5.96 g. (83%); m. p. 175°C; $[\alpha]_D^{20}$ −14.1° (*c* 2.35, dimethylformamide).

Found: C, 57.40; H, 7.94; N, 14.34. Calcd. for $C_{23}H_{37}O_6N_5$: C, 57.60; H, 7.78; N, 14.60%.

Benzyloxycarbonyl-D-phenylalanyl-L-proline Ethyl Ester (XI).—To a mixed anhydride prepared at −5°C from 4.0 g. (16.7 mmol.) of benzyloxycarbonyl-D-phenylalanine, 2.16 ml. (16.7 mmol.) of isobutyl chloroformate and 2.36 ml. (16.7 mmol.) of triethylamine in 25 ml. of chloroform, a chilled solution of 6.60 g. (20.9 mmol.) of L-proline ethyl ester *p*-toluenesulfonate[15] dissolved in a mixture of 2.93 ml. (20.9 mmol.) of triethylamine and 25 ml. of chloroform was added. After the reaction mixture had been allowed to stand overnight, it was evaporated in vacuo. The residue was dissolved in 80 ml. of ethyl acetate, and the solution was washed with 2 N hydrochloric acid, a 3% sodium bicarbonate solution and water, dried over sodium sulfate, and then evaporated to dryness in vacuo. The residual oil weighed 6.08 g. (86%). All attempts to crystallize this oil failed, so it was used as such for the next step.

D-Phenylalanyl-L-proline Ethyl Ester Hydrochloride (XII).—A solution of 5.80 g. (13.7 mmol.) of XI dissolved in a mixture of 12.7 ml. (15.0 mmol.) of 1.18 N dry hydrogen chloride in methanol and 30 ml. of methanol was hydrogenolyzed in the presence of palladium black. After 5 hr. the filtrate from the catalyst was evaporated to dryness in vacuo. The oil weighed 4.36 g. (98%). The homogeneity of this oil was certified by paper chromatography, in which only one spot was detected, R_f 0.88.[16]

Benzyloxycarbonyl-L-leucyl-D-phenylalanyl-L-proline Ethyl Ester (XIII).—This compound was prepared by the same anhydride method as has been described for the preparation of XI. Three and forty-four hundredths grams (13 mmol.) of benzyloxycarbonyl-L-leucine and 4.36 g. (13.4 mmol.) of XII gave 6.64 g. (95%) of XIII as an oily product.

L-Leucyl-D-phenylalanyl-L-proline Ethyl Ester Hydrochloride (XIV).—This compound was prepared by the same procedure as has been described for the preparation of XII. The hydrogenolysis of 3.37 g. (6.26 mmol.) of XIII in the presence of a 1.1 equivalent of hydrogen chloride afforded 2.59 g. (94%) of XIV as an oil. This gave only one spot in paper chromatography, R_f 0.92.[16] It was used for the next reaction without further purification.

***t*-Butyloxycarbonyl-L-valyl-δ-benzyloxycarbonyl-L-ornithyl-L-leucyl-D-phenylalanyl-L-proline Ethyl Ester (XV).**—A solution of 2.88 g. (6 mmol.) of X dissolved in a mixture of 8 ml. of dimethylformamide and 45 ml. of acetic acid was cooled to −5°C. To this, 6.6 ml. (6.6 mmol.) of N hydrochloric acid was added, followed by 2.2 ml. (6.6 mmol.) of 3 N sodium nitrite and then 6.6 ml. (6.6 mmol.) of N hydrochloric acid. After it had stood for 5 min. at this temperature, with occasional stirring, the solution was diluted with 250 ml. of water. The azide separated as a viscous mass was twice extracted with 40-ml. portions of ethyl acetate, and the combined ethyl acetate solution was washed thoroughly with a cold 3% sodium bicarbonate solution and cold water. After it had been dried over sodium sulfate for 10 min. at 0°C, this solution was added to a chilled (−5°C) solution of 2.70 g. (6.13 mmol.) of XIV dissolved in a mixture of 0.86 ml. (6.13 mmol.) of triethylamine and 15 ml. of dimethylformamide. After it had then been stirred for 2 days at 0°C, the solution was diluted with 20 ml. of ethyl acetate and washed successively with 0.5 M citric acid, a 3% sodium bicarbonate solution and water, dried over sodium sulfate, and then evaporated in vacuo. The resulting crystals were collected by filtration with the aid of petroleum ether (4.07 g.). The product was recrystallized from ethyl acetate - ether - petroleum ether. Yield, 3.53 g. (69%); m. p. 167—170°C; $[\alpha]_D^{20}$ −32.1° (*c* 2.05, dimethylformamide), R_f 0.96.[17]

Found: C, 63.28; H, 7.76; N, 10.17. Calcd. for $C_{45}H_{66}O_{10}N_6$: C, 63.51; H, 7.82; N, 9.88%.

***t*-Butyloxycarbonyl-L-valyl-δ-benzyloxycarbonyl-L-ornithyl-L-leucyl-D-phenylalanyl-L-proline (XVI).**—To a solution of 3.40 g. (4 mmol.) of XV dissolved in 30 ml. of methanol, 8 ml. (8 mmol.) of N sodium hydroxide was added. Saponification was carried out at room temperature, and the progress of the reaction was checked by thin-layer chromatography. The reaction was complete after 6 hr. The solution was evaporated in vacuo to a volume of about 12 ml., after which the residual solution was diluted with 40 ml. of water and then acidified with 10 ml. (10 mmol.) of M citric acid. The precipitated crystalline solid was taken up twice with 25-ml. portions of ethyl acetate, and the combined ethyl acetate solution was washed with water, dried over sodium sulfate, and then evaporated in vacuo.

15) T. Kato, S. Makisumi, M. Ohno and N. Izumiya, *J. Chem. Soc. Japan, Pure Chem. Sect. (Nippon Kagaku Zasshi)*, **83**, 1151 (1962).

16) The R_f value refers to the paper chromatography with the solvent system of *n*-butanol - acetic acid - pyridine - water (4 : 1 : 1 : 2 v/v).

17) The R_f value refers to the thin-layer chromatography using a solvent system of *n*-butanol - acetic acid - pyridine - water (4 : 1 : 1 : 2 v/v).

The resulting crystalline product was collected by filtration with the aid of a mixture of ether and petroleum ether (1 : 2) (3.06 g.). It was recrystallized from ethyl acetate - ether - petroleum ether. Yield, 2.92 g. (86%); m. p. 122—125°C; $[\alpha]_D^{20}$ −39.0° (*c* 2.05, dimethylformamide), R_f 0.82.[17]

Found: C, 62.42; H, 7.57; N, 10.14. Calcd. for $C_{43}H_{62}O_{10}N_6$: C, 62.75; H, 7.59; N, 10.21%.

L-Valyl-δ-benzyloxycarbonyl-L-ornithyl-L-leucyl-D-phenylalanyl-L-proline Hydrochloride (XVII).*—To a suspension of 1.24 g. (1.5 mmol.) of XVI in 5 ml. of ethyl acetate, 12 ml. (30 mmol.) of 2.5 N dry hydrogen chloride in ethyl acetate was added; meanwhile the material dissolved to form a clear solution. The solution was then allowed to stand at room temperature, and the reaction was followed by thin-layer chromatography. After 2 hr. the solution was evaporated in vacuo to afford crystals, which were then filtered off with the aid of ether and washed thoroughly with ether. Yield, 1.09 g. (95%); m. p. 195—200°C (decomp.); $[\alpha]_D^{20}$ −22.5° (*c* 2.12 dimethylformamide), R_f 0.66.[17]

Found: N, 10.89. Calcd. for $C_{38}H_{54}O_8N_6 \cdot HCl$: N, 11.07%. This product was used as such for the next reaction.

L-Valyl-δ-benzyloxycarbonyl-L-ornithyl-D-phenylalanyl-L-leucyl-L-proline Ethyl Ester Hydrochloride (XVIII).—To a suspension of 1.02 g. (1.2 mmol.) of XV in 6 ml. of ethyl acetate, 6 ml. (24 mmol.) of 4 N dry hydrogen chloride in ethyl acetate was added. The reaction mixture formed a clear solution. The solution was then allowed to stand at room temperature, and the progress of the reaction was checked by thin-layer chromatography. After 5 hr. the solution was evaporated to dryness in vacuo. The resulting oily residue was crystallized by the addition of ether (0.882 g.). The product was recrystallized from ethanol-ether. Yield, 0.811 g. (86%); m. p. 183—185°C; $[\alpha]_D^{20}$ −19.0° (*c* 2.1, dimethylformamide), R_f 0.73.[17]

Found: C, 60.65; H, 7.63; N, 10.78. Calcd. for $C_{40}H_{58}O_8N_6 \cdot HCl$: C, 61.01; H, 7.55; N, 10.67%.

***p*-Methoxybenzyloxycarbonyl-L-phenylalanyl-D-phenylalanyl-L-asparaginyl-L-glutaminyl-L-tyrosyl-L-valyl-δ-benzyloxycarbonyl-L-ornithyl-L-leucyl-D-phenylalanyl-L-proline Ethyl Ester (XX).**—A solution of 0.488 g. (0.5 mmol.) of IX dissolved in 6 ml. of dimethylformamide was cooled to −5°C. To this, 1.4 ml. (1.4 mmol.) of N hydrochloric acid was added, followed by 0.55 ml. (0.55 mmol.) of N sodium nitrite. After it had stood for 5 min. at −5°C, the solution was diluted with 50 ml. of cold water. The precipitated azide (XIX) was collected by filtration, washed with a cold 3% sodium bicarbonate solution and cold water, and then dried in vacuo at 0°C. The dried azide was added to a chilled (−5°C) solution of 0.394 g. (0.5 mmol.) of XVIII dissolved in a mixture of 0.07 ml. (0.5 mmol.) of triethylamine and 8 ml. of dimethylformamide; the solution was stirred for 2 days at 0°C, and then diluted with 80 ml. of water. The crystalline precipitate was collected by filtration and washed thoroughly with 0.5 M citric acid, a 3% sodium bicarbonate solution and water (0.596 g.). It was recrystallized from dimethylformamide-methanol-ether. Yield, 0.564 g. (70%); m. p. 242—243°C (decomp.); $[\alpha]_D^{20}$ −27.9° (*c* 0.62, dimethylformamide). The homogeneity was certified by thin-layer chromatography with regard to the hydrogenolyzed product, R_f 0.86.[17]

Found: C, 63.30; H, 6.80; N, 11.37. Calcd. for $C_{89}H_{107}O_{19}N_{13}$: C, 63.30; H, 6.56; N, 11.29%.

***p*-Methoxybenzyloxycarbonyl-L-phenylalanyl-D-phenylalanyl-L-asparaginyl-L-glutaminyl-L-tyrosyl-L-valyl-δ-benzyloxycarbonyl-L-ornithyl-L-leucyl-D-phenylalanyl-L-proline (XXI).**—The azide (XIX), which had been freshly prepared from 0.896 g. (1.0 mmol.) of IX by the procedure described just above, was added to a chilled (−5°C) solution of 0.911 g. (1.2 mmol.) of XVII dissolved in a mixture of 0.34 ml. (2.4 mmol.) of triethylamine and 8 ml. of dimethylformamide. The solution was then stirred for 2 days at 0°C, and the small amount of insoluble materials was filtered off. The filtrate was evaporated in vacuo, and the resulting semi-solid mass was triturated with a mixture of 15 ml. of ethyl acetate and 5 ml. of ether, and collected by filtration with the aid of ether. The solid mass crystallized when it was treated with a citric acid solution. The crystals were collected by filtration, and further washed with a dilute citric acid solution and then water (1.24 g.). The product was recrystallized from dimethylformamide-ether. Yield, 1.19 g. (75%); m. p. 233—236°C (decomp.); $[\alpha]_D^{20}$ −31.6° (*c* 0.58, dimethylformamide). The homogeneity of this product was established by thin-layer chromatography after hydrogenolysis, R_f 0.80.[17]

Found: C, 62.58; H, 6.57; N, 11.63. Calcd. for $C_{83}H_{103}O_{19}N_{13}$: C, 62.82; H, 6.57; N, 11.48%.

***p*-Methoxybenzyloxycarbonyl-L-phenylalanyl-D-phenylalanyl-L-asparaginyl-L-glutaminyl-L-tyrosyl-L-valyl-δ-benzyloxycarbonyl-L-ornithyl-L-leucyl-D-phenylalanyl-L-proline *p*-Nitrophenyl Ester (XXII).**—To a solution of 0.300 g. (0.189 mmol.) of XXI dissolved in 3.5 ml. of dimethylformamide, 5 ml. of anhydrous pyridine was added, followed by 0.612 g. (1.89 mmol.) of di-*p*-nitrophenyl sulfite. The faintly yellow solution was allowed to stand for 16 hr. at room temperature and then evaporated in vacuo. The oily residue was triturated with a mixture of ether and petroleum ether (1 : 1). The solid mass was collected by filtration and washed with a mixture of ether and petroleum ether (1 : 1) unitil the yellow color could not be discerned upon the addition of N sodium hydroxide to the filtrate. A faintly yellow product was thus obtained (0.325 g.). The *p*-nitrophenyl ester content of this product was estimated to be 110% by means of the method described by Schwyzer and Sieber,[5] except that a mixture of dimethylformamide and N sodium hydroxide (1 : 1) was used as the solvent and the absorption measurements were performed at the wavelength of 411 mμ. This product was used for the next reaction without further purification.

L-Phenylalanyl-D-phenylalanyl-L-asparaginyl-L-glutaminyl-L-tyrosyl-L-valyl-δ-benzyloxycarbonyl-L-ornithyl-L-leucyl-D-phenylalanyl-L-proline *p*-Nitrophenyl Ester Trifluoroacetate (XXIII).—To a mixture of 0.325 g. of XXII and 0.4 ml. of anisole, 4 ml. of anhydrous trifluoroacetic acid was added at −5°C. When swirled, the reaction mixture formed a solution after 10 min. The solution was then evaporated in vacuo at 0°C, and the resulting oily residue was triturated by

* An attempt to crystallize the HCl-free pentapeptide failed. When an aqueous solution of XVII was neutralized by the addition of triethylamine, the oil separated. This oil did not crystallize on prolonged standing in a refrigerator.

ether. The product was collected by filtration and washed with ether (0.292 g.). The *p*-nitrophenyl ester content of this product was estimated to be 95% by the procedure described in the preceding paragraph. This material was used as such in the next step.

Cyclo-L-phenylalanyl-D-phenylalanyl-L-asparaginyl-L-glutaminyl-L-tyrosyl-L-valyl-δ-benzyloxycarbonyl-L-ornithyl-L-leucyl-D-phenylalanyl-L-prolyl (XXIV).—A solution of 0.292 g. of XXIII dissolved in a mixture of 0.5 ml. of acetic acid and 10 ml. of dimethylformamide was stirred, drop by drop, into 100 ml. of anhydrous pyridine kept at 70—75°C over a 3.5-hr. period. The solution was further stirred for 1.5 hr. at this temperature, and then evaporated to dryness in vacuo. The resulting residue was collected by filtration with the aid of water, dried in vacuo (0.235 g.), and then dissolved in 50 ml. of a mixture of dioxane and water (5 : 2). This solution was passed successively through columns (2×4.5 cm.) of Dowex-50 (H^+ form) and Amberlite IR-4B (OH^- form) which had been washed with a mixture of dioxane and water (5 : 2). The columns were then washed with the same solvent. The filtrate and washings were combined (total 150 ml.) and lyophilized to afford the crystalline product (0.175 g.). It was recrystallized from dioxane-ether-petroleum ether. Yield, 0.160 g. (60% from XXI); m. p. 263—265°C (decomp.); $[\alpha]_D^{20}$ −111° (*c* 0.65, dimethylformamide). The homogeneity was certified by thin-layer chromatography, R_f 0.94.[17]

Found: C, 63.42; H, 6.86; N. 12.77. Calcd. for $C_{74}H_{93}O_{15}N_{13}$: C, 63.27; H, 6.67; N, 12.96%.

The molecular weight was measured on a vapor pressure osmometer of Mechrolab, Inc., model 301 A, using methanol as the solvent.* Found: 1422. Calcd. for the benzyloxycarbonyl-substituted cyclic decapeptide: 1405.

Cyclo-L-phenylalanyl-D-phenylalanyl-L-asparaginyl-L-glutaminyl-L-tyrosyl-L-valyl-L-ornithyl-L-leucyl-D-phenylalanyl-L-prolyl Hydrochloride (I_s).—A solution of 86.5 mg. (0.062 mmol.) of XXIV dissolved in a mixture of 0.32 ml. (0.064 mmol.) of 0.20 N dry hydrogen chloride in methanol and 3 ml. of methanol was hydrogenolyzed in the presence of palladium black. The progress of the reaction was checked by thin-layer chromatography. After 2.5 hr. the filtrate from the catalyst was concentrated to a small volume (0.1 ml.), and 2 ml. of ether was added to afford crystals; yield, 70 mg. Recrystallization from methanol-ether gave 65 mg. (74%) as the air-dried product (m. p. 239—240°C (decomp.)). Only one spot was obtained in thin-layer chromatography, R_f 0.76.[17] The elemental analysis was carried out using a desiccator-dried sample.

Found: C, 57.12; H, 6.96; N, 12.79. Calcd. for $C_{68}H_{87}O_{13}N_{13}\cdot HCl\cdot 5H_2O$: C, 56.75; H, 7.00; N, 13.03%.

When dried at 110°C (2 mmHg), this desiccator-dried sample lost 6.2% of its weight. Calcd. for $5H_2O$: 6.3%. On the other hand, the air-dried sample lost 8.8% of its weight after being dried for 2 hr. at 110°C (2 mmHg). Calcd. for $7H_2O$: 8.81%.

Amino acid analysis gave the molar ratios: leucine 1.0, phenylalanine 3.0, aspartic acid 1.0, glutamic acid 1.0, tyrosine 0.8, valine 1.0, ornithine 1.0, proline 1.0 and ammonia 2.1.

A Comparison of I_s and Natural Tyrocidine A Hydrochloride (I_n). — *(a) Paper Chromatography.* — This was carried out in two solvents. Both compounds gave a single spot and the same R_f values. R_f values of I_s: 0.92,[16] 0.95.[18] R_f values of I_n: 0.92,[16] 0.95.[18]

(b) Thin-layer Chromatography.—The R_f values of both compounds were exactly the same. R_f value of I_s: 0.76.[17] R_f value of I_n: 0.76.[17]

(c) Paper Electrophoresis.—This was carried out under the following conditions: paper, Toyo Roshi No. 52 chromatography paper; solvent, formic acid-acetic acid-methanol-water (1 : 3 : 6 : 10 v/v) (pH 1.8); voltage gradient, 17 V./cm.; charged period, 2.5 hr. Gramicidin S dihydrochloride was used as the reference compound. Figure 6 demonstrates the electrophoretic patterns of I_s, I_n and gramicidin S dihydrochloride. The mobility of I_s was indistinguishable from that of I_n.

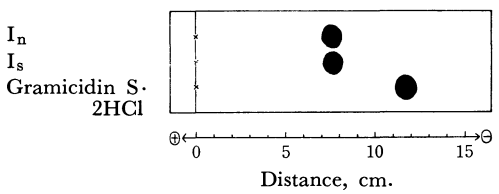

Fig. 6. Paper electrophoreses of I_s, I_n and gramicidin S dihydrochloride.

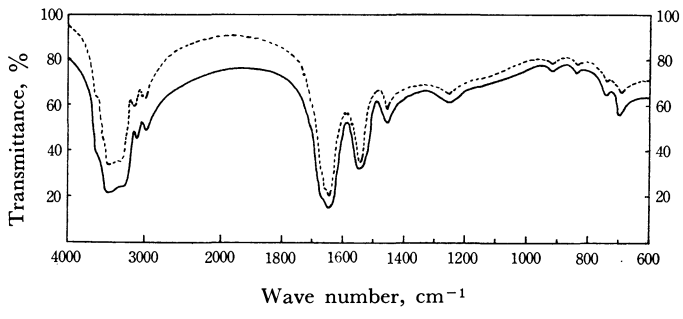

Fig. 7. Infrared spectra of I_s (——) and I_n (----).

* The atuhors are indebted to Mr. Michinori Waki of this laboratory for the molecular weight measurements.

18) The R_f value refers to paper chromatography with the solvent system of *t*-butanol-formic acid-water (75 : 15 : 10 v/v).

Table I. Inhibitory activity of I_s, I_n and gramicidin S on microorganisms
Minimum inhibitory concentrations, μg./ml.

A. Bouillon agar medium[a]

	Escherichia coli	*Proteus vulgaris*	*Staphylococcus aureus*	*Bacillus subtilis*	*Mycobacterium avium*	*Mycobacterium avium* (Streptomycin resistant St.)
I_s[b]	>100	>100	20	10	>100	>100
I_n[b]	>100	>100	20	10	>100	>100
Gramicidin S·2HCl	>100	>100	5—2	5—2	>100	>100

B. Synthetic medium[c]

	Escherichia coli	*Proteus vulgaris*	*Staphylococcus aureus*	*Bacillus subtilis*	*Mycobacterium avium*	*Mycobacterium avium* (Streptomycin resistant St.)
I_s[b]	>100	>100	20	10	>100	>100
I_n[b]	>100	50	20	20	>100	>100
Gramicidin S·2HCl	>100	>100	5	5	>100	>100

a) Usual bouillon agar medium, pH 7.0.
b) Air-dried samples were employed.
c) Stephenson-Whetham's medium (modified); K_2HPO_4 0.1%, NaCl 0.1%, $MgSO_4 \cdot 7H_2O$ 0.05%, Na-glutamate 0.4%, casamino acid 0.2%, yeast-extract 0.05% and agar 2.0%, pH 7.0.

(d) Infrared Spectra.—These were obtained on a Hitachi EPI-2 spectrophotometer. The spectra of both I_s and I_n are presented in Fig. 7. The spectrum of I_s is superimposable on that of I_n.

(e) Ultraviolet Spectra.—These were obtained on a Hitachi EPS-2 spectrophotometer using a pair of 1-cm. quartz cells. Figure 8 indicates the spectra of I_s and I_n in 50% ethanol; here their absorption maxima agree well with each other.

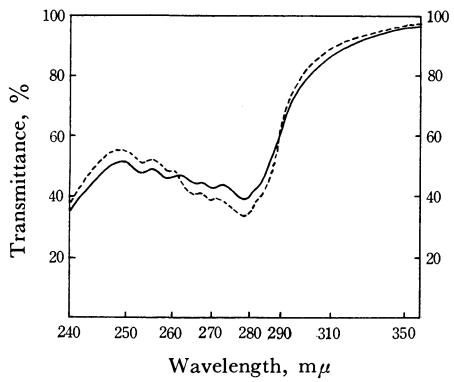

Fig. 8. Ultraviolet spectra of I_s (——) and I_n (----) in 50% ethanol; concentrations of I_s and I_n are 1.74×10^{-4} M and 1.85×10^{-4} M, respectively.

*(f) Carboxymethylcellulose (CMC) Column Chromatography.**—A 0.9×100 cm. CMC column was employed. The solvent used here was a methanol-containing (50%, v/v) 0.2 M pyridine-acetate buffer (pH 5.0). About 0.5 mg. of the sample was placed in 0.4 ml. of this solvent in the column, and the mixture was eluted with the same solvent. One milliliter fractions were collected at a flow rate of 7 ml. per hour. Each of them was kept for one hour at 90°C in order to remove methanol, and then 1 ml. of N sodium hydroxide was added to the residual solution and left to hydrolyze for 3 hr. at 90°C. After the solution had been neutralized by the addition of 0.5 ml. of 30% acetic acid, the components were determined by the Yemm-Cocking method.[19]

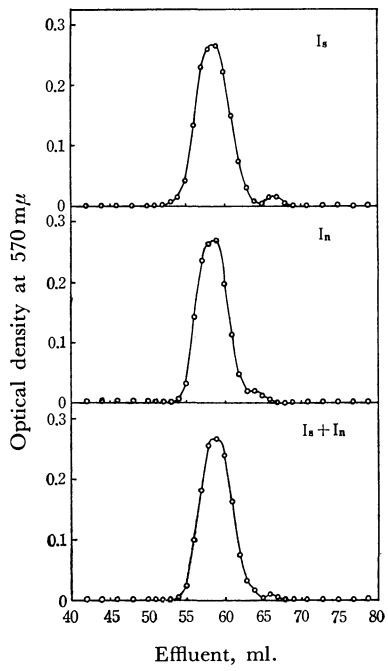

Fig. 9. CMC column chromatography of I_s, I_n and admixture of I_s and I_n.

* The authors are indebted to Mr. Haruhiko Aoyagi of this laboratory, who found the usefulness of the application of the CMC column chromatography in the separation of mixture of basic cyclic peptides.

19) E. W. Yemm and E. C. Cocking, *Analyst*, **80**, 209 (1955); *Biochem. J.*, **59**, xii (1954).

This procedure was applied to I_s, I_n and an equivalent admixture of I_s and I_n respectively. The results are shown in Fig. 9. The same chromatographic pattern was obtained in each of the three samples.

(g) Optical Rotation.—Air-dried samples were employed for the measurement, using 50% ethanol as the solvent: $[\alpha]_D^{20}$ of I_s $-108°$ (*c* 0.141); $[\alpha]_D^{20}$ of I_n $-108°$ (*c* 0.126). Lit.[1] $[\alpha]_D^{25}$ $-111°$ (*c* 1.37, 50% ethanol) for a sample dried at 110°C.

(h) Microbiological Assays.—The microorganisms employed are listed in Table I. The minimum amount of the compound necessary for the complete inhibition of growth was determined by a dilution method with a bouillon agar medium and with a synthetic medium. In addition to I_s and I_n, gramicidin S dihydrochloride was examined as a reference compound. Although, in the synthetic medium, small differences were observed in the effects of I_s and I_n on the *Proteus vulgaris* and *Bacillus subtilis*, the antibacterial spectra of the two compounds can be considered to be in agreement with one other.

The authors wish to express their thanks to Dr. Lyman C. Craig of Rockefeller Institute, U. S. A., for the generous gift of a smaple of the natural tyrocidine A hydrochloride. The authors are also much indebted to Dr. Motoo Shibata of Takeda Chemical Industries, Ltd. for the microbiological assays, and Kyowa Hakko Kogyo Co., Ltd. and Ajinomoto Co., Inc. for supplying some amino acids.

BULLETIN OF THE CHEMICAL SOCIETY OF JAPAN VOL. 39 1747—1753 (1966)

Studies of Peptide Antibiotics. V. Syntheses of Cyclic Penta- and Decapeptides with the L-Valyl-L-ornithyl-L-leucyl-D-phenylalanylsarcosyl Sequence

By Haruhiko AOYAGI and Nobuo IZUMIYA

Laboratory of Biochemistry, Faculty of Science, Kyushu University, Fukuoka

(Received November 15, 1965)

A cyclic decapeptide dihydrochloride cyclo-(L-valyl-L-ornithyl-L-leucyl-D-phenylalanylsarcosyl)$_2$·2HCl, which is an analog of gramicidin S and a cyclic pentapeptide monohydrochloride cyclo-L-valyl-L-ornithyl-L-leucyl-D-phenylalanylsarcosyl·HCl, were synthesized for the purpose of comparing their antibacterial activities with gramicidin S. The cyclic decapeptide dihydrochloride was obtained by hydrogenolysis in the presence of hydrogen chloride of a cyclic benzyloxycarbonyl-substituted decapeptide, which had been prepared by the cyclization of a corresponding linear decapeptide active ester. The cyclization reaction of a linear pentapeptide active ester yielded a mixture of a cyclic benzyloxycarbonyl-substituted pentapeptide as a major component, and a cyclic decapeptide and an unidentified cyclic peptide as minor components. The effects of two cyclic peptide hydrochlorides on bacterial growth were tested. The cyclic decapeptide was as active as gramicidin S; however, the cyclic pentapeptide showed no activity in relation to any of the microorganisms tested.

In connection with a series of studies in this laboratory on the significance of the chemical functional groups of gramicidin S (I) to its biological activities, the authors reported, in a previous paper, the synthesis of an analog of gramicidin S wherein proline residues in the 5 and 5′ positions of the molecule were replaced by glycines.[1] This 5, 5′-glycine-gramicidin S was found to possess approximately 10 times the antibacterial activity of natural gramicidin S in the test with a synthetic medium, while it possessed about half the activity of gramicidin S with a bouillon agar medium. In the light of the considerable antibacterial potency of this analog, the decision was made to investigate the effect of replacing the proline residues by sarcosines. The present paper will describe the syntheses and the antibacterial properties of this cyclic decapeptide, 5, 5′-sarcosine-gramicidin S (II), and of the cyclic pentapeptide, cyclo-L-valyl-L-ornithyl L-leucyl-D-phenylalanylsarcosyl (III), related to I and II.

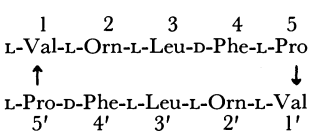

(I)

The structure of gramicidin S, with numbers indicating the positions of the individual amino acid residues.

1) H. Aoyagi, T. Kato, M. Ohno, M. Kondo, M. Waki, S. Makisumi and N. Izumiya, This Bulletin, **38**, 2139 (1965); H. Aoyagi, T. Kato, M. Ohno and N. Izumiya, *J. Am. Chem. Soc.*, **86**, 5700 (1964).

L-Val-L-Orn-L-Leu-D-Phe-Sar
↑ ↓
Sar-D-Phe-L-Leu-L-Orn-L-Val
(II)

L-Val-L-Orn-L-Leu-D-Phe-Sar
↑ |
|
(III)

The sequence of reactions employed for the synthesis of II is shown in Fig. 1. The condensation of the azide derived from acylpentapeptide hydrazide (XII) with pentapeptide (XI) gave acyldecapeptide (XIII) in a yield of 73%. The treatment of XIII with an excess of di-*p*-nitrophenyl sulfite gave an amorphous acyldecapeptide *p*-nitrophenyl ester (XIV). The *p*-methoxybenzyloxycarbonyl group of XIV was removed by the action of trifluoroacetic acid, and the decapeptide *p*-nitrophenyl ester trifluoroacetate (XV) thus obtained was treated with a large amount of hot pyridine for the cyclization reaction. The benzyloxycarbonyl-substituted cyclic peptide obtained in a yield of 45% (from XIII) was found to be a monomer, shown as XVI, from the result of the molecular weight determination. In this connection, it is of interest to note that the cyclization reaction of the decapeptide active ester yields monomer, cyclic decapeptide.[1,2] The final product (II·2HCl) was obtained as colorless

Fig. 1.

Z, benzyloxycarbonyl; DCC, dicyclohexylcarbodiimide; pMZ, *p*-methoxybenzyloxycarbonyl; ONP, *p*-nitrophenoxy ester; MA, mixed anhydride method. An amino acid residue except Sar and D-Phe is of L-configuration.

2) R. Schwyzer and P. Sieber, *Helv. Chim. Acta*, **40**, 624 (1957); **41**, 1582 (1958).

crystals containing seven moles of the water of crystallization. Its homogeneity was demonstrated by CM-cellulose column chromatography (Fig. 3) and paper electrophoresis (Fig. 4).

The synthesis of the protected cyclic decapeptide (XVI) was also attempted by the dimerization reaction of the pentapeptide active ester (XVIII). As is shown in Fig. 2, the treatment of the pentapeptide active ester (XVIII) gave a product (XX) with the character of benzyloxycarbonyl-substituted cyclic peptide in a fairly good yield. After the experiments of CM-cellulose column chromatography and paper electrophoresis (Figs. 3 and 4) with a hydrogenated material (XXI) of the product, this product (XX) was found to be a mixture of three components, namely, a protected cyclic pentapeptide (XIX) as a major component, and the protected cyclic decapeptide (XVI) and an unidentified cyclic peptide as minor components.

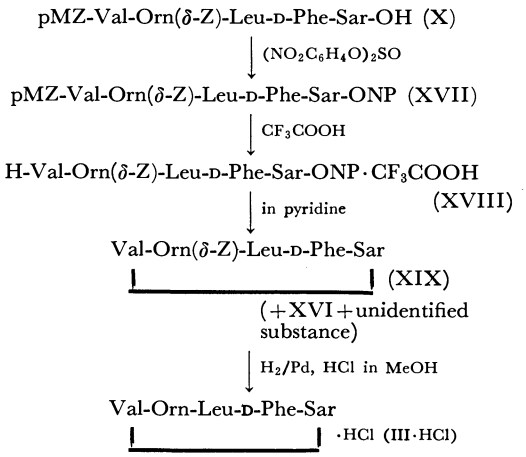

Fig. 2.

It was determined further, by analysis by means of the CM-cellulose column chromatography of the material (XXI) that the molar ratio between XIX and XVI was 92 : 8. The protected cyclic pentapeptide (XIX) in a pure state was obtained easily by several recrystallizations from methanol-ether of the product (XX); XIX was less soluble in methanol than XVI or the unidentified cyclic peptide. The fact that this major product is a monomer, shown as XIX, was denomstrated by the result of the molecular weight determination. The hydrogenation of XIX in the presence of equivalent hydrogen chloride yielded a cyclic pentapeptide hydrochloride (III·HCl) as colorless crystals, with three moles of the water of crystallization.

In a previous paper,[1] we observed that the cyclization reaction of the L-valyl-δ-benzyloxycarbonyl-L-ornithyl-L-leucyl- D - phenylalanylglycine active ester yielded a large amount of the pyridine-insoluble cyclic peptide, besides a small amount of the desired protected cyclic decapeptide. This pyridine-insoluble substance appears, from the results of the experiment of CM-cellulose chromatography, to be a cyclic benzyloxycarbonyl-substituted pentapeptide.[3] In this connection, it would be of interest to note that two reports have described that cyclization reaction of pentapeptide active esters, wherein *C*-terminal amino acid residues were glycine and isoleucine, yields a monomer cyclic pentapeptide.[4] On the contrary, several experiments have shown that the pentapeptide active ester, wherein the partial sequence at the *C*-terminal part is D - phenylalanyl - L - proline, yielded cyclic decapeptide by dimerization reaction.[5]

In order to ascertain whether or not the cyclic peptides, II and III, possess antibacterial activities, the effect of various levels of II and III on the growth of several microorganisms was examined (Table I). It was found that II was as active as gramicidin S in affecting several microorganisms. This result demonstrates further that the side chain of proline of gramicidin S is not absolutely required for its full activity. On the other hand, III exhibited no antibacterial activity in relation to any of the microorganisms tested. A communication from this laboratory has also described that a cyclic hexapeptide related to gramicidin S, cyclo-L-valyl-L-ornithyl- L - leucyl-D-phenylalanyl-L-prolylglycyl, showed no such activity either.[6] These results suggest that a certain ring size of a molecule, besides a specific amino acid sequence, will be necessary for the exhibition of activity.

Experimental

All melting points are uncorrected. Prior to analysis, the compounds were dried over phosphorus pentoxide at 80°C and 2 mmHg to a constant weight, except in the cases of II·2HCl and III·HCl.

Sarcosine Ethyl Ester *p*-Toluenesulfonate (IV). —This compound was prepared according to the general procedure of Kato et al.[7] A solution of sarcosine (4.0 g.) and *p*-toluenesulfonic acid monohydrate (9.4 g.) in a mixture of ethanol (20 ml.) and carbon tetrachloride (100 ml.) was refluxed, and the water thus liberated was removed as an azeotropic mixture. The reaction mixture was concentrated in vacuo, and the residual oil was treated with ether and petroleum ether. The product was very hygroscopic; yield, 12.0 g.

3) H. Aoyagi and N. Izumiya, unpublished.
4) G. W. Kenner and J. M. Turner, *Chem. & Ind.*, **1955**, 602; G. W. Kenner, P. J. Thomson and J. M. Turner, *J. Chem. Soc.*, **1958**, 4148; K. Isono and R. W. Curtis, *Phytochemistry*, **3**, 277 (1964).
5) R. Schwyzer and P. Sieber, *Helv. Chim. Acta*, **41**, 2186 (1958); German Patent, *Chem. Abstr.*, **57**, 949 (1962).
6) T. Kato, M. Kondo, M. Ohno and N. Izumiya, This Bulletin, **38**, 1202 (1965).
7) T. Kato, S. Makisumi, M. Ohno and N. Izumiya, *J. Chem. Soc. Japan, Pure Chem. Sect. (Nippon Kagaku Zasshi)*, **83**, 1151 (1962).

(92%); R_f 0.61.[8]

Benzyloxycarbonyl - D - phenylalanylsarcosine Ethyl Ester (V).—Into a solution of benzyloxycarbonyl-D-phenylalanine (6.71 g.) and IV (6.5 g.) in chloroform (80 ml.) there were stirred triethylamine (3.14 ml.) and dicyclohexylcarbodiimide[9] (4.61 g.) at 0°C. After it had been permitted to stand overnight at 0°C, the mixture was evaporated in vacuo and the residue was diluted with ethyl acetate; then the dicyclohexylurea thus precipitated was filtered off. The filtrate was washed successively with 4% sodium bicarbonate, 3% hydrochloric acid and water, and dried over anhydrous sodium sulfate. The filtered solution was evaporated in vacuo. The product was obtained as an oil; yield, 7.68 g. (86%); R_f 0.73.[8]

D-Phenylalanylsarcosine Ethyl Ester Hydrochloride (VI).—V (7.68 g.) was subjected to hydrogenolysis in the presence of palladium black and 0.44 N methanolic hydrogen chloride (46.5 ml.). The filtrate from the catalyst was evaporated to dryness in vacuo; yield of oil, 5.80 g. (100%); R_f 0.70.[8]

Benzyloxycarbonyl - L - leucyl - D - phenylalanylsarcosine Ethyl Ester (VII).—To a chilled solution of benzyloxycarbonyl-L-leucine (5.11 g.) and triethylamine (2.70 ml.) in tetrahydrofuran (40 ml.), isobutyl chloroformate (2.52 ml.) was added. After 15 min. a mixture of VI (5.80 g.), triethylamine (2.70 ml.) and chloroform (40 ml.) was added to the solution. The mixture was left overnight at room temperature, and then evaporated in vacuo. The residual oil was dissolved in ethyl acetate and treated as has been described in connection with the preparation of V. The oily residue wieghed 6.45 g. (66%); R_f 0.88.[8]

L-Leucyl-D-phenylalanylsarcosine Ethyl Ester Hydrochloride (VIII).—VII (2.96 g.) was subjected to hydrogenolysis in the presence of palladium black and 0.40 N methanolic hydrogen chloride (16.6 ml.), and then treated as has been described in connection with the preparation of VI. The yield of oily product was 2.28 g. (91%); R_f 0.59[8] and 0.62.[10]

***p*-Methoxybenzyloxycarbonyl-L-valyl - δ - benzyloxycarbonyl-L-ornithyl-L - leucyl - D - phenylalanyl - sarcosine Ethyl Ester (IX).**—The following operations were carried out in a cold room. To a chilled solution *p*-methoxybenzyloxycarbonyl-L-valyl-δ-benzyloxycarbonyl - L - ornithine hydrazide[6] (1.47 g.) in glacial acetic acid (30 ml.) there were stirred N hydrochloric acid (4.1 ml.) and sodium nitrite (210 mg.) in water (1 ml.). After 6 min., cold water (200 ml.) was added to the solution. The azide which thereupon precipitated as a white mass was collected by filtration and washed with water, 4% sodium bicarbonate and water, and then dried under a vacuum in a desiccator over phosphorus pentoxiede and potassium hydroxide. The azide was added to a solution of VIII (1.12 g.) and triethylamine (0.38 ml.) in dimethylformamide (20 ml.). The mixture was stirred for 3 days at 0°C and evaporated in vacuo. The precipitate which formed upon the addition of water (30 ml.) to the syrup was collected, wahsed with 4% sodium bicarbonate, 10% citric acid and water, and dried. It was recrystallized from methanol - ether - petroleum ether; yield, 1.82 g. (75%); m. p. 143—146°C; $[\alpha]_D^{26}$ —28.4° (*c* 0.5, acetic acid); R_f 0.73.[8]

Found: C, 62.79; H, 7.52; N, 9.70. Calcd. for $C_{47}H_{64}O_{11}N_6 \cdot {}^1/_2H_2O$: C, 62.86; H, 7.30; N, 9.40%.

***p*-Methoxybenzyloxycarbonyl- L -valyl- δ -benzyloxycarbonyl - L - ornithyl-L-leucyl -D- phenylalanyl-sarcosine (X).**—To a solution of IX (1.16 g.) in a mixture of methanol (30 ml.) and dioxane (10 ml.), 2 N sodium hydroxide (2 ml.) was added, and the solution was allowed to stand for 4 hr. at room temperature. After the addition of 10% citric acid (15 ml.) under cooling, the solution was concentrated in vacuo at a low temperature and the residue treated with water (100 ml.). After it had been stored in a refrigerator for several hours, the precipitate was collected by filtration, washed with water, and dried. The product was recrystallized from methanol - ether - petroleum ether; yield, 0.96 g. (86%); m. p. 151—153°C; $[\alpha]_D^{26}$ −26.8° (*c* 0.5, acetic acid); R_f 0.75.[8]

Found: C, 61.90; H, 7.20; N, 9.73. Calcd. for $C_{45}H_{60}O_{11}N_6 \cdot {}^1/_2H_2O$: C, 62.12; H, 7.07; N, 9.66%.

L -Valyl-δ-benzyloxycarbonyl-L-ornithyl-L-leucyl-D-phenylalanylsarcosine Hydrochloride (XI).—To a solution of X (1.64 g.) in dioxane (20 ml.), there was added 4.0 N hydrogen chloride in dioxane (20 ml.). After it had been permitted to stand for 2 hr. at room temperature, the solution was evaporated in vacuo. The residue was triturated with ether and washed repeatedly with ether by decantation. The crystalline product was collected by filtration with the aid of ether; yield, 1.38 g. (98%); m. p. 162°C; $[\alpha]_D^{20}$ −15.4° (*c* 0.5, acetic acid); R_f 0.67.[8]

Found: C, 58.69; H, 7.47; N, 11.31. Calcd. for $C_{36}H_{53}O_8N_6Cl$: C, 58.96; H, 7.28; N, 11.46%.

An attempt to crystallize the HCl-free pentapeptide failed.

***p*-Methoxybenzyloxycarbonyl- L -valyl- δ -benzyloxycarbonyl- L -ornithyl- L -leucyl- D -phenylalanyl-sarcosine Hydrazide (XII).**—To a solution of IX (2.30 g.) in dimethylformamide (10 ml.), hydrazine hydrate (2.5 ml.) was added and the solution was allowed to stand for 2 days at 30°C. The reaction mixture was then evaporated in vacuo. The hydrazide which precipitated upon the addition of water (30 ml.) was collected by filtration and dried; yield, 2.19 g. (98%); m. p. 172—175°C; $[\alpha]_D^{26}$ −32.8° (*c* 0.5, acetic acid); R_f 0.74.[8]

Found: C, 60.76; H, 7.18; N, 12.55. Calcd. for $C_{45}H_{62}O_{10}N_8 \cdot H_2O$: C, 60.52; H, 7.22; N, 12.55%.

***p* - Methoxybenzyloxycarbonyl -L-valyl-δ-benzyloxycarbonyl-L-ornithyl-L - leucyl - D - phenylalanyl-sarcosyl-L-valyl-δ- benzyloxycarbonyl-L-ornithyl-L-leucyl-D-phenylalanylsarcosine (XIII).** — Into a chilled solution of XII (0.79 g.) in a mixture of dimethylformamide (10 ml.) and glacial acetic acid (10 ml.), 1.2 N hydrochloric acid (2.4 ml.) and sodium nitrite (70 mg.) in water (4 ml.) were stirred. After 5 min., cold water (200 ml.) was added to the solution. The azide which thereupon precipitated was collected by

8) The R_f value refers to the thin-layer chromatography with Merck silica gel G and to the *n*-butanol - acetic acid - pyridine - water (4 : 1 : 1 : 2, v/v) system. Compounds possessing a free amino group were detected by spraying them with ninhydrin, and those with blocked amino groups, by spraying them with 47% hydrobromic acid, and then with ninhydrin.

9) J. C. Sheehan and G. P. Hess, *J. Am. Chem. Soc.*, **77**, 1067 (1955).

10) The R_f value refers to the paper chromatography on Toyo Roshi No. 52 with the *n*-butanol - acetic acid - pyridine - water (4 : 1 : 1 : 2, v/v) system.

filtration and treated as has been described in connection with the preparation of IX. The azide was added to a solution of XI (0.66 g.) in a mixture of dimethylformamide (20 ml.) and triethylamine (0.26 ml.), and the mixture was stirred for 3 days at 0°C. The insoluble material was removed by filtration, and the filtrate was evaporated in vacuo. The precipitate which formed upon the addition of 10% citric acid (30 ml.) was collected, washed with 10% citric acid and water and dried. Recrystallization from dioxane-ether gave 1.02 g. (73%) of XIII; m. p. 208—209°C; $[\alpha]_D^{26}$ −45.6° (*c* 0.5, acetic acid); R_f 0.76.[8]

Found: C, 62.44; H, 7.53; N, 10.82. Calcd. for $C_{81}H_{110}O_{18}N_{12}\cdot H_2O$: C, 62.45; H, 7.25; N, 10.79%.

Cyclo-(L-valyl-δ-benzyloxycarbonyl-L-ornithyl-L-leucyl-D-phenylalanylsarcosyl)$_2$ (XVI).—To a solution of XIII (467 mg.) in pyridine (6 ml.), di-*p*-nitrophenyl sulfite[11] (972 mg.) was added, and the reaction mixture was allowed to stand for 24 hr. at room temperature. After evaporation, the oily product was triturated with petroleum ether and washed repeatedly with a mixture of ether and petroleum ether (1 : 1) by decantation until no yellow color could be discerned on the addition of a sodium hydroxide solution to the washings. The product was collected by filtration, washed with a mixture of ether and petroleum ether, and dried. It weighed 444 mg. A small portion of this product (1.1 mg.) was dissolved in 25 ml. of dimethylformamide - N sodium hydroxide (1 : 1) (2.64×10^{-5} M/l.); the *p*-nitrophenyl ester content was estimated by measuring the optical density of the solution at 412 mμ.[2] The purity of the compound was estimated to be 88%.

To the *p*-nitrophenyl ester (XIV) (442 mg.), anisole (0.5 ml.) and trifluoroacetic acid (3.5 ml.) were added at 0°C. The solution was then evaporated in vacuo at 0°C, and the residue was triturated with ether. The decapeptide *p*-nitrophenyl ester trifluoroacetate (XV) was collected, washed with ether, and dissolved in dimethylformamide (9 ml.) containing glacial acetic acid (0.1 ml.). The solution was stirred, drop by drop, into pyridine (150 ml.) kept at 55—60°C over a period of 3.5 hr.; the stirring was then continued for an additional 2 hr. at the same temperature. After the solvent had been removed, the residual oil was dissolved in a mixture of methanol (100 ml.) and water (20 ml.). An insoluble substance was removed by filtration, and the filtrate was passed successively through columns of Dowex 1 (OH^- form, 2×10 cm.) and Dowex 50 (H^+ form, 2×7 cm.). The columns were washed with the same solvent (150 ml.), the combined effluent was evaporated to dryness in vacuo, and the product was suspended in water (50 ml.), collected by filtration, and dried (219 mg.). The product was recrystallized from methanol - ether - petroleum ether; yield, 186 mg. (45% from XIII); m. p. 165°C; $[\alpha]_D^{26}$ −139° (*c* 0.3, acetic acid); R_f 0.93.[8]

Found: C, 62.76; H, 7.61; N, 12.24. Calcd. for $C_{72}H_{100}O_{14}N_{12}\cdot H_2O$: C, 62.86; H, 7.47; N, 12.22%.

The molecular weight of XVI was determined by a Model 301 A Osmometer, Mechrolab Inc. (solvent: methanol).[12]

Found: 1240. Calcd. for $C_{72}H_{100}O_{14}N_{12}\cdot H_2O$: 1376.

Cyclo-(L-valyl-L-ornithyl-L-leucyl-D-phenylalanylsarcosyl)$_2$ Dihydrochloride (II·2HCl).—XVI (41 mg.), dissolved in methanol (0.6 ml.) and 0.24 N methanolic hydrogen chloride (0.3 ml.), was subjected to hydrogenolysis in the presence of palladium black. The solution, after being filtered from the calalyst, was evaporated to dryness in vacuo. The powder which remained was collected with the aid of ether; the yield of the air-dried product, 32 mg. (92%); m. p. 212—214°C; $[\alpha]_D^{20}$ −157° (*c* 0.3, ethanol); R_f 0.68,[8] 0.89,[10] 0.71[13] and 0.88.[14]

Found: C, 52.51; H, 7.87; N, 12.50. Calcd. for $C_{56}H_{90}O_{10}N_{12}Cl_2\cdot 7H_2O$: C, 52.20; H, 8.12; N, 13.05%.

The molecular weight was determined by the procedure described above (solvent: methanol).

Found: 510.[15] Calcd. for $(1/3)\times(C_{56}H_{90}O_{10}N_{12}Cl_2\cdot 7H_2O)$: 429.

The air-dried product lost 1.5% of its weight when it was left in a desiccator over calcium chloride at room temperature. Calcd. for H_2O: 1.4%. The air-dried product lost 7.4% of its weight after drying over phosphorus pentoxide for 3 hr. at 80°C (2mmHg), Calcd. for $5H_2O$: 7.0%. The product was treated with dinitrofluorobenzene in the manner described by Sanger et al.[16] After the hydrolysis of the dinitrophenylated compound (DNP-II), only one DNP-amino acid, identified as δ-DNP-ornithine, was detected on a paper chromatogram; R_f 0.68.[8]

Cyclo-L-valyl-δ-benzyloxycarbonyl-L-ornithyl-L-leucyl-D-phenylalanylsarcosyl (XIX).—To a solution of X (610 mg.) in pyridine (5 ml.), di-*p*-nitrophenyl sulfite (920 mg.) was added. The reaction mixture was allowed to stand for 24 hr. at room temperature and then treated as has been described in connection with the preparation of XVI. The product (XVII) obtained weighed 605 mg. The purity of the compound was estimated to be 107%. To the *p*-nitrophenyl ester (XVII) (600 mg.), anisole (0.5 ml.) and trifluoroacetic acid (3.5 ml.) were then added. The solution was evaporated in vacuo, and the residue was triturated with ether. The pentapeptide *p*-nitrophenyl ester trifluoroacetate (XVIII) was collected by filtration and dissolved in dimethylformamide (10 ml.) containing glacial acetic acid (0.1 ml.). The solution was then stirred, drop by drop, into pyridine (180 ml.) kept at 55—60°C over a period of 5 hr.; the stirring was then continued for an additional 2 hr. at the same temperature. After the solvent had been removed, the residual oil was dissolved in a mixture of methanol (100 ml.) and water (20 ml.). An insoluble substance was removed by filtration, and the filtrate was treated with the columns of Dowex 1 and 50 described in connection with the preparation of XVI. It weighed 183 mg. (XX). A few mg. of XX were subjected to hydrogenolysis; the hydrogenated material was designated as

11) B. Iselin and R. Schwyzer, *Helv. Chim. Acta*, **43**, 1760 (1960).

12) We are indebted to Mr. M. Waki of this laboratory for the molecular-weight determination.

13) The R_f value of the thin-layer chromatography with Merck silica gel G refers to the *t*-butanol - formic acid - water (75 : 15 : 10, v/v) system.

14) The R_f value refers to the paper chromatography on Toyo Roshi No. 52 with the *t*-butanol - formic acid - water (75 : 15 : 10, v/v) system.

15) This compound appears to dissociate into three molecules under the conditions under which the determination of the molecular weight was carried out.

16) F. Sanger and E. O. P. Thompson, *Biochem. J.*, **53**, 353 (1953).

XXI. XXI was found to be a mixture of II, III and an unidentified substance (XXII) (Figs. 3 and 4). Several recrystallizations of XX from methanol-ether gave 95 mg. (20% from X) of pure XIX; m. p. 224—227°C; $[\alpha]_D^{26}$ +0.7° (*c* 0.3, acetic acid); R_f 0.93.[8]

Found: C, 62.80; H, 7.50; N, 12.44. Calcd. for $C_{36}H_{50}O_7N_6 \cdot {}^1/_2H_2O$: C, 62.86; H, 7.47; N, 12.22%.

The molecular weight of XIX was determined by a Model 301 A osmometer (solvent: methanol).

Found: 750. Calcd. for $C_{36}H_{50}O_7N_6 \cdot {}^1/_2H_2O$: 689.

Cyclo - L - valyl - L - ornithyl- L -leucyl- D -phenylalanylsarcosyl Hydrochloride (III · HCl). — XIX (34.4 mg.) was dissolved in methanol (1.5 ml.) and 0.24 N methanolic hydrogen chloride (0.25 ml.) and treated as has been described in connection with the preparation of II·2HCl; yield, 22.4 mg. (77%); m. p. 198°C; $[\alpha]_D^{20}$ −26.8° (*c* 0.3, ethanol); R_f, 0.69,[8] 0.88,[10] 0.70[13] and 0.87.[14]

Found: C, 53.20; H, 7.94; N, 13.13. Calcd. for $C_{28}H_{45}O_5N_6Cl \cdot 3H_2O$: C, 52.94; H, 8.09; N, 13.23%.

The molecular weight was determined by the procedure described above (solvent: methanol).

Found: 340.[17] Calcd. for $(1/2) \times (C_{28}H_{45}O_5N_6Cl \cdot 3H_2O)$: 318.

The air-dried product lost 5.4% of its weight when it was left in a desiccator over calcium chloride at room temperature. Calcd. for $2H_2O$: 5.7%. The air-dried product lost 8.3% of its weight after having been dried over phosphorus pentoxide for 3 hr. at 80°C, 2 mmHg. Calcd. for $3H_2O$: 8.5%. After the hydrolysis of the dinitrophenylated compound (DNP-III), only δ-DNP-ornithine was detected on a paper chromatogram; R_f 0.68.[10]

Amino Acid Analyses of II and III.—A complete amino acid analysis except for the sarcosine of each compound was carried out according to the procedure described in a previous paper.[1] Amino acid determinations of II and III gave the molar ratios of 1.0 : 1.0 : 1.1 : 1.0 and 1.0 : 0.9 : 1.0 : 1.1 for valine, ornithine, leucine and phenylalanine respectively. In order to determine the sarcosine content, a mixture of sarcosine (0.5 μmol.) and leucine (0.5 μmol.) was dinitophenylated[18] and subjected to thin-layer chromatography.[19] Each band of DNP-sarcosine and DNP-leucine was eluted with methanol, the eluent was evaporated, and the residue was dissolved in 1% sodium bicarbonate (10 ml.) for spectrophotometric determination. It was found that the intensities at 380—385 mμ for DNP-sarcosine and at 360 mμ for DNP-leucine were almost the same. The same operations were carried out for the hydrolysates of II and III; the molar ratios for sarcosine and leucine are of 0.9 : 1.0 and 0.9 : 1.0 respectively.

Chromatography and Electrophoresis of II, III, XXI and Gramicidin S.—Carboxymethylcellulose column chromatography was performed as follows: Each portion (0.5—1 mg.) of hydrochlorides of II, III, XXI and gramicidin S was dissolved in 0.2—0.3 ml. of 0.2 M pyridinium acetate containing 30% methanol (pH 5.0), and then the solution was applied to a column (0.9×50 cm.) of carboxymethyl cellulose (Eastman Organic Chem. 7796). When elution was carried out with the same solvent at 20—25°C, and a flow rate was about 20 ml. per hr., 2 ml. fractions were collected. The peptide content in the fractions was determined by the method described by Yemm and Cocking.[20] Gramicidin S was used as a control. The results are shown in Fig. 3. In order to examine the molar ratio between XIX and XVI in the cyclization product (XX) from the pentapeptide active ester (XVIII), a solution containing 1 μmol. of III and 0.5 μmol. of II was subjected to column chromatography; the ratio of intensities resulting from ninhydrin between III and II was found to be 80 : 100 by calculating the areas on a chromatogram of the optical density-fraction number. By the use of the value obtained above, it was calculated from Fig. 3 that the molar ratio between III and II in XXI was about 92 : 8. Therefore, it was deduced that the cyclization reaction of the pentapeptide active ester (XVIII) gave the cyclic pentapeptide (XIX) predominantly. Their analyses were also carried out by electrophoresis. An appropriate amount of the material was placed on a paper of Toyo Roshi No. 52, and 500 V./30 cm. were applied for 3 hr. at room temperature, using a formic acid - acetic acid-methanol - water (1 : 3 : 6 : 10, v/v) system at pH

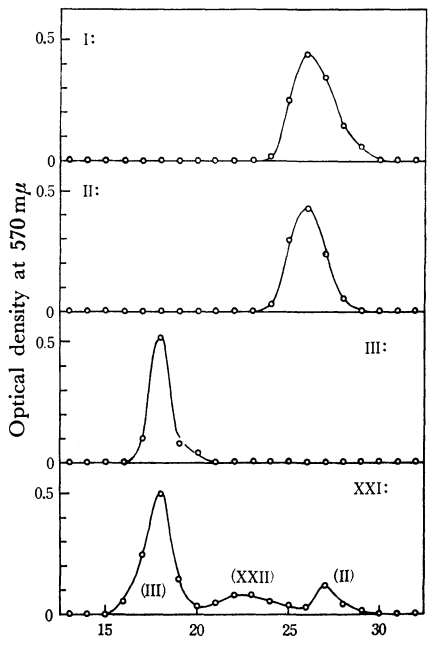

Fig. 3. CM-Column chromatography of hydrochlorides of gramicidin S (I), II, III and hydrogenated material (XXI) of the product (XX) obtained by cyclization reaction of pentapeptide active ester (XVIII). XXII is an unidentified cyclic peptide.

17) This compound appears to dissociate into two molecules under the conditions under which the determination of the molecular weight was carried out.

18) W. A. Schroeder and J. LeGette, *J. Am. Chem. Soc.*, **75**, 4612 (1953).

19) M. Brenner, N. Niederwieser and G. Pataki, *Experientia*, **17**, 145 (1961).

20) E. W. Yemm and E. C. Cocking, *Analyst*, **80**, 209 (1955); *Biochem. J.*, **58**, xii (1954).

Table I. Inhibitory activity of II, III and gramicidin S on microorganisms

Minimum inhibitory concentrations, μg./ml.

	Escherichia coli	*Proteus vulgaris*	*Staphylococcus aureus*	*Bacillus subtilis*	*Mycobacterium avium*	*Mycobacterium avium* (Streptomycin resistant St.)
A. Bouillon agar medium[a]						
II·2HCl	>100	>100	10	5	100	100
III·HCl	>100	>100	>100	>100	>100	>100
Gramicidin S·2HCl	>100	>100	5	5	>100	>100
B. Synthetic medium[b]						
II·2HCl	>100	>100	10	5	100	100
III·HCl	>100	>100	>100	>100	>100	>100
Gramicidin S·2HCl	>100	>100	5	5	>100	>100

a) Usual bouillon agar medium, pH 7.0.
b) Stephenson-Whetham's medium (modified); K_2HPO_4 0.1%, NaCl 0.1%, $MgSO_4 \cdot 7H_2O$ 0.05%, Na-glutamate 0.4%, casamino acid 0.2%, yeast-extract 0.05% and agar 2.0%, pH 7.0.

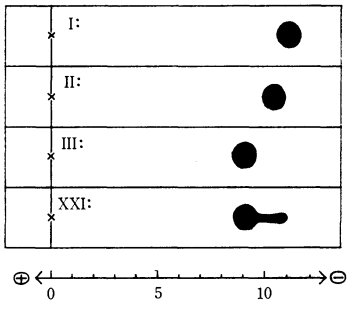

Fig. 4. Paper electrophoresis of hydrochlorides of gramicidin (I), II, III and XXI.

1.8 (Fig. 4). Figure 4 shows also that the cyclization product (XX) contained the cyclic pentapeptide (XIX) as a major component.

Microbiological Assays. — The microorganisms employed are shown in Table I. The minimum amount of the compounds needed for a complete inhibition of growth was determined by a dilution method with a bouillon agar medium and with a synthetic medium. As is shown in Table I, the cyclic decapeptide II was found to be as active as gramicidin S against *B. subtilis* and *Staph. aureus*. II appears to exhibit weak antibacterial activity against *Mycobact. avium* (streptomycin-resistant) and *Mycobact. avium*. The cyclic pentapeptide III exhibited no activity with relation to any of the organisms tested.

The authors wish to express their thanks to Dr. Motoo Shibata of Takeda Chemical Industries, Ltd., for the microbiological assays. Thanks are also due to the Ajinomoto Co., Inc., and to Kyowa Hakko Kogyo Co., Ltd., for supplying some of the amino acids.

BULLETIN OF THE CHEMICAL SOCIETY OF JAPAN VOL. 39 1754—1759 (1966)

The Knoevenagel Reaction between Hydroxybenzaldehydes and Ethyl Cyanoacetate

By Heinosuke YASUDA* and Hiroshi MIDORIKAWA

The Institute of Physical and Chemical Research, Bunkyo-ku, Tokyo

(Received November 30, 1965)

Substituted 2-hydroxybenzaldehydes react with two equivalents of ethyl cyanoacetate to give α-amino-β-(substituted 3-coumarinyl)-β-cyano-β-ethoxycarbonylethylenes in the presence of piperidine. When equivalent aldehyde and the cyanoacetate are used, substituted 2-imino-3-ethoxycarbonyl-2*H*-chromenes result, without the isolation of arylidenecyanoacetates. In *o*-hydroxyaryls, salicylic and *o*-thymotinic aldehydes, which give benzopyrane derivatives, are exceptional cases. 5-Phenylazo- and 5-nitro-2-hydroxybenzaldehydes result in the formation of coumarin derivatives. An abnormal condensation is also shown in the cases of 3, 5-dibromo-2, 4-dihydroxy-, 2-hydroxy-3-methoxy- and 2-hydroxy-4-methoxybenzaldehydes; i. e., the first one yields a 1 : 1-condensation product, while the last two give 3-cyanocoumarin derivatives, even with an excess of ethyl cyanoacetate. The condensation of *m*- and *p*-hydroxybenzaldehydes with ethyl cyanoacetate give the normally-expected arylidenecyanoacetates, even in the presence of a large excess of the cyanoacetate.

The base-catalyzed condensation of salicylaldehyde with ethyl cyanoacetate has already been described by Bechart[1] and by Knoevenagel et al.,[2] as giving an abnormal condensation product. They assigned the product to diethyl α, γ-dicyano-β-(2-hydroxyphenyl)-glutarate (Ia). Recently, however, Matsumura[3] established that this product has the structure of 2-amino-2-(cyano-ethoxycarbonylmethyl)-3-ethoxycarbonyl-α-benzopyrane (IIa) and not Ia. Sastry et al.[4] reported that ethyl 3-cyano-3, 4-dihydrocoumarin-4-cyanoacetate (III) was formed when Ia was refluxed in ethanol containing piperidine, but Matsumura gave the structure of α-amino-α-(3-coumarinyl)-β-cyano-β-ethoxycarbonylethylene (IV) instead of III.

The present investigation will be concerned with the condensation of various *o*-hydroxyaromatic aldehydes with ethyl cyanoacetate in the presence of piperidine. In addition, *m*- and *p*-hydroxyaryls will also be investigated.

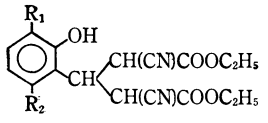

Ia, $R_1=R_2=H$
Ib, $R_1=i\text{-}C_3H_7$ $R_2=CH_3$

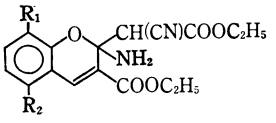

IIa, $R_1=R_2=H$
IIb, $R_1=i\text{-}C_3H_7$ $R_2=CH_3$

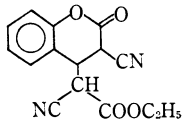

III

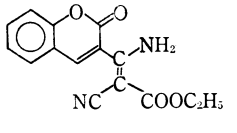

IV

* Present address; Laboratory of Chemistry, Utsunomiya University, Utsunomiya.

Results and Discussion

The condensation between salicylaldehyde and ethyl cyanoacetate was re-investigated. The condensation was attempted by heating the aldehyde with an equivalent amount of the cyanoacetate in ethanol containing piperidine or by letting the reactants stand; however, the required condensations could not be effected, and only negligible products were obtained.

The condensation was positive only with two equivalent amounts of the cyanoacetate; that is, only when the reaction mixture was heated for a short time at the boiling point of the solvent, two compounds (m. p. 239—240°C and m. p. 137.5—138.5°C) could be readily isolated.

On investigation, the product melting at 239—240°C was found to be devoid of saturated nitriles. This was confirmed by the infrared absorption spectrum, which showed no characteristic bands for the nitriles. However, two medium bands were shown near 3400 and near 3300 cm^{-1}, indicating a primary amino group; also, the spectrum exhibited an absorption near 2200 cm^{-1} for α, β-unsaturated nitrile. These facts, together with the analytical results, were in full agreement with the IV structure originally proposed by Matsumura. On the other hand, the spectrum of the compound melting at 137.5—138.5°C revealed two relatively intense bands near 3460

1) C. Bechart, *J. prakt. Chem.*, (2), **50**, 1 (1894).
2) E. Knoevenagel and R. Ornot., *Ber.*, **37**, 4496 (1904).
3) S. Matsumura, This Bulletin, **34**, 995 (1961).
4) V. D. N. Sastry and T. R. Seshadri, *Proc. Indian Acad. Sci.*, **16A**, 29 (1942).

TABLE I. α-AMINO-α-(SUBSTITUTED 3-COUMARINYL)-β-CYANO-β-ETHOXYCARBONYLETHYLENES

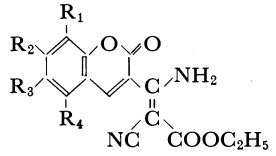

Compound	R_1	R_2	R_3	R_4	M.p. °C	Appearance[a]	Yield[b] %	Formula	C, % Calcd.	C, % Found	H, % Calcd.	H, % Found	N, % Calcd.	N, % Found
Va	H	H	Br	H	272—3 (decomp.)	SY Needles	53	$C_{15}H_{11}O_4N_2Br$	49.56	49.62	3.03	2.95	7.71	7.43
Vb	H	H	Cl	H	265—6	Y Needles	48	$C_{15}H_{11}O_4N_2Cl$	56.51	56.21	3.45	3.46	8.79	8.63
Vc	H	H	NO_2	H	238—9	Y Crystals	31	$C_{15}H_{11}O_6N_3$	54.71	54.30	3.37	3.36	12.76	12.89
Vd	H	H	H	CH_3	238—9	SY Needles	20	$C_{16}H_{14}O_4N_2$	64.42	64.59	4.73	4.58	9.39	9.28
Ve	H	OH	H	H	277—8 (decomp.)	Y Needles	49	$C_{15}H_{12}O_5N_2$	60.00	59.71	4.03	4.06	9.33	9.04
Vf	OCH_3	H	H	H	240—1	SY Needles	51	$C_{16}H_{14}O_5N_2$	61.14	60.85	4.49	4.43	8.91	8.80

a) S, Slightly; Y, Yellow.
b) Overall yield from the aldehyde used, and recrystallized from *n*-butanol.

TABLE II. INFRARED DATA OF α-AMINO-α-(SUBSTITUTED 3-COUMARINYL)-β-CYANO-β-ETHOXYCARBONYLETHYLENES

(in KBr disk)

Compound	Bonded NH_2 str.	Free NH_2 str.	C≡N str.	Ester C=O str.	Lactone C=O str.	C=C and NH_2 def.	(cm^{-1})
Va	3470m	3340m,br	2220 s	1720 s	1700 s	1620 s	
Vb	3470m	3330m	2220 s	1720 s	1700 s	1615m,sh	
Vc	3460m	3310m,br	2220 s	1715 s	1690 s	1615 s ,sh	
Vd	3420m	3290m,br	2220 s	1715 s	1695m	1615 s	
Ve	3460m	3300m,br	2220 s	1715 s	1700m	1635 s	
Vf	3440m	3370m	2220 s	1725 s,sh	1700 s	1620 s 1635 s	

Abbreviations: s, strong; m, medium; sh, shoulder; br, broad; str, stretching; def, deformation.

TABLE III. SUBSTITUTED 2-IMINO-3-ETHOXYCARBONYL-2*H*-CHROMENES

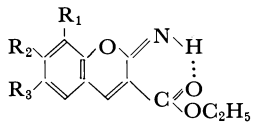

Compound	R_1	R_2	R_3	M. p. °C	Crystn. solvent	Appearance[a]	Yield[b] %
VIa	H	H	Cl	119—120	EtOH	YO Crystals	35
VIb	OH	H	H	179—180 (decomp.)	*n*-BuOH	Y Crystals	73
VIc	H	OH	H	182—183	*n*-BuOH	Y Needles	82
VId	H	H	OH	200—201	EtOH-H_2O	GY Crystals	84
VIe	Br	OH	Br	245—246 (decomp.)	*n*-BuOH	YO Needles	62
VIf	H	OH	NO_2	over 300	*n*-BuOH	YO Crystals	68

Compound	Formula	C, % Calcd.	C, % Found	H, % Calcd.	H, % Found	N, % Calcd.	N, % Found
VIa	$C_{12}H_{10}O_3NCl$	57.26	56.85	3.98	4.01	5.57	5.47
VIb	$C_{12}H_{11}O_4N$	61.80	61.79	4.75	4.72	6.01	5.95
VIc	$C_{12}H_{11}O_4N$	61.80	61.47	4.75	4.92	6.01	6.05
VId	$C_{12}H_{11}O_4N$	61.80	61.66	4.75	4.74	6.01	5.86
VIe	$C_{12}H_9O_4NBr_2$	36.83	36.61	2.30	2.36	3.58	3.59
VIf	$C_{12}H_{10}O_6N_2$	51.80	51.42	3.60	3.47	10.07	9.96

a) Y, Yellow; O, Orange; G, Green. b) Overall yield from the aldehyde used.

and near 3300 cm^{-1}; these were attributed to a primary amino group. The infrared and analytical data are in essential agreement with the IIa structure formulated by Matsumura.

The investigation was then extended to the action of the ethyl cyanoacetate on substituted 2-hydroxybenzaldehydes with the view of obtaining the IIa and/or the IV type. Using a 2 : 1 molar ratio of the aldehydes to the cyanoacetate, α-amino-α-(substituted 3-coumarinyl)-β-cyano-β-ethoxycarbonylethylenes (Va—Vf) (see Tables I and II), which very closely resemble the IV type, were regularly obtained, but the expected α-benzopyrane derivatives (the IIa type) could not be isolated; with a molar ratio of the aldehydes and the cyanoacetate, only the 1 : 1-condensation products were obtained.

The 1 : 1-condensation products mentioned above did not exhibit the characteristic C≡N stretching vibration in each infrared spectrum examined; therefore, the following structure, VI, was considered to hold for the products concerned.

Apparently, the spectrum of the 1 : 1-product obtained from 5-chlorosalicylaldehyde and ethyl cyanoacetate, for example, supported the structure

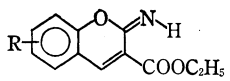

VI

of 2-imino-3-ethoxycarbonyl-6-chloro-2*H*-chromene (VIa), since three recognizable bands, at 3380, 1710 and 1635 cm^{-1} which due to an N–H, an α, β-unsaturated ester C=O and a C=N stretching vibrations respectively, were detected. A medium band at 1615 cm^{-1} attributable to the C=C stretching mode adjacent to the ester residue was also observed. Baker and Howea[5] have already inferred that, in the conversion of 2-hydroxybenzylidenecyanoacetic acid into 3-coumarincarboxylic acid in boiling water, an imino-lactone (VII) is the intermediate.

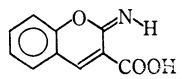

VII

The 1: 1-products investigated, accordingly, were considered to have the structure of 2-imino-3-ethoxycarbonyl-2*H*-chromenes (VIa—VIf) and not substituted arylidenecyanoacetates (see Tables III and IV). As may be seen in Table IV, α, β-unsaturated ester C=O bands of all the compounds measured in KBr disk are shifted to lower frequencies as compared with the normal spectral region of ester carbonyls vicinal to α, β-unsaturation. It is likely, judging from the infrared results, that these 2*H*-chromenes have the hydrogen-bonded chelate form in the solid state.

TABLE IV. INFRARED DATA OF SUBSTITUTED 2-IMINO-3-ETHOXYCARBONYL-2*H*-CHROMENES
(in KBr disk)

Compound	Bonded OH and NH str.	Ester C=O str.	C=N str.	C=C str. (cm^{-1})
VIa	3380 m	1710 s	1635 m	1615 m
VIb	3380 m	1700 s	1620 m	1610 s, sh
VIc	3310 m	1705 s	1630 s	1620 s, sh
VId	3320 m	1715 s	1620 m, sh	1610 m
VIe	3340 w	1715 s	1625 m, sh	1615 m
VIf	3390 m	1715 s	1645 s	1620 s, sh

Abbreviation: s, strong; m, medium; w, week; sh, shoulder; str, stretching

The problem of the mechanism of the formation of the β-ethoxycarbonylethylenes (Va—Vf) is reduced to the question of whether the condensation involves a self-condensation of the cyanoacetate forming an enamine-type dimer via a ketimine-type dimer following the dehydration reaction between the dimer and the aldehydes, or, alternatively, the formation of normal dehydration products without cyclization and a nucleophilic addition reaction by the cyanoacetate on the dehydration products. The two possibilities are illustrated in Scheme 1.

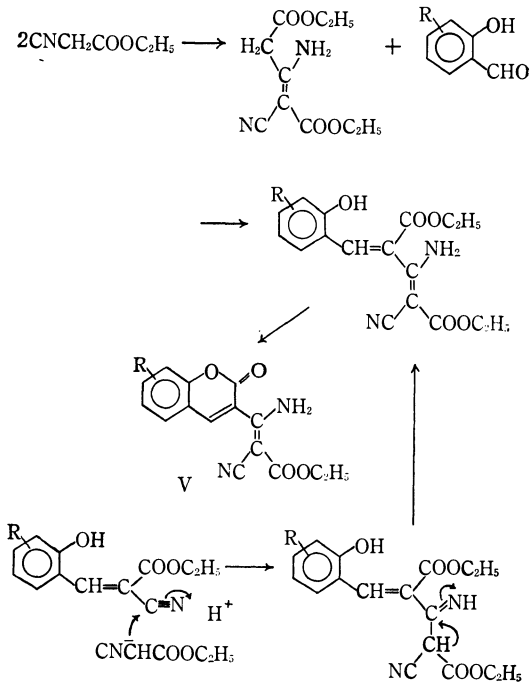

Scheme 1

When the *o*-hydroxyaryls were treated with an equivalent ethyl cyanoacetate, no β-ethoxycarbonylethylene derivatives occurred; only 1 : 1-products

5) W. Baker and C. S. Howea, *J. Chem. Soc.*, **1953**, 119.

TABLE V. SUBSTITUTED ETHYL *m*- OR *p*-HYDROXY-*α*-CYANOCINNAMATES

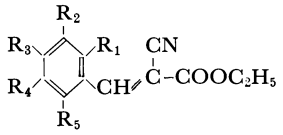

Compound	R_1	R_2	R_3	R_4	R_5	M. p. °C	Appearance[a]	Yield[b] %
IX	H	OH	H	H	H	91—92[c]	SY Needles	61
X	H	H	OH	H	H	171—172[d]	Y Needles	86
XI	H	OCH_3	OH	H	H	106—107[e]	YF Needles	79
XII	H	OC_2H_5	OH	H	H	76—77	Y Needles	82
XIII	H	CH_3	OH	H	H	220—221	SY Needles	78
XIV	H	CH_3	OH	CH_3	H	124—125	YM Crystals	95
XV	H	*i*-C_3H_7	OH	H	CH_3	190—191	Y Needles	80
XVI	H	Cl	OH	H	H	199—200	SY Needles	81
XVII	OCH_3	H	OCH_3	H	H	138—139[f]	Y Needles	89

Compound	Formula	C, % Calcd.	C, % Found	H, % Calcd.	H, % Found	N, % Calcd.	N, % Found
IX	$C_{11}H_{12}O_3N$					6.45	6.43
X							
XI							
XII	$C_{14}H_{15}O_4N$	64.36	64.47	5.79	5.63	5.36	5.37
XIII	$C_{13}H_{13}O_3N$	67.53	67.08	5.63	5.52	6.06	6.08
XIV	$C_{14}H_{15}O_3N$	68.55	68.06	6.16	6.09	5.71	5.60
XV	$C_{16}H_{19}O_3N$	70.33	69.77	6.96	6.74	5.13	5.07
XVI	$C_{12}H_{10}O_3NCl$	57.26	57.43	3.98	3.97	5.57	5.35
XVII							

a) F, Flattened; M, Micro; S, Slightly; Y, Yellow.
b) Overall yield from the aldehyde used, and recrystallized from ethanol-water.
c) Reported m. p. 98°C, K. P. Dave and K. S. Nargund, *J. Univ. Bombay*, **7**, 196 (1938); *Chem. Abstr.*, **33**, 3779 (1939).
d) Reported m. p. 173—174°C, F. D. Popp, *J. Org. Chem.*, **25**, 646 (1960).
e) Reported m. p. 108—109°C, reference as footnote d.
f) Reported m. p. 142—143°C, reference as footnote 5.

via intermediate arylidenecyanoacetates were obtained, as has been described above. These facts indicate that the latter mechanism, which involves the carbanion of the cyanoacetate attacking the possibly-polarized nitrile carbon atom of the resulting intermediates, may be more possible than the former mechanism. However, salicylaldehyde condensed with the dimer of ethyl cyanoacetate to give the β-ethoxycarbonylethylene (IV), as has been reported earlier.[3]

A definitive proof for the latter mechanism is lacking. Attempts to obtain the IV type by treating the appropriate 2*H*-chromene derivatives with ethyl cyanoacetate in boiling ethanol containing piperidine were unsuccessful.

5-Phenylazo-2-hydroxy- and 3, 5-dibromo-2, 4-dihydroxybenzaldehydes behaved "abnormally" in the condensation with an excess of ethyl cyanoacetate, giving ethyl 6-phenylazo-3-coumarincarboxylate (VIIa) and the 2*H*-chromene derivative (VIe) (see Table III), respectively. 5-Nitrosalicylaldehyde reacted with an equimolar ethyl cyanoacetate to yield an unexpected product, ethyl 6-nitro-3-coumarincarboxylate (VIIb); also, 2-hydroxy-3-methoxy- and 2-hydroxy-4-methoxybenzaldehydes resulted in the formation of 8-methoxy-3-cyanocoumarin (VIIIa) (C≡N stretching 2220 cm^{-1} in KBr disk) and 7-methoxy-3-cyanocoumarin (VIIIb) (C≡N 2220 cm^{-1}) respectively when an equimolar ethyl cyanoacetate was used. These were exceptional cases in the *o*-hydroxyaryl series.

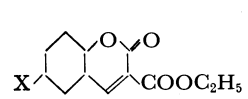

VIIa, X=Ph-N=N-
VIIb, X=NO_2

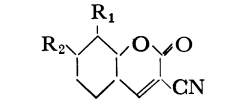

VIIIa, R_1=OCH_3 R_2=H
VIIIb, R_1=H R_2=OCH_3

The condensation of *m*- and *p*-hydroxybenzaldehydes with ethyl cyanoacetate gave the normally expected products, substituted ethyl *m*- and *p*-hydroxy-*α*-cyanocinnamates (IX—XVII), even with a large excess of the cyanoacetate. The results obtained are listed in Table V.

3, 4-Dihydroxybenzaldehyde reacted with an equivalent ethyl cyanoacetate to form ethyl α-cyano - β - hydroxy -β- (3, 4-dihydroxyphenyl)-propionate (XVIII); on subsequent treatment with acetic anhydride, this yielded ethyl α-cyano-3, 4-diacetyloxycinnamate (XIX). On the other hand, 2-imino-3-ethoxycarbonyl-7-hydroxy -2*H*- chromene (VIb), when refluxed with acetic anhydride, was converted into ethyl 7-acetyloxy-3-coumarincarboxylate (XX).

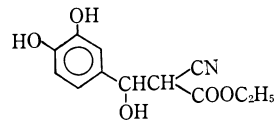

XVIII

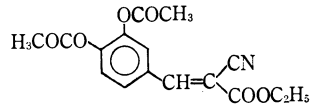

XIX

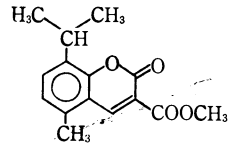

XXI

Previously, one of the present authors[6] has reported that the condensation between 2-hydroxy-3-isopropyl - 6 - methylbenzaldehyde, *o*-thymotinic aldehyde, gave mainly diethyl β, γ-dicyano-β-(2-hydroxy -3- isopropyl -6- methyl)-glutarate (Ib). The present infrared study shows that the condensation product formulated as Ib has the structure of 2-amino-2-(cyanoethoxycarbonylmethyl) -3-ethoxycarbonyl-5-methyl-8-isopropyl-α-benzopyrane (IIb). The infrared spectrum of Compound IIb exhibited characteristic absorption bands at 3460 and at 3380 cm^{-1} for the primary amino group; at 2245 cm^{-1} for the non-conjugated C≡N; at 1746 cm^{-1} for the saturated ester C=O; at 1645 cm^{-1} for the ester C=O conjugated with the unstauration bond and at 1640 cm^{-1} for an absorption attributable to NH_2 deformation vibration. This compound afforded methyl 5-methyl-8-isopropyl-3-coumarincarboxylate (XXI) in boiling methanol containing concentrated sulfuric acid.

Experimental*

Condensation of Salicylaldehyde and Ethyl Cyanoacetate.—Three grams (0.0246 mol.) of the aldehyde was dissolved in 15 ml. of ethanol containing 5.6 g. (0.0496 mol.) of the ester. To the refluxing solution was added one drop of piperidine. The solution was refluxed for an additional one hour and allowed to stand overnight at room temperature. The crude α-amino-α-(3-coumarinyl)-β-cyano-β-ethoxycarbonylethylene (IV) separated was collected, washed with ethanol and weighed 1.3 g. One recrystallization from ethanol gave slightly yellowish micro crystals melting at 245—246°C (Lit.,[3] 245—246°C). The initial filtrate and washings from crude IV were combined and diluted with water. An oily matter was extracted with ether, and ethreal extract was dried over sodium sulfate. The residual oil, on removal of the ether, was shaken with methanol, and the crude 2-amino-2-(cyanoethoxycarbonylmethyl) - 3 - ethoxycarbonyl - α - benzopyrane (IIa) was recrystallized from ethanol-water in almost colorless plates melting at 137.5—138.5°C, and which weighed 3.3 g. Lit.,[3] m. p. 137°C.

Synthesis of α-Amino-α-(6-bromo-3-coumarinyl)-β-cyano-β-ethoxycarbonylethylene (Va).—The preparation of this compound is typical of the preparation of the substituted β-ethoxycarbonylethylenes and is described in detail.

Two grams (0.01 mol.) of 5-bromo-2-hydroxybenzaldehyde was dissolved in 20 ml. of ethanol containing 2.3 g. (0.02 mol.) of ethyl cyanoacetate and one drop of piperidine. The mixture was warmed on a water-bath for 1 hr., and being allowed to stand overnight. The precipitates were collected, washed with ethanol and recrystallized from *n*-butanol, giving the required compound melting at 272—273°C with decomposition. The melting points and analytical data of the β-ethoxycarbonylethylenes are summarized in Table I.

Synthesis of 2-Imino-3-ethoxycarbonyl-6-chloro-2*H*-chromene (VIa).—The 2*H*-chromenes synthesized in this study are listed in Table III. All of these were prepared from ethyl cyanoacetate and the corresponding aldehyde. The physical properties are also included in Table III.

An example of the preparation of the 2*H*-chromenes is described.

5-Chloro-2-hydroxybenzaldehyde (0.18 g., 0.00115 mol.) and 0.13 g. (0.00115 mol.) of ethyl cyanoacetate were dissolved in 2 ml. of hot ethanol containing one drop of piperidine. The solution was allowed to stand overnight at room temperature. The precipitates were collected, washed with methanol and recrystallized from ethanol in yellowish micro crystals melting at 119—120°C. The resulting VIa weighed 0.1 g.

Synthesis of Ethyl 6-Phenylazo-3-coumarincarboxylate (VIIa).—5-Phenylazo-2-hydroxybenzaldehyde (0.5 g., 0.0022 mol.) and ethyl cyanoacetate (0.25 g., 0.0022 mol.) were mixed in 10 ml. of ethanol containing one drop of piperidine. The mixture was warmed on a water-bath for 1 hr., and being allowed to stand overnight. The crystals separated were collected, washed with ethanol and recrystallized from dioxane-water in lustrous yellowish brown needles melting at 153—154°C, and which weighed 0.2 g.

Found: C, 67.07; H, 4.48; N, 8.77. Calcd. for $C_{18}H_{14}O_4N_2$: C, 67.07; H, 4.38; N, 8.69%.

Synthesis of Ethyl 6-Nitro-3-coumarincarboxylate (VIIb).—To a solution of 0.24 g. of 5-nitro-2-hydroxybenzaldehyde and 0.16 g. of ethyl cyanoacetate in 2 ml. of ethanol was added one drop of piperidine. The solution was allowed to stand overnight at room temperature. The crude VIIb separated as a crystalline

6) H. Yasuda, *Sci. Papers Inst. Phys. Chem Res.* (*Tokyo*), **52**, 83 (1958).

* All melting points are uncorrected.

product was collected, washed with ethanol and recrystallized from *n*-butanol, giving almost colorless lustrous short needles melting at 193—194°C, and which weighed 0.27 g.

Found: C, 54.44; H, 3.49; N, 5.54. Calcd. for $C_{12}H_9O_6N$: C, 54.76; H, 3.45; N, 5.32%.

Synthesis of 8-Methoxy-3-cyanocoumarin (VIIIa).—A solution of 0.5 g. of 2-hydroxy-3-methoxybenzaldehyde and 0.4 g. of ethyl cyanoacetate in 5 ml. of ethanol containing one drop of piperidine was warmed on a water-bath for 20 min. The precipitates, on cooling, was collected, washed with ethanol and weighed 0.4 g. One recrystallization from *n*-butanol gave yellowish short needles melting at 222—223°C.

Found: C, 64.99; H, 3.48; N, 7.05. Calcd. for $C_{11}H_7O_3N$: C, 65.67; H, 3.51; N, 6.96%.

Synthesis of 7-Methoxy-3-cyanocoumarin (VIIIb).—2-Hydroxy-4-methoxybenzaldehyde (0.38 g.) was dissolved in 5 ml. of ethanol containing 0.28 g. of ethyl cyanoacetate and one drop of piperidine. The solution was allowed to stand overnight at room temperature. The solid separated was collected, washed with ethanol and recrystallized from *n*-butanol in slightly yellowish short needles melting at 218—219°C.

Found; C, 65.38; H, 3.72; N, 6.79. Calcd. for $C_{11}H_7O_3N$: C, 65.67; H, 3.51; N, 6.96%.

Synthesis of Ethyl *m*- or *p*-Hydroxy-α-cyanocinnamates (IX—XVII).—The method for the preparation of this series is illustrated by the synthesis of ethyl *m*-hydroxy-α-cyanocinnamate (IX). To a solution of 0.001 mol. of *m*-hydroxybenzaldehyde and 0.001 mol. of ethyl cyanoacetate in 5 ml. of ethanol was added one drop of piperidine. The solution was warmed on a water-bath for a few minutes, and being allowed to stand overnight at room temperature. The solid separated was collected, and recrystallized from ethanol-water. See Table V for the melting point and the analysis.

Condensation of 3, 4-Dihydroxybenzaldehyde and Ethyl Cyanoacetate.—To a solution of 1.0 g. of the aldehyde and 0.81 g. of the ester in 5 ml. of ethanol was added three drops of piperidine. After standing overnight, the solution was diluted with water, and the precipitates were recrystallized from ethanol-water to give yellowish needles melting at 166—167°C, and which weighed 1.5 g. The analytical values were identical with that of ethyl α-cyano-β-hydroxy-β-(3, 4-dihydroxyphenyl)-propionate (XVIII).

Found: C, 57.97; H, 5.08; N, 5.58. Calcd. for $C_{12}H_{13}O_5N$: C, 57.37; H, 5.22; N, 5.58%.

Reaction of XVIII and Acetic Anhydride to Ethyl α-Cyano-3, 4-diacetyloxycinnamate (XIX).—An appropriate amount of XVIII was refluxed with an appropriate amount of the anhydride for two hours, and then acetic acid and the anhydride were recovered under water-pump pressure. The residual solid was recrystallized from ethanol-water in colorless plates melting at 103—104°C. The analytical data were identical with that of XIX.

Found: C, 60.28; H, 4.74; N, 4.39. Calcd. for $C_{16}H_{15}O_6N$: C, 60.50; H, 4.77; N, 4.41%.

Conversion of 2-Imino-3-ethoxycarbonyl-7-hydroxy-2*H*-chromene (VIb) into Ethyl 7-Acetyloxy-3-coumarincarboxylate (XX).—An appropriate amount of VIb was heated to reflux with an appropriate amount of acetic anhydride for 1 hr. The residual solid, after removal of the anhydride, was recrystallized from methanol-water in slightly brownish needles melting at 147—148°C.

Found: C, 60.16; H, 4.46. Calcd. for $C_{14}H_{12}O_6$: C, 60.87; H, 4.38%.

Conversion of 2-Amino-2-(cyano-ethoxycarbonylmethyl)-3-ethoxycarbonyl-5-methyl-8-isopropyl-α-benzopyrane (IIb) into Methyl 5-Methyl-8-isopropyl-3-coumarincarboxylate (XXI).—One gram of IIb was refluxed with 10 ml. of ethanol containing 1 ml. of concentrated sulfuric acid for 1 hr. after which colorless crystals separated, on cooling, were collected, washed with water and recrystallized from methanol-water to give lustrous colorless needles melting at 120—120.5°C.

Found: C, 69.14; H, 6.23. Calcd. for $C_{15}H_{16}O_4$: C, 69.21; H, 6.20%.

The authors are indebted to Professor Taro Hayashi and Professor Tatsuo Takeshima for their advice, encouragement and suggestions during the course of this investigation.

We wish also to thank Dr. Haruo Homma, of this institute, for his microanalysis.

BULLETIN OF THE CHEMICAL SOCIETY OF JAPAN VOL. 39 1760—1764 (1966)

Studies on D-Glucosamine Derivatives. XII.*1 The Synthesis of *N*-Acetyl-3-*O*- and -4-*O*-aminoacyl-D-glucosamines

By Juji YOSHIMURA, Masuo FUNABASHI, Sadao ISHIGE and Tetsuo SATO

Department of Chemistry, Tokyo Institute of Technology, Ookayama, Meguro-ku, Tokyo

(Received December 9, 1965)

As a part of the investigation of the stabilities of the esters between *N*-acetyl-D-glucosamine and various amino acids, *N*-acetyl-3-*O*- and 4-*O*-aminoacyl-D-glucosamines were synthesized. Benzyl *N*-acetyl-4, 6-*O*-benzylidene-α- and -β-D-glucosaminide, and benzyl *N*-acetyl-3-*O*-benzyl-6-*O*-trityl-α- and -β-D-glucosaminide were condensed with *N*-benzyloxycarbonyl-amino acids by the dicyclohexylcarbodiimide method, followed by the step-by-step removal of the protecting groups. The α-Glycosidic benzyl group, however, could not be removed by the catalytic hydrogenolysis in the presence of oxalic acid, probably because of a steric hindrance.

In a previous report[1] of this series, 1, 2-dideoxy-1-glycylamino-2-acetamido-D-glucosamines have been synthesized. Such a *N*-acyl-glycosylamine linkage between sugars and amino acids has already been ascertained in glycoproteins[2] and in the process of the biological nucleotide synthesis[3].

However, the corresponding ester linkage[4] has been scarcely found, probably because of its instability. In order to examine the stabilities of the ester linkage between sugars and amino acids, we have synthesized the simple ester compounds between *N*-acetyl-D-glucosamine and various amino acids, of which the selective synthesis of *N*-acetyl-6-*O*-aminoacyl-D-glucosamines was reported in the previous paper.

In the present paper, the synthesis of 3-*O*- and 4-*O*-aminoacyl derivatives of *N*-acetyl-D-glucosamine will be described.

Results

The Synthesis of *N*-Acetyl-3-*O*-aminoacyl-D-glucosamines.—Kochetkov et al.[5] isolated 3-*O*-(*N*-benzyloxycabonyl*2-glycyl)-D-glucose as a by-product in the synthesis of 6-*O*-(*N*-Z-glycyl)-D-glucose from D-glucose and *N*-Z-glycine, while the homologues were synthesized by Muramatsu[6] by the condensation of 1, 2 ; 5, 6-di-*O*-isopropylidene-D-glucofuranose with *N*-Z-amino acids.

For the purpose of introducing the aminoacyl groups into the C-3 hydroxyl group of *N*-acetyl-D-glucosamine, we prepared benzyl *N*-acetyl-4, 6-*O*-benzylidene-α-[7] and -β-D-glucosaminide (A-I and B-I)*3 as starting materials.

The compound B-I was newly prepared by the benzylidenation of benzyl *N*-acetyl-β-D-glucosaminide, which had been isolated from the corresponding α, β-mixture[8] by the fractional crystallization of its acetate.

First of all, A-I was condensed with an equimolar amount of *N*-Z-amino acids (a: *N*-Z-glycine, b: *N*, *N'*-di-Z-L-lysine) in pyridine by dicyclohexylcarbodiimide (DCC) to give benzyl *N*-acetyl-3-*O*-(*N*-Z-aminoacyl)-4, 6-*O*-benzylidene-α-D-glucosaminides (A-II) in 72—84% yields. In the case of B-I, which is much less soluble than A-I in pyridine, such a condensation procedure as A-I gave the corresponding product in a low yield, accompanied by the ureide. In order to avoid the formation of the ureide,[9] a large quantity of *N*-Z-amino-acids (a, b, c; β-benzyl-*N*-Z-L-aspartate) were preliminary converted to the corresponding acid anhydrides by DCC in dioxane. After the dioxane had been removed, a solution of B-I in pyridine was added to the concentrated residue without isolating the acid anhydrides, and the mixed solution was allowed to stand at room temperature

*1 Part XI: *J. Chem. Soc. Japan, Pure Chem. Sect.* (*Nippon Kagaku Zasshi*), **85**, 511 (1964).

1) J. Yoshimura and H. Hashimoto, *J. Chem. Soc. Japan, Pure Chem. Sect.* (*Nippon Kagaku Zasshi*), **85**, 239 (1964).

2) I. Yamashina and M. Makino, *J. Biol. Chem.*, **51**, 359 (1962); V. Bogdanov, E. Kaverzneva and A. Andereyeva, *Biochim. Biopys. Acta*, **65**, 168 (1962); T. H. Jr. Plummer and C. H. W. Hirs, *J. Biol. Chem.*, **239**, 2530 (1964); K. Izumi, M. Makino and I. Yamashina, *J. Biochem.*, **51**, 365 (1962).

3) G. R. Greenberg, *J. Biol. Chem.*, **190**, 611 (1951).

4) A. Gottschalk and W. H. Murphy, *Biochem. Biophys. Acta*, **46**, 81 (1961).

5) N. K. Kochetkov, V. A. Derevitskaya, L. M. Likhosherstov, N. V. Molodtsov and S. G. Kara-Murza, *Tetrahedron*, **18**, 273 (1962).

*2 The benzyloxycarbonyl group is abbreviated as Z.

*3 The prefixes A and B are used for the α- and β-anomers respectively.

6) N. Muramatsu, *J. Chem. Soc. Japan, Pure Chem. Sect.* (*Nippon Kagaku Zasshi*), **84**, 861 (1963).

7) R. Kuhn and H. H. Baer, *Ann.*, **611**, 236 (1958).

8) J. Yoshimura, M. Funabashi, S. Ishige and T. Sato, *J. Chem. Soc. Japan, Pure Chem. Sect.* (*Nippon Kagaku Zasshi*), **85**, 142 (1964).

9) I. Muramatsu, ibid., **82**, 83 (1961).

for 24 hours. In this way benzyl *N*-acetyl-3-*O*-(*N*-Z-aminoacyl)-4, 6-*O*-benzylidene-β-D-glucosaminides (B-II) were obtained in 60—70% yields. The infrared spectra of A-II and B-II showed no absorption band of hydroxyl (at ca. 3500 cm^{-1}), but it did show absorption bands of ester carbonyl (at 1730—1750 cm^{-1}) and urethane carbonyl (at 1690—1710 cm^{-1}).

The next step, involving the hydrolysis of the benzylidene group of A-II and B-II with 70% acetic acid, gave benzyl *N*-acetyl-3-*O*-(*N*-Z-aminoacyl)-α- and -β-D-glucosaminides (A-III and B-III) in 60—75% yields.

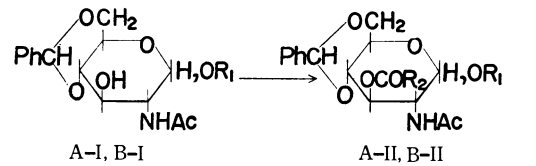

A-I, B-I A-II, B-II

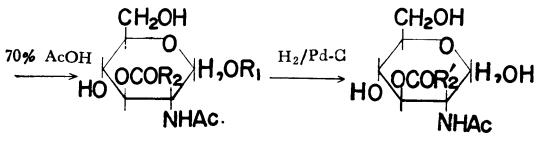

A-III, B-III IV

R_1 = $-CH_2C_6H_5$
Ph = $-C_6H_5$
Ac = $-COCH_3$
Z = $-COOCH_2C_6H_5$

a) $R_2 = -CH_2NHZ$
b) $R_2 = -CH(CH_2)_4NHZ$ (NHZ)
c) $R_2 = -CHCH_2COOCH_2C_6H_5$ (NHZ)

a) $R'_2 = -CH_2NH_2 \cdot 1/2(COOH)_2 \cdot 2H_2O$
b) $R'_2 = -CH(CH_2)_4NH_2 \cdot (COOH)_2 3H_2O$ (NH_2)
c) $R'_2 = -CHCH_2COOH \cdot 2H_2O$ (NH_2)

The hydrogenolysis of benzyl and benzyloxycarbonyl groups in A-III and B-III with palladium-charcoal (10%) gave 3-*O*-aminoacyl derivatives (IV) in ca. a 30% yield in the case of B-III, but the α-glycoside benzyl group of A-III could not be eliminated. This fact may be explained in terms of the steric hindrance of the C-2 *cis* acetamide group in the α-configuration, as was found in the case of phenyl 2, 3, 4, 6-tetra-*O*-acetyl-α- and -β-D-glucoside.[10]

The constants of the series of new compounds up to A, B-III and IV are shown in Tables I and II respectively.

The Synthesis of *N*-Acetyl-4-*O*-aminoacyl-D-glucosamines.—As a starting material to prepare 4-*O*-aminoacyl derivatives, benzyl *N*-acetyl-3-*O*-benzyl-6-*O*-trityl-α- and -β-D-glucosaminide (A-VII and B-VII) were synthesized in the following way.

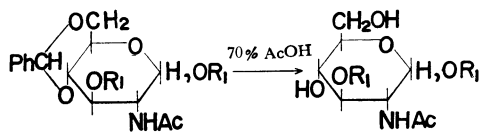

A-V, B-V A-VI, B-VI

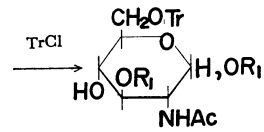

A-VII, B-VII

$Tr = -C(C_6H_5)_3$

Benzyl *N*-acetyl-3-*O*-benzyl-4, 6-*O*-benzylidene-α- and -β-D-glucosaminide (A-IV and B-IV) were obtained in 74—80% yields by reacting A-I or B-I with benzylchloride in dimethylformamide in the presence of potassium hydroxide respectively. When the benzylation of B-I was effected in dimethylsulfoxide with sodium hydride, the tribenzylated product (probably the *N*-benzylated derivative) was isolated as a by-product.

For the removal of the benzylidene group, A-V and B-V were then hydrolyzed in 70% acetic acid by refluxing them for an hour; this gave benzyl *N*-acetyl-3-*O*-benzyl-α- and -β-D-glucosaminide (A-VI and B-VI) in 72—85% yields. Finally, A-VII and B-VII were obtained by the triphenylmethylation of A-VI and B-VI in the usual method.

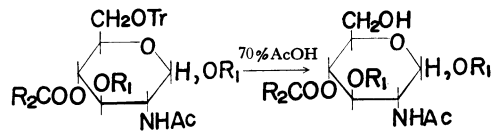

A-VIII, B-VIII A-IX, B-IX

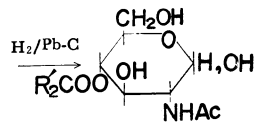

X

a) $R_2 = -CH_2NHZ$
b) $R_2 = -CH(CH_2)_4NHZ$ (NHZ)

a) $R'_2 = -CH_2NH_2 \cdot 1/2(COOH)_2 \cdot 2H_2O$
b) $R'_2 = -CH(CH_2)_4NH_2 \cdot (COOH)_2 \cdot 3H_2O$ (NH_2)

The condensation of A-VII and B-VI with an equimolar amount of *N*-Z-amino acids (a and b) was carried out in a small amount of pyridine using DCC to give benzyl *N*-acetyl-3-*O*-benzyl-4-*O*-(*N*-Z-aminoacyl)-6-*O*-trityl-α- and -β-D-glucosaminides (A-VIII and B-VIII).

The partial hydrolysis of A-VIII and B-VIII with 70% acetic acid at 100°C gave benzyl *N*-

10) C. E. Ballou, S. Roseman and K. P. Link, *J. Am. Chem. Soc.*, **73**, 1140 (1951).

TABLE I. BENZYL *N*-ACETYL-3-*O*-(*N*-Z-AMINOACYL)-D-GLUCOSAMINIDE DERIVATIVES

Compound	Molecular formula (Mol. wt.)	M.p., °C	$[\alpha]_{578}^{15}$	(*c*, solvent)	Found (Calcd.) C, %	H, %	N, %
A-IIa	$C_{32}H_{34}O_9N_2$ (590)	203—204	+77	(0.51, P*)	64.90 (65.07)	5.93 (5.80)	4.90 (4.74)
B-IIa	$C_{32}H_{34}O_9N_2$ (590)	250(decomp.)	−81	(0.50, P)	64.80 (65.07)	5.75 (5.80)	4.84 (4.74)
A-IIb	$C_{44}H_{49}O_{11}N_3$ (795)	195	+33	(0.51, P)	66.22 (66.40)	6.52 (6.21)	5.44 (5.28)
B-IIb	$C_{44}H_{49}O_{11}N_3$ (795)	208—210	−78	(0.50, P)	66.36 (66.40)	6.07 (6.21)	5.54 (5.28)
B-IIc	$C_{41}H_{42}O_{11}N_2$ (738)	185—186	−88	(0.50, P)	66.42 (66.65)	5.96 (5.73)	3.73 (3.80)
A-IIIa	$C_{25}H_{30}O_9N_2$ (502)	81—83	+79	(5.54, M**)	59.60 (59.75)	6.08 (6.02)	5.71 (5.58)
B-IIIa	$C_{25}H_{30}O_9N_2$ (502)	151—152	−30	(0.20, M)	58.95 (59.75)	6.28 (6.02)	5.48 (5.58)
A-IIIb	$C_{37}H_{45}O_{11}N_3$ (707)	151	+71	(0.51, M)	62.49 (62.76)	6.61 (6.40)	6.11 (5.93)
B-IIIb	$C_{37}H_{45}O_{11}N_3$ (707)	145	−23	(0.20, M)	62.29 (62.76)	6.46 (6.40)	6.17 (5.93)
B-IIIc	$C_{34}H_{38}O_{11}N_2$ (650)	158—159	−59	(0.22, M)	62.93 (62.74)	6.13 (5.89)	4.36 (4.30)

P*=Pyridine, M**=Methanol

TABLE II. *N*-ACETYL-3- AND 4-*O*-AMINOACYL-D-GLUCOSAMINES

Compound	Molecular formula	R_f	Found (Calcd.) C, %	H, %	N, %
IVa	$C_{10}H_{18}O_7N_2 \cdot 1/2(COOH)_2 \cdot 2H_2O$	0.19	37.77 (36.80)	6.42 (6.40)	7.40 (7.80)
IVb	$C_{14}H_{27}O_7N_3 \cdot (COOH)_2 \cdot 3H_2O$	0.10	38.64 (38.94)	6.79 (7.15)	8.37 (8.52)
IVc	$C_{12}H_{20}O_9N_2 \cdot 2H_2O$	0.15	39.32 (38.71)	6.35 (6.49)	7.22 (7.53)
Xa	$C_{10}H_{18}O_7N_2 \cdot 1/2(COOH)_2 \cdot H_2O$	0.16	37.31 (36.80)	5.92 (6.40)	7.88 (7.80)
Xb	$C_{14}H_{27}O_7N_3 \cdot (COOH)_2 \cdot 3H_2O$	0.12	39.95 (38.94)	7.35 (7.15)	8.24 (8.52)

TABLE III. BENZYL *N*-ACETYL-3-*O*-BENZYL-4-*O*-(*N*-Z-AMINOACYL)-D-GLUCOSAMINIDE DERIVATIVES

Compound	Molecular formula (Mol. wt.)	M.p., °C	$[\alpha]_{578}^{15}$	(*c*, methanol)	Found (Calcd.) C, %	H, %	N, %
A-VIIIa	$C_{51}H_{50}O_9N_2$ (834)	84—86	+77	0.54	73.48 (73.36)	6.06 (6.04)	3.61 (3.36)
B-VIIIa	$C_{51}H_{50}O_9N_2$ (834)	123—125	−6.5	0.47	73.68 (73.36)	6.24 (6.04)	3.50 (3.36)
A-VIIIb	$C_{63}H_{65}O_{11}N_3$ (1039)	82—84	+49	0.51	72.69 (72.74)	6.30 (6.30)	4.33 (4.04)
B-VIIIb	$C_{63}H_{65}O_{11}N_3$ (1039)	syrup	−6.9	0.44	72.54 (72.74)	6.60 (6.30)	4.22 (4.04)
A-IXa	$C_{32}H_{36}O_9N_2$ (592)	151—153	+107	0.50	64.70 (64.65)	6.07 (6.12)	4.97 (4.73)
B-IXa	$C_{32}H_{36}O_9N_2$ (592)	186—188	−15	0.20	64.54 (64.65)	6.03 (6.12)	4.90 (4.73)
A-IXb	$C_{44}H_{51}O_{11}N_3$ (797)	152	+49	0.51	66.11 (66.23)	6.58 (6.44)	5.33 (5.27)
B-IXb	$C_{44}H_{51}O_{11}N_3$ (797)	140	−16	0.40	66.22 (66.23)	6.66 (6.44)	5.48 (5.27)

acetyl-3-*O*-benzyl-4-*O*-(*N*-Z-aminoacyl)-α- and -β-D-glucosaminides (A-IX and B-IX) in 70—80% yields.

The glycosidic α-benzyl group of A-IX could not be removed by catalytic hydrogenolysis in the presence of oxalic acid, as has been shown in the case of A-III.

The protecting groups of B-VIII could be successfully eliminated, and 4-*O*-aminoacyl derivatives (X) could be isolated as oxalates.

The constants of the *N*-Z-aminoacyl compound of this series and X are shown in Tables III and II respectively.

Experimental

Melting points were uncorrected. Optical rotations were measured at 578 mμ with a Carl-Zeis Polarimeter. Paper chromatography was carried out by the ascending technique on Toyo Roshi No. 50 filter paper, using an upper layer of *n*-buthanol, acetic acid and water (4 : 1 : 5) as a developer, and a 0.1% ninhydrin solution in *n*-butanol as a spray reagent.

The Preparation of Benzyl *N*-Acetyl-β-D-glucosaminide.—Benzyl *N*-acetyl-α, β-D-glucosaminide (50 g.; ca. an equimolar mixture), prepared by the convenient glycosidation method[7] of *N*-acetyl-D-glucosamine, was dissolved in dry pyridine (100 ml.) and acetic anhydride (70 ml.), and then allowed to stand overnight at room temperature. The reaction mixture was then poured into a large amount of ice water. The precipitated crystal was filtered, washed several times with water, and dried in vacuo. The fractional crystallization of the crude product (70 g.) was repeated several times from methanol to give benzyl *N*-acetyl-3, 4, 6-tri-*O*-acetyl-β-D-glucosaminide (20 g.), m. p. 163—164°C (Lit.,[11] m. p. 165—167°C). The corresponding α-

11) R. Kuhn and W. Kirschenlohr, *Ber.*, **86**, 1331 (1953).

anomer (30 g.) was obtained from the mother liquor, m. p. 108°C, $[\alpha]_D^{20}$ +120° (*c* 1.0, methanol).

Found: C, 57.87; H, 6.21; N, 3.32. Calcd. for $C_{21}H_{27}O_9N$(437): C, 57.66; H, 6.22; N, 3.22%.

A more effective separation of the α, β-anomer is attained by a previous separation of the mixture by the decantation of the ether suspension, in which the β-anomer is much lighter than the α-anomer.

The β-acetate was then deacetylated with CH_3ONa to give benzyl *N*-acetyl-β-D-glucosaminide in a 85% yield. M. p. 203—204°C (Lit.,[11] m. p. 205—206°C).

Benzyl *N*-Acetyl-4, 6-*O*-benzyliden-β-D-glucosaminide (B-I).—A mixture of benzyl *N*-acetyl-β-D-glucosaminide (25 g.), freshly fused and powdered $ZnCl_2$ (25 g.), and benzaldehyde (90 ml.) was shaken at 60°C for an hour. The homogeneous reaction mixture was then agitated with petroleum ether.

The resulting crystalline mass was filtered, and washed several times with petroleum ether, with water, and then with a mixture of methanol and petroleum ether.

The dried crude product (36 g.) was recrystallized from methanol (800 ml.) and pyridine (200 ml.); yield, 26 g. m. p. 251—252°C (decomp.).

A small part was recrystallized twice from methanol. M. p. 260—261°C (decomp.) $[\alpha]_{578}^{20}$ −40° (*c* 0.50, pyridine).

Found: C, 65.87; H, 6.48; N, 3.56. Calcd. for $C_{22}H_{25}O_6N$: C, 66.15; H, 6.31; N, 3.51%.

This compound was converted to the corresponding 3-*O*-acetate by the usual acetylation method. M. p. 258—259°C (decomp.), $[\alpha]_{578}^{20}$ −56° (*c* 0.30, pyridine).

Found: C, 65.24; H, 5.98; N, 3.41. Calcd. for $C_{24}H_{27}O_7N$ (441): C, 65.29; H, 6.16; N, 3.17%.

Benzyl *N*-Acetyl-3-*O*-(*N*-benzyloxycarbonyl-aminoacyl)-4, 6-*O*-benzylidene-α-D-glucosaminides (A-II).—0.015 mol. of *N*-Z-amino acids (a; *N*-Z-glycine, b; *N*, *N'*-di-Z-L-lysine) and DCC (0.018 mol.) were added to a solution of benzyl *N*-acetyl-4, 6-*O*-benzylidene-α-D-glucosaminide (0.012 mol.) in pyridine (50 ml.), and the mixture was allowed to stand in a refrigerator overnight. The precipitate of dicyclohexylurea was filtered off, and the filtrate was concentrated under reduced pressure. The gelatinous residue was washed several times with ether and then dried in vacuo.

The crude product was recrystallized from ethanol and a small amount of pyridine; yield, 72—79%.

Benzyl *N*-Acetyl-3-*O*-(*N*-benzyloxycarbonyl-aminoacyl)-4, 6-*O*-benzylidene-β-D-glucosaminides (B-II).—0.03 mol. of *N*-Z-amino acids (a, b, c; β-benzyl *N*-Z-L-aspartate) and DCC (0.036 mol.) were dissolved in dry dioxane (40 ml.) and stirred at room temperature for 2 hr. The precipitate was filtered and washed twice with dry dioxane. The combined dioxane was evaporated in vacuo, a cold pyridine solution (160 ml.) of B-I was then added to the resulting residue, and the mixture was kept at room temperature overnight.

After the pyridine had been completely removed, the gelatinous residue was washed several times with ether or ethyl acetate. The semi-crystalline product was recrystallized from ethanol and pyridine (1 : 1); yield, 60—75%.

Benzyl *N*-Acetyl-3-*O*-(*N*-benzyloxycarbonyl-aminoacyl)-α- and -β-D-glucosaminides (A-III and B-III).—A-II or B-II (0.005 mol.) was suspended in 70% acetic acid (100 ml.) and heated on a boiling-water bath for 30 min. with occasional stirring. After the solution had been concentrated in vacuo, the gelatinous residue was then washed once with ether and recrystallized from ethanol, or from ethanol and ether; yield, 68—78%.

The Hydrogenolysis of Benzyl *N*-Acetyl-3-*O*-(*N*-benzyloxycarbonyl-glycyl)-α-D-glucosaminide (A-IIIa).—Three grams of A-IIIa and 0.45 g. of oxalic acid were dissolved in 50 ml. of methanol, and then 2 g. of Pd-C (5%) was added. The mixture was shaken at room temperature with hydrogen for about 5 hr. After the catalyst had been removed, the filtrate was concentrated in vacuo, and ethanol was added. The precipitate was filtered, washed with ethanol and dried in vacuo. The white amorphous powder (1.2 g.), which had a molecular formula consistent with $C_{17}H_{24}O_7N_2 \cdot 1/2(COOH)_2 \cdot 2H_2O$, did not reduce Fehling's solution.

Found: C, 48.24; H, 6.29; N, 5.63. Calcd.: C, 48.12; H, 6.50; N, 6.23%.

***N*-Acetyl-3-*O*-aminoacyl-D-glucosamines (IV).**—0.002 mol. of B-III and oxalic acid (0.003—0.004 mol.) were dissolved in 80% methanol (15—20 ml.), and 10% Pd-C (1.0—1.5 g.) was added. The mixture was then shaken at room temperature with hydrogen until the absorption had substantially ceased (20—48 hr.).

After the catalyst had been removed, ether was added to the filtrate and centrifugation was carried out to collect the precipitate. For the purification, the precipitated oil or solid was dissolved in several drops of water, reprecipitated with ethanol, centrifugated, and dried in vacuo. The amorphous hygroscopic powder, which reduced Fehling's solution and which gave a single ninhydrin positive spot in paper chromatography and paper electrophoresis, was obtained in ca. a 30% yield.

Benzyl *N*-Acetyl-3-*O*-benzyl-4, 6-*O*-benzylidene-α- and -β-D-glucosaminide (A-V and B-V).—(a) Into a mixture of 5 g. of A-I or B-I in dimethylformamide (100—150 ml.) and potassium hydroxide (3.5 g.), benzyl chloride (7.8 g.) was added drop-by-drop over a 15—20 min. period with vigorous stirring at 70—75°C. The reaction conditions were then maintained for a further 30 min. In the case of the compound A-I, the reaction solution was then poured into a large amount of ice water. The precipitate was filtered, washed several times with water and methanol, and dried in vacuo. The crude product (5.1 g.) was recrystallized from hot pyridine-water (100 ml.+50 ml.). Yield, 5 g. (80%).

In the case of B-I, the reaction solution was allowed to stand at room temperature. The crystalline product was filtered, washed several times with methanol and recrystallized from pyridine (70 ml.) and DMF (20 ml.); yield, 4.5 g. (74%).

A-V: m. p. 264—265°C (decomp.), $[\alpha]_{578}^{13}$ +85° (*c* 0.50, pyridine).

Found: C, 70.79; H, 6.79; N, 3.11%.

B-V: m. p. 266—267°C (decomp.), $[\alpha]_{578}^{17}$ −75° (*c* 0.20, dimethylformamide).

Found: C, 71.62; H, 6.31; N, 2.97. Calcd. for $C_{29}H_{31}O_6N$ (399): C, 71.74; H, 6.38; N, 2.86%.

(b) Compound B-I (10 g.) was dissolved in dimethylsulfoxide (150 ml.) at 60°C and NaH (2.5 g.) was gradually added. Into this opaque solution, benzylchloride (16 g.) was added drop-by-drop over a 10 min. period with stirring and with keeping the

temperature at 70—80°C. The reaction solution was then poured into a large amount of ice water, and the precipitate was filtered, washed several times with water, and then with methanol.

The crude product was recrystallized from pyridine (20 ml.) and DMF (40 ml.); yield, 7.0 g. (57%).

From methanol washings, a tribenzylated product (1 g.) which showed no infrared absorption band (1550 cm^{-1}) of the secondary amido, was obtained. M. p. 116—118°C, $[\alpha]_{578}^{15}$ −29° (*c* 0.56, pyridine).

Found: C, 74.81; H, 6.21; N, 2.51. Calcd. for $C_{36}H_{37}O_6N$ (579): C, 74.59; H, 6.43; N, 2.42%.

Benzyl *N*-Acetyl-3-*O*-benzyl-α- and -β-D-glucosaminide (A-VI and B-VI).—A-V or B-V (14 g.) was suspended in 400—500 ml. of 70% acetic acid and refluxed for an hour. The reaction solution was then concentrated under reduced pressure to a crystalline residue. The product was washed with ether and recrystallized from ethanol; yield, 72—85%.

A-VI: m. p. 178—179°C, $[\alpha]_{578}^{13}$ +165° (*c* 0.51, methanol).

Found: C, 65.69; H, 7.06; N, 3.71%.

B-VI: m. p. 169—170°C, $[\alpha]_{578}^{15}$ −20° (*c* 0.50, ethanol).

Found: C, 65.39; H, 6.81; N, 3.46. Calcd. for $C_{22}H_{27}O_6N$: C, 65.82; H, 6.78; N, 3.49%.

Benzyl *N*-Acetyl-3-*O*-benzyl-6-*O*-trityl-α- and -β-D-glucosaminide (A-VII and B-VII).—A-VI or B-VI (4 g.) and tritylchloride (3.3 g.) were dissolved in pyridine (30 ml.) and heated on a boiling-water bath for 2 hr. The reaction solution was then poured into ice water, and the gummy precipitate was extracted with methylene chloride, washed with water, and dried over sodium sulfate.

After the methylene chloride had been removed, the resulting syrup was crystallized from ethanol-petroleum ether. Yield, 70—72%.

A-VII: m. p. 169°C, $[\alpha]_{578}^{13}$ +85° (*c* 0.50, methanol).

Found: C, 76.38; H, 6.52; N, 2.39%.

B-VII: m. p. 143—145°C, $[\alpha]_{578}^{18}$ −19° (*c* 0.27, methanol).

Found: C, 76.16; H, 6.53; N, 2.14. Calcd. for $C_{41}H_{41}O_6N$ (643): C, 76.49; H, 6.42; N, 2.18%.

Benzyl *N*-Acetyl-3-*O*-benzyl-4-*O*-(*N*-benzyloxycarbonyl-aminoacyl)-6-*O*-trityl-α- and -β-D-glucosaminides. (A-VIII and B-VIII).—A-VII or B-VII (0.003 mol.), *N*-Z-amino acids (a or b, 0.003 mol.) and DCC (0.0036 mol.) were dissolved in dry pyridine (10 ml.) and then allowed to stand overnight in a refrigerator. The precipitate was filtered and washed with toluene. The filtrate and washings were concentrated in vacuo to a syrup. The product was dissolved in a small amount of ethanol, and treated with active carbon, and an equal amount of ether was added. Finally petroleum ether was added until a turbidity had appeared. Yield, 70—73%.

Benzyl *N*-Acetyl-3-*O*-benzyl-4-*O*-(*N*-benzyloxycarbonyl-aminoacyl)-α- and -β-D-glucosaminides (A-IX and B-IX).—A-VIII or B-VIII (0.005 mol.) was suspended in 70% acetic acid (30—50 ml.) and heated on a boiling-water bath while being stirred until it had dissolved completely. The reaction solution was then cooled with ice water to precipitate triphenyl carbinol, this was filtered off, and the filtate was concentrated in vacuo. The gelatinous residue was recrystallized from ethanol or ethanol and ether. Yield, 70—80%.

***N*-Acetyl-4-*O*-aminoacyl-D-glucosamines (X).**—B-IX (0.0012 mol.) and oxalic acid (0.0018—0.0036 mol.) were dissolved in 80% methanol (20 ml.), and 10% Pd-C (1.0—1.5 g.) was added. The reaction mixture was then shaken at room temperature with hydrogen until absorption had substantially ceased (20—24 hr.). After the catalyst had then been removed, a large amount of ether was added to the filtrate and centrifugation was carried out to collect the precipitate. The supernatant was removed, and the precipitate was dissolved in several drops of water, reprecipitated with ethanol, and centrifugated. The ethanol was decanted, and the resulting residue was dried in vacuo. The amorphous hygroscopic powder, which reduced Fehling's solution and which gave single ninhydrin-positive spot in paper chromatography and paper electrophoresis, was obtained. Yield, 39% (Xa), 51% (Xb).

The authors wish to thank the members of Laboratory of Organic Analysis for their elemental analyses.

BULLETIN OF THE CHEMICAL SOCIETY OF JAPAN VOL. 39 1765—1767 (1966)

The Reaction of 2-Cyclohexylimino-3-cyclohexyl-4, 5-diphenyl-4-oxazoline

By Takanobu KUMAMOTO, Takenori NAGAOKA and Teruaki MUKAIYAMA

Laboratory of Organic Chemistry, Tokyo Institute of Technology, Ookayama, Meguro-ku, Tokyo

(Received December 9, 1965)

The reaction of 2-cyclohexylimino-3-cyclohexyl-4, 5-diphenyl-4-oxazoline with isocyanate or isothiocyanate was studied. When the oxazoline was treated with isocyanate, an exchange reaction took place, thus forming new 2-imino-oxazoline and cyclohexyl isocyanate. Similarly, the reaction of the oxazoline with carbon disulfide resulted in the formation of 3-cyclohexyl-4, 5-diphenyl-4-oxazoline-2-thione and cyclohexyl isothiocyanate. Further, cyclohexyl isothiocyanate was obtained by the reaction of dicyclohexylcarbodiimide or cyclohexyl isocyanate with carbon disulfide.

It has recently been found[1] that 2-cyclohexylimino-3-cyclohexyl-4, 5-diphenyl-4-oxazoline was obtained in a good yield, along with triethyl phosphate, when a toluene solution of benzil, triethyl phosphite and dicyclohexylcarbodiimide was refluxed in the presence of copper powder. Further, it has been shown that the oxazoline gave the stable salts with protonic acids:

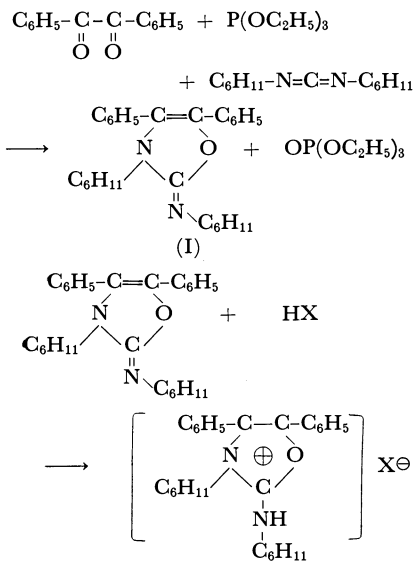

In the present study, it was found that the reactions of the oxazoline with isocyanate, isothiocyanate and carbon disulfide resulted in the formation of new oxazolines and oxazoline-2-thione. When a mixture of 2-cyclohexylimino-3-cyclohexyl-4, 5-diphenyl-4-oxazoline and phenyl isocyanate was stirred in petroleum ether at room temperature for 3 hr., 2-phenylimino-3-cyclohexyl-4, 5-diphenyl-4-oxazoline and cyclohexyl isocyanate were obtained in 72% and 69% yields respectively. These results show that the *exo*-imino group of the oxazoline is replaced by the phenylimino group of phenyl isocyanate:

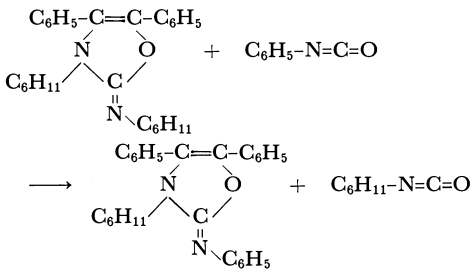

The same exchange reaction was expected to occur in the case of ethyl isocyanate, which is considered to have a more enhanced reactivity than the cyclohexyl isocyanate produced. Indeed, when oxazoline (I) and ethyl isocyanate were heated at 120°C for 4 hr. in a sealed tube, 2-ethylimino-3-cyclohexyl-4, 5-diphenyl-4-oxazoline was obtained in a 24% yield:

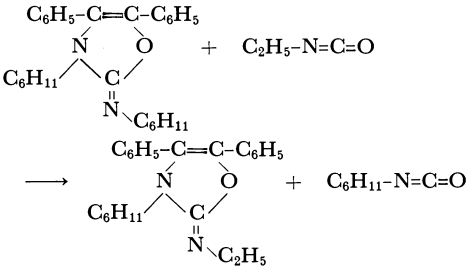

Further, when a solution of oxazoline (I) and phenyl isothiocyanate was stirred in petroleum ether at room temperature for 4 hr., 2-phenylimino-3-cyclohexyl-4, 5-diphenyl-4-oxazoline (80% yield) and cyclohexyl isothiocyanate (92% yield) were obtained:

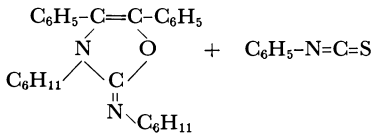

1) T. Mukaiyama, T. Kumamoto and T. Nagaoka, Part XVIII: Annual Meeting of The Chemical Society of Japan, Preliminary Issue (1965), p. 248.

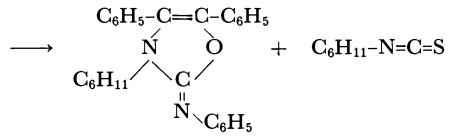

The above-mentioned exchange reactions are considered to proceed through the initial formation of an unstable four-membered intermediate (II) which is formed by the electrophilic attack of isocyanate or isothiocyanate on the *exo*-imino group of the oxazoline (I). By the transfer of electrons, II in turn changes into new 2-imino-oxazoline and cyclohexyl isocyanate or isothiocyanate:

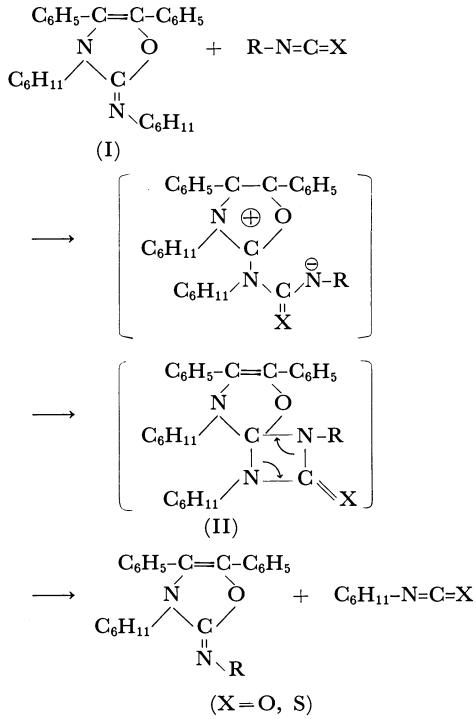

(I)

(II)

(X=O, S)

Concerning this type of exchange reaction, Bartoszewski and Jerzmanowska have already reported that[2] thiazoline-2-thione is produced by the reaction of 2-imino-thiazoline, the sulfur isomer of the oxazoline, with carbon disulfide:

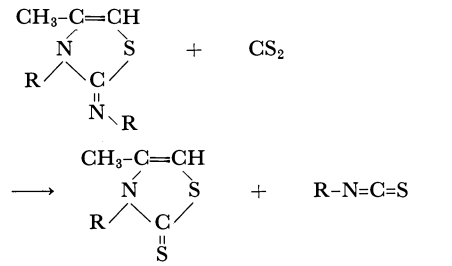

It was also established by the present experiment that the treatment of the oxazoline (I) with excess carbon disulfide at 150°C resulted in the formation of 3-cyclohexyl-4, 5-diphenyl-4-oxazoline-2-thione (90% yield) and cyclohexyl isothiocyanate (83% yield):

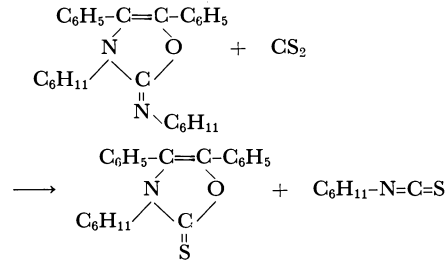

However, when 2-phenylimino-3-cyclohexyl-4, 5-diphenyl-4-oxazoline and carbon disulfide were heated under the same conditions, the expected products, 3-cyclohexyl-4, 5-diphenyl-4-oxazoline-2-thione and phenyl isothiocyanate, could not be obtained, only the starting materials were recovered.

Next, the reaction of dicyclohexylcarbodiimide and carbon disulfide was attempted in expectation that cyclohexyl isothiocyanate would be formed in a way similar to that described in the above exchange reaction. When they were heated at 150°C for 10 hr., cyclohexyl isothiocyanate was obtained in a 25% yield, and 55% of the dicyclohexylcarbodiimide was recovered:

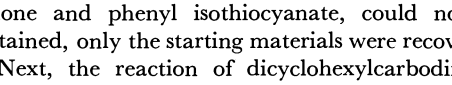

Further, it was established that cyclohexyl isothiocyanate was obtained in a 41% yield when a mixture of cyclohexyl isocyanate and carbon disulfide was heated under the same conditions in the presence of triethylamine:

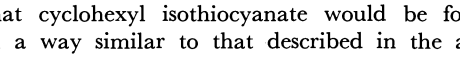

Experimental

The Reaction of 2-Cyclohexylimino-3-cyclohexyl-4, 5-diphenyl-4-oxazoline with Phenyl Isocyanate.—A solution of 2-cyclohexylimino-3-cyclohexyl-4, 5-diphenyl-4-oxazoline (2.00 g., 0.005 mol.) and phenyl isocyanate (0.60 g., 0.005 mol.) in petroleum ether was stirred for 3 hr. at room temperature. After the petroleum ether, had been removed, a white precipitate was obtained. It was recrystallized from ethyl acetate to give 2-phenylimino-3-cyclohexyl-4, 5-diphenyl-4-oxazoline, 1.98 g. (72%); m. p. 182—183°C.

Found: C, 81.82; H, 6.65; N, 7.34. Calcd. for $C_{27}H_{26}N_2O$: C, 82.20; H, 6.64; N, 7.10%.

The residue was distilled in vacuo, giving cyclohexyl isocyanate, 0.42 g. (63%); b. p. 62—67°C/20 mmHg.

The Reaction of 2-Cyclohexylimino-3-cyclohexyl-4, 5-diphenyl-4-oxazoline with Ethyl Isocyantate.—A mixture of 2-cyclohexylimino-3-cyclohexyl-4, 5-diphenyl-4-oxazoline (1.00 g., 0.0025 mol.) and an excess of ethyl isocyanate (0.71 g., 0.01 mol.) was heated at

2) J. Bartoszewski and Z. Jerzmanowska, *Roczniki. Chem.*, **37**, 11 (1963); *Chem. Abstr.*, **59**, 7510 (1963).

120°C for 4 hr. in a sealed tube. The removal of the excess ethyl isocyanate gave a white precipitate. It was then recrystallized from ethyl acetate, giving 2-ethylimino-3-cyclohexyl- 4, 5 - diphenyl - 4 - oxazoline, 0.21 g. (24%); m. p. 112—114°C.

Found: C, 79.42; H, 7.82; N, 8.30. Calcd. for $C_{23}H_{26}N_2O$: C, 79.73; H, 7.56; N, 8.09%.

The Reaction of 2-Cyclohexylimino-3-cyclohexyl-4, 5-diphenyl-4-oxazoline with Phenyl Isothiocyanate.—A solution of 2-cyclohexylimino-3-cyclohexyl-4, 5-diphenyl-4-oxazoline (2.00 g., 0.005 mol.) and phenyl isothiocyanate (0.68 g., 0.005 mol.) in petroleum ether was stirred at room temperature for 4 hr. After the solvent had been removed, a white crystalline solid was obtained. This was then filtered and recrystallized from ethyl acetate, giving 2-phenylimino-3-cyclohexyl-4, 5-diphenyl-4-oxazoline, 1.58 g. (80%); m. p. 183—184°C.

The fractional distillation of the residue gave cyclohexyl isothiocyanate, 0.51 g. (72%); b. p. 102—103°C/10 mmHg.

The Reaction of 2-Cyclohexylimino-3-cyclohexyl-4, 5-diphenyl-4-oxazoline with Carbon Disulfide.—A mixture of 2-cyclohexylimino-3-cyclohexyl-4, 5-diphenyl-4-oxazoline (4.00 g., 0.01 mol.) and an excess of carbon disufide (4 ml.) was heated at 150°C for 5 hr. in a sealed tube. The removal of the excess carbon disulfide gave a white precipitate. This was then recrystallized from ethanol, giving 3-cyclohexyl-4, 5-diphenyl-4-oxazoline-2-thione, 3.03 g. (90%); m. p. 201°C.

Found: C, 75.17; H, 5.96; N, 4.09. Calcd. for $C_{21}H_{22}NOS$: C, 75.00; H, 6.53; N, 4.19%.

The distillation of the residue under reduced pressure gave cyclohexyl isothiocyanate, 1.17 g. (83%); b. p. 101—104°C/10 mmHg.

The Reaction of Dicyclohexylcarbodiimide and Carbon Disulfide.—A mixture of dicyclohexylcarbodiimide (2.06 g., 0.01 mol.) and carbon disulfide (5 ml.) was heated at 150°C for 10 hr. in a sealed tube. After the excess carbon disulfide had been removed, cyclohexyl isothiocyanate, 0.75 g. (27%); b. p. 100—105°C/10 mmHg, was obtained, and 1.14 g. of dicyclohexylcarbodiimide (55%), b. p. 149—151°C/10 mmHg, was reccovered.

When dicyclohexylcarbodiimide (2.06 g., 0.01 mol.) and carbon disulfide (5 ml.) were heated in the presence of triethylamine (0.1 ml.) in a sealed tube at 150°C for 5 hr., cyclohexyl isothiocyanate, 0.36 g. (13%); b. p. 108—110°C/12 mmHg was obtained, and dicyclohexylcarbodiimide, 1.24 g. (60%); b. p. 152—154°C/12 mmHg, was recovered.

When a catalytic amount of boron trifluoride etherate was used in the above experiment, cyclohexyl isothiocyanate 0.20 g. (7%); b. p. 115—117°C/13 mmHg, was obtained, and 1.35 g. of dicyclohexylcarbodiimide (66%), b. p. 152—155°C/12 mmHg, was recovered.

The Reaction of Cyclohexyl Isocyanate with Carbon Disulfide in the Presence of Triethylamine.—A mixture of cyclohexyl isocyanate (2.50 g., 0.01 mol.), carbon disulfide (2 ml.) and triethylamine (2 ml.) was heated at 150°C for 5 hr. in a sealed tube. Distillation in vacuo gave cyclohexyl isothiocyanate, 1.17 g. (42%); b. p. 95—97°C/10 mmHg.

BULLETIN OF THE CHEMICAL SOCIETY OF JAPAN VOL. 39 1767—1773 (1966)

Rearrangement. IV.[1] Pyrolysis and Acetolysis of Some Sulfonic Esters

By Ryotaro KOTANI

Research Laboratory, Kureha Spinning Company, Ltd., Takatsuki, Osaka

(Received December 14, 1965)

The pyrolysis of cyclohexanemethyl methanesulfonate and 1-methylcyclohexanemethyl *p*-toluenesulfonate has been investigated, yielding predominantly rearranged cycloalkenes, with lesser amounts of cycloalkanes. The experiments support the suggestion that the pyrolysis may proceed, at least in part, through a free radical process. The methanesulfonic ester, on acetolysis in a 50% aqueous acetic acid solution, gave rearranged-unrearranged cycloalkenes and alcohols, and an unrearranged acetate, whereas the *p*-toluenesulfonic ester gave exclusively rearranged cycloalkenes, alcohols and acetates.

The availability of a *cis*-β-hydrogen in cyclohexanemethyl derivatives of acids or amines suggests that the pyrolysis of these compounds could involve a cis elimination,[2] giving predominantly methylenecyclohexane. Indeed, the pyrolysis of cyclohexanemethyl acetate[3] and *N*, *N*-dimethylcyclohexanemethylamine oxide[3,4] gave exclusively methylenecyclohexane; in contrast, however, cyclohexanemethyl borate[5] underwent pyrolytic change, chiefly into rearranged cycloalkenes, the formation of which was interpreted in terms of a carbonium ion-type rearrangement. Previous work in this

1) Part III: R. Kotani, *J. Chem. Eng. Data*, **11**, 248 (1966).

2) G. H. DePuy and R. W. King, *Chem. Revs.*, **60**, 431 (1960).

3) H. E. Baumgarten, F. A. Bower and T. T. Okamoto, *J. Am. Chem. Soc.*, **79**, 3145 (1957).

4) A. C. Cope, C. L. Bumgardner and E. E. Schweizer, ibid., **79**, 4729 (1957).

5) O. L. Chapman and G. W. Borden, *J. Org. Chem.*, **26**, 4193 (1961).

series[6] has shown that the pyrolysis of cyclohexanemethyl *p*-toluenesulfonate (I) at 200°C under reduced pressure gave predominantly rearranged cycloalkenes. The saturated hydrocarbon methylcyclohexane was also formed in a fairly high yield, whereas it was not mentioned as a pyrolytic product of the above acetate, amine oxide or borate. The nature of the pyrolysis of the sulfonate, however, remained to be determined, and such is the purpose of the present study.

Cyclohexanemethyl methanesulfonate (II) was pyrolyzed in the manner described earlier for I. No solvent was used. The crude product was analyzed by gas chromatography. Each component was separated by preparative-scale gas chromatography and identified by comparing its relative retention time and NMR spectrum with those of an authentic sample. The products were methylcyclohexane, 1-methylcyclohexene, 3-methylcyclohexene, methylenecyclohexane, cycloheptene, and cyclohexene. Except for the absence of toluene[7] the product composition was essentially the same as that obtained from I.

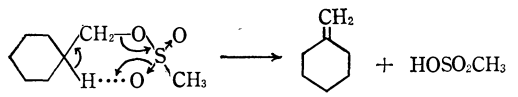

IV

It would not be unreasonable to expect that II might decompose predominantly, with the elimination of a *cis*-β-hydrogen through a quasi, six-membered ring (IV) as a transition state,[8] to give methylenecyclohexane, as has been observed in the runs with the acetate and amine oxide. That it does not do so is, however, evident from a consideration of the following facts: (1) the relative yield of methylenecyclohexane was only 1.1%; (2) rearranged cycloalkenes predominated (82.0%), and (3) a control experiment showed that the isomerization of exocyclic to endocyclic double bonds scarcely occurred under the experimental conditions employed.

1-Methylcyclohexanemethyl *p*-toluenesulfonate (III) was selected for study because it has no β-hydrogen for any possible participation in a cis elimination mechanism. Since III is a neoalkyl type of ester, it was expected that its pyrolysis would involve a complicated rearrangement of the carbon skeleton. Indeed, this was found. The product was separated into six fractions by preparative-scale gas chromatography; each fraction was characterized as has been described above under II. The products were methylcyclohexane, ethylcyclohexane, methylcycloheptane, 1-ethylcyclohexene, ethylidenecyclohexane, 1-methylcycloheptene, methylenecycloheptane, 1-methylcyclohexene, 3-methylcyclohexene, and an unidentified saturated compound (1.7%).[9]

The dehydration of cyclohexanemethanol and 1-methylcyclohexanemethanol was carried out at 150°C in the presence of oxalic acid to obtain an indication of the product ratios in a simple carbonium ion reaction. The dehydration of cyclohexanemethanol[10] gave 1-methylcyclohexene, 3-

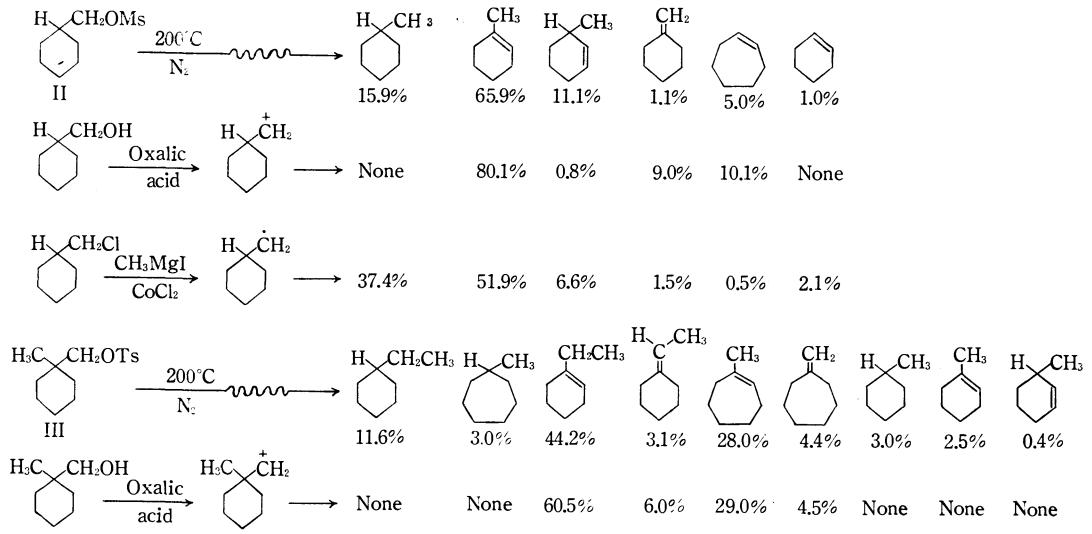

6) R. Kotani and S. Satoh, ibid., **30**, 3245 (1965).

7) The nonformation of toluene with II, but its formation with III, support the previous conclusion[6] that it arose from the *p*-toluenesulfonate group.

8) C. D. Hurd and F. H. Blunk [*J. Am. Chem. Soc.*, **60**, 2419 (1938)] first proposed a cyclic, concerted mechanism for stereospecific cis elimination.

9) A small amount of toluene was also formed. It obviously arose from the *p*-toluenesulfonate group, as has been discussed elsewhere.[6]

10) Chapman and Borden[5] reported that the dehydration of cyclohexanemethanol at 135°C in the presence of oxalic acid gave 1-methylcyclohexene (82.2%), methylenecyclohexane (10.2%), and cycloheptene (7.6%).

methylcyclohexene, methylenecyclohexane and cycloheptene, while that of 1-methylcyclohexanemethanol gave 1-ethylcyclohexene, ethylidenecyclohexane, 1-methylcycloheptene and methylenecycloheptane. No saturated hydrocarbon was formed from either alcohol; its nonformation was in contrast to its formation in the pyrolysis of the sulfonic esters.

A carbonium ion mechanism would account readily for the formation of cycloalkenes; it may, indeed, account for many of these products. It is questionable, however, if a carbonium ion intermediate participates in the formation of the observed cycloalkanes (16—20% yields), since this would require the unreasonable assumption of the abstraction of hydride ions from some other part of the reacting system.[6] The latter conclusion is supported experimentally by the absence of acetylenes or dienes in the products and by the nonformation of the cycloalkanes during the dehydration of the alcohols with oxalic acid.

The cycloalkanes could be explained readily by way of a radical mechanism; this idea was next explored. Some pyrolytic elimination reactions suggestive of or proceeding through a radical-chain process have been reported,[8,11] namely, the pyrolysis of carboxylic esters with no β-hydrogen and certain sorts of xanthates and sulfoxides.

The reaction of cyclohexanemethyl chloride with methylmagnesium iodide in the presence of cobalt(II) chloride was carried out in order to obtain an indication of the product ratios in a simple free radical process.[12] This reaction gave methylcyclohexane, 1-methylcyclohexene, 3-methylcyclohexene, methylenecyclohexane, cycloheptene, and cyclohexene. This composition was virtually the same as those obtained from I and II.

In an attempt to learn if free radicals participated in the present reactions, I, II and III were heated in the presence of a free radical inhibitor, and then in that of a free radical initiator. The addition of *p*-benzoquinone to I or II caused a change in the ratio of cycloalkane to cycloalkene (approximately 1 : 6.8 and 1 : 8.5 compared to 1 : 3.7 and 1 : 5.3, respectively), and also a decrease in the yield of the product (it was reduced by approximately 30% in both instances). The addition of *p*-benzoquinone to III exerted no appreciable influence on the product composition, but caused a decrease in its yield (approximately a 40% decrease). The decrease in yield and the change in product composition suggest that the free radicals formed would partially be trapped by the quinone. I, II or III, when heated with benzoyl peroxide at 100—105°C for a few minutes, yielded small amounts of cycloalkenes and cycloalkanes, whereas heating the sulfonic ester alone under the same conditions gave no product. No free radical chain reaction, however, was initiated by the addition of benzoyl peroxide.

III was selected for electron spin resonance (ESR) study because the nonavailability of a β-hydrogen would make its ESR spectrum simple. III was irradiated with ultraviolet rays for 1 hour at room temperature, and then it was cooled by liquid nitrogen. The ESR spectrum of its primary product showed a triplet with a relative intensity ratio of about 1 : 2 : 1. The spectrum suggests a free radical whose unpaired electron interacts equally with two protons; it was identified as the free radical V. The supperposed spectrum appearing in the central peak of V may be due to the free radical VI. When the irradiated III was taken out of the liquid nitrogen and kept at room temperature for a few minutes, the triplet spectrum changed into a poorly-resolved complex spectrum consisting of 15 hyperfine lines. The ESR spectrum of the free radical VII may consist of 7 hyperfine lines, and that of the free radical VIII, of 8 hyperfine lines. The observed change in the ESR

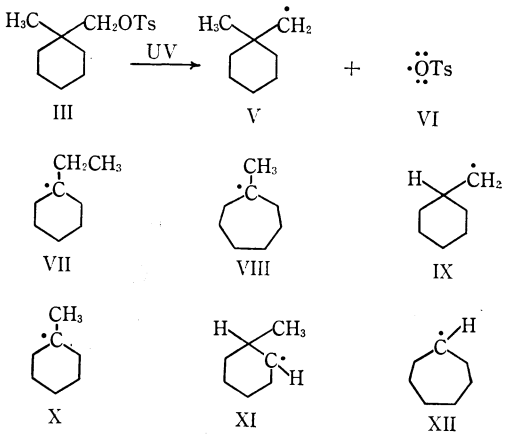

spectrum suggests the rearrangement of the less stable primary free radical, V, to the more stable tertiary free radicals, VII and VIII. The above ESR study also suggests indirectly, if not directly, the fate of the primary product of the pyrolysis of III.

The experimental data described above support the suggestion that the pyrolysis of I, II and III proceeds, at least in part, through a free radical process. I and II, on pyrolysis, would give a presumably less stable primary free radical (IX), which would predominantly rearrange to a presumably more stable tertiary free radical (X) by a 1, 2-hydrogen shift. Part of IX would give

11) a) E. M. Bilger and H. Hibbert, *J. Am. Chem. Soc.*, **58**, 823 (1936); b) C. A. Kingsbury and D. J. Cram, ibid., **82**, 1810 (1960); c) H. R. Nace, D. G. Manly and S. Fuso, *J. Org. Chem.*, **23**, 687 (1958); d) D. G. Botteron and G. P. Shulman, ibid., **27**, 2007 (1962).

12) M. S. Kharasch and W. H. Urry [*J. Org. Chem.*, **13**, 101 (1948)] investigated the reaction of alkylmagnesium halides with alkyl halides in the presence of cobalt(II) chloride.

methylenecyclohexane by the loss of a hydrogen. X would lose a hydrogen, thus yielding 1-methylcyclohexene and methylenecyclohexane, the former predominating. Part of X would subsequently rearrange to a presumably less stable secondary free radical (XI) through a 1, 2-hydrogen shift, which by the loss of hydrogen would yield 1-methylcyclohexene and 3-methylcyclohexene. The abstraction of hydrogen by IX, X or XI would give the saturated hydrocarbon methylcyclohexane. Another secondary free radical (XII) would also come from IX, but by ring enlargement rather than by hydrogen shift, and it would lead to cycloheptene. The primary product of III on pyrolysis would be the presumably less stable primary free radical V, which would subsequently rearrange to the presumably more stable tertiary free radicals, VII and VIII; this would be followed by the loss of hydrogen atoms, leading to the formation of the corresponding unsaturated hydrocarbons. The abstraction of hydrogen atoms by VII and VIII would yield the corresponding saturated hydrocarbons.

The acetolysis of II, III and 1-methylcyclohexanemethyl methanesulfonate (XIII) was carried out in a 50% aqueous acetic acid solution containing catalytic amounts of sodium acetate at reflux temperatures. From II there was formed 1-methylcyclohexene (27.3%), 3-methylcyclohexene (0.5%), methylenecyclohexane (0.5%), cycloheptene (1.5%), 1-methylcyclohexanol (15%), cyclohexanemethanol (7.0%), cycloheptanol (3.6 %), cyclohexanemethyl acetate (44.2%), and 1-methylcyclohexyl acetate (a trace). Bly and Dryden[13] have reported that II, when acetolyzed in the presence of acetic anhydride and an excess of sodium acetate, gave exclusively the unrearranged cyclohexanemethyl acetate, free from any cycloalkenes, alcohols or rearranged acetates. In contrast to this, the addition of water to the solvolysis system of II caused the formation of rearranged-unrearranged cycloalkenes and alcohols in about 30 and 26% yields. The formation of alcohols may be expected from the fact that water is much more nucleophilic than acetic acid.[14] The rearranged alcohols may be formed through rearrangement of the unstable primary carbonium ion initially formed to the more stable tertiary or secondary carbonium ions. The formation of the rearranged alcohols from the corresponding cycloalkenes and water in the presence of an acid may not be negligible.[15] The predominance of 1-methylcyclohexene among the cycloalkenes formed may be due to the relative stabilities of carbonium ions involved and to the acid-catalyzed exocyclic-endocyclic olefin isomerization. The experimental conditions used are quite favorable to such an isomerization.[15] No explanation is, however, apparent to account for cycloalkene formation in the presence of water, but its failure to be formed in the absence of water. It seems unlikely that the unrearranged acetate (44%) arose predominantly from the cyclohexanemethyl carbonium ion, because the unstable primary carbonium ions would mainly rearrange to the more stable tertiary or secondary carbonium ions, as evidenced by the formation of the rearranged alcohols (rearranged: unrearranged=2.7 : 1). The absence of rearranged acetate is in keeping with this suggestion. In view of these facts, the most probable conclusion is that two processes are competitively operative in the acetolysis of II under the conditions employed: (1) the S_N1 reaction, followed by rearrangement and elimination, and (2) the S_N2 displacement of the methanesulfonate group by solvents.

The products from III and XIII had essentially the same product composition; the products were 1-ethylcyclohexene (42.2 and 44.6%), ethylidenecyclohexane (1.3 and 0.6%), 1-methylcycloheptene (38.9 and 40.1%), methylenecycloheptane (1.3 and 1.4%), 1-ethylcyclohexanol (8.5 and 6.7%), 1-methylcycloheptanol (7.8 and 6.6%), and trace amounts of acetates of the above alcohols. Unrearranged alcohol or its acetate was not found in the products within the limits of detectability by gas chromatography under the conditions used. The addition of acetic anhydride and an excess of sodium acetate to III and XIII eliminated the formation of alcohols and acetates, but it gave exclusively rearranged cycloalkenes; the products were 1-ethylcyclohexene (52.5 and 50.0%), ethylidenecyclohexane (1.0 and 1.5%), 1-methylcycloheptene (45.5 and 47.5%), and methylenecycloheptane (1.0 and 1.0%).[16] The exclusive formation of the rearranged compounds in the acetolysis of III and XIII, neoalkyl-type esters, was in accord with that observed in the Demjanov rearrangement of 1-methylcyclohexanemethylamine, a neoalkyl-type amine.[17] The lack of unrearranged product may be explained in a manner similar to that presented in connection with the above amine.

Experimental[18]

Gas Chromatographic Analysis of Products.— The analysis was carried out using 500×0.35 cm. (A, B and D) and 1100×0.35 cm. (C) columns packed with 80—100 mesh Celite which was coated with the appropriate stationary phase. The stationary phases

13) R. S. Bly, Jr., and H. L. Dryden, Jr., *Chem. Ind. (London)*, **1959**, 1287.
14) C. G. Swain, R. B. Mosely and D. E. Bown, *J. Am. Chem. Soc.*, **77**, 373 (1955).
15) A. C. Cope, D. Ambros, E. Ciganek, C. F. Howell and Z. Jacura, ibid., **82**, 1750 (1960).
16) Bly and Dryden[13] have reported that XIII, when acetolyzed under the same conditions, gave ethylcyclohexane and methylcycloheptane (after the hydrogenation of the product cycloalkenes).
17) R. Kotani, *J. Org. Chem.*, **30**, 350 (1965).

employed were: (A) 30% (by weight) of a 40% solution of silver nitrate in tetraethylene glycol, (B) 25% (by weight) of octyl phthalate, (C) 30% (by weight) of polyethylene glycol, and (D) 30% (by weight) of Apiezon grease L. Columns A, B and C were used to analyze hydrocarbons at 60, 100 and 110°C respectively. Alcohols and acetates were analyzed using a column, D, at 150°C. The helium outlet flow rates were 45 (A), 55(B), 60(C), and 60(D) cc./min. The relative retention time is the ratio of the retention time of a substance to the retention time of benzene as measured from an air peak. Quantitative analysis was done as follows; the relative thermal conductivity cell response per mole of the authentic samples of the compounds under discussion was determined using benzene as an internal standard, following the procedure of Messner et al.[19] The mole ratio of the compounds in the product was determined from the above relative response and from the apparent peak area, which was obtained by half-width and peak-height measurements. The relative response of the unidentified compound obtained from the pyrolysis of III (1.7%) was arbitrarily assigned the value of 145 (100 for benzene, 145 for ethylcyclohexane, and so on).

NMR Analysis of Products.—The analysis was run at 25°C for cycloalkenes and at 70°C for alcohols in carbon tetrachloride (5—10%) on a Varian Associates Model V-4311 high resolution spectrometer operating at 60 Mc., using tetramethylsilane (τ 10.00) as an internal standard, unless otherwise noted. The resonance line shapes and chemical shifts (τ-value) used for the structural assignments[20] were as follows: cyclohexene (a triplet, 4.43 J=1.5 c. p. s., olefinic protons), 1-methylcyclohexene (an incompletely resolved multiplet,[21] 4.71, an olefinic proton; an incompletely resolved doublet, 8.40, methyl protons), 3-methylcyclohexene (a complex multiplet, three main lines, 4.44, 4.47 and 4.53, olefinic protons; an asymmetrical doublet, 9.00 and 9.11, J=6.6 c. p. s., methyl protons), methylenecyclohexane (a quintet, 5.47, terminal methylene protons), cycloheptene (a triplet, 4.30, J=3.7 c. p. s., olefinic protons), 1-ethylcyclohexene (an incompletely resolved multiplet, 4.65, an olefinic proton; a triplet, 9.03, methyl protons), ethylidenecyclohexane (two lines,[22] 4.90 and 4.99, an olefinic proton), 1-methylcycloheptene (a triplet, 4.51, an olefinic proton; an incompletely resolved doublet, 8.35, methyl protons), methylenecycloheptane (a quintet, 5.37, terminal methylene protons), methylcyclohexane (an asymmetrical doublet,[23] 9.07 and 9.14, J=4.2 c. p. s., methyl protons), cyclohexanemethanol (a doublet, 6.66, methylene protons of the $-CH_2OH$), 1-methylcyclohexanol (a singlet, 8.85, methyl protons), cycloheptanol (a broad absorption, 6.25, a methine proton), 1-ethylcyclohexanol[24] (a triplet, 9.14, methyl protons), and 1-methylcycloheptanol[24] (a singlet, 8.83, methyl protons).

ESR Analysis.—The ESR spectra were measured with a Varian x-band EPR spectrometer, Model V-4566, using field modulation at 100 kc./sec.

1-Methylcyclohexanemethyl *p*-toluenesulfonate was irradiated under nitrogen with ultraviolet rays for 1 hr. at room temperature, using a Toshiba SHLS-100 2B ultraviolet lamp set at the distance of 5 cm. from the sample. During the irradiation, the sample was dipped in liquid nitrogen to prevent heating, and then subjected to ESR spectroscopy.

Pyrolysis of Sulfonic Esters.—The pyrolysis was conducted in a 100-ml. flask equipped with a side arm for introduction of nitrogen. The flask was connected to a 40-cm. distilling column, which was connected in turn to a trap immersed in a dry ice-methanol bath, and then to a water pump. The flask was then charged with the sulfonic ester (0.03 mol. each), evacuated to 40 mmHg, and immersed in an oil bath. The bath was heated rapidly to 200—205°C. After a few minutes, the sulfonic ester began to decompose; this decomposition continued for 30—45 sec. The product in the trap was then taken up with ether, washed with a dilute sodium hydroxide solution and water, and dried over anhydrous magnesium sulfate, and the ether was removed, leaving a hydrocarbon mixture weighing between 1.92—2.19 (I), 1.71—1.98 (II), and 2.11—2.42 g. (III). Considerable amounts of tar-like substances remained in the reaction flask, but no attempt was made to identify them.

I, II and III (0.03 mol. each) were similarly pyrolyzed at 80 mmHg in the presence of *p*-benzoquinone (0.01 mol.), giving 1.15—1.40, 1.20—1.38, and 1.30—1.45 g. of hydrocarbons, respectively. I and II gave cyclohexene (2.1% and a trace), 1-methylcyclohexene (66.1 and 74.3%), 3-methylcyclohexene (9.7 and 9.3%), methylenecyclohexane (1.2 and 1.2%), cycloheptene (4.1 and 4.8%), methylcyclohexane (12.3 and 10.5%), and toluene (4.7% and none).

A mixture of I (0.03 mol.) and benzoyl peroxide (0.01 mol.) was rapidly heated to 100—105°C at 40 mmHg under nitrogen. II and III were treated in this way also. After 2 min. benzoyl peroxide began to decompose; this decomposition continued for several minutes. The heating was then discontinued. The products collected in the trap immersed in a dry ice-methanol bath weighed 0.38—0.42, 0.35—0.40, and 0.57—0.62 g., respectively. The residues consisted mainly of the unreacted sulfonic ester. I and II gave cyclohexene (a trace), 1-methylcyclohexene (5.5 and 5.3%), 3-methylcyclohexene (a trace), methylenecyclohexane (0.3 and 0.3%), methylcyclohexane (1.3

18) All melting points and boiling points are uncorrected.

19) A. E. Messner, D. M. Rosie and P. A. Argabright, *Anal. Chem.*, **31**, 230 (1959).

20) Signals due to the ring methylene protons are not described.

21) The signal determined at 40 Mc. was reported to be a triplet by G. V. D. Tiers, "Table of Characteristic NMR Shielding Values."

22) Since a sufficient quantity of ethylidenecyclohexane could not be isolated, its NMR spectrum was determined using a mixture of ethylidenecyclohexane and 1-ethylcyclohexene. The olefinic proton of the former would be expected to show a quartet by spin-spin coupling with methyl protons with the relative intensities of 1 : 3 : 3 : 1, but only two lines were detected. The proton showed a sharp single line (τ 4.95) when the spin-decoupling technique was applied.

23) The signal determined at 40 Mc. was reported to be a singlet.[21]

24) The NMR spectra of 1-ethylcyclohexanol and 1-methylcycloheptanol were determined at 120°C without a solvent and using cyclohexane (τ 8.56) as an internal standard.

and 1.1%), and benzene (92.7 and 93.3%), respectively. III gave 1-methylcyclohexene (a trace), 1-ethylcyclohexene (3.2%), 1-methylcycloheptene (2.5%), ethylcyclohexane (0.9%), and benzene (93.4%).

Evidence for the saturated compounds was obtained as follows: (1) the whole reaction product was treated with bromine in ether at 0°C, and then gas chromatographed; (2) the whole reaction product was analyzed on a 30 cm. column of 30% concentrated sulfuric acid on 40—60 mesh silica gel, which was connected to the end of the above octyl phthalate column; (3) by a comparison of the relative retention times with those of authentic samples (using an authentic sample alone and in admixture), and (4), in the case of the isolated methylcyclohexane or ethylcyclohexane, the NMR spectrum of each compound was exactly identical with that of an authentic sample, showing the absence of any resonance line due to olefinic protons.

Oxalic Acid-Catalyzed Dehydration of Cyclohexanemethanol and 1-Methylcyclohexanemethanol.—The dehydration was conducted following the procedure of Chapman and Borden.[5] A mixture of cyclohexanemethanol (0.05 mol.) or 1-methylcyclohexanemethanol (0.05 mol.) and oxalic acid (0.4 mol.) was heated to 150°C. The olefinic product was dried over anhydrous magnesium sulfate, and then analyzed by gas chromatography.

Cobalt(II) Chloride-Catalyzed Reaction of Cyclohexanemethyl Chloride.—In a 500-ml. three-necked flask fitted with a mechanical stirrer, a dropping funnel and a reflux condenser, there were placed magnesium (0.1 mol.) and 30 ml. of dry ether. Methyl iodide (0.1 mol.) in 20 ml. of dry ether was then added dropwise into the flask with stirring. Cyclohexanemethyl chloride (0.1 mol.) in 50 ml. of dry ether was then added. Cobalt(II) chloride (0.05 mol.) was added in portions into the reaction mixture with stirring. After the exothermic reaction had ceased, 20 ml. of water was added, and the ether layer was separated and dried over anhydrous magnesium sulfate. Distillation gave 3.5 g. of a hydrocarbon mixture. The mixture was analyzed by gas chromatography and NMR spectroscopy.

Acetolysis of Sulfonic Esters.—In a 500-ml. flask equipped with a reflux condenser, the top of which was connected to a trap immersed in a dry ice-methanol bath, there were placed the sulfonic ester (0.05 mol. each), sodium acetate (0.05 mol.), glacial acetic acid (1 mol.), and water (1 mol.). The flask was heated for 48 hr. in an oil bath under gentle reflux, and then cooled to 0—5°C. The contents were neutralized with a dilute sodium hydroxide solution and extracted with ether. The trap and condenser were rinsed with ether. The combined extracts were dried over anhydrous magnesium sulfate, and then fractionally distilled into 2 fractions. II gave 0.93 g. of a low-boiling fraction (b. p. 90—113°C) and 3.2 g. of a high-boiling fraction (b. p. 55°C at 20 mmHg to 85°C at 15 mmHg), while III gave 3.2 g. (b. p. 110—139°C) and 0.6 g. (b. p. 70—80°C at 20 mmHg) portions, and XIII, 3.6 g. (b. p. 110—139°C) and 0.6 g. (70—80°C at 20 mmHg) portions, respectively. No attempt was made to identify the residue.

III and XIII (0.05 mol. each) were similarly solvolyzed in glacial acetic acid (1 mol.) containing acetic anhydride (0.035 mol.) and sodium acetate (0.1 mol.); they gave 3.4 and 3.1 g. of cycloalkenes, respectively.

Preparation of Sulfonic Esters.—Cyclohexanemethyl *p*-toluenesulfonate, m. p. 32—33°C (lit.[25] m. p. 32—33°C), cyclohexanemethyl methanesulfonate, m. p. 43—44°C, 1-methylcyclohexanemethyl *p*-toluenesulfonate, m. p. 37—38°C (lit.[25] m. p. 37—38°C), and 1-methylcyclohexanemethyl methanesulfonate,[26] were prepared from the corresponding alcohols and methanesulfonyl or *p*-toluenesulfonyl chlorides in pyridine at room temperature. The crude products were then recrystallized twice from hexane, in 65—70% yields.

Preparation of Alcohols.—1-Methylcyclohexanol, b. p. 68°C at 20 mmHg (lit.[27] b. p. 72°C at 22 mmHg), 1-ethylcyclohexanol, b. p. 76.5°C at 20 mmHg (lit.[28] b. p. 77°C at 20 mmHg), and 1-methylcycloheptanol, b. p. 83—85°C at 20 mmHg (lit.[27] b. p. 82—85°C at 20 mmHg) were prepared following the directions of Mosher.[29] Cyclohexanemethanol, b. p. 91—92°C at 18 mmHg (lit.[30] b. p. 88—93°C at 18 mmHg), cycloheptanol, b. p. 184—185°C (lit.[31] b. p. 184—187°C), and 1-methylcyclohexanemethanol, b. p. 88°C at 17 mmHg (lit.[32] b. p. 85°C at 14 mmHg), were prepared by the methods of Gilman and Catlin, Matthews and Becker, and Koch and Haaf respectively.

Preparation of Acetates. — Cyclohexanemethyl acetate, b. p. 83—85°C at 15.5 mmHg (lit.[33] b. p. 199—201°C) at 740 mmHg, 1-methylcyclohexyl acetate b. p. 177°C (lit.[34] b. p. 178—179°C), 1-ethylcyclohexyl acetate, b. p. 190—192°C, and cycloheptyl acetate, b. p. 199°C (lit.[35] b. p. 199—200.5°C) were prepared from the corresponding alcohols and an excess of acetic anhydride in the presence of anhydrous sodium acetate.

Preparation of Cycloalkenes.— 1-Methylcyclohexanol, 1-ethylcyclohexanol, and 1-methylcycloheptanol were dehydrated following the method of Traynelis et al.,[36] thus yielding mixtures of 1-methylcyclohexene and methylenecyclohexane, (94 : 6), 1-ethylcyclohexene and ethylidenecyclohexane (95 : 5), and 1-methylcyclohexene and methylenecycloheptane (90 : 10) respectively. 1-Methylcyclohexene, b. p. 110°C (lit.[37] b. p. 110.2°C), methylenecyclohexane, b. p. 102°C (lit.[37] b. p. 102.5°C), 1-ethylcyclohexene,

---

25) C. F. Wilcox, Jr., and S. S. Chibber, *J. Org. Chem.*, **27**, 2332 (1962).
26) The methanesulfonate was solvolyzed without purification.
27) M. Barbier and M. F. Hügel, *Bull. Soc. Chim. France*, **1961**, 951.
28) H. B. Williams and W. R. Edwards, Jr., *J. Am. Chem. Soc.*, **69**, 336 (1947).
29) W. A. Mosher, ibid., **62**, 552 (1940).
30) H. Gilman and W. E. Catlin, "Organic Syntheses," Coll. Vol. I, 188 (1961).
31) D. N. Matthews and E. I. Becker, *J. Org. Chem.*, **21**, 1317 (1956).
32) H. Koch and W. Haaf, *Ann.*, **618**, 251 (1958).
33) A. Fawarsky and I. Borgmann, *Ber.*, **40**, 4865 (1907).
34) J. G. Traynham and O. S. Pascual, *J. Org. Chem.*, **21**, 1362 (1956).
35) N. A. Nelson, J. H. Fassnacht and J. U. Piper, *J. Am. Chem. Soc.*, **83**, 206 (1961).
36) V. J. Traynelis, W. L. Hergenrother, H. T. Hanson and J. A. Valicenti, *J. Org. Chem.*, **29**, 123 (1964).
37) R. B. Turner and R. H. Garner, *J. Am. Chem. Soc.*, **79**, 253 (1957).

b. p. 136°C (lit.[37] 136.2°C), 1-methylcycloheptene. b. p. 137°C (lit.[37] b. p. 136°C), and methylenecycloheptane, b. p. 136°C (lit.[37] b. p. 135°C), were isolated in the pure form by preparative-scale gas chromatography, and their structures were confirmed by their NMR spectra. Cycloheptanol and a mixture of *cis*- and *trans*-3-methylcyclohexanols were dehydrated by the method of Mosher,[29] thus yielding cycloheptene, b. p. 115°C (lit.[38] b. p. 115°C), and an olefinic mixture, respectively. Gas chromatographic analysis showed the olefinic mixture to consist of four components. The component corresponding to 3-methylcyclohexene was isolated by gas chromatography; its b. p. was 103°C (lit.[39] b. p. 104°C), and its structure was proved by NMR spectroscopy.

38) R. Willstätter, *Ann.*, **317**, 221 (1901).
39) N. D. Zelinsky, *Ber.*, **57**, 2055 (1924).

The author wishes to express his deep gratitude to Professor Charles D. Hurd of Northwestern University for his helpful suggestions and advice, to Dr. Takashi Kobayashi for his valuable discussions, and to Dr. Shiro Satoh for his NMR and ESR studies. The author is also indebted to Mr. Morio Yokawa for his ESR analysis and to Mr. Tadashi Ikegami for his assistance in the experimental work.

BULLETIN OF THE CHEMICAL SOCIETY OF JAPAN VOL. 39 1773—1775 (1966)

The X-Ray Structure Determination of Dihydroteleocidin B Monobromoacetate

By Hirokichi HARADA,* Noriyoshi SAKABE and Yoshimasa HIRATA

Chemical Institute, Faculty of Science, Nagoya University, Chigusa-ku, Nagoya

and Yujirō TOMIIE and Isamu NITTA

Faculty of Science, Kwansei Gakuin University, Nishinomiya

(Received December 15, 1965)

The structure of dihydroteleocidin B monobromoacetate, the derivative of a toxic substance teleocidin B produced by some streptomyces, has been determined by X-ray analysis. Crystals of the derivative, $C_{30}H_{44}O_3N_3Br$, are orthorhombic ($a=14.50$, $b=26.60$, $c=7.93$Å, $z=4$, the space group is $P2_12_12_1$). The intensities of 2053 reflections were measured using Cu$K\alpha$ radiation. The bromine position was determined by Patterson methods, and all the carbon, oxygen and nitrogen atoms were elucidated by three-dimensional minimum function methods. A three-dimensional Fourier synthesis and the least squares methods completed the refinement, giving a final R value of 16.4%. The derivative has a substituted indole nucleus with a nine-membered lactum ring.

Teleocidin B is one of the principal toxic elements isolated from the mycelia of some streptomyces.[1]

Recently, a structure containing a nine-membered lactum ring with a substituted indole nucleus has been suggested for dihydroteleocidin B,[2] which was derived from teleocidin B by catalytic hydrogenation.

In the course of that chemical investigation it, appeared desirable to confirm this rather unusual skeleton and the complete structure of this substance by X-ray crystallographic studies.

Dihydroteleocidin B monobromoacetate was selected for the X-ray crystal analysis. Three-dimensional Patterson and Fourier methods were employed for the determination of the crystal structure. Our results established the whole structure

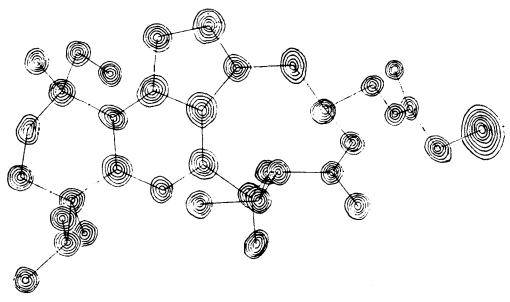

Fig. 1. The final three-dimensional electron density distribution viewed along the c axis.

* Present address: Research Laboratory, Fujisawa Pharmaceutical Co., Ltd., Higashi Yodogawa-ku, Osaka.

1) M. Takashima and H. Sakai, *Bull. Agr. Chem. Soc. Japan*, **24**, 647 (1960).

2) H. Harada, H. Nakata and Y. Hirata, *J. Chem. Soc. Japan, Pure Chem. Sect. (Nippon Kagaku Zasshi)*, **87**, 86 (1966).

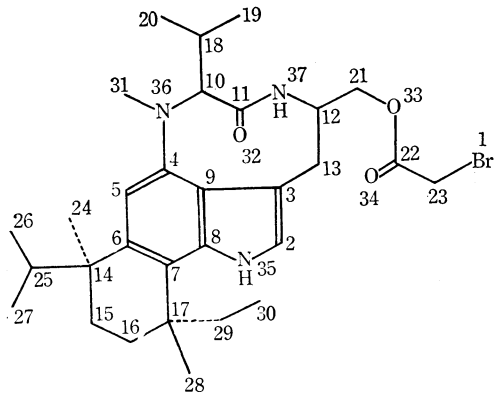

Fig. 2. The complete chemical formula of dihydroteleocidin B monobromoacetate.

TABLE I. ATOMIC CO-ORDINATES AND TEMPERATURE FACTORS

Atom	x/a	y/b	z/c	B
Br (1)	0.2987	0.0799	0.8767	5.354
C (2)	0.2285	0.4615	0.2991	3.760
C (3)	0.3216	0.4517	0.3396	3.561
C (4)	0.4040	0.3619	0.3245	2.717
C (5)	0.3888	0.3143	0.2753	3.423
C (6)	0.3001	0.2963	0.2215	2.898
C (7)	0.2260	0.3287	0.2038	3.550
C (8)	0.2428	0.3786	0.2584	2.963
C (9)	0.3319	0.3979	0.3108	2.867
C (10)	0.4958	0.4055	0.5438	3.464
C (11)	0.5742	0.4445	0.5196	3.477
C (12)	0.4810	0.4865	0.2717	4.005
C (13)	0.3855	0.4921	0.3800	3.662
C (14)	0.2918	0.2414	0.1917	2.920
C (15)	0.1913	0.2242	0.1637	4.743
C (16)	0.1393	0.2605	0.0478	4.850
C (17)	0.1327	0.3131	0.1302	4.322
C (18)	0.5186	0.3750	0.7147	3.828
C (19)	0.5057	0.4090	0.8800	5.626
C (20)	0.4495	0.3331	0.7329	4.444
C (21)	0.4916	0.5339	0.1656	3.849
C (22)	0.4158	0.0451	0.5930	3.901
C (23)	0.3229	0.0377	0.6663	4.728
C (24)	0.3459	0.2277	0.0169	4.351
C (25)	0.3362	0.2116	0.3527	4.660
C (26)	0.2965	0.2259	0.5311	5.301
C (27)	0.3293	0.1548	0.3262	5.487
C (28)	0.0576	0.3150	0.2862	5.337
C (29)	0.0966	0.3488	0.9714	5.202
C (30)	0.1702	0.3598	0.8305	6.372
C (31)	0.5709	0.3444	0.3390	4.151
O (32)	0.6491	0.4422	0.5974	4.275
O (33)	0.5794	0.5307	0.0717	4.497
O (34)	0.4831	0.0596	0.6881	6.232
N (35)	0.1804	0.4168	0.2564	4.295
N (36)	0.4937	0.3775	0.3755	2.903
N (37)	0.5602	0.4828	0.3989	4.011

of dihydroteleocidin B monobromoacetate to be as shown in Fig. 2.

TABLE II. INTERATOMIC DISTANCES AND ANGLES

(Bonded distances)

Bond	length, Å	Bond	length, Å
1—23	1.9496	12—13	1.6065
2— 3	1.4041	12—21	1.4872
2—35	1.4054	12—37	1.4903
3— 9	1.4514	14—15	1.5430
3—13	1.4552	14—24	1.5562
4— 5	1.3354	14—25	1.5660
4— 9	1.4231	15—16	1.4938
4—36	1.4188	16—17	1.5313
5— 6	1.4277	17—28	1.5907
6— 7	1.3842	18—19	1.5355
6—14	1.4817	18—20	1.5065
7— 8	1.4037	21—33	1.4570
7—17	1.5198	22—23	1.4656
8— 9	1.4403	22—34	1.2589
8—35	1.3617	25—26	1.4890
10—11	1.5478	25—27	1.5286
10—18	1.5361	29—30	1.5265
10—36	1.4505	31—36	1.4515
11—32	1.2289	17—29	1.5977
11—37	1.3709	22—33	1.2778

(Valency angles)

Bond	angle	Bond	angle
3— 2—35	111°	21—12—37	108°
9— 3—13	134	3—13—12	112
9— 3— 2	104	15—14—24	107
13— 3— 2	121	15—14—25	110
5— 4— 9	120	15—14— 6	113
5— 4—36	120	24—14—25	108
9— 4—36	120	24—14— 6	108
6— 5— 4	123	25—14— 6	111
7— 6—14	123	16—15—14	111
7— 6— 5	121	17—16—15	113
14— 6— 5	116	28—17— 7	110
8— 7—17	121	28—17—16	112
8— 7— 6	115	7—17—16	110
17— 7— 6	124	19—18—20	107
9— 8—35	109	19—18—10	109
9— 8— 7	125	20—18—10	109
35— 8— 7	126	33—21—12	107
3— 9— 4	133	23—22—34	123
3— 9— 8	107	1—23—22	112
4— 9— 8	116	26—25—27	111
11—10—18	107	26—25—14	113
11—10—36	105	27—25—14	112
18—10—36	116	2—35— 8	108
32—11—37	118	4—36—10	114
32—11—10	124	4—36—31	119
37—11—10	118	10—36—31	117
13—12—21	106	11—37—12	125
13—12—37	111		

Experimental and Structure Determination

Dihydroteleocidin B monobromoacetate, $C_{30}H_{44}O_3N_3Br$, was obtained from dihydroteleocidin B and monobromo-acetylbromide by the usual method. The crystals melt at 214—216°C. The crystal belongs to the orthorhombic system (space group $P2_12_12_1$), with four molecules in the unit cell with dimensions of $a=14.50\pm0.03$, $b=26.60\pm0.04$ and $c=7.39\pm0.03$ Å.

The intensities of the three-dimensional reflections were measured visually from integrated Weissenberg photographs around a and c axes taken by means of filtered Cu$K\alpha$ radiation. The relative values of the observed structure factors of 2053 reflections were then converted into the absolute scale by Wilson's method.[3] The position of the bromine atom was determined by the three-dimensional Patterson function. The three-dimensional minimum function[4] was calculated in order to elucidate the positions of light atoms. It seemed reasonable to regard several peaks found in this figure as light atoms. Then the projection of the electron density distribution was calculated along the b axis. However, since the distribution in some area is so complicated, another projection was calculated along the c axis, from which the positions of thirty-five atoms were determined. The structure so obtained was refined by three-dimentional Fourier syntheses and by the least-squares methods. The final atomic co-ordinates and temperature factors are listed in Table I. The interatomic distances and valency angles in Table II were then calculated.

The final R factor is 16.18%. The F_o-F_c values are shown in Table III.* Figure 1 shows the final three-dimentional electron density distribution viewed along the c axis, and Fig. 2, the complete chemical formula of dihydroteleocidin B monobromoacetate.

The calculations were performed on a NEAC-2206 electronic computer using our own programs.

The authors wish to express their deep thanks to the Takeda Chemical Industries, Ltd., for the computer used in this investigation.

3) A. J. C. Wilson, *Nature*, **150**, 152 (1942).
4) M. J. Buerger, *Acta Cryst.*, **4**, 531 (1951).

* The complete data of the F_o-F_c table are kept as Document No. 6601 at the office of the Bulletin of the Chemical Society of Japan. A copy may be secured by citing the document number and by remitting, in advance, ¥600 for photoprints. Pay by check or money order payable to: Chemical Society of Japan.

BULLETIN OF THE CHEMICAL SOCIETY OF JAPAN VOL. 39 1775—1778 (1966)

The Synthesis of 2, 7-Dideoxy-L-*manno*-heptose*[1]

By Juji YOSHIMURA, Hachiro KOMOTO,*[2] Hiroaki ANDO and Toshio NAKAGAWA

Laboratory of Organic Chemistry, Tokyo Institute of Technology, Ookayama, Meguro-ku, Tokyo

(Received December 17, 1965)

2, 7-Dideoxy-L-*manno*-heptose was synthesized from 1-*C*-nitro-1, 7-dideoxy-L-*glycero*-L-*talo*-heptitol by the elimination of the *C*-2 hydroxyl group (nitroolefin formation), by hydrogenation and by the Nef reaction. The corresponding ethyl α-glycoside, its acetate, and a few related 1-amino-1-deoxy derivatives were also described.

A number of dideoxy sugars, almost all of them belonging to the 2, 6-, 3, 6- and 4, 6-dideoxyaldohexoses,[1] have been found in numerous heterosides and antibiotics. The specific role of the sugars in relation to physiological activities remains, however, still unrevealed; knowledge of their synthesis is also limited.

In the course of their studies of nitrosugars, the present authors have synthesised 2, 7-dideoxy-L-*manno*-heptose; they would like to describe it in this paper. In a previous paper[2] some of the present authors reported a modification of Sowden's aldose-nitromethane condensation[3], using barium hydroxide instead of sodium alcoholate as a catalyst in a small amount of water; it was pointed out that the new method generally gave results equal

*1 A part of this work was presented at the 16th Annual Meeting of the Chemical Society of Japan, Tokyo, April, 1963.

*2 Present address: c/o Jeon Co., Takaoka, Toyama.

1) J. Stanek, M. Cerny, J. Kocourek and J. Pacak, "The Monosaccharides," Academic Press, New York (1963), p. 407.

2) J. Yoshimura and H. Ando, *J. Chem. Soc. Japan, Pure Chem. Sect. (Nippon Kagaku Zasshi)*, **85**, 138 (1964).

3) J. C. Sowden, "Advances in Carbohydrate Chemistry," Vol. VI, Academic Press, New York (1951), p. 291.

or superior to those obtained by Sowden's method, even when the amount of nitromethane used was less and the reaction time was shorter.

1-*C*-Nitro-1, 7-dideoxy-L-*talo*-heptitol (I), prepared thus from L-rhamnose, was converted to the corresponding acetate (II) and then heated in dried benzene with sodium bicarbonate[3] to give L-*manno*-3,4,5,6-tetra-*O*-acetyl-1-nitro-heptene-1 (III) as a sirup; this was identified by means of elementary analysis and a study of its infrared absorption spectra (–HC=CH– at 1660-cm^{-1}, $-NO_2$ at 1540 cm^{-1}). III was once subjected to high-vacuum distillation in order to purify it, but a considerable decomposition took place, and only a small amount of a distillate (b. p. 123—132°C/0.05 mmHg; m. p. 86—88°C) was obtained. The analytical values correspond with the formula $C_{13}H_{19}O_9N$, which is consistent with the one which results when one acetyl group is removed from III. Therefore, III was used without purification in the following experiments. The catalytic hydrogenation of III with palladium-charcoal, on the absorption of an equimolar amount of hydrogen, afforded 1-*C*-nitro-3, 4, 5, 6-tetra-*O*-acetyl-1, 2, 7-trideoxy-L-*manno*-heptitol (IV), which failed to crystallize. Infrared spectrometric analysis showed the disappearance of the double bond linkage in IV. On de-*O*-acetylation with sodium methoxide in absolute methanol, IV afforded crystalline 1-*C*-nitro-1, 2, 7-trideoxy-L-*manno*-heptitol (V). On the other hand, IV was converted to the corresponding 1-acetamido-heptitol (IX). The sodium salt of V was treated with sulfuric acid (Nef reactions) in the manner described by Sowden[4] for the preparation of 2-deoxy-D-ribose, the reaction mixture was neutralized with solid barium carbonate (pH 3.6) and the filtrate was concentrated to a sirup. On repeated evaporation with ethanol, it did not afford the expected heptose but a crystalline ethyl heptoside (VII), m. p. 152—154°C; $[\alpha]_D^{20}$ −129° (*c* 1.5, water). The product did not reduce the Fehling's solution, but after having been refluxed in 2 N sulfuric acid it showed a positive reaction.

The glycosidic configuration of VII was deduced to be α from the intensively negative rotational value, while the ring-size was determined by the cuprammonium-complex method.[5] If VII takes a furanoside ring, a cuprammonium-glycol complex should be formed with the hydroxyl groups on *C*-5 and *C*-6 out of the hemiacetal ring; therefore, one could not expect a dramatic change in the optical rotation. If it takes a pyranoside ring, on the other hand, the complex formation with the hydroxyl groups on *C*-3 and *C*-4 (equatorial and

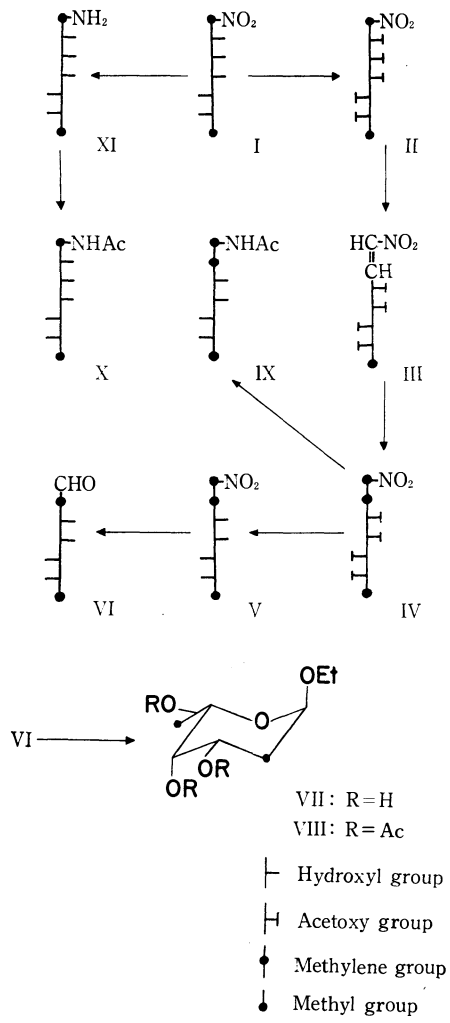

axial respectively) in the hemiacetal ring should change the rotational value strongly in the positive direction. The $\Delta[M]_{436}^{\text{Cupra A}}$ +318° and $\Delta[M]_{578}^{\text{Cupra A}}$ +345° values of VII were consistent with the latter results; consequently, VII was identified as ethyl 2, 7-dideoxy-α-L-*manno*-heptopyranoside. On acetylation, VII afforded the corresponding tri-*O*-acetate (VIII).

The direct formation of VII from V is caused by the remaining sulfuric acid; no crystalline product was obtained by a re-examination of the Nef reaction of V in which the acid was carefully neutralized with barium hydroxide. For the purposes of its hydrolysis to VI, the heptoside was dissolved in 2 N sulfuric acid and allowed to stand at room temperature. The specific rotation became more and more positive (−88° (13 min.); −83° (1 hr.); −63° (10 hr.); −50° (24 hr.)), until it reached to the equilibrated value of −40° (48 hr.). Then the solution was neutralised with 2 N barium hydroxide, filtered off, and the filtrate

4) J. C. Sowden, *J. Am. Chem. Soc.*, **71**, 1897 (1949); **72**, 808 (1950).

5) R. E. Reeves, "Advances in Carbohydrate Chemistry," Vol. VI, Academic Press, New York (1951), p. 107.

was completely deionized with a small amount of IRC-120. The removal of the solvent in vacuo left a colorless sirup ($[\alpha]_D^{21}$ −47.1° (*c* 1.72, water)), which showed no mutarotation. All the attempts to isolate the crystalline free heptose and its hydrazones have been in vain.

I and II were also converted to crystalline 1-amino- and 1-acetamide-1, 7-dideoxy-L-*glycero*-L-*talo*-heptitol (XI and X) respectively.

Experimental

1, 7-Dideoxy-1-*C*-nitro-2, 3, 4, 5, 6-penta-*O*-acetyl-L-*glycero*-L-*talo*-heptitol (II).—One drop of concentrated sulfuric acid from a capillary was added to a stirred suspension of compound I[2] (2.5 g.) in 25 ml. of acetic anhydride. The resulting solution was allowed to stand at room temperature for 4 hr. and then poured into ice water. It was extracted three times with chloroform, and the extract was washed with an aqueous solution of sodium bicarbonate, dried over anhydrous sodium sulfate, and concentrated to dryness in vacuo at 40°C, thus yielding colorless crystals. Two recrystallizations from ethanol gave 4.3 g. (86.8%) of plates with a m. p. of 133°C and $[\alpha]_D^{20}$ −3.0° (*c* 0.8, acetone).

Found: C, 46.62; H, 5.53; N, 3.30. Calcd. for $C_{17}H_{25}O_{12}N$ (435.38): C, 46.90; H, 5.79; N, 3.23%.

L-*manno*-3,4, 5, 6-Tetra-*O*-acetyl-1-nitroheptene-1 (III).—A solution of 2.5 g. of II in 50 ml. of dried benzene was refluxed for 2.5 hr. with 2.5 g. of sodium bicarbonate. After the mixture had then been cooled the precipitates were filtered off and the filtrate was concentrated to dryness in vacuo at 40°C thus giving a sirup (1.8 g., 83%). The sirup could not be crystallized, but its infrared absorptions and analytical values were consistent with those of III.

Found: C, 47.32; H, 5.85; N, 3.80. Calcd. for $C_{15}H_{21}O_{10}N$ (375.33): C, 48.00; H, 5.64; N, 3.73%.

The high-vacuum distillation of III gave, accompanied by a considerable decomposition, a small amount of a distillate, b. p. 123—132°C/0.05 mmHg, which crystallized on standing (m. p. 86—88°C). However, the analytical values (C, 46.93; H, 5.81; N, 4.42%) corresponded with the formula $C_{13}H_{19}O_9N$, which is consistent with the one which holds when one acetyl group is removed from III.

L-*C*-Nitro-3, 4, 5, 6-Tetra-*O*-acetyl-1, 2, 7-trideoxy-L-*manno*-heptitol (IV).—A crude sirup III (1.2 g.) was dissolved in 30 ml. of absolute alcohol and subjected to hydrogenation in the presence of 5% palladium-charcoal. The hydrogenation was stopped when the hydrogen-uptake reached an equimolar amount (79 ml.). The removal of the catalyst and the solvent left a colorless sirup (1.15 g., 95%), which failed to crystallize. Infrared spectrometric analysis showed the absence of a double-bond linkage.

1-*C*-Nitro-1, 2, 7-trideoxy-L-*manno*-heptitol (V).—To a solution of 2 g. of crude IV in 5 ml. of ethanol, 10 ml. of 0.65 N sodium methoxide in methanol was added drop by drop. The solution turned yellow, the temperature rose slightly, and colorless crystals appeared. After the solution had stood for 3 hr., 10 ml. of 2 N acetic acid were added to the mixture and the resulting clear solution was deionized with an ion exchanger, IR-120 (30 ml.).

The concentration of the solution gave 0.9 g. (59.7%) of crystals. It was recrystallized twice from ethanol; yield, 0.6 g.; m. p. 122.5—123.5°C; $[\alpha]_D^{21}$ −10.0° (*c* 1.8, ethanol).

Found: C, 40.09; H, 7.06; N, 6.86. Calcd. for $C_7H_{15}O_6N$ (209.20): C, 40.19; H, 7.23; N, 6.70%.

Ethyl 2, 7-Dideoxy-α-L-*manno*-heptopyranoside (VII).—a) Into a mixture of 10 ml. of concentrated sulfuric acid and 15 ml. of water, 4.4 g. of V in N sodium hydroxide (25 ml.) was swirled at 0°C. The reaction mixture was then diluted with 50 ml. of ice water and neutralized by stirring it with solid barium carbonate (pH 3.6). The mixture was filtered, and the filtrate was concentrated in vacuo to a sirup. By the repeated evaporation of the water with ethanol, it weighed 3.45 g. and crystallized from ethanol or ethanol-ether. After two recrystallizations from ethanol, it showed a m. p. of 152—154°C and $[\alpha]_D^{20}$ −129° (*c* 1.5, water). Yield, 1.1 g. (25.4%).

Found: C, 52.66; H, 9.11. Calcd. for $C_9H_{18}O_5$ (206.23): C, 52.41; H, 8.80%.

The product did not reduce the Fehling solution, but its hydrolysate in 2 N sulfuric acid showed a positive reaction. $\Delta[M]_{486}^{\text{Cupra A}}$ +318° or $\Delta[M]_{78}^{\text{Cupra A}}$ +345 means that VII has a pyranoside ring.

b) The glycosidation of VI with ethanol in the presence of a small amount of sulfuric acid in the usual manner gave the corresponding ethyl glycoside in a 75% yield; the m. p. was 153—154°C, and it showed no depression on admixture with an authentic sample.

Ethyl 2,7-Dideoxy-3,4,6-tri-*O*-acetyl-α-L-*manno*-heptopyranoside (VIII).—One hundred milligrams of VII was dissolved in a mixture of 3 ml. of anhydrous pyridine and 3 ml. of acetic anhydride. The solution was allowed to stand overnight at room temperature and then swirled into ice water. The crystals which appeared were filtered, dissolved in 3 ml. of ethanol, treated with charcoal, and then poured again into ice water to give colorless crystals, m. p. 90°C and $[\alpha]_D^{21}$ −157° (*c* 0.9, ethanol). Yield 110 mg. (68.2%).

Found: C, 54.25; H, 7.56. Calcd. for $C_{15}H_{24}O_8$ (332.34): C, 54.21; H, 7.28%.

2,7-Dideoxy-L-*manno*-heptose (VI).—One hundred and eighty milligrams of VII was allowed to dissolve in 8 ml. of 2 N sulfuric acid, and then left to stand for 2 days at room temperature while the change of the rotation was being traced. The acidic solution was then neutralized with 2 N barium hydroxide, the precipitates were filtered off, and the filtrate was exhaustly deionized with a small amount of IRC-120. The removal of the solvent in vacuo yielded a colorless sirup (86 mg.), which failed to crystallize. $[\alpha]_D^{20}$ −47.1° (*c* 1.72, water). No mutarotation was observed.

1-Acetamido-1, 2, 7-trideoxy-L-*manno*-heptitol (IX).—A solution of 2 g. of a crude sirup, IV, in 30 ml. of absolute ethanol was shaken with hydrogen in the presence of 0.2 g. of a platinum catalyst until the hydrogen uptake ceased. After the catalyst and the solvent had been removed, the sirup yielded was acetylated in the usual manner with 10 ml. of acetic anhydride and 10 ml. of pyridine, but the product failed to crystallize. Subsequently, it (1.4 g.) was subjected to de *O*-acetylation with sodium methoxide in absolute methanol. The concentration of the mixture in vacuo yielded crystals, which were then recrystallized from methanol; m. p. 140.5—141°C and

$[\alpha]_D^{20}$ −14.8° (*c* 1.0, water). Yield, 0.6 g. (52.5%).

Found: C, 49.04; H, 8.65; N, 6.25. Calcd. for $C_9H_{19}O_5N$(221.25): C, 48.85; H, 8.66; N, 6.33%.

1-Acetamido-1, 7-dideoxy-L-*glycero*-L-*talo*-heptitol (X).—a) Using the procedure described above, 2.8 g. of II was subjected to hydrogenation and then *N*-acetylation. Neither product could be crystallized. Then the latter was de-*O*-acetylated to give crystals; m. p. 202—204°C and $[\alpha]_D^{20}$ +31.0° (*c* 0.31, water). Yield, 0.6 g. (55.4%).

Found: C, 45.49; H, 8.26; N, 5.89. Calcd. for $C_9H_{19}O_6N$ (237.25): C, 45.56; H, 8.07; N, 5.90%.

b) The same product was obtained in a 80% yield by the *N*-acetylation of XI in the usual manner.

1-Amino-1, 7-dideoxy-L-*glycero*-L-*talo*-heptitol (XI).—A solution of 2 g. of I in 30 ml. of 80% ethanol was subjected to hydrogenation by the procedure described before. The crystals obtained were recrystallized from ethanol; m. p. 144—145°C and $[\alpha]_D^{20}$ +8.3° (*c* 0.24, methanol). Yield, 1.6 g. (92.4%).

Found: C, 42.82; H, 8.79; N, 6.86. Calcd. for $C_7H_{17}O_5N$ (195.21): C, 43.05; H, 8.78; N, 7.16%.

The authors would like to express their gratitude to Professor Tetsuo Sato of the Tokyo Institute of Technology for his encouragement throughout this work.

BULLETIN OF THE CHEMICAL SOCIETY OF JAPAN VOL. 39 1778—1782 (1966)

Organic Sulfur Compounds. IX. The Reactions of *N*-Sulfinylamines with Nitrogen Tetroxide and Nitrosyl Chloride

By Michio KOBAYASHI* and Koichi HONDA

Department of Chemistry, Yokohama City University, Mutsuura-machi, Kanazawa-ku, Yokohama

(Received January 5, 1966)

N-Sulfinylaniline reacted with nitrogen tetroxide to form the anhydrous benzenediazonium nitrate. The reactions of *N*-sulfinylaniline and several of its *p*-substituted derivatives with nitrosyl chloride also gave the anhydrous diazonium chlorides in the crystalline state. Aliphatic *N*-sulfinylamines reacted with nitrosyl chloride to form alkyl chlorides, probably by the decomposition of the initially-formed diazonium chlorides; during this reaction, no rearrangement of the alkyl group was observed.

Recent a short communication[1] which described the formation of benzenediazonium fluoroborate and hexafluoroantimonate from *N*-sulfinylaniline and, respectively, nitrosyl fluoroborate and hexafluoroantimonate prompted us to publish our similar studies of the reactions of *N*-sulfinylamines with nitrogen tetroxide or nitrosyl chloride.

Several addition reactions to *N*-sulfinylamines (I), in which a cationic part of the attacking reagent became attached to the nitrogen, and an anionoid part to the sulfur atoms, of I, have been known.[2,3]

$$R\text{-}N{=}S{=}O + ArSH \rightarrow R\text{-}\underset{\underset{H}{|}}{N}\text{-}\underset{\underset{O}{\downarrow}}{S}\text{-}S\text{-}Ar \qquad (1)$$

(I)

$$R\text{-}N{=}S{=}O + R'MgX \rightarrow R\text{-}\underset{\underset{XMg}{|}}{N}\text{-}\underset{\underset{O}{\downarrow}}{S}\text{-}R' \qquad (2)$$

On the other hand, many carbonyl compounds give condensation products with such reactive *N*-sulfinylamines as *N*-sulfinyl sulfonamides,[4] as shown below:

$$R\text{-}N{=}S{=}O + R'CHO \rightarrow R\text{-}N{=}CH\text{-}R' + SO_2 \qquad (3)$$

Analogous condensation between the nitroso compounds and *N*-sulfinylamines could take place according to the following equation:

$$R\text{-}N{=}S{=}O + X\text{-}NO \rightarrow R\text{-}N{=}N\text{-}X + SO_2 \qquad (4)$$

If X-NO is an ionic compound, which could dissociate to form a nitrosonium cation and an anion X^-, the above condensation would lead to the formation of the diazonium salts:

$$R\text{-}N{=}S{=}O + NO^+X^- \rightarrow [R\text{-}N{\equiv}N]^+X^- \qquad (5)$$

In the case of the aliphatic *N*-sulfinylamines, the primary product, alkyldiazonium salt with a well-known low stability, would decompose to RX and nitrogen:

$$[R\text{-}N{\equiv}N]^+X^- \rightarrow RX + N_2 \qquad (6)$$

These expectations have been fully realized, as will be described in this paper.

* To whom correspondence should be sent: Department of Chemistry, Faculty of Science, Tokyo Metropolitan University, Setagaya-ku, Tokyo.

1) K. Bott, *Angew. Chem.*, **77**, 132 (1965).

2) G. Kresze and H. P. Patzschke, *Chem. Ber.*, **93**, 380 (1960).

3) a) H. Gilman and H. L. Morris, *J. Am. Chem. Soc.*, **48**, 2399 (1926); b) D. Klamann, C. Sass and M. Zelenka, *Chem. Ber.*, **92**, 1910 (1959); c) W. T. Smith, Jr., P. A. Thio and M. Grasley, *J. Org. Chem.*, **27**, 692 (1962).

4) G. Kresze and R. Albrecht, *Angew. Chem.*, **74**, 781 (1962).

Results and Discussion

When an ether solution of *N*-sulfinylaniline was added to a solution of nitrogen tetroxide in ether at −10°C, the reaction started immediately, forming a white precipitate. The filtrate of this precipitate began to form a similar precipitate at once, and even after the second filtration of the second precipitate, a substantial amount of the fresh precipitate was obtained. These precipitates were shown, by their infrared spectra in a KBr disk, to be benzenediazonium nitrate. In the dry state, this compound tends to decompose violently upon a slight shock. It was easily soluble in water, and an aqueous solution gave a coupling product with an alkaline solution of β-naphthol. The ether filtrate of the diazonium nitrate smelled strongly of sulfur dioxide. Due to the hygroscopic and explosive nature of the diazonium salt, its exact yield could not be determined as such. In a separate experiment, the first, second and third precipitate were dissolved in water immediately after the filtration, and then subjected to a coupling reaction with β-naphthol to give α-phenylazo-β-naphthol, the combined yield of which was 80% of the theoretical yield based on *N*-sulfinylaniline. Since the third filtrate gave some diazonium nitrate too, the yield of the diazonium salt was considered to be almost quantitative. The third filtrate was mixed with water and sulfate anions were precipitated as barium sulfate, which amounted to 6% of the theoretical yield based on sulfinylaniline. Therefore, most of the sulfur of sulfinylaniline was converted into sulfur dioxide, of which only a small fraction underwent oxidation to a higher oxidation state such as nitrosyl sulfate by means of excess dinitrogen tetroxide. The above result may be formulated as below:

$$C_6H_5N{=}S{=}O + N_2O_4 \rightarrow C_6H_5N_2{}^+NO_3{}^- + SO_2 \quad (7)$$

When a solution of an equimolar nitrosyl chloride in carbon tetrachloride was added to an ether solution of sulfinylaniline cooled at −70°C, a white precipitate started to form immediately. After a few minutes this precipitate was filtered off and the filtrate was stored in a refrigerator overnight, during which time a considerable amount of the same precipitate was deposited. The infrared spectrum of this precipitate exhibited strong absorptions at 2270, 1570, 1456, 1303, 1080, and 760 cm^{-1}, just as authentic benzenediazonium chloride. The first precipitate gave α-phenylazo-β-naphthol in a 33% yield in a coupling reaction with β-naphthol.

In a similar manner, *p*-nitro-*N*-sulfinylaniline rapidly reacted with nitrosyl chloride at −70°C to form the copious precipitate of *p*-nitrobenzenediazonium chloride, which gave α-*p*-nitrophenylazo-β-naphthol upon coupling with alkaline β-naphthol.

p-Methoxy-*N*-sulfinylaniline reacted slowly with nitrosyl chloride at a low temperature. After the reaction mixture had been kept in a refrigerator for 3 days, the precipitated diazonium salt was filtered off and coupled with β-naphthol to give α-*p*-methoxyphenyl-β-naphthol in a 36% yield. The filtrate of the diazonium salt was then kept for another 3 days in a refrigerator; it thus gave the same precipitate, the yield of which was estimated to be 24% by the coupling method. The total yield of *p*-methoxybenzenediazonium chloride was over 60%. The crude diazonium salt exhibited an infrared absorption at 2225 cm^{-1} the same region as in an authentic specimen of *p*-methoxybenzenediazonium chloride.

In a similar way, *p*-chloro-*N*-sulfinylaniline reacted with nitrosyl chloride in an ether - carbon tetrachloride mixture to give a white precipitate, supposed to be *p*-chlorobenzenediazonium chloride, which coupled with β-naphthol to give α-chlorophenylazo-β-naphthol in a 44% yield based on sulfinylamine. The relative velocity of the reaction of the *p*-substituted sulfinylaniline derivatives with nitrosyl chloride, as judged from the apparent velocity of the precipitation of the diazonium salts, was:

$$p\text{-nitro} > p\text{-chloro} > H > p\text{-methoxy}.$$

In every case, the filtrate of the diazonium salt smelled strongly of sulfur dioxide.

On the basis of the above results, the reaction of *N*-sulfinylanilines with nitrosyl chloride can be expressed by the following formula, which is of the same type as is seen in the reaction with nitrogen tetroxide:

$$Ar{-}N{=}S{=}O + NOCl \rightarrow ArN_2{}^+Cl^- + SO_2 \quad (8)$$

Considering the possiblity of the equilibrium:

$$N_2O_4 \rightleftarrows NO^+NO_3{}^- \quad (9)$$

both reactions may be regarded as starting with the electrophilic attack of nitrosonium cations on the nitrogen atom of *N*-sulfinylanilines.

The facts that the amount of precipitated diazonium salt obtained by the first filtration did not exceed certain percentages of the theoretical yield, and that the fresh precipitate began to form immediately after the filtration, suggest the existence of some kind of equilibrium between the starting materials or one of the intermediates and the diazonium salt. A similar equilibrium phenomenon has been observed in the reaction of benzalaniline with nitrosyl chloride or nitrogen tetroxide to give the diazonium salts.[5]

The following reaction mechanism may be proposed:

5) J. Turcan, *Bull. soc. chim. France,* [5]**2**, 627 (1935); c. f. R. M. Scribner, *J. Org. Chem.,* **29**, 3429 (1964).

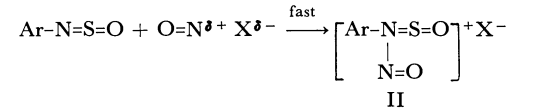

II (10)

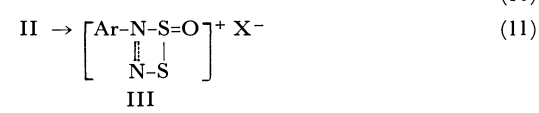

III (11)

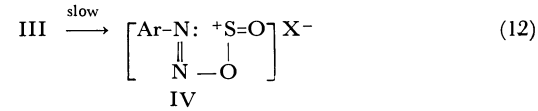

IV (12)

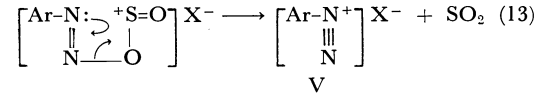

V (13)

Well-known reactions of the diazonium salts with sulfur dioxide in the presence of a copper catalyst to form the sulfinic acids or sulfonyl chlorides[6] may be attributed to the formation of IV by the reverse reaction of (13), which collapses, thus resulting in sulfonyl chloride (reaction 14) or in sulfinic acid, according to the reaction 15:

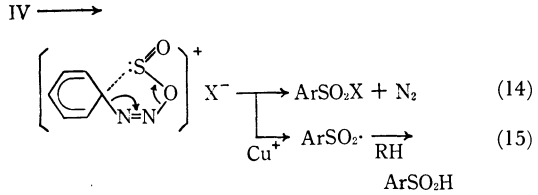

(14)

(15)

Reaction 10 seems to be very fast and irreversible, since the characteristic color of nitrosyl chloride faded almost instantly after the reactants were mixed. Only small fractions of the liberated sulfur dioxide were oxidized by nitrogen tetroxide to a higher oxidation state, suggesting that most of nitrogen tetroxide had been consumed, leaving only a small amount of it available for the oxidation when free sulfur dioxide was liberated in the reaction 13. Consequently, the reaction 10 could not be a rate determining step. Reactions 11 and 12 may form a concerted one-step process; they are probably the rate determining.

The order of the rate of the formation of the diazonium salt was *p*-nitro > *p*-chloro > unsubstituted > *p*-methoxy, as has been described above. Since the reaction 10 is a cationoid attack by nitrosonium ion, the reverse order would be expected if this reaction were the rate determining step. On the other hand, if the reaction 11 or 12, in which the adduct II rearranges to IV with a long conjugated system, is the rate determining step, the acceleration by an electron-attractive substituent is quite understandable.

6) H. Meerwein, G. Dittmar, R. Göllner, K. Hafner, F. Mensch and O. Steinfort, *Chem. Ber.*, **90**, 841 (1957).

Alkyldiazonium salts are known to be very unstable, and they have never been isolated. In this connection, the reaction mechanism of the aliphatic *N*-sulfinylamines with nitrosyl chloride seemed to be interesting. Although the reaction of *N*-sulfinylethylamine and nitrosyl chloride failed to give any definite product attributable to the diazonium salt formation, the reactions of *N*-sulfinyl-*n*-butylamine and *N*-sulfinyl-isobutylamine with nitrosyl chloride gave *n*-butyl chloride and isobutyl chloride respectively. In both cases, no isomeric chloride was observed to be formed.

These butyl chlorides are considered to be the decomposition products of the intermediate butyldiazonium chlorides. The above results definitely exclude the formation of a free butyl cation during the decomposition, since the *n*-butyl carbonium ion is known to rearrange readily to the *s*-butyl cation, and the isobutyl carbonium ion, to *s*-butyl and *t*-butyl cations.

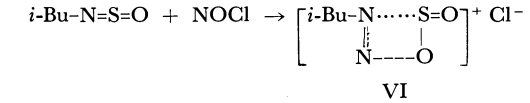

VI (16)

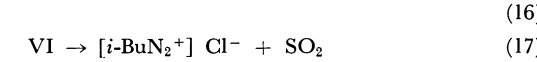

VII (17)

Therefore, the decomposition of the diazonium chloride VII to butyl chloride and nitrogen molecule must be a concerted process, in which the bond breaking between carbon and nitrogen and the bond forming between carbon and chlorine proceed simultaneously in an ion pair VII. The following two transition states, namely the S_N2 type (VIII) and the S_Ni type (IX), are conceivable for the last reaction:

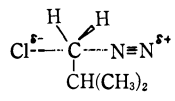

VIII

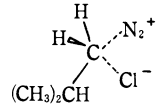

IX

Since the bond between carbon and the positively charged N_2^+ group is considered to be very weak, the nucleophilic assistance by the chloride ion in the splitting of this bond can not be important in any way. The rapid collapse of the tightly-bound ion pair VIII will result in the formation of either the inverted or the retained product, or both, depending on the location of the chloride ion in this ion pair intermediate.

In the reaction of the aliphatic amines with nitrous acid to give the alcohols, the rearrangement of the alkyl groups has been reported,[7]

7) V. Meyer, J. Barbieri and F. Forster, *Ber.*, **10**, 130 (1877); This problem has been discussed in great detail in lit. 9 and many examples are cited in that paper.

while their reactions with nitrosyl chloride to form the alkyl chlorides are accompanied by no such rearrangement,[8] just as in our case. The proposed explanation for the above difference was that the former reaction consisted of the reaction of the free alkyl carbonium ion, separated from the counter ion by a water molecule, whereas the latter reaction occurred within the ion pair in the early stage along the reaction coordinate.[9] Probably the same explanation is applicable in the present case.

Experimental

Materials.—Sulfinylaniline was prepared from aniline hydrochloride and thionyl chloride.[10] B. p. 88°C/12 mmHg. *p*-Nitro-*N*-sulfinylaniline[11] was prepared by refluxing *p*-nitroaniline with thionyl chloride in benzene. M. p. 70°C.

p-Methoxy-*N*-sulfinylaniline, b. p. 146.5°C/25 mmHg (lit.[12] b. p. 132°C/15 mmHg), and *p*-chloro-*N*-sulfinylaniline, b. p. 136°C/40 mmHg (lit.[13] b. p. 237°C), were prepared in a similar way. *N*-Sulfinylethylamine[14] was prepared as follows: To 15 g. of ethylamine cooled in ice water, there was added a solution of 46.5 g. of *N*-sulfinylaniline in 50 ml. of ether over a 30 min. period; the mixture was kept overnight at room temperature. After repeated fractional distillations, a fraction boiling 73—74°C was retained (6.5 g.).

***N*-Sulfinyl-*n*-butylamine.**—To an ice-cooled solution of 25 g. of *n*-butylamine in a mixture of 55 g. of dry pyridine and 50 ml. of ether, a solution of 41 g. of thionyl chloride in ether was slowly added; the reaction mixture was then stirred for 30 min., filtered, and vacuum-distilled to give 17 g. of sulfinyl-*n*-butylamine, b. p. 47°C/50 mmHg (lit.[15] 38°C/10 mmHg). *N*-Sulfinyl-isobutylamine was prepared from 25 g. of isobutylamine in a similar way. B. p. 44°C/60 mmHg; the yield was 26.8 g. (65%). Nitrogen tetroxide was obtained by the pyrolysis, at 260°C, of nitrogen pentoxide.[16] Nitrosyl chloride was generated from sodium nitrite and concentrated hydrochloric acid; dried by passing it over sodium nitrite, hydrated potassium chloride and calcium chloride successively,and finally purified by fractional distillation.[17]

The Reaction of *N*-Sulfinylaniline and Nitrogen Tetroxide.—i) A solution of 1 g. of nitrogen tetroxide in ether was cooled to −10°C. When a solution of 1 g. of sulfinylaniline in ether was added to this solution, drop by drop, a white precipitate began to form at once. As soon as this precipitate had been filtered off, a new precipitate started to form in the filtrate; from the second filtrate, third white crystalline precipitate was obtained. The infrared spectra of the first and second precipitates in the KBr disk completely coincided with that of the authentic benzenediazonium nitrate prepared by the diazotation of aniline nitrate with isoamyl nitrite.[18] When a minute crystal of the product was crushed on a porous plate, it exploded violently. The filtrate of the diazonium salt smelled strongly of sulfur dioxide. ii) In a similar way, 1.5 g. of sulfinylaniline and 1.3 g. of nitrogen tetroxide were mixed in ether and the successively-precipitating diazonium nitrate was taken off by filtration up to the third crop. The combined yield was estimated by coupling with β-naphthol to be 80% (α-phenylazo-β-naphthol, m. p. 206°C; 2.2 g.; identified by infrared spectrum). The filtrate of the third precipitate was mixed with water, and the ether was evaporated at room temperature. To the remaining solution the diluted hydrochloric acid was added and sulfur dioxide was expelled by warming the solution on a water bath. The addition of 0.1 N barium chloride to the above solution while it was hot gave 0.148 g. of barium sulfate, in 6% yield based on sulfinylaniline.

The Reaction of Sulfinylaniline with Nitrosyl Chloride.—When 1.0 g. of nitrosyl chloride (15 mmol.) in 8 ml. of carbon tetrachloride was added to a solution of 2.2 g. of sulfinylaniline (16 mmol.) in 10 ml. of ether, a white precipitate appeared immediately. After a few min., this precipitate was filtered through a fritted glass funnel, whereupon a new precipitate started to fill the filtrate. The first precipitate was dissolved in water and coupled with β-naphthol to give 1.2 g. of α-phenylazo-β-naphthol (33%).

The Reaction of *p*-Nitro-*N*-sulfinylaniline with Nitrosyl Chloride.—The reaction between 2.6 g. of *p*-nitrosulfinylaniline and 0.8 g. of nitrosyl chloride was carried out at −70°C in a similar way. The immediately-formed white precipitate was filtered off after a few minutes. Its infrared spectrum in a KBr disk was superimposable upon that of *p*-nitrobenzenediazonium chloride prepared by the diazotation of *p*-nitroaniline hydrochloride with isoamyl nitrite in acetic acid.[19] The coupling of the first precipitate with β-naphthol gave 1.5 g. of α-*p*-nitrophenylazo-β-naphthol (40%).

The Reaction of *p*-Methoxy-*N*-sulfinylaniline with Nitrosyl Chloride.—When 2.5 g. of *p*-methoxysulfinylaniline and 1.0 g. of nitrosyl chloride were treated at −70°C as above, the rate of the precipitation of the diazonium salt was much slower than the precipitation rates of the other diazonium salts described in this paper. After it had been stored for 3 days in a refrigerator, the reaction mixture was filtered off, and the precipitated diazonium chloride was dissolved

8) P. A. S. Smith, D. R. Baer and S. N. Ege, *J. Am. Chem. Soc.*, **76**, 4564 (1954).
9) R. Huisgen and C. Ruchardt, *Ann.*, **601**, 1 (1956). See also H. Zollinger, "Azo and Diazo Chemistry, Aliphatic and Aromatic Compounds," translated by H. E. Nursten, Interscience Publishers, N. Y. (1961), p. 123.
10) A. Michaelis and R. Herz, *Ber.*, **23**, 3480 (1890); A. Michaelis, ibid., **24**, 745 (1891).
11) G. Kresze and H. Smalla, *Chem. Ber.*, **92**, 1042 (1959).
12) O. Wichterle and J. Rocek, *Chem. Listy*, **47**, 1768 (1953); Ref. 11.
13) A. Michaelis and C. Hümme, *Ber.*, **24**, 754 (1891).
14) W. K. Glass and A. D. E. Pullin, *Trans. Faraday Soc.*, **57**, 546 (1961).
15) G. Zinner, *Chem. Ber.*, **91**, 971 (1958); Ref. 3b.
16) L. Hackspill and J. Besson, *Bull. soc. chim. France*, [5] **16**, 479 (1949).
17) W. A. Harrison, E. R. H. Jones, G. D. Meakins and P. A. Wilkinson, *J. Chem. Soc.*, **1964**, 3213; L. J. Beckham, W. A. Fessler and M. A. Kise, *Chem. Revs.*, **48**, 319 (1951).
18) E. Knoevenagel, *Ber.*, **23**, 2994 (1890).
19) A. Hantzsch and R. Jochem, ibid., **34**, 3338 (1901).

in water and subjected to a coupling reaction with β-naphtol to give 1.0 g. of α-*p*-methoxyphenylazo-β-naphthol (the total yield was 2.5 g.). Infrared absorption of this diazonium salt exhibited N≡N absorption at 2225 cm^{-1} in a KBr disk and coincided with that of the authentic specimen prepared from *p*-anisidine hydrochloride and isoamyl nitrite.[19]

The Reaction of *p*-Chloro-*N*-sulfinylaniline with Nitrosyl Chloride.—After a reaction mixture of 2.8 g. of *p*-chlorosulfinylaniline and 1.0 g. of nitrosyl chloride, treated as above at −70°C, was kept for a week in a refrigerator, the white precipitate was taken up by suction. Coupling with β-naphthol gave 1.7 g. of α-*p*-chlorophenylazo-β-naphthol in 44% yield. All the azo-β-naphthols described above were identified by means of their infrared spectrum.

The Reaction of *N*-Sulfinyl-*n*-butylamine with Nitrosyl Chloride.—To a solution of 8.5 g. of nitrosyl chloride in 20 ml. of ether, cooled at −70°C, there was added, drop by drop, a solution of 15.5 g. of sulfinyl-*n*-butylamine in 20 ml. of ether. The evolution of gas started immediately, accompanied by the copious formation of the white precipitate. When the reaction mixture was allowed to warm to room temperature, gas evolved vigorously from the precipitate, which turned into a spongy mass which floated over the surface and finally settled at bottom as a black oil. The reaction mixture smelled strongly of sulfur dioxide. The upper layer was separated, washed with water, dried over magnesium sulfate, and fractionally distilled to give 2 g. of a colorless liquid, b. p. 77.5°C, which was identified as *n*-butyl chloride by its infrared spectrum. No *s*-butyl chloride was detected. The yield was 20% of the theoretical.

The Reaction of *N*-Sulfinyl-isobutylamine with Nitrosyl Chloride.—The reaction of 9.0 g. of sulfinyl-isobutylamine with 16.5 g. of nitrosyl chloride was carried out in a way similar to that used for the *n*-butyl derivative. The white crystals which formed at −70°C decomposed at room temperature with the evolution of gas and gave white leaflet crystals and an oil layer, both insoluble in ether. This leaflet (0.5 g.), m. p. 157—159°C, was readily soluble in water and identified as isobutylamine hydrochloride by its infrared spectrum and by a Kjeldahl nitrogen determination (Found: N, 11.4%; Calcd. for $C_4H_9NH_3Cl$: 12.5%). The ether layer was washed with water and fractionally distilled to give 1.5 g. of isobutyl chloride, which was identified by means of its infrared spectrum and boiling point. No indication of the presence of *s*-butyl chloride or *t*-butyl chloride was observed by infrared spectroscopy or the gas liquid chromatography.

BULLETIN OF THE CHEMICAL SOCIETY OF JAPAN VOL. 39 1782—1784 (1966)

Organic Sulfur Compound. X. The Mechanism of the Carboxylic Ester Formation from Carboxylic Sulfurous Anhydrides

By Michio KOBAYASHI*

Department of Chemittry, Yokohama City University, Mutsuura-machi, Kanazawa-ku, Yokohama

and Reiko KIRITANI

Department of Chemistry, Radiation Center of Osaka Prefecture, Sakai, Osaka

(Received January 5, 1966)

Sodium benzoate-^{18}O reacts with methyl chlorosulfite to give methyl benzoate-^{18}O in a low yield; the excess ^{18}O content has been found to be exactly one-half of that in the starting benzoic acid. Another reaction of the labeled benzoic acid with phenyl chlorosulfite gives phenyl benzoate-^{18}O; its excess ^{18}O atom% is also one-half of that of benzoic acid. Both reactions are considered to proceed by way of the intermediate formation of the benzoic sulfurous mixed anhydrides, the decomposition of which by acyl-oxygen splitting affords the carboxylic esters labeled only in the carbonyl group.

The formation of the mixed anhydride (I) of the carboxylic acid and the sulfurous acid monoester (reaction 1) and its thermal decomposition at a relatively low temperature to give the carboxylic anhydride and the sulfurous acid diester (reaction 2) have been described in a preceding paper.[1] When the reaction mixture of the carboxylic acid salt with the chlorosulfite ester was heated at a high temperature until the evolution of sulfur dioxide was completed, the carboxylic ester has been reported to be formed in a good yield, probably by means of the intermediate formation of I (reaction 3):[2,3]

* Present address: Department of Chemistry, Faculty of Science, Tokyo Metropolitan University, Setagaya-ku, Tokyo.

1) Part II of this series. M. Kobayashi and A. Yamamoto, This Bulletin, **39**, 961 (1966).

2) P. Carré and D. Libermann, *Bull. soc. chim. France,* [4] **53**, 1050 (1933).

3) M. S. Newman and W. S. Fones, *J. Am. Chem. Soc.,* **69**, 1046 (1947).

$$RCO_2Na + Cl\text{-}S\text{-}OR' \longrightarrow R\text{-}\underset{\underset{O}{\|}}{C}\text{-}O\text{-}\underset{\underset{O}{\downarrow}}{S}\text{-}OR' \quad (1)$$

$$I \longrightarrow {}^1/_2(RCO)_2O + {}^1/_2(R'O)_2SO + {}^1/_2SO_2 \quad (2)$$

$$I \longrightarrow R\text{-}\underset{\underset{O}{\|}}{C}\text{-}OR' + SO_2 \quad (3)$$

It has not been established which bond in I is broken in the last reaction. Moreover, there is another possible course by which the carboxylic ester is formed from the salt of the carboxylic acid and the chlorosulfite ester—namely, a secondary reaction between two primary products of the decomposition reaction 2 of I, the carboxylic anhydride and sulfurous acid diester, — besides the direct decomposition of I (reaction 3) to the carboxylic ester. In order to obtain information about these points, the present investigation, using the ^{18}O-labeling method, was carried out.

Results and Discussion

The ^{18}O labeled sodium benzoate and methyl chlorosulfite were mixed, and the resulting jelly-like mixture was heated in an oil bath for 4 hr., until the evolution of sulfur dioxide had ceased. The products were then spearated by fractional distillation into benzoic anhydride (50% yield), dimethyl sulfite (25% yield) and methyl benzoate (about a 5% yield). The excess ^{18}O atom percentage of methyl benzoate was found to be exactly a half of that of the starting sodium benzoate. This reaction may be formulated as follows:

$$Ph\text{-}\underset{\underset{{}^{18}O}{\|}}{C}\text{-}{}^{18}O\text{-}\underset{\underset{O}{\downarrow}}{S}\text{-}OCH_3 \longrightarrow \quad (4)$$

Ia

$$Ph\text{-}\underset{\underset{{}^{18}O}{\|}}{C}\text{-}OCH_3 + SO^{18}O$$

Ethyl benzoyloxysulfinate Ib, which is a close analog of the methyl ester Ia postulated above, had previously been obtained in a solution or in the sirupy liquid state.[1] This compound has now been found to be distillable in a high vacuum with only slight decomposition. The infrared spectrum of the distillated sample was almost the same as that already reported.[1]

Equimolar amounts of the labeled benzoic acid and phenyl chlorosulfite were treated with triethylamine in ether, whereas triethylamine hydrochloride was precipitated quantitatively. The filtrate exhibited strong infrared absorption bands at 1729 cm^{-1} (C=O) and 1230 cm^{-1} (S-O), suggesting the formation of phenyl benzoyloxysulfinate Ic. The evaporation of ether in a vacuum gave a colorless residue; this residue was pyrolyzed at 90—140°C for 2 hr., until no more sulfur dioxide evolved. When the product mixture was treated with aniline in carbon tetrachloride, 55 mol.% of benzanilide was precipitated. The filtrate was then evaporated, and the remaining oil was chromatographed to give 20 mol.% of phenyl benzoate. Its excess ^{18}O atom% was again almost one-half of that in the original benzoic acid. Consequently, the decomposition of the intermediate Ic may be considered to proceed by the acyl-oxygen splitting shown below:

$$Ph\text{-}\underset{\underset{{}^{18}O}{\|}}{C}\text{-}{}^{18}O\text{-}\underset{\underset{O}{\downarrow}}{S}\text{-}OPh \longrightarrow$$

Ic

$$Ph\text{-}\underset{\underset{{}^{18}O}{\|}}{C}\text{-}OPh + SO^{18}O \quad (5)$$

The ^{18}O atom% of benzanilide should be the same as that of the carbonyl group of benzoic anhydride, which in turn may be expected to be the same as that in the original benzoic acid, provided this anhydride was formed straightforward, by disproportionation (6):

$$Ph\text{-}\underset{\underset{{}^{18}O}{\|}}{C}\text{-}{}^{18}O\text{-}\underset{\underset{O}{\downarrow}}{S}\text{-}OPh \longrightarrow {}^1/_2Ph\text{-}\underset{\underset{{}^{18}O}{\|}}{C}\text{-}{}^{18}O\text{-}\underset{\underset{{}^{18}O}{\|}}{C}\text{-}Ph$$

Ic

$$+ {}^1/_2(PhO)_2SO + {}^1/_2SO^{18}O \quad (6)$$

Actually, the ^{18}O atom % of benzanilide was found to be definitely lower than that of benzoic acid. This suggests that some kind of discrimination of the oxygen atoms must occur in the mixed anhydride, Ic.

If the ^{18}O atom% of the carbonyl group of benzoic anhydride could be postulated to be the same as that of benzanilide (1.29%), the ^{18}O atom % of phenyl benzoate, which would be formed by the interaction of two primary products (benzoic anhydride and diphenyl sulfite) in the reaction 7, as has been pointed out above, should be 0.75%:

$$Ph\text{-}\underset{\underset{{}^{18}O}{\|}}{C}\text{-}O\text{-}\underset{\underset{{}^{18}O}{\|}}{C}\text{-}Ph + (PhO)_2SO$$

$$\longrightarrow 2\,Ph\text{-}\underset{\underset{{}^{18}O}{\|}}{C}\text{-}OPh + SO^{18}O \quad (7)$$

(the ether oxygen atom of benzoic anhydride may contain ^{18}O. In the reaction 7, Ph-O bond is assumed to be reserved.)

Actually, the value found (0.98 atom%) was much higher than that, and it coincided rather well with the figure calculated on the basis of the reaction 5. Therefore, the carboxylic ester may be considered to be formed by the direct decomposition of the mixed anhydride Ic, not by a secondary reaction such as 7, at least not in this case.

Experimental

The Preparation of Benzoic Acid-^{18}O.—A mixture of 25 g. of benzotrichloride and 10 g. of $H_2{}^{18}O$

(1.52 atom%) was refluxed for 15 hr., protected against atmospheric moisture. The resultant crystalline mass was warmed under reduced pressure in a water bath for 2 hr. in order to expel the hydrogen chloride formed and excess water. The residue was dissolved in a solution of 8 g. of sodium hydroxide in 50 ml. of water and concentrated. The sodium benzoate thus separated was recrystallized once from the distilled water and dried in a vacuum for 2 hr. at 100°C. The white mass was powdered finely and dried once more in a vacuum at 100°C for a few hours to give about 15 g. of sodium benzoate-^{18}O (first crop). The concentration of the mother liquid gave another 9 g. of the same salt (2nd crop), which was dissolved in water and acidified with diluted hydrochloric acid to give 6 g. of benzoic acid-^{18}O. The ^{18}O atom% of the first crop was 1.49%.

Methyl Chlorosulfite.—To 40 g. of thionyl chloride 10 g. of anhydrous methanol was slowly added; the mixture was left at room temperature for several days. Distillation under reduced pressure gave 24 g. of a fraction boiling at 35—37°C/60 mmHg.

The Reaction of the Labeled Sodium Benzoate with Methyl Chlorosulfite.—To 10.0 g. of sodium benzoate-^{18}O (first crop) 16 g. of methyl chlorosulfite (2 mol.) was added, whereupon the exothermic reaction occurred. The milky reaction mixture was then heated in an oil bath at 110—130°C for 2 hr., during which time a vigorous evolution of sulfur dioxide was observed. The residue was refluxed for 2 hr., while the bath temperature was slowly raised to 190°C. The cooled reaction mixture was treated with ether and water; the ether layer was separated, washed with a sodium hydrogen carbonate solution, and dried over magnesium sulfate, and finally the solvent was removed in a vacuum. The residue was repeatedly fractionally distilled under reduced pressure to give 1 g. of dimethyl sulfite (b. p. 40—45°C/25 mmHg), 0.5 g. of methyl benzoate (the purity was checked by the infrared spectrum), and about 4 g. of benzoic anhydride. The acidification of the alkaline washing gave 0.8 g. of the unchanged benzoic acid. The ^{18}O atom% of methyl benzoate was 0.83%. (The calculated value on the basis of the formula 4 is 0.85%.)

The Reaction of Benzoic Acid-^{18}O with Phenyl Chlorosulfite.—To a solution of 3.0 g. of benzoic acid-^{18}O (^{18}O: 1.65 atom%) and 4.4 g. of phenyl chlorosulfite (equimolar) in 55 ml. of anhydrous ether, 2.5 g. of triethylamine in 10 ml. of ether was added, whereupon the reaction started at once, forming a white crystalline precipitate. After a half hour, the mixture was filtered; this precipitate was recrystallized from ethanol-ether, and identified by means its infrared spectrum as triethylamine hydrochloride (its yield of the crude state was almost the theoretical). The ether filtrate of this salt exhibited infrared absorption at 1729, 1590, 1230, 770, 710, and 690 cm^{-1} (the 1500—1300, and 1200—1000 cm^{-1} regions could not be measured because of the strong absorption of ether). No absorption of benzoic acid at 1690 cm^{-1} was observed. Since phenyl chlorosulfite has a strong absorption at 1228 cm^{-1} and diphenyl sulfite, at 1230 cm^{-1}, the 1230 cm^{-1} band of the product may be attributed to the S–O stretching vibration. Ether was expelled from this solution on a water bath (no sulfur dioxide evolution was observed), and the residue was heated in an oil bath at 80°C in the beginning and then at 140°C in the last stage of the reaction. During the last stage sulfur dioxide evolved vigorously. Finally the oily residue was treated with water and ether, and the ether layer was washed with alkali, dried, and evaporated, leaving about 4 g. of the colorless oil. Since its infrared spectrum indicated the presence of a large amount of benzoic anhydride, the oil was dissolved in carbon tetrachloride and treated with 3 g. of aniline. The separated crystals (3.2 g.) were washed with water and recrystallized from ethanol to give 1.3 g. of benzanilide (identified by its infrared spectrum and m. p.). The carbon tetrachloride filtrate was washed with a sodium hydrogen carbonate solution, water, and diluted hydrochloric acid successively, dried, and evaporated to give 3 g. of a colorless sirup. The chromatography of this sirup on alumina with benzene gave 1.0 g. of phenyl benzoate-^{18}O, m. p. 64°C. The ^{18}O atom% of this specimen was 0.98%. (The value calculated on the basis of the formula 5 was 0.93%.)

Ethyl Benzoyloxysulfinate.—To 5.5 g. of dried sodium benzoate, 7.0 g. of ethyl chlorosulfite was added, and the reaction mixture was vacuum distilled. A colorless liquid was obtained at 85°C/0.2 mmHg; this liquid contained a slight amount of the leaflet of benzoic acid. The infrared spectrum of this ester was almost superimposable upon that reported in the preceding paper.[1] The formation of some benzoyl chloride was noticed in a low-boiling fraction.

Ib: 84.43 mg.; $BaSO_4$: 78.94 mg.

Found: S, 12.8%. Calcd. for $C_9H_{10}O_4S$: 14.9%.

BULLETIN OF THE CHEMICAL SOCIETY OF JAPAN VOL. 39 1785—1787 (1966)

Organic Sulfur Compounds. XI. The Reactions of the Cyclic Sulfites with the Aromatic Aldehydes

By Michio KOBAYASHI* and Akira YABE

Department of Chemistry, Yokohama City University, Mutsuura-machi, Kanazawa-ku, Yokohama

and Reiko KIRITANI

Department of Chemistry, Radiation Center of Osaka Prefecture, Sakai, Osaka

(Received January 5, 1966)

The reactions of the cyclic sulfites with aldehydes to give the cyclic acetals have been investigated with the stereochemical and with the ^{18}O tracer technique. Both groups of evidence have indicated that the bonds broken are the S–O, not the C–O bond, of the sulfites.

The formation of the acetals from the aldehydes and alkyl sulfites has long been known.[1] Recently, the reaction of ethylene sulfite with the carbonyl compounds to give the cyclic acetals or ketals has also been described.[2] These reactions are catalyzed with hydrogen chloride, without which no reaction has been observed. In order to clarify the mechanism of the latter reaction, the present investigation has been carried out.

Results and Discussion

Stereochemical Study.—The reaction of *meso*-2, 3-butylene sulfite (2-oxo-4, 5-dimethyl-1, 3, 2-dioxothiolane) (I) with benzaldehyde was examined in an attempt to find which bond in the cyclic sulfite was broken in the acetal formation. I was prepared from thionyl chloride and *meso*-2, 3-butanediol. There could exist two configurational isomers in I, one with sulfoxide oxygen in an axial position, Ia, and the other with that oxygen in an equatorial position, Ib. This kind of problem has attracted much interest recently, and several studies by means of infrared spectroscopy or NMR have been published.[3,4] In the case of *meso*-diphenylethylene sulfite, these two isomers have been isolated in the crystalline state.[4] Indeed, it has been pointed out that the ordinary I is a mixture of Ia and Ib, which could be separated incompletely by the gas liquid chromatography.[4] However, these two isomerides, the existence of which depends on the pyramidal configuration of the sulfoxide group, would be tautomerized to each other in the presence of the acid catalyst, since the optically active sulfoxides have been reported to undergo racemization very easily in the presence of hydrochloric acid.[5] Therefore, no effort was made to use the pure configurational isomer in the present investigation. (Incidentally, the configuration of *dl*-2, 3-butanediol has been shown not to change during the formation of the cyclic sulfite, *dl*-2, 3-butylene sulfite.[4])

When I and benzaldehyde were refluxed in dioxane in the presence of hydrogen chloride, 2-phenyl-4, 5-dimethyl-1, 3-dioxolane (II) was obtained in a 50% yield. The identity of this product with 2-phenyl-*cis*-4, 5-dimethyl-1, 3-dioxolane IIa, prepared directly from *meso*-2, 3-butanediol and benzaldehyde, was established by the infrared spectroscopy and gas liquid chromatography. Symmetric structure of II was confirmed by NMR spectroscopy.

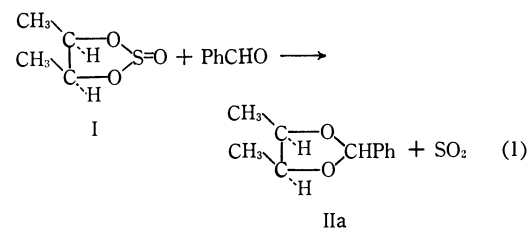

(1)

On the other hand, the reaction of *dl*-2, 3-butanediol with benzaldehyde gave 2-phenyl-*dl*-*trans*-4, 5-dimethyl-1, 3-dioxolane IIb, which exhibited the different NMR and infrared spectrum from those of the product II. The retention time of IIb in the gas liquid chromatography was shorter than that of II.

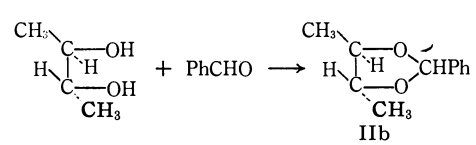

(2)

* To whom inquiries should be sent: Department of Chemistry, Faculty of Science, Tokyo Metropolitan University, Setagaya-ku, Tokyo.

1) W. Voss, *Ann.*, **485**, 283 (1931).

2) G. Hesse and M. Förderreuther, *Chem. Ber.*, **93**, 1249 (1960).

3) J. G. Pritchard and P. C. Lauterbur, *J. Am. Chem. Soc.*, **83**, 2105 (1961).

4) Q. E. Thompson, M. M. Crutchfield and M. W. Dietrich, *J. Org. Chem.*, **30**, 2698 (1965).

5) K. Mislow, T. Simmons, J. T. Melillo and A. L. Ternay, Jr., *J. Am. Chem. Soc.*, **86**, 1452 (1964).

Since it seems to be well understood that the C–O bond of the alcohols is retained in the acetal formation,[6] the above result may be considered to indicate the retention of the C–O bond in the cyclic sulfite in the reaction with aldehydes.

Isotope Tracer Study.—However, in the reaction described above, two successive inversions of the configuration around the asymmetric carbon atoms of the cyclic sulfite, one in each step involving C–O fission in the sulfite, could give *meso*-acetal from *meso*-sulfite. To confirm further the absence of the C–O bond fission of the sulfite in this type of reaction, the reaction of ethylene sulfite, IV, with *p*-nitrobenzaldehyde-[carbonyl-^{18}O] was examined. In the presence of hydrogen chloride, 2-*p*-nitrophenyl-1, 3-dioxolane III was produced in a 60% yield; this was found to contain no excess ^{18}O.

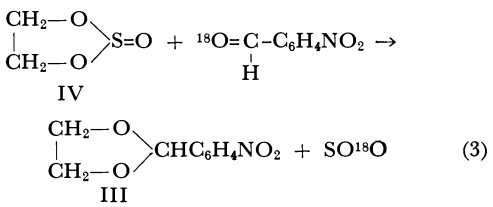

IV

III (3)

Consequently, from both of the stereochemical results and the isotope tracer study, it may be concluded that the C–O bond of the cyclic sulfite remained intact in the reaction with aldehydes to form the cyclic acetals.

The mechanism of the hydrolysis of the cyclic sulfites has been investigated kinetically,[7-8] with the ^{18}O tracer technique[10] and stereochemically;[11] it is now firmly established that S–O bonds are broken in the reaction under acidic conditions, and that C–O bond fission has never been observed. Also, the reaction of alcohols with the carbonyl compounds to form acetals or ketals,[6] and the hydrolysis of the acetals or ketals to reverse the above reaction,[12] are both considered to involve the retention of the C–O bond in the alcohol part. The formation of the cyclic acetals from the sulfites investigated in the present research seems to conform with these findings regarding related reactions.

The reaction of IV with benzaldehyde was carried out in the presence of boron trifluoride etherate or trifluoroacetic acid in order to examine their catalytic properties. In the presence of boron trifluoride, IV gave no cyclic acetal; instead, a large amount of the polymeric substance was produced. With trifluoroacetic acid, the formation of acetal, 2-phenyl-1, 3-dioxolane (V), was observed, but the yield was not improved over that obtained with hydrogen chloride.

The following reaction mechanism may tentatively be considered as one possibility for the reaction investigated in this paper:

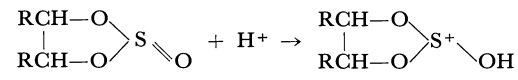

(4)

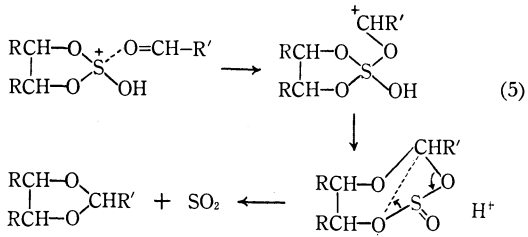

(5)

The addition of the proton to the cyclic sulfite (reaction 4) is a reversible, very fast step.[8] The attack on this protonated species by the nucleophilic reagent, somewhat as in the reaction 5, has been postulated to explain the catalytic property of the halides anion in the hydrolysis of the sulfites.[7,8]

Finally, it should be noticed that the following possibility can not be lightly excluded despite the denial of Hesse[2]—the possibility that the sulfite is hydrolyzed by a trace of water to give the glycols, which in turn react with aldehydes to form the cyclic acetals and to regenerate the equimolar water, with this water starting a new cycle. In the present stage of investigation, there is at least no definite evidence against this alternative.

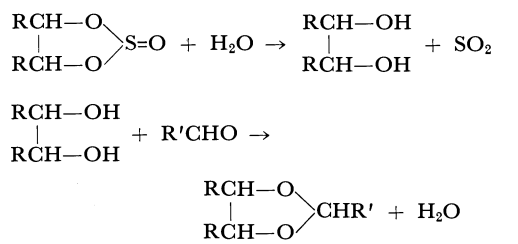

Experimental

***meso*-2, 3-Butylene Sulfite (I).**—The starting material, *meso*-2, 3-butanediol, was a commercial product and was purified by distillation twice before use; b. p. 65°C/7 mmHg; lit.[13] 89°C/16 mmHg; 127°C/101 mmHg.[10] It gave di-*p*-nitrobenzoate, m. p. 188°C,

6) J. Hine, "Physical Organic Chemistry," 2nd Ed., chapter 11, McGraw-Hill, N. Y. (1962).
7) C. A. Bunton, P. B. D. de la Mare and J. G. Tillett, *J. Chem. Soc.*, **1958**, 4754.
8) C. A. Bunton, P. B. D. de la Mare, A. Lennard, D. R. Llewellyn, R. B. Pearson, J. G. Pritchard and J. G. Tillett, *J. Chem. Soc.*, **1958**, 4761.
9) R. E. Davis, *J. Am. Chem. Soc.*, **84**, 599 (1962).
10) C. A. Bunton, P. B. D. de la Mare, P. M. Greaseley, D. R. Llewellyn, N. H. Pratt and J. G. Tillett, *J. Chem. Soc.*, **1958**, 4751.
11) H. K. Garner and H. J. Lucas, *J. Am. Chem. Soc.*, **72**, 5497 (1950).
12) M. M. Kreevoy, C. R. Morgan and R. W. Taft, Jr., ibid., **82**, 3064 (1960).
13) C. E. Wilson and H. J. Lucas, ibid., **58**, 2396 (1936).

in a yield more than 80%. *meso*-2, 3-Butylene sulfite was prepared from 17 g. of the above glycol and 23 g. of thionyl chloride at 40°C, and a fraction boiling at 83—85°C/35 mmHg was collected (lit.[10] b. p. 67°C/8 mmHg; 181—189°C[14]). The infrared spectrum of the product coincided with that in the literature,[10] except for the presence of a 1059 cm^{-1} absorption instead of the 1099 cm^{-1} in that paper.

2-Phenyl-*cis*-4, 5-dimethyl-1, 3-dioxolane (IIa).—A mixture of 5 g. of *meso*-2, 3-butanediol, 6 g. of benzaldehyde and a few drops of 40% sulfuric acid was warmed on a water bath for 28 hr. and extracted with benzene; the product was purified by the vacuum distillation twice. B. p. 97—99°C/5 mmHg; lit.[15] 109—110°C/10 mmHg.

The Reaction of *meso*-2, 3-Butylene Sulfite with Benzaldehyde.—Hydrogen chloride was bubbled into a mixture of 6 g. of I, 5 g. of freshly-distilled benzaldehyde and 10 ml. of purified dioxane.[16] After it had been refluxed for 25.5 hr., the mixture was diluted with benzene, washed with a sodium hydrogen carbonate solution, water, and a sodium hydrogen sulfite solution, warmed with a sodium hydroxide solution, dried, and finally vacuum distilled to give a fraction boiling at 93—94°C/4 mmHg. Its infrared spectrum was superimposable upon that of IIa.

dl-2, 3-Butanediol was prepared from the *meso*-isomer by the following reaction sequence: *meso*-glycol→*meso*-2, 3-diacetate (b. p. 90—93°C/20 mmHg; lit.[13] 66°C/5.5 mmHg)→*dl-threo*-3-chloro-2-butanol (b. p. 52°C/28—30 mmHg; lit.[17] 52°C/30 mmHg)→*cis*-2, 3-epoxybutane[17]→*dl-trans*-2, 3-butanediol (b. p. 71°C/4 mmHg; lit.[13] 86°C/16 mmHg). It gave *dl*-di-*p*-nitrobenzoate, m. p. 130°C; lit. 128.5°C.

2-Phenyl-*dl-trans*-4, 5-dimethyl-1, 3-dioxolane (IIb).—A mixture of 1.2 g. of *dl*-2, 3-butanediol, 1.48 g. of benzaldehyde, and one drop of 40% sulfuric acid was heated on a water bath for 26 hr. The reaction mixture was then treated as in the case of *meso*-isomer, and finally purified by chromatography on alumina with petroleum ether, followed by vacuum distillation; this gave 90 mg. of IIb as a colorless liquid.

Found: C, 74.43; H, 8.19. Calcd. for $C_{11}H_{14}O_2$: C, 74.13; H, 7.91%.

The Preparation of *p*-Nitrobenzaldehyde-[carbonyl-^{18}O].—To a solution of *p*-nitrobenzylidenaniline (10 g.), and 10 g. of $H_2{}^{18}O$ (1.52 atom%) in 80 ml. of anhydrous dioxane, 5 ml. of concentrated sulfuric acid was added. After the mixture had been warmed on a water bath, two layers were separated. After it had been diluted with 150 ml. of benzene, the organic layer was washed with a sodium hydrogen carbonate solution and water, dried over magnesium sulfate, and evaporated. The crystalline residue was purified from petroleum ether to give 5.5 g. of the labeled aldehyde (84%). Its ^{18}O atom% was 0.61%.

Ethylene Sulfite.—Prepared from ethylene glycol and thionyl chloride; b. p. 72°C/22 mmHg. Lit. 94°C/43 mmHg, 84°C/38 mmHg[9]; 88°C/52 mmHg[10]; 86—88°C/38 mmHg[18]; 90°C/42 mmHg[19]; 63°C/13 mmHg[3].

The Reaction of Ethylene Sulfite with *p*-Nitrobenzaldehyde-^{18}O.—Hydrogen chloride was introduced into a solution of 5 g. of the labeled aldehyde and 4 g. of ethylene sulfite in 20 ml. of anhydrous dioxane, and the mixture was refluxed in an oil bath for 34 hr. Dioxane was removed in a vacuum, and the residue was dissolved in 100 ml. of benzene, washed with aqueous sodium hydrogen carbonate, dried, and evaporated. The remaining crystals were purified by chromatography on alumina with benzene and recrystallization from petroleum ether or carbon tetrachloride to give 3.10 g. of 2-*p*-nitrophenyl-1, 3-dioxolane (III), m. p. 89—91°C, in a 46% yield. Its ^{18}O atom % was normal (0.21%). The infrared spectrum of this specimen was the same as that of the product, m. p. 90°C, prepared by warming 20 g. of ethylene glycol, 3 g. of *p*-nitrobenzaldehyde, and a few drops of 40% sulfuric acid for 33 hr. The ^{18}O atom% of the unchanged *p*-nitrobenzaldehyde recovered in a low yield, contaminated with some acetal (III), was 0.35%.

Gas liquid chromatography measurements were performed on Hitachi KGL-2 using 6 m column packed with silicone KF 54. The column was operated at 206°C with a flow of 30 ml. nitrogen per minute. Retention times were: II and IIa, 14.2 min; IIb, 12.0 min.

NMR spectra were run on a Varian A 60A NMR Spectrometer operating 60 Mc./sec. TMS was used as an internal standard for solutions in carbon tetrachloride. The chemical shift values of II was as shown below:

Chemical shift (τ)	Number of H	Splitting	Assignment
8.83	6	Doublet $J=6.0$ c/s	Methyl
5.83	2	Multiplet	H at C_4 and C_5
2.72	5	Multiplet	Aromatic

Thanks are due to Mr. Shozo Masuda of the Department of Chemistry, The University of Tokyo, for his elemental analyses.

14) F. M. Robertson and A. Neish, *Can. J. Research*, **25B**, 491 (1947).
15) J. Kovář, J. Šteffková and J. Jarý, *Collection Czech. Chem. Commun.*, **30**, 2793 (1965).
16) A. Weissberger and E. S. Proskauer, "Organic Solvents," 2nd Ed. (1955).
17) H. J. Lucas and C. W. Gould, Jr., *J. Am. Chem. Soc.*, **63**, 2451 (1941).
18) W. W. Carlson and L. H. Cretcher, ibid., **69**, 1954 (1947).
19) P. B. D. de la Mare, W. Klyne, D. J. Millen, J. G. Pritchard and D. Watson, *J. Chem. Soc.*, **1956**, 1813.

BULLETIN OF THE CHEMICAL SOCIETY OF JAPAN VOL. 39 1788—1791 (1966)

Organic Sulfur Compounds. XII. The Ultraviolet and Infrared Spectra of the Substituted Benzenesulfinic Acids and Their Esters

By Michio KOBAYASHI* and Nobuko KOGA

Department of Chemistry, Yokohama City University, Mutsuura-machi, Kanazawa-ku, Yokohama

(Received January 7, 1966)

The ultraviolet spectra of several substituted benzenesulfinic acids and their ethyl esters have been recorded, and the assignments of the absorption have been disucssed briefly.

There have been relatively few studies of the ultraviolet spectra of the sulfinic acids and their esters, although many systematic investigations have been published on the related sulfoxides, sulfones and sulfides.[1-3] Detoni and her collaborator[4] measured the ultraviolet spectra of benzenesulfinic acid and *p*-toluenesulfinic acid in ethanol, but no discussion was given. Bredereck et al.[5] studied the ultraviolet spectra of the above two compounds in heptane, methanol and water; they found that the spectra of the dissociated anion was overlapped on those of the free acid in the hydroxylic solvents. They pointed out the close similarity between the spectrum of the undissociated acid and that of the corresponding ester, and also the presence of a similar absorption band in the spectrum of the sulfoxide. Later, Ritchie[6] estimated the dissociation constants of several benzenesulfinic acid derivatives by the ultraviolet spectroscopic method, but he presented no details of the spectra themselves.

Results and Discussion

The ultraviolet Spectra of the Sulfinic Acids in Water.—The ultraviolet spectrum of the sulfinic acid in water is actually that of the completely dissociated anion, as has been pointed out by Bredereck,[5] since the sulfinic acid has a rather strong acid character. When the solution was increased in acidity by the addition of hydrochloric acid, the absorption spectrum of the undissociated acid appeared, making it possible to estimate the dissociation constant of the sulfinic acid. For example, the pK_a of *p*-chlorobenzenesulfinic acid could be estimated as 1.14 from the absorption curves shown in Fig. 1.

Aliphatic sulfinic acid exhibited no absorption maximum in the ordinary ultraviolet region, as may be seen in Fig. 2. This fact indicates that both the π-π^* and n-dπ transitions in the SO_2H or the SO_2^- group need high energies corresponding to absorptions well below 200 mμ; This situation may be easily understood by considering that the aliphatic sulfoxides have an n-dπ absorption at around 210 mμ.[1e]

The values of the absorption maxima of the substituted benzenesulfinic acids and their anion are listed in Table I.

The spectra of the anions are very close to those of the parent mono-substituted benzenes in the shape of the absorption curve and also in the wavelength of the band maximum. Only slight red shifts

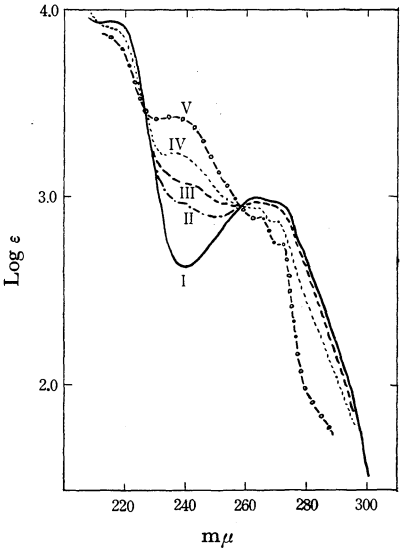

Fig. 1. Ultraviolet spectra of *p*-chlorobenzenesulfinic acid.
Solvent: I) H_2O, II) 0.01 N HCl, III) 0.02 N HCl, IV) 0.05 N HCl, V) 1.00 N HCl

* To whom inquiries should be addressed: Department of Chemistry, Faculty of Science, Tokyo Metropolitan University, Setagaya-ku, Tokyo.

1) H. P. Koch, *J. Chem. Soc.*, a) **1949**, 387; b) **1949**, 394; c) **1949**, 401; d) **1949**, 408; e) **1950**, 2892.
2) G. Leandri, A. Mangini and R. Passerini, ibid., **1957**, 1386.
3) a) C. C. Price and S. Oae, "Sulfur Bonding," Ronald Press, N. Y. (1962); b) N. Kharasch ed., "Organic Sulfur Compounds," Pergamon Press, Oxford (1961), Chapter 6 and 7; c) H. H. Jaffé and M. Orchin, "Theory and Applications of Ultraviolet Spectroscopy," J. Wiley & Sons, N. Y. (1962), p. 466.
4) S. Detoni and D. Hadži, *J. Chem. Soc.*, **1955**, 3163.
5) H. Bredereck, G. Brod and G. Höschele, *Chem. Ber.*, **88**, 438 (1955).
6) C. D. Ritchie, J. D. Saltiel and E. S. Lewis, *J. Am. Chem. Soc.*, **83**, 4601 (1961).

TABLE I. ULTRAVIOLET SPECTRA OF SUBSTITUTED BENZENESULFINIC ACIDS IN WATER
λ_{max} in mμ and log ε (in parenthesis)

Substituent	Acid			Anion	
	^1L_a	W	^1L_b	^1L_a	^1L_b
H	215** (3.8)	237 (3.4)	265 (2.8)	215 (3.9)	265 (2.9)
p-Methyl	223 (3.8)	240 (3.5)	265 (2.8)	223 (3.9)	265 (3.0)
p-Chloro	225 (4.3)	245 (4.0)	270 (3.2)	225 (4.2)	270 (3.2)
p-Bromo	230 (4.2)	~250 (3.8)	275** (2.9)	230 (4.2)	275 (3.2)
p-Methoxy	235* (4.1)		275 (3.1)	232 (4.1)	275 (3.3)
p-Acetamido	255* (4.2)			248 (4.2)	280* (~3)
p-Nitro	265* (4.0)			270* (4.0)	
o-Methyl	220 (3.8)	240 (3.5)	265 (3.0)	225 (3.9)	265 (3.5)
o-Methoxy	222 (3.8)	245 (3.3)	282 (3.5)	225 (3.9)	280 (3.5)
o-Nitro	265* (3.7)			265 (3.7)	
o-Carboxy	232 (3.7)		280 (3.2)	240 (3.5)**	278 (3.0)

* Superposition of several bands. See text.
** Shoulder.

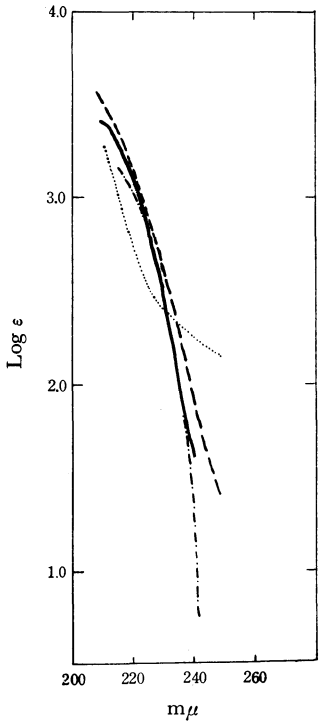

Fig. 2. Ultraviolet spectra of *n*-butanesulfinic acid and its ethyl ester.
—— Acid in H_2O
– – – Acid in 10^{-3} N NaOH
····· Acid in 1 N HCl
·—· Ethyl ester in 95% ethanol

are observed in the maximum of the ^1L_a band compared to those of the corresponding mono-substituted benzenes, suggesting the weakness of the interaction between the sulfinate anion group and the π-electron orbitals of the benzene ring.

The Stuart model of the molecule suggested the presence of a large steric interference between the sulfinate group and a bulky *o*-substituent. Although *o*-nitrobenzenesulfinic acid has almost the same absorption maximum as that of the *p*-isomer, its extinction coefficient is smaller by 0.3 unit in log ε, suggesting that the nitro group is rotated out of the benzene plane to some degree.

In the absorption spectra of the undissociated acids, the presence in 240—260 mμ of a new absorption should be noticed, an absorption which is not observed in the anion. Since similar absorptions are observed in the alkyl aryl sulfoxides, this band will here be designated as the W-band, according to the Jaffé's notation.[3c] A similar band exists in the spectrum of the corresponding ethyl sulfinates, as is shown in Table II. This W-band may be attributed to an excitation of the lone pair electrons of the sulfur atom into an antibonding orbital of the S–O bond or into a vacant 3d orbital of the sulfur atom (this difference depends only on the amount of the double bond character of the sulfoxide S–O bond; the exact estimation is still open to debate); the band appears in a longer wavelength region than the bands of the aliphatic sulfoxides, as a result of the conjugation to the benzene ring. Another postulation involving the excitation of a lone pair of the sulfur atom to an unoccupied orbitals of the aromatic electron system rather than to the sulfinyl group is also possible. With *p*-toluenesulfinic acid, this W-band shifts its maximum from 255 mμ in heptane,[5] over 245 mμ in ethanol to 240 mμ in diluted hydrochloric acid, and thus reveals its n-electron donating character. In the sulfinate anions, this W-band shifts to a much lower wavelength, under 200 mμ, as a result of the contribution of the negatively charged oxygen atom; this situation is the same as in the case of the carboxylic acid and its anion. Since *o*-toluenesulfinic acid, in which the sulfinoxy group is considered to rotate out of the benzene plane due to interaction with a bulky *o*-methyl group, shows its W-band at nearly the same wavelength as in the *p*-isomer, the coplanarity seems

not to be an important requirement in the conjugation between the sulfinyl group and the aromatic π-electron system, as is the case in the aromatic sulfones.[3a,3c,7,8] The existence of the W-band in nitro or carboxyl substituted benzenesulfinic acids is not clear due to the superposition of a strong charge transfer band in these compounds.

The Ultraviolet Absorption of the Ethyl Ester of the Substituted Benzenesulfinic Acids. —These are shown in Table II. Aliphatic sulfinate ester exhibited only an end absorption in the ultraviolet region, as in the free acid, indicating the high transition energy of the n-dπ excitation in the sulfinate ester group (Fig. 2).

TABLE II. ULTRAVIOLET SPECTRA OF ETHYL BENZENESULFINATES

λ_{max} (mμ) and log ε (in parenthesis)

Substituent	Solvent	^1L_a	W+^1L_b
H	Methanol	216 (3.89)	246 (3.52)
	n-Hexane	215 (3.96)	257 (3.46)
p-Methyl	Methanol	224 (3.95)	243 (3.70)
	n-Hexane	223 (4.00)	255 (3.51)
p-Chloro	Methanol	228 (4.13)	250 (3.73)
	n-Hexane	227 (4.14)	260 (3.58)
p-Bromo	Methanol	233 (4.17)	250 (3.80)
	Ether	232 (4.21)	258 (3.75)
	n-Hexane	232 (4.20)	260 (3.71)
p-Methoxy	Methanol	249 (4.13)*	
	n-Hexane	235 (4.07)	252 (3.94)
p-Cyano	Methanol	231 (4.24)	270 (3.64)
	n-Hexane	230 (4.18)	275 (3.50)
p-Nitro	Methanol	254 (4.03)**	280 (3.79)***
	n-Hexane	250 (4.07)	288 (3.63)

* Broad band, probably superposition of ^1L_a and W+^1L_b.
** Charge transfer band.
*** Shoulder.

There are two absorptions of distinctly different characters in the ultraviolet spectra of the substituted benzenesulfinic esters, one at a short wavelength, similar to the ^1L_a band of the corresponding mono-substituted benzenes, and the other in the long wavelength side. The shifts of the ^1L_a band from the position of the parent mono-substituted benzene are slightly larger than those in the sulfinate anion, suggesting a somewhat stronger interaction of the sulfinate ester group with the aromatic π-orbital than that of the sulfinate anion group, although the interaction is still weak compared with those of nitro or carbonyl groups.

The long wavelength band is considered to be an overlapping of the W-band and ^1L_b band. The optical active property of the W-band has been demonstrated clearly by optical rotatory dispersion and circular dichroism measurements of the optically active *l*-menthyl *p*-toluenesulfinate and *p*-methoxybenzenesulfinate,[7] thus confirming the assignment of this transition to a sulfinyl group origin, although in that earlier paper the long wavelength band has been postulated to be an overlapping of a pertubed ^1L_a benzene transition and the W-band. Discussing the problem of the stereochemistry of the sulfoxides and sulfinate esters, Mislow et al.[8b] assumed the long wavelength band to be arisen from the interaction of the ^1L_b band with the sulfoxide $(3sp^3)^2 \rightarrow (3sp^3)(3d)$ transition.

The absorption maximum of the long wavelength band does not vary much with the kind of substituent. In the *p*-methoxy derivative, the W-band shows slight blue shift, which is characteristic of n-π transition. In *p*-nitro and *p*-cyano derivatives, the existence of the W-band again becomes uncertain; probably it is covered by the absorption of the strong charge transfer band. The 250 mμ absorption of ethyl *p*-nitrobenzenesulfinate shows a red shift in a polar solvent, suggesting that this band is a charge transfer band, similar to that of nitrobenzene.[9] Since the absorption maximum of this compound does not differ much compared with that of nitrobenzene itself (252 mμ in heptane, 259.5 mμ in ethanol), the contribution of the lone pair of the sulfur atom could not be ascertained reliably, but the increased extinction coefficient of the long wavelength band suggests the overlapping of the W-band on the 280 mμ band of nitrobenzene or on the 271 mμ band of *p*-cyano derivative (both ^1L_b bands). The hypsochromic shift of these long wavelength bands in a polar solvent also supports this interpretation. If this could be true, the W-band may be said to show a large red shift upon coupling with an electron attractive substituent. On the other hand, the nearly-same position of the charge transfer excitation around 250 mμ seems to indicate the absence of a large contribution of the electrometric polar form in the excited state, as shown below:

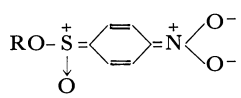

In this respect, the sulfinoxy group differs greatly from the sulfide group (for instance, *p*-nitrothioanisol has λ_{max} at 338 mμ, with log ε=4.12).

In conclusion, the sulfinoxy group and the alkoxysulfinyl group may be considered to have only a weak electron attractive conjugation property,

7) K. K. Andersen, W. Gaffield, N. E. Papanikolaou, J. W. Foley and R. I. Perkins, ibid., **86**, 5637 (1964).
8) a) K. Mislow, P. Schneider and A. L. Ternay, Jr., ibid., **86**, 2957 (1964). b) K. Mislow, M. M. Green, P. Laur, J. T. Melillo, T. Simmons and A. L. Ternay, Jr., ibid, **87**, 1958 (1965).
9) S. Nagakura and J. Tanaka, *J. Chem. Phys.*, **22**, 236 (1954); S. Nagakura, ibid., **23**, 1441 (1955).

and at the same time to be very weakly electron donating.

The Infrared Spectra of the Ethyl Esters of Substituted Benzenesulfinic Acids.—The spectra were measured in carbon tetrachloride and also in the pure liquid state. The wave numbers of the S–O stretching vibration are shown in Table III. The absorption maximum in the pure liquid is slightly lower in wave number (2—9 cm^{-1}) than that in a solution, probably because of the association. Ethyl *n*-butanesulfinate absorbs at 1132 cm^{-1} (CCl_4, and neat), which is almost the same as, or even rather lower than, the S–O stretching of ethyl benzenesulfinate. A similar phenomenon has been observed in the sulfoxides[10] and interpreted as indicating the absence of any strong conjugation between the aromatic ring and the sulfinyl group.

Table III. Infrared spectra of ethyl benzenesulfinates. S–O Stretching vibration in cm^{-1}

Substituent	H	*p*-CH_3	*p*-CH_3O	*p*-Cl	*p*-Br	*p*-NO_2
Neat	1132	1134	1126	1136	1138	1138
in CCl_4	1136	1136	1135	1142	1142	1149

The Hammett plot of the wave numbers of the S–O stretching against σ value shows a approximately linear correlation. Since there have been closely related studies of the methyl esters of the substituted benzenesulfinic acids,[11] further discussion will be omitted here.

Experimental

Materials.—*n*-Butanesulfinic acid was prepared from *n*-butyl bromide by the Grignard method.[12] Ethyl *n*-butanesulfinate was synthesized from sulfinyl chloride and ethanol, and boiled at 80°C/10 mmHg.[13] *o*-Toluenesulfinic acid, m. p. 80°C, was prepared from sulfonyl chloride by reduction with zinc. *p*-Chlorobenzenesulfinic acid, m. p. 93—94°C, was obtained by saturating a *p*-chlorobenzenediazonium chloride solution with sulfur dioxide.[14] *p*-Bromobenzenesulfinic acid, m. p. 114°C, was prepared by Friedel-Crafts' synthesis from bromobenzene and sulfur dioxide.[15] *p*-Methoxybenzenesulfinic acid, m. p. 97—98°C, was prepared from anisol in a similar way and was purified from water.[15] *o*-Methoxy derivative, m. p. 98—99°C, was prepared from diazotized *p*-anisidine.[16] *p*-Acetylaminobenzenesulfinic acid, m. p. 155°C (with decomposition), was prepared by reducing sulfonyl chloride with sodium sulfite.[17] *p*-Nitrobenzenesulfinic acid, m. p. 135°C, was obtained in a similar way.[18] *o*-Nitro-derivative, m. p. 130°C, was prepared by reducing sulfonyl chloride with stannous chloride and hydrochloric acid in ethanol.[19] *o*-Carboxybenzenesulfinic acid, m. p. 125°C, was obtained by the diazonium method and was recrystallized from acetic acid.[16] Ethyl esters of the benzenesulfinic acids was prepared by treating the sodium salt with ethyl chlorocarbonate in ethanol.[20]

The ultraviolet spectra were taken on a Beckmann DU quartz spectrophotometer. The concentration of the solution was 10^{-4}—10^{-5} mol./l. The infrared spectra were recorded with a Perkin-Elmer infrared spectrometer Model 21. The dissociation constants were calculated from the variation of the transmission with the change in pH. The pK_a values obtained for benzenesulfinic acid, *p*-toluenesulfinic acid and *p*-chlorobenzenesulfinic acid were 1.58, 1.70 and 1.14 respectively. The figures in the literature are 1.29,[21] 1.46,[22] 1.84,[23] 1.21[6] for the first compound; 1.60,[22] 1.99,[23] 1.24[6] for the second, and 1.09 for *p*-bromobenzenesulfinic acid.[6]

10) D. Barnard, J. M. Fabian and H. P. Koch, *J. Chem. Soc.*, **1949**, 2442.
11) S. Ghersetti and G. Modena, *Ann. Chim.* (Rome), **53**, 1083 (1963); B. Bonini, S. Ghersetti and G. Modena, *Gazz. Chim. ital.*, **93**, 1222 (1963).
12) H. G. Houlton and H. V. Tartar, *J. Am. Chem. Soc.*, **60**, 544 (1938).
13) J. v. Braun and G. Weissbach, *Ber.*, **63**, 2836 (1930).
14) M. E. Hanke, *J. Am. Chem. Soc.*, **45**, 1321 (1923).
15) E. Knoevenagel and J. Kenner, *Ber.*, **41**, 3315 (1908).
16) L. Gattermann, ibid., **32**, 1142 (1899).
17) Organic Syntheses, Coll. Vol. 1, 7 (1948).
18) T. Zincke and S. Lehnbardt, *Ann.*, **400**, 15 (1913); P. R. Carter and D. H. Hey, *J. Chem. Soc.*, **1948**, 147.
19) M. Claasz, *Ann.*, **380**, 303 (1911).
20) R. Otto, *Ber.*, **18**, 2504 (1885); Part VI of this series.
21) P. Rumpf and J. Sadet, *Bull. soc. chim. France*, **1958**, 447.
22) J. M. Loven, *Z. Physik. Chem.*, **19**, 456 (1896).
23) R. K. Burkhard, D. E. Sellers, F. DeCou and J. L. Lambert, *J. Org. Chem.*, **24**, 767 (1959).

BULLETIN OF THE CHEMICAL SOCIETY OF JAPAN VOL. 39 1792—1795 (1966)

Studies on Reactions of Polypropyrene. VI. The Thermal Degradation of Polypropylene Accelerated by the Fine Powdery Polymer with Closslinkage

By Yukio MIZUTANI, Keiichi YAMAMOTO and Seishiro MATSUOKA

Tokuyama Soda Co., Ltd., Tokuyama, Yamaguchi

(Received November 29, 1965)

The thermal degradation of polypropylene was investigated in the presence of the fine powdery polymer with crosslinkage by the use of an extruder under a nitrogen atmosphere. The fine powdery polymer was thus found to be effective as an accelerator for the thermal degradation of polypropylene. The fine powdery polymer used was prepared by the emulsion polymerization of some vinyl monomers and divinyl benzene or by the polymerization of glycidyl methacrylate and divinyl benzene in *n*-heptane. The fine powdery polymer consisting of glycidyl methacrylate and divinyl benzene was preferable to that with no reactive functional group, because of the reactivity of the glycidyl group. The polypropylene was modified and made dyeable by the thermal degradation accelerated by the fine powdery polymer.

It is well known that there are a few drawbacks to the practical uses of polypropylene; such as the poor flow properties resulting from its very high molecular weight, and the poor dyeability resulting from its nonpolarity and its high crystallinity. Therefore, many processes have been proposed to overcome these drawbacks.[1-10] In the thermal degradative process accelerated by such vinyl polymers as polystyrene and polymethyl methacrylate, graft or block copolymers were formed, and the poor dyeability of polypropylene could be modified.[11] However, some of the vinyl polymers used in this process were extractable by acetone, and it was considered to be undesirable for practical use.

In this paper, the fine powdery polymer with crosslinkage (FPC) was used as an accelerator for the thermal degradation of polypropylene. The thermal degradation was carried out by the use of an extruder, so this simple process should be practically useful.

Experimental

Materials.—The polypropylene (PP) powder used was under 30 mesh and contained no stabilizer. The properties of the polypropylene samples were as follows:

PP(A) melt index (at 230°C, load: 2.16 kg./cm.^{2}): 0.25 g./10 min., specific gravity: 0.912, and grain size: under 30 mesh.

PP(B) melt index (at 230°C, load: 2.16 kg./cm.^{2}): less than 0.01 g./10 min., specific gravity: 0.913, and grain size: under 30 mesh.

All the reagents, such as vinyl monomers, divinyl benzene (DVB), and solvents, were of chemical grade. The DVB content in commercial DVB was 50% by weight.

The Preparation of the Fine Powdery Polymer by the Emulsion Polymerization (EPC·E).—The vinyl monomers and DVB were polymerized by stirring at 80°C for 2—3 hr. under a nitrogen atomsphere. Then, the polymer was salted out, washed with water,

TABLE I. THE EXAMPLES OE THE PREPARATION OF FPC·E

Sample	Vinyl monomer, g.			DVB g.	Yield %
	Styrene	2-Methyl 5-vinyl pyridine	Methyl acrylate		
FPC·E-1	24	—	—	1	84
FPC·E-2	—	12	12	1	80
FPC·E-3	—	24	—	1	80
FPC·E-4	—	—	24	1	82

The quantities of water and Monogen-W were 300 cc. and 2 g. respectively.

Monogen-W was the emulsifier from Daiichi Kogyo Seiyaku Co., Ltd.

1) G. Natta, E. Beati and F. Seberini, *J. Polymer Sci.*, **34**, 685 (1959).
2) R. F. Stamm, E. F. Hosterman, C. D. Felton and C. S. Hsia Chen, *J. Appl. Polymer Sci.*, **7**, 753 (1963).
3) S. Torikai and E. Mukoyama, *Chem. High Polymers Japan (Kobunshi Kagaku)*, **19**, 337 (1962); **19**, 344 (1962).
4) Y. Iwakura, T. Kurosaki, K. Nagakubo, K. Takeda and M. Miura, This Bulletin, **38**, 1349 (1965).
5) P. Ginstiani, G. Natta and G. Mazzanti, U. S. Pat. 3115478.
6) M. Kubo and O. Fukumoto, Japanese Pat. 291 (1965).
7) M. Kubota, M. Katayama and O. Ishizuka, *J. Chem. Soc. Japan, Ind. Chem. Sect. (Kogyo Kagaku Zasshi)*, **66**, 725 (1963).
8) R. Oda and N. Takeda, Japanese Pat. 12170 (1965).
9) K. S. Minsker, I. Z. Shapiro and G. A. Razuvayev, *Polymer Sci., U. S. S. R.*, **4**, 1 (1963).
10) S. Morimoto, O. Ishiwari and S. Uchida, Japanese Pat. 4683; 4733 (1963).
11) Y. Mizutani, S. Matsuoka and K. Yamamoto, This Bulletin, **38**, 2054 (1965).

and dried at 70°C under a vacuum. An example of the polymerization is shown in Table I. Potassium persulfate was used as an initiator of the polymerization.

The Preparation of the Fine Powdery Polymer by the Polymerization of Glycidyl Methacrylate and DVB in *n*-Heptane (FPC·H).—Glycidyl methacrylate (GMA) and DVB were polymerized in *n*-heptane by stirring at 70°C for 5—6 hr. under a nitrogen atmosphere. Benzoyl peroxide was used as an initiator of the polymerization. The polymer prepared was filtered, washed with petroleum ether and dried under a vacuum. An example of the polymerization is shown in Table II.

Table II. The examples of the preparation of FPC·H

Sample	GMA g.	DVB g.	DVB*/(GMA+DVB)	*n*-Heptane cc.	BPO** g.	Yield %
FPC·H-1	190	10	0.025	2800	10	83
FPC·H-2	180	20	0.050	2800	10	82
FPC·H-3	170	30	0.075	2800	10	84

* Pure DVB
** Benzoyl peroxide

Blending.—FPC was dispersed in a solvent beforehand by the use of a mixer; then the polypropylene powder was added to the mixer, and the slurry was well mixed. The polymers were then filtered out and dried under a vacuum. The solvents used were methanol for FPC·E and *n*-heptane for FPC·H.

The Thermal Degradation.—The thermal degradation was carried out by the use of the extruder, which was a modification[11] of Type MK-1 from Modern Machinery Co., Ltd. The heating zone of the extruder was divided into three parts: T_1, T_2, and T_3, which show the temperatures of the three parts, the part near the sample inlet, the middle part, and the part near the sample outlet respectively, as has been shown in a preceding paper.[11]

The Determination of the Glycidyl Group Content.—The polymer extruded was powdered by reprecipitation; the polymer was then dissolved in hot *p*-xylene, and the hot solution was cooled slowly. Then the slurry obtained was stirred into methanol in a mixer. The powdered polymer was filtered, washed with methanol, and dried under a vacuum. The content of the glycidyl group was determined by the method used by Iwakura et al.[4] The powdered polymer (2 g.) was immersed in a solution of 25 ml. of dioxane and 20 ml. of a 0.1 N dioxane solution of hydrochloric acid. The mixture was then allowed to stand overnight, and the excess hydrochloric acid was titrated with a 0.1 N aqueous solution of sodium hydroxide, using phenolphthalein as an indicator.

Results and Discussion

The Thermal Degradation Accelerated by FPC·E.—It is beyond question that the change in intrinsic viscosity is the most preferable measure of the degree of the degradation, but the melt index was used in this study because FPC used was insoluble in any solvent.

Table III. The results of the thermal degradation of PP(A) accelerated by EPC·E

Sample	Reaction temp., °C T_1	T_2	T_3	Melt index g./10 min.
PP(A)	220	300	270	0.6
PP(A)	220	320	290	0.8
PP(A)-FPC·E-1	220	320	290	4.2
PP(A)-FPC·E-2	220	300	270	3.2
PP(A)-FPC·E-3	220	320	290	3.2
PP(A)-FPC·E-4	220	320	290	3.4

The quantity of FPC added was 5% by weight
The rotating speed of the screw shaft was 20 r.p.m.

Table III shows the results of the thermal degradation. It was established that FPC·E was effective as an accelerator for the thermal degradation of polypropylene. No vinyl polymer was extracted by acetone from the extruded polymer. This was considered to be reasonable, because FPC·E was crosslinked by DVB. However, although FPC·E was effective as an accelerator, FPC·E is practically inferior to FPC·H for the following reasons:

1) FPC·E is contaminated by the emulsifier, so the surface of FPC·E is hydrophilic and is therefore poor in affinity with polypropylene.

2) FPC·E is separated by salting-out from the emulsion and is strongly agglomerated; therefore, it is inferior to FPC·H because the blend of FPC·E to polypropylene is not easier than that of FPC·H.

3) FPC·E is prepared in water, so monomers with a reactive functional group can not be polymerized often.

The Thermal Degradation Accelerated by FPC·H.—In Table IV, it is shown that FPC·H was effective as an accelerator for the thermal degradation of polypropylene and that the degree of degradation increased with the elevating of the reaction temperature.

Table IV. The temperature effect on the thermal degradation of PP(B) accelerated by FPC·H-2

The quantity of FPC·H-2 added, %	Reaction temp., °C T_1	T_2	T_3	Melt index g./10 min.
0	220	325	280	0.01
6.5	220	280	280	0.12
6.5	220	310	280	0.6
6.5	220	325	280	2.6

The rotating speed of the screw shaft was 20 r.p.m.

Figure 1 shows the effect of the rotating speed of the screw shaft, which was related to the retention time of the polymer in the extruder. With the increase in the rotating speed, namely, with the decrease in the retention time of the polymer, the degree of degradation decreased. The shearing

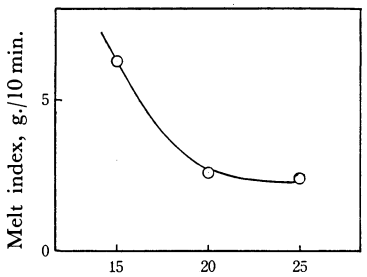

Fig. 1. The effect of the rotating speed of the screw shaft of the extruder on the thermal degradation of PP(B).
The content of FPC·H-2 added: 6.5%
Reaction temperature: T_1=230°C, T_2=325°C, and T_3=280°C
Retention time: about 5 min. for 15 r.p.m.
about 4 min. for 20 r.p.m.
and about 3 min. for 25 r.p.m.

effect of the screw shaft is negligible, because the shearing effect has a negative temperature coefficient;[12] no degradation of polypropylene ([η]: 4.3 dl./g. at 135°C in tetraline) was observed under the following conditions: T_1: 190°C, T_2: 240°C, T_3: 200°C, and the rotating speed of the screw shaft: 30 r. p. m.[11] The mixing effect of the screw shaft and the trace of oxygen due to the imperfect air-tightness of the extruder are questionable; however, they can not be explained in detail now.

Fig. 2 shows that with the increase in the FPC·H content, the melt index increased.

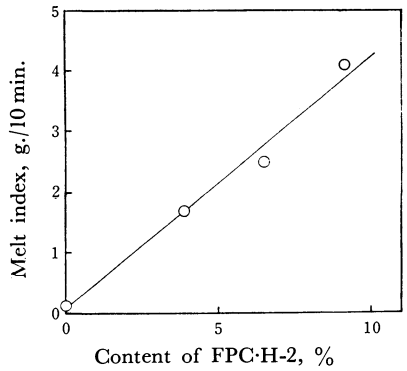

Fig. 2. The effect of the content of FPC·H-2 on the thermal degradation of PP(B).
Reaction temperature: T_1=220°C, T_2=325°C, and T_3=280°C
The rotating speed of the screw shaft: 20 r.p.m.

Figure 3 shows the effect of the DVB content of FPC·H. With the increase in the DVB content, the melt index decreased; namely, the accelerating effect of FPC·H decreased. This can be explained

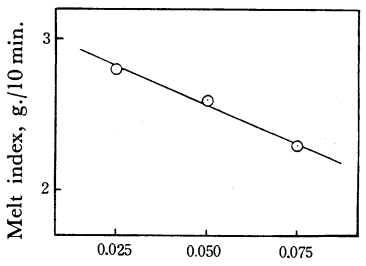

Fig. 3. The effect of the DVB content of EPC·H on the thermal degradation of PP(B).
The content of FPC·H: 6.5%
Reaction temperature: T_1=220°C, T_2=325°C, and T_3=280°C
The rotating speed of the screw shaft: 20 r.p.m.

in term of the fact that the rate of the degradation of polystyrene crosslinked by DVB decreases with the increase in the DVB content.[13]

As has been described above, FPC·H containing the glycidyl group was effective in accelerating the thermal degradation of polypropylene. Furthermore, the glycidyl group must survive after the degradation of polypropylene in order to hold its reactivity. Therefore, the change in the content of the glycidyl group was determined by measuring the contents before and after extruding. Table V shows that the greater part of the glycidyl group

TABLE V. THE GLYCIDYL GROUP CONTENTS BEFORE AND AFTER EXTRUDING

Sample	Reaction temp. °C			Glycidyl group content	Ratio of glycidyl group content S-2/S-1 or S-3/S-1
	T_1	T_2	T_3	mmol./g	
S-1	—	—	—	0.33	—
S-2	220	240	220	0.31	0.91
S-3	220	325	280	0.25	0.76

The rotating speed of the screw shaft was 20-r.p.m.
PP(B) and FPC·H-2 were used.

survived after extruding. This could be explained in terms of the fact that the glycidyl group generally reacts under ionic conditions and is not changed by the radical polymerization for the preparation of FPC·H or by the thermal degradation of polypropylene, which is also a radical reaction.[14]

Because the smell of glycidyl methacrylate was perceived during the extrusion, the degradation of FPC·H to the monomer seems to have occurred, although the quantity of the monomer liberated was probably not much. The active radical generated in the degradation of FPC to the monomer

12) R. J. Ceresa, "Block and Graft Copolymers," Butterworths, London (1962), p. 69.

13) H. H. G. Jellinek, "Degradation of Vinyl Polymers," Academic Press Inc., Publishers, New York (1955), p. 123.

14) F. Hamada, *Chem. High Polymers Japan* (*Kobunshi Kagaku*), **19**, 402 (1962).

may be effective in accelerating the thermal degradation of polypropylene, but the accelerating effect of FPC should be inferior to that of a linear vinyl polymer, as FPC was crosslinked by DVB, and the degradation rate of FPC should be slower than that of a linear vinyl polymer. Furthermore, interactions among the vinyl monomer liberated, FPC radicals, polypropylene radicals, and polypropylene molecules may be presumed to have occurred. This presumption is supported by the fact that, when a linear vinyl polymer was used in place of FPC, graft or block copolymer were detected.[11]

Dyeability.—The utility of a reactive polymer is well known.[15-17] The modification of polypropylene by glycidyl methacrylate has been reported already: the graft copolymer has been prepared[4] and the glycidyl methacrylate copolymer has been blended to polypropylene.[7] When the fiber of the modified polypropylene was dyed by a dye which has a functional group reactive with the glycidyl group, the dye could be perfectly fixed in the fiber, as determined by extraction with acetone.[7] The thin film (0.15 mm. in thickness) was molded from the extruded polymer and was dyed with such dispersion dyes as Estrol Fast Violet B, Estrol Orange 5R and Celliton Blue Extra by the ordinary method.[7] The film containg FPC·E was well dyed, but the dyed film was decolored by the extraction with acetone. On the other hand, the film containing the glycidyl group (FPC·H) was well dyed and the dyed film was not decolored with acetone. This fact was an evidence showing the utility of FPC·H as a reactive polymer. Also, it was elucidated by microscopic observation that FPC dispersed in polypropylene was well dyed, while polypropylene itself was not dyed.

15) M. Imoto, *J. Soc. Org. Syn. Chem. Japan* (*Yuki Gosei Kagaku Kyokaishi*), **15**, 325 (1957).
16) Y. Iwakura, ibid., **20**, 813 (1962).
17) W. Kern and R. C. Schulz, *Angew. Chem.*, **69**, 153 (1957).

Conclusion

The fine powdery polymer with crosslinkage was effective as an accelerator in the thermal degradation of polypropylene and also as a mordant in the dyeing of polypropylene. Among several polymeric systems, the fine powder of the glycidyl methacrylate - divinyl benzene polymer was preferable because of the reactivity of the glycidyl group.

The authors wish to thank for Professor Yoshinobu Takegami of Kyoto University; Mr. Haruo Nakazawa, Managing Director of Tokuyama Soda Co., Ltd., and Mr. Senpachi Miyoshi, Director of Tokuyama Soda Co., Ltd., for their discussions.

BULLETIN OF THE CHEMICAL SOCIETY OF JAPAN VOL. 39 1795—1800 (1966)

The Syntheses of Polypyromellitimide-amides*

By Motoo SAGA, Toshiyuki SHONO and Koichiro SHINRA

Department of Chemical Technology, Faculty of Engineering, Osaka University, Miyakojima-ku, Osaka

(Received December 6, 1965)

Dibasic acids containing a pyromellitimide ring were synthesized by the reaction of pyromellitic dianhydride with such ω-aminoacids as glycine, ε-amino-caproic acid and *p*-amino-benzoic acid. By the condensation polymerization of the dibasic acids obtained above with diamines, polypyromellitimide-amides were synthesized. The polymers were soluble in *m*-cresol and sulfuric acid, and the inherent viscosities of the polymers ranged from 0.21 to 0.42 (in *m*-cresol). The polymers were found to be considerably heat-stable.

It is generally recognized that the polymers with recurring aromatic units have a high thermal stability, and several synthetic studies of various polymers have been conducted. For example, the polypyromellitimide developed by the duPont Company and already commercialized as "H-film"[1] possesses an excellent heat-resistant property, a cold-proof property, a corrosion-resistant property for various chemicals, and a pronounced film-forming capability.

The method of synthesizing such material is shown as Formula 1 below:

* Presented at the 17th Annual Meeting of the Chemical Society of Japan, Tokyo, April, 1964.

1) L. E. Amborski, *Ind. Eng. Chem.*, **2**, 189 (1963).

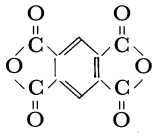
+ H_2NRNH_2 →

Aromatic diamine

Pyromellitic dianhydride

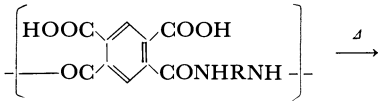

Polyamic acid

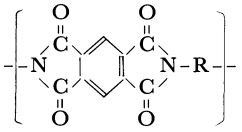
(1)

Polyimide

However, the polypyromellitimide has the disadvantage that it has no solubility in many organic solvents. One method of correcting this defect may be the introduction of the amide-linkages or straight-chain methylene groups into the polymer backbone, in addition to the imide-linkage.

In the present study, dibasic acids, as is generally shown by the Formula 2 were synthesized by the reaction of pyromellitic dianhydride with such ω-aminoacids as glycine, ε-amino-caproic acid and *p*-amino-benzoic acid. The polypyromellitimide-amides, generally shown by the Formula 3, were synthesized by the condensation polymerization of these dibasic acids with diamines.

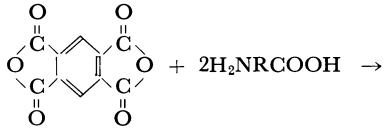
+ $2H_2NRCOOH$ →

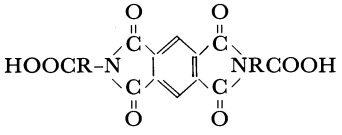
(2)

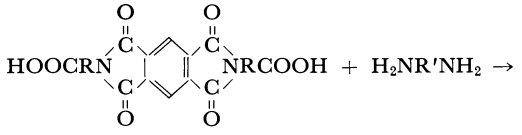
+ $H_2NR'NH_2$ →

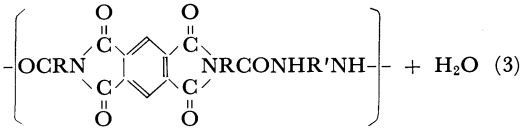
+ H_2O (3)

Polypyromellitimide-amide

The structures of these compounds were confirmed through elementary analyses and a study of the infrared absorption spectra.

On compounds similar to those reported here, some descriptions have appeared in the Japanese patents,[2] and there has been a brief report by K. Mienes.[3]

Experimental

The Synthesis of Pyromellitimide Caproic Acid (I).

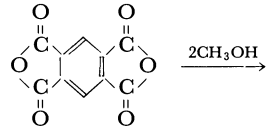
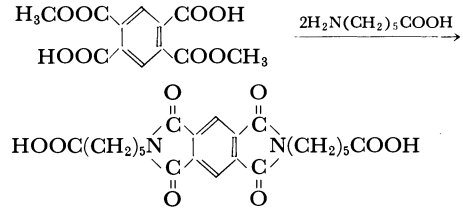
(I)

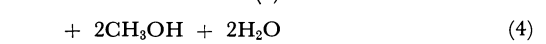
(4)

Pyromellitic Dianhydride. — Commercial pyromellitic dianhydride was recrystallized twice from acetic anhydride. This material was confirmed to be anhydride by study of its infrared absorption spectrum ($\nu_{C=O}$ 1775, and 1859 cm^{-1}). m. p. 285.5°C (lit.[4] m. p. 286°C).

ε-Amino-caproic Acid.—Synthesized from ε-caprolactam by the method described in Org. Synth.[5]:

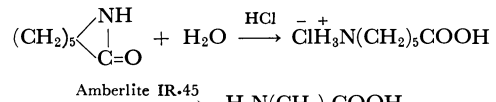
m. p. 202°C (lit.[5] m. p. 202°C)

Pyromellitic dianhydride (6.08 g. (0.0279 mol.)) and 30 ml. of anhydrous methanol were placed in a 100-ml. three-necked flask equipped with a drying tube. This mixture was then shaken by hand and gently warmed on a water bath until the solution became clear. After the reaction mixture had become transparent (in about 1 hour), 7.32 g. (0.0558 mol.) of ε-amino-caproic acid was added. The ε-amino-caproic acid immediately dissolved, and the solution became transparent again after it had been heated on a water bath for an hour. After this procedure the solvent was distilled off, and the product thus obtained was dried under reduced pressure for about 24 hr. The white product obtained was then recrystallized from acetic acid. The infrared absorption spectrum of the dibasic acid (I) is shown in Fig. 1. The characteristic absorption bands of the imide ring[6,7] were recognized at 730, 1380, and 1780 cm^{-1}.

2) Japanese Pat. 21500 (1963).
3) K. Mienes, *Kunststoffe*, **53**, 493 (1963).
4) J. Braun and G. Lemke, *Ber.*, **57**, 682 (1924).
5) A. H. Blatt, "Organic Syntheses," Coll. Vol. II, 28 (1963).
6) S. Nishizaki and A. Fukami *J. Chem. Soc. Japan, Ind. Chem. Sect. (Kogyo Kagaku Zasshi)*, **66**, 382 (1963).
7) S. D. Bruck, *J. Chem. Educ.*, **42**, 18 (1965).

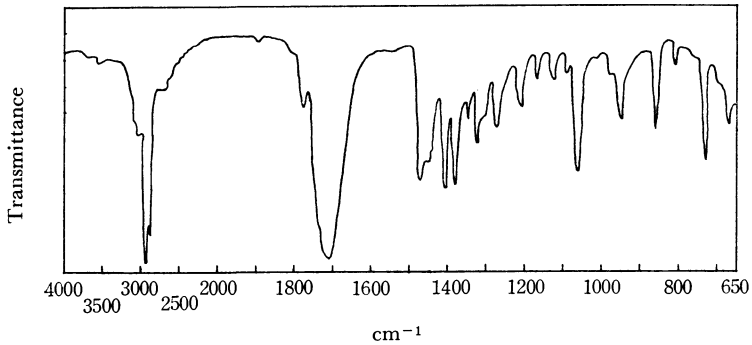

Fig. 1. Infrared spectrum of pyromellitimide caproic acid (I) (Nujol).

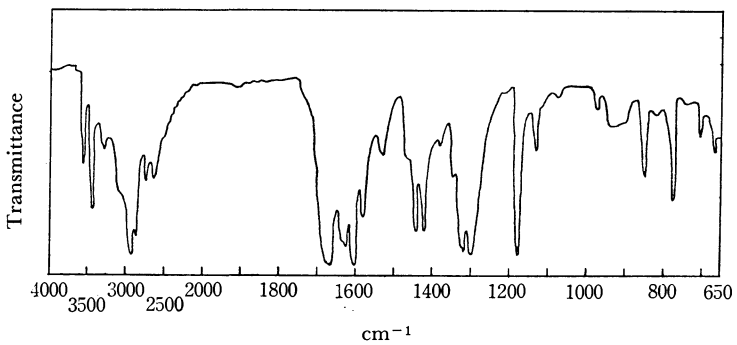

Fig. 2. Infrared spectrum of pyromellitimide benzoic acid (II) (Nujol). (unimidized)

Yield 88%; m. p. 231°C.

Found: C, 59.44; H, 5.41; N, 6.33. Calcd. for $C_{22}H_{24}O_8N_2$: C, 58.91; H, 5.49; N, 6.30%.

The Synthesis of Pyromellitimide Benzoic Acid (II).

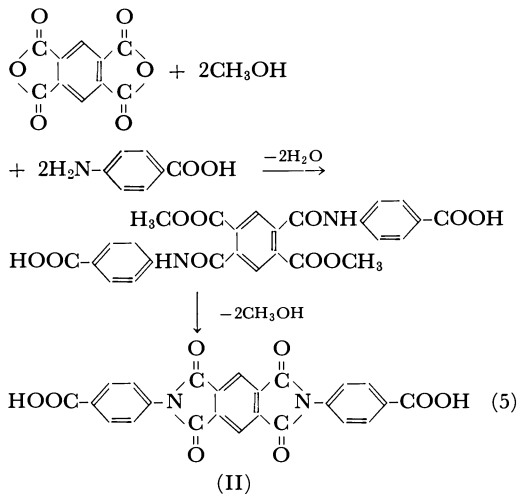

(II)

p-Amino-benzoic Acid.—Purified by recrystallization of the commercial-grade product from ethanol. White needles were thus obtained. m. p. 187°C (lit.[8] m. p. 187—187.5°C), II was prepared by a method similar to that used for pyromellitimide caproic acid I.

In this case, however, the imidization reaction could occur only with difficulty. A completely imidized substance was not obtained, even after drying under reduced pressure for several days at 60—70°C. By drying under reduced pressure at 250°C, a completely imidized substance was, however, obtained.

The pyromellitimide benzoic acid (II) obtained being insoluble in all organic solvents, the unreacted starting material was removed by extraction with glacial acetic acid and ethanol.

Yield 92%; m. p. 350°C.

Found: C, 62.73 H, 2.93. Calcd. for $C_{24}H_{12}O_8N_2$: C, 63.15 H, 2.65%.

The infrared absorption spectra of the dibasic acid (II) before and after the imidization reaction are shown in Fig. 2 and Fig. 3 respectively. The characteristic absorption bands due to amide CO and NH stretching vibration existing in the 1600—1650 and 3400—3500 cm^{-1} ranges before the imidization (Fig. 2) disappeared after imidization.

After imidization (Fig. 3), those which appear to have come from the characteristic absorption bands of the imide ring were recognized at 720, 1380, and 1780 cm^{-1}.

The material before the imidization reaction was a yellow powder and was soluble in many organic solvents, but after the imidization reaction it became a brown powder and was insoluble in an organic solvent.

The Synthesis of Pyromellitimide Acetic Acid (III).

8) N. A. Lange, "Hand Book of Chemistry," Ninth Edition, Hand Book Publishers, Inc. Sandusky, Ohio (1956), p. 399.

TABLE I. PREPARATION OF POLYPYROMELLITIMIDE-AMIDE

Polymer No.	Dibasic acid R*1	Diamine R'*2	Preparation method*3	Reaction condition		Yield %	Decomp. temp. °C	η_{inh}*4
				Temp. °C	Time hr.			
I	$-(CH_2)_5-$	$-(CH_2)_6-$	A	180	12	67.4	350	0.42
II	$-(CH_2)_5-$	$-(CH_2)_6-$	A	180	16	68.6	350	0.37
III	$-(CH_2)_5-$	$-(CH_2)_6-$	B	180	10	64.5	320	0.33
IV	$-(CH_2)_5-$	$-(CH_2)_{10}-$	A	180	12	64.3	255	0.28
V	$-(CH_2)_5-$	$-(CH_2)_{10}-$	A	180	16	67.7	270	0.36
VI	$-(CH_2)_5-$	$-(CH_2)_{10}-$	B	180	12	62.5	230	0.27
VII		$-(CH_2)_6-$	B	180	12	65.5	235	0.21
VIII		$-(CH_2)_6-$	B	180	12	58.3	220	0.23
IX	$-CH_2-$	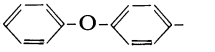	A	200	10	68.5	350	—
X	$-CH_2-$	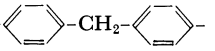	A	200	10	56.2	350	—

*1 R: 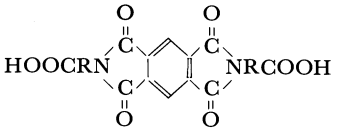

*2 R': $H_2NR'NH_2$

*3 A: Equimolar reaction between dibasic acid and diamine.
B: Nylon salts were employed.

*4 Measured at a concentration of 0.5 g./100 ml. *m*-cresol at 30°C.

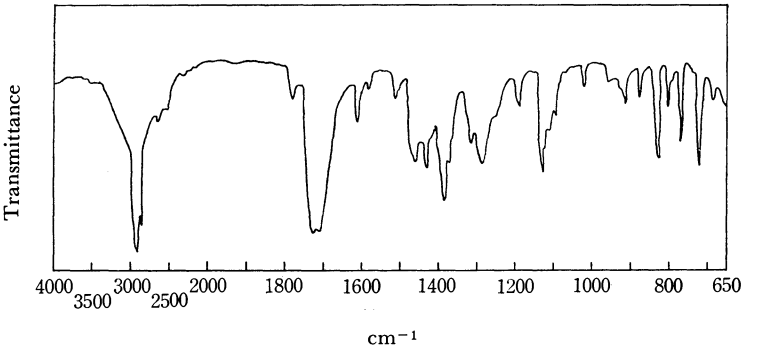

Fig. 3. Infrared spectrum of pyromellitimide benzoic acid II (Nujol). (imidized)

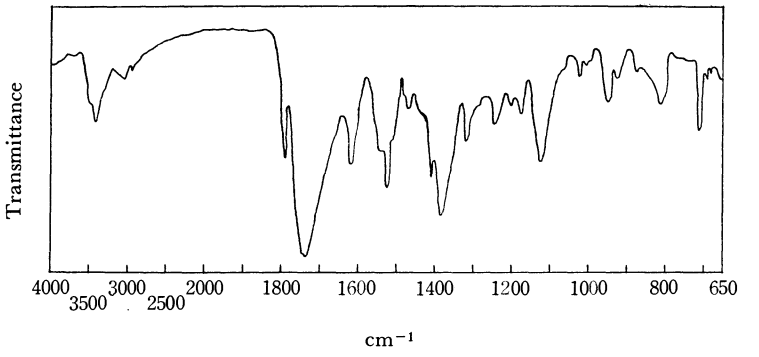

Fig. 4. Infrared spectrum of polymer I (KBr disk).

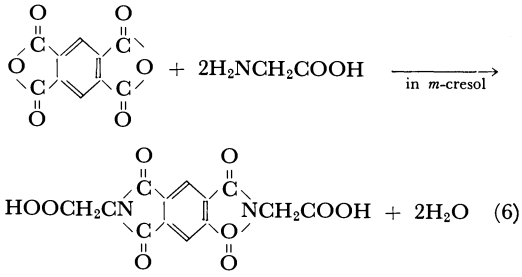

(III)

Glycine. — A commercial product was purified by recrystallization from methanol. *m*-Cresol (50 ml.) was taken into a 100-ml. three-necked flask, to which was then added 7.5 g. (0.1 mol.) of glycine. This mixture was heated to 100°C while being stirred. After the reaction had been completed, the product was recrystallized from dioxane, yielding light yellowish crystals.

The product obtained in this way was found by a study of its infrared absorption spectrum to be completely imidized.

Yield 81.3%; m. p.>320°C

Found: C, 50.72 H, 2.82. Calcd. for $C_{14}H_8O_8N_2$: C, 50.60 H, 2.55%.

The Synthesis of Nylon Salt.—In order to increase the degree of polymerization, and also in order to utilize the insoluble dibasic acid (II) as the polymer component, nylon salt was prepared by the following method.

To the dibasic acids suspended in hot water, diamines were added gradually. After the filtration of the transparent solution thus obtained, ethanol was added. Precipitated nylon salts were filtered and dried in a vacuum. The nylon salts obtained in this manner were as follows:

(a) Nylon salt derived from pyromellitimide caproic acid (I) and hexamethylene diamine:

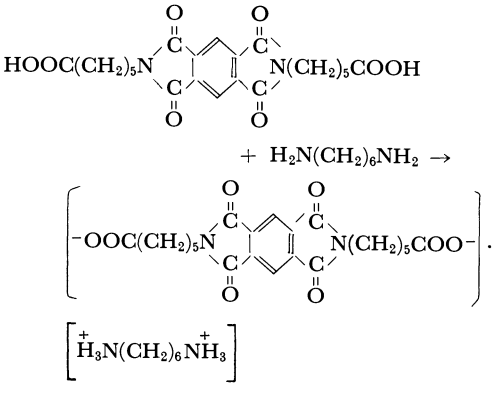

Found: N, 10.21. Calcd. for $C_{28}H_{40}O_8N_4$: N, 10.00%.

(b) Nylon salt derived from pyromellitimide benzoic acid (II) and hexamethylene diamines:

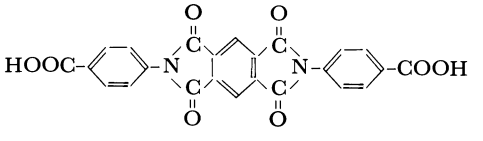

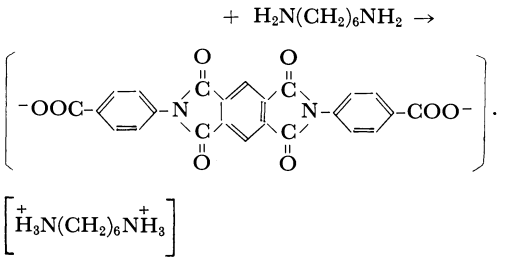

Found: N, 9.85. Calcd. for $C_{30}H_{28}O_8N_4$: N, 9.79%.

Condensation Polymerization between Dibasic Acids and Diamines.—An equimolar reaction between dibasic acid and diamine was carried out. 0.05 mol. of each component dissolved in 15 ml. of purified *m*-cresol was mixed in a thick test bube, the mixture was then heated under dry nitrogen.

When the nylon salts were employed, the condensation polymerization reaction was carried out in a similar way, dissolving 4—5 g. of nylon salts in 30 ml. of *m*-cresol.

The reaction temperature was gradually elevated for about one hour. Thereafter, the reaction was continued at 180°C until the viscosity of the reaction mixture seemed to have reached to the maximum. The polymer solution was then gradually dropped into methanol in order to precipitate the polymer. The precipitated polymer was filtered, and washed with water and acetone. The polymer was refined by repeating the procedure of dissolving the product into *m*-cresol, followed by reprecipitation. The results are shown in Table I.

The infrared absorption spectrum of the polymer I is shown in Fig. 4. In addition to the bands due to imide linkage, the characteristic absorption band for the amide NH stretching vibration was recognized near 3400 cm^{-1}.

The Heat Decomposition of the Polymers.—The thermal gravimetric analysis in atomospheric air of the polymer was undertaken by using a thermanobalance (Hitachi Thermano Balance Electric Furnace). The results of the measurements on the three types of polymers with different unit structures, are shown in Fig. 5.

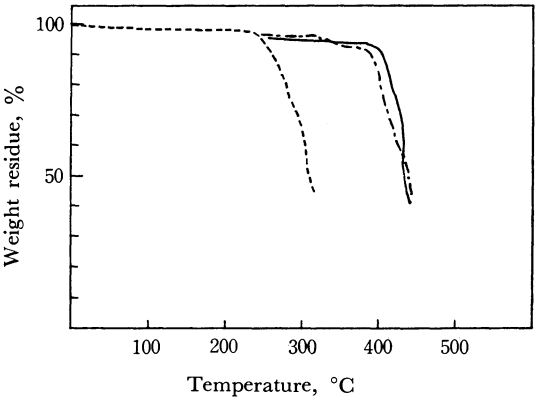

Fig. 5. Thermogravimetric analyses for polymers. ---- polymer I, ---- polymer IX, —— polymer X

Summary

Pyromellitimide caproic acid (I), pyromellitimide benzoic acid (II), and pyromellitimide acetic acid (III) have been synthesized in high yields by the reaction of pyromellitic dianhydride with three types of ω-amino acids, and their structures have been confirmed by elementary analyses and by a study of their infrared absorption spectra.

By the condensation polymerization between the dibasic acids described above and diamines, polypyromellitimide-amides with an imide ring and amide linkage in their molecule have been synthesized. The polymers obtained are generally soluble in *m*-cresol and sulfuric acid, but insoluble in other common organic solvents.

Such structures as the IX and X polymers in which the methylene chain in the molecule is short, and the aromatic unit is rich, were hard to dissolve in all the solvents mentioned above.

The results of the thermal gravimetric analyses indicated that, when the methylene chain is introduced into the polymer backbone, its heat stability appreciably decrease and that the polymer behaves like aliphatic polyamide. Those polymers such as the IX polymer which take a large part of the aromatic unit and a short methylene chain in repeating unit seem to have a good heat stability.

The authors wish to thank Dr. Yoshikazu Hachihama for his many helpful discussions and suggestions during this work.

BULLETIN OF THE CHEMICAL SOCIETY OF JAPAN VOL. 39 1800—1806 (1966)

Kinetics of the Hydrogenation of Aniline in the Vapor Phase on a Cobalt-Alumina Catalyst[1)]

By Hiroshi HAGIWARA,* Eiichi KOJIMA and Etsuro ECHIGOYA

Research Laboratory of Resources Utilization, Tokyo Institute of Technology, Ookayama, Meguro-ku, Tokyo

(Received December 7, 1965)

The kinetics of the catalytic hydrogenation of aniline with a cobalt-alumina catalyst in the temperature range from 160° to 210°C was studied by a differential flow reactor with a fixed bed. (1) The rate of reaction reaches a maximum in the 180—190°C range for the hydrogenation of aniline. From the thermodynamic calculations and the experimental results for a fluidized-bed reactor, the reverse reaction was found to be almost negligible below 200°C under the conditions of the reaction. This phenomenon was explained by the proposed kinetics of the reaction. (2) The initial rate of reaction without cyclohexylamine, and the rate when some cyclohexylamine was added to the reactants, were measured at atmospheric pressure over the following range of conditions of partial pressures; hydrogen 0.3—0.92 atm., aniline 0.05—0.2 atm., cyclohexylamine 0—0.24 atm. It was concluded that a plausible rate-controlling step was the surface reaction, i. e., the reaction between the adsorbed aniline and hydrogen on the surface of the catalyst. The equation for the vapor phase hydrogenation of aniline on a cobalt-alumina catalyst in the temperature range from 150°C to 210°C was determined to be:

$$r = k\frac{K_H^3 K_A P_H^3 P_A}{(1 + K_H P_H + K_A P_A + K_C P_C)^4}$$

No reports concerning the kinetic study of the catalytic hydrogenation of aniline in the vapor phase are to be found in the literature. We ourselves have, however, previously reported on our kinetic study of the catalytic hydrogenation of aniline on a nickel-diatomaceous earth catalyst.[2)] In the catalytic hydrogenation experiments, the highest conversion of aniline to cyclohexylamine was obtained in the temperature range from 180°C to 190°C.[3)] At higher temperatures, the degree of hydrogenation decreased. It is uncertain whether this phenomenon is caused by the nature of the chemical thermodynamic equilibrium or by the reaction kinetics. In order to clear up this point, the experiments reported here were planned.

Experimental

Catalyst Preparation.—The powdered alumina was added to a solution of cobalt nitrate, and the slurry was

* Present address: Yoshitomi Pharmaceutical Co. Ltd., Yoshitomi, Fukuoka

1) Presented at the 5th Symposium of the Chemical Reaction Engineering in Japan, Tokyo, October, 1965.

2) E. Echigoya, H. Hagiwara and K. Morikawa, presented on the 29th Annual Meeting of the Society of Chemical Engineers, Tokyo, March., 1964.

3) H. Hagiwara and E. Echigoya, *Shokubai* (*Catalyst*), **6**, 324 (1964).

stirred for some time; to it was then added, at room temperature, a 1 N ammonium carbonate solution in a slight excess. After it had been kept for one hour at 50°C without stirring, the slurry was filtered, and the filter cake was washed, dried at 100°C, and calcined at 500°C for 2 hr. The cobalt oxide content was about 20%. Before use, the catalyst was reduced at 450°C for 2 hr. with 250 ml./min. of hydrogen inside the same fixed-bed apparatus later used for the hydrogenation reaction. A series of experiments was carried out using powder of the 150—100-mesh range.

Reaction using Fluidized-bed Equipment.—The equipment used for the fluidization experiments consisted of a glass tube 90 cm. long and 5 cm. in diameter. The fluidized-bed runs were made over the temperature range from 150°C to 230°C, using 50—400 g. of 100—150-mesh-size catalysts. The average value of the minimum fluidization velocity used was 2 cm./sec. over the temperature range from 160 to 200°C. A detailed report will be presented in the near future.

Reaction using a Fixed Bed.—The apparatus is shown in Fig. 1. The mixture of reactants entered the

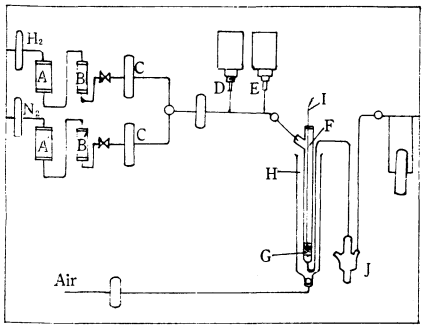

Fig. 1. Flow diagram.

A, A′: Deoxygenizer B, B′: Drying agent
C: Flow meter D: Aniline feeder
E: Cyclohexylamine feeder
F: Reactor G: Catalyst bed
H: Thermal fluidized bath
I: Thermocouple J: Cold trap

catalyst bed, which was maintained at the desired temperature by a solid-particle fluidized thermal bath. The gaseous products leaving the reaction zone were caught in a condenser trap cooled with a mixture of dry ice and methanol, from which condensates were drawn every thirty minutes for gas chromatographic analysis. The aniline and hydrogen concentrations in the reactants were varied by mixing in known amounts of nitrogen gas.

Results and Discussion

The Study of the Chemical Reaction Equilibrium for the Aniline Cyclohexylamine System.—Equilibrium constants for the aniline-cyclohexylamine system are little known compared with those of the benzene-cyclohexane system.[4]

Figure 2 shows the thermodynamic chemical

4) G. I. Janz, *J. Chem. Phys.*, **22**, 75 (1954).

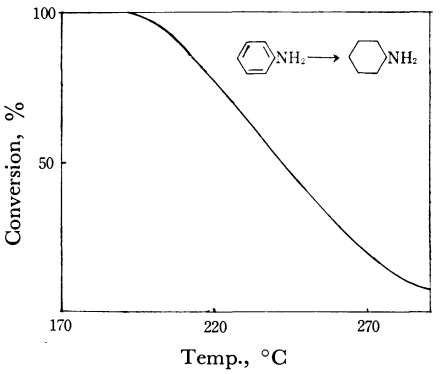

Fig. 2. Relationship between equilibrium conversion and reaction temperature $H_2/C_6H_5NH_2$ mole ratio 10.

equilibrium values calculated using Nernst's equation at a 10 to 1 mol. ratio of hydrogen to aniline. From Fig. 2, the dehydrogenation may be seen to be almost negligible below 200°C under these conditions. From the standpoint of the chemical reaction equilibrium, it is difficult to understand why the conversion obtained using a fixed-bed reactor should pass through a maximum value below 200°C. However, the hydrogenation reaction of aniline is an exothermic one. Thus it is difficult to measure a true reaction temperature in the fixed bed, which produces a large temperature gradient along its axial length. Accordingly, the fluidized bed, which has a large heat-transfer coefficient, was used to get a conversion at a true reaction temperature for this reaction.

The experimental results obtained at a uniform temperature within a fluidized bed are shown in Figs. 3 and 4. From the data, it may be seen that

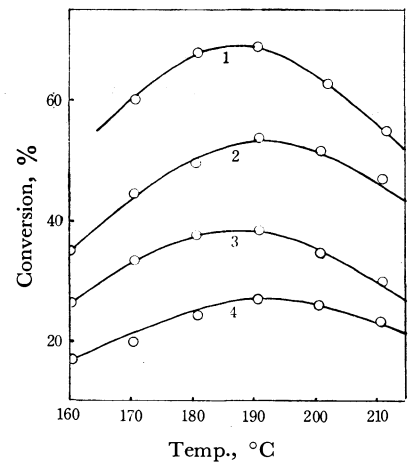

Fig. 3. Experimental data using a fluidized bed.
$H_2/C_6H_5NH_2$ mole ratio 15
Total feed mole 5.893 mol./hr.
Reaction diameter 2 inch.
Catalyst weights 1 266 g. 2 145 g.
3 98 g. 4 49 g.

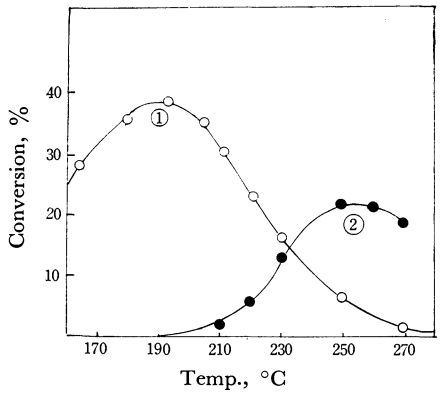

Fig. 4. Experimental data using a fluidized bed.

① 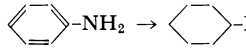 $-NH_2 \rightarrow$ 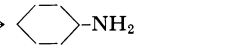 $-NH_2$

② 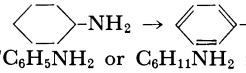 $-NH_2 \rightarrow$ 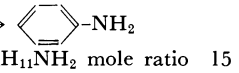 $-NH_2$

$H_2/C_6H_5NH_2$ or $C_6H_{11}NH_2$ mole ratio 15
$W/F=33.8$ $u/u_{mf}=2.15$

(1) the points of maximum conversion at the various space velocities were found in the temperature range from 180°C to 195°C, as in the fixed-bed experiments, and (2) the dehydrogenation reaction of cyclohexylamine was comparatively small below 210°C.

From the results obtained above, it may be assumed that the phenomenon of a negative temperature coefficient is caused by the reaction kinetics, not by chemical thermodynamic factors.

The following experiments were designed with this viewpoint in mind.

The Variation in the Catalyst Activity with the Reaction Time.—The changes in the catalyst's activity are shown in Fig. 5. The constant activity of the catalyst was obtained after about an hour and a half and did not change for about 6 hr., but then it gradually decreased. The catalyst was regenerated by passing hydrogen through it at 450°C for 1.5 hr.

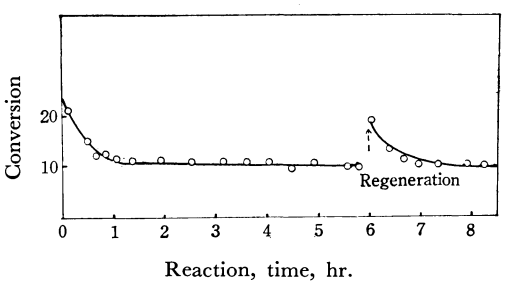

Fig. 5. Variation of catalyst activity with reaction time.
Temp. 180°C $H_2/C_6H_5NH_2$ molar ratio 10
$W/F \simeq 2$

The Dependency of the Fraction of Aniline Converted upon the Gas Space Velocity.—Experiments were first carried out to establish the range of conditions of the linear dependence between the reciprocal of space velocity and the conversion. The space velocity was here given as the volume (ml. at the reaction temperature) of gas coming in contact with 1 cc. of the catalyst per hour.

A series of runs were carried out under identical conditions, using powders of the 100—150-mesh-size range. In Fig. 6, the mole fraction of aniline converted against the reciprocal of space velocity was plotted, where F is a total flow rate [cc./hr]. The results obtained in this range could be treated as those of a differential reactor. A differential rate of reaction could then be calculated by the following approximate equation:

$$r = \Delta x_c/(W/f) \qquad (1)$$

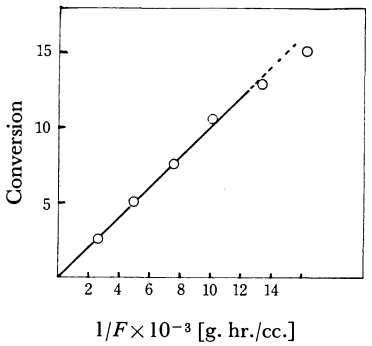

Fig. 6. Relationship between conversion vs. reciprocal of space velocity.
Reaction temp. 180°C
$H_2/C_6H_5NH_2$ mole ratio 10

where r: reaction rate [g.-mol./g. hr.], Δx_c: conversion in the differential reactor, W: catalyst weight [g.], and f: molar flow rate of an aniline-and-cyclohexylamine mixture [g. mol./hr.]. No by-products such as dicyclohexylamine could be found under these reaction conditions.

The Effects of Catalyst-particle Size.—The influence of the mass transfer on the over-all reaction rate was examined by using different sizes of catalyst (i. e., 100—150 mesh, 50—60 mesh, and 10—30 mesh). The results obtained were not at all different, and the effects of the mass transfer were concluded to be negligible.

The Initial Reaction Rate.—*The Dependence of the Initial Reaction Rate on Aniline and on the Hydrogen Partial Pressure.*—The experimental data obtained are summarized in Table I. The initial reaction rate can be expressed as follows:

$$r_0 = kP_A{}^{\alpha}P_H{}^{\beta}$$

where r_0: initial reaction rate, P_A and P_H: partial pressure of aniline and hydrogen, respectively [atm]. The order of the initial reaction as to aniline and to hydrogen partial pressure is given in Table II. From the table, it may be seen that the order

TABLE I. EXPERIMENTAL DATA OF THE INITIAL REACTION RATES

Temp. °C	P_H	P_A	x	r_0 (exp.) $\times 10^{-3}$	r_0 (cal.) by Eq. 2 $\times 10^{-3}$
165	0.91	0.09	7.65	3.6	3.3
	0.636	0.09	3.5	2.55	2.4
	0.454	0.09	1.0	1.80	1.16
	0.30	0.09	0.40	0.80	0.70
	0.80	0.200	11.5	2.90	2.71
	0.80	0.15	5.4	2.95	2.85
	0.80	0.101	3.6	2.93	3.30
	0.80	0.05	2.6	3.0	3.1
180	0.91	0.09	10.2	4.80	4.50
	0.636	0.09	4.0	2.95	2.9
	0.454	0.09	1.15	1.90	1.8
	0.30	0.09	0.46	0.85	0.86
	0.80	0.200	12.8	3.25	3.4
	0.80	0.15	5.9	3.2	3.5
	0.80	0.101	4.0	3.2	3.6
	0.80	0.05	2.5	2.8	3.1
195	0.91	0.09	8.95	4.2	3.9
	0.636	0.09	2.86	2.1	2.2
	0.454	0.09	0.665	1.2	1.2
	0.30	0.09	0.25	0.55	0.5
	0.80	0.20	12.6	3.2	2.85
	0.80	0.15	5.9	3.2	3.0
	0.80	0.101	3.88	3.1	3.02
	0.80	0.05	2.3	2.6	2.5
210	0.91	0.09	8.5	4.0	4.0
	0.636	0.09	3.0	2.2	1.8
	0.454	0.09	0.50	0.9	0.75
	0.30	0.09	0.15	0.30	0.25
	0.80	0.20	10.6	2.7	2.45
	0.80	0.15	4.7	2.55	2.7
	0.80	0.101	3.06	2.45	2.5
	0.80	0.05	1.86	2.1	2.1

TABLE II. THE ORDERS WITH RESPECT TO HYDROGEN PARTIAL PRESSURES AT VARIOUS TEMPERATURES

T °C	α Order with respect to hydrogen partial pressure	β Order with respect to aniline partial pressure
165	when $P_A=0.09$, 1.3	when $P_H=0.8$, ≈ 0
180	when $P_A=0.09$, 1.5	when $P_H=0.8$, ≈ 0.1
195	when $P_A=0.09$, 1.6	when $P_H=0.8$, ≈ 0.15
210	when $P_A=0.09$, 1.7	when $P_H=0.8$, ≈ 0.17

regarding the aniline partial pressure varied between 0 and 0.15 with the temperature, while the order regarding the hydrogen pressure varied between 1.3 and 1.7 with the temperature.

The Determination of the Rate Equation.—According to the Langmuir-Hinshelwood mechanism, the experimental data were discussed on the assumption that the surface reaction was the rate-controlling step. Different mechanisms may be presented for the hydrogenation of aniline, either the following possibilities or a combination of them:

1) Hydrogen is in the molecular state or is dissociated into atoms when adsorbed on the surface of a catalyst.

2) The mode of the addition of hydrogen to aniline is either step-by-step or simultaneous.

3) The adsorption of aniline and hydrogen takes place on the same active sites or on different ones.

4) Hydrogenation takes place between an aniline molecule in the gas phase and a hydrogen molecule adsorbed on the catalyst.

All the mechanisms were checked by comparing the experimental data on the initial rates with the characteristic curves of the modified rate equations. The results indicate that the data obtained can be fairly well correlated by the following rate equation:

$$r_0 = k \frac{K_A K_H^3 P_A P_H^3}{(1 + K_A P_A + K_H P_H)^4} \qquad (2)$$

where k: reaction rate constant [g.-mol./g. hr.],

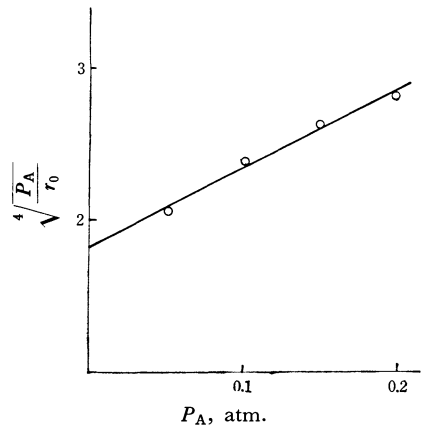

Fig. 7A. Verification of the Langmuir equation. Experiment at $P_H=0.8$ $T=180°C$ P_A variable

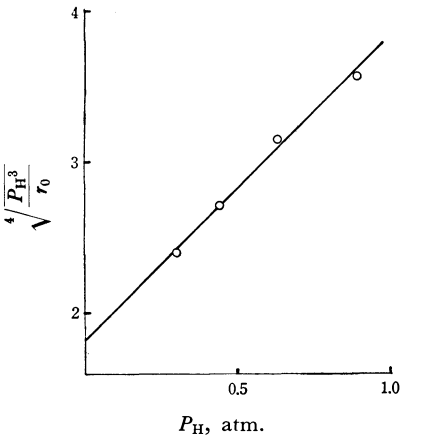

Fig. 7B. Verification of the Langmuir equation. Experiment at $P_A=0.09$ $T=180°C$ P_H variable

K_A and K_H: adsorption equilibrium constant of aniline and hydrogen, respectively [atm^{-1}].

In the above equation, when the hydrogen pressure, P_H, is constant, Eq. 2 can be transformed to the following:

$$\sqrt[4]{\frac{P_A}{r_0}} = \frac{1+K_AP_A+K_HP_H}{\sqrt[4]{kK_AK_H{}^3P_H{}^3}} = \varphi(P_A) \qquad (3)$$

This correlation is shown in Fig. 7A. A linear relationship was obtained between $\sqrt[4]{P_A/r_0}$ and P_A. At the constant aniline partial pressure, P_A, Eq. 2 can also be transformed into Eq. 4:

$$\sqrt[4]{\frac{P_H{}^3}{r_0}} = \frac{1+K_AP_A+K_HP_H}{\sqrt[4]{kK_AK_H{}^3P_A}} = \varphi(P_H) \qquad (4)$$

The correlation is shown in Fig. 7B. A linear relationship was obtained between $\sqrt[4]{P_H{}^3/r_0}$ and P_H. The values of K_H, K_A and k were obtained in the following manner. When P_H is constant, as in Fig. 7A, the gradient gives:

$$A = K_A/\sqrt[4]{kK_AK_H{}^3P_H{}^3}$$

and the point of intersection with the $\sqrt[4]{P_A/r_0}$ axis gives:

$$B = (1+K_HP_H)/\sqrt[4]{kK_AK_H{}^3P_H{}^3}$$

When P_A is constant, as in Fig. 7B, the gradient gives:

$$C = K_H/\sqrt[4]{kK_A{}^3K_H{}^3P_A}$$

and the point of intersection with the $\sqrt[4]{P_H{}^3/r_0}$ axis gives:

$$D = (1+K_AP_A)/\sqrt[4]{kK_AK_H{}^3P_A}$$

From A, B, C and D, the following equation is directly obtained:

$$\frac{B}{A} = \frac{1+K_HP_H}{K_A}, \quad \frac{D}{C} = \frac{1+K_AP_A}{K_H} \qquad (5)$$

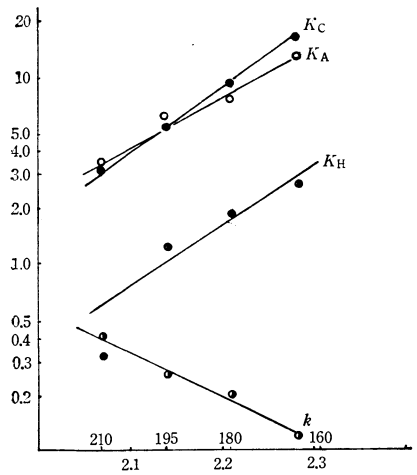

Fig. 8. Diagram showing the temperature dependence of rate constant and adsorption equilibrium constants.

TABLE III. THE VALUES OF THE ADSORPTION EQUILIBRIUM CONSTANTS AND RATE CONSTANT

	165°C	180°C	195°C	210°C	E or Q kcal./mol.
K_H	2.5	1.78	1.20	0.3	13.5
K_A	11.8	7.0	5.8	3.4	12.5
k	0.118	0.20	0.252	0.40	11
K_C	15.5	8.9	6.0	3.1	1.5

Using the above equations, the calculated values of K_A, K_H and k are shown in Table III. These values are reasonable for $K_A > K_H$, and the adsorption coefficient diminishes as the temperature becomes higher. The variation in k with the temperature yields an activation energy of 11.0 kcal./mol. The heats of adsorption of aniline and hydrogen are 12.5 kcal./mol. and 13.5 kcal./mol. respectively (Fig. 8).

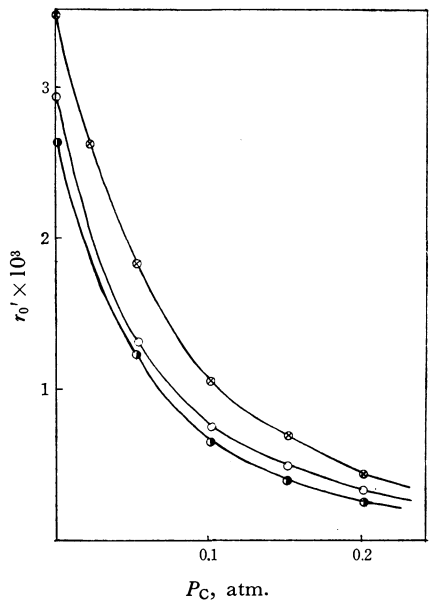

Fig. 9. Inhibition effect of cyclohexylamine. Reaction rate vs. cyclohexylamine partial pressure. $P_H=0.7$ $P_A=0.06$ P_C variable
○ 195°C, ⊗ 185°C ◑ 165°C

The Rate Equation with Cyclohexylamine. —The rate of reaction was measured by varying the cyclohexylamine concentration in the stream entering the reactor, while maintaining constant hydrogen and aniline partial pressures. The inhibition effect of cyclohexylamine was very clear throughout the whole range of temperatures (Fig. 9). The logarithmic transformation of this curve, $\log r_0' - \log P_C$, gave curves with negative gradients (Fig. 10). The value of K_C was obtained in the following way. The Langmuir rate equation might be written as follows:

$$r_0' = \frac{kK_AK_H{}^3P_AP_H{}^3}{(1+K_AP_A+K_CP_C+K_HP_H)^4} \qquad (6)$$

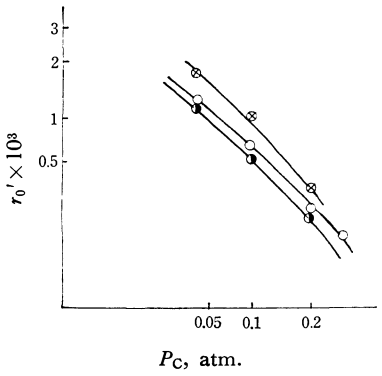

Fig. 10. Orders with respect to cyclohexylamine partial pressure.
○ 195°C ⊗ 180°C ◑ 165°C

where r_0': initial reaction rate with cyclohexylamine, P_C: partial pressure of cyclohexylamine [atm.] and K_C: adsorption equilibrium constant of cyclohexylamine [atm^{-1}]. The modified rate equation was obtained as follows:

$$\left(\frac{kK_H^3K_AP_H^3P_A}{r_0'}\right)^{1/4} = 1+K_AP_A+K_CP_C+K_HP_H \tag{7}$$

When P_A and P_H were kept constant, the following equation could be obtained:

$$\left(\frac{1}{r_0'}\right)^{1/4} = E+GP_C \tag{8}$$

$$\frac{E}{G} = \frac{1+K_AP_A+K_HP_H}{K_C} \tag{9}$$

The correlation in Eq. 8 was verified at a constant reaction temperature (Fig. 11). Using the values of K_A and K_H found before, the values of K_C were calculated. From the calculated value of K_C, the heat of adsorption of cyclohexylamine was found to be 15 kcal./mol.

As a final result, the following rate equation gives

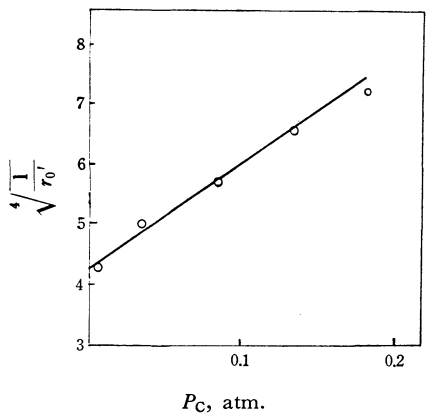

Fig. 11. Verification of the Langmuir equation.
Reaction temp. 180°C

the vapor-phase hydrogenation of aniline to cyclohexylamine on the cobalt-alumina catalyst:

$$r = k\frac{K_AK_H^3P_AP_H^3}{(1+K_HP_H+K_AP_A+K_CP_C)^4} \tag{10}$$

The average deviation of the proposed equation from the experimental values is about 10%.

A Test of the Rate Equation Obtained by the Differential-type Flow Reactor.—The conversion as a function of W/F (F: total flow rate [g.-mol./hr.]) was calculated numerically by Eq. 10, and it is plotted in Fig. 12. The data obtained using the integral-type flow reactor are superimposed on the plots in Fig. 12. Qualitatively the data and the plots show an approximate correspondence even though they have been determined by different methods.

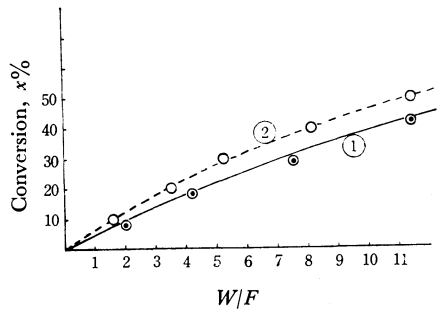

Fig. 12. Comparison of the conversion vs. W/F for the integral method data ① and the calculated values ②.
Reaction temp. 180°C
$H_2/C_6H_5NH_2$ mole ratio 15

Summary

1) The rate of reaction reaches a maximum value at about 180—190°C in the hydrogenation of aniline. According to thermodynamic calculation and experiments using a fluidized bed, the reverse reaction is almost negligible below 200°C under the conditions of the reaction. Therefore, this phenomenon has been assumed to be caused by the reaction kinetics.

2) The kinetics of the catalytic hydrogenation of aniline using a cobalt-alumina catalyst in the temperature range from 160 to 210°C was studied by a differential-type fixed-bed flow reactor. The initial rate of reaction without cyclohexylamine, and the rate when some cyclohexylamine was added to the reactants, were measured at atmospheric pressure over the following range of conditions:

hydrogen	0.3—0.92 atm.
aniline	0.05—0.2 atm.
cyclohexylamine	0—0.24 atm.

As a result of these experiments, it was concluded that the most plausible rate-controlling step was the surface reaction, i. e., the reaction between the

aniline and hydrogen adsorbed on the surface of the catalyst. The final equation for the vapor-phase hydrogenation of aniline on a cobalt-alumina catalyst in the temperature range from 150°C to 210°C was as follows:

$$r = k\frac{K_H{}^3 K_A P_H{}^3 P_A}{(1+K_H P_H+K_A P_A+K_C P_C)^4} \qquad (10)$$

Eq. 10 will be useful if it can be used to predict the rate over a wide range of conditions and, hence, be suitable for use in reactor design. However, it is not possible by kinetic study alone to determine the true mechanism of this reaction.

The authors wish to thank Professor Kiyoshi Morikawa for his useful discussions and guidance.

NOTES

Organic Photochemical Reactions. IV. Photoaddition Reactions of Various Carbonyl Compounds to Furan[1]

By Kensuke SHIMA and Hiroshi SAKURAI

The Institute of Scientific and Industrial Research, Osaka University, Sakai, Osaka

(Received September 13, 1965)

In an earlier paper dealing with the photoaddition of propionaldehyde or benzaldehyde to furan,[2] it was shown that this addition gives oxetanes (Ia, Ib) without the ketones which are formed by the addition of acyl radical to olefins. The present investigation was undertaken to extend this photoaddition to some aliphatic and alicyclic aldehydes, unsaturated aldehydes and several ketones.

In these experiments, ultraviolet light from a 350 W. high pressure mercury lamp was used. A mixture of the carbonyl compound and furan was placed in a 180-ml. reaction vessel and irradiated at 5—10°C in a nitrogen atmosphere[3]: the reaction product was then isolated by distillation under reduced pressure.

The reaction conditions and the yields of the products are summarized in Table I.

The distilled fraction in each case was identified as an oxethane on the basis of an elementary analysis, a molecular weight determination, and a study of the infrared and NMR spectra.[4]

These oxetanes showed a strong band in the infrared region near 980 cm^{-1}, and no absorption

Table I. The reaction conditions and yield of the products

Carbonyl compound used g. (mole)	Furan used g. (mole)	Irrad. time hr.	Product: Oxetane g.	Product: Residue g.
CH_3CHO 22(0.5)	136(2)	6	8.3	2.2
C_2H_5CHO 28(0.48)	126(1.85)	6	10.0	2.5
n-C_3H_7CHO 28.8(0.4)	109(1.6)	6	15.5	3.7
i-C_3H_7CHO 24(0.33)	136(2)	6	8.5	2.0
n-$C_5H_{11}CHO$ 33(0.33)	136(2)	6	10.7	2.1
n-$C_6H_{13}CHO$ 38(0.33)	136(2)	6	11.7	1.8
-CHO 37.3(0.33)	109(1.6)	6	16.1	3.5
C_6H_5CHO 42.5(0.4)	112(1.65)	6	24.5	3.5
CHO 15	160	10	4.2	1.5
CH_2=$CHCHO$ 10	150	9	2.5	2.2
CH_3CH=$CHCHO$ 10.5	136	10	2.3	1.7
CH_3COCH_3 29(0.5)	136(2)	6	1.1	1.4
$C_2H_5COCH_3$ 36(0.5)	136(2)	6	0.8	1.3
$C_6H_5COCH_3$ 48(0.4)	109(1.6)	6	0.7	0.3

1) Presented at Symposium on the Organic Radical Synthesis, Osaka, September, 1964.
Part III: Y. Sasajima, K. Shima and H. Sakurai, *J. Chem. Soc. Japan, Pure Chem. Sect.* (*Nippon Kagaku Zasshi*), in press.
2) S. Toki, K. Shima and H. Sakurai, This Bulletin, **38**, 760 (1965).
3) For the reaction apparatus, cf K. Shima, Y. Shigemitsu and S. Tsutsumi, ibid., **35**, 1728 (1962).
4) For an interpretation of the NMR spectra, see Ref. 2.

TABLE II. NMR SPECTRAL DATA*

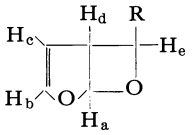

Compound		τ-Value	Multiplicity	Coupling constant c.p.s.
Ic	a	3.72	Doublet	J_{ab} 1.0
R=CH_3	b	3.40	Quartet	J_{ad} 4.3
	c	4.67	Triplet	J_{bc} 2.9
	d	6.51	Multiplet	J_{bd} 1.0
	e	5.31	Octet	J_{cd} 2.9
				J_{de} 3.1
Id	a	3.75	Quartet	J_{ab} 0.9
R=n-C_3H_7	b	3.41	Quartet	J_{ad} 4.3
	c	4.70	Triplet	J_{bc} 2.9
	d	6.59	Multiplet	J_{bd} 0.9
	e	5.47	Sextet	J_{cd} 2.9
				J_{de} 3.1
Ie	a	3.76	Doublet	J_{ab} 0.9
R=i-C_3H_7	b	3.37	Quartet	J_{ab} 4.2
	c	4.70	Triplet	J_{bc} 3.0
	d	6.53	Multiplet	J_{bd} 0.9
	e	5.77	Quartet	J_{cd} 3.0
				J_{de} 3.0
If	a	3.73	Quartet	J_{ab} 0.9
R=n-C_5H_{11}	b	3.41	Quartet	J_{ad} 4.2
	c	4.70	Triplet	J_{bc} 3.0
	d	6.59	Multiplet	J_{bd} 0.9
	e	5.48	Sextet	J_{cd} 3.0
				J_{de} 3.0
Ig	a	3.73	Quartet	J_{ab} 1.0
R=n-C_6H_{13}	b	3.40	Quartet	J_{ad} 4.2
	c	4.69	Triplet	J_{bc} 3.0
	d	6.59	Multiplet	J_{bd} 1.0
	e	5.48	Sextet	J_{cd} 3.0
				J_{de} 3.0
Ih	a	3.92	Doublet	J_{ad} 4.1
	b	3.49	Doublet	J_{bc} 3.0
R= 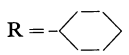	c	4.82	Triplet	J_{cd} 3.0
	d	6.59	Multiplet	J_{de} 3.0
	e	5.89	Quartet	
Ii	a	3.48	Doublet	J_{ab} 0.9
	b	3.33	Quartet	J_{ad} 4.2
R= 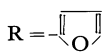	c	4.60	Triplet	J_{bc} 2.8
	d	6.06	Multiplet	J_{bd} 0.9
	e	4.60	Doublet	J_{cd} 2.8
				J_{de} 3.2

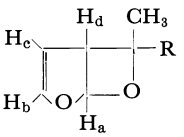

Compound		τ-Value	Multiplicity	Coupling constant c.p.s.
IIb	a	3.83	Doublet	J_{ab} 1.0
R=CH_3	b	3.42	Quartet	J_{ad} 4.2
	c	4.87	Triplet	J_{bc} 3.0
	d	6.46	Multiplet	J_{bd} 1.0
				J_{cd} 3.0
IIc**	a	3.83	Triplet	
R=C_2H_5	b	3.42	Quartet	
	c	4.89	Sextet	
	d	6.48	Multiplet	
IId	a	3.79	Doublet	J_{ab} 1.0
R=C_6H_5	b	3.31	Quartet	J_{ad} 4.2
	c	4.70	Triplet	J_{bc} 3.0
	d	6.18	Multiplet	J_{bd} 1.0
				J_{cd} 3.0

* Spectra were obtained on a Varian A-60 spectrometer using chloroform-d as solvent and tetramethylsilane as internal standard.

** NMR spectrum of this oxetane are different from others. The reason why proton a shows triplet (J=3.8 c.p.s.) and proton c shows triple-doublet (J=3.0 and 1.4 c.p.s.) are not clear.

of carbonyl or hydroxy groups was observed. The NMR spectral data are compiled in Table II.

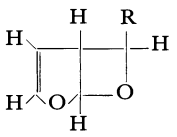

Ia	R=C_2H_5	g	R=n-C_6H_{13}
b	C_6H_5	h	
c	CH_3	i	
d	n-C_3H_7	j	CH_2=CH-
e	i-C_3H_7	k	CH_3CH=CH-
f	n-C_5H_{11}		

In the photoreaction of various aliphatic, alicyclic and unsaturated aldehydes with furan, oxetanes (Ic—Ik) were obtained. However, although in the case of n-butyraldehyde, acrolein and crotonaldehyde with furan, the main product was an oxetane, this fraction could not be purified by distillation. The properties of the oxetanes are shown in Table III.

Recently, Schenck et al.[5] reported that, in the photoreaction of dimethylmaleic anhydride with furan in the presence of benzophenone as a sensitizer,

5) G. O. Schenck, W. Hartmann and R. Steinmetz, *Chem. Ber.*, **96**, 498 (1963).

TABLE III. THE PROPERTIES OF OXETANES

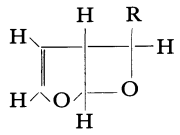

(I)

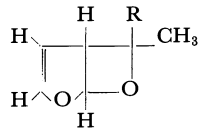

(II)

	b. p.	n_D	Anal.* C %	Anal.* H %
Ic, R=CH_3	41—42°C (11 mmHg)	1.4518 (20°C)	63.90 (64.27)	7.15 (7.19)
Ia, R=C_2H_5	74—75°C (30 mmHg)	1.4567 (20°C)	66.29 (66.64)	8.29 (7.99)
Id, R=n-C_3H_7	74—75°C (12 mmHg)	1.4518 (20°C)	70.38 (68.54)	9.02 (8.63)
Ie, R=i-C_3H_7	65—67°C (10 mmHg)		67.79 (68.54)	8.81 (8.63)
If, R=n-C_5H_{11}	106—108°C (12 mmHg)	1.4551 (20°C)	70.88 (71.39)	9.53 (9.59)
Ig, R=n-C_6H_{13}	81—82°C (1.5 mmHg)	1.4558 (20°C)	72.48 (72.49)	9.92 (9.96)
Ih, R=c-C_6H_{11}	86—87°C** (2 mmHg)		73.50 (73.30)	8.92 (8.95)
Ib, R=C_6H_5	104—105°C*** (1.2 mmHg)		76.12 (75.84)	6.02 (5.79)
Ii, R=C_4H_3O	80—83°C (1 mmHg)	1.5203 (16°C)	65.72 (65.85)	4.96 (4.91)
Ij, R=CH_2=CH	65—66°C (21 mmHg)	1.4728 (22.5°C)	66.28 (67.73)	6.62 (6.50)
Ik, R=CH_3CH=CH	86—90°C (17 mmHg)		68.27 (69.54)	7.21 (7.30)
IIb, R=CH_3	77—78°C (35 mmHg)	1.4510 (16.5°C)	66.64 (66.64)	8.20 (7.99)
IIc, R=C_2H_5	72—74°C (14 mmHg)	1.4552 (20°C)	68.67 (68.54)	8.77 (8.63)
IId, R=C_6H_5	86—87°C (1 mmHg)	1.5449 (11°C)	76.58 (76.57)	6.66 (6.43)

* The calculated values are in parentheses. ** m. p. 30°C. *** m. p. 49—50°C.

the oxetane (IIa) are formed. This structure was confirmed on the basis of its NMR spectrum by Gagnaire et al.[6] The photoreactions of acetone, methyl ethyl ketone and acetophenone with furan were undertaken to determine if these ketones would add to furan much as aldehydes adds to furan. It was observed that, in these photoreactions, the corresponding oxetanes (IIb—IId) are formed, but the yields of the oxetanes are very low compared with that of aldehydes to furan. It is interesting

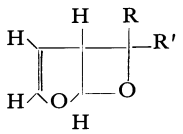

IIa R=R′=C_6H_5
b R=R′=CH_3
c R=CH_3, R′=C_2H_5
d R=CH_3, R′=C_6H_5

that there is a very large difference in the oxetane yield between benzaldehyde and acetophenone. Yang et al.[7] pointed out that, in the photoaddition reactions of benzaldehyde, acetophenone and benzophenone to 2-methyl-2-butene, the low-lying triplet states of these carbonyl compounds are $n\rightarrow\pi^*$ in nature, that they are the reactive species in these reactions, and that the quantum yield of the oxetane formation from benzaldehyde is 0.45, and 0.1, from acetophenone. However, they did not discuss the difference in the oxetane yield. Our results are comparable with theirs. We are now studying the reaction mechanism in order to clarify the reason why there is a difference in oxetane yield.

The authors with to thank Dr. Angelo A. Lamola (University of Notre Dame) for his helpful discussions.

6) D. Gagnaire and E. Payo-Subiza, *Bull. Soc. Chim. France*, **1963**, 2623.

7) N. C. Yang, M. Nussim, M. J. Jorgenson and S. Murov, *Tetrahedron Letters*, **1964**, 3657.

The Mass Spectrometric Determination of Gases Evolved in the Shell Mould Process for Iron Founding

By Hiroko HOSHINO, Nobuhide WASADA and Toshikazu TSUCHIYA

Government Chemical Industrial Research Institute, Tokyo, Shibuya-ku, Tokyo

(Received September 16, 1965)

Resins, such as phenol resin, are used as binders in order to form a shell mould for casting or to manufacture resin-bonded grinding wheels. When molten metal is poured into such a mould or when an article is ground with such a wheel, the binder is thermally decomposed and the decomposed gases contaminate the atmosphere of the work shop, unfavorably influencing the health of the workers.[1] The species of gases evolved are considered to depend to a large extent upon the nature of the binder used, upon the manufacturing process employed, and upon the operating condition of the mould or the grinding wheel.

Information about the evolved gases is necessary before proper measures can be taken to protect the workers from the noxious effects of the gases, but very little is known about them. Tubich et al.[2] have, however, reported that furfural, ammonia, phenol, aldehydes and carbon monoxide are evolved from shell moulds. We have now analysed the gases evolved from shell moulds in a foundry and have detected compounds which have not yet been reported.

The binder used in this mould was a kind of novolak resin. When molten iron was poured into a shell mould, an irritating gas evolved from the mould. The air around the surface was collected in a glass gas-collecting bottle which had been evacuated beforehand. The compounds present in the air of the bottle were then collected by the freeze-out technique reported previously.[3] The frozen-out substance was separated into three parts by isothermal distillation or by sublimation[4] at $-196°C$, $-78°C$ and room temperature. Each fraction was analysed by means of a CEC 21-103C mass spectrometer. The results are shown in Table I. When the gas was evacuated off, some residual substances remained in the sample bottle. After 60 days, appreciable amounts of ammonia and carbon dioxide were still found in the sample bottle. A part of the residue seems to have decomposed into these compounds.

TABLE 1. APPROXIMATE AMOUNT OF ORGANIC COMPOUNDS FOUND IN 760 mmHg OF AIR

Compound	Amount found in μHg
Benzene	8
Toluene	4
Xylene	<2
Phenol	2
Cresol	1
Benzaldehyde	trace

Those compounds which have a low boiling point, such as hydrogen, methane and carbon monoxide, may not be, or cannot be effectively collected by this freeze-out technique. Moreover, we cannot expect as reliable a result concerning those compounds which react with magnesium perchlorate, the drying agent for the isolated concentrate used in the procedure. That is, of the compounds detected, with benzaldehyde only a part of the amount originally present in the air may be collected. Though no acetone or alcohols were detected, it cannot be concluded legitimately that these compounds were not present in the air.

Considering the composition of novolak, it is not unreasonable for the compounds in the table to be detected. Actually, in a study of the mechanism of pyrolysis, between 500°C and 100°C, of novolak in a vacuum, we have identified all the compounds listed in the table as pyrolytic products of the resin,[5] though the mechanism of the production of the compounds in the foundry is considered to be somewhat different from that used under our experimental conditions, since the temperature of a part of the mould is much higher, moreover, the sand of the mould may act as a catalyst for the decomposition of the resin, and at least a part of the reaction proceeds in the presence of oxygen and water.

The authors are indebted to Dr. Hajime Matsufuji for bringing Refs. 1 and 2 to their attention, and to Mr. Ryuzo Shiota for his kind discussions and survey of the manuscript.

1) H. Matsufuji, T. Sakai, M. Kaneko, S. Mogi, S. Arai and M. Hosoya, *Tetsudo Rodo Kagaku*, **15**, 11 (1962) (Japanese).
2) G. S. Tubich, I. H. Davis and B. D. Bloomfield, *Arch. Indust. Health*, **21**, 424 (1960).
3) H. Hoshino, N. Wasada and T. Tsuchiya, This Bulletin **37**, 1310 (1964).
4) M. Shepherd, S. M. Rock, R. Howard and J. Stormes, *Anal. Chem.*, **23**, 1431 (1951).
5) To be published in this Bulletin.

The Solvent Extraction of Metal Ions in the Presence of Two Different Chelating Agents

By Hiroyuki YOSHIDA

Japan Atomic Energy Research Institute, Tokai-mura, Ibaraki

(Received September 27, 1965)

In the study of 2-thenoyltrifluoroacetone (TTA) solvent extraction, synergic effects were observed in the extraction of some metals in the presence of 8-quinolinol. Many studies of the synergic effects have been carried out. Most of these extraction systems contain complexing acids and other neutral ligands which form adduct compounds. The synergic effects in the presence of two different chelating agents are interesting,[1,2] because these agents can react as both chelate-forming and adduct-forming agents. In this paper, the extraction of uranyl and europium ions will be studied in the presence of TTA and 8-quinolinol and the stabilization factor will be calculated. It is well known that these metal ions are extracted into the organic phase as TTA[3] or 8-quinolinol[4] complexes under the present conditions.

Experimental

Reagents and Apparatus.—Uranium-237 was prepared by the (γ, n) reactions of natural uranium in a 20 MeV-electron linear accelerator of the Japan Atomic Energy Research Institute.[5] Europium-152+154 was supplied by the Radiochemical Centre, Amersham. Appropriate amounts of TTA and 8-quinolinol were dissolved in distilled benzene and were stored in a refrigerator. Radioactivity measurements were made with a Kobe Kogyo SA-230 scintillation counter.

The Determination of the Distribution Ratio.—Five ml. of an acetic acid - sodium acetate buffer solution (pH 3.5) and 1 ml. of the standard metal solution were transferred into a separatory funnel. Appropriate amounts of sodium perchlorate solution were then added to keep the ionic strength of the aqueous phase at 1 M. After the aqueous phase had been diluted to 10 ml. with water, TTA and 8-quinolinol solutions were added and the organic phase was diluted to 10 ml. with benzene. The system was then shaken for 5 min. at 25±2°C. The distribution ratio (D) was determined by the γ-counting of each phase. D was defined as the ratio of counts from the organic to those from the aqueous phase.

Results and Discussion

Determinations of D were carried out in the presence of TTA, 8-quinolinol, and a combination of the two. The results are shown in Tables I, II and III, respectively. $(D_M)_{TTA}$, $(D_M)_{OX}$ and $(D_M)_{TTA+OX}$ represent the distribution ratios of the elements in the presence of TTA, 8-quinolinol, and a combination of the two. β, the stabilization factors, $(D_M)_{TTA+OX}/((D_M)_{TTA}+(D_M)_{OX})$, are given in Tables II and III. The distribution ratio increases remarkably in the presence of two chelating agents. The extraction mechanism was not studied in this paper. Both agents (HA and HB) are able to form adduct compounds such as $MA_n(HA)_m$ with their acid forms as is shown in the extraction

Table I. Distribution ratio of uranium in the presenece of TTA and 8-quinolinol, respectively (7.2×10^{-5} mol. U, 0.1 M AcO^-)

TTA, M	$(D_U)_{TTA}$	8-Quinolinol, M	$(D_U)_{OX}$
1.0×10^{-2}	1.44	1.0×10^{-2}	0.061
6.0×10^{-3}	0.52	8.0×10^{-3}	0.034
4.0×10^{-3}	0.23	7.0×10^{-3}	0.025
3.0×10^{-3}	0.13	6.0×10^{-3}	0.018
2.0×10^{-3}	0.061	4.0×10^{-3}	0.007

Table II. Stabilization factor (7.2×10^{-5} mol. U, 0.1 M AcO^-)

Concn. of reagents, M TTA	8-Quinolinol	$(D_U)_{TTA+OX}$	β*
6.0×10^{-3}	4.0×10^{-3}	8.08	15.3
4.0×10^{-3}	6.0×10^{-3}	8.52	34.4
3.0×10^{-3}	7.0×10^{-3}	7.24	46.2
2.0×10^{-3}	8.0×10^{-3}	5.58	58.7

* $\beta = (D_U)_{TTA+OX}/((D_U)_{OX}+(D_U)_{TTA})$

Table III. Distribution ratio of europium and stabilization factor (10^{-8} mol. Eu, 1.0 M AcO^-)

Concn. of reagents, M TTA	8-Quinolinol	$(D_{Eu})_{TTA}$ or $(D_{Eu})_{OX}$	$(D_{Eu})_{TTA+OX}$	β*
0.20	—	6.55**	—	—
0.16	0.04	3.24**	21.35	6.6
0.12	0.08	1.38**	19.98	14.5
0.08	0.12	0.43**	11.87	27.6
0.04	0.16	0.052**	2.74	52.7
—	0.20	$<10^{-3}$***	—	—

* $\beta = (D_{Eu})_{TTA+OX}/((D_{Eu})_{TTA}+(D_{Eu})_{OX})$
** $(D_{Eu})_{TTA}$
*** $(D_{Eu})_{OX}$

1) T. Sekine and D. Dyrssen, *J. Inorg. Nuclear Chem.*, **26**, 1727 (1964).
2) T. Sekine and D. Dyrssen, ibid., **26**, 2013 (1964).
3) A. M. Poskanzer and B. M. Foreman, Jr., ibid., **16**, 323 (1961).
4) J. Stary, *Anal. Chim. Acta*, **28**, 132 (1963).
5) E. Akatsu, Private communication.

of uranium[3,6] with TTA or in the extraction of strontium with 8-quinolinol.[7] The synergic effects observed may be due to the mixed-ligand-complex formation of TTA and 8-quinolinol or to such adduct-compound formation as $MA_n(HB)_m$ or $MB_n(HA)_m$.

6) S. Peterson, *J. Inorg. Nuclear Chem.*, **14**, 126 (1960).
7) D. Dyrssen, *Svnesk Kem. Tidskr.*, **67**, 311 (1955).

The author is indebted to Mr. Hiroshi Okashita for his help in preparing the manuscript.

A Phase Transition in Phenanthrene Crystal*

By Shoichi MATSUMOTO

Central Research Laboratory, Tokyo Shibaura Electric Co., Ltd., Komukai, Kawasaki, Kanagawa

(Received October 19, 1965)

In a previous paper,[1] we reported that phenanthrene shows an anomaly at around 64—71°C in the temperature dependence of its electrical conductivity; the resistivity increases abruptly with the rising temperature and becomes 6—7 times greater than that below 64°C, while the linear relationship between the logarithm of resistivity and the reciprocal absolute temperature remains kept both below and above the anomaly. We also suggested in that paper that this anomaly may be attributed to a phase transition of the crystal.

In this paper, a differential thermal analysis and a dilatometric investigation of phenanthrene will be presented, and the phase transition confirmed by the results will be discussed.

Experimental

Material.—Phenanthrene of a chemical purpose-grade (Eastman Kodak Co.) was recrystallized three times from an ethanol solution, and then purified further by the zone-melting technique.

The recrystallized specimen was introduced into a Telex-glass tube with a diameter of 10 mm., and the tube was sealed under a vacuum after it had been evacuated for about 12 hr. Then the tube was subjected to forty-five passes in an automatic zone refiner, clamped in a vertical position. The molten zone about 5 mm. long was controlled to move downward at the speed of 20 mm. per hour.

Differential Thermal Analysis (DTA).—The measurements were performed with a recording differential thermal analysis apparatus (Shimadzu DT-10B), using α-alumina powder as the reference substance. In order to avoid possible effects by oxygen and humidity, the procedure was carried out, with nitrogen gas passed through slowly. For most measurements, the specimen was heated at the rate of 4—6°C per minute.

Dilatometric Measurements. — A dilatometric investigation was made by using a modified differential dilatometer of the type originated by Chevenard.[2] Our dilatometer was designed to magnify the differential expansion between a specimen and an equal length of fused silica used as the standard specimen 2000 times.

In this study, the heating rate was about 0.8°C per minute, except in the vicinity of the anomalous point, where temperature was raised as slowly as possible. The temperatures were measured by means of a calibrated chromel-alumel thermocouple; they were accurate to ±0.2°C.

Samples were prepared by casting molten rods of zone-refined phenanthrene, rods which were 9 mm. both in length and in diameter.

Results and Discussion

In the DTA investigation, upon heating we found a new endothermic peak at about 71°C on the thermogram of phenanthrene. A typical thermogram is shown in Fig. 1.

The endothermic peak at 71°C is very small, compared with the peak beginning at 100°C, which is the melting temperature of the substance, the area of this endothermic peak for each thermogram is approximately one-seventeenth of that for melting.

TABLE I. THE OBSERVED VALUES FOR ENDOTHERMIC PEAKS ON THE DTA THERMOGRAMS OF PHENANTHRENE

Trial	T_1, °C	T_p, °C	T_2, °C
Sample A-2	61	72	78
Sample A-3	59	70	76
Sample B-1	60	70	75
Mean	60	71	75

Table I lists the results observed in heating, where T_1 and T_2 show the temperatures at a point of intersection between the base line and the tangential line on the left side of the peak, and the

* Presented partly at the Symposium on Molecular Structure, Nagoya, October, 1965.

1) S. Matsumoto and T. Tsukada, This Bulletin, **38**, 2023 (1965).

2) P. Chevenard, *Rev. Met.*, **14**, 610 (1917).

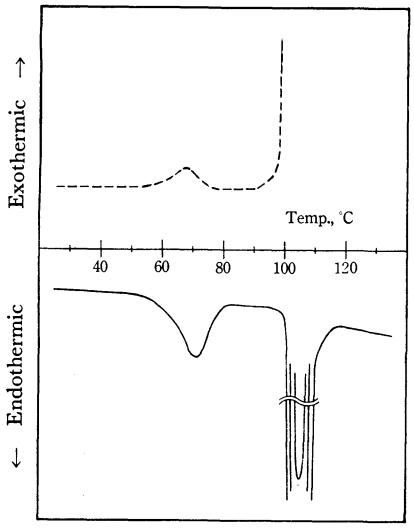

Fig. 1. A typical example of the thermogram of phenanthrene (Sample B-1 in Table I. The continuous curve for heating, the dashed one for cooling.

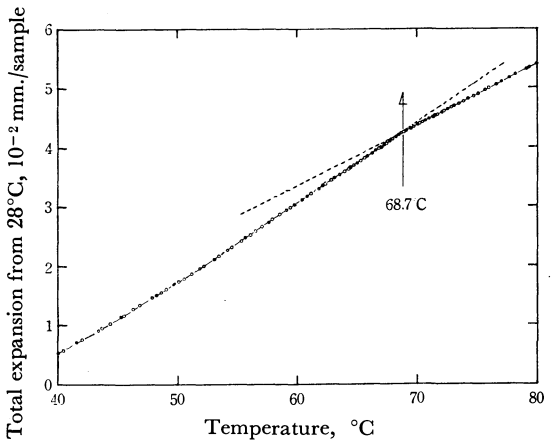

Fig. 2. The linear expansion-temperature relation of phenanthrene (sample 11-11 in Table II), showing a distinct discontinuity at 68.7°C. The open circles for heating, the black ones for cooling.

one on the right of it. T_p is the temperature at the vertex of the peak.

In the dilatometric study, we found a distinct discontinuity in the expansion-temperature relation of phenanthrene at 68.7°C. Figure 2 gives, as a typical example, a graphical representation of the total linear expansion of Sample 11-11 plotted aginst the temperature, where the curve consists of two distinct lines; the lines intersect at 68.7°C, although the slope below about 50°C gradually becomes smaller. These phenomena were quite reversible with the temperature. These features of the expansion-temperature relation show that the thermal expansion coefficient of

Table II. The mean coefficient of linear thermal expansion of phenanthrene measured with a dilatometer

Trial	$T_{tr.}$, °C	β_I	β_{II}
Sample 11-11	68.7	1.67×10^{-4}	1.05×10^{-4}
Sample 11-12	68.8	1.61×10^{-4}	1.08×10^{-4}
Sample 11-13	68.7	1.66×10^{-4}	1.03×10^{-4}
Average	68.7	1.65×10^{-4}	1.05×10^{-4}

the specimen is almost constant below or above 68.7°C, but that it undergoes a conspicuous, abrupt change at that temperature. Each expansion coefficient can be evaluated from the slope of each line. The results are summarized in Table II, where β_I is the mean coefficient of the linear thermal expansion between the temperature of 50°C and $T_{tr.}$, the transitional point, and where β_{II} is the coefficient between $T_{tr.}$ and 80°C.

Generally, a substance with a phase transition shows an endothermic peak corresponding to the transition on a thermogram of DTA, and the transition point exists between the T_i—T_p temperatures. The thermogram obtained for phenanthrene shows the presence of an endothermic peak with T_i=60°C and T_p=71°C, as is summarized in Table I. This result, in addition to the anomaly in the temperature dependence of the electrical conductivity,[1] reveals the presence of a phase transition in the phenanthrene crystal; this transition point is expected to exist between the temperature of 60 and 71°C.

The present attempt to make dilatometric measurements of phenanthrene indicates that the coefficient of the thermal expansion definitely undergoes a conspicuous change at 68.7°C; the value of 1.67×10^{-4} abruptly changes to 1.05×10^{-4} at this point, as is shown in Table II. This result shows that the transition point of phenanthrene crystal is 68.7°C.

In order to determine the heat associated with this phase transition, the ratio of the area of the endothermic peak at the transition to that for melting observed on the thermogram of DTA, 1 : 17, was conveniently applied. Phenanthrene melts at 100°C with a latent heat of fusion, ΔH= 4.45 kcal./mol.,[3] so the heat of the transition was evaluated as ΔH=0.26 kcal./mol., while the associated entropy change at the transition was estimated to be ΔS=0.77 e.u.

The estimated entropy change at this transition is much smaller than the change for the melting, ΔS=11.9 e. u. This indicates that the modification of phenanthrene above the transition point is at least not a so-called plastic crystal. It is not exactly clear at the present stage that what other kind of phase transition this transition belongs to, but as the shape of a graphical representation of

3) Landalt - Börnstein, Physikalisch - Chemischen Tabellen, 6 Auflage, II Band, 4 Teil.

the expansion plotted against the temperature and its reversibility with temperature, as is shown in Fig. 2, are characteristic of what is called a high-order transition, it seems that the phase transition of the phenanthrene crystal is not polymorphic.

For an accurate treatment of this transition from the point of view of structural chemistry, it is necessary to determine the crystal structure above the transition point. For this purpose, an X-ray analysis of the structure is now being made in our laboratory.

The Absorption Spectra of Bis(ethylenediamine)copper(II) Complexes in Various Solutions

By Kôzô Sone

Chemical Laboratory, Department of General Education, Nagoya University, Chikusa-ku, Nagoya

and Shunji Utsuno

Chemical Laboratory, Aichi Gakugei University, Higashi-ku, Nagoya

(Received December 4, 1965)

Recently we have carried out a series of measurements of the visible absorption spectra of bis(ethylenediamine)copper(II) complexes in a variety of solvents. Form the results, which are summarized in Table I, we can obtain some information on the states of the complex ion in these media.[1)]

Since the perchlorate ion is practically unable to form a complex in a solution, the complex $[Cuen_2](ClO_4)_2$ is considered to be the most favorable for studying the effects of various media on the bis(ethylenediamine)copper(II) ion. The absorption measurements of this complex in water, ethanol, acetone and nitromethane reveal that the λ_{max} and ε_{max} values are not very different in each case, and that the λ_{max} value is shifted toward a shorter wavelength in the order of water→(ethanol and acetone)→nitromethane. In an aqueous solution it may be assumed that two water molecules are loosely bound above and below the copper atom in each planar bis(ethylenediamine)copper(II) ion, forming an elongated octahedral structure; the same situation can also be assumed in ethanol and acetone solutions, but the bondings of the respective solvent molecules will be somewhat weaker than those in an aqueous solution. In a nitromethane solution, the additional coordination of the solvent molecules will be even weaker.[2)] Therefore, we can conclude that the weaker the bondings of the solvent molecules are, i. e., the higher the tetragonality of the bis(ethylenediamine)copper(II) ion in a solution is, the shorter will its λ_{max} value be.

Table I. Absorption maxima of $[Cu\ en_2]X_2$ in various solutions[a,b)]

X	Solvent	λ_{max}(mμ)	ε_{max}
ClO_4	H_2O	550	64
	C_2H_5OH*	547	63
	CH_3COCH_3	547	63
	CH_3NO_2	534	60
	$H_2O+NaClO_4$ (4M)	538	61
	$H_2O+NaClO_4$ (8M)	528	61
	$H_2O+Mg(ClO_4)_2$ (4M)	530	58
	C_5H_5N	582	96
NO_3	H_2O	550	64
	C_2H_5OH*	547	63
	$H_2O+NaNO_3$ (8M)	540	62
Cl	H_2O	550	64
	C_2H_5OH	575	84
	$H_2O+LiCl$ (10M)	553	73

a) Temp.: 20—25°C; chelate concentration: $7\times10^{-3}-8\times10^{-3}$ M (7×10^{-4} M in the cases marked with *).

b) Each absorption curve shows only a simple and approximately symmetrical absorption band.

Of special interest is the effect of concentrated aqueous solutions of sodium perchlorate and magnesium perchlorate. Here we can expect that most of the water molecules will be so strongly attracted by the ions of these salts that the bondings of water molecules above and below the bis(ethylenediamine)copper(II) ions will be more or less disturbed. In fact, we find that the λ_{max} values in these solutions are markedly smaller than that in pure water, and that the value in a 8 M solution of sodium perchlorate is even smaller than that in

1) A part of our conclusion does not agree with the opinion of C. K. Jørgensen, "Inorganic Complexes," Academic Press, New York (1963), p. 100. Cf. also F. Rosenblatt, *Z. anorg. u. allgem. Chem.*, **204**, 351 (1932) and H. Ojima and K. Sone, *Naturwiss.*, **51**, 105 (1964).

2) On the small coordination ability of nitromethane, cf. B. J. Hathaway and D. G. Holah, *J. Chem. Soc.*, **1964**, 2408.

nitromethane.[3] Similar effects can be found also in the case of $[Cu\ en_2](NO_3)_2$ in a concentrated sodium nitrate solution (see Table I), and also in solutions of some other copper complexes, e. g., $[Cu\ trien]^{2+}$ or $[Cu\ glycine_2]$ in the presence of a large amount of sodium perchlorate or sodium nitrate.[4,5]

In pyridine solutions of $[Cu\ en_2](ClO_4)_2$ and ethanol solutions of $[Cu\ en_2]Cl_2$ (see Table I), on the other hand, the λ_{max} and ε_{max} values are larger than those described above. In these cases, it is probable that the coordination of pyridine molecules or chloride ions to the bis(ethylenediamine)copper(II) ions takes place, giving the 5- or possibly 6-coordinated complexes, the tetragonalities of which are apparently much lower than those of the more or less solvated complex ions, as has been described above.[6] The spectrum of $[Cu\ en_2]Cl_2$ in concentrated lithium chloride shows, further, that chloro-complex formation also takes place to some extent in this medium.

In summing up all the data in Table I, we can conclude that the higher the tetragonality of the bis(ethylenediamine)copper(II) ion in a solution is, the shorter is its λ_{max} value. It is interesting to note that the powder reflection spectrum of $[Cu\ en_2](ClO_4)_2$ reported by Meek and Ehrhardt[7] shows the λ_{max} value of 525 mμ, which is still shorter than all the values in Table I; this indicates that the bis(ethylenediamine)copper(II) ion in this particular case is of the highest tetragonality, since the complex is in contact with only the perchlorate ions, which have only a negligible ability to coordinate.

3) In these solutions, and also in nitromethane, we can also expect that the dissociation of $[Cu\ en_2](ClO_4)_2$ into bis(ethylenediamine)copper(II) and perchlorate ions is hindered to some extent. However, it is quite certain that the bonding of a perchlorate ion above or below a planar complex ion is much weaker than that of a molecule of water, ethanol or acetone; therefore, we can assume that the tetragonality of the bis(ethylenediamine)copper(II) ions in an aqueous sodium (or magnesium) perchlorate solution or in nitromethane is, at any rate, much higher than that in water, ethanol or acetone (cf. the spectrum of solid $[Cu\ en_2](ClO_4)_2$ (see text)).

4) In the case of $[Cu\ glycine_2]$, for example, the λ_{max} and ε_{max} values in water are 630 mμ and 44, while in a 8 M solution of sodium perchlorate they are 602 mμ and 41 respectively.

5) A similar effect of sodium perchlorate on some nickel ammines has already been reported by C. K. Jørgensen, *Acta Chem. Scand.*, **11**, 399 (1957) and K. Sone and M. Kato, *Z. anorg. u. allgem. Chem.*, **301**, 277 (1959); in these cases, it was found also that the effect is intensified remarkably by heating. In the case of the bis(ethylenediamine)copper(II) ion, on the other hand, the effect of heating is not so large, and only comparatively small increases in λ_{max} and ε_{max} take place (the values in a 8 M solution of sodium perchlorate at 80°C are ca. 535 mμ and 65 respectively).

6) Cf. the spectra of $[Cu\ en_3]^{2+}$, $[Cu\ en_2NH_3]^{2+}$ and $[Cu\ en_2OH]^{+}$ reported by J. Bjerrum and E. J. Nielsen, *Acta Chem. Scand.*, **2**, 297 (1948) and H. B. Jonassen, R. E. Reeves and L. Segal, *J. Am. Chem. Soc.*, **77**, 2748 (1955).

7) D. W. Meek and S. A. Ehrhardt, *Inorg. Chem.*, **4**, 584 (1965). For the absorption spectra of single crystals of some bis(ethylenediamine)copper(II) complexes, see S. Yamada and R. Tsuchida, This Bulletin, **29**, 289 (1956).

The Heats of the Dilution of *cis*-Polybutadiene Solutions in Benzene and Toluene

By Akihiro KAGEMOTO, Sachio MURAKAMI and Ryoichi FUJISHIRO

Department of Chemistry, Faculty of Science, Osaka City University, Sumiyoshi-ku, Osaka

(Received December 6, 1965)

In a previous paper,[1] we measured the heats of the dilution of the atactic polystyrene solution and found that the interaction parameter, χ_H, between the polymer and the solvent depends on the concentration. In order to confirm this fact for other polymer solutions, the heats of dilution of which have not been directly determined, we measured the heats of the dilution of *cis*-polybutadiene, using toluene and benzene as a solvent.

The calorimeter used in this study has been described in the previous paper.[1] The *cis*-polybutadiene sample, the molecular weight of which was about 200000, was supplied by Dr. Toshio Yoshimoto of the Bridgestone Tire Co., Ltd.

The heats of the dilution of *cis*-polybutadiene solution were measured over the concentration range from 0.36 to 0.05 in a volume fraction of polymer at 25.0±0.01°C for the benzene solution, and at 26.0±0.01°C for the toluene solution, by adding the solvent in successive 10- or 20-ml. portions to a solution of a known concentration. The data obtained are shown in Table I. The *cis*-polybutadiene - toluene system is exothermic, while the benzene system is endothermic.

As was shown in the previous paper,[1] the heat of dilution, $\Delta\overline{H}_d$, is related to the initial volume fraction of the polymer, ϕ_2, and the final ϕ'_2 value as follows:

1) A. Kagemoto, S. Murakami and R. Fujishiro, This Bulletin, **39**, 15 (1966).

either $$\Delta\overline{H}_d = RT\chi_H\phi_2\phi'_2\Delta n_1 \quad (1)$$

when the interaction parameter, χ_H, is not dependent on the concentration,

or $$\Delta\overline{H}_d/RT\phi_2\phi'_2\Delta n_1 = \chi_1+\chi_2(\phi_2+\phi'_2)/2 \quad (2)$$

when χ_H depends linearly on the concentration, in conformity with the equation that $\chi_H=\chi_1+\chi_2\phi_2$. In these equations, Δn_1 is the number of moles of the solvent added.

By using the experimental data presented in Table I and Eq. 1, the interaction parameter has been obtained for each dilution process of each system; these values are given in the last column of the same table.

According to Eq. 1, $\Delta\overline{H}_d$ must linearly vary

TABLE I. HEATS OF DILUTION OF *cis*-POLYBUTADIENE SOLUTION

I. *cis*-Polybutadiene - Toluene at 26°C

V, cc.	ϕ_2	V', cc.	ϕ'_2	$-\Delta\overline{H}_d$, cal.	χ_H
20	0.318	30	0.212	0.154	−0.048
30	0.212	40	0.159	0.062	−0.032
40	0.159	50	0.127	0.040	−0.034
20	0.318	40	0.159	0.246	−0.042
20	0.318	50	0.127	0.286	−0.041
16	0.367	26	0.225	0.179	−0.038
26	0.225	46	0.127	0.070	−0.025
16	0.367	46	0.127	0.245	−0.032
50	0.127	70	0.091	0.049	−0.037
20	0.318	70	0.091	0.335	−0.040
15	0.318	25	0.190	0.080	−0.023
15	0.235	25	0.144	0.045	−0.024
25	0.141	55	0.064	0.037	−0.024
15	0.235	55	0.064	0.081	−0.024
55	0.064	85	0.041	0.010	−0.023
15	0.235	85	0.041	0.092	−0.023
25	0.134	35	0.096	0.021	−0.028

II. *cis*-Polybutadiene - Benzene at 25°C

V, cc.	ϕ_2	V', cc.	ϕ'_2	$\Delta\overline{H}_d$, cal.	χ_H
20	0.242	30	0.161	0.098	0.038
30	0.161	40	0.121	0.054	0.042
40	0.121	50	0.097	0.033	0.042
20	0.242	40	0.121	0.153	0.040
20	0.242	50	0.097	0.186	0.040
10	0.265	20	0.133	0.102	0.043
20	0.133	30	0.088	0.035	0.045
10	0.265	30	0.088	0.137	0.045
10	0.361	20	0.181	0.160	0.037
20	0.181	30	0.121	0.061	0.042
30	0.121	40	0.090	0.029	0.040
10	0.361	30	0.121	0.222	0.039
10	0.361	40	0.090	0.250	0.039
20	0.115	40	0.056	0.031	0.037
40	0.056	60	0.038	0.010	0.035
20	0.115	60	0.038	0.042	0.036
20	0.318	50	0.127	0.107	0.040
15	0.318	25	0.190	0.148	0.037
50	0.064	80	0.040	0.018	0.036

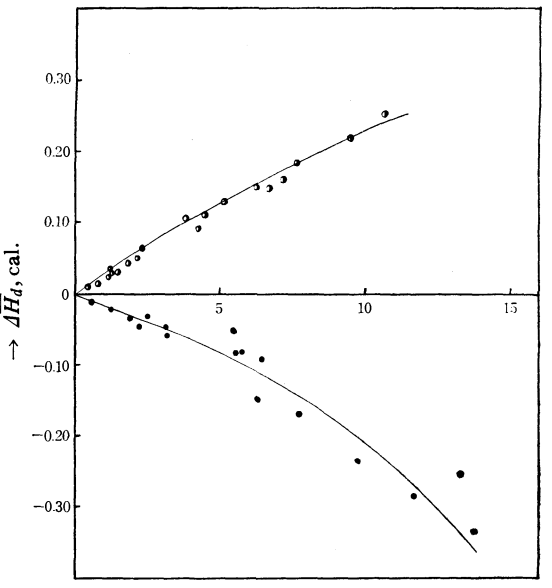

Fig. 1. $\Delta\overline{H}_d$ versus $\phi_2\phi_2'\Delta n_1$ data for *cis*-polybutadiene solution in benzene -◑- at 25°C and in toluene -●- at 26°C.
The curves are drawn according to Eq. 2 with the parameter of Table II.

TABLE II. VALUES OF INTERACTION PARAMETER $\chi_H=\chi_1+\chi_2\phi_2$

Solvent	χ_1	χ_2
Toluene	−0.019	−0.067
Benzene	0.039	−0.005

with the $\phi_2\phi'_2\Delta n_1$ value. However, as is shown in Fig. 1, those plots are not linear, indicating that χ_H depends on the concentration.

In order to obtain the dependence of the χ_H parameter on the concentration, a least-square analysis of the data were carried out according to Eq. 2; this gave the values of χ_1 and χ_2 summarized in Table II.

By using the values of χ_1 and χ_2 listed in Table II, the $\Delta\overline{H}_d-\phi_2\phi'_2\Delta n_1$ curve has been calculated for each system; this curve, shown by the full line in Fig. 2, is in good agreement with the experimental data for each system.

As is shown in Table II, the χ_H parameter in a good solvent (an exothermic system) is considerably dependent on the concentration, while in a poor solvent (an endothermic system) it depends hardly at all on the concentration.

Such a tendency was also seen in the polystyrene solution and explained by the use of the dilute solution theory.

The authors wish to thank Dr. Toshio Yoshimoto of the Bridgestone Tire Co., Ltd. for supplying the sample.

The Properties of Some Arjunolic Acid Derivatives

By Shin-ichi SASAKI, Hung Cheh CHIANG, Kazuo HABAGUCHI
Hong-Yen HSÜ and Koji NAKANISHI

Department of Chemistry, Tohoku University, Katahira-cho, Sendai

(Received December 20, 1965)

In connection with our investigations of South-East Asian plants,[1] the roots of *Psidium guaijava L.* ("banjiro" or "banzakuro") from Taiwan were studied because of the reputed cancerostatic activity of this Chinese herb. Since the ether extract was an intractable mixture, it was first methylated; the ester was then chromatographed and recrystallized. This ester eventually turned out to be methyl arjunolate,[2] the methyl ester of arjunolic acid (1).[3,4] Preliminary chemical and spectroscopic studies carried out prior to its identification, however, disclosed a few points worthy of comment; these points will be reported below.

Although the product obtained by the periodate oxidation of the ester 2 was analyzsed in the correct manner for a dialdehyde, it afforded only a mono-2, 4-dinitrophenylhydrazone, and its NMR spectrum showed only one aldehydic proton as a singlet (9.09 p. p. m.). Furthermore, the one-proton quartet (J 9.5 and 5 c. p. s.) that newly appeared at 5.12 p. p. m. in the oxidation product was shifted to 6.01 p. p. m. (J 9.1 and 5) in its acetate, a behavior which is characteristic of hemiacetals.[5] As has been mentioned above, the aldehyde proton signal is a singlet; therefore, the aldehyde group must be attached to a tertiary carbon atom. It follows that the structures of the oxidation product and its acetate should be 3 and 4 respectively, and that they are derived by means of hemiacetal formation between the primary hydroxyl group and the 2-aldehyde group. The C_2–H in Structures 3 and 4 is represented as β-axial in view of its 9.5- and 5-c. p. s. coupling constants.

The ester 2 afforded an acetonide 5 when reacted with acetone and cupric sulfate; the acetonide is formed between the 3-OH and 4-CH_2OH, as is evidenced by the appearance of a one-proton multiplet due to C_2-H at 5.5 p. p. m. in the NMR spectrum of the acetonide acetate 6.

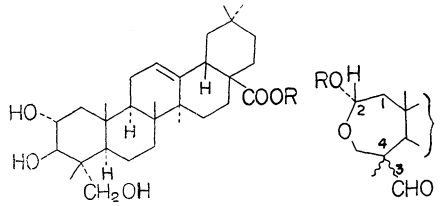

1 R=H 3 R=H } (C_{20} as COOMe)
2 R=Me 4 R=Ac }

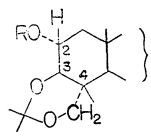

5 R=H } (C_{20} as COOMe)
6 R=Ac }

The mass spectra of methyl arjunolate 2, the hemiacetal 3, and the acetonide 5 are very similar in the high mass range in that they are characterized by peaks at *m/e* 262, 249, 203, 189 and 133, all derived from a retro-Diels-Alder-type cleavage of the β-amyrin skeleton.[6]

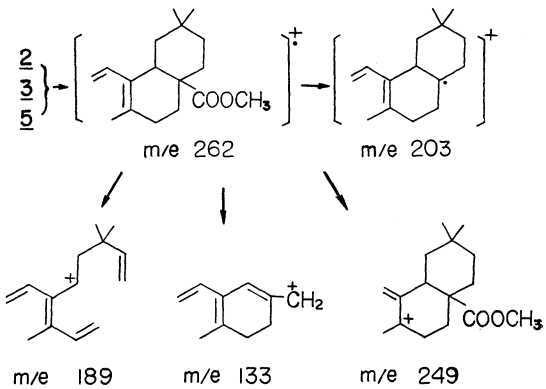

Experimental

The mass spectra were measured with a Hitachi RMU-6D model; ionization energy: 70 eV.; ionizing chamber heater: 250°C; evaporation temperature: 200°C.

1) Cf. K. Nakanishi, S. Sasaki, A. K. Kiang, J. Goh, H. Kakisawa, M. Ohashi, M. Goto, J. Watanabe, H. Yokotani, C. Matsumura and M. Togashi, *Chem. Pharm. Bull.* **13**, 882 (1965).
2) We are grateful to Professor R. E. Corbett, University of Otago, New Zealand, and Professor E. Ritchie, Department of Organic Chemistry, University of Sydney, Australia, for gifts of arjunolic acid derivatives.
3) F. E. King, T. J. King and J. M. Ross, *J. Chem. Soc.*, **1954**, 3995.
4) F. E. King, T. J. King and J. D. White, ibid., **1958** 2830.
5) For example: P. de Mayo, R. E. Williams and E. Y. Spencer, *Can. J. Chem.*, **43**, 1357 (1965).
6) H. Budzikiewicz, J. M. Wilson and C. Djerassi, *J. Am. Chem. Soc.*, **85**, 3688 (1963),

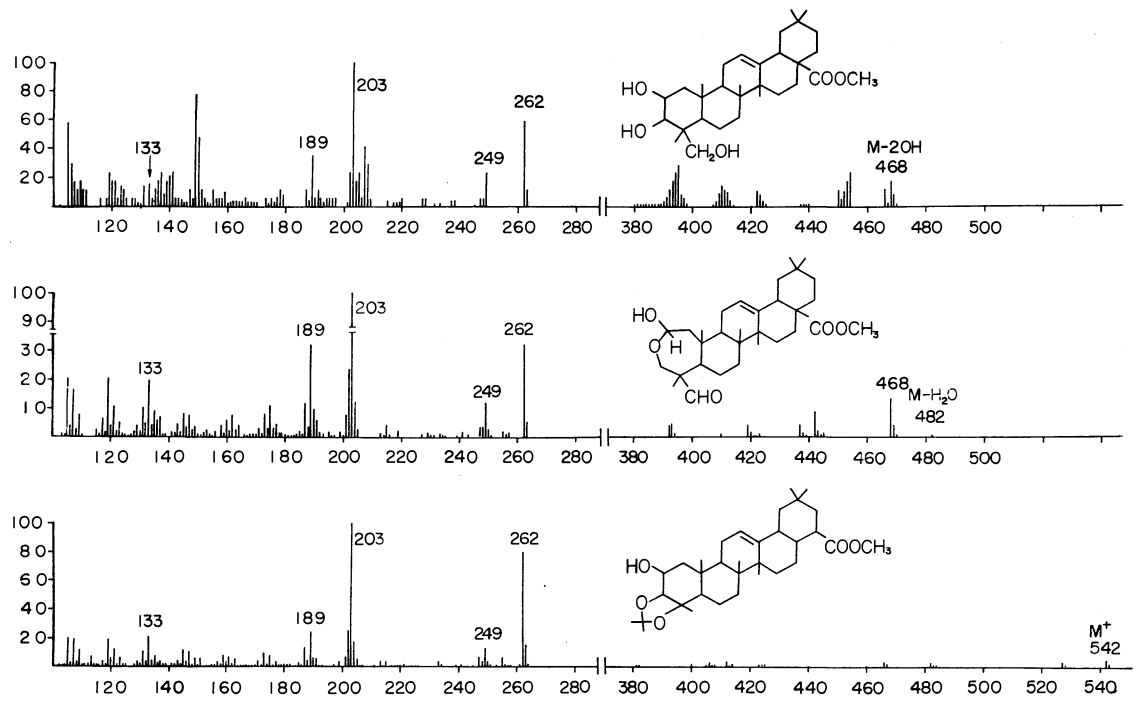

Fig. 1. Mass spectra of arjunolic acid derivatives.

The Extraction of Arjunolic Acid.—The roots (10 kg.) of pulverized *Psidium guaijava L.* were extracted continuously with ethanol to give 300 g. of a brown powder. After the powder had been extracted with petroleum ether, the residue was extracted with ether; when the ether extract was evaporated, 25 g. of a crude pale yellow residue was obtained. This was dissolved in methanol and treated with diazomethane; the solution was then passed through a column of silicic acid (1250 g., 100 mesh, Mallinckrodt) and eluted with chloroform to yield 2.5 g. of crude crystals. Several recrystallizations from acetone gave 2.0 g. of pure methyl arjunolate as white needles; m. p. 240—242°C, $[\alpha]_D$ 60.75° (*c* 1.0%, $CHCl_3$). ν_{max}^{KBr} 3425, 1730, 1460, 1385, 1365, 1040 cm^{-1}.

Found: C, 74.08; H, 10.01. Calcd. for $C_{31}H_{50}O_5$: C, 74.06; H, 10.03%.

The compound was identified as methyl arjunolate by a mixed melting point test and by a comparison of its IR spectrum with that of an authentic specimen.[2)]

The Periodate Oxidation of Methyl Arjunolate.—A solution of 100 mg. of the ester 2 in 20 ml. of ethanol was treated with 100 mg. of sodium periodate dissolved in 2 ml. of water; the mixture was then left in the dark for 24 hr. The crystalline precipitate was filtered and recrystallized several times from ethanol to give 60 mg. of needles; m. p. 200—201°C, $[\alpha]_D$ 191.8° (*c* 1.0% $CHCl_3$), ν_{max}^{KBr} 3530, 2720 1725 cm^{-1}.

Found: C, 74.50; H, 9.61. Calcd. for $C_{31}H_{48}O_5$; C, 74.36; H, 9.66%.

2, 4-*Dinitrophenylhydrazone;* m. p. 194—196°C.

Found: C, 65.54; H, 7.95; N, 8.08. Calcd. for $C_{37}H_{52}O_6N_4$: C, 65.59; H, 7.70; N, 8.23%.

The Acetate 4 (prepared by the treatment of 3 with acetic anhydride-pyridine): m. p. 197—198°C.

Found: C, 73.79; H, 9.31. Calcd. for $C_{33}H_{50}O_6$: C, 73.03; H, 9.31%.

The Acetonide 5.—The methyl ester 2 (200 mg.), dissolved in 40 ml. of anhydrous acetone, was treated with 1.8 g. of anhydrous cupric sulfate and the mixture was then stirred for 24 hr. at room temperature. The mixture was filtered, the filtrate was dried in vacuo, and the residual solid was dissolved in chloroform and chromatographed through silicic acid (100 mesh, Mallinckrodt) to yield the acetonide 5. The crude compound was recrystallized from ethanol and then from acetone to give 120 mg. of needles, m. p. 152—153.5°C.

Found: C, 74.45; H, 9.30. Calcd. for $C_{34}H_{54}O_5$: C, 75.23; H, 10.03%.

The Acetate 6: m. p. 197—200°C.

Found: C, 74.18; H, 9.77. Calcd. for $C_{36}H_{56}O_6$: C, 73.93; H, 9.65%.

We are grateful to the Toyo Rayon Company for the grant which enabled us to purchase the RMU-6D mass spectrometer.

The Preparation of Four Optically Active Isomers of 3-Methylmalic Acid

By Susumu TATSUMI, Masami IMAIDA and Yoshiharu IZUMI

Division of Organic Chemistry, Institute for Protein Research, Osaka University, Kita-ku, Osaka

(Received January 20, 1966)

3-Methylmalic acid contains two asymmetric centers and, hence, exists in two racemic forms — four optically active forms. Although there have been several reports[1-3] on the preparation of this hydroxy acid, these procedures all yield a mixture of the two isomeric racemates. Therefore, neither the two racemic forms nor their four optically active forms have yet been identified.

In the present work, the two racemic forms and four optically active forms were prepared. A mixture of isomeric racemates was synthesized from ethyl ethoxalyl propionate by Scherp's procedure,[2] and then it was separated into two racemic forms by means of the differential solubility of their barium salts in water. The less soluble salt yielded the racemic form with a m. p. of 115°C (I), while the more soluble one yielded the racemic form with a m. p. of 129°C (II). Then, their optical resolutions were performed by the usual method, using brucine as a resolving reagent. The values of the optical rotation of the optically active isomers were as follows:

(A) From the racemic form with the lower melting point (I):

(+)-isomer $[\alpha]_D^{20}$ +9.1° (*c* 3.7, water)

(−)-isomer $[\alpha]_D^{20}$ −8.9° (*c* 3.7, water)

(B) From the racemic form with the higher melting point (II):

(+)-isomer $[\alpha]_D^{20}$ +5.2° (*c* 3.2, water)

(−)-isomer $[\alpha]_D^{20}$ −5.3° (*c* 3.2, water)

The racemic form with the m. p. of 129°C (II) was assigned the threo form by the method of the nitrous acid deamination of DL-*threo*-3-methylaspartic acid, whose configuration had previously been proved by Baker et al.[4]

Experimental*

The Preparation of the Mixture of Isomeric Racemates.—The mixture of isomeric racemates was prepared from ethyl ethoxalylpropionate by the method of Scherp,[2] but using a Raney nickel catalyst in place of platinum oxide catalyst.

The Separation of the Mixture into Two Racemic Forms.—A very viscous colorless syrup of the mixture, weighing 148 g., was dissolved in 1000 ml. of water; the mixture was then adjusted to pH 8 with a 10% barium hydroxide solution. The resulting solution was stored overnight in a refrigerator. Then the salt which had precipitated was collected by filtration, washed several times with cold water, and dried in air at 80°C. Yield, 155 g. The salt was dissolved in 300 ml. of 6 N hydrochloric acid, and the resulting solution was then concentrated under reduced pressure. The residue was treated with a small amount of water, and the solution was again evaporated in vacuo to remove as much free hydrochloric acid as possible. This treatment was repeated several times to ensure the complete removal of the hydrochloric acid, and then the residue was extracted with six 30 ml. portions of acetone. The acetone extracts were combined and evaporated to a very viscous syrup. This was then dissolved in 100 ml. of ethyl acetate, and to the solution there was added 50 ml. of petroleum ether. This solution was stored in a refrigerator, and the precipitated crystalline product was collected by filtration. Yield, 65 g. The recrystallization of this product from ethyl acetate - petroleum ether (2 : 1) gave white crystals of I. Yield, 46 g. M. p. 113—115°C.

Found: C, 39.26; H, 5.51. Calcd. for $C_5H_8O_5$: C, 40.54; H, 5.44%.

The mother liquor of the barium salt of I was stored for a week, and a small amount of crystalline precipitate was filtered off. The clear solution was concentrated and decomposed with 120 ml. of concentrated hydrochloric acid, and then treated as has been described above. In this way, 28 g. of white crystals of II were obtained. M. p. 128—129°C.

Found: C, 39.81; H, 5.73. Calcd. for $C_5H_8O_5$: C, 40.54; H, 5.44%.

The Optical Resolution of I.—Thirty grams of I and 86 g. of brucine dihydrate were dissolved in 800 ml. of boiling water, and the resulting solution was allowed to stand overnight in an ice box. The crystals of the brucine salt which precipitated were collected by filtration; seven recrystallizations of this salt from ten parts of boiling water gave 25 g. of the pure brucine salt of I. This salt was suspended in 200 ml. of cold water and decomposed with 50 ml. of a N sodium hydroxide solution. The precipitated brucine was removed by filtration, and the alkaline filtrate was washed twice with 30 ml. portions of chloroform, neutralized with concentrated hydrochloric acid, and then evaporated to a syrup. To this a small amount of water was added, and the resulting solution was decolorized with charcoal and evaporated to dryness in order to remove the free hydrochloric acid. The residue was extracted several

1) E. B. Abbot and A. McKenzie, *Ber.*, **71**, 1214 (1938).
2) H. W. Scherp, *J. Am. Chem. Soc.*, **68**, 912 (1946).
3) H. Gault and H. Gotliniaux, *Compt. rend.*, **231**, 287 (1950).
4) H. A. Baker, R. D. Smyth, E. J. Wawszkiewicz, M. N. Lee and R. M. Wilson, *Arch. Biochem. Biophys.*, **78**, 468, (1958).

* All the melting points given in this paper are uncorrected values.

times with 20 ml. of acetone. The acetone extracts were combined and again evaporated to a syrup. The syrupy product was dried over sulfuric acid in a vacuum desiccator. In this way, white crystals of (+)-I were obtained. Recrystallization from 10 ml. of ethyl acetate - petroleum ether (1 : 1) gave 3.6 g. of optically-pure (+)-I. m. p. 107°C, $[\alpha]_D^{20}$ +9.1° (*c* 3.7, water).

Found: C, 40.36; H, 5.51. Calcd. for $C_5H_8O_5$: C, 40.54; H, 5.44%.

The mother liquor of the brucine salt of (+)-I was concentrated to a paste. After it had been stored for a week in an ice box, the brucine salt of (−)-I was collected. Optically-pure (−)-I was obtained from this salt by the procedure described above. Yield, 1.3 g. M. p. 106—107°C, $[\alpha]_{20}^{D}$ −8.9° (*c* 3.7, water). Found: C, 40.40; H, 5.24%.

The Optical Resolution of II.—Twenty grams of II and 58 g. of brucine dihydrate were dissolved in 900 ml. of boiling water, and then the resulting solution was treated as described for the resolution of I. Thus, 2.7 g. of optically pure (−)-II crystallized out. M. p. 111°C; $[\alpha]_{20}^{D}$ −5.3° (*c* 3.2, water).

Found: C, 40.32; H, 5.50. Calcd. for $C_5H_8O_5$: C, 40.54; H, 5.44%.

From the mother liquor of the brucine salt of (−)-II, 1.1 g. of optically pure (+)-II were obtained. M. p. 110—111°C, $[\alpha]_D^{20}$ +5.2° (*c* 3.2 water). Found: C, 40.54; H, 5.39%.

The Deamination of DL-*threo*-3-Methylaspartic Acid with Nitrous Acid.—Five grams of DL-*threo*-3-methylaspartic acid[4] were dissolved in 50 ml. of N hydrochloric acid, and the resulting solution was cooled to about 5°C in an ice bath. A solution of 3.5 g. of sodium nitrite in 30 ml. of water was then added slowly, with a continuous vigorous stirring and with cooling. (The addition required about 30 min.). After the addition, the reaction mixture was allowed to stand at 5°C for 1 hr., and then at room temperature overnight. To the reaction mixture, 50 ml. of concentrated hydrochloric acid were added, and the solution was evaporated to dryness in vacuo. Water was added, and the evaporation repeated. The yellowish residue was extracted several times with boiling acetone, and the white residue was discarded. The combined acetone extracts were evaporated under reduced pressure, and the resulting syrup was dissolved in a small amount of water. After decoloration with charcaol, the solution was again evaporated to a syrup; it was then allowed to stand in a refrigerator. The crystalline product was collected by suction, and two recrystallizations from ethyl acetate gave white crystals of II. Yield, 2.4 g.; m. p. 129°C. Found: C, 40.77; H, 5.59. Calcd. for $C_5H_8O_5$: C, 40.54; H, 5.44%.

This research has been supported by the Ajinomoto Co., Inc., Tokyo, to which the authors thanks are due. The authors wish also to express their sincere thanks to Miss Kiku Koike of this Institute for carrying out elemental analyses.

SHORT COMMUNICATIONS

Aluminum Chloride-Catalyzed Reactions of Organosilicon Compounds. A Rapid Redistribution Reaction of Chlorodisilanes

By Hideki SAKURAI, Kenji TOMINAGA and Makoto KUMADA

Department of Synthetic Chemistry, Kyoto University, Sakyo-ku, Kyoto

(Received May 11, 1966)

In recent years, considerable attention has been directed toward a study of the organopolysilanes.[1] An interesting example of this involves the reaction of organodisilanes with an electrophilic reagent.[2] During the course of an investigation of the reactivity of organopolysilanes toward electrophiles, we have found that methylchlorodisilanes readily undergo aluminum chloride-catalyzed redistribution reaction at room temperature, while the disproportionation of alkylchlorosilanes catalyzed by aluminum chloride has been reported to proceed slowly, even at much higher temperatures.[3,4]

$$(CH_3)_3SiSi(CH_3)_3 + Cl(CH_3)_2SiSi(CH_3)_2Cl \underset{\longleftarrow}{\overset{AlCl_3}{\longrightarrow}} 2(CH_3)_3SiSi(CH_3)_2Cl \quad (1)$$

When an equimolar mixture of hexamethyldisilane and 1, 2-dichlorotetramethyldisilane is stirred at room temperature in the presence of anhydrous aluminum chloride (0.05—0.25 mol./l.), the equilibrium is established between pentamethylchlorodisilane and its original components within 1.5 hr.[5]

As the equilibrium is established rapidly in favor of pentamethylchlorodisilane, the reaction can be applied in a preparative scale. In a typical experiment a mixture of 73.5 g. of hexamethyldisilane, 94.5 g. of tetramethyldichlorodisilane, and 5.5 g. of anhydrous aluminum chloride was stirred for about 2 hr. at room temperature. After 3 g. of acetone had been added to the mixture to deactivate the catalyst, the mixture was subjected to simple distillation under reduced pressure. The fractionation of the distillate gave 114 g. (68.5%) of pure pentamethylchlorodisilane.

In view of these finidings, it became of interest to investigate the aromatic substitution by a mixture of pentamethylchlorodisilane and aluminum chloride, since it is well known that halosilanes do not react with benzene in the presence of Lewis acid.[3,4]

Although an attempted silylation of benzene by a mixture of pentamethylchlorodisilane and aluminum chloride was unsuccessful, we have found that detrimethylsilylation was effected very rapidly by pentamethylchlorodisilane in the presence of a catalytic amount of aluminum chloride.

$$C_6H_5Si(CH_3)_3 + Cl\text{-}Si(CH_3)_2Si(CH_3)_3 \overset{AlCl_3}{\longrightarrow} C_6H_5Si(CH_3)_2Si(CH_3)_3 + Cl\text{-}Si(CH_3)_3 \quad (2)$$

Using competitive reaction conditions in benzene, we found that phenyltrimethylsilane underwent the reaction faster than *p*-chlorophenyltrimethylsilane and slower than *p*-methylphenyltrimethylsilane with pentamethylchlorodisilane.[6]

The order of substituent effects demonstrates the electrophilic nature of the reaction; it also confirms the present reaction to be a new class of aromatic electrophilic substitution.[7]

1) C. Eaborn, "Organosilicon Compounds," Butterworths Scientific Publications, London (1960), p. 351.

2) H. Sakurai, T. Imoto, N. Hayashi and M. Kumada, *J. Am. Chem. Soc.*, **87**, 4001 (1965).

3) H. Gilman and G. E. Dunn, *Chem. Revs.*, **52**, 77 (1953).

4) G. A. Russell, *J. Am. Chem. Soc.*, **81**, 4831 (1959), and references therein.

5) The apparent equilibrium constant, $K=[C_5H_{15}Si_2Cl]^2/[C_6H_{18}Si_2][C_4H_{12}Si_2Cl_2]$, was found to be 82.6 for the original mixture of 6.22 mmol. of hexamethyldisilane, 5.78 mmol. of tetramethyldichlorodisilane and 1 mmol. of aluminum chloride in 20 ml. of benzene. In chloroform, however, the reaction did not proceed even after one week at room temperature.

6) The apparent relative rates at an early stage of the reaction were found: $k_{p\text{-}CH_3}/k_H=2.0$ and $k_{p\text{-}Cl}/k_H=0.2$.

7) R. O. C. Norman and R. Taylor, "Electrophilic Substitution in Benzenoid Compounds," Elsevier Pubshing Co., Amsterdam (1965).

Novel Diphenylketene Derivatives of Dicyclopentadienyl-vanadium and -titanium

By Pang-bu HONG, Kenkichi SONOGASHIRA and Nobue HAGIHARA

The Institute of Scientific and Industrial Research, Osaka University, Sakai, Osaka

(Received May 18, 1966)

The interaction of cumulative carbon-carbon double bond systems with various organometallic compounds has been reported from this laboratory.[1] Because the comparison between the two kinds of interactions of ketene- and allene-systems with organometallic compounds is an interesting problem, we now wish to report on the isolation and on some properties of the diphenylketene derivatives of vanadium and titanium.

When a solution of diphenylketene (I) (3.7 g., 1.91 mmol.) and dicyclopentadienylvanadium (3.3 g., 1.82 mmol.) in toluene (20 ml.) was stirred under nitrogen at 60°C for 1 hr., the color of the reaction mixture changed from violet to dark green. After the mixture had then cooled to room temperature, dark green crystals separated. Recrystallization from toluene gave 5.5 g. (81% yield) of air-sensitive dark green crystals ((II); m. p. 159—163°C in a sealed tube under nitrogen). Found: C, 76.83; H, 5.30; mol. wt. (in benzene), 386. Calcd. for $C_{24}H_{20}OV$: C, 76.79; H, 5.37; mol. wt., 375. IR (KBr disk): 1618 and 1580 cm^{-1}, and no absorption in the region of 1620—2800 cm^{-1}.

II is paramagnetic; its electron paramagnetic resonance spectrum of a benzene solution shows a *g*-factor of 1.9976 and a ^{51}V hyperfine splitting of 45.5 gauss. This splitting and *g*-value are almost the same as those of the acetylene derivatives of dicyclopentadienylvanadium.[2] This fact suggests that the diphenylketene is bound to the metal as tightly as acetylene, although infrared data excludes such a cyclic structure as that of the acetylene derivatives. In view of the facts mentioned above, we postulate II as the most probable structure; in it the metal is coordinated through the C=C double bond in the ketene.

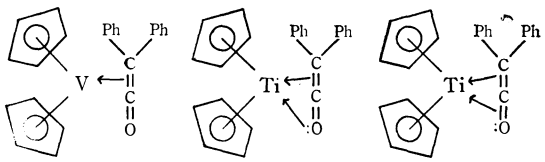

(II) (III-a) (III-b)

A similar reaction of I (1.4 g.) with dicyclopentadienyltitanium dicarbonyl (1.1 g.) in hexane has been found to form dicyclopentadienyl-diphenylketene-titanium (III) in a yield of 90%. III crystallizes as orange-yellow prisms from the reaction mixture, m. p. 215—217°C (decomp.), in a sealed tube under nitrogen. Found: C, 77.07; H, 5.49; O, 4.74; Ti, 13.6; mol.wt. 367 (vapor pressure osmometer, in benzene). Calcd. for $C_{24}H_{20}OTi$: C, 77.42; H, 5.41; O, 4.30; Ti, 13.0%; mol. wt. 372. IR (KBr disk): 1575 and 1555 cm^{-1}, and no absorption in the region of 1580—2800 cm^{-1}.

The NMR spectrum of III in methylene chloride or deuterochloroform shows that the relative intensity of π-cyclopentadienyl and phenyl protons is approximately 1 : 1. although the decomposition of the complex with the chlorinated solvents prevents precise measurements. To obtain the effective atomic number of krypton, the titanium atom must be supplied with 4 electrons from the π-complexed diphenylketene. Of the two most probable structures, a and b, the former, which involves the coordination of the diphenylketene group through the π-complexing C=C bond and the lone pair of the oxygen, is favored on the basis of a consideration of the steric requirement and its similarity with the cyanoamido complex.[3]

The reaction of II and III with such proton-donors as alcohol, hydrochloric acid, water and acetic acid were of considerable interest. These reagents decomposed the diphenylketene complexes, with the liberation of tetraphenylethane (IV). For example, when treated with glacial acetic acid, the III complex yielded IV, with a vigorous gas evolution, in a yield of 53%. Similarly, the vanadium complex, II, gave IV in a 25% yield, when treated with ethanol. The formation of IV in the above reactions suggests that the carbon-carbon double bond in the ketene is weakened by bonding to the metal.

Further work on the interaction of ketenes with organometallic π-compounds is in progress.

1) a) A. Nakamura, P.-J. Kim and N. Hagihara, *J. Organometal. Chem*, **3**, 7 (1965); ibid., **3**, 355 (1965). b) A. Nakamura, This Bulletin, **38**, 1868 (1965); **39**, 543 (1966).

2) R. Tsumura and N. Hagihara, ibid., **38**, 861 (1965).

3) H. Bock and H. Dieck, *Ber.*, **99**, 213 (1966).

The Copolymerization of Vinyl Chloride and Ethylene by a Ziegler-Natta Catalyst

By Akira MISONO and Yasuzo UCHIDA

Department of Industrial Chemistry, Faculty of Engineering, The University of Tokyo, Hongo, Tokyo

and Kunikazu YAMADA

Central Research Laboratory, Sekisui Chemical Co., Shimamoto-cho, Mishima-gun, Osaka

(Received June 3, 1966)

Recently, Yamazaki et al. have reported the copolymerization of vinyl chloride with propylene by the use of the catalyst systems consisting of $Ti(n\text{-}OBu)_4$ and organoaluminum compounds.[1] In the course of the studies of the copolymerization of vinyl chloride with ethylene, the present authors have also found that the same catalyst systems can copolymerize these monomers in a manner quite different from the radical copolymerization which they previously reported.[2] This paper will deal with the copolymerization by the use of the $Ti(n\text{-}OBu)_4$-$AlEtCl_2$ catalyst system.

The reaction was carried out in a stainless-steel autoclave equipped with an agitating device. The resultant copolymer was treated and purified in the usual manner. The composition of the product was calculated from the elemental analyses data. The reduced specific viscosity of the tetrahydrofuran-soluble polymer was measured using a 0.5 g./100 ml. cyclohexanone solution at 30.0°C.

Typical copolymerization results, including the results of successive solvent extraction, are shown in Table I. The copolymerizates obtained by the use of the present catalyst system were considerably richer in ethylene than those obtained in the radical copolymerization using trialkylboron-peroxide systems.[2] The copolymerizate became richer in ethylene with an increase in the aluminum/titanium molar ratio. At aluminum/titanium molar ratios higher than 5, only polyethylene was obtained at any composition of the monomer mixture.

In order to investigate the composition distribution of the copolymerizate, successive solvent extraction, using tetrahydrofuran and monochlorobenzene, of the products obtained at aluminum/titanium molar ratios of 1.8, 2.5 and 3 were carried out. These results are shown in Table I. The copolymerizates being extracted not only according to the difference in molecular weight, but also according to the difference in composition, it was considered that the copolymerizates consisted of copolymers of different compositions. There may exist several active sites in the catalyst system, each with different reactivity ratios and each producing its own type of polymer.

The catalyst system was active for vinyl chloride homopolymerization, but it showed little activity for ethylene at aluminum/titanium molar ratios lower than 2.5. However, the catalyst changed its activity for each monomer at an aluminum/titanium molar ratio slightly higher than 2.5. From the infrared spectroscopy of the extracted fractions of the copolymerizates, particularly investigating the 900—700 cm^{-1} region where absorptions due to the methylene rocking mode of polyvinyl chloride (833 cm^{-1}), the vinyl chloride-ethylene random copolymer (750 cm^{-1}) and polyethylene (730 and 720 cm^{-1}) are observed, it was proved that a random copolymer with a broad composition distribution was obtained at aluminum/titanium molar ratios lower than 2.5, whereas, at an aluminum/titanium molar ratio of 3, a block copolymer rich in ethylene was formed, along with a random copolymer rich in vinyl chloride.

Detailed experimental results and a discussion of the reaction mechanism will be reported in the near future.

TABLE I. COPOLYMERIZATION RESULTS WITH USE OF $Ti(n\text{-}OBu)_4$-$AlEtCl_2$ CATALYST SYSTEM

				THF extract			MCB extract		Residue	
Al/Ti	VCl mol.% in feed	yield %	VCl mol.% in product	wt.%	VCl mol.%	η_{sp}/C	wt.%	VCl mol.%	wt.%	VCl mol.%
1.8	40	5.97	44.85	40.12	66.41	0.1734	3.81	5.16	56.07	0
2.5	70	5.80	48.87	40.54	77.58	0.3068	42.40	20.42	17.06	—
3.0	90	8.22	53.26	43.76	77.49	0.4234	39.30	34.96	16.94	—
Polyvinyl chloride				100			0		0	
Polyethylene				2.47			29.63		67.90	

vinyl chloride + ethylene: 0.5 mol., $Ti(n\text{-}OBu)_4$: 2 mmol., $AlEtCl_2$: varied *n*-heptane: 50 ml., 50°C, 3 hr.

1) N. Yamazaki, M. Aritomi and S. Kambara, Preprint of the 19th Annual Meeting of the Chemical Society of Japan, Tokyo, 4T103 (1966).

2) A. Misono, Y. Uchida and K. Yamada, Preprint of the 19th Annual Meeting of the Chemical Society of Japan, Tokyo, 4U226 (1966).

Bismuth-Carbon Cleavage on Complex Formation

By Rokuro OKAWARA, Kiyoshi YASUDA and Masanobu INOUE

Department of Applied Chemistry, Osaka University, Higashinoda, Miyakojima, Osaka

(Received June 4, 1966)

Numerous investigations have been concerned with the preparation of triarylbismuths from diarylbismuth halides. Gilman et al.[1] have reported that the reaction of diphenylbismuth halides with hydrazine hydrate in refluxing alcohol gave triphenylbismuth and inorganic bismuth halides according to;

$$3Ph_2BiX \longrightarrow BiX_3 + 2Ph_3Bi \quad (1)$$

However, we have obtained monophenylbismuth compounds together with triphenylbismuth by the reactions of diphenylbismuth halides with pyridine at room temperature.

$$2Ph_2BiX \xrightarrow{py} PhBiX_2 \cdot 2py + Ph_3Bi \quad (2)$$

These compounds correspond to the hypothetical intermediate substances of the conversion reaction 1. Hartmann et al.[2] have assumed that analogous compounds are formed in the decomposition reactions of para-substituted phenylbismuth compounds.

Experimental.—Phenylbismuth Halides. — Ph_2BiX and $PhBiBr_2$ were prepared by the reaction[3] of Ph_3Bi and BiX_3 (X=Cl, Br), and purified by the recrystallization from dry benzene.

Phenylbismuth Dibromide Pyridine Adduct.—Method 1: A solution of 3 g. Ph_2BiBr in 50 ml. of dry pyridine was added dropwise to 150 ml. of petroleum ether. After filtering 0.2 gr. of white solid (A), m. p. 143—146°C, the filtrate was kept standing for a day at room temperature, and 1.1 gr. of pale yellow needle-like crystals (B) of $PhBiBr_2 \cdot 2py$ was obtained, m. p. 145—146°C. Yield (A+B) 62%.

Found: Bi, 34.72; C, 31.93; H, 2.33; N, 4.65; Br, 26.42. Calcd. for $C_6H_5BiBr_2 \cdot 2C_5H_5N$: Bi, 34.59; C, 31.81; H, 2.50; N, 4.64; Br, 26.46%.

Removal of the solvents under reduced pressure from the mother liquor gave 1.3 gr. of white solid, which was recrystallized from ethanol to give Ph_3Bi, m. p. 77—78°C. Yield 87%.

Method 2: On addition of a solution of $PhBiBr_2$ (1 g.) in 40 ml. of pyridine to 150 ml. of petroleum ether, a creamy precipitate of $PhBiBr_2 \cdot 2py$ (m. p. 145—146°C) was obtained almost quantitatively.

The infrared spectra and the mixed melting point showed that the complexes prepared by methods 1 and 2 were identical.

Phenylbismuth Dichloride Pyridine Adduct.—White needle crystals of $PhBiCl_2 \cdot 2py$ (m. p. 136—137°C) was prepared by the same procedure (method 1) used for the bromide. Yield 77%.

Found: Bi, 40.67; C, 37.83; H, 2.80; N, 5.46; Cl, 13.77. Calcd. for $C_6H_5BiCl_2 \cdot 2C_5H_5N$: Bi, 40.56; C, 37.30; H, 2.93; N, 5.44; Cl, 13.76%.

From the mother liquor a 95% yield of Ph_3Bi was obtained.

1) H. Gilman and H. L. Yablunky, *J. Am. Chem. Soc.*, **62**, 665 (1940).
2) H. Hartmann, G. Habenicht and W. Reiss, *Z. Anorg. Allg. Chem.*, **317**, 54 (1962).
3) H. Gilman, H. L. Yale, *Chem. Revs.*, **30**, 281 (1942).

The Photochemical Reactions of Ethyl Benzoylformate in Solution

By Tamotsu TOMINAGA, Yoshinobu ODAIRA and Shigeru TSUTSUMI

Department of Chemical Technology, Faculty of Engineering, Osaka University, Miyakojima-ku, Osaka

(Received June 8, 1966)

In an earlier paper dealing with photoethyl oxallylation,[1] the present authors reported that the direct introduction of ethyl oxallyl radicals, generated by the photolysis of diethyl oxalate or ethyl phenyl oxalate, into several hydrogen-donating solvents was successful, and that ethoxycarbonyl derivatives, i. e., esters, were always found to be the second principal product in a series of the above reactions.

Concerning the formation of esters, it seems more likely that the esters would be formed by a recombination between ethoxycarbonyl and solvent radicals. However, as has been previously pointed out,[2] ethoxycarbonyl radicals decompose exothermically because of their remarkable unstability and give rise to only carbon dioxide and ethyl radicals (quantitatively).

Meanwhile, in our photoreactions of the above oxalates in a solvent, carbon monoxide was invariably isolated as a major gaseous product; the ratio of the formation of carbon monoxide to that of carbon dioxide was approximately 4.5. From the above results, it may be considered that the reaction path for ester formation involving free ethoxycarbonyl radicals produced through the photolysis of the oxalate is not very significant. Subsequently, it seems that the esters may be formed by the secondary photolysis of the corresponding α-keto esters.

The photochemistry of α-keto esters in various media has been extensively studied recently by several investigators. Giving the photolysis of ethyl benzoylformate as an example, in an inert solvent such as benzene, ethyl benzoylformate is photodecarbonylated to afford benzaldehyde and acetaldehyde.[3] In alcoholic solvents at room temperature,[4,5] the formate is officiently photoreduced to the corresponding pinacol, while, on the other hand, at elevated temperature it undergoes intramolecular hydrogen abstraction, yielding acetaldehyde, the corresponding hydroxyketene, and the enol of phenylglyoxal. At any rate, the formation of esters from the α-keto esters by photodecarbonylation has not yet been reported.

In order to make sure of the feasibility of the formation of the ester from the α-keto ester, the photolysis of ethyl benzoylformate in solvents such as benzene and cyclohexane was undertaken.

The irradiation of a solution of ethyl benzoylformate (0.075 mole) in benzene (1.5 mole) with a light of approximately 3660 Å, provided by a 300 W. high-pressure mercury lamp through a suitable filter system, was carried out at 20°C for 7 days. As the photoproducts, ethyl benzoate (0.65 g.), ethyl mandelate (2.45 g.) and biphenyl (1.1 g.) were obtained, together with the products, such as benzaldehyde (0.5 g.) and acetaldehyde (0.1 g.), described above. Moreover, besides the above constituents, a small amount of a gaseous product consisting of carbon monoxide, carbon dioxide and ethane in the ratio of 19 : 6 : 1 was obtained.

In addition, the irradiation, at 20°C for 54 hr., of a solution of ethyl benzoylformate (0.1 mole) and cyclohexane (5.0 mole), using a 300 W. high-pressure mercury arc lamp, afforded the following various photoproducts: ethyl benzoate (1.0 g.), ethyl mandelate (1.6 g.), benzaldehyde (0.7 g.), biphenyl (0.4 g.), benzophenone (0.25 g.), ethyl cyclohexyl carboxylate (0.5 g.), and bicyclohexyl (1.8 g.), along with very small amounts of acetaldehyde, cyclohexyl methyl carbinol and cyclohexyl methyl ether. Most of the gaseous product obtained was composed of carbon monoxide. The conversion percentage of ethyl benzoylformate was 52%.

Although the present photochemical reaction is rather complex due to the many different radicals produced, the results show a plain demonstration of the possibility of ester formation from the α-keto ester by photodecarbonylation.

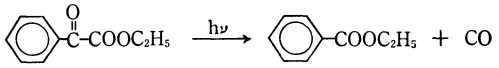

Details of this and further work will be reported shortly.

1) Y. Odaira, T. Tominaga, T. Sugihara and S. Tsutsumi, *Tetrahedron Letters*, **1964**, 2527; T. Tominaga, Y. Odaira and S. Tsutsumi, *J. Chem. Soc. Japan*, in press.
2) J. C. J. Thynne, *Pro. Chem. Soc.*, 18, **1961**; **1962**, 295.
3) P. A. Leermakers, P. C. Warren and G. F. Vesley, *J. Am. Chem. Soc.*, **86**, 1768 (1964).
4) E. S. Huyser and D. C. Neckers, *J. Org. Chem.*, **29**, 276 (1964).
5) N. C. Yang and A. Morduchowitz, ibid., **29**, 1654 (1964).

The Absolute Configuration of Pulegoneoxide

By Jun KATSUHARA

Sun Star Dentifrice Company, Akutagawa, Takatsuki, Osaka

(Received June 9, 1966)

Reusch and Johnson[1] recently reported on the configuration of diastereomeric pulegoneoxides and deduced that the (−)-pulegoneoxide which was derived from (+)-pulegone should be assigned the *cis* structure, and the (+)-pulegoneoxide, the *trans* structure, on the basis of IR, UV, NMR, and ORD data.

In contrast to the above deduction, Djerassi et al.[2] suggested that the assignment should be reversed in the light of his ORD investigations. The present paper will attempt to establish the absolute configuration of these pulegoneoxides by means of unequivocal chemical transformations of these oxides into diols with well-defined configurations.

(+)-(1R)-Pulegone (I) was oxidized with 30% hydrogen peroxide in a 30% sodium hydroxide solution to give a mixture of *cis*- and *trans*-pulegoneoxide, m. p. 43°C.

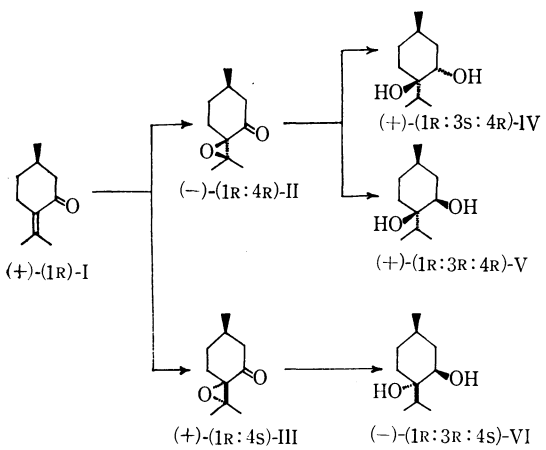

The fractional distillation, followed by the zone-melting purification, of the mixture afforded (−)-pulegoneoxide (II), m. p. 54°C, $[\alpha]_D^{20}$ −18.8° (ethanol), and (+)-*cis*-pulegoneoxide (III), m. p. 59°C; $[\alpha]_D^{20}$ +46.6° (methanol).

The (−)-diastereomer (II) was then reduced with lithium aluminum hydride in ether to give (+)-*trans*-4-hydroxyneomenthol (IV) in an 83% yield, m. p. 72°C; $[\alpha]_D^{20}$ +22.6° (chloroform), and (+)-*cis*-4-hydroxymenthol (V) in a 17% yield, m. p. 76°C; $[\alpha]_D^{20}$ +10.4° (chloroform).

These diols (IV and V) were identified as such by an IR-comparison with authentic (+)-(1R : 3s : 4R)-*trans*-4-hydroxyneomenthol[3] and (+)-(1R : 3R : 4R)-*cis*-4-hydroxy menthol[4] respectively.

The diastereomeric (+)-pulegoneoxide (III) was reduced with lithium aluminum hydride to give (−)-*trans*-4-hydroxyneoisomenthol (VI) in an almost quantitative yield, m. p. 76°C, $[\alpha]_D^{20}$ −22.0 (methanol). This was identified by a melting-point determination and by an IR comparison with authentic (−)-(1R : 3R : 4s)-*trans*-4-hydroxy-neoisomenthol.[4]

The results in the present study unambiguously settle the dispute about the absolute configuration of pulegoneoxides and support Djerassi et al.'s assignment based on the ORD investigations. The observed negative and positive Cotton effects of (−)-II and (+)-III respectively also suggest the reasonable applicability of the "reversed" Octant rule[2] to spiro [5, 2] systems. Further details will be reported elsewhere in the near future.

1) W. Reusch and C. K. Johnson, *J. Org. Chem.*, **28**, 2557 (1963).
2) C. Djerassi, W. Klyne, T. Norin, G. Ohloff and E. Klein, *Tetrahedron*, **21**, 163 (1965).
3) T. Suga, T. Shishibori and T. Matsuura, This Bulletin, **37**, 310 (1964).
4) W. Tagaki and T. Mitsui, *J. Org. Chem.*, **25**, 1476 (1960).

Studies on Amino-hexoses. XII. Crystalline Muramicitol and Its Use in a Study of the Lysozyme Action on the Cell Wall of Micrococcus Lysodeikticus

By Saburo HARA and Yoshio MATSUSHIMA

Department of Chemistry, Osaka University, College of Science, Toyonaka, Osaka

(Received June 11, 1966)

It has been concluded that the egg white lysozyme splits the polysaccharide part of the bacterial cell wall and that the di- and tetra-saccharides released have muramic acid as their reducing ends.[1] One of the structure analyses of these oligo-saccharides consisted of the reduction of the saccharides with borohydride and the examination of the subsequent hydrolysis mixture on chromatograms. As a result of a lack of the authentic muramicitol, 2-amino-3-*O*-(D-1'-carboxyethyl)-2-deoxy-D-glucitol, however, the above conclusion was drawn from the facts that muramic acid disappeared or diminished and that a new ninhydrin positive compound appeared on the chromatograms.

In order to gain a straight and positive conclusion, we have now prepared crystalline muramicitol and used it as the reference standard in a study of lysozyme action on the cell wall of M. lysodeikticus. As is shown in Table I, egg white lysozyme splits *N*-acetyl-muramide linkages only, leaving *N*-acetyl-glucosaminide linkages intact; this seems somewhat peculiar, because the same enzyme splits *N*-acetyl-glucosaminide linkages in chitin,[2] glycol chitin and carboxymethyl chitin.[3]

TABLE I. THE COMPOSITION OF THE ACID HYDROLYSATES (μmol./g.)

	Intact cell wall	Lysozyme digest treated with sodium borohydride
Muramic acid	597	169
Glucosamine	628	649
Muramicitol	0	360
Glucosaminitol	0	0
Glutamic acid	740	731
Glycine	765	729
Alanine	1635	1615
Lysine	697	688
Ammonia	763	832

The Preparation of Muramicitol.—Muramic acid[4] (150 mg.) was dissolved in 5 ml. of water, and to this solution there was then added 50 mg. of sodium borohydride while it was being stirred at room temperature. After the mixture had stood for 2 hr., its pH was adjusted to 5.6 by adding Amberlite IR-120 (H^+ form). The solution separated from the resins was concentrated to dryness in vacuo. To the residue 10 ml. of dry methanol was added, and the solution was evaporated to dryness in order to remove the methyl borate formed. This process was repeated three times. The residue was dissolved in 0.5 ml. of water, and to this solution 10 ml. of methanol was added. After the mixture had stood in a refrigerator, 90 mg. of colorless crystals were obtained. The specimen melted at 196°C (uncorr.) ($[\alpha]_D^{26}$ +44.9 (*c*, 0.423, water)). Found: C, 42.29; H, 7.72; N, 5.33. Calcd. for $C_9H_{19}O_7N$: C, 42.68; H, 7.56; N, 5.53%. The muramicitol thus obtained showed no reducing power against a ferricyanide reagent.[5] The ninhydrin color reaction was very weak, and the molar extinction coefficient was about 6% that of muramic acid. In a Stein-Moore column,[6] the specimen eluted before aspartic acid at pH 3.25 (0.2 N citrate).

The Lysozyme Action on the M. Lysodeikticus Cell Wall.—A cell wall (4.4 mg.) isolated from M. lysodeikticus by the usual bead-shaking method[7] was incubated with 0.5 mg.- of crystalline egg white lysozyme for 24 hr. at 37°C in 1.5 ml. of a M/15 phosphate buffer of pH 7.0. After the incubation had ended, the pH of the solution was adjusted to 9.0 by adding 0.1 N sodium hydroxide; then the mixture was treated with sodium borohydride for 24 hr. at room temperature. After lyophilization and hydrolysis with 6 N hydrochloric acid for 16 hr. at 100°C, an appropriate amount of the hydrolysate was run on a Stein-Moore column using an automatic instrument (Hitachi KLA-3). In Table I the results are shown and compared with the hydrolysate of the intact cell wall.

No correction was made for the degradation during acid hydrolysis, and the data for the minor-constituent amino acids are omitted.

This investigation was supported by U. S. Public Health Service Grant AI-04586-04.

1) M. R. J. Salton and J. M. Ghuysen, *Biochim. Biophys. Acta*, **36**, 552 (1959); ibid., **45**, 355 (1960); H. R. Perkins, *Biochem. J.*, **74**, 182 (1960); N. Sharon, T. Osawa, H. M. Flowers, and R. W. Jeanloz, *J. Biol. Chem.*, **241**, 223 (1966).

2) L. R. Berger and R. S. Weiser, *Biochim. Biophys. Acta*, **26**, 517 (1957).

3) Y. Matsushima, S. Hara, T. Miyazaki, and Y. Umemura, The 38th Annual Meeting of The Japanese Biochemical Society, October, 1965.

4) Y. Matsushima and J. T. Park, *J. Org. Chem.*, **27**, 3581 (1962).

5) J. T. Park and M. J. Johnson, *J. Biol. Chem.*, **181**, 149 (1949).

6) S. Moore and W. H. Stein, ibid., **192**, 663 (1951).

7) M. R. J. Salton and R. W. Horne, *Biochim. Biophys. Acta*, **7**, 177 (1951).

Dielectric Loss Measurement by Differential Thermal Analysis (DTA)

By Takasuke MATSUO, Hiroshi SUGA and Syûzô SEKI

Department of Chemistry, Faculty of Science, Osaka University, Toyonaka, Osaka

(Received June 15, 1966)

Dielectrics with an imaginary part, ε'', of electric susceptibility absorb energy proportional to $\varepsilon'' E_0^2 \omega$ per unit of time per unit of volume from an applied electric field, $E_0 \sin \omega t$. This suggests the possibility of measuring the dielectric loss factor of substances by temperature measurements. In fact, we observed this effect by the DTA technique which we have been developing.

The construction of the main part of the DTA apparatus has been reported elsewhere.[1] Electrodes for applying the field are a pair of 2.0-by-0.7 cm^2 aluminum foils attached to the outer surface of the DTA-specimen glass tube. The electrodes are electrically insulated from the copper block by a thin sheet of polyethylene, which also serves to keep the electrodes in place. A fine copper lead is pressed to the electrode beneath the polyethylene sheet.

The alternating voltage source is a 6CL6-807 high-frequency amplifier driven by a commercial test oscillator. A suitable output voltage was obtained by adjusting the position of the output tap of the 807-plate tank coil. The terminal voltage, usually 10—100 V., was monitored by a valve voltmeter. This assemblage worked satisfactorily between 200 kc. and 20 Mc.

As examples, results on glycerol and cyclohexanol are presented below. The dielectric properties of the former were studied extensively by Davidson and Cole[2] and by others. Our results are illustrated in Fig. 1 as a maximum-loss temperature-vs.-frequency relation.

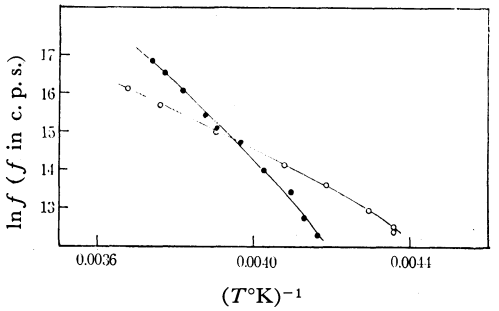

Fig. 1. Frequency vs. maximum-loss-temperature relation for glycerol and cyclohexanol.
—●— Glycerol —○— Cyclohexanol

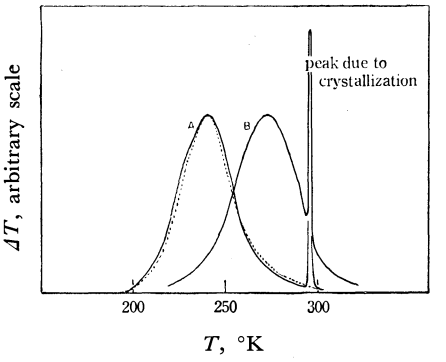

Fig. 2. ΔT vs. temperature plot for cyclohexanol.
A: At 0.81 Mc.
The broken line is the Debye type loss factor with $\tau = \tau_0 \exp(E/RT)$.
B: At 10.1 Mc.

The dielectric behavior of cyclohexanol has been reported on by several authors.[3] On cooling, the crystal takes a metastable form which shows a dielectric loss maximum. In Fig. 2, the ΔT value for this crystal is compared with a normalized Debye-type loss factor with a single $\tau = \tau_0 \exp(E/RT)$ ($\tau_0 = 1.38 \times 10^{-15}$ sec., $E = 9.78$ kcal./mol). The Arrhenius plot for the evaluation of τ_0 and E is given in Fig. 1. These values are in fair agreement with those given in the literature. An interesting feature of this crystal is seen in the ΔT curve for 10.1 Mc., in which the peak due to the crystallization is superposed on the higher-temperature side of the dielectric loss peak without breaking the continuity of the latter. This provides evidence that the mode of the rotational motion of the molecules does not change essentially upon crystallization.

Finally, it should be added here that recently the thermal method of detecting dielectric loss has been applied independently to barium titanate by Pilawski and Danielewicz.[4] Their method seems to be useful for substances with large ε'' values, while for those with smaller ε'' values, our method is more suitable.

1) H. Suga, H. Chihara and S. Seki, *J. Chem. Soc. Japan, Pure Chem. Sect.* (*Nippon Kagaku Zasshi*), **82**, 24 (1961).
2) D. W. Davidson and R. H. Cole, *J. Chem. Phys.*, **19**, 1484 (1951).
3) G. Corfield and M. Davies, *Trans. Faraday Soc.*, **60**, 10 (1964).
4) A. Pilawski and M. Danielewicz, *Acta Phys. Pol.*, **28**, 3 (1964).

The Crystal Structure of Ethylzinc *t*-Butoxide

By Yutaka MATSUI, Kazuhide KAMIYA and Masao NISHIKAWA

Research and Development Division, Takeda Chemical Industries, Ltd., Higashiyodogawa-ku, Osaka

and Yujiro TOMIIE

Faculty of Science, Kwansei Gakuin University, Nishinomiya

(Received June 15, 1966)

For several years one of the present authors has been sudying $ZnEt_2$ or its derivatives as catalysts for the polymerization of alkylene oxides; in these studies it has been assumed that RZnOR' plays an important role in $ZnEt_2$-alcohol-Al_2O_3 or RZnOR'-Al_2O_3 catalyst systems.[1]

Recently, Coates et al.[2] speculated about the structure of RZnOR' (I). This has prompted us to report our results, obtained through X-ray

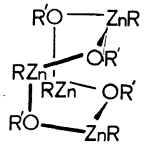

(I)

analysis which had been carried out in this laboratory. Since there seems to be some discrepancy between their results and ours, we want to publish a short account of our results now.

Ethylzinc *t*-butoxide was prepared by mixing *t*-butanol and $ZnEt_2$ (molar ratio: 1/1) in dry hexane under nitrogen; single crystals, as colorless prisms, were thus obtained.

The unit cell is monoclinic, with parameters of $a=16.96$ Å, $b=11.02$ Å, $c=10.06$ Å, and $\beta=119°$. The assumption of $(C_6H_{14}OZn)_8$ in a unit cell leads to a reasonable calculated density of 1.35 gcm^{-3}. Systematic extinctions of F_{obs} (h, k, l) when $h+k$ is odd, lead to a *C*-centered lattice, that is, *C*2, *Cm* or *C*2/*m*. A total of 740 independent reflections was recorded photographically with a Weissenberg camera; from these reflections the three-dimensional Patterson function was computed. The results show that a molecule consists of four $EtZnOBu^t$ and that it is in a form resembling a cube, its eight corners being occupied by four zinc and four oxygen atoms.

There are various cubic models that have a different arrangement of atoms. The analysis of the Patterson function alone is not enough to determine the true structure among them. Calculation was carried out by the least-squares method on the assumption of various arrangements of zinc and oxygen atoms in the molecule. However, the temperature factors of the atoms, which were assumed to be oxygen, came to have minus values. Thus, oxygen atoms should not be fixed at any four of the eight corners of the model. The reflection data can be explained most clearly on the hypothesis that the electron density at the eight corners is similar; i. e., the *R*-value reaches a minimum (23%) when such is the case. The structure could not be explained without a consideration of some kind of disorder. In this case, the most possible space group would be *C*2/*m* (*pseudo* symmetry) and the molecules would occupy the special position of 2/*m* in the unit cell. The bond distances and bond angles in this molecule are illustrated in Fig. 1.

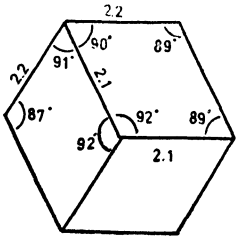

Fig. 1.

A disordered structure consisting of II and III is most probable, because bond distances between metals are usually above 2.5 Å, and the value of 2.15 Å obtained by our calculation is appropriate for Zn-O. In the disordered sturcture, it may be difficult to clarify the configuration of substituents. However, IV could presumably be assumed to be the structure of this molecule. At present, analysis is still under progress by means of the (F_o-F_c) synthesis to determine the configuration of ethyl and *t*-butoxyl groups.

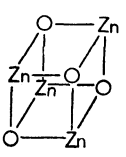

(II)

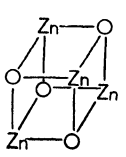

(III)

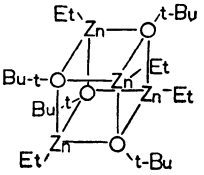

(IV)

Coates has estimated that six probable forms of I would interconvert rapidly, in which case the time-average structure would be cubic. However, it has been shown from the present study that the molecule takes a form resembling a cube, consisting of not three-, but of four-coordinated zinc and oxygen atoms. There is thus no necessity for assuming the time-average structure of I.

1) Y. Matsui, T. Saegusa and J. Furukawa, *J. Chem. Soc. Japan. Ind. Chem. Sect. (Kogyo Kagaku Zasshi)*, in press.
2) G. E. Coates and D. Ridley, *J. Chem. Soc.*, **1965**, 1870.

BULLETIN OF THE CHEMICAL SOCIETY OF JAPAN VOL. 39 1829—1836 (1966)

The Energy of the Excimer Luminescence of Naphthalene under a Variety of Geometrical Configurations

By Tohru AZUMI* and Hiroshi AZUMI

Department of Chemistry, Faculty of Science, Tohoku University, Katahira-cho, Sendai

(Received August 24, 1965)

A four-electron ASMO treatment of the interaction of two naphthalene molecules to yield excimers of D_{2h}, C_2, or S_4 is developed, and the energies of these excimers are calculated as a function of the angle, α, between corresponding bonds of the two molecules. It is shown that excimers are stable at two configurations, $\alpha=0°$ and $\alpha=75°$; that the excimer with $\alpha=0°$ does not emit because of the forbidden character of the transition, and that the excimer with $\alpha=75°$ emits and is considered to play a predominant role in the observed excimer fluorescence.

A large number of compounds exhibit, in a concentrated solution, a broad and structureless fluorescence about 6000 cm^{-1} to the red of the normal structured fluorescence. This broad fluorescence band is ascribed to the dimeric species produced by the photoassociation of one ground-state molecule and one excited-state molecule; the term "excimer fluorescence" has been used to describe this phenomenon. Although quite a lot of experimental information is available, theoretical interpretations of excimer fluorescence are scarce. Azumi and McGlynn[1] have suggested that the excimer state may be satisfactorily represented by a linear combination of molecular exciton states and charge resonance states. On the basis of this model, the energy of the excimer luminescence was calculated, by Azumi, Armstrong, and McGlynn,[2] for excimers of naphthalene, anthracene, pyrene, and perylene at the highest possible symmetry of excimer configuration (i. e., D_{2h}). Similar calculations have also been given by Murrell and Tanaka[3] and by Konijnenberg[4]. The agreement between the calculated and the experimental excimer energies strongly supports the above-mentioned idea and the general scheme of the calculation. There are, however, some pitfalls in the calculations which have been presented in the past. The calculations given by these three sets of authors were all carried out for an excimer configuration which may not exist in reality. The excimer configuration for which the calculations were carried out is such that one of the molecules which constitute an excimer is exactly superposed, at some distance, over the other. In an excimer of such a high symmetry, the transition between the lowest excimer state and the dimeric ground state is dipole-forbidden. On the other hand, as has been illustrated by Birks, Dyson, and King,[5] the lifetime of the excimer fluorescence is quite short, indicating the allowed character of excimer luminescence. In some cases, an excimer luminescence of a long duration is observed; however, it has been clarified that this duration is due to triplet-triplet annihilation, and not to the inherent forbidden character of the excimer luminescence.[6-10] All these experimental evidences seem to reveal that excimer luminescence is essentially allowed, and that, consequently, the excimer has a symmetry lower than D_{2h}.

Various geometrical configurations of sandwich-type excimers (in which two molecular planes are parallel) were analyzed group-theoretically by Azumi and McGlynn.[11] It was shown that excimer luminescence should be forbidden not only for the D_{2h} configuration, but also for the C_{2h}, C'_{2h}, or S_2 configurations of the excimer. That is, if the corresponding bonds of the two molecules that constitute an excimer are aligned parallel, excimer luminescence is invariably forbidden. In order for excimer luminescence to be an allowed transition, as seems to be the case, there must be some angle between the corresponding bonds of the two molecules. These are schematically represented in Fig. 1 for the naphthalene excimer.

* Postdoctoral fellow supported by the Japan Society for the Promotion of Science.

1) T. Azumi and S. P. McGlynn, *J. Chem. Phys.*, **41**, 3131 (1964).
2) T. Azumi, A. T. Armstrong and S. P. McGlynn, ibid., **41**, 3839 (1964).
3) J. N. Murrell and J. Tanaka, *Mol. Phys.*, **7**, 363 (1964).
4) E. Konijnenberg, Thesis, University of Amsterdam (1963).
5) J. B. Birks, D. J. Dyson and T. A. King, *Proc. Roy. Soc.*, **A277**, 270 (1964).
6) T. Azumi and S. P. McGlynn, *J. Chem. Phys.*, **39**, 3553 (1963).
7) C. A. Parker and C. G. Hatchard, *Trans. Faraday Soc.*, **59**, 284 (1963).
8) C. Tanaka, J. Tanaka, E. Hutton and B. Stevens, *Nature*, **198**, 1192 (1962).
9) C. A. Parker, ibid., **200**, 331 (1963).
10) F. J. Smith and S. P. McGlynn, *J. Chem. Phys.*, **42**, 4308 (1965).
11) T. Azumi and S. P. McGlynn, ibid., **42**, 1675 (1965).

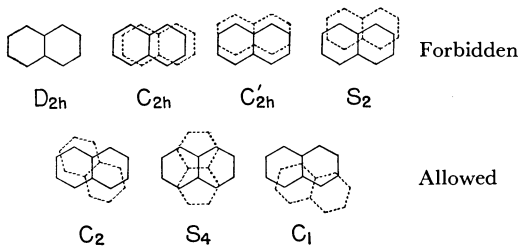

Fig. 1

This conclusion, arrived at group-theoretically, might, however, be hard to accept. First of all, it is against the intuition of chemists that a symmetrical configuration should be favored over an asymmetrical one. In addition, since in most aromatic crystals the two nearest molecules are aligned in the way of C_{2h} or S_2, there has been a suggestion that the excimer should have a similar configuration. It is, in this respect, desirable that some experimental or other kind of theoretical support of the above conclusion be obtained. Polarization measurements, conjoined with group theoretical analysis, would be most fruitful. Unfortunately, however, the polarization measurement of the excimer luminescence in a liquid solution is not possible because excimer formation is diffusion-controlled.[12] As a result, there has not been any experimental information thus far regarding the geometry of the excimer. Another way to approach this goal is to calculate the energy of the excimer luminescence for a variety of the geometrical configurations which give allowed dipole transitions and to see if there is any stable configuration among them. It is this which is effected in this paper.

In this paper, the effect of the angle, α, between the corresponding bonds of the two molecules is analyzed. Namely, excimers of D_{2h} ($\alpha=0°$), C_2 ($0°<\alpha<90°$), and S_4 ($\alpha=90°$) are considered, and the energy of the excimer luminescence is calculated as a function of the angle, α. (See Fig. 2.) Interest is focussed on the variation in energy with respect to the angle, α; in this respect, the separation of the two molecular planes is arbitrarily taken to be 3 Å.

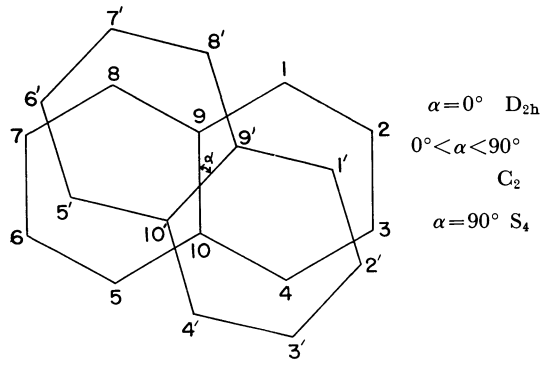

Fig. 2

12) J. B. Birks, D. J. Dyson and I. H. Munro, *Proc. Roy. Soc.*, **A275**, 575 (1963).

Zeroth-order Dimeric Wave Functions

The general scheme of calculation is essentially identical with those given by Azumi, Armstrong, and McGlynn,[2] since the methods employed by these authors proved satisfactory. The highest-occupied and the lowest-vacant molecular orbitals of one ground state molecule (say, Molecule A) are designated, respectively, as ϕ_1 and ϕ_2, and the corresponding orbitals of the other molecule (say, Molecule B), as θ_1 and θ_2. ϕ_1 and ϕ_2 are orthogonal, as are also θ_1 and θ_2. It is assumed that orthogonality exists between ϕ_1 and θ_2 and between θ_1 and ϕ_2; the overlap between these orbitals is not exactly zero in our overlap approximation (see below), but it is surely very small and may well be neglected. The overlap integrals between ϕ_1 and θ_1 and between ϕ_2 and θ_2 are designated, respectively, as S_1 and S_2; namely, in the bracket notation:

$$S_1 = (\phi_1 \mid \theta_1) \tag{1}$$

$$S_2 = (\phi_2 \mid \theta_2) \tag{2}$$

The zeroth-order dimeric wave functions of interest are, then, expressed in terms of these four molecular orbitals. The wave function for the dimeric ground state is:

$$\psi_G = (1 - 2S_1^2 + S_1^4)^{-1/2} \mid \phi_1\bar{\phi}_1\theta_1\bar{\theta}_1 \mid \tag{3}$$

where:

$$\mid abcd \mid = (4!)^{-1/2} \sum_p (-1)^p \mathbf{P} a(1)b(2)c(3)d(4) \tag{4}$$

The excitation of one electron to a higher orbital produces two molecular exciton states, ψ_A and ψ_B, and two charge resonance states, ψ_C and ψ_D.

The C_2 Excimer.—When an excimer is of the C_2 symmetry, it may easily be shown group-theoretically that all of the four wave functions form bases for the irreducible representation of B. The normalized wave functions are:

$$\psi_A = \{2(1 - S_1^2)\}^{-1/2}\{ \mid \phi_1\bar{\phi}_1\theta_1\bar{\theta}_2 \mid + \mid \phi_1\bar{\phi}_1\theta_2\bar{\theta}_1 \mid \} \tag{5}$$

$$\psi_B = \{2(1 - S_1^2)\}^{-1/2}\{ \mid \phi_1\bar{\phi}_2\theta_1\bar{\theta}_1 \mid + \mid \phi_2\bar{\phi}_1\theta_1\bar{\theta}_1 \mid \} \tag{6}$$

$$\psi_C = \{2(1 - S_1^2)\}^{-1/2}\{ \mid \phi_1\bar{\theta}_2\theta_1\bar{\theta}_1 \mid + \mid \theta_2\bar{\phi}_1\theta_1\bar{\theta}_1 \mid \} \tag{7}$$

$$\psi_D = \{2(1 - S_1^2)\}^{-1/2}\{ \mid \phi_1\bar{\phi}_1\phi_2\bar{\theta}_1 \mid + \mid \phi_1\bar{\phi}_1\theta_1\bar{\phi}_2 \mid \} \tag{8}$$

The D_{2h} Excimer.—When an excimer is of the D_{2h} symmetry, namely, when $\alpha=0°$, the two

wave functions ψ_{I} and ψ_{II} fall into the B_{3g} representation, and the two wave functions ψ_{III} and ψ_{IV} into the B_{2u} representation. These are, in terms of Eqs. 5—8;

$$\psi_{I} = \{2(1 + S_1S_2)\}^{-1/2}(\psi_{A} - \psi_{B}) \quad (9)$$

$$\psi_{II} = \{2(1 + S_1S_2)\}^{-1/2}(\psi_{C} - \psi_{D}) \quad (10)$$

$$\psi_{III} = \{2(1 - S_1S_2)\}^{-1/2}(\psi_{A} + \psi_{B}) \quad (11)$$

$$\psi_{IV} = \{2(1 - S_1S_2)\}^{-1/2}(\psi_{C} + \psi_{D}) \quad (12)$$

The S_4 Excimer.—When an excimer is of the S_4 symmetry, namely, when $\alpha=90°$, the two wave functions $\psi_{A}\pm i\psi_{B}$ fall into the degenerate E representation, and are also $\psi_{C}\pm i\psi_{D}$. When the configuration interaction between these two E states is considered, only one wave function from each E state may be taken. These are:

$$\psi_{\alpha} = 2^{-1/2}(\psi_{A} + i\psi_{B}) \quad (13)$$

$$\psi_{\beta} = 2^{-1/2}(\psi_{C} + i\psi_{D}) \quad (14)$$

Hamiltonian Matrix Elements

The Hamiltonian of the system is expressed in atomic units as:

$$H = \sum H_c(\nu) + \sum_{\nu<\mu} 1/r_{\nu\mu} \quad (15)$$

where $1/r_{\nu\mu}$ is the electrostatic repulsion between π electrons, ν and μ, and where $H_C(\nu)$ represents the effect of the core on the ν electron. In expressing integrals over molecular orbitals, the following notational simplification is made: ϕ_1 and ϕ_2 are designated as 1 and 2 respectively, and θ_1 and θ_2, as 1′ and 2′ respectively. Further,

$$(ij \mid kl) = \iint i(\nu)j(\nu)(1/r_{\nu\mu})k(\mu)l(\mu)\mathrm{d}\tau_{\nu}\mathrm{d}\tau_{\mu} \quad (16)$$

$$H^{c}_{ij} = \int i(\nu)H_c(\nu)j(\nu)\mathrm{d}\tau_{\nu} \quad (17)$$

The energy of the ground state, E_0, is then expressed as:

$$\begin{aligned}E_0 = {} & (1-2S_1^2+S_1^4)^{-1}[2(11 \mid 11) \\ & + (4-2S_1^2)(11 \mid 1'1') - 8S_1(11 \mid 11') \\ & + (-2+6S_1^2)(11' \mid 11') + (4-4S_1^2)H^{c}_{11} \\ & + (-4S_1+4S_1^3)H^{c}_{11'}] \end{aligned} \quad (18)$$

The other matrix elements are obtained similarly.

The C_2 Excimer.—The hamiltonian matrix elements are:

$$\begin{aligned}H_{AA} = {} & H_{BB} \\ = {} & (1-S_1^2)^{-1}[(11 \mid 11)+(11 \mid 22)+2(11 \mid 1'1') \\ & +(2-S_1^2)(11 \mid 2'2')+(12 \mid 12) \\ & -2S_1(11 \mid 11')-2S_1(11' \mid 22)-(11' \mid 11') \\ & -2S_1(12 \mid 1'2)+(-1+2S_1^2)(12' \mid 12') \\ & +(3-S_1^2)H^{c}_{11}+(1-S_1^2)H^{c}_{22}-2S_1H^{c}_{11'}] \end{aligned} \quad (19)$$

$$\begin{aligned}H_{CC} = {} & H_{DD} \\ = {} & (1-S_1^2)^{-1}[(11 \mid 11)+(2-S_1^2)(11 \mid 22) \\ & +2(11 \mid 1'1')+(11 \mid 2'2') \\ & +(-1+2S_1^2)(12 \mid 12)-2S_1(11 \mid 11') \\ & -2S_1(11' \mid 22)-(11' \mid 11')-2S_1(12 \mid 1'2) \\ & +(12' \mid 12')+(3-S_1^2)H^{c}_{11}+(1-S_1^2)H^{c}_{22} \\ & -2S_1H^{c}_{11'}] \end{aligned} \quad (20)$$

$$\begin{aligned}H_{AB} = {} & (1-S_1^2)^{-1}[-S_1S_2(11 \mid 1'1') \\ & +(2-S_1^2)(12 \mid 1'2')-2S_2(11 \mid 11') \\ & -2S_1(11 \mid 22')+3S_1S_2(11' \mid 11') \\ & +(-1+3S_1^2)(11' \mid 22')-2S_1(12 \mid 12') \\ & +S_1^2(12' \mid 1'2)-2S_1S_2H^{c}_{11}+(3S_1^2S_2-S_2)H^{c}_{11'} \\ & +(-S_1+S_1^3)H^{c}_{22'}] \end{aligned} \quad (21)$$

$$\begin{aligned}H_{AC} = {} & H_{BD} \\ = {} & (1-S_1^2)^{-1}[-S_1(11 \mid 22)-S_1(11 \mid 1'1') \\ & -S_1(11 \mid 2'2')-S_1(12 \mid 12)-2(11 \mid 11') \\ & +(3S_1^2-1)(11' \mid 22)+3S_1(11' \mid 11') \\ & +2(12 \mid 1'2)-S_1(12' \mid 12')-2S_1H^{c}_{11} \\ & +(-S_1+S_1^3)H^{c}_{22}+(-1+3S_1^2)H^{c}_{11'}] \end{aligned} \quad (22)$$

$$\begin{aligned}H_{AD} = {} & H_{BC} \\ = {} & (1-S_1^2)^{-1}[S_2(11 \mid 11)+2S_2(11 \mid 1'1') \\ & -S_1(12 \mid 1'2')-2S_1S_2(11 \mid 11') \\ & +(3-S_1^2)(11 \mid 22')-S_2(11' \mid 11') \\ & -2S_1(11' \mid 22')+2S_1^2(12 \mid 12') \\ & -S_1(12' \mid 1'2)+(3S_2-S_1^2S_2)H^{c}_{11} \\ & -2S_1S_2H^{c}_{11}+(1-S_1^2)H^{c}_{22'}] \end{aligned} \quad (23)$$

$$\begin{aligned}H_{CD} = {} & (1-S_1^2)^{-1}[-S_1S_2(11 \mid 1'1')+S_1^2(12 \mid 1'2') \\ & -2S_2(11 \mid 11')-2S_1(11 \mid 22') \\ & +3S_1S_2(11' \mid 11')+(-1+3S_1^2)(11' \mid 22') \\ & -2S_1(12 \mid 12')+(2-S_1^2)(12' \mid 1'2) \\ & -2S_1S_2H^{c}_{11}+(-S_2+3S_1^2S_2)H^{c}_{11'} \\ & +(-S_1+S_1^3)H^{c}_{22'}] \end{aligned} \quad (24)$$

Overlap matrix elements are:

$$S_{AB} = S_{CD} = -S_1S_2 \quad (25)$$

$$S_{AC} = S_{BD} = -S_1 \quad (26)$$

$$S_{AD} = S_{BC} = S_2 \quad (27)$$

The D_{2h} Excimer.—Hamiltonian and overlap matrix elements are expressed as follows. For B_{3g} states:

$$H_{I\,I} = (1 + S_1S_2)^{-1}(H_{AA} - H_{AB}) \quad (28)$$

$$H_{II\,II} = (1 + S_1S_2)^{-1}(H_{CC} - H_{CD}) \quad (29)$$

$$H_{I\,II} = (1 + S_1S_2)^{-1}(H_{AC} - H_{AD}) \quad (30)$$

$$S_{I\,II} = -(1 + S_1S_2)^{-1}(S_1 + S_2) \quad (31)$$

For B_{2u} states:

$$H_{III\,III} = (1 - S_1S_2)^{-1}(H_{AA} + H_{AB}) \quad (32)$$

$$H_{IV\,IV} = (1 - S_1S_2)^{-1}(H_{CC} + H_{CD}) \quad (33)$$

$$H_{III\,IV} = (1 - S_1S_2)^{-1}(H_{AC} + H_{AD}) \quad (34)$$

$$S_{III\,IV} = -(1 - S_1S_2)^{-1}(S_1 - S_2) \quad (35)$$

The S_4 Excimer.—The Hamiltonian and overlap matrix elements are:

$$H_{\alpha\alpha} = H_{AA} \quad (36)$$

$$H_{\beta\beta} = H_{CC} \quad (37)$$

$$H_{\alpha\beta} = H_{AC} \quad (38)$$

$$S_{\alpha\beta} = -S_1 \quad (39)$$

MO Integrals in Terms of AO Integrals

As bases molecular orbitals, ϕ_1, ϕ_2, θ_1, and θ_2, simple Hückel molecular orbitals are used. The differential overlap within any one molecule is neglected, since this approximation has been proved to be rather successful. No simplification is made for an intermolecular overlap integral (i. e., the overlap between two atomic orbitals which belong to different molecules.).

Hereafter, r, s, t, and u refer to atomic orbitals. The numbering r, s, t, or u, which designates the atom position within a molecule, is common to both Molecule A and Molecule B, and corresponding atoms on different molecules have the same number. Only when it is necessary specifically to indicate that the r atom is in Molecule A (or Molecule B) is the atomic orbital designated as r_A (or r_B) instead of just r.

The integrals over molecular orbitals are expressed in terms of integrals over atomic orbitals in the following way:

Overlap Integrals.—S_1 and S_2 are expressed as:

$$S_1 = \sum_r \sum_t C_{r1}C_{t1}(r_A \mid t_B) \quad (40)$$

$$S_2 = \sum_r \sum_t C_{r2}C_{t2}(r_A \mid t_B) \quad (41)$$

Electron Repulsion Integrals.—Mulliken's approximation[13] is applied consistently; it is set as:

$$r(\nu)t(\nu) = (1/2)(r \mid t)[r(\nu)r(\nu) + t(\nu)t(\nu)] \quad (42)$$

The electron repulsion integral is, then, expressed as:

$$(ij \mid kl) = (1/4) \sum_r \sum_s \sum_t \sum_u C_{ri}C_{sj}C_{tk}C_{ul}$$
$$(r \mid s)(t \mid u)[\gamma_{rt} + \gamma_{ru} + \gamma_{st} + \gamma_{su}] \quad (43)$$

where:

$$\gamma_{rt} = (rr \mid tt)$$

is the atomic Coulomb repulsion integral.

Core Integrals.—The core integral over molecular orbitals, i and j, is expressed as[2]:

$$H^c_{ij} = \sum_r \sum_t C_{ri}C_{tj}(r \mid t)[-A_c - (1/2)\sum_{q \neq t}\{(q:rr) + (q:tt)\}] - 2(11 \mid ij) - 2(1'1' \mid ij) \quad (44)$$

where summation over q should be carried out over all the carbon atoms in both Molecule A and Molecule B. A_c is the experimental electron affinity of the carbon atom in its valence state, and has the value[14] of:

$$A_c = 0.69 \text{ eV}.$$

and $(q : rr)$ is the Coulomb penetration integral.[15]

The Evaluation of AO Integrals

As basis functions for atomic orbitals, carbon 2p Slater orbitals are used. The appropriate choice of orbital exponent, Z, is a difficult task, but, in this paper, $Z=3.18$ is taken, since satisfactory results were obtained by Azumi, Armstrong, and McGlynn[2] with this Z value.

The integrals over atomic orbitals were evaluated in the following way:

Overlap Integrals.—As has been mentioned above, the differential overlap within any one molecule is neglected; namely, for the *intramolecular* overlap integral:

$$(r_A \mid t_A) = \delta_{rt} \quad (45)$$

The *intermolecular* overlap integral was evaluated by the formulas presented by Parr and Crawford[15];

$$(r_A \mid t_B) = S_\pi \cos^2\theta + S_\sigma \sin^2\theta \quad (46)$$

where

$$S_\pi = 240^{-1}\exp(-\rho/2)[240 + 120\rho + 12\rho^2 - 4\rho^3 - \rho^4] \quad (47)$$

$$S_\sigma = 120^{-1}\exp(-\rho/2)[120 + 60\rho + 12\rho^2 + \rho^3] \quad (48)$$

where:

$$\rho \equiv ZR \quad (49)$$

and where R is the distance, in atomic units, between two atoms, r_A and t_B. Furthermore, (see Fig. 3):

$$\cos\theta = v/R, \quad \sin\theta = h/R \quad (50)$$

Coulomb Repulsion Integrals.—The *intramolecular* Coulomb repulsion integral, $\gamma_{r_At_A}$, was taken from the table presented by Pariser.[16] These values were calculated from the Slater orbitals, with the exception of the one-center integral and the nearest neighbor two-center integrals; the latter values were obtained semi-empirically from the benzene spectrum.

13) R. S. Mulliken, *J. Chim. Phys.*, **46**, 497 (1949).

14) R. S. Mulliken, *J. Chem. Phys.*, **2**, 782 (1934).

15) R. G. Parr and B. L. Crawford, ibid., **16**, 1049 (1948).

16) R. Pariser, ibid., **24**, 324 (1956).

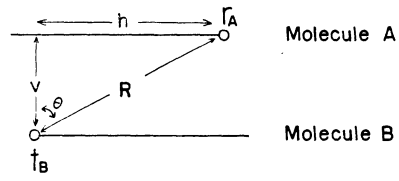

Fig. 3

Intermolecular Coulomb repulsion integrals were calculated, by the multiple expansion method proposed by Parr,[17] in atomic units[18];

$$\gamma_{r_A r_B} = R^{-1}[1 + (q/2R^2)(3\cos^2\theta - 1) + (3q^2/16R^4)(3 - 30\cos^2\theta + 35\cos^4\theta)] \quad (51)$$

where:

$$q = 24/Z^2 \quad (52)$$

Coulomb Penetration Integrals.—Since the penetration integral decreases very rapidly with the distance, some of the integrals may well be neglected, as is shown below.

The *intramolecular* Coulomb penetration integral, $(q_A : r_A r_A)$, is non-zero only when $q=r$ or q and r are adjacent. The integrals in these cases are evaluated by the formula given by Parr and Crawford[15]:

$$(q_A : r_A r_A) = (Z/3840)\exp(-\rho)[(4/7)\rho^5 + (67/7)\rho^4 + 86\rho^3 + 461\rho^2 + 1125(\rho+1)] \quad (53)$$

The *intermolecular* Coulomb penetration integral $(q_A : r_B r_B)$ is in all cases, neglected.

The Correction for Infinite Separation

The energies of the excited excimer states are obtained by solving secular equations of the form:

$$|\boldsymbol{H} - E\boldsymbol{S}| = 0 \quad (54)$$

where $\boldsymbol{H}$ and $\boldsymbol{S}$ represent, respectively, Hamiltonian and overlap matrices, the elements of which are given in Eqs. 19—39. It is convenient to calculate the energy with respect to the ground-state energy at $\alpha=0°$, E_0^0; for this purpose Eq. 54 is rewritten as:

$$|(\boldsymbol{H} - E_0^0\boldsymbol{S}) - E'\boldsymbol{S}| = 0 \quad (55)$$

where:

$$E' = E - E_0^0 \quad (56)$$

and where the calculated energy, E', is now the energy scaled from the ground state of the dimer of $\alpha=0°$.

The direct use of the theoretical Hamiltonian matrix elements reveals one significant difficulty. From the viewpoint of physical significance, $H_{AA}-E_0^0$ should converge on the ^1L_a excitation energy of the monomer at an infinite separation of the two molecules. As is evident from Eqs. 18 and 22, $H_{AA}-E_0^0$ equals (12|12) at an infinite separation. (12|12) is also the result of the theoretical evaluation of the ^1L_a monomer energy in a two-electron treatment; thus, H_{AA} extrapolates to a correct energy limit. However, the value of (12|12) is 0.491 eV., whereas ^1L_a is at 4.290 eV., and there exists great numerical discrepancy. This discrepancy, which may be due to the incompleteness of the simple four-electron treatment, needs to be calibrated. In this regard, the experimental ^1L_a monomer energy is obtained at an infinite separation. In other words, the monomer contribution is made as empirical as possible, while the dimerization effects are left in their fully theoretical form. This attitude is also adopted for charge resonance states. In sum, the $^1L_a-(12|12)$ term is added to all the diagonal terms of Eq. 55.

Results and Discussion

Calculations were carried out at intervals of five degrees in α. The lowest of the four excited states is the excimer state which is responsible for the excimer luminescence. The wave function of this state is expressed in the form of:

$$\psi = a\psi_A + b\psi_B + c\psi_C + d\psi_D \quad (57)$$

The energy of the excimer state, E', and the normalized mixing coefficients are summarized in Table I. The energy of the ground state scaled from that of $\alpha=0°$:

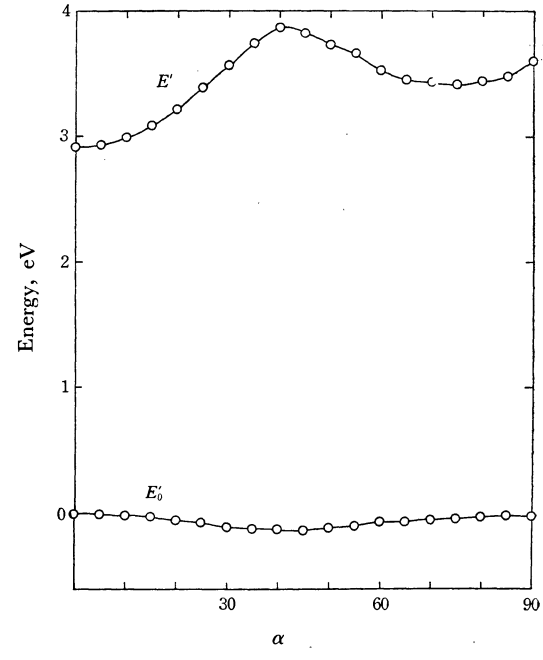

Fig. 4

17) R. G. Parr, ibid., **33**, 1184 (1960).
18) The unit of energy equals e^2/a_0, where e is the charge on an electron and a_0 is the Bohr radius.

Table I. Energy and mixing coefficients of naphthalene excimer

α	E', eV.	E_0', eV.	a	b	c	d
0	2.909	0	0.5461	−0.5461	0.3948	−0.3948
5	2.930	−0.009	0.5534	−0.5323	0.4471	−0.3479
10	3.005	−0.023	0.5565	−0.5362	0.4427	−0.3508
15	3.123	−0.042	0.5617	−0.5429	0.4349	−0.3548
20	3.278	−0.063	0.5696	−0.5535	0.4219	−0.3584
25	3.460	−0.084	0.5817	−0.5700	0.4003	−0.3581
30	3.659	−0.101	0.6023	−0.5970	0.3610	−0.3441
35	3.855	−0.123	0.6437	−0.6437	0.2799	−0.2798
40	3.992	−0.134	0.7091	−0.7002	0.0687	−0.0423
45	3.964	−0.139	0.6680	−0.6696	−0.2236	0.2169
50	3.851	−0.111	0.6142	−0.6195	−0.3586	0.2942
55	3.729	−0.098	0.5874	−0.5828	−0.4182	0.3212
60	3.622	−0.082	0.5741	−0.5553	−0.4489	0.3352
65	5.538	−0.064	0.5673	−0.5333	−0.4669	0.3458
70	3.482	−0.046	0.5638	−0.5145	−0.4787	0.3561
75	3.458	−0.031	0.5624	−0.4975	−0.4874	0.3669
80	3.466	−0.020	0.5627	−0.4806	−0.4953	0.3780
85	3.504	−0.014	0.5682	−0.4585	−0.5069	0.3852
90	3.622	−0.014	0.5372	$0.5372i$	0.4285	$0.4285i$

$$E_0' = E_0 - E_0^0 \tag{58}$$

is also shown in Table I. The calculated energies are also plotted in Fig. 4 as a function of α. It seems reasonable to assume that the mutual repulsion of the two cores, a repulsion which is not included in the present calculation, is nearly independent of α. Figure 4 may then be considered to be the potential energy diagram expressed as a function of α. As may be seen in Fig. 4, there are two minima in the potential of the excited states, one at $\alpha=0°$ and one at $\alpha=75°$; consequently, the excimer is stable at these two configurations. We assume that when two molecules approach, by diffusion, to form an excimer, there is no specific orientation of the two molecules. If this assumption is true, various configurations (namely, various α values) of the excimer are formed, with nearly equal probabilities. They will immediately undergo relaxation according to the potential of Fig. 4. The potential barrier of 0.5 eV. between the two stable configurations is too high compared with the thermal kinetic energy of $1.5\boldsymbol{k}T=0.04$ eV., and the mutual transformation of the two is impossible at ordinary temperatures. It may well, then, be said that at an equilibrium state two kinds of excimers exist; the one with $\alpha=0°$ is hardly ever interpreted as being responsible for excimer fluorescence because of the forbidden character of the transition, while the one with $\alpha=75°$ may contribute to the observed excimer fluorescence.

The calculated energy of excimer fluorescence at $\alpha=75°$,

$$E' - E_0' = 3.46 \text{ eV}.$$

may seem to be too high compared with the observed energy (3.13 eV.)[19] of the naphthalene excimer fluorescence. However, to discuss this discrepancy is trivial, since, in the present calculations, the interplanar distance of 3 Å and the orbital exponent of $Z=3.18$ have been tentatively chosen rather arbitrarily. If smaller values of Z are used, as has been suggested[3,20] the calculated energy would surely become lower, and an agreement with the observed energy might well be obtained.

Concluding Remarks

It has been shown that there is considerable configuration interaction between molecular exciton states and charge resonance states. As may be seen in Table I, all of the four zeroth order states, the two molecular exciton states and the two charge resonance states, contribute to the excimer states in nearly equal measure. It has also been shown that the energy of the excited state varies significantly with the α value, and a stable configuration may be obtained at $\alpha\neq0°$. It has been suggested that these configurations should, in general, be included in the calculation of this sort.

A number of questions remain. We have excluded the configuration of $\alpha=0°$ as the one responsible for excimer luminescence. Whether or not we are justified in doing so is a difficult question. Group theoretically, the excimer state at $\alpha=0°$ is of the B_{3g} symmetry in the D_{2h} point group,[11] and the transition to the A_g ground state is forbidden. Further, different from, say,

19) E. Döller and Th. Förster, *Z. Physik. Chem. N. F.*, **31**, 274 (1962).
20) G. C. Nieman and G. W. Robinson, *J. Chem. Phys.*, **37**, 2150 (1962).

the benzene fluorescence, there is no vibrational coupling to acquire an allowed transition moment in the excimer fluorescence, unless we consider hot bands, since the ground state is dissociative. These considerations favor our treatment; however, further investigations might be necessary. These will be the subject of ensuing publications.

In the present calculation we have considered only the excimer configurations in which two molecular planes are parallel and their principal axes coincide. This may actually seem rather a freakish situation. However, to treat excimers of random orientations is quite difficult, if not impossible; at any rate, it is beyond the limits of the present paper.

The present calculations are based upon the above-specified model, just one of many models we may think of; therefore, too much emphasis should not be placed upon our suggestion of the $\alpha=75°$ configuration. It is, however, of interest to add that our calculations on the radiative lifetime of the excimer fluorescence yield 6×10^{-6} sec. at $\alpha=75°$, which is in good agreement with the observed value[21] of $1.2-1.4\times10^{-6}$ sec. The details of the calculations will be published in the next paper.[22]

Table II. In-plane component of carbon-carbon distance, h

α	1-1′	1-2′	1-3′	1-4′	1-5′	1-6′	1-7′	1-8′	2-1′	2-2′
0	0	1.39000	2.40755	2.77999	3.67759	4.16999	3.67759	2.40755	1.39000	0
5	0.16041	1.23450	2.25429	2.67233	3.67409	4.21864	3.77348	2.52652	1.54887	0.21860
10	0.32052	1.08528	2.09814	2.55958	3.66359	4.25947	3.86248	2.64068	1.70914	0.43679
15	0.48002	0.94669	1.93974	2.44196	3.64613	4.29240	3.94441	2.74981	1.86939	0.65416
20	0.63860	0.82542	1.77986	2.31969	3.62172	4.31736	4.01908	2.85371	2.02855	0.87027
25	0.79597	0.73127	1.61945	2.19301	3.59042	4.33431	4.08636	2.95218	2.18577	1.08473
30	0.95183	0.67648	1.45975	2.06215	3.55228	4.34319	4.14609	3.04503	2.34038	1.29712
35	1.10587	0.67123	1.30248	1.92736	3.50738	4.34401	4.19815	3.13208	2.49178	1.50705
40	1.25781	0.71664	1.15005	1.78891	3.45580	4.33675	4.24244	3.21317	2.63947	1.71410
45	1.40735	0.80386	1.00611	1.64705	3.39765	4.32143	4.27886	3.28814	2.78301	1.91790
50	1.55421	0.92056	0.87620	1.50206	3.33303	4.29808	4.30735	3.35686	2.92200	2.11415
55	1.69812	1.05628	0.76867	1.35420	3.26206	4.26676	4.32783	3.41918	3.05607	2.31415
60	1.83879	1.20377	0.69500	1.20377	3.18489	4.22751	4.34027	3.47499	3.18489	2.50585
65	1.97596	1.35827	0.66710	1.05105	3.10165	4.18044	4.34464	3.52420	3.30813	2.69279
70	2.10938	1.51664	0.69077	0.89632	3.01250	4.12562	4.34094	3.56669	3,42552	2.87460
75	2.23877	1.67676	0.76105	0.73989	2.91763	4.06318	4.32917	3.60239	3.53679	3.05093
80	2.36391	1.83711	0.86622	0.58205	2.81720	3.99324	4.30936	3.63124	3.64169	3.22146
85	2.48454	1.99656	0.99464	0.42311	2.71140	3.91595	4.28155	3.65317	3.73999	3.38586
90	2.60045	2.15424	1.13765	0.26336	2.60045	3.83148	4.24579	3.66815	3.83148	3.54381

α	2-3′	2-5′	2-6′	2-7′	3-1′	3-2′	3-5′	3-6′	4-1′	4-5′
0	1.39000	4.16999	5.01171	4.81510	2.40755	1.39000	3.67759	4.81510	2.77999	2.40755
5	1.17864	4.11363	5.00694	4.87114	2.55737	1.59870	3.57502	4.74988	2.88236	2.28399
10	0.96504	4.04966	4.99264	4.91792	2.70329	1.80437	3.46600	4.67563	2.97925	2.15609
15	0.74961	3.97823	4.96884	4.95533	2.84487	2.00660	3.35077	4.59247	3.07046	2.02409
20	0.53274	3.89948	4.93557	4.98331	3.98173	2.20501	3.22958	4.50057	3.15583	1.88823
25	0.31487	3.81357	4.89291	5.00181	3.11353	2.39923	3.10272	4.40011	3.23519	1.74877
30	0.09639	3.72070	4.84094	5.01078	3.23992	2.58887	2.97050	4.29127	3.30839	1.60599
35	0.12226	3.62105	4.62658	4.65761	3.36062	2.77359	2.83322	4.17426	3.37529	1.46015
40	0.34068	3.51484	4.47733	4.46715	3.47535	2.95303	2.69127	4.04930	3.43577	1.31154
45	0.55846	3.40232	4.31991	4.27015	3.58384	3.12685	2.54501	3.91664	3.48971	1.16042
50	0.77518	3.28372	4.54215	4.95140	3.68585	3.29471	2.39487	3.77652	3.53701	1.00710
55	0.99042	3.15933	4.44544	4.91287	3.78117	3.45631	2.24135	3.62921	3.57757	0.85186
60	1.20377	3.02943	4.34027	4.86499	3.86959	3.61132	2.08500	3.47500	3.61132	0.69500
65	1.41483	2.89434	4.22683	4.80786	3.95092	3.75946	1.92644	3.31416	3.63820	0.53681
70	1.62320	2.75440	4.10535	4.74157	4.02499	3.90044	1.76647	3.14702	3.65815	0.37760
75	1.82848	2.60999	3.97606	4.66625	4.09164	4.03400	1.60607	2.97389	3.67114	0.21768
80	2.03028	2.46151	3.83919	4.58205	4.15073	4.15988	1.44650	2.79510	3.67714	0.05734
85	2.22821	2.30942	3.69502	4.48913	4.20215	4.27785	1.28952	2.61099	3.67614	0.10310
90	2.42191	2.15424	3.54381	4.38766	4.24579	4.38766	1.13765	2.42191	3.66815	0.26336

21) J. B. Birks and T. A. King, *Proc. Roy. Soc.* **A291**, 244 (1966).

22) T. Azumi and H. Azumi, This Bulletin, in press (1966).

The authors wish to express their appreciation to Dr. Yoshito Amako for his fruitful discussions.

The numerical calculations were carried out on the NEAC 2230 at the Computation Center, Tohoku University; the invaluable help in the programming provided by the staff is greatly appreciated.

Appendix I

Table II presents the in-plane components of distance, h, between two carbon atoms which belong to different molecules (see Fig. 3). These values are required in evaluating integrals over atomic orbitals. The atom positions are indicated by numbers, and those in different molecules are indicated by primed numbers, as is shown in Fig. 1. Since the Hückel coefficients for molecular orbitals, ϕ_1 or ϕ_2, are zero for atoms 9 and 10, the summation over r in Eqs. 40—44 may be carried out only from 1 to 8. There are still $8\times8=64$ pairs of carbons whose distances are required, but only twenty of these need be obtained; these are shown in Table II in Å units. Any other pair is identical to one of the pairs given in the table by symmetry considerations.

Appendix II

The numerical results for intramolecular and intermolecular MO integrals are tabulated in Tables III and IV. All integrals except the overlap integrals are in eV. units.

Table III. Intramolecular MO integrals

(11 | 11)	5.75862
(12 | 12)	0.94098
H_{11}^c	−21.37112

Table IV. Intermolecular MO integrals

α	S_1	S_2	(11 | 1'1')	(12 | 1'2')	(11 | 11')	(11 | 22')	(11' | 11')
0	−0.06685	−0.03690	3.71823	0.20429	−0.31670	−0.17524	0.02117
5	−0.06549	−0.03566	3.71887	0.20388	−0.31029	−0.16939	0.02033
10	−0.06193	−0.03247	3.71870	0.20060	−0.29360	−0.15442	0.01824
15	−0.05637	−0.02761	3.71782	0.19482	−0.26747	−0.13156	0.01519
20	−0.04908	−0.02147	3.71643	0.18705	−0.23317	−0.10265	0.01163
25	−0.04039	−0.01450	3.71474	0.17786	−0.19221	−0.06988	0.00801
30	−0.03064	−0.00720	3.71297	0.16778	−0.14616	−0.03554	0.00478
35	−0.02017	−0.00001	3.71376	0.15734	−0.09655	−0.00175	0.00227
40	−0.00929	0.00662	3.71374	0.14656	−0.04489	0.02949	0.00074
45	0.00167	0.01236	3.71421	0.13549	0.00736	0.05652	0.00031
50	0.01246	0.01682	3.70854	0.12366	0.05860	0.07751	0.00100
55	0.02275	0.01988	3.70861	0.11137	0.10771	0.09197	0.00268
60	0.03226	0.02133	3.70916	0.09805	0.15317	0.09891	0.00513
65	0.04073	0.02110	3.71008	0.08348	0.19370	0.09802	0.00805
70	0.04792	0.01924	3.71124	0.06735	0.22820	0.08948	0.01108
75	0.05367	0.01588	3.71251	0.04981	0.25581	0.07398	0.01387
80	0.05786	0.01130	3.71373	0.03099	0.27591	0.05270	0.01610
85	0.06039	0.00583	3.71482	0.01121	0.28813	0.02728	0.01754
90	0.06125	−0.00008	3.71570	−0.00907	0.29225	−0.00029	0.01804

α	(11' | 22')	(12 | 12')	(12 | 1'2)	(12' | 12')	(12' | 1'2)	H_{11}^c'	H_{22}^c'
0	0.01171	−0.02461	−0.03521	0.00165	0.00150	2.04484	1.13049
5	0.01109	−0.02376	−0.03461	0.00162	0.00139	2.00338	1.09260
10	0.00954	−0.02165	−0.03312	0.00158	0.00112	1.89523	0.99564
15	0.00737	−0.01843	−0.03075	0.00153	0.00074	1.72595	0.84762
20	0.00497	−0.01436	−0.02757	0.00146	0.00032	1.50388	0.66047
25	0.00272	−0.00974	−0.02362	0.00135	−0.00007	1.23889	0.44837
30	0.00097	−0.00490	−0.01897	0.00122	−0.00038	0.94129	0.22603
35	−0.00008	−0.00010	−0.01370	0.00105	−0.00054	0.62100	0.00722
40	−0.00038	0.00429	−0.00788	0.00087	−0.00056	0.28780	−0.19507
45	0.00000	0.00805	−0.00165	0.00073	−0.00044	−0.04901	−0.36998
50	0.00091	0.01083	0.00480	0.00064	−0.00024	−0.37948	−0.50590
55	0.00207	0.01277	0.01123	0.00063	0.00000	−0.69569	−0.59928
60	0.00320	0.01366	0.01739	0.00069	0.00024	−0.98822	−0.64389
65	0.00402	0.01346	0.02304	0.00083	0.00042	−1.24887	−0.63772
70	0.00433	0.01222	0.02795	0.00100	0.00052	−1.47061	−0.58189
75	0.00401	0.01003	0.03196	0.00118	0.00051	−1.64795	−0.48085
80	0.00307	0.00704	0.03491	0.00133	0.00040	−1.77702	−0.34236
85	0.00166	0.00349	0.03672	0.00143	0.00021	−1.85540	−0.17708
90	−0.00002	−0.00034	0.03734	0.00147	−0.00001	−1.88184	0.00220

BULLETIN OF THE CHEMICAL SOCIETY OF JAPAN VOL. 39 1837—1842 (1966)

The Reaction Rate of the Alkaline Hydrolysis of Ethyl Acetate

By Hiroo TSUJIKAWA and Hakuai INOUE

Department of Chemical Engineering, The University of Tokyo, Hongo, Tokyo

(Received November 11, 1965)

The reaction rate of the alkaline hydrolysis of ethyl acetate was studied by means of a continuous measurement of the electric conductivity change. The second-order rate constant decreased as the reaction proceeded. The decrease was evident when the initial concentrations of the ester and the base were close together. The initial rate constant at 25°C was measured as 0.1120 l./mol./sec. and the activation energy was 11.56 kcal./mol., values agreed well with those of previous studies. From the standpoint of the electronic theory of organic chemistry, Day and Ingold proposed a sequential reaction mechanism passing through an addition complex. The results of the approximate calculations to the pseudo-first-order reaction and the analog-computation of the exact models coincided with the experimental results. The difference in the activation energies of the forward and reverse reaction rates was calculated from the experimental data. At lower temperatures this reverse reaction rate was small, and the overall reaction rate was approximated as a pure second-order reaction. Other probable reasons for the rate constant decrease were also discussed.

The reaction rate of the alkaline hydrolysis of ethyl acetate has been well established to be a second-order reaction, and the mechanism has been discussed in detail.[1]

For the study of the performance of a flow-type stirred tank reactor, we carried out the hydrolysis reaction in it and analyzed the flow pattern in the reactor from the yield of the reaction. However, during the experiments, we found that the hydrolysis reaction could not satisfactorily be expressed as a second-order reaction. It was necessary to analyze the reaction rate more carefully. Therefore, we measured and analyzed the rate of the hydrolysis of ethyl acetate continuously. We will discuss the mechansim of the reaction kinetically.

Experimental

Apparatus.—The reaction was carried out in a batch-type reactor, and the electric conductivity of the reacting solution was measured with the time. The main apparatus is shown in Fig. 1. A 2-l. polyethylene beaker was used as the reaction vessel instead of a glass one, because in the case of a glass vessel some alkaline ions dissolved from the wall and so disturbed the exact measurement of the reaction rate.

During the reaction hydroxide ions are consumed and acetate ions are produced. This change in ion concentration results in a conductivity change in the solution, and by the measurement of this conductivity we could ascertain the degree of saponification.

The electrode used is shown in Fig. 2; it is set horizontally near the turbine so that the reactant flows thoroughly in it. The electrical circuits of the measuring system is shown in Fig. 3. A 0.8 V. a. c. current of

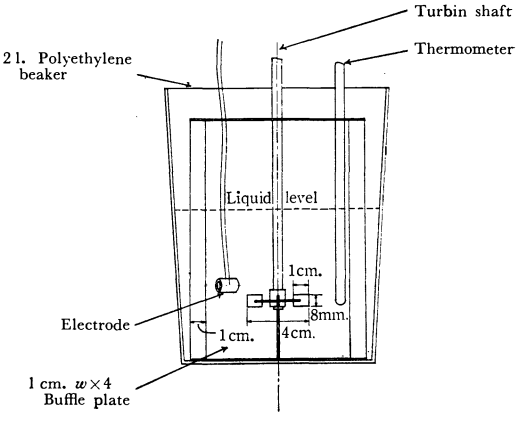

Fig. 1. The Experimental apparatus.

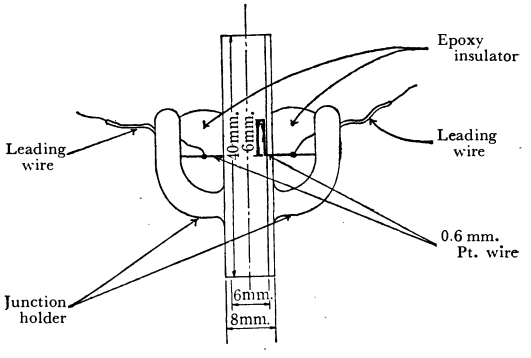

Fig. 2. The electrode.

1000 c/s is added at the electrode + a 5-ohm resistor in series. The voltage between the two sides of the resistor is amplified, converted into d. c., and recorded

1) M. L. Bender, *Chem. Revs.*, **60**, 53 (1960).

on a recording ammeter. Generally, the input-output characteristics of a diode are not linear, so the relation between the output current and the OH^-/CH_3COO^- ratio must be calibrated.[2] However, the negative feeding-back of the converted d. c. current to the intermediate part of the amplifier (the 15 kiloohm resistor and 10 microfarad condensor circuit of Fig. 3) forms a linear relationship between the current and the concentration ratio, as is shown in Fig. 4. By comparing the line in Fig. 4. with the conductivity of the reacting solution, in which the total concentration of OH^- and CH_3COO^- was about 0.02 N, we can calculate the degree of hydrolysis with the time.

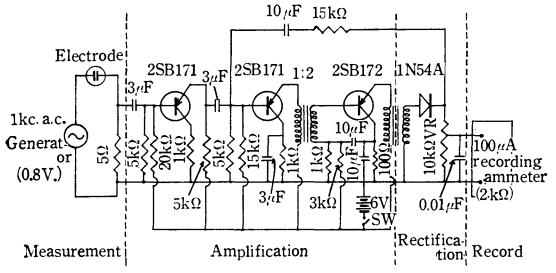

Fig. 3. The electric circuit for the electro-conductivity measurement.

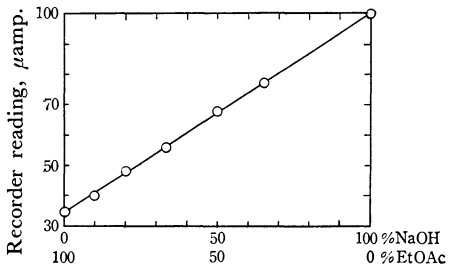

Fig. 4. The relationships between the ammeter reading and the reaction proceeding.

○ Total concentration of $Na^+ = 0.0200$ mol./l.
○ The ammeter was set 100 μamp. for 100% NaOH

Procedure.—A sodium hydroxide solution was prepared by dissolving sodium hydroxide (made by the Wako Pure Chemicals Co., Ltd., G. R. grade) in ion-exchange water with a relative resistance of more than 2×10^6 ohm-cm. The concentration was checked by an automatic titrater using a 0.1 N standard hydrochloric acid solution. Ethyl acetate (made by the Osaka Organic Chemicals Co., Ltd., G. R. grade) was used without any special processing; it yet gave a mean equilibrium conversion of 97%, which agrees with the theoretical equilirbium conversion.

To start the reaction, 994 ml. of a 0.02 N sodium hydroxide solution was poured into a beaker dipped in a water bath, and then vigorously stirred for more than 30 min., after which a definite volume of ethyl acetate was added to the solution under the stirring. The temperature of the mixture was kept constant during the reaction within a range of ±0.1°C.

Ethyl acetate dissolved into water within 10 sec., so the mixing time of the ester was negligible in comparison with the reacting time. During the reaction the conductivity of the solution was recorded continuously, and the degree of conversion was calculated. A small portion of the solution was sampled during the reaction and was acidified to stop the reaction rapidly; by the backtitration of the acid, the remaining hydroxide ions in the reacting system were determined. The concentration of hydroxide ions, as determined by this titration agreed well with that calculated from the conductivity measurements of the solution.

Results

Some results are shown in Fig. 5, where the concentration change is plotted as $(c_B - x_0)/(c_{A_0} - x)$ against the reaction time. The circled points in Fig. 5 stand for the experimental values, while the straight line in the figure shows the theoretical relation derived from the second order rate equation.

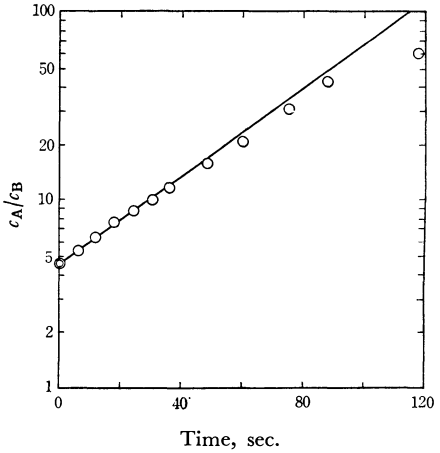

Fig. 5. Semi-logarithmic plot of experimental results.
Exptl. No. R-27 c_{A_0} 0.09897 N
Temp. 40.7°C c_{B_0} 0.02104 N
$k_{1\,obsd.}$ 0.337 l./mol. sec.

If the reaction is expressed as that of a complete second-order reaction, all the experimental values must be on the line. However the points obtained from the experiments deviate downwards from the linear relation. The deviation of the rate from the second-order rate equation becomes more remarkable as the initial concentrations of base and ester draw closer to each other.

Previous works on this kinetics did not analyze the rate in detail; usually only the mean initial rate constant has been obtained. The deviation from the second-order rate equation has never been analyzed in detail kinetically. Indeed, no such deviation has even been actually observed in the initial rate of the hydrolysis.

2) D. G. Flom and P. J. Elving, *Anal. Chem.*, **25**, 541 (1953).

We measured the initial rate constant by the addition of different amounts of the ester, and observed the rate constant independent of the concentration of the ester. These results coincided with those of previous works on the second-order rate equation. They are shown in Fig. 6, along with the inverse of the absolute temperature, $1/T$. The calculated activation energy of 11.56 kcal./mol. agrees well with those obtained in previous works; the rate constant at 25°C, 0.1125 l/N-sec., also agrees with them.[3-6]

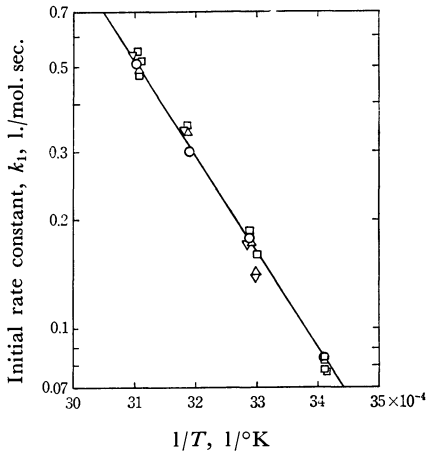

Fig. 6. The Arrhenius plots of the initial rate constants.
○ c_{A_0} about 0.02 mol./l.
□ c_{A_0} about 0.05 mol./l.
△ c_{A_0} about 0.10 mol./l.
▽ c_{A_0} about 0.25 mol./l.
E = 11.56 kcal./mol.

Analysis and Discussion

The mechanism of the basic hydrolysis of ester has been discussed hitherto, and it is well known that the mechanism may be expressed by the following reaction scheme:

$$\underset{\text{(A)}}{H_3C\text{-}\overset{\overset{O}{\|}}{C}\text{-}OC_2H_5} + \underset{\text{(B)}}{OH^-} \underset{[II]\ k_2}{\overset{[I]\ k_1}{\rightleftarrows}} \underset{\text{(C)}}{H_3C\text{-}\overset{\overset{O^-}{|}}{C}\text{-}OH\,(OC_2H_5)} \underset{[IV]\ k_4}{\overset{[III]\ k_3}{\rightleftarrows}}$$

$$\underset{\text{(D)}}{H_3C\text{-}\overset{\overset{O}{\|}}{C}\text{-}OH} + \underset{\text{(E)}}{C_2H_5O^-} \xrightarrow{[V]\ k_5} \underset{\text{(F)}}{C_2H_5OH} + \underset{\text{(G)}}{CH_3COO^-}$$

This mechanism of the basic hydrolysis of esters was proposed by Day and Ingold.[7] and since analyzed by Bender,[8] Swarts,[9] and many other investigators.[1] However, these studies were mainly from the viewpoint of organic chemistry; no detailed kinetic analysis of the hydrolysis of ethyl acetate has ever been made. Usually the reaction has been considered to be a second-order form, but, according to the above mechanism, the second-order rate equation is applicable only when the concentration of the addition complex C is very small and when the reverse reaction rate is negligible in comparison with the forward reaction rate.

In general, the total reaction path may be expressed by the following mathematical equations:

$$\frac{dc_A}{d\theta} = \frac{dc_B}{d\theta} = -k_1c_Ac_B + k_2c_C \tag{1}$$

$$\frac{dc_C}{d\theta} = k_1c_Ac_B - (k_2+k_3)c_C + k_4c_Dc_E \tag{2}$$

$$\frac{dc_D}{d\theta} = \frac{dc_E}{d\theta} = k_3c_C - (k_4+k_5)c_Dc_E \tag{3}$$

$$\frac{dc_F}{d\theta} = \frac{dc_G}{d\theta} = k_5c_Dc_E \tag{4}$$

where c means the concentrations of chemical compounds or ions, and where the suffixes A, B, C, ···denote the compounds or ions shown above. The k's indicates the reaction rate constants; k_1 and k_2 are the rate constants for the forward and reverse reactions of $A+B \rightleftarrows C$, k_3 and k_4 are the rate constants of the forward and reverse reactions of $C \rightleftarrows D+E$, and k_5 is that of the $D+E \rightarrow F+G$ reaction. The reaction rates were assumed to be proportional to the concentrations of all the reacting compounds. θ denotes the time.

The deviation from the second-order rate form which we observed seems to give the key to the analysis of the mechanism of the reaction. As the reaction proceeds, the concentration of the ester and hydroxide ions become very small; the effect of the reverse reaction rate of the addition complex on the total rate will therefore become remarkable.

Of course, there are many possible causes of the deviation of the rate from the second-order form. The $CH_3COOC_2H_5+H_2O \rightleftarrows CH_3COOH+C_2H_5OH$ equilibrium suggests the reverse reaction of the products. However, the deviation of the rate could not be due to this effect for the following reasons. According to the effect of this reverse reaction, the overall reaction rate would be retarded by the addition of the reaction product. We measured the reaction rate in the presence of

3) S. Lee and H. Kawakami, *Kogyo-Kagaku Zassi*, **43**, 551 (1940).
4) J. Murto, *Chem. Abstr.*, **55**, 24549 d (1961).
5) E. Tommila, ibid., **40**, 4591[4] (1946); E. Tommila and S. Hietara, ibid., **48**, 11888 e (1954).
6) H. A. Smith and H. S. Levenson, *J. Am. Chem. Soc.*, **61**, 1172 (1939).
7) J. N. E. Day and C. K. Ingold, *Trans. Faraday Soc.*, **37**, 686 (1941).
8) M. L. Bender, *J. Am. Chem. Soc.*, **73**, 1626 (1951).
9) F. Swarts, *Bull. soc. chim. Belges*, **35**, 414 (1926).

sodium acetate or ethanol. The addition of the products actually retarded the overall reaction rate, but it is too small to illustrate the deviation from the second-order form. Experimentally the deviation is most remarkable when the concentrations of the ester and the base are close. We tried to estimate the rate constant of the reverse reaction by making an analysis using an analog computer, this gave a good coincidence with the experimental results, but we could not obtain the rate constant independent of the change in the ester concentration.

Moreover, the salt effect of the sodium acetate produced, the solvent effect of the ethanol produced, and other effects due to the decrease in the concentration of the reactants were discussed and checked by experiments, although we could not illustrate the deviation of the reaction rate satisfactorily.

To analyze the above reaction path, it is necessary to solve the mathematical equations, 1, 2, 3, and 4, but it would be meaningless to solve the whole system by assuming many rate constants arbitrarily. It seems to be more reasonable to assume the following approximations, which are based on the usual consideration of ionic reactions. First, the rate of the reaction IV is very slow and negligible compared to the rate of the reaction III. Second, the reaction V is regarded to be very rapid.

Therefore, the overall reaction may be expressed more simply as follows:

$$\frac{dc_A}{d\theta} = \frac{dc_B}{d\theta} = -k_1 c_A c_B + k_2 c_C \quad (1)$$

$$\frac{dc_C}{d\theta} = k_1 c_A c_B - (k_2+k_3) c_C \quad (2')$$

$$\frac{dc_F}{d\theta} = \frac{dc_G}{d\theta} = k_3 c_C$$

If the stationary state approximation is applied, the overall rate may be written:

$$\frac{dc_A}{d\theta} = -k_1\left(1 - \frac{1}{k_2+k_3}\right) c_A c_B$$

and expressed as a second-order rate equation such as was obtained experimentally at the initial stage of the reaction.

However, as the concentration of the reactants becomes small, the balance of the addition complex concentration is gradually broken and the process is not expressed by the approximation any more. This discussion does not necessarily depend on the assumption of the existence of a large amount of the addition complex, but it does depend on the relative scale of $k_1 c_A$, k_2, and k_3.

Without the stationary state approximation, Eqs. 1 and 2′ are not solved analytically because of their nonlinearity.

If $c_A \gg c_B$, then the change of c_A on the right hand of Eqs. 1 and 2′ can be neglected and the equations can be approximated as:

$$\frac{dc_B}{d\theta} = -k_1 c_{A_0} c_B + k_2 c_C \quad (1')$$

$$\frac{dc_C}{d\theta} = k_1 c_{A_0} c_B - (k_2+k_3) c_C \quad (2'')$$

The initial conditions are:

$$\theta = 0 \qquad c_B = c_{B_0} \qquad c_C = 0 \quad (5)$$

$$\frac{dc_B}{d\theta} = -\frac{dc_C}{d\theta} = -k_1 c_{A_0} c_{B_0}$$

The solutions are:

$$c_B = \frac{k_1 c_{A_0} c_{B_0} - (\alpha-\beta) c_{B_0}}{2\beta} e^{-(\alpha+\beta)\theta} + \frac{-k_1 c_{A_0} c_{B_0} + (\alpha+\beta) c_{B_0}}{2\beta} e^{-(\alpha+\beta)\theta} \quad (6)$$

$$c_C = \frac{k_1 c_{A_0} c_{B_0}}{2\beta}\left(e^{-(\alpha-\beta)\theta} - e^{-(\alpha+\beta)\theta}\right) \quad (7)$$

where:

$$\alpha = (k_1 c_{A_0} + k_2 + k_3)/2 \quad (8)$$

$$\beta = (\alpha^2 - k_1 c_{A_0} k_3)^{1/2} \quad (9)$$

Fig. 7, where the experimental results when c_A—c_B are plotted on semi-logarhythmic graph paper, shows that the whole process may be expressed by two straight lines, at the initial and final stages. These results coincide with Eqs. 7.

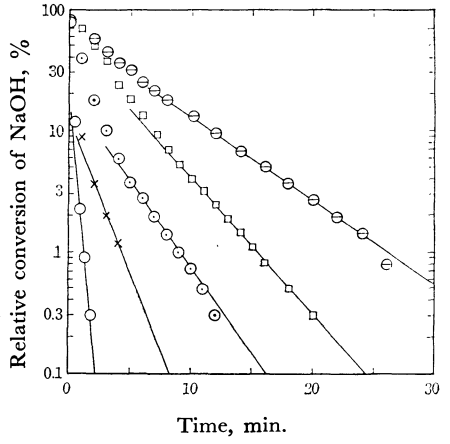

Fig. 7. Observation of $\alpha-\beta$ using the thermal rates of the reaction (temp. 30.5~30.7°C).

Initial ester concentration

⊖ 0.01985 mol./l. × 0.24211 mol./l.
□ 0.04959 mol./l. ○ 0.48422 mol./l.
⊙ 0.09897 mol./l.

Here let us survey the meaning of the time constants, $\alpha+\beta$ and $\alpha-\beta$. β has a rather complicated form, but noting $\alpha \gg k_1 k_3 c_{A_0}$ and using the Taylor expansion:

$$(1-x)^{1/2} = 1 - x/2 - x^2/8 + x^3/16 - x^4/128 + \cdots$$

β reduces to:

$$\beta \doteqdot \frac{k_1c_{A_0} + k_2 + k_3}{2} - \frac{k_1k_3c_{A_0}}{k_1c_{A_0} + k_2 + k_3} \quad (10)$$

Consequently:

$$\alpha+\beta \doteqdot k_1c_{A_0}+k_2+k_3 - \frac{k_1k_3c_{A_0}}{k_1c_{A_0}+k_2+k_3}$$

$$\doteqdot k_1c_{A_0}+k_2+k_3 \quad (11)$$

$$\alpha-\beta \doteqdot \frac{k_1k_3c_{A_0}}{k_1c_{A_0}+k_2+k_3} = \frac{1}{1/k_3+\frac{1}{k_1c_{A_0}}\left(1+\frac{k_2}{k_3}\right)} \quad (12)$$

If $k_3 \gg k_1c_{A_0}$ then:

$$\alpha-\beta \doteqdot \frac{k_1c_{A_0}}{1+k_2/k_3} \quad (13)$$

This is the time constant at the final stage of the reaction. The experimental measurements of $\alpha-\beta$ at 30°C are shown in Fig. 8. The k_2/k_3 values are calculated from Eqs. 11 at 30, 40, and 50°C and are shown in Fig. 9. The difference in the activation energies, k_2 and k_3, is obtained as 20 kcal./mol. from Fig. 9.

At lower temperatures, k_2/k_3 is small and the overall reaction rate is regarded as a second-order reaction, as uaual.[10]

The Confirmation of the Mechanism by an Analog Computer.—In order to confirm the above-mentioned mechanism at low concentrations of ester and base, Eqs. 1 and 2′ were solved directly by an analog computer. The boundary conditions were:

$$\theta=0 \qquad c_A=c_{A_0} \qquad c_B=c_{B_0} \qquad c_C=0 \quad (14)$$

The block diagram for the calculation is shown in Fig. 10. The "experimental chart reader" in Fig. 10 is used to read the results of the experiments into the computer and to compare them with the calculated results. An example of the calculation is shown in Fig. 11. In this calculation we must assume k_2 and k_3 respectively; the curve shown in Fig. 11 is an example. However, the main part of the curve is determined by the k_2/k_3 ratio, as may be understood from Eqs. 13; the absolute values of k_2 and k_3 in the reacting system could not be determined independently.

The calculated curve can be matched within a 3% error with such experiments.

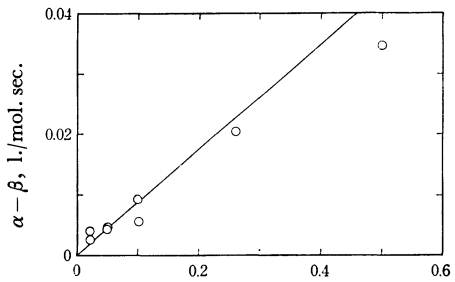

Fig. 8. The terminal reaction rate constants $\alpha-\beta$ (30.5—30.7°C)

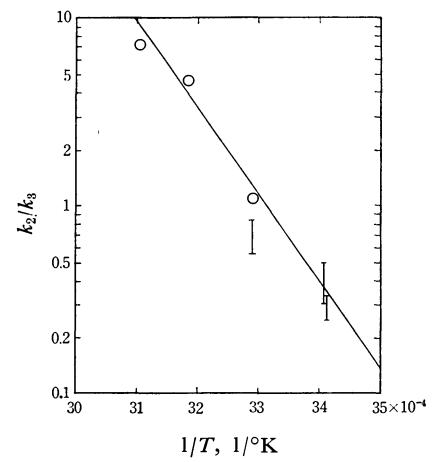

Fig. 9. The calculated values of k_2/k_3.

○ Means of all experiments

⊣⊢ Range of the calculated values for typical experiments (Calculated with an analog computer)

The difference of the activation energy $E_{k_2}-E_{k_3}=20$ kcal./mol.

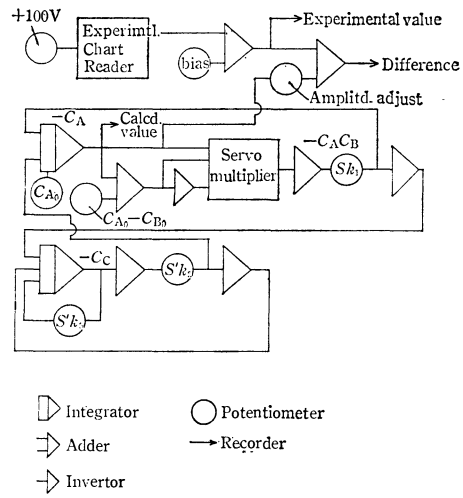

Fig. 10. The analog computer circuit for the calculation.

Calculation rate

c_A, c_B	1 mol./l. = 4000 V.
time	1 min. = 1.078 sec.

S(time scale factor) = 1.078

S'(time, concentration scale factor) = 1.078/4000

10) J. D. Potts, Jr., and E. S. Amis, *J. Am. Chem. Soc.*, **71**, 2112 (1949).

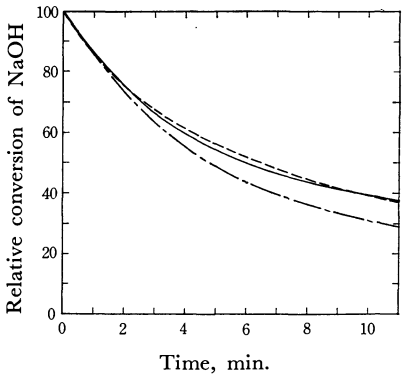

Fig. 11. Comparison of the experimental and the calculated curves of the reaction.

——— Experimental
— — — Theoretical as the pure 2nd order reaction.
- - - - Calculated with an analog computer ($k_2=2.0$, $k_3=7.2$ l./mol. sec.)

Conclusion

It has been observed that the reaction rate of the basic hydrolysis of ethyl acetate is not expressed satisfactorily by a second-order rate equation, and it has been proved, from the kinetic analysis of the reaction rate, that the mechanism of the hydrolysis is the sequential reaction process through the addition complex. We have obtained k_1 and k_2/k_3 values for several temperatures. These results correspond well with the conclusion obtained in the general nucleophilic reaction of carboxylic acid derivatives,[1] though the difference between the activation energies for k_2 and k_3 is too large in comparison with the results obtained by the hydrolysis of ethyl benzoate.[11] This may be due to the approximation used to get $\alpha-\beta$ from the experimental data.

11) M. L. Bender, R. D. Ginger and J. P. Unik, *J. Am. Chem. Soc.*, **80**, 1044 (1958).

BULLETIN OF THE CHEMICAL SOCIETY OF JAPAN VOL. 39 1842—1849 (1966)

Multiple Charge-transfer Bands of the Pyrene-Tetracyanoethylene Complex

By Haruo KURODA, Isao IKEMOTO and Hideo AKAMATU

Department of Chemistry, Faculty of Science, The University of Tokyo, Hongo, Tokyo

(Received November 18, 1965)

The polarized absorption spectra of the single crystal of the pyrene-tetracyanoethylene complex have been observed by means of a microspectrophotometer. It is shown that two absorption bands, at 12700 cm^{-1} and 20000 cm^{-1} respectively, are polarized along the *c*-axis, the direction connecting the molecular center of the donor and that of the acceptor; hence, both have been assigned to the charge-transfer bands. The interactions of 32 possible charge-transfer states with the no-bond state are discussed in terms of the simple molecular orbital theory, and their contributions to the energy of the complex formation are compared with each other. It is revealed that the interactions of higher charge-transfer states are relatively important and can not be neglected compared with that of the lowest charge-transfer state, and that the appearance of the multiple charge-transfer bands is a natural consequence of such a configurational interaction. It is also suggested that the ratio of the intensities of the first and the second charge-transfer bands may be a parameter that offers information on the orientation of the donor molecule to the acceptor molecule. A probable model is proposed for the structure of the pyrene-tetracyanoethylene complex formed in the solution.

Some charge-transfer complexes show two or three charge-transfer bands in their absorption spectra. The appearance of such multiplet charge-transfer bands has been ascribed to the difference between the donor and acceptor orbitals associated with the charge transfer.[1-4] Briegleb, Czekalla and Reuss[5] have shown that the energy difference between the first charge-transfer band and the second one is approximately equal to the excitation energy of the donor cation in the cases of the chloranil complexes and the tetracyanoethylene (TCNE) complexes which involve polycyclic

1) L. E. Orgel, *J. Chem. Phys.*, **23**, 1352 (1955).
2) A. Bier, *Rec. Trav. Chim. Pay-Bas*, **75**, 866 (1956).
3) R. E. Merrifield and W. D. Philips, *J. Am. Chem. Soc.*, **80**, 2778 (1958).
4) A. Kuboyama, *J. Chem. Soc. Japan, Pure Chem. Sect.* (*Nippon Kagaku Zasshi*), **81**, 558 (1960).
5) G. Briegleb, J. Czekalla and G. Reuss, *Z. Physik. Chem. N. F.*, **30**, 316 (1961).

aromatic hydrocarbons as the electron donor. Thus, the second charge-transfer bands in these cases can be assigned to the excitation associated with the charge transfer from the second highest occupied orbital of the donor to the lowest vacant orbital of the acceptor.

This interpretation, however, raises a question about the configuration of the complex. It is generally believed that a donor molecule takes an orientation relative to an acceptor molecule so as to give a maximum overlapping between the highest occupied orbital of the donor and the lowest vacant orbital of the acceptor. Such a structure is most favorable for the appearance of the first charge-transfer band, but it is not necessarily favorable for the second one since the symmetry of the second highest occupied orbital is usually different from that of the highest occupied orbital. In the case of the naphthalene-TCNE complex, for example, the first charge-transfer band should appear strongly when the molecules are stacked face-to-face, with their molecular centers directly over each other and with the central double bond of TCNE parallel to the long axis of naphthalene. However, the second charge-transfer band should be symmetry forbidden in this configuration. A similar situation may be expected also in the case of the pyrene-TCNE complex.

With these things in mind, Gott and Maish[6] suggested the presence of isomers which are different in the mutual orientations of the symmetry axes of the donor and acceptor. The presence of such orientational isomers has also been assumed by Zweig[7] as an explanation of the multiple charge-transfer bands of TCNE complexes of substituted benzenes.

In a previous paper,[8] we have shown, for several TCNE complexes, that the absorption bands corresponding to the first and second charge-transfer bands in the solution spectra appear in the absorption spectra of crystalline powders observed by means of the KBr pellet method. However, the possibility that the second absorption band found in a spectrum of crystalline powder is not a charge-transfer band, but a band associated with the excitation of the donor or acceptor, has not been conclusively ruled out. This point should be clarified by means of the observation of the polarized absorption spectra of the crystals.

In the present paper, the polarized absorption spectra of the crystal of the pyrene-TCNE complex will be shown in an attempt to prove that the multiple charge-transfer bands do really appear in the crystalline state as well as in the solution; then the interpretation of these bands will be discussed in detail in order to elucidate the general features of the multiple charge-transfer bands.

Experimental

Pyrene was purified by the successive application of recrystallization from a xylene solution, alumina column chromatography, and finally sublimation in vacuo. The purification of TCNE was accomplished by the sublimation in vacuo after the repetition of the recrystallization from a chlorobenzene solution. For the observation of the absorption spectrum of the complex crystal, minute single crystals of a lath shape, a few microns in width and in length and less than one micron thick, were prepared from a carbon tetrachloride solution.

The polarized absorption spectra were measured by means of a microspectrophotometer, a modification of the Olympus Model MSP-A-IV microspectrophotometer. An Xe-lamp of 500 W. was used as the light source. Although the technique of microspectrophotometry has been applied by other investigators to the observation of the spectra of organic crystals in the visible and ultraviolet regions, little has been done in the near infrared region because of the difficulty of finding a suitable detector. In the present experiment we have used a RCA 7102 photomultiplier tube as the detector in this region; it enables us to observe the absorption spectrum up to 1200 mμ.

Results and Discussion

(1) The Absorption Spectra and the Crystal Structure.—The visible absorption spectrum of a carbon tetrachloride solution of the pyrene-TCNE complex is shown in Fig. 1. The two broad bands at 13700 cm^{-1} and 19700 cm^{-1} are the first and the second charge-transfer bands respectively. The intensity ratio of these two bands remains constant over a wide temperature range. The oscillator strength of the first charge-transfer band is about 0.02.

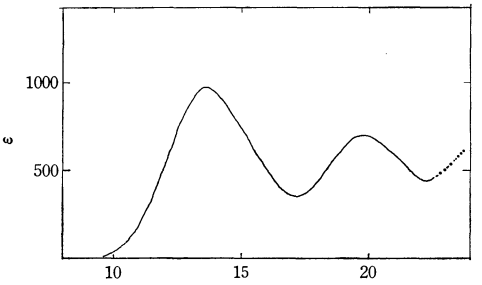

Fig. 1. The charge-transfer bands of pyrene-TCNE complex in carbon tetrachloride.

According to the results of the X-ray analysis of the crystal structure,[9] the crystal of the pyrene-TCNE complex has a monoclinic unit cell with

6) J. R. Gott and W. G. Maish, *J. Chem. Phys.*, **39**, 2229 (1963).
7) A. Zweig, *Tetrahedron Letters*, **1964**, 89.
8) H. Kuroda, M. Kobayashi, M. Kinoshita and S. Takemoto, *J. Chem. Phys.*, **36**, 457 (1962).
9) H. Kuroda, I. Ikemoto and H. Akamatu, This Bulletin, **39**, 547 (1966).

the lattice constants of $a=14.58$ Å, $b=7.34$ Å, $c=8.09$ Å and $\beta=92.4°$, and belongs to the $P2_1/a$ space group. Two pyrene and two TCNE molecules are contained in each unit cell. Pyrene and TCNE molecules are stacked alternately along the c-axis, their molecular planes parallel to each other so as to give a large overlap between their molecular orbitals. The crystals grown from a solution are either of lath-shape or are prisms elongated along the c-axis. In every case, the developed face is a (100) plane. Therefore, the b- and c-polarized spectra were observed in the direction perpendicular to the bc-plane with extremely thin crystals. The direction of the b-axis was determined by an examination with a polarizing microscope. The observed spectra are shown in Fig. 2.

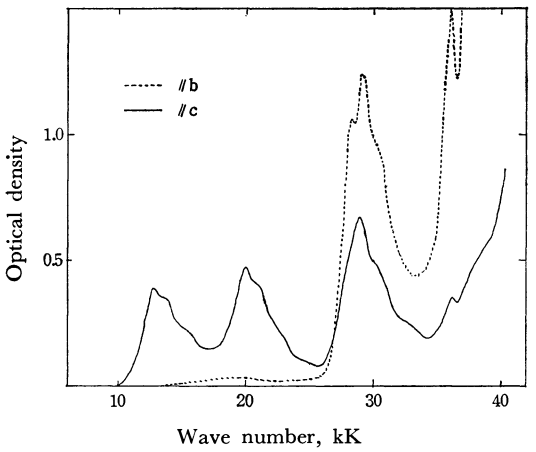

Fig. 2. The polarized absorption spectra of the crystal of pyrene-TCNE complex.

As can clearly be seen in Fig. 2, there are two absorption bands that are markedly polarized along the c-axis. The first band has the absorption maximum at 12700 cm^{-1}, and the second one, at 20000 cm^{-1}. No absorption band corresponding to the first one can be found in the b-polarized spectrum, but there is a very weak absorption with a maximum around 19000 cm^{-1}, which seems to correspond to the 20000 cm^{-1} band in the c-polarized spectrum. The third band in the c-polarized spectrum appears in the region of 25000 —35000 cm^{-1}, and the fourth begins from 35000 cm^{-1}. These bands are stronger in the b-polarized spectrum in contrast to the first and the second bands. Each band seems to have vibrational structures. The position of the peaks and the polarization ratio—the ratio of the integrated optical density of a band in the c-polarized spectrum to that in the b-polarized spectrum—are summarized in Table I.

The projection of the crystal structure along the a-axis onto the bc plane is shown in Fig. 3.

TABLE I. POLARIZATION RATIO AND POSITIONS OF PEAKS

Band	Polarization ratio of the band	Wave numbers of peaks cm^{-1}	
		b-polarized	c-polarized
I	>20		12700* 14000 15600
II	10	19500	20000* 21300
III	0.5	28900*	28400 29200* 31000
IV	0.2	>35000	>35000

* The maximum of the band.

It can readily be seen from this structure that, according to the oriented gas model, the short-axis polarized absorption of pyrene should be strongly polarized along the b-axis, while the long-axis polarized absorption may be exprected to show a polarization ratio of about unity. In any case, a large polarization ratio can hardly be expected for the local-excitation band. On the other hand, a charge-transfer excitation may be expected to be polarized along the c-axis, the direction connecting the centers of the pyrene and TCNE molecules stacked face-to-face. Thus, we can conclude that both the first and second absorption bands are charge-transfer bands, while the others are associated with the local excitations.

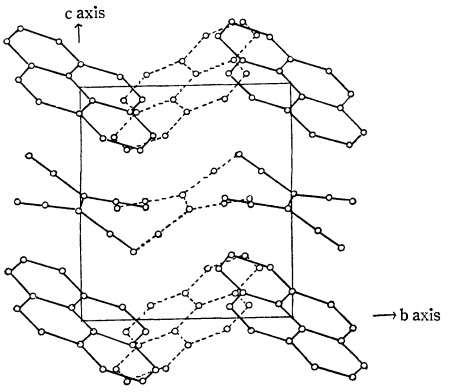

Fig. 3. The projection of the crystal structure of pyrene-TCNE complex along the a-axis on the bc plane.

The fact that the first band is exclusively polarized along the c-axis indicates that it is a pure charge-transfer band. The polarization ratio is a little lower for the second band. This could be due to mixing between the charge-transfer state and a local-excited state. Even if this is the case, however, the contribution of the local-excited state should

be quite small in order to give the observed polarization ratio. In the discussion below, therefore, we shall treat both of these absorption bands as pure charge-transfer bands, neglecting completely the interaction with any local excitation. The separation between the main peaks of the first and second charge-transfer bands is 7300 cm^{-1}, which approximately corresponds to the difference between the orbital energy of the highest occupied orbital and that of the second highest occupied orbital. It is most reasonable to presume that the first band is associated with a charge transfer from the highest occupied orbital of pyrene to the lowest vacant orbital of TCNE, and the second one, to that from the second highest occupied orbital. Interestingly, the integrated optical density is nearly the same for these two absorption bands in spite of the difference in the symmetry properties of these two molecular orbitals. The ratio of the integrated optical density of the first band to that of the second one is 0.94 in the c-polarized spectrum, and 1.3 in the solution spectrum. The significance of this ratio will be discussed later.

(2) Charge-transfer Interaction.—Since the experimental results described above indicate unambiguously that the first and second charge-transfer bands appear not only in the solution spectrum but also in the absorption spectrum of the crystal, where we can exclude the possibility of the presence of orientational isomers, the explanation for their appearance has to be found in the nature of the charge-transfer interaction between pyrene and TNCE, without assuming any orientational isomers. For the sake of simplicity, we shall consider here the interaction in a pair, a pyrene molecule and a TCNE molecule, stacked face-to-face as they are in the crystal, instead of the interaction in the crystalline state.

As is well known, the wave function of the ground state of a loosely-bounded molecular complex, or a weak complex, can be expressed as follows:

$$\Phi_N = a\phi_0(D\cdot A) + b\phi_1(D^+\cdot A^-) \qquad (1)$$

where $\phi_0(D\cdot A)$ and $\phi_1(D^+\cdot A^-)$ are the wave function of the no-bond structure and that of the dative structure respectively. Usually it is assumed that the wave function of the dative structure is satisfactorily expressed by the wave function of the lowest charge-transfer state where an electron has been transferred from the highest occupied orbital of the donor to the lowest vacant orbital of the acceptor, while the interactions of all the other, higher charge-transfer states are negligible. This approximation has been widely applied with success in the discussions of the charge-transfer bands, the dipole moment, and so on.[10] It can easily be seen, however, that the appearance of the second charge-transfer band can not be understood in terms of this approximation. We have to take into account the second chage-transfer state in which the donating orbital is the second highest occupied orbital of the donor. The energies of the Hückel orbitals of pyrene and TCNE are schematically shown in Fig. 4.* The molecular orbitals are numbered in the way shown in this figure.

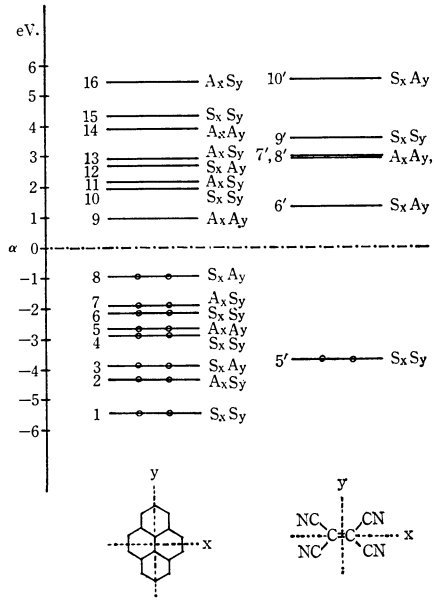

Fig. 4. The orbitals of pyrene and TCNE.

There can be a number of different charge-transfer states. In principle, all of them may interact with the no-bond state, and more or less contribute to the stabilization of the complex. The wave function of the ground state can be expressed generally as follows:

$$\Phi_N = a_0^0\phi_0(D\cdot A) + \sum_i\sum_j b_{ij}^0\phi_{ij}(D^+\cdot A^-) + \sum_k\sum_l c_{kl}^0\phi'_{kl}(D^-\cdot A^+) \qquad (2)$$

In Eq. 2, $\phi_{ij}(D^+\cdot A^-)$ is the wave function of a charge-transfer state where an electron has been transferred from the ith orbital of pyrene to the jth orbital of TCNE; $\phi'_{kl}(D^-\cdot A^+)$ is that of a state where an electron has been transferred from the lth orbital of TCNE to the kth orbital of pyrene, and a_0^0, b_{ij}^0 and c_{kl}^0 are the coefficients, generally $|a_0^0| \simeq 1$, $|b_{ij}^0| \ll 1$, $|c_{kl}^0| \ll 1$, for a weak complex such as pyrene-TCNE.

The energy of the ground state can be given by Eq. 3, using the approximation of the second-order perturbation theory:

10) See, for example, G. Briegleb, "Elektron-donator-acceptor-Komplexe" Springer-Varlay, Berlin, (**1961**).

* The value of β_{C-C} is assumed to be 2.16 eV.

$$W_N = W_0 - \{\sum_i\sum_j [H(0,ij) - W_0S(0,ij)]^2/(W_{ij} - W_0) + \sum_k\sum_l [H'(0,kl) - W_0S'(0,kl)]^2/(W'_{kl} - W_0)\} \quad (3)$$

where $H(0,ij) = \langle\phi_0|H|\phi_{ij}\rangle$, $H'(0,kl) = \langle\phi_0|H|\phi'_{kl}\rangle$, $S(0,ij) = \langle\phi_0 \mid \phi_{ij}\rangle$ and $S'(0,kl) = \langle\phi_0 \mid \phi'_{kl}\rangle$, and where W_0, W_{ij} and W'_{kl} are the energies of the ϕ_0,ϕ_{ij} and ϕ'_{kl} states respectively. If the wave functions of the complex are expressed in terms of the molecular orbitals of the donor and the acceptor, $S(0,ij)$ will be approximately equal to $\sqrt{2}\cdot S_{ij}$, where S_{ij} is the overlap integral between the donating and the accepting orbitals. Furthermore, it is possible to assume that $H(0,ij)$ is approximately proportional to $S(0,ij)$, and hence to S_{ij} also. Thus we can assume that $H(0,ij) - W_0S(0,ij) = -KS_{ij}$, where K is a constant. By using such approximations, Eq. 3 can be simplified to:

$$W_N = W_0 - K^2\{\sum_i\sum_j S^2_{ij}/(W_{ij} - W_0) + \sum_k\sum_l S'^2_{kl}/(W'_{kl} - W_0)\} \quad (4)$$

Therefore, the relative contribution of the interaction of a charge-transfer state, ϕ_{ij}, to the binding energy, $\Delta W = W_0 - W_N$, can be determined by comparing the values of $S^2_{ij}/(W_{ij} - W_0)$.

We have calculated S_{ij} as well as $S^2_{ij}/(W_{ij} - W_0)$ for a pair, a pyrene molecule and a TCNE molecule, stacked in the same way as they are in the crystal structure (Fig. 5). The distance between their molecular planes was taken to be 3.32 Å, the value determined by crystal structure analysis.

We have assumed the Hückel orbitals for the molecular orbitals of pyrene and TCNE, and the Slater functions with the orbital exponents of 1.64 and 2.13 a. u. for the 2p atomic orbitals of carbon and nitrogen respectively. It is known that a Slater function is not satisfactory for the tail of the atomic orbital, and it gives a markedly underestimated value in the calculation of an intermolecular integral.[11] In effect, the overlap integrals calculated in the present study will become nearly three times as large if the SCF atomic orbitals given by Roothaan, Clementi and Yoshimine[12] are used instead of the Slater orbitals. The use of a smaller orbital exponent has been recommended for the calculation of intermolecular integrals.[13] It can be shown, however, that the value of the overlap integral obtained by using SCF atomic orbitals is approximately proportional to the one obtained by using a Slater orbital for a given separation between the molecular planes of the donor and the acceptor which are stacked parallel to each other. Therefore, no essential difference is expected to occur in the estimation of the relative contributions of various charge-transfer states, even if SCF atomic orbitals are used, while the value of K is dependent on the atomic orbitals assumed. When Slater atomic orbitals are used, the value of K should be taken as 10—20 eV. in order to effect an agreement between the calculated binding energy and the observed one which is a few kcal./mol. The value of $W_{ij} - W_0$ was taken as equal to the energies of the first and second charge-transfer bands for the lowest charge-transfer state and the second one respectively. The values for the other states were estimated by using these values and the orbital energies.

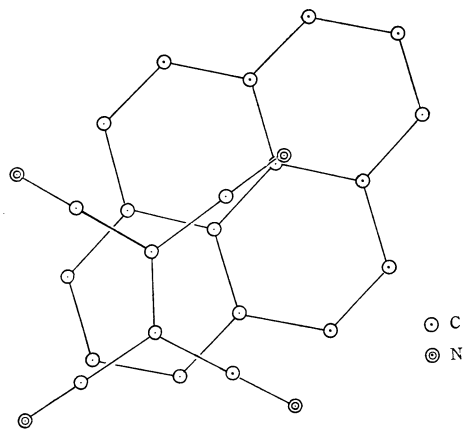

Fig. 5. The orientation of a pyrene molecule relative to the neighboring TCNE molecule in the crystal structure.

In Table II, the calculated values of S_{ij} and $S^2_{ij}/(W_{ij} - W_0)$ are given for 32 different charge-transfer states.* The charge-transfer states where the accepting orbitals are the 9′ orbital and the 10′ orbital of TCNE, and those where the donating orbitals are the 1′—4′ orbitals of TCNE, are omitted in this table because their contributions to ΔW are negligibly small. Generally, the lowest charge-transfer state is expected to play the most important role in the charge-transfer interaction. In the present case, this is the state where the donating orbital is the 8 orbital of pyrene and where the accepting one is the 6′ orbital of TCNE; we shall denote this state as [8→6′]. According to Table II, however, we have to give up such a preconception. The contribution of the lowest charge-transfer state to ΔW is by no means predominant in comparison with those of the other charge-transfer states. It can cover only 16 per cent of ΔW, while the contribution from the second charge-transfer state, [7→6′], is 19 per cent, and those

11) J. L. Katz, S. A. Rice, S. Choi and J. Jortner, *J. Chem. Phys.*, **39**, 1683 (1963).
12) E. Clementi, C. C. Roothaan and M. Yoshimine, *Phys. Rev.*, **127**, 1618 (1962).
13) J. N. Murrell and J. Tanaka, *Mol. Phys.*, **7**, 363 (1964).
* The overlap intergral was calculated by means of an PC-2 electronic computer, at University of Tokyo Data Processing Centre.

Table II (a). $[D^+ \cdot A^-]$ states

Donating orbital	Accepting orbital TCNE MO (j) 6′		7′		8′	
Pyrene MO (i)	S_{ij} ($\times 10^{-2}$)	$S^2_{ij}/W_{ij}-W_0$ ($\times 10^{-4}$)	S_{ij} ($\times 10^{-2}$)	$S^2_{ij}/W_{ij}-W_0$ ($\times 10^{-4}$)	S_{ij} ($\times 10^{-2}$)	$S^2_{ij}/W_{ij}-W_0$ ($\times 10^{-4}$)
8	+0.93487	0.585	+0.62951	0.127	+0.08169	0.002
7	−1.30721	0.703	+0.85602	0.180	+0.30725	0.023
6	+0.21919	0.018	−0.42038	0.041	+0.50695	0.059
5	−1.29369	0.519	−1.03604	0.221	−0.01051	0.000
4	+1.33335	0.517	−0.98549	0.192	+0.06040	0.001
3	+1.07578	0.262	+0.80119	0.106	+0.03828	0.000
2	−0.23324	0.011	+0.15216	0.004	−0.14353	0.003
1	−0.40761	0.028	+0.42446	0.024	−0.05253	0.000

Table II (b). $[D^- \cdot A^+]$ states

Accepting orbital	Donating orbital TCNE MO (l) 5′	
Pyrene MO (k)	S_{kl} ($\times 10^{-2}$)	$S^2_{kl}/W'_{kl}-W_0$ ($\times 10^{-4}$)
9	+0.21450	0.012
10	−0.26484	0.015
11	−0.53416	0.056
12	−0.17488	0.005
13	+0.03297	0.000
14	+0.07066	0.001
15	+0.05639	0.000
16	+0.02223	0.000

from the [5→6′] and [4→6′] states are both 14 per cent. It is thus revealed that the second charge-transfer state, as well as some of the much higher charge-transfer states, should be taken into account in discussions of the electronic states of the complex.

(3) **The Intensities of the Charge-transfer Bands.**—Corresponding to the expression of the wave function of the ground state given in Eq. 2, we can describe the wave function of a charge-transfer excited state associated with an electron transfer from the mth orbital of the donor to the nth orbital of the acceptor, as follows:

$$\Phi_E(mn) = a_0^{mn}\phi_0(D\cdot A) + b_{mn}^{mn}\phi_{mn}(D^+\cdot A^-) + \sum_{i\neq m}\sum_{j\neq n} b_{ij}^{mn}\phi_{ij}(D^+\cdot A^-) + \sum_k\sum_l c_{kl}^{mn}\phi'_{kl}(D^-\cdot A^+) \quad (5)$$

where $|a_0^{mn}|$, $|b_{ij}^{mn}|$ $(i\neq m,\ j\neq n)$, $|c_{kl}^{mn}| \ll 1$ and $|b_{mn}^{mn}| \simeq 1$. The transition moment of the charge-transfer excitation, $\Phi_E \leftarrow \Phi_N$, can then be approximately expressed by Eq. 6, neglecting all small terms and assuming that the dipole moment is zero in the no-bond state. The values of a_0^0 and b_{mn}^{mn} are taken as unity.

$$\mu(0, mn) = \langle\Phi_N|\mu|\Phi_E\rangle \simeq b_{mn}^0\langle\phi_{mn}|\mu|\phi_{mn}\rangle + \langle\phi_0|\mu|\phi_{mn}\rangle \quad (6)$$

where μ is the operator of the dipole moment. The dipole moment of the charge-transfer state, $\langle\phi_{mn}|\mu|\phi_{mn}\rangle$, is nearly the same for all the charge-transfer states; we shall denote it as μ_{CT}. We can also presume that the $\langle\phi_0|\mu|\phi_{mn}\rangle$ integral is roughly equal to $[S(0, mn)/2]\cdot\langle\phi_{mn}|\mu|\phi_{mn}\rangle$, according to Mulliken's approximation. Thus the following equations can be given for the transition moment:

$$\mu(0, mn) \simeq [b_{mn}^0 + S(0, mn)/2]\cdot\mu_{CT} \quad (7)$$

thus:

$$\mu(0, mn) \simeq [K/(W_{mn} - W_0) + 1/\sqrt{2}]\cdot S_{mn}\cdot\mu_{CT} \quad (8)$$

The ratio of the oscillator strength of the first charge-transfer band to that of the second one, f_1/f_2, can be roughly estimated by using Eq. 8. We obtained 0.8 for this ratio, assuming that $K \simeq 10$ eV. Since the observed value is 0.94 in the crystal spectrum and 1.3 in the solution spectrum, the agreement between the observed and the theoretical ratios seems satisfactory for such a rough approximation as we have made here.

We can predict that two charge-transfer bands associated with the charge-transfer states, [5→6′] and [4→6′], can be observed in the 25000—30000 cm^{-1} region with an oscillator strength comparable to the first charge-transfer band. The third band in the c-polarized spectrum could be due to these absorptions. The pyrene molecule has, however, ^1L_a and ^1L_b bands in this region. Therefore, we have to consider in this case the mixing of the local-excited states and the charge-transfer states. This problem will not be treated in this paper.

(4) **The Charge-transfer Bands and the Structure of the Complex.**—Hitherto we have assumed the orientation of the pyrene molecule to the TCNE molecule to be as it is in the crystal. However, the orientation could be different from this for the complex in solution. In the crystalline state, molecules would be arranged first of all in such a way that the crystal structure fulfills the condition of the closest packing. This leaves the possibility that molecules take an orientation

that is unfavorable for the charge-transfer interaction. On the other hand, molecules are supposed to take the most favorable orientation when they form a complex in a solution. It is worthwhile, therefore, to evaluate the binding energy associated with the charge-transfer interaction for various different orientations in order to ascertain the most stable structure.

Apparently the binding energy becomes quite small when the donor and acceptor molecules are not in close contact. We can safely ignore such a case, however, and can assume that the molecules are stacked face-to-face, so as to result in a large overlapping between their molecular orbitals. Then we have two variables; the one is the position of the symmetry center of TCNE relative to that of pyrene, and the other is the relative orientation of their molecular axes. We have made our calculation on the relative values of the binding energy, $\Delta W/K^2$, for the following two cases: [Model A], in which the symmetry centers are directly over each other (Fig. 6a), and [Model B], in which the relative positions of the centers are exactly the same as they are in the crystal structure (Fig. 6b). For each model, $\Delta W/K^2$ was evaluated by using Eq. 4 as a function of θ, the angle between the symmetry axes of the molecules, taking the 32 charge-transfer states into account. The results are shown in Fig. 7.

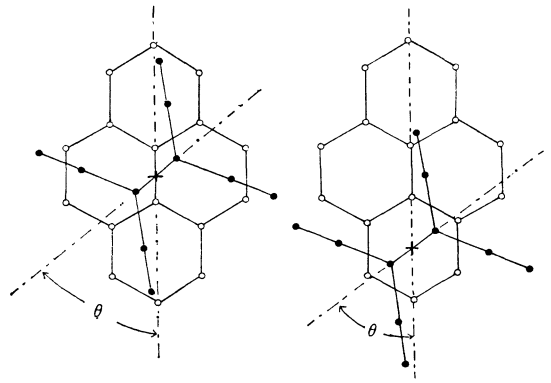

(a) Model A (b) Model B

Fig. 6. The models of pyrene-TCNE complex assumed for the calculation.

Interestingly, $\Delta W/K^2$ varies little with θ in either model. The difference between the largest value and the smallest one is less than 20 per cent of the mean value. This means that the rotation of the TCNE molecule around its symmetry axis perpendicular to the molecular plane would have a very low energy variation, less than 0.4 kcal./mol., as far as only the charge-transfer interactions are concerned. Therefore, we shall not be able to tell the value of θ for the most stable structure unless we have detailed information on other intermolecular interactions. This is a rather unexpected result, since we used to consider that the charge-transfer interaction would be the most strongly dependent on relative orientation of the molecules. Secondly, it may be seen in Fig. 7 that the value of $\Delta W/K^2$ is always larger in Model B than in Model A. This suggests that Model B is more acceptable for the stable structure than Model A.

The ratio of the oscillator strength of the first

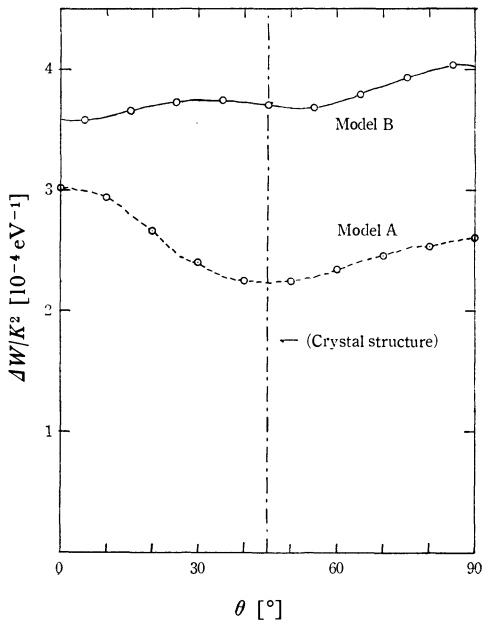

Fig. 7. The dependence of ΔW on the orientation of pyrene to TCNE.

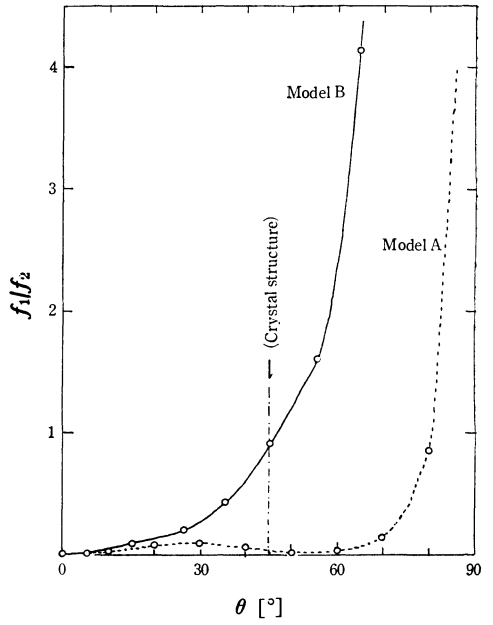

Fig. 8. The relation between the ratio of the oscillator strengths of the charge-transfer bands and orientation of pyrene to TCNE.

charge-transfer band to that of the second one may be theoretically estimated as a function of θ by means of Eq. 8. The results are shown in Fig. 8. It can be seen that the ratio varies markedly, depending on the θ value.

In the case of Model A, the f_1/f_2 ratio is very small except in the θ=80—90° region, where the magnitude of f_2 approaches zero. According to Eq. 8, the value of f_1 is smaller than 0.001 in this model; this is too small compared with the observed value, 0.02. On the other hand, f_1 and f_2 in Model B become comparable to each other in the θ=40—50° region, where the values of f_1 and f_2 are roughly estimated as 0.01, a value which is in agreement with the observed value. This structure corresponds to the one found in the crystal. Since the binding energy changes little with the θ value, we can not exclude the possibilities that the structures with different θ values co-exist, or that molecules rotate independently around their symmetry axes perpendicular to the molecular plane. In this case the oscillator strength, as well as the f_1/f_2 ratio, will be averaged over different values of θ. In Model A, the average f_1 value will be about 0.0005, and that of f_1/f_2, 0.06. Thus, it is impossible to explain the observed results with this model.

In Model B, however, the average value of f_1 is 0.01, and that of f_1/f_2, 0.9; these values are almost the same as those calculated for the orientation where the value of θ is fixed as 45°. The observed results can be explained well by means of this rotating model. Therefore, the following conclusions can be obtained from the results discussed above; (1) it is difficult to explain either the observed oscillator strengths of the charge-transfer bands or their ratio on the assumption of Model A, and (2) the oscillator strengths and their ratio can be reasonably explained using Model B if we assume either that θ=40—50°, or that the structures with different θ values co-exist with equal probability. In any case, it is Model B that seems more acceptable for the complex in solution.

Summary and Conclusion

We have shown, from the study of the polarized absorption spectra of the crystal of the pyrene-TCNE complex, that the first and second charge-transfer bands can be observed in the crystal spectra. A simple theoretical treatment has proved that the interactions of higher charge-transfer states make significant contributions to the stabilization of the complex. These interactions are by no means negligible; they thus should be taken into account in the discussions of the absorption spectra of the complex. If this has been done properly, the appearance of the multiple charge-transfer bands can be explained. We have pointed out the significance of the relative intensities of the first and the second charge-transfer bands for the purpose of ascertaining the structure of the complex.

We wish also to emphasize another important conclusion that has become clear in the present study. The structure of a charge-transfer complex has often been discussed by considering the symmetry properties of the highest occupied orbital of the donor and the lowest vacant orbital of the acceptor. However, this problem is not so simple. The interaction of the lowest charge-transfer state is not always predominant in the stabilization of the complex. When the interactions of the higher charge-transfer states are taken into account, however, the binding energy due to the charge-transfer interaction becomes rather insensitive to the change in the orientation of the molecular axes of the donor relative to those of the acceptor, provided that their molecular planes are parallel to each other and are in close contact. We can only predict the relative positions of the centers of the molecules in the case of the pyrene-TCNE complex. We have shown that the structure where the molecular centers are directly above each other is not likely to be the most stable structure because, in the first place, the binding energy will be relatively small in this case, and in the second place, the intensities of the observed charge-transfer bands can not be explained using this model. Thus, the relative positions of the centers as they are in the crystal seem to be acceptable also for the complex in solution. Although we have confined our discussion exclusively on the pyrene-TCNE complex, the general features of the conclusions, such as those on the origin of the multiple charge-transfer bands and on the nature of the charge-transfer interaction, can be extended to a number of the weak π-complexes that involve polycyclic aromatic compounds as the electron donors.

BULLETIN OF THE CHEMICAL SOCIETY OF JAPAN VOL. 39 1850—1854 (1966)

The Activation of Titanium Dioxide as a Decontaminant for Radioactive Contamination

By Toshiko TAKAMI and Tsunetaka SASAKI

Department of Chemistry, Faculty of Science, Tokyo Metropolitan University, Setagaya-ku, Tokyo

(Received November 19, 1965)

The decontamination efficiencies of treated and untreated titanium dioxide pastes were measured using ^{60}Co-contaminated surface of plastics, polyvinyl chloride. The titanium dioxides used were commercial titanium dioxide, hydrous titanium dioxide, titanium dioxide treated with sulfuric acid, and "Titanium Cake," an intermediate product of the titanium dioxide industry. Among these titanium dioxide decontaminants, titanium dioxide treated with sulfuric acid proved most effective in decontamination, even in neutral conditions, if activated properly. The optimum condition of activation was the 50% sulfuric acid treatment of commercial titanium dioxide at 50°C for 6 hr.

For the radioactive decontamination of a solid surface, we generally use radioactive decontaminants. These decomtaminants vary according to their purposes. In this connection, it is important to note that the residual contamination remaining even after a rough decontamination is often a matter of intense interest. Such a decontamination is often influenced by the nature and not by the amount of the decontaminant used. As for the decontaminants, such powdered substances as titanium dioxide,[1] alumina[1] and kaolin[2] are used. These substances are usually applied as pastes. Among these, titanium dioxide is comparatively effective and is widely used. However, little is known concerning its decontaminating action except for the facts that anatase is superior to rutile and the fresh precipitate is even more excellent.[1,3,4] However, it is troublesome to prepare a fresh precipitate from commercial titanium dioxide or a soluble titanium compound prior to each decontamination. It is, however, a usual practice in the preparation of an adsorbent to promote the adsorption capacity by the suitable treatment of its surface. Therefore, we desired to find a simple and effective method of activating a commercial titanium dioxide without complete dissolution, for the use as a decontaminant.

In the present investigation, the activation of titanium dioxide by sulfuric acid was undertaken for this purpose.

Experimental

Sample.—From the results of a preliminary experiment contaminating the solid surface of polyethylene, polystyrene and polyvinyl chloride, polyvinyl chloride was chosen as the test surface since it was comparatively more susceptible to contamination than the other specimens. A commercial product of polyvinyl chloride, 0.75 cm. thick and cut in a 2.5×2.5 cm. size, was used as the test piece. An aqueous solution of cobaltous chloride labeled with radioactive ^{60}Co was used as the contaminating solution, the concentration being 5.20×10^{-3} mol./l., and the specific activity, 19 c./mol. The titanium dioxide used as a decontaminant was a commercial product of the anatase type.

Experimental Procedure.—For the preparation of the contaminated sample, a test piece was soaked in a 0.5% solution of Epan 485 (a block copolymer composed of polyoxyethylene and polyoxypropylene, a Daiichi Kogyo Seiyaku product) to remove any oily contamination from the surface, rinsed with distilled water, and dried using filter paper. To contaminate the test piece, filter paper 2.0×2.0 cm. in size which had been soaked with 5 ml. of a radiaoactive $^{60}CoCl_2$ solution over a 24 hr. period, was placed on the sample for contamination. After an hour the filter paper was removed and the sample was immersed in water to rinse off the easily removable excess contaminant, the radioactivity was then measured using a Geiger-Müller counter (Aloka GP-1; window thickness: 1.4 mg./cm^2), with the sample placed 1 cm. below the counter tube. The amount of cobalt on the sample was calculated from this counting rate and the counting rate of a known amount of the cobaltous chloride, which was put in small droplets on a polyvinyl chloride sample and dried. Figure 1 shows the contamination remaining after such a treatment plotted against the time of washing. Here, the percentage of cobalt remaining on the surface was calculated from the counting rates observed for the test piece before and after the contamination. From this curve, it is difficult to distinguish between the contamination merely adhering to and that adsorbing on the solid surface. However, the initial, rapidly decreasing portion of the curve was

1) H. A. Künkel, *Strahlenther.*, **90**, 100 (1953); **91**, 326 (1954).
2) Ya. Nosek and V. Khemelorzh, *Med. Radiol.*, **4**, 74 (1954).
3) H. Hotta and H. Nakamura, *J. Chem. Soc. Japan, Pure Chem. Sect.* (*Nippon Kagaku Zasshi*), **81**, 1 (1960).
4) National Bureau of Standards Handbook U. S. A., 48 (1951).

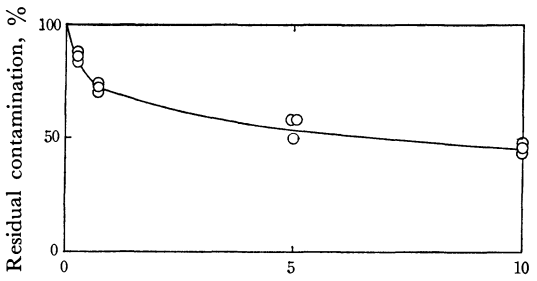

Time of washing, min.

Fig. 1. Residual contamination vs. time of washing by water.

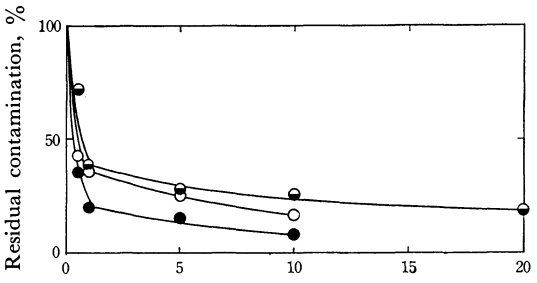

Time of decontamination, min.

Fig. 2. Residual contamination vs. time of decontamination.
○ Commercial titanium dioxide
● Hydrous titanium dioxide
◒ Distilled water alone

conveniently taken as due to the adhering contamination, and 1.5 minutes' washing was adopted for the preparation of a standard sample of the contamination. For further decontamination measurements, a 2 g. portion of titanium dioxide was mixed with 0.7 ml. of distilled water to make a paste, with which the sample was then put in close contact. After 5 min., the surface was rinsed with water for 30 sec. to remove the decontaminant, dried using filter paper, and the surface counting rate was measured. In these experiments, the pH of the paste was adjusted to 5.0—5.5 to avoid the co-operating action of hydrogen ions mentioned later. Also the mechanical action was not applied in order to study exclusively the chemical decontaminating action of the powder itself. In comparison with this, the decontamination experiment using distilled water without the powder was made in a shallow dish $2.4\times2.4\times0.3$ cm. in size. The sample was then similarly risned, and the amount of contamination was measured. Figure 2 shows the residual contaminations obtained with commercial titanium dioxide, hydrous titanium dioxide and distilled water without titanium dioxide, where the contaminations were plotted against the decontamination time. It may be seen in Fig. 2 that the residual contamination decreases rapidly in the initial one or two minutes, followed by a slow decrease in every case. Therefore, in the following experiments, the time of decontamination was properly chosen as 5 min., as has been mentioned above, after which the decrease in contamination was seen to be fairly slow. In discussing the effect of decontamination, the percentage of residual contamination,

$$\frac{\text{Residual contamination after 5 min.}}{\text{Initial contamination on standard sample}}\times 100$$

was used. All experiments were carrid out at room temperature (about 20°C).

Results

Decontamination by Commercial Titanium Dioxide and Hydrous Titanium Dioxide.— It is generally believed that freshly-precipitated titanium dioxide shows a strong decontamination power. Therefore, the hydrous titanium dioxide was prepared as follows.[5] About 24 g. of a commercial titanium dioxide was slowly dissolved in 60 ml. of concentrated sulfuric acid, stirred, and evaporated to dryness by heating it at 230°C for an hour. The product was then dissolved in 100 ml. of distilled water and filtered to remove any insoluble matter. The filtrate was neutralized with sodium hydroxide, and the precipitates formed were separated by decantation. It was then dried at 100°C for 24 hr., ground in a mortar, suspended in water, and heated to 70°C. The suspension was neutralized with hydrochloric acid, washed by repeated decantation using water, and dried. Thus, about 16 g. of neutral hydrous titanium dioxide was obtained.

Table I. Decontamination efficiency near neutral pH

Decontaminant	Initial contamination mol./4 cm² $\times 10^{10}$	Residual contamination mol./4 cm² $\times 10^{11}$	Residual contamination %
Water alone	1.11	3.31	29.8
Commercial titanium dioxide	1.92	3.95	20.5
Hydrous titanium dioxide	2.36	4.14	16.8
Titanium Cake A	1.88	4.76	25.3
Titanium Cake B	2.74	7.44	27.1

Table I shows the decontamination efficiency obtained for hydrous titanium dioxide, commercial titanium dioxide and water without titanium dioxide. It may be seen in this table that the addition of titanium dioxide to water evidently increases the decontamination efficiency and that the hydrous titanium dioxide shows a greater decontamination efficiency than the untreated one. The hydrous titanium dioxide reduced the remaining contamination to 50% of that obtained for the sample treated with distilled water alone. Therefore, hydrous titanium dioxide may be a better

5) W. B. Blumenthal, *Ceram. Age*, **51**, 320 (1948).

decontaminant than the untreated commercial product, which exhibits an 80% residual contamination, but it cannot be considered so effective a method of preparing a decontaminant, considering the concentrated sulfuric acid, the fairly high temperature and the exhaustive decantation required for the preparation of hydrous titanium dioxide.

Decontamination by Titanium Dioxide Treated with Sulfuric Acid.—We further attempted to prepare a more effective decontaminant by a more simple treatment of the commercial titanium dioxide powder, that is, by a mere surface treatment of titanium dioxide by sulfuric acid, without the total dissolution of the titanium dioxide.

Activation with Concentrated Sulfuric Acid.—About 20 g. of commercial titanium dioxide was treated with 20 ml. of concentrated sulfuric acid at 8, 20, 30, 50, 100 and 200°C for an hour, washed with water until it became neutral, and filtered. Table II shows the decontamination efficiencies for these samples. It may be seen in this table that the decontamination efficiency increased with the temperature of treatment, and that the maximum decontamination efficiency was attained above 50°C, regardless of the temperature. It was further confirmed that acid-treated titanium dioxide was more effective than hydrous titanium dioxide and, of course, than untreated titanium dioxide. In the above treatment, however, it was still troublesome to wash the treated sample with water alone, until it became neutral, although the time required for washing was remarkably shortened as compared with the case of the preparation of hydrous titanium dioxide mentioned above. Therefore, we further attempted to compare the difference in the decontamination efficiency of acid-activated (30°C, 1 hr.) titanium dioxide samples treated by the following three different methods of washing: washing until neutral with water alone; the addition of sodium hydroxide until the pH value of 2 was reached, followed by washing with water until neutral, and direct neutralization with sodium hydroxide. The results are shown in Table III.

TABLE II. EFFECT OF TEMPERATURE ON SULFURIC ACID TREATMENT OF TITANIUM DIOXIDE

Temp. °C	Initial contamination mol./4 cm² ×10¹⁰	Residual contamination mol./4 cm² ×10¹¹	Residual contamination %
8	6.74	9.99	17.4
20	2.21	2.58	11.7
30	2.78	3.30	11.0
50	1.44	1.30	9.0
100	8.07	7.38	9.1
200	7.25	7.21	9.8

TABLE III. EFFECT OF NEUTRALIZATION METHOD ON ACTIVATED TITANIUM DIOXIDE

Method	Initial contamination mol./4 cm² ×10¹⁰	Residual contamination mol./4 cm² ×10¹¹	Residual contamination %
Washing with water until neutral	2.78	3.30	11.0
Addition of NaOH until neutral	1.62	1.65	10.2
Addition of NaOH to pH 2 and washing with water	6.19	7.11	11.0

In this table, little difference in decontamination efficiency is seen amoung the treatments. From this, it may be concluded that direct neutralization by sodium hydroxide can be adopted to reduce remarkably the time of washing compared with mere washing with water. Therefore, the direct neutralization method was adopted in the following experiments.

Activation with Diluted Sulfuric Acid.—Attempt was then made to activate titanium dioxide with diluted sulfuric acid, since it is easier and desirable to use a diluted sulfuric acid than the concentrated one. The effects of the temperature and the time

TABLE IV. DECONTAMINATION EFFICIENCY OF ACTIVATED TITANIUM DIOXIDE UNDER VARIOUS CONDITIONS

Concn. of H_2SO_4 wt. %	Temp. °C	Time hr.	Initial contamination mol./4 cm² ×10¹⁰	Residual contamination mol./4 cm² ×10¹¹	Residual contamination %
15	50	6	2.45	2.88	13.0
15	50	24	1.52	1.90	12.5
30	50	6	2.44	3.12	13.1
30	50	24	2.76	3.92	10.7
40	50	6	3.48	3.77	10.9
40	50	24	3.26	3.26	10.0
50	50	6	1.15	1.07	9.3
50	30	1	2.86	5.25	18.4
50	30	3	1.61	1.97	12.2
50	30	6	1.60	1.91	11.9
50	30	24	0.937	1.04	11.1
75	30	1	5.60	6.99	13.9

of treatment on the decontamination efficiency under such conditions were examined. The results are shown in Table IV. From this table it may be seen that the temperature of treatment has a greater effect than the time of treatment above a 50% sulfuric acid activation. In the case of 30% sulfuric acid activation, the time of treatment is four times as long as that of the 50% sulfuric acid treatment needed to achieve the same decontamination efficiency. In the case of 15% acid activation, an even longer time is required.

Decontamination with "Titanium Cake."—The above experiments suggest that the so-called "Titanium Cake," that is, the wet intermediate product of the titanium dioxide industry, would be equally excellent as the acid-activated titanium dioxide in decontamination efficiency. Therefore, the decontamination efficiency was similarly examined with "Titanium Cake" with a pH value of about unity. The results are shown in Table I, where the pH of this paste was controlled with sodium hydroxide to 5.0—5.5. Contrary to the above expectations, "Titanium Cake" in a neutral-pH paste was little different in decontamination efficiency from distilled water alone, in spite of the wet nature of the "Titanium Cake."

Decontamination in an Acid Region.—It is further known that the decontamination efficiency of a decontaminant generally increases in an acid region, in addition to the action of the acid itself.[1] Therefore, the decontamination efficiencies of various titanium dioxide pastes were compared at a pH value of unity. The results are shown in

Table V. Decontamination efficiency in acid region

Decontaminant	Initial contamination mol./4 cm² $\times 10^{10}$	Residual contamination mol./4 cm² $\times 10^{11}$	Residual contamination %
Water alone	2.07	2.77	13.4
Commercial titanium dioxide	3.79	3.28	8.7
Activated titanium dioxide	9.14	2.90	3.2
Titanium Cake A	7.29	2.89	4.0
Titanium Cake B	8.80	5.00	5.7

Table V. Here, the pH values of "water alone" and commercial titanium dioxide were controlled with hydrochloric acid to unity, while acid-activated titanium dioxide was prepared under the optimum conditions of 50% sulfuric acid treatment at 50°C for 6 hr., followed by the addition of sodium hydroxide until a pH value of unity was reached, and the "Titanium Cake" with a pH value of unity was used without further control of the pH. These results confirm the view that the action of acid itself is remarkable in the decontamination, as can be seen from a comparison of the results of Tables IV and V. However, we can see a still further increase in the decontamination efficiency upon the addition of titanium dioxide; here again, acid-treated titanium dioxide proves to be best, as is to be expected.

Conclusion

It may be concluded from the results of the above investigation that an effective decontaminant for a surface of plastics contaminated with ^{60}Co is prepared by the surface treatment of titanium dioxide with sulfuric acid. The optimum conditions are treatment with 50% sulfuric acid at 50°C for 6 hr., but if we allow somewhat of a lowering of the decontamination efficiency, a 30% sulfuric acid treatment at 50°C for 24 hr. can also be recommended. These are more practicable conditions. The lowering of the temperature below 50°C resulted in a decrease in effect unrecoverable even by treatment over a prolonged time, this is in contrast to the decrease in efficiency produced by the lowering of the concentration of sulfuric acid which is recovered by a prolonged treatment. As for the pH dependence, it has been confirmed that the decontamination efficiency rises more remarkably in the acid region (pH unity) than near the neutral pH. "Titanium Cake," obtainable as a wet paste, is expected to be favorable for use as a decontaminant. The results of the measurements, however, show that in the neutral region, it is no more better than water without titanium dioxide, although it is nearly equal in its effect to acid-treated titanium dioxide in the acid region.

As for the titanium dioxide decontaminant, it is usually applied on a solid surface as a paste in 0.1 N hydrochloric acid. In this case the hydrogen ion and mechanical action during performance assist the decontaminating action, in addition tc the chemical action of titanium dioxide itself. However, it is not always allowable to lower the pH of the decontaminating solution and, further, to rub the surface effectively, because of the susceptibility to damage and the complicated shape of the solid surface. Also, the solid surface may often be scratched by rubbing, and thus, rendered to be liable to subsequent strong contamination. Consequencly, the titanium dioxide, even without such acid and mechanical actions, should have a good decontamination power in order to be effective under widely differing conditions of decontamination. In the present experiment, therefore, the mechanical effect of rubbing was avoided. The rubbing, if applied, would promote and make the decontamination efficiencies of almost all of the samples indistinguishable, but the subsequent contamination would become more marked. It

may be inferred, further, that the acid-treated titanium dioxide may be more highly recommended as a decontaminant than ordinary titanium dioxide, where a trace of residual radioactive contamination causes a serious problem, as in the case of skin contamination.

The authors are indebted to Mr. Tsutomu Seimiya of our laboratory for his assistance. They also thank Sakai Chemical Industry Co. Ltd., for titanium dioxide samples kindly given to them. The present study was made under the financial support of the Ministry of Education.

BULLETIN OF THE CHEMICAL SOCIETY OF JAPAN VOL. 39 1854—1857 (1966)

The Variation in Carbon-Halogen Bond Length with the Environment

By Arjun Singh RAJPUT and Suresh CHANDRA

Physics Department, University of Allahabad, Allahabad, India

(Received November 24, 1965)

The data on carbon-halogen bond lengths which have been obtained in recent years are summarized. It has been found that the interatomic distances corresponding to carbon-halogen bonds show a linear dependence on the number of adjacent atoms or bonds. Simple equations for these bond lengths are given to make it possible to estimate different carbon-halogen bond lengths empirically. It has been shown that this variation can be adequately explained on the basis of the hybridization effect. New values for the radii of the hybrid orbitals of carbon have been assigned and used to calculate the bond lengths in a variety of compounds. The agreement between calculated and experimental values is good.

As a result of the development of microwave spectroscopy for the study of the structure of the molecules, a large amount of information about interatomic distances in molecules has been accumulated. The accuracy of bond lengths determined experimentally depends upon the nature of the method used. The spectroscopic values for simple molecules are accurate to within ± 0.001 Å, while those for polyatomic molecules are somewhat less reliable. This accuracy has made it possible to derive relationships between bond lengths and various other bond properties. The dependence of the carbon-carbon and carbon-hydrogen bond lengths on the environment has been studied by many workers.[1-6] An analysis of these data has led to an empirical relationship for the C–C, C=C, C≡C and C–H bond lengths, which increase linearly with the increase in the number of adjacent bonds or atoms. This paper will deal with the carbon-chlorine, carbon-bromine and carbon-iodine bond lengths in simple polyatomic molecules. Recent experimental values for carbon-halogen bond lengths in polyatomic molecules seem to depend linearly on the environment. Simple empirical equations have been given to estimate the different carbon-halogen bond lengths. Many attempts[7-14] have been made to explain the variation in carbon-carbon and carbon-hydrogen bond lengths with the environment in terms of various descriptions of carbon atoms and their environment. It will be shown in this paper that the variation in carbon-halogen bond lengths can be explained on the basis of the hybridization effect. New values for the radii of the hybrid orbitals of carbon have been assigned, and these values have been used to calculate the bond lengths in a variety of compounds. It has been found that the calculated and the experimental values are in agreement.

A Summary of Carbon-Halogen Bond Lengths in Polyatomic Molecules.—The values of the bond lengths, the molecules from which they have been obtained, and the method by which they are determined are given in Table I. The quoted bond-length values may be supposed to be the best values available at the present time. Most of the

1) G. Herzberg, F. Patat and H. Verleger, *J. Phys. Chem.*, **41**, 123 (1937).
2) L. Pauling, H. D. Springall and K. J. Palmer, *J. Am. Chem. Soc.*, **61**, 927 (1939).
3) J. Overend and H. W. Thompson, *J. Opt. Soc. Am.*, **43**, 1065 (1953).
4) G. Herzberg and B. P. Stoicheff, *Nature (London)*, **175**, 79 (1955).
5) C. C. Costain and B. P. Stoicheff, *J. Chem. Phys.*, **30**, 777 (1959).
6) B. P. Stoicheff, *Tetrahedron*, **17**, 135, (1962).
7) M. J. S. Dewar and H. N. Schmeising, ibid., **5**, 166 (1959).
8) G. R. Somayajulu, *J. Chem. Phys.*, **31**, 919 (1959).
9) H. J. Bernstein, *J. Phys. Chem.*, **63**, 565 (1959).
10) R. S. Mulliken, *Tetrahedron*, **6**, 68 (1959).
11) L. S. Bartell, *J. Am. Chem. Soc.*, **81**, 3497 (1959).
12) B. Bak and L. Hansen-Nygaard, *J. Chem. Phys.*, **33**, 418 (1960).
13) J. K. Wilmshurt, ibid., **33**, 813 (1960).
14) D. R. Lide, Jr., *Tetrahedron*, **17**, 125 (1962).

values have been obtained from microwave spectroscopic methods; they have been reported to be accurate to about ±0.005 Å. Some values not available from microwave spectroscopic methods involve larger experimental errors because they are not independent of some assumptions. Moreover, a small amount of uncertainity is also involved as a result of zero point vibrations, as the data pertain to the ground vibrational state and are not equilibrium bond lengths. A few values obtained from X-ray and electron diffraction data are accurate to only ±0.04 Å and require rectification by means of microwave spectroscopic methods.

It may be seen that the data of carbon-chlorine, carbon-bromine and carbon-iodine bond lengths confirm the earlier conclusions[4-6] that the bond lengths increase linearly with the increase in the number of adjacent bonds or atoms. This may easily be seen in Fig. 1, where the bond lengths

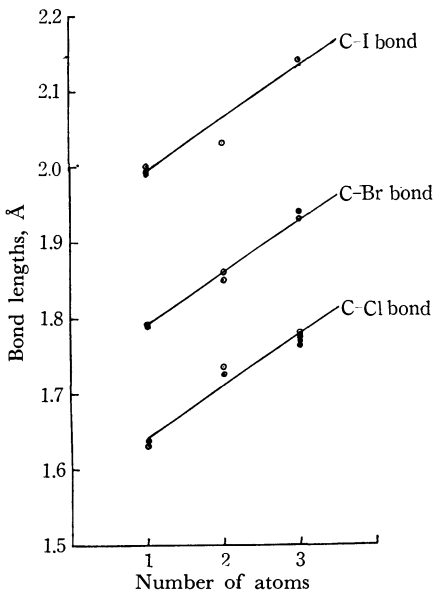

Fig. 1. A graph of carbon-chlorine, carbon-bromine and carbon-iodine bond lengths plotted against the number of adjacent atoms (or bonds).

are plotted against the number of adjacent bonds. In the figure all the bonds are equally well represented by lines with the slope of 0.070 n; i. e., all the lines are parallel. Most of the values for bond lengths lie within ±0.015 Å of the straight lines give by:

$$r(\text{C–Cl}) = 1.575 + 0.070\,n \quad (1)$$

$$r(\text{C–Br}) = 1.725 + 0.070\,n \quad (2)$$

$$r(\text{C–I}) = 1.925 + 0.070\,n \quad (3)$$

where n=1, 2 or 3.

Theory and Calculations

The properties of a bond depend upon the average number of electrons in it, their distribution among the molecular orbitals, and the concentration of the orbitals (as given by hybridization). Bond lengths are affected by changes in the hybridization of the orbitals forming the bond. Walsh[15] has pointed out that an increase in the s-character of the hybridization of carbon while passing from sp^3 to sp hybridization produces a stronger and shorter bond. Somayajulu[16] has shown that the strengths of the hybrid orbitals of carbon are in the order $sp > sp^2 > sp^3$; because stronger bonds are shorter, it is obvious that the radii of these orbitals will be in the order $sp^3 > sp^2 > sp$. Considering the CC "single bonds" it is evident from the accumulated structural data[6] that the best values for the lengths of the $\rangle$C-C$\langle$, $\rangle$C-C$\langle$ and ≡C-C≡ bonds are 1.534±0.005 Å, 1.472±0.005 Å and 1.378±0.005 Å respectively. If it is assumed that the $\rangle$C-C$\langle$, $\rangle$C-C$\langle$ and ≡C-C≡ bonds represent the tetrahedral (sp^3-sp^3) trigonal, (sp^2-sp^2) and digonal (sp-sp) bonds, we obtain for the radii of tetrahedral, trigonal and digonal carbon atoms the values of 0.767 Å, 0.736 Å and 0.689 Å respectively, which are very near to Lide's values (Ref. 14).

To account for the variation in carbon-chlorine, carbon-bromine and carbon-iodine bond lengths with the number of adjacent atoms or bonds, we have taken the covalent radii of chlorine, bromine and iodine to be 0.99, 1.14 and 1.33 Å respectively.[17] The values calculated for these bond lengths by the addition of the radii of hybrid orbitals of carbon and covalent radii of halogens and by applying of Schomaker-Stevensen correction[18] are given in Table I. Here the Schomaker-Stevensen coefficient has been given the value of 0.08.[17] It may be observed that in many instances the Schomaker-Stevensen correction gives a good agreement with the experimental values; in other instances, the additivity rule without this correction gives a better agreement. For example, the experimental values in ≡C-Cl, $\rangle$C-Br and ≡C-Br bands are fairly well reproduced by taking into account the Schomaker Stevensen correction, while in the case of $\rangle$C-Cl, $\rangle$C-Cl and $\rangle$C-Br bonds, the sum of the orbital radii gives a better agreement with the experimental values. It is not surprising that there are many exceptios to the Schomaker-Stevensen rule. In the case of carbon-iodine bonds, the Schomaker-Stevensen term becomes zero because the carbon and iodine have the same electronegativity value.

15) A. D. Walsh, *Trans. Faraday Soc.*, **43**, 60 (1947).
16) G. R. Somayajulu, *J. Chem. Phys.*, **28**, 814 (1958).
17) L. Pauling, "The Nature of the Chemical Bond," 3rd Ed., Cornell University Press, Ithaca, New York (1960).
18) V. Schomaker and D. P. Stevenson, *J. Am. Chem. Soc.*, **63**, 37 (1941).

TABLE I CARBON-CHLORINE, CARBON-BROMINE AND CARBON-IODINE BOND LENGTHS

Bond type	Sum of the orbital radii r_A+r_B Å	$r_A+r_B-0.08\lvert x_A-x_B\rvert$ Å	Obsd. length Å	Name of the substance	Formula	Method	Reference
$\rangle$C-Cl	1.757	1.717	1.781	Methyl chloride	CH_3Cl	MS	20
			1.78	Butyl chloride	$(CH_3)_3CCl$	MS	21,22
			1.778	Ethyl chloride	C_2H_5Cl	MS	23
			1.772	Methylene chloride	CH_2Cl_2	MS	24
			1.770	Trichloroacetonitrile	CCl_3CN	MS	22,25
			1.767	Chloroform	$CHCl_3$	MS	26,27
$>$C-Cl	1.726	1.686	1.726	Vinyl chloride	C_2H_3Cl	MS	28
			1.734	1,1-Dichlorocyclopropane	$C_3H_4Cl_2$	MS	29
≡C-Cl	1.679	1.639	1.630	Chlorocyanide	ClCN	MS	31
			1.637	Methylchloroacetylene	CH_3CCCl	MS	30
$\rangle$C-Br	1.907	1.883	1.940	Ethyl bromide	C_2H_5Br	MS	32
			1.94	Butyl bromide	$(CH_3)_3CBr$	MS	22
			1.939	Methyl bromide	CH_3Br	MS	20,33,34,35
			1.930	Bromoform	$CHBr_3$	MS	36,37
$>$C-Br	1.876	1.852	1.85	Vinylidene bromide	$C_2H_2Br_2$	ED	40
			1.86	Vinyl bromide	C_2H_3Br	ED	38,39,40
≡C-Br	1.829	1.805	1.789	Bromocyanide	BrCN	MS	41,42
			1.793	Methylbromoacetylene	CH_3CCBr	MS	43,44
$\rangle$C-I	2.097	2.097	2.14	Butyl iodide	$(CH_3)_3Cl$	MS	22
			2.139	Methyl iodide	CH_3I	MS	35,45
			2.139	Ethyl iodide	C_2H_5I	MS	46
$>$C-I	2.066	2.066	2.03	Vinyl iodide	C_2H_3I	ED	40
			2.03	Vinylidene iodide	$C_2H_2I_2$	ED	40
≡C-I	2.019	2.019	1.995	Iodocyanide	ICN	MS	41
			2.00	Iodocyanide		MS	47
			1.99	Methyliodoacetylene	CH_3CCl	MS	43

MS: Microwave spectroscopy ED: Electron Diffraction

20) W. Gordy, J. W. Simmons and A. G. Smith, *Phys. Rev.*, **74**, 243, 1246 (1948).
21) D. R. Lide and M. Jen, *J. Chem. Phys.* **38**, 1504 (1963).
22) J. Q. Williams and W. Gordy, ibid., **18**, 994 (1950).
23) R. S. Wagner and B. P. Dailey, ibid., **26**, 1588 (1957).
24) R. J. Myers and W. D. Gwinn, ibid., **20**, 1420 (1952).
25) J. G. Baker, D. R. Jenkins, C. N. Kenney and T. M. Sugden, *Trans. Faraday Soc.*, No, 419, **53**, part 11 (1957).
26) S. N. Ghosh, R. Trambarulo and W. Gordy, *J. Chem. Phys.*, **20**, 605 (1952).
27) R. R. Unterberger, R. Tramburalo and W. V. Smith, ibid., **18**, 565 (1950).
28) D. Kivelson, E. B. Wilson, Jr., and D. R. Lide, Jr., ibid., **32**, 205 (1960).
29) W. H. Flvgare, A. Narath and W. D. Gwinn, ibid., **36**, 200 (1962).
30) C. C. Costain, ibid., **23**, 2037 (1955).
31) A. G. Smith, H. Ring, W. V. Smith and W. Gordy, *Phys. Rev.*, **74**, 370 (1948).
32) R. S. Wagner, B. P. Dailey and N. Solimene, *J. Chem. Phys.*, **26**, 1993 (1957).
33) J. W. Simmons and W. E. Anderson, *Phys. Rev.*, **80**, 338 (1950).
34) J. W. Simmons and W. O. Swan, ibid., **80**, 289 (1950).
35) S. L. Miller, L. C. Aamodt, G. Dousmanis, C. H. Townes and J. Kraitchman, *J. Chem. Phys.*, **20**, 1112 (1952); *Phys. Rev.*, **82**, 327 (1952).
36) J. Sheridan and W. Gordy, *J. Chem. Phys.*, **20**, 591 (1952).
37) Q. Williams, T. Cox and W. Gordy, ibid., **20**, 1524 (1952).
38) J. A. C. Hugill, I. E. Coop, L. E. Sutton, *Trans. Faraday Soc.*, **34**, 1525 (1938).
39) H. W. Thompson, P. Torkington, *Proc. Roy. Soc.* (*A*), **21**, 184 (1945).
40) Z. G. Pinsker, "Electron Diffraction," Butterworths Scientific Publications, London (1953), p. 343.
41) A. G. Smith, H. Ring, W. V. Smith and W. Gordy, *Phys. Rev.*, **74**, 370 (1948).
42) C. H. Townes, A. N. Holden and F. R. Meritt, ibid., **74**, 1113 (1948).
43) J. Sheridan and W. Gordy, *J. Chem. Phys.*, **20**, 735 (1952).
44) J. Sheridan and W. Gordy, *Phys. Rev.*, **79**, 224 (1950).
45) J. W. Simmons and W. E. Anderson, ibid., **80**, 338 (1950).
46) T. Kasuya and T. Oka, *J. Phys. Soc. Japan*, **15**, 296 (1960).
47) W. Gordy, W. V. Smith, A. G. Smith and H. Ring, *Phys. Rev.*, **72**, 259 (1947).

Discussion

It may be seen from the table that the bond lengths for a given bond environment in different molecules vary slightly. This slight variation in the carbon-chlorine and carbon-bromine bond lengths for a given bond environment in different molecules may be explained on the basis of the effect of an electronegative atom attached to the carbon atom which induces partial double-dond characters in other bonds formed by the carbon atom. It has been observed that the carbon-chlorine bond distance in $C_2H_2Cl_2$ is less than that in CH_3Cl, and that this bond distance in $CHCl_3$ is less than that in $C_2H_2Cl_2$. Brockway[19] has attributed this difference to the effect of the double-bond character of one carbon-chlorine bond induced by the partial ionic character of another carbon-chlorine bond formed by the same carbon atom. This effect of the induction of a double-bond character by the partial ionic character of another bond is much more important for fluorine-substituted molecules than for molecules containing chlorine, bromine or iodine. This is partially due to the well-known fact that the C–F bond has a larger ionic character than the other carbon-halogen bonds. This well-known shortening of carbon-fluorine bond lengths upon the addition of F-atoms is a different phenomenon and is often larger than the shortening of carbon-fluorine bond lengths with the number of adjacent atoms or bonds. Therefore, we have not included the carbon-fluorine bonds in this study.

We wish to express our most sincere gratitude to Professor Krishnaji for his kind supervision of the work. The financial assistance from the National Bureau of Standards, U. S. A., is also thankfully acknowledged.

19) L. O. Brockway, *J. Phys. Chem.*, **41**, 185 (1937).

BULLETIN OF THE CHEMICAL SOCIETY OF JAPAN VOL. 39 1857—1861 (1966)

Molecular Vibrations and Structures of Polyalkyl Polysulfides. I. Polymethylene Disulfide

By Michiro HAYASHI, Yuji SHIRO and Hiromu MURATA

Department of Chemistry, Faculty of Science, Hiroshima University, Higashisenda-machi, Hiroshima

(Received December 4, 1965)

The polarized infrared spectra of oriented sheets of polymethylene disulfide were measured in the 4000—200 cm^{-1} region, and the fiber period was found to be 4.18 Å by X-ray diffraction. It was found that this polymer does not have the expected twofold symmetry axes intersecting the helical axis at right angles. The infrared active normal vibrations of two likely structural models were calculated by the use of a modified Urey-Bradley force field. The structure of polymethylene disulfide was concluded to be the GG'G conformation along the sequence of the $-S-CH_2-S-S-$ bonds of the 2_1 helical model.

Polyalkyl polysulfides $[(CH_2)_lS_m]_n$ are synthetic rubbers; one of them ($l=2$ and $m=4$) is commercially well known as Thiokol A. The present paper, the first of a series of reports on polyalkyl polysulfides, will deal with the molecular vibrations and the structure of polymethylene disulfide.

No studies have yet been reported on the molecular vibration and the structure of this substance. We therefore measured the polarized infrared spectra of an oriented sheet in the 4000—200 cm^{-1} region with a Perkin-Elmer 12C spectrometer. The fiber period of this substance was also measured by the X-ray diffraction method. The infrared active normal vibrations were calculated by the use of a modified Urey-Bradley force field, with the force constants transferred from the set obtained for simpler molecules with similar structures which we will report on separately.[1)]

Experimental

The sample was prepared by the reaction of dichloromethylene and an aqueous solution of sodium disulfide, using magnesium hydroxide as an emulsifying agent. About three times as much sodium disulfide as was really needed was used in order to prepare high-molecular-weight samples. The reaction products were purified by continuous extraction with absolute alcohol, so that impurities and lower-molecular-weight polymers were washed out. Solid sheets were prepared by

1) M. Hayashi, Y. Shiro and H. Murata, to be published.

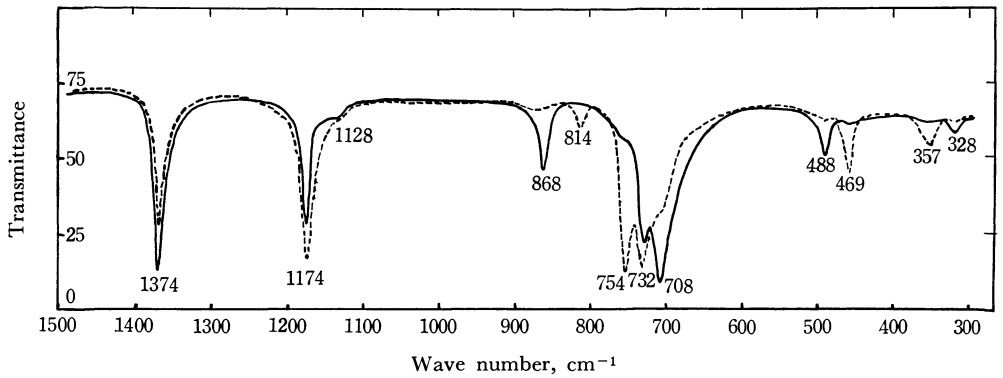

Fig. 1. Polarized infrared spectra of oriented film of polymethylene disulfide.
The solid curve was measured with the electric vector perpendicular and the broken curve with the electric vector parallel to the direction of orientation.

TABLE I. OBSERVED AND CALCULATED FREQUENCIES OF POLYMETHYLENE DISULFIDE (cm^{-1})

Observed*1	Calculated GG'G*2	Calculated TGG*3	Assignment*4
	A species		
2980 m	2968	2969	CH_2 str.
2920 m	2896	2896	CH_2 sym. str.
1374 s	1369	1366	CH_2 scissor.
1174 s	1204	1210	CH_2 wag.
1128 sh	1118	1122	CH_2 twist.
814 w //	783	785	CH_2 rock.
754 s //	715	720	CS asym. str.
732 s	655	669	CS sym. str. (85), SCS def. (14)
469 m //	475	510	SS str. (90),
357 m //	358	338	SCS def. (46), CSS sym. def. (41)
	240	254	CSS asym. def. (45), SCS def. (32)
	166	177	CSS asym. def. (68). SCS def. (18)
	96	115	SS torsion (74), CS torsion (21)
	B species	E species*5	
2980 m	2968	2968	CH str.
2929 m	2896	2896	CH str.
1374 s	1368	1366	CH_2 scissor.
1174 s	1204	1209	CH_2 wag.
1128 sh	119	1121	CH_2 twist.
868 m ∠	781	787	CH_2 rock.
732 s	714	721	CS asym. str.
708 s ∠	664	673	CS sym. str. (84), SCS def. (15)
488 w ∠	487	514	SS str. (90)
328 w ∠	339	320	SCS def. (43), CSS asym. def. (38)
	259	245	CSS asym. def. (38), SCS def. (30)
	115	167	CSS sym. def. (78), SCS def. (18)
	49	111	CS torsion (64)
		13*6	

*1 The dichroism is shown as // and ∠ only for the infrared bands which exhibit clearly.
*2 The helical model is taken as 2_1.
*3 The helical model is taken as 4_1.
*4 Diagonal elements of potential energy distributions of the structural model GG'G are given in parentheses for mixed vibrations. (%)
*5 The phase differences are 180° for the B species of the GG'G form and 90° for the E species of the TGG form.
*6 The corresponding frequency is absent for GG'G since the phase difference is 180° for this case.

hot pressing, and then they were uniaxially oriented. The fiber period of the sample was determined to be 4.17 Å from the first and second horizontal layer lines on an X-ray rotation photograph. The orientation of the solid sheets was not, however, high enough for us to obtain more detailed information. The polarized infrared spectra were observed to be as shown in Fig. 1 and Table I.

Discussion

There are three internal rotation angles per chemical unit of polymethylene disulfide $[CH_2SS]_n$, one around the C–S bond and the other two around the C–S bonds. If we may assume that every chemical unit has the same structure, one set of these internal rotation angles is sufficient for specifying the structure of the entire helical polymer. Experimental data for simpler molecules, such as sulfur monochloride[2] and dimethyl disulfide[3], indicate that the only stable conformation for the S–S bond is the gauche form, with the internal rotation angle of 90°. On the other hand, for the C–S bonds, there are three stable forms, as evidenced by the experimental data for simpler molecules such as methyl ethyl sulfide.[4] These are the trans (the internal rotation angle of ca. 180°) and the two gauche conformations (ca. ±60°).

We will hereafter use symbols such as TGG for the models of the helical polymer, according to the system of notation used by Miyazawa et al.[5] For example, TGG implies that the internal rotation conformations along the series of –S–CH_2–S–S– bonds are trans, gauche and gauche. The two gauche conformations which are obtained by clockwise and counterclockwise 60° rotations from the cis form are denoted as G and G′ respectively, while the rotation around the S–S bond is conventionally fixed as G (the internal rotation angle of 90°) throughout the treatment.

As Table II shows, there are six different possible helical conformations. In the same table are shown the expected fiber periods, the twofold symmetry properties, the number of repeating units, and the number of helical turns per fiber period. Two conformations, TTG and GGG, may be discarded, however, since the expected fiber periods are too much longer than the experimental value of 4.17 Å.

The fiber period of the TG′G conformation is calculated to be much longer than the measured value and to be a highly distorted structure. Therefore, this conformation may well be discarded also. As for the molecular vibrations of this substance, it is expected that, in general, there are twenty-six or twenty-seven infrared active vibrations, which may be classified into two different groups (the groups belonging to the A and E species, or to the A and B species, respectively).[5]

There are fourteen pairs of degenerate vibrations belonging to the E species for the TGG structural model. For the G′G′G and GG′G models, there are thirteen non-degenerate B vibrations (with a phase difference of $\delta=180°$) since these models are 2_1 helices. The bands due to these E or B vibrations exhibit a perpendicular dichroism.

On the other hand, the thirteen vibrations due to the A species exhibit parallel dichroism. However, if the conformation has twofold symmetry axes intersecting the helical axis at right angles, the vibrations belonging to the A species may be classified into two groups, A_1 and A_2, and the vibrations belonging to the A_1 species become infrared-inactive. There will then be seven A_1 and six A_2 vibrations.

As for the S–S stretching mode, there are, in general, one A vibration and one pair of E vibrations. If twofold symmetry axes exist, this A vibration belongs to the A_1 species and, hence, is infrared-inactive.

As is shown in Fig. 1 and Table I, however, we have observed two infrared bands around 470 cm^{-1} which can easily be assigned to the S–S stretching mode on the basis of the assignments given to simpler molecules, and also on the basis of the normal vibration calculations (to be described later). Since we expect no other vibration in this region, the above assignments of the observed infrared bands are reliable. The band at 488 cm^{-1} exhibits a perpendicular dichroism; it may be assigned to the E vibrations. On the other hand, the band at 469 cm^{-1} exhibits a parallel dichroism; it may be assigned to the A vibration.

As for the C–S stretching modes, we have two A vibrations and two pairs of E vibrations. If twofold symmetry axes exist, one of the two A vibrations belongs to the A_1 species and, hence, becomes infrared-inactive. In the expected region, we have observed three bands, at 754, 732 708 cm^{-1}. The band at 708 cm^{-1} clearly exhibits a perpendicular dichroism, but the band at 754 cm^{-1} clearly exhibits a parallel dichroism. Therefore, we may assign them to the E and A vibrations respectively. The band at 732 cm^{-1} also exhibits a parallel dichroism, but this band appears also to have a perpendicular component which shows up as a shoulder of the band at 708 cm^{-1} when the electric vector is perpendicular to the direction of orientation. Therefore, we may assign the band at 732 cm^{-1} to the A vibration, which is overlapped by the E vibrations. This assignment is also supported by the results of the normal vibration calculations.

2) E. Hirota, This Bulletin, **31**, 130 (1958).
3) M. Hayashi, *J. Chem. Soc. Japan, Pure Chem. Sect. (Nippon Kagaku Zassi)*, **78**, 101 (1958).
4) M. Hayashi, T. Shimanouchi and S. Mizushima, *J. Chem. Phys.*, **26**, 608 (1957).
5) T. Miyazawa, ibid., **35**, 693 (1961); *J. Polymer Sci.*, **55**, 214 (1961).
T. Miyazawa, K. Fukushima and Y. Ideguchi, *J. Chem. Phys.*, **37**, 764 (1962), ibid., **38**, 2709 (1963).

TABLE II. STRUCTURAL MODELS OF POLYMETHYLENE DISULFIDE

Model	Internal rotation axes			Twofold symmetry axis*3	Expected fiber period	$m_{/l}$*4
	S–C*1	C–S*1	S–S*1			
TTG	T	T	G	present	12 A	3_1
TGG	T	G	G	absent	4.18 A	4_1
TG'G	T	G'	G	absent	6.8 A	2_1
GGG	G	G	G	present	16 A	5_4
G'G'G	G'	G'	G	present	4 A	2_1
GG'G	G	G'	G	absent	4.18 A	2_1

*1 T, G and G' denote the internal rotation angles of 180°, 60° and −60°, respectively.
*2 G denotes the internal rotation angles of 90°.
*3 Twofold symmetry axes intersecting the helical axis as right angles.
*4 m: the number of repeating units per fiber period.
n: the number of helical turns per fiber period.

TABLE III. THE FORCE CONSTANTS ($F' = -0.1F$)

		(in md./Å)			
K(CH)	4.28	H(CSS)	0.15	F(CSS)	0.25
K(CS)	1.69	H(SCS)	0.15	F(SCS)	0.5
K(SS)	2.37	H(HCS)	0.15	F(HCS)	0.39
p(CH)	−0.13	H(HCH)	0.32	F(HCH)	0.2
		(in md./Å)			
$\kappa(CH_2)$	0.0	$l(CH_2)$	−0.01	Y(CS)	0.054
Y(SS)	0.147	t	0.07	g	−0.05

p: CH bond streching interaction constant.
l: angle interaction constants between SCH.
Y: torsional constants.
t, g: trans and gauche angle interaction constants between SCH and CSS.

As for the SCS skeletal deformation mode, there is one A vibration, plus one pair of E vibrations. If twofold symmetry axes exist, this A vibration belongs to the A_1 species and, hence, becomes infrared-inactive. However, we have observed in the expected region the bands at 357 and 328 cm^{-1}, which exhibit a parallel and a perpendicular dichroism respectively.

The observation of the parallel bands due to the S–S stretching and SCS deformation vibrations indicates that the helical conformation of polymethylene disulfide does not have twofold symmetry axes intersecting the helical axis at right angles; we may therefore discard three structural models, TTG, GGG and G'G'G. Since TG'G has already been discarded, TGG and GG'G remain as the possible structural models for this substance. GG'G is a 2_1 helical model. Although TGG has two possibilities, 4_1 and 5_1, we think that the 4_1 helix is the most possible model because we have no example of 5_1 helices for other polymers. The values of the internal rotation angles were calculated so as to reproduce the measured fiber period. Two sets of values (195°, 70°, 90°, and 68°, −68°, 90°) were obtained for TGG and GG'G respectively on the assumption of the values of the bond lengths of r(C–S) = 1.81 Å and r(S–S) = 2.08 Å, and the valency angles of α(CSS) = 105° and α(SCS) = 109°28'.

We have also attempted to calculate the normal vibrations in order to confirm the assignments of the observed infrared bands, and also in order to examine whch structural model is more likely, TGG or GG'G.

For the calculation of the inverse kinetic energy matrix, values of r (C–H) = 1.09 Å and α(HCH) = 109°28' were used besides the molecular parameters described for TGG and GG'G structural models. For the potencial energy matrix, a modified Urey-Bradley force field was used. This force field includes the same modifications as those used for simpler molecules such as dithiamethyl methane.[1] The modification terms are: (1) the torsional terms with the force constants Y; (2) the C–H bond interaction terms with the force constants p; (3) the angle interaction terms between the SCH angles with the force constants l, and (4) the angle interaction terms between the HCS and CSS angles with the force constants t and g. The last terms are the same type of correction terms as the trans and gauche interaction terms of the $-CH_2-CH_2-$ groups. For pairs of H and S atoms in the trans and gauche forms in the $-H_2CSS-$ group, the force constants t and g are used respectively. The force constants were all transferred from the set obtained for such simpler molecules as dimethyl disulfide and dithiamethyl methane.[1] They are listed in Table III. The method developed by

Miyazawa et al.[5] was used for the calculation. The results are shown in Table I.

First, it was found that the calculated frequencies agree satisfactorily with the observed frequencies in the higher frequency region. Second, significant differences are seen between the calculated low frequncies for the two possible structural models. For the S–S stretching vibrations, the calculated frequencies are 510 and 514 cm^{-1} for TGG, but they are 475 and 485 cm^{-1} for GG'G, while the observed frequencies are 469 and 488 cm^{-1}. The frequency agreements are much better for the GG'G model in their absolute values and also in the splitting of the A and E components. The same conclusion may be drawn from the analysis of one of the skeletal deformation modes and the C–S stretching modes. For other vibrations, such as the CH_2 deformation and C–H stretching modes, we did not find any essential differences between the different structual models.

Therefore, we may conclude that the polymethylene disulfide chain most probably has the 2_1 helical conformation of the GG'G type.

The assignments of the observed infrared bands are shown in Table I, together with the potential energy distributions.

For such other polymers as polyoxymethylene, the structural model, GG'G, has not been taken into consideration because of the intrachain steric impact.[6] It should be noted, however, that the situation is somewhat different for the polymethylene disulfide chain. The GG'G model is possible for this polymer because of the long bond lengths, r(S–S) and r(S–C), which tend to relax such steric impact.

The authers wish to express their gratitude to Professor Masamichi Tsuboi, Dr. Akiko Y. Hirakawa and Dr. Yoshimasa Kyogoku of the University of Tokyo for the use of their infrared spectrometer, and Mr. Tohoru Chiba of the Toho Rayon Company for his X-ray diffraction analysis. We also wish to thank Professor Tatsuo Miyazawa of the Institute for Protein Research, Osaka University, for his encouragement and invaluable advice throughout this work.

6) T. Shimanouchi, *Kobunshi (High Polymers, Japan)*, **13**, 954 (1964).

BULLETIN OF THE CHEMICAL SOCIETY OF JAPAN VOL. 39 1861—1866 (1966)

Molecular Vibrations and Structures of Polyalkyl Polysulfides. II. Polyethylene Disulfide

By Michiro HAYASHI, Yuji SHIRO and Hiromu MURATA

Department of Chemistry, Faculty of Science, Hiroshima University, Higashisenda-machi, Hiroshima

(Received December 4, 1965)

The polarized infrared spectra of oriented sheets of polyethylene disulfide were measured in the 4000—200 cm^{-1} region; the fiber period was thus found to be 8.8 Å by X-ray diffraction. It is found that this polymer does not have twofold symmetry axes intersecting the helical axis at right angles. The infrared-active normal vibrations of the four likely structural models were calculated by the use of a modified Urey-Bradley force field. The structure of polyethylene disulfide was concluded to be the GGG'G conformation along the sequence of the $-S-CH_2-CH_2-S-S-$ bonds of the 3_1 helical model. This model is very similar to the structure of polymethylene disulfide reported in the previous paper. The above structure was then discussed in comparison with two models proposed previously (J. R. Katz, *Trans. Faraday Soc.*, **32**, 77 (1936); Y. Minoura, *J. Soc. Rubber Ind. Japan*, **28**, 399 (1955)).

In the previous paper,[1] we have reported on the molecular vibrations and the structure of polymethylene disulfide. As a continuation of the researches, we will deal with the molecular vibrations and the structure of polyethylene disulfide in the present paper. This is the second of a series of papers on polyalkyl polysulfides.

For polyethylene disulfide, Katz[2] reported the results of X-ray studies and proposed a structural model. Minoura,[3] in discussing the structure of this substance, found that the structural model proposed by Katz is not unique, but that several different structural models possibly have the measured fiber period.

1) M. Hayashi, T. Shiro and H. Murata, This Bulletin, **39**, 1857 (1966).

2) J. R. Katz, *Trans. Faraday Soc.*, **32**, 77 (1936).

3) Y. Minoura, *J. Chem. Soc. Japan, Pure Chem. Sect. (Nippon Kagaku Zassi)*, **73**, 244 (1952); **75**, 869 (1954); *J. Soc. Rubber Ind. Japan*, **28**, 399 (1955).

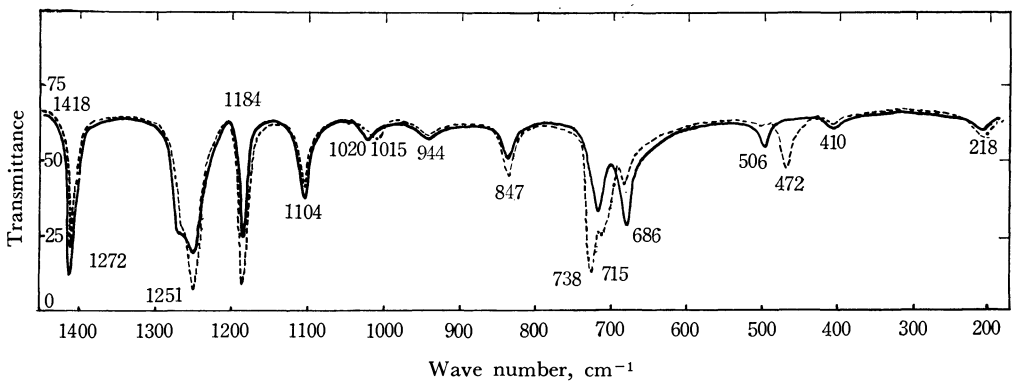

Fig. 1. Polarized infrared spectra of oriented film of polyethylene disulfide. The solid curve was measured with the electric vector perpendicular and the broken curve with the electric vector parallel to the direction of orientation.

We have measured the polarized infrared spectra of oriented sheets and have also remeasured the fiber period by X-ray diffraction. The infrared-active normal vibrations were calculated by the use of a modified Urey-Bradley force field, with the force constants transferred from the set obtained for simpler molecules with similar structures.[4]

Experimental

The sample used for the measurements was prepared by the reaction of 1, 2-dichloroethane and an aqueous solution of sodium disulfide, using magnesium hydroxide as an emulsifying agent. About a three-fold excess of sodium disulfide was used in order to obtain high-molecular-weight samples. The products were purified by continuous extraction with absolute alcohol; impurities and lower-molecular-weight polymers were thus washed out. The sheets were prepared by hot pressing and were subsequently uniaxially-oriented. The fiber period of the sample was measured as 8.8 Å on the X-ray rotation photograph; this value is in good agreement with the value reported previously.[2] The orientation of the solid sheets was not high enough for us to obtain more detailed information from the X-ray studies. The polarized infrared spectra of the oriented sheet were measured by a Perkin-Elmer 12C spectrometer; the results are shown in Fig. 1.

Discussion

There are four internal rotation angles per chemical unit of polyethylene disulfide $[-CH_2CH_2-SS-]_n$; one around the C–C bond, one around the S–S bond, and two around the two C–S bonds. As was described in the first paper of this series, the set of those four angles is sufficient to enable us to specify the structure of the entire helical polymer. As evidenced by the experimental data for simpler molecules,[5] there are three possible internal rotaion conformations around the C–C bond or the two C–S bonds, namely, the trans (180°) and the two gauche conformations (±60°), while the internal rotation angle around the S–S bond will be around 90°.

As in the previous paper, we will hereafter denote the structural models. For example, GTG'G is the structural model which consists of the gauche (60°), the trans (180°), the gauche prime (−60°) and the gauche (90°) internal rotation conformations along the sequence of the $-S-CH_2-CH_2-S-S-$ bonds. The angle around the S–S bond was fixed at 90° throughout the treatment.

As for molecular vibrations, it may be expected that, in general, there are twenty-two infrared active vibrations belonging to the A species. If the structural model has twofold symmetry axes intersecting the helical axis at right angles, these A vibrations can be classified into two groups (A_1 and A_2 species). We may expect a parallel dichroism for those vibrations, although the vibrations belonging to the A_1 species are infrared-inactive.

We have twenty-three pairs of degenerate vibrations belonging to the E species which exhibit a perpendicular dichroism. For 2_1 helical models, there are twenty-two B vibrations (with the phase difference of 180°) which give rise to perpendicular bands.

As for the S–S stretching mode, there is one A vibration and one pair of E vibrations. If twofold symmetry axes exist, the A vibration belongs to the A_1 species and, hence, becomes infrared-inactive. From the experimental data for such simpler molecules as dimethyl disulfide, we would expect, in the 500 cm^{-1} region, the bands due to

4) M. Hayashi, Y. Shiro, T. Oshima and H. Murata, This Bulletin, **38**, 1734 (1965); M, Hayashi, Y. Shiro, M. Murakami and H. Murata, ibid., **38**, 1740 (1965); M. Hayashi, Y. Shiro and H. Murata, ibid., **39**, 118 (1966).

5) E. Hirota, ibid., **31**, 130 (1958); M. Hayashi, *J. Chem. Soc. Japan, Pure Chem. Sect. (Nippon Kagaku Zassi)*, **78**, 101 (1958); M. Hayashi, T. Shimanouchi and S. Mizushima, *J. Chem. Phys.*, **26**, 608 (1957).

TABLE I. STRUCTURAL MODELS OF POLYETHYLENE DISULFIDE WITHOUT TWOFOLD SYMMETRY AXES INTERSECTING THE HELICAL AXIS AT THE RIGHT ANGLES

Model	Internal rotation axes*				Expected fiber period (Å)	m_n**
	S-C	C-C	C-S	S-S		
TTGG	T	T	G	G	8.8	2_1
TGGG	T	G	G	G	8.8	3_1
TG'G'G	T	G'	G'	G	6.5	3_1
TG'GG	T	G'	G	G	6.6	3_1
GTG'G	G	T	G'	G	8.8	4_1
GGG'G	G	G	G'	G	8.8	3_1
GG'G'G	G	G'	G'	G	2.0	2_1

* T, G and G' mean the internal rotation angles of 180°, 60° and −60°, respectively except for the angles around the S-S bond which are 90°.

** m: the number of repeating units per fiber period.
n: the number of helical turns per fiber period.

TABLE II. THE FORCE CONSTANTS ($F' = -0.1F$)

(md./Å)

K(C-H)	4.329	H(CSS)	0.15	F(CSS)	0.25
K(C-S)	1.8	H(HCS)	0.294	F(CSS)	0.192
K(S-S)	2.37	H(HCH)	0.331	F(HCH)	0.2
K(C-C)	2.2	H(CCS)	0.052	F(CCS)	0.056
P(CH)	−0.13	H(HCC)	0.156	F(HCC)	0.459

(md. Å)

Y(CS)	0.052	Y(SS)	0.147	Y(CC)	0.15
$\kappa(CH_2)$	0.058	$l(CH_2)$	0.057	t	0.136
g	−0.051				

P: CH bond stretching interaction constant.
l: angle interaction constants of CH_2 group.
Y: torsion constants.
t, g: trans and gauche angle interaction constants for the CH_2-CH_2 groups.

the S-S stretching modes, but no other bands. As is shown in Fig. 1 and Table III, we have observed two infrared bands, at 506 and 472 cm^{-1}, which exhibit a perpendicular and a parallel dichroism respectively. This indicates that the molecular conformation of this substance does not have twofold symmetry axes intersecting the helical axis at right angles.

In Table I, we have listed seven possible structural models (without twofold symmetry axes) and the expected fiber periods. Of these structural models, we may discard two of them (TG'G'G and TG'GG) since their expected fiber periods are quite different from the observed values. The GG'G'G conformation is not a likely model either, since, for this conformation, the steric hindrance is very large.

Four structural models (TTGG, TGGG, GTG'G and GGG'G) remain as the 2_1, 3_1, 4_1 and 3_1 helical conformations respectively. The values of internal rotation angles were calculated so as to reproduce the measured fiber periods.

By the use of the bond length values of r(S-S)= 2.08 Å, r(C-S)=1.81 Å, and r(C-C)=1.54 Å, and the valency angles of α(CSS)=105° and α(SCC)= 112°, the sets of internal rotation angles, (165°, 170°, 52.6°, 90°), (166°, 63°, 52°, 90°), (73°, 196°, −73°, 90°) and (71°, 68,° −71°, 90°) were obtained for TTGG, TGGG GTG'G and GGG'G respectively. The first two structural models have trans and gauche C-S bonds, but the last two have gauche and gauche prime C-S bonds. As for the C-C bond, the first and third model are in the trans form, while the second and last are in the gauche form.

It is well-known that the CH_2 rocking frequencies of the $-CH_2CH_2-$ groups exhibit frequency differences characteristic of the conformation around the C-C bond. For example, in the case of 1, 2-dithiamethyl ethane, the frequency differences for the trans and gauche isomers are found to be 271 cm^{-1} and 118 cm^{-1} respectively. The difference for the trans isomer is always found to be much larger than for the gauche isomer.

For polyethylene disulfide, we may expect four infrared bands due to the CH_2 rocking modes, that is, two parallel bands belonging to the A species and two perpendicular bands belonging to the E species. Judging from the results of the normal vibration calculation, the bands belonging to the E species are possibly overlapped with the bands belonging to the A species for any

TABLE III. OBSERVED AND CALCULATED FREQUENCIES OF POLYETHYLENE DISULFIDE (cm^{-1})

Observed*1	A species Calculated				Assignment*3
	TTGG*2	TGGG*2	GTG'G*2	GGG'G*2	
2980 s	2975	2972	2975	2972	CH str.
2980 s	2964	2968	2964	2967	CH str.
2920 vs	2929	2925	2929	2925	CH str.
2920 vs	2908	2911	2908	2911	CH str.
1418 s	1427	1427	1428	1427	CH_2 scissor.
1418 s	1424	1426	1424	1426	CH_2 scissor.
1272 s	1287	1301	1287	1301	CH_2 wag. (83), CH_2 scissor. (13)
1251 vs	1286	1290	1286	1291	CH_2 wag. (63), CH_2 twist. (22)
1184 s	1196	1168	1195	1167	CH_2 twist. (67), CH_2 wag. (12)
1104 m	1160	1139	1160	1140	CH_2 twist. (75), CH_2 wag. (12)
1015 w//	1038	1035	1042	1029	CC str. (54), CH_2 rock. (28)
944 vw	988	955	978	950	CH_2 rock. (63), CC str. (18)
847 m	733	868	721	872	CH_2 rock. (73), CH_2 wag. (11)
738 s //	702	664	715	666	CS asym. str.
686 m	691	641	692	646	CS sym. str.
472 m//	515	508	458	475	SS str.
410 vw	351	404	337	398	SCC asym. def. (62), CH_2 rock. (17)
	255	343	297	290	CCS asym. def. (36), CC torsion (28)
218 w	182	191	217	245	CSS syn. def. (69), CC torsion (10)
	113	147	163	193	CC torsion (47), CSS asym. def. (30)
	94	118	61	50	SS torsion (47), CC torsion (14)
	64	84	52	27	CS torsion

Observed*1	Calculated B species		E species		Assignment*3
	TTGG*2	TGGG*2	GTG'G*2	GGG'G*2	
2980 s	2975	2971	2975	2971	CH str.
2980 s	2963	2965	2964	2966	CH str.
2920 vs	2929	2919	2929	2918	CH str.
2920 vs	2908	2908	2909	2909	CH str.
1418 s	1427	1428	1428	1427	CH_2 scissor.
1418 s	1424	1427	1424	1426	CH_2 scissor.
1272 s	1287	1300	1288	1300	CH_2 wag. (85), CH_2 scissor. (11)
1251 vs	1286	1294	1285	1295	CH_2 wag. (66), CH_2 twist. (14)
1184 s	1196	1169	1198	1168	CH_2 twist. (63), CH_2 wag. (21)
1104 m	1160	1138	1164	1139	CH_2 twist. (78), CH_2 wag. (13)
1020 w∠	1038	1032	1043	1032	CC str. (56), CH_2 rock. (31)
944 vw	986	960	981	963	CH_2 rock. (65), CC str. (14)
847 m	735	869	721	870	CH_2 rock. (78)
715 sh∠	703	667	718	668	CS asym. str.
686 m	694	640	696	642	CS sym. str.
506 w∠	514	520	482	495	SS str. (92)
410 vw	319	420	351	420	SCC asym. def. (58), CSS sym. def. (10)
	263	326	279	278	CCS asym. def. (31), CC torsion (18)
218 w	195	208	242	218	CSS def. (53), SS torsion (10)
	174	195	151	140	CC torsion (30), SS torsion (18)
	107	106	93	85	SS torsion (58), CC torsion (23)
	79	43	72	60	CS torsion (41), SS torsion (10)
	—*4	29	43	18	CS torsion (53), SS torsion (15)

*1 The dichroism is shown as // and ∠ only for the infrared bands which exhibit clearly.
*2 The helical models are 2_1 for TTGG, 3_1 for TGGG and GGG'G.
*3 Diagonal elements of potential energy distributions of the structural model GGG'G are added in parentheses for mixed vibrrations. (%)
*4 This frequency is not existing since the phase difference is 180° for this model.

structural models, so that the dichroism of the band may not be expected to be high for the CH_2 rocking bands. In the region from 1050 to 700 cm^{-1}, we have observed seven infrared bands, at 1020, 1015, 944, 847, 738, 715 and 680 cm^{-1}. In the higher-frequency part of the region, we may also expect C–C stretching frequencies, while in the lower-frequency part of the region, we may also expect C–S stretching frequencies. Since we found C–C stretching frequncies around 1020 cm^{-1} for simpler molecules, such as 1, 2-ethanedithiol and 1, 2-dithiamethyl ethane, we may possibly assign the bands at 1020 and 1015 cm^{-1} to the C–C stretching frequencies. The band at 1020 cm^{-1} exhibits a highly perpendicular dichroism and so is assigned to the E species, whereas the band at 1015 cm^{-1} exhibits a highly parallel dichroism and is assigned to the A species.

We assign the band at 680 cm^{-1} to one of the C–S stretching frequencies, since this frequency is too low for the CH_2 rocking frequencies in comparison with the assignments given to simpler molecules. Since in no case are the C–S stretching frequencies higher than 750 cm^{-1}, we may assign the bands at 738 and 715 cm^{-1} to the C–S stretching frequencies also. We may assign the bands at 944 and 847 cm^{-1} to the overlapped CH_2 rocking frequencies. Their frequency difference is as great as 97 cm^{-1}, which is nearly equal to that for the gauche isomer of 1, 2-dithiamethyl ethane, This indicates that the conformation around the C–C bond of polyethylene disulfide is gauche; hence, the structural models TTGG and GTG'G may be eliminated from consideration.

We have calculated the infrared-active normal vibrations in order to confirm the assignments of the observed infrared bands, and also in order to examine which structural model is preferable, TGGG or GGG'G.

For the calculation of the inverse kinetic energy matrix, the bond length of $r(C–H)=109$ Å and the valency angle of $\alpha(HCH)=109°28'$ were used, besides the molecular parameters described above for TTGG, TGGG, GTG'G and GGG'G structural models. For the potential energy matrix, a modified Urey-Bradley force field was used. This force field includes the same modifications as were used for such simpler molecules as 1, 2-ethanedithiol and 1, 2-dithiamethyl ethane.[4] These modifications are: (1) torsional terms with the force constants Y, (2) C–H bond interaction terms with the force constants p, (3) angle interaction terms between the angles of one CH_2 group with the force constants, l, and (4) angle interaction terms between the angles of the CH_2–CH_2 group with the force constants t and g, which are usually called the trans and the gauche interaction terms.

The force constants were all transferred from the set obtained for simpler molecules. They are listed in Table II, while results are shown in Table III. The method developed by Miyazawa et al.[6] was used in the calculations.

First, from the calculation, it was found that the frequencies of the A and E vibrations due to the common vibrational modes, nearly coinciding except for the S–S stretching mode, some of the skeletal bending modes, and some of the torsional modes. Second, the calculated frequencies above 1000 cm^{-1} are not appreciably affected by the structural models, and the agreements between the observed and calculated frequencies are satisfactory for all structural models in this region. Third, the frequency differences of the two CH_2 rocking vibrations belonging to the same species exhibit behavior similar to that of simpler molecules; the trans conformation around the C–C bond produces a much larger frequency difference than that for the gauche conformation. From this reason too, as we have described before, we may discard the TTGG and GTG'G structural models from consideration.

Fourth, we found an appreciable frequency difference in the S–S stretching vibrations belonging to the A and E species for GTG'G and GGG'G, while the difference is very small for TTGG and TGGG. The observed S–S stretching frequencies and the difference in their A and E vibrations agree with the calculated frequencies of GTG'G and GGG'G much better than do the other models.

Furthermore, we found that the difference in the observed and the calculated frequencies of the CCS deformation vibration is much larger for the trans conformation of the C–C bond than that for the gauche conformation.

Therefore, we may conclude that the conformations of the –S–CH_2–CH_2–S–S– bond sequence are gauche, gacuhe, gauche prime and gauche; that is, the structural model of polyethylene disulfide is most probably the 3_1 helical model of the GGG'G type.

It may be seen in Table III that the calculated frequencies of two C–S stretching vibrations of both the A and E species do not agree very well with the observed frequencies. However, in previous papers on the vibrational assignments of such simpler molecules as 1, 2-dithiamethyl ethane, we have already pointed out that the calculated frequency differences of the two C–S stretching vibrations are much smaller than those of the observed values. We have concluded that this is due to imperfections in the force field; we therefore wish to modify the force field if sufficient observed data become available. In polyethylene disulfide

6) T. Miyazawa, *J. Chem. Phys.*, **35**, 693 (1961); *J. Polymer Sci.*, **55**, 214 (1961); T. Miyazawa, K. Fukushima and Y. Ideguchi, *J. Chem. Phys.*, **37**, 764 (1962); ibid., **38**, 2709 (1963).

also, we see a similar situation. The assignments of the observed infrared bands are shown in Table III, together with the potential energy distributions.

Such structural models as GGG'G have not been taken up for other polymers because of the steric impact between the atoms in the helix. However, as we described in the previous paper, the –S–S– structures reduce the steric impact and make these structural models possible for polyalkyl polysulfides. The structural model for polymethylene disulfide was determined to be GG'G in the previous paper. This model is very similar to the present model for polyethylene disulfide. Apparently, therefore, such models as GG'G and GGG'G are characteristic of polyalkyl polysulfides.

For the models proposed by Katz and by Minoura, the internal rotation conformations have not been described explicitly. Therefore, we are able to derive the conformations only from the pictures in their papers.

For Katz's model, the internal rotation conformations appear to be trans, trans, trans and cis along the $-S-CH_2-CH_2-S-S-$ bond sequence of the 2_1 helical model. The skeletal atoms are placed on one common plane and twofold symmetry axes (intersecting the fiber axis at right angles) exist, in contradiction with the results of the present infrared analyses.

In Minoura's model, the internal rotation conformations appear to be gauche, trans, gauche and gauche, and the internal rotation angle around the S–S bond is implicitly assumed to be around 100°C. The helical model of the conformation is 2_1, and twofold symmetry axes (intersecting the helical axis at right angles) again exist. As we have proved in the present work, however, the twofold symmetry axes actually do not exist. Therefore, neither of their models can be accepted.

The authers wish to express their gratitude to Professor Masamichi Tsuboi, Dr. Akiko Y. Hirakawa and Dr. Yoshimasa Kyogoku of the University of Tokyo for the use of their infrared spectrometer, and Mr. Tohoru Chiba of the Toho Rayon Company for measuring the fiber period of the substance. We wish also to thank Professor Tatsuo Miyazawa of the Institute for Protein Reseach, Osaka University, for his encouragement and his invaluable advice throughout this work.

BULLETIN OF THE CHEMICAL SOCIETY OF JAPAN VOL. 39 1866—1869 (1966)

Studies of Polybutenes. III. On the Molecular Motion Studied by Nuclear Magnetic Resonance*

By Shoichi KONDO,† Fumiaki ISHII,† Yasuo CHOKKI,†† Koji TANAKA† and Masatami TAKEDA†

† *Department of Chemistry, Faculty of Science, Tokyo College of Science, Shinjuku-ku, Tokyo*
†† *Takeda Chemical Industries Ltd., Osaka*

(Received December 18, 1965)

The molecular motion of polybutenes of low molecular weights has been studied by observing the NMR line widths and spin-lattice relaxation times at temperatures in the range from −180 to 200°C. The temperature dependence of these values is similar to that of polyisobutylene of a higher molecular weight. The correlation time spectra calculated from the spin-lattice relaxation time and the spin-spin relaxation time shift in the shorter-time direction with the decrease in the molecular weight. The dependence of the correlation frequency upon the temperature is also discussed in terms of the W. L. F. equation.

In previous papers[1,2] the molecular weight and its distribution in some polybutenes have been reported. The molecular weights from 300 to 10000 are situated between the typical high polymer and the monomer. Its chemical constituent is mainly polyisobutylene with some copolymer components of another butenes. It seems that it would be worthwhile to study the state of the molecular motion of these substances at low temperatures and to compare this motion with that of the polyisobutylene of a high molecular weight.[3]

* Presented at the International Symposium on Nuclear Magnetic Resonance, Tokyo, September, 1965.

1) R. Endo, K. Iimura and M. Takeda, This Bulletin, **37**, 950 (1964).

2) K. Iimura, R. Endo and M. Takeda, ibid., **37**, 874 (1964).

3) J. G. Powles, *Proc. Phys. Soc.*, **B 69**, 281 (1956): J. G. Powles and K. Luszczynski, *Physica*, **25**, 455 (1959).

In the present work line-widths and spin-lattice relaxation times were observed as functions of the temperature for three samples with different molecular weights. The glass transition temperatures were determined by dilatometry. On the basis of such observations, the possible transition of the mean correlation frequency with the temperature and the distribution spectra of the correlation frequency have been discussed.

Experimental

Samples.—The samples of the commercial polybutenes used were Indopol from Amoco and Vistanex from Esso Standard. Sample A: Indopol L-10 was selected as a sample of a lower molecular weight, sample B: Indopole H-300 of a medium molecular weight, and sample C: Vistanex LM-MH of a higher molecular weight. The molecular weights of the samples A and B were determined by a cryoscopic method using benzene as a solvent. The glass-transition temperature was determined with an improved dilatometer described by Bekkedahl.[4] *n*-Propylalcohol was used as a confining liquid from −150 to 0°C.

Equipment.—The nuclear magnetic resonance spectrometer used for the line-width measurement was a JNM-BL-1 type apparatus (Japan Electron Co. Ltd.) operating at a fixed frequency of 29 Mc./s. The measurement of the spin-lattice relaxation time was carried out with a spin-echo apparatus (Japan Electron Co. Ltd.) at the resonance frequency of 25 Mc./s. by applying 90°-90° pulse method.

Results and Discussion

Table I gives the molecular weights and the glass transition temperatures for the three samples. The high-resolution nuclear magnetic resonance spectrum of sample C was identical with that of polyisobutylene. The spectrum of the sample B was very similar to that of polyisobutylene except for the appearance of weak absorptions at higher magnetic fields. These absorptions are presented to a larger extent in the spectrum of the sample A.

Table I. Molecular weight and glass transition temperatures of polybutenes

	Sample	M_w	T_g, °C
A	Indopol L-10	310	−106
B	Indopol H-300	1100	−95
C	Vistanex LM-MH	11000	−85

The Temperature Dependence of Line Widths.—The first derivative curve of the absorption spectrum was recorded for the three samples at various temperatures from −180 to 0°C. The line width at the maximum slope is plotted against the temperature in Fig. 1. The general features

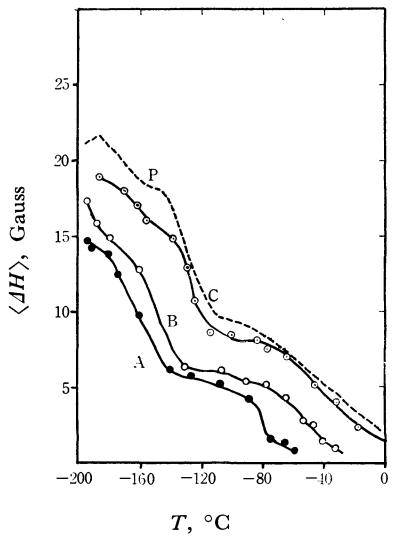

Fig. 1. Plots of line width vs. temperature. P: data by Powles.[3]

of these plots are similar to those of the plots observed on polyisobutylene by Powels.[3] Figure 1 shows two distinct narrowings on each curve. The low-temperature narrowing is due to the onset of a rotational motion around their three-fold axis of methyl groups. However, it may be seen that the temperature of this transition shifts lower as the molecular weight of the samples becomes smaller. This fact suggests that there is some coupling between the rotation of the methyl groups and some modes of the molecular motion of the main chain such as the rotational shear waves which have been suggested from the interpretation of the results of dynamic measurement at low temperatures. The high-temperature narrowing can be attributed to the onset of the segmental motion of these polymers. The temperatures defined as a narrowing center of the line width for samples A, B and C are −80, −54 and −38°C, respectively. The glass-transition temperatures are several tens of degrees lower than the temperatures of the narrowing center.

The Temperature Dependence of the Spin-Lattice Relaxation Time. — The spin-lattice relaxation time T_1 was measured for each sample over the temperature range from −50 to 200°C. An attempt to measure the T_1 at lower temperatures was unsuccessful for the sample C. Plots of the T_1 versus $1/T$ are given in Fig. 2. Two minima have been observed in both curves concerning samples A and B. The low temperature minima are probably associated with the methyl group motion which is in turn related to the above-mentioned line-width narrowing. The high temperature minima correspond to the segmental motion. The temperatures of the T_1 minima are shifted to the lower temperature side with the

4) N. Bekkedahl, *J. Research Natl. Bur. Standard*, **42**, 145 (1949).

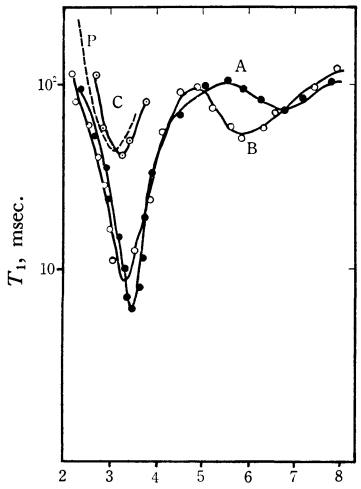

Fig. 2. Spin-lattice relaxation time as a function of temperature.

decrease in the molecular weight. The results of all the samples obtained are summarized in Table II.

TABLE II. TEMPERATURES AND VALUES OF T_1 MINIMA

Sample	T, °C	T_1, msec.	T, °C	T_1, msec.
A	12	6.4	−120	73.2
B	19	8.3	−90	65.4
C	44	42	—	—

The Temperature Dependence of the Correlation Frequency and Its Distribution.— The motional effects of the spin-lattice relaxation time T_1 and the spin-spin relaxation time T_2 for a coupling of nuclei were interpreted by the following equations:[5]

$$1/T_1 = 2/3 \cdot \Delta\omega_2^2\{\tau/(1+\omega^2\tau^2)+4\tau/(1+\omega^2\tau^2)\}$$

$$1/T_2 = \Delta\omega_2 \cdot 1/\alpha \cdot \tan^{-1}(\alpha\tau/T_2)$$

where α is the numerical coefficient nearly equal to unity and $\Delta\omega_2^2$ is the second moment in units of angular frequency. In the case of the polymers, however, a simple application of the above equations does not give a reasonable temperature dependence of the correlation frequency. One of the main reasons for this may be the neglect of the distribution of correlation frequencies. It is often necessary to postulate the distribution in order to explain the dynamic and dielectric behavior of the polymer. As the values of T_1 and T_2 as a function of the temperature were obtained from measurements at a fixed frequency, it is impossible to get the distribution from the isochronal NMR data alone. Therefore, we have to reduce the data of the temperature dependence to those of frequency dependence in some way. In dynamic and dielectric studies the relation between the frequency and the temperature can be explained by the W. L. F. equation which is widely used in discussing the segmental motion of the amorphous polymers. Slichter and Davis[6] have shown on the basis of their observation of the frequency dependence of the $T_{1\,\min}$ value for natural rubber, that the relation between the frequency and the temperature in the spin-lattice relaxation process can be explained by the W. L. F. equation. The shift factor which relates the correlation frequency at the temperature T with that at the reference temperature T_s can be expressed by the form:

$$\log a(T) = \log\{\tau(T)/\tau(T_s)\}$$
$$= -8.86(T-T_s)/101.6+T-T_s$$

where T_s is chosen 50°C higher than the glass-transition temperature. In Fig. 3, the smooth curves passing through the point of each T_2 show the temperature dependence of the correlation frequency using the shift factor. It may be seen that the application of the W. L. F. equation can not describe this case completely since all the ν_c points at $T_{1\,\min}$ appear somewhat below each curve. However, that equation can be used for most practical purposes.

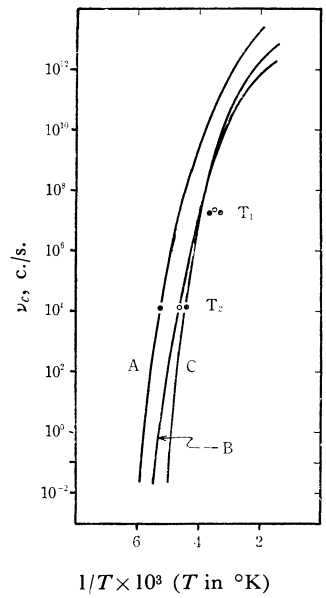

Fig. 3. Correlation frequencies as a function of temperature.

It has been proposed by Miyake[7] that the correlation-time spectra can be obtained from the

5) R. Kubo and K. Tomita, *J. Phys. Soc. Japan*, **9**, 888 (1954).
6) W. P. Slichter and D. D. Davis, *J. Appl. Phys.*, **34**, 98 (1963).
7) A. Miyake, *Rep. Prog. Poly. Phys. Japan*, **4**, 36 (1961).

observed values of T_1 and T_2 as a function of the temperature when the W. L. F. equation is applicable to the case of nuclear magnetic resonance. According to his method the correlation time spectra calculated from the observed values of T_1 and T_2 are shown in Fig. 5 using the following equation:

$$I\{\sqrt{1/2}\omega_0 a(T)\} \simeq 0.733\omega_0/\Delta\omega_2^2 T_1$$

$$I\{T_2/a(T)\} \simeq 4.60(T_2^\circ/T_2) \times \{1-\mathrm{d}\log a(T)/\mathrm{d}\log T_2\}^{-1}$$

in which T_2° is the particular value of T_2 when the temperature is sufficiently low and no motional narrowing is observed. It may be seen that the correlation time spectra for T_1 in Fig. 4 are slightly affected by the molecular weight while those of T_2 in Fig. 5 depend very much on the molecular weight. The dependence of the correlation-time spectra upon the molecular wieght seems to suggest that not only the micro-brownian motion but also the macro-brownian motion may be related to the distribution spectrum. This seems to be consistent with the fact that the curve of T_1 vs. $1/T$ in the sample A has a sharper and deeper minimum than in the sample C, and that the glass-transition temperature increases with the increase in the molecular weight.

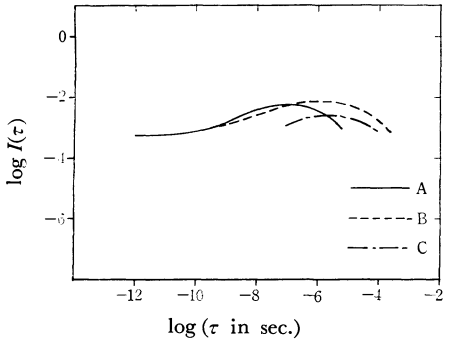

Fig. 4. Correlation time spectra calculated from spin-lattice relaxation time.

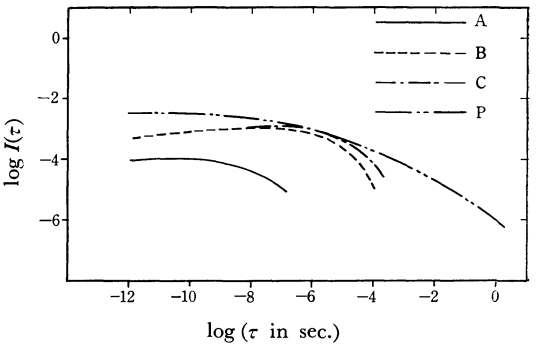

Fig. 5. Correlation time spectra calculated from spin-spin relaxation time.

The authors wish to thank Dr. Akira Miyake for his valuable discussions.

BULLETIN OF THE CHEMICAL SOCIETY OF JAPAN VOL. 39 1869—1873 (1966)

Kinetic Studies of the Oxidation of Uranium Iodides by Oxygen

By Muneo HANDA

Division of Fuel Research and Development, Japan Atomic Energy Research Institute, Tokai-mura, Ibaraki

(Received December 20, 1965)

The kinetics of the oxidations of uranium tetraiodide and of triiodide by oxygen were studied over the temperature ranges from 55.0 to 66.5°C and from 88.5 to 103.5°C respectively. The experiments were carried out with an apparatus in which the column of a gas chromatograph was replaced by an electric furance and traps of water vapor, oxygen and iodine. Most of the experiments were performed with the same partial pressure of oxygen (64 mmHg) and total flow rate (60 ml. per min.). The activation energies for the reaction of oxygen with uranium tetraiodide and triiodide were, respectively, 21.1 and 22.5 kcal. per mole. The rate of the formation of uranium trioxide was in agreement with the kinetics to be expected for reaction between a gas and a solid at a continuously diminishing spherical interface.

A study of the rates of reaction between uranium iodides and various gases, such as oxygen, hydrogen, and water vapor, provides information about the chemical behavior of fission iodine in a reactor fuel.[1-3] Before the present study was made, however, no fundamental data on the kinetics of

1) S. Yajima, K. Shiba and M. Handa, This Bulletin, **36**, 253 (1963).
2) S. Yajima, K. Shiba and M. Handa, ibid., **36**, 258 (1963).
3) S. Yajima, K. Shiba and M. Handa, ibid., **38**, 278 (1965).

the reaction were available, since uranium iodides are very unstable and must be handled in an inert gas atmosphere or in vacuo.[4]

The present work was therefore undertaken in an attempt to elucidate the kinetics and, if possible, the mechanism of the oxidation of uranium iodides by oxygen. The experiment was carried out with an apparatus in which the column of a gas chromatograph was replaced by an electric furnace and traps of water vapor, oxygen and iodine. This apparatus made it possible to carry out easily and precisely kinetic studies of a sample which could not be treated in the atmosphere.

From the X-ray analysis of the oxidation products, it was found that the reactions between uranium iodides and oxygen proceeded according to the following chemical equations:[5]

$$2UI_4 + 3O_2 = 2UO_3 + 4I_2 \quad (1)$$

$$2UI_3 + 3O_2 = 2UO_3 + 3I_2 \quad (2)$$

(The reaction temperature was below 200°C.)

$$3UI_4 + 4O_2 = U_3O_8 + 6I_2 \quad (3)$$

$$6UI_3 + 8O_2 = 2U_3O_8 + 9I_2 \quad (4)$$

(The reaction temperature was 600°C.)

Reaction 1 occurred with appreciable velocities when the temperature was raised to about 60°C. On the other hand, Reaction 2 proceeded rapidly at about 100°C or above. When uranium iodides were oxidized at 600°C in air, the uranium trioxide produced was decomposed to triuranium octoxide. The chemical reactions are shown in Eqs. 3 and 4. The kinetics of Reaction 1 has been studied over the temperature range from 55.0 to 66.5°C, and that of Reaction 2, over the range from 88.5 to 103.5°C. The rate of the formation of uranium trioxide was in agreement with the kinetics to be expected for a reaction between a gas and a solid at a continuously diminishing spherical interface. The activation energies for Reactions 1 and 2 were 21.1 and 22.5 kcal. per mole respectively.

Experimental and Results

The Preparation of the Samples.—*Uranium Tetraiodide Packed in a Silica Breakable.*—Uranium tetraiodide was prepared by the direct combination of uranium metal and iodine, using the method reported by Gregory.[6] The reaction was slow, but the product prepared in this way was pure uranium tetraiodide. The iodine/uranium ratio in the uranium tetraiodide was 4.00±0.02. The melting point of the uranium tetraiodide measured in an inert gas atmosphere was 506°C, a value approximately agreed with the 508°C reported in the literature.[4,7] The uranium tetraiodide was ground into powder of from 200 to 400 mesh with a glass mortar in a glove box filled with purified helium. About 200 mg. of the uranium tetraiodide was packed in a silica breakable in a way similar to that described in a previous paper.[3]

Uranium Triiodide Packed in a Silica Breakable.—Uranium triiodide was prepared by heating a stoichiometic mixture of the uranium tetraiodide and uranium metal powder at 750°C for 24 hr. The product was then purified by using a thermochromatograph[3] with pure helium as the carrier. The uranium triiodide deposited on the wall of the thermochromato-tube heated at 700—800°C

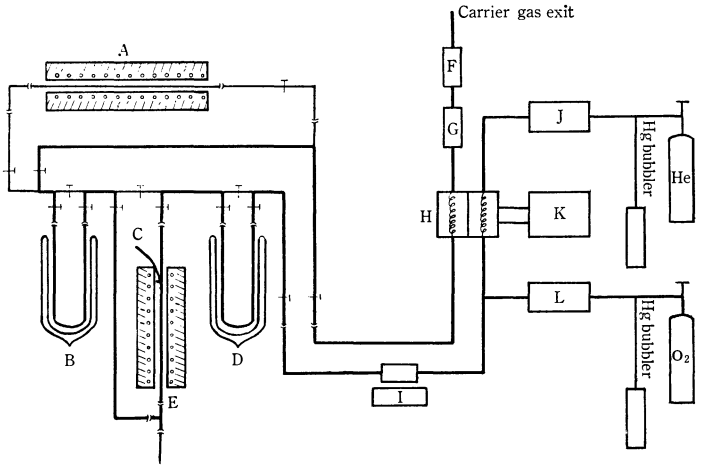

A: Oxygen trap (Uranium turnings: 300°C)
B: Iodine trap (−196°C)
C: Sample
D: Water trap (−196°C)
E: Reaction Furnace
F: Silica gel bed
G: Flow meter
H: Thermal conductivity cell
I: Gas mixing pump
J: Helium purifier
K: Recorder
L: Graphite bed

Fig. 1. Flow diagram of apparatus.

4) J. J. Katz and E. Rabinowitch, "The Chemistry of Uranium, The Element, Its Binary and Related Compounds," Dover Publications, New York (1951).
5) M. Handa, This Bulletin, submitted.
6) N. W. Gregory, UCRL, RL-4, 6, 272 (1944).
7) M. M. Popov and M. D. Senin, *Zhur. Neorg. Khim.*, **2**, 1479 (1957).

was taken out and transferred into a glove box. The uranium triiodide was then ground into powder of from 200 to 400 mesh and packed in a silica breakable in a way similar to that used for uranium tetraiodide. The iodine/uranium ratio in the uranium triiodide was 3.00±0.02. The melting point measured in an inert gas atmosphere was 788°C, nearly equal to the 780°C reported by other workers.[4,7]

Apparatus.—A flow diagram of the experimental apparatus is shown in Fig. 1. The column of a GC-1A Shimadzu-type gas chromatograph was replaced by an assembly of a reaction furnace, a water trap, an iodine trap, and an oxygen trap. Impurities in the helium were eliminated by passing it successively through a potassium hydroxide bed, a magnesium perchlorate bed, a copper gauze heated to 300°C, and uranium turnings heated to 800°C.

Purified helium was first made to flow through a standard thermal conductivity cell, and then oxygen was introduced into the helium stream. The two gases were completely mixed by a glass gas-mixing pump.[8] The water vapor in helium-oxygen gases was further eliminated by passing that gas through a water trap, which had been cooled by a liquid nitrogen at −196°C. After they had passed through the reaction furnace, the gases were introduced into the iodine trap in order to remove the iodine produced by the oxidation of uranium iodides in the reaction furnace. Then the gases were made to flow through a reference thermal conductivity cell, a flow meter, and a silica gel bed, and then released into the atmosphere. The flow rate and the partial pressure of oxygen in the carrier gas were controlled by changing the height of mercury in the bubblers.

The reaction furnace is shown in Fig. 2. A silica breakable containing the sample and a breaker (an iron bar sealed in a silica tube) were suspended in a silica tube in the furnace by a supporter (an iron bar sealed in the silica tube). The temperature of the furnace (a nichrome resistance furnace) was controlled by an S-175-type Chino temperature regulator which was able to maintain the temperature within 0.2% of its full scale and also to heat the sample at the desired rate. The temperature of the sample was measured by a copper-constantan thermocouple connected to a P-31-type Yokogawa potentiometer. A thermocouple to measure the reaction temperature was set beneath the sample in the silica tube.

The Heating Curves of Uranium Tetraiodide and Triiodide.—Most of the experiments were performed at the same partial pressure of oxygen (64 mmHg) and total flow rate (60 ml./min.).

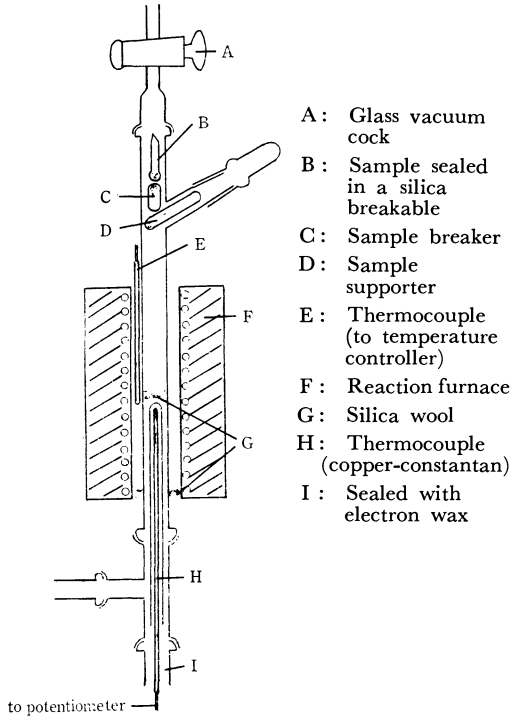

Fig. 2. Reaction Furnace.

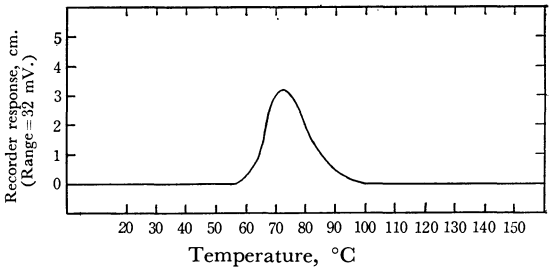

Fig. 3. Heating curve of uranium tetraiodide.
Sample weight: 0.145 g.
Carrier gas flow rate: 60 ml./min.
Partial pressure of oxygen: 64 mmHg
Rate of temperature increase: 2°C/min.

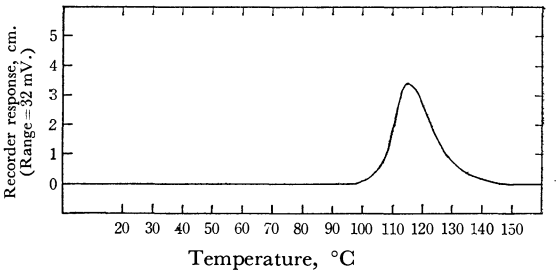

Fig. 4. Heating curve of uranium triiodide.
Sample weight: 0.175 g.
Carrier gas flow rate: 60 ml./min.
Partial pressure of oxygen: 64 mmHg
Rate of temperature increase: 2°C/min.

8) M. Handa, Y. Takahashi and K. Shiba, *Bunseki Kagaku (Japan Analyst)*, **13**, 1262 (1964).

When the base line of the recorder became constant, the breakable containing the sample was broken with a magnet and the sample was dropped into the center of the reaction furnace. Then the temperature of the furnace was raised at a constant rate 2°C/min. The heating curves for uranium tetraiodide and triiodide are shown in Figs. 3 and 4 respectively.

Isotherms for the Oxidation of Uranium Tetraiodide and Triiodide.—The heating curves of uranium tetraiodide and triiodide have peaks at 75 and 115°C respectively. Consequently, the isotherms for the oxidation of uranium tetraiodide and triiodide were determined in the vicinities of each peak.

The experiments were carried out in a similar way to that used for preparing the heating curves, except that the reaction furnace was kept at the given temperature before the sample was introduced into the furnace. Typical isotherm of uranium tetraiodide at 57.0°C is shown in Fig. 5.

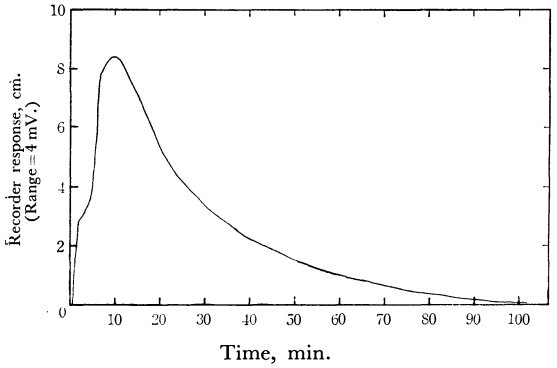

Fig. 5. Rate of oxidation of uranium tetraiodide.
Sample weight: 0.221 g.
Carrier gas flow rate: 60 ml./min.
Partial pressure of oxygen: 64 mmHg
Reaction temperature: 57.0°C

The X-Ray Analysis of the Oxidation Products.—A brown-colored material was obtained by isothermal experiments on both uranium tetraiodide and triiodide. The color turned yellow, however, when the material was taken out into the atmosphere. It was not soluble in water. When the brown material was heated in air at 600°C, the color changed from brown to black. The black material was also insoluble in water. An X-ray diffraction analysis indicated the brown material to be uranium trioxide and the black material to be triuranium octoxide.

The Kinetics of the Reaction.—A system of a solid and a gas may be idealized by assuming the solid to consist of a spherical particle of a uniform size, with the reaction starting on all particles. In such a reaction the following relationship can be deduced.[9-12]

$$(1 - F)^{1/3} = 1 - k't \quad (5)$$

$$F = (m_0 - m_t)/m_0 \quad (6)$$

where m_0 is the initial mass of the particle; m_t, the mass of the particle at time t, and k', the reaction rate constant. The amount of uranium iodide consumed by oxidation is directly proportional to the amount of oxygen consumed, because the oxidation reaction of uranium iodides proceeds according to Eq. 1 or 2. The amount of oxygen is directly proportional to the area of the recorder chart of the gas chromatograph, and the area is directly proportional to the weight of the piece cut off from the recorder chart. To simplify the calculation of the reaction kinetics, the amount of uranium iodide consumed by oxidation was replaced by the weight of the recorder chart.

All the isotherms reach a peak several minutes after the beginning of the experiment, as the temperature of the sample cannot reach the given temperature immediately after the sample is introduced in the furnace. Therefore, the data obtained before the peak of isothermal curve was reached has been omitted in the calculation of the reaction rate.

The plots of $(1-F)^{1/3}$ against the reaction time for uranium tetraiodide and triiodide are shown in Figs. 6 and 7 respectiveley. The experimental points lie on a straight line for each temperature, which is in agreement with Eq. 5, so that the reactions between uranium iodides and oxygen

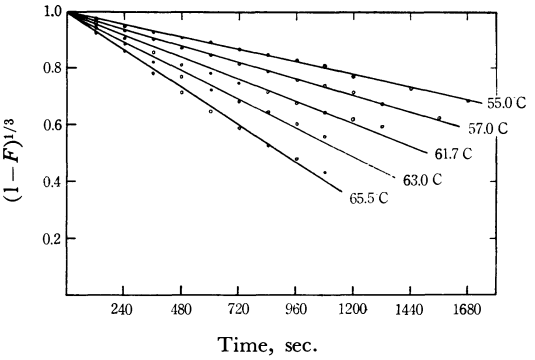

Fig. 6. Reaction of uranium tetraiodide with oxygen $(1-F)^{1/3}$ against time at various temperatures.
Sample weight: 0.223 g. (55.0°C), 0.221 g. (57.0°C), 0.194 g. (61.7°C), 0.143 g. (63.0°C), 0.171 g. (66.5°C)
Carrier gas flow rate: 60 ml./min.
Partial pressure of oxygen: 64 mmHg

9) V. Y. Labaton and K. D. B. Johnson, *J. Inorg. Nucl. Chem.*, **10**, 74 (1959).
10) C. E. Johnson and J. Fisher, *J. Phys. Chem.*, **65**, 1849 (1961).
11) R. L. Farrar, Jr., and H. A. Smith, ibid., **59**, 763 (1955).
12) J. S. Anderson, *Bull. Soc. Chim.*, **20**, 781 (1953)

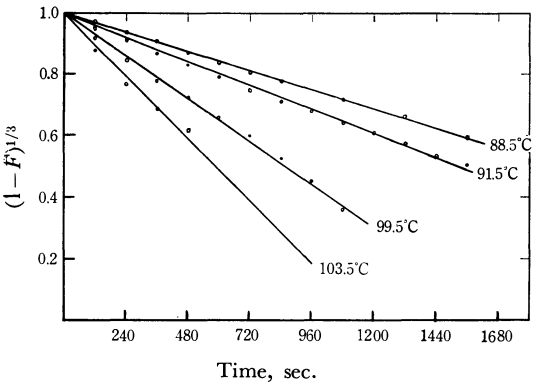

Fig. 7. Reaction of uranium triiodide with oxygen
$(1-F)^{1/3}$ against time at various temperatures.
Sample weight: 0.131 g. (88.5°C), 0.098 g. (91.5°C), 0.064 g. (99.5°C), 0.094 g. (103.5°C)
Carrier gas flow rate: 60 ml./min.
Partial pressure of oxygen: 64 mmHg

are governed by the linear law given by Anderson for a gas-solid reaction.[12]

The Effect of Oxygen Concentration.—Most of the runs were carried out with the same partial pressure of oxygen (64 mmHg) and total flow rate (60 ml./min.). In several runs, however, the partial pressure of oxygen was varied, the total flow rate of the carrier gas being kept approximately constant. Table I summarizes the effect of a variation in the partial pressure of oxygen. There is an approximately linear relationship between the reaction rate and the partial pressure of oxygen, as in the case of the fluorination of uranium tetrafluoride with fluorine.[9]

Table I. The effect of oxygen concentration on the rate constant at 61.5°C for uranium tetraiodide

Oxygen concn. in carrier gas %	Partial pres. (P_{O_2}) of oxygen mmHg	k' sec^{-1}	$k' \times 10^6/P_{O_2}$
8.50	64	3.20×10^{-4}	5.00
5.74	41	2.32×10^{-4}	5.66
4.50	34	1.80×10^{-4}	5.30

The Energy of Activation.—The reaction rate constant, k', was calculated from the slope in Figs. 6 and 7. The logarithm of the reaction rate constant, k', is plotted against the reciprocal of the absolute temperature, which is shown in Fig. 8. The slopes of the straight line in Fig. 8 are -4.6×10^3 and -4.9×10^3 for uranium tetraiodide and triiodide respectively, from which values the activation energies for their reactions with oxygen were estimated to be 21.1 and 22.5 kcal. per mole.

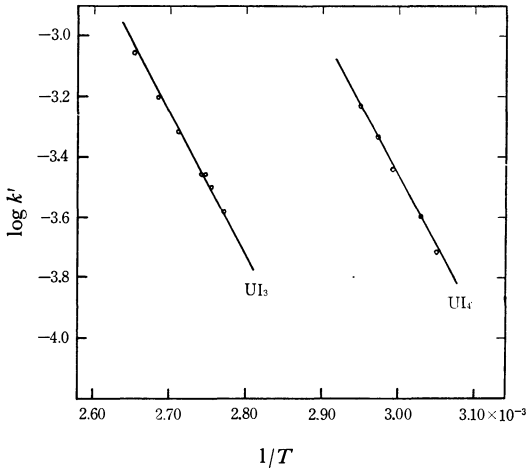

Fig. 8. Arrhenius plot for uranium tetraiodide and triiodide.

The author wishes to thank Professor Seishi Yajima and Mr. Koreyuki Shiba for their valuable discussions and suggestions, and Professor Takanobu Shiokawa for his continuing interest and encouragement during this work.

BULLETIN OF THE CHEMICAL SOCIETY OF JAPAN VOL. 39 1874—1877 (1966)

The π-Electronic Excitation Energies of Anthraquinone

By Akira KUBOYAMA and Kōichi WADA*

Government Chemical Industrial Research Institute, Tokyo, Shibuya-ku, Tokyo

(Received January 10, 1966)

Following our previous work on *o*-benzoquinone, the calculation of the π-electronic excitation energies of anthraquinone has been carried out with the Pariser-Parr-Pople method. The calculated excitation energies which correspond to the five distinct $\pi\rightarrow\pi^*$ bands have been obtained, though the agreement of the calculated excitation energies and the transition dipole-strengths with the observed energies and strengths are unsatisfactory. The π-electronic charge distribution in carbonyl groups of anthraquinone is almost the same as that of *p*-benzoquinone.

In our previous work,[1] the π-electronic excitation energies of *o*-benzoquinone were calculated using the Pariser-Parr-Popl method,[2,3] and from these results the $\pi\rightarrow\pi^*$ absorption bands of *o*-benzoquinone have been studied. In this paper, similar work on anthraquinone will be reported.

The Method of Calculation

The method of calculation was the same as that used in our previous work.[1] The integral values used have all been shown in our previous paper except for the core resonance integrals for carbon-carbon bonds.

The geometry of anthraquinone has been studied by Sen[4] by means of X-ray analysis. According to Sen's results, anthraquinone is planar, and its bond distances are as shown in Fig. 1.

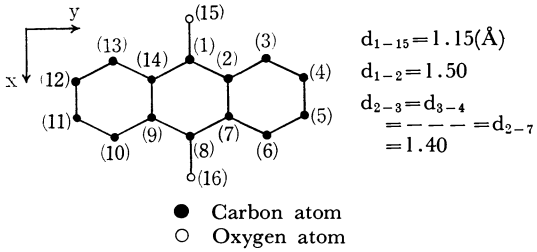

Fig. 1. Interatomic distances

In this work, these bond distances were used, and all the valence angles were assumed to be 120°. It was also assumed that anthraquinone is planar and that its symmetry group is D_{2h}.

As for the core resonance integral (β), the values of 1.45 eV. and 2.39 eV. were used for that over the atoms 1 and 2 and those of the benzene nuclei respectively, according to the method of Pariser and Parr.[2]

In the calculations, an electronic computor NEAC 2101 was used. The calculations were carried out in the same manner as in the previous work.[1]

Results

The molecular orbitals (ϕ_i) and their orbital energies (ε_i) are shown in Table I.[5] The excitation energies of the excited singlet and triplet configurations[6] less than 8 eV. are shown in Table II, along with the corresponding Coulomb and exchange integrals. Those of the orbitally-allowed and orbitally-forbidden transitions are shown in Table II (i) and II (ii) respectively.

The configuration interactions among the configurations in Table II were calculated. The obtained excited-state wave functions ($^{1,3}\Phi_i$), their excitation energies ($^{1,3}E_i-E_0$), the transition dipole-strengths from the ground state, and the interconfigurational matrix elements ($\Phi_{i\rightarrow j}|\mathbf{H}|\Phi_{k\rightarrow l}$) are shown in Table III.

In Table IV, the excitation energies, the transition dipole-strengths and the symmetry species of the excited states, experimentally determined,[7-9]

* Present address: The Yokohama Customs House, Naka-ku, Yokohama.

1) A. Kuboyama and K. Wada, This Bulletin, **38**, 1709 (1965).
2) R. Pariser and R. G. Parr, *J. Chem. Phys.*, **21**, 466, 767 (1953).
3) J. A. Pople, *Trans. Faraday Soc.*, **49**, 1375 (1953).
4) S. N. Sen, *Indian J. Phys.*, **22**, 347 (1948).

5) χ_i denotes the $2p\pi$ atomic orbital of *i*-atom.
6) Φ_0 and E_0 denote the wave function and the energy of the ground state respectively. $^1\Phi_{i\rightarrow j}$, $^1E_{i\rightarrow j}$ and $^3\Phi_{i\rightarrow j}$, $^3E_{i\rightarrow j}$ denote the wave functions and the energies of the singlet and triplet configurations, respectively, in which one electron is excited from an occupied orbital χ_i to an unoccupied orbital χ_j. The excitation energy of each excited configuration is given by the following formula.

$$\left.\begin{matrix}{}^1E_{i\rightarrow j}\\ {}^3E_{i\rightarrow j}\end{matrix}\right\}-E_0=(E_j-E_i)-(J_{ij}-K_{ij})\begin{cases}+K_{ij}\\ -K_{ij}\end{cases}$$

J_{ij} and K_{ij} denote Coulomb and exchange integrals over ϕ_i and ϕ_j respectively.

7) K. P. Popov and L. V. Smirnov, *Optics & Spectroscopy*, **13**, 155 (1962).
8) H. Labhart, *Chimia*, **15**, 20 (1961).
9) A. Kuboyama, Preprints of the International Conference on Photochemistry, Tokyo, p. 117 (1965) (The results obtained from the dichroism of phosphorescence excitation spectra.).

TABLE I. SCF MO's AND THEIR ENERGIES

Symmetry	SCF MO's	Orbital energies, eV.
b_{1u}	$\phi_1=0.4145\phi_1+0.6297\phi_2+0.4439\phi_3+0.3578\phi_4+0.3263\phi_5$	−13.818
b_{3g}	$\phi_2=0.5872\phi_6+0.5738\phi_7+0.5708\phi_8$	−13.144
b_{2g}	$\phi_3=0.6554\phi_9+0.2321\phi_{10}+0.1696\phi_{11}+0.0691\phi_{12}+0.6949\phi_{13}$	−12.326
b_{1u}	$\phi_4=0.4709\phi_1-0.0106\phi_2-0.3608\phi_3-0.5840\phi_4+0.5537\phi_5$	−11.964
b_{3g}	$\phi_5=0.7026\phi_6-0.0114\phi_7-0.7113\phi_8$	−9.934
a_u	$\phi_6=0.4210\phi_{14}+0.8125\phi_{15}+0.4031\phi_{16}$	−9.907
b_{2g}	$\phi_7=0.1066\phi_9-0.3744\phi_{10}-0.7907\phi_{11}-0.3962\phi_{12}+0.2569\phi_{13}$	−9.802
b_{1u}	$\phi_8=0.1808\phi_1-0.6460\phi_2-0.0538\phi_3+0.6003\phi_4+0.4318\phi_5$	−9.551
b_{2g}	$\phi_9=0.3567\phi_9+0.6119\phi_{10}-0.1288\phi_{11}-0.5217\phi_{12}-0.4575\phi_{13}$	0.546
b_{1u}	$\phi_{10}=0.2482\phi_1+0.3083\phi_2-0.7750\phi_3+0.3971\phi_4-0.2913\phi_5$	1.166
a_u	$\phi_{11}=0.7190\phi_{14}-0.0280\phi_{15}-0.6944\phi_{16}$	1.297
b_{3g}	$\phi_{12}=0.4017\phi_6-0.8188\phi_7+0.4099\phi_8$	1.404
b_{2g}	$\phi_{13}=0.5374\phi_9-0.1685\phi_{10}-0.3059\phi_{11}+0.6299\phi_{12}-0.4385\phi_{13}$	3.073
b_{1u}	$\phi_{15}=0.7155\phi_1-0.3014\phi_2+0.2628\phi_3-0.1123\phi_4-0.5616\phi_5$	3.179
a_u	$\phi_{15}=0.5529\phi_{14}-0.5822\phi_{15}+0.5960\phi_{16}$	4.572
b_{2g}	$\phi_{16}=0.3780\phi_9-0.6347\phi_{10}+0.4854\phi_{11}-0.4112\phi_{12}-0.2221\phi_{13}$	5.155

$$\phi_1=\frac{1}{\sqrt{2}}(\chi_1+\chi_8) \qquad \phi_9=\frac{1}{\sqrt{2}}(\chi_1-\chi_8)$$

$$\phi_2=\frac{1}{2}(\chi_2+\chi_7+\chi_9+\chi_{14}) \qquad \phi_{10}=\frac{1}{2}(\chi_2-\chi_7-\chi_9+\chi_{14})$$

$$\phi_3=\frac{1}{2}(\chi_3+\chi_6+\chi_{10}+\chi_{13}) \qquad \phi_{11}=\frac{1}{2}(\chi_3-\chi_6-\chi_{10}+\chi_{13})$$

$$\phi_4=\frac{1}{2}(\chi_4+\chi_5+\chi_{11}+\chi_{12}) \qquad \phi_{12}=\frac{1}{2}(\chi_4-\chi_5-\chi_{11}+\chi_{12})$$

$$\phi_5=\frac{1}{\sqrt{2}}(\chi_{15}+\chi_{16}) \qquad \phi_{13}=\frac{1}{\sqrt{2}}(\chi_{15}-\chi_{16})$$

$$\phi_6=\frac{1}{2}(\chi_2+\chi_7-\chi_9-\chi_{14}) \qquad \phi_{14}=\frac{1}{2}(\chi_2-\chi_7+\chi_9-\chi_{14})$$

$$\phi_7=\frac{1}{2}(\chi_3+\chi_6-\chi_{10}-\chi_{13}) \qquad \phi_{15}=\frac{1}{2}(\chi_3-\chi_6+\chi_{10}-\chi_{13})$$

$$\phi_8=\frac{1}{2}(\chi_4+\chi_5-\chi_{11}-\chi_{12}) \qquad \phi_{16}=\frac{1}{2}(\chi_4-\chi_5+\chi_{11}-\chi_{12})$$

TABLE II. EXCITATION ENERGIES AND TRANSITION DIPOLE-STRENGTHS OF THE CONFIGURATIONS AND ELECTRON REPULSION INTEGRALS

$i\rightarrow j$	Symmetry	$^1E_{i\rightarrow j}$-E_0, eV.	μ^2, Å^2	$^3E_{i\rightarrow j}$-E_0, eV.	J_{ij}, eV.	K_{ij}, eV.
(i) Orbitally allowed transitions						
8→ 9	B_{3u}	6.144	1.655	4.983	5.114	0.580
6→ 9	B_{2u}	6.153	0.999	5.738	4.716	0.208
8→12	B_{2u}	6.691	0.946	6.247	4.708	0.222
7→11	B_{2u}	6.820	1.061	6.309	4.792	0.255
5→10	B_{2u}	6.836	1.106	5.366	4.734	0.235
7→10	B_{3u}	6.959	0.519	6.096	4.873	0.431
5→11	B_{3u}	7.154	0.490	6.042	5.190	0.556
6→12	B_{3u}	7.341	0.972	6.302	5.010	0.520
(ii) Orbitally forbidden transitions						
5→ 9	B_{1g}	6.083		5.538	4.942	0.272
7→ 9	A_g	6.225		5.600	4.749	0.312
8→11	B_{1g}	6.498		5.840	5.009	0.329
8→10	A_g	6.605		5.981	4.736	0.312
6→11	A_g	7.133		6.345	4.861	0.394
6→10	B_{1g}	7.206		6.173	4.901	0.517
5→12	A_g	7.264		6.507	4.831	0.379
7→12	B_{1g}	7.360		6.268	4.939	0.546

TABLE III. WAVE FUNCTIONS, EXCITATION ENERGIES AND TRANSITION DIPOLE-STRENGTHS OF EXCITED STATES AND INTERCONFIGURATIONAL MATRIX ELEMENTS

(1) Singlet states

Symmetry		$^{1,3}E_i$-E_0, eV.	μ^2, Å^2
B_{3u}	$^1\Phi_1=0.3768^1\Phi_{8\to9}+0.5294^1\Phi_{6\to12}+0.6362^1\Phi_{7\to10}+0.4158^1\Phi_{5\to11}$	4.020	0.007
B_{2u}	$^1\Phi_2=0.4722^1\Phi_{8\to12}-0.5912^1\Phi_{6\to9}+0.4493^1\Phi_{5\to10}-0.4750^1\Phi_{7\to11}$	4.849	0.022
B_{2u}	$^1\Phi_3=0.5593^1\Phi_{8\to12}+0.6094^1\Phi_{6\to9}+0.4952^1\Phi_{5\to10}+0.2658^1\Phi_{7\to11}$	6.367	3.792
B_{3u}	$^1\Phi_4=0.9134^1\Phi_{8\to9}-0.2667^1\Phi_{6\to12}-0.3068^1\Phi_{7\to10}-0.0188^1\Phi_{5\to11}$	6.460	2.171
B_{2u}	$^1\Phi_5=0.0177^1\Phi_{8\to12}+0.5179^1\Phi_{6\to9}-0.2128^1\Phi_{5\to10}-0.8284^1\Phi_{7\to11}$	7.490	0.294
B_{3u}	$^1\Phi_6=0.1492^1\Phi_{8\to9}+0.4598^1\Phi_{6\to12}+0.0976^1\Phi_{7\to10}-0.8699^1\Phi_{5\to11}$	7.657	1.423
B_{2u}	$^1\Phi_7=0.6811^1\Phi_{8\to12}-0.1040^1\Phi_{6\to9}-0.7125^1\Phi_{5\to10}+0.1325^1\Phi_{7\to11}$	7.794	0.003
B_{3u}	$^1\Phi_8=0.0370^1\Phi_{8\to9}-0.6611^1\Phi_{6\to12}+0.7011^1\Phi_{7\to10}-0.2645^1\Phi_{5\to11}$	9.462	0.005
A_g	$^1\Phi_9=0.7716^1\Phi_{7\to9}-0.1461^1\Phi_{8\to10}+0.6020^1\Phi_{6\to11}-0.1440^1\Phi_{5\to12}$	4.902	Forbidden
A_g	$^1\Phi_{10}=0.1693^1\Phi_{7\to9}+0.7512^1\Phi_{8\to10}+0.1154^1\Phi_{6\to11}+0.6274^1\Phi_{5\to12}$	5.087	Forbidden
B_{1g}	$^1\Phi_{11}=0.7875^1\Phi_{5\to9}+0.1037^1\Phi_{6\to10}+0.6007^1\Phi_{8\to11}+0.0902^1\Phi_{7\to12}$	5.492	Forbidden
B_{1g}	$^1\Phi_{12}=0.1172^1\Phi_{5\to9}-0.7314^1\Phi_{6\to10}+0.0728^1\Phi_{8\to11}-0.6678^1\Phi_{7\to12}$	6.456	Forbidden

(2) Triplet states

B_{3u}	$^3\Phi_1=0.6812^3\Phi_{8\to9}+0.3788^3\Phi_{6\to12}+0.4244^3\Phi_{7\to10}+0.4608^3\Phi_{5\to11}$	3.847
B_{1g}	$^3\Phi_1=0.5123^3\Phi_{5\to9}+0.5209^3\Phi_{6\to10}+0.4583^3\Phi_{8\to11}+0.5061^3\Phi_{7\to12}$	4.200
A_g	$^3\Phi_3=0.6495^3\Phi_{7\to9}+0.4570^3\Phi_{8\to10}+0.4874^3\Phi_{6\to11}+0.3629^3\Phi_{5\to12}$	4.323
B_{1g}	$^3\Phi_4=0.5413^3\Phi_{5\to9}-0.4910^3\Phi_{6\to10}+0.4841^3\Phi_{8\to11}-0.4811^3\Phi_{7\to12}$	4.447
B_{3u}	$^3\Phi_5=0.4673^3\Phi_{8\to9}-0.5756^3\Phi_{6\to12}-0.5877^3\Phi_{7\to10}-0.3237^3\Phi_{5\to11}$	4.506
B_{2u}	$^3\Phi_6=0.2990^3\Phi_{8\to12}+0.7041^3\Phi_{6\to9}+0.2912^3\Phi_{5\to10}+0.5744^3\Phi_{7\to11}$	4.556

(3) Interconfigurational matrix elements

	Singlet state, eV.	Triplet state, eV.
$(\Phi_{8\to12}\|\mathbf{H}\|\Phi_{6\to9})$	0.333	−0.091
$(\Phi_{8\to12}\|\mathbf{H}\|\Phi_{5\to10})$	−1.019	−1.471
$(\Phi_{8\to12}\|\mathbf{H}\|\Phi_{7\to11})$	0.453	−0.023
$(\Phi_{6\to9}\|\mathbf{H}\|\Phi_{5\to10})$	0.385	−0.043
$(\Phi_{6\to9}\|\mathbf{H}\|\Phi_{7\to11})$	−0.928	−1.379
$(\Phi_{5\to10}\|\mathbf{H}\|\Phi_{7\to11})$	0.387	−0.100
$(\Phi_{8\to9}\|\mathbf{H}\|\Phi_{6\to12})$	−0.478	−0.091
$(\Phi_{8\to9}\|\mathbf{H}\|\Phi_{7\to10})$	−0.490	−0.275
$(\Phi_{8\to9}\|\mathbf{H}\|\Phi_{5\to11})$	−0.567	−1.350
$(\Phi_{6\to12}\|\mathbf{H}\|\Phi_{7\to10})$	−2.160	−1.903
$(\Phi_{6\to12}\|\mathbf{H}\|\Phi_{5\to11})$	−0.491	−0.130
$(\Phi_{7\to10}\|\mathbf{H}\|\Phi_{5\to11})$	−1.304	−0.100

TABLE IV. THE OBSERVED ABSORPTION BANDS OF ANTHRAQUINONE

	Excitation energy, eV.	μ^2, Å^2	Symmetry
Band I	3.8	∼0.3	$^1B_{3u}$
Band II	4.5	∼0.7	$^1B_{2u}$
Band III	4.9	∼1.8	$^1B_{3u}$
Band IV	6.1	∼0.7	?
Band V	∼6.7	>0.7	?

of the observed $\pi\to\pi^*$ absorption bands (I-V) of anthraquinone are shown.[10] The direction of the polarization of the transitions ($^1A_g\to{}^1B_{3u}$, $^1A_g\to{}^1B_{2u}$) are along the x and y axes in Fig. 1 respectively.

In Fig. 2(a) the π-electronic charge densities and π-bond orders of anthraquinone obtained are

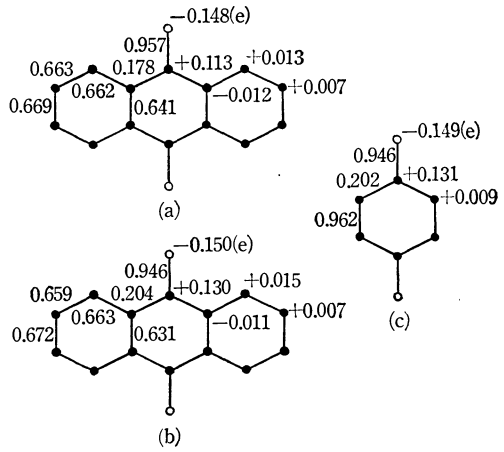

Fig. 2. Molecular diagrams.

10) Anthraquinone has an $n\to\pi^*$ band near 400 mμ.

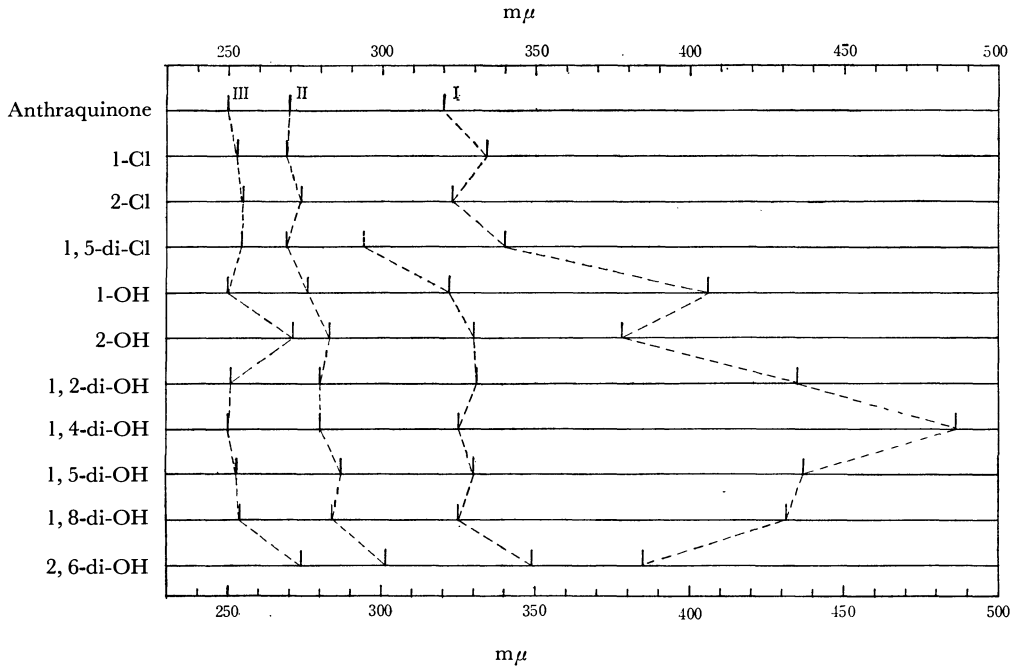

Fig. 3. Correspondence among $\pi \rightarrow \pi^*$ bands of anthraquinone and its chlorine or hydroxyl substitutes.

shown, while Fig. 2(b) shows those obtained using as the core resonance integral over the atoms 1 and 2 the value (1.68 eV.) which corresponds to the bond distance (1.47 Å). In Fig. 2(c) those of *p*-bnezoquinone calculated using the wave functions obtained by Sidman[11] are shown.

Discussion

Since all the intensities of Bands II—V in Table IV are strong, these absorption bands may reasonably be assigned to $\pi \rightarrow \pi^*$ allowed transitions. As for Band I, its intensity is not weak and it has a sharp peak at the longest wavelength edge in saturated hydrocarbons. Therefore, Band I may also reasonably be assigned to an allowed transition. From a comparison of Tables III and IV, Bands II and III may reasonably be assigned to the $E_0 \rightarrow {}^1E_3$ ($^1A_g \rightarrow {}^1B_{2u}$) and $E_0 \rightarrow {}^1E_4$ ($^1A_g \rightarrow {}^1B_{3u}$) transitions respectively. Bands IV and V may also reasonably be assigned to either one of the two transitions ($E_0 \rightarrow {}^1E_5$ ($^1A_g \rightarrow {}^1B_{2u}$) and $E_0 \rightarrow {}^1E_6$ ($^1A_g \rightarrow {}^1B_{3u}$)). Band I may be assigned to the $E_0 \rightarrow {}^1E_1$ ($^1A_g \rightarrow {}^1B_{3u}$), transition though the calculated dipole-strength of this transition is too small in comparison with that of Band I. The absorption band due to the $E_0 \rightarrow {}^1E_2$ ($^1A_g \rightarrow {}^1B_{2u}$) transition may be hidden in Band I. α- or β-Hydroxy-anthraquinone[12] has an absorption band between Bands I and II the intensity of which is nearly equal to that of Band I. This absorption band may be assigned to the $E_0 \rightarrow {}^1E_2$ transition. $\pi \rightarrow \pi^*$ bands of anthraquinone and its various chlorine[13] or hydroxyl[12] substitutes at the wavelengths longer than 240 mμ reasonably correspond to each other, as shown in Fig. 3. Those of various amino-anthraquinones[14] also correspond to those of the corresponding hydroxy-anthraquinones in Fig. 3 respectively.

The calculated singlet excitation energies of anthraquinone are much greater than the observed ones. A similar trend was observed in the *o*-[1] and *p*-benzoquinone[11] studied previously. In anthraquinone the agreement between the transition dipole-strengths calculated and those observed is also unsatisfactory. The alternate use of 1.68 eV. in place of 1.45 eV. as the core resonance integral over the atoms 1 and 2, or the use of −14.00 eV. in place of −13.00 eV. as U_{oo},[1] does not bring about any essential improvement in these points.

In Fig. 2 the charge distribution in carbonyl groups of anthraquinone is similar to those in *p*-benzoquinone and o-benzoquinone shown in our previous paper.[1] Especially it almost agrees with that in *p*-benzoquinone.

11) J. W. Sidman, *J. Chem. Phys.*, **27**, 429 (1957).

12) R. A. Morton and W. T. Earlam, *J. Chem. Soc.*, **1941**, 159. The solvent used was ethanol except for the case of 1, 4-dihydroxy-anthraquinone where hexane was used. The absorption-peak wavelengths of hydroxy-anthraquinones in ethanol and hexane are similar to each other.

13) A. Kuboyama, unpublished work. The solvent used was *n*-heptane except for the case of 1, 4-dichloro-anthraquinone where methylcyclohexane was used.

14) H. Hartmann and E. Lorenz, *Z. Naturforsh.*, **7b**, 360 (1952).

BULLETIN OF THE CHEMICAL SOCIETY OF JAPAN VOL. 39 1878—1886 (1966)

Correlations of the Structural Unit of Organic Compounds with the *G* Values of Thier Radiolytic Products

By Toshiro Isoya,* Kozo Hirota and Motoyoshi Hatada

Osaka Laboratories, Japanese Association for Radiation Research on Polymers, Neyagawa, Osaka (T. I., K. H., M. H.)
Department of Chemistry, Faculty of Science, Osaka University, Toyonaka, Osaka (K. H.)

(Received January 11, 1966)

Two correlations have been found between the *G* values of the radiolytic products and the number of the structural unit, *n*, in an organic molecule; (i) The *G* value from the homologous compounds has a linear relation to $1/n$ in the $n \leqq m$ region and is independent of *n* in the $n \geqq m$ region, where *m* is the number of the C–C bond through which the energy can be transferred, and (ii) the $G(CH_4)$ value from paraffin hydrocarbons, where the "terminal effect" is remarkable, has a linear relation to $1/n$ in both the $n \geqq m$ and $n \leqq m$ regions. These relations may be explained in terms of the energy transfer through C–C bonds.

Many studies have been carried out of radiation effects on chemical substances, but fewer investigations into correlations of the radiation effect on substances with their chemical structures have been made.[1-4]

In a previous paper,[5] the radiolysis of ethylene glycol diacetate was studied in order to investigate the effect of the number of ester groups in a molecule; it was found that the yields of gaseous products from ethylene glycol diacetate range from a half to one-third of those from methyl acetate. In the present paper, a similar method of research has been extended to other series of compounds in order to obtain a general rule which can predict the radiation effect for related compounds. Such research may also be useful for a better understanding of the mechanisms of the radiation effect on chemical substances in general.

Experimental

Commercially-available triacetin, glycerol, erythritol, and acetonylacetone were used without further purification.

In each run, each sample (2 ml., or 2 g. in the case of erythritol) was degassed by a conventional vacuum technique in a glass ampoule equipped with a breakable seal. Then the ampoule was sealed off and subjected to irradiation at room temperature with cobalt-60 gamma rays. The dose rate, which was determined by the use of a Fricke ferrous sulfate dosimeter, was 3.1×10^{15} eV. g^{-1} sec^{-1}.

The gaseous products were collected with a Toepler pump through traps at −196°C and −78°C; after their

Table I. *G* values from irradiated $-(-CHOOCCH_3-)-_n$

Compound	*n*	Radiation	Temp. °C	Phase	$G(H_2)$	$G(CH_4)$	$G(C_2H_6)$	$G(CO)$	$G(CO_2)$	Ref.
CH_3OOCCH_3	1	γ	R.T.	l.	0.87	2.07	0.27	1.57	0.78	6
	1	γ	27	l.	0.76	2.03	0.34	1.64	0.95	7
CH_2OOCCH_3 | CH_2OOCCH_3	2	γ	R.T.	l.	0.34	0.70	0.10	0.76	0.28	5
CH_2OOCCH_3 | $CHOOCCH_3$ | CH_2OOCCH_3	3	γ	R.T.	l.	0.11	0.27	0.05	0.46	0.26	This work

R.T.: Room temperature l.: liquid

* Present address: Technical Research Laboratory, Asahi Chemical Industry Co., Ltd., Itabashi-ku, Tokyo.

1) H. Yamazaki and S. Shida, *Isotopes and Radiation (Doitai to Hoshasen)*, **2**, 119 (1959).
2) K. Fueki and K. Hirota, *J. Chem. Soc. Japan, Pure Chem. Sect. (Nippon Kagaku Zasshi)*, **81**, 209 (1960).
3) K. L. Hall, R. O. Bolt and J. G. Carroll, "Radiation Effects on Organic Materials," Academic Press, New York (1963), p. 74.
4) T. J. Hardwick, *J. Phys. Chem.*, **66**, 1611 (1962).
5) T. Isoya, K. Hirota and M. Hatada, This Bulletin, **38**, 1722 (1965).
6) R. W. Hummel, *Trans. Faraday Soc.*, **56**, 234 (1960).
7) P. Ausloos and C. M. Trumbore, *J. Am. Chem. Soc.*, **81**, 3866 (1959).

amounts had been determined, they were subjected to mass spectrometry.

Results and Discussion

This general formula of the compounds can be presented: -(-CHR-)-$_n$; that is, n=1: CH_3R, n=2: CH_2RCH_2R, n=3: $CH_2RCHRCH_2R$,..... Tables I—IV show the G values of products from a series of esters (R=CH_3COO), alcohols (R=HO), ketones (R=CH_3CO), and paraffin hydrocarbons (R=H) respectively. In the tables, the G values of products from four irradiated compounds (tri-

TABLE II. G VALUES FROM IRRADIATED -(-CHOH-)-$_n$

Compound	n	Radiation	Temp. °C	Phase	$G(H_2)$	$G(CH_4)$	$G(CO)$	Ref.
CH_3OH	1	γ	R.T.	l.	4.0	0.24	0.16	8
	1	γ		l.	5.39	0.11	0.54	9
	1	γ		l.	4.1	1.23	0.15	10
	1	γ	20—25	l.	4.57	(0.36)*		11
	1	γ	19	l.	5.40	0.80	0.15	12
	1	γ	26	l.	5.66	0.57	0.45	13
	1	γ	20	l.	4.1	0.39	0.13	14
	1	γ		l.	4.99	0.44	0.12	15
	1	γ	20	l.	4.98	0.28	0.09	16
	1	γ	20	l.	4.60	0.31	0.15	16
	1	γ	22	g.	10.4	0.26	0.84	17
	1	γ	40—42	g.	10	0.5	1.0	18
CH_2OH | CH_2OH	2	γ	R.T.	l.	1.9	0.097	0.015	19
CH_2OH | $CHOH$ | CH_2OH	3	γ	R.T.	l.	1.8	0.002	0.034	This work
CH_2OH | $CHOH$ | $CHOH$ | CH_2OH	4	γ	R.T.	s.	1.1	0.000	0.000	This work

R.T.: Room temperature g.: gas l.: liquid s.: solid * $G(CH_4)+G(CO)$

TABLE III. G VALUES FROM IRRADIATED -(-CHCOCH$_3$-)-$_n$

Compound	n	Radiation	Temp. °C	Phase	$G(H_2)$	$G(CH_4)$	$G(CO)$	$G(C_2H_6)$	Ref.
CH_3COCH_3	1	γ	27	l.	0.88	2.62	0.83	0.48	20
	1	γ		l.	0.84	1.9	0.63	—	21
	1	γ	17	l.	0.85	1.84	1.70	0.43	22
	1	γ	28	l.	0.54	2.00	0.75	0.29	23
CH_2COCH_3 | CH_2COCH_3	2	γ	R.T.	l.	0.24	0.27	0.25	0.22	This work

R.T.: Room temperature l.: liquid

8) W. R. McDonell and S. Gordon, *J. Chem. Phys.*, **23**, 208 (1955).
9) G. Meshitsuka and M. Burton, *Radiation Research*, **8**, 285 (1958).
10) G. E. Adams and J. H. Baxendale, *J. Am. Chem. Soc.*, **80**, 4215 (1958).
11) N. N. Lichtin, *J. Phys. Chem.*, **63**, 1449 (1959).
12) J. H. Baxendale and F. W. Mellows, *J. Am. Chem. Soc.*, **83**, 4721 (1961).
13) R. H. Johnsen, *J. Phys. Chem.*, **65**, 2144 (1961).
14) E. Hayon and J. J. Weiss, *J. Chem. Soc.*, **1961**, 3970.
15) L. M. Theard and M. Burton, *J. Phys. Chem.*, **67**, 59 (1963).
16) M. Imamura, S. U. Choi and N. N. Lichtin, *J. Am. Chem. Soc.*, **85**, 3565 (1963).
17) J. H. Baxendale and R. D. Sedgwick, *Trans. Faraday Soc.*, **57**, 2157 (1961).
18) G. M. Meaburn, F. W. Mellows and A. Reiffsteck, *Nature*, **204**, 1301 (1964).
19) K. Hirota, K. Sando and M. Hatada, *J. Chem. Soc. Japan, Pure Chem. Sect. (Nippon Kagaku Zasshi)*, **81**, 29 (1960).
20) P. Ausloos and J. Paulson, *J. Am. Chem. Soc.*, **80**, 5117 (1958).
21) J. D. Strong and J. G. Burr, ibid., **81**, 775 (1959).
22) P. Ausloos, ibid., **83**, 1056 (1961).
23) R. Burker, *Trans. Faraday Soc.*, **59**, 375 (1963).

Table IV. G values from irradiated $-(-CH_2-)-_n$

Compound	n	Radiation	Temp. °C	Phase	$G(H_2)$	$G(CH_4)$	Ref.
CH_4	1	γ	22.5	g.	6.4		24
	1	α		g.	6.4*		25
	1	e		g.	5.7		26
	1	α		g.	4.8		27
	1	γ	25	g.	5.51		28
	1	x	25	g.	7.2		29
	1	γ	−196	s.	2.87		30
C_2H_6	2	γ	22.5	g.	6.8	0.6	24
	2	α		g.	5.0*	1.0*	25
	2	e	R.T.	g.	3.9	0.49	31
	2	γ	25	g.	8.8	0.39	32
	2	γ	25	g.	8.3	—	33
	2	γ		l.	7.00—8.60	—	34
C_3H_8	3	γ	22.5	g.	5.9	1.5	24
	3	α		g.	8.2	0.37	35
	3	α		g.	4.3*	1.2*	25
	3	γ		g.	6.25	—	36
	3	e	R.T.	g.	—	1.3	37
	3	γ		l.	5.50—7.45	—	34
C_4H_{10}	4	γ	170	g.	4.75—6.12	1.16—2.56	38
	4	α		g.	9.0	1.2	35
	4	α		g.	4.8*	0.89*	25
	4	γ		g.	4.92—5.41	—	34
	4	γ		g.	5.40	—	36
	4	γ	20	l.	4.05—4.50	0.42—0.49	38
	4	e	−30	l.	1.1	0.2	39
C_5H_{12}	5	e		g.	>6	0.7	40
	5	α		g.	7.3	0.81	35
	5	e	22	l.	4.2	0.22	41
	5	e		l.	4.2	0.4	42
	5	γ		l.	4.5	—	43
	5	x		l.	6.35	—	44
	5	e		l.	4.98	0.12	45
	5	γ	25	l.	4.17	0.22	46
	5	γ	R.T.	l.	5.04	0.25	47

24) K. Yang and P. J. Manno, *J. Am. Chem. Soc.*, **81**, 3507 (1959).
25) S. C. Lind and D. C. Bardwell, ibid., **48**, 2335 (1926).
26) F. W. Lampe, ibid., **79**, 1055 (1957).
27) R. E. Honig and C. W. Sheppard, *J. Phys. Chem.*, **50**, 119 (1946).
28) P. Ausloos, R. Gordon, Jr., and S. G. Lias, *J. Chem. Phys.*, **40**, 1854 (1964).
29) G. G. Meisels, W. H. Hamill and R. R. Williams, *J. Phys. Chem.*, **61**, 1456 (1957).
30) P. Ausloos, R. E. Rebbert and S. G. Lias, *J. Chem. Phys.*, **42**, 540 (1965).
31) L. M. Dorfmann, *J. Phys. Chem.*, **62**, 29 (1958).
32) K. Yang and P. L. Gant, ibid., **65**, 1861 (1961).
33) C. M. Nodetzki, P. A. McCusker and D. B. Peterson, ibid., **69**, 1056 (1965).
34) T. W. Woodward and R. A. Back, *Can. J. Chem.*, **41**, 1463 (1963).
35) R. A. Back and N. Miller, *Trans. Faraday Soc.*, **55**, 911 (1959).
36) R. A. Back, T. W. Woodward and K. A. McLachlan, *Can. J. Chem.*, **40**, 1380 (1962).
37) L. W. Sieck, N. K. Blocker and J. H. Futrell, *J. Phys. Chem.*, **69**, 888 (1965).
38) T. Miyazaki and and S. Shida, This Bulletin, **38**, 716 (1965).
39) V. J. Keeman, R. M. Lincoln, R. L. Rogers and H. Buroasser, *J. Am. Chem. Soc.*, **79**, 5125 (1957).
40) J. H. Frtrell, *J. Phys. Chem.*, **64**, 1634 (1960).
41) A. E. de Vries and A. O. Allen, ibid., **63**, 879 (1959).
42) H. A. Dewhurst, ibid., **61**, 1466 (1957).
43) P. J. Dyne and J. Denhartog, *Can. J. Chem.*, **40**, 1616 (1962).
44) T. J. Hardwick, *J. Phys. Chem.*, **66**, 1611 (1962).
45) P. Claes and S. Rzad, *Bull. Soc. Chem. Belg.*, **73**, 689 (1964).
46) J. W. Sutherland and A. O. Allen, *J. Am. Chem. Soc.*, **83**, 1040 (1961).
47) R. H. Schuler and R. R. Kunz, *J. Phys. Chem.*, **67**, 1004 (1963).

TABLE IV. (Continued)

Compound	n	Radiation	Temp. °C	Phase	$G(H_2)$	$G(CH_4)$	Ref.
C_6H_{14}	6	e		g.	4.3	0.5	48
	6	α		g.	5.6	0.78	35
	6	α		g.	3.5	0.44	51
	6	e	R.T.	g.	5.0	0.5	53
	6	e		l.	4.95	0.13	48
	6	e		l.	5.0	0.15	42
	6	e		l.	5.0	0.41	49
	6	e, γ		l.	4.0	0.12	50
	6	γ		l.	4.9	0.4	52
	6	γ		l.	5.1	—	43
	6	x		l.	5.28	0.11	44
	6	γ	20	l.	5.09	—	54
	6	γ	−196	s.	3.65	—	54
C_7H_{16}	7	e		l.	4.7	0.09	42
	7	e		l.	5.1	0.27	49
	7	γ	9	l.	4.9	0.22	55
	7	x	25—75	l.	5.2	—	56
	7	x		l.	6.06	—	44
C_8H_{18}	8	e		l.	4.8	0.08	42
	8	e		l.	4.7	0.17	49
	8	γ		l.	5.0	—	43
	8	x		l.	6.18	—	44
	8	γ	R.T.	l.	4.59	0.08	47
C_9H_{20}	9	e		l.	5.0	0.07	42
	9	γ		l.	4.9	—	43
	9	x		l.	6.05	—	44
$C_{10}H_{22}$	10	e		l.	5.2	0.06	42
	10	e		l.	4.2	0.11	49
	10	γ		l.	4.8	—	43
	10	x		l.	4.90	—	44
$C_{12}H_{26}$	12	e		l.	4.9	0.05	42
$C_{14}H_{30}$	14	e		l.	4.1	0.07	49
$C_{16}H_{34}$	16	e		l.	4.8	0.04	42
	16	e	19	l.	4.1	—	57
	16	e	4	s.	3.0	—	57
$C_{28}H_{58}$	28	e	25—50	s.	4.3	—	58
Polymethylene	∞	e	25—50	s.	5.4	0	58

* Calculated from author's data, assuming W=26.
R.T.: Room temperature. g.: gas l.: liquid s.: solid

48) J. H. Futrell, *J. Am. Chem. Soc.*, **81**, 5921 (1959).
49) C. S. Schoepf and C. H. Fellow, *Ind. Eng. Chem.*, **23**, 1396 (1931).
50) W. H. T. Davison, *Chem. Ind. (London)*, **1957**, 662.
51) V. P. Henri, C. R. Maxwell, W. C. White and D. C. Peterson, *J. Phys. Chem.*, **56**, 153 (1952).
52) F. H. Krenz, *Nature*, **176**, 1113 (1955).
53) H. A. Dewhurst, *J. Am. Chem. Soc.*, **83**, 1050 (1961).
54) L. Kevan and W. Fibby, *J. Chem. Phys.*, **39**, 1288 (1963).
55) A. M. Brodsky, U. A. Kolbanovsky, E. D. Filatova and A. S. Tchernyohevya, *Intern. J. Appl. Radiation and Isotopes*, **5**, 57 (1959).
56) D. F. Forsyth, E. N. Weber and R. H. Schuler, *J. Chem. Phys.*, **22**, 66 (1954).
57) R. Salovey and W. E. Falconer, *J. Phys. Chem.*, **69**, 2345 (1965).
58) A. A. Miller, E. J. Lawton and J. S. Balwit, ibid., **60**, 599 (1956).

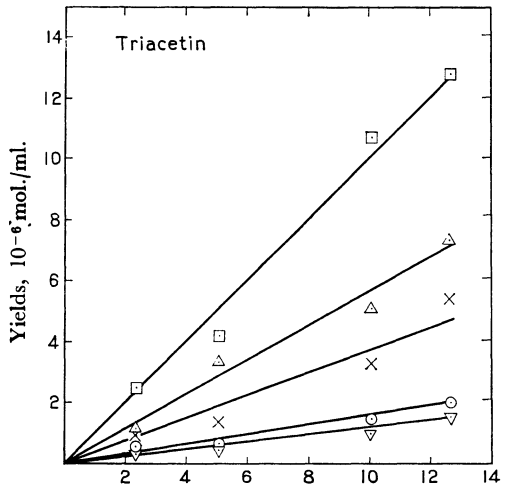

Fig. 1. Yields of gaseous products as a function of energy absorbed.

⊙ H_2, △ CH_4, ▣ CO, ▽ C_2H_6, × CO_2

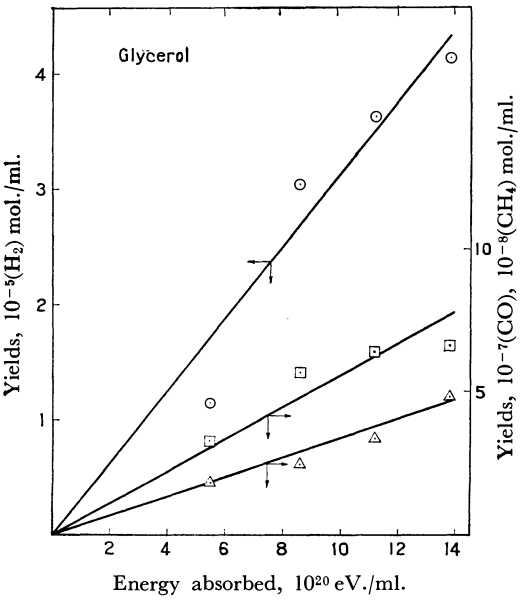

Fig. 2. Yields of geseous products as a function of energy absorbed.

⊙ H_2, △ CH_4, ▣ CO

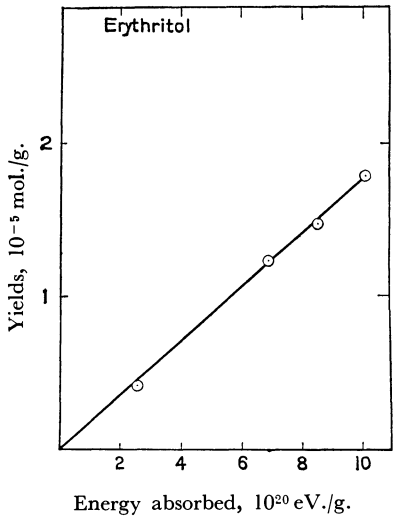

Fig. 3. Yields of hydrogen as a function of energy absorbed.

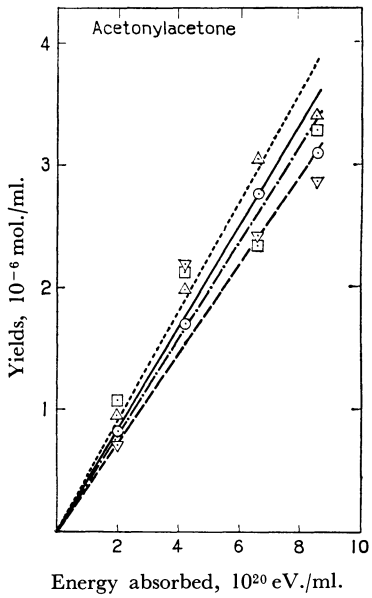

Fig. 4. Yields of gaseous products as a function of energy absorbed.

⊙ H_2, △ CH_4, ▣ CO, ▽ C_2H_6

acetin, glycerol, erythritol and acetonylacetone) were obtained, as usual, from the straight lines shown in Figs. 1, 2, 3 and 4. The G values of the others were obtained from the literature.

The G values for gaseous products from various series of compounds are plotted against the reciprocal of the number of the structural unit, $1/n$, in Figs. 5, 6 and 7. When the G values obtained from various authors are used for the sake of comparison, the differences in the experimental conditions, such as the types of radiation, the irradiation temperature, the dose rate, the dose, and the density of the samples, should be taken into consideration. Therefore, for the paraffin series, the G values which were obtained under the most similar experimental conditions are plotted in Figs. 8 and 9. The G values from gaseous substances are plotted in Figs. 8a and 9a, while those from liquid or solid substances are plotted in Figs. 8b and 9b. The G values obtained by different authors are

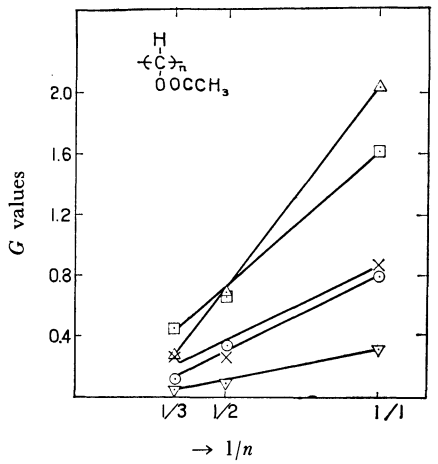

Fig. 5. G values vs. reciprocal of the number of the structural unit.

⊙ H_2, △ CH_4, ▣ CO, ▽ C_2H_6, × CO_2

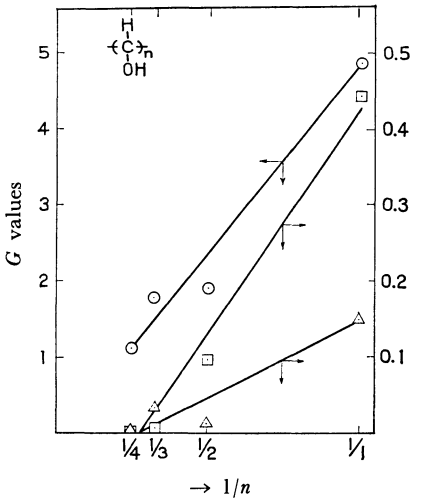

Fig. 6. G values vs. reciprocal of the number of the structural unit.

⊙ H_2, △ CH_4, ▣ CO

also plotted by the use of different symbols in Figs. 8c and 9c. The mean values were adopted as representative when different G values have been reported for a compound.

The G values have linear relations to the reciprocal of the number of the structural unit, $1/n$, in the R=CH_3COO, R=HO and R=CH_3CO series. In the series of paraffin hydrocarbons, R=H, $G(H_2)$ is independent of the structural unit in the $n \geqq$ ca. 6 region and has a linear relation to $1/n$ in the $n \leqq$ ca. 6 region as well as G values from the other series, while $G(CH_4)$ has an almost linear relation to $1/n$ in the two regions.

A schematic process of this radiation-chemical reaction may be presented as follows. The mole-

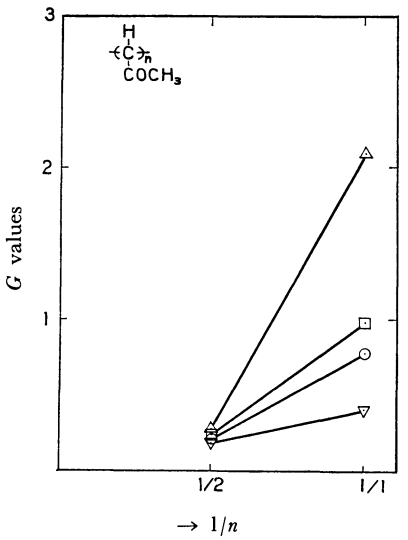

Fig. 7. G values vs. reciprocal of the number of the structural unit.

⊙ H_2, △ CH_4, ▣ CO, ▽ C_2H_6

cule which absorbs energy from ionizing radiations is excited or ionized:

$$A \rightsquigarrow \begin{bmatrix} A^+ + e^- \\ A^* \end{bmatrix} \quad (1)$$

Some produced ions turn finally into excited molecules by means of electron capture;

$$A^+ + e^- \longrightarrow A^* \quad (2)$$

Therefore the primary species correspond to excited molecules or molecular ions, which decompose into radicals and/or produce stable molecules through recombination, abstraction, disproportionation, and other reactions:

$$A^+, A^* \longrightarrow B + C \quad (3)$$

In short, a molecule which absorbs energy of radiation is excited or ionized, and these species decompose to radicals and/or stable products by the bond-rupture of the main or side chain. On the other hand, the overall yield of the product thus formed is generally expressed by the G value. The above relations between the structural units of the compounds and the G values of the products can be explained if the mechanism of the unimolecular decomposition of the excited molecule or molecular ion and the successive reactions are available.

It was proposed by Alexander and Charlesby[59] that the energy absorbed may be transferred over a comparatively far distance along the C–C chain; they based their proposal on their experimental findings that a copolymer of 20 per cent styrene

59) P. Alexander and A. Charlesby, *Nature*, **173**, 578 (1954).

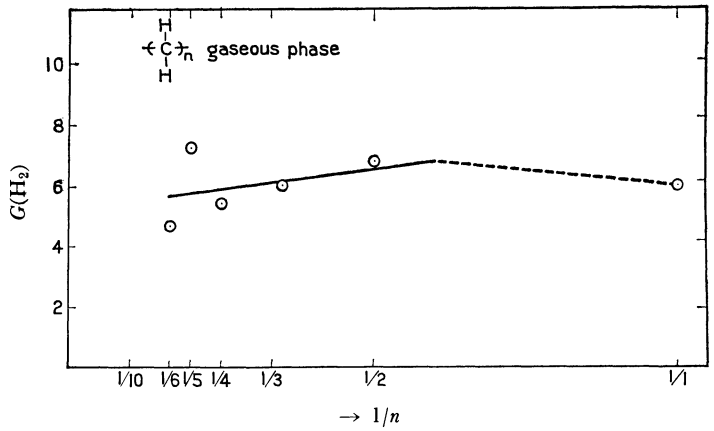

Fig. 8a. *G* values vs. reciprocal of the number of the structural unit.

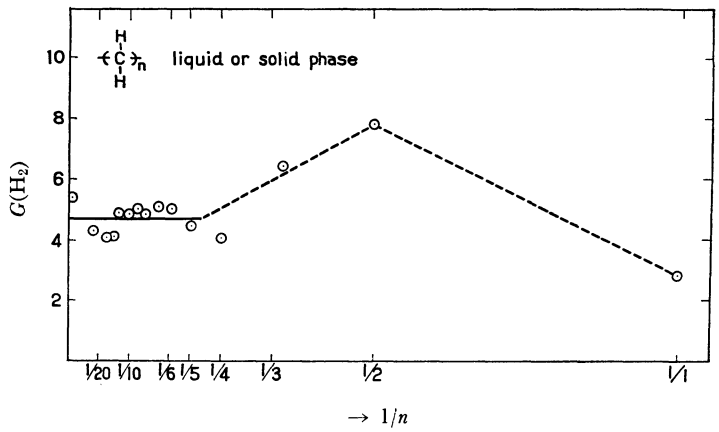

Fig. 8b. *G* values vs. reciprocal of the number of the structural unit.

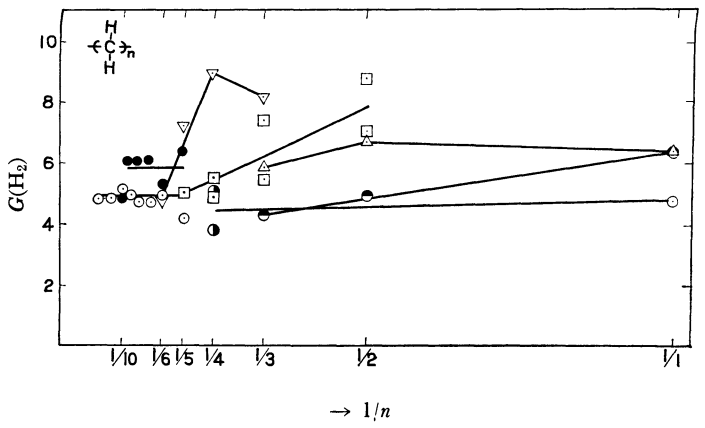

Fig. 8c. *G* values vs. reciprocal of the number of the structural unit.

⊙ Ref. 42, ⊡ Ref. 36, ● Ref. 44, ◓ Ref. 25,
△ Ref. 24, ▽ Ref. 35, ◑ Ref. 27

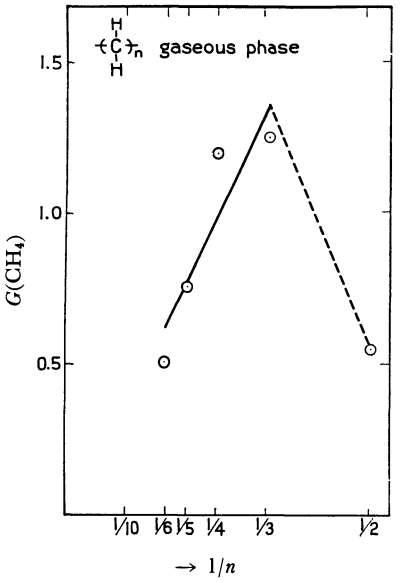

Fig. 9a. G values vs. reciprocal of the number of the structural unit.

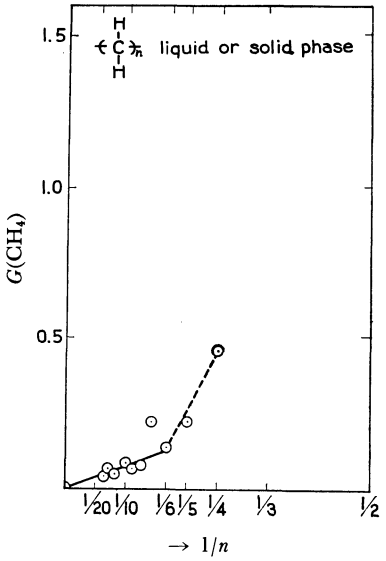

Fig. 9b. G values vs. reciprocal of the number of the structural unit.

and 80 per cent isobutylene is more resistant than the pure isobutylene, and that dose required to render a straight-chain hydrocarbon infusible is greatly increased by the presence of an aromatic ring.

It is interesting to compare the results of the following two systems; in one, (A) is a monomer, M, while in the other (B) is a polymer composed of such a monomer, the monomeric unit being assumed to have a similar chemical structure in both systems:

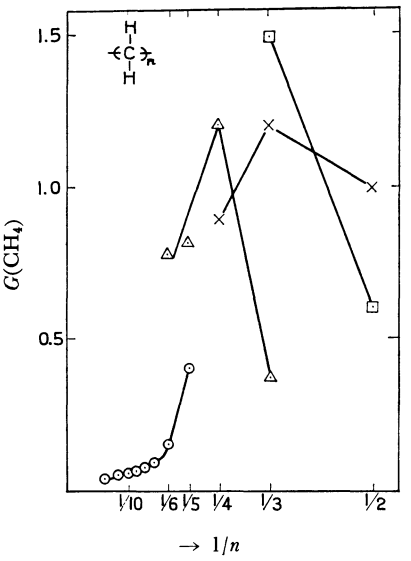

Fig. 9c. G values vs. reciprocal of the number of the structural unit.
⊙ Ref. 42, △ Ref. 25, ▣ Ref. 35, × Ref. 24

(A) M M M M* M M M M

(B) — M — M — M — M*— M — — M — M — M —

In the A system, the energy absorbed is localized on the excited molecule, M*, and enhances the probability of the decomposition of M*, although some part of the energy may be transferred to other molecules. On the other hand, in the B system, the energy absorbed is transferred away by an intramolecular process through the chemical bonds in addition to the intermolecular process. Therefore, the G values of decomposition may be expected to be larger in the A system than in the B system, and if homologous compounds are compared, their G values will decrease with an increase in the number of the monomeric unit, n, in a molecule. However, as the transfer of energy through chemical bonds may be restricted within several bonds, m, the G values of decomposition will be independent of n which is larger than m. This expectation is realized by Figs. 5, 6, 7 and 8, with the exception of $G(CH_4)$ from paraffins. The "m" number is evaluated in each series of -(-CHR-)-$_n$ to be as follows:

R	H	HO	CH_3CO	CH_3COO
m	ca. 6	>4	>2	>3

When R is H, that is, for hydrocarbons, m is given as ca. 6, while is not very different from the $m=12$ stated by Alexander and Charlesby.[59] The same reasoning may be applicable to the other series, in which the G values from monomeric compounds

Table V. A comparison of $G(H_2)$ values from monomers and polymers

Ethylbenzene[60]	$G(H_2)=0.18$
Polystyrene[61,62]	$G(H_2)=0.03$—0.04
Ethanol[63-72]	$G(H_2)=3.5$—5.53
Polyvinylalcohol[62]	$G(H_2)=1.6$
Polyethylene[73-75]	$G(H_2)=3.75$—6.0
Polymethylene[58]	$G(H_2)=5.4$

should be several times larger than those from the corresponding polymers. $G(H_2)$ from polyethylene is nearly equal to that obtained from polymethylene, as was to be expected. Table V compares the $G(H_2)$ values from monomers and polymers.

The curve of $G(CH_4)$ vs. $1/n$ for paraffins shows a different tendency from the curves of the others. This result may be explained similarly as far as the energy transfer is concerned, but the terminal effect must also be introduced. Methane is assumed to come from the rupture of the terminal C–C bonds, and it results only from the excitation of the $m/2$ carbon atoms from the terminal carbon atoms of both ends. Since the carbon atoms in the hydrocarbon molecule are assumed to be excited with an equal probability, the probability of the excitation of carbon atoms within $m/2$ from the terminals is m/n. If the G value of methane formation from hydrocarbons containing i carbon atoms is denoted by $G_i(CH_4)$, $G_n(CH_4)$ is expressed by the equation, $G_n(CH_4)=(m/n)G_m(CH_4)$, in the $n \geqq m$, region, and it decreases with an increase of n in the $n \leqq m$ region as well as the G values of the other products.

The authors are very grateful to Dr. Meiseki Katayama for his suggestions.

60) T. J. Sworski and M. A. Burton, *J. Am. Chem. Soc.*, **73**, 3790 (1951).
61) L. A. Hall and D. W. Brown, *J. Phys. Chem.*, **61**, 129 (1957).
62) A. Chapiro, "Radiation Chemistry of Polymeric Systems," Interscience Publishers, New York (1962), p. 358.
63) A. S. Newton and W. R. McDonell, *J. Am. Chem. Soc.*, **78**, 4554 (1956).
64) W. R. McDonell and A. S. Newton, ibid., **76**, 4651 (1954).
65) J. G. Burr, *J. Phys. Chem.*, **61**, 1477 (1957).
66) G. E. Adams, J. H. Baxendale and R. D. Sedgwick, ibid., **63**, 854 (1959).
67) E. Hayon and J. J. Weiss, *J. Chem. Soc.*, **1961**, 3962.
68) R. H. Johnsen, *J. Phys. Chem.*, **65**, 2144 (1961).
69) J. M. Ramaradhya and G. R. Freeman, *Can. J. Chem.*, **39**, 1836 (1961).
70) G. E. Adams and R. D. Sedgwick, *Trans. Faraday Soc.*, **60**, 865 (1964).
71) J. J. J. Myron and G. R. Freeman, *Can. J. Chem.*, **43**, 381 (1965).
72) J. J. J. Myron and G. R. Freeman, ibid., **43**, 1484 (1965).
73) E. L. Lawton, P. D. Zemany and J. S. Balwit, *J. Am. Chem. Soc.*, **76**, 3437 (1954).
74) T. F. Williams and M. Dole, ibid., **81**, 2919 (1959).
75) M. Dole and W. H. Howard, *J. Phys. Chem.*, **61**, 137 (1957).

BULLETIN OF THE CHEMICAL SOCIETY OF JAPAN VOL. 39 1886—1893 (1966)

The Effects of Polyamines on the Melting of Polyriboadenylic Acid Plus Polyribouridylic Acid Complexes in a Solution

By Shigesada HIGUCHI and Masamichi TSUBOI

Faculty of Pharmaceutical Sciences, University of Tokyo, Hongo, Bunkyo-ku, Tokyo

(Received January 17, 1966)

Ultraviolet absorptions of aqueous systems of polyriboadenylic acid (poly A) plus polyribouridylic acid (poly U) have been examined with various Na^+ and Mg^{2+} concentrations and at various temperatures. The transition temperatures (T_m) among the two-stranded conformation, poly(A+U), the three-stranded conformation, poly(A+2U), and the two single-stranded conformations, poly A and poly U, were determined. The effects upon the T_m of adding NH_3^+-$(CH_2)_nNH_3^+$-type diamines (n=2, 3, 4, 5, 6, and 8), spermine, and actinomycin D to the solutions were observed. It was found that these amines stabilize three-stranded poly(A+2U) more than they stabilize the two-stranded (poly(A+U)) and the single-stranded (poly A and poly U) conformations. Among the diamines examined, those with n=2 and 3 values show a greater effect than those with n=4, 5, 6, and 8 values.

This is our second paper on the effects of polyamines on the melting of synthetic nucleic acids. In our first paper[1] we dealt with an aqueous-solution system containing polyriboinosinic acid (poly I) and polyribocytidylic acid (poly C).

1) K. Matsuo and M. Tsuboi, This Bulletin, **39**, 347 (1966).

The word "melting" means a transition in the solution from the double-helical conformation of a 1 : 1 complex, poly(I+C), of these two polymers into random coils of poly I and poly C, i. e.:

$$\text{Poly(I+C)} \rightarrow \text{Poly I} + \text{poly C.} \quad (1)$$

In the present paper we will deal with a system containing polyriboadenylic acid (poly A) and polyribouridylic acid (poly U). Both of these two acids, like poly I and poly C, are synthetic polymers which have the same ribose-phosphate backbone as natural ribonucleic acid (RNA).[2] The system of poly A and poly U is, however, somewhat more complicated than the system of poly I and poly C. In the former, not only a double-helical complex[3] poly(A+U), but also a triple-helical complex[4] poly(A+2U), is formed. Not only a helix-to-random-coil transition, but also transitions of double-to-triple and triple-to-double helices, take place.[5,6] The transition temperatures are affected by the salt concentration in the system, and also by the polyamines added to the solution. The effects of these polyamines are the main subject of this paper.

Experimental

Two samples of polyriboadenylic acid (poly A) were used in the present study. One was purchased from the California Biochemicals Corporation, it showed 4S in an ultracentrifugal sedimentation experiment (Cal. Bio. poly A). The other, purchased from the Miles Chemical Company, showed 8.3S in an ultracentrifugal sedimentation experiment (Miles poly A). Polyribouridylic acid (poly U) was prepared by the use of polynucleotide phosphorylase obtained from *Azotobacter vinelandii*. The product was purified as follows: first it was precipitated by cold ethanol; then it was dissolved in water, deproteinized by chloroform, dialysed against an aqueous solution of 0.01 M ethylene diamine tetraacetate (pH 8), a 1.0 M sodium chloride solution, and distilled water successively, and finally lyophilized. Seven different samples were obtained: Nos. 24, 27, 38, 40, 47, 49, and 50. The sedimentation constants of these samples were, respectively, 8S, 6S, 3.6S, 5.0S, 4.1S, 3.5S, and 1.2S. The polynucleotide concentration in each standard solution was determined by measuring the phosphorous content.[7]

The samples of ethylenediamine dihydrochloride ($NH_3^+(CH_2)_2NH_3^+\cdot 2Cl^-$), 1, 3-diaminopropane dihydrochloride ($NH_3^+(CH_2)_3NH_3^+\cdot 2Cl^-$), 1, 4-diaminobutane dihydrochloride ($NH_3^+(CH_2)_4NH_3^+\cdot 2Cl^-$), 1, 5-diaminopentane dihydrochloride ($NH_3^+(CH_2)_5NH_3^+\cdot 2Cl^-$), 1, 6-diaminohexane dihydrochloride ($NH_3^+(CH_2)_6NH_3^+\cdot 2Cl^-$), 1, 8-diaminooctane dihydrochloride ($NH_3^+(CH_2)_8NH_3^+\cdot 2Cl^-$), and spermine tetrahydrochloride ($NH_3^+(CH_2)_3NH_2^+(CH_2)_4NH_2^+(CH_2)_3NH_3^+\cdot 4Cl^-$) used in this work are all the same as those used in the previous work.[1]

For tracing the conformational changes of the polymers, the ultraviolet absorptions were observed by the use of an Ito Spectrophotometer, Model QU-3. The temperature of the sample solution was controlled as described in our previous paper.[1]

Results and Discussion

1. Evidence of the Formation of a Two-stranded Complex and a Three-stranded Complex.—First, the following three preliminary examinations were made to ascertain whether our samples of poly A and poly U show evidence of forming a multi-stranded complex in solution, as previous investigators[3-6] have reported.

(*i*) *Ultracentrifugal Sedimentation.*—It has been shown that a 1 mole-to-1 mole mixture solution (in a 0.1 M sodium chloride + 0.01 M sodium citrate buffer, pH 7.0) of our poly A and poly U shows only one peak in an untracentrifugal sedimentation pattern (with Schlielen optics). This indicates that a 1 : 1 complex is formed. The sedimentation constant of the complex is found to be appreciably greater than those of the components. For example, the complex of poly A from the California Biochemicals Corp. with 4S and No. 38 poly U with 3.6S gives a sedimentation constant of 6.8S. The complex of Miles poly A with 8.3S and No. 49 poly U with 3.5S gives a sedimentation constant of 11.6S.

(*ii*) *Ultraviolet Absorptions.*—Poly A in a 0.15 M sodium chloride + 0.015 M sodium citrate buffer of pH 7.0 gives a spectrum with an absorption maximum at 257 mμ, and poly U in the same solvent gives a spectrum with an absorption maximum at 261 mμ, while a 1 : 1 mixture shows a spectrum with a maximum at 257 mμ. This spectrum was exactly the same as that reported by Warner.[8] On alkali hydrolysis a gerat hyperchromicity is observed in this absorption band.

(*iii*) *Mixing Curve.*—The absorbance was measured at 259 mμ for several mixtures (at 18±2°C) containing varying proportions of poly A and poly U, while the total nucleotide concentration was kept constant. The solvents examined were as follows:

a) 0.15 M NaCl plus a 0.015 M Na-citrate buffer (pH 7.0).

b) 0.025 M NaCl plus a 0.0005 M Na-citrate buffer (pH 7).

c) 0.015 M NaCl plus a 0.045 M glycylglycine buffer (pH 7.0).

d) 0.1 M NaCl plus a 0.01 M glycylglycine buffer (pH 7.1).

2) M. Grunberg-Manago, P. J. Ortiz and S. Ochoa, *Science*, **122**, 907 (1955).
3) A. Rich and D. R. Davies, *J. Am. Chem. Soc.*, **78**, 3548 (1956).
4) G. Felsenfeld, D. R. Davies and A. Rich, ibid., **79**, 2023 (1957).
5) J. R. Fresco, "Informational Macromolecules," Ed. by H. J. Vogel, V. Bryson and J. Q. Lampen, Academic Press, New York (1963), p. 121.
6) C. L. Stevens and G. Felsenfeld, *Biopolymers*, **2**, 293 (1964).
7) G. R. Bartlett, *J. Biol. Chem.*, **234**, 466 (1959).
8) R. C. Warner, ibid., **229**, 771 (1957).

Table I. A summary of what Stevens and Felsenfeld[6] found of the melting process in mixted solutions of poly A and poly U.

A : U mole ratio in the solution	Salt concn.		Melting process	At 259 mμ	At 280 mμ
1 : 1	Low	(A)	Poly(A + U) → poly A + poly U	hyper	no change
	High or + Mg^{2+}	(B)	2 poly(A + U) → poly(A + 2U) + poly A	no change	hypo
			→ 2 poly A + 2 poly U	hyper	hyper
1 : 2	Low	(C)	Poly(A + 2U) → poly(A + U) + poly U	hyper	hyper
			→ poly A + 2 poly U	hyper	no change
	High or + Mg^{2+}	(D)	Poly(A + 2U) → poly A + 2 poly U	hyper	hyper

(This is what Felsenfeld, Davies, and Rich[4] used.)

e) d) plus 0.00025 M ethylenediaminetetraacetic acid (EDTA).

f) d) plus 0.0016 M EDTA.

g) 3 ml. of d) plus 1 ml. of a 0.04 M EDTA solution.

h) d) plus 0.01 M EDTA.

In most cases the absorbance was observed immediately after the mixing of poly A and poly U. In the solvent d) however, the absorbance was observed not only immediately after the mixing, but also 25 min., 2 hr. and 54 hr. after the mixing. In the solvent g) the absorbance was observed 15 min. and 40 min. after the mixing, and also after the mixed solution had been kept overnight. The resulting mixing curve was always similar to what Felsenfeld, Davies, and Rich[4] observed in a solvent with 1.2×10^{-2} M magnesium chloride. It is composed of two straight lines which intersect sharply at a poly A : poly U mole ratio of 1 : 2, as is illustrated in Fig. 1. This indicates that,

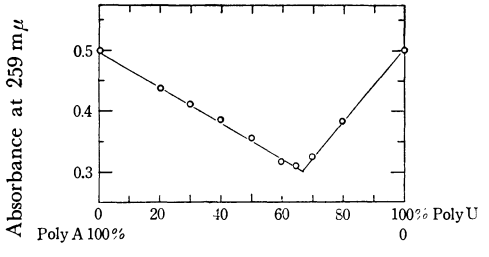

Fig. 1. A mixing curve for poly A and poly U. Solvent: 0.1 M NaCl plus 0.01 M glycylglycine buffer, pH 7.1. Temperature : 18±2°C. The absorbance at 259 mμ was observed at 54 hr. after every mixing of poly A and poly U.

in a mixture of 1 mole of poly A and 2 moles of poly U, a three-stranded complex, poly(A+2U), is formed under any of the above sets of conditions. What we observed in solvent d) is, however, different from what Felsenfeld, Davies, and Rich[4] observed. In this solvent, they observed a mixing curve composed of two straight lines which intersect at a mole ratio of 1 : 1. As will be shown below, this difference may be partly due to the difference in the temperature of the solution. They observed the mixing curve at 25°C, while we observed it at 18°C. On the basis of our rather detailed examination (see above), we may conclude that, at 18°C, a 1 mole-to-2 mole mixture of our poly A and poly U forms a three-stranded complex, poly(A+2U), even in a solvent with a low salt concentration.

2. The Melting Process of Poly(A+U) and Poly(A+2U).—A series of examinations were made to find out the conditions under which poly(A+U) and poly(A+2U) are stable and the process through which these complexes melt into random coils of poly A and poly U. As we were conducting our examinations, a paper of Stevens and Felsenfeld[6] reporting a similar attemt appeared. They showed that the melting process can be followed by tracing the absorbance at 260 mμ and that at 280 mμ. What they found is summarized in Table I. We found, as is illustrated in Fig. 2, that our samples of poly A and poly U show the same behavior as they found (compare Fig. 2 with Table I). On the basis of the results of other similar experiments of ours, as well as of a few previous works by others,[5,6] we have constructed diagrams shown in Figs. 3 and 4. These diagrams illustrate how the melting process in question depends upon the Na^+ concentration in the solvent. Because of an unknown factor, different batches of samples show some small but appreciable differences in melting temperatures. For example, poly(A+U) with No. 49 poly U shows a slightly but still appreciably higher T_m value than poly(A+U) with No. 47 poly U. The sedimentation constants of these two poly U's (No. 49 and 47) are 3.5S and 4.1S respectively, almost equal to each other. The transition temperatures of poly(A+2U) to poly(A+U) in the 1 mole-to-2 moles mixture of our samples are appreciably higher than those observed by Fresco[5] in a region with a lower salt concentration (see Fig. 4). As has been described in the preceding section, our sample does not form poly(A+U) at 18°C, even in a very low-salt environment. In general, the equilibrium of poly(A+U) and poly(A+2U) is a rather delicate one, as will be illustrated in the next section.

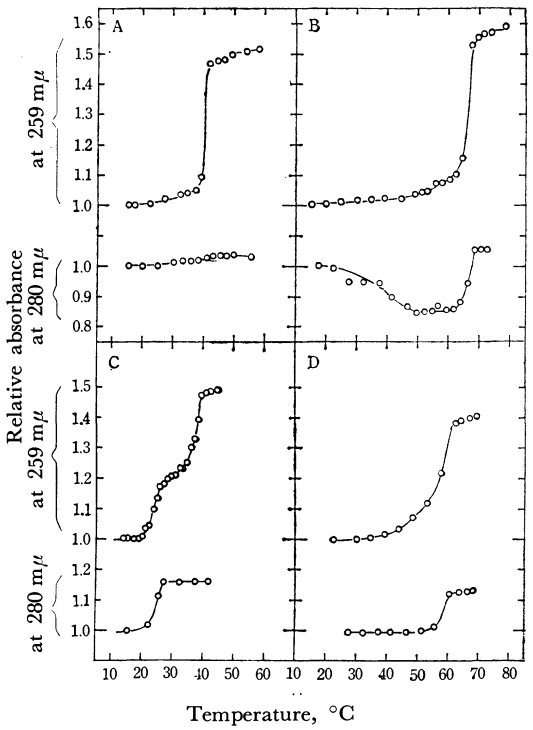

Fig. 2. Four types of melting process A, B, C, and D (See Table I) of helical complexes in mixed solution of poly A and poly U, as followed by observing the absorbance at 259 mμ and 280 mμ.

A: 1 mol. to 1 mol. mixture of Miles poly A and No. 49 poly U in 0.01 M NaCl+0.001 M Na-citrate buffer, pH 7

B: The same with A except +0.001 M $MgCl_2$

C: 1 mol. to 2 mol. mixture of Miles poly A and No. 50 poly U in 0.01 M NaCl+0.001 M Na-citrate buffer, pH 7

D: 1 mol. to 2 mol. mixture of Miles poly A and No. 50 poly U in 0.001 M $MgCl_2$+0.001 M Na-citrate buffer, pH 7

3. A Metastable Poly(A+2U).—In connection with the equilibrium between the two- and three-stranded complexes, we also noticed the following phenomenon.

Miles poly A plus No. 50 (or No. 47) poly U were dissolved, in a 1 : 1 mole ratio, into 0.01 M sodium chloride plus a 0.001 M sodium citrate buffer (pH 7), the solution was then heated. The absorbance at 259 mμ shows one-step melting at 39°C, while the absorbance at 280 mμ shows almost no change throughout the temperature range (15—45°C) examined. The solution of the melted polynucleotides was slowly cooled to 15°C (2 hr. for 45→15°C) and was then examined again as to its melting profile. The absorbance at 259 mμ shows two-step transitions at 26°C and 39°C, while the absorbance at 280 mμ shows a transition at 26°C. This melting profile is similar to

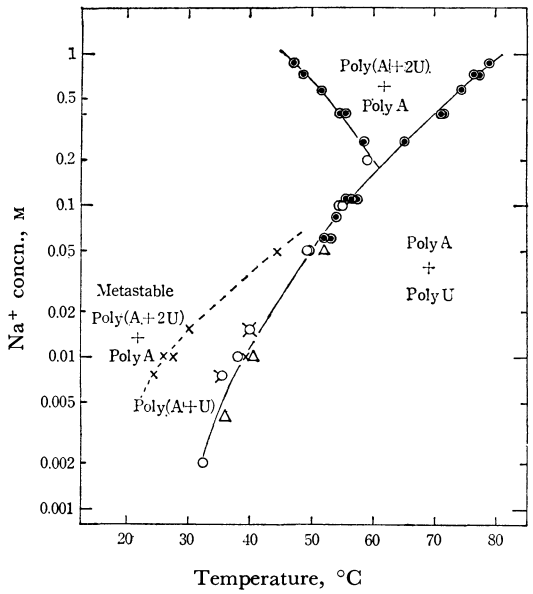

Fig. 3. Melting temperatures of poly(A+U) and poly(A+2U) in solutions with poly A and poly U in 1 : 1 mole ratio and with various Na^+ concentrations.

○: Miles poly A+No. 47 poly U
△: Miles poly A+No. 49 poly U
⊙: Observed by Stevens and Felsenfeld[6]
×: Observed for metastable poly(A+2U) (See section 3)

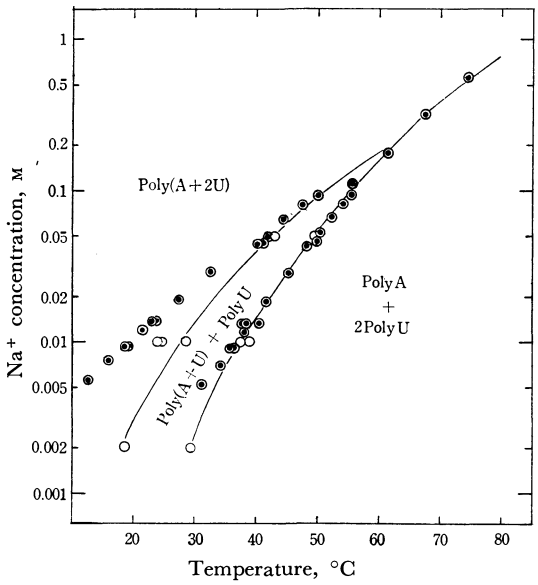

Fig. 4. Melting temperatures of poly(A+2U) and poly(A+U) in solutions with poly A and poly U in 1 : 2 mole ratio and with various Na^+ concentrations.

○: Miles poly A+No. 50 poly U
⊙: Observed by Fresco[5]

that of poly(A+2U) (the type C profile given in Table I or in Fig. 2).

This fact may be interpreted as indicating that the mixing of poly A and poly U (1 : 1) at room temperature causes this reaction:

$$\text{poly A} + \text{poly U} \rightarrow \text{poly(A + U)}, \quad (2)$$

However, the cooling of the melted poly A and poly U (1 : 1) mixture causes another reaction:

$$\text{poly A} + \text{poly U} \rightarrow {}^1/_2\,\text{poly(A + 2U)} + {}^1/_2\,\text{poly A}. \quad (3)$$

Support for this interpretations was obtained by another experiment. First, the three-stranded complex poly(A+2U) was formed in a solution, and then poly A was added to the solution so that the resulting total amounts of poly A and poly U became equivalent to each other (1 : 1 mole ratio). The resultant solution shows a melting profile similar to that of poly(A+2U) in a solution with a 1 : 2 mole ratio. Thus, the added poly A does not react with poly(A+2U); in other words, the reaction:

$${}^1/_2\,\text{poly(A + 2U)} + {}^1/_2\,\text{poly A} \rightarrow \text{poly(A + U)} \quad (4)$$

does not proceed in a low-salt-content environment.

Poly A does not form any highly-ordered conformation by itself at a neutral pH value. Therefore, at lower temperatures, poly(A+U) may be considered to be more stable than the partiallymelted form, 1/2 poly(A+2U) + 1/2 poly A. Thus, the poly(A+2U) resulting from reaction (3) may be considered to be in a metastable state.

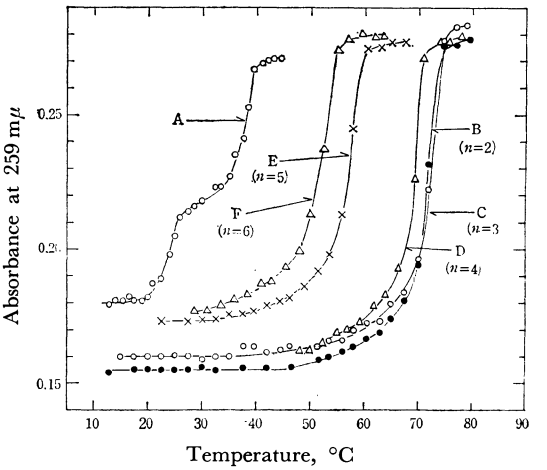

Fig. 6. The variation of the absorbance of Miles poly A plus No. 50 poly U (1 : 2) plus diamine ($NH_3^+(CH_2)_nNH_3^+$) solutions at 259 mμ with temperature.
Solvent: 0.01 M NaCl plus 0.001 M Na-citrate buffer, pH 7
A: No amine, B: 0.001 M $NH_3^+(CH_2)_2NH_3^+$, C: 0.001 M $NH_3^+(CH_2)_3NH_3^+$, D: 0.001 M $NH_3^+(CH_2)_4NH_3^+$, E: 0.001 M $NH_3^+(CH_2)_5NH_3^+$, F: 0.001 M $NH_3^+(CH_2)_6NH_3^+$

4. The Effects of Diamines.—When a $NH_3^+(CH_2)_nNH_3^+$-type diamine is added to a solution of poly(A+U) or poly(A+2U), an effect on the melting profile similar to that of an elevation of the salt concentration of a solution

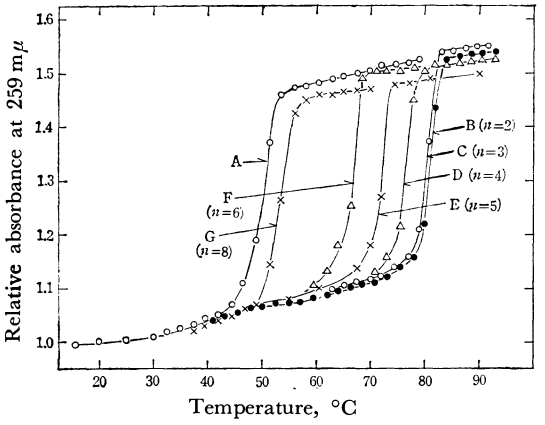

Fig. 5. The variation of the absorbance of Miles poly A plus No. 47 poly U (1 : 1) plus diamine ($NH_3^+(CH_2)_nNH_3^+$) solutions at 259 mμ with temperature.
Solvent: 0.05 M NaCl plus 0.001 M Na-citrate buffer, pH 6.5—7.0
A: No. amine, B: 0.01 M $NH_3^+(CH_2)_2NH_3^+$, C: 0.01 M $NH_3^+(CH_2)_3NH_3^+$, D: 0.01 M $NH_3^+(CH_2)_4NH_3^+$, E: 0.01 M $NH_3^+(CH_2)_5NH_3^+$, F: 0.01 M $NH_3^+(CH_2)_6NH_3^+$, G: 0.005 M $NH_3^+(CH_2)_8NH_3^+$

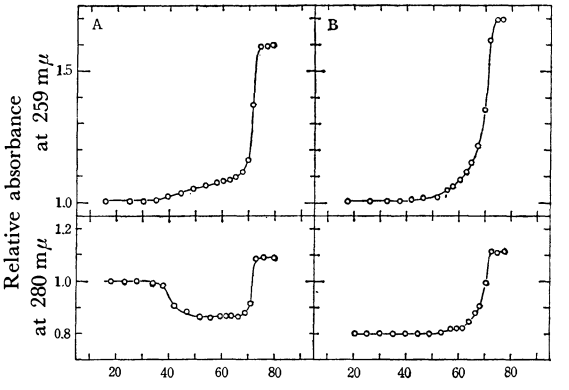

Fig. 7. The variation of the absorbance at 259 mμ and at 280 mμ of poly A plus poly U plus ethylenediamine dihydrochloride solutions with temperature.
Solvent: 0.001 M NaCl plus 0.001 M Na-citrate buffer, pH 7
A: Miles poly A plus No. 49 poly U in 1 : 1 mole ratio plus 0.001 M $NH_3^+(CH_2)_2NH_3^+$
B: Miles poly A plus No. 50 poly U in 1 : 2 mole ratio plus 0.001 M $NH_3^+(CH_2)_2NH_3^+$

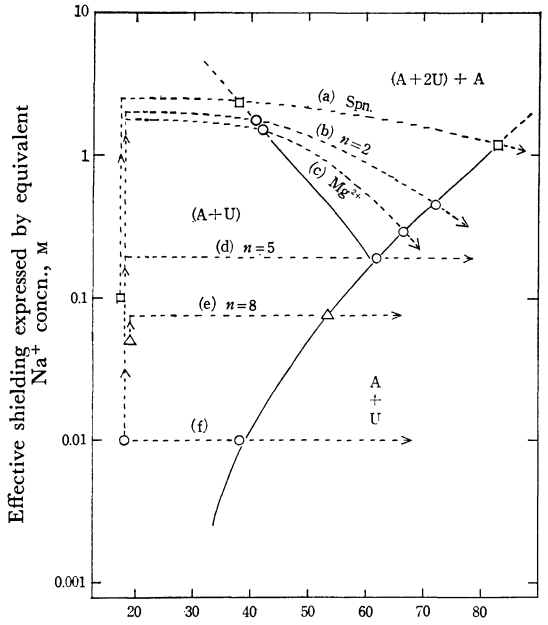

Fig. 8. Route of melting of poly(A+U) drawn on a phase diagram similar to Fig. 3, in a solution (a) with 0.001 M $NH_3^+(CH_2)_3NH_2^+(CH_2)_4NH_2^+(CH_2)_3NH_3^+$, (b) with 0.001 M $NH_3^+(CH_2)_2NH_3^+$, (c) with 0.001 M $MgCl_2$, (d) with 0.001 M $NH_3^+(CH_2)_5NH_3^+$, (e) with 0.005 M $NH_3^+(CH_2)_8NH_3^+$, or (f) without any divalent cation. The vertical dotted lines indicate the effect of the addition of divalent cations. The starting points of these lines indicate the Na^+ concentration of the solution before the addition of the divalent cations.

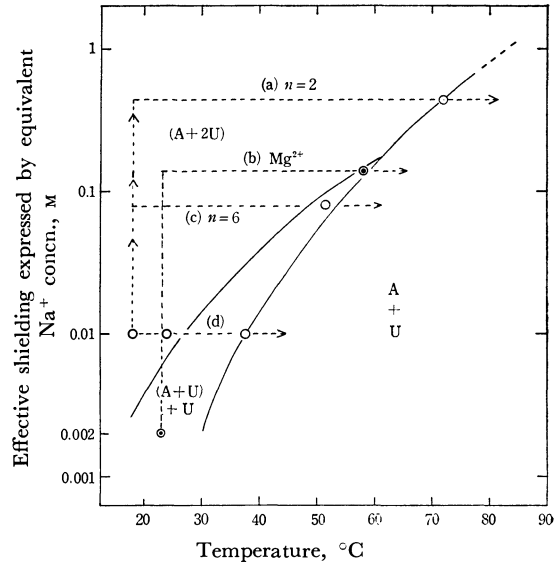

Fig. 9. Route of melting of poly(A+2U) drawn on a phase diagram similar to Fig. 4.
In a solution (a) with 0.001 M $NH_3^+(CH_2)_2NH_3^+$, (b) with 0.001 M $MgCl_2$, (c) with 0.001 M $NH_3^+(CH_2)_6NH_3^+$, or (d) without any divalent cation

is observed (Figs. 5 and 6). The melting temperature of poly(A+U) observed by the absorbance at 259 mμ is elevated (Fig. 5). The melting profile is changed from Type A into Type B (see Table I, Fig. 2, and Fig. 7, A). For poly(A+2U), the two-step melting profile traced by the absorbance at 259 mμ disappears; D-type melting profile is now observed (Fig. 6 and Fig. 7, B). This fact may be interpreted by considering that the effect of the diamine cation is essentially the same as the effect of Na^+, except that the former is much greater than the latter. In general, cations in the solution are considered to be bound by the PO_2^- group of the polynucleotide molecules and to shield the negative charge, so that the inter-strand repulsion is reduced in the two- or three-stranded complex. Therefore, it is probable that phase diagrams similar to those given in Figs. 3 and 4 are valid for every $NH_3^+(CH_2)_nNH_3^+$-type cation, if the ordinate, instead of the actual Na^+ concentration, is assumed to be a measure of the effectiveness of a certain amount of each cation in shielding the negative charge of the polynucleotide chains. On the basis of this interpretation, the effects of a few diamines are shown in Figs. 8 and 9, where the same phase diagrams as are given in Figs. 3 and 4 are used.

As may be seen in Fig. 8, the shielding effect of the $NH_3^+(CH_2)_2NH_3^+$ cation is slightly greater than that of Mg^{2+} for poly(A+U). For poly (A+2U), the shielding effect of $NH_3^+(CH_2)_2 \cdot NH_3^+$ is also somewhat greater than that of Mg^{2+} (see Fig. 9). These facts may be explained by considering that, while the shielding effect of the Mg^{2+} bound to the PO_2^- group may be greater than that of the $NH_3^+(CH_2)_2NH_3^+$, the binding constant of the $NH_3^+(CH_2)_2NH_3^+$ bound to polynucleotide is greater than that of the Mg^{2+}. The binding constant of a $NH_3^+(CH_2)_nNH_3^+$-type cation can be great if the distance of the two amino groups in the cation is nearly equal to the distance between two PO_2^- groups (or between two O^- atoms) in the secondary structure of the polynucleotide molecule in question. In a comparison of diamines with n values of 2, 3, 4, 5, 6, and 8 (cf. Fig. 5), the melting temperatures observed with the $n=2$ and $n=3$ diamines are almost equal to each other and are much higher than the melting temperatures observed with other diamines (see also Fig. 10, (b)). The melting temperature higher than 61°C observed in the system where poly A: poly U=1 : 1 (see Fig. 8) should correspond to the melting reaction:

$$\text{poly(A + 2U) + poly A} \rightarrow \text{2 poly A + 2 poly U} \quad (5)$$

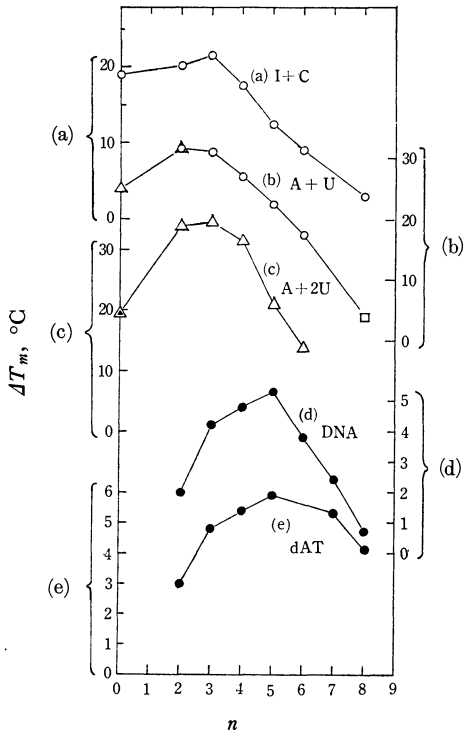

Fig. 10. A relative efficiency of diamines NH_3^+-$(CH_2)_nNH_3^+$ in stabilizing helical nucleic acids plotted against n, the number of the methylene groups placed between the two NH_3^+ groups. The stabilizing efficiency is expressed by an increment in the melting temperature, ΔT_m, of the nucleic acid solution caused by adding a certain amount of the diamine. For $n=0$, ΔT_m caused by Mg^{2+} was plotted. (a) poly(I+C),[1] (b) poly(A+U), (c) poly(A+2U), (d) calf thymus deoxyribonucleic acid,[9] and (e) alternating copolymer of deoxyadenylic acid and deoxythymidylic acid.[9]

○: ΔT_m observed with 0.01 M diamine or Mg^{2+} in 0.05 M NaCl plus 0.01 M Na-citrate buffer, pH 7.0.

△: ΔT_m observed with 0.001 M diamine or Mg^{2+} in 0.01 M NaCl plus 0.001 M Na-citrate buffer, pH 7.

▲: ΔT_m observed with 0.001 M Mg^{2+} plus 0.001 M Na-citrate buffer, pH 7.

□: ΔT_m observed with 0.005 M diamine in 0.05 M NaCl plus 0.001 M Na-citrate buffer, pH 7.

●: ΔT_m observed with 0.04 M diamine in 0.15 M NaCl plus 0.015 M Na-citrate buffer, pH 7.

Therefore, the $NH_3^+\cdots NH_3^+$ distance in the $n=2$ or $n=3$ diamine is considered to reflect a $PO_2^-\cdots PO_2^-$ distance (or $O^-\cdots O^-$ distance) in the three-stranded poly(A+2U) molecule. In the system where poly A : poly U=1 : 2, a melting temperature higher than 61°C should correspond to the melting reaction:

$$\text{poly (A + 2U)} \rightarrow \text{poly A + 2 poly U} \qquad (6)$$

In the comparison regarding this melting temperature shown in Fig. 6, the maximum is also observed around $n=2$ and $n=3$ (see Fig. 10, (c)). As has been described in a previous paper,[1] the maximum ΔT_m value was observed at $n=3$ for poly(I+C) (Fig. 10, (a)). For double-stranded deoxyribonucleic acids, on the other hand, the maximum ΔT_m value was observed at $n=5$[9] (Fig. 10, (d) and (e)). On the basis of what has been described above, these facts may be interpreted as indicating that the nearest $PO_2^-\cdots PO_2^-$ distance (or $O^-\cdots O^-$ distance) in two- or three-stranded-polyribonucleotide is smaller than that in double-stranded polydeoxyribonucleotide.

5. The Effect of Spermine.—The change in the melting profile of poly(A+U) caused by spermine is illustrated in Fig. 11. The melting profile observed with 0.001 M spermine belongs to the Type B in Table I; it is similar to the melting profile observed with 0.001 M Mg^{2+}. The first transition, however, takes place at a lower temperature (at 38°C) with spermine than with Mg^{2+}, while the second transition takes place at a higher temperature (at 83°C) with spermine than with Mg^{2+}. These facts indicate: (1) that spermine (like other cations) stabilizes the three-stranded poly(A+2U) more than it stabilizes the two-stranded poly(A+U) or single-chain poly A and poly U, and (2) that this function of spermine is stronger than that of Mg^{2+}. As may be seen

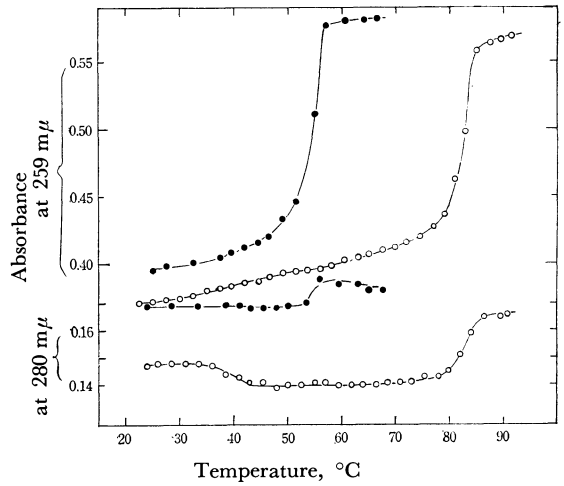

Fig. 11. The variation of the absorbance at 259 mμ and at 280 mμ of Miles poly A plus No. 48 poly U (1 : 1 mol. ratio) solutions with (○) and without (●) spermine (0.001 M).
Solvent: 0.1 M NaCl plus 0.001 M Na-citrate buffer, pH 7

9) H. R. Mahler and B. D. Mehrotra, *Biochim. Biophys. Acta*, **68**, 211 (1963).

in Fig. 8, the effect of spermine (0.001 M) is not only greater than that of Mg^{2+}, but also greater than that of ethylenediamine (0.001 M). This is understandable, because the spermine cation is tetra-valent and so its binding constant to the polynucleotide would be greater and its shielding effect would be greater than those of Mg^{2+} and $NH_3^+(CH_2)_2NH_3^+$. The effect of spermine on the poly A + poly U system may thus be explained qualitatively by considering only the ordinary effect of a cation. So far, it is not necessary to assume a so-called clamping function,[1,10] although it is still probable that spermine has this function also.

6. The Effect of Actinomycin D.—It has been found that 7γ/ml. of actinomycin D has no effect on the melting profile of a 1 : 1 mixture of poly A and poly U.

This work was supported by a grant from the United States Public Health Service (No. GM 10024-02) and a grant from the Ministry of Education of Japan.

10) M. Tsuboi, This Bulletin, **37**, 1514 (1964). (It should be pointed out here that there is a mistake in the DNA model shown in Fig. 11 of this paper.)

BULLETIN OF THE CHEMICAL SOCIETY OF JAPAN VOL. 39 1893—1897 (1966)

The Solvent Effect on the Interaction between Perylene and Antimony Pentachloride

By Haruo KURODA, Takako SAKURAI and Hideo AKAMATU

Department of Chemistry, Faculty of Science, The University of Tokyo, Hongo, Tokyo

(Received January 25, 1966)

The electronic spectrum of the mono-positive ions of perylene formed by the interaction of antimony pentachloride was examined in various solvents. The observed spectra may be classified into two types. The one is the spectrum observed when the solvent is of a high dielectric constant, a spectrum which almost coincides with the spectrum of perylene in sulfuric acid. The other is the spectrum observed for a solution in a solvent of a low dielectric constant, a spectrum consisting of broad absorption bands accompanied by an extra band at about 1200 mμ. The former type of spectrum may be attributed to the perylene ions in a free state stabilized by the solvation, and the latter to an associated state involving perylene and antimony pentachloride ions. It is suggested that, in the association of both kinds of ions, two or more perylene ions are in contact with each other, and that the interaction between them is responsible for the shift and broadening of the absorption bands of perylene ions, as well as for the appearance of the extra band.

Polycyclic aromatic hydrocarbons exhibit characteristic deep colors upon interaction with antimony pentachloride in a polar solvent. Aalbersberg, Hoijtink, Mackor and Weijland[1] have shown that this phenomenon is associated with the formation of positive ions of the hydrocarbons as a result of an electron transfer from the hydrocarbons to antimony pentachloride, which is known as a strong electron acceptor. The interaction between perylene and antimony pentachloride is a typical example of such electron transfer. In effect, as antimony pentachloride is added to a nitrobenzene solution of perylene, the absorption bands of the neutral perylene molecule are replaced with new absorption bands which coincide well with the spectrum of perylene in sulfuric acid. Apparently this change in the spectrum indicates the formation of perylene ions, since the spectrum of a sulfuric acid solution of perylene is known to be due to the mono-positive ions of perylene.[2-4] The electron transfer from perylene to antimony pentachloride also occurs in other solvents. We have noticed, however, that the absorption bands are shifted more or less depending on the solvent. This shift is quite remarkable in some cases, too large for the ordinary solvent effect, so that it seems questionable to regard the perylene ions formed by the interaction of antimony pentachloride as always in a free state

1) W. Ij. Aalbersberg, G. J. Hoijtink, E. L. Mackor and W. P. Weijland, *J. Chem. Soc.*, **1959**, 3055.

2) G. J. Hoijtink and W. P. Weijland, *Rec. trav. chim.*, **76**, 836 (1957).

3) Y. Yokozawa and I. Miyashita, *J. Chem. Phys.*, **25**, 796 (1956).

4) S. I. Weissman, E. de Boer and J. J. Conradi, ibid., **26**, 963 (1956).

in any kind of solvent. The present investigation was undertaken in order to elucidate the effect of solvents on the interaction between perylene and antimony pentachloride.

Experimental

Perylene obtained from the K & K Laboratory was purified by alumina column chromatography, and then by sublimation in vacuo. The following solvents were used: (1) *n*-heptane, (2) cyclohexane, (3) carbon tetrachloride, (4) benzene, (5) toluene, (6) carbon disulfide, (7) trichloroethylene, (8) chloroform, (9) *α*-chloronaphthalene, (10) bromobenzene, (11) chlorobenzene, (12) tetrachloroethane, (13) *cis*-dichloroethylene, (14) *o*-dichlorobenzene, (15) nitrobenzene, and (16) acetonitrile. A solution of perylene, about 10^{-5} mol./l., was prepared with each solvent after it had been well dried by using calcium chloride. Antimony pentachloride was added to the solutions until the absorption spectrum of the neutral perylene molecule was replaced almost completely with the spectrum of the perylene ion. This was usually made with an excess amount of antimony pentachloride. The solutions were not very stable since antimony pentachloride decomposes slowly in most solvents. Therefore, the spectrum was observed immediately after the preparation of each solution. The absorption spectrum in the visible and near-infrared region was measured by means of a Hitachi EPS-2U recording spectrophotometer.

Results and Discussion

The absorption spectra observed in the presence of an excess amount of antimony pentachloride can be classified into two types. The one type of the spectra, which we shall call "type A," has a weak band at about 740 mμ and a strong and sharp band in the 540—560 mμ region. An example of the type A spectrum is given in Fig. 1. This coincides very well with the spectrum of perylene in sulfuric acid (Fig. 2), except for the small red-

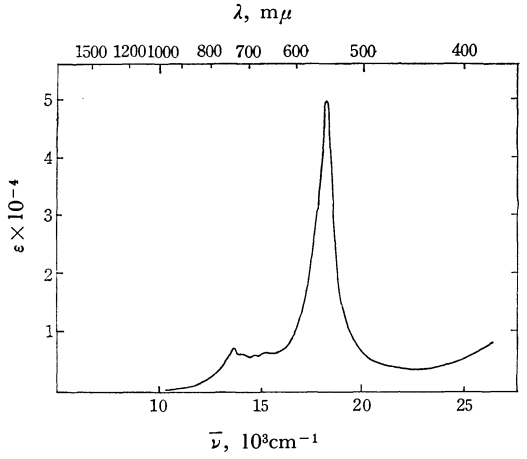

Fig. 1. Absorption spectrum of perylene-$SbCl_5$ in chlorobenzene.

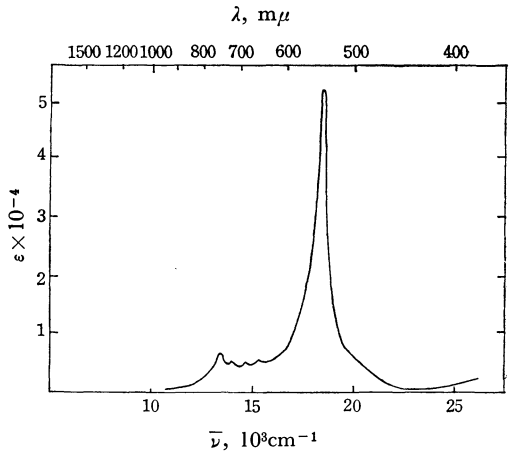

Fig. 2. Absorption spectrum of a sulfuric acid solution of perylene.

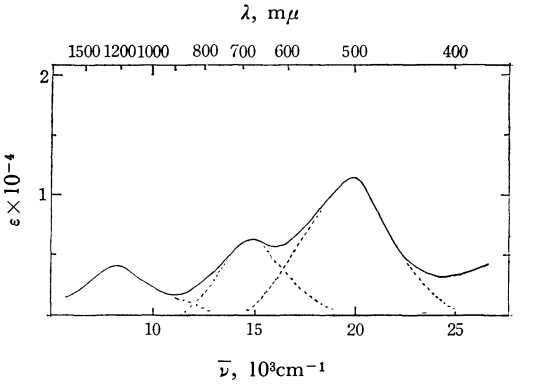

Fig. 3. Absorption spectrum of perylene-$SbCl_5$ in trichloroethylene.

shift of the strong band. The other type of spectrum, "type B", is shown in Fig. 3; this is observed for a trichloroethylene solution. A spectrum of this type is observed when the solvent is of a low dielectric constant. In this case, the absorption bands are appreciably broadened and, at the same time, the strong band of perylene ions at about 550 mμ is considerably blue-shifted. Interestingly, a broad absorption band appears at about 1200 mμ in the spectra of type B, a band which can never be found in the spectra of type A. The origin of this band will be discussed later. The observed wavelengths of the absorption bands are summarized in Table I.

Accoring to Bayliss' theory on the solvent effect,[5] the frequency difference in an absorption band between the gaseous state and the solution is approximately expressed by the following equation:

$$\Delta\nu = b(n^2 - 1)/(2n^2 + 1) \qquad (1)$$

where n is the refractive index of the solvent for the sodium-D line, and b is a constant dependent

5) N. S. Bayliss, *J. Chem. Phys.*, **18**, 292 (1950).

Table I. Absorption bands of perylene-$SbCl_5$ in various solvents

	Solvent	Wavelengths of absorption bands (mμ) I	II	III	Type of spectrum
(1)	*n*-Heptane	504 (b)	700 (b)	1200 (b)	B
(2)	Cyclohexane	512 (b)	710 (b)	1250 (b)	B
(3)	Carbon tetrachloride	521 (b)	700 (b)	1250 (b)	B
(4)	Benzene	510 (b)	710 (b)	1200 (b)	B
(5)	Toluene	517 (b)	710 (b)	1200 (b)	B
(6)	Carbon disulfide	508 (b)	650 (b)	1550 (b) (shoulder at 1200)	B*
(7)	Trichloroethylene	502 (b)	680 (b)	1250	B
(8)	Chloroform	545 (s)	742 (s)		A
(9)	α-Chloronaphthalene	558 (s)	755 (s)		A
(10)	Bromobenzene	562 (s)	748 (s)		A
(11)	Chlorobenzene	559 (s)	745 (s)		A
(12)	Tetrachloroethane	547 (s)	745 (s)		A
(13)	*cis*-Dichloroethylene	546 (s)	740 (s)		A
(14)	*o*-Dichlorobenzene	560 (s)	745 (s)		A
(15)	Nitrobenzene	556 (s)	740 (s)		A
(16)	Acetonitrile	538 (s)	735 (s)		A
(17)	Sulfuric acid**	540 (s)	735 (s)		A

b=broad. s=sharp

* This spectrum is appreciably different from other spectra of type B.

** The spectrum of perylene ion in sulfuric acid.

on the oscillator strength of the transition. In the more refined theories given by McRae[6] and Ooshika,[7] it is shown that the solvent shift depends not only on the refractive index, but also on the dielectric constant and other properties of the solvent. However, the Bayliss' relation would be approximately satisfied in the case of an absorption band of a non-polar molecule in a non-polar solvent. This relation can be extended even to the absorption band of a non-polar molecule in a polar solvent, but not to the band of a polar molecule.

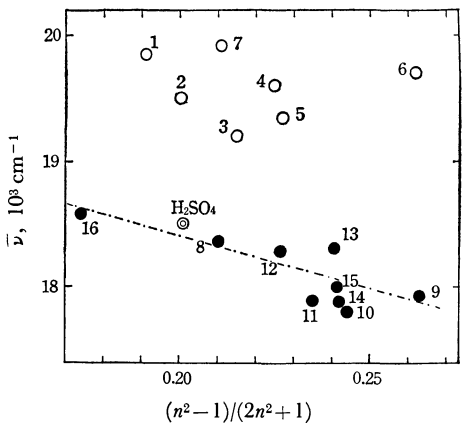

Fig. 4. Solvent shift of a strong absorption band of perylene ion at about 540 mμ. The number of each point indicates the solvent (see Table I).

In Fig. 4, the wave number of the strong band in the 500—560 mμ region is plotted against the value of $(n^2-1)/(2n^2+1)$. The points for the spectra of type A are shown by solid circles, and those for the spectra of type B, by open circles. The solid circles fall on a straight line, as is to be expected from Bayliss' relation. Clearly the solvent shift in the spectra of type A is one that can be understood without the consideration of any specific interaction of perylene ions with solvent molecules or with antimony pentachloride ions. In other words, we can assign the spectra of type A to monopositive ions of perylene in a relatively free state.

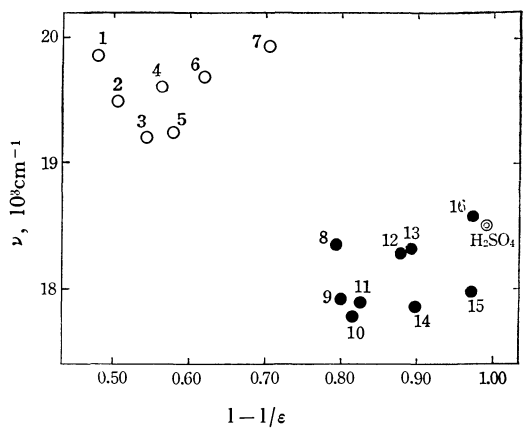

Fig. 5. Relation between the wave number of an absorption band of perylene ion and the dielectric constant of solvent.

6) E. G. McRae, *J. Phys. Chem.*, **61**, 562 (1957).
7) Y. Ooshika, *J. Phys. Soc. Japan*, **9**, 594 (1954).

On the other hand, in Fig. 4, the points for the spectra of type B deviate markedly from the regularity found for the spectra of type A. Apparently the shift of the peak is too large for a usual solvent shift. Hardly any simple relation can be found between the shift and the refractive index of the solvent in this case. These facts, as well as the broadness of the absorption band, suggest the presence of some specific interaction between a perylene ion and its surroundings in a case that exhibits a spectrum of type B.*

It should be noticed that the solvents which give spectra of type B are of a wide variety with respect to the electronic states. It is hard to expect that carbon tetrachloride, *n*-heptane and benzene will exhibit the same specific interaction with perylene ions. Therefore, we can exclude the possibility that the spectrum of type B is caused by a strong interaction between perylene ions and solvent molecules.

In a solution, perylene ions are stabilized by the solvation. The solvation energy which is associated with an electrostatic interaction of the electronic charge on a molecular ion with solvent molecules can be approximately expressed as follows:[9]

$$\Delta E \simeq \sum_i (q_i/2r)(1 - 1/\varepsilon) \qquad (2)$$

where q_i is the charge on the ith atom in the molecular ion; r is the effective interaction radius for the atomic centers, and ε is the dielectric constant of the solvent. Thus ΔE can be regarded as being proportional to $(1-1/\varepsilon)$. The wave number of the strong absorption band is plotted against $(1-1/\varepsilon)$ in Fig. 5. It can be seen that the spectra of type A and those of type B appear in different regions, the boundary between which is at the $(1-1/\varepsilon)$ value of about 0.75. The results described above suggest that, in a solvent with a high dielectric constant, a perylene ion is in a relatively free state as it is fully stabilized by the solvation, whereas in a solvent with a low dielectric constant the solvation energy is not large enough to free a perylene ion from an antimony pentachloride ion; this results in keeping them in an associated state involving the two kinds of ions. One may expect the presence of an equilibrium between the free ion state and the associated state when the dielectric constant of the solvent is a value intermediate between the two regions. In effect, such an equilibrium can be demonstrated by the spectra observed in the case of a mixed solvent consisting of benzene and chlorobenzene. The chlorobenzene solution gives a typical spectrum of type A, while the benzene solution gives a spectrum of type B. The spectra observed for the mixed solvent are shown in Fig. 6. The equilibrium of the two states appears when the volume ratio of chlorobenzene to benzene is 0.6—1.0. As we have already mentioned, the spectra of type B have an extra absorption band at about 1200 mμ which can not be found in the spectra of type A. Seemingly, this absorption band is due to the associated state, and it might be a charge-transfer band.

It is known that a solid complex can be obtained from the interaction between perylene and antimony pentachloride. Unfortunately, the crystal structure of this solid complex has not yet been determined. One could suppose, however, that the positive ions of perylene and the negative ions of antimony pentachloride are arranged alternately in the crystal. The minute crystals of the solid complex are formed when a chloroform solution of antimony pentachloride is sprayed onto the surface of a thin flake of perylene crystal. The difference between the absorption spectra of the crystal before and after the formation of a complex on its surface

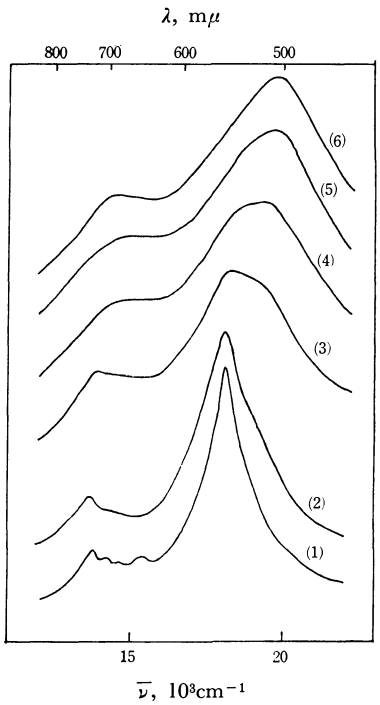

Fig. 6. Absorption spectrum of perylene-$SbCl_5$ in a mixed solvent, benzene-chlorobenzene. The volume ratio of chlorobenzene to benzene is: (1) 2.0, (2) 1.0, (3) 0.9, (4) 0.75, (5) 0.65 and (6) 0.5.

* The possibility of the formation of a covalent complex between perylene and antimony pentachloride can not be excluded, but it is not likely that the spectrum of type B is associated with the covalent complex, as it is quite different from the spectrum known for the proton complex.[8] The spectrum of type B is also different from the spectrum of a colloidal suspension of the solid complex reported by Blomgren and Kommandeur.[10]

8) W. Ij. Aalbergsberg, G. J. Hoijtink, E. L. Mackor and W. P. Weijland, *J. Chem. Soc.*, **1959**, 3049.
9) N. S. Hush and J. Blackledge, *J. Chem. Phys.*, **23**, 514 (1955).
10) G. F. Blomgren and J. Kommandeur, ibid., **35**, 1636 (1961).

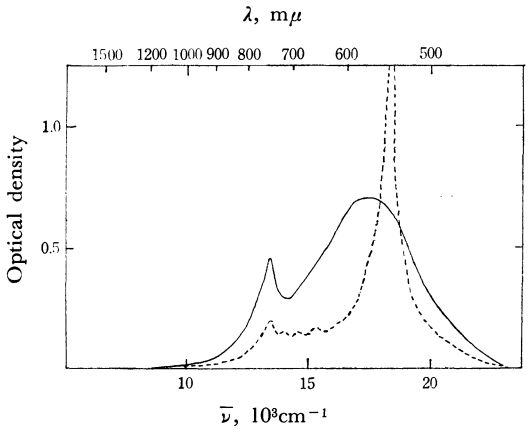

Fig. 7. Absorption spectrum of perylene-$SbCl_5$ solid complex. The broken line is the spectrum of perylene ion in sulfuric acid.

can be taken as the spectrum of the solid complex. The spectrum obtained in this way is shown in Fig. 7. The absorption spectrum of the solid complex has also been observed by Blomgren and Kommandeur[10] by using the KBr-pellet method; their spectrum is similar to the spectrum we show in Fig. 7.

The spectrum of the solid complex seems to correspond to the spectrum of type A rather than to that of type B, because: (i) the red-shift of the absorption peak from its position in a spectrum of type A is of the order that can be expected for the solid state, (ii) the band at 760 mμ is relatively sharp, while it is very broad in the spectra of type B, and (iii) the band at 1200 mμ is absent, or very weak. If we assume that the appearance of the spectrum of type B is due to the charge-transfer interaction between a perylene ion and an antimony pentachloride ion, the same type of spectrum could be expected for the solid complex. This is not the case, however, and the charge-transfer band due to the interaction between perylene and antimony pentachloride can not be observed for the solid complex. This leads to the conclusion that the spectrum of type B is caused by some specific interaction of perylene ions which does not take place in the free state nor in the crystal. Probably the large blue-shift and the marked broadening of the absorption bands in the spectrum of type B are due to the effect of interaction between perylene ions; the new band at 1200 mμ could be a charge-transfer band also caused by the interaction between perylene ions, not by the interaction between a perylene ion and an antimony pentachloride ion. This interpretation is possible if we suppose that the associated state formed in the solvents with low dielectric constants does not correspond to the pair of a perylene ion and an antimony pentachloride ion, but to an aggregate of two or more pairs, in which the arrangement of ions is quite different from that in the crystal, and in which perylene ions are in direct contact with each other. Thus the situation that gives the spectrum of type B seems similar to the dimer of radical ions as that has been presented by Hauser and Murrell[11] in the case of Wurster's blue perchlorate. Further evidence for the interaction between perylene ions might be obtained from a study of the electron spin resonance absorption.

11) K. H. Hausser and J. N. Murrell, ibid., **27**, 500 (1957).

BULLETIN OF THE CHEMICAL SOCIETY OF JAPAN VOL. 39 1898—1902 (1966)

Analytical Studies Using the Convection Electrode. XI. Cathodic Stripping Voltammetry of Chloride Ions with the Pushed-out Mercury Drop Convection Electrode

By Junsuke SUZUKI

Faculty of Education, Shizuoka University, Ooiwa, Shizuoka

(Received January 5, 1965)

The cathodic stripping voltammetry of chloride ions in a potassium nitrate or a nitric acid solution was studied by using the Pushed-out Mercury Drop Convection Electrode (PMDCE) (J. Suzuki and T. Ozaki, This Bulletin, **37**, 230 (1964)). The cathodic stripping peak current, i_p, depended upon the rotating rate of the disk, ω (600—1000 r. p. m.); the rate of voltage scan, v(100—300 mV./min.); the pre-electrolysis time, t (~3 min.), and the bulk concentration of chloride ions, C. It was concluded that the corresponding cathodic peak current, i_p, can be given by the equation:

$$i_p = kv\omega^{1/2}Ct^{2/3}$$

where k is the constant. In a 0.1 M nitric acid solution, it was possible to determine the chloride ions in so dilute a solution as 3×10^{-5} M with a good reproducibility.

A series of investigations of the stripping voltammetric analytical technique have shown that the method has a very high sensitivity in the determination of trace amounts of electroactive materials.

The anodic stripping analysis has been applied to the determination of those metal ions which can be deposited on the cathode as metals, and the cathodic stripping analysis, to the determination of those ions which can be precipitated on the surface of the anode as oxides or halides.

Recently, several applications of the mercury or silver electrode to the cathodic stripping analysis have been investigated for the determination of halide ions.[1-7] Ball et al.[1] and Shain and Perone.[5] reported that it was possible to determine chloride ions in solutions as dilute as 0.2 to 2γ/ml. with mercury electrode and iodide ions as dilute as 4×10^{-8} M by using the silver electrode. However, the reproducibilities obtained in these investigations were found not to be satisfactory. These unsatisfactory reproducibilities are considered to be caused by the irregularity of the flowing conditions of the solution during the electrolysis.

On the other hand, at the pushed-out mercury drop convection electrode (PMDCE), when a pulley-shaped disk was rotated near by, the reproducible flowing conditions of solution at the electrode surface were found to be achieved, as has been reported in the previous papers.[8]

In the present work, the PMDCE is applied to the cathodic stripping voltammetry in order to improve its reproducibility. The influences of the various factors upon the cathodic stripping peak current and the quantity of electricity involved in the reduction of the mercurous chloride produced on the surface of the electrode are investigated thoroughly. Also, the experimental equations of the peak current and the quantity of electricity at the PMDCE are derived. These results are described in detail below.

Experimental

Electrolytic Cell and Electrode.—The electrolytic cell used in the present experiment is the same as that described in the previous papers.[8] The electrode used is shown in Fig. 1.

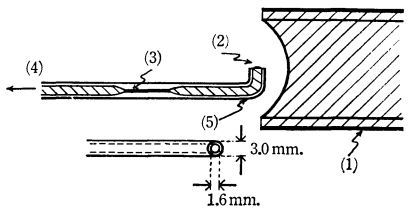

Fig. 1. Electrode and rotating disk.
(1) Rotating disk, (2) Electrode surface, (3) Capillary, (4) To the microsyringe, (5) Glass tube

1) R. G. Ball, D. L. Manning and O. Menis, *Anal. Chem.*, **32**, 621 (1960).
2) M. Ariel and U. Eisner, *J. Electroanal. Chem.*, **5**, 362 (1963).
3) W. L. Maddox, M. T. Kelley and J. A. Dean, ibid., **4**, 96 (1962).
4) K. Z. Braynina and E. M. Rozenblat, *Zavodskaya Lab.*, **28**, 21 (1962).
5) I. Shain and S. P. Perone, *Anal. Chem.*, **33**, 325 (1961).
6) W. Kemula, Z. Kublik and J. Taraszewska, *Acad. Poln. Sci.*, **8**, 269 (1960).
7) H. Specker and G. Schieve, *Z. anal. Chem.*, **196**, 1 (1963).
8) J. Suzuki and T. Ozaki, This Bulletin, **37**, 230, 789 (1964).

The renewal of the mercury drop surface of the electrode is carried out after each stripping analysis by pushing out one drop (volume: 0.0021 ± 0.0001 cc.) of mercury using a microsyringe. The peak height is found gradually to decrease when the same electrode surface is used repeatedly.

The cell and the saturated calomel reference electrode are connected through a salt bridge containing saturated potassium nitrate. Hence, cross-contaminations of the reference electrode and the sample can be prevented effectively.

The supporting electrolyte solution has a tendency to penetrate into the glass tube of the electrode. Therefore, the inside wall of the tube is coated with silicone film.

Apparatus.—The Shimadzu model RP-2 polarograph is employed for the measurements of stripping curves. The apparatus used for rotating the disk is the same as that used in the previous work.[8]

Reagents.—A nitric acid solution of an extra pure grade is used without further purification, and a potassium nitrate of an extra pure grade is purified by three recrystallizations. Also, a chloride solution is prepared from sodium chloride of an analytical reagent grade (99.99%). All the solutions are prepared with redistilled water.

Procedure.—About a 30-ml. portion of 0.1 M nitric acid or a 0.1 M potassium nitrate solution containing 3×10^{-5} M to 10×10^{-5} M of chloride ions is poured into the electrolytic cell.

The mercury surface of the electrode is renewed, and then mercurous chloride is deposited on the electrode surface by applying a potential of +0.4 V. vs. SCE for 1 min., while rotating the disk at 600 r. p. m. After this pre-electrolysis process, the disk is stopped and the electrolytic solution is allowed to stand for 15 sec.; then the deposited mercurous chloride is stripped polarographically by scanning the potential from +0.4 to 0 V. vs. SCE at a scanning rate of 200 mV./min., i. e., by a linearly-varying potential stripping method. A recorder sensitivity of 0.250 μamp./mm. is selected for recording the stripping curves. All the measurements are carried out at 25 ± 0.5°C.

The peak current, i_p, is measured as is illustrated in Fig. 2, and the quantity of electricity is obtained by measuring the area of the peak with a planimeter.

Results

The Reproducibility of the Peak Current.—A curve typical of those obtained is shown in Fig. 2. On the basis of the curve, the reproducibility of the peak current was investigated. A good reproducibility can always be obtained, with a mean error of $\pm 2\%$.

The Effect of the Pre-electrolysis Time.—By using a 0.1 M nitric acid solution containing 4×10^{-5} M chloride and a 0.1 M potassium nitrate solution containing 10×10^{-5} M chloride, the dependency of the peak current and the quantity of electricity on the pre-electrolysis time was investigated; the results are shown in Fig. 3 and Table I respectively. As can be seen from Fig. 3, the peak current gives a saturation curve with an increase in the pre-electrolysis time. As the pre-electrolysis time is longer than 5 min., the peak current is almost constant. However, in this case, it is necessary to remove the dissolved oxygen before the

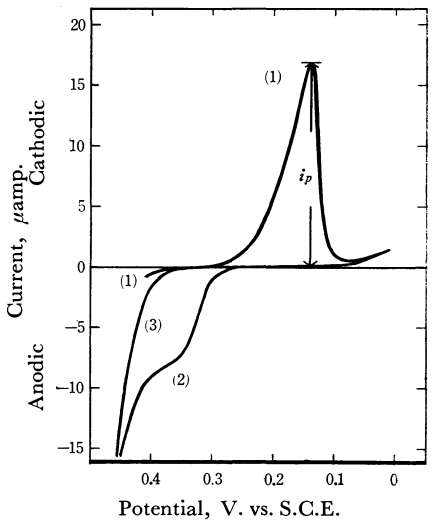

Fig. 2. Typical current-voltage curves of chloride ion in 0.1 M HNO_3 using the PMDCE.
(1) Cathodic stripping curve of 6×10^{-5} M Cl^-.
(2) D. C. polarogram of 1×10^{-4} M Cl^-.
(3) D. C. polarogram of 0.1 M HNO_3

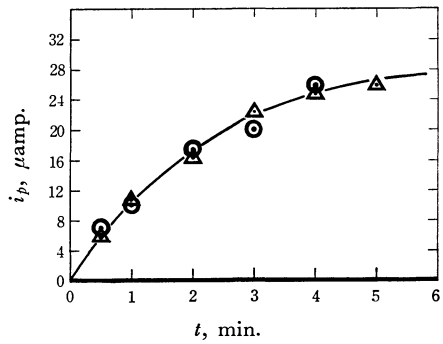

Fig. 3. Relations between the peak current i_p and the pre-electrolysis time t.
-△-: 4×10^{-5} M Cl^- in 0.1 M HNO_3
-⊙-: 1×10^{-4} M Cl^- in 0.1 M KNO_3

Table I. Effects of the pre-electrolysis time (t) on the quantity of electricity (Q) involved in the reduction of mercurous chloride (scanning rate: 200 mV./min.)

Pre-electrolysis time t, sec.	1×10^{-4} M Cl^- in 0.1 M KNO_3		4×10^{-5} M Cl^- in 0.1 M HNO_3	
	Q, μcoul.	Q/t	Q, μcoul.	Q/t
30	116.2	3.87	97.5	3.25
60	245.2	4.09	204.7	3.41
120	478.5	3.99	385.5	3.21
180	708.0	3.93	621.0	3.45
240	998.2	4.16	783.0	3.26
300	—	—	967.5	3.23

stripping, because the reduction of oxygen takes place before all the deposited mercurous chloride have been reduced.

The Influence of the Rotating Rate of the Disk during the Pre-electrolysis on the Peak Current and on the Quantity of Electricity.—The variations in the peak current and the quantity of electricity with the rotating rate (600—1000 r. p. m.) were investigated. The gradual increases in the peak current and in the quantity of electricity with the increase in the rotating rate were found to be as shown in Table II.

Table II. Effects of the rotating rate (ω) on the peak current (i_p) and on the quantity of electricity (Q) involved in the reduction of mercurous chloride (scanning rate: 200 mV./min.)

Stirring rate	1×10^{-4} M Cl^- in 0.1 M KNO_3		4×10^{-5} M Cl^- in 0.1 M HNO_3	
ω r.p.m.	i_p, μamp.	Q, μcoul.	i_p, μamp.	Q, μcoul.
600	9.93	245.3	11.18	204.8
800	11.17	294.8	12.73	261.8
1000	12.75	309.8	13.92	294.0

The Effects of the Voltage Scanning Rate on the Peak Current and on the Quantity of Electricity.—Three scanning rates, of 100 mV./min., 200 mV./min., and 300 mV./min., were investigated; the results are shown in Fig. 4. The figure shows that, as the rate of voltage scan was increased, the peak current increased linearly, but the quantity of electricity was almost constant at every scanning rate.

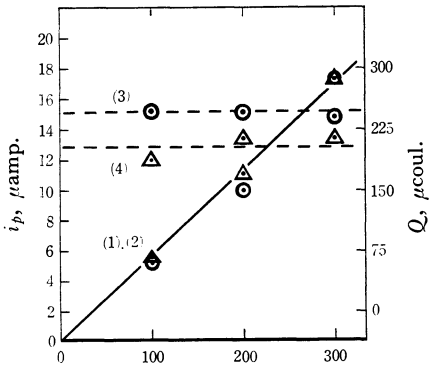

Fig. 4. Effects of the voltage scanning rate on the peak current i_p, and the quantity of electricity Q.
(1), (3): 1×10^{-4} M Cl^- in 0.1 M KNO_3
(2), (4): 4×10^{-5} M Cl^- in 0.1 M HNO_3
——: Peak current, ----: Quantity of electricity

Relations between the Concentration of Chloride and the Peak Current, and the Quantity of Electricity.—Several determinations of the peak current and the quantity of electricity were made at various concentrations of chloride; the results are shown in Fig. 5. It can be seen from the figure that satisfactory proportionalities between them are established.

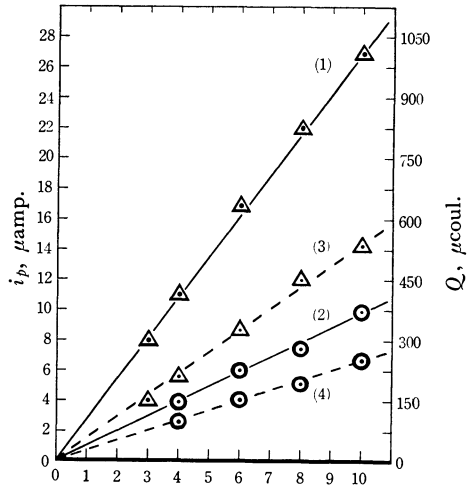

Fig. 5. Relations between the chloride concentration and the peak current i_p, and the quantity of electricity Q.
(1) (3): In 0.1 M HNO_3, (2) (4): In 0.1 M KNO_3
——: Peak current, ----: Quantity of electricity

Discussion

Pre-electrolysis Potential.—At any point on the anodic dissolution wave of mercury, the potential of mercury electrode can be expressed by:

$$E = E^0_{Hg} + 0.059/2 \log C^0_{Hg_2^{2+}} \quad \text{(at 25°C)} \quad (1)$$

where E^0_{Hg} is the standard potential of mercury-mercurous mercury couple (+0.553 V. vs. SCE) and $C^0_{Hg_2^{2+}}$ is the concentration of mercurous ions at the electrode surface. In the presence of chloride ions, however, the anodic wave of mercury shifts to more negative potentials. The anodic reaction can be expressed as follows:

$$2Hg + 2Cl^- = Hg_2Cl_2 + 2e \quad (2)$$

From the Nernst equation for the equilibrium potential[9] the following equation for the half-wave potential is obtained:

$$E_{1/2} = \text{const.} - 0.059 \log C_{Cl^-} \quad \text{(at 25°C)} \quad (3)$$

where C_{Cl^-} is the bulk concentration of chloride.

From Eq. 3, it follows that the $E_{1/2}$ value shifts to values more positive by about 60 mV. for each 10-fold decrease in the chloride concentration, until the chloride wave merges with the wave corresponding to the oxidation of mercury to mercurous

9) I. M. Kolthoff and J. J. Lingane, "Polarography," Vol. 2, Interscience, New York (1952), pp. 577—581.

ions. Therefore, the lower limit of the determination of chloride with the mercury electrode is found to be about 10^{-6} M.

As the solubility product of mercurous chloride is 6×10^{-19} at 25°C, the critical concentration of mercurous ions in a 1×10^{-6} M chloride solution becomes 6×10^{-7} M. By substituting this value into Eq. 1, the potential of the mercury electrode at this concentration is calculated to be:

$$E=0.553+0.030\log 6\times10^{-7}=+0.36 \text{ V. vs. SCE}$$

Consequently, in low concentrations of chloride it is necessary to apply a pre-electrolysis potential of about +0.4 V. vs. SCE. In the present investigation, a pre-electrolysis potential of +0.4 V. vs. SCE was applied.

Peak Current and Voltage Scanning Rate.—Randles[10] and Sevcik[11] independently derived an equation for the cathodic peak height in oscillographic polarography:

$$i_{max} = kAn^{3/2}v^{1/2}D^{1/2}C \qquad (4)$$

where k is the constant; A, the electrode area; n, the number of electrons involved in the reduction; v, the rate of voltage scan; D, the diffusion coefficient, and C, the bulk concentration.

The application of the Randles and Sevcik relationship to the anodic peak current obtained by the stripping method was studied by Nikelly and Cooke.[12] They found that the relation between the anodic peak current and the scanning rate was the same as in the above Eq. 4. Namely, the anodic peak current obtained by the stripping method is proportional to one-half the power of the scanning rate.

Therefore, in the stripping analysis, the selection of a voltage scanning rate is important. In general, the more rapid the rate of voltage scan, the sharper the peak. It is preferable that the scanning rate should be as rapid as possible.

As can be seen from Fig. 4, in contrast with the above finding of Nikelly and Cooke, the present result indicates the linear relation between the peak current and the scanning rate. Further studies are, however, necessary before any definite conclusion recording the disagreement between the Nikelly and Cooke result and the present author's can be drawn.

The Rotating Rate of the Disk.—One of the most important factors affecting the magnitude of the peak current and the quantity of electricity is the amount of mercurous chloride deposited on the electrode during the pre-electrolysis process. The amount of mercurous chloride deposited is governed by the rate of the diffusion of chloride ions toward the electrode surface, that is, the rate of convection caused by stirring the solution. Therefore, the stirring rate should carefully be kept constant; a rapid stirring of the electrolytic solution gives a high sensitivity. However, the effects of the rotating rate on the peak current and on the quantity of electricity have never been investigated.

Using the data in Table II, the relations between the logarithm of the rotating rate and that of the peak current, and that of the quantity of electricity were investigated. It can be seen that both the peak current and the quantity of electricity are proportional to the square root of the rotating rate.

The Pre-electrolysis Time.—The amounts of mercurous chloride deposited are governed by the pre-electrolysis time. Therefore, the peak current and the quantity of electricity depend on the pre-electrolysis time. As Table I shows, the quantity of electricity changes linearly with the increase in the pre-electrolysis time. This indicates that the amounts of mercurous chloride deposited increase linearly with the increase in the pre-electrolysis time. On the other hand, the peak current increases, not linearly, but gradually with the increase in the pre-electrolysis time. This slight deviation from linearity can be explained as follows. The longer the pre-electrolysis time, the larger the amounts of mercurous chloride deposited on the electrode surface. Therefore, at a long pre-electrolysis time, the larger amounts of chloride ions released at the electrode surface during the stripping change the equilibrium potential,[5] and then the dissolution curve obtained becomes broader.

This explanation is supported by the fact that the

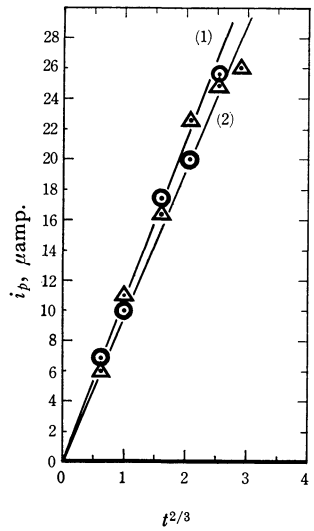

Fig. 6. Relations between the peak current i_p, and the two-thirds power of pre-electrolysis time t (min.).

(1) -△-: 4×15^{-5} M Cl^- in 0.1 M HNO_3
(2) -⊙-: 1×10^{-4} M Cl^- in 0.1 M KNO_3

10) J. E. B. Randles, *Trans. Faraday Soc.*, **44**, 327, 334 (1948).
11) A. Sevcik, *Collection Czechoslov. Chem. Commun.* **13**, 349 (1948).
12) J. G. Nikelly and W. D. Cooke, *Anal. Chem.*, **29**, 933 (1957).

larger peak current was obtained on rotating the disk during the stripping in order to remove the chloride ions released and eliminate the effect on equilibrium potential.

Experimental Equations of the Cathodic Peak Current and the Quantity of Electricity at the PMDCE.—As is shown in Fig. 3, the peak current obtained by the PMDCE increases gradually with the increase in the pre-electrolysis time. When the peak current is plotted against two-thirds the power of the pre-electrolysis time, the plots are found to be straight lines, as Fig. 6 shows.

Consequently, considering the effects on the peak current mentioned above, the cathodic peak current, i_p, at the PMDCE may be expressed by the following equation:

$$i_p = k'v\omega^{1/2}Ct^{2/3} \quad (5)$$

Similarly, the quantity of electricity, Q, at the PMDCE may be expressed by:

$$Q = k''\omega^{1/2}Ct \quad (6)$$

where k' and k'' are the constants; v, the rate of the voltage scan; ω, the rotating rate of the disk; t, the pre-electrolysis time, and C, the bulk concentration.

The author is grateful to Professor Tokuro Ozaki of Shizuoka University for his valuable discussions and suggestions, and to Mr. Yoshiya Suganuma for his earnest assistance.

BULLETIN OF THE CHEMICAL SOCIETY OF JAPAN VOL. 39 1902—1909 (1966)

The Polarographic Behavior of the Condensation Product of Glyoxal with *o*-Phenylenediamine, and Its Application to the Determination of Glyoxal

By Sôichirô MUSHA, Tamotsu WASA and Tameo NAITO*

Department of Applied Chemistry, College of Engineering, University of Osaka Prefecture, Sakai

(Received December 25, 1965)

In buffer solutions containing excess *o*-phenylene-diamine (OPD), glyoxal is condensed with OPD and the condensation product produces two diffusion-controlled reduction waves ($E_{1/2}=-0.211$ and -0.358 V. vs. SCE, pH=1.6) at pH values below 2.5 and a single well-defined reduction wave ($E_{1/2}=-0.782$ V., pH=8.5) at pH values above 2.5. In the pH range between 2 and 8, an ill-defined reduction wave, which seems to be a catalytic hydrogen wave brought about by the reduction product, is also observed at a more positive potential than a normal hydrogen wave. A linear relationship between the limiting current and the concentration of glyoxal has been obtained under the following conditions, which are recommended for the practical determination of glyoxal; $(1—2)\times10^{-2}$ M for the concentration of OPD, 7—10 for pH, 25°C for the temperature, and 30—60 min. for the condensation time. The application was made to the determination of the purity of a commercial glyoxal aqueous solution, and also to the determination of the glyoxal which is present in ethylene glycol as an impurity. A mechanism for the electrode reactions of the condensation product (i. e., quinoxaline) of glyoxal with OPD was postulated.

It was first reported by Winkel and Proske[1] that glyoxal shows an unstable reduction wave at -1.50 V. in an ammonium chloride solution. The half-wave potential was found by Mackinney and Temmer[2] to be -1.41 V. vs. SCE in a biphthalate buffer at pH 3.4. However, no remarks on the current were made in either paper. More detailed results on the polarographic behavior of glyoxal in various buffer solutions and the mechanisms of its electrolytic reduction have been reported by Elving and Bennett[3]; the reduction wave is typically kinetic-controlled in its character, and hence the limiting current varies with the temperature and with the pH of electrolytic solution, and also decreases with time in the alkaline region because of the instability of glyoxal. Therefore, strict experimental conditions seem to be required if this reduction wave is to be used in the polarographic determination of glyoxal.

* Present address: Yanagimoto Trading Co., Ltd., Shinonome-cho, Hiroshima.

1) A. Winkel and G. Proske, *Ber.*, **69**, 1917 (1936).

2) G. Mackinney and O. Temmer, *J. Am. Chem. Soc.*, **70**, 3586 (1948).

3) P. J. Elving and C. E. Bennett, ibid., **76**, 1412 (1954).

One of the present authors has previously reported that the condensation products of dehydro-L-ascorbic acid (DAA) and its related compounds with *o*-phenylenediamine (OPD) show diffusion-controlled reduction waves at a dropping mercury electrode, and that these reduction waves can be applied to the determination of DAA and its related compounds.[4]

An analogous study of glyoxal was made for the present work, and it was found that the condensation product of glyoxal with OPD gives a diffusion controlled reduction wave characteristic of glyoxal.

The present paper will describe the polarographic behavior of the condensation product and a method of analyzing glyoxal by using this reduction wave. Furthermore, some consideration will be given to the mechanism of the electrode reactions of the condensation product (i. e., quinoxaline) of glyoxal with OPD.

Experimental

Materials and Reagents.—The glyoxal was a commercial product (about a 40% aqueous solution) from Wako Pure Chemical Industries, Ltd.; it was used without further purification. Glyoxal-sodium bisulfite monohydrate was prepared according to the method of Ronzio and Waugh.[5] Quinoxaline was prepared by Jones and McLaughlin's method.[6]

Stock solutions of glyoxal and quinoxaline were prepared by using redistilled water or 99% ethanol as the solvent. As the standard solution of glyoxal, 1×10^{-2} M aqueous solution of the pure crystalline monohydrate of glyoxal-sodium bisulfite was used[7]; it was prepared by dissolving the specimen directly into redistilled water.

OPD was a commercial product; it was checked to give no reduction wave in the absence of glyoxal under the present experimental conditions. The stock solution (about 0.1 M) of OPD was prepared fresh daily by dissolving OPD directly in redistilled water. No maximum suppressor was used, since the condensation product showed no maximum under the present polarographic conditions. All the other chemicals were of the reagent grade or better.

Buffer Solutions.—Walpole's buffer for pH values from 1 to 2.5, an acetate buffer for pH 4.3, McIlvanie's buffer for pH 2.2 to 8.0, mixtures of disodium hydrogen phosphate with sodium hydroxide for pH above 8, and Britton-Robinson's buffer (BR buffer) for pH 1.8 to 12.0 were used for examining the effect of pH and, at the same time, for checking the effects of the components of the buffer solution.

Apparatus and Procedure.—The polarographic measurements were carried out with a Yanagimoto Automatic Recording Polarograph (Type PA 101). The characteristics of the capillary used were $m=1.14$ mg./sec. and $t=4.00$ sec./drop in the buffer solution (pH=4.0) when the height of the mercury reservoir was 71.0 cm. and when the applied potential was 0 V. vs. SCE at 25°C.

From the necessity of employing a thermostat for temperature control, a modified H-type electrolytic cell with a potasium nitrate-saturated agar bridge and a sintered glass disk was used. The accuracy of the temperature control was ±0.2°C. A saturated calomel electrode was used as the reference electrode. The cell resistance was less than 240 Ω. To check the potential at the dropping mercury electrode, a Shimadzu Potentiometer (Type 3P) was used, while the final pH of the polarographic solutions was measured with a Yanagimoto pH-meter (Type 42) after the polarographic measurements had been made, when necessary. For the experiments of controlled-potential electrolysis, a Yanagimoto Controlled-Potential Electrolyser (MFG. No. 258) was used.

The experimental procedure was as follows: a given volume (usually 1 to 4 ml.) of the glyoxal stock solution was placed in a 20-ml. volumetric flask; a given volume (usually 1 to 4 ml.) of a 0.1 M aqueous solution of OPD and 10 ml. of an appropriate buffer solution were added, and then the flask was filled up to the mark with redistilled water. A part of the mixture was transferred to an electrolytic cell, and the cell was kept in the thermostat for a given time to allow the condensation reaction to take place. At the same time the dissolved oxygen was removed by bubbling nitrogen gas. After this period of time, the polarograms are recorded.

Controlled-potential Electrolysis.—In order to get information concerning the reversibility of the electrode reaction and to ascertain the number of electrons

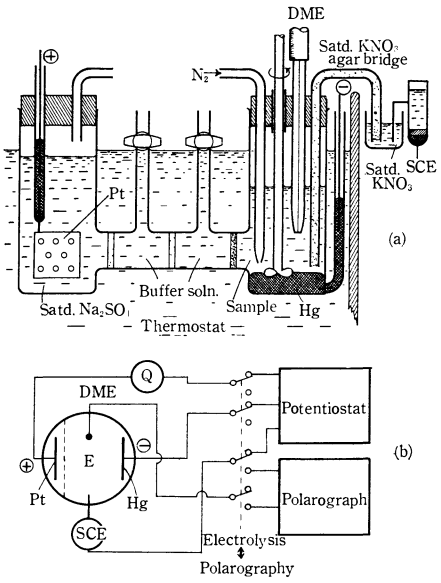

Fig. 1. Controlled-potential electrolysis.
(a) Electrolysis cell, (b) Schematical diagram of the circuit for the electrolysis and polarography.
E: Electrolysis cell (a), Q: gas coulometer.

4) T. Wasa, M. Takagi and S. Ono, This Bulletin, **34**, 518 (1961).
5) R. Ronzio and T. D. Waugh, "Organic Syntheses," **24**, 61 (1944).
6) R. G. Jones and K. C. McLaughlin, ibid., **30**, 86 (1950).
7) C. S. Wise, C. L. Mehltretter and J. W. Van Cleve, *Anal. Chem.*, **31**, 1241 (1959).

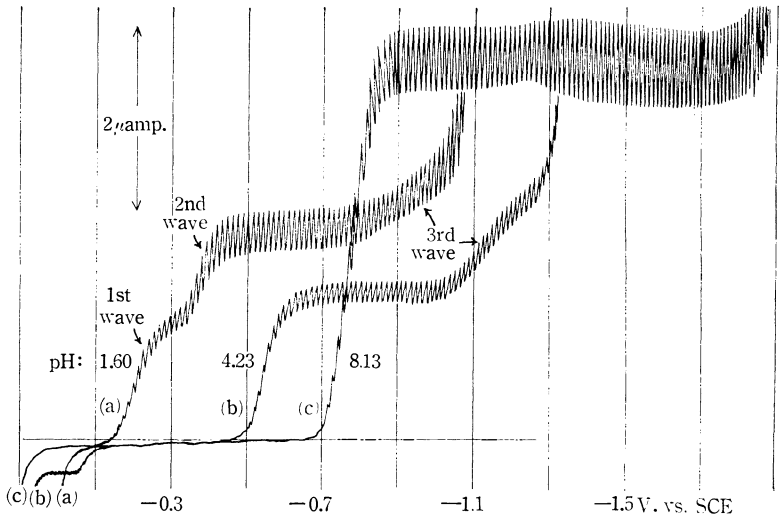

Fig. 2. Polarograms of condensation product in BR buffer at 25°C.
Glyoxal: 8×10^{-4} M, OPD: 1×10^{-2} M, Condensation: 60 min.

participating in the electrode reaction, controlled-potential electrolysis[8-10] was carried out by using the cell shown in Fig. 1.

The experimental procedure was as follows: about 45 ml. of a buffer solution (pH 8.9) was placed in the cathode compartment of the electrolytic cell, and the cell was placed in the thermostat. The solution and the mercury pool cathode (area, about 15 cm^2) were stirred vigorously with a glass propellor stirrer immersed in the mercury-solution interface, and the dissolving oxygen was removed by bubbling nitrogen gas. After the dissolved oxygen had been removed, electrolysis was carried on at a fixed cathode potential (e. g., −1.20 V. vs. SCE) until the current became negligibly small. The circuit was then connected to the polarograph, and 5 ml. of a quinoxaline solution of known concentration, which had been deaerated, was pipetted into the cell. After mixing, the inlet tube of nitrogen gas was pulled up and nitrogen gas was passed over the solution. The stirrer was stopped, and a polarogram was taken. The inlet tube of nitrogen gas was then pushed down again into the solution and the stirring was re-commenced; then the electrolysis was carried out at −1.20 V. vs. SCE, with automatic control, while nitrogen gas was being bubbled through the solution. After a given period, electrolysis was stopped, the electricity required for the electrolysis was measured by a gas coulometer,[10] and a polarogram was recorded according to the procedures described above. These procedures were repeated several times during the course of the electrolysis.

Results and Discussion

Reduction Waves of the Condensation Product of Glyoxal with OPD.—A well-defined reduction wave was obtained when glyoxal was treated with OPD in appropriate buffer solutions by the procedure described above, as may be seen in Fig. 2 (a, b and c). The reduction wave showed all the typical characteristics of a diffusion-controlled current: proportionality between the wave height and the square root of the height of the mercury reservoir (Fig. 3), and a small temperature

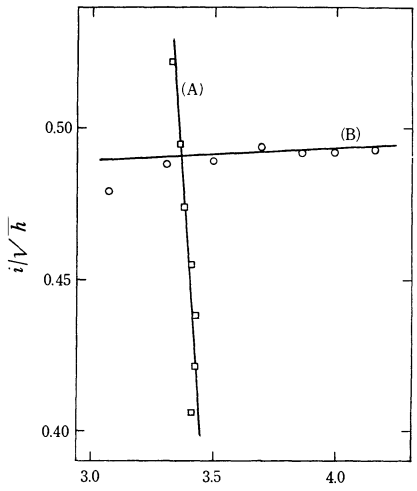

Fig. 3. Relationships between the limiting current (i) and the height (h) of mercury reservoir.
Glyoxal: (A) 3.2×10^{-2} M without OPD at pH 7.0, (B) 8×10^{-4} M with 1×10^{-2} M OPD at pH 8.0. Condensation: 60 min. at 25°C.

8) S. Ono, M. Takagi and T. Wasa, This Bulletin, **31**, 356 (1958).

9) N. Tanaka, T. Nozoe, T. Takamura and S. Kitahara, ibid., **31**, 327 (1958).

10) J. A. Page and J. J. Lingane, *Anal. Chim. Acta*, **16**, 175 (1957).

coefficient of 1.9%/deg. Figure 3 also includes the results obtained with glyoxal only.

The shape and the half-wave potential of this reduction wave were practically identical with those of the quinoxaline prepared by Jones and McLaughlin's method.[6] Therefore, the condensation product of glyoxal with OPD under the present experimental conditions is probably quinoxaline, as has been reported by Hinsberg[11] and Liebigs[12], and the reaction may be written as:

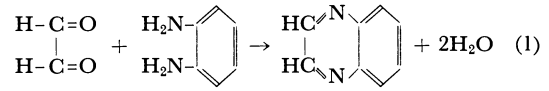

glyoxal OPD quinoxaline

The Stability of the Stock Solution of Glyoxal.— Figure 4 shows the change in the limiting currents of the condensation products with the time elapsed (at a room temperature of about 15°C) after the preparation of the stock solutions of glyoxal using 0.1 N sulfuric acid, 0.01 N sulfuric acid, water, or 99% ethanol. Figure 4 indicates that glyoxal in the ethanolic stock solution is the most stable; therefore, the ethanolic stock solution was used for the fundamental experiment. However, for analytical purposes the aqueous stock solution was also used, because the limiting current remained almost constant for a month or more when the condensation was carried out in an alkaline buffered solution.

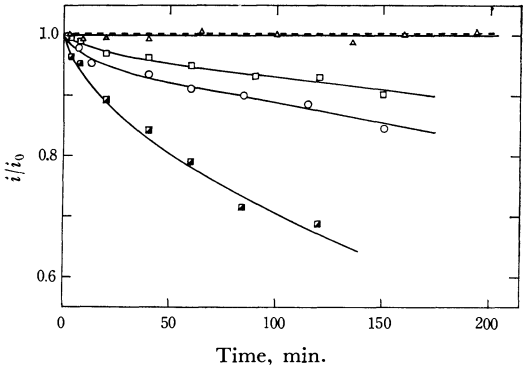

Fig. 4. Stability of the stock solution of glyoxal. Solvent of stock solution: △ 99% ethanol, ○ water, □ 0.01 N H_2SO_4, ◪ 0.1 N H_2SO_4. Condensation: 1×10^{-2} M OPD, 30 min. at 25°C in BR buffer. —— Condensation was carried out at pH 3.80, ---- at pH 8.90 with aqueous stock solution. i_0: initial wave height.

The Effect of pH.—In order to examine the effect of pH on the polarographic behavior of the condensation product of glyoxal with OPD, the concentrations of glyoxal and OPD were kept constant and only the pH of the mixture was changed (Fig. 5). The limiting currents of the condensation products were measured 60 min. after the addition of OPD at 25°C, since they increase with time during the first 40 min., attaining maximum values which remain almost constant for a further 24 hr. over all the pH range studied. Figure 5 shows that the limiting current of the condensation product shows its

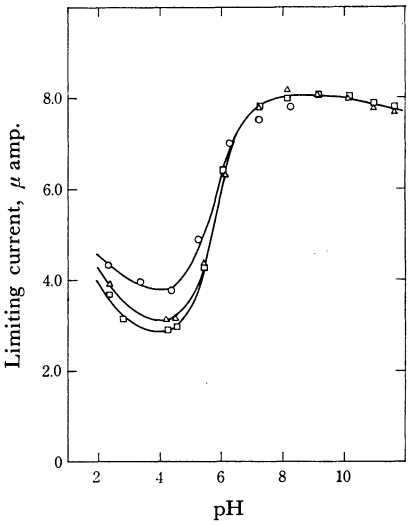

Fig. 5. pH-dependence of the limiting current of the condensation product at 25°C.
Condensation: 1.6×10^{-3} M glyoxal, 1×10^{-2} M OPD, 60 min. ○ one day after the preparation of ethanolic stock solution of glyoxal, △ 16 days, □ 21 days.

minimum value at pH about 4, and that it increases remarkably at pH above 5, reaching a maximum value in the pH of 7 to 10. The same behavior was not observed in the polarographic investigation of quinoxaline.[13] Also, Fig. 5 shows that the limiting current decreases slowly, at the rate of about 2%/day, in the pH range between 2 and 6 with the time elapsed after the preparation of the stock solution of glyoxal. These results seem to indicate that glyoxal in the stock solution changes into a form inactive (dimer or hydrate form) in the reaction with OPD and that this change is almost irreversible at a pH value of about 4, but that it becomes reversible and the rate of producing glyoxal from the inactive form increases upon either an increase or a decrease in pH from about 4.

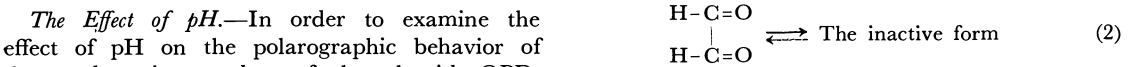

At pH values lower than 2.5 the splitting of the reduction wave into two waves which have almost equal heights was observed (Fig. 2). At the pH

11) O. Hinsberg, *Ber.*, **17**, 320 (1884).
12) H. Liebigs, *Ann. der Chem.*, **237**, 334 (1887).
13) M. Takagi, private communication to the authors.

between 2 and 8, an ill-defined and irreversible reduction wave was also observed at a more positive potential than the reduction wave of the hydrogen ion; it showed its maximum value at a pH value of about 4 and disappeared at pH values above 8. Further, when the condensation took place at a pH value of about 4, a small oxidation wave ($E_{1/2}=-0.07$ V. vs. SCE), which seems to be due to the condensation product of an aldehyde group of glyoxal with OPD, was observed (Fig. 2, b).

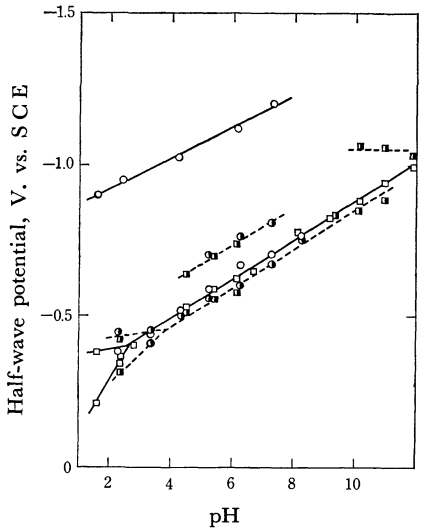

Fig. 6. pH-dependence of the half-wave (summit) potential.
○, ◑: McIlvaine buffer, □, ◧: BR buffer, -○-□-: half-wave potential, --◑--◧--: summit potential, 25°C.

The changes in the half-wave potentials of the condensation product with the pH value are presented in Fig. 6, in which the summit potentials ascertained by a. c. polarography are also shown. As may be seen in Fig. 6, a linear relationship has been obtained; its inclination was about 60 mV./pH at pH values above 2.5. Though no further experiments on the condensation product have been made by a. c. polarography, the changes in the summit potentials, the peak height and the shape of the peak with the pH value are obviously somewhat complicated. A typical a. c. polarogram was observed in the 8—10 pH range.

The influence of the components of buffer solutions on the half-wave potential, the wave height and the shape of the wave was examined, but no appreciable change has been observed.

The Effect of the Concentration of OPD.—Figure 7 shows the relationship at 25°C between the limiting current and the time elapsed after the addition of OPD to an electrolytic solution containing glyoxal and BR buffer with a pH value of 8.90, when the concentration of glyoxal was kept constant approximately at 8×10^{-4} M and the concentration of OPD was changed. With the increase in the concentration of OPD, the growing velocity of the wave increased, so the time required for the condensation was shortened.

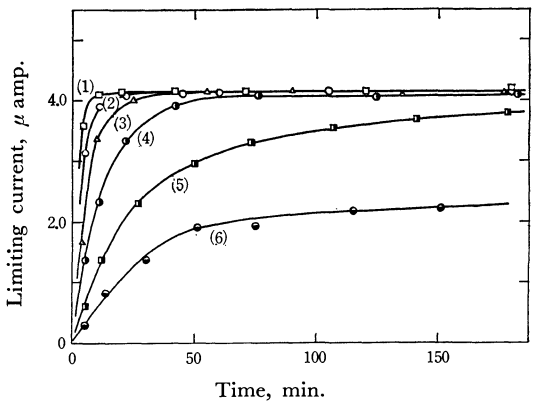

Fig. 7. Effect of the concentration of OPD.
OPD: (1) 2×10^{-2}, (2) 1×10^{-2}, (3) 5×10^{-3}, (4) 2×10^{-3}, (5) 1×10^{-3}, (6) 5×10^{-4} M.
Glyoxal: 8×10^{-4} M.
Condensation was carried out at pH 8.90 at 25°C.

The Effect of the Temperature.—Figure 8 shows the effect of the temperature on the reaction time. When the concentrations of glyoxal and OPD were kept constant and the experimental temperature was raised, the time required for condensation was shortened over all the pH range studied, while it was observed that the limiting current of the condensation product, after its maximum value was attained, decreased slightly with time at temperatures above 45°C.

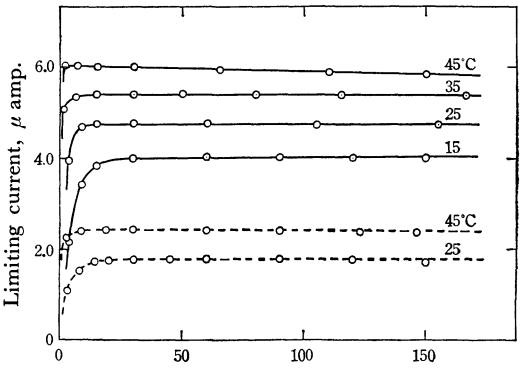

Fig. 8. Effect of the temperature.
Glyoxal: 9.3×10^{-4} M, OPD: 1×10^{-2} M
—— at pH 8.90, ---- at pH 3.80

Electrolysis and Coulometry at a Constant Potential.—Figure 9 shows the change in the polarograms of quinoxaline, the condensation product of glyoxal with OPD, during the course of electrolysis. In the early stages of electrolysis,

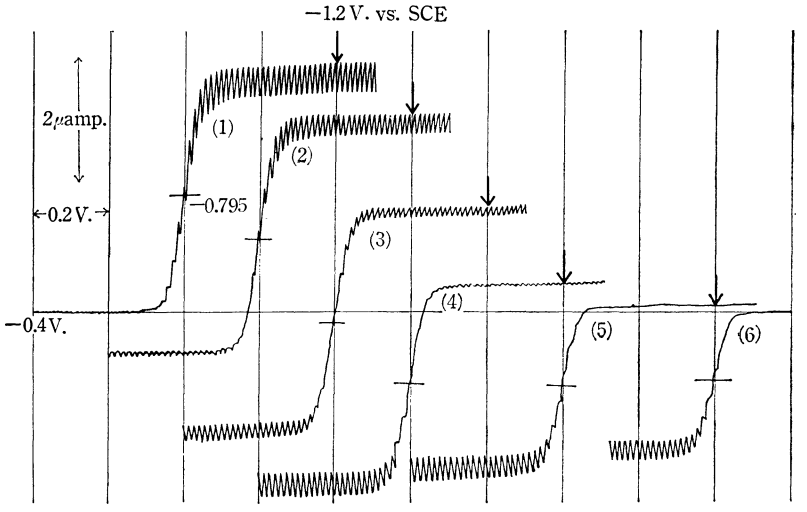

Fig. 9. Controlled-potential electrolysis of quinoxaline at −1.2 V. in BR buffer (pH 8.70) containing 10% ethanol.
Quinoxaline: 7.2×10^{-4} M. (1) before electrolysis, (2) after 5, (3) 15, (4) 25, (5) 35, and (6) 55 min. at 20°C.

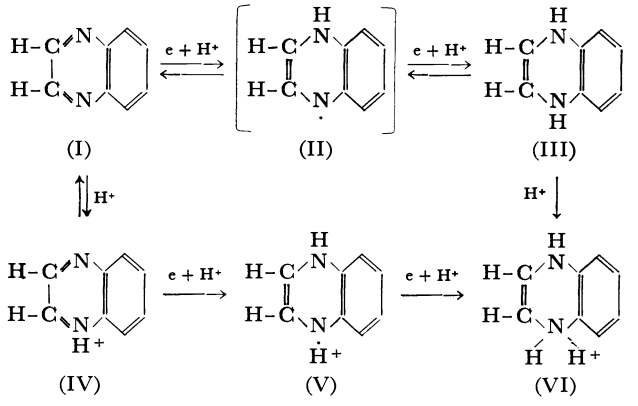

the anodic wave which is due to the oxidation of the electrolytic reduction product grows at the expense of the reduction wave of quinoxaline. On further electrolysis, the height of the anodic wave decreases slowly with time, and at the same time it is observed that the electrolytic solution becomes muddy; this is probably caused by the low solubility of the reduction product in an aqueous solution. However, the electrode reaction is reversible because the half-wave potential of the anodic wave is identical with that of the reduction wave of the condensation product (quinoxaline).

The results of the coulometric study are summarized in Table I. From this study one can conclude that the electrode reaction requires two electrons at pH 9.15.

The mechanism of the electrolytic reduction of quinoxaline is analogous to that of phenazine.[14,15] In strongly acidic solutions, the reduction of quinoxaline occurs in two well-separated steps

Table I. Estimation of the number of electrons required for the reduction of quinoxaline

Initial amount of quinoxaline: 4.985×10^{-5} mol. in 50 ml., pH 9.15, containing 10% alcohol, 20°C

Electrolysis time min.	Quantity of electricity consumed coulomb	Limiting current of quinoxaline μamp.	Amount of quinoxaline reduced $\times10^{-5}$ mol.	*n*
0	0	3.59		
5	1.144	3.14	0.623	1.903
10	2.178	2.78	1.127	2.003
20	3.425	2.29	1.805	1.966
25	3.991	2.10	2.069	1.999
35	4.862	1.74	2.567	1.963
55	6.132	1.33	3.141	2.023

14) R. C. Kaye and H. I. Stonehill, *J. Chem. Soc.*, **1952**, 3240.
15) Y. Asahi, *J. Pharm. Soc. Japan* (*Yakugaku Zasshi*), **80**, 679 (1960).

(see Fig. 2, a), each corresponding to the taking-up of one electron, since the two wave heights almost coincide with each other and the sum of the two wave heights is equal to that of the single wave in the neutral and alkaline ranges. As the pH increases, these waves move closer together, unitl at pH values higher than 2.5 they coalesce into a single two-electron step (see Fig. 2, b, c).

From the observation described above, it may be assumed that in acidic solutions of pH values lower than 2.5 a stable semiquinone (V) is formed in the first reduction step, and that its stability rapidly decreases as the pH value increases. The mechanisms of the electrolytic reductions may be expressed as follows:

$$\begin{array}{ccccc} O & \rightleftarrows & [O] & \rightleftarrows & O \\ \downarrow\uparrow & & & & \downarrow \\ O & \rightarrow & O & - & O \end{array}$$

The third wave (see Fig. 2), though no particular experiments have been made with this reduction wave, is considered to be a catalytic hydrogen wave of the protonated reduction product as in the case of the nitrogen-containing heterocyclic compounds.[16]

Application to the Determination of Glyoxal in Commercial Products.—On the basis of the above results, the following conditions may be recommended as the most practical conditions for the determination of glyoxal by utilizing the wave of the condensation product of glyoxal with OPD: $(1-2)\times10^{-2}$ M for the concentration of OPD, 7—10 for the pH range, 25°C for the temperature, and 30—60 min. for the condensation time. Under these conditions a linear relation was obtained between the concentration of glyoxal and the limiting current of the condensation product in the range of $(0.2—20)\times10^{-4}$ M, as is shown in Fig. 10.

For applying the present polarographic method to the determination of glyoxal in commercial products, the following procedure was employed: 1—5 g. of a commercial reagent (about 40% aqueous solution) was transferred to the 1 l. volumetric flask and diluted to the mark with distilled water. Then, in a run, 2 ml. of the diluted sample was placed in a 20-ml. volumetric flask, 10 ml. of a BR buffer with a pH value of 9.0 and 2 ml. of the aqueous solution of OPD (0.1 M) were added, and then the volume was made up to the mark with distilled water. A part of the mixture was taken in an electrolytic cell and immersed in a thermostat at 25°C for 45 min., during which time dissolved oxygen was removed by the bubbling nitrogen gas. After that, a ploarogram was taken in the usual way (A). In another run,

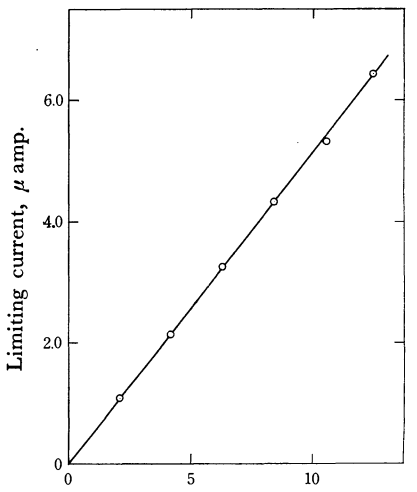

Fig. 10. Linear relationship between the limiting current of the condensation product and the concentration of glyoxal.

2 ml. of the diluted sample was placed in a 20 ml. volumetric flask, and 1 ml. of a standard solution containing glyoxal sodium bisulfite of 1×10^{-3} M, 10 ml. of a BR buffer of pH 9.0, and 2 ml. of the solution of OPD were added. After that, the same procedure as in the former run was followed, and a polarogram was recorded (B). By comparing the two polarograms, (A) and (B), the glyoxal content in the original sample was calculated. Some of the analytical results obtained are listed in Table II, together with those obtained by the titrimetric method[17] based on Cannizaro's reaction. The results obtained by the two methods are in good agreement with each other.

As another application, the determination of glyoxal in commercial products of ethylene glycol containing glyoxal and glycolaldehyde as impurities

Table II. The results of the determination of glyoxal in commercial product

Concn. of OPD: 1×10^{-2} M, pH 9.0, 25°C

Sample taken* g.	Polarographic		Titrimetric** content %
	Found g.	Content %	
1.267	0.539	42.5	42.8
1.259	0.530	42.1	
1.271	0.548	43.1	43.2
2.476	1.067	43.1	
2.481	1.052	42.4	

* Commercial product of glyoxal (about 40%).
** Determination by titration method based on Cannizaro's reaction.

16) P. Zuman, "Organic Polarographic Analysis," Pergamon Press, Oxford (1964), p. 100; see also M. Brezina and P. Zuman, "Polarography in Medicine, Biochemistry and Pharmacy," Interscience Publishers, New York (1958), p. 374.

17) J. G. Baldinus and I. Rothberg, *Anal. Chem.*, **32**, 1176 (1960).

was carried out. In this determination, the polarographic procedure described above was followed after the following pretreatment of the ethylene glycol sample: the sample was diluted to 2 to 5 times with distilled water, and the resulting diluted solution was allowed to stand overnight to effect hydrolysis, because glyoxal in concentrated ethylene glycol is considered to exist as acetal, which is inactive for OPD. The results obtained by the present polarographic method are given in Table III, together with those obtained by the titration method[18] using hydroxylamine hydrochloride. Though glycolaldehyde shows an anodic wave which is characteristic of monoaldehyde in the buffer solution containing OPD,* the presence of glycolaldehyde does not seriously interfere with the determination of glyoxal by the polarographic OPD method, because it does not give the waves in the potential range used for the determination of glyoxal. On the other hand, when the determination of glyoxal was carried out by the titration method, the presence of glycolaldehyde interfered seriously with the determination of glyoxal.

When such substances as methanol, ethanol, ethylene glycol, glycolic acid and acetone exist in the sample, the limiting current of the condensation product decreases slightly with an increase in the concentration of these substances. However, as long as the determination of the glyoxal is carried out by the standard addition method described above, these substances do not cause any interference, since the substances are not polarographically reducible under the present conditions.

Table III. The results of the determination of glyoxal in commercial ethylene glycol

Concn. of OPD: 1×10^{-2} M, pH 9.0, 25°C

Exp. No.	Content of glyoxal, %	
	Polarographic	Titrimetric*
1	0.0122	0.1979
2	0.0120	0.1975
3	0.0121	0.1983

* Hydroxylamine titration method (glyoxal + glycolaldehyde).

Aldehydes such as formaldehyde, acetaldehyde, propylaldehyde, butylaldehyde and glycolaldehyde give the anodic waves which have been described in the case of glycolaldehyde under the present experimental conditions, but they do not give reduction waves, whereas glyoxal does. Therefore, the presence of the aldehydes does not cause any interference with the determination of glyoxal. Furthermore, the presence of sulfite ion does not interfere, because electrolytic solutions are alkaline when they have pH values of 8—10.

Methylglyoxal, biacetyl and glyoxylic acid easily react with OPD under the present conditions and give reduction waves the half-wave potentials of which are −0.802, −0.851 and −0.830 V. respectively at pH 8.5. Therefore, the presence of these substances interferes with the determination of glyoxal.

The authors wish to express their thanks to Professor Sôzaburo Ono and Dr. Masanosuke Takagi of the College of Agriculture, University of Osaka Prefecture, for their kind advice and encouragement.

18) Sidney Siggia, "Quantitative Organic Analysis Via Functional Groups," Wiley, New York (1963). p. 73.

* The details of this kind of observations will be given elsewhere.

BULLETIN OF THE CHEMICAL SOCIETY OF JAPAN VOL. 39 1910—1915 (1966)

The Synthesis of 2-Alkyl-8-hydroxyquinolines and Their Chelating Behavior with Metal Ions[1,2]

By Hisamitsu KANEKO and Keihei UENO

Department of Organic Synthesis, Faculty of Engineering, Kyushu University, Fukuoka

(Received December 27, 1965)

2-Ethyl-, 2-*n*-propyl- and 2-*n*-butyl-8-hydroxyquinolines have been synthesized by the reactions of 8-hydroxyquinoline with alkyl-lithium. The dissociation constants and the chelate stability constants of these ligands with copper(II), zinc(II), nickel(II) and cadmium(II) have been measured in 50% v/v aqueous dioxane at 25.0±0.1°C with no additional electrolyte. Factors affecting the acid dissociation constants and the chelate stability constants will be discussed in this paper.

As a part of our investigations into the relationship between the chemical structure of a chelating agent and the metal chelate stability, a number of 8-hydroxyquinoline derivatives have been brought under investigation. 2-Methyl and 2-phenyl derivatives have been reported in the literature, and the selectivities of their metal chelate formation for certain metal ions have been discussed from theoretical and analytical standpoints.[3]

In this connection, our interest has been focused on the derivatives of 8-hydroxyquinoline with an alkyl group at the C-2 position. For this purpose, a general method for introducing an alkyl group to the C-2 position of 8-hydroxyquinoline has been developed. After investigating several reactions which seem to give the desired products,[4,5] we have finally chosen a method which is similar to the method used for the preparation of 2-phenyl-8-hydroxyquinoline; it consists of the reaction of 8-hydroxyquinoline with alkyl lithium in ether, followed by hydrolysis.[6,7] 2-Alkyl-8-hydroxyquinolines were isolated as hydrochloride because the free bases were difficult to purify because of their low melting points. The results of the syntheses are summarized in Table I. The attempted syntheses of isopropyl and *t*-butyl derivatives were not successful, as the reaction did not give enough yield for our purposes.

It is known that 2-methyl-8-hydroxyquinoline can not form a stable chelate with aluminum, and the selectivity of this reagent is understood to be caused by the steric hindrance of the 2-methyl group of this ligand around the aluminum ion, which has a relatively small ionic radius. Similarly, it may be expected that the introduction of a higher alkyl group to the C-2 position of 8-hydroxyquinoline would result in a different selectivity for metal ions. Thus, the chelate stability constants of 2-alkyl-8-hydroxyquinoline with copper(II), zinc(II), nickel(II) and cadmium(II) have been measured. As these ligands, as well as the metal chelate compounds, were not soluble in water, the acid dissociation constants and the chelate stability constants were measured in 50% v/v aqueous dioxane by the pH titration method.

Experimental

The Synthesis of Ligands.—As an example, the synthesis of 2-*n*-butyl-8-hydroxyquinoline will be described.

All the procedures until the hydrolysis step were conducted under dry nitrogen protected from atmospheric moisture. A solution of 13.6 g. (0.099 mol.) of *n*-butyl-bromide in 30 ml. of ether was dropped into a reaction flask containing 1.7 g. (0.245 mol.) of lithium covered with 50 ml. of ether. The bromide was then added over a 40 min. period, while the temperature was kept below −10°C. After this mixture had been stirred another 1.5 hr., a solution of 2.7 g. (0.019 mol.) of 8-hydroxyquinoline in 100 ml. of ether was dropped into the reaction flask over a 20 min. period. After the stirring had been continued for an additional 2 hr. at −10°C, the reaction product was hydrolyzed by pouring it onto ice chips. The ether layer was separated, and the ether was evaporated to obtain a yellow oil. The oil was taken into hydrochloric acid, and the resulting crystalline mass was repeatedly recrystallized from ethanol. Pale yellow crystals melting at 165.8—167.3°C were thus obtained. Yield: 2.0 g. (45%).

A similar procedure was followed for the synthesis

1) Contribution No. 69 from the Department of Organic Synthesis, Kyushu University.

2) This paper is taken, in part, from the Master of Engineering thesis of Hisamitsu Kaneko (1964), Kyushu University.

3) A. E. Martell and M. Calvin, "The Chemistry of Metal Chelate Compounds," Prentice-Hall, New York, N. Y. (1952).

4) I. G. Farbenindustrie, German Pat. 613066 (1935).

5) O. Döbner, *Ann.*, **242**, 265 (1887); ibid., **281**, 1 (1894).

6) H. Irving, E. J. Butler and M. F. Ring, *J. Chem. Soc.*, **1949**, 1489.

7) J. P. Phillips, R. L. Elbinger and L. L. Merritt, *J. Am. Chem. Soc.*, **71**, 3984 (1949).

Table I. Syntheses of 2-alkyl-8-hydroxyquinoline

Alkyl	Yield[a] %	M. p.[b] °C	Analytical data[c] C% Calcd.	C% Found	H% Calcd.	H% Found	N% Calcd.	N% Found
Ethyl	24	194.5—196.5	63.01	62.25	5.77	5.86	6.68	6.59
n-Propyl	26	161.5—163.0	64.43	63.96	6.31	6.72	6.26	6.11
n-Butyl	45	165.8—167.3	65.68	65.59	6.78	6.69	5.89	5.82

a) Based on 8-hydroxyquinoline.
b) The melting point and analytical data are those of hydrochlorides.
c) The Elementary analyses were carried out at the Elementary Analyses Center of Kyushu University.

of 2-ethyl and 2-*n*-propyl derivatives using the corresponding alkyl bromide. The yields, melting points and analytical data for the products are summarized in Table I.

Although tetrahydrofurane was used as a solvent in place of ether in the hope of improving the yield, the reaction did not proceed; only the starting material was recovered.

Chelate Stability Measurements.—*Materials.*—All the ligands were used as hydrochloride. Dioxane, of an analytical grade, was purified by refluxing it with 20% sulfuric acid, followed by repeated distillations.

An 0.1 N sodium hydroxide solution and 0.01 M metal ion solutions (nitrates) were prepared using 50% v/v aqueous dioxane as a solvent. The concentrations of metal ion solutions were determined by EDTA titration.

Apparatus and Procedure.—Potentiometric titration was carried out in a jacketed beaker equipped with a burett for the delivery of a sodium hydroxide solution, a glass electrode and a calomel electrode for pH measurement, and nitrogen inlet and outlet tubes.

The pH was measured with a Horiba-Hitachi Model P pH meter which had been standardized against the pK_a value[8,9] of acetic acid by titrating acetic acid in 50% v/v aqueous dioxane.

The titration was carried out on a solution with a ligand-to-metal ratio of 1 : 1 or 2 : 1, at 25.0±0.1°C and with no additional electrolyte. The titration curves for 2-*n*-butyl-8-hydroxyquinoline are shown in Figs. 1 and 2. The curves for the other ligands were found to be similar to those shown in Fig. 1.

Calculations

The Calculation of the Acid Dissociation Constants.—The acid dissociation constants were calculated from the titration curves of the ligands. The equilibrium constants may be expressed as follows:

$$H_2A^+ \rightleftarrows HA + H^+ \quad K_{NH} = \frac{[H^+][HA]}{[H_2A^+]} \tag{1}$$

$$HA \rightleftarrows H^+ + A^- \quad K_{OH} = \frac{[H^+][A^-]}{[HA]} \tag{2}$$

where H_2A^+ represents the protonated ligand (hydrochlolide).

As is shown in Fig. 1, the two buffer regions are so clearly separated that each dissociation stage can be treated independently. Thus, K_{NH} and K_{OH} can be expressed as follows, according to the standard treatment:

$$K_{NH} = \frac{[H^+](aT_A + [H^+])}{T_A - (aT_A + [H^+])} \tag{3}$$

$$K_{OH} = \frac{[H^+]\{(a-1)T_A - K_W/[H^+]\}}{T_A - \{(a-1)T_A - K_W/[H^+]\}} \tag{4}$$

where T_A and a represent, respectively, the total concentration of the ligand and the number of moles of the base added per mole of ligand, and where $K_W=[H^+]\cdot[OH^-]$.

Calculation of Chelate Stability Constants.—The step-by-step chelate formation constants of the reactions, may be expressed as:

$$M^{2+} + A^- \rightleftarrows MA^+ \quad K_{MA} = \frac{[MA^+]}{[M^{2+}][A^-]} \tag{5}$$

$$MA^+ + A^- \rightleftarrows MA_2 \quad K_{MA_2} = \frac{[MA_2]}{[MA^+][A^-]} \tag{6}$$

The stability constants were calculated by the least-squares method, using the data from 1 : 2 titrations.[10,11] The equation employed for this method was as follows:

$$\frac{\bar{n}}{(\bar{n}-1)[A^-]} = \frac{(2-\bar{n})[A^-]}{(\bar{n}-1)} K_{MA}\cdot K_{MA_2} - K_{MA} \tag{7}$$

where $\bar{n}$ is the average number of ligands bound per metal ion.

If, by replacing each term, one simplifies the above equation as:

$$Y = \frac{\bar{n}}{(\bar{n}-1)[A^-]} \tag{8}$$

$$X = \frac{(2-\bar{n})[A^-]}{(\bar{n}-1)} \tag{9}$$

$$a = -K_{MA} \tag{10}$$

8) H. S. Harned and B. B. Owen, "The Physical Chemistry of Electrolytic Solutions," 3rd. ed., Reinhold Publ. Corp., New York (1958), pp. 717, 756.
9) H. J. Harries, *J. Inorg. Nucl. Chem.*, **25**, 519 (1963).
10) H. Irving and H. S. Rossotti, *J. Chem. Soc.*, **1953**, 3397.
11) A. Albert and E. P. Serjeant, "Ionization Constants of Acid and Bases," 1st Ed. Methuen & Co., London, (1962), p. 158.

TABLE II. ACID DISSOCIATION CONSTANTS AND STABILITY CONSTANTS OF 2-ALKYL-8-HYDROXYQUINOLINE AT 25.0±0.1°C, $\mu \simeq 0$, $-\log K_W = 16.1$[9]

Ligand 2-R-8-HQ	Acid dissociation constant		Stability constant Ni(II)	Cu(II)	Zn(II)	Cd(II)
R=H	pK_{NH} (3.97)[a]	$\log K_{MA}$	(11.44)	(13.49)	(9.96)	(9.43)
	pK_{OH} (11.54)	$\log K_{MA_2}$	(9.94)	(12.73)	(8.90)	(7.68)
R=CH_3	pK_{NH} 4.63	$\log K_{MA}$	9.3_5	12.4_3	9.8_9	9.1_8
	pK_{OH} 11.83	$\log K_{MA_2}$	8.9_1	11.4_6	9.2_2	8.2_1
R=C_2H_5	pK_{NH} 4.47	$\log K_{MA}$	8.6_9	12.0_5	9.6_6	8.6_6
	pK_{OH} 11.86	$\log K_{MA_2}$	9.0_5	11.2_8	9.3_0	8.3_1
R=n-C_3H_7	pK_{NH} 4.44	$\log K_{MA}$	9.0_1	12.0_6	8.9_6	8.8_4
	pK_{OH} 11.95	$\log K_{MA_2}$	9.4_6	11.8_1	10.4_9	8.7_0
R=n-C_4H_9	pK_{NH} 4.41	$\log K_{MA}$	9.1_8	12.0_5	9.7_5	9.2_8
	pK_{OH} 12.07	$\log K_{MA_2}$	9.8_9	12.2_3	10.2_4	8.9_8

a) The values in parentheses have been taken from Ref. 13.

$$b = K_{MA} \cdot K_{MA_2} = \beta_2 \quad (11)$$

then the equations for the least-squares method can be written as follows:

$$\sum Y = na + b\sum X \quad (12)$$

$$\sum XY = a\sum X + b\sum X^2 \quad (13)$$

where n represents the number of observed points employed for each set of calculations. The experimental data corresponding to the $\bar{n}$ values of 0.95—1.05 were omitted in the calculations, because these values are very critical to the results. The results of the calculations[12] are summarized in Table II.

Results and Discussion

The Structural Proof for the Ligand.—In order to confirm the proposed structure for 2-alkyl-8-hydroxyquinoline, the NMR spectra were observed on the hydrochlorides in a deuterium oxide solution.

The spectra were measured at 60 Mc./sec., using tetramethylsilane as an internal standard. The results are summarized in Table III, along with their assignments. The table also includes the data for quinoline hydrochloride, 8-hydroxyquinoline hydrochloride and 2-methyl-8-hydroxyquinoline hydrochloride. The peaks at 1.43 τ of 8-hydroxyquinoline hydrochloride are assigned to the protons on C-2 and C-4; the decrease in the intensities of the corresponding peaks in the 1.4—1.6 τ region for the 2-alkyl derivatives indicates the elimination of a proton on either C-2 or C-4 by alkyl substitution. However, the spin-spin coupling constant of these peaks (8.5 c. p. s.) is closer to a J_{34} coupling constant of 7.3 c. p. s. than to the J_{23} coupling constant of quinoline[14]

TABLE III. ASSIGNMENTS OF NMR SPECTRA OF 2-ALKYL-HYDROXYQUINOLINE

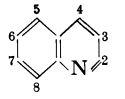

Compound	Peaks (τ)*	Intensity	Assignments of proton
Quinoline HCl	0.90	2	C-2, C-4
	1.95	5	C-3, C-5, C-6 C-7, C-8
8-Hydroxy-, HCl	1.43	2	C-2, C-4
	2.03	1	C-5
	2.93	2	C-6, C-7
	3.25	1	C-7
2-Methyl-	1.63	1	C-4
8-hydroxy-, HCl	2.50	1	C-3
	2.80	2	C-6, C-7
	3.07	1	C-3
	7.23	3	$-CH_3$
2-Ethyl-8-hydroxy-,	1.63	1	C-4
HCl	2.37	1	C-5
	2.88	2	C-6, C-7
	3.10	1	C-3
	6.97	2	$-CH_2-$
	8.65	3	$-CH_3$
2-n-Propyl-	1.50	1	C-4
8-hydroxy-, HCl	2.40	1	C-5
	2.73	2	C-6, C-7
	2.93	1	C-3
	6.95	2	$-CH_2-$ (α)
	8.27	2	$-CH_2-$ (β)
	9.00	3	$-CH_3$
2-n-Butyl-	1.47	1	C-4
8-hydroxy-, HCl	2.35	1	C-5
	2.68	2	C-6, C-7
	2.88	1	C-3
	6.93	2	$-CH_2-$ (α)
	8.50	4	$-CH_2-CH_2-$(β,γ)
	9.07	3	$-CH_3$

* The values listed in the table show the center of multiplet peaks.

12) Such calculations were carried out at the Computing Center of Kyushu University.

13) W. D. Johnston and H. Freiser, *J. Am. Chem. Soc.*, **74**, 5239 (1952).

14) J. A. Pople, W. G. Schneider and H. J. Bernstein, "High-resolution Nuclear Magnetic Resonance," McGraw-Hill, New York (1959), p. 269.

of 5.0 c. p. s., which was chosen as a model compound. Therefore, it is quite likely that the proton on C-2 is eliminated by the alkyl substitution, while the proton on C-4 remains unaltered.

Titration Curves.—The corrected potentiometric titration curves for 2-*n*-butyl-8-hydroxyquinoline, with or without an equivalent amount of metal ions, are given in Fig. 1.

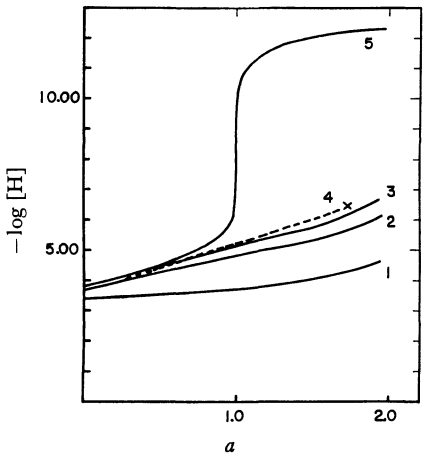

Fig. 1. Titration curves for 1:1 solution.
Concn. of ligand and metal ions: 1×10^{-3} M
1: Cu(II), 2: Zn(II), 3: Ni(II), 4: Cd(II), 5: ligand

The titration curves for the solutions with a 1 : 2 metal ligand ratio are illustrated in Fig. 2. It was noticed that some chelates began to precipitate at the point indicated by "X".

The curves of the other ligands are very similar to those of 2-*n*-butyl-8-hydroxyquinoline. The pK_{NH} and pK_{OH} values were calculated from the data of the titration curves of the ligands, in the ranges of $a=0.3$—0.7 and $a=1.3$—1.7 respectively.

Formation Functions and Equilibrium Constants.—The acid dissociation constants for 2-alkyl-8-hydroxyquinoline are shown in Table II. The pK_{NH} and pK_{OH} values stand for the dissociation of protons from the quinoline nitrogen and the phenolic oxygen respectively.

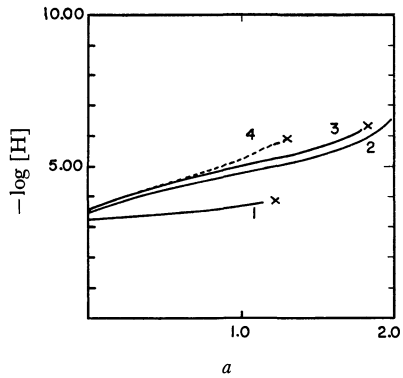

Fig. 2. Titration curves for 1:2 solution.
Concn. of ligand: 2×10^{-3} M
1: Cu(II), 2: Zn(II), 3: Ni(II), 4: Cd(II)

The chelate stability constants of these ligands with various metal ions are also shown in Table II. The reported values for 8-hydroxyquinoline, as well as those for 2-methyl-8-hydroxyquinoline,[13] are also included in the table for the sake of comparison. The chelate stability constants were computed by the least-squares method on the basis of the data on 1 : 2 titration described above. A typical example of calculations, those on the copper(II)-2-*n*-butyl-8-hydroxyquinoline system, is shown in Table IV. It may be seen from the table that fairly consistent stability constants are obtained over a wide range of $\bar{n}$ values, and that one could use the values of three significant figures in a meaningful discussion. These results are satisfactory if one considers the experimental conditions under which the titration was conducted in a non-aqueous solvent without an added electrolyte.

Table IV. Calculations of chelates stability constants on the system copper(II)-2-*n*-butyl-8-hydroxyquinoline (1:2 titration)

	[A]	$\bar{n}$	$X=\frac{(2-\bar{n})[A]}{(\bar{n}-1)}$	$Y=\frac{\bar{n}}{(\bar{n}-1)[A]}$	log K_{MA}	log β_2
1	0.19874×10^{-12}	0.2949	-0.48061×10^{-12}	-0.21045×10^{13}	12.07	24.31
2	0.24700×10^{-12}	0.3668	-0.63706×10^{-12}	-0.23451×10^{13}	12.05	24.28
3	0.29789×10^{-12}	0.4446	-0.83422×10^{-12}	-0.26870×10^{13}	12.04	24.27
4	0.34875×10^{-12}	0.5272	-0.10863×10^{-11}	-0.31967×10^{13}	12.05	24.28
5	0.40366×10^{-12}	0.6127	-0.14460×10^{-11}	-0.39195×10^{13}	12.07	24.29
6	0.46969×10^{-12}	0.6998	-0.20345×10^{-11}	-0.49639×10^{13}	12.04	24.28
7	0.52703×10^{-12}	0.7919	-0.30600×10^{-11}	-0.72217×10^{13}	12.14	24.30
8	0.61205×10^{-12}	0.8827	-0.58285×10^{-11}	-0.12291×10^{14}	12.07	24.28

$\sum X=-0.15407\times10^{-10}$ $\sum Y=-0.38729\times10^{14}$ log $K_{MA}=12.05$
$\sum X^2=0.52078\times10^{-22}$ $\sum XY=0.11772\times10^{3}$ log $\beta_2=24.28$

log $K_{MA}=12.09\pm0.05$
log $K_{MA_2}=12.20\pm0.07$
log $\beta_2=24.29\pm0.02$

and the early onset of precipitation. Therefore, the following discussion is based mainly on those values of three significant figures.

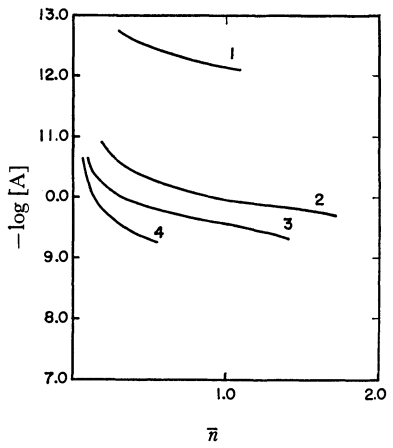

Fig. 3. Formation functions of some divalent metal chelates of 2-*n*-butyl-8-hydroxyquinoline.
Concn. of ligand: 2×10^{-3} M
Metal ions: 1×10^{-3} M
1: Cu(II), 2: Zn(II), 3: Ni(II), 4: Cd(II)

The Bjerrum's formation functions for the metal chelates of 2-*n*-butyl-8-hydroxyquinoline are shown in Fig. 3. Because of the early appearance of the precipitation, the formation curves only extended to $\bar{n}\approx0.6$ for cadmium(II) and $\bar{n}\approx1.0$ for copper(II). Only in the case of zinc(II) was a curve extending over almost the entire range found. Although the formation curve for a 1 : 1 or 1 : 2 chelate ratio has been shown to be symmetrical about $\bar{n}=1$, it does not seem likely in this case. The deviation from symmetry may be due to the easy precipitation.

The Effect of the Alkyl Group on the Chelate Stability.—As is shown in Table II, the pK_{NH} value is almost constant, regardless of the kind of alkyl groups, with the exception of the 2-methyl derivative, which shows a slightly higher pK_{NH} value than the rest of the ligands. On the other hand, the pK_{OH} value increases slightly with the increasing carbon number of the alkyl group.

Irving and Rossotti investigated the effect of alkyl substitution on the acid dissociation constant of 8-hydroxyquinoline; they found that pK_{OH} value increased and the pK_{NH} value decreased when the position of the methyl substitution moved from the C-2 to the C-7 position of the quinoline ring.[15] This effect is understood to be due to the *I*-effect of the methyl group. Similarly, one can expect an *I*-effect of the 2-alkyl group for the 2-alkyl-8-hydroxyquinolines, which have higher pK_{NH} values than 8-hydroxyquinoline, as is shown in Table II. However, the contribution of the *I*-effect of the 2-alkyl group to the pK_{NH} value may be partly cancelled by the steric effect of higher alkyl groups, which will interfere with the access of protonium ions to the quinoline nitrogen. Thus, the pK_{NH} value is highest for the 2-methyl derivative, while 2-ethyl, 2-*n*-propyl and 2-*n*-butyl derivatives have lower pK_{NH} values than the 2-methyl derivative. Regarding the pK_{OH} values, the access of protonium ions to the phenolate oxygen will not be interfered with by a 2-alkyl group. Therefore, pK_{OH} may be influenced only by the *I*-effect of the 2-alkyl group, although this influence may be fairly weak. The increase in the pK_{OH} value with the increase in the carbon number of the alkyl group supports this theory.

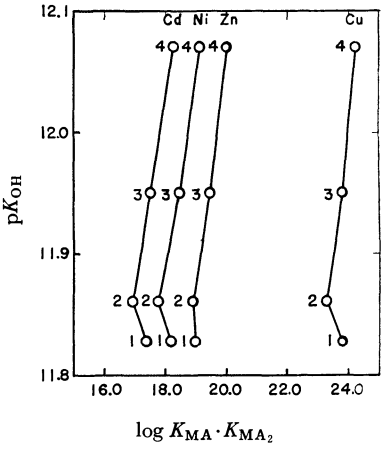

Fig. 4. Correlation between pK_{OH} and $\log K_{MA}\cdot K_{MA_2}$.
1: Me, 2: Et, 3: *n*-Pr, 4: *n*-Bu

As to the chelate stability constants, the values change rather slightly with the variation in alkyl group, as is shown in Table II. However, their differences seem to be large enough to allow us to make a meaningful interpretation of the results.

The order for the decreasing stability constants of 8-hydroxyquinoline was found to obey the Mellor-Maley order. However, the order of nickel and zinc was inverted in the case of 2-alkyl derivatives; thus: 8-hydroxyquinoline: Cu>Ni>Zn>Cd
2-alkyl derivative: Cu>Zn>Ni>Cd

The relationship between the overall stability constants and the acidity of the ligands is shown in Fig. 4. The $\log K_{MA}\cdot K_{MA_2}$ values are plotted against the pK_{OH} values, since the pK_{NH} values are almost contant for all the ligands except the 2-methyl derivatives. As expected, the overall stability constants increase linearly with the increase in the pK_{OH} values. However, in the case of the 2-methyl derivative, the relatively higher pK_{NH} value contributes to the overall stability constants, so that the values for the 2-methyl derivative deviate from linearity.

15) H. Irving and H. S. Rossotti, *J. Chem. Soc.*, **1954**, 2910.

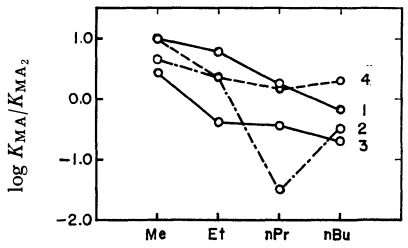

Fig. 5. Correlation for substituents.
1: Cu(II), 2: Zn(II), 3: Ni(II), 4: Cd(II)

The plots of log K_{MA}/K_{MA_2} against the carbon number of the alkyl group are shown in Fig. 5. It may be seen from this figure that the relative stability of 1 : 1 chelate to 1 : 2 chelate decreases with an increase in the carbon number of the alkyl group, with the exceptions of zinc and cadmium chelates of the 2-butyl derivative. This result is quite surprising, because it indicates that the formation of 1 : 2 chelate becomes more favorable when the higher alkyl group is introduced at the C-2 position of 8-hydroxyquinoline. The irregular behavior of zinc and cadmium may be partly explained in terms of the steric hindrance to the tetrahedral coordination structure; however, more experimental data will be needed before we can make a clear-cut explanation of the results obtained in this investigation.

The authors are greatful to the Ministry of Education, Japanese Government, for a grant in support of this work. They also thank to Dr. Kenji Motojima of Japan Atomic Energy Institute for his advice of the initiation of this work.

BULLETIN OF THE CHEMICAL SOCIETY OF JAPAN VOL. 39 1915—1922 (1966)

The Constitution, Reactivity and Thermal Change of Phosphate Ores

By Jumpei ANDO and Seiichi MATSUNO

Department of Industrial Chemistry, Faculty of Science and Engineering, Chuo University, Bunkyo-ku, Tokyo

(Received January 12, 1966)

Tests were made on twenty-five samples of phosphate ores from all over the world deposits. All of the samples consisted of apatite, plus small amounts of calcite and other minerals. The apatite crystals of the sedimentary ores ranged in size from around 0.05 μ (Gafsa, North Carolina, etc.) to around 0.5 μ (Taiba), while those of igneous ores reached 100 μ. The difference between the ores in their reactivity with citric, hydrochloric and nitric acid was mainly due to the difference in crystal size. The decomposition of the ores by a mixture of sulfuric and phosphoric acids was seriously affected by the coating of calcium sulfate crystals on the surface of the ores, and also by the aluminum and iron present in the acids and ores. The lattice constant, a_0, of the apatite of the ores ranged from 9.340 to 9.422 Å; it was generally smaller for the ores which had larger F_2/P_2O_5 ratios. Upon calcination above 500°C, the a_0 value of the apatite which had an excess of fluorine increased and approached that of true fluorapatite. The reactivity of the ores with the acids generally decreased upon calcination due to the sintering of the grains and the crystal growth. For ease of decomposition by a mixture of sulfuric and phosphoric acids, the calcined ore should contain a small amount of carbon dioxide. Tests also were made on the amount of organic matter and its decrease upon calcination.

Phosphate ores mined from various fields differ much in their nature. Moreover, it often happens that even ores which have been obtained from the same area and which have essentially the same chemical composition are significantly different in their behavior when treated with acids; this results in trouble for phosphate fertilizer plants. The reason for such differences is not clear.

Moreover, the calcination of ores which has recently been carried out in commercial-scale plants in order to increase the grade of the ores results in a further variation in the nature of the ores. Although many investigators[1-4] have reported on the phosphate ores, there is still much to study about the constitution and the nature of the ores.

1) J. H. Caro and W. L. Hill, *J. Agr. Food Chem.*, **4**, 684 (1961).
2) H. L. Marshall, L. F. Rader and K. D. Jacob, *Ind. Eng. Chem.*, **25**, 1253 (1933).
3) T. Noguchi, T. Hosoi and O. Kashimura, *J. Chem. Soc. Japan, Ind. Chem. Sect.* (*Kogyo Kagaku Zasshi*), **64**, 1892 (1961).
4) J. H. Caro and W. L. Hill, *J. Agr. Food Chem.*, **12**, 479 (1964).

TABLE I. CHEMICAL COMPOSITION OF SAMPLES

Sample	Chemical composition, %							Mole ratio		$KMnO_4$ consumption ml.
	BPL	P_2O_5	CaO	R_2O_3	SiO_2	F_2	CO_2	CaO/P_2O_5	F_2/P_2O_5	
Kola	85	39.1	51.1	1.8	3.2	2.8	0.1	3.31	0.27	2.6
Lao'Cay	87	40.2	—	0.9	—	3.7	0.1	—	0.34	—
Phallabowa	74	34.0	53.1	1.6	2.2	2.5	4.7	3.96	0.28	—
Florida	68	31.6	46.5	2.6	8.1	3.8	5.1	3.72	0.45	14.9
Florida	76	35.1	49.6	2.1	3.2	3.3	2.3	3.59	0.35	9.0
Florida	77	35.8	51.5	3.0	4.1	3.9	4.1	3.64	0.41	12.6
Calcined Florida	75	34.8	52.3	1.4	4.5	4.0	0.8	3.83	0.43	9.5
Calcined Florida	79	36.6	52.9	2.6	4.3	4.6	0.4	3.67	0.47	5.3
Calcined Florida	81	37.2	52.7	2.2	3.1	3.8	0	3.60	0.38	1.8
North Carolina	65	30.0	49.5	2.1	3.5	3.7	5.2	4.27	0.46	—
Taiba	80	36.9	50.0	2.0	3.6	—	—	3.44	—	17.3
Taiba	81	37.3	50.7	2.1	4.7	3.7	1.9	3.44	0.37	13.7
Taiba	82	37.9	52.6	2.2	2.2	3.3	1.8	3.51	0.33	—
Togo	79	36.7	53.2	1.5	3.8	3.0	1.8	3.67	0.31	—
Morocco	70	32.2	50.8	0.6	2.2	4.1	4.0	4.00	0.48	19.2
Morocco	73	33.6	51.2	0.7	1.4	4.2	6.3	3.86	0.47	10.2
Morocco	78	36.2	52.2	1.1	1.6	4.0	5.2	3.65	0.42	8.2
Kossier	61	28.4	47.3	1.5	7.9	3.4	6.3	4.22	0.45	66.0
Gafsa	55	25.5	43.2	3.4	—	3.2	4.2	4.29	0.46	—
Gafsa	64	29.8	49.1	1.2	10.8	3.7	4.2	4.17	0.46	41.5
Christmas	83	38.2	—	—	—	3.2	2.6	—	0.31	38.0
Christmas	84	38.9	—	3.0	0.2	1.1	1.5	—	0.11	18.0
Macatea	77	35.5	—	1.3	1.0	3.2	2.2	—	0.34	—
Macatea	80	37.0	52.0	1.0	0.4	3.2	2.7	3.56	0.32	43.2
Angaur	68	31.6	53.4	1.3	1.6	2.3	6.2	4.25	0.27	48.0
Synthetic HA*	89	40.9	53.8	0	0	0	0	3.33	0	0
Synthetic FHA**	89	41.1	53.9	0	0	1.8	0	3.32	0.16	0
Synthetic FA***	88	40.6	53.7	0	0	3.9	0	3.35	0.35	0
Theoretical FA	92	42.2	55.6	0	0	3.8	0	3.33	0.33	0

*Hydroxyapatite, **Fluorhydroxyapatite, ***Fluorapatite

The present authors[5-7] have recently studied many samples of ores by electron microscopy, X-ray diffraction, surface area measurement, differential thermal analysis and chemical analysis. In the present paper, the results of these studies will be summarized.

Samples

The chemical compositions of the samples of the ores and of the synthetic precipitated apatite are shown in Table I. Most of the ores were sedimentary ores; however, Kola, Lao'Cay and Phallabowa, were of igneous origin. Three ores, Christmas, Macatea and Angaur, were from ocean islands, while all of the others were from continents.

The three samples of calcined Florida ores were produced in commercial-scale plants. The reported calcination temperature was about 800°C for the BPL 75 sample and about 950°C for the others.

Three samples, FA, FHA and HA, were prepared by treating solutions of calcium chloride and sodium phosphate with or without sodium fluoride at 70°C at pH values from 8.0 to 8.6.

The principal mineral of all the ores was apatite. The F_2/P_2O_5 mol. ratios of several ores, such as Florida, Morocco and Gafsa, exceeded 0.33, which is the stoichiometric ratio for fluorapatite. As fluorite (CaF_2) was not detected in the ores, it may be considered that the excess fluorine is present in the apatite crystals, possibly in the form of CO_3F, which replaces PO_4. The ratio was smaller than 0.33 for a few ores, Kola, Phallabowa, Angaur and Christmas, this means that the shortage of fluorine ions had been covered by hydroxyl or other ions.

The ores contained more or less carbon dioxide, partly in the form of calcite and partly in the apatite as CO_3OH[8] or CO_3F, replacing PO_4^{3-}. Most of the carbon dioxide of three ores, Togo, Macatea and Taiba, seemed to be contained in the apatite,

5) J. Ando, S. Matsuno and T. Watanabe, *J. Chem. Soc. Japan, Ind. Chem. Sect* (*Kogyo Kagaku Zasshi*), **67**, 2014 (1964).
6) J. Ando and S. Matsuno, ibid., **68**, 1195 (1965).
7) J. Ando, S. Matsuno and S. Nishiyama, ibid., **69**, 12 (1966).

Table II. Results of the measurement

Mark	Sample	BPL	Crystal size μ	Citric solubility % 100 ml.	Citric solubility % 150 ml.	X-Ray peak height (222)	X-Ray peak height (123)	Specific surface area ($m^2/g.$)	Lattice constants, (Å) a_0	Lattice constants, (Å) c_0
△	Kola	85	0.5—100	6.4	10.7	48	55	0.9	9.405	6.908
▲	Lao'Cay	87	0.5—100	5.7	11.7	46	54	1.1	9.388	6.896
◬	Phallabowa	74	0.1 —20	17.2	21.6	38	48	10.7	9.409	6.904
◎	Florida	68	0.05— 0.5	26.0	37.4	29	36	13.7	9.355	6.908
◉	Florida	76	0.05— 0.5	—	34.7	29	38	—	9.361	6.904
○	Florida	77	0.05— 0.5	25.2	36.4	31	40	15.7	9.364	6.906
◬	Calcined Florida	75	0.1 — 1	—	28.0	39	47	—	9.378	6.904
△	Calcined Florida	79	0.1 —10	—	23.4	40	52	—	9.389	6.900
⚠	Calcined Florida	81	0.1 —10	—	20.8	43	53	—	9.391	6.899
●	North Carolina	65	0.02— 0.1	45.8	63.4	22	—	—	9.342	6.905
⊕	Taiba	80	0.05— 1	—	29.7	34	44	—	9.374	6.901
⊗	Taiba	81	0.1 — 1	20.0	29.2	33	42	12.2	9.374	6.904
⊘	Taiba	82	0.1 — 1	19.9	29.4	35	44	11.8	9.376	6.904
⊖	Togo	79	0.1 — 0.5	25.6	37.5	32	40	13.3	9.371	6.906
⊜	Morocco	70	0.05— 0.3	—	49.8	26	34	—	9.340	6.908
◐	Morocco	73	0.05— 0.2	35.5	50.2	28	37	22.0	9.355	6.910
◑	Morocco	78	0.1 — 0.5	25.7	35.6	30	38	14.6	9.364	6.906
⊙	Kossier	61	0.05— 0.2	32.4	46.5	26	35	20.6	9.359	6.907
◒	Gafsa	55	0.02— 0.1	44.7	64.4	23	31	26.4	9.344	6.911
◓	Gafsa	64	0.05— 0.2	39.7	57.5	25	32	21.8	9.345	6.911
◧	Christmas	83	0.05— 1	24.4	34.6	30	39	16.7	9.378	6.902
▬	Christmas	84	0.05— 1.5	35.5	48.4	30	37	19.1	9.422	6.899
▣	Macatea	77	0.05— 1	25.1	36.7	30	38	18.0	9.379	6.902
□	Macatea	80	0.05— 1	23.8	36.8	30	38	16.2	9.379	6.902
■	Angaur	68	0.05— 1	18.7	34.0	31	36	17.2	9.392	6.899
×	Synthetic HA*	89	0.05— 1.5	93.1	97.8	—	—	—	9.455	6.898
#	Synthetic FHA**	89	0.03— 1	—	62.3	—	—	—	9.429	6.902
+	Synthetic FA***	88	0.02— 0.5	44.0	57.5	—	—	—	9.406	6.904

*Hydroxyapatite, **Fluorhydroxyapatite, ***Fluorapatite

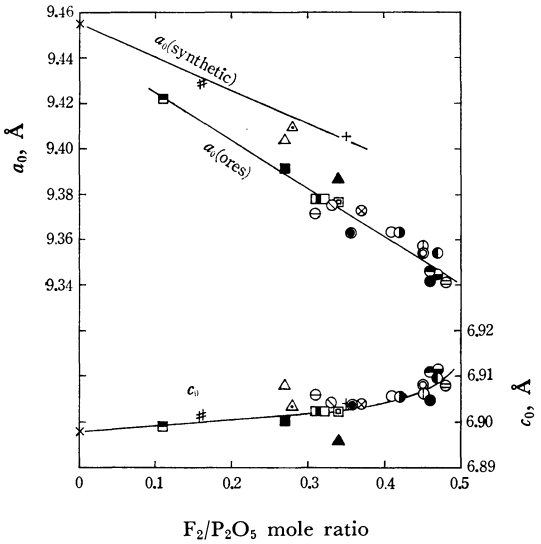

Fig. 1. Relation between the F_2/P_2O_5 ratio and the lattice constants. (The marks indicate the ores as shown in Table II.)

because the amount of calcite was very small in these ores.

The $KMnO_4$ (ml.) notations in Table I show the consumption of a N/10 potassium permanganate solution by 2-g. portions of the ores; this roughly indicates the relative amounts of organic matter, as will be described later.

Results and Discussion

The Relation between the F_2/P_2O_5 Ratio and the Lattice Constants of Apatite.—The lattice constants, a_0 and c_0, determined from (140) and (004) spacings are shown in Table II. The relation between the constants and the F_2/P_2O_5 mole ratio of the samples is shown in Fig. 1.

The a_0 constant was generally smaller when the F_2/P_2O_5 ratio was larger. Fluorapatite has a smaller a_0 value than does hydroxyapatite. An excess of fluorine made the a_0 value even smaller.

8) "DANA'S System of Mineralogy," Vol. II, (Seventh Ed.) John Wiley and Sons Inc., New York (1963), p. 882.

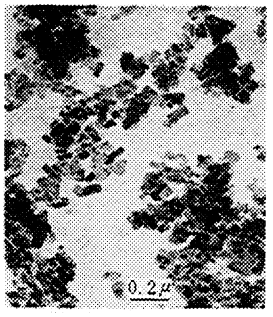

Photo. 1. Kossier (×25000)

Photo. 2. Christmas 84 (×25000)

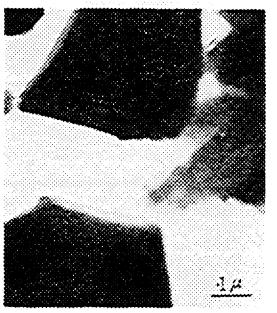

Photo. 3. Kola (×5000)

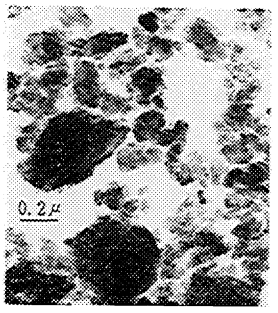

Photo. 4. Florida 77 (×25000)

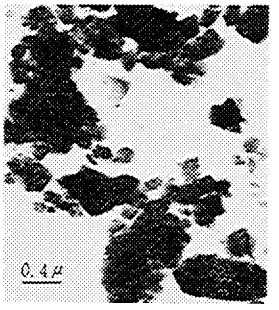

Photo. 5. Calcined Florida 75 (×12500)

Photo. 6. Calcined Florida 81 (×12500)

Electron microscope photographs

The constant of the ores was smaller than that of the synthetic precipitated apatite with an equal F_2/P_2O_5 ratio, presumably because of the effect of such impurities as CO_2 and R_2O_3 in the apatite. The c_0 constant increased slightly as the ratio increased from 0 to 0.33, and remarkably when the ratio exceeded 0.33, indicating the effect of excessive fluorine.

The Size and Shape of Apatite Crystals.—Apatite crystals of the samples ground to pass through 150 mesh (about 100 μ) were tested by both petrographic and electron microscopes. By the grinding, apatite crystals of the sedimentary ores were hardly destroyed at all because the crystals were generally smaller than 1 μ. The size range of most of the apatite crystals of each smaple is shown in Table II. Electron microscope photographs of typical samples are shown in Photos 1 to 6.

Most crystals of the sedimentary ores obtained from the continents (Florida, Morocco, etc.) were grainy or short-prism in shape, ranging in size from 0.02 to 1 μ. Of this sort of ores, Gafsa and North Carolina had the samllest crystal size, ranging from 0.02 to 0.1 μ, and Taiba had the largest size, ranging from 0.1 to 1 μ.

Most apatite crystals of the ores obtained from the ocean islands (Macatea, Angaur and Christmas) were prisms 0.05 to 0.2 μ in wide and 0.2 to 1 μ long. The igneous ores (Kola, Lao'Cay and Phallabowa) contained much larger crystals, up to 100 μ.

All of the synthetic apatite crystals were prism-shaped. The crystals of hydroxyapatite (HA) were much larger than those of fluorapatite (FA). Of the ores from the islands, the crystals of Christmas 84, which contained a particularly small amount of fluorine, were considerably larger than the others. Of the sedimentary ores from the continents, Gafsa and North Carolina, which had the largest F_2/P_2O_5 ratio, had the smallest crystal size. It seems that the presence of fluorine had depressed the growth of apatite crystals.

The Relation between Citric Solubility, the Height of X-ray Diffraction Peaks and the Specific Surface Area.—It has been reported that citric solubility is a good measure of the agronomic value of powdered phosphate ores.[1] Table II lists the citric solublity of the samples ground to pass through 150 mesh (300 mesh, 50% pass) tested in two ways: (1) 100 ml. of 2% citric acid was added to 1 g. of the sample and shaken for 30 min., and (2) 150 ml. of the acid was added to the sample and shaken for an hour.

The citric solubilities ranged from 5.7 to 45.8% in the 100 ml. method and from 10.7 to 64.4% in the 150 ml. method; they were generally higher for those ores which had smaller crystals and which gave shorter and broader X-ray diffraction peaks.

Figure 2 shows the relation between the height of the (222) peak ($2\theta=46.7°$ by CuKa) and the

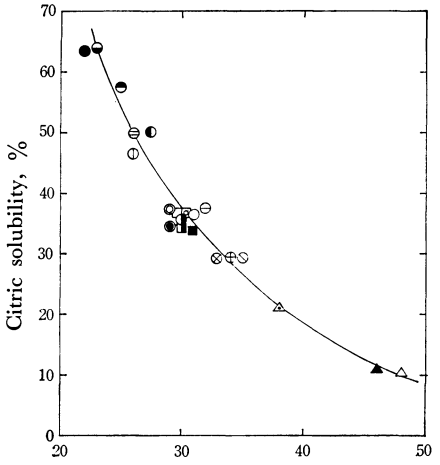

Fig. 2. Relation between the peak height and citric solubility of uncalcined ores. (The marks indicate the ores as shown in Table II.)

citric solubility as determined by the 150 ml. method. A similarly good correlation was found between the height and the solubility by the 100 ml. method, as well as found between the height of the (123) peak ($2\theta=49.5°$) and the solubility by both methods.

The peak height can be measured in several minutes; therefore, it would be useful for the rapid estimation of the nature of the ores. The peak height is related not only to the crystal size but also to the apatite content of the ore, both of which affect the citric solubility. The crystal size can be estimated more precisely by the measurement of the broadening of the diffraction peaks.

The specific surface area of the samples as measured by the nitrogen gas-absorption method is shown in Table II. The surface area was generally higher for the ores with larger citric solubilities; however, the correlation between the solubility and the X-ray peak heights was better than that between the solubility and the specific surface area[5].

Reactivity with Dilute Mineral Acids.—Tests were made on the reactivity of the ores with dilute hydrochloric, nitric, sulfuric and phosphoric acids. Figure 3 shows the relation between the decomposition ratio of the ores and the reaction time when 0.5 g. of the ore, ground to pass through 100 mesh (200 mesh, 70%; 300 mesh, 30% pass), was put into 37 to 40 ml. of N/4 hydrochloric acid (106% of the amount calculated to be needed to convert calcium, iron and aluminum into chlorides) and shaken for 10, 25 and 40 min. at 30°C.

The ease of the decomposition agreed with the fineness of the apatite crystals. The decomposition ratio of Kola was only about 70% when it was shaken for 40 min. Similar results were obtained

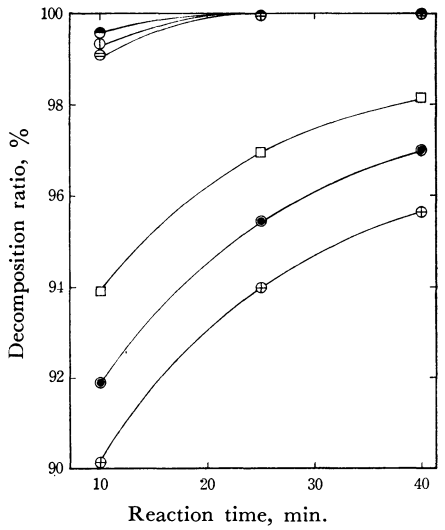

Fig. 3. Decomposition by N/4 hydrochloric acid. (30°C)
◓ Gafsa 64, ⦶ Kossier, ⊜ Morocco 70
□ Macatea 80, ◉ Florida 76, ⊕ Taiba 80

when N/4 nitric acid instead of the hydrochloric acid was used. Tests of the decomposition of Macatea ore by N/4 sulfuric acid showed that the decomposition ratio was close to that by the hydrochloric acid. The decomposition ratio by 1/4 mol. phosphoric acid was much lower.

Decomposition by a Mixture of Sulfuric and Phosphoric Acids.—These decomposition tests were made using a mixture of sulfuric and phosphoric acids at 90°C in a manner similar to that used in the production of wet-process phosphoric acid by the hemihydrate-dihydrate process. For each test, 50 g. of the ore ground to pass through 100 mesh (200 mesh, 70%; 300 mesh, 30% pass) or 150 mesh (200 mesh, 90%; 300 mesh, 50% pass) was used. Reagent-grade sulfuric acid, wet-process phosphoric acid prepared with the respective ore, and water were blended in such a way that, after the decomposition and the hydration of gypsum, the weight ratio of the liquid and the gypsum would be 65 : 35 and the product acid would contain 28% P_2O_5 and 4% SO_3. The decomposition was then carried out at a stirring rate of 120 r. p. m. in a covered glass container equipped with a condenser to prevent the loss o water during the decompostion. The decomposition ratio was mersured in a way similar to that reported by Murata and Noriyama.[9]

The relation between the reaction time and the ratio of the decomposition for several typical ores ground to pass through 100 mesh is shown in Fig. 4. The figure shows that Taiba was decomposed more quickly than was Morocco or

9) A. Murata and T. Noriyama, *Sekko to Sekkai*, No. 68, 9 (1964).

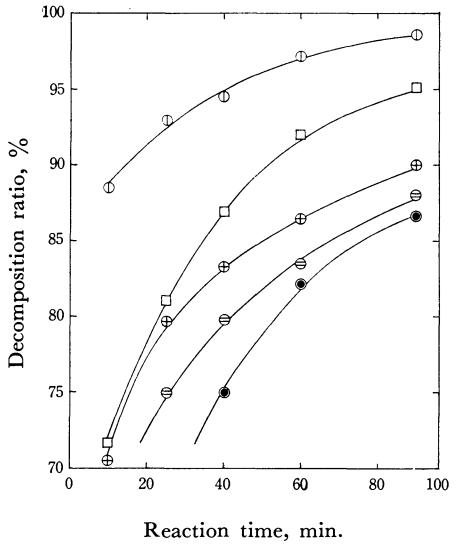

Fig. 4. Decomposition by the mixture of sulfuric and phosphoric acids. (−100 mesh, 90°C)
Ⓘ Kossier, □ Macatea 80, ⊕ Taiba 80, ⊖ Morocco, 70 ◉ Florida 76

Florida. The ease of the decomposition did not agree with the fineness of the apatite crystals of the ores.

Figure 4 also shows that the decomposition of the ores was much slower than when treated with dilute sulfuric or hydrochloric acid. The decomposition became still slower when an increasing amount of sulfuric acid was used. These characteristics of the decomposition by the mixed acid are mainly due to the coating by calcium sulfate hemihydrate crystals on the surface of the ores; this delays the decomposition seriously. The state of the coating differed considerably with different ores.

When the ores ground to pass through 150 mesh were treated in the same manner for 60 min., the decomposition ratio was about 98% for Kossier and Macatea (BPL 80), 95% for Taiba (BPL 80), and 93% for Florida (BPL 68 and 76) and Morocco (BPL 70). Kola was less reactive, and the decomposition ratio was 92% when the sample ground to pass through 150 mesh was reacted for 90 min.

The decomposition tests with the mixed acid were also made at 60°C, in the stable range of calcium sulfate dihydrate. The rate of the decomposition at 60°C was considerably larger than at 90°C for most ores which had been ground to pass through 100 mesh. However, for the ores which had been ground to pass through 150 mesh, the rates of the decomposition at 60°C and at 90°C were nearly equal. Presumably, the true of the reaction between the mixed acid and the ore is larger at 90°C than at 60°C; the effect of the coating by calcium sulfate is also larger at 90°C, and the effect of the coating is more remarkable when the coarser grains of the ore are used.

Carbon dioxide, especially when present in the apatite crystals, seems to promote the decomposition by breaking the calcium sulfate coating as it is released from the ore. The iron and aluminum, especially the latter, present in the ore and the acid delayed the decomposition of the ore.[7] Because of the effects of these many factors, the ease of decomposition can not be predicted on the basis of only the crystal-size measurement of the ores.

The Change in Apatite Crystals by Calcination.—The phosphate ores and synthetic apatite were heated at various temperatures between 500 and 1350°C for an hour. The lattice constant, a_0, of the apatite of most ores changed remarkably upon the heating. The change in typical samples is shown in Fig. 5.

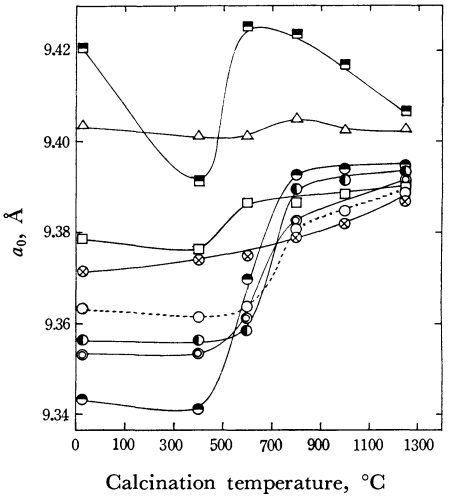

Fig. 5. Change of a_0 on the calcination. (The marks indicate the ores as shown in Table II.)

The a_0 constant of most ores increased when they were heated above 500°C. The increase was more remarkable for such ores as Morocco and Gafsa, which had larger amounts of excess fluorine and which had smaller a_0 values. The a_0 constant of synthetic apatite decreased upon the heating. After they had been heated above 900°C, the a_0 values of most ores, except Christmas 84 and Kola, were close to that of synthetic fluorapatite, 9.39 Å. Kola, which contained about 2% strontium, had larger a a_0, showing that strontium is present in the apatite, replacing calcium. The change of c_0 on the calcination was smaller.

On calcination at 500°C, the X-ray diffraction peak height of the apatite of most ores decreased by about 10%. This is probably caused by some

disorder in apatite crystals which occurred prior to the reorganization and crystal growth of apatite. When the ore was heated above 700°C, a crystal growth of apatite occurred, resulting in an increase in the X-ray diffraction peak height.

Tests with an electron microscope showed that in calcined Florida 81 (Photo. 6) the fine crystals of the initial ore (Photo. 4) began to combine with each other upon calcination at about 950°C, thus forming larger crystals (up to about 10 μ) which resemble those of Kola ore (Photo. 3).

The Change in the Reactivity to Acids on Calcination.—The citric solubility, the reactivity with dilute hydrochloric acid, and that with a mixture of sulfuric and phosphoric acids were tested in ores calcined at various temperatures.

The citric solubility of most ores decreased slightly upon calcination at 500°C, presumably because of the decrease in the porocity of the ores. The decrease in the citric solubility was remarkable upon calcination above 900°C as a result of the crystal growth. After the ores had been heated at 1350°C, the citric solubility of all the ores tested by the 150 ml. method was around 10%.

The decomposition tests by N/4 hydrochloric acid also showed a decrease in the reactivity upon calcination. For example, the decomposition ratios when Florida 76 ore ground to pass through 100 mesh after it had been calcined at 500, 700, 900 and 1100°C was treated for 25 min. were 95.2, 94.5, 93.0 and 91.8% respectively, while that of the uncalcined ore was 96.2%.

The rate of the decomposition by the mixture of sulfuric and phosphoric acids also decreased upon calcination. The decrease was remarkable when the ore had been calcined at above 900°C and had so lost nearly all of its carbon dioxide. Without carbon dioxide, the powdered ore had a tendency to form lumps when mixed with the acid; this caused a further delay in the decomposition. For example, the decomposition ratios of Florida 76 ore ground to pass through 100 mesh after the calcination at 500, 700, 900 and 1100°C were 81.1, 79.8, 71.3 and 69.1% respectively when it was treated with a mixture of reagent-grade sulfuric and phosphoric acids for an hour. The above-mentioned lumps were also formed in large-scale plants.

The decomposition tests with the mixed acid were also made with two samples of calcined Florida ores (79 and 81) produced at commercial-scale plants. In comparison with these, two samples of uncalcined Florida ores (68 and 76) were also tested. In these tests, the ores ground to pass through 150 mesh (200 mesh, 90%; 300 mesh, 50% pass), reagent-grade sulfuric acid and the wet-process phosphoric acid prepared with the respective ores were used. The rate of the decomposition of one of the calcined ores, BPL

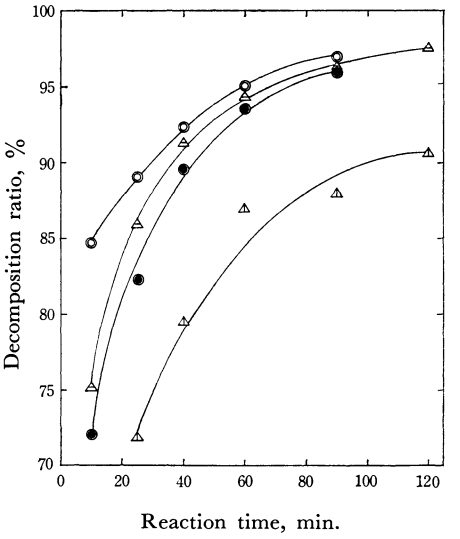

Fig. 6. Decomposition by the mixed acid of the calcined and uncalcined Florida ores.
◎ uncalcined 68, △ calcined 79
◉ uncalcined 76, △ calcined 81

79, was close to that of the uncalcined samples; however, another calcined sample, BPL 81, was decomposed much more slowly, as is shown in Fig. 6. The 81 sample contained no carbon dioxide and formed a considerable amount of lumps when treated with the acid. The 79 sample had a small amount of carbon dioxide (0.4%) and had little tendency to form lumps. The decomposition of this sample was a little quicker than that of the uncalcined ore (76). It is possible that, upon calcinaton at an adequate temperature, the alumina in the ore which usually depresses the rate of the decomposition becomes less reacitve and that in this manner the decomposition is promoted.

The amount of carbon dioxide has much to do with the decomposition. Too much carbon dioxide is not desirable because of too much effervescence. Carbon dioxide present in amounts 0.5 to 1% of the ore would be most desirable for the decomposition.

The Amount of Organic Matter and Its Decrease upon Calcination.—Organic matters contained in the ores are known to affect the nature of gypsum in the production of wet-process phosphoric acid.[10] As an approximate measure of the organic-matter content, the consumption of a potassium permanganate solution was determined on uncalcined and calcined ores in the following way: To 2 g. of a sample, 100 ml. of 3N sulfuric acid was added; they were stirred until the ore had been decomposed. An excess of a 0.1N potassium permanganate solution was then added.

10) K. Murakami and H. Tanaka, *Sekko to Sekkai*, No. 54, 207 (1961).

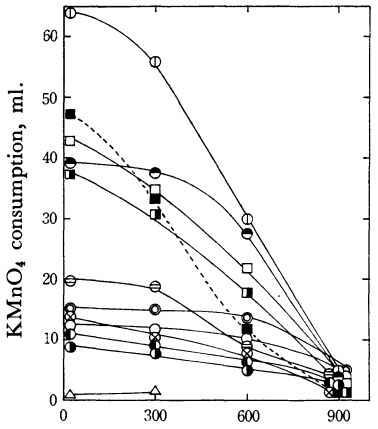

Fig. 7. Decrease of the consumption of $KMnO_4$ on the calcination. (The marks indicate the ores as shown in Table II.)

After the mixture had stood for 24 hr. at room temperature, the slurry was titrated with a 0.1 N sodium oxalate solution. The permanganate consumptions (ml.) by 2 g. portions of the samples are shown in Table I. The permanganate was mainly consumed by organic matter. The consumption by ferrous ions was minor in scale.

The samples of Kossier and Gafsa, the crystal size of which was the smallest, showed the highest consumption. The ores obtained from the ocean islands showed a relatively high consumption. The decrease in the consumption of several typical ores upon calcination is shown in Fig. 7. The manner of the decrease was considerably different for each sample. On heating at 300°C, the decrease was remarkable for Angaur, but it was only slight for the two Florida samples. Such a difference may indicate a difference in the type of organic compound.

Thermal analysis upon heating the ores showed exothermic reactions between 300 and 700°C for most ores. The amount of the exothermic heat was generally larger for those ores which consumed a larger amount of the permanganate, an indication that the exothermic reactions were mainly due to the burning of the organic matters.

BULLETIN OF THE CHEMICAL SOCIETY OF JAPAN VOL. 39 1922—1925 (1966)

The Isocyanurates. II. The Syntheses of Several Unsaturated Aliphatic Isocyanurates

By Fumio TANIMOTO, Takatomi TANAKA, Hisao KITANO and Kenichi FUKUI

Department of Fuel Chemistry, Faculty of Engineering, Kyoto University, Sakyo-ku, Kyoto

(Received August 16, 1965)

Triallyl, trimethallyl and tripropargyl isocyanurates were synthesized in good yields by the reaction of the corresponding halides with potassium cyanate in dimethylformamide or dimethyl sulfoxide. Allyl and ethyl isocyanates were easily trimerized in the presence of alkaline salts in dimethylformamide. Tris(1, 3-pentadienyl) isocyanurate was synthesized by the trimerization of 1, 3-pentadienyl isocyanate in a saturated solution of sodium benzoate in dimethylformamide. 1, 3-Butadienylene-1, 4-diisocyanate was also polymerized in the same solvent; it formed black solid mass, suggesting a polyisocyanurate structure of a low molecular weight.

In the literature considerable attention has been directed to the preparation[1] of and the properties[2] of unsaturated isocyanurates. A method of preparing triallyl isocaynurate from allyl chloride and alkali cyanates had early been patented by Kaiser,[3] but the method consisted of drastic reaction conditions and the yield of the isocyanurate was very poor. Himel and DePree[4] obtained isocyanurates by the reaction of organic halides with alkali cyanates catalyzed by

1) a) T. C. Frazier, *J. Org. Chem.*, **25**, 1944 (1960); b) A. A. Sayligh, *J. Chem. Soc.*, **1961**, 3148; c) E. C. Juenge and W. C. Francis, *J. Org. Chem.*, **26**, 3334 (1961); d) R. W. Cummins, ibid., **28**, 85 (1963); e) *Chem. Week*, Aug. **18**, 63 (1962); f) T. C. Frazier, U. S. Pat. 3065231 (1963); g) J. J. Tazuma and R. Miller, U. S. Pat. 3075979 (1963); h) E. D. Little and B. T. Poon, U. S. Pat. 3088948 (1963); i) F. E. G. Tate and J. H. Wild, Brit. Pat. 856372 (1960); j) W. C. Francis, Brit. Pat. 912964 (1962); k) H. France, Japanese Pat. 1963—6397; l) E. Nachbauer and W. Gottardi, *Monatsh. (3)*, **94**, *584 (1963)*.

2) R. W. Roth, *J. Polymer Sci.*, **55**, 41 (1961); *Chem. Week*, Apr. **25**, 127 (1964); K. Thinius, *Plaste und Kautschuk*, **6**, 275, 375, 439 (1959).

3) D. W. Kaiser, U. S. Pat. 2536849 (1951).

4) C. M. Himel and L. M. Richards, U. S. Pat. 2866802 (1958); D. O. DePree, U. S. Pat. 2866803 (1958).

Table I. Trimerization of allyl isocyanate

Allyl isocyanate g.	Solvent	g.	Catalyst	g.	Temp. °C	Time hr.	Yield %
10	PY.	(50)[1]	nil		15—20	700	0
10	TEA.	(50)[2]	nil		15—20	700	0
10	DMF[3]	50	nil		15—20	700	0
10	DMF	50	KOCN	1	15—20	500	75
10	DMF	50	K_2CO_3	1	15—20	500	70
10	DMF	50	CH_3COONa	1	100—110	4	94
10	DMF	50	C_6H_5COONa	1	100—110	4	97
10	DMF	20	PY.	9.5[4]	100—110	6	trace
10	DMSO[5]	20	KOCN	1	100—190[6]	0.5	75

1) 50 ml. of pyridine was used.
2) 50 ml. of triethylamine was used.
3) Dimethylformamide
4) Equivalent mol. of pyridine to the isocyanate.
5) Dimethyl sulfoxide
6) The temperature was raised by the reaction heat.

Table II. Trimerization of ethyl isocyanate

Ethyl isocyanate g.	Solvent	g.	Catalyst	g.	Temp. °C	Time hr.	Yield %
10	DMF	50	nil		10—20	2400	0
10	DMF	50	KOCN	1	10—15	500	80
10	DMF	50	K_2CO_3	1	10—15	500	57
10	DMF	50	PY.	(1)[1]	10—15	1000	trace
10	TOL.[2]	50	KOCN	1	100—110	4	trace
10	PY.	50	KOCN	1	100—110	4	7

1) 1 ml. of pyridine was used.
2) Toluene

tertiary amines.

The reaction of organic halides with alkal cyanates was systematically investigated in our laboratory[5]; it was found that the reaction could successfully be carried out in several aprotic solvents. In our previous paper[6] the physico-chemical properties of triallyl isocyanurate and its related compounds were partially discussed.

For the present paper, the preparation of several unsaturated isocyanurates was executed in detail. Triallyl, trimethallyl and tripropargyl isocyanurate were synthesized by the reaction of their corresponding halides with potassium cyanate in dimethylformamide or dimethyl sulfoxide. Tris-(1, 3-pentadienyl) isocyanurate and a polymer of 1, 3-butadienylene-1, 4-diisocyanate were prepared by the trimerization of their corresponding isocyanate in dimethylformamide.

In the reaction of the alkenyl halides with potassium cyanate, the nucleophilic substitution of the halide for the isocyanate was generally fast, while the trimerization of the isocyanate to the isocyanurate might be delayed, because of the reaction conditions. Various alkaline salts, such as potassium cyanate, potassium carbonate, sodium acetate, and sodium benzoate, were found to facilitate the trimerization in the aprotic solvent under anhydrous conditions, in spite of thier low solubility in the solvent (for example, the solubility of potassium cyanate in dimethylformamide was about 0.6 wt.% at 100°C). Potassium cyanate and potassium carbonate accelerated the trimerization of allyl isocyanate in dimethylformamide,[7] even at room temperature, as is shown in Table I; the effect of the same catalysts on ethyl isocyanate trimerization was also studied (cf. Table II). The isocyanurate formation from the isocyanate was deeply favored by the presence of the aprotic solvent and the alkaline salt, but the best-known solvents for isocyanates, toluene and pyridine, were not effective for the trimerization of the

5) K. Fukui and H. Kitano, Japanese Pat. 270734 (1960); 276856 (1960); 277389 (1961); 281924 (1961); 282405 (1961); Italian Pat. 60082 (1958); Brit. Pat. 858810 (1961); German Pat. 1124957 (1962); U. S. Pat. 3037979 (1962); Canadian Pat. 624454 (1964).

6) K. Fukui, H. Kato, T. Yonezawa, F. Tanimoto and H. Kitano, This Bulletin, **34**, 851 (1961).

7) W. J. Balon, Abst. Papers, 130th Meeting, Am. Chem. Soc., Atlantic City, N. J., Sept. 1956, p. 15; U. S. Pat. 2683144 (1954); I. C. Kogon, *J. Am. Chem. Soc.*, **73**, 4911 (1957); U. S. Pat. 2838511 (1958); Bolon demonstrated that the trimerization of aromatic diisocyanates was effectively catalyzed by sodium benzoate in dimethylformamide; Kogon also reported, with respect to the trimerization of aromatic isocyanates in ethyl alcohol, that the reaction was affected by the use of *N*-methylmorpholine as the catalyst. Aromatic or vinyl isocyanates are known to have a greater tendency to trimerize than allyl isocyanate.[1c]

isocyanate in the presence of the alkaline salt.

When a mixture of allyl, methallyl or propargyl halide and potassium cyanate was kept at 100—145°C in dimethylformamide or dimethyl sulfoxide, the reaction took place in a few minutes and was completed in 2—4 hr., giving the corresponding trialkenyl or trialkynyl isocyanurate in a good yield.

Some unsaturated aliphatic isocyanurates with carbon-carbon multiple bonds directly adjacent to the nitrogen atoms of the triazine ring were difficult to prepare by means of the reaction of corresponding halides with alkali cyanates. For this reason 1, 3-pentadienyl isocyanate and 1, 3-butadienylene-1, 4-diisoycanate were prepared by the Curtius rearrangement of the corresponding acid azide.[8,9]

1, 3-Pentadienyl isocyanate was treated with sodium benzoate in dimethylformamide to give tris(1,3-pentadienyl) isocyanurate. 1,3-Butadienylene-1, 4-diisocyanate was also treated with sodium benzoate in dimethylformamide. The product was a black solid mass which could be dissolved in dimethylformamide to form a black or a deep-colored solution. The analysis of the product suggested the formation of the low-molecular-weight isocyanurate polymer by the trimerization of the diisocyanate.

Experimental[10]

Triallyl Isocyanurate.—In a 1-l. flask 300 g. (4.1 mol.) of dimethylformamide and 200 g. (2.5 mol.) of potassium cyanate were placed. The mixture was then heated to 135°C while being stirred; 190 g. (1.5 mol.) of allyl bromide was then added through the dropping funnel over a period of 2 hr. After the bromide had been added, the reaction mixtute was kept between 135—140°C for an additonal hour. The mixture was then cooled to room temperature, mixed with about 200 ml. of anhydrous acetone, and left to stand overnight. The mixture was filtered, and the precipitate of inorganic salts was washed with acetone. The combined solution of the filterate and acetone was concentrated under reduced pressure. After the solvents had been removed, crude triallyl isocyanurate boiling at 130—145°C/4 mmHg was obtained in a 90% yield (based on the allyl bromide). This crude triallyl isocyanurate was then mixed with about 100 ml. of ligroin and left to stand overnight at 0—10°C. A small amount of white needles (1, 3-diallylurea) was filtered off, and the ligroin was evaporated from the filtrate. The residue was mixed with 50 ml. of petroleum ether, and the mixture was placed in an ice box for a day. Colorless hexagonal plates of pure triallyl isocyanurate were thus obtained in an 80% yield. M. p. 25.0—26.0°C; b. p. 144—146°C/4 mmHg; n_D^{25} 1.5110.

Found: N, 16.82. Calcd. for $C_{12}H_{15}O_3N_3$: N, 16.86%.

Trimethallyl Isocyanurate.—A mixture of 50 g. (0.6 mol.) of potassium cyanate and 110 g. (1.5 mol.) of dimethylformamide was heated to 140°C. Then 45 g. (0.5 mol.) of methallyl chloride was added in about a 1 hr. period. After the chloride had been added, the reaction was continued for 3 hr. at about 140°C. The reaction mexture was then cooled, diluted with 150 ml. of dry benzene, and poured into brine, and the benzene layer was separated. After the solvent had been removed, 47 g. of crude trimethallyl isocyanurate was obtained as a crystalline cake in a 97% yield. The recrystallization of the cake from methanol gave pure trimethallyl isocyanurate, m. p. 85—86°C.

Found: N, 14.38. Calcd. for $C_{15}H_{21}O_3N_3$: N, 14.42%.

Tripropargyl Isocyanurate.—Into a mixture of 27 g. (0.3 mol.) of potassium cyanate and 76 g. (1 mol.) of dimethyl sulfoxide, 24 g. of propargyl bromide (0.2 mol.) was stirred at room temperature. The exothermic reaction took place, and the mixture turned dark. The flask was then immersed in a water bath for 1 hr. to cool the mixture, and then it was warmed to 100°C. After the temperature had been maintained at about 100°C for an additional 3 hr. the mixture was treated as in the case of trimethallyl isocyanurate. The yield of crude tripropargyl isocyanurate was 34% (5.5 g.); the pure isocyanurate had a melting point of 160.5—161.0°C. The yield was increased to as high as 83% when dimethylformamide was used as the solvent.

Found: N, 17.10. Calcd. for $C_{12}H_9O_3N_3$: N, 17.28%.

The Trimerization of Isocyanates to Isocyanurates.—*Trimerization under High Pressure.*—In a 100 ml. autoclave, 10 g. (0.12 mol.) of allyl isocyanate and 50 ml. of anhydrous pyridine were charged and heated at 180—190°C for 10 hr. while being stirred. After it had cooled, the reaction mixture was distilled under reduced pressure in order to collect the fraction boiling at 139—144°C/3 mmHg. The distillate was triallyl isocyanurate, and the yield was about 15%. This material was characterized by infrared analysis, which showed the carbonyl peak at 5.9 μ and the isocyanurate peak at 13.04 μ.

Trimerization under Atmospheric Pressure.—The trimerization of allyl or ethyl isocyanate was carried out in a round-bottomed flask under suitable conditions, as is shown in Tables I and II. After the reaction had been completed, the reaction mixture was filtered. The unchanged isocyanate and the solvent were removed from the filtrate by evaporation under reduced pressure. The residual product was dissolved in benzene and washed with brine. The distillation of the solution under reduced pressure gave a product which was identified as the isocyanurate by infrared analysis.

Sorboyl Azide.—To a suspension of 19.5 g. (0.30 mol.) of activated sodium azide in 120 ml. of pure 1, 4-dioxane, there was added, drop by drop, 30 g. (0.28 mol.) of sorboyl chloride[11] (b. p. 55.5°C/6.5

8) E. W. Barret and C. W. Portar, *J. Am. Chem. Soc.*, **63**, 3434 (1941).

9) H. M. Singleton and W. R. Edwards, Jr., ibid., **60**, 540 (1938).

10) The boiling points and the melting points are uncorrected.

11) R. Adams and L. H. Ulich, *J. Am. Chem. Soc.*, **42**, 599 (1920); K. Taufel, Cl. Franzke and P. Dietze, *Fette, Seifen, Anstrichmittel*, **62**, 592 (1960).

mmHg, n_D^{19} 1.5771) at 10—14°C over a period of 1 hr. After the addition of the chloride had been completed, the mixture was stirred for 24 hr. at 10—14°C, with the subsequent addition of a further 6 g. (0.09 mol.) of sodium azide, and then it was stirred for an additional 24 hr. at that temperature. The reaction mixture was filtered to remove inorganic salt, and sorboyl azide was used without being separated from the dioxane solution.

1, 3-Pentadienyl Isocyanate.—The dioxane solution of sorboyl azide was warmed to 52°C under a slightly reduced pressure. The Curtius rearrangement took place gradually, and the temperature of the reaction mixture was slowly raised to 76°C so as to complete the rearrangement in the period of 4 hr. When the mixture was cooled, there precipitated a yellowish solid material, which was filtered off; the filtrate was distilled to give 1, 3-pentadienyl isocyanate boiling at 27—30°C/8—9 mmHg. The redistillation of the product afforded the pure isocyanate (b. p. 27—28°C/8 mmHg, in a 20% yield based on sorboyl chloride), which was highly reactive and so was converted into stable 1-benzyl-3-(1, 3-pentadienyl) urea, m. p. 157°C, by treatment with benzyl amine and then analyzed.

Found: C, 71.82; H, 7.20; N, 13.30. Calcd. for $C_{13}H_{16}ON_2$: C, 72.19; H, 7.39; N, 12.95%.

Tris(1, 3-pentadienyl) Isocyanurate.—A mixture of 5 g. (0.045 mol.) of 1, 3-pentadienyl isocyanate and 50 ml. of dimethylformamide was added carefully to 100 ml. of a saturated solution of sodium benzoate in dimethylformamide which had been chilled in an ice bath. An exothermic reaction took place immediately, and the solution turned pale yellow. The reaction mixture was then allowed to stand at 60—70°C for 5 hr. After the solvent had been evaporated under reduced nitrogen pressure, the residual mass was washed with water, alcohol, and ether, and then recrystallized from dimethylformamide to give pure tris(1, 3-pentadienyl) isocyanurate (m. p. 235—236°C, in a 90% yield). The isocyanurate was confirmed by infrared analysis.

Found: C, 65.77; H, 6.35; N, 13.14%. Calcd. for $C_{18}H_{21}O_3N_3$: C, 66.04; H, 6.47; N, 12.83%.

Muconyl Diazide.—Muconyl diazide was prepared from the reaction of sodium azide with muconyl dichloride[12] (m. p. 96°C) in a manner similar to that described for sorboyl azide. The dioxane solution of muconyl diazide without purification was used for the preparation of the isocyanate.[13]

1,3-Butadienylene-1,4-diisocyanate.—The Curtius rearrangement of muconyl diazide to the diisocyanate was carried out first at 40°C and then at 58°C and a 3 hr. period under slightly reduced pressure. Although the solution was considerably darkened during the reaction, no precipitation of a solid substance was observed. After two-thirds of the solvent had been removed, however, a yellow solid material was precipitated; this material was removed by filtration. The dioxane solution of the diisocyanate was submitted to isocyanate-group determination.[14] It was thus confirmed that 50 ml. of the solution contained 2 g. of the isocyanate. A small portion of the solution was treated with about two equivalent mol. of benzyl amine to afford 1,4-bis(3-benzylureido)-butadiene-1,3, which was then recrystallized from benzene to give colorless crystals melting at 278—279°C.

Found: C, 69.54; H, 6.53; N, 15.60. Calcd. for $C_{20}H_{22}O_2N_4$: C, 68.55; H, 6.33; N, 15.99%.

The Polymerization of 1, 3-Butadienylene-1, 4-diisocyanate.—To 100 ml. of a saturated solution of sodium benzoate in dimethylformamide, 50 ml. of a dioxane solution containing about 2 g. of the diisocyanate was added. The mixture soon darkened, and it turned almost black in a minute. After the solvents had been removed from the reaction mixture under reduced pressure, a small amount of ether was added to the residue and the black solid mass was triturated in the ether. The black powder was collected by filtration, dried over phosphorus pentoxide, and pulverized in a mortar. The powder was dissolved in dimethylformamide to afford a dark solution. The solution could not be decolorized with Norit Extra or other decolorizing agents. The black solution was then painted on a glass plate, and the solvent was evaporated under reduced pressure to give a dark brown film, which was insoluble in methanol, ethanol, gasoline and benzene. If the black polymer had isocyanuric rings connected with each other by conjugated double bonds, the polymer might have electrically-interesting characteristics.[15]

12) D. S. Bailey, *J. Am. Chem. Soc.*, **71**, 2370 (1949); **78**, 5905 (1956).

13) After the solvent had been removed, the pale yellow residue was recrystallized from methanol and ether to afford white leaflets of pure muconyl diazide, which decomposed explosively when heated to 80°C.

14) T. Yamabe, A. Nagasawa, H. Kitano and K. Fukui, *J. Chem. Soc. Japan, Ind. Chem. Sect. (Kogyo Kagaku Zasshi)*, **66**, 821 (1963).

15) The amounts of the polymeric products obtained were too small for them to be subjected to electrical tests.

BULLETIN OF THE CHEMICAL SOCIETY OF JAPAN VOL. 39 1926—1931 (1966)

Photochemical Reactions of Ethyl Chloroglyoxylate with Cyclohexane, Cyclohexene, and Toluene

By Chyongjin PAC and Shigeru TSUTSUMI

Department of Chemical Technology, Faculty of Engineering, Osaka University, Miyakojima-ku, Osaka

(Received September 30, 1965)

The photochemical reactions of ethyl chloroglyoxylate with cyclohexane, *cyclohexene,* and toluene have been carried out, and the reactivity of an alkyl radical towards ethyl chloroglyoxylate has been qualitatively discussed. A cyclohexyl radical attacks the carbonyl group of the acid chloride function in ethyl chloroglyoxylate to cause a chain reaction; cyclohexanecarbonyl chloride (51%) and ethyl cyclohexylglyoxylate (2—3%) are thus obtained, along with other minor products. On the other hand, a cyclohexen-3-yl or a benzyl radical might be unable to attack ethyl chloroglyoxylate under the conditions investigated.

In a previous paper,[1] it has been reported that the photolysis of ethyl chloroformate affords an ethoxycarbonyl radical in a selective manner, accompanied by the direct introduction of the radical into various hydrocarbons; carboxylated products are thus obtained. In such a photolysis, however, the carboxylated products do not form via any chain reactions.

The direct introduction of various carboxyl groups into hydrocarbons by means of radical reactions has received much attention recently.[2-7] Therefore, the photo- and peroxide-induced reactions of oxalyl chloride with a saturated hydrocarbons, such as cyclohexane, are of interest, since a characteristic chain reaction is operative in the formation of cyclohexanecarbonyl chloride.[8,9] To the related chain reactions, however, little attention has been paid.

In our preliminary report concerning the photochemical reactions of ethyl chloroglyoxylate (ECG) with olefins,[10] it has been suggested that the 1 : 1-adduct of ECG and an olefin might be formed via a chain reaction as follows;

$$\mathrm{ClCOCOOEt} \xrightarrow{h\nu} \cdot\mathrm{COCl} + \cdot\mathrm{COOEt}$$

$$>\mathrm{C{=}C}< + \cdot\mathrm{COOEt} \rightarrow -\overset{\cdot}{\underset{|}{\mathrm{C}}}-\underset{|}{\overset{|}{\mathrm{C}}}-\quad (\mathrm{COOEt})$$

$$-\overset{\cdot}{\underset{|}{\mathrm{C}}}-\underset{|}{\overset{|}{\mathrm{C}}}- + \mathrm{ClCOCOOEt} \rightarrow \quad (\mathrm{COOEt})$$

$$-\underset{|}{\overset{|}{\mathrm{C}}}-\underset{|}{\overset{|}{\mathrm{C}}}- + \cdot\mathrm{COOEt} \quad (\mathrm{COCl},\ \mathrm{COOEt})$$

The present paper will discuss whether or not an in situ-generated alkyl radical can attack ECG, and which site of ECG, if it is attacked, is reactive to the alkyl radical.

Results and Discussion

A mixture of ECG and a hydrocarbon placed in a quartz tube was irradiated with a high pressure-mercury arc without a filter. During the course of the irradiation, hydrogen chloride, carbon dioxide, carbon monoxide, ethane, and ethylene were evolved. Traces of ethyl chloride and acetaldehyde were trapped at −60°C at the end of the irradiation. In an attempt to obtain some information on the present photochemical reactions, the benzoyl peroxide-induced reaction of ECG with cyclohexane was carried out; it gave carbon dioxide and ethane, along with a trace of carbon monoxide as the gaseous products. The results concerning the gaseous products are summarized in Table I.

From the photochemical reaction of ECG with cyclohexane, a 51% yield of cyclohexanecarbonyl chloride was obtained; small amounts of the other products (ethyl cyclohexylglyoxylate, ethyl cyclohexanecarboxylate, and diethyl oxalate) were also detected (Table II).

1) C. Pac and S. Tsutsumi, This Bulletin, **38**, 1916 (1965).
2) L. Friedman and H. Shechter, *Tetrahedron Letters,* **1961**, 238; A. Rieche, E. Schmidtz and E. Gründeman, *Angew. Chem.,* **73**, 621 (1961).
3) D. Elad, *Proc. Chem. Soc.,* **1962**, 225.
4) D. Elad, *Tetrahedron Letters,* **1963**, 77.
5) D. Elad and J. Rochach, *J. Org. Chem.,* **29**, 1855 (1964).
6) C. Walling and E. S. Huyser, "Organic Reactions," Vol. 13, John Wiley & Sons, Inc., New York (1963), p. 111.
7) M. T. Ahmed and A. J. Swallow, *J. Chem. Soc.,* **1963**, 3918; D. R. Napier, *J. Org. Chem.,* **30**, 1305 (1965).
8) M. S. Kharasch, S. S. Kane and H. C. Brown, *J. Am. Chem. Soc.,* **62**, 454 (1940); **64**, 329 (1942).
9) F. Runge, *Z. Elektrochemie,* **56**, 779 (1952); **60**, 956 (1956).
10) C. Pac and S. Tsutsumi, *Tetrahedron Letters,* **1965**, 2341.

Table I. Ratios of gaseous products from photo- and peroxide-induced reactions of ECG with cyclohexane, cyclohexene, and toluene

ECG g.	Hydrocarbon g.	Reaction time hr.	Gaseous product: Volume[a] cc.	Ratio[b]: CO : CO_2 : C_2H_6 : C_2H_4
18	Cyclohexane, 40	5	2500	0.2 : 1 : 1 : —
25	Cyclohexane, 50[c]	19[c]	2000	trace : 1 : 0.8 : —
40	Cyclohexene, 60	25	80	d) : 1 : 0.3 : 0.2
27	Toluene, 62	41	50	1.1 : 1 : ca. 1 : —

a) Volumes of neutral gaseous products ($CO+C_2H_6+C_2H_4$)
b) The ratios were measured by gas chromatography.
c) Benzoyl peroxide-induced reaction
d) The ratio CO/C_2H_6 was not determined.

Table II. Liquid products formed by photo- and peroxide-induced reactions of ECG with cyclohexane, cyclohexene, and toluene

ECG g.	Hydrocarbon g.	Reaction time hr.	Conversion of ECG %	Product	Yield[a] %
18	Cyclohexane 40	5	83	Cyclo-$C_6H_{11}COCl$	51
				Cyclo-$C_6H_{11}COCOOEt$	2—3
				Cyclo-$C_6H_{11}COOEt$	<1
				Diethyl oxalate	<1
				Bicyclohexyl	b)
25	Cyclohexane[c] 50	19	80	Cyclo-$C_6H_{11}COCl$	49
				Cyclo-$C_6H_{11}COCOOEt$	5—6
				Bicyclohexyl	b)
40	Cyclohexene 60	25	25	Cyclo-$C_6H_{11}COOEt$	20
				Cyclo-C_6H_9-3-$COOEt$	1
				Diethyl oxalate	7
				3,3'-Bicyclohexenyl	(2.5 g.)
38	Cyclohexene 10	10	21	Cyclo-$C_6H_{11}COOEt$	d)
				Diethyl oxalate	d)
				3,3'-Bicyclohexenyl	d)
					ca. 10
27	Toluene 62	41	20	$C_6H_5CH_2COOEt$	ca. 10
				Diethyl oxalate	ca. 10

a) Yields were based on ECG not recovered.
b) The amounts were too small to be measured.
c) Dibenzoyl peroxide-induced reaction.
d) The amounts were not measured.
e) The final product after hydrolysis of the reaction-product.

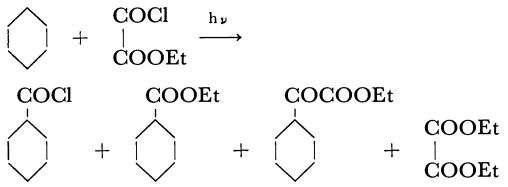

In contrast to the photochemical reaction, the benzoyl peroxide-induced reaction of ECG with cyclohexane gave no detectable amounts of ethyl cyclohexanecarboxylate and diethyl oxalate. The liquid products were cyclohexanecarbonyl chloride (49%), ethyl cyclohexylglyoxylate (—6%), and a trace of benzoyl chloride.

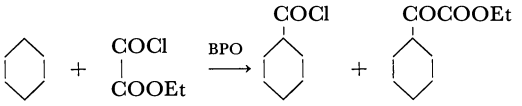

In both cases, the amount of bicyclohexyl formed was negligible. The liquid products are listed in Table II.

On the basis of the above results, the following scheme can be proposed:

a) Primary processes:

$$\mathrm{ClCOCOOEt} \longrightarrow \begin{cases} \longrightarrow \cdot\mathrm{COCl}\ (\mathrm{I}) + \cdot\mathrm{COOEt}\ (\mathrm{II}) & (1) \\ \longrightarrow \cdot\mathrm{Cl} + \cdot\mathrm{COCOOEt}\ (\mathrm{III}) & (2) \\ \longrightarrow \cdot\mathrm{COCOCl}\ (\mathrm{IV}) + \cdot\mathrm{OEt} & (3) \end{cases}$$

or

$$\mathrm{C_6H_5\overset{O}{\overset{\|}{C}}O\text{-}O\overset{O}{\overset{\|}{C}}C_6H_5} \longrightarrow 2\mathrm{C_6H_5CO_2}\cdot \quad (4)$$

b) The decomposition of radicals:

$$\mathrm{I} \longrightarrow \mathrm{CO} + \cdot\mathrm{Cl} \quad (5)$$

$$\mathrm{II} \longrightarrow \mathrm{CO_2} + \cdot\mathrm{C_2H_5} \quad (6)$$

$$\mathrm{III} \longrightarrow \mathrm{CO} + \mathrm{CO_2} + \cdot\mathrm{C_2H_5} \quad (7)$$

$$\mathrm{IV} \longrightarrow 2\mathrm{CO} + \cdot\mathrm{Cl} \quad (8)$$

$$2\ \mathrm{EtO}\cdot \longrightarrow \mathrm{EtOH} + \mathrm{CH_3CHO} \quad (9)$$

$$\mathrm{C_6H_5CO_2}\cdot \longrightarrow \cdot\mathrm{C_6H_5} + \mathrm{CO_2} \quad (10)$$

c) Chain initiation processes:

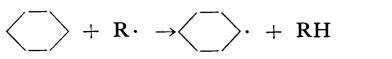

(11)

(R=Cl, $\mathrm{C_2H_5}$, EtO, $\mathrm{C_6H_5CO_2}$, and $\mathrm{C_6H_5}$)

d) Chain propagation processes:

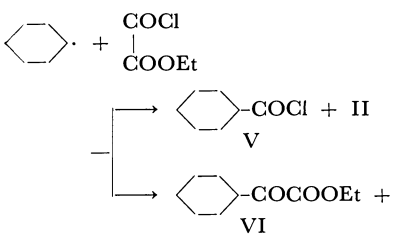

(12)

(13)

e) Chain termination processes:

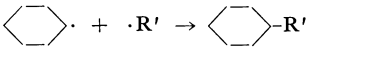

(14)

(R'=Cl, $\mathrm{C_2H_5}$, COOEt, COCl, and COCOOEt)

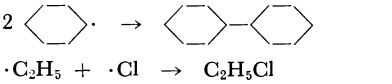

(15)

$$\cdot\mathrm{C_2H_5} + \cdot\mathrm{Cl} \rightarrow \mathrm{C_2H_5Cl} \quad (16)$$

f) Other reaction:

$$\mathrm{EtOH} + \mathrm{ClCOCOOEt} \rightarrow \mathrm{HCl} + \mathrm{C(COOEt)_2H} \quad (17)$$

It has been suggested that oxalyl chloride is photolyzed by the light in the 2537 Å region to cause a homolysis of the carbon-carbon bond, while the light in the 3650 Å region breaks down the chlorine-carbon bond.[11] In the present work, a high pressure-mercury arc was used without any filters; hence the primary processes 4 and 5 probably occur in a manner analogous to the photolysis of oxalyl chloride, though no efforts were made to clarify the primary processes of the photodecomposition of ECG. The formation of acetaldehyde suggests that an ethoxy radical might be generated; namely, the process 3 might take place.

The thermochemical data on the radicals I[12] and II[13] are known; the radicals will decompose as is shown in the processes 5 and 6 respectively. The radicals III and IV are likely to decompose as in the processes 7 and 8 respectively, though little is known of thier stability and their reactivity.

The irradiation in cyclohexane proceeds by a radical chain reaction. The gaseous products continuosly evolved for some time after the light source was shut off. In addition, the molar ratio of the cyclohexanecarbonyl chloride formed to the benzoyl peroxide used showed values of about six in the peroxide-induced reaction.

In the chain transfer process, however, three possible sites of ECG may be attacked; namely, the chlorine atom; the carbonyl group of the acid chloride function, and that of the ester function. The chlorine atom might be resistive to an attack by an alkyl radical, since no significant amounts of ethyl chloride and cyclohexyl chloride were produced. The liquid products from the photo- and the peroxide-induced reactions clearly show that the carbonyl group of the acid chloride function is attacked by a cyclohexyl radical, and that the ratio of the formation of the acid chloride V to the keto-ester VI may be controlled by the relative bond strength of the carbon-carbon, b, and the carbon-chlorine, a, bonds. Unfortunately, the

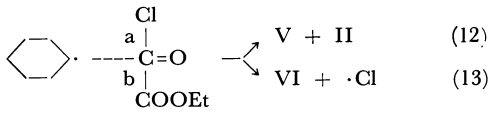

(12)

(13)

dissociation energies of the respective bonds in ECG have not appeared in any of the literature. Carson and Skinner have estimated the bond energy of the carbon-chlorine bond in acetyl chloride to be 76.7 kcal./mol.[14] Concerning the bond energy of the carbonyl-carbonyl bond in biacetyl, two values have been presented, 60 kcal./mol.[15] and 72 kcal./mol.[16] If the values for the dissociation energies of the C–Cl bond in acetyl chloride and of the C–C bond in biacetyl are used instead of those for the dissociation energies of the bonds a and b in ECG, the carbon-carbon fission 12 might be expected to be preferred over the carbon-chlorine fission 13 in the chain transfer process. This interpretation might be qualitatively consistent with the product-distribution.

11) K. B. Krauskopf and G. K. Rollefson, *J. Am. Chem. Soc.*, **58**, 443 (1936).

12) W. G. Burn and F. S. Dainton, *Trans. Farady Soc.*, **48**, 39 (1952).

13) P. Gray and J. C. J. Thynne, *Nature*, **191**, 1357 (1961).

14) A. S. Carson and H. A. Skinner, *J. Chem. Soc.*, **1949**, 936.

15) M. Szwarc, *Chem. Revs.*, **47**, 114 (1950).

16) J. G. Calvert and L. T. Gruver, *J. Am. Chem. Soc.*, **80**, 1313 (1958).

There is, however, a difference in the VI/V ratio between the photo- and the peroxide-induced reactions. In the photochemical reaction, the ratio was about one-third of that obtained from the peroxide-induced reaction. It has been reported that esters of α-keto acids, such as pyruvic and phenylglyoxylic acids, are rapidly photolyzed by light promising n–π^* excitation.[17] Since a high pressure-mercury arc was used as the light source, the α-keto ester VI is probable to decompose with ease. Thus, the decrease in the ratio might be ascribed to the photo-decomposition of VI during the irradiation. In fact, a prolonged irradiation causes a great decrease in VI.

The question, however arises as to whether the formation of ethyl cyclohexanecarboxylate from the photochemical reaction is caused by the attack of a cyclohexyl radical on the ester function in ECG, or by the radical coupling of a cyclohexyl radical with an ethoxycarbonyl radical. If the ester function is attacked, diethyl oxalate, an analogue of ECG, can react with a cyclohexyl radical; if so, ethyl cyclohexanecarboxylate and/or ethyl cyclohexylglyoxylate must be formed. Therefore, the benzoyl peroxide-induced reaction of diethyl oxalate with cyclohexane was carried out. Ethyl cyclohexanecarboxylate and the keto ester VI, however, were not detected in the products, whereas bicyclohexyl was obtained. Thus, it was established that the carbonyl group of the ester function in ECG was not attacked by a cyclohexyl radical. As has been suggested in a previous report,[1] the ethoxycarbonyl radical from the photolysis of ethyl chloroformate has a life long enough to associate with a cyclohexyl radical in a solvent cage at room temperature; hence, the formation of ethyl cyclohexanecarboxylate in the present photochemical reaction might be explained in terms of a radical coupling:

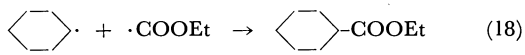

(18)

Diethyl oxalate was produced in the photochemical reaction, but not in the peroxide-induced reaction. Dimerization of ethoxycarbonyl radicals can not account for the formation of diethyl oxalate, since we have shown that the radical has not a life long enough to dimerize.[1] It is most reasonable that diethyl oxalate is produced by the reaction of ECG with ethanol as is shown in the process 17. The ethanol might be generated by the disproportionation between ethoxy radicals and/or the hydrogen abstraction of an ethoxy radical from a hydrogen donor. Therefore, it is comprehensible that diethyl oxalate is not produced by the peroxide-induced reaction, which might not involve the generation of ethoxy radicals.

17) P. A. Leermakers, P. C. Warren and G. F. Vesley, ibid., **86**, 1768 (1964).

The irradiation of ECG in an excess of *cyclohexene* gave no detectable amounts of an acid chloride. The liquid products obtained showed strong infrared absorption bands assignable to an ester, while no bands corresponding to an acid chloride were observed. As has been shown in Table II, the products mainly consisted of ethyl cyclohexanecarboxylate and 3, 3′-bicyclohexenyl; the amount of cyclohexene-3-carboxylate was small. From these results, it may be concluded that a cyclohexen-3-yl radical has no ability to attack ECG under the present conditions. The results may be interpreted as follows:

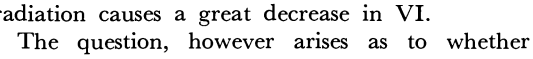

(19)

VII

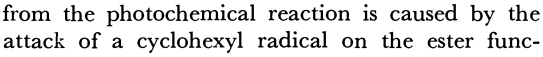

(20)

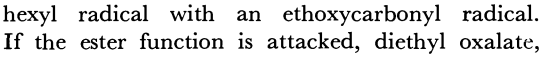

(21)

$R''=Cl$ and C_2H_5

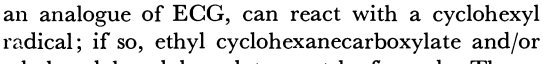

(22)

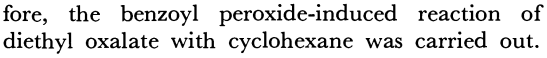

(23)

When an excess of *cyclohexene* was used, VII might predominantly abstract an allylic hydrogen atom of cyclohexene and might have less chance to attack ECG. When a smaller amount of cyclohexene was used than that of ECG, some of the derivative of cyclohexane-1, 2-dicarboxylic acid, VIII, were obtained. It might, therefore, be considered that VII attacks ECG to yield the product VIII.

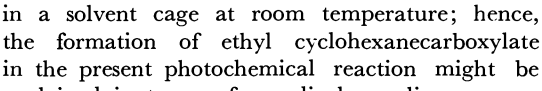

(24)

In the case of *toluene*, no significant amount of phenylacetyl chloride was formed. The liquid products from the photochemical reaction of ECG with toluene revealed strong bands of an ester in the infrared absorption spectra, whereas the absorption band at 1800 cm^{-1} was observed as the shoulder of the ester bands. Therefore, the amount of the acid chloride, if produced at all, was negligible. The above results suggest that a benzyl radical does not attack ECG, and the ethyl phenylacetate is formed via a radical-association reaction between a benzyl radical and an ethoxycarbonyl radical.

Experimental

Materials.—Cyclohexane, toluene, and diethyl oxalate were obtained commercially and purified in usual ways. Cyclohexene was prepared by the dehydration of cyclohexanol.[18] ECG was prepared by

18) G. H. Coleman and H. F. Johnstone, "Organic Syntheses," Coll. Vol. 1, 183 (1956).

the action of thionyl chloride on ethyl potassium oxalate according to the directions of Southwick.[19] The hydrocarbons were stored over sodium wire. All of the materials were distilled before use.

The Analysis of Gaseous Products and the Apparatus Used.—All of the photochemical reactions were carried out in a quartz tube (50 cm. long, 2 cm. in diameter) immersed in a water bath maintained at room temperature, and with a high pressure mercury arc (600 W.) mounted 1 cm. from the tube. The general procedures used for the analysis of gaseous and condensable products were identical with those described previously.[1] The ratios of the gaseous products were determined by gas chromatographic measurements under two sets of conditions (molecular-sieve 5A column: 2.5 m. at 63°C, and silica-gel column: 2.5 m. at 65°C). Under the former set of conditions, the ratio of carbon monoxide to ethane was determined, while that of carbon dioxide to C_2-hydrocarbons was measured under the latter set.

The gas-liquid chromatographic (g. l. c.) measurements of liquid products were carried out using a 5 mm. × 1 m. column packed with 5% of silicone DC 550 on Chromosorb (A) and a 5 mm. × 2 m. column packed with 5% of dioctyl sebatate on Chromosorb (B).

The Irradiation of ECG in Cyclohexane.—A mixture of ECG (18 g., 0.18 mol.) and cyclohexane (40 g., 0.5 mol.) was irradiated for 5 hr. in an atmosphere of nitrogen. During the course of the irradiation, 2500 cc. of neutral gases was evolved. After the irradiation, the evolution of gases had slowed sufficiently. After the unreacted cyclohexane (ca. 30 g.) had been removed from the irradiated mixture, the remaining oil was distilled under reduced pressure to yield the following fractions:

Fraction 1 (3 g.), b. p. 38—50°C/15 mmHg, which consisted largely of ECG, along with traces of ethylcyclohexane and cyclohexyl chloride, as determined by g. l. c. assay (A).

Fraction 2 (8 g.), b. p. 69—72°C/13 mmHg, which showed infrared absorption bands at 1790 (-COCl), 1770, 1750, and 1180 (-C(=O)-O-) cm^{-1}, and which was treated with aniline to give hexahydrobenzanilide, m. p. 143.5°C (Found: C, 76.52; H, 8.45. Calcd. for $C_{13}H_{17}ON$: C, 76.81; H, 8.43%).

After treatment with absolute methanol, the ratios of methyl cyclohexanecarboxylate to diethyl oxalate and to ethyl cyclohexanecarboxylate were determined by g. l. c. assay (A). Diethyl oxalate and ethyl cyclohexanecarboxylate were each contaminated less than 2%. It was confirmed that diethyl oxalate and ethyl cyclohexanecarboxylate in methanol were not cahnged significantly under the g. l. c. conditions.

Fraction 3 (1 g.), b. p. 103—113°C/13 mmHg, which showed infrared absorption bands assignable to an acid chloride (1790 cm^{-1}) and an ester (1730 and 1180 cm^{-1}). G. l. c. measurements (A) showed that this fraction consisted of ethyl cyclohexylglyoxylate, (ca. 0.7 g.), cyclohexanecarbonyl chloride (ca. 0.3 g.), and a trace of bicyclohexyl. The α-keto ester was identified by mixed melting point tests of its 2, 4-dinitrophenylhydrazone (2, 4-DNP), m. p. 159—159.5°C, which was recrystallized from ethanol (Found: C, 52.92; H, 5.53. Calcd. for $C_{16}H_{20}N_4O_6$: C, 52.74; H, 5.53%).

When the period of the irradiation described above was prolonged for 19 hr., a lower yield of the acid chloride (45%) was obtained, and the α-keto ester could not be isolated as its 2, 4-DNP, although its presence was confirmed by g. l. c. assay (A).

An authentic 2, 4-DNP of ethyl cyclohexylglyoxylate was prepared in the following way. The hydrogenation of mandelic acid on Adam's catalyst gave hexahydromandelic acid;[20] esterification with ethanol followed. A solution of ethyl hexahydromandelate (500 mg.) in acetic acid (50 ml.) was stirred with ice cooling, into which a solution of chromic acid (350 mg.) in acetic acid (50 ml.) was added drop by drop. After 5 hr. of stirring at room temperature, the evaporation of acetic acid in vacuo left a residue. To the residue there was added 100 ml. of water, and the aqueous solution was extracted three times with 100 ml. of ether. The etheral layer was washed with water, and dried over magnesium sulfate, and the solvent was evaporated in vacuo. The remainig, slightly yellow oil was treated with an aqueous solution of 2, 4-dinitrophenylhydrazine in 2 N hydrochloric acid, and then the resultant 2, 4-DNP was recrystallized from ethanol, m. p. 159.5°C (Found: C, 52.90; H, 5.55. Calcd. for $C_{16}H_{20}N_4O_6$: C, 52.74; H, 5.53%).

The Peroxide-induced Reaction of ECG with Cyclohexane.—A mixture of ECG (25 g., ca. 0.18 mol.) and cyclohexane (50 g., 0.6 mol.) containing benzoyl peroxide (2 g., 0.0083 mol.) was refluxed for 19 hr. at 84—85°C under an atmosphere of nitrogen. During the course of the reaction, 2000 cc. of neutral gases was evolved. After the unreacted cyclohexane (47 g.) and ECG (5 g.) had been removed, the remaining oil was distilled under reduced pressure to yield 8 g. of cyclohexanecarbonyl chloride, b. p. 68—72°C/15 mmHg, and 1.5 g. of ethyl cyclohexylglyoxylate, b. p. 112—115°C/15 mmHg. The former fraction showed no infrared absorption bands of esters. The fraction was converted to hexahydrobenzanilide, which was identified by a mixed melting point determination. The latter fraction showed strong bands of an ester and a moderate band of an acid chloride, and was found, by using a g. l. c. assay (A), to consist of ethyl cyclohexylglyoxylate (ca. 1.4 g.), cyclohexanecarbonyl chloride (ca. 0.1 g.) and a trace of bicyclohexyl.

The Peroxide-induced Reaction of Diethyl Oxalate with Cyclohexane.—A mixture of diethyl oxalate (17 g., ca. 0.12 mol.), cyclohexane (42 g., 0.5 mol.), and 2 g. of benzoyl peroxide was refluxed at 84—86°C for 26 hr. under an atmosphere of nitrogen. During the reaction, carbon dioxide was evolved. After the unreacted cyclohexane (38 g.) had removed, the remaining oil was distilled under reduced pressure to yield 15 g. of diethyl oxalate, b. p. 88—90°C/25 mmHg, and 2 g. of a fraction, b. p. 90—100°C/25 mmHg. The latter fraction was found, by g. l. c. assay (A), to consist largely of diethyl oxalate, plus a small amount of bicyclohexyl. No ethyl cyclohexanecarboxylate and ethyl cyclohexylglyoxylate could not be detected by g. l. c. assay (A).

19) P. L. Southwick and L. L. Seivard, *J. Am. Chem. Soc.*, **71**, 2535 (1949).

20) H. A. Smith, D. M. Alderman, Jr., C. D. Schacklett and C. M. Welch, ibid., **71**, 3772 (1949).

The Irradiation of ECG in Cyclohexene.—The irradiation of a mixture of ECG (40 g., 0.3 mol.) and cyclohexene (60 g., 0.8 mol.) for 25 hr. gave 80 cc. of neutral gases, unreacted cyclohexene (55 g.) and ECG (30 g.), plus the liquid fractions described below:

Fraction 1 (2.5 g.), b. p. 85—88°C/15 mmHg, which showed infrared absorption bands at 1770 (shoulder), 1740, and 1180 cm^{-1}, but no bands at 1790—1800 (COCl), 3100 (=C-H), and 1670 (C=C) cm^{-1}. The g. l. c. analysis (B) indicated that this fraction consisted of ethyl cyclohexanecarboxylate (1.6 g.), diethyl oxalate (0.7 g.), and ethyl cyclohexene-3-carboxylate[21] (0.2 g.).

Fraction 2 (3 g.), b. p. 100—108°C/15 mmHg, which showed infrared absorption bands assignable to a double bond at 3100 and 1670 cm^{-1}, in addition to the bands of an ester. The g. l. c. analysis (A) showed that this fraction consisted of ethyl cyclohexanecarboxylate (0.5 g.) and 3, 3'-bicyclohexeneyl (2.5 g.).

The remaining brownish oil was refluxed with absolute ethanol, and then distilled to give two fractions. One fraction (0.3 g.), b. p. 120—140°C/15 mmHg, showed six peaks in the gas chromatogram (B). The other (0.7 g.), b. p. 140—155°C/15 mmHg, showed five peaks in the gas chromatogram (B); one of these peaks had the same retention time as that of diethyl hexahydrophthalate, but it was very small. Further investigations were not carried out.

A mixture of ECG (38 g., 0.31 mol.) and cyclohexene (4 g., 0.05 mol.) was irradiated for 2.5 hr., and then another 2 g. of cyclohexene was added into the irradiated mixture. The irradiation was continued for an additional 3.5 hr., and then 4 g. of cyclohexene was added. The mixture was further irradiated for 7 hr. After the unreacted ECG (30 g.) and cyclohexene had removed, the remaining oil was distilled under reduced pressure to yield the following fractions:

Fraction 1 (0.2 g.), b. p. 50—60°C/0.9 mmHg, was found to be a mixture of ethyl cyclohexanecarboxylate, diethyl oxalate, and 3, 3'-bicyclohexenyl.

Fraction 2, (2.5 g.), b. p. 80—110°C/0.9 mmHg, was hydrolyzed with ethanolic potassium hydroxyde, and then acidified to give ca. 1 g. of a solid, which, when recrystallized from water, was found to have a m. p. of 223—224°C. This solid showed no melting point depression upon admixture with authentic *trans*-hexahydrophthalic acid prepared according to the method of Price and Szwarc.[22] (Found: C, 55.44; H, 7.36. Calcd. for $C_8H_{12}O_4$: C, 55.80; H, 7.03%).

The Irradiation of ECG in Toluene.—The irradiation of a mixture of ECG (27 g., 0.2 mol.) and toluene (62 g., 0.67 mol.) for 41 hr. gave 50 cc. of neutral gases. After the unreacted ECG (22 g.) and toluene (55 g.) had been removed, the distillation of the remaining oil afforded 1.5 g. of a fraction, b. p. 110—130°C/17 mmHg, which showed infrared absorption bands at 1770, 1750, and 1180 cm^{-1}, while the band at 1800 cm^{-1} (COCl) was observed on the shoulder of the 1750—1770 cm^{-1} region. Aromatic absorption bands at 3030, 1610, 1010, and 710 cm^{-1} were also observed. When this fraction was analyzed by g. l. c. (A), it was shown to consist of diethyl oxalate (0.5 g.) and ethyl phenylacetate (1 g.). This fraction was hydrolyzed with aqueous sodium hydroxide, and the resultant acid was identified as phenylacetic acid by a mixed melting point determination, m. p. and mixed m. p. 76—77.5°C (Found: C, 70.76; H, 5.88. Calcd. for $C_8H_8O_2$: C, 70.57; H, 5.92%).

21) An authentic sample was prepared according to the directions of Boorman and Linstead; *J. Chem. Soc.*, **1935**, 258.

22) C. C. Price and M. Szwarc, *J. Am. Chem. Soc.*, **62**, 2894 (1940).

BULLETIN OF THE CHEMICAL SOCIETY OF JAPAN VOL. 39 1931—1936 (1966)

Aminocyclitols. X. A Synthesis of Deoxyinosamine and Deoxyinosadiamine and Their Nuclear Magnetic Resonance Spectra

By Tetsuo SUAMI and Kenji YABE

Department of Applied Chemistry, Faculty of Engineering, Keio University, Koganei-shi, Tokyo

(Received November 9, 1965)

(±)-1-Deoxy-*muco*-inosamine-4, (±)-1-deoxy-*scyllo*-inosamine-2 and (±)-2-deoxy-*allo*-inosadiamine-3, 5 pentaacetates have been synthesized from 1-deoxy-*myo*-inositol (I). The hydroxyl groups of I are mesylated, and the mesyloxy groups are replaced by azido groups. The reduction of the azido compounds, followed by acetylation, gives the pentaacetyl-deoxyinosamines and deoxyinosadiamine. Their structures have been established by means of a study of the proton magnetic resonance spectra.

Although six deoxyinosamines have been described[1,6] recently, only one deoxyinosadiamine

1) M. Nakajima, A. Hasegawa and F. W. Lichtenthaler, *Ann.*, **680**, 21 (1964).

(deoxystreptamine) has been isolated from a biological origin (neomycin,[2] kanamycin,[3] paromomycin[4] and hygromycin B[5]).

In connection with previous papers of this series,[7] new deoxyinosamines and the deoxyinosadiamine have been synthesized, and their structures have been established by means of a study of the proton magnetic resonance spectra. In the present paper, (±)-1-deoxy-*myo*-inositol [(±)-*vibo*-quercitol] (I) is prepared by the method of McCasland et al.,[8] and then used as a starting material.

(±)-1-Deoxy-*muco*-inosamine-4.—I is heated in acetone in the presence of anhydrous zinc chloride and glacial acetic acid, and the product is subsequently acetylated to give (±)-4, 5, 6-tri-*O*-acetyl-1-deoxy-2, 3-isopropylidene-*myo*-inositol (II) in a 66% yield. Since the *O*-isopropylidene derivative of a vicinal glycol group on a six-membered ring is formed much more easily when the relationship between the hydroxyl group is cis than when trans,[9] the structure of II is assigned as described above; this assignment is confirmed by the further synthesis of the present study.

The *O*-isopropylidene group is easily removed by heating II in 80% aqueous acetic acid thus giving (±)-4, 5, 6-tri-*O*-acetyl-1-deoxy-*myo*-inositol (III) in a 55% yield. When III is reacted with one mole of methanesulfonyl chloride, (±)-4, 5, 6-tri-*O*-acetyl-1-deoxy-3-*O*-mesyl-*myo*-inositol (IV) is obtained in a 51% yield. IV is acetylated to give the tetra-*O*-acetyl derivative (V).

In a previous paper,[10] it has been described that methanesulfonyl chloride attacks an equatorial hydroxyl group selectively, rather than an axial one, in the *myo*-inositol derivative. Therefore, in the *vibo*-quercitol derivative, methanesulfonyl chloride is expected to behave in the same manner. This can be proved by establishing a structure of V, and the NMR spectrum gives an unequivocal confirmation of the structure. The NMR spectrum of V in deuteriochloroform, as Table I shows, exhibits a sharp signal at 6.99 τ which is ascribed to an equatorial mesyloxy group.[10] At 7.83, 7.93 and 7.97 τ, three sharp signals with a 1 : 1 : 2 intensity ratio appear; these signals are expected from one axial acetoxy group and three equatorial acetoxy ones.[11]

When V is treated with sodium azide in boiling aqueous 2-methoxyethanol for 51 hr., and subsequently acetylated with acetic anhydride in pyridine, (±)-4-azido-1, 4-dideoxy-*muco*-inositol tetraacetate (VI) is obtained in a 28% yield. The reduction of VI with Raney nickel in a hydrogen stream and subsequent acetylation give (±)-pentaacetyl-1-deoxy-*muco*-inosamine-4 (VII) in a 58% yield.

The structure of VII is substantiated by its NMR spectrum. The NMR spectrum in deuteriochloroform, as is given in Table I, exhibits three sharp signals, with a 2 : 1 : 1 intensity ratio, at 7.85, 7.96 and 7.98 τ; these signals correspond to two axial acetoxy groups (7.85 τ) and two equatorial ones (7.96 and 7.98 τ). There is also a sharp signal

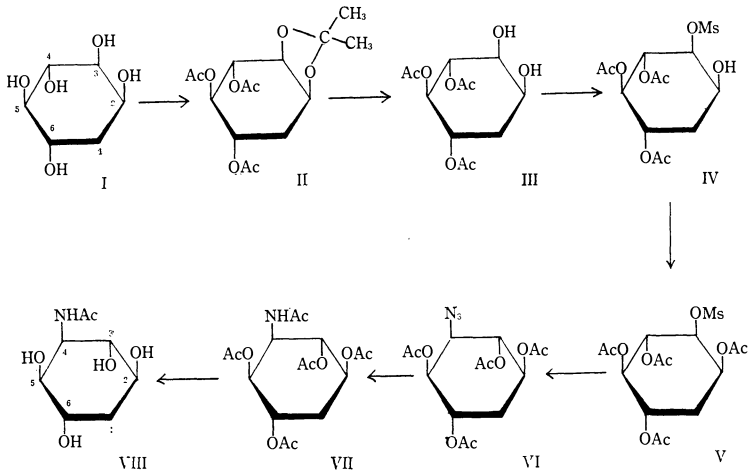

2) D. A. Kuehl, Jr., M. N. Bishop and K. Folkers, *J. Am. Chem. Soc.*, **73**, 881 (1951).
3) K. Maeda, M. Ueda, K. Yagishita, S. Kawaji, S. Kondo, M. Murase, T. Takeuchi, Y. Okami and H. Umezawa, *J. Antibiotics*, **A10**, 228 (1957).
4) T. H. Haskell, J. C. French and Q. R. Bartz, *J. Am. Chem. Soc.*, **81**, 3480 (1959).
5) P. F. Wiley, M. V. Sigal, Jr., and O. Weaver, *J. Org. Chem.*, **27** 2793 (1962).
6) M. Nakajima, A. Hasegawa and N. Kurihara, *Tetrahedron Letters*, **17**, 697 (1964).
7) T. Suami and S. Ogawa, This Bulletin, **37**, 1238 (1964); T. Suami and K. Yabe, ibid., **38**, 855 (1965); T. Suami, F. W. Lichtenthaler and S. Ogawa, ibid., **39**, 170 (1966).
8) G. E. McCasland and E. Clyde Horswill, *J. Am. Chem. Soc.*, **75**, 4020 (1953).
9) R. U. Lemieux, "Rearrangements and Isomerizations in Carbohydrate Chemistry," in "Molecular Rearrangements," Vol. II, Interscience Publishers, New York (1964), p. 731.
10) T. Suami, F. W. Lichtenthaler and S. Ogawa, This Bulletin, **38**, 754 (1965).
11) F. W. Lichtenthaler, *Chem. Ber.*, **96**, 2047 (1963).

at 8.09 τ which is expected to be from an equatorial acetamido group. Considering the reaction process employed, there are three possible structures for VII: a, b, and c.

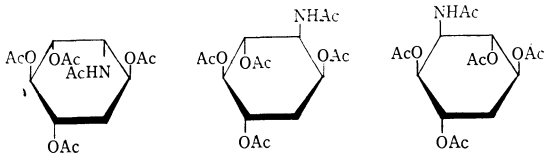

a b c

If the demesylation took place via a direct S_N2 mechanism, a would be obtained. b and c are anticipated only from an anchimeric mechanism, a neighboring-group participation. Since there is only one axial acetoxy group in both a and b, however a and b can be eliminated, and only c is compatible with the NMR spectrum. The possible mechanism of the reaction from V to VI is shown in the following scheme:

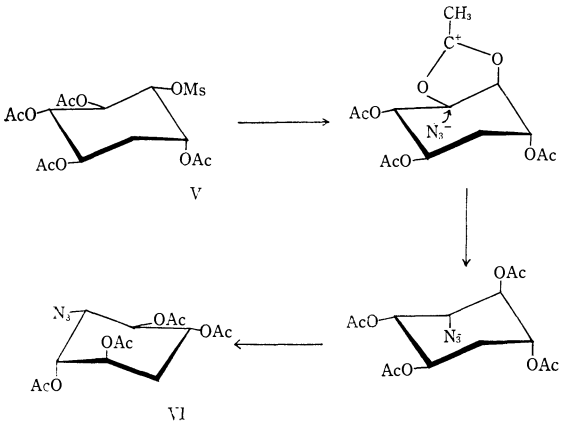

V VI

The elimination of the mesyloxy group takes place with a neighboring-group participation to form an intermediate acetoxonium ion, and then it is cleaved by an azide ion in a diaxial opening, as has been already observed in the replacement of the mesyloxy group in *myo*-inositol derivatives.[7]

(±)-1-Deoxy-*scyllo*-inosamine-2.—In analogy to the monomesylation of triacetyl deoxyinositol (III→IV), a selective monobenzoylation to the 3-*O*-benzoyl derivative should be possible under conditions analogous to those described in a previous paper.[7] When III is treated with one mole of benzoyl chloride in pyridine under ice cooling, the tri-*O*-acetyl-3-*O*-benzoyl derivative (IX) is obtained in a 58% yield. The mesylation of IX by an ordinary method gives (±)-4, 5, 6-tri-*O*-acetyl-3-*O*-benzoyl-1-deoxy-2-*O*-mesyl-*myo*-inositol (X) in a 87% yield. X is quite different in its physical properties from the (±)-4, 5, 6-tri-*O*-acetyl-2-*O*-benzoyl-1-deoxy-3-*O*-mesyl-*myo*-inositol (XIV) prepared by the benzoylation of IV. The NMR

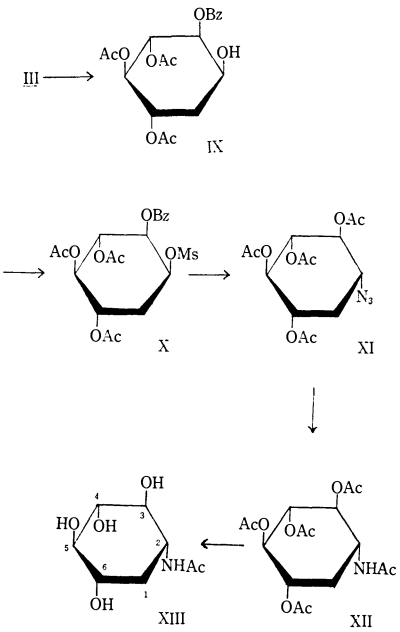

IX X XI XIII XII

spectrum of X (Table I) reveals a sharp signal at 6.97 τ corresponding to an axial mesyloxy group, while that of XIV (Table I) exhibits a sharp signal shifted to a slightly higher field (6.99 τ), as is to be expected from an equatorial mesyloxy group. Therefore, this presents another example of how benzoyl chloride attacks an equatorial hydroxyl group preferentially.[7]

Then X is treated with sodium azide as described above to give an azido compound (XI), which is hydrogenated and subsequently acetylated to yield (±)-pentaacetyl-1-deoxy-*scyllo*-inosamine-2 (XII). The NMR spectrum of XII, as is shown in Table I, exhibits two sharp signals, with a 2 : 2 relative intensity, at 8.02 and 8.06 τ; these signals correspond to four equatorial acetoxy groups. There is also a sharp signal at 8.22 τ which is to be ascribed to an equatorial acetamido group.

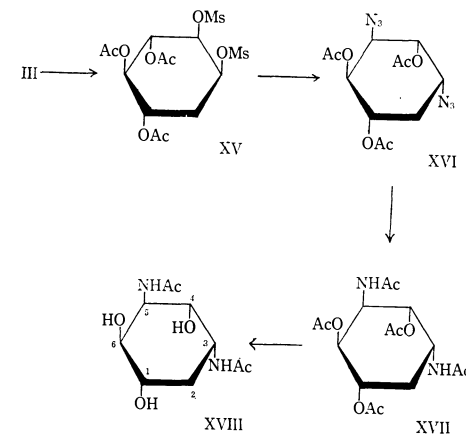

XV XVI XVIII XVII

TABLE I. SIGNALS OF PROTON MAGNETIC RESONANCE SPECTRA

Compound	Solvent	Protons of mesyloxy group axial	Protons of mesyloxy group equat.	Protons of acetoxy group axial	Protons of acetoxy group equat.	Protons of acetamido group axial	Protons of acetamido group equat.
V. 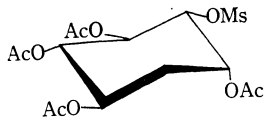	$CDCl_3$		6.99(1)	7.83(1)	7.93(1) 7.97(2)		
VII. 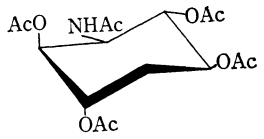	$CDCl_3$			7.85(2)	7.96(1) 7.98(1)		8.09(1)
X. 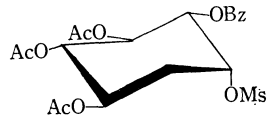	$CDCl_3$	6.97(1)			7.96(2) 8.06(1)		
XII. 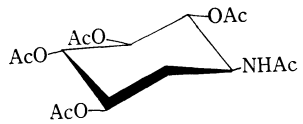	$(CD_3)_2SO$				8.02(2) 8.06(2)		8.22(1)
XIV. 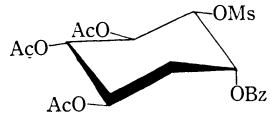	$CDCl_3$		6.99(1)		7.94(1) 7.95(1) 8.00(1)		
XV. 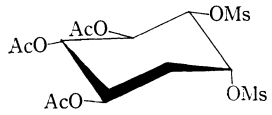	$CDCl_3$	6.82(1)	6.89(1)		7.92(1) 7.97(2)		
XVII. 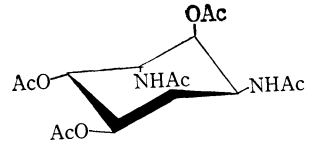	$(CD_3)_2SO$			7.90(1)	8.02(1) 8.13(1)	8.13(1)	8.23(1)
XVIII. 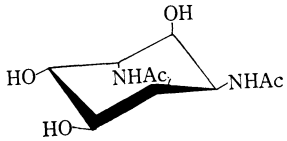	D_2O						7.92(1) 7.98(1)

Peak positions are given in τ values, and numbers in parentheses are relative intensities of the signals.

(±)-2-Deoxy-*allo*-inosadiamine-3, 5.— While III is treated with an excess amount of methanesulfonyl chloride in pyridine, the di-*O*-mesyl derivative (XV) is obtained in a 85% yield. The NMR spectrum of XV in deuteriochloroform, as is shown in Table I, exhibits two sharp signals, with equal intensities, at 6.82 and 6.89 τ for the protons of an axial and an equatorial mesyloxy group respectively.[10] Two sharp signals with a 1 : 2 relative intensity at 7.92 and 7.97 τ correspond to three equatorial acetoxy groups.[11]

When XV is heated with sodium azide in boiling aqueous 2-methoxyethanol for 41 hr. and subsequently acetylated by an ordinary method, diazido acetate (XVI) is obtained in a 17% yield. XVI is then hydrogenated in the presence of a catalyst in a hydrogen stream, and the reduction product is acetylated to afford pentaacetyl-deoxyinosadiamine (XVII) in a 68% yield. A selective de-*O*-acylation of XVII with ammonia in methanol yields the diacetamido derivative (XVIII). The structure of XVII is

substantiated by the NMR spectra of XVII in deuteriodimethyl sulfoxide and of XVIII in deuterium oxide. The NMR spectrum of XVIII, as is shown in Table I, shows two sharp signals, with equal intensities, at 7.92 and 7.98 τ, corresponding to an axial and an equatorial acetamido group respectively. The NMR spectrum of XVII, as may be seen in Table I, exhibits four sharp signals, at 7.90, 8.02, 8.13 and 8.23 τ (1 : 1 : 2 : 1), for the protons in an axial and an equatorial acetoxy group, another equatorial acetoxy group overlapped with an axial acetamido group, and an equatorial acetamido group respectively. Therefore, it might be reasonable to identify the structure of XVII as (±)-2-deoxy-*allo*-inosadiamine-3, 5. Considering the product obtained, the following reaction mechanism might be assumed: a mesyloxy group on C-3 is replaced by the participation of the neighboring acetoxy group in a trans position, thus forming an intermediate acetoxonium ion, and then the dioxolane-ring is attacked by a nucleophilic azide ion. The manner in which the ring is cleaved is considered to be the same diaxial opening described above and also observed in previous papers.[7,12] On the other hand, another mesyloxy group on C-2 might be replaced by an azide ion through a direct S_N2 mechanism. The behavior of the latter mesyloxy group is different from that of the mesyloxy group in an inositol derivative in an analogous situation;[7] this point must be studied further.

Experimental

The melting points were determined on a Mitamura Riken hot stage. The melting points marked with asterisks were measured in a liquid bath and are uncorrected. The NMR spectra of the samples were determined at a frequency of 60 Mc. p. s. with a Japan Electron Optics JNM-C-60 spectrometer in deuterium oxide, deuteriochloroform and deuteriodimethyl sulfoxide, using sodium trimethylsilylpropane-sulfonate or tetramethylsilane as an internal standard.

(±)-1-Deoxy-*myo*-inositol (I).—This substance was prepared from *myo*-inositol in a 30.4% yield by the method developed by McCasland et al.[8]

(±)-4, 5, 6-Tri-*O*-acetyl-1-deoxy-2 : 3-isopropylidene-*myo*-inositol (II).—A mixture of 10 g. of I, 50 g. of anhydrous zinc chloride, 50 ml. of glacial acetic acid and 400 ml. of acetone was heated to reflux for 36 hr. After the mixture had then cooled, 100 ml. of pyridine was added to the mixture and the precipitate was removed by filtration. The filtrate was evaporated under reduced pressure and the residue was acetylated overnight in a mixture of 60 ml. of acetic anhydride and 40 ml. of pyridine. After the precipitate had been removed, 150 ml. of chloroform was added to the filtrate. Then the solvent layer was washed with cold water, a 5% sodium carbonate solution and cold water successively. The solvent was evaporated, after drying over anhydrous sodium sulfate, to give 22 g. of an oily residue. The resiude was added to 300 ml. of ligroin and kept in a refrigerator overnight, thus yielding 14.7 g. of the crude product. The crude product was recrystallized from petroleum ether to give 12.8 g. (66.4%) of needles. m. p. *80—82°C. An analytical sample was obtained by a further recrystallization from petroleum ether. m. p. *82—83°C.

Found: C, 54.31; H, 6.62. Calcd. for $C_{15}H_{22}O_8$: C, 54.54; H, 6.71%.

(±)-4, 5, 6-Tri-*O*-acetyl-1-deoxy-*myo*-inositol (III).—A mixture of 2.3 g. of II and 100 ml. of 80% acetic acid was heated on a boiling water bath for two hours, and then evaporated under reduced pressure. The solid residue was recrystallized from ethanol to yield 1.3 g. of a crude product. The product was recrystallized from 5 ml. of ethanol, thus affording 1.1 g. (54.5%) of an analytically-pure product melting at 170—171°C.

Found: C, 49.70; H, 6.21. Calcd. for $C_{12}H_{18}O_8$: C, 49.65; H, 6.25%.

(±)-4, 5, 6-Tri-*O*-acetyl-1-deoxy-3-*O*-mesyl-*myo*-inositol (IV).—To a solution of 5.1 g. of III in 50 ml. of pyridine, 2.0 g. of methanesulfonyl chloride was added drop by drop under agitation at 0—5°C. After the solution had been stirred for two hours, it was left to settle in a refrigerator overnight. The crystals were then collected by filtration, 3.3 g. (50.9%) of the crude product, m. p. 131—131.5°C were thus obtained. An analytical sample was obtained by recrystallization from ethanol. m. p. 131—132°C.

Found: C, 42.54; H, 5.55; S, 8.31. Calcd. for $C_{13}H_{20}O_{10}S$: C, 42.39; H, 5.47; S, 8.70%.

(±)-2, 4, 5, 6-Tetra-*O*-acetyl-1-deoxy-3-*O*-mesyl-*myo*-inositol (V).—A 1.6 g. portion of IV was acetylated with acetic anhydride and pyridine. The crude product was recrystallized from ethanol to give 1.7 g. (95.4%) of crystals melting at *171—172°C.

Found: C, 43.97; H, 5.33; S, 7.78. Calcd. for $C_{15}H_{22}O_{11}S$: C, 43.90; H, 5.40; S, 7.81%.

(±)-2, 3, 5, 6-Tetra-*O*-acetyl-4-azido-1, 4-dideoxy-*muco*-inositol (VI).—A mixture of 0.5 g. of V, 0.25 g. of sodium azide and 30 ml. of 80% aqueous 2-methoxyethanol was heated to reflux for 51 hr. After the solvent had then been removed, a residue was acetylated with acetic anhydride and pyridine. The excess of the reagent was removed, and the residue was dissolved in 2 ml. of ethanol to yield 0.21 g. of the crude product. The crude product was recrystallized from ethanol to give 0.12 g. (27.6%) of crystals melting at 143—144°C.

Found: C, 47.28; H, 5.38; N, 11.63. Calcd. for $C_{14}H_{19}N_3O_8$: C, 47.06; H, 5.36; N, 11.76%.

(±)-Pentaacetyl-1-deoxy-*muco*-inosamine-4 (VII).—A 0.30 g. portion of VI was hydrogenated in 50 ml. of ethanol with Raney nickel T4[13] under a stream of hydrogen (50 p. s. i. g.). After the catalyst had then been removed, the solution was evaporated under reduced pressure. The residue was acetylated to yield 0.22 g. of the product. The crude product was recrystallized from ethanol to give 0.18 g. (57.5%) of plates melting at *215—216°C.

Found: C, 51.63; H, 6.38; N, 3.80. Calcd. for $C_{16}H_{23}NO_9$: C, 51.47; H, 6.21; N, 3.75%.

The hydrolysis of VII with 6 N hydrochloric acid for 6 hr. at 100°C gave the hydrochloride, which showed

12) T. Suami and S. Ogawa, This Bulletin, **38**, 2026 (1965).

13) S. Nishimura, This Bulletin, **32**, 61 (1959).

a single spot of R_f 0.25 (R_f of D-glucosamine hydrochloride: 0.27) in ascending paper chromatography in an acetic acid - ethyl acetate - pyridine - water (1 : 5 : 5 : 3) system[14] at 18—20°C. R_f/R_f glucosamine: 0.94.

(±)-*N*-Acetyl-1-deoxy-*muco*-inosamine-4 (VIII).—The selective de-*O*-acetylation of 0.63 g. of VII in methanol saturated with ammonia gave 0.17 g. of a crude product. The product was recrystallized from ethanol to yield 0.11 g. (32.6%) of crystals melting at 192—193°C.

Found: C, 46.61; H, 7.54; N, 6.69. Calcd. for $C_8H_{15}NO_5$: C, 46.82; H, 7.37; N, 6.83%.

(±)-4, 5, 6-Tri-*O*-acetyl - 3 - *O* -benzoyl - 1 - deoxy-*myo*-inositol (IX).—To a solution of 6.3 g. of III in 40 ml. of pyridine, 3.3 g. of benzoyl chloride was added drop by drop under ice cooling with agitation. After the mixture had settled at room temperature overnight, it was poured into 300 ml. of ice-cold water to give a precipitate which was then collected by filtration. The crude product was recrystallized from 100 ml. of ethanol to give 5.0 g. (58.2%) of crystals melting at *185—187°C.

Found: C, 57.85; H, 5.54. Calcd. for $C_{19}H_{22}O_9$: C, 57.86; H, 5.62%.

(±)-4, 5, 6-Tri-*O*-acetyl-3-*O*-benzoyl - 1 - deoxy-2-*O*-mesyl-*myo*-inositol (X).—A 3.1 g. portion of methanesulfonyl chloride was added to a solution of 7.1 g. of IX in 50 ml. of pyridine under ice cooling with agitation. Then the mixture was poured into ice-cold water to give 7.8 g. of a precipitate. The crude product was recrystallized from ethanol to give 7.4 g. (87.0%) of plates melting at 175—176°C.

Found: C, 50.65; H, 5.19; S, 6.83. Calcd. for $C_{20}H_{24}O_{11}S$: C, 50.84; H, 5.12; S, 6.79%.

(±)- 3, 4, 5, 6-Tetra-*O*-acetyl-2-azido-1, 2-dideoxy-*scyllo*-inositol (IX).—A mixture of 2.2 g. of X, 0.6 g. of sodium azide and 60 ml. of 80% aqueous 2-methoxyethanol was heated to reflux for 64 hr. Then the mixture was treated as has been described in the preparation of VI to give 1.0 g. of the crude product, which was then recrystallized from ethanol, giving 0.9 g. (55.1%) of needles melting at 137—138°C.

Found: C, 47.28; H, 5.35; N, 11.89. Calcd. for $C_{14}H_{19}N_3O_8$: C, 47.06; H, 5.36; N, 11.76%.

(±) - Pentaacetyl - 1 - deoxy - *scyllo*- inosamine-2 (XII).—A 0.95 g. portion of XI was hydrogenated in 30 ml. of ethanol with Raney nickel T4,[13] and then the reduction product was treated as has been described in the preparation of VII to give 0.51 g. of the crude product melting at 226—227°C. The crude product was recrystallized from ethanol to give 0.32 g. (32.7%) of crystals melting at 226—227°C.

Found: C, 51.57; H, 6.03; N, 3.61. Calcd. for $C_{16}H_{23}NO_9$: C, 51.47; H, 6.21; N, 3.71%.

Paper Chromatography.—The hydrochloride of XII was prepared and developed in paper chromatography using the procedure described above. It showed a single spot of R_f 0.14. R_f/R_f glucosamine: 0.52.

(±)-*N*-Acetyl-1-deoxy-*scyllo*-inosamine-2 (XIII).—The selective de-*O*-acetylation of 0.22 g. of XII by ammonia in methanol yielded 0.10 g. of the crude product, which was then recrystallized from a mixture of benzene and methanol to give 0.08 g. (72.7%) of crystals melting at 205—206°C.

Found: C, 47.31; H, 7.43; N, 6.63. Calcd. for $C_8H_{15}NO_5$: C, 46.82; H, 7.37; N, 6.83%.

(±)-4, 5, 6-Tri-*O*-acetyl-2-*O*-benzoyl - 1 - deoxy - 3-*O*-mesyl-*myo*-inositol (XIV).—A 0.6 g. portion of benzoyl chloride was added to a solution of 0.78 g. of IV in 20 ml. of pyridine; the mixture was then warmed for 30 min. and left to stand overnight at room temperature. Then the mixture was poured into ice-cold water to give 0.29 g. of needles melting at 151—152°C. For analysis the product was recrystallized twice from ethanol; yield, 0.17 g. (17.0%); m. p. 159—160°C.

Found: C, 50.97; H, 4.95; S, 6.39. Calcd. for $C_{20}H_{24}O_{11}S$: C, 50.84; H, 5.12; S, 6.79%.

(±)-4, 5, 6-Tri-*O*-acetyl-1-deoxy-2, 3-di-*O*-mesyl-*myo*-inositol (XV).—To a solution of 5.7 g. of III in 50 ml. of pyridine, 5.7 g. of methanesulfonyl chloride was added drop by drop with agitation at 0—5°C. After settling overnight in a refrigerator, the solution was poured into one liter of ice-cold water to obtain crystals, which were then collected by filtration. Yield, 7.4 g. (84.6%); m. p. 179—182°C. An analytical sample was obtained by recrystallizations from ethyl acetate. m. p. 181—182°C.

Found: C, 37.86; H, 4.80; S, 14.53. Calcd. for $C_{14}H_{22}O_{12}S_2$: C, 37.66; H, 4.97; S, 14.36%.

(±)-1, 4, 6 - Tri-*O*-acetyl-3, 5 - diazido - 2, 3, 5 - trideoxy-*allo*-inositol (XVI).—A mixture of 1.35 g. of XV, 1.2 g. of sodium azide and 40 ml. of 80% aqueous 2-methoxyethanol was heated to reflux for 41 hr. Then the mixture was treated as has been described in the preparation of VI to give 0.17 g. (16.5%) of crystals melting at 133—133.5°C.

Found: C, 42.61; H, 4.80; N, 24.45. Calcd. for $C_{12}H_{16}N_6O_6$: C, 42.35; H, 4.74; N, 24.70%.

(±)-Pentaacetyl-2-deoxy-*allo*- inosadiamine - 3, 5 (XVII).—A 1.03 g. portion of XVI was hydrogenated much as has been described in the preparation of VII to give 0.70 g. (67.6%) of crystals melting at *290—291°C.

Found: C, 51.40; H, 6.49; N, 7.43. Calcd. for $C_{16}H_{24}N_2O_8$: C, 51.60; H, 6.50; N, 7.52%.

XVII was hydrolyzed with 6 N hydrochloric acid, and the hydrochloride was developed by paper chromatography. The hydrochloride showed a single spot of R_f 0.14 at 18—20°C. R_f/R_f glucosamine: 0.52.

(±)-*N*, *N'*-Diacetyl - 2 - deoxy-*allo*-inosadiamine-3, 5 (XVIII).—The selective deacetylation of 0.53 g. of XVII as has been described in the preparation of VIII gave 0.16 g. (45.3%)of needles melting at 251—252°C.

Found: C, 49.00; H, 7.12; N, 11.25. Calcd. for $C_{10}H_{18}N_2O_5$: C, 48.77; H, 7.37; N, 11.38%.

The authors wish to thank Professor Sumio Umezawa for his helpful advice; Mr. Saburo Nakada and Miss Sumiko Uchida for their elemental analyses; Mr. Tatsuo Ishikawa for his technical assistance, and the Japan Electron Optics Co., Ltd., and the Research Laboratories of the Tanabe Seiyaku Co. for their measurements of the NMR spectra. This research has been supported in part by a grant of the Ministry of Education, to which the authors' thanks are also due.

14) F. G. Fischer and H. Dorfel, *Hoppe-Seyler's Z. Physiol. Chem.*, **301**, 224 (1955); F. W. Lichtenthaler, *Chem. Ber.*, **94**, 3071 (1961).

BULLETIN OF THE CHEMICAL SOCIETY OF JAPAN VOL. 39 1937—1941 (1966)

Solvent and Steric Effects on the Solvolysis of Polyvinylsulfonic Acid Esters[1]

By Sadao Yoshikawa, Oh-Kil Kim and Takeshi Hori

Department of Synthetic Chemistry, Faculty of Engineering, The University of Tokyo, Hongo, Tokyo

(Received November 16, 1965)

The solvolysis of ethanesulfonic acid esters followed closely first-order kinetics, while the case of polyvinylsulfonic acid esters gave strongly-curved first-order plots according to the solvent composition. With a high acetone content, the solvolysis rates of polymeric sulfonic esters decreased gradually with the lapse of time, while in a high water content, the solvolysis was suppressed at the beginning of the reaction but was accelerated remarkably with the reaction time. The former finding indicates the release from the steric congestion which contributed to the initial rate enhancement, while the latter indicates the aggregation of the polymer molecules owing to their strong hydrophobic character. The solvolysis rates, k_p, for polymeric sulfonic esters were much greater than those, k_m, for monomeric analogs in all cases except isopropyl and *n*-butyl esters in 20% aqueous acetone. The relative rate (k_p/k_m) increased with an increase in the acetone content and was apparently greater with the methyl ester than with the other esters, and the value of (k_p/k_m) in relation to the methyl ester in 80% acetone content reached 15. Furthermore, it was found that the proton catalysis by the neighboring sulfonic acid formed on the lapse of reaction time was absent, and also that the salt effect was negligibly small.

In previous papers[2] we have discussed the specific catalytic effects of polymeric sulfonic acids in the hydrolysis of esters in regard to the expansion of the polymer in solutions and to the geometrical distances between the nearest neighboring sulfonic acid groups on the polymer chain. It is the aim of the present paper to study the solvolysis of polyvinylsulfonic acid esters in various compositions of acetone-water mixtures in order to verify the previous assumption. Four kinds of polyvinylsulfonic esters were used: methyl, ethyl, isopropyl and *n*-butyl esters, the respective alkyl ethanesulfonates as the monomeric analog were also employed for the sake of comparison. While there has been no systematic study of the solvolytic reaction of the sulfonic esters comparable to the work on the organic halides, it has generally been accepted that the mechanism of the displacement involves the scission of the C–O bond, except for the special case of the phenyl ester,[3] which is known to be an S_N1-S_N2 borderline mechanism.[4]

Alkyl esters of sulfonic acids are much more reactive than alkyl bromide towards water, as a result of the greater strength of the sulfonic acid group.[5] Changes in the ester alkyl group, the solvent and the nucleophilic reagent alter the conditions, for example, from those favoring an S_N2 mechanism to those favoring the S_N1 mechanism; the substitution of α-alkyl groups increases the ionization tendency, so that in solvents of a high water content, the solvolytic reaction of the isopropyl ester of sulfonic acid is unaffected by hydroxide ions.[6]

The rates of the solvolysis of sulfonic esters as well as of alkyl halides are also dependent on the nature of the leaving group.[7] The case where the leaving group has a polymer chain has, however, hardly ever been studied.[8] A peculiar polymeric effect was found in this solvolytic reaction of polymeric sulfonic esters.

Experimental

Monomers.—A series of alkyl esters of vinylsulfonic acid was prepared by the method of Whitmore and Landau.[9] From 125 g. (1.0 mol.) of sodium sulfite and 285 ml. (3.30 mol.) of ethylene dibromide, there was obtained 275 g. of crude sodium β-bromoethanesulfonate, which, with 150 g. (0.73 mol.) of phosphorus pentachloride, yield 130.3 g. (65%) of β-bromoethanesulfonyl chloride (n_D^{20} 1.5242; b. p. 85°C/3 mmHg).

1) Dissertation submitted by Oh-Kil Kim in partial fulfillment of the requirements for the Ph. D. degree in the Graduate School of the University of Tokyo.
2) S. Yoshikawa and O-K. Kim, a) This Bulletin, **39**, 1515 (1966); b) ibid., **39**, 1729 (1966).
3) a) J. Fern and A. Lapworth, *J. Chem. Soc.*, **1912**, 273; b) C. A. Bunton and Y. F. Frei, ibid., **1951**, 1872.
4) R. E. Robertson, *Can. J. Chem.*, **31**, 589 (1953).
5) S. Winstein, E. Grunwald and H. W. Jones, *J. Am. Chem. Soc.*, **73**, 2700 (1951).
6) R. F. Hudson, G. M. Timmis and R. D. Marshall, *Biochem. Pharmacol.*, **1**, 48 (1958).
7) A. Streitwieser, Jr., "Solvolytic Displacement Reaction," McGraw-Hill Book Co., New York (1962). a) p. 82; b) p. 45.
8) H. Morawetz and P. E. Zimmering, *J. Am. Chem. Soc.*, **58**, 753 (1954).
9) W. F. Whitmore and E. F. Landau, ibid., **68**, 1797 (1946).

Methyl, ethyl, isopropyl and *n*-butyl vinylsulfonates were prepared from 0.11 mol. of β-bromoethanesulfonyl chloride and 0.1 mol. of the corresponding alcohol in the presence of pyridine. The sulfonic esters were redistilled immediately before use.

Polymers.—All the polyvinylsulfonic acid esters were prepared by the bulk polymerization of their respective monomers with γ-irradiation: ten grams of the monomer were poured into an ampoule and evacuated to 1 mmHg; the evacuation and pressuring with nitrogen repeated, and then it was sealed. The polymerization was carried out by exposing it to a ^{60}Co source yielding about 2×10^5 r./hr. for 72 hours at 0°C. The degree of polymerization was determined by the saponification of the polymers with sodium hydroxide into the respective poly-(sodium vinylsulfonate), which was precipitated from 70% methanol and dried in vacuo over phosphorus pentoxide; the value of the intrinsic viscosity[10] of respective poly-(sodium vinylsulfonate) in 0.5 N sodium chloride at 20°C was 10.0 ($\overline{M}_n=13000$) for the methyl ester, 8.2 ($\overline{M}_n=9400$) for the ethyl ester, 9.2 ($\overline{M}_n=11000$) for the isopropyl ester and 2.8 ($\overline{M}_n=1800$) for the *n*-butyl ester.

Other Materials.—Four alkyl (methyl, ethyl, isopropyl and *n*-butyl) ethanesulfonates were prepared from ethanesulfonyl chloride,[11] made from sodium ethanesulfonate[12] and phosphorus pentachloride, and the corresponding sodium alkoxide by modifying the method of Carius.[13] The esters so prepared were colorless liquids having the following boiling points: the methyl ester, 70—72°C/7 mmHg; the ethyl ester, 70—72°C/5 mmHg; the isopropyl ester, 71—73°C/5 mmHg; the *n*-butyl ester, 88—91°C/6 mmHg. The purity of the esters were ascertained by the value of saponification.

Solvolysis Procedure.—The concentrations of all the esters of sulfonic acids were initially adjusted to 7.5×10^{-3}, 1.2×10^{-2} and 3.0×10^{-2} mol./l. in acetone. The reaction mixture was prepared from 8 ml. of the adjusted 7.5×10^{-3} mol./l. ester and 2 ml. of water added from a microburette to make up an 80% acetone solution (v/v); from 5 ml. of the 1.2×10^{-2} mol./l. ester and 5 ml. of water to make up a 50% acetone solution, and from 2 ml. of the 3.0×10^{-2} mol./l. ester and 8 ml. of water to make up a 20% acetone solution. Five or six samples were employed in each run, and each sample, made up from 10 ml. of the mixture, was placed in a glass-stoppered tube placed in a thermostat regulated to 45±0.01°C. The reaction was followed by withdrawing samples from the bath at suitable intervals, and by titrating the liberated sulfonic acid with 0.02 N standard sodium hydroxide using a phenolphthalein indicator. The rate constants, *k*, for hydrolysis were calculated from the simple first-order equation and the individual rate constants in each run were averaged over the range of approximately 40—50% of the reaction.

Results and Discussion

The solvolysis of ethanesulfonic esters followed first-order kinetics closely as is exemplified in Table I, while those of polyvinylsulfonic acid esters obviously deviated from first-order kinetics depending upon the compositions of the acetone-water mixtures, as is illustrated in Figs. 1, 2, 3 and 4. A common tendency is seen in these figures; polyvinylsulfonic acid esters were solvolyzed more slowly with an increase in the acetone content of the mixed solvents as well as in the cases of monomeric sulfonic ester. The effect of adding water to acetone

Table I. Solvolysis rates of methyl ethanesulfonate and methyl polyvinylsulfonate in various ratios of acetone-water mixtures at 45°C

Solvent (acetone/water)	ESMe			PVSMe		
	Time min.	log (a/(a−x))	$10^3 k$ min^{-1}	Time min.	log (a/(a−x))	$10^3 k$ min^{-1}
20/80 (v/v)	63	0.0610	2.23	30	0.1114	8.58
	138	0.1290	2.15	73	0.2542	8.05
	232	0.2198	2.18	110	0.3440	7.22
	332	0.3167	2.20	225	0.6239	6.44
	446	0.4249	2.20			
50/50 (v/v)	200	0.0666	0.668	22	0.0775	7.12
	338	0.0989	0.675	120	0.2442	5.32
	392	0.1138	0.669	160	0.2964	4.27
	508	0.1477	0.671	220	0.3686	3.86
	632	0.1895	0.692			
80/20 (v/v)	544	0.0336	0.142	60	0.0730	2.79
	949	0.0573	0.139	140	0.1537	2.54
	1330	0.0784	0.136	267	0.2414	2.08
	1740	0.1022	0.138	360	0.2929	1.88

10) The molecular weight was calculated by K. Dialer and R. Kerber, *Makromol. Chem.*, **17**, 56 (1956).
11) W. Davies and J. H. Dick, *J. Chem. Soc.*, **1932**, 484.
12) H. G. Houlton and H. V. Tartar, *J. Am. Chem. Soc.*, **60**, 544 (1938).
13) L. Carius, *J. Prak. Chem.*, Band **2**, 270 (1870).

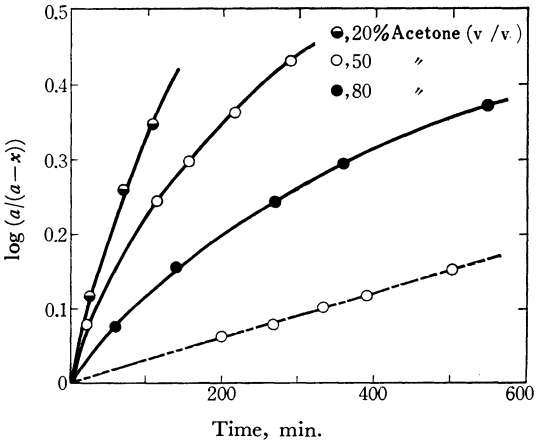

Fig. 1. Solvolysis of methyl polyvinylsulfonate (solid line) and methyl ethanesulfonate (dotted line) at 45°C.

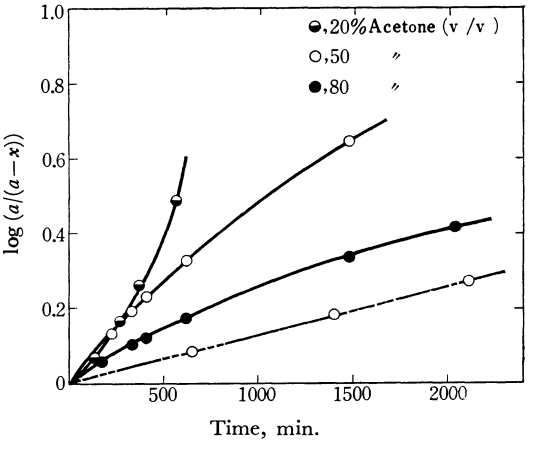

Fig. 2. Solvolysis of ethyl polyvinylsulfonate (solid line) and ethyl ethanesulfonate (dotted line) at 45°C.

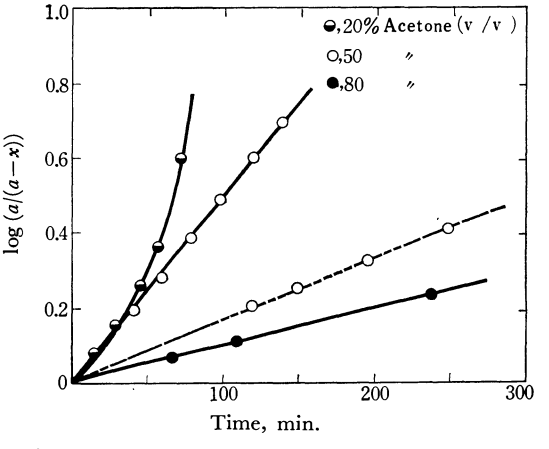

Fig. 3. Solvolysis of isopropyl polyvinylsulfonate (solid line) and isopropyl ethanesulfonate (dotted line) at 45°C.

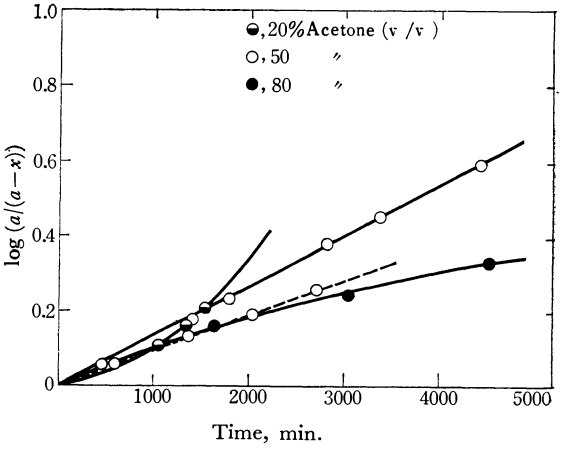

Fig. 4. Solvolysis of *n*-butyl polyvinylsulfonate (solid line) and *n*-butyl ethanesulfonate (dotted line) at 45°C.

is to increase the ionizing ability of the solvent and, thereby, to accelerate the solvolytic reaction, which depends on the stabilization of partial charges in the transition state.

However, in 20% acetone, an unusual phase was found in the solvolysis of polymeric esters. At the beginning of the reaction, the solvolysis rate was suppressed, but it was gradually accelerated remarkably with the lapse of time. Thus different aspects of the solvolytic behavior of polymeric sulfonic esters in a high water content are of interest when discussing the reactivity of the polymer in relation to the expansion in solutions rather than to the change in the reaction mechanism.

The solvolysis rates of polymeric sulfonic esters were much greater than that of the monomeric analog in all cases except those of isopropyl and *n*-butyl esters in 20% aqueous acetone. The relative rate between the polymeric ester and the monomeric analog (k_p/k_m) increased in proportion to an increase in the acetone content. It is also important to note that the ratios of the solvolytic rates between the methyl ester and other esters, $(k_R/k_{Me})_m$ for the monomeric analog and $(k_R/k_{Me})_p$ for the polymeric ester (Table II), decrease with the magnitude of ester alkyl except in the case of the isopropyl ester (because of its well-known high polar causes). The decrease in $(k_R/k_{Me})_m$ may be due mainly to the different polarity on the C–O bond which includes a alkyl group, while the decrease in $(k_R/k_{Me})_p$ may be due mainly to the differences in the polar and hydrophobic characters of the alkyl group on the polymer chain, since the steric factors of ethyl and *n*-butyl groups are considered to be of nearly the same magnitude.

Therefore, the relative value $(k_R/k_{Me})_p/(k_R/k_{Me})_m$ indicates the relative hydrophobic factor of the alkyl group of each polymeric ester in a

Table II. Solvolytic rate constants k (min^{-1}) and relative rates, k_p/k_m related to an peculiar polymeric effect and $(k_R/k_{Me})_{p \text{ or } m}$ to relative substituent effect in various acetone-water mixtures at 45°C

Ester	Solvent (acetone/water)		Me		Et		*i*-Pr		*n*-Bu	
			10^4k	k_p/k_m	10^4k	k_p/k_m	10^4k	k_p/k_m	10^4k	k_p/k_m
ES	20/80 (v/v)		22.3		13.0		299		8.34	
		$(k_R/k_{Me})_m$	(1.0)		(0.58)		(13.4)		(0.37)	
PVS			75.2	3.4	16.1	1.2	144	0.48	2.92	0.34
		$(k_R/k_{Me})_p$	(1.0)		(0.21)		(1.91)		(0.039)	
ES	50/50 (v/v)		6.68		2.97		40.0		2.08	
		$(k_R/k_{Me})_m$	(1.0)		(0.44)		(5.98)		(0.31)	
PVS			53.0	7.9	12.5	4.2	109	2.7	3.17	1.5
		$(k_R/k_{Me})_p$	(1.0)		(0.24)		(2.05)		(0.060)	
ES	80/20 (v/v)		1.36		0.515		4.69		0.298	
		$(k_R/k_{Me})_m$	(1.0)		(0.38)		(3.45)		(0.22)	
PVS			20.9	15.0	5.08	9.8	23.0	4.9	1.73	6.6
		$(k_R/k_{Me})_p$	(1.0)		(0.24)		(1.15)		(0.083)	

certain solvent composition. The values decrease with the number of alkyl carbon atoms and gradually increase with an increase in the acetone content of mixed solvents. Such changes in the relative values suggest the major importance of the expansion of polymers in solutions. This undoubtedly suggests that, in a solution of a high water content, the random-coiled molecules of the polymeric ester, especially isopropyl and *n*-butyl esters, are greatly aggregated, where the solvent ratio in the immediate neighborhood of the macromolecule may differ considerably from the bulk-average composition of the medium compared to their corresponding differences in other compositions of the solvent; that the conformational movements of the polymer are restricted by their strong hydrophobic character, and that, hence, the reaction probably occurs mainly on the outer layer of the random-coiled molecule.

This interpretation is clearly supported by the illustrations given in Figs. 5, 6, 7 and 8, where the

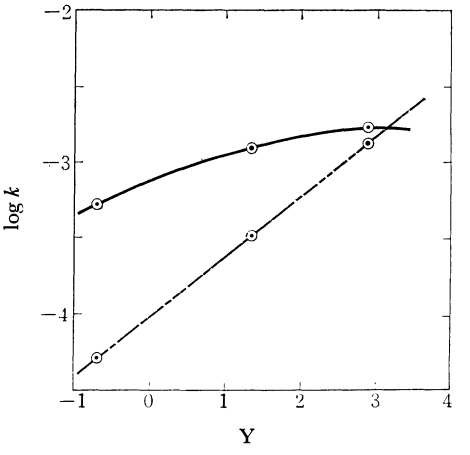

Fig. 6. Solvolysis rates of ethyl ethanesulfonate (dotted line) and ethyl polyvinylsulfonate (solid line) as a function of ionizing power Y.

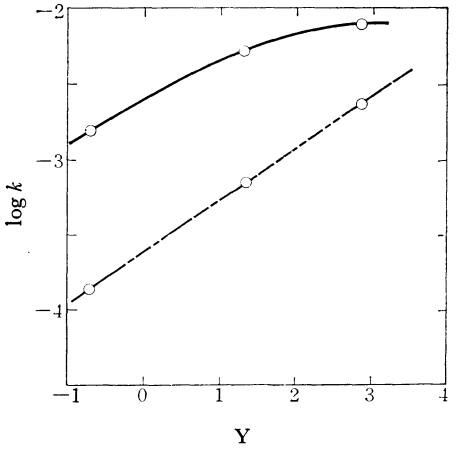

Fig. 5. Solvolysis rates of methyl ethanesulfonate (dotted line) and methyl polyvinylsulfonate (solid line) as a function of ionizing power Y.

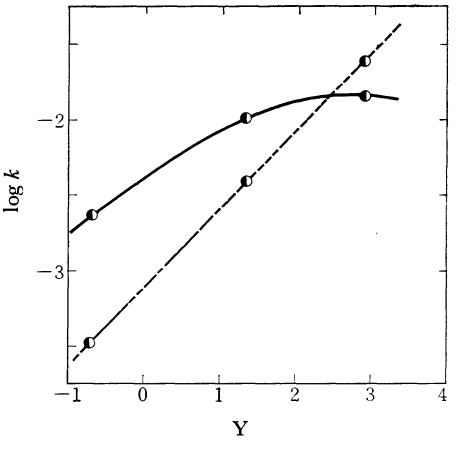

Fig. 7. Solvolysis rates of isopropyl ethanesulfonate (dotted line) and isopropyl polyvinylsulfonate (solid line) as a function of ionizing power Y.

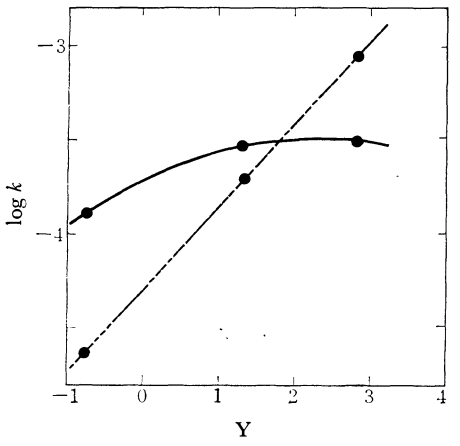

Fig. 8. Solvolysis rates of *n*-butyl ethanesulfonate (dotted line) and *n*-butyl polyvinylsulfonate (solid line) as a function of ionizing power Y.

Grunwald-Winstein correlation[14] is given:

$$\log k = mY + \log k_0$$

where Y is the measure of the ionizing power[15] of the solvent; k_0 is the rate of solvolysis in the standard solvent, and the slope m measures the susceptibility of the substrate to the ionizing power of the solvent. While the solvolysis of ethanesulfonic acid esters gives a linear correlation in Y, that of polymeric sulfonic esters deviates from linearity much more remarkably with the number of alkyl carbon atoms. The reaction rates were, however, accelerated by increasing the hydrophilic character of the polymer because of the sulfonic acid groups formed during the lapse of the reaction time.

On the other hand, the initial rate enhancement in the solvolysis of the polymeric ester in solvents of higher acetone contents may account for the major importance of the steric acceleration arising from the steric congestion by hydrophobic solvation on the polymer chain. This interpretation is also supported by the fact that solvolysis rates of polymer in 50% and 80% aqueous acetone (with the exception of 20% aqueous acetone, for the reason mentioned before) gradually became lower as a result of the release from the congestion between the immediate-neighboring alkyl groups with the lapse of reaction time. Steric assistance has been called[16] upon to explain the abnormally fast rate of the solvolysis of highly-branched tertiary alkyl halides. Such a phenomenon was also found in the solvolysis of cycloalkyl tosylate[17]; the solvolysis is accelerated by the steric interference of γ-opposed hydrogen with the tosylate group called non-bonding repulsion.

Furthermore, the ratio of the solvolysis rates between the series of alkyl polyvinylsulfonate and the corresponding ethanesulfonate (k_p/k_m), which indicates a positive polymeric effect, was much greater with the methyl ester than with the other esters and increased upon an increase in the acetone content of the mixed solvents in each run; the value of (k_p/k_m) towards the methyl ester in 80% acetone content attained 15, as is shown in Table II. These observations can be interpreted to suggest that the change in (k_p/k_m), which is dependent upon the alkyl structures of the polymer and the solvent compositions, involves a difference in the affinity of a substrate to a solvent. This may, in turn, cause the difference in the expansion or conformational movements of the polymer molecule.

A supplementary experiment was carried out with a partially-hydrolyzed polymeric ester to assure the absence of proton catalysis by the neighboring sulfonic acid present on the polymer chain. For example, initially 34% hydrolyzed *n*-butyl polyvinylsulfonate was hydrolyzed under the same conditions except that the solvent composition was 45% aqueous acetone; the rate constant was 3.09×10^{-4} (min^{-1}), which demonstrates that there is no intramolecular proton effect. Furthermore, the effect of added common and uncommon ions with both the polymeric ester and the monomeric analog in various systems showed the salt effect to be negligibly small for the noted concentration. The lack of sensitivity in the solvolyzing arylsulfonic esters (even in esters reacting by an apparent S_N1 mechanism) to the salt effect has also been noted by others.[4,18] In addition, solvolytic reactions of vinylsulfonic acid esters were also carried out in order to compare them with those of ethanesulfonic esters. The hydrolysis rates of the former were almost twice as much as the latter; the rate constants of methyl, isopropyl and *n*-butyl vinylsulfonates in 50% aqueous acetone at 45°C were 1.34×10^{-3}, 9.88×10^{-3} and 3.79×10^{-3} respectively. This magnitude in rates can be expected to result from the inductive electron withdrawal of the vinyl group.

14) E. Grunwald and S. Winstein, *J. Am. Chem. Soc.*, **70**, 846 (1948).
15) The values extracted from the data of Fainberg and Winstein are employed here: A. H. Fainberg and S. Winstein, ibid., **78**, 2770 (1956).
16) H. C. Brown and R. S. Fletcher, ibid., **71**, 1845 (1945) and ibid., **72**, 1223 (1950).
17) I. Moritani, S. Nishida and M. Murakami, ibid., **81**, 3420 (1959).
18) H. R. McCleary and L. P. Hammett, ibid., **63**, 2254 (1941).

BULLETIN OF THE CHEMICAL SOCIETY OF JAPAN VOL. 39 1942—1948 (1966)

Molecular Rearrangement in Polyphosphoric Acid. II. The Conversion of 1, 2-Dihydro-2-phenylimino-4*H*-3, 1-benzoxazin-4-one to 3-phenyl-2, 4(1*H*, 3*H*)-quinazolinedione[1,2]

By Masaru KURIHARA and Naoya YODA

Basic Research Laboratories, Toyo Rayon Co., Ltd., Tebiro, Kamakura

(Received November 18, 1965)

The treatment in polyphosphoric acid of the *N*-(phenylcarbamoyl)-anthranilic acid prepared by the reaction of anthranilic acid with phenyl isocyanate has been shown to yield 1, 2-dihydro-2-phenylimino-4*H*-3, 1-benzoxazin-4-one or 3-phenyl-2, 4(1*H*, 3*H*)-quinazolinedione, depending on the reaction temperature. An intramolecular rearrangement has been found to occur by the treatment of exocyclic iminobenzoxazinone with polyphosphoric acid to afford quinazolinedione. The mechanisms of conversion in polyphosphoric acid have been proposed to account for the experimental results, and the structure of 2-phenylimino-4*H*-3, 1-benzoxazin-4-one has been presumed by means of infrared and ultraviolet spectroscopies and elemental analyses. The products of the reaction of *N*-methylanthranilic acid with phenyl isocyanate have been shown to be 1-methyl-3-phenyl-2, 4(1*H*, 3*H*)-quinazolinedione, 1-methyl isatoic anhydride and *N*-methyl-2-(phenylcarbamoyl)-carbanilide. Furthermore, the formation of the mixed anhydride of carboxylic acid and phosphoric acid as a reaction intermediate has been postulated.

The most frequently reported use of polyphosphoric acid is cyclodehydration, or more specifically, intramolecular acylation.[3,4] To our knowledge no studies have been carried out in polyphosphoric acid on the conversion of compound I to quinazolone derivatives II. In connection with the solution polymerization, in polyphosphoric acid, of 4, 4'-diamino-biphenyl-3, 3'-dicarboxylic acid with diisocyanate by cyclopolycondensation reactions,[5] the cyclodehydration of *N*-(phenylcarbamoyl)-anthranilic acid in polyphosphoric acid[6] was studied; two condensation products, 1, 2-dihydro-2-phenylimino-4*H*-3, 1-benzoxazin-4-one (Ia) and 3-phenyl-2, 4(1*H*, 3*H*)-quinazolinedione (IIa) have been isolated, depending upon the reaction temperature. The authors also found that the intramolecular rearrangement in PPA of Ia to IIa occurs by heating Ia at 150°C through a phosphorylated reaction intermediate.

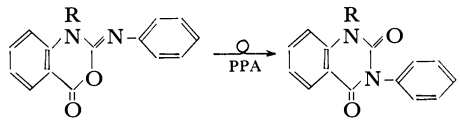

I II

(Ia R=H) (IIa R=H)
(Ib R=CH_3) (IIb R=CH_3)

In a previous paper[2] it has been shown that the reaction of anthranilic acid with aromatic isocyanate in the presence of PPA proceeded to the formation iminobenzoxazinone and quinazolinedione by way of phosphorylated intermediates. This type of rearrangement in PPA is especially notable because a possible mechanism for the cyclodehydration in PPA of *N*-(phenylcarbamoyl)-anthranilic acid involves phosphorylated reaction intermediates,[4] while the reaction in PPA afforded I and II, the former product arising from the presumed intermediate, V, via kinetic control, while the latter product was formed from V via thermodynamic control. The method of the synthesis of benzoxazinone (I), quinazolinedione (II) and related compounds is outlined in Scheme 1.

When *N*-(phenylcarbamoyl)-anthranilic acid (m. p. 186°C; from ethanol) is treated with PPA at 80—100°C for 1 hr., cyclodehydration occurs, thus yielding quantitatively 1, 2-dihydro-2-phenylimino-4*H*-3, 1-benzoxazin-4-one (Ia) (m. p. 193°C;

1) N. Yoda and M. Kurihara, presented in part at the 13th and 14th Meetings of the High Polymer Symposium of Japan, Tokyo, November, 1964, and Kyoto, October, 1965, and at the 18th Annual Meeting of the Chemical Society of Japan, Osaka, April, 1965.

2) M. Kurihara and N. Yoda, *Tetrahedron Letters*, **1965**, 2597.

3) a) For a recent review with references, see J. P. Marthe and S. Munavalli, *Bull. soc. chim. France*, **1963**, 2679. b) F. Uhlig and H. R. Snyder, "Advances in Organic Chemistry," Vol. I, Ed. by R. A. Raphael, E. C. Taylor and H. Wynberg, Interscience Publishers, New York, N. Y. (1960), p. 35.

4) D. M. Brown, "Advances in Organic Chemistry," Vol. III, Ed. by R. A. Raphael, E. C. Taylor and H. Wynberg, Interscience Publishers, New York, N. Y. (1963), p. 75.

5) N. Yoda, R. Nakanishi, M. Kurihara, Y. Bamba, S. Tohyama and K. Ikeda, *J. Polymer Sci.*, **B4**, 11 (1966).

6) A mixture of phosphoric acid and phosphorus pentoxide, hereinafter referred to as PPA. A chemically pure-grade reagent, PPA(P_2O_5 content; 84%), of Nippon Kagaku Kogyo, Ltd., was used.

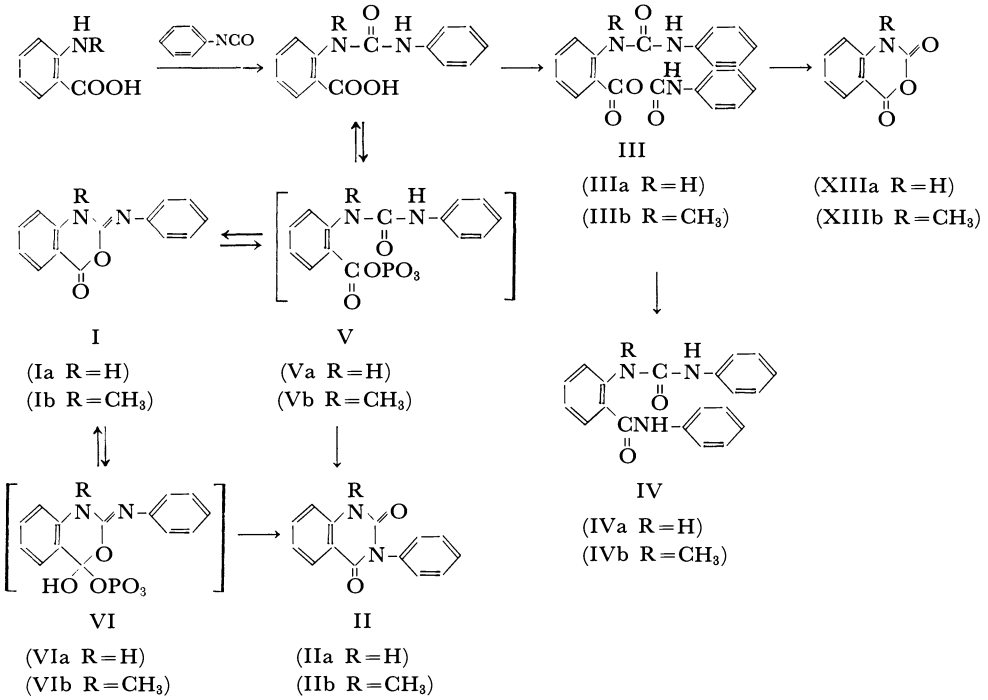

from chloroform), possibly through a phosphorylated reaction intermediate V. The OPO_3 fragment represents the phosphoric acid moiety, which is of an indefinite composition. A similar compound of phosphoric-carboxylic mixed anhydride was recently prepared by the reaction of silver dibenzyl phosphate with an alkyl chloroformate.[7] Conversion is effected by the treatment of Ia with PPA at 150°C for 1 hr.; this results in the formation of 3-phenyl-2, 4(1*H*, 3*H*)-quinazolinedione (IIa) (m. p. 281°C from ethanol) in an 80% yield.[8] The presumed reaction intermediate VIa is formed by the phosphorylation of the carbonyl group of benzoxazinone (Ia) in PPA, followed by ring opening to Va and recyclization, thus yielding quinazolinedione (IIa) by losing the polyphosphoric acid species. The direct cyclodehydration of *N*-(phenylcarbamoyl)-anthranilic acid is also effected by treatment with PPA at 150°C for 5 hr., thus affording quinazolinedione (IIa). When anthranilic acid was treated with an excess amount of phenyl isocyanate in bulk, 2-(phenylcarbamoyl)-carbanilide (IVa) was obtained quantitatively.[2,8d] The phosphorylation mechanism is supported by the experimental evidence of the polymerization reaction of 4, 4'-diamino-biphenyl-3, 3'-dicarboxylic acid with phenyl diisocyanate in PPA and by the successful isolation of the corresponding *phosphoric-carboxylic anhydride of polyurea acid.* The structure was determined by analyses of the phosphorus content by means of both colorimetry and emission X-ray measurements.

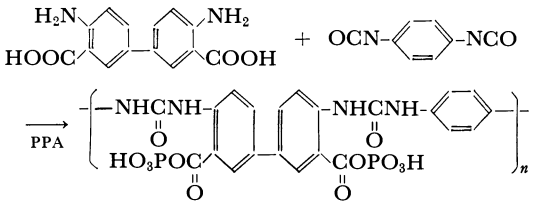

(2)

For a detailed account of the polymerization mechanism and a characterization of the resulting polymer of phosphoric-carboxylic anhydride, see another article.[5]

The tautomeric structure of benzoxazinone (I) is expressed in the following equation:

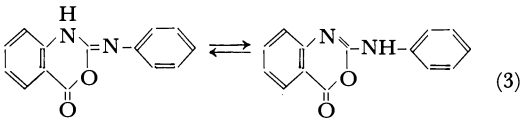

(3)

(Ia) (Ia')

It is also possible that the phosphorylated reaction intermediate (Va) exists in the following tautomeric forms:

7) D. L. Griffith and M. Stiles, *J. Am. Chem. Soc.*, **87**, 3710 (1965).

8) During the progress of this investigation, similar results have been obtained in different systems, such as in an alkaline solution or in a 10% sulfuric acid solution. a) G. Doleschall and K. Lempert, *Tetrahedron Letters*, **1963**, 1195. b) K. Lempert and G. Doleschall, *Monatsh. Chem.*, **95**, 950 (1964). c) G. Doleschall and K. Lempert, *Monatsh. Chem.*, **95**, 1068 (1964). d) J. C. Sheehan and G. D. Daves, Jr., *J. Org. Chem.*, **29**, 3599 (1964). e) H. Herlinger, *Angew. Chem.*, **76**, 437 (1964).

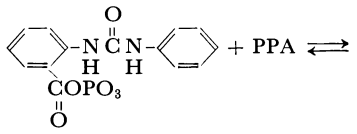

Va

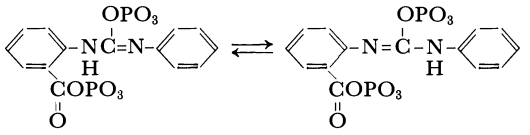

Va′ Va″

The infrared spectrum of I exhibits characteristic absorption bands of the carbonyl group at $\nu_{C=O}$ 1747 cm^{-1} and of the C=N double bond at $\nu_{C=N}$ 1644 cm^{-1} as is shown in Figs. 1 and 2. The ratios

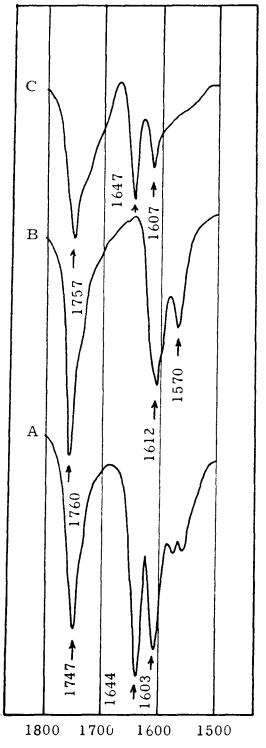

Fig. 1. Infrared spectra of benzoxazinone and related compounds (KBr).
(A) 1, 2-Dihydro-2-phenylimino-4*H*-3, 1-benzoxazin-4-one (Ia)
(B) 2-Phenyl-4*H*-3, 1-benzoxazin-4-one (VIII)
(C) 2-Methyl-4*H*-3, 1-benzoxazin-4-one (IX)[9]

of the extinction coefficients of the C=O absorption (ε_2) and C=N absorption (ε_1) are compared in various systems. The value in Ia is found to be $\varepsilon_2/\varepsilon_1=1.34$. In such compounds as 2-phenyl-4*H*-3, 1-benzoxazin-4-one (VII) and 2-methyl-4*H*-3, 1-benzoxazin-4-one (IX), the C=N double bond

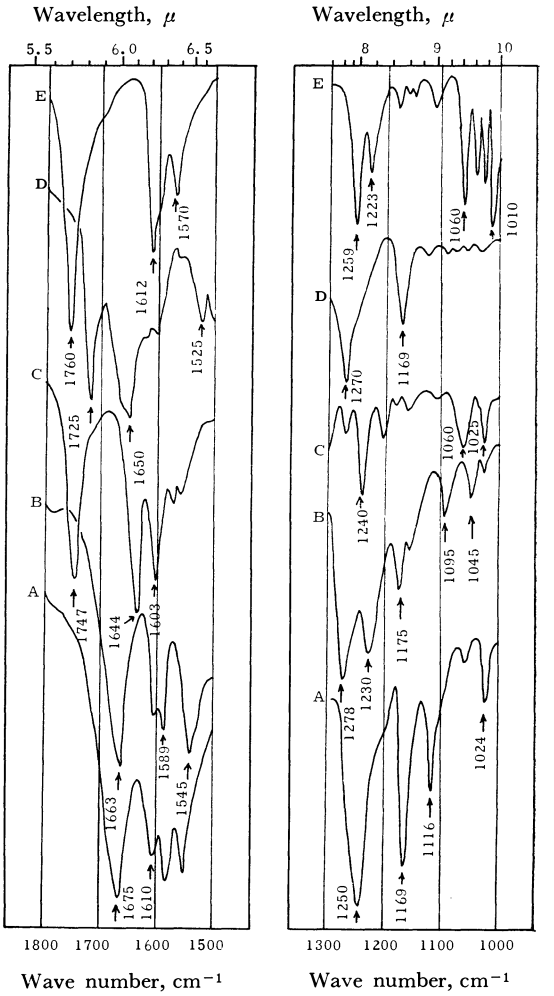

Fig. 2. Infrared spectra of quinazolinedione and related compounds (KBr).
(A) Anthranilic acid
(B) *N*-(Phenylcarbamoyl)-anthranilic acid[10]
(C) 1, 2-Dihydro-2-phenylimino-4*H*-3, 1-benzoxazin-4-one (Ia)
(D) 3-Phenyl-2, 4(1*H*, 3*H*)-quinazolinedione (IIa)[10]
(E) 2-Phenyl-4*H*-3, 1-benzoxazin-4-one (VIII)[11]

is endocyclic and the ratio of the ε values of the C=O and C=N absorptions are found to be $\varepsilon_2/\varepsilon_1=0.45$ and 0.82 respectively. It is clearly shown that the relative intensity of the C=N stretching vibration of Ia at 1644 cm^{-1}, is fairly strong as compared with the intensities of VIII and IX.[12] It has also been found that the

9) M. T. Bogert and H. M. Seil, *J. Am. Chem. Soc.*, **29**, 517 (1907).
10) C. Paal, *Ber.*, **27**, 977 (1894).
11) a) R. Anschutz and O. Schmidt, ibid., **35**, 3483 (1902). b) R. Snyder and R. H. Levine, *J. Am. Chem. Soc.*, **60**, 2025 (1938).
12) J. Fabian and M. Legrand, *Bull. soc. chim. France*, **1956**, 1461.

Table I. Ultraviolet absorption characteristics of benzoxazinone and related compounds

Compound	UV λ_{max} mμ [lit.]	Ext. coef. ε	log. ε
N-(Phenylcarbamoyl)-anthranilic acid	(1) 265[267][13,c]	37500	4.57[4.4][13,c]
	(2) 306[308][13,c]	9149	3.96[3.75][13,c]
1,2-Dihydro-2-phenylimino-4*H*-3, 1-benzoxazin-4-one (Ia)	(1) 244[c]	8160	3.91
	(2) 282	9200	3.96
	(3) 292[c]	8600	3.93
	(4) 332	2665	3.42
3-Phenyl-2, 4(1*H*, 3*H*)-quinazolinedione (IIa)	(1) 243[13][247][c]	11220	4.05[4.05][13,c]
	(2) 312[13][313][c]	3490	3.53[3.52][13,c]
2-(Phenylcarbamoyl)-carbanilide (IVa)	(1) 264[14][264]	34100	4.53[4.55][14]
	(2) 306[14][306]	9800	3.99[4.00][14]
2-Phenyl-4*H*-3, 1-benzoxazin-4-one (VIII)	(1) 241	22220	4.35
	(2) 275(sh)	16400	4.21
	(3) 285	21430	4.33
	(4) 298	19740	4.29
	(5) 321	11600	4.06
N-Dibenzylmethylene-2-phenylenediamine (X)	(1) 244[15]		3.83[15]
	(2) 275[15]		3.95[15]
	(3) 282[15]		3.90[15]

a) 99.5% ethanol, b) methanol, c) 95% ethanol

carbonyl absorption of Ia shows a bathochromic shift of 13 cm^{-1} as compared with the carbonyl absorption of the endocyclic C=N structure (IX); it is presumed that the exocyclic C=N structure is resonance stabilized because of the hybridization of π-electron orbitals of the C=N double bond with the phenyl group. The apparent stability of *N*-phenyliminobenzoxazinone (Ia) by resonance stabilization is supported by the fact that *N*-phenyliminobenzoxazinone (Ia) was isolated as a crystalline solid, whereas *N*-methyl imino and *N*-ethylimino derivatives are not stable enough to be isolated at 40—80°C; their presence was detected by thin-layer chromatography and by a study of the infrared spectrum at lower temperatures. The infrared data of these compounds will be compared elsewhere.

The absorption characteristics and the intensities of the ultraviolet spectra of benzoxazinone (Ia) and related compounds are summarized in Table I. The C=N double bond exhibits two characteristic absorption maxima in the 275—295 mμ range. The endocyclic C=N double bond of the VIII structure shows characteristic peaks at 285 and 298 mμ, and the Schiff base, *N*-benzylmethylene-2-phenylenediamine (X) has two characteristic C=N absorptions, at 275 and 282 mμ.[15] In the spectrum of benzoxazinone (Ia), characteristic maxima of the C=N bond are found at 282 mμ (9200) and 292 mμ (8600). Although the model compounds described in Table I, Fig. 1 and Fig. 2 may not represent exactly the fine structure of Ia, conclusive evidence was obtained by the direct comparison of the characteristic absorption bands of the infrared and ultraviolet spectra of Ia with those of Ib; these peaks of the C=N bond may be assigned to the exocyclic C=N bond on the basis of both the spectral comparison and the chemical reactivity of the compound Ia towards phenyl isocyanate.

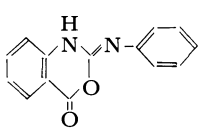

(Ia)

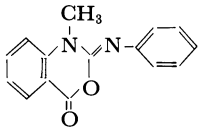

(Ib)

They show a bathochromic effect in the following increasing order (as is shown in Table I, the hyperchromic effect was observed in the same order):

noncyclic C=N < exocyclic C=N < endocyclic C=N

These effects are in good agreement with the results on the infrared spectral characteristics, and a tautomeric structure Ia was assigned to iminobenzoxazinone. In the exocyclic iminobenzoxazinone (Ia), the C=N double bond is conjugated not only with the benzene ring but also with the benzoxazinone ring through unshared electrons of ester oxygen and the carbonyl group; this may explain the apparent stability of Ia relative to the other tautomeric structure Ia'.

13) P. Grammaticakis, *Compt. rend.*, **247**, 2013 (1958).
14) P. Grammaticakis, *Bull. soc. chim. France*, **1962**, 487.
15) R. C. Elderfield and V. B. Meyer, *J. Am. Chem. Soc.*, **76**, 1887 (1954).

When *N*-methylanthranilic acid is treated with an equimolar amount of phenyl isocyanate, exocyclic iminobenzoxazinone (Ib) is the only possible product. It was found that it undergoes molecular rearrangement to form a thermodynamically-controlled product, 1-methyl-3-phenyl-2, 4(1*H*, 3*H*)-quinazolinedione (IIb), together with 1-methylisatoic anhydride (XIIIb) (m. p. 164—166°C) and *N*-methyl-2(phenylcarbamoyl)-carbanilide (IVb) (m. p. 252—253°C).

The treatment of exocyclic iminobenzoxazinone (I) with phenyl isocyanate failed to produce either 2-(phenylcarbamoyl)-phenylamino-4*H*-3, 1-benzoxazin-4-one (XI) or the other possible product (XII).

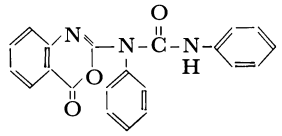

(XI)

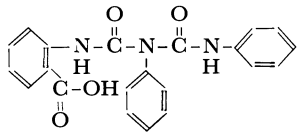

(XII)

A possible mechanism for the molecular rearrangement of iminobenzoxazinone (I) to quinazolinedione (II) in PPA involves the phosphorylated intermediates VI and VII; it is shown in the following scheme (2), which is based on the experimental evidence of the phosphoric-carboxylic mixed anhydride of polyurea acid.[1,4]

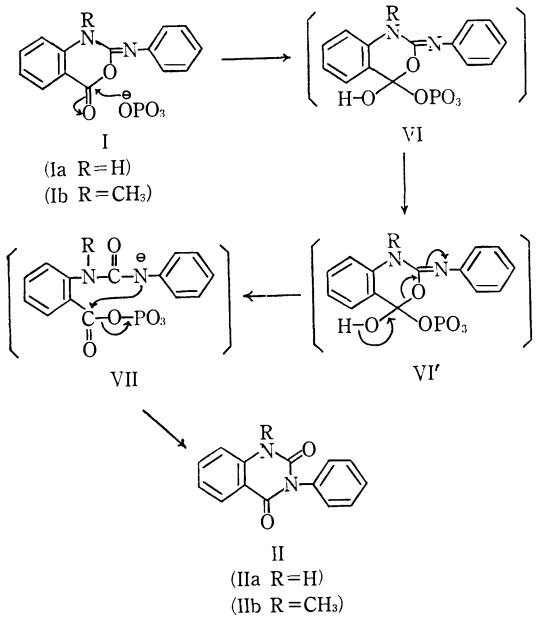

I
(Ia R=H)
(Ib R=CH_3)

VI

VII

VI'

II
(IIa R=H)
(IIb R=CH_3)

When I is treated with PPA at 150°C, the carbonyl group of benzoxazinone I is phosphorylated to form the reaction intermediate VI, followed by ring opening to form the mixed anhydride of carboxylic acid and phosphoric acid VII. The anion of ureido nitrogen attacks the carbonyl group of the mixed anhydride to cleave the phosphoric acid species. Recyclization is completed by quinazolinedione ring fromation II. A similar mechanism has been suggested for the hydrolysis of salicylphosphate, which involves the formation of a cyclic transition state.[16]

Experimental[17]

The Preparation of *N*-(Phenylcarbamoyl)-anthranilic Acid.—A 3.5 g. portion (0.03 mol.) of phenyl isocyanate was dissolved in 20 ml. of benzene. The solution was then gradually added into 40 mol. of a benzene solution containing 2.74 g. (0.01 mol.) of anthranilic acid at 50°C. After the mixture had been heated under reflux at 80°C for 1 hr., the precipitate was filtered and washed several times with benzene. Recrystallization from ethanol yielded needles which melted at 185—186°C (lit.[10] m. p. 183°C). The yield was 4.97 g. (97%). The infrared spectrum (KBr) shows a band at 3320 cm^{-1} (N-H stretching). The carbonyl stretching bands fall at 1675 cm^{-1} (carboxyl) and at 1663 cm^{-1} (ureido carbonyl).

Ultraviolet spectrum: λ_{max} 265 mμ (ε, 37500); 306 mμ (ε, 9149).

Found: C, 65.70; H, 4.72; N, 10.93. Calcd. for $C_{14}H_{12}O_3N_2$: C, 65.62; H, 4.72; N, 10.93%.

The Preparation of 3-Phenyl-2, 4(1*H*, 3*H*)-quinazolinedione (IIa). — A mixture of 3.00 g. (0.0117 mol.) of *N*-(phenylcarbamoyl)-anthranilic acid and 200 g. of PPA was placed in a three-necked flask fitted with a mechanical stirrer. The mixture was heated at 150°C for 5 hr., and the resulting solution was poured into 300 ml. of distilled water. The precipitate was filtered off and washed twice with a dilute aqueous sodium carbonate solution. Then it was washed thoroughly with water and dried. The yield was 2.38 g. (100%). It was recrystallized from ethanol to obtain needles, m. p. 280°C (lit.[10] 280°C). The infrared spectrum (KBr) showed bands at 3200 cm^{-1} (bonded N-H), 1725 cm^{-1} (4-carbonyl), 1650 cm^{-1} (2-carbonyl) and 1600 cm^{-1} (phenyl). The ultraviolet spectrum exhibited absorption maxima at λ_{max} 243 mμ (ε, 11200) and 312 mμ (ε, 3490).

Found: C, 70.33; H, 4.38; N, 11.76; mol. wt.,

16) J. D. Chanley, E. M. Gindler and H. Sobotka, *J. Am. Chem. Soc.*, **74**, 4347 (1952).

17) All the melting points were taken on a Büchi Melting Point Apparatus and are uncorrected. The microanalyses were carried out by the Microanalytical Section of these laboratories. The infrared spectal were recorded with Perkin-Elmer (Model 125) and Hitachi (Model EPI-S) recording spectrophotometers, using a potassium bromide disk or Nujol. The ultraviolet spectra were recorded with a Cary Model 14 recording spectrophotometer in ethanol. The molecular weights were determined with a Mechrolab Model 310A vapor pressure osmometer in benzene and ethyl methyl ketone.

241. Calcd. for $C_{14}H_{10}O_2N_2$: C, 70.58; H, 4.23; N, 11.48%; mol. wt., 238.

The Preparation of 1, 2-Dihydro-2-phenylimino-4*H*-3, 1-benzoxazin-4-one (Ia).—A 0.300 g. portion (0.00117 mol.) of *N*-(phenylcarbamoyl)-anthranilic acid was added to 20 g. of PPA, and then the mixture was heated at 80—100°C for 1 hr., and after the reaction, poured into 100 ml. of distilled water. It was then filtered, and washed with a 10% aqueous sodium caraonate solution and distilled water successively. Several recrystallizations from chloroform yielded needles, m. p. 193°C (lit.[8a,d,e] 192—193°C), in a 95% yield. The infrared spectrum (Nujol) shows absorption bands at 3300 cm^{-1} (N-H), 1747 cm^{-1} (lactone carbonyl), 1650 cm^{-1} (>C=N-) and 1240 cm^{-1} and 1060 cm^{-1} (C-O-C). The ultraviolet spectrum had absorption maxima at λ_{max} 244 mμ (ε, 8160), 282 mμ (ε, 9200), 292 mμ (ε, 8600) and 332 mμ (ε, 2665).

Found: C, 70.28; H, 4.25; N, 11.25; mol. wt., 237. Calcd. for $C_{14}H_{10}O_2N_2$: C, 70.58; H, 4.28; N, 11.48%; mol. wt., 238.

The Intramolecular Rearrangement of 1, 2-Dihydro-2-phenylimino-4*H*-3, 1-benzoxazin-4-one (Ia) to 3-Phenyl-2, 4(1*H*, 3*H*)-quinazolinedione (IIa).—A mixture of 0.200 g. (0.0084 mol.) of I and 20.0 g. of PPA was heated at 150°C for 5 hr. It was then poured into 100 ml. of distilled water, and the resulting precipitate was filtered and washed with a 10% aqueous sodium carbonate solution. It was then washed thoroughly with distilled water and dried. The yield was 0.140 g. (70%). It was recrystallized from ethanol to obtain colorless needles, m. p. 282°C. It was identified by a comparison of its infrared spectrum (KBr) with that of II prepared directly from *N*-(phenylcarbamoyl)-anthranilic acid in PPA. The infrared bands at 1240 cm^{-1} (-N=C-O-C-) and 1060 cm^{-1} (-C-O-C-) disappeared.

The Preparation of 2-Phenyl-4*H*-3, 1-benzoxazin-4-one (VIII).—A mixture of 3.40 g. (0.025 mol.) of anthranilic acid and 3.5 g. (0.025 mol.) of benzoyl chloride was dissolved into 115 g. of PPA; the solution was heated at 120 to 140°C for 12 hr., and then heated for 0.5 hr. It was then poured directly into 300 ml. of distilled water; the precipitate was filtered and washed thoroughly with distilled water to afford the product in a 99% yield. The product was recrystallized from ethanol to obtain colorless needles. It has a m. p. of 130.0—130.5°C. The infrared spectrum (KBr) shows carbonyl bands at 1760 cm^{-1} and 1060 cm^{-1} (C-O-C). The ultraviolet spectrum has bands at λ_{max} 241 mμ (ε, 22220), 275 mμ (ε, 16400) (shoulder), 285 mμ (ε, 21430), 298 mμ (ε, 19740) and 321 mμ (ε, 11600).

Found: C, 75.15; H, 4.03; N, 6.21; mol. wt., 230. Calcd. for $C_{14}H_9O_2N$: C, 75.32; H, 4.06; N, 6.28%; mol. wt., 223.

The Phosphorylated Intermediate of 4, 4'-Diamino-biphenyl-3, 3'-dicarboxylic Acid (BDC) with Phenyl Diisocyanate in PPA.—A 2.72 g. portion of purified BDC (0.01 mol.) and a 1.60 g. portion of phenyl diisocyanate (0.01 mol.) were dissolved in a 86 g. portion of PPA with vigorous mechanical stirring; the polymerization vessel was then heated at 90—100°C for 1 hr. After the completion of the reaction, the resulting polymer solution was poured into 300 g. of ice water and the precipitated polymer was filtered. It was washed several times with 50 ml. each of distilled water, and dried under a vacuum at 60°C. The phosphoric-carbonic anhydride of polyurea acid was obtained in 92% yield. The m. p. was above 350°C; the inherent viscosity measured in a 0.5% concentration at 25°C in concentrated sulfuric acid was found to be $\eta_{inh}=1.01$.

Found: C, 45.11; H, 2.82; N, 9.45; P*, 10.86. Calcd. for $(C_{22}H_{16}O_{12}N_4P_2)_n$: C, 44.79; H, 2.74; N, 9.50; P, 10.50%.

The Preparation of 2-Methyl-4*H*-3, 1-benzoxazin-4-one (IX).—A mixture of 2.74 g. (0.01 mol.) of anthranilic acid and 60 ml. of acetic anhydride was heated at 120°C under reflux for 5 hr. The solvent was then removed under reduced pressure, and the residue was recrystallized from petroleum ether to obtain colorless needles, m. p. 86—88°C (lit.[9] 80—81°C), in a 90% yield (3.45 g.).

The infrared spectrum (KBr) shows absorption band at 1757 cm^{-1} (carbonyl), 1647 (>C=N-), 1268 cm^{-1}, and 1054 cm^{-1} (=C-O-C).

The ultraviolet spectrum exhibits absorption maxima at λ_{max} 249 mμ (ε, 7160), 306 mμ (ε, 2900), and 315 mμ (ε, 2660).

Found: C, 67.15; H, 4.45; N, 8.70; mol. wt., 168. Calcd. for $C_9H_7O_2N$: C, 67.07; H, 4.38; N, 8.09%; mol. wt., 168.

The Reaction of *N*-Methylanthranilic Acid with Phenyl Isocyanate A).—A 3.02 g. (0.02 mol.) portion of *N*-methyl anthranilic acid (m. p. 186—187°C, recrystallized from aqueous ethanol) was dissolved into 100 ml. of benzene at 60°C for 20 min. To this solution there was they added a 2.38 g. (0.02 mol.) portion of phenyl isocyanate (b. p. 46—47°C/7 mmHg) in 10 ml. of benzene, and the mixture was refluxed at 80°C for 2.5 hr. After the mixture had been allowed to cool at room temperature, the precipitate was filtered, washed several times with distilled water, and dried. It was then recrystallized twice from ethyl acetate to obtain colorless needles in a 43% yield. M. p. 252—253°C. It was identified as *N*-methyl-2-(phenylcarbamoyl)carbanilide by a study of its infrared spectrum and by elemental analysis.

The infrared spectrum (KBr) shows absrotpion bands at 3300 cm^{-1} (N-H), and 1650 cm^{-1} (amide carbonyl). Ultraviolet spectrum: λ_{max} 210 mμ (ε, 29200), 257 mμ (ε, 33600).

Found: C, 73.49; H, 5.71; N, 12.60. Calcd. for $C_{21}H_{19}O_2N_3$: C, 73.02; H, 5.55; N, 12.17%.

The filtrate of the benzene solution was refluxed further at 80°C for 5 hr., and the benzene was removed under a vacuum to afford a cyclized reaction product. After recrystallization from a chloroform/cyclohexene (1 : 1) solution, colorless needles were obtained in 41% yield. M. p. 164—166°C. The product was found to be 1-methylisatoic anhydride by elemental analysis and by a study of its infrared spectrum. The infrared spectrum (KBr) shows absorption bands at 1770 cm^{-1} (carbonyl), 1720 cm^{-1} (carbonyl) and 1605 cm^{-1}.

The ultraviolet spectrum has bands at λ_{max} 223 mμ (ε, 49400), 248 mμ (ε, 17800), 252 mμ (ε, 17900), and 315 mμ (ε, 2730).

Found: C, 61.44; H, 4.40; N, 8.10; mol. wt., 177.

* The phosphorus was determined by colorimetry analysis with ammonium metavanadate and ammonium molybdate, and by emission X-ray analysis.

Calcd. for $C_9H_7O_3N$: C, 61.01; H. 3.98; N, 7.91%; mol. wt., 181.

B)—The reaction was carried out in tetrahydrofuran instead of benzene at −2°C for 1 hr., at 10°C for 1 hr., and at 20°C for 1 hr. successively. The solvent was then removed under a vacuum at 60°C, and the residue was extracted with 200 ml. of a 10% aqueous sodium carbonate solution. The product was precipitated by acidifying the solution with 12% hydrochloric acid. When the product was recrystallized from a chloroform/cyclohexane (1:1) solution, colorless needles were obtained in a 59.5% yield. M. p. 231—322°C. It was identified as 1-methyl-3-phenyl-2, 4(1*H*, 3*H*)-quinazolinedione (lit.[18] 229—230°C).

The infrared spectrum (KBr) shows characteristic carbonyl absorption bands of quinazoline-dione at 1706 cm^{-1}, 1680 cm^{-1}, 1658 cm^{-1} and 1610 cm^{-1}. The ultraviolet spectrum has absorption maxima at λ_{max} 245 mμ (ε, 5540) and 270 mμ (ε, 756).

Found: C, 71.08; H, 4.87; N, 10.80. Calcd. for $C_{15}H_{12}O_2N_2$: C, 71.41; H, 4.80; N, 11.11%.

The neutral fraction of the tetrahydrofuran solution was extracted with benzene, and a crystalline solid was obtained in a 14.5% yield; this was indentified as *N*-phenyl-2-(phenylcarbamoyl)carbanilide (m. p. 252—253°C) by a comparison of its infrared spectrum with that of an authentic sample and it was found to have no melting point depression on admixture.

The Attempted Cyclization of *N*-Phenyl-2-(phenylcarbamoyl)carbanilide with Polyphosphoric Acid.—A 1.0 g. portion of *N*-phenyl-2-(phenylcarbamoyl)carbanilide was added to 60 g. of polyphosphoric acid, and the mixture was heated at 140—150°C for 5 hr. After the reaction, the mixture was poured into 100 ml. of distilled water, washed with 50 ml. of 5% aqueous sodium carbonate, and filtered. The starting material was thus recovered almost quantitatively, m. p. 249—250°C.

Found: C, 73.44; H, 5.15; N, 12.50. Calcd. for $C_{21}H_{19}O_2N_3$: C, 73.02; H, 5.55; N, 12.17%.

The authors gratefully acknowledge the interest and encouragement of Drs. Toshio Hoshino and Ryoji Nakanishi of the Basic Research Laboratories, Toyo Rayon Company, Ltd. The authors are also indebted to Mr. Yasuyuki Ebata and his staff for their microanalyses, and Mr. Toshio Mizushima for his emission X-ray analysis.

18) C. M. Lee, *J. Heterocyclic Chem.*, **1**, 235 (1965).

BULLETIN OF THE CHEMICAL SOCIETY OF JAPAN VOL. 39 1948—1951 (1966)

The Synthesis of 5- and 6-Aminoazulene Derivatives from 5- and 6-Acetylazulene Derivatives

By Tetsuo Nozoe and Kahei Takase

Department of Chemistry, Faculty of Science, Tohoku University, Katahira-cho, Sendai

and Masao Tada

The Research Institute for Tuberculosis, Leprosy and Cancer, Tohoku University, Kitayoban-cho, Sendai

(Received November 19, 1965)

The Schmidt reactions on diethyl 5-acetyl-2-aminoazulene-1, 3-dicarboxylate and diethyl 6-acetyl-2-aminoazulene-1, 3-dicarboxylate afforded diethyl 2, 5-diaminoazulene-1, 3-dicarboxylate (I) and diethyl 2, 6-diaminoazulene-1, 3-dicarboxylate respectively. A preferential formation of the 5-acetamido-2-amino compound upon the mild acetylation of I, which contrasted with the preferential diazotization of the 2-amino group, was observed.

In a previous paper,[1] it was reported that 5- and 6-aminoazulene derivatives were synthesized by the reaction of 5-acetamidotropolone derivatives and ethyl cyanoacetate. 6-Aminoazulene derivatives were also synthesized from 6-bromoazulene derivatives by nucleophilic displacement with ammonia or amines.[2,3] In the present paper, the authors will described a third route of synthesizing aminoazulene derivatives, in which the aminoazulenes are synthesized from 5- and 6-acetylazulene derivatives[4] by the Schmidt reaction.

The treatment of diethyl 5-acetyl-2-aminoazulene-1, 3-dicarboxylate (I)[4] or its ethylene ketal (II)[4] with sodium azide in concentrated sulfuric acid gave two compounds, III and IV. One of these, III, was identical with the diethyl 5-acetamido-2-aminoazulene-1, 3-dicarboxylate which had already been obtained.[1] The other one, IV, was confirmed

1) T. Nozoe, K. Takase and M. Tada, This Bulletin, **36**, 1006 (1963).
2) T. Nozoe, K. Takase and M. Tada, ibid., **38**, 247 (1965).
3) M. Tada, ibid., **39**, 1954 (1966).
4) T. Nozoe, K. Takase and M. Tada, ibid., **36**, 1010 (1963).

to be diethyl 2, 5-diaminoazulene-1, 3-dicarboxylate from the facts that the acetylation of IV gave III and the mild alkaline hydrolysis of III gave IV. The further acetylation of III afforded a diacetamido compound V.

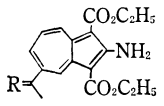

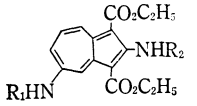

I: R=O

II: R=

III: R_1=$COCH_3$; R_2=H

IV: R_1=R_2=H

V: R_1=R_2=$COCH_3$

The same treatment of diethyl 5-acetylazulene-1, 3-dicarboxylate (VI)[4] with sodium azide and concentrated sulfuric acid afforded diethyl 5-aminoazulene-1, 3-dicarboxylate (VII). The acetylation of VII gave an acetamido compound VIII, which was also derived from III by deamination with isoamyl nitrite and sulfuric acid. When treated with isoamyl nitrite and sulfuric acid, the diamino compound IV gave the amino compound VII, in which the amino group at Position 2 was only deaminated. This fact shows that the basicity of the 2-amino group of IV is greater than that of the 5-amino group. The ultraviolet absorption spectra of the compounds, IV, V, VII and VIII, are shown in Fig. 1.

In an attempt to synthesize 2, 5-diaminoazulene

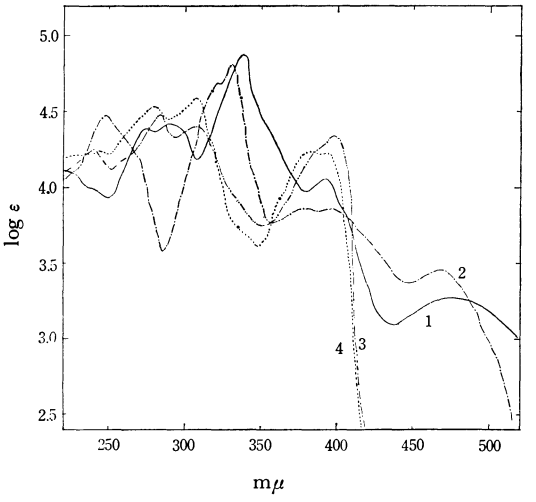

Fig. 1. Ultraviolet absorption spectra in methanol.

1. Diethyl 2, 5-diaminoazulene-1, 3-dicarboxylate (IV)
2. Diethyl 2, 5-diacetamidoazulene-1, 3-dicarboxylate (V)
3. Diethyl 5-aminoazulene-1, 3-dicarboxylate (VII)
4. Diethyl 5-acetamidoazulene-1, 3-dicarboxylate (VIII)

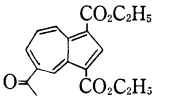

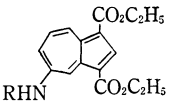

VI

VII: R=H

VIII: R=$COCH_3$

(IX), the corresponding dicarboxylic acid X obtained by the alkaline hydrolysis of III or IV was submitted to thermal decarboxylation, thus forming a dark tarry material from which none of the desired product was isolated.

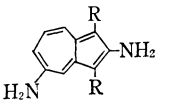

IX: R=H

X: R=COOH

The preferential formation of 5-acetamido-2-amino compound III on the mild acetylation of 2, 5-diamino compound IV, which contrasts with the preferential diazotization of the 2-amino group, can be explained by the operation of a steric hindrance caused by the presence of the two ethoxycarbonyl groups adjacent to the 2-amino group. Similar phenomena are also observed in the case of diethyl 2, 6 - diaminoazulene - 1, 3 - dicarboxylate (XI).[1] The Schmidt reactions on diethyl 6-acetyl-2-aminoazulene-1, 3-dicarboxylate (XII)[4] and its ethylene ketal (XIII)[4] afforded 2, 6-diaminoazulene derivative (XI). The reaction of diethyl 6-acetylazulene-1, 3-dicarboxylate (XIV)[4] gave both the 6-amino compound (XV) and the 6-acetamido compound (XVI).[1]

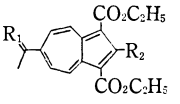

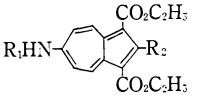

XII: R_1=O; R_2=NH_2

XIII: R_1= 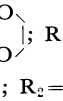 ; R_2=NH_2

XIV: R_1=O; R_2=H

XI: R_1=H; R_2=NH_2

XV: R_1=R_2=H

XVI: R_1=$COCH_3$; R_2=H

Experimental[5]

The Schmidt Reaction of Diethyl 5-Acetyl-2-aminoazulene-1, 3-dicarboxylate (I). — Into a solution of I (1.0 g.) in concentrated sulfuric acid (4 ml.), sodium azide (240 mg.) was added in small portions with stirring at room temperature. After having been stirred for 2 hr., the mixture was diluted with water (30 ml.), made slightly alkaline with 2 N sodium hydroxide, and allowed to stand in a cold place. The solid

5) All melting points are uncorrected. Shoulders in the UV spectral data are designated by "sh."

(600 mg.) which precipitated out was collected by filtration, washed with water, and recrystallized from ethanol to give yellow needles (300 mg.; m. p. 184—185°C), which showed no depression of melting point on admixture with diethyl 5-acetamido-2-aminoazulene-1, 3-dicarboxylate (III).[1)]

The residue obtained by the evaporation of the filtrate was dissolved in benzene, and the benzene solution was passed through a column of alumina. The column was eluted with benzene. The crude crystals (50 mg.) obtained from the effluent, were recrystallized from ethanol to give diethyl 2, 5-diaminoazulene-1, 3-dicarboxylate (IV) (40 mg.; m. p. 145—146.5°C) as dull orange micro-prisms.

Found: N, 9.32. Calcd. for $C_{16}H_{18}O_4N_2$: N, 9.27%.

λ_{max}^{MeOH} mμ (log ε): 220.5 (4.11), 235 (3.99) sh, 289 (4.43), 335 (4.88), 389 (4.07), 476 (3.28).

IR (Nujol): 3535, 3365, 3255, 1667, 1626 cm^{-1}.

The Dipicrate of IV.—Dark yellowish green micro-prisms (from ethanol); m. p. 147—148°C.

Found: C, 44.47; H, 3.17; N, 14.69. Calcd. for $C_{16}H_{18}O_4N_2$-$C_{12}H_6O_{14}N_6$: C, 44.22; H, 3.18; N, 14.74%.

When it was refluxed in acetic anhydride for 30 min., IV was acetylated to give III. This III (100 mg.) was then heated under reflux with potassium hydroxide (100 mg.) in 80% aqueous ethanol (5 ml.) for 3 hr.; by this procedure IV (20 mg.) was obtained.

The Schmidt Reaction of Diethyl 2-Amino-5-(1, 1-ethylenedioxyethyl)azulene-1, 3-dicarboxylate (II).—Into a solution of II (100 mg.) in concentrated sulfuric acid (1 ml.), sodium azide (25 mg.) was added in small portions with stirring at room temperature; the reaction mixture was then treated as in the above-mentioned method to give both III (35 mg.) and IV (4 mg.).

Diethyl 2, 5-Diacetamidoazulene-1, 3-dicarboxylate (V).—A solution of III (30 mg.) in acetic anhydride (1 ml.) was refluxed for 1 hr. The residue obtained by the evaporation of the solvent was recrystallized from aqueous ethanol to give V (20 mg.; m. p. 132—133°C) as brown micro-needles.

Found: C, 62.20; H, 5.71; N, 7.31. Calcd. for $C_{20}H_{20}O_6N_2$: C, 62.16; H, 5.74; N, 7.25%.

λ_{max}^{MeOH} mμ (log ε): 247.5 (4.47), 319 (4.70), 329 (4.82), 378 (3.86), 394 (3.86), 465 (3.46).

IR (Nujol): 3470, 3345, 1712, 1704, 1672 cm^{-1}.

By the same treatment, IV was acetylated to give V.

Diethyl 5-Aminoazulene-1, 3-dicarboxylate (VII).—*a) From Diethyl 5-Acetamido-2-aminoazulene-1, 3-dicarboxylate (III).*—A solution of III (200 mg.) in dioxane (12 ml.) and concentrated sulfuric acid (0.8 ml.) was warmed on a water bath for 10 min. and chilled. Into the solution, a solution of sodium nitrite (100 mg.) in water (4 ml.) was added with stirring without cooling. After the mixture had been stirred for 3 hr., a solution of sodium hypophosphite (1.6 g.) in water (10 ml.) was added. The mixture was stirred for a further 2 hr. and then allowed to stand overnight at room temperature. The reaction mixture was diluted with water and extracted with benzene. The extract was washed with water, dried over anhydrous sodium sulfate, and passed through a column of alumina. The column was eluted with benzene. From the effluent, the crude crystals (30 mg.) were obtained. Recrystallization from ethanol afforded VII (m. p. 157—158°C) as purple scales.

Found: C, 66.66; H, 5.69; N, 4.78. Calcd. for $C_{16}H_{17}O_4N$: C, 66.88; H, 5.96; N, 4.88%.

λ_{max}^{MeOH} mμ (log ε): 240 (4.24), 282 (4.47), 305 (4.40), 395 (4.32), 565 (3.20).

IR (Nujol): 3390, 3320, 3215, 1684, 1647 cm^{-1}.

b) From Diethyl 2, 5-Diaminoazulene-1, 3-dicarboxylate (IV).—To the diazotized solution of IV (200 mg.) with sodium nitrite (100 mg.), sodium hypophosphite (1.6 g.) was added, and the reaction mixture was treated as in a); VII (45 mg.) was thus obtained.

c) From Diethyl 5-Acetylazulene-1, 3-dicarboxylate (VI).—Into a mixture of VI (150 mg.) in chloroform (3 ml.) and concentrated sulfuric acid (2 ml.), sodium azide (70 mg.) was stirred in small portions without cooling. After the mixture had been stirred for 20 min., the acid layer was diluted with water and extracted with benzene. The extract was then washed with water, dried over anhydrous sodium sulfate, and passed through a column of alumina. The crystals obtained from the effluent were recrystallized from ethanol to give VII (8 mg.).

Diethyl 5-Acetamidoazulene-1, 3-dicarboxylate (VIII).—*a) From Diethyl 5-Acetamido-2-aminoazulene-1, 3-dicarboxylate (III).*—Into a solution of III (200 mg.) in dioxane (12 ml.) and concentrated sulfuric acid (1.2 ml.), a solution of sodium nitrite (100 mg.) in water (4 ml.) was gradually dropped with stirring under ice-water cooling. After the mixture had been stirred for 40 min. at room temperature, a solution of sodium hypophosphite (1.6 g.) in water (10 ml.) was added. The mixture was treated as in the case of VII-a) and gave reddish violet crystals (30 mg.). Recrystallization from a mixture of benzene and cyclohexane afforded VIII (20 mg.; m. p. 191—192°C) as pale purple scales.

Found: C, 65.58; H, 5.79; N, 4.30. Calcd. for $C_{18}H_{19}O_5N$: C, 65.64; H, 5.82; N, 4.25%.

λ_{max}^{MeOH} mμ (log ε): 235 (4.22) sh, 242 (4.23), 277 (4.53), 306 (4.59), 380 (4.24), 391 (4.23), 522 (2.96).

IR (Nujol): 3185, 1686, 1639 cm^{-1}.

b) From Diethyl 5-Aminoazulene-1, 3-dicarboxylate (VII).—A solution of VII (20 mg.) in acetic anhydride was warmed on a water bath for 5 min. The residue produced by the evaporation of the solvent was then recrystallized from aqueous methanol to give VIII (15 mg.).

2, 5-Diaminoazulene-1, 3-dicarboxylic Acid (X).—To a solution of III (200 mg.) in ethanol (6 ml.), a 10% potassium hydroxide aqueous solution (2 ml.) was added. The mixture was refluxed for 4 hr., concentrated to 2/3 volume under reduced pressure, diluted with water (20 ml.), and extracted with ethyl acetate. The extract was washed with water and dried over anhydrous sodium sulfate. The brownish black residue (45 mg.) obtained by the evaporation of the solvent was recrystallized from a mixture of benzene and cyclohexane to give X (30 mg.; m. p. above 285°C) as fine black crystals.

Found: N, 11.07. Calcd. for $C_{12}H_{10}O_4N_2$: N, 11.38%.

IR (Nujol): 3470, 3355, 3225, 1650, 1621 cm^{-1}.

IV was hydrolyzed to give X by the same treatment.

Diethyl 2, 6-Diaminoazulene-1, 3-dicarboxylate (XI).—Into a solution of diethyl 6-acetyl-2-aminoazulene-1, 3-dicarboxylate (XII) (1.0 g.) in concentrated sulfuric acid (4 ml.), sodium azide (240 mg.) was added in small portions with stirring without cooling; the reaction mixture was then treated as in the case of I to give the crude crystals (400 mg.). Recrystallization from benzene gave dull brown plates (290 mg.; m. p. 207—208°C), which showed no depression of melting point on admixture with XI[1]; the infrared spectrum was identical with that of XI.

XI (30 mg.) was also derived from diethyl 2-amino-6-(1, 1-ethylenedioxyethyl)azulene-1, 3-dicarboxylate (XIII) (100 mg.) by the same treatment.

The Schmidt Reaction of Diethyl 6-Acetylazulene-1, 3-dicarboxylate (XIV).—Into a mixture of XIV (70 mg.) in chloroform (3 ml.) and concentrated sulfuric acid (1.5 ml.), sodium azide (30 mg.) was added in small portions with stirring without cooling. After the mixture has been stirred for 30 min., the acid layer was diluted with ice-water and extracted with ethyl acetate. The extract was washed with water, dried over anhydrous sodium sulfate, and passed through a column of alumina. The column was eluted with ethyl acetate, and from the first effluent, XIV (3 mg.) was recovered. Orange leaflets (15 mg.; m. p. 220—221°C) from the second and orange scales (20 mg.; m. p. 235—236°C) from the third were obtained. The former showed no depression of melting point on admixture with diethyl 6-acetamidoazulene-1, 3-dicarboxylate (XVI),[1] and the latter showed no depression of melting point on admixture with diethyl 6-aminoazulene-1, 3-dicarboxylate (XV).[1]

Expenses for the present series of experiments were defrayed by grants-in-aid for Scientific Research from the Ministry of Education and from the Up. John Co., Ltd. The infrared spectra in this paper were measured by using a infrared spectrophotometer purchased by a grant-in-aid for Scientific Research from the Toyo Rayon Co., Ltd. The authors wish to express their deep gratitude for these contributions.

BULLETIN OF THE CHEMICAL SOCIETY OF JAPAN VOL. 39 1951—1953 (1966)

The Reaction of Methylchlorodisilanes with *t*-Butyl Hydroperoxide

By Kazuhisa KAWAZUMI and Bunjiro MURAI

Department of Material Technology and Technical Services, Central Research Laboratory
Tokyo Shibaura Electric Co., Ltd., Toshiba-cho, Kawasaki

(Received November 20, 1965)

The authors wished to get two new organosilyl peroxides with a silicon-silicon linkage, *t*-butylperoxypentamethyldisilane [$(CH_3)_3SiSi(CH_3)_2(OOC(CH_3)_3)$] and 1, 2-di-*t*-butylperoxytetramethyldisilane [$((CH_3)_3COO)(CH_3)_2SiSi(CH_3)_2(OOC(CH_3)_3)$], by the reaction of the corresponding chlorodisilanes with *t*-butyl hydroperoxide. The reaction, however, did not give the desired product; rather, it led to the formation of *t*-butoxypentamethyldisiloxane [$(CH_3)_3SiOSi(CH_3)_2(OC(CH_3)_3)$] and 1-*t*-butoxy-3-*t*-butylperoxytetramethyldisiloxane [$((CH_3)_3CO)(CH_3)_2SiOSi(CH_3)_2(OOC(CH_3)_3)$] respectively, substances which are believed to have resulted from the intramolecular rearrangement of the desired peroxydisilanes.

Chlorosilanes react readily with alkyl hydroperoxides to form fairly stable alkylperoxysilanes with the Si–O–O–C group. The literature on organosilicon compounds contains no example of a disilane with peroxy substituents. The present investigation was undertaken to prepare two derivatives of this class of compounds, *t*-butylperoxypentamethyldisilane (I) and 1, 2-di-*t*-butylperoxytetramethyldisilane (II), by treating the corresponding chlorodisilanes[1] with *t*-butyl hydroperoxide in the presence of pyridine:

$$Me_3SiSiMe_2Cl + HOOCMe_3 \xrightarrow{C_5H_5N} Me_3SiSiMe_2(OOCMe_3)$$
(I)

$$ClMe_2SiSiMe_2Cl + 2\,HOOCMe_3 \xrightarrow{C_5H_5N} (Me_3COO)Me_2SiSiMe_2(OOCMe_3)$$
(II)

However, these products were not obtained. The reaction between *t*-butyl hydroperoxide and pentamethylchlorodisilane gave a non-peroxidic compound, *t*-butoxypentamethyldisiloxane (III), the formation of which may well be ascribed to the intramolecular rearrangement of the unstable peroxide intermediate. Proof for the structure of

1) M. Kumada, M. Yamaguchi, Y. Yamamoto, J. Nakajima and K. Shiina, *J. Org. Chem.*, **21**, 1264 (1956).

III was afforded by its unambiguous synthesis from pentamethylchlorodisiloxane and *t*-butyl alcohol:

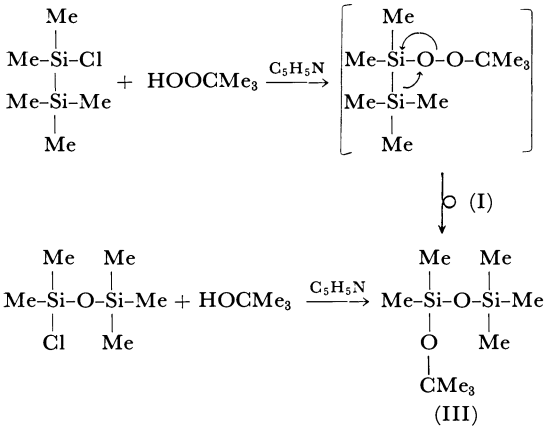

Similarly, from the reaction between 1, 2-dichlorotetramethyldisilane and *t*-butyl hydroperoxide, 1-*t*-butoxy-3-*t*-butylperoxytetramethyldisiloxane (IV) was obtained instead of the corresponding peroxidic compound (II). Apparently, the reaction proceeded as follows:

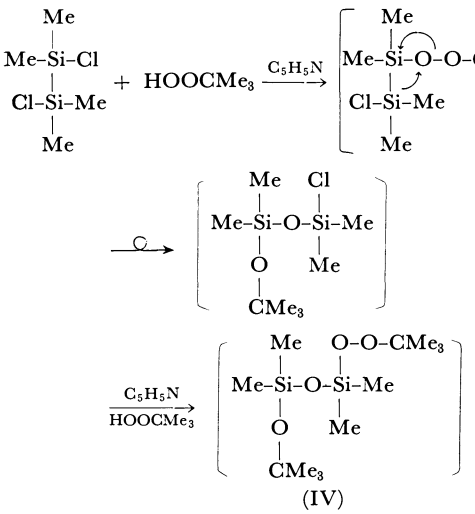

These results indicate that both silyl groups, Me_3Si and $ClMe_2Si$, have much greater migratory aptitudes than the methyl group, as was observed previously by Kumada and his collaborators[2] in the case of the intramolecular rearrangement of chloromethyldisilanes with anhydrous aluminum chloride:

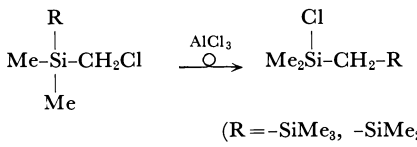

Intramolecular rearrangements of organosilyl peroxides have been reported by Buncel and Davies.[3] They observed the rearrangement only when they attempted to prepare acylperoxysilanes from the reaction between peroxybenzoic acid and trimethylchlorosilane or dimethylphenylchlorosilane:

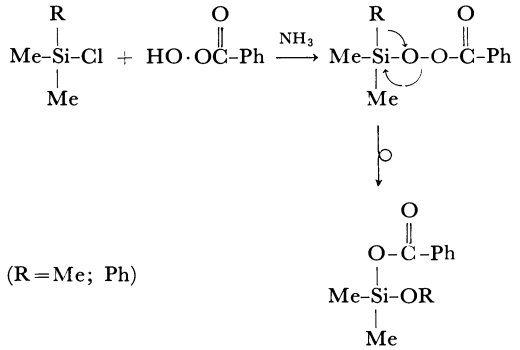

Similar nucleophilic 1, 2-rearrangements have been reported with other organometallic and organometalloidal compounds.[4,5]

Experimental

Starting Materials.—*Pentamethylchlorodisilane and 1, 2-Dichlorotetramethyldisilane.*—These were obtained by the method reported in detail by Kumada and his collaborators.[1]

t-Butyl Hydroperoxide.—The authors used *t*-butyl hydroperoxide-90, produced by Wallace & Tiernan, Inc., the purity of which is 90%.

Pentamethylchlorodisiloxane.—This was prepared from 1, 3-dichlorotetramethyldisiloxane ($ClMe_2SiOSiMe_2Cl$)[6,7] by methylation with the Grignard reagent.

The Reaction between Pentamethylchlorodisilane and *t*-Butyl Hydroperoxide.—A 500-ml. four-necked flask was fitted with an air-tight stirrer, a thermometer, a dropping-funnel and a reflux condenser with a calcium chloride tube. In the flask these were then placed 27 g. (0.27 mol.) of *t*-butyl hydroperoxide, 20 g. (0.253 mol.) of pyridine, and 200 ml. of petroleum ether. Into this mixture, a mixture of 41.7 g. (0.25 mol.) of pentamethylchlorodisilane and 50 ml. of petroleum ether was stirred over a 75-minute period. At once pyridine hydrochloride was precipitated. During the addition, the mixture was cooled with an ice-bath below 10°C. After the addition, the mixture was stirred over 5 hr. at room temperature. When the mixture was filtered, the organic layer was obtained. The ether was removed, and the residual oil was then distilled under reduced pressure to give 39 g. of a liquid boiling over the range from

2) M. Kumada, J. Nakajima, M. Ishikawa and Y. Yamamoto, *J. Org. Chem.*, **23**, 292 (1958).

3) E. Buncel and A. G. Davies, *Chem. & Ind.*, **1957**, 492.

4) A. G. Davies and J. E. Packer, *J. Chem. Soc.*, **1959**, 3164.

5) H. Hock and F. Ernst, *Chem. Ber.*, **92**, 2716 (1959).

6) W. I. Patnode and O. F. Wilcock, *J. Am. Chem. Soc.*, **68**, 358 (1946).

7) G. Greber and L. Metzinger, *Makromol. Chem.*, **39**, 167 (1960).

62°C/71 mmHg to 95°C/40 mmHg. The distillate was fractionally distilled through a 1.5×40 cm. Fenske column to give 22.1 g. of a colorless liquid (A), b. p. 55°C/18.5 mmHg. The yield was estimated to be 70—80% by gas chromatography. The physical properties and analytical data for this product A are listed in Table I.

Table I. Physical properties and analytical data for A and B

	Found A	Found B	Calcd. for I	Calcd. for III
b. p.	55°C/ 18.5 mmHg	155°C		
n_D^{20}	1.3910	1.3916		
d_4^{20}	0.8255	0.8233		
M. R.	63.5	63.7	68.0	63.6
M. W.	213.0	221.1	220.5	220.5
Active oxygen (%)	0.3		7.25	0
Analyses C	48.82	48.78	49.02	49.02
H	10.74	10.81	10.97	10.97
Si	25.5	25.0	25.47	25.47

t-Butoxypentamethyldisiloxane (III).—In a three-necked flask equipped with a stirrer, a dropping funnel and an efficient reflux condenser with a calcium chloride tube, 14.8 g. (0.2 mol.) of *t*-butyl alcohol was added to a mixture of 30 g. (0.164 mol.) of pentamethylchlorodisiloxane (Found: Cl, 19.3. Calcd. for $C_5H_{15}OSi_2$·Cl: 19.0%), 15.6 g. (0.197 mol.) of pyridine, and 200 ml. of dry ether. During the reaction, the mixture was cooled with an ice-bath below 10°C. After the addition of the *t*-butyl alchol, the reaction mixture was refluxed over a period of one hour with stirring. The pyridine hydrochloride was then removed by filtration. The evaporation of ether from the filtrate, followed by fractional distillation, gave 13.9 g. of a liquid, b. p. 47—49°C/14.5 mmHg. Redistillation under ordinary pressure gave a colorless liquid (B), b. p. 155°C. The physical properties and analytical data for this product B also are shown in Table I.

The Reaction between 1, 2-Dichlorotetramethyldisilane and *t*-Butyl Hydroperoxide.—This reaction was carried out in essentially the manner described above, except that 28.1 g. (0.15 mol.) of 1, 2-dichlorotetramethyldisilane was added to a mixture of 32.4 g. (0.324 mol.) of *t*-butyl hydroperoxide, 24 g. (0.3 mol.) of pyridine in 300 ml. of dry petroleum ether. We thus obtained 11.9 g. of a colorless liquid (C), b. p. 89—89.5°C/13 mmHg; its physical properties and analytical data are listed in Table II.

Table II. Physical properties and analytical data for C

	Found C	Calcd. for II	Calcd. for IV
b. p.	89—89.5°C/13 mmHg		
n_D^{20}	1.4016		
d_4^{20}	0.8889		
M. R.	80.6	84.9	80.5
M. W.	302.8	294.6	294.6
Active oxygen (%)	5.44	10.86	5.43
Analyses C	48.73	48.91	48.91
H	10.00	10.26	10.26
Si	18.9	19.07	19.07

Results and Discussion

From the two reactions of *t*-butyl hydroperoxide with pentamethylchlorodisilane and with 1, 2-dichlorotetramethyldisilane, two new compounds, III and IV, were isolated, but no organosilyl peroxide that contains both silicon-silicon and one or two peroxy groups was obtained.

Evidence for this conclusion was afforded by determinations of the active oxygen contents, the molecular refractions, and the retention times by means of gas chromatography and a study of the infrared spectra. The infrared spectrum of A agreed with that of B in all ranges. The retention time of A in the gas chromatogram agreed with that of B. The other physical properties (cf. Tables I and II) also supported these results.

Summary

Pentamethylchlorodisilane and 1, 2-dichlorotetramethyldisilane easily react with *t*-butyl hydroperoxide; they give not the corresponding peroxides with the silicon-silicon linkage, but *t*-butoxypentamethyldisiloxane and 1-*t*-butoxy-3-*t*-butylperoxytetramethyldisiloxane respectively. The formation of these two products through the intramolecular rearrangement of the unstable peroxy intermediates has been discussed.

The authors wish to express their hearty thanks to Professor Makoto Kumada and Dr. Mitsuo Ishikawa of Kyoto University for their valuable advice and discussions throughout this work.

BULLETIN OF THE CHEMICAL SOCIETY OF JAPAN VOL. 39 1954—1961 (1966)

The Anionoid Substitution Reaction of Diethyl 2-Acetamido-6-bromoazulene-1, 3-dicarboxylate

By Masao TADA

The Research Institute for Tuberculosis, Leprosy and Cancer, Tohoku University, Kitayoban-cho, Sendai

(Received November 24, 1965)

The bromine atom in diethyl 2-acetamido-6-bromoazulene-1, 3-dicarboxylate (I) is as reactive toward the anionoid reagents as in diethyl 6-bromoazulene-1, 3-dicarboxylate. Twenty-seven 6-substituted azulene derivatives have been synthesized from I by the nucleophilic substitution reaction. On one of them, diethyl 2-acetamido-6-diethylaminoazulene-1, 3-dicarboxylate, the removal of the 2-acetamido group has been carried out, giving diethyl 6-diethylaminoazulene-1, 3-dicarboxylate.

In a previous paper[1] dealing with anionoid substitution reactions on diethyl 6-bromoazulene-1, 3-dicarboxylate (I), it was shown that the bromine atom of I was easily displaced with various anionoid reagents, such as amines, alkoxide and mercaptide. In more recent work,[2] it was found that the bromine atom of diethyl 2-amino-6-bromoazulene-1, 3-dicarboxylate (II)[3,4a,b] was also displaced with alkoxide or mercaptide, but this reaction required much more severe conditions than those with I, and II did not react with amines. Such differences between the reactivities of I and II toward anionoid reagents may be attributed to the existence or nonexistence of the electron-releasing amino group which enhances the electron density at Position 6. The author's interest in the activity of the bromine atom in I and II has led to the suggestion that the bromine atom of diethyl 2-acetamido-6-bromoazulene-1, 3-dicarboxylate (III) will be reactive toward the anionoid reagents. The present paper will deal with reactions of III with various anionoid reagents.

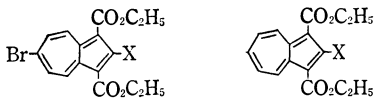

I: X=H
II: X=NH_2
III: X=$NHCOCH_3$
VII: X=$N(COCH_3)_2$

IV: X=NH_2
V: X=$NHCOCH_3$
VI: X=$N(COCH_3)_2$

It has been reported that the acetylation of diethyl 2-aminoazulene-1, 3-dicarboxylate (IV) was not achieved by heating IV in acetic anhydride for 3 hr.[4a] However, the heating of IV in acetic anhydride for 7—10 hr. gave a monoacetyl derivative V and a diacetyl derivative VI. When it was treated with acetic anhydride under the same conditions, the amino compound II gave a mixture of a monoacetyl derivative III and a diacetyl derivative (VII). The further acetylation of III afforded VII, while the alkaline or the acidic hydrolysis of VII gave a mixture of III and II. The relation among IV, V and VI was similar to that among 6-bromoazulene derivatives, II, III and VII. The ultraviolet spectra of these acetates are shown in Fig. 1.

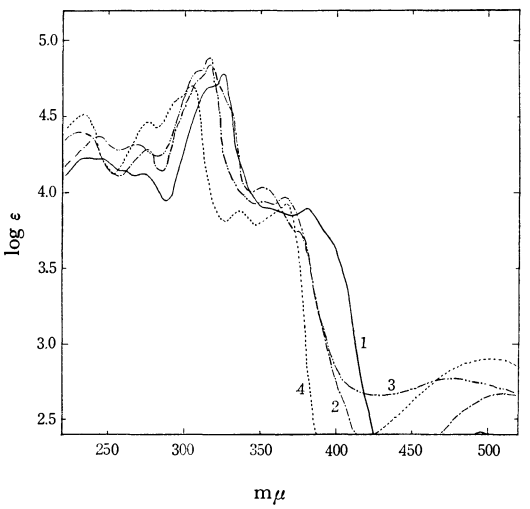

Fig. 1. Ultraviolet absorption spectra in methanol.
1. Diethyl 2-acetamido-6-bromoazulene-1, 3-dicarboxylate (III)
2. Diethyl 2-diacetylamino-6-bromoazulene-1, 3-dicarboxylate (VII)
3. Diethyl 2-acetamidoazulene-1, 3-dicarboxylate (V)
4. Diethyl 2-diacetylaminoazulene-1, 3-dicarboxylate (VI)

1) T. Nozoe, K. Takase and M. Tada, This Bulletin, **38**, 247 (1965).
2) T. Nozoe et al., unpublished data.
3) T. Nozoe, *Croat. Chem. Acta*, **29**, 20 (1957); T. Nozoe and S. Ito, *Chem. org. Naturstoffe*, **19**, 33 (1961).
4) a) T. Nozoe, S. Matsumura, Y. Murase and S. Seto, *Chem. & Ind.*, **1955**, 1257; T. Nozoe, S. Seto, S. Matsumura and Y. Murase, This Bulletin, **35**, 1179 (1962). b) T. Nozoe, S. Seto and S. Matsumura, ibid., **35**, 1990 (1962).

The treatment of III with aqueous ethanolic alkali afforded II and a hydroxyazulene derivative VIII, which in turn gave an acetoxy derivative ($\nu_{C=O}$ 1770 cm^{-1}) when heated with acetic anhydride. The treatment of III with ammonia or sodium azide (in the presence of dimethyl sulfoxide)[5] afforded diethyl 2-acetamido-6-aminoazulene-1, 3-dicarboxylate (IX). The alkaline hydrolysis of IX yielded diethyl 2, 6-diaminoazulene-1, 3-dicarboxylate (X), which had also been derived from diethyl 6-acetamido-2-aminoazulene-1, 3-dicarboxylate (XI).[6] The reaction of III

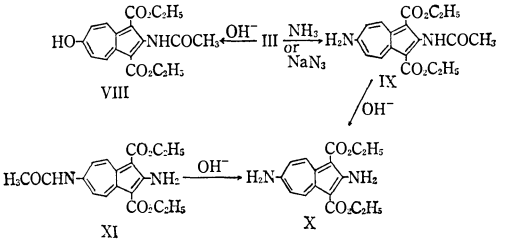

with sodium ethoxide in ethanol afforded diethyl 2-acetamido-6-ethoxyazulene-1,3-dicarboxylate (XII), and the treatment of III in ethanol with an aqueous solution of sodium hydrosulfide afforded the 6-mercapto derivative (XIII). The ultraviolet spectra of these derivatives are shown in Fig. 2.

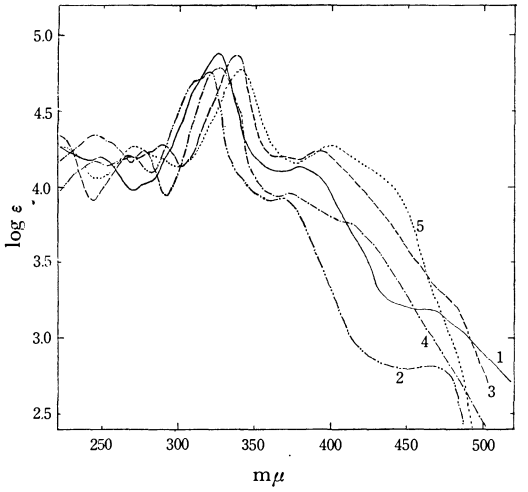

Fig. 2. Ultraviolet absorption spectra in methanol.

1. Diethyl 2-acetamido-6-hydroxyazulene-1,3-dicarboxylate (VIII)
2. Acetate of VIII
3. Diethyl 2-acetamido-6-aminoazulene-1,3-dicarboxylate (IX)
4. Diethyl 2-acetamido-6-ethoxyazulene-1,3-dicarboxylate (XII)
5. Diethyl 2-acetamido-6-hydrazinoazulene-1,3-dicarboxylate (XIV)

The reaction of III with hydrazine, phenylhydrazine, dimethylamine, diethylamine, 2-phenylethylamine, 2-hydroxyethylamine, di(2-hydroxyethyl)amine, 2-cyanoethylamine, di(2-cyanoethyl)amine, allylamine, diallylamine, ethyleneimine, pyrrolidine, piperidine, morpholine, 3-methoxypropylamine, 3-morpholinopropylamine, aniline, 2-aminopyridine, 3-methyl-2-aminopyridine, 4-aminopyridine, 2-aminoquinoline and 4-aminoantipyrine afforded, respectively, diethyl 2-acetamido-6-hydrazino- (XIV), -6-phenylhydrazino- (XV), -6-dimethylamino- (XVI), -6-diethylamino- (XVII), -6-(2-phenylethylamino)- (XVIII), -6-(2-hydroxyethylamino)- (XIX), -6-di(2-hydroxyethyl)-amino- (XX), -6-(2-cyanoethylamino)- (XXI), -6-di(2-cyanoethyl)amino- (XXII), -6-allylamino- (XXIII), -6-diallylamino- (XXIV), -6-ethyleneimino- (XXV), -6-pyrrolidino- (XXVI), -6-piperidino- (XXVII), -6-morpholino- (XXVIII),

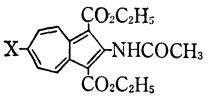

XII: X = OC_2H_5
XIII: X = SH
XIV: X = $NHNH_2$
XV: X = $NHNHC_6H_5$
XVI: X = $N(CH_3)_2$
XVII: X = $N(C_2H_5)_2$
XVIII: X = $NHC_2H_4C_6H_5$
XIX: X = NHC_2H_4OH
XX: X = $N(C_2H_4OH)_2$
XXI: X = NHC_2H_4CN
XXII: X = $N(C_2H_4CN)_2$
XXIII: X = $NHCH_2CHCH_2$
XXIV: X = $N(CH_2CHCH_2)_2$
XXV: X =
XXVI: X =
XXVII: X =
XXVIII: X =
XXIX: X = $NHC_3H_6OCH_3$
XXX: X = NHC_3H_6-
XXXI: X = NHC_6H_5
XXXII: X =
XXXIII: X =
XXXIV: X =
XXXV: X =
XXXVI: X =

5) K. Hafner, H. Patzelt and H. Kaiser, *Ann.*, **656**, 24 (1962).
6) T. Nozoe, K. Takase and M. Tada, This Bulletin, **36**, 1006 (1963).

-6-(3-methoxypropylamino)- (XXIX), -6-(3-morpholinopropylamino)- (XXX), -6-anilino- (XXXI), -6-(2-pyridylamino)- (XXXII), -6-(3-methylpyridin-2-yl)amino- (XXXIII), -6-(4-pyridylamino)- (XXXIV), -6-(2-quinolylamino)- (XXXV), and -6-(4-antipyrinylamino)azulene-1, 3-dicarboxylate (XXXVI).

It was mentioned in the previous report[1] that the reaction of 2-acetamido-6-bromoazulene (XXXVII)[4b] with amines did not afford any 6-aminoazulene derivatives. Therefore, it can be understood that the activity of the bromo group at Position 6 of III is enhanced by the presence of two ethoxycarbonyl groups at Positions 1 and 3, by which III is invested with reactivity towards anionoid reagents, thus giving some 6-substituted azulene derivatives.

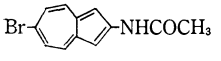

XXXVII

The acidic or the alkaline hydrolysis of XVII, XIX, XX, XXIV and XXVIII afforded 2-amino compounds XXXVIII, XXXIX, XL, XLI and XLII respectively; these deacetylations were more difficult than the deacetylation of the 6-acetamido-2-aminoazulene derivative XI.[6] The substituents were removed in XVII and XXXVIII; the diazotization reaction of XXXVIII was realized by sodium nitrite and an excess of sulfuric acid, while the decomposition of the diazonium salt formed was achieved on letting it stand in the presence of sodium hypophosphite. The reaction carried out in

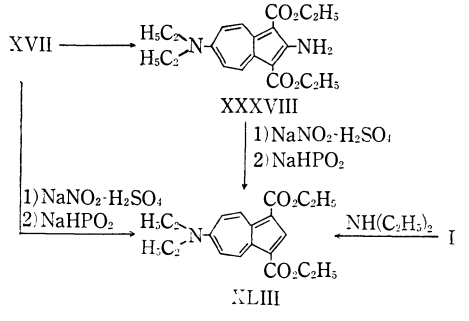

dioxane gave diethyl 6-diethylaminoazulene-1, 3-dicarboxylate (XLIII), which had also been derived from I.[1] An acetamido group in XVII, upon being hydrolyzed with the sulfuric acid, XLIII, was directly obtained from XVII. An attempt to derive 2-amino-6-diethylaminoazulene did not succeed. The ultraviolet spectra of XVII and XXXVIII are shown in Fig. 3.

Some compounds of these anionoid reaction products have been investigated in terms of the growth-inhibitory activity in relation to Crocker Sarcoma 180 and Bashford Carcinoma 63.[7]

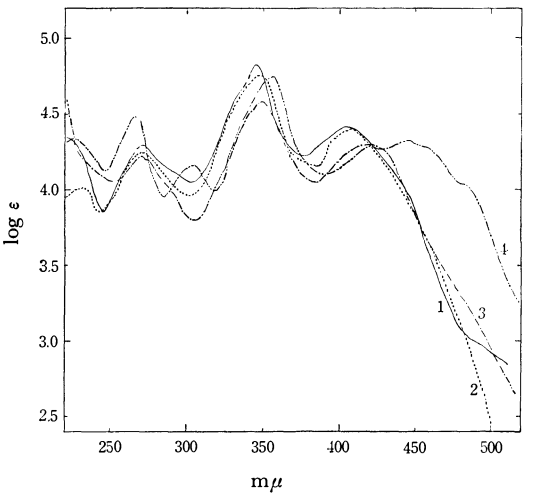

Fig. 3. Ultraviolet absorption spectra in methanol.

1. Diethyl 2-acetamido-6-diethylaminoazulene-1,3-dicarboxylate (XVII)
2. Diethyl 2-acetamido-6-morpholinoazulene-1,3-dicarboxylate (XXVIII)
3. Diethyl 2-acetamido-6-anilinoazulene-1,3-dicarboxylate (XXXI)
4. Diethyl 2-amino-6-diethylaminoazulene-1,3-dicarboxylate (XXXVIII)

Experimental[8]

The Reaction of Diethyl 2-Amino-6-bromoazulene-1, 3-dicarboxylate (II) and Acetic Anhydride.—A solution of II (5.0 g.) in acetic anhydride (8 ml.) was refluxed for 8 hr., and the residue produced by the evaporation of the excess of acetic anhydride under reduced pressure was dissolved in hot ethanol (60 ml.). The insoluble compound was recrystallized from ethyl acetate to give diethyl 2-acetamido-6-bromoazulene-1, 3-dicarboxylate (III) (m. p. 212—213°C; 4.0 g.) as pale red needles.

Found: C, 53.09; H, 4.37; N, 3.42. Calcd. for $C_{15}H_{18}O_5NBr$: C, 52.95; H, 4.44; N, 3.43%.

λ_{max}^{MeOH} mμ (log ε): 234 (4.23), 245 (4.22)sh, 272 (4.13), 314 (4.69)sh, 324 (4.78), 360 (3.87)sh, 379 (3.89), 496 (2.39).

IR (Nujol): 3270, 1718, 1658 cm^{-1}.

From the ethanol solution, brilliant red needles were obtained; these were recrystallized from ethanol to afford diethyl 2-diacetylamino-6-bromoazulene-1, 3-dicarboxylate (VII) (m. p. 141—142°C; 0.5 g.).

Found: C, 53.34; H, 4.42; N, 3.10. Calcd. for $C_{20}H_{20}O_6NBr$: C, 53.34; H, 4.48; N, 3.11%.

λ_{max}^{MeOH} mμ (log ε): 233 (4.39), 274 (4.28), 316 (4.83), 350 (4.03), 373 (3.75), 509 (2.69).

IR (Nujol): 1704, 1686 cm^{-1}.

Refluxing II (5.0 g.) in acetic anhydride for 12 hr. gave III (0.6 g.) and VII (4.1 g.), while refluxing III (50 mg.) in acetic anhydride for 1.5 hr. afforded VII (45 mg.).

The Hydrolysis of III.—a) A mixture of III (50

7) H. Endo and M. Tada, *Sci. Rep. Res. Inst. Tohoku Univ.(C)*, **11**, 377 (1964).

8) All melting points are uncorrected. Shoulders in the UV spectral data are designated by "sh."

mg.) in ethanol (8 ml.) and 6 N sulfuric acid (2 ml.) was refluxed for 1.5 hr. After the mixture had been cooled, the crystals precipitated gave II (20 mg.).

b) A mixture of III (100 mg.) in ethanol (6 ml.) and a 10% potassium hydroxide alcohol solution (6 ml.) was stirred for 2 hr. at room temperature; by this procedure II (20 mg.) was obtained.

The Hydrolysis of VII.—a) A mixture of VII (150 mg.) in ethanol (5 ml.) and 6 N sulfuric acid (1.5 ml.) was refluxed for 30 min. After it had cooled, III (130 mg.) precipitated out.

b) To a suspension of VII (1.0 g.) in ethanol (30 ml.) concentrated ammonia water (10 ml.) was added, and the mixture was warmed on a water bath for 5 min. At once III (850 mg.) was precipitated.

c) A mixture of VII (50 mg.) in ethanol (5 ml.) and 6 N sulfuric acid (3 ml.) was refluxed for 2 hr.; by this procedure II (15 mg.) was obtained.

Diethyl 2-Acetamidoazulene-1, 3-dicarboxylate (V).—A solution of IV (0.6 g.) in acetic anhydride (2 ml.) was refluxed for 7 hr., and the residue produced by the evaporation of the solvent was dissolved in benzene. The solution was then passed through a column of alumina and eluted with benzene. From the effluent, IV (50 mg.) was recovered; when the column was then further eluted with ethyl acetate, crude crystals were obtained. Recrystallization from methanol afforded V (m. p. 141—142°C; 0.4 g.) as red prisms.

Found: C, 65.94; H, 5.69; N, 4.28. Calcd. for $C_{18}H_{19}O_5N$: C, 65.64; H, 5.82; N, 4.25%.

λ_{max}^{MeOH} mμ (log ε): 243 (4.37), 268 (4.32), 306 (4.80)sh, 315 (4.88), 351 (3.95), 366 (3.98), 480 (2.77).

IR (Nujol): 3330, 1706, 1664 cm^{-1}.

Diethyl 2-Diacetylaminoazulene-1, 3-dicarboxylate (VI).—A solution of IV (0.6 g.) in acetic anhydride (3 ml.) was refluxed for 10 hr. The residue produced by the evaporation of the solvent was recrystallized from methanol to give VI (550 mg.; m. p. 138—138.5°C) as red needles.

Found: C, 64.85; H, 5.70; N, 3.63. Calcd. for $C_{20}H_{21}O_6N$: C, 64.68; H, 5.70; N, 3.77%.

λ_{max}^{MeOH} mμ (log ε): 234 (4.51), 275 (4.46), 304 (4.70), 337 (3.87), 366 (3.92), 505 (2.93).

IR (Nujol): 1727, 1689 cm^{-1}.

Diethyl 2-Acetamido-6-hydroxyazulene-1, 3-dicarboxylate (VIII).—A solution of III (0.2 g.) in ethanol (30 ml.) was added to a 10% potassium hydroxide aqueous solution (5 ml.), and the mixture was stirred for 1 hr. at room temperature. After the mixture had been allowed to stand overnight, the II (20 mg.) which precipitated was filtered off. The filtrate was diluted with water (20 ml.) and acidified with 6 N sulfuric acid. The crystals which separated were recrystallized from aqueous ethanol to give VIII (m. p. 217—218°C (decomp.); 0.1 g.) as dull yellow crystals.

Found: N, 4.14. Calcd. for $C_{18}H_{19}O_6N$: N, 4.06%.

λ_{max}^{MeOH} mμ (log ε); 234 (4.51), 275 (4.46), 304 (4.70), 337 (3.87), 366 (3.92), 505 (2.93).

IR (Nujol): 3410, 3155, 1706, 1647 cm^{-1}.

The Acetate of VIII: Obtained as reddish brown crystals by refluxing VIII in acetic anhydride for 15 min. (from aqueous ethanol); m. p. 137—138°C.

Found: N, 3.89. Calcd. for $C_{20}H_{21}O_7N$: N, 3.62%.

λ_{max}^{MeOH} mμ (log ε): 244 (4.18), 268 (4.20), 312 (4.72)sh, 318 (4.77), 368 (3.94), 465 (2.85).

IR (Nujol): 3270, 1770, 1715, 1664 cm^{-1}.

Diethyl 2-Acetamido-6-aminoazulene-1, 3-dicarboxylate (IX).—*a) From Liquid Ammonia.*—III (500 mg.) was added to an excess of liquid ammonia. After the mixture had stood for one week at room temperature, the residue obtained by the evaporation of the ammonia was dissolved in ethyl acetate. The solution was then passed through a column of alumina and eluted with ethyl acetate. From the first effluent, II (30 mg.) was obtained. From the second effluent, yellow crystals (310 mg.) were obtained; these were recrystallized from ethanol to give IX (m. p. 225—225.5°C) as yellow scales.

Found: C, 62.82; H, 5.54; N, 8.07. Calcd. for $C_{18}H_{20}O_5N_2$: C, 62.78; H, 5.85; N, 8.14%.

λ_{max}^{MeOH} mμ (log ε): 267 (4.20), 288 (4.27), 337 (4.85), 393 (4.23).

IR (Nujol): 3410, 3360, 3270, 1672, 1647 cm^{-1}.

The Picrate of IX: M. p. 155°C (decomp.); dull brown micro-prisms (from ethanol).

Found: N, 11.95. Calcd. for $C_{24}H_{23}O_{12}N_5$: N, 12.21%.

b) From Sodium Azide.—III (300 mg.) and sodium azide (1.0 g.) were added to dimethyl sulfoxide (10 ml.). The mixture was then heated on a water bath for 15 hr. After dilution with water (250 ml.), it was extracted with ethyl acetate. The extract was washed with 2 N acetic acid and water, and dried over anhydrous sodium sulfate. The extract was then passed through a column of alumina and eluted with ethyl acetate. From the effluent, IX (100 mg.) was obtained.

Diethyl 2, 6-Diaminoazulene-1, 3-dicarboxylate (X).—A mixture of IX (25 mg.) in ethanol (6 ml.) and 6 N sulfuric acid (1.5 ml.) was refluxed for 40 min., and the mixture was concentrated to half volume under reduced pressure. After the addition of water (6 ml.), the solution was neutralized with sodium hydrogen carbonate and the crystals thereby formed were recrystallized from benzene to give dull brown plates (m. p. 206—207°C; 10 mg.), which showed no depression of melting point on admixture with an authentic specimen[6] of X and which were identified with X by a comparison of their infrared spectra.

Diethyl 2-Acetamido-6-ethoxyazulene-1, 3-dicarboxylate (XII).—To a solution prepared from metallic sodium (20 mg.) and absolute ethanol (6 ml.), finely powdered III (200 mg.) was added. The mixture was then stirred for 5 hr. at room temperature. After it had stood overnight, it was diluted with water and the crystals thereby formed were recrystallized from aqueous ethanol to give XII (m. p. 116—117°C; 150 mg.) as yellow needles.

Found: C, 64.70; H, 6.58; N, 3.71. Calcd. for $C_{20}H_{23}O_6N$: C, 64.33; H, 6.21; N, 3.75%.

λ_{max}^{MeOH} mμ (log ε): 245 (4.34), 278 (4.24), 327 (4.79), 372 (3.97), 408 (3.77)sh.

IR (KBr): 3530, 3380, 1718, 1701, 1681, 1667 cm^{-1}.

Diethyl 2-Acetamido-6-mercaptoazulene-1, 3-dicarboxylate (XIII).—Into a suspension of III (50 mg.) in ethanol (10 ml.), a 27% sodium hydrosulfide aqueous solution (3 ml.) was added. The mixture was then stirred for 3 hr. at room temperature. After it had stood overnight, this mixture was diluted with water (40 ml.) and acidified with 6 N sulfuric acid. The

acidic solution was extracted with ethyl acetate. The extract was washed with water and dried over anhydrous sodium sulfate. The residue obtained by the evaporation of the solvent was recrystallized from benzene to yield XIII (m. p. 220—221°C; 20 mg.) as red micro-prisms.

Found: C, 61.05; H, 4.96; N, 3.68. Calcd. for $C_{18}H_{19}O_5NS$: C, 59.82; H, 5.30; N, 3.88%.

IR (Nujol): 3400, 3280, 1709, 1684, 1650 cm^{-1}.

Diethyl 2-Acetamido-6-hydrazinoazulene-1, 3-dicarboxylate (XIV).—Eighty per cent hydrazine hydrate (5 ml.) was added to a suspension of II (100 mg.) in methanol (10 ml.), and the mixture was stirred for 3 hr. at room temperature. After it had stood overnight, the reaction mixture was concentrated to half volume and added with water. The crystals thereby formed were recrystallized from ethanol to afford XIV (m. p. 203—204°C (decomp.); 60 mg.) as yellow micro-needles.

Found: C, 60.16; H, 5.63; N, 11.48. Calcd. for $C_{18}H_{21}O_5N_3$: C, 60.16; H, 5.89; N, 11.69%.

λ_{max}^{MeOH} mμ (log ε): 222 (4.27), 271 (4.26), 288 (4.19)sh, 341 (4.77), 399 (4.26).

IR (Nujol): 3340, 3320, 1667, 1645 cm^{-1}.

The Acetate of XIV: M. p. 234.5—235°C, pale brown micro-needles (from ethanol).

Found: N, 10.58. Calcd. for $C_{20}H_{23}O_6N_3$: N, 10.47%.

Diethyl 2-Acetamido-6-phenylhydrazinoazulene-1, 3-dicarboxylate (XV).—Into a solution of phenylhydrazine (3 ml.) in ethanol (10 ml.), III (300 mg.) was added. The mixture was then refluxed for 1 hr. and concentrated to 1/4 volume. After the addition of water (50 ml.) and 2 N acetic acid (5 ml.), the crystals thereby formed were recrystallized from ethanol to give XV (m. p. 218—219°C; 190 mg.) as brownish yellow micro-prisms.

Found: C, 66.00; H, 5.71; N, 9.54. Calcd. for $C_{24}H_{25}O_5N_3$: C, 66.19; H, 5.79; N, 9.65%.

λ_{max}^{MeOH} mμ (log ε): 270 (4.21)sh, 285 (4.22), 342 (4.75), 402 (4.31).

IR (KBr): 3380, 3330, 3290, 1701, 1647 cm^{-1}.

Diethyl 2-Acetamido-6-dimethylaminoazulene-1, 3-dicarboxylate (XVI).—To a mixture of a 40% dimethylamine aqueous solution (10 ml.) in methanol (20 ml.), III (500 mg.) was added, and the mixture was refluxed for 30 min. After the addition of water (40 ml.), the crystals thereby separated were recrystallized from methanol to give XVI (m. p. 179—180°C; 300 mg.) as yellow silky needles.

Found: C, 64.77; H, 6.19; N, 7.42. Calcd. for $C_{20}H_{24}O_5N_2$: C, 64.50; H, 6.50; N, 7.52%.

λ_{max}^{MeOH} mμ (log ε): 223 (4.27), 270 (4.28), 344 (4.82), 402 (4.37).

IR (Nujol): 3260, 1695, 1637 cm^{-1}.

Diethyl 2-Acetamido-6-diethylaminoazulene-1, 3-dicarboxylate (XVII).—III (500 mg.) was added to a mixture of diethylamine (5 ml.) and ethanol (6 ml.), and the mixture was refluxed for 1 hr. After the addition of water (30 ml.), the crystals which separated were recrystallized from ethanol to give XVII (m. p. 165—166°C; 320 mg.) as yellow micro-prisms.

Found: N, 6.85. Calcd. for $C_{22}H_{28}O_5N_2$: N, 7.00%.

λ_{max}^{MeOH} mμ (log ε): 271 (4.28), 290 (4.11)sh, 345.5 (4.82), 403 (4.41).

IR (Nujol): 3260, 1701, 1669, 1642 cm^{-1}.

Diethyl 2-Acetamido-6-(2-phenylethylamino)-azulene-1, 3-dicarboxylate (XVIII).—To a mixture of β-phenylethylamine (300 mg.) in ethanol (20 ml.), III (300 mg.) was added. The mixture was refluxed for 1 hr. and then concentrated to 1/3 volume. After the addition of water (30 ml.) and 2 N hydrochloric acid (3 ml.), the crystals thereby formed were recrystallized from aqueous ethanol to afford XVIII (m. p. 163—164°C; 210 mg.) as yellow leaflets.

Found: C, 69.39; H, 6.33; N, 5.95. Calcd. for $C_{26}H_{28}O_5N_2$: C, 69.62; H, 6.29; N, 6.25%.

λ_{max}^{MeOH} mμ (log ε): 270 (4.22), 290 (4.15), 343 (4.83), 399 (4.32).

IR (KBr): 3340, 3300, 1701, 1684, 1650 cm^{-1}.

Diethyl 2-Acetamido-6-(2-hydroxyethylamino)-azulene-1, 3-dicarboxylate (XIX).—III (80 mg.) was added to a solution of ethanolamine (2 ml.) in ethanol (5 ml.). The mixture was then refluxed for 30 min. and concentrated to 1/3 volume. After the addition of water (20 ml.), the crystals thereby obtained were recrystallized from aqueous ethanol to afford XIX (m. p. 207—208°C; 45 mg.) as yellow needles.

Found: N, 7.01. Calcd. for $C_{20}H_{24}O_6N_2$: N, 7.21%.

λ_{max}^{MeOH} mμ (log ε): 220 (3.99), 269 (4.17), 290 (4.13), 342 (4.78), 399 (4.27).

IR (Nujol): 3330, 3270, 1695, 1664 cm^{-1}.

Diethyl 2-Acetamido-6-[di(2-hydroxyethyl)-amino]azulene-1, 3-dicarboxylate (XX).—III (0.8 g.) was added to a solution of diethanolamine (5 ml.) in ethanol (10 ml.). The mixture was then refluxed for 1 hr. and concentrated to half volume. After the addition of water, the crystals which separated were recrystallized from aqueous methanol to XX (m. p. 210—211°C; 500 mg.) in the form of brownish yellow needles.

Found: C, 60.98; H, 6.49; N, 6.97. Calcd. for $C_{22}H_{28}O_7N_2$: C, 61.10; H, 6.53; N, 6.48%.

λ_{max}^{MeOH} mμ (log ε): 225 (3.97), 270 (4.25), 347 (4.77), 404 (4.38).

IR (Nujol): 3300, 1704, 1658 cm^{-1}.

Diethyl 2-Acetamido-6-(2-cyanoethylamino)-azulene-1, 3-dicarboxylate (XXI). — III (200 mg.) was added to a mixture of β-aminopropionitrile (2 ml.) and triethylamine (2 ml.) in ethanol (15 ml.). The mixture was then refluxed for 2 hr. and concentrated to 1/4 volume. After the addition of water, the reaction solution was neutralized with 2 N hydrochloric acid. The crystals thereby formed were recrystallized from aqueous ethanol to afford XXI (m. p. 105—106°C; 110 mg.) as yellowish orange leaflets.

Found: N, 10.39. Calcd. for $C_{21}H_{23}O_5N_3$: N, 10.58%.

λ_{max}^{MeOH} mμ (log ε): 268 (4.20), 289 (4.13), 342 (4.74), 398 (4.24).

IR (KBr): 3530, 3410, 3280, 2257, 1695, 1661 cm^{-1}.

Diethyl 2-Acetamido-6-[di(2-cyanoethyl)amino]-azulene-1, 3-dicarboxylate (XXII).—III (300 mg.) was added to a mixture of 3, 3′-iminodipropionitrile (3 ml.) and triethylamine (3 ml.) in ethanol (10 ml.). The mixture was then refluxed for 2.5 hr. and concentrated to 1/4 volume. After the addition of water (50 ml.),

the reaction mixture was extracted with benzene, and the extract was washed with 2 N hydrochloric acid and water. After being dried over anhydrous sodium sulfate, the benzene extract was passed through a column of alumina and eluted with benzene. From the effluent, III (80 mg.) was recovered; the column was then further eluted with a mixture of benzene and ethyl acetate. From the effluent, dull orange crystals were obtained; these were recrystallized from aqueous ethanol to give XXII (m. p. 136—138°C; 135 mg.) as brownish yellow micro-prisms.

Found: N, 12.60. Calcd. for $C_{24}H_{26}O_5N_4$: N, 12.44%.

λ_{max}^{MeOH} mμ (log ε): 270 (4.25), 288 (4.16)sh, 341 (4.83), 400 (4.32).

IR (KBr): 3510, 3360, 2247, 1689, 1656 cm^{-1}.

Diethyl 2-Acetamido-6-allylaminoazulene-1, 3-dicarboxylate (XXIII).—A mixture of III (200 mg.) and allylamine (2 ml.) in ethanol (10 ml.) was treated as in the case of XVII; by this procedure XXIII (m. p. 144—145°C; 110 mg.) was obtained as orangish yellow prisms (from ethanol).

Found: C, 65.47; H, 6.44; N, 7.19. Calcd. for $C_{21}H_{24}O_5N_2$: C, 65.61; H, 6.29; N, 7.29%.

λ_{max}^{MeOH} mμ (log ε): 270 (4.23), 289 (4.17), 342 (4.80), 399 (4.29).

IR (KBr): 3360, 1706, 1689 cm^{-1}.

Diethyl 2-Acetamido-6-diallylaminoazulene-1, 3-dicarboxylate (XXIV).—A mixture of III (200 mg.) and diallylamine (3 ml.) in ethanol (10 ml.) was treated as in the case of XVI; by this procedure XXIV (m. p. 158—159°C; 120 mg.) was obtained as orange needles (from methanol).

Found: N, 6.77. Calcd. for $C_{24}H_{28}O_5N_2$: N, 6.60%.

λ_{max}^{MeOH} mμ (log ε): 234 (3.99)sh, 248 (4.15), 257 (4.15), 275 (4.11), 324 (4.68), 342 (4.55), 389 (4.25).

IR (Nujol): 3250, 1721, 1701, 1678 cm^{-1}.

Diethyl 2-Acetamido-6-ethyleneiminoazulene-1, 3-dicarboxylate (XXV).—A mixture of III (60 mg.) and ethyleneimine (4 ml.) in methanol (4 ml.) was refluxed for 10 min. After the addition of water (40 ml.), the crystals thereby formed were recrystallized from methanol to give XXV (m. p. 164.5—165.5°C; 20 mg.) as orange micro-prisms.

Found: C, 64.68; H, 5.95; N, 7.43. Calcd. for $C_{20}H_{22}O_5N_2$: C, 64.85; H, 5.99; N, 7.56%.

λ_{max}^{MeOH} mμ (log ε): 238 (3.95), 268 (4.10), 334 (4.77), 367 (4.13)sh, 399 (4.21), 445 (3.17)sh.

IR (Nujol): 3175, 1701, 1692, 1642 cm^{-1}.

Diethyl 2-Acetamido-6-pyrrolidinoazulene-1, 3-dicarboxylate (XXVI).—A mixture of III (200 mg.) and pyrrolidine (2 ml.) in ethanol (10 ml.) was treated as in the case of XVIII to form XXVI (m. p. 182—183°C (decomp.); 100 mg.) as brilliant yellow micro-scales (from aqueous ethanol).

Found: C, 66.19; H, 6.72; N, 6.70. Calcd. for $C_{22}H_{26}O_5N_2$: C, 66.31; H, 6.58; N, 7.03%.

λ_{max}^{MeOH} mμ (log ε): 272 (4.26), 292 (4.10)sh, 347 (4.78), 402 (4.40).

IR (KBr): 3410, 1709, 1669 cm^{-1}.

Diethyl 2-Acetamido-6-piperidinoazulene-1, 3-dicarboxylate (XXVII).—A mixture of III (200 mg.) and piperidine (10 ml.) in methanol (20 ml.) was treated as in the case of XIV to form XXVII (m. p. 141—142°C; 130 mg.) as yellow needles (from ethanol).

Found: C, 66.85; H, 6.43; N, 6.82. Calcd. for $C_{23}H_{28}O_5N_2$: C, 66.97; H, 6.84; N, 6.79%.

λ_{max}^{MeOH} mμ (log ε): 270.5 (4.32), 274 (4.32), 347.5 (4.77), 410 (4.42).

IR (Nujol): 3250, 1706, 1639 cm^{-1}.

Diethyl 2-Acetamido-6-morpholinoazulene-1, 3-dicarboxylate (XXVIII).—A mixture of III (200 mg.) and morpholine (4 ml.) in ethanol (10 ml.) was treated as in the case of XVI, thus forming XXVIII (m. p. 205.5—206°C; 135 mg.) as yellow needles (from methanol).

Found: C, 63.65; H, 6.56; N, 6.60. Calcd. for $C_{22}H_{26}O_6N_2$: C, 63.75; H, 6.32; N, 6.76%.

λ_{max}^{MeOH} mμ (log ε): 233 (4.01), 271 (4.25), 347 (4.74), 409 (4.40).

IR (Nujol): 3280, 1718, 1701, 1647 cm^{-1}.

Diethyl 2-Acetamido-6-(3-methoxypropylamino)-azulene-1, 3-dicarboxylate (XXIX).—A mixture of III (200 mg.) and 3-aminopropyl methyl ether (2 ml.) in ethanol (10 ml.) was treated as in the case of XVIII to give XXIX (m. p. 157—158°C; 90 mg.) as brownish yellow prisms (from aqueous ethanol).

Found: C, 63.56; H, 6.73; N, 6.62. Calcd. for $C_{22}H_{28}O_6N_2$: C, 63.44; H, 6.78; N, 6.73%.

λ_{max}^{MeOH} mμ (log ε): 269 (4.25), 290 (4.28), 342 (4.81), 397 (4.32).

IR (KBr): 3290, 1706, 1678, 1647 cm^{-1}.

Diethyl 2-Acetamido-6-(3-morpholinopropylamino)azulene-1, 3-dicarboxylate (XXX).—A mixture of III (200 mg.) and 3-aminopropylmorpholine (2 ml.) in ethanol (12 ml.) was refluxed for 2 hr. and then concentrated to 1/4 volume under reduced pressure. After the addition of water, the solution was extracted with ethyl acetate. The extract was washed with 2 N acetic acid and water, and dried over anhydrous sodium sulfate. The residue obtained by the evaporation of the solvent was recrystallized from aqueous ethanol to afford XXX (m. p. 67—68°C; 60 mg.) as yellow micro-needles.

Found: N, 8.68. Calcd. for $C_{25}H_{33}O_6N_3$: N, 8.91%.

λ_{max}^{MeOH} mμ (log ε): 269 (4.10), 286 (4.03)sh, 343 (4.69), 399 (4.19).

IR (KBr): 3400, 3330, 1695, 1684, 1653 cm^{-1}.

Diethyl 2-Acetamido-6-anilinoazulene-1, 3-dicarboxylate (XXXI).—A mixture of III (500 mg.) and aniline (5 ml.) in ethanol (10 ml.) was treated as in the case of XXX to give XXXI (m. p. 233—234°C; 380 mg.) as yellow leaflets (from aqueous ethanol).

Found: C, 68.82; H, 5.84; N, 6.48. Calcd. for $C_{24}H_{24}O_5N_2$: C, 68.56; H, 5.75; N, 6.66%.

λ_{max}^{MeOH} mμ (log ε): 270 (4.21), 274 (4.20)sh, 348 (4.58), 417 (4.30).

IR (KBr): 3250, 3215, 1701, 1669, 1642 cm^{-1}.

Diethyl 2-Acetamido-6-(2-pyridylamino)azulene-1, 3-dicarboxylate (XXXII).—A mixture of III (200 mg.), 2-aminopyridine (1 g.), and triethylamine (2 ml.) in ethanol (10 ml.) was refluxed for 7 hr. and then concentrated to half volume. After the reaction mixture had been cooled, the III (80 mg.) which had precipitated was filtered off. The filtrate was acidified with 2 N hydrochloric acid and extracted with benzene. After being washed with water and dried over anhydrous sodium sulfate, the extract was passed through a column

of alumina and eluted with benzene. From the first effluent, III (30 mg.) was recovered, while from the second effluent, the crystals obtained were recrystallized from ethanol to give XXXII (m. p. 185—186°C; 15 mg.) as orange needles.

Found: 9.75. Calcd. for $C_{23}H_{23}O_5N_3$: N, 9.97%.

λ_{max}^{MeOH} mμ (log ε): 228 (4.27)sh, 271 (4.29), 303 (4.14)sh, 354 (4.69), 422 (4.57).

IR (KBr): 3360, 3230, 1701, 1669, 1647 cm^{-1}.

Diethyl 2-Acetamido-6-(3-methylpyridin-2-ylamino)azulene-1, 3-dicarboxylate (XXXIII). — A mixture of III (200 mg.), 2-amino-3-methylpyridine (2 ml.) and triethylamine (2 ml.) in ethanol (10 ml.) was treated as in the above experiment to form XXXIII (m. p. 110—112°C; 15 mg.) as yellow micro-prisms (from aqueous ethanol); III (20 mg.) was also recovered.

Found: N, 9.35. Calcd. for $C_{24}H_{25}O_5N_3$: N, 9.65%.

λ_{max}^{MeOH} mμ (log ε): 270 (4.23), 297 (4.16)sh, 344 (4.75), 400 (4.29).

IR (KBr): 3340, 3310, 1706, 1689, 1658, 1647 cm^{-1}.

Diethyl 2-Acetamido-6-(4-pyridylamino)azulene-1, 3-dicarboxylate (XXXIV).—A mixture of III (200 mg.), 4-aminopyridine (400 mg.) and triethylamine (2 ml.) in ethanol (10 ml.) was treated as in the case of XXXII to form XXXIV (m. p. 145—146°C; 35 mg.) as yellow needles (from ethanol); III (70 mg.) was also recovered.

Found: C, 65.56; H, 5.25; N, 9.69. Calcd. for $C_{23}H_{23}O_5N_3$: C, 65.54; H, 5.50; N, 9.97%.

λ_{max}^{MeOH} mμ (log ε): 232 (4.26), 278 (4.31), 324 (4.85), 369 (4.09), 439 (3.13).

IR (KBr): 3300, 1718, 1704, 1645 cm^{-1}.

Diethyl 2-Acetamido-6-(2-quinolylamino)-azulene-1, 3-dicarboxylate (XXXV). — A mixture of III (300 mg.), 2-aminoquinoline (300 mg.) and triethylamine (3 ml.) in ethanol (15 ml.) was treated as in the case of XXXII to form XXXV (m. p. 220—221°C; 20 mg.) as reddish yellow prisms (from ethanol); III (180 mg.) was also recovered.

Found: C, 68.53; H, 5.32; N, 8.66. Calcd. for $C_{27}H_{25}O_5N_3$: C, 68.78; H, 5.34; N, 8.91%.

λ_{max}^{MeOH} mμ (log ε): 230 (4.38)sh, 270 (4.33), 351 (4.66), 427 (4.51).

IR (KBr): 3340, 3280, 1695, 1664 cm^{-1}.

Diethyl 2-Acetamido-6-(4-antipyrinylamino)-azulene-1, 3-dicarboxylate (XXXVI).—A mixture of III (300 mg.), 4-aminoantipyrine (300 mg.) and triethylamine (3 ml.) in ethanol (15 ml.) was treated as in the case of XXXII to form XXXVI (m. p. 234—235°C; 80 mg.) as deep yellow micro-prisms (from ethanol).

Found: C, 65.55; H, 5.57; N, 10.38. Calcd. for $C_{29}H_{30}O_6N_4$: C, 65.65; H, 5.70; N, 10.56%.

λ_{max}^{MeOH} mμ (log ε): 277 (4.35), 282 (4.34)sh, 343 (4.69), 390 (4.36).

IR (KBr): 3230, 3165, 1709, 1689, 1672, 1661 cm^{-1}.

Diethyl 2-Amino-6-diethylaminoazulene-1, 3-dicarboxylate (XXXVIII).—A mixture of XVII (200 mg.) and 12 N sulfuric acid (1 ml.) in ethanol (5 ml.) was refluxed for 50 min. and then concentrated to half volume under reduced pressure. After the addition of water (40 ml.), the crystals thereby formed were dissolved in benzene. The benzene solution was passed through a column of alumina and eluted with benzene. From the effluent, crystals (80 mg.) were obtained; these crystals were recrystallized from ethanol to give XXXVIII (m. p. 153—154°C; 65 mg.) as brownish yellow prisms.

Found: C, 67.27; H, 7.00; N, 7.65. Calcd. for $C_{20}H_{26}O_4N_2$: C, 67.02; H, 7.31; N, 7.82%.

λ_{max}^{MeOH} mμ (log ε): 227 (4.33), 265.5 (4.49), 303 (4.16), 354.5 (4.74), 419 (4.28), 444 (4.32), 480 (4.05)sh.

IR (Nujol): 3530, 3370, 1715, 1678 cm^{-1}.

The Picrate of XXXVIII: M. p. 155—157°C, reddish brown prisms (from ethanol).

Found: C, 53.27; H, 4.56; N, 11.98. Calcd. for $C_{26}H_{29}O_{11}N_5$: C, 53.15; H, 4.98; N, 11.92%.

Diethyl 2-Amino-6-(2-hydroxyethylamino)azulene-1, 3-dicarboxylate (XXXIX). — A mixture of XIX (40 mg.) in ethanol (5 ml.) and 6 N sulfuric acid (1 ml.) was refluxed for 1 hr. After the addition of water, the crystals thereby precipitated were recrystallized from ethanol to yield XXXIX (m. p. 184—185°C; 15 mg.) as yellowish brown prisms.

Found: C, 62.17; H, 6.01; N, 7.84. Calcd. for $C_{18}H_{22}O_5N_2$: C, 62.41; H, 6.40; N, 8.09%.

λ_{max}^{MeOH} mμ (log ε): 252 (4.09), 297 (3.91)sh, 343 (4.76), 409 (4.24).

IR (Nujol): 3530, 3370, 3300, 1706, 1684, 1667, 1603 cm^{-1}.

Diethyl 2-Amino-6-[di(2-hydroxyethyl)amino]-azulene-1, 3-dicarboxylate (XL).—A 10% potassium hydroxide aqueous solution (1 ml.) was added to a solution of XX (100 mg.) in ethanol (5 ml.). The mixture was then refluxed for 10 min. and concentrated to half volume under reduced pressure. After the addition of water (30 ml.), the reaction solution was extracted with benzene. The benzene extract was washed with water and dried over anhydrous sodium sulfate. After the removal of the solvent, the crystals which remained were recrystallized from aqueous methanol to form XL (m. p. 146—147°C; 30 mg.) as orangish yellow prisms.

Found: N, 6.89. Calcd. for $C_{20}H_{26}O_6N_2$: N, 7.18%.

IR (Nujol): 3530, 3340, 1667, 1634 cm^{-1}.

Diethyl 2-Amino-6-diallylaminoazulene-1, 3-dicarboxylate (XLI).—A mixture of XXIV (150 mg.) in ethanol (6 ml.) and 6 N sulfuric acid (1 ml.) was treated as in the case of XXXVIII to give XLI (m. p. 123—124°C; 20 mg.) as brownish yellow micro-prisms (from a mixture of benzene and cyclohexane).

Found: N, 7.16. Calcd. for $C_{22}H_{26}O_4N_2$: N, 7.33%.

λ_{max}^{MeOH} mμ (log ε): 228 (4.31), 263 (4.47), 300 (4.13), 354 (4.72), 419 (4.22), 444 (4.24), 480 (3.98)sh.

IR (KBr): 3480, 3360, 1667, 1634 cm^{-1}.

Diethyl 2-Amino-6-morpholinoazulene-1, 3-dicarboxylate (XLII).—A solution of XXVIII (50 mg.) in ethanol (4 ml.) and 6 N sulfuric acid (1.5 ml.) was treated as in the case of XXXVIII to give XLII (m. p. 134—134.5°C; 10 mg.) as yellow needles (from methanol); then XXVIII (15 mg.) was also recovered.

Found: N, 7.13. Calcd. for $C_{20}H_{24}O_5N_2$: N, 7.52%.

λ_{max}^{MeOH} mμ (log ε): 260 (4.42), 293 (4.00), 349 (4.69), 428 (4.21), 480 (3.95)sh.

IR (Nujol): 3460, 3340, 1675, 1667, 1634 cm^{-1}.

The Picrate of XLII: M. p. 156—157°C, brownish black crystals (from ethanol).

Found: C, 52.12; H, 4.66; N, 11.50. Calcd. for $C_{26}H_{27}O_{12}N_5$: C, 51.91; H, 4.52; N, 11.64%.

Diethyl 6-Diethylaminoazulene-1, 3-dicarboxylate (XLIII).—*a) From XXXVIII.* — Into a solution of XXXVIII (180 mg.) and concentrated sulfuric acid (0.6 ml.) in dioxane (10 ml.), sodium nitrite (50 mg.) in water (2 ml.) was stirred at room temperature. After the mixture had been stirred for a further 30 min., sodium hypophosphite (1.5 g.) was added. The mixture was then stirred for a further 3 hr. and then allowed to stand overnight at room temperature. The reaction mixture was diluted with water and extracted with ethyl acetate. The extract was washed with water and dried over anhydrous sodium sulfate. It was then passed through a column of alumina and eluted with benzene. From the effluent, the crystals were obtained; they were then recrystallized from ethanol to give yellow needles (25 mg.), which showed no depression of melting point on admixture with an authentic specimen[1] of XLIII.

The water-layer was adjusted to a slightly alkaline state with a 10% potassium hydroxide aqueous solution and extracted with ethyl acetate. By the same purification, XLIII (5 mg.) was obtained.

b) From XVII.—A solution of XVII (200 mg.) and concentrated sulfuric acid (1 ml.) in dioxane (10 ml.) was warmed on a water bath for 15 min. and then treated as in a) to yield XLIII (35 mg.).

The author wishes to express his thanks to Professor Tetsuo Nozoe and Professor Kahei Takase, Faculty of Science, Tohoku University, for their kind guidance throughout the course of the present work. Thanks are also due to Professor Hideo Endo of the Institute for his interest and encouragement.

BULLETIN OF THE CHEMICAL SOCIETY OF JAPAN VOL. 39 1961—1967 (1966)

The Oxygen Exchange Reaction of Phenol in Acidic Media[1)]

By Shigeru OAE,† Reiko KIRITANI†† and Waichiro TAGAKI†

† *Department of Applied Chemistry, Faculty of Engineering, Osaka City University, Sumiyoshi-ku, Osaka*

†† *Department of Chemistry, Radiation Center of Osaka Prefecture, Sakai, Osaka*

(Received December 15, 1965)

The acid-catalyzed oxygen exchange reaction to a number of phenolic compounds that is, phenol, *o*- *m*- and *p*-hydroxy phenols, α- and β-naphthols, *o*- *m*- and *p*-nitrophenols, *o*- *m*- and *p*-aminophenols, *o*- and *p*-bromophenols, 2, 4, 6-tribromophenol, *o*- *m*- and *p*-cresols and 2, 4, 6-trimethylphenol, plus quinone for comparison with ^{18}O-enriched water was carried out under various conditions. A plot of the log k_x/k_h line against Hammett σ-constants in the substituted phenols gave a fairly good correlation line ($\rho=0.47$) except in the cases of *p*-bromophenol and *p*-aminophenol. The mechanism of these reactions has been discussed.

During the course of our study of the acid-catalyzed hydrolysis of phenyl benzenesulfonate with concentrated hydrochloric acid in ^{18}O-enriched water, we found that the phenol recovered was always incorporated with an excess of ^{18}O and that the amount of ^{18}O incorporation increased with prolonged heating.[2)] We have suggested that, in a strong acidic medium and at a high temperature, such as 180°C, phenol readily accepts a proton at either the *p*- or *o*- position to form a quasi-stable incipient carbonium ion intermediate (A) in which the original hydroxyl function acquires more of a carbonyl character, and hence the oxygen exchange is facilitated.

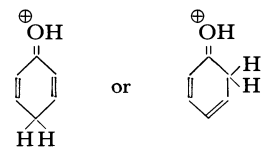

(A)

Gold and Satchell have proposed that phenolic compounds usually accept one proton at either the *o*- and *p*-position in a strong acidic medium to form the σ-complexes of the corresponding conjugate acids.[3)] Such a σ-complex has been shown by NMR and ultraviolet spectroscopic studies[4)] to exist in an appreciable concentration in the cases of phloroglucinol and its alkyl ethers. However,

1) The Reactions of Phenols and Phenolic Esters, Paper VII

2) a) S. Oae, T. Fukumoto and R. Kiritani, This Bulletin, **36**, 346 (1963); b) S. Oae and R. Kiritani, ibid., **37**, 770 (1964).

3) V. Gold and D. P. N. Satchell., *J. Chem. Soc.*, **1955**, 3619.

4) A. J. Kresge, G. W. Barry, K. R. Charles and Y. Chiany, *J. Am. Chem. Soc.*, **84**, 4343 (1962).

the ultraviolet spectra of phenol itself in concentrated sulfuric acid indicates that the major species is the oxygen-protonated phenol, while the so-called σ-complex is of only minor importance.[5]

Although the equilibrium concentration of such a σ-complex of phenol would be quite low around room temperature, it would definitely be increased at an elevated temperature. Moreover, even though its concentration would be low, the ring protonation is undoubtedly a very facile equilibrium reaction in view of the rapid hydrogen exchange reaction of phenol in strong acidic media; it would also be very important in the present oxygen exchange reaction. The ring protonation at the *o*- and *p*-positions to form the σ-complex causes the hydroxy group to acquire something of a carbonyl character, thus making the subsequent acid-catalyzed oxygen-isotopic exchange with ^{18}O-enriched water very facile. Incidentally, the carbonyl group of ketone or aldehyde is known to undergo very facile oxygen isotopic exchange with that of water in both acidic and alkaline media.[6] The overall picture of the reaction process is quite analogous to that of Bucherer-type reaction of naphthols. Naphthols, known to have something of a carbonyl character, undergo facile nucleophilic replacement reactions. Namely, β-naphthol is known to react with such nucleophilic reagents as sulfurous acid[7] and thioglycolic acid.[8] Here again these reactions are believed to proceed by the attack of the nucleophile at the carbonyl carbon of the quasi keto-form intermediate, formed by the ring protonation at either the *o*- or the *p*-position.

Therefore, the oxygen exchange reaction of phenol can best be understood when one assumes a mechanism involving a prior ring protonation and the subsequent nucleophilic attack of water at the carbonyl carbon. However, this somewhat unfamiliar idea has to be tested with more investigations in view of the fact that, although the hydroxylic proton of phenol has been shown to undergo a very facile D–H exchange in both acidic and alkaline aqueous media,[9] the oxygen exchange of the hydroxyl group with solvent water itself has been believed not to occur, even in a strong acidic medium.

This work was undertaken in order to determine the most suitable reaction conditions of oxygen exchange and in order to clarify the mechanism by examining the effect of the substituent on the rate of oxygen exchange.

Results and Discussion

The oxygen exchange reaction was tested at first under conditions similar to those used for the acid-catalyzed hydrolyses of phenyl benzenesulfonate[2] and *p*-nitrophenyl benzenesulfonate.[10] Phenol and 10 N hydrochloric acid, prepared by dissolving hydrogen chloride gas in ^{18}O-enriched water, were sealed in a glass tube, and the tube was heated under the conditions listed in Table I. The same procedure was also used for the solution 4.8 N hydrochloric acid. In a separate experiment, a mixture containing the same reactants was refluxed. The products, labeled phenols, were then recovered and subjected to ^{18}O analysis by the usual method.[11] The reaction conditions and the results are shown in Table I.

The phenols recovered were always incorporated with an excess of ^{18}O when the exchange reactions were carried out at 180°C in a sealed tube, the amount of ^{18}O incorporation increasing with an increase in the duration of heating. Since the reaction conditions used in this work were rather drastic, one might expect some possible rearrangement products from the phenols used. However, it was found that all the phenols used in this work, except for the isomeric nitrophenols, were recovered in almost quantitative yields. The purities of these recovered phenols were checked by infrared, ultraviolet and gas chromatographic analyses, and by the fractional recrystallization of the ester derived from the phenols, no rearranged phenol was detected from any of the phenols applied. Even in the case of the isomeric nitrophenols, where some severe decompositions were observed, the recovered phenols were identical to the starting phenols, although the yields of the recovered phenols were low. The change in the concentration of hydrochloric acid from 10 N to 4.8 N did not affect the extent of ^{18}O incorporation. However, both at 110°C in a sealed tube and under a reflux, no oxygen exchange was observed, even after 24 hr. These results can be explained by assuming either an increased concentration of the intermediate (A) at high temperatures, or an increased rate of the nucleophilic attack of water, or both.

The contribution of the quinoid structure A would be greater for the oxygen exchange of β-naphthol and related compounds than for that of phenol. Therefore, the oxygen exchange reactions of catechol, resorcinol, hydroquinone, quinone and both α- and β-naphthols were next investigated. The procedures for the preparation of the reaction mixtures and the reaction conditions were similar

5) E. M. Arnett and C. Y. Wu, ibid., **82**, 5660 (1960).
6) a) M. Cohn and H. C. Urey, ibid., **60**, 679 (1938); b) J. N. E. Day, *Science Progress*, **34**, 47 (1939).
7) See the Bucherer Reaction in "Organic Reaction," Vol. I, John Wiley & Sons, New York, N. Y. (1942), p. 105.
8) F. M. Furman, J. H. Thelin, D. W. Hein and W. B. Hardy, *J. Am. Chem. Soc.*, **82**, 1450 (1960).
9) a) C. K. Ingold, C. G. Raisin and C. L. Wilson, *J. Chem. Soc.*, **1936**, 1637; b) M. Koizumi and T. Titani, This Bulletin, **13**, 681 (1938); c) M. Koizumi, ibid., **14**, 353 (1939).
10) S. Oae and R. Kiritani, ibid., **38**, 765 (1965).
11) S. Oae, T. Kitao and Y. Kitaoka, *J. Am. Chem. Soc.*, **84**, 3359 (1962).

TABLE I. OXYGEN EXCHANGE REACTION OF PHENOL

Reaction condition			^{18}O Atom% of		Exchange
Concn. of HCl N	Time hr.	Temp. °C	Eq. HCl soln.	Recovered product	%
10	3	180	0.77	0.33	22.8
10	5	180	0.8	0.37	28.3
10	12	180	0.77	0.55	61.4
10	24	180	0.77	0.73	93.0
4.8	6	180	0.77	0.39	33.3
10	6	110	0.77	0.20	0
10	24	110	0.77	0.21	0
10	6	Reflux	0.77	0.20	0

TABLE II. OXYGEN EXCHANGE REACTION OF RELATED PHENOLS

Compound	Reaction condition		^{18}O Atom % of		Exchange
	Time hr.	Temp. °C	Eq. 10 N soln.	Product	%
Hydroxy phenols					
o-	6	180	0.74	0.37	31.5
	24	110	0.74	0.21	0
m-	6	180	0.77	0.53	57.9
	24	110	1.5	0.59	30.0
p-	6	180	0.74	0.50	55.6
	24	110	1.58	0.43	16.7
Quinone	6	180	0.74	0.52	59.3
	24	180	0.74	0.62	77.8
	24	110	1.5	0.58	29.2
Naphthols					
α-	6	180	0.77	0.54	59.7
	24	180	0.74	0.53	61.1
	24	110	1.5	0.74	41.5
β-	6	180	0.77	0.56	63.2
	24	180	0.74	0.56	66.7
	24	110	0.77	0.40	35.1

to those described in connection with the oxygen exchange of phenol (Table I). The results are shown in Table II.

Unlike the cases of monobasic phenols, the oxygen exchange of dibasic phenol listed in Table II took place not only at 180°C, but also at 110°C, except for the case of *o*-hydroxyphenol (catechol). The very facile oxygen exchange of both α- and β-naphthols is evident from their higher amounts of oxygen exchange, about 40%, even at 110°C. Here, the mechanism involving the quasi-quinoid intermediates appears to fit the experimental observations. It is interesting to note that the amount of ^{18}O incorporation was higher with resorcinol than those of the other *o*- and *p*-isomers. The same trend was observed in the cases of isomeric aminophenols.

We next carried out a series of experiments in the hope of obtaining more concrete information on the nature of this exchange reaction through comparing the substituent effects on the oxygen exchanges. This exchange reaction is considered to fall in the category of aromatic nucleophilic displacement reactions; it is also considered generally that the rate-determining step would be the addition of solvent water to the phenolic carbon. An important question is whether or not the quinoid structure A described before is well developed before the rate-determining step. If the hydroxyl group acquires a distinct carbonyl character before the actual oxygen-exchange reaction, the substituent effect represented by Hammett σ-values should nicely fit, just as in the cases of nucleophilic attack on a carbonyl carbon.

A similar substituent effect would be expected when the quinoid structure makes no contribution, with little assistance of ring protonation, and when the reaction proceeds directly through the nucleophilic attack on the aromatic carbon. However, in the latter case a strong electron-withdrawing substituent, such as the nitro group, would facilitate the exchange, especially by resonance, more than what may be expected from the σ- constant, and the substituent effect would be better expressed by σ^--constants. Furthermore, an important difference would be expected between the effects of *m*- and either the *o*- or *p*-OH and the NH_2 group. Ring protonation to form the quinoid structures would be favored for *m*-OH and *m*-NH_2 phenols because of the contribution of the following

TABLE III. OXYGEN EXCHANGE REACTION OF SUBSTITUTED PHENOLS

Compcund	Reaction condition Time, hr.	^{18}O Atom % of Eq. HCl soln.	^{18}O Atom % of Product	Exchange %
Nitrophenols				
o-	6	1.58	0.21	0
	24	1.58	0.21	0
m-	6	1.58	0.23 (0.30)	7.2
	24	1.58	0.24 (0.32)	8.7
p-	6	1.58	0.40 (0.80)	43.5
	24	1.58	0.37 (0.72)	37.7
Nitrobenzene	24	1.58	0.20	0
Aminophenols				
o-	6	0.74	0.21	0
	24	0.74	0.22	0
m-	6	0.74	0.41	38.9
	24	0.74	0.42	40.0
p-	6	0.74	0.24	7.4
	24	0.74	0.27	13.0
Bromophenols				
o-	6	0.74	0.32	22.2
	24	0.74	0.42	40.7
p-	6	0.77	0.30	17.5
	24	0.77	0.45	43.9
2,4,6-Tri-	6	0.77	0.21	0
	24	0.77	0.21	0
Cresols				
o-	6	0.77	0.26	10.5
	24	0.77	0.38	31.6
m-	6	0.77	0.30	17.5
	24	0.77	0.45	43.9
p-	6	0.77	0.26	10.5
	24	0.77	0.45	43.9
2,4,6-Tri-	6	0.77	0.22	0
	24	0.77	0.24	7.4

Reaction temp. 180°C.

Numerical values in parentheses represent the ^{18}O concentration of phenolic oxygen calculated from the concentration of whole molecule by neglecting the ^{18}O exchange of nitro group.

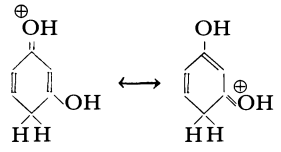

IIa IIb

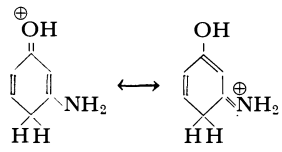

IIIa IIIb

resonance structures (IIa, IIb, IIIa, IIIb). Such a stabilization of quinoid structure is not expected for the corresponding *o*- and *p*-isomers. On the other hand, amino phenol is considered to be equilibrating with its *N*-protonated conjugate acid, and the *p*-ammonio group would strongly hinder the protonation at the same *p*-position, while the *m*-ammonio group would not much obstruct the protonation to the hydroxyl group at either the *o*- or the *p*-position. Both free amino and ammonio groups which are equilibrating thus favor the quinoid structure for the *m*-isomer much more than for the *p*-isomer. The same conclusions may be drawn for the hydroxyl group.

The results of the oxygen exchange reactions of isomeric nitrophenols, aminophenols, bromophenols and cresols are shown in Table III. The oxygen exchanges for cresol and bromophenol were the same or slightly less than that for unsubstituted phenol. Marked differences were observed for isomeric amino and nitro phenols. *p*-Nitrophenol showed an unusually high extent of oxygen exchange as compared to its *o*- and *m*-isomers, whereas the oxygen exchange of *m*-aminophenol was far greater than those of the *o*- and *p*-isomers. The same trend as in aminophenols, although less marked was observed for hydroxyphenols (Table II). Another remarkable observation is that practically no oxygen exchange takes place for *o*-isomers of amino-, hydroxy- and nitrophenol. Steric hindrance alone cannot explain such results, since the oxygen exchange was observed for *o*-cresol and *o*-bromophenols, although such exchange was smaller

than in the corresponding *m*- and *p*-isomers. Another responsible factor for the remarkable retardation of the ^{18}O exchange would be the intramolecular hydrogen bondings, which are expected for the former three phenols and which would stabilize the ground states much more than the transition states of the former three phenols.

Competitive Reaction—As is indicated in the runs of *p*-nitrophenol in Table III, the percentage of oxygen exchange was greater here despite the shorter reaction time. Since the reaction temperature was high and since the reactions were carried out in a sealed tube in an electric furnace, it was difficult to maintain the same reaction conditions. Therefore, we have carried out competitive reactions in order to eliminate other complicating factors and obtain at least a semi-quantitative measure of the relative reactivities of the isomeric phenols.

The reaction conditions and the procedures were essentially the same as those described above. A mixture of equimolar amounts of the unsubstituted reference phenol and a substituted phenol was sealed with a large excess of ^{18}O-enriched 10 N hydrochloric acid. The reaction products were then separated into phenol and substituted phenol by a combination of distillation, recrystallization and gas chromatography. The relative reactivity, k_x/k_h, was calculated using Eq. 3:

$$\frac{dX_t}{dt} k_x(X_\infty - X_t) \quad [H_2{}^{18}O] \tag{1}$$

$$\frac{dh_t}{dt} k_h(X_\infty - h_t) \quad [H_2{}^{18}O] \tag{2}$$

$$k_x/k_h = \log \frac{(X_\infty - X_0)}{(X_\infty - X_t)} \Big/ \log \frac{(X_\infty - h_0)}{(X_\infty - h_t)} \tag{3}$$

X_∞ : Calculated ^{18}O-atom% of the reaction mixture at equilibrium

X_t : Observed ^{18}O-atom% of the substituted phenol at the time *t*.

h_t : Observed ^{18}O-atom% of the unsubstituted phenol at the time *t*.

X_0 : Initial ^{18}O-atom% of substituted phenol ($t=0$).

h_0 : Initial ^{18}O-atom% of unsubstituted phenol ($t=0$).

Since Eq. 3 is derived from Eqs. 1 and 2, neglecting the reverse reaction, the k_x/k_h value depends on the extent of oxygen exchange; for more precise values, extrapolation to zero-time values is desirable. For a more precise ^{18}O-analysis, it is desirable that the atom % of the ^{18}O-enriched water be as high as possible. However, we had access to ^{18}O-enriched water of only 1.5% ^{18}O enrichment in the present work. Therefore, the values of k_x/k_h are unavoidably crude. In spite of these limitations, the two values of k_x/k_h for each isomer at different times were close to each other and, hence, may be used as reactivity measures of the isomeric phenols. The trends in Table IV are similar to those found in Table III. *m*-Aminophenol and *p*-nitrophenol are about three times more reactive than unsubstituted phenol. Methyl and bromo-substituents slightly decrease the reactivity, while *p*-aminophenol again shows an unusually low reactivity.

A plot of log k_x/k_h against Hammett σ-constants did not give a good correlation curve for isomeric methyl, bromo and *p*-nitro groups. Since aminophenol is considered to be an equilibrium mixture of free amino and ammonio species, it is difficult to assign any substituent constant to this group.

Table IV. Competitive reaction of phenol with related phenols

Compound mol. $\times 10^{-3}$	Reaction time hr.	^{18}O Atom % X_∞	h_t	X_t	k_x/k_h	log k_x/k_h
Aminophenol 7.33		1.533				
	4		0.50	0.87	2.760	0.441
m-	4		0.647	1.139	2.999	0.477
	7		0.816	0.395	0.268	−0.572
p-	8		0.786	0.497	0.250	−0.602
Nitrophenol 5.75		1.537				
p-	4		0.617	1.197	3.928	0.594
Cresol 7.39		1.532				
	4		0.440	0.272	0.569	
o-	8		0.783	0.319	0.308	
	4		0.619	0.606	0.971	−0.013
m-	8		0.726	0.66	0.869	−0.061
	4		0.462	0.416	0.879	−0.056
p-	8		0.583	0.565	0.959	−0.018
Bromophenol 4.62		1.540				
	8		0.545	0.491	0.874	
o-	24		1.074	0.931	0.733	
	25		0.936	0.848	0.835	
p-	8		0.578	0.532	0.896	−0.048

X_∞: ^{18}O Atom % of each compound when exchange reaction was taken place completely.

However, if the substituent constant of the trimethyl ammonio group, 0.904 for m-$\overset{\oplus}{N}(CH_3)_3$, is taken as the constant for m-$\overset{\oplus}{N}H_3$, and if $\sigma_p^-(=1.27)$ is used for p-nitrophenol, a fairly good correlation line ($\rho=0.47$) is obtained, as is shown in Fig. 1, although p-nitrophenol, p-bromophenol and, especially, p-aminophenol still greatly deviate from this line.

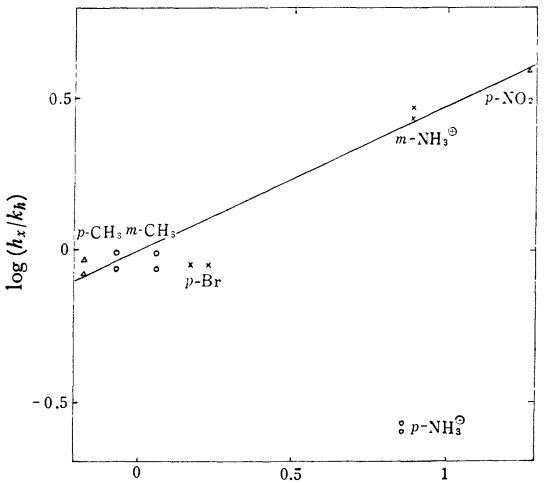

Fig. 1

A self-consistent explanation of all the above results is not easy. However, there are a few points of interest worthy of attention. The ρ value was found to be substantially smaller than that expected from ordinary aromatic nucleophilic substitutions. We believe that it is by no means a ρ value for a simple aromatic nucleophilic substitution, but a value that results from two succesive reactions with two different ρ values opposite in sign, i. e., the prior equilibrium reaction of protonation and the subsequent aromatic nucleophilic reaction. The small ρ value with a positive sign may indicate that the electronic effect of the substituent operates more at the second step, namely, the aromatic nucleophilic substitution, than at the prior protonation equilibrium reaction. The correlation of the reactivity of p-nitrophenol by the σ^--constant seems to indicate that the mechanism of the oxygen exchange of this phenol is different from those of the other phenols, as has been discussed before, the ring protonation to form the intermediate of the quinoid structure is not necessary, and the reaction may well proceed through direct nucleophilic displacement due to the strong electron-withdrawing ability of the p-nitro group (Eq. 4). This is consistent with our previous observations that the acid-catalyzed hydrolysis of p-nitrophenyl benzenesulfonate under strong acidic conditions proceeds partly through the fission of the phenolic C–O bond, while the hydrolysis of the unsubstituted phenyl benzenesulfonate proceeds by the fission of the S–O bond and practically no phenolic C–O bond fission was detected. The mechanism of the oxygen exchange of the other isomers seems to be better explained by assuming the quinoid structure A as the pre-equilibrium species which participates in the rate-determining step.

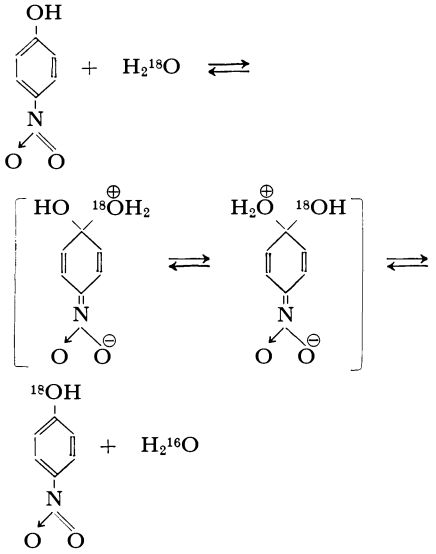

(4)

Only this mechanisms seems capable of explaining the large rate differences between p- and m-aminophenol presented before, irrespective of whether the contributing species is a free amino group or a protonated ammonio group. The usual unreactivity of p-aminophenol is undoubtedly due to the low concentration of the incipient quinoid intermediate A formed in the unfavored equilibrium of protonation, because the electron-withdrawing inductive effect of the ammonium group serves to deactivate the benzene ring for an electrophilic attack. The decreased reactivity of bromophenols is probably also due to the decreased concentration of the incipient intermediate A formed in the pre-equilibrium protonation, since the bromo group is known to deactivate the benzene ring for an electrophilic attack due to its strong electron-withdrawing inductive effect.

In conclusion, the mechanism involving the quinoid intermediate may be summarized as in Eq. 5:

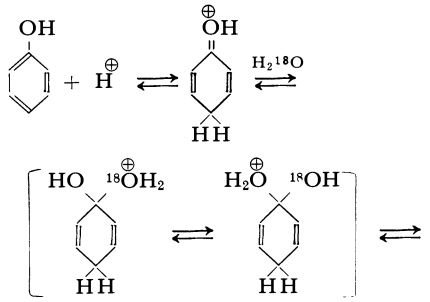

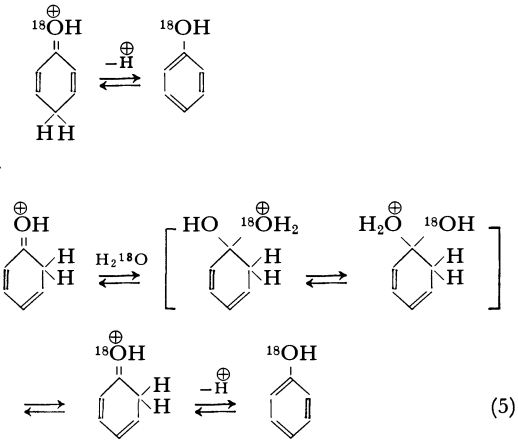

or

(5)

Experimental

The Oxygen Exchange Reaction of Substituted Phenols.—a) In a sealed tube, in 10 N hydrochloric acid: A phenol (1 g.) and 5 ml. of ^{18}O-enriched aqueous 10 N hydrochloric acid were sealed in a tube and heated at 110°C or 180°C for a suitable time. Then the sealed tube was broken, and all the contents except resorcinol, quinone and aminophenols were extracted with ether. The ether layer was dried over calcium chloride and concentrated, and the residue was treated in the following manner: Phenol was purified by distillation under reduced pressure or by reaction with bromine to give 2, 4, 6-tribromophenol, m. p. 96°C; catechol was recrystallized from alcohol, m. p. 105°C; hydroquinone was recrystallized from alcohol, m. p. 170—171°C; α-naphthol was purified by sublimation, m. p. 96°C; β-naphthol was purified by sublimation, m. p. 122—123°C; nitrophenols were purified by recrystallization or sublimation—*o*-nitrophenol (m. p. 44—45°C), *m*-nitrophenol (m. p. 97°C) and *p*-nitrophenol (m. p. 113—114°C); bromophenols were purified by distillation—*o*-bromophenol (b. p. 194°C) and *p*-bromophenol (b. p. 238°C, 92°C/24 mmHg); 2, 4, 6-tribromophenol was purified by sublimation, m. p. 96°C; and 2, 4, 6-trimethylphenol was recrystallized from ethanol, m. p. 75°C. Both resorcinol and quinone, after they had been subjected to the ^{18}O exchange experiments, were separated from the sealed tubes and collected by filtration. Resorcinol was purified by sublimation (m. p. 110—111°C), while quinone was recrystallized from alcohol, m. p. 115°C.

The aminophenols which separated as hydrochloride after the evaporation of the water from the reaction mixture were collected and recrystallized from water. The ammonium salts were neutralized with aqueous sodium hydroxide, and the free aminophenols which precipitated were filtered and recrystallized from ethanol—*o*-aminophenol (m. p. 170—174°C), *m*-aminophenol (m. p. 122—123°C) and *p*-aminophenol (m. p. 188°C). The reaction mixtures for isomeric cresols were separated into two layers. The upper, oily layer was distilled under reduced pressure, thus producing *o*-cresol (b. p. 191—192°C), *m*-cresol (b. p. 202°C) and *p*-cresol (b. p. 202°C).

Other Conditions for the ^{18}O Exchange.—b) In 4.8 N hydrochloric acid: The procedures were the same as in a).

c) Under reflux: The same reaction mixture of phenol and 10 N hydrochloric acid as was used in the above experiments was placed in a 20 ml. flask and refluxed for 6 hr. The procedure of the separation of phenol was the same as that described above.

All the results described in above (a), b) and c)) are shown in Tables, I, II and III.

When nitrobenzene was treated by the same procedure as in the reaction of nitrophenols, it was verified that the oxygen exchange of the nitro group did not take place.

Competitive Reactions.—a) Aminophenol: Phenol (0.800 g. (8.5×10^{-3} mol.)), *m*- or *p*-aminophenol (0.800 g. (7.33×10^{-3} mol.)) and 10 N hydrochloric acid containing excess ^{18}O (8.000 g. (0.444 mol.)) were sealed in a tube. The sealed tubes were then heated at 180°C for 4, 7 or 8 hr. The entire contents were extracted with ether and treated as above. Phenol was obtained from the ether layer, and aminophenol, from the aqueous layer.

b) *p*-Nitrophenol: Phenol (0.800 g. (8.5×10^{-3} mol.)), *p*-nitrophenol (0.800 g. (5.75×10^{-3} mol.)) and 10 N hydrochloric acid containing excess ^{18}O (8.000 g. (0.444 mol.)) were sealed in a tube. The sealed tubes were then heated at 180°C for 2 or 4 hr. The entire contents were extracted with ether, and the ether layer was dried over calcium chloride. The ether extract was then put into a sublimation apparatus to which a trap cooled with dry ice - acetone had been joined. When the sublimation apparatus was heated in vacuo, purified *p*-nitrophenol in the sublimation apparatus and phenol in the trap were simultaneously obtained.

c) Cresol: Phenol (0.800 g. (8.5×10^{-3} mol.), *o*-*m*- or *p*-cresol (0.800 g. (7.39×10^{-3} mol.)) and 10 N hydrochloric acid containing excess ^{18}O (8.000 g. (0.444 mol.)) were sealed in a tube. The sealed tubes were then heated at 180°C for 4 or 8 hr. The entire contents were extracted with ether, and the ether extracts were distilled. The distilled mixture was then separated to phenol and cresol by gas chromatography, using a 2 m. column of silicone 550, with nitrogen as the carrier gas (10—13 cc./min.), with a temperature of 160°C, and with a sensibility of 1.

d) Bromophenol: Phenol (0.800 g. (8.5×10^{-3} mol.)), *o*- or *p*-bromophenol (0.800 g. (4.62×10^{-3} mol.)) and 10 N hydrochloric acid containing excess ^{18}O (8.000 g. (0.444 mol.)) were sealed in a tube. The sealed tubes were then heated at 180°C for 8, 24 or 25 hr., and the entire contents were treated by the same procedure as was used for cresol.

All the phenols thus separated were subjected to ^{18}O analysis, and the k_x/k_h value was calculated according to Eqs. 1—3.

BULLETIN OF THE CHEMICAL SOCIETY OF JAPAN VOL. 39 1968—1971 (1966)

The Oxidation of Methyl Sorbate with Monoperphthalic Acid

By Yasuo SUHARA

Government Chemical Industrial Research Institute, Tokyo, Shibuya-ku, Tokyo

and Toshikatsu MINAMI

Chiba Institute of Technology, Narashino-shi, Chiba

(Received December 20, 1965)

The products obtained by treating methyl sorbate with monoperphthalic acid under various conditions were studied by chemical and spectroscopic procedures. From the results of chemical tests and spectroscopic observations in the infrared and ultraviolet regions, it was inferred that the product in all cases is methyl *trans*-4, 5-epoxy-*trans*-2-hexenoate. This inference was confirmed by NMR spectroscopy.

Epoxy compounds are, in general, prepared from non-conjugated fatty acids or their derivatives by treatment with organic peracids. However, some epoxy compounds can be prepared from conjugated unsaturated hydrocarbons by treatment with peracetic acid.[1] On the other hand, our previous study[2] has shown that the substances obtained by treating β-eleostearic acid (*trans*-9-*trans*-11-*trans*-13-octadecatrienoic acid) and its methyl ester with peracetic, perbenzoic, and monoperphthalic acids are not epoxy compounds but hydroxy-acyloxy compounds. Therefore, an investigation has been made to see whether methyl sorbate (*trans*-2-*trans*-4-hexadienoate) can be epoxidized by the action of an organic peracid. The results of this investigation will be described in this paper.

In the present study, methyl sorbate was treated with monoperphthalic acid under the conditions indicated in Table I.

The saponification values and the oxirane oxygen contents of the products were 396.8—401.7 and 10.3—11.0% respectively; these values agree with the theoretical values of methyl monoepoxyhexenoate (saponification value, 394.7; oxirane oxygen content, 11.3%). Although all the products had small peroxide values (10.3—13.3 meq./kg.), such values may be due to the presence of traces of monoperphthalic acid.

However, the oxidation products cannot be identified with methyl monoepoxyhexenoate on the basis of the above data alone. According to Bauer and Bähr,[3] an oxo compound (hexaoxostearic acid) is formed when a conjugated unsaturated fatty acid (eleostearic acid) is treated with perbenzoic acid. Hence, the products obtained in the present study may contain oxo groups.

The carbonyl values of the oxidation products were, therefore, determined by using hydroxylamine hydrochloride. The values obtained were 162.8—179.2. Also, the carbonyl values of methyl sorbate and crotonate, determined for purposes of comparison by the same method, were 175.6 and 101.0 respectively. On the other hand, in the test by Legal reaction with sodium nitroprusside, the oxidation products, methyl sorbate and crotonate, all gave negative results. From these observations it may be considered that the oxidation products do not contain oxo groups and that, in the determination of carbonyl values, hydroxylamine may have interacted with the carbon-carbon double bond presumed to exist in the products.

The fact that hydroxylamine interacts with the carbon-carbon double bond in an α-monoenoic fatty acid has already been reported.[4] This fact supports the above inference; it also suggests that the carbon-carbon double bond in the product of the oxidation of methyl sorbate exists in the position α to the carbonyl group.

This predicted position of the double bond was confirmed by ultraviolet spectroscopic studies. The molar absorbance of the product in a heptane solution at λ_{max} 217.7 mμ was 13700. The intense absorption at this wavelength arises from the conjugation of a double bond with a carbonyl group in hydrocarbon chains.[5]

1) V. I. Pansevich-Kolyada, T. S. Strigalova and Z. B. Idel'chik, *Sbornik Statei Obshchei Khim.*, **2**, 1418 (1953); *Chem. Abstr.*, **49**, 4615 (1955). V. I. Pansevich-Kolyada, *Zhur. Obshchei Khim.*, **26**, 2161 (1956); *J. Gen. Chem. U. S. S. R.*, **26**, 2413 (1956). A. V. Pudovik and B. E. Ivanov, *Zhur. Obshchei Khim.*, **26**, 2771 (1956); *J. Gen. Chem. U. S. S. R.*, **26**, 3087 (1956).

2) Y. Suhara and M. Nyui, *J. Japan Oil Chemists' Soc. (Yukagaku)*, **13**, 590 (1964).

3) K. H. Bäuer and O. Bähr, *J. prakt. Chem.*, **122**, 201 (1929).

4) N. E. Kologrivova and V. N. Belov, *Trudy Vsesoyuz. Nauch.-Issledovatel. Inst. Sintet. i Natural. Dushistykh Veshchestv*, **1958**, No. 4, 70; *Chem. Abstr.*, **53**, 14929 (1959).

5) C. F. Allen and J. Cason, *J. Biol. Chem.*, **220**, 407 (1956).

TABLE I. REACTION OF METHYL SORBATE WITH MONOPERPHTHALIC ACID

Monoperphthalic acid 0.30 mol.
Ether as solvent 280 ml.

Exp. No.	Condition: Methyl sorbate g.	Condition: Temp. °C	Condition: Time hr.	Result: Peracid consumption %	Result: Yield of product: Crude g.	Result: Yield of product: Purified g.
1	37.8	20—22	17	81.9	35.2	10.4
2	37.8	20—28 / 30 / 37	13 / 4 / 2	94.6	35.8	10.8
3	37.8	Room temp.	15 days	92.5	36.1	11.3
4	18.9	30—31 / 37	21 / 13	82.0	18.2	10.6

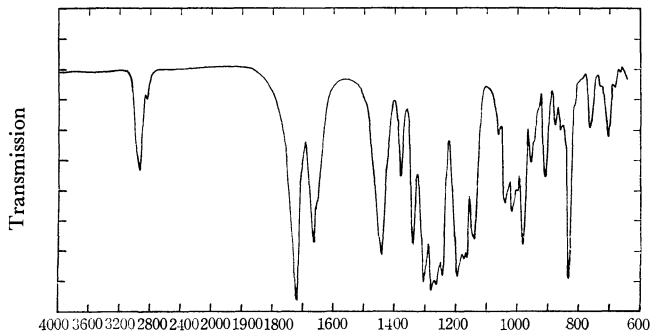

Fig. 1. Infrared absorption spectrum of the oxidation product.

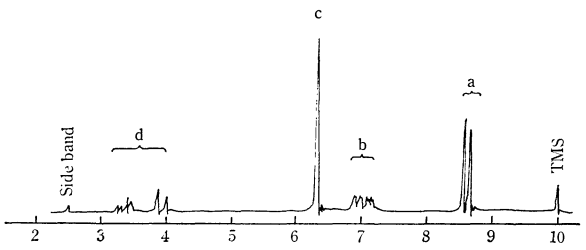

Sweep rate, 3.96 c.p.s./sec.; 100 Mc.; H_1, −70 db

Fig. 2. NMR spectrum of the oxidation product (0.1 g.) in carbon tetrachloride (1 ml.).

The structural characteristics of the oxidation products were further studied by infrared spectroscopy. In this case, the infrared spectra of methyl sorbate, crotonate and levulinate were also determined for purposes of comparison. The infrared spectra of the oxidation products were nearly all the same; one of them is presented in Fig. 1. The band at 980 cm^{-1} is due to the trans double bond existing in the position α to the carbonyl group in unsaturated fatty acids.[6] The absorption band exhibited by the oxidation products at 834 cm^{-1} may correspond to the band at 837 cm^{-1} in the spectrum of methyl crotonate.

The two bands at 1280 and 877 cm^{-1} in the spectrum of the product suggest the presence of *trans*-epoxy groups, because the literature[7] shows that many of the *trans*-epoxy compounds hitherto studied absorb near 1250 and 890 cm^{-1}. This spectroscopic information is in harmony with the results of the oxirane oxygen determination. The slight displacement of the observed bands

6) L. J. Bellamy, "The Infra-red Spectra of Complex Molecules," Methuen & Co. Ltd., London (1958), p. 45.

7) L. J. Bellamy, ibid., p. 115.

from the normal band positions may be due to the presence of a double bond near the epoxy group in the oxidation product.

The type of epoxy group suggested by the spectrum can be supported theoretically. From the stereochemical point of view, it is evident that the epoxy groups resulting from the reaction of methyl sorbate with paracids must exist in the trans-form, for methyl sorbate contains two trans-double bonds and, according to Lynch and Pausacker,[8] epoxidation with organic peracids always results in cis-addition.

Moreover, no absorption bands due to the conjugated double bond (1614 and 997 cm^{-1} [9]), the γ-keto carbonyl group (1736 cm^{-1} in the spectrum of methyl levulinate) and the hydroxyl group (near 3500 cm^{-1} [10]) appear in the spectrum of the oxidation products.

From the results of chemical tests and spectroscopic observations, it follows that the oxidation product obtained in each experiment contains neither a hydroxyl nor a keto carbonyl group, but an epoxy group and a double bond. As the ultraviolet and infrared spectra show, the double bond is in the position α to the ester carbonyl group; hence, the epoxy group is an α-epoxy group.

This conclusion was confirmed by NMR spectroscopy. The spectrum is presented in Fig. 2. As might be expected from the molecular structure suggested above, there appear four signals (mostly multiplets), which are marked a, b, c, and d in the figure. The chemical shift and signal intensity (peak area) measurements indicate that the signals, a, b, c, and d, are due to the groups

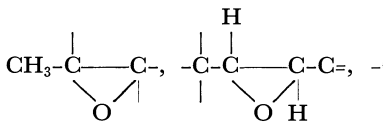

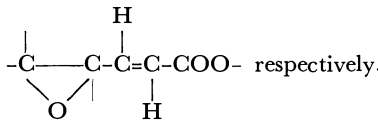

In a study similar to the present one, Smit[11] has stated that the product obtained by treating 9, 11-octadecadienoic acid with perbenzoic acid is a γ- or β-epoxide. Should the reaction of methyl sorbate with monoperphthalic acid proceed in nearly the same manner as the reaction of 9, 11-octadecadienoic acid with perbenzoic acid, one of the three epoxides represented below by formulas I, II, and III would be formed:

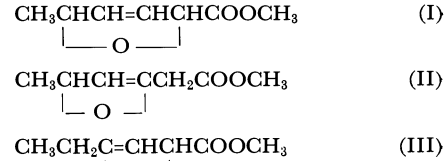

Whichever the product may be, the ultraviolet spectrum will show an absorption peak near 183 mμ (due to the isolated double bond[12]) and the infrared spectrum will show an absorption band in the 1070—1140 cm^{-1} range (associated with the larger ring of the cyclic ether group[7]). Moreover, if the product is epoxide II or III, the NMR spectrum will show five signals.

However, none of these characteristics have been observed in the present study. Hence, there is no possibility of the formation of γ- and β-epoxides under the conditions employed.

On the basis of the information obtained, it can be concluded that the product obtained in each of the present experiments is methyl *trans*-4, 5-epoxy-*trans*-2-hexenoate, and that the reaction of methyl sorbate with monoperphthalic acid proceeds as follows:

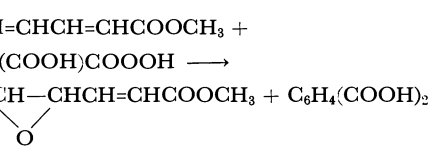

Even when the mole ratio of monoperphthalic acid to methyl sorbate is 2 to 1 (Exp. No. 4), the reaction does not give the diepoxide at all. (In this case, the yield of the monoepoxide is about twice the yield obtained when the mole ratio is 1 to 1.) This fact indicates that the double bond in the α position is resistant to the action of monoperphthalic acid.

Experimental*

Materials Used.—Monoperphthalic acid was prepared from phthalic anhydride by treatment with hydrogen peroxide in an ether solution according to the procedure of Goryaev et al.[13] Methyl sorbate, crotonate, and levulinate were prepared from the corresponding fatty acids by esterification with methanol in the presence of sulfuric acid as a catalyst.

Methyl sorbate: Purity: 98.2%. n_D^{25}: 1.5001. Acid value: 2.0.

8) B. M. Lynch and K. H. Pausacker, *J. Chem. Soc.*, **1955**, 1525.
9) L. J. Allan, G. D. Meakins and M. C. Whiting, ibid., **1955**, 1874.
10) L. J. Bellamy, "The Infra-red Spectra of Complex Molecules," Methuen & Co. Ltd., London (1958), p. 96.
11) M. W. C. Smit, *Rec. trav. chim.*, **49**, 675 (1930).
12) G. A. J. Pitt and R. A. Morton, "The Chemistry of Fats and Other Lipids," Vol. 4, Pergamon Press, London (1957), p. 229.
* All melting and boiling points are uncorrected.
13) M. I. Goryaev, G. A. Tolstikov and L. A. El'-chibekova, *Zhur. Priklad. Khim.*, **34**, 946 (1961); *J. Appl. Chem. U. S. S. R.*, **34**, 912 (1961).

Saponification value: Found, 447.3; Calcd., 444.8. UV ε: 23500 at λ_{max} 253.5 mμ in a heptane solution.

Analysis.—The consumption of monoperphthalic acid was determined by the method of Wheeler.[14]

The oxirane oxygen content was determined with a hydrogen bromide-glacial acetic acid solution by the method described in our previous paper.[15] The carbonyl values were determined by the method of Milewsky and Wentzel.[16]

The purity of the methyl esters noted above, and of the reaction products, was determined by gas-liquid chromatography. The instrument used was a Hitachi Gas-Liquid Chromatograph KGL-2 with a polyester column.

Spectroscopic Observation.—The ultraviolet absorption was measured in a heptane or ethanol solution with a Hitachi ESP-2U spectrophotometer.

The infrared absorption was measured in liquid films with a Shimadzu IR-27 infrared spectrophotometer, using sodium chloride cells.

The nuclear magnetic resonance spectrum was determined with a Varian HR-100 NMR spectrometer.

The Reaction of Methyl Sorbate with Monoperphthalic Acid.—Methyl sorbate (0.15 or 0.30 mol.) was added to a solution of monoperphthalic acid (0.30 mol.) in ether (280 ml.), and the mixture was stirred under the conditions indicated in Table I. After a specified period of time, the reaction mixture containing the precipitate formed by the reaction was filtered, and the ether in the filtrate was distilled off in vacuo. Chloroform was then added to the distillation residue. At this moment, a precipitate was again formed. The chloroform solution containing the precipitate was filtered; and the filtrate was washed with water and dried over anhydrous sodium sulfate. The chloroform was then distilled off in vacuo; the residue was subjected to vacuum distillation to yield a pure oxidation product of methyl sorbate.

Anal. (Purified Product in Table I, Exp. No. 2).—Found: C, 58.91; H, 7.12; O, 33.87. Calcd. for $C_7H_{10}O_3$: C, 59.14; H, 7.09; O, 33.77%; mol. wt., 142.16. Purity: 98.0%. n_D^{25}: 1.4619. B. p. 81—83°C/8 mmHg.

The precipitate separated from the reaction mixture and that separated from the chloroform solution were combined, and the whole was recrystallized from water. The recrystallization gave monoclinic crystals melting at 208—210°C. A mixture of the crystals with *o*-phthalic acid (m. p. 210—211.5°C) melted at 199.5—202°C. The analytical characteristics of the crystallized precipitate are as follows: Acid value: found, 681.6; calcd. for *o*-phthalic acid, 675.4. Saponification value (found): 678.4. UV ε: 1260 at λ_{max} 274 mμ in an ethanol solution. (The λ_{max} in a methanol solution[17] is 272 mμ.) Therefore, the precipitate is *o*-phthalic acid.

We are grateful to Dr. Osamu Yamamoto for determining the NMR spectrum, to Mr. Katsuhiko Higuchi for performing the gas-liquid chromatographic analysis, and to Mr. Heisuke Sugita for performing the elementary analysis.

14) D. H. Wheeler, *Oil and Soap*, **9**, 89 (1932).
15) Y. Suhara, *J. Japan Oil Chemists' Soc. (Yukagaku)*, **13**, 378 (1964).
16) R. Milewsky and H. Wentzel, *Fette, Seifen, Anstrichmittel*, **57**, 702 (1955).
17) Sadtler, 6272U (1960), Samuel P. Sadtler & Son, Inc., Philadelphia.

BULLETIN OF THE CHEMICAL SOCIETY OF JAPAN VOL. 39 1971—1974 (1966)

Studies of Thio Acids. VI.[1] The Electrolysis of Thiostearic Acid*1

By Yoshio HIRABAYASHI and Tetsuro MAZUME*2

Faculty of Engineering, Gifu University, Kagamigahara-shi, Gifu

(Received December 25, 1965)

Potassium thiostearate was electrolyzed in methanol in the presence of an excess of thiostearic acid by the use of platinum electrodes and a direct current. The product obtained by this electrolysis was found to consist of distearoyl disulfide, methyl stearate, stearic acid, and thiostearic acid. The mechanism of the formation of the above components was discussed in contrast with that of the Kolbe reaction of fatty acids.

Many studies of the Kolbe reaction of fatty acids have been made, whereas the studies of the electrolysis of thio acid have been very scanty, Bunge[2] reported that thioacetic acid (CH_3COSH) yielded diacetyl disulfide ($CH_3COSSOCCH_3$) on electrolysis, the reaction of which was different from the Kolbe reaction of fatty acids. However, no study of the electrolysis of higher aliphatic thio acids has yet been reported.

The present investigation was undertaken to

1) Part V of this series: Y. Hirabayashi, M. Mizuta and T. Mazume, This Bulletin, **38**, 1099 (1965).
2) N. Bunge, *Ber.*, **3**, 295, 911 (1870).

*1 Parts of this study were presented at the Symposium of Oils and Fats of the Chemical Society of Japan, Nagoya, November, 1958.
*2 Present address: Shimogamo-kishimotocho, Sakyo-ku, Kyoto.

obtain detailed knowledge of the electrolysis of thio acids. Potassium thiostearate was electrolyzed in methanol in the presence of an excess of thiostearic acid; then the reaction mechanism was discussed and the products investigated. The results will be described in this paper.

Experimental*3 and Results

Experimental Methods and Conditions.—After a solution of thiostearic acid (6 g.)*4 in absolute methanol (60 ml.) had been neutralized with ca. 1 N methanolic potassium hydroxide (21.75 ml.; concentration of methanol: 96 vol.%), thiostearic acid (5 g.) and methanol (40 ml.) were added; then the resulting solution was electrolyzed in an electrolytic cell, as is shown in Fig. 1,

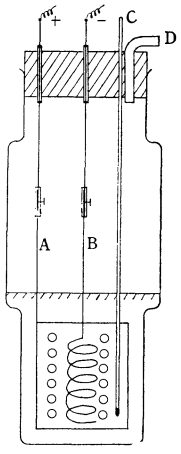

A: Anode
B: Cathode
C: Thermometer
D: Outlet tube of gas

Fig. 1. Electrolytic cell.

in which a platinum spiral wire was used as the cathode and a platinum cylinder with holes (4 cm. in diameter and 5 cm. high.) as the anode.

Conditions of electrolysis:
Direct current
Voltage: 11.0—11.5 V.
Current: 0.5 amp. (at the beginning)
Temperature of electrolyte: 50—55°C

A while after the electrolysis had started, a solid substance was gradually deposited on the anode; this substance disturbed the passage of the current through the solution, and the evolution of the gas (H_2) on the cathode was also gradually decreased. Then, after the electrolysis had occasionally been interrupted, the deposit on the anode was scraped off into the solution with a glass rod in order to expose the anode surface as much as possible and so facilitate continued electrolysis. A current of 0.5 amp. was again passed through the solution after the exposure of the anode surface. After 2 hr., thiostearic acid (5 g.) and methanol (10 ml.) were again added. Furthermore, after 3 hr., thiostearic acid (5 g.) and methanol (20 ml.) were again added in order to make the electrolysis continue for 5 more hours. The total period of the electrolysis was 10 hr.; the interruptions of electrolysis for the removal of the deposit mentioned above corresponded to one-third of the total period, although almost no interruption was required in the last 2 hr.

The Identification of the Products.—After the electrolysis had ended, the contents of the cell were diluted with warm water (600 ml.), acidified with dilute hydrochloric acid, and extracted with ether; then the ether layer was washed with water in order to remove the excess hydrochloric acid. The ether layer was dark yellow and turbid. The suspending ether-insoluble matter was filtered off; then the filtrate was dried over anhydrous sodium sulfate, and the ether was removed. The following parts were obtained: the

Table I. The characteristics of fractions obtained from the ether-insoluble part (5.5 g.)

Fraction	Yield, g.	M. p., °C	S(K), %
(1)	1.0	83.5—84.5	10.0
(2)	3.1	83.0—84.0	10.4
(3)	0.4	81.5—82.5	10.8
(4)	0.7	79 —81	10.7

S(K): sulfur content determined by Kitamura's method (by volumetric analysis)

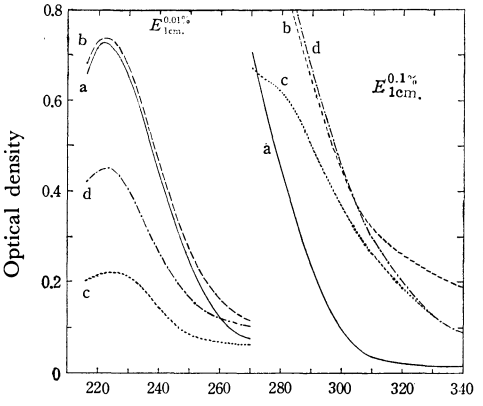

Fig. 2. Ultraviolet absorption spectra in cyclohexane.

a: Fraction 1, 2, or 3 in Table I
b: Fraction 4 in Table I
c: Fraction N-4 in Table II
d: Fraction A-3 in Table II

*3 All the melting points are uncorrected. The ultraviolet absorption spectra were measured with a Shimadzu quartz-spectrophotometer, model QB-50, and a silica cell (1 cm.).

*4 The characteristics of the thiostearic acid used in this experiments were as follows: m. p. 39.8—40.3°C; neutralization value, 185.8; sulfur content, 10.54 (iodine method), 10.62% (Kitamura's method).

ether-insoluble part, 5.5 g.; the ether-soluble part, 15.5 g.

The ether-insoluble part (5.5 g.) was repeatedly recrystallized from benzene to give, eventually, four fractions. Their characteristics and their absorption spectra are shown in Table I and Fig. 2.

The fractions, 1, 2, and 3, were identified as distearoyl disulfide by means of their characteristics and absorption spectra. Fraction 4 formed 3.3% of the total product. Its principal component was distearoyl disulfide, but it was supposed from its characteristics and absorption spectrum to contain a trace of an impurity. The saponification values of the above fractions were measured in order to determine whether or not hydrocarbons, formed by a reaction similar to the Kolbe reaction of fatty acids, were present. Their saponification values varied depending upon the heating time and the alkali concentration, but they were almost identical with the values determined by measuring an authentic distearoyl disulfide under the same conditions. Consequently, the presence of hydrocarbon in these fractions was unlikely.

The ether-soluble part (15.5 g.) was again dissolved in ether, washed thoroughly with a dilute solution of potassium hydroxide, and divided into neutral (N) and acidic (A) parts by the usual method. The contents of N and A in the total product were 64.8 and 9% respectively. Each part was repeatedly recrystallized from hexane and methanol, thus giving, eventually, four fractions (from N) or three fractions (from A). Their characteristics and ultraviolet absorption spectra are shown in Table II and Fig. 2.

Table II. The characteristics of fractions obtained from the ether-soluble part (15.5 g.)

Fraction	Yield, g.	M. p., °C	A.V.	S(J)
(N-1)	0.8	82 —83	—	—
(N-2)	4.4	38.7—39.2	0.7[a]	—
(N-3)	2.9	38.0—39.0	7.2	0
(N-4)	4.5	36 —37	4.8	0.1
(A-1)	0.6	69.5—70.5	197.2	—
(A-2)	0.2	69 —70	196.3	0.6
(A-3)	0.7	45 —50(60)	102.8	1.8[b]

A.V.: acid value, S(J): sulfur content determined by the iodine method, a): saponification value 188.2, b): S(K) 6.9%

These fractions were identified as follows:

N-1 was distearoyl disulfide which could not be separated out by the ether-extraction.

N-2, N-3, and N-4 were methyl stearate, judging from their characteristics; above all, N-2 was identified by a mixed melting point determination with an authentic sample, while it was known by their ultraviolet absorption spectra that they contained a trace of an impurity; above all, its content was highest in N-4.

A-1 was stearic acid.

A-3 was thiostearic acid, containing 30—40% of an unidentified substance.

As a result of the above investigations, the components and composition of the product were found to be approximately as follows:

Distearoyl disulfide+	31%
Methyl stearate	37
The part in which methyl stearate is the principal component+	24
Stearic acid	4
The part in which thiostearic acid is the principal component+	4

(+: Supposed to contain traces of unidentified substances).

Discussion

The electrolysis of potassium thiostearate in methanol (above 96 vol.%) in the presence of an excess of thiostearic acid at 50—55°C gave a product consisting of large amounts of distearoyl disulfide and methyl stearate, small amounts of stearic acid and thiostearic acid, and a trace of an unidentified substance. However, since hydrocarbons were not present in the product, the reaction mechanism of electrolysis of thio acids is considered to be different from that of the Kolbe reaction of fatty acids. Accordingly, more consideration will now be given to this subject.

The mechanism of the Kolbe reaction of fatty acids has been established to be as follows[3]: in the initial step, acyloxy radicals are formed by the discharge of a carboxylate anion on an anode; they decompose into alkyl radicals and carbon dioxide, and then the alkyl radicals yield saturated hydrocarbons, olefin, alcohol, and ester.

On the contrary, in the electrolysis of the potassium salt of thio acid, it may be considered that the acylthio radical ($RCOS\cdot$) is formed on an anode by the discharge of the carbothiolate anion ($RCOS^-$) formed from the potassium salt of thio acid; then the acylthio radical is dimerized to diacyl disulfide without being decomposed into alkyl radicals and carbon oxysulfide (Eq. 1). It is interesting that the electrolysis of thio acid is different from the Kolbe reaction of fatty acids in which various products are formed from acyloxy radicals. However, it is still unknown whether or not the difference between the two reactions is to be attributed to the difference in properties between $RCOO\cdot$ and $RCOS\cdot$. It may be also considered that two dimers, $(RCO)_2O_2$ and $(RCO)_2S_2$, are formed from $RCOO\cdot$ and $RCOS\cdot$ in the respective cases; the different products formed by the two reactions may be attributed to

3) E.g., C. L. Wilson and W. T. Lippincott, *J. Am. Chem. Soc.*, **78**, 4290 (1956).

the difference in stability between the two dimers*5: i. e., $(RCO)_2O_2$ proceeds to decomposition and $(RCO)_2S_2$ remains. In this case, the mechanism of the Kolbe reaction should be reconsidered by considering the results of this study.

On the other hand, it may also be considered that the formation of distearoyl disulfide is caused by the oxidation with oxygen generated at the anode by a trace of mixed water (Eq. 2). However, since it has been recognized that electrolysis in absolute methanol (CH_3OH–$C_{17}H_{35}COSK$–$C_{17}H_{35}COSH$ system) also gives distearoyl disulfide under the same conditions,*6 distearoyl disulfide is not formed by oxidation with the oxygen generated at the anode, but by the dimerization of the acylthio radicals, as has been mentioned above.

The reason for the formation of a large amount of methyl stearate is considered to be as follows: it has been recognized that distearoyl sulfide is formed by the elimination of hydrogen sulfide when thiostearic acid is heated in methanol at about 60°C; thiostearic acid and methyl stearate are then formed from the distearoyl sulfide and the methanol. Furthermore, the latter reaction is accelerated by the presence of a trace of alkali[1] (Eq. 3). On the other hand, it is also considered that methyl stearate is also formed by the direct reaction of thiostearic acid and methanol (Eq. 4). Accordingly, it may be concluded that methyl stearate is formed by the above reactions during a long-continued electrolysis in methanol, and that the formation of methyl stearate has no direct relation with the electrolysis.

A small amount of stearic acid may be formed by the change of thiostearic acid to stearic acid in the presence of a trace of water and alkali (Eq. 5).

The formation mechanism of the principal components was to be concluded as has been described. However, since unidentified substances were found in some fractions of the product, though present only in traces, and since an equilibrium between thiolic and thionic forms of the potassium salt of thio acid may exist in the solution, reactions other than above-mentioned may possibly occur. This situation will be clarified under other conditions by more detailed investigations in the near future.

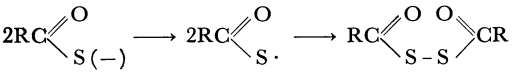

(1)

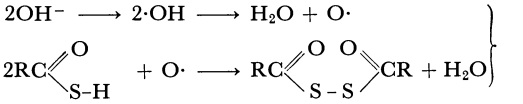

(2)

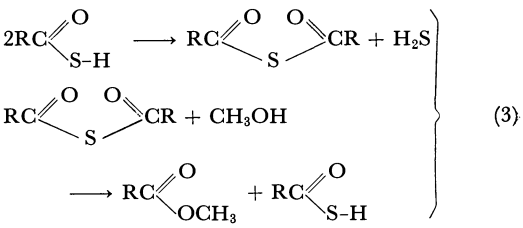

(3)

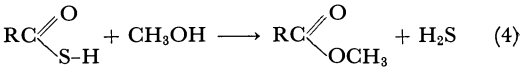

(4)

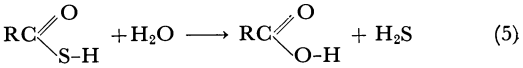

(5)

*5 In a study of the mechanism of the electrolysis of potassium caproate, Fichter et al. have stated that the decomposition of the primary electrolysis product, $(C_5H_{11}CO_2)_2$, is due to the evolution of heat at the cathode. (F. Fichter and R. Zumbrunn, *Helv. Chim. Acta*, **10**, 869 (1927).)

The good parallel between the products of Kolbe reactions and the decomposition of the corresponding diacyl peroxides suggests that the two processes have common paths or that peroxides are intermediates in the former. (S. Goldschmidt and M. Minsinger, *Chem. Ber.*, **87**, 956 (1954).)

*6 Not yet published.

BULLETIN OF THE CHEMICAL SOCIETY OF JAPAN VOL. 39 1975—1980 (1966)

Cyclopropene Derivatives. II.* The Reaction of Diazoketone with Triple Bond

By Naruyoshi OBATA and Ichiro MORITANI**

Department of Chemistry, Faculty of Engineering Science, Osaka University, Toyonaka, Osaka

(Received December 29, 1965)

The additions of some keto-carbene to a triple bond were studied. Since keto-carbene rearranges easily to a ketene derivative (Wolff rearrangement), the carbenic addition will always be in competition with the rearrangement. In the case of benzoylphenylcabene, the rearrangement is preferred, and no cyclopropene derivative is obtained. However, benzoyl and acetylcarbene, both having hydrogen instead of phenyl as a substituent, could be successfully added to diphenylacetylene and di-*n*-butylacetylene, thus giving 1, 2-disubstituted cyclopropene derivatives. Thus, it was found that the acylcyclopropenes were synthesized in a single step by the utilization of the carbenic addition of keto-carbene to a triple bond.

A very attractive way to synthesize cyclopropenylketone seems to be the addition of keto-carbene to a triple bond. It is well known, however, that the decomposition of diazoketone gives a ketene derivative, which is a product of Wolff rearrangement.[1] Actually, certain ketenes, such as diphenylketene, have already been prepared by this method.[2] Since, however, the intermediate of this Wolff rearrangement will presumably be keto-carbene,[3] the addition of keto-carbene to an olefinic bond will always be in competition with the Wolff rearrangement.

Another possible side reaction of keto-carbene will be the 1, 3-dipolar addition to an unsaturated bond. Huisgen and his co-workers[3,4] investigated this addition extensively. They studied the competition of the 1, 3-dipolar addition with the Wolff rearrangement and concluded that the rearrangement was much faster than the addition. In the presence of copper powder, however, they successfully directed the reaction to the 1, 3-dipolar addition route. Keto-carbene co-ordinated to copper, and its further rearrangement was prevented.

Several workers[5] have successfully investigated the addition of benzoylcarbene and acetylcarbene to an ordinary double bond and to isolated cyclopropane derivatives respectively. In general, however, a triple bond is less reactive toward electrophilic attack than is a double bond.[6] Since carbene is known as an electrophilic reagnet,[7] its addition to a triple bond will be more sluggish than to a double bond. In other words, the Wolff rearrangement will compete more strongly in the addition of keto-carbene to a triple bond.

In the present investigation, the addition of various keto-carbenes, phenylbenzoylcarbene, benzoylcarbene and acetylcarbene, to diphenylacetylene and di-*n*-butylacetylene was studied. The successful one-step synthesis of some acylcyclopropenes will here be reported.

Results and Discussion

The thermal decomposition of azibenzil (I) in diphenylacetylene produced 2, 3, 4-triphenyl-1-naphthyl diphenylacetate (IV) in a 46.2% yield. In the presence of copper powder, the yield of IV was 28.7%. The basic hydrolysis of IV gave 2, 3, 4-triphenyl-1-naphthol (V) and diphenylacetic acid (VI). No cyclopropene derivative (III) was detected among the products in this case. The formation of IV is undoubtedly due to the preferential rearrangement of I to diphenylketene (VII).

Smith and Hoehn studied the reaction of diphenylacetylene with diphenylketene and isolated the

* Part I: I. Moritani and N. Obata, *Tetrahedron Letters*, **1965**, 2817.

** All correspondence should be addressed to I. M.

1) L. Wolff, *Ann.*, **325**, 129 (1902); F. Weygand, *Angew. Chem.*, **72**, 535 (1960).

2) L. I. Smith and H. H. Hoehn, "Organic Syntheses," Coll. Vol. III, 356 (1955).

3) R. Huisgen, H. Konig, G. Binsch and H. J. Strum, *Angew. Chem.*, **73**, 368 (1961).

4) R. Huisgen, ibid., **67**, 439 (1955); *Proc. Chem. Soc.*, **1961**, 357; *Angew. Chem.*, **75**, 604, 742 (1963); R. Huisgen, G. Binsch and L. Chosez, *Chem. Ber.*, **97**, 2628 (1964).

5) K. B. Wiberg and T. W. Hutton, *J. Am. Chem. Soc.*, **76**, 5367 (1954); R. J. Bohrbacher and N. H. Cromwell, ibid., **79**, 401 (1957); P. Yates and T. J. Clark, *Tetrahedron Letters*, **1961**, 435; J. Novák, J. Satuský, V. Šneberk and F. Šorm, *Collection Czechoslov. Chem. Communs.*, **22**, 1836 (1957).

6) F. Bohlmann, *Angew. Chem.*, **69**, 82 (1957); M. Nakagawa, "Atarashii-Yuhkigosei-hannoh (New Synthetic Organic Reaction)," Kagaku Zohkan, 11, Kagaku Dohjin, Kyoto (1962), p. 35.

7) P. S. Skell and R. M. Etter, *Chem. Ind.*, **1958**, 624; W. Kirmse, "Carbene Chemistry," Academic Press, New York (1964).

same material.[8] In the present experiment, both materials, IV and V, showed satisfactory results of elemental analysis and molecular weights.

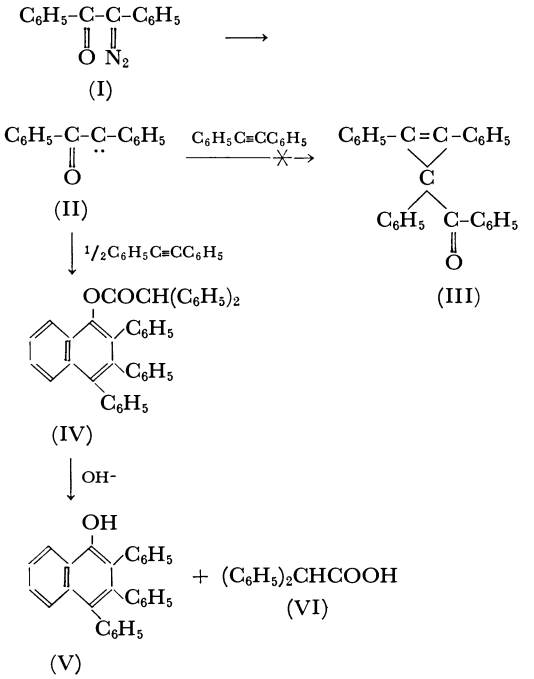

The structure of IV and V was further confirmed by the comparison of thier ultraviolet and proton magnetic resonance spectra with those of authentic 1, 2, 3-triphenyl-naphthalene. An attempt to transform V to a naphthalene derivative failed. *p*-Toluenesulfonate of V was treated with a large excess of Raney-nickel in ethanol,[9] but the tosyl group would not be removed.

Apparently, phenylbenzoylcarbene (II) rearranged preferentially; no carbenic addition product was detected. One possible reason for this preferential rearrangement could be a steric factor. It may be expected, therefore, that the replacement of the bulky phenyl group by hydrogen might make the carbenic addition to a triple bond possible. Thus, the thermal decomposition of diazoacetophenone, *p*-methoxy-diazoacetophenone and diazoacetone was investigated.

The decomposition of diazoacetophenone (VIII) in a large excess of diphenylacetylene resulted in the formation of two pure materials, X and XI. The infrared and ultraviolet spectra of X exhibited all of the characteristic absorptions of diphenylcyclopropene derivatives.[10] The results of the elemental analysis and the molecular weight determination were also in good agreement with the results for benzoyldiphenylcyclopropene.

Thus, compound X was identified as the desired cyclopropene derivative. Compound XI was found to be *trans*-1, 2, 3-tribenzoylcyclopropane on the basis of its melting point[11] and its infrared spectrum. The proton magnetic resonance spectrum was superimposable upon the reported one.[11c]

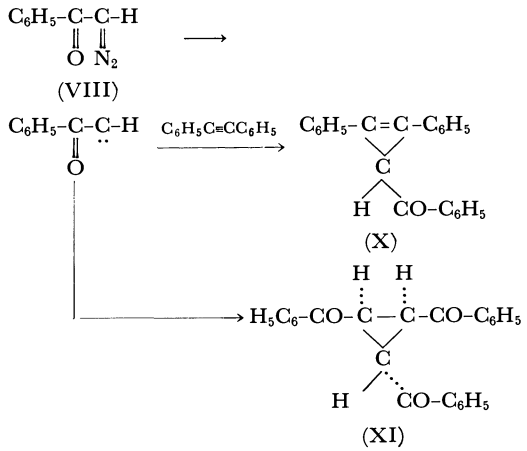

The structure of X was confirmed by the following observations. The permanganate oxidation of X produced tribenzoylmethane (XII) in a 57.1% yield. XII was identified by comparing it with an authentic sample.[12]

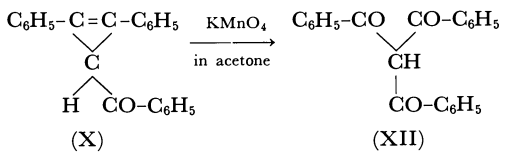

The reaction of 1, 2-diphenylcyclopropenylcarboxylic acid chloride, prepared via a different route,[13] with phenyl magnesium bromide gave an identical ketone (X).* Finally, the sodium borohydride reduction of X afforded phenyl-1, 2-diphenylcyclopropenyl carbinol in a very high yield.

The yields of X and XI were 1.2% and 7.8% respectively. The presence of copper powder markedly increased the yields, up to 8.1% for X and to 30.8% for XI.

Similarly, diazoacetophenone (VIII) was decomposed in di-*n*-butylacetylene, decyne-5, in the

8) L. I. Smith and H. H. Hoehn, *J. Am. Chem. Soc.*, **63**, 1180 (1941).
9) G. W. Kenner and M. A. Murray, *J. Chem. Soc.*, **1949**, Supplt. 178.
10) R. Breslow and Chin Yuan, *J. Am. Chem. Soc.*, **80**, 5991 (1958); R. Breslow, T. Eicher, A. Krebs, R. A. Peterson and J. Posner, ibid., **87**, 1320 (1965).
11) a) C. Grundmann, *Ann.*, **536**, 29 (1938); b) T. J. Clark and P. Yates, *J. Org. Chem.*, **27**, 286 (1962); c) J. A. Pople, W. G. Schneider and H. J. Bernstein, "High Resolution Nuclear Magnetic Resonance," McGraw-Hill Book Co., New York (1959), p. 289.
12) R. D. Abell, *J. Chem. Soc.*, **101**, 998 (1912).
13) R. Breslow, R. Boikess and M. Battiste, *Tetrahedron Letters*, **26**, 42 (1960).
* Breslow reported[13] the synthesis of X utilizing diphenylcadmium instead of phenyl magnesium bromide. The same reaction as the Breslow's was followed, but we could not obtained X.

presence of copper powder; 3-benzoyl-1, 2-di-*n*-butylcyclopropene-1 (XIII) was thus obtained in a 21.1% yield. A small amount of XI, 1.8%, was also formed.

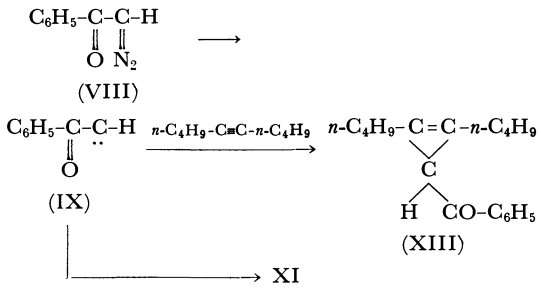

In the infrared region, compound XIII showed characteristic absorptions at 1667 cm^{-1} ($\nu_{C=O}$), and 1900 cm^{-1} ($\nu_{C=C}$). Its proton magnetic resonance spectrum is shown in Fig. 1. Aliphatic protons were separated nicely.

p-Methoxydiazoacetophenone (XIV) was also decomposed in diphenylacetylene in the presence of copper powder. The yield of 3-*p*-methoxybenzoyl-1, 2-diphenylcyclopropene-1 (XV) was 3.2%.

In a similar manner, diazoacetone (XVI) produced cyclopropene derivatives in both diphenyl acetylene and di-*n*-butylacetylene. The yields of XVII and XVIII was found to be 3.3% and 2.5% respectively.

All of the present results are summarized in Table I. The formation of *trans*-tribenzoylcyclopropane in a relatively large amount strongly suggests that the addition of acylcarbene to a triple bond is actually the case. It is known that the photodecomposition of pyrazolenine produces cyclopropene derivatives,[14] while thermally pyrazolenine is simply rearranged to aromatized pyrazol.[15] No example of its thermal decomposition to a cyclopropene derivative has yet been reported. Consequently, the intermediacy of pyrazolenine in the present study is practically out of the question.

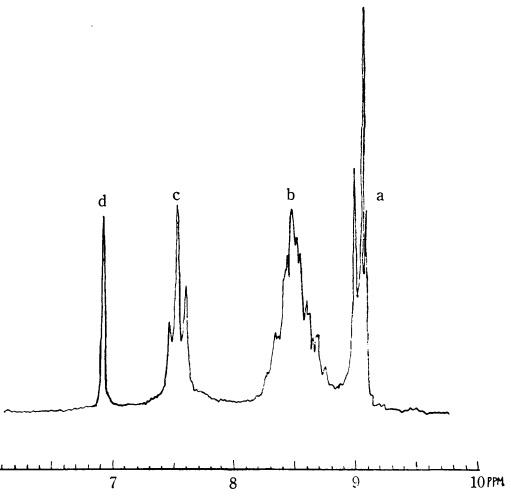

Fig 1. Proton magnetic resonance spectrum of 3-benzoyl-1, 2-di-*n*-butylcyclopropene-1.

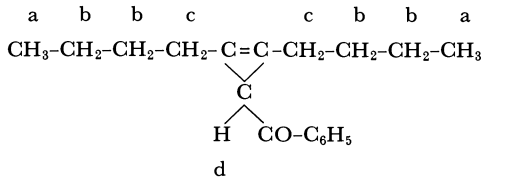

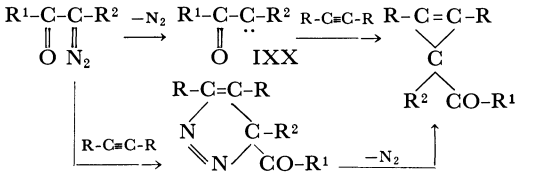

TABLE I. CYCLOPROPENE DERIVATIVES PRODUCED BY THE THERMAL DECOMPOSITION OF DIAZOKETONE IN THE PRESENCE OF COPPER POWDER AT 100°C

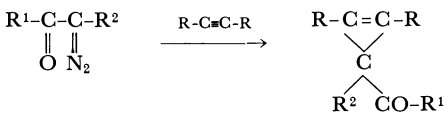

Run	Substituent		Acetylene	Solvent	Product, %	
	R^1	R^2			Cyclopropene	XI
1	C_6H_5	C_6H_5	Diphenyl	Diglyme	—	—
2	C_6H_5	H	Diphenyl	Diglyme	8.1	30.8
3	C_6H_5	H	Di-*n*-butyl	Diglyme	21.1	1.8
4	*p*-$CH_3OC_6H_4$	H	Diphenyl	Diglyme	3.2	—
5	CH_3	H	Diphenyl	Neat	3.3	—
6	CH_3	H	Di-*n*-butyl	Neat	2.5	—

14) G. L. Closs and W. A. Boll, *J. Am. Chem. Soc.*, **85**, 3904 (1963); G. Ege, *Tetrahedron Letters*, **1963**, 1667.

15) W. Kirmse and L. Horner, *Ann.*, **614**, 1 (1958); R. Hüttel, J. Riedl, H. Martin and F. Franke, *Chem. Ber.*, **93**, 1425 (1960); R. Hüttel, K. Franke, H. Martin and J. Riedl, ibid., **93**, 1433 (1960).

In the case of phenylcarbene, no addition to a triple bond occurred, whereas other carbenes IXX ($R^2=H$; $R^1=C_6H_5$, p-$CH_3OC_6H_4$, CH_3) added to a triple bond and produced yield. As is shown in Runs 2 and 3, the change in substituents on acetylene from the phenyl group to the *n*-butyl group resulted in a big increase in the yield of cyclopropene derivatives. This is understandable because of the difference in basicity between these two acetylenes. Substitution on carbene by more electron-releasing substituents, such as *p*-methoxybenzoyl and acetyl, instead of benzoyl reduced the yields of addition products. This is reasonable because of the electrophilic nature of the reacting carbene intermediate.

Experimental*

The Reaction of Azibenzil with Diphenylacetylene, 2, 3, 4-Triphenyl-1-naphthyl Diphenylacetate (IV).—A solution of azibenzil, m. p. 79—80°C with decomposition (reported m. p. 79°C (decomp.)[16]), 7.5 g. (0.034 mol.), in 25 ml. of digylme was added, drop by drop, to a solution of diphenylacetylene, 10.1 g. (0.057 mol.), in 5 ml. of diglyme at 140°C. The addition was completed after one and a half hours. The reaction mixture was then kept at 140°C for an additional 30 min. After it had cooled, the mixture was poured into a large amount of water. The organic material was extracted with ether three times. The combined ethereal solution (ca. 300 ml.) was washed successively with ten 50 ml. portions of water in order to remove the diglyme. After the solution had been dried with anhydrous magnesium sulfate, the ether was removed by evaporation and the residue was subjected to column chromatography. Activated alumina (250 g.) was used for this. Each fraction was analyzed by infrared and ultraviolet spectroscopy. Elution with petroleum ether afforded 8.65 g. (0.049 mol.) of recovered diphenylacetylene. Elution with benzene gave 4.4 g. (46.2%) of 2, 3, 4-triphenyl-1-naphthyl diphenylacetate, m. p. 169—170°C (chloroform) (reported m. p. 168—169°C[8]).

Found: C, 89.02; H, 5.34. Calcd. for $C_{42}H_{30}O_2$: C, 89.01; H, 5.34%. Mol. wt.: Found: 558, by freezing point-depression method in benzene. Calcd. for $C_{42}H_{30}O_2$: 556.7.

The characteristic infrared absorptions were 1760 cm^{-1} ($\nu_{C=O}$) and 1125 cm^{-1} (ν_{C-O}). The ultraviolet maxima in acetonitrile were 235 mμ (log ε 4.76) and 292 mμ (log ε 4.11). The NMR spectrum showed a multiplet (15 hydrogens) at 2.50—3.25τ and a singlet (1 hydrogen) at 5.02 τ.

In the presence of copper powder at 100°C, IV was obtained in a 28.7% yield.

2, 3, 4-Triphenyl-1-naphthol (V).—The hydrolysis of IV with pottasium hydroxide in a 50% water-ethanol mixture gave 2, 3, 4-triphenyl-1-naphthol, m. p. 162—163°C (ethanol) (reported m. p. 163°C[8]), in a 81% yield and diphenylacetic acid, m. p. 147—148°C (water) (reported m. p. 144—145°C[17]), in 74% yield. A mixed-melting-point determination of resultant diphenylacetic acid with an authentic material showed no depression.

The same naphthol derivative was also obtained by the reduction of diphenylacetate with litium aluminum hydride.

Found: C, 90.36; H, 5.42; O, 4.17; mol. wt., 326. Calcd. for $C_{28}H_{20}O$: C, 90.29; H, 5.42; O, 4.29%; mol. wt., 372.4.

The ultraviolet maxima in ethanol were 243 mμ (log ε 4.73), 260 mμ (log ε 4.58) and 310 mμ (log ε 3.95). The NMR spectrum showed a multiplet (19 hydrogens) at 1.65 —3.95τ, and a sharp singlet (1 hydrogen) at 4.61τ.

1, 2, 3-triphenylnaphthalene was prepared by following the known route[18]; m. p. 151.5—152.5°C. (ethanol-benzene) (reported m. p. 151°C[18]). Its UV and NMR spectra were very similar to those of V.

p-Toluenesulfonate of V was prepared by Tipson's method[19]; m. p. 171—172°C (ethanol). The *p*-toluenesulfonate (0.15 g.) thus obtained was treated with Raney nickel (5 g.) in ethanol (20 ml.) at the reflux temperature for 10 hr.[9] After the mixture had been worked up as usual the starting *p*-toluenesulfonate was obtained. Five days' refluxing gave the same results.

Found: C, 79.76; H, 4.91; S, 5.85. Clacd. for $C_{35}H_{26}O_3S$: C, 79.82; H, 4.97; S, 6.08%.

The Reaction of Diazoacetophenone with Diphenylacetylene, 3-Benzoyl-1, 2-diphenylcyclopropene (X).—A solution of diazoacetophenone, m. p. 46.5—47.5°C (reported m. p. 47—48°C[20]); 10.1 g. (0.069 mol.), in dried diglyme (40 ml.) was added, drop by drop, to a solution of diphenylacetylene (20.0 g. (0.11, mol.)) in dried diglyme (10 ml.) over a period of one and a half hours at 140°C. After the mixture had been worked up as in the former case, the reaction products were separated by alumina-column chromatography. After the recovered diphenylacetylene had been completely eluted out by petroleum ether, the eluent was changed to benzene. In relatively later fractions 3-benzoyl-1, 2-diphenylcyclopropene-1, 0.25 g. (1.2%); m. p. 152—153°C (ethanol), was obtained. After the eluent had been changed from benzene to ether, *trans*-1, 2, 3-tribenzoylcyclopropane, 0.55 g. (7.8%); m. p. 216—217°C (reported m. p. 215—217°C[11a,b]), was obtained in later fractions.

In a separate experiment, a mixture of 20.1 g. of diphenylacetylene, 9.95 g. of diazoacetophenone and 4.4 g. of copper powder was brought to reaction at 100°C. The yield of X was 1.62 g. (8.1%) and XI was 2.52 g. (30.8%).

The structure of X was identified on the basis of the following observations.

---

* Melting points are uncorrected. The molecular weights were determined by a vapor pressure osmometer unless otherwise stated. Diglyme (diethyleneglycol dimethyl ether) was dried over lithium aluminum hydride and distilled under reduced pressure.

16) C. D. Nenitzescu and E. Solomonica, "Organic Syntheses," Coll. Vol. II, 496 (1943).

17) C. S. Marvel, F. D. Hager and E. C. Caudle, ibid., Coll, Vol. I, 224 (1941).

18) L. I. Smith and H. H. Hoehn, *J. Am. Chem. Soc.*, **63**, 1184 (1941).

19) R. S. Tipson, *J. Org. Chem.*, **9**, 235 (1944).

20) P. Yates and B. L. Shapiro, *J. Am. Chem. Soc.*, **81**, 212 (1959).

Found: C, 89.10; H, 5.61; mol. wt., 280. Calcd. for $C_{22}H_{16}O$: C, 89.16; H, 5.44%; mol. wt., 296.3.

The infrared characteristic absorptions as a KBr pellet were 3060 cm^{-1}, 3020 cm^{-1} and 2990 cm^{-1} (ν_{C-H}), 1845 cm^{-1} ($\nu_{C=C}$) and 1668 cm^{-1} ($\nu_{C=O}$). The ultraviolet maxima were 228 mμ (log ε 4.39), 235 mμ (log ε 4.41), 244 mμ (log ε 4.28), 294 mμ(sh) (log ε 4.31), 308 mμ (log ε 4.40) and 321 mμ(sh) (log ε 4.24). NMR showed a multiplet (2 hydrogens) at 1.82τ, a multiplet (13 hydrogens) at 2.50τ, and a singlet (1 hydrogen) at 6.15τ.

2, 4-Dinitrophenylhydrazone of X was also prepared; m. p. 193—194°C (ethanol-benzene), Its infrared and ultraviolet spectra showed the presence of a cyclopropene skeleton.

Found: N, 11.85. Calcd. for $C_{28}H_{20}O_4N_4$: N, 11.76%.

trans-Tribenzoylcyclopropane (XI) gave the following results:

Found: C, 81.34; H, 5.21. Calcd. for $C_{24}H_{18}O_3$: C, 81.34; H, 5.12%.

NMR exhibited a multiplet (15 hydrogens) at 1.75 —2.80τ, a triplet (1 hydrogen) at 5.77τ, and a doublet (2 hydrogens) at 6.28τ.

The Oxidation of 3-Benzoyl-1, 2-diphenylcyclopropene, Tribenzoylmethane (XII).—Ketone X (0.230 g. (0.00077 mol.)) was dissolved in 10 ml. of acetone, and an acetone solution of potassium permanganate was then added to it drop by drop. The addition of permanganate was stopped when the solution did not discolor. After the filtration of manganese(IV) oxide, the reaction mixture was poured into a large amount of water, and the organic material was extracted with benzene three times. The combined benzene solution was then washed with water and dried over anhydrous magnesium sulfate. The evaporation of benzene gave a white solid material, tribenzoylmethane, m. p. 232—233°C (benzene) (reported 224 —226°C[12]); 0.145 g. (57.1%).

Found: C, 80.13; H, 5.01. Calcd. for $C_{22}H_{16}O_3$: C, 80.47; H, 4.91%.

The same material was prepared from dibenzoylmethane and benzoyl chloride.[12] The mixed melting point of two samples showed no depression. The infrared spectra of the two samples were superimposable.

The Reaction of Diphenylcyclopropenecarboxylic Acid Chloride with Phenyl Magnesium Bromide, 3-Benzoyl-1, 2-diphenylcyclopropene (X).—A mixture of 1.20 g. (0.0049 mol.) of 1, 2-diphenylcyclopropenecarboxylic acid, m. p. 208—209°C (reported m. p. 209—211°C),[21] and a large excess of oxalyl chloride was heated under refluxing for 2 hr.[22] The excess oxalyl chloride was removed by distillation. To the residue benzene and petroleum ether were added, and then they were removed under reduced pressure. The residual white solid material was dissolved in 50 ml. of absolute ether. To this solution there was added, drop by drop, a solution of a Grignard reagent, prepared from 1.6 g. of bromobenzene and 0.36 g. of magnesium in 20 ml. of absolute ether, at 0°C. After this mixture had been worked up as usual, there was obtained a white solid, 3-benzoyl-1, 2-diphenylcyclopropene, m. p. 152—153°C (no melting point was reported in the literature[13]); 0.64 g. (44.1%). This sample showed no melting point depression when mixed with the sample obtained above.

An attempt to follow Breslow's procedure,[13] utilizing diphenyl cadmium instead of a Grignard reagent, failed; the material isolated was the original carboxylic acid, m. p. 208—209°C.

The Sodium Borohydride Reduction of X, Phenyl - 1, 2 - diphenylcyclopropenyl Carbinol.—Benzoylcyclopropene (X) (0.327 g. (0.0011 mol.)) was reduced with sodium borohydride (0.053 g.) in ethanol (10 ml.) at reflux temperature for 3 hr. Carbinol, m. p. 84—85°C (petroleum ether); 0.265 g. (81%), was obtained.

Found: C, 88.73; H, 6.41. Calcd. for $C_{22}H_{18}O$: C, 88.56; H, 6.08%.

The infrared characteristic absorptions were 3200 cm^{-1} (ν_{O-H}) and 1810 cm^{-1} ($\nu_{C=C}$). The ultraviolet maxima in ethanol were 224 mμ (log ε 4.39), 230 mμ (log ε 4.44), 237 mμ (log ε 4.35), 310 mμ (log ε 4.30), 320 mμ (log ε 4.39) and 337 mμ (log ε 4.22). The NMR spectrum showed a multiplet (15 hydrogens) at 2.27—2.95τ, a doublet (1 hydrogen) at 5.54τ (J=7 c. p. s.), doublet (1 hydrogen) at 7.57τ (J=7 c. p. s.) and a singlet (broad, 1 hydrogen) at 7.94τ.

3-Benzoyl-1, 2-di-*n*-butylcyclopropene-1 (XIII).—Decyne-5[23] (15.25 g. (0.11 mol.)) and copper powder (7.35 g.) were placed in a reaction flask, and to them there was added 7.35 g. (0.0503 mol.) of diazoacetophenone[20] in 20 ml. of diglyme at 100°C were a period of two hours. After this mixture had been worked up as above, *trans*-tribenzoylcyclopropane (XI) was separated (0.314 g. (1.8%)). A fraction eluted with petroleum ether containing 10% ether was collected and distilled. 3-Benzoyl-1, 2-di-*n*-butylcyclopropene (XIII) boiled at 131—132°C (3×10^{-1} mmHg) (n_D^{20} 1.5202).

Found: C, 83.99; H, 9.59; mol. wt., 268. Calcd. for $C_{18}H_{24}O$: C, 84.32; H, 9.44%; mol. wt., 256.4.

The infrared characteristic absorptions were 1900 cm^{-1} ($\nu_{C=C}$) and 1667 cm^{-1} ($\nu_{C=O}$).

3-*p*-Methoxybenzoyl-1, 2-diphenylcyclopropene-1 (XV).—To a mixture of diphenylacetylene (18.15 g. (0.102 mol.)) and copper powder (3.8 g.) in 10 ml. of diglyme there was added 9.9 g. (0.056 mol.) of *p*-anisyl-diazomethane[24] in 30 ml. of diglyme over a two-hour period at 100°C. After this mixture had been worked up as above, 0.590 g. (3.2%) of 3-*p*-methoxybenzoyl-1,2-diphenylcyclopropene (XV) was obtained, m. p. 137—138°C (ethanol).

Found: C, 84.40; H, 5.54. Calcd. for $C_{23}H_{18}O_2$: C, 84.64; H, 5.56%.

The characteristic infrared peaks were 1840 cm^{-1} ($\nu_{C=C}$) and 1665 cm^{-1} ($\nu_{C=O}$). The ultraviolet maxima in ethanol were 223 mμ (log ε 4.57), 234 mμ (log ε 4.40), 292 mμ (log ε 4.64), 308 mμ (log ε 4.56) and 324 mμ (log ε 4.35). The NMR spectrum showed a doublet (2 hydrogens) at 1.90τ, a multiplet (10 hydrogens) at 2.30—2.80τ, a doublet (1 hydrogen) at 3.12τ, a singlet (3 hydrogen) at 6.18τ, and a singlet (1 hydrogen) at 6.30τ.

21) R. Breslow, R. Winter and M. Battiste, *J. Org. Chem.*, **24**, 415 (1959).
22) R. Breslow, J. Lockhart and A. Small, *J. Am. Chem. Soc.*, **84**, 2793 (1962).
23) E. A. Bride and G. F. Hennion, ibid., **59**, 1310 (1937).
24) A. C. Wilds and A. L. Meader, *J. Org. Chem.*, **13**, 763 (1948).

3-Acetyl-1, 2-diphenylcyclopropene-1 (XVII).—ω-Diazoacetone[24] (10.59 g. (0.110 mol.)) in 20 ml. of diglyme was added, drop by drop, to a mixture of 23.46 g. (0.132 mol.) of diphenylacetylene and 6.35 g. of copper powder in 10 ml. of diglyme at 100°C over the period of one hour. The reaction mixture was then treated in a manner similar to that described previously. From the fraction eluted out by an ether-benzene mixture, 3-acetyl-1,2-diphenylcyclopropene-1, m. p. 101—102°C (petroleum ether), was obtained in 3.3% yield.

Found: C, 87.12; H, 6.14; mol. wt., 230. Calcd. for $C_{17}H_{14}O$: C, 87.15; H, 6.14%; mol. wt., 234.3.

The infrared characteristic absorptions were 1840 cm^{-1} ($\nu_{C=C}$) and 1685 cm^{-1} ($\nu_{C=O}$). The ultraviolet maxima in ethanol were 226.5 mμ (log ε 4.37), 234 mμ (log ε 4.32), 283 mμ (log ε 4.24), 294 mμ (log ε 4.35), 318 mμ (log ε 4.38) and 330 mμ (log ε 4.34). The NMR spectrum exhibited a singlet (1 hydrogen) at 7.18τ, a singlet (3 hydrogens) at 8.25τ, and a multiplet (10 hydrogens) at 2.25—2.80τ.

2, 4-Dinitrophenylhydrazone of XVII melted at 210—211°C (decomp.) (an ethanol-benzene mixture).

Found: C, 66.96; H, 4.43. Calcd. for $C_{23}H_{18}O_4N_4$: C, 66.60; H, 4.38%.

p-Toluenesulfonylhydrazone of XVII was also prepared; m. p. 180—181°C (benzene).

Found: C, 71.86; H, 5.51. Calcd. for $C_{24}H_{22}O_2N_2S$: C, 71.61; H, 5.51%.

The Sodium Borohydride Reduction of XVII.—Ketone XVII (0.230 g.) was reduced by sodium borohydride (0.096 g.), in ethanol at the reflux temperature. Methyl-1, 2-diphenylcyclopropenyl carbinol, m. p. 78—79°C (petroleum ether), was obtained in a 96.1% yield.

Found: C, 85.99; H, 6.78. Calcd. for $C_{17}H_{16}O$: C, 86.40; H, 6.83%.

The characteristic infrared peaks were 3200 cm^{-1} (ν_{O-H}), 1810 cm^{-1} ($\nu_{C=C}$) and 1075 cm^{-1} (ν_{C-O}). The ultraviolet .maxima were 224 mμ (log ε 4.39), 230 mμ (log ε 4.44), 237 mμ (log ε 4.35), 310 mμ (log ε 4.30), 320 mμ (log ε 4.39), and 337 mμ (log ε 4.22). The NMR spectrum exhibited multiplet (10 hydrogens) at 2.25—2.90τ, a multiplet (1 hydrogen) at 6.12τ, a doublet (1 hydrogen) at 7.75τ, a broad singlet (1 hydrogen) at 8.20τ, and a doublet (3 hydrogens) at 8.80τ.

3-Acetyl-1, 2-di-*n*-butylcyclopropene-1 (XVIII).—A solution of ω-diazoacetone[24] (9.20 g. (0.11 mol.)) in 20 ml. of diglyme was added, drop by drop, to a mixture of 27.35 g. (0.197 mol.) of decyne-5 and 6.38 g. of copper powder at 100°C over a two-hour. After the usual treatment of the reaction mixture, fractions were eluted by a petroleum ether - ether mixture, collected, and distilled. 3-Acetyl-1, 2-di-*n*-butylcyclopropene-1, b. p. 77—78°C/0.3 mmHg; 0.485 g. (2.5%), was thus obtained.

Found: C, 79.91; H, 11.30. Calcd. for $C_{13}H_{22}O$: C, 80.35; H, 11.41%.

The infrared spectrum showed characteristic absorptions at 1895 cm^{-1} ($\nu_{C=C}$) and 1685 cm^{-1} ($\nu_{C=O}$). The NMR spectrum exhibited a triplet (4 hydrogens) at 7.58τ, a singlet (1 hydrogen) at 7.84τ, a singlet (3 hydrogens) at 8.16τ, a multiplet (8 hydrogens) at 8.52τ, and a triplet (6 hydrogens) at 9.06τ.

BULLETIN OF THE CHEMICAL SOCIETY OF JAPAN VOL. 39 1980—1988 (1966)

The Synthesis and Reactions of Benzo-1, 4-thiazinotropone Derivatives*[1]

By Tetsuo NOZOE, Toyonobu ASAO and Kazuko TAKAHASHI

Department of Chemistry, Faculty of Science, Tohoku University, Katahira-cho, Sendai

(Received December 29, 1965)

Three isomeric benzo-1, 4-thiazinotropones were obtained. Benzo-1, 4-thiazino[3, 2-b]tropones substituted with the chloro, the bromo, the nitro or the acetamido group at the seven-membered ring were synthesized by the reaction of di- or trihalotropolone, or 3-bromotropolones with the nitro or the acetamido group, with *o*-aminothiophenol. The bromination of benzo-1, 4-thiazino[3, 2-b]tropone (I) and its 8-isopropyl derivative (II) afforded 7- and/or 9-substituted compounds. In the case of nitration, 5-oxide and 5-oxide of 7-nitro derivative were obtained. The reaction of I or II with thionyl chloride unexpectedly gave the 7, 9-dichloro derivative of I, or four kinds of chloro derivatives of II.

The preparation of benzo[b]tropothiazine (cyclohepta[b]benzo[e]-1, 4-thiazine) (I), benzo-1, 4-thiazino[3, 2-b]tropone (cyclohepta[b]benzo-1, 4-thiazine-10(11*H*)-one) (II), and their alkyl and methoxyl derivatives by the reaction of 2-halotropones or 3-halotropolones with *o*-aminothiophenol has been reported.[1] The present paper will deal with the synthesis of the isomeric compounds and the various derivatives of II, and with some electrophilic substitution reactions of these compounds.

The condensation of 2-chloro-3-hydroxytropone[2]

*1 Presented at the 13th Annual Meeting of the Chemical Society of Japan, Tokyo, April, 1960.

1) T. Nozoe, T. Asao and K. Takahashi, This Bulletin, **34**, 146 (1961).

2) S. Seto, *Sci. Repts. Tohoku Univ.*, **I, 73**, 275 (1953).

with *o*-aminothiophenol (III) in methanol gave a small amount of a compound which could not be purified. However, when a solution of 2-chloro-3-methoxytropone (IV)[2] and III in methanol was allowed to stand in an ice bath, benzo-1, 4-thiazino[2, 3-b]tropone (V) was obtained as violet needles in a 23% yield. The condensation of 2-chloro-5-methoxytropone (VI; R=Me)[3] with III at 0°C gave an oily substance (VII). The analytical values of VII satisfied the formula, $C_{13}H_9ONS$, and the infrared and ultraviolet spectra of VII were completely in agreement with those of the product obtained from the reaction of 2-chloro-5-hydroxytropone (VI; R=H)[3] and III. These facts indicate that the methoxy group of 2-chloro-5-methoxytropone was hydrolyzed during the reaction with III.

It is known[1] that II exists as the keto form (IIa) rather than the enol form (IIb). The structure of V and VII were also examined for the

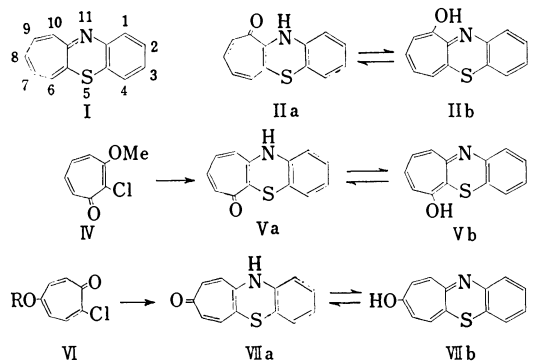

presence of any keto-enol tautomerism. The compounds V and VII were slightly soluble in an acidic medium but not in an alkaline medium, and they did not form any molecular compound such as a picrate.

The ultraviolet spectra (Fig. 1) of V in methanol and in an acidic medium are essentially similar to those of II, and the infrared spectrum of V displays

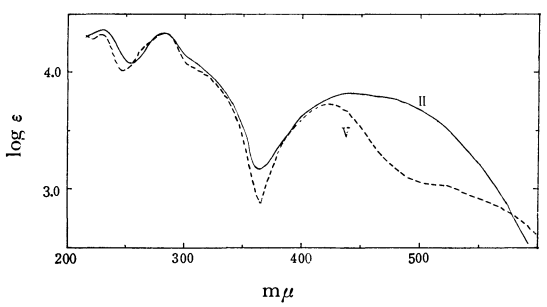

Fig. 1. Ultraviolet absorption spectra of II and V in MeOH.

3) T. Nozoe, T. Asao, E. Takahashi and K. Takahashi, This Bulletin, **39**, 1310 (1966).

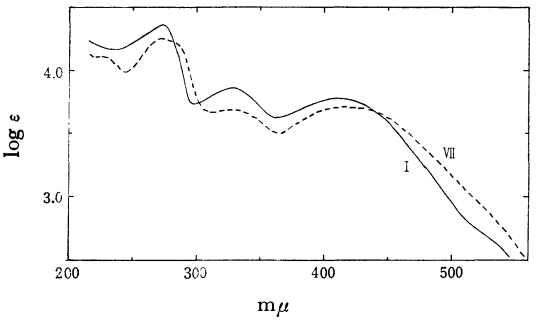

Fig. 2. Ultraviolet absorption spectra of I and VII in MeOH.

peaks at 3280, 3200, 1633 and 1615 cm^{-1} which are not observed in the spectrum of I. From these observations, it may be assumed that V exists as its keto form (Va) rather than as the enol form (Vb). The ultraviolet spectra (Fig. 2) of VII in methanol and in an acidic medium are similar to those of I rather than to those of II; however, the infrared spectrum of VII shows a peak at 1630 cm^{-1} (C=O). From these facts alone, it is difficult to draw any conclusions regarding the tautomerism of VII. A further, detailed investigation of the tautomerism of these isomeric thiazinotropones will, therefore, be carried out.

The reactions of *o*-aminothiophenol (III) with the following halotropolones have been studied. 3, 6-Dibromotropolone,[4] when treated with two molar equivalents of III in methanol, gave three compounds, as deep violet plates (VIII), red crystals (IX) and violet plates (X). From their analysis and absorption spectra, VIII was shown to be a pentacyclic compound formed by the condensation of two molecules of III with one molecule of 3, 7-dibromotropolone, as is shown in the scheme, while IX and X were shown to be the 9-*o*-aminophenylthio- and 9-bromo-derivatives of II respectively.

The application of one molar equivalent of III to 5, 7-dibromohinokitiol (3, 5 - dibromo - 6 -isopropyltropolone)[5] afforded the 7-*o*-aminophenylthio-8-isopropyl derivative of II (XI), plus a small amount of a compound which is assumed to be the 7-bromo-8-isopropyl derivative (XII). The 7-bromo-9-isopropyl derivative of II (XIII) was obtained by refluxing 5, 7-dibromo-α-thujaplicine (3, 5-dibromo-7-isopropyltropolone)[6] and III in methanol for 5 hr. However, 3-*o*-aminophenylthio - 5 - bromo - 7 - isopropyltropolone (XIV) was obtained in addition to XIII when the above mixture was refluxed for 2.5 hr.; XIV was

4) T. Nozoe, Y. Kitahara, K. Yamane and A. Yoshikoshi, *Proc. Japan Acad.*, **27**, 18 (1951).
5) T. Nozoe, K. Kikuchi and T. Ando, ibid., **26 (10)**, 32 (1950).
6) T. Nozoe, Y. Kitahara and T. Ikemi, ibid., **27**, 193 (1951).

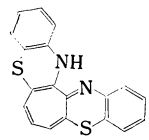

VIII

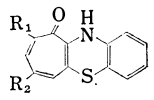

IX R_1=-S-, R_2=H (H_2N)

X R_1=Br, R_2=H

XIII R_1=isoPr, R_2=Br

XV R_1=R_2=Br

XVII R_1=R_2=Cl

XIX R_1=H, R_2=NO_2

XXII R_1=H, R_2=$NHCOCH_3$

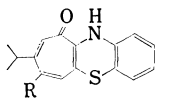

XI R=-S- (H_2N)

XII R=Br

XX R=NO_2

XXIII

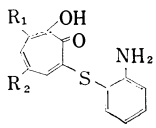

XIV R_1=isoPr, R_2=Br

XVI R_1=R_2=Br

XVIII R_1=R_2=Cl

XXI R_1=H, R_2=NH_2

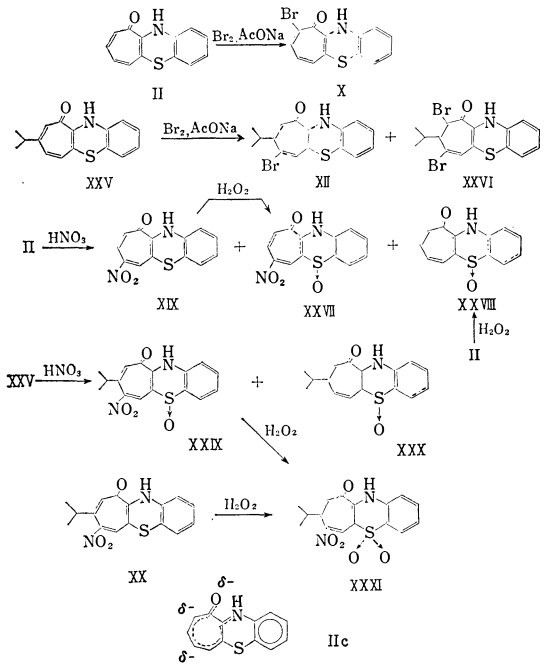

then converted into XIII by refluxing it in acetic acid. The difficulty in the cyclization of XIV is considered to be due to the steric interference and to the electron releasing effect of the isopropyl group.

On refluxing 3, 5, 7-tribromotropolone[7] and III in methanol, the 7,9-dibromo derivative XV was obtained in a good yield. On the other hand, when the reaction mixture was allowed to stand at room temperature, 3-*o*-aminophenylthio-5, 7-dibromotropolone (XVI) was obtained as the main product, in addition to some XV; XVI, on being heated above its melting point, afforded XV. Similar results were obtained in the reaction of 3, 5, 7-trichlorotropolone[8] and III, which afforded the 7, 9-dichloro derivative XVII as well as 3-*o*-aminophenylthio-5, 7-dichlorotropolone (XVIII). XVIII was converted into XVII on being heated above its melting point. When a mixture of 3-bromo-5-nitrotropolone[9] and III in methanol was allowed to stand at room temperature, the 7-nitro derivative of II (XIX) was obtained as black needles.

The nitration of 7-bromohinokitiol afforded two crystalline substances, m. p. 136°C and 111°C, which were considered to be stereoisomers of 7-bromo-5-nitrohinokitiol.[10] However, the latter compound has been shown recently[11] to be a mixture of 7-bromo-5-nitrohinokitiol and a small amount of 7-bromo-3-nitrohinokitiol. The application of III to each of these two substances afforded the same compound, the 7-nitro-8-isopropoyl derivative XX, but the isomeric 9-nitro-8-isopropyl derivative could not be isolated.

When 5-amino-3-bromotropolone[4,12] was allowed to react with III, only 5-amino-3-*o*-aminophenylthiotropolone (XXI) was obtained, even when the reaction mixture was refluxed. The compound XXI did not cyclize when heated above its melting point, and the starting material was recovered, while the *N, N'*-diacetyl derivative was formed when XXI was heated with acetic anhydride. This resistance to cyclization may be attributed to the electron-releasing resonance effect of the amino group in the tropolone nucleus. If this is so, cyclization may be expected to occur when 5-acetamido-3-bromotropolone is used instead of 5-amino-3-bromotropolone. Indeed, both the *N*-acetyl and *N, O*-diacetyl derivatives[4] of 5-amino-3-bromotropolone afforded the 7-acetamido derivative of II (XXII) when they were refluxed with *o*-aminothiophenol (III).

The reactions of 2, 3-, 2, 5- and 2, 7-dibromotropones with III gave no definite compound; only

7) T. Nozoe, S. Seto, Y. Kitahara, M. Kunori and Y. Nakayama, ibid., **26 (7)**, 38 (1950).

8) W. von E. Doering and L. H. Knox, *J. Am. Chem. Soc.*, **74**, 5683 (1952).

9) T Nozoe, Y. Kitahara, K. Doi and T. Arai, *Bull. Research Inst. Non-Aq. Solns., Thohoku Univ.*, **7**, 13 (1957).

10, T. Nozoe, Y. Kitahara, E. Kunioka and K. Doi, *Proc. Japan Acad.*, **26 (9)**, 38, 40 (1950).

11) L. C. Lin, T. Nozoe, T. Mukai and Y. Kitahara, *Sci. Repts. Tohoku Univ.*, **I, 48**, 96 (1964).

12) T. Nozoe, S. Seto, H. Takeda and T. Sato, ibid., **I, 35**, 274 (1952).

resinous products were obtained. The reactions of 7-amino-, 7-acetamido- and 7-diethylamino-2-bromotropone with III resulted in the complete recovery of the starting materials, whereas 7-benzamido-2-bromotropone yielded 7-benzamido-2-*o*-aminophenylthiotropone (XXIII), which did not afford any cyclization product, even when heated.

The general method utilized for the synthesis of phenothiazines, i. e., the reaction of diphenylamines and sulfur, was applied to 2-toluidinotropone, but the desired product was not obtained; only resinous products were formed.

The bromination of I in acetic acid in the presence of sodium acetate gave a poor yield of compound XXIV, assumed to be the tribromo derivative, in addition to a considerable amount of the recovered starting material. The ultraviolet spectrum*2 of XXIV shows a considerable hypsochromic shift. Furthermore, the 743 cm^{-1} band, due to the out-of-plane deformation of a 1, 2-disubstituted benzene, is present in the infrared spectrum of compound I, but not in the spectrum of XXIV. Therefore, it appears that some substitution must have occurred not only in the seven-membered ring but also in the benzene ring. However, the structure of XXIV could not be established.

The bromination of II afforded a monobromo derivative identical with the 9-bromo derivative X. The bromination of 8-isopropylbenzo-1, 4-thiazino[3, 2-b]tropone (XXV) afforded two products. One of the products was shown to be the 7-bromo derivative XII which had been obtained previously by the reaction of 5, 7-dibromohinokitiol and *o*-aminothiophenol. The structure of the second product, the analyses of which are in accord with those of a dibromo derivative of XXV, was deduced from the facts that its infrared spectrum shows absorption at 750 cm^{-1}, due to an out-of-plane deformation of a 1, 2-disubstituted benzene nucleus, and that its ultraviolet spectrum is similar to those of the 7, 9-dichloro- and the 7, 9-dibromo derivatives of II. This indicates that the compound is the 7, 9-dibromo derivative XXVI.

The nitration of I with fuming nitric acid did not give any definite product except the starting material. However, when II was treated with fuming nitric acid in acetic acid, three compounds were isolated. One of the compounds was found to be identical with the 7-nitro derivative XIX. The other two compounds (XXVII and XXVIII) have molecular formulae of $C_{13}H_9O_2NS$ and $C_{13}H_8O_4N_2S$ respectively, and they exhibit infrared absorption at 1026 and 1027 cm^{-1} respectively, due to a sulfoxide group[13]; therefore, they are considered to be the sulfoxide of II and its mononitro derivative respectively. Actually, XXVIII has also been obtained by the oxidation of II with hydrogen peroxide in acetic acid; this will be described in the following paper. The nitro group in XXVII must be located at the 7-position, since XXVII was also obtained by the oxidation of XIX. The nitration of XXV afforded two products XXIX and XXX. From their analyses and their infrared spectra, it was found that XXIX is the mononitro derivative of the simple sulfoxide XXX. In order to determine the position of the nitro group in XXIX, the authentic 7-nitro compound XX was oxidized with hydrogen peroxide. However, the product was not XXIX, but the sulfone XXXI, which shows absorptions due to a sulfone group[13] at 1295, 1284, 1151 and 1135 cm^{-1} in its infrared spectrum. However, the oxidation of XXIX in the same manner also gave XXXI, thus confirming that XXIX is the 7-nitro derivative of XXX. Similar examples of the oxidation of sulfide by nitric acid have often been observed with the phenothiazines. The oxidation of benzo-1, 4-thiazino[3, 2-b]tropones will be reported in the following paper.

From the results of the above electrophilic substitution reactions, it may be concluded that the ionic structure IIc of II contributes greately to these reactions.

Tropones condensed with some five-membered heterocycles, such as 3-phenylpyrrolo[2, 3-b]-tropone (XXXII)[14] and 2-hydroxyimidazolo-[5, 4-b]tropone (XXXIII)[15] which in part have a structural similarity to benzo-1, 4-thiazino-[3, 2-b]tropones, afforded their chloro derivatives, 8-chloro-3-phenyl-1-azaazulene and 2, 4-dichloro-1, 3-diazaazulene respectively, on treatment with phosphorus oxychloride or thionyl chloride. These reactions are considered to proceed through the enol forms. Although II is considered to exist as its keto form,[1] if II is able to assume the enol form, it may be expected that the 10-chloro derivative of I might be obtained by the reaction of II with some chlorinating reagents. The reaction of II with phosphorus oxychloride in pyridine resulted in the complete recovery of the starting material. However, on being treated with 1.25 molar equivalents of thionyl chloride in dry benzene, II afforded, as violet needles, a product which was not the expected 10-chloro derivative of I, but the 7, 9-dichloro derivative of II (XVII) obtained already by the reaction of 3, 5, 7-trichlorotropolone and *o*-aminothiophenol.

The reaction of XXV and thionyl chloride was carried out, and four products were obtained as

*2 See Experimental Section.

13) L. J. Bellamy, "The Infrared Spectra of Complex Molecules," Methuen and Co., London (1958), p. 350.

14) T. Nozoe, Y. Kitahara and J. Shin, to be published.

15) T. Nozoe, T. Mukai and K. Matsumoto, to be published.

follows. By heating XXV with 1.25 molar equivalents of thionyl chloride in dry benzene, red violet prisms (XXXIV), m. p. 156°C, and violet needles (XXXV), m. p. 156°C, were obtained, while from another run of the reaction, red violet plates (XXXVI), m. p. 149°C, were obtained in addition to the compound XXXV. Each of these products showed a depression in its melting point when mixed with any of the others. When XXV was treated with 2.5 molar equivalents of thionyl chloride, it yielded violet needles (XXXVII), m. p. 210°C. The yields of these four products in the crude state were moderate, but their purification proved difficult; consequently, the yields of the pure compounds were fairly low.

The structures of these four products were not determined chemically, but from a consideration of the results of their analyses and their ultraviolet and infrared spectra; the following conclusions were reached. The ultraviolet spectra of these four products show that they have not undergone any skeletal change. The infrared spectra of XXXIV, XXXV and XXXVI show peaks between 741—745 cm^{-1}, due to the out-of-plane deformations of a 1, 2-disubstituted benzene; therefore, it is considered that no substitution has taken place in the benzene rings of these three products. Analyses showed the molecular formulae of XXXIV—XXXVII to be $C_{16}H_{13}ONSCl_2$, $C_{16}H_{14}ONSCl$, $C_{16}H_{14}ONSCl$ and $C_{16}H_{12}ONSCl_3$, respectively. Since the ultraviolet spectrum of XXXIV is similar to those of the 7, 9-dihalo derivatives XV, XVII and XXVI, XXXIV is

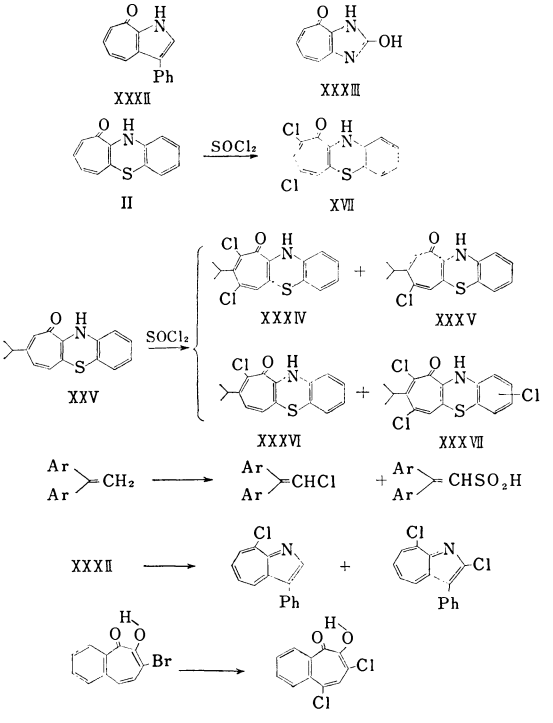

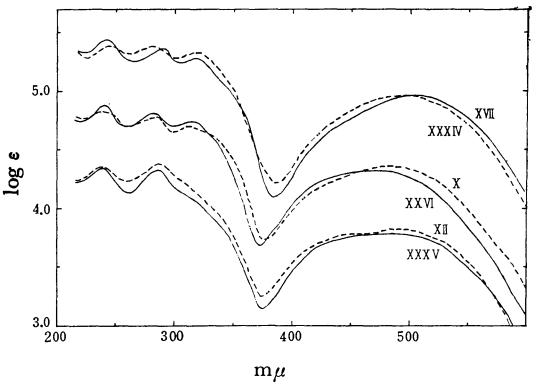

Fig. 3. Ultraviolet absorption spectra of X, XII, XVII, XXXIV, XXXV and XXXVI in MeOH.

assumed to be the 7, 9-dichloro derivative of XXV. The ultraviolet spectra of XXXV and XXXVI are similar to those of XII and X respectively; therefore, it is assumed that they are the 7-chloro and the 9-chloro derivatives of XXV respectively. Two of the three chlorine atoms in XXXVII are considered to be located at the 7- and 9- positions; since its infrared spectrum shows no absorption attributable to a 1, 2-disubstituted benzene, the remaining chlorine atom might be substituted in the benzene ring. However, its position could not be defined.

It is clear from the above that the reactions of benzo-1, 4-thiazino[3, 2-b]tropones with thionyl chloride result in the formation of products chlorinated at the 7- and/or the 9-positions. However, when the compound I was treated with thionly chloride, the reaction resulted in the recovery of the starting material and the formation of a small amount of an undefined, amorphous product.

Such substitutions involving the replacement of a hydrogen atom by the chlorine atom of thionly chloride, without the use of a catalyst, have also been observed in other cases. Patai and Bergmann[16] reported that the reaction of 1, 1-diarylethylene and thionyl chloride afforded mainly 1, 1-diaryl-2-chloroethylene and a small amount of 1, 1-diarylethylenesulfinic acid. Nozoe et al.[14] found that 2, 8-dichloro-3-phenyl-1-azaazulene and 8-chloro-3-phenyl-1-azaazulene were obtained from the reaction of XXXII with thionyl chloride, while Ebine[17] reported that the reaction of 7-bromo-3, 4-benzotropone with thionyl chloride gave an adduct which was converted into 5,7-dichloro-3, 4-benzotropone by recrystallization from ethanol.

Patai et al. has explained the mechanism of the above reaction by assuming that the reaction proceeds through the attack of an SOCl cation at

16) S. Patai and F. Bergmann, *J. Am. Chem. Soc.*, **72**, 1034 (1950).
17) S. Ebine, This Bulletin, **34**, 881 (1961).

a highly negative position, followed by the elimination of SO. Our results are inconsistent with the above mechanistic consideration, since, as has been mentioned previously, the position which undergoes chlorination with thionyl chloride is the same as that which is attacked by electrophilic reagents.

Experimental*3

Benzo-1, 4-thiazino[2, 3-b]tropone (V).—To a solution of 2-chloro-3-methoxytropone (IV) (100 mg.) in methanol (5 ml.), *o*-aminothiophenol (III) (80 mg.) was added; the mixture was then allowed to stand for 6 hr. in an ice box. The crystals which precipitated out were collected by filtration and recrystallized from a large amount of methanol, thus affording 30 mg. of V as black needles, m. p. 286°C (decomp.).

Found: C, 68.89; H, 4.03; N, 6.20. Calcd. for $C_{13}H_9ONS$: C, 68.72; H, 3.99; N, 6.17%.

λ_{max}^{MeOH} mμ (log ε): 230 (4.32), 285 (4.35), 320sh (3.96), 425 (3.71).

$\lambda_{max}^{0.1N\ HCl}$ mμ (log ε): 235 (4.28), 292 (4.41), 334 (3.90), 440 (3.74).

Benzo-1, 4-thiazino[4, 5-b]tropone (VII).—a) To a solution of 2-chloro-5-methoxytropone (VI; R=Me) (200 mg.) in methanol (8 ml.), III (167 mg.) was added; the mixture was then allowed to stand for 48 hr. in an ice box. The solvent was removed, the residue was dissolved in benzene, and the solution was washed with 2 N hydrochloric acid, followed with a 2 N sodium hydroxide solution and water, each three times, dried, and passed through an alumina column. Removing the solvent from the effluent gave 70 mg. of VII as a reddish oil.

Found: C, 68.91; H, 4.38; N, 5.68. Calcd. for $C_{13}H_9ONS$: C, 68.72; H, 3.99; N, 6.17%.

λ_{max}^{MeOH} mμ (log ε): 225 (4.24), 275 (4.25), 330 (3.69), 418 (3.70).

$\lambda_{max}^{0.1N\ HCl}$ mμ (log ε): 238 (4.20), 288 (4.13), 358 (3.95), 460—470 (3.46).

b) A solution of 2-chloro-5-hydroxytropone (VI; R=H) (110 mg.) and III (91.5 mg.) in methanol (15 ml.) was refluxed for one hour. The black resinous substance obtained by removing the solvent was dissolved in chloroform and passed through an alumina column; a reddish oily substance was thus obtained. Its infrared and ultraviolet spectra were superimposable upon those of VII obtained by procedure a).

The Reaction of 3, 7-Dibromotropolone with *o*-Aminothiophenol (III).—When a solution of 3, 7-dibromotropolone (280 mg.) and III (260 mg.) in methanol (8 ml.) was refluxed for 2.5 hr., 240 mg. of crude crystals were obtained. The crystals were separated into a soluble part A and an insoluble part B in benzene, and B was recrystallized from pyridine-ethanol, thus yielding VIII as deep violet plates, m. p. 175—176°C.

Found: C, 68.33; H, 3.42; N, 8.52. Calcd. for $C_{19}H_{12}N_2S_2$: C, 68.67; H, 3.64; N, 8.43%.

λ_{max}^{MeOH} mμ (log ε): 282 (4.51), 490—500 (4.00). In A, an insoluble part in methanol was recrystallized from pyridine, thus affording IX as reddish prisms, m. p. 251—252°C.

Found: C, 64.98; H, 3.80; N, 7.76. Calcd. for $C_{19}H_{14}ON_2S_2$: C, 65.15; H, 4.03; N, 8.00%.

λ_{max}^{MeOH} mμ (log ε): 245 (4.26), 280 (4.16), 355 (4.34), 470 (3.76). The part in A soluble in methanol was recrystallized from pyridine-methanol to give X as violet plates, m. p. 221—222°C.

Found: C, 50.93; H, 2.51; N, 4.62. Calcd. for $C_{13}H_8ONSBr$: C, 51.16; H, 2.31; N, 4.59%.

λ_{max}^{MeOH} mμ (log ε): 242 (4.32), 287 (4.28), 313 (4.19), 485 (3.86).

The Reaction of 5, 7-Dibromohinokitiol with III.—A solution of 5, 7-dibromohinokitiol (300 mg.) and III (124 mg.) in methanol (5 ml.) was refluxed for 2 hr. The solvent was removed, and the residue was dissolved in benzene, washed with water, and evaporated to leave a dark reddish oily substance. The crystals which were precipitated out by adding ether to the oil were filtered and recrystallized from ethanol to give 80 mg. of XI as reddish needles, m. p. 205°C.

Found: C, 66.99; H, 5.09; N, 7.12. Calcd. for $C_{22}H_{20}ON_2S_2$: C, 67.33; H, 5.14; N, 7.14%.

λ_{max}^{MeOH} mμ (log ε): 239 (4.64), 290 (4.34), 323 (4.22), 490 (3.86). The solvent of the filtrate was removed, and the residue was dissolved in benzene, washed with 6 N hydrochloric acid and a 10% sodium carbonate solution, and passed through an alumina column. From the effluent, XII was obtained as violet needles, m. p. 198—199°C.

Found: N, 4.46. Calcd. for $C_{16}H_{14}ONSBr$: N, 4.02%.

λ_{max}^{MeOH} mμ (log ε): 240 (4.26), 287 (4.27), 486—492 (3.73).

The Reaction of 5, 7-Dibromo-α-thujaplicine with III.—a) To a solution of 5, 7-dibromo-α-thujaplicine (1.66 g.) in methanol (20 ml.), III (1.33 g.) was added and the mixture was refluxed for 5 hr. The solvent was removed, leaving a reddish residue which was then dissolved in benzene. The solution was washed with a 2 N sodium hydroxide solution, followed by 2 N hydrochloric acid and water. The benzene solution was passed through an alumina column and eluted with benzene. 700 mg. of a reddish oil was obtained, it was then crystallized with ether. Recrystallization from methanol afforded XIII as reddish plates, m. p. 84—85°C.

Found: C, 55.44; H, 3.97; N, 3.98. Calcd. for $C_{16}H_{14}ONSBr$: C, 55.18; H, 4.05; N, 4.02%.

λ_{max}^{MeOH} mμ (log ε): 238 (4.38), 286 (4.28), 470—480 (3.86).

b) A solution of 5, 7-dibromo-α-thujaplicine (500 mg.) and III (404 mg.) in methanol (6 ml.) was refluxed for 2 hr. The crystals which separated out on cooling were filtered and recrystallized from methanol, yielding 230 mg. of XIV as pale yellow needles, m. p. 165°C. An ethanolic solution of XIV turned green when treated with ferric chloride.

Found: C, 52.48; H, 4.29; N, 4.24. Calcd. for $C_{16}H_{16}O_2NSBr$: C, 52.46; H, 4.40; N, 3.83%.

From the mother liquor, 264 mg. of hydrobromide of III and 80 mg. of XIII were obtained.

The Cyclization of XIV to XIII.—A solution of XIV (20 mg.) in acetic acid (3 ml.) was refluxed for 2.5 hr. The solvent was then distilled off in vacuo,

*3 All melting points are uncorrected.

the residue was dissolved in benzene, and the solution was washed with a 2 N sodium hydroxide solution, 2 N hydrochloric acid and water. By removing the solvent, 15 mg. of a reddish, oily substance was obtained. The ultraviolet and infrared spectra of this oil were superimposable upon those of XIII.

The Reaction of 3, 5, 7-Tribromotropolone with III.—To a solution of 3, 5, 7-tribromotropolone (360 mg.) in methanol (15 ml.), III (140 mg.) was added; when the solution was then allowed to stand for 2 hr. at room temperature, 170 mg. of crystals (A) were obtained. By letting the filtrate stand, 200 mg. of violet crystals (B), m. p. 228—230°C, were obtained. These crystals A were dissolved in chloroform and shaken with a 10% sodium carbonate solution; yellow sodium salt was thus obtained. From the chloroform layer, 50 mg. of violet crystals (C) were obtained. When the sodium salt was dissolved in water and acidified with 2 N hydrochloric acid, 85 mg. of yellow crystals were obtained. Recrystallization from chloroform-methanol afforded XVI as yellow prisms, m. p. 176°C.

Found: C, 38.44; H, 2.58; N, 3.29. Calcd. for $C_{13}H_9O_2NSBr_2$: C, 38.73; H, 2.25; N, 3.48%.

The combined crystals of B and C were recrystallized from chloroform, giving XV as reddish violet needles, m. p. 237—238°C.

Found: C, 40.62; H, 1.56; N, 3.29. Calcd. for $C_{13}H_7ONSBr_2$: C, 40.53; H, 1.83; N, 3.64%.

λ_{max}^{MeOH} mμ (log ε): 252 (4.30), 275 (4.31), 320 (4.18), 510—520(3.92). The heating of XVI over its melting point gave XV quantitatively.

The Reaction of 3, 5, 7-Trichlorotropolone with III.—To a solution of 3, 5, 7-trichlorotropolone (240 mg.) in methanol (4.5 ml.), III (150 mg.) was added; the solution was then allowed to stand at room temperature. After 2 hr. 110 mg. of yellow crystals were obtained by filtration. Recrystallization from chloroform-ethanol gave XVIII as orange yellow prisms, m. p. 178—179°C.

Found: C, 49.24; H, 2.84; N, 4.49. Calcd. for $C_{13}H_9O_2NSCl_2$: C, 49.99; H, 2.90; N, 4.48%.

From the filtrate obtained from the reaction mixture, 120 mg. of violet crystals were obtained. Recrystallization from chloroform gave XVII as violet needles, m. p. 237—238°C.

Found: C, 53.34; H, 2.09; N, 4.46. Calcd. for $C_{13}H_7ONSCl_2$: C, 53.06; H, 2.40; N, 4.76%.

λ_{max}^{MeOH} mμ (log ε): 242 (4.43), 290 (4.35), 315 (4.25), 500—510 (3.95). The heating of XVIII over its melting point gave XVII quantitatively.

7-Nitrobenzo-1, 4-thiazino[3, 2-b]tropone (XIX).—By allowing a solution of 3-bromo-5-nitrotropolone (322 mg.) and III (170 mg.) in methanol (8 ml.) to stand, 132 mg. of crystals were obtained. Recrystallization from acetone afforded XIX as black needles, m. p. 260°C (decomp.).

Found: C, 56.98; H, 3.11. Calcd. for $C_{13}H_8O_3N_2S$: C, 57.36; H, 2.96%.

λ_{max}^{MeOH} mμ (log ε): 232 (3.14), 295 (4.11), 366 (4.00), 553 (3.78).

8-Isopropyl-7-nitrobenzo-1, 4-thiazino [3, 2-b] tropone (XX).—*a) From 7-Bromo-5-nitrohinokitiol with a m. p. of 135°C.*—By allowing a solution of 7-bromo-5-nitrohinokitiol (410 mg.) and III (185 mg.) in methanol (9 ml.) to stand at room temperature for 10 hr., 150 mg. of crystals were obtained. Recrystallization from acetone gave 90 mg. of XX as black needles, m. p. 230°C.

Found: C, 61.00; H, 4.56; N, 8.79. Calcd. for $C_{16}H_{14}O_3N_2S$: C, 61.14; H, 4.49; N, 8.91%.

λ_{max}^{MeOH} mμ (log ε): 238 (4.36), 290 (4.32), 438—450 (3.74), 515 (3.79).

b) From 7-Bromo-5-nitrohinokitiol with a m. p. of 111°C.—The reaction of 7-bromo-5-nitrohinokitiol (170 mg.) and III (95 mg.) according to a method similar to that described above resulted in 54 mg. of XX, m. p. 230°C, which showed no depression of melting point on admixture with the sample obtained from the procedure a); moreover, the ultraviolet and infrared spectra of these two samples were superimposable upon one another.

5-Amino-3-(*o*-aminophenylthio)tropolone (XXI).—A solution of 5-amino-3-bromotropolone (300 mg.) and III (190 mg.) in ethanol (25 ml.) was refluxed for 2 hr. The reddish oil obtained by removing the solvent was dissolved in water, neutralized with sodium hydrogen carbonate, and extracted with ethyl acetate. From the extract, 320 mg. of crystals, m. p. 215—218°C, were obtained. Recrystallization from ethanol gave XXI as brown prisms, m. p. 218—219°C.

Found: C, 59.92; H, 4.56; N, 10.73. Calcd. for $C_{13}H_{12}O_2N_2S$: C, 59.99; H, 4.65; N, 10.77%.

Diacetate: pale brown crystals, m. p. 253—254°C.

Found: C, 59.20; H, 5.02; N, 8.00. Calcd. for $C_{17}H_{16}O_4N_2S$: C, 59.30; H, 4.68; N, 8.14%.

7-Acetamidobenzo-1, 4-thiazino[3, 2-b]tropone (XXII).—The reaction of 5-acetamido-3-bromotropolone (44 mg.) and III (27 mg.) in methanol gave 40 mg. of XXII, m. p. 251°C (from ethanol).

Found: C, 63.10; H, 4.39; N, 9.48. Calcd. for $C_{15}H_{12}O_2N_2S$: C, 63.38; H, 4.26; N, 9.86%.

λ_{max}^{MeOH} mμ (log ε): 235 (4.31), 286 (4.23), 318 (4.19), 477 (3.84). The compound XXII was also obtained from 5-acetamido-2-acetoxy-7-bromotropone and III by the method described above.

2-Benzamido-7-(*o*-aminophenylthio) tropone (XXIII).—A solution of 2-bromo-7-benzamidotropone (150 mg.) and III (70 mg.) in methanol (5 ml.) and benzene (1 ml.) was refluxed for 5 hr. The crystals which precipitated out were recrystallized from methanol, thus yielding XXIII as pale yellow crystals, m. p. 185—186°C.

Found: C, 68.78; H, 4.73; N, 7.86. Calcd. for $C_{20}H_{16}O_2N_2S$: C, 68.96; H, 4.63; N, 8.04%.

The Bromination of Benzo[b]tropothiazine (I).—To a solution of I (500 mg.) and sodium acetate (214 mg.) in acetic acid (25 ml.), bromine (470 mg.) in acetic acid (1 ml.) was added drop by drop at room temperature, and then the mixture was stirred for 1 hr. The precipitate was removed by filtration, the filtrate was concentrated, water was added, and the precipitate formed was filtered. A solution of the crude product in benzene was chromatographed on alumina and eluted with benzene. The crystals were recrystallized from ethanol to afford 60 mg. of XXIV as orange needles, m. p. 156.5°C.

Found: C, 35.17; H, 1.47; N, 2.88. Calcd. for $C_{13}H_6NSBr_3$: C, 34.81; H, 1.35; N, 3.12%.

λ_{max}^{MeOH} mμ (log ε): 225 (4.34), 255 (4.41), 355 (3.88).

The Bromination of Benzo-1, 4-thiazino[3, 2-b]-tropone (II).—To a stirred solution of II (500 mg.)

and sodium acetate (180 mg.) in acetic acid (25 ml.), these was added a solution of bromine (353 mg.) in acetic acid (0.5 ml.) under cooling with ice. The mixture was then stirred for a further 30 min. and allowed to stand overnight in an ice box. The crystals which separated out were filtered and purified by alumina chromatography, followed by recrystallization from pyridine, to give 190 mg. of reddish violet needles, m. p. 226—227°C; undepressed on admixture with a compound X prepared by the reaction of 3, 7-dibromotropolone with *o*-aminothiophenol.

The Bromination of 8-Isopropylbenzo-1, 4-thiazino[3, 2-b]tropone (XXV).—To a stirred solution of XXV (500 mg.) and sodium acetate (169 mg.) in acetic acid (30 ml.), these was added, drop by drop, a solution of bromine (365 mg.) in acetic acid (1 ml.) under cooling with ice. After this addition, the solution was stirred for 2 hr., and the solid thus precipitated was filtered and washed with methanol. Repeated recrystallizations of the more insoluble part of the solid from chloroform-methanol afforded 140 mg. of XXVI as reddish needles, m. p. 205—207°C.

Found: C, 45.28; H, 3.07; N, 3.22. Calcd. for $C_{16}H_{13}ONSBr_2$: C, 45.00; H, 3.07; N, 3.28%.

λ_{max}^{MeOH} mμ (log ε): 246 (4.31), 279 (4.27), 295 (4.27), 315(4.23), 470(3.80). The mother liquor of the recrystallization was evaporated to a small volume, water was added, and the solution was extracted with benzene. The dried benzene solution was then passed through an alumina column and eluted with benzene. The crystals (80 mg.) obtained from the effluent were recrystallized from methanol to give violet needles, m. p. 198°C. The ultraviolet and infrared spectra of these crystals were identical with those of XII, the 7-bromo derivative of XXV, obtained by the reaction of 5, 7-dibromohinokitiol with *o*-aminothiophenol.

The Nitration of Benzo-1, 4-thiazino[3, 2-b]tropone (II).—To a stirred solution of II (2.0 g.) in acetic acid (20 ml.), a solution of fuming nitric acid (0.6 ml.) in acetic acid (2 ml.) was added dropwise at 5—7°C over a period of 1.5 hr. After this addition, the reaction mixture was allowed to stand at room temperature for 4 hr. and then in an ice box overnight. Black crystals (720 mg.) were obtained by filtration. The crystals were chromatographed on an alumina column using chloroform and recrystallized from chloroform to give black needles, m. p. 262°C (decomp.). The ultraviolet and infrared spectra of these crystals are superimposable upon those of 7-nitrobenzo-1, 4-thiazino[3, 2-b]-tropone (XIX). The filtrate from the reaction mixture was diluted with water and extracted with chloroform, the solvent was removed, and the residue was washed with ether and then crystallized by the addition of chloroform. The crystals were filtered and recrystallized from acetic acid to give XXVII as yellow prisms (210 mg.), m. p. 273°C.

Found: C, 53.53; H, 2.93; N, 9.22. Calcd. for $C_{13}H_8O_4N_2S$: C, 54.17; H, 2.80; N, 9.72%.

λ_{max}^{MeOH} mμ (log ε): 234 (4.29), 435 (4.28). The above filtrate from the chloroform solution was then concentrated and passed through an alumina column. The crystals obtained from the first effluent by chloroform were recrystallized from benzene and then from dilute ethanol to afford 240 mg. of XXVIII as yellow prisms, m. p. 207°C.

Found: C, 64.27; H, 3.60; N, 5.65. Calcd. for $C_{13}H_9O_2NS$: C, 64.20; H, 3.73; N, 5.76%.

λ_{max}^{MeOH} mμ (log ε): 234 (4.42), 365 (4.22), 380 (4.22).

The Nitration of 8-Isopropylbenzo-1, 4-thiazino-[3, 2-b]tropone (XXV).—To a stirred solution of XXV (600 mg.) in acetic acid (6 ml.), a solution of nitric acid (144 mg.) in acetic acid (1 ml.) was added drop by drop under cooling with ice. After being allowed to stand at room temperature for 4 hr., the reaction mixture was diluted with water and extracted with chloroform. The extract was concentrated to a small volume, passed through an alumina column, and eluted with chloroform. The crystals obtained from the first effluent were recrystallized from methanol to afford 210 mg. of XXX as yellow prisms, m. p. 174°C.

Found: C, 67.21; H, 4.89; N, 4.89. Calcd. for $C_{16}H_{15}O_2NS$: C, 67.36; H, 5.30; N, 4.91%.

λ_{max}^{MeOH} mμ (log ε): 237 (4.43), 363 (4.20), 382 (4.23). The crystals obtained from the later effluent were recrystallized from methanol to give 32 mg. of XXIX as yellow prisms, m. p. 263°C.

Found: C, 58.21; H, 4.00; N, 8.26. Calcd. for $C_{16}H_{14}O_4N_2S$: C, 58.18; H, 4.27; N, 8.48%.

λ_{max}^{MeOH} mμ (log ε): 240 (4.40), 400 (4.26).

The Oxidation of 7-Nitrobenzo-1, 4-thiazino-[3, 2-b]tropone (XIX).—To a suspended solution of XIX (80 mg.) in acetic acid (1 ml.) 35% hydrogen peroxide (0.04 ml.) was added; the mixture was then allowed to stand at room temperature for a week, during which time it was occasionally stirred. Yellow brown crystals were filtered out, treated with charcoal in acetic acid, and recrystallized from the same solvent to give 50 mg. of yellow prisms, m. p. 273°C (decomp.). The ultraviolet and infrared spectra of this crystals were superimposable upon those of XXVII.

8-Isopropyl-7-nitrobenzo-1, 4-thiazino[3, 2-b]tropone 5, 5-Dioxide (XXXI).—a) A mixture of XX (80 mg.) and 35% hydrogen peroxide (0.1 ml.) in acetic acid (1 ml.) was allowed to stand at room temperature for 2 weeks. The crystals which precipitated out were then filtered and recrystallized from acetic acid affording XXXI as yellow needles, m. p. 295°C (decomp.).

Found: C, 56.90; H, 4.18; N, 7.15. Calcd. for $C_{16}H_{14}O_5N_2S$: C, 55.49; H, 4.08; N, 8.09%.

b) A mixture of XXIX (34 mg.) and 35% hydrogen peroxide (0.05 ml.) in acetic acid (1 ml.) was allowed to stand at room temperature for a week. The crystals which separated out were recrystallized from acetic acid to give yellow needles, m. p. 295°C (decomp.) which were identical with the XXXI obtained from XX.

The Reaction of Benzo-1, 4-thiazino[3, 2-b]tropone (II) with Thionyl Chloride.—After a solution of II (200 mg.) and thionyl chloride (130 mg.) in dry benzene (25 ml.) had been allowed to stand at room temperature for 30 min., the solution was refluxed for 3 hr.; then the solvent and excess of thionyl chloride were distilled off. The residue was washed with 2 N sodium hydroxide and water each three times, the benzene solution was dried over sodium sulfate, and the solvent was removed to give 150 mg. of a crude product. A benzene solution of the product was then passed through an alumina column, and the crystals obtained from the elute were recrystallized from benzene to yield violet needles, m. p. 223°C. This product was

identified as 7, 9-dichlorobenzo-1, 4-thiazino[3, 2-b]-tropone (XVII) by a mixed melting point determination and by a comparison of the ultraviolet and infrared spectra.

The Reaction of 8-Isopropylbenzo-1, 4-thiazino-[3, 2-b]tropone (XXV) with Thionyl Chloride.—a) A solution of XXV (500 mg.) and thionyl chloride (270 mg.) in dry benzene (30 ml.) was refluxed for 3 hr. After the evaporation of the solvent, the residue was dissolved in benzene, washed with water, dried, and passed through an alumina column. The crystals obtained from the first effluent were recrystallized from acetone, thus affording 20 mg. of XXXIV as violet prisms, m. p. 154—156°C.

Found: C, 55.55; H, 3.45; N, 4.11. Calcd. for $C_{16}H_{13}ONSCl_2$: C, 56.82; H, 3.87; N, 4.14%.

λ_{max}^{MeOH} mμ (log ε): 245 (4.35), 278 (4.35), 320 (4.32), 495 (3.90). The crystals obtained from the second effluent were recrystallized from acetone to give 60 mg. of XXXV as violet needles, m. p. 155—156°C, which showed a marked depression of melting point on admixture with another compound XXXIV.

Found: C, 62.84; H, 4.42; N, 4.89. Calcd. for $C_{16}H_{14}ONSCl$: C, 63.28; H, 4.65; N, 4.61%.

λ_{max}^{MeOH} mμ (log ε): 240 (4.38), 287 (4.36), 495 (3.81).

b) A solution of XXV (500 mg.) and thionyl chloride (270 mg.) in dry benzene (40 ml.) was allowed to stand for 4 hr. at room temperature, and then it was refluxed for 5 hr. After a work-up such as that described above, 30 mg. of XXXVI as reddish violet plates, m. p. 149°C (from acetone) were obtained from the first fraction of the chromatograph.

Found: C, 62.31; H, 4.18; N, 4.69. Calcd. for $C_{16}H_{14}ONSCl$: C, 63.21; H, 4.65; N, 4.61%.

λ_{max}^{MeOH} mμ (log ε): 240 (4.39), 280 (4.30), 313 (4.25), 470 (3.83). The crystals obtained from the second fraction were recrystallized from acetone to give 80 mg. of violet needles, m. p. 156°C; undepressed on admixture with XXXV.

c) A solution of XXV (2.0 g.) and thionyl chloride (2.2 g.) in dry benzene (20 ml.) was refluxed for 10 hr. The solvent was then distilled off, and the residue was recrystallized from benzene, thus yielding 410 mg. of XXXVII as violet needles, m. p. 208—210°C.

Found: C, 51.36; H, 3.31; N, 3.85. Calcd. for $C_{16}H_{12}ONSCl_3$: C, 51.60; H, 3.25; N, 3.78%.

λ_{max}^{MeOH} mμ (log ε): 250 (4.29), 265 (4.88), 320 (4.25), 490—500 (3.84).

The authors wish to express their gratitude to the Sankyo Co. for its donation of a research fund which covered a part of the expenses for this work. The infrared and ultraviolet spectrophotometers used in this study were purchased with a grant-in-aid for Fundamental and Technical Research from the Toyo Rayon Co., Ltd., to whom the authors are grateful.

BULLETIN OF THE CHEMICAL SOCIETY OF JAPAN VOL. 39 1988—1994 (1966)

Benzo-1, 4-thiazino[3, 2-b]tropone 5-Oxides and 5, 5-Dioxides*1

By Tetsuo NOZOE, Toyonobu ASAO and Kazuko TAKAHASHI

Department of Chemistry, Faculty of Science, Tohoku University, Katahira-cho, Sendai

(Received December 29, 1965)

The oxidation of benzo-1, 4-thiazino[3, 2-b]tropone and its 8-isopropyl derivative with hydrogen peroxide afforded the corresponding 5-oxides or 5, 5-dioxides. The stability of these oxides to heating, acid and alkali was examined. The bromination or nitration of these oxides gave mainly 9-bromo or 9-nitro derivatives. 7- or 9-Aminobenzo-1, 4-thiazino[3, 2-b]tropones were obtained by the reduction of the corresponding nitro compounds.

In their previous papers,[1,2] the present authors reported on the synthesis and some electrophilic substitution reactions of benzo-1, 4-thiazino-[3, 2-b]tropones (cyclohepta[b]benzo-1, 4-thiazin-10(11*H*)-ones). This study has now been extended to the oxidation of benzothiazinotropones; the present paper will deal with the formation and with the reactions of sulfoxides and sulfones of benzothiazinotropones.

The hydrogen peroxide oxidation of benzo[b]-tropothiazine (cyclohepta[b]benzo-1, 4-thiazine)[1] (I) yielded an amorphous, unidentified product, whereas the oxidation of benzo-1, 4-thiazino[3, 2-b]tropone (II)[1] with one molar equivalent of hydrogen peroxide in acetic acid easily afforded the corresponding sulfoxide (5-oxide) (III), as has been reported previously.[2] The treatment of III with a further mole of the reagent, or that of II with two molar equivalents of the reagent, gave the corresponding sulfone (5, 5-dioxide) (IV).

*1 Presented at the Local Meeting of the Chemical Society of Japan, Sendai, September, 1960.

1) T. Nozoe, T. Asao and K. Takahashi, This Bulletin **34**, 146 (1961).

2) T. Nozoe, T. Asao and K. Takahashi, ibid., **39**, 1980 (1966).

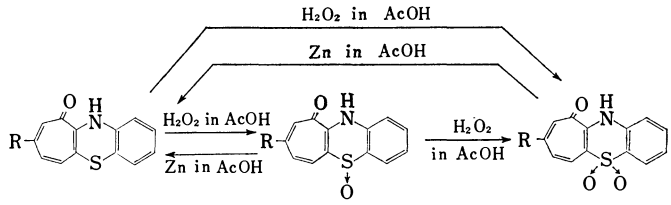

II R=H V R=isoPr III R=H VI R=isoPr IV R=H VII R=isoPr

The structure of IV is evident from the presence of bands characteristic of the sulfone group[3] at 1130 and 1189 cm^{-1} in its infrared spectrum. A similar oxidation of 8-isopropylbenzo-1, 4-thiazino-[3, 2-b]tropone (V) gave the corresponding sulfoxide (VI) and sulfone (VII).

The reduction of these oxidation products with zinc in acetic acid regenerated the corresponding thiazinotropones, II or V. These four oxidation products have higher melting points, lower solubilities in organic solvents, and shorter wavelength absorption maxima in the ultraviolet (Fig. 1) region, than do the corresponding starting materials, II or V.

Although II and V are weak bases, their sulfoxides and sulfones have an acidic character, as is shown

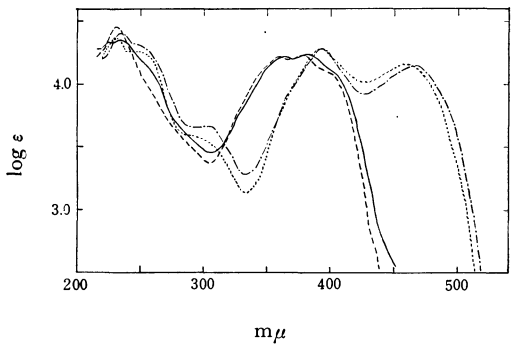

Fig. 1. Ultraviolet absorption spectra of III (—— in MeOH, —·— in 0.1 N NaOH) and IV (---- in MeOH, ····· in 0.1 N NaOH).

by their ultraviolet absorption spectra in an alkaline medium, which exhibit considerable bathochromic shifts as compared with those in methanol. Furthermore, III gave a sodium salt, as orange needles, which can be recrystallized from a 2 N sodium hydroxide solution, but which reverts to the parent acid, III, in water or in polar organic solvents. VI also gave a sodium salt, but it could not be successfully crystallized. Such an acidic character can obviously be attributed to the strong electronegativity of the sulfoxide or the sulfone groups.

In spite of their great stability to alkali, the sulfoxides, III and VI, are unstable to acids or to heating: when III or VI was heated at a temperature near its melting point for 10—15 min., its color changed from yellow to a reddish brown, decomposition occurred, and II or V was formed in about a 20% yield. Also, the attempted acetylation of III or VI with acetic anhydride at 140°C for one hour resulted in the formation of II or V respectively. The treatment of III or VI with 6 N sulfuric acid resulted in a dark brown coloration and in the formation of small amounts of II or V respectively, together with amorphous, unidentified substances. When heated with 10% hydrobromic acid for 2 hr., III gave II and reddish violet crystals of a halogenated compound (VIII) which has been shown to be the 9-bromo derivative of II.[2] Examples of the reduction and reductive halogenation of sulfoxides by acid have previously been observed with phenothiazine 5-oxide[4] and thianthrene 5-oxide.[5] The fact that VIII was also obtained[2] by the bromination of II is consistent with the mechanism proposed[6] for the reductive halogenation, which involves the initial reduction of the sulfoxide to the sulfide by acid, with the liberation of a mole of free halogen which subsequently attacks the heterocycle. In contrast to the sulfoxides, III and VI, the sulfones, IV and VII, were very stable to heat or to acids. This difference in the stability of sulfoxides and sulfones can be attributed to the difference in their S–O bond energies.[7]

As has already been reported,[1] the attempted alkylation of II or V with alkyl halide was unsuccessful. Since these oxidation products have an acidic character, one would expect alkylations or acylations of the OH or the NH group to be feasible. However, the attempted methylation of III or VI with methyl iodide, or the benzoylation with benzoyl chloride in pyridine, resulted

3) L. J. Bellamy, "The Infrared Spectra of Complex Molecules," Methuen and Co., London (1958), p. 360.

4) J. A. Smithe, *J. Chem. Soc.*, **95**, 349 (1909); H. J. Page and S. Smiles, ibid., **97**, 1112 (1910); A. C. Schmalz and A. Burges, *J. Am. Chem. Soc.*, **76**, 5455 (1954); E. N. Karaulova and G. D. Galpern, *Zhur. Obschshei. Khim.*, **29**, 3033 (1959); *Chem. Abstr.*, **54**, 12096 (1960).

5) H. Gilman and D. R. Swayampati, *J. Am. Chem. Soc.* **77**, 5944 (1955).

6) H. Gilman and J. Eisch, ibid., **77**, 3862 (1955).

7) D. Barnard, J. M. Fabian and H. D. Koch, *J. Chem. Soc.*, **1949**, 2442.

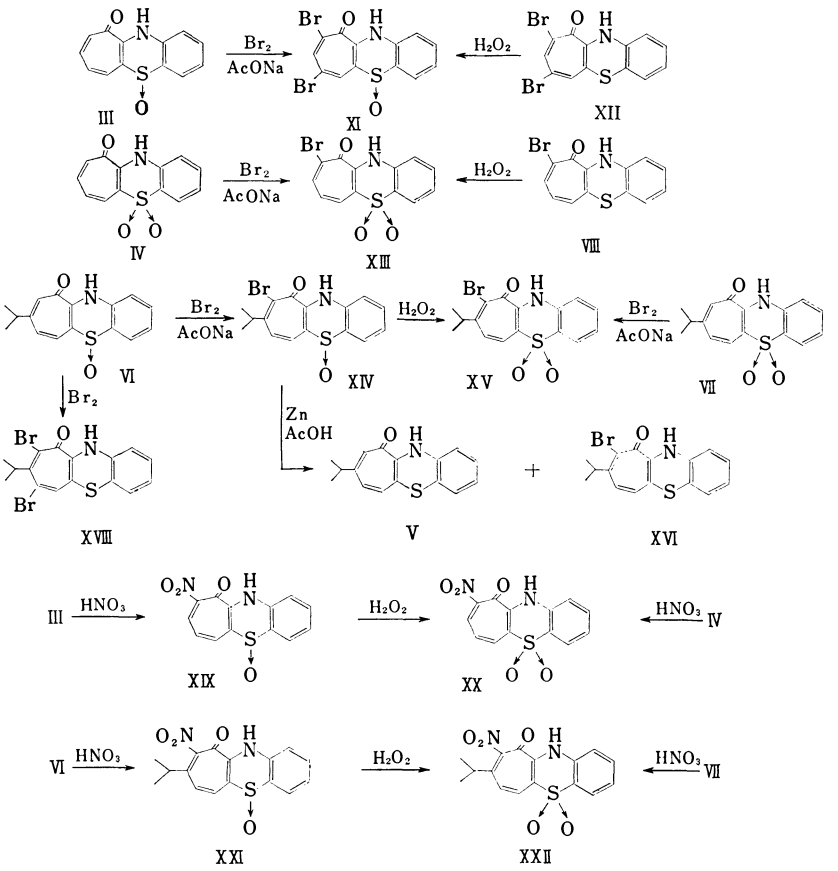

in the recovery of the starting materials, while the attempted acetylation with acetic anhydride resulted in the recovery of the starting materials or in the formation of decomposition products, II or V.

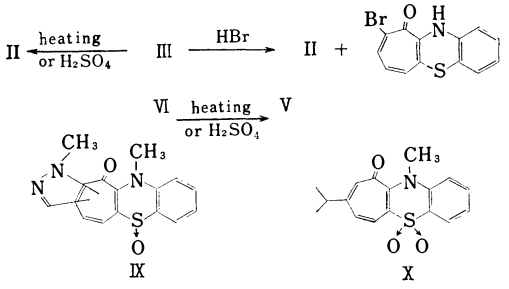

The reaction of the sodium salt of III with methyl iodide also did not afford any methylated product. However, the treatment of III with a large excess of diazomethane gave a small amount of yellow prisms (IX). From its analysis ($C_{16}H_{13}O_2N_3S$), and from the absence of an N–H stretching vibration band in its infrared spectrum, structure IX with a condensed pyrazole ring may be proposed for the compound. This is also supported by the fact that the reaction of tropones with diazomethane is known to give *N*-methylpyrazolotropones.[8] From the reaction of IV with diazomethane, a small amount of yellow crystals were obtained, but an attempt to purify them was not successful. When treated with diazomethane, VII yielded a small amount of a neutral yellow crystaline compound (X). From its analysis and from its infrared spectrum (no N–H band), X may be thought to be the simple *N*-methyl derivative, 8-isopropyl-11-methylbenzo-1, 4-thiazino[3, 2-b]tropone 5, 5-dioxide.

Sulfoxides or sulfones in the phenothiazine series undergo electrophilic substitution at the same position as does phenothiazine itself[9]; it is also known[2] that the bromination of II or V occurs at the 7- and/or the 9-positions, and that nitration occurs at the 7-position. Some electrophilic substitution reactions of the sulfoxides, III and VI, and the sulfones, IV and VII, were investigated for the sake of comparison with the above results.

The action of one molar equivalent of bromine

8) T. Nozoe, T. Mukai and T. Asao, to be published.
9) "Heterocyclic Compounds," Vol. VI, Ed. by R. C. Elderfield, John Wiley & Sons, New York (1957), p. 714.

on III in acetic acid in the presence of sodium acetate gave the dibromide XI, which was also obtained by the oxidation of 7, 9-dibromobenzo-1, 4-thiazino-[3, 2-b]tropone (XII).[2] The reaction of bromine and IV under the same conditions as in III gave monobromosulfone XIII, which was also obtained by the oxidation of 9-bromobenzo-1, 4-thiazino-[3, 2-b]tropone (VIII). Similarly, VI and VII yielded the monobromo compounds, XIV and XV, respectively. The fact that the location of the bromine atoms introduced into both compounds is the same as was established by the hydrogen peroxide oxidation of XIV, which afforded XV in a good yield. In order to determine the position of the bromine atoms, XIV was heated with zinc in acetic acid, thus obtaining two products, one of which was proved to be V. The ultraviolet absorption spectrum of the other product, red violet crystals (XVI), was different from that of 7-bromo-8-isopropylbenzo-1, 4-thiazino[3, 2-b]tropone, but it was similar to that of the 9-chloro derivative reported previously.[2] It is, therefore, clear from the above, and from the elemental analyses, that XVI is 9-bromo-8-isopropylbenzo-1, 4-thiazino-[3, 2-b]tropone; accordingly, XIV and XV are the sulfoxide and the sulfone, respectively, of XVI. When the bromination of VI was carried out without sodium acetate, a small amount of 7, 9-dibromo-8-isopropylbenzo-1, 4-thiazino[3, 2-b]tropone (XVIII) was obtained, together with unidentified products which were presumably formed by the decomposition of the sulfoxide with the hydrogen bromide liberated during the reaction of VI with bromine.

With the expectation that the bromine would be replaced by an ethoxy group, the sulfoxide XIV was heated with sodium ethoxide in a sealed tube; unexpectedly, however, VI was obtained, besides the recovery of the starting material.

The treatment of III in acetic acid with 1.5 molar equivalents of fuming nitric acid afforded a mononitro derivative XIX different from the 7-nitro derivative of III.[2] From the fact that no substitution had occurred in the benzene nucleus (the infrared spectrum of XIX exhibited a band at 770 cm^{-1} which is assigned to the out-of-plane deformation of a 1, 2-disubstituted benzene), and since the bromination of the sulfoxide occurs mainly at the 9-position, XIX is likely to be 9-nitrobenzo-1, 4-thiazino[3, 2 - b]tropone 5-oxide. The nitration of IV yielded a yellow mononitro compound XX, which was also obtained by the oxidation of XIX. It therefore, follows that the nitro group of XX is located at the 9-position.

Similarly, the nitration of VI and VII afforded the sulfoxide XXI and the sulfone XXII of 8-isopropyl-9-nitrobenzo-1, 4-thiazino[3,2-b]tropone respectively; the latter was also obtained by the oxidation of XXI. As a result of the effect of the nitro group, the ultraviolet spectra of XIX and

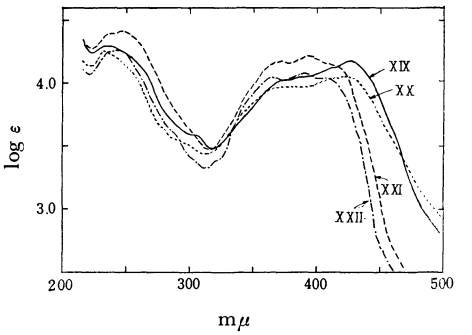

Fig. 2. Ultraviolet absorption spectra of XIX, XX, XXI and XXII in MeOH.

XX (Fig. 2) show considerable bathochromic shifts in comparison with those of III and IV. However, the spectra of the 8-isopropyl homologs (XXI and XXII) show only a small shift in comparison with those of VI and VII. This difference may be attributed to the decrease in the coplanarity of the nitro group and the benzothiazinotropone ring due to steric interference by the isopropyl groups at the position adjacent to the nitro groups in XXI and XXII.

The apparent reactivities of these sulfoxides and sulfones to the electrophilic reagents are greater than those of the benzothiazinotropones. It is considered that this is due to the greater electron density on the rings of the benzothiazinotropone 5-oxides or 5, 5-dioxides because of the easier deprotonation from N–H than on those of benzothiazinotropones.

It has been demonstrated[2] that the nitration of II or V introduces a nitro group at the 7-position, and that it simultaneously causes the oxidation of the sulfur atoms. In view of the nitration experiments described above, it is clear that, in the former cases, the nitration of the benzothiazinotropone rings occurs initially, and that this is followed by the oxidation of the nitrated products.

It has become clear from the above experiments that the bromination of sulfoxides and sulfones of benzothiazinotropone gives 7, 9-dibromo or 9-bromo derivatives, while their nitration produces 9-nitro derivatives exclusively.

When XIX and XXI were heated with zinc in acetic acid, 9-aminobenzo-1, 4-thiazino[3, 2-b]tropone (XXIII) and its 8-isopropyl homolog XXIV,

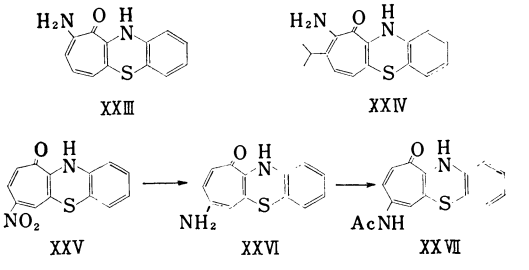

respectively, were obtained in good yields. The attempted reduction of 7-nitrobenzo-1, 4-thiazino-[3, 2-b]tropone (XXV)[2] by a similar method furnished a resinous product. However, the catalytic reduction of XXV in the presence of Pd-C gave an unstable 7-amino derivative (XXIV), the acetylation of which yielded 7-acetamidobenzo-1, 4-thiazino[3, 2-b]tropone (XXVII).[2]

Experimental*2

Benzo-1, 4-thiazino[3, 2-b]tropone 5-Oxide (III).—A solution of benzo-1, 4-thiazino[3, 2-b]tropone (II) (500 mg.) and hydrogen peroxide*3 (0.24 ml.) in acetic acid was allowed to stand at room temperature for a week. When water was then added to the solution, 490 mg. of yellow needles, m. p. 202°C, were obtained by filtration. Recrystallization from ethanol gave III as yellow needles, m. p. 207°C; a mixed m. p. determination with authentic III[2] showed no depression.

λ_{max}^{MeOH} mμ (log ε): 234 (4.42), 365 (4.22), 380 (4.22).

$\lambda_{max}^{0.1\ N\ NaOH}$ mμ (log ε): 233 (4.38), 393 (4.29), 466 (4.15).

Sodium salt: orange needles; m. p. 223—225°C (decomp.).

Found: C, 55.12; H, 3.19; N, 4.51. Calcd. for $C_{13}H_8O_2NSNa \cdot H_2O$: C, 55.12; H, 3.56; N, 4.95%.

Benzo-1, 4-thiazino[3, 2-b]tropone 5, 5-Dioxide (IV).—a) A solution of II (500 mg.) and hydrogen peroxide (0.7 ml.) in acetic acid (3 ml.) was allowed to stand for a week at room temperature. The crystals (490 mg.) which separated out were collected by filtration. Recrystallization from chloroform-methanol afforded yellow crystals (IV), m. p. 266°C.

Found: C, 60.30; H, 3.35; N, 5.48. Calcd. for $C_{14}H_9O_3NS$: C, 60.23; H, 3.50; N, 5.40%.

λ_{max}^{MeOH} mμ (log ε): 232 (4.44), 358 (4.20), 380 (4.21).

$\lambda_{max}^{0.1\ N\ NaOH}$ mμ (log ε): 232(4.35), 394(4.28), 459 (4.15).

b) A solution of III (500 mg.) and hydrogen peroxide (0.5 ml.) in acetic acid (3 ml.) was allowed to stand for 5 days at room temperature. The precipitated crystals were then recrystallized from chloroform-methanol, thus affording 450 mg. of IV, m. p. 266°C.

8-Isopropylbenzo-1, 4-thiazino[3, 2-b]tropone 5-Oxide (VI).—A solution of V (243 mg.) and hydrogen peroxide (0.11 ml.) in acetic acid (5 ml.) was allowed to stand at room temperature for 3 days. The solution was then diluted with water and extracted with chloroform. When the solvent was removed from the extract, and the residue was recrystallized from dilute methanol, VI (200 mg.) was afforded as yellow prisms, m. p. 174°C. This showed no depression of melting point on admixture with an authentic sample,[2] and their ultraviolet and infrared spectra are identical.

λ_{max}^{MeOH} mμ (log ε): 237(4.43), 363(4.20), 382(4.23).

$\lambda_{max}^{0.1\ N\ NaOH}$ mμ (log ε): 235(4.34), 250(4.30), 393 (4.21), 460 (4.06).

8-Isopropylbenzo-1, 4-thiazino[3, 2-b]tropone 5, 5-Dioxide (VII).—a) A solution of V (100 mg.) and hydrogen peroxide (0.1 ml.) in acetic acid (1 ml.) was allowed to stand at room temperature for a week. The precipitated crystals (86 mg.) were then recrystallized from methanol to give yellow crystals (VII), m. p. 195°C.

Found: C, 63.74; H, 5.10; N, 4.53. Calcd. for $C_{16}H_{15}O_3NS$: C, 63.78; H, 5.02; N, 4.65%.

λ_{max}^{MeOH} mμ (log ε): 234 (4.56); 360 (4.23), 377 (4.25).

b) A solution of VI (100 mg.) and hydrogen peroxide (0.1 ml.) in acetic acid (1 ml.) was allowed to stand for 5 days at room temperature. The precipitated crystals were then recrystallized from methanol to yield 80 mg. of VII, m. p. 195°C.

The Reductions of III, IV, VI and VII.—a) A mixture of III (65 mg.), acetic acid (3 ml.) and zinc (194 mg.) was heated at about 90°C for one hour. The excess of zinc was then filtered off, and the filtrate was diluted with water (20 ml.) and extracted three times with benzene. The solvent was removed, and the residue was recrystallized from methanol, thus affording 27 mg. of red needles, m. p. 158—160°C. This showed no depression of melting point on admixture with II.

b) A mixture of IV (100 mg.), acetic acid (5 ml.) and zinc (250 mg.) was heated at about 90°C for 2 hr. The excess of zinc was then filtered off, water was added, and the solution was extracted with benzene. The extract was chromatographed on alumina and then recrystallized from methanol to afford 20 mg. of II.

c) A mixture of VI (100 mg.), acetic acid (2.5 ml.) and zinc (100 mg.) was heated at about 90°C for one hour. When the mixture was then worked up as has been described above, 30 mg. of V, m. p. 94°C, were obtained.

The Thermal Decompositions of III and VI.—a) 5-Oxide (III) (25 mg.) was heated at around its melting point in a test tube for 10 min. The yellow color then gradually turned red. The resulting oil was dissolved in benzene and passed through an alumina column. From the effluent, 10 mg. of red crystals, m. p. 158°C, were obtained. The melting point of these crystals was not depressed by their admixture with II.

b) After VI (25 mg.) had been heated at around its melting point for about 10 min., the resultant red oil was distilled at 120°C/2 mmHg; 5 mg. of red crystals, m. p. 92°C, were thus obtained which showed no depression of melting point on admixture with V.

The Action of Acetic Anhydride to VI.—A solution of VI (150 mg.) in acetic anhydride (5 ml.) was heated at 140°C for one hour. Water was then added to the solution was extracted with benzene, and the extract was dried and passed through an alumina column. Red crystals (30 mg.), m. p. 92°C, were obtained, which showed no depression of melting point on admixture with V.

The Effect of 6 N Sulfuric Acid on III and VI.—a) By adding 6 N sulfuric acid to 5-oxide (III) (50 mg.), the compound was dissolved at once, and the color of the solution turned from brown to dark red. After being allowed to stand overnight, the solution was diluted with water, extracted with benzene, and purified by passing it through an alumina column; this gave 10 mg. of II.

b) After a solution of VI dissolved in 6 N sulfuric acid had been allowed to stand overnight, water was added, it was extracted with benzene, and the extract was passed through an alumina column; thus a small amount of V was afforded.

The Reaction of III with Hydrobromic Acid.—

*2 All melting points are uncorrected.

*3 The concentration of hydrogen peroxide used in all these experiments was 35%.

A solution of III (200 mg.) in 48% hydrobromic acid (2 ml.) was heated at about 90°C for 30 min. Water (30 ml.) was then added, the solution was extracted with chloroform, and the extract was washed with water and submitted to alumina chromatography. The first elution gave 40 mg. of red crystals, m. p. 158°C, after being recrystallized from methanol; undepressed on admixture with benzo-1, 4-thiazino[3, 2-b]tropone (II). The latter elution afforded 35 mg. of violet plates, m. p. 221°C; undepressed by admixture with 9-bromobenzo-1, 4-thiazino[3, 2-b]tropone (VIII).

The Reaction of III with Diazomethane.—To a solution of III (50 mg.) in methanol (30 ml.), 50 ml. of an ethereal solution of diazomethane prepared from 5 g. of *N*-nitrosomethylurea was added under cooling with ice; the mixture was then allowed to stand for 36 hr. in an ice box. After the insoluble starting material had been collected by filtration, the filtrate was evaporated to leave a red oil; this oil was dissolved in benzene and passed through an alumina column. From the effluent, 46 mg. of yellow prisms (IX), m. p. 194°C, were obtained after recrystallization from methanol.

Found: C, 61.56; H, 4.18; N, 12.95. Calcd. for $C_{16}H_{13}O_2N_3S$: C, 61,73; H, 4.21; N, 13.50%.

λ_{max}^{MeOH} mμ (log ε): 267 (4.26), 354 (4.03), 420 (3.84).

A considerable amount of a yellowish oily product was obtained besides IX, but it could not be purified.

The Reaction of VII with Diazomethane.—To a suspension of VII (100 mg.) in methanol (6 ml.), 10 ml. of an ethereal solution of diazomethane prepared from 1 g. of *N*-nitrosomethylurea was added under cooling by ice; the mixture was then kept in an ice box for 40 hr. The undissolved starting material was filtered off, and the residue obtained by removing the solvent from the filtrate was dissolved in chloroform and passed through an alumina column. From the effluent, 45 mg. of yellow crystals (X), m. p. 159—160°C, were obtained after recrystallization from methanol.

Found: C, 64.63; H, 5.37; N, 3.83. Calcd. for $C_{17}H_{17}O_3NS$: C, 64.75; H, 5.43; N, 4.44%.

λ_{max}^{MeOH} mμ (log ε): 236 (4.44), 368 (4.18).

7, 9-Dibromobenzo-1, 4-thiazino[3, 2-b]tropone 5-Oxide (XI).—a) To a stirred solution of III (200 mg.) and sodium acetate (74 mg.) in acetic acid (2 ml.) a solution of bromine (144 mg.) in acetic acid (1 ml.) was added under cooling by ice; the solution was then kept overnight in an ice box. The crystals (137 mg.) which separated out were collected, and recrystallized from chloroform-ethanol to afford orange plates (XI), m. p. 249°C (decomp.).

Found: C, 39.20; H, 1.96; N, 3.24. Calcd. for $C_{13}H_7O_2NSBr_2$: C, 38.94; H, 1.76; N, 3.49%.

λ_{max}^{MeOH} mμ (log ε): 236 (4.27), 268 (4.30), 380 (4.29).

b) A solution of 7, 9-dibromobenzo-1, 4-thiazino-[3, 2-b]tropone (XII) (60 mg.) and hydrogen peroxide (0.04 ml.) in acetic acid (4 ml.) was allowed to stand for 62 hr. at about 30°C. The crystals which separated out were filtered off and recrystallized from chloroform-ethanol to afford XI, m. p. 246°C (decomp.). The ultraviolet and infrared spectra of this compound are identical with those of the compound obtained in procedure a).

9-Bromobenzo-1, 4-thiazino[3, 2-b]tropone 5, 5-Dioxide (XIII).—a) To a stirred solution of IV (209 mg.) and sodium acetate (70 mg.) in a mixture of acetic acid (2 ml.) and chloroform (1.5 ml.), a solution of bromine (138 mg.) in acetic acid (1 ml.) was added under cooling by ice; the solution was then kept overnight in an ice box. The crystals which separated out were filtered and recrystallized from a large amount of acetic acid to give 150 mg. of yellow crystals (XIII), m. p. over 300°C.

Found: C, 46.31; H, 2.37; N, 4.16. Calcd. for $C_{13}H_8O_3NSBr$: C, 46.19; H, 2.39; N, 4.14%.

λ_{max}^{MeOH} mμ (log ε): 233 (4.28), 366 (4.18).

b) A solution of VIII (72 mg.) and hydrogen peroxide (0.2 ml.) in acetic acid (3 ml.) was allowed to stand for 5 days at about 30°C. Crystals (71 mg.), m. p. over 300°C, were obtained by filtration, followed by recrystallization from acetic acid. The ultraviolet and infrared spectra of this compound are identical with those of the compound obtained in a).

9-Bromo-8-isopropylbenzo-1, 4-thiazino[3, 2-b]-tropone 5-Oxide (XIV).—To a stirred solution of VI (200 mg.) and sodium acetate (65 mg.) in acetic acid (2 ml.), a solution of bromine (123 mg.) in acetic acid (1 ml.) was added. After it had been stirred for 2 hr., the solution was diluted with water and extracted with chloroform. The residue left by removing the solvent from the extract was crystallized by the addition of methanol. Recrystallization from acetone gave 126 mg. of yellow crystals (XIV), m. p. 224°C (decomp.).

Found: C, 52.83; H, 3.74; N, 3.58. Calcd. for $C_{16}H_{14}O_2NSBr$: C, 52.77; H, 3.87; N, 3.85%.

λ_{max}^{MeOH} mμ (log ε): 255 (4.33), 368 (4.13), 391 (4.11).

9-Bromo-8-isopropylbenzo-1, 4-thiazino[3, 2-b]-tropone 5, 5-Dioxide (XV).—a) To a stirred solution of VII (210 mg.) and sodium acetate (63 mg.) in a mixture of acetic acid (2 ml.) and chloroform (1.5 ml.), a solution of bromine (123 mg.) in acetic acid (1 ml.) was added. When the solution was left standing in an ice box for a day, 224 mg. of crystals were obtained. Recrystallization from a mixture of chloroform and methanol afforded yellow needles (XV), m. p. 272°C (decomp.).

Found: C, 50.40; H, 3.65; N, 3.86. Calcd. for $C_{16}H_{14}O_3NSBr$: C, 50.55; H, 3.71; N, 3.69%.

λ_{max}^{MeOH} mμ (log ε): 252 (4.30), 363 (4.25).

b) A solution of XIV (137 mg.) and hydrogen peroxide (0.1 ml.) in acetic acid (3 ml.) was allowed to stand for 4 days at about 30°C. The crystals which were precipitated were filtered and recrystallized from chloroform-methanol to give yellow needles, m. p. 270°C. The ultraviolet and infrared spectra of this crystals are superimposable upon those of the compound (XIV) obtained in a).

The Reduction of XIV.—A mixture of XIV (200 mg.), zinc (400 mg.) and acetic acid (4 ml.) was heated for 3 hr. at about 90°C. A solid was filtered off, and the filtrate was diluted with water and extracted with chloroform. The residue left by removing the solvent from the extract was dissolved in benzene and passed through an alumina column. From the first effluent, red violet crystals (XVI), m. p. 159—162°C, were obtained; the ultraviolet spectrum of these crystals (λ_{max}^{MeOH} mμ (log ε): 240 (4.38), 277 (4.30), 313 (4.25), 470 (3.83)) closely resembles that of 9-chloro-8-isopropylbenzo-1, 4-thiazino[3, 2-b]tropone.[2] From the latter effluent, red crystals, m. p. 95°C, were obtained; these crystals showed no depression of melting

point on admixture with 8-isopropyl-1,4-thiazino[3,2-b]-tropone (V).

9-Nitrobenzo-1, 4-thiazino[3, 2-b]tropone 5-Oxide (XIX).—To a stirred solution of III (200 mg.) in acetic acid (3 ml.), a solution of fuming nitric acid (80 mg.) in acetic acid (1 ml.) was added drop by drop. After the mixture had been allowed to stand overnight, 83 mg. of crystals were obtained; the recrystallization of these from acetic acid gave yellow crystals (XIX), m. p. 255°C (decomp.).

Found: C, 54.16; H, 2.82; N, 9.55. Calcd. for $C_{13}H_8O_4N_2S$: C, 54.17; H, 2.80; N, 9.72%.

λ_{max}^{MeOH} mμ (log ε): 235 (4.31), 370 (4.03), 427 (4.18).

$\lambda_{max}^{0.1\ N\ NaOH}$ mμ (log ε): 227 (4.29), 400 (3.81), 497 (4.27).

9-Nitrobenzo-1, 4-thiazino[3, 2-b]tropone 5, 5-Dioxide (XX). — a) To a stirred solution of IV (200 mg.) in a mixture of chloroform (1 ml.) and acetic acid (3 ml.), a solution of fuming nitric acid (100 mg.) in acetic acid (1 ml.) was added drop by drop at room temperature. After the mixture had stood for 36 hr. in an ice box, 130 mg. of crystals were obtained. Recrystallization from acetic acid afforded yellow crystals (XX), m. p. over 320°C.

Found: C, 51.20; H, 2.56; N, 9.33. Calcd. for $C_{13}H_8O_5N_2S$: C, 51.32; H, 2.65; N, 9.21%.

λ_{max}^{MeOH} mμ (log ε): 232 (4.25), 380 (3.98), 420 (4.05).

From the filtration of the products of the recrystallization, 97 mg. of the starting material were recovered.

b) A solution of XIX (100 mg.) and hydrogen peroxide (0.1 ml.) in acetic aicd (2 ml.) was allowed to stand for a week at room temperature. The crystals which separated out were then collected and recrystallized from acetic acid, thus affording yellow crystals (43 mg.), m. p. over 320°C. The ultraviolet and infrared spectra of these crystals are superimposable upon those of XX obtained in a).

8-Isopropyl-9-nitrobenzo-1, 4-thiazino[3, 2-b]tropone 5-Oxide (XXI). — To a stirred solution of VI (570 mg.) in acetic acid (6 ml.) a solution of fuming nitric acid (140 mg.) in acetic acid (1 ml.) was added; the mixture was then allowed to stand in an ice box overnight. When the crystals which separated out were collected and recrystallized from acetic acid, they gave 428 mg. of yellow crystals (XXI), m. p. 263°C (decomp.).

Found: C, 58.23; H, 4.12; N, 8.73. Calcd. for $C_{16}H_{14}O_4N_2S$: C, 58.18; H, 4.27; N, 8.48%.

λ_{max}^{MeOH} mμ (log ε): 223 (4.37), 247 (4.39), 370 (4.15), 395 (4.21).

8-Isopropyl-9-nitrobenzo-1, 4-thiazino[3, 2-b]tropone 5, 5-Dioxide (XXII).—a) To a stirred solution of VII (202 mg.) in a mixture of acetic acid (3 ml.) and chloroform (1 ml.), a solution of fuming nitric acid (90 mg.) in acetic acid (1 ml.) was added; the mixture was then allowed to stand in an ice box for 40 hr. The precipitated crystals (133 mg.) were collected and recrystallized from a large amount of acetic acid to give yellow crystals (XXII), m. p. 320°C (decomp.).

Found: C, 55.22; H, 4.04; N, 7.75. Calcd. for $C_{16}H_{14}O_5N_2S$: C, 55.49; H, 4.08; N, 8.09%.

λ_{max}^{MeOH} mμ (log ε): 243 (4.27), 365 (4.05), 390 (4.07).

b) A mixture of XXI (15 mg.), and hydrogen peroxide (0.05 ml.) in acetic acid (1 ml.) was allowed to stand at room temperature for 4 days. The crystals which separated out were recrystallized from acetic acid to give yellow crystals, m. p. 320°C (decomp.). The ultraviolet and infrared spectra of the crystals are superimposable upon those of XXII obtained in a).

9-Aminobenzo-1, 4-thiazino[3, 2-b]tropone (XXIII).—A mixture of XIX (200 mg.), and zinc (900 mg.) in acetic acid (6 ml.) was heated for 2 hr. at about 90°C. The excess of zinc was then filtered off, and the filtrate was diluted with water and extracted with chloroform. The extract was dried, passed through an alumina column, and eluted with chloroform. From the effluent, orange needles (XXIII) (27 mg.); m. p. 165°C, were obtained after recrystallization from benzene.

Found: C, 64.65; H, 4.37; N, 11.36. Calcd. for $C_{13}H_{10}ON_2S$: C, 64.46; H, 4.16; N, 11.57%.

λ_{max}^{MeOH} mμ (log ε): 238 (4.36), 349 (4.58), 440 (3.79).

9-Amino-8-isopropylbenzo-1, 4-thiazino[3, 2-b]-tropone (XXIV).—Orange needles (XXIV) (27 mg.); m. p. 136°C (from methanol), were obtained by the reduction of XXI (162 mg.) with zinc in acetic acid according to the procedure described above.

Found: C, 67.81; H, 5.77; N, 10.63. Calcd. for $C_{16}H_{16}ON_2S$: C, 67.59; H, 5.67; N, 9.85%.

λ_{max}^{MeOH} mμ (log ε): 239 (4.35), 348 (4.60), 435 (3.77).

The Reduction of 7-Nitrobenzo-1, 4-thiazino[3, 2-b]tropone (XXV).—A mixture of XXV (100 mg.), and 5% Pd-C (10 mg.) in acetic acid (10 mg.) was submitted to catalytic hydrogenation. After 27 ml. of hydrogen had been taken up, the catalyst was filtered off, and the filtrate was diluted with water and extracted with benzene and then with chloroform. The combined extracts gave reddish crystals (XXVI), m. p. 208°C, but they could not be purified. Acetic anhydride was added to the crystals, and the solution was heated gently. The violet needles (50 mg.) which separated out were recrystallized from methanol to afford deep reddish prisms, m. p. 251°C, which were identified with 7-acetamidobenzo-1, 4-thiazino[3, 2-b]tropone[2] (XXVII) by a mixed melting point determination and by a comparison of their ultraviolet and infrared spectra.

The authors wish to express their gratitude to the Sankyo Co. for its donation of a research fund which covered a part of the expenses for this work. The infrared and ultraviolet spectrophotometers used in this study were purchased with a grant-in-aid for Fundamental and Technical Research from the Toyo Rayon Co., Ltd., to whom the authors are grateful.

BULLETIN OF THE CHEMICAL SOCIETY OF JAPAN VOL. 39 1995—1998 (1966)

Vinylacetic Acid Ester Formation in the Reaction of Crotonoyl Chloride with Alcohol in the Presence of *t*-Amine

By Toshitsugu OZEKI and Masakatsu KUSAKA

Yokkaichi Laboratory, Daikyowa Petrochemical Co., Ltd., Daikyo-cho, Yokkaichi, Mie

(Received January 5, 1966)

In the esterification of crotonoyl chloride, vinylacetic acid ester was obtained predominantly, with an unusual double bond shift from the α, β- to the β, γ-position in the presence of a strong basic amine. In the case of ethyl alcohol, for example, the yields of ethyl vinylacetate were as follows (%): triethylamine (96.1), tributylamine (86.1), *N*-ethyl morpholine (74.6), *N*, *N*-diethyl aniline (0.1) and pyridine (0.9). The rest were *cis*- and *trans*-crotonic acid esters.

The interesting facts were found by the authors that, in the reaction of crotonoyl chloride with alcohol in the presence of a strong basic amine (the Einhorn reaction),[1] an unusual shifts of the double bond from the α, β- to the β, γ-position occurred and that vinylacetic acid ester was obtained predominantly (Eq. 1):

$$CH_3CH{=}CHCOCl + ROH + R_3'N \longrightarrow CH_2{=}CHCH_2COOR + CH_3CH{=}CHCOOR + R_3'N^+HCl^- \quad (1)$$

major product minor product

Although the double bond shift from the α, β- to the β, γ-position has been reported in the hydroformylation of ethyl crotonate and crotonamide,[2-4] such a double bond shift has not ever been reported in relation to the Einhorn reaction; the occurrence of a double bond shift from a conjugated to an unconjugated system in such a reaction is very interesting.

Experimental

Reagents.—All the reagents used except crytonoyl chloride were obtained commercially. The alcohols, amines and benzene were purified by fractional distillation after they had been treated with a drying agent. Crotonic acid, sodium hydroxide and sulfuric acid (98%), each available in a G. R. grade, were used without further purification. Crotonoyl chloride (b. p. 120—123°C, n_D^{18} 1.4598), prepared from crotonic acid and thionyl chloride, was identified by means of its NMR[5] and IR (960 cm^{-1}, $^{H}\rangle C{=}C\langle_{H}$ and 1768 cm^{-1}, C=CCOCl) spectra. The spectra are shown in Figs. 1 and 2.

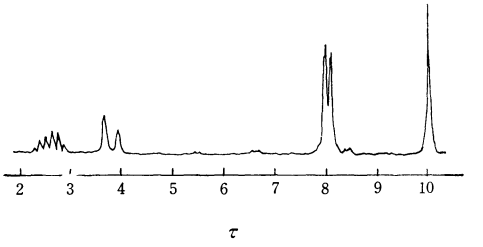

Fig. 1. NMR spectrum of crotonoyl chloride.
JNM-C-60
60 Mc., 20°C, Bulk
Stand. $(CH_3)_4Si$

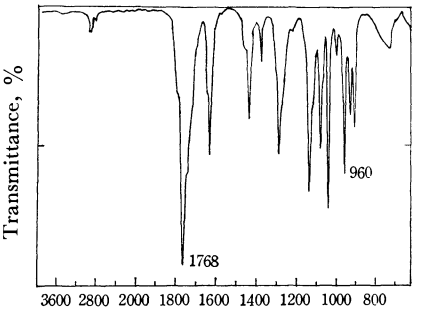

Fig. 2. IR spectrum of crotonoyl chloride.
Shimadzu IR-27
CCl_4 soln. (ca. 1.6%)
0.2 mm.

Procedure.—The alcohol, amine and solvent were placed in a flask fitted with a thermometer, a mechanical stirrer, a condenser, and a dropping funnel. Through the dropping funnel, crotonoyl chloride was then added slowly into the mixture with stirring at room temperature; after 15 min. the supernatant liquid of the reaction

1) H. Krauch and W. Kunz, "Organic Name Reactions", John Wiley & Sons, New York (1964), 141.
2) J. Falbe and F. Korte, *Angew. Chem.*, **74**, 900 (1962).
3) J. Falbe and F. Korte, *Chem. Ber.*, **95**, 2680 (1962).
4) J. Falbe, N. Huppes and F. Korte, ibid., **97**, 863 (1964).
5) H. Kashiwagi and J. Niwa, This Bulletin, **36**, 405 (1963).

Table I. Composition of products

Exp. No.	Alcohol	Base	Solvent	Reaction temp., °C	Product ratio, %*6 I	II	III
1*1	Methyl	TEA*5	Benzene	24—32	87.8	1.2	11.0
2*1	Ethyl	TEA	Benzene	24—28	96.1	0.6	3.3
3*1	Isopropyl	TEA	Benzene	26—30	96.6	0.8	2.7
4*1	*t*-Butyl	TEA	Benzene	23—28	96.9	1.2	1.9
5*1	*n*-Butyl	TEA	Benzene	24—28	95.4	0.7	3.8
6*1	Crotyl	TEA	Benzene	24—30	91.3	1.0	7.7
7*2	Isoamyl	TEA	Benzene	24—32	96.4	0.6	3.0
8*2	Methyl	TBA*5	Benzene	25—26	79.7	1.5	18.7
9*2	Ethyl	TBA	Benzene	25—27	86.1	0.9	13.1
10*2	Ethyl	EM*5	Benzene	24—26	74.6	3.5	21.9
11*2	Ethyl	Py*5	Benzene	25—27	0.9	5.9	93.2
12*2	Ethyl	DEA*5	Benzene	25—27	0.1	7.1	92.7
13*2	Ethyl	None	Benzene	23—26	3.2	9.5	87.3
14*3	Ethyl	NaOH	Benzene & Water	24—27	0.3	8.3	91.5
15*4	Ethyl	(H_2SO_4)	Benzene	Reflux	—	0.2	99.8

*1 Alcohol 0.75 mol., amine 0.5 mol., crotonoyl chloride 0.5 mol. and solvent 100 g. were used.
*2 Alcohol 0.35 mol., amine 0.25 mol., crotonoyl chloride 0.25 mol. and solvent 50 g. were used.
*3 Alcohol 17.2 g., NaOH 10 g., crotonoyl chloride 26.1 g., water 40 g. and benzene 40 g. were used.
*2 Alcohol 13.8 g., crotonic acid 8.6 g., benzene 20 g. and H_2SO_4 2 cc. were refluxed gently for 6 hr.
*5 TEA: triethylamine, TBA: tri-*n*-butylamine, Py: pyridine, DEA: diethylaniline and EM: *N*-ethyl morpholine.
*6 Total yields: 86—100% in Exp. 1—13 except Exp. 4, 65%.

Table II. Characteristic bands of IR (cm^{-1})*

	I_{Me}	I_{Et}	II_{Me}	II_{Et}	III_{Me}	III_{Et}
$\nu_{C=O}$	1742	1740	1720	1720	1727	1721
ν_{C-O-}	1170 1195	1177	1178 1200	1186	1179 1197	1184
$\nu_{C=C}$	1647	1646	1649	1652	1664	1666
$\nu_{=C-H}$	3085	3090	3030	3039	3062	3060
δ=C-H (in-plane)	1409	1407	1410	1414	—	—
δ=C-H (out-of-plane)	920 992	920 994	818	815	968	969

* Shimadzu IR-27, NaCl cell, liquid capillary.

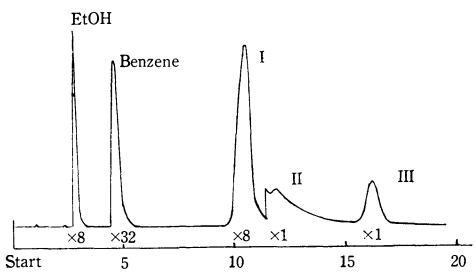

Time, min.

Fig. 3. Gas chromatogram for Exp. 2.

Shimadzu GC-2C
Tricresyl phosphate (10%, 5.25 m.)
100°C
H_2 10 cc./20 sec.

mixture was analyzed by gas chromatography in order to determine the product ratio. As amine hydrochlorides were soluble in benzene in Exp. 8, 9 and 12, an equal volume of *n*-hexane was added to the reaction mixture to precipitate them; thereafter an aliquot was withdrawn from the upper layer. In the Schotten-Baumann (Exp. 14) and Fisher (Exp. 15) methods, the benzene layer was submitted to analysis. A typical gas chromatogram for Exp. 2 is shown in Fig. 3. The results obtained are shown in Table I.

Identification

The products always consisted of three isomeric esters (denoted as I, II and III); they were isolated by fractional gas chromatography in some reactions (Shimadzu GC-11A; Tricresyl phosphate (20%) 4.5 m.; He; 100°C).

Table III. Chemical shifts and coupling constants of NMR*1

Ester	Chemical shift (τ-value)				Coupling constant (c.p.s.)*2					
	H_1	H_2	H_3	H_4	J_{12}	J_{13}	J_{14}	J_{23}	J_{24}	J_{34}
I_{Me}	4.1	4.9	4.9	7.0	9.5	17	6.4	—	1.3	1.3
I_{Et}	4.1	4.9	4.9	7.0	9.4	17	6.7	—	1.4	1.4
(Lit.)*3	(4.10)	(4.92)	(4.89)	(6.96)	(10.3)	(17.3)	(6.9)	(1.8)	(−1.5)	(−1.6)

	H_1	H_2	H_3	J_{12}	J_{13}	J_{23}
II_{Me}	4.2	3.7	7.9	12	1.4	7.0
II_{Et}	4.3	3.8	7.9	12	1.8	7.3
(Lit.)*4	(4.28)	(3.72)	(7.86)	(11.4)	(−1.82)	(7.27)

	H_1	H_2	H_3	J_{12}	J_{13}	J_{23}
III_{Me}	4.2	3.1	8.1	17	1.7	6.7
III_{Et}	4.2	3.1	8.1	15	1.6	6.8
(Lit.)*4	(4.24)	(3.10)	(8.12)	(15.5)	(−1.67)	(6.85)

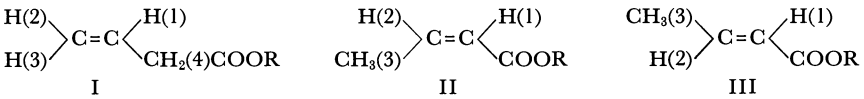

*1 Varian HR-100, 100 Mc., 10% CCl_4 soln., room temp., stand. $(CH_3)_4Si$.
*2 Absolute values. Not considered about the sign.
*3 Ref. 8.
*4 Ref. 5.

Table IV. Physical and chemical constants

Methyl esters	I_{Me}	II_{Me}	III_{Me}
Purity, %*1	100	99.0	99.8
B. p., °C/mmHg	53.8—4.0/106	—	68.8—9.6/118
(Lit.)*2	(108/774)	—	(119/768)
$n_D^{(t)}$	$1.4085^{(20.2)}$	$1.4258^{(20.0)}$	$1.4254^{(20.2)}$
(Lit.)*3	(1.4083)	(1.4223)	(1.4248)
Iodine value (calcd. 254)	245	—	248
Sapon. value (calcd. 561)	563	—	562
UV*4			
λ_{max}(mμ), (log ε_{max})	208 (3.47)	—	206 (4.16)
(Lit.)	(225_s) ((2.0))*5	—	(212) ((4.16))*6

Ethyl esters	I_{Et}	II_{Et}	III_{Et}
Purity, %*1	99.6	99.5	99.9
B. p., °C/mmHg	53.0—3.4/58	58.6—8.8/68	57.5—7.8/47
(Lit.)*2	(124/745)	—	(136.5/761)
$n_D^{(t)}$	$1.4109^{(19.8)}$	$1.4253^{(20.2)}$	$1.4251^{(19.8)}$
(Lit.)*2	(1.4110)	—	(1.4247)
Iodine value (calcd. 223)	221	216	216
Sapon. value (calcd. 492)	496	495	495

*1 By gas chromatographic analysis.
*2 Ref. 9.
*3 Ref. 10.
*4 Measured in 95% EtOH with ORD-UV-5 (JASCO).
*5 Values for ethyl ester in *n*-hexane (s: shoulder). J. C. Crawford, *J. Chem. Soc.*, **1953**, 2658.
*6 R. F. Rekker, P. J. Brombacher, H. Hamann and W. J. Nauta, *Rec. trav. chim.*, **73**, 410 (1954).

Characteristic infrared bands for methyl and ethyl esters are shown in Table II. These characteristic bands indicate the presence of the following functional groups[6];

in I	nonconjugated carbonyl group nonconjugated terminal vinyl group,
in II	conjugated carbonyl group conjugated cis-double bond,
and in III	conjugated carbonyl group conjugated trans-double bond.

NMR measurements for methyl and ethyl esters

6) L. J. Bellamy, "The Infrared Spectra of Complex Molecules," John Wiley & Sons, New York (1958), Chap. 3 and Chap. 11.

were carried out at 100 Mc.[7] The data are listed in Table III.

The spectra for II and III were analyzed and found to be of the ABX_3 type; their chemical shifts and coupling constants were consistent with the values given to *cis*- and *trans*-methyl crotonates in the literature.[5,8,9] It was reasonable to identify the spectra for I as the $ABCX_2$ type.[10] This result agreed well with the values for methyl vinylacetate.[11] These assignments were also supported by the proton ratios obtained by the integration of each signal.

The refractive index, the retention time in gas chromatography, and the infrared and ultraviolet spectra for I_{Me} were completely identical with those values for authentic methyl vinylacetate as prepared by Vogel's method.[12] Furthermore, the results of ozone oxidation, followed by the formaldehyde test using chromotropic acid, were positive, indicating the presence of a terminal vinyl group.

The physical and chemical constants for the isolated methyl and ethyl esters are shown in Table IV. Their iodine and saponification values were in agreement with the calculated values. The refractive indices were identical with the values in the literature.[12,13]

As to the other esters shown in Table I, analogous behavior in chemical and physical analysis was observed. Therefore, in all cases I, II and III were identified as the vinylacetic acid ester, the *cis*-crotonic acid ester and the *trans*-crotonic acid ester respectively.

Discussion

The absence of vinylacetyl chloride in crotonoyl chloride was confirmed by the absence of peaks at 1800 cm^{-1} (unconjugated acyl halide), 910 and 990 cm^{-1} (terminal vinyl) in IR, and by the near 6.5 τ-value (substituted methylene, $C{=}CCH_2{-}COX$) in NMR.

Regarding gas chromatography, the same results were obtained with both tricresyl phosphate and diethyleneglycol succinate columns; no isomerization was observed in either column. Therefore, the composition of the products must be correct.

It may be understood from Table I that the vinylacetic acid ester was formed predominantly in the presence of a strong basic amine (Exp. 1—10), with little dependence on the sort of alcohol, but that the crotonic acid ester was predominant in the presence of a weak basic amine (Exp. 11—12). In the reaction without amine or in Schotten-Baumann and Fisher reactions, however, the crotonic acid ester was formed predominantly. These facts suggest that the amine plays an important role in the formation of the vinylacetic acid ester.

The occurrence of an unusual double bond shift from a conjugated to an unconjugated system is very interesting. Hickmott has reported the following reaction (Eq. 2)[14]:

$$\begin{aligned} &RCH{=}CHCOCl + R'OH + R_3''N \longrightarrow \\ &\quad Cl^-R_3''N^+CHCH_2COOR' + \\ &\qquad\quad \underset{R}{|} \\ &\quad \text{main product} \\ &RCH{=}CHCOOR' + R_3''N^+HCl^- \qquad (2) \\ &\qquad\qquad (R{=}H,\ CH_3) \end{aligned}$$

This reaction may participate in the reaction mechanism of vinylacetic acid ester formation. Further investigation is now in progress and will be reported on at a later data.

The authors thank Dr. Shizuyoshi Sakai, Dr. Kenji Yokota and Dr. Ken Kanematsu of Nagoya University for their useful advices and Miss Kikuko Hayamizu of The Government Chemical Industrial Research Institute, Tokyo and Mr. Makoto Takeuchi of Japan Electron Optics Laboratory Co., Ltd. for NMR measurement and analysis.

7) NMR spectra at 100 Mc. were measured in The Government Chemical Industrial Research Institute, Tokyo. The NMR spectra at 60 Mc. were measured with a JNM 3H-60 (room temp.; bulk; stand. $(CH_3)_4$-Si) apparatus in the Japan Electron Optics Laboratory Co., Ltd.; the same results were obtained.

8) R. R. Fraser and D. E. McGreer, *Can. J. Chem.*, **39**, 505 (1961).

9) L. M. Jackman and R. H. Wiley, *J. Chem. Soc.*, **1960**, 2886.

10) R. M. Silverstein and G. C. Bassler," Spectrometric Identification of Organic Compounds, " John Wiley & Sons, New York (1963), pp. 83—89.

11) K. Hayamizu, unpublished data.

12) G. H. Jeffery and A. I. Vogel, *J. Chem. Soc.*, **1948**, 658.

13) D. E. McGreer. *J. Org. Chem.*, **25**, 852 (1960).

14) P. W. Hickmott, *J. Chem. Soc.*, **1964**, 883.

BULLETIN OF THE CHEMICAL SOCIETY OF JAPAN VOL. 39 1999—2000 (1966)

The Synthesis of γ-Alkylamides of L-Glutamic Acid. The Reactions of Metallic Salts of L-Pyrrolidonecarboxylic Acid with Primary Alkylamines

By Yoshitaka YAMADA, Moritaro SAKURAI and Yoshio TSUCHIYA

Central Research Laboratories, Ajinomoto Co., Inc., Kawasaki

(Received January 5, 1566)

L-Theanine, a principal component of flavors contained in green teas, and its homologs have been synthesized by the reactions of several metallic salts of L-pyrrolidonecarboxylic acid with primary alkylamines. Hitherto, γ-alkylamides of L-glutamic acid had been prepared in low yields by the reactions of L-pyrrolidonecarboxylic acid with anhydrous alkylamines. The use of metallic salts, especially cupric, zinc, and manganese salts, increased the yields of the γ-amides remarkably.

L-Theanine is a form of *N*-(γ-L-glutamyl)ethylamine known to be a principal component of the flavors contained in green teas, especially those of a higher grade.[1] Several procedures are available for the synthesis of L-theanine, e. g., the treatment of γ-ethyl *N*-benzyloxycarbonyl-L-glutamate with anhydrous ethylamine,[2] and that of L-pyrrolidonecarboxylic acid with aqueous[3] or anhydrous[4] ethylamine. The ring-opening reactions of pyrrolidonecarboxylic acid with primary alkylamines are equilibrium reactions and are remarkably affected by the solubilities of the products, γ-alkylamides of glutamic acid, in the reactant alkylamines.

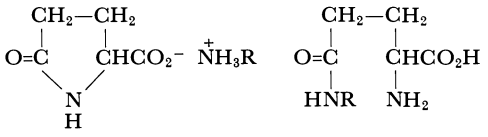

The yield of optically active L-theanine from L-pyrrolidonecarboxylic acid is compared with that of DL-theanine from DL-pyrrolidonecarboxylic acid in Fig. 1.

As a rule, the γ-alkylamides of racemic glutamic acid are less soluble in alkylamine than those of the optically active isomer. Consequently, if the L-amides produced could be made insoluble in the corresponding alkylamines by some means, the yields of the γ-amides might be increased. The present studies were initiated in search of a method which could displace the equilibrium and which would lead to complete conversion.

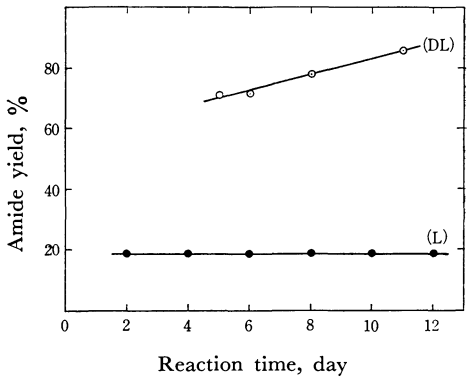

Fig. 1. The comparison of the yields of L- and DL-theanines. (Ethylamine and the respective acids were heated at 60°C in the molar ratio of 4 : 1.)

Experimental

Cupric L-Pyrrolidonecarboxylate.—Into a solution of 12.9 g. (0.1 mol.) of L-pyrrolidonecarboxylic acid in 100 ml. of water, basic cupric carbonate was added with stirring under a slight warming until the evolution of carbon dioxide ceased. After the mixture had then been filtered, the filtrate was concentrated under reduced pressure. The crystalline mass was filtered and then dried over sulfuric acid under reduced pressure. The yield of the cupric salt was 35.6 g. (91%); m. p. 190—210°C (decomp.).

Found: C, 30.50; H, 5.37; N, 7.42; Cu, 15.88. Calcd. for $C_{10}H_{12}O_6N_2Cu\cdot 4H_2O$: C, 30.65; H, 5.14; N, 7.15; Cu, 16.21%.

Zinc L-Pyrrolidonecarboxylate.—The zinc salt was prepared according to the procedure for the cupric salt described above.

Found: C, 33.62; H, 4.77; N, 7.61. Calcd. for $C_{10}H_{12}O_6N_2Zn\cdot 2H_2O$: C, 33.58; H, 4.51; N, 7.84%.

Manganese L-Pyrrolidonecarboxylate.—This was prepared in a similar manner, but attempts to crystallize the resultant syrup were unsuccessful.

1) Y. Sakato, *Nippon Nogeikagaku Zasshi*, **23**, 262 (1950).
2) Y. Sakato, T. Hashizume, Y. Kishimoto, ibid., **23**, 269 (1950).
3) N. Lichtenstein, *J. Am. Chem. Soc.*, **64**, 1021 (1942).
4) Y. Tuchiya, Japanese Pat. 197059.

L-Theanine, *N*-(γ-L-Glutamyl)ethylamine.— Thirty-two grams of anhydrous cupric L-pyrrolidonecarboxylate dried at 100°C under reduced pressure were treated with 51 ml. of anhydrous ethylamine for seven days at 70°C in a sealed glass tube. At the end of this time, the solution was concentrated to dryness under reduced pressure to yield the violet crystalline mass. The residue was suspended in 300 ml. of water, and then the cupric ions were removed by the usual method using hydrogen sulfide. The solution, now free from cupric ions, was decolorized with activated charcoal, concentrated under reduced pressure, and cooled. The colorless crystalline precipitate was collected and dried over concentrated sulfuric acid under reduced pressure.

Yield: 30.3 g. (87%); m. p. 214—215°C (decomp.).

Found: C, 48.06; H, 8.11; N, 16.05.

Calcd. for $C_7H_{14}O_3N_2$: C, 48.26; H, 8.10; N, 16.08%.

Cupric complexes of L-theanine prepared by the method described above were recrystallized from hot water before analysis.

Found: C, 40.79; H, 6.54; N, 13.31; Cu, 15.61. Calcd. for $C_{14}H_{26}O_6N_4Cu$: C, 41.01; H, 6.39; N, 13.66; Cu, 15.50%.

TABLE I. THE REACTIONS OF VARIOUS SALTS OF L-PYRROLIDONECARBOXYLIC ACID WITH ANHYDROUS ETHYLAMINE

Run[a]	Metallic Ion	Molar ratio[b]	Yield[c]	Solubility[d]
1	Ca^{2+}	10.0	0	Insol.
2	Cr^{2+}	5.0	0	Sol.
3	Mn^{2+}	7.8	80	Sol.
4	Co^{2+}	6.0	trace[e]	Sol.
5	Ni^{2+}	6.0	trace[e]	Sol.
6	Cu^{2+}	7.8	88	Sol.
7	Zn^{2+}	7.8	60	Sol.
8	Cd^{2+}	5.0	0	Sol.
9	Hg^{2+}	7.8	0[f]	Sol.
10	Pd^{2+}	10.0	0	Insol.

a) Experiments at 70°C for seven days.
b) Molar ratio of ethylamine to the metallic salt of L-pyrrolidonecarboxylic acid.
c) Yield of the metallic salt of L-theanine.
d) Solubility of the metallic salt of L-pyrrolidonecarboxylic acid in ethylamine.
e) A syrup was obtained from this run.
f) Metallic mercury was isolated from this run.

Results

The preliminary experiments have revealed that cupric, zinc and manganese salts of L-pyrrolidonecarboxylic acid are soluble in alkylamines, but the corresponding salts of the γ-alkylamides are insoluble. Thus, the use of these salts provides the best method for preparing γ-alkylamides of L-glutamic acid.

The experimental results of the reactions of various salts of L-pyrrolidonecarboxylic acid with anhydrous ethylamine are summarized in Table I. Similarly, the results of the reactions of zinc L-pyrrolidonecarboxylate with several primary alkylamines are given in Table II. The physical properties of the γ-alkylamides prepared are shown in Table III.

TABLE III. PHYSICAL PROPERTIES OF THE γ-ALKYLAMIDES OF L-GLUTAMIC ACID

$$RNHCOCH_2CH_2\underset{\displaystyle NH_2}{\underset{|}{C}}HCOOH$$

R	M. p., °C	$[\alpha]_D^{30}$ [a]	Taste
H	185—186	+6.1	nice and sweet
CH_3CH_2-	214—215	+6.1	↓
$CH_3CH_2CH_2-$	222—223	+5.8	↓
$CH_3(CH_2)_2CH_2-$	222—223	+5.7	↓
$CH_3(CH_2)_3CH_2$	207—208	+5.7	bitter

a) Specific rotation was measured in a neutral aqueous solution. (c 2, H_2O)

The L-Theanine thus prepared was identified by a comparison of its melting point, paper chromatographic behavior and infrared spectrum with those of an authentic sample prepared by the aminolysis of γ-ethyl *N*-benzyloxycarbonyl-L-glutamate with ethylamine, followed by hydrogenolysis.[2] Accordingly, it is evident that the alkylamino group is located in the γ-position of the L-glutamic acid residue.

We wish to express our deep thanks to Dr. Haruomi Oeda for his kind encouragement and valuable suggestions.

TABLE II. REACTIONS OF ZINC L-PYRROLIDONECARBOXYLATE WITH SEVERAL ALKYLAMINES

Run	Amine	Molar ratio	Temp. °C	Time day	Yield %	Analysis, % Calcd.	Found
1	NH_3	12	50	1	trace[a]		
2	Ethylamine	7.8	70	6	59	C 48.26 H 8.10 N 16.08	C 48.06 H 8.11 N 16.05
3	*n*-Propylamine	8	70	6	36	C 51.08 H 8.57 N 14.87	C 51.11 H 8.86 N 14.84
4	*n*-Butylamine	8	70	6	24	C 53.44 H 8.96 N 13.85	C 53.44 H 8.96 N 13.76
5	*n*-Amylamine	9	70	6	20	C 55.53 H 9.32 N 12.94	C 55.51 H 9.27 N 12.95

a) Identified by paper chromatography

BULLETIN OF THE CHEMICAL SOCIETY OF JAPAN VOL. 39 2001—2004 (1966)

The Reaction of Butadiene with Ethylene. I.* A New Synthesis of 3-Methyl-1, 4-pentadiene

By Masao IWAMOTO and Sadao YUGUCHI

Central Research Laboratories, Toyo Rayon Company, Ltd., Sonoyama, Otsu

(Received January 20, 1966)

3-Methyl-1, 4-pentadiene, 1, 4-hexadiene, and 1, 3-hexadiene were obtained, in the weight ratio of 2 : 1 : 2, by the use of a ternary catalyst consisting of a combination of ferric chloride and triethylaluminum, with triphenylphosphine as the third component. The products were identified by means of gas chromatography, infrared spectroscopy, mass spectroscopy, NMR, and hydrogenation. The effects of the catalyst compositions and the reaction conditions on the yield and the product composition were also studied. In order to obtain the C_6-dienes in the weight ratio described above, the following conditions are desirable; temperature 20—30°C, P/Fe mole ratio 1—2, Al/Fe mole ratio 3—5, and a high ethylene pressure. Although the use of several phosphorus compounds as the third component in the catalyst instead of triphenyl phosphine was investigated, these compounds were ineffective in the selective formation of C_6-dienes. It was suggested that the compound which serves as the third component in the catalyst plays an important role.

A linear dimerization of butadiene has been made by means of catalytic actions of cobalt complex catalysts[1-4] and a ternary catalyst consisting of a combination of ferric chloride and alkylaluminum compounds, with triphenyl phosphine as the third component.[5]

In the course of our study of the preparation of 1, 4-hexadiene from butadiene and ethylene, we have found that the ternary catalyst mentioned above catalyzed the formation of a mixture of C_6-dienes, i. e., 3-methyl-1, 4-pentadiene, 1, 4-hexadiene, and 1, 3-hexadiene. This paper will describe the identification of the reaction products and will study the factors affecting the reaction.

3-Methyl-1, 4-pentadiene was recently obtained by the thermally-initiated reaction of acetylene with 2-butene.[6] The preparation procedure described in this paper is also a convenient method to obtain the compound.

Experimental

Reagents.—Butadiene (purity: 98%) was purified by passing it through a series of columns filled with a ethyleneglycol-metallic sodium solution, potassium hydroxide pellets, activated alumina, and a triethylaluminum-liquid paraffin solution (about 10%) successively; it was then condensed in a measuring vessel kept in a dry ice - methanol bath. Ethylene (Nihon Petrochemical Co.) was used without further purification. Toluene (Udex grade) was purified by distillation under nitrogen. Anhydrous ferric chloride was sublimated in vacuo before use. The triphenyl phosphine and other compounds used as the third component in the catalysts were obtained commercially. Triethylaluminum (Ethyl Corp.) was uesd without purification.

Reaction Procedure.—A 200 ml. stainless steel autoclave equipped with a magnetic stirrer was used as the reactor. Calculated amounts of anhydrous ferric chloride, toluene, triphenyl phoshine, butadiene, and triethylaluminum were introduced, in that order, into the reactor, which had been flushed with nitrogen in advance. During the procedure, the reactor was kept at below −20°C to prevent the evaporation of butadiene. Then the reactor was closed and kept at reaction temperatures. The reaction was carried out under a constant ethylene pressure while the mixture was continuously being stirred. After a proper reaction time the catalyst was quenched by adding a small amount of methanol, and then the reaction mixture was washed with water containing a small amount of dilute hydrochloric acid.

The organic layer was thoroughly washed with water, dried with anhydrous sodium sulfate, and disitlled. A fraction which was distilled at bath temperature of up to 200°C was collected and analyzed by gas chromatography. The compositions of the products were calculated by the area ratios of the gas chromatogram. Higher boiling materials were recorded as a residue.

Analysis.—For the gas chromatographic analysis of the reaction products, copper tubing (4 mm. in diameter and 3 m. long) packed with Apiezon Grease L was used. For the hydrogenated product, a Golay column (45 m. long) coated with Apiezon Grease L was used. The purifications of 3-methyl-1, 4-pentadiene

* Presented at the 14th Symposium on Polymer Science, Kyoto, October, 1965.

1) S. Otsuka, T. Taketomi and T. Kikuchi, *J. Am. Chem. Soc.*, **85**, 3709 (1963).
2) S. Tanaka, K. Mabuchi and N. Shimazaki, *J. Org. Chem.*, **29**, 1626 (1964).
3) T. Saito, T. Ohno, Y. Uchida and A. Misono, *J. Chem., Soc. Japan, Ind. Chem. Sect. (Kogyo Kagaku Zasshi)* **66**, 1094 (1963).
4) D. Wittenberg, *Angew. Chem.*, **75**, 1124 (1963).
5) H. Takahashi, S. Tai and M. Yamaguchi, *Tetrahedron Letters*, **1964**, 3173.
6) N. F. Cywinski, *J. Org. Chem.*, **30**, 361 (1965).

and 1, 3-hexadiene in order to identify them were carried out after a preparative gas chromatography (Yanagimoto model GCS-1003). All analyses were carried out at 100°C, using helium as the carrier gas.

The infrared spectra of samples were determined by a Hitachi infrared spectrometer, model EPI-S. The NMR spectrum of 3-methyl-1, 4-pentadiene was obtained by a Varian A60 apparatus at 60Mc. Mass spectra were taken, in order to determine the molecular weight and in order to identify the skeletal structures of the hydrogenated products, by a Hitachi mass spectrometer, RMU-6.

Results and Discussion

The Identification of the Reaction Products. —The gas chromatogram (Fig. 1) of the reaction mixture indicates that it includes several components. The peaks 1, 2, 4, 6, 7, 8, and 9 in Fig. 1 were identified as air, unreacted butadiene, 1, 4-hexadiene, cyclohexene, 3-methyl-1, 4, 6-heptatriene, toluene, and 1, 3, 6-octatriene respectively by comparing their retention times with those of authentic samples. For the identification of the unknown products, each of the components of peaks 3 and 5 was collected by preparative gas chromatography. The infrared spectrum of the component of peak 3 showed the presence of a terminal double bond (910 and 992 cm^{-1}) and a methyl group (1377 cm^{-1}). The spectrum of the component of peak 5 showed the presence of a conjugated double bond (1600 and 1640 cm^{-1}), a trans-double bond (960 cm^{-1}), a terminal double bond (898 and 1002 cm^{-1}), and a methyl group (1374 cm^{-1}). Since both components had the same molecular peak, at *m/e* 82, in their mass spectra, these compounds must be hydrocarbons with the same six carbon atoms. The distillate, b. p. 45—60°C, was collected by distillation at atmospheric pressure and was hydrogenated at room temperature with hydrogen, using palladium black as the catalyst. Before the hydrogenation, the distillate contained three components and peaks 1′, 2′, and 3′ in Fig. 2A corresponded to the peaks 3, 4, and 5 respectively in Fig. 1. However, the hydrogenated product contained only two components (Fig. 2B). The area ratio of the peak 1′ to the two other peaks combined in Fig. 2A was about 1 to 2, and the ratio of the two peaks in Fig. 2B was about 1 to 1.8. It may be considered, therefore, that the components of the peaks 2′ and 3′ were hydrogenated to the same saturated hydrocarbon. Both components in the hydrogenated product had the same molecular peak, at m/e 86. This suggests that each of the components of peaks 3 and 5 in Fig. 1 has two double bonds, those of the component of peak 3 being of the vinyl type and those of the component of peak 5 being conjugated. The pattern coefficients of 3-methylpentane and *n*-hexane in API data agreed entirely with the mass spectral data of the two components of the hydrogenated product. In the NMR spectrum of the component of peak 3, the doublet at 8.9 τ indicates the presence of a secondary methyl group, while the multiplet at 7.14 τ indicates the presence of the following partial structure: $=CH-CH(CH_3)-CH=$.

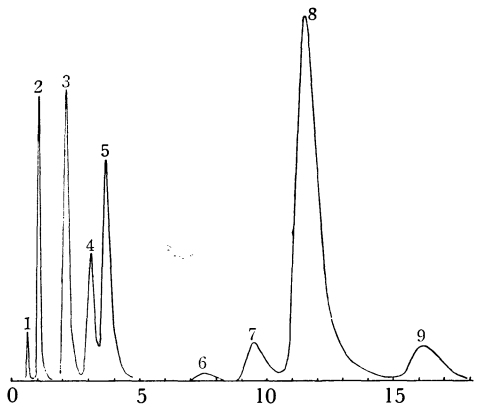

Fig. 1. Gas chromatogram of the reaction mixture of Exp. 5 in Table II.

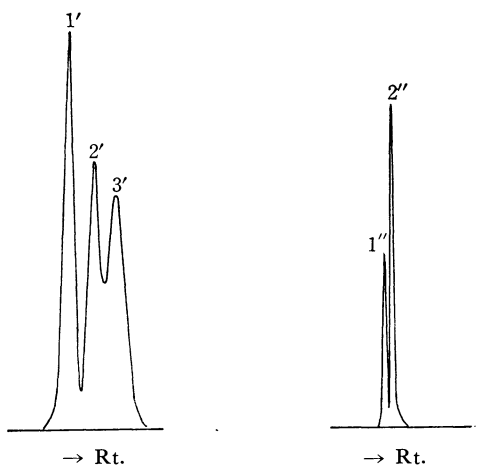

Fig. 2. Gas chromatograms, A: Before hydrogenation, B: After hydrogenation.

It is quite reasonable to conclude, from the evidence described above, that the component of peak 3 is 3-methyl-1, 4-pentadiene and that the component of peak 5 is 1, 3-hexadiene.

The Reaction of Butadiene with Ethylene. —The reaction of butadiene with ethylene can form the following four compounds as a 1 : 1 addition product; 3-methyl-1, 4-pentadiene, 1, 4-hexadiene, 1, 3-hexadiene, and cyclohexene.

The reaction conditions were examined using a catalyst consisting of a combination ferric chloride, triphenyl phosphine, and triethylaluminum. The catalyst containing no triphenyl phosphine was inactive in the reaction of butadiene with

Table I. Effect of the catalyst composition in $FeCl_3$-$P(C_6H_5)_3$-$(C_2H_5)_3Al$ system*1

Exp. No.	P/Fe mole ratio	Al/Fe mole ratio	Yield of product, g.			C_6-dienes composition, %*3		
			C_6-dienes	BD dimer*2	Residue	MPD	1,4-HD	1,3-HD
1	1	3.6	6.1	6.7	2.9	31	31	28
2	1.5	3.6	9.1	3.0	0.6	33.7	24.4	41.9
3	2	3.6	9.2	5.4	1.5	29.5	29.9	40.6
4	1.5	1	0.9	0.3	0.1	29.4	24.8	45.8
5	1.5	1.8	3.2	0.5	0.9	30.1	27.6	42.3
6	1.5	5	5.1	4.9	1.1	28.1	34.3	37.6
7	1.5	7.3	2.5	4.3	1.5	21.5	45	33.5

*1 Toluene 50 g., Butadiene 13.4 g., $FeCl_3$ 0.35 g., Ethylene pressure 40 kg./cm^2, 50°C, 3 hr.
*2 Butadiene linear dimers.
*3 MPD=3-methyl-1,4-pentadiene, 1,4-HD=1,4-hexadiene, 1,3-HD=1,3-hexadiene.

Table II. Effects of the reaction temperature

Exp. No.	1	2	3	4	5	6
$FeCl_3$ (g.)	0.32	0.32	0.32	0.32	0.52	0.35
$P(C_6H_5)_3$ (g.)	0.78	0.78	0.78	0.78	1.2	0.8
$(C_2H_5)_3Al$ (g.)	0.83	0.83	0.83	0.83	1.5	0.9
Toluene (g.)	50	50	50	66	16	50
Butadiene (g.)	13.4	13.4	13.4	27	46.9	30.1
Ethylene (kg./cm^2)	40	40	40	100	100	100
Temperature (°C)	20	50	70	20	30	30
Reaction time (hr.)	3	3	3	5	17.5	16.5
Product (g.)						
MPD	3.3	3.1	1.4	9.7	14.1	9.5
1,4-HD	1.7	2.2	1.6	4.9	7.8	5
1,3-HD	3.4	3.8	1.9	9.8	15	10.8
The others combined*1	6	4.8	6.8	8.6	18	10.2

*1 Cyclohexene, butadiene dimers, and residue are included.

Table III. Variation of the third component*1

Exp. No.	The third component	Mole ratio*2	Butadiene g.	Products, g.		
				C_6-dienes	BD dimers	Residue
1	$As(C_6H_5)_3$	1.5	30.1	0.25	0.5	1.8
2	$Sb(C_6H_5)_3$	1.5	24.1	0.22	trace	1.4
3	PCl_3	1.5	26.8	0.5	0.2	1.2
4	$POCl_3$	1.5	26.8	1.7	7.8	1.9
5	$P(OC_4H_9)_3$	1.5	26.8	0.3	20	5.1
6	$PO(C_6H_4)_3$	1.5	26.8	3.0	7.3	2.2
7	$P(OC_2H_5)_3$	1.5	13.4	0.8	8.9	4.5
8	$P(OC_6H_5)_3$	1	13.4	0.3	0.6	1.0
9	$P(OC_6H_5)_2(OC_6H_4CH_3)$	1	13.4	3.4	1.2	1.9
10	$P(C_4H_9)_3$	1	13.4	3.5	3.3	2.1

*1 $FeCl_3$ 0.32 g., $(C_2H_5)_3Al$ 0.83 g., Toluene 60 g.
Exp. No. 1—6 Ethylene pressure 60 kg./cm^2, 20°C, 5 hr.
Exp. No. 7—10 Ethylene pressure 100 kg./cm^2, 30°C, 16 hr.
*2 The third component/$FeCl_3$ mole ratio.

ethylene. The effects of the catalyst composition are shown in Table I. In all the runs, considerable side reactions of butadiene (the dienylation of butadiene) occurred, giving linear dimers as a by-product. The dienylation of ethylene gave 1, 3-hexadiene, which amounted to about 40 wt.% of the C_6-dienes obtained. The formation rate of 1, 3-hexadiene decreased slightly at higher Al/Fe mole ratios. A proper Al/Fe mole ratio of high activity probably exists in the range from two to five. The reaction temperature affected the yield of C_6-dienes and their composition (Table II). The reactions proceeded smoothly even at 20°C. More 3-methyl-1, 4-pentadiene than 1, 4-hexadiene was formed at lower reaction temperatures. The weight ratio of three C_6-dienes, i. e.,

3-methyl-1, 4-pentadiene, 1, 4-hexadiene, and 1, 3-hexadiene, in the products obtained at 20—30°C was about 2 : 1 : 2. The average formation ratio of C_6-dienes to butadiene dimers in ten runs under the same conditions was 4.5 to 1. Therefore, the average yield of 3-methyl-1, 4-pentadiene was about 25—30%. The condition of high ethylene pressure was advantageous to the formation of C_6-dienes. As the butadiene initially-charged increased, the yield of C_6-dienes decreased because more butadiene dimers and higher boiling materials were formed. As is shown in Table III, the butadiene dimers were predominantly formed by the catalysts containing phosphorus oxychloride, triphenyl phoshine oxide, tributyl phosphite or triethyl phosphite rather than triphenyl phoshine. Both triphenyl arsine and triphenyl stibine were ineffective. It may be considered that phosphorus compounds as the third component in the catalyst played an important role, one which might characterize the nature of the active site. These experimental results suggest that the variations in the reaction conditions affect the composition of the reaction products only slightly but that the third component affects it intensely. According to this suggestion, a search for the proper third component has been carried out and a new catalyst for the exclusive formation of 1, 4-hexadiene has been found. The details will be reported shortly.

In order to form the linear 1 : 1 addition products, a hydrogen atom transfer from either butadiene or ethylene is indispensable. The catalyst, consisting of cobalt compound and metal alkyl, studied by Wittenberg[4] promoted exclusively the hydrogen transfer from butadinene to give 1, 3-hexadiene; however, the catalyst, consisting of $Fe(C_5H_7O_2)_3$ and triethylaluminum, studied by Hata[7] promoted the transfer from ethylene to give 1, 4-hexadiene. In contrast, the ternary catalyst in this study can promote both reactions; further, the hydrogen which is transferred from ethylene adds to butadiene in two ways, that is, by 1, 2-addition to give 3-methyl-1, 4-pentadiene and by 1, 4-addition to give 1, 4-hexadiene. These ways are analogous to the linear dimerization of butadiene to give 3-methyl-1, 4, 6-heptatriene and 1, 3, 6-octatriene. The direction of the addition of hydrogen in all cases obeyed Markownikov's rule. Which monomers release a hydrogen atom is probably governed by the nature of the active site that is characterized by the combined effects of the catalyst components. Hydrogen transfer may occur in the same way as in the dimerzation of butadiene, through an intermediate with a hydrogen-metal bond.[8] However, it is not clear whether the hydrogen in the intermediate is a protonic or a hydride ion. Since a more detailed study of the mechanism of the hydrogen transfer reaction is required, this will be the subject of a future report.

The authors wish to express their thanks to Dr. H. Kobayashi for permission to publish this work. They wish also to thank Mr. I. Shionoya for his kindness in measuring the mass spectra.

7) G. Hata, *J. Am. Chem. Soc.*, **86**, 3903 (1964).
8) S. Otsuka and T. Taketomi, Abstracts of the Papers presented at the 18th Annual Meeting of the Chemical Society of Japan, Osaka, April, 1965, p. 446.

BULLETIN OF THE CHEMICAL SOCIETY OF JAPAN VOL. 39 2005—2008 (1966)

The Reactions of *N, N*-Dimethylbenzamide Diethylmercaptole

By Teruaki MUKAIYAMA and Tatsuaki YAMAGUCHI

Laboratory of Organic Chemistry, Tokyo Institute of Technology, Ookayama, Meguro-ku, Tokyo

(Received January 26, 1966)

The reactions of *N, N*-dimethylbenzamide diethylmercaptole with active methylene compounds, amines, hydrazines, benzaldoxime, benzhydroxamic acid and heavy metal salts have been studied. Active methylene compounds, hydroxylamine, hydrazine and phenylhydrazine were found to react with *N, N*-dimethylbenzamide diethylmercaptole to give the corresponding α-dimethylaminobenzylidene derivatives by eliminating ethyl mercaptan. In addition, such heterocyclic compounds as 2-phenylimidazoline, 2-phenyloxazoline and 2, 5-diphenyl-1, 3, 4-oxadiazole were derived from *N, N*-dimethylbenzamide diethylmercaptole by cyclization reactions with ethylenediamine, 2-aminoethanol and benzoylhydrazine respectively. Further, it was found that *N, N*-dimethylbenzamide diethylmercaptole reacted with benzaldoxime and benzhydroxamic acid to give the dehydrated products benzonitrile and phenyl isocyanate respectively. Finally, it was established that heavy metal salts, such as mercuric oxide, mercuric cyanide and silver cyanide, reacted with *N, N*-dimethylbenzamide diethylmercaptole to liberate heavy metal mercaptides, thus giving *N, N*-dimethylbenzamide, *N, N*-dimethylbenzamide dicyanide and *N, N*-dimethylbenzamide ethylmercaptocyanide respectively.

It was reported in a preceding paper[1] that *N, N*-dimethylbenzamide methylethylmercaptole had been derived from *N, N*-dimethyl-*S*-methylthiobenzamide iodide and sodium ethylmercaptide. In the present experiment, the reactions of *N, N*-dimethylbenzamide diethylmercaptole (I) with active methylene compounds, amines, hydrazines, benzaldoxime, benzhydroxamic acid and heavy metal salts were investigated.

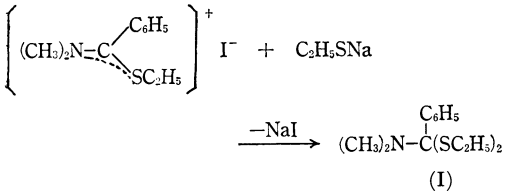

(I)

In the first place, it was found that the amide mercaptole (I) reacted with active methylene compounds to give the condensation products, i. e., α-dimethylaminobenzylidene derivatives (II) of the active methylene compounds, in fairly good yields, along with ethyl mercaptan. For example, malonitrile easily reacted with the amide mercaptole (I) at room temperature, with the evolution of ethyl mercaptan, and gave α-dimethylaminobenzylidene malonitrile (IIa) in a 71% yield; on the other hand, this compound could not be obtained from *N, N*-dimethyl-*S*-methylthiobenzamide iodide by the method mentioned in the previous paper.[1]

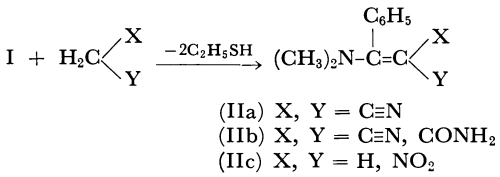

(IIa) X, Y = C≡N
(IIb) X, Y = C≡N, $CONH_2$
(IIc) X, Y = H, NO_2

Next, it was established that hydroxylamine, hydrazine and phenylhydrazine easily reacted with the amide mercaptole (I), resulting in the formation of the corresponding condensation products, i. e., *N, N*-dimethylbenzamidoxime, *N, N*-dimethylbenzamidazine and *N, N*-dimethylbenzamide phenylhydrazone respectively, in good yields. The *N, N*-dimethylbenzamide phenylhydrazone thus obtained was a red-brown oil which gradually turned dark-violet when it was exposed to the air. The electron-spin-resonance spectrum of the deep green oil which resulted from the treatment of *N, N*-dimethylbenzamide phenylhydrazone with

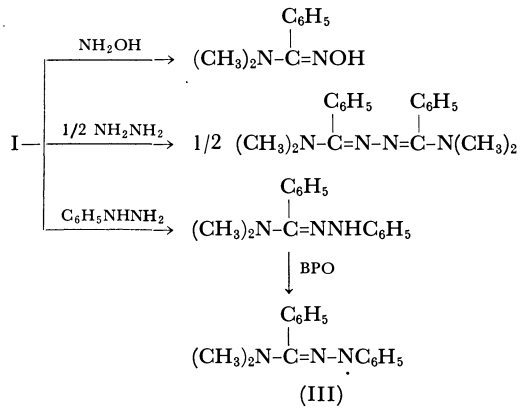

(III)

1) T. Mukaiyama, T. Yamaguchi and H. Nohira, This Bulletin, **38**, 2107 (1965).

benzoyl peroxide in benzene showed seven equally-spaced lines. This result would indicate that a stable free radical with a hydrazyl structure (III) exists in the above-mentioned oily substance.

When *N, N*-dimethylbenzamide diethylmercaptole (I) was treated with bifunctional active hydrogen compounds, such as ethylenediamine and 2-aminoethanol, heterocyclic compounds, i. e., 2-phenylimidazoline and 2-phenyloxazoline respectively, were given in good yields by means of the elimination of ethyl mercaptan and dimethylamine. In addition, the treatment of the amide mercaptole (I) with benzoylhydrazine in refluxing ethyl acetate gave an oily product which, on heating at 180°C, readily solidified to give 2, 5-diphenyl-1, 3, 4-oxadiazole in a 77.5% yield. The initially-obtained oily substance may be identified as *N, N*-dimethylbenzamide benzoylhydrazone (IV) because its infrared spectrum shows absorption bands at 3265 (NH), 2940 (CH_3), 1665 (C=O) and, 1640 cm^{-1} (C=N).

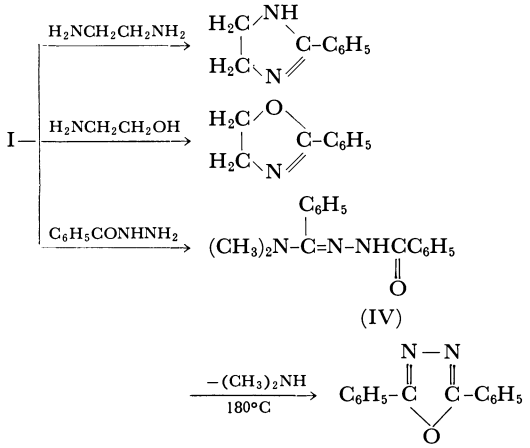

In the next place, since the amide mercaptole (I) is very easily hydrolyzed to *N, N*-dimethylbenzamide and ethyl mercaptan, intramolecular dehydration reactions of benzaldoxime and benzhydroxamic acid by means of the amide mercaptole (I) were attempted. Benzaldoxime reacted with the amide mercaptole (I) to give, as expected, benzonitrile in a good yield, together with *N, N*-dimethylbenzamide and ethyl mercaptan. On the other hand, when benzhydroxamic acid was mixed with the amide mercaptole (I), a vigorous evolution of ethyl mercaptan was observed; after this gas evolution had been ceased, a red-brown oil was obtained. This oily substance decomposed, upon being heated at 140—150°C, to yield phenyl isocyanate and *N, N*-dimethylbenzamide, while ethyl mercaptan was eliminated. The structure of the intermediate oil seems to be V; its infrared spectrum shows main absorption bands at 3250 (NH), 2915 (CH), 1620 (C=O) and 1510 cm^{-1} (CH).

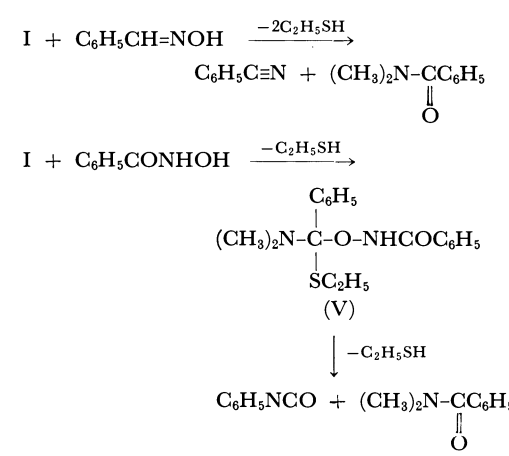

Since some of heavy metal salts can easily be converted to heavy metal mercaptides by treating them with mercaptans, reactions of the amide mercaptole (I) with heavy metal salts, such as mercuric oxide, mercuric cyanide and silver cyanide, were attempted. When mercuric oxide and mercuric cyanide were treated with the amide mercaptole (I), *N, N*-dimethylbenzamide and *N, N*-dimethylbenzamide dicyanide respectively resulted in good yields, while mercury ethylmercaptide was eliminated. In a similar fashion, the reaction of silver cyanide with the amide mercaptole (I) gave silver ethyl mercaptide and *N, N*-dimethylbenzamide ethylmercaptocyanide in fairly good yields.

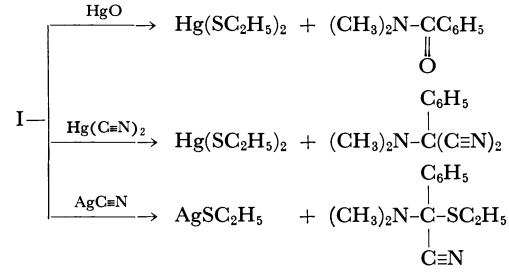

Further, it was established that the amide mercaptole (I) reacted with lead tetraacetate to give lead acetate, diethyl disulfide, acetic anhydride and *N, N*-dimethylbenzamide in good yields.

$$I + Pb(OCOCH_3)_4 \rightarrow Pb(OCOCH_3)_2 + CH_3COOCOCH_3 + C_2H_5SSC_2H_5 + (CH_3)_2NCOC_6H_5$$

These results showed that the amide mercaptole (I) was oxidized to *N, N*-dimethylbenzamide and diethyl disulfide, while lead tetraacetate was reduced to lead acetate. In the course of this oxidation-reduction reaction, acetic anhydride was produced in a good yield. The oxidation reactions of amide mercaptoles by means of other oxidizing reagents are now being investigated.

Experimental[2]

N, N-Dimethylbenzamide Diethylmercaptole (I).—A suspension of 64 g. (0.2 mol.) of *N*, *N*-dimethylbenzamide-*S*-ethylthiobenzamide iodide, prepared from *N*, *N*-dimethylthiobenzamide and ethyl iodide, and 17 g. (0.2 mol.) of sodium ethylmercaptide in dry ether (300 ml.) was stirred at room temperature for 3 hr. After the white precipitate of sodium iodide had been filtered off, the filtrate was concentrated; the distillation of the residual liquid gave 31 g. (63.5%) of *N*, *N*-dimethylbenzamide diethylmercaptole (I). B. p. 105—109°C/0.2 mmHg, n_D^{16} 1.5732; IR; 2950(s), 2850(s), 2760(m), 1480(m), 1445(s), 1260(m), 1010(s), 790(s), 730(s) and 700 cm^{-1}(s).

Found: C, 63.27; H, 8.20; N, 5.96. Calcd. for $C_{13}H_{21}NS_2$: C, 63.15; H, 8.19; N, 5.45%.

N, *N*-Dimethylbenzamide diethylmercaptole (I) is a pale yellow oil with a mercaptan odor; it turns red-brown after standing for a few days.

The Reaction of the Amide Mercaptole (I) with Malonitrile.—A solution of 2.50 g. (0.01 mol.) of the amide mercaptole (I) and 0.66 g. (0.01 mol.) of malonitrile in dry ether (30 ml.) was stirred at room temperature. The reaction soon started, with the evolution of ethyl mercaptan, and a white precipitate was separated from the solution. After the stirring had been continued for 2 hr., the white precipitate was filtered and recrystallized from 95% ethanol. Yield IIa, 1.40 g. (71%); m. p. 120—121°C.

Found: C, 73.14; H, 5.51; N, 21.28. Calcd. for $C_{12}H_{11}N_3$: C, 73.07; H, 5.62; N, 21.38%.

The infrared spectrum of this compound showed the absorption band at 2180 cm^{-1} assigned to the C≡N bond.

The Reaction of the Amide Mercaptole (I) with Cyanoacetamide.—When a mixture of 2.50 g. (0.01 mol.) of the amide mercaptole (I) and 0.85 g. (0.01 mol.) of cyanoacetamide was heated at 115°C, the evolution of ethyl mercaptan was observed. After 5 minutes' heating, the reaction mixture was cooled and triturated with dry ether. Then the ether was evaporated and the resulting solid was recrystallized from 95% ethanol. Yield (IIb), 0.7 g. (32.5%); m. p. 163—164°C.

Found: C, 67.06; H, 5.99; N, 19.45. Calcd. for $C_{12}H_{13}N_3O$: C, 66.95; H, 6.09; N, 19.52%.

The infrared spectrum of this compound showed absorption bands at 3370, 2160 and 1640 cm^{-1}.

The Reaction of the Amide Mercaptole (I) with Nitromethane.—A solution of 2.50 g. (0.01 mol.) of the amide mercaptole (I) and 0.65 g. (0.01 mol.) of nitromethane in benzene (10 ml.) was refluxed for an hour. After the benzene had been removed in vacuo, the resulting solid was recrystallized from benzene (or ethanol). Yield IIc, 1.00 g. (52%); m. p. 128°C. This material showed no depression in a mixed melting point determination with an authentic sample prepared by the previously reported method.[1]

The Reaction of the Amide Mercaptole (I) with Hydroxylamine.—Hydroxylamine was prepared from hydroxylamine hydrochloride by the method described in the literature.[3] M. p. 31—33°C. A benzene solution of 1.20 g. (0.005 mol.) of the amide mercaptole (I) and 0.175 g. (0.005 mol.) of hydroxylamine was refluxed for 2 hr. After this mixture had cooled, the solvent was removed in vacuo and the resulting *N*, *N*-dimethylbenzamidoxime was recrystallized from benzene. Yield, 0.82 g. (92%); m. p. 123—124°C.

Found: C, 65.76; H, 7.42; N, 16.89. Calcd. for $C_9H_{12}N_2O$: C, 65.83; H, 7.37; N, 17.06%.

The Reaction of the Amide Mercaptole (I) with Hydrazine.—Anhydrous hydrazine was prepared by the dehydration of hydrazine hydrate with sodium hydroxide. B. p. 114°C. A solution of 2.45 g. (0.01 mol.) of the amide mercaptole (I) and 0.16 g. (0.005 mol.) of hydrazine in dry benzene (20 ml.) was refluxed for 2 hr. After the benzene had been removed in vacuo, the resulting white solid was recrystallized from ethanol. Yield, 1.00 g. (68%); m. p. 137—138°C.

Found: C, 73.54; H, 7.47; N, 18.85. Calcd. for $C_{18}H_{22}N_4$: C, 73.43; H, 7.53; N, 19.03%.

The Reaction of the Amide Mercaptole (I) with Phenylhydrazine.—To a solution of the amide mercaptole (I) (2.50 g., 0.01 mol.) in dry benzene (20 ml.), there was added a solution of phenylhydrazine (1.08 g., 0.01 mol.) in dry benzene (10 ml.) under a nitrogen atmosphere. After it had been refluxed for 2 hr., the reaction mixture was concentrated and distilled in vacuo under nitrogen. Yield, 1.71 g. (71.5%); b. p. 127—129°C/0.03 mmHg.

Found: C, 73.83; H, 7.06; N, 17.36. Calcd. for $C_{15}H_{17}N_3$: C, 75.28; H, 7.16; N, 17.56%.

To a solution of 0.50 g. of *N*, *N*-dimethylbenzamide phenylhydrazone in dry benzene (15 ml.) there was added, drop by drop, a solution of 0.25 g. of benzoyl peroxide in dry benzene (10 ml.) under a nitrogen atmosphere. The dark-colored reaction mixture was stirred for an additional 30 min., and then the benzene was removed in vacuo at room temperature. The electron-spin-resonance spectrum of the resulting deep-green oil was recorded in the benzene solution.

The Preparation of 2-Phenylimidazoline and of 2-Phenyloxazoline.—A solution of 1.25 g. (0.005 mol.) of the amide mercaptole (I) and 0.30 g. (0.005 mol.) of anhydrous ethylenediamine in dry benzene (20 ml.) was refluxed for 3 hr. Then the benzene was removed under reduced pressure, and the resulting 2-phenylimidazoline was recrystallized from ethanol (or benzene). Yield, 0.70 g. (96%); m. p. 100—101°C (lit.[4] 101°C). A mixed melting point determination with an authentic sample showed no depression.

In a similar way, 2-phenyloxazoline was obtained in a 67% yield (b. p. 125—127°C/17 mmHg) when the amide mercaptole (I) and 2-aminoethanol were reacted in refluxing chloroform for 3 hr.

Found.: C, 73.00; H, 6.76; N, 9.47. Calcd. for C_9H_9NO: C, 73.45; H, 6.61; N, 9.52%.

The Reaction of the Amide Mercaptole (I) with Benzoylhydrazine.—A solution of 2.60 g. (0.01 mol.) of the amide mercaptole (I) and 1.36 g. (0.01 mol.) of benzoylhydrazine in 40 ml. of ethyl acetate was refluxed for 3 hr., and then the solvent was removed under reduced pressure. The resulting yellow oil was, in situ, heated to 180°C for a while; after it had cooled, it solidified to give 2, 5-diphenyl-1, 3, 4-oxadiazole (1.72 g.;

2) All melting points and boiling points are uncorrected.

3) H. S. Booths, "Inorganic Synthesis," Vol. I, McGraw-Hill Book Co. New York (1939), p. 87.

4) G. Forrsel, *Ber.*, **25**, 2135 (1892).

77.5%), which was then recrystallized from absolute ethanol. M. p. 136—137°C)lit.[5] 135—136°C).

Found: C, 75.61; H, 5.02; N, 12.41. Calcd. for $C_{14}H_{10}N_2O$: C, 75.65; H, 4.54; N, 12.61%.

The Reaction of the Amide Mercaptole (I) with Benzaldoxime.—A solution of 2.60 g. (0.01 mol.) of the amide mercaptole (I) and 1.21 g. (0.01 mol.) of *syn*-benzaldoxime in dry benzene (25 ml.) was refluxed for an hour. After the benzene had been removed, the residual liquid was distilled in vacuo to give 0.66 g. (67.5%) of benzonitrile (b. p. 88—93°C/22 mmHg), together with *N, N*-dimethylbenzamide (1.19 g., 80%; b. p. 93—98°C/1.0 mmHg). They were identified by comparing their infrared spectra with those of authentic samples.

The Reaction of the Amide Mercaptole (I) with Benzhydroxamic Acid.—When 2.60 g. (0.01 mol.) of the amide mercaptole (I) was mixed with 1.37 g. (0.01 mol.) of benzhydroxamic acid, an exothermic reaction soon took place and ethyl mercaptan was evolved violently. After the gas evolution had ceased, the resulting red-brown oil was, in situ, heated at 140—155°C; then it was distilled under reduced pressure to give 0.68 g. (57.5%) of phenyl isocyanate and 1.23 g. (82%) of *N, N*-dimethylbenzamide.

The Reaction of the Amide Mercaptole (I) with Mercuric Oxide.—Into a suspension of 2.16 g. (0.01 mol.) of meruric oxide in acetonitrile (25 ml.), there was added a solution of 2.60 g. (0.01 mol.) of the amide mercaptole (I) in acetonitrile (10 ml.). After the reaction mixture had then been stirred at room temperature for 30 min., it was heated at 50°C for an additional 30 min., cooled, and filtered to remove a white percipitate. After the filtrate had been concentrated, the resulting solid part was filtered, washed, and combined with the initial precipitate; this gave 1.20 g. (46%) of mercury ethylmercaptide (recrystallized from ethanol; m. p. 76—78°C; lit.[6] 76.5°C). The filtrate was concentrated and distilled to give 0.90 g. (60%) of *N, N*-dimethylbenzamide, b. p. 145—147°C/34 mmHg.

The Reactions of the Amide Mercaptole (I) with Mercuric Cyanide and Silver Cyanide.—A solution of 2.60 g. (0.01 mol.) of the amide mercaptole (I) in dry tetrahydrofuran (10 ml.) was added to a suspension of 2.52 g. (0.01 mol.) of mercuric cyanide in dry tetrahydrofuran (15 ml.); the mixture was then stirred at room temperature for an hour. After the solvent had been removed in vacuo, the resulting solid was recrystallized from acetonitrile (ca. 10 ml.); filtration gave 0.95 g. (72%) of mercury ethylmercaptide. The filtrate was concentrated and distilled to give 1.18 g. (64%) of *N, N*-dimethylbenzamide dicyanide, b. p. 100—103°C/5 mmHg.

Found: C, 71.44; H, 5.99. Calcd. for $C_{11}H_{11}N_3$: C, 71.33; H, 5.99%.

In a similar way, when silver cyanide was treated with the amide mercaptole (I) in refluxing tetrahydrofuran, pale yellow silver mercaptide was precipitated; this was then filtered off. The distillation of the filtrate gave a 46% yield of *N, N*-dimethylbenzamide ethylmercaptocyanide (b. p. 103—107°C/1.0 mmHg), which showed an infrared spectrum identical with that of the authentic sample derived by the previously-reported method.[1]

The Reaction of the Amide Mercaptole (I) with Lead Tetraacetate.—When a solution of 2.60 g. (0.01 mol.) of the amide mercaptole (I) and 4.43 g. (0.01 mol.) of lead tetraacetate in dry benzene (50 ml.) was heated at 60°C, a white precipitate was separated from the solution. After stirring had been continued for 2.5 hr., the white precipitate of lead acetate was filtered and dried. It weighed 2.28 g. (70%). The filtrate was then concentrated and fractionated, giving 0.80 g. (81%) of acetic anhydride (b. p. 65—67°C/57 mmHg), 0.43 g. (70%) of diethyl disulfide (b. p. 74—75°C/45 mmHg) and 1.07 g. (71%) of *N, N*-dimethylbenzamide (b. p. 130—133°C/17 mm Hg). They were identified by means of their infrared spectra.

The authors wish to thank Dr. Kazuo Shimogoshi for his analysis of the ESR spectrum.

5) E. Günther, *Ann.*, **254**, 64 (1889).
6) A. Gutmann, *Ber.*, **49**, 953 (1916).

BULLETIN OF THE CHEMICAL SOCIETY OF JAPAN VOL. 39 2009—2012 (1966)

Studies on D-Glucosamine Derivatives. XIII.*1 The Synthesis of *N*-Acetyl-1-*O*-aminoacyl-D-glucosamines

By Juji YOSHIMURA and Masuo FUNABASHI

Department of Chemistry, Tokyo Institute of Technology, Ookayama, Meguro-ku, Tokyo

(Received February 5, 1966)

For the purpose of examining the properties of the glycosidic ester linkage of sugars to amino acids, *N*-acetyl-1-*O*-aminoacyl-D-glucosamines were synthesized. *N*-Acetyl-4, 6-*O*-benzylidene-D-glucosamine was condensed with an equimolar amount of *N*-benzyloxycarbonyl amino acids by the dicyclohexylcarbodiimide method, followed by the hydrolytic and hydrogenolytic removal of the protecting groups. *N*-Acetyl-3-*O*-acetyl-D-glucosamine was also newly prepared as a contrast compound.

Though the presence of glycosidic ester lingkage between *N*-acetyl-D-galactosamine and L-glutamic acid in ovine submaxillary gland mucoprotein, reported by Gottschalk et al.,[1] is at present doubted by several workers,[2] it seems to be of interest to examine the properties of such a possible linkage.

The homologues, in which amino acids are linked to C-6, C-4, or C-3 positions of *N*-acetyl-D-glucosamine, were synthesized in previous experiments[3,4]; the present paper will describe the selective synthesis of *N*-acetyl-1-*O*-aminoacyl-D-glucosamines.

Results and Discussion

The glycosidic hydroxyl group in a sugar moiety is generally accepted to be much more reactive than the other groups, but few examples of the selective acylation of this hydroxyl group are known. Zervas[5] has reported the selective synthesis of 1-*O*-benzoyl-β-D-glucose by condensing sodium salt of 4, 6-*O*-benzylidene-D-glucose with an equimolar amount of benzoyl chloride, followed by hydrogenolysis.

In a similiar manner 1-*O*-glycyl-D-glucose sulfate[6] has been obtained from the sugar and *N*-benzyloxycarbonyl-glycyl chloride. On the other hand, it is known that the primary hydroxyl group of unprotected D-glucose or *N*-acetyl-D-glucosamine is directly acylated with an equimolar amount of *N*-Z*2-amino acids by the dicyclohexylcarbodiimide (DCC) method.[3,7]

In view of the facts mentioned above, *N*-acetyl-4, 6-*O*-benzylidene-D-glucosamine (I) was used as the starting material, in which the primary hydroxyl group is protected. The compound I was condensed with an equimolar amount of *N*-Z-amino acids (a, *N*-Z-glycine; b, *N*-Z-L-alanine; c, β-benzyl *N*-Z-L-aspartate) by DCC in pyridine or in a mixture of pyridine and dimethylformamide (DMF) to give *N*-acetyl-1-*O*-(*N*-Z-aminoacyl)-4,6-*O*-benzylidene-D-glucosamines (II) in a 40—50% yield. In order to remove the benzylidene group, II was then hydrolyzed with 70% acetic acid at 100°C for half an hour; *N*-acetyl-1-*O*-(*N*-Z-aminoacyl)-D-glucosamines (IIIa and IIIb) were isolated in ca. a 20% yield. Although the complete hydrolysis of *N*-Z-aminoacyl group was observed in the case of IIc, the catalytic hydrogenolysis of IIc in glacial acetic acid with palladium-charcoal (10%) could be directly carried out to give *N*-acetyl-1-*O*-(L-α-aspartyl)-D-glucosamine (IVc) in a 46% yield. The removal of the benzyloxycarbonyl group from IIIa and IIIb was also performed by palladium-catalyzed hydrogenolysis in the presence of oxalic acid, and *N*-acetyl-1-*O*-aminoacyl-D-glucosamines (IVa and were isolated as labile oxalates.

The infrared spectra of II and III showed the absorption band of ester carbonyl at 1730—1750 cm^{-1} and that of urethane carbonyl at 1690—1710 cm^{-1}. These compounds gave one spot in paper chromatography and showed no mutarotation, which indicates that the position of the ester linkage is at C-1. The anomeric structure of these compounds, which seems likely to depend on the solvent in the first condensation reaction, as will

*1 Part XII; This Bulletin, to be published.

1) A. Gottshalk and W. H. Murphy, *Biochem. Biophys. Acta*, **46**, 81 (1961).

2) W. Pigmann, *Exp. Ann. de Biochimie Medical*, **24**, 67 (1962); S. Harbon, G. Hermann Boussier and H. Clauser, *Bull. Soc. Chim. Biol.*, **45**, 1279 (1693).

3) J. Yoshimura, M. Funabashi, S. Ishige and T. Sato, *J. Chem. Soc. Japan, Pure Chem. Sect. (Nippon Kagaku Zasshi)*, **85**, 511 (1964).

4) Part XII.

5) L. Zervas, *Ber.*, **64**, 2289 (1931).

6) M. Bergmann, L. Zervas and J. Overhoff, *Z. Physiol. Chem.*, **224**, 52 (1934).

*2 The benzyloxycarbonyl group is abbreviated to Z hereafter.

7) K. Kochetkov, V. A. Derevitskaya, L. M. Linkhosherstov, N. V. Molodtsov and S. G. Kara-Murza, *Tetrahedron*, **18**, 273 (1962).

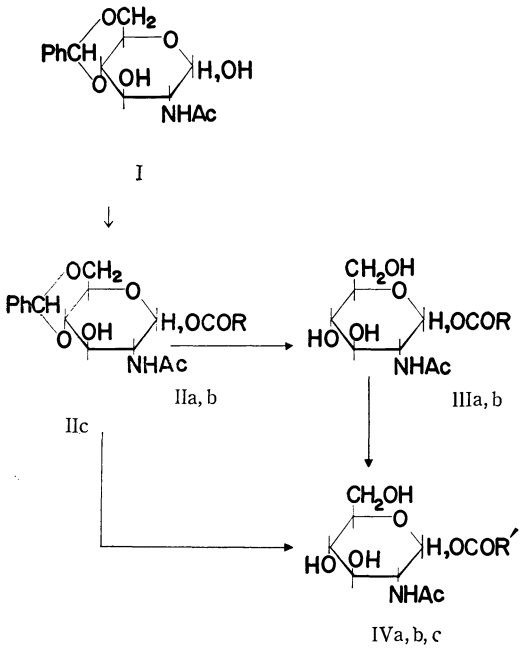

a) R=-CH_2NHZ
R'=-$CH_2NH_2 \cdot 1/2(COOH)_2 \cdot H_2O$
b) R=-$CH(CH_3)NHZ$
R'=-$CH(CH_3)NH_2 \cdot 1/2(COOH)_2 \cdot 2H_2O$
c) R=-$CHCH_2COOCH_2Ph$ (NHZ)
R'=-$CHCH_2COOH \cdot H_2O$ (NH_2)
(Z=-$COOCH_2Ph$)

be described in the Experimental Section, was deduced from the rotational values and the infrared spectra.

In order to compare the properties with III, *N*-acetyl-3-*O*-acetyl-D-glucosamine (V) was newly prepared by the hydrolytic and hydrogenolytic removal of benzylidene and benzyl groups from benzyl *N*-acetyl-3-*O*-acetyl-4, 6-*O*-benzylidene-β-D-glucosaminide.[4] In contrast with III, V showed mutarotation in water ($[\alpha]_{578}^{14}$ +89°—+44°). In the periodate oxidation of these compounds in an acetate buffer (pH 5.0) for 20 hr., overoxidation was observed in each case; for example, β-IIIa and V consumed, respectively, 5.0 and 3.4 mol. of periodates, as is shown in Fig. 1. Therefore, the periodate oxidation would not be adopted for determining the structure of *O*-acyl derivatives of *N*-acetyl-D-glucosamine as it is known in other amino sugar derivatives.[8]

However, the position of the ester linkage in II-IV is concluded to be at C-1 from the facts that the compounds do not show mutarotation

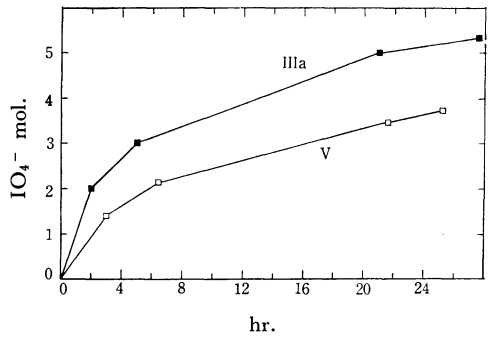

Fig. 1. Periodate Oxidation of *N*-acetyl-1-*O*-(*N*-benzyloxyloxycarbonylglycyl)-β-D-glucosamine (IIIa) and *N*-acetyl-3-*O*-acetyl-α-D-glucosamine (V).

and that 1-*O*-(*N*-Z-glycycl)-D-glucose, prepared by the procedure mentioned above, also showed no mutarotation and consumed 2 mol. of periodate, an amount consistent with the supposed structure.[9]

Experimental

All melting points are uncorrected. The optical rotations were measured at 578 mμ using a Carl-Zeiss polarimeter. Paper chromatography was carried out on Toyo Roshi No. 50 filter paper using the following solvent systems: A) isobutanol saturated with water, and B) *n*-butanol, acetic acid and water (4 : 1 : 5). An aqueous solution of 1% potassium iodide — 1% starch,[10] and a 0.1% ninhydrin solution in *n*-butanol were used as the spray reagents.

***N*-Acetyl-1-*O*-(*N*-benzyloxycarbonyl-glycyl)-4, 6-*O*-benzylidene-β-D-glucosamine (IIa).**—A solution of *N*-acetyl-4, 6-*O*-benzylidene-D-glucosamine (9.3 g.; 0.03 mol.) dissolved in a mixture of hot dry pyridine (80 ml.) and DMF (30 ml.) was cooled to room temperature. *N*-Z-Glycine (6.3 g.; 0.03 ml.) and DCC (8.0 g.; 0.039 mol.) were then added, and the mixture was allowed to stand overnight in a refrigerator. The precipitate of dicyclohexylurea was filtered off and washed with toluene. The filtrate and the washings were then concentrated to half their volume under reduced pressure and poured into ice water (300 ml.). The precipitate was filtered and washed several times with water.

The fractional recrystallization of the dry crude product was repeated several times from methanol in order to remove the unchanged starting material, I, which was recovered in ca. 30% yield. The final recrystallization from a mixture of methanol and pyridine (10 : 1) gave 4.1 g. (40%) of IIa, m. p. 180—182°C (decomp.), $[\alpha]_{578}^{20}$ −36° (*c* 0.49, pyridine).

Found: C, 60.04; H, 5.81; N, 5.36, Calcd. for $C_{25}H_{28}O_9N_2$ (500): C, 59.99; H, 5.64; N, 5.60%.

In another experiment, only dry pyridine (150 ml.)

8) A. B. Foster and D. Horton, "*Advances in Carbohydrate Chemistry*," XIV, Academic Press, New York (1959) p. 258.

9) Private communication from N. Muramatsu (Central Research Laboratory of Ajinomoto Co. Ltd.).

10) H. N. Rydon and P. W. Smith, *Nature*, **169**, 922 (1952).

was used as the solvent, and the filtrate was concentrated under reduced pressure to a gelatinous residue, which was then washed with ether or ethyl acetate.

After fractional recrystallization, 5.1 g. (49%) of the product was obtained. M. p. 178—181°C (decomp.); $[\alpha]_{578}^{15}$ −20° (*c* 0.51, pyridine).

Found: C, 59.93; H, 5.36; N, 5.48%.

The rotational value and the infrared spectrum indicate the product to be contaminated with the α-anomer.

N-Acetyl-1-O-(N-benzyloxycarbonyl-L-alanyl)-4, 6-O-benzylidene-α, β-D-glucosamine (IIb). — *N*-Benzyloxycarbonyl-L-alanine (6.1 g.) was condensed with I (4.5 g.) by DCC (4.8 g.) in dry pyridine (120 ml.). It was subsequently treated in the manner described above. Yield, 3.1 g.; m. p. 172—175°C (decomp.); $[\alpha]_{578}^{17}$ +23° (*c* 0.59, pyridine).

Found: C, 60.13; H, 6.29; N, 5.51. Calcd. for $C_{26}H_{30}O_9N_2$ (514): C, 60.69; H, 5.88; N, 5.45%.

N-Acetyl-1-O-(β-benzyl N-benzyloxycarbonyl-L-aspartyl)-4, 6-O-benzylidene-α, β-D-glucosamine (IIc).—The compound I (9.3 g.; 0.03 mol.) was condensed with β-benzyl *N*-benzyloxycarbonyl-L-aspartate (10.6 g.; 0.03 mol.) by DCC (8.0 g.; 0.039 mol.) in pyridine (150 ml.). Yield, 4.9 g.; m. p. 183—185°C (decomp.); $[\alpha]_{578}^{29}$ −9.8° (*c* 0.05, pyridine).

Found: C, 62.78; H, 5.49; N, 4.52. Calcd. for $C_{34}H_{36}O_{11}N_2$(648): C, 62.95; H, 5.59; N, 4.33%.

N-Acetyl-1-O-(N-benzyloxycarbonyl-glycyl)-β-D-glucosamine (IIIa).—A suspension of IIa (2.5 g.) in 70% acetic acid (60 ml.) was heated on a boiling water bath for 30 min. while being stirred. The solution was then concentrated under reduced pressure to a gelatinous residue, which was redissolved in water and extracted twice with ether. The aqueous layer was then extracted five times with *n*-butanol (10 ml.). The *n*-butanol extract was evaporated in vacuo to a crystalline residue. The recrystallization from ethanol and ether gave a compound IIIa with a m. p. of 178—180°C (decomp.). R_f 0.65 (Solvent A) and $[\alpha]_{578}^{16}$ −20° (*c* 0.2, water).

Found: C, 52.15; H, 5.92; N, 7.02. Calcd. for $C_{18}H_{24}O_9N_2$ (412): C, 52.42; H, 5.87; N, 6.79%.

The compound IIa which was condensed in pyridine was treated in the same manner to give a product with a m. p. of 153—155°C (decomp.) and a $[\alpha]_{578}^{23}$ −11° (*c* 0.41, water).

N-Acetyl-1-O-(N-benzyloxycarbonyl-L-alanyl)-α-D-glucosamine (IIIb).—A suspension of the crude IIb (4.2 g.) in 70% acetic acid (70 ml.) was heated on a boiling water bath for 30 min. while being stirred. The solution was diluted with water to 500 ml. and neutralized with sodium bicarbonate. The precipitate was filtered off, and the filtrate was extracted with ether (10 ml.×3). The aqueous layer was then extracetd with *n*-butanol (20 ml.×5), and the extract was concentrated in vacuo to a crystailline residue. Recrystallization from ethanol gave 0.43 g. of white needles with a m. p. of 165—167°C (decomp.). R_f 0.71 (Solvent A), $[\alpha]_{578}^{13}$ +80° (*c* 0.23, water).

Found: C, 53.75; H, 6.28; N, 6.53. Calcd. for $C_{19}H_{26}O_9N_2$ (426): C, 53.51; H, 6.15; N, 6.57%.

N-Acetyl-1-O-glycyl-β-D-glucosamine Oxalate (IVa).—A mixture of IIIa (620 mg.), oxalic acid dihydrate (190 mg.) and 0.6 g. of Pd-C (10%) in 70% methanol (10 ml.) was shaken with hydrogen until the absorption had substantially ceased.

After the catalyst had then been removed, ether was added to the filtrate and centrifugation was performed to collect a precipitate. For the purification the precipitated solid was dissolved in a few drops of water, reprecipitated with ethanol, centrifugated, and dried in vacuo. The amorphous hygroscopic powder, which is gradually decomposed with browning in moist air, gave a single ninhydrin positive spot on paper chromatography (R_f 0.19, solvent B). Yield, 310 mg. (60%); it gradually melts at ca. 82°C with decomposition. $[\alpha]_{578}^{15}$ −7.6° (*c* 0.53, water).

Found: C, 38.93; H, 7.08; N, 7.45. Calcd. for $C_{10}H_{18}O_7N_2 \cdot 1/2(COOH)_2 \cdot H_2O$: C, 38.71; H, 6.20; N, 8.21%.

N-Acetyl-1-O-(L-alanyl)-α-D-glucosamine Oxalate (IVb).—The compound IIIb (170mg.) was hydrogenated in 70% methanol (10 ml.) with 0.2 g. of Pb-C (10%) in the presence of oxalic acid dihydrate (40 mg.). The subsequent operations were performed in the same manner as with IVa. Yield, 52 mg. (37%); R_f 0.25 (solvent B). It melted gradually at ca. 70°C with decomposition; $[\alpha]_{578}^{15}$ +96° (*c* 0.25, water).

Found: C, 37.62; H, 6.53; N, 8.05. Calcd. for $C_{11}H_{18}O_6N_2 \cdot 1/2(COOH)_2 \cdot 2H_2O$; C, 38.58; H, 7.02; N, 7.88%.

N-Acetyl-1-O-(L-α-aspartyl)-α, β-D-glucosamine (IVc).—A mixture of IIc (1 g.) and 1 g. of Pd-C (10%) in glacial acetic acid (30 ml.) was shaken with hydrogen for 15 hr. After the catalyst had been removed, acetone (220 ml.) and ether (300 ml.) were added to the filtrate and centrifugation was performed to collect a precipitate. This was subsequently treated in the same manner as IVa. Yield, 240 mg. (46%); m. p. 149°C (decomp.); R_f 0.15 (Solvent B), $[\alpha]_{578}^{14}$ +9.4° (*c* 0.53, water).

Found: C, 40.62; H, 7.18; N, 8.03. Calcd. for $C_{12}H_{20}O_9N_2 \cdot H_2O$: C, 40.67; H, 6.21; N, 7.90%.

Benzyl N-Acetyl-3-O-acetyl-β-D-glucosaminide.—A suspension of benzyl *N*-acetyl-3-*O*-acetyl-4, 6-*O*-benzylidene-β-D-glucosaminide[4] (1.0 g.) in 70% acetic acid (40 ml.) was heated on a boiling water bath for half an hour. The solution was then concentrated in vacuo to dryness. The preduct was recrystallized from ethanol (17 ml.). Yield, 0.57 g. (72%); m. p. 201—203°C; R_f 0.72 (Solvent A) and $[\alpha]_{578}^{15}$ −66° (*c* 0.36, methanol).

Found: C, 57.98; H, 6.58; N, 3.85. Calcd. for $C_{17}H_{23}O_7N$(353): C, 57.78; H, 6.56; N, 3.96%.

N-Acetyl-3-O-acetyl-β-D-glucosamine (V). — A mixture of benzyl *N*-acetyl-3-*O*-acetyl-β-D-glucosaminide (0.71 g.), oxalic acid dihydrate (0.15 g.) and 0.7 g. of Pd-C (10%) in 60% methanol (20 ml.) was shaken with hydrogen at room temperature for 5 hr. After the catalyst had been removed, the filtrate was concentrated under reduced pressure to dryness. The paper chromatography of the product gave 3 spots (R_f 0.12, 0.35 and 0.71, solvent A), which correspond to *N*-acetyl-D-glucosamine, V and the starting material respectively. V was then separated with a column of magenesol-cerite (1 : 3) by eluting it with water-saturated isobutanol.

The recrystallization of the crude product from ethanol gave colorless needles with a m. p. of 159—161°C (decomp.). Yield, 0.21 g. (40%); R_f 0.35 (Solvent A); $[\alpha]_{578}^{14}$ +89° (after 5 min.)→ +44° (after 50 hr.) (*c* 0.48, water).

Periodate Oxidation.—The oxidation of *N*-acetyl-1-*O*-(*N*-benzyloxycarbonyl - glycyl) - β - D - glucosamine (IIIa), shown in Fig. 1, will be described as an example.

A solution of IIIa (41.5 mg.) in 20 ml. of an acetate buffer (pH 5.0) and 20 ml. of a sodium periodate solution (445.2 mg./40 ml.) were placed in a measuring flask. The flask was then allowed to stand in a refrigerator at 5°C and the solution was subjected to titration four times during a 30 hr. period. To 10 ml. of the sample there was added a 10 ml. portion of a 5% solution of borax and 0.5 g. of potassium iodide. Titration was performed with a 0.05 N sodium arsenite solution (F=1.050). A blank solution was used for correction.

BULLETIN OF THE CHEMICAL SOCIETY OF JAPAN VOL. 39 2012—2014 (1966)

The Synthesis of *dl*-α-Dihydrocaranone and γ-Lycorane

By Nasuo UEDA, Takashi TOKUYAMA and Takeo SAKAN

Department of Chemistry, Faculty of Science, Osaka City University, Sumiyoshi-ku, Osaka

(Received February 11, 1966)

dl-α-Dihydrocaranone (XII) has been synthesized stereoselectively, using the ring-closure reaction via benzyne intermediate of *N*-(2-bromo-4, 5-methylenedioxybenzyl)octahydroindole-6-one (X) with lithium piperidide in tetrahydrofuran. *dl*-γ-Lycorane (III) has been obtained by the Hauptmann reduction of XII.

The stereoisomers of lycorane derived from lycorine have been studied by Takeda and Kotera.[1] They established the stereochemistry of all of the possible isomers, α-, β-, γ- and δ-lycorane (I, II, III and IV). Recently, the stereoselective synthesis of *dl*-α- and β-lycorane has been reported by Hill,[2] but γ- and δ-lycorane have not yet been synthesized. The present investigation was undertaken in order to synthesize γ-lycorane stereoselectively, considering the biosynthesis[3] of the Amaryllidaceae alkaloids.

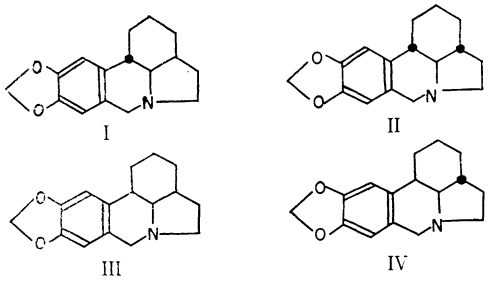

Fig. 1. The four stereoisomers of lycorane.

2-Bromo-4, 5-methylenedioxybenzyl bromide (V) was treated with 2, 5-dihydro-4-methoxyphenethylamine (VI) to give monobenzyl (VII) and di-benzyl (VIII) derivatives, which were then separated and purified by chromatography on silica gel. The ratio of VII to VIII was 3 : 1.

The monobenzyl derivative, VII, was hydrolyzed with 2 N hydrochloric acid into a 3-cyclohexenone

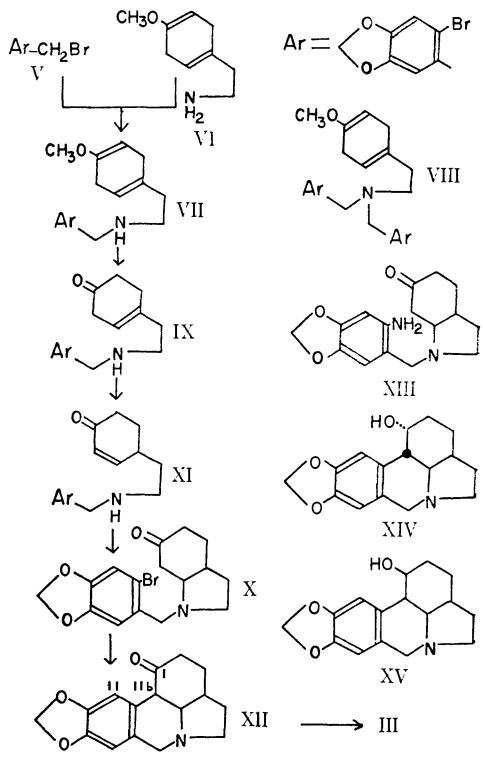

Fig. 2.

1) a) K. Takeda, K. Kotera, S. Mizukami and M. Kobayashi, *Chem. Pharm. Bull.*, **8**, 483 (1960); b) K. Kotera, *Tetrahedron*, **12**, 240 (1961); b) K. Kotera, ibid., **12**, 248 (1961).

2) R. K. Hill, J. A. Joule and L. J. Loeffler, *J. Am. Chem. Soc.*, **84**, 4951 (1962).

3) A. R. Buttersby, *Proc. Chem. Soc.*, **1963**, 189; D. H. R. Barton, ibid., **1963**, 293; A. R. Battersby, R. Binks, S. W. Breuer, H. M. Fales, W. C. Wildman and R. J. Highet, *J. Chem. Soc.*, **1964**, 1595.

(IX) hydrochloride, $C_{16}H_{18}NO_3 \cdot HCl$, m.p. 163°C. The NMR spectrum ($CDCl_3$) of the free base showed a vinyl proton multiplet at 4.35τ (1H) and a NH proton singlet at 5.2 τ (Fig. 3). The 3-cyclohexenone, IX, was refluxed in an 8 N hydrochloric acid - ethanol solution to yield *N*-(2-bromo-4, 5-methylenedioxybenzyl)-octahydroindole-6-one (X), which was then purified by chromatography on silica gel.

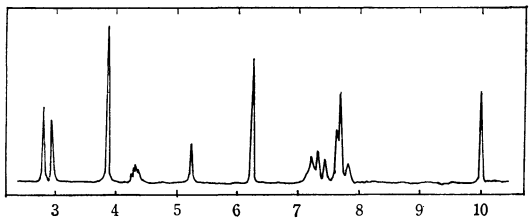

Fig. 3. NMR spectrum of XI (60 Mc.).

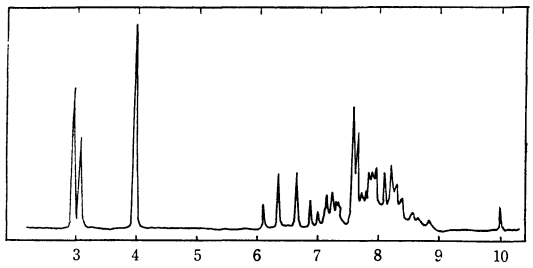

Fig. 4. NMR spectrum of X (60 Mc.).

The formation of the octahydroindole ring was deduced from the following facts. The NMR spectrum of this base showed a benzyl proton quartet at 6.4 τ (2H, AB type) (Fig. 4). The observed nonequivalence of the benzyl protons may arise from different magnetic shielding due to a molecular asymmetry resulting from the formation of the octahydroindole ring[4]. This base was then converted to its hydrochloride, $C_{16}H_{18}BrNO_3 \cdot HCl \cdot H_2O$, m.p. 123—125°C. The infrared spectrum of the hydrochloride exhibited the characteristic bands of an ammonium salt of the tertiary amine in the 2500—2700 cm^{-1} region. The more stable cis-fused octahydroindole ring may be obtained in this case.

The product obtained from α-dihydrocaranine (XIV) by Oppennauer oxidation was reported by Kotera[1] to be homogeneous α-dihydrocaranone (XII), which was isomeric at C_{11b} as compared with XIV. He suggested that another isomeric dihydrocaranone, the C_{11b} epimer of XII, might be unavailable due to non-bonded interaction between the C_{11}-aromatic proton and C_1-carbonyl-oxygen. Therefore, we considered the benzyl-octahydroindole, X, which has a cis-fused ring, would give XII upon treatment with strong bases.

Recently, Bunnett and his coworkers[5] reported many experiments on ring-closure reactions via benzyne intermediates. They mainly used potassium amide as the basic reagent.

The reaction of X with sodium or potassium amide in liquid ammonia did not give XII, but an amino-substituted derivative (XIII) solely. On the other hand, the treatment of X with lithium piperidide in tetrahydrofuran gave XII as the main product. This product was purified with chromatography over silica gel (35—40% yield) and recrystallized from methanol to give prisms, m.p. 147.5—149.5°C. The infrared spectrum in a chloroform solution was identical with that of the authentic *l*-α-dihydrocaranone.

dl-α-Dihydrocaranone, XII, was converted into its thioketal, m.p. 113.5—115°C, which was then desulfurized to *dl*-γ-lycorane, m.p. 101—102°C, by the method of Kotera.[1c]

The infrared spectrum of this compound was identical with that of the authentic *dl*-γ-lycorane. The reduction of XII with lithium aluminium hydride gave a mixture of two isomeric dihydrocaranines. The isomers were separated efficiently by silica gel chromatography into *dl*-1-epi-γ-dihydrocaranine, (XV), m.p. 135.5—136.5°C and *dl*-γ-dihydrocaranine, (C_1-epimer of XV), m.p. 180—181°C. The ratio of the isomers was 6 : 1. The infrared spectrum of the main product in a chloroform solution was identical with that of the authentic *l*-1-epi-γ-dihydrocaranine.

Experimental*1

2-Bromo - 4, 5 - methylenedioxybenzyl Bromide (V).*2—This was prepared by the method of Naik.[6]

2, 5-Dihydro-4-methoxyphenethylamine (VI).—This compound was prepared by a method similar to that described by Clarke.[7]

2-Bromo-4, 5 - methylenedioxybenzyl - (2, 5-dihydro-4-methoxyphenethyl)amine (VII).—A solution of 7 g. of V and 7.5 g. of VI in 500 ml. of absolute ethyl ether was kept at room temperature for one week. After the filtration of the deposited hydrobromide of VI, the solvent was removed under reduced pressure. The oily residue was then chromatographed over 130 g. of silica gel. Elution with a chloroform - ethyl ether solution (95 : 5 — 90 : 10) gave 2 g. of a dibenzyl derivative, VIII, as the first fraction. The product

4) Cf. R. K. Hill and T. H. Chan, *Tetrahedron*, **21**, 2015 (1965); G. M. Whitesides, J. J. Grocke, D. Holtz, H. Steinberg and J. D. Roberts, *J. Am. Chem. Soc.*, **87**, 1058 (1965); R. Grasky R. Huisgen, K. K. Sun and R. M. Moriarty, *J. Org. Chem.*, **30**, 74 (1965).

5) J. F. Bunnett and B. F. Hautfiord, *J. Am. Chem. Soc.*, **83**, 1691 (1961); J. F. Bunnett and J. A. Skorcz, *J. Org. Chem.*, **27**, 3836 (1962); J. F. Bunnett, T. Kato, R. R. Flynn and J. A. Skorcz, ibid., **28**, 1 (1963).

*1 All melting points are uncorrected.

*2 We are grateful to the Shiono-Koryo Co., Ltd., for its gift of piperonal for use as a starting material.

6) R. G. Naik and T. S. Wheeler, *J. Chem. Soc.*, **1938**, 1780.

7) C. B. Clark and A. R. Pinder, ibid., **1958**, 1967.

was then recrystallized from benzene - petroleum ether to give prisms, m. p. 88—89°C.

Found: C, 51.93; H, 4.48; N, 2.44. Calcd. for $C_{25}H_{25}O_5NBr_2$: C, 51.83; H, 4.35; N, 2.42%.

As a second fraction, 6 g. of a monobenzyl derivative (VII) were eluted.

4-[*N*-(2-Bromo-4, 5-methylenedioxybenzyl)-2'-aminoethyl]-3-cyclohexene-1-one (IX).—To a solution of 6.6 g. of the monobenzyl derivative (VII) in 150 ml. of ethanol, 300 ml. of a 2 N hydrochloric acid solution was added; the mixture was then allowed to stand at room temperature for 24 hr. The needles which thus formed were filtered (4.4 g.) and recrystallized from 1-propanol to give the 3-cyclohexenone (IX) hydrochloride, m. p. 163°C; infrared spectrum: ν_{max}^{Nujol} 1705 cm^{-1} (C=O), 2740 cm^{-1} (NH_2^+).

Found: C, 49.63; H, 4.95; N, 3.57. Calcd. for $C_{16}H_{19}NO_3BrCl$: C, 49.44; H, 4.93; N, 3.60%.

***N*-(2-Bromo-4, 5-methylenedioxybenzyl)octahydroindole-6-one (X).**—A solution of 4.5 g. of 3-cyclohexenone IX, or its hydrochloride in 200 ml. of ethanol and 200 ml. of 8 N hydrochloric acid was refluxed for 6—7 hr. The solvent was then evaporated under reduced pressure. The residue was dissolved in 100 ml. of water, and the solution was basified with a 10% sodium hydroxide solution and extracted with chloroform. The chloroform extract was washed with water, dried over sodium sulfate, and evaporated to dryness. The residue was chromatographed over silica gel. Elution with a chloroform-methanol-triethylamine solution (98.5 : 1 : 0.5) gave 3.7 g. of oily octahydroindolone, X. Its hydrochloride shows a m. p. of 123—125°C (infrared spectrum: ν_{max}^{Nujol} 1705 cm^{-1} (C=O), 2650 cm^{-1} (NH^+)).

Found: C, 46.97; H, 5.35; N, 3.44. Calcd. for $C_{16}H_{18}BrNO_3 \cdot HCl \cdot H_2O$: C, 47.25; 5.21; N, 3.20%.

The Reaction of Octahydroindolone (X) with Sodium Amide.—A solution of 360 mg. of the octahydroindolone, X, in 20 ml. of absolute ethyl ether was treated with a solution of sodium amide, prepared from 0.2 g. of sodium metal in 200 ml. of liquid ammonia, for 2.5 hr. After the addition of 0.3 g. of ammonium chloride and 30 ml. of ethyl ether, the ammonia was evaporated. Cold water was added to the mixture, and it was extracted with ether. The ethereal extracts were washed with water, dried, and evaporated to dryness. The residue was then chromatographed over a silica gel column. Elution with a chloroform-methanol-triethylamine solution (98.5 : 1.0 : 0.5) gave 250 mg. of an oily amino-substituted derivative, XIII, which was then derived to its acetate, prisms, m. p. 143—144°C.

Found: C, 65.62; H, 6.62; N, 8.53. Calcd. for $C_{18}H_{22}N_2O_4$: C, 65.44; H, 6.71; N, 8.48%.

The Reaction of Octahydroindolone (X) with Lithium Piperidide.—Into 580 mg. of octahydroindolone, X, in 120 ml. of tetrahydrofuran, a tetrahydrofuran solution of lithium piperidide, which had been prepared from 1 ml. of piperidine and 2 ml. of 4 N *n*-butyllithium in hexane, was added at 40—45°C with stirring under a nitrogen stream over about a one-hour period. After the mixture had then been stirred for a further 10—12 hr., the orange-yellow reaction mixture was cooled to 10°C, neutralized with ammonium chloride. After the addition of water, the resulting two layers were separated and the aqueous layer was extracted with ether. The tetrahydrofuran layer and the extracts were combined, and washed with a saturated aqueous solution of sodium chloride. The solvent was removed under reduced pressure, and the residue was chromatographed over 10 g. of silica gel. Elution with a chloroform - ethyl ether - methanol solution (94 : 5 : 1) gave 180 mg. of XII, which was then recrystallized from methanol to give prisms, m. p. 147.5—149.5°C.

Found: C, 70.94; H, 6.35; N, 5.34. Calcd. for $C_{16}H_{17}NO_3$: C, 70.83; H, 6.32; N, 5.16%.

The authers express their thanks to Dr. Kenichi Takeda and Dr. Katsumi Kotera for their helpful advice and for infrared identification.

BULLETIN OF THE CHEMICAL SOCIETY OF JAPAN VOL. 39 2014—2017 (1966)

Studies of Aminosugars. XIII. The Synthesis of Paromamine*

By Sumio UMEZAWA and Shinkiti KOTO

Department of Applied Chemistry, Faculty of Engineering, Keio University, Koganei, Tokyo

(Received December 25, 1965)

Paromamine has been synthesized by condensing the *N*, *N'*-dinitrophenyl derivative of deoxystreptamine with the *N*-dinitrophenyl derivative of acetobromoglucosamine in nitromethane in the presence of mercuric salts, and by then removing the protecting groups by treatment with methanolic ammonia and hydrolysis with Dowex 1X2. The synthetic sample was shown to be identical with natural paromamine by a comparison of their infrared spectra and by microbiological assay. The identity was also proved by the determination of the $\Delta[M]_{CuAm}$ values of the tri-*N*-acetate of the synthetic and natural specimens by the copper-complex methods.

Paromamine,[1] an aminoglucoside, has received wide attention in recent years in the field of chem-

* Part XXVI of "Studies on Antibiotics and Related Substances," by S. Umezawa.

1) T. H. Haskell, J. C. French and Q. R. Bartz, *J. Am. Chem. Soc.*, **81**, 3480 (1959).

istry of antibiotics, since it shows antibacterial activity[2] and is a common moiety of such useful antibiotics as paromomycin I, II and kanamycin C.[3] We now know three examples of aminoglucosides, composed of two carbohydrate moieties, which exert antibiotic action on bacteria, i. e., paromamine, neamine[4] and 4-*O*-(6-amino-6-deoxy-α-D-glucopyranosyl)-deoxystreptamine[5]; however, they have never been synthesized.

The present paper will present the details of our work on the synthesis of paromamine, work which was announced previously in a preliminary communication,[6] as well as details of some additional related studies.

The acetohalogeno derivatives of glucosamine, hitherto successfully used to synthesize α-glucosaminides of bulky alcohols, are 3, 4, 6-tri-*O*-acetyl-2-(2, 4-dinitroanilino)-2-deoxy-α-D-glucopyranosyl bromide[7] (I) and 3, 4, 6-tri-*O*-acetyl-2-(*p*-methoxybenzylidenamino)-2-deoxy-α-D-glucopyranosyl bromide[8]; however, to our knowledge, no α-glucosaminide of any kind of cyclic secondary alcohol has ever been synthesized with these acetobromo derivatives of glucosamine. Since deoxystreptamine is lacking in reactivity, and since, consequently, the conditions of glucosidation inevitably become drastic, a preliminary condensation of the more stable bromide (I) with cyclohexanol by Helferich's method[9] has been tested: Cyclohexyl 3, 4, 6-tri-*O*-acetyl-2-(2, 4-dinitroanilino)-2-deoxy-α-D-glucopyranoside (II) and its β-isomer (III) have been successfully obtained. An analogous reaction was then applied to the synthesis of paromamine.

The condensation of bis-*N*, *N'*-(2, 4-dinitrophenyl)-deoxystreptamine[10] with I in nitromethane in the presence of mercuric cyanide and bromide, gave a mixture of glucosides. The acetylation of the mixture and separation by TLC gave 4-*O*-[3, 4, 6-tri-*O*-acetyl-2-(2, 4-dinitroanilino)-2-deoxy-α-D-glucopyranosyl]-5, 6-di-*O*-acetyl-*N*, *N'*-bis-(2, 4-dinitrophenyl)-deoxystreptamine (IV).

On the other hand, paromamine was converted into tris-*N*-(2, 4-dinitrophenyl)-paromamine; when further acetylated, it gave penta-*O*-acetyl-tris-*N*-(2, 4-dinitrophenyl)-paromamine.

The infrared spectrum of IV could be completely superimposed on that of the above mentioned derivative of natural paromamine. The melting point of IV was not depressed by admixture with the derivative of natural paromamine.

The hydrolysis of IV with methanolic ammonia, followed by treatment with Dowex 1 X2 (OH^-), gave a crude base, which was then chromatographed on a column of cellulose powder. Finally, the ninhydrin-positive fraction was rechromatographed on Dowex 1 X2 (OH^-) to give a crystalline free base of 4-*O*-(2-amino-2-deoxy-α-D-glucopyranosyl)-deoxystreptamine (V).

Paper chromatography of the synthetic product V illustrated that its R_f value corresponds to that of paromamine. A paper chromatographic study of the synthetic product hydrolyzed by refluxing it with 3 N hydrochloric acid showed just three spots, those of D-glucosamine, deoxystreptamine and the unchanged material.

Finally, the absolute configuration of the synthetic product and its identity with the natural paromamine were confirmed by a modified method[11] using cuprammonium-glucoside complexes.[12] Tri-*N*-acetylparomamine includes two pairs of adjacent hydroxyl groups which make projected angles of about +60° and −60°, one in the glucosamine moiety and other in the deoxystreptamine moiety. Accordingly, the $\Delta[M]_{CuAm}$ of tri-*N*-acetyl paromamine may be expected to be nearly zero as a result of internal compensation. The free base V was acetylated and de-*O*-acetylated to afford 4-*O*-(2-acetamido-2-deoxy-α-D-glucopyranosyl)-*N*, *N'*-diacetyl-deoxystreptamine (VI).

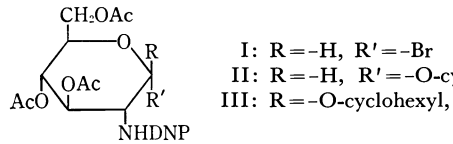

I: R=-H, R'=-Br
II: R=-H, R'=-O-cyclohexyl
III: R=-O-cyclohexyl, R'=-H

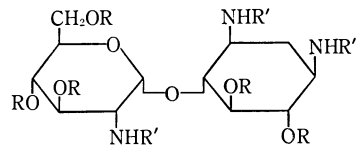

IV: R=-Ac, R'=-DNP
V: R=R'=-H (Paromamine)
VI: R=-H, R'=-Ac

Ac=-$COCH_3$, DNP=- 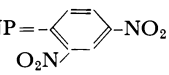

Fig. 1

2) T. Wakazawa and S. Fukatsu, *J. Antibiotics*, **A15**, 225 (1962).
3) M. Murase, ibid., **A14**, 367 (1961).
4) B. E. Leach and C. M. Teeters, *J. Am. Chem. Soc.*, **73**, 2794 (1951); H. E. Carter, J. R. Dyer, P. D. Shaw, K. L. Rinehart, Jr., and M. Hichens, ibid., **83**, 3723 (1961).
5) S. Umezawa and T. Tsuchiya, *J. Antibiotics*, **A15**, 51 (1962).
6) S. Umezawa and S. Koto, ibid., **A19**, 88 (1966).
7) P. F. Lloyd and M. Stacey, *Chem. & Ind.*, **1955**, 917.
8) E. F. Hardy, J. G. Buchanan and J. Baddiley, *J. Chem. Soc.*, **1963**, 3360.
9) B. Helferich and J. Zirner, *Chem. Ber.*, **95**, 2604 (1962).
10) S. Umezawa and S. Koto, *J. Antibiotics*, **A17**, 186 (1964).
11) S. Umezawa, T. Tsuchiya and K. Tatsuta, This Bulletin, **39**, 1235 (1966).
12) R. E. Reeves, "Advances in Carbohydrate Chemistry," Vol. VI, Academic Press, New York (1951), p. 107; M. Hichens and K. L. Rinehart, Jr., *J. Am. Chem. Soc.*, **85**, 1547 (1963).

The determination of the $\Delta[M]_{CuAm}$ values of the synthetic product and the corresponding tri-*N*-acetyl derivative of natural paromamine gave values of +191 and +13 respectively. If VI were a 5-*O*- or 6-*O*-linked derivative of deoxystreptamine, instead of the 4-*O*-linked derivative mentioned above, the $\Delta[M]_{CuAm}$ values would be +2000 or +4000 respectively. The observed values for $\Delta[M]$'s of VI and tri-*N*-acetyl paromamine agree within the range of experimental error. Thus, the synthetic product, VI, was proved to be identical with the *N*-acetyl derivative of natural paromamine.

In the above-mentioned synthesis, the DNP group appears to have played an important role in the α-glucoside formation, for the dinitrophenylamino group would not be expected to exert a considerable anchimeric affect on the anomeric center. It is also conceivable that the plane of the phenyl group occupies a position almost perpendicular to the sugar body in the transition state; therefore, it is not so much of a steric hindrance, while the anchimeric effect of the 6-*O*-acetyl group[13] has a favorable influence on the formation of α-linkage in the polar solvent, nitromethane.

The synthetic product V behaved in conformity with natural paromamine in antibiotic spectra and minimal inhibitory concentrations (MIC) as is shown in Table I.

Table I. The MIC's of the synthetic (V) and natural paromamine as determined by the dilution method in bouillon

Test organisms		MIC μg./ml. V	MIC μg./ml. Paromamine
Bacillus subtilis PCI 219	(24 hr.)	125	125
Mycobacterium tuberculosis 607	(96 hr.)	>1000	>1000

In view of the established method of synthesis of deoxystreptamine by Nakajima et al.,[14] the above synthesis may be regarded as a total synthesis of paromamine.

It has been reported[15] that a kind of diastereoisomer of paromamine can be obtained from a crude product by acid reversion or, alternatively, by the reaction mentioned above, but no definite configurational assignment could be made at that time. Subsequently, the diastereoisomer was proved to be 5-*O*-(2-amino-2-deoxy-α-D-glucopyranosyl)-deoxystreptamine.[16]

13) P. F. Lloyd and G. P. Roberts, *J. Chem. Soc.*, **1963**, 2962.
14) M. Nakajima, A. Hasegawa and N. Kurihara, *Tetahedron Letters*, **1964**, 967.
15) T. Tsuchiya, H. Fujita and S. Umezawa, *J. Antibiotics*, **A17**, 181 (1964).
16) S. Umezawa, T. Tsuchiya and H. Fujita, ibid., **A19**, 222 (1966).

Experimental

General Procedures.—TLC was performed on "Silica-Rider for TLC" (Dai-ich Pure Chemicals Co.) using three solvent systems, (a) benzene: MEK=4 : 1, (b) benzene : MEK=10 : 3, and (c) ethyl acetate : methanol=1 : 1, as the mobile phase. The DNP derivatives were visualized directly on an air-dried plate as yellow spots or bands, while others were detected by spraying a dried chromatogram with 50% sulfuric acid and heating it at 90—100°C. The extraction from Silica Rider was carried out with excess acetone. Paper chromatography was performed on Toyo filter paper No. 51, using the (d) solvent system (*n*-butanol : pyridine : water : acetic acid=6 : 4 : 3 : 1); ninhydrin (0.25%) in pyridine was sprayed on.

Cyclohexyl 3, 4, 6-Tri-*O*-acetyl-2-(2, 4-dinitroanilino)-2-deoxy-α-D-glucopyranoside (II). — To a solution of I (534 mg., 1 mmol.) and cyclohexanol (0.31 ml., 3 mmol.) in nitromethane (21 ml.), there was added mercury(II) cyanide (130 mg., 0.5 mmol.) and mercury(II) bromide (180 mg., 0.5 mmol.); the mixture was then stirred at 27—29°C for 6 days. The reaction mixture was evaporated, and the dark residue (1.19 g.) was treated with chloroform. The filtrate was washed with 10% aqueous potassium bromide (10 ml.×4) and distilled water (10 ml.×3), dried over sodium sulfate, and evaporated to give a reddish brown sirup (709 mg.). This was extracted with boiling ethanol (20 ml.), and then the solution was allowed to stand at room temperature overnight, thus precipitating a yellow crystalline solid (375 mg.). Two recrystallizations from ethanol gave crystals of cyclohexyl 3, 4, 6-tri-*O*-acetyl-2-(2, 4-dinitroanilino)-2-deoxy-α-D-glucopyranoside (II), m. p. 201.5°C, $[\alpha]_D^{17}$ +43° (*c* 0.81, chloroform). IR spectrum (KBr): 3320, 3100, 1620, 1590, 1530, 1332 (NH–DNP); 2910, 2840 (cyclohexyl); 1750, 1225 (O–Ac), 850 cm^{-1} (type 2a of the pyranose ring).

Found: C, 51.77; H, 5.21; N, 7.49. Calcd. for $C_{24}H_{31}N_3O_{12}$ (553): C, 52.07; H, 5.65; N, 7.59%.

The mother liquor separated from II further deposited yellow needles (200 mg.), m. p. 179—179.5°C, $[\alpha]_D^{26}$ −53° (*c* 1.0, chloroform). The optical rotation and the infrared spectrum of the product showed that it is cyclohexyl 3, 4, 6-tri-*O*-acetyl-2-(2, 4-dinitroanilino)-2-deoxy-β-D-glucopyranoside (III).

Found: C, 52.10; H, 5.68; N, 7.49. Calcd. for $C_{24}H_{31}N_3O_{12}$ (553): C, 52.07; H, 5.65; N, 7.59%.

4-*O*-[3, 4, 6-Tri-*O*-acetyl-2-(2, 4-dinitroanilino)-2-deoxy-α-D-glucopyranosyl]-5, 6-di-*O*-acetyl-*N*, *N'*-bis-(2, 4-dinitrophenyl)-deoxystreptamine (IV).—A suspension of I (5.0 g., 9.4 mmol.), bis-*N*, *N'*-(2, 4-dinitrophenyl)-deoxystreptamine[12] (3.1 g., 6.3 mmol.), mercury(II) cyanide (1.2 g., 4.8 mmol.) and mercury-(II) bromide (1.7 g., 4.8 mmol.) in nitromethane (15 ml.) was heated at about 95°C for 50 hr. while occasionally being stirred. The reaction mixture was then diluted with chloroform (100 ml.), and the dark brown filtrate was dried up in vacuo to give a residue (8.0 g.) which left a hard gummy substance (fraction A) (3.1 g.) when extracted with hot chloroform (50 ml.). The evaporation of the chloroform solution gave a dark residue (fraction B) (4.0 g.). Fraction B was chromatographed on silicon dioxide (170 g., 3.8×24 cm.) with benzene-ethanol (10 : 1, v/v) to give a yellow solid

(fraction B') (0.91 g.). Fraction A was again dissolved in ethyl acetate, filtered and evaporated to afford a brown residue (fraction A') (2.9 g.). Fractions A' and B' were combined and chromatographed on thin layer plates (20×20×0.05 cm; 160 sheets) with the a a solvent system; the distance of development was 10 cm. Three fractions, C, D and E (0.93 g., 0.83 g., and 1.58 g.), were obtained; the rate of flow of C was the largest. The fraction C was then further separated into two nearly equal fractions by preparative TLC using the b solventsystem. A yellow homogeneous substance (270 mg.) was obtained from the fraction with the smaller R_f value. The product was then acetylated with acetic anhydride (4 ml.) and pyridine (4 ml.) overnight at room temperature. The crude acetate was subjected to preparative TLC using the b solvent system; the distance of development was 17 cm. Extraction with acetone from the main band gave a yellow solid. This solid was taken up in acetone and filtered, and an excess of ethanol was added to afford fine yellow needles of the title compound (IV), m. p. 275—280°C (decomp.; sintered at about 200°C). $[\alpha]_D^{24}$ +250° (*c* 0.9, acetone). IR spectrum (KBr): 3345, 3100, 1628, 1593, 1525, 1336, 745 (NH–DNP); 1758, 1220 cm^{-1} (O–Ac).

Found: C, 46.47; H, 4.21; N, 12.37. Calcd. for $C_{40}H_{41}N_9O_{24}$ (1031): C, 46.56; H, 4.01; N, 12.22%.

4-*O*-(2-Amino-2-deoxy-α-D-glucopyranosyl)-deoxystreptamine (V).—A sample (30 mg.) of IV was dissolved by gently stirring into methanolic ammonia (40 g.) saturated at 0°C and then kept standing at room temperature overnight. Evaporation in vacuo was followed by letting the mixture stand under reduced pressure for several hours in order to remove the acetamide. The red residue was then dissolved in an acetone-water mixture (1 : 1), and an excess of Dowex 1X2 (OH^-) was added to the yellow solution. The mixture was shaken at room temperature overnight, and filtered, and the colorless filtrate was evaporated in vacuo. The product (10 mg.) was mixed with cellulose powder (200 mg.), placed on a column of cellulose powder (4.0 g.; 18×1.05 cm.), and eluted with the d solvent mixture, the fractions being cut into 20-ml. portions. The appearance of the product was examined by means of ninhydrin coloration. After the evaporation of the solvent at about 25°C, the fractions of tube Nos. 3—4 afforded a colorless sirup (8 mg.); this sirup was deionized with Dowex 1X2 (OH^-) and distilled water. The evaporation of drop Nos. 15—45 gave the pure free base (V), 7.0 mg. (74% from IV), $[\alpha]_D^{24}$ +111° (*c* 0.75, water).

Found: C, 44.15; H, 7.64; N, 12.67. Calcd. for $C_{12}H_{25}N_3O_7$ (323.5): C, 44.57; H, 7.79; N, 13.00%.

Descending paper chromatography of the synthetic product illustrated that its R_f value corresponded well with that of paromamine as ascertained by ninhydrin coloration.

4-*O*-(2-Acetamido-2-deoxy-α-D-glucopyranosyl)-*N*, *N'*-diacetyl-deoxystreptamine (VI).—A sample (11 mg.) of V was acetylated with acetic anhydride (1 ml.) and pyridine (1 ml.) at about 30°C for one week; then, after the evaporation of the excess reagent, the crude product was de-*O*-acetylated with methanolic sodium methylate (4 ml., 0.02%) at room temperature overnight. Neutralization with Amberlite IR 120 (H^+), followed by evaporation, gave a colorless residue which was then deionised by the use of Dowex 1X2 (0.8×8 cm.) and Dowex 50WX8 (0.3×4 cm.) successively, and developed with water. The elute was evaporated to yield a crystalline solid (4.7 mg.); $[\alpha]_D^{15}$ +110° (*c* 0.34, water), $[\alpha]_{436}^{15}$ +200° (*c* 0.34, water), $[\alpha]_{436}^{15}$ +243° (*c* 0.33, CuAm), $\Delta[M]_{CuAm}$ +191. The R_f value of the product, as ascertained using the c solvent system, corresponded well with that of tri-*N*-acetyl paromamine obtained by the same procedure of acetylation and de-*O*-acetylation.

Found: C, 47.87; H, 6.92; N, 9.41. Calcd. for $C_{18}H_{31}N_3O_{10}$ (449.5): C, 48.10; H, 6.95; N, 9.35%.

Penta-*O*-acetyl-tris-*N*-(2, 4-dinitrophenyl)-paromamine.—A suspension of paromomycin sulfate (Sankyo Co.) (1.0 g.) in methanol (25 ml.) containing concentrated hydrochloric acid (1 ml.) was refluxed gently for 8 hr. The resulting colorless crystals were then collected and washed with methanol; yield, 356 mg. The crude product (340 mg.) was dissolved in distilled water (1.0 ml.), put on the Dowex 1×2 (OH^-) column (1×13 cm.), and developed with distilled water, the fractions being cut into 5-ml. portions. The evaporation of the fraction of tube Nos. 2—4, which was detected by ninhydrin coloration, followed by crystallization from methanol, gave a sample of chromatographically-pure paromamine (190 mg.).

Found: C, 44.36; H, 7.59; N, 12.86. Calcd. for $C_{12}H_{25}N_3O_7$ (323.5): C, 44.57; H, 7.79; N, 13.00%.

A mixture of the paromamine (163 mg.) and sodium bicarbonate (193 mg.) in water (6 ml.) was stirred for a while. To the solution there were then added 2, 4-dinitrofluorobenzene (308 mg.) and ethanol (3.5 ml.), after which the mixture was stirred for about 6 hr. at 29—30°C, until the yellow gummy product initially formed became powdery; yield, 350 mg. (85%). The crude product of tris-*N*-(2, 4-dinitrophenyl)-paromamine was acetylated with acetic anhydride (5 ml.) and py-pyridine (5 ml.). The resulting yellow glass was crystallized from acetone as fine needles by the gradual addition of ethanol. Two recrystallizations from an acetone-ethanol mixture gave a chromatographically-pure product, m. p. 275—280°C (decomp.; sintered at about 200°C); $[\alpha]_D^{24}$ +262° (*c* 0.9, acetone).

Found: C, 46.23; H, 3.98; N, 12.24. Calcd. for $C_{40}H_{41}N_9O_{24}$ (1031): C, 46.56; H, 4.01; N, 12.22%.

The infrared spectra of the product and of IV were identical.

The authors wish to thank Mr. Saburo Nakada for his microanalyses, Mrs. Michiko Ishizawa for her infrared analyses, and Mr. Hiroyuki Odawara and Miss Mizuko Handa for their technical assistances.

BULLETIN OF THE CHEMICAL SOCIETY OF JAPAN VOL. 39 2018—2020 (1966)

Organoboron Compounds. XI.* The Polymerization of Vinylboronic Acid

By Seiji KATO,** Keiko KIMURA, Katsuhisa NAGATA and Yojiro TSUZUKI

Department of Chemistry, Tokyo College of Science, Kagurazaka, Shinjuku-ku, Tokyo

(Received February 22, 1966)

It has been found that potassium persulfate is a good initiator for the polymerization of vinylboronic acid. With this initiator the polymerization has been studied in acidic as well as in basic medium, and the best conditions for the polymerization have been established with the help of molecular weight determination of the products. The highest molecular weight has been observed in basic medium to be about 7000. A mixed solvent (1 : 1) of ether and acetone has been used as the precipitant. The variation in the rate of polymerization and the boron content has been investigated in a narrow range of pH, from 6 to 8.

In the course of our investigation of some boronic acids we observed that boronic acids with an alkyl or an aryl group attached to the boron atom can be converted, on oxidation and hydrolysis, into the corresponding alcohol and boric acid. In the case of vinylboronic acid, where a vinyl group is linked with the boron atom, it is to be expected that polyvinyl alcohol may eventually be produced by its polymerization, oxidation and hydrolysis, as is formulated below:

$$RX \longrightarrow RB(OH)_2 \xrightarrow[\text{Hydrolysis}]{\text{Oxidation}} ROH + B(OH)_3$$

$$CH_2{=}CH \longrightarrow \underset{\displaystyle X}{\overset{\displaystyle |}{CH_2{-}CH}} \longrightarrow -\left[\underset{\displaystyle B(OH)_2}{\overset{\displaystyle |}{CH_2{-}CH}}\right]_n-$$

$$\xrightarrow[\text{Hydrolysis}]{\text{Oxidation}} -\left[\underset{\displaystyle OH}{\overset{\displaystyle |}{CH_2{-}CH}}\right]_n- + B(OH)_3$$

Ritter et al.[1,2] and Matteson[3] have, however, pointed out that a resonance stabilization of the intermediate radical would result from the carbon-boron π-bonding when the vinyl group is one of the three groups bonded to the boron atom:

$$\underset{\displaystyle B}{\overset{\displaystyle |}{>C{=}C-}} \longleftrightarrow \underset{\displaystyle B^-}{\overset{\displaystyle \|}{>C^+{-}C-}}$$

In general, there are two processes in the vinyl-type polymerization, namely, ionic and radical polymerization. As a result of the mesomeric effect described above, and as a result of the great difficulty encountered in removing the free water from vinylboronic acid, it is probable that no ionic initiator has any influence on opening the vinyl group. In fact, no polymerization was effected when a solution of vinylboronic acid was treated with ionic initiators, but radical polymerization really occurred when potassium persulfate was used as an initiator.

Vinylboronic acid and its butyl ester were prepared by Normant[4] and by Matteson[5], who reported that polymerization readily set in during the synthesis. The present paper will deal with more detailed experiments carried out on the polymerizing factor of vinylboronic acid; the results of these experiments are shown in Tables I—IV.

As regards the polymerization in an aqueous solution, some instances have been known, such as those of itaconic acid[6] and acrylic acid, both of which use potassium persulfate as the initiator. On the other hand, *p*-vinylbenzeneboronic acid has been found to enter into polymerization by the same initiator in *t*-butyl alcohol.[7] Vinylboronic acid can be polymerized to higher-molecular substances in a dilute solution of sodium hydroxide rather than in a dilute solution of hydrochloric acid.

The polyvinylboronic acids of higher degrees of polymerization are soluble in water, and the lower polymers are soluble in an extremely dilute alkaline solution. All of them are insoluble in common organic solvents with the exception of tetrahydrofuran.

It has been established experimentally that the best conditions for polymerization are when the concentration of the medium is 0.11 N alkali, the concentration of the initiator is 4% (weight percent based on the monomer), and the temperature is 50°C. The rate of polymerization and the boron content were investigated in a narrow pH range, from 6 to 8, with the specimens of polyvinylboronic acids obtained under the conditions described above. The results are shown in Fig. 1.

* Part X: This Bulletin, **39**, 1582 (1966).

** Died April 9, 1965.

1) T. D. Parsons, M. B. Silverman and D. M. Ritter, *J. Am. Chem. Soc.*, **79**, 5091 (1957).

2) T. D. Parsons and D. M. Ritter, ibid., **76**, 1710 (1954).

3) D. S. Matteson, ibid., **81**, 5004 (1959).

4) H. Normant, *Compt. rend.*, **248**, 828 (1959).

5) D. S. Matteson, *J. Am. Chem. Soc.*, **82**, 4228 (1960).

6) C. S. Marvel and T. H. Shepherd, *J. Org. Chem.*, **24**, 599 (1959).

7) J. Pellon, L. H. Schwind, M. J. Guinard and W. M. Thomas, *J. Polymer Sci.*, **55**, 161 (1961).

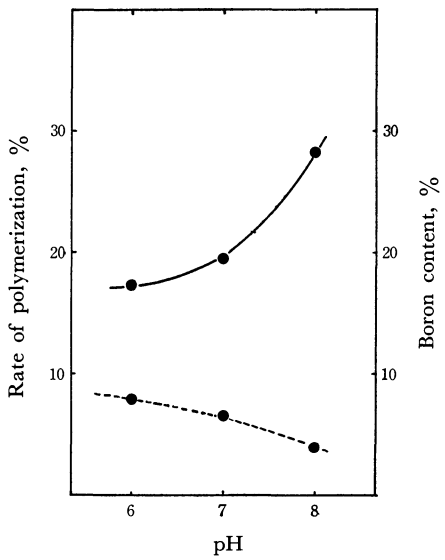

Fig. 1. The rate of polymerization and the boron content of the products in the range of pH 6—8.
—— rate of polymerization, ---- born content

The rate of polymerization becomes higher with an increase in the pH value, but the boron content decreases. This may show that the cleavage of the carbon-boron bond has really occurred.

The infrared spectra of the products obtained in an acidic medium show absorptions of 3500 cm^{-1} (O–H), 1300—1400 cm^{-1} (B–O), 1000—1100 cm^{-1} (B–C) and 2900 cm^{-1} (CH, CH_2), while those of the products obtained in a basic medium resemble the spectra of polyvinyl alcohol.

Since their structure is similar to that of polyvinyl alcohol, the average molecular weight was roughly estimated from the following equation (I), using the constants of polyvinyl alcohol ($K=8.5\times10^{-4}$ and $\alpha=0.62$ at 20°C),[8] the molecular weight being about 7000 (maximum) in a basic medium and from 500 to 1000 in an acidic medium:

$$[\eta] = KM^{\alpha} \qquad (I)$$

The intrinsic viscosity was measured in water and found to be in the range from 0.04 to 0.2 at 20°C, so the products should be called "oligomers" rather than "polymers."

Experimental Results

The Preparation of Vinylboronic Acid.—The method used here was practically identical with that of Matteson,[4] who prepared vinylboronic acid from vinylmagnesium bromide and trimethyl borate, but the procedure of crystallization was somewhat modified. After acidifing the solution of vinylboronic acid sodium salt with phosphoric acid, and extracting it with ether, the ethereal solution was concentrated. The vinylboronic acid was then precipitated by pouring a concentrated ethereal solution of it into a large quantity of *n*-hexane before using it; it was dried in a vacuum oven within five minutes, m. p. 83°C. Yield 35%.

Selection of Initiator.—The initiators used in the experiments are listed in Table I. A solution of 2 g. of the monomer in 10 ml. of the solvent was prepared. This solution was then introduced in seven 20-ml. sealed tubes, each containing 0.05 g. of the initiator. All the tubes were deaerated and sealed under reduced presure. Samples 1—3 were kept at a constant temperature of 80°C for 24 hr., and samples 4—7, at −70°C in a dry ice - acetone bath for 48 hr. From sample 3 a polymer was isolated by adding a mixed ether-acetone solvent (1 : 1 by volume), while no polymer was obtained from the others with any kind of precipitating reagent.

Table I. Initiators and solvents of polymerization

No.	Initiator	Solvent	Type of polymerization
1	Benzoic peroxide	*t*-Butylalcohol	Radical
2	Azobisisobutylonitrile	*t*-Butylalcohol	Radical
3	Potassium persulfate	Water	Radical
4	Sodium naphthalene	Glycoldimethyl ether	Ionic
5	Ethyllithium	Ethyl ether	Ionic
6	Sodium cyanide	Dimethylformamide	Ionic
7	Sodium triphenylmethane	Ethyl ether	Ionic

Polymerization of Vinylboronic Acid.—Further polymerization experiments employing potassium persulfate initiation were carried out both in basic medium of an aqueous solution of sodium hydroxide and in acidic medium of an aqueous solution of hydrochloric acid.

Table II. Rate of polymerization and normality of medium[a]

Acidic medium[b]			Basic medium[c]			
No.	Normality of HCl	Pr %	No.	Normality of NaOH	Pr %	Pd %
1	0.25	3.2	1	0.065	62.5	14
2	0.05	4.5	2	0.11	64.5	77
3	0.0025	8.5	3	0.55	—*	—
4	0.0005	16.0	4	1.11	—	—

a) All sealed tubes were kept at 50°C in a bath for 48 hr.
b) Monomer (1.25 g.) was introduced each in four sealed tubes each with 10 ml. of water containing hydrochloric acid of the specified normal concentration and with 0.05 g. of initiator.
c) Monomer concentration was 0.8 g. per 10 ml. of water containing sodium hydroxide of the specified normal concentration. Initiator (0.016 g.) was added.
* Not precipitated in a mixture of ether-acetone (1 : 1 by volume).

8) H. Staudinger and H. Warth, *J. prakt. Chem.*, **155**, 261 (1940).

TABLE III. RATE OF POLYMERIZATION AND CONCENTRATION OF INITIATOR[a]

Acidic medium[b]			Basic medium[c]			
No.	Quantity of initiator[d] %	Pr %	No.	Quantity of initiator[d] %	Pr %	Pd %
1	0.5	5.0	1	1.0	64.0	93
2	1.0	6.5	2	2.0	64.5	77
3	2.0	10.5	3	4.0	65.8	54
4	4.0	16.0	4	8.0	53.3	40

a) All sealed tubes were kept at 50°C in a bath for 48 hr.
b) A stock solution of the monomer was prepared, which contained 1.25 g. of the sample in 10 ml. of hydrochloric acid of concentration 5×10^{-4} N.
c) Solvent was a sodium hydroxide solution of 0.11 N. A solution of the monomer was of the concentration corresponding to the acidic medium.
d) Expressed by the number of grams per 100 g. of vinylboronic acid taken.

The relations of the rate of polymerization to the normality of the medium, the concentration of the initiator, and the temperature of polymerization were investigated. The experimental methods employed were described below each of Tables II—IV. All the tubes used in the experiments were dearated and sealed under a vaccum. A tetrahydrofuran solution of the polymer was precipitated and purified in a mixed solvent of ether and acetone (1 : 1 by volume). The rate of polymerization was determined by weight percent based on the monomer. The polymerization degree was measured at 20°C using a dilute-type Ubbelohde viscosimeter. The symbols used in Tables II—IV are as follows: (Pr)—the rate of polymerization, and (Pd)—the degree of polymerization.

Determination of Boron.—Although a number of methods have been proposed for the analysis of boron, they are for the most part troublesome. Our modification of the method of Martin[9] has been proved to be easier and more practical.

TABLE IV. RATE OF POLYMERIZATION AT VARIOUS TEMPERATURES

Acidic medium[a]			Basic medium[b]			
No.	Temp. °C	Pr %	No.	Temp. °C	Pr %	Pd %
1	0	10.0	1	0	10.0	—*
2	15	12.0	2	20	35.0	78
3	30	16.0	3	30	62.0	77
4	50	16.5	4	50	69.0	99

a) Monomer (1.25 g.) was placed in each tube with 10 ml. of 5×10^{-4} N of hydrochloric acid and with 0.05 g. of potassium persulfate.
b) Monomer solution consists of 0.8 g. per 10 ml. of water containing 0.11 N of sodium hydroxide. Concentration of initiator was fixed at 2%, namely 2 g. per 100 g. vinylboronic acid taken.
* Not precipitated in a mixture of ether-acetone (1: 1 by volume).

The sample is refluxed with a sodium peroxide solution for several hours until it is dissolved. The solution is then exactly neutralized to pH 6.9 with hydrochloric acid by the help of a pH-meter; when mannitol is added, the solution is titrated back with a standard solution of sodium hydroxide until the pH-meter indicates 6.9 exactly. The boron content (%) is given by the following equation (II):

$$B\% = \frac{10.8}{W} \times \frac{NV}{V_t} \qquad \text{(II)}$$

where N and V are the normality and the used volume of a standard solution of sodium hydroxide respectively, where V_t is the final volume of the solution of the sample, and where W is the number of grams of the weighed sample.

9) J. R. Martin, *Anal. Chem.*, **24**, 182 (1952).

BULLETIN OF THE CHEMICAL SOCIETY OF JAPAN VOL. 39 2021—2023 (1966)

The Dimerization of Ethylene Using Palladous Chloride as the Catalyst

By Yasuo KUSUNOKI*, Ryokei KATSUNO, Noboru HASEGAWA, Susumu KUREMATSU, Yoshio NAGAO, Kanzi ISHII and Shigeru TSUTSUMI

Department of Chemical Engineering, Faculty of Engineering, Osaka University, Miyakojima-ku, Osaka

(Received September 21, 1965)

The dimerization of ethylene was carried out using palladous chloride as the catalyst. Acetic acid, ethylene dichloride, ethylene tetrachloride, benzene, chlorobenzene, triethyleneglycol, acetic acid esters, chloroform, cyclohexane and ethanol were employed as the reaction solvents, and the effects of these solvents on the reaction were investigated. The best yield of butylene (about 1500 mol.% to palladous chloride) was obtained, when acetic acid was used as the solvent; the yield decreased gradually following the above order of solvents until, when ethanol was used as the solvent, it yielded only 96 mol.%. However, in all solvents dimerization was carried out predominantly, and only a few higher polymers were obtained. It is very interesting that the solvent effect mentioned above was different from the effect of solvents in the isomerization of olefin when metal carbonyl was used as the catalyst. To explain these results, a hydride ion-shift mechanism has been proposed.

Recently, many reports have been published on the polymerization or isomerization of olefins, using Ziegler-Natta catalysts or metal carbonyls.[1] In these reactions the intermediate formation of a π-complex between olefin and catalyst was assumed. The present study will deal with the dimerization of ethylene using palladous chloride, which easily forms a complex with ethylene and which gives butylenes in a fairly good yield. Although the dimerization proceeded with few side reactions, the effects of solvents on this reaction were comparatively great. Some solvents, e. g., acetic acid or halogenated hydrocarbons, led to excellent yields of the dimerization products, whereas others, e. g., ethanol, led to lower yields. The maximum yield of butylenes (about 1500 mol.% to the palladous chloride based on the ethylene) was obtained in the case of the acetic acid solvent.

From these results it may be considered that this dimerization reaction is similar to a Friedel-Crafts-type reaction.

Results and Discussion

The experimental conditions are shown in Table I, while the results are summarized in Table II; it is clear from Table II that the highest yield of butylenes is obtained when acetic acid is used as a solvent, and that the yield decreases in the order of the solvents as they are listed in this table, from dichloroethane to ethanol. It may generally be said that the ratio of butylene-2 to butylene-1 decreases with the decrease in the yield of butylenes.

As a by-product, a small amount of hexene was detected in every case; octene or isobutyl chloride was also detected in some cases. However, when an acetic acid ester was used as a solvent, the formation of isobutyl chloride was remarkable. The fact that, in an ethanol solvent, small amounts of ethyl vinyl ether and acetal were detected by gas chromatography, agrees with the observations by Stern and Spector,[2] and Moiseef et. al.[3]

As has been described above, the dimerization of ethylene proceeds predominantly with a palladous chloride catalyst; the formation of higher olefins is negligible. The relation between the yield of butylenes and the kind of solvent is quite contradictory to Mannel's results[4] on the isomerization of olefin with a metal carbonyl catalyst; Mannel obtained good results by using methanol, ethanol, acetone and benzene solvents, while he regarded acetic acid, carbon tetrachloride and acid chlorides as unsuitable solvents. As the mechanism of these isomerizations, the formation of the so-called π-en-yl-type complex by way of a proton shift from a π-complex may be described. Huettel[5] has already pointed out that the hydrogen

* Present address: Yawata Chemical Industry Co., Ltd., Tobata-ku, Nakabaru, Kitakushu City.

1) E. Lutz, *J. Am. Chem. Soc.*, **83**, 2551 (1961); J. Rose, *J. Chem. Soc.*, **1960**, 60; B. Franzus, *J. Am. Chem. Soc.*, **81**. 1514 (1959); J. Harris, *J. Org. Chem.*, **25**, 633 (1960); J. Sauer, *J. Am. Chem. Soc.*, **79**, 2659 (1957); L. Meriwether, *J. Org. Chem.*, **26**, 5155, (1961); G. Hata, *Chem. & Ind.*, **1965**, 223.

2) E. W. Stern and M. L. Spector, *Proc. Chem. Soc.*, **1961**, 370.

3) I. I. Moiseef, M. N. Vargaftik and Ya. K. Syrkin, *Doklady Akad. Nauk U. S. S. R.*, **133**, 377 (1960).

4) T. A. Mannel, *J. Org. Chem.*, **27**, 3941 (1962).

5) R. Huttel, J. Kratzer and M. Bechter, *Chem. Ber.*, **94**, 766 (1961).

TABLE I. REACTION CONDITIONS

Solvent	React. temp. °C	React. time hr.	Note
Acetic acid	70—100	4.5	additional C_2H_4 43 kg./cm$_2$
Dichloroethane	70— 90	9.0	
Tetrachloroethane	80— 95	4.5	
Benzene	85—100	7.0	additional C_2H_4 61 kg./cm$_2$ (twice)
Chlorobenzene	70— 90	3.0	
Triethylene glycol	95—100	2.5	
Methyl acetate	80—100	3.0	
Butyl acetate	80—100	3.0	
Chloroform	100—150	4.0	
Cyclohexane	110—200	4.5	
Ethanol	100—200	6.0	

$PdCl_2$: 8.8 g. (0.05 mol.), solvent: 40 c.c.,
C_2H_4: 60 kg./cm^2 (initial pressure at room temperature)
Numbers on the left in the temperature column indicate the temperature at which absorption of ethylene began.

TABLE II. EXPERIMENTAL RESULTS

Solvent	Butylene yield		Ratio[b]		By-products[c]
	g.	%[a]	C_4H_8-1	C_4H_8-2	
Acetic acid	20.8	1488	12	88	Hexene
Dichloroethane	13.0	930	9	91	—
Tetrachloroethane	11.9	852	5	55	Hexene, Octene, Isobutyl chloride
Benzene	8.0	552	12	88	Hexene, Isobutyl chloride
Chlorobenzene	8.7	620	6	94	Hexene, Isobutyl chloride
Triethylene glycol	6.1	436	9	91	—
Methyl acetate	6.7	480	9	91	Isobutyl chloride (3.8 g.)
Butyl acetate	5.4	390	7	93	Isobutyl chloride (5.0 g.)
Chloroform	5.2	372	21	79	Hexene
Cyclohexane	3.4	244	12	88	Hexene
Ethanol	1.4	96	38	62	Ethyl vinyl ether, Acetal

a) Calculated as follows: $\frac{\text{mol. of butylene produced} \times 2}{\text{mol. of } PdCl_2 \text{ used}} \times 100$

b) Given as percentage of respective peak area in gas chromatography.

c) The amounts of by-products are generally too small to be determined quantitatively.

chloride from Zeise's salt was eliminated and that a complex of another type was formed as:

$$(C_nH_{2n}\cdot PdCl_2)_2 \rightarrow (C_nH_{2n-1}\cdot PdCl)_2 + 2HCl$$

In our experiments the formation of hydrogen chloride was clearly detected. Therefore, considering the Friedel-Crafts-type reaction caused by a palladous chloride - hydrogen chloride system, as in the case of aluminum chloride, these dimerization reactions may be explained as:

$$CH_2{=}CH_2 \xrightarrow[HCl]{PdCl_2} [CH_3{-}\overset{\oplus}{C}H_2][\overset{\ominus}{PdCl_3}] \xrightarrow{CH_2=CH_2} [CH_3{-}CH_2{-}CH_2{-}\overset{\oplus}{C}H_2][\overset{\ominus}{PdCl_3}] \xrightarrow{H^-\text{-shift}} CH_3{-}CH_2{-}\overset{\oplus}{C}H{-}CH_3$$

$$\longrightarrow \begin{cases} \xrightarrow{-H^+} \begin{cases} CH_3{-}CH{=}CH{-}CH_3 \\ CH_3{-}CH_2{-}CH{=}CH_2 \end{cases} \\ \xrightarrow{CH_3\text{-shift}} CH_2{-}\underset{CH_3}{\underset{|}{CH}}{-}CH_3 \xrightarrow{Cl^-} ClCH_2CH\begin{matrix} CH_3 \\ CH_3 \end{matrix} \end{cases}$$

Although the reaction may be explained by the proton - shift mechanism in the case of a metal carbonyl catalyst, the hydride-ion-shift mechanism seems adequate for a palladous chloride catalyst, considering that the effects of solvents on the reaction are quite opposite. Moreover, the fact that the yield of butylene decreases upon a decrease in the dielectric constant of solvents agrees with Pepper's work.[6] However, such polar solvents as acetic acid or ethanol, which have a cocatalytic character in themselves showed either an exceptionally large or an exceptionally small yield of butylene. On the other hand, esters would have a peculiar solvent effect, resulting in a remarkable yield of isobutyl chloride.

Experimental

Apparatus.—A stainless-steel autoclave equipped with a magnetic stirrer was used.

6) D. C. Pepper, *Trans. Faraday Soc.*, **45**, 397 (1949).

Reagents.—Palladous chloride: A commercial product of an extra pure grade was used.

Ethylene: Commercial ethylene in a cylinder was used.

Solvents: Commercial solvents were purified and dried as usual before use.

Palladous chloride (8.8 g.; 0.05 mol.) and 40 ml. of solvent were charged into the autoclave and compressed to 60 kg./cm^2 (at room temperature) with ethylene. The autoclave was stirred at room temperature for about half an hour to dissolve the ethylene in the solvent sufficiently, heated to a desired temperature, and again stirred during the reaction. Table I summarizes the reaction conditions for each solvent.

In these cases where a violent absorption of ethylene was observed, additional ethylene was charged in. After the reaction had ended, the autoclave was cooled to room temperature, the pressure read, and the autoclave was again heated to about 50°C while being stirred in order to expel the gaseous products. The gas was passed through cold a trap cooled with dry ice - methanol and a washing bottle containing distilled water to absorb the hydrogen chloride, and then collected in a gas holder. The liquid condensed in the cold trap was vaporized at room temperature after it had been weighed and they collected in another gas holder. The gases were analyzed by gas chromatography (T. C. P. column, 3 m.; temperature, 40°C.; H_2 flow rate, 17.5 cc./min.).

The liquid product was separated from the catalytic residue by filtration and distilled. The distillates were analyzed by gas chromatography, using such proper column packing materials as tricresyl phosphate, polyethylene glycol, and dinonyl phthalate.

BULLETIN OF THE CHEMICAL SOCIETY OF JAPAN VOL. 39 2023—2026 (1966)

The Cyclisation of Anthrimides to Carbazoles. III.* The Structure of Indanthrene Gray A

By K. S. NAIR and K. H. SHAH

Department of Chemical Technology, University of Bombay, Matunga, Bombay 19, India

(Received September 24, 1965)

The anthraquinonyl amino group of the 1, 2'-dianthrimide type, when included in the complex structure of vat dyes, does not cyclise to yield a carbazole structure, with alkali, under the conditions of isoviolanthrone formation; rather, it cleaves to yield an alizarin-type derivative under the conditions of violanthrone formation. The constitution assigned to Indanthrene Gray A (Colour Index No. 60020) has thus been confirmed.

An anthraquinonyl amino group of the 1, 2'-dianthrimide type, when included in the complex structure of such vat dyes as Indanthrene Gray M and Indanthrene Olive T, has been proved to be present as such and not as carbazole (a cyclised structure) during their formation by means of mild treatment with alcoholic alkali.[1] The action of alkali on the 1, 2'-dianthrimide type under conditions of isoviolanthrone and violanthrone fusion needs to be studied further, for 1, 1'-dianthrimide is known to cyclise to a carbazole at 180—230°C.[2]

The Action of Alkali under Conditions of Isoviolanthrone Fusion.—Indanthrene Gray A (Colour Index No. 60020) is manufactured by the condensation of bis (9-bromo-3-benzanthronyl) sulphide (Ib) with two moles of 1-aminoanthraquinone to yield (Ic), and by subsequent fusion with alkali. The dye is assigned the IIIc structure, which contains an isoviolanthrone nucleus and 1, 2'-dianthrimide-type groups.

Isoviolanthrone is formed from bis (3-benzanthronyl) sulphide (Ia) by treatment with isobutanolic alkali at 140°C.[3] Therefore, the assumption of the formation of isoviolanthrone in this case is justified. The dye is obsolete, however, and no manufacturing details are available. The following process was standardised in order to obtain an authentic specimen of the dye. 9-Bromo-3-nitrobenzanthrone, upon being heated with sulphur in trichlorobenzene, gave bis (9-bromo-3-benzanthronyl) disulphide (IIb)[4], which was converted to sulphide (Ib) upon being heated with phenol.[5] The sulphide was condensed with 1-amino-anthraquinone to yield (Ic). The authentic

* Part II: *Indian J. Chem.*, **3**, 273—275 (1965).

1) S. R. Koppikar, K. H. Shah and K. M. Shah, *Indian J. Chem.*, **2**, 361-64 (1964).

2) W. Bradley and C. R. Thitchener, *J. Chem. Soc.*, **1953**, 1085.

3) British Intelligence Objectives Sub-committee, Final Report No. 1363 (Catholic Press India), **35**, (1949).

4) P. Nawiasky, E. Holzapfeb and O. Braunsdorf, D. R. Pat. 443021 (To I. G. Farbenindustrie AKT-GES), March 31, 1927: *Friedlaender*, **15**, 727 (1927).

5) P. Nawiasky, E. Holzappel and O. Braunsdorf, D. R. Pat. 441465 (To I. G. Farbenindustrie AKT-GES), Feb. 17, 1927; *Friedlaender*, **15**, 730 (1927).

dye was obtained by treating (Ic) with isobutanolic potassium hydroxide at 140°C for two hours. It was a dark blue powder which dissolved in concentrated sulphuric acid with a deep olive green colour and dyed cotton from an alkaline dithionite vat a grayish blue. It did not contain sulphur. It was analysed as $C_{62}H_{30}N_2O_6$ and exhibited λ_{max} at 250, 275, 310, 360, 410, 660, 730 mμ in sulphuric acid and two bands at 1675 and 1645 cm^{-1} in its infrared spectrum.

Bradley[6] has recorded the spectral characteristics of violanthrone (λ_{max} at 223, 385, 573, 760, and 845 mμ) and isoviolanthrone (λ_{max} at 220, 270, 390, 668, 732 mμ) in sulphuric acid. The spectra of the dye indicated the presence of an isoviolanthrone nucleus in the dye.

Venkataraman[7] has observed that anthrimides exhibit an λ_{max} in the 360 mμ region and two bands at 1670—1664 and 1665—1630 cm^{-1} in their infrared spectra, and carbazoles, a broad band in the 508 mμ region and one band at 1666 cm^{-1} in their infrared spectra. On this basis the spectrum of the dye indicated the presence of uncyclised anthrimide groups.

An unambiguous synthesis of the structure IIIc was carried out by condensing 2, 11-diamino isoviolanthrone with 1-chloroanthraquinone in naphthalene in the presence of copper oxide. The product exhibited chemical and spectral properties identical with those of the above product. The compound IIIc was cyclised with aluminium chloride in nitrobenzene. Crystallisation from nitrobenzene gave blue black needles which dissolved in concentrated sulphuric acid with a bluish green colour and which had no affinity for cotton from an alkaline dithionite vat. It exhibited λ_{max} at 270, 310, 380, 410, 500, 665, and 735 mμ and a band at 1670 cm^{-1} in the infrared spectrum and so can be assigned the structure IV.

The Action of Alkali under Conditions of Violanthrone Fusion.—Fierz-David[8] has suggested the structure V for the product obtained by the alkali fusion of 9-(1-anthraquinonyl amino) benzanthrone (VIc). The structure assumes the formation of a carbazole ring and a violanthrone nucleus. Fierz-David assumes cyclisation to take place at the 2, 13-positions of the violanthrone nucleus. However, 1, 2'-dianthrimide cyclises at 1', 2-positions with titanium tetrachloride.[9] Therefore, the cyclisation probably takes place at 4, 11-positions, as in VII.

Bradley[2] has observed that the action of fused alkali on 1, 2'-dianthrimide yields alizarin as the main product. 1, 2'-Dianthrimide type structures, unlike 1, 1'-dianthrimide, do not cyclise under the conditions of alkali fusion to yield carbazole, but they cleave to yield alizarin-type derivatives. Therefore, confirmation is essential for the structure V.

The fusion of VIc with potassium hydroxide at 220°C gave a violet substance which did not contain nitrogen; it was analysed as $C_{34}H_{16}O_6$, and its infrared spectra indicated the presence of the

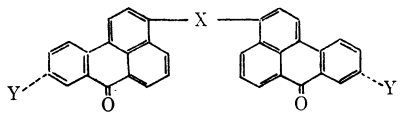

(I) X=-S- ; (II) X=-S-S-

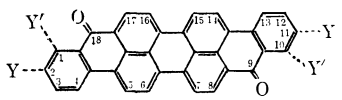

(III)

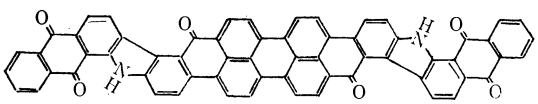

(IV)

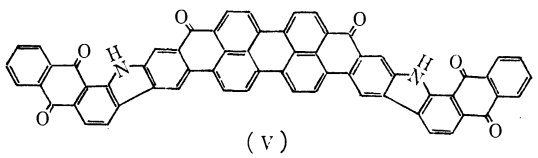

(V)

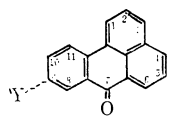

(VI)

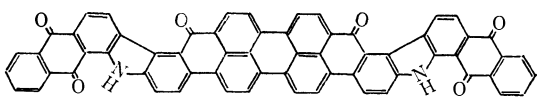

(VII)

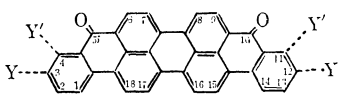

(VIII)

a, Y=H
b, Y=Br
c, Y=1-anthraquinonyl amino
Y'=H if present
d, Y=Y'=-OH

6) W. Bradley and F. K. Sutcliffe, *J. Chem. Soc.*, **1952**, 2118.
7) K. Venkataraman, *J. Indian Chem. Soc.*, **1961**, 205.
8) H. Fierz-David, *Friedlaender*, **16**, 1159 (1927).
9) H. J. Lecher, M. Scalera and W. S. Forster, U. S. Pat. 2416931 (To American Cyanamide Co.); *Chem. Abstr.*, **41**, 5151-i (1947).

hydroxyl group. It showed λ_{max} in sulphuric acid at 385, 500, 580, 630, 765, 845 mμ, indicating the presence of a violanthrone nucleus, and gave a tetrachloroacetoxy derivative. This substance can be assigned the structure VIIId. It dyed cotton a greenish violet from an alkaline dithionite vat and dissolved in concentrated sulphuric acid with a greenish blue colour.

Similarly, the fusion of Ic with caustic potash at 220°C gave a product which did not contain nitrogen. It was analysed for $C_{34}H_{16}O_6$ and gave a tetrachloroacetoxy derivative. It exhibited λ_{max} in sulphuric acid at 380, 490, 635, 670 and 740 mμ, showing the presence of isoviolanthrone, and its infrared spectrum indicated the presence of a hydroxyl group. It dissolved in concentrated sulphuric acid with a bluish green colour and dyed cotton from an alkaline dithionite vat a greenish violet. It can be assigned the structure IIId.

An authentic specimen of VII was obtained as follows: 3, 12-Diamino violanthrone was condensed with 1-chloroanthraquinone. The product exhibited two bands at 1675 and 1650 cm^{-1} in its infrared spectrum and λ_{max} at 315, 365, 385, 405, 570, 765 and 845 mμ. It dyed cotton a grayish blue and dissolved in concentrated sulphuric acid with a dark bluish green colour: it was analysed as $C_{62}H_{30}N_2O_6$(VIIIc). Treatment with aluminium chloride gave a product exhibiting a band at 1660 cm^{-1} in the infrared spectrum and λ_{max} in sulphuric acid at 310, 395, 405, 510, 570, 765 and 840 mμ. It gave a greenish blue colour in concentrated sulphuric acid and had no dyeing property. This shows that the cyclisation has taken place as in VII.

Experimental

Bis(9-bromo-3-benzanthronyl) Sulphide (Ib).—9-Bromo-3-nitrobenzanthrone (5 g.) was stirred under reflux with sulphur (15 g.) in trichlorobenzene (120 g.) for three hours. The trichlorobenzene was then steam-distilled, and the product IIb was collected. Crystallisation from *o*-dichlorobenzene gave yellow plates, m. p. 320° (3 g.). The above product (3 g.) was then stirred with phenol (15 g.) for 8 hr. at 180°C. The yellow product (2 g.) obtained after dilution with alcohol (30 ml.) was crystallised from *o*-dichlorobenzene in the form of yellow needles, m. p. above 300°C.

Found: S, 4.5. Calcd. for $C_{34}H_{16}Br_2O_2S$: S, 4.9%.

Bis- 9, 9'-di(1-anthraquinonylamino) - 3 - benzanthronyl Sulphide (Ic).—Ib (1.7 g.), 1-aminoanthraquinone (1.2 g.), anhydrous sodium carbonate (0.60 g.), and a trace of copper oxide were stirred under reflux in naphthalene (12 g.) for 24 hr. The product (2.5 g.) was collected after the naphthalene had been removed by steam distillation and the copper oxide had been removed by washing it with dilute hydrochloric acid. Crystallisation from nitrobenzene gave deep brown needles.

Found: N, 3.4; S, 3.3. Calcd. for $C_{62}H_{32}N_2O_6S$: N, 3.0; S, 3.4%.

Indanthrene Gray A.—One gram of Ic was added to a mixture of caustic potash (2 g.) in isobutanol (4 g.) at 70°C and the mixture was then stirred at 140°C for 2 hr. After dilution with water and air oxidation, a blue black residue was collected. Crystallisation from nitrobenzene gave blue black needles. They dissolved in concentrated sulphuric acid with a deep olive green colour and dyed cotton from an alkaline dithionite vat a grayish blue. λ_{max} in concentrated sulfuric acid: 250, 275, 310, 360, 410, 660, 730 mμ. IR: 1675 and 1645 cm^{-1}.

Found: C, 82.7; H, 3.0; N, 2.7. Calcd. for $C_{62}H_{30}N_2O_6$: C, 82.9; H, 3.3; N, 3.1%.

2, 11-Bis(1-anthraquinonylamino)isoviolanthrone (IIIc).—2, 11-Diamino isoviolanthrone (2 g.), 1-chloroanthraquinone (2 g.), anhydrous sodium carbonate (0.8 g.) and traces of copper oxide were stirred under reflux in naphthalene (25 g.) for 48 hr. The product, collected after steam distillation, was washed free of copper. It crystallised from nitrobenzene in the form of blue-black needles. It showed spectral properties and colour reactions identical to those of the above product.

Found: C, 82.5; H, 3.5; N, 3.4. Calcd. for $C_{62}H_{30}N_2O_6$: C, 82.9; H, 3.3; N, 3.1%.

The Cyclisation of IIIc.—One gram of IIIc was stirred with anhydrous aluminum chloride (4 g.) and nitrobenzene (25 ml.) at 140°C for six hours. The resulting mixture was steam-distilled to remove the nitrobenzene. The product gave blue-black needles on crystallisation from nitrobenzene. It dissolved in concentrated sulphuric acid with a bluish green colour and had no affinity for cotton from an alkaline dithionite vat. λ_{max} in concentrated sulphuric acid at 270, 310, 380, 410, 500, 665 and 735 mμ. IR.; 1670 cm^{-1}.

Found: N, 2.9. Calcd. for $C_{62}H_{26}N_2O_6$: N, 3.1%.

3, 4, 11, 12-Tetrahydroxy Violanthrone (VIIId).—9-(1-Anthraquinonyl amino) benzanthrone (1 g.) was added to molten caustic potash (8 g.) at 220°C, and then the mixture was stirred for 30 min. at the same temperature. The product was collected after dilution with water and aerial oxidation for one hour. Repeated crystallisations from nitrobenzene gave bluish-violet needles (0.35 g.). The product dissolved in concentrated sulphuric acid with a blue colour and dyed cotton from an alkaline dithionite vat a greenish violet. λ_{max} in sulphuric acid at 385, 500, 580, 630, 765, and 845 mμ, and IR: 3350 cm^{-1}.

Found: C, 78.6; H, 4.0. Calcd. for $C_{34}H_{16}O_6$: C, 78.5; H, 3.1%.

The Chloroacetoxy Derivative of VIIId. — The above compound (1 g.) and chloroacetyl chloride (6 ml.) were stirred under reflux for 8 hr. The resulting product (1.2 g.) was collected after dilution with water. Crystallisation from nitrobenzene gave brownish-black needles which dissolved in concentrated sulphuric acid with a greenish blue colour and which dyed cotton from an alkaline dithionite vat a greenish violet.

Found: Cl, 17.6. Calcd. for $C_{42}H_{20}Cl_4O_{10}$: Cl, 17.2%.

1, 2, 10, 11-Tetrahydroxy Isoviolanthrone (IIId).—One gram of Ic was added to molten caustic potash at 220°C and the mixture was stirred for 30 min. The residue was collected after dilution with water and air oxidation. Crystallisation from nitrobenzene gave

blue-black needles (0.30 g.). They dissolved in concentrated sulphuric acid with a bluish green colour and dyed cotton from alkaline dithionite vat a greenish violet. The product did not contain nitrogen; λ_{max} in sulphuric acid at 380, 490, 635, 670 and 740 mμ, and IR: 3350 cm^{-1}.

Found: C, 78.2; H, 3.8. Calcd. for $C_{34}H_{16}O_6$: C, 78.5; H, 3.1%.

The Chloroacetoxy Derivative of IIId.—The above product, IIId (1 g.), was refluxed with chloroacetyl chloride (6 ml.) for 8 hr. The resulting product (1.1 g.) was collected after dilution with water. It crystallized from nitrobenzene in brownish-blue needles which dissolved in sulphuric acid with a greenish blue colour and which dyed cotton from an alkaline dithionite vat a greenish violet.

Found: Cl, 16.8%. Calcd. for $C_{42}H_{20}Cl_4O_{10}$: Cl, 17.2%.

3, 12 - Bis(1 - anthraquinonylamino)violanthrone (VIIIc).—3, 12-Diaminoviolanthrone (2 g.), 1-chloroanthraquinone (2 g.), anhydrous sodium carbonate (0.80 g.), and a trace of copper oxide were stirred under reflux in naphthalene for 48 hr. The product was collected after steam distillation.

It crystallised from nitrobenzene in the form of grayish blue needles which dissolved in concentrated sulphuric acid with a greenish blue colour. It dyed cotton from an alkaline dithionite vat a grayish blue. λ_{max} in sulphuric acid: 315, 365, 385, 405, 570, 765, and 845 mμ. IR: 1675, 1650 cm^{-1}.

Found: C, 82.6; H, 3.2; N, 2.8. Calcd. for $C_{62}H_{30}N_2O_6$: C, 82.9; H, 3.3; N, 3.1%.

The Cyclisation of VIIIc.—The substance VIIIc (2 g.) and anhydrous aluminum chloride (8 g.) and nitrobenzene (40 ml.) were stirred at 140°C for 6 hr. The product obtained after steam distillation gave a blue-black powder from nitrobenzene. It dissolved in concentrated sulphuric acid with a greensish blue colour and had no dyeing property. λ_{max} in sulphuric acid at 310, 395, 405, 510, 570, 765 and 845 mμ IR: 1660 cm^{-1}.

Found: N, 2.8. Calcd. for $C_{68}H_{26}N_2O_6$: N, 3.1%.

BULLETIN OF THE CHEMICAL SOCIETY OF JAPAN VOL. 39 2026—2040 (1966)

The Effects of Magnesium Fluoride on the Thermal Behavior of Serpentine*

By Hanzo MASE and Tomoyuki FUKUDA

Department of Applied Chemistry, Faculty of Industry, Iwate University, Ueda, Morioka

(Received October 7, 1965)

By means of thermogravimetric, differential thermal, and X-ray diffraction techniques, the thermal behavior of a mixture of serpentine (heated at 730°C for 1 hr.) with 31 per cent magnesium fluoride and or mixtures of serpentine with 10, 15.5, 20, 31, 40, and 62 per cent magnesium fluoride were examined at various temperatures up to 1450°C and for various heating periods. The presence of magnesium fluoride affects the shapes of serpentine thermogravimetric and differential thermal curves, but it hardly affects the starting temperatures of the dehydroxylation of the serpentine (730°C) at all. The thermogravimetric curves showed a gradual weight loss above the dehydroxylation temperature of serpentine. In the differential thermal curves, the height reduction of two serpentine exothermic peaks (830°C and 1100°C), and the appearance of two or three endothermic peaks above 1000°C were observed; moreover, a mixture of the preheated serpentine with 31 per cent magnesium fluoride showed a new exothermic peak at 775°C. These effects of magnesium fluoride were discussed. The main heating products of serpentine in the presence of magnesium fluoride were fluorine norbergite, forsterite, magnesioferrite, and magnesium oxide, whereas those of serpentine alone were forsterite and enstatite.

It is well known that the formation of mullite from kaolinite occurs above 1000°C. Recently Bien and Keyser[1] have shown that mullite can be formed at a temperature as low as 600°C (i. e., immediately after the dehydroxylation of kaolinite) through the action of aluminum fluoride. Locsci[2,3] has also elucidated that aluminum fluoride reacts with kaolinite via an intermediate, topaz $Al_2(F, OH)_2SiO_4$, below 575°C to form $Al_6F_6Si_2O_9$ (veszpremite, metakaolinite fluoride), which decomposes rapidly at 800°C to 900°C to form mullite.

Crystallographically speaking, serpentine is composed of magnesium hydroxylphyllosilicate and is very similar to kaolinite, which is composed of

*1 Part XII of "Studies of the Utilization of Serpentine and Olivine."

1) A. Bien and W. L. Keyser, *Mineral. Mag.*, **4**, 80 (1963).

2) B. P. Locsci, *Veszpremi Vegyip. Egyet. Kozlemin.*, **6** (3), 217 (1962), *Chem. Abstr.*, **60**, 10250f (1964).

3) B. P. Locsci, *Keram. Z.*, **16** (6), 350 (1964); *Interceram.*, **1964**, No. 1, 28—29.

aluminum hydroxylphyllosilicate. Therefore, it seems reasonable to assume that magnesium fluoride might contribute to the formation of forsterite and enstatite, which are the stable high-temperature phases of the silica-magnesia system, at a relative lower temperature on the thermal decomposition of serpentine.

Experimental

Materials.—The serpentine used was rock from Kuroishimori (Iwate Prefecture) crushed to powder passable through a 200 mesh sieve with the composition: SiO_2 39.29, Fe_2O_3 7.09, Al_2O_3 2.54, CaO 1.10, MgO 38.02 (ignition loss 12.51, moisture 1.20 per cent). Its thermal behavior was determined by following the thermogravimetric analysis (TGA) and differential thermal analysis (DTA) (Figs. 1 and 2 respectively).

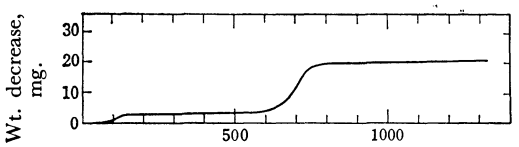

Fig. 1. TGA curve of serpentine.
Sample: 0.3 g.

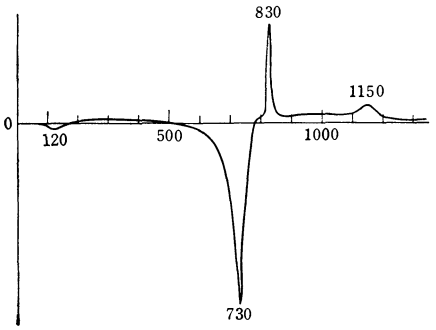

Fig. 2. DTA curve of serpentine.
Sample: 0.890 g.

Figures 1 and 2 indicate that serpentine was endothermally dehydroxylated between 500 and 700°C, and that its original structure was destroyed with a loss in weight and changed exothermally to forsterite and silica at about 800°C without a weight loss.[4-6]

The magnesium fluoride employed was of a G. R. grade of commercial origin (Morita Chemicals Co., Ltd.). Its thermal behavior was shown by TGA and DTA curves (Figs. 3 and 4 respectively), which indicated that the magnesium fluoride hardly changes in weight

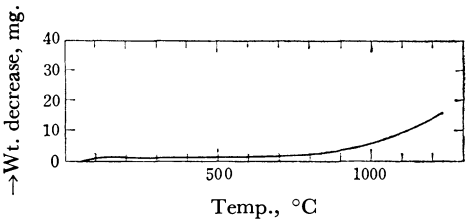

Fig. 3. TGA curve of magnesium fluoride.
Sample: 0.4137 g.

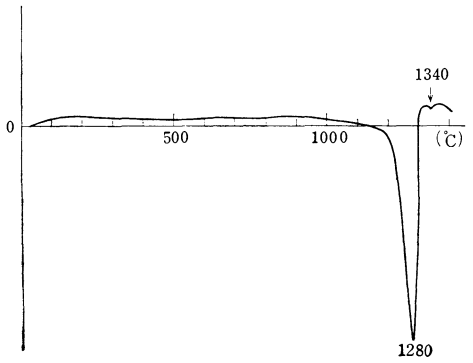

Fig. 4. DTA curve of magnesium fluoride.
Sample: 0.850 g.

up to about 790°C, but that it gradually decreases in weight above 790°C and begins to melt at about 1180°C.

Six mixtures of serpentine were prepared, with 10, 15.5, 20, 31, 40, and 62 per cent mangesium fluoride respectively. Moreover, a mixture of the serpentine (heated at 730°C for 1 hr.) was prepared with 31 per cent magnesium fluoride (hereafter referred to as the preheated mixture (31 per cent). These powdered mixtures were homogenized in a dry state. Of these mixtures, those containing 15.5, 31, and 62 per cent magnesium fluoride (hereafter referred to as the 15.5, 31, and 62 per cent mixtures respectively) give materials with the following compositions if it is assumed that serpentine reacts stoichiometrically with magnesium fluoride:

(15.5 per cent) $2\,Mg_3Si_2O_5(OH)_4 + 2\,MgF_2 \rightarrow 3\,Mg_2SiO_4 + 2\,MgO + SiF_4 + 4\,H_2O$

(31 per cent) $Mg_3Si_2O_5(OH)_4 + 2\,MgF_2 \rightarrow Mg_2SiO_4 + 3\,MgO + SiF_4 + 2\,H_2O$

(62 per cent) $Mg_3Si_2O_5(OH)_4 + 4\,MgF_2 \rightarrow 7\,MgO + 2\,SiF_4 + 2\,H_2O$

The ignition losses calculated from these idealized chemical equations are 25.94, 34.87, and 46.38 per cent respectively.

Methods.—A Shimadzu X-ray Diffractometer (GX-A type) with a Geiger Counter was used with Cu$K\alpha$ radiation. The operating conditions were as follows:

Target, Cu; Scatter slit, Not placed;
Filter, Ni; Full scale count, 500 or 1000 c. p. s.;
Voltage, 35 kV.; Scanning speed, 2deg./min.;

4) H. Heraldsen, *C. Min. A.*, **1928**, 311; S. Caillire, *Compt. rend.*, **196**, 628 (1933).
5) R. Kiyoura and Y. Ito, *J. Ceram. Assoc. Japan (Yogyo Kyokai Shi)*, **16**, 525 (1953).
6) H. Mase, *J. Chem. Soc. Japan, Ind. Chem. Sect. (Kogyo Kagaku Zasshi)*, **60**, 1502 (1957); **62**, 793, 895 (1959).

Current, 15 m amp.; Time constant, 5 sec.;
Divergence slit, 1 mm.;
2θ range measured, 16—70°;
Receiving slit, 0.25 mm.; Chart speed, 20 mm./min.

The TGA and DTA measurements of the mixtures (15.5 and 31 per cent) were carried out at the Shimadzu Analytical Centre. The operating conditions were as follows:

	TGA	DTA
Neutral material	—	α-Al_2O_3
Atmosphere	Air	Air
Sensitivity	200 mg./full scale	100 μV.
Chart speed	2 min./div.	2 min./div.
Heating velocity	12°C/min.	12°C/min.
Sample holder	TB-2S	BHL-2IV.

However, the sample with 62 per cent magnesium fluoride was measured with a Shimadzu Recording Differential Thermal Analysis Apparatus and its attached Thermobalance (DT-2A and TB-2 types, respectively) in our laboratory. The operating conditions were the same as the above except for the following factors:

	TGA	DTA
Sensitivity	100 mg./full scale	—
Chart speed	4 min./div.	4 min./div.
Heating velocity	10°C/min.	10°C/min.

Results and Discussion

Weight Losses During Heating.—Three mixtures (15.5, 31, and 62 per cent) were examined by TGA. The results obtained are shown in Fig. 5, together with that for a preheated mixture (31 per cent). Figure 5 shows that both the mixtures (15.5 and 31 per cent) have two weight losses in the region up to about 800°C—namely, the dehydration of serpentine and magnesium fluoride between 30 and 130°C, and the dehydroxylation of serpentine starting at about 580°C. When these mixtures are heated above 750°C, gradual weight losses are observed up to about 1450°C, whereas pure serpentine shows no weight loss in this temperature region (Fig. 1). These results suggest that magnesium fluoride may affect the starting temperature of the dehydroxylation of serpentine hardly at all, and that a weight loss above 750°C may be closely related to the thermal changes of magnesium fluoride.

Differential Thermal Analysis and X-Ray Diffraction Analysis.—The presence of magnesium fluoride markedly affects the height of the serpentine endothermic and exothermic peaks. This is well shown by the DTA curves in Fig. 6 obtained for the mixtures with magnesium fluoride. These curves and that for serpentine alone (Fig. 2) resemble one another very closely up to 750°C; in this region, endothermic effects due to the dehydration of serpentine and magnesium fluoride and to the dehydroxylation of serpentine were observed. An increase in the amount of magnesium

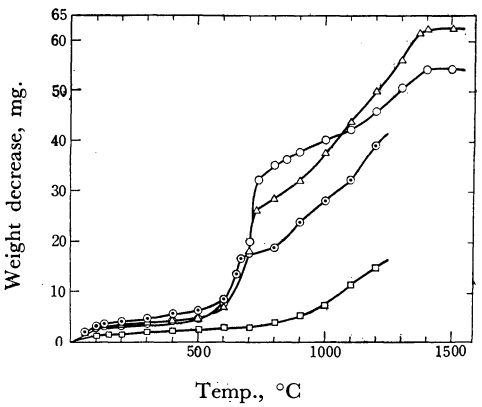

Fig. 5. TGA curves of mixtures of serpentine with magnesium fluoride.
○ 15.5% MgF_2; △ 31% MgF_2;
◉ 62% MgF_2; □ Preheated mixture (31%)
Sample: 0.3 g.

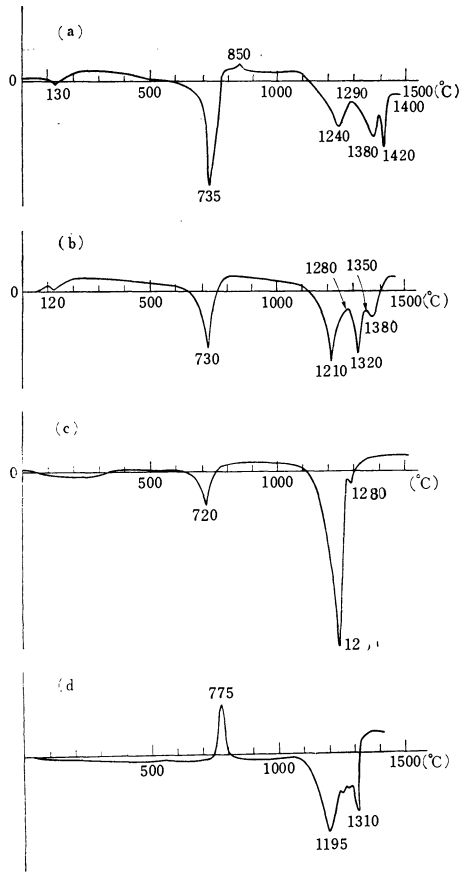

Fig. 6. DTA curves of mixtures of serpentine with magnesium fluoride.
(a) 15.5% MgF_2; Sample: 0.896 g.
(b) 31% MgF_2; Sample: 0.896 g.
(c) 62% MgF_2; Sample: 0.8841 g.
(d) Preheated mixture (31% MgF_2); Sample: 0.805 g.

fluoride markedly reduced the height of the endothermic peak at about 730°C.

With the 15.5 and 31 per cent mixtures, three endothermic peaks appear above 1000°C. Each of these 15.5 per cent mixture peaks was situated at higher temperatures than those of the 31 per cent mixture. On the other hand, the 62 per cent mixture shows a sharp and large endothermic peak near 1250°C and a weak and small endothermic one at 1290°C.

The preheated mixture (31 per cent) shows no endothermic peak below 1000°C, because the serpentine has been completely dehydroxylated, but it does show an exothermic peak at 775°C and two endothermic peaks above 1000°C, which are situated at lower temperatures than those of the 31 per cent mixture. In order to make clear the crystallographic significance of these peaks, each of the

Table I. Results of X-ray diffraction analysis for mixtures of serpentine of preheated serpentine with various percentages of magnesium fluoride and their products heated at various temperatures and for various periods*

(1) 10% MgF_2

Raw sample			700°C, 1 hr.			700°C, 2 hr.			800°C, 1 hr.		
19.75°	w	S	19.70°	w	S	17.4°	vw	F	17.4°	w	F
$_{1}$24.65	s	S	$_{1}$24.6	s	S	23.0	vw	F	$_{7}$23.0	m	F
$_{5}$27.4	m	M	$_{4}$27.5	w	M	25.6	vw	F	$_{10}$25.6	w	F
$_{3}$35.75	m	S	$_{2}$36.1	w	S	27.1	vw	M	27.35	vw	M
$_{2}$36.0	m	S	$_{3}$36.9	w	S	$_{5}$32.4	w	F	$_{3}$32.4	m	F
$_{4}$36.8	m	S	40.7	vw	M	$_{1}$35.9	m	F, MF	$_{2}$35.85	m	F, MF
40.6	w	M	53.75	w	M	$_{2}$36.6	m	F	$_{1}$36.65	m	F
53.75	w	M	$_{5}$60.4	w	S	39.9	w	F	$_{6}$39.9	m	F
60.3	w	S	68.3	w	M	$_{3}$40.1	m	M	$_{5}$40.2	m	N
60.7	w	M				40.4	m	M	$_{8}$40.4	m	M
68.35	vw	M				$_{4}$52.6	m	F	41.95	vw	F
						62.1	vw	MF	$_{4}$52.5	m	F
						62.9	w	F	53.65	vw	M
						67.25	vw	F	62.25	w	F
									$_{9}$63.0	w	MF
									67.35	w	F

(2) 15.5% MgF_2

Raw sample			700°C, 1 hr.			800°C, 1 hr.			1070°C, 1 hr.		
19.7°	w	S	19.7°	w	S	17.4°	vw	F	17.4°	w	F
$_{1}$24.6	s	S	$_{1}$24.65	m	S	$_{6}$23.0	w	F	$_{8}$23.0	m	F
$_{2}$27.45	m	M	$_{2}$27.65	w	M	25.75	vw	F	24.0	w	F
$_{4}$36.0	w	S	36.25	w	S	$_{9}$27.35	w	M	$_{10}$29.3	vw	N
36.75	w	S	$_{4}$36.9	w	S	$_{10}$29.3	vw	N	27.0	w	N
$_{3}$40.6	w	M	$_{3}$40.7	m	M	29.9	vw	F	29.85	w	F
43.8	w	M	44.0	w	M	$_{7}$32.4	w	F	30.40	vw	MF
$_{5}$53.75	w	M	$_{5}$53.75	w	M	34.1	vw	N	$_{5}$32.45	m	F
56.5	vw	M	56.5	vw	M	$_{1}$35.85	m	F, MF	$_{1}$35.8	m	F, MF
60.45	w	S	60.5	w	S	$_{2}$36.65	m	F	$_{4}$36.60	m	F
60.8	w	M	60.8	w	M	38.55	vw	N	38.45	vw	N
68.3	w	M	68.3	w	M	39.8	vw	F	39.0	vw	N
						$_{4}$40.15	w	N	$_{9}$39.8	w	F
						$_{3}$40.5	w	M	$_{2}$40.15	m	N
						41.85	vw	F	41.9	vw	F
						43.8	vw	M	$_{7}$52.4	w	F
						$_{5}$52.55	w	F	$_{3}$52.8	m	N
						53.6	w	N	55.1	vw	F
						55.15	vw	F	57.1	vw	N
						$_{8}$63.00	w	MF	57.6	w	MF
						68.25	vw	M	58.95	vw	F, N
						69.75	vw	F	62.05	vw	F
									$_{6}$63.0	w	MF
									67.2	w	F
									69.75	w	F

(TABLE I. continued)

1290°C, 1 hr.			1380°C, 1 hr.			1420°C, 1 hr.		
17.4°	w	F	17.45°	w	F	17.45°	m	F
$_4$22.95	w	F	$_4$23.0	m	F	$_5$22.9	m	F
23.95	w	F	23.95	w	F	$_9$23.95	m	F
$_9$25.65	w	F	$_8$25.6	m	F	$_8$25.65	m	F
29.9	w	F	29.9	w	F	29.9	w	F
30.4	vw	MF	30.4	vw	MF	30.4	vw	MF
$_3$32.4	m	F	$_3$32.45	m	F	$_3$32.35	s	F
$_1$35.85	s	F, MF	$_1$35.8	s	F, MF	$_1$35.85	s	F, MF
$_2$36.65	s	F	$_2$36.65	s	F	$_2$36.65	s	F
38.4	vw	N	38.4	vw	N	38.4	w	N
$_7$39.8	m	F	$_7$39.8	m	F	$_6$39.8	m	F
$_8$40.15	m	N	$_6$40.15	m	N	$_7$40.15	m	N
41.9	w	F	41.9	w	F	41.95	w	F
43.5	vw	MF	43.5	vw	MF	43.5	w	MF
$_5$52.4	m	F	$_5$52.45	m	F	$_4$52.45	m	F
55.0	vw	F	55.0	vw	F	55.0	w	F
56.35	vw	F	56.3	w	F	56.35	w	F
57.0	vw	F, N	56.9	w	F, N	56.9	w	F, N
58.9	vw	F, N	58.8	vw	F, N	58.9	w	F, N
$_{10}$62.1	w	F	$_9$62.05	w	F	62.1	m	F
$_6$63.0	m	MF	$_{10}$62.95	w	MF	$_{10}$63.0	m	MF
67.25	w	F	67.20	w	F	67.2	w	F
69.8	w	F	69.95	w	F	69.65	w	F

(3) 20% MgF_2

Raw sample			700°C, 1 hr.			800°C, 1 hr.		
19.75°	w	S	19.75°	w	S	17.40°	w	F
$_1$24.6	s	S	$_1$24.6	s	S	$_{10}$23.0	w	F
$_2$27.4	m	M	$_2$27.4	m	M	24.0	vw	F
$_4$35.9	w	S	$_5$35.9	w	S	25.5	vw	F
36.8	w	S	36.8	w	S	$_5$27.3	m	M
$_3$40.6	m	M	$_3$40.6	m	M	29.25	w	N
43.8	vw	M	43.8	w	M	29.9	vw	F
$_5$53.75	m	M	$_4$53.75	m	M	$_6$32.4	w	F
56.35	w	M	56.35	vw	M	34.05	vw	N
60.45	w	S	60.45	w	S	$_3$35.80	m	F, MF
60.75	w	M	60.75	w	M	$_2$36.55	m	F
68.3	w	M	68.3	vw	M	$_4$40.15	m	N
						$_1$40.50	m	M
						41.80	vw	F
						43.80	vw	M
						$_7$52.50	w	F
						$_8$53.50	w	M
						56.25	w	M
						57.10	vw	F, N
						60.75	vw	M
						62.10	vw	F
						$_9$63.0	w	MF
						68.20	w	M

(TABLE I. continued)

(4) 31% MgF_2

Raw sample			700°C, 1 hr.			800°C, 1 hr.			1070°C, 1 hr.		
19.6°	w	S	23.1°	vw	F	17.4°	w	F	17.25°	vw	N
$_{2}$24.55	m	S	$_{10}$24.6	w	S	20.4	w	N	20.3	vw	N
$_{1}$27.5	s	M	$_{1}$27.4	m	M	21.6	w	N	23.0	vw	F
$_{5}$35.75	m	S	32.5	vw	F	23.0	w	F	24.15	vw	F
36.0	m	S	$_{4}$35.8	S	S	24.0	w	F	25.10	vw	F
$_{3}$36.8	w	S	$_{7}$36.6	w	S	24.2	w	F	25.70	vw	F
$_{3}$40.6	m	M	39.8	vw	F	25.75	w	F	27.65	w	N
43.95	w	M	$_{2}$40.5	m	M	26.9	w	N	$_{6}$29.25	w	N
$_{4}$53.75	m	M	$_{5}$43.8	w	M	$_{6}$27.3	w	M	$_{8}$29.75	w	F
56.5	w	M	52.6	vw	F	$_{2}$29.3	m	N	$_{10}$32.4	w	F, N
60.75	w	M	$_{3}$53.6	w	M	32.4	w	F, N	$_{9}$33.95	w	N
68.25	w	M	$_{8}$56.5	w	M	$_{5}$34.1	w	N	$_{7}$34.5	w	N
			$_{9}$60.8	w	M	$_{10}$35.75	w	F, MF	$_{5}$35.8	m	F, MF
			$_{6}$68.4	w	M	$_{8}$36.6	w	F	36.6	w	F
						37.4	w	N	37.3	vw	N
						38.6	w	N	38.5	vw	N
						$_{4}$40.1	w	N	38.9	w	N
						$_{1}$40.5	m	M	39.25	w	N
						42.0	w	F	$_{1}$40.1	m	N
						43.75	w	M	$_{4}$40.4	m	N
						46.75	w	F, N	46.8	w	F, N
						49.5	w	N	$_{2}$52.75	m	N
						52.4	w	F	57.15	vw	N
						$_{3}$53.2	w	N	57.65	vw	MF
						$_{7}$53.5	w	N	$_{3}$63.0	w	MF
						56.4	w	M	67.0	w	F
						$_{9}$63.2	w	MF			
						68.2	w	M			

1240°C, 1 hr.			1320°C, 1 hr.			1380°C, 1 hr.		
17.6°	vw	F	17.45°	w	F	17.45°	m	F
22.9	vw	F	$_{3}$23.0	m	F	$_{3}$23.0	m	F
$_{10}$24.2	w	F	23.95	w	F	24.0	m	F
25.15	w	F	25.7	w	F	25.65	m	F
$_{9}$25.7	w	F	29.8	w	F, N	29.9	m	F
26.3	vw	N	$_{4}$32.4	w	F, N	$_{4}$32.5	m	F, N
27.8	vw	N	$_{1}$35.8	s	F, MF	$_{2}$35.8	s	F, MF
$_{8}$29.75	w	F	$_{2}$36.65	s	F	$_{1}$36.65	s	F
30.3	vw	MF	38.35	vw	N	38.4	vw	N
$_{6}$32.45	w	F, N	39.0	vw	N	39.0	vw	N
$_{5}$34.5	m	N	$_{7}$39.8	m	F	$_{7}$39.9	m	F
$_{3}$35.8	m	F, MF	$_{8}$40.1	w	N	$_{10}$40.2	m	N
36.6	vw	F	41.9	w	F	42.0	w	F
38.25	vw	N	$_{6}$43.1	m	O	$_{5}$43.2	m	O
39.0	w	N	$_{5}$52.45	m	F	44.7	vw	N
$_{1}$40.1	m	N	55.0	w	F	47.0	vw	F, N
42.1	vw	F	56.3	w	F	48.6	vw	F
$_{7}$43.0	w	O	56.9	w	N	50.5	vw	F
45.5	vw	N	58.75	vw	F, N	$_{6}$52.5	m	F
46.9	vw	F, N	62.1	w	F	55.1	vw	F
48.2	vw	F	$_{10}$62.5	m	O	56.25	w	F
51.0	vw	N	$_{9}$62.8	m	MF	57.0	w	N
$_{2}$52.75	m	N	67.2	w	F	58.8	vw	F, N
57.6	w	N	69.8	w	F	62.25	m	F
62.05	w	F				$_{9}$62.55	m	O
62.4	w	O				$_{8}$62.85	m	MF
$_{4}$63.0	m	MF				67.2	w	F

(TABLE I. continued)

(5) 40% MgF_2

Raw sample			700°C, 1 hr.			1070°C, 1 hr.			1210°C, 1 hr.		
19.6°	w	S	20.9°	vw	N	20.25°	w	N	17.55°	w	F
$_{3}$24.6	m	S	23.0	vw	F	26.7	w	N	18.5	w	F
$_{1}$27.35	s	M	$_{1}$27.35	s	M	$_{9}$27.5	w	N	$_{10}$23.1	w	F
36.0	w	S	32.45	vw	F	$_{1}$29.2	s	N	24.15	w	F
$_{2}$40.5	s	M	$_{8}$35.3	w	M	$_{10}$29.7	w	N	25.8	w	F
43.95	w	M	$_{7}$35.8	w	F, MF	$_{5}$33.9	m	N	26.5	vw	N
$_{4}$53.7	m	M	$_{9}$36.7	w	F	$_{7}$35.8	w	F, MF	30.0	w	F
56.4	w	M	$_{2}$40.5	s	M	$_{8}$37.3	w	N	$_{7}$32.6	w	F
60.75	w	M	$_{5}$43.8	w	M	38.4	w	N	33.8	w	N
$_{5}$68.3	w	M	52.45	vw	F	39.2	vw	N	$_{2}$36.0	m	F, MF
			52.7	vw	N	$_{4}$40.0	m	N	$_{6}$36.8	m	F
			53.05	vw	N	$_{2}$40.4	m	N	37.5	w	N
			$_{3}$53.7	m	M	43.0	vw	O	39.2	w	N
			$_{6}$56.35	w	M	$_{6}$52.75	m	N	$_{9}$39.9	w	F
			$_{10}$60.8	w	M	$_{3}$53.0	m	N	$_{3}$40.15	m	N
			$_{4}$68.25	w	M	53.75	w	N	42.2	vw	F
									$_{1}$43.1	m	O
									52.6	w	N
									$_{4}$52.9	m	N
									54.5	vw	N
									55.1	vw	F
									$_{8}$62.55	w	O
									$_{5}$63.0	w	MF
									69.8	w	F

(6) 62% MgF_2

600°C, 5 hr.			700°C, 1 hr.			1070°C, 1 hr.			1250°C, 1 hr.		
24.5°	w	S	23.0°	vw	F	20.25°	w	N	17.5°	vw	N
$_{1}$27.3	s	M	$_{1}$27.3	s	M	20.7	vw	N	20.4	vw	N
35.3	w	M	32.25	vw	N	26.75	w	N	20.8	vw	N
35.9	w	S	$_{7}$35.25	w	M	$_{3}$27.2	m	M	26.9	vw	N
36.75	vw	S	$_{9}$35.75	w	MF, F	$_{8}$27.8	w	N	$_{3}$27.3	m	M
$_{2}$40.5	s	M	$_{10}$36.7	w	F	$_{2}$29.2	s	N	27.75	m	N
$_{5}$43.85	w	M	$_{2}$40.5	s	M	32.25	vw	N	$_{2}$29.3	s	N
$_{3}$53.65	m	M	$_{5}$43.8	w	M	32.9	vw	N	32.4	vw	N
56.3	w	M	52.5	vw	F	$_{4}$33.85	m	N	$_{4}$34.0	m	N
60.8	w	S	$_{3}$53.65	m	M	35.85	vw	F, MF	35.25	vw	M
63.8	vw	M	$_{6}$56.3	w	M	36.3	vw	N	35.8	vw	F, MF
$_{4}$68.3	m	M	$_{8}$60.75	w	M	$_{9}$37.3	w	N	36.6	vw	N
			63.7	vw	M	$_{10}$38.4	w	N	37.5	w	N
			$_{4}$68.2	w	M	$_{7}$39.85	w	F	38.7	w	N
						$_{1}$40.5	s	M	$_{8}$40.1	m	N
						42.9	vw	O	$_{1}$40.5	s	M
						43.75	w	M	$_{9}$43.0	m	O
						46.75	vw	F, N	43.9	w	F, N
						49.5	vw	N	46.9	vw	F, N
						52.8	w	N	52.9	w	N
						$_{5}$53.0	m	N	$_{5}$53.25	m	N
						$_{6}$53.4	m	M	$_{6}$53.6	m	M
									56.3	vw	M
									57.9	vw	MF
									62.4	w	O
									$_{7}$63.1	m	MF
									64.2	w	M
									$_{10}$68.2	w	M

(TABLE I. continued)

(7) Heated Serpentine + MgF_2 (31%)

Raw sample			775°C, 1 hr.			1075°C, 1 hr.			1195°C, 1 hr.		
17.4°	vw	F	17.4°	vw	F	17.35°	w	F	17.4°	w	F
$_{9}$23.0	w	F	20.5	vw	N	20.5	w	N	18.4	w	N
24.0	vw	F	21.0	vw	N	20.8	w	N	$_{8}$23.05	m	F
25.6	vw	F	23.0	w	F	24.4	vw	F	24.0	w	F
$_{1}$27.4	s	M	24.05	vw	F	26.95	w	N	25.7	w	F
30.0	vw	F	25.65	w	F	27.4	w	M	26.45	vw	N
$_{10}$32.5	w	F	26.85	vw	N	$_{10}$27.8	w	N	29.3	w	N
$_{6}$35.8	w	F, MF	$_{2}$27.35	m	M	$_{1}$29.35	s	N	30.4	w	MF
$_{5}$36.7	w	F	$_{6}$29.3	w	N	32.5	vw	F, N	$_{5}$32.5	m	F, N
39.85	w	F	29.85	w	N	$_{4}$34.1	s	N	33.75	w	N
$_{3}$40.5	s	M	$_{8}$32.5	w	F, N	35.85	w	F, MF	34.85	w	F
41.9	vw	F	34.1	w	N	36.55	w	N	$_{1}$35.85	s	F, MF
$_{7}$43.8	w	M	$_{5}$35.85	w	F, MF	$_{8}$37.5	w	N	$_{4}$36.7	m	F
52.45	w	F	$_{4}$36.7	m	F	$_{9}$38.7	w	N	38.45	vw	N
$_{2}$53.75	s	M	37.6	vw	N	39.35	w	N	39.1	w	N
$_{8}$56.4	w	M	38.6	vw	N	$_{5}$40.15	vw	N	$_{9}$39.8	w	F
60.8	w	M	$_{7}$40.2	w	N	$_{2}$40.6	s	M	$_{2}$40.2	m	N
63.8	vw	MF	$_{1}$40.6	s	M	44.75	vw	N	42.0	w	F
$_{4}$68.25	w	M	41.9	vw	F	46.95	w	N	$_{7}$43.1	m	O
			$_{10}$43.95	w	M	49.75	w	F, N	46.9	vw	F, N
			$_{9}$52.6	w	F	52.6	w	F	48.65	vw	F
			53.3	w	N	$_{7}$53.0	w	N	$_{3}$52.85	m	F
			$_{3}$53.65	m	M	$_{3}$53.3	s	N	55.1	vw	F
			55.15	vw	F	55.8	vw	N	56.35	vw	M
			56.35	w	M	56.3	vw	M	57.1	w	N
			60.8	vw	M	57.95	w	N, F	59.0	vw	N, F
			63.15	w	MF	58.6	w	M	62.15	w	F
			68.25	w	M	60.85	vw	M	$_{10}$62.45	w	O
						$_{6}$63.15	m	F	$_{6}$63.0	m	MF
						68.25	w	M	67.25	w	F
									69.35	w	F

* In this table, the very weak diffraction lines were omitted except when the special need was not seen. Moreover, the figures prefixed in small prints stand for the order in intensity for the main ones. For each specimen:
ffrst column: 2 (°),
second column: intensity of diffraction
(abbr.) s, strong; m, middle; w, weak; vw, very weak
third column: identifiication
(abbr.) S, serpentine; M, magnesium fluoride; F, forsterite;
MF, magnesioferrite; N, fluorine norbergite; O, magnesium oxide
X-ray diffraction data for the raw sample with 62 per cent magnesium fluoride were omitted because those were almost identical with the raw sample with 40 per cent magnesium fluoride.

mixtures was heated at various temperatures and for various heating periods, and then quenched in air. These were then examined by X-ray diffraction analysis. The results are illustrated in Table I.

An Endothermic Effect between 600 and 800°C.—As has been mentioned above, no changes occur below about 600°C except for the dehydration of mixtures occurring below about 200°C. In the case of the 62 per cent mixture, no changes occurred even when it was heated at 600°C for 5 hr. (Table I).

As is generally known, the principal reaction occurring between 600 and 800°C is the dehydroxylation of serpentine; however, in the presence of magnesium fluoride, the following reactions appear to occur successively.

The Formation of Fluorine Norbergite ($Mg_2SiO_4 \cdot MgF_2$).[7]—All the mixtures always gave the characteristic diffraction peaks of fluorine norbergite

7) W. Eitel, "The Physical Chemistry of the Silicates," The University of Chicago Press, Chicago (1952), p. 873.

Table II. The X-ray diffraction data of the products heated immediately below and beyond an exothermic peak (775°C) of a mixture of the preheated serpentine with 31 per cent magnesium fluoride*

700°C			850°C		
17.5°	vw	F	17.4°	vw	F
			20.3	vw	N
			20.7	vw	N
			21.5	vw	N
22.95	vw	F	23.0	w	F
23.85	vw	F	24.0	w	F
25.6	vw	F	25.6	vw	F
			26.8	vw	N
$_{1}$27.3	s	M	$_{2}$27.3	m	M
			29.25	w	N
29.9	vw	F			
30.1	vw	MF			
32.3	vw	F	$_{8}$32.4	w	N, F
			33.25	vw	N
			34.0	vw	N
$_{9}$35.3	w	M	35.3	vw	M
$_{6}$35.8	w	F, MF	$_{5}$35.8	w	F, MF
$_{4}$36.8	w	F	$_{4}$36.75	w	F
			37.4	vw	N
			38.5	vw	N
39.75	vw	F			
			$_{9}$40.1	w	N
$_{2}$40.5	m	M	$_{1}$40.5	m	M
			41.8	vw	F
$_{7}$43.85	w	M, MF	43.85	vw	MF
47.2	vw	M	47.0	vw	M
$_{10}$52.4	w	F	$_{6}$52.5	w	F
			$_{7}$53.2	w	N
$_{3}$53.65	m	M	$_{3}$53.85	w	M
54.9	vw	F			
$_{8}$56.3	w	M	$_{10}$56.3	w	M
			57.0	vw	F
60.75	w	M			
			62.1	vw	F
			63.05	vw	MF
63.7	vw	M			
$_{5}$68.2	w	M	68.2	vw	M
69.5	vw	F	69.6	vw	F

* The figures and abbreviations are all the same as those in Table I.

when heated at 700°C or 800°C for 1 hr. The mixtures with higher contents of magnesium fluoride (e. g., 40 or 62 per cent) formed fluorine norbergite at 700°C for 1 hr., while, on the contrary, those with lower contents of magnesium fluoride (10, 15.5, 20, or 31 per cent) formed fluorine norbergite at 800°C for 1 hr. However, even in the latter cases, the serpentine has been dehydroxylated by heating at 700°C and above for 2 hr. Therefore, it is evident that a larger amount of magnesium fluoride facilitates the formation of fluorine norbergite at lower temperatures. As is shown in Table I, the number and intensity of the characteristic peaks of fluorine norbergite decrease with the amount of magnesium fluoride and with the rise in the heating temperatures; namely, its diffraction peaks were intensified as the heating temperature was elevated, showing maximum values at about 1000°C, but being generally reduced above 1070°C. However, the 62 per cent mixture formed a product chiefly consisting of fluorine norbergite when treated even at 1250°C for 1 hr., although the 10 per cent mixture gave a product mainly consisting of forsterite when treated at 800°C for 1 hr.

The preheated mixture (31 per cent) displayed an exothermic peak at 775°C, without any endothermic effect below 1000°C on its DTA curve. The product heated at 775°C for 1 hr. clearly showed the presence of fluorine norbergite; furthermore, the product heated immediately beyond the exothermic peak temperature (850°C) showed the absence of fluorine norbergite (Table II). Therefore, the formation of fluorine norbergite appears to be exothermic.

As has been mentioned above, the endothermic peak due to the dehydroxylation of serpentine at about 730°C was reduced with an increase in the amount of magnesium fluoride. This seems to be due not only to the decreased amount of serpentine, but also, at the same time, to the overlapping of the exothermic effect of the formation of fluorine norbergite. In other words, the forsterite formed endothermally on the dehydroxylation of serpentine probably immediately combines with magnesium fluoride under the evolution of heat. The forsterite which is then formed, at the moment of the birth (in statu nascendi), appears to be in a specially active state. From this point of view, the mixtures of serpentine with magnesium fluoride appear to form fluorine norbergite at a temperature lower than 775°C—immediately after the dehydroxylation of serpentine.

$$2\ Mg_3Si_2O_5(OH)_4 \rightarrow 3\ Mg_2SiO_4 + SiO_2 + 4\ H_2O \quad (1)$$

$$Mg_2SiO_4 + MgF_2 \rightarrow Mg_2SiO_4 \cdot MgF_2 \quad (2)$$

The Formation of Magnesioferrite ($MgFe_2O_4$).— Magnesioferrite was formed from all the mixtures of serpentine with magnesium fluoride at about 700°C or 800°C for 1 hr., and from serpentine alone at 730°C for 1 hr. The formation temperature of magnesioferrite agreed approximately with those of forsterite and fluorine norbergite. In general, the characteristic X-ray diffraction peaks of magnesioferrite were observed more clearly and more sharply in the presence of magnesium fluoride than those of serpentine alone. It seems likely that magnesium fluoride may accelerate the crystal growth of magnesioferrite.

Magnesioferrite is formed principally according to the following reaction:

$$MgO + Fe_2O_3 \rightarrow MgFe_2O_4 \quad (3)$$

where magnesium oxide is a component of the intermediate, unstable phase ($Mg_3Si_2O_7$) which had resulted from the dehydroxylation of serpentine,[4,6] and where ferric oxide is one of the impurities of serpentine.

Various Reactions between 800 and 1100°C.—As is generally known, serpentine shows two exothermic peaks in this temperature region; the first one, at about 830°C, is attributed to the crystal growth of forsterite, and the second, at about 1100°C, to the formation of enstatite. In the presence of magnesium fluoride, both these exothermic peaks exhibit a tendency to be reduced or to disappear with an increase in the amount of magnesium fluoride.

The disappearance of the first peak is due to Reaction 2—the conversion of forsterite into fluorine norbergite—at about 775°C.

The Hydrolysis of Magnesium Fluoride and Related Phenomena.—A plausible explanation for the disappearance of the second peak is as follows.

The water vapor evolved on the dehydroxylation of serpentine—Reaction 1—appears to react with a part of the magnesium fluoride to produce magnesium oxide, together with hydrogen fluoride, which perhaps successively attacks the serpentine

Table III. Weight losses and X-ray diffraction data for the heated products of some mixtures of raw and heated serpentine with magnesium fluoride*

(1) 15.5% MgF_2

Heating temp., °C			1000			1290			1400			1450		
Weight loss, %			12.20			17.22			18.24			21.95		
Difference in weight loss, %					5.02			1.02			3.71			
X-Ray diffraction data														
1000°C			1290°C			1400°C			1450°C					
17.4°	w	F	17.4°	w	F	17.4°	w	F	17.4°	m	F			
20.6	vw	N				20.7	vw	N	20.7	vw	N			
$_6$23.0	m	F	$_3$22.9	m	F	$_3$23.0	m	F	$_4$22.95	m	F			
23.9	w	F	$_{10}$23.9	w	F	23.9	w	F	23.95	w	F			
$_{10}$25.7	w	F	25.6	w	F	$_9$25.6	w	F	$_{10}$25.6	w	F			
27.3	vw	M												
29.25	vw	N												
29.9	w	F	29.9	w	F	29.85	w	F	29.9	w	F			
			30.4	vw	MF	30.4	vw	MF	30.5	vw	MF			
$_3$32.4	m	F, N	$_4$32.3	m	F, N	$_4$32.4	m	F, N	$_3$32.4	s	F, N			
34.0	vw	N												
$_1$35.8	m	F, MF	$_1$35.75	s	F, MF	$_2$35.8	s	F, MF	$_2$35.8	s	F, MF			
$_2$36.7	m	F	$_2$36.6	s	F	$_1$36.7	s	F	$_1$36.65	s	F			
38.4	vw	N	38.4	vw	N	38.4	vw	N	38.4	vw	N			
39.25	vw	N	38.9	vw	N	39.0	vw	N	38.9	vw	N			
$_7$39.8	w	F	$_6$39.8	m	F	$_6$39.8	m	F	$_6$39.75	m	F			
$_4$40.1	m	N	$_7$40.15	m	N	$_7$40.1	m	N	$_7$40.15	m	N			
40.5	w	M												
41.9	vw	F	41.8	w	F	41.9	w	F	41.8	w	F			
			43.0	vw	O	43.0	vw	O	43.0	vw	O			
			43.4	vw	MF	43.4	vw	MF	43.6	vw	MF			
44.7	vw	F, N	44.75	vw	F, N	44.6	vw	F, N	44.75	vw	F, N			
46.8	vw	F, N	46.7	vw	F, N	46.6	vw	F, N	46.75	vw	F, N			
			48.6	vw	F	48.6	vw	F	48.5	vw	F			
$_5$52.5	m	F	$_5$52.4	m	F	$_5$52.4	m	F	$_5$52.4	m	F			
55.1	vw	F	55.1	vw	F	55.1	vw	F	55.1	vw	F			
57.0	vw	F, N	57.0	vw	F, N	56.9	vw	F, N	57.0	vw	F, N			
						57.5	vw	MF	57.5	vw	MF			
58.75	vw	F, N	58.7	vw	F, N	58.75	vw	F, N	58.75	vw	F, N			
$_9$62.15	vw	F	$_9$62.0	w	F	$_8$62.0	w	F	$_9$62.1	w	F			
$_8$62.9	vw	MF	$_8$62.8	w	MF	$_{10}$63.0	w	MF	$_8$62.8	m	MF			
64.0	vw	M												
67.2	vw	F	67.2	vw	F	67.2	vw	F	67.2	vw	F			
69.75	vw	F	69.8	vw	F	69.6	w	F	69.8	w	F			

(TABLE III. continued)

(2) 31% MgF_2

Heating temp., °C	1000	1280	1350	1440
Weight loss, %	12.61	20.19	20.42	20.50
Difference in weight loss, %	7.56	0.32	0.08	

X-Ray diffraction data

1000°C			1280°C			1350°C			1440°C		
17.25°	vw	N									
17.4	w	F	17.4°	w	F	17.4°	w	F	17.4°	w	F
20.4	vw	N									
			20.7	vw	N	20.7	vw	N	20.7	vw	N
21.4	vw	N									
22.9	vw	F	$_{8}$22.9	m	F	$_{3}$22.9	m	F	$_{3}$22.95	m	F
23.9	vw	F	24.0	w	F	23.9	w	F	23.95	w	F
25.45	vw	F									
			25.7	w	F	25.6	w	F	25.6	w	F
26.8	vw	N									
27.3	vw	M									
27.7	vw	N									
$_{2}$29.25	m	N									
29.8	vw	F	29.9	w	F	29.9	w	F	29.9	w	F
			30.3	vw	MF	30.3	vw	MF	30.3	vw	MF
$_{10}$32.4	vw	F, N	$_{4}$32.4	m	F, N	$_{4}$32.4	m	F, N	$_{4}$32.4	m	F, N
33.25	vw	N									
$_{6}$34.0	m	N									
$_{8}$35.8	w	F, MF	$_{1}$35.8	s	F, MF	$_{2}$35.75	s	F, MF	$_{1}$35.8	s	F, MF
$_{9}$36.8	vw	F	$_{2}$36.7	s	F	$_{1}$36.6	s	F	$_{2}$36.6	s	F
37.4	vw	N									
38.5	vw	N	38.4	vw	N	38.3	vw	N	38.35	vw	N
			39.0	vw	N	38.9	vw	N	39.05	vw	N
39.25	vw	N									
			$_{7}$39.8	m	F	$_{7}$39.75	m	F	$_{8}$39.8	m	F
$_{3}$40.15	m	N	$_{6}$40.1	m	N	$_{8}$40.1	m	N	$_{9}$40.1	m	N
$_{1}$40.4	m	M, N									
41.9	vw	F	41.9	w	F	41.9	w	F	41.9	w	F
			$_{8}$43.1	m	O	$_{6}$43.0	m	O	$_{6}$43.1	m	O
44.7	vw	N	44.7	vw	N	44.7	vw	N	44.6	vw	N
46.8	vw	F, N	46.75	vw	F, N	46.75	vw	F, N	46.75	vw	F, N
			48.55	vw	F	48.6	vw	F	48.55	vw	F
49.6	vw	M									
									50.6	vw	F
			51.0	vw	N	51.1	vw	N	51.0	vw	N
$_{5}$52.6	m	F	$_{5}$52.5	m	F	$_{5}$52.4	m	F	$_{5}$52.4	m	F
$_{4}$53.2	m	M									
			55.0	vw	F	55.0	vw	F	55.0	vw	F
56.4	vw	F	56.3	w	F	56.2	vw	F	56.25	vw	F
57.1	vw	N	57.0	w	N	56.9	vw	F	56.95	vw	F
									57.6	vw	MF
			58.9	vw	F, N	58.8	vw	F, N	58.9	vw	F, N
62.25	vw	F	62.1	w	F	62.2	w	F	62.25	w	F
			$_{10}$62.5	w	O	$_{10}$62.5	w	O	$_{10}$62.6	m	O
$_{7}$63.0	w	MF	$_{9}$62.9	m	MF	$_{9}$62.8	m	MF	$_{7}$62.85	m	MF
64.0	vw	M									
			67.2	vw	F	67.2	vw	F	67.15	w	F
			69.8	w	F	69.75	w	F	69.8	w	F

(TABLE III. continued)

(3) 62% MgF_2

Heating temp., °C			1050			1280			1360		
Weight loss, %			5.50			18.67			19.50		
Difference in weight loss, %			13.17			0.83					
X-Ray diffraction data											
1050°C			1280°C			1360°C					
17.3°	vw	N, F	17.3°	w	N, F	17.3°	w	N, F			
20.3	vw	N	20.35	vw	N	20.4	vw	N			
20.8	vw	N	20.75	vw	N	20.85	vw	N			
21.5	vw	N	21.5	vw	N						
						25.7	vw	F			
26.8	w	N	26.8	w	N	26.8	vw	N			
$_{2}$27.3	s	M, N	27.3	w	N, M	27.3	vw	N, M			
$_{8}$27.65	m	N	27.7	w	N	27.7	vw	N			
$_{4}$29.3	m	N	$_{2}$29.3	s	N	$_{7}$29.3	m	N			
						29.75	vw	F			
32.4	vw	N, F	32.35	vw	N, F	32.5	w	F, N			
$_{5}$34.0	m	N	$_{6}$34.0	m	N	$_{10}$34.0	w	N			
35.25	vw	M									
35.75	vw	F, MF	35.65	w	F, MF	35.85	w	F, MF			
36.4	vw	N, F	36.5	vw	N, F	36.6	vw	F, N			
			37.0	vw	O	37.1	w	O			
37.4	w	N	$_{10}$37.5	w	N	37.4	vw	N			
38.5	w	N	38.6	w	N	38.6	vw	N			
39.3	vw	N	39.3	vw	N	39.3	vw	N			
$_{7}$40.0	w	N	$_{8}$40.1	m	N	$_{6}$40.2	m	N			
$_{1}$40.5	s	M	$_{3}$40.5	m	M	$_{2}$40.45	m	M, N			
			41.4	vw	N						
			$_{1}$43.05	s	O	$_{1}$43.05	s	O			
43.8	w	M	43.8	w	M, MF	43.8	vw	MF, M			
44.75	vw	N	44.6	vw	N						
46.7	vw	N	46.75	w	N	46.9	w	N			
49.4	vw	N	49.4	vw	N						
52.8	w	N, F	$_{9}$52.95	w	N, F	$_{9}$52.85	m	F, N			
$_{6}$53.2	m	M, N	$_{5}$53.3	m	N, M	$_{8}$53.2	m	N, M			
$_{3}$53.6	m	N	53.6	m	N	53.6	m	N			
						53.9	w	MF			
55.7	vw	N, M	55.75	vw	N, M						
56.4	w	M	56.4	vw	M						
57.25	vw	N	57.25	vw	N	57.2	vw	N			
58.5	vw	N, F	58.6	vw	N, F	58.5	vw	N, F			
60.7	w	M	60.75	vw	M	60.7	vw	M			
						$_{4}$62.4	m	F			
			$_{4}$62.55	m	O	$_{3}$62.5	m	O			
$_{9}$63.1	w	MF	$_{7}$63.15	m	MF	$_{5}$63.05	m	MF			
64.1	w	M	64.15	w	M	64.0	vw	M			
66.75	vw	M									
			66.9	vw	F	67.0	vw	F			
67.8	vw	M	67.8	vw	M						
$_{10}$68.2	vw	M	68.3	vw	M	68.3	vw	M			
			69.4	vw	F	69.4	vw	F			

(TABLE III. continued)

(4) Heated serpentine with 31% MgF_2

Heating temp., °C			1000			1280			1350
Weight loss, %			4.24			7.67			7.90
Difference in weight loss, %				3.43			0.23		
X-Ray diffraction data									
1000°C			1280°C			1350°C			
17.3°	vw	F, N	17.4°	w	F	17.4°	w	F
20.35	vw	N						
22.95	vw	F	$_3$22.9	m	F	$_3$23.0	m	F
23.9	vw	F	23.95	w	F	24.0	w	F
25.7	vw	F	25.65	w	F	25.7	w	F
27.1	w	M						
27.7	vw	N						
$_2$29.25	m	N						
			29.85	w	F	29.9	w	F
30.3	vw	MF	30.4	vw	MF			
32.4	vw	N, F	$_4$32.4	m	F, N	$_4$32.4	w	F, N
33.25	vw	N						
$_7$34.0	m	N						
$_8$35.8	w	F, MF	$_1$35.8	s	F, MF	$_2$35.8	s	F, MF
$_9$36.6	w	F	$_2$36.65	s	F	$_1$36.7	s	F
37.4	vw	N						
38.5	vw	N	38.35	vw	N	38.4	vw	N
			39.0	vw	N	39.0	vw	N
			$_9$39.8	w	F	$_7$39.8	m	F
$_4$40.15	m	N	$_7$40.15	m	N	$_8$40.15	m	N
$_1$40.5	m	M						
41.85	vw	F	41.9	vw	F	41.9	w	F
			$_6$43.15	m	O	$_6$43.1	m	O
43.85	vw	M						
44.7	vw	N	44.9	vw	N	44.75	vw	N
46.75	vw	N	46.8	vw	N	46.75	vw	N
						48.5	vw	F
49.7	vw	N						
						50.4	vw	F
$_5$52.5	m	F	$_5$52.5	m	F	$_5$52.4	m	F
$_3$52.85	m	N						
$_{10}$53.15	m	N						
53.5	w	N						
55.0	vw	F	55.2	vw	F	55.0	w	F
			56.4	vw	F	56.3	w	F
57.2	vw	N	57.0	vw	F	57.0	w	F
			57.6	vw	MF, N	57.6	vw	MF, N
58.4	vw	N						
			58.75	vw	F	58.9	vw	F
59.65	vw	N						
60.75	vw	M						
			62.1	w	F	62.25	w	F
			$_{10}$62.5	w	O	$_{10}$62.5	m	O
$_6$63.1	m	MF	$_8$62.95	m	MF	$_9$62.8	m	MF
67.1	vw	F	67.2	vw	F	67.15	w	F
69.7	vw	F	69.85	w	F	69.8	w	F

* The figures and abbreviations used in X-ray diffraction data are all the same as those in Table I.

or amorphous silica and forsterite resulting from Reaction 1:

$$MgF_2+H_2O \rightarrow MgO+2\ HF \quad (4)$$

$$SiO_2+4\ HF \rightarrow SiF_4+2\ H_2O \quad (5)$$

$$Mg_2SiO_4+8\ HF \rightarrow 2\ MgF_2+SiF_4+4\ H_2O \quad (6)$$

$$Mg_3Si_2O_5(OH)_4+14\ HF \rightarrow 3\ MgF_2+2\ SiF_4+4\ H_2O \quad (7)$$

The following reaction also appears to occur at that time:

$$2\ MgO+SiO_2 \rightarrow Mg_2SiO_4 \quad (8)$$

This reaction is a combination of magnesium oxide and silica in the amorphous state, and it appears to be accelerated by the hydrogen fluoride and silicon tetrafluoride resulting from Reactions 4—7.[8] The product, forsterite, successively reacts with magnesium fluoride to form fluorine norbergite —Reaction 2, or with hydrogen fluoride—Reaction 6.

According to Sychev,[8] pure magnesium fluoride does not show any volatilization between 800 and 1300°C, but water vapor present in the furnace atmosphere hydrolyzes it rapidly, forming magnesium oxide. Therefore, Reaction 4—the hydrolysis of magnesium fluoride—was expected to progress rapidly, but magnesium fluoride remained in the free state when heated up to 1070°C for 1 hr. In addition, the preheated mixture (31 per cent) also contained the free magnesium fluoride, even when heated at 1075°C for 1 hr., because the constitutional water of serpentine had almost all been lost.

The X-ray diffraction data of the heated mixtures (Table I) showed that magnesium fluoride exists partly in the form of fluorine norbergite and partly in the free state. However, the free magnesium fluoride disappeared entirely at about 1070°C, except for the 62 per cent mixture. It is worth noticing that the X-ray diffraction peaks of magnesium oxide distinctly appeared immediately after the magnesium fluoride had disappeared. This indicates that the hydrolysis of magnesium fluoride—Reaction 4—progresses completely in practice at 1070°C for 1 hr., and that the thermal change of magnesium fluoride is very closely related to the formation of magnesium oxide. However, this reaction seems to progress gradually to a slight degree in the region between about 730 and 1070°C, as is shown by the gradual weight decrease above 730°C on the TGA curves (Fig. 5).

The Formation of Magnesium Oxide and Forsterite. —The mixtures with comparatively large amounts of magnesium fluoride formed magnesium oxide above about 1070°C. The X-ray diffraction peaks of magnesium oxide were especially clearly confirmed in the mixtures with 31 per cent and more magnesium fluoride; on the contrary, its formation was not clear in the mixtures with 20 per cent and less magnesium fluoride. In the case of serpentine alone, no formation of magnesium oxide was observed in this temperature region. Thus magnesium oxide results from the hydrolysis of magnesium fluoride according to Reaction 4, and a part of it successively reacts with the amorphous silica formed on the dehydroxylation of serpentine —Reaction 1 — to produce forsterite according to Reaction 8.

The disappearance of the second exothermic peak of serpentine at 1100°C seems to be caused by the interaction of amorphous silica with magnesium oxide or hydrogen fluoride—Reaction 8 or 5, because the amorphous silica plays an important role in the formation of enstatite ($SiO_2+Mg_2SiO_4 \rightarrow 2\ MgSiO_3$).

Two or Three Endothermic Effects above 1000°C.—In order to elucidate these effects, the 15.5, 31, and 62 per cent mixture and the preheated mixture (31 per cent) were heated just below and beyond these peak temperatures. They were then examined in term of their weight losses (and fluorine contents in the case of the 31 per cent mixture only), and by X-ray diffraction. The results are summarized in Table III.

Table III shows that the first endothermic peak in the temperature region above 1000°C is most closely related to the remarkable decrease in weight (and the fluorine contents*). Moreover, just beyond these peak temperatures, none of the mixtures contained magnesium fluoride except for the 62 per cent mixture, and none formed magnesium oxide except for the 15.5 per cent mixture.** Therefore, it can be concluded that these first endothermic effects are to be attributed to the hydrolysis of magnesium fluoride by the water vapor according to Reaction 4, which leads to the evolution of hydrogen fluoride and silicon tetrafluoride. It should be noted that, besides the constitutional water of serpentine and the moisture of the furnace atmosphere, the water vapor resulting from Reactions 5—7 participates in Reaction 4.

The second endothermic effect may perhaps be attributed to the melting of magnesium fluoride (m. p. 1265°C). This is deduced from the fact

8) M. M. Sychev, *Trudy Leningrad Tekhnol. Inst. im Lensoveta,* **1955**, No. 34, 29—31; *Chem. Abstr.*, **50**, 12434d.

* When the 31 per cent mixture was heated for 1 hr. at the following temperatures, the fluorine contents of the products were as follows:

	1075°C	1210°C	1280°C	1320°C	1350°C
F, %	7.84	5.59	0.65	0.46	0.33

were 1210°C and 1320°C correspond to the first and second peaks respectively.

** In the 15.5 per cent mixture, the characteristic peaks of magnesium oxide were too weak for its presence to be concluded.

that the product heated immediately beyond the peak temperature was sintered. However, at about 1250°C (its first peak) and above, the 62 per cent mixture gave the sintered mass, which was shrunked and cracked. Furthermore, the intensities of the first and second peaks of both the 15.5 and 31 per cent mixtures exhibit a tendency to increase and to approach nearer toward each other with an increase in the amount of magnesium fluoride. These appear to indicate that its first endothermic peak between 1060 and 1280°C is to be attributed to the melting of magnesium fluoride in addition to its hydrolysis; namely, in this temperature region, the melting of magnesium fluoride occurs simultaneously with its hydrolysis. From this point of view, the second endothermic peak of a mixture (62 per cent) probably corresponds to the third ones for both the mixtures (15.5 and 31 per cent). Moreover, in this mixture, the existence of the free magnesium fluoride in the temperature region above the first endothermic peak is also probably caused by the melting of magnesium fluoride, which results from a decrease in the contact area between the magnesium fluoride and the water vapor.

The third endothermic peak of the preheated mixture (31 per cent) was not found in the region above the second one. Moreover, the intensity of the third endothermic peak decreases with an increase in the amount of magnesium fluoride. The reason for these results is not yet evident. Further work is required to explain fully the second and third effects.

Furthermore, the weight losses during heating were by far smaller than the calculated values (Table III). This is probably due to the formation of fluorine norbergite, which is more thermally stable than magnesium fluoride.

The Mineral Composition of the Heated Products.—The color of the heated products of all the mixtures generally vary from brownish white to dark brown as the temperature is raised. This is mainly caused by the formation and the crystal growth of magnesioferrite, and of the ferric oxide resulting from the oxidation of ferrous oxide, which is one of the impurities of serpentine.

Independent of the amount of magnesium fluoride, the products heated above the first endothermic peak temperature mainly consist of similar components—forsterite, magnesioferrite, fluorine norbergite, and magnesium oxide. The amount of the latter two increases with an increase in the amount of magnesium fluoride; especially in the case of the mixture with 62 per cent magnesium fluoride, its product when it is heated at 1250°C for 1 hr. is composed chiefly of magnesium oxide and fluorine norbergite, accompanied by a small amount of magnesioferrite—it contains almost no forsterite (Table I). On the other hand, forsterite is the principal component of the heated products with a decrease in the amount of magnesium fluoride. Moreover, among these components, the amount of fluorine norbergite tends to decrease in the temperature region above 1070°C; on the contrary, the three others are thermally stable.

The authors wish to express their gratitude to Mr. Shiro Saito for his help with the X-ray diffraction, the differential thermal, and the thermogravimetric analyses.

NOTES

The Cyclisation of Anthrimides to Carbazoles. IV.* The Cyclisation of 4, 4'-Dibenzamido Dianthrimides

By K. H. SHAH and K. M. SHAH

Department of Chemical Technology, University of Bombay, Matunga, Bombay 19, India

(Received September 24, 1965)

Indanthrene Corinth RK (C. I. No. 65020), containing only one benzamido group in the 4th position, does not cyclise to a carbazole, but hydrolyses with sulphuric acid at 100°C.[1] The cyclisation of a dianthrimide to a carbazole with sulphuric acid is successful only when two benzamido groups are present in 4, 4'- or 4, 5'- or 5, 5'-positions. E.g., Indanthrene Gray K, 4, 4'-dibenzamido-1, 1'-dianthrimide, cyclises to the corresponding carbazole, Indanthrene Olive R.

In order to confirm this observation and to compare the reactivity of 1, 1'- and 1, 2'-dianthrimides, 4, 4'-dibenzamido-1, 2'-dianthrimide was prepared by the condensation of 1-benzamido-3-bromoanthraquinone with 1-amino-4-benzamido anthraquinone. The product exhibited λ_{max} values at 290, 325—330 and 455 mμ. When treated with sulphuric acid at 26—30°C for about three hours while being stirred, it changed to another compound which exhibited λ_{max} values at 280, 360—380, 570 mμ. Indanthrene Gray K exhibits λ_{max} values at 250—260, 335—340 and 435 mμ. Indanthrene Olive R exhibits λ_{max} values at 225, 260—270, 360—380, 548, and 580 mμ. From these changes it is evident that 4, 4'-dibenzamido-1, 2'-dianthrimide cyclises to a carbazole under this treatment.

The spectral study of the rates of cyclisation with sulphuric acid (see attached graphs) of 4, 4'-dibenzamido-1, 1'-dianthrimide and 4, 4'-dibenzamido-1, 2'-dianthrimide indicated that the former compound cyclised readily in almost 50 min., while the latter compound cyclised very slowly (in about three hours) in an unstirred, 1 cm. long cell on a recording spectrophotometer (C ϕ-C 10). Therefore, 1, 1'-dianthrimide derivative cyclises more readily than the corresponding 1, 2'-dianthrimide derivative.

One point to be noted is that dianthrimides without benzamido groups exhibit λ_{max} values at 360 mμ, those with a benzamido group in the 4-position exhibit λ_{max} values at 390—405 mμ,[1] and those with two benzamido groups in the 4, 4'-positions exhibit λ_{max} values at 435—455 mμ. The corresponding carbazoles containing benzamido group in the 4 or 4, 4'-positions exhibit λ_{max} values at 360—380 mμ.[1] This does not apply to carbazoles containing benzamido groups in 4, 5'- or 5, 5'-positions. Indanthrene Brown FFR or R, obtained by the cyclisation of 4, 5'-dibenzamido-1,1'-dianthrimide, exhibits λ_{max} values at 343, 560 and 605 mμ.[2] Indanthrene Golden Orange 3G, obtained by the cyclisation of 5, 5'-dibenzamido-1, 1'-dianthrimide, exhibits λ_{max} values at 323 and 640 mμ.[2]

Experimental

Ultraviolet and visible spectra were taken on a Carl-Zeiss spectrophotometer, while the rate of cyclisation was studied on a Recording Spectrophotometer (C ϕ-C 10). Analar sulphuric acid was used.

The Purification of Indanthrene Gray K.—The commercial dye (4 g.), after water and alcohol solubles had been removed, crystallised from nitrobenzene as blue needles; these needles gave a green color when dissolved in concentrated sulphuric acid. UV: $\lambda_{max}^{H_2SO_4}$ mμ: 250—260, 335—340, 430—440.

Found: C, 75.5; H, 3.9; N, 6.6. Calcd. for $C_{42}H_{25}N_3O_6$: C, 75.6; H, 3.8; N, 6.8%.

The Cyclisation of Indanthrene Gray K.—The above dye (1.2 g.) was stirred with concentrated sulphuric acid (8 g. of 96%) for two hours at 26—28°C. The olive dye which precipitated when the solution was then poured on ice was collected. It crystallized from nitrobenzene as microcrystals. UV: $\lambda_{max}^{H_2SO_4}$ mμ 262, 360—375, 538—545, and 580. In 50 min. Indanthrene Gray K was cyclised to Indanthrene Olive R by "Analar" sulphuric acid at 23°C; this was indicated by the recording spectrophotometer (see attached graph).

The Purification of Commercial Indanthrene Oilve R.—The commercial dye (2 g.), after water and alcohol solubles had been removed, crystallised from nitrobenzene as microcrystals which gave a red color

* Part III: K. S. Nair and K. H. Shah, This Bulletin, **39**, 2023 (1966).

1) K. H. Shah and K. M. Shah, *Indian J. Chem.*, **1965**, 273.

2) W. Bradley and J. V. Butcher, *J. Chem. Soc.*, **1954**, 2317.

4, 4'-dibenzamido-1, 1'-dianthrimide

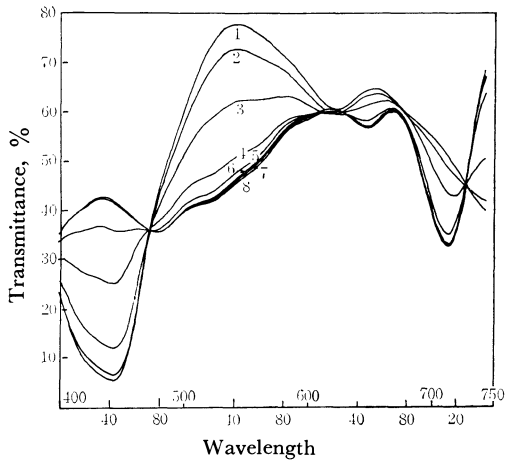

4, 4'-dibenzamido-1, 2-dianthrimide

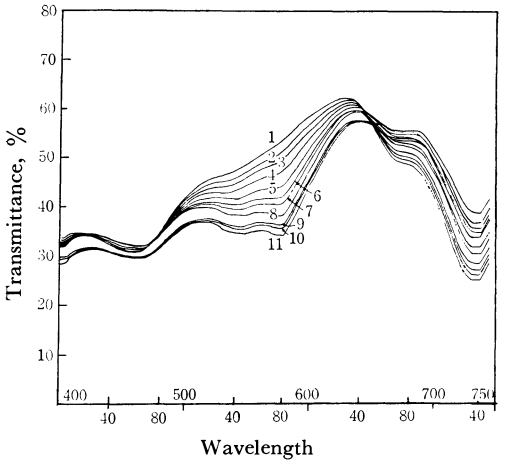

when dissolved in concentrated sulphuric acid. UV: $\lambda_{max}^{H_2SO_4}$ mμ: 225, 260—270, 360—380, 548, 580.

4, 4'-Dibenzamido-1, 2'-dianthrimide. — *1-Benzamido-3-bromoanthraquinone.*—A mixture of crystallised 1-amino-3-bromoanthraquinone[3] (1.5 g.), benzoyl chloride (2 ml.), and *o*-dichlorobenzene (13 ml.) was refluxed while being stirred for two hours. The product was then collected; it crystallised from benzene as yellowish-green needles.

Found: N, 3.9. Calcd. for $C_{21}H_{12}BrNO_3$: N, 3.5%.

4, 4'-Dibenzamido-1, 2'-dianthrimide. — A mixture of crystallised 1-amino-4-benzamido anthraquinone (0.6 g.), 1-benzamido-3-bromoanthraquinone (0.75 g.), sodium acetate (0.2 g.), soda-ash (0.2 g.), copper powder (0.07 g.), copper acetate (0.01 g.) and naphthalene (8.0 g.) was refluxed while being stirred for eight hours. The product (1.1 g.) was collected after steam distillation. It separated from nitrobenzene as blackish-gray microcrystals; these gave a greenish-yellow colour when dissolved in concentrated sulphuric acid. UV: $\lambda_{max}^{H_2SO_4}$ mμ: 290, 325—330, 455.

Found: C, 74.0; H, 3.7; N, 5.6. Calcd. for $C_{42}H_{25}N_3O_6 \cdot 0.5H_2O$: C, 74.5; H, 3.8; N, 6.2%.

The Cyclisation of 4, 4'-dibenzamido-1, 2'-dianthrimide.—The above dye (0.6 g.) was stirred with concentrated sulphuric acid (8 ml.) for 3.5 hr. at 25—30°C. The black compound which precipitated when the solution was then poured on ice crystallised from nitrobenzene as black needles; when dissolved in concentrated sulphuric acid, these needles gave a reddish-violet colour. UV: $\lambda_{max}^{H_2SO_4}$ mμ 280, 360—380, 570.

Found: C, 74.4; H, 3.7. Calcd. for $C_{42}H_{23}N_3O_6 \cdot 0.5H_2O$: C, 74.8; H, 3.6%.

4, 4'-Dibenzamido-1, 2'-dianthrimide was cyclised in three hours by "Analar" sulphuric acid at 23°C, as was indicated by a recording spectrophotometer (see attached graph).

Recording Spectrophotometer (C ϕ-C 10)
Temperature 23°C

Rate of cyclisation of Indanthrene Gray K (4, 4'-Dibenzamido-1, 1'-dianthrimide)

Indanthrene Gray K 0.0132 g./l.

Graph No.	Time interval	
	min.	sec.
1	6	15
2	13	45
3	22	00
4	27	15
5	29	40
6	34	55
7	42	10
8	50	45

Rate of cyclisation of 4, 4'-dibenzamido-1, 2'-dianthrimide; concentration, 0.0132 g./l.

Graph No.	Time interval		
	hr.	min.	sec.
1		10	15
2		18	30
3		26	45
4		39	00
5		58	15
6	1	15	30
7	1	32	45
8	1	55	00
9	2	6	15
10	2	28	30
11	3	15	45

Summary

Cyclisation of a dianthrimide to a carbazole with sulphuric acid is successful only when two benzamido groups are present. The spectral study of rates of cyclisation with sulphuric acid indicates that 4, 4'-dibenzamido-1, 1'-dianthrimide cyclises more readily than 4, 4'-dibenzamido-1, 2'-dianthrimide.

3) F. Ullmann and O. Eiser, *Chem. Ber.*, **49**, 2156 (1916).

Studies on Reactions of Polypropylene. VII. The Modification of Polypropylene by Making Use of Oxidation and Treatment with Toluylene Diisocyanate

By Yukio MIZUTANI, Keiichi YAMAMOTO and Shigeo HISANO

Tokuyama Soda Co., Ltd., Tokuyama, Yamaguchi

(Received November 29, 1965)

It is well-known that there are a few drawbacks in the practical use of polypropylene, including its poor dyeability and its susceptibility to oxidation. In this work, the latter drawback was utilized in order to improve the former. Namely, polypropylene (PP) was oxidized in order to introduce the hydroperoxide group[1,2] or the carbonyl group,[3] and then these groups were reduced to the hydroxyl group.

$$\text{PP} \xrightarrow{\text{air}} \text{PP-OOH} \xrightarrow{AlEt_3} \text{PP-OH} \xrightarrow{\text{TDI}}$$

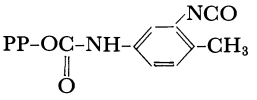

(PP-TDI)

When PP–OH prepared is dipped in toluylene diisocyanate (TDI), one of the two isocyanate groups of TDI may react with the hydroxyl group of PP–OH and TDI may be fixed to the polypropylene chain. The other isocyanate group may still be reactive and may react with a dye in the dyeing process. The film of PP–OH was dipped in TDI at room temperature for 8 days; then the film of PP-TDI was washed with dry acetone untill no TDI was detected in acetone. Absorption bands were detected at 4.5 μ and 5.9—6.7 μ in the infrared spectrum of this film (Fig. 1). On the other hand, these bands were not detected in the spectrum of the film of PP similarly treated.

From the fact that the film of PP-TDI was perfectly soluble in hot *p*-xylene and that the isocyanate group was present in the film, as is indicated by the absorption band at 4.5 μ, it is clear that, while one of two isocyanate groups of TDI reacted with the hydroxyl group on the polypropylene chain, the other group remained reactive. The band at 4.5 μ disappeared when the film was treated with dry methanol, but it could survive the dipping of the film in water for two days, although the film then became a cloudy white. It seems likely that the isocyanate group is protected from water by the water-repelling property of polypropylene. As the removal of TDI soaked in the polymer was not needed practically, the TDI content of the PP-TDI film was weighed without any special treatment other than wiping of TDI on the surface of the film with a filter paper. The results are shown in Table I.

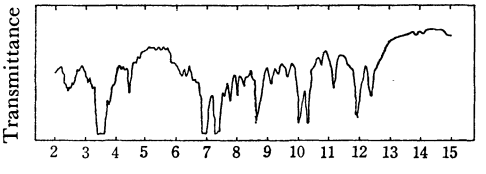

Fig. 1. The infrared spectrum of PP-TDI after acetone-extraction.

Table I. The TDI content of the film of PP-TDI

Dipping time in TDI, day	2	4	6	8
TDI content, %	1—3	2—4	3—5	4—7

For comparison, the film of PP was dipped in TDI for 8 days. The final TDI content was only about 1% and was less than those listed in Table I, because the film of PP containing no hydroxyl group could not fix the TDI in the film.

The films and fibers of PP–OH were dipped in TDI for 8 days, washed quickly with dry acetone, and dyed by the ordinary method with such dispersed dyes as Duranol Red X3B, Celliton Blue Extra, and Estrol Fast Violet B. They were dyed deeply, clearly, and homogeneously to the inner part (Photo 1).

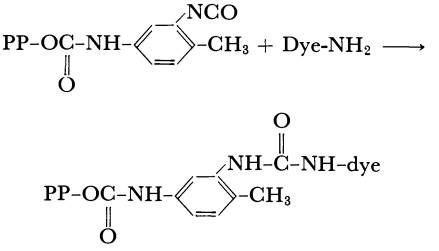

The dyed fiber was not decolored by extraction with acetone. This was evidence of the perfect fixation of the dye in the fiber, as had been elucidated by

1) K. S. Minsker, I. Z. Shapiro and G. A. Razuvayev, *Polym. Sci. U. S. S. R.*, **4**, 112 (1963).
2) G. Natta, E. Beati and F. Severini, *J. Polym. Sci.*, **34**, 685 (1959).
3) S. S. Stivala, R. Reich and P. G. Kelleher, *Makromol. Chem.*, **59**, 28 (1963).

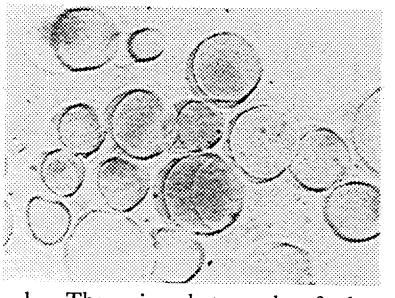

Photo. 1. The microphotograph of the cross-section of the dyed fiber.
Magnification: 250

Kubota et al.[4] Since the isocyanate group is protected from water, as has been described above, and since it reacts with amino groups more rapidly than with water,[5] the addition reaction between the isocyanate group and amino groups of the dyes should occur in the dyeing process. When the film of PP-TDI was treated with dry methanol, the isocyanate group in the film was killed. Accordingly, this film was dyeable with the dispersed dye, but it was easily decolored by acetone.

PP-OH could be prepared also by the relatively severe oxidation of polypropylene to introduce the carbonyl group and then by reduction with lithium aluminum hydride. The film thus treated acted in a manner similar to that of the film described above, except that the film became partially insoluble in hot *p*-xylene when dipped in TDI at room temperature for 7 days. This can be explained as resulting from the crosslinking behavior of TDI and the much greater content of the hydroxyl group in the film.

4) M. Kubota, M. Katayama and O. Ishizuka, *J. Chem. Soc. Japan Ind. Chem. Sect. (Kogyo Kagaku Zasshi)*, **66**, 725 (1965).

5) J. H. Saunders and K. C. Frisch, "Polyurethanes, Chemistry and Technology Part I Chemistry," Interscience Publishers, New York (1962), p. 181.

Experimental

Materials.—The powdery polypropylene used contained no stabilizer and its properties were as follows: melt index (at 230°C, load: 2.16 kg./cm.^{2}): 2.5, and specific gravity (at 23°C): 0.912. The film about 0.2 mm. thick was molded under a nitrogen atmosphere, and the fiber was spun at 270°C under a nitrogen atmosphere by the use of a spinneret 0.5 mm. in diameter.

The Preparation of PP-OH.—(1) The powdery sample was oxidized at 70°C for 7 hr. under air in order to introduce the hydroperoxide group. The oxidized sample (4 g.) was dipped in a 2% *n*-heptane solution of aluminum triethyl (70 cc.) at 20°C for 24 hr., then hydrolyzed with a 0.1 N aqueous solution of hydrochloric acid, and washed with water. The hydroxyl group to be introduced was limited to be about 0.3%.[1] (2) The powdery sample was oxidized at 125°C for 2 hr. under air in order to introduce the carbonyl group. The oxidized sample (1 g.) was refluxed for 4 hr. in an ether solution of lithium aluminum hydride (1.9 g./200 cc.) under a nitrogen atmosphere, then washed with methanol, a 15% aqueous solution of sodium hydroxide and water.

The Effect of the Temperature on the Fluidization of Supported Metal Catalysts

By Etsuro ECHIGOYA, Hiroshi HAGIWARA* and Akio SAKURAI

Research Laboratory of Resources Utilization, Tokyo Institute of Technology, Ookayama, Meguro-ku, Tokyo

(Received December 8, 1965)

The fluidization technique has become a widely-used method for solid-gas contact operations in the chemical industry. In general, metal powder shows agglomeration when it is heated in a hydrogen stream.[1,2] In hydrogenation experiments using a fluidized bed appearatus, it is necessary to find a metal powder catalyst which is stable without agglomeration under the reaction conditions. The aim of the present experiments is to find such a catalyst, on which shows stable fluidization characteristics under the operating conditions.

Experimental Method

Metal Powders for the Fluidization Experiments.—Commercial-grade metal powders of silver, copper, nickel, iron and stainless steel were used.

The Preparation of Supported Nickel and Cobalt Catalysts for the Fluidization Experiment.—30% *Nickel-Diatomaceous Earth.*—Powdered diatomaceous earth was added to a solution of a 1 N nickel nitrate solution to the slurry; then these was slowly added, at 20°C, an equivalent quantity of ammonium carbonate dissolved in water. The precipitate, after being filtrated and washed, was dried at 100°C and calcined at 400°C for 2 hr.

---

* Present address; Yoshitomi Pharmaceutical Ind., Yoshitomi, Fukuoka.

1) E. Echigoya and G. L. Osberg, *Can. J. Chem. Eng.*, **38**, 43 (1960).

2) E. Echigoya presented in part at 2nd Meeting of Chemical Reaction Eng. Osaka (1960), p. 11.

TABLE I. THE AGGLOMERATION TEMPERATURES OF VARIOUS KINDS OF METAL POWDERS IN A STREAM OF HYDROGEN OR IN AIR

Metal	Size, mesh	Fluidizing gas	Agglomeration temperature, °C	M. p., °C
Ag	−100+200	Air	85	960.8
Cu	−100+200	H_2	250	1083
Cu	−100+200	Air	>400	
Ni	−150+300	H_2	325	1455
Fe	−100+300	H_2	345	1535
Fe	−100+150	H_2	>420	
Stainless steel	−150+200	H_2	>390	

10% Nickel-Silica Catalyst.[3]—This catalyst was prepared by the super-coprecipitation method from a mixed-solution of nickel nitrate and sodium silicate, using ammonium carbonate at 20°C, and with vigorous stirring. The precipitate was washed with distilled water on the filter, dried at 100°C, and calcined at 550°C for 2 hr.

20% Nickel-Alumina and 20% Cobalt-Alumina.—The powdered alumina was added to a solution of cobalt nitrate. The slurry was stirred for some time, and to it these was then slowly added, at 20°C, a quantity of dissolved ammonium carbonate in a slight excess; the mixture was then heated and kept at 60—70°C for 5 hr. After it had been filtrated and washed, the precipitate was dried at 100°C and calcined at 500°C for 2 hr. The structure and properties of the catalysts were described in a previous report.[4]

The Fluidization Test.—An experimental method reported before[1] was used for the fluidization tests. The bed temperatures were measured with a thermocouple immersed in the bed. Fluidizing difficulties due to agglomerate formation were directly visible through the pyrex tube, but they could also be readily deduced from the pressure-drop readings.

Results and Discussion

(1) Metal powders showed agglomeration when heated in a stream of hydrogen. The experimental results are shown in Table I. The agglomeration temperature was influenced by many factors, such as the particle size and the kinds of gas used. In the case of silver, agglomeration was observed even in air at 85°C.

(2) The nickel-diatomaceous earth catalyst ceased to be fluidized after a few hours. The agglomerates which formed were of a relatively low mechanical strength. Cooling the bed to room temperature, while maintaining the gas flow, was sufficient to bring about fluidization again. If this cycle of heating and cooling was repeated several times, a gradual lowering of the agglomeration temperature, characterized by the cessation of fluidization, was observed, but after a still larger number of cycles this temperature appeared to tend toward a constant value (Table II, B).

TABLE II. INDUCTION PERIOD DATA OF THE AGGLOMERATION PROCESS OF Ni-DIATOMACEOUS EARTH

Catalyst	Run	Reaction temp., °C	Induction period, t, min.
(A)	1	350	20
New	2	350	30
Cat.	3	300	140
	4	325	30
	5	275	155
(B)	6	350	2
Repeated	7	325	6
catalyst	8	275	35
	9	275	24

When a fresh sample of nickel-diatomaceous earth powder was maintained at a constant temperature under the fluidizing conditions, difficulties due to agglomeration did not occur immediately. A time interval which depended on the bed temperature was observed. The "induction period" was, therefore, defined as the time interval between the beginning of fluidization and the first major decrease in pressure drop, a decrease which culminated in complete bed immobility. Such induction periods were not observed with the other catalyst compositions, but the possibility of their occurance after lengths of time greater than those used in our experiments (about 40 hr.) can not be ruled out. The induction-period data of the agglomeration process is given in Table II, A for the nickel-diatomaceous earth. The Arrehenius plot correlated the induction period as a function of the reciprocal bed temperature, so the data may be represented by an empirical equation:

$$\frac{1}{t} = A \exp\left(-\frac{\Delta E}{RT}\right) \qquad (1)$$

Where t is the induction period (min.); T is the bed temperature, °K and A and E are experimental constants. E is regarded as the activation energy for the overall agglomeration process. The activation energy calculated from the slope of these line was about 22 kcal.

3) T. Shirasaki, R. Shioda, H. Hagiwara, G. Shin, M. Kato and K. Morikawa, *J. Chem. Soc. Japan Ind. Chem. Sect. (Kogyo Kagaku Zasshi)*, **68**, 279 (1965).
4) H. Hagiwara and E. Echigoya, This Bulletin, **38**, 2163 (1965).

(3) At the reaction temperature, cobalt-alumina, nickel-alumina and nickel-silica catalyst powders could be fluidized satisfactorily for 40 hr. of continuous operation.

It was found from the above results that the nickel-diatomaceous earth catalyst in which the nickel is not combined with the carrier forms agglomerates under the reaction conditions, while the cobalt or nickel catalysts in which the metal forms a complex with the carrier resists the formation of agglomerates.

The cobalt-alumina catalyst found in this experiment was used for the experiments on the hydrogenation of aniline with a fluidized bed; good results were thus obtained.[5]

The agglomeration phenomena might be explained by connecting it with the sintering process of the metal.[6-8]

The authors wish to thank Professor Kiyoshi Morikawa for his valuable discussion and constant guidance.

5) E. Echigoya, H. Hagiwara and A. Sakurai, to be submitted.
6) W. D. Kingery and M. Berg, *J. App. Phys.*, **26**, 1205 (1955).
7) A. L. Pranatis and L. Seigle, *Powder Metallurgy*, **1**, 53 (1961).
8) G. C. Kuczinsky, *Acta Met.*, **4**, 58 (1956).

Acetamide as the *N*-Methylaminating Reagent. The Reaction of Halogenonitrobenzenes with Acetamide

By H. L. SHARMA, V. N. SHARMA and R. L. MITAL

Department of Pharmacology, S. M. S. Medical College, Jaipur, India
Department of Chemistry, University of Rajasthan, Jaipur, India

(Received January 20, 1966)

During an attempt to develop a new method for the synthesis of nitrobenzoxazoles, required for pharmacological work, from halogenonitrobenzenes and acetamide, we came across an interesting reaction which indicates the possible use of acetamide as a *N*-methylaminating reagent, a use which has not been reported hitherto. It has been found that when halogenonitrobenzenes are heated under reflux in the presence of copper sulphate, the halogen activated by the nitro groups is replaced by a methylamino group, thus yielding nitro-*N*-methylanilines.

The compound obtained by treating 1-chloro-2, 4-dinitrobenzene (I) with acetamide by this method was found to be homogeneous by thin-layer chromatography (Silica gel G, activated at 110°C for 24 hr.) using a benzene-ethanol mixture (1 : 1, v/v) which had been purified before use by standard methods. Its structure has been identified as 2, 4-dinitro-*N*-methylaniline, as it exhibits bands at 1515 cm^{-1} and 1351 cm^{-1} corresponding to asymmetric and symmetric stretching valence vibrations of the NO_2-group, and bands at 3350 cm^{-1} and 1645 cm^{-1} corresponding to N–H stretching and deformation vibrations of the secondary amino group. Moreover, it has been found to be identical with the product obtained by treating 2, 4-dinitrochlorobenzene with methylamine.[1]

The reaction was further studied with 3-chloro-1-iodo-(II), 3-chloro-1-bromo-2, 6-dinitro-4-methylbenzene (III) and with some other halogenonitrobenzenes (IV—VI).

Both the halogen atoms in compounds II and III are likely to be reactive, as they have two nitro groups, either in both the ortho positions or in the ortho and para positions. Neither of them, however, is replaced in this reaction. The products obtained in both cases are identical and invariably contain chlorine, indicating that in this reaction only halogen at position 1 is substituted.

This preferential replacement of the halogen atom can be explained by considering the spatial details of the halogen atom at position 3. The spatial consideration reveals that the NO_2 group at position 2 in compounds II and III is effectively held out of the plane of the ring by the bulky halogen atoms. Moreover, the "H" atoms of the methyl group are tetrahedrally placed. Therefore, the approach of the attacking reagent at position 3 is inhibited due to the *nonbonded interaction* of the tetrahedrally-placed "H" atoms of the methyl group on the side and the "O" atom of the twisted nitro group on the other side; hence, its replacement by the $NH–CH_3$ group is inhibited.

A detailed investigation of the mechanism of this reaction is in progress; it will be communicated separately in the near future.

1) P. Leymann., *Ber.*, **15**, 1234 (1882).

Table I

S. No.	Halo-nitrobenzenes used	*N*-Methylaniline formed $R_1=-NH\cdot CH_3$	Time reflux hr.	Yield %	Colour	M. p.* °C	Formula	N% Found	N% Calcd.
1.	$R_1=Cl$; $R_2=H$; $R_3=CH_3$, $R_4=R_5=NO_2$	$R_2=H$; $R_3=CH_3$ $R_4=R_5=NO_2$	13	51	Yellow	172[3]	$C_8H_9N_3O_4$	19.50	19.90
2.	$R_1=Cl$; $R_3=R_4=H$; $R_2=R_5=NO_2$	$R_3=R_4=H$; $R_2=R_5=NO_2$	13	52	Orange	105[4]	$C_7H_7N_3O_4$	21.02	21.31
3.	$R_1=Cl$; $R_2=F$; $R_3=H$; $R_4=R_5=NO_2$	$R_2=F$; $R_3=H$; $R_4=R_5=NO_2$	10	62	Dirty yellow	126[5]	$C_7H_6FN_3O_4$	19.31	19.53
4.	$R_1=Br$; $R_3=Cl$; $R_4=CH_3$ $R_2=R_5=NO_2$	$R_3=Cl$; $R_4=CH_3$; $R_2=R_5=NO_2$	14	55	Orange	159[6]	$C_8H_5ClN_3O_4$	16.86	17.10
5.	$R_1=I$; $R_3=Cl$; $R_4=CH_3$ $R_2=R_5=NO_2$	$R_3=Cl$; $R_4=CH_3$; $R_2=R_5=NO_2$	13	56	Orange	159[6]	$C_5H_5ClN_3O_4$	16.89	17.10

* Lit. m. p. 173, 106—107, 128, 160 and 160°C respectively.

Experimental

2, 4-Dinitro-*N*-methylaniline.[2]—A mixture of 1 chloro-2,4-dinitrobenzene (2.0 g., 0.01 mol.), copper sulphate (0.1 g., 0.004 mol.) and acetamide (8.0 g.) was refluxed with stirring for about 10 hr. The melt was then poured into ice cold water (ca. 30 ml.). The solid thus separated was filtered and extracted with ethanol. The residue obtained after evaporating the ethanol was crystallised by water in the form of yellow crystals, m. p. 175°C (Found: C, 42.34; H, 3.51; N, 20.98. Calcd. for $C_7H_7O_4N_3$: C, 42.64; H, 3.55; N, 21.31%). (Lit.[2] m. p. 176°C, undepressed on admixture with the the sample obtained above.)

Following the above procedure, a few halogenonitrobenzenes were successfully converted into the respective *N*-methylanilines[3-6] (Table I). In a few cases the product was isolated by extracting the diluted reaction mixture with benzene.

The authors wish to express their grateful thanks to Dr. R. M. Kasliwal, Principal, S. M. S. Medical College, Jaipur, and to Professor Dr. R. C. Mehrotra, Head of the Chemistry Department, University of Rajasthan, Jaipur, for providing facilities.

2) P. Van. Romburgh, *Chem. Ztg.*, **35**, 200 (1922).

3) E. L. Brown and N. Campbell, *J. Chem. Soc.*, **1937**, 1169.

4) R. Meldola and W. F. Holley, ibid., **107**, 617, (1915).

5) D. S. Deorha and H. L. Sharma, *J. Indian Chem. Soc.*, **40**, 973 (1963).

6) D. S. Deorha and H. L. Sharma, ibid., **40**, 894 (1963).

The Effect of Thermal Treatment on the Electric Conductivity of Muscovite

By Michio ASHIDA, Teizo WATANABE and Wasaburo JONO

Department of Industrial Chemistry, Faculty of Engineering, Kobe University, Nada-ku, Kobe.

(Received January 25, 1966)

It is well known that large, well-crystallized sheets of muscovite are resistant to thermal decomposition at temperatures above 500°C. According to Grim and Bradley,[1] the differential thermal curves for coarse-grained muscovite showed only a single dehydration reaction, beginning at about 800°C with a peak at about 900°C. On the other hand, Roy[2] reported that the dehydration curve for muscovite showed a slow, relatively gradual loss of water up to about 800°C, without any restricted interval of large water loss, and that its differential thermal curve was characterized by the lack of a definite peak. Gaines and Vedder[3] demonstrated the loss of structual hydroxyl groups

1) R. E. Grim and W. F. Bradley, "X-ray Identification and Structure of the Clay Minerals," Mineralogical Society of Great Britain Monograph, (1951), p. 147.

2) R. Roy, *J. Am. Ceram. Soc.*, **32**, 202 (1949).

3) G. L. Gaines., Jr., and W. Vedder, *Nature*, **201**, 495 (1964).

by infrared spectroscopy when a thin sheet of muscovite was heated for a long enough time at 600°C. Arizumi and Maekawa[4] investigated the mechanism of gas evolution from muscovite in vacuo and suggested that there were two sources of gas evolution, one of which was a surface contamination and the other was the OH^- ion, a component of the crystal network. They reported that the temperature at which muscovite became opaque was between 720°C and 750°C, and that dehydration began to take place at the lower temperature. It is clear, therefore, that the dehydration process occurs in muscovite without a general destruction of the crystal lattice. The primary step in this process is the formation of water molecules from structural OH^- groups. Fripiat and Toussaint[5] investigated the dehydroxylation of kaolinite by conductivity measurements.

As is well known, muscovite is a good electric insulator. However, when muscovite sheets were heated at high temperatures in vacuo, it behaved characteristically in its conductivity. In this paper, the conductivity will be measured in order to explain some behavior associated with the dehydroxylation.

Experimental

A large well-crystallized sheet of muscovite was cut into pieces 20 mm. square. The thickness of the sheet was in the range from 0.05 to 0.1 mm. Aluminum metal was evaporated onto the freshly-cleaved surface as electrodes. For the surface electrical conductivity measurements, the distance between electrodes was 10 mm. in width and 0.5 mm. in length. For the volume conductivity measurements, electrodes were prepared on both planes of the muscovite sheet by the evaporation of metal. The diameter of the electrodes was 10 mm., and the distance from an electrode to the guard ring was 8 mm. The crystallographic principal axes of muscovite were determined in its basal plane by the use of a polarizing microscope. The muscovite sheets thus prepared were placed in a Pyrex glass tube of 30 mm. in diameter. The glass tube was wrapped with a grounded copper foil in order to keep it from the stray electric field and then inserted in an electric furnace. The conductivity was measured at a pressure of about 5×10^{-5} mmHg with a vibration-reed electrometer apparatus. Since the plate of methacrylic resin which was used as an insulator in the conductivity apparatus had a resistivity of about 10^{15} Ω, it was impossible to measure a higher resistivity than 10^{16} Ω·cm. for the specimen.

Results

The muscovite sheets were heated up to temperatures below 450°C, held at that temperature, and then cooled to room temperature in vacuo. The temperature dependencies of the surface and volume conductivities were measured by continuous heating and cooling. Figure 1 shows the change in the volume conductivity observed when the temperature of muscovite is increased and decreased.

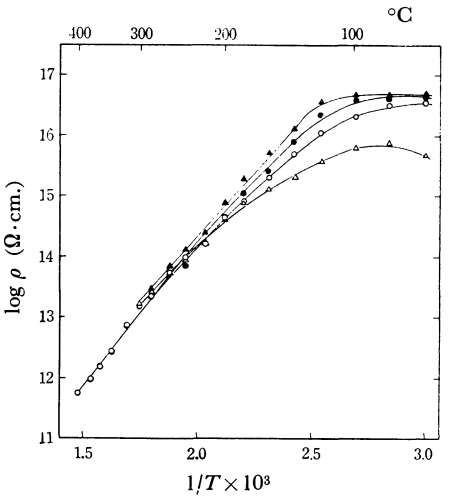

Fig. 1. Temperature dependency of volume conductivity.
Heat treatment up to 300°C:
△, heating process; ▲, cooling process
Heat treatment up to 400°C:
○, heating process; ●, cooling process

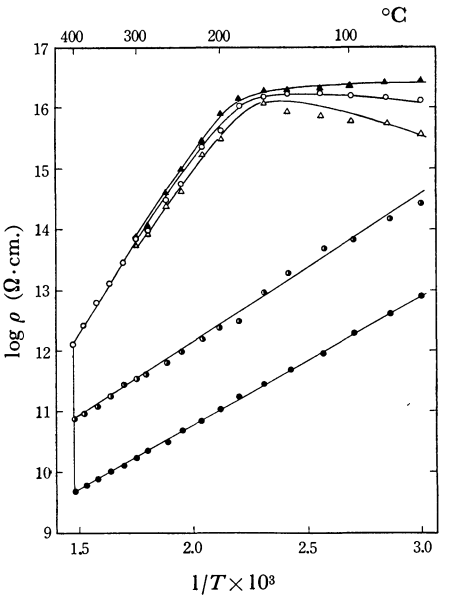

Fig. 2. Temperature dependency of surface conductivity.
Heat treatment up to 300°C:
△, heating process; ▲, cooling process
Heat treatment up to 400°C:
○, heating process; ◑, cooling process along the a-axis; ●, cooling process along the b-axis.

4) T. Arizumi and S. Maekawa, *Oyo Butsuri*, **23**, 150 (1954).
5) J. J. Fripiat and F. Toussaint, *J. Phys. Chem.*, **67**, 30 (1963).

A linear increase of the log ρ versus the reciprocal absolute temperature curve was observed in the range from 150°C to 450°C. While the sheet was kept at a temperature lower than 300°C for one hour, the conductivity remained constant. The conductivity in the cooling process decreased in accordance with the same curve as that in the heating process. When the specimen was held at 400°C for one hour, the conductivity increased a little, while on cooling the curve decreased along the curve with a slope similar to that of the heating curve. In this case, the conductivites in the heating and cooling processes were of the same order, and the discrepancy between them was very slight. In contrast to the volume conductivity, the surface conductivity exhibited a characteristic behavior in the same range of temperatures. Figure 2 shows the changes in the surface conductivity along the a- and b-axes of muscovite caused by the thermal treatment. When a specimen was heated to 300°C, held at that temperature for one hour, and then cooled to room temperature, no apparent change was observed between the heating and cooling curves on the surface conductivity. On the contrary, it should be noted that the surface conductivity gradually increased and then became constant after about one hour while the specimen was kept at 400°C, and that the relatively high conductivity still remained after the cooling process. Although no discrepancy between the values obtained along the a-axis and those along the b-axis was observed in the heating curve, the conductivity along the b-axis increased considerably more than that along the a-axis while the specimen was kept at 400°C. The linear relations of the log ρ versus the reciprocal T curve in both cooling curves have similar inclinations, which are different from that in the heating curve. The activation energy was determined from the inclination to be 0.43—0.47 eV. for the former and about 1.08 eV. for the latter. This suggests that the surface conduction mechanism of muscovite was changed by the thermal treatment at 400°C.

Discussion

The crystal lattice of muscovite is characterized by the repetition of so-called subcells about 10 Å thick, with two sheets of oxygentetrahedron with a silicon or aluminum atom at the center, as is shown in Fig. 3. The triangular basal planes of tetrahedral sit on a plane of the cleavage face and are linked to one another to form a hexagonal network as a whole. Above each center of the hexagonal space formed by the six tetrahedra, a K^+ ion is located. On the other side of the layer, the centers of the hexagon defined by the tetrahedron apexes are filled with OH^- ions, forming a dioctahedral layer between two opposite-facing

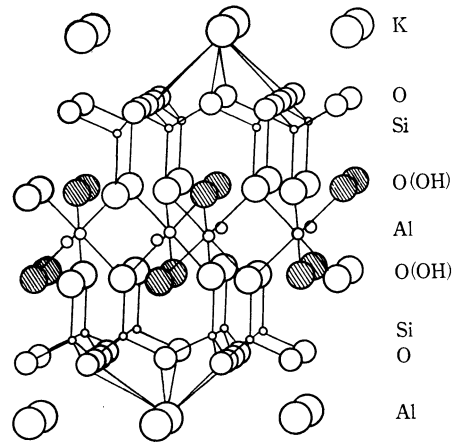

Fig. 3. Muscovite structure.

tetrahedron sheets. Although each layer has its own hexagonal symmetry, a monoclinic configuration is found in the subcell and a plane of symmetry passes through the OH^- ions perpendicularly to the layer. Tsuboi[6] and Vedder et al.[7,8] investigated the behavior of OH^- ions by infrared spectroscopy. Vedder and McDonald[7] concluded from the pleochroism of the OH^- stretching band that the vibrational transition moments are tilted out of the cleavage plane by about 16°. Their projection onto the cleavage plane makes an angle of about 32° with the b-axis. At 400°C, the surface conductivity along the a-axis was different from that along the b-axis. This finding suggested that the compositions included not only in the top layer but also in the subcells contribute to the surface conductivity. It is reasonable to postulate that the variation in muscovite structure occurred only in layers near the surface, since no apparent change was observed in the volume conductivity at this temperature.

Fripiat and Toussaint[5] observed that when kaolinite was heated, the process corresponding to a slow increase in conductivity appeared between 100°C and 360°C. They suggested that this process was due to the delocalization of protons which involve the free hydrid orbitals of octahedral oxygens. Finely-divided muscovite begins to lose its structural water at an appreciable rate at temperatures as low as 450°C (Ref. 2).

By taking these facts into account, the dehydroxylation of muscovite may be explained as follows. The protons in the dioctahedral layer increase the delocalization with a rise in the temperature up to 300°C, thus giving rise to a slow increase in the conductivity. When the temperature of muscovite

6) M. Tsuboi, This Bulletin, **23**, 83 (1950).
7) W. Vedder and R. S. McDonald, *J. Chem. Phys.*, **38**, 1583 (1963).
8) W. Vedder, *Am. Mineralogist*, **49**, 736 (1964).

reaches about 400°C, a water molecule is formed from the structural hydroxyl group and the dehydroxylation of muscovite begins, without a general destruction of the crystal lattice by the diffusion of the water molecules. In this process, lattice defects which are caused in layers near the surface by dehydroxylation contribute to an increase in the surface conductivity. The anisotropy of the conductivity is assumed to be due to the anisotropic arrangement of hydroxyl ions in the crystal lattice.

The authors wish to express their hearty thanks to Professor Eiji Suito and Dr. Natsu Uyeda of the Institute for Chemical Research, Kyoto University, for their many valuable discussions and suggestions.

The Pyrolysis of Organodisilanes

By Hideki SAKURAI, Ryongsu KOH, Akira HOSOMI and Makoto KUMADA

Department of Synthetic Chemistry, Kyoto University, Sakyo-ku, Kyoto

(Received February 3, 1966)

It has previously been reported[1] that hexamethyldisilane undergoes rearrangement at 600°C to give trimethyl(dimethylsilylmethyl)silane. The experiments described below will deal with the analysis of the products of this reaction, together with related investigations.

After hexamethyldisilane was passed slowly through a quartz tube heated at 600°C, the reaction products were collected in a trap immersed in a liquid-nitrogen bath. The careful examination of the reaction mixture by gas chromatography revealed that there were two main products, trimethylsilane (I) and trimethyl(dimethylsilylmethyl)-silane (II), along with unchanged hexamethyldisilane. The formation of these compounds is consistent with the reaction scheme we proposed earlier:

$$(CH_3)_3Si\text{–}Si(CH_3)_3 \rightarrow 2(CH_3)_3Si\cdot$$

$$(CH_3)_3Si\cdot + (CH_3)_3SiSi(CH_3)_3 \rightarrow (CH_3)_3SiH + (CH_3)_3SiSi(CH_3)_2CH_2\cdot \quad (2)$$

(I)

$$(CH_3)_3SiSi(CH_3)_2CH_2\cdot \rightarrow \cdot Si(CH_3)_2CH_2Si(CH_3)_3 \quad (3)$$

$$\cdot Si(CH_3)_2CH_2Si(CH_3)_3 + (CH_3)_3SiSi(CH_3)_3 \rightarrow (CH_3)_3SiCH_2Si(CH_3)_2H + (CH_3)_3SiSi(CH_3)_2CH_2\cdot \quad (4)$$

(II)

The ratio of the amount of II to that of I was found to be approximately 4 : 1 by gas chromatographic analysis. Accordingly, this value indicates that the average kinetic chain length of the reaction is about 4.

In this connection, a typical free radical reaction initiated by benzoyl peroxide in hexamethyldisilane was investigated at 80°C. The main products of the reaction between hexamethyldisilane and benzoyl peroxide were benzene, benzoic acid, 1, 2-bis(pentamethyldisilanyl)ethane (III), benzylpentamethyldisilane, and a small amount of an unidentified compound. No rearranged product, II, was formed. Therefore, in a solution at a low temperature, the pentamethyldisilanylmethyl radical does not undergo rearrangement as in the pyrolysis. Only dimerization was the main fate of this free radical.

$$2(CH_3)_3SiSi(CH_3)_2CH_2\cdot \rightarrow (CH_3)_3SiSi(CH_3)_2CH_2CH_2(CH_3)_2SiSi(CH_3)_3$$

(III)

Judging from this fact, the reaction 3 seems to be rate-determining and to require a higher activation energy than the other processes.

Finally, it is interesting to note that 1, 2-diphenyltetramethyldisilane did not undergo rearrangement at 600°C. The recovered material was essentially as pure as the starting material. Apparently, the substitution of phenyl groups increases the dissociation energy of the silicon-silicon bond.

Experimental

Trimethylsilane (I).—This was prepared from trimethylchlorosilane by reduction with lithium aluminum hydride in di-*n*-butyl ether.

Trimethyl(dimethylsilylmethyl)silane (II).—This was prepared from trimethyl(dimethylchlorosilylmethyl)silane by reduction with lithium aluminum hydride in ether. To a stirred suspension of 4.4 g. (0.11 mol.) of lithium aluminum hydride in 200 ml. of dry ether, there was added, drop by drop, 25 g. (0.138 mol.) of trimethyl(dimethylchlorosilylmethyl)-silane dissolved in 100 ml. of ether. During the addition, a gentle reflux of the ether was observed to take place. The reaction mixture was heated to reflux for 7 hr. and then submitted to distillation under reduced pressure. After the solvent had been removed, the mixture was fractionally distilled to give 12 g. (59%)

1) K. Shiina and M. Kumada, *J. Org. Chem.*, **23**, 139 (1958).

of II boiling at 118°C, n_D^{20} 1.4168. Topchiev et al.[2] prepared II from dichloro(trichlorosilylmethyl)silane, b. p. 119—20°C, n_D^{20} 1.4158.

The Pyrolysis of Hexamethyldisilane.—Hexamethyldisilane (40 g., 0.27 mol.) was passed slowly through a 3.7×50 cm. quartz tube mounted in a thermostatted furnace at 600°C. The reaction products, with unchanged hexamethyldisilane, were collected in a trap which was directly linked with the quartz tube and immersed in a liquid-nitrogen bath. The amount of material recovered was 38 g. The mixture was then analyzed on a gas chromatographic column packed with Apiezon L on Celite 545. The components were eluted on this column in the order of I (4.3 mol.%), a trace of an unidentified component, hexamethyldisilane (78.2 mol.%), II (17.5 mol.%), and a trace of another unidentified component.

The Attempted Pyrolysis of 1, 2-Diphenyltetramethyldisilane.—Diphenyltetramethyldisilane (20 g.; 0.074 mol.) was evaporated at reduced pressure (2 mmHg) and then passed slowly through the quartz tube described above at 600°C. The material thus recovered (17 g.) was analyzed on a gas chromatographic column packed with Apiezon L on Celite 545; this disclosed a single peak of the starting material.

The Decomposition of Benzoyl Peroxide in Hexamethyldisilane.—To a 200 ml. four-necked flask equipped with a mechanical stirrer, a reflux condenser, a thermometer, and a gas inlet tube, there were added 15 g. (0.062 mol.) of benzoyl peroxide and 100 g. (0.683 mol.) of hexamethyldisilane. The mixture was then heated at 100°C, stirred for 6 hr. under a slow stream of nitrogen, and cooled. The reaction mixture was washed with a saturated sodium bicarbonate solution and with water. The organic layer was dried and subjected to distillation. The fraction boiling at temperatures up to 110°C and that boiling at 110—113°C were mainly composed of recovered hexamethyldisilane and a small amount of benzene. The fraction boiling over the range from 100 to 120°C at 18 mmHg was found to consist mainly of 1, 2-bis(pentamethyldisilanylmethyl)ethane,[3] plus a small amount of benzylpentamethyldisilane. Both compounds were separated by gas chromatography (Silicone DC 550 on Celite 545) and identified by comparing their infrared spectra and retention times with those of authentic samples.

The research was supported in part by a grant-in-aid of the Ministry of Education and by the Kawakami Memorial Foundation, to both of which institutions the authors' thanks are due.

2) A. V. Topchiev, N. S. Nametkin and L. S. Povarov, *Doklady Akad. Nauk S. S. S. R.*, **97**, 99 (1954).

3) H. Sakurai, T. Kishida, A. Hosomi and M. Kumada, *J. Organometal. Chem.* in press.

The Electron Spin Resonance of Irradiated Single Crystals of Dichloroacetamide

By Michio KASHIWAGI

Basic Research Laboratories, Toyo Rayon Company, Ltd., Kamakura

(Received March 5, 1966)

Although there have been many ESR studies of irradiated single crystals, only Pooley and Whiffen[1] have reported the chlorine coupling constant in organic radicals. We will here report the chlorine coupling found in X-irradiated single crystals of dichloroacetamide. Simultaneously we will report on the hyperfine couplings for N and H nuclei of the amide group, which have not been investigated so far.

Single crystals of dichloroacetamide were prepared from methanol solutions by slow evaporation. The crystals were prismatic, with a well-developed face. An orthogonal axis system, xyz, was defined for the sake of convenience. The x and the y axes were selected in the developed face, with the x axis parallel to the elongated direction of the crystal. The y axis was found by ESR measurements to be along the monoclinic unique axis.[2] The crystals were X-irradiated at room temperature to 1 Mrad. The ESR spectra of the irradiated crystals were measured at 9.5 kMc./sec.

Figure 1 shows a typical ESR spectrum of the irradiated single crystals of dichloroacetamide. The spectrum is a septet with an ill-resolved substructure and with an intensity ratio of approximately 1 : 2 : 3 : 4 : 3 : 2 : 1. The septet is to be expected for a radical with two equally coupling chlorine (spin 3/2) nuclei; this indicates that the radicals produced in dichloroacetamide are of the form;

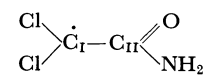

A similar radical, $F_2C_IC_{II}ONH_2$, was found in

1) D. Pooley and D. H. Whiffen, *Spectrochim. Acta*, **18**, 291 (1962).

2) C. Bodewig, *Z. Krist.*, **5**, 554 (1881).

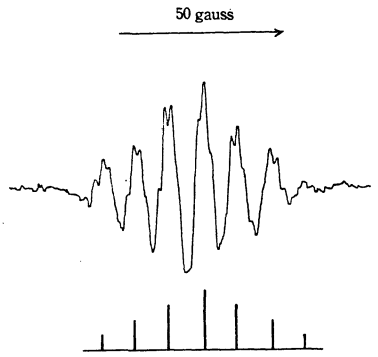

Fig. 1. Second-derivative ESR spectrum of an X-irradiated single crystal of dichloroacetamide for the magnetic field making an angle of 75° with the x axis in the xz plane.

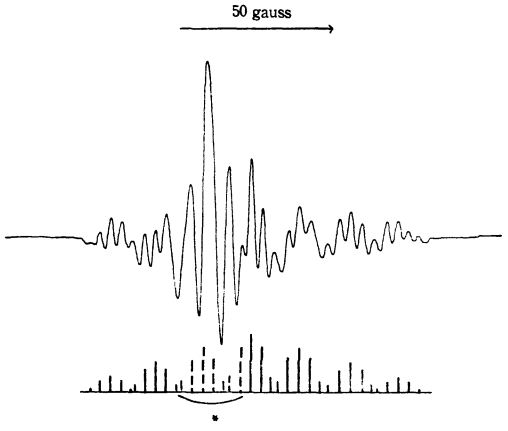

Fig. 2. Second-derivative ESR spectrum of an irradiated single crystal of dichloroacetamide for the magnetic field along the direction (0.28 0.63 0.72).
* There are overlapping lines due to alternative radicals whose orientations are related by the symmetry operations to each other.

TABLE I. PRINCIPAL VALUES AND DIRECTION COSINES FOR A^{Cl} OF THE RADICAL Cl_2CCONH_2

Principal values		Direction cosines with respect to the xyz axis system		
A_1^{Cl}	3G	0.96	$\mp$0.20	−0.20
A_2^{Cl}	5G	0.02	$\pm$0.75	−0.66
A_3^{Cl}	14G	0.28	$\pm$0.63	0.72

irradiated trifluoroacetamide,[3] where the radial is planar and where the F_2CCON skeleton is in the nodal plane of a π orbital on C_I. The fluorine coupling constant has a cylindrical symmetry, with the cylindrical axis perpendicular to the radical plane. A similar situation may be anticipated in the case of dichloroacetamide. However, the chlorine quadrapole coupling gives rise to a breakdown in the usual selection rule, $\Delta M_I=0$; this makes it difficult to analyze the ESR spectra. Measurements show that the ESR spectra exhibit a considerably different appearance from the simple septet when the coupling constant of the chlorine is smaller than about 7 *G*.[4] A crude estimation has been made of the principal values of the coupling constant by a least-squares analysis of the angular dependence of coupling constants larger than 7 *G*. The results are shown in Table I; these results can be used in considering the radical orientation, but they are too rough to make it possible to discuss the electronic structure of the radical in detail.

The substructure of the septet is resolved into a quintet for a magnetic field perpendicular to the radical plane. The substructure is different from the superposition of the hyperfine structure due to ^{35}Cl and ^{37}C.[5] This can well be explained by equal couplings of one N and two H nuclei of the amide group, as is shown in Fig. 2. There is some delocalization of the unpaired electron in the π system from the carbon C_I to the nitrogen, and the unpaired electron would couple with N and H nuclei. The calculation of Hückel MO[6] shows that the spin density on the nitrogen of the amide group increases in the order of: F_2CCONH_2[3] < $Cl_2CCONH_2 \approx FHCCONH_2$[7] < R_2CCONH_2 (R:H, CH_2 or CH_3). This indicates that $FHCCONH_2$ should give N and H couplings with the same order of magnitude as those in Cl_2CCONH_2. Moreover, R_2CCONH_2 and F_2CCONH_2 should give couplings with larger and smaller magnitudes respectively. The experimental data[3,6,8] are consistent with the prediction; this supports the preceding mechansim of the N and H couplings. The couplings will be treated in detail in discussing irradiated succinamide.[8]

3) R. J. Lontz and W. Gordy, *J. Chem. Phys.*, **37**, 1357 (1962). According to this paper, the N and H couplings are too small to be detected.

4) The quadrapole effect is very intense when the quadrapole coupling is of a magnitude comparable to that of the hyperfine coupling. From this fact it may be inferred that the quadrapole coupling, $3eqQ/4I(2I-1)$, is$\sim 7G$(20 Mc.) and that, therefore, $eqQ=\sim 80$ Mc. in this radical.

5) T. G. Castner and W. Känzig, *J. Phys. Chem. Solids*, **3**, 178 (1957).

6) M. Kashiwagi, unpublished results.

7) R. J. Cook, J. R. Rowlands and D. H. Whiffen, *Mol. Phys.*, **7**, 31 (1963—1964). In this paper it is left undecided whether or not the observed couplings are due to N and H nuclei of the amide group.

8) M. Kashiwagi, *J. Chem. Phys.*, **44**, 2823 (1966).

SHORT COMMUNICATIONS

A New Chelating Agent, α, α'-Diamino-*o*-xylene-*N*, *N*, *N'*, *N'*-tetraacetic Acid

By Takeshi ANDO and Keihei UENO*

The Chemical Laboratory, General Education Department, Kyushu University, Otsubo-Machi, Fukuoka

(Received June 15, 1966)

A large number of ethylenediaminetetraacetic acid (EDTA) derivatives have been known in the literatures, and it is therefore, possible to study the influence of electronic and steric variations on their chelating behaviors toward metal ions. However not many informations are available about the EDTA derivatives containing the benzene ring. We are now successful to synthesize α, α'-diamino-*o*-xylene-*N*, *N*, *N'*, *N'*-tetraacetic acid, (*o*-XyDTA) which is a new complexane containing benzene ring.

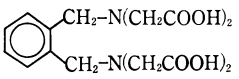

The tetramethyl ester of this acid was prepared by the condensation of α, α'-dibromo-*o*-xylene (0.01 mol.) with iminodiacetic acid dimethyl ester (0.06 mol.) in dry acetone at 70—80°C, with refluxing for 8 hr. After the reaction, the precipitated iminodiacetic acid dimethyl ester hydrobromide was filtered off and the crude tetra ester was obtained from the filtrate after distilling off acetone under reduced pressure. The ester was hydrolyzed with 10% sodium hydroxide at 70°C for 8 hours. After cooling, the pH of the solution was adjusted to about 1. The precipitated crude acid was recrystallized from hot water: yield about 20%. It decomposed at 226—229°C.

Found: C, 52.27; H, 5.53; N, 7.64%.[1] Calcd. for $C_{16}H_{20}N_2O_8$: C, 52.17; H, 5.53; N, 7.64%.

Pure acid is slightly soluble in water (about 0.4 g./1000 ml. H_2O).

The acid dissociation constants were determined by the potentiometric method at 25°C, in a medium of ionic strength of 0.10, with sodium hydroxide as a titrant. The titration curve is essentially the same as that of EDTA. The constants of this acid were calculated by the method of Schwarzenbach et al.[2] except that an algebraic method of solution was used instead of a graphical one. The results are $pk_1=2.0$: $pk_2=2.71$: $pk_3=5.99$: $pk_4=10.88$. The values of k_1, k_2, k_3 are similar to those of EDTA, but k_4 is fairly less than EDTA.

This acid showed similar chelating behavior to EDTA on the qualitative test using metal indicators such as Erio T (pH 10, Ca, Mg) or xylenol Orange (pH 5—6, Zn).

The chelating behavior toward metal ions in aqueous solution is now under study. The results of the detailed investigation on this ligand will be published later.

* Present address: The Department of Organic Synthesis, Faculty of Engineering, Kyushu University, Hakozaki, Fukuoka.

1) Elementary analysis was carried out at the Service Center of Elementary Analysis of Organic Compounds of Kyushu University.

2) G. Schwarzenbach, A. Willi and R. O. Bach, *Helv. Chim. Acta*, **30**, 1303 (1947).

On the Hyperfine Structure of the ESR Spectra of Copper(II) Complexes

By Hiroshi Yokoi and Taro Isobe

The Chemical Research Institute of Non-Aqueous Solutions, Tohoku University, Katahira-cho, Sendai

(Received May 17, 1966)

The solvent effects on the ESR spectra of several copper(II) complexes have been investigated in order to examine the theoretical basis of the ESR of copper(II) complexes. When planar 4-coordinated copper(II) complexes are dissolved in basic solvent, one or two of the basic solvent molecules are known to coordinate to the complexes along the axis normal to the molecular plane; spectroscopical studies of these phenomena have been carried out by several authors.[1] For this work the ESR spectra of cupric bis-acetylacetone chelate (I) and cupric bis-acetylacetone-ethylenediimine chelate (II) were measured in various solvents; the ESR spectra of II in all the solvents used show a clearly-resolved extra hyperfine structure due to the two nitrogen nuclei of ligand. The magnetic parameters determined are listed in Table I.

It is shown in Table I that the g values increase and the absolute A values decrease remarkably when the basicity of the solvent used is increased. The odd electron is placed in the antibonding B_{1g} molecular orbital, in which the coefficient of $d_{x^2-y^2}$ is taken as α. The values of α^2 were evaluated from copper hyperfine interaction by the usual procedures;[2] they are listed in the last column of Table I, from which it may be seen that α^2 decreases as the solvent basicity increases. However, it is reasonable to consider that α^2 should increase in basic solvents for the following reasons: First, the covalency of the metal-ligand bonding should decrease upon the coordination of basic solvent molecules because of the repulsion between the 3d electrons and the electrons which come from the solvent molecules, and the increase of α^2 is theoretically consistent with the tendency for $g_{\parallel}$ to increase. Second, the extra hyperfine interaction energy of the ligand nitrogen nuclei in II decreases in basic solvent; this fact definitely indicates that α^2 increases in basic solvents. It may be concluded from the above discussion that there is some uncertainty as to the theoretical basis of the ESR of copper(II) complexes.

The Fermi contact term, k_0, arises from the spin polarization of s-electrons and has been assumed to be constant.[3] In the case of planar copper(II) complexes in basic solvents, the 4s-orbital of the copper atom interacts with the σ-orbitals of solvent molecules; the degree of their mixing depends on the basicity of the solvents. Therefore, the spin polarization of the 4s-electrons contributes to the value of k_0 to a varying extent, and k_0 is not exactly constant. It seems that the above mentioned uncertainty can be ascribed to this property of k_0. Recently, Kivelson and Lee reported k_0 to vary in vanadyl complexes.[4] Some other copper(II) complexes show the same solvent effects as the complexes under discussion. Details will be published elsewhere.

Table I. Magnetic[a] and bonding parameters

Copper complex	Solvent[b]	$g_{\parallel}$	$g_{\perp}$	$A_{\parallel}\times10^4$ (cm^{-1})	$A_{\perp}\times10^4$ (cm^{-1})	$A_N\times10^4$ (cm^{-1})	α^2
I	A[c]	2.256	2.056	197	22		0.86
	B	2.309	2.070	167	14		0.84
	C	2.322	2.071	158	14		0.83
II	A	2.191	2.05	207		12.9	0.83
	B	2.218	2.06	195		12.2	0.82
	C	2.230	2.06	186		12.2	0.81

a) All ESR spectra were measured in ca. 0.01 M solution at 77°K.

b) Solvent A: toluene. Solvent B: 10% pyridine, 90% toluene. Solvent C: 10% piperidine, 90% toluene. Magnetic parameters did not depend on the mixing ratio of two solvents in solvents B and C.

c) Although the solubility of I in toluene is very small, the magnetic parameters of I in toluene could be determired from the ESR spectrum measured in toluene-chloroform solvent. Details will be published elsewhere.

1) R. L. Belford, C. Calvin and G. Belford, *J. Chem. Phys.*, **26**, 1165 (1957); D. P. Graddon and E. C. Watton, *Nature.*, **187**, 1022 (1960).

2) A. H. Maki and B. R. McGarvey, *J. Chem. Phys.*, **29**, 31, 35 (1958); D. Kivelson and R. Neiman, ibid., **35**, 149 (1961).

3) A. Abragam, J. Horowitz and M. H. L. Pryce, *Proc. Roy. Soc.*, **A230**, 169 (1955); R. E. Watson and A. J. Freeman, *J. Appl. Phys.* (*Suppl.*), **32**, 118 (1961).

4) D. Kivelson and S. Lee, *J. Chem. Phys.*, **41**, 1896 (1964).

The Novel Transesterification of Quaternary Ammonium Dithiocarbonates and Thiolesters

By Hiroshi YOSHIDA, Saburo INOKAWA and Tsuyoshi OGATA

Department of Synthetic Chemistry, Faculty of Engineering, Shizuoka University, Hamamatsu

(Received July 6, 1966)

It is well known that transesterification occurs when an ester is heated with an alcohol in the presence of acid or a base.

In the previous papers[1] the present authors have reported that methylxanthates reacted with trimethylamine at room temperature to form quaternary ammonium dithiocarbonates, as in Eq. 1.

$$MeOCS_2R + Me_3N \rightarrow \underset{(I)}{Me_4\overset{+}{N}\overset{-}{S}COSR} \qquad (1)$$

When the ammonium salts were mixed with esters in acetonitrile, transesterification was observed; this reaction will be described in this communication.

Reactions were carried out in acetonitrile homogeneously for about 20 min. at room temperature. After the solvent had been evaporated in vacuo, the residue was separated into an ether-soluble part (A) and an insoluble part (B). A was a mixture of esters, and B was a mixture of quaternary ammonium dithiocarbonates. B was then treated with methyl iodides, as has previously been reported.[1] The products were identified through comparison with authentic samples via their gas chromatographic retention times (silicone grease column, 130—180°C). The results are shown below.

$$\left.\begin{array}{l} I(R=Me) + MeSCOSEt^{1a)} \\ I(R=Et) + MeSCOSMe^{1a)} \\ I(R=Et) + MeSCOSEt \end{array}\right\} \rightarrow$$

$$MeSCOSMe + MeSCOSEt + EtSCOSEt + I(R=Me) + I(R=Et) \qquad (2)$$

$$I(R=Et) + MeSCSSMe^{2)} \rightarrow MeSCSSMe + MeSCSSEt^{3)} + I(R=Me) + I(R=Et) \qquad (3)$$

$$I(R=Et) + C_6H_5COSMe^{4)} \rightarrow C_6H_5COSMe + C_6H_5COSEt^{4)} + I(R=Me) + I(R=Et) \qquad (4)$$

Reactions 2—4 showed that almost all of the ethyl radicals of I(R=Et) were transferred to the esters and that a large amount of I(R=Me) was found in the residual ammonium salts. Although thiolesters reacted easily with I(R=Et), esters such as methyl benzoate, dimethyl carbonate[5] did not react under similar reaction conditions.

These experimental results show that I(R=Me) is more stable than I(R=Et), that carbonyl-SR bond fisson may occur, and that then mercapto groups may exchange with each other.

1) a) H. Yoshida et al., *J. Chem. Soc. Japan, Pure Chem. Sect.* (*Nippon Kagaku Zasshi*), **86**, 950, 1179 (1966); b) H. Yoshida, S. Inokawa and T. Ogata, unpublished.

2) E. Wertheim, *J. Am. Chem. Soc.*, **48**, 826 (1926).

3) Du Pont de Nemours & Co., A. Pat. 2313871 (1938).

4) L. S. Pratt and E. E. Reid, *J. Am. Chem. Soc.*, **37**, 1937 (1915).

5) B. Röse, *Ann.*, **205**, 236 (1880).

Rotatory Dispersions and Circular Dichroisms of Platinum(II) Complexes

By Haruko Ito (née Sugi), Junnosuke Fujita and Kazuo Saito

Department of Chemistry, Faculty of Science, Tohoku University, Katahira-cho, Sendai

(Received July 27, 1966)

For square-planar complexes, various schemes for orbital energies have been proposed (Fig. 1), but they all make the practical assignment of the absorption bands of platinum(II) complexes difficult. Several attempts have been made to overcome this problem,[1] but it still remains unsolved.

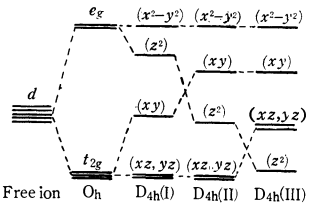

Fig. 1. Probable modes of orbital splitting in square-planar D_{4h} complex.

Table I. The symmetries of the excited states, the magnetic moment and the electric moment brought about by stretching vibrations (D_{4h})

	Excited configuration	Magnetic polarization	Vibronic (stretching) polarization
$d_{xy} \rightarrow d_{x^2-y^2}$	A_{2g}	μ_z	r_x, r_y
$d_{xz}, d_{yz} \rightarrow d_{x^2-y^2}$	E_g	μ_x, μ_y	r_x, r_y, r_z
$d_{z^2} \rightarrow d_{x^2-y^2}$	B_{1g}	—	r_x, r_y

We have measured the R. D. and C. D. spectra of platinum(II) complexes containing *l*-propylenediamine and studied the splitting of the d orbitals on the basis of an analysis of these spectra. Table I shows the symmetries of the excited states, the magnetic moment, and the electric moment brought about by stretching vibrations for a planar complex with D_{4h} symmetry.

It can be seen that only the $d_{xy} \rightarrow d_{x^2-y^2}$ and d_{xz}, $d_{yz} \rightarrow d_{x^2-y^2}$ transitions have magnetic moments. In the former transition, however, the electric moment and the magnetic moment are perpendicular to each other. This selection rule still holds for symmetries lower than D_{4h}, so far as the stretching vibration alone is considered. Therefore, only the transition to the E_g state should be optically active.

The maxima of the absorption frequencies and the $\varepsilon_l - \varepsilon_r$ values are shown in Table II. The C. D. spectra due to the vicinal effects of propylenediamine have positive signs in all the complexes studied. The fact that only the bands 2 and 4 are optically active supports the idea that both transitions are $A_{1g} \rightarrow E_g$ ($d_{xz}, d_{yz} \rightarrow d_{x^2-y^2}$), the lower frequency band involving the triplet, and the other, the singlet state. The ordering of D_{4h}(III) in Fig. 1 can account for these results. The rotatory strength of [Pt *l*-pn$_2$]Cl$_2$ is just twice that of [Pt *l*-pn en]Cl$_2$. This indicates that the magnitude of the Cotton effect due to the vicinal effect is proportional to the number of optically active ligands; there is no appreciable interaction between the ligands.

Table II. Experimental results

	Band 1	Band 2			Band 3		Band 4			
	Absorption*	Absorption*		C. D.*		Absorption*		Absorption*		C. D.*	
	ν_{max}	log ε	ν_{max}	log ε	ν_{max}	$\varepsilon_l - \varepsilon_r$	ν_{max}	log ε	ν_{max}	log ε	ν_{max}	$\varepsilon_l - \varepsilon_r$
$K_2[PtCl_4]$	~18	~0.7	21.0	1.18			25.7	1.78	30.5	1.80		
[PtCl$_2$ *l*-pn]			27.3	1.56	27.0	0.15	33.1	2.37	~37	2.10	37.2	0.38
[Pt *l*-pn$_2$]Cl$_2$			35.7	1.65	35.7	0.54	41.6	1.00**	44.6	2.68	45.2	1.03
[Pt *l*-pn en]Cl$_2$			35.7	1.61	35.7	0.29	~41.7		44.6	2.65	45.1	0.54
[Pt *l*-pn(NH$_3$)$_2$]Cl$_2$			35.2	1.60	35.2	0.22	~41.4		45.3	2.64	44.8	0.51

* ν in 10^3 cm^{-1}, ** Obtained from Gaussian analysis

1) J. Chatt, G. A. Gamlen and L. E. Orgel, *J. Chem. Soc.*, **1958**, 486; R. F. Fenske, D. S. Martin, Jr., and K. Ruedenberg, *Inorg. Chem.*, **1**, 411 (1962); H. B. Gray and C. J. Ballhausen, *J. Am. Chem. Soc.*, **85**, 260 (1963); D. S. Martin, Jr., and C. A. Lenhardt, *Inorg. Chem.*, **3**, 1368 (1964); D. S. Martin, Jr., M. A. Tucker and A. J. Kassman, ibid., **4**, 1682 (1965); D. S. Martin, Jr., J. G. Foss, M. E. McCarville, M. A. Tucker and A. J. Kassman, ibid., **5**, 491 (1966).

BULLETIN OF THE CHEMICAL SOCIETY OF JAPAN VOL. 39 2057—2062 (1966)

The Effect of Substituents on the Half-Wave Potential of the Polarographic Reduction of Pyridine *N*-Oxide Derivatives[1]

By Tanekazu KUBOTA and Hiroshi MIYAZAKI

Shionogi Research Laboratory, Shionogi & Co., Ltd., Fukushima-ku, Osaka

(Received March 23, 1965)

Polarograms of twenty-three pyridine *N*-oxide derivatives substituted at γ- and β-positions were extensively measured at various pH's. The half-wave reduction potential, $E_{1/2}$, was expressed by the form $-E_{1/2}=a\,[\mathrm{pH}]+b$. The wave height due to the reduction of the $\rangle N\rightarrow O$ group decreased with an increase in the pH in a pH region over ~6. This phenomenon was common to all the compounds studied here; it was thought to be useful in identifying an aromatic *N*-oxide group by the polarographic method. The $E_{1/2}$ plot against Hammett's σ value of the substituent satisfied a linear relation well, and the slope of Hammett's ρ value was positive. This indicates that the reduction process is nucleophilic. The linear relation was explained qualitatively on the basis of the MO theory by applying the second-order perturbation method.

In a previous paper[2] concerning the pH dependence of the polarographic reduction wave of pyridine *N*-oxide, we showed that the reduction wave is actually due to the 2-electron reduction of the protonated *N*-oxide; we also determined the rate constant, k_r; in the proton addition process (1) using the equation derived by Koutecky[3] and by Matsuda[4]:

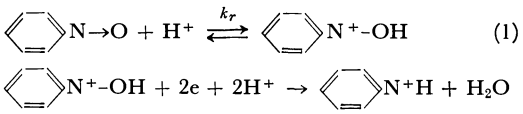

(1)

In the present study, polarographic measurements will be extended to twenty-two substituted pyridine *N*-oxides, and the relationship between their half-wave potential values ($E_{1/2}$) and Hammett's substituent constants (σ) will be discussed in terms of the lowest vacant MO energy of the substituted pyridine *N*-oxides and their protonated species predicted by the second-order perturbation method.

Experimental

Measurements.—The polarograms were recorded with two Yanagimoto polarographs, Model PA-102 and PB-4. The pH values were determined with a Beckman pH meter, Model G. The capillaries used for the dropping mercury electrode had the following values of m and t at an open circuit: (A) $m=1.23$ mg./sec. and $t=4.35$ sec. at $h=65$ cm., and (B) $m=0.879$ mg./sec. and $t=4.48$ sec. at $h=70$ cm. Capillary A was used in measurements with compounds I, IV, V, VI, and VII, and capillary B, with the other eighteen compounds. All the polarographic measurements were made at 25 ± 0.1°C in a suitable buffer solution after bubbling purified nitrogen in for about 10 min. in order to remove the oxygen dissolved in the solution. The buffer solutions were the same as those employed in the previous report.[2] The ionic strength of the sample solution was adjusted to 0.45 by the addition of an appropriate amount of sodium chloride. A saturated calomel electrode was used as the external reference electrode. Measurements were made with about a 5×10^{-4} mol./l. solution containing an accurately-weighed sample, and the values obtained from three separate measurements were averaged.

Materials.—The compounds investigated in the present study are listed in Table I. Compounds II, VIII, XII, XIV, and XXIII were kindly supplied by Dr. Sadazi Kaziwara of our laboratory, and III, by Professor Yutaka Mori of Osaka Gakugei University. Compounds IV, V, IX, and X were synthesized by respective substitution reactions[5] from γ-nitropyridine *N*-oxide (XIII), which had been prepared by the nitration of pyridine *N*-oxide.[5] Compounds I, VI, VII, XI, XV, XVI, XVII, XVIII, XIX, XX, XXI, and XXII were prepared from the corresponding substituted pyridines by hydrogen peroxide oxidation in acetic acid. β-Fluoro-,[6] β-chloro,[7] and β-bromo[7] pyridines were prepared according to the literature, while β-methoxypyridine was prepared by the decomposition of diazotized β-aminopyridine in the presence of methanol.*1 The other substituted pyridines used for the above-mentioned *N*-oxide preparations were commercial products and were purified by a conventional method. All the compounds used for polarographic measurements were purified by at least three recrystallizations, and their purities were checked

1) The Polarographic Study of Aromatic *N*-Oxides. Part II. Presented at the meeting of "The Symposium on Polarography" held by the Chemical Society of Japan, Kyoto, October 1962.

2) T. Kubota and H. Miyazaki, This Bulletin, **35**, 1549 (1962).

3) J. Koutecky, *Collection Czech. Chem. Commun.*, **18**, 183, 597 (1953); **19**, 857 (1954).

4) H. Matsuda and Y. Ayabe, This Bulletin, **28**, 422 (1955).

*1 This is a modification of the method of Ref. 7.

5) E. Ochiai, *J. Org. Chem.*, **18**, 534 (1953).

6) A. Roe and G. F. Hawkins, *J. Am. Chem. Soc.*, **69**, 2443 (1947).

7) C. Räth, *Ann.*, **486**, 95 (1931).

TABLE I. SUBSTITUTED PYRIDINE *N*-OXIDES INVESTIGATED, WITH THEIR MELTING POINTS AND THEIR HALF-WAVE REDUCTION POTENTIALS AT pH 5.0

Compound No.	γ-Substituent	M. p., °C	$E_{1/2}$, V.
I	H	b. p. 138—140°C/15 mmHg	−1.281
II	NH_2	181—182 (HCl salt)	−1.465
III	NHOH	149—150 (decomp.) (HCl salt)	−1.434
IV	OCH_3	83	−1.416
V	OC_2H_5	119	−1.396
VI	CH_3	184—185	−1.357
VII	C_2H_5	108—109	−1.331
VIII	$NHCOCH_3$	266—267	−1.189
IX	Cl	163 (decomp.)	−1.174
X	Br	180 (decomp.)	−1.094
XI	$COOC_2H_5$	69	−0.862
XII	CN	225—226	−0.857
XIII	NO_2	163	−0.204, −1.436 *
	β-Substituent		
XIV	NH_2	153 (HCl salt)	−1.280
XV	OCH_3	115—116 (HCl salt)	−1.168
XVI	CH_3	149.5—150.5 (HCl salt)	−1.272
XVII	C_2H_5	84 (HCl salt)	−1.246
XVIII	$NHCOCH_3$	215	−1.129
XIX	F	143—144 (HCl salt)	−1.144
XX	Cl	164.5—165 (HCl salt)	−1.071
XXI	Br	187—188 (HCl salt)	−1.040
XXII	$COOC_2H_5$	103	−0.992
XXIII	CN	175—176	−0.943

* Two waves were observed: −0.204 V. and −1.436 V. attributed to reduction steps of NO_2 and $\rangle N\rightarrow O$ groups, respectively.

by ultraviolet and infrared spectral methods and by elementary analyses.

Results and Discussion

The Polarographic Behavior of Substituted Pyridine *N*-Oxides.—First let us discuss the polarographic behavior of pyridine *N*-oxides substituted by NH_2, NHOH, OCH_3, OC_2H_5, CH_3, C_2H_5, and $NHCOCH_3$ at the γ-position and by NH_2, OCH_3, CH_3, C_2H_5, $NHCOCH_3$ and F at the β-position. A typical example of their polarograms is shown in Fig. 1 (b). All the compounds of this group showed a one-step reduction wave in the pH region studied (pH > 1.0). The wave height corresponded to a 2-electron reduction in an acidic medium according to the Ilkovic equation, using the same constants as those used in the previous paper,[2] but the wave decreased rapidly with an increase in pH in the pH range over ~6. These phenomena are just the same as those observed in the reduction of pyridine *N*-oxide (I),[2] whose polarogram is also shown in Fig. 1 (a). Thus the wave corresponds to the 2-electron reduction of the protonated N→O group, and the behavior observed in the pH region over ~6 is probably due to the wave including the kinetic current arising from the proton addition to the N→O group in the molecules.[2] This type of pH dependence was also observed with all the other substituted pyridine *N*-oxides studied here and with some nitrone derivatives;[8] hence it may be thought to be characteristic of the reduction of aromatic *N*-oxides, and it would be very useful for the identification of an aromatic *N*→O group by the polarographic method. The variation in the half-wave potential, $E_{1/2}$, with pH can be expressed by Eq. 2 in the pH region from 1 to 8 with all the compounds of this group except for the two amino derivatives.*2 The slopes, *a*, were almost all of the same order, as can be seen from Table II.

$$-E_{1/2} = a[\mathrm{pH}] + b \qquad (2)$$

In the polarograms of γ-chloro- and γ-bromopyridine *N*-oxides, the maximum shown by the

*2 We obtained two straight lines, crossing at pH = 2.60 and 4.50 for II and XIV respectively. It should be noted that these values do not coincide with the pK_a's values (3.65 and 1.47 respectively).[9] At the present time, no satisfactory explanation for this fact can be given.

8) T. Kubota, H. Miyazaki and Y. Mori, Part III, to be published.

9) H. H. Jaffé and G. O. Doak, *J. Am. Chem. Soc.*, **77**, 4441 (1955).

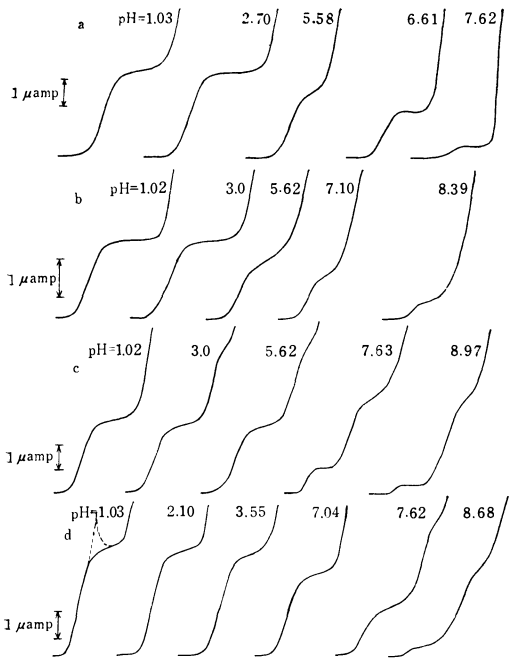

Fig. 1. Typical polarograms of some pyridine *N*-oxides in various pH solutions.
a : Pyridine *N*-oxide (I) (5.28×10^{-4} mol./l.)
b : β-$NHCOCH_3$ derivative (XVIII) (4.40×10^{-4} mol./l.)
c : β-Cl derivative (XX) (4.78×10^{-4} mol./l.)
d : γ-Br derivative (X) (5.19×10^{-4} mol./l., 0.005% gelatin added)
The dotted line in (d) represents the maximum wave which always appeared in reduction of γ-halogen derivatives in measurements without gelatin.

dotted line in Fig. 1 (d) was always observed over a wide pH range, although this maximum disappeared upon the addition of small amount (0.005%) of gelatin to the electrolytic solution. It should be noted, however, that the wave height of the γ-substituted halogen compounds was a little higher than that for the compounds discussed in the foregoing paragraph. On the other hand, no maximum was found with the β-chloro or the β-bromo derivatives. The polarograms of the former are shown in Fig. 1(c). The pH dependences of $E_{1/2}$ of the four halogen-substituted pyridine *N*-oxides also satisfied Eq. 2.

Cyano and carboethoxy derivatives (XI, XII, XXII and XXIII) exhibited somewhat different polarographic behavior. Thus, the polarograms of these compounds always showed two-step reduction waves.*3 The pH dependence of the first wave height was similar to that for the common

*3 Two waves also appeared in the polarographic reduction of halogen-substituted pyridine *N*-oxides, but the separation of the two was ambiguous.

Table II. The values of a and b in Eq. 2, $-E_{1/2}=a[\mathrm{pH}]+b$, which holds in the pH region from 1.5 to 7-8 except where indicated

Substituent	a	b	
H	0.0865	0.849	
γ-NH_2	0.074	1.026	(pH 1—2.6)
	0.1023	0.953	(pH 2.6—7)
γ-NHOH	0.069	1.089	
γ-OCH_3	0.094	0.946	
γ-OC_2H_5	0.0963	0.914	
γ-CH_3	0.0948	0.883	
γ-C_2H_5	0.0933	0.864	
γ-$NHCOCH_3$	0.0788	0.795	
γ-Cl	0.087	0.739	
γ-Br	0.0975	0.606	
γ-$COOC_2H_5$	0.058	0.572	
γ-CN	0.057	0.572	(pH 4—9)
γ-NO_2	0.04	0.004	(for the first wave)
	0.096	0.956	(for the second wave)
β-NH_2	1.095	0.75	(pH 1—4.5)
	0.074	0.91	(pH 4.5—8)
β-OCH_3	0.0785	0.775	
β-CH_3	0.0816	0.864	
β-C_2H_5	0.081	0.841	
β-$NHCOCH_3$	0.072	0.769	
β-F	0.0795	0.7465	
β-Cl	0.0793	0.674	
β-Br	0.0778	0.651	
β-$COOC_2H_5$	0.0665	0.659	
β-CN	0.0713	0.586	

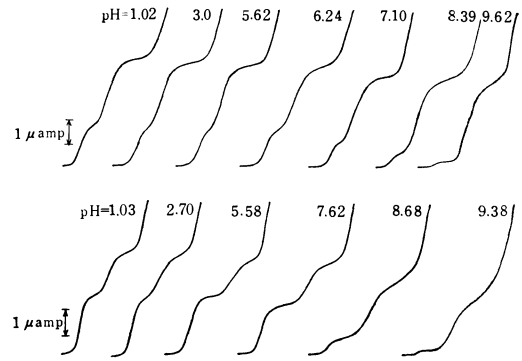

Fig. 2. Typical polarograms of some pyridine *N*-oxides showing 2-step reduction waves.
Upper: γ-$CO_2C_2H_5$ derivative (5.11×10^{-4} mol./l., 0.005% gelatin added)
Lower: β-CN derivative (5.26×10^{-4} mol./l.)

pyridine *N*-oxides discussed earlier, while the second wave height held almost unchanged over a wide pH range. Therefore, only one wave, which corresponds to the second one in the acidic solution measurements, was observed in measurements at a higher pH value. The situation may be demonstrated well by Fig. 2. It would be reasonable to identify the first wave as the reduction of the protonated cation ($\rangle N^+-OH$) on the basis of its

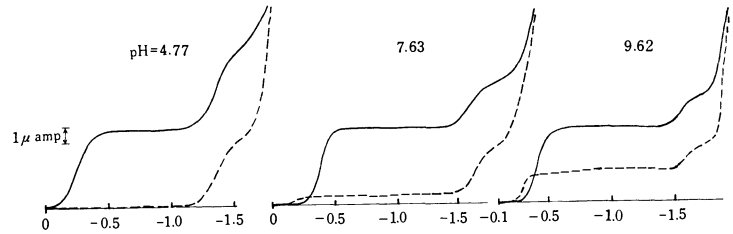

Fig. 3. Polarograms of γ-NO_2 (5.49×10^{-4} mol./l., 0.005% gelatin added, ——) and γ-NHOH (4.73×10^{-4} mol./l., ----) derivatives of pyridine *N*-oxide.

pH dependence and of the relation of its $E_{1/2}$ value to Hammett's σ, which will be discussed below. A plausible assignment of the second wave can not be attained at the present time. It was difficult to establish the relationship between $E_{1/2}$ and pH for XII in the lower pH region because of the ambiguous separation of the two waves, but a good linear plot was obtained in the 4—9 pH region, where the separation was clear.

The polarogram of γ-nitropyridine *N*-oxide (XIII) shown in Fig. 3 is of special interest. It was found that the compound shows two reduction waves, the first of which corresponds to an approximately four-electron reduction on the basis of the Ilkovic equation,[2] and that its wave height is almost independent of the pH value. On the other hand, the second wave height decreased as the pH increased. This two-step reduction can be reasonably explained as follows. At first the nitro group of the compound is reduced to NHOH by the first 4-electron reduction, and then the γ-hydroxyaminopyridine *N*-oxide (III) formed is subjected to $\rangle$N→O-group reduction. This assumption is based on the facts that: (i) the second reduction wave of the nitro derivative (XIII) appeared at nearly the same $E_{1/2}$ value as that of the hydroxyamino derivative (III), and (ii) the pH dependence of its wave height was a typical one associated with the $\rangle$N→O-group reduction discussed before. Moreover the $E_{1/2}$-σ plot falls right on the straight line in Fig. 4 if we plot the $E_{1/2}$ of the second wave of XIII against the σ value for γ-NHOH instead of that for NO_2, a fact suggesting that the second reduction wave of XIII is that of III to γ-hydroxyaminopyridine. However, an alternative possibility for the intermediate cannot be ruled out, for some other chemical evidence on pyridine *N*-oxide[5] would suggest that the intermediate produced by the first 4-electron reduction is 4, 4'-azopyridine 1, 1'-dioxide. However, the polarographic measurement of this azo compound, m. p. 246°C (decomp.); (5.09×10^{-4} mol./l., 0.005% gelatin added) showed two reduction waves. One was a wave of $E_{1/2}=-1.266$ V., and the limiting current was $i_l=3.79$ μamp. at pH=4.80, both $E_{1/2}$ and i_l being pH-dependent, and i_l decreased in the alkaline region. The other was a wave at about −0.01 V. at pH 4.80 continuing from an anodic wave. The former wave may be due to the reduction of an *N*-oxide group, but no further conclusive discussion can be made, since Hammett's σ values of the *p*-azo group are not known.*4

The Relationship between the Reduction Potentials of Substituted Pyridine *N*-Oxides and Hammett's σ Constants.—The plotting of $E_{1/2}$ versus Hemmett's σ constant of substituted pyridine *N*-oxides is of special interest in understanding the effect of substituents on $E_{1/2}$ and in elucidating the reduction mechanism.

As is apparent from Table II, the pH dependence of $E_{1/2}$ is nearly of the same order, and so we would expect straight lines with roughly equal slopes for the above plotting made at different pH's. Table I and Table III show the $E_{1/2}$ values observed at pH=5.0 and the selected σ values, cited mainly from Jaffé's review,[10] repectively. The plots of $E_{1/2}$ at pH=5.0 vs. σ are depicted in Fig. 4, where we can see that a good linear relation holds between them. The linear relation was also obtained for the values at different pH's, as had been expected. The slopes, that is, the ρ's of Hammett's equation, are: +0.457, 0.495 and 0.584 at pH values of 3.0, 4.0 and 5.0 respectively.

The plot for γ-NH_2 using the value of $\sigma=-0.66$ derived by Jaffé[10] deviated largely from the straight line in Fig. 4; the reduction actually took place at a more positive potential than that to be expected from the σ value. Zuman[11] found a similar trend of the *p*-NH_2 value in the polarographic reduction of other systems, and he set σ as −0.13 in order to fit the polarographic reduction potential data. This σ value is better than Jaffé's, −0.66, for the present system, but it is not close enough

*4 In the meanwhile it would be worthwhile to point out that the γ-NHOH derivative (III) showed two waves in the alkaline region (see Fig. 3, the dotted curves). The first wave may be due to an azo-type compound formed from III in an alkaline solution.[5] In fact, the solution of III becomes more yellowish at a higher pH value.

10) H. H. Jaffé, *Chem. Revs.*, **53**, 191 (1953); *J. Org. Chem.*, **23**, 1790 (1958).

11) P. Zuman, *Collection Czech. Chem. Commn.*, **25**, 3225 (1960).

TABLE III. SELECTED SUBSTITUENT CONSTANTS

Substituent	σ[a]
γ-NH_2	$\begin{cases}-0.660\\-0.13^{b}\end{cases}$
γ-NHOH	−0.339
γ-OCH_3	−0.268
γ-OC_2H_5	−0.250
γ-CH_3	−0.170
γ-C_2H_5	−0.151
$NHCOCH_3$	−0.015
γ-Cl	+0.227
γ-Br	+0.232
γ-$COOC_2H_5$	+0.678[c]
γ-CN	+0.660[d]
γ-NO_2	$\begin{cases}+0.778\\+1.270^{c}\end{cases}$
β-NH_2	−0.161
β-OCH_3	+0.115
β-CH_3	−0.069
β-C_2H_5	−0.043
β-$NHCOCH_3$	+0.154[e]
β-F	+0.337
β-Cl	+0.373
β-Br	+0.391
β-$COOC_2H_5$	+0.398
β-CN	+0.56[d]

a) These σ-values were cited from Jaffé's review[10] unless otherwise noted.
b) See Ref. 11.
c) These are Jaffé's σ^* (σ^-) values.[10]
d) D. H. McDaniel and H. C. Brown, *J. Org. Chem.*, **23**, 420 (1958).
e) See Ref. 9.

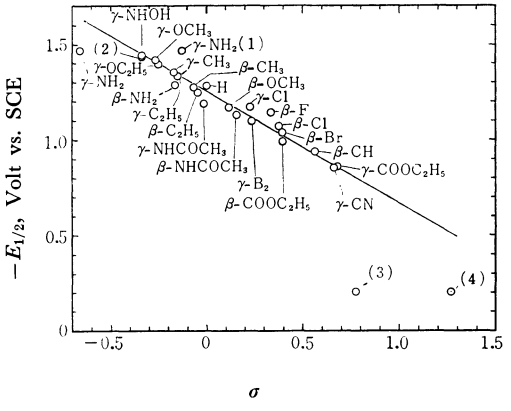

Fig. 4. The plot of $E_{1/2}$ against Hammett's σ. The points indicated by 1, 2, 3 and 4 represent, respectively, the plots of $E_{1/2}$ for II against Zuman's σ of γ-NH_2 (point 1), $E_{1/2}$ for the second wave of XIII against σ of γ-NHOH (point 2), and $E_{1/2}$ for the first wave of XIII against σ (point 3) and σ^- (point 4) of γ-NO_2 group.

to fit straight line, as do the other substituents. Another exceptional case is that of an NO_2 group. We can see from Fig. 4 that the plots of $E_{1/2}$'s corresponding to the first and the second waves of γ-nitropyridine *N*-oxide deviate eminently from the straight line, regardless of the choice of convertional σ or σ^- values for the γ-NO_2 group. This situation has been explained above.

Now it should be noted that the ρ value is positive. This means that the more electron-releasing a substituent is, the more negative is the $E_{1/2}$ value. From this we can say that the first process which occurred on the cathode was an electron transfer from a dropping-mercury electrode to the active center of the molecule to be reduced ($\rangle N^+$-OH), in which process the electron on the dropping mercury electrode acted as a nucleophilic reagent. The same conclusion was also drawn by Zuman for other systems.[11]

A Consideration of the Relationship between $E_{1/2}$ and Hammett's σ in Terms of the Lowest Vacant MO Energy Qualitatively Predicted by the Second-Order Perturbation Method.—It would be noteworthy if we could point out that the MO theory gives some basis for the interpretation of the above-mentioned relationship between $E_{1/2}$ and Hammett's σ, as well as of the well-known relationship between $E_{1/2}$ and the lowest vacant orbital energy.

For the sake of convenience, a substitued pyridine oxide is divided into two composite systems, as is shown in Fig. 5, where R and S represent a pyridine oxide part and a substituent located at the β or γ position*5 respectively. If we pick substituents having only one π-MO, such as CH_3, OCH_3, or NH_2, the lowest vacant orbital energy, E_{iR}, of pyridine oxide will change to E_{iR} according to Eq. 3, which was derived by the second-order perturbation mehtod;[12]

$$E_{iR} = E^{\circ}_{iR} + \frac{(C_{iR})^2\beta^2_{r-s}}{E^{\circ}_{iR} - E^{\circ}_{S}} \qquad (3)$$

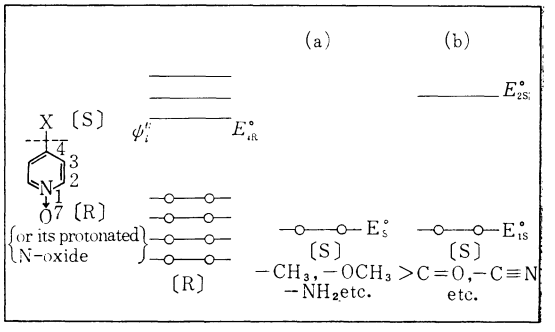

Fig. 5. Schematic diagram of MO for substituted pyridine *N*-oxides.

*5 The atom at which the substituent is attached is designated as r.

12) K. Higashi and H. Baba, "Quantum Organic Chemistry," Asakura Publishing Co., Tokyo (1956), p. 164 (in Japanese).

Here C_{iR}, β_{r-s}, and E_S° represent, respectively, the coefficient on the atom r in MO ϕ_i, the resonance integral between the atom r in a pyridine oxide part and the atom s in a substituent, and the energy of the highest-filled MO of the substituent. As β_{r-s} can be assumed to be a constant as the first approximation, the smaller the $|E_S^\circ|$ value or the larger the $|C_{ir}|$ value is, the smaller is the $|E_{iR}|$.*6 If we use the naive MO's parameter, δ in our discussion,*6 we can say that $E_{1/2}$ should move towards more negative values with a decrease in the δ of the substituent.[13] The order of estimated δ values appearing in the literature[14] is $CH_3>OH—OR>NH_2—NR_2$; therefore, the order of $-E_{1/2}$ should be the reverse. This predicted order of $-E_{1/2}$, $NH_2>OCH_3>CH_3$ agrees with the order predicted from σ values using Fig. 4. However, for the case of halogen substituents, a similar teatment was not successful, probably because of their fairly large σ inductive effects, as well as because of intramolecular charge transfer from MO's of R to, for example, the 3-d atomic orbital of chlorine. These electron-withdrawing effects would be a reason why halogens have positive values of Hammett's σ's and why halogen-substituted pyridine oxides showed an easier reduction.

Let us now consider the term C_{ir}. Our previous MO calculations[15] on pyridine oxide and its proton addition compound always resulted in a larger coefficient on the 4-position than on the 3-position as to the lowest vacant MO (symmetry b_2); $|C_4|>|C_3|$. This suggests that the substituted pyridine oxide at the 4-position should have a larger $-E_{1/2}$ value than that at the 3-position for the same substituent. This prediction agreed with the observed $E_{1/2}$ data.

For a substituent having two or more π-MO's, like $>C=O$, $-C\equiv N$, etc., Eq. 3 is rewritten as:

$$E_{iR} = E_{iR}^\circ + \sum_{j=1}^{n} \frac{(C_{ir}\cdot C_{js})^2\cdot\beta_{rS}^2}{E_{iR}^\circ - E_{jS}} \qquad (4)$$

Generally speaking, however, the orbital (E_{iR}°) interacts more strongly with the vacant orbital of the substituent (E_{2S}° or higher) because of a smaller energy difference, as may be understood from Fig. 5; consequently, the level will be lowered. This stabilization results in an easier reduction (a smaller $-E_{1/2}$) of the substituted pyridine oxide compared with its mother compound. This also coincides with the tendency to be expected from Hammett's σ values.

In the case of nitropyridine *N*-oxide, the $-E_{1/2}$ value due to an NO_2 group reduction is much lower than that due to $\rangle N\rightarrow O$-group reduction. This indicates that the lowest empty orbital of the compound originates from the nitro group.

The authors wish to express their deep thanks to Professor Emeritus Eiji Ochiai of The University of Tokyo and to Professor Shinzi Koide of Mukogawa Women's University in Nishinomiya for their valuable advice. Thanks are also due to Professor Mitsugi Senda of Kyoto University and Professor Saburo Nagakura of the Institute for Solid State Physics, The University of Tokyo, for their helpful discussions, and to Professor Yutaka Mori of Osaka Gakugei University and Dr. Sadazi Kaziwara of our laboratory for supplying some samples and for their discussions.

*6 If we put $E_S^\circ=\alpha+\delta\beta$, δ is the parameter which is now being discussed. In addition, E, α, and β are negative values, and $-E_{iR}^\circ<-E_S^\circ$.

13) For the relationship between $E_{1/2}$ and the lowest vacant MO, see (a) A. Streitwieser, Jr., "Molecular Orbital Theory for Organic Chemists," John Wiley & Sons, New York, N. Y. (1961), p. 173; (b) S. Koide, *J. Elect ochem. Soc. Japan (Denki Kagaku)*, **23**, 485 (1955).

14) H. Baba, This Bulletin, **34**, 76 (1961); H. Baba and S. Suzuki, ibid., **34**, 82 (1961); Ref. 12, p. 150.

15) T. Kubota, *J. Chem. Soc. Japan, Pure Chem. Sect. (Nippon Kagaku Zasshi)*, **80**, 578 (1959); This Bulletin, **35**, 946 (1962); T. Kubota and H. Watanabe, ibid., **36**, 1093 (1963), etc.

BULLETIN OF THE CHEMICAL SOCIETY OF JAPAN VOL. 39 2063—2066 (1966)

A Phtometric Particle-size Analyzer with a Moving Light Flux

By Yoshihide KOTERA, Kazuo SATO and Akihiro MIYAYAMA

Government Chemical Industrial Research Institute, Tokyo, Shibuya-ku, Tokyo

(Received September 2, 1965)

A recording, photometric, particle-size analyzer has been developed which is useful in measuring the particle-size distributions of powdered materials in the subsieve range. Provision for continuously moving the optical system upwards allows for rapid analysis of the finer particles, while by moving the system downwards accurate analysis of the particles with a larger density is possible. It was ascertained that the movement of the optical system has no effect on the results obtained.

The photo-extinction method of size-frequeny determination offers great possibilities, as has been pointed out by Rose,[1] for the development of a precise and convenient technique applicable to both routine and research investigations. As a matter of fact, however, this method takes a long time for a routine application, just as do the other sedimentation methods of size-frequency determination. Talcite and Paulus[2] constructed a recording, photometric, particle-size analyzer which has a provision for continuously varying the sedimentation depth so that the analysis can be carried out within an hour. However, they did not clarify how the movement of the sedimentation vessel affects the results obtained, and their system may be accompanied by trouble resulting from the movement of the vessel. We have now constructed an analyzer provided with an apparatus for continuously moving the light flux upwards or downwards, in order thus to carry out a rapid analysis of the finer particles or an accurate analysis of the particles with a larger density. The optical system designed to move smoothly allows a complete, accurate analysis to be made within an hour. The comparison of the results obtained by means of an apparatus with a moving light flux with those obtained by the ordinary static method makes it clear that the movement of the optical system has no effect on the analysis.

Principles.—The principles of the photo-extinction method have been published elsewhere.[1] The absorbance of a powder suspension is related to its concentration by an extension of the Lambert-Beer law:

$$\ln (I_0/I) = kcl \sum_{d_0}^{d_1} K_x n d_x^2 \qquad (1)$$

where I_0=the intensity of the incident light; I=the intensity of the transmitted light; k=a factor equal to A_p/d_x^2, where A_p is the projected area of a particle, and d_x, the diameter; c=the concentration of the powder suspension (g./ml.); l=the length of the cell; K_x=the extinction coefficient, that is, the ratio of the light-obscuring power of a particle to that for the same particle if the "square law" of geometrical optics were applicable, and n=the number of particles, whose diameter is d_x, per gram of powder. When we begin with a uniform suspension and a transverse light beam at a fixed depth below the surface, no change in the absorbance of the suspension will occur until the largest particles in the suspension fall from the surface to the level of the measuring beam. At this time the absorbance will decrease by an amount proportional to the concentration of the largest particles. Any point on the absorbance-vs.-time curve represents, then the concentration of particles smaller than the particle which would fall the distance, h, from the surface to the measuring beam during the time, t. When the light flux moves upwards or downwards, two cases may be considered:

a) when the light flux moves upwards with a constant velocity, v_0, from a point whose depth is b below the surface of the suspension, then:

$$h = b - v_0 t$$

and: $$d_x = K\sqrt{v} = K\sqrt{h/t};$$

Then: $$t = K^2 b/(d_x^2 + K^2 v_0);$$

b) when the flux moves downwards with a constant velocity, v_1, from a point whose depth is b below the surface of the suspension and when, after a time, t_1, it moves upwards with the same velocity, then:

$$h = v_1 t + b \quad \text{for} \quad t < t_1$$
$$t = K^2 b/(d_x^2 - K^2 v_1)$$

or: $$h = v_1(2t_1 - t) + b \quad \text{for} \quad t > t_1$$
$$t = K^2(2v_1 t_1 + b)/(d_x^2 + K^2 v_1)$$

where: $K^2 = 18\eta/g(\rho_p - \rho)$,

and η=the viscosity of the medium (poise), ρ_p=the density of the particle (g./ml.), ρ=the density

1) H. E. Rose, "Measurement of Particle Size in Very Fine Powders," Constable, London (1954).
2) N. A. Talvite and H. J. Paulus, *Rev. Sci. Instr.*, **27**, 763 (1956).

of the medium (g./ml.), and g=the gravitational constant (cm./sec./sec.).

A size-distribution based on the weight is expressed in the form of:

$$F_x = \frac{d_m}{K_m}(\ln I_1 - \ln I_2) \Big/ \sum_0^\infty \frac{d_m}{K_m}(\ln I_1 - \ln I_2),$$

where I_1 or I_2 is the intensity of the transmitted light for the suspension containing the powder whose diameters are in the range from 0 to d_1 or d_2 respectively. d_m is the mean of d_1 and d_2, and the K_m is the K_x value for d_m. I_1 and I_2 are proportional to the photocurrents, M_1 and M_2, from the photomultiplier.

Thus a size-distribution curve is obtained with an absorbance coordinate representing the concentration of particles less than the stated size and a time ordinate representing the particle size in terms of the Stokes diameter.

Design Constructions.—The analyzer is arranged as shown in the schematic diagram of Fig.

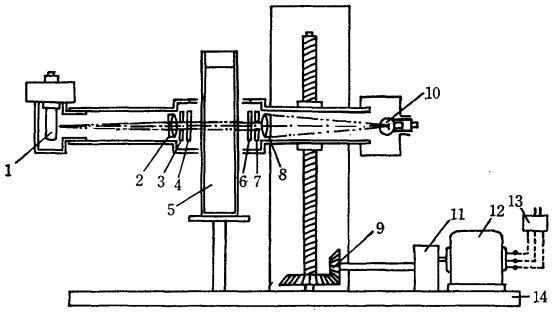

Fig. 1. Schematic diagram of the photometric particle-size analyzer.
1: Photomultiplier
2: Telescope lens
3: Slits
4: Absorption filter
5: Sedimentation cell
6: Monochrome filter
7: Slit
8: Collimeter lens
9: Gear for movement of light flux
10: Light source
11: Gear box
12: Synchronous motor
13: Reversing Switch
14: Base

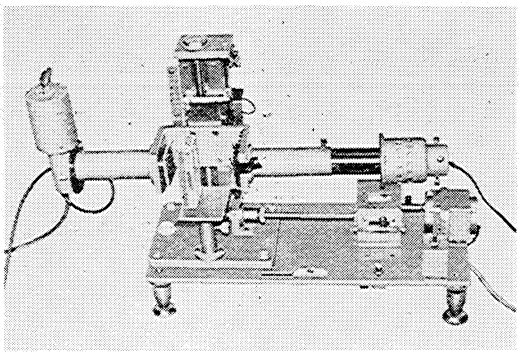

Fig. 2. Picture of the analyzer.

1. The apparatus is pictured in Fig. 2. The light source is a 5-amp., 6-V. bulb with a straight coiled filament and operated at a rated voltage from a 6-V. storage battery, the current being controlled with a rheostat. The collimation of a light beam is required for accurate analysis; therefore, the beam is made parallel by a condenser lens at its focal distance from the light source, while a slit immediately before the sedimentation cell limits the dimensions and angular divergence of the beam. A second slit following the cell cuts off the scattered light. A filter mount is located between the cell and the second slit, and a neutral filter is used for the control of the light intensity, while an interference filter is mounted when monochromatic light is required. The distance from the light source to the sedimentation cell is 33 cm., and that from the cell to the surface of the photomultiplier is 22 cm. The sedimentation cell must have parallel sides; its usual size is $40 \times 15 \times 100$ mm. The applied voltage for the photomultiplier, RCA-931A, is 700 V. to 770 V. The photocurrent is recorded by a Honeywell recorder.

The slit width is fixed at 25 mm., while its height may be varied in two fixed steps; 1 mm. and 2 mm. The optical system, including the light source, the lens, the slits and the photomultiplier, is mounted on a steel base arm and is fastened to a vertical brass slide. It can be raised or lowered by means of a standard micrometer head; this micrometer is coupled, by way of a set-screw clutch and right-angle drive, to a synchronous motor geared to raise or lower the

TABLE I. EXPERIMENTAL CONDITIONS

Exp. No.	Sample	Density of powder in the suspension wt.%	Conditions for movement of light flux					
			Movement	Velocity cm./sec.	Position of start cm.	Position of reverse cm.	Position of stop cm.	Time for measurement, min.
305	Silica powder	0.5	Fixed	0	4	—	4	30
306	Silica powder	0.5	Down- and upwards	0.0111	2	4	0	9
309	Silica powder	0.5	upwards	0.0333	10	no reverse	0	5
311	Silica powder	0.5	upwards	0.0111	6	no reverse	0	9

TABLE II. CALCULATING PROCESS OF RESULT OBTAINED

d_x, μ	0	5	10	15	20	25	30	35	40	45	50	
K_m		2.70	2.10	1.95	1.80	1.65	1.50	1.45	1.40	1.35	1.3	1.2
t, sec.		725.8	466.3	292.2	191.9	113.2	73.78	52.28	39.12	30.44	24.39	
M_x	8.19	7.50	6.87	4.32	3.70	3.42	3.25	3.17	3.12	3.095	3.08	3.04
$\log M_x$	0.9133	0.8751	0.8370	0.6355	0.5682	0.5340	0.5119	0.5011	0.4942	0.4907	0.4886	0.4829
$\log \frac{M_{x-1}}{M_x}$		0.0382	0.0381	0.2015	0.0673	0.0342	0.0221	0.0108	0.0069	0.0035	0.0021	0.0057
$\frac{1}{K_m}\bar{d}_x \log \frac{M_{x-1}}{M_x}$		0.035	0.136	1.292	0.654	0.466	0.405	0.242	0.185	0.110	0.077	0.285
$\sum_{\bar{d}_x}^{\infty}\left(\frac{1}{K_m}\bar{d}_x \log \frac{M_{x-1}}{M_x}\right)$		3.887	3.852	3.716	2.424	1.770	1.304	0.899	0.657	0.472	0.362	0.285
$\Sigma/\Sigma t \times 100$		99.1	95.6	62.4	45.5	33.5	23.1	16.9	12.1	9.3	7.3	
F_x		0.9	3.5	33.2	16.9	12.0	10.4	6.2	4.8	2.8	2.0	7.3

Temp.: 25.0°C

optical system. The rate may be varied in three fixed steps; 0.033 cm./sec., 0.011 cm./sec., and 0.0037 cm./sec. A reverse microswitch automatically changes the movement of the optical system from downwards to upwards when the system reaches the surface of the fixed height in the sedimentation cell, while a second microswitch shuts off the motor at the end of the run and may also shut off the paper drive of the recorder.

A 50 cm. × 26 cm. × 1 cm. structural, channel-steel plate forms the base of the analyzer; a rigid mounting surface for the sedimentation cell is fixed upon this base.

Operation.—Silica sand (density: 2.66) and tungsten carbide powder (density: 14.0) were used as the two samples for the test of the analyzer. The mixing of the suspension, whose concentration of solids was varied in several steps, was accompanied by quick inversions and agitations of the cell and by returning it to the cell component without delay. Sodium hexametaphosphate (0.2% of the total volume) was added to the suspension prior to the mixing in order to obtain a good dispersion. The intensity of the light beam was adjusted and the recorder chart and the mechanism which moves the optical system were actuated beforehand in order for the record to begin to operate at the instant when the cell was returned to its compartment. The chart speed was 0.0423 cm./sec. When the optical system is lowered in the first period of the experiment, the reverse switch changes the movement at the time of the arrival of the system at the fixed surface, its height from the surface of the suspension being measured before the start of the experiments. On the arrival of the light flux at the suspension surface, the measurement is finished.

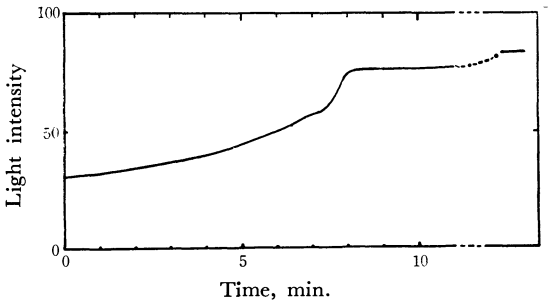

Fig. 3. Example of the chart obtained.

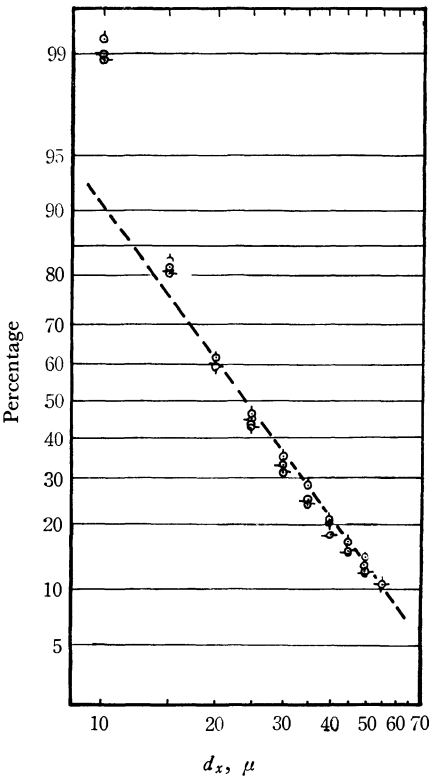

Fig. 4. Typical curves of particle-size distribution.
⊙ : A Fixed light flux.
⊙-: B Moved upwards $b=6$ cm.
⊙ : C Down- and upwards
-⊙ : D Moved upwards $b=10$ cm.

Performance.—The experimental data obtained under the conditions shown in Table I were calibrated in terms of Stokes' diameter. A typical procedure is shown in Table II, which relates the description to the principles. The values of K_m, the extinction coefficient, are those published by Rose, while M_x is the reading of the photocurrent for the suspension of the powder whose diameter is d_x. The summation of the values of $\{1/K_m \cdot d_x \cdot \log(M_{x-1}/M_x)\}$ was carried out from right to left in the table, that is, beginning with the value for the largest particles. The chart obtained in the experiments is shown in Fig. 3. Typical curves of particle-size distribution are shown in Fig. 4. In this figure it may be seen that the movement of the light flux has no effect upon the particle-size distribution curves. The deviation of the measured values with the movement of the light flux against those in the case of a fixed flux was very small and was estimated to be within the range of experimental error. It might be due to the disturbance of the suspension which remains immediately after the mixing of the powder suspension; this may cause the portion with the smaller diameter to increase. Such a deviation may occur when the analysis is carried out without taking the precaution of suppressing the disturbance of the suspension. Experiments are now being carried out in our laboratory in order to clarify this phenomenon. The fluctuations rise from other sources than the movement of the light flux, such as the inhomogeneity of the dispersion and the fluctuation of the cell temperature. The result for tungsten carbide powder seems to be more accurate in the subsieve range when the light flux is moved downwards at the beginning of the measurement than in the case of a fixed flux. In this case it was possible to shorten the measuring time to 9 min. by moving the flux, while the measurement with a fixed flux takes 30 min. All the measurements shown in Table I were carried out in 10 min., and the calculation for one measurement was about 10 min. longer than in the case of a fixed flux. The latter would be shortened by the use of an appropriate calculating chart.

BULLETIN OF THE CHEMICAL SOCIETY OF JAPAN VOL. 39 2066—2071 (1966)

Studies of the Surface Oxide Layer of Platinum Electrode

By Kunio OHASHI, Kazuo SASAKI* and Shigeo NAGAURA

Faculty of Engineering, Osaka City University, Sumiyoshi-ku, Osaka

(Received September 29, 1965)

The formation and reduction rates of the oxide layer of the platinum electrode were investigated by triangular-wave voltammetry and chronopotentiometry. A rate equation for the anodic process has been proposed in order to describe the fact that the electrode potential increases linearly with an increase in the surface concentration of oxygen. The cathodic reduction of surface oxide obeys the second-order rate law with respect to the amount of oxide covering the surface.

It has commonly been accepted that, in the electrolysis of an aqueous solution, an oxide layer is formed on the surface of the platinum electrode before any oxygen evolves. The chemical properties of the oxide and the kinetics of this electrode process have been studied by many workers.[1-16]

The present investigation has been carried out by means of chronopotentiometry and triangular wave voltammetry in order to understand the

* Present address: Faculty of Engineering, Hiroshima University, Hiroshima.

1) A. Hickling, *Trans. Faraday Soc.*, **41**, 333 (1945).
2) S. E. S. El Wakkad and S. H. Emara, *J. Chem. Soc.*, **1952**, 461.
3) I. M. Kolthoff and N. Tanaka, *Anal. Chem.*, **26**, 632 (1954).
4) F. Anson and J. J. Lingane, *J. Am. Chem. Soc.*, **79**, 4901 (1957).
5) K. J. Vetter and D. Berndt, *Z. Elektrochem.*, **62**, 378 (1958).
6) J. Giner, ibid., **63**, 386 (1959).
7) F. C. Will and C. Knorr, ibid., **64**, 258, 270 (1960).
8) J. Giner, ibid., **64**, 491 (1960).
9) H. A. Laitinen and C. G. Enke, *J. Electrochem. Soc.*, **107**, 773 (1960).
10) M. W. Breiter and J. L. Weininger, ibid., **109**, 1135 (1962).
11) S. Shibata, This Bulletin, **37**, 410 (1964).
12) S. Gilman, *Electrochim. Acta*, **9**, 1025 (1964).
13) W. Visscher and M. A. V. Devanathan, *J. Electroanal. Chem.*, **8**, 127 (1964).
14) K. Ohashi, K. Sasaki and S. Nagaura, *J. Electrochem. Soc. Japan (Denki Kagaku)*, **32**, 515 (1964).
15) J. S. Mayell and S. H. Langer, *J. Electrochem. Soc.*, **111**, 438 (1964).
16) S. W. Feldberg, C. G. Enke and C. E. Bricker, ibid., **110**, 826 (1963).

formation and reduction kinetics of the oxide, in a 1 N sulfuric acid solution. In a previous paper,[14] it was pointed out that the formation rate of the oxide can be elucidated by one of the following assumptions, either (a) or (b): (a) the apparent rate constant, k, of the electron transfer step obeys the equation: $k=k_0\exp(-g\theta)$, where θ is the surface coverage of the oxide layer, and g, a constant, or (b) the reaction involves the rate-determining adsorption step of the discharged species, which obeys Elovich's rate equation.[17] In this paper, the rate equation previously proposed for the anodic process[14] has been re-examined for a wider range of current density. For the cathodic process, a rate equation has been proposed.

Experimental

All the experiments were conducted at 25°C in 1 N aqueous sulfuric acid solutions prepared by mixing distilled water (sepcific resistance $>1\times10^6$ ohm·cm.) and concentrated pure sulfuric acid which had been obtained from the Wako Pure Chemical Ind. Co. (Osaka). For all experiments, the solutions were deaerated by nitrogen gas.

Two kinds of platinum electrode were used. One was a wire electrode of 0.1 cm. in diameter and about 1 cm. long, while the other was the same in platinum, a cross-sectional area of which was exposed. Before each run of measurements, the electrode was cleaned by dipping it in a chromic acid mixture and washed with distilled water. Finally, it was subjected to alternate anodic and cathodic polarizations in the 1 N sulfuric acid solution. A saturated calomel electrode was used as the reference electrode.

Chronopotentiometry.—A series of experiments was carried out by using the chronopotentiometric technique, with a current reversal. An electronic pen-recorder (Model EPR-2TB, Toa Electronics Ltd.; pen speed, 0.5 sec. for the full span; input impedance, 1.8 MΩ) was used to record the potential-time curve at low current densities of about 100 μamp./cm^2 or less, whereas at higher current densities a cathode ray oscilloscope (Model 502-A, Matsushita Communication Ind. Co., Ltd.; input impedance, 1 MΩ) was employed. The electrolytic current passing through the cell was switched by means of a mercury switching device.

Triangular Wave Voltammetry.—An electronic potentiostat (Model N-EP-2, Nichia Keiki, Sapporo) was used in this experiment. The electrolytic current was recorded by means of the electronic pen-recorder. The maximum sweep rate was limited by the response of the pen-recorder; it was about 0.4 V./sec.

Results and Discussion

The Anodic Chronopotentiogram and the Potential-Current Curve.—A typical chronopotentiogram obtained at the current density of 32 μamp./cm^2 is shown in Fig. 1. The oxide layer was formed in the region C and reduced in C'. Since the potential-time curve was almost linear in C, the increment of surface oxide with the electrode potential, dq/dE, was determined in this region. The results are listed in Table I in terms of $n\boldsymbol{F}(dq/dE)$*1.

The transition time in C, τ_a, was always greater than that in C', τ_c. The ratio of τ_a to τ_c was, for instance, about 1 : 0.8 at the current density of 32 μamp./cm^2. The cause of this discrepancy is not certain, but this problem will be referred to again at the end of this article.

A typical current-potential curve obtained at the sweep rate of 0.2 V./sec. is illustrated in Fig. 2. The curve shows two peaks in the region A, where the ionization of chemisorbed hydrogen occurs.[7]

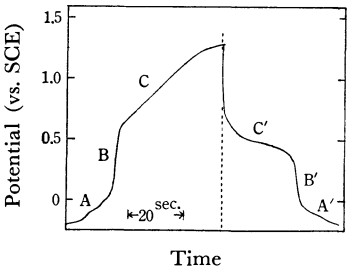

Fig. 1. Chronopotentiogram of platinum electrode in 1 N sulfuric acid solution.
Current density: 32 μamp./cm^2

Table I. The values of $n\boldsymbol{F}(dq/dE)$ at various current densities

Current density mamp./cm^2	$n\boldsymbol{F}(dq/dE)$ μF/cm^2
0.032	1.5×10^3
0.23	1.3
0.45	1.3
0.91	1.2
2.2	1.3
8.9	1.1
22	1.1

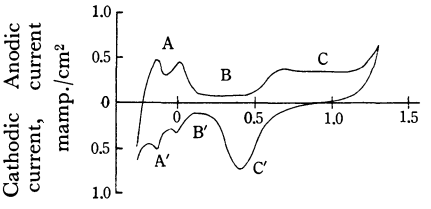

Fig. 2. Current-potential curve obtained by the potential sweep experiment with platinum electrode in 1 N sulfuric acid solution.
Sweep rate: 0.2 V./sec.

17) S. Yu. Elovich and G. M. Zhabrova, *Zhur. Fiz. Khim.*, **13**, 1761, 1775 (1939).

*1 The value of q is in mol./cm^2. The number of electrons, n, involved in the reaction concerned was assumed to be 2.

The regions denoted by C and C′ correspond to those denoted by the same notations in Fig. 1. The amount of charge (Q_H) required in A was graphically determined to be 4.0×10^2 μcoul./cm.^{2} while that (Q_O) required in C′ was 8.2×10^2 μcoul./cm^2. Thus, the ratio Q_H/Q_O was almost 1/2. This value coincides with that obtained by Will and Knorr,[7] who suggested a one-to-one correspondence between hydrogen and oxygen atoms on the surface of the platinum electrode.

The Rate Equation for the Anodic Process. —The anodic formation rate of the surface oxide obeys the following equation, as was pointed out in a previous paper.[14]

$$i_a = n\boldsymbol{F}k_a \exp(\beta n\boldsymbol{F}E/\boldsymbol{R}T-\lambda_a q) \qquad (1)$$

where i_a is the anodic current density; k_a and λ_a, constants; q, the amount of oxygen deposited to form the oxide layer (in mol./cm^2), and where the other symbols have their usual significance. The electrode potential, E, referred to the normal hydrogen electrode (NHE), was used in Eq. 1 instead of the overpotential.

Since in the experimental conditions $di_a/dt=0$ in the chronopotentiometry, Eq. 1 may be simplified as follows;

$$dq/dt = \frac{\beta n\boldsymbol{F}}{\lambda_a\boldsymbol{R}T}\cdot\frac{dE}{dt} \qquad (2)$$

This equation indicates that dq/dE should be constant, regardless of the current density. In fact, the experimentally-determined values of $n\boldsymbol{F}(dq/dE)$ were approximately constant even though the current densities employed were in a wide range, as may be seen in Table I. The slight decrease in $n\boldsymbol{F}(dq/dE)$ with an increase in the current density may be caused by another reason.*2

In Eq. 1, there is an additional exponential term describing the current dependence upon the amount of surface oxide deposited. Such a form of rate equation has often been found in the chemisorption process,[18,19] in which the activation energy, ε, of chemisorption increases linearly with an increase in the surface coverage, θ, of adsorbed species, as is shown by:

$$\varepsilon = \varepsilon_0 + r\theta$$

Since the surface coverage, θ, can be given by q/q_s, in which q_s is the amount of oxygen at the full coverage, the following equation can be written in analogy to Eq. 1:

$$i_a = n\boldsymbol{F}k_a \exp\{(\beta n\boldsymbol{F}E - r\theta)/\boldsymbol{R}T\} \qquad (3)$$

A rate equation of this form has also been applied to some electrode processes involving the chemisorption of reactant or intermediate product.[20]

Although Eq. 1 is analogous to Eq. 3 in form, it is hard to say whether the process concerned is the chemisorption of oxygen or the surface oxide formation.

For this reason, the term "surface oxide" has been used in the present article without any specification of its physico-chemical nature.

The Rate Equation for the Cathodic Process. —Since no rate equation has been strictly confirmed so far, the following equation will be assumed for the time being;

$$i_c = n\boldsymbol{F}k_c q^m \exp(-\alpha n\boldsymbol{F}E/\boldsymbol{R}T+\lambda_c q) \qquad (4)$$

where i_c is the cathodic current density, and k_c and λ_c are constants. In contrast to Eq. 1, the variable, q, which describes the surface concentration of oxygen is included in both the pre-exponential and the exponential terms in order to see the effect of this variable. In addition, the number of the reaction order, m, was introduced.

The time derivative of Eq. 4 is:

$$\frac{di_c}{dt} = i_c\left\{\left(\frac{m}{q}+\lambda_c\right)\frac{dq}{dt} - \frac{\alpha n\boldsymbol{F}}{\boldsymbol{R}T}\cdot\frac{dE}{dt}\right\} \qquad (5)$$

For the chronopotentiometric experiment, where the current is kept constant, Eq. 5 can be written as:

$$\frac{dE}{dt} = -\frac{\boldsymbol{R}T}{\alpha n\boldsymbol{F}}\left\{\frac{m}{\tau_c-t}+\frac{\lambda_c i_c}{n\boldsymbol{F}}\right\} \qquad (6)$$

by using the relations of $n\boldsymbol{F}q=(\tau_c-t)\cdot i_c$ and $i_c=-n\boldsymbol{F}\,dq/dt$. The slope, dE/dt, at the midpoint of the cathodic transition wave is:

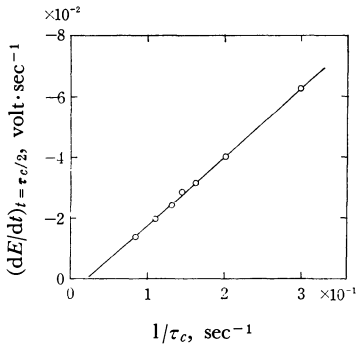

Fig. 3. Slope at the midpoint of the cathodic transition wave plotted against the reciprocal of the transition time (examination Eq. 7). The current density was kept at 1.8×10^2 μamp./cm^2 and the potential at which the anodic current as was reversed to cathodic one was changed.

*2 This behavior may be related to the fact that τ_a was greater than τ_c. If a part of the oxide dissolves chemically from the electrode surface, the value of dq/dE should decrease with an increase in the current density.

18) G. C. Bond, "Catalysis by Metals," Academic Press, London (1962), p. 105.

19) B. M. W. Trapnell, "Chemisorption," Butterworths Sci. Pub., London (1957).

20) B. E. Conway and E. Gileadi, *Can. J. Chem.*, **42**, 90 (1964).

$$\left(\frac{dE}{dt}\right)_{\tau_c/2} = -\frac{RT}{\alpha nF}\left\{\frac{2m}{\tau_c} + \frac{\lambda_c i_c}{nF}\right\} \quad (7)$$

Eq. 7 is examined in Fig. 3, where the slope of the potential-time curve determined at $\tau_c/2$ is plotted against the reciprocal of the transition time. The linearity is very good. It must be noted that the straight line crosses an ordinate near the point of origin. This shows a small value of λ_c (about 2% of λ_a). Therefore, the exponential contribution of q in Eq. 4 is negligible, and the term can safely be dropped. The slope of Fig. 3 should give $2mRT/\alpha nF$. Assuming $n=2$,*3 α/m is found to be 0.13.

Since, in the potential sweep experiment, the sweep rate is constant and di_c/dt is zero at the point of the cathodic current peak, the following equation can be obtained from Eq. 5:

$$\frac{1}{i_{max}} = \frac{RT}{\alpha(nF)^2 v}\left\{\frac{m}{q_{max}} + \lambda_c\right\} \quad (8)$$

where v is the sweep rate in V./sec. ($v=-dE/dt$ for the cathodic potential sweep) and where the subscript *max* denotes the values of each quantity observed at the current peak.

It was observed that the peak current value decreases with the decrease in the amount of oxide layer deposited anodically. In Fig. 4, the reciprocal of the peak current, $1/i_{max}$, is plotted against $1/q_{max}$. The value of q_{max} is the amount of oxide yet remaining unreduced until the potential of current peak is reached. Each q_{max} value was obtained by the graphical integration of the current-potential curve. The straight line intersects the ordinate at the point of origin, thus confirming the negligible value of λ_c. From the slope, α/m was found to be 0.13.

The reaction order, m, can be determined from the potential sweep experiment. The results obtained are shown in Fig. 5, where ($\log i_c - m \log q$)

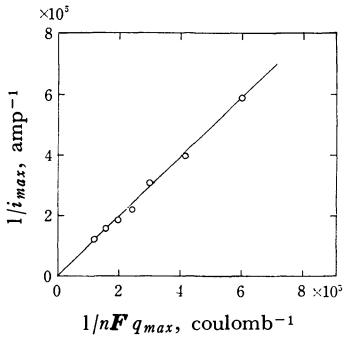

Fig. 4. The reciprocal of the peak current (i_{max}) is plotted against the reciprocal of the amount of oxide yet remained at the potential of current peak (examination of Eq. 8).
Sweep rate: 0.1 V./sec.
Electrode area: 7.8×10^{-3} cm²

*3 Cf. the reaction scheme proposed below.

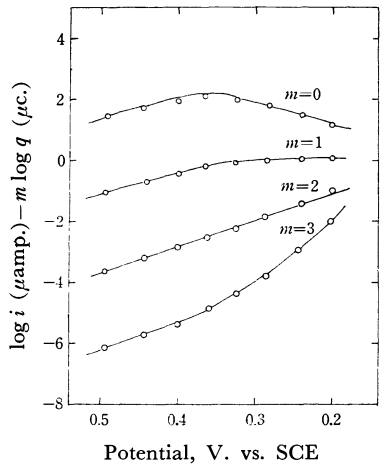

Fig. 5. The determination of the number of reaction order.
Sweep rate: 54 mV./sec.
Electrode area: 0.41 cm²

is plotted against the electrode potential. Four curves correspond to the arbitrary values of $m=$ 0, 1, 2 and 3 respectively. A straight line was obtained over the whole range of the cathodic reduction (C′ in Fig. 2) only when $m=2$. Accordingly, it can be concluded that the cathodic process is a second-order reaction with respect to the surface concentration. Therefore, the proper rate equation for the cathodic process becomes:

$$i_c = nFk_c q^2 \exp(-\alpha nFE/RT) \quad (9)$$

Another indication that the reaction order should be of the second-order was obtained by the following examination.

If the exponent of the amount of the oxide is unity instead of two, the following equation can be written as in Eq. 9, under the conditions of the potential sweep experiment, i. e., $dE/dt=-v=$ constant:

$$i_c = nFk_{c,I}\, q \exp\left\{-\frac{\alpha_I nF}{RT}(E_{t=0} - vt)\right\} \quad (10)$$

where the I subscript refers to the first-order reaction and where $E_{t=0}$ denotes the potential at which the direction of the potential sweep is reversed. By writing Eq. 10 as;

$$i_c = nFk_I q \exp\left(\frac{\alpha_I nF}{RT} vt\right) \quad (10')$$

and by integrating, using the relation $-nFdq/dt = i_c$,

$$i_c = nFk_I q_0 \exp\left(\frac{k_I}{P_I}\right)\exp\left\{x - \frac{k_I}{P_I}\exp(x)\right\} \quad (11)$$

where q_0 is the total amount of oxide to be reduced and where the other notations are:

$$P_I = \frac{\alpha_I nFv}{RT} \quad \text{and} \quad x = P_I t$$

Since $di_c/dt=0$ at the current peak,

$$P_I t_{max} = \ln \frac{P_I}{k_I} \tag{12}$$

By introducing Eq. 12 into Eq. 11, one can obtain an expression of the peak current, i_{max}:

$$i_{max}=nFq_0 P_I \exp\left\{\frac{k_I}{P_I}-1\right\} \tag{13}$$

Assuming $k_I P_I \ll 1$*4

$$i_{max}=\frac{\alpha_I (nF)^2 q_0 v}{eRT} \tag{14}$$

From the last equation, the transfer coefficient, α_I, can be determined by using the peak value of the current as determined experimentally. Once α_I is obtained, k_I is determined using Eq. 12.

If, however, the rate is second-order with respect to the surface concentration, Eq. 9 can be expressed in terms of time, i. e.,;

$$i_c = nFk_{II}q^2 \exp\left(\frac{\alpha_{II} nFvt}{RT}\right)$$

After similar treatment, as has been done with the equations from 11 to 14, the following relation are obtained:

$$i_c = nFk_{II}\left[\frac{P_{II}q_0}{k_{II}q_0\{\exp(x)-1\}+P_{II}}\right]^2 \exp(x) \tag{15}$$

$$P_{II}t_{max} = \ln\left(\frac{P_{II}}{k_{II}q_0}\right) \tag{16}$$*4

and by inserting Eq. 16 into Eq. 15:

$$i_{max} = \frac{\alpha_{II}(nF)^2 q_0 v}{4RT} \tag{17}$$

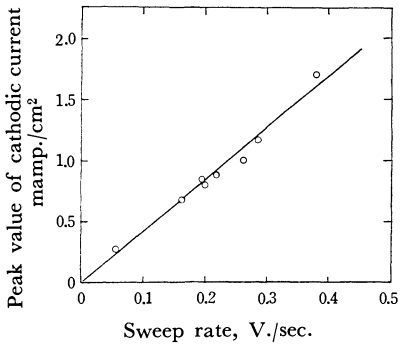

Fig. 6. Plot of cathodic peak current against sweep rate.

The α_{II} and k_{II} parameters can be determined by means of Eqs. 17 and 16. Equation 14 or 17 shows that the peak value of the current should be proportional to the sweep rate. This is confirmed in Fig. 6.

The values of kinetic parameters determined for the first- and second-order reactions are listed in Table II, where α_I and α_{II} were determined from Fig. 6 using either Eq. 14 or 17. The validity of the drived equations, 11 and 15, is examined in Fig. 7. It can easily be seen that the curve drived from Eq. 15 coincides with the experimental curve depicted for the sake of comparison. In the foregoing examination, the value of α/m was found to be 0.13, which is just half as much as the value of $\alpha_{II}=0.26$ determined for the second-order reaction (see Table II). This may, again, give the value of m to be two. The apparent rate constant, k_c, in Eq. 9 was determined as 5×10^{13} cm²/mol. sec. at 0 V. (vs. NHE).

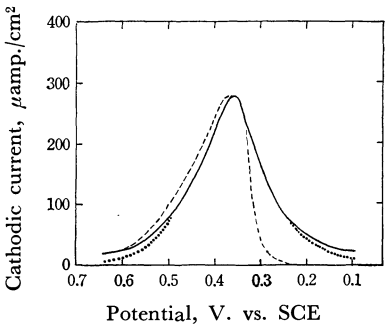

Fig. 7. Cathodic current-potential curves for the reduction of surface oxide;
—— Experimental curve sweep rate: 5.4×10^{-2} V./sec.)
---- Calculated from Eq. 11
····· Calculated from Eq. 15

Vetter[5] once suggested that hydrogen peroxide might be produced during the cathodic reduction of the surface oxide of the platinum electrode. According to him, the number of electrons, n, involved in the anodic oxide formation must be two per atom of oxygen deposited, whereas n is unity if the cathodic reduction product is hydrogen peroxide. Hence, in this case the quantity of charge observed in the anodic oxide formation should be twice as much as that in the cathodic reduction. Although Vetter's assumption was not based upon

TABLE II. NUMERICAL VALUES OF PARAMETERS REQUIRED IN THE CALCULATION OF EQS. 11 AND 15
Apparent rate constants, k_I and k_{II}, refer to 1.30 V. (SCE), at which the direction of the potential sweep was reversed. The value of q_0 was found as 5.1×10^{-9} mol./cm².

	m	α	k_I or k_{II}		v
1st order	1	0.18	1.9×10^{-6}	(sec^{-1})	0.054 (V./sec.)
2nd order	2	0.26	1.3	($cm^2 sec^{-1} mol^{-1}$)	0.054 (V./sec.)

*4 The validity of this assumption was confirmed by the derived result, $(k_I/P_I)=1.4\times 10^{-7}/v$. A similar assumption made in deriving Eq. 16 was confirmed by the result, $(k_{II}q_I/P_{II})=3.2\times 10^{-10}/v$.

any direct proof of the formation of hydrogen peroxide, its formation has recently been confirmed by Peters and Mitchell,[21] and also by Bianchi and Mussini.[22] They observed that hydrogen peroxide is produced with a high current efficiency during the cathodic reduction of the dissolved oxygen on the platinum electrode. Although Liang and Juliard[23] reported that no hydrogen peroxide was detected in the same system, this discordant finding, in our opinion, might have arisen from the different surface states of the electrode used.

Since, at the platinum electrode, the cathodic reduction of the dissolved oxygen and the surface oxide take place voltammetrically in one step,[24,25] the mechanism of the cathodic reduction of these two species will be quite similar. Therefore, it is probable that hydrogen peroxide will be produced intermediately during the reduction of surface oxide. If this is the case, the second-order rate law observed by the authors seems to favor the elucidation of the hydrogen peroxide formation. This problem, together with the reactions of dissolved oxygen and hydrogen peroxide, will be discussed elsewhere.[25]

The discrepancy found between τ_a and τ_c can be attributed partly to the intermediate formation of hydrogen peroxide. The reaction scheme may be written, for instance.*5 as:

$$\left.\begin{array}{l} \rightarrow 2PtO + 2H^+ + 2e \rightarrow 2Pt + H_2O_2 \quad (I) \\ \quad Pt + H_2O_2 \rightarrow PtO + H_2O \quad (II) \end{array}\right\}$$

If a part of the hydrogen peroxide formed by the bimolecular step (step I) diffuses away from the platinum surface without oxidative decomposition (step II), τ_c must be less than τ_a.

21) D. G. Peters and R. A. Mitchell, *J. Electroanal. Chem.*, **10**, 306 (1965).
22) G. Bianchi and T. Mussini, *Electrochim. Acta*, **10**, 445 (1965).
23) C. C. Liang and A. L. Juliard, *J. Electroanal. Chem.*, **9**, 390 (1956).
24) J. J. Lingane, ibid., **5**, 441 (1963).
25) K. Sasaki, K. Ohashi, M. Ioi and S. Nagaura, to be published in *J. Chem. Soc. Japan*.

*5 The reactions scheme presented here is the simplest one among the several possible reaction paths.

BULLETIN OF THE CHEMICAL SOCIETY OF JAPAN VOL. 39 2071—2085 (1966)

A New Method of Quantitative Differential Thermal Analysis

By Takeo OZAWA

Electrotechnical Laboratory, Tanashi-machi, Kitatama-gun, Tokyo

(Received October 26, 1965)

This paper presents a rigorous new theory of differential thermal analysis, taking account of the temperature gradient in the sample. From this consideration, a new quantitative method is proposed, where a solid-cell holder of low thermal conductivity is set between a sample cell and a metal block, and a thermocouple is inserted tightly between the outside wall of the cell and the cell holder. By means of this arrangement, the peak area becomes proportional to the heat of transformation, irrespective of the kinds and the states of samples and operational variables. The experimental verification using various samples and the effect of several operational variables, such as the heating rate, the concentration of a diluent, the packing density, and the depth of the packing sample, are also shown; satisfactory results are obtained. Two new concepts, the sensitivity and the response time of the system, are proposed and evaluated. Conventional methods are criticized, and the inherent limitations of differential thermal analysis are discussed.

Differential thermal analysis has been widely used in scientific and engineering fields to study clays, soaps, polymers and various other organic and inorganic materials[1-3] since Le Chaterier's first employment of its prototype in 1887.[4] By this method we can record the temperature difference between a sample and a thermally-inert reference material heated at a constant rate by an external furnace, and thermal transformations occurring in the sample can thus be recognized as deviations from the base line in the record of the temperature difference against the time, which forms a differential thermogram.

1) W. J. Smothers and Yao Chiang, "Differential Thermal Analysis: Theory and Practice," Chemical Publishing Co., Inc., New York (1958).

2) B. Ke, "Organic Analysis," Vol. 4, Ed. by J. Mitchel, Jr., I. M. Kolthoff, E. S. Proskauer and A. Weissberger, Interscience Publishers, New York (1960): B. Ke, "Newer Methods of Polymer Characterization," Interscience Publishers, New York (1964).

3) W. W. Wendlandt, "Thermal Methods of Analysis," Interscience Publishers, New York (1964).

4) H. Le Chaterier, *Z. physik. Chem.*, **1**, 396 (1887).

Although numerous reports have hitherto been published, there remain problems about the quantitative differential thermal analysis, namely, the method of estimating the heat of transformation by differential thermal analysis. In order to evaluate the heats of transformation from differential thermograms, Vold[5] suggested a theory which requires a knowledge of the heat capacity of the sample. If her theory is further developed, a relation can be derived which corresponds to the theories of Kerr and Kulp;[6] Speil, Swerdlow, Pask and Davices;[7] Evans, Hutton and Mathews,[8] and so on, who all indicate that the area enclosed by the peak and the base line in a differential thermogram is proportional to the heat of transformation. However, in these theories the experimental condition for the constant of the proportionality between the heat and the area is not shown to be independent of the sorts of the samples and other experimental factors, because the effects of the volume and the shape of the sample are neglected in the theories.

On the other hand, considering these effects Soulé[9] and Nagasawa[10] suggested that the proportionality constant contains the apparent density and apparent thermal conductivity of the sample; furthermore, Boersma[11] pointed out, for the same reasons, that quantitative differential thermal analysis by the conventional methods is inherently impossible, because the proportionality constant becomes a function of the apparent thermal conductivity of the sample. Soulé thus suggested a method which makes the proportionality constant independent of the thermal conductivity of the sample and other operational factors, but his method has not yet been developed. Strum[12] extended Boersma's theory and introduced a method of quantitative differential thermal analysis, but it is a rather complicated one. Otsubo and Yamaguchi[13] also published their rigorous treatment of heat conduction within the apparatus of differential thermal analysis and devised an approximate method of estimating the heat; their theory is, however, essentially equivalent to Vold's theory, and also the value of the specific heat of the sample is needed if we are to analyze the data. Naturally, therefore, the theory is limited in application. Strella[14] recently proposed a new method, but it is a complicated one and seems to contain some rough assumptions. Therefore, quantitative differential thermal analysis has not yet been established.

Recently Speros and Woodhouse[15] reported on "quantitative differential thermal analysis," but theirs is essentially a differential enthalpic analysis,[16] one which has different theoretical bases, different advantages, and a limited application, because the temperature difference between the sample and the reference material must be nullified and the error of such operation has a serious effect at a higher temperature; this is also the case in an adiabatic calorimeter.

Although the direct measurement of the specific heat by an adiabatic calorimeter (or differential enthalpic analysis) is an absolute, excellent method, the differential thermal analysis has the following advantages over it: (1) the simplicity and ease of the operation and the analysis of the data; (2) its applicability to cooling processes and to measurements under a high pressure[17] and/or at a higher temperature, and (3) its applicability to chemical reactions and exothermic phenomena such as crystallization.[18] Therefore, it is still important to establish quantitative differential thermal analysis.

In the present paper, the author will report a theory of broad vision from which he has derived a new, simple and convenient method of estimating the heat of transformation by differential thermal analysis; the experimental verification of the method will also be shown. From these considerations we can elucidate the sensitivity of the apparatus, the resolution of the peaks, the influence of some operational factors on the differential thermograms, and the inherent limitations of differential thermal analysis.

Theoretical Considerations

As has been mentioned above, there have been no rigorous treatments of the temperature gradient in the sample in the previous theories of differential thermal analysis. Now, an exact elucidation of the temperature gradient should be attempted. In a conventional apparatus, the sample and the reference material are packed in a pair of cavities of a metal block, and a temperature-detection device is inserted into the center of each cavity. In some cases,[19] the sample and reference cells with the

5) M. J. Vold, *Anal. Chem.*, **21**, 683 (1949).
6) P. F. Kerr and J. L. Kulp, *Am. Mineralogist*, **33**, 387 (1948).
7) S. Speil, S. B. Swerdlow, J. Pak and B. Davices, *Bureau of Mines, Technical Paper*, **664**, (1945).
8) D. Evans, J. F. Hutton and J. B. Mathews, *J. Appl. Chem.*, **2**, 252 (1952).
9) J.-L. Soulé, *J. phys. rad.*, **13**, 516 (1952).
10) K. Nagasawa, *J. Earth Sci., Nagoya Univ.*, **1**, 156 (1953).
11) S. L. Boersma, *J. Am. Ceram. Soc.*, **38**, 281 (1955).
12) E. Strum, *J. Phys. Chem.*, **65**, 1935 (1961).
13) Y. Otsubo and K. Yamaguchi, *Bull. Sci. and Eng. Res. Lab., Waseda Univ.*, No. 19, 58 (1962).
14) S. Strella, *J. Appl. Polymer Sci.*, **7**, 1281 (1963).
15) D. M. Speros and R. L. Woodhouse, *J. Phys. Chem.*, **67**, 2164 (1963); *Nature*, **197**, 1261 (1963).
16) C. Eyraud, *Compt. rend.*, **238**, 1511 (1954).
17) B. Wunderlich, *Rev. Sci. Instr.*, **32**, 1424 (1961); R. C. Newton, A. Jayaraman and G. C. Kennedy, *J. Geophys. Res.*, **67**, 2559 (1962).
18) N. D. Scott, *Polymer*, **1**, 114 (1960).
19) C. J. Penther, S. T. Abrams and F. H. Stross, *Anal. Chem.*, **23**, 1459 (1951).

temperature-detection devices are inserted in the cavities of the metal block without touching the walls at all. In the method described in this paper, the sample and reference cells are put into cell-holders set in the cavities of the metal block, while the temperature-detection devices are located between the cells and the cell holders. These arrangements are illustrated in Fig. 1. The cell holder is made of thermally-inert solid material of a low thermal conductivity in which a temperature gradient develops corresponding to the heat flow into the sample, as will be seen later.

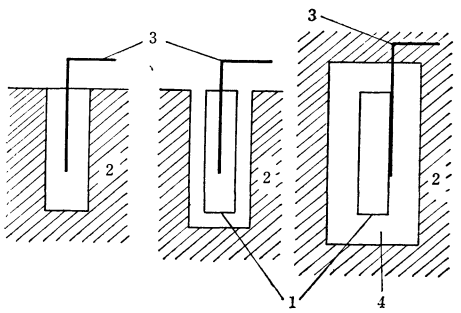

Fig. 1. The three types of the arrangements of the cell (1), the metal block (2), the temperature detection device (3) and the cell holder (4).

Now, let us consider the temperature gradient in the sample, the reference material and the cell holders. We can derive the equations of the heat flow for these materials by assuming that the heat transfers by conduction only, that the heat is not lost at the interface between the cell holder and the cell, and that the temperature of the inner surface of the cell holder is equal to that of the surface of the cell. The metal block is heated at a constant rate, a, of heating (or cooling). It is also assumed that the metal block has so large a heat capacity and thermal conductivity, and/or that it is controlled so strictly in its heating rate, that the heating rate of the metal block is not disturbed by the heat of transformation occurring in the sample. For the sake of simplicity the shape of the cell is cylindrical and it is long enough for us to be able to neglect the heat flow through the ends. The heat loss through the temperature-detection device is also neglected.

Within the sample:

$$\lambda_s \nabla T_s = c_s \rho_s \frac{\partial T_s}{\partial t} + \rho_s \Delta H \frac{\partial m}{\partial t} \tag{1}$$

and within the cell holder:

$$\lambda_h \nabla T_h = c_h \rho_h \frac{\partial T_h}{\partial t} \tag{2}$$

where:

∇ = a Laplacian

λ = the thermal conductivity

T = the temperature

c = the specific heat

ρ = the apparent density

t = the time

ΔH = the heat of the transformation of the sample per unit mass

$\frac{\partial m}{\partial t}$ = the rate of the transformation in mass,

and where the subscripts s and h denote the sample and the cell holder.

The boundary and initial conditions of the above equations are as follows:

$$T = at \qquad \text{at } r = R_o \tag{3}$$

$$\lambda_s \frac{\partial T_s}{\partial r} = \lambda_h \frac{\partial T_h}{\partial r} \qquad \text{at } r = R_i \tag{4}$$

$$T_s = T_h \qquad \text{at } r = R_i \tag{5}$$

and

$$T_s = T_h = 0 \qquad \text{at } t = 0 \tag{6}$$

where

r = the distance from the central axis

R_o = the outer radius of the cell holder

R_i = the inner radius of the cell holder

= the radius of the cell

These equations can be applied to other arrangements of the sample. Namely, if R_o is made equal to R_i, the solution becomes one for a conventional appearatus. In an apparatus such as (b) in Fig. 1, the temperature is measured at the center of the sample, and the solution of the equations can be applied if one neglects the heat transfer by convection and radiation in the air gap between the cell and the metal block.

Assuming a cylindrical symmetry, we have the next solutions of Eqs. 1 and 2, when the transformation does not occur in the sample; i. e., $\partial m/\partial t = 0$ (see in Appendix).

$$T_s = at - \frac{a}{4\lambda_h}\left[c_h\rho_h(R_o^2 - R_i^2) + 2R_i^2(c_s\rho_s - c_h\rho_h)\log\frac{R_o}{R_i}\right] - \frac{ac_s\rho_s}{4\lambda_s}(R_i^2 - r^2) + \sum_{n=0}^{\infty} \boldsymbol{A}_n(r)\exp\left(-\frac{t}{\tau_n}\right) \tag{7}$$

$$T_h = at - \frac{a}{4\lambda_h}\left[c_h\rho_h(R_o^2 - r^2) + 2R_i^2(c_s\rho_s - c_h\rho_h)\log\frac{R_o}{r}\right] + \sum_{n=0}^{\infty} \boldsymbol{B}_n(r)\exp\left(-\frac{t}{\tau_n}\right) \tag{8}$$

where $\boldsymbol{A}_n(r)$'s and $\boldsymbol{B}_n(r)$'s are functions of r only, and where τ_n's are the roots of the equation:

$$\sqrt{\lambda_h c_h \rho_h}\boldsymbol{J}_0\left(R_i\sqrt{\frac{c_s\rho_s}{\lambda_s\tau_n}}\right)\Big[\boldsymbol{J}_1(R_ix)\boldsymbol{Y}_0(R_ox) - \boldsymbol{J}_0(R_ox)\boldsymbol{Y}_1(R_ix) = \sqrt{\lambda_s c_s \rho_s}\boldsymbol{J}_1\left(R_i\sqrt{\frac{c_s\rho_s}{\lambda_s\tau_n}}\right) \times [\boldsymbol{J}_0(R_ix)\boldsymbol{Y}_0(R_ox) - \boldsymbol{J}_0(R_ox)\boldsymbol{Y}_0(R_ix)] \quad (9)$$

where x is equal to $\sqrt{c_h\rho_h/\lambda_h\tau_n}$, where $\boldsymbol{J}_0$ and $\boldsymbol{J}_1$ are Bessel functions of the zero and 1st orders respectively, and where $\boldsymbol{Y}_0$ and $\boldsymbol{Y}_1$ are Neuman functions of the zero and 1st orders respectively.

The following equations are derived analogously for the reference material and its cell holder:

$$T_r = at - \frac{a}{4\lambda_h}\left[c_h\rho_h(R_o^2 - R_i^2) + 2R_i^2(c_r\rho_r - c_h\rho_h)\log\frac{R_o}{R_i}\right] - \frac{ac_r\rho_r}{4\lambda_r}(R_i^2 - r^2) + \sum_{n=0}^{\infty}\boldsymbol{C}_n(r)\exp\left(-\frac{t}{\tau_n'}\right) \quad (10)$$

$$T_{h'} = at - \frac{a}{4\lambda_h}\left[c_h\rho_h(R_o^2 - r^2) + 2R_i^2(c_r\rho_r - c_h\rho_h)\log\frac{R_o}{r}\right] + \sum_{n=0}^{\infty}\boldsymbol{D}_n(r)\exp\left(-\frac{t}{\tau_n'}\right) \quad (11)$$

where the subscripts r and h' denote the reference material and its cell holder respectively, where $\boldsymbol{C}_n(r)$'s and $\boldsymbol{D}_n(r)$'s are functions of r only, and where τ_n''s are the roots of the equation:

$$\sqrt{\lambda_h c_h \rho_h}\boldsymbol{J}_0\left(R_i\sqrt{\frac{c_r\rho_r}{\lambda_r\tau_n'}}\right)[\boldsymbol{J}_1(R_ix')\boldsymbol{Y}_0(R_ox') - \boldsymbol{J}_0(R_ox')\boldsymbol{Y}_1(R_ix')] = \sqrt{\lambda_r c_r \rho_r} \times \boldsymbol{J}_1\left(R_i\sqrt{\frac{c_r\rho_r}{\lambda_r\tau_n'}}\right)[\boldsymbol{J}_0(R_ix')\boldsymbol{Y}_0(R_ox') - \boldsymbol{J}_0(R_ox')\boldsymbol{Y}_0(R_ix')] \quad (12)$$

where x' is equal to $\sqrt{c_h\rho_h/\lambda_h\tau_n'}$.

The last terms of Eqs. 7, 8, 10 and 11 form the Bessell-Fourier series expressing the transient temperature; they are related to the temperature distribution in the steady state.

As the temperatures are measured at the interfaces between the cells and the cell holders in the present method, the temperature difference between the sample and the reference material, ΔT, is given by:

$$\Delta T = T_s - T_r = \Delta T_b + \sum_{n=0}^{\infty}\boldsymbol{A}_n(R_i)\exp\left(-\frac{t}{\tau_n}\right) - \sum_{n=0}^{\infty}\boldsymbol{C}_n(R_i)\exp\left(\frac{t}{\tau_n'}\right) \quad (13)$$

where:

$\Delta T_b = a(C_r - C_s)/K$

$K = 2\pi l\lambda_h/\log(R_o/R_i)$

$C_s = \pi R_i^2 c_s\rho_s l$ = the heat capacity of the sample plus the cell

$C_r = \pi R_i^2 c_r\rho_r l$ = that of the reference material plus the cell

l = the length of the cell.

The height of the base line is ΔT_b, and the other terms give the transient temperature.

From Eq. 13 it is apparent that it is necessary for the heat capacity of the reference material to be equal to that of the sample, as has already been pointed out by Vold[5]; the necessity of this remains in our method derived by the rigorous treatment. The differential method eliminates the error due to the fluctuation of the base line caused by the fluctuating rate of heating, if the above necessity is fulfilled, and it is preferable that τ_n''s be nearly equal to τ_n's; i. e., it is preferable that the reference material have a similar effective thermal conductivity. The role of the reference material is neither more nor less than this elimination.

The values of $\boldsymbol{A}_n(r)$'s, $\boldsymbol{B}_n(r)$'s, $\boldsymbol{C}_n(r)$'s and $\boldsymbol{D}_n(r)$'s do not play an important role in the measurement, and so we need not know their exact values, because these series converge to zero in the intervals of the order of $5\tau_n$ and $5\tau_n'$, which are important ones. It is necessary to know. The largest values of τ_n's and τ_n''s, τ_0 and τ_0' are the response times of the system, and they give the order of the time necessary for the system to attain to a steady state. If the values of τ_0 and τ_0' are large, the measurement of the transformation occurring at a lower temperature becomes obscure, because the system has not attained to the steady state before it reaches the transformation temperature. It should be noted that τ_n and τ_n' do not depend on the point of the temperature measurement and the heating rate, but on the thermal properties and the geometry of the system. It should also be pointed out that τ_n is important to the measurement in yet another way, as will be discussed below.

We should now like to discuss the other transient state after the transformation. Suppose that the transformation in the sample is completed at $t = t_c$ and that the temperature distribution is different from that of the steady state. As the same equations, 1 and 2, and the same boundary conditions, 3, 4 and 5, hold for this case, the transient temperature distribution is given corresponding to different initial conditions, because the temperature distribution at the steady state and the τ_n's are determined irrespective of the initial temperature distribution (see Appendix).

$$T_s = at - \frac{a}{4\lambda_h}\left[c_h\rho_h(R_0^2 - R_i^2) + 2R_i^2(c_s\rho_s - c_h\rho_h)\log\frac{R_0}{R_i}\right] - \frac{ac_s\rho_s}{4\lambda_s}(R_i^2 - r^2) + \sum_{n=0}^{\infty} \boldsymbol{E}_n(r)\exp\left(-\frac{t-t_c}{\tau_n}\right) \quad (14)$$

$$T_h = at - \frac{a}{4\lambda_h}\left[c_h\rho_h(R_0^2 - r^2) + 2R_i^2(c_s\rho_s - c_h\rho_h)\log\frac{R_0}{r}\right] + \sum_{n=0}^{\infty} \boldsymbol{F}_n(r)\exp\left(-\frac{t-t_c}{\tau_n}\right) \quad (15)$$

where the last terms are the Bessell-Fourier series related to the temperature distribution at t_c, and where the τ_n's are, as before, the roots of Eq. 9.

Thus, the transient temperature disappears in the time interval of the order of $5\tau_0$, which determines the resolution of the adjacent peaks and which should be called "the response time" determining the resolving power of the system. It is of interest to note that the response time of the system is not given in the dimension of temperature but in that of time, and that, if the second transformation occurs within the temperature range of the order of $5a\tau_0$, the peaks may overlap. These facts suggest the advantage of a low heating rate. However, there is a possibility of resolving these overlapped peaks in a different way. If τ_0 is large enough compared to the other τ_n's, which may be true in most cases, the transient temperature of the Bessell-Fourier series can be approximated by a single exponential function. Thus, if one plots the logarithm of $(\Delta T - \Delta T_b)$ against the time beginning at the top of the peak, the points lie on a straight line after the completion of the transformation. Such a procedure not only resolves the overlapped peaks, but also gives, though only approximately, the time of the completion of the transformation, the determination of which is important in the measurements of binary mixtures, high polymeric samples, and chemical reactions, because these changes occur over a wide range of temperature. This linearity can also be used to separate the peaks. For example, in order to ascertain the melting behavior of high polymers, one must plot the change in the crystallinity against the temperature. By using differential thermal analysis, this can be done by separating the peaks with these exponentially-decaying curves. Ke[20] divided the peak into components, but his method of division should be revised on the basis of the present facts. The above-mentioned linear relationship was pointed out and shown experimentally by Vold[5] and by Otsubo et al.,[13] but it should be noted that τ_0 determines the resolving power and that it can be estimated by Eq. 9 in designing the apparatus.

20) B. Ke, *J. Polymer Sci.*, **42**, 15 (1960).

Finally we consider the area under the peak, for which the relation (see Appendix) holds:

$$\Delta H \cdot M = K \cdot A \quad (16)$$

where M is the mass of the sample and A is the area of the peak. The proportionality coefficient, K, is given above; it is related to the geometry and thermal conductivity of the cell holder, not to the thermal properties of the sample. Therefore, the coefficient is the constant characteristic of the apparatus. This fact is the basis of this quantitative differential thermal analysis; the cell holder serves as the heat-flow-meter, developing within itself the proportional magnitude of the temperature gradient to be measured. The proportionality coefficient can be evaluated by the measurement of a sample of a known heat of transformation. As it is related to the thermal conductivity, it would be a function of the temperature and one needs to measure the transition of the known latent heat over the workable temperature range in order to evaluate the proportionality coefficient.

As has already been pointed out by Boersma,[11] in the conventional method, the sample plays two quite different parts, parts which conflict with each other: (a) a producer of heat to be measured, and (b) a heat measureing resistance in which the heat flow develops a temperature gradient necessary for the measurement. Thus, in the conventional model, the temperature gradient within the sample is essential. However, in the present method the temperature gradient within the sample can be reduced without sacrificing the sensitivity of the apparatus. If one introduces a certain device to diminish the temperature gradient within the cell, the peaks will be sharpened, and the accuracy of the temperature measurement and the resolution of the peaks may even be increased.

Essentially, this method of quantitative differential thermal analysis is a technique for measuring the heat by the temperature gradient existing in the given inert material, through which the heat flows into the sample cell.

Let us now discuss the optimum design of the

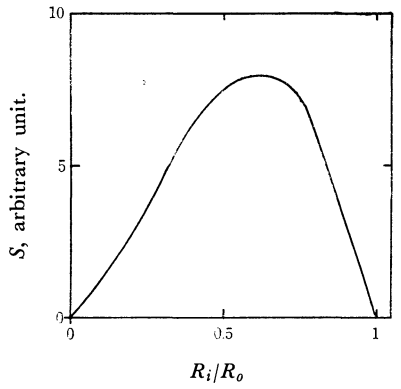

Fig. 2. The sensitivity versus the ratio, R_i/R_0.

cell holder. The "sensitivity" of the apparatus, S, could be defined as the peak area per the unit heat of transformation occurring in the unit volume of the sample:

$$S = A/\rho_s \Delta H = V_s/K \tag{17}$$

Namely,

$$S = R_i^2 \log (R_o/R_i)/2\lambda_h \tag{18}$$

The sensitivity increases with the second power of the radius of the cell. It may easily be seen that, for a given R_o, the optimum ratio of R_i to R_o is $e^{-1/2}$; the sensitivity is plotted against the ratio in Fig. 2. If R_i is fixed, the sensitivity increases logarithmically with an increase in R_o.

For a glass transition[21-24] or a second-order transition, where the specific heat of the sample changes without latent heat, a step-by-step change in the base line is recorded as being due to the change in the heat capacity of the sample. The height of the step-by-step change is derived:

$$\Delta T_{b2} - \Delta T_{b1} = aS\Delta c_s \rho_s \tag{19}$$

where ΔT_{b1} and ΔT_{b2} are the temperature differences in the steady state before and after the transition respectively, and where Δc_s is the change in the specific heat of the sample. In this case, the change in the base line depends on the sensitivity and the heating rate, and thus higher heating rates are preferred. The response time to the new base line would also be of the order of $5\tau_0$.

Thus, we have a theoretical basis for estimating the heat of transformation by differential thermal analysis, and the expressions of the response time and the sensitivity have been given. The inherent limitations of the differential thermal analysis should now be considered. In the derivation given above, the heat capacity of the sample is implicitly assumed to be constant. If the heat capacity changes at the thermal transformation, the base line must change after the peak; the estimation of the peak area should suffer from these changes. The theoretical treatment can be derived considering these changes in the thermal properties of the sample; the corrected area is shown in Fig. 3, where the time interval, τ_c, has the following value (see Appendix):

$$\tau_c = c_h \rho_h \left(R_o^2 - R_i^2 - R_i^2 \log \frac{R_o}{R_i} \right) \Big/ 4\lambda_h \log \frac{R_o}{R_i} + c_s' \rho_s' R_i^2 \log \frac{R_o}{R_i} \Big/ 4\lambda_h \tag{20}$$

where c_s' and ρ_s' are the specific heat and the density of the sample after the transition, and where τ_c contains those unknown values. Therefore,

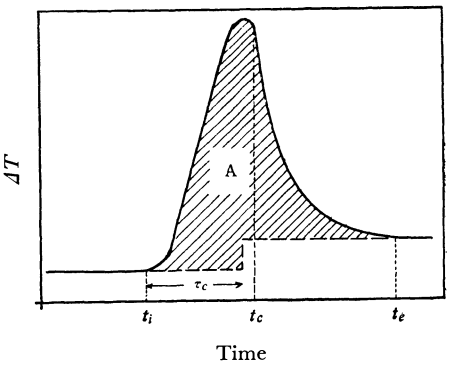

Fig. 3. The corrected peak area.

no accurate correction can be made unless those values are known. Strella[14] suggested a method of correction, but his theory contains rough assumptions and it seems that, using it, the error due to the assumptions would become larger than the correction.

The end effect neglected in the theory should also be considered; this effect would add some terms to the proportionality coefficient and could be decreased if the length of the cell is large enough in comparison with its diameter. The heat flow through the leads of the temperature-detection device is also neglected; it would also add some correction terms to the proportionality coefficient if the leads pass through the metal block and if the heat flows into the cell through the leads not from the outside but from the metal block.

Finally, let us give the proportionality coefficient, the sensitivity and the response time for other types of arrangements and discuss them briefly. For the most conventional type (as is shown in (a) of Fig. 1), because $R_o = R_i = R$ and $r = 0$ (see Appendix):

$$K = 4\pi l \lambda_s \tag{21}$$

$$S = R^2/4\lambda_s \tag{22}$$

and:

$$J_0(R\sqrt{c_s \rho_s/\lambda_s \tau_n}) = 0 \tag{23}$$

For the type shown in (b) of Fig. 1 (see Appendix):

$$K = 4\pi l/[1/\lambda_s + (2/\lambda_a) \log (R_o/R_i)] \tag{24}$$

$$S = R_i^2[1/4\lambda_s + (1/2\lambda_a) \log (R_o/R_i)] \tag{25}$$

Here the τ_n's are the roots of an equation similar to Eq. 9, where λ_h, c_h and ρ_h are replaced with those of air, λ_a, c_a and ρ_a respectively. If λ_s is much larger than λ_a,

$$K \fallingdotseq 2\pi l \lambda_a / \log (R_o/R_i) \tag{26}$$

The proportionality coefficient becomes the coefficient independent of the kind and the state of the sample, but the heat exchange by radiation and convection disturbs the proportionality, especially above 300°C.

21) M. L. Dannis, *J. Appl. Polymer Sci.*, **7**, 231 (1963).
22) S. Strella, ibid., **7**, 569 (1963).
23) B. Wunderlich, D. M. Bodily and M. H. Kaplan, *J. Appl. Phys.*, **35**, 95 (1964).
24) A. R. Haly and M. Dole, *J. Polymer Sci.*, B, **2**, 285 (1964).

Experimental

Apparatus.—In designing the apparatus, the assumptions made in the mathematical derivations must be taken into account, besides the arrangement of the cell, the cell holder and the temperature-detection device; the metal block must have a large enough heat capacity and heat transfer coefficient; it is preferable that the thermal conductivity of the cell holder be low and have a small temperature dependency; the solid cell holder must cover the entire surface of the cell; it should make a good, reproducible thermal contact with the surface of the cell if possible, and the temperature gradient in the system has a cylindrical symmetry (in other words, the length of the cylinder must be long enough compared with its radius). The temperature gradient in the metal block must be negligibly small. The response time and sensitivity must also be taken into account.

The purpose of constructing our apparatus is to study the thermal behavior of high polymeric meterials. Hence, the apparatus is expected to be operated up to 600°C and it must be suitable to a sample with a low thermal conductivity. The following apparatus is constructed for the above purpose, but the principles of the design considered in this research are essentially applicable to other fields of research.

According to the above considerations, the apparatus shown in Figs. 4 and 5 is constructed. The metal block consists of three separable parts, which cover the cell holders, as is shown in Fig. 4; these are made of nickel because of its thermal stability. Although copper and aluminum are preferred because of their higher thermal conductivities, these metals are not stable at high temperatures. In the block are drilled six cylindrical cavities, in which are inserted the cell holders, the cells, and the thermocouples. In two of the six cavities are set reference cells with the same heat capacity as that of the sample; in three of them, a sample cell, and in the sixth and last one a reference cell with a half-amount of the reference material. The temperature difference between the last reference cell and the ordinary reference cell serves as a monitor to indicate the false deflection of the base line due to the fluctuation of the heating rate or other accidential causes. The other three temperature differences between the three sample cells and the two reference

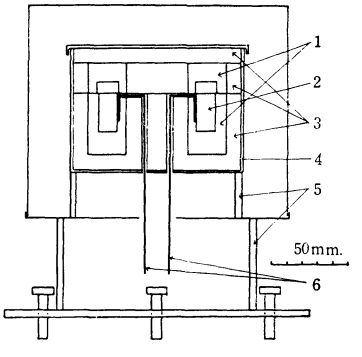

Fig. 4. The apparatus.

1 Cell holder 2 Cell
3 Metal block 4 Heater
5 Quartz support 6 Thermocouple

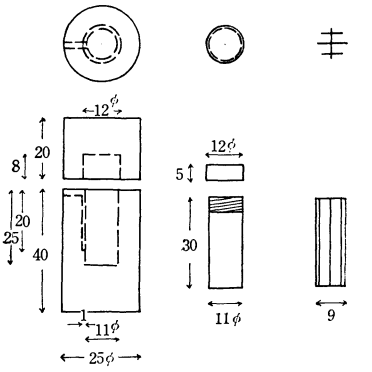

Fig. 5. The cell holder, the cell and the heat distributor.

cells are recorded. This arrangement makes possible the simultaneous measurement of three samples.

The block is inserted into a furnace made of a nickel cylinder. Nichrome wire about 0.3 mm. in diameter is wound on the mica film with which the side and bottom of the furnace are convered. As the heat capacity of the block is several hundreds times as large as that of the sample and the reference materials plus the cells, the linear heating of the block would not be disturbed by the heat of transformation occurring in the sample. Therefore, the control of the temperature of the furnace, not of the block itself, is suitable in this case in order to reduce the fluctuation of the heating rate, because of the faster response to control; furthermore, the narrow air gap between the block and the furnace absorbs the fluctuation of the short period and plays a role analogous to an electrical smoothing circuit.

Fused quartz is chosen as the material of the cell holder for the reasons mentioned above and because of its strength. The transition at 573°C of quartz has had little effect on the thermograms previously obtained, probably because of its small heat effect and its differential use. The shape of the holder is shown in Fig. 5. The thermocouple is inserted through the side groove. In determining the dimensions and the material of the holder, the proportionality coefficient, K, is calculated to be about 6 cal./°C min. at 100°C; the response times, τ_0's are also calculated and tabluated in Table I. These values are satisfactory, because $5a\tau_0$ is about 2°C at the heating rate of 30°C/hr. except for water.

The cell is made of stainless steel, SUS 27, or nickel;

Table I. The response times of systems*

$\sqrt{\lambda_s/c_s\rho_s}$	$\sqrt{\lambda_s c_s \rho_s}$	τ_0	τ_1	Corresponding substances
4	2	0.6	0.2	Metals
0.65	0.356	0.7	0.2	Inorganic salts
0.1	0.1	0.8	0.3	Organic substances
0.3	0.1	5.7	1.1	Water

* The cell holder is made of fused quartz; $\sqrt{\lambda_h/c_h\rho_h}=0.65$ and $\sqrt{\lambda_h c_h \rho_h}=0.356$. The dimensions of the quantities are expressed by cm., g., min., cal. and °C.

TABLE II. THE RESULTS OF THE MEASUREMENTS OF THE TRANSFORMATIONS

Sample*	The temp. of transformation, °C obt.	lit.	K**	σ***	ΔH_{lit} cal./g.	Ref.
KNO_3 (a, GR)	135	128	2.09	0.07	12.8	25),26)
	337	338	2.70	0.06	25.2	27),28)
Ag_2S (a, EP)	177	179	2.60	0.12	4.076	26)
$KClO_4$ (a, GR)	304	299.8	2.84	0.07	23.7	29)
$NaNO_3$ (b, GR)	310	306.2	2.50	0.09	41.3	26),30),31)
C_2Cl_6 (c, EP)	49	44.9	1.85	0.20	2.59	32)
	75	71.2	2.53	0.28	8.295	32)
Pentaerythritol (c, GR)	191	187.8	2.53	0.20	77.1	32)
CBr_4 (a, GR)	49	47	1.71	0.07	4.81	33)
	97	90.1	2.13	0.04	2.9	27)
$K_2Cr_2O_7$ (e, GR)	401	398	2.53	0.07	28.9	27)
Stearic acid (d)	69	69	1.87	0.12	47.5	32)
Palmitic acid (d)	60	62.5	2.03	0.11	51.2	34)
Benzophenone (c, GR)	46	48.2	1.85	0.09	23.5	32)
$PbCl_2$ (a, EP)	500	498	3.87	0.16	20.9	27)
$AgNO_3$	168	160	2.56	0.13	3.47	35),36)
	213	211	2.75	0.12	17.6	36)
Benzoic acid (GR)	125	123.2	2.14	0.09	3.48	32),37),38)
Phenanthrene (c, EP)	100	99.3	2.64	0.16	25.0	32)
NH_4NO_3 (f, GR)	89	84.2	2.15	0.20	4.0	27)
	130	125.2	2.36	0.12	12.6	27),32)
Azoxybenzene (c, EP)	35	34.6	1.76	0.10	21.6	32)
Bibenzoyl (c, GR)	98	94.9	1.74	0.12	22.2	32)
Biphenyl (c, EP)	70	69.8	2.00	0.22	28.7	32)
p-Nitroaniline (c, GR)	152	147.5	2.34	0.30	36.5	32)
Hexamethylbenzene (c, EP)	110	110.9	2.40	0.20	2.59	32)
	164	163.9	2.67	0.27	30.3	32)
trans-Cinnamic acid (c, GR)	137	133	2.13	0.07	36.5	39)
Azobenzene (c, GR)	69	69.1	1.98	0.07	28.9	32)
Li_2SO_4 (a, EP)	580	575	4.87	0.21	62	27)
Na_2WO_4 (a, EP)	583	587.8	4.85	0.16	28.4	29)
	586	589				
Sn (g, EP)	235	232	2.38		15.1	27),40)
Pb (a, GR)	332	327.6	2.70		5.50	27)
α-Naphthol (a, GR)	80	95	2.37	0.19	38.8	32)
LiBr (a, GR)	553	550	3.43	0.27	36	41)

* The manufacturer and the grade of the samples are described in the parenthesis: a refers to Kanto Chemical Co., Ltd., b, Showa Chemical Co., Ltd., c, Tokyo Chemical Co., Ltd., d, purified sample kindly supplied by professor Kambe of the Institute of Space and Aeronautical Science, The University of Tokyo, e, Kokusan Chemical Co., Ltd., f, Tomiyama Pure Chemical Industrial Co., Ltd., g, Sumida Chemical Co., Ltd.

** The dimension of K is cal./°C min.

*** The standard deviation of K.

25) A. Mustajoki, *Ann. Acad. Sci. Fennicae Ser. A,* **VI**, 99, 11pp (1962); *Chem. Abstr.*, **57**, 5365e (1962).
26) A. Arell, *Ann. Acad. Sci. Fennicae Ser. A,* **VI**, 101, 3pp (1962); *Chem. Abstr.*, **57**, 2941g (1962).
27) K. K. Kelley, *Bull. U. S. Bur. Mines,* **584** (1960).
28) V. A. Sokolov and N. E. Shmidt, *Izvest. Sektora Fiz.-Khim. Anal., Inst. Obshchei i Neorg. Khim., Akad. Nauk S. S. S. R.,* **27**, 217 (1956); *Chem. Abstr.*, **50**, 15200b (1956).
29) F. D. Rossini, D. D. Wagman, W. H. Evans, S. Levine and I. Jaffe, *Circular Natl. Bur. Standards,* **C500** (1952).
30) A. Mustajoki, *Ann. Acad. Sci. Fennicae Ser. A,* **VI**, No. 5, 17pp (1957); *Chem. Abstr.*, **52**, 5111g (1958).
31) V. A. Scokolov and N. E. Shmidt, *Izvest. Sektora Fiz.- Khim. Anal., Inst. Obshchei i Neorg. Khim., Akad. Nauk S. S. S. R.,* **26**, 123 (1955); *Chem. Abstr.*, **50**, 3059i (1956).
32) Chem. Soc. Japan, Ed., "Kagaku Benran," 2nd ed., Maruzen, Tokyo (1958).
33) J. G. Marshall, L. A. K. Staveley and K. R. Hart, *Trans. Faraday Soc.,* **52**, 19 (1956); *Chem. Abstr.,* **50**, 13588c (1956).
34) T. L. Ward and W. S. Singleton, *J. Phys. Chem.,* **56**, 696 (1952); *Chem. Abstr.*, **46**, 9930c (1952).
35) A. Arell, *Ann. Acad. Sci. Fennicae Ser. A,* **VI**, No. 100, 3 (1962); *Chem. Abstr.*, **57**, 2941d (1962).
36) G. J. Janz and F. J. Kelly, *J. Phys. Chem.*, **67**, 2848 (1963).
37) G. T. Furukawa, R. E. McCoskey and G. J. King, *J. Res. Natl. Bur. Standards,* **47**, 256 (1951); *Chem. Abstr.*, **46**, 4348g (1952).
38) A. A. Sklyankin and P. G. Strelkov, *Zhur. Priklad. Mekh. i Teck. Fiz.,* No. 2, 100 (1960); *Chem. Abstr.*, **56**, 5464f (1962).
39) Chem. Soc. Japan, Ed., "Kagaku Benran," 1st ed., Maruzen, Tokyo (1952).
40) K. G. Khomyakov, V. A. Kholler and S. A. Zhvanko, *Vestnik Moskov. Univ.,* **7**, No. 3, *Ser. Fiz.-Mat. i Estestven. Nauk,* No. 2, 41 (1952); *Chem. Abstr.*, **46**, 9404g (1952).
41) M. Blanc, *Compt. rend.,* **246**, 570 (1958); *Chem. Abstr.*, **52**, 9741g (1958).

its shape is shown in Fig. 5, which also shows the heat distributor, which is put into the cell to reduce the temperature gradient in the cell, to sharpen the peak, and to increase its accuracy and resolving power.

The whole system mentioned above is covered with a shield case preventing heat loss to the outside, and the apparatus is placed in a vacuum chamber.

As is shown in Fig. 4, the thermocouple leads pass through the metal block and the cell holder and are inserted between the interface and into the groove cut on the inner surface of the cell holder. These passages prevent the heat from flowing directly to the outside through the leads. The heat flows from the metal block into the sample cell through the thermocouple leads, but the proportionality of the peak area to the heat of transformation could be said to hold, taking account of this heat flow, which would add a certain correction term to the proportionality coefficient, because no heat flows into the cell from other parts of the apparatus. If a similar thermocouple and a similar insulating tube are always used, this heat flow occurs reproducibly.

An alumel-chromel thermocouple 0.3 mm. in diameter, manufactured by Hoskins Mfg. Co., is used with an alumina insulating tube 1 mm. in outer diameter. As the electromotive force of the thermocouple increases almost linearly with an increase in the temperature, the thermocouple is preferable for differential thermal analysis.

A cam-driven program controller of the three-position action type, purchased from the Chino Works, Ltd. (model E 142), is used to control the furnace temperature from 0 to 600°C; the power supplied to the furnace is controlled by the three-position action of the controller. Furthermore, the voltage of the supplied power is increased at the heating cycle with a synchronous motor when the temperature is not higher than the set point, and decreased at the cooling cycle when the temperature is not lower. A multipoint recorder with a 250 mm.-wide strip-chart, a d. c. amplifier (model AM101) and a relay-box (Ohkura Electric Co., Ltd.) recorded the four temperature differences and the temperature of the reference material as functions of the time. The full-scale span of the recorder corresponds to 60 μV. of the output of the differential thermocuples when fed through the d. c. amplifier at its highest sensitivity; it also corresponds to a 600°C rise in the temperature of the reference material. The dotting period for each point is 36 sec. Almost all runs are made at a heating rate of 30°C/hr. under an ambient pressure.

Materials.—The materials to be tested are used without purification. The manufacturer and the grade are listed in Table II. The 200—300 mesh powder of α-alumina from Nishio Kogyo Co., Ltd. is used as the reference material. Quartz sand of a 99.8% purity, occurring in Fukushima Prefecture and supplied by Nihon Optical Co., Ltd., is used as the diluent.

Results

To prove the validity of the theory, we should be able to show experimentally that the proportionality coefficient, K, does not depend on the sample and the operational variables, but on the temperature. Two types of experiments are made. (1) The measurements to obtain the proportionality coefficient are done on various kinds of samples of known heats of transition, including organic materials, inorganic salts and metals. The smoothed curve of the coefficients must be drawn against the temperature. (2) The coefficient is obtained for the transition of potassium perchlorate at 299.8°C, changing such operational variables as the heating rate, the packing density, the concentration of the diluent, and the depth of packing the sample. The same value of the coefficient must be obtained irrespective of the values of the variables.

First, the difference in the base line between the beginning and the end of the peak must be considered. As has been pointed out in connection with theoretical considerations, no true correction of the difference can be made unless the specific heat and the density of the sample are known. Therefore, the base line under the peak is taken as a straight line between the base line at the beginning and that at the end. Any error due to the above approximation would be small, because the differences in the base line, even if they exist, are small compared with the peak areas in most of the cases described below.

Next, we must check the reproducibility of the data which are obtained in investigations of the transitions of ammonium nitrate at 84°C and 125°C by the method of an analysis of the variance, where the elements are the cell holder, the cell, and the cylindrical cavity. The results of the analysis shows that the variance in the proportionality coefficient contains the variance of the cell holder because of the poor interchangeability, which is presumably due to the low precision of the machining. The standard deviation due to the experimental error amounts of about 7%; if one uses a given cell holder and measures the heat with this apparauts, the error of a single measurement may be 7%. In the following experiment three cell holders are used; they show middle values of the proportionality coefficient among the twelve and do not differ appreciably from one another.

Three methods of determing the temperature of the transformation have been used: the temperature is obtained at the point where the peak starts to develop, or at the top of the peak, or at the intersection of the line extrapolating the steeply-rising portion of the peak to the initial base line. The choice of method depends on the particular apparatus. The best estimate of the temperature of the transformation with our apparatus is obtained at the intersection. The temperatures obtained by this estimation are included in Table II. The average deviation of the measured temperature from the reported temperature is +2°C. A typical peak is reproduced in Fig. 6.

The results of Experiment (1) are tabulated in

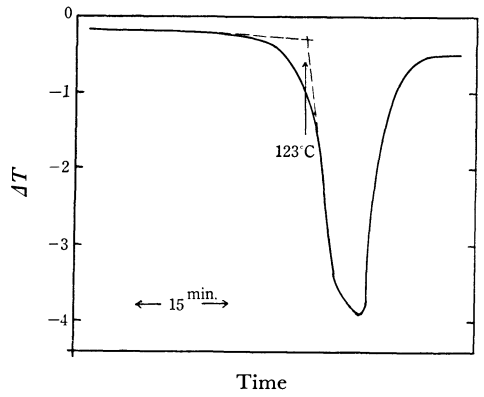

Fig. 6. A typical peak of benzoic acid.

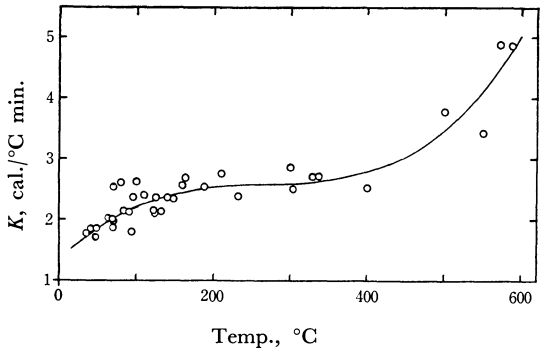

Fig. 7. The proportionality coefficient versus the temperature.

Table II, which also lists the measured temperatures of transformation, their literature values, and the literature heats of transformation, ΔH_{lit}. The proportionality coefficients are plotted in Fig. 7; the best fit was obtained by the method of the least squares, with a confidence limit of 95%. The formula of the smoothed curve is:

$$K = 1.507259 + 8.782709 \times 10^{-3}\, T - 1.808468 \times 10^{-5}\, T^2 + 6.324056 \times 10^{-14}\, T^4 \qquad (27)$$

where T is the temperature in °C. Considering the great variety of samples, their thermal conductivities, and particle sizes, Fig. 7 is sufficient to indicate that the proportionality coefficient is a function of the temperature only and that it is independent of the kinds and states of the samples. The standard deviations of the mean values of the proportionality coefficient of three or more measurements are 2% to 13%, as is shown in Table II; these errors are caused partly by the difference in the cell holders. Large deviations are found in the measurements of organic samples, presumably because of their broad peaks. The scattering of the points about the smoothed curve in Fig. 7 is due to the random error of the measurements, the difference in the cell holders, and the error in the reported values of the heat of transformation. The variance in the points is the sum of the three variances.

Now, we observe the dependency of the proportionality coefficient on the operational variables. The effects of the heating rate, the packing density, the concentration of the diluent and the depth of packing the sample are shown in Figs. 8, 9, 10 and 11 respectively. The packing density is varied as follows: for the most densely packed one, the powder sample is tamped into the cell as tightly as possible; for the second, the sample is poured into the cell, tapping the cell repeatedly; for the third, the sample is poured and tapped slightly, and for the most loosely packed one, the sample is poured lightly. To vary the concentration of the diluent, the weighed amounts of the powder sample and the diluent are mixed in a mortar and packed into the cell with a similar density. Except for the last effect, the operational variables have no effect on the proportionality coefficient.

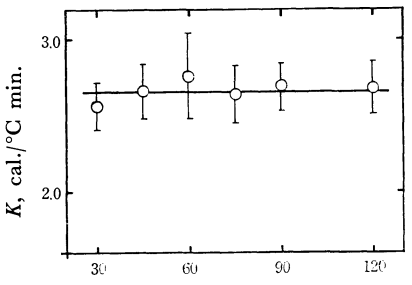

Fig. 8. The effect of heating rate. The range shown is the standard deviation.

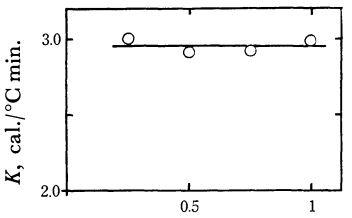

Fig. 9. The effect of packing density.

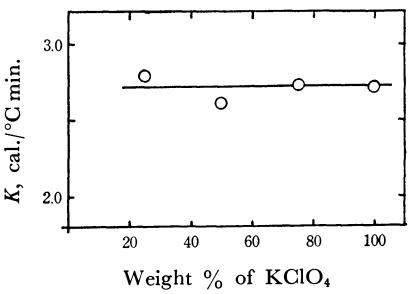

Fig. 10. The effect of diluent.

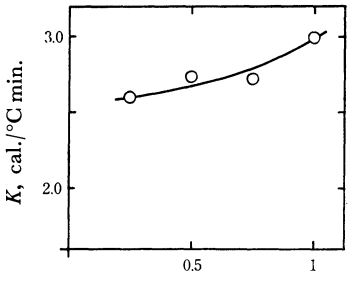

Fig. 11. The effect of the depth of packing the sample. The ratio of the depth of packing the sample to the depth of the cell is abscissa.

as has been expected in the theoretical considerations. The last effect would disturb the heat flow of the cylindrical symmetry and the consequent temperature gradient along the cylindrical axis would change the value of the proportionality coefficient. This finding suggests that the sample must be filled up to the top of the cell, even though loosely.

Besides these experiments, the effect of the diluent is tested by using the reference material of alumina as the diluent; the proportionality coefficient varies in this case. Alumina does not seem suitable as a diluent, probably because of the intereaction between the sample and the diluent.

These results shown above give an assurance of validity of the theory. We may conclude that the proportionality coefficient does not depend on the kind and state of the sample, but that it depends on the temperature only, as has been expected in the theoretical considerations, and that the estimation of the heat of transformation occurring in the sample is possible by this type of quantitative differential thermal analysis.

It would be explained by loose thermal contact due to a little air gap between the cell and the cell holder that the value of the proportionality coefficient obtained is smaller than the expected one of 6 cal./°C min. The linear relation of $\log(\Delta T - \Delta T_b)$ against the time after the completion of the transformation is verified experimentally; it is shown in Fig. 12. The response times, τ_0's, are also examined on some organic and inorganic samples and found to be about 1.5 min. for most samples. A reasoning similar to the above explanation of the proportionality coefficient applies to the discrepancy between the obtained response time and the calculated ones in Table I. It should also be noted that the effect of the heat distributor in the cell is neglected in the calculation of the response times.

To show an effect of the metal heat distributor in the cell, the peaks with or without the distributor are compared. The peak area does not change, but the peak becomes broader without the distributor. The transition of potassium perchlorate is completed 12 min. after the peak is reached without the distributor, but it is completed after 3 min. at the same heating rate when the distributor is used. The time of the completion is almost the same for different samples.

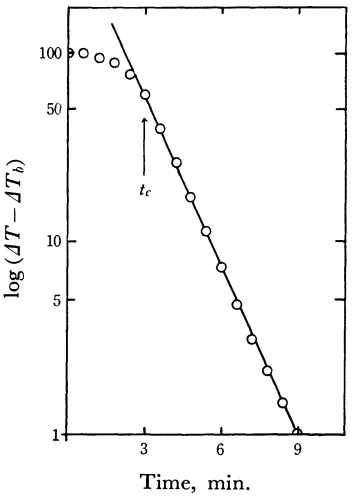

Fig. 12. The change of the temperature difference after the completion of the transformation of potassium perchlorate.

Discussion

Even after Boersma's suggestion of the inherent impossibility of quantitative differential thermal analysis, there have still been published a number of papers on the theme. For example, on the effect of the heating rate on the peak area, Barrall et al.[42] found, on several kinds of samples, that the peak area is decreased by a decrease in heating rate, showing zero area at a zero heating rate, with the type of apparatus where the microsample cell is suspended in an air oven. On the other hand, with a different type of apparatus such as (b) of Fig. 1, Barrall et al.[43] found a similar but more complicated dependency of the peak area of the mixture of silver nitrate; in this case the area is proportional to the heat of transition of the silver nitrate present when the areas at different heating rates are extrapolated to a zero heating rate. Ke[44] found the area of the melting of annealed Marlex 6000 to be independent of the heating rate. Suga et al.[45] reported similar findings except in the case of very low heating rates. In the cases mentioned

42) E. M. Barrall II, R. S. Porter and J. F. Johnson, *Anal. Chem.*, **36**, 2172 (1964).
43) E. M. Barrall II and L. B. Rogers, ibid., **34**, 1101 (1962).
44) B. Ke, *J. Polymer Sci.*, A, **1**, 1453 (1963).
45) H. Suga, H. Chihara, S. Seki, K. Nakatsuka and T. Shinoda, *J. Chem. Soc. Japan, Pure Chem. Sect. (Nippon Kagaku Zasshi)*, **82**, 24 (1961).

above, the area is compared among transitions of a single sample; therefore, the same sampling procedure should give the same proportionality coefficient.

The effect of the diluent is such that, if the sample content is low and if the packing state is changed slightly from run to run by fixing the particle size and the manner of packing the mixture, then the thermal conductivity and consequently the proportionality coefficient will become nearly constant. This effect was noted in the paper of Barrall et al.[43] on salicylic acid diluted with carborundum, and in Yamamoto's paper[46] on benzoic acid diluted with fused silica powder. However, as the diluent has other effects (e. g., the interaction with sample, resulting in a false peak),[47,48] the quantitative differential thermal analysis by using a diluent has limitations, besides the facts that the manner of packing has an influence on the area[46] and the sensitivity decreases because of a diluted active component.

With the type of apparatus in which the sample cell with the thermocouple on its outside is suspended in an air oven, Barrall et al.[42] found that the proportionality coefficient, calibrated with a few materials, shows a linear dependency on the temperature as has been observed in the present paper. David[49] compared with reported values the heats of the transition of eight samples calculated from the area and the proportionality coefficient calibrated on tin; he obtained satisfactory agreements with a similar apparatus. It should be noted here that, in the two papers[42,49] mentioned above, the thermocouple is located on the outside of the cell, that the air gap is between the cell and furnace wall, and that the observed transitions occur below 300°C. In these cases, the air gap would play the same role as the cell holder in the present paper if convection and radiation could be neglected. The results would be less satisfactory if the measurement were made above 300°C, where radiation transfers heat and David's theory would not hold.

Recently, Yagfarov[50] proposed a method of thermography with which one can obtain the values of specific heat, thermal conductivity and thermal diffusivity simultanously. The peak is obtained at the transformation of the sample by the principles of conventional differential thermal analysis; he postulated that the heat of transformation can be estimated from the peak and the thermal conductivity thus obtained. However, the thermal conductivity can not be obtained in the peak region because the thermal conductivity and the state of the packing of the sample have a tendency to change during the transformation. These difficulties were not discussed, and the heat of transformation estimated experimentally was not described, in his paper.

The results obtained in this research can not be of a very high precision, but they do seem encouraging. If the low interchangeability of the cell holder and its poor thermal contact with the block and the cell could be improved, the accuracy would be improved appreciably. In fact, a preliminary experiment with a ceramic cell holder shows an improved reproducibility, for the standard deviation is 3.3% for an average measurement.

However, the most serious defect of the differential thermal analysis as a technique for measuring the heat of transformation is the necessity of calibrating it with a sample of a known heat of transformation. Hence, the accuracy of the method depends on that of the other absolute method of heat measurement. In order to bring out the unique merits of differential thermal analysis, it should be applied to the field of higher temperatures and high pressures; research for developting the absolute differential thermal analysis is now keenly needed.

As an analytical technique, the method proposed in this paper seems to have fair advantages over the other types of differential thermal analysis, because it does not suffer from operational variables and because it improves the reproducibility of the peak of the thermogram. The new concepts presented in this paper, i. e., the response time and the sensitivity, would be helpful for designing new apparatuses.

Attempts are now in progress in our laboratory to improve the apparatus and to make the method an absolute one; this work will be reported on shortly. These improvements will reduce the differential thermal analysis to a dynamic operation of a calorimeter of Calvet's type;[51] it will be a calorimeter with unique features and unique applicability. Both this apparatus and Calvet's are based on the same theoretical back-grounds, so the theory can also be applied to a calorimeter of Calvet's type.

The capable assistance of Hiroshi Isozake in the assembly and operation of the apparatus is gratefully acknowledged. Thanks are also due to Professor Hirotaro Kambe of the Institute of Space and Aeronautical Science, The University of Tokyo, for his encouraging discussions.

Appendix

To derive the temperature change in the sample cell and the cell holder, the temperature is divided into three parts:

46) A. Yamamoto, *Japan Analyst*, **12**, 26 (1963).
47) H. Morita and H. M. Rice, *Anal. Chem.*, **27**, 336 (1955).
48) E. M. Barrall II and L. B. Rogers, ibid., **34**, 1106 (1962).
49) D. J. David, ibid., **36**, 2162 (1964).
50) M. S. Yagfarov, *Russ. J. Inorg. Chem.* (English translation), **6**, 1236 (1961).
51) E. Calvet, *Compt. rend.*, **226**, 1702 (1948); ibid., **236**, 486 (1953).

$$T = T_1 + T_2 + T_3 \tag{A-1}$$

where T_1 represents the temperature at the steady state, where T_1+T_2 is the initial transient temperature, and where T_3 is the additional temperature due to the heat of transformation. First, the temperature gradient at the steady state is considered; then the transient state and the peak are calculated by using the linearity of differentiation, which makes possible the above separation of the temperature. All these temperatures must be derived as functions of the coordinate for the arrangement of (c) in Fig. 1.

If we designate by q the heat flowing into the inner part per unit time through a cylindrical plane of a unit length, and the radius by r, q is the heat necessary to heat up the inner part at the rate of a at the steady state, and the temperature gradient at r occurs by the necessity of letting the heat q flow. Then, for $0 \leq r \leq R_i$:

$$q = \int_0^r 2\pi r a c_s \rho_s \mathrm{d}r \tag{A-2}$$

and for $R_i \leq r \leq R_o$:

$$q = \int_{R_i}^r 2\pi a c_h \rho_h \,\mathrm{d}r + \pi R_i^2 a c_s \rho_s \tag{A-3}$$

The temperature gradient is:

$$q = 2\pi r \lambda_s \partial T_{s1}/\partial r \qquad \text{for } 0 \leq r \leq R_i \tag{A-4}$$

and:

$$q = 2\pi r \lambda_h \partial T_{h1}/\partial r \qquad \text{for } R_i \leq r \leq R_o \tag{A-5}$$

By combining Eqs. A-2 and A-4, and Eqs. A-3 and A-5, the integration of them gives T_{s1} and T_{h1}: for $0 \leq r \leq R_i$:

$$T_{s1}(r) - T_{s1}(R_i) = a c_s \rho_s (r^2 - R_i^2)/4\lambda_s \tag{A-6}$$

and for $R_i \leq r \leq R_o$:

$$T_{h1}(r) - T_{h1}(R_o) = a c_h \rho_h (r^2 - R_o^2)/4\lambda_h + a R_i^2 \log (r/R_o)(c_s \rho_s - c_h \rho_h)/2\lambda_h \tag{A-7}$$

As the temperature of the metal block, $T_{h1}(R_o)$, is equal to at,

$$T_{s1}(r) = at - \frac{a}{4\lambda_h}\left[c_h \rho_h (R_o^2 - R_i^2) + 2R_i^2 (c_s \rho_s - c_h \rho_h) \log \frac{R_o}{R_i}\right] - \frac{a c_s \rho_s}{4\lambda_s}(R_i^2 - r^2) \tag{A-8}$$

$$T_{h1}(r) = at - \frac{a}{4\lambda_h}\left[c_h \rho_h (R_o^2 - r^2) + 2R_i^2 (c_s \rho_s - c_h \rho_h) \log \frac{R_o}{r}\right] \tag{A-9}$$

Secondly, the initial transient period must be taken into account. For this period, the next differential equations hold, because conditions and solutions must be added to those of the steady state to fulfil the overall conditions.

$$\lambda_s \nabla T_{s2} = c_s \rho_s \partial T_{s2}/\partial t \tag{A-10}$$

$$\lambda_h \nabla T_{h2} = c_h \rho_h \partial T_{h2}/\partial t \tag{A-11}$$

with the boundary conditions:

$$T_{h2} = 0 \qquad \text{at } r = R_o \tag{A-12}$$

$$\lambda_s \partial T_{s2}/\partial r = \lambda_h \partial T_{h2}/\partial r \qquad \text{at } r = R_i \tag{A-13}$$

$$T_{s2} = T_{h2} \qquad \text{at } r = R_i \tag{A-14}$$

and with the initial conditions:

$$T_{s2} = \frac{a}{4\lambda_h}\left[c_h \rho_h (R_o^2 - R_i^2) + 2R_i^2 (c_s \rho_s - c_h \rho_h) \log \frac{R_o}{R_i}\right] + \frac{a c_s \rho_s}{4\lambda_s}(R_i^2 - r^2) \tag{A-15}$$

$$T_{h2} = \frac{a}{4\lambda_h}\left[c_h \rho_h (R_o^2 - r^2) + 2R_i^2 (c_s \rho_s - c_h \rho_h) \log \frac{R_o}{r}\right] \tag{A-16}$$

Assuming the cylindrical symmetry, the solutions of the above partial differential equations are typical;[52] they are given below:

$$T_{s2} = \sum_{n=0}^{\infty} \alpha_n \boldsymbol{J}_0\left(r\sqrt{\frac{c_s \rho_s}{\lambda_s \tau_n}}\right)[\boldsymbol{J}_0(R_i x)\boldsymbol{Y}_0(R_o x) - \boldsymbol{J}_0(R_o x)\boldsymbol{Y}_0(R_i x)] \exp\left(-\frac{t}{\tau_n}\right) \tag{A-17}$$

$$T_{h2} = \sum_{n=0}^{\infty} \beta_n \boldsymbol{J}_0\left(R_i\sqrt{\frac{c_s \rho_s}{\lambda_s \tau_n}}\right)[\boldsymbol{J}_0(rx)\boldsymbol{Y}_0(R_o x) - \boldsymbol{J}_0(R_o x)\boldsymbol{Y}_0(rx)] \exp\left(-\frac{t}{\tau_n}\right) \tag{A-18}$$

where x is equal to the x used in Eq. 9, and where α_n's and β_n's are constants. In order to fulfil the boundary and initial conditions, A-12, A-13, A-14, A-15 and A-16, τ_n's are defined by the roots of Eq. 9, and α_n's and β_n's are determined to express the initial temperature distribution. By adding Eq. A-8 to Eq. A-17, and Eq. A-9 to Eq. A-18, we obtain Eqs. 7 and 8.

Thirdly, the other transient temperature is derived. The temperature distribution at the time of the completion of the transformation, t_c, can be expressed as a certain function of r, which is the initial condition for this case. As the same expressions of Eqs. A-10 to A-14 are applicable, the solutions, i. e., Eqs. 14 and 15, are derived similarly to Eqs. 7 and 8. It is apparent from the above considerations that T_3 is diminished to a negligibly small value, after a long enough time has elapsed, and then the additional temperature due to the heat of transformation reaches a form of peak.

Finally, the peak area from the beginning of the peak, t_i, to its end, t_e, is calculated.

$$\lambda \nabla T_3 = c\rho \partial T_3/\partial t + \Delta H \rho \partial m/\partial t \tag{A-19}$$

The initial and final conditions are as follows:

$$T_3 = 0 \qquad \text{at } t = t_i \tag{A-20}$$

$$T_3 = 0 \qquad \text{at } t = t_e \tag{A-21}$$

and the boundary conditions are:

$$T_3 = 0 \qquad \text{at } r = R_o \tag{A-22}$$

$$T_{s3} = T_{h3} \qquad \text{at } r = R_i \tag{A-23}$$

and:

$$\lambda_s \partial T_{s3}/\partial r = \lambda_h \partial T_{h3}/\partial r \qquad \text{at } r = R_i \tag{A-24}$$

The integration of Eq. A-19 from t_i to t_e gives:

$$\lambda \int_{t_i}^{t_e} \nabla T_3 \,\mathrm{d}t = c\rho \int_{t_i}^{t_e} \mathrm{d}T_3 + \rho \Delta H \tag{A-25}$$

52) H. S. Carslaw and J. C. Jaeger, "Conduction of Heat in Solids," Oxford University Press, Oxford (1959).

According to the initial and final conditions,

$$c\rho\int_{t_i}^{t_e} dT_3 = 0 \qquad \text{(A-26)}$$

and the integration of T_3 from t_i to t_e is the desired peak area, A. Then, the integration of Eq. A-25 over the volume, V, as with Boersma,[11] gives:

$$\lambda\int_V dV\Delta A = \int_V \rho\Delta H\, dV \qquad \text{(A-27)}$$

Namely,

$$\lambda\int_F dF\, \boldsymbol{grad}\, A = \rho V\Delta H \qquad \text{(A-28)}$$

where F is the surface of the cylinder; considering the cylinderical symmetry, we have:

$$F\lambda\frac{\partial A}{\partial r} = \rho V\Delta H \qquad \text{(A-29)}$$

Taking into account that the heat is produced or consumed in the sample only, Eq. A-29 is separated into two equations: for $R_i \leq r \leq R_o$:

$$\frac{\partial A(r)}{\partial r} = \rho_s\Delta H V_s/\lambda_h F(r) \qquad \text{(A-30)}$$

where V_s is the volume of the sample, and for $0 \leq r \leq R_i$:

$$\frac{\partial A(r)}{\partial r} = \rho_s\Delta H V(r)/\lambda_s(r) \qquad \text{(A-31)}$$

As $T_3=0$ at $r=R_o$, for $R_i \leq r \leq R_o$:

$$A(r) = \frac{M\Delta H \log(R_o/r)}{2\pi l\lambda_h} \qquad \text{(A-32)}$$

and for $0 \leq r \leq R_i$:

$$A(r) = \frac{M\Delta H}{2\pi l}\left[\frac{\log(R_o/R_i)}{\lambda_h} + \frac{(R_i^2-r^2)}{2\lambda_s R_i^2}\right. \qquad \text{(A-33)}$$

All the derived equations are functions of r, the position of the temperature-detection device, and if we let r equal R_i, i. e., if the temperature-detection devices are inserted at R_i, the equation becomes equal to Eq. 16. If r is made equal to 0 and if the radiation and convection can be neglected, the equation becomes applicable to the type (b) of Fig. 1. Equation applicable to the conventional method is also derived, when R_o is made equal to R_i and r, equal to 0.

Let us consider the case where the specific heat, the density, and the heat conductivity change abruptly to new values, c_s', ρ_s' and λ_s', at the temperature of transformation, T_t. The base line after the peak becomes different from the one prior to the peak, reflecting this change in thermal properties; Eq. 16 can not be applied to this case; for it, however, an expression can be derived for the apparatus of the type (c) in Fig. 1.

The heat flowing through the cylindrical plane in the cell holder with the radius of r, into the cell and the inner part of the cell holder from t_i to t_e is equal to the heat necessary to heat the inner part from the temperature distribution at t_i to the new temperature distribution at t_e, plus the heat of transformation. The temperature distributions at t_i and t_e must first be derived. As the sample at the outermost part of the cell begins to be transformed at t_i, the temperature at this point is equal to the temperature of the transformation. Therefore, for $0 \leq r \leq R_i$:

$$T_s = T_t - \frac{ac_s\rho_s}{4\lambda_s}(R_i^2 - r^2) \qquad \text{at } t = t_i \qquad \text{(A-34)}$$

and for $R_i \leq r \leq R_o$:

$$T_h = T_t + \frac{a}{2\lambda_h}R_i^2(c_s\rho_s - c_h\rho_h)\log\frac{r}{R_i} + \frac{ac_h\rho_h}{4\lambda_h}(r^2 - R_i^2) \qquad \text{at } t = t_i \qquad \text{(A-35)}$$

when $t=t_e$, at $r=R_o$:

$$T_h = T_t + a(t_e - t_i) + \frac{a}{2\lambda_h}R_i^2(c_s\rho_s - c_h\rho_h)\log\frac{R_o}{R_i} + \frac{ac_h\rho_h}{4\lambda_h}(R_o^2 - R_i^2) \qquad \text{(A-36)}$$

for $R_i \leq r \leq R_o$:

$$T_h = T_t + a(t_e - t_i) + \frac{a}{2\lambda_h}R_i^2(c_s\rho_s - c_h\rho_h)\log\frac{R_o}{R_i} + \frac{ac_h\rho_h}{4\lambda_h}(R_o^2 - R_i^2) - \frac{ac_h\rho_h}{4\lambda_h}(R_o^2 - r^2) - \frac{a}{2\lambda_h}R_i^2(c_s'\rho_s' - c_h\rho_h)\log\frac{R_o}{r} \qquad \text{(A-37)}$$

and for $0 \leq r \leq R_i$:

$$T_s = T_t + a(t_e - t_i) + \frac{a}{2\lambda_h}R_i^2(c_s\rho_s - c_h\rho_h)\log\frac{R_o}{R_i} + \frac{ac_h\rho_h}{4\lambda_h}(R_o^2 - R_i^2) - \frac{a}{4\lambda_h}R_i^2(c_s'\rho_s' - c_h\rho_h)\log\frac{R_o}{R_i} - \frac{ac_h\rho_h}{4\lambda_h}(R_o^2 - R_i^2) - \frac{ac_s'\rho_s'}{4\lambda_s}(R_i^2 - r^2) \qquad \text{(A-38)}$$

The heat necessary to bring the system from the state described by Eqs. A-34 and A-35 to the state described by Eqs. A-37 and A-38 includes the following: (1) the heat to heat up the sample from the initial temperature (Eq. A-34) to T_t with the specific heat of c_s and the density of ρ_s; (2) the heat of the transformation of the sample, $M\Delta H$; (3) the heat to raise the temperature of the sample from T_t to the temperature distribution of Eq. A-38 with the specific heat of c_s' and the density of ρ_s', and (4) the heat necessary to heat the cell holder from the state of Eq. A-35 to Eq. A-37. Now suppose that the transformation did not take place. Then, the base line would not change and the heat flowing through the cylindrical plane, with the radius r, during the interval is $a(t_e - t_i)[\pi R_i^2 c_s\rho_s + \pi(r^2 - R_i^2)c_h\rho_h]$. Therefore, it we represent the additional temperature due to the transformation by ΔT_t, which is the temperature difference between the peak and the extrapolated initial base line,

$$2\pi r\lambda_h\frac{\partial}{\partial r}\int_{t_i}^{t_e}\Delta T_t(r,t)\,dt = a(t_e - t_i)\pi R_i^2(c_s'\rho_s' - c_s\rho_s) + \frac{a\pi c_s'\rho_s'}{4\lambda_h}R_i^4\log\frac{R_o}{R_i}(c_s\rho_s - c_s'\rho_s') + \frac{a\pi}{8\lambda_s}R_i^4[(c_s\rho_s)^2 - (c_s'\rho_s')^2] + \Delta H\pi R_i^2\rho_s + \frac{ac_h\rho_h\pi}{4\lambda_h}(c_s\rho_s - c_s'\rho_s')(2r^2\log R_o + r^2 - 2r^2\log r - R_i^2) \qquad \text{(A-39)}$$

By integrating Eq. A-39 and making r equal to R_i, we obtain:

$$\int_{t_i}^{t_e} \Delta T_t \, dt = \frac{R_i^2 \rho_s \Delta H}{2\lambda_h} \log \frac{R_o}{R_i} + \frac{a(t_e - t_i)}{2\lambda_h} R_i^2 \log \frac{R_o}{R_i} (c_s' \rho_s' - c_s \rho_s) + \frac{a c_h \rho_h}{8\lambda_h^2} R_i^2 (c_s \rho_s - c_s' \rho_s') \left(R_o^2 - R_i^2 - R_i^2 \log \frac{R_o}{R_i} \right) + \frac{a R_i^4}{16 \lambda_s \lambda_h} \log \frac{R_o}{R_i} (c_s^2 \rho_s^2 - c_s'^2 \rho_s'^2) + \frac{a c_s' \rho_s'}{8\lambda_h^2} R_i^4 (c_s \rho_s - c_s' \rho_s') \left(\log \frac{R_o}{R_i} \right)^2 \quad \text{(A-40)}$$

The left side of Eq. A-40 is the area enclosed by the peak, the extrapolated initial base line and the straight line drawn perpendicularly at $t = t_e$. This equation can be converted to the next one by considering Eqs. 16 and 19:

$$M \Delta H = K \left[\int_{t_i}^{t_e} \Delta T_t \, dt - (\Delta T_{b2} - \Delta T_{b1}) \{ (t_e - t_i) - \tau_c \} \right] + a\pi R_i^4 \left(\frac{c_s^2 \rho_s^2}{\lambda_s} - \frac{c_s'^2 \rho_s'^2}{\lambda_s'} \right) \quad \text{(A-41)}$$

If some devices are used to decrease the temperature gradient in the cell, the last term of Eq. A-41 due to the change in the temperature distribution in the cell may be neglected; the corrected peak area is as is shown in Fig. 3 and Eq. 20.

BULLETIN OF THE CHEMICAL SOCIETY OF JAPAN VOL. 39 2085—2094 (1966)

The Deterioration of Oxidative Polymerized Films

By Leo-Wang CHEN and Ju KUMANOTANI

The Engineering Research Institute, Faculty of Engineering, The University of Tokyo, Hongo, Tokyo

(Received November 24, 1965)

The deterioration of oxidative polymerized films, such as films of polymerized oils, alkyd resins, and phenolic varnishes, was studied by means of dynamic-mechanical measurements, in addition to such conventional methods as infrared spectral and elementary analysis. The visco-elastic changes induced by thermo-oxidation were correlated with the network structure of the films. The baked films are more stable than the air-dried films. The aliphatic chains decomposed more easily when a comparison was made among air-dried film and baked film of alkyd resin modified by unsaturated fatty acid; this is because of the existence of more hydroperoxyl and conjugated carbonyl groups and the effect of the drying agent contained in the air-dried film. After thermo-oxidation, the glass-transition temperature and the degree of crosslinking of the film showed an increase, an increase which is considered to be the result of the oxidative decomposition and crosslinking of aliphatic chains. It was also observed that the impact strength of baked film decreased upon thermo-oxidation.

Polymerized oils, alkyd resins, and phenolic varnishes are representative of oxidative polymerizable prepolymers widely employed in the coating industry. The film formation is proceeded by the formation of hydroperoxide and then its decomposition leading to a network structure. The autoxidation being complicated, the film structure is much affected by such conditions as the temperature, the catalyst, and the time under which the varnish or film is treated. With this reaction complexity and the easy chemical modification of prepolymers, this is a field of study which correlates the physical properties and the structure of the crosslinking polymer. Not only practical requirements but also the study of the polymer reaction needs such investigation, but the reaction complexity and the difficulty of handling the network structure somewhat affect the carrying-out of this study.

The authors measured the viscoelastic properties, the line-width of the NMR spectra, and the molecular weight between crosslinks, besides such conventional analytical methods as infrared spectral and elementary analysis, in their study. Some information has already been obtained, such as the effect of chemical factors on the glass-transition temperature and the degree of crosslinking of alkyd films,[1] the correlation of the glass transition temperature measured by the dynamic-mechanical method and the line-width measurement (NMR) in relation to the chemical structure,[2] and the chemical and physical behavior of phenolic resins in films of phenolic varnishes.[3]

In this report, the deterioration of oxidative polymerized films induced by thermo-oxidation will be studied by means of dynamic-mechanical

1) J. Kumanotani, L. W. Chen and T. Kuwata, This Bulletin, **35**, 8, 1341 (1962).
2) L. W. Chen and J. Kumanotani, *J. Appl. Polymer Sci.*, **9**, 3519 (1965).
3) L. W. Chen and J. Kumanotani, ibid., **9**, 2785, (1965).

measurements made in combination with infrared spectral analysis and other methods.

As the deterioration of polymer is of importance in respect to its polymer reactions and its practical requirements, several papers[4-7] regarding the degradation of oxidative polymerized films have been reported. These studies have involved degradation by ultraviolet rays, thermo-oxidative degradation, or aging, and have been carried by means of the analysis of infrared absorption spectra, oxygen absorption, and volatile materials, or by means of the mechanical-property measurement of films, independently or sometimes in combination.

As to the thermo-oxidative degradation of oxidative polymerized films, the films prepared from polymerized oil, alkyd resin, and phenolic varnishes will be studied, and air-dried and baked films will be compared as well.

Their viscoelastic change in correlation with the network structure will also be investigated in this report.

Experimental

Raw Materials.—*Drying Oil (O).*—A mixture of tung oil (iodine value 168, Wijs method) and linseed oil (iodine value 187) (1 : 1) was used.

Phenol Resins.—*p-t*-Butylphenol-formaldehyde resins were prepared by the conventional method; the oil-reactive resin (R) had a molecular weight of 650, as measured by a vapor pressure osmometer (Mechrolab, Inc.) m. p. 65—72°C, while the oil-nonreactive resin (N) had a molecular weight of 375, m. p. 55—62°C.

Linseed Oil Fatty Acid.—Commercially-available: iodine value 187.

Glycerol and Phthalic Anhydride.—They were chemically pure.

The Preparation of Prepolymers.—*Polymerized Oil.*—The drying oil was heated in air at 210°C for 5.5 hr. The heating was stopped near gelation, and the mixture was dissolved in an equal weight of mineral turpentine after it had been cooled to room temperature.

Phenolic Varnishes.—A mixture of oil and resin (6 : 4) was heated in air at 210°C. The heating was stopped near gelation, and the mixture was dissolved in an equal weight of mineral turpentine. The reaction time was 8 hr. for the oil-nonreactive resin (N–O), and 3 hr. for the oil-reactive resin (R–O). Another varnish was prepared by dissolving at room temperature, a mixture of polymerized oil and oil-nonreactive resin (6 : 4) in an equal weight of mineral turpentine containing 2—3% methyl ethyl ketone (N+PO).

Alkyd Resin.—An Equimolar mixture of linseed oil fatty acid, glycerol, and phthalic anhydride was put in a four-necked 500-ml. flask equipped with a sealed glass stirrer, a thermometer, a nitrogen gas inlet tube, and a Stark & Dean trap, and heated in an oil bath at 230°C for 9 hr. The varnish was prepared by dissolving the prepolymer ($\bar{M}_n$, 1710) in an equal weight of xylene.

Conditions of Film Formation.—*Polymerized Oil Film.*—The varnish, containing drying agents, naphthenates of cobalt (0.02%) and manganese (0.02%) was coated on tin plates, the coating and heating at 80°C for 2 hr. were repeated 10 times.

Films of Phenolic Varnishes.—The varnishes, containing drying agents, naphthenates of cobalt (0.02%) and manganese (0.02%), were coated on tin plates. For air drying, the procedure of coating and standing for one day at room temperature was repeated 10 times. For baking, the same procedure was used as with polymerized oil film.

Alkyd Films.—In the case of air drying, the varnish containing drying agents, naphthenates of cobalt (0.04%), manganese (0.04%), and lead (0.2%), was coated on tin plate and left to stand at room temperature two days. This procedure was repeated 4 times. In the case of baking, the varnish, without any drying agent being added, was coated on tin plate and heated at 105°C for 2 hr. in air. This procedure was repeated 4 times. The films were then stripped off by an amalgam method.

The Conditions of Thermal Treatment.—*Polymerized Oil Film.*—After it had stood in air for 3 months, the film was heated in air at 150°C for 3 hr., and then subsequently heated at 200°C for 3 hr.

Films of Phenolic Varnishes.—After they had stood in air for 3 months, the films were submitted to heating, just as in the case of the polymerized oil films.

Alkyd Films.—After it had stood in air for 2.5 months, the air-dried film was heated in air at 105°C for 5 hr., while the baked film, after it had stood in air a week, was submitted to heating just as in the case of the polymerized oil film.

The Dynamic-mechanical Measurement of Films.—The temperature (t) dependence of the shear modulus (G) and the logarithmic decrement (λ) of the film were measured by the torsional pendulum method.[8] The data obtained from the G-t and λ-t curves included the glass transition temperature as measured by the dynamic-mechanical method $(T_g)_d$; the temperature at which λ reaches a maximum (λ_{max}). As the frequency of measurement is in the range of 0.1-1 cycle/sec., the $(T_g)_d$ value is not far from that obtained by the dilatometric method.[9]

Shear modulus at high temperatures G_h; This is the shear modulus obtained from the plateau region at high temperatures. It is a measure of the degree of the crosslinking of film.[10-12] Shear modulus at room temperature G_r; This is the shear modulus at 20°C, noted as a measure of the rigidity of the film at room temperature.

Infrared Spectral Analysis of Films.—The change in the functional group in the process of film degradation was examined by the measurement of the infrared spectra.

4) E. B. FitzGerald, *A. S. T. M. Bull.*, **65**, TP 137—48 (1955).
5) C. D. Miller, *Ind. Eng. Chem.*, **50**, 125 (1958).
6) A. L. Smith, ibid., **49**, 1903 (1957).
7) T. Imai, *J. Japan Soc. Colour Material, (Shikizai)* **30**, 6, 216 (1957).
8) Y. Inoue, *J. Soc. Polymer Sci., Japan (Kobunshi Kagaku)*, **10**, 140 (1953).
9) L. E. Nielsen, "Mechanical Properties of Polymers", Reinhold, New York (1962), p. 162.
10) H. F. Drum, C. W. H. Dodge and L. E. Nielsen, *Ind. Eng. Chem.*, **48**, 76 (1956).
11) K. Ueki, *J. Chem. Soc. Japan, Ind. Chem. Sect. (Kogyo Kagaku Zasshi)*, **65**, 137 (1962).
12) D. Katz and A. V. Tobolsky, *J. Polymer Sci.*, **A2**, 1587 (1964).

A rock salt was coated with varnish and dried, and then thermo-treated under specified conditions, as mentioned previously, the infrared spectra were then measured. The chemical change in functional groups is reflected in changes in the optical density (D) or the ratio of those of related functional groups.

In infrared spectral analysis, the characteristic absorption bands employed are: ν_{3570} cm^{-1}: hydroxyl, hydroperoxyl, or carbonyl; ν_{2850} cm^{-1}: methyl or methylene of aliphatic chains; ν_{1590} cm^{-1}: the carbon-to-carbon linkages of phthalate; and ν_{980} cm^{-1}, trans ethylenic double bond, while D_{2850}/D_{1590} is expressed as a measure of the ratio of the aliphatic to the phthalate in films.

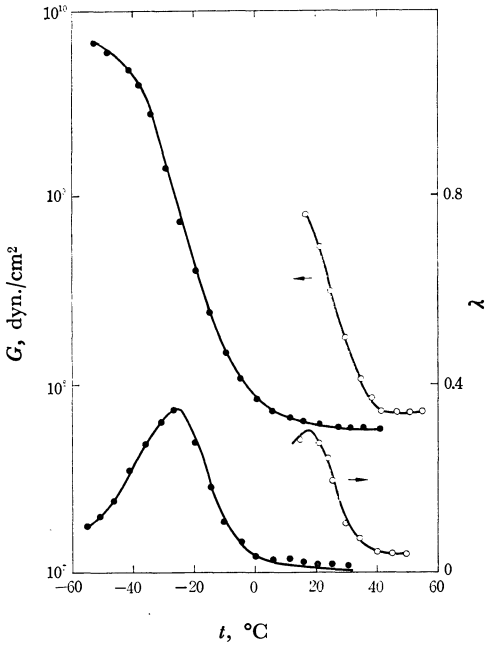

Fig. 1. Thermo-oxidative degradation of polymerized oil film observed in G-t, λ-t curves.
● Original film
○ After heating at 150°C for 3 hr.

The Degree of Swelling and the Soluble Portion of the Film.—The degree of swelling and the soluble portion of film were measured as follows:

The film (W_0) was dipped in chloroform at room temperature for more than a week; then the swollen film was weighed in another covered weighing bottle filled with chroloform until the weight was constant (W_s). The degree of swelling is expressed by $(W_s/W_0) \times 100$.

The swollen film was then dried in a vacuum (W_d), and the soluble portion of film was expressed by $(W_0 - W_d)/W_0 \times 100$.

Other measurements of the properties of the film, such as elementary analysis, thermograms*1 and impact strength*2 were also carried out.

Results and Discussion

The Thermo-oxidative Degradation of Polymerized Oil Film.—The G-t and λ-t curves of polymerized oil film are shown in Fig. 1, while the infrared spectra are shown in Fig. 2. The results are summarized in Table I.

It was observed when the baked polymerized oil film was thermo-treated in air that:

1) The $(T_g)_d$, G_r, and G_h of the film increased; namely, the hardness of film and the degree of the crosslinking of the film increased:

2) D_{2850}, D_{3570}, and D_{980} decreased; and

3) The weight loss amounted to 8.7% when the film was treated at 150°C for 3 hr. in air.

The Thermo-oxidative Degradation of Films of Phenolic Varnishes.—The G-t and λ-t curves of films of phenolic varnishes are shown in Fig. 3 and Fig. 4. The results are summarized in Table II.

It was observed when the films of phenolic varnishes were thermo-treated in air that:

1) The $(T_g)_d$, G_r, and G_h values of the films increased, and

2) The weight loss amounted to 10% or more

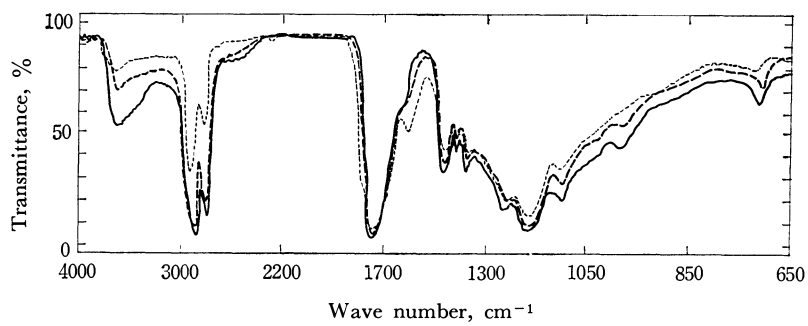

Fig. 2. Thermo-oxidative degradation of polymerized oil film observed in infrared spectra.
—— Original film ---- After heating at 150°C for 3 hr.
····· After heating at 200°C for 3 hr.

*1 Measured by a DTA apparatus Shimadzu Type 1A, in air.

*2 Measured by a du Pont Impact Tester.

TABLE I. THERMO-OXIDATIVE DEGRADATION OF BAKED FILM OF POLYMERIZED OIL

Film	$(T_g)_d$ °C	G_r dyn./cm²	G_h dyn./cm²	D_{2850}	D_{3570}	D_{980}	Weight loss %
Baked film (exposed in air for 33 months)	−27	6.0×10^7	5.8×10^7	0.847	0.213	0.062	
Above film heated at 150°C for 3 hr.	15	6.0×10^8	7.2×10^7	0.662	0.104	0.031	8.7
Above film heated at 200°C for 3 hr.				0.227	0.063	0.06	

TABLE II. THERMO-OXIDATIVE DEGRADATION OF AIR-DRIED FILM OF PHENOLIC VARNISHES

Film	$(T_g)_d$ °C	G_r dyn./cm²	G_h dyn./cm²	Weight loss %
Air-dried film of oil reactive phenolic varnish	32	3.4×10^9	3.0×10^7	
Above film heated at 150°C for 3 hr.	67	3.8×10^9	4.3×10^7	10.4
Air-dried film of nonreactive phenolic varnish (cold blend)	20	2.4×10^9	3.5×10^7	
Above film heated at 150°C for 3 hr.	75	5.5×10^9	4.5×10^7	12.3

TABLE III. THERMO-OXIDATIVE DEGRADATION OF AIR-DRIED FILM OF PHENOLIC VARNISHES
(Infrared spectra)

Film	Thermal treating condition	D_{2850}	D_{3570}	D_{980}
Air-dried film of oil reactive phenolic varnish	(dried for 2 days)	0.296	0.089	0.032
	Heated at 80°C for 10 hr.	0.264	0.069	0.022
	Heated at 150°C for 3 hr.	0.179	0.043	0.017
	Heated at 200°C for 3 hr.	0.148	0.02	0.007
Air-dried film of oil nonreactive phenolic varnish (cold blend)	(dried for 2 days)	0.460	0.140	0.077
	Heated at 80°C for 10 hr.	0.394	0.108	0.040
	Heated at 150°C for 3 hr.	0.390	0.08	0.021
	Heated at 200°C for 3 hr.	0.153	0.03	0

TABLE IV. THERMO-OXIDATIVE DEGRADATION OF AIR-DRIED FILM OF ALKYD RESIN

Thermal treating condition	$(T_g)_d$ °C	G_r dyn./cm²	G_h dyn./cm²	λ	Weight loss, %	Elementary analysis C%	H%	O%
2 weeks after drying						63.78	7.46	28.76
2.5 months after drying	5	1.5×10^8	$<5.7\times10^7$	0.62				
Above film heated at 105°C for 2 hr.	41	3.0×10^9	8.6×10^7	0.36	7	63.39	7.19	29.42
Above film heated at 105°C for 5 hr.								

Thermal treating condition	D_{2850}	D_{1590}	D_{2850}/D_{1590}	D_{3570}	D_{3570}/D_{1590}	D_{980}
2 weeks after drying	0.448	0.090	4.99	0.167	1.85	
2.5 months after drying	0.431	0.092	4.62	0.200	2.22	0.085
Above film heated at 105°C for 2 hr.	0.240	0.090	2.67	0.046	0.51	0.034
Above film heated at 105°C for 5 hr.	0.238	0.090	2.64	0.054	0.60	

when the film was treated at 150°C for 3 hr. in air.

The infrared spectra changes involved in the thermal treating are shown in Figs. 5 and 6, and in Table III. The films prior to thermal treatment were a little different from that used for viscoelastic measurement; namely, each of the varnishes was coated on rock salt and dried for two days, followed by heating at 80°C for 10 hr. and subsequent heating at 150°C for 3 hr. and at 200°C for 3 hr. in air.

It was observed that D_{2850}, D_{3570}, and D_{980} decreased in this thermal treating.

The Thermo-oxidative Degradation of Alkyd Films.—The G-t and λ-t curves, the infrared spectra, and the thermogram of air-dried film are shown in Figs. 7, 8, and 9 respectively. The results are summarized in Table IV.

It was observed when the air-dried film was

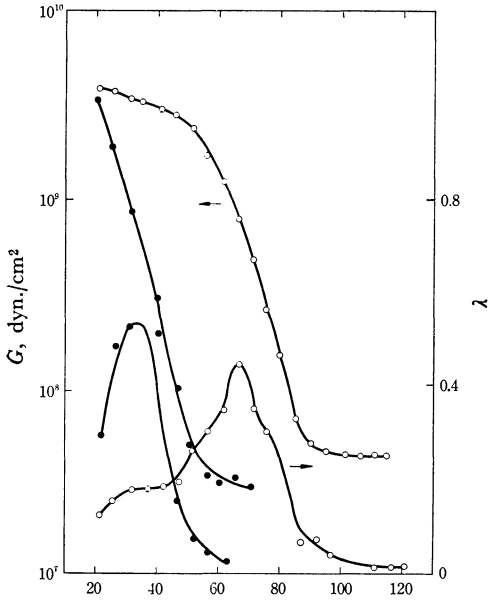

Fig. 3. Thermo-oxidative degradation of air-dried film of phenolic varnish (R-O) observed in *G-t*, *λ-t* curves.
● Original film, R-O
○ After heating at 150°C for 3 hr.

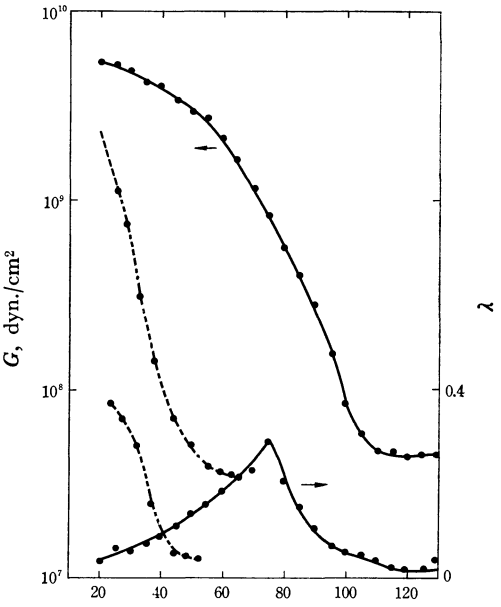

Fig. 4. Thermo-oxidative degradation of air-dried film of phenolic varnish (N+PO) observed in *G-t*, *λ-t* curves.
---- Original film
—— After heating at 150°C for 3 hr.

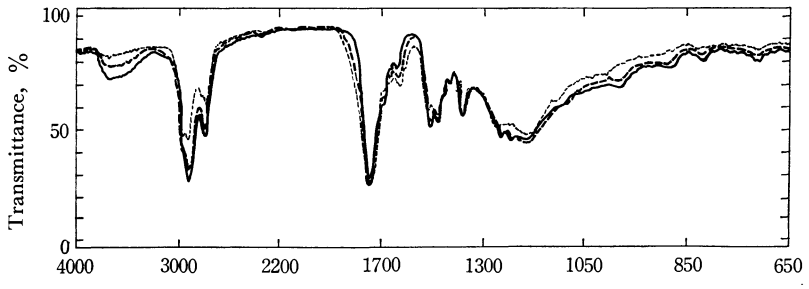

Fig. 5. Thermo-oxidative degradation of air-dried film of phenolic varnish (R-O) observed in infrared spectra.
—— Original film
---- After heating at 150°C for 3 hr.
····· After heating at 200°C for 3 hr.

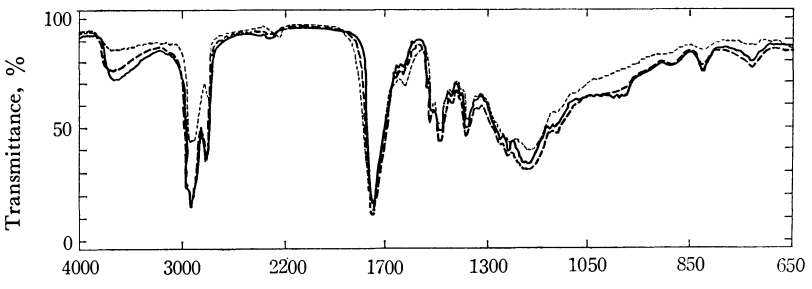

Fig. 6. Thermo-oxidative degradation of air-dried film of phenolic varnish (N+PO) observed in infrared spectra.
—— Original film
---- After heating at 150°C for 3 hr.
····· After heating at 200°C for 3 hr.

TABLE V. THERMO-OXIDATIVE DEGRADATION OF BAKED FILM OF ALKYD RESIN

Thermal treating condition	$(T_g)_d$ °C	G_r dyn./cm²	G_h dyn./cm²	λ	Weight loss, %	Elementary analysis C%	H%	O%
Baked film laid in air for one week	4	4.6×10^7	3.7×10^7	0.89		64.29	7.39	28.32
Above film heated at 150°C for 3 hr.	25	8.0×10^8	4.8×10^7	0.99	2.5	65.20	7.33	27.47
Above film heated at 200°C for 3 hr.	55	5.0×10^9	1.1×10^8	0.62	14.0	63.86	6.60	29.54

Thermal treating condition	D_{2850}	D_{1590}	$\frac{D_{2850}}{D_{1590}}$	D_{3570}	$\frac{D_{3570}}{D_{1590}}$	D_{980}	Degree of swelling %	Chloroform soluble portion of film, %	Impact strength (by du Pont Impact Tester)
Baked film laid in air for one week	0.551	0.110	5.02	0.139	1.26	0.081	530	17.3	1/16″×1kg ×50cm.
Above film heated at 150°C for 3 hr.	0.437	0.106	4.12	0.121	1.14	0.058	450	11.9	1/8″×1kg ×50cm.
Above film heated at 200°C for 3 hr.	0.304	0.091	3.34	0.080	0.83	0.037	Disparted	0.4	1/4″×0.5kg ×50cm.

TABLE VI. WEIGHT LOSS OF FILMS OF PHENOLIC VARNISHES DURING THERMO-OXIDATIVE TREATING

	Film of nonreactive phenolic varnish (N-O)	Film of nonreactive phenolic varnish (cold blend) (N+PO)	Film of reactive phenolic varnish (R-O)	Film of reactive phenolic varnish (cold blend) (R+PO)
Air-dried film	9.3*1	12.3	10.4	18.0
Baked film	5.6	8.1	5.8	13.3

*1 Expressed as

$$\left(\frac{\text{film weight prior to thermal treating-film weight after thermal treating}}{\text{film weight prior to thermal treating}}\right)\times 100$$

TABLE VII. ELEMENTARY ANALYSIS OF AIR-DRIED AND BAKED FILMS OF ALKYD RESIN

Film	Elementary analysis C%	H%	O%	C : H : O (in atoms)			C : H : O (in atoms) (reduced*2)			Number of oxygen atoms combined per aliphatic chain*3
Air-dried film*1	63.78	7.46	28.76	5.31	7.46	1.80	29.0	40.8	9.80	2.80
Baked film	64.29	7.39	28.32	5.35	7.39	1.77	29.0	40.0	9.60	2.60

*1 Laid in air for weeks after drying.
*2 The ratio of C, H, and O (in atoms) in prepolymer which contained one aliphatic chain is 29 (C): 41 (H): 7 (O)
*3 No scission of acyl group taking place during film formation is assumed.

TABLE VIII. EFFECT OF DRYING AGENT ON DECOMPOSITION OF ALIPHATIC CHAINS

Film	Drying temperature	Heating time	Times of coating	Addition of drying agents	D_{2850}/D_{1590}*	D_{3570}/D_{1590}*	Chloroform soluble portion of film %
1	Room temperature	2 days	6	Co 0.02% Mn 0.02%	3.8	1.29	46
2	105°C	2 hr.	6	none	4.3	1.49	16.5
3	105°C	2 hr.	6	Co 0.02% Mn 0.02%	3.4	1.18	8.4
4	105°C	8 hr.	6	none	4.1	1.41	3.8
5	105°C	8 hr.	6	Co 0.02% Mn 0.02%	2.9	1.03	

* IR spectra were measured by KBr disk method.

thermo-treated in air that:

1) The $(T_g)_d$, G_r, and G_h values of the film increased, and the λ-t curve was broadened:

2) The weight loss amounted to 7% when the film was treated at 150°C for 3 hr. in air, and

3) D_{2850}/D_{1590} and D_{3570}/D_{1590} decreased intensively, whereas D_{1590} unchanged.

The G-t and λ-t curves, the infrared spectra, and the thermogram of baked film are shown in Figs. 10, 11, and 9 respectively. The results are

summarized in Table V. The results concerning the degree of swelling and the soluble portion of film, and impact strength of films are also tabulated in Table V.

It was observed when the baked film was heated in air that:

1) The $(T_g)_d$, G_r, and G_h values of the film increased:

2) D_{2850}/D_{1590} and D_{3570}/D_{1590} decreased less than in the case of air-dried film, and D_{1590} decreased also, and

3) The D_{980} decreased also.

It was generally observed when the oxidative polymerized films were thermo-treated that the glass transition temperature and the degree of the crosslinking of the film increased accompanying a decrease in the aliphatic chains and the trans ethylenic double bonds.

The increase in $(T_g)_d$ is considered to be the result of the oxidative decomposition and crosslinking of aliphatic chains. In relation to the network structure, the free aliphatic chains functioned as internal plasticizers; such a function was decreased by the oxidative decomposition of the aliphatic chain induced by thermal treating. Moreover, it may be suggested that such oxidative decomposition induces the decrease in the impact strength of the film.

A Comparison of Thermo-oxidative Degradation of Air-dried and Baked Films.— Smith[6] reported that the baked film alkyd resin (175°C-1 hr.) decomposed and dissipated completely after being heated at 200°C for 5 days. Miller[5] reported that the phthalate also suffered decomposition after the baked film of alkyd resin had been exposed (120°C; 1 hr. without the addition of any drying agent) to ultraviolet rays, they described the conjugated carbonyl as especially unstable, as had been recognized by others. FitzGerald[4] reported that the phthalates decomposed when the baked film of alkyd resin (175°C; 20 min., with the

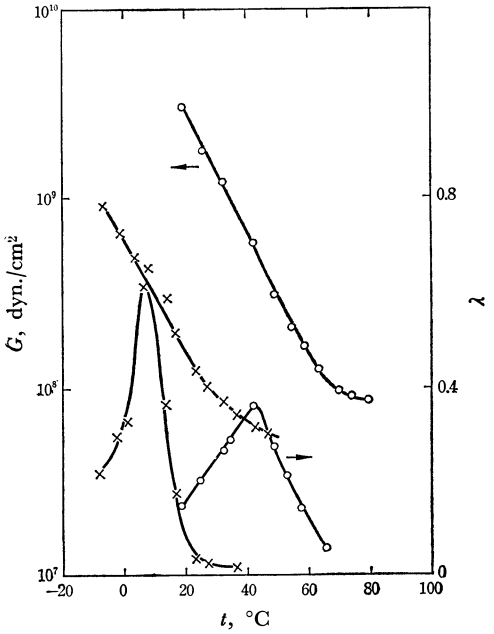

Fig. 7. Thermo-oxidative degradation of air-dried film of unsaturated fatty acid modified alkyd resin observed in G-t, λ-t curves.
× Original film
○ After heating at 105°C for 2 hr.

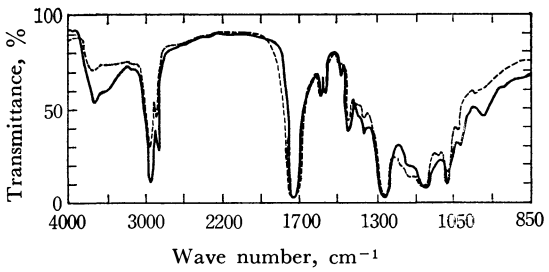

Fig. 8. Thermo-oxidative degradation of air-dried film of unsaturated fatty acid modified alkyd resin observed in infrared spectra.
—— Original film
---- After heating at 105°C for 2 hr.

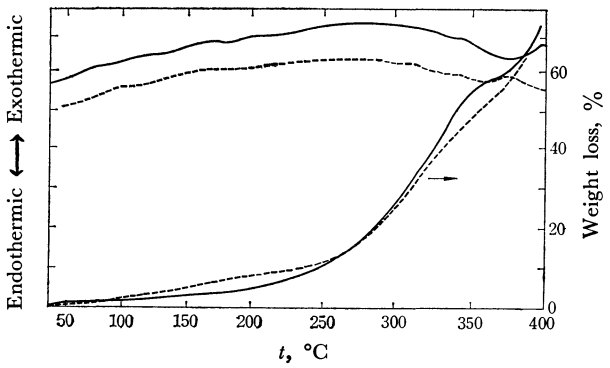

Fig. 9. Thermograms of films of unsaturated fatty acid modified alkyd resin.
---- Air-dried film, —— Baked film

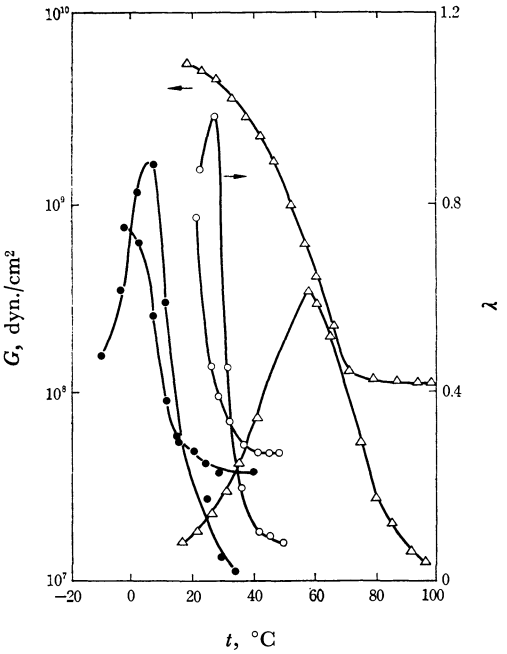

Fig. 10. Thermo-oxidative degradation of baked film of unsaturated fatty acid modified alkyd resin observed in G-t, λ-t curves.
● Original film
○ After heating at 150°C for 3 hr.
△ After heating at 200°C for 3 hr.

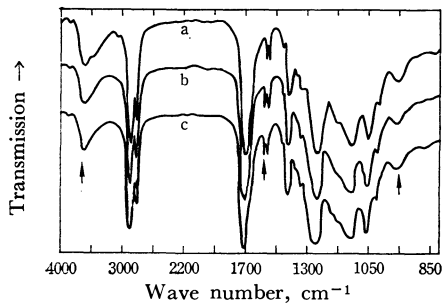

Fig. 11. Thermo-oxidative degradation of baked film of unsaturated fatty acid modified alkyd resin observed in infrared spectra.
a Original film
b After heating at 150°C for 3 hr.
c After heating at 200°C for 3 hr.

addition of a drying agent: stored in air for one month) was thermo-treated (120°C-72 hr.), or exposed to ultraviolet rays. Such a decomposition was initiated at the unsaturated part of aliphatic chains and propagated to the glyceride part and the phthalate part; as a result, the alkyd molecules decomposed and dissipated.

When the thermo-oxidative degradations of air-dried and baked alkyd films were compared, it was found the aliphatic chain decomposed more in the case of air drying; nevertheless, it was treated

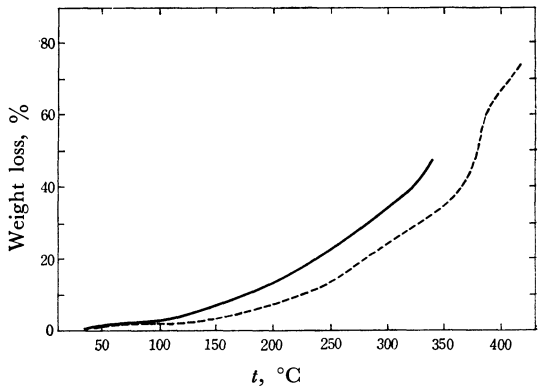

Fig. 12. Thermograms of polymerized oil films (PO).
—— Air-dried film, ---- Baked film

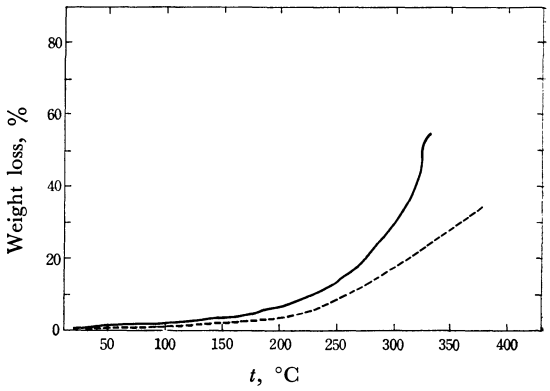

Fig. 13. Thermograms of films of phenolic varnish (R-O).
—— Air-dried film, ---- Baked film

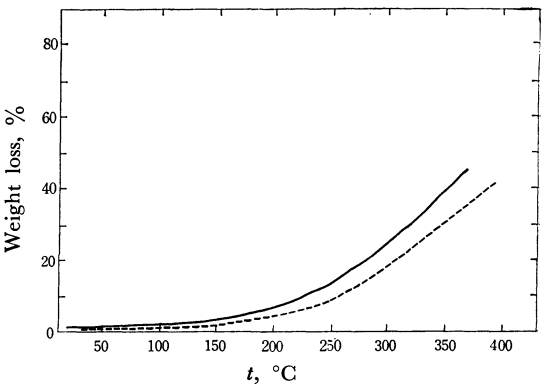

Fig. 14. Thermograms of films of phenolic varnish (N+PO).
—— Air-dried film, ---- Baked film

mildly, and the phthalate was unchanged.

As to baked film, the phthalate dissipated after this thermal treating; this result accorded with those obtained by others.

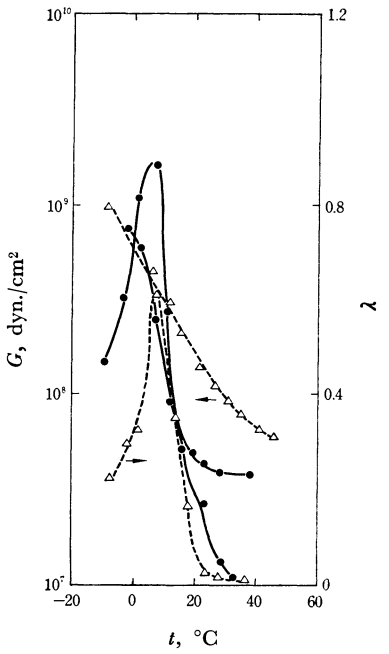

Fig. 15. Comparison of G-t, λ-t curves of air-dried and baked film of unsaturated fatty acid modified alkyd resin prior to thermo-oxidative degradation.
--△-- Air dried film, —●— Baked film

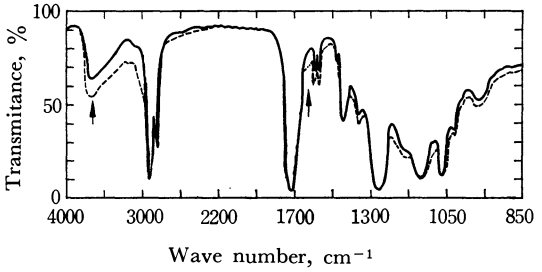

Fig. 16. Comparison of infrared spectra of air-dried and baked film of unsaturated fatty acid modified alkyd resin prior to thermo-oxidative degradation.
---- Air-dried film, —— Baked film

The easy decmoposition of air-dried film is also observed in films of phenolic varnishes and polymerized oil films (see Figs. 12, 13, and 14 and Table VI). Table VI is a comparison of the weight loss during thermal treatment, and Figs. 12—14 are thermograms of air-dried and baked films of phenolic varnishes or polymerized oil exposed in air for the same time and thermal treated under the same conditions.

The infrared spectra, G-t and λ-t curves, and elementary analysis of alkyd films prior to thermal treatment were compared. It was found that:

1) The absorptions near 3500 cm^{-1} and near 1600 cm^{-1}, which are due to conjugated carbonyl, of air-dried film were more intensive (see Fig. 16):

2) The $(T_g)_d$ values are the same, and the shear modulus of plateau region was not observed in air-dried film. The degree of crosslinking of air-dried film is small, suggesting a less crosslinked network structure (see Fig. 15), and

3) The oxygen combined per acyl group in film is nearly the same (see the last column of Table VII).

In combination with these results and the application of the mechanism of autoxidation, it may be suggested that the amount of hydroperoxyl group in air-dried film is more than that in baked film.

Another factor which should be taken account of in connection with easy decomposition of aliphatic chains in the network structure is the effect of drying agents. In this connection, the following five were prepared from a varnish of a composition similar to that of the varnish used in the above experiment.

Film 1.—The varnish, with drying agents (Co 0.02%, Mn 0.02%) added, was coated every other day (6 times) at room temperature.

Film 2.—The varnish, without any drying agents added, was coated and heated at 105°C for 2 hr.; this procedure was also repeated 6 times.

Film 3.—As with Film 2, except that drying agents were added (Co. 0.02%, Mn 0.02%).

Film 4.—The varnish, without any drying agents added, was coated and heated at 105°C for 8 hr.; this procedure was repeated 6 times.

Film 5.—As with Film 4 except that drying agents were added (Co 0.02%, Mn 0.02%).

And their D_{2850}/D_{1590} and D_{3570}/D_{1590} values are compared in Table VIII.

There is an effect of drying agents on the decomposition of aliphatic chains, but the decrease in D_{2850}/D_{1590} is less than that in the thermal treatment of air-dried film.

Therefore, it may be concluded that the easy decomposition of the aliphatic chain, without an accompanying dissipation of the phthalate in air-dried film, is due to the networks containing more hydroperoxyl and conjugated carbonyl groups and their consequent instability, as well as to the presence of drying agents.

From the above results, the extent to which autoxidation is induced by air-drying and baking, and how the structure of the network affects the thermo-oxidative degradation of oxidative polymerized films, have been established.

Summary

1) The aliphatic chains decomposed more easily, and the phthalate was rather more stable in oxidative thermal treatment in air-dried film than in baked film of unsaturated fatty acid-modified alkyd resin.

2) This is a result of the presence of more hydroperoxy and conjugated carbonyl groups, and of the drying agent in air-dried film.

3) After the thermo-oxidation of oxidative polymerized films, the glass transition temperature, the hardness of film, and the degree of crosslinking of film showed an increase: this is considered to be the result of the oxidative decomposition and crosslinking of aliphatic chains. It has been observed also that the impact strength of baked film decreased upon thermo-oxidation.

4) The drying agents contained in film accelerated the decomposition of aliphatic chains during thermal treatment.

BULLETIN OF THE CHEMICAL SOCIETY OF JAPAN VOL. 39 2094—2101 (1966)

A Theoretical Interpretation of the Substituent Effects in Argentation Equilibria of Aromatic Hydrocarbons*

By Takayuki FUENO, Tadashi OKUYAMA and Junji FURUKAWA

Department of Synthetic Chemistry, Kyoto University, Sakyo-ku, Kyoto

(Received December 6, 1965)

The effects of ring substituents on the stability of silver ion complexes of benzene and styrene are discussed in terms of the delocalization energies as calculated by the simple LCAO MO method. It is demonstrated that the delocalization energy responsible for the formation of the σ-type molecular bond can predict the relative stabilities of the complexes; the calculated energies are linearly correlated with Hammett's sigma values. The π-type molecular bond energy arising from the delocalization of silver d-electrons decreases linearly with the increase in the σ-type bond energy. In cases where the two energies are comparable in magnitude, the substituent effects may well be controlled by the entropy term, as has previously been demonstrated experimentally. This apparent paradox encountered in the interpretation of substituent effects may best be reconciled by assuming that the behavior of the silver 4d-orbital in complexation is more closely associated with the entropy change than that of the 5s-orbital of the same atom.

Since Winstein and Lucas[1] first revealed evidence for the formation of silver ion complexes of olefins in the aqueous phase, the nature of such complexes has received considerable attention from physical and organic chemists. Thus, Andrews and Keefer[2] performed extensive measurements of the equilibrium constants for the silver ion complexation (argentation) of aromatic as well as olefinic compounds, hoping thereby to clarify the relation between the substrate structure and the complex stability. More light has recently been shed on these complexes through the structural studies of the isolated silver salt—substrate complexes, using the X-ray diffraction method[3,4] and the ultraviolet,[5,6] infrared[6,7] and NMR[5,8] spectroscopic techniques.

Admittedly, however, little is known about the nature of the complexation bonds formed between the silver ion and substrates. Dewar[9] proposed a complexation model in which the two components are bound by two types of molecular bonds; one is a *σ-type* bond formed by the delocalization of the carbon 2pπ electrons of the substrates onto a vacant 5s-orbital of the silver ion, while the other is a *π-type* bond formed by the *backward* delocalization of the silver 4d-electrons onto a vacant pπ* antibonding orbital of the substrates. Although there has been a growing tendency to accept the above customary picture, no direct confirmation of the role of the d-electrons has ever been provided.

Recently, Hosoya and Nagakura[6] made a theoretical analysis of the electronic structure of the cyclohexene - silver ion complex by evaluating the interactions among several possible electronic

*1 The Structure—Stability Relationship of the Metal Ion Complexes of Unsaturated Compounds. II. Reference 12 is the Paper I of this series.

1) S. Winstein and H. J. Lucas, *J. Am. Chem. Soc.*, **60**, 836 (1938).

2) a) L. J. Andrews and R. M. Keefer, ibid., **71**, 3644 (1949); b) ibid., **72**, 3113 (1950); c) ibid., **72**, 5034 (1950).

3) R. E. Rundle and J. H. Goring, ibid., **72**, 5337 (1950); H. G. Smith and R. E. Rundle, ibid., **80**, 5075 (1958).

4) F. S. Mathews and W. N. Lipscomb, *J. Phys. Chem.*, **63**, 845 (1959).

5) D. B. Powell and N. Sheppard, *J. Chem. Soc.*, **1960**, 2519.

6) H. Hosoya and S. Nagakura, This Bulletin, **37**, 249 (1964).

7) H. J. Taufen, M. J. Murray and F. F. Cleveland, *J. Am. Chem. Soc.*, **63**, 3500 (1941).

8) D. F. R. Gilson and C. A. McDowell, *J. Chem. Phys.*, **39**, 1825 (1963).

9) M. J. S. Dewar, *Bull. soc. chim. France*, **18**, C79 (1951).

configurations of the components. From the results of this analysis, they drew the conclusion that the *d*-electrons of the silver ion contribute appreciably to the stabilization of the ground state of the complex. On the other hand, Fukui et al.[10] used the simple LCAO MO approximation to calculate the delocalization energies of $2p\pi$ electrons alone and demonstrated that such energies could be used as a measure of the relative stability of the 1 : 1 argentation complexes of aromatic hydrocarbons.

It is to be expected that, in substituted aromatic hydrocarbons, the relative effects of substituents on the complex stability will be reversed, depending on which type of molecular bond is the more predominant, the σ-type or the π-type. According to Andrews and Keefer,[2b] the substituent effects in the case of benzene can roughly be interpreted in terms of the Hammett $\rho\sigma$ relationship;[11] the first equilibrium constants, K_1, of substituted benzenes are larger as the substituents are more electrondonating. A similar trend has been observed in our previous experimental work on substituted styrenes.[12] It would seem, then, that only the σ-type bond formation is important in the stabilization of complexes. However, it must be cautioned that, more precisely, such comparisons of substituent effects between theory and experiment should be directed toward the free-energy change in the complex formation rather than toward the enthalpy change, particularly when these changes are relatively small.

In the present paper, we will attempt to make theoretical examinations of the substituent effects observed for the stability of argentation complexes of benzene and styrene. The simple LCAO MO approximation will be used throughout in appreciation of its considerable simplicity. First, the above-mentioned simple delocalization model of Fukui et al.[10] will be tested for the substituted compounds. Second, a suggestion will be made as to the extent to which the d-electrons of silver would participate in the formation of argentation complexes. Finally, consequences of the above suggestion will be discussed, and the empiricism inherent in the present treatment will be assessed.

The pπ-Electron Delocalization Energies of the Complexes

In an attempt to interpret the relative stabilities of silver ion complexes of different aromatic hydrocarbons, Fukui et al.[10] have adopted Dewar's "bond-delocalization model" of the π-complex[13] in which only a pair of $2p\pi$ carbon orbitals of a particular unsaturated bond overlap longitudinally with a vacant orbital of a complexing ion located equidistant from the two carbons. Assuming that the interaction is sufficiently small, they applied the perturbation technique to calculating, within the framework of the simple LCAO MO approximation, the stabilization energy of the complex due to the delocalization of $p\pi$ electrons. The result was expressed in the form:

$$\Delta E_{rs}^{(p)} = 2\sum_{j}^{occ.} \frac{(c_{jr}+c_{js})^2}{m_j}\left(-\frac{\gamma^2}{\beta}\right) \qquad (1)$$

Here, r and s signify the carbon atoms constituting the bond at which the complexation takes place; γ is the resonance integral for the two weak bonds formed between the ion and the carbons, r and s; and the other symbols, which are associated with the isolated aromatic molecules,

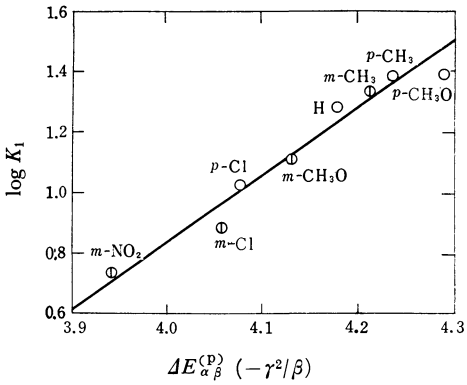

Fig. 1. Plots of the $p\pi$-delocalization energies of argentation complexes of substituted styrenes against log K_1.

have their usual meanings. The energy, $\Delta E_{rs}^{(p)}$, calculated from Eq. 1 has proven capable of providing a successful account of the relative stabilities of the silver ion complexes of aromatic hydrocarbons. The quantity, $\Delta E_{rs}^{(p)}$, will henceforth be referred to as the $p\pi$-delocalization energy.

In the silver ion complexes of substituted styrenes, there are good reasons for believing that the primary center for the coordination of the silver ion is an extracyclic double bond, i. e., the α-β bond.[12] Using Eq. 1, the $p\pi$-delocalization energies of the complexes of substituted styrenes are computed for the α-β bonds. The integral

10) K. Fukui, A. Imamura, T. Yonezawa and C. Nagata, This Bulletin, **34**, 1076 (1961).
11) L. P. Hammett, "Physical Organic Chemistry," McGraw-Hill Book Co., New York, N. Y. (1940), Chapter 7.
12) T. Fueno, T. Okuyama, T. Deguchi and J. Furukawa, *J. Am. Chem. Soc.*, **87**, 170 (1965).
13) M. J. S. Dewar, *Discussions Faraday Soc.*, **2**, 50 (1947). He calculated a $p\pi$-delocalization energy which is the same in principle as that of Fukui et al., but different numerically, because he solved the secular equations for the complexes in which the resonance integrals for the new bonds were assumed to have the value β.

TABLE I. THE pπ-DELOCALIZATION ENERGIES AND THE EQUILIBRIUM CONSTANTS FOR ARGENTATION COMPLEXES OF SUBSTITUTED STYRENES

Substituent	K_1[a] l./mol.	$\Delta E_{\alpha\beta}^{(p)}$, $-\gamma^2/\beta$	$S_\alpha^{(E)}$	$S_\beta^{(E)}$	$S_{\alpha\beta}^{(E)}$
H	19.1(18.2[b])	4.1775	0.9113	1.2662	1.0000
p-CH_3	24.2	4.2357	0.9112	1.3055	1.0095
m-CH_3	21.7	4.2122	0.9113	1.2890	1.0059
p-CH_3O	24.2	4.2899	0.9084	1.3612	1.0101
m-CH_3O	12.9	4.1308	0.9115	1.2361	0.9916
p-Cl	10.6	4.0774	0.9088	1.2096	0.9795
m-Cl	7.58	4.0567	0.9111	1.1890	0.9783
m-NO_2	5.45	3.9413	0.9103	1.1174	0.9568

a) K_1 is the equilibrium constant at 25°C for the following reaction (Ref. 12):
$Ag^+ + St \rightleftarrows AgSt^+ \quad K_1 = [AgSt^+]/[Ag^+][St]$.
b) Andrews and Keefer (Ref. 2c).

TABLE II. THE pπ-DELOCALIZATION ENERGIES AND THE EQUILIBRIUM CONSTANTS FOR ARGENTATION COMPLEXES OF SUBSTITUTED BENZENES

Substituent	K_1[a] l./mol.	$\Delta E_{om}^{(p)}$ $-\gamma^2/\beta$	$\Delta E_{mp}^{(p)}$ $-\gamma^2/\beta$	$S_o^{(E)}$	$S_m^{(E)}$	$S_p^{(E)}$
H	2.41	2.6667	2.6667	0.8333	0.8333	0.8333
CH_3	2.95	2.7356	2.7430	0.8734	0.8561	0.8730
CH_3O	2.50	2.7086	2.7537	0.9487	0.8021	0.9397
Cl	0.69	2.5042	2.5093	0.7938	0.7553	0.7857
F	0.46	2.5449	2.5769	0.8412	0.7605	0.8323
$COCH_3$	0.54	2.5014	2.4458	0.7427	0.7683	0.7296
$COOC_2H_5$	0.56	2.4843	2.4359	0.7408	0.7633	0.7301
NO_2	0.19	2.3221	2.2566	0.6761	0.6944	0.6552

a) K_1 is the equilibrium constant at 25°C for the following reaction (Ref. 2b):
$Ag^+ + Bz \rightleftarrows AgBz^+ \quad K_1 = [AgBz^+]/[Ag^+][Bz]$.

parameters[14] used for the various heteroatoms and bonds are those given in a previous paper.[15] For *m*-nitrostyrene, the inductive model with $k = -1.1$ was used for the nitro group.

The calculated values of $\Delta E_{\alpha\beta}^{(p)}$ are listed in Table I, together with the first argentation constants, K_1, measured at 25°C.[12] Plots of log K_1 against $\Delta E_{\alpha\beta}^{(p)}$ give a good linear correlation, as is shown in Fig. 1; the larger the $\Delta E_{\alpha\beta}^{(p)}$ value, the more stable are the complexes.

For the silver ion - substituted benzene complexes, Andrews and Keefer[2a,b] suggested a structure in which the silver ion is located above the plane of the ring at a position equidistant from the six ring carbon atoms, forming covalent bonds with any of these six carbons. However, it has been confirmed by the X-ray diffraction studies that, in the silver perchlorate - benzene complex salt, the silver ion is located above a carbon-carbon bond of the benzene plane and that it interacts primarily with the two nearest carbon atoms.[3]

Although the structure is not known for the complexes formed from substituted benzenes, we have assumed the bond-delocalization model as depicted above and have calculated the pπ-delocalization energies, $\Delta E_{om}^{(p)}$ and $\Delta E_{mp}^{(p)}$, for ortho-meta and meta-para bonds, respectively, of substituted benzenes. The results of the calculations are given in Table II.

Table II shows that, for a given benzene derivative, the pπ-delocalization energies for ortho-meta and meta-para bonds are nearly equal in magnitude. Since these bonds are little hindered sterically, it may reasonably be assumed that ortho-meta and meta-para bonds contribute equally to the coordination of the silver ion. On the other hand, since the steric effects on argentation are fairly large for the bonds adjacent to the carbon-substitutent bonds,[1] a neglect of the coordination of the silver ion on such bonds will not cause an appreciable error. Thus, the number, *n*, of the bonds effective for silver ion complexation may be assumed to be 4 for all the monosubstituted benzenes considered, while it is 6 for benzene itself.

If the above assumptions are basically correct, all the plots of $\log(K_1/n)$ against $\Delta E_{om}^{(p)}$ and $\Delta E_{mp}^{(p)}$ would fall in the vicinity of a single line. This has been roughly substantiated, as can be seen

14) The π-electron densities, q_r, calculated for the meta and para ring carbons by the use of our parameters are in a linear correlation with Taft's σ°-values[16] of the substituents:
$\sigma_r^\circ = 9.68(1 - q_r)$[15]
15) T. Fueno, T. Okuyama and J. Furukawa, This Bulletin, **39**, 569 (1966).

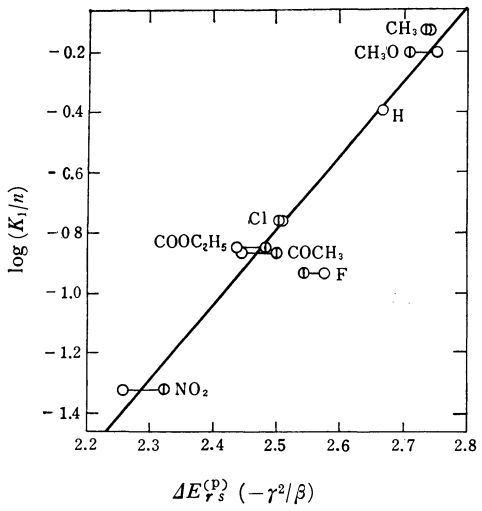

Fig. 2. Plots of the pπ-delocalization energies of argentation complexes of substituted benzenes against log (K_1/n).
n denotes the number of the bonds effective for the complexation. ⓘ, $\Delta E^{(p)}_{om}$; ○, $\Delta E^{(p)}_{mp}$

in Fig. 2. These results may be taken as suggesting the validity of our proposal on the structure of the silver ion - benzene complexes. The value, $\Delta E^{(p)}_{om} + \Delta E^{(p)}_{mp}$, may therefore be regarded as a measure of the relative stabilities of the silver ion complexes of substituted benzenes.

The Correlation of $\Delta E^{(p)}_{rs}$ with π-Electron Distributions

The pπ-delocalization energy, $\Delta E^{(p)}_{rs}$, can be transformed into[10]

$$\Delta E^{(p)}_{rs} = \{S^{(E)}_r + S^{(E)}_s + 2S^{(E)}_{rs}\}(-\gamma^2/\beta) \quad (2)$$

where $S^{(E)}_r$ and $S^{(E)}_s$ are the superdelocalizabilities for an electrophilic attack at the rth and sth carbon atoms respectively, and where $S^{(E)}_{rs}$ is a "bond-delocalizability" defined as[17]

$$S^{(E)}_{rs} = 2\sum_j^{occ.} c_{jr}c_{js}/m_j \quad (3)$$

Thus, the pπ-delocalization energy does not depend upon only the $S^{(E)}_r$ and $S^{(E)}_s$; an important contribution comes into play from the $S^{(E)}_{rs}$ as well.

When the substituents are located sufficiently far from the r-s bonds,[20] the sum of the bond terms, $S^{(E)}_{rs}$, with respect to the s atoms adjacent to a fixed atom, r, becomes identical with the π-electron density, q_r, at the position r. That is,

$$\sum_s{}' S^{(E)}_{rs} = 2\sum_j^{occ.}\sum_s{}' c_{jr}c_{js}/m_j = q_r \quad (4)$$

where the simple LCAO MO relation:

$$-c_{jr}m_j + \sum_s{}' c_{js} = 0 \quad (5)$$

valid under the above conditions, has been utilized.

In the case of ring-substituted styrenes, $S^{E}_{\alpha\beta}$ is in itself equal to the π-electron density on the β-carbon:

$$S^{(E)}_{\alpha\beta} = 2\sum_j^{occ.} c_{j\beta}{}^2 = q_\beta \quad (6)$$

Similarly, it can be shown that $S^{(E)}_\alpha$ is identical with Coulson's π-bond order, $p_{\alpha\beta}$, of the α-β bond:

$$S^{(E)}_\alpha = 2\sum_j^{occ.} c_{j\alpha}c_{j\beta} = p_{\alpha\beta} \quad (7)$$

According to the results of numerical calculations, the values of $S^{(E)}_\alpha$ are nearly constant, irrespective of the sort of ring substituents. On the other hand, $S^{(E)}_\beta$ increases almost linearly with

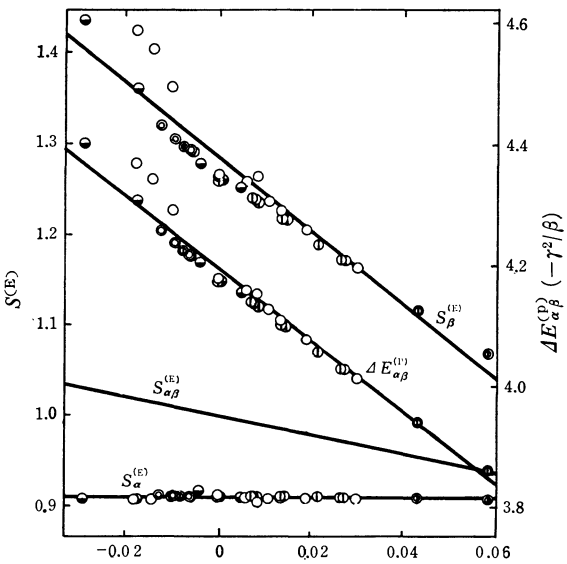

Fig. 3. Linear relationships between the β-carbon electron density and various π-delocalization quantities for substituted styrenes.
Calculations have been performed for various combinations of Coulomb and resonance integrals and the inductive parameters, δ. ○ and ⓘ correspond to para and meta substituents of the methylene-anion type with $\delta=0.3$; ◒ and ◓, to para and meta substituents of the same type with $\delta=0.1$; and ◎ and ⓟ indicate para and meta inductive-model substituents.

16) R. W. Taft, Jr., *J. Phys. Chem.*, **64**, 1805 (1960).
17) According to Ham and Ruedenberg,[18] the non-dimensional bond quantities defined by Eq. 3 are intermediate in nature between "molecular-orbital" bond orders and bond populations. Further, it has been shown by Ham[19] that, in the case of even alternant hydrocarbons, the above bond quantities are mathematically identical with Pauling's "resonance-theory" bond orders.
18) N. S. Ham and K. Ruedenberg, *J. Chem. Phys.*, **29**, 1215 (1958).
19) N. S. Ham, ibid., **29**, 1229 (1958).

an increasing q_β value. These trends were not affected by the type (methylene-anion type or nonconjugative) or the position (meta or para) of the substituents investigated, nor did they depend on the integral parameters, which were arbitrarily chosen for the substituents (see Fig. 3). The net result is, then, that the calculated values of $\Delta E_{\alpha\beta}^{(p)}$ and q_β are inherently in linear correlation with each other.

When we used the substituent parameters which had previously been adopted for the calculation of charge distributions in benzene derivatives,[15] the magnitudes of the imparted quantities, $S_\alpha^{(E)}$, $S_\beta^{(E)}$ and $S_{\alpha\beta}^{(E)}$, for substituted styrenes were found to be such as are listed in Table I. Comparisons of the $S_{\alpha\beta}^{(E)}$, i. e., q_β, with Hammett's σ-values revealed a satisfactory linear relationship between them, as is illustrated in Fig. 4.[21] Since the q_β in turn is in linear correlation with $\Delta E_{\alpha\beta}^{(p)}$, as has been stated above, the $\Delta E_{\alpha\beta}^{(p)}$ must also be linearly correlated with the σ-values (see Fig. 4). If the pπ-delocalization energy is a primary quantity governing the relative stabilities of the silver ion complexes, then the linearity found above between $\Delta E_{\alpha\beta}^{(p)}$ and σ will suffice to explain our previous observations that the argentation equilibria of ring-substituted styrenes fit the Hammett $\rho\sigma$ relation.[12]

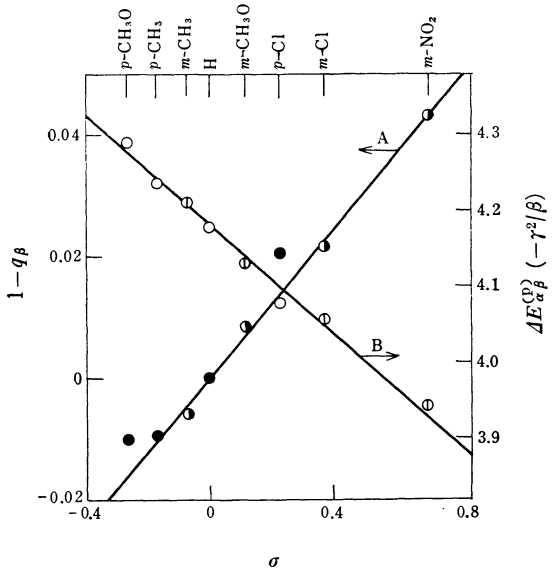

Fig. 4. Correlations of q_β and $\Delta E_{\alpha\beta}^{(p)}$ of substituted styrenes with the Hammett σ.
A, plots of $1-q_\beta$ vs. σ: ●, para; ◑, meta
B, plots of $\Delta E_{\alpha\beta}^{(p)}$ vs. σ: ○, para; ⓘ, meta

In the case of substituted benzenes, we may write the following identities:

$$\Delta E_{om}^{(p)} = (S_o^{(E)} + S_m^{(E)} + 2S_{om}^{(E)})(-\gamma^2/\beta)$$
$$\Delta E_{mp}^{(p)} = (S_m^{(E)} + S_p^{(E)} + 2S_{mp}^{(E)})(-\gamma^2/\beta) \quad (8)$$

where the subscripts o, m and p refer, respectively, to the ortho, meta and para ring positions with respect to the substituents. Again, from Eq. 4, we may write, to a good approximation, the equality:

$$S_{om}^{(E)} + S_{mp}^{(E)} = q_m \quad (9)$$

where q_m is the π-electron density on meta carbons.

The values of $S_o^{(E)}$, $S_m^{(E)}$ and $S_p^{(E)}$ were calculated for several monosubstituted benzenes. The results are included in Table II, where it may be seen that $S_o^{(E)}$ nearly equals $S_p^{(E)}$ with each compound. Aside from the p-CH_3O group, plots of $S_m^{(E)}$ and $S_p^{(E)}$ against the corresponding σ-values give a single straight line, as can be seen in Fig. 5.

Also plotted in Fig. 5 are the $\Delta E_{rs}^{(p)}$ values; for the sake of convenience, the $\Delta E_{om}^{(p)}$ values are plotted against σ_m, while the $\Delta E_{mp}^{(p)}$ values are plotted against σ_p. The differences between $\Delta E_{om}^{(p)}$ and $\Delta E_{mp}^{(p)}$ for given substituents are, on the whole, smaller than the differences of either $\Delta E_{om}^{(p)}$ or $\Delta E_{mp}^{(p)}$ between different substituents. If we assume, as before, that ortho-meta and meta-para bonds contribute equally to the complexation, then an average of the two energies may

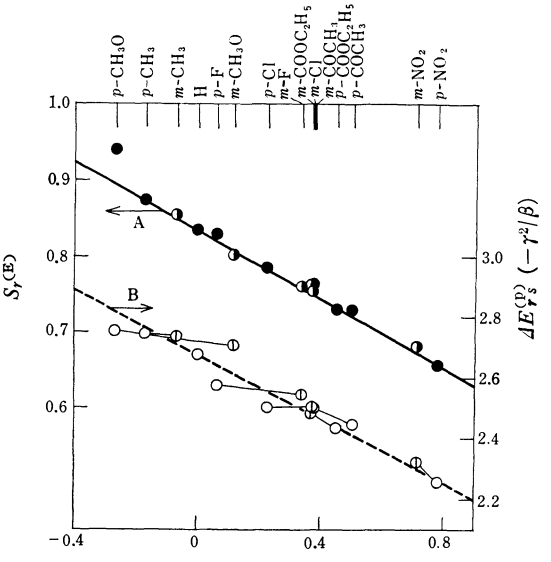

Fig. 5. Correlations of $S_r^{(E)}$ and $\Delta E_{RS}^{(p)}$ of substituted benzenes with the Hammett σ.
A, plots of $S_r^{(E)}$ vs. σ: ●, para; ◑, meta
B, plots of $\Delta E_{rs}^{(p)}$ vs. σ: ○, $\Delta E_{mp}^{(p)}$; ⓘ, $\Delta E_{om}^{(p)}$
For the sake of convenience, $\Delta E_{om}^{(p)}$ are plotted against σ_m and $\Delta E_{mp}^{(p)}$, against σ_p.

20) The condition is fulfilled if the substituents and reaction centers are spatially separated to the extent that the auxiliary inductive effect of substituents on the Coulomb integral of the carbon in question is negligibly small.

21) Deviations in the p-chloro and p-methoxy points from Line A may suggest that the linearity between q_β and σ is only approximate and that it tends to be violated by the methylene-anion type para substituents.

perhaps be a convenient measure of the complexation ability. Thus, by combining Eqs. 8 and 9 with the approximation $S_o^{(E)} \simeq S_p^{(E)}$, we can write:

$$\langle E^{(p)} \rangle \equiv (\Delta E_{om}^{(p)} + \Delta E_{mp}^{(p)}) / 2 \simeq (S_p^{(E)} + S_m^{(E)} + q_m)(-\gamma^2 / \beta) \quad (10)$$

Equation 10 allows us to infer that, insofar as the pπ-delocalization energies in benzene complexes are concerned, the contribution of meta substituent effects might more or less outweigh that of para substituent effects. According to the results of numerical calculations, however, the variation in q_m with σ is less sensitive than that of $S_p^{(E)}$ and $S_m^{(E)}$, so that $\langle E^{(p)} \rangle$ is fairly well correlated with $(\sigma_m + \sigma_p)/2$. Such a relationship is marked with a broken line in Fig. 5. Thus, it may be more reasonable to correlate[22] $\log (K_1/n)$ with $(\sigma_m + \sigma_p)/2$ than to relate $\log K_1$ directly to σ_m, as Andrews and Keefer did previously.[2b]

At this point it is worthwhile to compare the slopes of the $\Delta E^{(p)}$-σ lines for substituted styrenes and benzenes, i. e., Lines B of Figs. 4 and 5. The slope ratio is 1 : 1.46, which is qualitatively understandable because the effects of substituents should increase as the distance between the substituents and the reaction center decreases. Interestingly, this ratio is close to the corresponding ρ ratio, -0.766[12]: -1.36[22]$=1 : 1.78$, derived from the Hammett plots of the argentation equilibrium constants.

The Contribution of the Silver *d*-Electrons

So far, the relative stabilities of the silver ion complexes have been considered in terms of the delocalization energies of pπ-electrons alone. The complexation model underlying the treatments has been a simplification of the Dewar model[9] in that the participation of the silver d-electrons in the complex formation has been ignored. In the case of unsubstituted hydrocarbons, the contribution of these d-electrons to the complex stabilities will parallel that of the pπ-electrons hitherto considered, because, in the Hückel approximation, the bonding and antibonding π-orbitals of the isolated hydrocarbons are spaced in pairs and the distributions of the phantom electrons in the antibonding π-orbitals are the same as in the pairing bonding orbitals. In substituted compounds, however, this parity of orbitals breaks down, and the relative effects of substituents on the complex stability may be reversed, depending on which electrons, pπ or d, exert the more predominant contribution to the complex formation. According to the recent work of Hosoya and Nagakura,[6] the two contributions are almost equally important to the stabilization of the ground state of silver-monoolefin complexes.

If the energy level of the 5s-orbital of the silver ion is $h_s\beta$ relative to the 2pπ Coulomb integral of a benzene carbon, Eq. 1 should be modified to

$$\Delta E_{rs}^{(p)} = 2 \sum_j^{occ.} \frac{(c_{jr} + c_{js})^2}{h_s - m_j} \left(-\frac{\gamma^2}{\beta}\right) \quad (11)$$

Likewise, we may express the delocalization energy, $\Delta E_{rs}^{(d)}$, of a pair of electrons originally belonging to the $4d_{xz}$ atomic orbital of the silver ion as

$$\Delta E_{rs}^{(d)} = 2 \sum_j^{unocc.} \frac{(c_{jr} - c_{js})^2}{h_d - m_j} \left(-\frac{\gamma_d^2}{\beta}\right) \quad (12)$$

where $h_d\beta$ is the energy level of the $4d_{xz}$ orbital of the silver ion in the complex relative to the Coulomb integral of a benzene carbon; γ_d is the resonance integral for the bonds formed by the overlap of the silver $4d_{xz}$ orbital and the $2p_z$ orbitals of the rth and sth carbon atoms of the substrate molecules; and the summation extends over the unoccupied π-orbitals of the substrates. The energy, $\Delta E_{rs}^{(d)}$, may be referred to as the d-delocalization energy.

In order to evaluate these delocalization energies exactly, it is necessary to know the precise values of the energy level quantities, h_s and h_d, for the silver ion in the complexes. At the level of the present approximations, however, little can be predicted for these values. Yet, it is merely the relative effects of various substituents that we are primarily concerned with here. Thus we have decided to avoid the difficulty by proceeding, for the time being, by assuming somewhat arbitrary values for h_s and h_d.

To begin with, we calculated the d-delocalization energies for the various styrenes, assuming that $h_d=0$. The results are given in the third column of Table III. Comparisons of these $\Delta E_{\alpha\beta}^{(d)}$ values with the $\Delta E_{\alpha\beta}^{(p)}$ values previously obtained (Table I) show that there exists a linear correlation between them, as can be seen in Fig. 6. Since the slope of this linearity is negative, the relative effects of substituents in relation to the strengths of the σ- and π-type complexation bonds would tend to act in directions to cancel each other out. Thus a question remains whether the variation in the total complexation *energy* from one substituted styrene to another should parallel that of $\Delta E_{\alpha\beta}^{(p)}$, which has previously been used as a measure of the complex stability. This point will be discussed in the following section.

Next, we calculated the pπ- and d-delocalization energies for styrenes, varying the magnitudes of h_s and h_d. Table III lists the results obtained

22) In fact, plots of $\log (K_1/n)$ against the average sigma result in as satisfactory a linear relation as the plots of $\log K_1$ vs. σ_m, within the limits of the accuracy of experimental data. This new linearity gives a reaction constant of $\rho=-1.36$, while the Andrews and Keefer value is $\rho=-1.60$.

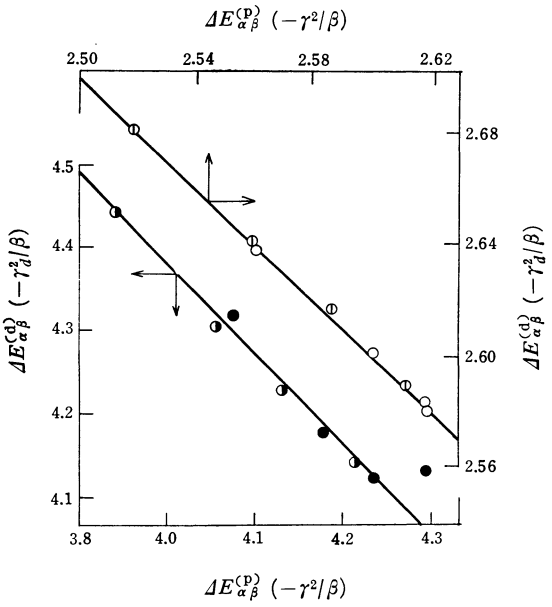

Fig. 6. Linear relationships between the pπ- and d-delocalization energies of silver ion - substituted styrene complexes.
●, para; ◑, meta, calculated with $h_s=0$ and $h_d=0$.
○, para; ⦶, meta, calculated with $h_s=-0.5$ and $h_d=0.5$.

from the choices of $h_s=-0.5$ and $h_d=0.5$ and 1. Comparisons of the $\Delta E^{(p)}_{\alpha\beta}$ values calculated for $h_s=-0.5$ with those previously obtained with $h_s=0$ (Table I) show that these two sets of data run linear. The same is found to be true among the three sets of $\Delta E^{(d)}_{\alpha\beta}$ values (Table III), except for some minor irregularities. This implies that we may expect a linearity of the type given in Fig. 6 without a loss of generality, as long as the d—s separation energy for the complexed silver ion is such that $-0.5<h_s<0<h_d<1$.

Table III. The delocalization energies for the silver ion complexes of substituted styrenes:— Effects of energy levels of the orbitals of silver ion

Substituent	$\Delta E^{(p)}_{\alpha\beta}$, $-\gamma^2/\beta$	$\Delta E^{(d)}_{\alpha\beta}$, $-\gamma_d^2/\beta$		
	$h_s=-0.5$	$h_d=0$	$h_d=0.5$	$h_d=1$
H	2.6004	4.1775	2.6004	1.9114
p-CH_3	2.6182	4.1224	2.5823	1.9017
m-CH_3	2.6112	4.1412	2.5884	1.9048
p-CH_3O	2.6186	4.1318	2.5794	1.8983
m-CH_3O	2.5861	4.2297	2.6163	1.9200
p-Cl	2.5604	4.3210	2.6347	1.9293
m-Cl	2.5595	4.3055	2.6409	1.9328
m-NO_2	2.5188	4.4440	2.6810	1.9534

Similar considerations hold for benzene derivatives. The results are found to be much the same as have been described for styrene derivatives.

Discussion and Conclusions

As has already been mentioned, the relative effects of substituents on the σ- and π-types of complexation energies act in opposite directions. If these effects are of comparable importance, as seems to be the case, it is conceivable that, in effect, the two contributions cancel each other out, so that the total complexation energies change but little within a given series of substituted compounds. This view is consistent with our previous observation that, for a few substituted styrenes, the differences in the enthalpy changes with respect to substituents, $\delta\Delta H$, are quite small despite the sensible differences in free energy change, $\delta\Delta F°$, the substituent effects thus being entropy-controlled in the ordinary temperature region.[12] A similar trend can be noticed in inspecting the argentation data for various α-olefins recently reported by Cvetanović et al.[25]

Nonetheless, it does appear that, at least in the cases of benzene and styrene, the effects of substituents on the stabilities of the silver ion complexes can be interpreted in terms of the pπ-delocalization energy, $\Delta E^{(p)}$, a contribution to the enthalpy change, ΔH. This apparent paradox may best be reconciled by invoking the conventionally accepted concept of the isokinetic relationship.[26] That is, the calculated $\Delta E^{(p)}$ somehow reflects the entropy contribution. In argentation equilibria of substituted compounds, the relationship is perhaps such that, the tighter a complexation bond, the greater is the accompanying entropy loss, $-\Delta S$, which in turn controls the substituent effects in prevalence over the contribution of ΔH.[12] Since $\Delta E^{(p)}$ is correlated with σ, whereas it antiparallels $\Delta E^{(d)}$, the entropy loss associated with $\Delta E^{(d)}$ should be a quantity which parallels σ. This would imply that the observed entropy loss is isokinetically associated more directly with $\Delta E^{(d)}$ than with $\Delta E^{(p)}$. It is, of course, hard to justify this implication theoretically. Offhand, however, this seems to be likely because of the directional properties of the silver d-orbitals in the complexes.

In conclusion, the pπ-delocalization energy, $\Delta E^{(p)}$, can successfully interpret the observed substituent effects on the argentation equilibria

23) Considering the singlet d-s separation energy (5.7 eV.[24]) of the free silver ion, we may guess that the difference between h_s and h_d for a complexed silver ion will be of the order of unity.

24) C. E. Moore, "Atomic Energy Levels," Vol. III, National Bureau of Standards, Washington, D. C. (1958).
25) R. J. Cvetanović, F. J. Duncan, W. E. Falconer and R. S. Irwin, *J. Am. Chem. Soc.*, **87**, 1827 (1965).
26) J. E. Leffler, *J. Org. Chem.*, **20**, 1202 (1955); J. E. Leffler and E. Grunwald, "Rates and Equilibria of Organic Reactions," John Wiley and Sons, Inc., New York (1963), Chapter 9.

of benzene and styrene despite some warnings raised against the Hückel calculations of π-complex stability.[27] However, the conclusion is only ostensibly correct, because the binding energy arising from the contribution of silver d-electrons, $\Delta E^{(d)}$, is of comparable importance, as is $\Delta E^{(p)}$, and because the two energies join together to suppress the enthalpy contribution to the relative substituent effects. The indications of such simple treatments may naturally be crude, but they seem to be significant so long as complexes merely of identical geometry are being compared. It seems, then, that only by assuming an isokinetic correlation between $\Delta E^{(d)}$ and ΔS can the observed substituent effects be cast into such a semiempirical theory of the free energy correlations as has been developed previously.[15]

27) C. A. Coulson and M. J. S. Dewar, *Discussions Faraday Soc.*, **2**, 54 (1947).

BULLETIN OF THE CHEMICAL SOCIETY OF JAPAN VOL. 39 2101—2104 (1966)

Catalytic Activities of Metal Oxides in the Oxidation of Propylene

By Toyosaburo TAKEUCHI, Michiaki HONMA* and Hideo TAKEDA

Faculty of Literature and Science, Toyama University, Gofuku, Toyama

(Received December 9, 1965)

The catalytic oxidation of propylene by the flow method was carried out in order to investigate the correlation between the activity and the physical properties of the catalyst, using the oxides of zinc, copper, nickel, cobalt, iron, manganese, chromium, vanadium and titanium, all of which were supported with alumina. The analysis by means of gas chromatography indicated that the main products of the reaction were carbon dioxide and water. An abrupt increase in the rate of conversion against the temperature, denoted by C_T, was irrespective of the amount of oxide and was characteristic of each oxide. The C_T was expressed as a function of the % d character of the metal of the oxide, as well as a function of the heat of formation per gram-atom of oxygen in the oxide. The mechanism of the abrupt change in the rate of conversion was discussed in relation to the ability of oxygen to be removed from the oxide and the amount of propylene adsorbing on the oxide during the reaction.

The usefulness of metal oxides in the catalytic oxidation of hydrocarbons has been extensively investigated by many workers.[1-5] However, many problems still remain for the establishment of the correlation between the physical properties of metal oxide and the catalytic activity. Recently, Kwan and his co-workers[6] have presented a rule of the catalytic activity of metallic oxides by the use of the experimental results given by Popovskii and Boreskov,[7] who studied the catalytic oxidation of hydrogen. Their rule claims that the activity of the oxidation can be expressed by a function of the heat of formation per gram-atom of the oxygen of the oxide.

This study will deal with the oxidation of propylene on various metallic oxides in order to ascertain whetehr the rule can be applicable to the oxidation of hydrocarbon. The catalytic activities of the oxides will also be discussed from the standpoint of the electronic property of the metal atom of the oxides. The % d character of the metal of the oxide will be taken into consideration for this purpose. The metallic oxides used were titanium(IV) oxide, vanadium(V) oxide, chrome(III) oxide, manganese(IV) oxide, iron(III) oxide, nickel(II) oxide, copper(II) oxide and zinc oxide.

Experimental

The test of the catalytic activity was carried out by a flow method using air. The apparatus used is shown in Fig. 1, where A is the reaction tube, whose diameter and length are 12 mm. and 200 mm. respectively. P is a premixer, and C is a damper of air coming from the compresser, D. F is a flow meter of the soap film. M is an oil manometer, and T is a trap cooled by a mixture of ice and sodium chloride in order to remove the water vapor present in a mixture of propylene and air. The volume of the reaction tube,

* Present address: Nikki Chemical Co., 2-4 Ootemachi, Chiyodaku, Tokyo.

1) G. Parravano and M. Boudart, "Advances in Catalysis," Academic Press, **7**, 50 (1955).
2) E. R. S. Winter, ibid., **10**, 196 (1958).
3) J. K. Dixon, "Catalysis," Reinhold Pub., **7**, 183 (1960).
4) F. S. Stone, "Advances in Catalysis," **13**, 1 (1962).
5) G. K. Boreskov, ibid., **15**, 286 (1964).
6) I. Komuro, H. Yamamoto and T. Kwan, This Bulletin, **36**, 1532 (1963).
7) V. V. Popovskii and G. K. Boreskov, *Probl. Kinetiki; Kataliza, Akad. Nauk. SSSR.*, **10**, 67 (1960).

including an oil manometer of the U-type portions was about 200 cc.

0.5 g. of the oxide was used; it was replaced afresh for each run of the test. The glass fiber was packed at both sides of the catalyst. The ratio of propylene to air was always kept at 0.04—0.05. The flow rate of the mixed gas in the reaction tube was in the range from 100 to 120 cc./min. The analysis of the reaction products was made by means of gas chromatography, using helium as the carrier. The intervals of every analysis were 30 or 60 min. The fluctuation in the amounts of products could be found over about a 30 min. period in the initial stage. The average was taken for the evaluation of the activity. It was calculated from the values measured for five hours, except for the initial hour.

The catalysts, except for those of titanium dioxide and vanadium pentoxide, were prepared from the nitrates. 30—50 mesh γ-alumina was used as the carrier. It was immersed into about a 2 N solution of each nitrate for about 48 hr. at room temperature; then the precipitate was separated from the solution and ignited at 550°C in a furnace. Vanadium pentoxide was prepared by immersing alumina in a solution of meta-ammonium vanadate, which had been dissolved in nitric acid. Titanium dioxide was prepared by immersing alumina into the solution of titanium, which had been dissolved in hydrofluoric acid; then the precipitate was separated from the solution and ignited at 550°C.

Five oxides, i. e., cupric oxide, vanadium pentoxide, zinc oxide and chromium trioxide, were tested without a carrier in order to investigate the influence of the carrier on the oxidation of propylene. The powder of about 50 mesh was selected by sifting it before use. The B. E. T. areas of the catalysts were determined by using nitrogen or methane at −196°C. Nitrogen was used for the supported catalysts, while methane was used for the unsupported catalysts.

Results

The products of the oxidation of propylene were, in most cases, carbon dioxide and water. The products of the oxidation in the presence of vanadium pentoxide gave a stimulant smell. The gas chromatogram of the products, however, gave only the patterns of carbon dioxide and water.

The activity was represented as a percentage of the amount converted, which was determined from the amount of carbon dioxide produced. The results are summarized in Figs. 2 and 3. In Fig. 3, the results on pure alumina are also shown for the purpose of comparison. The alumina used for this purpose was prepared by heating it in vacuo at 450°C. The figures indicate that the percentage of the conversion on the oxides of nickel, manganese, chromium, iron, cobalt and vanadium changes markedly in a certain temperature range. However, no such remarkable change could be found either on pure alumina or on the supported oxides of copper, zinc and titanium. The temperature of the remarkable change was independent of the amount of the catalyst. It can be said, therfore, that the temperature is characteristic of each oxide. The inclination of the line at a point of remarkable change for the pure oxides (unsupported catalysts), except vanadium oxide, is steeper than those for the oxides combined with alumina (a supported catalyst). We denote the temperature of the remarkable change as C_T. The figures indicate that the C_T of chromium oxide and that of vanadium oxide are lowered by the presence of the carrier, while, C_T of cupric oxide is raised. The influence of the carrier is very small in the case of zinc oxide.

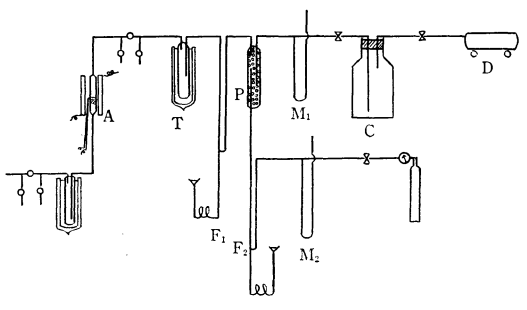

Fig. 1. Apparatus for oxidation of propylene.

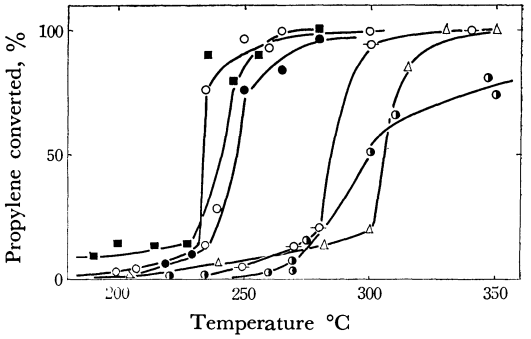

Fig. 2. Result of the oxidation of propylene.
■ NiO, ● MnO_2, ○ Cr_2O_3, -○- Fe_2O_3, △ V_2O_5, ◑ Co_3O_4.

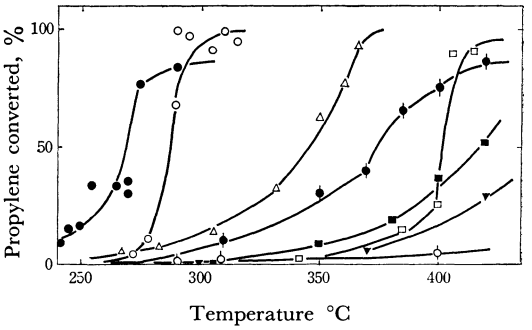

Fig. 3. Result of the oxidation of propylene.
○ unsupported Cr_2O_3, ● unsupported CuO, △ unsupported V_2O_5, □ unsupported ZnO, ● CuO, ■ ZnO, ▼ TiO_2, ○ γ-Al_2O_3.

Figure 4 shows the correlation between C_T and ΔH, the heat of formation per gram-atom of the oxygen of the corresponding oxide. The figure shows that an approximate linear relation can be established for all the oxides except for the supported cupric oxide and chromium oxide. The rates of reaction were calculated by the following equation:

$$V = rFX/(1 + r)S$$

where V is the rate of reaction, X is the percentage of the propylene converted, and F is the space velocity of gas. S and r are the surface area of the catalyst and the mole ratio of propylene to air, (O_2 in air)/(propylene), respectively.

Figure 5 shows the correlation between log V and the reciprocal of the reaction temperature. The correlations are represented by broken lines, suggesting that the activation energies below and above C_T differ from each other. However, no systematic correlation between the activation energy and ΔH could be found in either temperature range, as has previously reported by Morooka and Ozaki.[8]

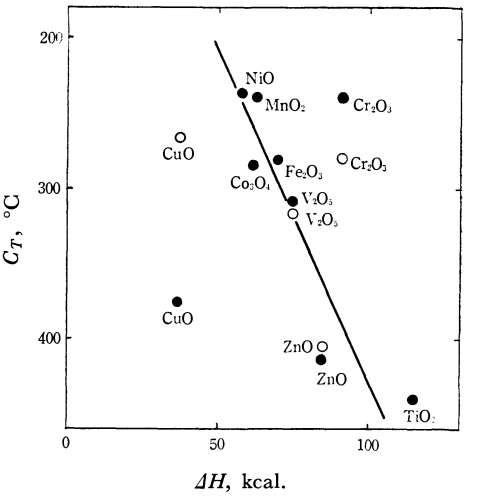

Fig. 4. Correlation between C_T and ΔH.
○ indicates unsupported oxide.

Discussion

The change of catalytic activity in the presence of alumina may suggest that a change of structure of oxide occurs. An experimental confirmation of the structural change of each supported oxide could not be made, nevertheless, the oxide whose activity is changed may be considered to have the spinel structure from the standpoint of valency.

The rates of the reaction in the temperature range above C_T could not be known accurately. The temperature would rise due to the accumulation of heat by the explosive fast reaction which could be supposed to occur, though the thermometer of the reaction tube always showed a constant temperature. Whatever may be the accurate value of the reaction rate above C_T, the change in the activation energy below and above C_T may suggest a change in the mechanism of the reaction, as is clear from the results in Fig. 5.

Hofer et al.[9] investigated the oxidation of ethylene and carbon monoxide on cupric oxide, cobalt

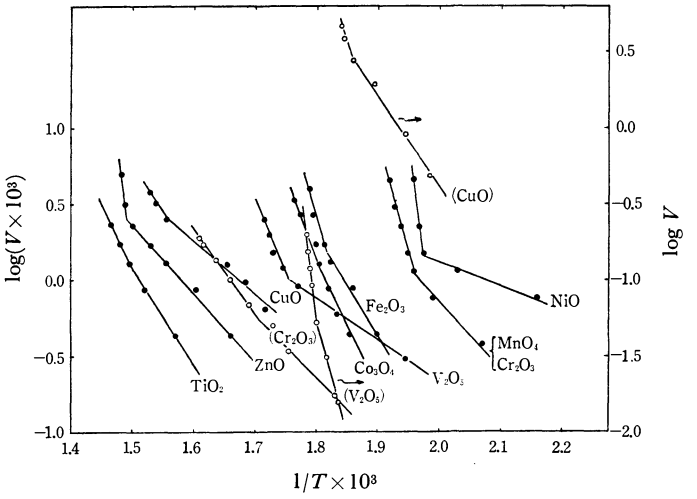

Fig. 5. Temperature dependence of rate of reaction.
The unit of the rate V is cc./min.m^2.
Bracket indicates unsupported oxide.

8) Y. Morooka and A. Ozaki, *Shokubai*, **6**, 27 (1964).

9) L. J. E. Hofer, P. Gussey and R. B. Anderson, *J. Catalysis*, **3**, 451 (1964).

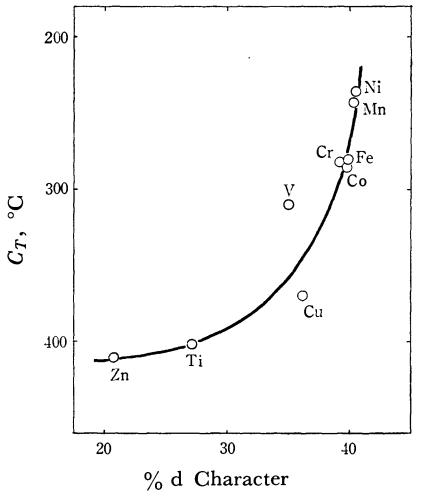

Fig. 6. Correlation between C_T and % d character of metal of oxide.

oxide and chromium oxide by means of gas chromatography; they reported the dependence of the amount of the product and that of the reactants adsorbed on the oxide upon the reaction temperature. Evidently from their data, a remarkable change in the amount of conversion takes place at the temperature where the amount of the reactants adsorbed on the oxide becomes nearly zero, though they put no scuh interpretation on thier results. An exception is found, however, in the reaction on copper oxide. They reported that the amounts of reactants adsorbed on the cupric oxide were nearly zero in the temperature range investigated. The extremely small value obtained from the measurement of adsorption on the copper oxide seems to result from the difficulty of accurate measurement of the amount of adsorption, because the surface of the copper oxide is particularly small, about 1/20 that of the other oxides. Considering from their results, the remarkable increase of the amount of conversed propylene may be due to the decrease of the adsorbed propylene to a certain concentration at the temperature of C_T. The ability of gas to be adsorbed on the metal oxides can be estimated from the heats of adsorption on them. Unfortunately, no information on the heats of adsorption of propylene on metal oxides has appeared in literatures so far. However, the heats of adsorption on oxides may be estimated, if we assume that the propylene is adsorbed on the metal atoms of the oxide, and that the cohesive binding between metal and oxygen occurs by the shift of the valence electron of 4p orbitals of the metal atom to oxygen, without affecting the d electron of the metal atom. By applying the valence bond theory of Pauling[10] to the metal oxides and the proposal by Beeck,[11] who found the correlation between the heat of adsorption and the % d character of metal, the correlation between the % d character of the metal atom of each oxide and C_T can be obtained. The results are shown in Fig. 6, where the % d character of all the metal atoms except for zinc are quoted from the list given by Pauling. The % d character of zinc was calculated by assuming 4.56 for its valence[12] and the resonance structure of $V(2)$ and $V(6)$, where V indicates the valence of the metal. The correlation in the figure seems to be more satisfactory than that between ΔH and C_T, because the deviation is smaller. The figure indicates that C_T increases with decreasing % d character. Since the heat of adsorption is connected with the ability of adsorption and since it decreases with increasing % d character of metal atom,[11] it can be said that the oxide of the lower C_T value has a smaller ability of adsorption of propylene than the oxide of the higher C_T value and that the surface of the catalyst would be covered more densely with oxygen than with propylene.

The reaction mechanism of the oxidation of hydrocarbon proposed by Bretton et al.[13] was the removal of hydrogen from the hydrocarbon at its first step. The same proposal has been made by Sachtler and De Boer[14] and by Adams and Jennings[15] for the oxidation of propylene. A satisfactory explanation of the difference in the mechanisms of the oxidation in the two temperature ranges below and above C_T is far from having been established at present. However, it can be concluded that the difference in C_T of various metal oxides may be due to the ability of oxygen to be removed from the oxide and that of propylene to be adsorbed on the metal atom of the oxide.

10) L. Pauling, *J. Am. Chem. Soc.*, **69**, 542 (1947); *Proc. Roy. Soc.*, **A196**, 343 (1949).
11) O. Beeck, *Discussions Faraday Soc.*, **8**, 118 (1950).
12) L. Pauling, "The Nature of the Chemical Bond", Cornell U. P. and O. U. P., 3rd ed., Ithaca, N. Y. (1960), p. 396.
13) R. H. Bretton, S. U. Wan and B. F. Dodge, *Ind. Eng. Chem.*, **44**, 594 (1952).
14) W. H. N. Sachtler and N. H. De Boer, "Proc. 3rd Intern. Cong. Catalysis," North Holland Pub. Co. (1964), p. 252.
15) C. R. Adams and T. J. Jennings, *J. Catalysis*, **3**, 549 (1964).

BULLETIN OF THE CHEMICAL SOCIETY OF JAPAN VOL. 39 2105—2109 (1966)

The Diffusion of Gases at High Pressures. I. The Self-diffusion Coefficient of Carbon Dioxide

By Shinji TAKAHASHI and Hiroji IWASAKI

Chemical Research Institute of Non-Aqueous Solutions, Tohoku University, Katahira-cho, Sendai

(Received December 9, 1965)

The self-diffusion coefficients of carbon dioxide were measured over a pressure range from 2 to 250 atm. at 25, 50, and 75°C. The measurements of self-diffusion through a plug of porous bronze were made using the radioactive tracer technique. The products of the density and the diffusion coefficient increase slightly with the density in the region of lower density, below about 10 mol./l., for both isotherms at 50 and 75°C, but they decrease in the region of higher density. These results agree with the results obtained by O'Hern et al., but not with Enskog's dense gas theory, and not with the values calculated by the generalized chart of Slattery et al.

The diffusion coefficient of gases at high pressure is not only an interesting physical property from the standpoint of the kinetic theory of gases, but it is also an important property for the analysis of the operations and design of apparatus in the chemical industry. Enskog[1,2] made some theoretical studies of the diffusion process in developing his kinetic theory of non-uniform gases, based on the assumption of a rigid spherical molecule. Slattery et al.[3] prepared a generalized chart for the self-diffusion coefficient of gases at high densities using Enskog's theoretical relations on transport properties and experimental data on the viscosity.

There have been some recent reports[4] on the gaseous diffusion coefficient at high densities measured by the use of either the radioactive or the stable isotope-tracer technique. However, the results have not indicated a definite relation between $D\rho$ and ρ (D: diffusion coefficient, ρ: density). For example, in the case of the self-diffusion coefficient of carbon dioxide, Drickamer et al. concluded that $D\rho$ decreases in accordance with Enskog's theory until $\rho = 0.067$ g./cc., whereas O'Hern et al. stated that $D\rho$ is constant independent of the density, and Becker et al. showed that $D\rho$ increases with the density. Thus, further investigation seems to be necessary in order to clarify the relation between $D\rho$ and the density in the high pressure range.

Additional measurements of the diffusion coefficient in the $^{14}CO_2$-$^{12}CO_2$ system, by a method similar to that of O'Hern et al., will be reported here. These measurements were made at pressures up to 50 atm. at 25°C, and up to 250 atm. at 50 and 75°C. The results will be compared with the values obtained by other investigators and with the values calculated by Enskog's equation and the generalized chart.

Apparatus

The diffusion cell, the major part of the apparatus, was nearly identical with that used by O'Hern et al., Mifflin et al., and Durbin et al., as is shown in Fig. 1. The principle of measurement procedure was as follows: a diffusion path, B, composed of porous metal was placed between two chambers, C and D, equal in volume. The concentration gradient of $^{14}CO_2$ was created between these two chambers through the porous plug, and the diffusion coefficient, D_{12}, in the $^{14}CO_2$-$^{12}CO_2$ system was calculated from the measurements of the change in the concentration of $^{14}CO_2$ with time.

Each chamber had a volume of 35 cc. and was connected to the diffusion path, B, which had a length of 40 mm. and a diameter of 18 mm. The diffusion path was a plug of sintered bronze powder; two types of plugs were used, one with a grain size of ϕ160—250 μ (I) and the other, with a grain size of ϕ60—70 μ (II). The concentration of $^{14}CO_2$ was measured by means of the ionization current in the chamber. The collecting electrode, I ($20\phi \times 15$ mm.), was made of invar

1) S. Chapman and T. G. Cowling, "The Mathematical Theory of Non-Uniform Gases," Cambridge University Press, London (1939).

2) J. O. Hirschfelder, C. F. Curtiss and R. B. Bird, "Molecular Theory of Gases and Liquids," John Wiley & Sons, Inc., New York (1954).

3) J. Slattery and R. B. Bird, *A. I. Ch. E. Journal*, **4**, 137 (1958).

4) K. D. Timmerhaus and H. G. Drickamer, *J. Chem. Phys.*, **19**, 1242 (1951); W. L. Robb and H. G. Drickamer, ibid., **19**, 1504 (1951); K. D. Timmerhaus and H. G. Drickamer, ibid., **20**, 981 (1952); Q. R. Jeffries and H. G. Drickamer, ibid., **21**, 1358 (1953), ibid., **22**, 436 (1954); H. A. O'Hern and J. J. Martin, *Ind. Eng. Chem.*, **47**, 2081 (1955); C. Chou and J. J. Martin, ibid., **49**, 758 (1957); E. Becker, W. Vogell and F. Zigan, *Z. Naturforsch.*, **8a**, 686 (1953); T. R. Mifflin and C. O. Bennett, *J. Chem. Phys.*, **24**, 975 (1958); V. Berry and R. Koeller, *A. I. Ch. E. Journal*, **6**, 274 (1960); L. Durbin and R. Kobayashi, *J. Chem. Phys.*, **37**, 1643 (1962); H. H. Reamer and B. H. Sage, *J. Chem. Eng. Data*, **8**, 34 (1963); I. F. Golubev and A. G. Bondarenko, *Gaz. Prom.*, **8**, 46 (1963).

steel and was insulated from the stainless steel plug, F, by a surface-polished quartz disk, E ($30\phi \times 15$ mm.). The collecting electrode, the quartz disk, and the plug were cemented together by epoxy resin. The quartz disk had a 3ϕmm. hole in its center through which the lead-in wire, H, used for measuring the ionization current, projected. The lead-in wire was insulated from the steel pipe, not shown in Fig. 1, with metharylate resin insulators and was connected to a dynamic condenser electrometer manufactured by the Okura Electric K. K. The applied voltage was maintained at about 540 V., using 12 layer-built dry cells of 45 V. each. The quantity of $^{14}CO_2$ used for each measurement was in the range of 0.01—1 μCi, and the ionization current was in the range of 10^{-13}—10^{-11} amp. The results of a preliminary experiment* are shown in Fig. 2 and Fig. 3. As is apparent in these figures, a linear relationship exists between the amount of $^{14}CO_2$ and the ionization current under these experimental conditions. The ionization currents in each of the two chambers were measured by two electrometers, and the readings were recorded during the experiment.

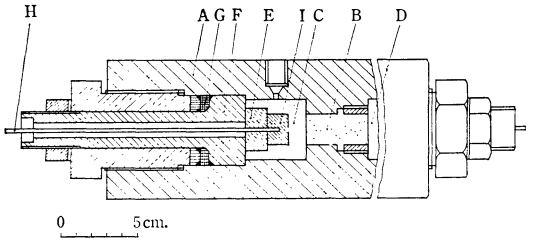

Fig. 1. Diffusion cell.

A: body, B: diffusion path, C and D: ionization chamber, E: quartz disk, F: stainless steel plug, G: teflon packing, H: lead-in wire, I: collecting electrode.

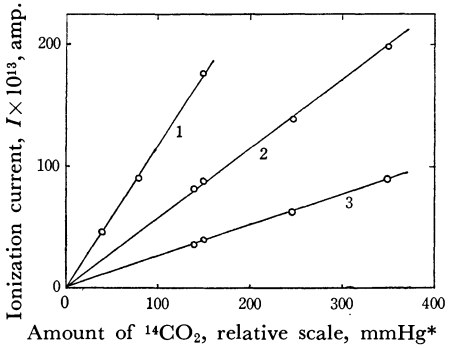

Fig. 2. Relations between the amount of $^{14}CO_2$ and ionization current at 25°C.
1: 8 atm., 2: 20 atm., 3: 50 atm.

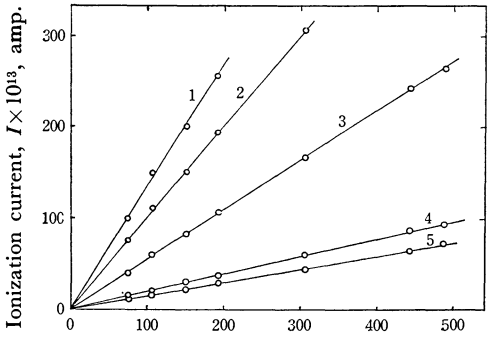

Fig. 3. Relations between the amount of $^{14}CO_2$ and ionization current at 50°C.
1: 10 atm., 2: 20 atm., 3: 50 atm., 4: 100 atm., 5: 200 atm.

An air thermostat was used. The temperature was kept within ±0.1°C by a combination of a platinum resistance thermometer, a Wheatstone bridge, and a photoelectric cell circuit,[5] and was measured by a platinum resistance thermometer calibrated against the freezing and boiling points of water and a PTR thermometer. The pressure was measured by a Bourdon gauge calibrated against a pressure balance of a free-piston type. The errors in pressure measurements were within ±0.02 atm. up to 20 atm., ±0.1 atm. in the 10—50 atm. range, and ±0.5 atm. in the 50—250 atm. range.

The radioactive $^{14}CO_2$ was generated by adding 60% $HClO_4$ to $Ba^{14}CO_3$; its specific radioactivity was approximately 1 μCi/cc. at N.T.P. The non-radioactive carbon dioxide, with a purity of over 99.9% and with a water content of less than 0.04%, was used after it had been dried over phosphorus pentoxide.

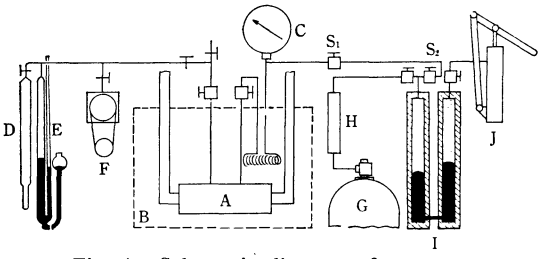

Fig. 4. Schematic diagram of apparatus.

A: diffusion cell, B: air thermostat, C: pressure gauge, D: $^{14}CO_2$ container, E: gas burette, F: vacuum pump, G: $^{12}CO_2$ cylinder, H: drying tube, I: intensifier, J: oil pump, S_1 and S_2: valves

* The experimental procedures were as follows: after the ionization chamber had been evacuated, a mixture of $^{14}CO_2$ and $^{12}CO_2$ was introduced into the chamber (70—500 mmHg). These pressures are shown as abscissae in Fig. 2 and Fig. 3. The amounts of $^{14}CO_2$ are proportional to these pressures. Then, the pressure of the chamber was raised to 10—200 atm. by introducing $^{12}CO_2$, and the ionization current was measured.

5) K. Date, G. Kobuya and H. Iwasaki, *Bulletin of The Chemical Research Institute of Non-Aqueous Solutions, Tohoku Univ.*, **10**, 67 (1961).

Experimental

The arrangement of the experimental apparatus is shown in Fig. 4. An air thermostat was adjusted to a pre-determined temperature and allowed to stand for approximately 24 hr. Cell A was then evacuated to approximately 10^{-2} mmHg by a vacuum pump, F. A suitable quantity of $^{14}CO_2$ was introduced through the gas burette, E, from the $^{14}CO_2$ container, D, into the left chamber in the cell. The non-radioactive carbon dioxide was introduced into the right chamber from the cylinder, G, through the drying tube, H, and compressed to a given pre-determined pressure by the oil pump, J. In this way a major portion of the $^{14}CO_2$ was collected in the left chamber and a large concentration gradient of $^{14}CO_2$ was created between the two chambers through the porous plug. Then, the diffusion cell was disconnected from the pressure system between the two valves, S_1 and S_2, and the voltage was applied to cell, A; the resulting ionization current was measured and recorded. An example is shown in Fig. 5.

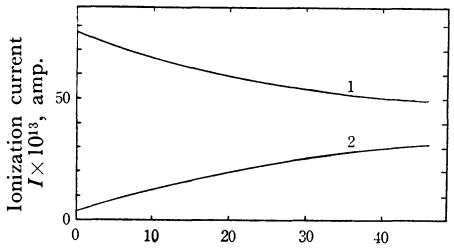

Fig. 5. The variation of ionization current with time at 50°C, 84.2 atm.
1: I_1, 2: I_2

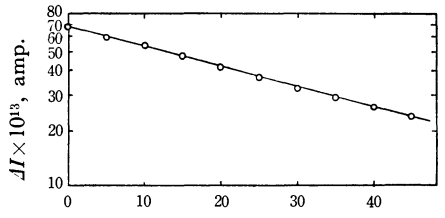

Fig. 6. Semilog plot of current difference ΔI vs. time at 50°C, 84.2 atm.

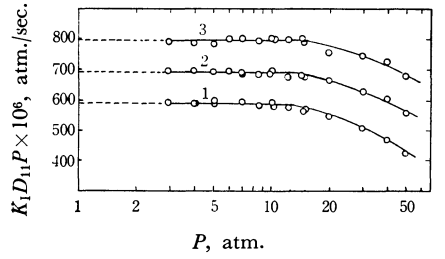

Fig. 7. Relations between $K_1D_{11}P$ and P.
1: 25°C, 2: 50°C, 3: 75°C

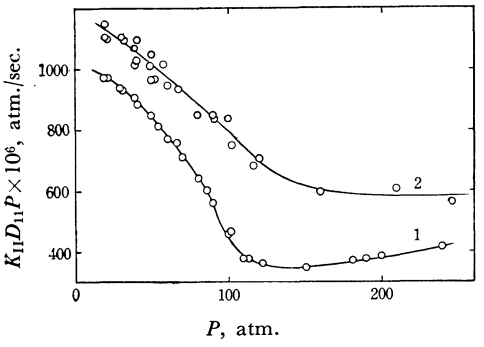

Fig. 8. Relations between $K_{II}D_{11}P$ and P.
1: 50°C, 2: 75°C

Calculation

Assuming that the concentration gradient of $^{14}CO_2$ in the diffusion path is linear and that the concentration in each chamber is uniform, the following equations are obtained:

$$\ln(C_1 - C_2) = -KD_{12}t + \text{constant} \quad (1)$$

$$K = \frac{A}{L}\left(\frac{1}{V_1} + \frac{1}{V_2}\right) \quad (2)$$

where C_1 and C_2 are concentrations of $^{14}CO_2$ in chamber 1 and chamber 2, shown as C and D, respectively in Fig. 1, where D_{12} is the mutual diffusion coefficient in the $^{14}CO_2$-$^{12}CO_2$ system, and where t is the time. K is an apparatus constant; it is given by Eq. 2, where A and L are the effective cross section and the effective length of the diffusion path and where V_1 and V_2 are the volumes of chamber 1 and chamber 2 respectively. Since a linear relationship holds between the concentration of $^{14}CO_2$ and the ionization current, Eq. 1 may be written as:

$$\ln \Delta I = -KD_{12}t + \text{constant} \quad (3)$$

$$\Delta I = I_1 - \gamma I_2$$

$$\gamma = I_1'/I_2'$$

where I_1 and I_2 are the ionization currents in chamber 1 and chamber 2 respectively. I_1' and I_2' are the ionization currents in chamber 1 and chamber 2 respectively, when $^{14}CO_2$ is introduced into the chambers at the same concentration. According to Eq. 3, ln ΔI should be linear with t; this was experimentally proved, as is shown in Fig. 6, where common logarithms are used. If ΔI at time t_i and t_f are designated as $(\Delta I)_i$ and $(\Delta I)_f$ respectively, KD_{12} can be calculated by the following equation:

$$KD_{12} = \frac{6.3961\times10^{-4}}{\Delta t}\log\frac{(\Delta I)_i}{(\Delta I)_f} \quad (4)$$

where the terms are expressed as follows: K; 1/cm², D_{12}; cm²/sec., Δt; hr., and ΔI: amp. Hutchinson[6]

6) F. Hutchinson, *J. Chem. Phys.*, **17**, 1081 (1949).

verified the following relationship between the self-diffusion coefficient, D_{11}, and the mutual diffusion coefficient, D_{12} at normal pressure:

$$\frac{D_{11}}{D_{12}}=\left[\left(\frac{m_1m_2}{m_1+m_2}\right)\left(\frac{m_1+m_1}{m_1m_1}\right)\right]^{1/2}=\left(\frac{2m_2}{m_1+m_2}\right)^{1/2} \quad (5)$$

where m_1 and m_2 are masses of gaseous molecular species containing isotopes. Assuming that the above relationship also holds in the high pressure region, the D_{11} value in the $^{12}CO_2$ system was obtained by multiplying the D_{12} measured in this work by 1.011.

Results

When Diffusion Path I was Used.—In the 2—50 atm. pressure range, a type-I porous plug was used as the diffusion path. The values of $K_ID_{11}P$ obtained are shown in Fig. 7. The values of K_ID_{11} at 1 atm. were then obtained by extrapolation using the observed values of $K_ID_{11}P$. The apparatus constant, K_I was determined by the use of the values of D_{11} reported by Amdur et al.[7] at 1 atm. These are shown in Table I. The values of D_{11} calculated using K_I, which is given in Table I, are shown in Table II. The smoothed values of D_{11} obtained from the values in Table II are shown in Table III. The deviation of the

TABLE I. DETERMINATION OF APPARATUS CONSTANT K_I

Temp. °C	P atm.	$K_ID_{11}P\times10^6$ atm./sec.	$D_{11}\times10^3$* cm²/sec.	$K_I\times10^3$ 1/cm²
25	1.0	591	114.0	5.19
50	1.0	689	132.7	5.20
75	1.0	795	152.3	5.22

* Measured by Amdur et al.[7]

TABLE II. EXPERIMENTAL RESULTS FOR DIFFUSION PATH I

25°C		50°C		75°C	
P atm.	$D_{11}\times10^3$ cm²/sec.	P atm.	$D_{11}\times10^3$ cm²/sec.	P atm.	$D_{11}\times10^3$ cm²/sec.
2.91	39.1	2.91	45.8	2.91	52.1
2.91	39.2	3.91	34.2	3.91	38.7
3.91	29.0	4.91	26.9	4.91	30.7
3.91	28.7	5.89	22.7	5.89	26.1
4.91	23.5	6.81	19.4	6.87	22.4
4.91	23.2	6.87	19.1	8.74	17.4
6.81	16.7	8.74	15.0	10.68	14.4
8.74	12.8	10.3	12.8	11.4	13.5
10.30	11.0	10.68	12.5	12.61	12.1
10.68	10.4	12.61	10.3	14.55	10.6
12.61	8.78	14.55	8.98	15.3	9.81
14.55	7.43	15.3	8.50	20.5	7.09
15.3	7.15	20.5	6.21	30.4	4.71
20.5	5.12	30.4	3.98	40.4	3.45
30.4	3.20	40.4	2.88	50.5	2.59
40.4	2.23	50.4	2.13		
50.4	1.61				

TABLE III. SMOOTHED VALUE OF $D_{11}\times10^3$, cm²/sec.

P, atm.	25°C	50°C	75°C
10.0	11.2	13.2	15.2
20.0	5.30	6.35	7.48
30.0	3.26	4.05	4.81
40.0	2.25	2.90	3.51
50.0	1.62	2.18	2.71

TABLE IV. DETERMINATION OF APPARATUS CONSTANT K_{II}

Temp. °C	P atm.	$K_{II}D_{11}P\times10^6$ atm./sec.	$K_{II}\times10^3$ 1/cm²
50	20	970	7.64
50	30	930	7.65
50	40	880	7.59
50	50	830	7.61
			Average 7.62
75	20	1130	7.55
75	30	1090	7.57
75	40	1050	7.49
75	50	1005	7.42
			Average 7.51

TABLE V. EXPERIMENTAL RESULTS FOR DIFFUSION PATH II

50°C		75°C	
P atm.	$D_{11}\times10^3$ cm²/sec.	P atm.	$D_{11}\times10^3$ cm²/sec.
19.2	6.62	20.2	7.20
22.4	5.69	20.3	7.22
29.9	4.11	21.1	7.24
30.3	4.00	30.3	4.84
40.0	2.95	32.3	4.52
40.8	2.83	40.1	3.40
49.8	2.21	40.1	3.54
53.1	1.99	40.4	3.33
58.8	1.70	41.2	3.54
67.1	1.47	50.1	2.77
70.9	1.31	50.2	2.67
80.7	1.03	50.2	2.54
86.7	0.907	50.5	2.49
92.5	0.792	58.1	2.33
98.0	0.678	61.0	2.06
101.7	0.600	67.4	1.85
102.2	0.595	81.5	1.42
109.5	0.453	91.5	1.23
113.2	0.436	92.5	1.20
123.3	0.379	99.4	1.12
150.3	0.297	103.5	0.956
182.5	0.266	117.5	0.770
189.4	0.260	123.1	0.759
199.4	0.250	158.5	0.503
240.0	0.228	208.3	0.386
		245.6	0.303

7) I. Amdur, J. W. Irvine, Jr., E. A. Mason and J. Ross, *J. Chem. Phys.*, **20**, 436 (1952).

experimental value from the smoothed value reaches a maximum of 3.6%; on the average it is 0.9%.

When Diffusion Path II was Used.—When the type-I porous plug was used for the measurements at pressures over 100 atm., the plot of $\log \Delta I$ against t presented a convex curve downwards; thus, the assumption made for the derivation of Eq. 1 became invalid. However, a type-II porous plug gave no such trouble during experiments at higher pressures.

The values of $K_{II}D_{11}P$ obtained at 50 and 75°C and in the range of 20—250 atm. are shown in Fig. 8. From the smooth curves, the smoothed values of $K_{II}D_{11}P$ at 20, 30, 40, and 50 atm. were obtained; they are shown in the third column of Table IV. By using the smoothed values of D_{11} at 20—50 atm. shown in Table III, K_{II} was calculated; it is shown in the last column of Table IV. The values of D_{11} calculated using these K_{II} values are shown in Table V.

Discussion

From the standpoint of the kinetic theory of gases, Enskog[1,2] derived the following equations for the diffusion coefficient of gases at high pressures, assuming a rigid sphere as the molecular model:

$$D = (D_{11})^\circ/\chi \tag{6}$$

$$(D_{11})^\circ = \frac{3}{8}\sqrt{\frac{\boldsymbol{k}T}{\pi m}}\frac{1}{n\sigma^2\Omega^{(1,1)*}} \tag{7}$$

$$\chi = 1 + 0.625\left(\frac{2}{3}\pi n\sigma^3\right) + 0.2569\left(\frac{2}{3}\pi n\sigma^3\right)^2 + 0.115\left(\frac{2}{3}\pi n\sigma^3\right)^3 + \cdots \tag{8}$$

where $(D_{11})^\circ$ is a value which can be calculated from the relationship applicable at the normal pressure and which is approximately given by Eq. 7, where χ is the correction factor due to the pressure rise and is given by Eq. 8, where $\boldsymbol{k}$ is Boltzmann's constant, where m is the mass of the molecule, where n is the number of molecules in a unit volume, where $\Omega^{(1,1)*}$ is the reduced collision integral, and where σ is a constant related to the intermolecular potential. It can be seen from Eq. 7 that $(D_{11})^\circ$ is a function of the temperature alone in the vicinity of the normal pressure. By Enskog's theoretical equation (6), $D_{11}\rho = (D_{11})^\circ\rho/\chi$ and $D_{11}\rho$ is dependent not only on the temperature, but also on χ, that is, on ρ. Therefore, it is convenient to study the relationship between $D_{11}\rho$ and ρ.

In Fig. 9, $D_{11}\rho$ is plotted against ρ. The values of ρ were calculated by using the compressibility data of Michels et al.[8] The plot shows a close similarity to that of the results obtained by O'Hern et al. The values at 35°C, which were interpolated from our experimental values, were always higher than their experimental values, but the differences were never more than 5%. On the other hand, there were large deviations in the experimental values of Drickamer et al., and so their values could not be used for an accurate comparison. The relative values of $D_{11}\rho$, obtained by Becker et al., were expressed as 1.00 at 20°C and 15 atm., 1.08 at 40 atm., and 1.26 at 50 atm., and they showed a rapid increase with the pressure, thus indicating an entirely different tendency from the results obtained by the present authors.

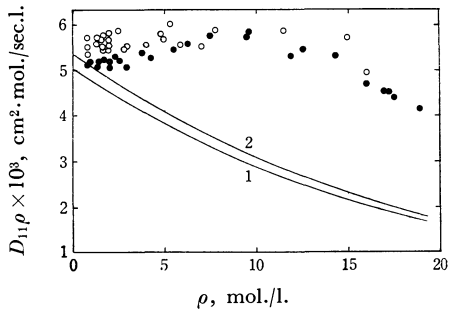

Fig. 9. Comparison of the measured values with the values calculated by Enskog's theory.
Experimental: ●—50°C, ○—75°C
Theoretical: 1—50°C, 2—75°C

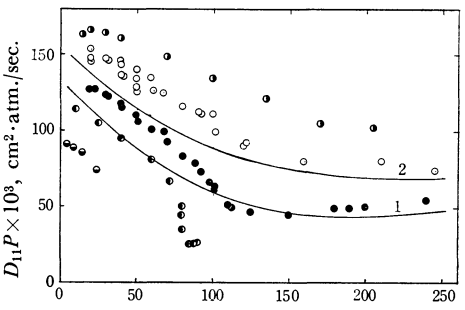

Fig. 10. Comparison of the measured values with the values calculated by the generalized chart.
Present work: ●—50°C, ○—75°C
O'Hern et al.: ◑—100°C, ◐—35°C, ◒—0°C
Calculated: 1—50°C, 2—75°C

The values calculated by substituting $\sigma = 3.996$ Å in Eq. 8 are shown as solid lines in Fig. 9. The deviations increase with the pressure, amounting to approximately 50% when $\rho = 10$ mol./l. Even if the decrease in σ with the pressure was taken into account in Eq. 8, in accordance with the consideration of O'Hern et al., a theoretical relation which fits the experimental values could not be obtained.

The values of $D_{11}P$ calculated from the generalized chart are shown as solid lines in Fig. 10. The deviation from our experimental values is approximately 20% in the vicinity of 50 atm., but it decreases over 100 atm.

8) A. Michels and C. Michels, *Proc. Royal Soc.*, **A153**, 201 (1936); **A160**, 348 (1937).

BULLETIN OF THE CHEMICAL SOCIETY OF JAPAN VOL. 39 2110—2114 (1966)

A Molecular Orbital Treatment of ^{13}C–H Spin-Spin Coupling Constants

By Teijiro YONEZAWA, Isao MORISHIMA and Mutsuo FUJII

Faculty of Engineering, Kyoto University, Sakyo-ku, Kyoto

(Received December 24, 1965)

A molecular orbital interpretation of the directly-bonded ^{13}C–H spin-spin coupling constant without the concept of hybridization is presented. The observed values of J_{C-H} for some saturated and conjugated compounds are shown to be proportional to the square of the bond order between the 1S atomic orbital of the hydrogen atom and the 2S atomic orbital of the carbon atom, P^2, which is calculated using the extended Hückel molecular orbital method.

In a preliminary communication,[1] we pointed out that a molecular orbital method is successful in interpreting the ^{13}C–H spin-spin coupling constants of some aliphatic cyclic and unsaturated compounds. In the present paper, the full details of an MO treatment of ^{13}C–H spin-spin coupling constants will be presented.

Several investigators have directed their attention towards the elucidation of the factors affecting proton-^{13}C spin-spin coupling. Especially, the directly-bonded proton-^{13}C coupling constant, J_{C-H}, has been studied extensively.[2-7] These investigations have led to the conclusions that the Fermi contact term may play an essential role in the coupling, and that J_{C-H} depends solely upon the fractional S-character of the carbon hybrid atomic orbital.

The relation between J_{C-H} and the fractional S-character, ρ_{C-H}, of the carbon hybrid orbital used in the C–H bond may be expressed as Eq. 1 on the basis of semiempirical studies.[2,6]

$$J_{C-H} = 500\,\rho_{C-H}\ \text{c.p.s.} \qquad (1)$$

The additivity relation of substituent effects on J_{C-H} in substituted methanes and formyl compounds has been discussed by the aid of Eq. 1. Besides this relation, the relations between J_{C-H} and the C–C–C internuclear bond angle in the C–CH–C systems,[8,9] the C–H bond distances[2] and the electronegativity of the substituent have been investigated by several authors. Goldstein and Hobgood[7] and Veillard and Del Re[10] have calculated the fractional S-character, ρ_{C-H}, by the maximum overlap orbital method; they found that the ρ_{C-H} so obtained paralleled that estimated from the experimental J_{C-H} value obtained with Eq. 1.

In this paper, an attempt will be made to calculate the J_{C-H} values *ab initio* using the extended Hückel MO[11] method in which the parameters affecting the J_{C-H} value, that is, the bond distance, the bond angle and the electronegativity, are involved.

Theoretical

A molecular orbital treatment of spin-spin coupling was presented by McConnell[12] for proton-proton spin systems; this treatment gave a positive value for every J_{H-H} value, and was found to be less valuable than a valence bond treatment. Recently, Pople and Santry[13] have extended the MO theory of spin-spin coupling and have pointed out that the coupling constants calculated by an MO theory are not always positive. In fact, they obtained a negative J_{H-F} coupling constant in hydrogen fluoride without the introduction of an "average triplet excitation energy," ΔE. It has also been shown recently[14] that the geminal proton-proton coupling constnats in various systems can be interpreted well by this molecular orbital theory. However, since the J_{C-H} value for directly-bonded C–H is believed to be positive in sign, McConnell's procedure, as simplified by adopting an average excitation energy, ΔE, may be used.*

1) T. Yonezawa, I. Morishima, M. Fujii and K. Fukui, This Bulletin, **38**, 1224 (1965).
2) N. Muller and D. E. Pritchard, *J. Chem. Phys.*, **31**, 768, 1471 (1959).
3) M. Karplus and D. M. Grant, *Proc. Natl. Acad. Sci.* (U. S.), **45**, 1269 (1959).
4) N. Muller, *J. Chem. Phys.*, **36**, 359 (1962).
5) H. Dreeskamp and E. Sackmann, *Z. Physik. Chem.*, **34**, 273 (1962).
6) C. Juan and H. S. Gutowsky, *J. Chem. Phys.*, **37**, 2198 (1962).
7) J. H. Goldstein and R. T. Hobgood, Jr., ibid., **40**, 3592 (1964).
8) S. S. Foote, *Tetrahedron Letters*, No. 9, 579 (1963).
9) K. Mislow, ibid., No. 22, 1415 (1964).
10) A. Veillard and G. Del Re, *Theoret. Chim. Acta.*, **2**, 55 (1964).
11) R. Hoffmann, *J. Chem. Phys.*, **39**, 1397 (1963); K. Morokuma, H. Kato, T. Yonezawa and K. Fukui, This Bulletin, **38**, 1263 (1965).
12) H. M. McConnell, *J. Chem, Phys.*, **24**, 460 (1956).
13) J. A. Pople and D. P. Santry, *Mol. Phys.*, **8**, 1 (1964).
14) J. A. Pople and A. A. Bothner-By, *J. Chem. Phys.*, **42**, 1339 (1965).

* This point will be checked in the final section of the present paper.

Table I. Coulomb integral of various atomic orbitals (eV.)

Atom	Orbital				
	1S	2S	2P	3S	3P
Hydrogen	−13.60	—	—	—	—
Carbon	—	−21.43	−11.42	—	—
Oxygen	—	−35.30	−17.76	—	—
Nitrogen	—	−27.50	−14.49	—	—
Chlorine	—	—	—	−25.26	−15.09

In a molecular orbital treatment of the C^{13}–H spin-spin coupling proposed by Muller[2] or Pople and Santry[13], they used a two-center molecular orbital localized in the C–H bond. On the other hand, in order to take into account the effect of neighboring atoms, (the bond distance, the valence angle, and so on,) on the electronic structure of the C–H bond, we used a delocalized molecular orbital obtained by a linear combination of the valence atomic orbitals of all the atoms in the molecule.

When we assume that J_{C-H} is exclusively determined by the Fermi contact term, it may be expressed by the equation[12]:

$$J_{C-H} = (1/h)(2\beta h)^2\gamma_C\gamma_H(1/\Delta E)(2\pi^2/3)P^2 \times (2S_C|\delta|2S_C)(1S_H|\delta|1S_H) \quad (2)$$

where $P=2\sum_i^{occ} a_{1S_H}b^i{}_{2S_C}$ and $a^i{}_{1S_H}$ and $b^i{}_{2S_C}$ are coefficients of the hydrogen 1S and the carbon 2S orbitals in the ith molecular orbital respectively.** ΔE is the mean excitation energy, which is assumed to be constant throughout this treatment. Then Eq. 2 may then be simply written as:

$$J_{C-H} = AP^2 \quad (3)$$

where A is a constant. It may be seen that J_{C-H} is proportional to the square of the bond order, P^2. In the present method, a molecular orbital is represented by a linear combination of valence atomic orbitals, that is, the 1S orbital of the hydrogen atom, the 2S, $2P_x$, $2P_y$ and $2P_z$ orbitals of the carbon, oxygen, nitrogen atoms and so on.[11] The orbital energy is given by solving the secular equation:

$$\det|H_{rs} - \varepsilon S_{rs}| = 0 \quad (4)$$

where H_{rs} is a matrix element and S_{rs} is the overlap integral between the rth and the sth atomic orbitals. The Coulomb integral, H_{rr}, of an atomic orbital is the negative value of the ionization potential[15] of the valence state of the neutral atom, which is tablulated in Table I, the resonance integral, H_{rs}, is expressed as:

** The bond order, P, used in Eq. 2 is related to that between the 1S atomic orbital of the hydrogen atom and the 2S atomic orbital of the carbon atom and so should be referred to as the "partial bond order."

15) H. O. Pritchard and H. A. Skinner, *Chem. Revs.*, **55**, 745 (1955).

Table II. Calculated values of p^2 and observed $J_{^{13}C-H}$

No.	Compound		P^2	J_{C-H} c. p. s.	Ref.
	Group a		Cycloalkanes and some other heterocylic compounds		
1	Ethylene oxide		0.0810	175	a
2	Ethyleneimine		0.0693	168	b
3	Cyclopropane		0.0677	161	c
4	Cyclobutane		0.0600	134	d
5	Cyclobutanone	β	0.0585	136	d
6		α	0.0525	131	d
7	Norbornadiene-7[i]		0.0548	135.5	e
8	Cyclopentane		0.0524	128	c
9	Cyclohexane		0.0515	124	c
	Group b		Halmothanes and ethane		
1	Chloroform		0.0605	209	a
2	Dichloromethane		0.0517	178	a
3	Monochloromethane		0.0447	150	a
4	Ethane		0.0441	126	a
5	Methane		0.0380	125	a
	Group c		Unsaturated compounds		
1	Acetylene		0.0942	248	a
2	Norbornadiene[i]		0.0763	172	e
3	Norbornene[j]		0.0745	166	e
4	Benzene		0.0671	159	a
5	Ethylene		0.0620	157	a
6	Allene		0.0508	166	f
	Group d		$-^{13}$CHO Compounds		
1	Formic acid		0.1156	215	g
2	Formate ion		0.1123	195	h
3	Formamide		0.0855	192	g
4	Benzaldehyde		0.0841	174	g
5	Acetaldehyde		0.0835	172	g

a) F. C. Nachod and W. D. Phillips, "Determination of Organic Structures by Physical Methods," Vol. 2, Academic Press, New York (1962).
b) F. S. Mortier, *J. Mol. Spectry.*, **5**, 199 (1960).
c) Ref. 2.
d) Ref. 8.
e) K. Tori, R. Muneyuki and H. Tanida, *Can. J. Chem.*, **41**, 3142 (1963).
f) R. M. Lynden-Bell and N. Sheppard, *Proc. Roy. Soc.*, **A 269**, 385 (1962).
g) Ref. 4.
h) R. M. Hammaker, *J. Mol. Spectry.*, **15**, 506 (1965).
i), j) Bond distances and bond angles are referred to C. F. Wilcox, *J. Am. Chem. Soc.*, **82**, 414 (1960).

TABLE III. CALCULATED VALUES OF P^2 AND OBSERVED $J_{^{13}C-H}$

Compounds	Position		P_2	J_{C-H}, (c. p. s.)	Ref.
Group a Aromatic compound					
Nitrobenzene	*o*		0.0610	170	a
	m		0.0655	164	a
	p		0.0650	162	a
Pyridine	2		0.0660	179	b
	3		0.0691	163	b
	4		0.0685	152	b
Pyrrole	2		0.0840	182	c
	3		0.0703	169	c
Pyrimidine	1		0.0740	206	d
	3		0.0625	182	d
	4		0.0652	168	d
		(I)[h]	(II)[i]		
Azulene	1,3	0.0718	0.0558	165	e
	2	0.0708	0.0875	183	e
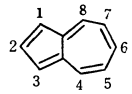	4,8	0.0615	0.0580	158	e
	5,7	0.0630	0.0674	161	e
	6	0.0630	0.0560	158	e
Group b					
Vinyl chloride	1		0.0620	161	f
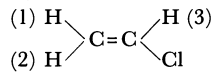	2		0.0581	160	f
	3		0.0734	195	f
Group c				$\lvert J_{^{15}N-H} \rvert$, c. p. s.	
Formamide	1		0.0492	92	g
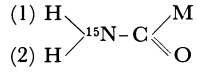	2		0.0420	88	g

a) P. C. Lauterbur, *J. Chem. Phys.*, **38**, 1432 (1963).
b) L. Z. Malinowski, L. Z. Pollara and J. P. Larmann, *J. Am. Chem. Soc.*, **84**, 2649 (1962).
c) K. Tori and T. Nakagawa, *J. Phys. Chem.*, **68**, 3163 (1964).
d) G. S. Reddy, R. T. Hobgood and J. H. Goldstein, *J. Am. Chem. Soc.*, **84**, 336 (1962).
e) H. Spiesecke and W. G. Schneider, *Tetrahedron Letters*, No. 14, 468 (1961).
f) G. J. Karabatsos and C. E. Orzech, Jr., *J. Am. Chem. Soc.*, **86**, 3574 (1964).
g) G. Brinsch, J. B. Lambert, B. W. Roberts and J. D. Roberts, ibid., **86**, 5564 (1964).
h) Calculated assuming regular pentagon and heptagon R(C-C)=1.40 Å, R(C-H)=1.10Å
i) $\angle C_3-C_2-C_1=95°$, $R(C_9-C_{10})$ bond distance=1.48 Å, R(C-H)=1.10 Å other R(C-C)=1.40 Å

$$H_{rs} = 0.5K(H_{rr} + H_{ss})S_{rs} \qquad (5)$$

where the value of K is taken as 1.75 as in a paper reported by Hoffmann,[11] and the values of S_{rs} are obtained by Mulliken's Table.[16] The interatomic distances and bond angles of several compounds required for the calculation were referred to Sutton's compilation.[17] For the other compounds, references are cited in the footnote of Tables II and III.

16) R. S. Mulliken, C. A. Rieke, D. Orloff and H. Orloff, *J. Chem. Phys.*, **17**, 1248 (1949).
17) L. E. Sutton, "Interatomic Distances," The Chemical Socieyt, London (1958).

Results

The values of the calculated P^2 values and the observed J_{C-H} values are cited in Tables II and III. In Table II, the compounds are classified systematically in four groups, a to d. In group a, saturated cyclic compounds are listed. Since cyclobutane is non-planar and has two groups of nonequivalent C–H bonds, the mean value of these two bond orders is indicated in the table. For the sake of simplicity, the calculation of J_{C-H} is carried out with respect to only one configuration, the chair form, for cyclohexane and the staggered form for ethane. In each group, a, b, c,

and d, one can find a linear relation between the calculated valued of P^2 and the observed J_{C-H} values, with a few discrepancies as to acetylene and allene in group c. These linear relations are exemplified in Fig. 1 and Fig. 2 for group a and group b respectively. We find also some discrepancies between different groups. For example, the nearly constant values of J_{C-H}/P^2 in group a and group b, the average values of which are obtained from Figs. 1 and 2, are not equal. The values of J_{C-H}/P^2, which is equal to the A constant, are estimated to be 2200 (c. p. s.) and 3600 (c. p. s.) for group a and group b in Table II respectively. The A value of group b is exceptionally large. It might be attributed to the parametrization of H_{rr}, H_{rs} or to the assumption of a constant excitation energy, ΔE; this question will be discussed in a later part.

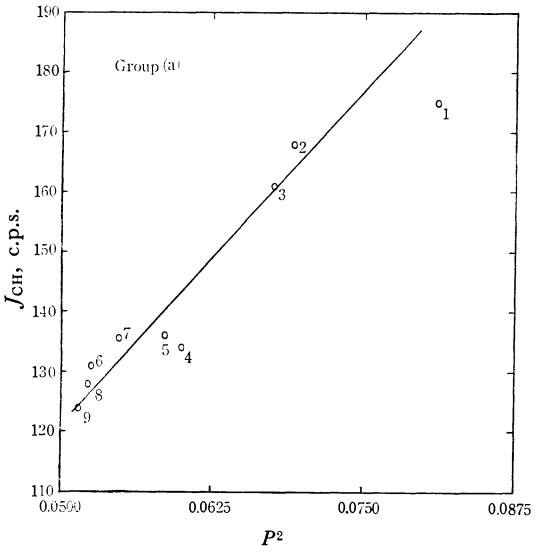

Fig. 1. A plot of the calculated values of P^2 versus observed J_{CH} for compounds of group a in Table II.

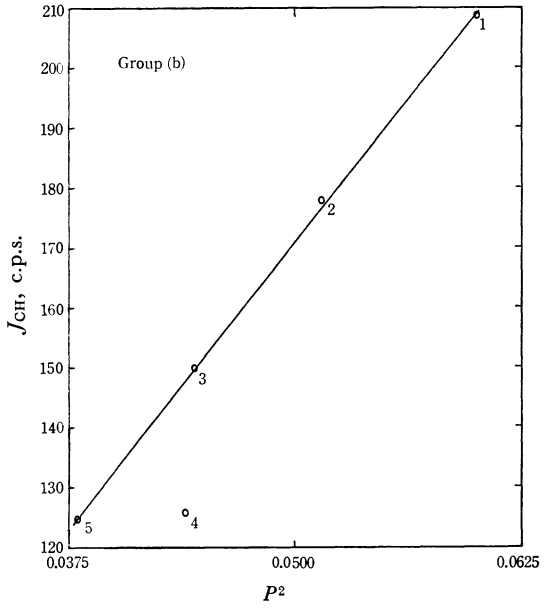

Fig. 2. A plot of the calculated values of P^2 versus observed J_{CH} for compounds of group b in Table II.

In Table III, in order to compare the J_{C-H} values, at the different positions in a molecule, we present the calculated P^2 values and the observed J_{C-H} values of aromatic compounds in group a and vinyl chloride compound in group b. In each compound, there seems to be a linear relation between P^2 and J_{C-H}. However, the interpretation of J_{C-H} for the C–H bond adjacent to the heteroatom is difficult by the present treatment. For example, the J_{C-H} for the ortho position of nitrobenzene, the $J_{C(2)-H}$ for pyridine, and the $J_{C(3)-H}$ for pyrimidine are all too large for the calculated P^2 value. In azulene, calculation is done in two ways. In Calculation I, the molecular shape for the azulene is assumed to be a regular pentagon and heptagon with the bond distances of R(C–C) = 1.40 Å and R(C–H) = 1.10 Å, while in Calculation II, we assume that the bond distances for $R(C_9–C_{10})$, other R(C–C) and R(C–H) are 1.48 Å, 1.40 Å, and 1.10 Å respectively, and that the $C_3–C_2–C_1$ bond angle is 95°. An exceptionally large J_{C-H} value at position 2 can be interpreted by the method of Calculation II, in which the bond angle at the carbon 2 is more acute than in Calculation I. On the contrary, for other positions the results by Calculation I seem to be better than those of Calculation II. Therefore, a more satisfactory agreement may be expected when the calculation is carried out assuming that the $C_3–C_2–C_1$ bond angle at position 2 is slightly more obtuse than 95°. At any rate, however, the molecular shape of azulene has not been definitely determined; the validity of the present results should be examined by future experiments.

Vinyl chloride in group b of Table III is given as an example to show the difference between the $J_{C-H(2)}$ value *cis* and the $J_{C-H(1)}$ value *trans* to the chlorine atom. In group c, we applied the present treatment to formamide-^{15}N in order to explain the difference between $J_{N-H(1)}$ and $J_{N-H(2)}$. Assuming that the magnitude of the coupling between nitrogen-15 and directly-bonded hydrogen is determined by the contact interaction, as in the case of ^{13}C–H coupling, the ^{15}N–H coupling constnat should be expressed by a relation similar to Eq. 2. The constant A in Eq. 3 for nitrogen–15 and hydrogen coupling no doubt differs from that for ^{13}C–H, since the product of the gyromagnetic ratios and the mean triplet

excitation energy are different for each coupling case.

Discussion

In the present treatment, only one coupling mechanism, the Fermi term, and the approximation of the mean excitation energy are assumed. Nuclear spin-spin interactions have been proposed to proceed by three different mechanisms, mechanisms which arise from: (1) the Fermi contact interaction, (2) the nuclear spin-electron orbital interaction, and (3) the electron-nuclear dipole-dipole interaction. It has been shown that[13] the coupling of protons with other directly-bonded nuclei derives principally from the contact term. In a molecular orbital treatment,[12,13] the contact term may be further divided into one- and two-electron contributions; the former has been commonly neglected.[12,13] However, the deviations from the linear relationship expressed by Eq. 1 have been observed, and the validity of the S-character calculated from the experimental J_{C-H} value with Eq. 1 has been criticized by Karabatsos.[18] This deviation may be attributed to the breakdown of one or more assumptions involved in Eq. 1 or to the neglect of another coupling mechanisms, such as the dipole-dipole interaction and the spin-orbital term.[18,19] The deviations from the linear correlation represented by Eq. 3 which are found in compounds of group c and group a in Table II might be partly due to this.

The second assumption, the mean excitation energy, ΔE, was taken only for the sake of simplicity in our work. Recently, this point has been reexamined by Pople and Santry[13] for proton-proton coupling[13] and F-H coupling; they showed that an MO treatment is successful in interpreting the sign of the coupling constant for each case. For C-H coupling, we also examined the sign of the $\pi_{SA,SB}$ term in Pople's equation[15] instead of $P^2/\Delta E$, where $\pi_{SA,SB}$ is written as:

$$\pi_{SA,SB}=4\sum_{i}^{occ}\sum_{j}^{unocc}(E_i-E_j)^{-1}C_{iSA}C_{iSB}C_{jSA}C_{jSB}$$

For a directly-bonded C-H spin-spin system, the sign of the calculated value of $\pi_{SC,SH}$ is positive for most compounds,* this leads to the positive value of J_{C-H}. From these considerations, the approximation of the mean exictation energy, ΔE, in the present treatment is rather crude, but it is qualitatively valid so far as the sign of J_{C-H} is concerned. These points should be investigated in future studies.

A few discrepancies found in Tables II and III may also be attributed partly to this assumption of the constant mean excitation energy. Namely, in Table II the fact that the J_{C-H}/P^2 for group b is larger than that for groups a, c and especially d means that the mean excitation energy of the compounds in groups a, c and d should decrease. Finally, the disagreement as to heterocyclic compounds in Table III may be partly attributed to the parametrization of Hoffmann's extended Hückel molecular orbital.

The calculations were carried out on the IBM 7090 at Japan IBM Co., with the permission of the UNICON Committee, whose help we hereby acknowledge.

18) G. J. Karabatsos, *J. Am. Chem. Soc.*, **86**, 3574 (1964).
19) N. Muller, *J. Chem. Phys.*, **42**, 4309 (1965).
* Details of this point will be published in the near future.

BULLETIN OF THE CHEMICAL SOCIETY OF JAPAN VOL. 39 2114—2116 (1966)

The Relation between Ultrasonic Velocity and Viscosity in Aqueous Solutions of Electrolytes

By Satya PRAKASH, Som PRAKASH and Shobhay LAXMI

Ultrasonic Laboratories, Department of Chemistry, Allahabad University, India

(Received January 6, 1966)

From the experimental data on the ultrasonic velocity and viscosity of thorium nitrate, lanthanum acetate and lanthanum chloride, it has been found that the product of adiabatic compressibility and viscosity is fairly constant over the concentration range studied. From those data the relation between ultrasonic velocity and viscosity has been derived which can explain the variation in sound velocity with the concentration.

Prakash and Srivastava,[1] from their ultrasonic velocity and viscosity measurements in aqueous

1) S. Prakash and S. P. Srivastava, *Indian J. Chem.*, **2**, 499 (1964).

solutions of silver nitrate, have explained the decrease in sound velocity with the concentration as due to the relative variation in density and viscosity parameters. These conclusions were drawn from an empirical equation obtained from the experimental data on sound velocity and viscosity in aqueous solutions of silver nitrate. Here in this present work we have again found that the variation in ultrasonic velocity with the concentration can be explained on the basis of the proposed empirical equation. No theoretical explanation of this relation can, however, be given at this time.

Experimental

Ultrasonic velocities at the frequency of 5 Mc./sec. have been measured by the light diffraction method introduced by Debye and Sears.[2] The source of the ultrasonic waves was a generator comprising of an oscillator and a quartz transducer unit, operating at either of two frequencies, 1 Mc./sec. or 5 Mc./sec. The output of sound energy at 5 Mc./sec. was 3.5 W.; all the work was done at this frequency.

Solutions of thorium nitrate, lanthanum acetate and lanthanum chloride were prepared by dissolving pure substances (B. D. H. analar) in doubly-distilled water. The densities of these solutions were measured with the help of a relative density bottle, while the viscosities were measured with an accurate Ostwald viscometer. The errors in the measurement of the density and viscosity were 0.02 and 0.4 per cent respectively. The adiabatic compressibility, β, was calculated using the equation:

$$\beta = \frac{1}{V^2\rho}$$

where V is the ultrasonic velocity and ρ, the density of the solution.

The probable errors involved in the measurement of sound velocity and adiabatic compressibility are 0.13 and 0.24 percent respectively.

Results and Discussion

Several workers have reported that the presence of a heavy or complex ion in a solution decreases the ultrasonic velocity. Here thorium nitrate, lanthanum acetate and lanthanum chloride all have a heavy ion; nevertheless, it is interesting to note, the ultrasonic velocity does not decrease, but instead increases linearly with the increase in concentration.

Whenever an electrolyte is dissolved in water, its compressibility is decreased. This lowering in compressibility may be attributed due to the influence of the electrostatic pressure of the ions on the surrounding water molecules, thus increasing the total internal pressure and making the solution harder to compress. The variation of adiabatic compressibility in all the cases is quite normal. It decreases regularly with the increase in concentration.

The values of the velocity, adiabatic compressibility, density and viscosity are given in Tables I, II and III.

Table I. Thorium nitrate
Temp.: 35±0.1°C

Sample No.	Concn. mol./l.	Velocity m./sec.	Adiabatic compressibility β cm²/dyne $\times 10^{12}$	Viscosity centipoise η	$\beta\times\eta\times 10^{12}$
1	0.020	1512	43.39	1.014	43.99
2	0.040	1513	42.98	1.022	43.92
3	0.050	1514	42.78	1.026	43.89
4	0.062	1515	42.45	1.030	43.72
5	0.100	1516	41.98	1.032	43.86
6	0.125	1518	41.32	1.056	43.63
7	0.250	1525	39.50	1.109	43.80
8	0.500	1532	35.47	1.230	43.61

Table II. Lanthanum acetate
Temp.: 30±0.1°C

Sample No.	Concn. mol./l.	Velocity m./sec.	Adiabatic compressibility β cm²/dyne $\times 10^{12}$	Viscosity centipoise η	$\beta\times\eta\times 10^{12}$
1	0.006	1535.0	42.49	1.023	43.46
2	0.007	1536.7	42.46	1.024	43.49
3	0.008	1538.2	42.34	1.026	43.44
4	0.009	1541.0	42.24	1.028	43.42
5	0.010	1545.0	42.23	1.030	43.46
6	0.020	1546.6	41.93	1.038	43.45
7	0.030	1547.1	41.79	1.040	43.46
8	0.040	1548.0	41.66	1.043	43.50
9	0.050	1548.5	41.64	1.044	43.49
10	0.080	1550.2	41.45	1.052	43.46
11	0.090	1551.3	41.33	1.059	43.42

Table III. Lanthanum chloride
Temp.: 30±0.1°C

Sample No.	Concn. mol./l.	Velocity m./sec.	Adiabatic compressibility β cm²/dyne $10\times^{12}$	Viscosity centipoise η	$\beta\times\eta\times 10^{12}$
1	0.042	1556.0	41.11	1.038	42.65
2	0.049	1556.5	40.96	1.043	42.74
3	0.056	1557.5	40.88	1.061	43.38
4	0.084	1564.0	40.42	1.070	43.27
5	0.112	1567.0	39.96	1.082	43.25
6	0.126	1569.0	39.53	1.096	43.31
7	0.140	1571.5	39.23	1.106	43.38

From the last column of the tables it can be seen that the product of adiabatic compressibility and viscosity is fairly constant over the concentration range studied. The average value of the constant is 43.38×10^{-12} cm²/dyne.

It follows, therefore that:

2) P. Debye and F. N. Sears, *Proc. Natl. Acad. Sci., U. S.*, **18**, 410 (1932).

$$\beta \times \eta = K \tag{1}$$

By combining the equation with the well-known equation:

$$\beta = \frac{1}{V^2\rho}$$

we have:

$$\frac{1}{V^2\rho} \times \eta = K \tag{2}$$

or:

$$V = \sqrt{\eta/K\rho}$$

or:

$$V = K'\sqrt{\eta/\rho} \tag{3}$$

where K' is another constant equal to $\sqrt{1/K}$. By differentiating Eq. 3 with respect to the concentration, we get;

$$\frac{1}{V_\infty} \cdot \frac{dV}{dC} = \frac{1}{2}\left[\frac{1}{\eta_\infty}\frac{d\eta}{dC} - \frac{1}{\rho_\infty}\frac{d\rho}{dC}\right] \tag{4}$$

This equation indicates that the variation in the ultrasonic velocity depends upon the magnitude of the viscosity and density parameters. Equation 4 can explain the anomalous variation in ultrasonic velocity with the concentration. Prakash and Srivastava[1] have explained the decrease in ultrasonic velocity in aqueous solutions of silver nitrate as due to the value of $1/\rho_\infty \cdot d\rho/dC$ being greater than $1/\eta_\infty \cdot d\eta/dC$.

The increase in ultrasonic velocity in thorium nitrate, lanthanum acetate and lanthanum chloride solutions can also be explained, on the basis of the above equation, as being due to the greater value of $1/\eta_\infty \cdot d\eta/dC$ than $1/\rho_\infty \cdot d\rho/dC$.

These experimental results indicate that the variation in ultrasonic velocity with the concentration is governed by two factors, the viscosity and the density of the medium.

This work was supported by a junior fellowship from C. S. I. R., New Delhi, to S. P. S. and by a S. R. T. Scholarship to S. L. K.

3) S. V. Subrahamanyam, *Trans. Faraday Soc.*, **56**, 971 (1960).
4) R. Barthel, *J. Acoust. Soc. Am.*, **260**, 227 (1954).
5) C. G. Balchandran, *Nature*, **187**, 136 (1960).

BULLETIN OF THE CHEMICAL SOCIETY OF JAPAN VOL. 39 2116—2126 (1966)

Sigma-Pi Interaction Accompanied by Stereoselection

By Kenichi FUKUI and Hiroshi FUJIMOTO

Faculty of Engineering, Kyoto University, Sakyo-ku, Kyoto

(Received January 7, 1966)

A simple molecular orbital theoretical treatment of the sigma-pi interaction caused by chemical reactions of planar-conjugated systems has been developed. The problem of the streo-selection of the two alternative directions of configuration altering due to the hybridization change at the centers of interaction has been considered by means of a simple perturbation treatment. Two theoretical indices, which represent the conjugation stabilization by way of the sigma-pi and reagent-pi interactions, have been introduced for this purpose. The theoretical results are consistent with the results of experience so far accumulated in various organic reactions, such as additions, eliminations, substitutions, and rearrangements, of conjugated molecules.

The electronic wave function for planar-conjugated molecules is divided into the so called sigma and pi parts. The former is composed of the molecular orbitals (MO) which are symmetric with respect to the molecular plane and have the direction of extension on that plane, while the latter consists of the MO's antisymmetric with respect to that plane, to which their direction of maximum extension is perpendicular. The condition of this separability has been thoroughly discussed by Lykos and Parr.[1] When such a planar system is exposed to a certain perturbation, say, for instance, to a chemical interaction due to the approach of atoms, molecules, radicals, or ions from definite sides of the plane toward definite positions of the molecule, both the sigma and pi MO's will be affected. The change in MO's as well as in energies is obtainable from the usual perturbation calculation on an assumption of an unchanged molecular configuration.[2] However, the actual effect will cause a change in the nuclear distances

1) P. G. Lykos and R. G. Parr, *J. Chem. Phys.*, **24**, 1166 (1956); **25**, 1301 (1956).

2) Hosoya and Nagakura (H. Hosoya and S. Nagakura, Preprint of Symposium on Molecular Structure, Japan (1962), p. 48 (in Japanese)) calculated the deformation of MO's with the mixing of the 3s orbital with the $2p\pi$ orbitals due to the approach of a point charge to an ethylenic bond.

and valence angles near the center of approach, giving rise to changes in the hybridization of carbon atoms. Such an altering in the molecular configuration is not calculable by a mere perturbation treatment. The most favorable configuration would be obtained as the one which gives the minimum adiabatic potential due to the Born-Oppenheimer approximation adopted for the perturbed system. This procedure is not, however, simple enough to be practical for organic chemists.

This paper will present a simple MO treatment of organic chemical processes in planar-conjugated molecules, thus providing a method by which we can discuss very simply the direction of the configuration-altering of molecules associated with the hybridization change in carbon atoms. This configuration's frequent alterations arise stereospecifically; it is the purpose of the present paper to elucidate the rule which governs this stereoselection.

Simple Perturbation Treatment

Let us consider a planar-conjugated hydrocarbon molecule having several carbon $2p\pi$ atomic orbitals (AO). The carbon atom, t, has one π orbital, ϕ_t, and three sp^2 hybridized σ orbitals, χ_t, $\chi_{t'}$, and $\chi_{t''}$, to combine with neighboring carbon sp^2 orbitals or otherwise with hydrogen 1s orbitals, ζ_p's. The direction of the extension of these real hybridized orbitals conforms to the direction of bonding, so that they have always positive values in the region of their maximum extension (Fig. 1). All $2p\pi$ orbitals are taken as

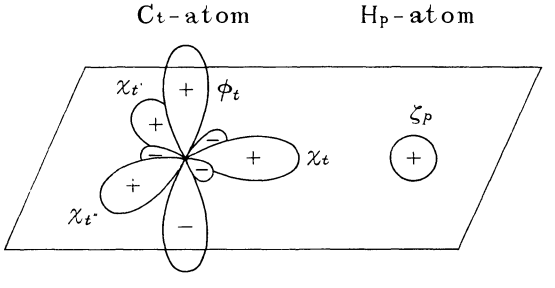

Fig. 1. The atomic orbitals.

having the same sign on the same side of the molecular plane. The total unperturbed wave function is assumed to be a product of the π part and the σ part, both of which are represented by a mere product of the usual simple Hückel MO's, which are written as:

$$\psi_i = \sum_t c_t^i \phi_t \qquad \text{for the } \pi \text{ part, and} \quad (1a)$$

$$\varphi_k = \sum_t b_t^k \chi_t + \sum_p d_p^k \zeta_p \qquad \text{for the } \sigma \text{ part,}^{3)} \quad (1b)$$

where ψ_i and φ_k are ith π MO and kth σ MO respectively. The first term on the right side of the latter equation signifies the summation with respect to each of three σ hybrids, namely:

$$\sum_t (b_t^k \chi_t + b_t^{k'} \chi_{t'} + b_t^{k''} \chi_{t''})$$

Instead of proceeding with the usual perturbation concept, we may here adopt the "method of perturbed secular determinant."[4)]* This method is suitable for calculating the energy difference between two systems for which the secular determinants differ slightly. The characteristic feature of this method is that it makes possible the calculation of the changes in energy, electron density, bond order, and other MO-theoretical quantities without an explicit knowledge of the change in the Hamiltonian operator or in that of wave functions.

The nonperturbed MO's of the π part are orthogonal to those of the σ part. The resonance integral between ϕ_t and χ_t's for the nonperturbed field is, of course, zero. Let us consider the configuration alteration which is indicated in Fig. 2, corresponding to the hybridization change due to chemical interaction with conjugated molecules. Figure 2 illustrates the case of a two-center interaction. Since, in all cases, our interest is limited to the direction of configuration alteration, each carbon atom is assumed to change its hybridized state from sp^2 to sp^x, where x is a definite number between 2 and 3. With this change the Coulomb integrals of a π orbital and a σ hybrid vary by $(\Delta\alpha)_\pi$ and $(\Delta\alpha)_\sigma$ respectively. The changes in the resonance integrals between a varied and the neighboring π AO's, and between a varied and the neighboring σ hybrids, are $(\Delta\beta)_\pi$ and $(\Delta\beta)_\sigma$ respectively, while the change in the resonance integral between the two σ hybrids of the same carbon atom[3)] is $(\Delta\beta)_\sigma'$. The resonance integral between the π orbital and a σ hybrid of the same carbon atom, say t, is designated by γ_t^σ. Since the way of taking the sign of basis orbitals is as illustrated in Fig. 1, we have two cases with respect to the value of γ^σ: namely, the one is the case of the carbons t and u of Fig. 2(i) (or the carbon t of ii), and the other is the case of the carbon u of Fig. 2(ii).

3) a) K. Fukui, H. Kato, T. Yonezawa, K. Morokuma, A. Imamura and C. Nagata, This Bulletin, **35**, 38 (1962); b) see also K. Fukui, H. Kato and T. Yonezawa, ibid., **34**, 442, 1111 (1961); **35**, 1475 (1962); T. Yonezawa, H. Kato, H. Saito and K. Fukui, ibid., **35**, 1814 (1962); K. Morokuma, K. Fukui, T. Yonezawa and H. Kato, ibid., **36**, 47 (1963); H. Kato, K. Fukui and T. Yonezawa, ibid., **38**, 189 (1965).

4) K. Fukui, C. Nagata, T. Yonezawa, H. Kato and K. Morokuma, *J. Chem. Phys.*, **31**, 287 (1959); K. Fukui, K. Morokuma, T. Yonezawa and C. Nagata, This Bulletin, **33**, 963 (1960).

* The term "perturbation" is here employed to imply the origin of the change in particular parameters in the secular determinant. The change in any quantum-mechanical quantity derived by solving it can be obtained by a procedure similar to the usual perturbation calculations.

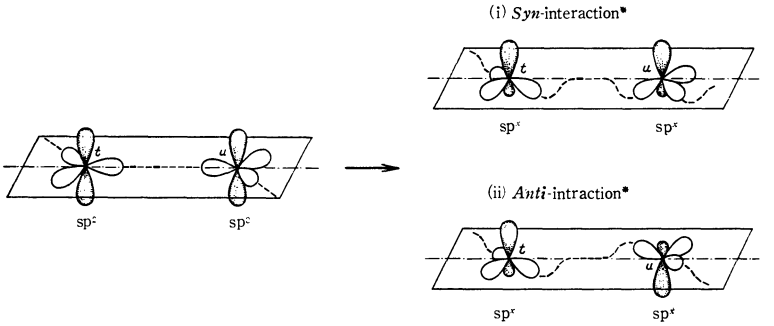

(x: a number between 2 and 3)

Fig. 2. A schematic representation of the mode of two-center σ-π interaction with a conjugated molecule.
* The terms *syn-* and *anti-* are used in order to evade confusion with *cis-* and *trans*-configurations of the remaining double bonds.

In the former case γ^{σ} is clearly negative, while in the latter it is positive. In addition, we have to consider the interaction with the reagent system. The resonance integral for the overlapping at the rth π orbital of the conjugated molecule with the reagent system (mostly one or two independent systems) is denoted by γ_r^{R}.

The increase in the total energy, ΔE, is thus represented by the following equations:[4]

$$\Delta E = (\Delta E)_{\sigma} + (\Delta E)_{\pi} + (\Delta E)_{\mathrm{R}} + (\Delta E)_{\sigma\pi} + (\Delta E)_{\mathrm{R}\pi} \tag{4}$$

$$\begin{aligned}(\Delta E)_{\sigma} &= 2\sum_{k}^{\mathrm{occ}}\sum_{t}(b_t^k)^2(\Delta\alpha)_{\sigma} \\ &+ 4\sum_{k}^{\mathrm{occ}}\sum_{t}\left\{\sum_{u}^{nei} b_t^k b_u^k(\Delta\beta)_{\sigma} + \sum_{t'}^{\mathrm{sam}} b_t^k b_{t'}^k(\Delta\beta)_{\sigma}'\right\} \\ &+ 2\sum_{k}^{\mathrm{occ}}\sum_{l}^{\mathrm{uno}}\frac{1}{\eta_k-\eta_l}\left\{\sum_{t} b_t^k b_t^l(\Delta\alpha)_{\sigma}\right. \\ &+ \sum_{t}\sum_{u}^{\mathrm{nei}}(b_t^k b_u^l + b_u^k b_t^l)(\Delta\beta)_{\sigma} \\ &\left.+ \sum_{t}\sum_{t'}^{\mathrm{sam}}(b_t^k b_{t'}^l + b_{t'}^k b_t^l)(\Delta\beta)_{\sigma}'\right\}^2\end{aligned} \tag{5}$$

$$\begin{aligned}(\Delta E)_{\pi} &= 2\sum_{i}^{\mathrm{occ}}\sum_{t}(c_t^i)^2(\Delta\alpha)_{\pi} \\ &+ 4\sum_{i}^{\mathrm{occ}}\sum_{t}\sum_{u}^{\mathrm{nei}} c_t^i c_u^i(\Delta\beta)_{\pi} \\ &+ 2\sum_{i}^{\mathrm{occ}}\sum_{j}^{\mathrm{uno}}\frac{1}{\varepsilon_i-\varepsilon_j}\left\{\sum_{t} c_t^i c_t^j(\Delta\alpha)_{\pi}\right. \\ &\left.+ \sum_{t}\sum_{u}^{\mathrm{nei}}(c_t^i c_u^j + c_u^i c_t^j)(\Delta\beta)_{\pi}\right\}^2\end{aligned} \tag{6}$$

$$(\Delta E)_{\sigma\pi} = 2\left(\sum_{i}^{\mathrm{occ}}\sum_{k}^{\mathrm{uno}} - \sum_{k}^{\mathrm{occ}}\sum_{i}^{\mathrm{uno}}\right)\frac{1}{\varepsilon_i-\eta_k} \times\left(\sum_{t} c_t^i b_t^k \gamma_t^{\sigma}\right)^2 \tag{7}$$

$$\begin{aligned}(\Delta E)_{\mathrm{R}\pi} &= 2\left(\sum_{i}^{\mathrm{occ}}\sum_{l}^{\mathrm{uno}} - \sum_{l}^{\mathrm{occ}}\sum_{i}^{\mathrm{uno}}\right)\frac{1}{\varepsilon_i-e_l} \\ &\times\left(\sum_{r} c_r^i d_{r'}^l \gamma_r^{\mathrm{R}}\right)^2 + 2\left(\sum_{i}^{\mathrm{occ}}\sum_{l'}^{\mathrm{uno}} - \sum_{l'}^{\mathrm{occ}}\sum_{i}^{\mathrm{uno}}\right) \\ &\times\frac{1}{\varepsilon_i-e_{l'}}\left(\sum_{s} c_s^i d_s^{l'}\gamma_s^{\mathrm{R}'}\right)^2 + \cdots\end{aligned} \tag{8}$$

In addition to the right-side terms in Eq. 4, there may happen to exist zero-order terms which have no connection with stereochemical problems.

We may proceed further without mentioning the modification well-known to be necessary for the case of any type of degeneracy with respect to MO energies which may yield first-order terms in these equations in lieu of the corresponding second-order terms. The terms $(\Delta E)_{\sigma}$, $(\Delta E)_{\pi}$ and $(\Delta E)_{\mathrm{R}}$ signify the change in energy due to the interaction in the sigma, pi, and reagent parts respectively, while $(\Delta E)_{\sigma\pi}$ and $(\Delta E)_{\mathrm{R}\pi}$ are the conjugation stabilizations through sigma-pi and reagent-pi interactions respectively. In these equations occ and uno mean all the occupied and unoccupied MO's respectively, while nei and sam imply all neighboring orbitals and all hybrids of the same carbon atom respectively. When a radical plays a part, the terms due to the half-occupied orbital must not be doubled. The energy of ith π-MO and kth σ-MO are denoted by ε_i and η_k respectively. The summation with respect to t on the right sides of Eqs. 5 and 7 has the same meaning as in Eq. 1b. For the reagent part, e_l and $d_{r'}^l$ are the energy and the coefficient of r'th AO (at which the overlapping takes place with the rth π orbital of the reactant) of the Reagent System 1 (which is, of course, not limited to a conjugated system). Similarly, $e_{l'}$ and $d_s^{l'}$ are for Reagent System 2, and so forth. The term $(\Delta E)_{\mathrm{R}}$ represents the energy change in the reagent, which may have a form similar to $(\Delta E)_{\sigma}$ and $(\Delta E)_{\pi}$.

The stereoselectivity of this type of reaction is thus governed by the terms of $(\Delta E)_{\sigma\pi}$ and $(\Delta E)_{R\pi}$ since, in such a problem, $(\Delta E)_{\sigma}$, $(\Delta E)_{\pi}$ and $(\Delta E)_{R}$ are deemed as common in the two opposite configurations in Fig. 2. In addition, the geometrical circumstances in the interaction of the reagent system with the reactant system, or the interesting effect of neighboring-group participation, should never be left out of account; however, this is obviously a problem to be discussed in a separate paper.

The Parametrization

In order to calculate the value of ΔE, we need to evaluate the integrals of both σ and π parts on a unified basis. These we have already made available in several of our previous papers,[3] and also summarized in a recent paper in which we adopted a slightly different estimation.[5] In the present paper we will use the latter values, with slight modifications, plus the values of newly-evaluated integrals for aromatic skeletons, as are listed in Table I. These numerical values have been determined with reference to the analytical form of the Slater orbitals and the theoretical evaluation of the overlap integrals in order to be consistent with various empirical data.

Table I. The parameters employed for hydrocarbons

Coulomb integrals:
- for carbon p orbital: $\alpha-0.15\beta$
- sp^3 hybrid: $\alpha-0.10\beta$
- sp^2 hybrid: α
- sp hybrid: $\alpha+0.10\beta$
- for all hydrogens: $\alpha-0.20\beta$

Resonance integrals:
- for C–C single bonds:
  - sp^3-sp^3: 0.84β sp^3-sp^2: 0.88β sp^3-sp: 0.96β
  - sp^2-sp^2: 0.92β sp^2-sp: 0.98β sp-sp: 1.04β
- for C–C double bonds:
  - p-p (π): 0.30β
  - sp^2-sp^2 (σ): 1.00β sp^2-sp (σ): 1.04β
  - sp-sp (σ): 1.08β
- for C–C triple bonds:
  - p-p (π): 0.35β
  - sp-sp (σ): 1.13β
- for aromatic C–C bonds:
  - sp^2-sp^2: 0.96β
- for C–C bonds of polyenyl radicals:
  - sp^2-sp^2: 0.96β
- for two σ hybrids belonging to the same carbon:
  - sp^3-sp^3: 0.30β sp^2-sp^2: 0.38β sp-sp: 0.60β
- for C–H bond:
  - sp^3 carbon: 0.90β
  - sp^2 carbon: 0.94β
  - sp carbon: 0.96β

(α: the Coulomb integral of a carbon sp^2 hybrid
β: the resonance integral for two bonding carbon sp^2 hybrids in the ethylenic double bond.)

(The resonance integrals for C–C single bond other than sp^3-sp^3 are given for the single bonds of such types as C–C= (sp^3-sp^2), C–C≡ (sp^3-sp); =C–C= (sp^2-sp^2), and so on. Such a clasification obviously does not possess any essential meaning. The slight difference in these resonance integrals does not affect seriously the result.)

The Sigma-pi Interaction

The quantity, $(\Delta E)_{\sigma\pi}$, which has been introduced above is useful in various problems in which the hybridization change participates. We assume, in this connection, that the arbitrary value of r_t^{σ} in Eq. 7 is to be regarded as equal to $g_t\gamma^{\sigma}$, in which g_t is $+1$ (as in the case of the carbons t and u of Fig. 2(i) and the carbon t of ii) and -1 (in the case of the carbon u of Fig. 2 (ii) and γ^{σ} is a negative constant; thus we may difine a new index, which we tentatively denote by $h_{tu\cdots}$, as:

$$h_{tu\cdots} = (\Delta E)_{\sigma\pi}\beta/(\gamma^{\sigma})^2 = 2\left(\sum_i^{\text{occ}}\sum_k^{\text{uno}} - \sum_k^{\text{uno}}\sum_i^{\text{occ}}\right)\frac{(-\beta)}{\eta_k-\varepsilon_i} \times (c_t^i c'^k_t g_t + c_u^i c'^k_u g_u + \cdots\cdots)^2 \quad (9)$$

where $c'^k_t = b^k_t + b^k_{t'} + b^k_{t''}$, where β is the resonace integral between two bonding carbon sp^2 hybrids in the ethylene double bond, and where t, u,$\cdots$ imply the carbon atoms at which the hybridization change takes place.* Several of the simplest cases are specified by:

$$h_t = 2\left(\sum_k^{\text{occ}}\sum_i^{\text{uno}} - \sum_i^{\text{occ}}\sum_k^{\text{uno}}\right)\frac{(-\beta)}{\varepsilon_i-\eta_k}(c_t^i)^2(c'^k_t)^2 \quad (10a)$$

$$h_{tu}^{(syn)} = 2\left(\sum_k^{\text{occ}}\sum_i^{\text{uno}} - \sum_i^{\text{occ}}\sum_k^{\text{uno}}\right)\frac{(-\beta)}{\varepsilon_i-\eta_k} \times (c_t^i c'^k_t + c_u^i c'^k_u)^2 \quad (10b)$$

$$h_{tu}^{(ant)} = 2\left(\sum_k^{\text{occ}}\sum_i^{\text{uno}} - \sum_i^{\text{occ}}\sum_k^{\text{uno}}\right)\frac{(-\beta)}{\varepsilon_i-\eta_k} \times (c_t^i c'^k_t - c_u^i c'^k_u)^2 \quad (10c)$$

For the systems having a half-occupied level, i, the terms due to that level must not be doubled but must be summed over all the k's.

The index h_t represents the ease of hybridization of the tth π orbital, namely, the ease of mixing the s-nature into the p AO; thus we may refer to

5) K. Fukui in "Modern Quantum Chemistry," Vol. I, Ed. by O. Sinanoglu, Academic Press, New York (1965), p. 49.

* In the two-center interaction at the equivalent positions (t, u) of a molecule with C_{2h}-symmetry, in which we assume that $|g_u| = a|g_t|$ ($a>0$), it is easy to show that:

$$h_{tu}^{(syn)} - h_{tu}^{(ant)} = a\,[h_{tu}^{(syn)} - h_{tu}^{(ant)}]_{a=1}$$

it as the "hybridizability" of the tth pπ atomic orbital. This quantity is closely related to the problem of olefinicity (and, therefore, also to that of aromaticity), which will be discussed elsewhere.

The index h_{tu} is connected with the stability of the activated complex of the two-center reactions of conjugated molecules, a discussion of which will immediately follow.

Acyclic Two-center Interactions

Let us proceed further by dividing the problem into two cases, those of cyclic and of acyclic interactions. Also, let us limit the discussion to the two-center interaction only.

By an "acyclic two-center interaction" we mean a simultaneous or quasi-simultaneous interac-

TABLE II. THE COMPARISON OF $h_{tu}^{(syn)}$ AND $h_{tu}^{(anti)}$ FOR NONCYCLIC TWO-CENTER INTERACTIONS IN SEVERAL CONJUGATED HYDROCARBONS

Conjugated hydrocarbons	Positions of interaction, tu	$h_{tu}^{(syn)}$	$h_{tu}^{(anti)}$	Favorable configurations
(I) α,β-Interaction				
Ethylene	1,2	3.1194	5.5244	*anti*
(excited)		(8.9912)	(5.5180)	(*syn*)
Butadiene	1,2	3.2486	5.4947	*anti*
Hexatriene	1,2	3.2994	5.4671	*anti*
Benzene	1,2	3.4428	5.0468	*anti*
Styrene	α,β	3.2301	5.5457	*anti*
Naphthalene	1,2	3.3883	5.2540	*anti*
Anthracene	1,2	3.3728	5.3021	*anti*
Acenaphthylene*1	1,2	3.4096	5.4107	*anti*
Fulvene*1	1,2	3.4124	5.3581	*anti*
(II) α,γ-Interaction				
Allyl cation	1,3	5.0844	4.7323	*syn*
Pentadienyl cation	1,3	4.7313	4.5092	*syn*
Allyl	1,3	4.7528	5.1758	*anti*
Pentadienyl	1,3	4.5738	4.9189	*anti*
Allyl anion	1,3	4.4212	5.6192	*anti*
Pentadienyl anion	1,3	4.4163	5.3286	*anti*
(III) α,δ-Interaction				
Butadiene	1,4	4.6130	4.4241	*syn*
Hexatriene	1,4	4.5679	4.3888	*syn*
Benzene	1,4	4.3817	4.1079	*syn*
Naphthalene	1,4	4.5559	4.2012	*syn*
Anthracene	1,4	4.5840	4.2128	*syn*
Anthracene	9,10	4.8058	4.3194	*syn*
Fulvene	1,4	4.2373	4.7009	*anti**2
(IV) α,ε-Interaction				
Pentadienyl cation	1,5	4.7367	4.7737	*anti*
Pentadienyl	1,5	4.8185	4.7737	*syn*
Pentadienyl anion	1,5	4.9002	4.7737	*syn*
(V) α,ζ-Interaction				
Hexatriene	1,6	4.5570	4.5775	*anti*

*1 Numbering for acenaphthylene and fulvene:

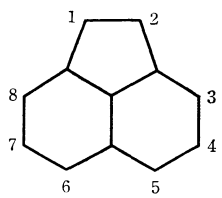

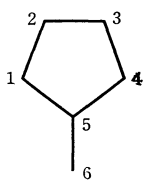

*2 The prediction of *anti*-predominance of 1,4-interaction in fulvene may be attributed to the odd-membered ring, in which this interaction is regarded also as α,γ-.

TABLE III. THE FAVORABLE MODE OF CYCLIC INTERACTIONS AS BASED UPON $(\Delta E)_{R\pi}$ (1)

Conjugated systems	Positions of interaction *rs*	$(\Delta E)_{R\pi}(\beta'/(\gamma^R)^2)$*1		Favorable configuration
		syn	*anti*	
Case Ia. The reagent is a vacant single orbital.				
Ethylene	1,2	3.4286	0.0000	*syn*
Butadiene	1,2	3.4757	0.1937	*syn*
	1,4	0.6195	3.6886	*anti*
Hexatriene	1,2	3.5307	0.3237	*syn*
	1,4	0.6599	3.5654	*anti*
	1,6	3.7701	0.9883	*syn*
Benzene*2	1,2	2.3297	0.5714	*syn*
	1,4	0.6154	2.2857	*anti*
Styrene	α,β	3.4606	0.1480	*syn*
Naphthalene	1,2	2.6992	0.4561	*syn*
	1,4	0.6024	2.7136	*anti*
Anthracene	1,2	2.8563	0.4232	*syn*
	1,4	0.5941	2.8733	*anti*
	9,10	0.5729	3.4608	*anti*
Acenaphthylene	1,2	3.4126	0.4886	*syn*
Fulvene	1,2	3.4243	0.5648	*syn*
Case Ib. The reagent is a half-occupied single orbital.*4				
Allyl	1,3	1.2651	16.9705	*anti*
Pentadienyl	1,3	1.2186	16.5163	*anti*
	1,5	16.3511	1.7143	*syn**3
Heptatrienyl	1,3	1.2134	12.9885	*anti*
	1,5	12.5808	1.6210	*syn*
	1,7	1.9770	12.6326	*anti*
Cyclopropenyl	1,2	1.6000	4.8000	*anti*
Cyclopentadienyl	1,2	3.4075	1.4089	*syn**3
	1,3	1.1279	3.6886	*anti*
Cycloheptatrienyl	1,2	3.2612	6.3476	*anti*
	1,3	1.5412	8.0676	*anti*
	1,4	7.2086	2.4002	*syn*
Indenyl	1,2	3.6098	1.7058	*syn*
	1,3	1.1597	5.6332	*anti*
Case Ic. The reagent is a doubly-occupied single orbital.				
Ethylene	1,2	0.0000	4.8000	*anti*
Butadiene	1,2	0.3066	5.5024	*anti*
	1,4	6.4126	0.7618	*syn*
Hexatriene	1,2	0.6629	6.2231	*anti*
	1,4	7.2193	0.8341	*syn*
	1,6	1.2933	8.0676	*anti*

*1 The value of $(\Delta E)_{R\pi}$ depends on the reagent orbital. The values presented here are tentatively calculated for the case of hydrogen migration.
The quantity β' corresponds to the resonance integral of an ethylenic p-p(π) bond. ($=0.3\beta$)

*2 This case corresponds to the 5,6-proton migration of cyclohexa-1,3-dienyl cation. Other cases are also to be interpreted similarly.

*3 The cyclic and acyclic cases were not distinguished in the theory of Woodward and Hoffmann (Ref. 16); namely e. g. the cases of 1,5-migrations of cyclopentadiene and all-*cis*-pentadiene. The former corresponds to the case of 1,2-interaction of cyclopentadienyl and the latter to that of 1,5-interaction of pentadienyl in this table.

*4 The values in case Ib are given for the systems each of which is composed of a vacant single orbital and the anion corresponding to the original reactant except the cases of cyclopropenyl and cycloheptatrienyl. In these two cases, the values are for a doubly-occupied single orbital with cyclopropenyl cation or cycloheptatrienyl cation. The zero-order terms due to electron transfer interaction are deemed as common both in *syn*- and *anti*-interactions.

Table IV. The favorable mode of cyclic interactions as based upon $(\Delta E)_{R\pi}$ (2)

Conjugated systems	Positions of interaction *rs*	$(\Delta E)_{R\pi}(\beta'/(\gamma^R)^2)$*1 *syn*	*anti*	Favorable configuration
Case II. The reagent is ethylenic.				
Ethylene	1,2	0.0000	2.0000	*anti*
Allyl anion*2	1,3	2.4142	0.4142	*syn*
Butadiene	1,2	0.1056	1.8945	*anti*
	1,4	1.7889	0.4223	*syn*
Hexatriene	1,2	0.1500	1.8711	*anti*
	1,4	1.6560	0.4503	*syn*
	1,6	0.6218	1.6570	*anti*
Benzene	1,2	0.3333	1.4444	*anti*
	1,4	1.3333	0.4444	*syn*
Naphthalene	1,2	0.7668	2.0701	*anti*
	1,4	1.4491	0.4300	*syn*
Anthracene	1,2	0.2500	1.6036	*anti*
	1,4	1.4748	0.4243	*syn*
	9,10	1.6163	0.4041	*syn*
Pleiadiene*3	7,10	1.5269	0.4715	*syn*
Pleiadylene*3	5,8	1.4291	0.5330	*syn*

*1 The values are calculated for the case of reagent of ethylene. $\beta'=0.3\beta$.
*2 This case presents a model for the 1,3-dipolar additions (R. Huisgen, *Proc. Chem. Soc.*, **1961**, 357).
*3 The numbering is:

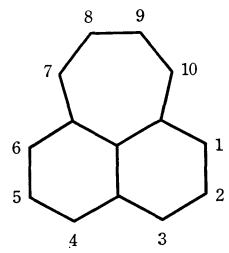

Pleiadiene

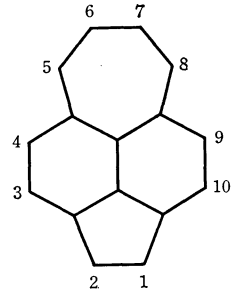

Pleiadylene

Table V. The favorable mode of cyclic interactions as based upon $(\Delta E)_{R\pi}$ (3)

Conjugated systems	Positions of interaction *rs*	$(\Delta E)_{R\pi}(\beta'/(\gamma^R)^2)$*1 *syn*	*anti*	Favorable configuration
Case IIIa. The reagent is an allyl cation.				
Ethylene	1,2	0.4142	2.4142	*anti*
Butadiene	1,4	2.7889	0.7889	*syn*
Case IIIb. The reagent is an allyl.				
Allyl	1,3	2.0000*3	0.0000*3	*syn**2
Case IIIc. The reagent is an allyl anion.				
Ethylene	1,2	2.4142	0.4142	*syn*
Butadiene	1,4	0.7889	2.7889	*anti*
Naphthalene	1,4	0.7175	2.0508	*anti*
Anthracene	9,10	0.7245	2.7245	*anti*
Acenaphthylene	1,2	2.6915	0.4818	*syn*

*1 $\beta'=0.3\beta$
*2 This case corresponds to Cope rearrangements. The intramolecular rearrangements like that of *cis*-1,2-divinyl cyclobutane to cycloöcta-1,5-diene (cf. E. Vogel, *Ann.*, **615**, 1 (1958)) are also essentially a Cope rearrangement.
*3 These values correspond to the first order terms, $2|c_rc_r'\pm c_sc_s'|$ between two half-occupied orbitals in γ^R.

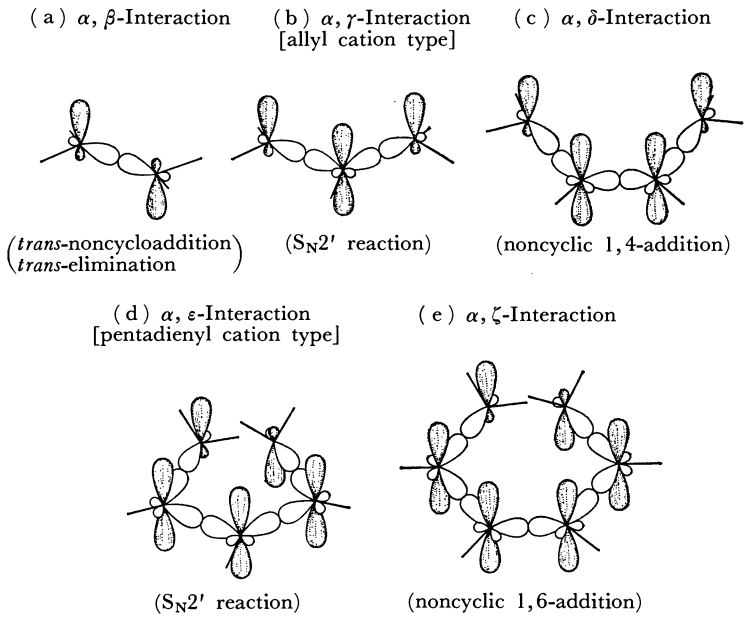

Fig. 3. A schematic representation of favorable configurations in noncyclic two-center interactions of conjugated molecules.

tion of two independent reagents with each of two positions of the reactant conjugated system. To this group may belong additions, eliminations, substitutions, rearrangements, and so forth. In such a case, if we concentrate our attention on the qualitative direction of the configuration alteration, *syn*- or *anti*- in Fig. 2, it is evident that we need to compare the magnitudes of the term $(\Delta E)_{\sigma\pi}$ only, since $(\Delta E)_{R\pi}$ is as an approximation common in these two configurations. A qualitative determination of the preferable configuration may be possible by a comparison of $h_{tu}^{(syn)}$ and $h_{tu}^{(ant)}$ of Eq. 10.

α, β-Interaction.—The two carbon atoms under consideration, neighboring each other in a conjugated system, are designated as α and β. Let us take the ethylene molecule as an example. The values of $h_{12}^{(syn)}$ and $h_{12}^{(ant)}$ are 3.1194 and 5.5244 respectively; thus, they exhibit the predominance of *anti*-interaction.[6] This is consistent with a number of well-known experimental results of *trans*-noncycloadditions[7] and *trans*-eliminations.[8] The results for the α, β-interactions in other conjugated systems are listed in Table II (I); all of them demonstrate the *anti*-interaction to be favorable.[9]

α, γ-Interaction.—Similarly, we can discuss the α, γ-interactions. The essential feature of S_N2' reactions is regarded as 1, 3-noncyclointeraction of the allyl cation type, because the leaving group takes off two electrons.* These reactions are known to proceed by means of a *syn*-configuration;[10] this is in accordance with the theoretical results obtained in Table II (II).

α, δ-, α, ε-, and α, ζ-Interactions. — These cases seem not yet to have been experimentally established. The theoretical results, however, predict the dominant configurations indicated in Fig. 3, a configuration which corresponds to the calculations of Table II (III, IV, V).

It may be noteworthy that, as is shown in Table II, the differences in the values of $h_{tu}^{(syn)}$ and $h_{tu}^{(ant)}$ become smaller as the two reaction centers become farther apart. Thus, in noncyclic 1, 6-additions, high stereospecificity is not to be expected.

6) With respect to the MO-theory of the stereoselectivity of additions, see also K. Fukui, This Bulletin, **39**, 498 (1966).

7) E. S. Gould, "Mechanism and Structure in Organic Chemistry," Henry Holt & Co., New York (1959), p. 514, 732 ff.; B. A. Bohm and P. I. Abell, *Chem. Revs.*, **62**, 599 (1962).

8) E. Frankland, *J. Chem. Soc.*, **1912**, 654; D. Y. Curtin and D. B. Kellom, *J. Am. Chem. Soc.*, **75**, 6011 (1953); see also many examples indicated by Gould Ref. 7.

9) The predominance of *trans*-addition has also been discussed as an orientation problem. See K. Fukui, *Tetrahedron Letters*, No. 28, 2427 (1965); see also a paper of the present authors to be published in the near future.

10) H. L. Goering, T. D. Nevitt and E. F. Silversmith, *J. Am. Chem. Soc.*, **77**, 4042 (1955); G. Stork and W. N. White, ibid., **78**, 4609 (1956). One of the present authors (K. F.) is grateful to Professor Stork for his private communication.

* The hybridized state of β-carbon is assumed to stay unchanged during the course of this reaction. A similar assumption is made in the discussion of other, more distant two-center interactions, and in cyclic cases.

Cyclic Two-center Interactions

The term "cyclic two-center interaction" signifies a chemical interaction corresponding to the transition state in which a conjugated reactant system interacts simultaneously at two positions with one "connected" reagent system. Thus, for instance, if we regard a diene in the Diels-Alder reaction as a conjugated reactant system, the associated dienophile is a reagent, while if we regard a dienophile as a conjugated reactant system, the associated diene is a reagent. The reagent is, of course, not necessarily a conjugated system; it may be any other system which is capable of interacting simultaneously with two positions of a conjugated system. It may be a proton in a protonated ethylene molecule, a phenyl cation in a phenonium ion, osmium tetroxide in an adduct to conjugated hydrocarbons, and so forth.[11]

MO-theoretical treatments for interactions of such a kind are not new.[12] To such treatments may belong the theoretical studies of the well-known Diels-Alder reaction, the Claisen and the Cope rearrangements, the 1, 3-dipolar cycloadditions, and so on. The significance of the symmetry of the highest-occupied (HO) MO and the lowest-vacant (LV) MO in the problem of selection rule for the Diels-Alder reaction was first pointed out by one of the present authors.[13] Hoffmann and Woodward discussed a similar selection rule for the occurrence of cycloadditions more generally, from the point of view of the MO symmetry conservation.[14]

The problem of the stereoselectivity of these reactions is presented in terms of $(\Delta E)_{R\pi}$ and $(\Delta E)_{\sigma\pi}$ in Eq. 4. However, it seems likely that, in this cyclic case, $(\Delta E)_{R\pi}$ is in general more determinative than $(\Delta E)_{\sigma\pi}$. The term $(\Delta E)_{R\pi}$ in Eq. 8 is reduced to the following form:

$$(\Delta E)_{R\pi} = \sum_i \sum_l \frac{\nu_i - \nu_l}{\varepsilon_i - e_l} \left(\sum_r c_r^i d_r^l \gamma_r^R \right)^2 \qquad (11)$$

where ν_i and ν_l are the numbers of electrons occupying the ith and the lth MO in the reactant and the reagent systems respectively. The sigma-type overlap stabilization of this type has already been discussed in several papers.[13,15] Several important cases will now be treated.

Case I. The reagent orbital is a single s orbital:

(Ia) When the reagent orbital is vacant:

$$(\Delta E)_{R\pi} = \sum_i \frac{\nu_i}{\varepsilon_i - e} (c_r^i \pm c_s^i)^2 (\gamma^R)^2 \qquad (12a)$$

(Ib) When the reagent orbital is half-occupied:

$$(\Delta E)_{R\pi} = \frac{1}{2} \left\{ \sum_i \frac{\nu_i}{\varepsilon_i - e} - \sum_i \frac{(2-\nu_i)}{\varepsilon_i - e} \right\} \times (c_r^i \pm c_s^i)^2 (\gamma^R)^2 \qquad (12b)$$

(Ic) When the reagent orbital is doubly-occupied:

$$(\Delta E)_{R\pi} = -\sum_i \frac{2-\nu_i}{\varepsilon_i - e} (c_r^i \pm c_s^i)^2 (\gamma^R)^2 \qquad (12c)$$

where ν_i is the number of π electrons occupying the ith MO of the reactant system, and where r and s are the centers of interaction. It is assumed that the absolute values of γ_r^R and γ_s^R are equal in the transition state, so that the upper and lower signs in parentheses are for *syn*- and *anti*-interactions respectively.

Case I, in particular the hydrogen migration belonging to Case Ib, was very recently discussed theoretically by Woodward and Hoffmann from a different point of view.[16] By Eqs. 12a—c, the results listed in Table III are obtained for the favorable mode of interaction in the ground-state reactions. The stabilization in some "nonclassical" carbonium ions, and also such reactions as the proton or carbonium cation migration in protonated conjugated hydrocarbons or carbonium cations, are covered by Case Ia; similarly, anion migrations belong to Case Ic. The well-known experimental results so far available are consistent with the theoretical results.

The reagent orbital is frequently a single p orbital. Similar arguments can easily show that such an orbital, when it is vacant, is allowed to enter into interaction simultaneously with two π orbitals of the reactant, for which the most favorable configuration is demonstrated to be "*syn*" in Table III, Case Ia. The well-known

11) For the discussion of such cases, see also the description of *cis*-1, 2-addition in Ref. 6.

12) See the many examples given, for example, in A. Streitwieser, Jr., "Molecular Orbital Theory for Organic Chemists," John Wiley & Sons, New York (1961).

13) K. Fukui, "Molecular Orbitals in Chemistry, Physics, and Biology," Ed. by P.-O. Löwdin and B. Pullman, Academic Press, New York (1964), p. 513.

14) R. Hoffmann and R. B. Woodward, *J. Am. Chem. Soc.*, **87**, 2046 (1965).

15) K. Fukui, *Tetrahedron Letters*, No. 24, 2009 (1965); cf. also Refs. 4 and 6.

16) R. B. Woodward and R. Hoffmann, *J. Am. Chem. Soc.*, **87**, 2511 (1965): These innovators have, no doubt, brought the first streaks of dawn into the field of theoretical stereochemistry through their elegant generalization (see Ref. 14 and also R. B. Woodward and R. Hoffmann, *J. Am. Chem. Soc.*, **87**, 395 (1965)). However, from the quantum-chemical point of view, their papers seem to leave a few points open to criticism. One of the present authors has recently made a comment (Ref. 15). In their discussion of "sigmatropic" reactions (*J. Am. Chem. Soc.*, **87**, 2511 (1965)), to take another instance, they determined the expected steric course by considering only the highest-occupied orbital (HO) symmetry, even in excited states. As was pointed out in Ref. 15, such a discrimination of HO would require proper grounds. Thus, the results of the prediction of excited-state reactions would probably be unreliable. Excited-state radical reactions are mostly too complicated to be treated by simple MO theories. In the ground-state reactions, the prediction by HO symmetry only almost coincides with that which is made by Eq. 12b.

Table VI. The favorable mode of cyclic interactions as based upon $(\Delta E)_{R\pi}$ (4)

Conjugated systems	Positions of interaction *rs*	$(\Delta E)_{R\pi}(\beta'/\gamma^R)^2)$*1 *syn*	*anti*	Favorable configuration
Case IV. The reagent is butadienic.				
Ethylene	1,2	1.7889	0.4223	*syn*
Butadiene	1,2	1.7441	0.4919	*syn*
	1,4	0.7155	1.7888	*anti**2
Benzene	1,2	1.3333	0.6111	*syn*
Naphthalene	1,2	1.4540	0.5731	*syn*
	1,4	0.6577	1.4266	*anti*
Anthracene	1,2	1.4913	0.5627	*syn*
	1,4	0.6565	1.4599	*anti*

*1 $\beta'=0.3\beta$

*2 After E. Vogel (*Ann.*, **615**, 1 (1958)), cycloöcta-1,5-diene from catalytic dimerization of butadiene is not likely to come through the direct 1,4-1',4'-interaction.

Table VII. The favorable mode of cyclic interactions as based upon $(\Delta E)_{R\pi}$ (5)

Conjugated systems	Positions of interaction *rs*	$(\Delta E)_{R\pi}(\beta'/(\gamma^R)^2)$*1 *syn*	*anti*	Favorable configuration
Case V. The reagent is of the osmium tetroxide*2,*3 type (including permanganate and manganate anions, MnO_4^- *4 and MnO_4^{2-} *5).				
Ethylene	1,2	0.6317	0	*syn*
Butadiene	1,2	0.6095	0.0340	*syn*
	(1,4)	(0.1256)	(0.6025)	(*anti*)
Benzene	1,2	0.4449	0.1053	*syn*
Naphthalene	1,2	0.4934	0.0840	*syn*
Anthracene	1,2	0.5083	0.0784	*syn*
Phenanthrene	9,10	0.5318	0.0642	*syn*

*1 $\beta'=0.3\beta$

*2 R. Criegee, *Ann.*, **522**, 75 (1936); R. Criegee, B. Marchand and H. Wannowius, idid., **550**, 99 (1938).

*3 These values are for the case of interaction with MnO_4^- (cf. C. J. Ballhausen and H. B. Gray, "Molecular Orbital Theory," W. A. Benjamin, New York (1964), p. 126). In these cases, only the z-components of the two adjacent oxygen atomic orbitals of the degenerate highest occupied orbitals are tentatively taken for the simplicity of calculation. The lowest vacant orbitals which belong to *E* are in favor of *syn* interaction except the case of butadiene 1,4.

*4 J. Boeseken, *Rec. trav. chim.*, **40**, 553 (1921); **47**, 683 (1928); K. B. Wiberg and K. A. Saegebarth, *J. Am. Chem. Soc.*, **79**, 2822 (1957).

*5 J. S. F. Pode and W. A. Waters, *J. Chem. Soc.*, **1956**, 717.

formation of phenonium ions and the singlet-state addition of carbenes, as well as the addition of atomic carbon to olefins,[17] which has recently been found, may involve this type of interaction.

When the reagent p orbital is half-occupied, too, the *syn* addition takes place if the symmetry relation is favorable. The formation of some epoxides, or the reaction with ozone may belong to this case.

Case II. The reagent orbitals are two bonding orbitals, which are equivalent to each other and which can enter into interaction with two orbitals of the reactant. Therefore, we have:

$$(\Delta E)_{R\pi} = \frac{1}{2}\left\{\sum_i \frac{\nu_i}{\varepsilon_i - e'}(c_r^i \mp c_s^i)^2 - \sum_i \frac{2-\nu_i}{\varepsilon_i - e}(c_r^i \pm c_s^i)^2\right\}(\gamma^R)^2 \qquad (13)$$

for the case of a reagent composed of two ethylenic π orbitals, where e and e' are the energies of bonding and antibonding orbitals respectively. The upper and lower signs stand for the *syn*- and *anti*-configurations respectively.

A comparison of the $(\Delta E)_{R\pi}$ values for two configurations of several conjugated systems indicates the dominant direction of change listed in Table IV; this is in agreement with our experience in dienes in Diels-Alder reactions, which belong to this case and which have already been treated by one of the present authors.[13] Excited-state reactions, in which the electron configuration of the reactant is assumed, can also be easily discussed in terms of Eq. 13.

Case III. The reagent orbitals are three

17) P. S. Skell and A. Y. Garner, *J. Am. Chem. Soc.*, **78**, 5430 (1956); P. S. Skell and R. R. Engel, ibid., **87**, 1135, 2493 (1965).

allylic π orbitals, two terminal orbitals of which interact with two reactant π orbitals. The well-known Claisen[18a] and Cope rearrangements[18b] are examples of this case. The $(\Delta E)_{R\pi}$ values in Table V demonstrate that, in experimentally-known cases, the theoretically-favorable configuration is *syn*. The 1, 3-dipolar addition occurs at *cis*- with respect dipolarophiles.

Case IV. The reagent orbitals are butadiene-type π orbitals, two terminal orbitals of which interact with two reactant π orbitals. The theoretical results are listed in Table VI. The Diels-Alder reaction is known to take place at *cis* positions in dienophiles.

Case V. The reagent is of another type. The additions of osmium tetroxide, manganate and permanganate anions, and so forth involve transition states in which the reagent system is considered to belong to none of cases, I to IV. The values of $(\Delta E)_{R\pi}$ are calculable separately by Eq. 11, leading to the conclusions indicated in Table VII, which are consistent with experience.

Through all these cases of cyclic interactions, the spatial circumstances of the transition state evidently require *syn* interaction in order for the reaction actually to take place. Therefore, the conclusion obtained in Tables III—VII affords a stereoselection rule: *syn* stands for the "sterically-allowed" case, and *anti*, the "streically-forbidden."

The explanation as to why the dimerization of butadiene yields 1, 2-divinyl cyclobutane compounds only, and not 1, 3-divinyl compounds,[19] is also an interesting example of Eq. 11, which gives a far larger $(\Delta E)_{R\pi}$ value for the formation of 1, 2- than 1, 3-divinyl compounds.

In all the cases mentioned above, we can easily see that the theoretical conclusion obtained from Eq. 11 for the ground-state reactions is in excellent agreement with that from the consideration of HO and LV only.[6] These orbitals are nothing but the frontier MO's, which are known to play a significant role in various reactions of organic molecules.

Thus, Eq. 11 has a wide applicability to various other problems of reactivity in conjugated systems, problems which are too manifold to systematize in a single paper. Considerations of them are to be published henceforth in sequence.

18) a) P. de Mayo, "Molecular Rearrangements," Interscience Publishers, New York (1963); b) E. N. Marvell, J. L. Stephenson and J. Ong, *J. Am. Chem. Soc.*, **87**, 1267 (1965).

19) E. Vogel, *Ann.*, **615**, 1 (1958).

BULLETIN OF THE CHEMICAL SOCIETY OF JAPAN VOL. 39 2126—2132 (1966)

Spectroscopic Studies of Dialkylaluminum Alkoxides and the Trialkylaluminum-Ether Complex. II. Assignments of Observed Frequencies

By Ryokichi TARAO

Research Center, Chisso Co., Ltd., Kanazawa-ku, Yokohama

(Received January 20, 1966)

The polarization data on the Raman lines of $Al(CH_3)_3 \cdot (CH_3)_2O$, $[Al(CH_3)_2OCH_3]_3$, $[Al(C_2H_5)_2OCH_3]_3$, and $[Al(C_2H_5)_2OC_2H_5]_2$ have been obtained in the 3100—130 cm^{-1} region. Most of the infrared absorption bands and Raman lines of these four compounds in the skeletal vibration region (720—130 cm^{-1}) have been tentatively assigned with the aid of these polarization data and on the assumption that the symmetries of these four compounds are as given in the previous paper. The Raman spectra of $Al(CH_3)_3 \cdot (CD_3)_2O$, $[Al(CH_3)_2OCD_3]_3$, and $[Al(C_2H_5)_2OC_2D_5]_2$ have been measured in the 3100—130 cm^{-1} region. Most of the infrared absorption bands and Raman lines of $Al(CH_3)_3 \cdot (CH_3)_2O$, $[Al(CH_3)_2OCH_3]_3$, $[Al(C_2H_5)_2OCH_3]_3$, and $[Al(C_2H_5)_2OC_2H_5]_2$ in the CH-stretching region (3100—2700 cm^{-1}) have been assigned with the aid of the spectroscopic data of the above-mentioned partly-deuterated substances.

In a previous paper,[1] the author showed that dimethylaluminum methoxide $[Al(CH_3)_2OCH_3]_3$ and diethylaluminum methoxide $[Al(C_2H_5)_2OCH_3]_3$ take trimeric structures with the D_{3h} symmetry, that diethylaluminum ethoxide $[Al(C_2H_5)_2OC_2H_5]_2$ takes a dimeric structure with the V_h symmetry and that the trimethylaluminum-dimethyl ether complex, $Al(CH_3)_3 \cdot (CH_3)_2O$, takes the structure with the C_s symmetry; these assignments were made by comparing the infrared and Raman spectra of these four compounds in the skeletal vibration region (720—300 cm^{-1}). (The

1) R. Tarao, This Bulletin, **39**, 725 (1966).

assignments of the observed frequencies were impossible at that time except for $Al(CH_3)_3 \cdot (CH_3)_2O$.[2] The present paper will describe the results of the qualitative measurements of the degree of the depolarization of the Raman lines of these four compounds. The Raman spectra of three partly-deuterated substances, $Al(CH_3)_3 \cdot (CD_3)_2O$, $[Al(CH_3)_2OCD_3]_3$, and $[Al(C_2H_5)_2OC_2D_5]_2$, will also be measured. The tentative assignments for the infrared absorption bands and Raman lines of $Al(CH_3)_3 \cdot (CH_3)_2O$, $[Al(CH_3)_2OCH_3]_3$, $[Al(C_2H_5)_2OCH_3]_3$, and $[Al(C_2H_5)_2OC_2H_5]_2$ will be made with the aid of the polarization data and the spectroscopic data of the above-mentioned partly-deuterated substances.

Experimental

$Al(CH_3)_3 \cdot (CH_3)_2O$, $[Al(CH_3)_2OCH_3]_3$, $[Al(C_2H_5)_2OCH_3]_3$, and $[Al(C_2H_5)_2OC_2H_5]_2$ were prepared by the method described in the previous paper.[1] Deuterated materials (dimethyl-d_6-ether, methanol-d_3, and ethanol-d_5) were purchased from the Volk Co. (isotopic purity> 99%). $Al(CH_3)_3 \cdot (CD_3)_2O$ was prepared by the reaction of trimethylaluminum with dimethyl-d_6-ether, b. p. 72—73°C/42 mmHg. $[Al(CH_3)_2OCD_3]_3$ was prepared by the reaction of trimethylaluminum with methanol-d_3, b. p. 70.5—72°C/3.5 mmHg. $[Al(C_2H_5)_2OC_2D_5]_2$ was prepared by the reaction of triethylaluminum with ethanol-d_5, b. p. 114—116°C/12 mmHg. The Raman spectra were measured by the method described in the previous paper.[1] The polarization data of Raman lines

Table I. The number of skeletal normal vibrations of $Al(CH_3)_3 \cdot (CH_3)_2O$ (C_s)

Mode of vibration	A′	A″	Total
Activity {IR	+	+	
Activity {Raman	+	+	
AlC_3 stretching	2	1	3
AlC_3 deformation	2	1	3
AlC_3 rocking	1	1	2
AlC_3 torsion		1	1
AlO stretching	1		1
CO stretching	1	1	2
OC_2 scissors	1		1
OC_2 wagging	1		1
OC_2 rocking		1	1
Total	9	6	15

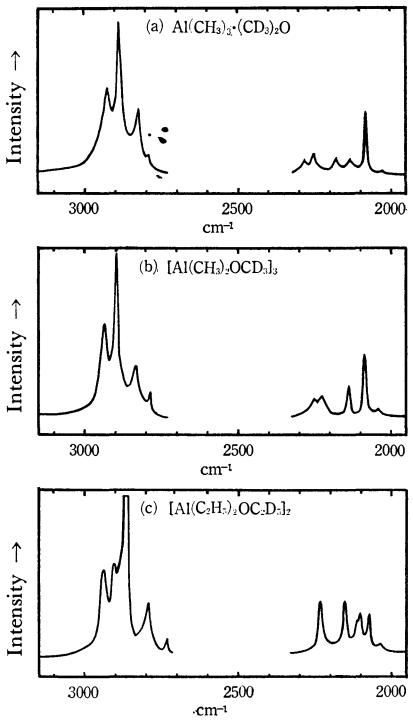

Fig. 1. The Raman spectra of partly deuterated substances in the CH and CD stretching region.

Table II. The number of skeletal normal vibrations of $[Al(CH_3)_2OCH_3]_3$ and $[Al(C_2H_5)_2OCH_3]_3$*1 (D_{3h})

Mode of vibration	A_1'	A_2'	E′	A_1''	A_2''	E″	Total
Activity { IR	−	−	+	−	+	−	
Activity { Raman	+	−	+	−	−	+	
AlC_2 stretching	1		1		1	1	4
AlC_2 scissors	1		1				2
Ring stretching	1	1	2				4
Ring in-plane deformation	1		1				2
Ring out-of-plane deformation					1	1	2
AlC_2 wagging		1	1				2
AlC_2 rocking					1	1	2
AlC_2 twisting				1		1	2
CO stretching	1		1				2
CO in-plane bending		1	1				2
CO out-of-plane bending					1	1	2
Total	5	3	8	1	4	5	26

*1 For $[Al(C_2H_5)_2OCH_3]_3$, C_2H_5 group is treated as a single particle to simplify the discussion.

2) S. Takeda and R. Tarao, ibid., **38**, 1567 (1965).

TABLE III. THE NUMBER OF SKELETAL NORMAL VIBRATIONS OF $[Al(C_2H_5)_2OC_2H_5]_2$*1 (V_h)

Mode of vibration	A_g	A_u	B_{1g}	B_{1u}	B_{2g}	B_{2u}	B_{3g}	B_{3u}	Total
Activity IR	−	−	−	+	−	+	−	+	
Activity Raman	+	−	+	−	+	−	+	−	
AlC_2 stretching	1			1	1			1	4
AlC_2 scissors	1							1	2
Ring stretching	1		1			1			3
Ring deformation	1							1	2
AlC_2 wagging			1			1			2
AlC_2 rocking				1	1				2
AlC_2 twisting		1					1		2
Ring puckering				1					1
CO stretching	1					1			2
CO in-plane bending			1					1	2
CO out-of-plane bending				1			1		2
Total	5	1	3	4	2	3	2	4	24

*1 C_2H_5 group is treated as a single particle to simplify the discussion.

TABLE IV. OBSERVED FREQUENCIES OF $Al(CH_3)_3\cdot(CH_3)_2O$ AND $Al(CH_3)_3\cdot(CD_3)_2O$ IN cm^{-1} AND VIBRATIONAL ASSIGNMENT*1,*2

$Al(CH_3)_3\cdot(CH_3)_2O$ IR	$Al(CH_3)_3\cdot(CH_3)_2O$ Raman	$Al(CH_3)_3\cdot(CD_3)_2O$ Raman	Assignment
3028 w	−3035 w D		CH_3 degenerate str. (OCH_3)
2983 m	−2989 vw		
2953 sh	−2957 m P		Overtone of CH_3 deform. (OCH_3)
2925 s	−2926 m D	2925 m D	CH_3 degenerate str. ($AlCH_3$)
2889 m	−2887 s P	2887 s P	CH_3 symmetric str. ($AlCH_3$)
2847 w	−2842 m P		CH_3 symmetric str. (OCH_3)
2820 vw	−2820 m P	2820 m P	Overtone of CH_3 deform. ($AlCH_3$)
	2787 vw P	2790 vw P	
		2282 w D	
		2250 m D	CH_3 degenerate str.
		2175 w P	
		2131 w P	Overtone of CD_3 deform.
		2081 s P	CD_3 symmetric str.
		2025 vw	
1462 s	−1460 m D	1436 m D	CH_3 degenerate deform. ($AlCH_3$), CH_3 degenerate deform., CH_3 symmetric deform. (OCH_3)
1250 w			
1185 vs	−1190 m P	1189 m P	CH_3 symmetric deform. ($AlCH_3$), CH_3 rock (OCH_3)
1153 m			
		1123 w P	CD_3 symmetric deform.
1046 vs	−1052 w D	1062 m D	CO antisymmetric str. A''
891 s	− 894 m P	861 w	CO symmetric str. A'
710 s	− 716 m D	714 m D	AlC_3 degenerate str. A'', CH_3 rock ($AlCH_3$)
		684 w D	
622 m	− 625 m D	627 m D	AlC_3 degenerate str. A'
	576 w D	594 m P	
525 m	− 525 vs P	527 vs P	AlC_3 symmetric str. A'
473 m	− 470 w	456 m P	AlO str. A'
		414 vw	OC_2 scissors A'
		312 m D	
	233 w D	224 w D	AlC_3 symmetric deform. A'
	154 s D	152 s D	AlC_3 degenerate deform. A''

*1 m, medium; s, strong; w, weak; v, very. *2 P, polarized; D, depolarized.

TABLE V. OBSERVED FREQUENCIES OF $[Al(CH_3)_2OCH_3]_3$ AND $[Al(CH_3)_2OCD_3]_3$ IN cm^{-1} AND VIBRATIONAL ASSIGNMENT

$[Al(CH_3)_2OCH_3]_3$ IR	$[Al(CH_3)_2OCH_3]_3$ Raman	$[Al(CH_3)_2OCD_3]_3$ Raman	Assignment
	3064 vw		CH_3 degenerate str. (OCH_3)
2988 sh			
2954 sh	—2953 m P		Overtone of CH_3 deform. (OCH_3)
2934 s	—2935 m D	2935 m D	CH_3 degenerate str. ($AlCH_3$)
2895 w	—2894 s P	2895 s P	CH_3 symmetric str. ($AlCH_3$)
2853 m	—2854 m P		CH_3 symmetric str. (OCH_3)
2829 vw	—2828 w P	2831 m P	Overtone of CH_3 deform. ($AlCH_3$)
	2785 vw P	2785 vw P	
		2250 vw D	CD_3 degenerate str.
		2227 m P	
		2139 m P	Overtone of CD_3 deform.
		2086 s P	CD_3 symmetric str.
		2039 vw	
1457 m	—1458 w D	1434 w D	CH_3 degenerate deform. ($AlCH_3$), CH_3 degenerate deform., CH_3 symmetric deform. (OCH_3)
		1407 vw	
1256 vw			
1200 vs	—1201 m P	1207 m P	CH_3 symmetric deform. ($AlCH_3$), CH_3 rock (OCH_3)
		1140 vw	CD_3 degenerate deform.
		1069 w D	
1019 vw	—1018 m P	1000 m P	CO symmetric str. A_1'
987 vs	— 994 w D	981 w D	
		904 w	
686 vs	— 687 m D	685 m D	AlC_2 symmetric str. E', CH_3 rock ($AlCH_3$)
642 s			AlC_2 antisymmetric str. A_2''
	596 s P	598 s P	AlC_2 symmetric str. A_1'
567 vw	— 569 vw D	566 vw	Ring degenerate str. E'
437 m	— 440 vw	435 vw	
	380 s P	372 s P	Ring symmetric str. A_1'
305 m	— 309 vw	303 vw	Ring degenerate deform. E'
	251 vw	244 vw	
	207 vw	203 vw	
	141 m D	140 m D	AlC_2 degenerate deform. E'

were taken by the use of parallel and perpendicular Polaroid cylinders placed alternately over the Raman tube.

Results and Discussion

$Al(CH_3)_3 \cdot (CH_3)_2O$.—In Table I the expected types of skeletal vibrational modes and the number of skeletal vibrations in each species are shown. All of the 15 possible skeletal vibrations are both infrared- and Raman-active. The tentative assignments in the skeletal vibration region (720—130 cm^{-1}) are given in Table IV. The infrared and Raman intensities and polarization data of the Raman lines support these assignments. The assignments in the 720—350 cm^{-1} region agree precisely with those assignments which have been made by comparing the infrared spectra of several related substances.[2]

Onishi showed that, for $Al_2(CH_3)_6$ and $Al_2(CH_3)_4Cl_2$, CH_3 symmetric deformation bands appear near 1200 cm^{-1} and that CH_3 rocking bands appear near 700 cm^{-1};[3] in accordance with these assignments, the bands near 1185 cm^{-1} and 710 cm^{-1} of $Al(CH_3)_3 \cdot (CH_3)_2O$ may be assigned to the CH_3 symmetric deformation ($AlCH_3$), superposed by CH_3 rocking (OCH_3), and to the AlC_3 degenerate stretching (A''), superposed by CH_3 rocking ($AlCH_3$), respectively.

As is shown in Table IV, $Al(CH_3)_3 \cdot (CH_3)_2O$ has seven to eight infrared bands and Raman lines in the 3100—2700 cm^{-1} region. These are very likely to be CH_3 degenerate stretchings, CH_3 symmetric stretchings, and overtones of CH_3 deformations of the $Al(CH_3)_3$ part and the $(CH_3)_2O$ part. The six Raman lines of $Al(CH_3)_3 \cdot (CD_3)_2O$ in the 2300—2000 cm^{-1} region are mainly due to

3) T. Onishi, Dissertation, The University of Tokyo (1964).

TABLE VI. OBSERVED FREQUENCIES OF $[Al(C_2H_5)_2OCH_3]_3$ IN cm^{-1} AND VIBRATIONAL ASSIGNMENT

IR	Raman	Assignment
2989 sh		CH_3 degenerate str. (OCH_3)
2941 s	—2937 m P	CH_3 degenerate str. (AlC_2H_5), Overtone of CH_3 deform. (AlC_2H_5, OCH_3)
2901 s	—2897 w D	CH_2 antisymmetric str. (AlC_2H_5)
2865 s	—2865 s P	CH_3 symmetric str. (AlC_2H_5, OCH_3)
2796 m	—2792 m P	CH_2 symmetric str. (AlC_2H_5)
2731 w	—2730 vw P	
1467 m, 1454 m	—1464 s D	CH_3 degenerate deform., CH_3 symmetric deform. (AlC_2H_5, OCH_3)
1411 m	—1414 m D	CH_2 scissors (AlC_2H_5)
1376 w	—1381 vw	
1254 w		
1223 w		
1197 s	—1195 s P, 1134 vw, 1099 w	CH_2 wag, CH_2 twist (AlC_2H_5), CH_3 rock (AlC_2H_5, OCH_3)
1019 vw	—1016 vw	CO symmetric str. A_1'
984 vs	— 988 s D	CC str.
956 w	— 962 vw	
918 m		
885 w		
848 w		
655 vs	— 650 m D	AlC_2 symmetric str. E', CH_2 rock (AlC_2H_5)
632 m		AlC_2 antisymmetric str. A_2''
	568 s P	AlC_2 symmetric str. A_1'
540 vw	— 536 vw	Ring degenerate str. E'
460 m	— 449 w	
	393 s P	Ring symmetric str. A_1'
351 m	— 339 vw	Ring degenerate deform. E'

CD stretchings of the $(CD_3)_2O$ part (Fig. 1a). The infrared and Raman spectra of $(CD_3)_2O$ and their assignments have been reported by Kanazawa and Nukada.[4] They assigned the Raman lines at 2230, 2202, and 2185 cm^{-1} to CD asymmetric stretchings; a strongly polarized line of a medium intensity at 2137 cm^{-1} to an overtone or to a combination of CD_3 deformation vibrations, and a strongly polarized line of a very strong intensity at 2053 cm^{-1}, to CD_3 symmetric stretching. By taking their assignments into consideration, four principal Raman lines of $Al(CH_3)_3\cdot(CD_3)_2O$ in the 2300—2000 cm^{-1} region may be assigned as is shown in Table IV. This assignment explains the intensity and polarization data satisfactorily. The 2175 cm^{-1} line (CH_3 degenerate stretching) is polarized; this may be due to the possible superposition of one of the overtones of the CD_3 deformations. Four lines, those at 3035, 2989, 2957, and 2842 cm^{-1}, of the eight Raman lines of $Al(CH_3)_3\cdot(CH_3)_2O$ in the 3100—2700 cm^{-1} region disappear in the spectrum of $Al(CH_3)_3\cdot(CD_3)_2O$. These four lines are evidently due to CH stretchings of the $(CH_3)_2O$ part. The remaining four lines, those at 2926, 2887, 2820, and 2787 cm^{-1}, which exist also in $Al(CH_3)_3\cdot(CD_3)_2O$, are due to CH stretchings of the $Al(CH_3)_3$ part. The 2926, 2887, and 2820 cm^{-1} lines are assigned to CH_3 degenerate stretching, CH_3 symmetric stretching, and an overtone of CH_3 deformation of the $Al(CH_3)_3$ part respectively. These considerations lead to the assignments in the 3100—2700 cm^{-1} region given in Table IV.

$[Al(CH_3)_2OCH_3]_3$.—Table II shows the expected types of skeletal vibrational modes and the number of skeletal vibrations in each species. The assignments in the skeletal vibration region (720—130 cm^{-1}) may be made tentatively as in Table V. The selection rule, the infrared and Raman intensities and the Raman polarization data support these assignments. The same consideration as in the case of $Al(CH_3)_3\cdot(CH_3)_2O$ leads to the identification of the bands near 1200 cm^{-1} and 686 cm^{-1} of $[Al(CH_3)_2OCH_3]_3$ as a CH_3 symmetric deformation ($AlCH_3$), superposed by CH_3 rocking (OCH_3) and an AlC_2 symmetric stretching (E'), superposed by CH_3 rocking ($AlCH_3$), respectively.

The infrared and Raman spectra of $[Al(CH_3)_2OCH_3]_3$ and $[Al(CH_3)_2OCD_3]_3$ in the 3100—2700 cm^{-1} region are quite similar to the spectra of $Al(CH_3)_3\cdot(CH_3)_2O$ and $Al(CH_3)_3\cdot(CD_3)_2O$ discussed above (Fig. 1b). Analogous considerations lead to the assignments in the 3100—2700 cm^{-1}

4) Y. Kanazawa and K. Nukada, This Bulletin, **35**, 612 (1962).

Table VII. Observed frequencies of $[Al(C_2H_5)_2OC_2H_5]_2$ and $[Al(C_2H_5)_2OC_2D_5]_2$ in cm^{-1} and vibrational assignment

$[Al(C_2H_5)_2OC_2H_5]_2$ IR	$[Al(C_2H_5)_2OC_2H_5]_2$ Raman	$[Al(C_2H_5)_2OC_2D_5]_2$ Raman	Assignment
2977 m	—2974 w D		CH_3 degenerate str. (OC_2H_5)
2939 s	—2930 m P	2936 m P	CH_3 degenerate str. (AlC_2H_5), Overtone of CH_3 deform. (AlC_2H_5, OC_2H_5)
2901 s	—2898 w D	2901 w D	CH_2 antisymmetric str. (AlC_2H_5, OC_2H_5)
2864 s	—2865 s P	2867 s P	CH_3 symmetric str. (AlC_2H_5, OC_2H_5)
2791 w	—2791 w P	2790 m P	CH_2 symmetric str. (AlC_2H_5, OC_2H_5)
2727 w	—2729 w P	2730 w P	
		2231 s D	CD_3 degenerate str.
		2152 s P	Overtone of CD_3 deform.
		2113 sh	CD_2 antisymmetric str.
		2103 m P	CD_3 symmetric str.
		2073 m P	CD_2 symmetric str.
		2036 vw	
1482 w, 1462 sh, 1451 s	—1458 s D	1468 m D	CH_3 degenerate deform., CH_3 symmetric deform. (AlC_2H_5, OC_2H_5), CH_2 scissors (OC_2H_5)
1409 s	—1410 m D	1410 m D	CH_2 scissors (AlC_2H_5)
1394 s			
1288 m	—1295 w D		CH_2 wag, CH_2 twist (OC_2H_5)
1254 w			
1222 w			
1193 s	—1193 s P	1193 s P	CH_2 wag, CH_2 twist (AlC_2H_5),
1100 s	—1118 w P	1123 w	CH_3 rock (AlC_2H_5, OC_2H_5)
1058 vs	—1084 w D	1050 w D	CO asymmetric str. B_{2u}
985 s	— 990 m P	993 m P	CC str.
948 m	— 955 w P	953 w P	
914 w	— 928 w P	918 w P	
894 s			
806 s			
652 s			AlC_2 antisymmetric str. B_{1u}, CH_2 rock (AlC_2H_5)
	634 m D	644 m D	AlC_2 antisymmetric str. B_{2g}
		580 m D	
481 w			AlC_2 symmetric str. B_{3u}
	462 m P	439 s P	AlC_2 symmetric str. A_g
	380 m P	372 w P	Ring symmetric str. A_g

region described in Table V.

$[Al(C_2H_5)_2OCH_3]_3$.—In Table II the expected types of skeletal vibrational modes and the number of skeletal vibrations in each species are shown. The tentative assignments in the skeletal vibration region (720—130 cm^{-1}) are shown in Table VI. The selection rule, the infrared and Raman intensities and the Raman polarization data support these assignments. Although no deuterated compound such as $[Al(C_2H_5)_2OCD_3]_3$ has been studied, the assignment in the 3100—2700 cm^{-1} region may be made with certainty by taking the assignments of $[Al(CH_3)_2OCH_3]_3$ and $[Al(C_2H_5)_2OC_2H_5]_2$ (discussed below) into consideration (Table VI).

$[Al(C_2H_5)_2OC_2H_5]_2$.—In Table III the expected types of skeletal vibrational modes and the number of skeletal vibrations in each species are shown. The tentative assignments in the skeletal vibration region (720—130 cm^{-1}) shown in Table VII may be made. In assigning 652, 634, 481, and 462 cm^{-1} vibrations to AlC_2 stretchings B_{1u}, B_{2g}, B_{3u}, and A_g respectively, the assignments made by Onishi and Shimanouchi for $Al_2(C_2H_5)_6$ are taken into consideration (AlC_2 stretchings of $Al_2(C_2H_5)_6$: A_g 564 cm^{-1}, B_{1u} 662 cm^{-1}, B_{2g} 643 cm^{-1}, B_{3u} 546 cm^{-1}).[5] The selection rule, the infrared and Raman intensities and the Raman polarization data support these assignments. Hoffmann showed that, for $Al_2(C_2H_5)_6$, CH_2 rocking bands appear near 626 cm^{-1};[6] in accordance with this assignment, the infrared band at 652 cm^{-1} is assigned to AlC_2 antisymmetric stretching superposed by CH_2 rocking (AlC_2H_5).

As is shown in Table VII, $[Al(C_2H_5)_2OC_2H_5]_2$

5) T. Onishi and T. Shimanouchi, *Spectrochim. Acta*, **20**, 325 (1964).
6) E. G. Hoffmann, *Z. Elektrochem.*, **64**, 616 (1960).

has six infrared bands and Raman lines in the 3100—2700 cm^{-1} region. These are very likely to be CH_3 degenerate stretchings, CH_2 antisymmetric strechings, CH_3 symmetric stretchings, CH_2 symmetric stretchings, and overtones of CH_3 deformations of the $Al(C_2H_5)_2$ part and the OC_2H_5 part. The six Raman lines of $[Al(C_2H_5)_2OC_2D_5]_2$ in the 2300—2000 cm^{-1} region are mainly due to CD stretchings of the OC_2D_5 group (Fig. 1c). These lines may be tentatively assigned as in Table VII. This assignment explains satisfactorily the intensity and polarization data. Only one Raman line at 2974 cm^{-1} among six Raman lines of $[Al(C_2H_5)_2OC_2H_5]_2$ in the 3100—2700 cm^{-1} region disappears in the spectrum of $[Al(C_2H_5)_2OC_2D_5]_2$. Four Raman lines, those at 2936, 2901, 2867, and 2790 cm^{-1}, of $[Al(C_2H_5)_2OC_2D_5]_2$ are assigned to CH_3 degenerate stretching superposed by an overtone of CH_3 deformation, CH_2 antisymmetric stretching, CH_3 symmetric stretching, and CH_2 symmetric stretching of the C_2H_5 group attached to aluminum respectively. This assignment explains satisfactorily the infrared and Raman intensities and polarization data. These consideration lead to the assignments in the 3100—2700 cm^{-1} region given in Table VII.

The author is indebted to Professor Takehiko Shimanouchi of the University of Tokyo and to Mr. Saburo Takeda for their valuable discussions throughout this work, and to Dr. Hiroshi Suzuki of the University of Tokyo for reading the manuscript and for advice.

BULLETIN OF THE CHEMICAL SOCIETY OF JAPAN VOL. 39 2132—2134 (1966)

The Infrared and Raman Spectra of the Trimethylaluminum - Dimethyl Sulfide Complex

By Ryokichi TARAO

Research Center, Chisso Co., Ltd., Kanazawa-ku, Yokohama

(Received January 20, 1966)

The infrared and Raman spectra of a mixture of trimethylaluminum and dimethyl sulfide (molar ratio, 1 : 1) have been measured (IR: 3100—300 cm^{-1}, Raman: 3100—130 cm^{-1}). The spectra obtained are entirely different from the superposition of the spectra of the two components. Tentative assignments for most of the infrared bands and Raman lines have been suggested. The CS stretching vibration lines of dimethyl sulfide shift to frequencies lower by about 5 cm^{-1} when it is mixed with trimethylaluminum. These findings, together with the measurement of the Raman spectrum of the mixture in a 10-volume-percent benzene solution, indicate that the 1 : 1 mixture of trimethylaluminum and dimethyl sulfide forms a pure coordination complex, $Al(CH_3)_3 \cdot (CH_3)_2S$, which does not dissociate into its components appreciably in either the liquid state or the benzene solution.

Dimethyl sulfide forms a coordination complex when mixed with trimethylaluminum. It is known that the Al←S bond in this complex is much weaker than the Al←O bond in the trimethylaluminum - dimethyl ether complex, and that in the vapor phase the trimethylaluminum - dimethyl sulfide complex partially dissociates into trimethylauminum and dimethyl sulfide.[1] To make sure whether, in the liquid state, the mixture of trimethylaluminum and dimethyl sulfide (molar ratio, 1 ; 1) forms a pure coordination complex or whether it contains three chemical species (complex, trimethylaluminum, and dimethyl sulfide) as a result of the partial dissociation, as in the vapor phase, the infrared and Raman spectra of the complex (a 1 : 1 mixture) in the liquid state will be measured. Qualitative polarization data on Raman lines will also be obtained. No infrared or Raman spectrum of any trialkylaluminum - dialkyl sulfide complex has ever been reported, as far as the author is aware.

Experimental

When trimethylaluminum was mixed with dimethyl sulfide in a molar ratio of 1 : 1, considerable heat evolution was observed. Six milliltrters of the mixture was then transferred into a flask, distilled in vacuo into a Raman tube with a volume of 6 ml., and sealed off under reduced pressure. The Raman spectrum was measured in the 3100—130 cm^{-1} region in the liquid state with a Shimadzu GRS Raman spectrophotometer. The polarization data were taken by the use of parallel

1) N. Davidson and H. C. Brown, *J. Am. Chem. Soc.*, **64**, 316 (1942).

Table I. Observed Raman frequencies of $(CH_3)_2S$, $Al_2(CH_3)_6$, and $Al(CH_3)_3 \cdot (CH_3)_2S$ in cm^{-1} *1,*2

$(CH_3)_2S$*3			$Al_2(CH_3)_6$*4			$Al(CH_3)_3 \cdot (CH_3)_2S$		
						3003	m	D
2980	s	D	2936	m	D	2934	vs	P
2911	vs	P	2892	vs	P	2886	s	P
2832	w	P	2825	w	P	2819	w	P
1609	vw							
						1437	w	D
1426	m	D	1434	w	D	1340	vw	
1325	w	P						
1224	vw		1257	vw	D			
			1203	m	P	1188	m	P
			1137	vw	P	1129	vw	
1041	vw					1031	vw	
						987	vw	
						958	vw	
919	vw					926	vw	
						835	vw	
742	s	D				738	m	D
			722	vw	D	719	vw	D
690	vs	P	685	m	D	685	s	P
						624	m	D
			592	s	P	574	w	D
						521	vs	P
480	vw		495	w	P	465	vw	
			453	s	P			
			311	s	P			
285	s	P				283	w	
						244	vw	
						195	vw	D
						154	s	D
			148	s	D			

*1 m, medium; s, strong; w, weak; v, very.
*2 P, polarized; D, depolarized.
*3 Cited from R. Fonteyne, *J. Chem. Phys.*, **8**, 60 (1940).
*4 Values listed are obtained by the present author.

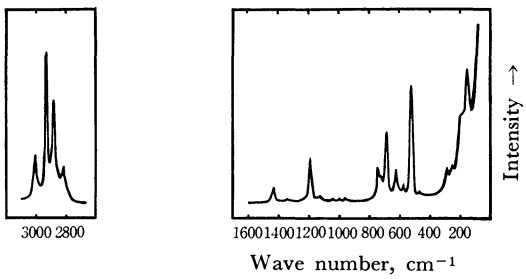

Fig. 1. The Raman spectrum of $Al(CH_3)_3 \cdot (CH_3)_2S$.

and perpendicular Polaroid cylinders placed alternately over the Raman tube. Table I shows the results of these measurements, along with those of trimethylaluminum and dimethyl sulfide. Figure 1 shows the Raman spectrum chart of the trimethylaluminum-dimethyl sulfide complex. The Raman spectrum of the trimethylaluminum - dimethyl sulfide complex was also measured in the 10-volume-percent benzene solution. The infrared spectrum was measured in the 3100—300 cm^{-1} region in the liquid state with a Japan Spectroscopic Co. Model DS-402G infrared spectrophotometer. The procedure described before was used.[2]

Results and Discussion

As is shown in Table I, the Raman spectrum of the trimethylaluminum-dimethyl sulfide complex is quite different from the superposition of the spectra of trimethylaluminum and dimethyl sulfide. Not even very strong Raman lines of these components (592 and 311 cm^{-1} lines of trimethylaluminum, 2980 and 2911 cm^{-1} lines of dimethyl sulfide) can be found in the spectrum of the complex.

The principal infrared bands and Raman lines in the 3100—130 cm^{-1} region are tentatively assigned in Table II, taking the assignment for the trimethylaluminum - dimethyl ether complex[2,3] and Goggin and Woodward's assignment for the $[CH_3\text{-}Hg\text{-}S(CH_3)_2]^+$ ion[4] into consideration. The AlC_3 skeletal vibrations (three AlC_3 stretchings and two AlC_3 deformations) appear at practically the same frequencies, with the same intensities and with the same degree of depolarization (Raman) as in the case of the trimethylaluminum - dimethyl ether complex. Similarly, the CS stretchings, SC_2 scissors, and SC_2 wagging appear at almost the same frequencies as in the case of $[CH_3Hg\text{-}S(CH_3)_2]^+$ ion. Both the CS antisymmetric stretching (742 cm^{-1}) and the CS symmetric stretching vibration line (690 cm^{-1}) of dimethyl sulfide shift to frequencies lower by about 5 cm^{-1} when a complex is formed with trimethylaluminum (Table III). This corresponds closely with the shifts of the CO stretchings of dimethyl ether on forming a complex with trimethylaluminum.[2] The magnitudes of shifts are smaller than in the case of $[CH_3Hg\text{-}S(CH_3)_2]^+$.

The Raman spectrum of the trimethylaluminum - dimethyl sulfide complex in the 10-volume-percent benzene solution is merely a superposition of the spectrum of the complex and that of benzene. No line except for the lines of the complex and benzene is found. The positive evidence for the existence of an equilibrium formulated as follows:

$$Al(CH_3)_3 \cdot (CH_3)_2S \rightleftarrows 1/2\ Al_2(CH_3)_6 + (CH_3)_2S,$$

which exists in the vapor phase, is not found in either the liquid state or the benzene solution.

These findings suggest that the 1 : 1 mixture of trimethylaluminum and dimethyl sulfide forms a pure coordination complex, $Al(CH_3)_3 \cdot (CH_3)_2S$, which does not dissociate appreciably into its components in either the liquid state or the benzene solution. It is reasonable to assume that the complex takes a structure similar to that of trimethylaluminum - dimethyl ether complex, in which an unshared pair of electrons of the sulfur atom coordinates to the aluminum atom.

2) S. Takeda and R. Tarao, This Bulletin, **38**, 1567 (1965).
3) R. Tarao, This Bulletin, 39, 2126 (1966).
4) P. L. Goggin and L. A. Woodward, *Trans. Faraday Soc.*, **58**, 1495 (1962).

TABLE II. OBSERVED FREQUENCIES OF $Al(CH_3)_3 \cdot (CH_3)_2S$ IN cm^{-1} AND VIBRATIONAL ASSIGNMENT*1,*2

IR		Raman			Assignment
2999	w	—3003	m	D	CH_3 degenerate str. (SCH_3)
2929	vs	—2934	vs	P	CH_3 degenerate str. ($AlCH_3$), CH_3 symmetric str. (SCH_3)
2888	s	—2886	s	P	CH_3 symmetric str. ($AlCH_3$)
2860	w				Overtone of CH_3 deform. (SCH_3)
2821	w	—2819	w	P	Overtone of CH_3 deform. ($AlCH_3$)
1433	s	—1437	w	D	CH_3 degenerate deform. ($AlCH_3$, SCH_3)
1337	vw	—1340	vw		CH_3 symmetric deform. (SCH_3)
1312	w				
1256	w				
1185	vs	—1188	m	P	CH_3 symmetric deform. ($AlCH_3$)
		1129	vw		
1035	m	—1031	vw		CH_3 rock (SCH_3)
984	m	— 987	vw		
949	vw	— 958	vw		
916	vw	— 926	vw		
851	vw	— 835	vw		
		738	m	D	CS antisymmetric str. A
716	vs	— 719	vw	D	AlC_3 degenerate str. A'', CH_3 rock ($AlCH_3$)
678	s	— 685	s	P	CS symmetric str. A'
623	m	— 624	m	D	AlC_3 degenerate str. A'
		574	w	D	
521	s	— 521	vs	P	AlC_3 symmetric str. A'
457	vw	— 465	vw		
437	w				
287	w	— 283	w		SC_2 scissors A'
		244	vw		AlC_3 symmetric deform. A'
		195	vw	D	SC_2 wag A'
		154	s	D	AlC_3 degenerate deform. A''

*1 m, medium; s, strong; w, weak; v, very.

*2 P, polarized; D, depolarized.

TABLE III. SHIFTS OF THE C–S VIBRATION LINES ON COMPLEX FORMATION

	ν_{as}(CS) (cm^{-1})			ν_s(CS) (cm^{-1})		
$(CH_3)_2S$*1	742	s	D	690	vs	P
$Al(CH_3)_3 \cdot (CH_3)_2S$	738	m	D	685	s	P
$CH_3Hg\text{-}S(CH_3)_2^+$*2	729	mw	D	675	m	P

*1 Cited from R. Fonteyne, loc. cit.

*2 Cited from P. L. Goggin and L. A. Woodward, Ref. 4.

The author is indebted to Professor Takehiko Shimanouchi of the University of Tokyo and to Mr. Saburo Takeda for their valuable discussions throughout this work, and to Dr. Hiroshi Suzuki of the University of Tokyo for reading the manuscript and for his advice.

BULLETIN OF THE CHEMICAL SOCIETY OF JAPAN VOL. 39 2135—2140 (1966)

The Exchange Reaction of Oxygen Atoms between Oxygen and Carbon Dioxide on Metal Oxides of the Fourth Period of the Periodic System*

By Tadamitsu KIYOURA

Department of Chemistry, Faculty of Science, Tokyo Metropolitan University, Setagaya-ku, Tokyo

(Received January 24, 1966)

The exchange reactions of oxygen atoms between oxygen and carbon dioxide on metal oxides were studied by the static batch method in the temperature range from 150 to 600°C. The order of the catalytic activity of the oxides in the reaction was found to be; (higher activity) $Co_3O_4 > MnO_2 > NiO > Fe_2O_3 > Cr_2O_3 > V_2O_5 > TiO_2$. A very close similarity of the change in the reactivity of these oxides was found in the exchange between oxygen and oxides. There is an approximately linear relationship between the catalyst activity of the metal oxides and the heat of the formation of these oxides. At any temperature examined, carbon dioxide exchanged their oxygen atoms with those of oxide rapidly. The rate of isotopic exchange decreased in the following order on any oxide examined: CO_2-Oxide > O_2-Oxide > O_2-CO_2 on oxide. The exchange between oxygen and carbon dioxide was observed only when the exchange between oxygen and oxide took place. According to these results, it was concluded that the exchange between oxygen and carbon dioxide takes place through the exchange between these gases and oxygen atoms of oxide, and that the rate-determining step is the exchange with oxygen.

About twenty-five years ago Titani and his collaborators[1-3] investigated the isotopic oxygen exchange reaction between oxygen and water vapor on various kinds of metal oxides. They found that there is a regular relationship between the catalyst activity of the metal oxide and the position where the metal element is placed in the periodic system. From group to group, there is a progressive shift of the catalyst activity. For instance, in the case of the fourth-period elements, titanium oxide (the fourth group) has the lowest activity, and manganese oxide (the seventh group) has the highest activity, with the catalyst activity of the other fourth-period elements arranged in good order between these two elements. Recently Boreskov et al.[4,5] studied the homomolecular oxygen exchange reaction on metal oxides of the fourth-period elements, and discussed the relations between the catalyst activity and the physical and chemical properties of the oxides. However, to the author's knowledge, no systematic investigation has been made into the exchange reaction between oxygen and carbon dioxide on metal oxides. The present author has, therefore, investigated the exchange reaction between oxygen and carbon dioxide on metal oxides of the fourth period of the periodic system, hoping thereby to give an order of the catalyst activity of the oxides and a general picture of the reaction. In the isotopic exchange reaction $\Delta H \fallingdotseq 0$, so the influence of the heat of reaction can be ignored in the comparison of the catalyst activity. It is of interest to study the possible relations between the exchange reaction and the other oxidation reactions on an oxide catalyst. In the exchange reaction between oxygen and carbon dioxide on metal oxides, it may be expected that the catalyst activity of the metal oxides will show the same regular relations as that reported by Titani and his collaborators[1-3] and by Boreskov et al.[4,5] However, such a conclusion could hardly be regarded as certain before experiments have been performed to test this point. The results of the present experiment show that, in the exchange between oxygen and carbon dioxide, there is a regular relation in the catalyst activity of the metal oxides. In the investigation of the oxygen exchange reaction on an oxide catalyst, the measurement of the oxygen exchange between a reactant and an oxide catalyst provides a strong clue to the mechanism of the reaction; therefore, the exchange between oxygen and oxides, and that between carbon dioxide and oxides were studied in the initial step.

Experimental

Gases.—Heavy oxygen, $O^{18}O$, was prepared in our laboratory by the thermal diffusion method;[6] its concentration was 1.81 atom%. Carbon dioxide labeled with ^{18}O (1.79 atom%) was prepared by equilibrating samples of water enriched with ^{18}O

* Presented partly at the 18 th Annual Meeting of the Chemical Society of Japan, Osaka, April, 1965.

1) N. Morita, H. Nakata and T. Titani, This Bulletin, **14**, 9 (1939).

2) N. Morita, ibid., **15**, 47 (1940).

3) N. Morita, ibid., **15**, 71 (1940).

4) A. P. Dzisjak, G. K. Boreskov and L. A. Kasatkina, *Kinetika i Kataliz*, **3**, 81 (1962).

5) G. K. Boreskov, A. P. Dzisjak and L. A. Kasatkina, ibid., **4**, 388 (1963).

6) Y. Horibe, *Isotopes and Radiation*, **2**, 25 (1959).

TABLE I. OXIDE CATALYSTS

Oxide	Method of preparation	Specific surface area, m^2/g.	Amount of oxide used, mg.
TiO_2	Hydrolysis of $TiCl_4$	14	215
V_2O_5	Thermal decomposition of NH_4VO_3	2.5	300
Cr_2O_3	Thermal decomposition of hydroxide	15	200
MnO_2	Thermal decomposition of nitrate	18	170
Fe_2O_3	Thermal decomposition of hydroxide	10	300
Co_3O_4	Thermal decomposition of nitrate	16	200
NiO	Thermal decomposition of carbonate	31	100

with tank carbon dioxide of a natural isotopic composition prepurified by pumping off the vapors not condensable at the temperature of liquid nitrogen. All the gases used were dried through a train of traps immersed in solid carbon dioxide. A search for impurities in the gases after purification was made by a mass spectrometer up to mass 100; it was found that they were mass-spectrometrically pure, except for traces of other inert gases.

Oxide Catalysts.—The methods of preparation and the specific surface area of the oxides are shown in Table I, together with the amount of the oxides used for the reaction.

For the purpose of comparing the catalyst activity of these oxides, the following precaution was taken, The amount of oxide used for the reaction was adjusted in order to give a fixed total surface area for the different oxides; therefore, the total surface area of a single portion of each oxide used for the reaction was about 3 m^2 except in the case of vanadium pentoxide.

Procedure.—The reaction was carried out by the static batch method. The reaction vessel was made of pyrex or of fused silica glass. In order to maintain a constant pressure of the gas at each reaction temperature (14 cmHg for CO_2–Oxide, and O_2–Oxide; 27 cmHg for O_2–CO_2 on oxide), reaction vessels of different volumes were chosen for the different reaction temperatures. A single portion of each oxide used for the reaction is listed in the last column of Table I. For the exchange between carbon dioxide and oxides or that between oxygen and oxides, a weighed amount of oxide was placed in the reaction vessel and then outgassed at 550°C for 3 hr., using a mercury diffusion pump, through a liquid nitrogen trap. (Manganese dioxide was, however, outgassed at 200°C for 1 hr.) Then the temperature of the reaction vessel was adjusted to the desired temperature, and 1.8 ml. (NTP) of the enriched carbon dioxide or heavy oxygen was introduced. At desired time intervals, the entire amount of gas was collected and the ^{18}O content of the gas was analyzed by the use of a mass spectrometer. For the exchange between oxygen and carbon dioxide on oxides, a 3.4-ml. portion (NTP) of the gas mixture of heavy oxygen and normal carbon dioxide in a ratio of 1 to 1 was used. The weight of oxides used, the outgassing and the other procedures were the same as those used in investigation of the exchange between gases and oxides.

Results and Discussion

The Isotopic Oxygen Exchange between Gases and the Reaction Vessel, and the Catalytic Action of the Reaction Vessel.—Within the limits of experimental error, the surface of the reaction vessel did not participate in the exchange reaction.

The Exchange between Carbon Dioxide and Metal Oxides in the Absence of Oxygen, and between Oxygen and Metal Oxides in the Absence of Carbon Dioxide.—The exchange reaction between carbon dioxide and oxides proceeded rapidly, and the quantitative measurement of the reaction rate was difficult in the ordinary static method. In any of the oxides examined, carbon dioxide actively exchanged its oxygen atoms with those of oxide, even below the temperature at which no exchange between oxygen and oxides was observed. As an example of the experimental results, the exchange between carbon dioxide and chromic oxide, and that between oxygen and chromic oxide are graphically shown in Fig. 1. From the shapes of the curves shown in Fig. 1, the temperature dependence of the rate of the exchange with carbon dioxide may be seen to be not very appreciable; therefore, the apparent energy of activation can be estimated within a few kcal./mol. Within ten minutes after introduction of the enriched carbon dioxide into the reaction vessel, the ^{18}O content of the carbon dioxide reached a definite value. This value was characteristic of the reaction temperature. At this stage of the reaction, an isotopic equilibrium was established

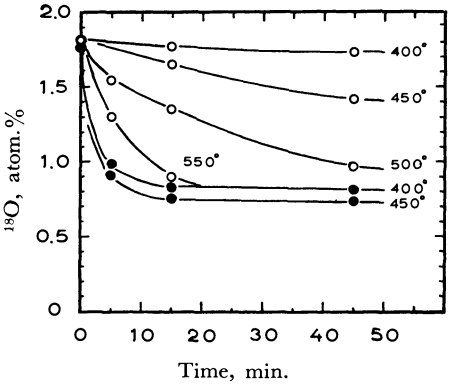

Fig. 1. Extent of the exchange reaction between $CO^{18}O$ and Cr_2O_3, $O^{18}O$ and Cr_2O_3.

Open circle, $O^{18}O$ and Cr_2O_3
Filled circle, $CO^{18}O$ and Cr_2O_3

TABLE II. THE VALUES OF n_s AT DIFFERENT TEMPERATURES
(The numerals in parentheses are the reaction temperatures, °C)

Oxide	n_s (g. atom/g. of oxide)				
Co_3O_4	3.0×10^{-5} (100)	5.1×10^{-5} (150)	7.8×10^{-5} (200)	9.3×10^{-5} (250)	1.5×10^{-4} (300)
MnO_2	2.5×10^{-4} (200)	3.4×10^{-4} (250)	4.1×10^{-4} (300)	4.5×10^{-4} (350)	4.9×10^{-4} (400)
NiO	1.5×10^{-4} (200)	3.2×10^{-4} (250)	4.8×10^{-4} (300)	6.0×10^{-4} (350)	7.0×10^{-4} (400)
Fe_2O_3	5.4×10^{-5} (300)	9.3×10^{-5} (350)	1.6×10^{-4} (400)	2.0×10^{-4} (450)	2.3×10^{-4} (500)
Cr_2O_3	7.4×10^{-4} (350)	9.4×10^{-4} (400)	1.1×10^{-3} (450)	1.2×10^{-3} (500)	1.3×10^{-3} (550)
V_2O_5	5.9×10^{-5} (450)	9.4×10^{-5} (500)	1.4×10^{-4} (550)	3.5×10^{-4} (600)	
TiO_2	3.5×10^{-4} (450)	4.8×10^{-4} (500)	6.1×10^{-4} (550)	6.7×10^{-4} (600)	

between the carbon dioxide in the gas phase and a certain part of the oxide. After the fast initial reaction had finished, there was a slow downward drift of the ^{18}O content of the carbon dioxide. From Fig. 1, the definite ^{18}O content may be obtained by the extrapolation of the drift line to time zero. From this quantity, and from the amount of carbon dioxide and chromic oxide used, we calculated the amount of rapidly-exchangeable oxygen of the oxide, n_s (gram atom per gram of oxide). It was assumed that the ^{18}O content of the exchangeable part of the oxide becomes equal to that of the ambient gas. The values of n_s at different temperatures are tabulated in Table II. The n_s values of these oxides are in the order of 10^{-5} g. atom/m^2, and there is not very remarkable difference in these values in each oxide. The density of the oxygen atoms on the surface of the oxides is in the order of 10^{-5} g. atom/m^2; this agrees with the n_r values.

The surface area of these oxides was measured at the beginning and at the end of the reaction; the difference was within 15%.

As is shown in Fig. 1, the exchange with oxygen proceeded more slowly than that with carbon dioxide. The same results were obtained with the other oxides examined. We have calculated F_1, the fractional attainment of the equilibrium of the exchange reaction between oxygen and oxides, from Eq. 1, where $^{18}O_0$, $^{18}O_t$, and $^{18}O_\infty$, are the initial, at time t, and equilibrium ^{18}O contents of the oxygen gas respectively.

$$F_1 = [(^{18}O_0 - {}^{18}O_t)/(^{18}O_0 - {}^{18}O_\infty)]\times 100 \qquad (1)$$

A random distribution of ^{18}O between the oxygen gas and the exchangeable surface oxygen of the oxide being assumed, the value of $^{18}O_\infty$ was calculated through the value of n_s and through the amount of heavy oxygen and the oxide used. The value of $^{18}O_\infty$ is characteristic of the reaction temperature because the value of n_s depends on the temperature. The results obtained with chromic oxide are shown in Table III.

The rate of the exchange, R (g. atom/min.), is expressed by Mckay's equation:

$$R = -2.303[(a\cdot b)/(a+b)] \log (1-F_1/100)/t \qquad (2)$$

where a and b are the amount of heavy oxygen gas used and the amount of exchangeable surface oxygen of the oxide used respectively, where t

TABLE III. THE EXCHANGE BETWEEN $O^{18}O$ AND Cr_2O_3

[The initial ^{18}O contents in O_2 and Cr_2O_3 are 1.81 and 0.204 atom.% respectively.]

Temp. °C	Time min.	^{18}O atom% in O_2	F_1 %
400	15	1.77	4.3
400	45	1.72	11
400	∞	0.87	100
450	15	1.65	15
450	45	1.42	41
450	∞	0.79	100
500	5	1.54	17
500	15	1.37	42
500	45	0.970	89
500	∞	0.760	100
550	5	1.30	48
550	15	0.891	86
550	∞	0.74	100

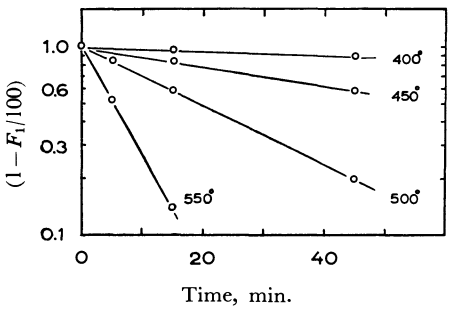

Fig. 2. Exchange between $O^{18}O$ and Cr_2O_3. Semilogarithmic plot of one minus fractional exchange versus time.

TABLE IV. THE APPARENT ENERGY OF ACTIVATION OF THE EXCHANGE REACTION BETWEEN OXYGEN AND OXIDE

Oxide	TiO_2	Cr_2O_3	MnO_2	Fe_2O_3	V_2O_5	Co_3O_4	NiO
A, kcal./mol.	39	31	16	21	41	14	15

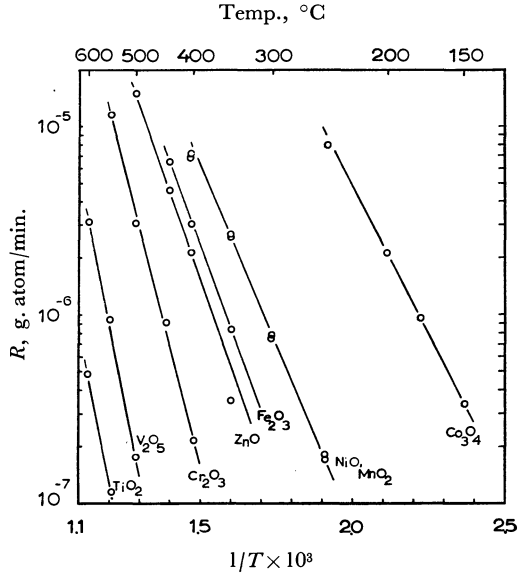

Fig. 3. Temperature dependence of rate of the exchange reaction between oxygen gas and various oxides.

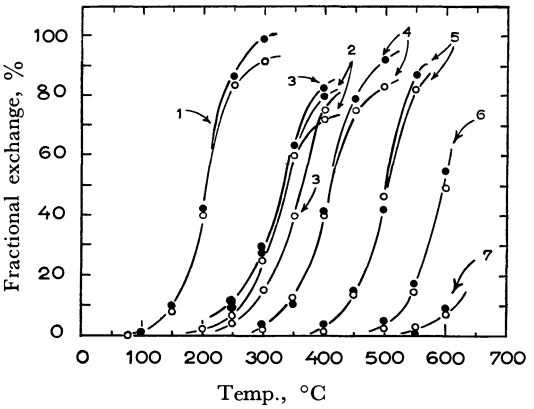

Fig. 4. Fractional attainment of the exchange reaction vs. reaction temperature.

Open circle, $O^{18}O$-CO_2
Filled circle, $O^{18}O$- Oxide
1, Co_3O_4; 2, MnO_2; 3, NiO; 4, Fe_2O_3; 5, Cr_2O_3; 6, V_2O_5; 7, TiO_2

is the reaction time, and where F_1 is the fractional attainment of the exchange reaction.

Equation 2 requires a linear relationship between $\log(1-F_1/100)$ and t, which are shown in Fig. 2. The values of R, which are calculated from the slopes of Fig. 2, are shown in Fig. 3, together with those of the other oxides examined. The apparent energies of activation, A, were obtained from the slopes of Fig. 3; they are listed in Table IV.

The values of F_1 at various temperatures, 15 min. after the beginning of the reaction are shown in Fig. 4. From Fig. 4, the reactivity of the oxides was estimated by means of the temperature threshold of the reaction. The order of reactivity of these oxides in relation to the exchange with oxygen is in the following sequence:

(Higher activity) $Co_3O_4 > MnO_2 = NiO > Fe_2O_3 > Cr_2O_3 > V_2O_5 > TiO_2$

As is shown in Fig. 4, the temperature threshold of the reaction is characteristic of each metal oxide. Above this temperature, the chemisorbed state of oxygen is probably in the form of O^-. In the case of exchange reaction between oxygen and zinc oxide,[7] the temperature threshold is about 350°C. Kwan et al.[8] studied the adsorbed state of oxygen on zinc oxide by the ESR method; they reported that at about 370°C the adsorbed state is in the form of O^-.

The Exchange between Oxygen and Carbon Dioxide on Metal Oxides.—As an example, the case of chromic oxide used as a catalyst is shown in Fig. 5 and Table V. The exchange of oxygen occurred at a measureable rate around 400°C. This result is similar to that shown in Fig. 1. The number of ^{18}O that the carbon dioxide had gained was less than that the oxygen had lost. This difference may be ascribed to the

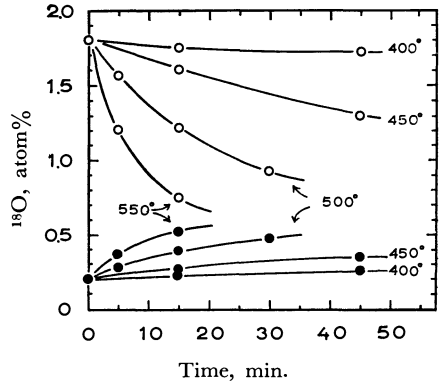

Fig. 5. Extent of the exchange reaction between $O^{18}O$ and CO_2 on Cr_2O_3.

Open circle, Decrease of ^{18}O in O_2
Closed circle, Increase of ^{18}O in CO_2

7) T. Titani, T. Kiyoura and A. Adachi, This. Bulletin, **38**, 2075 (1965).
8) M. Sedaka and T. Kwan, ibid., **38**, 1414 (1965).

TABLE V. THE EXCHANGE BETWEEN $O^{18}O$ AND CO_2 ON Cr_2O_3

(The initial $O^{18}O$ contents in O_2 and CO_2 are 1.81 and 0.204 atom% respectively.)

Temp. °C	Time min.	^{18}O atom% in CO_2	F_2 %
400	15	0.221	3.5
400	45	0.261	12.0
400	∞	0.685	100
450	15	0.264	14.0
450	45	0.366	38.9
450	∞	0.620	100
500	5	0.280	19.5
500	15	0.393	47.1
500	30	0.492	72.0
500	∞	0.607	100
550	5	0.383	44.0
550	15	0.527	83.2
550	∞	0.594	100

exchange with oxide. We have calculated F_2, the fractional attainment of the equilibrium of the reaction, from Eq. 3, where $CO^{18}O_t$ is the ^{18}O content of the carbon dioxide at time t, where $CO^{18}O_\infty$ is the ^{18}O content of the carbon dioxide when the reaction attains equilibrium, and where the numerical constant, 0.204, is the natural abundance of ^{18}O.

$$F_2=[(CO^{18}O_t-0.204)/(CO^{18}O_\infty-0.204)]\times 100 \quad (3)$$

A random distribution of ^{18}O among the oxygen, the carbon dioxide, and the exchangeable surface oxygen of the metal oxide being assumed, the value of $CO^{18}O_\infty$ was calculated using the amounts of the gases and the oxide used. The values of F_2 at different temperatures, 15 min. after the beginning of the reaction are shown in Fig. 4, together with those of the other oxides examined.

Using the results shown in Fig. 4, $\log[-\log(1-F_2/100)]$ was plotted against $1/T$. As is shown in Fig. 6, the plots give straight lines. The apparent energies of activation, obtained from the slopes of Fig. 6, are listed in Table VI. These values are very similar to those shown in Table IV.

For a measure of the catalytic activity of the oxides, the temperature threshold for the reaction was chosen. From Fig. 4, the temperatures

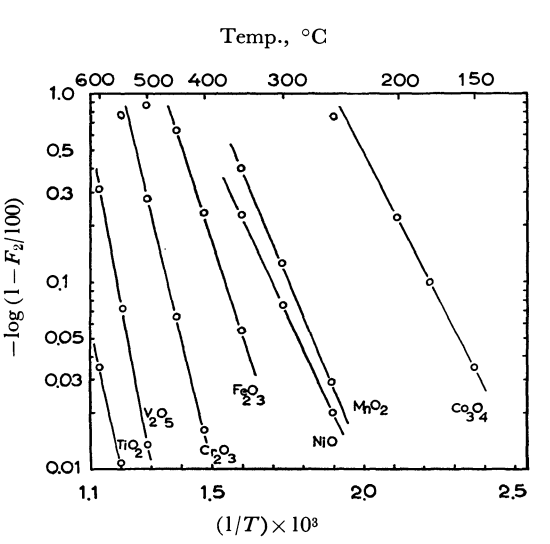

Fig. 6. Temperature dependence of $\log[-\log(1-F_2/100)]$.

at which the F_1 and F_2 reached 10% for the respective oxide, $t(10\%)$°C, may be obtained; these temperatures are summarized in Table VII. From Fig. 4 and Table VII, the order of the catalytic activity of these oxides in the reaction is found to be:

(Higher activity) $Co_3O_4>MnO_2>NiO>Fe_2O_3>Cr_2O_3>V_2O_5>TiO_2$

This is very close to the experimental results of the exchange between oxygen and oxide.

The following questions have been raised concerning the reaction mechanism:

(a) Does the reaction proceed through the interaction of the chemisorbed oxygen and the chemisorbed carbon dioxide?

(b) Does the reaction proceed through the exchange between these gases and the oxygen atoms of metal oxide ?

(c) Does the reaction proceed through both mechanisms a and b ?

As is shown in Table VII, the $t(10\%)$°C value was similar in both reactions, and the exchange between oxygen and carbon dioxide was observed only when the exchange between oxygen and oxide took place. The rate of the isotopic exchange

TABLE VI. THE APPARENT ENERGY OF ACTIVATION OF THE EXCHANGE BETWEEN $O^{18}O$ AND CO_2 ON VARIOUS OXIDES

Oxide catalyst	TiO_2	Cr_2O_3	Fe_2O_3	V_2O_5	Co_3O_4	NiO	MnO_2
A, kcal./mol.	41	30	24	41	15	15	17

TABLE VII. THE $t(10\%)$°C VALUES OF VARIOUS OXIDES

Oxide	TiO_2	V_2O_5	Cr_2O_3	Fe_2O_3	MnO_2	NiO	Co_3O_4
$t(10\%)$°C of F_1	605	530	440	345	260	260	150
$t(10\%)$°C of F_2	610	535	440	350	265	280	155

decreased in the following order on all the oxides examined:

$$CO_2\text{-Oxide} > O_2\text{-Oxide} \geq O_2\text{-}CO_2$$

Moreover, the apparent energies of activation, shown in Tables IV and VI, are similar in the two reactions. According to these results, it is natural to think, that the reaction proceeds through the b mechanism; that is, the reaction consists of two consecutive and simultaneous reactions, 4 and 5, with Reaction 5 being far more rapid than Reaction 4, where MO represents metal oxide.

$$O^{18}O + MO = O_2 + M^{18}O \quad (4)$$

$$CO_2 + M^{18}O = CO^{18}O + MO \quad (5)$$

The c mechanism was excluded, because $\log[-\log(1-F_2/100)]$ against $1/T$ gives straight lines over an appreciable wide range of reaction temperature (Fig. 6).

The catalytic activity of the oxides with respect to the exchange between oxygen and water vapor[1-3] is in the following sequence:

(Higher activity) $MnO_2 > Fe_2O_3 > Cr_2O_3 > NiO > V_2O_5 > TiO_2$

This is similar to the exchange between oxygen and carbon dioxide, with the exception of nickel oxide. A similar change in the catalyst activity of the oxides with respect to the homomolecular oxygen exchange,[4,5] the oxidation of hydrogen,[9] the oxidation of carbon monoxide,[10,11] and the oxidation of hydrocarbon[12] has been reported. The concept that the catalyst activity of the oxide is related to the heat of formation of the corresponding oxide was recently advanced by Tamaru[13] and by Kwan and his collaborators[14]. We also attempted to plot the $t(10\%)$°C (the measure of the catalyst activity) against the heat of formation of these oxides. The plots thus obtained are shown in Fig. 7. As this figure shows, there is an approximately linear relationship between the catalyst activity of the oxides and the heat of formation of these oxides. In other words, the weaker the oxygen bond of the metal oxide, the faster the rate of oxygen exchange reaction.

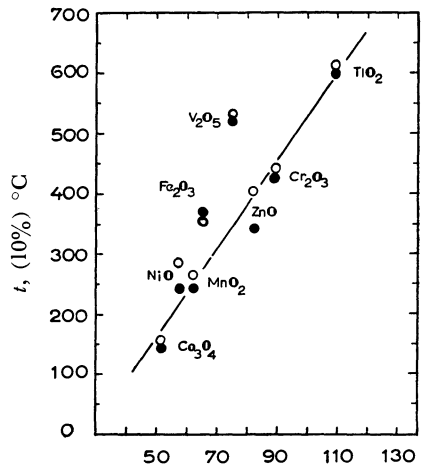

Fig. 7. The relation between the catalytic activity of metal oxides and the heat of formation of metal oxides.
Open circle, $O^{18}O$-CO_2 on oxide
Filled circle, $O^{18}O$-Oxide

The author wishes to express his deep thanks to Professor Toshizo Titani for his suggestions and guidance.

9) V. V. Popovsky and G. K. Boreskov, *Probl. Kinetika i Kataliza, Akad. Nauk SSSR*, **10**, 67 (1960).
10) O. V. Krilov, *Kinetika i Kataliz*, **3**, 502 (1962).
11) F. S. Stone, "Chemistry of the Solid State," Butterworths, London (1955), p. 397.
12) K. C. Stein, I. I. Feenan, G. P. Thompson, I. F. Shutts, L. J. E. Hofer and R. S. Anderson, *Ind. Eng. Chem.*, **52**, 113 (1960).
13) K. Tanaka and K. Tamaru, *Catalyst (Shokubai)*, **4**, 328 (1962).
14) I. Komuro, H. Yamamoto and T. Kwan, This Bulletin, **36**, 1532 (1963).

BULLETIN OF THE CHEMICAL SOCIETY OF JAPNA VOL. 39 2141—2144 (1966)

Studies of the Alkaline Earth Complexes in Various Solutions. I. Barium(II) Complexes with Sulfate and Oxalate Ions in 1M Sodium Perchlorate Media

By Tatsuya SEKINE, Mitsuo SAKAIRI and Yuko HASEGAWA

Department of Chemistry, Tokyo College of Science, Kagurazaka, Shinjuku-ku, Tokyo

(Received January 25, 1966)

The distribution of barium(II) at a very low concentration was determined between a carbon tetrachloride solution of 0.1 M thenoyltrifluoroacetone and 0.2 M tributylphosphate and aqueous solutions of 1 M $Na(ClO_4)$ at 25°C. The net distribution ratio is decreased when a part of the perchlorate ions are replaced by sulfate or oxalate ions. This decrease was explained in terms of the complex formation of Ba^{2+} with these ligands. The stability constants were determined graphically from the experimental data as follows:

Ligand	$\log \beta_1$	$\log \beta_2$
SO_4^{2-}	0.66	1.42
$C_2O_4^{2-}$	0.58	2.20

(1 M $Na(ClO_4)$, 25°C)

The solubility of barium sulfate and oxalate has been reported by many authors, but the complex formation of barium ion with these anions in an aqueous solution has not been studied very much.[1] This may be due to the fact that the concentration of barium ions in sulfate or oxalate solutions is too low to be studied by such methods as the e.m.f. measurement, conductometry and spectropothometry.

In the present work, the authors studied the complex formation of barium with sulfate and oxalate ions in sodium perchlorate media at 25°C. A carrier-free radioactive barium-140 tracer was used to keep the barium concentration very low in order to prevent the formation of precipitates. The decrease in the free barium ion concentration in the aqueous phase caused by the complex formation was determined by a solvent extraction technique recently developed in our laboratory.[2] The stability constants were determined by a graphical method from the distribution data.

Experimental

Tracer.—Barium-140 was obtained from the Radiochemical Center, Amersham, England. It was diluted with a mixture of 0.1 M perchloric acid and 0.9 M sodium perchlorate.

Reagents.—All of the reagents used were of analytical grade. Thenoyltrifluoroacetone (TTA) was obtained from the Dojin Yakukagaku Co. Tributylphosphate (TBP) was obtained from the Tokyo Kasei Co. The TBP was washed with 0.1 M perchloric acid, water, 0.1 M sodium hydroxide, and several times with water respectively, and was finally equilibrated with a 1.0 M sodium perchlorate solution. Sodium perchlorate was prepared from sodium carbonate and perchloric acid and was recrystallized two times from water. The concentration of the stock sodium sulfate solution was determined from the weight of the residue left after a portion of the solution had been dried up in an air bath at 120°C. The stock sodium oxalate solution in 1 M $Na(ClO_4)$ was prepared by dissolving a weighed portion of sodium oxalate crystals in a sodium perchlorate solution.

Procedures.—All of the procedures were carried out in a thermostatted room at 25°C. Stoppered glass tubes (volume: 20 ml.) were used to equilibrate the organic and the aqueous phases. The tracer solution, various amounts of a sodium sulfate or sodium oxalate solution, a buffer solution, a sodium perchlorate solution and the organic solution were placed in the tubes. The aqueous phase was maintained at 1.0 M $Na(ClO_4)$; the aqueous phase always contained 1.0 M sodium ions and various amounts of sulfate or oxalate ions, together with perchlorate ions. A small amount of triethanolamine or sodium acetate (the initial concentration was 0.01 M) was added to the aqueous phase to buffer the hydrogen ion concentration. The organic phase was a mixture of 0.1 M TTA and 0.2 M TBP in carbon tetrachloride. The initial volume of the two phases was always 5.0 ml.

The two phases in the tubes were vigorously agitated by a mechanical shaker for fifteen minutes and then centrifuged for three minutes at 2000 r. p. m. A 2.0-ml. portion was pipetted from the two phases and transferred into small, stoppered glass test tubes for the measurement of the γ-radioactivity. Another portion of the aqueous phase was transferred into small glass vessels, and the hydrogen ion concentration was determined

1) L. G. Sillén and A. E. Martell, "Stability Constants," Spec. Pub. 17, The Chemical Society, London (1964).

2) T. Sekine, S. Obuchi and M. Sakairi, This Bulletin, to be published.

potentiometrically using 0.0100 M $HClO_4$ + 0.99 M $NaClO_4$, as the standard of $-\log[H^+] = 2.00$. The solutions in the small glass test tubes were let stand for more than seventeen days, until the decay equilibrium was reached between barium-140 (the half life is 12.80 days) and lanthanum-140 (the half life is 40.22 hr.); the γ-radioactivity was then measured with a well-type (NaI) scintillation counter.

Statistical Treatment

The nth step of the complex formation of a dipositive metal ion, M^{2+}, with a dinegative ligand ion, L^{2-}, may be described as:

$$M^{2+} + nL^{2-} \rightleftarrows ML_n^{2-2n} \quad (1)$$

$$\beta_n = [ML_n^{2-2n}]/[M^{2+}][L^{2-}]^n \quad (2)$$

The distribution of this metal ion between an organic phase with an organophilic chelating acid, HA, and an aqueous phase with no complex-forming ligands may be described as:

$$M^{2+} + 2HA(org) \rightleftarrows MA_2(org) + 2H^+ \quad (3)$$

$$K = [MA_2]_{org}[H^+]^2/[M^{2+}][HA]_{org}^2 \quad (4)$$

Here the subscript "*org*" denotes a chemical species in the organic phase.

The net distribution ratio of the metal ion between the organic and the aqueous phase may be defined as:

$$D = [M(II)]_{org,\ total}/[M(II)]_{total} \quad (5)$$

The extraction constant may be defined as:

$$K_{ex} = D[H^+]^2[HA]_{org}^{-2}$$

When there is no complex-forming ligand in the aqeuous phase, the distribution ratio of the metal ion may be described as:

$$D_0 = [MA_2]_{org}/[M^{2+}] \quad (7)$$

The extraction constant is then:

$$K_{ex_0} = ([MA_2]_{org}/[M^{2+}])[H^+]^2[HA]_{org}^{-2} \quad (8)$$

Here the subscript "0" denotes a system where the ligands, L^{2-}, are absent in the aqueous phase. We see that the K_{ex_0} in Eq. 8 equals the K in Eq. 4; therefore, K_{ex_0} should give a constant value at a certain temperature.

When there is the complex-forming ligand in the aqueous phase at a certain concentration $[L^{2-}]$, the distribution ratio may be described from Eqs. 2 and 5 as:

$$D = [MA_2]_{org}/([M^{2+}]+[ML]+[ML_2^{2-}]+\cdots)$$

$$= ([MA_2]_{org}/[M^{2+}])(1+\sum_1^n \beta_n[L^{2-}]^n)^{-1} \quad (9)$$

The extraction constant is then:

$$K_{ex} = ([MA_2]_{org}/[M^{2+}])[H^+]^2[HA]_{org}^{-2} \times (1 + \sum_1^n \beta_n[L^{2-}]^n)^{-1} \quad (10)$$

By dividing Eq. 10 by Eq. 8, we obtain the following equation:

$$\frac{K_{ex}}{K_{ex_0}} = (1 + \sum_1^n \beta_n[L^{2-}]^n)^{-1} \quad (11)$$

Thus we may determine the stability constants, β_n, from Eq. 11.

When an organophilic neutral ligand, N, is added to the organic phase and the metal chelate forms adducts with N, the equilibrium may be described as:

$$MA_2(org) + lN(org) \rightleftarrows MA_2N_l(org) \quad (12)$$

$$\beta_{a,l} = [MA_2N_l]_{org}/[MA_2]_{org}[N]_{org}^l \quad (13)$$

When there is no complex-forming ligand, L^{2-}, in the aqueous phase and when there is an adduct-forming ligand in the organic phase at a constant concentration, $[N]_{c,\ org}$, the distribution ratio and the extraction constant are:

$$D = ([MA_2]_{org} + [MA_2N]_{org} + [MA_2N_2]_{org} + \cdots)/[M^{2+}]$$

$$= ([MA_2]_{org}/[M^{2+}]) \times (1 + \sum_1^l \beta_{a,l}[N]_{c,org}^l) \quad (14)$$

$$K_{ex_0} = ([MA_2]_{org}/[M^{2+}])[H^+]^2[HA]_{org}^{-2} \times (1 + \sum_1^l \beta_{a,l}[N]_{c,org}^l) \quad (15)$$

The extraction constant in Eq. 15 is $1+\sum_1^l \beta_{a,l}[N]_{c,org}^l$ times the constant in Eq. 8, but the former should also give a constant value at a certain temperature as long as the concentration of N is kept constant.

When there is a complex-forming ligand in the aqeuous phase at a concentration, $[L^{2-}]$, we may introduce the following equation by the same procedure;

$$K_{ex} = ([MA_2]_{org}/[M^{2+}])[H^+]^2[HA]_{org}^{-2} \times (1 + \sum_1^l \beta_{a,l}[N]_{c,org}^l) \times (1 + \sum_1^n \beta_n[L^{2-}]^n)^{-1} \quad (16)$$

From Eqs. 15 and 16 we may also see that Eq. 11 is valid even in a solvent extraction system where the distribution ratio is enhanced by the adduct formation (synergism).

The stability constants can be determined from the distribution data by a curve-fitting method[3-5] using Eq. 11.

It may be possible to discuss the problem more

3) L. G. Sillén, *Acta Chem. Scand.*, **10**, 186 (1956).
4) F. Rossotti and H. Rossotti, "The Determination of Stability Constants," McGraw-Hill Book Co., New York (1961).
5) T. Sekine and Y. Hasegawa, This Bulletin **39**, 240 (1966).

generally, but here we assume that only the first and the second complexes, ML and ML_2^{2-}, are formed in the aqueous solution.

When we replace K_{ex}/K_{ex_0}, $\beta_2^{1/2}[L^-]$ and $\beta_1\beta_2^{-1/2}$ with y, a and R respectively, we obtain the following equation instead of Eq. 11:

$$y = (1 + Ra + a^2)^{-1} \quad (17)$$

By introducing various values into R in Eq. 17, a family of standard curves represented by the following equations are obtained:

$$\begin{aligned} Y &= \log y = -\log(1 + Ra + a^2) \\ X &= \log a \end{aligned} \quad (18)$$

One of these curves will be found to fit the plot of the experimental data, $\log(K_{ex}/K_{ex_0})$ vs. $\log[L^{2-}]$. Since $\log a$ equals $^1/_2\log\beta_2+\log[L^{2-}]$, the value of $\log\beta_2$ can be obtained from the position of the experimental plot, $\log(K_{ex}/K_{ex_0})$ vs. $\log[L^{2-}]$, on the $\log a$ axis, and R equals $\beta_1\beta_2^{-1/2}$; that is, $\log\beta_1$ equals $\log R+^1/_2\log\beta_2$, then the β_1 value can be calculated from the values R and β_2.

Results

Perchlorate System.—It was concluded from another study[6] that the main barium complex species in a carbon tetrachloride solution of 0.1 M TTA (HA) and various amounts of TBP (L) is BaA_2L_2 in the higher TBP-concentration region. Therefore, the distribution equilibrium can be written as:

$$Ba^{2+} + 2HA(org) + 2L(org) \rightleftarrows BaA_2L_2(org) + 2H^+$$

Figure 1 gives the dependence of the distribution ratio of barium ions on the hydrogen ion concentration when the organic phase is a carbon tetrachloride solution of 0.1 M TTA and 0.2M TBP and when the aqueous phase is 1.0 M sodium perchlorate.

The plot falls on a straight line with a +2 slope, and the extraction constant calculated from the nineteen points in Fig. 1 is:

$$\log D_0[H^+]^2[HA]_{org}^{-2} = -10.01$$

These results seem to show that: (i) there is no complex formation of barium with TTA in the aqueous phase, and (ii) there is no extraction of barium complexes with perchlorate ions into the organic phase.

Thus we may conclude that the K_{ex_0} value obtained from these results can be used for the calculation of the stability constants by means of Eq. 11 (cf. Ref. 7).

Sulfate System.—The distribution ratio of barium(II) is decreased by the addition of sodium sulfate to the aqueous phase. Figure 2 gives the decrease in the extraction constant as a function of $\log[SO_4^{2-}]$. In these experiments the analytical concentration of sodium sulfate in the aqueous phase can be regarded as the concentration of sulfate ions, $[SO_4^{2-}]$, because the $-\log[H^+]$ was kept between 6.4 and 6.6 and the pK_a value of sulfuric acid in 1 M $Na(ClO_4)$ at 25°C is 1.02.[8]

The plot was found to fit a standard curve, $Y=-\log(1+0.9a+a^2)$, $X=\log a$. This indicates that

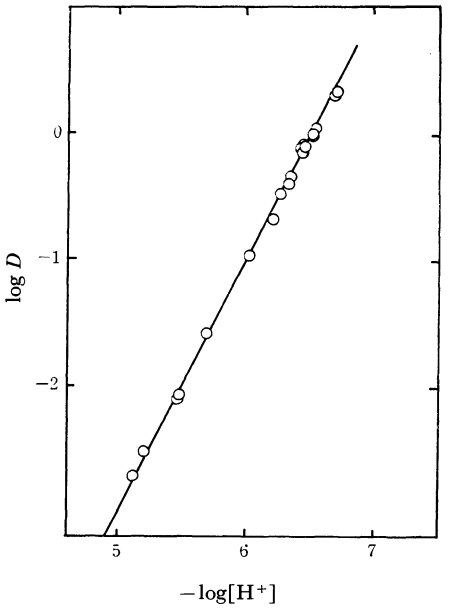

Fig. 1. Distribution ratio of barium(II) between 0.1 M TTA + 0.2 M TBP - carbon tetrachloride and 1.0 M $NaClO_4$, at 25°C. The straight line gives $\log D=-2\log[H^+]-12.01$. The extraction constant;
$\log K_{ex_0}=D[H^+]^2[HA]_{org}^{-2}=-10.01$

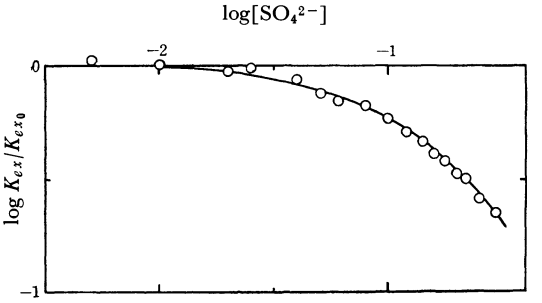

Fig. 2. Decrease in the extraction constant of barium(II) as a function of sulfate ion concentration. The solid curve was calculated by the following equation.
$Y=-\log(1+4.60[SO_4^{2-}]+26.3[SO_4^{2-}]^2)$;
$X=\log[SO_4^{2-}]$

6) T. Sekine and M Sakairi, in press.

7) T. Sekine, M. Sakairi, F. Shimada and Y. Hasegawa, This Bulletin **38**, 847 (1965).

8) E. Eichler and S. Rabideau, *J. Am. Chem. Soc.*, **77**, 5501 (1955).

both the $BaSO_4$ and $Ba(SO_4)_2^{2-}$ complexes are formed. The stability constants finally determined are given in Table I.

TABLE I. STABILITY CONSTANTS OF BARIUM(II) COMPLEXES IN 1 M $Na(ClO_4)$ AT 25°C

$\beta_n=[BaL_n^{2-2n}]/[Ba^{2+}][L^{2-}]^n$

Ligand	$\log \beta_1$	$\log \beta_2$
SO_4^{2-}	0.66	1.42
$C_2O_4^{2-}$	0.58	2.20

Oxalate System.—The distribution ratio of barium(II) is also decreased by the addition of sodium oxalate to the aqueous phase. Figure 3 gives the decrease in the extraction constant as a function of $\log[C_2O_4^{2-}]$. In these experiments, the analytical concentration of sodium oxalate in the aqueous phase can be regarded as the concentration of oxalate ions, $[C_2O_4^{2-}]$, because the $-\log[H^+]$ value was kept between 6.4 and 6.6 and because the pK_{a_2} value of oxalic acid in 1 M $Na(ClO_4)$ at 25°C is 3.54.[9] It was not possible to obtain a higher oxalate concentration, because the solubility of sodium oxalate in 1 M sodium perchlorate is not large.

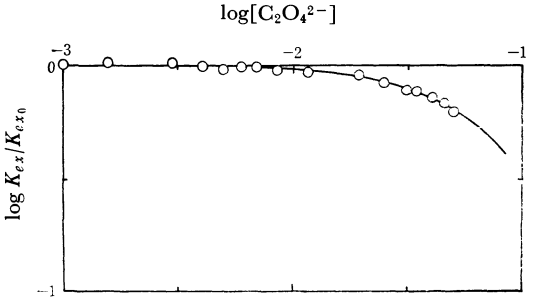

Fig. 3. Decrease in the extraction constant of barium(II) as a function of oxalate ion concentration. The solid curve was calculated by the following equation.
$Y=-\log(1+3.80[C_2O_4^{2-}]+159[C_2O_4^{2-}]^2)$;
$X=\log[C_2O_4^{2-}]$

The plot was found to fit a standard curve, $Y=-\log(1+0.3a+a^2)$, $X=\log a$. This indicates that both BaC_2O_4 and $Ba(C_2O_4)_2^{2-}$ complexes are formed. The stability constants finally determined are given in Table I.

Discussion

The solubility of barium sulfate and oxalate is very small. The previous data on the solubility products in dilute ionic media were around 10^{-10} for barium sulfate and around 10^{-8} for barium oxalate.[1,10]

Money and Davies[11] gave a stability constant for the barium oxalate complex at an infinite dilution at 18°C as $[BaC_2O_4]/[Ba^{2+}][C_2O_4^{2-}]=$ca. $10^{2.31}$, but this data canhot be compared directly with the present results because the concentrations of the electrolytes in the solutions are different. No data seem to have been presented on the stability of barium sulfate complexes.

In the present study, carrier-free barium-140 was always employed as the tracer, and the concentration of barium(II) was calculated to be less than 10^{-12} M if the barium impurity in the solution was neglected. It is difficult to estimate the amount of non-radioactive barium impurities in the system. However, we may conclude that the coprecipitation of the radioactive barium with the non-radioactive barium impurities in the system is negligible, because the recovery of the radioactivity from the two phases was always quantitative and the results in Figs. 2 and 3 are reproducible and reasonable.

The results in the table indicate that the stabilities of the barium complexes with these anions are much smaller than those of lanthanide and actinide complexes.[9,12] This seems to agree with the fact that the solubilities of barium sulfate and oxalate are not very much increased by an excess of these anions in aqueous solutions.

The authors are very grateful to Dr. Yukio Murakami of the Japan Atomic Research Institute for the offer of some materials. They are also grateful to Mr. Satoru Obuchi of the present laboratory for his experimental aid. This research was partly supported by the Matsunaga Science Foundation.

9) T. Sekine, *Acta Chem. Scand.*, **19**, 1476 (1965).

10) W. M. Latimer, "Oxidation Potentials," 2nd ed. Prentice-Hall, Englewood Cliffs (1964).

11) R. W. Money and C. W. Davies, *Trans. Faraday Soc.*, **28**, 609 (1932).

12) T. Sekine, *Acta Chem. Scand.*, **19**, 1469 (1965).

BULLETIN OF THE CHEMICAL SOCIETY OF JAPAN VOL. 39 2145—2152 (1966)

Physical Chemistry of Binary Plastic Crystals. I. The System of Carbon Tetrachloride and *t*-Butyl Iodide*

By Hideaki CHIHARA, Masako OTSURU** and Syûzô SEKI

Department of Chemistry, Faculty of Science, Osaka University, Toyonaka, Osaka

(Received February 18, 1966)

The binary system, carbon tetrachloride-*t*-butyl iodide, was studied by the proton magnetic resonance, the dielectric measurements and the X-ray diffraction. The complete phase diagram, constructed by the differential thermal analysis, shows a solid solution region where carbon tetrachloride is more than 50 mole%. Detailed studies of the solid solution containing 6.6 mole% of *t*-butyl iodide reveals that the solution can be described by the theory of regular solutions; its molecular polarization above the transition temperature obeys the Debye formula giving the dipole moment of *t*-butyl iodide a value of 1.6 debye units. The high-resolution nuclear magnetic resonance experiments with the same phase shows that carbon tetrachloride molecules diffuse in the solid solution with an energy of activation of 6.8 kcal./mole. The transition temperature varies with the composition, and below it the rotational motion of the solute molecules is more hindered. Pure *t*-butyl iodide shows motional narrowing around −150°C in the NMR line shape, above which temperature a reorienting molecular model can account for the magnitude of second moment of the nuclear magnetic resonance absorption.

Plastic crystals[1] are a class of molecular crystals which show enhanced plasticity in a temperature region below the melting point. Except in the case of inert monatomic crystals, they undergo one or more phase transitions accompanied with a large increase in entropy, due primarily to the acquisition of the molecular rotational or orientational degrees of freedom.

Thus, carbon tetrachloride is one of typical plastic crystals, having a phase transition at −47.7°C (225.5°K) with the entropy of transition, 4.86 cal./deg. mole. In its plastic phase between −47.7° and −22.9°C (m. p.), the molecules in solid carbon tetrachloride are in the state of hindered rotation, its potential barrier being estimated to be 2.4 kcal./mole.[2] The crystal structure in this plastic phase is that of face-centered cubic.[3]

If a compound having a permanent dipole moment is dissolved in a matrix of carbon tetrachloride and if they form a plastic solid solution, there will be a possibility of obtaining some information about the crystal field in the matrix compound by dielectric measurements. In the present study, *t*-butyl iodide was chosen as such a solute in the hope that one might get at an anomalous dispersion in a convenient radio-frequency region. The result turned out not to be the case, but instead, the plastic phase was found to be close to an ideal liquid solution and to be described by the theory of regular solutions. Some results obtained by proton magnetic resonance techniques will also be reported.

Similar studies have been described for the systems, CCl_4–$C(CH_3)_4$[4] and CCl_4–$C(CH_3)_3Cl$[5-7].

Experimental

Meterials.—Commercial special grade carbon tetrachloride was distilled after drying over calcium chloride; m. p. −22.9°C. The *t*-butyl iodide prepared by the method of Stone and Schechter[8] was purified through fractional distillation under reduced pressure and further under vacuum over mercury to minimize decomposition: Semi-microanalysis gave C, 26.21%; H, 4.94%; I, 68.63% (calcd. C, 26.10; H, 4.93; I, 68.97 %), a purity of some 99.5%; n_D^{20} 1.4920 (literature value 1.4890) and m. p. −37.0°C. NMR spectrum and gas chromatography detected no impurities. The X-ray powder diffraction spacings taken at −78°C are given in Table I.

Equipments.—The high-resolution NMR spectra were recorded on a Varian A-60 analytical spectrometer combined with an attachment for temperature variation.

The broad-line NMR spectra were obtained with a Robinson-type autodyne oscillator-detector operated at about 20 Mc./s. The temperature of the specimen was

* Presented before the 18th Annual Meeting of the Chemical Society of Japan, Osaka, April, 1965.

** Present address: Shionogi Research Laboratory, Shionogi & Co., Ltd., Fukushima, Osaka.

1) See for example, *J. Phys. Chem. Solids*, **18**, No. 1 (1961).

2) H. Chihara and T. Shinoda, This Bulletin, **37**, 125(1964).

3) B. Post, *Acta Cryst.*, **12**, 349 (1959).

4) E. Chang and E. F. Westrum, Jr., *J. Phys. Chem.*, **69**, 2176 (1965).

5) A. Turkevich and C. P. Smyth, *J. Am. Chem. Soc.*, **62**, 2468 (1940).

6) W. P. Conner and C. P. Smyth, ibid., **63**, 3424 (1941).

7) J. G. Powles and H. S. Gutowsky, *J. Chem. Phys.*, **24**, 1061 (1956).

8) H. Stone and H. Schechter, *J. Org. Chem.*, **15**, 491 (1950).

TABLE I. X-RAY DIFFRACTION SPACINGS OF SOLID *t*-BuI AT −78°C (in Å)

d	*I*	*d*	*I*	*d*	*I*
5.04	w	2.22	s	1.47	f
4.45	s	2.07	m	1.45	f
4.04	f	2.01	f	1.42	f
3.85	f	1.92	w	1.38	w
3.75	w	1.88	m	1.36	f
3.61	s	1.79	w	1.33	f
3.36	w	1.74	m	1.30	f
3.08	m	1.71	f	1.28	f
2.70	s	1.65	w	1.26	f
2.61	m	1.59	f	1.23	w
2.53	f	1.53	f		
2.24	w	1.51	f		

s: strong, m: moderately strong, w: weak, f: faint

determined with a Chromel-P-constantan thermocouple attached at the bottom of the specimen tube. The temperature drifted by about 2°C during a single sweep of magnetic field through resonance.

X-Ray powder diffraction photographs were taken by a camera of 35 mm. in diameter. The sample in a Li glass capillary (0.5 mm. in diameter) was chilled with a cold stream of nitrogen from its top. The temperature of the specimen was held constant to within a few degrees during exposure to nickel-filtered Cu$K\alpha$ radiation, ranging from 2.6 hr. for *t*-butyl iodide to 8—16 hr. for carbon tetrachloride or the mixtures.

The dielectric constant and loss were measured with the same equipments as have been described previously.[9] The sample container (see Fig. 1) consists of coaxial cylinders of Telex glass fitted inside with cylinders of platinum which serve as the measuring electrodes. The air capacitance of the cell is about 21 pF. This was inserted into a hole drilled through a heavy copper block to aid in slow change of the temperature. The specimens were frozen so as not to develop fissures or vapor snakes while freezing. The plastic nature of the crystal allowed its close fitting between the electrodes if maintained some degrees below the melting point. The dielectric constant of pure carbon tetrachloride agreed satisfactorily with the values obtained by Guillien[10] over the range of temperature examined. When the specimen was frozen quickly or was not annealed in the plastic phase, its dielectric constant appeared smaller.

The apparatus of the differential thermal analysis is the same as the one reported earlier.[11]

Results and Discussion

Pure *t*-Butyl Iodide.—The differential thermal analysis showed no solid-state transition between −196°C and the melting point, −37.0°C.

The temperature dependence of the dielectric constant ε' and the loss factor ε'' was measured between 1 kc./s. and 1 Mc/s. showing no discontinuity nor anomalous dispersion. Absolute values of ε' and ε'' were poorly reproducible because the crystal tended to fissure between the electrodes. ε'' increased toward the lower frequency: It gives linear plots against the reciprocal of the frequency, $1/f$, as shown in Fig. 2. The figure indicates that

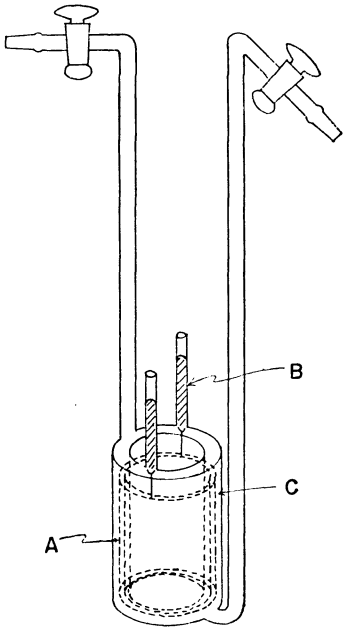

Fig. 1. The dielectric cell.
A's are the cylindrical platinum electrodes, B's are mercury terminals and C is the space for specimen.

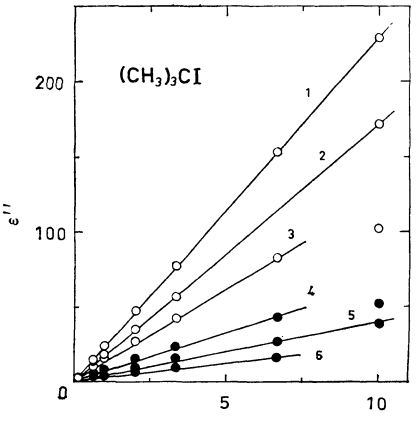

Fig. 2. The dielectric loss factor ε'' of *t*-BuI vs. the reciprocal of the frequency for two different coolings (open and closed circles);
1. −59°C, 2. −67°C, 3. −74°C, 4. −75°C, 5. −81°C, 6. −87°C.

9) H. Chihara, S. Okawa and S. Seki, This Bulletin, **37**, 1373 (1964).
10) R. Guillien, *J. phys. radium*, **1**, 29 (1940).
11) H. Suga, H. Chihara and S. Seki, *J. Chem. Soc. Japan, Pure Chem. Sect.* (*Nippon Kagaku Zasshi*), **82**, 24 (1961).

the real part of the complex conductivity γ' obeys the formula

$$\gamma' = \varepsilon'' f / 1.8 \times 10^{12},$$

suggesting also that the low-frequency loss is due to d. c. conductivity. By fitting the Arrhenius type of equation

$$\gamma' = \gamma_0' \exp(-E/\boldsymbol{R}T),$$

the activation energy E was estimated to be 3.8 to 6.8 kcal./mole, varying from specimen to specimen, probably because it depends on the crystal packing between the electrodes, the size of crystallites, or the extent of dislocations. These values of E are rather small for the activation energy of diffusion through crystal lattice; the charge carriers may be small fragments of *t*-butyl iodide molecules produced by photochemical processes, moving through dislocations.

The proton magnetic resonance line shapes are reproduced in Fig. 3 at two representative temperatures. Figure 4 is a graph of the second moment plotted as a function of the temperature. It is 27.8 gauss^2 at -160°C and decreases to 2.4 gauss^2 at -100°C. Above the melting point, the observed resonance line was as narrow as the inhomogeneity of the magnet. To compare with these figures, theoretical values of the second moments were calculated by the method of Van Vleck.[12] The molecular parameters employed were H–H 1.79 Å, C–H 1.10 Å, and C–C 1.54 Å, the bond angles being assumed all tetrahedral. The contribution of the iodine spins was ignored. The dipolar interaction between three methyl groups was calculated as if the three protons of a methyl group collapsed into the center of the equilateral proton triangle. Table II is the result of such calculations.

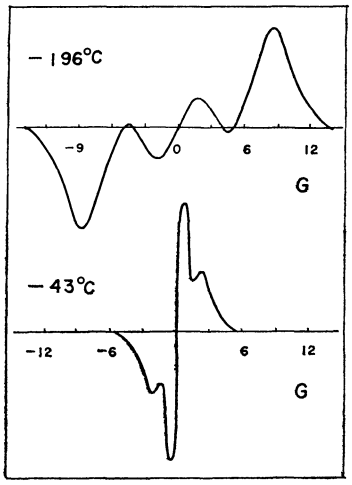

Fig. 3. The proton magnetic resonance (derivative) line shapes of *t*-BuI.

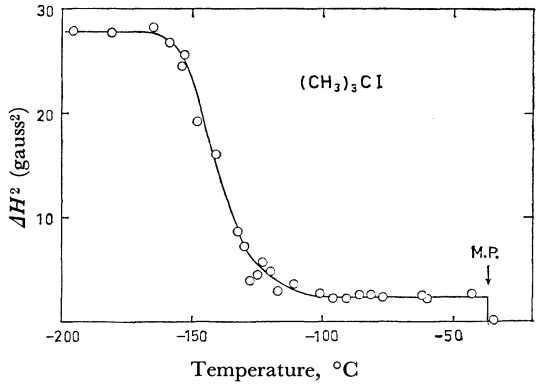

Fig. 4. Temperature dependence of the second moment of the proton magnetic resonance absorption of *t*-BuI.

Table II. Theoretical estimates of the second moments of solid *t*-butyl iodide in gauss^2

	Intra-methyl contribution (A)	Inter-methyl contribution in a molecule (B)	(A)+(B)
Rigid lattice	21.7	3.48	25.2
C_3-Rotation*	5.43	3.48	8.91
C_3'-Rotation*	0.64	0.87	1.51

* C_3-Rotation denotes the rotation of methyl groups around the C–C bonds.
C_3'-Rotation denotes the axial rotation of a whole molecule around the C–I axis.

The comparison between the observed and the theoretical values of the second moment shows that the lattice is rigid at the lowest temperature and undergoes a change through motional narrowing to a state in which are taking place not only the rotation*[1] of the methyl groups around the C–C axes but also the axial rotation of the entire molecule around the C–I axis. This does not contradict with non-existence of phase transition of this solid because a cooperative effect must be involved if a transition is to be seen by thermal measurements. The NMR experiments thus indicate that no bulk diffusion is occurring in solid *t*-butyl iodide.

The Phase Diagram of the System, Carbon Tetrachloride-*t*-Butyl Iodide.—The phase diagram of the binary system was constructed by means of a series of differential thermal analysis (DTA) runs at different compositions. The heating rate was about 0.7—1.0°C/min. The phase diagram as well as typical DTA curves are shown in Figs. 5A and 5B in which capital letters indicate points and lower-case letters indicate areas on the phase diagram. Where the concentration was near the eutectic point C, the endothermic anomalies in the DTA curves were poorly resolved and therefore their temperatures are not very precise. While

*[1] No discrimination of the words, rotation or reorientation, is made in this paper.[2]

12) J. H. Van Vleck, *Phys. Rev.*, **74**, 1168 (1948).

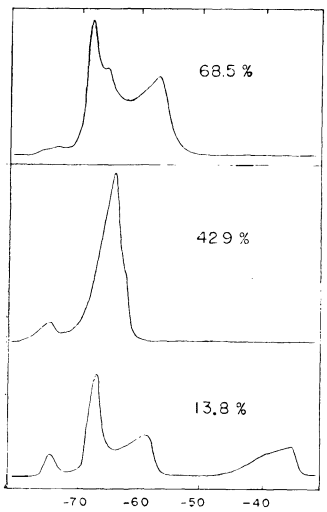

(A)

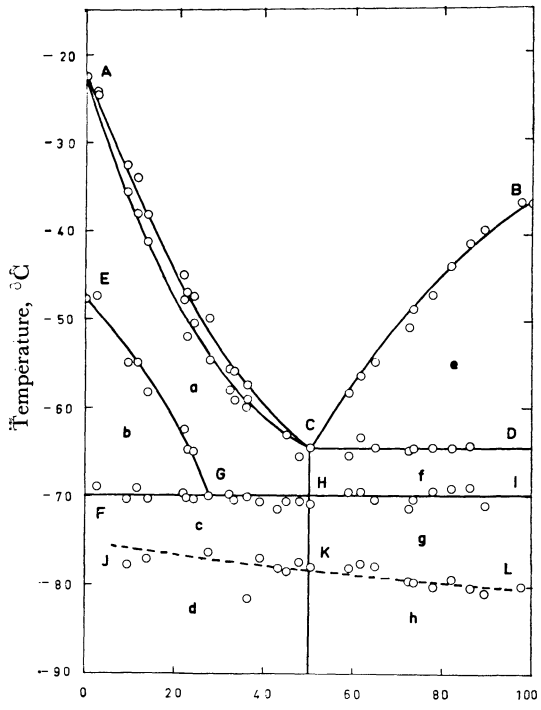

(B)

Fig. 5. Some typical DTA curves (A) and the phase diagram (B) of the system, CCl_4 - *t*-BuI.

the state of aggregation in each area will be discussed in later Sections, it suffices here to mention that within a limited range of the concentration (carbon tetrachloride richer than about 50 mole%), the system forms a solid solution, and also that a phase transition corresponding to that of pure carbon tetrachloride may be seen at a lower temperature. Therefore in such a concentration range, it is expected that the solute, *t*-butyl iodide, behaves as a built-in probe to study the molecular motions in the binary solid.

The areas on the phase diagram will now be briefly characterized. The area a corresponds to the solid solution. The point E is the transition temperature of pure carbon tetrachloride and the line EG shows its variation with the composition. In the area b, pure carbon tetrachloride coexists with the solid solution having varying composition. At the line FI, phase separation into pure components occurs. The origin of the thermal anomaly* corresponding to the line JL is not apparent but it does not appear in either of the pure components and its magnitude on the DTA curves is not perfectly reproducible. While the DTA curves in Fig. 5A may be taken as indicating that the anomaly is more prominent nearer the point J, there is no such definite tendency. Since complete phase separation occurs below −70°C, this anomaly must be associated with some effect of the interface or boundary of phases. The point C is a kind of eutectic point and the system is invariant here. The area, f, therefore, represents the solid solution of the composition C and pure *t*-butyl iodide.

A few words must be added here about the possibility of the existence of a phase transition in solid *t*-butyl iodide. Baker and Smyth[13] reported the existence of a phase change at −75°C through their measurements of the dielectric constant. However, in the present study, no anomaly was observed at this temperature in the differential thermal analysis, the nuclear magnetic resonance, or the X-ray diffraction. Our measurements of

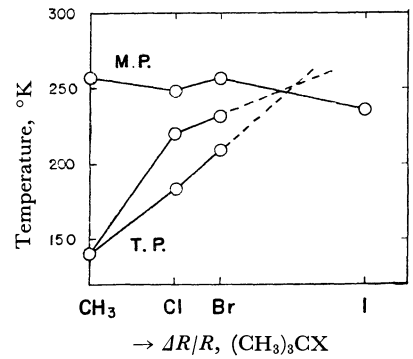

Fig. 6. Correlations between the temperatures of phase changes and the dissymmetry of molecules of $(CH_3)_3CX$.

* The shape of the thermal anomaly is not a fixed one; it is sometimes a sharp peak and sometimes a broad maximum or a lambda-type anomaly. The temperatures at which these anomalies occur also show considerable scatter on either side of the line JL.

13) W. O. Baker and C. P. Smyth, *J. Am. Chem. Soc.*, **61**, 2798 (1936).

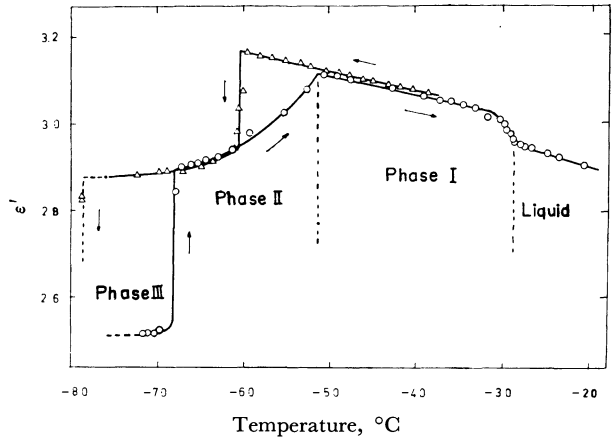

Fig. 7. Temperature dependence of the dielectric constant of a solid solution containing 6.6 mole % *t*-BuI at 15 kc./s.

the dielectric constant were not extended to a low enough temperature to show this because the contact of the specimen with the electrodes became poorer as we went down to lower temperatures. A comparison of the *t*-butyl compounds yields, however, an interesting diagram as shown in Fig. 6. Here, the melting point and the transition point are plotted as a function of the asymmetry parameter η of the molecules. The η is defined by

$$\eta = (R - R')/R = \Delta R/R$$

where R is the radius of the molecular sphere and R' is the distance from the central carbon atom to the periphery of the molecular sphere. Figure 6 suggests that *t*-butyl iodide would not have a transition in the solid state. A similar conclusion may be drawn from the type of analysis Miller and Smyth[14] developed for tetrahalomethanes.

A Solid Solution Containing 6.6—6.8 mole% of *t*-Butyl Iodide.—The solid solution containing 6.6—6.8 mole% of *t*-butyl iodide was chosen for detailed study because the peaks in the DTA curve are well resolved at such a concentration.

The precision of the equipments for the dielectric measurements did not permit us to work with a lower concentration of *t*-butyl iodide. The regions a, b, and c in the phase diagram (Fig. 5) will be referred to as the phases I, II, and III respectively.

Phase I.—The dielectric constant ε' at 15 kc./s. of the solid solution containing 6.6 mole% *t*-butyl iodide is shown in Fig. 7 through different phases. A good reproducibility of the ε' values indicates that close filling of the measuring cell with specimen has been attained. No dielectric dispersion and absorption were observed in the frequency range examined, therefore the results presented in Fig. 7 may be considered to represent the static dielectric constant.

We will first discuss the behavior of the system in Phase I. The negative slope in Phase I region in Fig. 7 is the same as in liquid solution phase. This is analogous to the case of many plastic crystals[1] in which the molecular rotational (or reorientational) degrees of freedom are fully excited, opposing the effect of electric field that tends to orient the molecular dipoles in its direction and decreasing the molecular polarization. There is small but definite change in ε' in going from Phase I to the liquid over a narrow temperature region between the solidus and the liquidus lines of the phase diagram, in accordance with the change in the density upon melting. The rotational motion of the *t*-butyl iodide molecules in the carbon tetrachloride matrix is not perfectly free in Phase I but must see a finite potential energy barrier hindering general rotation.[2] The X-ray diffraction pattern of Phase I was essentially the same as that of the Phase I of solid carbon tetrachloride which is known to be a plastic phase. This means that, so far as the orientational degrees of freedom are concerned, Phase I may be approximately regarded as a liquid solu totion; it is, therefore, of interest to examine what extent it may be.

The interactions between the solute molecules being ignored, the molecular polarization P_{12} of a dilute solution of polar molecules (suffix 1) in a non-polar solvent (suffix 2) is given by

$$P_{12} = \frac{\varepsilon - 1}{\varepsilon + 2} \cdot \frac{1}{d}(c_1M_1 + c_2M_2)$$

$$= \frac{4\pi N}{3}(c_1\alpha_1 + c_2\alpha_2) + \frac{4\pi Nc_2}{9kT} \cdot \mu^2$$

where c_1 and c_2 are mole fractions, M_1 and M_2 are the molecular weights, α_1 and α_2 are the optical polarizabilities, d is the density of the solution, and μ is the dipole moment of the solute molecule. Figure 8 shows a graph of the P_{12}

14) R. C. Miller and C. P. Smyth, ibid., **79**, 20 (1957).

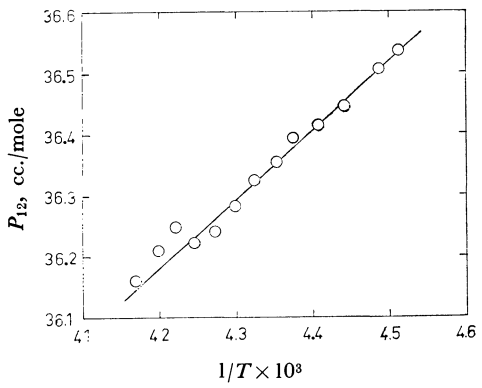

Fig. 8.

values plotted against the reciprocal of the temperature. In calculating P_{12} the density of the solution was assumed to be equal to that of pure carbon tetrachloride at corresponding temperature and evaluated from ε' values for pure carbon tetrachloride under the assumption of the temperature-independence of the molecular polarization of pure carbon tetrachloride. The plot is a good straight line, yielding a value of $\mu = 1.6 \times 10^{-18}$ e.s.u. for the dipole moment of *t*-butyl iodide. There are no literature values to be compared with this dipole moment but the C–I bond moment has been estimated to be about 1.2×10^{-18} e.s.u. The difference is small and it is hard to decide if the difference is a real one.

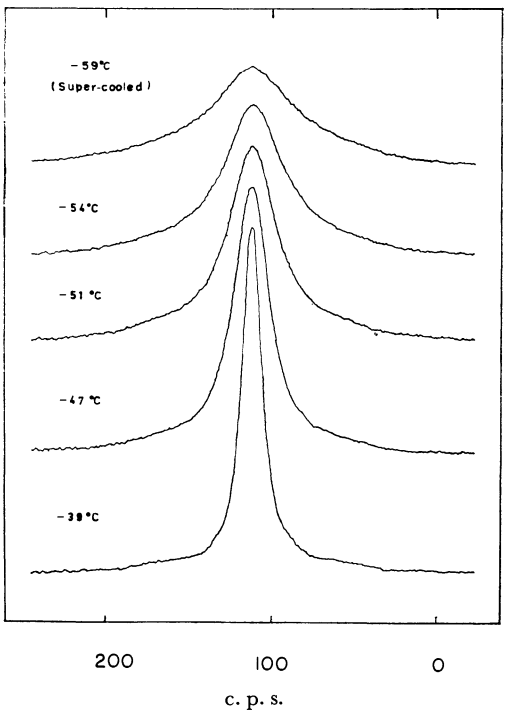

Fig. 9. High-resolution proton NMR of *t*-BuI in Phase I of the solid solution.

Having seen that the system may be regarded as a liquid solution with regard to molecular orientation, an attempt was made to study the proton magnetic resonance in the hope that we might see the effect of self-diffusion in Phase I.[15] Figure 9 shows the temperature dependence of the high-resolution NMR line shape for the sample containing 6.8 mole% *t*-butyl iodide. The experiment started from −59.5°C (with the supercooled Phase I) upwards. The line-width is so narrow as to indicate that the reorientational motion of *t*-butyl iodide molecules is fully excited; its variation with the temperature must then be due to diffusion of molecules in the solid solution. If one assumes, as is done frequently, that the line-width is determined by the spin-spin interaction time T_2, the half-peak width is inversely proportional to T_2. The time T_2 is now related to the diffusion coefficient D through Torry's equation[16]

$$T_2 = \frac{1}{c} \cdot b^4 D$$

By virtue of the relations[17]

$$D = b^2 \nu_D \cdot \exp(-\Delta G_d / \boldsymbol{R}T)$$
$$= D_0 \exp(-\Delta H_d / \boldsymbol{R}T)$$

we have

$$cT_2/b^4 = D_0 \exp(-\Delta H_d / \boldsymbol{R}T)$$

where ΔG_d is the Gibbs energy of activation, ν_D is the Debye cut-off frequency of the solid, c is a material constant independent of the temperature, b is the lattice parameter of the face-centered cubic lattice to which the equation is applicable. Because of the narrow temperature range studied, the b may be taken as a constant. The linear dependence of log T_2 on $1/T$ in Fig. 10 gives a value of 6.8 kcal./mole for ΔH_d of diffusion.

The origin of the residual line-width (Fig. 9)

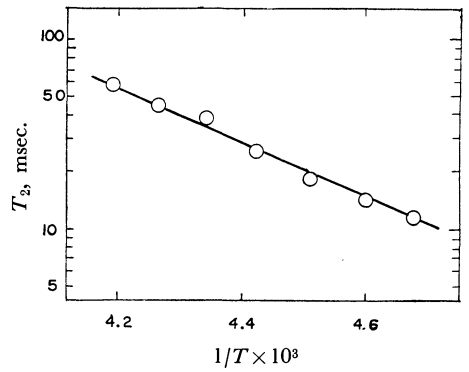

Fig. 10.

15) See for example, H. Suga and S. Seki, This Bulletin, **35**, 1905 (1962).
16) Quoted by H. A. Resing, *J. Chem. Phys.*, **37**, 2175 (1962).
17) C. Zener, *J. Appl. Phys.*, **22**, 372 (1951).

must now be investigated more closely. The state of distribution of *t*-butyl iodide in the carbon tetrachloride matrix is not at once obvious: The solute molecules possibly form small aggregates by dipole-dipole forces in order to relax the local distortion of the matrix lattice and thus to minimize the total strain energy. Because no bulk seggregation was observed in Phase I, there must be an equilibrium set of concentrations for single solute molecules, pairs of molecules, etc. Judging from the case of vacancy pairs in inert gas solid,[18] the concentration of the pairs and the higher multiples of molecules will be less than a few tenth of one per cent. Therefore, it will be safe to assume that most of the solute is distributed uniformly throughout the solid solution. A uniform distribution means that an average *t*-butyl iodide molecule is separated from other nearest *t*-butyl iodide molecules by about 300 Å and that each *t*-butyl iodide molecule sees only carbon tetrachloride molecules at its neighbors. The proton-chlorine interactions thus contribute predominantly to the residual line-width; the second moment contributed by this type of interaction is greater than that by the intermolecular proton-proton interaction by a factor of 10^2, by a rough computation. Another order-of-magnitude estimate can be made with regard to the line-width itself. The maximum local magnetic field which a proton sees is about 80 c. p. s. due to chlorine nuclei, whereas the field due to other protons amounts only to 20 c.p.s., assuming that the nuclei are bound rigidly at the f. c. c. lattice points. The observed line-width ranges between 15 and 60 c. p. s.

These arguments suggest that what is being observed is the narrowing of proton resonance caused by the diffusion of the carbon tetrachloride molecules. Therefore, the observed heat of activation, 6.8 kcal./mole, is that for diffusion of carbon tetrachloride relative to *t*-butyl iodide molecules. Here the *t*-butyl iodide molecules behave like a built-in probe to study the motion of the non-magnetic or weakly magnetic molecules (carbon tetrachloride).

There are no other experimental or theoretical values available for comparison with this value of ΔH_d, but it seems to be a reasonable value in view of the low value of the rotational potential barrier height, 2.4 kcal./mole.[2] In the case of metals, Nachtrieb[19] demonstrated a proportionality relation between ΔH_d and the heat of fusion ΔH_f with an empirical constant of proportion:

$$\Delta H_d = 16.5\ \Delta H_f$$

This relation gives ΔH_d a value of 9.9 kcal./mole for carbon tetrachloride. The reason for the observed value to be smaller is not immediately apparent; the small observed value may show failure of the Nachtrieb's relation in the case of molecular crystals or it may be an indication of local distortion of the carbon tetrachloride host lattice in the vicinity of the solute molecules.

The direct determinations of the relaxation times T_1 and T_2 at this and still lower concentrations of *t*-butyl iodide, and also similar investigations using other *t*-butyl halides will be helpful in a more quantitative understanding of the molecular motion. Studies along these lines are being undertaken.

Phases II and III.—The Phase II of the binary solid is an inhomogeneous phase because pure carbond tetrachloride (of the low-temperature modification) keeps segregating upon cooling below the transition temperature. This is seen by the X-ray diffraction pattern which is a super-impose of the low-temperature pattern of carbon tetrachloride and the pattern of the solid solution.

The dielectric constant ε' is still large in Phase II, although its temperature coefficient is positive in contrast to the case of Phase I, showing that the molecular reorientation tends to be restricted progressively upon cooling. The reason for this is two-fold: One is the effect of smaller kinetic energy at lower temperatures and the other is the increase in the solute concentration in the solid solution part. In conformity with such view, there is a Maxwell-Wagner type of absorption in ε'' at −68°C at low frequency side of Fig. 11. An anomalous absorption extends towards higher frequencies, showing a possibility of finding a maximum in ε'' between 10^8 and 10^9 c. p. s. The reorientational motion of *t*-butyl iodide in Phase II is apparently more heavily restricted than in Phase I but is easier than in pure *t*-butyl iodide in which the dispersion is considered to occur around 5×10^4 c.p.s.

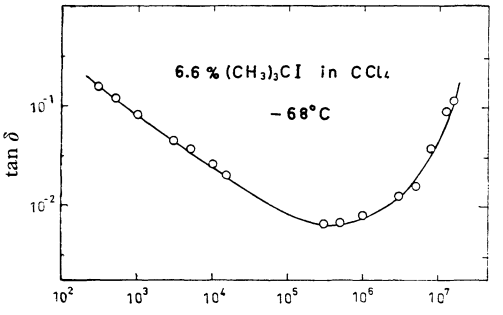

Fig. 11.

In Phase III the two components are completely separated (by X-ray diffraction). The dielectric constant changes discontinuously at the eutectic point (−70°C). The value of ε' (2.5) in this

18) K. Iwamura, *Busseiron Kenkyu*, [2] **9**, 311 (1961); see also O. G. Peterson, D. N. Batchelder and R. O. Simmons, *Phil. Mag.*, **12**, 1193 (1965).

19) N. H. Nachtrieb and G. S. Handler, *Acta Met.*, **2**, 797 (1954). N. H. Nachtrieb, J. A. Weil, E. Catalano and A. W. Lawson, *J. Chem. Phys.*, **20**, 1189 (1952).

phase is comparable to the high frequency limit (2.6) for pure *t*-butyl iodide and the low temperature limit (2.4) for pure carbon tetrachloride.

Comparison of the Systems CCl_4 - *t*-BuX where X is CH_3, Cl or I.—The published phase diagrams for the systems carbon tetrachloride - $C(CH_3)_4$[4] and carbon tetrachloride - *t*-butyl chloride[7] differ in many respects from the diagram given in Fig. 5 of the present paper. Only portion that may be compared is where the transition point of carbon tetrachloride varies with the concentration of the second component. This portion is

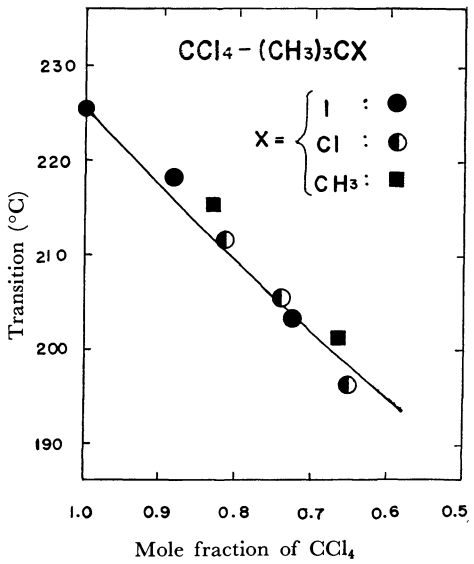

Fig. 12. Transition point lowering of CCl_4. The solid line corresponds to a theoretical prediction for a regular solution case with $w=350$ cal./mol.

depicted in Fig. 12. The solid line in the figure gives what one would expect if it is assumed that the plastic solid phase (Phase I) forms a regular solution; i. e. the equation of the solid line in the figure is given by

$$RT_0 \ln x + w(1-x)^2 = \Delta H\left(1-\frac{T_0}{T}\right)$$

and

$$w = 350 \text{ cal./mol.}$$

where x is the mole fraction of carbon tetrachloride, T_0 is the transition temperature of pure carbon tetrachloride, ΔH is its heat of transition, and T is the observed transition temperature. The parameter w is related to the heat of mixing of the two components. The deviation of the observed points from the solid line is small, which fact shows that the plastic crystals are good solid solvents and they are 'liquids' at least with regard to the molecular orientation.[20] Similar finding has also been obtained for the solid system, CO-N_2.[21]

The authors are grateful to Professor Masazumi Nakagawa and Mrs. Noriko Sorai of Osaka University for their kind advice and help in the synthesis of the *t*-butyl iodide. This research was supported by the Government Special Equipment Funds which were acknowledged with gratitude.

Dedication

This paper is dedicated to Professor Masao Kotani of Osaka University in celebration of his sixtieth birthday, who has a world-wide reputation for his scientific activity in so many different branches of physics and chemistry.

20) J. A. Pople and F. E. Karasz, *J. Phys. Chem. Solids*, **18**, 28 (1961).
21) E. K. Gill and J. A. Morrison, unpublished work.

BULLETIN OF THE CHEMICAL SOCIETY OF JAPAN VOL. 39 2153—2156 (1966)

Effect of Temperature on the Molecular Structure of Iodine Observed by Gas Electron Diffraction

By Takeshi UKAJI* and Kozo KUCHITSU

Department of Chemistry, Faculty of Science, The University of Tokyo, Hongo, Tokyo

(Received March 18, 1966)

The bond distance and its mean square amplitude for the iodine molecule were measured at 80°C, 300°C, and 500°C by gas electron diffraction. The observed temperature dependences of the above parameters were in good agreement with those calculated on the basis of an anharmonic-oscillator model and experimental spectroscopic constants.

Recent development in the technique of gas electron diffraction has made it possible to measure small changes in internuclear distances and mean square amplitudes with temperature. As first demonstrated for phosphorus(III) chloride by Hedberg and Iwasaki,[1] studies of this sort can be used effectively for investigating the effect of intramolecular vibrations on structure and for assessing the accuracy of the diffraction experiments made at high temperatures. The present study has been carried out as a primary step toward this goal.

Iodine is one of the most suitable molecules for the examination of the temperature effect because of its low vibrational frequency (214 cm^{-1}) and its chemical stability to several hundred degrees. Therefore, the bond distance and its mean square amplitude observed at different temperatures have been compared with those calculated from spectroscopic data. The results of the least-squares analysis have been tested by using theoretical molecular intensity function based on the probability distribution function of a one-dimensional anharmonic oscillator expanded to the fourth order.

Experimental and Analysis

Electron diffraction photographs were taken at 80°C, 300°C, and 500°C by the use of a diffraction unit with a high temperature nozzle, which has been reported elsewhere.[2] The accelerating voltage was 41.04 kV. Five plates for each temperature were selected for analysis. The temperature was measured by a thermocouple attached to the nozzle assembly. In order to measure the temperature of the vapor at the nozzle tip, the thermocouple was calibrated by the following procedure. Fine pieces of crystals of known melting points, such as 2-aminodiphenylamine [80°C], anthraquinone [286°C], and zinc iodide [445°C], were placed on top of the nozzle capillary, through which the iodine vapor was emitted into the diffraction chamber while the temperature was raised gradually. Melting of a fine edge of the crystal was observed under a microscope. It was found that the temperature of the vapor measured by the above procedure agreed with that of the nozzle indicated by the thermocouple within a few degrees.

Photographic densities were measured by a self-recording microphotometer with spinning of the plate around the center of the halos at about 600 r. p. m. The microphotometer charts were analyzed by the method described in previous papers.[3]

The bond distance r_a, the mean amplitude l_m, the phase parameter κ, and the index of resolution i were obtained from a least-squares analysis.[3] The experimental reduced molecular intensity was fitted to the following theoretical equation:

$$M(s) = iAC \exp(-l_m^2 s^2/2) \sin[s(r_a - \kappa s^2)]/sr_a \quad (1)$$

where A is a normalization constant, nearly equal to unity, which appears in the probability distribution function described below, and C is a known function of s related to the elastic and inelastic scattering factors of the iodine molecule. The mean internuclear distance r_g was calculated from the experimental r_a distance by

$$r_g = r_a + l_m^2/r_a \quad (2)$$

The probability distribution function for a one-dimensional anharmonic oscillator at the absolute zero temperature has been given by Kuchitsu and Bartell.[4] This function has recently

* Permanent address: Ikutoku Polytechnic Institute, Atsugi, Kanagawa.

1) K. Hedberg and M. Iwasaki, *J. Chem. Phys.*, **36**, 589 (1962).

2) Y. Morino, T. Ukaji and T. Ito, This Bulletin, **39**, 64 (1966).

3) Y. Morino, K. Kuchitsu, T. Iijima and Y. Murata, *J. Chem. Soc. Japan, Pure Chem. Sect.* (*Nippon Kagaku Zasshi*), **83**, 803 (1962); Y. Murata, T. Ito and K. Kuchitsu, *Bussei*, **5**, 91 (1964). Y. Morino, K. Kuchitsu and Y. Murata, *Acta Cryst.*, **18**, 549 (1965).

4) K. Kuchitsu and L. S. Bartell, *J. Chem. Phys.*, **35**, 1945 (1961).

been extended in order that the equation may be valid for any nonzero temperature[5] by using a harmonic mean amplitude l_h^2 in place of the corresponding zero-point amplitude l_a^2 defined in Ref. 4,

$$P(x) = A(2\pi l_h^2)^{-1/2}(1+\sum_{n=1}^{\infty} c_n x^n)\exp(-x^2/2l_h^2) \quad (3)$$

where $x = r - r_e - \delta r$ (4)

$$l_h^2 = l_a^2(1+\chi)/(1-\chi) \quad (5)$$

$$l_a^2 = \hbar/8\pi^2\mu c\omega_e \quad (6)$$

and $\chi = \exp(-hc\omega_e/kT)$ (7)

The coefficients c_n in Eq. 3 can be calculated by a second-order perturbation method on the basis of a fourth-order potential function.[5,6] Numerical values of c_n for iodine, listed in Table I, were obtained by using the experimental values of ω_e, α_e, and x_e determined by ultraviolet spectroscopy.[7] The correction for the centrifugal distortion, δr, is equal to $kT/2\pi^2\mu c^2\omega_e^2 r_e$.

TABLE I. VALUES OF c_n (in Å^{-n} units)

c_n	80°C	300°C	500°C
c_0	0.997	0.996	0.995
c_1	0.256	0.105	0.059
c_2	−0.324	−0.163	−0.097
c_3	2.227×10^2	1.531×10^2	1.171×10^2
c_4	-8.828×10^2	-1.042×10^2	-0.900×10^2
c_5	0	0	0
c_6	2.480×10^4	1.172×10^4	0.686×10^4

The reduced molecular intensity of scattered electrons,

$$M(s) = C\int_{-\infty}^{\infty} P(x)dx[\sin s(r_e+\delta r+x)]/s(r_e+\delta r+x) \quad (8)$$

can be written in terms of c_n as

$$M(s) = AC(\sigma_1^2+\sigma_2^2)^{1/2}\exp(-l_h^2s^2/2)\sin[s(r_a+\phi(s))]/sr_e \quad (9)$$

where σ_1 and σ_2 are infinite polynomial functions of c_n given by

$$\sigma_1 = \sum_{n=0}^{\infty}(-1)^n\varepsilon_{2n+1}(l_h^2s)^{2n+1} \quad (10)$$

$$\sigma_2 = \sum_{n=0}^{\infty}(-1)^n\varepsilon_{2n}(l_h^2s)^{2n} \quad (11)$$

$$\varepsilon_n = \sum_{m=0}^{\infty}[(n+2m)!/2^m n!m!]d_{n+2m}l_h^{2m} \quad (12)$$

$$d_n = c_n - d_{n-1}/r_e \quad (13)$$

5) K. Kuchitsu This Bulletin, to be published.
6) A. Reitan, *Det Kgl. Norske Videnskabers Selskabs Skrifter* (1958), NR 2.
7) R. D. Verma, *J. Chem. Phys.*, **32**, 738 (1960).

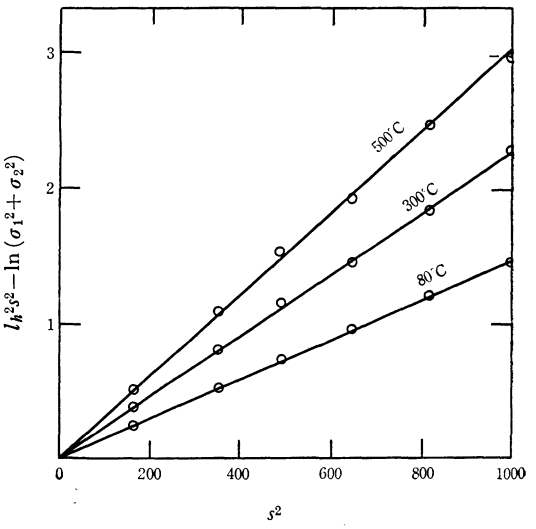

Fig. 1. Plots of $l_h^2s^2-\ln(\sigma_1^2+\sigma_2^2)$ vs s^2; calculated values are shown in open circles.

and $d_0=1$. The present calculation for iodine indicates the following features of Eq. 9. First, each polynomial function ε_n converges so rapidly that the summation of the first few terms of the series is sufficient for the calculation of $M(s)$. Second, the term $(\sigma_1^2+\sigma_2^2)^{1/2}\exp(-l_h^2s^2/2)$ can be substituted for nearly exactly by $\exp(-l_m^2s^2/2)$ with a parameter l_m taken as constant. The effective mean amplitude l_m can thus be given by

$$l_m \approx [l_h^2 - s^{-2}\ln(\sigma_1^2+\sigma_2^2)]^{1/2} \quad (14)$$

The plots of $l_h^2s^2-\ln(\sigma_1^2+\sigma_2^2)$ against s^2, shown in Fig. 1, can be approximated by straight lines for the temperature range studied. Third, the phase function $\phi(s)$ can be approximated by a quadratic function of s,

$$\phi(s) = (1/s)\arctan(\sigma_1/\sigma_2) - r_a = -\kappa s^2 + \cdots \quad (15)$$

The constant phase parameter κ can further be represented by[5]

$$\kappa \approx (1/6)a_3 l_h^4[1+8\chi/(1+\chi)^2] \quad (16)$$

in terms of a cubic anharmonic parameter a_3 of the potential function,[8]

$$V(x) = (1/2)f(x^2 - a_3x^3 + \cdots) \quad (17)$$

and the Boltzmann factor χ for temperature T. The plots of $\phi(s)$ at 80°C, 300°C, and 500°C against s^2 are shown in Fig. 2; they are found to be linear, except for a slight deviation found in the 500°C curve beyond 25 in the s-value. The values of κ predicted by Eq. 16 are practically equal to those obtained from the slopes of the $\phi(s)$ vs. s^2 curves shown in Fig. 2. It has thus been shown that Eq. 1 is a good approximation

8) K. Kuchitsu and Y. Morino, This Bulletin, **38**, 805 (1965).

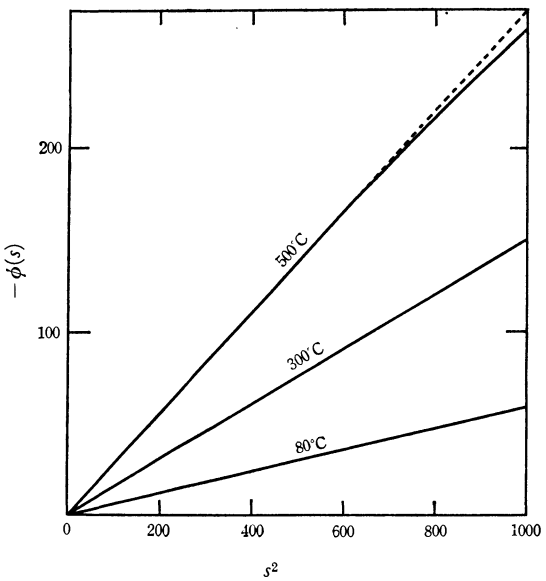

Fig. 2. Curves of $-\phi(s)$ (10^{-4} Å) of Eq. 9 plotted against s^2 for 80°C, 300°C and 500°C.

of Eq. 9 for iodine even at a temperature as high as 500°C.

Results and Discussion

The experimental r_g values derived from the least-squares analysis (exp) are compared in Table II with the corresponding values (calc) calculated by[5]

$$r_g = r_e + [(\varepsilon_0 + \varepsilon_1 r_e + 2\varepsilon_2 l_h^2)/(\varepsilon_0 r_e + \varepsilon_1 l_h^2)]l_h^2 \quad (18)$$

The values of l_m (calc) in Table II are determined from the slopes of the curves shown in Fig. 1, while that of κ(calc) in the same table are calculated by Eq. 15.

Table II. Comparison of the observed structural parameters with theoretical values

	80°C	300°C	500°C
r_g(calc)	2.6756 Å	2.6808 Å	2.6855 Å
r_g(exp)[a]	2.672_3 $\pm 0.003_4$	2.679_0 $\pm 0.001_8$	2.687_2 $\pm 0.002_3$
l_m(calc)	0.0551 Å	0.0691 Å	0.0796 Å
l_m(exp)	0.061_5 $\pm 0.005_2$	0.070_5 $\pm 0.004_3$	0.077_1 $\pm 0.005_1$
κ(calc)	59 10^{-7}Å^3	152 10^{-7}Å^3	275 10^{-7}Å^3
κ(exp)	39±84	100±112	130±102
i(exp)	0.986 ±0.051	1.003 ±0.093	0.924 ±0.105

a) Experimental errors represent the estimated limit of systematic errors plus 2.5 times the standard error obtained from the least-squares analysis. See Ref. 3.

A comparison of the observed molecular intensity (80°C) with the corresponding calculated intensity based on the optimized set of the parameters is illustrated in Fig. 3.

The least-squares fit to the observed molecular intesity is based on Eq. 1 with the structural parameters r_a, l_m, κ, and i. Since this procedure depends on the approximations stated above, it was thought desirable to examine the validity of this procedure. Iodine is a suitable molecule for this test, because the molecule is simple and its molecular parameters necessary for the calculation of the molecular intensity are precisely known.

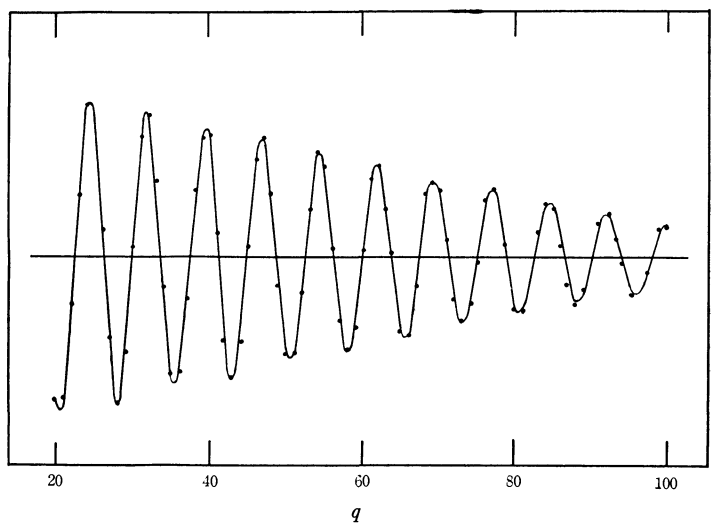

Fig. 3. Comparison of the observed and calculated molecular intensities plotted against $q=10s/\pi$. The solid line shows the experimental molecular intensity curve. The dots are the best-fit molecular intensities obtained from the least-squares analysis.

TABLE III. RESULTS OF THE LEAST-SQUARES ANALYSIS OF THE THEORETICAL $M(s)$ FUNCTION

	80°C	300°C	500°C
r_a(calc)	2.6745 Å	2.6789 Å	2.6830 Å
r_a(LS)	2.6745 ±0.0001	2.6789 ±0.0001	2.6828 ±0.0002
l_e(calc)	0.0562 Å	0.0713 Å	0.0835 Å
l_m(calc)	0.0551	0.0691	0.0796
l_m(LS)	0.0556 ±0.0001	0.0692 ±0.0001	0.0795 ±0.0002
k(calc)	59 10^{-7}Å^3	152 10^{-7}Å^3	275 10^{-7}Å^3
κ(approx)	60	153	260
κ(LS)	60±2	157±4	282±8

r_a(calc), l_e(calc): Average values based on the probability function given in Eq. 3.
l_m(calc): Effective amplitudes estimated from Eq. 14.
κ(approx): Calculated by Eq. 16.
(LS): Outputs of the least-sqares analyses of the theoretical $M(s)$ function given by Eq. 9.

Accordingly, the molecular intensity was calculated by Eq. 9 for integral q values ($q=10s/\pi$) in the region where the experimental data are present, and a least-squares fit was made to those calculated values as if they were experimental data. The output structural parameters thus obtained are compared in Table III with the corresponding rigorous values derived directly from the original equations 14, 15, and 18. The agreement indicates that in this case the present method of least-squares analysis should result in nearly exact estimates for the effective parameter values if it is applied to a perfect set of experimental data.

The experimental bond distance r_g agrees with the calculated values to within 0.1% for the three temperatures. The agreement of the experimental and calculated mean amplitudes is also satisfactory, except for a slight discrepancy in the value for 80°C. The observed values of the phase parameter κ for 80°C and 300°C are comparable with the theoretical counterparts within large experimental errors, while the discrepancy in the value at 500°C is even larger, probably because a systematic error is involved in the experimental molecular intensity for s beyond 25. No evidence was observed in the present study for the s-independent phase shift reported by Karle.[9]

The above comparison shows that the temperature effects on r_g and l_m as observed by the present experiment are for the most part in agreement with those expected by theory. Further efforts are being made to reduce experimental standard errors and to make similar high-temperature measurements on the structural parameters of other molecules.

The authors are indebted to Professor Yonezo Morino for his helpful advice. Their thanks are also due to Dr. Hideo Inuzuka of the Central Research Laboratory, Toshiba Electric Co. for his help in the construction of the high-temperature nozzle, and to the Ministry of Education for the financial support.

9) I. L. Karle, *J. Chem. Phys.*, **23**, 1739 (1955); A. Almenningen, O. Bastiansen, L. Fernholt and M. Traetteberg, ibid., **32**, 616 (1960); I. L. Karle, ibid., **32**, 617 (1960).

BULLETIN OF THE CHEMICAL SOCIETY OF JAPAN VOL. 39 2157—2160 (1966)

Dielectric Relaxation and Molecular Structure. II. Notes on Analysing Dielectric Data of Dilute Solutions

By Keniti HIGASI

Research Institute of Applied Electricity, Hokkaido University, Sapporo

(Received March 25, 1966)

Dielectric data from dilute solution studies consist of two slopes, a' and a'', as defined by $\varepsilon'=\varepsilon_1'+a'c_2$ and $\varepsilon''=a''c_2$. In this article it is shown that the Debye equations for dilute solutions can be described by the use of a' and a''. These equations are obtained by replacing dielectric constant and loss, ε' and ε'' in Debye's equations for polar liquids by a' and a''. As applications of these new equations based on a' and a'' following topics are discussed: Symth's a', a'' plot in the complex plane; Scaife's method of polarizability plot; the familiar loss tangent method originated by Debye for obtaining the relaxation time in solution; and Gopola Krishna's new method for the same purpose.

To avoid the much disputed ambiguity[1] concerning the internal field correction, the dielectric relaxation time of a polar molecule is preferrably measured in dilute solutions of a non-polar solvent. However, the theoretical basis of the dilute solution method has not been well established. For instance, Smyth and his co-workers[2] in Princeton obtain two slopes, a' and a'', for dilute solutions of a polar substance in a non-polar solvent and make a plot of a' and a'' in the complex plane instead of the ε' and ε'' plot for the pure liquid. This procedure was justified graphically, that is, by plotting the dielectric constants and losses of solutions in the complex plane they obtained semi-circles which differed in size according to the concentration of the solute but had exactly the same shape with the semi-circle obtained by the a' and a'' plot. This proof is suggestive but may be better replaced by a mathematical expression in order to have a wider application of the a', a'' plot.

Thirty years ago Debye[3] devised a method of evaluating the relaxation time from the $\tan\vartheta$ values of dilute solutions. A number of researchers[4] have used the latter method since; however, it has not been made clear whether there is any correlation between the two methods, i. e., between the loss tangent method of Debye and the slope method by Smyth.

In this short article it is shown that by the use of two slopes, a' and a'', one can describe the equations of Debye for dielectric relaxation, and that the Smyth procedure of the a' and a'' plot can be examined from this result. Furthermore, the loss tangent method originated by Debye and also the new method proposed by Gopola Krishna[5] can be derived from the equations based on two slopes; and Scaife's method of the polarizability plot[6] will become equivalent to the dielectric constant plot for dilute solution if the two slopes are used in the analysis of dielectric data.

General Theory

With the use of complex dielectric constant, $\varepsilon^*=\varepsilon'-i\varepsilon''$, the complex polarizability $p(\omega)$ is defined by*

$$p(\omega) = p' - ip'' = \frac{\varepsilon^*-1}{\varepsilon^*+2} \tag{1}$$

Consider a dielectric system consisting of dilute solution of a polar substance in a non-polar solvent. If this system is provided with a single relaxation time τ which arises from the polar solute molecules, the dependence of $p(\omega)$ upon the angular frequency ω will be described by

$$p(\omega) = p(\infty) + \frac{p(0)-p(\infty)}{1+i\omega\tau} \tag{2}$$

where

1) C. P. Smyth, "Dielectric Behavior and Structure," McGraw Hill Book Co., New York (1955), Chapter 2; C. J. F. Böttcher, "Theory of Electric Polarisation," Elsevier Publishing Co., Amsterdam (1952), Chapter 6; R. H. Cole, *J. Chem. Phys.*, **43**, 637 (1965).

2) A. D. Franklin, W. M. Heston, Jr., E. J. Hennelly and C. P. Smyth, *J. Am. Chem. Soc.*, **72**, 3447. W. F. Hasel, M. D. Magee, S. W. Tucker and S. Walker, *Tetrahedron*, **20**, 2137 (1964).

3) P. Debye, *Physik. Z.* **35**, 101 (1934).

4) W. Jackson and J. G. Powles, *Trans. Faraday Soc.*, **42A**, 101 (1946) and several papers in the same appendix; C. P. Smyth, loc. cit., p. 64; C. J. F. Böttcher loc. cit., p. 375.

5) K. V. Gopola Krishna, *Trans. Faraday Soc.*, **53**, 767 (1957).

6) B. K. P. Scaife, *Proc. Phys. Soc.*, **81**, 124 (1963).

* The molecular polarization $P(\omega)=p(\omega)M/d$, in which M is the average molecular weight and d is density, is frequently used instead. See Ref. 1, C. P. Smyth, p. 59, Eq. (2.37) and Ref. 1, C. J. F. Böttcher, p. 356, Eq. (10.44).

$$\left.\begin{aligned} p(\infty) &= \frac{\varepsilon_\infty - 1}{\varepsilon_\infty + 2} \\ p(0) &= \frac{\varepsilon_0 - 1}{\varepsilon_0 + 2} \end{aligned}\right\} \quad (3)$$

in which ε_0 is the static dielectric constant and ε_∞ is the dielectric constant measured at frequencies so high that the permanent dipoles are unable to rotate. Since both ε_0 and ε_∞ are real, $p(0)$ and $p(\infty)$ are both real quantities while $p(\omega)$ has the real and the imaginary parts which are given by

$$\left.\begin{aligned} p' &= \frac{(\varepsilon'-1)(\varepsilon'+2)+\varepsilon''^2}{(\varepsilon'+2)^2+\varepsilon''^2} \\ p'' &= \frac{3\varepsilon''}{(\varepsilon'+2)^2+\varepsilon''^2} \end{aligned}\right\} \quad (4)$$

And from Eq. 2

$$\frac{(p'-ip'')-p(\infty)}{p(0)-p(\infty)} = \frac{1}{1+i\omega\tau} \quad (5)$$

If the dielectric system has a distribution of relaxation times, the right side of Eq. 5 should be duly amended.

The so-called "slopes" a' and a'' are defined in the usual way.[2] The dielectric constant ε' and loss ε'' of the dilute solutions are assumed to be represented by the empirical equations:

$$\left.\begin{aligned} \varepsilon' &= \varepsilon_1' + a'c_2 \\ \varepsilon_0 &= \varepsilon_{10} + a_0c_2, \quad \varepsilon_\infty = \varepsilon_{1\infty} + a_\infty c_2 \\ \varepsilon'' &= a''c_2 \end{aligned}\right\} \quad (6)$$

in which subscript 1 refers to the pure solvent and 2 to the solute while subscript 0 refers to the zero frequency measurement in the static field and ∞ to the infinite frequency measurement (at a very high frequency). The concentration of the solute c_2 has been usually expressed in the units of mole fraction[2] but it will be seen later that any concentration units can be used instead.

From Eqs. 6 and Eqs. 4 the following relations are obtained since the square terms such as $(a'c_2)^2$, $(a''c_2)^2$ are negligible for dilute solutions.

$$\left.\begin{aligned} p' &= p_1' + b'c_2 \\ p'' &= b''c_2 \end{aligned}\right\} \quad (7)$$

and

$$\left.\begin{aligned} b' &\simeq \frac{3a'}{(\varepsilon_1'+2)^2\left[1+\frac{2a'c_2}{\varepsilon_1'+2}\right]} \\ &\simeq \frac{3a'}{(\varepsilon_1'+2)^2} \\ b'' &\simeq \frac{3a''}{(\varepsilon_1'+2)^2\left[1+\frac{2a'c_2}{\varepsilon_1'+2}\right]} \\ &\simeq \frac{3a''}{(\varepsilon_1'+2)^2} \end{aligned}\right\} \quad (8)$$

Consequently, there exists a simple relation:

$$\frac{b''}{a''} \simeq \frac{b'}{a'} \quad (9)$$

If we write for $p(0)$ and $p(\infty)$ which are both real

$$\left.\begin{aligned} p(0) &= p_1(0) + b_0c_2 \\ p(\infty) &= p_1(\infty) + b_\infty c_2 \end{aligned}\right\} \quad (10)$$

we obtain

$$b_0 \simeq \frac{3a_0}{(\varepsilon'_{10}+2)^2}, \quad b_\infty \simeq \frac{3a_\infty}{(\varepsilon'_{1\infty}+2)^2}$$

Since

$$\varepsilon_1' \simeq \varepsilon_{10} \simeq \varepsilon_{1\infty} \quad (11)$$

$$\frac{b_0}{a_0} \simeq \frac{b_\infty}{a_\infty} \simeq \frac{b'}{a'} \quad (12)$$

Relations 9 and 12 are important and will be discussed later. Introducing Eqs. 7 and 10 into Eq. 5, the left side of Eq. 5 becomes

$$\frac{(p'-ip'')-p(\infty)}{p(0)-p(\infty)} = \frac{p'_1-p_1(\infty)+c_2(b'-b_\infty-ib'')}{p_1(0)-p_1(\infty)+c_2(b_0-b_\infty)} \quad (13)$$

For non-polar solvents which have no dielectric loss, there is an approximate relation

$$p_1' \simeq p_1(0) \simeq p_1(\infty) \quad (14)$$

which arises from Eq. 11. Both Eqs. 11 and 14 are not rigorously valid for any non-polar solvent; but observed deviations are usually very small to be ignored.

By the use of Eqs. 9 and 12

$$\frac{b'-b_\infty-ib''}{b_0-b_\infty} = \frac{a'-a_\infty-ia''}{a_0-a_\infty} \quad (15)$$

From Eqs. 5, 13, 14 and 15 one obtains for the system of a single relaxation time

$$\frac{a'-a_\infty-ia''}{a_0-a_\infty} = \frac{1}{1+i\omega\tau} \quad (16)$$

Equation 16 becomes

$$\frac{a^*-a_\infty}{a_0-a_\infty} = \frac{1}{1+i\omega\tau} \quad (17)$$

in which a complex slope a^* introduced.

$$a^* = a' - ia'' \quad (18)$$

The usual Debye equation for the polar liquid is

$$\frac{\varepsilon^*-\varepsilon_\infty}{\varepsilon_0-\varepsilon_\infty} = \frac{1}{1+i\omega\tau_M} \quad (19)$$

where the complex dielectric constant ε^*, the static dielectric constant ε_0 and the high frequency dielectric constant ε_∞ are used in places of a^*, a_0 and a_∞ in Eq. 17.

The macroscopic relaxation time τ_M differs from τ defined by Eq. 2;[7]

7) C. J. F. Böttcher, Ref. 1, p. 357, Eq. (10.51)

$$\tau_M = \tau \frac{\varepsilon_0+2}{\varepsilon_\infty+2} \tag{20}$$

However, τ_M becomes identical with τ for dilute solutions in a non-polar solvent (cf. Eq. 11).

Debye Equations

From the real part of Eq. 16 we obtain

$$\frac{a'-a_\infty}{a_0-a_\infty} = \frac{1}{1+\omega^2\tau^2} \tag{21}$$

From the imaginary part

$$\frac{a''}{a_0-a_\infty} = \frac{\omega\tau}{1+\omega^2\tau^2} \tag{22}$$

Equations 21 and 22 provide two independent values of the relaxation times for a solute molecule from the measured values of a' and a'' at a single frequency in the dispersion range.

Combination of these equations will lead to a set of two equations which are independent to each other.

$$a' = a_\infty + \frac{1}{\tau}\left(\frac{a''}{\omega}\right) \tag{23}$$

and

$$a' = a_0 - \tau(\omega a'') \tag{24}$$

The latter equations are useful in checking the validity of the Debye equations of a single relaxation time.

If the Debye equation of a single relaxation time is valid for the system under consideration and if the measurement is conducted with sufficient accuracy, we would be able to determine the relaxation time by use of any equation above mentioned. Accuracy of such a procedure was carefully examined for a few examples by Higasi and Kiyohara.[8]

The equation derived originally by Debye for the same purpose is

$$\tan\vartheta = \frac{\varepsilon''}{\varepsilon'} \simeq \frac{(\varepsilon_1'+2)^2}{\varepsilon_1'} \frac{4\pi\mu^2 c_2}{2700\boldsymbol{k}T} \boldsymbol{N} \frac{\omega\tau}{1+\omega^2\tau^2} \tag{25}$$

in which c the molar concentration and $\boldsymbol{N}$ is the Avogadro number. Equation 25 is a modified form of Eq. 22. Since there is a relation[9] between the dipole moment μ and the two slopes a_0 and a_∞

$$\mu^2 \simeq B^2(a_0-a_\infty) \tag{26}$$

where

$$B^2 = \frac{1}{(\varepsilon_1'+2)^2} \frac{2700\boldsymbol{k}T}{4\pi\boldsymbol{N}} \tag{27}$$

Assuming $\varepsilon''=a''c_2$, $\varepsilon'=\varepsilon_1'$ for dilute solution Eq. 25 is shown to be identical with Eq. 22.

Gopola Krishna[5] proposed a new method of determining the relaxation time from microwave measurement at a single frequency. His equation is:

$$x = P + \frac{1}{\omega\tau} y \tag{28}$$

in which

$$x = p', \quad y = p'' \text{ and } P = p(\infty) \tag{29}$$

Cf. Eqs. 3 and 4. τ is calculated from the slope of the graph, x against y.

For dilute solutions of a non-polar solvent we have the following equations (cf. Eqs. 7 and 10).

$$p' = p_1' + b'c_2, \quad p'' = b''c_2$$

and

$$p(\infty) = p_1(\infty) + b_\infty c_2$$

Hence Eq. 28 can be rewritten

$$\frac{1}{\omega\tau} = \frac{x-P}{y} = \frac{p_1'-p_1(\infty)+(b'-b_\infty)c_2}{b''c_2}$$

And from Eqs. 9, 12 and 14

$$\frac{1}{\omega\tau} = \frac{a'-a_\infty}{a''} \tag{30}$$

Eq. 30 is identical with Eq. 23.

Concluding Remarks

1) In obtaining slopes a' and a'' as defined

$$\left.\begin{aligned}\varepsilon' &= \varepsilon_1' + a'c_2\\ \varepsilon'' &= a''c_2\end{aligned}\right\} \tag{6}$$

there is no restriction on the choice of the concentration unit for the solute since the linear relationship is little affected by such a choice.[10] Gram fraction, volume fraction or mole/litre can be used in place of the mole fraction usually employed. This will be evident at the inspection of Eq. 15 where all the c_2s are cancelled.

2) If a_0 is measured and a_∞ is estimated with reasonable accuracy, the relaxation time τ will be calculated either from the a' value or from a'' value measured at a single frequency in the dispersion range.

$$\tau = \frac{1}{\omega}\sqrt{\frac{a_0-a'}{a'-a_\infty}} \tag{31}$$

$$\tau = \frac{1}{\omega}[A \pm \sqrt{A^2-1}] \tag{32}$$

where

$$A = \frac{a_0-a_\infty}{2a''} \tag{33}$$

8) K. Higasi and O. Kiyohara, *Bull. Inst. Appl. Elec.*, **18**, 24 (1966).
9) K. Higasi, ibid., **4**, 231 (1952); *Bull. Inst. Phys. Chem. Research*, **22**, 865 (1943).
10) K. Higasi and K. Uchiyama, *Bull. Inst. Appl. Elec.*, **17**, 164 (1965).

If both a' and a'' are measured at a single frequency, τ will be calculated together with a_0 or a_∞.

$$\tau = \frac{1}{\omega}\frac{a_0 - a'}{a''} \tag{34}$$

$$\tau = \frac{1}{\omega}\frac{a''}{a' - a_\infty} \tag{35}$$

These equations are applicable only to the dilute solution system with a single relaxation time.

3) The ε', ε'' plot is based on the Cole-Cole equation:[11]

$$\frac{\varepsilon^* - \varepsilon_\infty}{\varepsilon_0 - \varepsilon_\infty} = \frac{1}{1 + (i\omega\tau_0)^{1-\alpha}} \tag{36}$$

where τ_0 is the most probable relaxation time and α is the Cole-Cole parameter for representing the distribution of the relaxation times. Similarly the a', a'' plot is based on the following equation;

$$\frac{a^* - a_\infty}{a_0 - a_\infty} = \frac{1}{1 + (i\omega\tau_0)^{1-\alpha}} \tag{37}$$

Equation 37 will be obtained from Eq. 5, if the right side of Eq. 5 is assumed to be equal to $1/[1+(i\omega\tau_0)^{1-\alpha}]$.

11) K. S. Cole and R. H. Cole, *J. Chem. Phys.*, **9**, 341 (1941).

From a measurement of a' and a'' at a single frequency in the dispersion region, one is able to find τ_0 and α by the following equations[12] which are derived from Eq. 37.

$$\tau_0 = \frac{1}{\omega}\left(\frac{A^2 + B^2}{C^2}\right)^{\frac{1}{2(1-\alpha)}} \tag{38}$$

$$1 - \alpha = \frac{2}{\pi}\tan^{-1}\frac{A}{B} \tag{39}$$

where

$$\left.\begin{aligned} A &= a''(a_0 - a_\infty) \\ B &= (a_0 - a')(a' - a_\infty) - a''^2 \\ C &= (a' - a_\infty)^2 + a''^2 \end{aligned}\right\} \tag{40}$$

Equations 38 and 39 for the Cole-Cole distribution are to be used only when all the values, a', a'', a_0 and a_∞ are obtained with high accuracy.

4) Compare the polarizability plot of $p' = p_1' + b'c_2$ vs. $p'' = b''c_2$ with the Cole-Cole plot of $\varepsilon' = \varepsilon_1' + a'c_2$ vs. $\varepsilon'' = a''c_2$. One will find that two semi-circles for dilute solutions should have the same shape, because there are proportionality relations between b''/a'', b'/a', etc. See Eqs. 9 and 12. Consequently the a', a'' plot becomes equivalent to the p', p'' plot[6] in this case.

12) See also G. L. Clark, ibid., **25**, 125 (1956).

BULLETIN OF THE CHEMICAL SOCIETY OF JAPAN VOL. 39 2160—2168 (1966)

Dielectric Relaxation and Molecular Structure. III. Relaxation Times of Aniline Derivatives in Benzene and Dioxane

By Kazuo CHITOKU and Keniti HIGASI

Research Institute of Applied Electricity, Hokkaido University, Sapporo

(Received March 25, 1966)

A brief description is made of the experimental methods for measuring microwave dielectric constants and losses of solutions in the frequency range 10—50 Gc./sec. Dielectric data obtained in this experiment were analysed from the viewpoint of molecular interaction between the solute and the solvent molecules. Six benzene derivatives with the amino group, aniline (A), *N*, *N'*-dimethylaniline (B), *N*, *N'*-diethylaniline (C), 2, 6-dimethylaniline (D), *p*-nitroaniline (E) and *N*-methylaniline (F) were chosen as solutes. Benzene and dioxane were used as solvents. The relaxation times of A, D and E obtained in dioxane are about three or five times larger than the corresponding relaxation times in benzene. The relaxation times of B and C in dioxane were about twice or one and half of the corresponding values obtained in benzene. The dielectric behavior of F is intermediate between A and B. These results are attributable to the hydrogen-bond formation between an oxygen atom of the dioxane molecule and an amino-hydrogen atom (F) or atoms (A, D and E).

According to Eyring[1,2] the process of molecular rotation requires an activation energy sufficient to overcome the energy barrier separating the two mean equilibrium positions with opposite directions of the dipole; and hence, the relaxation time τ is given by the rate expression

1) S. Glasstone, K. J. Laidler and H. Eyring, "The Theory of Rate Processes," McGraw-Hill, New York (1941), Chapter 9.

2) W. Kauzmann, *Rev. Mod. Phys.*, **14**, 12 (1942).

Table I. Relaxation times τ (p. sec.) measured in cyclohexane and carbon tetrachloride and differences in free energies $\Delta F_2^* - \Delta F_1^*$ (cal./mole)

Substance	t, °C	CCl_4	C_6H_{12}	τ_2/τ_1	$\Delta F_2^* - \Delta F_1^*$
Chlorobenzene	25	12.8[a]	7.6[a]	1.68	310
Nitrobenzene	25	19.6[a]	11.8[a]	1.66	300
t-Butyl chloride	20	3.4[b]	1.6[c]	2.12	440
Chloroform	20	5.0[d]	3.2[d]	1.56	260
Camphor	20	10.7[d]	7.1[d]	1.51	240
Cyclohexyl chloride	25	14.3[a]	9.2[a]	1.55	260
Cyclohexanone	25	8.7[e]	4.4[e]	1.98	400
Pyridine	25	7.8[a]	5.3[a]	1.47	230

a) H. Hase, *Z. Naturforsch.*, **8a**, 695 (1953).
b) A. T. Curtis, P. L. McGeer, G. B. Rathmann and C. P. Smyth, *J. Am. Chem. Soc.*, **74**, 644 (1952).
c) A. D. Franklin et al., Ref. 12.
d) D. H. Whiffen, *Trans. Faraday Soc.*, **46**, 130 (1950).
e) F. Dieringer, *Z. Physik*, **145**, 184 (1956).

$$\tau = \frac{h}{kT}\exp\left(\frac{\Delta F^*}{RT}\right) = \frac{h}{kT}\exp\left(\frac{-\Delta S^*}{R}\right)\exp\left(\frac{\Delta H^*}{RT}\right) \quad (1)$$

where h is the Planck constant, k is the Boltzmann constant, T is the absolute temperature, R is the gas constant; ΔF^*, ΔH^* and ΔS^* are the free energy, the enthalpy, and the entropy, of activation for dipole relaxation.

If two relaxation times τ_1 and τ_2 of the same substance are obtained at the same temperature in two different solvents 1 and 2, the ratio τ_2/τ_1 will be given by Eq. 2.

$$\frac{\tau_2}{\tau_1} = \exp\left(\frac{\Delta F_2^* - \Delta F_1^*}{RT}\right) = \exp\left(\frac{\Delta S_1^* - \Delta S_2^*}{RT}\right)\exp\left(\frac{\Delta H_2^* - \Delta H_1^*}{RT}\right) \quad (2)$$

in which ΔF_1^* and ΔF_2^* are the free energies of activation in the two solvents 1 and 2; and similarly, ΔS_1^*, ΔS_2^*, ΔH_1^* and ΔH_2^* represent the entropies and the enthalpies in the corresponding solvents.

In contrast to this, the familar Debye-Stokes equation[3] is expressed by

$$\tau = \frac{4\pi\eta a^3}{kT} \quad (3)$$

in which η is the viscosity of the liquid and a is the radius of the polar spherical molecule. This equation fails to explain why the relaxation time of a given polar molecule obtained in carbon tetrachloride differs from that obtained in cyclohexane in spite of the fact that these solvents have almost the same viscosity (Table I).

On the basis of Eq. 2, however, we can explain the observed difference between two relaxation times as indicating that ΔF_2^* in carbon tetrachloride is much larger than ΔF_1^* in cyclohexane. If ΔS_1^* is not much different from ΔS_2^*, the energy term ΔH^* in the activation process will become larger in carbon tetrachloride. One may say from this that carbon tetrachloride hinders much more effectively the rotation of the solute dipole than cyclohexane does. Perhaps the forces acting between the solute and carbon tetrachloride molecules are fairly large;* indeed, some molecular compounds with appreciable heats of formation have been detected in systems with carbon tetrachloride.[4] It is to be noted in this connection that the difference of ΔF^* by a few hundreds calories per mole results in a considerable difference in dielectric relaxation times.

For this reason dielectric relaxation times might be considered useful clue for studying interactions between the solute and solvent molecules. The present paper deals with an examination on this possibility.

Experimental Apparatus

Dielectric constants and losses are measured at four frequencies, 1 Mc./sec., 9.33 Gc./sec., 24.15 Gc./sec. and 48.00 Gc./sec. The detailed description of the apparatus and the experimental procedure is given in the following. The measurements at 1 Mc./sec. are based on the usual heterodyne beat method.

Measurements at Frequencies 9.33 and 24.15 Gc./sec.—Figure 1 shows the block diagram of 24.15 Gc. apparatus which is based on the standing wave method as developed by Heston, Franklin,

3) P. Debye, "Polar Molecules," Chemical Catalogue, New York (1929), Chapter 5.

* Or, one may consider cyclohexane an anomalous solvent instead (F. Hufnagel and H. Klip, *Z. Naturforsch.*, **18a**, 769 (1963).

4) A. Kuboyama, *Symposium on Electronic States*, **9**, 13 (1954); W. F. Wyatt, *Trans. Faraday Soc.*, **24**, 429 (1928), **25**, 43, 49 (1929); P. Traynard, *Bull. Soc. Chim.*, **12**, 98 (1945).

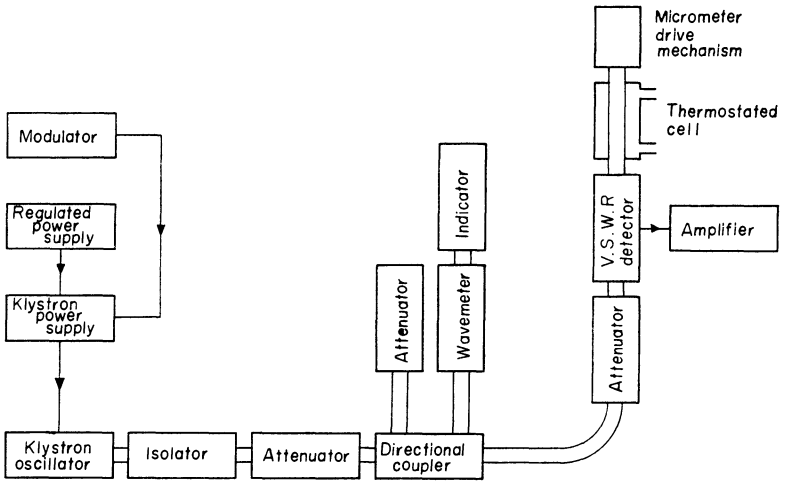

Fig. 1. Block diagram of 24 Gc. apparatus.

Hennelly and Smyth.[5] It consists of a klystron as the energy source, wave guides for transmitting the energy, and a traveling probe for detecting the energy (Fig. 1). A mica window is used in a wave guide to separate the wave guide into two parts, the top part of which forms the dielectric cell into which is put the solution being measured. A micrometer driven plunger is mounted in this cell (Fig. 2). The energy wave entres the wave guide, passes through the liquid, and then comes in contact with open circuited plunger, which reflects the wave back into the wave guide and produces a standing wave.

The experimental process is as follows. With the liquid in the cell and the plunger at the cell window, the traveling probe is set to a minimum

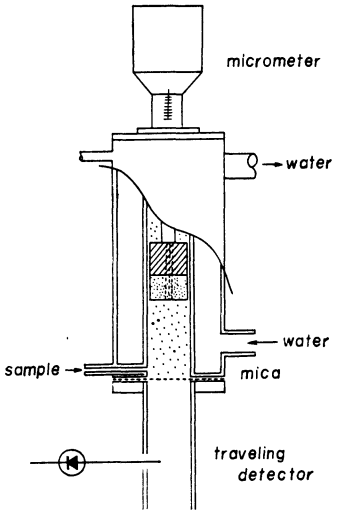

Fig. 2. Dielectric cell for use at 24 Gc.

power position. Then the plunger is turned upward, increasing the depth of the liquid, until another power minimum is noticed, i. e., a second node. The distance between two minima is equal to $\lambda_d/2$. For low loss materials the dielectric constant ε' is given by

$$\varepsilon' = \left(\frac{\lambda_0}{\lambda_d}\right)^2 + \left(\frac{\lambda_0}{\lambda_c}\right)^2 \qquad (4)$$

where λ_c is the cut-off wavelength, λ_0 is the free space wavelength, and λ_d is the wavelength in the dielectric filled guide of the cell.

The dielectric loss is determined by bringing the plunger down to the window and minimizing the powder with the probe. Then the plunger is brought up to the various successive minimum positions and the standing wave ratio, ρ, is measured from the width of the minimum. Values of ρ increase for successive minimum settings n. The dielectric loss factor ε'' is approximated by

$$\varepsilon'' = \frac{\lambda_0^2}{\lambda_d} \cdot \frac{2}{\pi\lambda_g} \cdot \frac{\partial(1/\rho_n)}{\partial n} \qquad (5)$$

Loss Measurements as Frequency of 48 Gc./sec.—The dielectric constants of solutions at this frequency have been measured by the same principle using an apparatus similar to that described in Fig. 1. The dielectric losses at this frequency are measured by use of the transmission method[6] (see Fig. 3). The dielectric cell is made of an inclined rectangular wave guide with a mica window down (Fig. 4). The power transmitted through the dielectric cell filled with solution is measured and compared with the original power

$$T = \frac{\text{Power transmitted}}{\text{Power received}} = e^{-sl} \qquad (6)$$

5) W. M. Heston, Jr., A. D. Franklin, E. J. Hennelly and C. P. Smyth, *J. Am. Chem. Soc.*, **72**, 3443 (1950).

6) D. H. Whiffen and H. W. Thompson, *Trans. Faraday Soc.*, **42a**, 114 (1946).

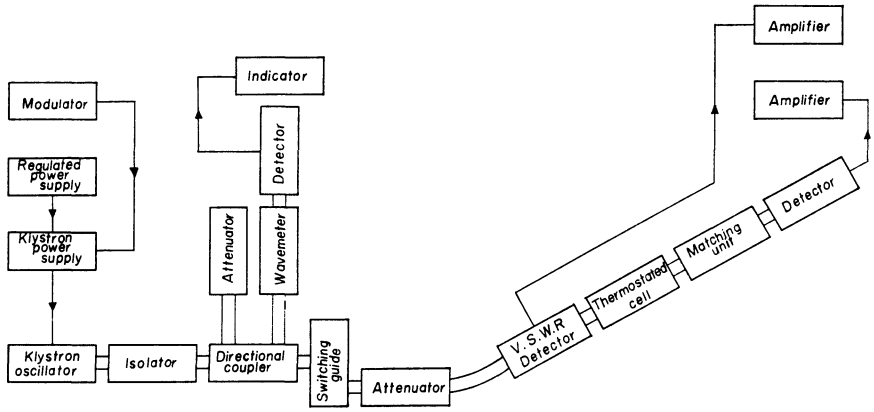

Fig. 3. Block diagram of 48 Gc. apparatus.

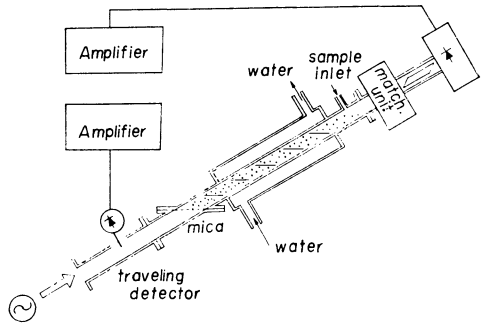

Fig. 4. Dielectric cell for use at 48 Gc.

in which S is defined the attenuation coefficient and l is the depth of the liquid in the cell which can be measured accurately. From values of S the dielectric loss is calculated by

$$\tan \delta = \frac{\varepsilon''}{\varepsilon'} = S \cdot Q \tag{7}$$

and Q is calculable, e. g., for the H_{10} mode

$$Q = \frac{\beta}{(\pi/a)^2 + \beta^2}$$

where β is the propagation constant $2\pi/\lambda_d$ and a is a constant depending on the dimension of the wave guide. From Eq. 6 one obtains

$$S = \frac{1}{l} \ln\left(\frac{1}{T}\right) \tag{8}$$

In order to eliminate the effects due to the meniscus of the liquid surface and the attenuation of the empty cell the measurements were made varying both the liquid depth and the concentration. By use of the attenuation coefficient, T_0, for the empty cell, values $\ln(T_0/T)$ are considered instead of $\ln(1/T)$ and the difference in $\ln(T_0/T)$ between the solution and the solvent is taken always. From these data one is able to calculate the effective value of S in Eq. 8 from which the desired difference in the $\tan \delta$ values between the solution and the solvent is obtained.

Experimental Materials

Aniline was kept in a cold, dark place with sodium hydroxid for several days and distilled under vacuum-(b. p. 81.0°C at 19 mm., n_D^{20} 1.5860). *p*-Nitroaniline was recrystallized with water and completely dried (m. p. 149.6—149.8°C). These materials were purchased from Wako Pure Chemical Industries (G. R. Grade). *N*, *N'*-Dimethylaniline (b. p. 72.3°C at 9 mmHg., n_D^{20} 1.5585), *N*, *N'*-diethyl aniline (b. p. 89.0°C at 8 mmHg., n_D^{20} 1.5420), 2, 6-dimethylaniline (b. p. 92.0°C at 9 mmHg, n_D^{20} 1.5610) and *N*-methylaniline (b. p. 75.0°C at 8 mmHg, n_D^{20} 1.5704) were distilled under vacuum. These four materials were obtained from Tokyo Kasei Kogyo Co., Ltd.

p-Dioxane was first boiled with HCl and water, then was treated with potassium hydroxide, completely dried with sodium and distilled at 101.4°C. n_D^{20} 1.4224, η 1.2836 cp. and ε'/1 Mc. 2.215 at 20°C. Because of the existence of wall losses ε'' were not measured exactly: estimated values are $\varepsilon'' \simeq$ 0.002/9 Gc., 0.004/24 Gc. and 0.005/48 Gc. Benzene was purified and sistilled in a usual manner at 80.3°C. n_D^{20} 1.5011, η 0.6466 cp. and ε' 2.282 at 20°. Apparent ε'' values were 0.0008/9 Gc., 0.003/24 Gc. and 0.004/48Gc. which are due partly to the wall loss and partly to the trace of water which can only be removed by weeks or months of drying treatment.[7] *n*-Hexane was purified and distilled with sodium at 67.8—68.0°C. n_D^{20} 1.3775, η 0.3238 cp. and ε' 1.9016 at 20°C. All these solvents are of G. R. Grade, Wako Chemical Industries.

Experimental Results

For dilute solutions with small concentration range ($c_2 \leq 0.05$), dielectric constant and loss

7) L. Hartshorn, J. V. L. Parry and L. Essen, *Proc. Phys. Soc.*, **68**, 422 (1955).

TABLE II. SLOPES FOR DEPENDENCE OF DIELECTRIC CONSTANT AND LOSS UPON CONCENTRATION (GRAM FRACTION), AT 20°C

Frequency/sec.	a'	a''
Aniline-Benzene		
1 Mc.	2.93	—
9.33 Gc.	2.65	0.69_7
24.15 Gc.	1.96	0.92_6
48.00 Gc.	1.55	0.82_2
Aniline-Dioxane		
1 Mc.	4.63	—
9.33 Gc.	2.84	1.42
24.15 Gc.	1.80	0.91_6
48.00 Gc.	1.65	0.72_5
Aniline-Hexane		
1 Mc.	2.10	—
9.33 Gc.	2.05_1	0.22_7
24.15 Gc.	1.67_0	0.45_4
48.00 Gc.	1.42	0.46
***N,N'*-Dimethylaniline - Benzene**		
1 Mc.	2.49	—
9.33 Gc.	1.60	0.94
24.15 Gc.	0.83_6	0.67
48.00 Gc.	0.55_6	0.47_6
***N,N'*-Dimethylaniline - Dioxane**		
1 Mc.	3.18	—
9.33 Gc.	1.45	1.07
24.15 Gc.	1.05	0.55_5
48.00 Gc.	0.84	0.37_5
***N,N'*-Diethylaniline - Benzene**		
1 Mc.	2.56	—
9.33 Gc.	0.87	0.94
24.15 Gc.	0.52	0.46
48.00 Gc.	0.40	0.29_2
***N,N'*-Diethylaniline - Dioxane**		
1 Mc.	3.24	—
9.33 Gc.	0.95_5	0.79
24.15 Gc.	0.62_5	0.30_3
48.00 Gc.	0.54	0.24_2
2,6-Dimethylaniline - Benzene		
1 Mc.	2.59	—
9.33 Gc.	2.07	0.80_5
24.15 Gc.	1.24	0.68
48.00 Gc.	0.91	0.58_7
2,6-Dimethylaniline - Dioxane		
1 Mc.	4.02	—
9.33 Gc.	1.88	1.21
24.15 Gc.	1.16	0.64
48.00 Gc.	1.08	0.47_6
***p*-Nitroaniline - Benzene**		
1 Mc.	31.40	—
9.33 Gc.	12.6_7	12.6_7
24.15 Gc.	5.5_7	7.20
48.00 Gc.	3.3_8	4.4_8
***p*-Nitroaniline - Dioxane**		
1 Mc.	43.7	—
9.33 Gc.	4.20	9.5_7
24.15 Gc.	3.0_7	4.72
48.00 Gc.	2.4_3	2.8_9
***N*-Methylaniline - Benzene**		
1 Mc.	3.03	—
9.33 Gc.	1.98	1.01
24.15 Gc.	1.15	0.75
48.00 Gc.	0.89	0.54
***N*-Methylaniline - Dioxane**		
1 Mc.	4.41	—
9.33 Gc.	1.66	1.25
24.15 Gc.	0.92	0.61
48.00 Gc.	0.78	0.41

ε' and ε'' can be expressed as linear functions of concentration.[8]

$$\left.\begin{aligned}\varepsilon' &= \varepsilon_1' + a'c_2\\ \varepsilon'' &= \varepsilon_1'' + a''c_2\end{aligned}\right\} \quad (9)$$

in which c_2 is the weight fraction of a polar solute and ε_1'' is usually considered zero for a non-polar solvent. The polarity of *p*-dioxane is sometimes in question; two values are reported of either zero of 0.3—0.4 D.[9] The ε_1'' values for benzene and *p*-dioxane are insignificant.

The Debye equation for dilute solutions in a nonpolar solvent is expressed as[10]

$$\frac{a^*-a_\infty}{a_0-a_\infty} = \frac{1}{1+i\omega\tau} \quad (10)$$

in which ω is the angular frequency, τ is the relaxation time, a^* is the complex quantity defined by

$$a^* = a' - ia'' \quad (11)$$

And a_0 and a_∞ are the slopes a' at the static frequency and at the very high frequency, respectively. The equation representing a system with the Cole-Cole distribution of relaxation times is as follows.[10]

$$\frac{a^*-a_\infty}{a_0-a_\infty} = \frac{1}{1+(i\omega\tau_0)^{1-\alpha}} \quad (12)$$

in which τ_0 is the most probable relaxation time and α is the Cole and Cole parameter of distribution.

If the dielectric system under consideration is a

8) K. Higasi and K. Uchiyama, *Bull. Inst. Appl. Elec.*, **17**, 1641 (1965).
9) A. L. McClellan, "Tables of Experimental Dipole Moments," Freemen and Co., San Francisco (1963).
10) K. Higasi, This Bulletin, **39**, 2157 (1966).

TABLE III. AVERAGE RELAXATION TIMES τ_0, DISTRIBUTION CONSTANTS α, AND DIPOLE MOMENTS (20°C)
Units of τ_0: p. sec.

Solute	Solvent	τ_0	Parameter α	Dipole moment (Debye)
Aniline	Benzene	6.7	0	1.50
	Dioxane	19.4	0.0_8	1.75
	Hexane	5.0	0.0_7	1.48
N, *N'*-Dimethylaniline	Benzene	14.5	0.0_6	1.5_9
	Dioxane	30.4	0	1.6_6
N, *N'*-Diethylaniline	Benzene	33.2	0	1.81
	Dioxane	47.4	0.1_2	1.89
2,6-Dimethylaniline	Benzene	11.0	0	1.61
	Dioxane	30.1	0.0_8	1.88
p-Nitroaniline	Benzene	24.5	0.0_5	6.2_3
	Dioxane	113.5	0	6.8_4
N-Methylaniline	Benzene	15.0	0.09	1.65
	Dioxane	$33._1$	0.17	1.80

superposition of two independent Debye dispersions, that is, if it has two relaxation times, τ_1 and τ_2, we have the following expression.

$$\frac{a^*-a_\infty}{a_0-a_\infty} = \frac{c_1}{1+i\omega\tau_1} + \frac{c_2}{1+i\omega\tau_2} \tag{13}$$

and

$$c_1 + c_2 = 1 \tag{14}$$

Dielectric data concerning aniline and its derivatives are often examined on the assumption of existence of two relaxation times.[11] Equation 13 might preferably be chosen for this reason if there were no risk of arbitrariness in such an analysis.

In the present paper, however, the usual a' and a'' plot[10,12] based on Eq. 12 is used to obtain τ_0 and α values. This is not to say that the Cole-Cole distribution better represents the actual situation. In fact, the a' and a'' plot is a preliminary step taken in view of a small number of data points, but it well afford a clue for finding an average effect of the dielectric relaxation.

Table II shows the values of two slopes, a' and a'', of six substances obtained in dilute solutions of either benzene or dioxane. By the use of a' and a'' recorded in Table II the a', a'' plot in the complex plane was made for each system and thus the average relaxation time τ_0 and the distribution constant α are obtained (see Table III). Dipole moments are also calculated by the Halverstadt-Kumler approximate equation[13] from the measurements at 1 Mc./sec.

It will be seen at the inspection at Table III that the distribution parameter α is not much different from zero throughout; one would feel that the Debye equations for a single relaxation time may be valid. The Debye equations based on a' and a'' are:[10]

$$\frac{a'-a_\infty}{a_0-a_\infty} = \frac{1}{1+\omega^2\tau^2} \tag{15}$$

$$\frac{a''}{a_0-a_\infty} = \frac{\omega\tau}{1+\omega^2\tau^2} \tag{16}$$

Combination of Eqs. 15 and 16 gives another set of equations:

$$\tau = \frac{1}{\omega}\frac{a_0-a'}{a''} \tag{17}$$

$$\tau = \frac{1}{\omega}\frac{a''}{a'-a_\infty} \tag{18}$$

The values of τ of aniline and 2, 6-dimethylaniline, both in benzene, calculated by use of these equations are recorded in Table IV.

It is interesting to find a gradual decrease of

TABLE IV. RELAXATION TIMES (p. sec.) CALCULATED FROM MEASUREMENTS AT A SINGLE FREQUENCY BY Eqs. 15—18

Equation	Data used	Frequency (Gc./sec.) 9.33	24.15	48.00
Aniline in benzene ($a_\infty=1.07$)				
I (Eq. 15)	$a'a_0\,a_\infty$	7.1_8	6.8_8	5.6_2
II (Eq. 16)	$a''a_0\,a_\infty$	7.6_9	7.2_3	5.5_1
III (Eq. 17)	$a'a''a_0$	6.8_5	6.9_0	5.5_7
IV (Eq. 18)	$a'a''\,a_\infty$	7.5_2	6.8_6	5.6_8
2,6-Dimethylaniline in benzene ($a_\infty=0.80$)				
I (Eq. 15)	$a'a_0\,a_\infty$	10.9_1	11.5_4	12.9_6
II (Eq. 16)	$a''a_0\,a_\infty$	10.6_7	14.3_1	8.8_7
III (Eq. 17)	$a'a''a_0$	11.0_2	13.0_8	9.4_9
IV (Eq. 18)	$a'a''a_\infty$	10.8_1	10.1_9	17.6_9

11) E. L. Grubb and C. P. Smyth, *J. Am. Chem. Soc.*, **83**, 4879 (1961); H. Kramer, *Z. Naturforsch.*, **15a**, 974 (1960); P. Knobloch, ibid., **20a**, 854 (1965).
12) A. D. Franklin, W. M. Heston, Jr., E. J. Hennelly and C. P. Smyth, *J. Am. Chem. Soc.*, **72**, 3447 (1950).
13) I. F. Halverstadt and W. D. Kumler, *J. Am. Chem. Soc.*, **64**, 2988 (1942).

the values of aniline with increase in the frequency; this tendency suggests that there may be another dispersion in the range of higher frequency which the a', a'' plot fails to detect. The observed a'' value at 48 Gc./sec. being too large the a', a'' plot is not satisfactory for 2, 6-diemthylaniline. An examination of τ values in Table IV shows that Eqs. 16 and 17 based on the use of a'' give smaller values of about 9 p. sec. This result is just as expected, however, the use of Eqs. 15 and 18 gives even a higher value than τ_0 11.0 p.sec.*

Discussion

The relaxation times of aniline measured in three solvents increase in the order: hexane 5.0 p.sec., benzene 6.7 p.sec. and dioxane 19.4 p.sec. This trend in τ values is in accordance of the order of viscosities of the solvent, hexane 0.3238 cp., benzene 0.6466 cp., and dioxane 1.2836 cp. which are approximately in the ratio of 1 : 2 : 4. It may be noticed, however, that the change of viscosity from hexane to benzene does not produce much change in relaxation time while its further change to *p*-dioxane resulted in a significant increase.

The effects of viscosity on the relaxation time have been studied in great detail,[14] and it has been confirmed that they are not usually so great as expected from Eq. 3. The observed increase of τ values from hexane to benzene may be regarded as normal.** On the contrary the appreciable increase of τ in dioxane may be considered anomalous, that is, this is an indication, one may infer, that there exists some other factor than the viscosity effect which contributes to the large value of aniline in dioxane.***

In order to examine the above point in more detail the ratio of the relaxation time τ_D obtained in dioxane to that of τ_B in benzene is calculated for six substances (A, B, C, D, E and F) and the result is shown in Table V.

It will be seen that the lowest τ_D/τ_B values are found in *N, N'*-dimethylaniline (B) and *N, N'*-diethylaniline (C). In these molecules two hydrogen atoms of the NH_2 group in aniline are replaced by two methyl or two ethyl radicals, both being inactive in the hydrogen-bonding effect.

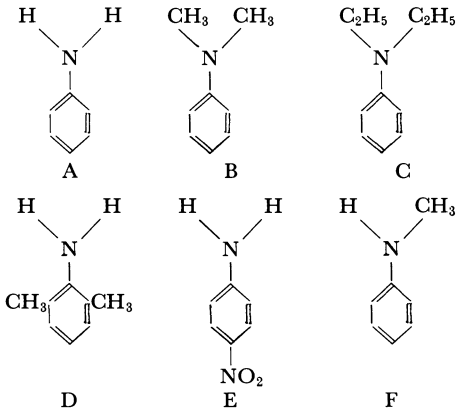

TABLE V. RATIOS OF RELAXATION TIMES, DIFFERENCES OF DIPOLE MOMENTS AND INTERACTION ENERGIES

Substance	τ_D/τ_B	$\mu_D-\mu_B$	ΔF^* cal./mol.
Aniline (A)	2.90	0.25	640
N, N'-Dimethylaniline (B)	2.10	0.07	430
N, N'-Diethylaniline (C)	1.43	0.08	210
2,6-Dimethylaniline (D)	2.74	0.27	590
p-Nitroaniline (E)	4.63	0.61	900
N-Methylaniline (F)	2.21	0.15	460

In *N*-methylaniline (F) one finds the ratio τ_D/τ_B to be intermediate between that of aniline (A) and those of *N, N'*-disubstituted anilines (B and C). These results seem to indicate the formation of bonds between amino-hydrogen atoms in aniline and an oxygen atom of the dioxane molecule which leads to a high relaxation time in dioxane.

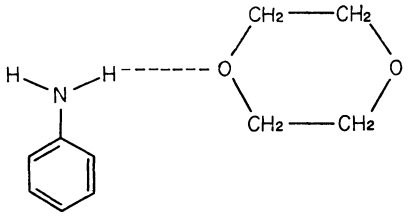

(I)

The hydrogen bond between the solute and the solvent becomes stronger with an increase in the electropositive nature of the aminohydrogen atoms. Indeed, this occurs in *p*-nitroaniline (E), because the molecule has a considerable contribution from the resonance structure II which has the formal positive unit charge at the nitrogen atom of the amino group.[15] Consequently the hydrogen

* The values a_∞ used in the above estimation of τ are obtained from intercepts of the a', a'' plot (Fig. 5)—it should be noted that a proper choice of a_∞ is very important in this calculation. See K. Higasi and O. Kiyohara, *Bull. Inst. Appl. Elec.*, **19**, 24 (1966).

** This statement is only approximately true, because interaction between solute and benzene is sometimes appreciable.

*** The hydrogen bonding of aniline has been studied by several workers, e. g., from ultraviolet study, J. C. Dearden and W. F. Forbes, *Can. J. Chem.*, **38**, 896 (1960); H. Baba, Private communication; By N. M. R., B. N. Rao et al., ibid., **40**, 963 (1962), and by dipole moment see Refs. 16 and 17.

14) See, for instance, K. Chitoku and K. Higasi, This Bulletin, **36**, 1064 (1963); K. Higasi, "Dipole Molecules and Chemistry," Hokkaido University, Sapporo (1965), Chapter 1; Krishnaji and A. Mansingh, *J. Chem. Phys.*, **42**, 2503 (1965).

15) Y. Tsuzuki and K. Higasi, *Sci. Papers Inst. Phys. Chem. Res.*, **39**, 185 (1941).

bonding with dioxane is much stronger, producing the highest ratio of τ_D/τ_B for E in Table V.

Contrary to this the resonance structure III for D is less stabilized because of the steric effect of methyl groups. A slightly smaller ratio τ_D/τ_B for 2,6-dimethylaniline than that of aniline may be accounted for by this reason. To sum up, one would expect from the tendency of hydrogen bonding that the ratio τ_D/τ_B will have the order E>A>D>F>B≃C, while the observed order is: E>A>D>F>B>C, in good accord with the anticipation.

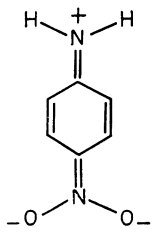

(II)

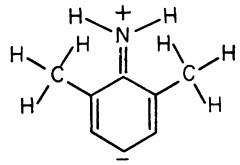

(III)

In Table V the differences between the dipole moments of the same substances measured in dioxane and benzene are recorded. It will be seen that the differences, $\mu_D-\mu_B$, has the order E>A≃D>F>B≃C again in fair agreement with the observed order of τ_D/τ_B. The values $\Delta\mu=\mu_D-\mu_B$ obtained by Smith and his co-workers[16] are E 0.62D>A 0.24D>F 0.18D>B 0.06D again in good agreement with the corresponding values in Table V.

The dipole moments of the 1 : 1 complex of aniline-dioxane is estimated as about 1.88D.[17] On forming a hydrogen bond between aniline and dioxane the apparent dipole moment increases on account of the electron migration effect from the benzene nucleus toward the amino group.[16] And this migration is most pronounced in *p*-nitroaniline (E), next in aniline (A) or in 2, 6-dimethylaniline (D) and then in *N*-methylaniline (F) while no such migration is possible in the remaining substances (B and C).

Next we shall turn to a question what we can conclude from this study on the binding energy of the hydrogen bond between the solute and solvent. By the use of Eq. 2 the value $(\Delta F_2^*-\Delta F_1^*)=\Delta\Delta F^*$ is obtained from τ_D/τ_B—this would represent $\Delta\Delta H^*\simeq\Delta H_2^*-\Delta H_1^*$ if $\Delta S_1^*\simeq\Delta S_2^*$. For aniline (A) $\Delta\Delta F^*$ amounts to 640 cal./mol. which must be associated with both the hydrogen bonding and the viscosity effects. If the latter effect is estimated as about 300 cal./mol., (an average of $\Delta\Delta F^*$ values for two non-hydrogen-bonding substances, B and C) the remaining value 340 cal./mol. may be regarded as arising chiefly from the hydrogen-bonding interaction between the solute and solvent molecules. The same estimation is made for other molecules with the result:

E 600 cal./mol.>A 340 cal./mol.>

D 290 cal./mol.>F 160 cal./mol.

The system of aniline and *p*-dioxane was studied by Few and Smith[17] by the polarization method. According to their estimate about 65% of the aniline is in the form of 1 : 1 complex with dioxane at infinite dilution in dioxane. The measured value $\Delta\Delta F^*$ is associated with the equilibrium mixture; and the energy difference for the complex $\Delta\Delta F^*$ (or possibly $\Delta\Delta H^*$) would be of the order of about 500 cal./mol.

Feodosév and Andreeva[18] found the heat of formation of the aniline-dioxane complex as 0.72 kcal./mol. from an isothermal calorimetric measurement of mixing heats. It is of interest to note that these values, $\Delta\Delta F^*$ (or $\Delta\Delta H^*$) and ΔH are of the same magnitude, although they refer to different mechanisms of the same origin. Both ΔF^* and ΔH^* are associated with the activation for dipole rotation[2] and even $\Delta\Delta H^*$ is not equal to ΔH in this sense, because the former is a part of the hydrogen-bonding energy effective in hindering the dipole rotation.

In Table VI the slopes a_0, a_∞ and a_D are recorded. The a_0 and a_∞ values, which are defined as the slopes a' at the static field and at the very high frequency, respectively, are obtained from the two intercepts of the semi-circles of the a', a'' plot with the abscissa in the complex plane (Fig. 5). The a_D values are obtained from refractivity measurements of dilute solutions and are given by $n^2=n_1^2+a_Dc_2$. Compare this equation with Eq. 9.

It will be seen at Table VI that the differences, $a_\infty-a_D$, are fairly large in some substances (A, D, E, etc.) in which they are not so small as expected to be arising from atomic polarizations.

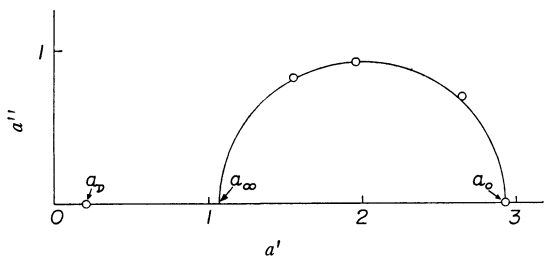

Fig. 5. The a', a'' plot of aniline in benzene.

16) J. W. Smith, "Electric Dipole Moments," Butterworths Sci. Publ., London (1955), p. 313, Table 49. See also C. Curran and G. K. Estok, *J. Am. Chem. Soc.*, **72**, 4575 (1950); K. Kimura and R. Fujishiro, This Bulletin, **32**, 433 (1959).

17) A. V. Few and J. W. Smith, *J. Chem. Soc.*, **1949**, 2781.

18) N. N. Feodosév and T. A. Andreeva, *Chem. Abstr.*, **57**, 144 (1962).

TABLE VI. SLOPES, a_0, a_∞, AND a_D, AND DIFFERENCE $a_\infty - a_D$, CONCENTRATION UNITS BEING THE WEIGHT FRACTION (20°C)

Solute	Solvent	a_0	a_∞	a_D	$a_\infty - a_D$
Aniline (A)	Benzene	2.93	1.07	0.20	0.87
	Dioxane	4.63	1.37	0.49	0.88
N,*N'*-Dimethylaniline (B)	Benzene	2.49	0.41	0.16	0.25
	Dioxane	3.18	0.79	0.40	0.39
N,*N'*-Diethylaniline (C)	Benzene	2.56	0.36	0.10	0.26
	Dioxane	3.24	0.50	0.38	0.12
2,6-Dimethylaniline (D)	Benzene	2.59	0.80	0.14	0.66
	Dioxane	4.02	0.93	0.43	0.50
p-Nitroaniline (E)	Benzene	31.4	2.60	0.67	1.93
	Dioxane	43.7	2.15	0.70	1.45
N-Methylaniline (F)	Benzene	3.03	0.68	0.22	0.46
	Dioxane	4.41	0.62	0.47	0.15

The dipole moment of a polar molecule is approximately given by

$$\mu = B(a_0 - a_D)^{1/2} \tag{19}$$

where

$$B = \frac{1}{2(\varepsilon_1 + 2)} \sqrt{\frac{27 M_2 \boldsymbol{k} T}{\pi \boldsymbol{N} d_1}} \tag{20}$$

when the concentration c_2 is expressed in the units of weight fraction.[19] The symbols M_2, d_1, $\boldsymbol{k}$, T, $\boldsymbol{N}$, etc. have the usual significance.

If the dipole moment associated with τ_0 and α is expressed by μ_0, one may calculate μ_0 by

$$\mu_0 = B(a_0 - a_\infty)^{1/2} \tag{21}$$

and one will find that μ_0 is smaller than μ, sometimes beyond the possible errors. If this difference is anomalously large, we shall suspect whether or not there is another dielectric absorption in the region of the higher frequency. Should such an extra absorption exist, the extra component of the molecular dipole moment would be estimated by

$$\mu^2_{\text{extra}} = \mu^2 - \mu_0^2 = B^2(a_\infty - a_D) \tag{22}$$

The value B of aniline in benzene is about 1.0D at room temperature and hence, μ_{extra} amounts to 0.9D. Caution must be taken if we find a large difference, $a_\infty - a_D$; this point is very important requiring for more detailed analysis. For instance. aniline is believed to have an absorption in the region of a very short wavelength of about 1 mm.[20]; and also from the present measurement at 48 Gc./sec. a very small value of about 1 p.sec. for aniline in benzene is calculated by use of $a_D = 0.20$ and Eq. 16. More experimental data in the millimetre wave region are desirable to characterize the dispersion of a very small relaxation time.

The present work has dealt with the "probable" relaxation time in the main dispersion region and found that this relaxation time becomes much larger when a hydrogen bond is formed between the solute and solvent molecules.

Thanks are due to Professor Hiroaki Baba for helpful discussion and Mr. Kiyoshi Uchiyama for measurements of static dielectric constant, density and refractive index.

19) K. Higasi, *Bull. Inst. Appl. Elec.*, **4**, 231 (1952); *Bull. Inst. Phys. Chem. Res.*, **22**, 865 (1943).

20) C. P. Smyth, Private communications. See also Ref. 11, P. Knobloch who gives $\mu_{\text{extra}} \simeq \mu_2 = 0.9$D with $\tau_2 = 0.5$ p.sec. by use of a_D.

BULLETIN OF THE CHEMICAL SOCIETY OF JAPAN VOL. 39 2169—2172 (1966)

The Simultaneous Extraction and Spectrophotometric Determination of Rhodium(III) with 2-Thenoyltrifluoroacetone

By Asha V. RANGNEKAR and S. M. KHOPKAR

Department of Chemistry, Indian Institute of Technology, Bombay, India

(Received September 8, 1965)

A method has been described for the extractive spectrophotometric determination of rhodium(III) with 2-thenoyltrifluoroacetone (TTA) in an acetone-xylene mixture. The bright yellow rhodium(III)-TTA chelate solution in an acetone-xylene solvent mixture obeys Beer's law over the concentration range of 1.95—19.5 μg. of rhodium per ml. Around pH 6.0 quantitative extraction is possible with 0.015 M TTA - acetone - xylene. The colour of the complex is quite stable up to 72 hr. Rhodium(III) can be extracted in the presence of a large number of ions.

Of the β-diketones used as chelating agents, 2-thenoyltrifluoroacetone (TTA) has proved to be one of the most versatile chelating and extracing agents for the liquid-liquid extraction and spectrophotometric determination of numbers of elements.[1] During the solvent extraction studies of palladium[2] with this reagent, it was found that rhodium(III) also gives a bright yellow-coloured complex in a TTA-acetone mixture in the presence of xylene.

The separation of rhodium from iridium, lanthanum, cerium and zirconium was accomplished by using pyridine.[3] Similarly, the pyridine-thiocyanate complex[4] in hexone was measured spectrophotometrically at 380 mμ. The extractive separation of rhodium from iridium in a hydrobromic-perchloric acid solution was carried out with isopentyl alchool.[5] The separation of rhodium(III) from platinum and palladium was done with diantipyrylpropyl methane.[6] Linder[7] attempted the extraction of rhodium with 0.50 M TTA - acetone - benzene solutions, but the method proved to be laborious and time consuming. So far no systematic work has been carried out on the simultaneous extraction and spectrophotometric determination of rhodium with TTA.

In this paper a method will be described for the liquid-liquid extraction of rhodium at micro-levels with a 0.015 M TTA - acetone - xylene solution. The optinum conditions, as established from the critical investigation of various influencing factors, will also be presented.

Experimental

Apparatus and Reagents.—A type C♯ϕ 4 quartz spectrophotometer with 10-mm. quartz cells and a Cambridge pH meter (Marshal model were used).

2-Thenoyltrifluoroacetone (B. D. H. Anal R), about a 0.015 M solution in acetone, was used. A stock solution of of rhodium(III) was prepared by dissolving one gram of $RhCl_3 \cdot 3H_2O$ (Johnson Matthey and Co., Ltd., London) in 500 ml. of water containing ~0.5% hydrochloric acid. The solution, on standardization,[8,9] was found to contain 78.2 μg. of rhodium per ml.

General Procedure.—An aliquot of a rhodium chloride solution containing about 78.2 μg. of rhodium per ml. was taken. Then 0.1 ml. of 60 per cent perchoric acid was added to the solution. The pH of the solution was then adjusted to the desired pH by the addition of 0.01 M hydrochloric acid or 0.01 M sodium hydroxide. The final volume of the aqueous phase was made up to 25 ml. in each case.

During the studies of the effect of salting-out agents or diverse ions, each one of them was added to the solution before the adjustment of the pH value.

The solution, after adjustment to pH=6.0 unless otherwise specified, was transfered to a 250-ml. separatory funnel. Then 10 ml. of 0.015 M TTA in acetone was added to it. Immediately after the addition of the reagent, 10 ml. of xylene was added to the mixture. After the separatory funnel had been properly stoppered, it was shaken briskly for about 10 min. The layers were then allowed to settle and separate. The organic phase was carefully withdrawn to a 10-ml. volumetric flask. The absorbance of a bright yellow-coloured complex was measured at 430 mμ against the

1) S. M. Khopkar and A. K. De, *J. Sci. and Ind. Res.*, **21A**, 131 (1962).
2) A. V. Rangnekar and S. M. Khopkar, This Bulletin, **38**, 1696 (1965).
3) N. E. Ballou, "Radiochemical Studies—The Fission Products," McGraw Hill Book Co. Inc., New York (1951), p. 1563.
4) J. H. W. Forsythe, R. J. Magee and C. L. Wilson, *Talanta*, **3**, 330 (1960).
5) G. G. Tertipis and F. E. Beamish, *Anal. Chem.*, **34**, 623, (1962).
6) A. I. Busev and V. A. Akimov, *Zh., Analit. Khim.*, **18**, 610 (1963); *Chem. Abstr.*, **59**, 4527 (1963).
7) M. Linder, U. S. Atomic Energy Commission Report UCRL-4377.
8) A. K. De, "Separation of Heavy Metals," Pergamon Press Ltd., London (1961), p. 234.
9) K. Watanabe, *J. Chem. Soc. Japan, Pure Chem. Sect.* (*Nippon Kagaku Zassi*), **77**, 1008 (1956).

reagent blank. The amount of rhodium present was calculated from the Beer's law plot.

The reagent blank was prepared as follows, 10 ml. of 0.015 ml. TTA - acetone was equilibrated with 10 ml. of xylene. The phases were then allowed to settle and to separate. The organic phase was used directly as the reagent blank.

Results and Discussion

Absorption Spectra.—The absorption spectrum of the solution of the rhodium(III)-TTA complex (Rh=7.60×10^{-6} M) is shown in Fig. 1. The

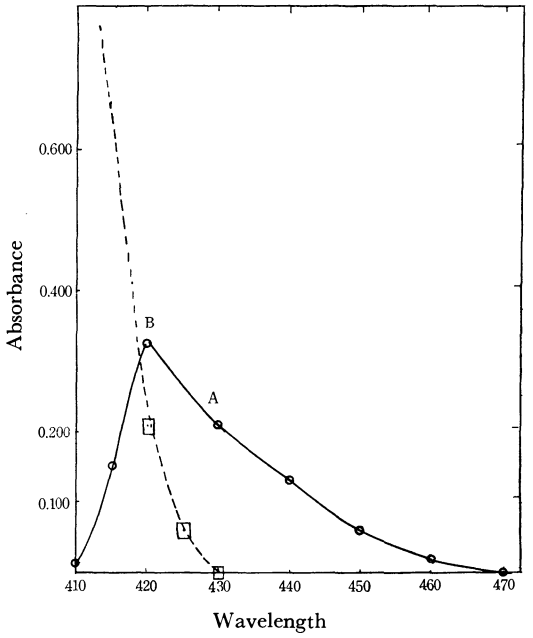

Fig. 1. Absorption spectra.
A. Absorption spectrum of Rh(III) - 2-Thenoyltrifluoroacetone chelate in acetone-xylene mixture. Rh(III)=7.60×10^{-6} M, TTA=1.5×10^{-3} M, pH=6.0 versus reagent blank.
B. Absorption spectrum of the reagent blank solution versus solvent mixture.

bright yellow rhodium(III)-TTA solution absorbs strongly around 420 mμ. The reagent blank at this wavelength also shows some absorbance. The absorbance of the complex gradually decreases, until it becomes negligible beyond 480 mμ. The reagent itself shows an insignificant absorbance at 430 mμ; hence, all the absorbance measurements were carried out at this wavelength. The molecular extinction coefficient at 430 mμ, on the basis of rhodium contents, is 276±9.5. On account of strong absorbance of the reagent itself, tests were not made below 410 mμ.

The Effect of the Amount of Acetone in the Solvent Mixture.—The complex of rhodium with TTA is soluble in acetone and, although very little, in xylene. The addition of xylene to the aqueous phase extracts the complex into the organic phase. Acetone is miscible only in the aqueous phase. The solubility of the acetone in the organic phase at the pH of extraction is practically negligible. Hence, for all practical purposes, it may be assumed that the volume of an organic phase, namely, 10 ml. of xylene, is the same both before and after the extraction of rhodium.

For the clean-cut separation of two layers, the ratio of acetone to xylene must, however, be controlled. From the experimental observations it was found that the optimum ratio of acetone to xylene is 1 : 1 (by volume). If the ratio is changed from 1 : 1 to 1 : 2 or 1 : 3 or even more at the time of extraction, the enhanced volume of xylene in the organic phase produces turbidity and inhibits the colorimetric determination of rhodium.

The Effect of the pH Value.—The solvent extraction behaviour of the rhodium(III)-TTA system was studied over the pH range from 1.0 to 7.0. On plotting the graph of the percentage extraction as the function of pH (Fig. 2), it was observed that the extraction commences around pH ~2.0; then it steadily increases, becoming quantitative around pH=6.0. In the pH region of 2.5—3.5, the extraction is quite large, but incomplete, while in the pH region from 5.2 to 6.2 the extraction tends to be complete. It is possible to extract rhodium(III) quantitatively at pH 6.0 with 0.015 M TTA - acetone in the presence of

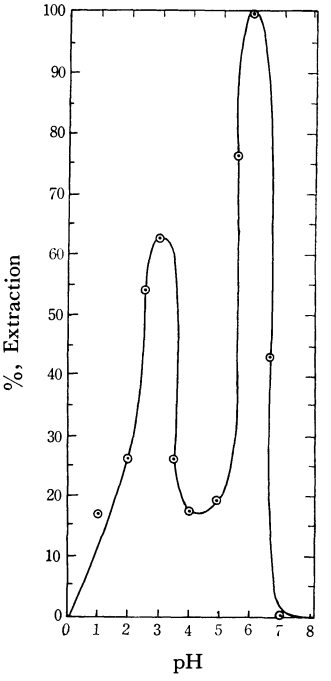

Fig. 2. Extraction of Rh(III)-TTA complex with acetone-xylene as the function of pH.

xylene. It is not worthwhile attempting extraction at pH >6.5, however, as rhodium may precipitate as the hydroxide. Furthermore, the extraction curve drops sharply beyond pH 6.5 and terminates at pH 7.0; the pH of the solution remains unaltered after extraction in the pH region of 1.0—7.0. Moreover, the reagent, TTA, possesses the advantage of being very effective in the acid regions as compared with other β-diketones.[10]

The Effect of Salting-out Agents.—Such salting-out agents as chlorides of magnesium, barium, sodium and potassium were tested in order to observe their effect on the extraction of rhodium by TTA (Table I). It was found that

Table I. Effect of salting-out agents

Salting-out agent	Concn.	Absorbance at 430 mμ	% Extraction
None	—	0.210±0.010	100
$MgCl_2$	1 M	0.155	73.8
$BaCl_2$	1 M	0.100	47.6
NaCl	1 M	0.210	100
KCl	1 M	0.100	47.6
$HClO_4$ 60%	0.10 ml.	0.210	100
	0.15 ml.	0.195	92.8
	0.2 ml.	0.195	92.8

none of them have a pronounced effect upon the extractability of rhodium. The effect of the addition of different volumes of 60% perchloric acid on the extractability of rhodium was also studied. The presence of perchloric acid in the aqueous phase enhances the extraction. This may be explained as follows:—

i) It might provide a higher concentration of the complexing anion in the system, a concentration which, by mass action, would increase the concentration of the complex and enhance the extraction, or

ii) The dielectric constant of the aqueous phase might decrease with an increase in the ionic concentration, or

iii) By binding of the water molecules by the anions, it might become unavailable as a free solvent, or

iv) It may have a pronounced effect upon the activity coefficient of the ions participating in the formation of the complex.

In general, large ionic size and the charge of an ion such as the perchlorate ion play an important role in enhancing the extraction.

Beer's Law Plot.—The absorbance of different amounts of rhodium(III) extracted at pH 6.00 were noted against the reagent blank at 420, 430, and 440 mμ. The results in Table II show that

Table II. Beer's law

Rhodium(III) taken, μg.	420 mμ	430 mμ	440 mμ
62.56	0.260	0.170	0.120
78.20	0.310	0.210	0.130
101.66	0.430	0.280	0.200
117.30	0.490	0.320	0.250

the system conforms to Beer's law at 430 mμ over the concentration range of 1.95—19.5 μg. of rhodium per ml.

The Stability of the Colour of the Complex.—The absorbance of an acetone-xylene solution of a rhodium-TTA complex was measured at 430 mμ at lapsed times of 1, 2, 4, 7, 16, 24, 48, 72 and 96 hr. The corresponding absorbances were 0.210, 0.210, 0.210, 0.210, 0.210, 0.210, 0.210, 0.215 and 0.220. This clearly shows that the colour of the complex is quite stable up to 72 hr. It undergoes about a 2.1% decomposition beyond this time.

The Effect of Different Concentration and Volumes of the Reagent.—The effect of varying volumes as well as varying concentrations of the reagent on the extraction behaviour was studied. The results in Table III show that in no case does acetone play a vital role in influencing the extractability of rhodium, either at varying volumes and at varying concentrations of the reagent. It can be also seen that the use of 5, 10 or 20 ml. of 0.015 M TTA gives a constant value for the absorbance when the rhodium concentration is kept constant. This amply supplements the above observation.

Table III. Effect of different volume and concentration of the reagent
(Rh=78.2 μg., pH=6.0)

TTA concn. M	TTA added ml.	Absorbance at 430 mμ
0.015	10	0.210±0.010
0.015	20	0.210
0.015	5	0.210
0.015	2	0.0
0.0015	10	0.030
0.0075	10	0.080
0.010	10	0.150
0.025	10	0.220
0.050	10	0.235

Since the absorbance at 0.015 M TTA is quite large, it is recommended that this concentration be used in all the determinations in preference to the higher concentration of the reagent. Moreover, the latter are also uneconomical.

The use of lower concentrations, such as 0.0075 and 0.0015 M, are unsuitable, as very little of the reagent is actually available for the complete

10) G. H. Morrison and H. Freiser, "Solvent Extraction in Analytical Chemistry," John Wiley & Co., New York (1957), p. 27.

Table IV. Diverse ions
(Rh(III)=78.2 μg.; pH=6.0, TTA=0.015 M)

Foreign ion	Added as	Amount added	Absorbance at 430 mμ
None	—	—	0.210 ±0.010
Tl^+	Tl_2SO_4	150	0.240[a]
Pb^{2+}	$Pb(CH_3COO)_2$	300	0.205
Cu^{2+}	$CuSO_4 \cdot 5H_2O$	78	Colour[b]
Pd^{2+}	$PdCl_2 \cdot 2H_2O$	78	Colour[a]
Fe^{3+}	$FeCl_3$	78	Colour[b]
Al^{3+}	$AlCl_3 \cdot 3H_2O$	78	0.220
Cr^{3+}	$CrCl_3 \cdot 6H_2O$	39	Colour[a]
Th^{4+}	$Th(NO_3)_4$	78	0.200
UO_2^{2+}	$UO_2(NO_3) \cdot 2H_2O$	39	Colour
Ce^{4+}	$Ce(SO_4)_2$	39	Colour
Be^{2+}	$Be(NO_3)_2$	150	0.215
Zn^{2+}	$ZnSO_4 \cdot 7H_2O$	78	0.180[a]
Mn^{2+}	$MnCl_2 \cdot 2H_2O$	39	Colour[a]
Co^{2+}	$Co(NO_3)_2 \cdot 2H_2O$	39	Colour[b]
Ni^{2+}	$NiSO_4 \cdot 5H_2O$	39	Colour[b]
Ca^{2+}	$CaCl_2 \cdot 2H_2O$	75	0.195
CH_3COO^-	CH_3COONH_4	150	0.220[c]
$Malonate^{2-}$	$CH_2(COOH)_2$	75	0.215
$EDTA^{3-}$	EDTA (disodium salt)	80	0.210
$C_2O_4^{2-}$	$H_2C_2O_4 \cdot 2H_2O$	78	0.210
PO_4^{3-}	Na_2HPO_4	78	0.215
$S_2O_3^{-2}$	$Na_2S_2O_3 \cdot 5H_2O$	80	0.210

a) Interference eliminated by complexation with EDTA.
b) Interference eliminated by formation of cyanide complexes.
c) Interference eliminated by anion exchange resin.

complexation of the metal ion, resulting in incomplete extraction.

The Effect of Diverse Ions.—The effect of the presence of diverse ions on the extraction of rhodium was also studied. It was seen that lead, aluminum, beryllium, thorium, thiosulphate, EDTA(-disodium salt), acetate, oxalate, phosphate showed no interference (Table IV). However, the ions giving characteristic colour reactions with TTA, such as copper, cerium, uranium, iron, cobalt, nickel and chromium, interfere. The interferences due to common cations, such as copper, cobalt, iron, and nickel, can be eliminated by converting them into suitable anionic cyanide complexes, which, in general, are not extracted by this reagent. Similarly, the interferences due to such ions as thallium, chromium, zinc, and manganese can be eliminated by converting them to suitable anionic EDTA complexes. The interferences due to a few anions can be eliminated by passing the solution over a strongly basic anion exchange resin such as Dowex 1-X8 before the extraction step.

About 78.2 μg. of rhodium was taken up and extracted as per the "general procedure" at pH 6.0. The organic phase was separated, and the absorbance of a bright yellow-coloured complex was measured at 430 mμ. From eight runs with 78.2 μg. of rhodium(III), the absorbance noted was 0.210+0.010. The standard deviation was ±1.2%. The method permits the simultaneous extraction and spectrophotometric determination of rhodium within 30 min. As little as 76 γ of rhodium per ml. can be detected.

BULLETIN OF THE CHEMICAL SOCIETY OF JAPAN VOL. 39 2173—2178 (1966)

Continuous Determination of Nitric Oxide and Nitrogen Dioxide in the Atmosphere

By Saburo YANAGISAWA,*1 Noboru YAMATE,*2 Shumpo MITSUZAWA*3 and Masaki MORI*4

Department of Applied Chemistry, Faculty of Engineering, Keio University, Koganei, Tokyo

(Received October 9, 1965)

Continuous determinations of nitric oxide and nitrogen dioxide in the atmospheric air by the use of a modified Saltzman reagent will be described. Measurement was made intermittently, once every 30 min., by an automatic continuous analyzer equipped with a single-path colorimeter. The response of the analyzer was obtained as an average of the concentration of nitrogen oxides over a period of 25 min. Two bubblers were used for absorbing nitrogen oxides into the modified Saltzman reagent, whose transmittance was measured for the determination. One bubbler was designed to absorb nitrogen dioxide, and the other, nitric oxide plus nitrogen dioxide after the oxidation of the nitric oxide by permanganate. The oxidizing efficiency of the permanganate was 96—100 per cent. The acetic acid in the Saltzman reagent was replaced with *n*-propyl alcohol in the modified Saltzman reagent; the spontaneous coloration and corrosive quality of the reagent was decreased by this substitution. The concentration of nitric oxide was obtained from the difference between the two responses of the analyzer, while the concentration of nitrogen dioxide could be read directly from the indication of the recorder. The transmittance ratio method was applied to the measurements, accurate determinations were possible, even at high blank values. Therefore, the reagent was used repeatedly by cycling it on the basis of measuring the difference in the coloration of the reagent before and after the absorption of nitrogen oxides. The analyzer could be used for a long period without changing the reagent.

The maximum allowable concentration and the warning concentration of nitrogen dioxide are 5 p. p. m. and 0.5 p. p. m. respectively,[1] but those of nitric oxide are not known in the present stage of our knowledge. As these oxides are interchangeable under atmospheric conditions, the determination of nitric oxide should be made together with that of nitrogen dioxide for purposes of air-pollution control.

Some apparatuses for the determination of nitrogen dioxide have been designed by several researchers.[2,3] Among these Thomas and his coworkers developed a continuous-determination apparatus for both nitrogen oxides provided with a triple-path colorimeter.[4] A continuous analyzer for nitrogen oxides equipped a single-path colorimeter will be described in this paper.

This analyzer determines the amoung of nitrogen oxides once every 30 min. by integrating them in the liquid absorber, whose transimittance is measured for the determination of the nitrogen oxides. A transmittance ratio method developed by Hisky[5] and by Bastian[6] was applied to the analyzer accurate measurements were then possible, even at high values of the blank. The absorber can be repeatedly used in the system, and the differences in the transmittances of the liquid, before and after the absorption of the gases, indicate the average concentrations of the nitrogen oxides during the period being considered.

Nitrogen dioxide gives color to the color-developing reagent, which is simultaneously the absorber of the gas, and nitric oxide reacts with the reagent after being oxidized to nitrogen dioxide by a sulfuric acid solution of potassium permanganate. Saltzman reagent was modified and successfully used for this purpose.

Reagents

The Modified Saltzman Reagent.—The absorbing and color-developing reagent: Disslove100

*1 Present address: Department of Applied Chemistry, Faculty of Engineering, Keio University, Koganei-shi, Tokyo.

*2 Present address: National Institute of Hygienic Science, Steagaya-ku, Tokyo.

*3 To whom correspondence should be sent: Department of Chemistry, Faculty of Science, Tokai University, Hiratsuka, Kanagawa.

*4 Present address: Denki Kagaku Keiki Co., Musashino-shi, Tokyo.

1) *Am. Ind. Hyg. Assoc. J.*, **23**, 419 (1962).

2) F. E. Adley and C. P. Skillerm, ibid., **19**, 233 (1958).

3) S. Yanagisaws, S. Mitsuzawa, A. Hirose and M. Arai, *Japan Analyst (Bunseki Kagaku)*, **12**, 1937 (1963).

4) M. D. Thomas and J. A. Macleod, *Anal. Chem.*, **28**, 1810 (1956).

5) C. F. Hisky, ibid., **21**, 1440 (1949).

6) R. Bastian, ibid., **22**, 160 (1950).

g. of sulfanilic acid, 1 g. of *N*-(1-naphthyl)-ethylenediamin dihydrochloride, and 200 ml. of *n*-propyl alcohol (or *s*-butyl alcohol) into distilled water, and then make up the volume to 20 l.

Standard Solution.—Dissolve 0.154 g. of sodium nitrite, which has been dried at 105—110°C for 3 hr., into distilled water, and make up the volume to 1 l.; then dilute 10 ml. of this solution to 1 l. Each milliliter of the solution thus prepared is equivalent to 0.001 ml. of nitrogen dioxide gas in the standard state (0°C, 760 mmHg).

Oxidizing Solution.—Dissolve 25 g. of potassium permanganate in 500 ml. of a 2.5% solution of sulfuric acid.

The Modification of Saltzman Reagent

Saltzman reagent[7] is prepared by dissolving 100 g. of sulfanilic acid, 1 g. of *N*-(1-naphthyl)-ethylenediamine dihydrochloride and 100 ml. of acetic acid into distilled water, and making up the volume to 20 l. This reagent is colored spontaneously over a long period; this color interferes with the measurement of the absorbance of the reagent-NO_2 complex. This reagent also corrosively attacks the metallic and plastic parts of the analyzer. Thus, acetic acid was eliminated from the reagent in order to avoid the corrosion of the apparatus. On the other hand, 200 ml. of *n*-propyl alcohol (or *s*-butyl alcohol) was tentatively added to lower the surface tension of the reagent and to increase its gas-collection efficiency, for the reason that the acetic acid was added to Saltzman reagent was to minimize the surface tension of the reagent. Moreover, the acetic acid in Saltzman reagent lowers the pH of the solution. However, it was found that the pH of the solution was sufficiently low even if acetic acid was omitted, as it was 1.5.

The changes in the spontaneous coloring with the time of Saltzman reagent and the modified reagent are shown in Table I. It is believed that the discoloration is accelerated by the light and the temperature. In view of this, the reagent solution tanks in the equipment were all made dark boxes.

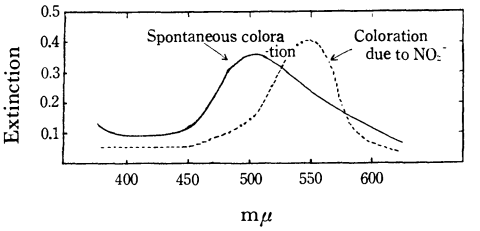

Fig. 1. Spontaneous coloring of Saltzman reagent.

Saltzman reagent and the modified reagent take, respectively, 12 min. and 15 min. to reach a full color development at 20°C. The gradient of the working curve resulting from the modified reagent was 10.6 % lower than that from Saltzman reagent.

Oxidation of Nitric Oxide

The reagent is colored by a coupling reaction with nitrogen dioxide, but not by nitric oxide, so nitric oxide must be oxidized before the reaction with the reagent.

There have previously been established three ways to oxidize nitric oxide; gas-phase oxidation, by a solid catalyzer, and liquid-phase oxidation. It is known that the oxygen-oxidation or air-oxidation method is effective in oxidizing nitric oxide

TABLE I. CHANGE IN SPONTANEOUS COLORING WITH TIME OF THE ABSORBING AND COLOR DEVELOPING REAGENT

(Reference: distilled water, 540 mμ, 20 mm.-cell, Transmittance—%)

Storage container, 500 ml.	No. of days				
	0	3	10	20	30
SALTZMAN'S REAGENT					
White polyethylene bottle	99.7	94.3	85.5	80.2	76.3
Brown polyethylene bottle	99.7	95.8	89.0	86.0	84.0
Brown polyethylene bottle (in refrigarator)	99.7	79.5	94.0	93.5	91.3
White polyethylene bottle (25°C)	99.7	87.0	81.6	75.4	72.0
MODIFIED REAGENT					
White polyethylene bottle	99.7	99.5	99.0	98.3	97.2
Brown polyethylene bottle	99.7	99.7	99.4	99.0	98.0
White polyethylene bottle (25°C)	99.7	96.7	93.4	90.0	86.0

7) B. E. Saltzman, *Anal. Chem.*, **32**, 135 (1960).

of a higher concentration,[8] but the reaction takes place very slowly for nitric oxide of a lower concentration, such as one in atmospheric air; this method of oxidation, therefore, is not applicable to the continuous determination of nitric oxide in atmospheric air.[9] Thomas reported that an ozone concentration of 0.3 p. p. m. was suitable for oxidizing the air sample in his continuous analyzer,[4] but it is not easy to keep the concentration of ozone constant, and, furthermore, ozone decomposes the reagent sometimes it even oxidizes the atmospheric nitrogen. Therefore, the ozone-oxidation method was not used in this research.

Silica gel and active carbon are often used as oxidizing agents of nitric oxide,[10] but they are not preferably used because they are effective only for nitric oxide of a higher concentration, and also because they absorb nitrogen dioxide. Among the liquid-phase oxidizing agents, potassium permanganate in a sulfuric acid solution, potassium bichromate in a sulfuric acid solution, and hydrogen peroxide in a sulfuric acid solution, etc., 2.5% of potassium permanganate dissolved in 2.5% sulfuric acid has been used by several researchers for the oxidation of nitric oxide with Saltzman reagent.[11,12]

The oxidizing agant is placed in a vessel made of glass, and the air sample is bubbled through a ball filter of fritted glass (G-1), 30 mm. in outside diamater.

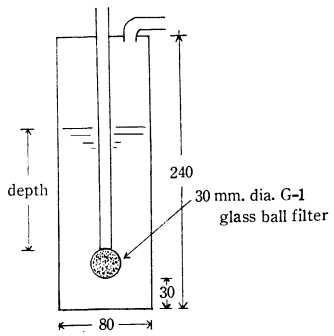

Fig. 2. The oxidation vessel.

The relation between the oxidizing efficiency and the depth of the oxidizing liquid is shown in Table II.

Table II. The relation between the depth of the oxidizing liquid and the oxidizing efficiency

Depth of liquid cm.	Volume of liquid ml.	Oxidizing efficiency: 2.5% $KMnO_4$-2.5% H_2SO_4 solution	Oxidizing efficiency: 2.5% $KMnO_4$-15% H_2SO_4 solution
5	270	96%	100%
9	560	100%	100%
15	840	100%	100%

In these experiments 2.7 p. p. m. of nitric oxide in nitrogen was passed through at a rate of 150 ml./min. for 5 min. As is shown in Table II, the oxidizing efficiency is higher at higher concentrations of sulfuric acid, at which concentrations the oxidizing reagent decomposes itself over a long period. 2.5% sulfuric acid was used for the practical oxidation by placing a glass tube with a ball filter of fritted glass deeper than 10 cm. below the surface of the oxidizing liquid, through this tube the air sample was dispersed into the liquid.

Apparatus

A schematic diagram of the gas and liquid flow system is show in Fig. 3, while the program of the operation of the analyzer is shown in Table III. The valves (V_1—V_5) are operated for the periods indicated in Table III; the analysis operation advances toward the right with the passage of time, and the solenoid valves, the timer, the piston pump and the programmer motor are actuated in the framed parts.

The gas-absorbing bubbler is shown in Fig. 4. The air sample is introduced into the absorbing bubbler, which contains 50 ml. of the reagent,

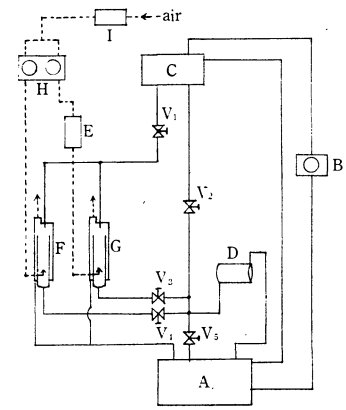

Fig. 3. Diagram of gas and liquid flow system in the nitric oxide - nitrogen dioxide analyzer. V_1—V_5, solenoid valves; A, solution tank (20 l.); B, solution pump; C, head tank; D, cell; E, oxidation vessel; F, NO_2 bubbler; G, $NO+NO_2$ bubbler; H, air pump; I, dust filter

8) S. W. Nicksic and J. Harkins, ibid., **34**, 985 (1962).
9) O. Tada, *J. of Science of Labour (Rodo Kagaku)*, **40**, 185 (1964).
10) T. Kiba, "Shokubai Kagaku Gairon" (Outline of Catalytic Chemistry), Kyoritsu Shuppan, Tokyo (1956), p. 212.
11) M. B. Jacobs, "The Chemical Analysis of Air Pollutants," Interscience Publishers, New York (1960), p. 215.
12) Second Subcommittee. Japan Society of Air Pollution, "Taikiosen no Sokutei" (Determination of Air Pollutants), Corona Sha, Tokyo (1962), p. 159.

TABLE III. ANALYSIS PROGRAM

Analysis operations	Measure reaction solution	Introduce sample air	Fill cell	Zero point check	Liquid discharge	Fill cell	$NO+NO_2$ determ.	Liquid discharge	Fill cell	NO_2 determ.	Liquid discharge
Time, min.	0.5	25	0.5	0.5	0.5	0.5	0.5	0.5	0.5	0.5	0.5
Programer moter	ROTATE	—	ROTATE								
Timer	—	ROTATE	—	—	—	—	—	—	—	—	—
Solution valves V_1	OPEN	—	—	—	—	—	—	—	—	—	—
Solution valves V_2	—	—	OPEN	—	—	—	—	—	—	—	—
Solution valves V_3	—	—	—	—	—	OPEN			—	—	—
Solution valves V_4	—	—	—	—	—	—	—	—	OPEN		
Solution valves V_5	—	—	—	—	OPEN	—	—	OPEN	—	—	OPEN
Gas pump	GAS SUCTION		—	—	—	—	—	—	—	—	—

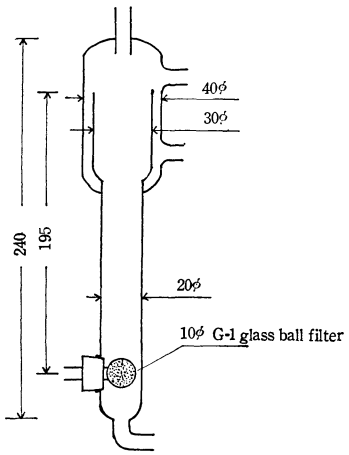

Fig. 4. The absorbing bubbler.

the volume being measured by an over-flow system. The absorbing efficiency of this bubbler by gas sample was 96—98% under the actual conditions of analysis.

The air sample is divided into two parts, one is led into the first bubbler directly, while the other is led through the oxidizing liquid to the second bubbler. The air sample is bubbled for 25 min. at a constant rate of 150 ml./min. by means of a piston pump. The nitrogen dioxide in the air sample is integrated during a 25 min. period in the first bubbler, and both nitric oxide and nitrogen dioxide, in the second bubbler. Then, the transmittances of the reagents for the determinations of nitrogen oxides are measured in a colorimetric cell in the order of the reagent blank, the reagent colored by nitrogen dioxide, and that colored by both nitrogen dioxide and nitric oxide. The ratios of the transmittances of the working reagents, which show the concentrations of nitrogen dioxide and of nitric oxide plus nitrogen dioxide, are plotted on the recorder in a logarithmic scale as the averages of 25-min. measurements. The concentration of nitric oxide is obtained by subtracting the concentration of nitrogen dioxide from that of the sum of nitric oxide and nitrogen dioxide.

Thomas used the reagent repeatedly by treating it with active carbon,[4] but generally the reagent used for the continuous determination is discarded without re-processing.[2,3] In this experiment, the reagent was not re-processed and used repeatedly, and the reagent blank was determined in each determination, for the re-processing system was considered not very reproducible and it might make the apparatus rather complicated. Correct determinations can be made in the range of the linear part of the calibration curve, even if the reagent itself is colored; therefore, a transmittance-ratio method[5,6] was applied to the analyzer, and accurate measurements were possible even at higher values of the blank. The larger volume of the reagent reservoir could be helpful for a long-run determination. The reagent was replaced when it reached a definite absorbance, as was determined by monitoring by an absolute transmittance meter.

The electric circuit is shown in Fig. 5.

In the first step, the blank reagent is led into the colorimetric cell, and the switch, S, is connected to (1); at this stage a voltage corresponding to a

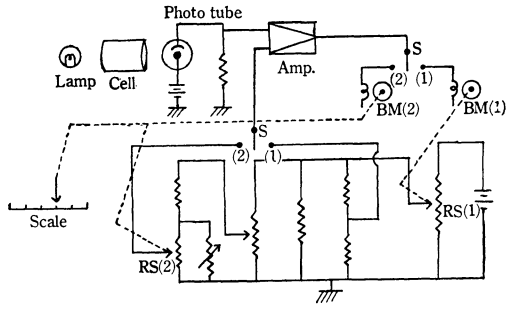

Fig. 5. Diagram of instrument circuit.

photo-current appears at both ends of the sliding resistance, RS(2), as a result of automatical balancing by RS(1). Then, the reagent colored is led to the cell; a voltage corresponding to the photo-current in this stage is represented by the position of the contact point of the sliding resistance when the switch, S, is connected to (2). The transmittance ratio of two optical measurements are represented by the voltages in this stage of the resistances. Then, each transmittance ratio of the reagents, that of nitrogen dioxide to the blank and that of nitrogen dioxide plus nitric oxide to the blank, is plotted on the recorder separately, and the indications are read out in a logarithmic scale graduated from 0 to 5 p. p. m.

Examples

Three of these analyzers are used at the National Institute of Hygienic Science, Tokyo.

Analytical data on nitrogen dioxide and nitric oxide collected at the Continuous Air-monitoring Station of the Institute, Kasumigaseki, Tokyo, from January through December, 1964, are shown in Table IV. An example of the determination

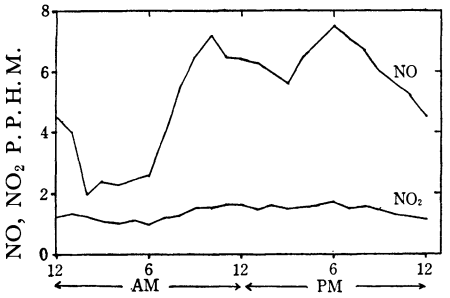

Fig. 6. An example of analysis of the atmospheric air.

is shown in Fig. 6, in which the average concentrations of the nitrogen oxides during the period from January to March, 1964, is graphically displayed, along with the time of day. The avarage concetration of nitric oxide was several times that of nitrogen dioxide; it seems that these results were intensely affected by pollution from the automobiles near the Monitoring Station.

This analyzer has played an improtant role in monitoring air pollution and in analyzing the mechanism of that pollution in Japan.

Table IV. Analytical data of nitrogen dioxide and nitric oxide in Tokyo
(Continuous air monitoring station at Kasumigaseki, Tokyo)

Nitrogen dioxide (p. p. h. m.)

Date	Number of determination	Each determination		Hour-average		Day-average		Average	Standard deviation
		min.	max.	min.	max.	min.	max.		
1964. 1	685	0.5	4.0	0.9	1.5	0.4	2.4	1.3	0.62
2	605	0.5	5.0	1.0	1.6	1.0	1.9	1.3	0.56
3	520	0.5	3.5	1.2	1.8	1.0	2.2	1.5	0.53
4	650	0.5	4.0	1.8	2.4	1.6	2.5	2.1	0.64
5	612	0.5	4.0	1.5	2.2	1.6	3.0	2.0	0.33
6	622	0.5	4.0	1.6	2.4	1.8	2.6	2.0	0.61
7	657	0.5	5.0	1.8	2.4	2.0	2.4	2.1	0.13
9	586	0.5	5.0	1.7	2.6	2.0	2.5	2.2	0.72
10	638	1.0	5.0	1.8	2.4	2.0	2.6	2.2	0.29
11	648	1.0	6.0	1.9	3.0	2.0	3.2	2.3	0.82
12	616	1.0	5.0	2.0	2.7	1.9	3.2	2.4	0.64

Nitric oxide (p. p. h. m.)

Date	Each determination		Hour-average		Day-average		Average	Standard deviation
	min.	max.	min.	max.	min.	max.		
1964. 1	0.5	32.0	2.2	9.7	2.6	10.5	6.7	4.93
2	0.5	21.0	1.2	6.6	0.7	9.8	4.1	3.91
3	1.0	30.0	2.0	6.8	2.3	10.8	4.8	3.37
4	1.0	15.0	1.9	5.5	2.5	9.8	4.2	2.41
5	0.5	15.0	1.9	4.5	1.0	9.7	3.2	2.76
6	0.5	6.0	0.9	2.5	0.8	3.3	1.8	1.25
7	1.0	8.0	1.2	3.3	1.1	4.7	2.4	1.52
9	0.5	21.0	1.3	7.5	1.0	10.6	4.9	4.44
10	1.0	24.0	1.3	9.2	2.6	9.6	5.6	4.01
11	1.0	21.0	1.4	7.2	1.8	9.9	4.5	3.54
12	1.0	51.0	1.5	13.3	2.2	15.1	7.2	6.27

Conclusions

Saltzman reagent has been modified and acetic acid has been replaced with *n*-propyl alcohol (or *s*-butyl alcohol) as a surface-active agent, decreases in the spontaneous coloration and in the corrosive quality of the reagent have resulted, and better results of the determination have been obtained in the continuous analysis.

The intermittent measurement system of the continuous analyzer has made the apparatus simpler, and the data obtained are convenient for statistical data processing.

The re-cycling of the reagent has made it possible to run a continuous determination for a long time, even for more than a month in the winter time.

BULLETIN OF THE CHEMICAL SOCIETY OF JAPAN VOL. 39 2178—2180 (1966)

The Direct Complexometric Titration of Thallium(III) Using Iron(III)-Sulfosalicylate Complex as Metal Indicator

By R. C. AGGARWAL and A. K. SRIVASTAVA

Chemistry Department, Lucknow University, Lucknow (U. P.), India

(Received December 28, 1965)

The iron(III)-sulfosalicylate complex has been used as the indicator for the direct complexometric determination of thallium(III). This indicator permits the rapid and accurate determination of both micro and macro quantities of thallium(III). The titrations are best carried out at about pH 2.6. Most of the divalent cations, such as calcium, strontium, barium, magnesium, manganese and mercury, and trivalent cations, such as chromium and aluminum, do not interfere in the determination.

Thallium(III) reacts with ethylenediaminetetraacetic acid (EDTA) to form a 1 : 1 complex. This reaction has been recently used as the basis for both the direct[1,2] and the indirect[3,4] titrimetric determination of thallium(III) using such metal indicators as xylenol orange, 1-(2-pyridylazo)-2-naphthol (PAN) and 4-(2-pyridylazo)resorcinol (PAR). In a previous communication[5] we reported on the use of familiar dyes, methylene blue and methyl violet, as metal indicators for the direct complexometric determination of thallium(III). Since colored-metal complexes were not used as indicators earlier in the titrimetric determination of thallium(III), a direct complexometric titration of it has been carried out using the iron(III)-sulfosalicylate complex as an indicator; the results obtained will be described in this communication. The use of sulfosalicylic acid for the indirect complexometric determination of thallium(III) has been previously reported.[6]

The determination of thallium(III) using the iron(III)-sulfosalicylate complex as an indicator is based on the facts that in spite of the greater stability of the iron(III)-EDTA complex[7] as compared with the thallium(III)-EDTA complex,[8] EDTA combines with free thallium(III) ions in preference to the iron(III) present as the sulfosalicylate complex, and that when all the thallium(III) ions have combined with EDTA, the violet color of the indicator is discharged due to the formation of the almost colorless iron(III)-EDTA complex, which is much more stable than the iron(III)-sulfosalicylate complex.

Experimental and Results

A 0.05 M solution of the disodium salt of EDTA was prepared by dissolving 18.615 g. of this salt in doubly-distilled water and by then making up the volume to a liter. The strength of the solution was checked by titrating it against calcium carbonate, using calcon as the metal indicator.

A stock solution of thallium(III) nitrate was prepared by dissolving thallium metal in nitric acid and by then oxidizing it to thallium(III)

1) A. I. Busev and V. G. Tiptsova, *Zh. Analit. Khim.*, **15**, 573 (1960); *Chem. Abstr.*, **55**, 15223 (1961).
2) A. I. Busev, L. L. Talipova and V. M. Ivanov, *Zh. Khim. Obshch.*, **6**, 598 (1961); *Chem. Abstr.*, **56**, 5398 (1962).
3) H. Flaschka, *Mikrochemie ver Mikrochim. Acta*, **40**, 42 (1952).
4) W. T. Foley and R. F. Pottie, *Anal. Chem.*, **28**, 1101 (1956).
5) R. C. Aggarwal and A. K. Srivastava, *Indian J. Chem.*, in press.
6) A. I. Busev and V. G. Tiptsova, *Zh. Analit. Khim.*, **16**, 275 (1961); *Chem. Abstr.*, **56**, 4096 (1962).
7) F. J. Welcher, "Analytical Uses of EDTA," D. Van Nostrand Co., Princeton, New Jersey (1957), p. 6.
8) A. I. Busev, V. G. Tiptsova and T. K. Sokolova, *Zh. Neorgan. Khim.*, **5**, 2749 (1960); *Chem. Abstr.*, **56**, 4360 (1962).

TABLE I. EFFECT OF HYDROGEN ION CONCENTRATION ON THE TITRATION OF THALLIUM(III)

Thallium(III) solution taken=30.66 mg.; EDTA solution=0.05 M
Volume of indicator used=0.5 ml.; EDTA used for blank=0.05 ml.

pH	1.5	2.0	2.3	2.6	2.8	3.0	3.2	3.5
Volume of EDTA used, ml.	2.80	2.90	3.00	3.00	3.00	3.00	2.80	2.65
Thallium(III) found, mg.	28.61	29.63	30.66	30.66	30.66	30.66	28.61	27.08

Note: 1 The volumes of EDTA given in Table I and the succeeding Tables II and III are corrected for blank.
2 The data recorded in Tables I, II and III represent the mean value of the multiple determination, standard deviation being within 0.5%.

with alkaline bromine. The thallium(III) hydroxide thus precipitated was washed well with water and dissolved in a minimum quantity of dilute nitric acid. The solution was then shaken with an excess of thallium(III) hydroxide in order to minimize the acidity of the solution. The thallium content of the solution was estimated by titrating it with a EDTA solution standardized as above, using xylenol orange as the metal indicator.

The iron(III)-sulfosalicylate complex indicator was prepared by mixing 10 ml. of a 0.05 M ferric alum solution and 30 ml. of 0.05 M sulfosalicylic acid, and by then making up the volume to 100 ml. Five-hundredths milliliters of this indicator was used throughout the experiment.

Buffer solutions with pH values in the 2.2—4.00 range were made by mixing requisite quantities of 0.01 M solutions of potassium hydrogen phthalate and hydrochloric acid.

The solutions of various metal ions used for interference studies were prepared by dissolving the requisite amounts of analytical-grade reagents in doubly-distilled water; they were standardized, where necessary, by the determination of their metal contents by usual methods.

The Effect of pH.—Determinations of thallium(III) were carried out at various pH values (adjusted with a pH meter using glass and calomel electrodes) in order to find out the optimum hydrogen ion concentrations for titration. The data recorded in Table I show that the indicator is pH-dependent and that it works well only in a limited pH range, from 2.3 to 3.0.

Titration Procedure.—A solution containing 10.22 to 91.98 mg. of thallium (III) was taken and diluted to about 20 ml. with doubly-distilled water; its pH was adjusted to about 2.6 by potentiometric titrations with dilute ammonium hydroxide; a requisite amount of a buffer solution was added to maintain the pH; 0.5 ml. of the iron(III)-sulfosalicylate complex indicator was added,

TABLE II. DETERMINATION OF THALLIUM(III) WITH EDTA USING IRON(III)-SULFOSALICYLATE COMPLEX INDICATOR AT pH 2.6

Volume of indicator used=0.5 ml.
EDTA used for blank=0.05 ml.

Th(III)* taken, mg.	Volume of EDTA used, ml.	Th(III)* found, mg.	Error %
10.22	1.00	10.22	—
20.44	2.00	22.44	—
30.66	3.00	30.66	—
40.88	4.00	40.88	—
51.10	5.00	51.10	—
61.32	6.00	61.32	—
71.54	7.05	72.05	+0.71
81.76	8.00	81.76	—
91.98	8.95	91.46	−0.57

* See Note 2 in Table I.

TABLE III. EFFECT OF FOREIGN IONS

Thallium(III) taken=40.88 mg.=4.00 ml. of 0.05 M thallium(III)
pH of the soln.=2.6; EDTA soln.=0.05 M

Foreign cation	Wt. of foreign cation, mg.	Volume of EDTA used, ml.	Th(III)* found, mg.
Ca^{2+}	40.00	4.00	40.88
Sr^{2+}	43.80	4.00	40.88
Ba^{2+}	34.31	4.00	40.88
Mg^{2+}	30.40	4.00	40.88
Zn^{2+}	32.68	5.55	56.12
Pb^{2+}	51.80	5.25	53.65
Cd^{2+}	41.90	5.10	52.12
Mn^{2+}	41.13	4.00	40.88
Hg^{2+}	38.90	4.00	40.88
Cu^{2+}	31.76	Interferes**	—
Ni^{2+}	44.01	Interferes**	—
Co^{2+}	43.32	Interferes**	—
Al^{3+}	33.70	4.00	40.88
Cr^{3+}	28.88	4.00	40.88
Bi^{3+}	46.55	Interferes	—
Ga^{3+}	34.86	Interferes**	—
In^{3+}	34.41	Interferes**	—
Ce^{3+}	35.30	Interferes**	—
Ce^{4+}	35.30	Interferes**	—

* See Note 2 in Table I.
** No sharp end point was obtained, therefore, the amount of EDTA used could not be recorded.

and the solution was titrated with a 0.05 M EDTA solution until the violet color of the solution was discharged. A blank titration with 0.5 ml. of the indicator was also carried out under similar conditions, and the necessary correction was made in the determinations. The blank correction amounted to 0.05 ml. of the 0.05 M EDTA solution. The results obtained are shown in Table II.

The Effect of Foreign Ions.—Since EDTA forms fairly stable complexes with large number of cations, many of them may be expected to interfere in the titrimetric determination of thallium(III). The determination of thallium(III) was carried out at pH 2.6 in the presence of almost equivalent amounts of many di- and tervalent cations; the results obtained are recorded in Table III. The divalent metal ions, such as calcium, strontium, barium, magnesium, manganese, and mercury, and the tervalent metal ions, such as chromium and aluminum, do not interfere, but gallium, indium, bismuth, cerium and most of the colored metal ions interfere in the determination of thallium(III).

The authors' grateful acknowledgements are due to the Head, Chemistry Department, Lucknow University, Lucknow, for providing laboratory facilities, and to the Council of Scientific and Industrial Research, New Delhi, for awarding a junior Research Fellowship to one of them (A. K. S.).

BULLETIN OF THE CHEMICAL SOCIETY OF JAPAN VOL. 39 2180—2183 (1966)

Proton Magnetic Resonance Spectra of Cobalt(III) Hexammine-type Polyamine Complexes[1)]

By Hayami YONEDA

Chemistry Department, Wakayama University, Masago-cho, Wakayama

and Yukiyoshi MORIMOTO

Research Laboratories, Fujisawa Pharmaceutical Company, Higashiyodogawa-ku, Osaka

(Received January 31, 1966)

The proton magnetic resonance spectra of [Co *en*$_3$]Cl$_3$, [Co *tn*$_3$]Cl$_3$, [Co *pn*$_3$]Cl$_3$ and [Co *den*$_2$]Cl$_3$ (*den*=diethylenetriamine) dissolved in trifluoroacetic acid were measured. All of the observed spectra consist of broad bands, which were assigned on the basis of intensity considerations and by comparing them with the spectra of the corresponding deuterated species. In case of the ethylenediamine complex, the double-resonance method was applied, measurements at different temperatures were made, and the origin of the breadth of the bands was discussed. The NH_2 signals of the ethylenediamine and trimethylenediamine complexes show AB-type features. This was confirmed by comparing the spectra obtained at 60 Mc. and at 100 Mc. The AB-type features of the NH_2 signal were explained in terms of the crystal structure of the complex.

Although the study of Werner-type complexes by the use of the proton magnetic resonance technique is an attractive subject to the coordination chemist, relatively few works have been reported. This is because most of Werner-type complexes are not soluble in ordinary organic solvents, and because in aqueous solutions, the strong signal of water prevents the observation of the signals of ligands and, moreover, rapid proton exchange makes it difficult to pick up the signals of ligands separately. To avoid this difficulty, Clifton and Pratt[2)] measured the proton magnetic resonance spectra of several cobalt(III) ammine complexes dissolved in acidified heavy water; they thus succeeded in obtaining fairly satisfactory results.

Recently we found that an acid itself, if it is a liquid and dissolves a sample, could be used for the NMR measurement of the complex.[3)] Among the several acids we tried, trifluoroacetic acid proved to be the most suitable for this purpose. In this paper we should like to report on several interesting features of the NMR spectra of cobalt(III) polyamine complexes.

1) A part of this article was presented at the 15th Symposium of Coordination Chemistry, Kanazawa University, October, 1965.

2) P. Clifton and L. Pratt, *Proc. Chem. Soc.*, **1963**, 339. S. Hayashi made the same kind of measurements using heavy water; *J. Chem. Soc. Japan, Pure Chem. Sect. (Nippon Kagaku Zasshi)*, **85**, 256 (1964); **86**, 364 (1965).

3) During this work we learned that W. L. Jolly, A. D. Harris and T. S. Briggs had reported the use of concentrated sulfuric acid as a solvent for NMR studies of cobalt(III) ammine complexes; *J. Inorg. Chem.*, **4**, 1064 (1965).

Experimental

The complexes used in the measurement were tris-ethylenediamine cobalt(III) chloride [Co *en*$_3$]Cl$_3$, tris-trimethylenediamine cobalt(III) chloride [Co *tn*$_3$]Cl$_3$, tris-propylenediamine cobalt(III) chloride [Co *pn*$_3$]Cl$_3$ and bis-diethylenetriamine cobalt(III) chloride [Co *den*$_2$]Cl$_3$. The spectra of the free ethylenediamine as well as of its trifluoroacetic acid salt were also measured. The trifluoroacetic acid used in the measurement is of the spectrograde (Merck Company).

The apparatus used was a Varian A60 Analytical NMR spectrometer. In some cases, a Varian HR100 NMR spectrometer was also used. Tetramethylsilane was used as the internal standard throughout the measurements.

Results and Discussion

The NMR spectrum of the free ethylenediamine dissolved in carbon tetrachloride consists of two sharp signals of an equal intensity; the peak appearing in the higher field (−64 c. p. s.) is assigned to the NH_2 protons, and the other, in the lower field (−156 c. p. s.), to the CH_2 protons. (The NH_2 protons of alkylamine dissolved in carbon tetrachloride have their signals in higher fields than the CH_3 and CH_2 protons.) However, this situation is reversed in the case of the protonated ethylenediamine dissolved in an acid. By protonation the NH_2 group becomes the NH_3^+ group, and its signal is shifted to −459 c. p. s. On the other hand, the CH_2 signal is shifted to −237 c. p. s. (The assignment of the signals can easily be made from intensity consideration.) The spectrum of the [Co *en*$_3$]$^{3+}$ complex is expected to have a character intermediate between those of the free and protonated ethylenediamine species. Actually, it has two signals of an equal intensity. While the signal in the higher field (−190 c. p. s.) shows no fine structure, the other in the lower field, has a doublet structure (−292 and −310 c. p. s.), and each doublet component carries a shoulder. In order to assign these signals, the spectrum of the amino-deuterated complex was also measured. In the deuterated complex, the NH_2 group is converted to the ND_2 group, and the signal due to the NH_2 protons should disappear. In the actual deuterated complex, the signal in the lower field disappears. Therefore, this is assigned to the NH_2 protons. Consequently, the signal in the higher field is assigned to the CH_2 protons. The general features of the spectrum are rather coloser to those of the protonated ethylenediamine than to those of the free ethylenediamine. Therefore, we assume that the nature of the coordinated ethylenediamine is closer to that of the protonated ethylenediamine.

In Fig. 1, the NMR spectra of [Co *tn*$_3$]Cl$_3$, [Co *pn*$_3$]Cl$_3$ and [Co *den*$_2$]Cl$_3$ are also shown. Of these, the spectrum of [Co *tn*$_3$]Cl$_3$ is similar to that of [Co *en*$_3$]Cl$_3$. The signal on the left-hand side (−282 and −267 c. p. s.) has a doublet structure and disappears in the deuterated species. Therefore, it is assigned to NH_2. The middle one (−170 c. p. s.) and the one on the right-hand side in the spectrum (−130 c. p. s.) are assigned to the CH_2 adjacent to NH_2 and to the middle CH_2 respectively. The spectrum of the [Co *pn*$_3$]$^{3+}$ complex has five bands which correspond to CH_3 (−92 c. p. s.), CH_2 (−185 c. p. s.), CH (−210 c. p. s.), and two kinds of NH_2 (ca. −280 and ca. −310 c.p.s.). The spectrum of the [Co *den*$_2$]$^{3+}$ complex has the most diffuse pattern among the four complexes. From intensity considerations, the bands are assigned to CH_2 (−205 c. p. s.), NH_2 (−280 and −310 c. p. s.), and the middle NH (−435 c. p. s.).

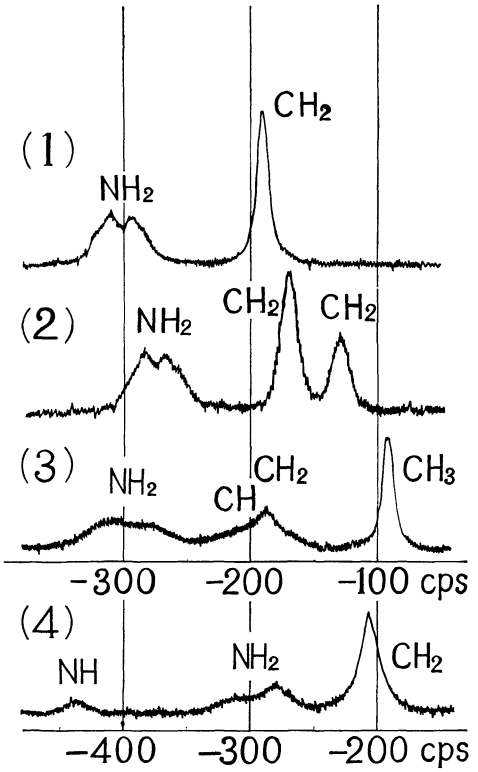

Fig. 1. NMR spectra of four complexes.
(1) [Co *en*$_3$]Cl$_3$, (2) [Co *tn*$_3$]Cl$_3$, (3) [Co *pn*$_3$]Cl$_3$, (4) [Co *den*$_2$]Cl$_3$

All these spectra consist of broad bands. This seems to be characteristic of polyamine complexes. In polyamine complexes, there are several kinds of possibilities which cause signal broadening. To obtain a deeper insight, further experiments were made involving the [Co *en*$_3$]$^{3+}$ complex. First, the NMR spectra of the complex at 70 and 10°C were measured. Though the temperature effect is very small within this temperature range, we can clearly observe a definite tendency for the bands to be broadened at low temperatures and to be sharpened at high temperatures. Secondly,

TABLE I. NH_2 SIGNALS OF [Co *en*$_3$]Cl_3 AND [Co *tn*$_3$]Cl_3 MEASURED AT 60 AND 100 Mc. (c. p. s. UNIT)

		Shoulder	Main peaks		Shoulder
[Co *en*$_3$]Cl_3	60 Mc.	−284	−292	−310	−319
	100 Mc.	−476.5	−485	−520.6	−529
		Coupling constant 8.5 c. p. s.			
		Chemical shift 0.43 p. p. m.			
[Co *tn*$_3$]Cl_3	60 Mc.	−257	−267	−282	−292
	100 Mc.	−431	−440	−473	−483
		Coupling constant 9.5 c. p. s.			
		Chemical shift 0.40 p. p. m.			

the double resonance technique was applied to the pair of CH_2 and NH_2 signals (more exactly, a component of the NH_2 signal). The irradiation of either signal causes a slight sharpening of the other. In the case of the CH_2 band, the value of the half-width decreases to nearly 60% of the original. (Similarly, a sharpening of the CH_2 band takes place in the deuterated [Co *en*$_3$]$^{3+}$ complex. In this case, the value of the half-width is approximately one half of the original.) Therefore, the spin-spin coupling between the CH_2 and NH_2 protons is one of the origins of the band-broadening. In addition, in polyamine complexes, many protons which are magnetically different and crowded around the central metal ion and fixed in a relatively rigid, cage-like framework. The situation is somewhat like that in a solid. Therefore, a complete time-averaging of local fields is not realized. The authors should like to regard this situation as the main origin of band-broadening. The tendency of the temperature effect is consistent with this view. In the case of the NH_2 signal, the irradiation of the CH_2 signal does not change the essential features of the band. Consequently, the diffuse pattern may be attributed mainly to the quadrupole relaxation of the nitrogen nucleus.

The NH_2 signal of the [Co *en*$_3$]$^{3+}$ and [Co *tn*$_3$]$^{3+}$ complexes seems to have the characteristics of the AB-type pattern. To confirm this point, the NMR spectra of both the complexes at 100 Mc. were also measured. The results are listed, along with those obtained at 60 Mc., in Table I. As expected, at 100 Mc. the separation between the main peaks of the doublet components increases, while the separation between the main peak and its shoulder is kept constant. This is characteristic of the AB-type. Thus, it has been proved that two kinds of magnetically-unequivalent protons exist in the NH_2 group.

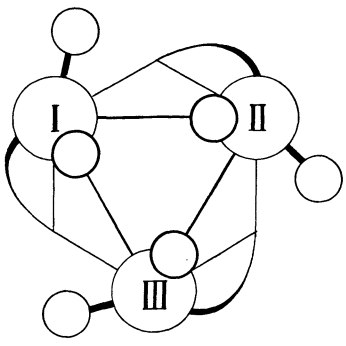

Fig. 2. Structure of the [Co *en*$_3$]$^{3+}$ complex.
Small circles represents hydrogens.
Large circles represents nitrogens.

The structure of the [Co *en*$_3$]$^{3+}$ complex was analyzed by Nakatsu et al.[4] According to their report, the complex has a threefold axis, and all three ethylenediamine ligands coordinated to the cobalt(III) ion have a nonplanar twisted structure of optically the same configuration.[5] In this structure, if we assume the nitrogen atom to have a regular tetrahedral configuration, we can easily distinguish two kinds of protons attached to it. The situation is illustrated in Fig. 2, which shows the upper part of the complex viewed along the threefold axis. Among the six N–H bonds in Fig. 2, three are directed upwards from the N(I)-N(II)N(III) plane and the other three outwards nearly perpendicularly to the threefold axis. In this way the upper three H(A) atoms form a regular triangle, while the lower three H(B) atoms form a larger, regular triangle. The same situation holds in the lower part of the complex. Although the structure of the [Co *tn*$_3$]$^{3+}$ complex has not yet been elucidated by X-ray analysis, a similar situation may be assumed. Here it is worth noting that this kind of doublet pattern does not appear in an aqueous solution. In an acidified aqueous solution, the NH_2 signal appears as a broad single band with no fine structure. This indicates that

4) K. Nakatsu, Y. Saito and H. Kuroya, This Bulletin, **29**, 428 (1956); **30**, 158 (1957).

5) When the ethylenediamine molecule takes a twisted structure, two optically-isomeric forms are possible, as is shown below. These are figures viewed along the C–C axis. The full lines represent the upper side of the molecule, the dotted lines, the lower side.

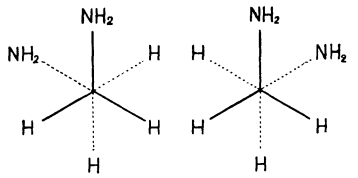

k form *k'* form

a frequent flipping[6] of the coordinated ethylenediamine takes place, through which all the NH_2 protons are magnetically equalized. Such a flipping is presumed to be eased by proton dissociation from the NH_2 group. The feature of the NH_2 signal in an aqueous solution can thus be understood. On the contrary, neither proton dissociation nor proton exchange takes place in trifluoroacetic acid solution (the spectrum of the deuterated complex in trifluoroacetic acid solution does not show a time-change). Therefore, no flipping of the coordinated ethylenediamine occurs.

6) By "flipping" we mean that the coordinated ethylenediamine turns over from the *k* form to *k'*, and vice versa, keeping its two coordination positions fixed.

Last, it must be added that two kinds of the CH_2 protons also exist in the above-mentioned stereomodel of the $[Co\ en_3]^{3+}$ complex. Therefore, the doublet pattern of the CH_2 signal should be observed. However, this is not the case. This is probably either because the relative chemical shift is too small to be observed, or because all the CH_2 protons are equalized through the rocking motion of the CH_2 group.

The authors would like to express their thanks Dr. Kenkichi Nukada, Basic Research Laboratory, Toyo Rayon Company for his measurement at 100 Mc. They also wish to express their thanks to Dr. Masao Ohara, Head of Research Laboratories, Fujisawa Pharmaceutical Company for his encouragement during this work.

BULLETIN OF THE CHEMICAL SOCIETY OF JAPAN VOL. 39 2183—2187 (1966)

The Separation of Zirconium and Hafnium by Tributyl Phosphate - Celite Reversed-phase Partition Chromatography*

By Kaoru UENO and Michio HOSHI

Japan Atomic Energy Research Institute, Tokai, Ibaraki

(Received February 22, 1966)

The distribution ratios, K_d, for zirconium and hafnium were measured in the hydrochloric acid - TBP - celite system, the acid concentration being varied from 5 N to 8 N. The data obtained showed that the separation factor for the above elements, $K_{d_{Zr}}/K_{d_{Hf}}$, is fairly high, —4, in the 7—8 N hydrochloric acid range. Thus, the separation of these elements was carried out in 7.1 N hydrochloric acid by the use of a TBP-celite column.

Recently the technique of reversed-phase partition chromatography has been increasingly used for the separation of metal ions of similar chemical behavior. Fiedelis and Siekierski[1,2] demonstrated the application of this technique to the separation of the rare earth metals, using tributyl phosphate absorbed on kieselguhr as the stationary phase and nitric acid in various concentrations as the eluant. Crawley[3] used tributyl phosphate on kieselguhr for the separation of zirconium and hafnium in a nitric acid solution. The decontamination factor of zirconium in the recovery of 90% of the hafnium, calculated on the basis of his experimental data, was within 10^2, although hafnium was separated from zirconium excellently.

The present paper will show the mutual separation of zirconium and hafnium by reversed-phase partition chromatography, performed using tributyl phosphate absorbed on the celite as the stationary phase and hydrochloric acid as the mobile phase in order to obtain purified zirconium and hafnium.

Experimental

Reagents.—Commercial-quality tributyl phosphate was purified in the usual way.[4] Zirconium and hafnium chloride solution were prepared from analytical reagent-quality zirconium oxide and hafnium oxide respectively. All the other reagents used were of an analytical grade. hafnium-181 and zirconium-95 free from niobium-95 were chosen as the radioactive tracers for hafnium and zirconium respectively.

Batch Equilibrations.—A half grams of the TBP-celite was placed into a cylindrical vessel, then 5 ml. portions of hydrochloric acid in various concentrations were added, and finally a known quantity of zirconium-95 or hafnium-181 solution. The vessels were then closed and shaken vigorously at room temperature for 10, 30 and 60 min.

* Reported at the 8th Discussion Meeting on Radiochemistry, Osaka, November, 1964.

1) S. Siekierski and I. Fidelis, *J. Chromatog.*, **4**, 60 (1960).

2) I. Fidelis and S. Siekierski, ibid., **5**, 161 (1961).

3) R. H. A. Crawley, *Nature*, **197**, 377 (1963).

4) D. F. Peppard, W. J. Driscoll and J. L. Maier, *J. Inorg. Nucl. Chem.*, **3**, 215 (1956).

After that, the aqueous layers were taken and centrifuged. Activities in 1 ml. aliquots of aqueous solutions, the equilibrium activities, C_f, were measured for the given systems. The distribution ratios, K_d, were obtained from the following equation: $K_d = \frac{C_0/5 - C_f}{C_0/5} \times 2$, where C_0 is the initial activity of the zirconium-95 or hafnium-181 added to the system. According to the equation given above, K_d values represent the ratios of activities of metal ions per gram of celite to that per milliliter of the solution.

Column Separation.—The column studies of zirconium and hafnium were carried out with a TBP-treated celite bed 0.8 cm. in diameter and 10.5 cm. high.

The material, TBP-celite, was transferred into a column, and the bed was pressed with a glass rod to eliminate air bubbles. The column was then conditioned with the same concentration of hydrochloric acid as the eluant. When one milliliter of the labeled zirconium or hafnium solution was placed on the top of the bed, it adsorbed completely. Then elution was started with eluants composed of various concentrations of hydrochloric acid. The elution rate was held at 1 ml./cm²/min.

The activity of 2 ml. samples of the eluate was determined by counting γ-rays with a well-type scintillation counter.

Results

The Separation Factor for Zirconium and Hafnium.—The first tests were made of the shaking-time dependence of the distribution ratios, K_d, between TBP-celite—hydrochloric acid with tracer-scale zirconium and hafnium in different concentrations of hydrochloric acid. As is shown in Fig. 1, the K_d values of these ions became almost constant in a shaking time of less than 10 min. Therefore, the batch equilibrium of both ions is attained in 10 min.

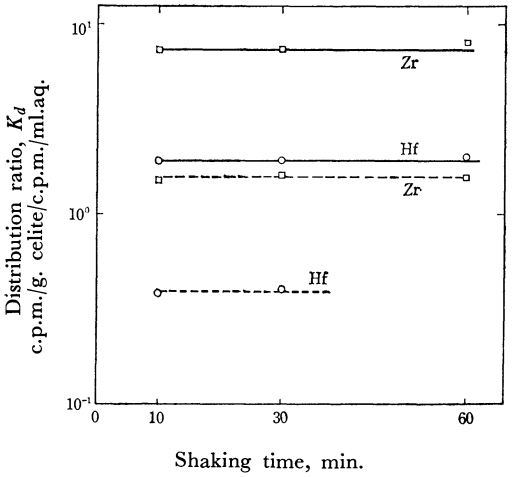

Fig. 1. Shaking time dependence of distribution ratio.
—— 7.35 N HCl
---- 6.85 N HCl
Weight ratio: TBP (1:2) celite

The K_d values of zirconium and hafnium as a function of the acid concentration are shown in Fig. 2. From these data, it may be seen that the K_d values of zirconium and hafnium increase linearly within the concentration of from 7 to 8 N of hydrochloric acid, and that hafnium is eluted more easily than zirconium by the eluant. The separation factor of these ions, $K_{d_{Zr}}/K_{d_{Hf}}$, is about 4 at each point of this acidity range.

The Loading Capacity of TBP-Celite.—The loading capacity of TBP-celite with the weight ratio of 1 : 2 was determined by the batch-equilibrium method described above. In this case, the

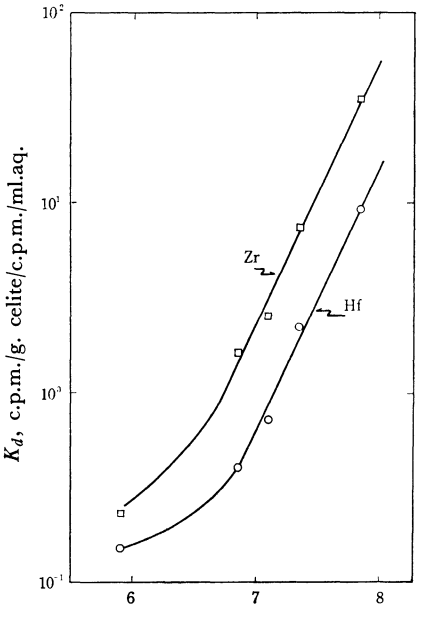

Fig. 2. K_d values of Zr and Hf dependent on HCl concentration.
Weight ratio: TBP (1:2) celite

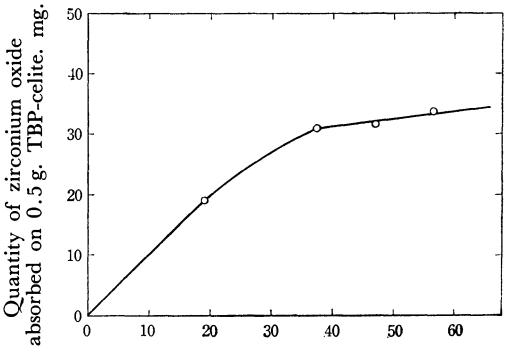

Fig. 3. The loading capacity of TBP-celite.
Weight ratio: TBP(1:2) celite

quantity of zirconium oxide in the solution was changed, while the acid concentration was kept at 9 N hydrochloric acid. As is shown in Fig. 3, the loading capacity is about 70 mg. zirconium oxide per 1 gr. TBP-celite. This number agrees with the value calculated on the assumption that the composition of the complex is $ZrO(NO_3)_2$-$(TBP)_2$.

The Separation of Zirconium and Hafnium by the Column Method.—*Acid Dependence.*—Figure 4 shows elution curves for both hafnium and zirconium. The curves for hafnium were obtained with 6.85, 7.10 and 7.35 N hydrochloric acid, and those for zirconium, with 6.85 and 7.10 N. Factors other than the acidity were kept constant. With an increase in the hydrochloric acid concentration, the curve becomes broader and the peak eluate positions are shifted to the right. Figure 5 shows the linear relationship between the peak eluate volumes in TBP-celite-reversed phase chromatography and the corresponding distribution ratio, K_d, obtained by the batch method. The values obtained fall along straight lines, with very little deviation. This fact shows the good reliability of the TBP-celite reversed-phase chromatography.

The Effect of the Amount of TBP Absorbed on the Celite.—In order to check this effect, TBP-celite absorbents with the weight ratios of 1 : 1, 1 : 2 and 1 : 4 were prepared. Figure 6 shows the relationships between the weight ratio of TBP-celite and the peak eluate volumes in this reversed-phase chromatography. The column with increasing TBP weight ratios makes the elution curve broader, and the peak eluate position shifts right for both zirconium and hafnium. This results is

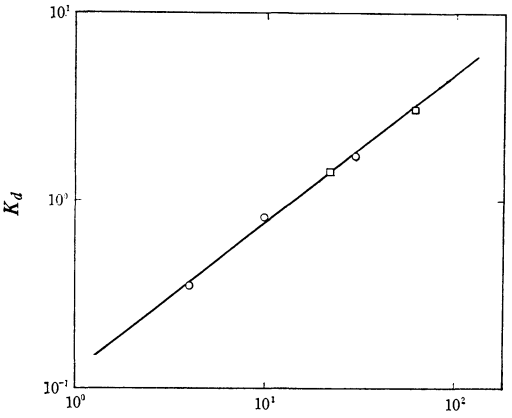

Peak eluate volume, ml.

Fig. 5. Relationship between K_d values and peak eluate volume.
○ Hf □ Zr

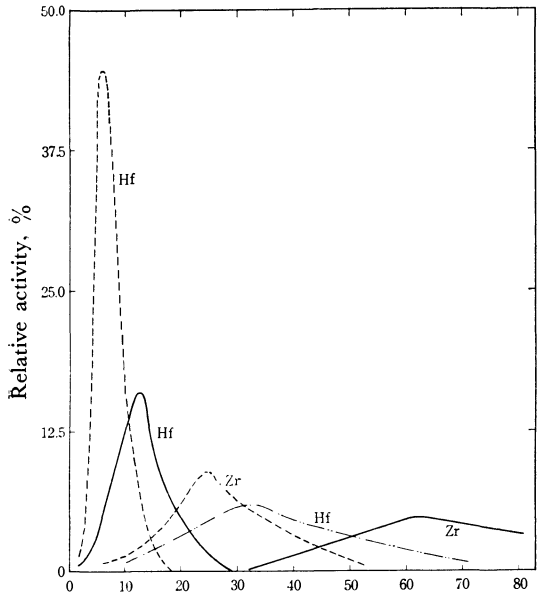

Volume of eluate, ml.

Fig. 4. Elution curves of Zr and Hf from TBP-celite with 6.85—7.35 N HCl.
Eluant
---- 6.85 N HCl
—— 7.10 N HCl
-·-·- 7.35 N HCl
Column ϕ=0.8 cm. h=10.5 cm. weight ratio, TBP (1:2) celite

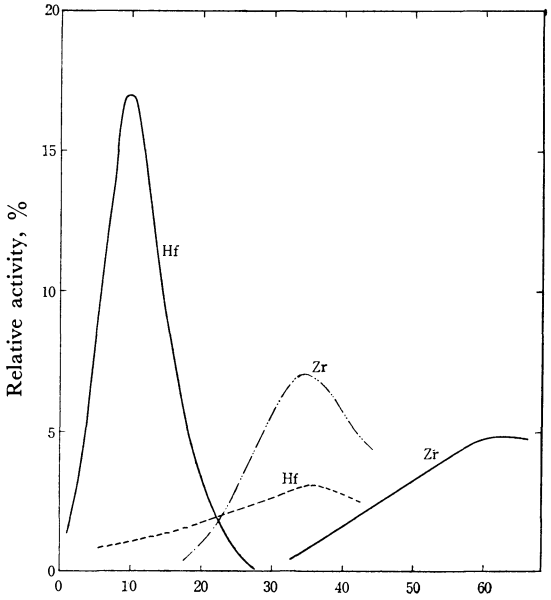

Volume of eluate, ml.

Fig. 6. Elution curves dependent on the weight ratio of TBP to celite.
Weight ratio of TBP to celite
—— TBP (1:2) celite
---- TBP (1:1) celite
-·-·- TBP (1:4) celite
Column ϕ=0.8 cm. h=10.5 cm. eluant, 7.10 N HCl

similar to those obtained from a study of the hydrochloric acid concentration dependence on the elution curves.

Miscellaneous Conditions for the Separations of Zirconium and Hafnium.—In the course of this work it has been observed that the peak eluate volumes of zirconium and hafnium for a 1 : 2-weight-ratio TBP-celite column are almost independent of the amounts of these elements in the range from tracer scale to 50 mg./ml. of hydrochloric acid. After these experiments, using 7.1 N hydrochloric acid as the eluant, the separation was checked in detail with 10 mg. of zirconium and a small quantity of hafnium labeled with Hf-181. The radioactivities of hafnium in the eluate became detectable at 4 ml.; the concentration in the eluate rose to a maximum at 14 ml. and then fell off roughly symmetrically to an undetectable level.

The mutual separation of 10 mg. of hafnium and a small amount of zirconium labeled with zirconium-95 was effected, using 7.1 N hydrochloric acid as the eluant. The activities of zirconium in the eluate began to come through at 30 ml., reaching a maximum at 65 ml. and then falling gradually.

These elution curves of hafnium or zirconium are very similar to the curves obtained with pure hafnium or zirconium respectively. Several column tests like these two showed that mixtures of the two ions in weight ratios, Zr/Hf, from 1 : 1000 to 1000 : 1 bring about no change in the shapes and locations of the elution curves of zirconium and hafnium.

Finally, other factors, such as the grain size of the celite or the conditioning time with water or hydrochloric acid, were also examined. No remarkable difference caused by these factors was observed. Hafnium is separated with hydrochloric acid, leaving zirconium in the column; the zirconium remaining is easily eluted with less than

TABLE I. DECONTAMINATION FACTOR

Column: $\phi = 0.8$ cm. $h = 10.5$ cm.
Weight ratio: TBP(1:2) celite

Eluant	Taken		Recovery, %		Decontamination factor	
HCl concn., N	HfO_2, mg.	ZrO_2, mg.	Hf	Zr	Zr for Hf	Hf for Zr
6.95	10	10	100		1.8×10	
			99		7.0×10	
			98		1.5×10^2	
			96		5.8×10^2	
			95		$>10^3$	
6.95	10	10		100		1.1×10
				99		7.2×10
				98		2.0×10^2
				96		$>10^3$
				95		$>10^3$
7.10	100	0.01	100		8.7×10	
			99.5		4.5×10^2	
			99		$>10^3$	
7.10	100	0.01		100		9.9×10
				99.5		9.9×10^2
				99		$>10^3$
7.10	10	10	100		1.6×10^2	
			99.5		$\sim10^3$	
			99		$>10^3$	
7.10	10	10		100		2.2×10^2
				99.5		7.1×10^2
				99		$>10^3$
7.10	0.01	100	100		1.3×10^2	
			99.5		6.6×10^2	
			99		$>10^3$	
7.10	0.01	100		100		7.2×10
				99.5		8.3×10^2
				99		$>10^3$
7.10	0.01	0.01	100		5.7×10	
			99.5		1.1×10^2	
			99		2.0×10^2	
7.10	0.01	0.01		100		2.5×10
				99.5		1.1×10^2
				99		3.6×10^2

0.01 N of oxalic acid, which is also very effective in stripping zirconium from the TBP-celite column.

From the results described above, the decontamination factors of zirconium or hafnium were calculated. These values are shown in Table I, in which values higher than 10^3 indicate that no detailed calculations could be made because of the statistical error of the counting method.

Conclusion

The mutual separation of zirconium and hafnium with reversed-phase partion chromatography, using 7.1 N hydrochloric acid as the eluant and 1 : 2-weight-ratio TBP-celite as the stationary phase, can be carried out very simply.

The authors wish to express their gratitude to Dr. Tomitaro Ishimori for his kind guidance, and to Drs. Kan Kimura and Eiko Akatsu and Mr. Kenju Watanabe for the valuable advice and discussion given during this work.

BULLETIN OF THE CHEMICAL SOCIETY OF JAPAN VOL. 39 2187—2190 (1966)

Infrared Spectroscopic Study on Ion Association of Hexacyanoferrate(III) and Hexacyanoferrate(II) Ions

By Nobuyuki TANAKA, Yumiko KOBAYASHI and Minoru KAMADA

Department of Chemistry, Faculty of Science, Tohoku University, Katahira-cho, Sendai

(Received February 25, 1966)

The ion association of hexacyanoferrate(III) and hexacyanoferrate(II) anions with univalent or bivalent cations in aqueous solutions has been studied by the measurement of the infrared absorption band due to the C≡N stretching vibrations. All the solutions measured in which ion-pairs with hexacyanoferrates(III) predominated gave an absorption maximum at 2121 cm^{-1}, and those in which ion-pairs with hexacyanoferrates(II) predominated, at 2020 cm^{-1}, although hexacyanoferrates(III) and hexacyanoferrates(II) of potassium and alkaline earth metals gave different spectra from each other in solid state. No difference in absorption band obtained with different solutions was supported by the distance between two ions in ion-pair, which was estimated from the structures of hexacyanoferrate(III) and hexacyanoferrate(II) ions and the closest approach of the ion-pair; this indicates that there is no direct interaction between the complex anion and the cation, but one or more water molecules interpose between the two ions.

A number of investigations on ion-pair formation in solutions have been made by the conductometric method, but only a few, by the measurements of Raman and infrared spectra. Hester and Plane[1] measured Raman spectra of aqueous solutions of some metal nitrates, sulfates and perchlorates and discussed on the interionic (inner-sphere) association of metal ions with these anions from the change in the symmetry and the force constant estimated from the Raman spectra. Fronaeus and Larsson[2,3] obtained infrared spectra of some metal thiocyanato complexes both in solution and in solid state and correlated the changes in absorption frequency and intensity with the structure and the bonding characteristics of the complexes. Larsson studied[4] also on the infrared spectra of hexamminecobalt(III) ions in aqueous solutions of some electrolytes in order to know of the kind of the bonding forces of the outer-sphere complexes.

This investigation was undertaken for the purpose of obtaining some information of the bonding character of the outer-sphere ion association of hexacyanoferrate(III) and hexacyanoferrate(II) ions with univalent and bivalent cations.

Experimental

Materials.—Magnesium, calcium and barium hexacyanoferrates(III) were prepared from potassium hexacyanoferrate(III) by the following procedure. More than three equivalents of perchloric acid was

1) R. E. Hester and R. A. Plane, *Inorg. Chem.*, **3**, 769 (1964).
2) S. Fronaeus and R. Larsson, *Acta Chem. Scand.*, **16**, 1433 (1962).
3) S. Fronaeus and R. Larsson, ibid., **16**, 1447 (1962).
4) R. Larsson, ibid., **16**, 2460 (1962).

TABLE I. WAVE NUMBERS OF ABSORPTION BAND DUE TO THE C≡N STRETCHING VIBRATION OF AQUEOUS SOLUTIONS OF POTASSIUM HEXACYANOFERRATE(III) OF VARIOUS CONCENTRATIONS

Concn. of $K_3[Fe(CN)_6]$ added, mol./l.	K_c	Concn. of $K^+[Fe(CN)_6]^{3-}$, mol./l.	Degree of ion-pair formation, %	Wave number of $\nu_{C\equiv N}$, cm^{-1}
0.02	7.0	0.006	30	2121
0.05	5.1	0.02	43	2121
0.10	4.5	0.06	57	2121
0.25	4.5	0.19	78	2121
1.00	4.5	0.93	93	2121

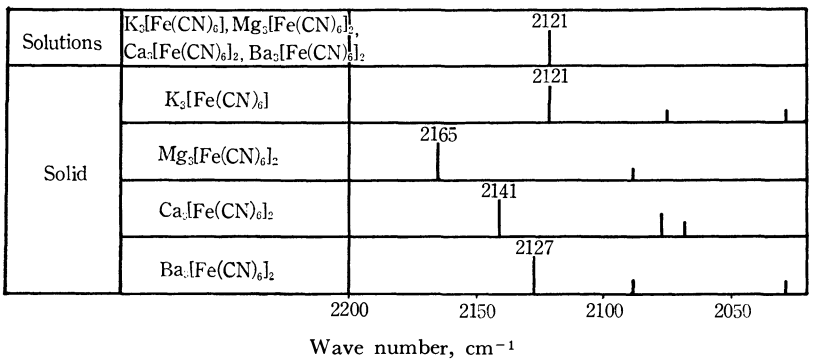

Fig. 1. Wave numbers of the absorption bands of hexacyanoferrates(III) in aqueous solution and in solid state. Solutions contain each complex by 0.02 M up to saturation. For solid state, crystalline water is not described.

added to one equivalent of potassium hexacyanoferrate(III) to precipitate potassium perchlorate. The solution of hydrogen hexacyanoferrate(III) thus obtained was neutralized with magnesium hydroxide, and then magnesium hexacyanoferrate(III) was precipitated by the addition of magnesium chloride in excess. Calcium and barium hexacyanoferrates(III) were prepared in the same way. All the materials obtained were recrystallized three times from water and washed by water, ethanol and ether. Calcium hexacyanoferrate(II) was obtained from potassium hexacyanoferrate(II) in a similar way.

Measurements of Infrared Spectra.—Infrared spectra were measured by using a Hitachi EPI-2G infrared spectrophotometer equipped with a potassium bromide foreprism and a grating double monochrometer. Cells with windows of sodium chloride and those of calcium fluoride were used. In the former case, polyethylene pouch was used to prevent the dissolution of the window material. Platinum foil of 0.05 mm. thick was used for a spacer. Infrared spectra of solid samples were measured by the potassium bromide disk method and the Nujol mull method. The spectra were precisely recorded in the region of 1900 to 2300 cm^{-1}. The internal standard method was adopted when the accurate determination of relative wave numbers was required.

Results

Infrared absorption due to the C≡N stretching vibration was measured with the solutions of potassium hexacyanoferrate(III) of various concentrations. The concentration of ion-pair $K^+[Fe(CN)_6]^{3-}$ present in the solution was calculated in the following way. The concentration association constant of potassium hexacyanoferrate(III), K_c, was calculated from the reported value of the thermodynamic association constant ($\log K_a = 1.3$[5]), using activity coefficients which were obtained from the diagram given by Ringbom.[6] In order to increase the accuracy in the measurements of wave numbers, an absorption band due to the C N stretching vibration of potassium hexacyanoferrate(II) at 2047 cm^{-1} was used as the internal standard, to which the C≡N stretching bands of all hexacyanoferrates(III) were referred. The results obtained with aqueous solutions of potassium hexacyanoferrate(III) are shown in Table I. Absorptions due to the C≡N stretching vibration gave maxima at 2121 cm^{-1} in all cases.

The solutions which contained 0.04 M potassium hexacyanoferrate(III) and 0.2 M magnesium, calcium or barium chloride, and the saturated solutions of magnesium, calcium and barium hexacyanoferrates(III) gave also the absorption due to the C≡N stretching vibration at 2121 cm^{-1}. In the former solutions 70—80% of hexacyanoferrate(III) ions present in the solutions existed in the form of ion-pairs $M^{2+}[Fe(CN)_6]^{3-}$. The calculation was made with the same procedure as in the case of ion-pairs $K^+[Fe(CN)_6]^{3-}$, using the

5) J. C. James and C. B. Monk, *Trans. Faraday Soc.*, **46**, 1041 (1950).
6) A. Ringbom, "Complexation in Analytical Chemistry," Interscience, New York (1964), p. 24.

TABLE II. CLOSEST APPROACH AND DISTANCE FOR HYDRATED METAL IONS WITH HEXACYANOFERRATES(III) AND HEXACYANOFERRATES(II)

Ion-pair	log K_a	Closest approach (a), Å	Available distance for hydrated metal ions (l),* Å	Hydrated metal ion radius, Å
$K^+[Fe(CN)_6]^{3-}$	1.3	7.7	5.3	2.18
$Mg^{2+}[Fe(CN)_6]^{3-}$	2.79	7.1	4.7	1.50
$Ca^{2+}[Fe(CN)_6]^{3-}$	2.83	6.8	4.4	1.84
$Ba^{2+}[Fe(CN)_6]^{3-}$	2.88	6.4	4.0	2.20
$K^+[Fe(CN)_6]^{4-}$	2.3[10]	4.5	2.4	2.18
$Ca^{2+}[Fe(CN)_6]^{4-}$	3.77[11]	5.8	3.7	1.84

* See Fig. 3 for l.

concentration association constants of $M^{2+}[Fe(CN)_6]^{3-}$ which were converted from the thermodynamic association constants[7] of $10^{2.79}$ for Mg^{2+}-$[Fe(CN)_6]^{3-}$, $10^{2.83}$ for $Ca^{2+}[Fe(CN)_6]^{3-}$ and $10^{2.88}$ for $Ba^{2+}[Fe(CN)_6]^{3-}$. The absorption spectra of potassium, magnesium, calcium and barium hexacyanoferrates(III) in solid state were measured and compared with the spectra of the solutions of those compounds. They are shown in Fig. 1.

The solutions of hexacyanoferrate(II) salts were also subjected to the measurements of absorption spectra, and compared with each other. The absorption spectra of these solutions were also compared with those of the solids. In this measurement the absorption at 2349 cm^{-1} of carbon dioxide was taken as the internal standard. In the case of the solutions only one absorption band was observed at 2020 cm^{-1} with all the solutions of various concentrations both for potassium and calcium hexacyanoferrates(II). In solid state, however, the spectra of the calcium salt differed from those of the potassium salt. The results are shown in Fig. 2.

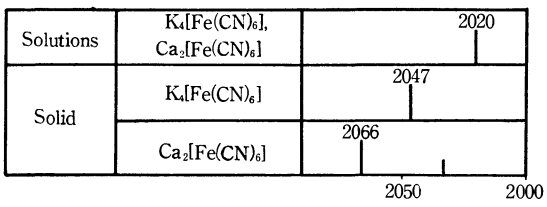

Fig. 2. Wave numbers of the absorption bands of hexacyanoferrates(II) in aqueous solution and in solid state. Solutions contain each complex by 0.02 M up to saturation. For solid state, crystalline water is not described.

Discussion

The solutions of various hexacyanoferrates(III) gave the same frequency and shape of absorption band due to the C≡N stretching vibration under widely different conditions, although these compounds gave different absorption spectra from each other in solid state. The same was found with hexacyanoferrates(II). The absoprtion bands due to the C≡N stretching vibration observed in solid state were at higher frequencies than those observed with the solutions in all cases except potassium hexacyanoferrate(III). One of the explanations of the phenomena is that the complex anion has no direct interaction with a metal cation but it forms an ion-pair with a hydrated metal cation.

Fronaeus and Larsson state[8] in their report that, because a sulfate ion bonds to a metal ion in the form of outer-sphere complex, the disturbance of the symmetry may be so small that its spectra will be identical with those of the free sulfate ion. Since no non-aqueous solvent in which hexacyanoferrates(II) and hexacyanoferrates(III) are soluble in required concentrations was found, an experimental approach to the examination of direct interaction of a complex anion and a metal cation was not successful. Alternatively, the possibility of existence of one or more water molecules between the complex anion and the metal cation was examined by the calculation of the distance of these two ions in ion-pair.

The relation between the closest approach of two ions in ion-pair, a, and the association constant, K, is given by the equations,[9]

$$K = \frac{4\pi N}{1000}\left(\frac{|z_i z_j| e^2}{\varepsilon \boldsymbol{k} T}\right)^3 Q(b) \qquad (1)$$

$$Q(b) = \int_2^b x^{-4} \exp(x)\, dx \qquad (2)$$

where

$$x = \frac{|z_i z_j| e^2}{r \varepsilon \boldsymbol{k} T} \qquad (3)$$

and

7) C. W. Gibby and C. B. Monk, *Trans. Faraday Soc.*, **48**, 632 (1952).

8) S. Fronaeus and R. Larsson, *Proc. 8 ICCC (1964)*, p. 383.

9) C. W. Davies, "Ion Association," Butterworths, London (1962), p. 164.

10) C. W. Davies, *J. Am. Chem. Soc.*, **59**, 1760 (1937).

11) C. W. Davies, *J. Chem. Soc.*, **1945**, 460.

$$b = \frac{|z_i z_j| e^2}{a\varepsilon \boldsymbol{k} T} \quad (4)$$

N represents the Avogadro number, ε dielectric constant, z the charge of ion, $\boldsymbol{k}$ the Boltzmann's constant and r the distance between two ions in ion-pair. For infinitely dilute aqueous solutions at 25°C, Eqs. 1. and 4 are written as,

$$\log K = 0.4386 + 3\log|z_i z_j| + \log Q(b) \quad (5)$$

$$\log a = \log|z_i z_j| - 7.1468 - \log b \quad (6)$$

The values of a for various ion-pairs of hexacyanoferrate(III) and hexacyanoferrate(II) ions with the metal cations were calculated with Eqs. 5 and 6, and given in Table II.

The positions of water molecule interposing between a complex anion and a metal cation is assumed to be located on the face of the octahedron of a hexacyanoferrate ion as shown in Fig. 3.[12]

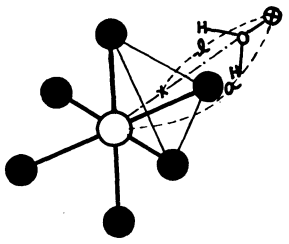

Fig. 3. The possible position of a hydrated metal ion forming an ion-pair with a hexacyanoferrate ion. ○ indicates Fe atom, ● C≡N group and ⊗ a center of a hydrated metal cation.

From the crystal structure of potassium hexacyanocobaltate(III)[13] similar to hexacyanoferrate(III), the Fe-C distance is estimated to be about 2.5 Å and the C-N distance about 1.15 Å. In the case of hexacyanoferrates(II), Marcus[14] reported that the Fe-C distance in the iron cyanide ions may be assumed to be 1.85 Å, which equals the Fe-C bond distance in $Fe(CNCH_3)_6^{2+}$. This value agrees with the Fe-C distance calculated from the crystal structure of potassium hexacyanoferrate(II)[15]; the Fe-C and the C-N distance were calculated to be about 1.9 Å and 1.18 Å, respectively. Using these distances and the values for the closest approach the available distance for the hydrated metal ion, l, was calculated for the univalent and bivalent cations, which are given in Table II. The ionic radii of hydrated metal ions were considered to be the ionic radii of the metal ions plus 0.85 Å.[16] From these values and the available distance for the hydrated metal ions given in Table II, it may be concluded that a water molecule or molecules interpose between the metal cation and the complex anion when they are in the state of ion-pair. This, in turn, suggests that there is no direct interaction between univalent and bivalent cations and hexacyanoferrate(III) and hexacyanoferrate(II) ions.

The authors wish to thank the Ministry of Education for the financial support granted for this research.

12) B. E. Conway and J. O'M. Bockris, *Electrochim. Acta*, **3**, 340 (1961).
13) H. Kuroya and Y. Saito, "Mukikagakuzensho, Sakuen," Ed. by K. Yamasaki and T. Inoue, Maruzen, Tokyo (1959), p. 220.
14) R. A. Marcus, *J. Chem. Phys.*, **26**, 867 (1957).
15) V. A. Pospelov and G. S. Zdanov, *Z. Fiz. Khim. SSSR*, **21**, 405, 521, 879 (1947).
16) W. M. Latimer, K. S. Pitzer and G. M. Slansky, *J. Chem. Phys.*, **7**, 108 (1939).

BULLETIN OF THE CHEMICAL SOCIETY OF JAPAN VOL. 39 2191—2194 (1966)

The Radiation-Induced Addition Reaction of Thiols to Chlorofluoroolefins

By Kan INUKAI, Teruo UEDA and Hiroshige MURAMATSU

Government Industrial Research Institute, Nagoya, Kita-ku, Nagoya

(Received August 23, 1965)

The addition of thiols to chlorofluoroethylenes was carried out under γ-ray irradiation; chlorofluoroethyl alkyl sulfides were thus obtained. Chlorofluoroethyl alkyl sulfoxides and sulfones were prepared by the oxidation of the sulfides. The dehydrohalogenation of chlorofluoroethyl alkyl sulfides yielded chlorofluorovinyl alkyl sulfides, whose structure indicated that the thiyl radical attacked the difluoromethylene side of the asymmetrical dichlorodifluoroethylene. Chlorofluorovinyl sulfoxides and sulfones were also synthesized from the sulfides by oxidation with hydrogen peroxide.

The free radical addition of thiols to olefins[1] is well known, and a variety of sulfur-containing compounds, such as thiols[2] and hydrogen sulfide[3], have been added to fluoroolefins using peroxide, or under ultraviolet or X-ray irradiation. The base-catalyzed addition of thiols[4,5] to fluoroolefins has also been studied extensively.

In this paper, the addition of RSH, where R is methyl, ethyl, or isopropyl, to 1, 1, 2-trichloro-2-fluoroethylene, 1, 2-dichloro-1, 2-difluoroethylene, and 1, 1-dichloro-2, 2-difluoroethylene will be described. By the oxidation of 1 : 1 adducts (the chlorofluoroethyl alkyl sulfides), both the corresponding chlorofluoroethyl alkyl sulfoxides and sulfones were prepared. The chlorofluorovinyl alkyl sulfides, sulfoxides, and sulfones were also synthesized by the dehydrohalogenation of the 1 : 1 adducts, followed by oxidation.

The reactants were irradiated in a glass tube at a rate of $0.6—0.7\times10^5$ r./hr. for a period of 3—4 weeks at room temperature. The irradiation conditions of each run are listed in Table I, along with the yields as calculated on the basis of the amounts of olefins added. The addition to 1, 2-dichloro-1, 2-difluoroethylene and 1, 1-dichloro-2, 2-difluoroethylene gave mainly 1 : 1 adducts in appreciable yields. Since a mixture of thiols and chlorofluoroethylenes gave no products upon standing in a dark at room temperature for a month, the reactions under the radiation seem to be through a free-radical mechanism. The general reaction is:

$$RSH + CFX{=}CClX \xrightarrow{\gamma\text{-ray}} RSCFXCHClX$$

where X=F or Cl; R=CH_3, C_2H_5, or i-C_3H_7.

Table I. Irradiation conditions in addition of RSH to chlorofluoroolefins

R	Molar ratio of RSH to olefin[a]	Total dose r.	Yield[b] of 1 : 1 adduct g.(%)	RSSR, g.	$(RS)_2C{=}CFCl$ g.
		$CFCl{=}CFCl$			
C_2H_5	1.0	2.2×10^7	12.5(17.0)	3.8	2.0
C_2H_5	1.5	3.5×10^7	17.5(23.9)	3.5	10.5
i-C_3H_7	1.0	3.5×10^7	13.5(17.2)		2.0
		$CF_2{=}CCl_2$			
CH_3	1.0	2.2×10^7	48.2(71.0)	1.5	
C_2H_5	1.0	2.2×10^7	44.5(61.0)	2.5	
i-C_3H_7	1.0	3.5×10^7	57.5(73.3)		

a) Fifty grams of the olefin were used in each run.

b) Based on the amounts of olefin added.

The reaction of trichlorofluoroethylene and tetrachloroethylene with thiols gave no addition products, and the yields of the addition products with 1, 1-dichloro-2, 2-difluoroethylene were higher than those of 1, 2-dichloro-1, 2-difluoroethylene. These facts seem to indicate that asteric interference between the bulky sulfur and chlorine atom may have an effect on the reactivity of olefins. The physical properties of the 1 : 1 adducts are shown in Table II.

The alkyl disulfides, which were identified by a comparison of their infrared spectra and gas chromatogram with those of authentic samples, were generally formed as by-products. In the reaction of 1, 2-dichloro-1, 2-difluoroethylene with thiols, an appreciable amount of a viscous compound was obtained, together with the 1 : 1 adduct and alkyl disulfide. Further, the amount of the compound increased with an increase in the ratio of the thiol to the ethylene. From its infrared spectrum, molecular weight, and elemental analysis,

1) C. Walling, "Free Radicals in Solution," John Wiley & Sons, Inc., New York (1957), p. 313.

2) J. F. Harris, Jr., and F. W. Stacey, *J. Am. Chem. Soc.*, **83**, 840 (1961).

3) J. F. Harris, Jr., and F. W. Stacey, ibid., **85**, 749 (1963).

4) W. T. Miller, U. S. Pat. 2864867 (1958).

5) I. L. Knunyants and A. V. Fokin, *Izv. Akad. Nauk SSSR, Otdel Khim. Nauk*, **1952**, 261; *Chem. Abstr.*, **47**, 3221 (1953).

TABLE II. CHLOROFLUOROETHYL ALKYL SULFIDES

R	B. p. °C(mmHg)	n_D^{20}	d_4^{20}	MR_D Found	MR_D Calcd.	Cl, % Found	Cl, % Calcd.	F, % Found	F, % Calcd.
			$RSCF_2CCl_2H$						
CH_3	48—50(20)	1.4525	1.460	33.47	33.75	38.8	39.2	20.7	21.0
C_2H_5	61—62(20)	1.4531	1.372	38.43	38.37	35.7	36.4	19.3	19.5
i-C_3H_7	70—71(20)	1.4535	1.311	43.12	42.98	33.6	34.0	18.2	18.2
			RSCFClCFClH						
C_2H_5[a]	60—61(20)	1.4548	1.361	38.85	38.37	35.9	36.4	19.5	19.5
i-C_3H_7[b]	63—65(20)	1.4586	1.273	44.84	42.98				

a) Lit[5] b. p. 138°C, n_D^{20} 1.4612, d_5^{20} 1.425.
b) Though the gas chromatogram (column packed with Silicone DC-550 or PEG-400) showed a single peak, the compound seems to contain the disulfide as an impurity.

TABLE III. CHLOROFLUOROVINYL ALKYL SULFIDES

R	B. p. °C(mmHg)	n_D^{20}	d_4^{20}	MR_D Found	MR_D Calcd.	Cl, % Found	Cl, % Calcd.	F, % Found	F, % Calcd.	$\nu_{C=C}$ cm^{-1}
			$RSCF=CCl_2$							
CH_3	45—46(20)	1.5062	1.427	33.53	33.20	43.7	44.1	11.9	11.8	1605
C_2H_5	52—54(20)	1.4458	1.337	38.24	37.82	40.1	40.6	10.6	10.9	1601
i-C_3H_7	67—68(20)	1.4896	1.269	43.03	42.44	37.2	37.6	9.6	10.1	1599
			RSCF=CFCl							
C_2H_5[a]	116—118	1.4455	1.255	33.65	33.03	22.1	22.4	23.7	24.0	1661
i-C_3H_7[b]	53—56(50)	1.4480	1.200	38.47	37.65	20.5	20.6	21.8	22.0	1658

a) Lit.[5] b. p. 106—107°C, n_D^{20} 1.4385, d_4^{20} 1.282.
b) Lit.[5] b. p. 135°C, n_D^{20} 1.4178, d_4^{20} 1.275.

TABLE IV. CHLOROFLUOROETHYL AND CHLOROFLUOROVINYL SULFOXIDES

R	B. p. °C(mmHg)	n_D^{20}	d_4^{20}	MR_D Found	MR_D Calcd.	Cl, % Found	Cl, % Calcd.	F, % Found	F, % Calcd.	$\nu_{S=O}$ cm^{-1}	$\nu_{C=C}$ cm^{-1}
			$RSOCF_2CCl_2H$								
CH_3[a]						35.6	36.0	18.9	19.3		
C_2H_5	105—106(20)	1.4678	1.484	39.50	39.76	33.0	33.7	17.9	18.0	1030	
i-C_3H_7	75—77(3)	1.4676	1.423	43.93	44.38	31.1	31.6	16.4	15.9	1033	
			RSOCFClCFClH								
C_2H_5	93—94(15)	1.4711	1.483	39.78	39.76	32.8	33.7	17.6	18.0	1030	
i-C_3H_7	79—81(6)	1.4698	1.414	44.37	44.38	30.8	31.6	16.2	16.9	1033	
			$RSOCF=CCl_2$								
CH_3	115—117(15)	1.5224	1.565	34.51	34.59	39.7	40.1	10.3	10.7		1620
C_2H_5	101—103(15)	1.5107	1.472	38.86	39.21	36.6	37.2	9.4	10.0	1030	1620
i-C_3H_7	91—92(5)	1.5059	1.386	43.93	43.83	34.1	34.6	9.2	9.3	1033	1618
			RSOCF=CFCl								
C_2H_5	67—69(5)	1.4738	1.419	34.55	34.42	20.3	20.3	21.5	21.8	1030	1670
i-C_3H_7	70—73(3)	1.4509	1.409	39.08	39.61	17.2	17.4	18.3	18.6	1033	1669

a) M. p. 75—76°C.

the structure of the compound was determined to be $(RS)_2C=CFCl$. The formation of the compound is probably a result of the sequence of the radical dehalogenation. The radical dehalogenations from the intermediate radicals with bulky neighboring groups were often observed in radical-induced addition reactions, in, for example, those of polyhalobutene,[6] 1, 2-dichlorotetrafluorocyclobutene, and 1, 2-dichlorohexafluorocyclopentene.[7]

The direction of the attack of the thiyl radical on asymmetrical dichlorodifluoroethylene was determined by the dehydrohalogenation of the 1 : 1 adduct with potassium hydroxide; chlorofluorovinyl alkyl sulfide was thus yielded. The formation of

6) H. Muramatsu and P. Tarrant, *J. Org. Chem.*, **29**, 1796 (1964).
7) H. Muramatsu and K. Inukai, ibid., **31**, 544, 2546 (1965).

Table V. Chlorofluoroethyl and chlorofluorovinyl alkyl sulfones

R	B. p. °C(mmHg)	n_D^{20}	d_4^{20}	MR_D Found	MR_D Calcd.	Cl, % Found	Cl, % Calcd.	F, % Found	F, % Calcd.	ν_{SO_2} cm^{-1}	$\nu_{C=C}$ cm^{-1}
				$RSO_2CF_2CCl_2H$							
CH_3	103—104(15)	1.4510	1.635	33.08	35.71	33.2	33.3	17.7	17.9	1162, 1352	
C_2H_5	103—105(15)	1.4548	1.541	39.96	40.33	31.1	31.3	16.7	16.7	1155, 1348	
i-C_3H_7	86—88(3)[a]					29.4	29.5	15.4	15.8	1149, 1345	
				$RSO_2CFClCFClH$							
C_2H_5	90—100(15)	1.4536	1.511	40.64	40.33	31.2	31.3	16.7	16.7	1150, 1350	
i-C_3H_7	86—88(3)	1.4568	1.465	44.80	44.95	28.7	29.5	15.3	15.8	1147, 1343	
				$RSO_2CF=CCl_2$							
CH_3	113—114(15)[b]					37.3	36.8	9.5	9.8	1166, 1348	1618
C_2H_5	106—108(15)	1.4896	1.526	39.20	39.78	34.2	34.3	9.1	9.2	1155, 1348	1610
i-C_3H_7	98—100(5)	1.4852	1.440	43.92	44.40	32.1	32.1	8.6	8.6	1148, 1345	1605
				$RSO_2CF=CFCl$							
C_2H_5	76—78(5)	1.4527	1.489	34.57	34.99	18.2	18.6	19.8	20.0	1142, 1350	1670
i-C_3H_7	70—73(3)	1.4509	1.409	39.08	39.61	17.2	17.4	18.3	18.6	1145, 1345	1662

a) M. p. 32—34°C. b) M. p. 44—46°C.

1-fluoro-2, 2-dichlorovinyl alkyl sulfides showed that the RS radical was added to the CF_2 side. If the thiyl radical would attack the CCl_2 side, 1-chloro-2, 2-difluorovinyl alkyl sulfides would be obtained. The physical properties of the chlorofluorovinyl alkyl sulfides prepared are shown in Table III.

The chlorofluoroethyl alkyl sulfoxides and sulfones were synthesized by the oxidation of the corresponding chlorofluoroethyl alkyl sulfides with hydrogen peroxide in acetic acid, at 40—45°C and at 75—80°C respectively. The oxidation of the chlorofluorovinyl alkyl sulfides run under similar conditions yielded the corresponding chlorofluorovinyl alkyl sulfoxides and sulfones.

$$RSCFXCHClX \xrightarrow[AcOH]{H_2O_2} \begin{cases} \rightarrow RSOCFXCHClX \\ \rightarrow RSO_2CFXCHClX \end{cases}$$

$$RSCFXCHClX \xrightarrow{KOH} RSCF=CClX \xrightarrow[AcOH]{H_2O_2} \begin{cases} \rightarrow RSOCF=CClX \\ \rightarrow RSO_2CF=CClX \end{cases}$$

Attempts to dehydrohalogenate the chlorofluoroethyl alkyl sulfoxides and sulfones were found to lead to the decomposition of the sulfoxides and sulfones. The physical properties of chlorofluoroethyl and chlorofluorovinyl alkyl sulfoxides and sulfones are listed in Tables IV and V respectively.

Experimental[8]

The Addition Reactions of Thiols to Chlorofluoroolefins.—A mixture of 23.5 g. (0.38 mol.) of ethanethiol and 50 g. (0.38 mol.) of 1, 1-dichloro-2, 2-difluoroethylene was sealed in a glass tube (ca. 300 ml. in capacity) and irradiated to a total dosage of 2.2×10^7 r. The contents of the tube were then washed out with a diluted solution of sodium hydroxide and extracted with ether. The distillation of the extract under reduced pressure gave 44.5 g. (0.22 mol., 61% yield) of 1, 1-difluoro-2, 2-dichloroethyl ethyl sulfide, b. p. 61—62°C/20 mmHg, and 2.5 g. of ethyldisulfide, which was identified by a comparison of its infrared spectra and gas chromatogram with those of an authentic sample.[9] The addition reactions of thiols to 1, 2-dichloro-1, 2-difluoroethylene were carried out under similar conditions. In these cases, appreciable amounts of the viscous compounds were obtained, together with the 1 : 1 adduct and alkyl disulfide. In the addition of ethanethiol, a compound with a b. p. of 87—89°C/10 mmHg, $\nu_{C=C}$ 1587 cm^{-1}, n_D^{20} 1.5215, d_4^{20} 1.207, was isolated using a preparative gas chromatograph. From its infrared spectrum, molecular weight, and elemental analysis, the structure was assumed to be $(C_2H_5S)_2C=CFCl$.

Found: MR_D 50.64; F, 9.2; Cl, 18.2; mol. wt. 200.[10] Calcd. for $C_6H_{10}FClS_2$: MR_D 49.99; F, 9.5; Cl, 17.7; mol. wt. 200.5.

The irradiation conditions and yields are summarized in Table I.

The Dehydrohalogenation of Chlorofluoroethyl Alkyl Sulfides.—A mixture of 30.0 g. (0.15 mol.) of 1, 1-difluoro-2, 2-dichloroethyl ethyl sulfide and 17.5 g. (0.31 mol.) of powdered potassium hydroxide in a 100 ml. flask equipped with a reflux condenser and a stirrer was heated at 120—125°C for 1.5 hr. The reaction mixture was then poured into water and extracted with ether. The extract was dried and distilled to give 22.0 g. (0.13 mol., 82% yield) of 1-fluoro-2, 2-dichlorovinyl ethyl sulfide, b. p. 52—54°C/20 mmHg.

In a similar manner, the other chlorofluoroethyl alkyl sulfides were treated with potassium hydroxide; they thus gave the corresponding halovinyl alkyl sulfides, whose physical properties are shown in Table III.

8) All temperature readings are uncorrected.

9) E. Miller, F. S. Crossley and M. L. Moore, *J. Am. Chem. Soc.*, **64**, 2323 (1942).

10) Determined by a mass spectrometer.

The Oxidation of Chlorofluoroethyl Alkyl Sulfides and Chlorofluorovinyl Alkyl Sulfides.— In a 100 ml. flask equipped with a stirrer and a reflux condenser were placed 12.0 g. (0.058 mol.) of 1, 1-difluoro-2, 2-dichloroethyl isopropyl sulfide and 8.0 g. (0.071 mol.) of hydrogen peroxide (30% aqueous solution) in acetic acid (50 ml.). The mixture was then stirred for 5 hr. at 40—45°C. After the acetic acid had been distilled off, the reaction mixture was washed with a sodium carbonate solution and extracted with ether. The extract was dried and distilled to give 11.5 g. (0.051 mol., 89% yield) of 1, 1-difluoro-2, 2-dichloroethyl isopropyl sulfoxide, b. p. 75—77°C/3 mmHg, ν_{SO} 1033 cm^{-1}.

Using the same procedure, the other chlorofluoroethyl and chlorofluorovinyl alkyl sulfides were oxidized to the corresponding sulfoxides in yields of about 70%.

In a 200 ml. flask there was placed 23.0 g. (0.11 mol.) of 1, 1-difluoro-2, 2-dichloroethyl isopropyl sulfide in acetic acid (20 ml.). Fifty grams (0.44 mol.) of hydrogen peroxide (30% aqueous solution) in 100 ml. of acetic acid were then added drop by drop over a period of 1 hr. After it had been continuously stirred for an additional 4 hr. at 75—80°C, the mixture was washed with an aqueous sodium carbonate solution and extracted with ether. The distillation of the extract gave 23.5 g. (0.098 mol., 92% yield) of 1, 1-difluoro-2, 2-dichloroethyl isopropyl sulfone, b. p. 86—88°C/3 mmHg; m. p. 32—34°C.

By the same procedure, the other chlorofluoroethyl and chlorofluorovinyl sulfides were oxidized to the corresponding sulfones in yields of about 80%.

BULLETIN OF THE CHEMICAL SOCIETY OF JAPAN VOL. 39 2194—2201 (1966)

The Isomers of the Hydrogenation Products of Bisphenol A. The Separations and Configurations of Three Isomers of 2, 2-Bis-(4-hydroxycyclohexyl)propane and Two of 2-(4-Hydroxy-cyclohexyl)-2-(*p*-hydroxyphenyl)propane[1]

By Akira TERADA

Government Industrial Research Institute, Osaka; Oyodo-ku, Osaka[2]

(Received October 20, 1965)

Hydrogenations of bisphenol A (I) over Raney nickel (W-1) and Urushibara nickel A and B have been carried out, and three stereoisomers of 2,2-bis(4-hydroxycyclohexyl)propane (II) and two of 2-(4-hydroxycyclohexyl)-2-(*p*-hydroxyphenyl)propane (III) have been isolated from the products. The configurations and the preferred conformations of the II isomers, *cis-cis* (m. p. 174—175°C), *cis-trans* (164—165.5°C) and *trans-trans* (188—189°C), and of the III isomers, *cis* (159—161°C) and *trans* (150.5—151.5°C), have been determined by means of the infrared and nuclear magnetic resonance spectra, inversions over sodium to the stable isomers, and other methods. When heated with purified methanol, 2, 2-bis(4-ketocyclohexyl)propane prepared from the chromium trioxide oxidation of an isomeric mixture of II afforded 2, 2-bis(4, 4-dimethoxycyclohexyl)propane, m. p. 140.5—141.5°C. The recrystallization of III_t from benzene yielded $III_t \cdot C_6H_6$. Treating III_c with acetic anhydride gave 2-(3-cyclohexenyl)-2-(*p*-hydroxyphenyl)propane (where *c*: *cis* and *t*: *trans*).

The catalytic hydrogenation of 2, 2-bis(*p*-hydroxyphenyl)propane, bisphenol A (I), under high pressure gives an isomeric mixture of 2, 2-bis(4-hydroxycyclohexyl)propane (II) and 2-(4-hydroxycyclohexyl)-2-(*p*-hydroxyphenyl)propane (III). This reaction was discussed by Jordan in 1925, who mentioned that, under 10—15 atm. of hydrogen pressure using a less active nickel catalyst, the compound III was mainly obtained as a glassy solid, besides the recovered starting material, while none of the saturated compound II was observed.[3] However, he also observed that the use of a colloidal palladium catalyst gave an oily mixture with an aromatic odor and containing the II isomers. Braun also used a less active nickel catalyst at the temperature of 260°C and under 50 atm. of hydrogen pressure for this reaction; he obtained only hydrogenolysis products, which were presumably cyclohexanol, 4-isopropylcyclohexanols, phenol and *p*-isopropylphenol. However, using decalin as a solvent and using a more active nickel catalyst, he succeeded

1) Presented at the Hokkaido Meeting of the Chemical Society of Japan, Hakodate, July, 1962.

2) Present address: Department of Industrial Chemistry, Kyushu Institute of Technology, Tobata-ku, Kitakyushu.

3) H. Jordan, *Chem. Zentr.*, II, 1587 (1926); Brit. Pat. 252594 (1925).

in preparing III in a good yield, besides a small amount of II.[4]

After these investigations it seems that there have been no other reports concerning the preparation of II,[5] and that no investigator has isolated the isomers of II and III, or discussed the configurations.[7] The present study was undertaken in order to isolate these isomers and in order to determine the configuration of the hydroxyl groups, preferred conformations and chemical behavior. These compounds are particularly useful in the production of polyester resins as polyalcohol components.[8]

The above-quoted reports and reports of other analogous hydrogenations have suggested that the use of a more active catalyst[9] and a higher hydrogen pressure would be necessary, and that this would increase the yield of II rather than that of III and prevent the formation of the hydrogenolysis products. Accordingly, the experiments herein are carried out under about 100 kg./cm^2 of initial hydrogen pressure over each of three kinds of nickel catalyst, Raney nickel (W-1), and Urushibara nickel A and B,[12] all of which can easily be prepared and all of which possess considerably high activities.

With regard to the aspects of the hydrogenation, the reaction temperatures and the pressure changes were measured to elucidate the mechanism of the hydrogen absorption. By hydrogenation up to 210°C using a large amount of Urushibara nickel A or B, only products containing III as a major component were obtained, and even at temperatures as high as 260°C the hydrogenations were not completed, whereas over Raney nickel at 260°C, the hydrogen absorption was completed, giving II in an almost theoretical yield. These observations led us to conclude that the hydrogenation takes place step-by-step on each of the phenolic benzene rings, as has generally been recognized hitherto in the usual hydrogenations of biphenyl compounds,[10,13] we also concluded that Urushibara nickel A and B were unsuitable for the hydrogenation of a benzene nucleus of this kind.

Usually a glassy solid was obtained as the hydrogenation product after the resulting solution had been filtered to remove the catalyst and then concentrated to dryness. The residue was spearated into the components either by fractional crystallization or by extraction with aqueous alkali, as is summarized in Fig. 1 and as is described in the Experimental section.

Since analogous compounds, like the II diols, often produce the molecular compound among their stereoisomers, for instance, in the cases of bis(4-hydroxycyclohexyl)[14] and 4-cyclohexylcyclohexanol,[16] each of the products, II_I, II_{II} and II_{III}, obtained here was confirmed to be a single compound through the regenerative hydrolysis of the diacyl compound to the original diol.

The assignment of the configurations of the hydroxyl groups in II_I, II_{II} and II_{III} was initially given from their infrared spectra. The band positions of the secondary alcohol groups in many cyclohexane rings of such compounds as steroids,[17,18] 2-decalols[17] and alkylcyclohexanols[19] generally differ according as it is axial or equatorial. The equatorial hydroxyl groups in such alicyclic ring systems absorb in the 1040—1050 cm^{-1} region, and the axial, at 1000—1010 and 950—960 cm^{-1}. Also, the axial and equatorial acetates both show absorption peaks in the region of about 1230 cm^{-1}, but the axial one shows more complex bands than the equatorial.[17,18] II_I had bands at 1072 and 1048; II_{II}, at 1062, 1020 and 952; and II_{III}, at 1011 and 958 cm^{-1}. The

4) J. v. Braun, *Ann.*, **472**, 65 (1929).

5) Kalina and Brůthans have reported on this hydrogenation after this investigation was completed. They used various cyclohexanol derivatives as solvents and obtained a white, transparent mass as the product.[6]

6) M. Kalina and V. Brůthans, Czech. Pat. 103572 (1962); *Chem. Abstr.*, **58**, 13846 (1963).

7) The *trans-trans* ($II_{t\text{-}t}$), *cis-trans* ($II_{c\text{-}t}$) and *cis-cis* ($II_{c\text{-}c}$) forms of II, and the *trans* (III_t) and *cis* (III_c) of III are considered to be their configurations between the hydroxyl and isopropylidene groups.[3]

8) Brit. Pat. 464762 (1937); 792485 (1958); 808485 (1958); German Pat. 1011148 (1957); Belgian Pat. 546375 (1959); U. S. Pat. 2828278 (1958).

9) Many examples of the hydrogenation procedure for hydroxybiphenyl compounds and many studies of the activities of various nickel catalysts in analogous reactions have been reported. For instance, Yoshitake[10] examined in detail the activities of several kinds of nickel catalysts in the case of the hydrogenation of *o*-phenylphenol; he reported that the activity sequence was in the following order: Raney nickel>stabilized nickel>flaked nickel>reduced nickel. Morita[11] used Urushibara nickel B and nickel Kieselguhr for the hydrogenation of *o*- and *p*-phenylphenols and observed that only the phenolic nuclei were saturated when the former catalyst was used, and that the latter catalyst was not suitable for his purpose because of its low activity.

10) H. Yoshitake, "The Hydrogenation of 2-Phenylphenol, and Chemical Studies of the Products", the Thesis of the Doctor of Pharmacy to Kyoto University, (1961), p. 37; *J. Pharm. Soc. Japan*, **83**, 532, 542 (1963).

11) E. Morita, *The Reports of the Asahigarasu Kogyo Gijitsu Shoreikai*, **6**, 253 (1960).

12) Y. Urushibara and S. Nishimura, "Synthetic Methods of Organic Compounds (Yuuki Kagobutsu Goseiho)," Vol. XI, The Society of Organic Synthetic Chemistry, ed., Gihodo Co., Tokyo (1959), p. 124.

13) S. Kimura, *J. Soc. Org. Synth. Chem. Japan*, **22**, 132 (1964).

14) A. L. Wilds, C. H. Shunk and C. H. Hoffman, *J. Am. Chem. Soc.*, **76**, 1737 (1954).

15) H. E. Ungnarde and A. Ludutsky, *J. Org. Chem.*, **10**, 307 (1945).

16) H. E. Ungnarde, ibid., **13**, 361 (1948).

17) E. A. Braude and E. S. Waight, "Progress in Stereochemistry," Vol. I, W. Klyne, ed., Butterworths, London (1954), p. 167.

18) M. Ōhashi and K. Nakanishi, "Infrared Spectra," Vol. VI, T. Shimanouchi, Y. Mashiko and K. Nakanishi, ed., Nankodo, Tokyo (1958), p. 15.

19) W. Hückel and Y. Riao, *Ann.*, **637**, 33 (1960).

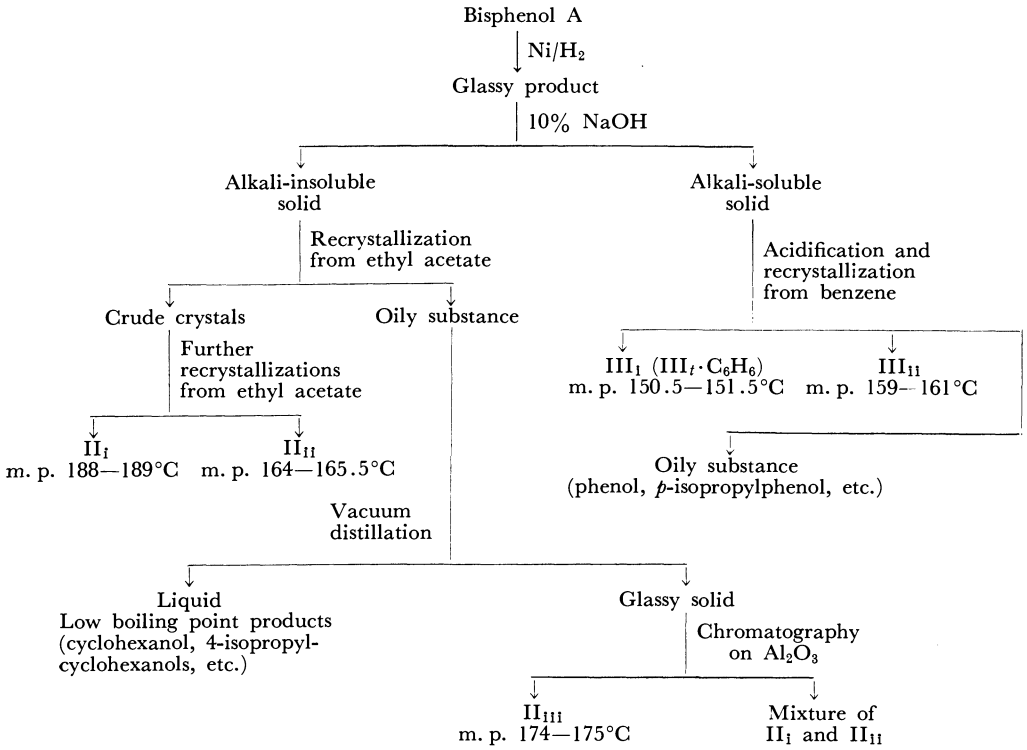

Fig. 1. Separation procedure.

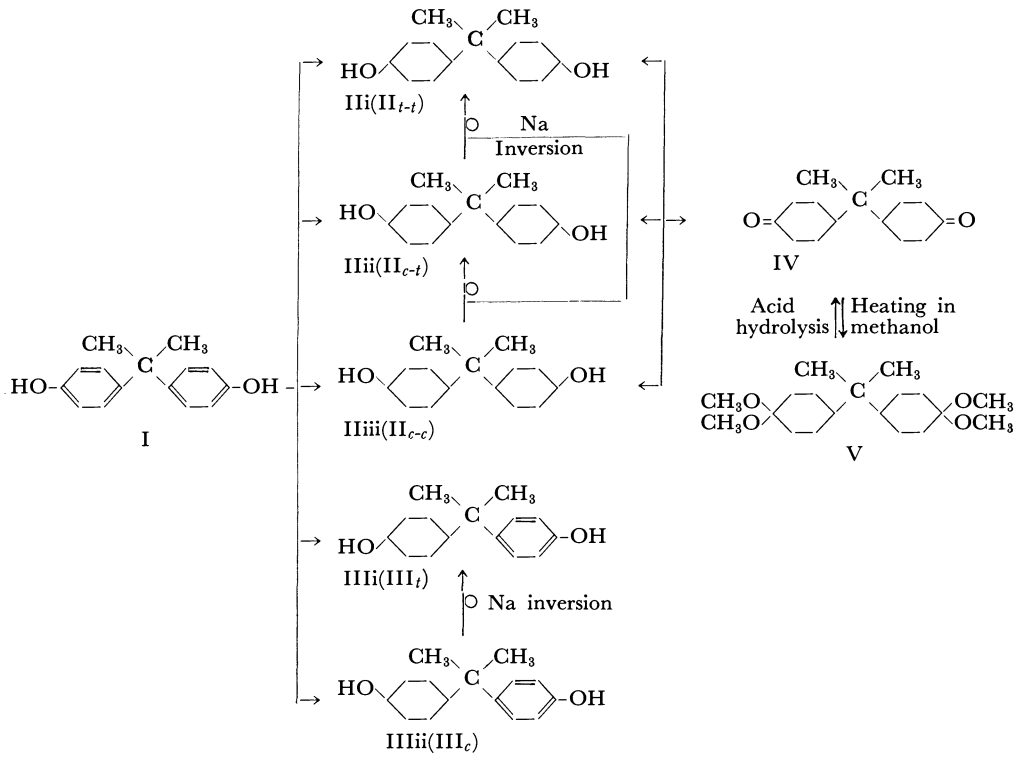

Fig. 2

diacetate of II_{III} showed the most complex absorption bands among the three isomers, that of II_{II} was next, and that of II_I was the simplest. Therefore, the two hydroxyl groups at C_4 and C_4' of II_I were concluded to be both equatorial; one of those of II_{II} was equatorial and another axial, and all of those of II_{III} were axial.

Generally, the cyclohexanes having equatorial hydroxyl groups are more stable than the corresponding axial isomers; therefore, when a polycyclic secondary alcohol is equilibrated with alkali metal, the isomer which is preponderant in the reaction product will be that which has equatorial hydroxyl.[10,15,20] When II_{II} and II_{III} were each heated with sodium, II_I was preferentially obtained. Since it is most probable that the isopropylidene groups attached to both C_1 and C_1' of the two cyclohexane rings of II isomers are arranged equatorially, the configurations of the hydroxyl groups in II_I with respect to the isopropylidene should be both *trans* ($II_{t\text{-}t}$), *cis* and *trans* ($II_{c\text{-}t}$) in II_{II}, and all *cis* ($II_{c\text{-}c}$) in II_{III}. The adsorption of these isomers on activated aluminum oxide also indicated the same conclusion, that to be expected from the above results. The *cis*, *cis* isomer was least strongly adsorbed, followed by the *cis*, *trans*, and *trans*, *trans* isomers in that order.[21] Thus, the above-mentioned conclusions from the infrared spectrum studies were also supported by these other results, as well as by the nuclear magnetic resonance spectra of the diacetates, as will be shown in the Experimental section.

The oxidation of the isomeric mixture of II with chromium trioxide gave the diketone compound IV in a good yield. The recrystallization of this diketone from purified methanol afforded the tetramethyl diketal, 2, 2-bis(4, 4-dimethoxycyclohexyl)propane, while when other carbinols, such as absolute ethanol or propanol, were used, no formation of ketal was observed.

The diketone IV promptly absorbed two moles of hydrogen on hydrogenation over a platinum catalyst and gave a mixture of the diol containing $II_{c\text{-}t}$ mainly, plus $II_{c\text{-}c}$ and $II_{t\text{-}t}$ in minor amounts in that order.

On the acidification of the alkali extract of the hydrogenation product with mineral acid, a mixture of phenolic compounds was deposited as a glassy solid mass. Crystallization from benzene yielded a phenolic material, III_I, m. p. 150.5—151.5°C. The infrared spectrum of III_I showed the absorption peaks of phenolic groups, *p*-disubstituted benzene and equatorial ring alcohol, while its ultraviolet spectrum showed a peak of the phenolic compound at 278 mμ, the intensity of which was approximately half that of bisphenol A. These results led us to the conclusion that III_I still possessed a phenolic benzene ring, besides a cyclohexanol ring. Drying III_I in vacuo at the boiling point of xylene quantitatively removed one mole of the benzene, but the melting point was unchanged. It was, therefore, concluded that the benzene was the solvent of crystallization and that the molecular formula of III_I was $C_{15}H_{22}O_2 \cdot C_6H_6$, while III_I was concluded to be the *trans* isomer, III_t, by the above spectral analysis. The diacetate was also prepared in order to confirm that the III_t was a single compound.

Crystals of III_{II} were deposited from the mother liquor, from which III_t had completely been removed. Recrystallization from benzene gave the other isomer, III_{II}, melting at 159—160°C; this was concluded to be the *cis* isomer, III_c. The configuration of the hydroxyl group was also recognized as axial by means of a study of the infrared spectrum and by the sodium inversion to III_t. The acetylation of III_c using acetic anhydride in the presence of potassium acetate gave an oily mixture whose infrared spectrum showed strong bands of hydroxyl, and weak bands of acetyl groups and also of the carbon-carbon double bond. After the phenyl urethane formation, it was found that the main product in the acetylation was 2-(3-cyclohexenyl)-2-(*p*-hydroxyphenyl)propane. The following explanation was proposed for the formation of this dehydrated compound. Since the hydroxyl group in the cyclohexane ring of III_c was axial, it was easily dehydrated and gave the cyclohexene derivative rather than the diacetoxyl compound.[22]

As to the preferred conformations of both the cyclohexane rings to the isopropylidene group in II isomers, the following remarks may be made. If it can be assumed that all of the energy barriers of internal rotation among the methyl, methylene and methylidene groups are equivalent by neglecting the detailed stereochemical factors, the conformations II: A (*gauche*)[23] and II: B (*anti*),[23] (Fig. 3) each of which has four *gauche* interactions like *n*-butane, are less strained than the other possible conformations. However, if one of the cyclohexane rings is placed as II: A with respect to the isopropylidene group, and another ring, as II: B (i. e., II: A + II: B = II: D), the internuclear distance between the two carbon atoms, C-2 and C-6', will approach about 2.5 Å, and the axial hydrogen atom attached to C-2 and the equatorial atom attached to C-6' must face each other at about 0.73 Å.[24] On the other hand, when both the

20) W. Klyne, Ref. 17, p. 57.
21) Analogous facts were observed by Ungnarde[16] and Wilds et al.[14] in the cases of hydrodiethylstilbestrols and bis(4-hydroxycyclohexane).
22) Some analogous examples can be found in the case of *cis*, *cis*-perhydrodiethylstilbestrol.[15]
23) Correlations between isopropylidene methyls and the two bonds of the cyclohexane ring (C-1–C-2, and C-1–C-6).
24) Measured by Dreiding molecular models.

cyclohexane rings are "*anti*" configurations with respect to the isopropylidene group (II:C), each of the two pairs of the methylene carbon atoms, C-2:C-6′ and C-6:C-2′, will also approach each other at a distance of about 2.5 Å, and the four axial hydrogen atoms attached to these four carbon atoms must face each other in each pair. Therefore, these two steric arrangements, II:C and II:D, are actually impossible and the other conformation, II:E, is the most probable. The II:E conformation is a combination of two II:A conformations, where the two chair cyclohexane rings are contrarily twisted 60° (the projected valency angles about the carbon-carbon bonds between the isopropylidene and each of the rings) from the completely-eclipsed situations with the isopropylidene methyls. The two bonds, C-1-C-6 and C-1′-C-6′, and the bisector of the bond angle of CH_3–C–CH_3 should, therefore, be coplanar.

Regarding the preferred conformation of III, if it can also be assumed that all the steric strains among the methyl, methylene, and the carbon atoms at the junction of the benzene ring are equivalent, as in II isomers, the conformations of III:A and III:B shown in Fig. 3 should have equal relative stabilities and be more probable than the other possible conformations. However, while only one methylene group (C-2) in III-C is near to the hydrogen atom attached to an ortho position of the benzene ring, two of the methylene groups in III:D (C:2 and C:6) will approach two of the ortho hydrogens. Hence, a whole-molecular conformation such as III:C is energetically more probable.

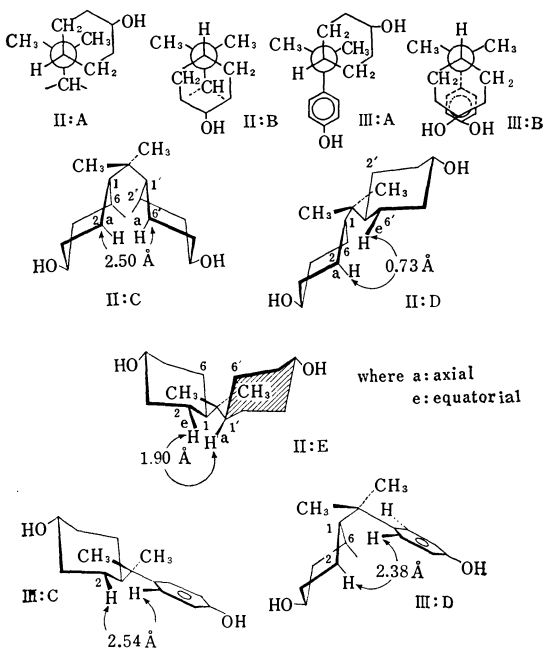

Fig. 3

Experimental

The Hydrogenation of Bisphenol A over Raney Nickel Catalyst (W-1).—Fifty grams of bisphenol A dissolved in 120 ml. of absolute ethanol and 20 ml.[25] of Raney nickel (W-1) were charged in a one-liter stainless-steel autoclave and shaken under 94 kg./cm² of initial hydrogen pressure. The temperature was allowed to rise up to 260°C during a period of 120 min. in order to complete the hydrogen absorption. The resulting solution was filtered, and the solvent was removed under diminished pressure. The obtained glassy solid was refluxed and stirred in 400 ml. of 10% sodium hydroxide for 5 hr. in order to remove any phenolic component; then the remaining crystalline solid was repeatedly washed with large amounts of hot water. This yielded 51.0 g. (96%) of an isomeric mixture of II, m. p. 133—153°C.

$II_{t\text{-}t}$. — One recrystallization of the above-obtained crystalline mixture from ethyl acetate gave 35.1 g. of the first crop, which had a melting point of 147—183°C. From the mother liquor 10.0 g. of other crystals, the second crop, m. p. 133—153°C, were recovered. The further recrystallization of the first crop from the same solvent gave an analytical sample of II_1 ($II_{t\text{-}t}$), m. p. 188—189°C.

Found: C, 74.94; H, 11.75. Calcd. for $C_{15}H_{28}O_2$: C, 74.95; H, 11.74%.

ν_{max}^{Nujol} 3310 (OH); 1072, 1048 cm^{-1} (equatorial alcohol).

$II_{c\text{-}t}$.—Repeated recrystallizations of the second crop, obtained above, from ethyl acetate gave an analytical sample of II_{II} ($II_{c\text{-}t}$), m. p. 164—165.5°C. The melting point was depressed when it was mixed with $II_{t\text{-}t}$.

Found: C, 74.75, 74.91; H, 11.68, 11.58. Calcd. for $C_{15}H_{28}O_2$: C, 74.95; H, 11.74%.

ν_{max}^{Nujol} 3360 (OH); 1062 (equatorial alcohol); 1020, 952 cm^{-1} (axial alcohol).

All the mother liquors from the above recrystallization procedures were combined separately with the corresponding fractions of the other experimental runs described later, and stored for used in the detection of $II_{c\text{-}c}$.

III_t.—Upon acidification with dilute hydrochloric acid of the alkaline extract obtained above, a viscous oil was isolated. After sufficient washings with hot water, 2.0 g. of powder were obtained. Crystallization from benzene gave 0.15 g. of III_i ($III_t \cdot C_6H_6$), m. p. 150.5—151.5°C.

Found: C, 80.18, 80.35; H, 9.27, 9.15; C_6H_6; 26.42;[26] mol. wt. (Rast), 170. Calcd. for $C_{15}H_{22}O_2 \cdot C_6H_6$: C, 80.74; H, 9.02; C_6H_6, 26.28%; mol. wt., 312.46.

ν_{max}^{KBr} 3454, 3130 (OH, broad); 1961, 1813 (benzene); 1612, 1595, 1518 (phenyl); 1242 (phenol); 1046 (equatorial alcohol); 832 cm^{-1} (*p*-disubstituted benzene).

λ_{max}^{EtOH} 224.1, 255, 278 mμ (ε, 10600, 1080, 2300).

The drying course using a thermobalance under

25) Measured in the volume as a precipitate in absolute ethanol.

26) Weight loss upon drying at the boiling point of xylene under a vacuum until a constant weight was obtained.

atmospheric pressure showed that the dissociation temperature of the benzene was as low as below 80°C.

ν_{max}^{KBr} of benzene-free III_t: 3410, 3240 (OH, broad); 1878, 1613, 1596, 1517 (phenyl); 1250 (phenol); 1060 (equatorial alcohol); 831 cm^{-1} (*p*-disubstituted benzene).

The mother liquor collected and gathered from the above recrystallization procedures of $III_t \cdot C_6H_6$ was combined with similar fractions of the later experimental runs, and they stored for use in the detection of III_c.

The Hydrogenation of Bisphenol A with Urushibara Nickel-A.—*Reduction up to 220°C.*—The hydrogenation of 50.0 g. of I in 100 ml .of absolute ethanol over 10 ml.[25] of a U-Ni-A catalyst was carried out under 100 kg./cm^2 of initial hydrogen pressure, with the temperature rising up to 220°C over a period of 225 min. After working-up as usual, a sirupy product was obtained; this was, as usual, separated into alkali-insoluble and soluble portions. The crystallization of the insoluble part from ethyl acetate gave the following crops: (a) m. p. 141—170°C; 15.0 g. (28.5%); (b) m. p. 140.5—149°C; 7.45 g. (14.1%), and (c) m. p. 130—140°C; 2.07 g. (3.9%); the total of 24.5 g. (46.5%). These crops were identified as follows; the fraction a consisted mainly of $II_{t\text{-}t}$, and the b, of $II_{c\text{-}t}$, as was confirmed by mixed-melting-point tests.

The acidification of the alkali-soluble portion with hydrochloric acid gave 6.5 g. of crude crystals of III, which were mostly III_t.

Reduction up to 260°C.—This was carried out under 100 kg./cm^2 of initial hydrogen pressure, using 30 ml. of a U-Ni-A. The reaction temperature was raised up to 260°C over a period of 195 min. After working up as usual, 18.5 g. (35%) of crystals insoluble in alkali were obtained, m. p. 142—150°C, 17.9 g., these crystals contained mainly $II_{c\text{-}t}$, with $II_{t\text{-}t}$ the remainder.

From the alkaline solution, a solid mass (phenolic material) was recovered on acidification. Crystallization from benzene-acetone gave 30 g. of a crude crystalline mixture with a melting point of 97°C. Another recrystallization from benzene yielded 19.1 g. (27.9%) of a pure sample of $III_t \cdot C_6H_6$.

The Hydrogenation of Bisphenol A over Urushibara Nickel-B.—*Reduction up to 220°C.*—This was carried out as usual, using 70 ml. of a U-Ni-B[12] under 92 kg./cm^2 of initial hydrogen pressure. The temperature was allowed to rise up to 220°C over a period of 135 min. After working-up as usual and subsequent crystallization from benzene, 33.5 g. of crystals were obtained, m. p. 97—137°C. This product was easily soluble in ethyl acetate and in alkali, and gave no crystals from the ethyl acetate solution on cooling. Therefore, this fraction consisted of phenolic compounds and no saturated ones. Recrystallization from benzene-acetone gave 21.1 g. (32%) of $III_t \cdot C_6H_6$.

The concentration of the above-obtained mother liquor gave 2.4 g. (4.6%) of other crystals, m. p. 173—185°C, a crude $II_{t\text{-}t}$.

The finally-remaining oily substance (29 g.) was stored for use in the detection of the other isomers of II and III.

Reduction up to 260°C.—This was carried out as usual under a 103 kg./cm^2 initial hydrogen pressure, using 82 ml. of a U-Ni-B. The temperature was allowed to rise up to 263°C over a period of 195 min. Working-up as usual yielded 43 g. (81%) of an alkali-insoluble product, m. p. 122—148°C. Recrystallization from ethyl acetate gave the following crops: (a) m. p. 167—182°C, 15 g. (28%), which mainly consisted of $II_{t\text{-}t}$; (b) m. p. 156—159°C, 13 g. (24%), almost all $II_{c\text{-}t}$; and (c) m. p. 132—150°C, 4.4 g. (8%).

The Diacetate of $II_{t\text{-}t}$.—A mixture of 1.0 g. of $II_{t\text{-}t}$, 0.2 g. of anhydrous sodium acetate, and 1.67 g. of acetic anhydride was heated in a boiling-water bath for 5 hr. After cooling, the solution was poured into ice-water and neutralized with sodium bicarbonate powder. The white precipitate was then collected on a filter, washed with water, and dried to give the crude crystals, 1.30 g. (96%). Recrystallization from methanol gave the analytical sample, m. p. 136—138°C.

Found: C, 70.32; H, 9.92. Calcd. for $C_{19}H_{32}O_4$: C, 70.33; H, 9.94%.

ν_{max}^{Nujol} 1736, 1730 (C=O, acetate); 1259, 1244 (acetate); 1038, 1019 cm^{-1} (C–O).

NMR[27], (70 mg./0.45 ml. of CCl_4): 5.58 τ (axial hydrogens at C-4 and C-4').

The Dibenzoate of $II_{t\text{-}t}$. — One gram of $II_{t\text{-}t}$, 3 g. of pyridine, 5 ml. of dioxane, and 3 g. of benzoyl chloride were mixed and heated under reflux for 2 hr. This mixture, after the usual work-up, gave 1.45 g. (78%) of the dibenzoate of $II_{t\text{-}t}$ as white needles, m. p. 192—193°C, these needles were insoluble in both ethanol and methanol.

Found: C, 77.61; H, 7.99. Calcd. for $C_{29}H_{36}O_4$: C, 77.64; H, 8.09%.

ν_{max}^{Nujol} 1708 (C=O, benzoate); 1274 cm^{-1} (benzoate).

The Hydrolysis of the Diacetate of $II_{t\text{-}t}$.—A mixture of 0.15 g. of the diacetate in 3 ml. of methanol with 0.3 g. of sodium hydroxide in 2 ml. of water was refluxed for 3.5 hr. After concentration and then dilution with water, white crystals (0.10 g., 90%) separated out; these crystals melted at 188—189°C and did not depress the melting point of an authentic sample of $II_{t\text{-}t}$.

The Diacetate of $II_{c\text{-}t}$.—This was prepared as has been described in the case of $II_{t\text{-}t}$. After working-up, 1.35 g. of the crude diacetate melting at 70—74°C were obtained. Recrystallization from ethanol gave 1.05 g. (77%) of the analytical sample, m. p. 75.5—76.5°C.

Found: C, 70.44; H, 9.83. Calcd. for $C_{19}H_{32}O_4$: C, 70.33; H, 9.94%.

ν_{max}^{Nujol} 1742, 1730 (C=O, acetate); 1266, 1243, 1221 (acetate); 1039, 1019 cm^{-1} (C-O).

NMR, 70 mg./0.45 ml. of CCl_4): 5,10 τ (equatorial hydrogen at C-4); 5.58 τ (axial hydrogen at C-4').

The Dibenzoate of $II_{c\text{-}t}$. — One gram of the diol was benzoylated in the same manner as $II_{t\text{-}t}$. After working-up as usual the resulting oil was crystallized from methanol to give a crude dibenzoate of $II_{c\text{-}t}$. Another recrystallization from methanol gave 1.4 g. (76%) of the analytical sample, melting at 105—105.5°C.

Found: C, 77.51; H, 8.08. Calcd. for $C_{29}H_{36}O_4$: C, 77.64; H, 8.09%.

ν_{max}^{Nujol} 1710 (C=O, benzoate); 1276 cm^{-1} (benzoate).

The Hydrolysis of Diacetate of $II_{c\text{-}t}$.—A sample

27) The nuclear magnetic resonance spectra were obtained by Dr. Keishi Kotera, the Osaka Research Laboratory of Tanabe Seiyaku Co., on a Japan Electron Optics Laboratory 60 MC spectrometer, using dilute solutions in carbon tetrachloride, with tetramethylsilane as an internal standard.

of 0.30 g. of the diacetate of II_{c-t} was hydrolyzed as in the case of that of II_{t-t}; this gave 0.21 g. (94%) of II_{c-t}, m. p. 163—164°C. This sample showed no melting-point depression on admixture with the original sample of II_{c-t}.

The Isolation of II_{c-c}. — A mother liquor obtained from all the separation procedures for II_{t-t} and II_{c-t} was concentrated under reduced pressure, and then heated in methanol with an excess of sodium ethoxide in order to remove the still-remaining phenolic compounds as water-soluble sodium salts.

After the removal of the solvent and sufficient washings with hot water, the remaining glassy solid was dissolved in benzene and passed through an activated-aluminum oxide column; this gave crystals from an elute using ethyl acetate. Recrystallization from ethyl acetate gave a sample melting at 167—170°C. The melting point was depressed on admixture with II_{t-t} or II_{c-t}. Therefore, this was confirmed to be the last isomer of II, II_{c-c}.

Found: C, 75.10, 75.14; H, 11.85, 11.78. Calcd. for $C_{15}H_{28}O_2$: C, 74.95, H, 11.74%.

The Diacetate of II_{c-c}. — This was prepared as that of II_{t-t}, using 0.5 g. of II_{c-c}; 0.68 g. (theoretical yield) of white crystals, m. p. 113.5—115°C, was thus obtained. Another recrystallization from methanol gave the analytical sample, m. p. 117—117.5°C.

Found: C, 70.33, H, 9.97. Calcd. for $C_{19}H_{32}O_4$: C, 70.33, H, 9.94%.

ν_{max}^{Nujol} 1735 (broad, C=O, acetate); 1260, 1251, 1220, 1217, 1209 (acetate); 1009 cm^{-1} (C–O).

NMR, (75 mg./0.45 ml. of CCl_4): 5.15 τ (equatorial hydrogens at C-4 and C-4').

The Dibenzoate of II_{c-c}.—A sample of 0.5 g. of II_{c-c} was benzoylated as usual. The recrystallization of the product from methanol gave white needles (0.66 g., 71%), m. p. 152—153°C.

Found: C, 77.61; H, 8.07. Calcd. for $C_{29}H_{36}O_4$: C, 77.64; H, 8.09%.

ν_{max}^{Nujol} 1710 (C=O, benzoate); 1608, 1589 (phenyl); 1280, 1272 cm^{-1} (benzoate).

The Hydrolysis of the Dibenzoate of II_{c-c}.— A solution of 0.24 g. of the dibenzoate in 4 ml. of acetone, and 2 ml. of water containing 0.10 g. of sodium hydroxide were mixed and refluxed for 6 hr. After the solvent had been removed, the resulting crystals were gathered on a glass filter, washed with water, and dried. Recrystallization from benzene - petroleum benzine gave 0.10 g. (77%) of II_{c-c}, m. p. 174—175°C.

Found: C, 74.86, 75.04; H, 11.71, 11.62. Calcd. for $C_{15}H_{28}O_2$: C, 74.95; H, 11.74%.

ν_{max}^{Nujol} 3380 (OH); 1012, 959 cm^{-1} (axial alcohol).

The Sodium Inversion of II_{c-t} to II_{t-t}. — One gram of II_{c-t} was dissolved in 1 ml. of xylene. To this solution at 160°C, 0.4 g. of sodium was added in small portions. The reaction system evolved hydrogen gas, and after a while it precipitated some solids. After reaction at 180°C for 12 hr., the reaction mixture was decomposed by the drop-by-drop addition of ethanol and water. The precipitate was gathered on a glass filter, washed with water, dried, and weighed (0.96 g. (96%)), m. p. 175—184°C. Recrystallization from ethyl acetate gave an analytical sample, m. p. 188—189°C, which was identical with an authentic sample of II_{t-t}.

The Sodium Inversion of II_{c-c} to II_{t-t}. — This was carried out as above, using 0.50 g. of II_{c-c}; it gave 0.35 g. (70%) of a pure sample of II_{t-t}.

2, 2-Bis(4-ketocyclohexyl)propane (IV)[28]. — An isomeric mixture of II (54.0 g., m. p. 150—178°C) was dissolved in 250 ml. of glacial acetic acid. To this solution, under stirring and cooling at 17—18°C, there was added, drop by drop over a period of about 2 hr., 55.0 g. of chromium trioxide in a dilute acetic acid (250 ml. of glacial acetic acid and 40 ml. of water). After another one hour's reaction, 275 ml. of isopropyl alcohol was added under water-cooling; the solution was then allowed to stand overnight. Concentration under reduced pressure and the pouring of the remaining product into water precipitated powdery white crystals. After filtration and drying, 41.0 g. (78%) of the crude diketone, m. p. 159—163°C, was obtained. Recrystallization from benzene raised the melting point to 162.5—163°C (lit.,[4] m. p. 158—160°C).

Found: C, 76.36; H, 10.18. Calcd. for $C_{15}H_{24}O_2$: C, 76.23; H, 10.24%.

ν_{max}^{Nujol} 1718 cm^{-1} (six-membered-ring ketone).

Disemicarbazone.—This was prepared as usual, m. p. 220—223°C (decomp.) (lit.,[4] 220—223°C). Another melting point, 238—239°C (decomp.), was observed when the disemicarbazone was measured with a rapid temperature rise.

The Formation of 2, 2-Bis(4, 4-dimethoxycyclohexyl)propane (V) and the Regeneration of the Original Diketone IV by Acid Hydrolysis.—When the diketone IV was heated in purified methanol and the solution was concentrated, fair white plates of the tetramethyl diketal, m. p. 140.5—141.5°C, were obtained in a theoretical yield.

Found: C, 69.11; H, 10.80. Calcd. for $C_{19}H_{36}O_4$: C, 69.47; H, 11.05%.

ν_{max}^{Nujol} no peak in the region of six-membered-ring ketone; 1161, 1100, 1040 cm^{-1} (tetramethyl diketal).

Similar procedures using other alcohols, such as ethanol or propanol, gave no reaction, and only the original diketone was recovered.

The tetramethyl diketal (1.00 g.) in a mixed solution of 15 ml. of acetone and 5 ml. of water containing 2.0 ml. of concentrated hydrochloric acid was refluxed for 2 hr. After the addition of 15 ml. of water to the reaction system and the removal of the acetone by distillation, crystals of IV were recovered.

The Rapid Hydrogenation of the Diketone IV over Platinum Black Catalyst.—A solution of 1.00 g. of IV in 35 ml. of glacial acetic acid was shaken with 0.37 g. of a platinum black catalyst and hydrogen under atmospheric pressure at room temperature. After 55 min., 110% of the theoretical amount of hydrogen was absorbed. Working-up as usual gave 1.05 g. of a sirup which was subsequently separated chromatographically, using 120 g. of an activated aluminum oxide, into three main fractions. The first fraction, eluted with ether-methanol, was 200 mg. (19.7%) of crude crystals, containing II_{c-c} mainly. The second was 636 mg. (62.5%) of a sirup consisting mainly of II_{c-t}, plus some II_{t-t}. These two fractions were confirmed

28) This procedure followed the analogous method by Wilds et al. used for the preparation of bicyclohexyl-4, 4'-dione.[14]

by a study of their infrared spectra and by mixed-melting-point tests with authentic samples after repeated recrystallizations from benzene. The third fraction consisted of 32 mg. (3.1%) of almost pure crystals of $II_{t\text{-}t}$, m. p. 183—185°C.

The Diacetate of III$_t$.—A solution of 1.33 g. of $III_t \cdot C_6H_6$ in 2.0 g. of acetic anhydride containing two drops of concentrated sulfuric acid was heated in a boiling-water bath for 1.5 hr. After working-up as usual and recrystallization from methanol, 0.67 g. (49%) of crystals melting at 108—109.5°C was obtained.

Found: C, 71.75; H, 8.30. Calcd. for $C_{19}H_{26}O_4$: C, 71.67; H, 8.23%.

ν_{max}^{Nujol} 1760, 1227 (phenyl acetate); 1730, 1249 (acetate of secondary alcohol); 1610, 1511 (phenyl); 1039, 1022 (C–O); 841 cm^{-1} (*p*-disubstituted benzene).

The Isolation of III$_c$.—The mother liquor collected from the purification of the alkali-soluble product, which was almost free from III_t, was repeatedly extracted with a hot alkali solution in order to separate it from alkali-insoluble materials. On acidification, from the extract there separated a viscous oil which deposited crystals when left standing. Recrystallization from benzene gave an analytical sample melting at 159—161°C, this was concluded to be III_c by a mixed-melting-point test with an authentic sample of III_t and by the following analyses.

Found: C, 76.82; H, 9.51. Calcd. for $C_{15}H_{22}O_2$: C, 76.88; H, 9.46%.

ν_{max}^{Nujol} 3445, 3220 (OH); 1613, 1597, 1509 (phenyl); 1231 (phenol); 1008, 944 (axial alcohol); 825 cm^{-1} (*p*-disubstituted benzene).

The Sodium Inversion of III$_c$ to III$_t$.—A sample of 0.50 g. of III_c in 0.50 g. of xylene was refluxed with 0.20 g. of sodium at 180°C for 10 hr. After the solution had been treated with ethanol and then water, and acidified with dilute hydrochloric acid, the isolated product was worked-up as usual and recrystallized from benzene-acetone to give 0.21 g. (42%) of crystals melting at 147.5—150°C. Further recrystallization gave an analytical sample which was found to be identical with an authentic sample of III_t by a mixed-melting-point test.

The Reaction of III$_c$ with Acetic Anhydride.—A mixture of 0.20 g. of III_c and 0.1 g. of potassium acetate in 1.0 ml. of acetic anhydride was heated in a boiling-water bath for 10 hr., and then poured into ice-water and neutralized with sodium bicarbonate. The oily product which separated was taken up in benzene, washed with water, and dried over anhydrous sodium sulfate. After the removal of the solvent, there was obtained 0.34 g. of an oily mixture which did not crystallize upon the usual treatment. This mixture was, therefore, vacuum-distillated in order to purify it; it gave one fraction, boiling in the range of 120—160°C/0.55 mmHg without decomposition. The distillate almost entirely solidified like a wax after it had stood for a while, but it still was not pure enough to analyze. Therefore, a chromatographic separation of this distillate through a silica gel column was carried out. Elution with benzene-ether (2 : 3) gave 240 mg. (76%) of crude crystals melting below 60°C; these crystals were concluded, by the following tests, to be 2-(3-cyclohexenyl)-2-(*p*-hydroxyphenyl)propane formed by the dehydration, not the diacetate of III_c.

Found: C, 82,13, 82.10; H, 9.31, 9.29. Calcd. for $C_{15}H_{20}O$: C, 83.28; H, 9.32%.

ν_{max}^{Liquid} 3330 (OH); 3040, 2990 (=CH); 1230 (phenol); 827 cm^{-1} (*p*-disubstituted benzene).

Phenyl Carbamate.—This was prepared as usual from 200 mg. of the above-obtained crude sample and 0.50 g. of phenyl isocyanate; it was obtained as a waxy crystalline product melting at 100—110°C. By a chromatographic separation using a silica gel column and subsequently-repeated recrystallizations from petroleum benzine and then ethanol-water, the melting point was raised to 116—117.5°C, 2-(3-cyclohexenyl)-2-(*p*-phenylaminocarboxyphenyl)propane.

Found: C, 78.53; H, 7.73; N, 4.35. Calcd. for $C_{22}H_{25}NO_2$: C, 78.77; H, 7.51; N, 4.18%.

ν_{max}^{KBr} 3350 (bonded NH); 3057, 3018 (unsaturated CH); 1740—1709 (amide I); 1652 (RHC=CHR', *cis*); 1615, 1600, 1500 (phenyl); 1543 (amide II); 848 cm^{-1} (*p*-disubstituted benzene).

The author wishes to thank Dr. Isao Shiihara, Government Industrial Research Institute of Osaka, for his excellent aid to this research, and Mrs. Masako Hayashi for the elemental analyses.

BULLETIN OF THE CHEMICAL SOCIETY OF JAPAN VOL. 39 2202—2205 (1966)

Studies of *C*-Substituted Tartaric Acid. II. On the Configurations of Isomeric 2-Methyltartaric Acids, 1, 2-Dihydroxycyclohexane-1, 2-dicarboxylic Acid and 2, 3-Dimethyltartaric Acids

By Susumu TATSUMI

Division of Organic Chemistry, Institute for Protein Research, Osaka University, Kita-ku, Osaka

(Received November 5, 1965)

The assignments of the erythro-threo configuration to isomeric 2-methyltartaric acids and the cis-trans configuration to isomeric 1, 2-dihydroxycyclohexane-1, 2-dicarboxylic acids were made on the basis of the infrared absorption spectra of their calcium salts. Thus, the isomer of 2-methyltartaric acid, with a m. p. of 146°C, corresponds to the erythro form, and the other isomer, with a m. p. of 161°C, to the threo form; also the one isomer of isomeric 1, 2-dihydroxycyclohexane-1, 2-dicarboxylic acids with a m. p. of 154°C corresponds to the cis (meso) form, and the other, with a m. p. of 180°C, to the trans (racemic) form. The configurations of the compounds are discussed in comparison with those of tartaric acid and 2, 3-dimethyltartaric acid, the latter of which was recently decided by optical resolution by present author (S. Tatsumi, This Bulletin, in press.).

2-Methyltartaric acid, 1, 2-dihydroxycyclohexane-1, 2-dicarboxylic acid and 2, 3-dimethyltartaric acid are interesting substances in relation to tartaric acid from the stereochemical point of view. In the previous paper[1] it has been reported that two racemic forms of 2-methyltartaric acid, the melting points of which are 146°C (Ia) and 161°C (Ib), were prepared and that both racemic substances were then resolved into their optically active isomers. In an earlier publication from our laboratory,[2] it was also reported that a Raney nickel catalyst treated with aqueous solutions of these optically active hydroxy acids has an asymmetric activity in the hydrogenation of methyl acetoacetate to methyl 3-hydroxybutyrate, and that a high asymmetric activity is obtained when the catalyst is treated with optically active Ib, while opticallyactive Ia has only a low asymmetric effect on Raney nickel under the same conditions. Thus it has been supposed that the difference in the asymmetric effects of Ia and Ib depends upon their erythro-threo isomerism. However, there have been no reports on the configurations of isomeric 2-methyltartaric acids.

1, 2-Dihydroxycyclohexane-1, 2-dicarboxylic acid,*1 which is a kind of *C*, *C'*-disubstituted tartaric acid, was prepared from 1, 2-cyclohexanedione and then separated into two optically inactive isomeric forms, the melting points of which are 154°C (IIa) and 180°C (IIb).*1 It is, however, unknown at the present time which steric isomer is cis (meso) and which is trans (racemic).

On the other hand, the present author and others[1] have reported that 2, 3-dimethyltartaric acid has two optically inactive modifications, the melting points of which are 180°C (IIIa) and 187°C (IIIb), and that IIIb could be resolved into two optically active isomers, while IIIa could not. This shows clearly that IIIb corresponds to the threo (racemic) form and IIIa, to the erythro (meso) form.

In the present study, the configurations of the isomeric 2-methyltartaric acids and 1, 2-dihydroxycyclohexane-1, 2-dicarboxylic acids were assigned on the basis of a study of the infrared spectra of their calcium salts in comparison with the configurations of meso and racemic tartaric acid (IVa and IVb) and those of meso and racemic 2, 3-dimethyltartaric acid. There have been several reports[3] on the configurations of aliphatic or alicyclic diol, but these cannot always be applied to an α, α'-dihydroxydicarboxylic acid. In the present paper, the configurations of isomeric *C*-substituted and *C*, *C'*-disubstituted tartaric acids are also predicted.

The physical constants and analytical data of the acids and their salts used in the present work are listed in Table I.

Experimental

Materials.—Ia (or Ib) and IIIa (or IIIb) were prepared from α-acetoxyacetoacetate and diacetyl respectively by the method described in the previous

1) S. Tatsumi, Y. Izumi, M. Imaida, Y. Fukuda and S. Akabori, This Bulletin, in press.

2) Y. Izumi, S. Tatsumi, M. Imaida, Y. Fukuda and S. Akabori, ibid., in press.

*1 The preparation of this hydroxy acid and its separation into the two isomeric forms will be described in this Bulletin in the near future.

3) L. P. Kuhn, *J. Am. Chem. Soc.*, **74**, 2492 (1952); **76**, 4323 (1954); **80**, 5950 (1958); N. Mori, S. Omura and Y. Tsuzuki, This Bulletin, **38**, 1037 (1965).

TABLE I. MELTING POINTS AND ANALYTICAL DATA ON THE ACIDS USED AND ON THEIR SALTS

Acid and salt	M. p., °C	Empirical formula	Anal. {Calcd. (%) {Found (%) C	H
2-Methyltartaric acid (Ia)	146	$C_5H_8O_6$	36.59 36.73	4.91 4.89
2-Methyltartaric acid (Ib)	161	$C_5H_8O_6$	36.59 36.53	4.91 4.93
1,2-Dihydroxycyclohexane-1,2-dicarboxylic acid (IIa)	154	$C_8H_{12}O_6$	47.06 47.14	5.92 5.96
1,2-Dihydroxycyclohexane-1,2-dicarboxylic acid (IIb)	180	$C_8H_{12}O_6$	47.06 46.72	5.92 5.97
meso-2,3-Dimethyltartaric acid (IIIa)	180	$C_6H_{10}O_6$	40.45 40.31	5.66 5.64
DL-2,3-Dimethyltartaric acid (IIIb)	187	$C_6H_{10}O_6$	40.45 41.00	5.66 5.60
meso-Tartaric acid (IVa)	140	$C_4H_6O_6$	32.01 32.11	4.03 4.00
DL-Tartaric acid (IVb)	206	$C_4H_6O_6$	32.01 32.09	4.03 3.99
Ia-Ca	—	$C_5H_6O_6Ca\cdot 2H_2O$	25.21 25.17	4.23 4.34
Ib-Ca	—	$C_5H_6O_6Ca\cdot 2H_2O$	25.21 25.08	4.23 4.17
IIa-Ca	—	$C_8H_{10}O_6Ca\cdot H_2O$	36.91 37.66	4.65 4.70
IIb-Ca	—	$C_8H_{10}O_6Ca$	39.66 39.57	4.16 4.20
IIIa-Ba	—	$C_6H_8O_6Ba\cdot 2H_2O$	20.62 20.31	3.46 3.54
IIIb-Ba	—	$C_6H_8O_6Ba\cdot 2H_2O$	20.62 20.39	3.46 3.66
IVa-Ba	—	$C_4H_4O_6Ba\cdot H_2O$	15.83 15.60	1.99 2.07
IVb-Ba	—	$C_4H_4O_6Ba\cdot 5H_2O$	12.79 13.08	3.76 3.36

paper.[1] IIa*[1] (or IIb*[1]) was prepared from 1,2-cyclohexanedione, and IVa (or IVb) was prepared from glyoxal by Pollak's procedure.[4]

The calcium salts were obtained by the neutralization of aqueous solutions containing the acids and an equimolar amount of calcium chloride, with a sodium hydroxide solution. The barium salts were obtained similarly by the neutralization of aqueous solutions of the acids with a barium hydroxide solution. The data for these acids and salts are listed in Table I.

Spectra.—The infrared spectra were recorded using a Shimadzu IR spectrophotometer; further details were also recorded using a Perkin-Elmer Model 221 spectrophotometer equipped with a lithium fluoride prism.

Results and Discussion

The Infrared Spectra of the Salts.—The spectra of Ia-calcium salt (Ia-Ca) and Ib-calcium salt (Ib-Ca) are shown in Fig. 1.

A characteristic difference between the spectrum of Ia-Ca and that of Ib-Ca was observed in the region around 3600 cm^{-1}. In this region Ia-Ca had a single sharp band, while Ib-Ca did not. A similar difference between the spectra of IIa-Ca and IIb-Ca was also observed, as is shown in Fig. 2. It is likely that these differences depend on the erythro-threo or meso-racemic (cis-trans) configurations of the salts.

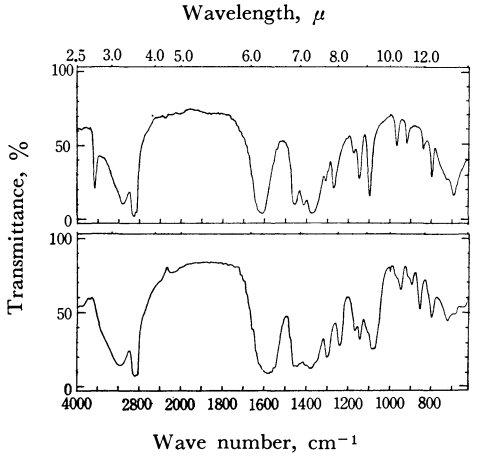

Fig. 1. Infrared spectra (Nujol) of:
Ia-Ca (upper curve)
Ib-Ca (lower curve)

4) F. Pollak, *Monatsh.*, **15**, 469 (1894).

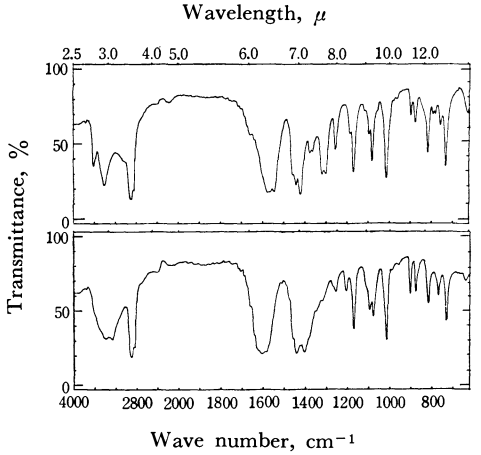

Fig. 2. Infrared spectra (Nujol) of:
IIa-Ca (upper curve)
IIb-Ca (lower curve)

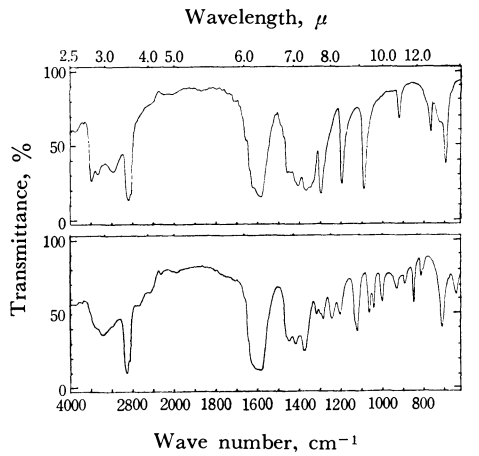

Fig. 4. Infrared spectra (Nujol) of:
IVa-Ba (upper curve)
IVb-Ba (lower curve)

To explain the configurations of these substances, the spectra of IIIa-Ba, IIIb-Ba, IVa-Ba and IVb-Ba, the configurations of which are well known, were measured and compared with the results described above. The spectra of these compounds of known configurations are shown in Figs. 3 and 4.

As is shown in Figs. 3 and 4, both IIIa-Ba and IVa-Ba had sharp bands similar to those of Ia-Ca and IIa-Ca shown in Figs. 1 and 2 in the region around 3600 cm^{-1}. IIIb-Ba and IVb-Ba did not have these bands, however, and thus were like Ib-Ca and IIb-Ca in this characteristic point.

On the other hand, as has been reported in the previous paper[1], IIIa and IIIb correspond to the erythro (meso) and threo (racemic) forms respectively; the optical resolution of the former is possible, but that of the latter is impossible. Moreover, IVa is the erythro (meso) form, and IVb is the threo (racemic) form.

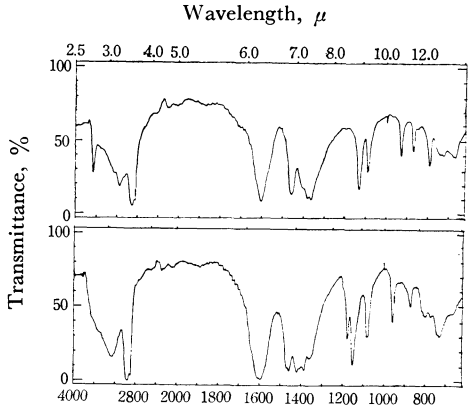

Fig. 3. Infrared spectra (Nujol) of:
IIIa-Ba (upper curve)
IIIb-Ba (lower curve)

Thus, from the configurations of these acids and the spectra of their salts, it may be supposed that both Ia and IIa are to be assigned to the same erythro or meso (cis) configuration as IIIa and IVa, and both Ib and IIb*2, to the same threo or racemic (trans) configuration as IIIb and IVb.

For further details of the spectrum in the 3600 cm^{-1} region, measurements were made of the spectra of the salts using a lithium fluoride prism. The observed frequencies were then calibrated against that of atmospheric vapor. Sharp bands of Ia-Ca, IIa-Ca, IIIa-Ba and IVa-Ba were observed at 3597, 3546, 3605 and 3554 cm^{-1} respectively, and no regular change in the intensity ratio with the concentration was observed. However, there were no similar bands in the spectra of Ib-Ca, IIb-Ca, IIIb-Ba and IVb-Ba. Hence, these bands must be due to intramolecular hydrogen bonds, which appear clearly only in the

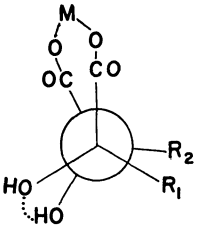

Fig. 5. Projections of the salts of:
Ia-Ca; M=Ca, $R_1=CH_3$ $R_2=H$
IIa-Ca; M=Ca, $(R_1)\text{-}CH_2\text{-}CH_2$ / $(R_2)\text{-}CH_2\text{-}CH_2$
IIIa-Ba; M=Ba, $R_1=R_2=CH_3$
IVa-Ba; M=Ba, $R_1=R_2=H$

*2 Subsequently, IIb corresponding to the racemic form was resolved into the optically active isomers and the present assignment was proved to be correct. Details of this work will be published in this Bulletin in the near future.

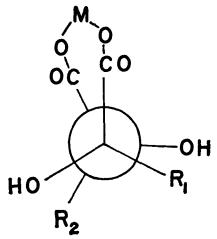

Fig. 6. Projections of the salts of:
Ib-Ca; M=Ca, $R_1=CH_3$, $R_2=H$
IIb-Ca; M=Ca, $\begin{matrix}(R_1)\text{-}CH_2\text{-}CH_2\\ \quad\quad\quad\quad\quad\quad|\\ (R_2)\text{-}CH_2\text{-}CH_2\end{matrix}$
IIIb-Ba; M=Ba, $R_1=R_2=CH_3$
IVb-Ba; M=Ba, $R_1=R_2=H$

erythro- or cis-type salts because of the definite conformational structure formed by the fixing of two carboxyl groups to a calcium or a barium metal, and by two fixing groups, carboxyl-metal and the alicyclic ring, as is shown in Fig. 5. It is likely that Ib-Ca, IIb-Ca, IIIb-Ba and IVb-Ba, which do not have intramolecular hydrogen bonds, have the threo or trans form and that they have the conformation shown in Fig. 6.

The configurations of isomeric 2-methyltartaric acids given above support the findings on their asymmetric hydrogenation effects upon a Raney nickel catalyst obtained in previous work.[2]

Summary

The configurations of isomeric 2-methyltartaric acids and 1, 2-dihydroxycyclohexane-1, 2-dicarboxylic acids have been determined on the basis of a study of the infrared spectra of their calcium salts in comparison with those of the barium salts of isomeric tartaric acids and 2, 3-dimethyltartaric acids, the configurations of which were already known. Both barium meso tartaric acid and barium meso 2, 3-dimethyltartaric acid have a sharp band due to intramolecular hydrogen bonds; however, the racemic salts do not. Similar differences have been observed in the spectra of the calcium salts prepared from isomeric 2-methyltartaric acids and isomeric 1, 2-dihydroxycyclohexane-1, 2-dicarboxylic acids. It has been concluded that these are due to a definite conformational structure caused by the fixing of two carboxyl groups with a metal. Thus, the form of 2-methyltartaric acid, with a m. p. of 146°C, was identified as the erthro form, and the form with a m. p. of 161°C, as the threo form. Further, the form of 1, 2-dihydroxycyclohexane-1, 2-dicarboxylic acid, with a m. p. of 154°C, was identified as the cis or meso form, and the other form, with a m. p. of 180°C, as the trans or racemic form.

The author wishes to express his hearty thanks to Dr. Yoshiharu Izumi of this Institute for his constant guidance throughout this study. He is also much indebted to Professor Tatsuo Miyazawa of the Molecular Biophysics Division of this institute for his valuable advice and discussion on the infrared spectra. He wishes to thank to Mr. Masami Imaida for experimental help, and Miss. Kiku Koike for elemental microanalyses. This research was made possible by the support of Ajinomoto Co., Inc., Tokyo.

BULLETIN OF THE CHEMICAL SOCIETY OF JAPAN VOL. 39 2206—2211 (1966)

Vinyl Polymerization. CXLVI.[1] The Influence of Dibenzoyl Disulfide Derivatives on Radical Polymerizations

By Kazuichi TSUDA and Takayuki OTSU

Faculty of Engineering, Osaka City University, Sumiyoshi-ku, Osaka

(Received November 19, 1965)

In order to study the effects of aromatic sulfur derivatives on radical polymerizations, dibenzoyl disulfide (DBDS) and its derivatives were prepared and used as initiators or chain transfer agents for the polymerizations of styrene and methyl methacrylate. All of these derivatives failed to act as initiators of thermal polymerizations, but they did prove effective photosensitizers. The rates of polymerizations were found not to be proportional to the square-root concentration of the initiator (DBDS) used. The sulfur radical derived from the photo-dissociation of DBDS affected not only the initiation reaction, but also the termination reaction. The chain transfer constants to DBDS derivatives in the polymerization of styrene and methyl methacrylate showed no linear relationship with Hammett's equation ($\log C/C_0=\rho\sigma$), but a linear relationship was obtained when a modification of Hammett's equation ($\log C/C_0=\rho\sigma+\gamma E_R$) was applied. From the plot obtained by the use of $\log C/C_0=\rho\sigma+\gamma E_R$, the γ value, which indicates the extent of resonance stabilization in the transition state was found to be 6.0 upon the polymerization of styrene at 60°C. Under similar conditions, however, the γ-value for benzoyl peroxide was calculated as 3.0 from the results of Cooper. This difference may be explained from an increased 3d-orbital resonance stabilization of DBDS in the transition state.

Several studies of the decomposition of organic peroxides have been made in order to clarify the relation between the structure of the peroxides and the abilities of their spontaneous and induced decompositions into free radicals. Not many systematic studies have yet been made, however, of the radical decomposition of organic peroxides. Pierson[2,3] reported the influence of several aromatic disulfides on the polymerization of styrene initiated by 2, 2'-azobisisobutyronitrile. Further studies were carried out by Otsu[4] on the use of diphenyl disulfide derivatives as chain-transfer agents in the polymerization of styrene. Tsuda et al.[5] have studied the influence of several sulfur compounds, which correspond to oxygen compounds, on radical polymerizations of styrene and methyl methacrylate.

The present paper will deal with the effect of the structure of di-substituted DBDS on their spontaneous decomposition (initiating activity) and induced decomposition (chain transfer ability) in the thermal or photo-polymerization of styrene and methyl methacrylate.

The nuclear-substituted DBDS substances used in this study have the following substituents: *p,p'*-OCH_3, *p,p'*-CH_3, *p,p'*-H, *p,p'*-Cl, *p,p'*-Br, *p,p'*-CN and *p,p'*-NO_2.

Experimental

The Preparation of *p, p'*-Disubstituted DBDS.—*Dibenzoyl Disulfide (DBDS).*—The preparation of DBDS was carried out according to the method of Frank and Blegen,[6] m. p. 128.0—128.5°C. (Found: C, 61.21; H, 3.80; S. 23.38. Calcd. for $C_{14}H_{10}O_2S_2$: C, 61.28; H, 3.67; S, 23.37%.)

p,p'-Dibromodibenzoyl Disulfide (Br-DBDS).—Br-DBDS was prepared from *p*-bromobenzoic acid which had been obtained from *p*-nitrotoluene,[7] the same as in the case of DBDS; m. p. 146.0—147.0°C. (Found: C, 39.05; H, 1.97; S, 14.90; Br, 37.15. Calcd. for $C_{14}H_8O_2S_2Br_2$: C, 38.91; H, 1.87; S, 14.84; Br, 36.83%.)

p,p'-Dichlorodibenzoyl Disulfide (Cl-DBDS).—Cl-DBDS was prepared from *p*-chlorobenzoic acid which had been obtained by the oxidation of *p*-chlorotoluene,[8] the same as in the preparation of DBDS; m. p. 122.5—123.0°C. (Found: C, 49.26; H, 2.45; S. 18.39; Cl, 20.60. Calcd. for $C_{14}H_8O_2S_2Cl_2$: C, 48.99; H, 2.35; S, 18.68; Cl, 20.65%).

p,p'-Dimethoxydibenzoyl Disulfide (MeO-DBDS).—Commercial anisic acid was recrystallized (m. p. 183.0—183.5°C), and MeO-DBDS was obtained by the same manner as DBDS. The MeO-DBDS thus obtained was light pink in color; m. p. 119.0—120.0°C. (Found:

1) Vinyl Polymerization. CXLV: S. Aoki, T. Otsu and M. Imoto, *Makromol. Chem.*, in press.
2) R. M. Pierson, A. J. Costanza and A. H. Weinstein, *J. Polymer Sci.*, **17**, 221 (1955).
3) A. J. Costanza, R. J. Coleman, R. M. Pierson, C. S. Marvel and C. King, ibid., **17**, 319 (1955).
4) T. Otsu and H. Motooka, *J. Chem. Soc. Japan, Ind. Chem. Sect. (Kogyo Kagaku Zasshi)*, **62**, 287 (1959).
5) K. Tsuda, S. Kobayashi and T. Otsu, This Bulletin, **38**, 1517 (1965).
6) R. L. Frank and J. R. Blegen, "Organic Syntheses", Coll. Vol. 3, 116 (1955).
7) L. A. Bigelow, ibid., Coll. Vol. I, 136 (1941).
8) C. S. Marvel and S. M. McElvain, ibid., Coll. Vol. I, 170 (1941).

C, 57.38; H, 4.30; S, 18.97. Calcd. for $C_{16}H_{14}O_4S_2$: C, 57.47; H, 4.22; S, 19.18%.)

p, p' - Dimethyldibenzoyl Disulfide (Me - DBDS). — *p*-Toluic acid, an oxidation intermediate of *p*-xylene to telephthalic acid, was recrystallized first from toluene and then from benzene; m. p. 178.5—179.0°C. Me-DBDS was prepared from *p*-toluic acid by the same manner as DBDS; m. p. 118.0—119.0°C. (Found: C, 63.30; H, 4.70; S, 21.09. Calcd. for $C_{16}H_{14}O_2S_2$: C, 63.55; H, 4.67; S, 21.15%.)

p, p'-Dinitrodibenzoyl Disulfide (NO_2-DBDS). — According to the method mentioned above, NO_2-DBDS was prepared from *p*-nitrobenzoic acid. This material was yellow in color and was an amorphous substance; m. p. 183.0—183.5°C. with decomp. (Found: C, 46.40; H, 2.40; S, 17.47; N, 7.64. Calcd. for $C_{14}H_8O_6N_2S_2$: C, 46.15; H, 2.22; S, 17.60; N, 7.68%.)

p, p'-Dicyanodibenzoyl Disulfide (CN-DBDS).—From *p*-cyanobenzoic acid,[9] CN-DBDS was prepared by the same manner as DBDS. The CN-DBDS thus obtained was orange in color and was an amorphous material; m. p. 179.5—180.0°C with decomp. (Found: C, 58.87; H, 2.59; S, 19.15; N, 8.47. Calcd. for $C_{16}H_8O_2N_2S_2$: C, 59.24; H, 2.49; S, 19.77; N, 8.64%.)

The Purification of Materials.—It was rather difficult to remove impurities from the DBDS derivatives thus obtained, so recrystallization was repeated from 5 to 10 times in dichloroethane or ethyl acetate.

The 2, 2'-azobisisobutyronitrile (AIBN) which was used as the initiator was purified by recrystallization three times from ethanol; m. p. 102.0—102.5°C.

Styrene (St) and methyl methacrylate (MMA) were purified by the ordinary method.

Polymerization Procedure.—Bulk polymerization by the ordinary glass-tube method was employed. In the case of NO_2-DBDS, however, benzene solution polymerization was adopted, because this disulfide was not dissolved in these monomers.

Thermal polymerizations were conducted at 60°C, under shaking and in the absence of light. Photopolymerizations were done at 25°C, using ultraviolet-ray irradiation. None of the polymerizations were allowed to proceed beyond 10% conversion. It was noted that the addition of NO_2-DBDS or CN-DBDS caused the mixture to grow yellowish-white during the polymerization. After polymerization, the polymer was precipitated by the addition of an excess of methanol, washing with methanol, and then drying under a vacuum. A trace of a yellow substance similar to sulfur was obtained when the polymer, monomer and methanol precipitant were removed. No further examination of this substance was made.

The Determination of the Chain Transfer Constant.—The intrinsic viscosity $[\eta]$ was determined in benzene at 30°C by using Ubbelohde's viscometer. The number-average degree of polymerization ($\overline{P_n}$) was calculated by Eqs. 1 and 2;

For polystyrene[10]: $\log \overline{P_n} = 3.205 + 1.37 \log [\eta]$ (1)

For polymethyl methacrylate[11]:

$$\log \overline{P_n} = 3.420 + 1.13 \log [\eta] \quad (2)$$

The chain transfer constants (C) to DBDS derivatives were calculated by Mayo's equation (3):

$$1/\overline{P_n} = 1/\overline{P_0} + C \cdot [S]/[M] \quad (3)$$

where [S] and [M] are the initial concentrations of the DBDS derivatives and the monomers respectively.

Results

DBDS Derivatives Used as Initiators in Thermal Polymerization.—Table I shows the results of the thermal polymerization of St and MMA when DBDS derivatives were employed as initiators at 60°C.

As is shown in Table I, it may safely be said that DBDS derivatives do not act as initiators in the thermal polymerizations of St and MMA. Recently, it has been found that DBDS derivatives also do not act as initiators of the thermal polymerization of St and MMA at 80°C and 100°C.[12]

Table I. Thermal polymerization in the presence of DBDS derivatives (60°C)

Concn. of DBDS mol./l.	3.1×10^{-3}	1.0×10^{-2}	3.0×10^{-3}	1.0×10^{-2}
Subst. of DBDS	Rate of polymerization, %/hr. St		MMA	
MeO	0.10	0.10	0.14	0.14
Me	0.10	0.10	0.10	0.10
H	0.10	0.10	0.19	0.19
Cl	0.11	0.10	0.13	0.13
Br	0.10	0.10	0.13	0.13
CN	0.16	0.16	0	0.06
NO_2	0	0	0	0
None*	0.12	0.11	0.13	0.13

* Absence of DBDS.

DBDS Derivatives as Chain-transfer Agents in Thermal Polymerizations Initiated by AIBN.—Thermal polymerizations were conducted by adding DBDS derivatives to the systems whose initiator was AIBN. R_0 and R stand for the rate

Table II. Chain-transfer constants to DBDS at 60°C

Subst. of DBDS	St	MMA
MeO	9.60×10^{-3}	1.46×10^{-3}
Me	4.63×10^{-3}	1.10×10^{-3}
H	3.60×10^{-3}	1.00×10^{-3}
Cl	1.96×10^{-2}	1.00×10^{-3}
Br	7.45×10^{-2}	1.67×10^{-3}
CN	3.19×10^{-1}	2.90×10^{-2}
NO_2	(6.65×10^{-1})	(6.94×10^{-2})

9) E. P. Valby and H. J. Lucas, *J. Am. Chem. Soc.*, **51**, 2718 (1929).

10) F. R. Mayo, R. A. Gregg and M. S. Mathieson, ibid., **73**, 1691 (1951).

11) B. Baysal and A. V. Tobolsky, *J. Polymer Sci.*, **9**, 171 (1952).

12) K. Tsuda, N. Kita and T. Otsu, *Memoires of the Faculty of Engineering, Osaka City University*, **7**, 103 (1965).

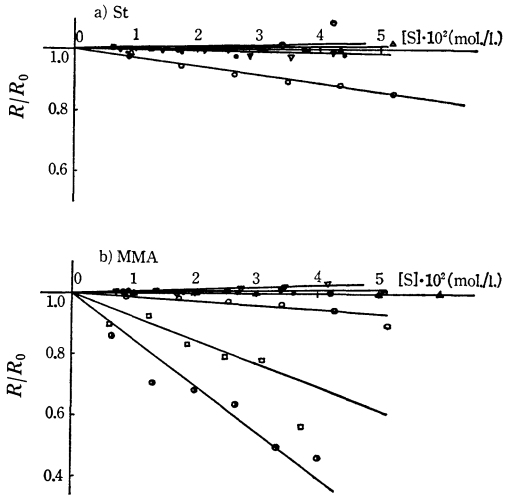

Fig. 1. Effects of DBDS derivatives on the rate of polymerization of St and MMA initiated by AIBN (3.1×10^{-3} mol./l.) at 60°C.
-●- H -△- Cl -▽- Br -◑- NO_2
-◒- MeO -○- Me -□- CN

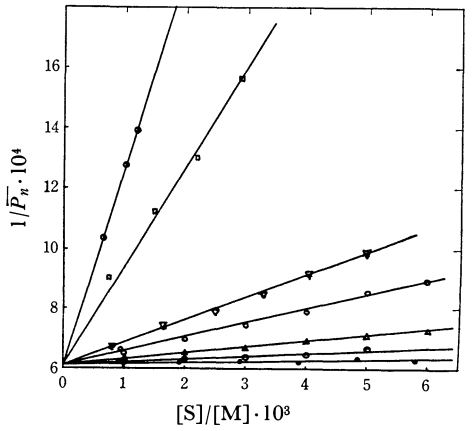

Fig. 2. Relationship between $1/\overline{P_n}$ and [S]/[M] in the polymerization of St initiated by AIBN at 60°C. Marks are the same as in Fig. 1.

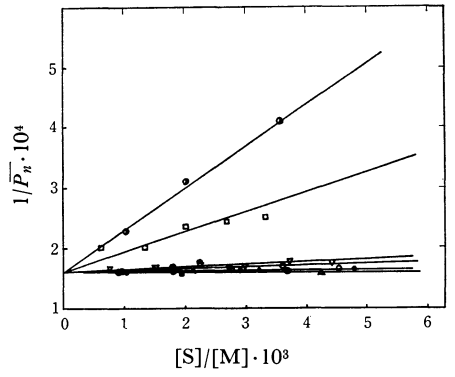

Fig. 3. Relationship between $1/\overline{P_n}$ and [S]/[M] in the polymerization of MMA initiated by AIBN at 60°C. Marks are the same as in Fig. 1.

of polymerization in the absence and in the presence of DBDS derivatives. Figure 1 shows the correlation between R/R_0 and the concentration of the DBDS derivatives. It may be seen that CN-DBDS and NO_2-DBDS remarkably retard the polymerization of MMA. These facts agree with the results shown in Table I. In order to estimate the chain transfer constants of DBDS derivatives, the plots obtained by Eq. 3 are shown in Figs. 2 and 3. The chain transfer constants to DBDS derivatives are shown in Table II.

The Photo-polymerization of DBDS Derivatives. — The results of the photo-polymerization of St and MMA conducted using DBDS derivatives as photo-sensitizers are shown in Table III.

Table III. Photo-polymerization using DBDS derivatives as photo-sensitizers at 25°C
[DBDS] = 1.0×10^{-2} mol./l.

Subst. of DBDS	Rate of polymerization, %/hr. St	MMA
MeO	0.95	3.83
Me	0.95	3.91
H	0.81	3.84
Cl	0.98	3.55
Br	0.99	—
CN	0.97	3.09
NO_2	0	0
None*	0.08	0.23

* Absence of DBDS

As may be clearly seen from Table III, the DBDS derivatives employed here were effective sensitizers in the photo-polymerizations of both monomers. The relations between the concentrations of the DBDS derivatives employed as sensitizers and the rates of polymerizations are shown in Fig. 4. Unlike as in the ordinary radical polymerizations, the rate of polymerization had no linear relationship depending on the square-root concentration of the DBDS derivatives; it gave a maximum, indicating that the sulfur radical produced by the photo-decomposition of DBDS derivatives acts as both initiator and terminater of the polymerization.

Similar phenomena were observed in the photo-polymerization of these monomers in the presence of AIBN. The results are shown in Fig. 5.

Discussion

As is clear from Table I, DBDS derivatives do not serve as initiators of the thermal polymerization of St and MMA. It is obvious from this finding that DBDS derivatives, unlike benzoyl peroxide, do not decompose into free radicals under the present conditions. This may be attributable to the difference between the bond-dissociation energy

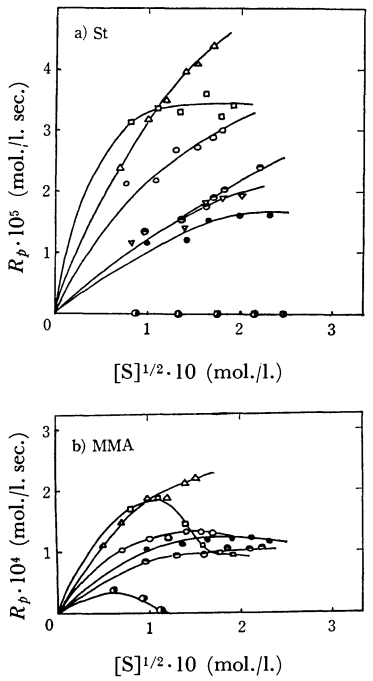

Fig. 4. Effects of DBDS on the rate of photo-polymerization of St and MMA at 25°C.
Marks are the same as in Fig. 1.

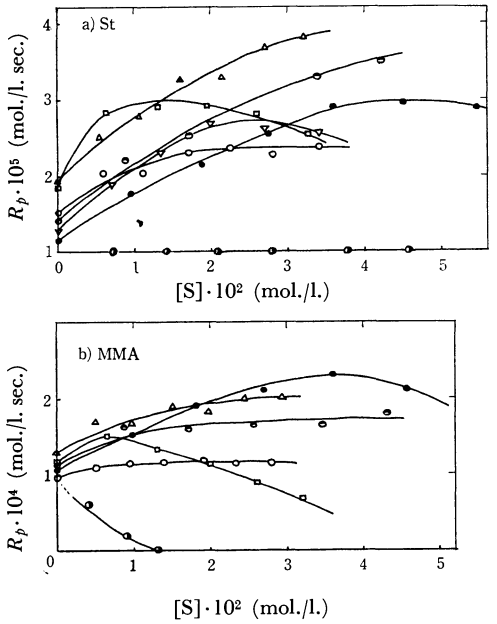

Fig. 5. Effects of DBDS on the rate of photo-polymerization of St and MMA sensitized by AIBN at 25°C.
Marks are the same as in Fig. 1.

of the –O–O– linkage in benzoyl peroxide (about 30 kcal./mol.) and that of the –S–S– linkage in alkyl disulfide (about 70—73 kcal./mol.). As

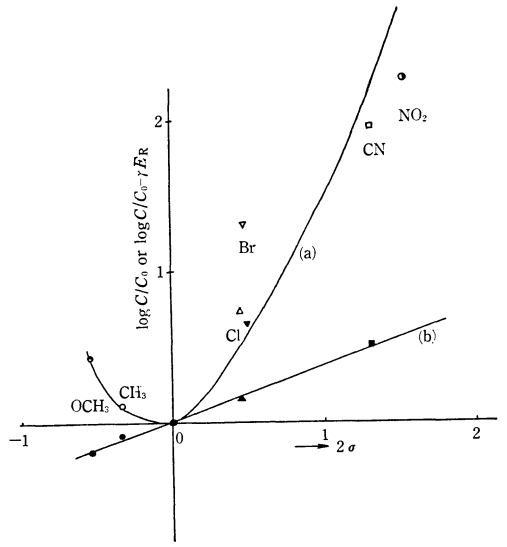

Fig. 6. Plots by Eqs. 4 and 5 for the chain transfer to DBDS in the polymerization of St.

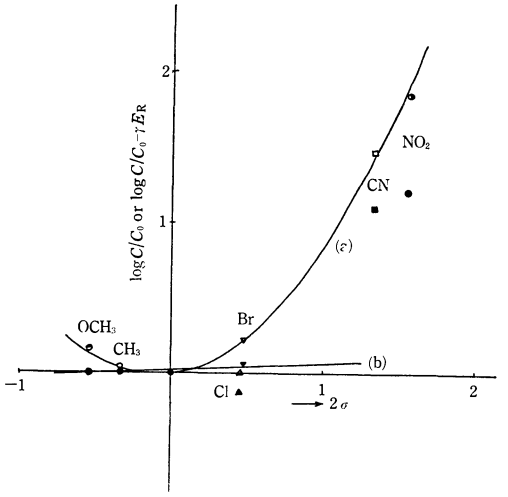

Fig. 7. Plots by Eqs. 4 and 5 for the chain transfer to DBDS in the polymerization of MMA.

shown in Table III, all DBDS derivatives except NO_2-DBDS could act as effective sensitizers of the photo-polymerization of these monomers. NO_2-DBDS was found to inhibit thermal and photo-polymerizations.

Contrary to the ordinary kinetic behavior, an abnormal correlation between the rate of polymerization and the concentration of DBDS derivatives in the photo-polymerizations was observed, as is shown in Figs. 4 and 5. These results can be explained by noting that the sulfur radical produced by the application of ultraviolet rays can not only initiate but also terminate the polymerization. Almost the same behavior was observed in

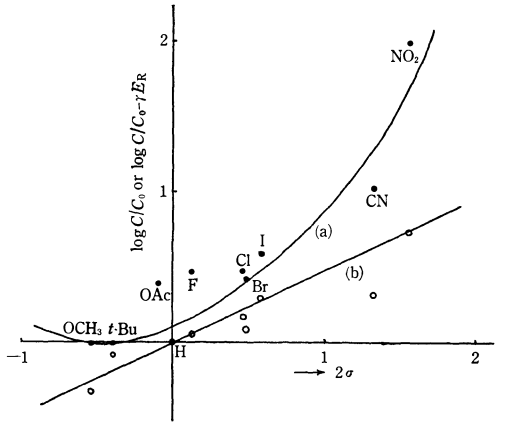

Fig. 8. Relationship between $\log C/C_0$ or $\log C/C_0 - \gamma E_R$ and σ constants calculated from the chain transfer to benzoyl peroxide derivatives in the polymerization of St:
a) plotted by Eq. 4, b) plotted by Eq. 5.

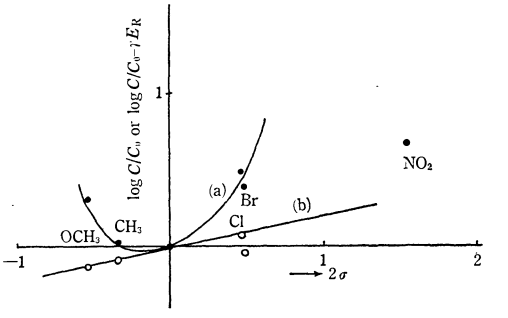

Fig. 9. Relationship between $\log C/C_0$ or $\log C/C_0 - \gamma E_R$ and σ constants calculated from the chain transfer to diphenyl disulfide derivatives in the polymerization of St:
a) plotted by Eq. 4. b) plotted by Eq. 5.

the polymerization of MMA initiated by tetraethyl thiuram disulfide.[13]

In order to clarify the relation between the reactivites of DBDS derivatives toward the attack of radicals and their structures, especially those of their substituents, the chain-transfer constants of those derivatives were plotted with the σ values, according to Hammett's equation (4);

$$\log C/C_0 = \rho\sigma \qquad (4)$$

were C and C_0 are the chain-transfer constants of substituted and of unsubstituted DBDS, respectively, σ is Hammett's substituent constant, and ρ is the reaction constant. The results are shown in Figs. 6 and 7; they do not give a straight line. Such parabola-type relations have been observed in many radical reactions.[14,15]

Recently, Yukawa and Tsuno[16] have derived a modified Hammett's equation by considering the resonance contribution in electrophilic ionic reactions. On the other hand, Yamamoto et al.,[17] who are now working in our laboratory, have proposed another modified Hammett's equation (5) for radical reactions:

$$\log C/C_0 = \rho\sigma + \gamma E_R \qquad (5)$$

where the γ value is the extent of the resonance stabilization and E_R is the resonance substituent constant, as was estimated by Yamamoto et al.[15,17] ρ is the reaction constant, and σ is Hammett's polar term. It was then shown that Eq. 5 could be nicely applied in various types of radical reactions (over 120 examples).

When Eq. 5 was applied to the present chain-transfer reactions of DBDS derivatives, the fairly good straight lines illustrated in Figs. 6 and 7 were obtained. From these figures, the values of γ and ρ were obtained as follows:

For St: $\gamma = 6.0$ $\rho = 0.36$

For MMA: $\gamma = 1.5$ $\rho = 0.07$

In 1952, Cooper[18] determined the chain-transfer constant to substituted benzoyl peroxides in the polymerization of St. When Cooper's results are plotted by Hammett's equation (4) and Yamamoto's equation (5), Fig. 8 is obtained. Figure 9 is obtained by the same plots of the chain-transfer constants to substituted diphenyl disulfides.[4] The ρ and γ values from Figs. 8 and 9 are summarized in Table IV.

TABLE IV. γ, ρ VALUES FOR CHAIN TRANSFER REACTION

Attacking radical	Chain transfer agent	γ	ρ
PSt	DBDS	6.0	0.36
PMMA	DBDS	1.5	0.07
PSt	BPO*	3.0	0.38
PSt	DPDS**	4.0	0.23

* BPO: Benzoyl peroxide
** DPDS: Diphenyl disulfide

The value of DBDS toward the attack of a polystyryl radical is larger than that of benzoyl peroxide, because the resonance stabilization of sulfur is exceedingly strong. As has been pointed out by Oae,[19] the resonance stabilization in the reactions involving a sulfur compound may be considered

13) T. Otsu, ibid., **3**, 201 (1961).
14) Y. Yukawa and T. Tsuno, "Progress in Organic Reaction Mechanisms," **Ed.** by M. Murakami, Vol. I, Maki, Tokyo (1958), p. 1.
15) T. Otsu and T. Yamamoto, *J. Soc. Org. Synth. Chem. Japan*, **23**, 643 (1965).
16) Y. Yukawa and T. Tsuno, This Bulletin, **32**, 972 (1960); Y. Yukawa, *J. Soc. Org. Synth. Chem. Japan*, No. 232, p. 69 (1963).
17) T. Azumi and T. Yamamoto, *Reports of Himeji Institute of Techn.*, **11**, 152 (1960).
18) W. Cooper, *J. Chem. Soc.*, **1952**, 2408.
19) C. C. Price and S. Oae, "Sulfur Bonding," Ronald Press, New York (1962); S. Oae, *Chemistry*, **18**, 1028 (1963); W. Tagaki, *Kagaku-no-Ryoiki*, **17**, 349 (1963).

to be made greater by the existence of the 3d orbital resonance of the sulfur atom in the transition state than those involving an oxygen compound.

The decrease in γ values for the attack of the PMMA radical compared with that of the PSt radical may be considered to reflect the difference in the degree of contribution of the resonance effect in their transition states, but this point is not clear at the present time.

The ρ values obtained are positive, indicating that the –S–S– linkage in DBDS is $\delta+$ as is shown below;

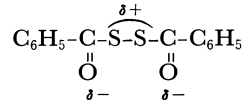

This is also true in benzoyl peroxide, as was pointed out by Imoto et al.[20] The fact that almost the same ρ values were obtained in both DBDS and benzoyl peroxide (Table IV) might indicate that the polar contribution of the two compounds in their transition states did not differ from each other.

20) M. Imoto and S. Choe, *J. Polymer Sci.*, **15**, 485 (1955).

BULLETIN OF THE CHEMICAL SOCIETY OF JAPAN VOL. 39 2211—2215 (1966)

The Autoxidation of *p*-Xylene Catalyzed with Cobalt Monobromide in Acetic Acid

By Yoshio KAMIYA, Tadahiko NAKAJIMA and Kōichiro SAKODA

Department of Fuel Technology, The University of Tokyo, Hongo, Tokyo

(Received November 26, 1965)

The rate of the cobalt-catalyzed autoxidation of *p*-xylene by adding sodium bromide reaches the steady state within several minutes and increases remarkably at high cobalt concentrations. Although *p*-tolualdehyde as well as water, the main oxidation products of *p*-xylene at the initial stage, strongly affect the rate of oxidation, the apparent rate is kept constant over a long period. When cobalt dibromide is used, a pronounced induction period can be observed at high cobalt concentrations, and the rate of oxidation starts to decrease after a short while. The effect of the ratio of sodium bromide to cobalt has shown that cobalt monobromide is an effective catalyst for the propagation step. The rate of the oxidation of *p*-xylene is found to be of the order of from 1.5 to 2.0 with respect to cobalt at concentrations from 10^{-3} to 5×10^{-2} mol./l. and at temperatures from 65 to 95°C, and to be first-order with respect to the *p*-xylene concentration; these findings show excellent agreement with the theory. When cobalt is partly replaced by manganese, a strong synergistic effect can be observed.

Although several papers[1-5] have been published on the autoxidation of methyl-substituted benzene catalyzed with cobalt bromide, the reaction mechanism is still far from certain. We have shown very recently that the rate of the cobalt-catalyzed autoxidation of tetralin[6] in acetic acid is increased remarkably in the presence of sodium bromide and have kinetically proved that this effect can be attributed to the participation of a new type of propagation reaction between cobalt monobromide and the tetralyl peroxy radical; the kinetic scheme can be represented as follows:

$$\mathrm{ROOH} + (\mathrm{Co})_2 \xrightarrow{k_1'} \text{radical} \xrightarrow{\mathrm{RH}} \mathrm{R}\cdot \quad (1)$$

$$\mathrm{R}\cdot + \mathrm{RH} \xrightarrow{k_2} \mathrm{RO_2}\cdot \quad (2)$$

$$\mathrm{RO_2}\cdot + \mathrm{RH} \xrightarrow{k_3} \mathrm{ROOH} + \mathrm{R}\cdot \quad (3)$$

$$\mathrm{RO_2}\cdot + \mathrm{Co^{2+}BrH} \xrightarrow{k_3'} \text{products} + (\mathrm{Co^{2+}} + \mathrm{Br}\cdot) \quad (4)$$

$$(\mathrm{Co^{2+}} + \mathrm{Br}\cdot) + \mathrm{RH} \xrightarrow{k_4} \mathrm{Co^{2+}BrH} + \mathrm{R}\cdot \quad (5)$$

$$\mathrm{RO_2}\cdot + \mathrm{RO_2}\cdot \xrightarrow{k_6} \text{products} + \mathrm{O_2} \quad (6)$$

$\mathrm{Co^{2+}BrH}$ represents the cobalt-hydrogen bromide complex, which we suggest is the effective catalyst

1) D. A. S. Ravens, *Trans. Faraday Soc.*, **55**, 1768 (1959).
2) N. Ohta, E. Takahashi and H. Horikiri, *J. Chem. Soc. Japan, Ind. Chem. Sect.* (*Kogyo Kagaku Zasshi*), **65**, 1353 (1962).
3) M. Shigeyasu, ibid., **67**, 1396 (1694).
4) A. Suzuki, K. Iwasa and J. Nakamura, ibid., **67**, 1550 (1964).
5) Y. Takegami, T. Okano, T. Fujii, S. Uemura and S. Okaya, *J. Japan Petrol. Inst.*, **7**, 560, 723, 727 (1964).
6) Y. Kamiya, *Tetrahedron*, **22**, 2029 (1966).

for the propagation and the alternative structure of cobalt monobromide in acetic acid.

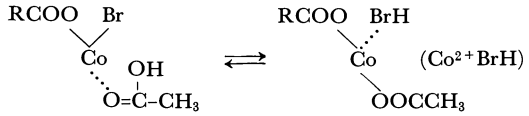

However, the reaction scheme in the autoxidation of *p*-xylene catalyzed with cobalt bromide should be considerably different from the one shown above; the rate of the cobalt-catalyzed autoxidation of *p*-xylene in acetic acid is extremely slow at temperatures as low as 80°C, even at the cobalt concentration of 5×10^{-2} mol./l., and so the rate of propagation step must be very slow. Previously,[6] it has been suggested that another propagation reaction 7 between $Co^{2+}BrH$ and the peroxy radical, proceeds to a minor extent as compared with Eq. 4, because the steady state concentration of tetralin hydroperoxide observed increases a little when sodium bromide is added to the solution.

$$RO_2\cdot + Co^{2+}BrH + RH \xrightarrow{k_3''} ROOH + (Co^{2+} + Br\cdot) + R\cdot \qquad (7)$$

When the hydroperoxide is formed by Eq. 7 instead of Eq. 4, and when k_2 and k_4 are large enough compared with k_3' and k_3'', the overall rate of oxidation under stationary-state conditions is given by:

$$-dO_2/dt = [k_3' + k_3''(RH)](k_1'/2k_6)^{1/2}\cdot (Co)(Co^{2+}BrH)(ROOH)^{1/2} \qquad (8)$$

When the rate of hydroperoxide decomposition equals its rate of formation,

$$-dO_2/dt = k_3''(RH)[k_3' + k_3''(RH)]\cdot (Co^{2+}BrH)/2k_6 \qquad (9)$$

Provided k_3' is much larger than $k_3''(RH)$, as in the case of tetralin autoxidation,

$$-dO_2/dt = k_3'k_3''(RH)(Co^{2+}BrH)^2/2k_6 \qquad (10)$$

Experimental

The experimental techniques[7] have been described previously. *p*-Xylene was oxidized at 65, 80 or 95°C using a 50-ml. long-necked flask in a 1 : 1 (by volume) acetic acid - *p*-xylene solution except when noticed. The bromides used were sodium or ammonium bromides and cobalt dibromide. Cobalt, manganese and copper were used as decanoates. The amount of *p*-tolualdehyde was determined by gas chromatography using 2.5 m. of a PEG succinate ester column at 180°C. The *p*-toluic acid was titrated with an aqueous solution of sodium hydroxide in the presence of EDTA as a chelating reagent after drying off the solvent with an infrared lamp.

7) Y. Kamiya, S. Beaton, A. Lafortune and K. U. Ingold, *Can. J. Chem.*, **41**, 2034 (1963).

Results and Discussion

Oxygen Absorption Curve.—The rate of cobalt-catalyzed autoxidation of *p*-xylene in acetic acid increases slowly as the oxidation proceeds and as *p*-tolualdehyde is accumulated in the solution. On the other hand, when sodium bromide is added the rate reaches the steady state in several minutes and is increased by a factor of three hundred at cobalt concentration of 5×10^{-2} mol./l. and at the sodium bromide concentration of 1×10^{-1} mol./l. Typical oxygen absorption curves are shown in Fig. 1 at the cobalt concentration of

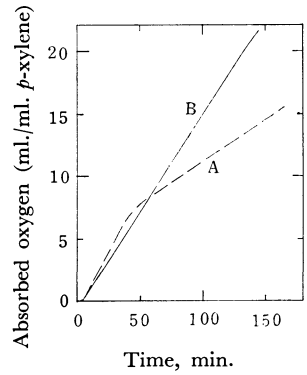

Fig. 1. Oxygen absorption curves in the autoxidation of *p*-xylene in acetic acid catalyzed with 10^{-2} mol./l. $CoBr_2$ (A) and with 10^{-2} mol./l. $CoDe_2$ and 2×10^{-2} mol./l. NaBr (B) at 80°C.

2×10^{-2} mol./l. With cobalt decanoate and sodium bromide, the rate of oxidation is kept constant over a long period. Generally, the addition of ammonium bromide instead of sodium bromide results in about a 10% lower rate. On the other hand, with cobalt dibromide the initial rate is about 20% higher than that obtained with cobalt and sodium bromide, but the rate suddenly decreases after 30 min. (that is, the catalyst is deactivated). Hay and Blanchard[8] obtained similar results in the autoxidation of cumene. They concluded that these results can be attributed to the formation of phenol due to the decomposition of cumene hydroperoxide by hydrogen bromide. However, in the case of *p*-xylene almost no phenolic inhibitor is formed by the decomposition of *p*-xylene hydroperoxide. In the present state these peculiar results remain unclarified.

Benzyl bromide, reported by Takegami[5] and his coworkers to be one of the most effective organic bromides for the oxidation of *p*-toluic acid, has been shown to have a moderate effect on the rate of oxidation, showing the value of 1.9×10^{-4} mol./l.sec. compared with 8.0×10^{-4} mol./l.sec. in the case of NaBr at cobalt 5×10^{-2} mol./l. and at the bromide-to-cobalt ratio of 3.0.

8) A. S. Hay and H. S. Blanchard, ibid., **43**, 1306 (1965).

A high concentration of cobalt dibromide shows a very pronounced induction period, during which the rate of oxygen absorption is extremely small. This induction period can be increased by increasing the concentration of cobalt dibromide as well as by decreasing the temperature; it can become, for example, 37 min. at cobalt 2×10^{-2} mol./l., and more than 120 min. at cobalt 1×10^{-1} mol./l. at 65°C. The induction period due to cobalt dibromide can be entirely eliminated in the presence of an equimolar amount of sodium acetate; this shows that cobalt monobromide is the effective catalyst, as has been observed in the autoxidation of tetralin. As is shown in Fig. 2,

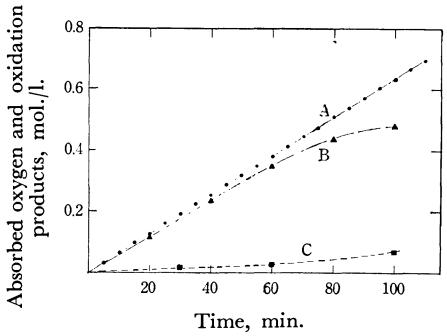

Fig. 2. Absorbed oxygen (A) and oxidation products, *p*-tolualdehyde (B) and *p*-toluic acid (C), as a function of time in the oxidation of *p*-xylene in acetic acid with 2×10^{-2} mol./l. cobalt and 4×10^{-2} mol./l. NaBr at 65°C.
—— O_2 ---- *p*-Tolualdehyde
····· *p*-Toluic acid

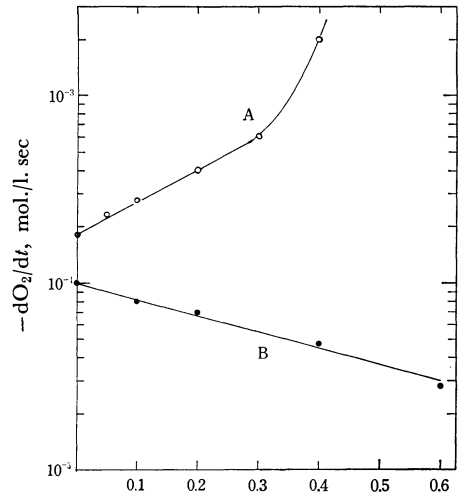

Fig. 3. The effect acid of *p*-tolualdehyde (A) at 80°C and of *p*-toluic acid (B) at 65°C.
○ *p*-Tolualdehyde, 80°C, Co: 2×10^{-2} mol./l., NaBr: 4×10^{-2} mol./l.
● *p*-Toluic acid, 65°C, Co: 2×10^{-2} mol./l., NaBr: 4×10^{-2} mol./l.

the oxidation products at the initial stage are mainly composed of *p*-tolualdehyde, accompanied by an equimolar amount of water and relatively small amounts of *p*-toluic acid and *p*-toluyl alcohol. The rate of oxidation should be increased as the aldehyde is accumulated, since the effect of aldehyde on the rate is remarkable, as Fig. 3 shows. On the other hand, water is found to deactivate the catalyst strongly; i. e., the rate is decreased by a factor of three by adding 0.69 mol. of water to 1.0 mol. of *p*-xylene at 2×10^{-2} mol./l. of cobalt and 4×10^{-2} mol./l. of sodium bromide, but it is not affected when 0.069 mol. of water is added. Moreover, as *p*-xylene is consumed the rate of oxidation should tend to decrease, because the rate is proportional to *p*-xylene, as Figs. 3 and 7 show. In spite of various effects, however, the apparent rate of oxidation is kept constant over a long period. Therefore, the rate of autoxidation of *p*-xylene catalyzed with cobalt monobromide is apparently independent of the hydrocarbon concentration in the course of oxidation, and it is first-order with respect to the initial hydrocarbon concentration (see Fig. 7).

The Ratio of Sodium Bromide to Cobalt.— The effect of the ratio of sodium bromide to cobalt is shown in Figs. 4 and 5. Just as in the case of tetralin oxidation, the rate shows a limiting value at a 1 : 2 ratio of sodium bromide to cobalt at temperatures below 80°C. It is confirmed that the increase in the rate of oxidation upon the addition of bromide is due not to free hydrogen bromide but to cobalt monobromide, since the rate reaches a limit or nearly so at sodium bromide/cobalt 1.0. At this ratio, the concentration of free hydrogen bromide should be extremely low, because most of the bromide can be complexed with cobalt and the equilibrium constant of Eq. 11 is very small:

$$CH_3COOH + NaBr \rightleftarrows HBr + CH_3COONa \quad (11)$$

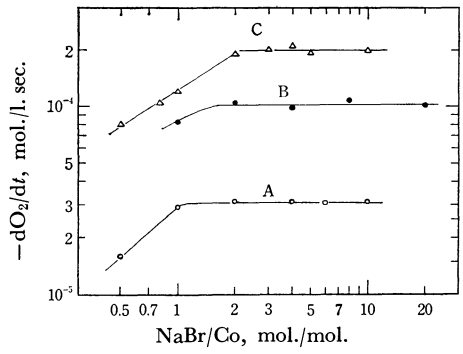

Fig. 4. The steady rate of oxidation of *p*-xylene in acetic acid as a function of the ratio of NaBr/Co, with 5×10^{-2} mol./l. cobalt at 65°C (A), with 2×10^{-2} mol./l. cobalt at 65°C (B) and with 2×10^{-2} mol./l. cobalt at 80°C (C).

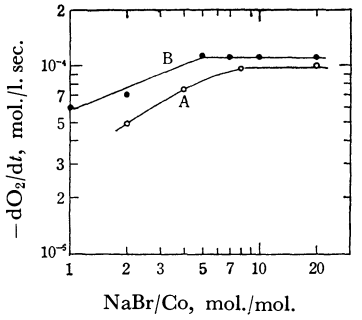

Fig. 5. The steady rate of oxidation of *p*-xylene as a function of the ratio of NaBr/Co in acetic acid with 1×10^{-2} mol./l. cobalt at 95°C (A) and in butyric acid with 5×10^{-2} mol./l. cobalt at 80°C (B).

Although, at 95°C, the rate of oxidation tends to increase until sodium bromide/cobalt is reached at 8.0, as is shown in Fig. 5, the rate has shown a limiting value at sodium bromide/cobalt 2.0 at such higher cobalt concentrations as 5×10^{-2} mol./l. These results might be due to the decrease of the concentration of hydrogen bromide by the formation of inactive organic bromides. The organic bromides can be expected to increase at high temperatures, but the influence on the rate of oxidation will be small at high concentrations of sodium bromide.

It has already been proved that hydrogen bromide is not effective in the initiating reaction, since with just the addition of hydrogen bromide to the solution, in the absence of metal salt or an initiator, the oxidation of tetralin[6] does not proceed, and the induction period[8] due to a phenol can not be decreased.

The Effect of Cobalt Concentration.—The limiting rates of the oxidation of *p*-xylene, as the ratio of sodium bromide to cobalt is varied, are plotted against the cobalt concentration at temperatures from 65°C to 95°C in Fig. 6. At all temperatures the curves show the same characteristics. The rate of oxidation is nearly second-order with respect to cobalt at concentrations below 2×10^{-2} mol./l.; the order in cobalt tends to decrease to the extent of 0.75 as the cobalt is increased. (Incidentally, quite a similar relation was obtained at the *p*-xylene concentration of 1.22 mol./l.). The rate of oxidation is required to be second-order with respect to cobalt according to Eqs. 8 and 10, provided $Co^{2+}BrH$ is proportional to cobalt. Therefore, $Co^{2+}BrH$ seems to be almost proportional to cobalt at low concentrations, but the order of $Co^{2+}BrH$ with respect to cobalt seems to decrease a little as the amount of cobalt is increased.

The Effect of the *p*-Xylene Concentration.—The rate of the autoxidation of *p*-xylene is plotted against the concentration of *p*-xylene in

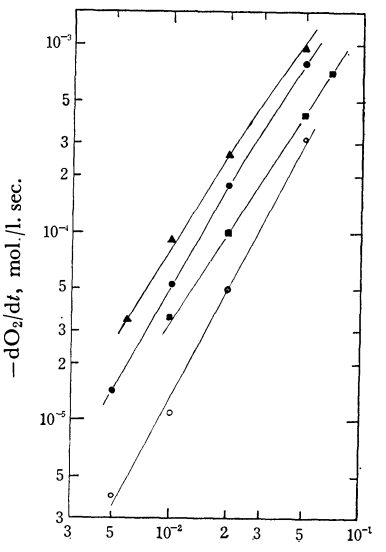

Fig. 6. The maximum rate of oxidation of *p*-xylene in acetic acid in the presence of NaBr as the ratio of NaBr/Co is varied as a function of cobalt concentration.

- ■ 65°C, *p*-xylene/acetic acid 1/1 (ml./ml.) NaBr/Co 2
- ● 80°C, *p*-xylene/acetic acid 1/1 (ml./ml.) NaBr/Co 2
- ▲ 95°C, *p*-xylene/acetic acid 1/1 (ml./ml.) NaBr/Co 8
- ○ 80°C, *p*-xylene/acetic acid 1/5 (ml./ml.) NaBr/Co 2

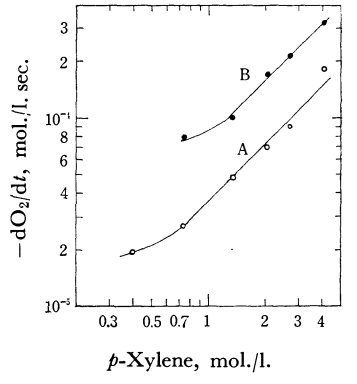

Fig. 7. The steady rate of oxidation of *p*-xylene in acetic acid as a function of *p*-xylene concentration with 2×10^{-2} mol./l. cobalt and 4×10^{-2} mol./l. NaBr at 80°C (A) and with 5×10^{-2} mol./l. cobalt and 1×10^{-1} mol./l. NaBr at 65°C (B).

Fig. 7 at 65°C and 80°C; it is found to be exactly first-order with respect to *p*-xylene, as is required by Eq. 10, showing excellent agreement with the theory. On the other hand, the rate tends to be independent of *p*-xylene at low concentrations; this result suggests that the following reaction

becomes more important than Eq. 7 at low concentrations of *p*-xylene:

$$Co^{2+}BrH + RO_2\cdot \xrightarrow{k_3'''} (Co^{2+} + Br\cdot) + ROOH \qquad (12)$$

When Eq. 7 is replaced by Eq. 12, the rate of oxidation, instead of with Eq. 10, can be represented by:

$$-dO_2/dt = k_3'k_3'''(Co^{2+}BrH)^2/2k_6 \qquad (13)$$

The Effect of Acid Strength.—When a higher fatty acid is used instead of acetic acid, the rate of oxidation shows a lower value as the carbon number of the fatty acid is increased. However, further experiments show that the rate reaches a limit at a higher ratio of sodium bromide to cobalt in a higher fatty acid solvent. For example, at a cobalt concentration of 2×10^{-2} mol./l., the rate of oxidation in butyric acid shows a maximum value of 1.1×10^{-4} mol./l.sec. at the sodium bromide/cobalt ratio of 4.0 as compared with the maximum rate of 1.8×10^{-4} mol./l.sec. at a sodium bromide/cobalt ratio of 2.0 in acetic acid. When bromoacetic or chloroacetic acids are used instead of acetic acid, the initial rate of oxidation results in a small decrease (about 10%), and the catalyst is gradually deactivated as the reaction proceeds.

The Synergistic Effect of the Metal Catalyst.—When 20% of the cobalt is replaced by manganese, an approximately five-fold increase in the rate of the oxidation of *p*-xylene was observed, showing that the metals are strongly synergistic, as is shown in Fig. 8. As has previously been suggested,[9] manganeous salt easily reacts with peroxy radicals and terminates the chain. Therefore, the synergistic effect may occur when manganese increases the rate of Eq. 7 because of a strong affinity to the peroxy radical. However, the synergistic effect due to manganese and the rate of oxidation catalyzed with manganese bromide are rapidly decreased as oxidation proceeds; i. e., the manganese is found to be deactivated easily. In contrast to the synergistic effect of manganese, cupric salt has shown a very strong antagonistic effect, showing that the rate of the oxidation of *p*-xylene is reduced by a factor of ten when 20% of the cobalt is replaced by copper.

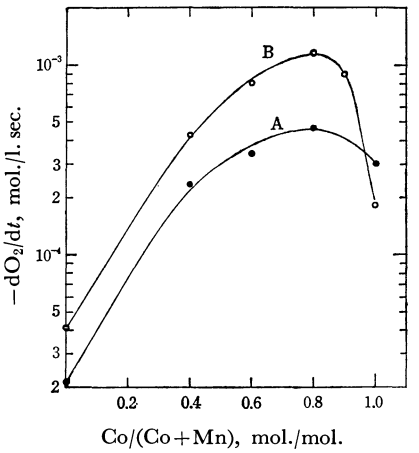

Fig. 8. The mixing effect of cobalt with manganese at 5×10^{-2} mol./l. of total metal concentration and 1×10^{-1} mol./l. NaBr at 65°C (A) and at 2×10^{-2} mol./l. of total metal concentration and 4×10^{-2} mol./l. NaBr at 80°C (B).

The authors wish to express their thanks to Professor Singo Ando for his continued advice and encouragement throughout the course of this work.

9) Y. Kamiya and K. U. Ingold, ibid., *Can. J. Chem.*, **42**, 1027 (1964).

BULLETIN OF THE CHEMICAL SOCIETY OF JAPAN VOL. 39 2216—2219 (1966)

Studies of Thio Acids. VII.[1] The Synthesis of Thiopalmitic Acid and Thiomyristic Acid*[1]

By Yoshio HIRABAYASHI, Masateru MIZUTA and Tetsuro MAZUME*[2]

Faculty of Engineering, Gifu University, Kagamigahara-shi, Gifu

(Received December 25, 1965)

Thiopalmitic acid, $C_{15}H_{31}COSH$ (m. p. 30.8—31.3°C), and thiomyristic acid, $C_{13}H_{27}COSH$ (m. p. 19.8—20.3°C), were synthesized by the reaction of sodium hydrogen sulfide in ethanol with palmitoyl and myristoyl chlorides respectively. The infrared absorption spectra of thiopalmitic and thiomyristic acids indicate that both acids assumed the thiolic acid form. Dipalmitoyl disulfide (m. p. 76.0—76.5°C) and ethyl palmitate, and dimyristoyl disulfide (m. p. 70.5—71.5°C) and ethyl myristate were isolated as by-products.

Auger et al.[2] reported that the melting point of thiopalmitic acid ($C_{15}H_{31}COSH$) was 71°C, while the melting point of thiomyristic acid ($C_{13}H_{27}COSH$) was lower than 25°C. On the other hand, in a previous paper of this series,[3] it was reported that the melting point of thiostearic acid was 39.8—40.3°C. Such an irregular relationship between the number of carbon atoms and the melting point in the homologous series of higher aliphatic thio acids seems doubtful considering the fact that, in the series of higher fatty acids having odd or even carbon atoms, the melting point rises monotonically with the increasing number of carbon atoms.

For the purpose of solving the above question and obtaining extensive knowledge of the properties of the above thio acids, the present authors made the synthesis of thiopalmitic and thiomyristic acids by a method different from that of Auger et al. and then studied the properties of these thio acids and by-products.

Palmitoyl or myristoyl chloride prepared from palmitic or myristic acid and thionyl chloride by the usual method was added, drop by drop, to an ethanol solution of sodium hydrogen sulfide (prepared from metallic sodium, absolute ethanol, and hydrogen sulfide) with heating. The resulting solution was acidified to produce the crude product. By the fractional crystallization of the crude product from palmitoyl chloride, thiopalmitic acid was obtained in the form of colorless crystals (m. p. 30.8—31.3°C), together with small amounts of dipalmitoyl disulfide (colorless crystals of m. p. 76.0—76.5°C) and ethyl palmitate. On the other hand, the crude product from myristoyl chloride was divided into an acidic fraction and a neutral fraction. By the fractional crystallization of the acidic fraction, thiomyristic acid was obtained in the form of colorless crystals (m. p. 19.8—20.3°C), together with small amounts of dimyristoyl disulfide (colorless crystals of m. p. 70.5—71.5°C) and ethyl myristate. The neutral fraction was confirmed to consist mainly of ethyl myristate.

The separation of thiopalmitic or thiomyristic acid from the respective by-products was achieved by fractional crystallization from petroleum ether or hexane; it was difficult to achieve it by fractional crystallization from other solvents or by fractional distillation under reduced pressure. The quantities of the by-products depended upon the conditions of the reaction. In particular, the formation of

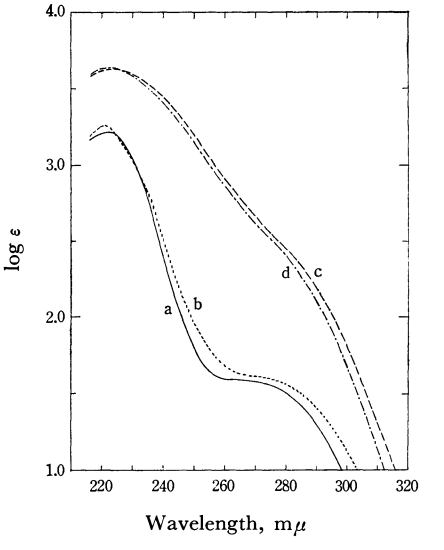

Fig. 1. Ultraviolet absorption spectra in cyclohexane.
a : Thiopalmitic acid c : Dipalmitoyl disulfide
b : Thiomyristic acid d : Dimyristoyl disulfide

1) Part VI of this series: Y. Hirabayashi and T. Mazume, This Bulletin, **39**, 1971 (1966).

*1 Parts of this study were presented at the 11th Annual Meeting of the Chemical Society of Japan, Tokyo, April, 1958, and at the Symposium of Oils and Fats of the Chemical Society of Japan, Nagoya, November, 1958.

*2 Present address: Shimogamo-Kishimotocho, Sakyo-ku, Kyoto.

2) V. Auger and M. Billy, *Compt. rend.*, **136**, 555 (1903).

3) Y. Hirabayashi, M. Mizuta and T. Mazume, This Bulletin, **37**, 1002 (1964).

ethyl palmitate or myristate made the separation of the corresponding thio acid difficult in fractional crystallization. The mechanism of the formation of these by-products may be similar to that of the synthesis of thiostearic acid.[3]

The ultraviolet absorption spectra of thiopalmitic and thiomyristic acids in cyclohexane solutions*3 are shown in Fig. 1. Thiopalmitic acid shows a band at $\lambda_{max}=221.5$ mμ ($\varepsilon=1670$), while thiomyristic acid shows a band at $\lambda_{max}=$ 221.0 mμ ($\varepsilon=1740$). Both the spectra indicate inflections at longer wavelengths and are nearly identical with that of thiostearic acid in shape.[3]

In the infrared absorption spectrum of thiopalmitic acid measured by the potassium bromide-disk method (Fig. 3), an absorption band for the S–H group appears at 2545 cm^{-1} and an absorption band for the C=O group appears at 1665 cm^{-1}. On the other hand, in the infrared absorption spectrum of thiomyristic acid as measured by the liquid film method (Fig. 4), an absorption band for the S–H group appears at 2548 cm^{-1} and an absorption band for the C=O group appears at 1708 cm^{-1}. However, in the spectra of both acids, no absorption bands for the C=S group are observed. These facts indicate that the synthesized thiopalmitic and thiomyristic acids assume the thiolic acid form; this is in accordance with the view of Sheppared[4] and Crouch[5] that thioacetic acid has the thiolic acid form, and with the view of Hirabayashi et al.[3] that thiostearic acid also has the thiolic acid form.

As has been mentioned above, Auger et al. reported that thiopalmitic acid which was synthesized by the phenyl ester-sodium hydrogen sulfide method had the melting point of 71°C. As has previously been reported,[6] in this synthetic method a large quantity of diacyl disulfide is produced. Accordingly, judging from the melting point and synthetic method described by Auger et al., the substance which was reported to be thiopalmitic acid by Auger et al. is really dipalmitoyl disulfide or some substance in which dipalmitoyl disulfide is a principal component.*5 As a result of the present experiments, the melting point of thiopalmitic acid*6 should be corrected to 30.8—31.3°C, and the melting point of thiomyristic acid, which has been ambiguous, has been determined to be 19.8—20.3°C.

The relations between the number of carbon atoms and the melting point of higher aliphatic thio acids and diacyl disulfides are shown in Fig. 2.

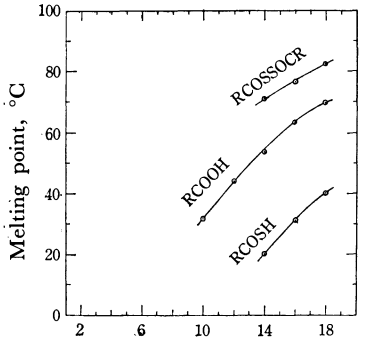

Number of carbon atom
(Half the number in RCOSSOCR)

Fig. 2. Relations between number of carbon atoms and melting points of RCOSH and RCOSSOCR.

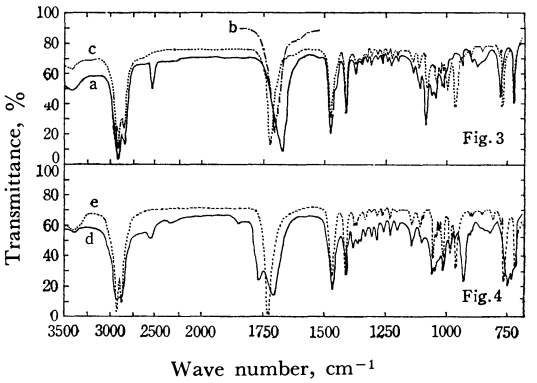

Wave number, cm^{-1}

Fig. 3. Infrared absorption spectra.
a : Thiopalmitic acid (——) in KBr disk (1.50 mg./200 mg. KBr)
b : Thiopalmitic acid (—·—) in a chloroform solution
c : Dipalmitoyl disulfide (----) in KBr disk (1.30 mg./200 mg. KBr)

Fig. 4. Infrared absorption spectra.
d : Thiomyristic acid (——) in a liquid film
e : Dimyristoyl disulfide (----) in KBr disk (1.40 mg./200 mg. KBr)

*3 The ultraviolet absorption spectra were measured by using a Shimadzu Quartz spectrophotometer, model QB-50, and silica cells (1 cm.).

4) N. Sheppared, *Trans. Faraday Soc.*, **45**, 693 (1949).

5) W. W. Crouch, *J. Am. Chem. Soc.*, **74**, 2926 (1952).

*4 Since the calculated amounts of each element in thiopalmitic acid and dipalmitoyl disulfide are nearly equal to each other, it is very difficult to distinguish and identify the one from the other by the results of elementary analysis. In the report of Auger et al., only the value of sulfur obtained by elementary analysis is described; the neutralization value for distinguishing them is not described. Moreover, it must be taken into consideration that it is possible to convert thiopalmitic acid into dipalmitoyl sulfide by the elimination of hydrogen sulfide during recrystallization or storage.

*5 E. g., in "Beilstein, Handbuch der Organischen Chemie," or E. E. Reid, "Organic Chemistry of Bivalent Sulfur IV," Chemical Publishing, New York (1962), p. 61, etc., the melting point of thiopalmitic acid has been given as 71°C, as given by Auger et al.

6) Y. Hirabayashi, M. Mizuta and T. Mazume, This Bulletin, **38**, 320 (1965).

Experimental

The Synthesis of Palmitoyl Chloride and Myristoyl Chloride.—The synthetic method used here was essentially identical with that described earlier for stearoyl chloride.[3]

Palmitoyl chloride (100 g.), with a b. p. of 148—149°C/2 mmHg, was synthesized in a 93.0% yield by the reaction of palmitic acid (100 g.; m. p. 61.5—62.0°C; neutralization value, 218.2) with freshly-distilled thionyl chloride (100 g.).

Myristoyl chloride (86 g.), with a b. p. of 145—148°C/5 mmHg, was synthesized in a 93.5% yield by the reaction of myristic acid (85 g.; m. p. 53.5—54.0°C; neutralization value, 245.9) with freshly-distilled thionyl chloride (85 g.).

The Preparation of a Sodium Hydrogen Sulfide-Ethanol Solution.—This was carried out according to the method described in a previous paper.[3]

The Synthesis of Thiopalmitic Acid.—The palmitoyl chloride (85 g.) was added, drop by drop and over a period of several minutes, to the above sodium hydrogen sulfide - ethanol solution (prepared from 20.0 g. of metallic sodium, 300 ml. of absolute ethanol, and hydrogen sulfide) while the solution was being vigorously stirred and heated at 65—70°C (molar ratio; $C_{15}H_{31}COCl$: NaSH=1 : 2.8). Then the mixture was refluxed on a water bath for 1 hr., after which the ethanol was separated under a vacuum in the current of hydrogen to give a white jelly residue. The residue was dissolved in 1 l. of water, acidified with dilute hydrochloric acid, and extracted with ether. The ether layer was washed with water in order to remove the excess hydrochloric acid. An insoluble white matter suspended between the ether and the water was filtered off (0.8 g. (A)). The ether layer was dried over anhydrous sodium sulfate, and a crude product (78.0 g.) (B) was obtained by distilling off the ether (light yellow colored; m. p. 28—29°C (partly 45°C); neutralization value, 180.4; and sulfur content, 10.2 (by the iodine method) or 10.8% (by Kitamura's method)). By the fractional crsytallization of the product B (77.0 g.) from benzene, thiopalmitic acid (43.9 g., m. p. 30.8—31.3°C) was obtained as colorless crystals.

Found: neutralization value, 205.8; C, 70.26; H, 11.95; S, 11.64 (the iodine method), 11.80 (Kitamura's method).

Calcd. for $C_{16}H_{32}OS$: neutralization value, 205.9; C, 70.52; H, 11.84; S, 11.77%.

From the higher-melting point fraction and the product A, dipalmitoyl disulfide (3.4 g.) was obtained as colorless crystals (from benzene); m. p. 76.0—76.5°C, undepressed on admixture with an authentic specimen. (Found: S, 11.80. Calcd. for $C_{32}H_{62}O_2S_2$: S, 11.81 %. UV, Fig. 1; IR, Fig. 3).

From the lower-melting point fraction, ethyl palmitate was isolated.

As a result of the fractional crystallization, the compositions of the products (A and B) were found to be as follows: thiopalmitic acid 82.5%, dipalmitoyl disulfide 5.0%, and ethyl palmitate 12.5%.

The Synthesis of Thiomyristic Acid.—The myristoyl chloride (86.0 g.) was added, drop by drop and over about a 10-min. period, to the above sodium hydrgoen sulfide - ethanol solution (prepared from 32.0 g. of metallic sodium, 320 ml. of absolute ethanol, and hydrogen sulfide) while it was being vigorously stirred and heated at 70—75°C (molar ratio; $C_{13}H_{27}COCl$: NaSH=1 : 3.7). Then, the mixture was refluxed on a water bath for 1 hr., after which the ethanol was separated under a vacuum in the current of hydrogen to give a white jelly residue. Water (1.5 l.) was added to the residue, and the ether-soluble matter (neutral fraction) therein was extracted several times with ether. Concurrently, the aqueous layer was acidified with dilute hydrochloric acid and extracted with ether (acidic fraction). Each ether layer was washed with water and dried over anhydrous sodium sulfate. When the ether was distilled off, there remained the neutral fraction (6.5 g.; m. p., below 25°C; neutralization value, 42.6; S, 2.4 (by the iodine method) or 2.5% (by Kitamura's method)) and the acidic fraction (78.0 g.; m. p., below 25°C; neutralization value, 221.9; S, 12.1 (by the iodine method) or 12.4% (by Kitamura's method)). By the fractional crystallization of the acidic fraction (70.0 g.) from hexane, thiomyristic acid (48.5 g.; m. p. 19.8—20.3°C) was obtained as colorless crystals.

Found: neutralization value, 228.8; C, 68.51; H, 11.70; S, 12.94 (the iodine method); 13.10 (Kitamura's method). Calcd. for $C_{14}H_{28}OS$: neutralization value, 229.5; C, 68.79; H, 11.55; S, 13.12%.

From the lower-melting point fraction, ethyl myristate was isolated, while from the higher-melting point fraction dimyristoyl disulfide (2.2 g.) was obtained as colorless crystals (from hexane), m. p. 70.5—71.5°C; undepressed on admixture with an authentic specimen. (Found: S, 13.20. Calcd. for $C_{28}H_{54}O_2S_2$: S, 13.17 %. UV, Fig. 1; IR, Fig. 4).

As a result of the fractional crystallization, the compositions of the acidic part were found to be as follows: thiomyristic acid 87.5%, dimyristoyl disulfide 3.5%, and ethyl myristate 9.0%.

On the other hand, the neutral fraction was confirmed by further recrystallization to consist of ethyl myristate (81.6%) and thiomyristic acid (18.4%).

The Synthesis of Dipalmitoyl Disulfide and Dimyristoyl Disulfide.—An iodine solution (ca. 1 N) was added, drop by drop, to a solution of thiopalmitic acid (3.0 g.) or thiomyristic acid (3.0 g.) in ether (20 ml.)-ethanol (20 ml.) until coloring was observed; the reaction mixture was then kept at room temperature for 1 hr.. The deposit was filtered off and thoroughly washed with ethanol to give a crude product.

The crude product from thiopalmitic acid was recrystallized repeatedly from benzene to give colorless, flaky crystals (2.5 g.) with a m. p. of 76.0—76.5°C.

Found: C, 70.59; H, 11.66; S, 11.80 (Kitamura's method). Calcd. for $C_{32}H_{62}O_2S_2$: C, 70.79; H, 11.51; S, 11.81%. UV (cf. Fig. 1): $\lambda_{max}^{cyclohexane}$, 224 mμ ($\varepsilon$=4260).

The crude product from thiomyristic acid was recrystallized repeatedly from hexane to give colorless, flaky crystals (2.5 g.) with a m. p. of 70.5—71.5°C.

Found: C, 68.83; H, 11.38; S, 13.20 (Kitamura's method). Calcd. for $C_{28}H_{54}O_2S_2$: C. 69.08; H, 11.18; S, 13.17%. UV (cf. Fig. 1): $\lambda_{max}^{cyclohexane}$, 223 mμ ($\varepsilon$=4260).

Infrared Absorption Spectra.—The infrared absorption spectra of thiopalmitic acid, dipalmitoyl disulfide, thiomyristic acid, and dimyristoyl disulfide are

shown in Figs. 3 and 4. A Hilger H-800 infrared spectrophotometer was used for the measuring.

Thiopalmitic Acid.—In the spectrum measured by the potassium bromide-disk method, the S–H stretching band appeared at 2545 cm^{-1} and the C=O stretching band appeared at 1665 cm^{-1}. An absorption band, probably due to the S–H group, appeared at around 862 cm^{-1}. In the spectrum measured by the Nujol-mull method,*6 the S–H stretching band was not evident; however, the C=O stretching band shifted to 1714 cm^{-1}. In the spectrum measured in a chloroform solution, the C=O stretching band shifted to 1707 cm^{-1}.

Thiomyristic Acid.—In the spectrum measured by the liquid film method, the S–H stretching band appeared at 2548 cm^{-1} and the C=O stretching band appeared at 1708 cm^{-1}. Since the thiomyristic acid used in the measuring was retained in the liquid state in a vacuum desiccator for a considerable period after the isolation from the reaction product, a part of the converted product, dimyristoyl sulfide, was contained in the sample.*7 Accordingly, absorption bands appeared at 1763 and 926 cm^{-1} which did not appear in the spectra of such homologues as thiostearic or thiopalmitic acid; the two bands corresponded to the high-intensity absorption bands at 1766 and 932 cm^{-1} which appeared in the spectrum of distearoyl sulfide ($C_{17}H_{35}COSOCC_{17}H_{35}$).[7]

Dipalmitoyl Disulfide and Dimyristoyl Disulfide.—In the spectra measured by the potassium bromide-disk method, the C=O stretching bands appeared at 1712 in dipalmitoyl disulfide and at 1715 cm^{-1} in dimyristoyl disulfide.

*6 A part of the sample is melted or dissolved in Nujol in the preparation of paste because of its low melting point.

*7 When thiomyristic acid was retained in a vacuum desiccator in the liquid state, it was converted into dimyristoyl sulfide by the elimination of hydrogen sulfide. This will be reported on later in detail.

7) Y. Hirabayashi, M. Mizuta and T. Mazume, This Bulletin, **38**, 1099 (1965).

BULLETIN OF THE CHEMICAL SOCIETY OF JAPAN VOL. 39 2219—2223 (1966)

Studies of Thio Acids. VIII.[1] The Reaction of Thiostearic Acid with Alcohols*1

By Yoshio HIRABAYASHI, Masateru MIZUTA and Tetsuro MAZUME*2

Faculty of Engineering, Gifu University, Kagamigahara-shi, Gifu

(Received December 29, 1965)

The products obtained by heating thiostearic acid in methanol, aqueous methanol, ethanol, or aqueous ethanol have been found to consist of hydrogen sulfide, distearoyl sulfide, methyl or ethyl stearate, thiostearic acid, and stearic acid, the last of which has been detected only in the case of aqueous alcohols. On the basis of the above results, the following scheme may be involved, at least in part, in the formation of carboxylic ester and hydrogen sulfide by heating the thio acid in alcohols:

$$2RCOSH \rightarrow RC\overset{O}{\diagdown}\underset{S}{\diagup}\overset{O}{\diagup}CR + H_2S$$

$$RC\overset{O}{\diagdown}\underset{S}{\diagup}\overset{O}{\diagup}CR + R'OH \rightarrow RCOOR' + RCOSH$$

Reid et al.[2] have reported that hydrogen sulfide and a normal ester (C_6H_5COOR) were formed by the reaction of thiobenzoic acid with a primary alcohol, while water and a thiol ester (C_6H_5COSR) were formed by the reaction of benzoic acid with a primary mercaptan. On the other hand, Stewart and McKinney[3] have reported that the reaction of thioacetic acid with primary, secondary, or tertiary alcohols in benzene solutions proceeds by either or one of the two ways shown by Eqs. A and B:

$$RCOSH + R'OH \rightarrow RCOOR' + H_2S \quad (A)$$

$$RCOSH + R'OH \rightarrow RCOSR' + H_2O \quad (B)$$

*1 Parts of this study were presented at the Symposium of Oils and Fats of the Chemical Society of Japan, Nagoya, October, 1957.

*2 Present address: Shimogamo - kishimotocho, Sakyo-ku, Kyoto.

1) Part VII of this series: Y. Hirabayshi, M. Mizuta and T. Mazume, This Bulletin, **39**, 2216 (1966).

2) E. E. Reid, *Am. Chem. J.*, **43**, 489 (1910); L. S. Pratt and E. E. Reid, *J. Am. Chem. Soc.*, **37**, 1934 (1915); J. H. Sachs and E. E. Reid, ibid., **38**, 2746 (1916); J. W. Kimball and E. E. Reid, ibid., **38**, 2757 (1916); E. M. Faber and E. E. Reid, ibid., **39**, 1930 (1917).

3) F. B. Stewart and P. V. McKinney, ibid., **53**, 1482 (1931).

The present paper relates to a study of the detection of additional products obtained on heating thiostearic acid in alcohol. This study suggests that the reaction of thiostearic acid with alcohol may also proceed by way of an intermediate (distearoyl sulfide), and that the production of hydrogen sulfide is not so simple as is shown in the reaction of Eq. A. Namely, when the thio acid is heated in an alcohol, diacyl sulfide is formed as an intermediate, together with hydrogen sulfide; the diacyl sulfide may then give carboxylic ester and thio acid in the reaction with the alcohol.[4] Accordingly, the formation of hydrogen sulfide and the carboxylic ester may not undergo the reaction of Eq. A alone. On the other hand, the formation of thiol ester (Eq. B) could not be verified in this study.

Experimental*3 and Results

The Heating of Thiostearic Acid in Alcohols.—Experimental Method.—A mixture of thiostearic acid with absolute methanol, aqueous methanol, absolute ethanol, or with aqueous ethanol (in accordance with corresponding experiments) was placed in a round-bottomed flask (500 ml.) fitted with a reflux condenser with a calcium chloride tube; the mixture was then heated for 20 hr. on a water bath, with a gradual passing of dried nitrogen gas through the mixture (solution). Hydrogen sulfide was evolved during the heating in each experiment. After the heating had stopped, the alcohol or the water immediately distilled off under reduced pressure at below 60°C, and a reaction product was obtained (only when aqueous methanol was used, was the reaction product extracted with ether when the distillation had been nearly completed). The conditions of each experiment are shown in Table I.

TABLE I. THE EXPERIMENTAL CONDITIONS

Exp.	$C_{17}H_{35}COSH$[a] g.	ROH, ml.	Heating-temp., °C
I	5.0	abs. CH_3OH, 340	65
II	3.0	88% CH_3OH, 553[b]	
III	4.5	abs. C_2H_5OH, 450	78
IV	4.5	85% C_2H_5OH, 450	

a) The characteristics of thiostearic acid used in the experiments were as follows: m.p 39.8—40.3°C; neutralization value 185.4; sulfur content 10.55% (Kitamura's method).
b) A minimum quantity was used for the dissolution of thiostearic acid at the heating-temperature.

The Investigation of the Products.*4—*Exp. I.*—The characteristics of the reaction product I were as follows: m.p. 59—63°C, N.V. 121.7, $S(J)_{NV}$ 6.32%, S(K) 8.24%.

Its ultraviolet absorption spectrum is shown in Fig. 1, in which the intensity of the absorption maximum at 221 mμ is lower and the absorption in the region of 240—250 mμ is intensified as compared with the ultraviolet absorption spectrum of thiostearic acid.[5]

The reaction product I (2.6 g.) in an ether solution was separated into an acidic part (A) and a neutral part N by treating it with an aqueous solution of potassium carbonate. The characteristics of each part were as follows:

(A): Y 1.7 g., N.V. 162.4, $S(J)_{NV}$ 8.91%, S(K) 9.02%
(N): Y 0.9 g., N.V. 63.3, $S(J)_{NV}$ 2.94%.

The ultraviolet absorption spectrum of A was essentially identical with that of thiostearic acid, and that of N exhibited an absorption maximum at 238 mμ (Fig. 1). Therefore, each part was repeatedly recrystallized from benzene and hexane to give, eventually, the several fractions shown in Table II; their ultraviolet absorption spectra are given in Fig. 1.

The results of the above experiments, confirm that N-1 was distearoyl sulfide (no depression of melting point was observed when its further recrystallized product was admixed with a synthesized authentic sample; the two substances exhibited identical ultraviolet absorption spectra) and that A-2 was thiostearic acid (its characteristics and ultraviolet absorption spectrum were identical with those of thiostearic acid); A-3 was mostly thiostearic acid. It was found from the characteristics that N-3 consisted of an ester (about 85%), distearoyl sulfide, and thiostearic acid, which could not be separated by the above treatment. If the ester be methyl thiostearate ($C_{17}H_{35}COSCH_3$), a high-intensity absorption should appear in the neighborhood of 230 mμ,[6] but it was not actually shown in the absorption

TABLE II. THE CHARACTERISTICS OF THE FRACTIONS OBTAINED FROM THE PRODUCT I (2.6 g.)

F	Y, g.	M.p., °C	N.V.	$S(J)_{NV}$, %
N-1	0.2	79.5—80.5	104.1	5.49[a]
N-2	0.4	76—79.5	—	—
N-3	0.2	34—35	28.9[b]	2.12
A-1	0.05	55—60	115.0	0.91
A-2	0.8	39.5—40.5	184.8	10.37[c]
A-3	0.6	35.5—37.0	161.1	9.04

a): S(K) 5.62%. b): S.V. 192.4. c): S(K) 10.53%

*3 All melting points are uncorrected. The ultraviolet absorption spectra were measured by using a Shimadzu Quartz spectrophotometer, Model QB-50, and a silica cell (1 cm.).

4) Y. Hirabayashi, M. Mizuta and T. Mazume, This Bulletin, **38**, 1099 (1965).

*4 The following notations will be used hereafter; F: fraction; Y: yield; S.V.: saponification value: N.V.: neutralization value; S(J): sulfur content as determined by the iodine mehtod; $S(J)_{NV}$: sulfur content as determined by titrating the solution with an iodine solution after the N.V. has been determined; S(K): sulfur content as determined by Kitamura's method. (It was assumed for the purposes of calculation that stearic acid and sulfuric acid were produced by thiostearic acid in the case of mixtures; S(K) was determined by volumetric analysis, which was not always accurate.)

5) Y. Hirabayashi, M. Mizuta and T. Mazume, This Bulletin, **37**, 1002 (1964).

6) Y. Hirabayashi and T. Mazume, This Bulletin, **38**, 171 (1965).

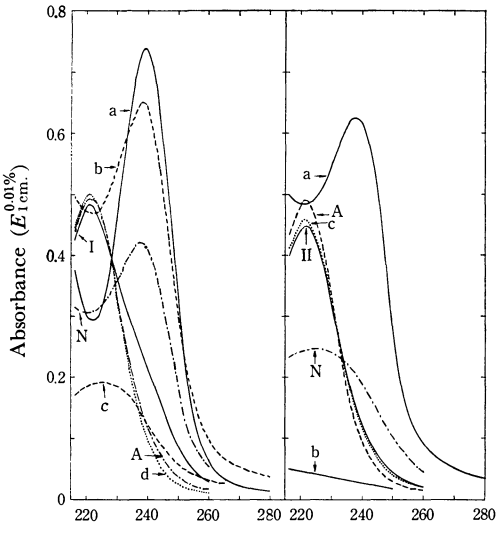

Fig. 1. Fig. 2.

Fig. 1. Ultraviolet absorption spectra of product I and its fractions (shown in Table II) in cyclohexane.

I; product I, A; acidic part A of I, N; neutral part N of I
a; fraction N-1, b; fraction N-2, c; fraction N-3, d; fraction A-3

Fig. 2. Ultraviolet absorption spectra of product II and its fractions (shown in Table III) in cyclohexane.

II; product II, A; acidic part A of II, N; neutral part N of II
a; fraction 1, b; fraction 2, c; fraction 6

curve. The ester was identified as methyl stearate on further recrystallization.

Exp. II.—The characteristics of the reaction product II were as follows:

m. p. 38—42°C, N. V. 137.0, $S(J)_{NV}$ 7.51%, S(K) 8.49%.

Its ultraviolet absorption spectrum is shown in Fig. 2, which is essentially identical with that of the reaction product I.

The reaction product II (2.5 g.) was then separated into an acidic part (A) and a neutral part (N) by the same treatment as was used in Exp. I. The ultraviolet absorption spectrum of A was essentially identical with that of thiostearic acid, while that of N did not exhibit a sharp absorption maximum at 238 mμ and so was different from that of the N of the reaction product I (Fig. 2). Since N was obtained in a small amount, it was again combined with A; the combination was repeatedly recrystallized from benzene and hexane to give, eventually, the several fractions shown in Table III. Their ultraviolet absorption spectra are shown in Fig. 2.

As a result of the above experiments, it was found that the main component of 1 was distearoyl sulfide; that of 2 was stearic acid, and that of 3, 4, 5, and

Table III. The characteristics of the fractions obtained from the product II (2.5 g.)

F	Y, g.	M. p., °C	N. V.	$S(J)_{NV}$, %
1	0.2	76.5—78	—	—[a]
2	0.15	68.5—69.5	196.5	0.21
3	1.1	38—40	177.2	9.71[b]
4	0.4	38.5—39.5	158.9	9.32[c]
5	0.3	37—38	155.2	8.99
6	0.2	34.5—35.5	144.1	7.37

S(K): a) 8.61; b) 10.14; c) 9.47%.

especially 6 was thiostearic acid, containing an ester. This ester is assumed to be methyl stearate from its characteristics and from the ultraviolet absorption spectra of the fractions; the approximate contents of methyl stearate in 3, 4, 5, and 6 were 4, 14, 16, and 22% respectively.

Exp. III.—The characteristics of the reaction product III were as follows:

m. p. 36—40°C, N. V. 129.7, $S(J)_{NV}$ 7.21%, S(K) 7.90%.

Its ultraviolet absorption spectrum is shown in Fig. 3, in which the intensity of the absorption maximum at 221 mμ is lower and that of the absorption in the 240—250 mμ region is higher than in the ultraviolet absorption spectrum of thiostearic acid.

The distearoyl sulfide present in I and II might be decomposed in the treatment with alkali.[4] Hence, the separation of the product into neutral and acidic parts was omitted, and the reaction product III (3.8 g.) was repeatedly recrystallized from benzene and hexane to give, eventually, the several fractions shown in Table IV (cf. Fig. 3).

Table IV. The characteristics of the fractions obtained from the product III (3.8 g.)

F	Y, g.	M. p., °C	N. V.	$S(J)_{NV}$ %	S(K) %
1	0.45	80.5—81.5	—	—	6.01
2	0.2	76—78	—	—	7.67
3	0.3	60—70	165.5	5.53	7.69
4	0.9	38—40	173.5	10.24	10.42
5	0.3	32.5—34.5	—	—	—
6	1.5	30.5—31.5	106.5	5.77	6.14

As a result of the above experiments, it was found that 1 was distearoyl sulfide, 2 was distearoyl sulfide containing a small amount of thiostearic acid, 4 was thiostearic acid, and 5 and 6 were mixtures of thiostearic acid and an ester. The fraction 6 is assumed not to be a mixture of thiostearic acid and ethyl thiostearate, judging from its characteristics; it is reasonable to consider that the ester part consists of ethyl stearate similar to the methyl stearate in the reaction products I and II; the ethyl stearate content in 6 was about 43%.

Exp. IV.—The characteristics of the reaction product IV were as follows:

m. p. 55—60°C, N. V. 95.9, $S(J)_{NV}$ 3.59%, S(K) 4.51%.

Its ultraviolet absorption spectrum, shown in Fig. 4, is very different from those of the reaction products I, II, and III.

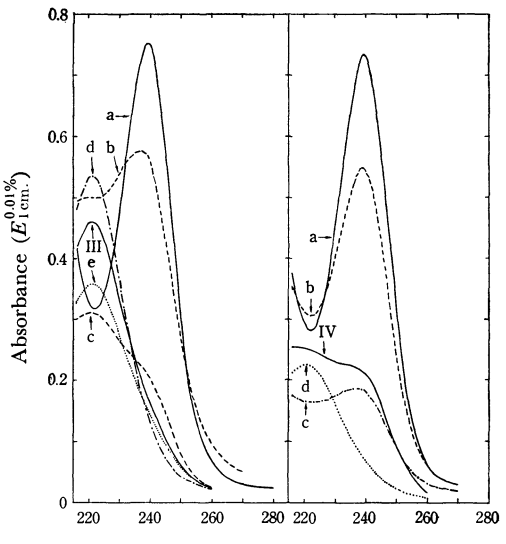

Fig. 3. Fig. 4.

Fig. 3. Ultraviolet absorption spectra of product III and its fractions (shown in Table IV) in cyclohexane.

III; product III, a; fraction 1, b; fraction 2, c; fraction 3, d; fraction 4, e; fraction 6

Fig. 4. Ultraviolet absorption spectra of product IV and its fractions (shown in Table V) in cyclohexane.

IV; product IV, a; fraction 1, b; fraction 2, c; fraction 3, d; fraction 5

The reaction product IV (3.8 g.) was repeatedly recrystallized from benzene and hexane to give, eventually, the several fractions shown in Table V. Their ultraviolet absorption spectra are shown in Fig. 4.

As a result of the above experiments, it was found that 1 was distearoyl sulfide, 2 was mostly distearoyl sulfide, 3 was stearic acid containing a small amount of distearoyl sulfide, and 5 was a mixture of ethyl stearate (about 65%), thiostearic acid, and distearoyl sulfide (a trace).

TABLE V. THE CHARACTERISTICS OF THE FRACTIONS OBTAINED FROM THE PRODUCT IV (3.8 g.)

F	Y g.	M. p. °C	N. V.	$S(J)_{NV}$ %	S(K) %
1	0.9	80.5—81.5	—	—	6.08
2	0.2	76—80	—	—	—
3	0.8	68—69	160.8	1.42	1.52
4	0.1	60—63	—	—	—
5	1.7	29.5—31	44.5—68.6	2.59—3.61	4.41

Discussion

When thiostearic acid was heated in methanol, ethanol, aqueous methanol, or aqueous ethanol, hydrogen sulfide was evolved, and the products consisted of distearoyl sulfide, methyl or ethyl stearate, thiostearic acid, and stearic acid (the last product was obtained only in the case of aqueous alcohols). These results are summarized in Table VI.

TABLE VI. THE COMPONENTS OF THE PRODUCTS OBTAINED BY HEATING THIOSTEARIC ACID IN ALCOHOLS

Alcohol	Component of product ($R=C_{17}H_{35}-$, $R'=CH_3-$ or C_2H_5-)				
	RCOSOCR	RCOSH	RCOOR′	RCOOH	RCOSR′
abs. CH_3OH	○	○	○	×	×
aq. CH_3OH	○	○	○	○	×
abs. C_2H_5OH	○	○	○	×	×
aq. C_2H_5OH	○	○	○	○	×

The mark " ○ " means presence and " × " means absence.

On the basis of the above data, it may be concluded that the reaction consists of the following processes:

1. Distearoyl sulfide is formed according to Eq. 1.
2. Thiostearic acid is re-formed from the distearoyl sulfide and the alcohol according to Eq. 2, by which the stearic ester is also formed, whereas the formation of the thiolester according to Eq. 3 does not occur.
3. The re-formed thiostearic acid repeats the reaction of Eqs. 1 and then that of 2.
4. When aqueous alcohol is treated, thiostearic acid is re-formed, together with the stearic acid formed by partial reaction with water, as is shown in Eq. 4.

$$2RCOSH \rightarrow RC(=O)S(=O)CR + H_2S \quad (1)$$

$$RC(=O)S(=O)CR \xrightarrow{R'OH} RCOSH + RCOOR' \quad (2)$$

$$RC(=O)S(=O)CR \xrightarrow{R'OH} \not\rightarrow \quad (3)$$

$$RC(=O)S(=O)CR \xrightarrow{H_2O} RCOSH + RCOOH \quad (4)$$

$$RCOSH + R'OH \longrightarrow RCOOR' + H_2S \quad (5)$$

$$RCOSH + R'OH \longrightarrow RCOSR' + H_2O\ (?) \quad (6)$$

As has been described in a previous paper,[4] the reaction of Eq. 2 has been confirmed by investigating the properties of distearoyl sulfide. Accordingly, it is not reasonable to say that hydrogen sulfide and the carboxylic ester are formed only in the reaction of thio acid with alcohol (Eq. 5); they may be formed by the two reaction processes, Eqs. 1 and 2, and 5.

The above reaction mechanisms are not confined to the reaction of thiostearic acid only, but could be applied equally well to that of other thio acids.

Stewart and McKinney[3] have reported that Eqs. 5 and/or 6 occurred when thioacetic acid was heated with methanol, ethanol, isopropanol, or triphenylcarbinol in benzene. Their experiments

and discussion were based on the assumptions that hydrogen sulfide was produced according to Eq. 5 alone and that the acid (thioacetic acid) disappeared according to both Eqs. 5 and 6; if both reactions of Eqs. 5 and 6 took place simultaneously, the amount of hydrogen sulfide formed would be less than that of the acid disappearing.

However, the following facts have been confirmed in the reaction of thiostearic acid with alcohol: the evolution of hydrogen sulfide is due to the formation of an intermediate, diacyl sulfide, and/or to the reaction of Eq. 5; the thio acid and the carboxylic ester are formed by the reaction of the diacyl sulfide with an alcohol[4]; the thiol ester is not identified in the product. Stewart and McKinney assumed the occurrence of the reactions of Eqs. 5 and 6 by the estimation of hydrogen sulfide and residual acid without considering the formation and behavior (measurements for the estimate of residual acid) of the diacyl sulfide; they then discussed the mechanism of the esterification of the alcohol with the carboxylic acid, but it seems to be important to consider the presence of diacyl sulfide as an intermediate.

BULLETIN OF THE CHEMICAL SOCIETY OF JAPAN VOL. 39 2223—2226 (1966)

Asymmetric Hydrogenation with Modified Raney Nickel. VIII

By Yoshiharu IZUMI, Susumu TATSUMI and Masami IMAIDA

Division of Organic Chemistry, Institute for Protein Research, Osaka University, Kita-ku, Osaka

(Received January 6, 1966)

Asymmetric hydrogenation catalysts were prepared by modifying Raney nickel with aqueous solutions of D-tartaric acid, monomethyl D-tartrate, L-*erythro*- and D-*threo*-2, 3-dihydroxybutyric acid, L-malic acid, (+)-*erythro*- and (−)-*threo*-3-methylmalic acid, L-citramalic acid and L-methylsuccinic acid. Their asymmetric activities in the hydrogenation of methyl acetoacetate to methyl 3-hydroxybutyrate were compared with each other in order to study the effect of the chemical structure of the modifying reagent on the activity. Monomethyl D-tartrate, L-*erythro*- and D-*threo*-2, 3-dihydroxybutyric acid are less effective in asymmetric activity than D-tartaric acid. On modification with these three reagents, optimum asymmetric activities were obtained under acidic conditions. With D-tartaric acid, however, while high asymmetric activities were obtained at pH 5—9, there was a considerable decrease in activity at lower pH values. This suggests that the β-carboxyl group of tartaric acid plays an important role in the modification. (−)-*threo*-3-Methylmalic acid is more effective in asymmetric activity than L-malic acid, while (+)-*erythro*-3-methylmalic acid and L-citramalic acid are less effective. It has been suggested that these differences are related to hindrances due to the methyl groups on the α- or β-asymmetric centers, and also related to the correlations of the configurations of the asymmetric centers of 3-methylmalic acids. L-Methylsuccinic acid has little asymmetric effect on Raney nickel.

Previous papers in this series[1-7] have reported on the asymmetric hydrogenation of methyl acetoacetate to methyl 3-hydroxybutyrate using Raney nickel catalysts modified with various optically active 2-amino acids and 2-hydroxy acids. High asymmetric activities were generally observed when Raney nickel was modified with such optically active dihydroxy dicarboxylic acids as D-tartaric acid, (+)-*threo*-2-methyltartaric acid and (+)-*threo*-2, 3-dimethyltartaric acid.[6] An especially high asymmetric activity was obtained by modification with (+)-*threo*-2-methyltartaric acid. On the contrary, optically active hydroxy monocarboxylic acids had rather low asymmetric effects upon Raney nickel.[3]

In the present work, the asymmetric activities of Raney nickel catalysts modified with monomethyl D-tartrate, L-*erythro*- and D-*threo*-2, 3-dihydroxybutyric acid were tested and compared with that of the catalyst modified with D-tartaric acid; this was done in order to study the role of the β-carboxyl group of D-tartaric acid and in order to elucidate the difference in the asymmetric effects

1) Y. Izumi, M. Imaida, H. Fukawa and S. Akabori, This Bulletin, **36**, 21 (1963).
2) Y. Izumi, M. Imaida, H. Fukawa and S. Akabori, ibid., **36**, 155 (1963).
3) S. Tatsumi, M. Imaida, Y. Fukuda, Y. Izumi and S. Akabori, ibid., **37**, 846 (1964).
4) Y. Izumi, S. Akabori, H. Fukawa, S. Tatsumi, M. Imaida, Y. Fukuda and S. Komatsu, *Proceedings of the 3rd International Congress on Catalysis*, **2**, 1364 (1964).
5) Y. Izumi, S. Tatsumi, M. Imaida, Y. Fukuda and S. Akabori, This Bulletin, **38**, 1206 (1965).
6) Y. Izumi, S. Tatsumi, M. Imaida, Y. Fukuda and S. Akabori, ibid., in press.
7) Y. Izumi, S. Tatsumi and M. Imaida, ibid., to be published.

Table I. The optical rotation of modifying reagent

Modifying reagent	Optical rotation, $[\alpha]_D^{20}$	Value in literature
(+)-*erythro*-3-Methylmalic	+9.1° (*c* 3.7, H_2O)	—
(−)-*threo*-3-Methylmalic acid	−5.3° (*c* 3.2, H_2O)	—
L-Citramalic acid	+23.2° (*c* 3, H_2O)	+23.2° (*c* 4.4, H_2O)[8]
L-Methylsuccinic acid	−11.5° (*c* 5, H_2O)	−11.7° (*c* 3, H_2O)[12]
Monomethyl D-tartrate monohydrate	+18.1° (*c* 3, H_2O)	+18.4° (*c* 10, H_2O)[10]
L-*erythro*-2, 3-Dihydroxybutyric acid	+10.3° (*c* 3.2, H_2O)	+8.8° (—, H_2O)[13]
D-*threo*-2, 3-Dihydroxybutyric acid	+15.9°(*c* 2.1, H_2O)	+15.5° (—, —)[14]

of a hydroxy dicarboxylic acid and a hydroxy monocarboxylic acid.

In spite of the high asymmetric effect with (+)-*threo*-2-methyltartaric acid, only a very low effect was observed on modification with (−)-*erythro*-2-methyltartaric acid.[6] It was suggested that the difference in the effects of these two reagents on Raney nickel is related to the erythro-threo isomerism, that is, that it results from the configurational difference between the two diasymmetric centers in these molecules.

In the present work, the asymmetric activities of catalysts modified with (+)-*erthro*- and (−)-*threo*-3-methylmalic acid were also compared with each other, and with that of a catalyst modified with L-malic acid, in order to study the effect of the configuration of the modifying reagent upon the catalyst. Raney nickel was also modified with L-citramalic acid, in which the hydrogen atom on the asymmetric α-carbon of malic acid is replaced by a methyl group, in order to study the role of an α-substituted group in the formation of an asymmetric catalyst. L-Methylsuccinic acid was also tested as a modifying reagent.

The optical purities of the modifying reagents used in the present study are listed in Table I.

Experimental

The methods of the preparation of the Raney nickel catalyst, the hydrogenation of methyl acetoacetate, and the measurement of the asymmetric activity of the catalyst were as described in a previous paper.[3]

Modifying Reagents. — (+)-*erythro*-3-Methylmalic acid,* (−)-*threo*-3-methylmalic acid,* L-citramalic acid[8] and L-methylsuccinic acid[9] were prepared from the corresponding racemic acids. Monomethyl D-tartrate monohydrate was prepared by a slight modification of Markward's procedure.[10] L-*erythro*-2, 3-Dihydroxybutyric acid and D-*threo*-2, 3-dihydroxybutyric acid were prepared from L-allothreonine and D-threonine respectively.[11]

Results and Discussion

Modifications with Monomethyl D-Tartrate Monohydrate, L-*erythro*- and D-*threo*-2, 3-Dihydroxybutyric Acid.—Measurements were made of the asymmetric activities of catalysts modified at 0°C with aqueous solutions of monomethyl D-tartrate monohydrate, L-*erythro*- and D-*threo*-2, 3-dihydroxybutyric acid, the pH values of which had been adjusted to specified values with a sodium hydroxide solution.

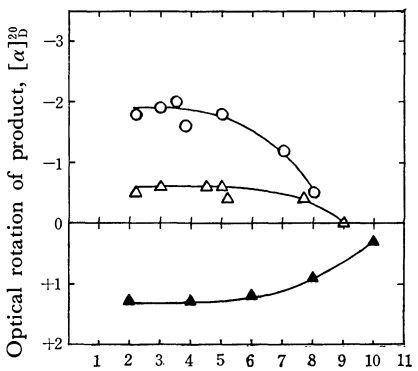

Fig. 1. Modifications with monomethyl D-tartrate, L-*erythro*- and D-*threo*-2, 3-dihydroxybutyric acid. (Modified at 0°C for 15 min.)

○ Monomethyl D-tartrate
△ D-*threo*-2, 3-Dihydroxybutyric acid
▲ L-*erythro*-2, 3-Dihydroxybutyric acid

As is shown in Fig. 1, the catalysts modified with monomethyl D-tartrate monohydrate and D-*threo*-2, 3-dihydroxybutyric acid gave levorotatory products predominantly, while that modified with L-*erythro*-2, 3-dihydroxybutyric acid gave dextrorotatory products. In all cases, the optimum asymmetric activity was observed under acidic condi-

* Details of the preparation of the racemic acid, its separation into the two isomeric forms, the optical resolutions of the isomers, and the determination of their configurations have recently been reported by the present authors. This Bulletin, in press.

8) M. J. Coon, "Biochemical Preparations," Vol. IX, John Wiley & Sons, New York (1962), p. 21.

9) A. Ladenberg, *Ber.*, **28**, 1170 (1895).

10) W. Markward and L. Karczag, ibid., **42**, 1518 (1909).

11) C. E. Meyer and W. C. Rose, *J. Biol. Chem.*, **115**, 721 (1936).

tions, and there was a considerable decrease in activity under alkaline conditions. These asymmetric activity curves were similar in character to those obtained on modifications with optically active monohydroxy monocarboxylic acids[3]; however, they were quite different from that obtained with D-tartaric acid.**

On modification with D-tartaric acid, optimum asymmetric activities were observed at pH 5—9; there was a considerable decrease in activity at both lower and higher pH values, as is shown in Fig. 2.

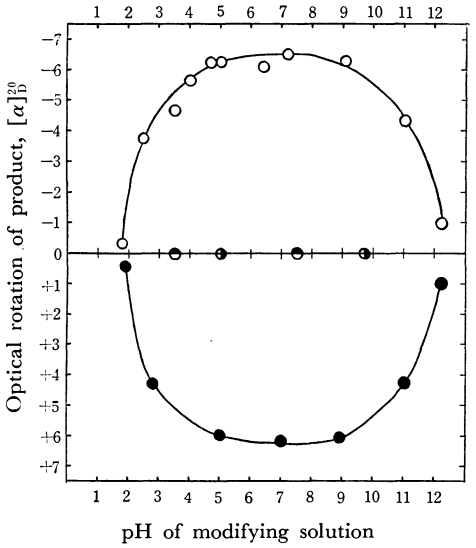

Fig. 2. Modifications with optically active and inactive tartaric acid. (Modified at 0°C)

○ D-Tartaric acid ◑ DL-Tartaric acid
● L-Tartaric acid ◓ *meso*-Tartaric acid

Both monomethyl D-tartrate and D-*threo*-2, 3-dihydroxybutyric acid are characterized by the lack of the free β-carboxyl group of D-tartaric acid. Therefore, in the modification with D-tartaric acid, the diminution of asymmetric activity under acidic conditions is clearly due to the free β-carboxyl group of the reagent. It is likely that both carboxyl groups of D-tartaric acid are adsorbed freely on the surface of nickel metal in the absence of alkali, and that with a decrease in acidity one is desorbed from the nickel metal and then produces a massive steric hindrance which regulates the approach of the hydrogenation substrate to the catalyst. On the other hand, in modifications with monomethyl D-tartrate and D-*threo*-2, 3-dihydroxybutyric acid, their adsorption forms on the surface of the metal similarly under all acidic conditions, since the ester and methyl groups are less affected by the modifying conditions.

Modifications with L-Malic Acid, (+)-*erythro*- and (−)-*threo*-3-Methylmalic Acid.— Raney nickel was modified with L-malic acid, (+)-*erythro*- and (−)-*threo*-3-methylmalic acid in order to study the role of a β-substituted methyl group and the effect of the configuration at the β-carbon of the modifying reagent upon asymmetric hydrogenation. The asymmetric activities of the resulting catalysts were then compared. The results are shown in Fig. 3.

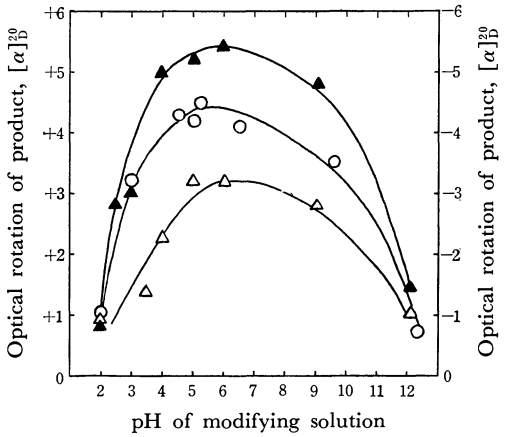

Fig. 3. Modifications with L-malic acid, (+)-*erythro*- and (−)-*threo*-3-methylmalic acid. (Modified at 0°C)

The left scale is used for L-malic acid, and the right scale for (+)-*erythro*- and (−)-*threo*-3-methylmalic acid.

○ L-Malic acid
▲ (−)-*threo*-3-Methylmalic acid
△ (+)-*erythro*-3-Methylmalic acid

The catalysts modified with (+)-*erythro*- and (−)-*threo*-3-methylmalic acid produced levorotatory methyl 3-hydroxybutyrate predominantly, while that modified with L-malic acid produced dextrorotatory methyl 3-hydroxybutyrate. Optimum asymmetric activities were obtained under nearly neutral modifying conditions; there was a considerable diminution in activity under both acidic and alkaline conditions, as was observed upon modification with D-tartaric acid. Moreover, (−)-*threo*-3-methylmalic acid was more effective in asymmetric hydrogenation than was L-malic acid, while (+)-*erythro*-3-methylmalic acid was less effective. The difference between these reagents is clearly due to the β-methyl group of the modifying reagent. On the other hand, by

12) M. Naps and I. B. Johns, *J. Am. Chem. Soc.*, **62**, 2450 (1940).
13) E. Hoff-Jörgensen, *Z. physiol. Chem.*, **268**, 194 (1941).
14) I. W. E. Glattfeld and J. W. Chittum, *J. Am. Chem. Soc.*, **55**, 3663 (1933).

** The modification with D-tartaric acid had already been reported on in Part II of this series.[2] Subsequent studies of modifications with optically active and inactive tartaric acid gave the results shown in Fig. 2.

referring to the findings of Baker,[15] the same configuration can evidently be assigned to the α- and β-asymmetric centers of (−)-*threo*-3-methylmalic acid, while those of (+)-*erythro*-3-methylmalic acid are opposite in configuration. Accordingly, it is likely that the difference between (−)-*threo*-3-methylmalic acid and (+)-*erythro*-3-methylmalic acid is related to the above different configurations of the modifying reagents.

Modification with L-Citramalic Acid (L-2-*C*-Methylmalic Acid).—Modification with L-citramalic acid was performed at 0°C; the asymmetric activity of the resulting catalyst was then compared with that of the catalyst modified with L-malic acid in order to study the effect of an α-*C*-substituted group on the asymmetric hydrogenation. The results are shown in Fig. 4.

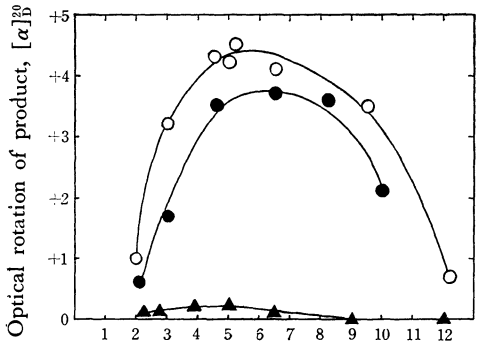

Fig. 4. Modifications with L-malic acid, L-citramalic acid and L-methylsuccinic acid. (Modified at 0°C)
○ L-Malic acid
● L-Citramalic acid
▲ L-Methylsuccinic acid

L-Citramalic acid was less effective in asymmetric hydrogenation than was L-malic acid. The difference is evidently caused by the methyl group on the asymmetric α-carbon atom of L-citramalic acid. Similar differences were observed between the modifications with glutamic acid and α-*C*-substituted glutamic acids.[5] These results clearly show that, to obtain an effective asymmetric catalyst, the α-asymmetric carbon atom of the modifying reagent should not possess a bulky substituted group in addition to the hydroxyl group, carboxyl group and β-carbon chain.

Modification with L-Methylsuccinic Acid.—The asymmetric activity of the catalyst modified with an aqueous solution of L-methylsuccinic acid was also measured.

As is shown in Fig. 4, L-methylsuccinic acid had little or no effect upon Raney nickel under any of the acidic and alkaline conditions tested. These results are in marked contrast to the high asymmetric activities obtained on modification with L-malic acid. Since in L-methylsuccinic acid the hydroxyl group of L-malic acid is replaced by a methyl group, it is clear that the α-hydroxyl group of the modifying reagent plays an important role in the asymmetric modification, and that it is indispensable for the preparation of a catalyst possessing a high asymmetric activity.

This research was supported by Kawaken Fine Chemicals Co., Ltd., Tokyo, and Ajinomoto Co. Inc., Tokyo.

15) H. A. Baker, R. D. Smyth, E. J. Wawszkiewicz, M. N. Lee and R. M. Wilson, *Arch. Biochem. Biophys.*, **78**, 468 (1958).

BULLETIN OF THE CHEMICAL SOCIETY OF JAPAN VOL. 39 2227—2229 (1966)

The Nitration and Halogenation of Palladium Acetylacetonate*

By Akira KASAHARA, Katsuyasu UJI-IE and Keiko TANAKA

Department of Chemistry, Faculty of Liberal Arts and Science, Yamagata University, Yamagata

(Received January 11, 1966)

The pseudo-aromatic divalent palladium acetylacetonate has been found to undergo electrophilic substitution at the central carbon of the chelate ring. The mononitro (decomp. p. 240—245°C, λ_{max} 325 mμ) and dinitro (decomp. p. 250—255°C, λ_{max} 324 mμ) palladium acetylacetonates were prepared by treating palladium acetylacetonate with a mixture of copper nitrate trihydrate and acetic anhydride; they were characterized by their infrared and NMR spectra. The halogenation of palladium acetylacetonate was accomplished with *N*-halosuccinimides in chloroform. Dichloro (decomp. p. 205—210°C, λ_{max} 345 mμ), dibromo (decomp. p. 240—245°C, λ_{max} 345 mμ) and diiodo (decomp. p. 195—200°C, λ_{max} 324 mμ) derivatives were isolated and characterized by their spectra.

Recently, a variety of electrophilic substitutions at the central carbon atoms of metal acetylacetonates and related chelate systems have been reported by several authors[1-16]; these substitutions indicate the conspicuous pseudo-aromatic nature of the six-membered rings. By such a process, chloro,[6,13,15] bromo,[6,13] iodo,[6] thiocyano,[7,14] nitro,[4,11,15] acetyl,[4,14] butyryl,[14] benzoyl,[14] formyl,[11] dimethylaminomethyl,[16] chloromethyl,[16] phenylthio[14] and chlorothio[14] groups have been introduced into the stable rings of tris-acetylacetonates of chromium(III), cobalt(III) and rhodium(III).

Previously, Nakamoto, McCarthy and Martell[17] have discussed the relationships between the infrared spectra and the stability of the divalent acetylacetonate; they claimed that the stability of the divalent acetylacetonates decreased in the order of palladium>copper>nickel>cobalt>zinc, and that the stability of the palladium derivative is to be attributed to the exceeding delocalization of the π-electrons as well as of the α-electrons of the metal around all the chelate rings (cf. Fig. 1).

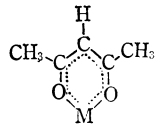

Strong chelate
M=Pd(II)

Fig. 1.

This consideration suggests that palladium acetylacetonate has the pseudo-aromatic structure and may undergo electrophilic substitutions.

This paper will describe the nitration and halogenation of this relatively stable divalent acetylacetonate of palladium. Although palladium acetylacetonate was destroyed by mineral acids, this acetylacetonate was stable in glacial acetic acid. The attempted nitration of palladium acetylacetonate (I) with N_2O_4 in methylene chloride resulted in the destruction of the chelate ring, but a mixture of copper nitrate trihydrate in acetic anhydride proved very effective in the nitration of palladium acetylacetonate (I), and the pure dinitro-chelate (II) was isolated in a high yield by the hydrolysis of the reaction mixtures. The treatment of palladium acetylacetonate (I) with a limited amount of this nitrating agent at 0°C for 4 hr. afforded a 46% yield of mononitro-chelate (III). These nitro-acetylacetonates (II

* Presented partly at the Tohoku Local Meeting of the Chemical Society of Japan, Morioka, October, 1964.

1) K. Yamakawa, *Kagaku no Ryo-iki*, **16**, 905 (1962).
2) J. P. Collman, "Reactions of Coordinated Ligands and Homogeneous Catalysis," Ed. by R. F. Gould, Advances in Chemistry Series, No. 37, American Chemical Society, Washington D. C. (1963), p. 78.
3) J. P. Collman, *Angew. Chem.*, **77**, 154 (1965).
4) J. P. Collman, R. A. Moss, S. D. Goldby and W. S. Trahanovsky, *Chem. & Ind. (London)*, **1960**, 1213.
5) R. W. Kluiber, *J. Am. Chem. Soc.*, **82**, 4839 (1960).
6) J. P. Collman, R. A. Moss, H. Maltz and C. C. Heindel, ibid., **83**, 531 (1961).
7) R. W. Kluiber, ibid., **83**, 3030 (1961).
8) J. P. Collman and E. T. Kittleman, ibid., **83**, 3529 (1961).
9) J. P. Collman, R. P. Blair, A. L. Slada and R. L. Marshall, *Chem. & Ind. (London)*, **1961**, 141.
10) J. P. Collman and E. T. Kittleman, *Inorg. Chem.*, **1**, 499 (1962).
11) J. P. Collman, R. L. Marshall, W. L. Young, III, and S. D. Goldby, ibid., **1**, 704 (1962).
12) J. P. Collman, R. L. Marshall and W. L. Young, III, *Chem. & Ind. (London)*, **1962**, 1380.
13) J. P. Collman, R. P. Blair, R. L. Marshall and L. Slade, *Inorg. Chem.*, **2**, 576 (1963).
14) J. P. Collman, R. L. Marshall, W. L. Young, III, and C. T. Sears, Jr., *J. Org. Chem.*, **28**, 1449 (1963).
15) J. P. Collman and M. Yamada, ibid., **28**, 3017 (1963).
16) R. H. Barker, J. P. Collman and R. L. Marshall, ibid., **29**, 3216 (1964).
17) K. Nakamoto, P. J. McCarthy and A. E. Martell, *J. Am. Chem. Soc.*, **83**, 1272 (1961).

and III) were characterized by analyses and by infrared and nuclear magnetic resonance spectroscopy.

It has been reported that the strong doublet in the 1500—1600 cm^{-1} region of the infrared spectra of metal acetylacetonate is usually united into a singlet by the replacement of the hydrogen at the central carbon by other groups.[6,8,11] On the other hand, the dinitro-chelate (II) exhibits two strong bands in this region. The lower band, at 1525 cm^{-1}, seems to arise from an asymmetric nitro-stretching frequecny. There are no absorption peaks at 1200 cm^{-1} in the spectra of this dinitro-chelate (II). The medium band at 1199 cm^{-1} in the spectra of palladium acetylacetonate (I) has previously been assigned to the bending mode of the hydrogen at the central carbon atom,[17] and Collman et al.[11] have claimed that the absence of this peak is an excellent measure of the complete replacement of metal acetylacetonates at the central carbon.

The proton spin-resonance spectra summarized in Table I provide conclusive proof of the structure assigned to the dinitro-chelate (II). The dinitro-chelate (II) exhibits only one signal, at 7.73τ, whereas the unsubstituted palladium acetylacetonate (I) gives signals at 7.97τ and 4.65τ, with integrated intensities of 6 : 1. The higher field signal (7.97τ) may thus be assigned to the methyl protons, and the lower signal, to the ring hydrogen. The presence of electronegative nitro groups is probably responsible for the shift to a lower field of the methyl proton signal (7.73τ) in the dinitro-chelate (II).

TABLE I. PROTON MAGNETIC RESONANCE SPECTRA AT 60 Mc./sec.

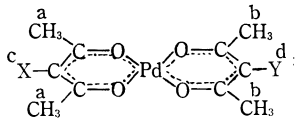

compound	Substituent X	Substituent Y	H_a	H_b	H_c	H_d
I	H	H	7.97(6)		—	—
II	NO_2	NO_2	7.73		—	—
III	H	NO_2	7.92(6)	7.75(6)	4.56(1)	—
IV	Cl	NO_2	7.69(1)	7.76(1)	—	—
V	Br	NO_2	7.58(1)	7.75(1)	—	—
VI	Cl	Cl	7.69		—	—
VII	Br	Br	7.55		—	—
VIII	I	I	7.52		—	—

NMR data is presented as τ value and deuteriochloroform was used as solvent.
Relative peak intensities in parentheses.

The structure of the mononitro-chelate (III) was confirmed by its nuclear magnetic resonance spectra (cf. Table I). The mononitro-chelate (III) exhibits proton signals at 7.92, 7.75 and 4.56τ, with relative intensities of 6 : 6 : 1. These signals are assigned to the methyl groups on the unsubstituted ring, the methyl groups on the nitrated ring, and the hydrogen on the unsubstituted chelate ring respectively. A further support for the assigned structure of the mononitro-chelate (III) was obtained from the infrared spectrum. The nitro group gave rise to an asymmetric nitro-stretching frequency at about 1520 cm^{-1}, whereas the appearance of a band at 1200 cm^{-1} indicated the presence of at least one unsubstituted chelate ring. A doublet at 1584 and 1550 cm^{-1} also indicated that not all acetylacetonate rings were substituted at the central carbon.

The structure of the mononitro derivative was further confirmed by the replacement of the other ring by electrophiles. The mixed ligand chelates IV and V were obtained by the chlorination and bromination of the mononitro-chelate (III).

Also, the introduction of halogen into the palladium acetylacetonate ring has been studied. The treatment of a glacial acetic acid solution of palladium acetylacetonate (I) with bromine resulted in the decomposition of the chelate ring. Collman et al.[6] have reported previously that *N*-halosuccinimides are effective halogenating agents for metal acetylacetonates in glacial acetic acid or in chloroform. The treatment of palladium acetylacetonate (I) with *N*-halosuccinimides in chloroform gave dichloro-, dibromo- and diiodochelate (VI, VII and VIII respectively) in high yields. These halogenated chelates showed only one signal, at about 7.5 τ, in their nuclear magnetic resonance spectra. The infrared spectra of these chelates (VI, VII and VIII) exhibit a single peak in the 1500—1600 cm^{-1} region and no absorption at 1200 cm^{-1}, providing further evidence of the complete replacement of all chelate rings at the central carbon.

Experimental[18]

Palladium Acetylacetonate (I).—This compound was prepared by the procedure of Grinberg.[19]

Bis(3-nitro-2, 4-pentanediono)-palladium (II). — A mixture of 2.4 g. (10 mmol.) of copper nitrate trihydrate and 70 ml. of acetic anhydride was stirred for 45 min. at 0°C. At the end of this time, a portion of the copper nitrate had been dissolved to form a deep blue solution. To this solution there was then added one gram (3.3 mmol.) of palladium acetylacetonate (I), and the resulting mixture was stirred for 4 hr. at 0°C, and then for one more hr. at room temperature.

18) All melting points are uncorrected. The infrared spectra were measured in KBr disks with a Hitachi EPS-2 infrared spectrometer, while the ultraviolet absorption spectra were measured in a chloroform solution with a Hitachi recording spectrophotometer, model EPU-2.

19) A. A. Grinberg and I. Simonova, *Zhur. Priklad. Khim.*, **26**, 880 (1953); *Chem. Abstr.*, **47**, 11060 (1953).

The solution was decomposed by stirring it for two hr. with 500 ml. of 1 : 1 ice-water which had been buffered with 10 g. of sodium acetate. The fine pale yellow precipitate was collected on a filter, washed with water, and then recrystallized from benzene. The yield of bis(3-nitro-2, 4-pentanediono)-palladium (II) was 0.97 g. (72%). It darkened from about 220°C and decomposed at 250—255°C. IR spectrum (KBr): 1581, 1525 (NO_2), 1468, 1420, 1346, 1102, 932, 826 (NO_2) and 702 cm^{-1}; UV spectrum ($CHCl_3$): λ_{max} mμ (log ε) 324 (3.95).

Found: C, 30.46; H, 3.01; N, 6.85. Calcd. for $C_{10}H_{12}O_8N_2Pd$: C, 30.45; H, 3.06; N, 7.09%.

(2, 4-Pentanediono) - (3 - nitro-2, 4-pentanediono)-palladium (III). — A mixture of 0.79 g. (3.3 mmol.) of copper nitrate trihydrate and 20 ml. of acetic anhydride was stirred for 45 min. at 0°C. To this solution there was then added one gram (3.3 mmol.) of palladium acetylacetonate (I). The resulting mixture was stirred for 4 hr. at 0°C, allowed to come to room temperature, and then stirred for one more hour. The reaction mixture was poured into a mixture of 100 g. of ice, 100 ml. of water, and 5 g. of sodium acetate, and then stirred for one hour. The water layer was extracted three times with chloroform, and the combined chloroform extracts were washed with a 5% aqueous sodium bicarbonate solution and then water. After solution had been dried over sodium sulfate, the solvent was removed under a vacuum. The resulting yellow residue was purified by recrystallization from benzene and obtained in a 46% yield (0.65 g.). It darkened at about 190°C and decomposed at 240—245°C. The purity of this product was checked by the chromatography of a small portion on alumina, using chloroform as the eluent. IR spectrum (KBr): 1584, 1550, 1520 (NO_2), 1475, 1370, 1345, 1200 (C–H bending), 1078, 823 (NO_2) and 745 cm.$^{-1}$. UV spectrum ($CHCl_3$): λ_{max} mμ (log ε) 325 (396).

Found: C, 34.95; H, 3.91; N, 4.12. Calcd. for $C_{10}H_{13}O_6NPd$: C, 34.35; H, 3.75; N, 4.00%.

Bis(3-chloro-2, 4-pentanediono)-palladium (VI). —A solution of 600 mg. (2.0 mmol.) of palladium acetylacetonate (I) and 1.06 g. (8.0 mmol.) of *N*-chlorosuccinimide in 50 ml. of chloroform was heated at reflux for 20 min., washed with a 5% aqueous sodium sulfite solution, and then washed with water. After the organic layer had been dried over sodium sulfate, the solvent was removed under a vacuum. The residue was recrystallized from benzene, and 580 mg. (77%) of bis(3-chloro-2, 4-pentanediono)-palladium (VI), m. p. 205—210°C (decomp.), was obtained. IR spectrum (KBr): 1550, 1452, 1367, 1041, 928 and 690 cm^{-1}. UV spectrum ($CHCl_3$): λ_{max} mμ (log ε) 345 (4.09).

Found: C, 32.19; H, 3.38; Cl, 18.64. Calcd. for $C_{10}H_{12}O_4Cl_2Pd$: C, 32.13; H, 3.21; Cl, 19.01%.

Bis(3-bromo-2, 4-pentanediono)-palladium (VII). —A mixture of *N*-bromo-succinimide (1.424 g., 8.0 mmol.) and palladium acetylacetonate (I) (600 mg., 2.0 mmol.) in 50 ml. of chloroform was boiled for ten minutes, washed with an aqueous sodium sulfite solution, and then washed with water. The chloroform solution was dried over sodium sulfate, the chloroform was removed, and the resulting solid was recrystallized from benzene. The yield of bis(3-bromo-2, 4-pentanediono)-palladium was 630 mg. (68%). It decomposed at 240—245°C. IR spectrum (KBr): 1545, 1445, 1347, 1025, 927 and 694 cm^{-1}. UV spectrum ($CHCl_3$): λ_{max} mμ (log ε) 345 (3.94).

Found: C, 26.10; H, 2.81; Br, 33.92. Calcd. for $C_{10}H_{12}O_4Br_2Pd$: C, 25.97; H, 2.61; Br, 34.63%.

Bis(3-iodo-2, 4-pentanediono)-palladium (VIII). —A mixture of *N*-iodo-succinimide (1.8 g., 8.0 mmol.) and palladium acetylacetonate (600 mg., 2.0 mmol.) in 70 ml. of chloroform was stirred at room temperature for one hour, washed with an aqueous sodium bisulfite solution, and then washed with water. After the chloroform solution had been dried, the solvent was removed under a vacuum and the resulting solid was recrystallized from benzene. Yellow crystals (650 mg., 60%) of bis-(3-iodo-2, 4-pentanediono)-palladium were obtained. They decomposed at 195—200°C. IR spectrum (KBr): 1548, 1445, 1351, 1025, 927 and 691 cm^{-1}. UV spectrum ($CHCl_3$): λ_{max} mμ (log ε) 324 (3.84).

Found: C, 21.13; H, 1.87; I, 45.62. Calcd. for $C_{10}H_{12}O_4I_2Pd$: C, 21.97; H, 2.19; I, 46.51%.

(3-Chloro-2, 4 - pentanediono)(3 - nitro - 2, 4-pentanediono)-palladium (IV).—This compound was prepared from (2, 4-pentanediono)(3-nitro-2, 4-pentanediono)-palladium (III) and *N*-chloro-succinimide in chloroform by the usual manner (70% yield). The yellow crystals darkened at 193—198°C and decomposed at 230°C. IR spectrum (KBr): 1523 (NO_2), 823 (NO_2) and no peak at 1200 cm^{-1}. UV spectrum ($CHCl_3$): λ_{max} mμ (log ε) 325 (4.08).

Found: C, 30.41; H, 2.96; N, 3.47. Calcd. for $C_{10}H_{12}O_6NClPd$: C, 31.25, H, 3.12; N, 3.62%.

(3 - Bromo - 2, 4 - pentanediono) (3 - nitro-2, 4-pentanediono)-palladium (V).—This compound was prepared from mononitro-chelate (III) and *N*-bromo-succinimide in chloroform by the usual manner (75% yield). It darkened at 190—195°C and decomposed at 220—225°C. IR spectrum (KBr): 1524 (NO_2), 826 (NO_2) and no peak at 1200 cm^{-1}. UV spectrum ($CHCl_3$): λ_{max} mμ (log ε) 235 (4.11).

Found: C, 28.55; H, 3.01; N, 3.37. Calcd. for $C_{10}H_{12}O_6NBrPd$: C, 28.03; H, 2.80; N, 3.27%.

The authors wish to express their deep gratitude to Professor Sekio Mitsui of Tohoku University for his helpful discussions and to the Kawaken Fine Chemicals Co., Ltd., for the donation of palladium chloride.

BULLETIN OF THE CHEMICAL SOCIETY OF JAPAN VOL. 39 2230—2233 (1966)

Studies of Organic Catalytic Reactions. IV.[1] A Redox Reaction between Unsaturated Organic Compounds and Primary Alcohols in the Presence of Nickel Catalysts

By Koji SAKAI, Takehiko ITO and Ken-ichi WATANABE

Department of Chemistry, Faculty of Science, Tokyo Metropolitan University, Setagaya-ku, Tokyo

(Received January 17, 1966)

Styrene, mesityl oxide, benzonitrile and nitrobenzene are reduced when heated with primary alcohols, such as methanol, ethanol, 1-butanol and benzyl alcohol, in the presence of nickel catalysts. On the other hand, aldehydes are obtained by the dehydrogenation of the primary alcohols. The relative reactivity of the functional groups for the reduction is as follows: $C=C > C\equiv N > NO_2 > C=O$. The carbonyl group and the benzene nucleus can not be reduced under these reaction conditions. A selective reduction occurs in the reaction with mesityl oxide. The lower limit of the reaction temperature depends on the combination of the two species of the hydrogen donor (primary alcohol) and the acceptor compounds. The use of a large excess of alcohols for the reduction is effective in this redox reaction. In the reaction between styrene and benzyl alcohol, the ratio of the decreased amount of styrene to the increased amount of ethylbenzene is always 1 : 1, as determined by gas chromatographic analysis.

It has been found that a redox reaction occurs between some kinds of unsaturated organic compounds and primary alcohols when they are heated in the presence of nickel catalysts. The ethylenic bond is reduced to the saturated bond, while nitrile and nitro groups are reduced to the corresponding amino groups. The carbonyl group and the benzene nucleus can not be reduced under these reaction conditions. A trace of benzyl alcohol was obtained in the reaction with benzaldehyde. On the other hand, primary alcohols afford the corresponding aldehydes by dehydrogenation. When primary alcohols alone are refluxed with the catalysts, the velocity of dehydrogenation is extremely slow. Of course, this redox reaction does not proceed without catalysts.*1

It is well-known that secondary alcohols are excellent hydrogen donors in the reaction with metallic catalysts. Some studies of the redox reaction with metallic catalysts have been reported in which 2-propanol,[2] cholesterol[3] and benzhydrol[3] are employed. Borneol is also useful.*2 Newham and Burwell[2] reported that, in the presence of large amounts of hydrogen at temperatures of 115—150°C, the reaction 2-propanol + 2-butanone = acetone + 2-butanol occurs as a coupled surface reaction on metallic copper at about 2.5 times the rate of the net hydrogenation. The redox reaction between cholesterol and cyclohexanone with Raney nickel affords cholestenone in 80% yield.[3]

In the present paper, it may be concluded that primary alcohols may generally be used for the reduction of some types of organic compounds, though the reactivity is lower than when secondary alcohols are used. On the other hand, this redox reaction is specifically useful for the preparation of aldehydes from primary alcohols under mild reaction conditions.

Styrene, mesityl oxide, benzonitrile, nitrobenzene, acetophenone and benzaldehyde were used as the hydrogen acceptors, while methanol, 1-butanol and benzyl alcohol were used as the hydrogen donors. Ethanol could also be used. In order to investigate the reaction process, the use of benzyl alcohol was advantageous. The catalysts used were Raney nickel W-7 (R-Ni), Urushibara nickel-B

1) Paper III: "The Hydration Mechanism of Nitriles to Amides with Nickel Catalysts," K. Watanabe and K. Sakai, This Bulletin, **39**, 8 (1966).

*1 Braude and Linstead established that high-potential quinones are hydrogen acceptors for unsaturated primary alcohols or secondary alcohols without metallic catalysts. E. A. Braude and R. P. Linstead, *J. Chem. Soc.*, **1956**, 3070.

2) J. Newham and R. L. Burwell, Jr., *J. Am. Chem. Soc.*, **86**, 1179 (1964); K. Tarama, S. Teranishi, T. Kubomatsu and S. Kishida, *Catalyst (Shokubai), Japan*, **7**, 289 (1965).

3) E. C. Kleiderer and E. C. Kornfeld, *J. Org. Chem.*, **13**, 455 (1948).

*2 Unpublished: The redox reaction between borneol and carbonyl compounds has been studied in our laboratory with regard to the studies of the dehydrogenation and dehydration of exo- and endo-borneol on metallic catalysts. When borneol and cyclohexanone are heated in xylene (140°C) in the presence of nickel catalysts, the redox reaction occurs predominantly.

(U-Ni-B)*3 and a stabilized nickel (S-Ni)*4, all can also be used for the catalytic hydrogenation. The use of a large excess of alcohols for the reaction seems to be useful for the effective reduction of the organic compounds.

Results and Discussion

The results of the experiments are shown in Table I. As is shown in Exp. Nos. 5, 11 and 12, the reduction of carbonyl groups hardly ever proceeds under these reaction conditions. This may be due to the oxidation-reduction potentials of the correlating compounds (donor-acceptor) in the reactions. A study of oxidation-reduction potentials in the catalytic reactions was presented by Adkins and his co-workers.[4] With regard to the reaction temperatures, their lower limits depend on the combination of the two species. When the reaction temperature is lower than the limit for the reaction, only a little reduction takes place with the adsorbed hydrogen on the catalysts used.

According to Table I, it may be concluded that the relative reactivity of the functional groups for the reduction is as follows: C=C>C≡N>NO_2>C=O. The selective reduction can be applied

Table I. The redox reaction between organic compounds and primary alcohols in the presence of nickel catalysts

Exp. No.	Catalysts	Nickel content g.	Compound (sample)	g.	Solvent (alcohol)	ml.	Reaction time hr.	Reaction temp. °C
1	U-Ni-B	4	Styrene	25	Benzyl alcohol	50	5	100
2	R-Ni	4	Styrene	25	Benzyl alcohol	50	6	100
3	R-Ni	10	Styrene	10	Benzyl alcohol	100	11	100
4	R-Ni	4	Styrene	10	Methanol	100	20	Reflux
5	R-Ni	4	Mesityl oxide	25	Benzyl alcohol	50	15	100
6	U-Ni-B	4	Benzonitrile	25	Benzyl alcohol	50	10	160
7	U-Ni-B	4	Benzonitrile	20	1-Butanol	80	14	Reflux
8	S-Ni	12.5	Benzonitrile	20	Benzyl alcohol	100	12	160
9	U-Ni-B	4	Nitrobenzene	20	Benzyl alcohol	80	15	180
10	R-Ni	4	Nitrobenzene	10	1-Butanol	100	20	Reflux
11	U-Ni-B	4	Acetophenone	20	Benzyl alcohol	80	8	100
12	R-Ni	4	Benzaldehyde	20	1-Butanol	80	8	Reflux

Exp. No.	Main product	Recovered* sample g.	(%)	%	Aldehyde* produced	g.	By-products
1	Ethylbenzene*	14	(55)	45	Benzaldehyde	9	Toluene* (trace)
2	Ethylbenzene*	17.5	(68.5)	31	Benzaldehyde	15	Toluene* (trace)
3	Ethylbenzene*	9.8	(95)	trace	Benzaldehyde	10	Toluene* (trace)
4	Ethylbenzene*	14	(55)	45	Formaldehyde	+	
5	Isobutyl methyl ketone*	17	(66.5)	32	Benzaldehyde	17.5	Toluene* (trace)
6	Amines-HCl	10		13	Benzaldehyde	5.2	Toluene* (trace), Benzamide 3 g.
7	Amines-HCl	15		37	*n*-Butyraldehyde	+	Toluene* (trace), Benzamide 0.4 g.
8	Amines-HCl	19.5		trace	Benzaldehyde	20	Benzene*, Toluene,* Benzylidenebenzylamine
9	Aniline	3.5	(23.2)	30	Benzaldehyde	10	Toluene* (trace), Benzylideneaniline
10	Aniline	1.2	(7.9)	48	*n*-Butyraldehyde	+	
11	—			100	Benzaldehyde	6.8	Toluene* (trace)
12	Benzyl alcohol*	(trace)		95	*n*-Butyraldehyde	+	

* Approximate value calculated from the gas chromatographic analysis.

*3 The nickel precipitated on the zinc dust from a nickel chloride solution, treated with a sodium hydroxide solution and water, is as active as Raney nickel. K. Watanabe, This Bulletin, **37**, 1325 (1964); Y. Urushibara and S. Nishimura, ibid., **27**, 480 (1954); **28**, 446 (1955).

*4 Obtained from the Nikko Scientific & Chemical Co., Ltd., Tokyo, this is kind of nickel-kieselguhr catalyst (50%) prepared from nickel formate, stabilized with inert gas. It is used directly for the reaction without any treatment.

4) H. Adkins, R. M. Elofson, A. G. Rossow and C. C. Robinson, *J. Am. Chem. Soc.*, **71**, 3622 (1949).

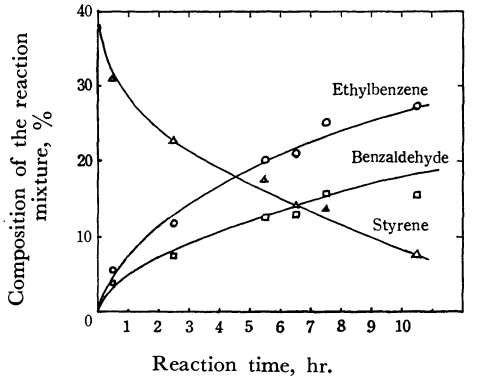

Fig. 1. The redox reaction between styrene and benzyl alcohol in the presence of U-Ni-B.
Sample: Styrene 25 g. and benzyl alcohol 50 ml.
Catalyst: U-Ni-B containing 4 g. Ni
Reaction temperature: 100°C

to compounds that have both C=C and C=O groups together.

The Reduction of Styrene and Mesityl Oxide.—With a combination of styrene and benzyl alcohol, the reaction occurred preferably at 100°C, no reaction took place below 80°C, and the polymerization of styrene occurred at 120°C. When the mole ratio of styrene to benzyl alcohol was ca. 1 : 2 (Exp. Nos. 1 and 2, Table I, Fig. 1), unreacted styrene was recovered even after twelve hours' reaction. When about ten times as much alcohol as styrene was used (Exp. No. 3), almost all the styrene was reduced in eleven hours in the presence of much more of the catalyst than in other cases. Methanol was not a suitable hydrogen donor for styrene (Exp. No. 4). The formaldehyde formed by the dehydrogenation of methanol was expelled out of the reaction system during the refluxing. Isobutyl methyl ketone was mainly obtained by the selective reduction of mesityl oxide (Exp. No. 5).

The Reduction of Benzonitrile and Nitrobenzene.—The reaction with the combination of benzonitrile and benzyl alcohol took place above 160°C, but with 1-butanol instead of benzyl alcohol, the reaction proceeded at the reflux temperature (ca. 120°C). A mixture of primary and secondary amines was obtained by the reduction of benzonitrile. The activity of S-Ni is relatively low, so much more of it should be used than when other catalysts are used (Exp. No. 8). It may be presumed that a part of the benzylamine reacts with aldehydes to form the corresponding Schiff base during the reaction. However, the formation and existence of the aldehyde as the free form were confirmed by gas chromatographic analysis, and also by the formation of 2, 4-dinitrophenylhydrazone from the reaction mixture. In Exp. Nos. 6 and 7, benzamide was obtained in varying amount. The U-Ni-B used in these reactions may have contained some water that remained after the preparation process, even though the catalyst was washed with alcohols. It has been reported[1,5] that nitriles are hydrated to the corresponding amides when refluxed in water with catalysts for hydrogenation (the nickel catalysts are the best), in which case no acid or base is necessary. Therefore, water should be excluded from the reaction system as far as possible. The reduction of nitrobenzene seemed to proceed slowly. Even after a twenty-hour reaction with an excess of alcohol, the yield of aniline was low (Exp. No. 9). Amines formed by the reduction of benzonitrile and nitrobenzene may be adsorbed on the catalysts and may interfere with the adsorption of the alcohols. This may be one of the reasons for their low reactivity.

The Combination of Hydrogen Donor and Acceptor.—On the whole, it may be concluded that a suitable combination of the two species of hydrogen donor and acceptor compounds in the reaction is essential if we are to expect successful redox reactions to occur. Further, this combination may determine the preferable temperature in the individual reaction. Actually, the effect of the reaction temperature on the reactions is delicate; its lower limit depends on the combination of species employed.

The Investigation of the Reaction Process.—During the reaction between styrene and benzyl alcohol, the diminution of styrene and the formation of ethylbenzene and benzaldehyde were investigated by gas chromatographic analysis (Fig. 1). In Fig. 1, the quantity percentage of styrene indicates ca. 37 when the reaction starts, which means that ca. 63 per cent of the reaction mixture is benzyl alcohol. After the reaction has proceeded for four hours, about a half of the styrene remains (ca. 18 per cent as determined by gas chromatographic analysis, Fig. 1), while about an equal percentage of ethylbenzene is formed. According to the graphic curves of styrene and ethylbenzene, the ratio of the decreased amount of styrene to the increased amount of ethylbenzene throughout the reaction is always ca. 1 : 1. This fact indicates that the reduction proceeds almost quantitatively. On the other hand, benzaldehyde is formed by the dehydrogenation of benzyl alcohol, and the proportion of the benzaldehyde formed to the ethylbenzene should be 1 : 1 if no other reaction occurs. However, some hydrogen adsorbed on the catalysts works for the formation of ethylbenzene. The shapes of the graphic curves show this.

Experimental

The Reduction of Styrene (Exp. No. 2).—In a 200-ml. three-necked, round flask equipped with a reflux

5) K. Watanabe, This Bulletin, **32**, 1280 (1959); **37**, 1325 (1964).

condenser, a stirrer and a thermometer, were placed 25 g. of styrene, 50 ml. of benzyl alcohol and 4 g. of Raney nickel. The contents were then stirred for 6 hr. at 100°C. After the reaction had been completed, the catalyst was separated by filtration. A part of the filtrate was analyzed by gas chromatography. The yield of ethylbenzene was 68.6%; unreacted styrene, benzaldehyde, and a trace of toluene were detected. When the filtrate was distilled, ca. 17.5 g. of the crude ethylbenzene fraction was obtained, b. p. 129—131°C. The ethylbenzene was also identified by infrared spectrum analysis. Benzaldehyde was identified as 2, 4-dinitrophenylhydrazone, m. p. 237°C, from an aliquot of the filtrate. The latter was recrystallized from ethanol and identified by infrared spectrum analysis, too. Gas chromatography: column, 30% Carbo-wax 1500 on Celite 30—40 mesh; length, 2 m.; temp., ca. 180°C; flow rate, 14—20 cm./sec.; carrier gas, H_2; relative retention times of the components: ethylbenzene 1, styrene 1.33, benzaldehyde 2.83, benzyl alcohol 7.29, and (toluene 0.9). Gas chromatograph apparatus: Yanagimoto-GCG 220 Type, Yanagimoto Mfg. Co., Ltd., Kyoto, Japan.

The Reduction of Mesityl Oxide (Exp. No. 5).—The reaction procedure was almost the same as in Exp. No. 2. After fifteen hours' reaction at 100°C, the reaction mixture was analyzed by gas chromatography as follows: the column and the conditions of analysis were the same as in Exp. No. 2; relative retention times of the components: isobutyl methyl ketone 1, mesityl oxide 1.27, benzaldehyde 3.42, and benzyl alcohol 8.79. The yeild of the reduction product, isobutyl methyl ketone, was 66.5%.

The Reduction of Benzonitrile (Exp. No. 6).—The reaction procedure was almost the same as in Exp. No. 2. After ten hours' reaction at 160°C, the catalyst was separated by filtration. A part of the filtrate was then analyzed by gas chromatography. The column and the conditions of analysis were the same as in Exp. No. 2; relative retention times of the components: benzaldehyde 1, benzonitrile 1.26, benzyl alcohol 2.54, and (toluene 0.29). The filtrate was acidified with concentrated hydrochloric acid, and then extracted with ether. From the ether extract, 3 g. of benzamide were obtained, m. p. 127—128°C. When the acidic solution was carefully evaporated to dryness, 10 g. of amine salt were obtained. The amine salt was decomposed with an alkaline solution, benzylamine was obtained as an acetyl derivative, 6.5 g.; m. p. 58.3—59.8°C. Dibenzylamine was detected by Hinsberg's method.[6] The quantity of the primary amine in the amine product obtained was ca. 60%. When 1-butanol was used instead of benzyl alcohol (Exp. No. 7), *n*-butyraldehyde was obtained as 2, 4-dinitrophenylhydrazone, recrystallized from ethanol, m. p. 119—120°C; it was also identified by infrared spectrum analysis.

The Reduction of Nitrobenzene (Exp. No. 9).—The reaction procedure was also the same as in Exp. No. 2. After fifteen hours' reaction at 180°C, the catalyst was separated by filtration. A part of the filtrate was then analyzed by gas chromatography. The column and the conditions of analysis were the same as in Exp. No. 2; relative retention times: benzaldehyde 1, nitrobenzene 1.26, benzyl alcohol 2.6, and (toluene 0.27). A very small quantity of a precipitate was obtained from the filtrate. It was washed with water and then identified as benzylideneaniline by infrared spectrum analysis. The filtrate was acidified with concentrated hydrochloric acid, and then extracted with ether to take off the unreacted nitrobenzene, benzyl alcohol, and benzaldehyde. When the water part (acidic) was evaporated to dryness, amine salt was obtained. It was decomposed with an alkaline solution and extracted with ether. From the ether solution, 3.5 g. of aniline were obtained by distillation, b. p. 182—184°C.

The authors wish to express their hearty thanks to Professor Kazuo Hata for his kind advice.

6) R. L. Shriner, R. C. Fuson and D. Y. Curtin, "The Systematic Identification of Organic Compounds," Asian Edition, Maruzen Co., Tokyo (1956), p. 103.

BULLETIN OF THE CHEMICAL SOCIETY OF JAPAN VOL. 39 2234—2242 (1966)

Studies of Peptide Antibiotics. VI. Syntheses of Cyclic Penta and Decapeptides with a Glycyl-L-ornithyl-L-leucyl-D-phenylalanylglycyl Sequence

By Michio KONDO, Haruhiko AOYAGI, Tetsuo KATO and Nobuo IZUMIYA

Laboratory of Biochemistry, Faculty of Science, Kyushu University, Fukuoka

(Received January 17, 1966)

A cyclic decapeptide dihydrochloride, cyclo-(glycyl-L-ornithyl-L-leucyl-D-phenylalanylglycyl)$_2$·2HCl, which is an analog of gramicidin S, and a cyclic pentapeptide monohydrochloride, cyclo-glycyl-L-ornithyl-L-leucyl-D-phenylalanylglycyl·HCl, were synthesized in order to compare their antibacterial activities with that of gramicidin S. The cyclization reaction via two linear decapeptide active esters was found to yield the same cyclic bezyloxycarbonyl-substituted decapeptide; this was converted by hydrogenolysis to the cyclic decapeptide dihydrochloride mentioned above. The cyclization reaction of a linear pentapeptide active ester, in which the glycines are both terminal amino acid residues, yielded a cyclic benzyloxycarbonyl-substituted pentapeptide exclusively. When another linear pentapeptide active ester and a pentapeptide azide were also subjected to cyclization reaction, they afforded the same cyclic benzyloxycarbonyl-substituted pentapeptide; this was then hydrogenolyzed to the corresponding cyclic pentapeptide monohydrochloride. The effects of the two cyclic peptide hydrochlorides on the bacterial growth were tested; no retardation of growth was observed with any of the microorganisms tested.

For a study of the relationsihp between the chemical structure and the biological activity of such antibacterial cyclic peptides as gramicidin S (I) and tyrocidine A, various cyclic peptides which possess several characteristic features have been prepared and their biological activities have been tested, as has been described in previous papers from this laboratory. It was observed that some of them,[1] such as a cyclic hexapeptide related to gramicidin S, were devoid of antibacterial activity, but an analog of gramicidin S, 5, 5'-sarcosine-gramicidin S,[2] was as active as gramicidin S against several microorganisms. Furthermore, 5, 5'-glycine-gramicidin S was found to possess approximately 10 times as much activity as gramicidin S in a synthetic medium.[3] The result shows that the replacement of the proline residues by glycines or sarcosines in the sequence of gramicidin S does not reduce the activity, and that the side chain of proline is not indispensable to its full activity. In order to investigate whether or not the valine residues in the 1- and 1'-positions of gramicidn S might be replaced by an amino acid of a smaller molecule, glycine, without a decrease in the antibacterial activity, we attempted to prepare 1, 1', 5, 5'-glycine-gramicidin S (II). The present paper will describe the syntheses and antibacterial properties of this cyclic decapeptide (II) and of the cyclic pentapeptide, cyclo-glycyl-L-ornithyl-L-leucyl-D-phenylalanylglycyl (III), which is related to II.

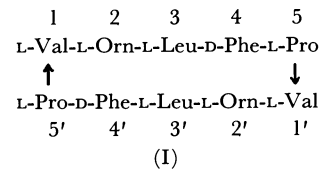

(I)

The structure of gramicidin S, with numbers indicating the positions of the individual amino acid residues.

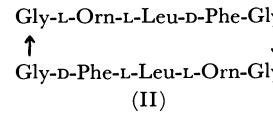

(II)

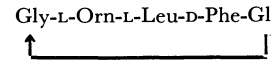

(III)

The protected cyclic decapeptide (XXVI), which was converted to II by hydrogenolysis, was synthesized via two different routes, shown in Figs. 1 and 2.

Figure 1 indicates one route for the synthesis of XXVI via the linear decapeptide active ester (XXV), in which glycylglycine is the C-terminal

1) N. Izumiya, T. Kato, Y. Fujita, M. Ohno and M. Kondo, This Bulletin, **37**, 1809 (1964); T. Kato, M. Kondo, M. Ohno and N. Izumiya, ibid., **38**, 1202 (1965).

2) H. Aoyagi and N. Izumiya, ibid., **39**, 1747 (1966).

3) H. Aoyagi, T. Kato, M. Ohno, M. Kondo, M. Waki, S. Makisumi and N. Izumiya, ibid., **38**, 2139 (1965); H. Aoyagi, T. Kato, M. Ohno, M. Kondo and N. Izumiya, *J. Am. Chem. Soc.*, **86**, 5700 (1964).

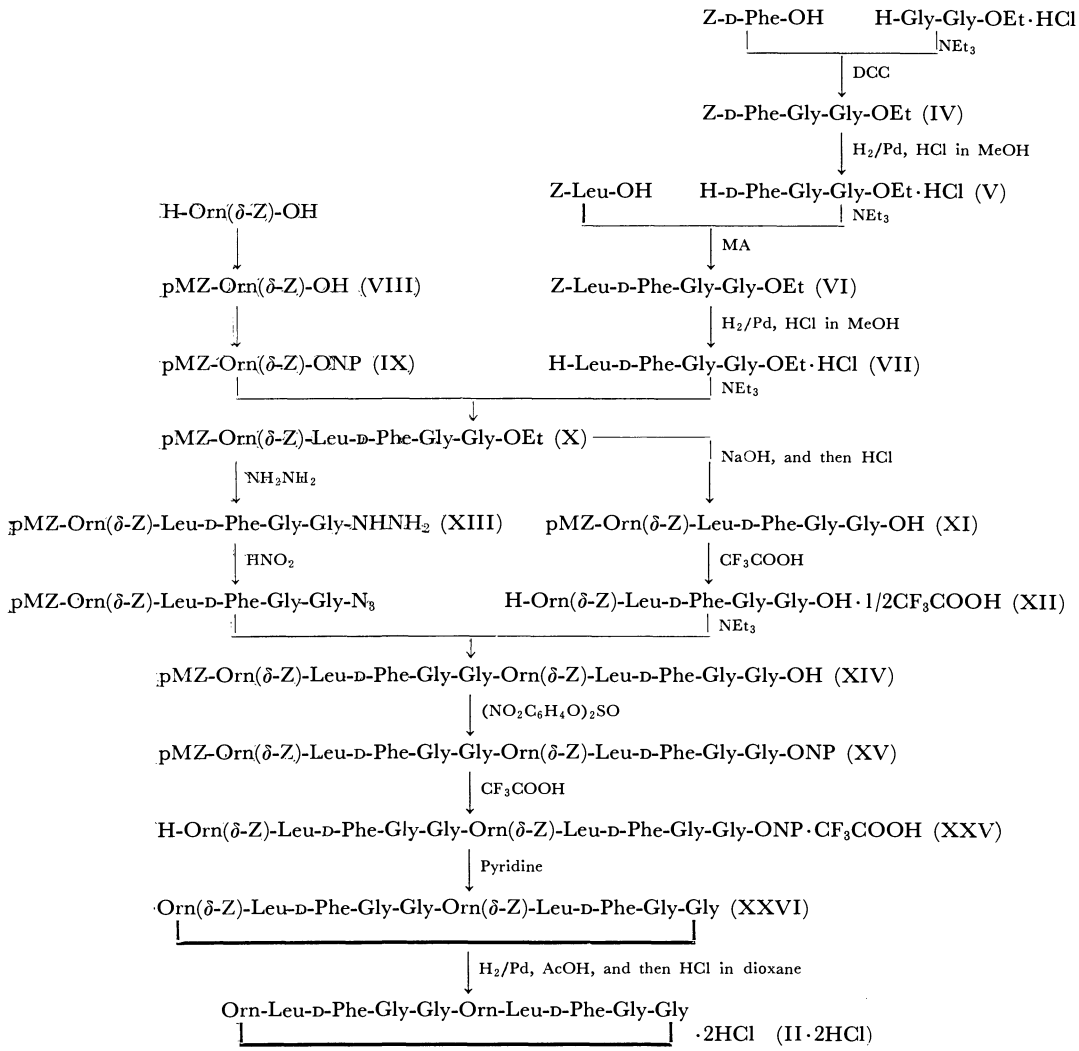

Fig. 1.

Z, benzyloxycarbonyl; DCC, dicyclohexylcarbodiimide; pMZ, *p*-methoxybenzyloxycarbonyl; ONP, *p*-nitrophenoxy ester; MA, mixed anhydride method. An amino acid residue except Gly and D-Phe is of L-configuration.

sequence. The *C*-terminal tetrapeptide derivative (VI) was prepared by a step-by-step elongation by means of the dicyclohexylcarbodiimide method and the mixed anhydride method. Syntheses of *p*-methoxybenzyloxycarbonyl-δ-benzyloxycarbonyl-L-ornithylglycine benzyl ester by the coupling of diacylornithine (VIII) with the glycine ester were attempted by several methods as a preliminary experiment for the preparation of diacylpentapeptide ester (X) by the coupling of VIII with the tetrapeptide ester (VII); it was found that the reaction of the diacylornithine active ester (IX) with the glycine ester gave the pure compound in the best yield. In fact, the reaction of IX with VII afforded the crystalline pentapeptide derivative (X) in a good yield. The azide, which was derived from XIII, was then made to react with XII to give the protected decapeptide (XIV) in a 68% yield. XIV was converted to the *p*-nitrophenyl ester (XV) by the action of di-*p*-nitrophenyl sulfite, and the removal of the *p*-methoxybenzyloxycarbonyl group from XV with trifluoroacetic acid gave the amorphous decapeptide *p*-nitrophenyl ester trifluoroacetate (XXV). The cyclization reaction of XXV in pyridine gave the crude benzyloxycarbonyl-substituted cyclic peptide (XXVI), which was then purified by passing it through columns of acidic and basic ion exchangers; the yield of the crystalline XXVI from XIV was found to be 21% after recrystallization. The molecular weight determination by the micro Rast method demonstrated that the molecular size of this compound corresponded to that of cyclic decapeptide (XXVI).

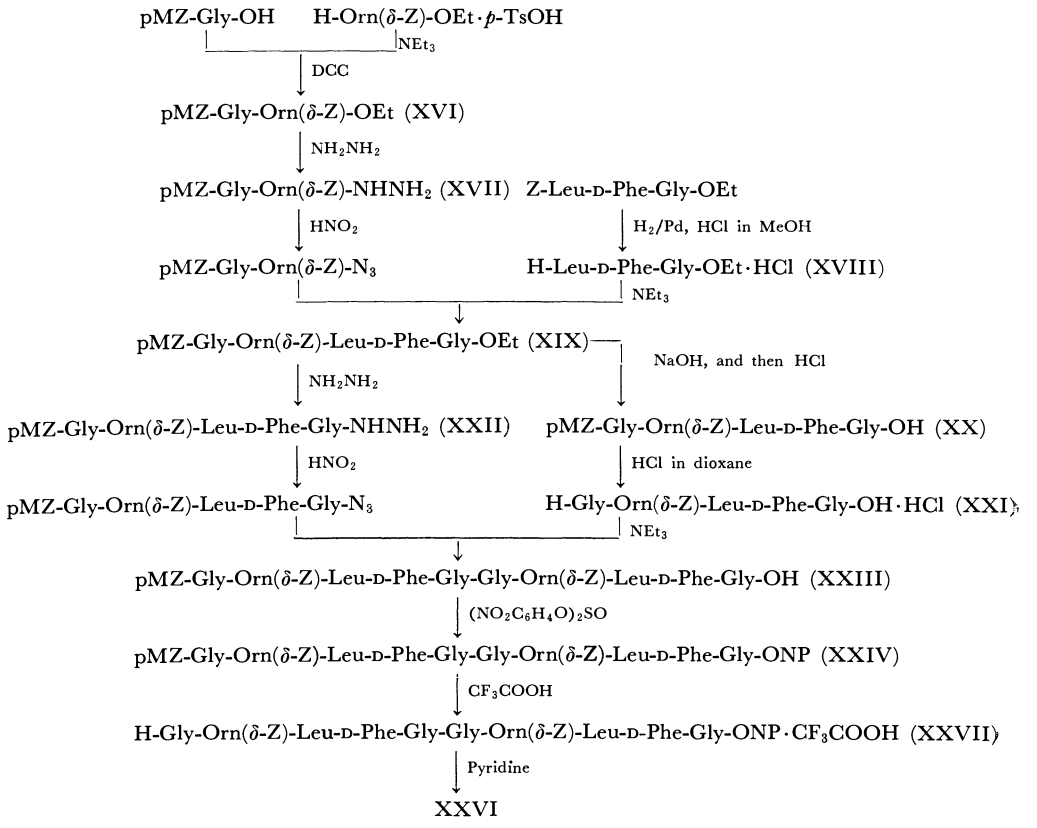

Fig. 2.

The final product (II·2HCl) was obtained as colorless crystals containing four moles of the water of crystallization. Its homogeneity was demonstrated by carboxymethyl(CM) cellulose column chromatography (Fig. 6) and by paper electrophoresis (Fig. 7).

The protected cyclic decapeptide (XXVI) was obtained again via another route, this time from the linear decapeptide active ester (XXVII), as is shown in Fig. 2, in which the glycines are the *N*- and *C*-terminal amino acid residues. It should be noted that the sequence of reactions presented in Fig. 2 is similar to that used for the preparation of 5, 5'-sarcosine-gramicidin S.[2] The cyclization reaction of XXVII gave the crystalline product (XXVI) in a yield of 36% from XXIII. From a comparison of melting points and specific rotations, this product is demonstrated to be identical with the protected cyclic decapeptide (XXVI) prepared from XXV.

The synthesis of the protected cyclic decapeptide (XXVI) was further attempted by the dimerization reaction of a pentapeptide active ester (XXX). However, the benzyloxycarbonyl-substituted cyclic peptide obtained in a yield of 23% from XI was found to be a monomer, shown as XXXI, by the results of the molecular weight determination.

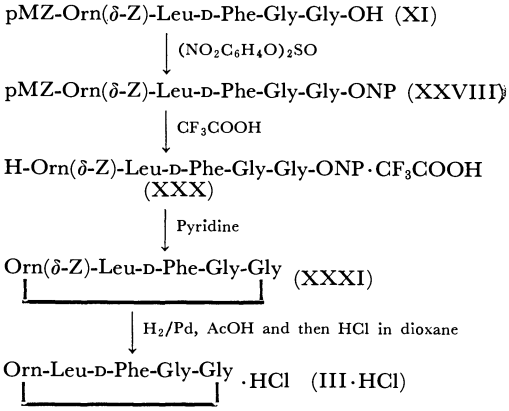

Fig. 3.

The hydrogenolysis of XXXI in the presence of an equivalent amount of hydrogen chloride yielded a cyclic pentapeptide hydrochloride (III·HCl). The experiments of CM-cellulose column chromatography showed that the product (III·HCl) gives only one peak, which is at a position different from that of the cyclic decapeptide (II·2HCl).

The cyclizations of pentapeptides via different routes were also performed, as Figs. 4 and 5 show. Although it has been reported that cyclic hexa-

glycyl was obtained in a good yield from triglycine azide,[4] the linear pentapeptide azide, which was derived from XXXII, gave only a very small amount of the protected cyclic pentapeptide (XXXI) (Fig. 4). It should be noted, in this connection, that a paper from this laboratory has reported that the yield of the cyclization of pentaglycyl-ε-benzyloxycarbonyl-L-lysine azide attempting to obtain the corresponding cyclic hexapeptide was very poor.[5]

pMZ-Orn(δ-Z)-Leu-D-Phe-Gly-Gly-$NHNH_2$ (XIII)
↓ CF_3COOH
H-Orn(δ-Z)-Leu-D-Phe-Gly-Gly-$NHNH_2 \cdot 2CF_3COOH$ (XXXII)
↓ HNO_2
H-Orn(δ-Z)-Leu-D-Phe-Gly-Gly-N_3
↓ $NaHCO_3$
XXXI

Fig. 4.

pMZ-Gly-Orn(δ-Z)-Leu-D-Phe-Gly-OH (XX)
↓ $(NO_2C_6H_4O)_2SO$
pMZ-Gly-Orn(δ-Z)-Leu-D-Phe-Gly-ONP (XXIX)
↓ CF_3COOH
H-Gly-Orn(δ-Z)-Leu-D-Phe-Gly-ONP·CF_3COOH (XXXIII)
↓ pyridine
XXXI

Fig. 5.

Figure 5 shows the reaction sequence for the cyclization of the pentapeptide active ester, in which the glycines are both terminal amino acid residues. The cyclization reaction of the pentapeptide active ester (XXXIII) in a large amount of pyridine gave crude, protected cyclic peptide (XXXIV), which was found to contain only protected cyclic pentapeptide (XXXI), and not even a trace of the protected cyclic decapeptide (XXVI), from the criteria of CM-cellulose chromatography and paper electrophoresis of the hydrogenolyzed material of XXXIV. The protected cyclic pentapeptide (XXXI) in an analytically-pure state was obtained in a yield of 37% (from XX) after the recrystallization of XXXIV from methanol and ether. This result is of great interest, for it is in contrast with the fact that the cyclization reaction of L-valyl-δ-benzyloxycarbonyl-L-ornithyl-L-leucyl-D-phenylalanyl-glycine (or -sarcosine) active ester[2,3] yielded an appreciable amount of the protected cyclic decapeptide by the dimerization reaction, besides a large amount of the monomeric cyclic pentapeptide.

The antibacterial activities of 1, 1', 5, 5'-glycine-gramicidin S (II) and cyclic pentapeptide (III) toward several microorganisms were also examined. Neither compound had any retarding effect on the growth of the microorganisms, even at so high level as 100 γ per ml. of assay medium. From these findings, it appears that the valine residues in the gramicidin S sequence are of importance for the activity, for 5, 5'-glycine-gramicidin S showed a strong activity. In this connection, it is of interest to note that 1, 1'-glycine-2, 2'-lysine-gramicidin S, which has a structure similar to that of II, was found to possess some antibacterial activity.[6]

To clarify the effectiveness of the valine residues in gramicidn S further, the syntheses of several analogs of gramicidin S in which the valine residues are replaced by appropriate amino acids are in progress in this laboratory.

Experimental

All the melting points are uncorrected. The optical rotations were measured on a Yanagimoto Photometric Polarimeter, OR-20 type. Prior to analysis, the compounds were dried to a constant weight over phosphorus pentoxide at 80°C and 2 mmHg, except in the case of II·2HCl and III·HCl.

Benzyloxycarbonyl-D-phenylalanylglycylglycine Ethyl Ester (IV).—To a solution of benzyloxycarbonyl-D-phenylalanine (6.0 g.), glycylglycine ethyl ester hydrochloride (3.9 g.) and triethylamine (2.8 ml.) in chloroform (80 ml.), dicyclohexylcarbodiimide[7] (4.12 g.) was added at 0°C. The reaction mixture was stirred for 2 hr. at 0°C and then kept overnight in a refrigerator. The mixture was evaporated in vacuo, and the residue was extracted with ethyl acetate (120 ml.). After the dicyclohexylurea thus formed was filtered off, the filtrate was washed successively with a 4% sodium bicarbonate solution, 3% hydrochloric acid, and water, and then dried over anhydrous sodium sulfate. The filtered solution was evaporated in vacuo; the residual oil solidified after ether had been added. Recrystallization from ethyl acetate-ether gave 5.9 g. (67%); m. p. 95—96°C; $[\alpha]_D^{20}$ +17.3° (*c* 2, dimethylformamide).

Found: C, 62.36; H, 6.19; N, 9.63. Calcd. for $C_{23}H_{27}O_6N_3$: C, 62.57; H, 6.16; N, 9.52%.

D-Phenylalanylglycylglycine Ethyl Ester Hydrochloride (V).—IV (8.83 g.) was subjected to hydrogenolysis in the presence of palladium black and 0.43 N methanolic hydrogen chloride (50.6 ml.). The filtrate from the catalyst was then evaporated to dryness in vacuo; yield of oil, 6.9 g. (100%); R_f 0.85.[8]

Benzyloxycarbonyl-L-leucyl-D-phenylalanylglycylglycine Ethyl Ester (VI).—To a chilled solution of benzyloxycarbonyl-L-leucine (5.17 g.) and triethylamine (2.72 ml.) in tetrahydrofuran (40 ml.), isobutyl

4) J. C. Sheehan and W. L. Richardson, *J. Am. Chem. Soc.*, **76**, 6329 (1954); **77**, 6391 (1955).
5) M. Ohno and N. Izumiya, This Bulletin, **38**, 1839 (1965).
6) German Patent, *Chem. Abstr.*, **57**, 949 (1962).
7) J. C. Sheehan and G. P. Hess, *J. Am. Chem. Soc.*, **77**, 1067 (1955).
8) The R_f of the paper chromatography with Toyo Roshi No. 52 refers to the *n*-butanol-acetic acid-pyridine-water (4 : 1 : 1 : 2, v/v) system.

chloroformate (2.52 ml.) was added. After 15 min., a mixture of V (6.9 g.), triethylamine (2.72 ml.), and chloroform (40 ml.) was added to the solution. The reaction mixture was allowed to stand overnight and then evaporated to dryness in vacuo. The residual oil was dissolved in ethyl acetate (150 ml.), and the solution was wahsed successively with 4% sodium bicarbonate, 3% hydrochloric acid and water, dried over sodium sulfate, and then evaporated to dryness in vacuo. The product was obtained as an oil; yield, 8.32 g. (75%).

L-Leucyl-D-phenylalanylglycylglycine Ethyl Ester Hydrochloride (VII).—VI (6.1 g.) was treated as has been described in the case of V. The product was obtained as a hygroscopic powder; yield, 4.7 g. (94%); R_f 0.87.[8]

p-Methoxybenzyloxycarbonyl-δ-benzyloxycarbonyl-L-ornithine (VIII).—A mixture of δ-benzyloxycarbonyl-L-ornithine (2.67 g.), sodium bicarbonate (2.52 g.), water (100 ml.), dioxane (150 ml.), and *p*-methoxybenzyloxycarbonyl azide[9] was stirred for 60 hr. at room temperature. The solution was then evaporated in vacuo in order to remove dioxane. After it had been extracted with ether, the solution was acidified with 0.5 M citric acid (40 ml.) and then extracted with ethyl acetate. The organic layer was dried over sodium sulfate and evaporated to dryness in vacuo. The residual oil was solidified by the addition of petroleum ether; yield, 3.42 g. (79%). For analysis, a part of the product was recrystallized from ethyl acetate-petroleum ether; m. p. 73—75°C; $[\alpha]_D^{20}$ −2.3° (*c* 2, dimethylformamide).

Found: C, 60.96; H, 6.22; N, 6.77. Calcd. for $C_{22}H_{26}O_7N_2$: C, 61.38; H, 6.09; N, 6.51%.

p-Methoxybenzyloxycarbonyl-δ-benzyloxycarbonyl-L-ornithine p-Nitrophenyl Ester (IX).—To a stirred solution of VIII (3.34 g.) and *p*-nitrophenol (1.31 g.) in ethyl acetate (25 ml.), dicyclohexylcarbodiimide (1.60 g.) was added at 0°C. The stirring was continued for 2 hr. at 0°C, and then for 3 more hours at room temperature. The dicyclohexylurea which precipitated was filtered off and washed with ethyl acetate, and the combined filtrates were evaporated to dryness. The cyrstalline residue was recrystallized from hot ethanol; yield, 3.34 g. (78%); m. p. 123—124°C; $[\alpha]_D^{20}$ −14.1° (*c* 2, dimethylformamide).

Found: C, 60.63; H, 5.25; N, 7.80. Calcd. for $C_{28}H_{29}O_9N_3$: C, 60.97; H, 5.30; N, 7.62%.

p-Methoxybenzyloxycarbonyl-δ-benzyloxycarbonyl-L-ornithylglycine Benzyl Ester.—*a) MA Method.*—The mixed anhydride prepared from VIII (1 mmol.) was coupled with the glycine benzyl ester (1 mmol.), following the procedure used in the preparation of VI. The crude product was recrystallized from ethyl acetate-ether; yield, 60 mg. (21%); m. p. 141—143°C. The melting point of this product was not depressed by admixture with the product (m. p. 143—144°C) obtained by the ONP-method.

b) DCC Method.—The same product was obtained by the carbodiimide method in the usual manner; yield, 144 mg. (50%); m. p. 141—143°C.

c) ONP Method.—The product was prepared with IX (1mmol.) and the glycine benzyl ester in the usual manner; yield, 188 mg. (65%); m. p. 143—144°C; $[\alpha]_D^{20}$ −3.0° (*c* 2, dimethylformamide).

Found: C, 64.44; H, 6.47; N, 7.53. Calcd. for $C_{31}H_{35}O_8N_3$: C, 64.46; H, 6.11; N, 7.28%.

p-Methoxybenzyloxycarbonyl-δ-benzyloxycarbonyl-L-ornithyl-L-leucyl-D-phenylalanylglycylglycine Ethyl Ester (X).—To a solution of VII (4.7 g.) and triethylamine (1.87 ml.) in dimethylformamide (14 ml.), IX (5.68 g.) was added, and the solution was allowed to stand overnight at room temperature. Cold water (100 ml.) was then added slowly to it, and the mixture was kept in a refrigerator for several hours. The crystals were collected by filtration and washed with 4% sodium bicarbonate, M citric acid, and water. They were then recrystallized from dioxane-ether; yield, 6.12 g. (71%); m. p. 172—174°C; $[\alpha]_D^{16}$ +1.5° (*c* 2, dimethylformamide); R_f 0.92.[10]

Found: C, 61.60; H, 6.58; N, 10.01. Calcd. for $C_{43}H_{56}O_{11}N_6$: C, 62.00; H, 6.78; N, 10.09%.

p-Methoxybenzyloxycarbonyl-δ-benzyloxycarbonyl-L-ornithyl-L-leucyl-D-phenylalanylglycylglycine (XI).—To a solution of X (510 mg.) in methanol (8 ml.), 1.03 N sodium hydroxide (0.71 ml.) was added. The solution was then allowed to stand overnight at room temperature. After the addition of water (60 ml.), the solution was concentrated in vacuo in order to remove methanol. It was extracted with ether and acidified with 1.22 N hydrochloric acid (0.61 ml.) under cooling. After they had been stored in a refrigerator for several hours, the crystals were collected by filtration, washed with water, and dried. Recrystallization from methanol-ether gave 420 mg. (84%); m. p. 190—192°C; $[\alpha]_D^{16}$ −0.7° (*c* 2, dimethylformamide); R_f 0.72.[10]

Found: C, 60.10; H, 6.66; N, 10.49. Calcd. for $C_{41}H_{52}O_{11}N_6 \cdot H_2O$: C, 59.84; H, 6.61; N, 10.21%.

δ-Benzyloxycarbonyl-L-ornithyl-L-leucyl-D-phenylalanylglycylglycine Hemitrifluoroacetate (XII).—To a mixture of XI (916 mg.) and anisole (0.4 ml.), trifluoroacetic acid (4 ml.) was added at 0°C. After it had been permitted to stand for 40 min. at 0°C, the solution was evaporated in vacuo. The residue was triturated with ether (20 ml.) and washed repeatedly with ether by decantation. Crystals were filtered off with the aid of ether; yield, 783 mg. (96%); m. p. 183—184°C; $[\alpha]_D^{20}$ +13.2° (*c* 2, dimethylformamide). R_f 0.85[8] and 0.64.[10]

Found: C, 54.28; H, 6.68; N, 11.71. Calcd. for $C_{32}H_{44}O_8N_6 \cdot 1/2CF_3COOH \cdot 2H_2O$: C, 54.10; H, 6.66; N, 11.45%.

An attempt to crystallize the CF_3COOH-free pentapeptide failed.

p-Methoxybenzyloxycarbonyl-δ-benzyloxycarbonyl-L-ornithyl-L-leucyl-D-phenylalanylglycylglycine Hydrazide (XIII).—A solution of X (440 mg.) and hydrazine hydrate (0.53 ml.) in dimethylformamide (4 ml.) was allowed to stand for 2 days at 30°C. The solution was then concentrated in vacuo to a small volume. The hydrazide which precipitated upon the

9) F. Weygand and K. Hunger, *Chem. Ber.*, **95**, 1 (1962).

10) The R_f of the thin-layer chromatography with Merck silica gel G refers to the *n*-butanol-acetic acid-pyridine-water (4 : 1 : 1 : 2, v/v) system. Compounds possessing a free amino group were detected by spraying with ninhydrin, and those with blocked amino groups, by spraying with 47% hydrobromic acid and then with ninhydrin.

addition of water (20 ml.) was collected and recrystallized from methanol-ether; yield, 352 mg. (80%); m. p. 201—202°C; $[\alpha]_D^{16}$ +2.1° (*c* 2, dimethylformamide).

Found: C, 59.76; H, 6.60; N, 13.36. Calcd. for $C_{41}H_{54}O_{10}N_8$: C, 60.13; H, 6.65; N, 13.68%.

***p*-Methoxybenzyloxycarbonyl-δ-benzyloxycarbonyl-L-ornithyl-L-leucyl-D-phenylalanylglycylglycyl-δ-benzyloxycarbonyl-L-ornithyl-L-leucyl-D-phenylalanylglycylglycine (XIV).** — The following operations were carried out in a cold room. Into a chilled solution of XIII (820 mg.) in dimethylformamide (12 ml.), 1.22 N hydrochloric acid (2.45 ml.) and sodium nitrite (83 mg.) in water (2 ml.) were stirred. After 5 min., cold water (80 ml.) was added to the solution. The azide, which precipitated as a white mass, was collected by filtration and washed with cold water, 4% sodium bicarbonate, and water, and then dried under a vacuum in a desiccator. The azide was added to a solution of XII (735 mg.) and triethylamine (0.28 ml.) in dimethylformamide (15 ml.). The mixture was stirred for 3 days at 0°C and then evaporated in vacuo. The precipitate which formed upon the addition of ethyl acetate (8 ml.) and ether (4 ml.) was collected, washed with 0.5 M citric acid, and water, and dried. Recrystallization from dioxane-ether did not raise the melting point. The yield was 971 mg. (66%); m. p. 235°C (decomp.); $[\alpha]_D^{16}$ +0.4° (*c* 2, dimethylformamide); R_f 0.87,[10] R_f of the hydrogenolyzed product of XIV, 0.52[10] and 0.69[8].

Found: C, 60.44; H, 6.50; N, 11.63. Calcd. for $C_{73}H_{94}O_{18}N_{12}\cdot 2H_2O$: C, 60.31; H, 6.59; N, 11.56%.

***p*-Methoxybenzyloxycarbonyl-δ-benzyloxycarbonyl-L-ornithyl-L-leucyl-D-phenylalanylglycylglycyl-δ-benzyloxycarbonyl-L-ornithyl-L-leucyl-D-phenylalanylglycylglycine *p*-Nitrophenyl Ester (XV).**—To a solution of XIV (855 mg.) in a mixture of dimethylformamide (4.5 ml.) and pyridine (1.46 ml.), di-*p*-nitrophenyl sulfite[11] (1.94 g.) was added. After the mixture had then been allowed to stand for 20 hr. at room temperature, the solvent was removed in vacuo and the residual oil was solidified by the addition of a mixture of ether and petroleum ether (1 : 1). The product was collected by filtration and washed with a mixture of ether and petroleum ether (1 : 1) until no yellow color could be discerned upon the addition of N sodium hydroxide to the filtrate. The yield was 920 mg. The *p*-nitrophenyl ester content in this product was spectrophotometrically estimated to be 98% by measuring the optical density of the compound at 412 mμ.[5,12]

***p*-Methoxybenzyloxycarbonylglycyl-δ-benzyloxycarbonyl-L-ornithine Ethyl Ester (XVI).** — *p*-Methoxybenzyloxycarbonylglycine[5] (1.19 g.) was coupled with δ-benzyloxycarbonyl-L-ornithine ethyl ester *p*-toluenesulfonate[1] (2.32 g.) by dicyclohexylcarbodiimide (1.03 g.), following essentially the same procedure as that employed in the preparation of IV. As a minor alternation, however, 0.5 M citric acid was used instead of 2% hydrochloric acid to wash the reaction mixture. Recrystallization from ethyl acetate-ether gave 1.59 g. (62%); m. p. 102°C; $[\alpha]_D^{20}$ −6.0° (*c* 2, dimethylformamide).

Found: C, 60.44; H, 6.29; N, 7.89. Calcd. for $C_{26}H_{33}O_8N_3$: C, 60.57; H, 6.45; N, 8.15%.

***p*-Methoxybenzyloxycarbonylglycyl-δ-benzyloxycarbonyl-L-ornithine Hydrazide (XVII).**—XVI (1.38 g.) was converted to the hydrazide (XVII) as has been described in the case of XIII; yield, 1.21 g. (90%). For analysis, a part of the product was recrystallized from dioxane-ether; m. p. 170—171°C; $[\alpha]_D^{20}$ −1.3° (*c* 2, dimethylformamide).

Found: C, 57.42; H, 6.13; N, 13.96. Calcd. for $C_{24}H_{31}O_7N_5$: C, 57.47; H, 6.23; N, 13.97%.

L-Leucyl-D-phenylalanylglycine Ethyl Ester Hydrochloride (XVIII).—Benzyloxycarbonyl-L-leucyl-D-phenylalanylglycine ethyl ester[3] (3.98 g.) was subjected to hydrogenolysis as has been described in the case of V. The oily residue was crystallized by the addition of ether; yield, 3.14 g. (97%); m. p. 182—184°C; $[\alpha]_D^{20}$ +68.8° (*c* 0.5, dimethylformamide); R_f 0.90[8] and 0.75[10].

Found: C, 55.65; H, 7.74; N, 10.27. Calcd. for $C_{19}H_{30}O_4N_3Cl\cdot 1/2H_2O$: C, 55.80; H, 7.64; N, 10.28%.

XVIII had been obtained in this laboratory as an oily product earlier.[3]

***p*-Methoxybenzyloxycarbonylglycyl-δ-benzyloxycarbonyl-L-ornithyl-L-leucyl-D-phenylalanylglycine Ethyl Ester (XIX).**—XVII (3.77 g.), in a mixture of glacial acetic acid (30 ml.) and 3.0 N hydrochloric acid (7.6 ml.), was treated with an aqueous solution of sodium nitrite (570 mg.) at −5°C. After 5 min., cold water (100 ml.) was added to the mixture. The azide was then extracted with ethyl acetate, and the organic layer was washed with 4% sodium bicarbonate and water, and dried over sodium sulfate. The filtered solution was added to a solution of XVIII (3.07 g.) and triethylamine (1.05 ml.) in dimethylformamide (15 ml.). The mixture was stirred for 3 days at 0°C and then evaporated in vacuo to a small volume. The precipitate which formed upon the addition of water was collected, washed with 0.5 M citric acid, 4% sodium bicarbonate, and water, and dried. Recrystallization from methanol-dixoane-ether gave 4.90 g. (78%) of XIX; m. p. 180—181°C; $]\alpha]_D^{20}$ +1.0° (*c* 2, dimethylformamide); R_f 0.90[10]; R_f of hydrogenolyzed product of XIX, 0.74[8] and 0.68[10].

Found: C, 61.67; H, 6.76; N, 10.14. Calcd. for $C_{43}H_{56}O_{11}N_6$: C, 62.00; H, 6.67; N, 10.09%.

***p*-Methoxybenzyloxycarbonylglycyl-δ-benzyloxycarbonyl-L-ornithyl-L-leucyl-D-phenylalanylglycine (XX).**—To a solution of XIX (1.67 g.) in a mixture of methanol (10 ml.) and dioxane (5 ml.), 2 N sodium hydroxide (1.1 ml.) was added. After the solution had then been allowed to stand overnight at room temperature, the desired product was obtained by the procedure described in the case of XI. It was recrystallized from dioxane-ether; yield, 1.50 g. (93%); m. p. 157—159°C; $[\alpha]_D^{20}$ −1.5° (*c* 2, dimethylformamide); R_f 0.74.[10]

Found: C, 60.60; H, 6.45; N, 10.43. Calcd. for $C_{41}H_{52}O_{11}N_6\cdot 1/2H_2O$: C, 60.50; H, 6.56; N, 10.33%.

Glycyl-δ-benzyloxycarbonyl-L-ornithyl-L-leucyl-D-phenylalanylglycine Hydrochloride (XXI).—To a solution of XX (1.29 g.) and anisole (0.4 ml.) in dioxane (8 ml.), 3.9 N hydrogen chloride in dioxane (8 ml.) was added at room temperature. After 2 hr., the solution was evaporated to dryness in vacuo and the residue was collected with the aid of ether; yield,

11) B. Iselin and R. Schwyzer, *Helv. Chim. Acta*, **43**, 1760 (1960).

12) R. Schwyzer and P. Sieber, ibid., **40**, 624 (1957).

1.10 g. (98%); m. p. 188—191°C; $[\alpha]_D^{20}$ −7.6° (*c* 2, dimethylformamide); R_f 0.87[8] and 0.69[10].

Found: C, 55.48; H, 6.96; N, 12.12. Calcd. for $C_{32}H_{45}O_8N_6Cl \cdot H_2O$: C, 55.28; H, 6.82; N, 12.09%.

***p*-Methoxybenzyloxycarbonylglycyl-δ-benzyloxycarbonyl-L-ornithyl-L-leucyl-D-phenylalanylglycine Hydrazide (XXII).**—XIX (1.67 g.) was converted to the hydrazide (XXII) as has been described in the case of XIII; yield, 1.60 g. (97%). For analysis, a part of the product was recrystallized from methanol-ether; m. p. 163—164°C; $[\alpha]_D^{20}$ −2.5° (*c* 2, dimethylformamide).

Found: C, 59.47; H, 6.65; N, 13.38. Calcd. for $C_{41}H_{54}O_{10}N_8 \cdot 1/2H_2O$: C, 59.48; H, 6.67; N, 13.54%.

***p*-Methoxybenzyloxycarbonylglycyl-δ-benzyloxycarbonyl-L-ornithyl-L-leucyl-D-phenylalanylglycylglycyl-δ-benzyloxycarbonyl-L-ornithyl-L-leucyl-D-phenylalanylglycine (XXIII).**—To XXII (828 mg.) in dimethylformamide (10 ml.), 1.22 N hydrochloric acid (2.45 ml.) and sodium nitrite (83 mg.) in water (1 ml.) water added at 0°C. After 7 min., cold water (70 ml.) was added to the solution. The azide which formed was extracted with ethyl acetate (100 ml.), and the extract was treated as has been described in the case of XIX. The solution of the azide was added to a solution of XXI (695 mg.) and triethylamine (0.28 ml.) in dimethylformamide (25 ml.). Then, the desired acyldecapeptide (XXIII) was obtained by the procedure used in the preparation of XIV. It was recrystallized from dioxane-ether; yield, 1.01 g. (70%); m. p. 239—242°C; $[\alpha]_D^{20}$ −0.6° (*c* 2, dimethylformamide); R_f 0.75[10]; R_f of hydrogenolyzed product of XXIII, 0.68[8] and 0.35[10].

Found: C, 60.92; H, 6.68; N, 11.78. Calcd. for $C_{73}H_{94}O_{18}N_{12} \cdot H_2O$: C, 60.65; H, 6.62; N, 11.63%.

***p*-Methoxybenzyloxycarbonylglycyl-δ-benzyloxycarbonyl-L-ornithyl-L-leucyl-D-phenylalanylglycylglycyl-δ-benzyloxycarbonyl-L-ornithyl-L-leucyl-D-phenylalanylglycine *p*-Nitrophenyl Ester (XXIV).**—A solution of XXIII (723 mg.) and di-*p*-nitrophenyl sulfite (1.62 g.) dissolved in pyridine (7.5 ml.) was allowed to stand overnight at room temperature and then treated in the manner described in the case of XV. The powder obtained weighed 770 mg. The *p*-nitrophenyl-ester content of this product was estimated to be 81%. The product was used for the next reaction without further purification.

Cyclo-(glycyl-δ-benzyloxycarbonyl-L-ornithyl-L-leucyl-D-phenylalanylglycyl)$_2$ (XXVI). — *a) From XV.*—To XV (890 mg.) and anisole (0.5 ml.), trifluoroacetic acid (4 ml.) was added at −5°C. After 20 min., the solution was evaporated in vacuo at 0°C, and the residue was triturated with ether. The decapeptide *p*-nitrophenyl ester trifluoroacetate (XXV) was collected in a cold room by filtration, washed with ether, and dissolved in dimethylformamide (18 ml.) containing glacial acetic acid (0.4 ml.). The solution was then stirred, drop by drop, into pyridine (180 ml.) which had been kept at 60—65°C over a period of 6 hr.; the stirring was then continued for an additional 2 hr. at the same temperature. After the solvent had been removed, the residue was dissolved in a mixture of methanol (200 ml.) and water (80 ml.). The insoluble substance was removed by filtration, and the filtrate was passed successively through columns (2.5×10 cm.) of Dowex 1 (OH^- form) and Dowex 50 (H^+ form). The columns were then washed with the same solvent (300 ml.), the combined effluents were evaporated to dryness in vacuo, and the product was suspended in water (20 ml.), collected by filtration, and dried (174 mg.). This substance was then recrystallized from methanol-ethyl acetate-ether; yield of the air-dried product, 153 mg. (21% from XIV); m. p. 274—275°C (decomp.); $[\alpha]_D^{20}$ −5.0° (*c* 0.51, dimethylformamide); R_f 0.90.[10]

Found: C, 60.56; H, 6.83; N, 13.31. Calcd. for $C_{64}H_{84}O_{18}N_{12} \cdot H_2O$: C, 60.83; H, 6.86; N, 13.30%.

The air-dried product lost 1.40% of its weight after it had been dried for 2 hr. at 115°C, 2 mmHg. Calcd. for H_2O: 1.43%. The molecular weight[13] was determined by the micro Rast method using a solvent of hexahydro-*p*-aminobenzoic acid lactam.[14]

Found: 1100. Calcd. for $C_{64}H_{84}O_{18}N_{12}$: 1245.

b) From XXIV.—XXIV (765 mg.) was converted to the decapeptide active ester trifluoroacetate (XXVII) as has been described above. XXVII was allowed to react in pyridine (180 ml.), after with a treatment similar to that mentioned above was further carried out to give a crude cyclic product (284 mg.). This was recrystallized from methanol-ethyl acetate-ether; yield of the air-dried product, 233 mg. (36% from XXIII); m. p. 274—276°C (decomp.); $[\alpha]_D^{20}$ −4.9° (*c* 1, dimethylformamide); R_f 0.90.[10]

Found: C, 60.70; H, 6.82; N, 13.35. Calcd. for $C_{64}H_{84}O_{14}N_{12} \cdot H_2O$: C, 60.83; H, 6.86; N, 13.30%.

The molecular weight was determined by the micro Rast method described above. Found: 1030. Calcd. for $C_{64}H_{84}O_{14}N_{12}$: 1245.

Cyclo-(glycyl-L-ornithyl-L-leucyl-D-phenylalanylglycyl)$_2$ Dihydrochloride (II·2HCl). — A solution of XXVI (84 mg.) in glacial acetic acid (2 ml.) was subjected to hydrogenolysis in the presence of palladium black. The filtrate from the catalyst was evaporated to dryness in vacuo. The residue was dissolved in a mixture of methanol (1 ml.) and dioxane (1 ml.), and then 0.4 N hydrogen chloride in dioxane (0.5 ml.) was added to the solution. After the solution had then been evaporated in vacuo, the resulting crystals were filtered with the aid of a mixture of ether and petroleum ether (1 : 1); yield of the air-dried product, 59 mg. (84%); m. p. 239—242°C (decomp.); $[\alpha]_D^{20}$ −42.0° (*c* 0.5, acetic acid); R_f 0.88[8] and 0.65.[10] The amino acid analysis[3] gave the molar ratio of 1.9 : 1.1 : 1.0 : 1.1 for glycine, ornithine, leucine and phenylalanine.

Found: C, 51.52; H, 7.47; N, 14.91. Calcd. for $C_{48}H_{74}O_{10}N_{12}Cl_2 \cdot 4H_2O$: C, 51.37; H, 7.37; N, 14.98%.

The air-dried product lost 6.6% of its weight after it had been dried over phosphorus pentoxide for 3 hr. at 80°C; 2 mmHg. Calcd. for $4H_2O$: 6.4%.

***p*-Methoxybenzyloxycarbonyl-δ-benzyloxycarbonyl-L-ornithyl-L-leucyl-D-phenylalanylglycylglycine *p*-Nitrophenyl Ester (XXVIII).**—To a solution of XI (393 mg.) in a mixture of dimethylformamide (1 ml.) and pyridine (1,2 ml.), di-*p*-nitrophenyl sulfite

13) The molecular weight determination by the use of an osmometer of Mechrolab, Inc., could not be applied to the protected cyclic decapeptide (XXVI) and pentapeptide (XXXI) because these products are insoluble in methanol or dioxane at room temperature.

14) G. Went, *Ber.*, **75**, 425 (1942).

(640 mg.) was added. The mixture was then allowed to stand overnight at room temperature. After evaporation, the residual oil was triturated with petroleum ether and washed with a mixture of ether and petroleum ether (1 : 1) by decantation until no yellow color could be discerned on the addition of a sodium hydroxide solution to the washings. The product was collected by filtration and dried. It weighed 373 mg. The *p*-nitrophenyl ester content of this product was estimated to be 70%.

***p*-Methoxybenzyloxycarbonylglycyl-δ-benzyloxycarbonyl-L-ornithyl-L-leucyl-D-phenylalanylglycine *p*-Nitrophenyl Ester (XXIX).**—A solution of XX (403 mg.) and di-*p*-nitrophenyl sulfite (975 mg.) dissolved in pyridine (3 ml.) was allowed to stand overnight at room temperature; then it was treated as above. The *p*-nitrophenyl ester content of this product was estimated to be 94%.

Cyclo-glycyl-δ-benzyloxycarbonyl-L-ornithyl-L-leucyl-D-phenylalanylglycyl (XXXI). — *a) From XXVIII.*—XXVIII (368 mg.) and anisole (0.2 ml.) were dissolved in trifluoroacetic acid (1 ml.) at −5°C. After 20 min., the solution was concentrated to a small volume in vacuo at 0°C, and then the residue was triturated with ether. The *p*-nitrophenyl ester trifluoroacetate (XXX) collected was dissolved in dimethylformamide (4 ml.) containing glacial acetic acid (0.1 ml.). The solution was stirred, drop by drop, into pyridine (80 ml.), which had been kept at 55—60°C over a period of 4 hr.; the stirring was then continued for an additional 2 hr. at the same temperature. After the solvent had been removed, the residue was dissolved in a mixture of methanol (50 ml.) and water (20 ml.). The insoluble substance was filtered off, and the filtrate was passed through columns of Dowex 1 and Dowex 50. The columns were eluted with the same solvent, the combined effluents were evaporated to dryness in vacuo, and the residue was collected by filtration with the aid of water (77 mg.). It was recrystallized from methanol-ether; yield, 71 mg. (32% form XI); m. p. 282—283°C (decomp.); $[\alpha]_D^{15}$ −49.7° (*c* 1.01, dimethylformamide); R_f 0.79.[10]

Found: C, 61.63; H, 6.67; N, 13.41. Calcd. for $C_{32}H_{42}O_7N_6$: C, 61.72; H, 6.80; N, 13.50%.

The molecular weight was determined by the micro Rast method. Found: 600. Calcd. for $C_{32}H_{42}O_7N_6$: 623.

b) From XIII.—To XIII (234 mg.) and anisole (0.1 ml.), trifluoroacetic acid (0.32 ml.) was added at −5°C. After 30 min., the solution was evaporated in vacuo at 0°C, and the residue was triturated with ether. The hydrazide ditrifluoroacetate (XXXII) was collected by filtration. To a solution of XXXII in water (2 ml.), 0.1 N hydrochloric acid (3.1 ml.) and sodium nitrite (22.3 mg.) in water (0.5 ml.) were added at −5°C. After 15 min., the reaction mixture was added to a solution of water (200 ml.) containing sodium bicarbonate (1.2 g.) and dioxane (100 ml.) at 0°C. The mixture was stirred for 2 days at 0°C; then it was brought to pH 5.0 with N hydrochloric acid. The mixture was evaporated in vacuo, and the residue was collected by filtration with the aid of 5 ml. of water (120 mg.). This was treated in a mixture of methanol (90 ml.) and water (30 ml.). The insoluble substance was filtered off, and then the filtrate was passed through columns, as has been mentioned above. The combined effluents were evaporated in vacuo to dryness; yield of crude product, about 8% from XIII. A solution, after the hydrogenolysis of the crude product in methanol containing hydrogen chloride, showed only one spot on paper and thin-layer chromatograms, a spot which was in a position identical with that of III·HCl obtained from XXX or XXXIII.

c) From XXIX.—XXIX (460 mg.) was converted to the pentapeptide active ester trifluoroacetate (XXXIII) by the method described for XXX. XXXIII was allowed to react in pyridine (160 ml.), and the reaction mixture was treated as has been described in the case of XXXI a). The combined effluents obtained after passing through the ion-exchangers were evaporated to dryness; the crude product which resulted weighed 136 mg. (XXXIV). A few mg. of XXXIV was subjected to hydrogenolysis, and the solution was submitted to CM-cellulose column chromatography and paper electrophoresis. The chromatography showed only one peak or spot resulting from presence of III. Therefore, it was concluded that the product (XXXIV) contains only protected cyclic pentapeptide (XXXI). XXXIV was recrystallized from methanol-ether; yield, 115 mg. (37% from XX); m. p. 281—282°C (decomp.); $[\alpha]_D^{20}$ −50.1° (*c* 1, dimethylformamide); R_f 0.80.[10]

Found: C, 61.70; H, 7.04; N, 13.35. Calcd. for $C_{32}H_{42}O_7N_6$: C, 61.72; H, 6.80; N, 13.50%.

The molecular weight was determined by the micro Rast method. Found: 610. Calcd. for $C_{32}H_{42}O_7N_6$: 623.

Cyclo-glycyl-L-ornithyl-L-leucyl-D-phenylalanylglycyl Hydrochloride (III·HCl).—A solution of XXXI (53.2 mg.) in glacial acetic acid (1 ml.) was subjected to hydrogenolysis in the presence of palladium black, and then treated with the method which has been described in the case of II·2HCl. Yield of the air-dried product, 38.2 mg. (85%); m. p. 270—272°C (decomp.); $[\alpha]_D^{20}$ −54.4° (*c* 0.5, acetic acid); R_f 0.81[8] and 0.61.[10] The amino acid analysis[3] gave the molar ratio of 1.9 : 1.1 : 1.0 : 1.0 for glycine, ornithine, leucine and phenylalanine.

Found: C, 53.47; H, 7.09; N, 15.17. Calcd. for $C_{24}H_{37}O_5N_6Cl\cdot H_2O$: C, 53.08; H, 7.23; N, 15.47%.

The air-dried product lost 3.19% of its weight after it had been dried over phosphorus pentoxide 3 hr. at 80°C; 2 mmHg. Calcd. for H_2O: 3.31%.

Chromatography and Electrophoresis of II, III and Gramicidin S (I).—A sample (0.5—1 mg.) was dissolved in 0.2—0.3 ml. of 0.2 M pyridinium acetate containing 30% methanol (pH 5.1); the solution was then applied to a column (0.9×50 cm.) with carboxymethyl cellulose (Eastmen Organic Chem. 7796), and development was continued with the same solvent. Two-ml. fractions were collected at a flow rate of 20 ml. per hour. The peptide content in the fractions was determined by the method described by Yemm and Cocking.[15] Gramicidin S was used as a control. The results are shown in Fig. 6. In order to determine the sensibilities for ninhydrin with the cyclic peptides, II and III, a solution containing 1 μ mole of III and 0.5 μ mole of II was also submitted to column chromatography; the ratio of intensities caused by ninhydrin between III and II was found to be 5 : 4 by calculating

15) E. W. Yemm and E. C. Clcking, *Analyst*, **80**, 209 (1955); *Biochem. J.*, **58**, xii (1954).

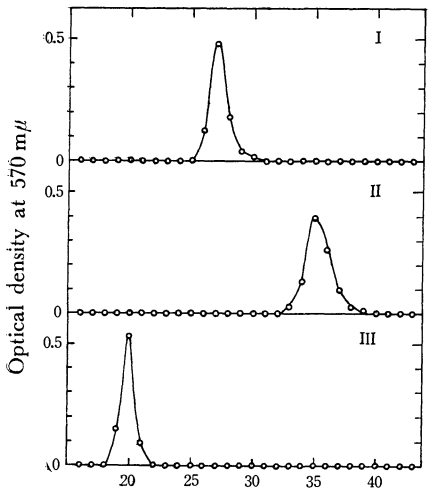

Fig. 6. Carboxymethylcellulose column chromatography of II, III and gramicidin S (I).

the areas in a chromatogram of the optical density-fraction number.

Electrophoresis on Toyo Roshi No. 52 paper was carried out with a formic acid - acetic acid - methanol - water (1 : 3 : 6 : 10, v/v; pH 1.8) solvent system for 3 hr. at 500 V./30 cm. The peptides were detected with ninhydrin. Figure 7 shows that II migrates faster toward the cathode than III, and that the mobility of

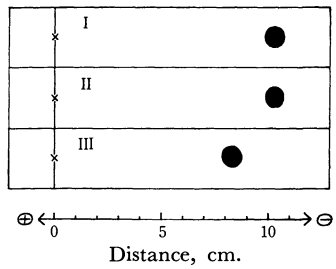

Fig. 7. Paper electrophoresis of II, III and gramicidin S (I).

II is indistinguishable from that of gramicidin S (I).

Microbiological Assays. — The microorganisms employed are *E. coli*, *P. vulgaris*, *S. aureus*, *B. subtilis* and *M. avium*. A minimum amount of compound for complete inhibition of growth was determined by a dilution method with a bouillon agar medium and with a synthetic medium. Synthetic cyclic peptides II and III exhibited no antibacterial activity against any of the microorganisms tested even at levels of 100 γ per ml. of assays medium, whereas gramicidin S exhibited considerable activity against some of the microorganisms.

The authors wish to express their thanks to Dr. Motoo Shibata of Takeda Chemical Industries, Ltd. for the microbiological assays. The authors are also indebted to Ajinomoto Co., Inc. and Kyowa Hakko Kogyo Co., Ltd. for supplying some amino acids.

BULLETIN OF THE CHEMICAL SOCIETY OF JAPAN VOL. 39 2242—2249 (1966)

Studies of Peptide Antibiotics. VII. The Synthesis of Cyclo-D-phenylalanyl-D-leucyl-L-ornithyl-L-valyl-D-ornithyl-L-prolyl

By Tetsuo KATO and Nobuo IZUMIYA

Laboratory of Biochemistry, Faculty of Science, Kyushu University, Fukuoka

(Received March 14, 1966)

A cyclic hexapeptide, cyclo-D-phenylalanyl-D-leucyl-L-ornithyl-L-valyl-D-ornithyl-L-prolyl, was once reported to be an antibiotic gramicidin J_2, and the synthesis of the compound was described also. However, the natural occurrence of gramicidin J_2 was denied recently. For the purpose of comparing its antibacterial activity, if any, with gramicidin S, the synthesis of this compound was carried out. *p*-Methoxybenzyloxycarbonyl-D-phenylalanyl-D-leucyl-*δ*-benzyloxycarbonyl-L-ornithyl-L-valyl-*δ*-benzyloxycarbonyl-D-ornithyl-L-proline *p*-nitrophenyl ester was prepared, and, after the selective cleavage of *p*-methoxybenzyloxycarbonyl group, the hexapeptide ester was transformed to the cyclic benzyloxycarbonyl hexapeptide, which was then hydrogenated to afford the desired cyclic hexapeptide as dihydrochloride. The effects of the synthesized cyclic peptide on bacterial growth have been examined. No antibacterial activities were observed in reaction to the microorganisms utilized here.

A number of polypeptide antibiotics, such as gramicidin S, have three characteristic features in common; namely, the occurrence of D-amino acids, basic amino acids, and a cyclic structure in the molecule. For a study of the relationship between the chemical structure and the biological activities of peptide antibiotics, some dipeptide anhydrides, which are the simplest compounds possessing the characteristics mentioned above, were synthesized; however, these were all devoid

of any antibacterial activity.[1] A cyclic hexapeptide, cyclo-L-valyl-L-ornithyl-L-leucyl-D-phenylalanyl-L-prolylglycyl, which contains the partial amino acid sequence found in gramicidin S and tyrocidines, was then prepared, and its biological activity examined. However, in spite of its apparent resemblance to those natural antibiotics, this compound also was found to be inactive.[2] Thus, it was concluded that even the occurrence of a hexapeptide ring structure may not be a sufficient condition for a molecule to exhibit antibacterial activity. These results prompted the present study of another cyclic hexapeptide, cyclo-D-phenylalanyl-D-leucyl-L-ornithyl-L-valyl-D-ornithyl-L-prolyl (XXIV), which has been demonstrated to be an antibiotic named gramicidin J_2.[3]

D-Phe-D-Leu-L-Orn-L-Val-D-Orn-L-Pro

XXIV

Previously Noda[3] isolated an antibiotic peptide from a culture of *Bacillus brevis Nagano* and proposed its chemical structure to be that shown as XXIV. He furthermore reported a method of the chemical synthesis of the compound corresponding to XXIV, and described that the product synthesized was identical with natural gramicidin J_2.[4] Nevertheless, Kurahashi[5] and Otani and Saito[6] reported that natural gramicidin J_2 is the same compound as gramicidin S, a cyclic decapeptide.

To elucidate the ambiguity described above, the present authors attempted to synthesize the cyclic hexapeptide with the structure of XXIV and to test its antibacterial activity.

The sequence of reaction employed for the synthesis of the acylhexapeptide ester (XVII) is indicated in Figs. 1 and 2. The proline residue was selected as the *C*-terminal amino acid in a linear hexapeptide in order to avoid otherwise possible racemization. *p*-Methoxybenzyloxycarbonyl and benzyloxycarbonyl groups were employed for the selective blocking of the *N*-terminal amino group and the δ-amino group of ornithine residue respectively.

As is shown in Fig. 1, the *C*-terminal dipeptide derivative, the *t*-butyloxycarbonyl-δ-benzyloxycarbonyl-D-ornithyl-L-proline ethyl ester (IV), was prepared via three different methods: (a) the mixed anhydride method,[7] (b) the active ester method using the diacyl D-ornithine *p*-nitrophenyl ester (III),[8] and (c) the dicyclohexylcarbodiimide method.[9] The last method gave the highest yield. The protected tripeptide ester (IX) was secured via two ways; (a) stepwise elongation from *C*-terminal amino acid, and (b) fragment condensation via the azide method. The former method gave a slightly better yield, but the latter method furnished two well-defined crystalline intermediate compounds, VII and VIII.

As is shown in Fig. 2, the *N*-terminal tripeptide derivative, the *p*-methoxybenzyloxycarbonyl-D-phenylalanyl-D-leucyl-δ-benzyloxycarbonyl-L-ornithine ethyl ester (XV), was obtained via stepwise elongation and converted to the corresponding hydrazide (XVI). However, the protected hexapeptide ester (XVII), derived from the azide of XVI and X, showed resistance to saponification. Hence, the preparation of the protected hexapeptide (XX) was carried out as is shown in Fig. 3.

Figure 3 indicates the route for the synthesis of the cyclic hexapeptides (XXIII, XXIV). XX was prepared by the coupling reaction of tripeptide azide (from XVI) with neutral free tripeptide (from XIX), and then XX was converted to the protected hexapeptide *p*-nitrophenyl ester (XXII). The removal of the *p*-methoxybenzyloxycarbonyl group from XXII by treatment with trifluoroacetic acid yielded the hexapeptide *p*-nitrophenyl ester trifluoroacetate. The cyclization reaction of the trifluoroacetate in pyridine gave the benzyloxycarbonyl-substituted cyclic peptide (XXIII), which was then purified by passing it through columns of Dowex 50 (H^+ form) and Dowex 1 (OH^- form). The molecular-weight determination using a vapor pressure osmometer demonstrated that the molecular size of XXIII corresponds to that of cyclic hexapeptide. The final product, XXIV, was obtained, upon the hydrogenolysis of XXIII in the presence of two equivalents of hydrogen chloride, as crystalline dihydrochloride, with five moles of water. The treatment of XXIII with hydrogen bromide in acetic acid furnished the corresponding cyclohexapeptide hydrobromide (the hydrobromide of XXIV). The homogeneity and identity of the two products ($XXIV \cdot 2HCl \cdot 5H_2O$ and hydrobromide of XXIV) was established by paper, thin-layer, and carboxymethyl cellulose column chromatography and by paper electrophoresis.

The chromatographic behavior and several other characteristics of the synthesized product, $XXIV \cdot 2HCl \cdot 5H_2O$, were compared with those

1) N. Izumiya, T. Kato, Y. Fujita, M. Ohno and M. Kondo, This Bulletin, **37**, 1809 (1964).
2) T. Kato, M. Kondo, M. Ohno and N. Izumiya, ibid., **38**, 1202 (1965).
3) Y. Noda, *J. Chem. Soc. Japan, Pure Chem. Sect. (Nippon Kagaku Zasshi)*, **79**, 662 (1958).
4) Y. Noda, ibid., **80**, 411 (1959).
5) K. Kurahashi, *J. Biochem.*, **56**, 101 (1964).
6) S. Otani and Y. Saito, ibid., **56**, 103 (1964).
7) J. R. Vaughan, Jr., *J. Am. Chem. Soc.*, **73**, 3547 (1951); J. R. Vaughan, Jr., and J. A. Eichler, ibid., **75**, 5556 (1953); R. A. Boissonnas, *Helv. Chim. Acta*, **34**, 874 (1951); T. Wieland, W. Kern and R. Sehring, *Ann.*, **569**, 117, 122 (1950).
8) M. Bodansky, *Nature*, **175**, 685 (1955); M. Bodansky and V. du Vigneaud, *J. Am. Chem. Soc.*, **81**, 5688 (1959).
9) J. C. Sheehan and G. P. Hess, ibid., **77**, 1067 (1955).

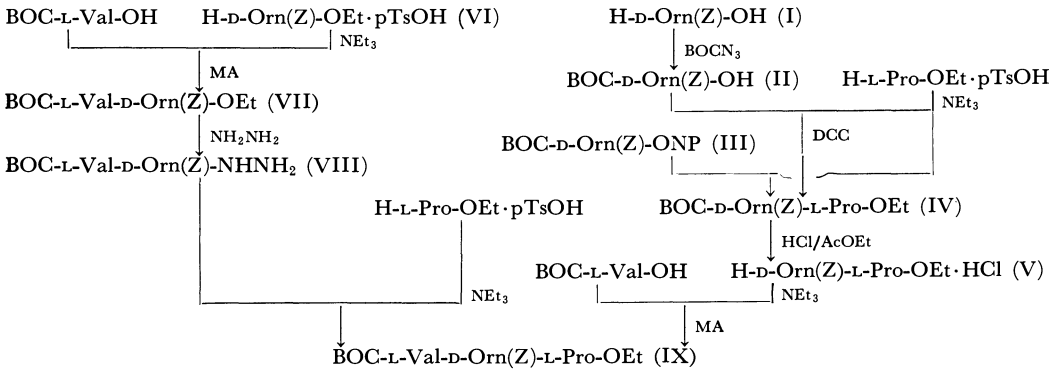

Fig. 1. The abbreviations used are: BOC, *t*-butyloxycarbonyl; Z, benzyloxycarbonyl; pMZ, *p*-methoxybenzyloxycarbonyl; NEt_3, triethylamine; DCC, dicyclohexylcarbodiimide; MA, mixed anhydride; OEt, ethyl ester; ONP, *p*-nitrophenyl ester; pTsOH, *p*-toluenesulfonic acid.

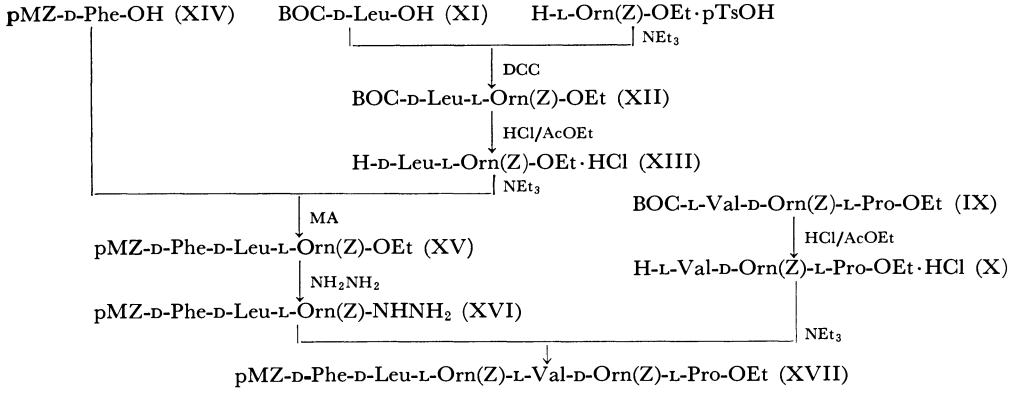

Fig. 2.

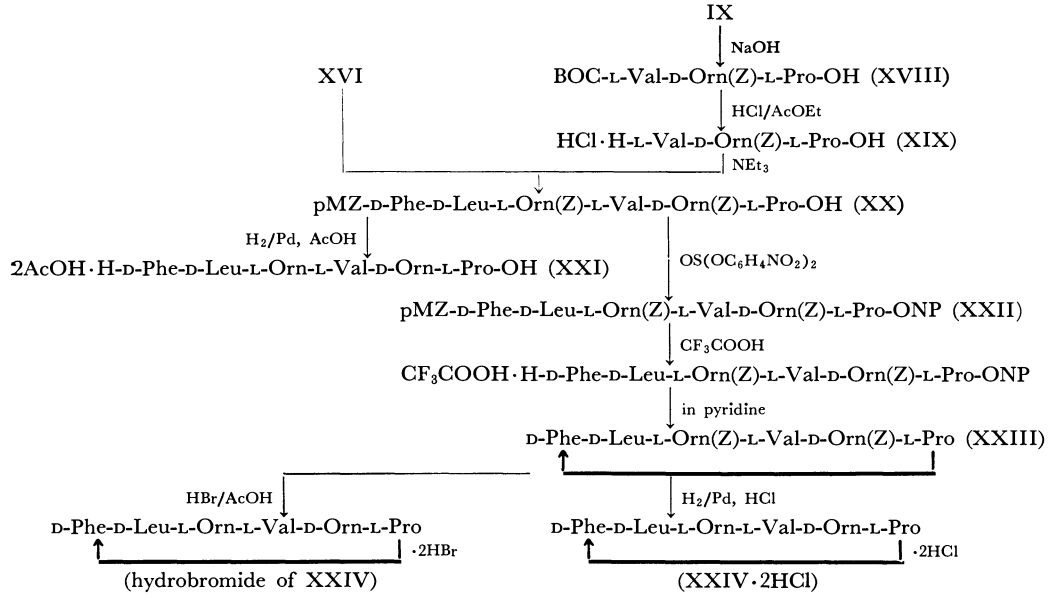

Fig. 3.

Table I. Comparison of XXIV with gramicidin S

	XXIV·2HCl·5H$_2$O	XXIV·2HCl by Noda[4]	Gramicidin S
Melting point	242—244°C (decomp.)	279—280°C (decomp.)	277—278°C (decomp.)[a,10]
Specific rotation	$+15.3°\left(\begin{smallmatrix}c\ 0.3,\ \mathrm{EtOH}\\ t=18°\mathrm{C}\end{smallmatrix}\right)$	$-313.1°\left(\begin{smallmatrix}c\ 0.4,\ \mathrm{EtOH}\\ t=14°\mathrm{C}\end{smallmatrix}\right)$	$-295°\left(\begin{smallmatrix}70\%\ \mathrm{EtOH}\\ t=21°\mathrm{C}\end{smallmatrix}\right)^{a,11}$
R_f on silica gel	0.69		0.80[b]
on paper[c]	0.64	0.90	0.94[b]
Electrophoretic mobility (related to lysine) in solvent (i) pH 1.8	0.64		0.60[b]
in solvent (ii) pH 7.0	0.95		0[b]

a) Reported value for gramicidin S dihydrochloride.
b) Observed value for gramicidin S sulfate octahydrate, Astra Co., U.S.A.
c) The solvent used in this case was *n*-butanol - acetic acid - water (4: 1: 1, v/v).

of gramicidin S. These two cyclic peptides were quite different from each other in chromatographic behavior. Moreover, such constants as the specific rotation of XXIV·2HCl·5H$_2$O observed were quite different from those of XXIV·2HCl reported by Noda.[4] Table I compares the physical constants and R_f values of XXIV·2HCl·5H$_2$O synthesized in this paper and described by Noda,[4] and those of gramicidin S.

The antibacterial activity of XXIV·2HCl·5H$_2$O and gramicidin S in reaction to several microorganisms were examined. XXIV·2HCl·5H$_2$O had no retarding effect on the growth of the microorganisms, even at so high a concentration as 100γ per ml. of the assay medium. Gramicidin S, however, showed substantial activity under these conditions. It should be noted that the antibacterial activity of the product, XXIV·2HCl, synthesized by Noda[4] was reported to be the same as that of gramicidin S.

The findings described in this paper are in marked disagreement with the observations of Noda.[4] The authors have no explanation for the discrepancy between their results and those of Noda.[4,12]

Experimental

All the melting points are uncorrected. The paper chromatography was carried out on Toyo Roshi No. 52 paper. The thin-layer chromatography was carried out on Merck silica gel G. The developing solvent commonly used was *n*-butanol - acetic acid - pyridine - water (4 : 1 : 1 : 2 v/v). Spots of materials possessing a free amino group on a thin-layer plate were detected by spraying ninhydrin, and those of the amino-group-blocked materials, by spraying 47% hydrobromic acid and then ninhydrin. Prior to analysis, the compounds were dried over phosphorus pentoxide to a constant weight at 80°C and 2 mmHg.

Amino Acids.—The amino acids used were as follows: D-phenylalanine, $[\alpha]_D^{24}$ +33.5° (*c* 2, water) (lit. for the L-isomer, −34.5°[13]), was obtained from acetyl-DL-phenylalanine through the asymmetric hydrolytic action of hog renal acylase.[14] D-Leucine, $[\alpha]_D^{24}$ +15.5° (*c* 2, 5 N HCl) (lit. for L-isomer −16.0°[13]), L-ornithine hydrochloride, $[\alpha]_D^{24}$ +21.8° (*c* 2, 5 N HCl) (lit. +22.2°[13]), L-valine, $[\alpha]_D^{24}$ +27.7° (*c* 2, 5 N HCl) (lit. +28.3°[13]), and L-proline, $[\alpha]_D^{24}$ −59.7° (*c* 2, 5 N HCl) (lit. −60.4°[13]), were commercial products. D-Ornithine hydrochloride, $[\alpha]_D^{24}$ −22.6° (*c* 2, 5 N HCl) (lit. for L-isomer +22.2°[13]), was obtained from DL-ornithine hydrochloride through optical resolution, using D-glutamic acid as the resolving reagent.[15]

δ-Benzyloxycarbonyl-D-ornithine (I).—This compound was obtained according to the procedure for the L-isomer.[16] Yield, 87%; m. p. 255°C; $[\alpha]_D^{24}$ −21.1° (*c* 1, 6 N HCl), −21.3° (*c* 1, 50% acetone + 2 eq. HCl) (lit. for L-isomer +17.0°[16]).

Found: C, 58.47; H, 6.85; N, 10.53. Calcd. for $C_{13}H_{18}O_4N_2$: C, 58.63; H, 6.81; N, 10.52%.

α-*t*-Butyloxycarbonyl - δ - benzyloxycarbonyl - D - ornithine (II).—To a stirred solution of I (2.295 g., 8.6 mmol.) and sodium bicarbonate (2.94 g., 35 mmol.) in water (50 ml.) at 50°C, a solution of *t*-butyloxycarbonyl azide[17] (2.419 g., 17 mmol.) in dioxane (50 ml.) was added. After 2 days' stirring at 45°C, the reaction mixture was evaporated to a half volume and extracted with ether. The aqueous layer was then acidified and extracted with ethyl acetate, and the organic layer was dried and evaporated. The residual oil weighed 2.574 g. (82%).

α-*t*-Butyloxycarbonyl - δ - benzyloxycarbonyl - D - ornithine *p*-Nitrophenyl Ester (III).—A solution of II (733 mg., 2 mmol.), dicyclohexylcarbodiimide[9] (412 mg., 2 mmol.) and *p*-nitrophenol (333 mg., 2.4 mmol.) in tetrahydrofuran was stirred for 3 hr. at 0°C, and then for 2.5 hr. at room temperature. After filtration,

10) R. Schwyzer and P. Sieber, *Helv. Chim. Acta*, **40**, 624 (1957).
11) R. L. M. Synge, *Biochem. J.*, **39**, 363 (1945).
12) It may be pointed out that in his paper Noda reported that he had used di-*p*-nitrophenyl sulfide instead of di-*p*-nitrophenyl sulfite in the preparation of the *p*-nitrophenyl ester of trityl-D-phenylalanyl-D-leucyl-δ-tosyl-L-ornithyl-L - valyl - δ - tosyl - D - ornithyl-L-proline, and cited the literature (Org. Syntheses, Vol. 28, p. 82) on the synthesis of di-*p*-nitrophenyl sulfide.
13) J. P. Greenstein and M. Winitz, "The Chemistry of Amino Acid," John Wiley & Sons, New York (1961).
14) S. M. Birnbaum, L. Levintow, R. B. Kingsley and J. P. Greenstein, *J. Biol. Chem.*, **194**, 455 (1952).
15) M. Kondo and N. Izumiya, unpublished.
16) J. I. Harris and T. S. Work, *Biochem. J.*, **46**, 582 (1950).
17) R. Schwyzer, P. Sieber and H. Kappeler, *Helv. Chim. Acta*, **42**, 2622 (1959).

the solution was evaporated to an oil. After the addition of a mixture of ether and petroleum ether (1 : 1, 4 ml.), the solution was stored in a refrigerator overnight. The crystals were filtered off, washed with a mixture of ether and petroleum ether (1 : 1), and dried (683 mg.). Recrystallization from ethyl acetate - ether - petroleum ether gave 611 mg. (63%); m. p. 108°C.

Found: C, 59.13; H, 6.00; N, 8.62. Calcd. for $C_{24}H_{29}O_8N_3$: C, 59.23; H, 5.99; N, 8.69%.

α-*t*-Butyloxycarbonyl-δ-benzyloxycarbonyl-D-ornithyl-L-proline Ethyl Ester (IV).—*a) The Dicyclohexylcarbodiimide Method.*[9]—To a solution of II (1.042 g., 2.85 mmol.), L-proline ethyl ester *p*-toluenesulfonate[18] (967 mg., 3 mmol.), and triethylamine (0.46 ml.) in tetrahydrofuran (6 ml.), dicyclohexylcarbodiimide (618 mg.) was added at 0°C. After the stirring had been continued for 2 hr. at 0°C, and for more 2 hr. at room temperature, the mixture was left to stand overnight. The mixture was then evaporated in vacuo, and the residue was diluted with ethyl acetate (20 ml.). The solution which was separated from the dicyclohexylurea by filtration was washed successively with water, a 4% sodium bicarbonate solution, water, 10% citric acid, and water, and then dried over anhydrous sodium sulfate. The filtrate separated from the salt was evaporated in vacuo. The residual oil weighed 1.316 g. (89%).

b) The p-Nitrophenyl Ester Method.—A solution of III (488 mg., 1 mmol.), L-proline ethyl ester *p*-toluenesulfonate[18] (378 mg., 1.2 mmol.), and triethylamine (0.15 ml.) in chloroform (4 ml.) was prepared and treated as usual.[8] Yield, 266 mg. (53%).

δ-Benzyloxycarbonyl-D-ornithyl-L-proline Ethyl Ester Hydrochloride (V).—To a solution of IV (488 mg., 1 mmol.) in ethyl acetate (5 ml.), 4.38 N hydrogen chloride in ethyl acetate (5 ml.) was added; the reaction mixture was then allowed to stand for 2 hr. at room temperature. After it had been evaporated to dryness, the residual oil weighed 377 mg. (88%).

δ-Benzyloxycarbonyl-D-ornithine Ethyl Ester *p*-Toluenesulfonate (VI).—This compound was prepared according to the procedure of Kato et al.[1] Yield, 80%; $[\alpha]_D^{21}$ −8.9° (*c* 2, dimethylformamide) (lit. for L-isomer +8.9°[1]).

Found: C, 56.47; H, 6.67; N, 5.95. Calcd. for $C_{22}H_{30}O_7N_2S$: C, 56.63; H, 6.48; N, 6.01%.

***t*-Butyloxycarbonyl-L-valyl-δ-benzyloxycarbonyl-D-ornithine Ethyl Ester (VII).**—To a freshly-prepared mixed anhydride of *t*-butyloxycarbonyl-L-valine[17] (2.004 g., 9.22 mmol.), triethylamine (1.29 ml., 9.22 mmol.) and isobutyl chloroformate (1.20 ml., 9.22 mmol.)[7] in tetrahydrofuran (20 ml.), a solution of VI (4.301 g., 9.22 mmol.) and triethylamine (1.29 ml.) in chloroform (20 ml.) was added. The mixture was then washed and dried as has been described for IV. To the dried solution, a mixture of ether and petroleum ether was added, and the solution was stored in a refrigerator. The crystals which precipitated were collected and dried (3.97 g.). Recrystallization from ethyl acetate - ether - petroleum ether gave 3.505 g. (77%); m. p. 123—125°C; $[\alpha]_D^{20}$ −8.2° (*c* 1, acetic acid).

Found: C, 60.70; H, 7.73; N, 8.30. Calcd. for $C_{25}H_{39}O_7N_3$: C, 60.83; H, 7.96; N, 8.51%.

***t*-Butyloxycarbonyl-L-valyl-δ-benzyloxycarbonyl-D-ornithine Hydrazide (VIII).**—A solution of VII (987 mg., 2 mmol.) and hydrazine hydrate (2 ml., 40 mmol.) in dimethylformamide (4 ml.) was allowed to stand for 2 days at room temperature. Upon the addition of water (40 ml.), colorless crystals of VIII were precipitated; these were filtered off, washed with water, and dried (912 mg., 95%); m. p. 174°C; $[\alpha]_D^{20}$ −9.6° (*c* 1, ethanol).

Found: C, 57.60; H, 7.61; N, 14.33. Calcd. for $C_{23}H_{37}O_6N_5$: C, 57.60; H, 7.78; N, 14.60%.

***t*-Butyloxycarbonyl-L-valyl-δ-benzyloxycarbonyl-D-ornithyl-L-proline Ethyl Ester (IX).** — *a) From V and t-Butyloxycarbonyl-L-valine.*—To a freshly-prepared mixed anhydride gel of *t*-butyloxycarbonyl-L-valine[17] (100 mg., 0.46 mmol.), triethylamine (0.064 ml.), and isobutyl chloroformate (0.060 ml.) in tetrahydrofuran (2 ml.), a solution of V (205 mg., 0.46 mmol.) and triethylamine (0.064 ml.) in chloroform (3 ml.) was added. The mixture was treated as has been described for VII. The oily residue obtained weighed 215 mg. (79%).

b) From VIII and L-Proline Ethyl Ester. — The following operations were carried out in a cold room. Into a chilled solution of VIII (735 mg., 1.53 mmol.) in a mixture of glacial acetic acid (2 ml.) and dimethylformamide (4 ml.), N hydrochloric acid (1.7 ml.), 116 mg. of sodium nitrite, and additional N hydrochloric acid (1.7 ml.) were stirred. After 7 min., cold water (40 ml.) was added. The azide which was precipitated as a white mass was extracted thrice with ethyl acetate; the combined extract was washed successively with cold water, a saturated sodium bicarbonate solution, and water, and then dried over anhydrous sodium sulfate. The filtered azide solution was added to a solution of L-proline ethyl ester *p*-toluenesulfonate[18] (483 mg., 1.53 mmol.) and triethylamine (0.21 ml.) in dimethylformamide (10 ml.), and the mixture was stirred for 3 days at 0°C. The solution was evaporated and washed successively with water, a 4% sodium bicarbonate solution, water, 10% citric acid, and water, and then dried over anhydrous sodium sulfate. The filtrate was evaporated in vacuo; the oily residue weighed 728 mg. (81%).

L-Valyl-δ-benzyloxycarbonyl-D-ornithyl-L-proline Ethyl Ester Hydrochloride (X).—A solution of IX (215 mg., 0.36 mmol.) in 2.6 N hydrogen chloride in ethyl acetate (2.8 ml., 7.2 mmol.) was allowed to stand for 2 hr. at room temperature, and then evaporated to dryness in vacuo; the residue weighed 194 mg. Recrystallization from acetone-ether gave 148 mg. (77%) as hygroscopic crystals. R_f 0.93 on paper.

***t*-Butyloxycarbonyl-D-leucine (XI).** — This compound was prepared according to the general procedure of Schwyzer et al.[17] As a slight alteration, sodium bicarbonate was used instead of magnesium oxide, and a 1.2 equivalent of *t*-butyloxycarbonyl azide was utilized per equivalent of amino acid; yield, 76% (lit. for L-isomer 73%,[17] 72%,[19]); m. p. 84°C (lit. for L-isomer 78—81°C[17] 74—80°C[19]); $[\alpha]_D^{21}$ +25.2° (*c* 2, acetic acid) (lit. for L-isomer −24.0°C[19]).

Found: C, 53.04; H, 9.39; N, 5.73. Calcd. for

18) T. Kato, S. Makisumi, M. Ohno and N. Izumiya, *J. Chem. Soc. Japan, Pure Chem. Sect. (Nippon Kagaku Zasshi)*, **83**, 1151 (1962).

19) F. C. Mckay and N. F. Albertson, *J. Am. Chem. Soc.*, **72**, 4648 (1957).

$C_{11}H_{21}O_4N \cdot H_2O$: C, 52.99; H, 9.30; N, 5.62%.

***t*-Butyloxycarbonyl-D-leucyl-δ-benzyloxycarbonyl-L-ornithine Ethyl Ester (XII).**—To a solution of XI (2.493 g., 10 mmol.) and dicyclohexylcarbodiimide[9] (2.06 g., 10 mmol.) in absolute tetrahydrofuran (20 ml.) at 0°C, a solution of δ-benzyloxycarbonyl-L-ornithine ethyl ester *p*-toluenesulfonate[11] (4.665 g., 10 mmol.) and triethylamine (1.4 ml., 10 mmol.) in chloroform (20 ml.) was added. The mixture was stirred for 3 hr. at 0°C and then allowed to stand overnight at room temperature. After the solvent had been removed by evaporation in vacuo, the resultant oily residue was dissolved in ethyl acetate (50 ml.) and the mixture was stored in a refrigerator for several hours. After it had been filtered from the formed dicyclohexylurea, the solution was washed and dried as has been described for IV(a). The filtrate was evaporated in vacuo, and the residual oil was solidified after pertoleum ether (20 ml.) had been added and the mixture had been stored in a refrigerator for several days. Recrystallization from ethyl acetate-petroleum ether gave 3.913 g. (77%); m. p. 88°C; $[\alpha]_D^{21}$ +11.0° (*c* 2, acetic acid).

Found: C, 61.77; H, 8.05; N, 8.46. Calcd. for $C_{26}H_{41}O_7N_3$: C, 61.52; H, 8.14; N, 8.28%.

D-Leucyl-δ-benzyloxycarbonyl-L-ornithine Ethyl Ester Hydrochloride (XIII).—To a solution of XII (254 mg., 0.5 mmol.) in ethyl acetate (2 ml.), 4.38 N hydrogen chloride in ethyl acetate (2.3 ml., 10 mmol.) was added. When, after 3 hr. at room temperature, the solution was evaporated to dryness in vacuo, hygroscopic crystals were obtained (211 mg., 96%). R_f 0.93 on paper.

***p*-Methoxybenzyloxycarbonyl-D-phenylalanine (XIV).**—To a solution of D-phenylalanine (1.652 g., 10 mmol.) and sodium bicarbonate (2.52 g., 30 mmol.) in water (30 ml.), a solution of *p*-methoxybenzyloxycarbonyl azide[20] (2.693 g., 13 mmol.) in dioxane (30 ml.) was added; the reaction mixture was stirred for 48 hr. at room temperature, and then evaporated in vacuo. The residual aqueous solution was extracted twice with ether (20 ml. each) and acidified with 10% citric acid (40 ml.). The acidified mixture was extracted thrice with ethyl acetate (30 ml. each), and the combined extract was washed with water, dried over sodium sulfate, and evaporated. The residual oil solidified upon the addition of petroleum ether. Recrystallization from ethyl acetate-petroleum ether gave 2.555 g. (77%); m. p. 81—88°C; $[\alpha]_D^{24}$ −5.7° (*c* 2, acetic acid) (lit. for L-isomer +5.7°[20]).

Found: C, 65.61; H, 6.05; N, 4.53. Calcd. for $C_{18}H_{19}O_5N$: C, 65.64; H, 5.82; N, 4.25%.

***p*-Methoxybenzyloxycarbonyl-D-phenylalanyl-D-leucyl-δ-benzyloxycarbonyl-L-ornithine Ethyl Ester (XV).**—To a solution of XIV (988 mg., 3 mmol.) and triethylamine (0.42 ml.) in tetrahydrofuran (10 ml.), isobutyl chloroformate (0.4 ml., 3 mmol.) was added at 0°C. After 20 min., a solution of XIII (1.40 g., 3 mmol.) and triethylamine (0.42 ml.) in chloroform (10 ml.) was added thereto, and the reaction mixture was allowed to stand overnight at room temperature. The mixture was then concentrated in vacuo, and water (100 ml.) and petroleum ether were added. The crystals were collected by filtration, washed with 10% citric acid, water, a 4% sodium bicarbonate solution, and water, and then dried; 1.598 g. (74%). Recrystallization from ethanol-ether-petroleum ether gave 1.394 g. (65%); m. p. 159°C; $[\alpha]_D^{21}$ +8.4° (*c* 2.01, acetic acid).

Found: C, 64.84; H, 6.95; N, 7.86. Calcd. for $C_{39}H_{50}O_9N_4$: C, 65.16; H, 7.01; N, 7.82%.

***p*-Methoxybenzyloxycarbonyl-D-phenylalanyl-D-leucyl-δ-benzyloxycarbonyl-L-ornithine Hydrazide (XVI).**—XV was converted to the hydrazide as in the case of VIII. Yield, 97%; m. p. 205°C; $[\alpha]_D^{24}$ +9.7° (*c* 1.0, dimethylformamide).

Found: C, 63.10; H, 6.94; N, 11.95. Calcd. for $C_{37}H_{48}O_8N_6$: C, 63.05; H, 6.86; N, 11.93%.

***p*-Methoxybenzyloxycarbonyl-D-phenylalanyl-D-leucyl-δ-benzyloxycarbonyl-L-ornithyl-L-valyl-δ-benzyloxycarbonyl-D-ornithyl-L-proline Ethyl Ester (XVII).**—Into a chilled solution of XVI (310 mg., 0.44 mmol.) in a mixture of glacial acetic acid (2.5 ml.) and dimethylformamide (2 ml.), 1.09 N hydrochloric acid (0.5 ml.), 33 mg. of sodium nitrite, and additional 1.09 N hydrochloric acid were stirred. After 6 min., cold water (20 ml.) was added. The azide which precipitated was filtered off, washed successively with cold water, a sodium bicarbonate solution, and water, and then dried under a vacuum in a desiccator. The azide was added to a solution of X (236 mg., 0.44 mmol.) and triethylamine (0.061 ml.) in dimethylformamide (4 ml.), and the mixture was stirred for 3 days at 0°c. The insoluble substance was removed by filtration. The precipitate which formed upon the addition of water (40 ml.) to the filtrate was collected, washed with 0.5 M citric acid, a 4% sodium bicarbonate solution and water, and dried. Recrystallization from dioxane-ether gave 366 mg. (71%); m. p. 168—170°C; $[\alpha]_D^{22}$ −14.4° (*c* 2, acetic acid).

Found: C, 63.02; H, 7.06; N, 9.51. Calcd. for $C_{62}H_{82}O_{14}N_8 \cdot H_2O$: C, 63.03; H, 6.99; N, 9.49%.

XVII was only partially saponified, even if it was treated with ten equivalents of alkali for 48 hr. at 30°C.

***t*-Butyloxycarbonyl-L-valyl-δ-benzyloxycarbonyl-D-ornithyl-L-proline (XVIII).**—To a solution of IX (728 mg., 1.23 mmol.) in methanol (6 ml.), N sodium hydroxide (1.61 ml.) was added; the solution was then allowed to stand for 3 hr. at room temperature. After the addition of water (6 ml.), the solution was evaporated in vacuo. After filtration, the solution was acidified with 0.5 M citric acid (6 ml.) and extracted with ethyl acetate three times (20 ml. each); then the combined extract was dried over anhydrous sodium sulfate. The filtrate from the salt was evaporated in vacuo to yield an oily product; 654 mg. (94%).

L-Valyl-δ-benzyloxycarbonyl-D-ornithyl-L-proline Hydrochloride (XIX).—To a solution of XVIII (654 mg., 1.16 mmol.) in dioxane (2 ml.), 4.2 N hydrogen chloride in dioxane (5.5 ml.) was added. After 2 hr. at room temperature, the solution was evaporated in vacuo to afford hygroscopic powder. Yield, 522 mg. (90%); R_f 0.61 on paper, 0.54 on silica gel.

***p*-Methoxybenzyloxycarbonyl-D-phenylalanyl-D-leucyl-δ-benzyloxycarbonyl-L-ornithyl-L-valyl-δ-benzyloxycarbonyl-D-ornithyl-L-proline (XX).**—The powder of azide drived from XVI (895 mg., 1.27 mmol.), N hydrochloric acid (2.8 ml.), and sodium nitrite

20) F. Weygand and K. Hunger, *Chem. Ber.*, **95**, 1 (1962).

(97 mg.) in a mixture of acetic acid (8 ml.) and dimethylformamide (2 ml.) were collected, washed, and dried as in the case of XVII. Then the azide was added to a solution of XIX (619 mg., 1.21 mmol.) and triethylamine (0.169 ml.) in dimethylformamide (10 ml.), and the mixture was stirred for 3 days at 0°C. Then the filtered solution was evaporated in vacuo, and the residual oil solidified upon the addition of ethyl acetate (4 ml.) and ether (20 ml.). The collected precipitate was washed with 10% citric acid and water. Recrystallization from dioxane - methanol - ether gave 893 mg. (65%); m. p. 163°C; $[\alpha]_D^{21}$ −15.7° (*c* 2, acetic acid).

Found: C, 63.26; H, 7.01; N, 9.77. Calcd. for $C_{60}H_{78}O_{14}N_8$: C, 63.47; H, 6.93; N, 9.87%.

D-Phenylalanyl-D-leucyl-L-ornithyl-L-valyl-D-ornithyl-L-proline Diacetate (XXI). — XX (9.0 mg., 0.007 mmol.), dissolved in a mixture of methanol (0.5 ml.), acetic acid (0.2 ml.) and water (0.3 ml.), was subjected to hydrogenolysis in the presence of palladium black. After being filtered from the catalyst, the solution was evaporated to dryness in vacuo. The hygroscopic powder which remained was collected with the aid of ether; yield, 6.3 mg.; R_f 0.43 on paper, and 0.47 on silica gel. The amino acid analysis gave the molar ratio of 1.0 : 1.0 : 2.2 : 0.8 : 1.1 for phe : leu : orn : val : pro.

***p*-Methoxybenzyloxycarbonyl-D-phenylalanyl-D-leucyl-δ-benzyloxycarbonyl-L-ornithyl-L-valyl-δ-benzyloxycarbonyl-D-ornithyl-L-proline *p*-Nitrophenyl Ester (XXII).**—To a solution of XX (795 mg., 0.7 mmol.) in pyridine (14 ml.), di-*p*-nitrophenyl sulfite[21] (1.814 g., 5.6 mmol.) was added. The reaction mixture was allowed to stand for 24 hr. at room temperature. After the solvent had been evaporated, the oily product was triturated in petroleum ether and washed repeatedly with a mixture of ether and petroleum ether (1 : 1) by decantation. The residual solid was filtered off and washed with a mixture of ether-petroleum ether until no yellow could be discerned upon the addition of N sodium hydroxide to the filtrate. The yield was 826 mg. The *p*-nitrophenyl-ester content in this product was spectrophotometrically estimated to be 80% by measuring the optical density of the compound at 412 mμ.[10,22]

Cyclo-D-phenylalanyl-D-leucyl-δ-benzyloxycarbonyl-L-ornithyl-L-valyl-δ-benzyloxycarbonyl-D-ornithyl-L-proyly (XXIII).—Anisole (0.5 ml.) and trifluoroacetic acid (4 ml.) were added to XXII (826 mg.) below 0°C. The solution was then evaporated in vacuo at 0°C, and the residue was triturated with ether. The hexapeptide *p*-nitrophenyl ester trifluoroacetate was collected in a cold room, washed with a mixture of ether and petroleum ether and dried in vacuo. The dried trifluoroacetate was then dissolved in dimethylformamide (10 ml.) containing 0.2 ml. of acetic acid, and the solution was stirred, drop by drop, into pyridine (200 ml.) which had been kept at 60°C over a period of 4 hr.; the stirring was then continued for an additional 2 hr. at the same temperature. After the solvent had been removed, the residue was dissolved in a mixture of methanol (50 ml.) and water (20 ml.). The insoluble substance was removed by filtration, and the filtrate was passed successively through the columns (2×10 cm. each) of Dowex 1 (OH^- form) and Dowex 50 (H^+ form). The columns were washed with the same solvent (140 ml.), and the collected effluent was evaporated to dryness in vacuo. The residual product was dissolved in methanol, and the solution was evaporated. The residue was triturated and pulverized in a mixture of ether and petroleum ether (1 : 1). Recrystallization from ethyl acetate - ether - petroleum ether gave 322 mg. (48% form XX); m. p. 184°C; $[\alpha]_D^{24}$ +7.3° (*c* 1.01, acetic acid).

Found: C, 64.22; H, 7.59; N, 11.26. Calcd. for $C_{51}H_{68}O_{10}N_8$: C, 64.26; H, 7.19; N, 11.75%.

The molecular weight of XXIII was determined by a model 301 A Osmometer, Mechrolab Inc. (solvent methanol).[23]

Found: 955. Calcd. 953.

Cyclo-D-phenylalanyl-D-leucyl-L-ornithyl-L-valyl-D-ornithyl-L-prolyl Dihydrochloride (XXIV·2HCl).—XXIII (48.6 mg., 0.05 mmol.), dissolved in methanol (0.5 ml.) containing 0.48 N methanolic hydrogen chloride (0.23 ml.), was subjected to hydrogenolysis in the presence of palladium black. After being filtered from the catalyst, the solution was evaporated to dryness in vacuo. The residual crystals were then collected with the aid of a mixture of acetone and ether, and dried in air. Yield, 37.4 mg. (81%); m. p. 242—244°C (decomp.); $[\alpha]_D^{23}$ +6.6° (*c* 1.02, acetic acid); R_f 0.73 on paper, 0.69 on silica gel. The amino acid analysis gave the molar ratio of 1.0 : 1.1 : 2.3 : 1.0 : 1.2 for phe, leu, orn, val, and pro.

Found: C, 49.79; H, 7.90; N, 12.88. Calcd. for $C_{35}H_{58}O_6N_8Cl_2\cdot 5H_2O$; C, 49.58; H, 8.08; N, 13.22%.

The air-dried product lost 8.8% of its weight after being dried over phosphorus pentoxide at 80°C (2 mmHg) to a constant weight. Calcd. for $4H_2O$: 8.5%.

The molecular weight of XXIV·2HCl·$5H_2O$ was determined by the procedure described above (solvent methanol).[23]

Found: 340. Calcd. for $1/3\times(C_{35}H_{56}O_6N_8\cdot 5H_2O\cdot 2HCl)$: 283.[24]

Cyclo-D-phenylalanyl-D-leucyl-L-ornithyl-L-valyl-D-ornithyl-L-prolyl Hydrobromide (Hydrobromide of XXIV).—Ten mg. of XXIII was dissolved in 2 N hydrogen bromide in acetic acid (0.2 ml.). After 45 min., the reaction mixture was evaporated in vacuo, and acetic acid (0.2 ml.) and ether (0.5 ml.) were added. The precipitate was filtered off, repeatedly washed with ether, and dried in vacuo. The hygroscopic powder obtained weighed 6.6 mg. Its homogeneity was established by paper (R_f 0.73), thin-layer (R_f 0.68), and carboxymethyl cellulose column chromatography (Fig. 4), and by paper electrophoresis (Fig. 5).

The Chromatography and Electrophoresis of XXIV and Related Compounds.—A sample (0.5 mg. —1mg.) was dissolved in 0.2—0.3ml. of 0.2M pyridinium acetate contining 30% methanol (pH 5.0); the solution was then applied to a column (0.9×50 cm.) with carboxymethyl cellulose (Eastman Organic Chem. 7796),

21) B. Iselin and R. Schwyzer, *Helv. Chim. Acta*, **43**, 1760 (1960).

22) M. Ohno and N. Izumiya, This Bulletin **38**, 1839 (1965).

23) The authors are indebted to Mr. Michinori Waki of this laboratory for the molecular-weight determination.

24) This compound appears to dissociate into three molecules under the conditions under which the determination of the molecular weight was carried out.

TABLE II. INHIBITORY ACTIVITY OF XXIV·2HCl·5H$_2$O AND GRAMICIDIN S ON MICROORGANISMS

Minimum inhibitory concentrations, μg./ml.

	Escherichia coli	*Proteus vulgaris*	*Staphylococcus aureus*	*Bacillus subtilis*	*Mycobacterium avium*
XXIV·2HCl·5H$_2$O	>100	>100	>100	>100	>100
Gramicidin S·H$_2$SO$_4$·8H$_2$O	>100	>100	5	5	>100

Medium used was Stephenson-Whetham's medium (modified); K_2HPO_4 0.1%, NaCl 0.1%, $MgSO_4 \cdot 7H_2O$ 0.05%, Na-glutamate 0.4%, casamino acid 0.2%, yeast-extract 0.05% and agar 2.0%, pH 7.0. The same results were obtained on bouillon agar medium.

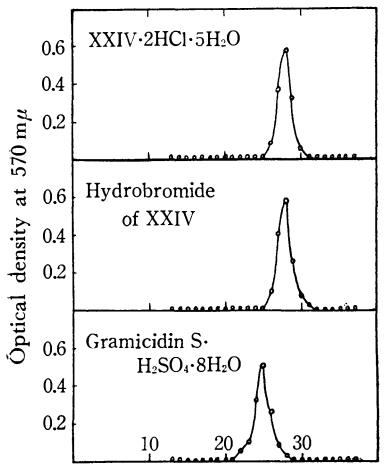

Fig. 4. Carboxymethyl cellulose column chromatography of three compounds.

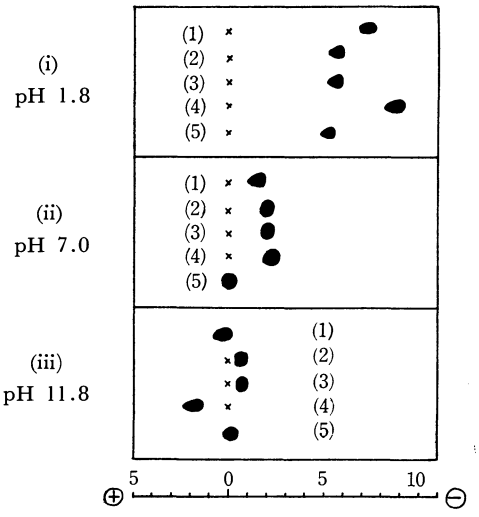

Fig. 5. Paper electrophoresis of (1) XXI, (2) XXIV·2HCl·5H$_2$O, (3) hydrobromide of XXIV, (4) L-lysine hydrochloride, and (5) gramicidin S·H$_2$SO$_4$·8H$_2$O.

and development was continued with the same solvent. Two milliliter fractions were collected at a flow rate of 20 ml. per hour. The peptide content of the fractions was determined by the method described by Yemm and Cocking.[25] Gramicidin S was used as the control. As is shown in Fig. 4, the same chromatographic pattern was obtained for XXIV·2HCl·5H$_2$O and for the hydrobromide of XXIV.

Paper electrophoresis was carried out under these conditions: paper, Toyo Roshi No. 52; voltage gradient, 500 V./30 cm.; charged period, 2 hr.; solvent system, (i) formic acid - acetic acid - methanol - water (1 : 3 : 6 : 10, v/v) (pH 1.8), (ii) 0.02 M sodium citrate buffer - methanol (1 : 1, v/v) (pH 7.0), and (iii) triethylamine - concentrated ammonium hydroxide - methanol - water (1 : 1 : 20 : 40, v/v) (pH 11.8). L-Lysine hydrochloride and gramicidin S sulfate were used as the reference compounds. Figure 5 demonstrates the electrophoretic patterns of XXI, XXIV·2HCl·5H$_2$O, the hydrobromide of XXIV, lysine and gramicidin S. The mobility of XXIV·2HCl·5H$_2$O with relation to lysine was 0.64 in solvent i, and 0.95 in solvent ii; it was indistinguishable from one of the hydrobromides in each solvent.

Microbiological Assays. — The microorganisms employed are shown in Table II. The minimum amount of the compounds needed for the complete inhibition of growth was determined by a dilution method with a bouillon agar medium and with a synthetic medium. As Table II shows, the cyclic hexapeptide XXIV·2HCl·5H$_2$O was found to be devoid of activity in reaction against any of the microorganisms utilized, even at high concentrations of the test compound, whereas gramicidin S exhibited considerable activity in reaction against some of the microorganisms at substantial concentrations.

The authors wish to express their thanks to Dr. Motoo Shibata of Takeda Chemical Industries, Ltd., for his microbiological assays. Thanks also due to Ajinomoto Co., Inc., and Kyowa Hakko Kogyo Co., Ltd., for supplying some amino acids.

25) B. W. Yemm and E. C. Cocking, *Analyst*, **80**, 209 (1955); *Biochem. J.*, **58**, xii (1954).

BULLETIN OF THE CHEMICAL SOCIETY OF JAPAN VOL. 39 2250—2255 (1966)

Cyclopropene Derivatives. IV.*1 The Reactions of Acylcyclopropene

By Naruyoshi OBATA and Ichiro MORITANI*2

Department of Chemistry, Faculty of Engineering Science, Osaka University, Toyonaka, Osaka

(Received January 24, 1966)

The reactions of acylcyclopropenes, such as 3-benzoyl-1, 2-diphenyl- and 3-acetyl-1, 2-diphenyl-cyclopropene, were investigated. These ketones gave normal hydrazones with 2, 4-dinitrophenylhydrazine. With *p*-toluenesulfonylhydrazine, the acetyl compound gave ordinary hydrazone, but the benzoyl derivative did not give its hydrazone. The reaction with hydrazine hydrate caused the expansion of the cyclopropene ring and produced pyridazine derivatives in both the ketones. The carbenic decomposition of 3-acetyl-1, 2-diphenylcyclopropene *p*-toluenesulfonylhydrazone with sodium methoxide in diglyme gave diphenylacetylene and 3, 4-diphenyl-6-methylpyridazine. On irradiation with ultraviolet light, 3-benzoyl-1, 2-diphenylcyclopropene produced 1, 2, 4, 5-tetraphenylbenzene. In the case of 3-acetyl-1, 2-diphenylcyclopropene, the same benzene derivative and 1, 2, 4, 5-tetraphenyl-3, 6-diacetyltricyclo[3, 1, 0, $0^{2,4}$]hexane were obtained. The latter material was transformed into a benzene derivative upon further irradiation. Tricyclohexane could be an intermediate in the transformation of ketones to a benzene derivative.

A series of investigations of the cyclopropenyl derivatives have been made by Breslow and his co-workers.[1] They report the facile ring expansion of the cyclopropene in a number of cases.[1] Since it is known that the olefinic group plays an important role in a carbene reaction[2] and in the photochemical reaction[3], the reaction of cyclopropenylcarbene and the photochemistry of cyclopropenylketone are of great interset. Unusual reaction products other than the ring-expanded one might be formed. In this respect, the thermal decomposition of 1, 2-diphenylcyclopropenyldiazoethane and the photochemical reaction of 3-acyl-1, 2-diphenylcyclopropene will be investigated here.

The Reaction of Methyl-1, 2-diphenylcyclopropene-3-yl Carbene.—It has been shown[4] that the reaction of 3-benzoyl-1, 2-diphenylcyclopropene with hydrazine hydrate gives a ring-expanded isomer, dihydropyridazine, whereas the reaction with hydroxylamine gives an unrearranged cyclopropenyl oxime. It seems, therefore, that a ring expansion in the hydrazone formation is not inevitable in the cyclopropenyl ketone. Accordingly, the reactions of 3-benzoyl-1, 2-diphenylcyclopropene (Ia) and 3-acetyl-1, 2-diphenylcyclopropene (Ib) with some hydrazines were investigated.

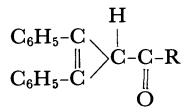

Ia: R=C_6H_5

Ib: R=CH_3

The reaction of ketone Ia with hydrazine hydrate gave a mixture of yellow and white materials. The yellow material gradually changed to the white one during recrystallization from ethanol or benzene. The white material was purified and identified as 3, 4, 6-triphenylpyridazine (IIIa), m. p. 171—172°C. The spectral study of a crude yellow material, m. p. 167—178°C, showed that the material contained the N-H group and a less extended conjugating system. Therefore, the yellow material could be the dihydropyridazine (IIa) reported by Breslow.[4],*3 It seems that IIa is formed by the reaction of ketone Ia with hydrazine hydrate, but that IIa is oxidized to IIIa, presumably by oxygen in the air, during the recrystallization. Such an easy oxidation of the dihydropyridazine to the pyridazine is observed in many cases.[5]

*1 Part III of this series: N. Obata and I. Moritani, *Tetrahedron Letters*, in press.

*2 All correspondence should be addressed to I. M.

1) a) R. Breslow, J. Lockhart and A. Small, *J. Am. Chem. Soc.*, **84**, 2793 (1960). b) R. Breslow and M. Battiste, ibid., **82**, 3626 (1960). c) R. Breslow in P. de Mayo, ed., "Molecular Rearrangement," Vol. I, John Wiley & Sons, New York (1963), Chapter 4.

2) For summaries Re: carbene chemistry see: a) J. Hine, "Divalent Carbon," The Ronald Press Co., New York, N. Y. (1964). b) W. Kirmse, "Carbene Chemistry," Academic Press, New York, N. Y. (1964).

3) a) W. A. Noyes, Jr., G. S. Hammond and J. N. Pitts, Jr., ed., "Advances in Photochemistry," Vol. I, Interscience Publishers, New York (1963). b) P. de Mayo in R. A. Raphael, E. C. Taylor and H. Wynberg, ed., "Advances in Organic Chemistry," Vol. II, Interscience Publishers, New York (1960), p. 367.

4) R. Breslow, R. Boikess and M. Battiste, *Tetrahedron Letters*, **26**, 42 (1960).

*3 Breslow did not give the melting point of IIa.

5) See, for example, C. Paal and E. Dencks, *Ber.*, **36**, 495 (1903); K. Alder and H. Niklas, *Ann.*, **585**, 6 (1954).

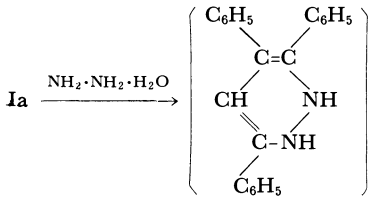

(IIa)

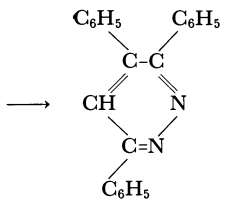

(IIIa)

The same result was also obtained in the reaction of ketone Ib with hydrazine hydrate.

Unlike the reaction with hydrazine, however, ketone Ia and Ib gave 2, 4-dinitrophenylhydrazone with no skeletal rearrangement.[6] The existence of the 1, 2-diphenylcyclopropenyl group in the resulting hydrazones was clearly shown by the characteristic patterns in infrared and ultraviolet spectra.[7] The 2, 4-dinitrophenyl group might diminish the nucleophilic character of β-nitrogen and prevent its further attack on a cyclopropene ring. In a similar way, the reaction of ketone Ib with *p*-toluenesulfonylhydrazine also gave an unrearranged cyclopropenylhydrazone. However, ketone Ia failed to react under the same reaction conditions.

Since the preparation of the hydrazone without any ring expansion was successful, the reaction of cyclopropenylcarbene was also studied. A solution of *p*-toluenesulfonylhydrazone (IVb) of ketone (Ib) in diglyme was added dropwise to a solution of sodium methoxide in diglyme at 140°C. Gas was evolved gently. The collected gas was analyzed by means of a mass spectrometer. A mother peak for C_3H_4, probably methylacetylene and/or allene, was found in addition to a large amount of nitrogen. The reaction products were isolated and separated by alumina-column chromatography. From a hydrocarbon fraction, diphenylacetylene (VII) was obtained in a 28.4% yield. No other hydrocarbon could be detected in the products. From a later fraction of the chromatography, 3, 4-diphenyl-6-methylpyridazine (IIIb) was isolated in a 26.1% yield.

The diazo compound V of the desired structure, formed by the base catalyzed decomposition of *p*-toluenesulfonylhydrazone (IVb), produced methyl-1, 2-diphenylcyclopropene-3-yl carbene (VI), which then splits into two olefinic materials, diphenylacetylene (VII) and C_3H_4. If a ring expansion in carbene VI occurs, the compound derived from cyclobutadiene might be formed. If the intramolecular addition of carbene VI to a double bond occured, the tetrahedrane derivative might be formed. However, such was not the case in the present experiment. A pyridazine, IIIb, was formed by the ring expansion of the diazo compound V.

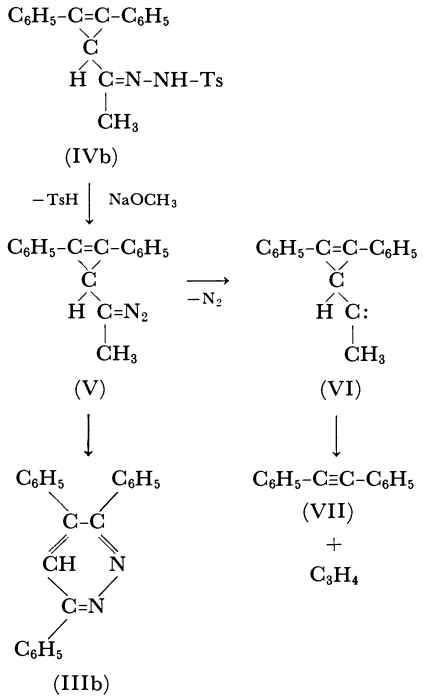

(IVb)

(V)

(VI)

(VII)

(IIIb)

A similar splitting of the three-membered ring in the carbene reaction has been reported by Friedman and Shechter.[8] Cyclopropylcarbene, prepared similarly from the corresponding *p*-toluenesulfonylhydrazone, gave ethylene, acetylene and cyclobutene.

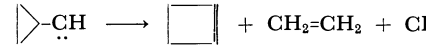

Recently, Masamune and Kato[9] decomposed 3-formyl-1, 2-diphenylcyclopropene *p*-toluenesulfonylhydrazone with sodium methoxide at −20°C under irradiation with ultraviolet light. The major reaction product was also diphenylacetylene in this case, but a tetrahedrane derivative was also obtained in a 0.05—0.1% yield. In the present experiment, *p*-toluenesulfonylhydrazone (IVb) was investigated under very similar conditions, but

6) N. Obata and I. Moritani, This Bulletin, in press.

7) The 1, 2-Diphenylcyclopropene skeleton exhibits very characteristic absorptions in the IR and UV regions; see R. Breslow and Chin Yuan, *J. Am. Chem. Soc.*, **80**, 5991 (1958); R. Breslow, T. Eicher, A. Krebs. R. A. Peterson and J. Posner, ibid., **87**, 1320 (1965),

8) L. Friedman and H. Shechter, *J. Am. Chem. Soc.*, **82**, 1002 (1960).

9) S. Masamune and M. Kato, ibid., **87**, 4190 (1965).

no evolution of nitrogen gas was observed at such a low temperature. Sodium salt of *p*-toluenesulfonylhydrazone was apparently formed, but its decomposition to a diazo compound might require a much higher temperature. In the present study we failed to obtain the tetrahedrane derivative.

The Photochemical Reaction of 3-Acyl-1, 2-diphenylcyclopropene.—A solution of 3-acylcyclopropene in tetrahydrofuran was irradiated by a high-pressure mercury lamp. The products were then separated by means of alumina-column chromatography. 3-Benzoyl-1, 2-diphenylcyclopropene (Ia) gave a hydrocarbon when eluted by petroleum ether and a glassy material when eluted by benzene or ether. The structure of the hydrocarbon was established to be 1, 2, 4, 5-tetraphenylbenzene (VIII) by comparison with an authentic material prepared through a known route.[10] The yield of VIII was 25.3%.

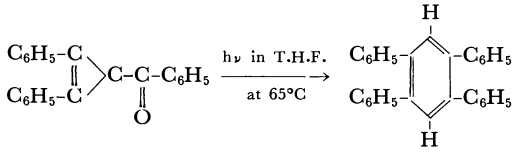

(Ia) (VIII)

Under the same conditions, the 3-acetyl derivative (Ib) gave a new compound IX in addition to tetraphenylbenzene (VIII), biacetyl (X), and a glassy material. When IX was dissolved in tetrahydrofuran and irradiated further under the same conditions, VIII was formed in a 43.4% yield, besides a glassy material. Consequently, it is clear that IX is the intermediate in the transformation of a cyclopropenyl ketone (Ib) to 1, 2, 4, 5-tetraphenylbenzene (VIII).

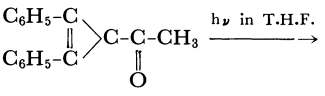

(Ib)

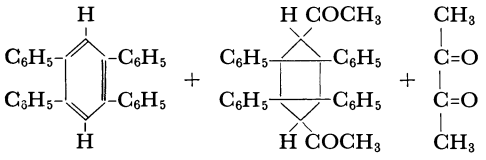

(VIII) (IX) (X)

Compound IX is considered to be 1, 2, 4, 5-tetraphenyl-3, 6-diacetyltricyclo[3, 1, 0, $0^{2,4}$]hexane on the basis of the following observations.[11] The spectral study of IX in the infrared and ultraviolet region shows clearly that the 1, 2-diphenylcyclopropene skeleton is absent in the compound IX. The analytical results and the molecular weight determination indicate that IX must be a dimeric material of the Ib ketone. Since IX has been found to be a precursor of VIII, it should have a structure which gives 1, 2, 4, 5-tetraphenylbenzene. Therefore, the compound IX may be considered to be either 1, 2, 4, 5-tetraphenyl-3, 6-diacetyltricyclo[3, 1, 0, $0^{2,4}$]hexane (IXa) or 1, 2, 4, 5-tetraphenyl-3, 6-diacetylcyclohexa-1, 4-diene (IXb):

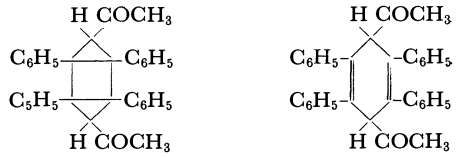

(IXa) (IXb)

In the infrared region, IX exhibited characteristic absorptions at 1700 cm^{-1} and at 1020 cm^{-1}. The carbonyl stretching frequency observed corresponds to that expected for cyclopropylketone.[12] The 1020 cm^{-1} absorption is due to the cyclopropane skeleton. The ultraviolet absorption spectrum of IX showed a broad maximum at 226 mμ (log ε 4.21) and a shoulder at 275 mμ (log ε 3.74). It has been reported that 1, 2-diphenylcyclopropane[13] exhibits maxima at 234 mμ (log ε 4.10) and at 275 mμ (log ε 3.95), whereas *cis*-α, α'-dimethylstilbene[14] shows a maximum at 252 mμ (log ε 3.94). The proton magnetic resonance spectrum of IX exhibited a multiplet (20 hydrogens) at 2.85 τ, a singlet (2 hydrogens) at 4.80 τ*4 and a singlet (6 hydrogens) at 8.25 τ. Chemically, IX did not discolor a solution of potassium permanganate in acetone at room temperature after one hour, whereas *cis*-stilbene did. All these results are consistent with the tricyclohexane structure (IXa). The stereochemistry of this compound is not yet known. The yield was 6.7%.

Consequently, it may be suggested that the cyclopropenylketone Ib dimerizes preferentially to the cyclobutane derivative, IX. Further irradiation caused an α-cleavage and produced a biradical of a tricyclohexane, which then rearranged to a benzene derivative.

In an attempt to produce a cyclopropenyl radical, Breslow[16] obtained a dimer, bis-cyclopropenyl. This dimer rearranges to benzene derivatives on

10) W. Dilthey and G. Hurtig, *Ber.*, **67**, 2004 (1934).
11) N. Obata and I. Moritani, *Tetrahedron Letters*, in press.
12) L. J. Bellamy, "The Infra-red Spectra of Complex Molecules," John Wiley & Sons, New York (1958).
13) S. G. Beech, J. H. Turfull and W. Wilson, *J. Chem. Soc.*, **1952**, 4686.
14) H. Suzuki, This Bulletin, **33**, 396 (1960).
*4 This absorption was identified as a tertiary proton in the tricyclohexane structure. Though similar proton appeared at a higher field (6.73—7.82 τ)[15] in methyl *trans, cis*-1, 2-diphenylcyclopropane-1-carboxylate, the deshielding effect might be more effective in IX because of the rigid ring system.
15) J. K. Blatchford and M. Orchin, *J. Org. Chem.*, **29**, 839 (1964).
16) R. Breslow, P. Gal, H. W. Chang and L. J. Altman, *J. Am. Chem. Soc.*, **87**, 5139 (1965).

heating, by irradiation or by treatment with potassium amide.

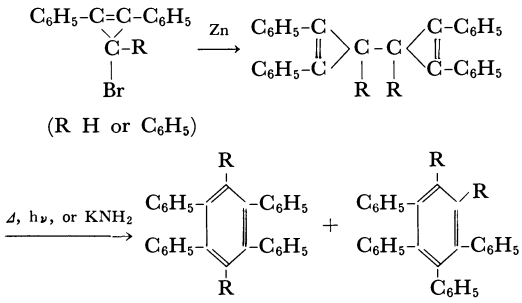

From a structural consideration, the ketones Ia and Ib in the present experiment are also capable of taking such a dimerization route, because one of the common photoreactions of the ketone is the α-cleavage.[17] When a carbon-carbon bond on one side of a calbonyl group is preferentially cleaved, a cyclopropenyl radical is produced; it may dimerize as above, or it may abstract a hydrogen from the solvent. However, this was not the case in the ketones Ia and Ib. In a hydrocarbon fraction of the product none of the monomeric or dimeric hydrocarbons were detected other than a tricyclohexane and tetraphenylbenzene. Moreover, the isolation of a tricyclohexane as an intermediate clearly established that the reaction path was the preferential dimerization of the double bond in a cyclopropene skeleton. The α-cleavege followed it. A similar photodimerization of a cyclopropene derivative has recently been reported.[18] Irradiation with ultraviolet light on 1, 3, 3-trimethylcyclopropene-1 in acetone in the presence of benzophenone results in the formation of two stereoisomeric dimers, tricyclo[3, 1, 0, $0^{2,4}$]hexanes.

There is an interesting possibility for this dimerization, that is, the carbonyl group may be absorbing most of the light, while the double bond is doing most of the reaction, as has been found in some other cases.[19] In the present experiment, no evidence is available as a basis for deciding whether most of the light is absorbed by the carbonyl or by the double bond. However, the diphenylcyclopropene system absorbs the light at an appreciably longer wavelength with a high intensity.[6,7] It is more likely, therefore, that the double bond in a diphenylcyclopropene is more easily excited than a carbonyl group and forms a cyclobutane ring. The cycloaddition of two double bonds under irradiation is well known and has been discussed recently by Hoffmann and Woodward.[20]

In conclusion, the carbene reaction and photochemical reactions of the cyclopropene derivatives did not give simply ring-expanded materials as have been observed in many reactions. Cyclopropenylcarbene split into two olefinic compounds. Ultraviolet light caused a dimerization of olefin in the cyclopropene ring. Tricyclohexane derivatives were intermediates for the transformation of cyclopropenylketone to a benzene derivative.

Experimental*5

The Reaction of 3-Benzoyl-1, 2-diphenylcyclopropene (Ia) with Hydrazine Hydrate, 3, 4, 6-Triphenylpyridazine (IIIa).—A mixture of 1.07 g. (3.6 mmol.) of 3-benzoyl-1, 2-diphenylcyclopropene and 1.08 g. (21 mmol.) of hydrazine hydrate in 20 ml. of ethanol was heated under reflux for 15 hr. After the solution had cooled down, a mixture of yellow and white crystals, m. p. 135—175°C, was obtained. Repeated recrystallization of a mixture from ethanol-benzene gave white crystals, 3, 4, 6-triphenylpyridazine (IIIa), m. p. 171—172°C (reported 171°C)[21]; 0.75 g. (66.8%).

Found: C, 85.49; H. 5.17; N, 9.12; mol. wt. 299,
Calcd. for $C_{22}H_{16}N_2$: C, 85.69; H, 5.23; N, 9.09%; mol. wt. 308.4.

In the infrared region, two characteristic peaks of IIIa were observed at 1560 cm^{-1} and 1580 cm^{-1}. The ultraviolet maximum in ethanol was 269 mμ (log ε 4.3) reported 273 mμ (log ε 4.4).[22] A three-hour reaction caused a recovery of the starting material. The same material was prepared from ω-desylacetophenone and hydrazine hydrate.[21] A mixed melting point determination of two samples showed no depression. The infrared and ultraviolet spectra of two samples were superimposable, also. The attempted recrystallization of yellow crystal gave a material which melted at 167—178°C, and which showed peaks at 3300 cm^{-1} (νN–H), 1635 cm^{-1} and 1590 cm^{-1} in the infrared spectrum. The ultraviolet spectrum of this impure yellow material showed broad maxima at 250 mμ and 310 mμ.

The Reaction of 3-Acetyl-1, 2-diphenylcyclopropene (Ib) with Hydrazine Hydrate, 3, 4-Diphenyl-6-methylpyridazine (IIIb).—A solution of hydrazine hydrate (0.23 g. (4.4 mmol)), and 3-acetyl-1, 2-diphenylcyclopropene (Ib) (0.46 g. (1.9 mmol.)) in 4 ml. of ethanol was heated under reflux for 20 hr. After the solution had cooled down, yellow crystal, m. p. 135—149°C, was obtained. This compound could not be purified by repeated recrystallization from ethanol or benzene. The evaporation of the mother liquid gave white crystals, 2, 4-diphenyl-6-methylpyridazine (IIIb), m. p. 122—123°C (petroleum ether); 0.15 g.

17) O. L. Chapman, in W. A. Noyes, Jr., G. S. Hammond and J. N. Pitts, Jr., ed., "Advances in Photochemistry," Vol. I, Interscience Publishers, New York (1963), p. 323; R. Srinivasan, ibid., p. 83.
18) H. H. Stechl, *Chem. Ber.*, **97**, 2681 (1964).
19) Z. J. Barneis, D. M. S. Wheeler and T. H. Kinsle, *Tetrahedron Letters*, **1965**, 275; H. Morison, ibid., **1964**, 3653.
20) R. Hoffmann and R. B. Woodward, *J. Am. Chem. Soc.*, **87**, 2047 (1965); see also G. W. Griffin, A. F. Vellturo and K. Furukawa, ibid., **83**, 2725 (1961).
*5 All melting points were uncorrected. The IR spectrum was recorded by the use of EPI-S2. The UV spectrum was recorded by the use of EPS-2U. The NMR spectrum was recorded by the use of JNM-4H-100. The molecular weight was determined by the use of a vapor pressure osmometer.
21) A. Smith, *Ann.*, **289**, 316 (1896).
22) C. F. H. Allen and J. A. Vanallan, *J. Am. Chem. Soc.*, **73**, 5850 (1951).

(36.3%). Moreover, a solution of the yellow crystals in ether was gradually discolored in two days and 3, 4-diphenyl-6-methylpyridazine was obtained quantitatively. The structure of IIIb was established by the following observation.

Found: C, 82.75; H, 5.78; N, 11.35; mol. wt. 242. Calcd. for $C_{17}H_{14}N_2$: C, 82.90; H, 5.73; N, 11.67%; mol. wt. 246.3.

The characteristic infrared absorptions were at 1565 cm^{-1} and 1580 cm^{-1}. The ultraviolet maximum in ethanol was at 242 mμ (log ε 4.1). The NMR showed a multiplet (11 hydrogens) at 2.80 τ and a singlet (3 hydrogens) at 7.13 τ. Characteristic IR peaks of the impure yellow crystals, m. p. 150—156°C, were shown at 3300 cm^{-1} (νN–H), 1630 cm^{-1} and 1590 $cm.^{-1}$

2, 4-Dinitrophenylhydrazone of Ia and Ib.—The preparation of materials has already been described.[6] The characteristic infrared absorptions of 2, 4-dinitrophenylhydrazone of Ia, m. p. 193—194°C, were at 3250 cm^{-1} (νN–H) and 1825 cm^{-1} (νC=C in cyclopropene). The ultraviolet maxima of this compound in ethanol were at 228 mμ (log ε 4.25), 235 mμ (log ε 4.32), 296 mμ (log ε 4.25), 315 mμ (log ε 4.30) and 332 mμ (log ε 4.29). 2, 4-Dinitrophenylhydrazone of Ib, m. p. 210—211°C, showed characteristic IR peaks at 3300 cm^{-1} (νN–H) and 1830 cm^{-1} (νC=C in cyclopropene). The ultraviolet maxima of this compound in ethanol were at 228 mμ (log ε 4.33), 236 mμ (log ε 4.30), 295 mμ (log ε 4.24), 312 mμ (log ε 4.28) and 330 mμ (log ε 4.26).

3-Acetyl-1, 2-diphenylcyclopropene *p*-Toluenesulfonylhydrazone (IVb).—A solution of 3-acetyl-1, 2-diphenylcyclopropene (Ib) (0.14 g. (0.6 mmol.)) and *p*-toluenesulfonylhydrazine (0.16 g. (0.86 mmol.)) in 5 ml. of ethanol was heated under reflux for 0.5 hr. The product was then collected and recrystallized from benzene, m. p. 180—181°C (decomp.) The yield was 0.22 g. (93.0%).

Found: C, 71.86; H, 5.51. Calcd. for $C_{24}H_{22}N_2SO_2$: C, 71.61; H, 5.51%.

In the infrared spectrum the characteristic absorptions were observed at 3200 cm^{-1} (νN–H), 1820 cm^{-1} (νC=C in cyclopropene) and 1160 cm^{-1} (νSO_2). The ultraviolet maxima in ethanol were at 227 mμ (log ε 4.34), 234 mμ (log ε 4.32), 294 mμ (log ε 4.26), 302 mμ (log ε 4.36), 312 mμ (log ε 4.39) and 329 mμ (log ε 4.25).

At room temperature, a starting material was recovered after one day, whereas acetone and acetophenone reacted successfully.

The Reaction of 3-Benzoyl-1, 2-diphenylcyclopropene (Ia) with *p*-Toluenesulfonylhydrazone.—A solution of 3-benzoyl-1, 2-diphenylcyclopropene (Ia) (0.089 g. (0.30 mmol.)) and *p*-toluenesulfonylhydrazine (0.057 g. (0.32 mmol.)) in 5 ml. of ethanol was heated under reflux for 24 hr. After cooling, the precipitated material was found to be a starting ketone. After one week under reflux, however, no crystalline material was separated from the solution any more. The removal of the solvent gave a tarry material; *p*-toluenesulfonylhydrazone could not be obtained. In a separate experiment, the reaction was carried out in acetic acid at 90°C for 10 hr., but a tarry material resulted here also.

The Carbenic Decomposition of 3-Acetyl-1,2-diphenylcyclopropene *p*-Toluenesulfonylhydrazone (IVb) in the presence of Sodium Methoxide.—A solution of 3-acetyl-1, 2-diphenylcyclopropene *p*-toluenesulfonylhydrazone (IVb) (2.04 g. (5.1 mmol.)), in dry diglyme (40 ml.), was added drop by drop to a solution of sodium methoxide (0.31 g. (5.9 mmol.)), in dry diglyme (40 ml.), over a period of two hours at 120°C, at which temperature nitrogen gas was evolved gradually. Nitrogen gas and the volatile material was collected in a gas buret, and the latter was analyzed by mass spectrometer. We observed a mother peak corresponding to the C_3H_4 fragment in the mass spectrum. After it had cooled down, the reaction mixture was poured into a large amount of water. The organic material was extracted with ether several times. The combined ether solution was washed successively with ten 30-ml. portions of water to remove most of the diglyme. After the solution had been dried with anhydrous magnesium sulfate, the ether was removed by evaporation and the residue was subjected to column chromatography. Activated alumina (100 g.) was used. Elution with petroleum ether resulted in 0.26 g. (28.4%) of diphenylacetylene (VII), m. p. 59—60°C (reported 61°C).[23] Elution with ether gave 0.33 g. (26.1%) of 3, 4-diphenyl-6-methylpyridazine (IIIb), m. p. 123—123.5°C (petroleum ether). In a separate experiment, *p*-toluenesulfonylhydrazone (IVb) was decomposed in the presence of copper powder at 120°C. The result was the same; the yields of VII and IIIb were 24.3 and 11.1% respectively.

The Photochemical Transformation of 3-Benzoyl-1, 2-diphenylcyclopropene (Ia).—3-Benzoyl-1, 2-diphenylcyclopropene (Ia) (0.602 g. (2.03 mmol.)), was dissolved in dry tetrahydrofuran (400 ml.) and irradiated by a high-pressure mercury lamp. The reaction was followed by a study of the ultraviolet spectrum. After the solution had been irradiated one and a half hours, the characteristic ultraviolet peaks near 300 mμ present in the staring ketone disappeared. The tetrahydrofuran was evaporated, and the residue was subjected to column chromatography. Activated alumina (90 g.) was used. Elution with petroleum ether gave 0.098 g. (25.3%) of 1, 2, 4, 5-tetraphenylbenzene (VIII), m. p. 260—261°C (petroleum ether) (reported 262—263°C).[10]

Found: C, 93.86; H, 5.84. Calcd. for $C_{30}H_{22}$: C, 94.20; H, 5.80%.

The ultraviolet maxima in ethanol were at 252 mμ (log ε 4.65) and 282 mμ (log ε 4.24).

The same material was prepared from 3, 4-diphenylcyclopentadienon and diphenylacetylene at 275°C.[10] A mixed melting point determination of the two samples showed no depression. The infrared and ultraviolet spectra of the two samples were also superimposable. Elution with benzene, followed by that with ether, resulted in a glassy material (0.32 g.) which was not studied further.

The Photochemical Transformation of 3-Acetyl-1, 2-diphenylcyclopropene (Ib).—3-Acetyl-1, 2-diphenylcyclopropene (Ib) (0.78 g. (3.3 mmol.)) was dissolved in dry tetrahydrofuran (350 ml.) and irradiated by a high-pressure mercury lamp at 65°C. After two hours of irradiation, most of the solvent was removed by evaporation; and the separated solid was collected

23) L. F. Fieser, "Experiments in Organic Chemistry," Maruzen Co., Tokyo, Japan (1963), p. 181.

from the oily residue. The recrystallization of the solid material from ligroin-benzene resulted in 0.052 g. (7.6%) of 1, 2, 4, 5-tetraphenyl-3, 6-diacetyl-tricyclo-[3, 1, 0, $0^{2,4}$]hexane (IX), m. p. 285—287°C (with decomp.)

Found: C, 87.13; H, 6.10; mol. wt. 451. Calcd. for $C_{34}H_{28}O_2$: C, 87.15; H, 6.02%; mol. wt. 468.6.

In the infrared region, IX exhibited its characteristic absorptions at 1700 cm^{-1} and at 1020 cm^{-1}. The ultraviolet maxima in ethanol were at 226 mμ (log ε 4.21) and a shoulder at 275 mμ (log ε 3.74). The NMR showed a multiplet (10 hydrogens) at 2.85τ, a singlet (1 hydrogen) at 4.80, and a singlet (3 hydrogens) at 8.25τ.

The concentration of the mother liquid of recrystallization gave a material melting at 260—261°C, 1, 2, 4, 5-tetraphenylbenzene (VIII). The combined residue of recrystallization was subjected to column chromatography. From the hydrocarbon fraction, additional portions of VIII were obtained. The yield of VIII was 0.133 g. (20.3%).

The Photolysis of 1, 2, 4, 5-Tetraphenyl-3, 6-diacetyl-tricyclo[3, 1, 0, $0^{2,4}$]hexane (IX).—Tricyclohexane (IX) (25 mg. (0.053 mmol.)) was dissolved in dry tetrahydrofuran (300 ml.), and the solution was irradiated by a high-pressure mercury lamp for 4.5 hr. The temperature of the solution was kept at 50°C during the photolysis. Tetrahydrofuran was removed, and the residue was subjected to column chromatography. Activated alumina (30 g.) was used. Elution with petroleum ether gave 8.9 mg. (43.4%) of 1, 2, 4, 5-tetraphenylbenzene (VIII). Elution with ether resulted in a glassy material, but this was not studied further.

BULLETIN OF THE CHEMICAL SOCIETY OF JAPAN VOL. 39 2255—2256 (1966)

The Reaction of *p*-Methoxystyrene-α-^{14}C with Lead Tetraacetate

By Yasuhide YUKAWA and Nobuyoshi HAYASHI

The Institute of Scientific and Industrial Research, Osaka University, Sakai, Osaka

(Received January 27, 1966)

The reaction of *p*-methoxystyrene with lead tetraacetate in glacial acetic acid should proceed mainly through the rearrangement of the carbon skeleton. The possibility of the hydrogen migration can not be ruled out, but its extent should be only 7% even if it is involved.

It has been known that lead tetraacetate is an effective oxidizing reagent not only for the fission of 1, 2-glycols, but also for the introduction of acetoxy groups into unsaturated compounds. The mechanism of the reaction of lead tetraacetate on the olefinic compounds is not so straightforward. There is a considerable variation in the products depending on the olefin used and on the conditions of the reaction. The normal reaction should be the addition of two acetoxy groups to a carbon-carbon double bond, but an abnormal reaction giving the rearranged product has usually been observed.

Criegee et al.[1] reported that the reaction of *p*-methoxystyrene in glacial acetic acid with lead tetraacetate gave *p*-methoxyphenylacetaldehyde diacetate. The most plausible mechanism of this reaction is the 1, 2-nucleophilic rearrangement of the *p*-anisyl group, as has been suggested by Criegee:

$$CH_3OC_6H_4CH{=}CH_2$$
(I)

$$\xrightarrow[AcOH]{Pb(OAc)_4} CH_3OC_6H_4\underset{\displaystyle OAc}{\underset{|}{CH}}\text{-}CH_2Pb(OAc)_3$$

$$\longrightarrow CH_3OC_6H_4\underset{\displaystyle OAc}{\underset{|}{CH}}\text{-}CH_2\overset{\oplus}{}$$

$$\longrightarrow \overset{\oplus}{C}H\text{-}CH_2C_6H_4OCH_3 \quad (\text{OAc})$$

$$\longrightarrow (AcO)_2CH\text{-}CH_2C_6H_4OCH_3$$
(II)

However, it can just as well be explained by the 1, 2-migration of hydrogen. The following mechanisms may, therefore, be suggested:

$$CH_3OC_6H_4CH{=}CH_2$$
(I)

$$\xrightarrow[AcOH]{Pb(OAc)_4} CH_3OC_6H_4\overset{\oplus}{C}H\text{-}CH_2Pb(OAc)_3$$

$$\longrightarrow CH_3O_6H_4CH_2\text{-}\overset{\oplus}{C}HPb(OAc)_3$$

$$\longrightarrow CH_3OC_6H_4CH_2\underset{\displaystyle Pb(OAc)_3}{\underset{|}{CH}}OAc$$

$$\longrightarrow CH_3OC_6H_4CH_2CH(OAc)_2$$
(II)

1) R. Criegee, P. Dimroth, K. Noll, R. Simons and C. Weis, *Chem. Ber.*, **90**, 1070 (1957).

$$CH_3OC_6H_4CH{=}CH_2 \quad \text{(I)}$$

$$\xrightarrow[AcOH]{Pb(OAc)_4} CH_3OC_6H_4CH(Pb(OAc)_3)-CH_2OAc$$

$$\longrightarrow CH_3OC_6H_4CH_2-\overset{\oplus}{C}HOAc$$

$$\longrightarrow CH_3OC_6H_4CH_2CH(OAc)_2 \quad \text{(II)}$$

In the present paper, the confirmation of the actual migrating group by means of the carbon-14 tracer technique will be reported.

It was found that styrene itself gives phenylacetaldehyde diacetate with lead tetraacetate in acetic acid. However, *p*-methoxystyrene was selected as the starting material in view of the powerful migrating aptitude of the *p*-anisyl group and the experimental convenience of the separation and purification of the reaction product. *p*-Methoxystyrene-α-^{14}C (I) was obtained, through *p*-anisaldehyde-carbonyl-^{14}C, from *p*-anisic acid-carbonyl-^{14}C, which had been prepared from *p*-methoxyphenyl magnesium bromide and carbon dioxide-^{14}C.

The treatment of *p*-methoxystyrene-α-^{14}C with lead tetraacetate in glacial acetic acid gave *p*-methoxyphenylacetaldehyde-diacetate-^{14}C, namely, 2-methoxyphenylethyl-1, 1-diol diacetate-^{14}C (II), as white needles. The specific radioactivity of II was 2.53 μc./mmol.

On the oxidation of II with an aqueous solution of potassium permanganate, followed by acidification, the fission products, carbon dioxide and anisic acid, were obtained. The specific activity of the carbon dioxide was 2.15 μc./mmol., which corresponds to 85% of the activity of the reaction product, II. This indicates that the rearrangement of the anisyl group is the major process of the reaction. The specific activity of anisic acid was 0.16 μc./mmol. This corresponds to 6.7% of the activity of II, suggesting the rearrangement of anisyl group up to 93.3%. The decrease in the activity of the carbon dioxide can be attributed to the formation of low-activity carbon dioxide by the further oxidation of anisic acid by permanganate. The activity of the anisic acid suggests hydrogen migration to a maximum extent of 7%.

In conclusion, the reaction of *p*-methoxystyrene with lead tetraacetate in glacial acetic acid should proceed mainly through the rearrangement of the carbon skeleton. The possibility of the hydrogen migration can not be ruled out, but its extent should be only 7% even if it is involved.

Experimental

The Preparation of *p*-Methoxystyrene-α-^{14}C. — *p*-Anisic acid-carboxyl-^{14}C was prepared by the Grignard carboxylation of *p*-bromoanisole (15 mmol.) with carbon dioxide liberated from barium carbonate (10 mmol.) (labeled: 1 mc./8.5 mg; unlabeled; 1.97 g.) by the usual method.[2] The acid was obtained in a 60% yield, m. p. 182—183°C; 0.9 g. The specific radioactivity was determined to be 90 μc./mmol.; total activity 533 μc. by the Van-Slyke-Folch wet combustion method.[3]

The labeled anisic acid was converted into the acid chloride with thionyl chloride, and the chloride was reduced to the aldehyde by the Rosenmund method. The resultant aldehyde, diluted to 15 g. with the unlabeled aldehyde, was then added to the Grignard solution from 17 g. of methyl iodide. This mixture was allowed to stand overnight and decomposed with ice and diluted sulfuric acid. The ethereal layer was separated, dried, and evaporated. On the distillation of the residue, 7.4 g. of the styrene (I), b. p. 92—97°C/16 mmHg was obtained.

The Reaction of *p*-Methoxystyrene with Lead Tetraacetate.—*p*-Methoxystyrene-α-^{14}C (2.7 g.) was added to a suspension of 10 g. of lead tetraacetate in 20 ml. of acetic acid. The mixture was then stirred for 2 hr. at room temperature and poured onto ice water. The oil which separated was taken up into ether, and the solvent was evaporated. The residue was solidified on keepting it in an ice-box and recrystallized from petroleum ether, giving fine needles of II, m. p. 49—50°; 1.9 g. The specific activity of the II obtained was 2.53 μc./mmol.

The diacetate II (0.4 g.) was oxidized in the usual manner by boiling it for 2 hr. in an aqueous acetone solution of alkaline potassium permanganate. After the manganese dioxide was been removed by filtration, the filtrate was acidified and the carbon dioxide liberated was absorbed into a barium hydroxide solution. The barium carbonate obtained showed a specific activity of 2.15 μc./mmol. By ether extraction, 0.1 g. of the anisic acid was obtained from the above acidified filtrate. The specific activity of this product was 0.16 μc./mmol.

2) A. Murray, III, and D. L. Williams, "Org. Synth. with Isotopes," Part I, Interscience Publishers, New York (1958), p. 86.

3) D. D. Van Slyke and J. Folch, *J. Biol. Chem.*, **136**, 509 (1940); D. D. Van Slyke, J. Plazin and J. R. Weisiger, ibid., **191**, 299 (1951).

BULLETIN OF THE CHEMICAL SOCIETY OF JAPAN VOL. 39 2257—2260 (1966)

The Relative Reactivities of Alkyl Acrylates in Their Radical Copolymerizations*

By Takayuki Otsu, Toshio Ito, Tomiya Fukumizu and Minoru Imoto

Faculty of Engineering, Osaka City University, Sugimoto-cho, Sumiyoshi-ku, Osaka

(Received February 3, 1966)

In order to clarify the effect of the alkyl groups in alkyl acrylates (RA) on their reactivities to the attack of a radical, the copolymerization of RA (M_2) with styrene (M_1) has been carried out at 60°C. From the results obtained, the monomer reactivity ratios and the Q_2 and e_2 values were determined. It was found that the relative reactivities ($1/r_1$) of RA to a polystyryl radical were correlated only by the polar substituent constant (σ^*) of the alkyl group in RA, not by their steric substituent constant (E_s) in Taft's equation:

$$\log(1/r_1) = \rho^*\sigma^* + \delta E_s$$

According to the above equation, the ρ^* and δ values were obtained as 0.56 and 0, respectively. It was also observed that the Q_2 and e_2 values for RA were correlated by Taft's σ^* substituent constant.

In a previous paper,[1,2] it has been reported that the relative reactivities of alkyl methacrylates to attack by polymer radicals are correlated only by the polar substituent constants (σ^*) of their alkyl groups in Taft's equation (1)[3]:

$$\log(\text{rel. reactivity}) = \rho^*\sigma^* + \delta E_s \qquad (1)$$

where E_s indicates the steric substituent constants of alkyl groups, and where ρ^* and δ are reaction constants. This result strongly indicated that the relative reactivities of alkyl methacrylates depended on the polar character of their alkyl groups, not on their steric characters.

Recently, we have obtained the same linear correlations between the reactivities of alkyl acrylates (RA) or nuclear-substituted phenyl methacrylates to attack by a polystyryl radical and the σ^* constants of alkyl groups or σ constants of para and meta substituents on the benzene ring, respectively. Some of these results have been reported in a previous short communication.[4] The present paper will present detailed results of the copolymerization of some RA with styrene. The RA used in this study were as follows: ethyl acrylate (EA), isopropyl acrylate (IPA), benzyl acrylate (BzA), 2-chloroethyl acrylate (CEA), and 2-cyanoethyl acrylate (CNEA).

Experimental

Materials.—The commercial EA was used after purification by the ordinary method. The other RA were prepared by the esterification of acrylic acid, methyl acrylate or acroyl chloride with the corresponding alcohols. The products thus obtained were distilled under reduced pressure until the absorption of unreacted alcohols disappeared in the infrared spectra. These RA were then used after redistillation in a nitrogen atmosphere. The physical constants of the RA used are shown in Table I.

Table I. Physical properties of RA monomers

RA	b. p. °C/mmHg	n_D^{20}	d_4^{20}
EA	99/760	1.4020	0.913[a]
IPA	52/100	1.4070	0.893[a]
BzA	65/1	1.5180	1.057[a]
CEA	60/19	1.4487	1.121
CNEA	64/2	1.4417	1.062[b]

a) From data summarized by Clarke.[5]
b) Data of Rehberg et al.[6]

The styrene used as a reference monomer in the copolymerization was purified by the ordinary method and was distilled before used.

2, 2'-Azobisisobutyronitrile (AIBN), a radical initiator, was recrystallized twice from ethanol.

Benzene, methanol, petroleum ether, and the other solvents were purified by the usual technique.

Copolymerization Procedure.—The copolymerizations of RA (M_2) with styrene (M_1) were carried out in an ordinary sealed-glass tube in the presence of 6.1

*1 Vinyl Polymerization. 153.

1) T. Otsu, T. Ito, and M. Imoto, *J. Polymer Sci.*, **B3**, 113 (1965).

2) T. Otsu, T. Ito and M. Imoto, Preprints of International Symposium on Macromolecular Chemistry, Prague (August, 1965), p. 254.

3) R. W. Taft, Jr., in "Steric Effect in Organic Chemistry," Ed. by M. S. Newman, Wiley, New York (1956), p. 556.

4) T. Otsu, T. Ito and M. Imoto, *J. Polymer Sci.*, **A4**, 733 (1965).

5) J. T. Clarke, in "Monomers," Ester of Acrylic Acid, Ed. by E. R. Blout and H. Mark, Interscience, New York (1951), p. 22.

6) C. E. Rehberg, M. B. Dixon and W. A. Faucette, *J. Am. Chem. Soc.*, **72**, 5199 (1950).

$\times 10^{-3}$mol./l. of AIBN at 60°C. The resulting copolymer was precipitated by the addition of a large amount of methanol or petroleum ether, and then reprecipitated from the benzene - petroleum ether system for the copolymer of EA and IPA, or the benzene-methanol system for the other copolymers. Most of the copolymerizations were run to five percent conversion.

The composition of the copolymer was determined from chlorine analysis (CEA copolymer), nitrogen analysis (CNEA copolymer), and carbon analysis (other copolymers). The monomer reactivity ratios, r_1 and r_2 were calculated by the method of Fineman and Ross.[7]

Results and Discussion

The results of the copolymerizations of RA with styrene are summarized in Table II. From this table, it may be observed that the rate of these copolymerizations increases with an increase in the concentration of RA in the monomer mixture. The monomer reactivity ratios, r_1 and r_2, and Alfrey-Price Q_2 and e_2 values of RA were found to be as is shown in Table III.

As can be seen from Table III, the relative reactivities, $1/r_1$, of RA toward the attack of a polystyryl radical increased with the increase in the electron-attracting nature of their alkyl substituents. When $\log(1/r_1)$ were plotted against the σ^* constant of the alkyl group according to Eq. 1, a straight line, with $\rho^*=0.56$ was obtained, as Fig. 1 shows.

However, the plot of $\log(1/r_1)-\rho^*\sigma^*$ (where $\rho^*=0.56$) against the E_s constant of the alkyl group also gave a straight line, with $\delta=0$, as is shown in Fig. 2. This result strongly indicated that the relative reactivities of RA toward a polystyryl radical were dependent on the polar character of their alkyl substituents, not on their steric characters. A similar correlation was also observed for the relative reactivities of alkyl methacrylates;[1,2] in this case, the ρ^* and δ values were found to be 0.33 and 0 respectively. The increased ρ^* value in this case might be understood from the fact that the e_2 values for RA were larger than those for alkyl methacrylates.

Figure 3 shows the relationship between the Q_2

Table II. The results of copolymerizations of RA (M_2) with styrene (M_1) at 60°C

RA (M_2)	$[M_2]$ in comonomer, mol.-fraction	Time min.	Conversion %	C (%) in copolymer	$[M_2]$ in copolymer mol.-fraction
EA	0.205	60	2.9	86.51	0.214
	0.325	60	2.6	82.37	0.319
	0.508	60	3.0	80.03	0.390
	0.657	60	3.1	77.15	0.480
	0.805	60	3.4	73.59	0.589
IPA	0.183	110	4.1	86.27	0.195
	0.278	100	3.9	84.24	0.260
	0.473	80	3.1	80.12	0.399
	0.574	60	1.9	78.82	0.443
	0.677	50	0.9	76.86	0.510
	0.890	40	1.8	71.33	0.705
BzA	0.158	100	5.8	86.84	0.229
	0.287	100	6.4	85.24	0.308
	0.428	80	5.4	83.17	0.418
	0.581	60	4.5	82.07	0.483
	0.749	60	4.3	80.48	0.582
CEA	0.160	60	3.6	6.50[a]	0.200
	0.389	60	3.3	12.07[a]	0.391
	0.555	60	4.6	14.48[a]	0.480
	0.724	60	4.4	15.98[a]	0.537
	0.899	60	2.3	19.20[a]	0.667
CNEA	0.147	30	2.2	3.11[b]	0.243
	0.289	30	2.8	4.26[b]	0.340
	0.443	30	3.1	5.13[b]	0.415
	0.592	30	4.0	5.85[b]	0.479
	0.745	30	4.2	6.79[b]	0.564
	0.898	30	4.3	7.89[b]	0.843

a) Chlorine % in the copolymers.
b) Nitrogen % in the copolymers.

7) M. Fineman and S. D. Ross, ibid., **5**, 269 (1950).

Table III. Monomer reactivity ratios for styrene (M_1) - RA (M_2) copolymerizations and Q_2, e_2 values of RA

RA	σ^* constant of R in RA	r_1	r_2	$1/r_1$	Q_2	e_2
MA[a]	0.1	0.75	0.18	1.34	0.42	0.60
EA	−0.100	0.77	0.17	1.30	0.42	0.62
n-BA[b]	−0.130	0.82	0.21	1.22	0.43	0.53
IPA	−0.190	0.76	0.26	1.32	0.48	0.45
s-BA[b]	−0.210	0.97	0.28	1.03	0.41	0.34
BzA	0.215	0.55	0.20	1.82	0.53	0.69
CEA	0.385	0.43	0.12	2.33	0.58	0.93
CNEA	0.46*	0.40	0.13	2.50	0.63	0.92

a) From Young's table for copolymerization.[8]
b) Data of Rohm & Haas Co.[9]
* Calculated from σ^* value for $CNCH_2$-group.

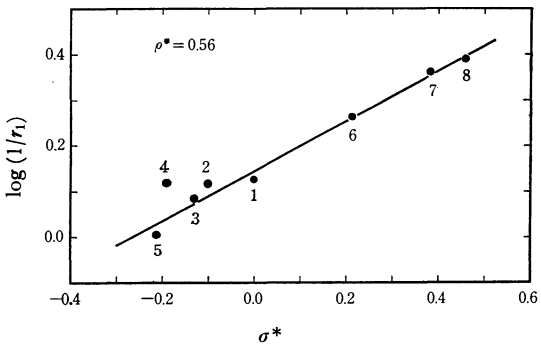

Fig. 1. The correlation between the relative reactivities of RA toward a polystyryl radical and σ^* constants of alkyl groups: 1, CH_3; 2, C_2H_5; 3, *n*-C_4H_9; 4, *i*-C_3H_7; 5, *s*-C_4H_9; 6, $C_6H_5CH_2$; 7, $ClCH_2CH_2$; 8, $CNCH_2CH_2$.

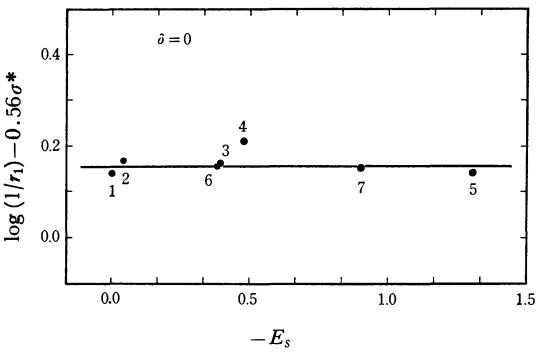

Fig. 2. The correlation between $\log(1/r_1) - \rho^*\sigma^*$ and E_s constants of alkyl groups: 1, CH_3; 2, C_2H_5; 3, *n*-C_4H_9; 4, *i*-C_3H_7; 5, *s*-C_4H_9; 6, $C_6H_5CH_2$; 7, $ClCH_2CH_2$.

and e_2 values of RA and the σ^* constant of the alkyl groups. From this figure, it is obvious that both Q_2 and e_2 values for RA increase as a function of the electron-attracting nature of the alkyl substituents, as in the case of alkyl methacrylates.[1,2] As compared with both acrylate and methacrylate series, it was observed that the change in the Q_2 values of RA effected by the σ^* constant of the alkyl groups was smaller than that of alkyl methacrylates, while the change in e_2 values was larger. These differences are perhaps understandable from the consideration that the effects of hyperconjugation and the electron-releasing nature due to the α-methyl group in alkyl methacrylates were important factors.

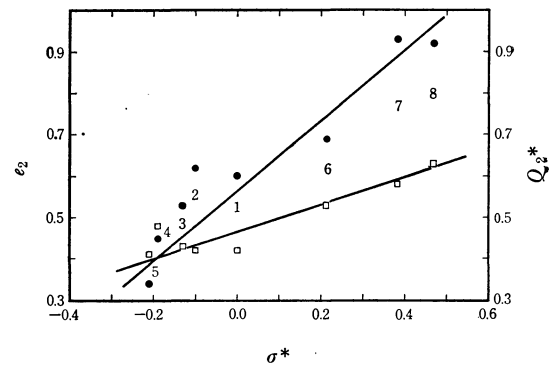

Fig. 3. The correlation between Q_2, e_2 values of RA and σ^* constants of alkyl groups: 1, CH_3; 2, C_2H_5; 3, *n*-C_4H_9; 4, *i*-C_3H_7; 5, *s*-C_4H_9; 6, $C_6H_5CH_2$; 7, $ClCH_2CH_2$; 8, $CNCH_2CH_2$.

Table IV shows the results of the measurement of the infrared spectra of RA monomers in liquid film. From this table, it was observed that the carbonyl-streching frequencies in RA were shifted

Table IV. Infrared spectroscopic data of RA*

RA	σ^* of R	$\nu_{C=O}$	$\nu_{C=C}$	ν_{C-O}
IPA	−0.190	1723	1640, 1622	1204
EA	−0.100	1726	1638, 1622	1197
BzA	0.215	1726	1634, 1621	1186
CEA	0.385	1727	1636, 1621	1185
CNEA	0.46	1728	1631, 1619	1186

* Determined with a Hitachi EPI-2 infrared spectrophotometer.

8) L. J. Young, *J. Polymer Sci.*, **54**, 411 (1961).
9) "Encyclopedia of Polymer Science and Technology," Vol. 1, Interscience, New York (1964), p. 246.

to longer wavelengths roughly as the electron-releasing character of the alkyl substituent increased. The same behavior has also been observed in a number of aliphatic or aromatic aldehydes, ketones, and acid esters.[10] Accordingly, the introduction of an electron-releasing substituent in RA makes their carbonyl groups more polar, and enhances the nature of the single-bonding of their carbonyl groups, as is shown in Eq. 2.

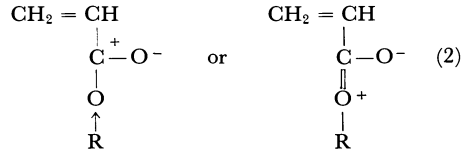

(2)

This contribution leads to the isolation of the vinyl group from its conjugated structure with the carbonyl group, and results in a decrease in Q_2 values, as well as of the e_2 values of RA as a function of the electron-releasing nature of their alkyl substituents. Such a consideration was supported by the results of ultraviolet spectroscopic study of RA and other vinyl monomers.[11]

10) M. St. Flett, *Trans. Faraday Soc.*, **44**, 767 (1948); N. Fuson, M.-L. Josien, and E. M. Shelton, *J. Am. Chem. Soc.*, **76**, 2526 (1954); H. H. Freedman, ibid., **82**, 2454 (1960); W. H. T. Davidson, *J. Chem. Soc.*, **1951**, 2456; E. J. Bourne, M. Stacey, J. C. Tatdow and R. Worrall, ibid., **1958**, 3268; M.-L. Josien, N. Fuson, J.-M. Lebas and T. M. Gregory, *J. Chem. Phys.*, **21**, 331 (1953); M. M. Morgoshes, F. Fillealk, V. A. Fassel and R. E. Randle, ibid., **22**, 281 (1954); G. Berthier, B. Pullman and J. Pontis, *J. Chim. Phys.*, **49**, 367 (1952); R. E. Kagarise, *J. Am. Chem. Soc.*, **77**, 1377 (1955).

11) T. Ito, T. Otsu and M. Imoto, *J. Polymer Sci.*, in press.

BULLETIN OF THE CHEMICAL SOCIETY OF JAPAN VOL. 39 2260—2263 (1966)

The Mechanism of the Alkaline Fusion of Diphenylsulfone[1]

By Shigeru OAE and Naomichi FURUKAWA

Department of Applied Chemistry, Faculty of Engineering, Osaka City University, Sumiyoshi-ku, Osaka

(Received February 7, 1966)

Diphenylsulfone-1-^{14}C was treated with fused potassium hydroxide at 300°C for 7 hr. in a sealed metal tube. The yield of phenol, as determined by the isotope dilution technique, was found to be almost quantitative. The distribution of ^{14}C in the resulting phenol was determined by degradating it by the usual method. Practically all the activity of ^{14}C in the phenol was found at the position 1, which corresponded to the originally-labeled position in the diphenylsulfone-1-^{14}C used. This indicates that the mechanism of the alkaline fusion of diphenylsulfone proceeds thruogh a simple S_N2-type mechanism, not the elimination-addition mechanism.

The treatment of diphenylsulfone with potassium hydroxide at a high temperature was first performed several decades ago by Otto,[2] who claimed to have obtained diphenyl and phenol as the main final products of the reaction. Many years later, Ingold and Jessop[3] studied the reaction more precisely; they observed that the main products of this reaction were benzene and benzenesulfonic acid. From the product analysis, they suggested that the mechanism of the reaction involved the primary attack of the hydroxide ion on the sulfur atom, thus expanding the valence shell to decet and forming an incipient complex that collapsed immediately to form the sulfonic acid and benzene, as is shown below.

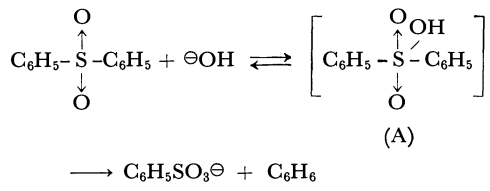

(A)

$\longrightarrow C_6H_5SO_3^{\ominus} + C_6H_6$

Although the hypothesis of valence-shell expansion in the sulfur atom is very attractive in view of the many well-elucidated examples in other reactions,[4] it has to be tested with more rigorous experiments. We have previously investigated this reaction using ^{18}O-labeled potassium hydroxide[5] in order to test Ingold's mechanism; we found that there was no simultaneous ^{18}O incorporation in diphenyl sulfone during the reaction. This suggested that the reaction was a simple synchronous S_N2-type displacement reaction at the sulfur

1) Phenols and Phenolic Esters. XII.
2) R. Otto, *Chem. Ber.*, **19**. 2425 (1886).
3) C. K. Ingold and J. A. Jessop, *J. Chem. Soc.*, **1930**, 708.
4) C. C. Price and S. Oae, "Sulfur Bonding," Ronald Press, New York (1962).
5) D. R. Christman and S. Oae, *Chem. & Ind.*, **1959**, 1251.

atom. However, all these past experiments do not give any hint as to the mechanism of the formation of phenol.

A question still remains whether phenol is formed directly by the nucleophilic attack on the sulfone group by the hydroxide anion (Mechanism I), or through the initial formation of benzenesulfonic acid, followed by substitution with the hydroxide anion (Mechanism II). Moreover, in such strong alkaline conditions as were used in the reaction, the elimination-addition mechanism involving a benzyne-type intermediate[6] also has to be considered (Mechanism III).

The three different mechanisms conceivable for the reaction may be summarized as follows:

I. Simple S_N2-type mechanism:

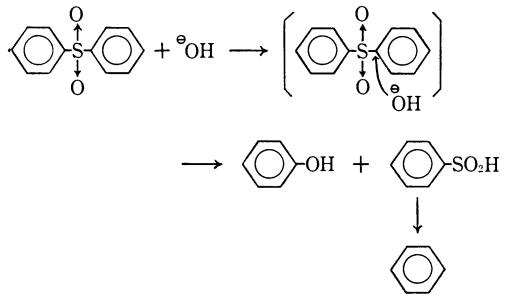

II. Through-sulfonic-acid mechanism:

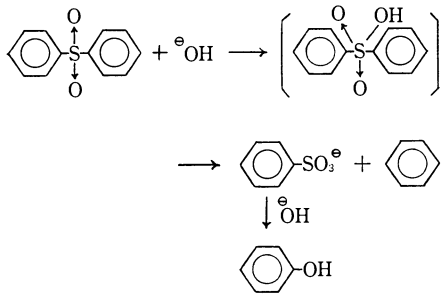

III. Elimination-addition mechanism:

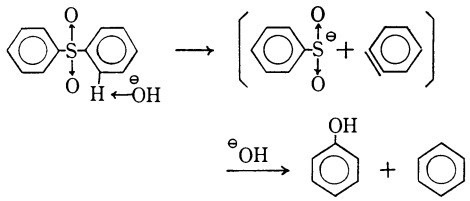

Both the mechanisms I and III involve the formation of phenol and sulfinic acid, which eventually give benzene and which are quite reasonable since benzenesulfinic acid is known to decompose to benzene when treated with molten alkali at a relatively low temperature.[7] According to the mechanism II, benzene is formed, together with benzenesulfonic acid, which is then converted directly to phenol through a simple S_N2-type mechanism.[8] In this paper, we wish to present a detailed account of the mechanistic investigation of the alkaline fusion of diphenyl sulfone using the sulfone labeled with ^{14}C at position 1 of the benzene ring. When the reaction proceeds through the mechanism I or II, the ^{14}C activity in the phenol will be found only at the 1 position, whereas if the reaction proceeds through the mechanism III, half of the total ^{14}C activity in the phenol may be expected to be found at the 1 position, while the remaining 50% should be distributed equally between the 2 and 6 positions.

Results and Discussion

Diphenyl sulfone-1-^{14}C was synthesized according to the following scheme (Fig. 1):

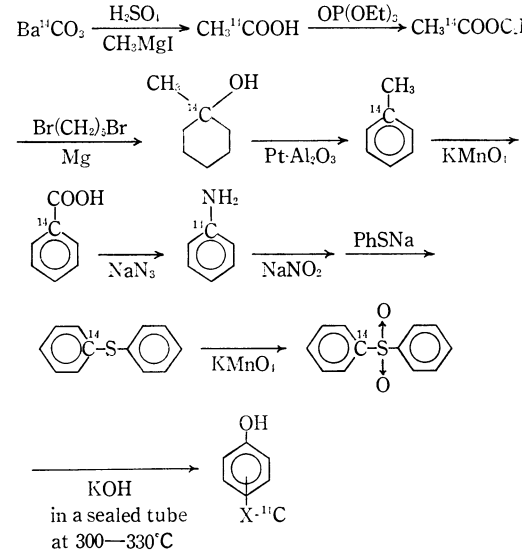

Fig. 1.

The method of degrading phenol is illustrated schematically in Fig. 2. A detailed account of the scheme has been presented elsewhere.[8] The yield of phenol was determined by the conventional isotopic dilution technique, which will be described in detail in the Experimental section.

The results of the degradation of the resulting phenol are shown below:

The results clearly indicate that all the ^{14}C activities of the phenol were found at position 1 of the sulfone where ^{14}C was originally labeled. This

6) See, for example, J. D. Roberts, H. E. Simmons, Jr., C. A. Carlsmith and C. W. Vaughan, *J. Am. Chem. Soc.*, **75**, 3290 (1953).

7) R. Otto, *Ann*, **145**, 322 (1868).

8) S. Oae, N. Furukawa, M. Kise and M. Kawanishi, This Bulletin, **39**, 1212 (1966).

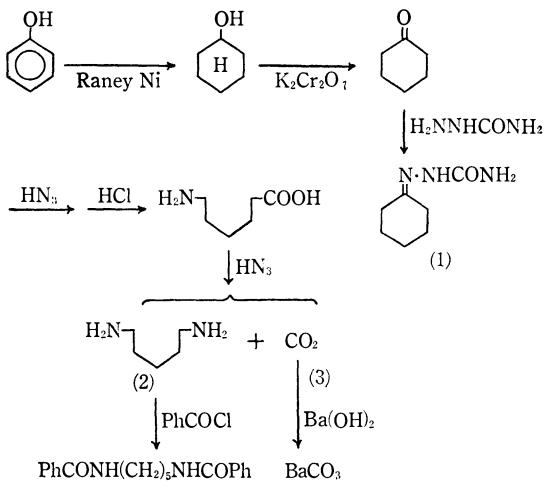

Fig. 2.

Table I. Counting data

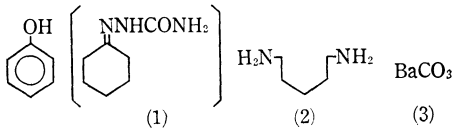

	(1)	(2)	(3)
c. p. m.	625 (729)[a]	0	4215 (703)[b]
%	100	0	96.4
c. p. m.	426 (497)[a]	—	2903 (484)[b]
%	100	—	97.4

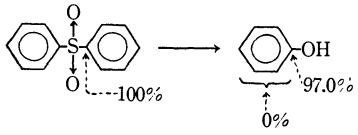

a, b) The counts were corrected for background. The counts were recalculated as follows; for example, $625\times7/6=729$ and $4215\times1/6=703$.

excludes the elimination-addition mechanism involving a benzyne-type intermediate, since the mechanism requires half of the ^{14}C activities to be at the position 1, while the remaining half are divided equally between the two ortho positions.

Now that the mechanism III is excluded from the ^{14}C tracer experiment, the next problem is to make a choice between the mechanisms I and II. Earlier works related to nucleophilic substitutions on various aryl arylsulfonates suggest that the hydroxide ion prefers to attack the sulfone group rather than the aryl carbon.[9,10] Although a reaction in a fused alkali may be somewhat different from that in aqueous media, the same trend of nucleophilic selectivity would be found in both reactions, since the negative hydroxide ion attacks the positively-charged sulfur atom of the sulfone group more readily than the neutral benzene carbon. Moreover, the successful isolation of benzenesulfonic acid in the reaction by Ingold and his group, as well as by us, appears to suggest strongly that the hydroxide ion preferentially attacks at the sulfone group, as is illustrated by mechanism II.

9) C. A. Bunton and Y. F. Frei, *J. Chem. Soc.*, **1956**, 3240.
10) S. Oae and R. Kiritani, This Bulletin, **38**, 765 (1965).

Experimental

The Preparation of Diphenylsulfone

Aniline-1-^{14}C.—Aniline-1-^{14}C was synthesized starting from barium carbonate-^{14}C through 7 steps. The synthetic method has been described previously.[8]

Diphenylsulfide-1-^{14}C.—Thiophenol (3.0 g.) was dissolved in 40 ml. of a 20% potassium hydroxide solution. To this solution there was added benzenediazonium chloride-1-^{14}C prepared from 1.9 g. of aniline and 1.7 g. of sodium nitrite in 8 ml. of water, with the temperature kept at 70°C with vigorous stirring. After the addition had been completed, the mixture was stirred for 2 more hr. at the same temperature. Then the solution was extracted with ether. The ether solution was washed with water and dried over magnesium sulfate. After the ether had been evaporated, the residue was distilled under reduced pressure. Diphenylsulfide-1-^{14}C (2.8 g.) was thus obtained in a 76% yield (b. p. 124°C/3 mmHg).

Diphenylsulfone-1-^{14}C.—Diphenylsulfide-1-^{14}C (2.8 g.) was oxidized with 4.4 g. of potassium permanganate in 15 ml. of acetic acid. After the addition of potassium permanganate, the reaction mixture was warmed on a water bath for 1 hr. at 50°C. Then the mixture was quenched with a large amount of water. To this solution sulfur dioxide gas was introduced in order to decompose the excess potassium permanganate. The precipitate was then filtered and washed with water. The crude diphenylsulfone was recrystallized from *n*-hexane - benzene. The yield was 2.6 g. in a 81% yield (m. p. 128°C).

The Alkaline Fusion of Diphenylsulfone-1-^{14}C.—Diphenylsulfone-1-^{14}C (1.00 g.) was fused with 3.0 g. of potassium hydroxide in a small nickel tube which had a cork stopper equipped with a capillary tube to collect the benzene evolved. The tube was immersed in a potassium nitrate salt bath at the initial temperature of 240°C. Then the temperature was raised gradually to 300—330°C, at which temperature the reaction tube was kept for 7 hr. The reaction began at 250°C. After cooling, the reaction mixture was dissolved in water. To this mixture authentic phenol was added as a carrier. The mixture was acidified with concentrated hydrochloric acid, and then steam-distilled. The distillate was saturated with sodium chloride and extracted with ether, and the etheral solution was dried over magnesium sulfate. After the ether had evaporated off, the residue was distilled; phenol-*x*-^{14}C boiling at above 180°C was thus collected. The yield was determined by the isotope dilution method using the equation:

$$xS_0 = (a - x)S \qquad x = \frac{aS}{S_0 - S}$$

where x is the unknown weight of the phenol produced, where S_0 and S are the ^{14}C activities in the initial and diluted phenol respectively, where S_0 represents the activity of the diphenyl sulfone-1-^{14}C available in the reaction, and where a is the authentic, weighed amount of pure phenol for dilution.

From the experimental figure (S_0: 9738 c. p. m.; S: 1448 c. p. m; a: 2.22 g.), x was calculated to be 0.39 g. (91% of the theoretical yield).

The Degradation of Phenol-x-^{14}C.—The degradation of phenol-x-^{14}C was carried out following a method described previously.[8]

The counting of ^{14}C was performed according to the conventional Van-Slyke wet combustion method. The activities were measured for cyclohexanonesemicarbazone, barium carbonate and dibenzoyl pentamethylenediamine, with pellets of these samples weighing 132 mg., 181 mg., and 218 mg. respectively. The measurements of ^{14}C was performed with an Aloka 2π-gas flow G. M. counter, using Q-gas as the counting gas. The data are shown in Table I.

BULLETIN OF THE CHEMICAL SOCIETY OF JAPAN VOL. 39 2263—2265 (1966)

The Reaction of Organodisilanes with *N*-Bromosuccinimide[1)]

By Hideki SAKURAI, Akira HOSOMI, Jun-ichi NAKAJIMA and Makoto KUMADA

Department of Synthetic Chemistry, Kyoto University, Sakyo-ku, Kyoto

(Received February 17, 1966)

The reactions of three hexaorganodisilanes with *N*-bromosuccinimide in carbon tetrachloride or in chloroform were carried out. Hexamethyldisilane afforded trimethylbromosilane (82.9—100%) and *N*-trimethylsilylsuccinimide (73.5—79.5%). No bromomethylpentamethyldisilane was obtained. Similarly, 1, 2-diphenyltetramethyldisilane gave phenyldimethylbromosilane and a small amount of bromobenzene. The *N*-silyl compound could not be isolated, but succinimide was obtained as a decomposition product. Phenylpentamethyldisilane gave trimethylbromosilane and phenyldimethylbromosilane in 67.4 and 12.3% yields respectively. A possible reaction mechanism was discussed.

N-Bromosuccinimide (NBS) is known as an efficient brominating agent, especially for allylic carbons;[2)] it may react via a free radical chain mechanism in non-hydroxylic solvents.

Since the introduction of a halogen into a methyl group of hexamethyldisilane or other related compounds is a highly desirable operation in the field of organosilicon chemistry, we have investigated the reaction of hexamethyldisilane with NBS, primarily in the hope of preparing (bromomethyl)-pentamethyldisilane. However, contrary to our expectation, the reaction led to a cleavage of the silicon-silicon bond, even in non-polar solvents. In view of these findings, it became of interest to investigate the reaction for variously substituted disilanes, since NBS is known to react as a positive halogen donor to an olefin only in polar protic solvents.[3)]

While the present work was in progress, Calas, Frainnet and Dentone[4)] have also briefly described the formation of methyldiethylbromosilane and *N*-methyldiethylsilylsuccinimide by the reaction of 1, 2-dimethyltetraethyldisilane with NBS.

In the present paper, we wish to report some of our own results especially from the mechanistic point of view.

Results and Discussion

The reaction of the three organodisilanes employed here with NBS leads to the cleavage reaction, giving bromosilanes and *N*-silylsuccinimides instead of (bromomethyl)disilanes. The results are summarized in Table I. It is interesting to note that trimethylbromosilane was a major product in the reaction of phenylpentamethyldisilane with NBS.

NBS has been considered to undergo a reaction in which the initial attack on the substrate in the bromination is possibly by the succinimido radical and in which the chain-propagating step is the attack on the second NBS molecule by the resulting carbon radical.[5)]

Hydrogen atoms of hexamethyldisilane have been

1) Preliminary experiments were cited in M. Kumada and R. Okawara, "Yukikeiso Kagaku (Organosilicon Chemistry)," Maki, Tokyo (1959), p. 74.

2) C. Djerassi, *Chem. Revs.*, **43**, 271 (1948).

3) L. Horner and E. H. Winkelmann, *Angew. Chem.*, **71**, 349 (1959).

4) R. Calas, E. Frainnet and Y. Dentone, *Compt. rend.*, **259**, 3777 (1964).

5) C. Walling, "Free Radicals in Solutions," John Wiley & Sons, New York (1957).

TABLE I. THE REACTION OF ORGANODISILANES WITH *N*-BROMOSUCCINIMIDE[a]

Disilanes	Solvent	Product	(% yield)
$(CH_3)_3SiSi(CH_3)_3$	$CHCl_3$	$(CH_3)_3SiN(COCH_2)_2$	(79.5)
		$(CH_3)_3SiBr$[b]	(82.9)
$(CH_3)_3SiSi(CH_3)_3$	CCl_4	$(CH_3)_3SiN(COCH_2)_2$	(73.5)
		$(CH_3)_3SiBr$[b]	(100)
$C_6H_5(CH_3)_2SiSi(CH_3)_3$	CCl_4	$(CH_3)_3SiBr$[b]	(67.4)
		$C_6H_5(CH_3)_2SiBr$[b]	(12.3)
		C_6H_5Br, small amount	
		$(CH_2CO)_2NH$[c]	(77.1)
$C_6H_5(CH_3)_2SiSi(CH_3)_2C_6H_5$	CCl_4	$C_6H_5(CH_3)_2SiBr$[b]	(76.6)
		C_6H_5Br, small amount	
		$(CH_2CO)_2NH$[c]	(67.7)

a) Equimolar amount of NBS to disilanes was employed.
b) Determined by titration.
c) Possibly, decomposition compound of $C_6H_5(CH_3)_2SiN(COCH_2)_2$.

shown to be abstracted by a number of electron-seeking radicals, such as benzoyloxy,[6] *t*-butoxy[7] and trichloromethyl[7] radicals. Therefore, it may be expected that hexamethyldisilane can be brominated by chain reactions involving homolytic hydrogen abstraction by succinimido radicals in non-polar solvents. Accordingly, the reaction of hexamethyldisilane with NBS does not involve this sort of free-radical-chain mechanism.

Alternatively, recent evidence[8,9] indicates that the mechanism of NBS bromination may actually involve bromine molecules rather than NBS as the chain-carrying species; namely, NBS may function only by producing bromine molecules at a low concentration:

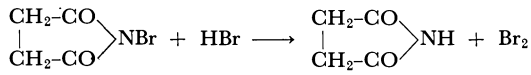

$$Br_2 \rightleftarrows 2Br\cdot$$

$$Br\cdot + RH \longrightarrow HBr + R\cdot$$

If this is the case, the cleavage of the silicon-silicon bond may be expected, since hexaalkyldisilanes are considerably reactive towards bromine molecules.[10] In fact, immediately after a first portion of hexamethyldisilane had been added to a cold suspension of NBS, a red color of bromine developed throughout the reaction. Moreover, the fact that diphenyltetramethyldisilane requires a higher temperature to complete the reaction may indicate that some sort of electrophilic attack on the silicon-silicon bond occurs.[10]

However, such a mechanism is not sufficient to account for the formation of *N*-silylsuccinimides. The simplest mechanism consistent with the facts seems to be one in which an intermediate of a four-center type is involved. In general, the silicon-silicon bond undergoes a variety of electrophilic and oxidative cleavage reactions. Many examples suggest that the cleavage reactions may resemble the corresponding electrophilic addition reactions to the carbon-carbon double bond.[11] *N*-Bromoamides are also known to have a tendency to form an addition compound with a carbon-carbon double bond; some of these addition compounds have been isolated.[2]

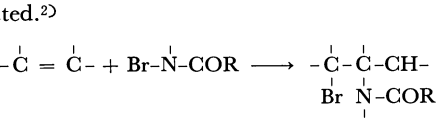

Therefore, although the possibility of a mechanism involving molecular bromine can not be excluded, the product distribution in the reaction of phenylpentamethyldisilane with NBS suggests that the probable mechanism for this reaction is the direct attack of NBS on the silicon-silicon bond through a four-center transition state. Such a process must be likely in carbon tetrachloride or chloroform, since the solvents have no nucleophilic power and since no separation of ions, which is improbable in a weakly polar reaction, is necessary.

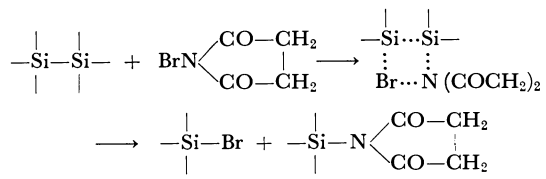

The bromine atom may orient to the more negative silicon atom, so that trimethylbromosilane is formed as a major product in the reaction of phenylpentamethyldisilane with NBS.

6) H. Sakurai, R. Koh, A. Hosomi and M. Kumada, This Bulletin, **39**, in press.
7) H. Sakurai, T. Kishida, A. Hosomi and M. Kumada, *J. Organometal. Chem.*, in press.
8) R. E. Pearson and J. C. Martin, *J. Am. Chem. Soc.*, **85**, 354 (1963).
9) G. A. Russell C. Deboer and K. M. Desmore, ibid., **85**, 365 (1963).
10) C. Eaborn, "Organosilicon Compounds," Butterworths, London (1960), Chapt. 12.
11) H. Sakurai, T. Imoto, N. Hayashi and M. Kumada, *J. Am. Chem. Soc.*, **87**, 4001 (1965).

Experimental

Materials.—NBS,[12] hexamethyldisilane,[13] phenylpentamethyldisilane,[14] and 1, 2-diphenyltetramethyldisilane[15] were prepared by the reported procedure.

The Reaction of Hexamethyldisilane with NBS in Chloroform.—To a stirred and externally-cooled suspension of 37.5 g. (0.21 mol.) of NBS in 50 ml. of dry chloroform, there was added, drop by drop, 34 g. (0.23 mol.) of hexamethyldisilane. Immediately after a first portion of hexamethyldisilane had been added, the red color of bromine developed. After the addition had been completed, the solution was stirred at room temperature for 1 hr., then an almost complete decolorization occurred. The mixture was then submitted to distillation to give the following fractions: (a) chloroform and trimethylbromosilane, boiling up to 80°C (110 g.); and (b) fraction boiling at 120°C (18 mmHg) (27 g.). The redistillation of Fraction a through a 35 cm. column packed with glass helicoils gave 31 g. of trimethylbromosilane, b. p. 80°C, contaminated with a small amount of chloroform. The mixture was analyzed by titrating the hydrolyzable bromine and so estimated to contain 26.8 g. (0.175 mol., 82.9%) of trimethylbromosilane. Fraction b was quite hygroscopic and decomposed to succinimide, m. p. 123—125°C, and hexamethyl disiloxane upon treatment with water. The redistillation of Fraction b gave pure *N*-trimethylsilylsuccinimide, n_D^{20} 1.4732, d_4^{20} 1.0684, MR_D 44.99 (calcd. 45.18).

Found: Si, 16.7. Calcd. for $C_7H_{13}O_2NSi$: Si, 16.4%.

The Reaction of Hexamethyldisilane with NBS in Carbon Tetrachloride.—To a stirred suspension of 37.5 g. (0.21 mol.) of NBS in 50 ml. of dry carbon tetrachloride, 31 g. of hexamethyldisilane was added in virtually the manner described above. After work-up, *N*-trimethylsilylsuccinimide (25 g., 73.5%) and trimethylbromosilane (33.7 g., 100% by titration) were obtained.

The Reaction of 1, 2-diphenyltetramethyldisilane with NBS in Carbon Tetrachloride.—1, 2-Diphenyltetramethyldisilane (20 g., 0.074 mol.) in 100 ml. of dry carbon tetrachloride was added to a stirred suspension of 13 g. of NBS (0.073 mol.) in 30 ml. of carbon tetrachloride. External heating was necessary to keep the reaction proceeding. After the addition was complete, the reaction mixture was submitted to distillation. After the carbon tetrachloride has been removed, b. p. 75°C, a fraction boiling at 118—125°C (50 mmHg) (12.5 g.) was obtained. The gas chromatographical analysis of the fraction indicated the presence of phenyldimethylbromosilane (main component) and bromobenzene. The amount of phenyldimethylbromosilane was determined by titration to be 12.0 g. (yield 76.6%). The distillation residue, possibly *N*-phenyldimethylsilylsuccinimide, could not be distilled off successfully, but 4.9 g. (67.7%) of succinimide was obtained as a decomposition product, b. p. 148°C (2 mmHg).

The Reaction of Phenylpentamethyldisilane with NBS in Carbon Tetrachloride.—Phenylpentamethyldisilane (15 g., 0.072 mol.) was allowed to react with NBS (13 g., 0.073 mol.) in carbon tetrachloride in the same manner. Moderate heating was necessary to initiate the reaction. After work-up as described above, 74 g. of a mixture of carbon tetrachloride and trimethylbromosilane, b. p. 75—78°C, 3 g. of a mixture of phenyldimethylbromosilane and bromobenzene, 63°C (31 mmHg), and 5.5 g. (77.1%) of succinimide were obtained. The amounts of trimethylbromosilane and phenyldimethylbromosilane were determined by titration to be 7.4 g. (67.4%) and 1.9 g. (12.3%) respectively.

The authors are indebted to the Tokyo Shibaura Electric Co., Ltd., for its gifts of chlorosilanes and a methylchlorosilane residue.

This research was supported in part by a grant-in-aid of the Ministry of Education and by the Kawakami Memorial Foundation, to which the authors' thanks are due.

12) K. Ziegler, A. Späth, E. Schaaf, W. Schmann and E. Winkelmann, *Ann.*, **551**, 109 (1942).
13) M. Kumada, M. Yamaguchi, Y. Yamamoto, J. Nakajima and K. Shiina, *J. Org. Chem.*, **21**, 1264 (1956).
14) E. A. Chernychev, N. G. Tolstikova, A. A. Ivashenko, A. A. Zelenetskoya and L. A. Leites, *Izv. Akad. Nauk S. S. S. R., Otd. Khim. Nauk*, **1963**, 660.
15) H. Gilman, G. D. Lichtenwalter and D. Wittenberg, *J. Am. Chem. Soc.*, **81**, 5320 (1959).

BULLETIN OF THE CHEMICAL SOCIETY OF JAPAN VOL. 39 2266—2269 (1966)

The Reactions of Oximes with Lead Tetraacetate. The Scope of the Reactions

By Yasuhide YUKAWA, Mitsuru SAKAI and Shigeo SUZUKI

The Institute of Scientific and Industrial Research, Osaka University, Sakai, Osaka

(Received March 7, 1966)

A detailed study of the reaction of oximes by lead tetraacetate has been made. It has been found that the reaction gave nitrogen and the respective aldehydes or ketones in good yields. In the reaction, which can be applied to general oximes, the order of yields was: aliphatic aldoximes > aliphatic ketoximes > alicyclic ketoximes > aromatic ketoximes > aromatic aldoximes. Some limited mechanistic implications are presented and discussed on the basis of the results obtained. Stoichiometrically, it has been found that 2 moles of oxime react with 1 mole of lead tetraacetate to produce 2 moles of aldehyde or ketone and 1 mole of nitrogen.

Many interesting results of the reactions with lead tetraacetate have been observed in a wide variety of organic substrates. In addition to its utility in cleaving glycols and in oxidizing alcohols to aldehydes, lead tetraacetate can be used to introduce methyl or acetoxy groups into suitably-activated positions in organic compounds.[1] More recently, we have found that 1, 2-dioximes could be dehydrogenated and cyclized to form furoxane derivatives quantitatively by adding the dioxime to an acetic acid solution of lead tetraacetate.[2] In the last few years, we have been interested in the reactions of lead tetraacetate, particularly those with olefins and oximes.[3] A thorough search of the literature has revealed that lead tetraacetate-oxime reactions had not previously been investigated in detail. Iffland and Criner,[4] for instance, reported that lead tetraacetate was capable of oxidizing cyclohexanone oxime. Their study was carried out at 0°C for 5 hr. in dichloroethane. They supposed that this reaction product was 1-acetoxy-1-nitrosocyclohexane, but they gave no evidence for this assignment.

In the present paper, we wish to report the results of lead tetraacetate-oxime reaction. The interaction between the two species yields aldehyde or ketone, lead acetate and acetic acid. The scopes, limitations, and synthetic applications of various lead tetraacetate-oxime reactions will be presented in this paper. The kinetic and mechanistic aspects of these reactions will be discussed in a succeeding paper.

Results

The reaction of aldoximes or ketoximes in acetic acid with lead tetraacetate proceeds smoothly, with the evolution of nitrogen, to give the corresponding carbonyl compounds in good yields. The procedure consists of stirring the reactants at 70°C in acetic acid and quenching the reaction mixture by pouring in cold water. A reasonable equation for the over-all reaction seems to be Eq. 1:

$$\begin{matrix} R \\ R' \end{matrix}\!\!>\!C{=}NOH + \frac{1}{2}Pb(OAc)_4 \longrightarrow \begin{matrix} R \\ R' \end{matrix}\!\!>\!C{=}O + \frac{1}{2}N_2 + \frac{1}{2}Pb(OAc)_2 + AcOH \quad (1)$$

Standard conditions, a one-hour heating at 70°C with a half-equivalent of lead tetraacetate, were employed throughout the present work in order to compare the reactions of different oximes. Product assignments were made by a comparison of the infrared spectra and vapor-phase chromatogram of the products with those of authentic samples. The products were also isolated from the reaction mixture by means of distillation and vapor-phase chromatography. The analytical gas chromatography of nitrogen was performed, using helium as the carrier gas, on a column of Molecular sieve 13X at 25°C.

The reaction was applied to more than thirty oximes of various types. The pertinent data are summarized in Table I.

As is indicated in Table I, seven aliphatic aldoximes, seven aromatic aldoximes, ten aliphatic

1) R. Criegee, *Angew. Chem.*, **70**, 173 (1958); G. W. K. Cavill and D. H. Solomon, *J. Chem. Soc.*, **1954**, 3943; R. Criegee, *Ann.*, **481**, 263 (1930); R. F. Brown and L. S. Yee, *J. Am. Chem. Soc.*, **67**, 874 (1945); L. F. Fieser and S. T. Putnum, ibid., **69**, 1038 (1947); L. F. Fieser and E. B. Hershberg, ibid., **60**, 1893, 2542 (1938).

2) Y. Yukawa and M. Sakai, *J. Chem. Soc. Japan, Pure Chem. Sect. (Nippon Kagaku Zasshi)*, **87**, 79, 81, 84 (1966).

3) Y. Yukawa and M. Sakai, This Bulletin, **36**, 761 (1963).

4) D. C. Iffland and G. X. Criner, *Chem. & Ind.*, **1956**, 176.

Table I. Deoximation by lead tetraacetate

Oxime 0.05 mol.; Lead teteaacetate 0.025 mol.; Acetic acid 50 ml.; Temp. 70°C; Time 30 min.

Oxime	M. p., °C	Carbonyl compd. Yield, %
$CH_3(CH_2)_4CH=NOH$	51	69
$CH_3(CH_2)_6CH=NOH$	60	85
$CH_3(CH_2)_7CH=NOH$	63.5	94
$CH_3(CH_2)_8CH=NOH$	67.8	92
$CH_3(CH_2)_9CH=NOH$	71	91
$CH_3(CH_2)_{10}CH=NOH$	72	90
Citral oxime	b. p. 130°C/10 mmHg	75
$C_6H_5CH=NOH$	35	91
p-$CH_3OC_6H_4CH=NOH$	60	90
p-$(CH_3)_2CHC_6H_4CH=NOH$	60	76
$C_6H_5CH=CHCH=NOH$	136	89
$C_6H_5CH=CCH=NOH$ $\quad\quad\quad

TABLE III. THE OXIDATION OF ACETOPHENONE OXIME BY VARIOUS OXIDANTS

Acetophenone oxime, 0.05 mol.; Oxidants, 0.03 mol.; Solvents, 50 ml.

Oxidant	Solvent	Temp., °C	Time, hr.	Yield, % Acetophenone	N_2
Lead tetraacetate	Acetic acid	70	2	92	95
Periodic acid	Dioxane	25	0.5	43	20
Potassium ferricyanide	H_2O-EtOH	60	4	0	0
Sodium bismuthate	Acetic acid	25	0.5	70	60
Mercuric sulfate	Acetic acid	120	2	35	—
Cupric sulfate	Pyridine	80	2	30	15
Potassium dichromate	Acetic acid	80	2	40	45
Mercuric acetate	Acetic acid	80	2	20	5
Cerium nitrate	Acetic acid	25	1	41	20
None	Acetic acid	120	2	1.5	0

The reactions of the unsaturated oximes are interesting because lead tetraacetate can easily attack unsaturated compounds. However the presence of a double bond does not affect the reaction so seriously, though it does lower the yield. It appears to be necessary to choose suitable conditions in such a case. The reaction of citral oxime with lead tetraacetate was investigated under various conditions, which are summarized in Table II.

In these studies, a slight modification of the usual reaction conditions was employed. The best yield of citral (82%) was obtained when acetic acid was used as a solvent and an equivalent mole of anhydrous sodium acetate was added. The yield dropped to 45% when pyridine was employed. In this reaction, lead tetraacetate would act toward oximes as an oxidizing agent, but not as a hydrolyzing agent. It was desirable to compare it with other oxidizing agents. The reactions of acetophenone oxime with periodic acid, potassium ferricyanide, sodium bismuthate, mercuric sulfate, mercuric acetate and cerium nitrate were therefore carried out. The reaction conditions employed and the results obtained are summarized in Table III. Lead tetraacetate and sodium bismuthate were more efficient oxidizing agents than either periodic acid or cerium nitrate. In the absence of an oxidizing agent, only a small percentage of the acetolysis product was obtained. The above results indicated that lead tetraacetate is a suitable oxidizing agent for the conversion of acetophenone oxime to acetophenone.

Experimental

All melting points and boiling points are uncorrected. The melting points were taken on a Yanagimoto melting-point apparatus. The infrared spectra were determined using a Hitachi double-beam spectrophotometer. The vapor-phase chromatographic analyses were carried out on a Yanagimoto Model GCG-3 vapor fractometer. The elemental analyses were performed by the Micro-analytical Laboratories of our Institute.

Materials.—The glacial acetic acid was purified with chromium trioxide as before.[6] All of the oximes were prepared in the same manner, using the corresponding carbonyl compounds, hydroxylamine hydrochloride and sodium bicarbonate. The melting points of these oximes are given in Table I.

General Procedure.—Lead tetraacetate was prepared according to the method of Dimroth and Schweizer.[7] It was moistened with acetic acid for storage. The reagent was filtered under suction and dried in a vacuum-desiccator over potassium hydroxide pellets for 6 hr. The resulting white crystalline material was then usually about 98% pure, as estimated by iodometric titration. When reactions were carried out in a solvent other than acetic acid, the lead tetraacetate obtained as above was repeatedly washed with the appropriate solvent and, after filtration, was dried in a vacuum desiccator: in these cases, a brownish material was obtained.

Oximes (0.05 mol.) in glacial acetic acid (30 ml.) was added, drop by drop over a 1 hr. period, to a stirred suspension of lead tetraacetate (0.025 mol.) in glacial acetic acid (20 ml.). The addition of an oxime to lead tetraacetate in acetic acid at room temperature caused an immediate green coloration of the solution. During the addition the reaction mixture was kept at 70°C, and the reaction proceeded rapidly with the evolution of nitrogen. The analytical gas chromatography of nitrogen was performed on a Yanagimoto Model GCG-3, with helium as the carrier gas on a column of Molecular sieve 13X at 25°C. The green reaction mixture gradually turned into a clear yellow solution. After stirring had continued for an additional hour, the solution was poured into ether (50 ml.) and 20 ml. of water was added. The resultant precipitates in the etheral solution had dissolved into the washing water, and no lead dioxide was observed. The etheral layer was washed with 20 ml. of water, six 20 ml. portions of 5% sodium bicarbonate, and two 20 ml. portions of water. The ethereal solution was dried over magnesium sulfate. The ether was removed, and the remaining liquid was distilled through a spinning-band column.

The Reaction of Menthone Oxime with Lead Tetraacetate in Dichloroethane.—To a stirred

6) E. Berliner and M. C. Beckett, *J. Am. Chem. Soc.*, **79**, 1425 (1957).

7) O. Dimroth and R. Schweizer, *Ber.*, **56**, 1375 (1923).

solution of 3.5 g. (0.021 mol.) of menthone oxime in 50 ml. of dichloroethane, 10.0 g. (0.023 mol.) of lead tetraacetate was added. The temperature was maintained at 0—5°C with cooling. After about 1 hr. of stirring, the solution was deep blue. The resulting mixture was poured into cold water. The dichloroethane layer was separated and dried, and the dichloroethane was evaporated under reduced pressure. The distillation of the residue gave 4.0 g. (85%) of 1-acetoxy-1-nitroso-2-isopropyl-5-methylcyclohexane, b. p. 92°C/3.5 mmHg, $\lambda_{max}^{alc.}$ 680 mμ (ε 18).

Found: C, 63.62; H, 9.70. Calcd. for $C_{12}H_{21}NO_3$; C, 63.41; H, 9.31%.

We wish to thank the Shiono-koryo Company for the kindness of providing us with samples of citral, menthone, carbomenthone and pulegone. We are also indebted to Mr. Tsuneyo Shishido and Takuzo Fujino of the Microanalytical Section of this laboratory for microanalyses.

BULLETIN OF THE CHEMICAL SOCIETY OF JAPAN VOL. 39 2269—2273 (1966)

The Rotatory Dispersion and Stereochemistry of Organic Compounds. XII.[1] The Circular Dichroism of Hexose Nitrates

By Yojiro TSUZUKI, Koko TANABE, Kikuhiko OKAMOTO and Noriko YAMADA

Department of Chemistry, Tokyo College of Science, Kagurazaka, Shinjuku-ku, Tokyo

(Received March 19, 1966)

Circular dichroism has been measured of eighteen nitrates of hexoses (glucose, mannose and altrose), and its correlation with the rotatory dispersion as well as the ultraviolet absorption has been established, verifying even a number of suggestions made as regards the sign of some ambiguous Cotton effects (Tsuzuki et al., This Bulletin, **39**, 1391 (1966)), which has eventually led to some significant conclusions.

It was reported for the first time by Mitchell[2] that nitrochromophore ($-NO_2$) is of significance in the studies of rotatory dispersion (RD). Some interesting results were really shown with several nitro-compounds,[3,4] and recently investigations were made on the rotatory dispersion, circular dichroism (CD) and ultraviolet absorption (UV) of a number of compounds containing nitrochromophore.[5,6] Thanks to these studies, the NO_2-chromophore proved to be quite useful in investigating configurational problems for organic compounds. Particularly comparison of CD and UV was found advantageous to the analysis of complex or obscure Cotton effects.

As already reported,[1,7-9] the nitrate chromophore exhibited an optically active absorption and proved to be of great use to the configurational studies of sugars and hydroxy-carboxylic acids, especially with respect to the conformation and optical contribution of the hydroxyl groups.

The rotatory dispersion of compounds with nitrate chromophore exhibits a Cotton effect around 300 mμ, but its absorption is so weak that it becomes often difficult in sugar derivatives to discern the character of the Cotton effect, since it is overlapped by the strong, background optical rotation, particularly due to the C_1- and C_2 groups.

In a previous paper[1] some RD curves were analyzed and the Cotton effects were characterized with the help of the corresponding CD studies. The present authors will deal in this paper with CD measurement of a number of related compounds shown in Table I, whose RD studies were already published, and will confirm their views expressed on the correlation between the rotatory dispersion and stereochemistry of these compounds by studying comparatively the RD and CD curves together with the ultraviolet absorption curves, and further will inquire into the relation between the ultraviolet absorption and the steric influence.

1) Part XI. Y. Tsuzuki, K. Tanabe, K. Okamoto and N. Yamada, This Bulletin, **39**, 1391 (1966).
2) S. Mitchell and R. R. Gordon, *J. Chem. Soc.*, **1936**, 853.
3) N. Kornblum, L. Fishbein and R. A. Smiley, *J. Am. Chem. Soc.*, **77**, 6261 (1955).
4) A. Bowers, M. B. Sanchez and H. T. Ringold, ibid., **81**, 3702 (1959).
5) K. Mislow, E. Bunnenberg, R. Records, K. Wellman and C. Djerassi, ibid., **85**, 1342 (1963).
6) C. Djerassi, H. Wolf and E. Bunnenberg, ibid., **85**, 2835 (1963).
7) Y. Tsuzuki, K. Tanabe and K. Okamoto, This Bulletin, **38**, 274 (1965).
8) Y. Tsuzuki, K. Tanabe and K. Okamoto, ibid., **39**, 1387 (1966).
9) Y. Tsuzuki, K. Tanabe, K. Okamoto and M. Fukubayashi, ibid., **39**, 1391 (1966).

Results and Discussion

In Fig. 1 are given the RD and CD curves of the α-C_1-nitrate of glucopyranose (I), where those of galactopyranoside (II)[1] are reproduced for comparison's sake. The agreement of these two compounds in sign of circular dichroism undoubtedly indicates that the Cotton effect is due to the α-C_1-ONO_2 chromophore. That the peak of CD (II, 263.5 mμ) is a little red-shifted as compared with that of CD (I, 273 mμ) is to be attributed to the steric effect of the C_4-OAc group of L-configuration in the galactoside (II).

In Fig. 2 are shown the RD and CD curves of 1, 3, 4, 6-tetra-*O*-acetyl-2-*O*-nitro-α-D-glucopyranoside (III) and those of its anomer (IV). The CD (III) has a negative sign, which confirms the view[7] that the RD curve (III) shows a negative Cotton effect. The CD (IV) exhibits a positive sign in agreement with the positive Cotton effect (IV). The CD curves III and IV are nearly equal in optical rotatory strength, both originating in the C_2-ONO_2 chromophore of D-type, but they are opposite in sign, that is undoubtedly attributed to the respective α- and β-form of the C_1-OAc

Table I. Nitrate compounds

Number	Name
I[1]	2,3,4,6-Tetra-*O*-acetyl-1-*O*-nitro-α-D-glucopyranose
II[8]	2,3,4,6-Tetra-*O*-acetyl-1-*O*-nitro-α-D-galactopyranose
III[7]	1,3,4,6-Tetra-*O*-acetyl-2-*O*-nitro-α-D-glucopyranose
IV[8]	1,3,4,6-Tetra-*O*-acetyl-2-*O*-nitro-β-D-glucopyranose
V[8]	Methyl 4 : 6-*O*-ethylidene-β-D-glucopyranoside 3-nitrate
VI[1]	1,2:5,6-Diisopropylidene-3-*O*-nitro-α-D-glucofuranose
VII[1]	Methyl 4 : 6-*O*-benzylidene-α-D-altropyranoside 3-nitrate
VIII[8]	Methyl 2,3,6-tri-*O*-acetyl-4-*O*-nitro-β-D-glucopyranoside
IX[8]	Methyl 2,3,4-tri-*O*-acetyl-6-*O*-nitro-α-D-glucopyranoside
X[8]	Methyl 4 : 6-*O*-ethylidene-α-D-glucopyranoside 2 : 3-dinitrate
XI[8]	Methyl 4 : 6-*O*-ethylidene-β-D-glucopyranoside 2 : 3-dinitrate
XII[1]	Methyl 4 : 6-*O*-ethylidene-α-D-mannopyranoside 2 : 3-dinitrate
XIII[1]	Methyl 4 : 6-*O*-benzylidene-α-D-altropyranoside 2 : 3-dinitrate
XIV[1]	Methyl 6-*O*-acetyl-2,3,4-tri-*O*-nitro-β-D-glucopyranoside
XV[8]	Methyl 2,3-di-*O*-acetyl-4 : 6-di-*O*-nitro-β-D-glucopyranoside
XVI[1]	Methyl 2,3,4,6-tetra-*O*-nitro-β-D-glucopyranoside
XVII[1]	Methyl 2,3,4,6-tetra-*O*-nitro-α-D-glucopyranoside
XVIII	1,2,3,4,6-Penta-*O*-nitro-α-D-glucopyranose

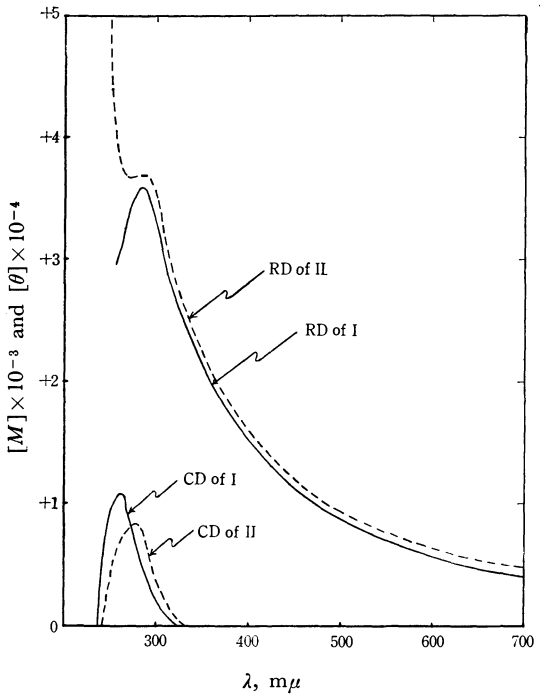

Fig. 1. RD and CD of C_3-nitrates of glucose (I) and galactose (II).

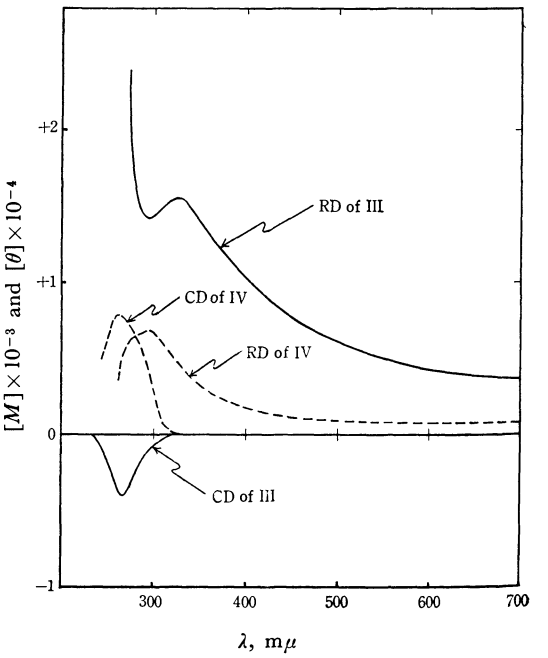

Fig. 2. RD and CD of C_2-nitrate of glucose.

group, which predominates over others in optical rotation.

Figure 3 shows the CD curves of three C_3-nitrates (V-VII), and reproduces their RD curves. Small as its ellipticity is, the CD curve (V) of methyl 4 : 6-*O*-ethylidene-β-D-glucopyranoside is negative in sign. The RD curve was discussed in a previous paper[8] to have a negative Cotton effect by analyzing the curve with the help of Drude equation as well as configurational studies.

The positive CD (VI) of 1, 2 : 5, 6-diisopropylidene-3-*O*-nitro-α-D-glucofuranose is consistent

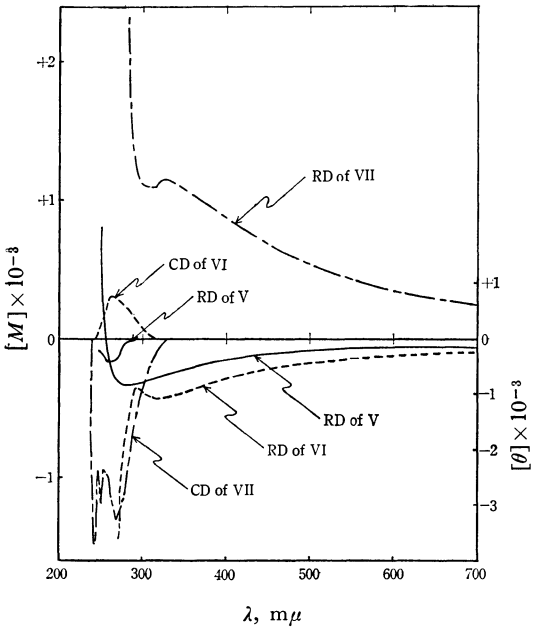

Fig. 3. RD and CD of C_3-nitrate of hexoses.

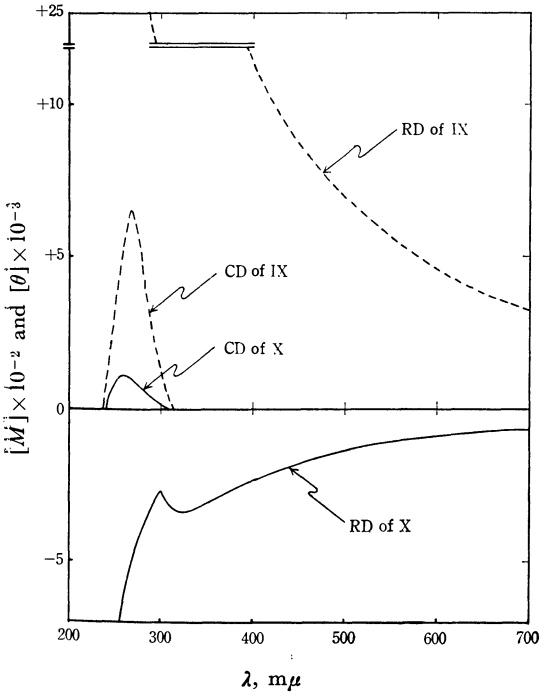

Fig. 4. RD and CD of C_4-nitrate (VIII) and C_5-nitrate (IX) of glucose.

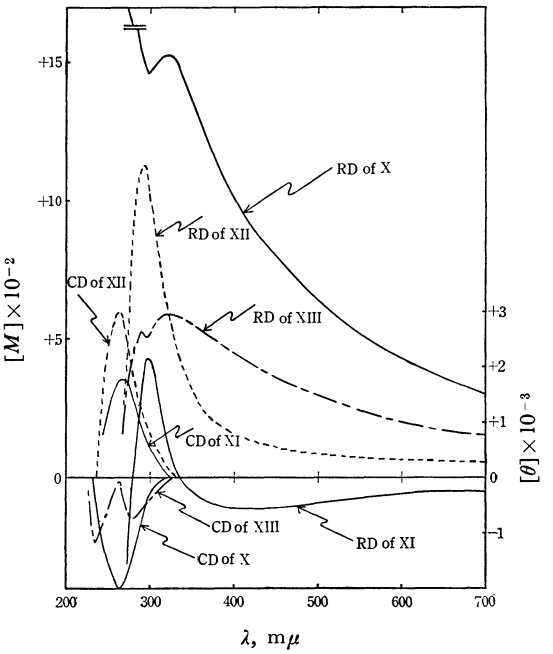

Fig. 5. RD and CD of 2,3-dinitrates of hexoses.

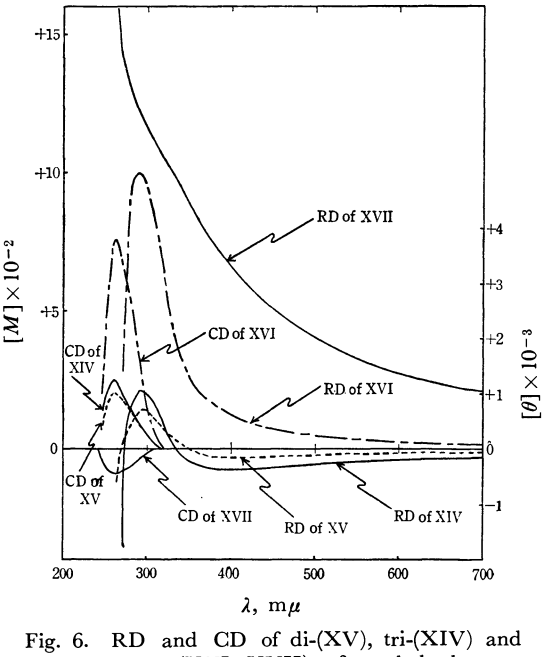

Fig. 6. RD and CD of di-(XV), tri-(XIV) and tetranitrates (XVI, XVII) of methyl glucopyranosides.

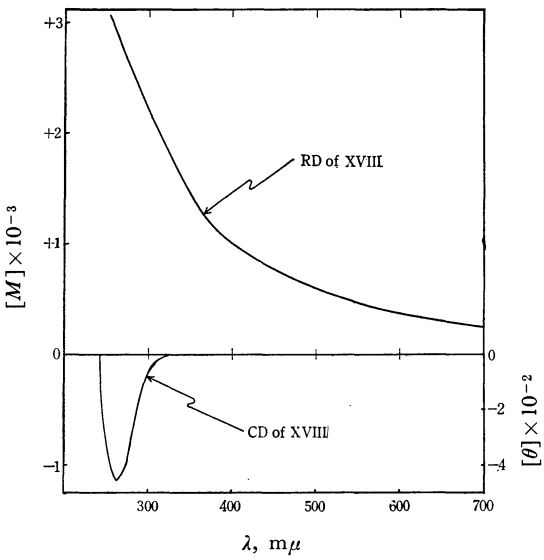

Fig. 7. RD and CD of pentanitrates of glucopyranose.

with the weakly positive Cotton effect (RD VI). The ellipticity is smaller in C_3-nitrates (V and VI) than in C_1-nitrate (Fig. 1) and in C_2-nitrate (Fig. 2). The complex circular dichroism of 4 : 6-*O*-benzylidene-α-D-altropyranoside 3-nitrate (VII) has a negative sign, one of the peaks of which (270 mμ) may be associated with the negative Cotton effect appearing in the RD curve as already demonstrated.[1] The negative maximum 242 mμ exhibited in the CD curve (VII) is due to the benzylidene radical, qualified by the D-configuration of C_4.[10]

In Fig. 4 are exhibited the RD and CD of glucopyranose C_4-nitrate (VIII) and C_6-nitrate (IX). The positive circular dichroism (VIII) now justifies the dicision of the weak Cotton effect (RD VIII) to be positive in sign.[8]

As already reported, the C_6-nitrate (IX) shows a nearly plain dispersion curve[8] and only a shoulder in the UV absorption spectrum in the region 265 to 280 mμ, but displays a distinct circular dichroism of positive sign at 267 mμ. This suggests the existence of an optically active absorption in this region, although hidden by the strong background rotation of α-methylglucopyranoside.

The positive sign of this "hidden" Cotton effect can be expected from the rule proposed by the present authors in a previous paper,[1] which states that the Cotton effect due to a nitrate of the β-configuration in α-glucosides is positive, for the C_6-nitrate in this case is linked to the β-configurated C_5-atom.

In Fig. 5 are given the RD and CD curves of some C_2, C_3-dinitrates of hexose derivatives (X-XIII). As already demonstrated[1,8] the sign of the Cotton effect due to the chromophore is controlled and determined in di-, tri- as well as tetranitrates always by the configuration of the asymmetric center, which contributes most strongly to optical rotation. The rotatory dispersion of methyl 4 : 6 - *O* -ethylidene - α - D-glucopyranoside 2 : 3-dinitrate (X) exhibits a weakly negative Cotton effect[8] because of the C_2-chromophore of D-configuration in the α-series, regularly contributing to negative rotation. And the distinct, negative circular dichroism really supports this conclusion.

On the contrary its anomer (XI) shows a positive Cotton effect,[8] being dominated by the C_2-chromophore in the β-series, quite in harmony with the positive circular dichroism (XI).

By comparing the compounds X and XI with each other in circular dichroism, it will be noted that their CD curves take a form of symmetry, because they are associated primarily with the optically active absorption due to the C_2-chromophore. However, methyl 4 : 6-*O*-ethylidene-α-D-mannopyranoside 2 : 3-dinitrate (XII) exhibits a positive Cotton effect,[1] which is further evidenced by the positive circular dichroism (Fig. 5).

The ellipticity of compound XII is large as compared with that of compound XI, since the C_2- and C_3-chromophores both contribute to positive rotation in compound II, while the C_2- and C_3-chromophores of compound XI are respectively a positive and a negative contributor, so that its circular dichroism becomes less positive.

In Fig. 5 are reproduced the RD and CD curves of methyl 4 : 6-*O*-benzylidene-α-D-altropyranoside 2 : 3-dinitrate (XIII) already reported.[1] Here it should be pointed out that a negative maximum appears in circular dichroism at 240 mμ characteristic of the benzylidene group, which may be due to the C_4-contribution, as observed in another benzylidene derivative (VII, Fig. 3).

Figure 6 exhibits the RD and CD curves of the di-, tri- and tetra-nitrates of glucopyranose (XIV—XVII). The positive circular dichroism (XIV) confirms the sign of the Cotton effect (RD XIV) of methyl 6-*O*-acetyl-2, 3, 4-tri-*O*-nitro-β-D-glucopyranoside (XIV) which was determined to be positive. This rotatory dispersion was dominated by the dextro-rotatory C_2-chromophore, which is characteristic of the D-configuration in the β-glucoside. Methyl 2, 3-di-*O*-acetyl-4, 6-di-*O*-nitro-β-D-glucopyranoside (XV) also shows a positive Cotton effect, the sign of which is verified by the positive circular dichroism (XV). This Cotton effect can be explained in the following way: in the α-glucoside the D-configurated C_4-chromophore contributes to positive rotation, and although the C_5-asymmetric center contributes to negative one, as may be expected from the behavior of

10) The RD of compounds containing benzene ring has recently been reported to display Cotton effect in the region 258 to 260 mμ. L. Verbit, *J. Am. Chem. Soc.*, **87**, 1617 (1965).

C_6-nitrate (IX), the former predominates over the latter in the absorption region. The positive Cotton effect of methyl 2, 3, 4, 6-tetra-*O*-nitro-β-D-glucopyranoside (XVI)[1] agrees, as shown in Fig. 6, with the CD (XVI) in sign, and its anomer (XVII) on the contrary exhibits a negative circular dichroism (267 mμ). Although the RD curve (XVII) presents only a slight shoulder in the region from 285 to 325 mμ, it was interpreted to have a negative Cotton effect due to the C_2-ONO_2 chromophore overlapped by the stronger α-glucosidic positive rotation. Thus the interpretation has now been confirmed by the CD measurement.

In Fig. 7 is given the RD curve of penta-*O*-nitro-α-D-glucopyranose (XVIII), which shows a more or less apparent anomaly about 285 to 315 mμ, though no distinct Cotton effect can be observed. The compound XVIII exhibits a negative circular dichrosim (Fig. 7), probably because the dominant C_2-ONO_2 effect in this α-glucoside series becomes negative in sign.

As may be seen from Figs. 5, 6 and 7 the C_2-chromophore always determines the circular dichroism as well as the rotatory dispersion excepting the cases where steric hindrance interferes, since the C_2-group is most influential in the optical rotation of these sugars.

Conclusions

1) Anomalous rotatory dispersion curves of sugar nitrates have been analyzed and verified by CD measurement, the wavelength of CD_{max} always coinciding with the region of the ultraviolet absorption.

2) The CD_{max} of sugar nitrates lies in the region 260 to 270 mμ, and is red-shifted by steric hindrance.

3) The C_6-nitrates of the α-series (glycosides) exhibit positive circular dichroism, in accordance with the rule found by the present authors,[1] since the C_5-configuration is of L-type.

4) Each anomer has an ellipticity of nearly equal strength.

5) The contribution to the ellipticity conforms to the order of the rotatory contribution, namely,

$$C_2 > C_3 > C_4 > C_5$$

Experimental

The circular dichroism was measured with a JASCO optical rotatory dispersion recorder of the ORD/UV-5 type at 25° to 30°C in chloroform (but XVIII in ethanol) in the wavelength region from 350 to 230 mμ. The rotatory dispersion was measured with a Rudolph spectropolarimeter.

2, 3, 4, 6-Tetra-*O*-acetyl-1-*O*-nitro-α-D-galactopyranose (compound I): $[\theta]_{330}$ 0, $[\theta]_{300}$ +9.37, $[\theta]_{270}$ +25.4, $[\theta]_{250}$ +4.67, $[\theta]_{248}$ 0 (*c*, 0.2356).

2, 3, 4, 6-Tetra-*O*-acetyl-1-*O*-nitro-α-D-glucopyranose (compound II): $[\theta]_{330}$ 0, $[\theta]_{300}$ +18.1, $[\theta]_{267}$ +64.1, $[\theta]_{250}$ +25.7, $[\theta]_{240}$ 0 (*c*, 0.3901).

1, 3, 4, 6-Tetra-*O*-acetyl-2-*O*-nitro-α-D-glucopyranose (compound III): $[\theta]_{315}$ 0, $[\theta]_{300}$ −7.35, $[\theta]_{266}$ −56.7, $[\theta]_{250}$ −42.9, $[\theta]_{240}$ 0 (*c* 0.3205).

1, 3, 4, 6-Tetra-*O*-acetyl-2-*O*-nitro-β-D-glucopyranose (compound IV): $[\theta]_{330}$ 0, $[\theta]_{300}$ +17.2, $[\theta]_{260}$ +39.5, $[\theta]_{250}$ +33.4 (*c* 0.7534).

Methyl 4 : 6-*O*-ethylidene-β-D-glucopyranoside 3-nitrate (compound V): $[\theta]_{290}$ 0, $[\theta]_{270}$ −1.93, $[\theta]_{260}$ −2.42 (*c* 0.4382).

1, 2 : 5, 6-Diisopropylidene-3-*O*-nitro-α-D-glucofuranose (compound VI): $[\theta]_{320}$ 0, $[\theta]_{300}$ +2.91, $[\theta]_{262}$ +26.3, $[\theta]_{250}$ +8.30, $[\theta]_{248}$ 0, (*c* 0.7362).

Methyl 4 : 6-*O*-benzylidene-α-D-altropyranoside 3-nitrate (compound VII): $[\theta]_{330}$ 0, $[\theta]_{300}$ −4.45, $[\theta]_{270}$ −12.4, $[\theta]_{255}$ −6.68, $[\theta]_{244}$ −14.2, $[\theta]_{240}$ 0 (*c* 0.3681).

Methyl 2,3,6-tri-*O*-acetyl-4-*O*-nitro-β-D-glucopyranoside (compound VIII): $[\theta]_{315}$ 0, $[\theta]_{300}$ +5.00, $[\theta]_{260}$ +31.5 (*c* 0.4755).

Methyl 2,3,4-tri-*O*-acetyl-6-*O*-nitro-α-D-glucopyranoside (compound IX): $[\theta]_{310}$ 0, $[\theta]_{290}$ +4.42, $[\theta]_{267}$ +9.95, $[\theta]_{250}$ +5.54, $[\theta]_{240}$ 0 (*c* 4.944).

Methyl 4 : 6-*O*-ethylidene-α-D-gluxopyranoside 2 : 3-dinitrate (compound X): $[\theta]_{320}$ 0, $[\theta]_{300}$ −6.83, $[\theta]_{263}$ −61.1, $[\theta]_{250}$ −50.8, $[\theta]_{240}$ −17.6 (*c* 0.6358).

Methyl 4 : 6-*O*-ethylidene-β-D-glucopyranoside 2 : 3-dinitrate (compound XI): $[\theta]_{325}$ 0, $[\theta]_{300}$ +13.4, $[\theta]_{265}$ +55.2, $[\theta]_{250}$ +44.2, $[\theta]_{240}$ +22.7 (*c* 0.6610).

Methyl 4 : 6-*O*-ethylidene-α-D-mannopyranoside 2 : 3-dinitrate (compound XII): $[\theta]_{330}$ 0, $[\theta]_{300}$ +17.4, $[\theta]_{261}$ +90.5, $[\theta]_{250}$ +66.7, $[\theta]_{240}$ 0 (*c* 0.4293).

Methyl 4 : 6-*O*-benzylidene-α-D-altropyranoside 2 : 3-dinitrate (compound XIII): $[\theta]_{310}$ 0, $[\theta]_{300}$ −2.84, $[\theta]_{280}$ −11.2, $[\theta]_{267}$ −2.65, $[\theta]_{258}$ +2.00, $[\theta]_{250}$ −9.86, $[\theta]_{240}$ −74.0, $[\theta]_{235}$ 0 (*c* 0.9829).

Methyl 6-*O*-acetyl-2, 3, 4-tri-*O*-nitro-β-D-glucopyranoside (compound XIV): $[\theta]_{330}$ 0, $[\theta]_{300}$ +6.65, $[\theta]_{260}$ +32.7, $[\theta]_{253}$ +30.4 (*c* 0.6596).

Methyl 2, 3-di-*O*-acetyl-4, 6-di-*O*-nitro-β-D-glucopyranoside (compound XV): $[\theta]_{340}$ 0, $[\theta]_{300}$ +6.04, $[\theta]_{258}$ +31.4, $[\theta]_{254}$ +30.9 (*c* 0.7627).

Methyl 2, 3, 4, 6-tetra-*O*-nitro-α-D-glucopyranoside (compound XVI): $[\theta]_{310}$ 0, $[\theta]_{300}$ −3.19, $[\theta]_{270}$ −20.2, $[\theta]_{250}$ −16.0, $[\theta]_{243}$ 0 (*c* 0.5860).

Methyl 2, 3, 4, 6-tetra-*O*-nitro-β-D-glucopyranoside (compound XVII): $[\theta]_{322}$ 0, $[\theta]_{300}$ +8.68, $[\theta]_{260}$ +30.8 (*c* 0.4740).

1, 2, 3, 4, 6-Penta-*O*-nitro-α-D-glucopyranose (compound XVIII):[11] Colorless syrup. The RD was measured at 22°C in ethanol (*c* 0.9852). $[\alpha]^{22}_{700}$ +69.7°, $[\alpha]_{589}$ +99.1°, $[\alpha]_{500}$ +143°, $[\alpha]_{400}$ +244°, $[\alpha]_{360}$ +318°, $[\alpha]_{320}$ +439°, $[\alpha]_{300}$ +524°, $[\alpha]_{290}$ +556°, $[\alpha]_{280}$ +597°.

$[\theta]_{312}$ 0, $[\theta]_{310}$ −13.8, $[\theta]_{290}$ −138, $[\theta]_{260}$ −468, $[\theta]_{245}$ 0.

The authors owe the CD measurement to the Japan Spectroscopic Co., Ltd.

11) W. Will and F. Lenze, *Ber.*, **31**, 74 (1898).

BULLETIN OF THE CHEMICAL SOCIETY OF JAPAN VOL. 39 2274—2286 (1966)

Resonance Effect in Hammett Relationship. IV. Linear Free Energy Relationship based on the Normal Substituent Constants*

By Yasuhide YUKAWA, Yuho TSUNO and Masami SAWADA

The Institute of Scientific and Industrial Research, Osaka University, Higashiasakayama, Sakai

(Received April 7, 1966)

A set of normal substituent constants, σ^0, was derived from the rates of alkaline hydrolysis of *m*- and *p*-substituted ethyl phenylacetates in 60% (v/v) aqeuous acetone at 25.0°C. The obtained values of σ^0-constants were generally identical with Taft's values within experimental uncertainty. On the basis of the derived σ^0, substituent effects on the general electrophilic reactions were correlated excellently by the equation, $\log k/k_0=\rho(\sigma^0+r\Delta\bar{\sigma}_R^+)$, where $\Delta\bar{\sigma}_R^+$ corresponds to the exaltation of Brown and Okamoto's σ^+ from σ^0. The similar treatment could be applied also to the nucleophilic reactions. The utility of this equation for the estimation of resonance contribution and for the consideration of reaction mechanisms are discussed.

The general failure of the Hammett equation[1] to correlate electrophilic reactivities led to the suggestion of the use of alternate substituent constants, denoted by σ^+, derived from the substituent effect in an electrophilic reaction.[2-5] Various authors proposed their own set of σ^+ values from the individual reference reaction.[3-5] Later, Brown and Okamoto have proposed the familiar σ^+ constants, defined by the substituent effects on the solvolysis rates of phenyldimethylcarbinyl chlorides, and demonstrated the utility of their σ^+ to the prediction of electrophilic reactivities.[5] The exalted contribution of electron releasing *para* substituents can be attributed to the additional delocalization by resonance of the positive charge produced at the reaction site. The σ^+ treatment stands on an assumption that the substituent constant in electrophilic reactions remains a constant relative to the marked change in ρ. However, the degree of the resonance delocalization must depend on the amount of charge produced or the electron deficiency of the reaction site. Accordingly, the σ^+ of respective *para* substituents should be subject to variation with reactions. It should be inevitably required for *para* substituents to add a second term, taking into account such an exalted resonance contribution.[3,6]

At this point of view, the relationship (1) was proposed[6] for the correlation of substituent effects on general electrophilic reactions,

$$\log k/k_0 = \rho(\sigma + r\Delta\sigma_R^+) \qquad (1)$$

where r is a constant depending on the resonance effect in the reaction, and $\Delta\sigma_R^+$ measures the capacities of substituents to supply electrons by resonance. $\Delta\sigma_R^+$ values were defined by the increments of Brown and Okamoto's σ^+ from σ. The applicability of Eq. 1 was demonstrated in the original paper[6] with the excellent results for 35 representative electrophilic reactivities. Thereafter, Eq. 1 has been utilized in order to correlate various reactivities and elucidate the reaction mechanism by a number of investigators.[7,8] These are reviewed entirely in several recent articles.[9-11] Analogous equations have been proposed[7a,12,13] in these few years, but none of them appears more useful practically or more

* Presented in summary at the Japanese-American Seminar in Physical Organic Chemistry, Kyoto, Japan, April, 1965.

1) L. P. Hammett, *J. Am. Chem. Soc.*, **59**, 96 (1937); "Physical Organic Chemistry," McGraw-Hill, New York (1940), Chapt. 7, p. 184.

2) For the review, see, P. R. Wells, *Chem. Revs.*, **63**, 171 (1963).

3) Y. Tsuno, T. Ibata and Y. Yukawa, This Bulletin, **32**, 960 (1959); Y. Yukawa and Y. Tsuno, ibid., **32**, 965 (1959).

4) D. E. Pearson, J. F. Baxter and J. C. Martin, *J. Org. Chem.*, **17**, 1151 (1952); J. K. Kochi and G. S. Hammond, *J. Am. Chem. Soc.*, **75**, 3445 (1953); N. C. Deno and A. Schriesheim, ibid., **77**, 3051 (1955); N. C. Deno and W. L. Evans, ibid., **79**, 5804 (1957); J. Miller, *Austral. J. Chem.*, **9**, 61 (1956).

5) H. C. Brown and Y. Okamoto, *J. Am. Chem. Soc.*, **79**, 1913 (1957); ibid., **80**, 4979 (1958); H. C. Brown, "Advances in Physical Organic Chemistry," Vol. 1, Academic Press, New York (1963), Chapt. 2, p. 34.

6) Y. Yukawa and Y. Tsuno, This Bulletin, **32**, 971 (1959).

7) a) J. D. Dickinson and C. Eaborn, *J. Chem. Soc.*, **1959**, 3036. b) C. Eaborn and J. A. Waters, ibid., **1961**, 542; C. Eaborn and R. Taylor, ibid., **1961**, 1012; R. Baker, R. W. Bott, C. Eaborn and P. P. M. Greasley, ibid.,, **1964**, 627; R. W. Bott, C. Eaborn D. R. M. Walton, ibid., **1965**, 384.

8) R. Taylor, G. G. Smith and W. H. Wetzel, *J. Am. Chem. Soc.*, **84**, 4817 (1962); R. Taylor and G. G. Smith, *Tetrahedron*, **19**, 937 (1963); T. Inukai, This Bulletin, **35**, 400 (1962); L. A. Singer, and D. J. Cram, *J. Am. Chem. Soc.*, **85**, 1080 (1963); T. I. Crowell, C. E. Bell, Jr., and D. H. O'Brien, ibid., **86**, 4973 (1964); W. P. Jencks, "Progress in Physical Organic Chemistry," Vol. II, Interscience, New York (1964), p. 110.

general to cover a wide variety of reactions.

While the relationship (1) is conventionally based on the σ-standard and the resonance parameter $\Delta\sigma_R^+$ was defined originally by $\sigma^+ - \sigma$, it is evidently known that the Hammett σ-constant involves in itself the σ^+-type exalted resonance contribution to a considerable extent. Taft[14,15] and Wepster[16] have proposed independently that the unexalted or normal substituent constants, σ^0 or σ^n, should be taken as the standard of the benzene subtituent contribution instead of σ. Of course, for the practical purpose, it is believable that the original definition of the relationship (1) must be the best choice of the standard.[17] However, in view of further development of this type of approach and performing the theoretical analysis of the substituent effect, the additional resonance contribution to the unexalted effect, σ^0, should be fully included into the additional resonance term corresponding to $r\Delta\sigma_R^+$. It was therefore attempted to develop an alternate treatment of substituent effects based on the σ^0-standard.

In this connection, σ and σ^+ on which our original treatment is based are the most familiar to the organic chemist and well established sets of substituent constants. While the σ^0-constant was derived by Taft[14,15] statistically from the reactions free from the mutual conjugative interaction between substituent and the reaction site, the numerical values do not appear to be so precise because of the lack of sufficient data available at that time. As similar to the pK_a of benzoic acids for σ, the σ^0 should be defined by the substituent effect on the dissociation of phenylacetic acids. In practice, however, the effects are so small relative to the experimental uncertainty to evaluate the precise constants. Accordingly, first of all, the more reliable experimental σ^0-values have been determined on the basis of the substituent effects on alkaline hydrolysis of ethyl phenylacetates. In the present paper are reported and discussed the determination of σ^0-constants and the development and generality of the alternate treatment based on the σ^0-constants obtained.

Experimental

Most of phenylacetic acids were prepared by the Willgerodt reaction of the appropriate acetophenones.[18] The modified procedure using sulfur and morpholine was employed; the morpholides were separated, washed and hydrolyzed with concentrated potassium hydroxide solution. This method was generally successful except for *p*-chloro and *p*-bromo derivatives. Another method generally employed was the hydrolysis of the nitriles prepared from the correspondingly substituted benzyl halides. *m*-Fluoro and *m*-chloro derivatives were obtained from the corresponding benzoic acids by the Arndt-Eistert reaction.[19] The other substituted derivatives were prepared by the convenient method in the literature (see Table I). The acids were purified by the recrystallization or the distillation of the esters, followed by the recrystallizations of regenerated acids. The acids were esterified by the standard method and finally the esters were fractionated or recrystallized immediately before the rates of their hydrolysis were measured. Any impurities or undesirable isomers were not detected by vapor phase chromatography. The physical constants of these materials were listed in Table I.

Acetone which had been treated with potassium permanganate was distilled, dried over potassium carbonate and fractionated. It was diluted with freshly boiled, deionized water to give a 60% (v/v) aqueous acetone.

Kinetic Measurement.—The rates of the hydrolysis of all these phenylacetic esters were determined in 60% aqueous acetone solution at 25.00±0.01 °C by following the decrease of conductance of the solution. The procedure employed for this measurement was essentially the same as that described by Hancock.[20] The initial concentrations of alkali and the ester were precisely equal (0.01—0.005 M) and the reaction was followed up to the extent of 90% reaction. The initial conductance was determined by the reading of conductance of alkaline solution alone. All runs showed strictly second order kinetics, while in some cases slight deviations from the kinetic plot was observed in the initial 5—10% reaction period. The rate constants from different runs agreed within 1% except for *p*-bromo derivative, which did not give a precise second order rate constant and the average deviation of repeated runs was about 3% for this derivative. The rate constants obtained are listed in Table II.

Of the slow reacting derivatives, the rates were determined also by means of the titration method under the same condition as the above. The procedure employed was essentially the same as that described in

9) R. O. C. Norman, "Electrophilic Substitution in Benzene Compounds," Elsevier (1965).
10) J.E. Leffler and E. Grunwald, "Rates and Equilibria of Organic Reactions," John Wiley, New York (1963), Chapt. 6, p. 128.
11) Y. Yukawa and Y. Tsuno, *J. Chem. Soc. Japan, Pure Chem. Sect. (Nippon Kagaku Zasshi)*, **86**, 873 (1965).
12) J. R. Knowles, R. O. Norman and G. K. Radda, *J. Chem. Soc.*, **1960**, 4885.
13) R. E. Dessy and J. Y. Kim, *J. Am. Chem. Soc.*, **82**, 686 (1960); J. Hine, ibid., **82**, 4877 (1960).
14) R. W. Taft, Jr., *J. Phys. Chem.*, **64**, 1805 (1960).
15) R. W. Taft, Jr., I. C. Lewis, *J. Am. Chem. Soc.*, **80**, 2436 (1958); ibid., **81**, 5343 (1959); R. W. Taft, Jr., S. Ehrenson, I. C. Lewis and R. E. Glick, ibid., **81**, 5354 (1959).
16) H. van Bekkum, P. E. Verkade and B. M. Wepster, *Rec. Trav. Chim.*, **78**, 815 (1959).
17) In the original paper (Ref. 6), we used the σ-values from Jaffé's compilation (H. H. Jaffé, *Chem. Revs.*, **53**, 191 (1953)), but it should be better to utilize the σ-values from the pK_a values of benzoic acids. Thus a little change in the original parameters has to be necessary for some substituents.
18) E. Schwenk and E. Bloch, *J. Am. Chem. Soc.*, **64**, 3051 (1942); M. Carmack and D. F. DeTar, ibid., **68**, 2029 (1946).
19) W. E. Bachmann and W. S. Struve, "Organic Reactions," Vol. I, John Wiley, New York (1942), Chapt. 2, p. 38.
20) C. K. Hancock, E. A. Meyers and B. J. Yager, *J. Am. Chem. Soc.*, **83**, 4211 (1961).

TABLE I. PHENYLACETIC ACIDS AND ETHYL PHENYLACETATES

Substituent	Acid		Ethyl ester	
	M. p., °C	Method[a]	B. p., °C/mmHg	M. p., °C
p-CH_3O	88—88.5[d,e]	W	117.5/3.5[l]	
p-CH_3S	99—100[f]	W		57—57.5[n]
p-C_6H_5O	79.5	W	150/0.7[o]	
p-C_6H_5	161—161.5[d]	W	167—168/3.5	Solid
p-CH_3	92—93[e,f]	W	112—112.5/9.5[e]	
p-C_2H_5	91.5—92[g]	W	143/22[p]	
p-*i*-C_3H_7	51.5—52.5[h]	W	144.5—145/19[q]	
p-*t*-C_4H_9	82—83[i]	W	126.5/6[j]	
p-F	84.5[f,i]	A	103—104/10[e]	34.5—35.5[e]
p-Cl	105[e,i]	N(W)	110—111/4	33—34[j]
p-Br	114—114.5[d]	N(W)	143.5—144/11	27—29[e]
p-CH_3CO		b		61—62[b,e]
p-NO_2	153[c,i]	c		64.5—65[e]
β-Napht.	140.5—141[j,k]	W	148.5/3.5	32—33[j]
Unsubst.	77—77.5		83.5—84/4	
m-CH_3	63.5—64[e,f]	N	119—119.3/13[e]	
m-F		A	98—98.5/10[j]	
m-Cl		A	118—118.5/7.5[l]	
m-Br	101—101.5[l]	W	145.5/14[r]	
m-CH_3CO	104—104.5[b]	b	138/3.5	
m-NO_2	118.5—119[e,m]	N	142—142.5/3[e]	

a) The method of preparation: W, Willgerodt reaction (Ref. 18); A, Arndt-Eistert reaction (Ref. 19); N, nitrile synthesis. b) Preparation by acetylation of ethyl phenylacetates; D. Papa, E. Schwenk and A. Klingsberg, *J. Am. Chem. Soc.*, **68**, 2133 (1946). c) Nitration of phenylacetonitrile; "Org. Synthesis," Coll. Vol. I, 396 (1956). d) E. Schwenk and D. Papa, *J. Org. Chem.*, **11**, 798 (1946). e) Ref. 22. f) R. C. Elderfield and K. L. Burgess, *J. Am. Chem. Soc.*, **82**, 1975 (1960). g) *Anal.*, Found: C, 73.10; H, 7.33. Calcd. for $C_{10}H_{12}O_2$: C, 73.15; H, 7.37%. h) *Anal.*, Found: C, 74.23; H, 8.06. Calcd. for $C_{11}H_{14}O_2$: C, 74.13; H, 7.92%. i) Ref. 24. j) Ref. 23. k) E. Schwenk and E. Bloch, *J. Am. Chem. Soc.*, **64**, 305 (1942). l) C. D. DePuy and D. H. Froemsdorf, ibid., **79**, 3710 (1957). m) D. L. Yabroff and C. W. Porter, ibid., **54**, 1199 (1932). n) *Anal.*, Found: C, 62.76; H, 6.71; S, 15.12. Calcd. for $C_{11}H_{14}O_2S$: C, 62.83; H, 6.71; S, 15.25%. o) *Anal.*, Found: C, 75.25; H, 6.49. Calcd. for $C_{16}H_{16}O_3$: C, 74.98; H, 6.29%. p) *Anal.*, Found: C, 75.18; H, 8.61. Calcd. for $C_{12}H_{16}O_2$: C, 74.97; H, 8.39%. q) *Anal.*, Found: C, 75.75; H, 8.92. Calcd. for $C_{13}H_{18}O_2$: C, 75.69; H, 8.80%. r) *Anal.*, Found: C, 49.58; H, 4.72; Br, 32.53. Calcd. for $C_{10}H_{11}O_2Br$: C, 49.41; H, 4.56; Br, 32.87%.

TABLE II. RATE CONSTANTS OF HYDROLYSIS OF SUBSTITUTED ETHYL PHENYLACETATES IN 60% AQUEOUS ACETONE AT 25°C

Subst.	$10^2 \times k_2$	Subst.	$10^2 \times k_2$
p-CH_3O	3.50	β-Napt.	5.03
p-CH_3	3.30	Unsubst.	4.36
p-C_2H_5	3.26	*m*-CH_3	3.71
p-*i*-C_3H_7	3.80	*m*-F	9.67
p-*t*-C_4H_9	2.96	*m*-Cl	9.33
p-C_6H_5	4.78	*m*-Br	9.64
p-F	7.07	*m*-CH_3CO	10.50
p-Cl	8.23	*p*-CH_3CO	13.2
p-Br	8.7	*m*-NO_2	21.8
p-C_6H_5O	5.17	*p*-NO_2	27.0
p-CH_3S	5.27		

the literature.[21] The equal initial concentration of round 0.01 M for alkali and ester was employed for all runs. The aqueous acetone solution of sodium hydroxide was frequently prepared and standardized. More than triplicated runs were carried out for respective esters. The respective run, which involved more than 12 measurements convering two half-lives, followed the second order kinetic law, with slight fluctuation of few points. The average deviation of a run was estimated to be within 2%, and the reproducibility of repeated runs to be ±3%. The aveaged rate constants obtained were identical within experimental uncertainty with those by means of the conductivity measurement.

21) D. P. Evans, J. J. Gordon and H. B. Watson, *J. Chem. Soc.*, **1937**, 1430.

Results and Discussion

The Standard σ^0-Constnat.—A difficulty in the determination of precise σ^0-constants arises from the low susceptibility to the substituent change of the insulated reactivity, the reactivity free from the mutual conjugative interaction between substituent and reaction site. In view of comparatively large substituent effects, alkaline hydrolysis of substituted phenylacetic esters is

the most appropriate reference reaction of σ^0-constants. While the rates of alkaline hydrolysis of ethyl phenylacetates were available in the literature[22] for several derivatives in 60% aqueous acetone solution, data were not enough to determine precise σ^0-constants. Thus the more extensive study of this reaction was carried out for a variety of substituted derivatives in order to derive a reliable set of σ^0-constants. According to the preliminary experiments, the reaction proceeded rather too fast in this solvent at 25°C to follow by the usual titration method. This might cause the large experimental error in the results. Therefore the rates were determined by following the change in electric conductivity of the solution during reaction. The results were satisfactory in all the case. When we had finished the series of experiments, additional data for the same reaction by means of titration method were published.[23] They agreed to our results for most of derivatives but did not for several derivatives, such as *p-t*-butyl and *m*-nitro derivatives. Accordingly, the re-examination was undertaken for slow reacting derivatives by means of titration method, while this confirmed our results from the conductivity measurement, which appeared to give more accurate results in comparison with the other method. The disagreement of highly reactive derivatives, especially a large deviation of *m*-nitro derivative,[22] might be responsible to the experimental difficulty in titration measurement. The recent data on the alkaline hydrolysis of the same esters in aqueous alcohol,[24] in which the reaction proceeds considerably slow (ca. 5 times), are much closely related to the present results in spite of different solvents. For the other derivatives, the excellent reproducibility of data from the repeated runs evidently estimates the high reliability of our results due to conductivity measurements. The further support of our results is the fact that the effects of substituents, $\log k/k_0$,

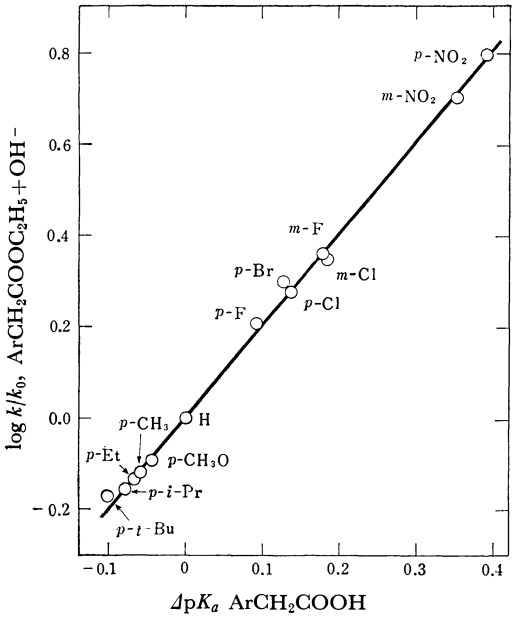

Fig. 1. Linear free energy relation between dissociation of phenylacetic acids and hydrolysis of ethyl phenylacetates.

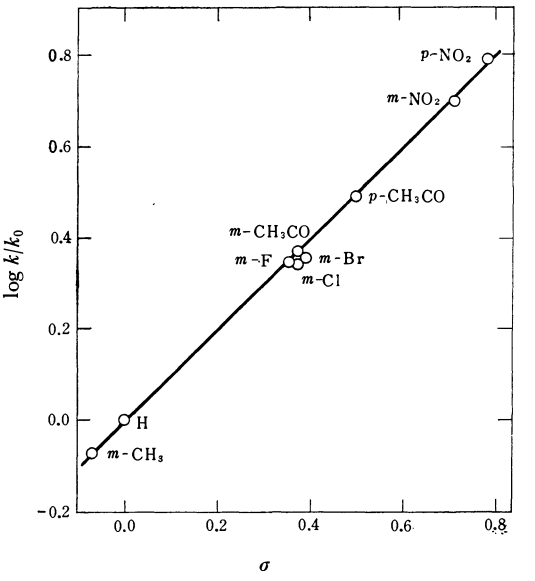

Fig. 2. Hammett plot of the alkaline hydrolysis of ethyl phenylacetates.

Table III. Substituent parameters

p-Substituent	σ^0	$\Delta\bar{\sigma}_R^+$
CH_3O	−0.100	−0.678
CH_3	−0.124	−0.187
C_2H_5	−0.131	−0.164
i-C_3H_7	−0.156	−0.124
t-C_4H_9	−0.174	−0.082
C_6H_5	0.039	−0.218
F	0.212	−0.285
Cl	0.281	−0.167
Br	0.30	−0.15
β-Napht.	0.062	−0.197
CH_3S	0.083	−0.68
C_6H_5O	0.076	
HO	−0.16*	−0.82
NH_2	−0.36*	−1.00
$N(CH_3)_2$	−0.48*	−1.30

* Derived from other reactivities statistically.

22) R. O. C. Norman, G. K. Radda, D. A. Brimacombe, P. D. Ralph and E. M. Smith, ibid., **1961**, 3247.

23) R. O. C. Norman and P. D. Ralph, ibid., **1963**, 5431.

24) J. G. Watkinson, W. Watson and B. L. Yates, ibid., **1963**, 5437.

TABLE IV. SUMMARY OF CORRELATIONS OF σ^0-TYPE REACTIVITIES[a]

Reaction	ρ	s[b]	R[c]	n[d]
pK_a, Phenylacetic acids, water, 25°C[e]	0.502	0.013	0.998	12
Phenylacetic acids with diphenyldiazomethane, ethanol, 35.6°C[f]	0.347	0.011	0.997	8
Saponification, ethyl arylacetates, 85.4% aq. ethanol, 24.8°C[g]	1.092	0.031	0.998	9
Saponification, ethyl arylacetates, 87.8% aq. ethanol, 30°C[h]	1.020	0.022	0.999	7
Saponification, ethyl arylpropionates, 87.8% aq. ethanol, 30°C[i]	0.639	0.013	0.999	7
Saponification, substituted-benzyl benzoates, 70% aq. acetone, 25.0°C[j]	0.990	0.017	0.999	14
Saponification, benzyl acetates, 60% aq. acetone, 25°C[k]	0.793	..017	0.998	9
pK_a, Benzylammonium ions, water, 25°C[l]	1.087	0.031	0.996	12
Benzoic acids with diphenylguanidine, benzene, 25°C[m]	2.10	0.086	0.993	17
pK_a, Ar-PO_3H^-, water, 25°C[n]	1.104	0.038	0.997	11
Alkaline hydrolysis, ArO-Si$(C_2H_5)_3$, 51.4% aq. ethanol, 25°C[o]	1.976	0.019	0.999	6
pK_a, *trans*-Arylcyclopropylcarboxylic acids, 50% aq. ethanol, 25°C[p]	0.515	0.045	0.996	8
Saponification, ethyl arylcyclopropylcarboxylates, 87.8% aq. ethanol, 30°C[i]	0.873	0.030	0.996	8

a) The Hammett type correlation based on σ^0 values obtained in the present investigation. b) Standard deviation. c) Correlation coefficient. d) The number of substituents involved in the calculation. e) Ref. 25. f) R. M. O'Ferrall and S. I. Miller, *J. Am. Chem. Soc.*, **85**, 2440 (1963). g) Ref. 24. h) K. Kindler, *Ann.*, **452**, 90 (1927); A. Fischer, J. Packer, J. Vaughan, A. F. Wilson and E. Wong, *J. Org. Chem.*, **24**, 155 (1959): For the rate of the unsubstituted derivative, 12.2×10^{-3} reported by the latter was used. i) R. Fucks and J. J. Bloomfield, *J. Org. Chem.*, **28**, 910 (1963). j) Y. Yukawa, Y. Tsuno and M. Sawada, Unpublished. k) E. Tommila and C. N. Hinshelwood, *J. Chem. Soc.*, **1938**, 1801; E. Tommila, *Ann. Acad. Sci. Fennicae*, **59**, No. 4 (1942): The unsubstituted derivative was omitted from the correlation. l) L. F. Blackwell, A. Fischer, R. D. Topsom and J. Vaughan, *J. Chem. Soc.*, **1964**, 3588: *p*-Fluoro group was not included in the calculation. m) M. M. Davis and H. H. Hetzer. *J. Res. Natl. Bur. Standards*, **60**, 569 (1958). n) H. H. Jaffé, L. D. Freedman and G. O. Doack, *J. Am. Chem. Soc.*, **75**, 2209 (1953). o) E. Aekerman, *Acta Chem. Scand.*, **11**, 373 (1957). p) R. Fucks, C. A. Kaplan, J. J. Bloomfield and L. F. Hatch, *J. Org. Chem.*, **27**, 733 (1962).

obtained can be correlated linearly with those on the dissociation of phenylacetic acids[25] as illustrated in Fig. 1. This can be compared with the linear free energy correlation between hydrolysis of benzoic esters and the pK_a of benzoic acids.

As would be anticipated, for all *meta* substituents and conjugatively electron attracting *para* substituents, a precisely linear Hammett correlation was obtained (Fig. 2). The ρ value is equal to 0.978 with standard deviation of +0.010 and the correlation coefficient 0.999. On the basis of this correlation, the apparent substituent constants of this reaction were calculated. The resulted constants are generally identical with Taft's σ^0 values within usual uncertainty, and expected to be more reliable than the latter. This set of substituent constants in Table III can correlate precisely the substituent effects on the hydrolysis of substituted benzyl benzoates.[26] The unexalted reactivities which recently have become available in the literature can be also correlated excellently with the above set, as summarized in Table IV. The excellent results in the table indicate that the present set can be generally utilized as the standard σ^0-constant. In the following treatment therefore the values in Table III will be used as the standard σ^0-constants.

It is of interest to note that the effects of alkyl groups in the present reaction follow clearly the inductive order, while they appear to follow the Baker-Nathan order in aqueous alcohol.[24] The analogous behavior of alkyl groups was also noted in the saponification of benzoic esters,[27] and also in the other reactions.[23,28] The substituent effect is sensitive to conditions of reaction.[15,16] Taft has suggested the solvent dependency of σ^0-constants of particular substituents, such as *p*-methoxy group,[14] but this was not distinctly significant in the reactivities sited. The further investigation of the dependency of σ^0-constants upon reactions, solvents and the other conditions is under progress in this laboratory[26] and will be published in near furure.

Correlations of Reactivities.—In view of the general utility of Eq. 1 using $\Delta\sigma_R^+$ as the resonance substituent constants, the increment of Brown and Okamoto's σ^+ to the σ^0 is expected

25) J. F. J. Dippy and R. H. Lewis, ibid., **1936**, 644; J. F. J. Dippy and F. R. Williams, ibid., **1934**, 161; J. F. J. Dippy and J. E. Page, ibid., **1938**, 357; A. Fischer, B. R. Mann and J. Vaughan, ibid., **1961**, 1093.

26) Y. Yukawa, Y. Tsuno and M. Sawada, Unpublished.

27) E. Berliner, M. C. Beckett, E. A. Blommers and B. Newman, *J. Am. Chem. Soc.*, **74**, 4940 (1952).

28) V. J. Shiner, Jr., and C. J. Verbanic, ibid., **79**, 369 (1957).

TABLE V. CORRELATIONS OF ELECTROPHILIC REACTIVITIES

A. Side Chain Reaction

No.	Reaction	ρ	r	s[1]	R[2]	Ref.[3]
1	Brown and Okamoto's σ^+	(1.000)	(1.000)			
2	Pinacol rearrangement, tetraphenylpinacols	−2.83	1.24	0.15	0.991	5
3	Solvolysis, phenylethyl chlorides, in 80% aq. acetone, 45°C	−4.95	1.161	0.044	1.000	6
4	Solvolysis, anisylarylcarbinyl chlorides, in 85% aq. ethanol, 0°C	−2.643 −3.02	1.176 1.043	0.105 0.058	0.998 0.999	7 7a
5	Solvolysis, benzhydryl chlorides, in 70% aq. acetone, 0°C	−4.583	1.140	0.102	0.997	8
6a	Solvolysis, benzhydryl chlorides, in ethanol, 25°C	−3.806	1.172	0.22	0.989	9
6b	Solvolysis, benzhydryl chlorides, in ethanol, 25°C	−4.126	1.172	0.125	0.998	10
7	Solvolysis, 9-arylfluorenyl chlorides, in 90% methanol - acetone, 25°C	−3.420	1.016	0.103	0.997	11
8	Pyrolysis, α-arylethyl acetates, 600°K	−0.643	0.998	0.022	0.997	12
9	Ion pair formation, triphenylmethyl chlorides, in SO_2, 0°C	−4.043	0.885	0.048	0.998	13
10	Hydration, arylacetylenes, 50.2°C	−4.453	0.867	0.094	0.998	14
11	Protodegermylation, arylethynyl-triethylgermanes, perchloric acid, 29°C	−3.294	0.755	0.067	0.999	15
12	t-Stilbenes with perbenzoic acid	−1.095	0.718	0.043	0.999	16
13	Acetolysis, ω-diazoacetophenones, 40°C	−0.818	0.667	0.011	1.000	17
14	Rearrangement, arylpropenylcarbinols	−3.705	0.650	0.023	1.000	18
15	Acetolysis, neophyl brosylates, 70°C	−3.745	0.612	0.025	1.000	19
16	Rearrangement, acetophenone oximes, in sulfuric acid, 51°C	−1.938 −1.930	0.658 0.632	0.110 0.116	0.995 0.996	20 20a
17	Rearrangement, acetophenone-oxime-picrates, in dichlorobutane, 70°C	−4.116	0.600	0.150	0.995	21
18	Solvolysis, biphenylyl dimethylcarbinyl chlorides, in 90% aq. acetone, 25°C	−1.526	0.589	0.089	0.991	22
19	Benzoic acids with diphenyldiazomethane, in ethanol, 30°C	−0.908 −0.913	0.289 0.280	0.026 0.022	0.998 0.999	23 23a

B. Aromatic Substitution

No.	Reaction	ρ	r	s	R	Ref.
20	Molecular bromination	−9.49	1.418	0.194	0.999	24
21	Molecular chlorination	−7.79 −7.95	1.239 1.221	0.110 0.100	0.993 0.994	24 24a
22	Protodeboronation	−4.94	1.091	0.163	0.998	25
23	Mercuration	−3.974	1.050	0.120	0.997	26
24	Acetylation	−9.52	0.813	0.336	0.992	27
25	Bromodesilylation	−6.62	0.808	0.21	0.991	28
26	Ethylation, ethyl bromide - gallium bromide, in ethylene dichloride	−2.647	0.774	0.090	0.991	29
27a	Protodesilylation, sulfuric acid	−4.942	0.761	0.021	1.000	30
27b	Protodesilylation, perchloric acid	−5.318 −5.283	0.734 0.732	0.045 0.058	0.999 1.000	31 31a
28a	Protodegermylation, sulfuric acid	−4.333	0.744	0.052	1.000	32
28b	Protodegermylation, perchloric acid	−4.629	0.727	0.039	1.000	33
29	Protodeplumbylation	−2.419	0.664	0.059	0.999	34
30	Protodemercuration	−2.87	0.61	0.29	0.981	35
31	Protodestannylation	−3.723	0.561	0.015	0.999	36
32	Protodesilylation, biphenyls	−1.325	0.424	0.024	0.999	37

C. Equilibrium

No.	Reaction	ρ	r	s	R	Ref.
33	pK_R^+, Benzhydrols	−9.37 −9.59	1.078 1.143	0.44 0.49	0.995 0.999	38 38a
34	pK_{BH^+}, Benzaldehydes	−1.764	1.164	0.099	0.996	39

No.	Reaction	ρ	r	s	R	Ref.
35	pK_{BH^+}, Benzalacetophenones	−1.339	0.872	0.024	1.000	40
36	pK_{BH^+}, Azobenzenes	2.238	0.849	0.27	0.998	41
37	pK_{R^+}, Triarylcarbinols	−11.39	0.787	0.49	0.999	38
		−11.50	0.768	0.73	0.997	42a
		−11.37	0.742	0.51	0.998	42b
38	pK_{BH^+}, Acetophenones	2.200	0.760	0.070	0.998	43
39	pK_{BH^+}, Benzoic acids	1.167	0.558	0.057	0.992	44
		1.146	0.553	0.053	0.993	44a
40	pK_{BH^+}, Pyridine oxides	2.684	0.550	0.14	0.996	45
41	Aryltropylium ions	2.055	0.464	0.083	0.993	46
42	pK_{BH^+}, Benzamides	1.243	0.364	0.058	0.992	47
43	pK_a, Benzoic acids, in water, 25°C	1.000	0.272	0.012	1.000	48
44	pK_a, Benzoic acids, in methanol	1.415	0.274	0.029	0.999	49
45	pK_a, Benzoic acids, in ethanol	1.515	0.253	0.043	0.997	50
46	pK_a, Benzoic acids, in *n*-propanol	1.569	0.237	0.025	0.999	51
47	pK_a, Benzeneboronic acids, in water	2.141	0.222	0.036	0.999	52

D. Non-reactivity Data

No.	Reaction	ρ	r	s	R	Ref.
48	F^{19} chemical shift, *p*-fluorobenzophenones in sulfuric acid	7.469	1.068	0.019	0.998	53
49	Ionization potential, benzyl radicals	1.140	1.015	0.082	0.999	54
50a	F^{19} chemical shift, *p*-fluorobenzophenone - BCl_3 complexes, dichloromethane	7.410	0.797	0.18	0.999	55
50b	F^{19} chemical shift, *p*-fluorobenzophenone - BF_3 complexes, dichloromethane	6.592	0.797	0.18	0.998	55
51	F^{19} NMR chemical shift, *p*-fluorobenzophenones, dichloromethane	2.398	0.325	0.064	0.998	55
52	UV $1/\lambda_{max}$, malachite green, in acetic acid	6.13	0.752	0.3	0.997	56

a) The summary of the results of the least squares application of Eq. 2. Substituents generally included were the selected groups; *p*-methoxy, *p*-alkyl, *p*-phenyl, *p*-halogens, well behaving *metas* substituents and *para*+*R* substituents, otherwise noted.

b) Reference numbers in the last column refer to those bellow the table rather than those in the text. 1) Standard deviation. 2) Correlation coefficient. 3) Literatures and remarks; reference numbers refer to the following rather than those cited in the text. 4) Ref. 5 in the text. 5) W. E. Bachmann and E. H. Mosher, *J. Am. Chem. Soc.*, **54**, 1124 (1932); W. E. Bachmann and J. W. Ferguson, ibid., **56**, 2081 (1934). 6) Y. Yukawa, Y. Tsuno and Y. Kusuyama, Unpublished. 7) J. R. Fox and G. Kohnstam, *Proc. Chem. Soc.*, 115 (1964). 7a) *p*-Nitro group was excluded from the calculation. 8) G. Kohnstam, **1960**, 2066; V. J. Shiner, Jr. and C. J. Verbanic, *J. Am. Chem. Soc.*, **79**, 369 (1957). 9) J. F. Norris and C. Banta, ibid., **50**, 1804 (1928); J. F. Norris and J. T. Blake, ibid., **50**, 1808 (1928). *p*-Methoxy group was not included into the calculation. 10) S. Nishida, privte communication; J. Packer, J. Vaughan and A. F. Wilson, *J. Org. Chem.*, **23**, 1215 (1958). 11) R. Bolton, N. B. Chapman and J. Shorter, *J. Chem. Soc.*, **1964**, 1895. 12) Ref. 38 in the text. 13) N. N. Lichtin and M. J. Vignale, *J. Am. Chem. Soc.*, **79**, 579 (1957); N. N. Lichtin and P. D. Bartlett, ibid., **73**, 5530 (1951); N. N. Lichtin and H. Glanzer, ibid., **73**, 5537 (1951); N. N. Lichtin and H. P. Leftin, *J. Phys. Chem.*, **60**, 164 (1956). 14) R. W. Bott, C. Eaborn and D. R. M. Walton, *J. Chem. Soc.*, **1965**, 384. 15) R. W. Bott, C. Eaborn and D. R. M. Walton, *J. Organometallic Chem.*, **1**, 420 (1964). 16) B. M. Lynch and K. H. Pausacker, *J. Chem. Soc.*, **1955**, 1525. 17) Ref. 3 in the text. 18) E. A. Braude and E. S. Stern, *J. Chem. Soc.*, **1947**, 1096. 19) R. Heck and S. Winstein, *J. Am. Chem. Soc.*, **79**, 3432 (1957). 20) D. E. Pearson, J. F. Baxter and J. C. Martin, *J. Org. Chem.*, **17**, 1151 (1952); D. E. Pearson and J. D. Burton, ibid., **19**, 957 (1954). 20a) Based on the data reported in, P. J. McNulty and D. E. Pearson, *J. Am. Chem. Soc.*, **81**, 612 (1959). 21) R. Huisgen, J. Witte, H. Walz and W. Jira, *Ann.*, **604**, 191 (1957). 22) T. Inukai, This Bulletin, **35**, 400 (1962). 23) J. D. Roberts, E. A. McElhill and R. Armstrong, *J. Am. Chem. Soc.*, **71**, 2923 (1949); R. A. Benkeser, G. E. Deboer, R. E. Robinson and D. H. Sauve, ibid., **78**, 682 (1956); N. B. Chapman, J. Shorter and J. H. P. Utley, *J. Chem. Soc.*, **1962**, 182. 23a) Correlation with the exclusion of *p*-fluoro group. 24) Data taken from, L. M. Stock and H. C. Brown, *J. Am. Chem. Soc.*, **84**, 1661 (1962). 24a) The correlation excluding *m*-bromo group. 25) H. G. Kuivila, *J. Am. Chem. Soc.*, **83**, 2167 (1961). 26) H. C. Brown and G. Goldman, ibid., **84**, 1650 (1962). 27) H. C. Brown and G. Marino, ibid., **84**, 1658 (1962). 28) C. Eaborn and D. E. Webster, *J. Chem. Soc.*, **1957**, 4449. 29) H. C. Brown and A. H. Neyens, *J. Am. Chem. Soc.*, **84**, 1655 (1962). 30) F. B. Deans and C. Eaborn, *J. Chem. Soc.*, **1959**, 2299. 31) C. Eaborn, ibid., **1956**, 4858. 31a) *p*-Dimethyamino-, *p*-hydroxy- and β-naphthyl-groups were included into the calculation. 32) C.

Eaborn and K. C. Pande, *J. Chem. Soc.*, **1961**, 5082. 33) C. Eaborn and K. C. Pande, ibid., **1961**, 297. 34) C. Eaborn and K. C. Pande, ibid., **1961**, 3715. 35) R. E. Dessy and J. Y. Kim, *J. Am. Chem. Soc.*, **82**, 686 (1960). 36) C. Eaborn and J. A. Waters, *J. Chem. Soc.*, **1961**, 542. 37) R. Baker, R. W. Bott, C. Eaborn and P. M. Greasley, ibid., **1964**, 627. 38) N. C. Deno and A. Schriesheim, *J. Am. Chem. Soc.*, **77**, 3051 (1955); N. C. Deno and W. L. Evans, ibid., **79**, 5804 (1957). 38a) *p*-Dimethylamino group was included. 39) K. Yates and R. Stewart, *Can. J. Chem.*, **37**, 664 (1959). 40) D. S. Noyce and M. J. Jorgenson, *J. Am. Chem. Soc.*, **84**, 4312 (1962). 41) H. H. Jaffé and R. W. Gardner, ibid., **80**, 319 (1958). 42a) The correlation including *p*-dimethylamino, *p*-amino and *p*-hydroxy groups. 42b) The correlation including *p*-dimethylamino and *p*-hydroxy groups. 43) R. Stewart and K. Yates, *J. Am. Chem. Soc.*, **80**, 6355 (1958). 44) R. Stewart and K. Yates, ibid., **82**, 4059 (1960). 44a) *m*-Chloro group was excluded. 45) H. H. Jaffé and G. O. Doak, *J. Am. Chem. Soc.*, **77**, 4441 (1955); J. N. Gardner and A. R. Katritzky, *J. Chem. Soc.*, **1957**, 4375; C. D. Johnson, A. R. Katritzky, B. J. Ridgewell, N. Shaker and A. M. White, *Tetrahedron*, **21**, 1055 (1965). 46) C. Jutz and F. Voithenleitner, *Chem. Ber.*, **97**, 29 (1964). 47) J. T. Edward, H. S. Chang, K. Yates and R. Stewart, *Can. J. Chem.* **38**, 1518 (1960). 48) Data taken from, D. H. McDaniel and H. C. Brown, *J. Org. Chem.*, **23**, 420 (1958); *p*-Dimethylamino, *p*-amino and *p*-hydroxy groups were included. 49) J. H. Elliot and M. Kilpatrick, *J. Phys. Chem.*, **45**, 454 (1941). 50) J. H. Elliott and M. Kilpatrick, ibid., **45**, 466 (1961). 51) J. H. Elliott, ibid., **46**, 221 (1942). 52) G. E. K. Branch, D. L. Yabroff and B. Bettman, *J. Am. Chem. Soc.*, **56**. 937 (1934); ibid., **56**, 1865 (1934); ibid., **56**, 1850 (1934). 53) R. W. Taft and Y. Tsuno, unpublished. 54) A. G. Harrison, P. Kebarle and F. P. Lossing, *J. Am. Chem. Soc.*, **83**, 777 (1961). 55) R. W. Taft, unpublished. 56) C. C. Barker, M. H. Bride, G. Hallas and A. Stamp, *J. Chem. Soc.*, **1961**, 1285.

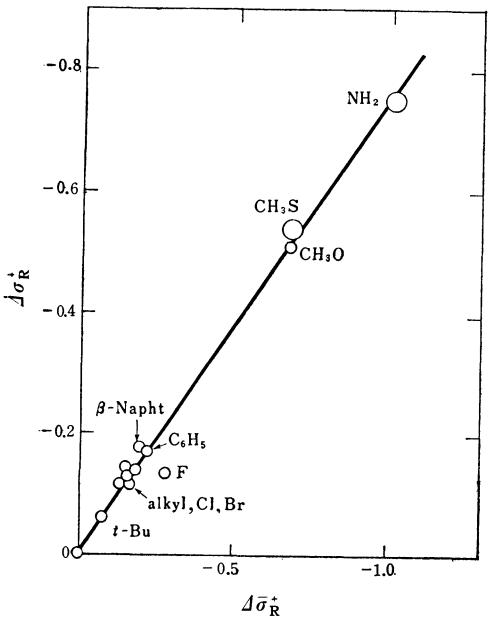

Fig. 3. Relation between $\Delta\sigma_R^+$ and $\Delta\bar{\sigma}_R^+$.

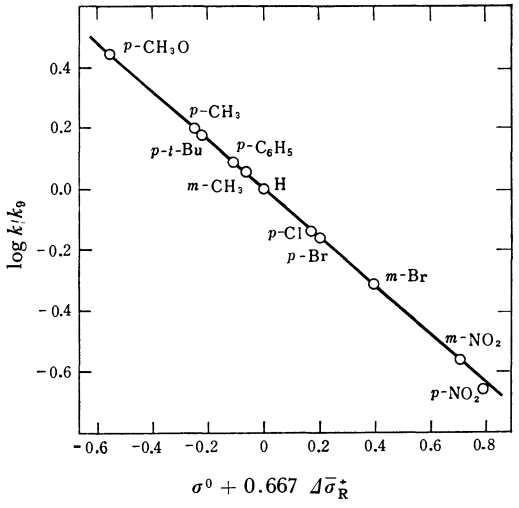

Fig. 4. Application of Eq. 2 to the decomposition of ω-diazoacetophenones in acetic acid at 40°C.

to be capable of being the resonance substituent constant. The increment $\sigma^+ - \sigma^0$ in fact runs precisely parallel to $\Delta\sigma_R^+$ for corresponding substituents, as shown in Fig. 3. The correlation can be given by :

$$\Delta\sigma_R^+ = 0.74(\sigma^+ - \sigma^0).$$

The quantity, $\sigma^+ - \sigma^0$, can correlate also linearly the exalted resonance contribution involved in Hammett σ-values, $\sigma - \sigma^0$, with a proportionality constant of 0.26.[29] These facts evidently suggest that the individual set of these increments is measuring in the different scale the identical quantities capable of being the resonance substituent parameter. The replacement of the standard from σ to σ^0 does not result the change in the form of the equation. Thus the alternate relationship can be represented by Eq. 2,

$$\log k/k_0 = \rho(\sigma_0 + r\Delta\bar{\sigma}_R^+) \qquad (2)$$

where a new set of resonance substituent parameters, $\Delta\bar{\sigma}_R^+$, was defined by $\sigma^+ - \sigma^0$ in Brown and Okamoto's scale.

29) An anomaly arises in *p*-fluoro group in this correlation; only fluoro group deviates measurably from the correlation line. A satisfactory explanation of the deviation is not immediately available, but the deviation of this group is not significant in the other benzoic reactivities, such as hydrolysis of benzoic esters or the reaction of benzoic acids with diphenyldiazomethane. Therefore, the deviation does not deny the applicability of the present treatment for fluoro group.

Equation 2 has been applied successfully to correlate representative electrophilic reactivities including the benzoic reactivities, by using the method of least squares. The results are summarized in Table V and several examples are illustrated in figures. Our previous result on the decomposition of diazoacetophenones in acetic acid[3] was correlated excellently with an r-value of 0.667 as shown in Fig. 4. For our recent data of the hydrolysis of m- and p-substituted α-phenylethyl chlorides in 80% aqueous acetone at 45°C,[30] Hammett equation resulted a scattered plot but Eq. 2 gave an excellent straight line for the same data using an r of 1.16. This can be compared in Figs. 5 and 6. The precision of the correlations can be easily estimated by standard deviations and correlation coefficients in Table V. The excellent result covering a wide variation of ρ and a variety of reactions evidently confirms the generality of this empirical relationship (2).

Most of the correlations in Table V were obtained primarily on the basis of reactivities of selected substituents. Dimethylamino-, amino, hydroxy-, and some others were not included into the calculations of correlations, because σ^0 and $\Delta\sigma_R^+$ values for these groups are not equivalently reliable as those for the other well-behaving substituents. Whereas the inclusion of these groups into calculations usually did not result the significant change in the correlation.

ρ and r in Eq. 2 might be practically covariant and compensate for variations of each other. Our treatment is essentially based as the standard.

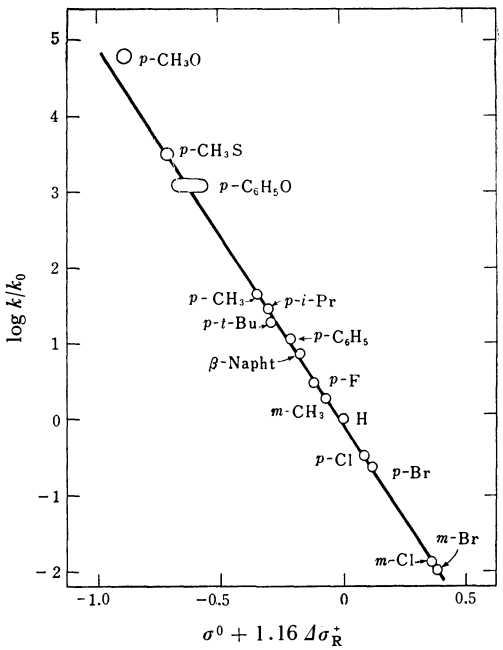

Fig. 6. Application of Eq. 2 to the solvolysis of α-arylethyl chlorides.

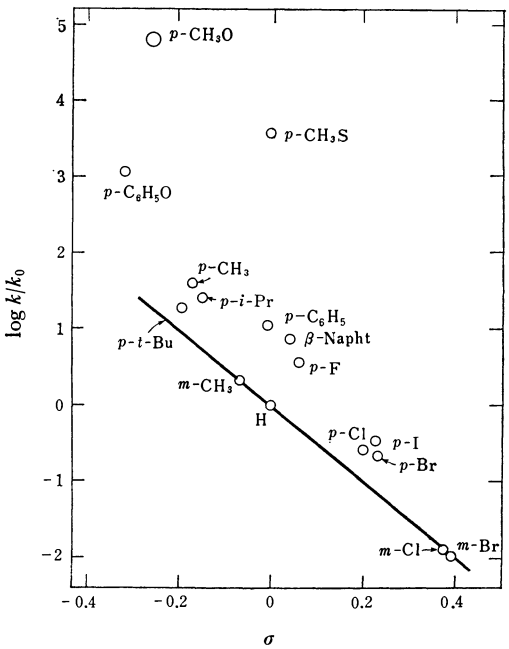

Fig. 5. Hammett plot of solvolysis of α-arylethyl chlorides.

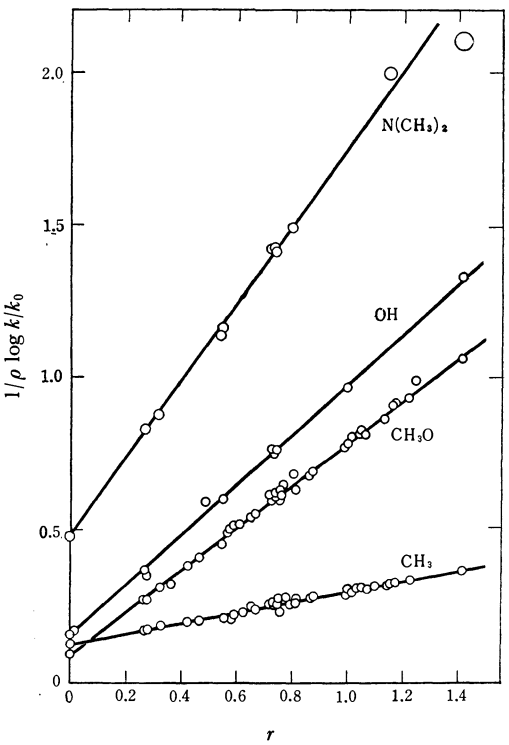

Fig. 7. Dependency of the effects of *para* substituents on r.

30) Y. Yukawa, Y. Tsuno and Y. Kusuyama, to be published.

on the ρ_m value, which should be the general basis of the Hammett type linear free energy correlations.[3,15,16] Certainty of the resulted correlation or r must depend on the reliability of ρ-value, and accordingly depend on the number of *meta* substituents involved in the series. ρ values obtained by the least squares application of Eq. 2 were generally found to agree with values calculated from *meta* reactivities alone. This should be an important fact to support our treatment, and thus r-value is not merely a mathematical compensating parameter but appears to be a parameter characteristic of the reaction practically independent of ρ-value.

Figure 7 illustrates the variation of apparent substituent constants, $1/\rho \log k/k_0$, of respective groups as a function of r for varied reactions. The respective substituents indicates clearly the first order dependence upon r. Since the gradient corresponds to $\Delta\bar{\sigma}_R^+$ and the intercept to σ^0 of respective substituents, the linear dependency is an evidence for the constancy of $\Delta\bar{\sigma}_R^+$ parmameters of these groups independent of reactions. Dimethylamino and hydroxy groups also indicate clearly the linear dependency covering over a remarkable variation of reactivities. Here again it should be mentioned that these groups were not included in the calculation of r values. Thus this should be the strong support to the certainty of the present relationship for a wide variety of substituents including these strongly conjugative substituents. Unfortunately, data are not sufficiently available in the literature for *p*-amino, *p*-methylmercapto and *p*-phenoxy groups to examine the validity of parameters. Additional data must be awaited.

The present type equation is expected to be applied for the correlation of conjugatively electron attracting *para* substituents in the nucleophilic reactions.[31] This can be realized by Eq. 3,

$$\log k/k_0 = \rho(\sigma^0 + r\Delta\bar{\sigma}_R^-) \qquad (3)$$

using the difference, $\sigma^- - \sigma^0$, as the resonance substituent constant, $\Delta\bar{\sigma}_R^-$. The dissociation of phenols or anilines will be perhaps the extreme case of this equation; these were referred to $r=1$. The linear correlation in Fig. 8 is illustrating the application of Eq. 3 to the dissociation of substituted thiophenols[32] which requires $r=0.52$. NMR chemical shifts of the acetylenic proton of substituted phenylacetylenes[33] resulted an excellent correlation in terms of r of 0.63 for *para* electron attracting groups. Yoshioka et al.[34] reported

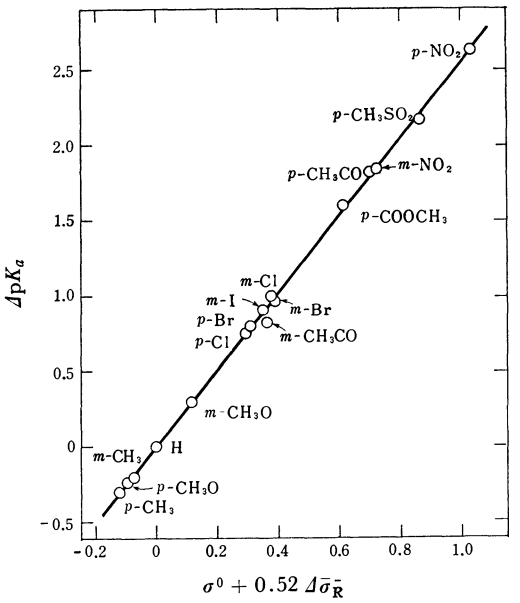

Fig. 8. Application of Eq. 3 to the dissociation of substituted thiophenols.

that the dissociations of several series of sulfonanilides were correlated linearly, giving r's close to 0.5. Although further examination may have to be required for Eq. 3, few other data of this reactivity class are available in the literature. However, these results may be sufficient to suggest that the present type treatment can be applicable not only to electrophilic but nucleophilic reactions.

From the general success of the present type and original treatments, and also from a precise proportionality between $\Delta\sigma_R^+$ and $\Delta\bar{\sigma}_R^+$, it can be conclusive that there should exist a general measure of the resonance capacity of substituents. The substituent effect on reactivities can be represented by the generalized form,

$$\log k/k_0 = \rho(\sigma^0 + \phi) \qquad (4)$$

where ϕ represents the exalted contribution of *para* substituents, exclusively attributable to the resonance contribution. The present result shows that ϕ can be given by

$$\phi = r\Delta\bar{\sigma}_R^+ \quad \text{and/or} \quad = r\Delta\bar{\sigma}_R^- \qquad (4')$$

for conjugatively electron releasing *para* substituents in electrophilic reactions and electron attracting *para* substituents in nucleophilic reactions, respectively. This is an actual establishment of the linear free energy relationship for the exalted resonance contribution. Equation 4 associated with 4' is in the other view the separation of substituent effect into the substituted phenyl polarity and the polarizability effects.

31) Y. Yukawa, *J. Soc. Org. Synth. Chem. Japan, sp. ed.*, 69 (1962).
32) F. G. Bordwell and H. H. Andersen, *J. Am. Chem. Soc.*, **75**, 6019 (1953); G. Schwarzenbach and H. A. Egli, *Helv. Chim. Acta*, **17**, 1176 (1934).
33) Y. Yukawa and H. Yamada, *J. Chem. Soc. Japan, Pure Chem. Sect., (Nippon Kagoku Zasshi)*, **85**, 501 (1964).
34) M. Yoshioka, K. Hamamoto and T. Kubota, This Bulletin, **35**, 1723 (1962); A. Willi, *Helv. Chim. Acta.* **39**, 49 (1956).

As pointed out frequently,[11,14,15,35] ψ term is susceptible to various factors such as the loss of resonance due to steric inhibition, specific solvation, and beyond the question experimental errors. An excellent result with the present treatment should be an evidence supporting that only the polar contribution, inductive and resonance contributions, is the dominant factor of the given reactivity. The ordinary effects, such as the dependency of resonance upon solvation or desolvation, will be included in r and also in ρ as a common factor. On the other hand, the deviation from the correlation should be taken as an evidence for the existence of some specific effects of particular substituents. An illustrative example of the case is the bromination of polymethylbenzenes. Illuminati reported the substituent effect on the nuclear bromination of substituted durenes, isodurenes and mesitylenes, where only the desired attacking nuclear position is opened.[36] On the basis of Eq. 2, the additional resonance contribution, ψ, to this reaction is separated using $\rho = -8.69$. Figure 9 shows the plot of ψ-values against

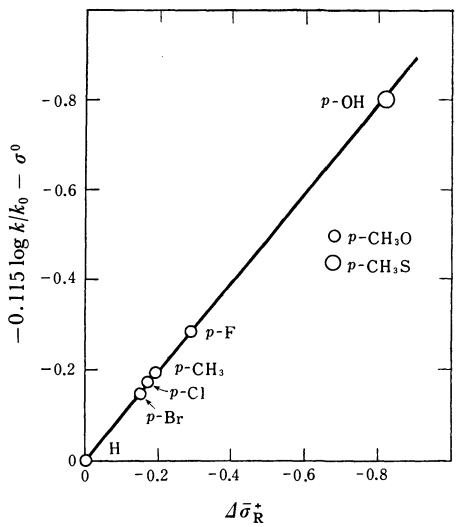

Eig. 9. Resonance contribution in the bromination of polymethylbenzenes.

$\Delta\bar{\sigma}_R^+$. The points for alkyl- and halo-groups fall on a line giving an r of 1.00 whereas methoxy and methylmercapto groups deviate from the line. The deviation might be attributed to the steric loss of resonance interaction with the ring due to the twisting from the coplanarity by adjacent methyl groups. The resonance contribution of the other groups may not be affected sterically, so that they satisfy the linear relation with $\Delta\bar{\sigma}_R^+$. *p*-Hydroxy groups, of which the rate is estimated from that of the 2, 6-dimethyl derivative,[12] is also usually free from such an effect and thus satisfies the correlation. Illuminati has pointed out the inhibition of resonance only for *p*-nitro group on the basis of the Hammett correlation, while he did not verify that of methoxy or methylmercapto group, simply because the lack of any reliable standard correlation. The considerably lower r than that of the bromination of monosubstituted benzenes can be explained reasonably in terms of the incorporated stabilization of the transition state by the electron releasing methyl groups in the polymethylbenzene case. The slightly low ρ value is referred to the same reason and also to the steric contribution of methyl groups to the reaction center.

One of the characteristic features of our treatment is the introduction of the variable r for variations of resonance from reaction to reaction. In our concept, r must be a measure of the degree of resonance interaction between substituent and reaction site. As mentioned previously,[6,11] r remains approximately a constant for reactions which have the closely similar structure of the transition state. In the case of dissociations of substituted benzoic acids, ρ-parameter varies considerably with respect to the change in the condition such as solvent change, whereas r remains so constant as to give a constant σ-value for respective substituents. In the carbonium ion reactions, trityl derivatives gave an approximately constant r of 0.8, and the benzhydryl provided r-value close to 1.1.

In the series of solvolysis reactions, cumyl chlorides have an r-value of unity by the definition, α-phenylethyl chlorides provide a precise r value of 1.16, and benzyl derivatives r-value round 1.5.[37] The changes of r can be attributed to variations of the degree of aryl participation in competition with electron donation by the adjacent methyl group. The variation in ρ does not provide any useful indication.

In the case of Beckmann rearrangement of acetophenone oximes (16 and 17), the change of the leaving group resulted the distinctly different ρ values but comparable r values. Closeness of r might be a suggestion of the close similarity of the transition state. Change in ρ provides few information about the mechanism. On the contrary, the solvolysis of cumyl and neophyl

36) G. Illuminati, *J. Am. Chem. Soc.*, **80**, 4941 (1958); ibid., **80**, 4945 (1958); E. Baciocchi and G. Illuminati, ibid., **86**, 2677 (1964).

35) C. D. Ritchie and W. F. Sager, "Progress in Physical Organic Chemistry," Vol. II, Interscience, New York (1964), Chapt. 6, p. 323.

37) The definite r-value can not be determined for this reactivity; as for example, the solvolysis of benzyl tosylates appears to involve the change in the reaction mechanism due to substituent changes. Accordingly, even ρ_m value can not be accurately determined for this reaction. (J. K. Kochi and G. S. Hammond, *J. Am. Chem. Soc.*, **75**, 3445 (1953); F. T. Fang, J. K. Kochi and G. S. Hammond, ibid., **80**, 563 1958).

derivatives (1 and 15) resulted comparable ρ-values but different r-values, suggesting the different structures of transition states.

The gas phase pyrolysis of substituted α-phenylethyl acetates, studied by Smith et al.,[38] can be compared interestingly with the solvolysis of phenylethyl chlorides in an aqueous acetone.[30] The pyrolysis of acetates gave a remarkably small ρ but a comparable r value with that for the solvolysis of the chlorides indicating the resemblance of the transition states of both reactions.

In the series of the protonation equilibria of the benzoyl derivatives (No. 34, 38, 39 and 42),

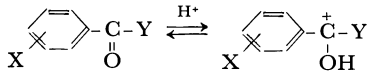

where Y's are H, CH_3, OH and NH_2, r-value decreases from 1.16 to 0.36 in the increasing order of electron donating capacities of Y-substituents. This can be explained reasonably in terms of the competitive participation of aryl and Y-substituent groups. ρ parameter appears to be a complicated resultant of the pertinent factors, while the condition of reactions is nearly the same. From these facts, r-parameter can be discernible as the more appropriate measure of the electronic requirement of the transition state than ρ-parameter.

A theoretical approach to the present-type linear free energy relationship (2 and 3) has been recently carried out by Fueno and Furukawa.[39] Hammett σ and various σ^+-type substituent constants were calculated as the delocalization energy changes of substituted benzyl-type carbonium ions by the perturbation and also variation methods.[40] The results suggested that the variation of estimated Coulomb parameter k in $\alpha+k\beta$ for the reaction site, assumed as a heteroatom ion, was proportional to the change in r of the present study. Thus the experimental r, the degree of resonance contribution, appears to be compatible with the degree of delocalization estimated from M. O. approximation.

Theoretically both r and ρ should be responsible to the variation of electron density at the reaction site, accordingly, both parameters might be correlated in some way with each other. Norman[12] has proposed recently Eq. 5 for the correlation of aromatic electrophilic reactions,

$$1/\phi \log k/k_0 = \sigma_G + \phi\sigma_P \qquad (5)$$

where ϕ is the electron demand constant, σ_G is a measure of the ground state polarization and σ_P the polarizability constant of a substituent. In view of the formal similarity to our relationship, he has attempted to rationalize his Eq. 5 in terms of our parameters.[41] σ_G can be equated to σ^0. σ_P might correspond to our resonance parameter in its concept and reasonably be expected to be proportional to the latter. Further correspondence requires that r value has to be parallel to ρ values of various reactions, provided ϕ being equal to ρ. In view of the nature of ρ, such a parallelism will be observable only in the closely limited reaction series. Norman has demonstrated the existence of linearity between both parameters for 6 aromatic electrophilic substitution reactions. Whereas, Eaborn has indicated the other examples against this.[42] In Fig. 10 are figured out both parameters

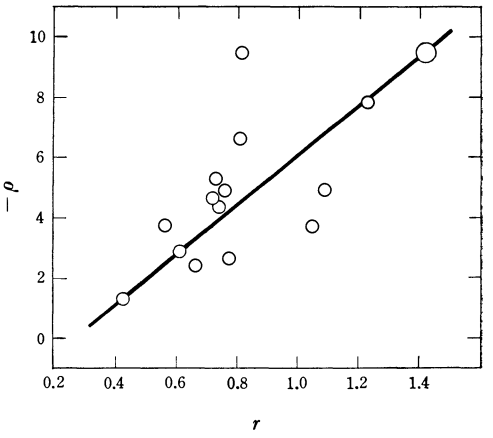

Fig. 10. Relation between ρ and r of aromatic electrophilic substitutions.

for aromatic substitutions obtained in the present investigation. The resulted correlation is clearly far out of the accuracy of usual linear free energy correlations, even if a linearity may exist. Generally the present result does not necessarily agree with Norman's assumption. Norman equation appears to be describing the limited theoretical model of the ideal aromatic substitution reaction, while such an ideal series of reactions can not easily be observed experimentally.

Of the empirical treatments of the substituent effect, Taft equation[14,15] has been most generally accepted.[2] The separation of the substituent effect into inductive and resonance effects appears to be most likely and physically meaningful. His equation is often employed in the literature

38) R. Taylor, G. G. Smith and W. H. Wetzel, *J. Am. Chem. Soc.*, **84**, 4817 (1962).

39) T. Fueno and J. Furukawa, private communication. Authors are indebted to their invaluable advices and discussions.

40) The integral parameters for substituents were determined in such a way as to give the calculated pi-electron change densities being proportional to the corresponding σ^0-constants, and these fixed parameters were employed for the calculation of other sets of substituent constants.

41) R. O. C. Norman and G. K. Radda, *Tetrahedron Letters*, **1962**, 125.

42) R. W. Bott and C. Eaborn, *J. Chem. Soc.*, **1963**, 2130.

to electrophilic reactivities as the form,[43]

$$\log k/k_0 = \rho_I\sigma_I + \rho_R\sigma_R^0 \qquad (6)$$

where σ_R^0 may be replaced by σ_R or σ_R^+. The precision of the fit is usually comparable with that of the present treatment. According to Taft's definition,[14] σ_I is a constant of respective substituents independent of reactions, and ρ_I has to be equal to ρ_m value. However, on applying Eq. 6 to -R *para* substituents in the electrophilic reaction, it is found that the best ρ_I value obtained is not always equal to ρ_m value.[44] The statistically most probable ρ_I of a given reaction significantly varies depending on the choice of his resonance parameters. For instance, the application of Eq. 6 to Brown's reference reaction of σ^+[5] results the ratios of σ_I/σ_m of 1.00 (by definition), 1.35 and 1.50, dependent on the use of σ_R^+, σ_R and σ_R^0, respectively. These variations exceed distinctly the limit of the common uncertainty; more interestingly, they are rather systematic. The similar difficulties are not rarely observed in Taft's treatment, and are inevitable from the mutual non-linearity of his resonance parameters for respective substituent. Thus, any set of his resonance parameters can not accomplish generally the linear resonance free energy relationship. These treatments might be perhaps the overextension or a kind of incorrect use of Taft equation. As Taft mentioned by himself,[14,15] individual set of his resonance parameters should be employed limitedly for its appropriate reactivity class, otherwise, the correlation obtained means merely a mathematically best result and either ρ_I or ρ_R resulted will lend little help to the elucidation of the mechanism of a given reaction. While Taft equation is conceptually reasonable and meaningful, the present treatment (4) togehter with (4') has the advantage of Taft's one in the view point of the linear resonance free energy relationship.

The insulated aryl reactivities can be separated conceptually into mesomeric and inductive effects. Accordingly, Eq. 4 for general reactivities can be rewritten in the form,

$$\log k/k_0 = \boldsymbol{I} + \boldsymbol{R}_0 + \boldsymbol{\Psi} \qquad (7)$$

where $\boldsymbol{I}$ and $\boldsymbol{R}_0$ represent the inductive and mesomeric effects in the insulated reactivities. Either $\boldsymbol{R}_0$ or $\boldsymbol{\Psi}$ is essentially responsible to the inherent resonance capacity of respective substituents. Hence it might be plausible to expect that both $\boldsymbol{R}_0$ and $\boldsymbol{\Psi}$ terms can be described by a common resonance parameter inherent in the individual substituent. As usual, $\boldsymbol{R}_0$ could be replaced by Taft's σ_R^0, whereas, σ_R^0 is not exactly proportional to $\Delta\bar{\sigma}_R^+$ and is incapable of being linear free energy description of $\boldsymbol{\Psi}$ contributions. The general applicability of our $\Delta\bar{\sigma}_R^+$ for the $\boldsymbol{\Psi}$ contribution would lead to the expectation that a measure of the conceptual $\boldsymbol{R}_0$ will be practically realizable from our resonance parameters. The estimated $\boldsymbol{R}_0$-parameter might not be exactly equal to Taft's σ_R^0 parameter, and as a sequence, this might estimate a different scale of the inductive effect for the aryl-residue from Taft's σ_I scale. Such an analysis of the substituent effect should be of great importance and interest, to obtain some informations about the essential implication of the present treatment and also the nature of the substituent effect. The analysis along this line has been recently carried out in this laboratory and will be the subject of a forthcoming publication.

Authors are indebted to Professor J. E. Leffler and Professor G. S. Hammond for helpful discussions. Special thanks are due to Professor R. W. Taft who has always encouraged us and also has given us invaluable suggestions and advices to this work.

43) A. Bryson, *J. Am. Chem. Soc.*, **82**, 4862 (1960); *Austral. J. Chem.*, **16**, 401 (1963); I. R. Fox, P. L. Levins and R. W. Taft, Jr., *Tetrahedron Letters*, **1961**, 249; R. R. Fraser, *Can. J. Chem.*, **38**, 2226 (1960).

44) To be discussed in the forthcoming paper.

BULLETIN OF THE CHEMICAL SOCIETY OF JAPAN VOL. 39 2287—2289 (1966)

The Synthesis, Resolution and Configuration of β-Hydroxyvaline[1]

By Jun-ichi OH-HASHI and Kaoru HARADA

Institute of Molecular Evolution and Department of Chemistry, University of Miami, Coral Gables, Florida, U. S. A.

(Received April 9, 1966)

DL-β-Hydroxyvaline was synthesized from sodium β, β-dimethylglycidate by aminolysis with benzylamine, followed by hydrogenolysis. *N*-Benzoyl-DL-β-hydroxyvaline was resolved by use of (−)-α-methylbenzylamine to yield (−)-*N*-benzoyl-β-hydroxyvaline. The configuration of VI was determined by converting it to methyl *N*-benzoyl-β-chlorovalinate (I) and subsequent hydrogenolysis of I yielded (−)-methyl *N*-benzoylvalinate (II). From II, optically pure D-(−)-valine was obtained upon hydrolysis.

The finding of β-hydroxyvaline in nature has been reported.[2-4] However, later investigations showed that the natural occurrence of the amino acid was questionable.[5-8] Syntheses of the racemic amino acid have been reported by use of the addition reaction of mercuric acetate and bromine to β, β-dimethylacrylic acid.[5,9-11] Ammonolysis of ethyl β, β-dimethylglycidate resulted in β-amino α-hydroxy derivative.[12-14] Recently Kaneko and Inui[15] synthesized and characterized racemic β-hydroxyvaline and an α-hydroxy-β-aminoisovaleric acid which were separated from the reaction mixture of ammonolysis of sodium β, β-dimethylglycidate (I).

Optically active β-hydroxyvaline has not been prepared. In this investigation, DL-β-hydroxyvaline was prepared by treatment of I with benzylamine in aqueous condition in a way similar to the method employed by Liwschitz et al.[16,17] in which they obtained only α-amino β-hydroxy

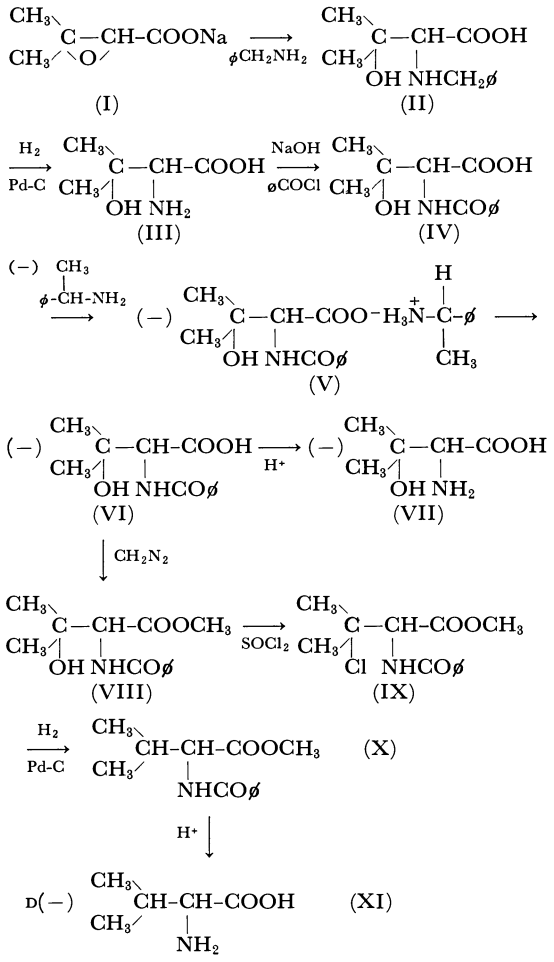

Fig. 1. Schematic route of synthesis, resolution and configuration determination of β-hydroxyvaline.

1) Contribution No. 054 of the Institute of Molecular Evolution, University of Miami.
2) S. B. Schryver and H. W. Buston, *Proc. Roy. Soc.*, **B99**, 476 (1925—26).
3) E. J. Czarnetsky and C. L. A. Schmidt, *J. Biol. Chem.*, **92**, 453 (1931).
4) M. A. B. Brazier, *Biochem. J.*, **24**, 1188 (1930).
5) E. Adberhalden and K. Heyns, *Ber.*, **67**, 530 (1934). *Z. Physiol. Chem.*, **229**, 236 (1934).
6) A. J. Martin, R. L. M. Synge and F. O. Bell, *Biochem. J.*, **35**, 294 (1941).
7) C. M. Stevens and P. E. Halpern, *J. Biol. Chem.*, **179**, 389 (1949).
8) B. H. Nicolet and L. A. Shinn, ibid., **142**, 139 (1942).
9) W. Schrauth and H. Geller, *Ber.*, **55**, 2783 (1922).
10) S. Tatsuoka, T. Ueno and K. Hirata, *Yakugaku Zasshi*, **70**, 229 (1950).
11) K. Rutenacht, *Helv. Chim. Acta*, **35**, 762 (1952).
12) S. N. Danilov and V. F. Martynov, *Zhur. Obschei Khim.*, **22**, 1572 (1952).
13) O. von Schickh, German Pat. 583243 (1933), [*Chem. Abstr.*, **28**, 260 (1934)].
14) V. F. Martynov, *Doklady Akad. Nauk U. S. S. R.*, **89**, 869 (1953).
15) T. Kaneko and T. Inui, *J. Chem. Soc. Japan, Pure Chem. Sect.* (*Nippon Kagaku Zasshi*), **82**, 743 (1961).
16) Y. Liwschitz, Y. Rabinsohn and D. Perera, *J. Chem., Soc.* **1962**, 1116.
17) Y. Liwschitz, Y. Rabinsohn and A. Haber, ibid., **1962**, 3589.

acids. The resulting *N*-benzyl-β-hydroxyvaline (II) was debenzylated by hydrogenolysis with palladium on charcoal. The prepared DL-β-hydroxyvaline (III)[18] was benzoylated and was resolved by (−)-methylbenzylamine[19,20] to yield (−)-*N*-benzoyl-β-hydroxyvaline (−)-amine salt (V). From the salt V, (−)-*N*-benzoyl-β-hydroxyvaline (VI) was isolated. Free (−)-β-hydroxyvaline (VII) was obtained by hydrolysis of VI. To determine the configuration of the resolved (−)-β-hydroxyvaline (VII), (−)-*N*-benzoyl-β-hydroxyvaline (VI) was converted to the methyl ester (VIII) by the use of diazomethane. The ester VIII was treated with thionyl chloride to convert VIII to β-chloro ester (IX). The β-chloro ester was catalytically hydrogenolyzed by the use of palladium on charcoal to yield methyl *N*-benzoyl-valinate (X) as was done in the study of β-phenylserine.[21] The ester X was hydrolyzed and optically pure D (−)-valine (XI) was obtained. Accordingly, the α-carbon atom of (−)-β-hydroxyvaline is assigned the D-configuration. The schematic route of this work is shown in Fig. 1.

Attempts to obtain active glycidic acid by resolution were unsuccessful, because of instability of the free glycidic acid.

Experimental[22]

DL-*N*-Benzyl-β-hydroxyvaline (II).—A mixture of sodium β, β-dimethylglycidate (I),[15] 6.9 g. (0.05 mol.), water, 7 ml., and benzylamine, 8.0 g., was heated under reflux for 6 hr. After cooling, the excess of benzylamine was removed by distillation in vacuo. The pH of the aqueous solution was adjusted to 5.5 with concentrated hydrochloric acid. The precipitated crystals of DL-*N*-benzyl-β-hydroxyvaline (II) were separated by filtration and washed with acetone, then ether. The crude product, 7.6 g. (68%), was recrystallized from *N*, *N*-dimethylformamide. Yield, 6.9 g. (62%), m. p. 204°C.

Found: C, 64.38; H, 7.80; N, 6.35. Calcd. for $C_{12}H_{17}NO_3$: C, 64.55; H, 7.67; N, 6.27%.

DL-β-Hydroxyvaline (III).—DL-*N*-Benzyl-β-hydroxyvaline (II), 2.2 g. (0.01 mol.), was dissolved in 50 ml. of 50% methanol. To this solution, 1.0 g. of 5% palladium on charcoal was added and the hydrogenolysis was carried out at room temperature. When the hydrogen uptake ceased, the catalyst was removed by filtration. The filtrate was concentrated in vacuo. The crystalline residue was recrystallized from water and methanol. Yield, 1.21 g. (93%). This was further purified from water and ethanol, 1.13 g. (85%), m. p. 218°C (decomp.), [reported m. p. 226—227°C (decomp.)[15]]. Infrared spectrum showed[15] absorption bands at 1670, 1620, 1600, 1560, 1420 cm^{-1} (amino acid), 1145 cm^{-1} ($\rangle$C–OH). R_f value 0.44, BuOH : AcOH : H_2O=4 : 1 : 2. The compound showed a single peak in the Phoenix model K-5000 automatic amino acid analyzer.

Found: C, 45.12; H, 8.57; N, 10.42. Calcd. for $C_5H_{11}NO_3$: C, 45.10; H, 8.33; N, 10.52%.

DL-*N*-Benzoyl-β-hydroxyvaline (IV).—DL-β-Hydroxyvaline (III), 6.65 g. (0.05 mol.), was dissolved in 25 ml. of 2 N sodium hydroxide solution. The solution was chilled in an ice bath and benzoylated in the usual Schotten-Baumann method with a total of 7.0 g. of benzoyl chloride and 25 ml. of 2 N sodium hydroxide solution. Upon completion of the addition of reagents, the reaction mixture was shaken for 15 min. at room temperature and then acidified to pH 3.0 under cooling with concentrated hydrochloric acid. DL-*N*-Benzoyl-β-hydroxyvaline (IV) was extracted with ethyl acetate 2 times (100 ml.×2) and this ethyl acetate layer was washed with water. The ethyl acetate solution was dried with anhydrous sodium sulfate. After evaporation of ethyl acetate in vacuo, 8.9 g. (75%) of crude IV was obtained. Contaminating benzoic acid was removed from the product by boiling with 30 ml. chloroform and subsequently filtering this mixture. These crystals were purified by recrystallization from ethanol and ether. Yield, 8.3 g. (70%), m. p. 156°C (decomp.), [reported 155—157°C (decomp.)[15]]. Infrared spectrum showed bands at 1720 cm^{-1} (–COOH), 1635; 1520 cm^{-1} (–CONH–); 1152 cm^{-1} ($\rangle$C–OH). The benzoyl derivative seems to correspond to the stable form of IV reported by Kaneko and Inui.[15] (The unstable form was reported m. p. 135—136°C.[15])

Found: C, 60.73; H, 6.53; N, 5.80. Calcd. for $C_{12}H_{15}NO_4$: C, 60.75; H, 6.37; N, 5.90%.

(−)-α-Methyl Benzylamine Salt of *N*-Benzoyl-β-hydroxyvaline (V). — DL-*N*-Benzoyl-β-hydroxyvaline (IV), 94.8 g. (0.4 mol.), and (−)-α-methylbenzylamine, 48.4 g. (0.4 mol.), ($[\alpha]_D^{25}$=42.3°, benzene), were dissolved in 50 ml. methanol. The solvent was evaporated in vacuo. The residual syrup was dissolved in hot acetone (150 ml.). After cooling, crystallization of (−)-α-methylbenzylamine salt (V) began by seeding with an authentic specimen which was obtained in another crystallization experiment. After standing overnight in a refrigerator, the crystals were filtered and washed with cold acetone. The crystals, 51.8 g. (72%), were purified from a hot mixture of methanol and acetone (5 : 95). Yield, 47.3 g. (66%), m. p. 155°C, $[\alpha]_D^{25}$= −22.9° (*c* 2.32, water).

Found: C, 67.12; H, 7.43; N, 7.64. Calcd. for $C_{20}H_{26}N_2O_4$: C, 67.02; H, 7.31; N, 7.82%.

(−)-*N*-Benzoyl-β-hydroxyvaline (VI).—(−)-α-Methylbenzylamine salt (V), 36.0 g. (0.1 mol.), was dissolved in 100 ml. of water. To this solution, 110 ml. of 2 N sodium hydroxide was added. The alkaline solution was extracted with ether twice (100 ml.×2) to remove (−)-α-methylbenzylamine. Concentrated hydrochloric acid was added to the aqueous solution to bring the pH to 3.0. (−)-*N*-Benzoyl-β-hydroxyvaline (VI) was extracted with ethyl acetate (100 ml.×2).

18) III showed a single spot in paper chromatography and also showed a single peak in the Phoenix model K-5000 automatic amino acid analyzer.
19) W. Theilacker, *Chem. Ber.*, **87**, 690 (1954).
20) W. Leither, ibid., **64**, 2831 (1931).
21) K. Vögler, *Helv. Chim. Acta*, **33**, 2111 (1950).
22) All temperature measurements are uncorrected. All optical rotation measurements were carried out by the use of the Rudolph model 80 polarimeter with PEC-101 photometer. Elemental analyses were carried out by Micro-Tech Laboratories, Inc., Skokie, Illinois, U. S. A. Infrared absorption spectra were recorded by the use of the Perkin Elmer Model 137 B Infracord Spectrophotometer.

The ethyl acetate solution was washed with water and dried with anhydrous sodium sulfate. After evaporation of ethyl acetate in vacuo, 20.7 g. (87%) of crude VI was obtained. This was recrystallized from methanol and ether. Yield, 19.7 g. (83%), m. p. 112°C, $[\alpha]_D^{25} = -30.5°$ (*c* 2.01, ethanol). Infrared spectrum showed bands at 1745 cm^{-1} (–COOH); 1645, 1550 cm^{-1} (–CONH–); 1150 cm^{-1} (>C–OH). The optically active *N*-benzoyl-β-hydroxyvaline also showed polymorphism which was detected by infrared spectrographically as was reported for DL-*N*-benzyl-β-hydroxyvaline.[15]

Found: C, 60.85; H, 6.32; N, 5.70. Calcd. for $C_{12}H_{15}NO_4$: C, 60.75; H, 6.37; N, 5.90%.

(—)-β-Hydroxyvaline (VII).—A mixture of (—)-*N*-benzoyl-β-hydroxyvaline (VI), 2.37 g. (0.01 mol.), and 5 N hydrochloric acid, 50 ml., was refluxed for 5 hr. After cooling, the precipitated benzoic acid was separated by filtration. The filtrate was extracted with chloroform (50 ml.×2) to remove the residual benzoic acid. After evaporation of the hydrochloric acid solution under reduced pressure, the residual syrup was dissolved in 50 ml. of water. The solution was treated with silver carbonate to remove hydrogen chloride. This mixture was filtered and washed with water. Hydrogen sulfide gas was bubbled through the solution. Silver sulfide was removed by filtration. The filtrate was concentrated in vacuo. A yield of 1.18 g. of (89%) of crude VII was obtained. This was recrystallized from water and ethanol, 0.997 g. (75%), m. p. 208°C (decomp.), $[\alpha]_D^{25} = -13.5°$ (*c* 4.82, 5 N HCl). Infrared spectrum showed bands at 1660, 1600, 1555, 1418 cm^{-1} (amino acid), 1145 cm^{-1} (>C–OH). R_f value 0.44, BuOH : AcOH : H_2O=4 : 1 : 2. The phenomenon of polymorphism of the compound was also observed by infrared spectra. Infrared absorption curve varied depending on the ratio of water and ethanol in the recrystallization.

Found: C, 45.08; H, 8.31; N, 10.69. Calcd. for $C_5H_{11}NO_3$: C, 45.10; H, 8.33; N, 10.52%.

***N*-Benzoyl-β-hydroxyvaline Methyl Ester (VIII).**—(—)-*N*-Benzoyl-β-hydroxyvaline (VI), 2.37 g. (0.01 mol.), was dissolved in 20 ml. of methanol. To this solution, diazomethane in ether solution was added. After the reaction was completed, excess diazomethane was decomposed by adding 5 per cent acetic acid in methanol solution. After evaporation of the solvent under reduced pressure, the residual syrup was dissolved in ethyl acetate. The solution was washed with sodium bicarbonate, then water. The ethyl acetate solution was dried with anhydrous sodium sulfate. After evaporation of the solution in vacuo, an oily residue was obtained. This did not crystallize.

(±)-*N*-Benzoyl-β-hydroxyvaline methyl ester, (±)-VIII, was obtained from IV by diazomethane. Yield, 92%, m. p. 105°C.

Found: C, 62.36; H, 6.75; N, 5.55. Calcd. for $C_{13}H_7NO_4$: C, 62.14; H, 6.82; N, 5.57%.

***N*-Benzoyl-β-chlorovaline Methyl Ester (IX).**—*N*-Benzoyl-β-hydroxyvaline methyl ester (VIII) (oil obtained above) was chilled in an ice bath and 1.2 ml. of thionyl chloride was added. This mixture was warmed in a water bath (about 40°C) to dissolve the oil. After 4 hr., 10 ml. of water was added to the reaction mixture to decompose the excess thionyl chloride. The mixture was extracted with ethyl acetate. The ethyl acetate layer was washed with water, aqueous sodium bicarbonate, and water. The ethyl acetate solution was dried with anhydrous sodium sulfate. After evaporation of ethyl acetate in vacuo, a yellow oil was obtained. This did not crystallize.

(±)-IX was obtained from (±)-VIII by treatment with thionyl chloride under the same conditions as above.

***N*-Benzoylvaline Methyl Ester (X).**—The yellow oil IX was dissolved in 50 ml. of 80% methanol. To this solution, 2.0 g. of sodium acetate, 2.0 ml. of acetic acid, and 2.0 g. of 5% palladium on charcoal were added and the hydrogenolysis was carried out at room temperature. When hydrogen uptake ceased, the catalyst was removed by filtration. The filtrate was concentrated in vacuo. This residue was dissolved in water and extracted with ethyl acetate. The ethyl acetate layer was washed with aqueous sodium bicarbonate and then with water. The ethyl acetate layer was dried with anhydrous sodium sulfate. After evaporating the ethyl acetate in vacuo, 1.5 g. (63.8% based on VI) of *N*-benzoylvaline methyl ester (X) was obtained. This was recrystallized from ethanol and ether. Yield, 1.3 g. (55% based on VI), m. p. 128°C. The specific rotation is too samll to measure in alcohol or in chloroform. The direction of rotation seems to be slightly (+).

Found: C, 66.29; H, 7.33; N, 6.01. Calcd. for $C_{13}H_{17}NO_3$: C, 66.36; H, 7.28; N, 5.95%.

N-Benzoyl-DL-valine methyl ester, (±)-X, was obtained from (±)-IX. Yield, 64.2% [based on (±)-VIII], m. p. 86°C.

Found: C, 66.10; H, 7.23; N, 5.97%.

D(—)-Valine (XI).—The mixture of *N*-benzoylvaline methyl ester (X), 4.7 g. (0.02 mol.), and 5 N hydrochloric acid, 50 ml., was refluxed for 6 hr. After cooling, the precipitated benzoic acid was separated by filtration. The filtrate was extracted with chloroform (50 ml.×2) to remove the residual benzoic acid. After evaporating the hydrochloric acid solution in vacuo, residual crystals were dissolved in a minimum amount of absolute alcohol at room temperature and pyridine was added to the solution. Crude D-(—)-valine (XI), 1.78 g., was obtained. This was recrystallized from water and ethanol. Yield, 1.50 g. (65%), m. p. 310°C (sublimation, sealed capillary), $[\alpha]_D^{25} = -28.7°$ (*c* 2.92, 5 N HCl).[23]

Found: C, 51.05; H, 9.68; N, 12.01. Calcd. for $C_5H_{11}NO_2$: C, 51.26; H, 9.46; N, 11.96%.

In a similar way, DL-valine was obtained from (+)-X. Yield, 75%. Found: C, 51.02; H, 9.47; N, 11.80%.

This work was supported by Grant No. NsG-689 of the National Aeronautics and Space Administration, U. S. A. The authors wish to express their thanks to Dr. S. W. Fox for his discussion and encouragement.

23) L-Valine, $[\alpha]_D^{25} = +28.2°$ (5 N HCl). J. P. Greenstein and M. Winitz, "Chemistry of the Amino Acids," Vol. 3, John Wiley & Sons, Inc., New York (1961), p. 2368.

BULLETIN OF THE CHEMICAL SOCIETY OF JAPAN VOL. 39 2290—2294 (1966)

The Effects of Some Antioxidants on the Elastomers Derived from Carboxy-terminated Polybutadiene

By Harusuke Tokui

Daicel, Ltd., Yuraku-cho, Chiyoda-ku, Tokyo

and Kiroku Yamazaki

Institute of Space and Aeronautical Science, The University of Tokyo, Komaba, Meguro-ku, Tokyo

(Received March 18, 1966)

The capability of several sorts of conventional antioxidants was studied by means of the tensile and the swelling tests of the elastomers derived from the carboxy-terminated polybutadiene prepolymer. When exposed for one year, the elastomers containing no antioxidants deteriorated remarkably; they became brittle and, without exception, no longer looked like the so-called "elastomers." Many kinds of the antioxidants worked out and were found to be effective; their capabilities were evaluated as almost the same as far as the tensile properties of the exposed material were concerned. The changes in the reciprocal value of the average chain length between cross-links, $1/M_c$, in the course of the exposure, however, would be a convenient semi-quantitative measure of the induced cross-linking reaction. With this assumption, the swelling test might prove that, among the additives covered, the amine-type antioxidants were most effective in preventing the deterioration induced by the over-cross-linking reaction of the elastomer. The relationship between the amount of the sol-fraction and the cross-linking density for the exposed specimens was fitted to that of the random cross-linking and the scission of the polymer with a random distribution of chain lengths.

The conventional composite propellants are composed of an inorganic oxidizing material, several sorts of additives, and a polymeric resin fuel. The fuel resin also acts as a binder; a lot of solid materials are finely dispersed therein. It should give the grain of good mechanical properties as well as of high energy. It is quite difficult, however, to combine good mechanical properties with the conventional resinous materials, since the required quantities of solid ingredients usually amount to 75—85% or more of the grain.

On the other hand, from the point of view of energy, fuel binders of a low heat of formation, and the low molecular weight of the burnt gas are plausible.

The starting materials should be liquid at an ambient temperature; they should be able to be cured after the solid components are dispersed therein. From these standpoint, the synthesized elastomeric materials (such as polysulfide, polyurethane and polybutadiene rubbers) are at present preferred as fuel binders for composite propellants.

Work on the cross-linking reactions of carboxy-terminated polybutadiene, which is believed to be an excellent fuel binders, has been reported by the present authors.[1] It may deteriorate easily on aging, and then cause physical or chemical changes which would offer serious problems, especially for storability, since it is a kind of diene-type rubber.

The changes in tensile properties and the values of the equilibrium swelling in the course of the one-year exposure were determined in order to evaluate the capability of the antioxidants.

The effect of some conventional antioxidants will also be described.

Materials

The following antioxidants were tested:

	Commercial name	Maker*
(Amine Type)		
N, N'-Diphenyl-*p*-phenylenediamine	Nocrac DP	O
N, N'-Di-(2-naphthyl)-*p*-phenylenediamine	Nocrac White	O
Phenyl-α-naphthylamine	Nocrac PA	O
Phenyl-β-naphthylamine	Nocrac D	O
Blend of phenyl-β-naphthylamine and diphenyl-*p*-phenylenediamine	Nocrac HP	O
Blend of phenyl-α-naphthylamine and diphenyl-*p*-phenylenediamine	Nocrac 500	O
Octyl diphenylamine	D. D. A.	Bayer

1) K. Yamazaki and H. Tokui, This Bulletin, **38**, 2172 (1965).

(Phenol Type)		
2, 6-Di-*t*-butyl-*p*-cresol	Ionol	Shell
1, 1'-Bis-(4-hydroxyphenyl)cyclohexane	Antigene W	S
4, 4'-Thiobis-(6-*t*-butyl-3-methylphenol)	Antigene WX	S
Derivative of 6-*t*-butyl-3-methylphenol	Antigene WL	S
Styrenated phenol	Antigene S	S
(Reaction Products of Amine and Aldehyde)		
Aldol-α-naphthylamine	Nocrac C	O
(Reaction Products of Amine and Ketone)		
6-Ethoxy-2, 2, 4-trimethyl-1, 2-dihydroquinoline	Nocrac AW	O
Reaction product of diphenylamine and acetone	Nocrac B	O
(Benzimidazoles)		
2-Mercaptobenzimidazole	Antigene MB	S
Zinc salt of 2-mercapto-benzimidazole	Antigene MBZ	S
(Others)		
Tri-(nonyl phenyl) phosphite	Antigene TNP	S
Di-lauryl-thiodipropionate	Antigene TPL	S
Nickel dibutyl dithiocarbamate	Antigene NBC	S
——	Polygard C	N
——	Flexzone	N

* O: Ouchi Shinko Chem. Co., Ltd.
S: Sumitomo Chem. Co., Ltd.
N: Naugatuck Chem. Div., U. S. Rubber Co.

The antioxidants, the carboxy-terminated prepolymers, HC-434 (Thiokol Chem.) and Butarez CTL (Phillips Petr. Co.), and the cross-linking agent, tris[1-(2-methyl)aziridinyl]phosphine oxide [MAPO] (Interchemical Co.), were used as received.

Experimental

The polybutadiene prepolymer, MAPO, an accelerator, and the antioxidant were mixed thoroughly and then cured as an elastomer sheet 2 mm. thick. While the quantities of the prepolymer, the curing agent and the accelerator were kept constant, the quantity of the antioxidant recommended by the maker was added.

Dumbbell-shaped specimens (JIS-K-6301, No. 3-type) were die-cut from the sheet and used for both the tensile and the exposure tests.

The details of the elastomer preparation, the tensile test, and the process of the equilibrium swelling have already been described.[1]

The specimens were fixed on polyethylene-lined plywood plates which faced south and which were inclined at a 30° angle. They were then exposed on the roof of the Central Research Laboratory of Daicel, Ltd. (171 Ohi-mura Tsuruoka, Iruma-gun, Saitama Pref., Japan; longitude 139°30′ E; latitude 35°52′ N). The weathering test was carried out from Oct. 29, 1964, to Oct. 30, 1965. After the samples had been exposed, both the tensile and the swelling tests were performed again with the aged specimens.

Results and Discussion

Table I illustrates the changes in the tensile properties upon exposure. Obviously, the specimens containing no antioxidant deteriorated most. They were no longer the so-called "elastomeric material" after the exposure; they turned very brittle, and showed an extremely poor elongation. The elastomers with the antioxidant still retained the elongation values of 100—150% at the breaking point for the exposed specimens; they thus proved the capability of the antioxidant.

It is an interesting fact that the former faded from brown to light yellow and increased in transparency, while the latter did not, but became rather opaque and turned dark brown upon exposure.

After the specimens had been exposed for one year, their tensile moduli were increased remarkably. This seems undoutedly due to the cross-linking reaction caused by sunlight and air. It could not be a measure of the deterioration of the material, however, because almost all of the exposed specimens produced small cracks upon being stretched. These cracks should cause a local concentration of the stress and so induce failure.

From the results of the tensile tests, it may be concluded roughly that the effectiveness of these additives against aging are all nearly the same.

The swelling data are compiled in Table II.

The content of the sol in the elastomer, and the average molecular weight of the chain between cross-links, M_c, decreased after exposure, while the density of the polymer increased slightly. Indeed, some of the specimens were warped concave to the exposed surface in the course of the exposure.

These results show that the cross-linking reaction of the chains of the network structure, and that of the residual impregnated sol fraction, took place.

Assuming that the density of the elastomer is unity, and that $1/M_c$ equals the moles of the effective chain of the network per unit mass; then the change of $1/M_c$ caused by the exposure would be proportional to the number of sites where the cross-linking reaction has occurred.

Charlesby[2] defined the cross-linking density, q, as in Eq. 1:

$$q = k M_0/M_c \quad (1)$$

where M_0 is the molecular weight of the monomer unit.

2) A. Charlesby and S. H. Pinner, *Proc. Royal Soc.*, **A249**, 367 (1959).

Table I. Changes in tensile properties of the elastomers caused by the exposure

No.	Composition*	Before or after exposure	Tensile strength kg./cm²	Elongation at break point %	Stress at 100% elongation kg./cm²	Stress at 300% elongation kg./cm²	Hardness	Appearances after exposure
1	Nocrac DP 1.00	before	8.7	400	3.5	7.2	24.8	turned dark brown
		after	10.0	150	8.7	—	46.2	
2	Nocrac White 1.00	before	9.5	350	4.1	8.4	30.5	turned dark brown
		after	10.2	110	10.1	—	51.0	
3	Nocrac White 2.00	before	8.9	380	3.7	7.4	23.8	turned dark brown
		after	9.1	120	8.6	—	48.5	
4	Nocrac PA 2.00	before	11.1	500	3.8	7.3	26.0	turned dark brown
		after	8.9	220	6.5	—	41.8	
5	Nocrac D 1.00	before	11.9	450	4.3	8.5	29.9	turned dark brown
		after	8.2	150	7.4	—	44.3	
6	Nocrac HP 1.00	before	9.8	390	4.1	8.0	28.7	turned dark brown
		after	7.4	170	6.4	—	44.3	
7	Nocrac 500 1.00	before	11.5	320	5.6	11.1	35.5	turned dark brown
		after	10.6	150	8.8	—	50.4	
8	D.D.A. 2.00	before	9.2	420	3.8	7.4	29.1	turned dark brown
		after	8.1	120	7.8	—	47.9	
9	Ionol 2.00	before	11.2	370	4.8	9.5	31.0	turned dark brown
		after	8.6	100	8.5	—	50.8	
10	Antigene W 1.00	before	10.1	290	5.3	—	34.0	turned dark brown
		after	9.8	90	—	—	52.6	
11	Antigene WX 2.00	before	12.5	370	5.6	10.6	34.5	turned dark brown
		after	9.3	110	9.1	—	52.2	
12	Antigene WL 2.00	before	10.1	400	4.3	8.2	30.0	turned dark brown
		after	8.8	120	8.7	—	50.0	
13	Antigene S 2.00	before	8.7	330	4.1	8.1	29.1	turned dark brown
		after	8.6	90	—	—	50.8	
14	Nocrac C 2.00	before	10.7	480	4.0	7.6	29.2	turned dark brown
		after	7.7	120	7.5	—	44.9	
15	Nocrac AW 2.00	before	10.2	480	3.6	7.0	26.5	turned dark brown
		after	7.6	160	6.9	—	42.0	
16	Nocrac B 1.00	before	12.0	410	4.6	9.1	30.0	turned dark brown
		after	8.7	110	8.5	—	49.8	
17	Nocrac-White 1.00 Antigene MB 1.00	before	11.8	450	4.5	8.7	30.9	turned dark brown
		after	6.9	160	6.5	—	43.1	
18	Nocrac-White 1.00 Antigene MBZ 1.00	before	11.7	450	4.4	8.5	30.4	turned dark brown
		after	8.0	130	7.7	—	50.2	
19	Antigene TNP 2.00	before	11.4	420	4.5	8.7	30.6	turned dark brown
		after	7.7	120	7.5	—	46.5	
20	Antigene TPL 2.00	before	10.6	420	4.1	8.0	28.5	turned dark brown
		after	7.8	120	7.5	—	45.5	

Table I (Continued)

No.	Composition*	Before or after exposure	Tensile strength kg./cm²	Elongation at break point %	Stress at 100% elongation kg./cm²	Stress at 300% elongation kg./cm²	Hardness	Appearances after exposure
21	Antigene NBC 2.00	before	10.6	360	4.5	9.0	34.1	turned dark brown, bloomed remarkably
		after	9.5	110	9.4	—	53.3	
22	Polygard C 2.00	before	10.9	370	4.8	9.4	33.1	turned dark brown
		after	7.0	110	6.9	—	46.4	
23	Flexzone 2.00	before	9.6	500	3.5	6.5	25.8	turned dark brown
		after	7.8	150	7.1	—	46.7	
24	No Antioxidant	before	10.1	420	4.2	8.0	26.3	faded to light yellow, became brittle
		after	5.8	8	—	—	55.9	
25	No Antioxidant	before	10.5	490	3.8	7.1	27.8	turned dark brown
		after	7.5	110	7.3	—	47.7	
26	No Antioxidant	before	9.2	420	3.7	7.2	25.5	faded to light yellow, became brittle
		after	6.5	14	—	—	53.3	
27	No Antioxidant	before	6.3	440	2.4	4.6	17.3	faded to light yellow, became brittle
		after	6.2	25	—	—	52.3	

* No. 1—24: HC-434 100, MAPO 9.8, Accelerator 5 (parts)
No. 25 : Butarez CTL 100, MAPO 5.3, Accelerator 5
No. 26 : Butarez CTL 100, MAPO 7.9, Accelerator 5
No. 27 : Butarez CTL 100, MAPO 10.5, Accelerator 5

Table II. Changes in swelling data of the elastomers caused by the exposure

No.	ρ*	ρ'	S**	S'	M_c	M_c'	$(1/M_c'-1/M_c)$
1	0.947	0.954	11.14	4.70	10100	6390	0.5748×10^{-4}
2	0.947	0.954	—	—	—	—	—
3	0.975	0.953	—	—	—	—	—
4	0.946	0.956	19.96	6.56	17860	8060	0.6808
5	0.946	0.955	15.30	5.50	13580	7580	0.5829
6	0.943	0.954	11.85	5.99	12490	8040	0.4432
7	0.943	0.952	9.83	4.78	10640	6480	0.6034
8	0.947	0.957	9.36	4.84	10500	6230	0.6527
9	0.942	0.957	13.60	3.11	13680	5270	1.1665
10	0.944	0.956	12.05	2.27	13340	4560	1.4434
11	0.945	0.958	10.20	2.68	12550	4990	1.2072
12	0.943	0.955	8.49	2.71	9610	4870	1.0127
13	0.942	0.955	9.01	3.38	9805	4670	1.1214
14	0.939	0.960	14.15	4.83	14480	6440	0.8622
15	0.945	0.954	15.29	5.06	17720	7690	0.7361
16	0.945	0.958	12.59	3.57	14350	5580	1.0952
17	0.947	0.959	13.66	5.06	16690	7320	0.7669
18	0.946	0.959	14.81	3.96	18300	6470	1.0088
19	0.943	0.958	7.78	3.97	9560	5540	0.7595
20	0.940	0.959	16.34	3.49	18050	5710	1.1973
21	0.944	0.963	13.18	2.22	13720	5340	1.1438
22	0.945	0.959	8.13	5.19	9550	6320	0.5353
23	0.945	0.954	15.50	3.86	18590	6620	0.9727
24	0.942	0.968	7.21	—	9040	3650	1.6337
25	0.936	0.956	10.07	3.14	14540	6110	0.9489
26	0.939	0.966	—	—	—	—	—
27	0.940	0.970	14.67	4.03	14130	4600	1.4662

* Density of the polymer
** Solfraction of the polymer
(Dashed notation means the states of the postexposure)

k means the average number of cross-links per effective chain. When two functional carboxy-terminated polybutadienes are cured with a trifunctional compound, MAPO, in such a manner that no terminal sections result, the k-value should be 2/3, while in the case of conventionally-cured rubbers with sulfur or peroxides, that value should be 1.0. In this study, the degree of the cross-linking reaction during the exposure is defined as $(q'-q)$. (The dashed notation means the state of the post-exposure.)

Since the quantity of the cross-linked sol fraction caused by the exposure is relatively small, it might be assumed that k' is nearly equal to k. On this assumption, $(q'-q)$ is represented by Eq. 2:

$$(q' - q) = k M_o (1/M_c' - 1/M_c) \quad (2)$$

The values of $(1/M_c - 1/M_c')$, tabulated in Table II, is proportional to the degree of the cross-linking reaction; the smaller the value, the lower the degree of cross-linking. This should be a semi-quantitative measure of the effectiveness of the antioxidants in preventing the cross-linking reaction.

Apparently, the amine-type antioxidants are the most effective. It should be noticed, however, that the capability of the antioxidants can not be evaluated only from the effect in preventing the cross-linking reaction.

Antigene NBC was not compatible in the pre-cured medium, and it bloomed remarkably on the elastomer surface.

The relationship between the quantity of the sol fraction, S, and the cross-linking density, q, has been studied by Charlesby[2] and by Bristow[3,4]. For the random cross-linking and the scission of a polymer having a random distribution of chain lengths, they deduced the following Eq. 3:

$$S + S^{1/2} = p/q + 1/q\,\overline{Y}_n \quad (3)$$

where p: the density of the main fracture of the chain.

$\overline{Y}_n$: the number average chain length of the polymer.

Assuming that the k-value in Eq. 1 is 2/3, the quantity of $(S+S^{1/2})$ is plotted versus $1/q$ in Fig. 1. A good linearity was observed for the exposed elastomers. The cross-linking and scission processes occurred at random in the system, so that the initial polymer should have a random distribution of chain lengths; this connection, however, is not very stringent, because the cross-linking reaction can occur optionally at any site of the network structure.

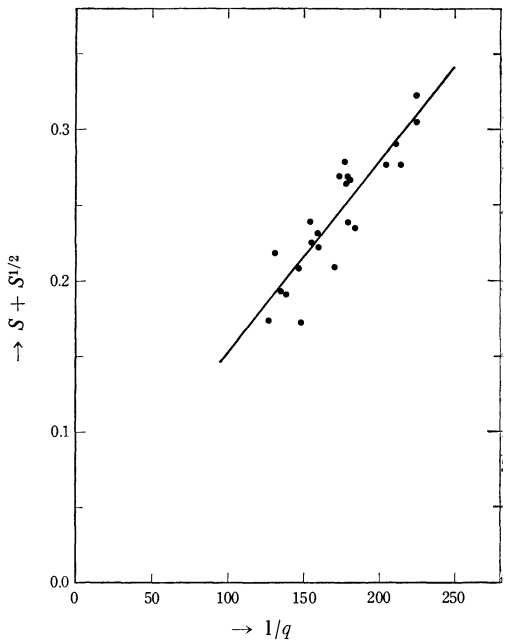

Fig. 1. Plot of $S+S^{1/2}$ versus $1/q$ for exposed elastomers.

The plot of $(S+S^{1/2})$ versus $1/q$ for the unexposed elastomer deviated from the line remarkably, since the cross-linking took place only at aboth ends of the prepolymer chain. From these facts, it may be assumed that the cross-linking reaction caused by the exposure was so effective that it randomized the relatively regular distribution of the initial cross-linking sites.

Conclusions

The elastomer derived from the carboxy-terminated polybutadiene prepolymer (cured with MAPO) showed a fatal deterioration tendency in the course of a one-year exposure test. Several sorts of antioxidants were tested; it was found that they were all effective as far as the experiments showed.

From the tensile data, it was roughly observed that all these antioxidants were almost equally effective; the swelling test, however, proved that the amine-type compounds were most effective among the antioxidants tested in preventing the cross-linking reaction caused by the exposure.

The plot of $(S+S^{1/2})$ versus $1/q$ for the exposed elastomers showed a good linearity, proving that the random crosslinking and scission of the polymer resulted from the exposure.

The authors offer their deep thanks to Mr. Toshimitsu Iwase for his assistance in the experiment.

3) G. M. Bristow, *J. Appl. Pol. Sci.*, **7**, 1023 (1963).
4) G. M. Bristow, ibid., **8**, 1696 (1964).

NOTES

The Water Penetration of Emulsion Polymer Films

By Soichi MUROI

Pioneering Research Laboratories, Asahi Chemical Industry, Co., Ltd., Nakadai, Itabashi-ku, Tokyo

(Received October 4, 1965)

Many studies[1-4] have been made of the mechanism of polymer film formation from emulsions, but little attention has been paid to the mechanism of water penetration into emulsion films.[5] The properties of the films deposited from polymer emulsions may be said to be essentially different from those of solution-cast or milled polymer films, considering the fact that the emulsion films more easily undergo several changes when exposed to water or water vapor a swelling and whitening of the films, accompanied by a deterioration of the mechanical properties and a decrease in adhesion to the substrate.

The present study was made in order to clearly establish the mechanism of water penetration into emulsion films. For this purpose vinyl acetate (VAc)-butyl acrylate (BA) copolymer emulsions were selected as samples because of their enormous consumption in the paint industry and in other fields.

Experiments

Materials.—Emulsions were prepared by the usual method. They were prepared by using 2% of sodium polyoxyethylene nonylphenyl sulfate as an emulsifier and 0.3% of ammonium persulfate (based on the monomer) as an initiator.

Solid polymers free from water-soluble substances were obtained as follows: an emulsion state was destroyed by freezing; small masses of the polymer so obtained were then washed with water for 7 days and dried at 50°C for 4 days.

The films used in the study were prepared by drying the chosen emulsion or solution on a leveled glass plate. The films so obtained then were left to stand at 20°C under 65% R. H. for more than 4 days.

Methods.—The weight of the water absorbed (Q) was determined as follows. Samples (4×5 cm.) were cut from the film and weighed on a direct reading balance. They were then immersed in water at 20°C, taken out at appropriate intervals, blotted quickly with a hard filter paper, and weighed. Five samples were used for each measurement, and the values obtained were averaged. The films 70±10 micron thick were used for the measurements. The film thickness was measured by a thickness gauge.

Results and Discussion

The Water-Absorption Behavior of Emulsion Film in Aqueous Solutions.—When an emulsion is dried, its particles approach each other and eventually touch, thus forming a continuous polymer network. The spherical particles deform, flow together and interpenetrate, leaving small deposits of water which contain the water-soluble substances originally present in the emulsion. As the last water evaporates through the polymer network and the spaces between the fused particles (channels), small clots of the water-soluble substances remain behind.[5,6]

Water penetrates into the clots through the polymer network and channels when the emulsion film is immersed in water. Simultaneously, the polymer network absorbs water to attain an equilibrium. Therefore, it is reasonable to consider that the driving force for the water penetration is given by the difference between the vapor pressure inside the film and that of the external phase to which the film is exposed.

To check this assumption, the films deposited from the VAc-BA (75 : 25) copolymer emulsion were immersed in aqueous solutions of various concentrations of ammonium chloride, sucrose and glucose. The value of Q is plotted against the square root of the time in Fig. 1.

The diagram shows that Q initially increases linearly as a whole with the square root of the time, and that it then gradually approaches an equilibrium value. Although Q soon reaches the equilibrium in a rather concentrated solution, it continues to increase slowly in water or in a diluted

1) R. E. Dillon, L. A. Matheson and E. B. Bradford, *J. Colloid Sci.*, **6**, 108 (1951).
2) W. A. Henson, D. A. Taber and E. B. Bradford, *Ind. Eng. Chem.*, **45**, 735 (1953).
3) G. L. Brown, *J. Polymer Sci.*, **22**, 423 (1956).
4) S. S. Voyutskii, "Autohesion and Adhesion of High Polymer," Interscience Pub., New York (1963), p. 63.
5) G. L. Brown and J. P. Scullin, *Ind. Eng. Chem.*, **45**, 743 (1953).
6) H. Fikentscher, H. Gerrens and H. Schuller, *Angew. Chem.*, **72**, 856 (1960).

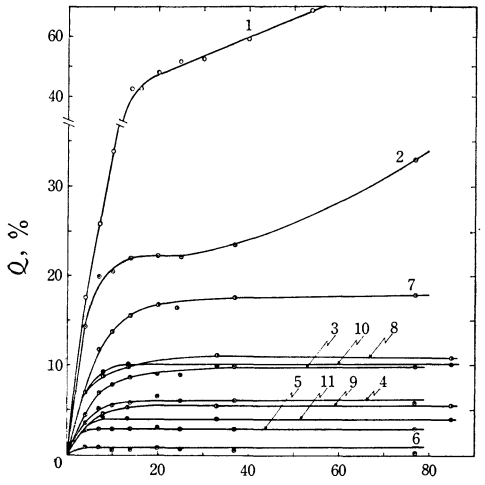

Fig. 1. Effect of concentration of aqueous solutions on water absorption behaviors of emulsion films. (1) water, (2) 0.1 N ammonium chloride, (3) 0.5 N ammonium chloride, (4) 1 N. ammonium chloride, (5) 2 N ammonium chloride, (6) 5 N ammonium chloride, (7) 0.5 N sucrose, (8) 1 N sucrose, (9) 2 N sucrose, (10) 1 N glucose, (11) 2 N glucose

solution, even after an extended time of immersion. The values of Q after a sufficient time of immersion decrease with an increase in the concentration of the solutions, approaching zero as the concentration of the solutions approaches saturation.

The results obtained here suggest that, as expected, the force for water penetration decreases with a reduction in the activity of the external phase (the vapor pressure of the external phase). This may be seen distinctly in Fig. 2, which gives the relationship between the activity of water in the external phase and the value of Q after 100 min. The activity was determined by calculation. Figure 2 shows that Q begins to increase rapidly beyond the activity value of 0.9, almost regardless of the solute nature. This may show that the water-soluble substances contain some water and that, consequently, the activity of water inside the film is rather high.

Another experiment determined the Q of the film deposited from an emulsion which had been dialyzed in a cellophane dialysis tube for 7 days. The dialysis of the emulsion was conducted under such conditions that the emulsifier in the emulsion was not removed; the resulting emulsion was stable. The value of Q for the film after immersion for 7 days ($\sqrt{\text{min.}} \fallingdotseq 100$) was only 18%, against 87% for the untreated emulsion film (it must be noted that these values involve the weight of the water absorbed by the copolymer itself 6.8% as is seen in Table I). On the basis of the results obtained here, it can be said that even a small amount of

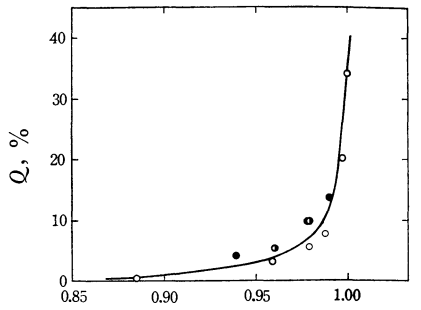

Fig. 2. Relationship between activity of water in aqueous solutions and Q after 100 min. ○: ammonium chloride solution, ●: sucrose solution, ◑: glucose solution.

the salts present in the film, salts which are derived from the initiator and the impurities contained in the emulsifier, may play a leading role for water penetration, whereas the emulsifier may have rather less effect. This may be attributed to the difference in their solubilities in the copolymer.

In a subsequent experiment, films which had been 60% pre-swollen by immersing in water for about 48 hr. ($\sqrt{\text{min.}} \fallingdotseq 54$) were dehydrated by immersing them in aqueous solutions of different concentrations. The dehydration rates of the pre-swollen films are much higher than their water absorption rates, as is shown in Fig. 3. For example, it takes about 48 hr. for the original emulsion film to absorb 60% of the water, as has been mentioned above, while the pre-swollen film is almost completely dehydrated in about 36 min. in 5 N aqueous ammonium chloride. This fact indicates that, in water absorption, water must penetrate into a film against the resistance of the polymer

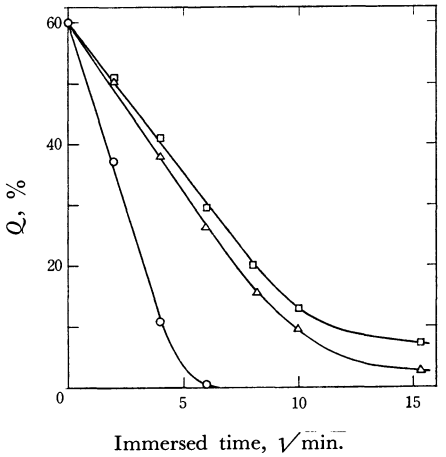

Fig. 3. Dehydration of pre-swollen emulsion films in aqueous ammonium chloride at different concentrations.
○: 5 N, △: 0.5 N, □: 0.1 N

network, while in dehydration there is no such resistance.

The Effect of the Modulus of the Polymer Network on Water-Absorption Behavior.—The water-absorption behavior of the films with different moduli, prepared from the emulsions of VAc with BA in different copolymerization compositions, was determined over extremely extended immersion periods. The results are shown in Fig. 4. The moduli of the copolymers are expressed in terms of Young's moduli of solution-cast films, which have the copolymerization compositions corresponding to those of the respective emulsion films and are free from water-soluble substances, as Table I shows.

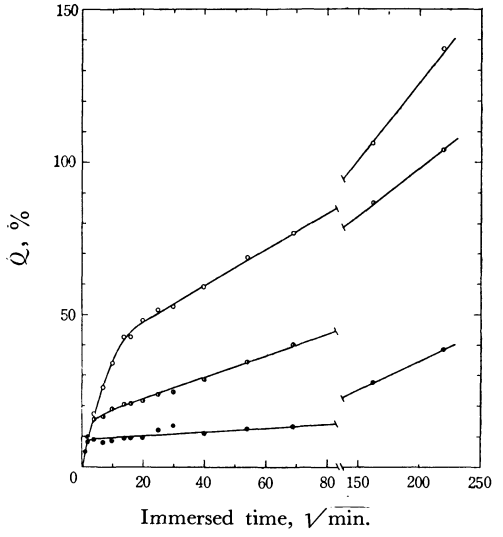

Fig. 4. Effect of modulus of polymer network on water absorption behavior.
●: PVAc, ◑: VAc/BA 90/10, ○: VAc/BA 75/25

TABLE I. YOUNG'S MODULUS AND WATER ABSORPTIVITY OF SOLUTION-CAST FILMS FREE FROM WATER SOLUBLE SUBSTANCES

VAc : BA	Young's modulus (dyne/cm²)10⁹	Q after 7 days, %
100 : 0	9.6	13.7
90 : 10	4.2	9.9
75 : 25	1.4	6.8

The values of Q for all emulsion films initially increase at the same rate linearly against the square root of the time, but the rate sharply decreases at a certain Q, in correspondence with the modulus of the film (polymer network). The values of the breaks increase with a decrease in the modulus of the polymer network. The water absorptivity of the film increases with the reduction in its modulus, that is, with the increase in the BA component in the copolymer. On the other hand, the solution-cast film free from water-soluble substances, contrary to the tendency of the emulsion film, shows a small decrease in Q (after 7 days' immersion) with an increase in the BA component, as Table I shows.

It is evident from the results obtained here that the resistance to water penetration is due to the resistance of a polymer network to deformation. On the other hand, it is of great interest to note that Q did not attain an equilibrium but continued to increase slowly, even after one month ($\sqrt{\text{min.}} \fallingdotseq 208$).

The Water-Absorption Behavior of Solution-Cast Film Prepared from Emulsion Film.—The water-absorption behavior of the emulsion film and the solution-cast film, which have exactly the same composition, is compared in Fig. 5. The cast film was deposited from the solution which had been prepared by dissolving the VAc-BA (75 : 25) copolymer emulsion film in ethyl acetate.

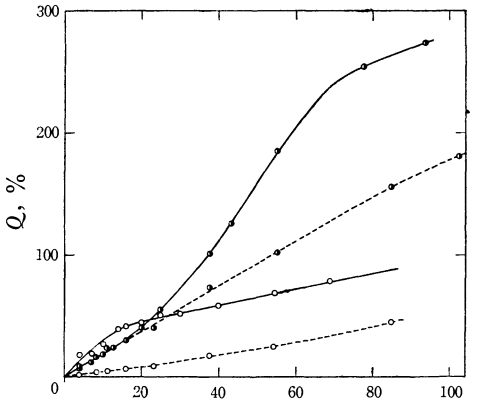

Fig. 5. A comparison between water absorption behavior of emulsion film and that of solution-cast film prepared from the emulsion film.
——: original film, ----: film after a water absorption-redrying cycle, ○: emulsion film, ◑: solution-cast film

The water absorption rate in the initial stage is more rapid for the emulsion film than for the cast film, but in the later stage the Q of the cast film is a few times of that of the emulsion film.

The cast film may show such high water absorptivity because the clots of the water-soluble substances originally present in the emulsion film are kept undissolved in ethyl acetate and, consequently, the film prepared from this solution has the same structure as that of the original emulsion film. In addition, less water-soluble substances might be extracted from the cast film than from the emulsion film because the former has fewer channels. For such reasons, the cast film would ultimately absorb much more water than the emulsion film.

In order to verify this assumption, the weight of the film before and after immersion-redrying were ascertained. The films were immersed in

water until the water absorption rates broke. It took about 400 hr. to reach that stage for the cast film, and 24 hr. for the emulsion film. Then they were redried at 20°C under 65% R. H. for 4 days. The weight reductions of the films, based on the original weight, were 0.6% for the cast film and 1.9% for the emulsion film.

The water-absorption behavior of the redried films was then again ascertained. The water absorptivities of the films are markedly lowered, as is shown by the dotted lines in Fig. 5. Obviously, this results from the decrease in the water-soluble substances in the films.

In a subsequent experiment, the water absorptivities of solution-cast films prepared from solutions of the VAc-BA (75 : 25) copolymer emulsion films in various solvents were determined. The results are shown in Table II.

TABLE II. EFFECT OF SOLVENTS USED FOR DISSOLUTION OF EMULSION FILM ON WATER ABSORPTIVITY OF RESULTING CAST FILM

Solvent	Q after 7 days, %
Carbon tetrachloride	110
Toluene	137
Acetone	140
Methanol	58
Formic acid	63

According to the values of Q in Table II, they may be classified into two groups; the first group showing higher values, and the second, lower values, than that of the emulsion film. The former films are prepared by those solvents which dissolve salts only with difficulty, while the latter are prepared by those solvents which dissolve salts to some extent.

It seems that in the film of the lower-Q value group the water-soluble substances are dispersed unimolecularly, while in the film of the higher-Q value group, they are dispersed as clots, as has been mentioned above. This difference in film structure may affect the water absorptivity. It is not known, however, how the difference in film structure can be related to that in water absorptivity.

Conclusion

From the results obtained so far, it can be understood that there is no essential difference between the water absorption behavior of emulsion films and that of solution-cast films. Emulsifiers and salts are necessarily attendant on emulsion films, and, consequently, they absorb extremely much water. Furthermore, emulsion films are obliged to have a rather low modulus because of their forming mechanism. On the other hand, solution-cast or milled films have no limitation on their formation, and films of a rather high modulus are often used. Emulsion films may generally be regarded to absorb water much more easily than solution-cast or milled films because of the difference in the factors mentioned above.

As far as the present study has so far discovered, the water-resistance of PVAc emulsion film cannot be improved by the copolymerization of a higher acrylic ester.

The author is indebted to Mr. Shoji Sakai for his technical assistance.

Octahedral Complexes of Nickel(II) Formate with Amines

By Gopal NARAIN

Department of Chemistry, University of Lucknow, Lucknow (U. P.), India

(Received November 4, 1965)

Three hexaco-ordinated complexes of nickel-(II) formate with ammonia, ethylenediamine and propylenediamine have been prepared. Conductivity measurements indicate the complexes to be non-electrolytes. Molecular weight measurements confirm this. The visible absorption spectrophotometric measurements show a number of bands corresponding to the various permitted transitions of the metal. A discussion of the structure in the light of these transitions is presented.

A large number of nickel ammine complexes of inorganic salts have been prepared, but comparatively very little work has been done on organic salts of nickel.[1-3] Moreover, the nature of the anion is found to be a contributing factor to the stability of the complexes.[4] An attempt has, therefore, been made to prepare some amine complexes of nickel(II) formate and to study their absorption spectra and the effect of formate ions on the properties of the complexes.

1) H. Grossmann and G. Jagar, *Z. anorg. Chem.*, **73**, 48 (1912).
2) C. S. Shaw, *Z. Physik. Chem.*, **204**, 194 (1955).
3) P. Shukla et al., *Z. anorg. u. allgem. Chem.*, **333**, 165 (1964).
4) T. Moeller, "Inorganic Chemistry" (1st. Indian printing) (1962), p. 237.

No.	Formula	In alcohol		In formamide	
		λ_{max}, mμ	Approximate frequency, cm^{-1}	λ_{max}, mμ	Approximate frequency, cm^{-1}
1	$[Ni(HCOO)_2(NH_3)_4]^0$	Insoluble		345	29000
				555	18020
				825	13000
				928	10700
2	$[Ni(HCOO)_2(en)_2]^0$	340	29400	350	28600
		550	18000	560	18700
		820	12200	825	13000
		915	10930	935	10700
3	$[Ni(HCOO)_2(pn)_2]^0$	355	28600	360	28600
		555	18000	560	18000
		825	13000	825	13000
		925	10700	925	10800

Experimental and Results

Synthesis.—*i) Biformatotetra(ammine)nickel(II).*—Five hundred milligrams of nickel(II) formate was placed in a calcium chloride tube fitted with a cotton wool plug at the bottom. The tube was then attached to the neck of a flask containing an excess of liquid ammonia and left overnight. The tube was taken out in the morning, and dried first over calcium chloride and then over phosphorus(V) oxide. The complex is blue in colour and is soluble in formamide. (Found: Ni, 26.89; N, 25.66; NH_3, 31.06. Mol. wt., 201. Cond., 0.43 mhos. Calcd. for $C_2H_{14}O_4N_4Ni$: Ni, 27.08; N, 25.8; NH_3, 31.33%. Mol. wt., 216.7)

ii) Biformatobis(ethylenediamine)nickel(II).—A five hundred milligrams portion of nickel(II) formate was shaken in acetone with a calculated quantity of amine for two hours; the reaction mixture was then left overnight, filtered the next morning, and dried over phosphorus(V) oxide. The complex is violet in color and is soluble in formamide and alcohol. (Found: Ni, 21.65; N, 20.58, en, 44.19. Mol. wt, 253. Cond., 0.51 mhos. Calcd. for $C_6H_{18}O_4N_4Ni$: Ni, 21.84; N, 20.84; en, 44.67%. Mol. wt, 268.7)

iii) Biformatobis(propylenediamine)nickel(II).—This was prepared as ii). The complex is violet in colour and is soluble in formamide and alcohol (Found: Ni, 19.4; N, 18.58; pn, 49.44. Mol. wt., 278. Cond., 0.26 mhos. Calcd. for $C_8H_{22}O_4N_4Ni$: Ni, 19.79; N, 18.87; pn, 49.9%. Mol. wt., 296.7)

The Determination of the Base and the Molecular Weight.—The methods used have already been outlined by the author.[5]

Visible Absorption Spectra.—The spectra were recorded on a Unicam S. P. 500 spectrophotometer in formamide and in alcohol.

Discussion

The results of analysis show the molecular formulae to be $Ni(HCOO)_2(am)_4$ and $Ni(HCOO)_2(am)_2$, where am represents ammonia, ethylenediamine and propylenediamine. The conductivity and molecular weight measurements in formamide indicate the complexes to be non-electrolytes; hence, it is suggested that formate ions, besides neutralizing the charge of the metal, are also coordinated to it. The formulae of the complexes are thus to be written as $[Ni(HCOO)_2(am)_4]^0$ and $[Ni(HCOO)_2(am)_2]^0$. The coordination number thus becomes six in all the cases. The violet colour of the bidentate amine complexes is in contrast with the blue or green colour observed for all other octahedral complexes. It is known that the greater the strength of the coordinate bond between a nickel atom and a ligand, the greater is the deviation from the usual colour.[6]

The terms arising from the d^8 ground state are:

$$3d^8 = F, P, G, D \text{ and } S$$

Ballhausen,[7] on the basis of a series of calculations, found that at least three of four transitions are to be expected for octahedral complexes. The complexes presently under investigation also show four sharp bands in alcohol and formamide. In alcohol the bands occur in the vicinity of 345, 550, 815 and 920 mμ while in formamide, they occur near 350, 560, 825 and 925 mμ. The slight positive shift in the positions of the bands results from the higher polarity of formamide; this changes the energies, which in their turn change the frequencies of the absorption bands.

Further, the comparison of these spectra with the spectra of other known octahedral nickel complexes (bands in the vicinity of 350, 550, 800 and

5) G. Narain, *Z. anorg. u. allgem. Chem.*, to be published.

6) R. S. Nyholm, *Chem. Revs.*, **53**, 263 (1953).

7) C. J. Ballhausen, *Dan. Mat-fys. Medal*, **29**, No. 4 (1954).

925 mμ) shows a fair agreement between the two. Moreover, as has been reported by Frenelius,[8] the ν_3/ν_1 ratio is 1.82 for all octahedral nickel(II) complexes irrespective of the ligands used for coordination. If the 925 mμ band in this case is considered to be the ν_1 band, the ν_3/ν_1 ratio also turns out to be 1.82.

8) C. Fernelius and W. Manch, *J. Chem. Ed.*, **38**, 192 (1961).

The four absorption bands arise from the following transitions of the electrons:

Position of the absorption band	Transition
925 mμ (ν_1)	$A_{2g} \rightarrow T_{2g}$
825 mμ (ν_2)	$A_{2g} \rightarrow E_g$
560 mμ (ν_3)	$A_{2g} \rightarrow T_{1g(F)}$
350 mμ (ν_4)	$A_{2g} \rightarrow T_{1g(P)}$

Drynap Reduction. II.* The Reduction of Nitrobenzene with a Commercial Sodium-Lead Alloy

By Katsumi TABEI and Kuniomi NATOU

Tokyo College of Pharmacy, Kashiwagi 4, Shinjuku-ku, Tokyo

(Received November 29, 1965)

Recently the commercial sodium-lead alloy, "Drynap," was introduced and recommended by one of the present authors as a mild reducing agent in place of sodium amalgam.[1] Nitrobenzene was submitted to Drynap reduction under various conditions.

Acetic acid or hydrochloric acid was chosen as the neutralizing agent, while ethanol or water was used as the reaction solvent. The reduction products were separated through an alumina column and checked by thin-layer chromatography. The product in each experiment was identified by mixed-melting-point determination.

As expected, aniline (over 70% yield; m. p. 114°C; as acetanilide) was the main product of the reduction of nitrobenzene in an aqueous suspension with the alloy and hydrochloric acid. The yield was rather poor (about 20%) with an ethanol solvent, and a large amount of nitrobenzene (about 70%) was recovered. The above-mentioned decrease in the yield may be due to the production of insoluble lead chloride, which covers the surface of the alloy. A small amount of azobenzene (m. p. 68°C; below 3% yield) and hydrazobenzene (m. p. 125—126°C; below 1% yield) was detected as a by-product in the above two experiments.

By using acetic acid as the neutralizing agent, however, nitrobenzene was reduced to azobenzene in a yield greater than 45%, while the yield of aniline decreased (about 25%) either in ethanol or in a water solvent. Efficient stirring, a higher temperature, and a longer reaction time seemed to raise the yield of aniline. Azoxybenzene (m. p. 36°C; yield 3—10%) and hydrazobenzene (below 1% yield) were obtained as by-products.

Without using an acid, nitrobenzene was also reduced to azobenzene in 60—80% yields by vigorously stirring Drynap into an ethanolic solution or an aqueous suspension. In this experiment, small amounts of hydrazobenzene and azoxybenzene were obtained as by-products.

From the above results, it may be concluded that the Drynap reduction of nitrobenzene in a hydrochloric acid solution gives the same product as in an ordinary reduction with mineral acid and such metals as zinc, iron, and tin, and that, in acetic acid or a neutral solution, the reaction gives the same results as in the case of sodium amalgam or sodium ethoxide.[2,3]

Experimental

Materials.—Nitrobenzene and aniline of G. R. grade were used after distillation. Azobenzene, hydrazobenzene, azoxybenzene, and phenylhydroxylamine were derived from nitrobenzene by the usual method[4] and were purified.

Reduction Procedure.—Five grams (0.04 mol.) of nitrobenzene dissolved in 80 ml. of ethanol or suspended in 80 ml. of water was reduced by the addition of 50 g. (corresponding to 0.2 atom of sodium metal) of Drynap (in small portions) at 35—40°C. In acidic reduction, 0.5 mol. of an acid was also added.

After one hour, the ethanol was removed with an

* A previous report, Ref. 1, represents Part I of the series.

1) K. Tabei, H. Hiranuma and N. Amemiya, This Bulletin, **39**, 1085 (1966).

2) V. O. Lukashevich, *Ann.*, **521**, 198 (1936).

3) H. S. Fry and J. J. Cameron, *J. Am. Chem. Soc.*, **49**, 864 (1927).

4) L. Gattermann, "Die Praxis des Organischen Chemikers," 36. Aufl., 161, 163 (1954); H. Gilman, "Organic Syntheses", Coll. Vol. I, 445 (1956).

Table I. Drynap reduction of nitrobenzene

Expt. No.	Solvent	Acid	Product	Yield, %	By-product*
1	Water	HCl	Aniline	70—80	AB, HAB
2	Ethanol	HCl	Aniline	20—25	AB, HAB
3	Water	AcOH	Azobenzene	45—65	HAB
			Aniline	10—25	
			Azoxybenzene	~10	
4	Ethanol	AcOH	Azobenzene	45—65	AOB
			Aniline	~25	
5	Water	—	Azobenzene	~70	HAB, AOB
6	Ethanol	—	Azobenzene	60—70	HAB, AOB

* AB represents azobenzene, HAB: hydrazobenzene, AOB: azoxybenzene.

ethanol solvent, and the reduction mixture was extracted with ether. The ether extract was washed with water (and a 5% sodium hydrogen carbonate solution) and dried over sodium sulfate.

After the evaporation of the ether, the extract was dissolved in benzene, and a small portion of the benzene solution was subjected to thin-layer chromatography in order to check the reduction product. Most of the benzene solution was passed through an alumina column, and each reduction product was collected as a fraction.

In the case of an aqueous suspension, the reaction mixture was extracted with ether and the extract was treated in the way described above.

Each product was purified by recrystallization or by distillation, and was identified by means of mixed-melting-point determination and by thin-layer chromatography. The results are tabulated in Table I.

Thin-layer Chromatography. — The thin-layer chromatoplate (0.5 mm.) used for the check of the product was made with Wako Gel B-10 (silica gel). The spot of the sample was developed with benzene at 18—20°C. The spot of each component developed was detected either by exposing the plate to iodine vapor or by letting the plate stand under ultraviolet light after spraying sulfuric acid on it and heating it at 105°C for 15 min. The R_s values (the ratio of the R_f value to that of azobenzene) were compared with those of the authentic compounds: azobenzene: 1.00; nitrobenzene: 0.97; *p*-hydroxyazobenzene: 0.95; azoxybenzene: 0.89; hydrazobenzene: 0.79; aniline: 0.35; phenylhydroxylamine: 0.15.

The authors wish to thank the Wako Pure Chemical Co., Ltd., for its gift of Drynap.

The Infrared Spectra of *S*-Alkylisothiouronium Salts

By Masahisa HASHIMOTO and Satoshi ARAKAWA

Research Laboratory, Dainippon Pharmaceutical Co., Ltd., Ebie, Fukushima-ku, Osaka

(Received January 6, 1966)

The infrared spectra of thiourea[1,2] and its metal co-ordination complex[3] have been examined by several authors. Kutzelnigg and Mecke made the vibration assignment of the isothiouronium ion.[4] Stam examined the crystal structure of *S*-methylisothiouronium sulfate by X-ray analysis.[5] However, no reports on the characteristic absorption bands of *S*-alkylisothiouronium salts and their deuterated compounds have yet appeared.

The infrared spectra of *S*-alkylisothiouronium salts ($R\text{-}S\text{-}C\langle^{NH_2}_{NH}\cdot HX$) have two characteristic absorption bands in the region from 1675 to 1420 cm^{-1}. On deuteration, they shift to a lower frequency, and two new bands appear in the region from 1198 to 1140 cm^{-1}. These bands were observed in almost the same region when the alkyl groups and salts of *S*-alkylisothiouronium compounds were substituted. Isothiouronium compounds are important as agents protecting against radiation and as the medium of the sulfur-containing compounds. In this note the characteristic absorption bands of *S*-alkylisothiouronium compounds will be presented.

Experimental

The Preparation of Compounds.—Most of the compounds used in this experiment were prepared by

1) J. E. Stewart, *J. Chem. Phys.*, **26**, 248 (1957).
2) R. M. Badger and R. D. Waldron, ibid., **26**, 255 (1957).
3) A. Yamaguchi, R. B. Penland, S. Mizushima, T. J. Lane, C. Curran and J. V. Quagliano, *J. Am. Chem. Soc.*, **80**, 527 (1958).
4) W. Kutzelnigg and R. Mecke, *Spectrochim. Acta*, **17**, 530 (1961).
5) C. H. Stam, *Acta Cryst.*, **15**, 317 (1962).

Table I. The characteristic absorption bands of *S*-alkylisothiouronium salts (cm^{-1})*

Compound						
S-Methyl	iodide	1639 (s)		1427 (m)		
	deuterated	1577 (s)		1393 (m)	1189 (m)	1142 (m)
	difference	62		34		
S-Methyl	sulfate	1675 (s)	1642 (m)	1435 (m) 1420 (m)		
	deuterated	1587 (s)		1397 (m)	1182 (m)	—
	difference	88	55	38 23		
S-Ethyl	iodide	1642 (s)	1635 (sh)	1433 (m)		
	deuterated	1575 (s)		1391 (s)	1188 (m)	1155 (m)
	difference	67	60	42		
S-Ethyl	bromide	1645 (s)	1637 (sh)	1453 (m) 1431 (m)		
	deuterated	1563 (s)		1399 (s)	1198 (m)	1143 (m)
	difference	82	74	54 32		
S-Ethyl	chloride	1658 (sh)	1647 (s)	1447 (m) 1427 (m)		
	deuterated	1563 (s)		1399 (s)	1195 (m)	1143 (m)
	difference	95	84	48 28		
Ethylene-di-	bromide	1639 (s)		1435 (s)		
	deuterated	1565 (s)		1389 (s)	1192 (m)	1140 (m)
	difference	74		56		
1-Phenyl-	chloride	1645 (s)		1439 (s)		
propenyl	deuterated	1582 (s)		1391 (s)	1193 (m)	1140 (m)
	difference	63		48		
O-Methyl-	chloride	1692 (s)		1580 (m)		
isouronium	deutrated	1631 (s)		1543 (m)	1233 (m)	1067 (m)
	difference	61		37		

* (s); strong, (m); medium, (sh); shoulder

the method described in "Organic Syntheses."[6,7] Their purity was examined by elementary analysis. 1-Phenyl-propenylisothiouronium chloride and ethylene-diisothiouronium bromide were obtained from Dr. Nishimura of this laboratory.[8] Deuterated compounds were obtained by the treatment with deuterium oxide in a sealed tube and by drying in vacuo.

Infrared Spectra.—The infrared spectra were recorded on a Perkin-Elmer model 21 infrared spectrophotometer, equipped with a sodium chloride prism, in the region from 5000 to 650 cm^{-1}. The spectra of crystals were measured in a potassium bromide disk. Deuterated compounds should be measured in either hexachlorobutadiene paste or Nujol mull, but the compounds used in this study did not disperse homogeneously in these media; therefore, the measurements of spectra were carried out in a potassium bromide disk which had been carefully prepared in a simple dry box.

Results and Discussion

Several spectra of *S*-alkylisothiouronium salts are illustrated in Fig. 1, while the observed frequencies of the characteristic absorption bands of *S*-alkylisothiouronium salts are shown in Table I. The two characteristic absorption bands of

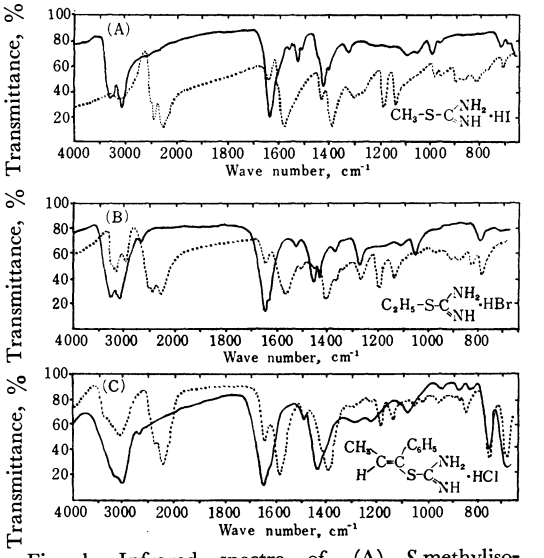

Fig. 1. Infrared spectra of, (A) *S*-methylisothiouronium iodide, (B) *S*-ethylisothiouronium bromide, and (C) 1-phenylpropenylisothiouronium chloride; ——, normal comound, ----, deuterated compound.

S-alkylisothiouronium salts were observed in the 1675—1635 cm^{-1} and 1455—1420 cm^{-1} regions. On deuteration, they shift to the lower frequency regions of 1590—1565 cm^{-1} and 1400—1390 cm^{-1} respectively, as is shown in Table I. The band

6) E. Brand and F. C. Brand, "Organic Syntheses," Coll. Vol. III, 440 (1955).
7) F. Kurzer and A. Lawson, ibid., Coll. Vol. IV, 645 (1963).
8) H. Nishimura, *J. Pharm. Soc. Japan (Yakugaku Zasshi)*, **84**, 930 (1964).

observed at about 1650 cm^{-1} may correspond to the two kinds of NH_2 scissoring vibrations, one of which is coupled with the out-of-phase N–C–N stretching vibration because it is shifted by only 50—90 cm^{-1} on deuteration. The increase in frequency of the out-of-phase N–C–N stretching vibration compared with that (A_2, 1470 cm^{-1}) of thiourea[3] may be explained as resulting from the greater double-bond character of the N–C–N bond; this has been confirmed by X-ray analysis in *S*-methylisothiouronium sulfate.[5] In the metal thiourea complex, the above situation has been reported for the same vibration.[3]

The band observed at about 1440 cm^{-1} may correspond to the band of thiourea at 1417 cm^{-1} (A_1), which has been assigned to the NH_2 rocking vibration coupled with the N–C–N and C=O stretching vibrations. For some compounds, each of the two characteristic absorption bands described above splits into two components, as Table I shows. A quantitative discussion of the nature of these characteristic vibrations could be made possible only by an appropriate normal coordinate treatment. The deuterated compounds give a pair of new bands with a medium intensity at around 1190 cm^{-1} and 1140 cm^{-1}; these bands can be assigned to the ND_2 scissoring vibrations.

Both characteristic absorption bands of *S*-alkylisothiouronium compounds exist in a narrow frequency region when their alkyl groups and their salts are replaced by other groups and salts. *S*-Alkylisothiouronium salt can be distinguished from *O*-alkylisouronium salt, which gives these characteristic absorption bands at slightly higher frequencies. An examination has been made by means of infrared absorption measurements as to whether an interaction of those compounds with alkali halide takes place. However, no change was found in the spectra when those compounds were mixed with alkali halides.

Though only a limited number of compounds were examined, it can be concluded that *S*-alkylisothiouronium salts have their characteristic absorption bands in the 1675—1635 cm^{-1} and 1455—1420 cm^{-1} regions. On deuteration, they shift to 1590—1565 cm^{-1} and 1400—1390 cm^{-1}, and give the two bands in the 1200—1180 cm^{-1} and 1155—1140 cm^{-1} regions. These characteristic absorption bands are expected to be useful for the determination of the *S*-alkylisothiouronium group involved in unknown compounds.

The authors wish to express their gratitude to Drs. Shinsuke Ose, Hideji Takamatsu and Kiyoshi Nakamura of this laboratory for their encouragement. We are also grateful to Dr. Haruki Nishimura for supplying some of the materials.

The Fluorination of Chloromethane, Chlorodifluoromethane and Dichlorofluoromethane*

By Shunji NAGASE, Hajime BABA and Takashi ABE

Government Industrial Research Institute, Nagoya, Kita-ku, Nagoya

(Received January 7, 1966)

The previous papers in this series[1,2] have shown that organic gases which are not very soluble in hydrogen fluoride can be fluorinated controllably by electrochemical fluorination. A good deal has been learned about the electrochemical fluorination of liquid halogenohydrocarbons, including unsaturated ones,[3-8] but no detailed report has yet been made on gaseous compounds.[9]

This paper will deal with the electrochemical fluorination of chloromethane. Such halogenomethanes as chlorodifluoromethane and dichlorofluoromethane were also fluorinated for the sake of comparison.

Chloromethane yielded all the expected fluorinated methanes (tetrafluoromethane, chlorotrifluoromethane, trifluoromethane, chlorodifluoromethane, difluoromethane, chlorofluoromethane and monofluoromethane) in a substantial total yield and with reasonable current efficiency. Chlorination reaction took place to a slight extent during the fluorination, giving traces of dichlorodifluoromethane and dichlorofluoromethane.

Tetrafluoromethane, chlorotrifluoromethane, and trifluoromethane were formed from chlorodifluoromethane, and tetrafluoromethane, chlorotrifluoromethane, trifluoromethane, dichlorodifluoromethane, and chlorodifluoromethane, from dichlorofluoromethane, in reasonable total yields, but with low current efficiencies.

The reaction conditions used for respective samples and the results obtained are summarised

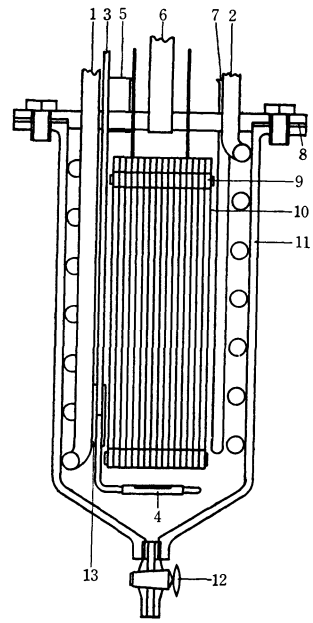

Fig. 1. Electrolytic fluorination cell and bubbler.

1,2 Inlet and outlet of cooling spiral for temperature regulation
3 Sample feed tube
4 Bubbler
5 Inlet for sodium fluoride addition
6 Lowest part of reflux condenser
7 Thermometer well
8 Neoprene packing
9 Polytetrafluoroethylene spacers between anodes and cathodes
10 Electrodes
11 Cell body
12 Valve for draining
13 Polyethylene tube connector

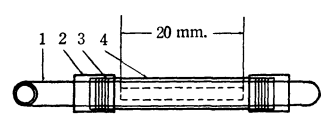

Fig. 2. Bubbler.

1 Copper tube
2 Polyethylene sheet
3 Copper wire
4 Polytetrafluoroethylene filter paper

---

* "The Electrochemical Fluorination of Gases," Part III. Presented in part at the 18th Annual Meeting of the Chemical Society of Japan, Osaka, April, 1965.

1) S. Nagase, K. Tanaka and H. Baba, This Bulletin, **38**, 834 (1965).
2) S. Nagase, K. Tanaka, H. Baba and T. Abe, ibid., **39**, 219 (1966).
3) British Thomson-Houston Co. Ltd., Brit. Pat. 668609 (1952).
4) Farbenfabriken Bayer A.-G., Brit. Pat. 740723 (1955).
5) Farbenfabriken Bayer A.-G., Brit. Pat. 741399 (1955).
6) General Electric Co., Brit. Pat. 758492 (1956).
7) H. Schmidt and H. D. Schmidt, *J. Prakt. Chem.*, **2**, 250 (1955).
8) R. N. Haszeldine and F. Nyman, *J. Chem. Soc.*, **1956**, 2684.
9) M. Schmeisser and P. Sartori, *Chemie-Ing.-Techn.*, **36**, 9 (1964). A review.

TABLE I. THE FLUORINATION OF CHLOROMETHANE[a]

Run No.	Sample[b] feed rate ml./min.	Total amount of sample fed mol.	Electricity passed amp. hr.	NaF used g.	He used ml./min.	Temp. °C	Total[c] yield mol.%	Total[d] current eff. %
1	30	0.448	111	10	0	5—6	85.4	45.2
2	52	0.607	86	10	0	5—6	61.5	52.5
3	71	0.482	49	10	0	5—6	36.5	41.1
4	52	0.525	76	50	0	5—6	50.2	32.4
5	52	0.527	76	10	104[e]	5—6	74.7	56.1
6	52	0.502	70	10	0	—10[f]	33.1	27.8
7	52	0.568	80	10	0	16	75.0	76.6

Run No.	Product compn., mol.%						
	CF_4	$CClF_3$	CHF_3	$CHClF_2$	CH_2F_2	CH_2ClF	CH_3F
1	18.3	13.2	35.2	17.0	8.7	4.4	3.2
2	15.5	11.2	25.3	20.1	15.4	7.8	4.7
3	17.2	10.5	22.0	12.5	10.7	19.9	7.2
4	7.7	2.2	16.4	22.6	17.6	20.8	12.7
5	6.0	5.2	37.5	14.9	19.3	7.5	9.6
6	14.6	6.5	35.4	11.6	18.4	4.5	9.0
7	13.6	6.7	22.9	22.0	17.6	6.9	10.3

a) All the experiments were carried out with the anodic current density of 2.2 amp./dm^2.
b) Gas volume is expressed in normal condition in this table and in Table II.
c) Calculation of yield of fluorinated product was based on the amount of CH_3Cl fed. A trace of chlorinated by-products, CCl_2F_2 and $CHCl_2F$ was neglected in quantitative calculation.
d) Total current efficiency shown was the sum of the current efficiency of each component based on the following equations, ($n=1, 2$, or 3).

$$CH_3Cl + 2nF = CH_{3-n}F_nCl + nHF \quad (1)$$

$$CH_3Cl + (2n+1)F = CH_{3-n}F_{n+1} + nHF + Cl \quad (2)$$

e) Dilution ratio (CH_3Cl : He) is 1 : 2 by volume.
f) The cell temperature was raised to 6°C at the end of the reaction.

TABLE II. THE FLUORINATION OF CHLORODIFLUOROMETHANE AND DICHLOROFLUOROMETHANE[a]

Run No.	Sample feed rate ml./min.	Total amount of sample fed mol.	Electricity passed amp. hr.	Temp. °C	Total[b] yield mol.%	Total[c] current eff. %	Product compn., mol. %				
							CF_4	$CClF_3$	CHF_3	CCl_2F_2	$CHClF_2$
				Chlorodifluoromethane							
1	27	0.410	117	5—6	55.4	12.6	58.4	24.6	17.0		
2	52	0.502	70	5—6	43.2	19.4	48.0	37.3	14.7		
3	69	0.580	58	5—6	42.6	24.9	33.4	52.0	14.6		
4	52	0.502	68	—10[d]	48.3	14.5	8.4	33.8	57.8		
5	52	0.404	57	—2[d]	53.8	19.0	21.0	42.1	36.9		
6	52	0.502	70	12—13	49.1	21.5	44.6	38.2	17.2		
				Dichlorofluoromethane[e]							
1	23	0.240	77	5—6	76.0	15.5	23.1	12.4	1.7	49.0	13.8
2	55	0.239	32	5—6	60.6	26.1	12.5	11.2	6.9	51.9	17.5
3	56	0.240	33	—9[d]	37.6	14.5	1.2	12.0	18.4	49.2	19.2
4	55	0.155	21	10	59.5	27.9	18.9	12.6	1.8	55.3	11.4

a) All the experiments were carried out with the anodic current density of 2.2 amp./dm^2, with the addition of 10 g. of NaF.
b) Calculation of yield was based on the amount of $CHClF_2$ and $CHCl_2F$ fed, respectively.
c) Calculation of the current efficiency was made with the similar way to that for chloromethane.
d) The cell temperature was raised to 6°C at the end of the reaction.
e) This was introduced together with the carrier of helium (rate at 35 ml./min.) into the cell through the bubbler.

n Tables I and II. It is apparent that the milder fluorination reaction proceeded with an increased sample feed rate, as has also been observed in the fluorination of methane[1] and of ethylene and ethane[2].

Helium appeared to serve satisfactorily as a diluent, and the addition of an increased amount of sodium fluoride resulted in a milder reaction in chloromethane.

The total yield and the current efficiency, as well as the composition of the products, were much affected by the electrolysis temperature.

The order of the facility of replacement between hydrogen and chlorine by fluorine seemed to be indefinite in chloromethane under the fluorination conditions used. In chlorodifluoromethane, the replacement of hydrogen was usually favored over the replacement of chlorine; it yielded a larger amount of chlorotrifluoromethane than that of trifluoromethane.

At lower temperatures, however, this apparent relation was reversed. A similar tendency was observed in dichlorofluoromethane.

Experimental

Apparatus.—Fluorination units, which mainly consisted of an electrolytic cell (1 l. in capacity), a safety tube dipped in mercury, a hydrogen fluoride absorber, an oxygen difluoride absorber, and condensing traps, were virtually identical with those described earlier,[1] but the position of the bubbling arrangement (the bubbler) in the cell and its shape were modified, as is illustrated in Figs. 1 and 2 respectively.

Figure 1 shows a sectional view of the cell with the bubbler, while the plan of the bubbler is shown in Fig. 2. The bubbler consisted of an L-shaped copper tube about 100 mm. in total length and 4 mm. in diameter. At the horizontal portion (about 60 mm. in length) of the tube, a slit-like hole of 2×20 mm. was opened toward the direction of the lower end of the nickel electrodes (the effective surface area of the electrodes was 9.2 dm^2). The hole was wrapped with a filter paper made of polytetrafluoroethylene fiber (Daikin Industries Co.), which was fixed with a copper wire and a polyethylene sheet. The distance between the hole and the lower end of the electrodes was about 8 mm. One end of the copper tube was closed, while the other end was connected to the sample feed tube.

The sample introduced through the sample feed tube was led to the bubbler and came out as a number of minute bubbles in hydrogen fluoride.

Materials and Procedure.—Chloromethane (99.5 %) was obtained from the Matheson Co. Chlorodifluoromethane and dichlorofluoromethane from a commercial cylinder were used after purification by distillation.

The operating procedures used in the fluorination were essentially the same as those described previously.[2] Low-temperature distillation and gas chromatography (a silica gel column was employed) were used for the quantitative analysis of the products. Infrared measurements were frequently carried out in order to identify the components.

A Novel Type of Differential Thermogram Revealed in Potassium Molybdate

By Hiroshi Isozaki and Takeo Ozawa

Electrotechnical Laboratory, Tanashi-machi, Kitatama-gun, Tokyo

(Received January 31, 1966)

Differential thermal analysis experiments have been carried out on anhydrous potassium molybdate, and differential thermograms with novel and interesting features have been obtained. These experiments were conducted in air on a powdered sample packed tightly in a sample cell, by using a new quantitative type apparatus with high sensitivity and resolution.[1] It was previously reported that there are several transition temperatures on anhydrous potassium molybdate;[2-4] 323, 458, 480 and 926°C. In the heating stage, the usual sharp peaks were obtained in our thermograms, as is shown in Fig. 1. The experiments were made up to 500°C; the temperatures and the heats of the transitions were estimated to be 283°C, 8.3±0.1 cal./g. and 457°C, 0.64±0.03 cal./g., respectively, but the third transition, previously reported to occur at 480°C, was not detected. The method of estimating the heats has been described elsewhere.[1]

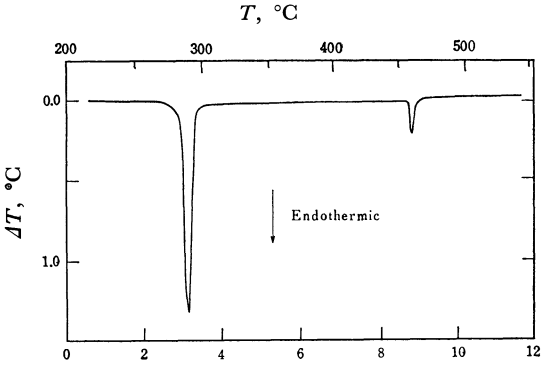

Fig. 1. Differential thermogram of K_2MoO_4 at heating stage in air.
Heating rate, 30°C/hr.

When the sample was heated to about 600°C and then left to be cooled, the transition at 457°C was reversed as a normal peak at the same temperature; however, for the transition at lower temperature, the novel and interesting thermogram which is reproduced in Fig. 2 was obtained. As may be seen in Fig. 2, a saw-tooth-like curve is revealed instead of the usual sharp peak; the transition was supercooled to the temperature range from 152 to 148°C, in comparison with the temperature of the transition, 283°C, in the heating stage. These saw-tooth-like curves are reproducible in nature whenever the sample is cooled after the transition at 283°C, and if one heats the sample up again immediately after the completion of the saw-tooth-like transition, the normal sharp peak is reproduced at 283°C without any change in the peak area. Similar thermograms can be obtained on the same sample by using another type of differential thermal-analysis apparatus with open sample cells.

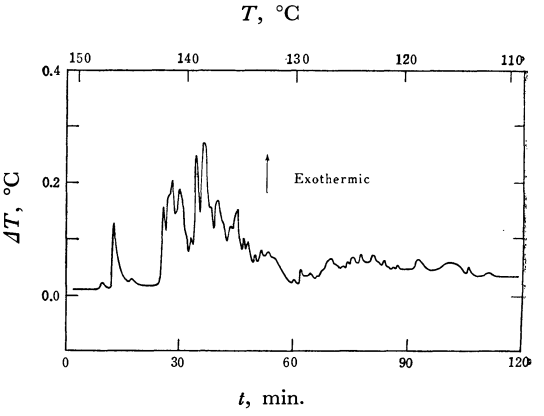

Fig. 2. Differential thermogram of K_2MoO_4 at cooling stage in air.
Cooling rate, about 25°C/hr.

The heats of the transitions in the cooling stage were also estimated. The heat at 457°C was 0.74±0.05 cal./g., somewhat larger than the heats in the heating stage, but the heats of the saw-tooth-like transition were estimated to be about 3.4 cal./g., though the peak area was rather ambiguous and though the recorder did not follow the change exactly because of the long responce time.

Similar thermograms were also obtained in the cooling stage of powdered tin heated to about 450°C. The saw-tooth-like change in the differential temperature began at about 230°C, followed by the usual peak. When the sample was heated again, the usual peak was obtained,

1) T. Ozawa, This Bulletin, **39**, 2071 (1966).
2) F. D. Rossini, *Circular Natl. Bur. Standards*, **C500** (1952).
3) I. M. Kuleshov, *Zhur. Neorg. Khim.*, **1**, 2011 (1956).
4) G. Petit and J. Mireille, *Compt. rend.*, **244**, 1900 (1957).

and the thermogram was reproduced on the same sample at the second cooling. In this case, oxidation seemed to occur; any oxide would have affected the solidification of the tin.

As may be apparent in its great tendency to supercool, the lower transition is difficult to reverse by cooling, and the transformation could not be propagated beyond the crystalline boundary. Hence, any sample particles would be transformed independently, without influencing each other; this behavior might produce a saw-tooth-like curve. If a differential thermal-analysis apparatus with a high resolution and with a micro amount of a sample were constructed, interesting kinetic aspects of transitions such as this would be elucidated.

The apparatus used has been described elsewhere.[1] Briefly, cylindrical sample cells with threaded lids are inserted in ceramic sample holders set in a metal block, and alumel-chromel thermocouples are inserted between the cells and the cell holders. This arrangement makes the quantitative heat measurement possible.[1] The rates of heating are 60°C/hr. and 30°C/hr.; they are controlled with a PI-type program controller and a SCR regulator. The temperature and the differential temperatures are recorded against the time on a six-point recorder. The sample is of a G. R. grade; it is used without further purification, dried at about 120°C for more than 6 hr., and kept in a desiccator above silica gel. The reference material is calcined alumina.

Studies of Copolymers Containing L-Proline Residue as a Main Constituent. I. The Synthesis of Copolymers of L-Proline with the γ-Ester of L-Glutamic Acid

By Rume SAKAI, Shoichi IKEDA and Toshizo ISEMURA

Department of Biology, Faculty of Science and Institute for Protein Research, Osaka University, Kita-ku, Osaka

(Received March 1, 1966)

Polyamino acids are very useful as a model for elucidating the physico-chemical properties of proteins.[1] Many investigators have studied collagen, the major protein component of the connective tissues, which is very specific because of its amino acid composition and structure. The vertebrate collagen contains about 30% glycine residues and more than 20% L-proline residues, inclusive of L-hydroxyproline residues, and its molecular structure is similar to that of poly-L-proline II.[2] Therefore, it is interesting to investigate how the conformation of copolypeptide containing L-proline changes with the L-proline content. We have studied polyamino acids which contain L-proline residue as the main constituent.

In the present communication, the synthesis of copolypeptides with proline will be described. The other constituent is γ-methyl-L-glutamate (γMLG) or γ-benzyl-L-glutamate (γBLG). Some properties of the copolypeptides obtained will also be described briefly. The reason why we have chosen γMLG or γBLG as the other constituent in the copolypeptides is that poly-γ-methyl-L-glutamate (PMLG) and poly-γ-benzyl-L-glutamate (PBLG) have already been thouroghly studied by many investigators.[3] Moreover, the copolypeptides which contain these constituents can be readily converted to water-soluble copolypeptides by the cleavage of γ-ester groups in side chains.

We have carried out the copolymerization in various solvents, including dioxane, pyridine, acetonitrile and nitrobenzene, and have found that nitrobenzene is a solvent suitable for the preparation of copolymers of L-proline with γMLG or γBLG at various molar ratios.

To prepare the copolymers, about 4 g. of *N*-carboxy anhydrides (NCA's) of L-proline and L-glutamate in a desired molar ratio were dissolved or suspended in 100 ml. of a polymerization solvent. Sodium methoxide was used as the initiator for the polymerization. The solution was left standing for about a month. The solution, excepting that in nitrobenzene, became turbid with time, and a precipitate separated out in the course of the reaction. The precipitate thus separated is designated as a precipitate a. After the precipitate had been removed, ethyl ether was added to the solution. Then further precipita-

1) E. Katchalski and M. Sela, "Advances in Protein Chemistry," XIII, Academic Press, New York (1958), p. 243.

2) W. F. Harrington and P. H. von Hippel, ibid., XVI (1961), p. 1.

3) E. R. Blout, R. H. Karlson, P. Doty and B. Hargitay, *J. Am. Chem. Soc.*, **76**, 4492 (1954); P. Doty, J. H. Bradbury and A. M. Holtzer, ibid., **78**, 947 (1956).

Table I. Properties of polypeptides

Polypeptide	Content of L-proline			$[m']^*_{546}$	$[\eta]^{***}$ dl./g.
	at polymerization	from amino acid analysis	from absorption of benzyl residue		
Poly-L-proline	1.0	—	—	−41°**	0.436
Copoly-3:1-(L-proline, γ-benzyl-L-glutamate)	0.75	0.767	0.756	−74°	0.251
Copoly-1:1-(L-proline, γ-benzyl-L-glutamate)	0.50	0.535	0.528	−89°	0.165
Copoly-1:3-(L-proline, γ-benzyl-L-glutamate)	0.24	0.274	0.26	−50°	0.150
Poly-γ-benzyl-L-glutamate	0	—	0	+16°	0.405

* Measured in 1,2-dichloroethane.
** Measured in 1,2-dichloroethane - acetic acid (99.5—0.5%).
*** Measured in dichloroacetic acid at 25°C.

tion occurred. This precipitate is designated as the precipitate b. On the other hand, the solution in nitrobenzene remained clear throughout the reaction. When ether was added to the solution, the precipitate separated out as well. The precipitate thus obtained was different in composition from the precipitates a and b. In fact, the specific rotation at 546 mμ in dichloroacetic acid was −376° for the precipitate a and −266° for the precipitate b, when the NCA's of L-proline and γMLG were copolymerized in dioxane at a molar ratio of 4:1. As the specific rotation of PMLG was found to be −37°, and that of poly-L-proline, −510°, in dichloroacetic acid, the precipitate a would contain more proline residues than b. Copoly-1:1-(L-proline, γMLG) which was prepared in nitrobenzene was found to be readily soluble in chloroform, although both poly-L-proline and PMLG were insoluble in it.

Copolymerizations at different L-proline-to-γBLG ratios were performed in nitrobenzene. The amino acid compositions of these copolypeptides were determined by amino acid analysis and by means of studying the ultraviolet absorption at 258 mμ. It was found that the composition is as is shown in Table I.

Poly-L-proline, PBLG and the copolymers obtained above were all soluble in *m*-cresol, dichloroacetic acid and nitrobenzene. In chloroform, PBLG, copoly-1:3-(L-proline, γBLG) and copoly-1:1-(L-proline, γBLG) were soluble, whereas copoly-3:1-(L-proline, γBLG) was soluble in this solvent if the temperature of solution was raised. However, poly-L-proline was not soluble in chloroform. On the other hand, poly-L-proline is the only water-soluble polypeptide among these substances. When copoly-1:1-(L-proline, γBLG) was shaken with a water-chloroform system, no significant amount of the copolymer was found in the water layer. All of these polypeptides excepting poly-L-proline were soluble in 1,2-dichloroethane. Poly-L-proline was soluble in 1,2-dichloroethane containing only 0.5% acetic acid. This solution showed little mutarotation, just as the solutions of other copolymers in 1,2-dichloroethane. The final values of the effective mean residue rotation at 546 mμ are also shown in Table I. As is well known, poly-L-proline can exist in two different forms in solution according to the nature of the solvent.[4] One of these is designated as poly-L-proline I, the specific rotation of which at 546 mμ is about +40°. The other, namely, poly-L-proline II, has its specific rotation of about −500°. Acetic acid is a solvent converting poly-L-proline I to II. Consequently, 1,2-dichloroethane may be a solvent which stabilizes Form I of poly-L-proline. It has already been reported by Katchalski et al.[5] that copolymers can be formed in dioxane with great difficulty. They assumed that the marked tendency of the terminal prolyl residue of a growing chain to react with the NCA of L-proline in preference to the NCA of γBLG was the cause.

However, all the findings reported here support the conception that the true copolypeptides of L-proline with γ-L-glutamate can be formed when nitrobenzene is used as the polymerization solvent.

The authors wish to thank Mr. Keishiro Wada for performing the amino acid analysis.

4) I. Z. Steinberg, W. F. Harrington, A. Berger, M. Sela and E. Katchalski, ibid., **82**, 5263 (1960).
5) E. Katchalski, A. Berger and J. Kurtz, "Aspects of Protein Structure," Ed. by G. N. Ramachandran, Academic Press, New York (1963), p. 205.

The Isolation of the Four Isomers of Tris-(L(+)-valinato)cobalt(III)[1]

By Muraji SHIBATA, Hiroaki NISHIKAWA and Yuzo NISHIDA

Department of Chemistry, Faculty of Science, Kanazawa University, Kanazawa

(Received March 9, 1966)

Lifschitz[2] isolated α and β forms of tris-(alaninato)cobalt(III) from a reaction mixture of cobalt(III) hydroxide with dextro-alanine, and also separated the α forms into two isomers, α and α'. Recently, Douglas and Yamada[3] found a fourth isomer, β', along with the other three isomers (α, α' and β), in the cobalt(III) complexes of D- and L-alanine. At almost the same time, Dunlop and Gillard[4] reported the isolation of the four isomers of tris-(L(+)-alaninato)-cobalt(III). We have now succeeded in obtaining the analogous four isomers (α, α', β and β') of tris-(L(+)-valinato)cobalt(III).

Following the usual procedure of Ley and Winkler[5] freshly-prepared $Co(OH)_3$ (9.2 g.) was treated with L-valine (34 g.). Red forms (β and β') of the complex precipitated from the reaction mixture as a brown solid containing unreacted $Co(OH)_3$. When the precipitates were extracted with hot water and the solution was evaporated, the more soluble β' isomer crystallized. When the residue from the above was treated with SO_2-water, the β isomer remained as undissolved material. This was then recrystallized from 50% sulfuric acid.

On the other hand, a mother liquor from the reaction mixture was evaporated to dryness, and the resulting solid was treated with ethanol; unreacted L-valine was thereby left. The complex was then taken up in ethanol. The alcohol solution was concentrated under reduced pressure

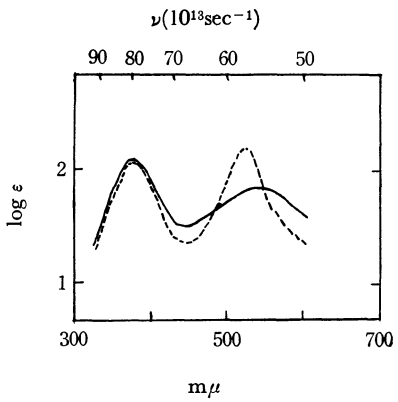

Fig. 1. Absorption spectra of
—— α-[Co(L-val)$_3$], ---- β-[Co(L-val)$_3$].

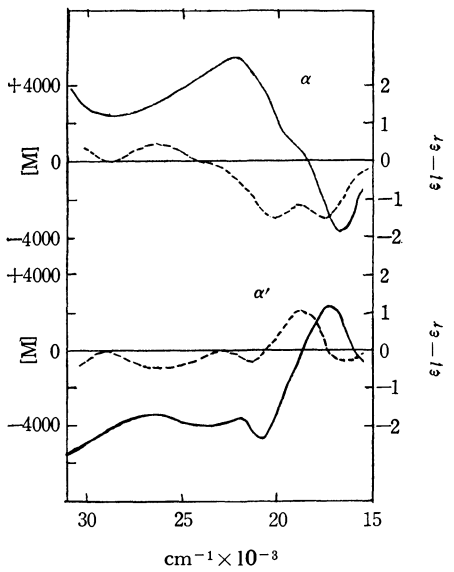

Fig. 2. Rotatory dispersion (——), and circular dichroism (----) of α- and α'-[Co(L-val)$_3$].

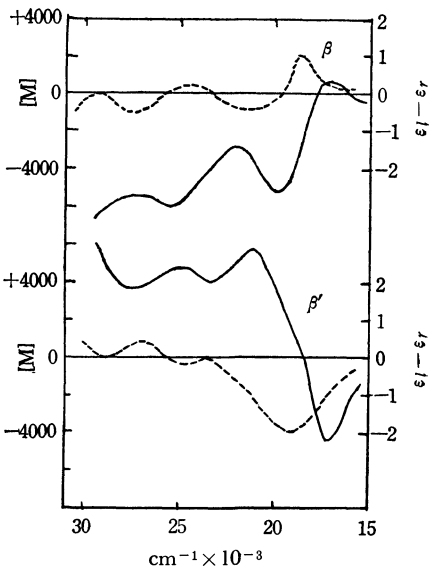

Fig. 3. Rotatory dispersion (——) and circular dichroism (----) of β- and β'-[Co(L-val)$_3$].

1) Presented at the 15 th Symposium on Coordination Chemistry, Kanazawa, October, 1965.
2) J. Lifschitz, *Z. physik Chem.*, **114**, 403 (1925).
3) B. E. Douglas and S. Yamada, *Inorg. Chem.*, **4**, 1561 (1965).
4) J. H. Dunlop and R. D. Gillard, *J. Chem. Soc.*, **1965**, 6531.
5) H. Ley and H. Winkler, *Ber.*, **42**, 3894 (1909).

and then left to stand overnight to precipitate some of the β' isomer. After the β' had been removed, the solution was added to an alumina column previously washed with ethanol. When ethanol was passed through the column, violet forms (α and α') of the complex were eluted out, while a trace amount of the β' remained at the top of the column. The eluted solution was concentrated to a small volume, and then acetone was added to make an ethanol-acetone (1 : 2) solution. The mixed solvent solution was then again chromatographed by using ethanol-acetone (1 : 2) as the eluent. Two violet bands separated completely, and the α and α' were obtained from the first and the second fractions respectively, by evaporation.

Yield: α and α', about 10%; β and β', about 5%.

Found: C, 44.5; H, 7.5; N, 9.4. Calcd. for α-[Co(L-val)$_3$]·1/2H$_2$O: C, 44.5; H, 7.8; N, 10.3%. Found: C, 43.5; H, 7.7; N, 9.4. Calcd. for α'-[Co(L-val)$_3$]·H$_2$O: C, 43.6; H, 7.7; N, 10.2%. Found: C, 39.3; H, 7.5; N, 9.21. Calcd. for β-[Co(L-val)$_3$]·3H$_2$O: C, 40.0; H, 8.0; N, 9.40%. Found: C, 43.2; H, 7.3; N, 10.0. Calcd. for β'-[Co(L-val)$_3$]·H$_2$O: C, 43.6; H, 7.7; N, 10.2%.

The absorption curves are given for only two isomers (α and β) in Fig. 1, since the curves are essentially the same for the others (α' and β'). From these spectra, the α and α' are identified as the 1, 2, 6 (mer) isomer, and the β and β', as the 1, 2, 3 (fac) isomer. The optical rotatory dispersion and circular dichroism curves are given in Figs. 2—3. For the β and β' isomers belonging to the point group C_3, the configurations can be tentatively identified as Λ(D) for the β and Δ (L) for the β' by comparing the C. D. and O. R. D. curves of the present isomers with those of the Λ(D)-tris-(ethylenediamine)cobalt(III) ion.

Optical Resolution and Configuration of *trans*-2, 3-Epoxybutyric Acid[1,2]

By Kaoru HARADA and Jun-ichi OH-HASHI

Institute of Molecular Evolution and Department of Chemistry, University of Miami, Coral Gables, Florida, U.S.A.

(Received March 15, 1966)

The direct epoxidation of the double bond of α, β-unsaturated acids by peroxy acid or by hydrogen peroxide has been known to be generally very slow. (±)-*trans*-2, 3-Epoxybutyric acid (epoxy acid I) was successfully synthesized from crotonic acid (*trans*) by epoxidation with hydrogen peroxide and sodium tungstate.[3] Liwschitz et al.[4] reported the amination of I by treating with benzylamine or ammonia in which they reported the synthesis of (±)-allothreonine.

In the present study, the epoxy acid (I) was resolved by brucine. To determine the configuration of the resolved (−)-*trans*-2, 3-epoxybutyric acid [(−)-epoxy acid] (III), it was treated with benzylamine or ammonia, as was done by Liwschitz et al. The resulting *N*-benzyl allothreonine (IV) was hydrogenolyzed by the use of palladium on charcoal. The isolated amino acid was found to be optically pure (+)-allothreonine (V) and it did not contain any threonine or other amino acid, even in the reaction mixture. This was examined paper chromatographically[5] and also by the automatic amino acid analyzer. This fact suggests that the amination proceeds with a typical S_N2 mechanism and no racemization occurs during the reaction. The configuration of the resulting (+)-allothreonine (V) is known as: 2(s), 3(s). Therefore, the configuration of (−)-*trans*-2, 3-epoxybutyric acid would be 2(R), 3(s). The reaction products of epoxy acid and ammonia showed a large allothreonine peak and a little peak at about the alanine area in the automatic amino acid analyzer, (ratio allo : unknown=99.4 : 0.6). The latter peak might be α-hydroxy β-amino butyric acid (isothreonine) which is a possible ammonolysis product. Attempts to obtain optically active α-hydroxybutyric acid by reduction of (−)-epoxy acid (III) with sodium borohydride and by catalytic hydrogenation were unsuccessful. In each case, mainly β-hydroxybutyric acid was isolated by column chromatography.[6]

1) Stereochemistry of Glycidic Acid. II, Part I of this series, K. Harada, *J. Org. Chem.*, **31**, 1407 (1966).

2) Aided by Grant no. NsG-689 of the National Aeronautics and Space Administration. Contribution No. 061 of the Institute of Molecular Evolution, University of Miami.

3) G. B. Payne and Paul H. Williams, *J. Org. Chem.*, **24**, 54 (1959).

4) Y. Liwschitz, Y. Rabinsohn and D. Perera, *J. Chem. Soc.*, **1962**, 1116.

5) K. N. F. Shaw and S. W. Fox, *J. Am. Chem. Soc.*, **75**, 3421 (1953). *n*-butanol : acetone : conc. ammonia : H_2O=100 : 12.5 : 12.5 : 75.

6) E. F. Phares, E. H. Mosbach, F. W. Denison, Jr., S. F. Carson, M. V. Long and B. A. Gwin, *Anal. Chem.*, **24**, 660 (1952).

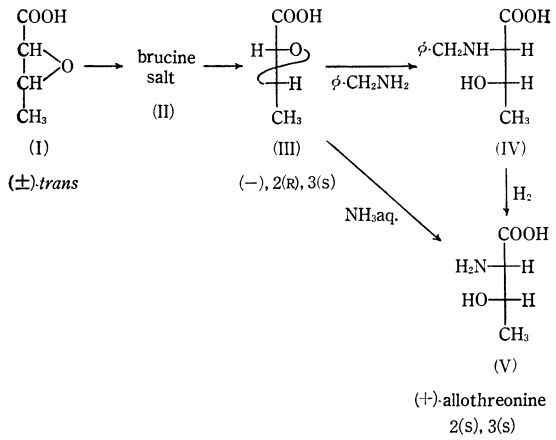

Fig. 1.

Experimental

(±)-*trans*-2, 3-Epoxybutryic Acid (I).—The epoxy acid was prepared by the method of Payne and Williams.[3] M. p. 83°C.

Brucine Salt of (+)-*trans*-2, 3-Epoxybutyric Acid (II).—Epoxy acid (I), 20.4 g. (0.2 mol.), and brucine, 78.8 g. (0.2 mol.), were dissolved in 200 ml. of hot methanol. The solution was filtered and the solvent was evaporated in vacuo. The residual syrup was dissolved in a hot mixture of methanol (20 ml.) and acetone (180 ml.). After cooling, crystallization of brucine salt began by seeding with an authentic specimen which was obtained in another crystallization experiment. After standing overnight at room temperature, the crystals were filtered and were washed with cold acetone. The crystals, 35.0 g., were recrystallized from a hot mixture of methanol (5 ml.) and acetone (95 ml.). Yield, 32.0 g., m. p. 173°C, $[\alpha]_D^{25}=-26.0°$ (*c* 2.1, H_2O).

(−)-*trans*-2, 3-Epoxybutyric Acid (III).—Brucine salt (II), 14.3 g. (0.03 mole), was dissolved in 100 ml. of water. To this solution, 1 N sodium hydroxide solution, 33 ml., was added. The precipitated brucine was separated by filtration. The filtrate was extracted with benzene three times to remove the residual brucine. Concentrated hydrochloric acid was used to bring the pH of the aqueous solution to 2.5. After saturation of the solution with sodium chloride, the epoxy acid was extracted with ether five times (100 ml.×5). The ether solution was dried with anhydrous sodium sulfate. After evaporation of ether, 1.80 g. (60%) of crude III was obtained. This was recrystallized from benzene. 1.20 g. (40%), m. p. 61°C. $[\alpha]_D^{25}=-82.5°$ (*c* 0.59, benzene). Neut. equiv. Found: 102. Calcd. for $C_4H_6O_3$.

(+) *N*-Benzyl-allothreonine (IV).—A mixture of III, 1.53 g., water, 5 ml., and benzylamine, 2 ml., was refluxed for 2 hr. After cooling, the excess benzylamine was removed by ether extraction and the pH of the aqueous solution was brought to 5.5 by the addition of concentrated hydrochloric acid. Precipitated IV was washed with acetone and then with ether. The crude product, 2.2 g. (70%), was recrystallized from *N, N*-dimethylformamide. Yield, 2.0 g. (67%). m. p. 245°C (decomp.), $[\alpha]_D^{25}=+12.2°$ (*c* 1.9, 5 N hydrochloric acid).

Found: C, 63.42; H, 7.20; N, 6.68. Calcd. for $C_{11}H_{15}O_3N$: C, 63.14; H, 7.23; N, 6.69%.

(+)-Allothreonine (V). — (+)-*N*-Benzyl-allothreonine (IV), (2.09 g.), was dissolved in 50 ml. of 50% ethanol. To this solution, 1.0 g. of 5% palladium on charcoal was added and the hydrogenolysis was carried out at room temperature. When the hydrogen uptake ceased, the catalyst was removed by filtration. The filtrate was concentrated in vacuo. The crystalline residue was recrystallized from water and ethanol. Yield, 1.13 g. (95%). This was repurified from water (1) and ethanol (9). Yield, 0.95 g. (80%). M. p. 285°C, $[\alpha]_D^{25}=+32.9°$ (*c* 1.9, N hydrochloric acid).[7]

Found: C, 40.09; H, 7.48; N, 11.57. Calcd. for $C_4H_9O_3N$: C, 40.33; H, 7.62; N, 11.76%.

(+)-Allothreonine (V) by Ammonolysis of III.—A mixture of 1.53 g. (0.015 mol.) of III and 50 ml. of concentrated ammonia (sp. gr. 0.90) was kept at room temperature. After 4 days the reaction mixture was concentrated in vacuo. A weight of 1.43 g. (80%) of crude V was obtained.[8] This was recrystallized from water. Yield, 0.50 g. (28%). m. p. 285°C (decomp.), $[\alpha]_D^{25}=+33.5°$ (*c* 2.0, N hydrochloric acid).[7]

7) D. F. Elliot, *J. Chem. Soc.*, **1950**, 62. (+)-Allothreonine, $[\alpha]_D^{25}=+32.5°$ (*c* 8.2, N HCl).

8) The crude V contains some impurity which is ninhydrin negative. It decomposes at 238°C and shows specific rotation $[\alpha]_D^{25}=+27.2°$ (*c* 2.1, N HCl).

Triterpenoids from the Leaves of *Ilex latifolia* Thunberg

By Shozo YAMADA

Osaka City Institute of Hygiene, Kita-ku, Osaka

(Received March 31, 1966)

From the leaves of *Ilex latifolia* Thunberg, ursolic acid has been isolated by Kariyone et al.[1] and by Takemoto et al.[2] The present paper will deal with the isolation and identification of β-amyrin, lupeol, taraxerol, uvaol and β-sitosterol, besides that of ursolic acid, and with the isolation of an unknown triterpenoid acid, $C_{30}H_{48}O_3$, m. p. 296—298°C (decomp.), from the leaves of this plant. In this experiment, α-amyrin,[3] which has been isolated from the bird-lime of this plant, was not found. The structure of the triterpenoid acid is now being elucidated.

Experimental*

The Isolation and Identification of β-Amyrin, Lupeol, Teraxerol, Uvaol and β-Sitosterol.—Fresh leaves (6 kg.), collected in Kyoto Prefecture in August of 1963, were cut into chops and percolated with alcohol (55 l.) at room temperature for a week. The evaporation of the alcoholic extract afforded a tarry mass, which was then treated with water. A dark green, oily mass then separated, along with a greenish-white, amorphous material, from a turbid tan brown solution (a). The dark green, oily mass gave, after having been treated with a 50% alcoholic solution, a greenish-white amorphous material. The alcoholic filtrate was again evaporated to dryness and treated with water; the aqueous solution was then combined with the foregoing solution a. Both greenish-white, amorphous materials were continuously extracted with hexane. The unextracted amorphous material was found to be almost pure ursolic acid after purification through its potassium salt. The hexane solution was evaporated to dryness, and the residual resinous matter was divided into neutral and acidic fractions. From the acidic fraction, ursolic acid was isolated. When the crystallized neutral fraction was triturated with hexane and recrystallized from 80% alcohol, it afforded needles, m. p. 220—222°C; the identity of which with uvaol which had been synthesized by the lithium aluminium hydride reduction of methyl ursolate was estabished by a mixed melting point determination and an infrared comparison.

From the mother liquor of uvaol needles, m. p. 258—266°C, were separated. These were purified by silica-gel chromatography, giving needles, m. p. 272—274°C, which were found to be identical with taraxerol by a mixed melting point determination and an infrared comparison.

The mother liquor of taraxerol was mixed with silica gel and was fractionated by silica-gel chromatography, using a *n*-hexane - ethyl acetate mixture as the elution solvent.

Fractions showing R′ values of 0.80—0.82 on TLC were collected and recrystallized from alcohol or acetone to afford fine needles, m. p. 148—167°C. These were then acetylated with acetic anhydride and concentrated sulfuric acid, and the acetate mixture was fractionally recrystallized from ethyl acetate. The less soluble part of acetate in ethyl acetate gave flat rectangular plates, m. p. 293—294°C; undepressed after admixture with an authentic sample of taraxeryl acetate; its identity was confirmed by an infrared comparison.

The more soluble part gave, after tedious recrystallization from ethyl acetate, rods, m. p. 234—236°C, and floculent needles, m. p. 211—213°C. The former and its deacetylated alcohol (m. p. 195—196°C) were shown to be identical with β-amyrin acetate and β-amyrin, respectively, by a mixed melting point determination and an infrared comparison. The deacetylation of the latter gave microneedles, m. p. 210—211°C, from acetone. Its benzoate showed a m. p. of 263°C (from ethyl acetate). The identities of the alcohol and its benzoate were confirmed by a mixed melting point determination and by an infrared comparison with authentic samples of lupeol and its benzoate.

From the fractions showing an R_f value of 0.70, glistening leaflets, m. p. 135—136°C, undepressed after admixture with an authentic sample of β-sitosterol, were obtained.

Uvaol was also obtained from the fractions showing an R_f value of 0.50—0.53.

Some crystalline materials were obtained from the fractions showing lower R_f values, but they were not determined.

The Isolation of a Triterpenoid Acid, $C_{30}H_{48}O_3$.—The aqueous solution a was extracted with ether and, after the ether had been removed, was treated with a neutral lead acetate solution. The precipitated yel-

1) T. Kariyone, Y. Hashimoto and T. Kikuchi, *Yakugaku Zasshi*, **69**, 314 (1949).

2) T. Takemoto and K. Takahashi, *Yakugaku Kenkyu*, **22**, 301 (1952).

3) K. Yagishita, *Bull. Agr. Chem. Soc. Japan*, **21**, 157 (1957).

* The melting points are uncorrected. The microanalyses and the measurement of the infrared spectra were made by M. Goda and his associates of Osaka City University. Throughout this work the content and homogeneity of each material were checked by thin-layer chromatography (TLC) with a *n*-hexane: ethyl acetate=7 : 3 solvent.

The author is indebted to Professor Syun Iseda of Kumamoto Women's University for providing β-amyrin, lupeol and their derivatives, to Professor Hiroyuki Inoue of Kyoto University for providing the ursolic acid, β-sitosterol and their derivatives, and to Dr. Yoshisuke Tsuda of Osaka University for providing the taraxerol and its acetate. The author is also indebted to Mr. Tsugio Baba of this laboratory for collecting the plants, and to him and Miss Nobuko Edamura of Mukogawa Women's University for their assistance in the experimental work.

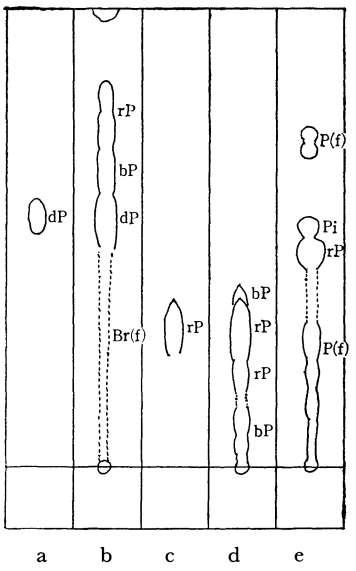

Fig. 1. Thin layer chromatogram of
a) a glucoside, m. p. 220—222°C
b) a glucoside mixture
c) a triterpenoid acid, m. p. 296—298°C
d) an acidic fraction of hydrolysate of b
e) a neutral fraction of hydrolysate of b.
Solvent: *n*-buthanol : acetic acid : water = 4:1:1 (a and b), *n*-hexane : ethyl acetate = 7 : 3 (c, d and e)
Development of color: 10% sulfuric acid
dP: dark purple, rP: reddish purple,
bP: bluish purple, P: purple, Pi: pink,
Br: brown, f: faint

lowish-white mud was dried and extracted repeatedly with boiling alcohol. The combined alcohol extracts were evaporated under reduced pressure to afford yellowish-white powder upon drying. This powder was crystallized from pyridine when small portions of water were added; then it was recrystallized from a diluted methanol or ethanol solution to give fine needles, m. p. 220—222°C. This compound afforded, on hydrolysis with 6 N hydrochloric acid in methanol, a triterpenoid acid, m. p. 296—298°C (decomp.); $[\alpha]_D^{12}$ +283° (*c* 1.03, chloroform : methanol = 1 : 1), whose R_f value on TLC was 0.32—0.33* (Fig. 1). Liebermann-Burchard reaction: purple; tetranitromethane test: yellow.

Found: C, 79.08, 78.94; H, 10.18, 10.07;. Calcd. for $C_{30}H_{48}O_3$: C, 78.90; H, 10.59%.

The acetylation of the acid with acetic anhydride and pyridine gave a reversible acetate, m. p. 262—264°C (decomp.).

Found: C, 77.12, 77.12; H, 9.66, 9.81. Calcd. for $C_{32}H_{50}O_4$: C, 77.06; H, 10.11%.

When the aqueous solution a (2 l.) stood after acidification with hydrochloric acid, there was precipitated a large amount of a reddish-tan resinous matter which solidified upon being dried (31 g.). This was found to be a mixture of glucosides containing the above-mentioned glucoside, m. p. 220—222°C; on hydrolysis with hydrochloric acid, it gave the above-mentioned triterpenoid acid and several neutral compounds (Fig. 1).

Grateful acknowledgement is hereby made to Dr. Nobumasa Nakayama and Dr. Yoshio Kurayuki of this Institute for their interest and encouragement throughout the progress of this work.

* On the same TLC, ursolic acid showed an R_f value of 0.35—0.36 and oleanolic acid, one of 0.38.

SHORT COMMUNICATIONS

The Formation of Uranium Trioxide by the Oxidation of Uranium Iodides at Low Temperatures

By Muneo HANDA

Division of Fuel Research and Development, Japan Atomic Energy Research Institute, Tokai-mura, Ibaraki

(Received December 6, 1965)

The oxidations of uranium tetraiodide and triiodide by oxygen were studied using a special experimental apparatus, in which the column of a gas chromatograph was replaced with an electric furnace and traps of water vapor, oxygen, and iodine. With this apparatus, studies can be made easily and accurately of chemical reactions between gases and solids, even when such solids cannot be treated in the air. This is because measurements can be made on the gases consumed or released during the reaction. The heating curves (the rate of temperature increase: 2°C/min.) obtained for the reactions between uranium iodides and oxygen are shown in Fig. 1. The peaks appearing in the heating curves correspond to the

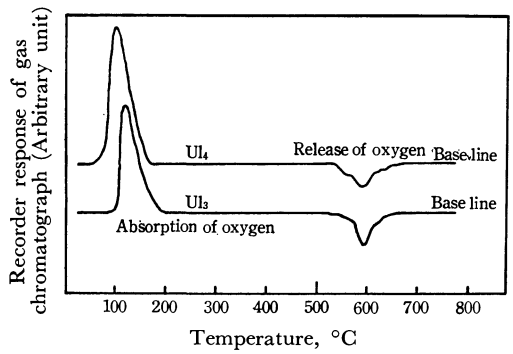

Fig. 1. Heating curves of uranium iodides.
Sample weight UI_4: 0.152 g.
UI_3: 0.141 g.
Partial pressure of oxygen: 1/10 atm.
Rate of temperature increase: 2°C/min.

absorption of oxygen, while the valleys correspond to the release of oxygen during the reaction. The oxidations of uranium tetraiodide and of uranium triiodide by oxygen, whose partial pressure was one-tenth of the atmosphere, started at temperatures of about 60 and 100°C respectively. When the temperatures were raised to about 600°C, the products resulting from the oxidations of uranium iodides released oxygen; the volume of oxygen released was about one-tenth of that absorbed in the oxidation. The colors of the compounds obtained by the oxidations of uranium tetraiodide and triiodide were both brown. When these brown-colored compounds were heated to about 600°C, oxygen was released and they turned black at the same time. The brown and the black compounds were then taken out from the apparatus for chemical and X-ray analyses; these analyses showed that the brown compounds were uranium trioxide and the black compounds, triuranium octoxide. Therefore, the peaks of the absorption of oxygen in the heating curves for uranium iodides appeared when the uranium iodides were oxidized to uranium trioxide; the valleys of the release of oxygen, on the other hand, were caused by the decomposition of uranium trioxide to triuranium octoxide. The reactions involved are as follows:

$$\overset{60°C}{2UI_4 + 3O_2 = 2UO_3 + 4I_2} \quad (1)$$

$$\overset{100°C}{2UI_3 + 3O_2 = 2UO_3 + 3I_2} \quad (2)$$

$$\overset{600\text{—}700°C}{3UI_4 + 4O_2 = U_3O_8 + 6I_2} \quad (3)$$

$$\overset{600\text{—}700°C}{6UI_3 + 8O_2 = 2U_3O_8 + 9I_2} \quad (4)$$

It has been reported by Foster and Tvrzicky[1] that oxygen or dry air converts uranium iodides to triuranium octoxide at elevated temperatures, and to uranyl iodide (UO_2I_2) or uranous oxyiodide (UOI_2) at room temperature. An attempt was therefore made by the present author to obtain the same compounds at various temperatures and at various oxygen partial pressures using the same method; however, his experiments all failed to produce such compounds. In the course of the experiments, however, he observed the reaction in which the oxidation proceeded in two stages as the temperature was raised. The oxidations of uranium iodides at low temperatures, represented by the two chemical equations, 1 and 2, may be useful for the preparation of pure uranium trioxide.

1) In J. J. Katz and E. Rabinowitch, ed., "The Chemistry of Uranium: The Element, Its Binary and Related Compounds," Dover Publications, New York (1951) p. 538.

The Proton Magnetic Resonance of Thianaphthenes. IV. The Estimation of the Chemical Shifts of Thianaphthene by Partial Deuteration

By Kensuke TAKAHASHI, Ichi ITO and Yasuo MATSUKI

The Chemical Research Institute of Non-Aqueous Solutions, Tohoku University, Katahira-cho, Sendai

(Received August 1, 1966)

In our previous communications[1-3] we have discussed some long-range coupling constants observed in thianaphthenes. The spectrum of thianaphthene itself is too complex to analyze. Therefore we tried to prepare the 5-, 6- and 7-deuterothianaphthenes and to analyze their proton spectra. Deuteration was done by the reduction of the corresponding bromothianaphthenes. The reduction was carried out by zinc and deuterated acetic acid. Details of the preparation will be published later somewhere. The spectra of the deuterated products are shown in Fig. 1. Spectra were taken in 5 mole per cent solutions in carbon tetrachloride, in cyclohexane and in acetone, with a small amount of tetramethylsilane as an internal reference. The first-order analyses are possible in the cases of 5- and 6-deuterothianaphthenes but not in the case of 7-deuterothianaphthene. The spectrum of 7-deuterothianaphthene is an ABX type which is very close to AA'X type. The results of the chemmical shifts obtained are shown in Table I. Agreement of the chemical shifts given for three deuterated

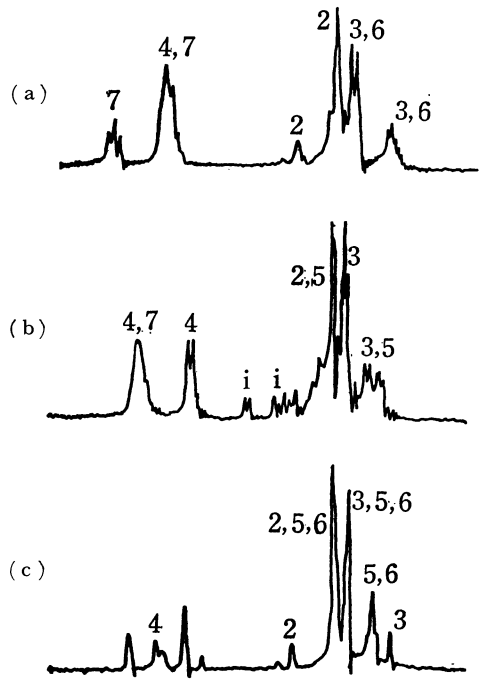

Fig. 1. The PMR spectra of some deuterated thianaphthenes in carbon tetrachloride at 60 Mc.p.s. Applied magnetic field increases from left to right and the number on each peak shows the assignment.
(a) 5-Deuterothianaphthene,
(b) 6-Deuterothianaphthene,
(c) 7-Deuterothianaphthene

TABLE I. CHEMICAL SHIFTS OF SOME THIANAPHTHENE DERIVATIVES IN CARBON TETRACHLORIDE, REFERRED TO TMS AT 60 Mc.p.s.

Substituent	Assignment					
	2-H	3-H	4-H	5-H	6-H	7-H
5-D	7.33	7.23	7.72_5	—	7.24	7.78_5
6-D	7.34_5	7.21_5	7.72_5	7.25	—	7.79
7-D	7.30_5	7.22_5	7.71	7.26	7.23	—
— (Estimated)	7.33	7.22	7.72	7.26	7.24	7.79

compounds is good enough to estimate the chemical shifts of thianaphthene, as is shown in the lowest line in Table I. A characteristic point of thianaphthene is that the chemical shifts of the 5- and the 6-hydrogens are almost the same but the former seems to be a little larger than the latter. The difference of the chemical shifts of about 0.5 p. p. m. between the 4- and 5- or between the 6- and 7-hydrogens will be explained by the ring current effect similar to that of natpthalene but it is somewhat larger than that of naphthalene.[4] Therefore the whole part of the difference can not be explained by only the ring current effect. The chemical shift of the 7-hydrogen is larger than that of the 4-hydrogen. This may be due to the magnetic anisotropy or electronic effect of the sulfur atom. Approximate values of the coupling constants between ring hydrogens for deuterothianaphthenes are following: $J_{23}=5._5$, $J_{26}=0.5$, $J_{37}=0.7_5$, $J_{45}=J_{67}=8._0-7._5$, $J_{56}=7._5-7._0$, $J_{46}=J_{57}=1._5-1._0$, $J_{47}=0.7$ c. p. s. respectively. Some of the coupling constants were determined only approximately because of the broadness of the lines caused by the interaction with the deuterium.

1) K. Takahashi, T. Kanda and Y. Matsuki, This Bulletin, **37**, 768 (1964).
2) K. Takahashi, T. Kanda, F. Shoji and Y. Matsuki, ibid., **38**, 508 (1965).
3) K. Takahashi, T. Kanda and Y. Matsuki, This Bulletin, **38**, 1799 (1965).
4) N. Jonathan, S. Gordon and B. P. Dailey, *J. Chem. Phys.*, **36**, 2443 (1962); B. P. Dailey, ibid., **41**, 2304 (1964).

BULLETIN OF THE CHEMICAL SOCIETY OF JAPAN VOL. 39 2317—2320 (1966)

The Lifetime of Excimer Fluorescence of Naphthalene

By Tohru AZUMI* and Hiroshi AZUMI

Department of Chemistry, Faculty of Science, Tohoku University, Katahira-cho, Sendai

(Received December 6, 1965)

The radiative lifetimes of the excimer fluorescence of naphthalene are calculated for excimers of various geometrical configurations. The results vary, to a great extent, with the configurations, but with a previously-suggested configuration the calculated lifetime is 6×10^{-6} sec. This is within a factor of 5 of the experimental results.

The lifetime of the excimer fluorescence has been a subject of dispute for a long time. Williams,[1] in an attempt to interpret the delayed fluorescence he observed from the vapor of several aromatic compounds, assumed the production of an excimer, which, after several milliseconds, dissociates into a monomer ground-state molecule and a monomer excited-state molecule. This idea was also incorporated by Stevens, Hutton, and Porter[2] in their interpretation of the delayed fluorescence of phenanthrene species observed from anthracene vapor. These interpretations received some support from the theoretical considerations of Hoijtink,[3] who showed that if the excimer has center of symmetry, excimer luminescence is forbidden and that, hence, apart from radiationless conversion to the ground state, the only way of losing its excess energy is the dissociation to monomers. However, this simple treatment does not satisfactorily explain the fact that excimer fluorescence is indeed observed for a number of molecules. Questions have, therefore, arisen as to whether the excimer fluorescence is a dipole-allowed transition or an environmentally-allowed forbidden transition. Azumi and McGlynn[4] observed delayed excimer fluorescence in rigid glass media, and, in view of their experimental evidence, interpreted this duration as being due to the inherent forbidden character of excimer luminescence. Later work by Smith and McGlynn,[5] however, revealed that the delayed excimer luminescence is due to an excimer produced by triplet-triplet annihilation; namely, the duration of the excimer luminescence is ascribed to the delay in the production of excimer species, and not to the delay in the luminescence itself. In addition to these studies, recent studies of delayed fluorescence have thrown some doubt on the earlier interpretations given by Williams[1] and by Stevens et al.[2] As Azumi and McGlynn[6] suggested, the vapor-delayed fluorescence reported by these researchers might also be interpreted in terms of triplet-triplet annihilation, in which case there is no necessity of assuming any excimer formation. In this way it became questionable whether an excimer of a long duration really exists or not. Things have, however, become clearer since excellent lifetime measurements of excimer fluorescence were reported by Birks, Dyson, and King.[7] The resluts show that the lifetime of excimer fluorescence is quite short—in fact, shorter than the lifetime of normal monomer fluorescence.

In a previous paper[8] the present authors calculated the energy of the excimer luminescence of naphthalene with a variety of geometrical configurations. Starting from the excimer of such a configuration that one of the molecules which constitute an excimer is exactly superposed, at some distance, over the other, the authors examined the effect of the rotation of one molecule with respect to the other on the energy of the excimer luminescence. The principal axes of the two molecules were kept common, and the intermolecular distance was chosen as 3 Å. The excimer configuration for which the calculations were carried out is schematically represented in Fig. 1. It was shown that excimer is stable when the angle, α, of rotation is 75 degrees; this configuration was proposed as the one responsible for excimer fluorescence.

In this paper, the radiative lifetime of naphthalene excimer fluorescence will be calculated for excimers of the same geometrical configurations as in the previous paper[8] (i. e., those represented in Fig. 1). It will also aim to check if the previously-developed

* Postdoctoral fellow supported by the Japan Society for the Promotion of Science.

1) R. Williams, *J. Chem. Phys.*, **28**, 577 (1958).
2) B. Stevens, E. Hutton and G. Porter, *Nature*, **185**, 917 (1960).
3) G. J. Hoijtink, *Z. Elektrochem.*, **64**, 156 (1960).
4) T. Azumi and S. P. McGlynn, *J. Chem. Phys.*, **39**, 3533 (1963).
5) F. J. Smith and S. P. McGlynn, ibid., **42**, 4308 (1965).
6) T. Azumi and S. P. McGlynn, ibid., **39**, 1186 (1963).
7) J. B. Birks, D. J. Dyson and T. A. King, *Proc. Roy. Soc.*, **A277**, 270 (1964).
8) T. Azumi and H. Azumi, This Bulletin, **39**, 1829 (1966).

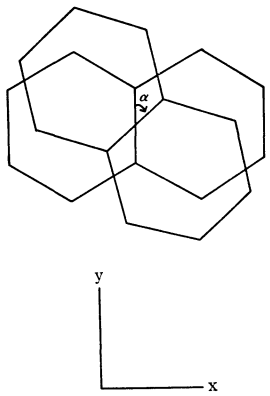

Fig. 1

model of an excimer, which gives satisfactory energy data, also gives reasonable lifetime data.

The Method of Calculation

The general scheme of calculation is identical to that developed in previous papers.[8,9] The highest-occupied and the lowest-vacant molecular orbitals of one ground state molecule (say, molecule A) are designated, respectively, as ϕ_1 and ϕ_2, and the corresponding orbitals of the other molecule (say, molecule B), as θ_1 and θ_2. ϕ_1 and ϕ_2 are orthogonal, as are also θ_1 and θ_2. It is assumed that an orthogonality exists between ϕ_1 and θ_2 and between θ_1 and ϕ_2. The overlap integral between ϕ_1 and θ_1 is designated by S_1.

Wave Functions.—The dimeric wave function for the ground state is:

$$|G\rangle = (1 - 2S_1^2 + S_1^4)^{-1/2}|\phi_1\bar{\phi}_1\theta_1\bar{\theta}_1| \quad (1)$$

The wave function for the excimer state is expressed as a linear combination of four zeroth-order wave functions:

$$|E\rangle = a\psi_A + b\psi_B + c\psi_C + d\psi_D \quad (2)$$

where:

$$\psi_A = \{2(1-S_1^2)\}^{-1/2}\{|\phi_1\bar{\phi}_1\theta_1\bar{\theta}_2| + |\phi_1\bar{\phi}_1\theta_2\bar{\theta}_1|\} \quad (3)$$

$$\psi_B = \{2(1-S_1^2)\}^{-1/2}\{|\phi_1\bar{\phi}_2\theta_1\bar{\theta}_1| + |\phi_2\bar{\phi}_1\theta_1\bar{\theta}_1|\} \quad (4)$$

$$\psi_C = \{2(1-S_1^2)\}^{-1/2}\{|\phi_1\bar{\theta}_2\theta_1\bar{\theta}_1| + |\theta_2\bar{\phi}_1\theta_1\bar{\theta}_1|\} \quad (5)$$

$$\psi_D = \{2(1-S_1^2)\}^{-1/2}\{|\phi_1\bar{\phi}_1\phi_2\bar{\theta}_1| + |\phi_1\bar{\phi}_1\theta_1\bar{\phi}_2|\} \quad (6)$$

The mixing coefficients, a, b, c, and d, at different α values were evaluated in a previous paper[8]; they are tabulated in Table I of Ref. 8.

9) T. Azumi, A. T. Armstrong and S. P. McGlynn, *J. Chem. Phys.*, **41**, 3839 (1964).

Transition Moment.—The transition moment length for the excimer luminescence is expressed as:

$$\begin{aligned}\mu_E &= \langle G|\boldsymbol{R}|E\rangle \\ &= \{2(1 - S_1^2)/(1 - 2S_1^2 + S_1^4)\}^{1/2} \\ &\quad \times [\langle\phi_1|\boldsymbol{R}|\phi_2\rangle\{(a + b) - S_1(c + d)\} \\ &\quad + \langle\phi_1|\boldsymbol{R}|\theta_2\rangle\{(c + d) - S_1(a + b)\}]\end{aligned} \quad (7)$$

μ_E is calibrated by taking the experimental transition moment length for the monomer ^{1}A-^{1}L$_a$ transition, μ_M, as a standard, so that the correct transition moment be obtained at an infinite separation of the two molecules. A theoretical evaluation of μ_M yields:

$$\mu_M = \sqrt{2}\,\langle\phi_1|\boldsymbol{R}|\phi_2\rangle \quad (8)$$

μ_E is then calculated by the equation:

$$\begin{aligned}\mu_E = \mu_M^{exp}&\{(1-S_1^2)/(1-2S_1^2+S_1^4)\}^{1/2} \\ &\times[(a+b)-S_1(c+d)+\{(c+d)- \\ &S_1(a+b)\}\langle\phi_1|\boldsymbol{R}|\theta_2\rangle/\langle\phi_1|\boldsymbol{R}|\phi_2\rangle]\end{aligned} \quad (9)$$

where μ_M^{exp} is the experimental transition moment length for the monomer ^{1}A-^{1}L$_a$ absorption and has the value:

$$\mu_M^{exp} = 0.6923\,\text{Å} \quad (10)$$

The lifetime of the excimer luminescence is then evaluated by the equation:

$$\tau_E = \frac{3h}{64\pi^4\tilde{\nu}^3e^2\mu_E^2} \quad (11)$$

MO Integrals in Terms of AO Integrals.—The MO overlap integral, S_1, is evaluated by:

$$S_1 = \sum_r\sum_s C_{r1}C_{s1}\langle r_A \mid s_B\rangle \quad (12)$$

where C_{r1} is the Hückel coefficient of the atomic orbital, r, in ϕ_1, $\langle r_A|s_B\rangle$ is the overlap integral between the atomic orbital, r, in the A molecule and the atomic orbital, s, in the B molecule, it is evaluated by the formulas given by Parr and Crawford.[10]

The intermolecular transition moment length $\langle\phi_1|\boldsymbol{R}|\theta_2\rangle$ is expressed as:

$$\langle\phi_1|\boldsymbol{R}|\theta_2\rangle = [\langle\phi_1|\boldsymbol{x}|\theta_2\rangle^2+\langle\phi_1|\boldsymbol{y}|\theta_2\rangle^2]^{1/2} \quad (13)$$

where x and y axes are along the long and short axes of one molecule, as are shown in Fig. 1. The z axes component need not be considered, since the group theoretical treatment[11] shows that the excimer fluorescence is invariably polarized in-plane when the principal axes of the two molecules which constitute an excimer are common. The x component is further expressed in the following way:

10) R. G. Parr and B. L. Crawford, ibid., **16**, 1049 (1948).

11) T. Azumi and S. P. McGlynn, ibid., **42**, 1675 (1965).

$$\langle\phi_1|\boldsymbol{x}|\theta_2\rangle = \sum_r\sum_s C_{r1}C_{s2}\langle r_A|\boldsymbol{x}|s_B\rangle$$
$$= (1/2)\sum_r\sum_s C_{r1}C_{s2}\langle r_A|s_B\rangle$$
$$\times\{x(r_A) + x(s_B)\} \quad (14)$$

where C_{s2} is the Hückel coefficient of atomic orbitals in ϕ_2 (or θ_2), and where $x(r_A)$ and $x(s_B)$ are the x coordinates of r_A and s_B respectively. Here, the center of the naphthalene molecule is taken as the origin of the coordinate, and axes are chosen along the molecular axes of the A molecule (Fig. 1). Then,

$$x(s_B) = \cos\alpha\, x(s_A) + \sin\alpha\, y(s_A) \quad (15)$$

Consequently,

$$\langle\phi_1|\boldsymbol{x}|\theta_2\rangle = (1/2)\sum_r\sum_s C_{r1}C_{s2}\langle r_A|s_B\rangle$$
$$\times\{x(r_A)+\cos\alpha x(s_A)+\sin\alpha y(s_A)\} \quad (16)$$

The y component is obtained similarly:

$$\langle\phi_1|\boldsymbol{y}|\theta_2\rangle = (1/2)\sum_r\sum_s C_{r1}C_{s2}\langle r_A|s_B\rangle$$
$$\times\{y(r_A)-\sin\alpha x(s_A)+\cos\alpha y(s_A)\} \quad (17)$$

The intramolecular transition moment, $\langle\phi_1|\boldsymbol{R}|\phi_2\rangle$, in Eq. 9 is similarly obtained; the result is:

$$\langle\phi_1|\boldsymbol{R}|\phi_2\rangle = 0.8137\,\text{Å} \quad (18)$$

Results and Discussion

The calculated lifetimes at different configurations are shown in Table I. The only results of any physical significance are those around the stable configurations, $\alpha=75°$ and $\alpha=0°$. The excimer is most unstable around $30°<\alpha<50°$ (see Fig. 4 of the previous paper[8]); the calculated values in Table I for such unstable configurations are those of virtual states and are thus, in fact, meaningless. The fact that quite unreasonable data are obtained around $30°<\alpha<50°$ configurations of the excimer is consistent with the potential energy diagram obtained in the previous paper. At the previously suggested stable configuration, $\alpha=75°$, the calculated lifetime is 6.3×10^{-6} sec.

The lifetimes of the naphthalene excimer fluorescence recently observed by Mataga, Tomura, and Nishimura[12] are $\sim10^{-7}$ sec, but the contribution of the radiative decay is unknown and a direct comparison with the calculated result is impossible. There are, unfortunately, no other experimental data on the lifetime of the naphthalene excimer. However, lifetime data for 1, 6-dimethylnaphthalene were obtained by Birks and King.[13]

Table I. Lifetimes of excimer fluorescence at variety of geometrical configurations

α	μ_E, Å	Lifetime, sec.
0	0	—
5	-2.69×10^{-2}	2.84×10^{-5}
10	-2.54×10^{-2}	3.18×10^{-5}
15	-2.29×10^{-2}	3.92×10^{-5}
20	-1.89×10^{-2}	5.75×10^{-5}
25	-1.31×10^{-2}	1.20×10^{-4}
30	-5.57×10^{-3}	6.61×10^{-4}
35	-1.57×10^{-5}	8.30×10
40	-8.63×10^{-3}	2.76×10^{-4}
45	-1.53×10^{-3}	8.77×10^{-3}
50	-5.88×10^{-3}	5.94×10^{-4}
55	2.83×10^{-3}	2.57×10^{-3}
60	1.58×10^{-2}	8.25×10^{-5}
65	2.97×10^{-2}	2.33×10^{-5}
70	4.35×10^{-2}	1.08×10^{-5}
75	5.71×10^{-2}	6.30×10^{-6}
80	7.17×10^{-2}	4.00×10^{-6}
85	9.49×10^{-2}	2.28×10^{-6}
90	5.91×10^{-1}	5.89×10^{-8}

Since the excimer fluorescence of dimethyl derivatives of naphthalene behaves quite like that of naphthalene,[14] it is reasonable to assume that the lifetime also does not differ much. Radiative rate parameters for the excimer fluorescence of 1, 6-dimethylnaphthalene[13] is $1.4\times10^6\,\text{sec}^{-1}$ in an n-heptane solution and $2.2\times10^6\,\text{sec}^{-1}$ in pure liquid. When calibration is made to a medium whose reflactive index is unity, the rate parameters are $0.73\times10^6\,\text{sec}^{-1}$ for the former, and $0.85\times10^6\,\text{sec}^{-1}$ for the latter. These data correspond to radiative excimer lifetimes in vacuo of $1.2-1.4\times10^{-6}$ sec. Hence, the lifetime calculated in this paper, 6.3×10^{-6} sec., is within a factor of 5 of the experimental value. The fairly good agreement with the experimental value is another support of the excimer configuration suggested in a previous paper.[8]

The above consideration is confined to the lifetime at one of the two stable configurations, i. e., $\alpha=75°$. We have disregarded the lifetime at the other stable configuration, i. e., at $\alpha=0°$, since excimer luminescence is forbidden there. It might be argued that the allowed component may arise by the thermal motion of the two molecules of the excimer. In order to check this, let the thermal motion be confined to the thermal vibration needed to change the angle, α. It may then be seen, from the energy data given in the previous paper, that the α which can be changed by the energy of the thermal motion, $1.5kT=0.04$eV., is approximately 5°. Even though there is a considerable increase in the transition probability for this change of α, the calculated lifetime

12) N. Mataga, M. Tomura and H. Nishimura, *Mol. Phys.*, **9**, 367 (1965).
13) J. B. Birks and T. A. King, *Proc. Roy. Soc.*, **A291**, 244 (1966).
14) J. B. Aladekomo and J. B. Birks, ibid., **A284**, 551 (1965).

at $\alpha=5°$ of 3×10^{-5} sec., which is 20 times larger than the experimental value, still can not account for the observed lifetime of the excimer fluorescence.

The present calculations were carried out for excimers in which the two molecular planes are parallel and which have principal axes in common. This is, in fact, rather a freakish situation. To treat the excimers of random orientations, however, is quite difficult, if not impossible, and, at any rate, beyond the range of the present paper. The present treatment may, therefore, only be considered as a prototype calculation. Our suggestion that the excimer of $\alpha=75°$ is responsible for the excimer fluorescence is valid only within the framework of the above specified model. The only conclusion of any general validity may be that the geometrical configuration of the excimer which is responsible for excimer fluorescence is definitely different from the one of the highest symmetry.

The numerical calculations were carried out on the NEAC 2230 at the Computation Center, Tohoku University.

The authors wish to express their appreciation to Dr. John B. Birks of Manchester University for valuable discussions and for supplying them his lifetime data prior to publication. They are also indebted to Dr. Yoshito Amako for fruitful discussions.

BULLETIN OF THE CHEMICAL SOCIETY OF JAPAN VOL. 39 2320—2322 (1966)

The Electronic Spectra of 1, 1'-Dianthrylpoly-ynes[1)]

By Kichisuke NISHIMOTO*

Mellon Institute, Pittsburgh, Pa., U. S. A.

and Ryoichi FUJISHIRO

Department of Chemistry, Faculty of Science, Osaka City University, Sumiyoshi-ku, Osaka

and Shuzo AKIYAMA and Masazumi NAKAGAWA

Department of Chemistry, Faculty of Science, Osaka University, Toyonaka, Osaka

(Received January 18, 1966)

The electronic spectra of 1, 1'-dianthrylpoly-ynes have been studied by Hückel MO theory on the basis on various approximations for resonance integrals. A good agreement between theoretical and experimental values is obtained from a modified bond-alternation approximation. This result shows that the contribution of a cumulene-type ionic structure to the ground state of the molecule increases with an increase in the number of the triple bonds.

Recently, two of the present authors (S. A. and M. N.)[2)] found a peculiar spectral shift in the electronic absorption spectra of 1, 1'-dianthryl-poly-ynes (I). In this series, the maxima of the longest wave length absorptions increase linearly with the square of the number of the triple bonds. This fact forms a striking contrast to a well-known spectral shift in the series of linear polyenes or linear poly-ynes, in which the square of the absorption maxima, λ^2_{max}, varies linearly with the number of the conjugated multiple bonds.[3,4)] In order to elucidate this interesting spectral shift, we have carried out some MO calculations of the electronic structure of 1, 1'-dianthrylpoly-ynes.

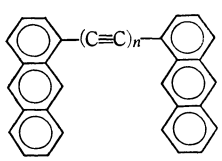

(I)

Calculation

The calculations were carried out in the framework of the Hückel MO theory. All interpretations of the spectra of polyenes by the wave-mechanical method have hitherto required that there should be an alternation of double and single

1) Presented at the Symposium on Molecular Structure and Spectroscopy, The Ohio State University, Columbus, U. S. A., June 15—19, 1964.

* Present address: Department of Chemistry, Faculty of Science, Osaka City University, Sumiyoshi-ku, Osaka.

2) S. Akiyama and M. Nakagawa, *Tetrahedron Letters*, No. **13**, 719 (1964).

3) F. Bohlmann, *Angew. Chem.*, **65**, 385 (1953).

4) J. B. Armitage, N. Entwistle, E. R. H. Jones and M. C. Whiting, *J. Chem. Soc.*, **1954**, 147.

bonds along the polyene chain.[5-9] This requirement is most important for the interpretation of the spectra of poly-ynes. It is, however, desirable to carry out calculations on the basis on the following approximations: All conventional Coulomb integrals are assigned the same value, α. According to the study by Hinze and Jaffe,[10] the valence-state electronegativity of the carbon π-orbital is practically independent of its hybridization, so the constant Coulomb integral approximation is reasonable. The resonance integral associated with the aromatic carbon-carbon bond is assigned a constant value, β. On the other hand, there is at present no definite method for the estimation of the resonance integrals associated with a triple and a single bond of the polyacetylene system. In this paper, the following approximations will tentatively be used;

I Constant β approximation

$$\beta_{C\equiv C} = \beta_{C-C} = 1.0\,\beta$$

II Bond alternation 1

$$\beta_{C\equiv C} = 1.1\,\beta,\ \beta_{C-C} = 0.9\,\beta$$

III Bond alternation 2

$$\beta_{C\equiv C} = 1.2\,\beta,\ \beta_{C-C} = 0.8\,\beta$$

IV Modified bond alternation

$$\beta_{C\equiv C} = (1 + 1/(n+4))\beta$$

$$\beta_{C-C} = (1 - 1/(n+4))\beta$$

Approximation I is most usual. Approximation II is suitable for polyenes.[11] The value of 1.2β in Approximation III was estimated for acetylene from an empirical relation.[12] Approximation IV is proposed with the following points in mind; for 1, 1'-dianthrylpoly-yne, we can write down twenty-five cumulene-type ionic structures (II), in which the formal charges move in the anthracene nuclei:

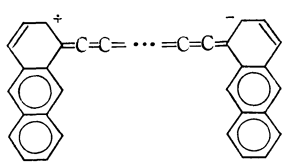

(II)

In structure I, the bond alternation in poly-yne chain might be present. However, a rather uniform electron distribution may be expected in the cumulene chain in structure II. Therefore, the energy difference between the structure I and a given cumulene-type ionic structure may be given by;

$$\Delta E = I_C - A_C - n\Delta\gamma + C$$

where I_C and A_C are the ionization potential and the electron affinity of the carbon atom respectively. The core energy difference between the two structures is included in the correction term, C. $\Delta\gamma$ measures the energy difference between the electron repulsions in a classical triple bond, γ_t, and those in a cumulene-type bond, γ_c. It is natural that γ_t should be larger than γ_c, because in the classical triple bond the four electrons are packed in a small space. Therefore, the contributions of the cumulene-type ionic structures to the ground state of the molecule would increase with the number of the triple bonds, n, because the energy difference between the ionic and the non-ionic structures decreases with n. This situation might be characteristic of a poly-yne system. In order to take this situation into account, the values of $\beta_{C\equiv C}$ and β_{C-C} are varied with n, The longest-wavelength absorption in anthracene is polarized in the direction of the molecular short axis (^1L_a species).[13] Similarly, the absorptions of poly-ynes are also polarized in this direction. It is, therefore, reasonable to assign the longest-wavelength absorption of 1, 1'-dianthrylpoly-yne to the ^1L_a species. The absorption wavelengths of a conjugated system can be calculated by the Hückel MO theory, using very simple correlation equations.[12] The equation for the ^1L_a species is expressed by;

$$\lambda(^1L_a) = 474(\Delta m)^{-1/2} - 145\ m\mu$$

where $\lambda(^1L_a)$ is the absorption wavelength. Δm is the energy difference expressed in β between the highest-occupied and the lowest-vacant orbitals of the molecule. The calculated $\lambda(^1L_a)$'s for the various approximations are given in Table I and in Fig. 1, together with the experimental values.

Table I. Calculated and observed absorption wavelengths of 1,1'-dianthrylpoly-ynes

n	$\lambda(^1L_a)$ in mμ Approximation I	II	III	IV	Obs.[2]
1	490	468	430	430	—
2	531	466	427	437	428
3	573	476	424	449	437
4	616	486	421	465	450
5	658	495	419	483	466
6	699	503	418	503	487
7	—	—	416	525	—

5) S. F. Mason, *Quart. Revs.*, **15**, 287 (1961).
6) H. Labhart, *J. Chem. Phys.*, **27**, 957, 963 (1957).
7) M. Tsuji, S. Fujinaga and T. Hashino, *Rev. Modern Phys.*, **32**, 425 (1960).
8) Y. Ooshika, *J. Phys. Soc. Japan*, **12**, 1238, 1246 (1957).
9) H. C. Longuet-Higgins and L. Salem, *Proc. Roy. Soc.*, **A251**, 172 (1959); **A257**, 445 (1960).
10) J. Hinze and H. H. Jaffe, *J. Am. Chem. Soc.*, **84**, 540 (1962).
11) A. Streitwieser, Jr., "Molecular Orbital Theory for Organic Chemists," John Wiley & Sons, New York (1961), p. 135.
12) K. Nishimoto, This Bulletin, **39**, 645 (1966).
13) K. Nishimoto and L. S. Forster, *Theor. Chim. Acta (Berl.)*, **3**, 407 (1965).

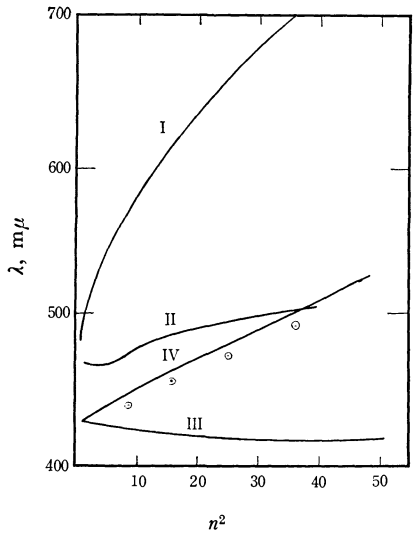

Fig. 1. The predicted and observed absorption wavelengths in the 1-1'-dianthrylpoly-ynes.

As Fig. 1 shows, the calculated results based on Approximation IV and the experimental data agree well. It should be noted that Approximation III leads to the very strange result that the $\lambda(^1L_a)$ value should decrease with n.

Conclusion

The present study has shown that the interpretation of the peculiar spectral shift in a series of 1, 1'-dianthrylpoly-ynes in the visible region requires a modified bond-alternation approximation which assumes that the contribution of cumulene-type ionic structures to the ground state of the molecule increases with an increase in the number of triple bonds. All other approximations give unsatisfactory results.

We are grateful to Professor Kenzo Jo of Osaka University for providing machine time of the NEAC 2203 there. One of authors (K. N.) wishes also to acknowledge the most generous financial support of the Mellon Institute.

BULLETIN OF THE CHEMICAL SOCIETY OF JAPAN VOL. 39 2322—2331 (1966)

The Crystal and Molecular Structure of 8, 8-Dicyanoheptafulvene

By Hirotaka SHIMANOUCHI,* Tamaichi ASHIDA, Yoshio SASADA and Masao KAKUDO

Institute for Protein Research, Osaka University, Kita-ku, Osaka

and Ichiro MURATA and Yoshio KITAHARA

Department of Chemistry, Faculty of Science, Tokoku University, Katahira-cho, Sendai

(Received February 3, 1966)

Crystals of 8, 8-dicyanoheptafulvene, $C_{10}H_6N_2$, are monoclinic, with two molecules in a unit cell with the dimensions $a=7.84$, $b=13.14$, $c=3.99$ Å, and $\beta=97.9°$; the space group is $P2_1/m$. The intensities were recorded on multiple-film equi-inclination Weissenberg photographs and measured visually against a standard scale. A trial structure was constructed from the Patterson projections, $P(u, v)$ and $P(u, w)$, and a Harker section, $P(u, 1/2, w)$. The atomic coordinates and anisotropic temperature factors were refined by the least-squares method. The final R factor for (hkl) reflections is 0.107. A considerable bond alternation in the conjugated seven-membered ring has been observed. The average long and short bond lengths in the ring are 1.44 and 1.34 Å respectively. The shortest C=C bond measures 1.31 Å, which is shorter than that in ethylene. The exocyclic C=C bond length is 1.42 Å, suggesting a considerable dipolar resonance structure, one which may be responsible for the stability of the compound. The C≡N bond length is 1.13 Å. The molecule deviates slightly from being planar; it lies nearly parallel to the (101) plane. All the intermolecular separations correspond to normal van der Waals interactions; the perpendicular distance between the molecular planes is 3.4 Å. The thermal motion was interpreted in terms of rigid body vibrations, and the bond lengths and angles were corrected for the rotational oscillations.

Recently 8, 8-dicyanoheptafulvene $C_{10}H_6N_2$ (I), a derivative of the non-alternant hydrocarbon

* On leave from Department of Chemistry, Faculty of Science, Tohoku University.

heptafulvene, has been synthesized in several laboratories.[1-3]

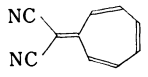

I

While heptafulvene itself decomposes at room temperature and cannot be isolated,[4] this derivative is very stable at temperatures up to 300°C, and reacts neither with dienophiles nor with electrophilic reagents. It will be interesting to ascertain the structural basis of this high stability. The present work has been underatken out of our general concern with the molecular geometry of aromatic seven-membered ring compounds, which should give fundamental information for investigating quantitatively the physical and chemical properties of such systems.

A preliminary report on the structure has already been published.[5]

Experimental

8, 8-Dicyanoheptafulvene (I) was prepared by the method given by Kitahara and Doi (1959).[6] It crystallizes from a methanol solution in the form of red needles elongated along the c axis.

The crystallographic and physical data obtained are: 8, 8-Dicyanoheptafulvene $C_{10}H_6N_2$, m. p. 199—200°C; Monoclinic, $a=7.84$ Å, $b=13.14$ Å, $c=3.99$ Å, and $\beta=97.9°$. Absent spectra, $(0k0)$ when k is odd. Space group, $P2_1$ or $P2_1/m$. Two molecules per unit cell. Volume of the unit cell; 407.1 Å^3 Density (by flotation); 1.27_2 g. cm^{-3}. Density (calculated); 1.26_4 g. cm^{-3}. Linear absorption coefficient for Cu$K\alpha$ radiation; $\mu=6.31$ cm^{-1}. Total number of electrons per unit cell; $F(000)=160$.

Equi-inclination Weissenberg photographs for 0—3 layers were taken around the c axis, using Cu$K\alpha$ radiartion at room temperature. Precession photographs for $(h0l)$ zone were also taken, using Cu$K\alpha$ and Mo$K\alpha$ radiations, in order to determine the relative scales among the layers. The crystal used was square in cross-section, with rectangular dimensions: 0.02×0.01 cm.

Intensities were estimated by visual comparison with a standard scale prepared with the same crystal. The multiple-film technique was applied to correlate strong and weak reflections, ranging in relative intensity from 10000 to 1. Reflections from 514 planes were observed out of 930 accessible (hkl)'s. The corrections for Lorentz and polarization factors were made in the usual way, while that for absorption was omitted. Tentative scale and temperature factors were obtained by Wilson statistics,[7] the latter being $B=2.0$ Å.^{2}

Structure Determination

The sharpened Patterson projection, $P(u, v)$, shown in Fig. 1, was calculated with the relative intensities of 100 observed $(hk0)$ reflections. A planar molecular model was set up by assuming plausible bond distances and angles, the hydrogen atoms being ignored. The molecular orientation was obtained by seeking the best fit of the intramolecular vector sets with the Patterson function. The long axis of the molecule is perpendicular to the b axis, and the molecule lies nearly parallel to the (101) plane. Vector sets at the best fit are indicated by the spots in Fig. 1. This orientation was also supported by another Patterson projection, $P(u, w)$, shown in Fig. 2.

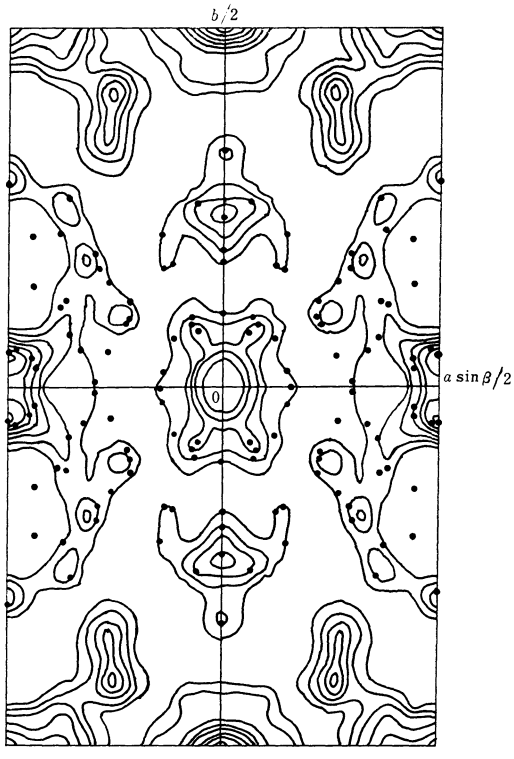

Fig. 1. Patterson projection $P(u, v)$. The contours are at equal arbitrary intervals and those at the origin are omitted. The spots show the intramolecular vector sets at the best fit.

If the space group is $P2_1$, the y coordinate of an atom can be arbitrarily chosen. Therefore, approximate y coordinates of the other atoms were

1) T. Nozoe, T. Mukai, K. Osaka and N. Shishido, This Bulletin, **34**, 1384 (1961).
2) K. Hafner, H. W. Riedel and M. Danielisz, *Angew. Chem.*, **75**, 344 (1963); *Angew. Chem. internat. Edit.*, **2**, 215 (1963).
3) C. Jutz, *Chem. Ber.*, **97**, 2050 (1964).
4) W. v. E. Doering and D. W. Wiley, *Tetrahedron*, **11**, 183 (1960).
5) H. Shimanouchi, T. Ashida, Y. Sasada, M. Kakudo, I. Murata and Y. Kitahara, This Bulletin, **38**, 1230 (1965).
6) Y. Kitahara and K. Doi, ibid., to be published.
7) A. J. C. Wilson, *Nature*, **150**, 152 (1942).

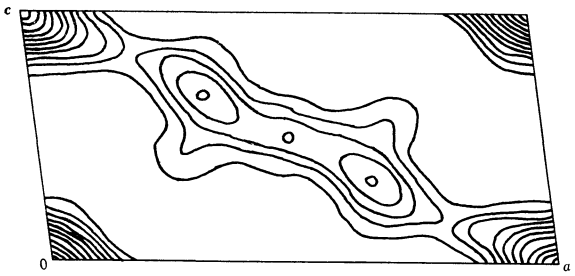

Fig. 2. Patterson projection $P(u, w)$. The contours are at equal arbitrary intervals.

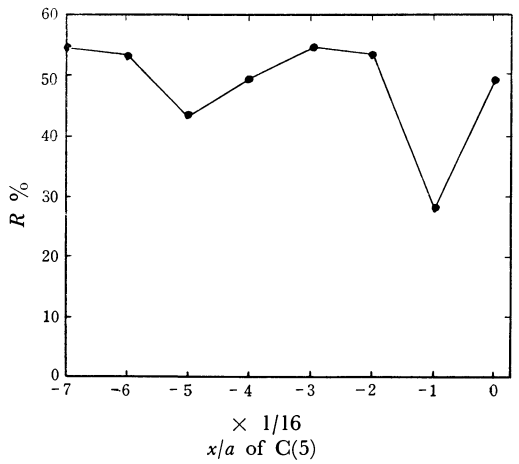

Fig. 3. One dimensional R map computed with all $(hk0)$ reflections.

given by the model. The x coordinates were obtained by a one-dimensional minimum residual calculation,[8] where the discrepancy factor, $R=\Sigma||F_o|-|F_c||/\Sigma|F_o|$, was computed for all $(hk0)$ reflections. Figure 3 shows the variation of R against the x coordinate of the reference atom, C(5). The first electron density projection, $\rho(x, y)$, was computed with phases based on these parameters. It clearly showed a definite molecular shape, without any ghost peaks. The atomic coordinates read off from the Fourier synthesis were refined by the block-diagonal matrix least-squares method. After five cycles of the refinement, the R factor reached 0.078 for the observed reflections. The atomic arrangement in the unit cell thus obtained suggested the existence of a mirror plane perpendicular to the b axis, within the limits of error. Moreover, the pyroelectricity test and the statistical investigation of the intensity data,[9] $|F_o(hk0)|^2$'s and $|F_o(hk1)|^2$'s respectively, showed that the crystal should be centrosymmetrical. Therefore, the space group of this crystal was chosen to be $P2_1/m$ for the subsequent studies.

8) A. K. Bhuiya and E. Stanley, *Acta Cryst.*, **17**, 746 (1964).
9) E. R. Howells, D. C. Phillips and D. Rogers, ibid., **3**, 210 (1950).

In order to obtain the z coordinates, a sharpened Harker section, $P(u, 1/2, w)$, was calculated, as is shown in Fig. 4. There were two rows of peaks parallel to the (101) plane. The high peaks near the c axis were interpreted as follows. If the y coordinates of the two atoms are euqal, the non-Harker peak due to these atoms should be placed at the midpoint of their Harker peaks and be doubly weighted.[10] In the tentative structure of 8, 8-

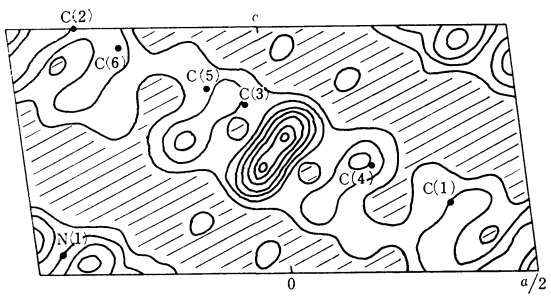

Fig. 4. Harker section $P(u, 1/2, w)$. The contours are at equal arbitrary intervals. The region lower than the starting contour is indicated by oblique lines. The spot shows the position of the expected Harker peak of each atom.

dicyanoheptafulvene, there were three pairs of atoms at the same y level; i. e., C(4) and C(5), C(1) and C(6), and C(1′) and C(6′), their corresponding Harker peaks being indicated by the spots in Fig. 4. The non-Harker peaks due to these atoms pairs were situated at nearly the same position and gave the considerably high peaks mentioned above.

The coordinates thus obtained were then refined by the block-diagonal matrix least-squares method with anisotropic temperature factors, all (hkl) reflections being used. The parameters of the hydrogen atoms were also refined; they were first located at a distance of 1.0 Å outward radially

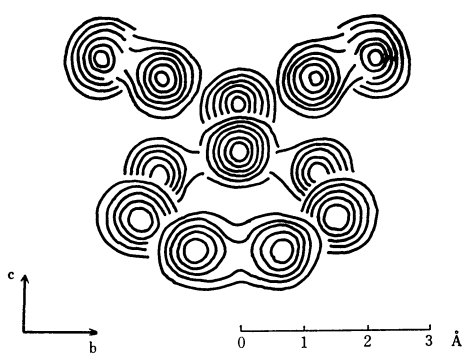

Fig. 5. Composite electron density diagram of sections parallel to (100). The contours are at intervals of 1.0 e.Å^{-3} starting with 2.0 e.Å^{-3}.

10) G. Albrecht and R. B. Corey, *J. Am. Chem. Soc.*, **61**, 1087 (1939).

TABLE I. OBSERVED AND CALCULATED STRUCTURE FACTORS

H	10FO	10FC
K,L=	0,	0
1	202	177
2	212	-196
3	316	-292
4	126	-109
5	19	8
6	42	46
7	23	28
8	51	-49
9	16	9
K,L=	1,	0
1	152	-137
2	244	233
3	110	-88
4	14	12
5	0	-2
6	67	60
7	35	-29
8	16	13
9	25	21
K,L=	2,	0
0	370	-408
1	69	-55
2	251	-229
3	92	76
4	88	82
5	61	51
6	23	22
7	20	-29
8	25	17
9	0	-2
K,L=	3,	0
1	109	108
2	103	105
3	31	-22
4	183	-178
5	56	43
6	0	7
7	29	-18
8	30	-24
9	0	-1
K,L=	4,	0
0	288	-305
1	15	4
2	326	309
3	103	91
4	31	30
5	37	-40
6	109	-101
7	31	-29
8	0	7
9	0	8
K,L=	5,	0
1	145	135
2	55	-47
3	97	-90
4	0	2
5	13	14
6	57	58
7	55	49
8	0	-0
9	22	-22
K,L=	6,	0
0	0	-8
1	82	-74
2	10	6
3	75	-60
4	85	-79
5	0	3
6	78	70
7	65	67
8	0	6
K,L=	7,	0
1	28	-21
2	19	4
3	26	18
4	68	66
5	55	-47
6	48	-52
7	19	-22
8	0	0
K,L=	8,	0
0	49	50
1	78	71
2	0	-11
3	73	65
4	19	-24
5	57	-54
6	0	10
7	15	-13
8	0	-7
K,L=	9,	0
1	103	-100
2	26	-28
3	78	74
4	0	0
5	37	32
6	16	-19
7	0	-4
8	18	17

H	10FO	10FC
K,L=	10,	0
0	90	-84
1	93	-89
2	0	7
3	14	19
4	66	62
5	26	25
6	30	-31
K,L=	11,	0
1	20	-25
2	0	8
3	18	-13
4	0	-0
5	16	-18
6	14	11
K,L=	12,	0
0	82	73
1	78	78
2	14	-13
3	55	-57
4	19	-19
5	17	12
K,L=	13,	0
1	42	37
2	0	-7
3	0	-4
4	0	3
5	0	4
K,L=	14,	0
0	13	10
1	17	-16
2	27	-27
3	17	-14
4	0	0
5	14	15
K,L=	15,	0
1	14	16
2	0	5
3	0	-9
4	8	-6
K,L=	16,	0
0	13	-8
1	0	-5
2	27	18
K,L=	0,	1
0	53	68
1	490	-473
2	0	-23
3	167	173
4	0	1
5	0	11
6	13	10
7	18	22
8	32	-27
-1	192	-219
-2	242	250
-3	126	121
-4	24	-24
-5	132	-140
-6	24	16
-7	34	40
-8	52	-45
K,L=	1,	1
0	165	-250
1	687	-697
2	28	-26
3	26	-25
4	124	136
5	35	47
6	16	15
7	21	-30
8	0	-4
-1	147	151
-2	177	161
-3	152	136
-4	18	1
-5	19	15
-6	49	-60
-7	56	58
-8	0	6
-9	19	17
K,L=	2,	1
0	147	-137
1	153	134
2	65	71
3	38	41
4	26	-26
5	55	-69
6	0	3
7	13	-15
8	0	9
-1	140	127
-2	35	-42
-3	123	113
-4	54	-55
-5	0	-11
-6	15	14
-7	0	17
-8	29	29
K,L=	3,	1

H	10FO	10FC
0	27	27
1	109	-99
2	17	4
3	152	156
4	0	9
5	20	22
6	37	-47
7	25	-34
8	0	3
-1	399	374
-2	91	90
-3	148	-150
-4	32	-48
-5	73	-82
-6	0	7
-7	16	-13
-8	0	-3
K,L=	4,	1
0	16	-12
1	99	101
2	0	8
3	136	-135
4	0	-23
5	31	42
6	0	-0
7	34	39
8	31	27
-1	32	-39
-2	0	7
-3	142	-139
-4	29	32
-5	38	42
-6	43	-39
-7	29	-30
-8	0	11
K,L=	5,	1
0	29	25
1	100	88
2	72	-70
3	59	-59
4	24	-24
5	36	-42
6	0	14
7	43	44
8	0	18
-1	142	-134
-2	134	-127
-3	80	-89
-4	0	-3
-5	140	146
-6	109	117
-7	0	5
-8	21	-35
-9	17	-23
K,L=	6,	1
0	132	130
1	25	-14
2	42	-46
3	17	7
4	57	59
5	34	43
6	23	-27
7	47	-52
8	32	-34
-1	0	-9
-2	66	-64
-3	44	-43
-4	47	47
-5	56	68
-6	16	18
-7	0	-12
-8	16	-22
K,L=	7,	1
0	51	53
1	36	44
2	50	49
3	0	-12
4	40	39
5	0	-7
6	0	-8
7	0	-7
8	17	-16
-1	0	-17
-2	70	65
-3	87	87
-4	48	-50
-5	61	-63
-6	72	-71
-7	0	-15
-8	0	9
-9	14	20
K,L=	8,	1
0	27	32
1	11	-18
2	70	-76
3	0	6
4	0	5
5	0	-8
6	58	57
7	0	2

H	10FO	10FC
-1	45	41
-2	77	-83
-3	26	31
-4	13	-11
-5	23	-25
-6	0	3
-7	0	-14
-8	0	-3
K,L=	9,	1
0	97	-105
1	49	-54
2	20	-21
3	0	8
4	28	-31
5	40	44
6	0	13
7	0	-11
-1	25	-25
-2	0	4
-3	39	53
-4	86	88
-5	35	-47
-6	0	-18
-7	0	12
-8	27	32
K,L=	10,	1
0	0	-0
1	23	22
2	55	57
3	0	0
4	27	-32
5	18	-20
6	20	-19
7	14	18
-1	21	-22
-2	46	47
-3	16	-18
-4	0	9
-5	0	-7
-6	0	-1
-7	21	22
K,L=	11,	1
0	64	75
1	82	81
2	59	73
3	18	-23
4	25	-33
5	26	-27
-1	0	-1
-2	55	-64
-3	37	-42
-4	0	-8
-5	32	28
-6	0	-8
-7	0	-1
K,L=	12,	1
0	64	-73
1	0	-15
2	0	10
3	17	-0
4	0	14
-1	0	5
-2	32	33
-3	0	13
-4	18	-22
-5	0	-1
-6	0	-8
K,L=	13,	1
0	21	-23
1	29	-24
2	53	-49
3	0	-1
4	17	16
-1	15	-15
-2	15	17
-3	0	5
-4	0	0
-5	19	19
-6	21	21
K,L=	14,	1
0	12	8
1	0	-3
2	0	5
3	0	12
-1	0	0
-2	0	9
-3	0	10
-4	0	-5
K,L=	15,	1
0	0	4
1	16	-15
2	0	-4
3	21	20
-1	33	29
-2	38	51
-3	0	2
-4	17	-24
K,L=	16,	1
0	18	15
1	0	-6
-2	15	-17

H	10FO	10FC
K,L=	0,	2
0	145	177
1	441	-411
2	231	-235
3	14	-6
4	20	-17
5	52	68
6	15	22
7	0	5
-1	48	52
-2	49	57
-3	20	-7
-4	64	72
-5	50	-60
-6	32	39
-7	29	32
-8	0	12
-9	27	27
K,L=	1,	2
0	57	44
1	19	11
2	254	262
3	0	9
4	19	-21
5	25	-35
6	15	-25
7	0	-9
-1	114	-116
-2	89	-74
-3	24	1
-4	49	60
-5	29	36
-6	52	-58
-7	47	46
-8	0	-9
-9	0	5
K,L=	2,	2
0	41	50
1	125	114
2	72	76
3	11	4
4	28	27
5	19	-26
6	0	3
7	18	-17
-1	24	-26
-2	171	-161
-3	15	-13
-4	37	-37
-5	31	37
-6	31	-38
-7	29	-34
-8	0	-11
-9	0	-1
K,L=	3,	2
0	101	-116
1	40	36
2	14	19
3	25	-23
4	68	-76
5	15	11
6	15	20
7	0	8
-1	39	-30
-2	79	-67
-3	39	46
-4	92	97
-5	35	-37
-6	29	-38
-7	0	-13
-8	32	30
-9	0	-3
K,L=	4,	2
0	156	-148
1	29	22
2	47	40
3	31	-31
4	23	-23
5	0	-5
6	15	-22
7	14	20
-1	120	-113
-2	60	60
-3	0	3
-4	80	90
-5	87	86
-6	30	28
-7	15	-21
-8	0	-14
-9	25	-17
K,L=	5,	2
0	47	52
1	42	46
2	59	-55
3	0	-2
4	47	49
5	22	27
6	12	10
7	12	-15
-1	0	-7

H	10FO	10FC
-2	58	62
-3	29	22
-4	26	-30
-5	0	-15
-6	0	5
-7	0	-8
-8	0	7
K,L=	6,	2
0	26	26
1	26	-24
2	0	7
3	33	37
4	0	6
5	0	6
6	0	-0
7	0	-2
-1	77	80
-2	118	115
-3	12	-13
-4	118	-135
-5	111	-128
-6	13	-17
-7	42	48
-8	25	29
K,L=	7,	2
0	21	23
1	34	-37
2	0	-14
3	20	-22
4	0	5
5	25	-25
6	0	-7
7	18	20
-1	22	-26
-2	0	1
-3	0	-1
-4	28	-32
-5	24	23
-6	0	9
-7	0	6
-8	16	-16
K,L=	8,	2
0	33	-30
1	57	-62
2	23	-28
3	0	6
4	0	-1
5	16	-17
6	16	21
7	0	6
-1	29	-26
-2	73	77
-3	24	15
-4	0	7
-5	16	24
-6	18	21
-7	27	-24
K,L=	9,	2
0	20	-22
1	0	9
2	30	34
3	48	49
4	0	-9
5	0	-4
6	19	-17
7	55	56
-1	15	-21
-2	34	-37
-3	47	38
-4	17	21
-5	0	1
-6	13	23
-7	0	-4
K,L=	10,	2
0	25	26
1	61	66
2	39	46
3	0	12
4	0	-11
5	0	-1
6	14	-16
-1	48	-49
-2	36	-39
-3	50	-51
-4	40	45
-5	14	16
-6	16	-18
-7	31	-33
K,L=	11,	2
0	0	2
1	52	-55
2	29	-30
3	25	-29
4	0	7
5	16	19
-1	22	27
-2	27	29
-3	0	-11
-4	0	-16
-5	0	7
K,L=	12,	2
0	0	-11

H	10FO	10FC
1	18	-13
2	47	-37
3	41	-40
-1	29	23
-2	18	13
-3	0	5
-4	0	-1
-5	29	27
K,L=	13,	2
0	0	6
1	39	34
-1	24	-18
-2	0	-1
-3	0	10
-4	0	-9
K,L=	14,	2
0	19	22
-1	12	12
-2	0	-1
-3	0	-13
-4	19	-21
K,L=	15,	2
-1	20	-25
K,L=	0,	3
0	51	-56
1	21	-22
2	70	64
3	135	154
4	0	0
5	0	-7
6	23	-28
-1	75	-75
-2	0	6
-3	27	29
-4	48	56
-5	77	-77
-6	31	25
-7	0	1
-8	14	-6
K,L=	1,	3
0	0	13
1	50	-30
2	94	94
3	21	17
4	0	1
5	0	4
6	0	-16
-1	49	-40
-2	12	-7
-3	56	-52
-4	20	17
-5	0	-0
-6	63	-58
-7	0	-6
-8	27	-24
K,L=	2,	3
0	0	1
1	33	-37
2	26	-23
3	61	-65
4	0	-11
5	0	-16
6	0	18
-1	54	41
-2	17	12
-3	47	38
-4	44	-42
-5	0	15
-6	0	-14
-7	30	22
-8	0	0
K,L=	3,	3
0	57	-52
1	38	-34
2	20	-22
3	0	-5
4	0	-9
5	0	5
6	0	2
-1	69	73
-2	0	5
-3	0	11
-4	48	37
-5	42	41
-6	24	21
-7	0	-13
-8	13	-8
K,L=	4,	3
0	38	33
1	70	72
2	0	-2
3	26	-26
4	19	16
5	36	32
6	0	2
-1	0	12
-2	0	-11
-3	42	-40
-4	24	-22
-5	20	17

H	10FO	10FC
-6	0	12
-7	16	-9
-8	14	12
K,L=	5,	3
0	69	63
1	30	30
2	28	-25
3	0	6
4	0	17
5	0	-4
6	0	-1
-1	28	24
-2	0	-1
-3	73	-75
-4	107	-101
-5	34	-32
-6	43	41
-7	27	24
-8	16	10
K,L=	6,	3
0	16	-19
1	16	-20
2	0	-17
3	0	7
4	0	-11
5	0	-12
6	14	-14
-1	41	-34
-2	0	-2
-3	26	30
-4	61	55
-5	16	13
-6	0	-11
-7	28	-26
K,L=	7,	3
0	16	-12
1	22	-25
2	0	-6
3	0	-8
4	0	1
-1	56	-51
-2	28	24
-3	80	71
-4	48	47
-5	18	20
-6	0	-13
K,L=	8,	3
0	24	22
1	0	-6
2	19	24
3	22	25
4	16	16
-1	0	8
-2	49	-45
-3	0	13
-4	0	-7
-5	0	0
-6	0	-9
K,L=	9,	3
0	34	-30
1	40	31
2	43	37
3	14	14
4	0	-11
-1	0	-3
-2	47	-37
-3	0	2
-4	30	18
-5	28	-29
-6	33	-30
K,L=	10,	3
0	0	10
1	0	-1
2	40	-35
3	37	-32
4	20	-22
-1	25	25
-2	40	27
-3	31	-30
-4	0	-5
-5	0	-9
K,L=	11,	3
0	0	13
1	0	-16
2	0	-11
3	24	-21
-1	0	11
-2	22	20
-3	15	-9
-4	0	4
-5	16	13
K,L=	12,	3
0	31	-25
1	14	10
2	31	24
-1	20	-16
-2	0	7
-3	0	8
-4	15	-14

from each carbon atom in the ring, with an isotropic temperature factor of 3.5 Å.[2] After five cycles of the refinement, the decreasing rate of the R factor seemed to slow down and no significant shifts in the parameters were observed. The final R factor reached 0.107 for the observed reflections. The atomic scattering factors for carbon and nitrogen given by Berghuis, Haanappel, Potters, Loopstra, MacGillavry and Veenendaal,[11] and for hydrogen given by McWeeny,[12] were used

11) J. Berghuis, IJ. M. Haanappel, M. Potters, B. O. Loopstra, C. H. MacGillavry and A. L. Veenendaal, *Acta Cryst.*, **8**, 478 (1955).

12) R. McWeeny, ibid., **4**, 513 (1951).

Table II. Final atomic coordinates and temperature factors

The anisotropic temperature factors are expressed in the form of $\exp-(B_{11}h^2+B_{22}k^2+B_{33}l^2+B_{12}hk+B_{13}hl+B_{23}kl)$

Atom	x	y	z	B_{11}	B_{22}	B_{33}	B_{12}	B_{13}	B_{23}
C(1)	0.16973	0.15379	0.15405	0.018504	0.006258	0.058048	−0.000558	0.015398	0.000036
C(2)	0.31773	0.13101	0.03132	0.023291	0.007359	0.076423	0.005206	0.008958	−0.006962
C(3)	0.44187	0.20011	−0.08203	0.018138	0.011003	0.067218	0.003689	0.022888	−0.005383
C(4)	0.09801	0.25000	0.22205	0.018590	0.005645	0.027213	0	0.006040	0
C(5)	−0.06160	0.25000	0.35357	0.020446	0.005034	0.057056	0	0.011879	0
C(6)	−0.14449	0.15722	0.44395	0.016152	0.006619	0.082259	0.004031	0.021257	−0.002280
N(1)	−0.20917	0.08564	0.51663	0.023228	0.006313	0.131942	−0.000560	0.046332	0.007021

Atom	x	y	z	B(Å^2)
H(1)	0.1153	0.0917	0.2180	2.97
H(2)	0.3355	0.0574	0.0294	4.72
H(3)	0.5398	0.1701	−0.1674	3.35

Table III. Estimated standard deviations ($\sigma(x)$,$\sigma(y)$ and $\sigma(z)$ in Å, $\sigma(B)$ in Å^2)

Atom	$\sigma(x)$	$\sigma(y)$	$\sigma(z)$	$\sigma(B_{11})$	$\sigma(B_{22})$	$\sigma(B_{33})$	$\sigma(B_{12})$	$\sigma(B_{13})$	$\sigma(B_{23})$
C(1)	0.0061	0.0066	0.0061	0.001286	0.000457	0.005195	0.001338	0.003935	0.002637
C(2)	0.0071	0.0074	0.0070	0.001516	0.000531	0.005990	0.001532	0.004656	0.003063
C(3)	0.0061	0.0075	0.0064	0.001388	0.000676	0.005924	0.001473	0.004333	0.003070
C(4)	0.0087	0	0.0080	0.001780	0.000587	0.006256	0	0.005013	0
C(5)	0.0092	0	0.0089	0.002017	0.000582	0.007830	0	0.006022	0
C(6)	0.0062	0.0069	0.0067	0.001179	0.000475	0.005949	0.001332	0.004128	0.002884
N(1)	0.0058	0.0059	0.0066	0.001329	0.000419	0.006627	0.001312	0.004744	0.002931

Atom	$\sigma(x)$	$\sigma(y)$	$\sigma(z)$	$\sigma(B)$
H(1)	0.055	0.063	0.060	1.55
H(2)	0.063	0.069	0.066	1.86
H(3)	0.057	0.060	0.058	1.63

throughout this structure determination. The observed and calculated structure factors are listed in Table I. The final atomic coordinates and the temperature factors are given in Table II, and their standard deviations, in Table III. The final three-dimensional electron-density distribution, calculated with signs based on these atomic coordinates, is shown in Fig. 5.

The computations were done on a NEAC 2101 computer in the Institute, with programs written by Takano and Nishi, and on an IBM 7090 computer through "UNICON" project, with programs written by one of the present authors (T. A.).

Discussion

Molecular Geometry.—The intramolecular bond lengths and angles are illustrated in Fig. 6 and are listed in Table IV.

All the bond distances in the dicyanomethylene group are nearly equal to those of the corresponding bonds in 7, 7, 8, 8-tetracyanoquinodimethane[13] (TCNQ) (C≡N=1.140 Å and C-C=1.441 Å). They slightly differ from those in pyridinium dicyanomethylide[14] (C≡N=1.13 Å and C-C=1.41Å), and TCNQ in a 1 : 1 complex of TCNQ

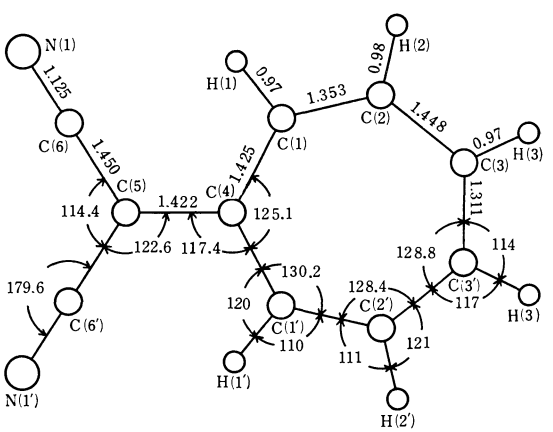

Fig. 6. Bond length (Å) and angles (degrees), without libration corrections.

and *N, N, N', N'*-tetramethyl-*p*-phenylenediamine (TMPD)[15] (C≡N=1.160 Å and C–C=1.412 Å). On the other hand, the length between C(4) and C(5), 1.422 Å, is significantly longer than that of TCNQ, and slightly longer than that of TCNQ in a 1 : 1 complex with TMPD. A comparison of these values with the normal C–C bond lengths seems to suggest a considerable contribution of

13) R. E. Long, R. A. Sparks and K. N. Trueblood, ibid., **18**, 932 (1965).
14) C. Bugg and R. L. Sass, ibid., **18**, 591 (1965).
15) A. W. Hanson, ibid., **19**, 610 (1965).

TABLE IV. BOND LENGTHS AND ANGLES WITH THEIR e.s.d.'s

Numbers in parentheses are after corrections for libration.
The e.s.d.'s do not include estimated error in libration corrections.

	Distance (Å)		e.s.d.		Angle (deg.)		e.s.d.
C(4)-C(1)	1.425	(1.432)	0.011	C(1)-C(4)-C(1′)	125.1	(125.1)	0.7
C(1)-C(2)	1.353	(1.357)	0.010	C(4)-C(1)-C(2)	130.2	(130.1)	0.7
C(2)-C(3)	1.448	(1.450)	0.011	C(1)-C(2)-C(3)	128.4	(128.3)	0.7
C(3)-C(3′)	1.311	(1.314)	0.015	C(2)-C(3)-C(3′)	128.8	(129.0)	0.7
C(4)-C(5)	1.422	(1.426)	0.013	C(1)-C(4)-C(5)	117.4	(117.4)	0.7
C(5)-C(6)	1.450	(1.454)	0.012	C(4)-C(5)-C(6)	122.6	(122.6)	0.7
C(6)-N(1)	1.125	(1.128)	0.010	C(6)-C(5)-C(6′)	114.4	(114.5)	0.7
C(1)-H(1)	0.97		0.07	C(5)-C(6)-N(1)	179.6	(179.6)	0.7
C(2)-H(2)	0.98		0.07	H(1)-C(1)-C(4)	120		4
C(3)-H(3)	0.97		0.06	H(1)-C(1)-C(2)	110		4
				H(2)-C(2)-C(1)	111		4
				H(2)-C(2)-C(3)	121		4
				H(3)-C(3)-C(2)	117		4
				H(3)-C(3)-C(3′)	114		4

TABLE V. COMPARISON OF BOND LENGTH IN THE LINEAR AND RING CONJUGATED COMPOUNDS

Compound	Average bond lengths			Ref.
	C-C	C=C	Mean	
15, 15′-Dehydro-β-carotene	1.456Å*	1.345Å*	1.401Å*	21
Vitamine-A acid	1.452*	1.361*	1.407*	22
β-Ionyliden crotonic acid	1.466*	1.343*	1.405*	23
7, 7, 8, 8-Tetracyanoquinodimethane	1.448	1.346	1.397	13
p-Benzoquinone	1.477	1.322	1.400	24
Cyclooctatetraenecarboxylic acid	1.470	1.322	1.396	25
Dimethylfulvene	1.438	1.346	1.392	18
1, 2, 3, 4-Tetrachlorobenzo[g]sesquifulvalene	1.45	1.37	1.41	19
1, 2, 3-Tribromo-6-(*o*-methoxyphenyl)fulvene	1.48**	1.31**	1.40**	20
8, 8-Dicyanoheptafulvene	1.437	1.339	1.388	

* These values were obtained from the trans-chain parts.
** These values were obtained from the five-membered ring.

the following dipolar resonance form to the structure:

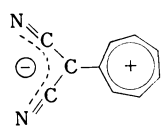

Thus, the present analysis supports the idea that this dipolar structure must be responsible for the stability of the molecule.[1-3,16,17]

The bond alternation, as suggested by its Kekule formula, is observed in the seven-membered ring. Similar bond alternation has been reported in other non-benzenoid aromatic compounds, dimethylfulvene,[18] 1, 2, 3, 4-tetrachlorobenzo[g]sesquifulvalene,[19] and 1, 2, 3-tribromo-6-(*o*-methoxyphenyl)fulvene.[20] To investigate the extent of bond alternation, average single and double bond lengths in the conjugated cyclic molecules were compared with those in molecules with an all-trans conjugated polyene chain (cf. Table V). The average lengths of single bonds and those of double bonds are approximately constant in the various linear polyenes. On the other hand, these values spread out over a wider range in the cyclic molecules. This may occur as a result of intramolecular strain. However, it may be pointed out that the mean values between the average single and double bond lengths show nearly the same value, 1.40 Å, throughout all the compounds given in Table V.

16) D. J. Bertelli, C. Golino and D. L. Dreyer, *J. Am. Chem. Soc.*, **86**, 3329 (1964).
17) M. Yamakawa, H. Watanabe, T. Mukai, T. Nozoe and M. Kubo, ibid., **82**, 5665 (1960).
18) N. Norman and B. Post, *Acta Cryst.*, **14**, 503 (1961).
19) Y. Nishi, Y. Sasada, T. Ashida and M. Kakudo, This Bulletin, **39**, 818 (1966).
20) Y. Kato, Y. Sasada and M. Kakudo, ibid., **38**, 1761 (1965).
21) W. G. Sly, *Acta Cryst.*, **17**, 511 (1964).
22) C. H. Stam and C. H. MacGillavry, ibid., **16**, 62 (1963).
23) E. L. Eichhorn and C. H. MacGillavry, ibid., **12**, 872 (1959).
24) J. Trotter, ibid., **13**, 86 (1960).
25) D. P. Shoemaker, H. Kindler, W. G. Sly and R. C. Srivastava, *J. Am. Chem. Soc.*, **87**, 482 (1965).

Even after the rotational corrections, as will be shown later, the C(3)-C(3′) distance is apparently shorter than the C=C distance in ethylene (1.337±0.003 Å).[26] Similar situations have been observed elsewhere; a C=C bond distance in *p*-benzoquinone[24] is 1.322±0.008 Å, the shortest bond distance in pyrene[27] is 1.315±0.020 Å without rotational corrections and 1.320±0.020 Å with the corrections, and the shortest double bond distance in cyclooctatetraenecarboxylic acid[25] is 1.310±0.007 Å, while its average double bond distance is 1.322 Å. These values suggest that the C=C distance in ethylene can not be taken as the normal double bond distance in the molecules of this type.[28]

Planarity.—The 8, 8-dicyanoheptafulvene molecule is approximately planar, as may be expected from the chemical formula. The detailed analysis of the atomic coordinates shows, however, a slight but significant deviation from this planarity. The equation for the best plane of the molecule, calculated with all twelve heavy atoms equally weighted, is:

$$Z = -0.6048X + 1.2571$$

where $X=ax\sin\beta$, $Y=by$, and $Z=cz+ax\cos\beta$. The large deviations from this plane are 0.059 Å for C(5), −0.040 Å for N(1), and 0.024 Å for C(1). On the other hand, the eight atoms, C(1)-C(5), all lie, within the range of 0.014 Å, on the plane:

$$Z = -0.5834X + 1.2081$$

as is illustrated in Fig. 7. The linear C(5)-C(6)-N(1) unit thus makes an angle of about 2° with this plane. A similar non-planarity has also been

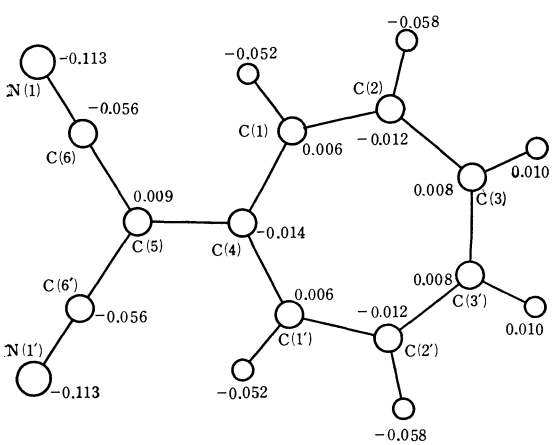

Fig. 7. The deviations (Å) of the atoms from the least-squares plane through atoms C(1)—C(5).

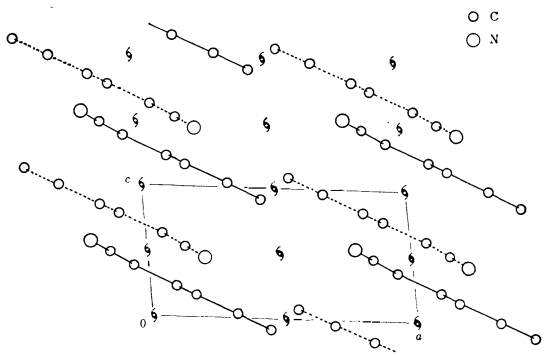

Fig. 8. The crystal structure projected along the b axis. The molecules drawn with brokn lines lie down half-period of the b axis.

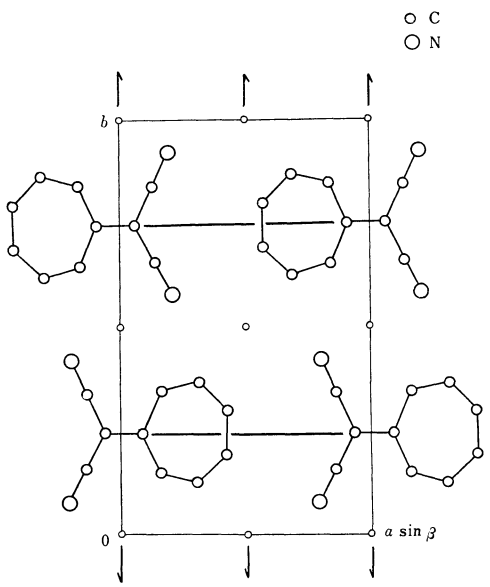

Fig. 9. The crystal structure projected along the c axis.

TABLE VI. SHORT INTERMOLECULAR DISTANCES (Å)

	Atom (molecure 1)	to Atom in Molecule		Distance
C···C	C(3)	C(6)	4	3.66
C···N	C(1)	N(1′)	2	3.41
	C(2)	N(1′)	2	3.54
	C(2)	N(1′)	3	3.62
	C(3)	N(1)	4	3.70
N···H	H(1)	N(1′)	2	2.62
	H(2)	N(1′)	2	2.88
	H(2)	N(1′)	3	2.94

Molecule	1	x	y	z
	2	$-x$	$1/2+y$	$1-z$
	3	$-x$	$1/2+y$	$-z$
	4	$1+x$	y	z

reported for the pyridinium dicyanomethylide carbanion[14] and TCNQ in a 1 : 1 complex with

26) H. C. Allen and E. K. Plyler, ibid., **80**, 2673 (1958).
27) A. Camerman and J. Trotter, *Acta Cryst.*, **18**, 636 (1965).
28) D. W. J. Cruickshank, *Tetrahedron*, **17**, 155 (1962).

TMPD[15]. In TCNQ,[13] however, the molecule is planar within the limit of errors. It may be anticipated that, because of the dipolar resonance structure, the electronic state of the C(5) significantly deviates from the sp^2 hybridization.

Crystal Structure.—The packing diagrams of the crystal of 8, 8-dicyanoheptafulvene viewed along the b and c axes are shown in Figs. 8 and 9 respectively. Short intermolecular distances are listed in Table VI. There are no abnormal intermolecular approaches displayed in the crystal. This compound has the high dipole moment of 7.49 D (in dioxane at 25°C).[17] The arrangement of the molecules appears to be favorable enough to compensate for this high dipole moment.

The molecule lies nearly parallel to the (101) plane at an intermolecular spacing of 3.41 Å, which corresponds to the normal van der Waals contact between the benzenoid rings.

Anisotropic Thermal Motion.—The anisotropic thermal parameters, B_{ij}, were transformed to U tensors referred to the molecular axes, 1, 2 and 3, shown in Fig. 10, the origin of the coordinate system lay at the center of gravity of the molecule. The direction cosines of the molecular axes referred to the orthogonal axes (a*, b, c) are:

Table VII. Observed and calculated U_{ij}, the latter being evaluated with T and ω in Table VIII (Values in 10^{-2}Å^2)

Atom	U_{11}		U_{22}		U_{33}		U_{12}		U_{13}		U_{23}	
	Obs.	Calcd.	Obs.	Calcd.	Obs.	Calcd.	Obs.	Calcd.	Obs.	Calcd.	Obs.	Calcd.
C(1)	4.38	4.64	5.47	5.45	5.94	6.09	−0.13	0.34	1.21	0.98	−0.07	0.14
C(2)	6.26	4.81	6.44	6.17	6.95	8.25	1.62	−0.11	1.02	0.92	−0.09	0.18
C(3)	3.97	4.41	9.62	7.33	6.95	7.21	1.18	0.11	1.15	0.99	−0.11	0.24
C(4)	4.43	4.33	4.94	5.34	3.51	3.80	0	0.52	1.89	1.04	0	0.06
C(5)	5.04	4.33	4.40	5.70	5.80	4.31	0	0.52	1.38	1.01	0	0.09
C(6)	3.90	4.62	5.79	6.23	7.55	7.06	1.06	1.03	0.31	1.02	0.28	0.06
N(1)	4.82	5.25	5.52	6.83	12.74	12.14	−0.58	1.69	0.60	1.01	0.72	−0.12

Table VIII. Values of T_{ij}, ω_{ij} and their e.s.d.'s, when the rigid body contains twelve atoms
T_{ij} and $\sigma(T_{ij})$ in 10^{-2}Å^2, ω_{ij} and $\sigma(\omega_{ij})$ in deg^2

$$T = \begin{pmatrix} 4.33 & 0.52 & 1.04 \\ & 5.34 & 0.06 \\ & & 3.80 \end{pmatrix} \qquad \omega = \begin{pmatrix} 43.86 & -0.01 & 0.92 \\ & 9.19 & -0.40 \\ & & 6.46 \end{pmatrix}$$

$$\sigma(T) = \begin{pmatrix} 0.27 & 0.25 & 0.28 \\ & 0.35 & 0.36 \\ & & 0.47 \end{pmatrix} \qquad \sigma(\omega) = \begin{pmatrix} 5.61 & 1.34 & 2.40 \\ & 2.50 & 1.79 \\ & & 1.70 \end{pmatrix}$$

Table IX. Values of T_{ij}, ω_{ij} and their e.s.d.'s, when the rigid body contains only seven atoms of the ring
T_{ij} and $\sigma(T_{ij})$ in 10^{-2}Å^2 ω_{ij} and $\sigma(\omega_{ij})$ in deg^2

$$T = \begin{pmatrix} 4.33 & 0.76 & 1.28 \\ & 5.29 & -0.05 \\ & & 3.94 \end{pmatrix} \qquad \omega = \begin{pmatrix} 29.97 & 0.00 & 1.07 \\ & 8.20 & 0.20 \\ & & 12.15 \end{pmatrix}$$

$$\sigma(T) = \begin{pmatrix} 0.27 & 0.26 & 0.29 \\ & 0.35 & 0.35 \\ & & 0.58 \end{pmatrix} \qquad \sigma(\omega) = \begin{pmatrix} 9.46 & 2.00 & 3.68 \\ & 2.16 & 1.85 \\ & & 1.81 \end{pmatrix}$$

Table X. Observed and calculated U_{ij}, the latter being evaluated with T and ω in table IX (Values in 10^{-2}Å^2)

Atom	U_{11}		U_{22}		U_{33}		U_{12}		U_{13}		U_{23}	
	Obs.	Calcd.	Obs.	Calcd.	Obs.	Calcd.	Obs.	Calcd.	Obs.	Calcd.	Obs.	Calcd.
C(1)	4.38	4.93	5.47	5.49	5.94	5.54	−0.13	0.42	1.21	1.24	−0.07	0.01
C(2)	6.26	5.24	6.44	6.84	6.95	7.23	1.62	−0.42	1.02	1.21	−0.09	0.01
C(3)	3.97	4.49	9.62	9.03	6.95	6.86	1.18	−0.01	1.15	1.27	−0.11	−0.05
C(4)	4.43	4.33	4.94	5.29	3.51	3.95	0	0.76	1.89	1.28	0	−0.05
C(5)	5.04	4.33	4.40	5.96	5.80	4.40	0	0.76	1.38	1.26	0	−0.06
C(6)	3.90	4.88	5.79	6.96	7.55	6.43	1.06	1.72	0.31	1.21	0.28	−0.15
N(1)	4.82	6.06	5.52	8.08	12.74	10.08	−0.58	2.96	0.60	1.12	0.72	−0.37

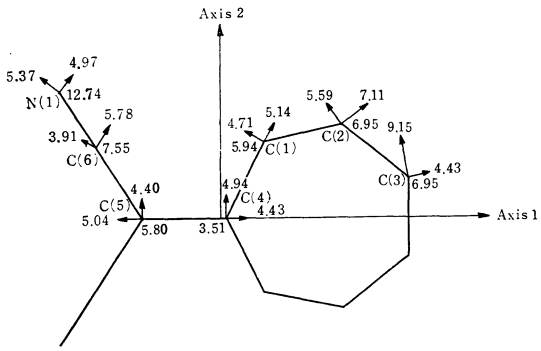

Fig. 10. The values of $\bar{u}^2$ (in unit 10^{-2}Å^2) in the directions radial and tangential to the center, and perpendicular to the molecular plane.

axis 1 : +0.8717, 0, −0.4900
axis 2 : 0, 1, 0
axis 3 : +0.5175, 0, +0.8557

The values of the six independent U_{ij}'s for each atom are shown in Table VII in the columns headed 'Obs.' The values of the mean-square oscillation, $\bar{u}^2$, in the directions radial and tangential to the center, and perpendicular to the molecular plane were derived from the U_{ij}'s,[29] as is shown in Fig. 10.

If a molecule is rigid-body, the molecular vibration can be expressed in terms of two symmetric tensors, T and ω, the former giving the translational vibrations of the mass center, and the latter the angular oscillations about the axes through the center.[30] Given the U tensors for a number of atoms, the T and ω tensors may be determined by the method of least-squares. The resulting T and ω tensors for 8, 8-dicyanoheptafulvene are given in Table VIII. The r. m. s. amplitudes of translational oscillation in the directions of the molecular axes, obtained from the square roots of the diagonal elements of T, are 0.21, 0.23 and 0.19 Å respectively. The corresponding r. m. s. amplitudes of angular oscillation obtained from ω are 6.5°, 3.0° and 2.5°.

While the r. m. s. amplitudes of translational oscillation are nearly equal to each other, those of angular oscillation are different for the three axes. This may be interpreted as indicating a

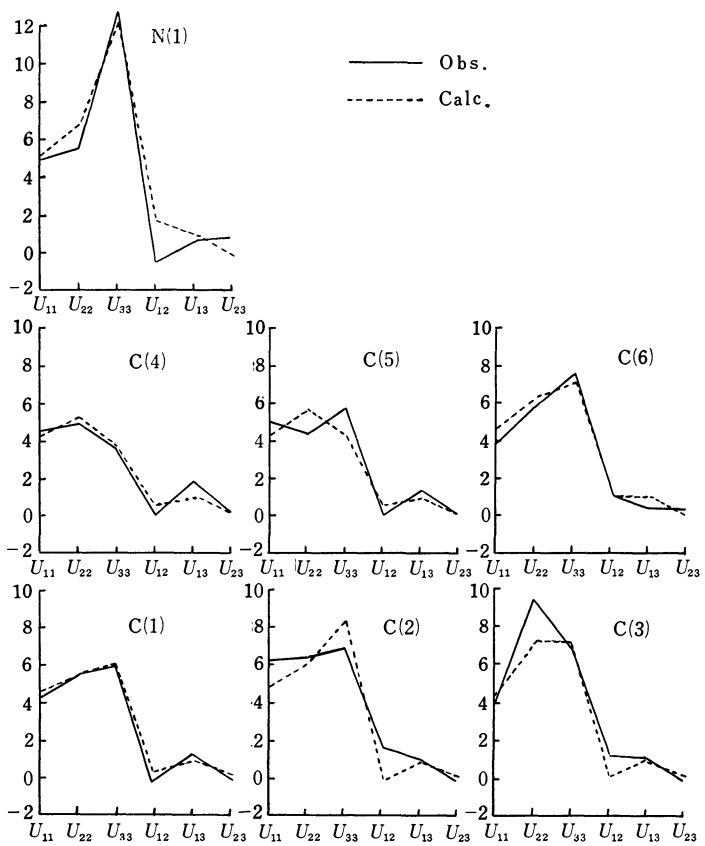

Fig. 11. Comparison between observed and calculated U_{ij}, the latter being evaluated with T and w in Table VIII.

29) D. W. J. Cruickshank, *Acta Cryst.*, **9**, 747 (1956).
30) D. W. J. Cruickshank, ibid., **9**, 754 (1956).

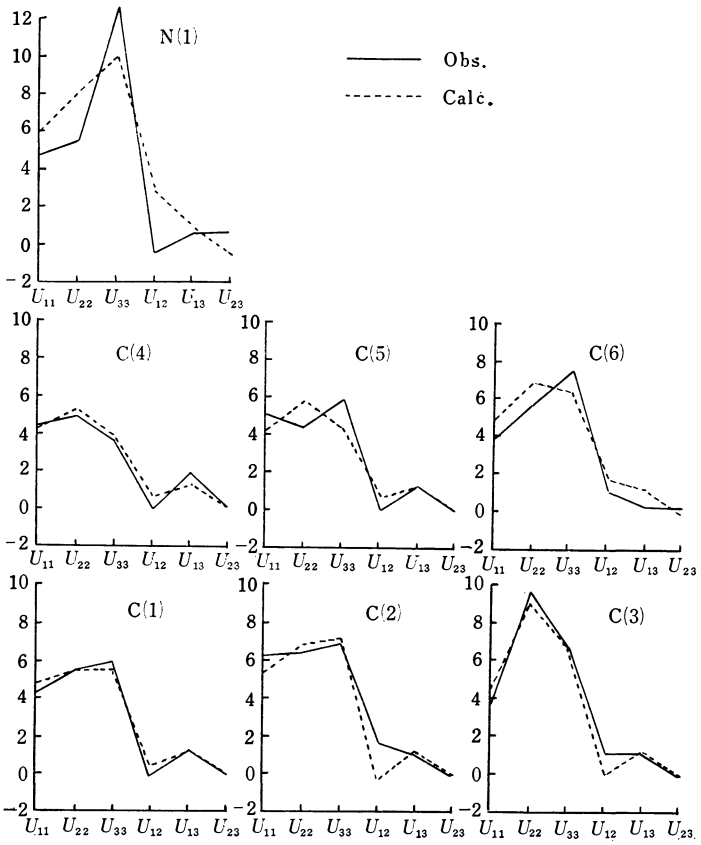

Fig. 12. Comparison between observed and calculated U_{ij}, the latter being evaluated with T and w in Table IX.

difference in the moments of inertia of the molecule around the three axes. The moments of inertia are $I_1=274$, $I_2=698$ and $I_3=972$ g.Å^2/mol. around the 1, 2 and 3 axes respectively. The larger the moment, the smaller the amplitude becomes.

In order to examine the validity of the rigid-body approximation, the U_{ij} values calculated with T and ω are listed in Table VIII in the column headed 'Calcd.' while the observed and calculated U_{ij}'s are compared in Fig. 11. Considerable discrepancies are observed for C(2), C(3) and C(5), which may be due to equal weights for all the atoms in the evaluation. T and ω tensors were, therefore, calculated with only seven atoms in the ring weighted equally, as is shown in Table IX, and the U_{ij}'s were then calculated using these values, as is shown in Table X. The observed and calculated U_{ij}'s are compared in Fig. 12. Good agreements are observed within the seven-membered ring, but in the dicyanomethylene group there are large discrepancies. This may be due to the twisting and scissoring of the exocyclic group.

It is necessary to allow for the angular oscillations causing the atoms to appear too close to the center of the molecule.[31] The radial error in the position of an atom is given by:

$$1/2r\{s^2/(1+s^2/q^2)+t^2/(1+t^2/q^2)\},$$

where s^2 and t^2 are the mean-square amplitudes of the angular oscillation in the molecular plane and in the direction perpendicular to it respectively, where q^2 is the Gaussian peak-width parameter for an atomic peak without the angular oscillations, and where r is the distance from the point of origin. The two mean-square amplitudes, s^2 and t^2, were calculated from ω_{ij}'s by Cruickshank's equation.[30] Using a value of q^2, 0.112 Å^2, the corrected bond distances and angles were calculated to be as shown in parentheses in Table IV. The corrected C(3)-C(3′) distance is still shorter than the C=C distance in ethylene, as has been stated above.

The authors wish to express their deep thanks to Mrs. Yoriko Nishi and Dr. Tsunehiro Takano for their assistance in the use of the electronic computer. The computing time of IBM 7090 was made available to the authors through the "UNICON" project.

31) D. W. J. Cruickshank, ibid., **9**, 757 (1956).

BULLETIN OF THE CHEMICAL SOCIETY OF JAPAN VOL. 39 2332—2335 (1966)

Studies of the Aqueous Solution of a Surface Active Substance by Means of an Ultrasonic Interferometer. II. The Effects of Added Electrolytes on the Dissolved State of Sodium Alkyl Sulfate

By Koji SHIGEHARA*

Department of Chemistry, Faculty of Science, Tokyo Metropolitan University, Setagaya-ku, Tokyo

(Received February 8, 1966)

The sound velocity (U) and the density of aqueous solutions of sodium dodecyl (SDS) and octyl (SOS) sulfates with inorganic electrolyte have been measured by using a differential ultrasonic interferometer and a float balance respectively, and the compressibility (β) has then been calculated from these results. The CMC's of SDS solutions of various concentrations of sodium salts have been determined from U-vs.-SDS and β-vs.-SDS concentration (C_2) diagrams. The results show a linear relationship between the logarithm of CMC and the logarithm of the concentration of sodium ions. The values of $d\beta/dC_2$ below CMC are affected by the addition of electrolytes, while the values above CMC are almost not affected at all by the addition of electrolytes. The diagrams of $d\beta/dC_2$ of alkyl sulfate vs. the number of carbon atoms in alkyl sulfate molecules with varying concentrations of added electrolytes showed straight lines which all passed through the same point when extrapolated to a zero number of carbon atoms. These results have been explained by taking account of the dissolved state of a surface active substance under the builder action of added inorganic electrolytes, which action decreases not only the mutual repulsion of the ionized-head group of a surface active substance but also the non-ionic hydration of the CH_2-chain of the surface active substance.

In previous papers,[1] it has been shown that differential ultrasonic interferometry is one of the most useful methods for the study of aqueous solutions of surface active substances. The sound velocity measurements by this method, together with the density measurements, has made possible the calculation of the compressibility and the critical micelle concentrations (CMC) of aqueous solutions of several alkyl sulfates, and from these data the compressibility, the molar volume, and the hydration number of the ionic micelle were determined. It was concluded therefrom that the hydrocarbon interior of an ionic micelle assumes a liquid-like structure rather than a solid-like one.

It has been well known that the addition of some inorganic salts, often called the "builders," enhances the surface activity. This effect can also be well studied by hydration measurements using differential ultrasonic interferometry. Hitherto little has been known experimentally, however, about the hydration of surface active substances in connection with the builder action. The present paper will describe the results of measurements of the sound velocity, the density, and the compressibility of aqueous solutions of sodium alkyl sulfates containing inorganic electrolytes. The CMC, the hydration, and the compressibility of single molecules and micelles of alkyl sulfates in the presence of the added electrolytes will also be discussed.

Experimental

Sodium *n*-dodecyl (SDS) and *n*-octyl (SOS) sulfate were prepared from the respective alcohols and purified as usual. The sodium chloride, sodium sulfate, and magnesium chloride used to study the builder action were purified from commercial products by recrystallization.

The method of measuring the small changes in the sound velocity (ΔU) due to the small changes in the concentrations (C_2) of the alkyl sulfates by the differential ultrasonic interferometer was the same as that reported in previous papers.[1] The concentration of the added inorganic electrolytes was kept constant during the measurements. The sound velocity of an aqueous solution containing the inorganic electrolyte alone was also measured. The measurements were carried out in a thermostat at 30.00 ± 0.003°C. The frequency of the ultrasonic wave was 1.432 Mc./sec., and the error in the measurement of ΔU was ±3 cm./sec.

The density of the solution at 30°C was determined by the float-balance method.[2] As the standard,[3]

* Present address: Ocean Research Institute, University of Tokyo, Nakano-ku, Tokyo.

1) T. Sasaki and K. Shigehara, IVth International Congress of Surface Activity, B/IV. 13, Brussels, Belgium (1964); K. Shigehara, This Bulletin, **38**, 1700 (1965).

2) T. W. Richards and J. W. Shipley, *J. Am. Chem. Soc.*, **34**, 599 (1912); T. W. Richards and G. W. Harris, ibid., **38**, 1000 (1916).

3) "International Critical Tables," Vol. III, McGraw-Hill Book Co., New York (1928), p. 51.

the aqueous solution of the inorganic electrolyte was used, and the change in density ($\Delta\rho$) caused by the addition of alkyl sulfates was measured. The thermostat used was controlled to ± 0.001°C. The accuracy of the measurements was $\pm 10^{-6}$ g./cc.

The compressibility (β) of the solution was calculated from the sound velocity (U) and the density (ρ) by using the Laplace equation:

$$\beta = 1/U^2\rho$$

Results and Discussion

In Figs. 1 and 2, the change in sound velocity (ΔU) is plotted against the concentration of alkyl sulfates (C_2), while in Figs. 3 and 4, the change in compressibility ($\Delta\beta$) is plotted against the concentration of aqueous solutions of SOS and SDS, with and without the addition of inorganic electrolytes. As may be seen in Figs. 2 and 4, the diagrams for SDS solutions consist of two linear portions with a sharp break point between them; this break point may reasonably be ascribed to the CMC of SDS, as will be mentioned later. The change in density ($\Delta\rho$)-vs.-SDS concentration diagrams show similar break points corresponding to CMC, but they are not shown in this paper.

The change in the value of CMC with the concentration of sodium chloride and sulfate is shown in Fig. 5. As may be seen in Fig. 5, the logarithm of CMC changes linearly with the logarithm of the concentration of sodium ions; a similar linear relationship has been reported by Corrin and

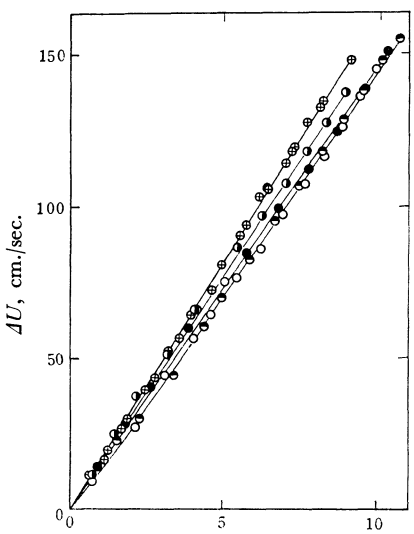

Fig. 1. ΔU vs. C_2 diagram for SOS solution.

⊕ without electrolyte ◑ 0.05 N NaCl
○ 0.1 N NaCl ◓ 0.5 N NaCl ● 0.05 N Na_2SO_4

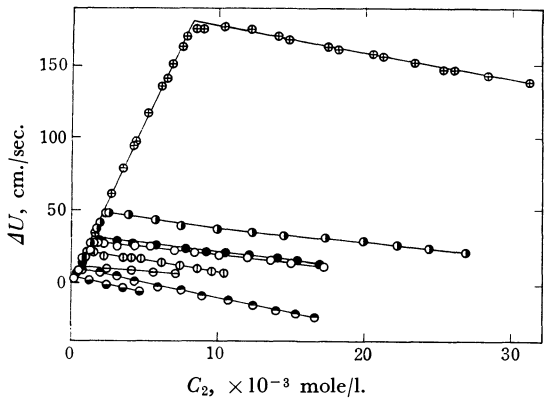

Fig. 2. ΔU vs. C_2 diagram for SDS solution.

⊕ without electrolyte ◑ 0.05 N NaCl
○ 0.1 N NaCl ◓ 0.5 N NaCl ◒ 1 N NaCl
● 0.1 N Na_2SO_4 ⊕ 0.05 N $MgCl_2$
⊖ 0.1 N $MgCl_2$

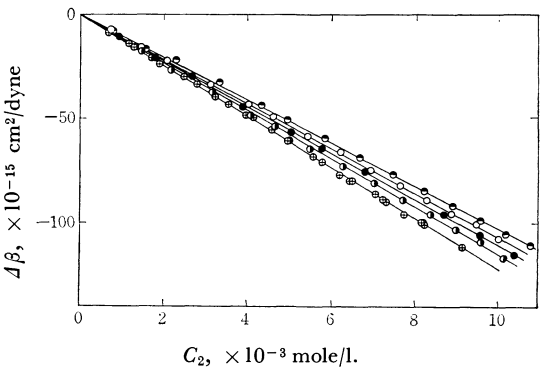

Fig. 3. $\Delta\beta$ vs. C_2 diagram for SOS solution.

⊕ without electrolyte ◑ 0.05 N NaCl
○ 0.1 N NaCl ◓ 0.5 N NaCl ● 0.05 N Na_2SO_4

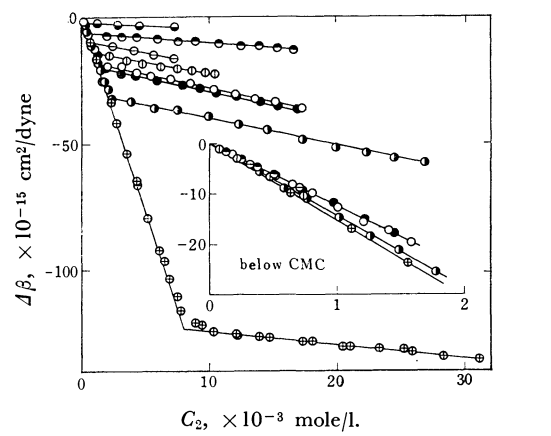

Fig. 4. $\Delta\beta$ vs. C_2 diagram for SDS solution.

⊕ without electrolyte ◑ 0.05 N NaCl
○ 0.1 N NaCl ◓ 0.5 N NaCl ◒ 1 N NaCl
● 0.1 N Na_2SO_4 ⊕ 0.05 N $MgCl_2$
⊖ 0.1 N $MgCl_2$

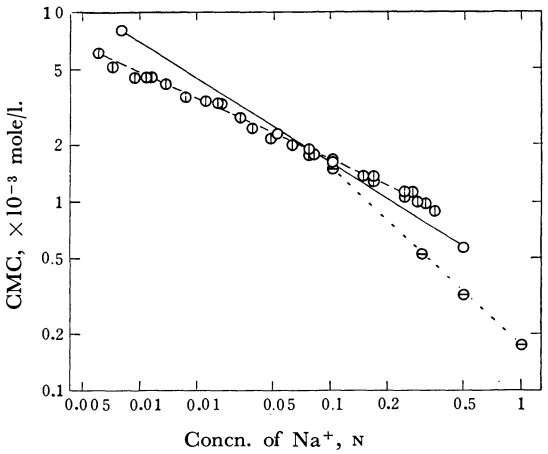

Fig. 5. CMC vs. concentration of Na^+.
○ and solid line, the present author
◐ and broken line, Corrin and Harkins, by dye solubilization method
⊖ and dotted line, Matuura et al., by surface tension method

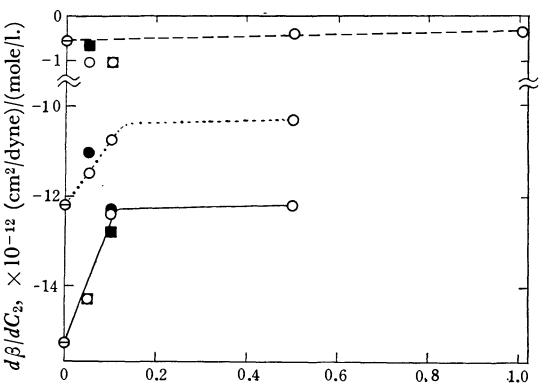

Fig. 6. $d\beta/dC_2$ vs. concentration of added electrolyte.
solid line, SDS solution below CMC
dotted line, SOS solution below CMC
broken line, SDS solution above CMC
⊖ without electrolyte
○ presence of sodium chloride
● presence of sodium sulfate
■ presence of magnesium chloride

Harkins[4] and by Matuura et al.[5]

In the diagrams of $\Delta\rho$ vs. C_2, the slopes were not affected by the addition of inorganic electrolytes. This shows that the molar volume of alkyl sulfate in the dissolved state is not affected by the addition of inorganic electrolytes. This fact is consistent with the findings of Hutchinson and Mosher[6] on the partial molal volume of sodium decyl sulfate above CMC.

The increase in $\Delta\beta$ with C_2 ($d\Delta\beta/dC_2$ or $d\beta/dC_2$) for solutions of SOS and SDS is plotted against the concentration of the added electrolyte in Fig. 6. In this figure, the $d\beta/dC_2$ increases with the concentration of the electrolyte up to CMC. This result may be ascribed to the dehydration of SOS and SDS by the added electrolytes. After the CMC, the value of $d\beta/dC_2$ is almost independent of the concentration of inorganic electrolytes.

Figure 7 shows the plots of $d\beta/dC_2$ vs. the number of carbon atoms (N) in the solute molecule. As may be seen in Fig. 7, the values of $d\beta/dC_2$ change linearly with N when sodium chloride is added to the solution. The values without the addition of sodium chloride reported in previous papers[1] also fall on straight lines. From this figure, the values of $d\beta/dC_2$ for the solutions of various NaCl contents at the zero carbon number were estimated by extrapolation below and above CMC. These values all fall at the same point. This suggests that the hydration characteristics of the SO_4Na radical of alkyl sulfates are independent of the carbon number as well as of the presence of the builder and of the micellization. The contribution of each CH_2-chain in the solute molecule to the value of $d\beta/dC_2$ is independent of the total number of

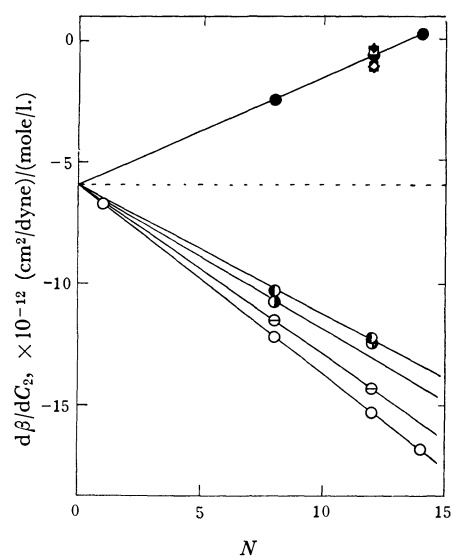

Fig. 7. $d\beta/dC_2$ vs. N.

below CMC:	above CMC:
○ without electrolyte	● without electrolyte
⊖ 0.05 N NaCl	■ 0.05 N NaCl
◑ 0.1 N NaCl	◇ 0.1 N NaCl
◐ 0.5 N NaCl	□ 0.5 N NaCl
	◆ 1 N NaCl

4) M. L. Corrin and W. D. Harkins, *J. Am. Chem. Soc.*, **69**, 683 (1947).
5) R. Matuura, H. Kimizuka, A. Matsubara, K. Matsunobu and T. Matsuda, This Bulletin, **35**, 552 (1962).
6) E. Hutchinson and C. S. Mosher, *J. Colloid Sci.*, **11**, 352 (1956).

carbon atoms in its molecule, but it is changed by the addition of electrolytes. As has been pointed out in the previous papers,[1] the value of $d\beta/dC_2$ obtained by the extrapolation to $N=0$ shows a compressibility decrease due to the introduction of one mole of Na^+ and $-SO_4^-$ each in water. The decrease in this value with respect to N for the solution below CMC, namely, the vertical difference between the dotted horizonatal line and the straight line for the solution below CMC in Fig. 7, shows an additional decrease in compressibility due to the dissolution of one mole of alkyl chains of the respective carbon numbers in a molecule in the state of molecular dispersion in water; the increase for the solutions above CMC, namely, the vertical difference between the dotted horizontal line and the upper straight line, shows a similar increase in compressibility due to the introduction of one mole of alkyl chains in micelles. Therefore, the fact that the $d\beta/dC_2$ value above CMC was almost unchanged by the addition of the electrolyte indicates that the compressibility of micelles is presumably not affected by the addition of an inorganic electrolyte.

It may be inferred from these results that the non-ionic hydration of the CH_2-chain, together with ionic hydration, is one of the important factors in the dissolution of surface active substance into water, and that the builder action of inorganic electrolytes is due not only to the decrease in the mutual repulsion of the ionized head group of the surface active substance by the gegen-ion attachment, as may be understood from Fig. 5, but also to the decrease in the non-ionic hydration of the CH_2-chain of the surface active substance.

The author wishes to express his deep gratitude to Professor Tsunetaka Sasaki of our University for his kind direction and valuable criticism. The cost of this research has been defrayed by a grant of the Ministry of Education given to Professor Sasaki.

BULLETIN OF THE CHEMICAL SOCIETY OF JAPAN VOL. 39 2335—2340 (1966)

Properties of Dilute Solutions of Polyurethanes. I. Linear Polymers

By Hiroshi SATO

Research Laboratory, Mitsubishi Rayon Co., Ltd., Otake, Hiroshima

(Received February 10, 1966)

Polyurethanes were prepared from polycaprolactone, 4, 4'-diphenylmethane diisocyanate, and ethylene diamine. Two kinds of polymers were used for the present experiments. One contained polycaprolactone with the number-average molecular weight, $\overline{M}_n$, of 1.30×10^3, while the other contained polycaprolactone with an $\overline{M}_n$ value of 2.80×10^3. Each polymer was fractionated from a dimethyl acetamide solution by progressive precipitation with a mixture of *n*-heptane and ethyl ether, and the fractions were characterized in terms of viscosity and sedimentation. The relations between the intrinsic viscosity and the molecular weight were found in DMF at 25°C to be:

$$[\eta] = 5.52\times10^{-4}M^{0.66}$$

for the polymer containing polycaprolactone ($\overline{M}_n=1.30\times10^3$) and

$$[\eta] = 7.71\times10^{-4}M^{0.62}$$

for the polymer containing polycaprolactone ($\overline{M}_n=2.80\times10^3$). The viscosities of the solutions of the polymers were measured in several solvents at different temperatures, and the polymer-solvent interaction parameters were obtained by using the Fixman theory for the expansion factor. The molecular-weight distribution of the polymer containing polycaprolactone ($\overline{M}_n=1.30\times10^3$) was obtained from the distribution of the sedimentation coefficient, while the value of $\overline{M}_w/\overline{M}_n$ was calculated from the distribution curve to be 1.95.

Recently a number of studies have reported on the elastic properties of polyurethanes. As is well known, the elastic properties of polymers depend on their polymer characteristics, such as their molecular weight and its distribution. As polyurethane used for fiber-forming has no cross-link in the molecule, the characteristics of the polymer exert a great influence on its behavior in the fiber-forming process and on the elastic properties of the fiber. Little information[1] has,

1) J. Moacanin, *J. Appl. Polymer Sci.*, **1**, 272 (1959); M. Nishide and M. Sera, *J. Chem. Soc. Japan, Ind. Chem. Sect. (Kogyo Kagaku Zasshi)*, **63**, 189 (1960).

however, been found about the characteristics of the polymer.

On the other hand, it is of great interest from the point of view of physical chemistry to study polyurethane as a kind of block copolymer.

The present investigation has, therefore, been carried out in an attempt to establish the relation between the intrinsic viscosity and the molecular weight and to obtain knowledge of the molecular-weight distribution and the thermodynamic properties of solutions of polyurethane consisting of polycaprolactone, diphenylmethane diisocyanate, and ethylene diamine.

Experimental

Polymer.—One mole of polycaprolactone (PCL) was treated with 2 moles of 4, 4'-diphenylmethane diisocyanate (MDI) in bulk for 110 min. at 75°C in order to prepare the prepolymer. The prepolymer thus obtained was then dissolved in dimethyl acetamide and was extended into polyurethane by reaction with the equivalent moles of ethylene diamine (ED) at 40°C.

The solution thus obtained was spun into water in order to obtain the coagulated polymer, which was then dried in a vacuum at room temperature.

In this manner, two kinds of polyurethanes were prepared. One contained PCL with a number-average molecular weight, $\overline{M}_n$, of 1.30×10^3; it was designated as the polymer B. The other contained PCL with an $\overline{M}_n$ value of 2.80×10^3; it was designated as the polymer C.

The polymer may be symbolized as follows:

$$-(-\text{MDI}-\text{PCL}-\text{MDI}-\text{ED}-)_{\overline{n}}$$

Solvents.—Dimethyl formamide (DMF), dimethyl acetamide (DMAA), and dimethyl sulfoxide (DMSO) were purified by the usual method.

Fractionation.—Each polymer was fractionated from a 1% solution in DMAA by precipitation fractionation, using a mixture of *n*-heptane and ethyl ether as the precipitant at 25°C. The gel-like precipitate was then dissolved in a small amount of DMAA, and the resulting solution was added, drop by drop, into an excess of water. Thus, the polymer B was divided into 13 fractions, which were designated as UB(1300), and the polymer C, into 12 fractions, designated as UC(2800). Each fraction was dried in a vacuum at room temperature.

In the other runs of fractionation, both of the polymers B and C were divided into 3 fractions; the middle fractions were designated UB-T(1300) and UC-T(2800) respectively.

Viscosity.—A modified Ubellohde viscometer was used to measure the viscosity of polymer solutions.

Partial Specific Volume.—The density of solutions was determined over the concentration range from 0.5 to 3.0 wt. % by using a 10-cc. Ostwald picnometer at 25°C; the partial specific volume was then calculated from the density data.

Ultracentrifugation.—The sedimentation velocity was measured with a Hitachi analytical ultracentrifuge, Model UCA-1, equipped with Schlieren optics and a phase plate. The rotor temperature was maintained at 25°C, and the rotor speed was 55430 r. p. m. throughout the experiments.

TABLE I. PROPERTIES OF POLYMER B

Fraction	$[\eta]$	k'	$S_0\times10^{13}$	k_s	$k_s/[\eta]$	$\overline{M}\times10^{-4}$	N%
UB-1	1.262	0.406	2.41	1.94	1.54	12.8	4.63
3	1.650	0.406	2.79	2.85	1.72	18.4	4.50
5	1.478	0.397	2.55	2.45	1.66	15.1	4.46
7	1.243	0.421	2.28	2.11	1.70	11.8	4.47
9	1.031	0.417	2.05	1.76	1.71	9.39	4.32
10	0.875	0.420	1.91	1.45	1.66	7.16	
11	0.659	0.413	1.51	1.07	1.63	4.61	4.30
12	0.485	0.430	1.13	0.825	1.70	2.62	
Original	1.279	0.419	2.59	2.12	1.67	13.5	4.45*
UB-T	1.211					11.5	

* The calculated value is 4.52%.

TABLE II. PROPERTIES OF POLYMER C

Fraction	$[\eta]$	k'	$S_0\times10^{13}$	k_s	$k_s/[\eta]$	$\overline{M}\times10^{-4}$	N%
UC-1	1.190						2.74
3	1.748	0.395	3.08	3.08	1.76	26.6	2.46
4	1.215	0.390	2.29	2.05	1.69	14.2	
5	1.165	0.392	2.25	1.93	1.65	13.5	2.44
8	0.930	0.385	1.87	1.56	1.68	9.07	
9	0.820	0.400	1.74	1.37	1.67	7.71	2.40
10	0.652	0.408	1.51	1.14	1.74	5.56	
11	0.447	0.405	1.14	0.81	1.80	3.06	2.38
Original	1.244	0.390	2.66	2.19	1.76	18.3	1.43*
UC-T	1.177					13.8	

* The calculated value is 2.50%.

Results and Discussion

The Constitution of the Polymer. — The nitrogen content of the original polymer, as determined by the micro-Kjeldahl method, was less than the calculated value for both polymers B and C. This may mean that a small amount of water reacted with isocyanate groups in the polymerization process, resulting in the inhomogeniety in the composition (cf. Tables I and II).

The Relation between the Intrinsic Viscosity and the Molecular Weight.—From the plots of the reduced viscosity (η_{sp}/C) against the concentration (expressed in g./100 cc.), as is shown in Fig. 1, the intrinsic viscosity and the Huggins constant, k', were obtained by using the following equation:

$$(\eta_{sp}/C) = [\eta] + k'[\eta]^2C \qquad (1)$$

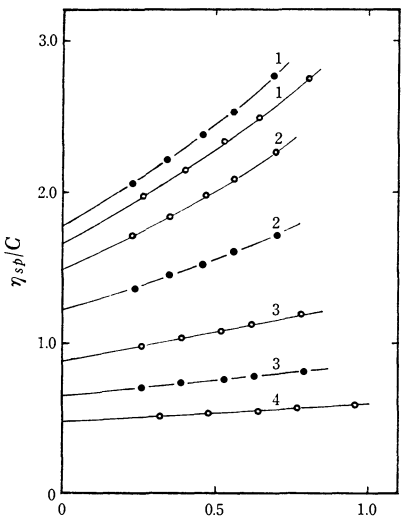

Fig. 1. (η_{sp}/C) vs. C of polymer fractions in DMF at 25°C.
Open circles, 1: UB-3, 2: UB-5, 3: UB-10, 4: UB-12
Solid circles, 1: UC-3, 2: UC-4, 3: UC-10

As the plots became curved in the higher-molecular weight fractions, the values of $[\eta]$ and k' for these fractions were estimated from the straight lines obtained from the plots of the inherent viscosity ($\ln \eta_r/C$) against the concentration by applying the following equation:

$$(\ln \eta_r/C) = [\eta] - (0.5 - k')[\eta]^2C \qquad (2)$$

The results are given in Tables I and II for the UB(1300) and UC(2800) polymer fractions respectively.

The Huggins constant, k', slightly decreases with an increase in the molecular weight of PCL.

The reciprocals of the sedimentation coefficients, $1/S$, were plotted against the concentration (expressed in g./100 cc.), as is shown in Fig. 2. The sedimentation coefficient at the infinite dilution, S_0, and the constant, k_s, were obtained from the empirical equation:

$$1/S = (1/S_0)(1 + k_sC) \qquad (3)$$

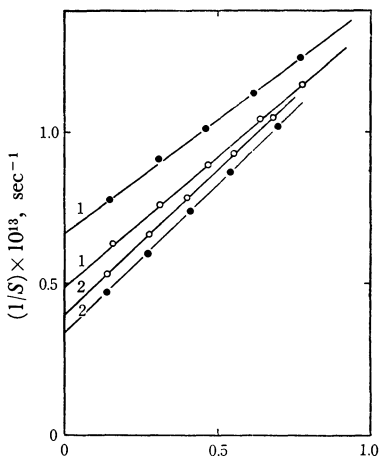

Fig. 2. ($1/S$) vs. C of polymer fractions in DMF at 25°C.
Open circles, 1: UB-9, 2: UB-5
Solid circles, 1: UC-10, 2: UB-5

Wales[2] has proposed this relation between the constant, k_s, and the intrinsic viscosity:

$$k_s/[\eta] = 1.66 \qquad (4)$$

Yamakawa[3] has theoretically estimated the ($k_s/[\eta]$) ratio to be about 1.7 in good solvent systems. The ratio obtained in the present study is also about 1.7, as may be seen in column 6 of Tables I and II. Wales' equation can, therefore, be applied to the case of these block copolymer solutions.

The molecular weight of each fraction, M, was calculated from the intrinsic viscosity and the sedimentation coefficient by using the Mandelkern-Flory equation[4]:

$$S_0[\eta]^{1/3}/M^{2/3} = (\boldsymbol{\Phi}^{1/3}\boldsymbol{P}^{-1})(1-\bar{v}\rho)/\eta_0\boldsymbol{N}_A \qquad (5)$$

where $\boldsymbol{\Phi}$ and $\boldsymbol{P}$ are universal constants; $(\boldsymbol{\Phi}^{1/3}\boldsymbol{P}^{-1})$ takes the value of 2.5×10^6; $\bar{v}$ is the partial specific volume of the polymer in solution; ρ and η_0 are the density and the viscosity of solvent respectively, and $\boldsymbol{N}_A$ is Avogadro's number.

The partial specific volumes of the polymers in DMF at 25°C were calculated from the data of density to be as follows:

2) M. Wales and K. E. Van Holde, *J. Polymer Sci.*, **14**, 81 (1964).
3) H. Yamakawa, *J. Chem. Phys.*, **36**, 2995 (1962).
4) L. Mandelkern, W. R. Krigbaum, H. A. Scharaga and P. J. Flory, ibid., **20**, 1392 (1952).

$\bar{v} = 0.8480$ for the polymer B

$\bar{v} = 0.8745$ for the polymer C

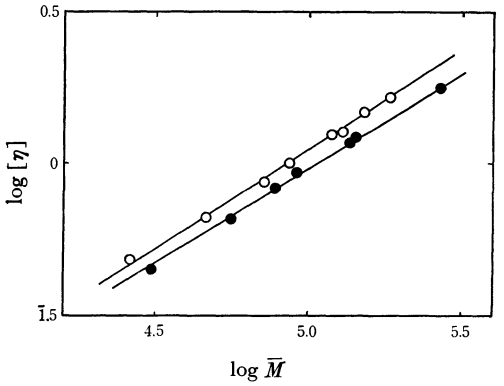

Fig. 3. Log $[\eta]$ vs. log $\bar{M}$ of polymer fractions in DMF at 25°C.
Open circles: UB(1300), Solid circles: UC(2800)

The intrinsic viscosities are plotted logarithmically against the molecular weight in Fig. 3. From this figure, the following two equations, 6 and 7, are obtained for the UB(1300) and UC(2800) polymer fractions respectively in DMF at 25°C:

$$[\eta] = 5.52 \times 10^{-4} M^{0.66} \quad (6)$$

$$[\eta] = 7.71 \times 10^{-4} M^{0.62} \quad (7)$$

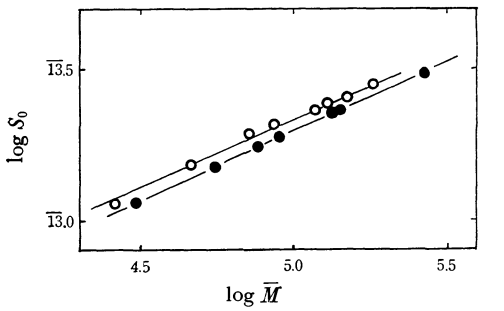

Fig. 4. Log S_0 vs. log $\bar{M}$ of polymer fractions in DMF at 25°C.
Open circles: UB(1300), Solid circles: UC(2300)

The relation between the sedimentation coefficient and the molecular weight was derived from the double logarithmic plots in Fig. 4; it was found in DMF at 25°C to be:

$$S_0 = 1.36 \times 10^{-15} M^{0.44} \quad (8)$$

for the UB(1300) polymer fractions and

$$S_0 = 9.86 \times 10^{-16} M^{0.46} \quad (9)$$

for the UC(2800) polymer fractions.

Polymer-Solvent Interaction Parameters.— The intrinsic viscosity depends on the molecular weight of the polymer in accordance with the relationship:

$$[\eta] = KM^{1/2}\alpha^3 \quad (10)$$

where $K = \Phi(\bar{r}_0^2/M)^{3/2}$, $\bar{r}_0^2$ is the mean square end-to-end distance for an unperturbed chain and α, the viscosity expansion factor.

Stockmayer and Fixman[5] have proposed the simple relation:

$$[\eta] = KM^{1/2} + 0.66\Phi BM \quad (11)$$

by combining Eq. 10 with the following Fixman equation[6] for the excluded volume effect:

$$\alpha^3 = 1 + 2z \quad (12)$$

where $z = (3/2\pi)^{3/2}(\bar{r}_0^2/M)^{-3/2}BM^{1/2}$;
$B = 2(\bar{v}^2/V_1N_A)\psi_1(1-\Theta/T)$; V_1 is the molar volume of the solvent; ψ_1, the entropy term of Flory's polymer-solvent interaction parameter, and Θ, Flory's temperature.

Hence, a plot of $[\eta]/M^{1/2}$ vs. $M^{1/2}$ will be linear in a given solvent at a particular temperature. The value of K is determined by the intercept. Thus, the value of α^3 can be evaluated by putting the value of K into Eq. 10. $(\alpha^3-1)M^{-1/2}$ should give a straight line when plotted against $1/T$, and both Θ and ψ_1 for any given solvent can be evaluated.

The values of K were obtained by using Eq. 11 in DMF at 25° and 70°C for UB(1300) and UC-(2800) fractions respectively; a small decrease in K with an increase in the temperature was observed for both polymers. The decrease in K with the temperature was, then, assumed to be linear between 25°C and 70°C, and the α for each polymer-solvent-temperature combination was calculated from the intrinsic viscosity by using Eq. 10 and the interpolated value of K at the temperature, T.

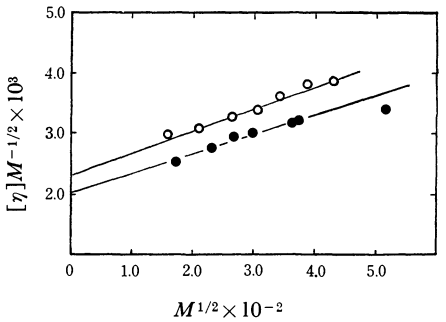

Fig. 5. $([\eta]/M^{1/2})$ vs. $M^{1/2}$ of polymer fractions in DMF at 25°C.
Open circles: UB(1300), Solid circles: UC(2800)

Figure 5 shows the Stockmayer-Fixman plots. The relations obtained from the straight lines are as follows:

$$[\eta] = 2.29 \times 10^{-3} M^{1/2} + 3.64 \times 10^{-6} M \quad (13)$$

for UB(1300), and

5) W. H. Stockmayer and M. Fixman, *J. Polymer Sci.*, Part C, No. 1, 137 (1963).
6) M. Fixman, *J. Chem. Phys.*, **36**, 3123 (1962).

$$[\eta] = 2.02\times10^{-3} M^{1/2} + 3.20\times10^{-6} M \quad (14)$$

for UC(2800), both being measured in DMF at 25°C.

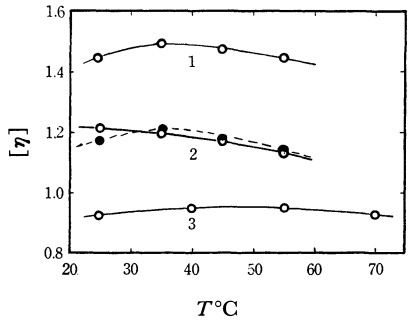

Fig. 6. Dependence of $[\eta]$ on temperature in various solvents.
Open circles: UB-T (solvent 1: DMAA, 2: DMF, 3: DMSO)
Solid circles: UC-T (solvent: DMF)

Figure 6 shows the temperature dependence of the intrinsic viscosities of the UB-T(1300) and UC-T(2800) polymers plotted against the temperature in several solvents.

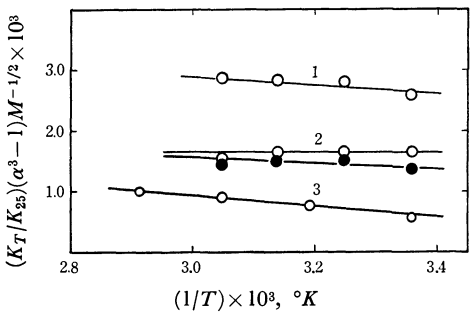

Fig. 7. Plots of $(K_T/K_{25})(\alpha^3-1)M^{-1/2}$ vs. $(1/T)$ for polymer fractions in various solvents.
Open circles: UB-T (solvent 1: DMAA, 2: DMF, 3: DMSO)
Solid circles: UC-T (solvent: DMF)

The plots of $(K_T/K_{25})(\alpha^3-1)M^{-1/2}$ against $1/T$ are given in Fig. 7. K_T/K_{25}, the ratio of K at T to K at the reference temperature, 25°C, was introduced in view of the temperature dependence of $(\bar{r}_0^2/M)^{3/2}$.

The results are given in Table III, where the heat term, κ_1, at 25°C was calculated by the relation:

Table III. Thermodynamic parameters

Polymer	Solvent	ψ_1	Θ°K	κ_1^{25}	χ_1^{25}
UB-T(1300)	DMAA	0.35	141	0.17	0.32
UB-T(1300)	DMF	0.10	0	0	0.40
UB-T(1300)	DMSO	0.21	235	0.16	0.45
UC-T(2800)	DMF	0.17	158	0.09	0.42

$$\kappa_1 = \psi_1\Theta/T \quad (15)$$

and where the polymer-solvent interaction parameter, χ_1, at 25°C was evaluated from the following relation:

$$(1/2) - \chi_1 = \psi_1 - \kappa_1 \quad (16)$$

For the solutions of UB-T(1300), the heat of dilution behaves athermally in DMF and endothermally in DMAA and DMSO. The cohesive energy densities (CED) of these solvents are 123, 147 and 170 cal./cc. for DMAA, DMF and DMSO respectively. The value of κ_1 is related to the solubility parameter, δ, which is the square root of CED, through the following Hildebrand equation:

$$\kappa_1 = (V_1/\boldsymbol{R}T)(\delta_1-\delta_2)^2 \quad (17)$$

where $\boldsymbol{R}$ is the gas constant and where the suffixes 1 and 2 represent the solvent and the polymer respectively. Consequently, the value of CED for the polymer B lies between those for DMAA and DMSO, and is nearly the same as that for DMF.

The constant, a, of the Mark-Houwink equation and the long-range interaction term of the Stockmayer-Fixman equation decrease in DMF solutions with an increase in the molecular weight of PCL, as has been shown above. When the long-range interaction term is separated into two terms, the heat and the entropy of dilution, the heat term, κ_1, increases with the molecular weight of PCL.

These results lead us to the conclusion that the PCL segments may mix endothermally with such a polar solvent as DMF, although the value of CED for the copolymer may be obtained as the average of the values of two sorts of segments and although the values of CED have not been obtained for each segment of the polymers used in the present study.

Molecular-weight Distribution.—The distribution of the limiting sedimentation coefficient, S_0, for the polymer B was evaluated by making corrections for both diffusion and concentration, and the transformation from the distribution of the sedimentation coefficient to the molecular-weight distribution was made by using Eq. 8. The results are given in Fig. 8.

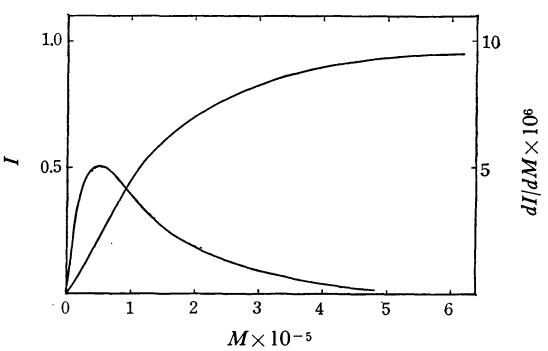

Fig. 8. Molecular weight distribution of polymer B.

The ratio of the weight-average molecular weight, $\overline{M}_w$, to the number-average, $\overline{M}_n$, was calculated from the distribution curve. The value of 1.95 for the $\overline{M}_w/\overline{M}_n$ ratio agrees fairly well with the value of 2.0 for the "*most probable distribution*" which can be expected in the addition polymerization.

On the other hand, the distribution estimated from the data of precipitation fractionation seems to be narrower than that obtained by the sedimentation method. This may be caused by insufficient effectiveness of fractionation.

The author wishes to express his hearty thanks to Professor Masaji Miura of Hiroshima University and to Dr. Toshizo Isoshima and Dr. Nobuo Yamada of this laboratory for their encouragement and useful discussions throughout this work.

BULLETIN OF THE CHEMICAL SOCIETY OF JAPAN VOL. 39 2340—2344 (1966)

Properties of Dilute Solutions of Polyurethanes. II. Branched Polymers

By Hiroshi SATO

Research Laboratory, Mitsubishi Rayon Co., Ltd., Otake, Hiroshima

(Received February 10, 1966)

Linear and branched polyurethanes, both of which contained polycaprolactone ($\overline{M}_n = 1.80 \times 10^3$), were prepared. Each polymer was fractionated from a dimethyl acetamide solution by precipitation with a mixture of *n*-heptane and ethyl ether, and the fractions were characterized by viscosity and sedimentation. The degree of branching for the fractions of the branched polymer was estimated by using the relation between viscosity and branching, derived by Flory. The ratio of the concentration dependence of the sedimentation coefficient k_s to $[\eta]$ was about 1.7 for the linear polymer, but the $k_s/[\eta]$ value increased with an increase in the degree of branching for the branched polymer. The Huggins constant, k', seems to be independent of the degree of branching.

In a previous paper,[1] the properties of dilute solutions of polyurethanes were investigated in an attempt to establish the relation between the intrinsic viscosity and the molecular weight and to obtain knowledge of the molecular weight distribution and the thermodynamic properties of solutions.

As linear polyurethane is usually prepared from a long chain diol, a diisocyanate, and a so-called chain-extender, such as diamine, a rather well-characterized branched polymer can easily be obtained by substituting triol for a part of the diol.

The purpose of the present paper is to estimate the degree of branching for branched polymers and to investigate the dependence of the properties of polymer solutions on the degree of branching.

The degree of branching can be estimated by several measurements, such as of the "*radius of gyration*" of the polymer chain,[2] the osmotic second virial coefficient,[3] the intrinsic viscosity, and the sedimentation.[4,5] The methods used here consist of measuring the viscosity and the sedimentation, as these measurements are rather more accurate than the others.

Experimental

Polymer.—One mole of polycaprolactone (PCL), the number-average molecular weight of which was 1.80×10^3, was treated with 2 moles of 4, 4'-diphenylmethane diisocyanate (MDI) in bulk at 65°C for 2 hr. to form a prepolymer. The prepolymer thus obtained was then dissolved in dimethyl acetamide and extended into polyurethane by reaction with equivalent moles of ethylene diamine (ED) at 40°C for 1 hr.

The polyurethane obtained in this manner was designated as the linear polymer E.

The branched polymers were prepared as follows. A mixture of PCL ($\overline{M}_n = 1.80 \times 10^3$) and a small amount of trimethylol ethane (TME) was treated with MDI in bulk at 65°C for 2 hr. to form a prepolymer, where the molar ratio of the isocyanate group to the hydroxyl group was 2. The prepolymer was extended into branched polyurethane with ED under the same conditions as in the case of the linear polymer. Thus, two kinds of branched polymers were obtained.

1) H. Sato, This Bulletin, **39**, 2335 (1966).
2) C. D. Thurmond and B. H. Zimm, *J. Polymer Sci.*, **8**, 477 (1952).
3) W. R. Krigbaum and Q. A. Trementozzi, ibid., **28**, 295 (1958).
4) L. D. Moore, Jr., G. R. Greear and J. O. Sharp, ibid., **59**, 333 (1962).
5) J. Blachford and R. F. Robertson, ibid., **A3**, 1289 (1965).

Table I. Solution properties of fractions of linear polymer E

Fraction	Weight, g.	$[\eta]$	k'	$S_0\times10^{13}$	k_s	$k_s/[\eta]$	$\bar{M}\times10^{-4}$
UE-2	2.958	1.340	0.407	2.46	2.35	1.75	14.64
3	1.061	1.245	0.405	2.35	2.16	1.74	13.20
4	2.295	1.210	0.393	2.22	2.08	1.72	11.95
5	1.247	1.150	0.366	2.21	1.94	1.68	11.60
6	2.311	0.880	0.400	1.84	1.45	1.65	7.69
7	2.184	0.701	0.400	1.55	1.22	1.70	5.25
8	2.232	0.310	0.395	0.92	0.55	1.70	1.79

Table II. Solution properties of fractions for branched polymers F and G

Fraction	$[\eta]_b$	k'_b	$S_{0b}\times10^{13}$	k_{sb}	$k_{sb}/[\eta]_b$	$\bar{M}\times10^{-4}$	$[\eta]$
UF-4	1.505	0.387	2.91	2.92	1.94	20.0	1.647
UF-7	0.947	0.414	2.10	1.76	1.86	9.67	1.029
UG-3	1.120	0.413	2.50	2.43	2.17	13.7	1.292
UG-6	0.748	0.404	1.85	1.59	2.15	7.12	0.847

The molar ratios of PCL to the trifunctional component (TME) in the polymers were as follows:

Branched polymer F (PCL : TME=70 : 1)

Branched polymer G (PCL : TME=42 : 1)

The linear polymer E is symbolized as follows:

$$-(-\text{MDI-PCL-MDI-ED-})_{\bar{n}}$$

whereas the branched polymer contains trifunctional groups:

-(-MDI-TME-MDI-ED-)-
MDI-ED-)-

Fractionation.—In the same manner as in the previous paper,[1] the linear polymer E was divided into 9 fractions, while the branched polymers F and G were divided into 8 fractions.

Viscosity and Sedimentation.—Viscosity and sedimentation measurements were carried out as in the previous paper.[1]

Results and Discussion

The UE-2-8, UF-4, UF-7, UG-3 and UG-6 fractions were selected from the fractions of the linear polymer E and the branched polymers F and G, because the Schlieren patterns for these fractions were narrow enough for an accurate determination of the sedimentation coefficient.

The data of viscosity in dimethyl formamide (DMF) at 25°C, shown in Figs. 1 and 2, were treated in accordance with the complementary relationships for intrinsic viscosity:

$$\eta_{sp}/C = [\eta] + k'[\eta]^2C \quad (1)$$

$$(\ln \eta_r)/C = [\eta] - (0.5 - k')[\eta]^2C \quad (2)$$

where η_r and η_{sp} are the relative and specific viscosities respectively, and where k' is the Huggins constant. The values of $[\eta]$ and k' derived therefrom are listed in Tables I and II.

The reciprocals of the sedimentation coefficients, $1/S$, are plotted against the concentration in Figs. 3—5; the sedimentation coefficients at an infinite dilution, S_0, were estimated from

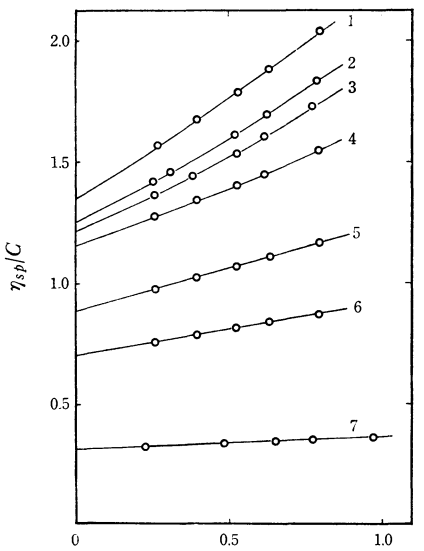

Fig. 1. (η_{sp}/C) vs. C of polymer fractions for linear polymer E in DMF at 25°C.
1: UE-2, 2: UE-3, 3: UE-4, 4: UE-5, 5: UE-6, 6: UE-7, 7: UE-8

the intercepts of the straight lines, while the values of k_s were calculated from the relation:

$$1/S = (1/S_0)(1 + k_sC) \quad (3)$$

Results are presented also in Tables I and II.

Figure 6 shows the plot of log S_0 against log $[\eta]$ for the fractions of the linear polymer E in DMF at 25°C, where the solid line through the points corresponds to the equation:

$$S_0 = 2.02\times10^{-13}[\eta]^{0.693} \quad (4)$$

In addition, the molecular weight, M, of each fraction was calculated according to the Mandelkern-Flory equation:[6]

6) L. Mandelkern, W. R. Krigbaum, H. A. Scheraga and P. J. Flory, *J. Chem. Phys.*, **20**, 1392 (1952).

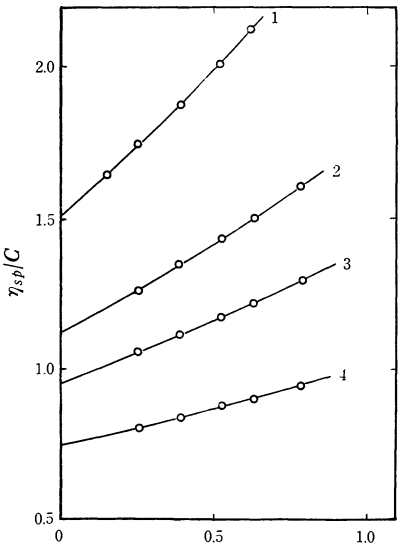

Fig. 2. (η_{sp}/C) vs. C of polymer fractions for branched polymers F and G in DMF at 25°C.
1: UF-4, 2: UG-3, 3: UF-7, 4: UG-6

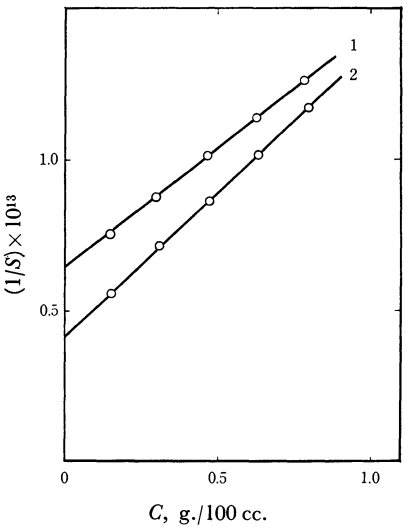

Fig. 3. $(1/S)$ vs. C of polymer fractions for linear polymer E in DMF at 25°C.
1: UE-7, 2: UE-2

$$S_0[\eta]^{1/3}/M^{2/3} = \Phi^{1/3}\boldsymbol{P}^{-1}(1-\bar{v}\rho)/\eta_0\boldsymbol{N}_A \qquad (5)$$

where Φ and $\boldsymbol{P}$ are constants, ρ and η_0 are the density and the viscosity of the solvent respectively, $\boldsymbol{N}_A$ is Avogadro's number, and $\bar{v}$ is the partial specific volume, which was calculated from the data of density to be 0.8581 cc./g.

The relation between the intrinsic viscosity and the molecular weight and that between the sedimentation coefficient and the molecular weight

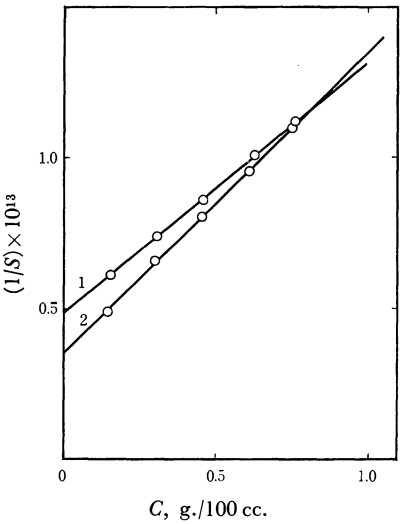

Fig. 4. $(1/S)$ vs. C of polymer fractions for branched polymer F in DMF at 25°C.
1: UF-7, 2: UF-4

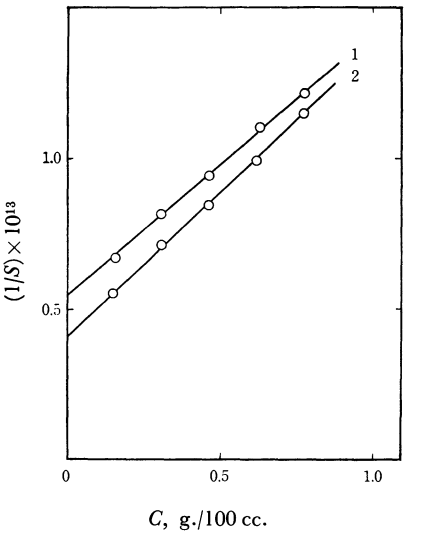

Fig. 5. $(1/S)$ vs. C of polymer fractions for branched polymer G in DMF at 25°C.
1: UG-6, 2: UG-3

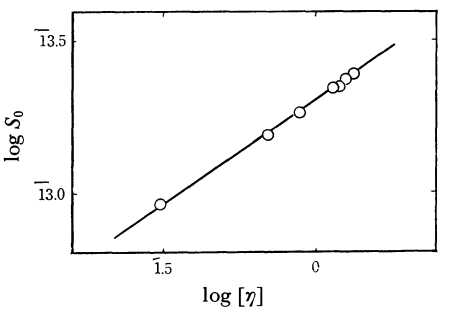

Fig. 6. Log S_0 vs. log $[\eta]$ of polymer fractions for linear polymer E in DMF at 25°C.

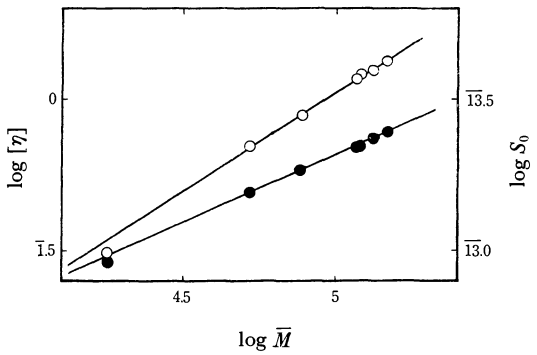

Fig. 7. Log [η] vs. log $\overline{M}$ (open circles) and log S_0 vs. log $\overline{M}$ (solid circles) of polymer fraction for linear polymer E in DMF at 25°C.

for the linear polymer E were derived from double logarithmic plots, shown in Fig. 7, as follows:

$$[\eta] = 5.90\times 10^{-4}M^{0.65} \quad (6)$$

$$S_0 = 1.18\times 10^{-15}M^{0.45} \quad (7)$$

in DMF at 25°C.

The ratio of the mean-square radius of gyration of a branched molecule, $\bar{r}_b^2$, to that of a linear molecule, $\bar{r}^2$, of the same molecular weght is defined by g:

$$g = \bar{r}_b^2 / \bar{r}^2 \quad (8)$$

where g is related to the number of branches per molecule, m, according to Zimm and Stockmayer's theory.[7]

For a branched molecule, the intrinsic viscosity, $[\eta]_b$, and the sedimentation coefficient, S_{0b}, are expressed by the following equations:

$$[\eta]_b = g'[\eta] = g'\Phi 6^{3/2}(\bar{r}^2)^{3/2}/M \quad (9)$$

$$S_{0b} = M(1-\bar{v}\rho)/N_A\eta_0 hP 6^{1/2}(\bar{r}^2)^{1/2} \quad (10)$$

where $[\eta]$ is the intrinsic viscosity of a linear molecule having the same molecular weight as the branched polymer and where the g' and h factors are a function of g.

Several theories[8-10] have been proposed to relate g' to g. According to the Flory theory, g' and h are related to g as follows:

$$g' = g^{3/2} \quad (11)$$

$$h = g^{1/2} \quad (12)$$

The combination of Eqs. 9—12 leads us to the following equation:

$$S_{0b}[\eta]_b^{1/3}/M^{2/3} = \Phi^{1/3}P^{-1}(1-\bar{v}\rho)/\eta_0 N_A \quad (13)$$

For the calculation of the g factor, intrinsic viscosities measured at Θ-temperature should be used in principle, as the g factor in the Zimm-Stockmayer theory[7] is defined for unperturbed quantities. Many experimental results[2,11,12] show, however, that the value of g' is nearly the same for both good and Θ-solvents. Consequently, the estimation of the value of g' from intrinsic viscosities measured at non-Θ-temperature is permissible.

When the value of M is the same in Eq. 5 for the linear molecule and in Eq. 13 for the branched molecule, the following equation can be derived:

$$S_{0b}[\eta]_b^{1/3} = S_0[\eta]^{1/3} \quad (14)$$

The substitution of Eq. 4 for the linear polymer into Eq. 14 then gives:

$$S_{0b}[\eta]_b^{1/3} = 2.02\times 10^{-13}[\eta]^{1.03} \quad (15)$$

Thus, the value of $[\eta]$ for a linear polymer having the same molecular weight as a branched polymer can be evaluated with $[\eta]_b$ and S_{0b} in accordance with Eq. 15.

The values of $[\eta]$ thus calculated are listed in column 2 of Table III, while calculated values of g' are given in column 3 of that table.

The values of g were calculated in accordance with Eq. 11, they are presented in column 4 of Table III.

Table III. Degree of branching

Fraction	$[\eta]$	g'	g	m
UF-4	1.647	0.914	0.942	0.58
UF-7	1.029	0.921	0.947	0.52
UG-3	1.292	0.868	0.910	0.90
UG-6	0.847	0.883	0.920	0.78

The value of m in Table III is the number of branches per molecule which are estimated to be trifunctional branches of random lengths by Zimm and Stockmayer.[7]

Many investigators have discussed the dependence of the Huggins constant, k', of a branched polymer on the degree of branching. Orofino[11] has shown that k' in a good solvent is not affected by branching, but in a Θ-solvent the k' value for a branched polymer is slightly larger than that for the corresponding linear polymer. Morton[12] has observed, however, that for a branched polymer the values of k' are slightly larger than that for a linear polymer in both good and Θ-solvents. In Pollock's work,[13] there is no evidence for such a difference in k' due to branching. Blachford et al.[5] have observed that the value of k' for a branched polymer increases with the increase in the degree of branching in a good solvent.

7) B. H. Zimm and W. H. Stockmayer, ibid., **17**, 1301 (1949).
8) W. H. Stockmayer and M. Fixman, *Ann. N. Y. Acad. Sci.*, **57**, 334 (1953).
9) B. H. Zimm and R. W. Kilb, *J. Polymer Sci.*, **37**, 19 (1959).
10) K. Katsuura, *J. Phys. Soc. Japan*, **15**, 2310 (1960).
11) T. A. Orofino and F. Wenger, *J. Phys. Chem.*, **67**, 566 (1963).
12) M. Morton, T. E. Helminiak, S. D. Gadkary and F. Bueche, *J. Polymer Sci.*, **57**, 471 (1962).
13) D. J. Pollock, L. J. Elyash and T. W. DeWitt, ibid., **15**, 335 (1955).

In the present work, the viscosity data on branched polymers in a rather poor solvent give values of k' experimentally indistinguishable from those obtained for the linear polymers. As many factors, such as the molecular weight distribution, may affect k', it is difficult to determine whether the value of k' depends on the degree of branching or not.

Wales[14] has proposed the following relation between k_s and $[\eta]$:

$$k_s/[\eta] = 1.66 \tag{16}$$

This relation has been supported by many investigations for linear polymers. For branched polymers, however, a larger $k_s/[\eta]$ value has been reported.[6]

For the fractions of the linear polymer E, the values of $(k_s/[\eta])$ were about 1.7, but the values for the branched polymer, as may be seen in column 6 of Table II, are higher than that for the linear polymer and it seems that the ratio of k_s to $[\eta]$ increases with the increase in the degree of branching. The larger values of $(k_s/[\eta])$ may suggest that the dependence of k_s on the degree of branching is less than that of $[\eta]$.

The degrees of polymerization of the fractions for the branched polymers are about 85, 41, 62 and 30 for UF-4, UF-7, UG-3 and UG-6 respectively. If the polymer molecules contain trifunctional groups (TME) in proportion to the molar ratio of TME to PCL, then the numbers of branches per molecule may be 1.21, 0.59, 1.47 and 0.71 for UF-4, UF-7, UG-3 and UG-6 respectively. The initial two fractions obtained by precipitation fractionation, however, contained many micro gel particles for both of the branched polymers, F and G. This might mean that the trifunctional groups are localized upon the initial few fractions having high molecular weights. It may be reasonable, therefore, that the degrees of branching for the fractions measured in this study were less than the above-calculated values.

The authors wishes to express his hearty thanks to Professor Masaji Miura of Hiroshima Univeristy, and to Dr. Toshizo Isoshima and Dr. Nobuo Yamada of this laboratory for their encouragement and useful discussions throughout this work.

14) M. Wales and K. E. VanHold, *J. Polymer Sci.* **14**, 81 (1954).

BULLETIN OF THE CHEMICAL SOCIETY OF JAPAN VOL. 39 2344—2346 (1966)

The Reactions of t-$C_4H_9^+$ in the Radiolysis of Neopentane in the Gas Phase

By Tetsuo MIYAZAKI and Shoji SHIDA

Laboratory of Physical Chemistry, Tokyo Institute of Technology, Ookayama, Tokyo

(Received March 1, 1966)

The yields and reactions of t-$C_4H_9^+$ produced in the radiolysis of neopentane in the gas phase have been studied by the use of ammonia. The yields of *iso*-C_4H_8 increase sharply upon the addition of a small amount of ammonia in the radiolysis of neopentane and show a constant value upon the further addition of ammonia (more than 10 mol.%). Since this increase is due to the following reaction:

$$t\text{-}C_4H_9^+ + NH_3 \rightarrow iso\text{-}C_4H_8 + NH_4^+$$

we get $G(t\text{-}C_4H_9^+)=1.76$ by assuming the increment of *iso*-C_4H_8 to be equal to the yield of t-$C_4H_9^+$. This value is consistent with the value expected from the mass spectrum of neopentane. It has, therefore, been concluded that the ammonia method is a very effective general method for studying the reactions of ions. It is applicable to the study of ions under high pressures, ions which can not be studied by a mass spectrometer. It is especially effective in the study of less reactive ions.

In order to study ionic reactions in general, it is desirable to devise a general method which can easily and definitely discriminate the reactions of ions from those of neutral active species. Ausloos[1] studied ionic reactions using deuterated compounds and radical scavengers in the radiolysis of hydrocarbons. However, the application of his method is limited to highly reactive ions.

The present authors showed in a previous

1) R. P. Borkowski and P. J. Ausloos, *J. Chem. Phys.*, **39**, 818 (1963).

TABLE I. EFFECT OF AMMONIA IN THE RADIOLYSIS OF NEOPENTANE

Yields of products at 180 mmHg of neopentane

Run	Additive[a]		Product[a]					
	C_5H_{10}-1	NH_3	H_2	CH_4	C_2[b]	C_3H_6	*iso*-C_4H_{10}	*iso*-C_4H_8
6	0	0	2.07	3.43	4.38	0.87	1.65	0.82
28	50	0	2.43	3.42	5.09	0.71	0.40	1.09
8	50	0	2.08	3.04	4.41	0.64	0.32	1.12
11	50	9.21	2.20	3.19	4.11	0.64	0.38	2.14
13	50	18.4	2.11	3.31	3.68	0.46	0.40	3.03
14	50	40.9	2.73	3.43	4.01	0.63	0.34	4.23
15	50	77.4	2.36	3.44	4.21	0.64	0.44	4.59
23	50	151	2.04	3.15	3.30	0.50	0.38	4.82
29	50	246	2.21	3.18	3.40	0.44	0.46	5.28
9	50	487	2.57	3.41	3.60	0.36	0.51	5.16

a) Moles per 1000 mol. of *neo*-C_5H_{12}.
b) C_2 represents the sum of C_2H_6, C_2H_4 and C_2H_2.

paper[2] that ammonia is a very effective reagent for studying the reactions of ions in the radiolysis of *n*-butane and that this method can also be applied to the study of an unreactive ion, such as *sec*-$C_4H_9^+$. Though the *t*-$C_4H_9^+$ ion is the most abundant ion in the mass spectrum of neopentane, the yield and the reaction of this ion in the radiolysis of neopentane have not been decided, since *t*-$C_4H_9^+$ does not produce C_4-products directly because of its low reactivity. Here we have studied the reaction of *t*-$C_4H_9^+$ in the radiolysis of neopentane by the use of the ammonia method.

Experimental

Most of the experimental procedures were identical with those described in the previous study.[2] Neopentane was supplied by the Takachiho Shoji Co.; its gas chromatographic analysis showed the presence of 0.05% *n*-pentane as an impurity. C_5H_{10}-1, used as a radical scavenger, was 99.99% pure. NH_3 was also of a high purity. The samples were irradiated at room temperature with γ-rays from Cs-137 of 5000 c. The total dose was 2.4×10^{21} eV.g^{-1}, and the dose rate was 8.9×10^{18} eV. g^{-1} hr^{-1} The reaction vessel was a glass cylinder (2.0 cm. in external diameter, 15 cm. high, and with a volume of about 50 cc.). The analytical procedures were identical with those described before.[3] C_2–C_4 hydrocarbon products were analysed by gas chromatography (dimethyl sulfolane column, 15 m.).

Results and Discussion

The effect of ammonia on the radiolysis of neopentane in the gas phase is shown in Table I and in Fig. 1. Though H_2, CH_4 and C_2 Products are not significantly affected by ammonia, *iso*-C_4H_8 increases markedly upon the addition of ammonia even only a small percentage, and becomes constant at a high concentration of ammonia. These phenomena are thought to be due to the following reactions, as in the radiolysis of the *n*-C_4H_{10}–NH_3 system[2]:

$$neo\text{-}C_5H_{12} \xrightarrow{I} t\text{-}C_4H_9^+ + CH_3 \qquad (1)$$

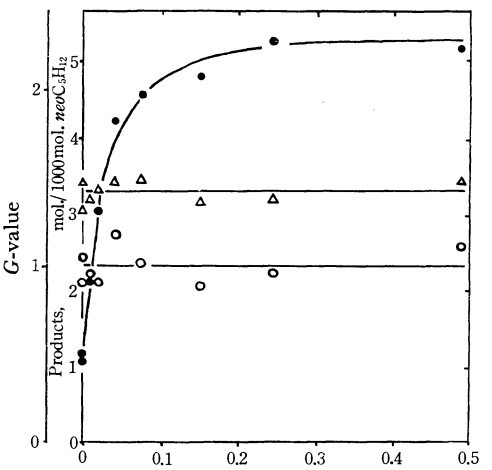

Fig. 1. Effect of ammonia in the radiolysis of *neo*-C_5H_{12}
H_2 ○, CH_4 △, *iso*-C_4H_8 ●

$$t\text{-}C_4H_9^+ \xrightarrow{k_2} P \qquad (2)$$

$$t\text{-}C_4H_9^+ + NH_3 \xrightarrow{k_3} iso\text{-}C_5H_8 + NH_4^+ \qquad (3)$$

(I: Rate of reaction 1; k: Rate constant)

t-$C_4H_9^+$ cannot produce *iso*-C_4H_{10} by the following hydride ion transfer reaction with neopentane, because this reaction is endothermic by about 20 kcal.[4]:

2) T. Miyazaki and S. Shida, This Bulletin, **38**, 2114 (1965).
3) T. Miyazaki, S. Arai, S. Shida and S. Sunohara, ibid., **37**, 1352 (1964).
4) S. G. Lias and P. Ausloos, *J. Chem. Phys.*, **43**, 2748 (1965).

$$t\text{-}C_4H_9^+ + neo\text{-}C_5H_{12} \longrightarrow iso\text{-}C_4H_{10} + C_5H_{11}^+ \quad (4)$$

From a kinetic treatment similar to one described before,[2] we get $k_2/k_3=11.5$ mol./1000 mol. *neo*-C_5H_{12}. If k_3 is taken as 2×10^{-9} cc.molecule^{-1} sec^{-1},[5] we get $k_2=1.38\times10^8$ sec^{-1}. Therefore, the life time of t-$C_4H_9^+$ is about 7×10^{-9} sec., which is the same order of magnitude as the life time of the *sec*-$C_4H_9^+$ produced in the radiolysis of *n*-butane.[2] Since the life time of t-$C_4H_9^+$ is much shorter than the time of neutralization ($10^{-2}-10^{-3}$ sec.),[6] and the time of diffusion to wall of the vessel (about 10^{-1} sec.),[7] t-$C_4H_9^+$ may be consumed by the addition to C_5H_{10}-1;

$$t\text{-}C_4H_9^+ + C_5H_{10}\text{-}1 \longrightarrow C_9H_{19}^+ \quad (5)$$

Then, $k_2=k_5[C_5H_{10}\text{-}1]$. Therefore, we get $k_5=0.45\times10^{-9}$ cc. molecule^{-1} sec^{-1}, which is similar to the ordinary rate constant of ion-molecule reactions. Since the total dose was large in this work and since an unsaturated product, such as *iso*-C_4H_8, may react with radicals, C_5H_{10}-1 was added as a radical scavenger. However, we found that C_5H_{10}-1 may react also as an ion-scavenger. Since *iso*-C_4H_{10} is formed in considerable amounts in the absence of C_5H_{10}-1 in the radiolysis of neopentane (Table I), the neutralization of t-$C_4H_9^+$ may produce the t-C_4H_9 radical as follows:

$$t\text{-}C_4H_9^+ + e \longrightarrow t\text{-}C_4H_9 \quad (6)$$

$$t\text{-}C_4H_9 + neo\text{-}C_5H_{12} \longrightarrow iso\text{-}C_4H_{10} + C_5H_{11} \quad (7)$$

$$t\text{-}C_4H_9 + R \longrightarrow P \quad (8)$$

(R: a radical; P: the products of Reaction 8, a combination- and disproportionation reaction between t-C_4H_9 and a radical of the system.)

In the mass spectrum of neopentane, the fraction of t-$C_4H_9^+$ amounts to 41% of all the ions. Taking $W_{neo\text{-}C_5H_{12}}$ as 24 eV., it may be expected that $G(t\text{-}C_4H_9^+)=1.7$. Since the increment of *iso*-C_4H_8 is equal to the yield of t-$C_4H_9^+$ in the present work, we get $G(t\text{-}C_4H_9^+)=1.76$ in the radiolysis of neopentane; this is in good agreement with the mass spectrometric value. Recently Ausloos reported that the $G(iso\text{-}C_4H_8)$ value in the radiolysis of *neo*-C_5H_{12}–NO in a stainless-steel reaction vessel differs from that in a graphite-coated reaction vessel.[4] Assuming this difference to be equal to t-$C_4H_9^+$, he obtained $G(t\text{-}C_4H_9^+)=1.23$. However, this value seems to be an underestimate.

It can be concluded that ammonia is a very effective reagent for studying the reaction of ions, especially that of the unreactive ions in the radiolysis of hydrocarbon, and that ionic reactions at high pressures, which can not be studied by a mass spectrometer, can be studied easily by the ammonia method.

The authors appreciate the help of Dr. Toshio Sugiura and others of the Japan Atomic Energy Institute in performing the work.

5) M. S. B. Munson and F. H. Field, *J. Am. Chem. Soc.*, **87**, 4242 (1965).
6) D. P. Stevenson, *J. Phys. Chem.*, **61**, 1453 (1957).
7) C. N. Hinshelwood, "The Kinetics of Chemical Change in Gaseous Systems," Claredon Press, Oxford (1933), p. 29.

BULLETIN OF THE CHEMICAL SOCIETY OF JAPAN VOL. 39 2346—2351 (1966)

Nuclear Magnetic Resonance Studies of the Intermolecular Interaction of Amides and Some Other Related Dipolar Molecules

By Teijiro YONEZAWA and Isao MORISHIMA

Department of Fuel Chemistry, Faculty of Engineering, Kyoto University, Sakyo-ku, Kyoto

(Received March 5, 1966)

The chemical shifts for *N*, *N*-disubstituted amides and some other isoelectronic compounds as pure liquid and in dilute solutions in CCl_4 are reported. The characteristic shifts generally observed on going from a CCl_4 solution to pure liquid are explained in terms of specific self-association in the pure liquid.

Rotation about the central C–N bond of substituted amides is hindered, and two resonance peaks, those of protons of R_2 at site A and of R_3 at site B, are observed.

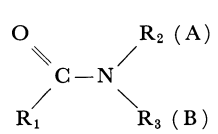

I

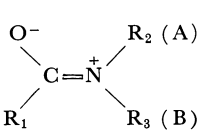

II

From the temperature dependence of the proton magnetic resonance spectra of substituted amides, the energy barriers restricting the internal rotation about the central C–N bond have been obtained.[1-5]

The barrier height strongly depends on the nature of the solvent and on the concentration when these substances are studied in solution.[4,5] This has been attributed to the changes of a partial double-bond character in the C–N bond arising from the intermolecular interactions. Whittaker and Siegel[5] showed evidence of the dipolar association of *N*, *N*-dimethylformamide (DMF) from their NMR study of solvent effects on the hindered internal rotation about the C–N bond.

However, there has been no dispute over the nature of the self-association which takes place between amide molecules in the pure liquid. Recently, there has been a considerable amount of work on the specific intermolecular interaction by the NMR method; for example, the solvent-solute interaction between benzene and amide.[6] the self-association of azabenzene[7] and of pyrrole[8] have been discussed, along with the configuration or the mode of the interacting molecules. Hence, in the present paper, a detailed investigation of dipolar interactions of highly-polar molecules, amides and some other related dipolar molecules will be made by examining the concentration effect on the proton chemical shifts of amide and some other carbonyl compounds.

It will be made clear that the dilution shift and the change in the proton-proton coupling constant in solution can be interpreted in terms of a "head-to-tail" type of association between amide molecules.

Experimental

Materials.—*N*, *N*-Dimethylformamide (DMF), *N*, *N*-dimethylacetamide (DMAC), *N*, *N*-diethylformamide (DEF), *N*-methyl-2-pyrrolidone, and some other carbonyl compounds listed in Table II were obtained from commercial sources. The remaining compounds were prepared as follows. *N*-Formylpiperidine was prepared from the reaction of piperidine with chloral.[9] *N*, *N*-Dimethylglycolamide (DGA) was prepared by the aminolysis of methyl glycolate. These compounds were so pure that they showed no impurity lines when the spectrometer gain was near its maximum; hence, no further purification of the samples was carried out.

NMR Spectra.—The chemical shifts were measured in c.p.s. from internal tetramethylsilane with a Varian A-60 analytical spectrometer operating at 60 Mc. at a temperature of about 35°C. The precision of the measurement of chemical shifts was within about ±0.3 c. p. s.

Results and Discussion

The Chemical Shift and the Proton-proton Coupling Constant.—The amides studied in this work are listed in Table I, together with the chemical shifts and the association shift, which is defined as the difference between the chemical shifts in the neat liquid and in the carbon tetrachloride solution ($\delta_{\text{in neat}} - \delta_{\text{in CCl}_4}$). The notations used to distinguish the various protons in the groups attached to the nitrogen atom are shown in III; each proton is referred to as *cis* or *trans* with respect to the carbonyl oxygen.

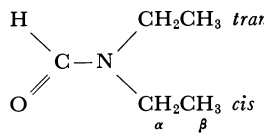

III

The NMR spectra of several amides are given in Fig. 1. The peaks in the NMR spectrum have been assigned by two different methods. The first one utilizes the difference in the long-range coupling constant between the protons of R_1 and R_2 or R_3; the *trans* coupling is believed to be larger than the *cis*.[10-12] The other method makes use of the change in the NMR spectrum of amides when they are diluted with benzene.[6,12] Hatton and Richards[6] proposed a specific interaction between benzene and the amide molecule in which the negatively-charged carbonyl oxygen was located as far away from the center of the benzene ring as possible.[12,13] We will now present our experimental results on the change in the proton-proton coupling constants and proton chemical shifts for each compound.

As to *N*, *N*-dimethylformamides, the magnitude of the long-range coupling constant between the formyl proton and the *N*-methyl protons decreases upon dilution with carbon tetrachloride (as is shown in Fig. 1). With higher concentrations,

1) H. S. Gutowsky and C. H. Holm, *J. Chem. Phys.*, **25**, 1228 (1956).
2) G. Fraenkel and C. Franconi, *J. Am. Chem. Soc.*, **82**, 4478 (1960).
3) M. T. Rogers and J. C. Woodbrey, *J. Phys. Chem.*, **66**, 540 (1962).
4) J. C. Woodbrey and M. T. Rogers, *J. Am. Chem. Soc.*, **84**, 13 (1962).
5) A. G. Whittaker and S. Siegel, *J. Chem. Phys.*, **42**, 3320 (1965).
6) J. V. Hatton and R. E. Richards, *Mol. Phys.*, **3**, 253 (1960); ibid., **5**, 139 (1962).
7) J. N. Murrel and V. M. S. Gil, *Trans. Faraday Soc.*, **61**, 402 (1965).
8) H. J. Anderson, *Can. J. Chem.*, **43**, 2387 (1965).
9) F. F. Blicke, *J. Am. Chem. Soc.*, **74**, 3933 (1952).
10) D. G. de Kowalewski, *Arkiv Kemi.*, **16**, 373 (1960). *J. Phys. Radium*, **23**, 255 (1962); V. J. Kowalewski and D. G. de Kowalewski, *J. Chem. Phys.*, **32**, 1272 (1960).
11) E. W. Randall and J. D. Baldeschwieler, *J. Mol. Spectry.*, **8**, 365 (1962).
12) L. A. LaPlanche and M. T. Rogers, *J. Am; Chem. Soc.*, **85**, 3728 (1964).
13) G. J. Karabatsos and R. A. Taller, ibid., **86**, 4373 (1964).

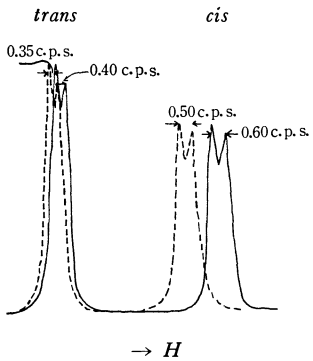

Fig. 1. *N*-Methyl signals of *N*,*N*-dimethylformamide ——: pure liquid, ----: 10% CCl_4 solution.

the polar structure, II, is favored by a dipolar-type interaction and a double-bond character between C and N serves to increase the long-range coupling constant between the formyl proton and the *cis* methyl proton J_{12}, or between the formyl proton and the *trans* methyl proton J_{13}. This may be seen obviously from the value of J_{12} or J_{13} given in Fig. 1. From the chemical shift data of DMF in Table I, it may be seen that the *cis* methyl signal shifts upfield as the concentration increases, while the *trans* methyl signal remains almost constant.

For *N*, *N*-dimethylacetamide, the two *N*-methyl signals are not equally sharp, with the higher field line being broader (as is shown in Fig. 2);

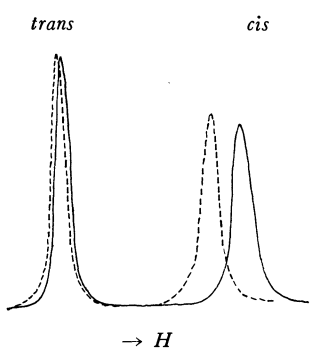

Fig. 2. *N*-Methyl signals of *N*,*N*-dimethylacetamide ——: pure liquid. ----: 10% CCl_4 solution.

the increased breadth of the high field line indicates that this line has a larger unresolved hyperfine interaction between *N*-methyl protons and *C*-methyl protons. When diluted with an inert solvent, carbon tetrachloride, the higher-field *N*-methyl signal line becomes sharp due to the diminution in the long-range coupling with *C*-methyl protons, as is also shown from the change in the H_{cis}/H_{trans} value given in Table I. Here, H_{cis} and H_{trans} indicate the height of the *cis* and *trans* methyl signals, and the H_{cis}/H_{trans} ratio is proportional to the ratio of the two long-range coupling constants, J_{12}/J_{13}. The large double-bond character of the C–N bond in the pure liquid makes J_{13} (*trans* coupling) larger, in turn resulting in a broad *cis* *N*-methyl signal line, that is, a decrease in the H_{cis}/H_{trans} value. This result also demonstrates the dipolar association for DMAC when the concentration increases. The *cis* *N*-methyl proton signal exhibits a larger upfield shift than the *trans* where there is a remarkable dipolar association of amide, as in the case of DMF. On the other hand, *C*-methyl protons show a downfield shift, much as that observed in the case of the formyl proton in DMF. In *N*-methyl-2-pyrolidone, in which rotation about the C–N bond is restricted, an upfield shift of the methyl proton resonance when the concentration is increased is also observed. On the other hand, α-methylene protons resonate downfield at higher concentrations; this is also attributed predominantly to the increment of the polar structure II, as is observed with the formyl proton in DMF and with the *C*-methyl protons in DMAC.

N, *N*-Diethylformamide (DEF) and *N*-formylpiperidine are used to examine the concetration effect on the proton shift. In DEF and *N*-formyl piperidine, compared to DEF, it is very interesting that α-methylene protons exhibit shifts to a lower field in pure liquid than in a carbon tetrachloride solution, while β-methyl protons show an upfield shift in pure liquid, as is the case for *cis* methyl protons in DMF, DMAC, and *N*-methyl-2-pyrrolidone. It is also interesting to note that the β-methyl protons *trans* to the carbonyl bond show a larger downfield shift than the *cis* protons. These interesting results will be discussed below.

In *N*, *N*-dimethylglycolamide (DGA), anomalous[14] chemical shifts of methyl protons have been observed, the methyl signal line at lower field being broader (Fig. 3). When we assumed that the *trans* coupling is larger than the *cis*, as is the case for DMF and DMAC, it follows that the resonance of *cis* methyl protons occurs at a lower field in DGA.

This larger breadth of the lower-field resonance line may be expected to arise from the larger long-range coupling between *cis* *N*-methyl protons and the methylene protons in the methylol group than that for *trans* methyl protons. This is justified from the spin-spin decoupling experiment. The methyl proton signal at a lower field is sharpened by methylene proton decoupling (Fig. 3-a and 3-b). In this compound, as is shown in Table I, the

14) Similar anomalous features are not observed for similar hydroxyl amides, *N*, *N*-dimethylhydracrylamide and *N*, *N*-dimethyllactamide. The details of the NMR spectra of these compounds, together with those of DGA, will be published elsewhere.

Table I. Chemical shifts[a] of amides

	Compound	Solvent	$H_\alpha(CH_3)$ cis	$H_\alpha(CH_3)$ trans	$H_\alpha(CH_2)$ cis	$H_\alpha(CH_2)$ trans	$H_\beta(CH_3)$ cis	$H_\beta(CH_3)$ trans	H or CH_3 (α to C=O)	H_{cis}/H_{trans}
1	*N*,*N*-Dimethylformamide	Neat	167.5	177.5	—		—		—	—
		CCl_4[b]	160.0	177.2	—		—		—	—
		CCl_4+MeOH[c]	171.2	179.2	—		—		—	—
2	*N*,*N*-Dimethylacetamide	Neat	170.0	180.2	—		—		119.5	0.75
		CCl_4[b]	171.0	180.2	—		—		117.0	0.82
		CCl_4+MeOH[c]	175.1	181.6	—		—		—	—
3	*N*-Methyl-2-pyrrolidone	Neat	163.5	—	—		—		—	—
		CCl_4[b]	165.0	—	—		—		—	—
4	*N*,*N*-Dimethylglycolamide	CCl_4 (30 w/v %)	176.0	172.0	—		—		—	0.71
		CCl_4 (5 w/v %)	179.0	173.0	—		—		—	0.87
5	*N*,*N*-Diethylformamide	Neat	—	—	201.0[d]		64.0	68.5	484.0	—
		CCl_4[b]	—	—	196.0[d]		65.5	71.5	476.0	—
6	*N*-Formylpiperidine	Neat	206.0	210.0	—		95.0		480.0	—
		CCl_4[b]	204.0	210.0	—		98.0		472.0	—

a) Chemical shifts are in c. p. s. from internal tetramethylsilane.
b) 10±1% solution.
c) Methanol is added to a CCl_4 solution.
d) *Cis* and *trans* signals are superposed.

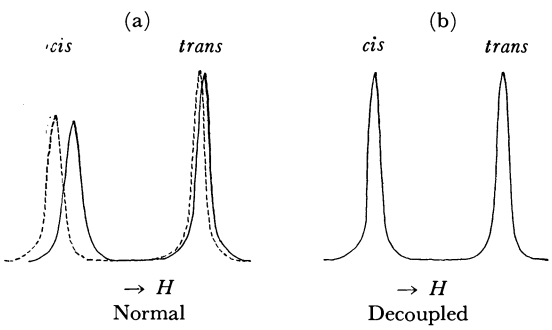

Fig. 3. *N*-Methyl signals of *N*,*N*-dimethylglycolamide, ——: 30% CCl_4 solution, ----: 5% CCl_4 solution.

proton signal of the *cis* methyl group also shifts upfield as the concentration increases.

The Nature of the Association of Amides.— The dilution of amides with CCl_4 may change the electronic distribution of the amide molecules, the diamagnetic anisotropy effect of the carbonyl bond, and the energy barrier of internal rotation about the C–N bond. All of these effects may cause a change in the proton chemical shift.

The association shift of methyl protons of DMF, DMAC, *N*-methyl-2-pyrrolidone, and DGA, together with β-methyl and methylene protons of DEF and *N*-formylpiperidine, probably does not result from the changes in charge distribution, since, if so, the methyl signal would move to a lower field; this is in contrast with those experiments in which the concentration increases, whereupon the polar structure II is favored due to the dipolar interaction, and the positively-charged nitrogen atom withdraws the σ-electron in the C–H bond.

When the energy barrier restricting the hindered internal rotation about the C–N bond increases with the amide concentration,[4,5] the separation between two methyl proton signals of DMF increases, and the symmetrical shift of two methyl proton signals can be observed. This internal rotation effect, however, will not contribute to the upfield shift of methyl protons of *N*, *N*-dimethylamides at high concentrations, because one of the two methyl proton signals at the higher field shifts upfield more than that of the lower-field methyl signal, resulting in an asymmetrical shift (Fig. 1). In fact, in *N*-methyl-2-pyrrolidone, which has a rigid structure and in which the methyl resonance is not affected by the internal rotation about the C–N bond, the upfield association shift is also observed for *N*-methyl protons. Thus, the upfield association shift is attributable to the long-range shielding effect of the carbonyl group. Two possible explanations of this behavior of chemical shifts come to mind; (1) a dipolar association may modify the magnetic anisotropy of the carbonyl bond, which in turn should change the chemical shift of the *N*-methyl protons. (2) This association may also decrease the average distances between amide molecules, and the proton resonances

of one amide molecule may be affected by the magnetic anisotropy of the carbonyl bond of neighbouring amide molecules. These two effects are referred to as the intramolecular and the intermolecular long-range diamagnetic anisotropic shielding effect (abbreviated as the intra- and intermolecular anisotropic effects respectively). In fact, there may be a superposition of these two effects.

The intramolecular anisotropic effect of the carbonyl group can be ruled out as a main factor from the following considerations. First, a dipolar association like the hydrogen bonding at the carbonyl oxygen[15] enhances the charge polarization of the carbonyl bond. However, when the hydrogen bonding occurs, as is shown in Table I, the *cis* methyl proton resonance shows a larger downfield shift than does the *trans*. Therefore, the upfield shift of *cis* methyl protons as the concentration increases may be due to the intermolecular anisotropic effect. Second, α-methyl proton resonance of DEF and *N*-formylpiperidine show a downfield shift as the concentration of amides increases. If the intramolecular anisotropic effect is the main factor in the association shift, this contrary tendency of the association shift is in contrast to the shift for methyl protons of DMF and DMAC. Thus, not the intra- but the intermolecular anisotropic effect is believed to be mainly responsible for the concentration effect of the chemical shifts of protons neighboring the carbonyl bond.

The anisotropic shielding effect of the carbonyl double bond has been exhibited in amides,[15-17] α, β-unsaturated carbonyl compounds, a series of steroids,[18] and α-methylenecycloketones.[19] In each of these cases, the chemical shift data indicate that the resonance spectra of magnetic nuclei shift to a higher field when the nuclei are constrained to a position in a conical region above and below the carbonyl bond.[20]

In the qualitative sense, it then follows that the association shift to the higher field indicates that the methyl group is in a conical region above or below the carbonyl double bond of another amide molecule. Thus, the structure of the dipolar association of the type demonstrated in Fig. 4 (the "head-to-tail" type of dipolar interaction) is probably favored for DMF, DMAC, *N*-methyl-2-pyrolidone, and DGA.

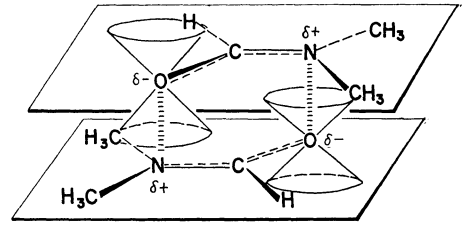

Fig. 4. The proposed model of the specific dipolar association of *N*, *N*-dimethylformamide.

In order to investigate further this type of association for other, similar carbonyl compounds, we measured the association shift of mesityl oxide and phorone. The results are listed in Table II; also shown is the chemical shift change effected by the hydrogen bond. The association shifts of these two carbonyl compounds are also upfield for the *trans* methyl proton; this reveals the same type of dipolar association as when the amides exist.

Table II. Chemical shifts[a] of α, β-unsaturated carbonyl compounds

	Compound	Solvent	Methyl protons	
1	Mesityl oxide[b,d]	Neat	125.2	110.7
		10% CCl_4	125.3	111.7
		10% CCl_4 +MeOH[e]	126.3	113.5
2	Phorone[c,d]	Neat	129.5	111.1
		10% CCl_4	128.8	112.9
		10% CCl_4 +MeOH	128.7	114.3

a) Chemical shifts are in c. p. s. from internal tetramethylsilane.

b)
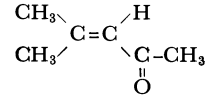

c)
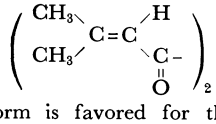

d) S-cis form is favored for these compounds from the infrared spectra (Ref. 21), dipole moment measurements (Ref. 22) and carbon-13 magnetic resonance spectroscopy (Ref. 23).

e) The concentration of MeOH is about 5%.

From the above qualitative considerations as to the chemical shift change of the protons neighboring the carbonyl bond effected by the dipolar

15) More quantitative discussions on the hydrogen bonding effects on the proton chemical shifts of carbonyl compounds will be published in the near future.
16) P. T. Narasimhan and M. T. Rogers, *J. Phys. Chem.*, **63**, 1388 (1959).
17) D. L. Hooper and R. Kaiser, *Can. J. Chem.*, **43**, 2363 (1965).
18) L. Chapman, H. G. Smith and R. W. King, *J. Am. Chem. Soc.*, **85**, 806 (1963); A. D. Cross and I. T. Harrison, ibid., **86**, 3223 (1963); D. H. Williams, N. S. Bhacca and C. Djerassi, ibid., **85**, 2810 (1963).
19) R. Kaiser and D. L. Hooper, *Mol. Phys.*, **8**, 403 (1964); G. Klose, ibid., **6**, 585 (1963).
20) L. M. Jackman, "Applications of Nuclear Magnetic Resonance Spectroscopy in Organic Chemistry," Pergamon Press, New York (1959).
21) R. L. Erskine and E. S. Waight, *J. Chem. Soc.*, **1960**, 3425.
22) J. B. Bentley, K. B. Everard, R. J. B. Marsden and L. E. Sutton, ibid., **1949**, 2957.
23) J. B. Stothers and P. C. Lauterbur, *Can. J. Chem.*, **42**, 1563 (1964).

Table III. Chemical shiets[a] of nitrosamines

Compound R_1R_2 NNO		Solvent	$H_\alpha(CH)$		$H_\alpha(CH_2)$		$H_\alpha(CH_3)$		$H_\beta(CH_3)$		Ref.
R_1	R_2		cis	trans	cis	trans	cis	trans	cis	trans	
C_2H_5	C_2H_5	Neat	—	—	271.0	251.5	—	—	62.0	82.0	Present work
		CCl_4	—	—	210.5	247.5	—	—	62.5	84.0	
CH_3	CH_2CH_3	Neat	—	—	215.4	250.2	180.0	223.2	61.2	79.8	24)
		CCl_4	—	—	211.2	249.0	175.8	222.6	63.0	82.8	
CH_3	$CH(CH_3)_2$	Neat	301.8	289.8	—	—	177.0	219.6	67.2	84.6	24)
		CCl_4	301.8	291.0	—	—	172.2	217.2	65.4	85.2	

a) Chemical shifts are in c. p. s. from internal T. M. S.

association mentioned above, we propose the dipolar association of the type given in Fig. 4 for amide and other carbonyl compounds. The structure of the dipolar association also indicates that *cis* methyl protons will show a large shielding effect of the carbonyl bond of neighboring amide molecule than those *trans* to the carbonyl bond; this finding is compatible with the experimental.

For *N*, *N*-diethyl amides and *N*-formylpiperidine the upfield shift of the β-proton and the downfield shift of α-protons by the association leads us to the inferences that β-protons may be in the conical region above or below the carbonyl bond and that the α-protons are nearly all in the remaining region of the carbonyl bond. If this model is valid, similar association shifts should be observed for the equimolecular and isoelectronic compounds, and *N*, *N*-diethylnitrosamine, in which the two methylene signals (for *cis* and *trans*) are well separated, unlike DMF. The experimental results are given in Table III for several nitrosamines. An inspection of the data will reveal that the chemical shift of β-protons goes upfield with an increase in the concentration of nitrosamine, while that of α-protons shows a downfield shift. The configuration of the dipolar-associated dimer of *N*, *N*-diethylnitrosamines is considered to be similar to that of *N*, *N*-diethylformamide.

We may summarize our conclusions as follows. In the pure liquid amides and some other isoelectronic compounds, i. e., α, β-unsaturated carbonyl compounds and nitrosamines, it is probable that the high-charge polarization of these molecules favors a structure of dipolar self-association in which the positively-charged nitrogen (or carbon) of one molecule is directly over the negative oxygen atom of the other.

24) C. J. Karabatsos and R. A. Taller, *J. Am. Chem. Soc.*, **86**, 4373 (1964).

BULLETIN OF THE CHEMICAL SOCIETY OF JAPAN VOL. 39 2352—2355 (1966)

Kinetic Studies of Ammonia Oxidation in Shock Waves. II. The Rate of Ammonia Consumption*

By Tetsu TAKEYAMA and Hajime MIYAMA

Basic Recearch Laboratories, Toyo Rayon Company, Ltd., Tebiro, Kamakura, Kanagawa

(Received March 5, 1966)

An investigation was made of ammonia oxidation in shock waves at temperatures from 2100 to 2600°K by monitoring the ultraviolet absorption of ammonia at 2245 Å. The absorption coefficient of ammonia was measured at various temperatures; the rate constant of the decomposition reaction at higher temperatures with a mixture of 1% NH_3 and 99% Ar was found to be in good agreement with the results of other studies. By using several mixtures of ammonia and oxygen highly diluted with argon, the rate of ammonia consumption immediately after an induction period was found to be expressed by:

$$-\left(\frac{d[NH_3]}{dt}\right)_0 = k_0[NH_3]^{1.5}[O_2]^{0.5}[Ar]^{0.5}$$

where: $\log k_0(l^{1.5}mole^{-1.5}sec^{-1}) = 12.77 \pm 0.10 + (-8488 \pm 573)/T$. This corresponds to an apparent activation energy of 38.8±2.6 kcal./mole.

In a preceding paper[1] on the ammonia-oxygen reaction, we reported the results obtained from measurements of the induction periods and time histories of various intermediate species, and a reaction mechanism for the induction period was proposed.

Now, a challenging problem is to study the early stage of the reaction which follows the induction period. We will describe here results obtained from measurements of ammonia absorption at 2245 Å over the range of conditions $2100 \leq T \leq 2600$°K, $2.1 \leq p \leq 5.4$ atm., $0.5 < [NH_3]/[O_2] \leq 2$, and $1.0 \times 10^{-4} \leq [O_2]$, $[NH_3] \leq 4.1 \times 10^{-4}$ mol./l.

Experimental

The experimental details have been described previously.[2] In brief, the velocity of an incident shock wave was measured with two thin-film thermometers, which were placed at a distance of 139.0 mm. from each other, and with an electronic counter. One of the thermometers was placed 5.0 mm. from the endplate where the observation windows of quartz were set.

An ultraviolet absorption of ammonia was measured at 2245 Å.[3] The slit width of a monochrometer was set at 0.6 mm., which allowed a band pass of 7 Å.

The procedures of preparing reaction mixtures as well as the materials used were the same as those described in a previous paper.[1]

Results and Discussion

The Extinction Coefficients of Ammonia at 2245 Å.—The extinction coefficient at room temperature was determined from the decrease in photocurrent when the shock tube (7.6 cm. in internal diameter) was filled with pure ammonia. The absorption of ammonia agreed well with Beer's law up to a pressure of 700 mmHg, which was the upper limit of our glass gas-handling system. The decadic extinction coefficients found were 3.42 and 4.15 l. $mole^{-1}$, at 295 and 300°K respectively.

The extinction coefficients at high temperatures were determined from the initial decreases in photocurrent immediately after the passage of the incident and reflected shock waves, by using mixtures of 1, 2, or 3% ammonia and argon. The absorption increased linearly with the concentration of ammonia up to about a 90% absorption. The extinction coefficients as a function of the temperature are plotted in Fig. 1, which shows a rather definite decrease in their value above 3000°K. This may be due to a rapid decomposition of ammonia at these high temperatures. The solid line in the figure was obtained by a multiple regression analysis, while the dashed line was obtained by Michel and Wagner[4] at 2300 Å. The latter line was calculated from their Arrhenius-type expression up to 3000°K, though its effective temperature range was not explicit in their paper. The difference between these two data is large at lower temperatures;

* Presented at the 19th Annual Meeting of the Chemical Society of Japan, Tokyo, April, 1966.

1) T. Takeyama and H. Miyama, This Bulletin, **38**, 1670 (1965).

2) T. Takeyama and H. Miyama, ibid., **38**, 936 (1965).

3) R. W. B. Pearse and A. G. Gaydon, "The Identification of Molecular Spectra," Chapman & Hall, London (1950), p. 180.

4) K. W. Michel and H. Gg. Wagner, "Tenth Symposium (International) on Combustion," The Combustion Institute, Pittsburgh (1965), p. 353.

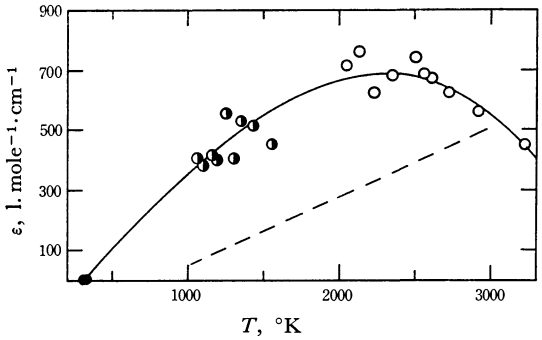

Fig. 1. Temperature dependence of the NH_3 extinction coefficient at 2245Å.
●, measured by static method at room temperature; ◑, measured in incident shock waves, ○, measured in reflected shock waves. Solid line is the best fit to the points by multiple regression analysis. Dashed line is a result of Michel and Wagner[4] at 2400A.

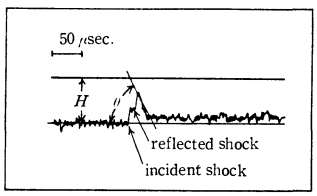

Fig. 2. Typical oscillogram showing NH_3 absorption vs. time.
1%NH_3-99%Ar; p_1, 51.0 mmHg: w_r, 1122 m./sec.; T_5, 2790°K; P_5, 7.3 atm.; [NH_3], 2.05×10^{-4} mole/l.

they differ by a factor of ten at 1000°K. This can be attributed to the strong wavelength dependence of extinction coefficients at lower temperatures.[5]

The Pyrolysis of Ammonia.—Oscillographic records obtained in the measurements of the extinction coefficients of ammonia showed that a detectable amount of decomposition started only after a temperature-dependent induction period at lower temperatures (<2400°K). Therefore, the initial rates of the decomposition of ammonia were determined for higher-temperature runs, in which no induction period was observed, as is shown in Fig. 2. Here, mixture of 1% ammonia and argon were used. The equation used was[6]:

$$-\frac{d[NH_3]}{dt}=\frac{\tan\theta\exp(\varepsilon l[NH_3])}{Hw\varepsilon l} \qquad (1)$$

where ε denotes the extinction coefficient in l. mole^{-1} cm^{-1}; l, the optical length (7.6 cm.), and w, the sweep velocity on the record (sec. cm^{-1}). The height, H, is assumed to be the deflection for 100% absorption, since the room temperature

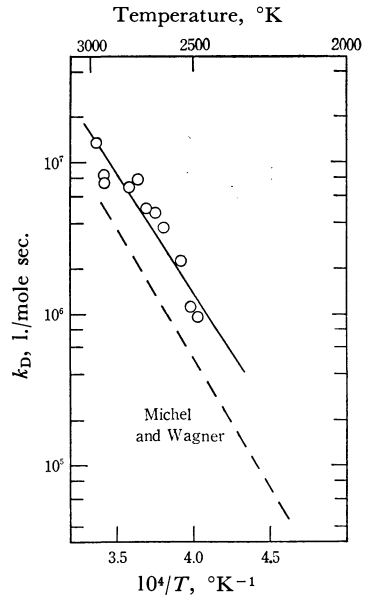

Fig. 3. Second-order rate constants for decomposition of ammonia.

absorption of ammonia is negligibly small, as was described above. The tangent of the angle θ gives the initial rate of change of absorption by ammonia. θ was estimated within a range not exceeding a 10% decomposition of ammonia. Therefore, as an approximation, the authors did not include in Eq. 1 such corrections brought about by the reaction as the temperature decrease, the density increase, and the change in the extinction coefficient.

Thus, the decomposition rate constant, k_D, of the first order with respect to ammonia and argon,* was determined from the initial rate. The results are presented in Fig. 3 as an Arrhenius plot. The solid line obtained by a least-squares calculation is expressed by:

$$\log k_D\ (\text{l. mole}^{-1}\,\text{sec}^{-1})=(12.36\pm0.15)-(71100\pm9200)/2.303RT \qquad (2)$$

For the purposes of comparison, the results of Michel and Wagner[4] obtained from the measurement of the ultraviolet absorption of ammonia at 2300 Å are also shown in the figure. There exists a good agreement among the data of the two groups; this confirms the reliability of the present measurements.

The Rate of Ammonia Consumption in the Oxidation Reaction.—The oxidation of ammonia was studied over the temperature range from 2100

5) H. Gg. Wagner, private communication.
6) H. B. Palmer and D. F. Hornig, *J. Chem. Phys.*, **26**, 98 (1957).

* Michel and Wagner[4] used the second-order expression, $k_D[NH_3][Ar]$, though Jacob[7] obtained $k_D[NH_3]^{1.5}[Ar]^{0.5}$. Although our data are not enough to determine which of these expressions is right, the former expression was used for the sake of simplicity. Even when the latter is applied, however, our data agree well with those of Jacob.
7) T. A. Jacob, *J. Phys. Chem.*, **67**, 665 (1963).

TABLE I. INITIAL RATES OF AMMONIA CONSUMPTION DETERMINED AT 2255±10°K WITH VARIOUS REACTION MIXTURES

Reaction mixture	Number of runs	Composition % NH_3	O_2	Ar	P_4 atm.	P_1 mmHg	T_5 °K	$[NH_3]$ 10^{-4} mole/l.	$[O_2]$ 10^{-4} mole/l.	[Ar] 10^{-2} mole/l.	v_0 mole l^{-1}. sec^{-1}
I	5	2.0	1.0	97.0	5.0	50.3±0.1	2255±10	3.91±0.01	1.96±0.00	1.90±0.00	19.0±2.6
II	6	1.0	1.0	98.0	5.0	53.3±0.3	2255±15	2.01±0.01	2.01±0.01	1.97±0.01	4.9±0.7
III	2	0.5	1.0	98.5	5.0	54.3±0.1	2260± 0	1.01±0.00	2.01±0.00	1.98±0.00	1.9±0.0
IV	4	1.0	2.0	97.0	5.0	53.6±0.1	2265±15	2.05±0.00	4.10±0.01	1.99±0.00	7.1±0.5
V	5	1.0	0.5	98.5	5.0	53.4±0.2	2255±15	2.00±0.01	1.00±0.00	1.97±0.01	3.5±0.3
VI	7	0.8	0.8	98.4	7.3	78.7±0.3	2250± 0	2.40±0.01	2.40±0.01	2.88±0.01	7.6±2.0
VII	5	1.0	1.0	98.0	6.0	63.8±0.4	2250±15	2.40±0.02	2.40±0.02	2.35±0.02	10.2±1.1
VIII	7	1.2	1.2	97.6	5.0	52.2±0.1	2250± 0	2.38±0.01	2.38±0.01	1.93±0.00	7.1±1.2
IX	9	2.0	2.0	96.0	3.0	29.2±0.4	2260± 0	2.31±0.03	2.31±0.03	1.11±0.02	5.9±1.2

Note; P_4, P_1, and T_5 are pressure of driver section, initial pressure of test section, and temperature immediately behind reflected shock wave respectively.

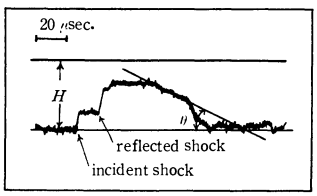

Fig. 4. Oscillographic record showing the change in NH_3 absorption during oxidation reaction.
0.82%NH_3-0.82%O_2-98.36%Ar; P_1, 97.1 mmHg; w_r, 978.9 m./sec.; T_5, 2160°K; P_5, 5.14 atm.; $[NH_3]$ and $[O_2]$, 2.38×10^{-4} mole/l.

to 2600°K. A typical oscillogram is shown in Fig. 4. An appreciable amount of reaction starts after an induction period, which becomes shorter at higher temperatures, with an initial rate of v_0. Then, the rate increases to a final rate, v, as the reaction proceeds further. As the temperature increases, the v_0 rate becomes greater until finally it coalesces with v. The initial rates were calculated by the procedure used in the preceding section. The order of reaction was determined in the following manner; for example, for the determination of the order with respect to ammonia, the initial rates were measured by using different mixtures, in which only the ammonia content was varied, keeping

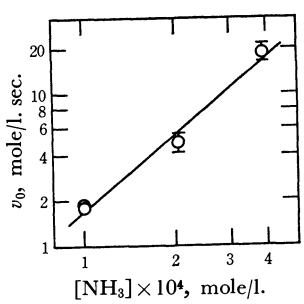

Fig. 5. Dependence of rate on ammonia concentration.
T_5, 2255±10°K; $[O_2]$, $(1.99\pm0.02)\times10^{-4}$ mole/l.
[Ar], $(1.94\pm0.03)\times10^{-2}$ mole/l.

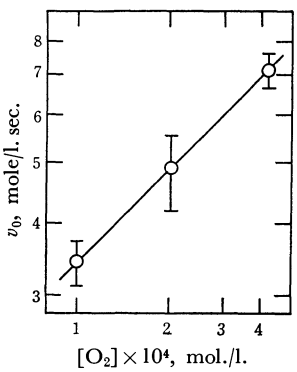

Fig. 6. Dependence of rate on oxygen concentration.
T_5, 2260±15°K;
$[NH_3]$, $(2.01\pm0.02)\times10^{-4}$ mole/l.
[Ar], $(1.97\pm0.01)\times10^{-2}$ mole/l.

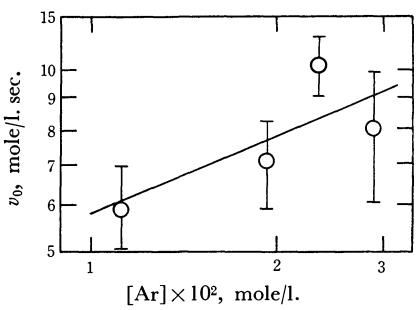

Fig. 7. Dependence of rate on argon concentration.
T_5, 2255±10°K;
$[NH_3]$ and $[O_2]$, $(2.28\pm0.10)\times10^{-4}$ mole./l.

those of oxygen and argon unchanged, and by adjusting the pressures of the driving helium and of the reaction mixtures so that a constant temperature was obtained. The results obtained at 2255±10°K are summarized in Table I and shown graphically in Figs. 5, 6, and 7. The reaction orders with respect to ammonia, oxygen, and argon were found

from least-squares calculation to be 1.70±0.06, 0.51±0.01, and 0.42±0.08* respectively. Thus, the initial rate of ammonia consumption may approximately be expressed by the following equation:

$$v_0 = -\left(\frac{d[NH_3]}{dt}\right)_0 = k_0[NH_3]^{1.5}[O_2]^{0.5}[Ar]^{0.5} \quad (3)$$

Next, the rate constant, k_0, was determined over the 2100—2600°K temperature range and the 2.1—5.4 atm. pressure range by using mixtures of 1% ammonia, 1% oxygen, and 98% argon, on the assumption that the rate equation (3) is valid. The results are shown in Fig. 8 as an Arrhenius plot. The solid line calculated by a least-squares method is expressed as follows:

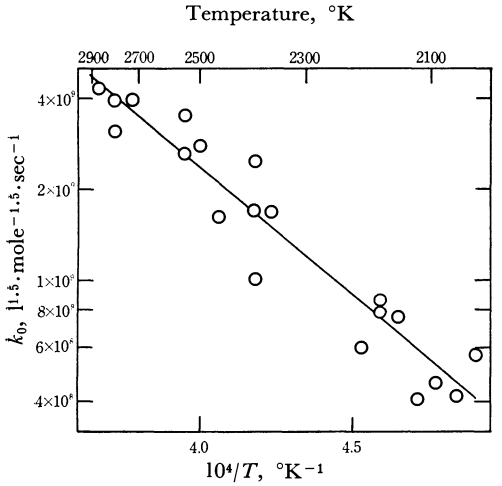

Fig. 8. Arrhenius plot for the rate constants of ammonia consumption in 1%NH_3-1%O_2-98%Ar mixture.

$$\log k_0\ (l.^{1.5}mole^{-1.5}sec^{-1}) = (12.77\pm0.10) + (-8488\pm573)/T \quad (4)$$

The temperature dependence corresponds to an apparent activation energy of 38.8±2.6 kcal./mole. On the other hand, the values of activation energy obtained at lower temperatures[8-10] were in the range of 30—50 kcal./mole. However, a comparison of the present value with those at lower temperatures is useless because the rate expressions in the latter cases are more complicated due to the wall effect.

Also, we were not successful in finding a reasonable chain-branching mechanism to fit the rate expression (3) by using the present and other available data. However, concerning the thermal decomposition of ammonia in shock waves, Jacob[7] obtained the following relation:

$$-d[NH_3]/dt = k[NH_3]^{1.5}[Ar]^{0.5} \quad (5)$$

Here, $k=2.5\times10^{13}\exp(-77\ \text{kcal./}\boldsymbol{R}T)$ l. mole^{-1}· sec^{-1}. In order to explain this relation, Avery and Bradley[11] proposed this reaction scheme:

$$NH_3 + Ar \xrightarrow{k_1} R_1 + \cdots + Ar \quad (I)$$

$$R_1 + NH_3 \xrightarrow{k_2} [R_2 + \cdots] \rightarrow R_1 + \cdots \quad (II)$$

$$R_1 + R_1 \xrightarrow{k_3} \text{stable products}, \quad (III)$$

The assumption of a stationary-state concentration of the R_1 radical leads to a corresponding kinetic expression with $k=k_2k_1^{1/2}/k_3^{1/2}$. If the initiation step I is replaced with the following steps in the case of ammonia oxidation, the rate expression (6) is easily derived by a stationary-state assumption:

$$NH_3 + O_2 \rightleftarrows [NH_3\cdots O_2]$$

equilibrium constant K

$$[NH_3\cdots O_2] + Ar \xrightarrow{k_1'} R_1 + \cdots$$

$$-d[NH_3]/dt = \frac{k_2k_1'^{1/2}K^{1/2}}{\sqrt{2}k_3^{1/2}} \times [NH_3]^{1.5}[O_2]^{0.5}[Ar]^{0.5} \quad (6)$$

This agrees with experimental equation (3). However, the scheme described above is one of many possibilities of explaining the present results; the actual situation in the high-temperature oxidation of ammonia will not be so simple.

In order to explain the present experimental results, it is desirable to compare them with the theoretical rate law and the activation energy, which can be predicted by an analytical solution of several linear differential equation for an appropriate chain-branching scheme. However, no detailed data on elementary reactions are available for this purpose, and so the solution of this problem must be postponed.

The authors wish to express their thanks to Messrs. Kazutoshi Sugiyama and Akio Sawa for their help in the experiment.

*2 Least-squares calculation by using all the data in Table I also gives a reaction order of about 0.5 with respect to argon. However, for the sake of simplicity, typical runs, all conducted under almost the same conditions, except for the argon concentration, in order to keep the effect of the ammonia and oxygen concentrations as small as possible, are shown in Fig. 7.

8) E. R. Stephens and R. H. Pease, *J. Am. Chem. Soc.*, **74**, 3480 (1952).
9) E. R. Stephens and R. H. Pease, ibid., **72**, 1188 (1950).
10) J. Vervimp and A. Van Tiggelen, *Bull. Soc. Chim. Belg.*, **62**, 205 (1953).
11) H. E. Avery and J. N. Bradley, *Trans. Faraday Soc.*, **60**, 857 (1964).

BULLETIN OF THE CHEMICAL SOCIETY OF JAPAN VOL. 39 2356—2361 (1966)

An NMR Study of Proton Exchange in Alcohols. I. Oxygen Effects in Methanol*1

By Shizuo FUJIWARA, Yuzuru FUJIWARA*2 and Makoto NAGAI*3

Department of Chemistry, Faculty of Science, The University of Tokyo, Hongo, Tokyo

(Received March 23, 1966)

Molecular interactions between oxygen and organic molecules are investigated in detail. It was confirmed that the broadening of spectral lines due to oxygen is appreciable only with hydroxyl protons. This effect is attributed to the enhancement of the proton exchange of OH groups by oxygen. Detailed investigation was made with methanol-oxygen system. In relation with this, a new method is proposed which makes the measurement of heat of dissolution of oxygen in methanol possible.

It has long been known that the line widths of the electron spin resonance are much broadened by oxygen, but not by nitrogen, argon, and hydrogen.[1] This oxygen effect has tentatively been ascribed to a dipolar broadening of the line from adsorbed paramagnetic oxygen. The reversible interaction of carbon-free radicals with molecular oxygen has also received considerable attention.[2-6]

A similar broadening effect is assumed to exist in high-resolution NMR spectra. Chiarotti and Giulotto made an effort to obtain the T_1 of water which is completely free of oxygen.[7] Gaven, Stockmeyer, an Waugh referred the oxygen effect in the T_1's of methane and other diamagnetic gases.[8] They interpreted the oxygen effect in the same way as in ESR, in terms of local magnetic fields which alter the lifetimes of nuclear-spin states.

However, so far as we know, there is no evidence which shows that the observed line-width broadening with oxygen is mainly due to paramagnetic dipolar interactions. On the contrary, in our preliminary experiment, we encountered several cases where the paramagnetic dipolar broadening due to oxygen is relatively small. The broadening effect is, indeed, so small in several cases that it is only detectable in the wiggles, or in the hyperfine structure. Figure 1 shows the resonance lines of methine protons in degassed and in un-degassed

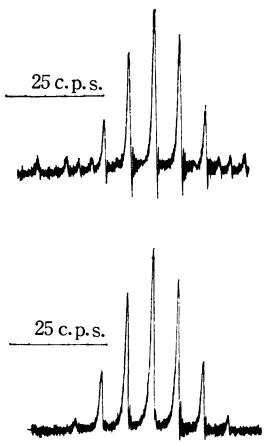

Fig. 1. NMR of methine protons in isopropyl chloride (at 100 Mc).
a) upper: degassed b) lower: undegassed

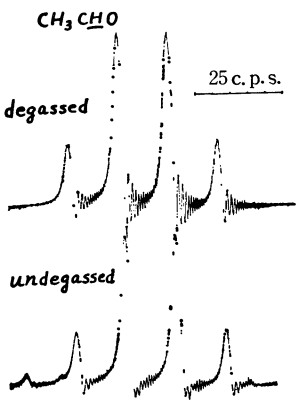

Fig. 2. NMR of active protons in acetaldehyde (at 100 Mc).

*1 Presented at the 1st International Symposium on Novel Applications of Nuclear Magnetic Resonance, Tokyo, September, 1965.

*2 On leave from the Kurashiki Rayon Company, Kurashiki, Okayama.

*3 On leave from the Central Research Laboratory, Mitsui Chemical Company, Tokyo.

1) R. C. Fehel, *Phys. Rev.*, **114**, 1219 (1959).
2) D. J. E. Ingram and J. G. Tapley, *Chem. & Ind.* **1955**, 568.
3) J. Uebersfeld and E. Erb, *J. Phys. Radium*, **16**, 340 (1955).
4) D. E. G. Austen and D. J. E. Ingram, *Chem. & Ind.* **1956**, 981.
5) J. E. Uebersfeld, *C. R. Acad. Sci., Paris*, **241**, 371 (1955).
6) L. S. Singer and W. T. Spry, *Bull. Am. Phys. Soc.*, **1956**, 214.
7) G. Chiarotti and L. Giulotto, *Phys. Rev.*, **93**, 1241 (1954).
8) V. J. Gaven, W. H. Stockmayer and J. S. Waugh, *J. Chem. Phys.*, **37**, 1188 (1962).

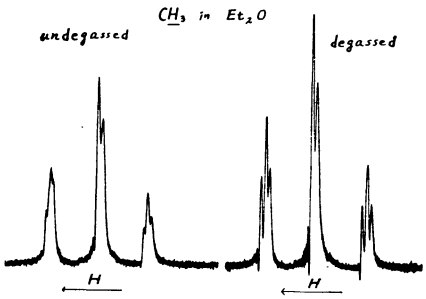

Fig. 3. NMR of methyl protons in ethyl ether at 40 Mc.
(By courtesy of Dr. Hayashi of the Japan Electron Optics Company.)

isopropyl chloride. The line width of the degassed sample is slightly narrower than that of the undegassed sample, as may be deduced by the large amplitude of wiggles. A similar fact may be deduced from the resonance lines of the active protons of acetaldehyde (cf. Fig. 2). Figure 3 presents another case where the small difference in line-widths is observed in the change in line shapes of the hyperfine structure. The left-hand-side signal refers to the methyl proton signal at 40 Mc. in un-degassed ethyl ether, and the right-hand side signal, to that in the degassed sample. The line-widths of the degassed sample is smaller than that of the un-degassed one.

It should be noticed that all the compounds referred to above are those which do not contain exchangeable protons. According to the results of these measurements, we may conclude that the dipolar broadening effect of oxygen, present in the liquid in a concentration of a magnitude of contamination, is only about 0.1, or 0.2 cycles per second at room temperature.

This value is about two hundredths of the value calculated by the equation for paramagnetic dipolar broadening derived by Bloembergen[9] with the use of the value of the specific susceptibility of oxygen[10] as $+3449\times10^{-6}$ (293°K), and taking the oxygen content in water or in other liquids, which is in equilibrium with air, as 20 p. p. m. in weight. The latter value was determined by the use of an oxymeter of Magna Corp.[11] On the other hand, those compounds which contain hydroxyl groups give line-widths larger than those which can be ascribed to simple electron paramagnetic dipolar or contact interactions. Typical examples are obtained with methyl alcohol, ethyl alcohol, isopropyl alcohol, aquated acetaldehyde, and hemiacetal.

9) N. Bloembergen, E. M. Purcell and R. V. Pound, *Phys. Rev.*, **73**, 679 (1948).
10) "Handbook of Chemistry and Physics," Chemistry and Rubber Publishing Company, 44th Ed., P. 2731.
11) Oxymeter Model 1070, Magna Corporation, Santa Fe, New Mexico.

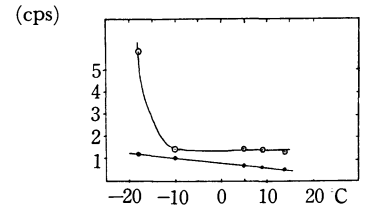

Fig. 4a. NMR in 40% aqueous solution of acetaldehyde.
-○- hydrated molecule
-●- non hydrated molecule

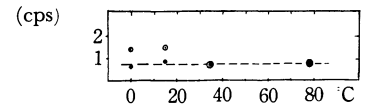

Fig. 4b. NMR in acetaldehyde dissolved in methyl alcohol.
⊙; CH_3 of hemiacetal, $CH_3(CH)(OH)(OCH_3)$
●; CH_3 of acetal, $CH_3(CH)(OCH_3)_2$
---- instrumental line width

Figure 4(a) shows the spectrum of a proton resonance in an aqueous solution of acetaldehyde. The aquated molecule is coexistent in the same capillary tube with a molecule of pure acetaldehyde. The spectral lines of the two molecular species are distinguished from each other by separate lines which refer to each species. The line-widths of the spectrum of the hydrated molecule are, as shown in the figure, larger than those of the pure acetaldehydre by about 0.5 cycles per second.

Figure 4(b) presents the line-widths of acetaldehyde in a methyl alcohol solution. The width of the methyl signal of hemiacetal, which contains a hydroxyl group, is larger than that of acetal, which does not contain a hydroxyl group. It should be noted that these differences refer to differences between molecular species which are coexistent in the same capillary.

Degassed ethyl alcohol reveals hyperfine structures for all the groups, OH, CH_2, and CH_3, as is shown in Fig. 5. However, in the spectra of the un-degassed sample, the second-order hyperfine structure of CH_2 proton signal, which is observable in the degassed sample, is missed. It must be noted

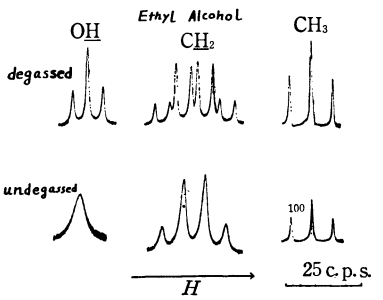

Fig. 5. Hfs. in degassed ethyl alcohol.

that the half-maximum line-widths of one component of the hyperfine lines of the methyl signal is only a few tenths cps. larger in the un-degassed sample than in the degassed sample. This implies that the paramagnetic dipolar or contact broadening effect of oxygen is very small, even in systems which contain hydroxyl protons. It is, therefore, apparent that the large broadening effect which is observed in alcohols and other related compounds is due to the effect of air and to the chemical exchange of hydroxyl protons.

Methyl alcohol is taken as the sample for detailed investigation because it is the simplest alcohol, and a strong oxygen effect is observed in it.

Experimental

Measurements were made at 60 Mc./sec. with a C-60 spectrometer of the Japan Electron Optics Laboratory, and at 100 Mc./sec. with an HA-100 spectrometer of Varian Associates. The sample temperature could be varied from $-100°$ to $+80°C$ with an accuracy of $\pm 1°C$. The line-width was measured in the lower temperature range as the half-maximum line width of one component of the spectra's hyperfine structure. In the higher temperature range, where the hyperfine structure is smeared out, the half-maximum line-widths of the whole envelope of the spectrum was measured. In the intermediate range, measurements were made in line with the nature of the spectrum, according to the method proposed by Alexander.[12]

About twenty samples were prepared and used in the present experiment. They differ according to the procedure used to purify them and according to the impurity concentration. For convenience, however, they may be classified into four groups: (a) the purest one, prepared from anhydrous methanol by a three-stage distillation over magnesium; (b) those prepared by twice distilling them over magnesium: (c) commercial methanol, of the purest guaranteed grade, used as the starting material for the other distillations, and (d) the one prepared by saturating the degassed sample, (a), with one atmosphere of oxygen. Sample (d) will be referred to as "the oxygen sample" in later discussions. As will be shown, these samples show remarkable differences in their chemical shifts and in the exchange rate of their OH protons. It was noticed during the experiment that the spectrum of each sample changed considerably with time. As this happened in sealed-glass tubes, we assumed it to be due to impurities coming from the walls of the glass tubes. Because of this sensitivity in the spectral features, all the results reported here have been obtained from freshly prepared samples.

Degassing was carefully done by repeated freezing and melting, either under a vacuum or under a nitrogen atmosphere. The latter procedure was most effective in removing oxygen.

The chemical shift was measured in two ways: one, by using tetramethyl silane as an internal reference, and the other, by locking the CH_3 signal without any addition of tetramethyl silane. By the former method, the CH_3 signal was found to be independent of the temperature and to be effectively constant, regardless of the presence of oxygen. Figure 6 shows the results of measurements where the methyl signal of tetramethyl silane is locked as the internal standard. It was noticed that tetramethyl silane affects the exchange rate of hydroxyl protons; therefore, precise measurements of the line shape and of the chemical shift of OH protons were made by the latter method. The chemical shift of OH protons in the purest methanol is taken to be -300 ± 1 c. p. s. at 100 Mc., or -3.00 ± 0.01 p. p. m. from CH_3. The fluctuation in this value of ± 1 c. p. s. is due to contamination by trace amounts of oxygen. Contamination by other impurities, such as water and alkali, produces much larger fluctuations. In practice, the chemical shift and the line shape measurements reveal the difficulty of obtaining pure methanol.

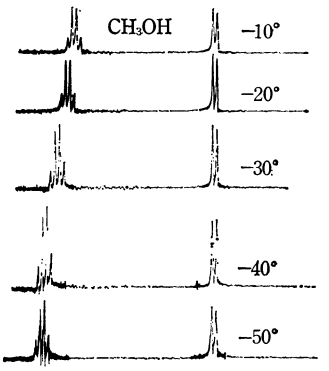

Fig. 6. Chemical shift of OH of MeOH as the function of temperature.

The chemical shift of OH protons is a linear function of the temperature, as has been reported already.[13] The chemical shift of OH protons in the purest methanol can be used as an accurate control of the temperature of an NMR sample.[14]

Results and Discussion

Line-widths.—The line shapes of the proton resonance in methanol are temperature-dependent; they can be divided into three types according to the temperature; one, a single line at a high temperature; two, a well-separated hyperfine structure at a low temperature; and three, a collapsing hyperfine structure at an intermediate temperature. Figures 7 and 8 present typical examples of the temperature dependence of the line shapes of OH protons. The relative position of each spectrum along the horizontal line is with reference to the chemical shift to the temperature at which the spectrum was measured. It may be seen in Fig. 7 that the hyperfine structure begins to appear between 10 and 20°C, and that the components of the quadruplet's structure are well separated at about $-20°C$.

12) S. Alexander, *J. Chem. Phys.*, **37**, 967, 974 (1962).

13) J. T. Arnold and M. E. Packard, ibid., **19**, 507 (1951).

14) This technique was also referred to independently by Prof. L. W. Reeves at the NMR Symposium held in Tokyo in 1965.

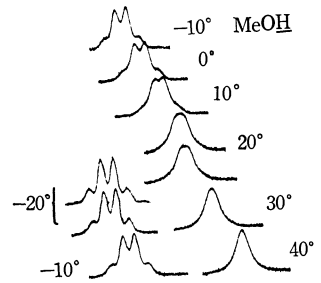

Fig. 7. Temperature dependence of the line shapes of OH protons in MeOH undegassed.

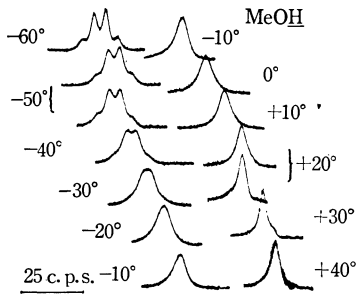

Fig. 8. Temperature dependence of the line shapes of OH protons in MeOH saturated with 1 atmospheric O_2.

However, in Fig. 8, in the oxygen sample the hyperfine structure begins to appear as low as at from −30 to −40°C, and a quadruplet is well separated at −60°C. This is surprising, because both samples have been prepared from the same purified methanol at the same time; they differ only in the concentration of oxygen. If we define T_{hfs} and T_{quad} as the temperature where the hyperfine structure begins to appear and that where the quadruplet structure begins to be well separated respectively, the observed differences in T_{hfs} and T_{quad} between the two samples must be attributed to the effect of oxygen. It may clearly be seen that the critical temperatures for the vacuum-degassed and the nitrogen-degassed samples are lowered by about 5°C in the un-degassed sample. This lowering may also be attributed to the effect of oxygen. It should especially be noted that the observed effect is not due to nitrogen. These results suggest that the lowering of the critical temperature, which is equivalent to the enhancement of the proton exchange between hydroxyl groups, is caused by oxygen.

In order to interpret this effect, we must investigate the interaction of oxygen with methanol. We will do by the method used to investigate the interactions between methanol and transition metal ions,[15] with necessary modifications being made in the course of interpretation. We assume a model which represents the system to be investigated. The system to be considered here consists of two nuclear environments, the coordination sphere of paramagnetic oxygen and the bulk solvent. The two environments are designated by the indices M and A. We will treat a special case where the number of protons in the A environment is much larger than that in the M environment; the ratio of M protons is written as pq, where p is the number of oxygen molecules per solvent molecule, and q, the solvation number of oxygen. Hence, $pq \ll 1$.

The magnetic resonance of A and M protons are characterized by the relaxation times, T_{1A}, T_{2A}, T_{1M}, and T_{2M} respectively. The difference in Larmor frequencies between the two environments is designated by $\Delta\omega$. Protons can be exchanged between the two environments at a rate characterized by the average residence time of a proton in the M environment, τ_M. In fact, we can not assume, in the lower temperature range, a diffusional motion of molecules which produces exchange between bonded and free molecules.

The NMR spectrum actually observed consists essentially of a single peak; i. e., A and M protons do not show separate peaks. We assume that this is not due to the low concentration of oxygen, but to the rapid motion of oxygen, which averages out the resonant sites of all protons in the medium. In such a case, the line-widths of the bonded molecule is related to the electron relaxation time, τ_s, and the hyperfine interaction constant, A. The behavior of the OH and CH_3 peaks is similar, and the same remarks apply to both. At low temperatures, the exchange of molecules between the bulk methanol and the coordination sphere is too slow to affect the spectrum. We assume that the peaks of the bulk methanol are characterized by equal longitudinal and transverse relaxation times, which change little with the temperature.

As the temperature is increased, exchange sets in and the line width increases. It reaches a maximum, and then decreases with an increase in the temperature. This movement is attributed to the exchange between OH protons, resulting in an averaging of the hyperfine lines. It must be noted that the temperature where the maximum width occurs is the same for both the OH and CH_3 signals, and that it depends upon the character of the sample, i. e., the concentration of impurities.

In the lower temperature range, we take the electron spin relaxation time, τ_s, for the correlation time of the interaction between the paramagnetic oxygen and methanol molecules. Kinetic parameters are calculated for molecular interactions in this range by the use of Eqs. 1 to 4. They were originally derived by Solomon and Connick[15] and used by Meiboom.[16]

15) T. J. Swift and R. E. Connick, *J. Chem. Phys.*, **37**, 308 (1962).

16) Z. Luz and S. Meiboom, ibid., **40**, 1058, 1066, 2686 (1964).

$$1/T_{2M}=pq/T_{2M} \quad (1)$$

$$\Delta\omega=pq\Delta\omega_M/[(\tau_M/T_{2M}+1)^2+\tau_M^2(\Delta\omega_M)^2] \quad (2)$$

$$\Delta\omega_M/\omega_I=\frac{s(s+1)}{3kT}\frac{g|\beta|}{\gamma_I}A \quad (3)$$

$$1/T_{2M}=\frac{4}{3}\frac{s(s+1)\gamma_I^2g^2\beta^2}{\gamma^6}\tau_s+\frac{2}{3}\frac{s(s+1)}{\hbar^2}A^2\tau_s^2 \quad (4)$$

In practice, we assume, regarding the relations between τ_s, τ_M, $\Delta\omega_M$, that $\tau_{2M}\gg\tau_M$ and that $\tau_M\Delta\omega_M\simeq 1$. We also assume that r, the distance between oxygen and a methanol molecule, is equal to 3 Å. In Eq. 1, $1/T_2$ is taken to be 0.2 c. p. s. or less, while $\Delta\omega$, in Eq. 2, is taken to be less than 1 c. p. s. The latter is the value for the sample which is saturated with one atmosphere of oxygen; the p value for this solution is found to be 1×10^{-4} from the solubility data. The values obtained are $1/T_{2M}\leqq 500$ c. p. s., $\Delta\omega_M\leqq 1\times10^4$ c. p. s., $A/h=2.3\times10^2$ c. p. s., and $\tau_s=1.5\times10^{-12}$ sec. These values may be compared with those obtained for the methanol-metal ion interactions.[16] It is noted that τ_s is shorter than the correlation time of methanol, which is expected to be about 3×10^{-11} sec., and about the same as that for transition metal ions in methanol. The hyperfine interaction constant is smaller than that of the methanol-metal ion system by a factor of two or three.

The apparent activation energy for the relaxation rate in this range, when calculated from the slope of the temperature dependence of the line widths, is found to be less than several tenths of kcal./mol. This value is about the same order of magnitude as that of the methanol-metal ion system, 0.9 kcal./mol.; it is significantly less than the activation energy for diffusion. This low value of the activation energy may be assumed to be related to the mechanism of relaxation, where the electronic interactions between oxygen and methanol are transmitted rapidly through the methanol medium.

In the higher temperature range, where the hyperfine structure begins to smear out, the activation energy for the change in line width is found, from spectra showing the hyperfine structure, to be about 3 kcal./mol. This coincides with the value generally adopted as the activation energy for the molecular diffusion of methanol; it suggests that the smearing of the hyperfine structure is due to the diffusional or rotational motion of methanol.

Oxygen Effect.—According to the results given previously, it is clear that the oxygen effect in methyl alcohol is far less than expected with regard to paramagnetic dipolar or contact broadening. However, the proton exchange between hydroxyl groups is strongly enhanced by oxygen. This effect may clearly be seen in Figs. 7 and 8; it will be expressed in terms of the exchange rate of hydroxyl protons, $1/\tau$, which is calculated using the data obtained from Figs. 7 and 8. The half-maximum line-width of one component of the spectra showing hyperfine structure is measured and designated as $1/T_2$. The measured line-width parameter, $1/T_2$, is related to the following equation, $1/T_2=1/T_{20}+1/\tau+1/T_1$, where $1/T_{20}$ is the linewidth of the spectrum for the state where there is no proton exchange, and where $1/T_1$ is the contribution of the spin-lattice relaxation of paramagnetic oxygen. The last term can not be neglected in principle; however, its contribution is assumed to be negligible in methyl alcohol which contains oxygen, since the line-width of the un-degassed sample is only by one- or two-tenths cycle per second larger than that of the degassed sample in the lower temperature range where there is no proton exchange. Similarly, the line-widths of methyl proton signals in un-degassed and in degassed ethyl alcohol differ from each other by only one or two cycles per second.

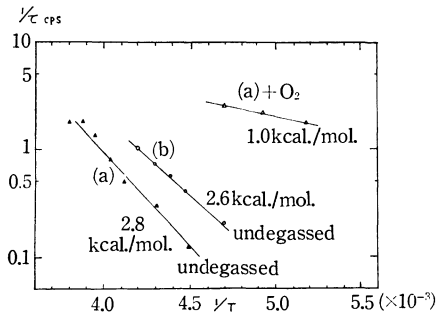

Fig. 9

The Arrhenius plots of the exchange rates obtained are shown in Fig. 9; the activation energy for the exchange, ΔE, is obtained as, for example, ca. 1.0 kcal./mol., and ca. 3 kcal./mol. for the with-oxygen and the un-degassed methyl alcohol respectively. The difference, ΔE, between these two samples may be ascribed to the energy evolved by the dissolution of oxygen in methyl alcohol. This can be done in view of the following considerations. As is clear from the results of Fig. 4 on ethyl alcohol, the molecular interaction between alcohol and oxygen is not homogeneous over a molecule of alcohol, and the oxygen relaxes more strongly at the site of a hydroxyl group than at that of a methyl group. This refers to the specific interaction between hydroxyl protons and oxygen, which results in the evolution of a heat of interaction as well as in an elongation of the OH distance. The latter situation is related to the enhancement of the proton exchange between the hydroxyl group and to the reduction of the apparent activation energy of the proton exchange, ΔE.

We may conclude that the results obtained here suggest a new method of measuring the heat of solution of oxygen in methyl alcohol, Q, which has not yet been made available in the literature. In practice, we could not find any significant difference

in ΔE between degassed and un-degassed methyl alcohol; all differences were within the limits of experimental error. We found $Q=3-1=2$ kcal./mole.

As may be seen in Figs. 7 and 8, the enhancement of the proton exchange between hydroxyl groups is clearly seen in the temperature range where the quadruplet structure begins to be unobservable; that is at -30 or -40°C for the with-oxygen sample, and at 10 or 20°C for the un-degassed sample. A lowering by about 5°C is observed between the degassed and the un-degassed samples. These results refer to the difference in frequency factors, ν_1 assuming a constant activation energy, ΔE. For example, we take:

ν(oxygen sample) $\exp(-3/233\,k)=\nu$(un-degassed) $\exp(-3/293\,k)$.

Hence,

ν(oxygen sample)/ν(un-degassed)$=4.5$

Similarly,

ν(un-degassed)/ν(degassed)$=1.4$

The catalytic effect of trace amounts of oxygen may be related to the short relaxation time of the electronic spin of oxygen; it suggests a very rapid transportation of the spin energies of oxygen. We will not here give a more detailed interpretation of this mechanism of transportation. However, we will note a case of molecular interaction between water and ammonia as an example of how a trace amount of impurity (water) dominates the orientation of the nuclear spins of ammonia.

Summary

1) The dipolar broadening effect of oxygen is small in NMR.

2) The proton exchange rate for hydroxyl groups is enhanced appreciably by the presence of oxygen. This may be attributed to an increase in the frequency factor of the exchange rate.

3) A new method has been proposed for the determination of the heat of the solution of oxygen; this method is based on the oxygen effect referred to in 2).

BULLETIN OF THE CHEMICAL SOCIETY OF JAPAN VOL. 39 2361—2364 (1966)

The Superstructure in Fine Aragonite Particles

By Yuzuru HIRAGI,† Sukeji KACHI,† Toshio TAKADA†† and Norihiko NAKANISHI†

†*Department of Chemistry, Faculty of Science, Kyoto University, Sakyo-ku, Kyoto*
††*Institute for Chemical Research, Kyoto University, Sakyo-ku, Kyoto*

(Received April 9, 1966)

An electron diffraction study was done with fine aragonite particles about 0.5 to 1.0 μ in size. The specimens were obtained by mixing a boiled calcium chloride solution (0.1 N) with 0.1 N of an ammonium carbonate solution. Extra spots were observed with half-integer indices $\{1/2, 1/2, l\}$. This suggests the existence of a structure that differs from that of normal aragonite. From an X-ray diffraction study of the specimen, a $\{1/2, 3/2, 0\}$ diffraction was also observed. The structure for explaining these half-integer diffractions is presented as a superstructure of aragonite; it belongs to the space group of D_{2h}^{15}-*Pbca*, with cell dimensions of $A=8.420$ Å, $B=9.385$ Å, and $C=5.741$ Å, and it containes 8 formula units in a unit cell. A dark-image photograph shows this anomalous area to be comparatively wide and suggests that the anomalous area is dominant in a crystal. The authors conclude that rapidly-precipitated aragonite powders contain a small quantity of the repeatedly-twinned crystals mentioned above.

There are, as is well known, three modifications of calcium carbonate; calcite with a rhombohedral structure, aragonite with an orthorhombic structure, and vaterite with a hexagonal structure. Furthermore, many investigations of polymorphism in calcite have revealed the existence of calcite I, II and III,[1] which differ from each other only in the orientation of their carbonate groups.[2,3]

However, no such anomalous structure has yet been reported for aragonite except for the twin structure proposed by Bragg.[4] This twin structure is made up of two crystals intersecting on the (110) plane, arrangements of the cabonate group being symmetrical with this plane.

In the course of a study of the phase transformation of aragonite to calcite,* the present authors

1) P. W. Bridgeman, *Am. Jour. Sci.*, **237**, 7 (1939).
2) J. J. Lander, *J. Chem. Phys.*, **17**, 892 (1949).
3) J. C. Jamieson, *J. Geol.*, **65**, 334 (1949).
4) W. L. Bragg, *Proc. Roy. Soc.*, **A-105**, 16 (1924).
* Y. Hiragi, N. Nakanishi, T. Takada and S. Kachi, to be published.

found a new structure of aragonite. The electron diffraction patterns taken from fine crystals of aragonite exhibited extra spots involving half-integer indices which cannot be explained by the ordinary structures. As a result of the analysis, the new structure was found to correspond to a superstructure with regard to the orientation of the carbonate ion group.

Experimental

To obtain fine particles of aragonite suitable for electron diffraction, the following procedure was carried out: Equal volumes of solutions of calcium chloride (0.1 N) and of ammonium carbonate (1.0 N) were prepared; then both were boiled to 100°C and mixed together to precipitate calcium carbonate. The precipitate was soon filtrated and dried. Although it is difficult to obtain pure and fine aragonite powders, almost 100 percent of the aragonite was precipitated under these conditions. The water suspension of the particles was dispersed by ultrasonic waves to obtain pieces of aragonite crystals, which were a few μ long and a few thousands of Å wide and thick.

They were examined by the direct transmission of a selected area in an electron microscope with an applied voltage of 50 kV. It generally happens that the thickness of the particles is so large that the electron beam can not easily penetrate the particles. However, one can get the diffraction pattern by searching out a thin plate. The X-ray diffraction study was also made by the Debye-Scherrer method, using a diffractometer.

Results and Discussion

Figure 1 (a) and (b) show an electron micrograph and a diffraction pattern taken from aragonite involving half-integer indices. The net diffraction pattern shows that the particle is a single crystal and that it has an orthorhombic lattice. Figure 2 shows the indices of the diffraction pattern, based on the normal aragonite lattice. The results of the analysis are shown in Table I, in which the $d_{calc.}$ values were calculated from the cell dimensions given on the A. S. T. M. card 5—0453. Figure 3 (a) and (b) show an electron micrograph and dark-image photographs of a fine aragonite particle. Figure 4 shows a part of the X-ray diffraction chart of the aragonite powder; the (1/2, 3/2, 0) diffraction was observed as well as the diffraction from normal aragonite.

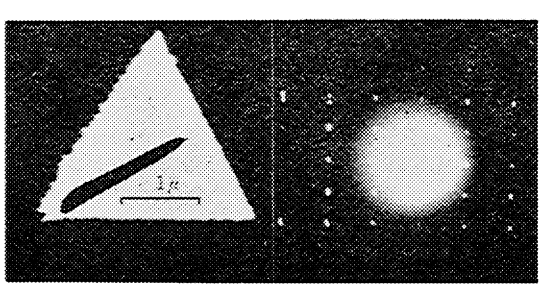

Fig. 1. Electron micrograph and diffraction pattern of super structure of aragonite fine particle.

Table I. The indexing of the diffracted spots based on the lattice of normal aragonite and the interplanar spacings compared with the calculated values

$\{h, k, l\}$	$d_{obs.}$	$d_{calc.}$
1/2, 1/2, 0	8.45	8.420
0, 0, 1	5.95	5.741
1/2, 1/2, 1	4.84	4.744
1, 1, 0	4.26	4.210
1, 1, 1	3.44	3.395
0, 0, 2	2.93	2.871
3/2, 3/2, 0	2.85	2.804
1/2, 1/2, 2	2.78	2.714
3/2, 3/2, 1	2.55	2.521
1, 1, 2	2.43	2.372
2, 2, 0	2.12	2.105
3/2, 3/2, 2	2.05	1.965
2, 2, 1	1.99	1.976
0, 0, 3	1.97	1.914
1/2, 1/2, 3	1.91	1.792
1, 1, 3	1.78	1.742

In the case of electron diffraction, the planes which satisfy the diffraction conditions are parallel to the incident electron beam. Hence, it necessarily follows from the analysis of the pattern that the plate of aragonite must have been oriented to the (001) and (110) planes parallel to the direction of the electron beam; judging from the dark image photographs, the [001]axis is parallel to the length of the plate.

The half-integer indices on the electron diffraction and X-ray diffraction patterns cannot be accounted for by a normal aragonite structure. The normal aragonite structure belongs to the space group D_{2h}^{16}-*Pmcn*,[4] for which the following conditions limit the possible reflections: for *hkl*: no condition; *hko* : $h+k=2n$, and for *hol* : $l=2n$. Nevertheless, in the present electron diffraction pattern, there appear several forbidden spots which do not satisfy the rule; for example, $(00\bar{3})$, $(00\bar{1})$, (001)...; spots which are denoted by in Fig. 2 cannot satisfy the rule. This observation indicates that the double diffraction occurs in a fairly thick crystal, because generally the electron beam strongly interacts with materials. However, the half-integer indices, whose spots are denoted by ⊠, cannot be accounted for by the normal structure of aragonite, even if the double diffraction effect is taken into account. The half-integer spots can be seen along the [110] axis of the reciprocal lattice shown in Fig. 2. Therefore, the periodicity of the (110) plane must be twice as large as that of normal aragonite; i. e., reflections with $\{1/2, 1/2, l\}$ indices suggest a superstructure which has a repeating unit twice as large as that of normal aragonite. In view of the fact that the l indices still remain integers in both electron and X-ray diffraction

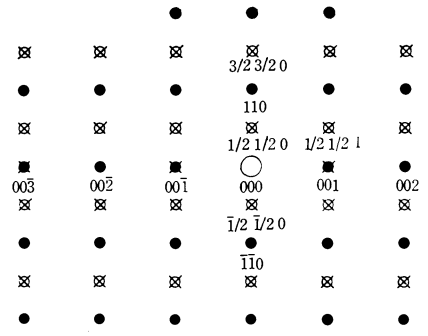

Fig. 2. Indexing of diffraction pattern of Fig. 1.
● Diffraction spots of normal aragonite.
◙ Double diffraction spots of normal aragonite.
⊠ Double diffraction spots of superstructure.

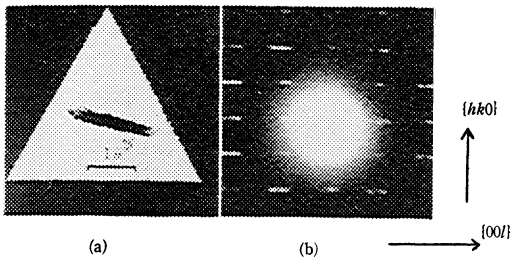

Fig. 3. Electron micrograph and dark image photographs of superstructure of aragonite fine particle.

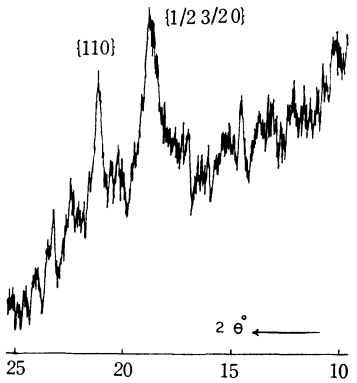

Fig. 4. X-ray diffraction chart, with CuKα radiation, of aragonite fine particles including superstructure of aragonite.

patterns, it must be added that there is no anomaly in the direction of the 'c' axis.

The model for such a structure is presented in the form of the (001) projection in Fig. 5, where only one-half of the structure along the 'c' axis is drawn. The superstructure is constructed so as to repeat the twinning every two layers of carbonate ions on (110) planes; this is called polysynthetic twinning by mineralogists. In Fig. 5, solid lines show the two unit cells of the repeated twinning

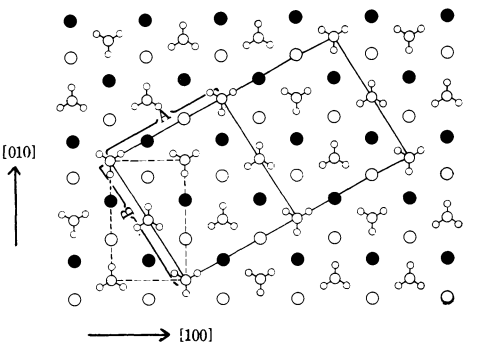

Fig. 5. The (0 0 1) plane projection of the model for superstructure, in which is drawn the position of atoms from 0 to $c/2$. The rigid lines show the unit cells of the superstructure, and broken lines a unit cell of normal aragonite. There is no longer the periodical structure within the broken lines.

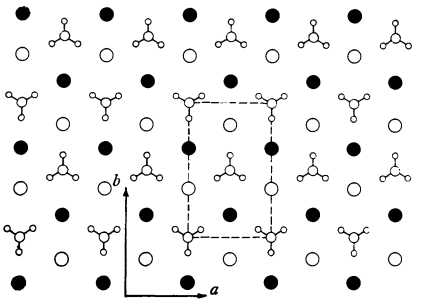

Fig. 6. The structure of normal aragonite projected on (0 0 1) plane.

structure, while the broken lines show a unit cell of normal aragonite. We can see that a periodic structure is lacking within the lines.

For comparison, Fig. 6 shows a (001) projection of the normal aragonite. As can be seen, all CO_3 groups which lie in a row parallel to the 'a' axis are similarly oriented, whereas groups which lie in a row parallel to the (110) plane point alternate ways. Meanwhile, in the superstructure, as Fig. 5 shows, every two CO_3 groups in the row parallel to the 'a' axis of normal aragonite orient in alternate ways, and the groups which lie in a row parallel to the (110) plane of normal aragonite similarly orient in alternate ways, like the case of normal aragonite.

This model is still aragonite, for it has the same layer structure as normal aragonite. It belongs to the space group of D_{2h}^{15}-*Pbca*, with cell dimensions of A=8.420, B=9.385 and C=5.741, and it containes 8 formula units in a unit cell. The relation of normal aragonite to the twinned structure is given by:

$$\boldsymbol{A} = \mathbf{a} - \mathbf{b} \qquad H = h - k$$

$$\boldsymbol{B} = \frac{3}{2}\mathbf{a} + \frac{1}{2}\mathbf{b} \quad K = \frac{3}{2}h + \frac{1}{2}k$$

$$\boldsymbol{C} = \mathbf{c} \qquad L = l$$

where $\boldsymbol{A}$, $\boldsymbol{B}$, $\boldsymbol{C}$, and H, K, L are, respectively, the unit lattice vector and the Miller indices of the superstructure, and where $\mathbf{a}$, $\mathbf{b}$, $\mathbf{c}$ and h, k, l are those of the normal aragonite.

The content of twinned particles is so small compared to the normal aragonite that the diffraction from the twinned structure is very weak in X-ray diffraction studies. Hence, it is necessary to distinguish carefully the diffracted peaks from the backgrounds. In the present experiments both Fe$K\alpha$ and Cu$K\alpha$ radiations were used to take X-ray diffraction patterns. In the pattern of the diffraction with Cu$K\alpha$ radiation shown in Fig. 4, the (1/2, 3/2, 0) diffraction was observed. It must also be added that this peak is also observed in diffractometry using Fe$K\alpha$ radiation. These findings support the theory of the presence of a superstructure and the appropriateness of the model.

The dark-image photographs show that the area of the superstructure is comparatively large; however, it is still not clear whether or not this area covers all the crystal, for it is generally difficult to get a clear dark-image photograph. Nevertheless, as the superstructure region requires a different structure, one may call this another phase, i. e., aragonite II.

The authors are grateful to Dr. Tsuneo Seto of Tokyo Metropolitan University for determining the space group, and to Prof. Hatsujiro Hashimoto of Kyoto Technical University and Dr. Takeo Ueda of our university for their helpful suggestions. They are also grateful to Dr. Yasumasa Goto and Mr. Koji Kosuge of our laboratory for their fruitful discussions. One of them (Y. H.) wishes to express his gratitude to Mr. Shigeki Shimidzu of the Toda Industry Co., Ltd., and Mr. Shigeo Horii of the Reikoo Co., Ltd., for their support during the work.

BULLETIN OF THE CHEMICAL SOCIETY OF JAPAN VOL. 39 2364—2368 (1966)

The Vibrational Assignments of Sulfuryl-Fluoride, -Chloride and -Fluorochloride and Their Transferable Force Constants

By Hiroshi Toyuki and Kazuhiro Shimizu

Osaka Municipal Technical Research Institute, Kita-ku, Osaka

(Received April 13, 1966)

A normal coordinate treatment has been carried out on the basis of the Urey-Bradley force field in order to obtain a set of the most probable assignments and the transferable force constants for the sulfuryl fluoride, the chloride and the fluorochloride series. The assignments selected and the force constants obtained have been satisfactory. The potential energy distributions have been calculated and the vibrational modes have been estimated for each molecule.

Several infrared and Raman spectra of sulfuryl fluoride[1-3] and chloride[3-7] have already been recorded; their normal coordinate treatments have been made on the basis of the valence force field (VFF).[2,8-10]

Siebert[8] assumed the same angular geometry for both molecules and used a seven-parameter VFF. Stammrich et al.[9] simply reported $\nu_5(A_2) < \nu_9(B_2) < \nu_7(B_1)$ as holding for sulfuryl fluoride and $\nu_5(A_2) < \nu_7(B_1) < \nu_9(B_2)$ as holding for sulfuryl chloride, in connection with a normal coordinate analysis of chromyl chloride. Hunt et al.[10] applied the VFF described by Siebert to both the molecules and calculated several corresponding sets of force constants for probable sets of assignment of each molecule by using the correct geometry and the redundant condition. They could find a probable set of the force constants which predicted the fundamental frequencies for an assignment

1) G. R. Hunt and M. K. Wilson, *Spectorchim. Acta*, **16**, 570 (1960).
2) W. D. Perkins and M. K. Wilson, *J. Chem. Phys.*, **20**, 1791 (1952).
3) R. J. Gillespie and E. A. Robinson, *Can. J. Chem.*, **39**, 2171 (1961).
4) P. Bender and J. M. Wood, *J. Chem. Phys.*, **23**, 1313 (1955).
5) R. Vogel-Högler, *Acta. Phys. Austriaca*, **1**, 323 (1948).
6) K. C. Schreiber, *Anal. Chem.*, **21**, 1168 (1949).
7) D. E. Martz and R. T. Lagemann, *J. Chem. Phys.*, **22**, 1193 (1954).
8) H. Siebert, *Z. anorg. u. allegem. Chem.*, **257**, 210 (1954).
9) H. Stammreich, K. Kawai and Y. Tavares, *Spectrochim. Acta*, **15**, 438 (1959).
10) G. R. Hunt and M. K. Wilson, ibid., **18**, 959 (1962).

of sulfuryl chloride, but they could not find a suitable one for the fluoride. However, one of the assignments for the fluoride unsuccssefully treated by Hunt et al. was recently supported, after a useful study of the microwave spectrum, by Lide et al.[11] For this reason, a normal coordinate treatment for both the molecules on the basis of the force field other than the VFF may be useful in the choice of probable assignments. Thus, we will try to carry out the treatment by using the simple Urey-Bradley force field (SUBFF). If necessary, the modified Urey-Bradley force field (MUBFF) will also be employed.

When the force constants obtained for sulfuryl fluoride and chloride predict satisfactorily the observed fundamental frequencies of corresponding molecules, consist with any tentative expectation and moreover they are transferable to sulfuryl fluorochloride, the assignment used is taken as the most probable one for each molecule.

Calculations

Sulfuryl fluoride and chloride both have a tetrahedral configuration and belong to the point group C_{2v}.[12,13] The nine normal vibrations of each molecule are distributed among the four symmetry species: four of the A_1 species, one of the A_2 species, two of the B_1 species, and two of the B_2 species. The A_2 mode is active only in Raman spectra, while the A_1, B_1 and B_2 are both infrared- and Raman- active.

Though we have, unfortunately, no configuration data on sulfuryl fluorochloride, the molecule is supposed to have a configuration similar to that of sulfuryl fluoride and chloride. If the OSO plane is assumed to be at right angles to the FSCl plane, the configuration belongs to the point group C_s. The nine normal vibrations are nondegenerate— six of the A′ species and three of the A″ species. All the vibrations are both infrared- and Raman-active.

The following symmetry coordinates are used for the transformation into the factored $\boldsymbol{F}$ and $\boldsymbol{G}$ matrices defined by Wilson[14]:

For sulfuryl fluoride and the chloride:

$$A_1:\ S_1 = (1/\sqrt{2})(\Delta R_1+\Delta R_2)$$
$$S_2 = (1/\sqrt{2})(\Delta r_3+\Delta r_4)$$
$$S_3 = (1/\sqrt{P})(A\Delta\alpha_{12}-\Delta\theta_{13}-\Delta\theta_{14}-\Delta\theta_{23}-\Delta\theta_{24})$$
$$S_4 = (1/\sqrt{Q})(B\Delta\beta_{34}-C\Delta\alpha_{12}-\Delta\theta_{13}-\Delta\theta_{14}-\Delta\theta_{23}-\Delta\theta_{24})$$
$$S_r = (1/\sqrt{R})(\gamma_1\Delta\alpha_{12}+\gamma_2\Delta\beta_{34}+\Delta\theta_{13}+\Delta\theta_{14}+\Delta\theta_{23}+\Delta\theta_{24})\equiv 0$$

$\gamma_1=2\cos(\beta/2)\sin(\alpha/2)/\sin\theta$, $\gamma_2=2\cos(\alpha/2)\sin(\beta/2)/\sin\theta$, $A=4/\gamma_1$, $B=(4+\gamma_1^2)/r_2$, $C=\gamma_1$, $P=A^2+4$, $Q=B^2+C^2+4$, $R=\gamma_1^2+\gamma_2^2+4$

$$A_2:\ S_5 = (1/2)(\Delta\theta_{13}-\Delta\theta_{14}-\Delta\theta_{23}+\Delta\theta_{24})$$
$$B_1:\ S_6 = (1/\sqrt{2})(\Delta R_1-\Delta R_2)$$
$$S_7 = (1/2)(\Delta\theta_{13}+\Delta\theta_{14}-\Delta\theta_{23}-\Delta\theta_{24})$$
$$B_2:\ S_8 = (1/\sqrt{2})(\Delta r_3-\Delta r_4)$$
$$S_9 = (1/2)(\Delta\theta_{13}-\Delta\theta_{14}+\Delta\theta_{23}-\Delta\theta_{24})$$

and for sulfuryl fluorochloride,

$$A':\ S_1 = (1/\sqrt{2})(\Delta R_1+\Delta R_2)$$
$$S_2 = \Delta r_3$$
$$S_3 = \Delta d_4$$
$$S_4 = (1/\sqrt{S})(D\Delta\alpha_{12}-\Delta\theta_{13}-\Delta\theta_{14}-\Delta\theta_{23}-\Delta\theta_{24})$$
$$S_5 = (1/\sqrt{T})(E\Delta\beta_{34}-F\Delta\alpha_{12}-\Delta\theta_{13}-\Delta\theta_{14}-\Delta\theta_{23}-\Delta\theta_{24})$$
$$S_6 = (1/2)(\Delta\theta_{14}+\Delta\theta_{24}-\Delta\theta_{13}-\Delta\theta_{23})$$
$$S_r = (1/\sqrt{U})(\delta_1\Delta\alpha_{12}+\delta_2\Delta\beta_{34}+\Delta\theta_{13}+\Delta\theta_{14}+\Delta\theta_{23}+\Delta\theta_{24})\equiv 0$$

$\delta_1=2\cos(\beta/2)\sin(\alpha/2)/\sin\theta$, $\delta_2=2\cos(\alpha/2)\sin(\beta/2)/\sin\theta$, $D=4/\delta_1$, $E=(4+\delta_1^2)/\delta_2$, $F=\delta_1$, $S=D^2+4$, $T=E^2+F^2+4$, $U=\delta_1^2+\delta_2^2+4$,

$$A'':\ S_7 = (1/\sqrt{2})(\Delta R_1-\Delta R_2)$$
$$S_8 = (1/2)(\Delta\theta_{13}-\Delta\theta_{23}+\Delta\theta_{14}-\Delta\theta_{24})$$
$$S_9 = (1/2)(\Delta\theta_{14}-\Delta\theta_{24}-\Delta\theta_{13}+\Delta\theta_{23})$$

The internal coordinates used above are shown in Fig. 1.

The molecular constants of sulfuryl fluorochloride must be estimated because there are no experimental constants. The values of the equilibrium distance, S–F and S–Cl, are assumed to be equal to the corresponding one of sulfuryl fluoride and chloride. The S–O distance and the OSO angle proposed by Gillespie et al.[15] are used. This value of the OSO angle and the values of the OSF angle of sulfuryl fluoride and of the OSCl angle of sulfuryl chloride cause the FSCl angle to be 104.1 deg. On the other hand, an arithmetical mean value of the FSF and ClSCl angles shows the FSCl angle to be 103.9 deg. As a result, we regard the value of the FSCl angle as 104 deg. Since the difference between the observed angle, OSF (108.3 deg.), of sulfuryl fluoride and the OSCl angle (106.4 deg.) of the chloride is less than 2 deg., the bond angles, OSF and OSCl, in sulfuryl fluorochloride can be assumed to be equal in a normal coordinate treatment. The

11) D. R. Lide, Jr., D. E. Mann and J. J. Comeford, ibid., **21**, 497 (1965).
12) D. R. Lide, Jr., D. E. Mann and R. M. Fristrom, *J. Chem. Phys.*, **26**, 734 (1957).
13) K. J. Palmar, *J. Am. Chem. Soc.*, **60**, 2360 (1938).
14) E. B. Wilson, *J. Chem. Phys.*, **9**, 76 (1941).
15) R. J. Gillespie and E. A. Robinson, *Can. J Chem.*, **41**, 2074 (1963).

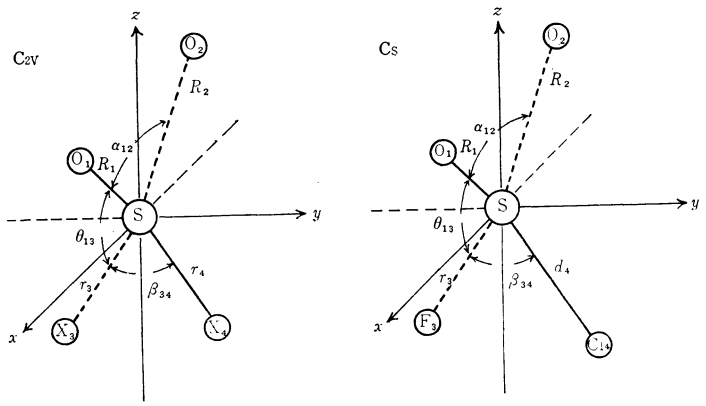

(X=F or Cl)

Fig. 1. The internal coordinates.

symmetry coordinates of sulfuryl fluorochloride have been made in accordance with these assumptions. The molecular constants of each molecule are summarized in Table I.

Table I. The molecular constants used in calculations

	SO_2F_2[12]	SO_2Cl_2[13]	SO_2FCl
R(S-O)Å	1.405	1.43	1.41[15]
r(S-F)Å	1.530		1.530
r(S-Cl)Å		1.99	1.99
∠OSO deg.	123.9	119.8	122[15]
∠FSF deg.	96.1		
∠ClSCl deg.		111.2	
∠FSCl deg.			104
∠OSF deg.	108.3		107.4
∠OSCl deg.		106.4	107.4

For the purpose of obtaining the force constants of sulfuryl fluoride and chloride in order to fit the calculated frequencies to the observed, the method of the minimization of functions described by Shimanouchi et al.[16] is used, because the usual adjustment of least-squares was inadequate for these molecules. At the beginning of the calculation of force constants, the trial set of force constants are transferred from corresponding ones of thionyl halides, sulfur trioxide, sulfate ions, etc. The force constant, F', is assumed to be equal to $-0.1F$, as usual. The observed frequencies of sulfuryl fluoride assigned obviously by Lide et al. and those of sulfuryl chloride which were discussed by Hunt et al. are used in the calculations.

The calculation of the vibrational frequencies of sulfuryl fluorochloride are also carried out by the use of force constants transferred or predicted by applying the usual additive property from the values of sulfuryl fluoride and chloride. The results of calculation are then compared with the observed frequencies.

16) T. Shimanouchi and I. Suzuki, *J. Mol. Spectroscopy*, **8**, 222 (1962).

Results and Discussion

The convergence of force constants for sulfuryl fluoride is obtained readily in the SUBFF. Although Hunt et al. failed to make a normal coordinate analysis of this assignment with the VFF, we have obtained a good agreement between the calculated and the observed frequencies, as is shown in Table II. Moreover, the values of the force constants obtained are reasonable, as Table III shows.

On the other hand, the calculations on the basis of the SUBFF for Hunt et al.'s and our assignments of sulfuryl chloride show no great difference in the average deviation between the observed and the calculated frequencies. These results are listed as the set I and the calc.(1) of set II in Tables II and III. The values of the force constants obtained are reasonable, except for κ in set I having a large negative value. Since the deviation between the observed and the calculated frequencies in set I is found to be not great in the modes related by the κ, this exceptional value of κ in set I can not be corrected through a modification of the potential function. On the other hand, the calc.(1) of set II in Table II shows a great deviation in the rocking mode; this deviation can be corrected by applying the following modified UBFF (MUBFF), in which the l_{ijk} is the interaction force constant:

$$V = (\text{SUBFF}) + \sum l_{ijk}(\Delta\theta_{ij})(\Delta\theta_{ik})$$

The results of the calculation are shown in calc.(2) of set II in Tables II and III. It is not clear why such extra terms are necessary for sulfuryl chloride but unnecessary for sulfuryl fluoride.

The nonbonded O···O distances and the repulsion constants, F(OO)'s, picked up from previous reported data are shown together with our data in Table IV. The value of the constant obtained

Table II. The observed and calculated frequencies for SO_2F_2 and SO_2Cl_2 (cm^{-1})

	SO_2F_2			SO_2Cl_2 Set I		Set II			
	obs.	calc.*	modes	obs.[10]	calc.*	obs.	calc.(1)*	calc.(2)**	modes
$A_1\nu_1$	1269	1290	$\nu_s(SO_2)$	1205	1223	1205	1231	1235	$\nu_s(SO_2)$
ν_2	848	852	$\nu_s(SF_2)$	577	578	577	571	569	$\delta(OSO)+\nu_s(SCl_2)$
ν_3	544	542	$\delta(OSO)+\delta(FSF)$	406	429	406	418	414	$\nu_s(SCl_2)+\delta(OSO)$
ν_4	384	382	$\delta(FSF)+\delta(OSO)$	209	205	209	208	206	$\delta(ClSCl)$
$A_2\nu_5$	388	393	twist.	363	349	280	274	280	twist.
$B_1\nu_6$	1502	1480	$\nu_{as}(SO_2)$	1434	1409	1434	1403	1402	$\nu_{as}(SO_2)$
ν_7	539	533	$r(SO_2)$	388	394	388	412	389	$r(SO_2)$
$B_2\nu_8$	885	887	$\nu_{as}(SF_2)$	586	560	586	587	599	$\nu_{as}(SCl_2)+w(SO_2)$
ν_9	553	543	$w(SO_2)$	280	281	363	333	351	$w(SO_2)+\nu_{as}(SCl_2)$

* SUBFF
** MUBFF
Set I: Hunt et al. supported from calculations using the VFF.[10]
Set II: This work.

Table III. The force constants of SO_2F_2 and SO_2Cl_2

	SO_2F_2	SO_2Cl_2 Set I	Set II (1)	Set II (2)
K(SO)(md./Å)	11.01	10.43	10.30	10.31
K(SF)	4.38			
K(SCl)		2.13	2.08	1.97
F(OO)	0.725	0.425	0.610	0.655
F(FF)	0.381			
F(ClCl)		0.190	0.141	0.148
F(OF)	0.566			
F(OCl)		0.293	0.402	0.437
H(OSO)	0.617	0.553	0.536	0.549
H(FSF)	0.460			
H(ClSCl)		0.150	0.165	0.166
H(OSF)	0.512			
H(OSCl)		0.376	0.290	0.285
κ (md.Å)	0.428	−0.634	0.119	0.173
l(OOCl)				0.025
l(ClClO)				0.001
l(OClCl)				−0.135
l(ClOO)				0.054

Table IV. The nonbonded distances and F(OO)

	q(OO)Å	F(OO)(md./Å)	Ref.
HCO_2^{2-}	2.24	3.00	17
CO_3^{2-}	2.27	1.72	18
BO_3^{3-}	2.36	1.05	18
H_3N^+-SO_3^-	2.43	0.76	19
SO_2F_2	2.47	0.725	This work
SO_2Cl_2	2.47	0.655(0.425)*	This work
SO_3	2.48	0.555	18
SiO_4	2.56	0.530	20
OsO_4	2.61	0.510	20
CrO_4	2.65	0.504	20
SeO_4	2.68	0.342	20
IO_4	2.87	0.226	20

* The value is calculated from the assignment-set I of SO_2Cl_2.

from our assignment of sulfuryl chloride seems to be adequate. The corresponding force constants between F and F and between Cl and Cl are approximately equal to the values calculated from the Lennard-Jones 6–12 potential; therefore, they may be considered to be appropriate. (As the force constants for other assignments of sulfuryl chloride treated by Hunt et al.[10] show inadequate values, their results are not reprinted here.)

In Table II, our assignment of sulfuryl chloride, shown as set II, is found to be more suitable than the assignment shown as set I in view of the force constants transferring from sulfuryl fluoride and chloride to sulfuryl fluorochloride, as is shown in Table V. We recorded the infrared spectrum of liquid sulfuryl chloride in the range from 400 cm^{-1} to 200 cm^{-1} with a Japan Spectroscopic spectrophotometer-402G. We can find no band near 280 cm^{-1}, and we find near 350 cm^{-1} the weak band observed at 363 cm^{-1} in the Raman spectrum.* This means that the Raman band at 280 cm^{-1} belongs to the infrared inactive A_2 species. These facts show that our assignment of sulfuryl chloride can be considered satisfactory. Therefore, the force constants of this molecule, listed in column 2 of set II in Table III, seem to be appropriate.

Gillespie et al.[21] reported a Raman band of sulfuryl fluorochloride at 195 cm^{-1} as one of

* The far infrared spectrum in the gaseous state is now being studied; it will be reported on later.

17) T. Miyazawa, *J. Chem. Soc. Japan, Pure Chem. Sect. (Nippon Kagaku Zasshi)*, **77**, 381 (1956).
18) G. J. Janz and Y. Mikawa, *J. Mol. Spectroscopy*, **1**, 92 (1960).
19) M. J. Schmelz, T. Miyazawa, T. J. Lane and J. V. Quagliano, *Spectrochim. Acta*, **9**, 51 (1957).
20) K. Venkateswarlu and R. Thanalakshmi, *J. Sci. Ind. Res. (India)*, **21B**, 461 (1962).
21) R. J. Gillespie and E. A. Robinson, *Spectrochim. Acta*, **18**, 1473 (1962).

deformations connected with the chlorine atom, but, judging from our calculations, this frequency seems to be unsuitable as a fundamental one. We employ the Raman band at 308 cm^{-1} instead of that at 195 cm^{-1} and identify it as the FSCl deformation, $\nu_6(A')$, superimposed on the twisting, $\nu_9(A'')$, deformation, as is shown in Table V. The band at 195 cm^{-1} might rise from a difference between two vibrations.

Table V. The observed and calculated frequencies of SO_2FCl (cm^{-1})

	obs.[21]	calc. (Set I)	calc. (Set II)	modes
A' ν_1	1224	1257	1263	$\nu_s(SO_2)$
ν_2	823	848	858	ν(SF)
ν_3	627	604	616	ν(SCl)+$r(SO_2)$+δ(OSO)
ν_4	505	519	522	δ(OSO)+$r(SO_2)$
ν_5	430	380	407	ν(SCl)+$r(SO_2)$
ν_6	308	315	300	δ(FSCl)
A'' ν_7	1455	1447	1442	$\nu_{as}(SO_2)$
ν_8	480	505	486	$w(SO_2)$+twist.
ν_9	308	374	326	twist.+$w(SO_2)$

Table VI. The estimated force constants of SO_2FCl

K(SO)	10.66 (md./Å)	κ	0.301 (md.Å)
K(SF)	4.38	l (OOCl)	0.025
K(SCl)	1.97	l (FClO)	0.000
F(OO)	0.690	l (ClFO)	0.000
F(OF)	0.566	l (OFCl)	-0.068
F(OCl)	0.437	l (ClOO)	0.054
F(FCl)	0.256	l (OOF)	0
H(OSO)	0.583	l (FOO)	0
H(OSF)	0.512		
H(OSCl)	0.285		
H(FSCl)	0.313		

Table VII. The potential energy distribution $F_{ii}L_{ia}^2/\lambda_a$ for the normal vibrations of SO_2F_2

A_1 Vibration

	ν_1	ν_2	ν_3	ν_4
S_1	0.99	0.02	0.00	0.00
S_2	0.05	0.89	0.08	0.00
S_3	0.02	0.07	0.57	0.39
S_4	0.01	0.05	0.18	0.80

B_1 Vibration

	ν_6	ν_7
S_6	1.00	0.01
S_7	0.05	0.96

B_2 Vibration

	ν_8	ν_9
S_8	0.92	0.10
S_9	0.22	0.80

The force constants which lead to a good agreement between the observed and the calculated frequencies, as is shown in set II of Table V, are listed in Table VI. The assumed molecular constants of sulfuryl fluorochloride might not be so far from the true values.

The potential energy distributions for sulfuryl fluoride, chloride and fluorochloride are listed in Tables VII, VIII and IX respectively, while the vibrational modes for each molecule are added to Tables II and V.

Table VIII. The potential energy distribution $F_{ii}L_{ia}^2/\lambda_a$ for the normal vibrations of SO_2Cl_2

A_1 Vibration

	ν_1	ν_2	ν_3	ν_4
S_1	1.02	0.00	0.00	0.00
S_2	0.01	0.29	0.66	0.07
S_3	0.16	0.69	0.27	0.09
S_4	0.00	0.05	0.02	0.95

B_1 Vibration

	ν_6	ν_7
S_6	1.00	0.01
S_7	0.02	0.99

B_2 Vibration

	ν_3	ν_9
S_8	0.76	0.30
S_9	0.54	0.52

Table IX. The potential energy distribution $F_{ii}L_{ia}^2/\lambda_a$ for the normal vibration of SO_2FCl

A' Vibration

	ν_1	ν_2	ν_3	ν_4	ν_5	ν_6
S_1	1.00	0.01	0.00	0.00	0.00	0.00
S_2	0.02	0.93	0.00	0.06	0.00	0.00
S_3	0.00	0.01	0.42	0.01	0.58	0.02
S_4	0.01	0.02	0.22	0.57	0.08	0.05
S_5	0.01	0.00	0.10	0.01	0.00	0.90
S_6	0.00	0.10	0.39	0.35	0.21	0.04

A'' Vibration

	ν_7	ν_8	ν_9
S_7	1.00	0.00	0.00
S_8	0.03	0.62	0.38
S_9	0.00	0.25	0.76

The authors wish to thank Professor Haruo Shingu of Kyoto University and Professor Hiromu Murata of Hiroshima University for their many valuable discussions. The authors also wish to express their gratitude to Dr. Yoshifumi Kato of Kobe University for his help in the measurement of the far infrared spectrum.

BULLETIN OF THE CHEMICAL SOCIETY OF JAPAN VOL. 39 2369—2378 (1966)

The Crystal Structures of L-Tryptophan Hydrochloride and Hydrobromide

By Takaji TAKIGAWA,* Tamaichi ASHIDA, Yoshio SASADA and Masao KAKUDO

Institute for Protein Research, Osaka University, Kita-ku, Osaka

(Received April 26, 1966)

The hydrochloride and hydrobromide of L-tryptophan crystallize in the monoclinic space group $P2_1$. The cell dimensions of the hydrochloride are: $a=7.45$, $b=5.30$, $c=14.67$ Å, $\beta=98.80°$, and those of the hydrobromide are: $a=7.64$, $b=5.41$, $c=14.58$ Å, $\beta=100.47°$. There are two molecules in the unit cell. The two compounds are isomorphous. The crystal structure of the hydrobromide was first determined by the heavy atom method with two-dimensional data, and then that of the hydrochloride was refined by three-dimensional least-squares procedure. The molecular and crystal structure is mainly discussed for the hydrochloride here. The average of six C–C bond lengths in the benzene ring is 1.396 Å, that of C–N bond lengths in the indole ring is 1.384 Å. In the carboxyl group, one C–O bond length, 1.147 Å and two O–C–C angles, 106.8° and 125.7° are significantly different from those reported for amino and carboxyl acids so far investigated. The molecule consists of two planes of the carboxyl group and of the indole ring, the planes making an angle of 70.6° with each other. As to the conformation about the C(α)–C(β) bond, C(γ) lies at the gauche position with both of the carboxyl and the amino groups. The molecules are arranged in double layers parallel to the ab plane; the polar layer is held together by a network of the three N–H··· Cl^- hydrogen bonds, 3.17, 3.19 and 3.24 Å and one O–H···Cl^-, 3.04 Å, and in the non-polar layer, the indole rings are packed mainly by van der Waals forces, the shortest C···C and C···N contacts being 3.74 and 3.42 Å respectively.

The three-dimensional structures of the amino acids have been studied by many authors to furnish the structural basis for protein research.[1] Out of twenty-odd naturally occurring amino acids, some seventeen compounds have been determined by X-ray analysis so far. Although the preliminary examination was reported for DL-tryptophan dihydrochloride by Dawson and Mathieson,[2] detailed X-ray analysis for tryptophan has not yet been published. This paper deals with X-ray analysis of the crystal structures of L-tryptophan hydrochloride and hydrobromide.

Experimental

L-tryptophan hydrochloride and hydrobromide,

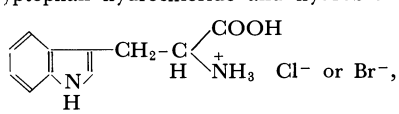

were obtained in the form of needle-like crystals by dissolving L-tryptophan in concentrated hydrochloric and hydrobromic acid respectively at room temperature and by standing them at 5°C.

Rotation, Weissenberg and precession photographs showed the crystals to be monoclinic, the unique b being coincident with the needle axis. The unit-cell dimensions were determined from zero layer Weissenberg photographs taken about three crystallographic axes with standard aluminum powder reflections. The densities were measured by flotation in a benzene-carbon tetrachloride mixture.

Crystal data so obtained are:

For hydrochloride,

$a=7.45\pm0.02$, $b=5.30\pm0.01$, $c=14.67\pm0.02$ Å, $\beta=98.80\pm0.07°$, $D_m=1.394$, $D_c=1.396$ g. cm^{-3}, $Z=2$,

$\mu=29.1$ cm^{-1} for Cu$K\alpha$ radiation.

For hydrobromide,

$a=7.64\pm0.02$, $b=5.41\pm0.01$, $c=14.58\pm0.02$ Å, $\beta=100.47\pm0.10°$, $D_m=1.594$, $D_c=1.597$ g. cm^{-3} $Z=2$,

$\mu=49.0$ cm^{-1} for Cu$K\alpha$ and 37.6 cm^{-1} for Mo$K\alpha$ radiation.

The only systematic absence in these two crystals is observed for (0k0) reflections with k odd. The space group was determined to be C_2^2-$P2_1$, an alternative centrosymmetric space group C_{2h}^2-$P2_1/m$ being excluded because of the asymmetry of the molecule.

Somewhat different crystal was obtained by dissolving L-tryptophan in dilute hydrobromic acid (1 N). The cell constants with less accuracy are $a=31.30$, $b=13.86$, $c=5.73$ Å, space group being $P2_12_12_1$. Density was measured to be 1.444 g. cm^{-3}. Elementary analysis and the crystal data indicated that the asymmetric unit consisted of 2tryptophan·HBr·1/2H_2O. No further study was attempted for this crystal.

* Present address: Faculty of Pharmaceutical Sciences, Osaka University, Toyonaka, Osaka.

1) e. g., A. Rich and D. W. Green, *Ann. Rev. Biochem.*, **30**, 93 (1961).

2) B. Dawson and A. Mathieson, *Acta Cryst.*, **4**, 475 (1951).

For the hydrochloride, three-dimensional intensity data were collected by equi-inclination Weissenberg procedure with nickel-filtered Cu$K\alpha$ radiation. Photographs were taken for layers ($h0l$) to ($h4l$) and ($0kl$) to ($5kl$) by the multiple-film technique. Out of 1387 accessible reflections, 1258 non-zero reflections were observed and they amount to 80% of the reciprocal lattice points within the limiting sphere for Cu-$K\alpha$ radiation.

For the hydrobromide, only intensity data for ($h0l$) and ($0kl$) zones were recorded on Weissenberg and precession photographs respectively, the latter being taken with zirconium-filtered Mo$K\alpha$ radiation.

Intensities were estimated visually against the standard scale and they were corrected for Lorentz and polarization factors. For the equi-inclination Weissenberg data, a correction for spot-shape was made according to Phillips' equation.[3] Sizes of crystals used in the experiment were: $0.10\times0.15\times2.0$ mm. and $0.15\times0.15\times0.40$ mm. for the b and a axis photographs of the hydrochloride respectively, $0.15\times0.15\times2.5$ mm. for the b axis photographs of the hydrobromide.

Three-dimensional structure factors were put on a common scale by comparing data from photographs of the different axis. Estimated errors in the scaling were less than 10%.

Since the a axis data seemed to be less accurate than the b axis data, the former was only used, in the subsequent analysis, for reflections unaccessible by the b axis photographs.

Structure determination

Hydrobromide.—A modified Patterson projection along the b axis was constructed for the hydrobromide. From a heavy Patterson peak, the x- and z-coordinates of the bromide ion were determined to be 0.100 and 0.125 respectively. Based on the signs of the bromide ion, Fourier summation was carried out. Almost all the atoms were resolved on the resulting Fourier projection, and it was not difficult to give approximate coordinates even for a few overlapped atoms. Succesive Fourier refinement was made until the discrepancy factor, $R=\sum||F_o|-|F_c||/\sum|F_o|$, became 0.19, the overall temperature factor $B=4.0$ Å^2 being applied. A least-squares refinement was then proceeded using 240 independent ($h0l$) reflections. Anisotropic temperature factors were applied only for the bromide ion. After three cycles of the refinement, the R factor dropped to 0.086.

In the a axis projection with the plane group pg, the y coordinate of the bromide ion was arbitrarily fixed at 1/4. On the Fourier projection based on the phases of the bromide ion only, much overlapping was observed, since it involved an additional mirror symmetry. With the aid of the molecular model of tryptophan and the b axis projection, the Fourier projection on (100) was interpreted reasonably and approximate y coordinates of all the atoms were obtained. Successive Fourier refinement decreased the R factor to 0.196. Further refinement was carried out by least-squares refinement, and after three cycles the R factor became 0.101.

Hydrochloride.—As seen from Fig. 1, the modified Patterson projections of hydrochloride and hydrobromide were similar to each other in general feature. This observation and approximately the same unit cell dimensions of the two crystals suggested that these two were isomorphous. The x- and z-coordinates of the chloride ion were determined to be 0.100 and 0.122 respectively from the Patterson projection. Fourier projections on (010), (100) and (001) were made with phases which were derived by assuming that the coordinates of the non-hydrogen atoms except the chloride ion were the same as those in the hydrobromide. The approximate coordinates of all the atoms were obtained from these Fourier projections and they were improved by three-dimensional Fourier synthesis.

The refinement of the structure was carried out by three-dimensional least-squares procedure. The least-squares program was constructed with the block-diagonal matrix approximation. In the earlier stage, temperature factor for each atom was taken as isotropic.

Three cycles of the refinement deduced the

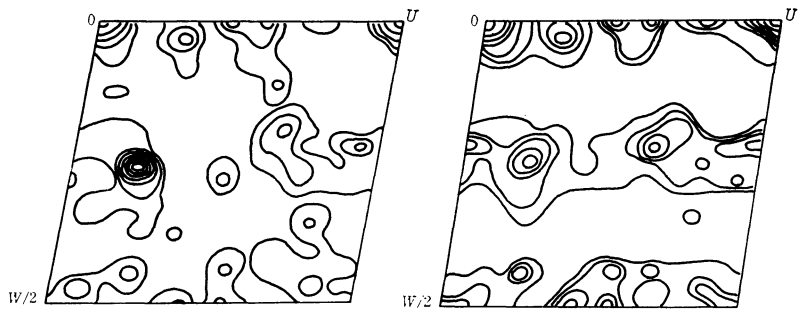

Fig. 1. Patterson projection on (010), modified by the factors of $M(\sin\theta)=\exp\{8(\sin\theta/\lambda)^2\}$
a) of the hydrobromide b) of the hydrochloride

3) D. C. Phillips, Acta Cryst., **7**, 746 (1954).

R factor from 0.193 to 0.131. Disagreement between the observed and calculated structure factors increased with increasing k values. It was suggested that the anisotropic thermal vibration should be taken into account. Three cycles of least-squares refinement, with the anisotropic temperature factors for all the atoms, deduced the R factor to 0.117. Since the systematic disagreement remained, interlayer scales of the b axis data were adjusted by comparing the observed and

Table I. The final fractional coordinates and the estimated standard deviations (in Å).

Atom	x/a	$\sigma(x)$	y/b	$\sigma(y)$	z/c	$\sigma(z)$
C(1)	0.5668	0.009	0.5872	0.010	0.1091	0.008
C(2)	0.6900	0.009	0.8211	0.009	0.1262	0.008
C(3)	0.7266	0.008	0.9126	0.010	0.2270	0.009
C(4)	0.8132	0.008	0.7138	0.011	0.2956	0.008
C(5)	0.7321	0.009	0.5178	0.010	0.3309	0.009
C(6)	1.0224	0.010	0.4963	0.011	0.3963	0.009
C(7)	1.0026	0.008	0.7009	0.009	0.3372	0.008
C(8)	1.1515	0.009	0.8579	0.011	0.3273	0.009
C(9)	1.3164	0.009	0.7833	0.014	0.3789	0.009
C(10)	1.3375	0.010	0.5813	0.011	0.4396	0.009
C(11)	1.1890	0.010	0.4255	0.011	0.4475	0.009
N(1)	0.8669	0.007	0.7554	0.011	0.0943	0.007
N(2)	0.8534	0.008	0.3816	0.009	0.3920	0.008
O(1)	0.4185	0.007	0.6361	0.009	0.1456	0.008
O(2)	0.5996	0.006	0.4068	0.008	0.0717	0.007
Cl	0.1130	0.002	0.2500	0.004	0.1202	0.002
H(1)	0.326	0.11	0.486	0.13	0.135	0.12
H(2)	0.647	0.09	0.949	0.11	0.074	0.09
H(3)	0.869	0.09	0.747	0.16	0.025	0.09
H(4)	0.947	0.10	0.581	0.13	0.105	0.10
H(5)	0.950	0.09	0.901	0.11	0.103	0.10
H(6)	0.642	0.09	1.051	0.11	0.249	0.09
H(7)	0.817	0.09	1.064	0.11	0.231	0.09
H(8)	1.136	0.10	1.013	0.11	0.280	0.10
H(9)	1.423	0.10	0.890	0.12	0.371	0.10
H(10)	1.467	0.12	0.506	0.13	0.481	0.11
H(11)	1.200	0.09	0.263	0.14	0.490	0.09
H(12)	0.826	0.10	0.213	0.14	0.429	0.10
H(13)	0.600	0.10	0.456	0.12	0.312	0.10

Table II. The final anisotropic temperature factors in the form of $\exp\{-(B_{11}h^2+B_{22}k^2+B_{33}l^2+B_{12}hk+B_{13}hl+B_{23}kl)\}$ and their standard deviations ($\times 10^4$)

Atom	B_{11}	$\sigma(B_{11})$	B_{22}	$\sigma(B_{22})$	B_{33}	$\sigma(B_{33})$	B_{12}	$\sigma(B_{12})$	B_{13}	$\sigma(B_{13})$	B_{23}	$\sigma(B_{23})$
C(1)	177	19	255	34	34	4	−63	44	12	15	13	21
C(2)	157	17	284	40	35	4	12	40	−10	14	1	20
C(3)	150	17	236	32	44	5	−39	45	26	14	−43	22
C(4)	160	16	277	40	37	4	−15	46	50	13	−42	23
C(5)	157	18	347	41	47	5	−63	48	55	16	−39	25
C(6)	213	21	300	38	36	4	−12	48	59	16	−20	21
C(7)	188	17	245	40	27	4	− 9	42	37	13	−50	19
C(8)	207	21	387	44	33	4	−42	52	28	15	−25	24
C(9)	176	19	526	58	53	5	−117	66	36	16	−13	34
C(10)	187	20	398	44	42	5	130	54	22	16	19	26
C(11)	226	22	357	42	32	4	170	55	8	16	11	25
N(1)	188	15	386	32	41	3	−24	54	44	11	13	27
N(2)	236	19	369	37	45	4	−45	48	53	14	− 1	23
O(1)	181	15	523	40	77	5	−133	41	42	14	−82	24
O(2)	204	15	347	30	70	4	−31	40	57	13	−84	21
Cl	181	4	325	8	46	1	−118	15	33	3	22	7

calculated structure factors. The contributions from hydrogen atoms were introduced at this stage. Hydrogen atoms were placed in such a way to give the bond distances, 1.09 Å for C–H, 1.01 Å for N–H and 0.97 Å for O–H, and bond angles in accord with the probable trigonal or tetrahedral arrangement of the bonds. Three hydrogens on the amino nitrogen and one on

TABLE III. THE OBSERVED AND THE FINAL CALUCULATED STRUCTURE FACTORS

L	FO	FC	L	FO	FC	L	FO	FC	L	FO	FC	L	FO	FC	L	FO	FC	L	FO	FC
H,K= 0			9	151	160	-17	14	8	9	72	61	0	92	96	-6	70	76	17	27	36	C	17	18
3	57	50	9	71	44	-18	36	34	1	55	56	1	174	180	-7	81	95	H,K=	1	2	1	89	87
4	456	463	10	41	40	H,K=	4	C	10	73	25	2	45	55	-8	37	43	C	285	297	2	55	56
5	445	419	11•	0	17	-1	177	175	11	96	62	3	44	43	-9	74	92	1	58	95	3	24	31
6	168	185	12	71	67	-2	197	180	12•	0	10	4	87	89	-10	54	57	2	173	163	4	19	18
7	95	88	13	12	24	-3	293	263	13	30	33	5	100	109	-11	26	26	3	71	82	5	37	35
8	132	143	H,K=	6	0	-4	316	289	14	56	53	6	53	62	-12	18	20	4	233	224	6	62	60
9	247	243	0•	0	11	-5	248	222	15	55	55	7	10	14	-13	58	68	5	125	116	7	13	18
10	57	57	1	111	122	-6	153	161	16	40	34	8	30	34	-14	85	77	6	80	77	8•	0	3
11	92	88	2	51	61	-7	217	205	17	32	35	9	62	57	-15•	0	12	7	57	61	9	17	25
12	75	78	3	61	74	-8	35	42	18	33	29	10	24	27	-16•	0	13	8	88	88	H,K=	8	2
13•	0	15	4	40	52	-9	76	109	H,K=	1	1	11•	C	8	-17	34	30	9	74	78	C	23	24
14	59	67	5•	C	5	-10	105	113	0	236	228	H,K=	7	1	H,K=	5	1	10	52	50	1	47	41
15	32	39	6	27	34	-11	59	68	1	402	458	0	54	56	-1	86	91	11	23	29	2	45	42
16	34	34	7•	0	4	-12	77	85	2	302	306	1	45	47	-2	73	96	12	42	43	3•	0	11
17•	0	3	8	19	17	-13	17	23	3	373	354	2	31	35	-3	71	91	13	71	74	4	28	24
18	89	78	9•	C	1	-14	22	28	4	275	281	3	24	25	-4	64	69	14	46	48	5	38	33
H,K=	1	C	10•	0	0	-15•	0	8	5	415	414	4	26	28	-5	42	42	15	24	24	H,K=	1	2
C	268	259	11	28	29	-16	90	84	6	209	210	5	43	39	-6	110	117	16•	6	11	-1	318	342
1	44	36	H,K=	7	0	-17•	0	10	7	84	82	6•	C	13	-7	50	57	17	17	22	-2	154	159
2	52	48	0	108	120	H,K=	5	C	8	169	173	7•	C	3	-8	32	39	H,K=	2	2	-3	210	206
3•	8	0	1	34	53	-1	114	117	9	257	256	9•	C	12	-9	52	56	0	185	169	-4	59	62
4	109	107	2	58	74	-2•	0	17	10	149	154	9	37	29	-10	68	78	1	132	126	-5	403	394
5	45	57	3•	0	6	-3	89	94	11	95	98	10	25	26	-11	48	55	2	192	194	-6	72	65
6	149	150	4	61	63	-4	64	67	12	77	92	H,K=	8	1	-12	29	41	3	41	36	-7	226	220
7	28	40	5	73	82	-5	32	33	13	109	112	0	32	35	-13	50	48	4	122	119	-8	44	39
8	25	28	6	69	67	-6	86	86	14	43	41	1•	C	17	-14	73	71	5	94	99	-9	207	207
9	21	22	7	51	55	-7	48	63	15	91	78	2	56	47	-15•	20	19	6	184	190	-10	66	75
10	51	41	8	53	49	-8	38	47	16	19	26	3	46	42	-16	29	27	7	101	95	-11•	0	21
11	18	19	9	59	52	-9	127	124	17	73	64	4	33	38	-17	27	28	8	57	54	-12	44	39
12	70	72	10	36	42	-10	126	130	H,K=	2	1	5•	C	9	H,K=	6	1	9	51	54	-13	49	57
13•	0	3	H,K=	8	0	-11	35	52	0	461	445	6	48	44	-1	67	70	10	161	171	-14	62	69
14	41	44	0•	0	17	-12	20	24	1	394	400	7	38	40	-2	91	95	11	97	95	-15	39	40
15	99	96	1	43	55	-13	72	71	2	283	280	H,K=	9	1	-3	116	136	12	20	25	-16	17	14
16	26	29	2•	0	19	-14	42	47	3	199	196	0•	C	6	-4	158	161	13	79	38	-17	27	31
17	15	C	3	35	35	-15	51	41	4	168	163	1	28	27	-5	73	73	14	69	67	H,K=	2	2
18	32	34	4	18	14	-16	31	33	5	202	192	2	32	32	-6	23	24	15	46	46	-1	133	115
H,K=	2	0	5•	0	0	-17	19	17	6	99	102	H,K=	1	1	-7	25	31	16•	C	14	-2	184	178
C	145	143	6•	0	10	H,K=	6	C	7	193	184	-1	220	213	-8	98	102	H,K=	3	2	-3	105	111
1	65	69	7	38	40	-1	141	155	8	87	85	-2	428	458	-9	91	101	C	146	146	-4	120	112
2	243	240	H,K=	9	0	-2	35	48	9	40	49	-3	514	553	-10•	0	23	1	237	231	-5	161	152
3	124	131	0	27	27	-3	87	79	10	24	32	-4	363	349	-11	27	29	2	194	184	-6	146	138
4	342	328	1•	0	15	-4	25	35	11	98	105	-5	198	215	-12	38	37	3	73	76	-7	158	155
5•	0	4	2•	C	10	-5	88	101	12	92	92	-6	222	235	-13	45	41	4	38	30	-8	97	106
6	176	175	3	14	22	-6	51	59	13	54	50	-7	350	339	-14	57	56	5	120	116	-9	211	226
7	15	22	H,K=	1	0	-7•	0	15	14	28	29	-8	48	41	-15	30	23	6	192	192	-10	71	78
8	193	182	-1	414	338	-8	52	60	15	35	32	-9	64	59	-16	13	15	7	32	35	-11	67	68
9	98	94	-2	210	174	-9	40	47	16	16	17	-10	51	57	H,K=	7	1	8	95	100	-12	57	64
10	113	120	-3	465	386	-10•	0	C	17	35	36	-11	132	130	-1	25	31	9	63	67	-13	68	73
11	21	28	-4	578	496	-11•	0	5	H,K=	3	1	-12	85	86	-2	25	27	10	106	104	-14	83	79
12	16	16	-5	173	174	-12•	0	6	0	82	78	-13•	0	5	-3	27	32	11	45	53	-15	36	31
13	20	24	-6	175	176	-13	53	60	1	51	58	-14	40	52	-4	82	88	12	51	46	-16	32	35
14	71	73	-7	110	106	-14•	0	18	2	140	138	-15	52	52	-5	24	34	13	56	45	-17	15	19
15	92	86	-8	116	122	-15	16	19	3	215	216	-16	28	37	-6	25	26	14	49	43	H,K=	3	2
16•	0	16	-9	211	223	-16	18	18	4	31	16	-17	47	35	-7	25	18	15	38	43	-1	145	139
17•	0	6	-10	145	152	H,K=	7	0	5	11	14	-18	25	27	-8	104	106	H,K=	4	2	-2	159	188
H,K=	3	0	-11	42	53	-1•	0	19	6	120	118	H,K=	2	1	-9	41	42	0	164	179	-3	217	215
0	75	75	-12	36	49	-2	129	135	7	138	127	-1	188	188	-10•	0	9	1	135	133	-4	65	64
1	312	295	-13	83	99	-3•	0	8	8	93	96	-2	85	87	-11	18	13	2	48	54	-5	79	71
2	70	77	-14	77	91	-4	97	107	9	52	59	-3	178	168	-12	23	20	3	126	132	-6	83	81
3	125	129	-15	11	16	-5	21	30	10•	0	7	-4	280	263	-13	68	57	4	108	108	-7	127	127
4	64	76	-16•	0	7	-6	105	108	11	39	48	-5	209	287	-14	28	27	5	87	96	-8	17	10
5	337	330	-17	29	24	-7	20	22	12	48	49	-6	144	161	H,K=	8	1	6	88	88	-9	21	28
6	129	138	-18•	8	20	-8•	0	14	13	28	30	-7	152	152	-1	69	64	7	57	62	-10	89	99
7	49	50	H,K=	2	0	-9•	0	4	14	15	15	-8	79	73	-2	40	41	8	65	69	-11	78	84
8	18	29	-1	373	338	-10	26	31	15	41	39	-9	80	86	-3	39	32	9	55	57	-12	38	49
9	114	118	-2	552	478	-11	123	105	H,K=	4	1	-10	26	27	-4	42	37	10	48	50	-13	43	50
10	177	191	-3	31	42	-12•	0	1	C	113	117	-11	17	23	-5	75	71	11•	C	11	-14	31	34
11	40	47	-4	38	33	-13	24	27	1	21	35	-12	78	74	-6	52	46	12	23	31	-15	42	43
12	53	58	-5	70	80	-14•	0	2	2	114	110	-13	24	25	-7	32	31	13	24	29	-16	27	33
13	23	29	-6	192	182	H,K=	8	C	3	142	135	-14•	0	13	-8	55	50	14•	8	18	-17	24	28
14	69	72	-7	30	48	-1•	0	11	4	83	88	-15•	C	10	-9	34	27	H,K=	5	2	H,K=	4	2
15	25	30	-8	111	105	-2	19	29	5	84	83	-16	53	50	-10	28	22	0	119	114	-1	40	33
16•	0	1	-9•	0	7	-3	24	28	6	96	94	-17•	C	23	-11	37	37	1	88	99	-2	43	41
H,K=	4	0	-10	190	191	-4	24	37	7	72	78	-18	16	15	-12	11	13	2	76	82	-3	109	97
0	245	249	-11	21	25	-5	28	35	8	55	66	H,K=	3	1	H,K=	9	1	3	103	101	-4	184	188
1	230	236	-12	50	66	-6•	0	11	9•	4	18	-1	268	254	-1•	0	5	4	90	101	-5	74	72
2	40	49	-13	43	57	-7•	0	1	10	93	91	-2	29	36	-2	29	23	5•	0	10	-6	53	58
3	14	15	-14	129	140	-8	51	50	11	95	93	-3	108	104	-3	14	11	6	69	71	-7	39	43
4	111	112	-15	30	36	-9	37	40	12•	0	4	-4	318	304	-4	22	27	7	50	56	-8	135	145
5	88	99	-16	26	35	-10•	0	14	13	16	18	-5	228	215	-5	17	18	8	74	77	-9	73	83
6	56	58	-17	19	23	-11	36	30	14	59	49	-6	136	145	-6	28	26	9•	C	5	-10	84	99
7	25	20	-18	53	44	-12•	0	15	15	57	54	-7	72	67	H,K=	0	2	10	22	24	-11	51	58
8	72	74	H,K=	3	0	H,K=	9	C	H,K=	5	1	-8	104	109	C	230	247	11	18	18	-12	83	87
9	17	22	-1	152	147	-1	19	22	0	34	26	-9	202	215	1	207	256	12	31	32	-13•	8	12
10•	C	8	-2	71	63	-2	19	24	1	162	172	-10	155	146	2	68	69	13	15	16	-14	65	60
11	58	66	-3	26	38	-3	29	35	2	67	70	-11	53	52	3	125	124	H,K=	6	2	-15	20	20
12	18	26	-4	98	87	-4	29	34	3	34	31	-12	45	48	4	253	252	C	28	32	-16	29	30
13	24	17	-5	49	61	-5	15	19	4•	0	9	-13	104	124	5	273	260	1	44	53	-17	23	24
14•	0	2	-6	125	139	-6	21	24	5	155	156	-14	93	96	6	130	117	2	25	30	H,K=	5	2
15	13	11	-7	91	93	-7	19	29	6	73	87	-15	59	58	7	158	142	3	82	81	-1	83	80
H,K=	5	C	-8	21	28	-8	43	47	7	99	98	-16	52	47	8	175	161	4•	0	11	-2	87	95
0	20	21	-9	75	98	H,K=	0	1	8	25	32	-17	33	24	9	91	86	5	41	45	-3	109	123
1	18	20	-10	73	93	1	308	412	9	25	42	-18	31	35	10	63	62	6	19	26	-4	161	171
2•	0	5	-11	10	21	2	230	240	10	54	54	H,K=	4	1	11	17	29	7	68	65	-5	67	65
3	60	68	-12	14	6	3	436	514	11	36	35	-1	236	232	12	76	75	8	11	20	-6	74	82
4	89	88	-13	14	24	4	169	166	12•	9	9	-2	125	123	13	88	86	9•	C	18	-7	83	85
5•	0	20	-14	24	23	5	122	117	13	18	16	-3	72	65	14•	0	13	10	27	29	-8	143	156
6	12	21	-15•	9	6	6	35	30	14	16	21	-4	134	123	15	25	32	11	27	29	-9	58	64
7•	0	7	-16	16	14	7	176	170	H,K=	6	1	-5	125	108	16	31	30	H,K=	7	2	-10	32	33

TABLE III (Continued)

L	FC	FC	L	FO	FC	L	FO	FC	L	FO	FC	L	FC	FC	L	FO	FC	L	FO	FC	L	FO	FC
-11	72	74	15	16	16	1	12	13	H,K=	6	3	2	45	48	-5	45	44	0	96	104	-6	45	39
-12	93	92	16*	0	9	2	11	11	-1	37	31	3	54	50	-6	39	36	1	56	64	-7	44	42
-13	21	33	H,K=	2	3	3	12	19	-2	47	51	4	59	52	-7	101	120	2	39	44	-8	14	23
-14	60	57	0	180	191	H,K=	1	3	-3	84	71	5	103	100	-8	22	33	3	43	56	-9	24	21
-15	17	18	1	130	135	-1	112	139	-4	80	79	6	76	68	-9	37	37	4	64	64	-10	34	31
-16	30	40	2	70	59	-2	74	82	-5*	0	7	7	38	33	-10	29	28	5	64	59	H,K=	5	5
H,K=	6	2	3	52	55	-3	63	60	-6	22	29	8*	0	8	-11	29	28	6	12	17	-1*	0	7
-1	68	77	4	167	189	-4	172	186	-7	93	91	9	30	27	-12	71	68	7*	8	19	-2	75	68
-2	28	32	5	136	143	-5	105	106	-8	64	58	10	32	28	-13	14	22	8	46	37	-3*	0	17
-3	36	45	6	110	112	-6	34	32	-9	19	22	11	62	55	-14	74	69	9	40	31	-4	40	39
-4	91	88	7	22	27	-7	98	105	-10*	0	18	12	42	35	H,K=	4	4	10	16	15	-5*	0	11
-5*	0	19	8	167	178	-8	52	54	-11	56	52	13	10	22	-1	53	58	11*	7	11	-6	34	40
-6	80	82	9	77	76	-9	37	37	-12	20	21	H,K=	4	4	-2	16	28	H,K=	3	5	-7	34	42
-7*	0	14	10	87	84	-10	47	52	-13	31	35	0	13	19	-3	85	86	0	91	89	-8	19	16
-8	61	57	11	20	16	-11	49	43	H,K=	7	3	1	126	134	-4	63	61	1	35	40	H,K=	0	6
-9	13	19	12	36	31	-12*	0	14	-1	75	73	2	21	17	-5	45	35	2	29	26	0	73	78
-10	63	56	13	60	53	-13*	0	9	-2	58	54	3	78	72	-6	20	16	3	66	62	1	59	54
-11	53	49	14	44	38	-14	46	44	-3	53	47	4	42	46	-7	38	38	4	71	68	2	33	28
-12	32	33	15	36	26	-15	45	36	-4	75	73	5	83	77	-8	60	59	5	37	41	3	64	67
-13	32	27	H,K=	3	3	-16	28	27	-5	57	49	6	42	47	-9	46	39	6	11	8	4	15	16
-14	39	33	0	186	198	H,K=	2	3	-6	47	45	7	25	25	-10	12	23	7	30	35	5	30	42
-15	22	32	1	72	72	-1	96	95	-7*	0	13	8	80	73	-11*	0	13	8	74	64	6	57	51
H,K=	7	2	2	67	69	-2	97	99	-8	36	33	9	67	57	-12	44	39	9	20	25	7	15	15
-1	46	50	3	93	106	-3	90	96	-9	48	38	10	24	25	-13	27	23	10	24	21	8	31	24
-2	30	29	4	131	136	-4	136	152	-10	35	31	11	14	11	-14	19	13	H,K=	4	5	H,K=	1	6
-3	66	65	5	64	64	-5	115	121	-11	29	29	H,K=	5	4	H,K=	5	4	0	30	24	0	25	28
-4	50	50	6	22	25	-6	44	50	H,K=	8	3	0	109	94	-1	66	68	1	49	50	1	20	22
-5	43	45	7	86	89	-7	92	107	-1	24	22	1	66	61	-2	35	38	2	59	52	2	31	35
-6	80	73	8	70	67	-8	122	126	-2*	0	4	2	35	42	-3	36	45	3*	0	15	3	54	64
-7	28	30	9	22	13	-9	77	77	-3	32	24	3	52	49	-4	86	78	4*	0	4	4*	0	11
-8	20	23	10	30	40	-10	134	154	-4*	0	18	4	73	73	-5	108	104	5	44	36	5*	0	4
-9	21	27	11	60	55	-11	117	128	-5*	0	14	5	21	22	-6*	0	12	6	62	62	6	49	51
-10	69	63	12*	0	12	-12	84	87	-6	32	25	6	12	17	-7	28	36	7	48	28	7	14	21
-11	22	21	13	27	23	-13	20	24	-7*	0	6	7	17	19	-8	67	57	8	18	21	8	20	18
-12	11	12	14	53	49	-14	86	77	-8	19	22	8	17	16	-9	80	68	H,K=	5	5	H,K=	2	6
-13	15	22	H,K=	4	3	-15	24	24	H,K=	0	4	9	15	22	-10	16	23	0	32	19	0*	0	10
H,K=	8	2	0	48	45	-16	18	22	0	58	68	H,K=	6	4	-11	12	16	1	27	28	1*	0	9
-1	27	31	1	29	29	H,K=	3	3	1	21	36	0*	0	5	-12	35	29	2	51	45	2	55	49
-2	41	39	2	20	17	-1	108	113	2*	9	16	1	39	36	-13	35	35	3	12	18	3	25	27
-3	65	60	3	93	102	-2	92	89	3	29	37	2	31	30	H,K=	6	4	4	9	4	4	24	29
-4	35	30	4	25	23	-3	41	42	4	83	93	3	18	26	-1	20	19	5	62	54	5	32	29
-5	18	17	5	73	76	-4	50	44	5	82	80	4	17	15	-2	57	53	6	41	37	6	43	41
-6	17	18	6	74	75	-5	148	163	6	27	6	5	32	31	-3	12	15	H,K=	1	5	7	30	32
-7	60	52	7	68	60	-6	61	55	7	42	46	6	42	40	-4	49	49	-1*	0	13	H,K=	3	6
-8*	0	11	8	35	29	-7	47	44	8	69	78	7	38	37	-5	30	28	-2	23	42	0	47	43
-9	51	44	9	47	42	-8	69	82	9	42	35	H,K=	7	4	-6	54	50	-3	73	69	1	19	22
-10	17	18	10	83	70	-9	98	103	10	44	50	0*	0	8	-7	41	29	-4	77	81	2	35	31
H,K=	9	2	11	21	22	-10	54	50	11*	0	8	1	23	18	-8*	0	5	-5	31	30	3	43	35
0	35	45	12	52	44	-11	68	70	12	37	34	2	57	51	-9	68	62	-6	28	34	4	60	59
-1	20	24	13	24	22	-12	58	66	13	55	49	3	11	15	-10	29	23	-7	27	35	5	25	26
-2	14	15	H,K=	5	3	-13	16	22	14	24	26	H,K=	1	4	-11	35	32	-8	39	49	H,K=	4	6
-3	19	21	0	105	114	-14	92	75	15*	0	12	-1	100	147	H,K=	7	4	-9	27	31	0	54	58
-4	33	30	1	99	109	-15	26	29	H,K=	1	4	-2	77	98	-1	16	17	-10	16	16	1	48	36
-5	22	27	2	27	31	-16*	8	18	0	143	164	-3	38	46	-2	44	35	-11	23	27	2	49	48
H,K=	0	3	3	32	38	H,K=	4	3	1	65	83	-4	145	150	-3*	0	9	-12	20	29	H,K=	1	6
1	43	63	4	18	20	-1	47	44	2	64	77	-5	94	107	-4	16	14	H,K=	2	3	-1	40	43
2	207	211	5	66	60	-2	97	101	3	113	131	-6	54	54	-5	26	18	-1	36	41	-2*	0	9
3	49	44	6	90	85	-3	63	61	4	69	75	-7	62	68	-6	40	36	-2	20	31	-3	12	19
4	93	85	7*	0	3	-4	44	52	5	82	74	-8	53	59	-7	15	20	-3	46	41	-4	31	32
5	95	105	8	14	16	-5	113	125	6	73	80	-9	96	103	-8*	0	8	-4	71	74	-5	48	34
6	139	139	9	59	55	-6	126	135	7	127	139	-10	49	48	H,K=	0	5	-5	84	91	-6	34	41
7	44	47	10	69	66	-7	48	52	8	44	47	-11	43	43	1	43	38	-6	25	32	-7	21	27
8	43	46	11	17	17	-8	25	34	9*	0	13	-12	44	43	2	91	100	-7	30	33	-8	27	29
9	80	78	12*	0	11	-9	129	136	10*	0	10	-13	51	35	3	97	102	-8	18	26	H,K=	2	6
10	130	153	H,K=	6	3	-10	60	63	11	67	61	-14	50	45	4*	0	26	-9	52	48	-1	48	52
11	37	46	0	53	44	-11	40	48	12	34	26	-15	27	27	5	50	54	-10	18	16	-2	58	62
12	28	27	1	97	94	-12	40	43	13	18	27	H,K=	2	4	6	62	71	-11	14	18	-3	17	26
13	27	26	2	55	57	-13	86	71	14*	0	9	-1	23	30	7	31	39	-12	20	24	-4	16	16
14	57	47	3	37	35	-14	82	71	H,K=	2	4	-2	45	51	8*	0	3	H,K=	3	3	-5	37	46
15	52	47	4	64	61	-15	43	40	0	28	13	-3	78	84	9	35	30	-1	73	75	-6	19	16
16	47	41	5	75	70	-16	15	27	1	66	61	-4	95	96	10	66	54	-2	16	12	-7	13	21
H,K=	1	3	6	31	32	H,K=	5	3	2	44	50	-5	63	66	11	43	15	-3	30	32	-8	14	21
0	120	164	7*	0	12	-1	72	76	3	55	57	-6	95	108	12	18	20	-4	77	84	H,K=	3	6
1	98	113	8	22	20	-2	58	58	4	68	64	-7	60	58	H,K=	1	5	-5	54	58	-1	13	9
2	158	162	9	46	40	-3	53	57	5	126	121	-8	60	62	0	76	93	-6	66	56	-2	16	16
3	93	96	10	19	22	-4	92	91	6	17	21	-9	59	65	1	104	105	-7	42	41	-3	29	13
4	77	75	H,K=	7	3	-5	57	60	7	50	56	-10	71	76	2	50	50	-8	40	41	-4	34	30
5	142	146	0	63	56	-6	60	65	8	31	23	-11	43	44	3	28	31	-9	47	43	-5	16	17
6	67	57	1	23	19	-7	19	26	9	45	43	-12	38	36	4	49	44	-10	55	53	-6	15	9
7	47	45	2*	0	8	-8	54	55	10	41	38	-13	34	32	5	72	74	-11	19	13	-7	29	32
8	19	23	3	20	25	-9	49	57	11	61	58	-14	63	59	6	42	43	-12*	7	15	H,K=	4	6
9	50	55	4	54	46	-10	35	30	12*	0	15	-15	29	33	7*	0	14	H,K=	4	5	-1*	0	2
10	69	64	5	17	18	-11	30	24	13	26	24	H,K=	3	4	8	19	17	-1	64	72	-2	18	16
11	27	28	6*	0	4	-12*	8	11	14	25	27	-1	58	56	9	55	57	-2	44	37	-3	32	34
12	36	34	7*	0	10	-13	21	17	H,K=	3	4	-2	38	37	10	56	56	-3	37	39	-4	68	71
13	74	66	H,K=	8	3	-14*	8	5	0	38	37	-3	134	145	11*	0	12	-4	18	23	-5*	9	13
14	48	38	0	13	18	-15	17	12	1	125	134	-4	30	35	H,K=	2	5	-5	40	34			

the carboxyl group were put on the lines to the chloride ions with which they hydrogen-bonded. After three cycles of the least-squares refinement, average shifts in the coordinates of the non-hydrogen atoms were $\Delta x/a=0.0003$, $\Delta y/b=0.0006$ and $\Delta z/c=0.0001$ and their maximum shifts were 0.0008, 0.002 and 0.004 respectively, and the R factor dropped to 0.087. Additional two cycles of the least-squares were made in order to adjust the interlayer scale factors, leaving coordinates and temperature factors fixed. The R factor was 0.088 and $\sum|F_c|/\sum|F_o|$ for each k value converged fairly to the unity. The weights in the least-squares calculation were given systematically as a function of the absolute values of the structure factors. Damping factors for the shifts were as follows; 0.7 in the overall scale factor, 0.5 in the overall temperature factor, 0.7 in the coordinates of non-hydrogen atoms, 0.5 in the anisotropic temperature factors of non-hydrogen atoms, and 0.1 in the coordinates and isotropic temperature factors of hydrogen atoms. The atomic scattering

factors were taken from the International Tables for X-ray Crystallography.[4]

The final atomic coordinates with their standard deviations are listed in Table I and the anisotropic temperature factors are given in Table II. The estimated standard deviations were caluculated by the Cruickshank's formula.[5] A list of the observed and the final caluculated structure factors is given in Table III, in which reflections with asterisk were omitted in the least-squares refinement. The final superimposed sections of electron density distribution cut through the every atomic centers are shown in Fig. 2.

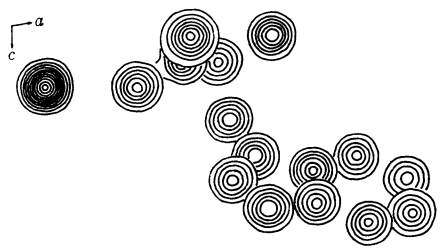

Fig. 2. The final three-dimensional Fourier synthesis. Sections passing approximately through the center of the atoms are superimposed on (010). Contour intervals of 1.5 e.Å^{-3} for light atoms and 3.0 e.Å^{-3} for the chloride ion; the first contour begins at 1.5 e.Å^{-3}.

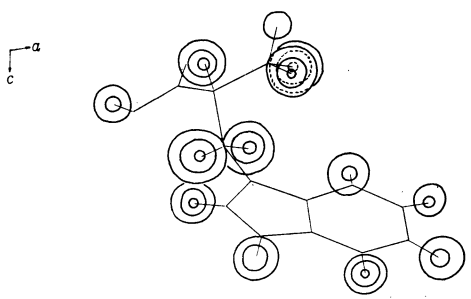

Fig. 3. The three-dimensional (F_o-F_c) synthesis. Sections passing approximately through the center of the hydrogen atoms are superimposed on (010). Contour intervals of 0.2 e.Å^{-3}, the first contour begins at 0.2 e.Å^{-3}. The dotted contours are in the lower section.

A three-dimensional (F_o-F_c) synthesis was then caluculated where F_c did not include the contributions from the hydrogen atoms, and phase was that of F_c. Fourier synthesis in this manner gives somewhat modified electron density distribution for hydrogen atoms.

In the resulting map as shown in Fig. 3, peaks were found in positions which could associate with the thirteen hydrogen atoms, their coordinates and heights being shown in Table IV. Maximum difference between the coordinates from the difference synthesis and those from the least-squares is 0.23 Å.

TABLE IV. THE COORDINATES AND PEAK HEIGHTS OF HYDROGEN ATOMS OBTAINED FROM THE THREE-DIMENSIONAL (F_o-F_c) SYNTHESIS

Atom	x/a	y/b	z/c	peak heights (in e.Å^{-3})
H(1)	0.347	0.479	0.126	0.36
H(2)	0.642	0.956	0.080	0.59
H(3)	0.897	0.760	0.037	0.22
H(4)	0.939	0.608	0.118	0.60
H(5)	0.947	0.908	0.106	0.69
H(6)	0.637	1.033	0.236	0.64
H(7)	0.798	1.050	0.238	0.68
H(8)	1.133	1.008	0.296	0.51
H(9)	1.400	0.900	0.377	0.44
H(10)	1.440	0.513	0.472	0.46
H(11)	1.189	0.268	0.486	0.58
H(12)	0.834	0.246	0.427	0.45
H(13)	0.623	0.450	0.319	0.60

Bond lengths (in Å)

O(1)-H(1)	1.01	C(8)-H(8)	0.91
C(2)-H(2)	1.01	C(9)-H(9)	0.88
N(1)-H(3)	0.90	C(10)-H(10)	0.90
N(1)-H(4)	0.98	C(11)-H(11)	1.00
N(1)-H(5)	1.00	N(2)-H(12)	0.91
C(3)-H(6)	0.97	C(5)-H(13)	0.90
C(3)-H(7)	0.90		

TABLE V. INTRAMOLECULAR DISTANCES BETWEEN NON-BONDED ATOMS (in Å)

O(1)···O(2)	2.22
O(1)···C(2)	2.30
O(2)···C(2)	2.40
O(2)···N(1)	2.70
C(1)···C(3)	2.60
C(1)···N(1)	2.45

All the numerical computations were done on a NEAC 2101 of this laboratory, a NEAC 2206 of the computing center of Osaka University, a HITAC 5020 of the computing center of the University of Tokyo and an IBM 7090 of Japan IBM Co. Ltd. Main programs used are 'NLP-W-01-T' for Lorentz polarization and spot shape correction written by Nobuo Tanaka, 'FR-S-01-T' for the two-dimensional Fourier synthesis by Tsunehiro Takano and Yoriko Nishi, 'HBLS' for the least-squares by Tamaichi Ashida and 'SFFR' for three-dimensional Fourier synthesis by Yoshio Sasada.

Discussion of the structure

The present structure determination of L-tryptophan hydrohalides has revealed that the

4) "International Tables for X-ray Crystallography," Vol. III, Kynoch Press, Birmingham (1962), p. 202.
5) ibid., Vol. II, Kynoch Press, Birmingham (1959), p. 330.

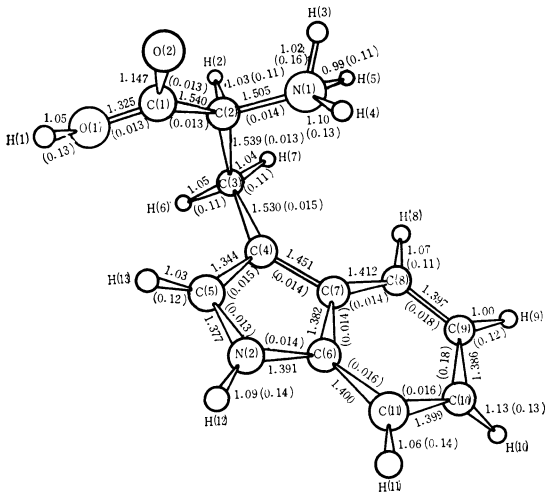

(a)

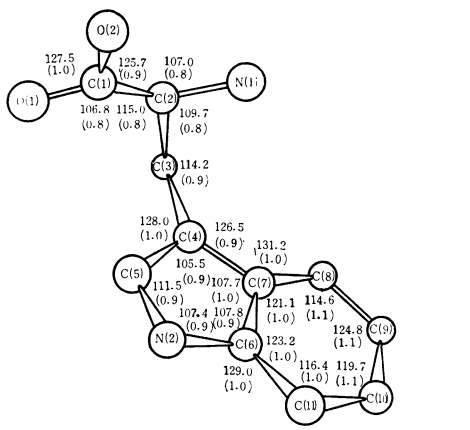

(b)

Fig. 4. (a) Bond lengths and their standard deviations in parentheses (in Å).
(b) Bond angles and their standard deviations in parentheses (in degree).

crystals of the hydrochloride and hydrobromide are isomorphous with each other and conformation of the tryptophan cations is essentially the same in both crystals. As the accuracy of the analysis of the hydrobromide is not so high, the crystal and molecular structure of the hydrochloride will be mainly discussed here.

All the interatomic bond distances and angles caluculated from the final coordinates are shown in Fig. 4, together with their standard deviations. Some of the important intramolecular distances between non-bonded atoms are given in Table V.

Carboxyl and Amino Group.—The planarity of the carboxyl group with α-carbon atom has been established in many investigations. For the present molecule, the equation for this median plane is determined to be

$$1.112X - Y + 2.090Z = 3.522$$

where X, Y and Z in Å refers to the crystallographic a^*, b and c axes respectively and coefficients were obtained by the least-squares method. The deviations of all the atoms from the least-squares plane are less than 0.0001 Å and they are strictly coplanar. The amino nitrogen is 0.154 Å out of the plane, the C–N bond making an angle of 6° with the plane.

The deviations of the amino nitrogen range from 0.00 to 0.82 Å for the amino acids so far investigated. The C–N distance 1.505 Å coincides well with those in, e. g., histidine hydrochloride monohydrate[6] (1.495 Å). Two C–O bond lengths are 1.325 and 1.147 Å and three angles around the C(1) atom are O(1)–C(1)–O(2) = 127.5°, O(1)–C(1)–C(2) = 106.8° and O(2)–C(1)–C(2) = 125.7°. This short C–O bond length 1.147Å and two O–C–C angles, 106.8° and 125.7° differ significantly from those reported for amino acids so far. Hahn's treatment[7] for the relation between bond lengths and angles of the carboxyl groups can not be applied in the present case.

Indole Ring.—The median plane through the atoms in the indole ring with the methylene carbon attached to it can be described by the equation,

$$0.3349X - Y - 1.3642Z = -6.3687$$

The plane forms a dihedral angle of 70.6° with that of the carboxyl group described above. The deviations of the atoms from the least-squares plane are listed in Table VI. The maximum deviation from the plane is 0.019 Å and the average 0.009 Å. It is concluded that the atoms are on nearly the same plane within the limit of error, as in the related compounds, glycyl-L-tryptophan dihydrate[8] and 3-indolylacetic acid[9]. Bond lengths in the indole ring are tabulated in Table VII-a with those of the compounds quoted above. The average of six C–C bond lengths in the benzene ring is 1.396 Å, while that of C–N bond lengths in the indole ring is 1.384 Å respectively. The bond lengths found in the present molecule are all in good agreement with those of 3-indolylacetic acid[9] within the limit of error.

Longuet-Higgins and Coulson[10] have determined the mobile bond orders of the indole molecule by the molecular orbital treatment. Theoretical bond lengths derived from the bond orders by the empirical equation (Coulson,[11] Cox and

6) J. Donohue and A. Caron, *Acta Cryst.*, **17**, 1178 (1964).
7) T. Hahn, *Z. Krist.*, **109**, 438 (1957).
8) R. A. Pasternak, *Acta Cryst.*, **9**, 341 (1956).
9) I. L. Karle, K. Britts and P. Gum, ibid., **17**, 496 (1964).
10) H. C. Longuet-Higgins and C. A. Coulson, *Trans. Faraday Soc.*, **43**, 87 (1947).
11) C. A. Coulson, *Proc. Roy. Soc.*, **A 207**, 91 (1951).

Table VI. Deviation from the least-squares plane (in Å)

Atom	
C(3)	−0.020
C(4)	−0.001
C(5)	+0.000
C(6)	−0.004
C(7)	+0.006
C(8)	−0.008
C(9)	+0.014
C(10)	−0.019
C(11)	+0.015
N(2)	−0.003
Mean	0.009

Table VII. The dimensions of the indole group

a) Bond lengths (in Å)

	I	II	III	IV	V
C(3)-C(4)	1.530	1.514	1.534		
C(4)-C(5)	1.344	1.342	1.338	1.36	0.812
C(4)-C(7)	1.451	1.470	1.418	1.42	0.498
C(5)-N(2)	1.377	1.401	1.430	1.36	0.412
N(2)-C(6)	1.391	1.385	1.307	1.37	0.381
C(6)-C(7)	1.382	1.407	1.388	1.41	0.565
C(7)-C(8)	1.412	1.434	1.405	1.41	0.574
C(8)-C(9)	1.397	1.409	1.411	1.38	0.709
C(9)-C(10)	1.386	1.396	1.353*	1.40	0.626
C(10)-C(11)	1.399	1.409	1.390*	1.38	0.699
C(11)-C(6)	1.400	1.422	1.399	1.40	0.604
σ (mean)	0.015	0.018	0.014		

b) Bond angles (in degree)

	I	II	III
C(2)-C(3)-C(4)	114.2	114.7	115.1
C(3)-C(4)-C(5)	128.0	127.2	127.3
C(3)-C(4)-C(7)	126.5	125.2	124.7
C(5)-C(4)-C(7)	105.5	107.1	108.0
C(4)-C(5)-N(2)	111.5	110.3	106.9
C(5)-N(2)-C(6)	107.4	108.2	109.3
N(2)-C(6)-C(11)	129.0	128.2	127.9
N(2)-C(6)-C(7)	107.8	108.2	108.8
C(7)-C(6)-C(11)	123.2	123.5	123.1
C(4)-C(7)-C(8)	131.2	134.1	134.3
C(4)-C(7)-C(6)	107.7	106.1	106.9
C(6)-C(7)-C(8)	121.1	119.8	118.8
C(7)-C(8)-C(9)	114.6	116.7	117.4
C(8)-C(9)-C(10)	124.8	122.2	122.1*
C(9)-C(10)-C(11)	119.7	122.5	121.5*
C(6)-C(11)-C(10)	116.4	115.2	116.4*
σ (mean)	1.0	1.3	1.0

I ; L-tryptophan hydrochloride
II ; 3-indolylacetic acid[9]
III ; glycyl-L-tryptophan dihydrate[8]
IV ; theoretical value[10-12]
V ; mobile bond order[10]
* Pasternak points out that the coordinates of C(10) is less accurate than the other atoms.

Jeffrey[12]) are given in Table VII-a. The bond lengths in the indole ring of L-tryptophan hydrochloride agree well with the theoretical values within the limit of error.

But in glycyl-L-tryptophan dihydrate,[8]) some bond lengths, especially C(6)–N(2), differ from those in L-tryptophan hydrochloride. Significantly short C(6)–N(2) bond, 1.307 Å of length, in glycyl-L-tryptophan dihydrate[8]) may suggest that in this compound the contribution from the resonance of ortho- or para-benzoquinone type increases.

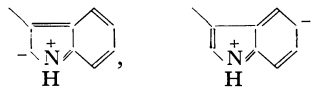

It will be interesting that the conformation changes as a result of introduction of glycyl residue, as shown in Fig. 5.

Bond angles in the indole ring are also shown in Table VII-b. Bond angles in the indole ring of the present molecule show the fairly good agreement with those of the related compounds and those in the benzene ring do not deviate from 120°.

Conformation about the C(α)-C(β).—Figure 5 shows the conformation about the C(α)–C(β) bond in the present molecule by the stereographic projections together with those in histidine hydrochloride monohydrate,[6]) glycyl-L-tryptophan dihydrate[8]) and L-tyrosine hydrobromide[13]). In the present molecule, C(γ) lies at gauche position with both of carboxyl and amino group. The same conformation has been found in the crystal of histidine hydrochloride monohydrate,[6]) whose

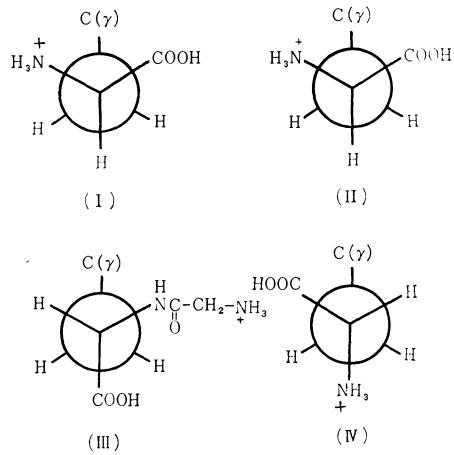

Fig. 5. Stereographic projection of the conformation about the C(α)-C(β) bond.
I; histidine hydrochloride monohydrate
II; L-tryptophan hydrochloride
III; glycyl-L-tryptophan dihydrate
IV; L-tyrosine hydrobromide

12) E. G. Cox and G. A. Jeffrey, ibid., **A207**, 110 (1951).
13) R. Srinivasan, *Current Sci. (India)*, **27**, 46 (1958).

Table VIII. Intermolecular distances less than 4.0 Å

From atom in molecule M	to atom	in molecule	distance (in Å)		angle (in degree)
a) Hydrogen bond					
O(1)	Cl	M	3.04	C(1)-O(1)···Cl	118.3
N(1)	Cl	M′	3.17	C(2)-N(1)···Cl	119.1
N(1)	Cl	A	3.24	C(2)-N(1)···Cl	131.5
N(1)	Cl	B	3.19	C(2)-N(1)···Cl	106.7
b) Other short contact					
C(4)	C(11)	M′	3.93		
C(5)	C(11)	M′	3.87		
N(2)	C(11)	M′	3.77		
C(6)	C(11)	M′	3.74		
C(7)	C(11)	M′	3.85		
C(9)	N(2)	M′	3.80		
C(10)	N(2)	M′	3.43		
C(11)	N(2)	M′	3.42		

Molecule M is at (x, y, z), M′ at $(1-x, 1/2+y, -z)$, A at $(1+x, y, z)$ and B at $(1+x, 1+y, z)$.

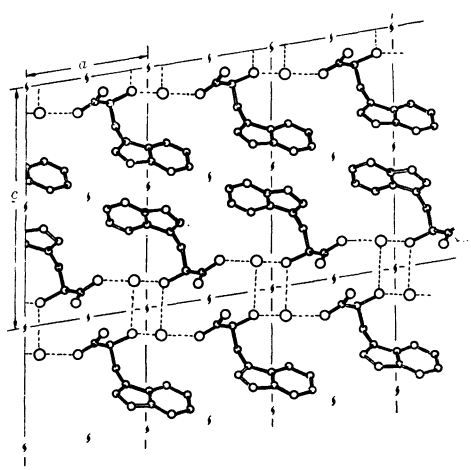

(a)

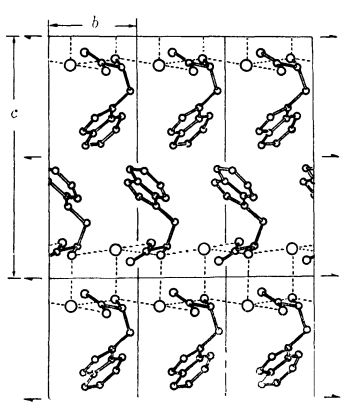

(b)

Fig. 6. (a) A projection of the structure along the *b* axis.
(b) A projection of the structure along *a* axis. Hydrogen bonds are indicated by the broken lines.

molecule also includes the five-membered ring next to C(β), while Ramachandran and Lakshminarayanan[14] have pointed out that in tyrosine and phenylalanine, both of which contain benzene ring, C(γ) goes only to the position at trans with the nitrogen and gauche with the carboxyl group.

The enviroment of the molecule.—Views of the crystal structure along the b and a axes are shown in Fig. 6 and intermolecular distances less than 4.0 Å and angles including hydrogen bonds are given in Table VIII. An amino nitrogen atom forms three N–H···Cl⁻ hydrogen bonds, in lengths of 3.17, 3.19 and 3.24 Å; three acceptor halogen atoms are approximately at three vertices of regular tetrahedron centered around the nitrogen atom, with the α-carbon atom directed toward the fourth vertex. The fourth hydrogen bond is O–H···Cl⁻ in length of 3.04 Å. Similar hydrogen bond distances are reported for N–H···Cl⁻, 3.08, 3.25 and 3.27 Å, and for O–H···Cl⁻, 2.98 Å in L-cystine hydrochloride.[15]

In L-tryptophan hydrobromide, the corresponding distances between nitrogen and bromide ion are 3.30, 3.31 and 3.35 Å, although the accuracies of these values are not so high. These values are comparable to those found in the other hydrobromide; 3.28, 3.41 and 3.42 Å in L-cystine dihydrobromide.[16] One O···Br⁻ approach of 3.13 Å in the present crystal is similar to a value; 3.17 Å in L-cystine dihydrobromide.[16]

Molecular arrangement in the crystal can be well described as double-layered system parallel to the ab plane, which is characteristic for a structure

14) G. N. Ramachandran and A. V. Lakshminarayanan, to be published in *Biopolymers*.
15) L. K. Steinrauf, J. Peterson and L. H. Jensen, *J. Am. Chem. Soc.*, **80**, 3835 (1958).
16) J. Peterson, L. K. Steinrauf and L. H. Jensen, *Acta Cryst.*, **13**, 104 (1960).

containing polar and non-polar groups together. The polar layer is held together by a network of the hydrogen bonds, as described above, between the chloride ions and amino nitrogen and between the chloride ion and carboxyl group. In the non-polar layer, the indole rings are packed mainly by van der Waals forces, in a manner similar to that found for the typical aromatic molecule. No unusually short contacts between non-bonded atoms are found in the crystal structure, and the shortest C···C and C···N distances are 3.74 and 3.42 Å respectively. The weakly basic nitrogen atom of the indole ring does not take part in the hydrogen bond. This structure well interprets the observed cleavage in the ab plane.

We wish to express our deep thanks to all our collaborators for their helpful discussions and for permission to use the computer programs. Thanks are also due to the staffs of Computing Centers of Osaka University and of the University of Tokyo for numerical computation. The computing time of IBM 7090 was made available to us through the project of 'UNICON'.

BULLETIN OF THE CHEMICAL SOCIETY OF JAPAN VOL. 39 2378—2385 (1966)

Diffusion in Glassy Polymers. III. Temperature Dependence and Solvent Effects

By Hisashi ODANI, Shigeru KIDA and Mikio TAMURA

Department of Industrial Chemistry, Faculty of Engineering, Kyoto University, Yoshida, Kyoto

(Received May 12, 1966)

Absorption and desorption of benzene and ethyl acetate by atactic polystyrene (A-PS) were studied at various temperatures below the glass transition point of the polymer. In the A-PS+benzene system raising temperature did not alter the general feature of the family of successive differential absorption curves, but merely compressed the whole family of curves towards a low concentration region. The critical concentration of penetrant at which the transition from non-Fickian to Fickian behavior occurred became lower in the order benzene, ethyl methyl ketone, and ethyl acetate. The logarithm of the time, t_*, which specifies the inflection point of the second stage on the two-stage absorption curve, were linearly dependent on the initial concentration of penetrant, C_i, and the correlation lines between $\log t_*$ and C_i obtained for various combinations of temperature and solvent were nearly parallel with one another. The features of integral absorptions were essentially the same in all cases, and the absorption curves showed a pronounced dependence on concentration.

Recent studies of absorption and desorption of organic vapors by amorphous polymers have shown that when the polymer is in the glassy state these processes do not conform to the Fickian type; that is, the Fick diffusion equation with a concentration dependent diffusion coefficient and with the usual boundary conditions is not obeyed.[1] It is generally accepted that these non-Fickian processes are controlled not only by the ordinary diffusion mechanism but also by the relaxation mechanism of polymer network chains. When the polymer is in the glassy state the rate at which the network of polymer chains responds to the osmotic swelling pressure is so slow that the rate of absorption or desorption of organic vapors by the polymer may depend markedly upon both temperature and penetrant concentration. However, our present knowledge[2-6] about this problem is insufficient or otherwise incomplete. For example, data on the temperature dependence of the successive differential absorption are as yet not available. The first purpose of the present work is to find out how the behavior of successive absorption processes in systems of amorphous polymer and organic vapor is affected by temperature. To this end we have studied the system atactic polystyrene (A–PS) and benzene.

In a recent publication,[7] we showed that the general features of the family of successive

1) For a review of recent studies in the field, see H. Fujita, *Fortschr. Hochpolymer.-Forsch.*, **3**, 1 (1961).

2) G. S. Park, *Trans. Faraday Soc.*, **46**, 684 (1950).

3) A. T. Hutcheon, R. J. Kokes, J. L. Hoard and F. A. Long, *J. Chem. Phys.*, **20**, 1232 (1952).

4) R. J. Kokes, F. A. Long and J. L. Hoard, ibid., **20**, 1711 (1952).

5) F. A. Long and R. J. Kokes, *J. Am. Chem. Soc.*, **75**, 2232 (1953).

6) R. J. Kokes and F. A. Long, ibid., **75**, 6142 (1953).

7) H. Odani, J. Hayashi and M. Tamura, This Bulletin, **34**, 817 (1961).

differential absorption curves for the A-PS+ethyl methyl ketone system was similar to those obtained for the A-PS+benzene system. However, for the ethyl methyl ketone system, the critical concentration at which the polymer-penetrant mixture underwent glass transition at the temperature of the experiment was lower than that for the benzene system, and the characteristic variation of the types of successive differential absorption curves occurred in a relatively lower concentration region. In either of these systems, the second stage portion of the two-stage process shifted rapidly to the short time region as the initial concentration of each step was increased. To express this rate of shift the time t_* for the inflection point of each differential absorption curve was taken as the measure of the location of the second stage portion on the time axis. The plots of the logarithm of t_* against the initial concentration C_i was linear. The slopes of the lines were nearly the same. Ethyl methyl ketone and benzene have nearly the same molar valumes, but the former is less soluble in A-PS than is the latter. To confirm these features and other effects of polymer-penetrant interaction upon absorption and desorption kinetics, we have made similar measurements with the system A-PS and ethyl acetate and have compared the results with our previous results with the benzene system and the ethyl methyl ketone system. These three penetrants have about the same molar volumes, but have different solvent powers for A-PS. The values of the interaction parameter χ_1 of A-PS at 25°C are 0.55, 0.53, and 0.45 for ethyl acetate, ethyl methyl ketone, and benzene, respectively.[8] Thus the solvent power for A-PS becomes larger in the order ethyl acetate, ethyl methyl ketone, and benzene.

Experimental

The atactic polystyrene (A-PS) used was the same as that described previously.[9] Its viscosity-average molecular weight was 2.2×10^5. The films used for sorption measurements were approximately 2.4×10^{-3} cm. thick. Benzene and ethyl acetate used as organic penetrants were of G. R. grade, and no attempt was made to effect further purification. The temperatures at which the sorption measurements were performed were 25, 35, and 50°C for A-PS+benzene and 25°C for A-PS + ethyl acetate. These temperatures are well below the glass transition temperature of the dry polymer.[10]

Results and Discussion

Absorption Isotherms.—Absorption isotherm data for the system A-PS+benzene at 25, 35, and 50°C are given in Fig. 1. Here the ordinate

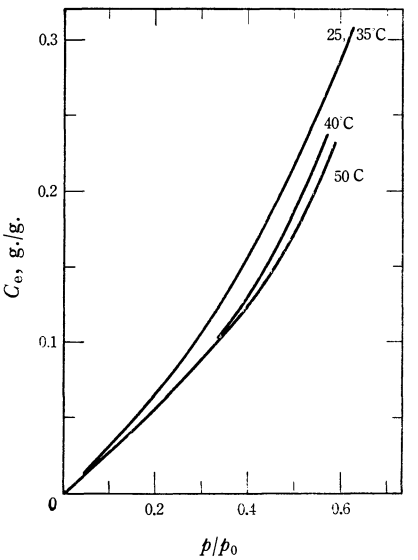

Fig. 1. Absorption isotherms of A-PS+benzene at 25, 35, and 50°C.

represents the mass of absorbed vapor in grams per unit gram of dry polymer and the abscissa the relative pressure of the vapor in the external phase. Although the individual points are not given in the figure, at a given relative pressure the differences in equilibrium gain between integral and differential absorption experiments were negligible at the three temperatures examined (Data at 25°C are shown later in Fig. 2.). It is seen that the data for 25 and 35°C are nearly represented by a single curve, indicating that the isotherms are practically independent of temperature within this narrow range of temperature. The data of Long and Kokes at 40°C[5] are also included in the figure for comparison. Formal application of the Flory-Huggins thermodynamic equation of polymer solutions, with the assumption that no volume change occurs on mixing, shows that at each temperature the interaction parameter χ_1 increases slightly with increase of equilibrium vapor concentration. The average values of χ_1 over the concentration range studied, except at very low penetrant concentrations, were 0.14, 0.14, and 0.32 at 25, 35, and 50°C, respectively. The average value of χ_1 evaluated from the data of Long and Kokes[5] was 0.27 at 40°C.

Figure 2 compares absorption isotherm data for the system A-PS+ethyl acetate, the system A-PS+benzene, and the system A-PS + ethyl methyl ketone,[7] all at 25°C. As expected, it can be seen that the equilibrium mass of absorbed penetrant

8) R. F. Boyer and R. S. Spencer, *J. Polymer Sci.*, **3**, 97 (1948).

9) A. Kishimoto, H. Fujita, H. Odani, M. Kurata and M. Tamura, *J. Phys. Chem.*, **64**, 594 (1960).

10) H. Mark and A. V. Tobolsky, "Physical Chemistry of High Polymeric Systems," Interscience Pub. Inc., New York (1950), p. 347.

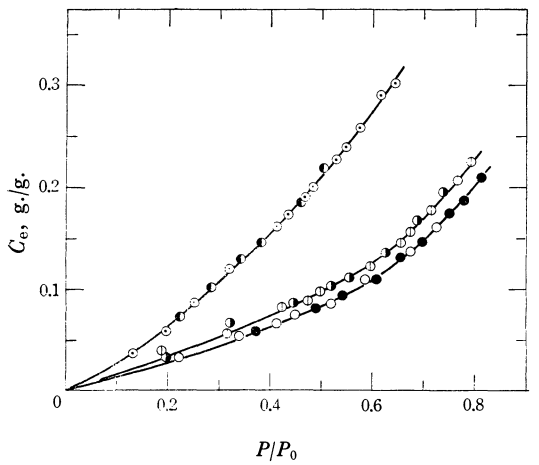

Fig. 2. Absorption isotherms of A-PS+ethyl acetate, A-PS+benzene, and A-PS+ethyl methyl ketone at 25°C.

	Integral absorption	Differential absorption
A-PS+ethyl acetate	○	●
A-PS+benzene	⊙	◐
A-PS+ethyl methyl ketone	◫	◑

becomes less in the order benzene, ethyl methyl ketone, and ethyl acetate when compared at the same relative vapor pressure of penetrant. That is, at a given relative vapor pressure, the poorer the solvent power to a given polymer the lower is the equilibrium vapor absorption. The values of the interaction parameter χ_1 calculated from these isotherm data at 25°C were 0.97 and 0.78 for A-PS+ethyl acetate and A-PS+ethyl methyl ketone, respectively.

Successive Differential Absorptions.— Figure 3 gives the data of successive differential absorptions for the system A-PS+benzene at 35°C in the medium and high concentration regions. The increments of benzene concentration in successive steps were kept about 0.01 g. penetrant per gram of dry polymer, which was almost the same as those used in our previous experiments.[7,9] Although the results in the low penetrant concentration region are not given in the figure, the general character of the absorption steps in this region was quite similar to that for the system polymethyl methacrylate+methyl acetate at 30°C.[9] That is, the absorption behavior was of the sigmoid type. The inflection point characteristic of the sigmoid curve shifted toward the short time region and the initial rate of each absorption increased as the initial concentration was increased. The first step in Fig. 3 exhibits a sigmoid character, and the subsequent absorption curves change their type according to the following scheme: pseudo-Fickian→two-stage→ Fickian. As noted in the previous paper,[9] the data for the A-PS+benzene system did not show a pseudo-Fickian process in the transition from the two-stage to the normal Fickian process.

With increasing temperature the concentration at which the absorption curve change their type from sigmoid to pseudo-Fickian behavior shifted toward low concentration values, and this was also the case with the initial concentration at which the transition from the pseudo-Fickian to the two-stage and from the two-stage to the Fickian occurred. In other words, raising temperature did not alter the general features of the family of successive differential absorption curves but merely compressed the whole family of curves to a lower concentration region. It has been demonstrated

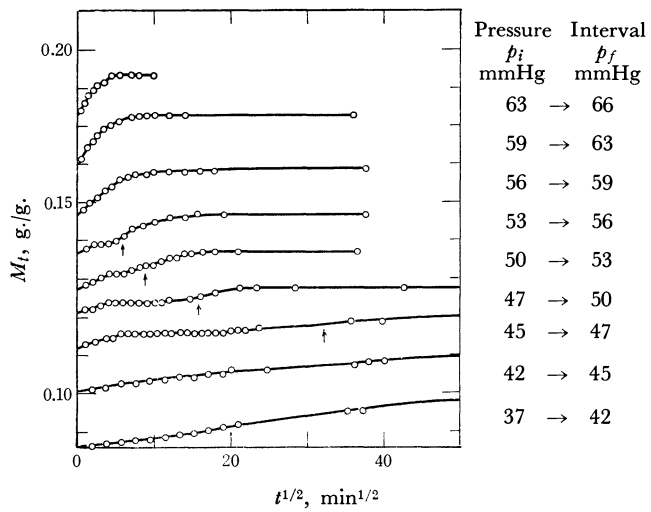

Fig. 3. Successive differential absorptions of A-PS+benzene at 35°C. Initial and final pressures, p_i and p_f, of each step are given in the right columns.

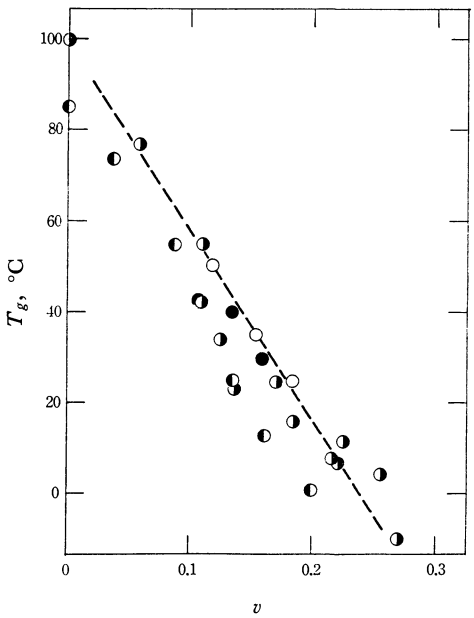

Fig. 4. Comparison of volume fraction for glass transition with critical volume fraction for diffusion.
○, Differential absorption experiments;
●, Sorption experiments by Long and Kokes[5];
◑, Dilatometric studies by Fox[11];
◐, Refractive index studies by Jenckel and Heusch.[12]

in the previous papers[7,9] that successive differential absorption curves change their type from non-Fickian to Fickian when the penetrant concentration reaches a value at which the polymer-penetrant mixture undergoes glass transition at the temperature of the experiment. From differential absorption data obtained with concentration intervals of nearly the same magnitude as those shown in Fig. 3, we estimated such a critical concentration for the A-PS+benzene system to be 0.150 at 35°C and 0.113 at 50°C in grams of benzene per gram of dry polymer. At 25°C the critical concentration of benzene was 0.191 g./g.[9] In Fig. 4 the values for the critical volume fraction calculated from these data are compared with the results obtained from dilatometric studies by Fox,[11] from refractive index studies by Jenckel and Heusch,[12] and from sorption experiments by Long and Kokes.[5] It can be seen that the points from different experimental techniques fall satisfactorily on a single line, indicating that the glass transition is closely related to the molecular mechanism which distinguishes Fickian absorption behavior of an amorphous polymer-penetrant system from non-Fickian.

The successive differential absorption data for A-PS+ethyl acetate at 25°C showed features which were quite similar to those of A-PS+ethyl methyl ketone at 25°C investigated previously.[7] That is, the successive curves change their type with increasing penetrant concentration according to the scheme: sigmoid→pseudo-Fickian→two-stage→pseudo-Fickian→Fickian. However, for A-PS+ethyl acetate the critical concentration was 0.112 in grams of ethyl acetate per gram of dry A-PS. This value is well consistent with the data interpolated from refractive index measurements of Jenckel and Heusch,[12] but lower than 0.139 g./g. obtained previously for ethyl methyl ketone at the same temperature. In the previous paper,[7] from comparison of the critical concentrations of ethyl methyl ketone and of benzene, we suggested that for an amorphous polymer at a given temperature a penetrant of poorer solubility gives a lower critical concentration if comparison is made for penetrants of about the same molar volumes. As described in the foregoing lines, the molar volumes of ethyl acetate, ethyl methyl ketone, and benzene are nearly the same. Thus we find that the present result with the system A-PS+ethyl acetate is in line with the deduction from our previous results.[7,9]

Concentration Dependence of the Second Stage Mechanism.—It is generally accepted[7,9] that the rate-determining factor for the second stage portion of the two-stage absorption is the rate at which polymer chains rearragne themselves in the presence of penetrant molecules, while the first stage involves the purely Fickian process. In accordance with the treatment presented in previous studies,[7,9] we here use the time t_* to characterize the position of the second stage portion on the time axis, where t_* is the time corresponding to the inflection point of a differential absorption curve of the two-stage type. The previous study[13] demonstrated for the system A-PS+benzene at 25°C that the value of t_* for a given initial concentration, C_i, increased with decreasing concentration increment and converged to a limiting value taken as characteristic of the given C_i. This was also the case with the A-PS+benzene at 35 and 50°C. The values of t^* characteristic of a given C_i for the system A-PS+benzene at 25, 35, and 50°C are plotted semilogarithmically against C_i in Fig. 5. We see that the plots for different temperatures are linear and nearly parallel with one another, indicating that for a given amorphous polymer the slope of $\log_{10} t_*$ vs. C_i plot is approximately independent of temperature. Thus the plots for $\log_{10} t_*$ vs. C_i at different temperatures may be superimposed with one another by shifting each plot along the

11) T. G. Fox. *Phys. Rev.*, **86**, 652 (1952).
12) E. Jenckel and R. Heusch, *Kolloid Z.*, **130**, 89 (1953).
13) H. Odani, S. Kida, M. Kurata and M. Tamura, This Bulletin, **34**, 571 (1961).

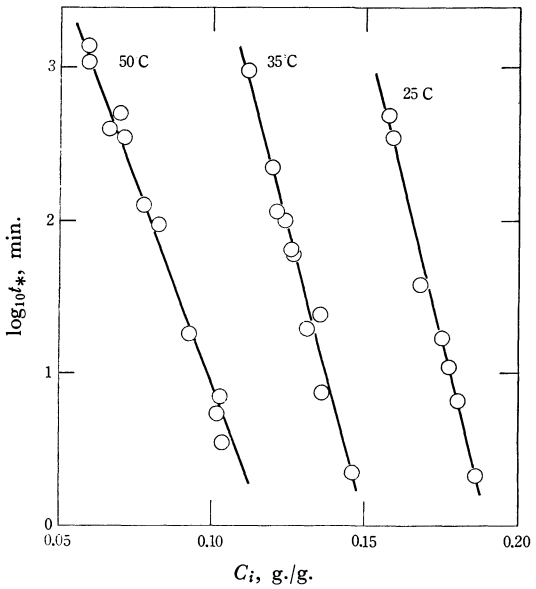

Fig. 5. Logarithmic correlation plots of t_* and initial concentration C_i for A-PS+benzene at 25, 35, and 50°C. t_* is the time corresponding to the inflection point of the second stage of the two-stage process.

ordinate to a particular temperature chosen as reference. This behavior bears resemblance to the time-concentration reduction scheme which was shown to be obeyed by stress-relaxation behavior of polymer-diluent systems in nearly the same concentration regions.[14] In this connection, it is worth-while to note the correlation between t_* and the mean relaxation time or, more properly, retardation time. We have shown for the system A-PS+benzene that the values of the mean retardation time, evaluated from the tensile creep measurements, and their dependence upon C_i are closely correlated with the values of t_* and their dependence upon C_i*. These results lend support to the argument that the second stage of a two-stage absorption process is primarily caused by the slow rearrangements of polymer network chains. Plots for $\log_{10} t_*$ vs. C_i at higher temperatures appear in the region of lower values of C_i. This is the reflection of the fact that the value of C_i at which the transition from pseudo-Fickian to two-stage type absorption occurred shifts toward the lower concentration region with increasing temperature. The values of the apparent activation energy were estimated at $C_i=0.115$ and 0.110 g./g. based on the assumption that the temperature dependence of t_* follows the Arrhenius type equation. They were 64 and 46 kcal./mol., respectively. These values compare favorably with those obtained from the time-temperature shift factor for linear visco-elastic behavior of amorphous polymers in the temperature region near glass transition.

Plots of $\log_{10} t_*$ vs. C_i for the system A-PS+ethyl acetate at 25°C are illustrated in Fig. 6. For the sake of comparison, the corresponding data for A-PS+benzene, A-PS+ethyl methyl ketone, and cellulose nitrate+acetone are included in the figure. The slope of the line for A-PS+ethyl acetate is nearly the same as those for A-PS+benzene and A-PS+ethyl methyl ketone. These slopes for A-PS systems are greater than that for cellulose nitrate. In the previous paper,[7] it was argued that the slopes of $\log_{10} t_*$ vs. C_i plot for a given polymer must be independent of penetrant species, because the second stage absorption primarily reflects the characteristic relaxation-motion of the network chains. Data for A-PS+ethyl acetate establish firmly this view. This, together with the results for the temperature dependence of $\log_{10} t_*$ vs. C_i plots shown in Fig. 5, clearly indicates that the second stage of the

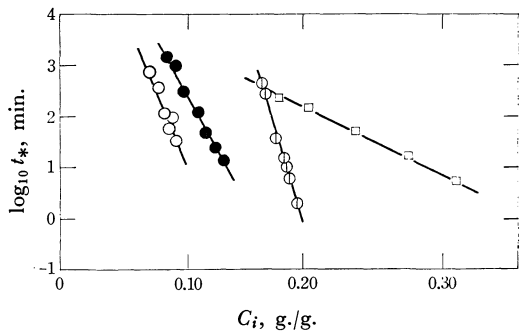

Fig. 6. Logarithmic correlation plots of t_* and initial concentration C_i for some polymer+vapor systems at 25°C.
○, A-PS+ethyl acetate;
⊖, A-PS+benzene;
●, A-PS+ethyl methyl ketone;
□, Cellulose nitrate+acetone.

two-stage process is governed by the rate at which the network of polymer chains change its conformation under the osmotic swelling pressure.

Integral Absorptions and Desorptions.— The measurements of integral absorption and desorption with various pressure differences were carried out from and back to zero penetrant concentration. The general features of the integral absorption and desorption processes for A-PS+benzene at 35 and 50° were quite similar to those obtained previously at 25°C.[13] That is, the integral absorption curves were sigmoid for all pressure intervals investigated. On the other hand, the integral absorption curves were concave to the $t^{1/2}$ axis, no linear portion was observed in

14) H. Fujita and A. Kishimoto, *J. Polymer Sci.*, **28**, 547 (1958).

* Preliminary report of the tensile creep behavior of the system A-PS+benzene appeared in "*Rep. Progr. Polymer Phys. Japan*," **6**, 163 (1963). Detail will be reported in a forthcoming publication.

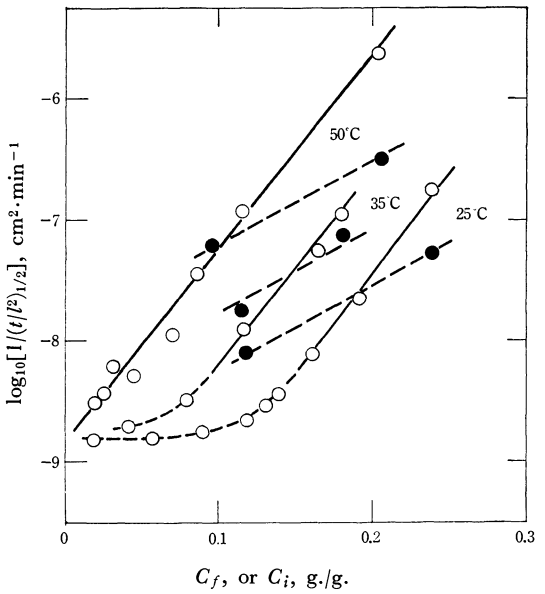

Fig. 7. Logarithmic correlation plots of $1/(t/l^2)_{1/2}$ and final equilibrium concentration, C_f, for absorption or initial concentration, C_i, for desorption for A-PS+benzene at 25, 35, and 50°C. $(t/l^2)_{1/2}$ is the value t/l^2 when the amount of vapor in polymer reaches one half of the final equilibrium value; l is the thickness of film and t is time. ○, absorption. ●, desorption.

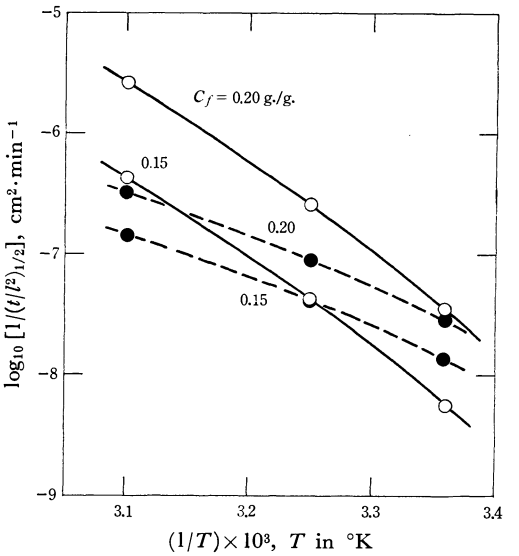

Fig. 8. Logarithmic correlation plots of $1/(t/l^2)_{1/2}$ and reciprocal absolute temperature for A-PS+benzene at $C_f=0.15$ and 0.20 g./g. ○, absorption. ●, desorption.

the initial stage, and the slope of the curve decreased continuously from the origin. The desorption curve had a much higher initial rate than that of the corresponding absorption and intersected with the latter in the later stage. At 35 and 50°C the absorption curves showed a pronounced dependence on the pressure difference and the general feature of this dependence was similar to that observed at 25°C. As noted in the previous report,[13] the absorption processes from zero to equilibrium concentrations above the critical concentration exhibited non-Fickian features contrary to the data of Long and Kokes,[5] who observed Fickian absorption curve in such cases. This was also the case at 35 and 50°C, and the non-Fickian behavior still persisted at the highest equilibrium concentration studied. At the highest concentration, which was far above the critical concentration, the polymer films hardly supported its own weight from the spring balance.

In the case when absorption and desorption curves do not conform to normal Fickian features, we are not able to evaluate the mutual diffusion coefficient of the system by using the methods which utilize data for the initial slope of the absorption curve. In such a case, as in the previous treatment,[7,13] we may be content with the reciprocal of $(t/l^2)_{1/2}$ being taken as a quantitative measure of the overall rate of an absorption or desorption curve, where l is the thickness of the film and $(t/l^2)_{1/2}$ is the value of t/l^2 for the time t at which the amount of penetrant in the film reaches one half the final equilibrium value. The values of $1/(t/l^2)_{1/2}$ for the system A-PS+benzene, determined from integral absorptions from and to zero penetrant concentration, are plotted semi-logarithmically against the equilibrium concentration, C_f, in Fig. 7. It is seen that at 25 and 35°C the plots from absorption data are convex to the concentration axis in the low concentration region and are linear at medium and high values of C_f. At 50°C. the plots increase linearly with increasing C_f over the entire range investigated. In the linear portion the plots for the three temperatures are nearly parallel and their slopes are larger than those for integral desorption. From this latter behavior it follows that the temperature dependence of sorption rate is greater for absorption than for desorption at fixed values of C_f, and it may be expected that for a glassy polymer the apparent activation energy for absorption is larger than that for desorption.

For a quantitative representation of the temperature dependence of the overall rate of absorption or desorption, we determined the apparent activation energy from the slope of a plot for the logarithm of $1/(t/l^2)_{1/2}$ against reciprocal absolute temperature. Figure 8, which illustrated such plots for A-PS+benzene at $C_f=0.15$ and 0.20 g./g., indicates that for both absorption and desorption the values of $\log_{10}[1/(t/l^2)_{1/2}]$ decrease nonlinearly with increasing $1/T$. This similar feature has been reported for diffusion coefficients of gases

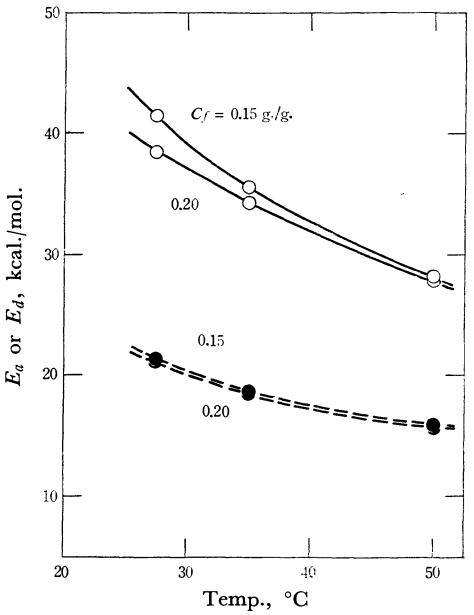

Fig. 9. Temperature dependence of the apparent activation energy for absorption, E_a, or for desorption, E_d, for A-PS+benzene at C_f=0.15 and 0.20 g./g. ○, absorption. ●, desorption.

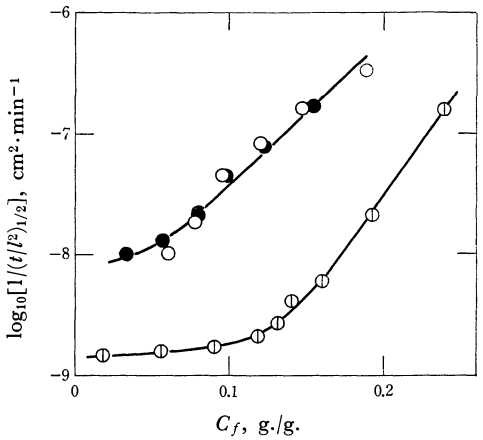

Fig. 10. Logarithmic correlation plots of $1/(t/l^2)_{1/2}$ and final equilibrium concentration C_f for A-PS +ethyl acetate, A-PS+benzene, and A-PS+ ethyl methyl ketone at 25°C.
○, A-PS+ethyl acetate;
Ⓘ, A-PS+benzene;
●, A-PS+ethyl methyl ketone.

or vapors in elastomers.[15-18]

An apparent activation energy for absorption, E_a, may be defined by the equation:

$$E_a = -Rd\{\ln[1/(t/l^2)_{1/2}]_a\}/d(1/T),$$

where $[1/(t/l^2)_{1/2}]_a$ is the value of $1/(t/l^2)_{1/2}$ for absorption. Similarly, an apparent activation energy for desorption, E_d, may be defined. The values of E_a and E_d calculated from Fig. 8 are plotted as a function of temperature in Fig. 9. It is seen that E_a are greater than E_d in the temperature region studied.

For the system A-PS+ethyl acetate integral absorptions and desorptions from and to zero concentration were studied at 25°C in the same range of penetrant concentration as in the case of A-PS+benzene[13] and A-PS + ethyl methyl ketone.[7] The curves obtained had exactly the same features as those for A-PS+benzene mentioned above. Figure 10 gives the plots of $\log_{10}[1/(t/l^2)_{1/2}]$ vs. C_f for A-PS+ethyl acetate at 25°C. For the sake of comparison, the data for the benzene system and the ethyl methyl ketone system at the same temperature are also illustrated in the figure. It is seen that the plots for ethyl acetate and ethyl methyl ketone are almost represented by a single curve. This suggests that the values of diffusion coefficient and its dependence upon penetrant concentration for A-PS+ethyl acetate are nearly the same as those for the system A-PS+ethyl methyl ketone.

Summary

The successive differential absorptions for the A-PS+benzene system at 25, 35, and 50°C change with the initial concentration according to the scheme: sigmoid type→pseudo-Fickian type→two-stage type→Fickian type. The last transition, from two-stage to Fickian types, occurs at a lower concentration as the temperature of the experiment is raised. The values of the critical concentration for this transition are well compared with those for glass transition of the system. The successive differential absorptions for the A-PS+ethyl acetate system change their type with the increase of initial concentration according to the scheme, which is typical of systems of amorphous polymer+ organic vapor; that is, sigmoid→pseudo-Fickian→ two-stage→pseudo-Fickian→Fickian. The critical concentration for the last transition becomes lower in the order benzene, ethyl methyl ketone, and ethyl acetate. For all systems investigated the second stage portion of the two-stage process shifts rapidly to the short time regions as the initial concentration of each step increases. For A-PS+ benzene the dependence of the rate of this shift upon intial concentration is very similar at 25, 35, and 50°C. For A-PS + ethyl acetate the rate of the shift depends upon initial concentration in nearly the same manner as in the A-PS+benzene system and the A-PS+ethyl methyl ketone system.

The general features of integral absorptions for

15) R. M. Barrer and G. Skirrow, *J. Polymer Sci.*, **3**, 549 (1948).
16) van Amerongen, ibid., **5**, 307 (1950).
17) M. J. Hayes and G. S. Park, *Trans. Faraday Soc.*, **51**, 1134 (1955).
18) H. Fujita, A. Kishimoto and K. Matsumoto, ibid., **56**, 424 (1960).

the A-PS+benzene system at 25, 35, and 50°C are very similar, and the absorption curves show a pronounced dependence on concentration. At 25 and 35°C the logarithmic correlation plots of the overall rate of absorption and final equilibrium concentration are linear at the medium and high values of equilibrium concentration, and at 50°C the plots are linear over a nearly entire range of concentration studied. An apparent activation energy for absorption is greater than that for desorption in the temperature region investigated. The general feature of integral absorptions for the A-PS+ethyl acetate system is very similar to those for benzene and ethyl methyl ketone systems, irrespective of the difference in the penetrant-polymer interaction among these systems. The dependence of absorption rate upon concentration is also similar in general character to that for benzene and ethyl methyl ketone systems.

We wish to thank Professor Hiroshi Fujita of Osaka University and Professor Michio Kurata of this University for advice given during the course of this study. Thanks are also due to Mr. Munetada Kanaya for his aid in making various experiments.

BULLETIN OF THE CHEMICAL SOCIETY OF JAPAN VOL. 39 2385—2395 (1966)

Non-Debye Reorientation Processes of Molecules. Correlation Functions and Spectral Densities for Spherical Molecules

By Hiroshi SHIMIZU*

Department of Chemistry, Stanford University, Stanford, California, U. S. A.

(Received May 16, 1966)

The non-Debye reorientation processes in which the Debye equation is inapplicable are studied for spherical molecules by using an equation proposed by the author. The physical meaning of the angular correlation in the non-Debye processes is discussed in detail. It is shown that in the non-Debye processes the non-dissipative decay of the mutual-phase correlation of rotating molecules must be taken into account, in addition to the dissipative decay due to molecular collisions, and that the use of the "microscopic viscosity" in the Debye equation is not plausible. It is also shown that, in contrast to the Debye processes, there is no one-to-one correspondence between the correlation time for molecular reorienation and the mean life time of the rotation, since the contribution from the nondissipative decay should be considered also. The vector and the tensor correlation functions,

$$\langle \cos\theta(0)\cos\theta(t)\rangle \quad \text{and} \quad \langle (1/2)\{3\cos^2\theta(0)-1\}\{(1/2)3\cos^2\theta(t)-1\}\rangle,$$

and the corresponding spectral densities, the band shapes of infrared and Raman spectra respectively, are obtained theoretically for various conditions and are shown graphically. As illustravtie examples of the treatment, methane and deutero methane molecules are studied. Vector correlation functions are obtained from the observed band shapes of the infrared spectra of these molecules. Comparing the theoretical correlation functions with experimental ones, it is shown that a reasonable agreement between theory and experiment is obtained and that methane molecules have a typical non-Debye reorientation process even below the freezing point. Some characteristic features of the non-Debye process are also discussed.

The observed correlation times for the reorientation of molecules are, in general, shorter than those derived from Debye's theory of the reorientation of spherical particles in liquids.[1] In particular, for light molecules such as substituted benzenes or some of the lower ethers or alcohols, the observed correlation times, τ_1 and τ_2, for the vector and the tensor correlation function:

$$\Phi_1(t) = N_1\langle \cos\theta(0)\cos\theta(t)\rangle \tag{1}$$

and

$$\Phi_2(t) = N_2\langle \frac{1}{2}\{3\cos^2\theta(0)-1\}\frac{1}{2}\{3\cos^2\theta(t)-1\}\rangle \tag{2}$$

are shorter by a factor of 10—100.[2,3] In these

* On leave of absence from Department of Chemistry, Chiba University, Chiba, Japan.

1) P. Debye, "Polar Molecules," Chemical Catalog Company, New York (1929).

2) K. Higasi, "Dipole, Molecule and Chemistry," Research Institute of Applied Electricity, Hokkaido University, Sapporo (1965).

3) W. B. Moniz and H. S. Gutowsky, *J. Chem. Phys.*, **38**, 1155 (1963).

equations, for instance in (1), $\langle\ \rangle$ refers to the average of the products, $\cos\theta$ at $t=0$ times $\cos\theta$ at $t=t$, over the ensemble, where θ is the angle between a vector fixed on a molecule and the z-axis of a space-fixed laboratory frame. N_1 is a normalization constant which makes $\Phi_1(0)$ unity.

The serious disagreement between the theoretical and the experimental correlation times may be attributed to the use of the macroscopic viscosity, η, in the Debye equation:[1,4]

$$\tau_j = \frac{4\pi\eta a^3}{3kT}(1+\delta_{1j}) \tag{3}$$

In this equation, a refers to the radius of the molecule; $\delta_{1j}=1$ for $j=1$ and is otherwise zero. Since no medium is continuous or homogeneous on the molecular scale, the effective viscosity for molecular reorientation, the microscopic viscosity, must be, in general, different from the macroscopic one. However, the use of the microscopic viscosity in (3) may not be a sufficient improvement on Debye's theory. As is shown below, the disagreement arises from the basic inapplicability of Debye's scheme to the substances mentioned above.

The Debye equation is derived on the assumption that random reorientations of molecules can be described in terms of a diffusion equation.[1,4] Therefore, a molecular reorientation with a finite and large angle is assumed to appear as a result of many rotations which occur successively in time.[4] This situation may be compared with the translational diffusion of molecules in a three-dimensional space, where a molecule moves step by step, at random and in all directions.[5] The assumption of a continuous medium is consistent with the basic concept of the diffusion: the continuous liquid *constantly* exerts against a rotating molecule. This force leads to two important sequences through *constantly* exerts a resistive force against a rotating molecule. This force leads to two important sequences through the reduction of the angular velocity of the rotating molecule: (1) it reduces the magnitude of a step of the tiny rotation, and (2) fluctuating forces must be supplied constantly from the outside in order to keep the average rotational energy constant against the friction.

On the other hand, the discrete and inhomogeneous nature of the medium may not result in a diffusion process, at least not when the medium molecules move at random at a rate that is comparable with that of the rotation of the solute molecule. A fluctuation in the positions of the medium molecules may temporarily give the solute molecule a vacant space and allow it to rotate relatively freely as in the gas phase. Since the duration of such a "vacant" space is fairly close to the mean period of the rotation of the solute molecule, a step of a single rotation must be so large that the reorientation of the solute molecule cannot be related to a diffusion process. Moreover, the appearance of the nature of the "free" rotation in liquids clearly makes the correlation times very short.

The use of the Debye equation, which is equivalent to the assumption of the existence of a well-defined diffusion process in the liquid, is not appropriate in those many cases where we really use a microscopic viscosity instead of η in order to reduce the large disagreement between theory and experiment. We may call such fast reorientation processes "non-Debye processes."

A further step in the study of the random reorientation of molecules has been made in a paper by Gordon.[6] He showed that a tensor correlation function could be obtained from a Raman spectrum as the Fourier transform of the band-shape function whose structures are originally due to the rotation-vibration interaction. In other words, the band shape itself represents the spectral density of the random reorientation of a molecule. This idea was soon extended by Gordon[7] to the infrared case: vector correlation functions were obtained similarly from infrared spectra. He discussed briefly the form of the correlation functions corresponding to a non-Debye process. The correlation functions for CO and CH_4 molecules clearly showed that the reorientation processes for these molecules are non-Debye, even in solution.

A general theory of the random reorientation of molecules, including non-Debye processes, was proposed by Shimizu[8]; he also obtained vector and tensor correlation functions theoretically. Then, by using the theory of linear response,[9] it was shown that band-shape functions corresponding to various kinds of spectra, including infrared, Raman, and dielectric relaxation, could be obtained in terms of the Fourier transform of the theoretical correlation functions, and vice versa. The theory was found to be reasonable from a comparison with the correlation functions obtained experimentally from the infrared spectrum of *trans*-dichloroethylene.

In the present paper, the nature of the non-Debye reorientation of a spherical rotor will be discussed, using as a typical example the methane molecule. Graphical representations of the correlation functions and the corresponding spectral densities will

4) H. Frohlich, "Theory of Dielectrics" Clarendon Press, Oxford, (1958).
5) S. Chandrasekhar, *Rev. Modern Phys.*, **15**, 1 (1943).
6) R. G. Gordon, *J. Chem. Phys.*, **42**, 3658 (1965).
7) R. G. Gordon, ibid., **43**, 1307 (1965).
8) H. Shimizu, ibid., **43**, 2453 (1965). The terms "the Debye limit" and "the inertial limit" were used there. It was assumed that, in the Debye limit, the correlation function with the correlation time τ_j given by the Debye equation holds. In this paper "the Debye process" means the molecular reorientation process within the Debye limit.
9) R. Kubo, *J. Phys. Soc. Japan*, **12**, 570 (1957).

be given from the theory. The relations between the band shapes of the infrared and Raman spectra and the random reorientation process of molecules will be automatically discussed in the present paper, since the spectral densities corresponding to a vector correlation function and tensor correlation function are equivalent to the band shape of infrared and Raman spectra respectively.[6-8] No effort will be made to discuss the accurate form of the correlation functions. Our principal aim is to show the properties of non-Debye processes in terms of simple physical concepts and straightforward mathematical expressions.

The Correlation Functions for Non-Debye Processes

Though the general form of the correlation functions for non-Debye reorientation processes have already been discussed,[8] the correlation functions for spherical rotors were only briefly given. Therefore, a detailed discussion of the form of the correlation functions and the spectral densities of spherical molecules will be given in this and the next section in order to illustrate the general features of non-Debye processes.

The correlation function for non-Debye processes, more accurately, for the inertial limit, may be approximately given by[8]:

$$\Phi_j(t) = a_j(t)\Phi_j^{(0)}(t) + b_j(t)\Phi_j^{(p)}(t) \qquad (4)$$

with $j = \begin{cases} 1 & \text{for the vector correlation function} \\ 2 & \text{for the tensor correlation function,} \end{cases}$

where $\Phi_j^{(0)}(t)$ is the correlation function for "free" molecules. The perturbed correlation function, $\Phi_j^{(p)}(t)$, is related to the reorientation of the molecule under the perturbation due to the interaction with the neighboring molecules. We may assume that the perturbed correlation function has an exponential form when $t \gg \tau_f$.[8,10] Here the mean period of rotation, τ_f, is a function of the absolute temperature, T, and the moment of inertia, I, of the molecule:

$$\tau_f = (I/\boldsymbol{k}T)^{1/2}$$

For example, we may assume[8,11]:

$$\Phi_j^{(2)}(t) = \exp\left\{-\Delta_j^2 \int_0^t \mathrm{d}t'(t-t') \exp\left(-|t|/\tau_{rj}\right)\right\} \qquad (5)$$

as a first-order approximation, where τ_{rj} is the life time of the rotation. The modulation amplitude is a function of the magnitude of the fluctuation of the angular velocities of the rotating molecules, velocities arising from the perturbation from the neighboring molecules. Equation 5 corresponds an assumption that the fluctuation of the angular velocities is a Gaussian process.[10] A strong collision assumption leads to a simple form[8]:

$$\Delta_1^2 = 3/\tau_f^2 \qquad (6)$$

The Δ_2^2 quantity was not discussed before. Hence, we will give it here. We may assume that a non-Debye process approaches a Debye process as $\tau_{rj}/\tau_f \to 0$, where, due to frequent collisions with the neighboring molecules, the (solute) molecules are allowed such small rotations as occur in rotational diffusion. Debye's theory gives:

$$\tau_1/\tau_2 = 3 \qquad (7)$$

On the other hand, the effective correlation time for $\Phi_j^{(2)}(t)$ is given by[8]:

$$\tau_j' \cong (\Delta_j^2 \tau_{rj})^{-1} \qquad (8)$$

Thus, naively assuming $\tau_{r1} = \tau_{r2}$, we obtain:

$$\Delta_2^2 = 9/\tau_f^2 \qquad (9)$$

from (6)—(8). The modulation amplitude, (6) or (9), was obtained by assuming that the magnitude of the angular momentum was changed at each collision.[8] If only the orientation of the angular momentum is changed by collisions, the correlation function, $\Phi_j^{(2)}(t)$, is improper. A detailed discussion of the correlation function will be presented in the near future. Qualitatively, the nature of the reorientation processes determines the magnitude of the modulation amplitude.

The simplest assumption as to the form of the adjusting functions will be taken as[8]:

$$\left.\begin{aligned} b_j(t) &= 1 - \exp\left(-|t|/\tau_{bj}\right) \\ a_j(t) &= \exp\left(-|t|/\tau_{aj}\right) \end{aligned}\right\} \qquad (10)$$

The time constants, τ_{aj} and τ_{bj}, are roughly the lifetime of rotation.

By using a very simple assumption:

$$\tau_{rj} = \tau_{aj} = \tau_{bj} \equiv \tau_r$$

vector and tensor correlation functions were calculated by varying τ_r/τ_f. The results are shown graphically in Figs. 1 and 2, where the unit of the time scale is τ_f. The correlation functions are not exponential, unless τ_r/τ_f is much smaller than unity. For $\tau_r/\tau_f \gtrsim 1$, the nonexponential contribution of $\Phi_j^{(0)}(t)$ to $\Phi_j(t)$ is appreciable.

An Interpretation of the Form of Correlation Functions

We choose the local frame or the local coordinate system of each molecule in such a way that their

10) R. Kubo, "Fluctuation, Relaxation, and Resonance in Magnetic System," Oliver and Boyd, Ltd., London (1962).

11) The use of (5) is correct only when the random process of ω-fluctuation is a Gaussian process. Therefore, the physical meaning of Eq. 4 with 5 is that all the molecules start to rotate in phase at $t=0$ and then, regarding the molecules which have had more than one collision since $t=0$, the initial memory of the phases of rotation is randomized. Therefore, after a collision the molecular reorientation process may be regarded as a Gaussian process with random phases. This process is given by (5).

origins are common with that of the laboratory frame. A local frame of a molecule coincides with the corresponding molecular frame at $t=0$, except for the origin. One can thus transform between the two frames by a pure translation. The Eulerian angles between a local frame and the laboratory frame may be written as $\Omega\equiv(\alpha, \theta(0), \gamma)$. By introducing Wigner's rotation matrix, $D_{mm'}^{(1)}(\Omega)$, of the first order, the direction cosines between the z-axes of the molecular and the laboratory frames may be written as:

$$\cos\Theta(t) = \sum D_{mo}^{(1)}(\alpha, \theta(0), \gamma) y_m(\Theta(t), \Psi(t)) \tag{11}$$

where $y_m(\Theta, \Psi)$ are the reduced spherical harmonics relating the spherical coordinates of the z-axis of the molecular frame as observed in the local frame;

$$\left.\begin{aligned} &y_1(\theta(t), \Psi(t)) \\ &\quad = -\frac{1}{\sqrt{2}}\sin\Theta(t)\exp\{i\Psi(t)\} \\ &y_0(\Theta(t), \Psi(t)) = \cos\Theta(t) \\ &y_{-1}(\Theta(t), \Psi(t)) \\ &\quad = \frac{1}{\sqrt{2}}\sin\Theta(t)\exp\{-i\Psi(t)\} \end{aligned}\right\} \tag{12}$$

From (11)—(12), with the assumption $\Theta(0)=\Psi(0)=0$;

$$\begin{aligned} \langle\cos\theta(0)\ \cos\theta(t)\rangle &= \langle\cos\theta(0)\cdot\cos\theta(0)\cos\Theta(t)\rangle \\ &+ \langle\cos\theta(0)\cdot\sin\theta(0)\sin\Theta(t)\cos(\Psi(t) \\ &- \alpha(0))\rangle \qquad (13) \\ &= \langle\cos^2\theta(0)\rangle\langle\cos\Theta(t)\rangle \qquad (14) \end{aligned}$$

where the last expression is only when the system is spatically isotropic. In fact, for an isotropic system the statistical average of a physical quantity of an ensemble must be independent of the directions of the coordinate axis of the laboratory frame. From this it follows that the average over the fraction of the molecules, $f(\theta, \varphi)\sin\theta d\theta d\varphi$, is independent of θ and φ, provided that the magnitude of the solid angle, $\sin\theta d\theta d\varphi$, is properly chosen. The $f(\theta, \varphi)$ function is a normalized distribution function of the molecular axis (the z-axis of the molecular frame) in terms of the spherical coordinates defined with respect to the laboratory frame. The ensemble average is, in general, equivalent to the average over the molecules in an arbitrary fraction, $f(\theta, \varphi)\sin\theta d\theta d\varphi$. In Function 13, the averages of $\cos\Theta$ and $\sin\Theta$ are independent of $\theta(0)$. Hence, the functions of $\theta(0)$ and Θ may be averaged independently. Denoting the average over the molecules whose initial orientations are in a small solid angle, $d\Omega$, around $\theta(0)=0$ as $\langle\ \rangle_{\theta(0)=0}$, we may obtain:

$$\Phi_1(t) = \langle\cos\theta(t)\rangle_{\theta(0)=0} \tag{15}$$

since in an isotropic system it is clear that:

$$\begin{aligned} &\langle\cos\theta(0)\cos\theta(t)\rangle_{\theta(0)=0} = \langle\cos\theta(t)\rangle_{\theta(0)=0} \\ &\quad = \langle\cos\Theta(t)\rangle_{\theta(0)=0} = \langle\cos\Theta(t)\rangle = \Phi_1(t) \end{aligned}$$

The definition of the correlation function, 15, was used in a previous paper[8] without explicit proof. The use of the new definition (15) instead of (1) has the great advantage that a correlation function may be discussed in terms of a simple model of molecular motion. For instance, it immediately turns out from (15) that the $\Phi_1(t)$, correlation function, is a periodic function of the time, when all the molecules rotate with a uniform frequency and phase. On the other hand, if the phases of the rotating molecules are random, the correlation function decays in a monotonic manner. The $\Phi_1^{(0)}(t)$ correlation function in Fig. 1 is interesting from this point of view, since it is a hybrid of these two extremes.

As an introductory example, the $\Phi_1^{(0)}(t)$ function for diatomic molecules will be discussed first and then the discussion will be extended to spherical molecules. Molecules whose initial orientations are not in the solid angle, $d\Omega$, around $\theta(0)=0$ will not be explicitly discussed. This does not, however, imply that we assume that all the molecules in the system have the same orientation at $t=0$. In the discussion below the word "molecules" in quotation marks refers to the molecules characterized by $\theta(0)=0$.

The correlation function may be given in terms of two different representations, the orientation representation by Debye and the angular momentum representation by Schwinger.[12] The latter representation was used in the discussion of the nuclear magnetic relaxation of hydrogen molecules in the gas phase. There the Hamiltonian

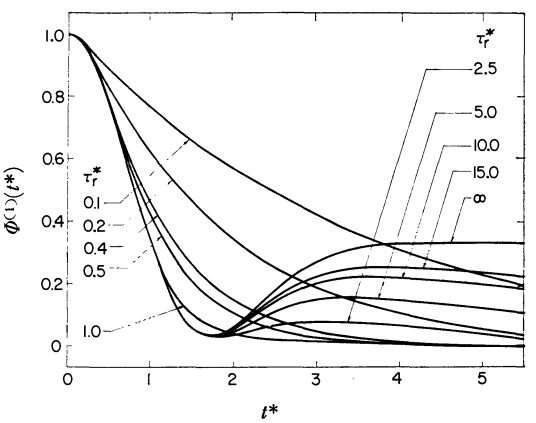

Fig. 1. The vector correlation functions for a spherical rotor obtained by using Eq. 4. The asterisks on t and τ_r indicate that these quantities are measured on the τ_f-scale. Note that $\Phi_1^{(0)}(t^*)=\Phi_1(t^*)$ for $\tau_r^*=\infty$.

12) Referred to in N. Bloembergen, E. M. Purcell and R. V. Pound, *Phys. Rev.*, **73**, 679 (1948). Schwinger's theory is cited in this paper.

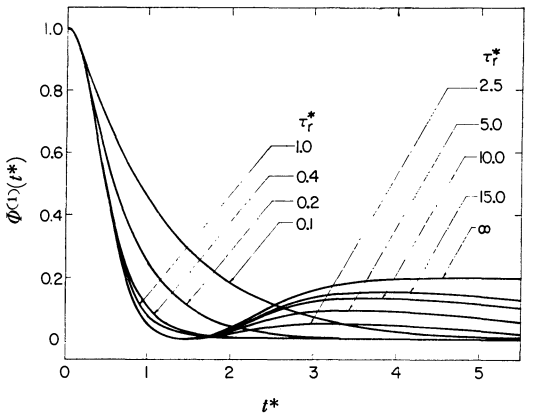

Fig. 2. The tensor correlation fractions, $\Phi_2(t^*)$, for a spherical rotor obtained by using Eq. 4. Note that $\Phi_2^{(0)}(t^*)=\Phi_2(t^*)$ for $\tau_r^*=\infty$.

for the magnetic dipolar coupling between two protons was given in terms of the angular momentum vector of the molecule by replacing the interatomic vector by the angular momentum vector using the Wigner-Eckart theorem.

The vector correlation function in the orientation representation may be given as:

$$\Phi_1^{(0)}(t) = \cos \omega_0 t \tag{16}$$

for the *free* "molecules" with a uniform frequency, ω_0, and a uniform phase. Since the "molecules" have two rotational degrees of freedom, they rotate around the uniformly-distributed axes in the x-y plane. The 16 function never decays, since the mutual phase correlations among the "molecules" are never randomized. In the angular momentum representation, the abovementioned correlation function should be a constant:

$$\Phi_{1J}^{(0)}(t) = 1 \tag{17}$$

because the angular momenta of the "molecules" are never changed. In order to get a better image of the angular momentum representation, we will introduce a description of the molecular motion in terms of the rotating coordinate system; each "molecule" is observed from the corresponding rotating frame, where the axis of rotation is the same as that of the observed "molecule." Moreover, the angular frequency, ω_0, of the rotation of the frame is the same as that of the "molecule." Therefore, the "molecules" are fixed on the rotating frames, where the z-axes are chosen parallel to the μ vectors on the "molecules." We assume that the fraction of the "molecules" whose axes of rotation are in $d\varphi$ around φ' can be observed from the same rotating frame, $S_R(\omega_0;\ \theta,\ \varphi)= S_R(\omega_0;\ \pi/2,\ \varphi')$. We choose the value of $d\varphi$ so that the statistical behavior of the "molecules" in such a fraction is independent of φ. It is clear that the description of the motion of molecules in terms of the angular momentum representation is basically equivalent to that in the rotating frames, provided that ω_0 is proportional to the magnitude of angular momentum and provided that the direction specified by θ and φ is parallel to the direction of angular momentum. We thus obtain:

$$\Phi_{1R}^{(0)}(t) = 1 \tag{18}$$

in a rotating frame, for instance, in $S_R(\omega_0;\ \pi/2,0)$. For the "molecules" which are fixed in the laboratory frame, we obtain:

$$\left.\begin{aligned} \Phi_1(t) &= 1 \\ \Phi_{1J}(t) &= \Phi_{1R}(t) = \cos \omega_0 t \end{aligned}\right\} \tag{19}$$

The relationship between the two representations is not straightforward, as is shown above, if the "molecules" have nonuniform angular velocities. Even in such a case, however, the 17 correlation function is valid for the free "molecules." However, in a rotating frame, $S_R(\omega_0:\ \pi/2,\ \varphi)$, the correlation function, $\Phi_{1R}^{(0)}(t)$, is, in general, not so simple as in (18), because there are many "molecules" whose angular frequency is different from ω_0. In general, the "molecule" has the angular frequency of $\omega-\omega_0$ in $S_R(\omega_0:\ \pi/2,\ \varphi)$. As a result, the "molecules" with $\omega>\omega_0$ and $\omega<\omega_0$ rotate in positive and negative directions respectively. Hence, the directions of the vectors $\boldsymbol{\mu}$ in S_R will gradually be randomized.

To treat this process more explicitly, we will consider a subensemble of the "molecules" whose rotation is to be described in $S_R(\omega_0:\ \pi/2,\ 0)$, The distribution of ω may be given by the Boltzmann distribution, $\exp(-I\omega^2/2\boldsymbol{k}T)$. If ω_0 is defined by the equation:

$$\int_0^\infty \exp\left(-I\omega^2/2\boldsymbol{k}T\right) \sin\left(\omega-\omega_0\right)d\omega=0 \tag{20}$$

or, more explicitly, by:

$$\omega_0(t) = \frac{1}{t}\tan^{-1}\left\{\frac{2}{\sqrt{\pi}}E_{rf}(t/\sqrt{2}\tau_f)\right\} \tag{21}$$

then the expectation value of the vector sum of each vectors, $\boldsymbol{\mu}$, over the subensemble in the rotating frame, $S_R(\omega_0:\ \pi/2,0)$, is always parallel to the z-axis of $S_R(\omega_0:\ \pi/2,0)$. The $\omega_0(t)$ frequency is roughly independent of the time:

$$\omega_0(0) = \frac{\tau_f}{\sqrt{2\pi}} \tag{22}$$

for small t values and gradually decreases with time. As has been mentioned before, the phase correlations among the vectors $\boldsymbol{\mu}$ in $S_R(\omega_0:\ \pi/2,0)$ eventually vanish and the directions of the vectors are eventually randomized. Hence, the $\Phi_{1R}^{(0)}(t)$ function, which is proportional to the z-component of a vector-sum, $\boldsymbol{p}$, of the vectors, $\boldsymbol{\mu}$, on each member of subensemble "molecules," decreases with time. It can be shown that:

$$\Phi_{1R}^{(0)}(t)=\int_0^\infty \exp(-I\omega^2/2\boldsymbol{k}T)\cos(\omega-\omega_0)t\mathrm{d}\omega$$
$$=\frac{\sqrt{2}}{\tau_f}\mathrm{e}^{-t^2/2\tau_f^2}\{\sqrt{\pi}\cos\omega_0 t + E_{rf}(t/\sqrt{2}\tau_f)\sin\omega_0 t\} \quad (23)$$

from which $\Phi_{1R}^{(0)}(t)\to 0$, as $t\to\infty$ is clear. Thus, roughly speaking, the mean period of rotation, τ_f, is the relaxation time of $\Phi_{1R}^{(0)}(t)$, namely, the relaxation time of $\Phi_1^{(0)}(t)$. To facilitate discussion, we will call the vectors on each "molecules" the μ-vectors, and the sum of the μ-vectors on all the "molecules," the $\boldsymbol{P}$-vectors.

The decay of $\Phi_{1R}^{(0)}(t)$ due to the loss of the phase correlation of the μ-vectors in the rotating frame may be compared to the free-induction decay of a macroscopic magnetization vector, $\boldsymbol{M}$, which was discussed by Hahn,[13] namely, the decay of the magnetization vector after a 90°-pulse. This pulse changes the direction of the magnetization vector by 90°. Then the vector begins to precess in a plane perpendicular to the direction of the magnetic field. In properly-chosen rotating frames, the motion of an ensemble of the μ-vectors with a uniform angular frequency may be compared to that of an ensemble of the noninteracting microscopic magnetization vectors, $\boldsymbol{m}$, in a homogeneous magnetic field. In both cases the $\boldsymbol{P}$ and $\boldsymbol{M}$ vectors are constant in the rotating frames. The motion of the $\boldsymbol{M}$-vector in an inhomogeneous field is similar to that of the $\boldsymbol{P}$-vector when the molecules have nonuniform frequencies; the phase memory among the $\boldsymbol{m}$-vectors is gradually lost as a result of the inhomogeneity of the magnetic field, which gives nonuniform frequencies to the precessing $\boldsymbol{m}$-vectors. It should be noted that no energy exchange process is involved here between the microscopic vectors, or between the microscopic vectors and the external degrees of freedom. In any case, the $\boldsymbol{P}$ vector relaxes or goes to zero, efficiently. Though the existence of this mechanism in the relaxation of the correlation function has not yet been noticed explicitly, it must be one of the important relaxation mechanisms, even when interactions are introduced among the molecules. This decay process may be tentatively called a *non-dissipative process,* though it must be more properly named in the future. The correlation function in the Debye representation is given, in terms of $\Phi_{1R}(t)$, as:

$$\Phi_1(t) = \Phi_{1R}(t)\cos\omega_0 t \quad (24)$$

where ω_0 is a function of the time as shown by (21).

The constant term, 1/3, in the correlation function, $\Phi_1^{(0)}(t)$, for spherical molecules results from three rotational degrees of freedom of spherical molecules. In other words, the "molecules" can rotate around any arbitary axes. For example, for the fraction of "molecules" whose axis of rotation is parallel to the z-axis, the μ-vectors are constants of motion. Thus, the $\Phi_1^{(0)}(t)$ function must have a constant term, which is contributed by the "molecules" to be described in the $S_R(\omega_0;\ \theta\neq\pi/2,\ \varphi)$ rotating frames.

Summarizing the discussions given above, we may describe the characteristic features of the $\Phi_1^{(0)}(t)$ correlation function for free spherical molecules as follows: (a) it is a periodic function of time; (b) however, the frequency of the periodicity, ω_0, is a function of time and is inversely proportional to t in a rough sense of the word; and (c) as a result of the existence of a non-dissipative process, the function relaxes, with a relaxation time of the order of τ_f, to a constant value which, qualitatively, arises from the fraction of "molecules" whose axis of rotation is parallel to the z-axis of the laboratory frames. The correlation function, $\Phi_1^{(0)}(t)$, shown in Fig. 1 has all these features.

We may use a similar argument for interacting molecules, or when there are collisions amoung the molecules in the system. The magnitude and the direction of the angular momentum of a "molecule" will be changed when it collides with other molecules. The transition of a μ-vector from one rotating frame to another is involved when the orientation of the angular momentum is changed. Thus, we may assume that the orientation of the μ-vectors after a collision may be randomized in the y-z plane of the rotating frames. As a result, the magnitude of $\boldsymbol{p}$ is reduced. This process of the relaxation of the angular correlation may be called a *dissipative process,* one which gives a non-periodic decay of the correlation function. In general, to $\Phi_1(t)$, correlation function is decreased by two causes which reduce the phase correlations among the rotating "molecules", the dissipative and the non-dissipative processes. Using the analogy of the free induction decay, we may compare these relaxation processes with the phase memory relaxation of the $\boldsymbol{m}$-vectors due to the spin-relaxation and due to the inhomogeneties of the external field.

When $\tau_r \gg \tau_f$, the correlation function has an extra maximum between $t=2\tau_f$ and $5\tau_f$. The decay before the maximum is mainly due to the non-dissipative process, while the one after the maximum is due to the dissipative process, where, qualitatively speaking, the orientation of the vectors which were parallel or nearly parallel to the z-axis at $t=0$ is changed by collisions. Quite similar discussions may be applied to the tensor correlation functions.

The form of the correlation functions near $t=\tau_f$ sharply depends on the τ_r/τ_f ratio when $\tau_r/\tau_f=0.5$—2.5, in other words, when τ_r is of the order of magnitude of τ_f. It is insensitive when

13) E. L. Hahn, *Phys. Rev.*, **77**, 297 (1950); **80**, 580 (1950).

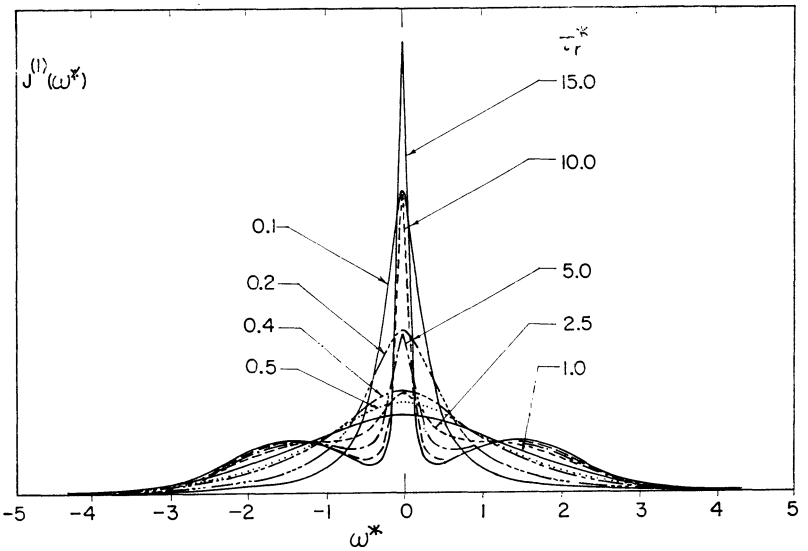

Fig. 3. The spectral densities or the infrared band spectrum for a spherical rotor, $J_1(\omega^*)$, obtained by using Eqs. 4 and 17. The asterisk on ω indicates that it is given in units of $1/\tau_f$. An arbitrary units is used for the ordinate.

$\tau_r/\tau_f \geqslant 10$. There is no bump in the correlation function when $\tau_r/\tau_f \leqslant 1.0$.

The Spectral Density and the Band Shape of Spectra

Spectral Densities.—The spectral densities corresponding to the correlation functions discussed above may be defined by[8]:

$$J_j(\omega) = \frac{1}{2}\int_{-\infty}^{\infty} \Phi_j(t) e^{-i\omega t} dt \qquad (25)$$

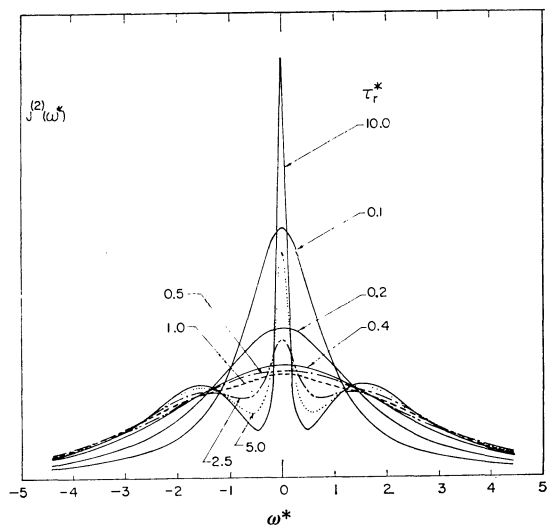

Fig. 4. The spectral densities or the Raman band spectrum of a spherical rotor, $J_2(\omega)$, obtained by using Eqs. 4 and 25.

The forms of the $J_1(\omega)$ and $J_2(\omega)$ functions are given in Figs. 3 and 4 respectively, where $1/\tau_f$ is chosen as the unit of the angular frequency These figures also show the band shapes of respectively, the infrared and Raman spectra of spherical molecules.

For $\tau_r/\tau_f \gg 1$, the spectral density is composed of three distinguishable parts, that is, the so-called P, Q, and R branches.[14] The spectral density, $J_j^{(0)}(\omega)$ for a free rotor has a δ-function-like line at $\omega=0$; this line results from the constant term in the $\Phi_j^{(0)}(t)$ correlation function. Collisions give a finite width to this line. When $\tau_r/\tau_f \gg 1$, the width of the central line is roughly the inverse of the "relaxation time" for the decay of the correlation function after the bump, that is, the relaxation time for the dissipative process. Mathematically, the bump of the correlation function gives bumps in the corresponding spectral density, or vice versa. Hence, when there is no bump in the correlation function, we cannot distinguish the P, Q, and R branches in the spectral density. When $\tau_r/\tau_f \ll 1$, the shape of the spectral density is close to a Lorentz form.

Correlation Times.—The correlation time for a $\Phi_j(t)$ correlation function may be defined as:[6,8,9]

$$\tau_j \equiv \frac{1}{2} J_j(0) = \frac{1}{2}\int_{-\infty}^{\infty} \Phi_j(t) dt \qquad (26)$$

Fig. 6 shows the dependence of the normalized correlation times, $\tau_j^* \equiv \tau_r/\tau_f$, on the normalized

14) C. Herzberg, "Molecular Spectra and Molecular Structure. I. The Spectra of Diatomic Molecules," D. Van Nostrand Company, Princeton (1950).

lifetime of the rotation, $\tau_r^* \equiv \tau_r/\tau_f$. On a semilogarithmic scale, τ_i^* is almost symmetric with respect to $\tau_r^* = 1$. This is also appproximately true for τ_2^*. In the Debye process there is a one-to-one correspondence between τ_r and τ_j, while in the non-Debye process this is not true, because of contributions from the non-dissipative decay of the angular correlation. Therefore, the reorientation rate cannot be determined by measuring only the correlation times. In particular, it is difficult to determine the value of τ_r^* from τ_2^* when τ_r^* is between 0.3—1.2.

Reorientation of Methane Molecules

It has been shown experimentally[15,16] that methane molecules have a non-Debye reorientation process in the liquid state. To show this clearly, vector correlation functions are obtained from the observed infrared spectra of methane molecules by the relation:[6-8]

$$\Phi_1(t) = \int_{-\infty}^{\infty} \omega^{-1}\sigma_1(\omega) \exp(i\omega t)\mathrm{d}\omega \qquad (27)$$

where $\sigma_1(\omega)$ is the band-shape function. The results are shown in Fig. 5, where τ_f is chosen as the time unit. Clearly, the functions are not exponential; this suggests non-Debye processes in the molecules. The characteristic features of the experimental functions are quite well approximated by Eq. 4, as is shown in Fig. 5. One of the remarkable points of Fig. 5 is that the vector correlation functions for CH_4 and CD_4 in the liquid state of 104°K are fairly close. The molecular structures of CH_4 and CD_4 were studied by Kuchitsu and Bartell[18] by means of the electron diffraction. The values of $r_0 = 1.0940$ Å and $r_e = 1.0850$ Å were reported for the C–H bond, and $r_0 = 1.0918$ Å and $r_e = 1.0850$ Å for the C–D bond, where r_0 and r_e refer to the bond lengths corresponding to the minimum potential and the equilibrium distance respectively. In our calculation we roughly assumed that $r_e(\mathrm{C\text{-}H}) = r_e(\mathrm{C\text{-}D}) = 1.085$Å at various temperatures, since there were no serious results of this assumption in the final results.

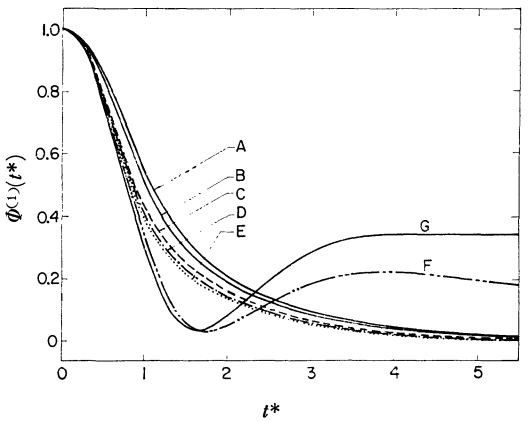

Fig. 5. The vector correlation functions $\Phi_1(t^*)$ for methane or deuteromethane molecules. The functions were obtained from experimental IR spectra by using Eq. 27, where the band shape functions for A—E and for F were, respectively, taken from Ewig's[14] and Armstrong and Welsch's[17] data. A=(CD_4 in CH_4, liquid at 104°K), B=(CD_4 in CD_4, liquid at 104°K), C=(CH_4 in CH_4, liquid at 104°K), D=(CH_4 in CH_4, liquid at 98°K), E=(CH_4 in CH_4, solid at 95°K), F=(CH_4 in He, gas at 294°K, 201 Amag.), and G=$\Phi_1^{(0)}(t)$. In this figure the wiggles which appear after a long time in the correlation functions are properly smoothed out.

It should be noted that the time scale in Fig. 5 has a unit of $\tau_f = (I/kT)^{1/2}$; the length of the time unit in Fig. 5 for the CD_4-function is larger than that for the CH_4-function by about 1.4 times. If we assume that the Debye equation is reasonable for the reorientation processes of methane molecules, there must be no significant difference between the CH_4- and CD_4- correlation functions, and the two functions must be quite different in Fig. 5. In addition, in contrast to Fig. 5, the CD_4-function must be inside the CH_4-function. Hence, it is clear that Debye's picture is entirely inapplicable to methane molecules.

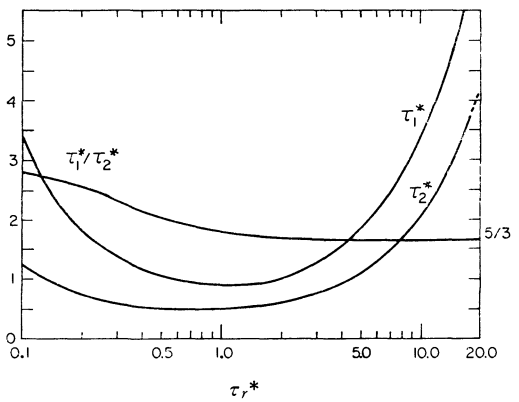

Fig. 6. Dependences of τ_1^*, τ_2^*, and τ_1^*/τ_2^* on τ_r^*. These curves were obtained by using Eq. 4.

The above-mentioned difficulties in Fig. 5 may be interpreted as follows. In Fig. 5, the unperturbed functions, $\Phi_1^{(0)}(t)$, for CH_4 and CD_4 are equivalent. In other words, the contribution from the nondissipative process to the correlation functions, $\Phi_1(t^*)$, of CH_4 and CD_4 are the same in Fig. 5. Hence, the observed small differences

15) G. E. Ewing, *J. Chem. Phys.*, **40**, 179 (1964).
16) G. A. deWit and M. Bloom, *Can. J. Phys.*, **43**, 986 (1965).
17) R. L. Armstrong and H. L. Welsch, *Spectrochim. Acta*, **16**, 840 (1960).
18) K. Kuchitsu and L. S. Bartell, *J. Chem. Phys.*, **36**, 2470 (1962).

among the $\Phi_1(t^*)$ correlation functions may be attributed to the differences in $\tau_r^*=\tau_r/\tau_f$, the normalized mean lifetime of the rotation. For the sake of convenience, the notation $\Phi_{CH_4/CD_4}(t;\ 100°K)$ will be used for the vector correlation function of CH_4 measured at 100°K in a CD_4 solution. The times, τ_f and τ_r, corresponding to this correlation function may be denoted as $\tau_f(CH_4/CD_4;\ 100°K)$ and $\tau_r(CH_4/CD_4;\ 100°K)$. Comparing Fig. 5 with Fig. 1, we have:

$$\tau_r^*(CH_4/CH_4:\ 104°K)>\tau_r^*(CD_4/CD_4:\ 104°K)>\tau_r(CD_4/CH_4:\ 104°K) \quad (28)$$

Qualitatively, this relation may be proved as follows. We may assume that the translational energy of a molecule is so much larger than the rotational energy that the rate of the change in the rotation of molecules depends only on the collision frequency. Therefore, $1/\tau_r$, the rate of the change in the rotational motion of molecules, is proportional to the frequency of collisions per second.

The total number of N_{12} collisions occuring per unit volume and per unit of time between pairs of the 1 and 2 gas molecules whose masses are, respectively, m_1 and m_2, is given by[19]:

$$N_{12}=2n_1n_2\sigma_{12}^2\left[\frac{2\pi kT(m_1+m_2)}{m_1m_2}\right]^{1/2} \quad (29)$$

where n_1 and n_2 are the number of the 1 and 2 molecules in a unit of volume, and where σ_{12} is the mean diameter of the molecules and is given in terms of the diameters of the 1 and 2 molecules, σ_1 and σ_2, by:

$$\sigma_{12}=\frac{1}{2}(\sigma_1+\sigma_2)$$

We may also consider other models of collisions. For example, we may treat molecules as harmonic oscillators which are restricted to their equilibrium positions. The frequencies of oscillators are inversely proportional to the square root of the m_1 or m_2 masses. We may assume that a collision occurs when one of the oscillating molecules is at the maximum deviation from its equilibrium position. Hence, we obtain:

$$N_{12}\propto\left(\frac{1}{\sqrt{m_1}}+\frac{1}{\sqrt{m_2}}\right) \quad (30)$$

In any case, the reduced lifetime of the rotation, τ_r^*, is portional to:

$$\tau_r^*\propto\sqrt{I}N_{12} \quad (31)$$

By neglecting the contribution from CD_4–CD_4 collision to $\tau_r^*(CD_4/CH_4)$ and by using (29) or (30), the inequality (28) is obtained. From (29) and (30) we obtain $\tau_r^*(CH_4/CH_4)$: $\tau_r^*(CD_4/CD_4)$: $\tau_r^*(CD_4/CH_4)=1:.79:.72$ and $1:.79:.75$ respectively. The difference between $\tau_r^*(CD_4/CD_4)$ and $\tau_r^*(CD_4/CH_4)$ is very small in the latter case.

Another interesting feature is that the Φ_{CH_4/CH_4} $(t:95°K)$ correlation function obtained from the infrared spectrum of solid methane is very close to those Φ_{CH_4/CH_4} $(t:98°K)$ and Φ_{CH_4/CH_4} $(t:104°K)$. Ewing[14] discussed this point in terms of the infrared spectra. It was also pointed out by deWit and Bloom[16] after their measurement of the nuclear magnetic relaxation of methane and deuteromethane. The latter found that there was no discontinuity in the nuclear magnetic relaxation time, T_1, just before and after the melting point of the solid methane. In addition, the temperature dependence of the relaxation time, T_1, was much weaker than that predicted by Debye's theory. From Fig. 5 we may say that the reorientation process of methane near the melting point is a non-Debye process. The $\Phi_{CH_4/He}$ $(t:294°K)$ correlation function shows very clearly that the decay of the angular correlation is caused by two different effects, the dissipative and the nondissipative processes.

By comparing Figs. 1 and 5, we find that $\tau_r^*(CH_4/CH_4:\ 95°K)$, $\tau_r^*(CH_4/CH_4;\ 98°K)$ and $\tau_r^*(CH_4/CH_4:\ 104°K)$ are of the order of 0.4—0.5, that $\tau_r^*(CD_4/CD_4:\ 104°K)$ and $\tau_r^*(CD_4/CH_4:\ 104°K)$ are roughly equal to 0.3—0.4, and that $\tau_r^*(CH_4/He_4:\ 294°K)=5.0$—10.0, as is suggested by a rough estimation that the rotational states of methane molecules are changed at each collision.

Discussion

The characteristic differences between the Debye and the non-Debye processes may be observed in the following phenomena: (a) the temperature dependence of the correlation function or of the correlation time, (b) the dependence of these quantities on the moment of inertia of molecules, and (c) the deviation of the form of correlation functions from an exponential one. Of course, it is also clear that the correlation function depends on the macroscopic viscosity, η, quite differently from what is predicted by the Debye equation. However, we do not wish to become involved in a discussion of ways of improving the Debye model by simply introducing the concept of the microscopic viscosity or that of the effective molecular radius.

The Temperature Dependence.—If we use the reduced time, t^*, whose unit is chosen as τ_f, the correlation functions for the free rotor, $\Phi_f^{(0)}(t^*)$, will be independent of the temperature. This is because τ_f is the correlation time corresponding to the $\Phi_f^{(0)}(t)$ function and, in addition, the temperature dependence of this function comes only through τ_f. In the inertial limit the temperature

19) S. Chapman and T. G. Cowling, "The Mathematical Theory of Non-Uniform Gases," Cambridge University Press, London (1952).

dependence of the $\Phi_j(t^*)$ function is given only through τ_r^*. For example, when τ_r is proportional to τ_f, that is, when it is proportional to $T^{-1/2}$, the $\Phi_j(t^*)$ correlation function is independent of the temperature. Such a case is given when (29) is satisfied. Then, the spectral density,

$$J_j(\omega^*) \equiv \frac{1}{2}\int_{-\infty}^{\infty} \Phi_j(t^*)e^{-i\omega^* t^*}dt^* \qquad (32)$$

must also be independent of the temperature where $\omega^* = |\tau_f|\omega$. The dimensionless quantity, $|\tau_f|$, is used to indicate that ω^* is measured in units of $1/\tau_f$. From (25) and (32) we obtain:

$$J_j(\omega) = |\tau_f| J_j(\omega^*/|\tau_f|) \qquad (33)$$

which gives the temperature dependence of the spectral density. Similarly, we obtain from (33) and (26):

$$\tau_j = \frac{1}{2}|\tau_f| J_j(0^*) \qquad (34)$$

Of course, (32)—(34) are valid only in a limited range of temperature, and a phase transition must not be involved in such a temperature range. Equation 34 gives a weaker temperature dependence of the correlation time than the Debye equation (3). The motional narrowing effect of the anisotropic potential due to the motion of the solvent molecules[8,20] has another effect on τ_j. If this effect is included, the $J_j(0^*)$ quantity becomes a function of the temperature; $J_j(0^*)$ will be increased when the temperature is raised.[8,20] Therefore, the temperature dependence of τ_j through $|\tau_f|$ is partially cancelled by this effect. Hence, we have here a weaker temperature dependence than that obtained from (34).

The Dependence on the Moment of Inertia.—In the Debye process the correlation time depends on the viscosity and on the size of the molecule. Hence, the effect of the isotopic substitution on the correlation time is, in general, so small that we can neglect it for all practical purposes. On the other hand, in the non-Debye process, the isotopic effect must be fairly large, as it is clearly shown in (34). Note that the *reduced* correlation function for the free rotor is independent of the moment of inertia.

The Form of Correlation Functions.—Correlation functions do not have an exponential form when the nondissipative loss of the phase correlation is appreciable. Experimentally, this can be checked by two different methods; from the infrared or Raman spectra, and from the nuclear magnetic relaxation. In the former experiment, the band shape of a spectrum must be quite different from a Lorentz form, provided that the nondissipative loss is appreciable. The measurement of the nuclear magnetic relaxation due to the spin-rotation interaction is also very helpful, because we can estimate the lifetime of the rotation, τ_r directly. If τ_r is comparable with or larger than τ_f, the form of the correlation function must not be exponential.

Effective Viscosities.—It is not accidental that methane shows non-Debye processes. This is because of the highly symmetric structure of this molecule. In general, rotational motions of molecules are perturbed by the anisotorpic part, V_{aniso}, of the intermolecular potential, but not by the isotropic part, V_{iso}, which perturbs the translational motion. Since the macroscopic viscosity for translational diffusions is used in the Debye equation (3), a necessary condition for Debye's theory must be $V_{\text{aniso}} \fallingdotseq V_{\text{iso}}$. Clearly this is not true for methane molecules. The concept of the effective viscosity for a given effective radius of a molecule or that of the effective radius for a given viscosity is nonsense in the strict sense of the words in non-Debye processes: the correlation times, τ_1 and τ_2, for which the τ_1/τ_2 ratio is not equal to 3 result in different viscosities or in effective radii from those produced by the Debye equation. In other words, these phenomenological quantities depend on the methods of measurement. Note Fig. 6

Conclusion

If the correlation time, τ_j, obtained from the experimental data is quite different from the corresponding one obtained from the Debye equation (3), there is a high possibility that the molecular reorientation is of a non-Debye process, where the nondissipative decay of angular correlation is not negligible. Therefore, the use of the Debye equation with an effective viscosity or microscopic viscosity is physically nonsense in such processes. However, it may not always be true that any non-Debye process gives a very much smaller correlation time than the corresponding Debye process. In the non-Debye processes correlation times may have a weaker temperature dependence than in the Debye processes, and they depend on the moment of inertia of the molecule. Often the forms of the correlation functions are different from the exponential ones as a result of the existence of the nondissipative decay of angular correlation, as we showed in the case of methane.

When the correlation functions of spherical particles for non-Debye processes are needed, we may conveniently use Eq. 4 as an approximate expression. It has been proved that (4) is a reasonably simplified expression for the correlation function of non-Debye processes, being related to the two kinds of decays of angular correlation. Or, experimentally, the vector and the tensor

20) M. Bloom, to be published.

correlation functions may be obtained from infrared and Raman spectra respectively in terms of the Fourier transform of the band-shape functions. Fourier transform of the band-shape functions. Conversely, the infrared and Raman spectra can be calculated from Function 4 by means of the Fourier transformation. Therefore, the theory of the band shape of the vibrational spectra is basically equivalent with the theory of the angluar correlation of molecules. Information on the reorientation process is obtained through the measurements of the vibrational spectra or of the nuclear magnetic relaxation due to the spin-rotation interaction.

The present work was supported by NIH Grant-GM-13545-01. For priceless 7094 computer time (the problem number N-4210) the author wishes to thank the M. I. T. Computation Center. Without this grant, many of the problems presented here could not have been solved. The author was also partly helped in his calculation by the Stanford University Computation Center, which gave him free 7090 computer time under Account Number F134. Deep thanks are also due Professor Baldeschwieler for his warm hospitality to the author.

BULLETIN OF THE CHEMICAL SOCIETY OF JAPAN VOL. 39 2395—2399 (1966)

Studies of the Formation of Condensed Phosphates Containing Alkyl-groups*

By Shiro UEDA and Mitsuyasu TADA**

Department of Industrial Chemistry, Faculty of Engineering, Chiba University, Yayoicho, Chibashi

(Received September 9, 1965)

Alkyl ammonium polyphosphate (AAPP) was prepared readily by a thermal reaction of alkyl (ethyl, *n*-propyl, *n*-butyl) dihydrogen phosphate and urea at temperatures ranging from 120°C to 200°C. At the same time, a small amount of cyanuric acid was obtained as a by-product. 1) AAPP was confirmed, from a study of the data of infrared spectroscopy, paper chromatography and chemical analysis, to have a long-chain structure possessing P–O–P linkage. The three types of AAPP were of almost the same form, according to the X-ray diffraction patterns. 2) AAPP was more or less hygroscopic, although the hygroscopicity of AAPP decreased with an increase in the carbon number of the alkyl group. 3) AAPP is reasonably stable, keeping a P–O–P linkage even upon degradation in an acidic aqueous solution.

In a previous paper,[1] the present authors reported that when a mixture of phosphoric acid and urea was heated at 140—160°C, the decomposition of urea and the condensation and neutralization of phosphoric acid took place simultaneously. The products formed were ammonium polyphosphate and a small amount of cyanuric acid.

By a method similar to those used in preparing ammonium polyphosphate, the reaction of urea with alkyl dihydrogen phosphates was investigated. Alkyl phosphates with two hydroxyl radicals were thus found to bring about a poly condensation reaction with urea, giving alkyl ammonium polyphosphate (hereinafter this compound will simply be abbreviated as AAPP). All of the reaction products were identified by infrared absorption, X-ray diffraction, paper chromatography and quantitative chemical analysis. Several properties of AAPP were also investigated.

Experimental

The Formation of Alkyl Dihydrogen Phosphate.—Ethyl, *n*-propyl and *n*-butyl alcohol was reacted with phosphorus oxychloride at about 25°C. Alkyl phosphorodichloridate was obtained in about a 75—85% yield by means of vacuum distillation in each case. Alkyl phosphorodichloridates were hydrolyzed with water,[2] and de-hydrogenchloride carried out by blowing dry air into a volumetric flask under reduced pressure. The alkyl dihydrogen phosphate thus obtained was a light yellow, transparent liquid.

The Reaction of Alkyl Dihydrogen Phosphate with Urea.—Alkyl dihydrogen phosphates and urea were mixed so that the molar ratio of phosphorus pentoxide to urea in each alkyl dihydrogen phosphate corresponded to 1 : 2. The mixture was then gradually heated until the urea dissolved completely into the

* Presented at the 18th Annual Meeting of the Chemical Society of Japan, April, 1965.

*1 Present address: Reitaku University, Kashiwashi, Chiba.

1) S. Ueda, K. Oyama and K. Koma, *J. Chem. Soc. Japan, Ind. Chem. Sect. (Kogyo Kagaku Zasshi)*, **66**, 586 (1963); S. Ueda, T. Nakagawa and K. Koma, ibid., **66**, 589 (1963).

2) G. M. Kosolapoff, "Organo Phosphorus Compounds," John Wilely & Sons, Inc., New York. (1950).

alkyl dihydrogen phosphate. The reaction proceeded rapidly; a stimulative gas which contained carbon dioxide was evolved at about 130—135°C. At the initial stage of the reaction, the reaction product was remarkably expanded, and within several minutes the reaction was completed, the end point of the reaction being indicated by the formation of solid matter. Also, at the end of the reaction, a small amount of ammonia gas was generated. The resultant product was a light yellow, humid substance containing small amounts of unreacted urea and a water-insoluble substance.

The reaction product was then dissolved in water, and the insoluble substance was filtered off. Three times as much acetone as mother liquor was added to the latter, with constant stirring.

A white crystalline phosphate was separated as a precipitate, the urea remaining in the mother liquor. The precipitate was then again filtered off. After having been washed with anhydrous ethanol and acetone, the purified reaction product was dried using silica-gel under reduced presure.

Paper Chromatography.[3]—Paper chromatography was carried out in a constant-humidity cabinet manufactured by the Mitamura Co., Ltd.

The solvent used for the development consisted of:

isopropyl alcohol	735 ml.
trichloroacetic acid	50 g.
distilled water	265 ml.
concentrated ammoniacal water	2.5 ml.

A spray reagent was prepared by mixing 5 ml. of 60% perchloric acid, 1 ml. of hydrochloric acid, and 1 g. of ammonium molybdate, and by then diluting this mixture to 100 ml. with water. Toyo filter paper No. 53 were used, and the development was conducted for 4—5 hr. at room temperature.

Chemical Analysis.—Ammonia was analyzed by a conventional chemical method. The phosphorus was spectrophotometrically determined at the 410 mμ wavelength, using a vanadomolybdate as the color reagent.[4] The alkoxyl groups were analyzed by the Zeisel method.[5]

X-Ray Diffraction.—The X-ray diffraction of samples was carried out with a Rigaku-Denki, D-2F unit using a nickel filter and copper K_α radiation. The unit was operated with a voltage of 30 kV., a current of 15 mamp., a scale factor of 400, a time constant of 2/sec., and a scanning speed of 2°/min.

Infrared Spectroscopy.—All of the spectra were recorded over the range from 4000 to 700 cm^{-1}, using a Hitachi EPIS-11 Double beam Spectrometer. The infrared spectra of the samples were taken both by potassium bromide pellet and by Nujol mull methods.

Results and Discussion

All of the resulting products were obtained as colorless crystalline substances. These products was of a somewhat hygroscopic nature and seemed to have a good solubility in water. The hygroscopicity of the products containing *n*-butyl and *n*-propyl groups were less pronounced than that containing the ethyl group.

The Composition of the Reaction Products.—Analytical results of the reaction products obtained from alkyl dihydrogen phosphates and urea are given in Table I. Small amounts (0.5—1.8%) of cyanuric acid as an insoluble substance in water, the identity of which was established by X-ray diffraction, were also obtained.

These phosphate polymer contained considerable amounts of water. In calculating the number average chain length, we disregarded the water in the phosphate.

M^1 stands for the mono-valency cation. The amonia and alkyl groups were expressed as $(NH_4)_2O$ and A_2O respectively in calculating the composition of the phosphates.

The nitrogen exists in phosphate as an ionized ammonium radical; this is confirmed by the fact that a barium salt prepared by adding barium chloride to an aqueous solution of phosphate does not contain the nitrogen.

As is shown in Table I, the molar ratio of $M^1{}_2O$ to P_2O_5 is approximately unity. The composition of poly-condensed phosphate can be expressed as $xM^1{}_2O{\cdot}yP_2O_5$, corresponding to the molar ratio of $R=x/y$. The general formula for the long-chain polyphosphates is usually given as:

$$\lim_{n\to\infty} M^1{}_{n+2}P_nO_{3n+1} = M_nP_nO_{3n}$$

For linear polymers, molar ratio, R, approaches 1 for sufficiently long chains. Judging from the analytical results, AAPP can, therefore, be thought of as being a long chain phosphate.

The average chain length of the polyphosphate can be determined by calculating the molar ratio, R. It is well known that the average chain length, $\bar{n}$, of polyphosphates is given by the equation:

$$R = M^1{}_2O/P_2O_5 = (n+2)/n$$

As the molar ratio, R, approaches unity, $\bar{n}$ approaches infinity. From the data in Table I,

Table I. Analytical results of the reaction products

Alkyl dihydrogen phosphate	$(NH_4)_2O$ wt. %	A_2O* wt. %	P_2O_5 wt. %	$(NH_4)_2O/A_2O$ mole ratio	$M^1{}_2O/P_2O_5$** mole ratio	pH of 1% solution
Ethyl	15.3	2.1	47.2	9.1	1.0	5.9
n-Propyl	19.3	4.4	52.5	8.6	1.1	5.7
n-Butyl	20.6	7.6	58.0	6.8	1.1	5.9

* Alkyl ** $M^1{}_2O=(NH_4)_2O+A_2O$

3) A. S. T. M. Designation D 501-58 T (1958).
4) O. B. Michelsen, *Anal. Chem.*, **29**, 60 (1957).
5) "Hand book of Analytical Chemistry," Maruzen Book Co., Tokyo (1961), p. 538.

we can calculate the average chain length, $\bar{n}$, of AAPP as having a value of more than 20.

Paper Chromatography. — Chromatograms and R_f values are shown in Fig. 1 and Table II respectively. When alkyl dihydrogen phosphate was used, almost all the phosphates produced were high polymers which could not be developed by paper chromatography. Even though a two dimensional development technique was used, no evidence of the formation of a ring-form phosphate was obtained.

In Fig. 2 are illustrated chromatograms of the hydrolysis products of AAPP, which were produced in an aqueous solution at pH 2.5 (adjusted by hydrochloric acid) and at 60°C.

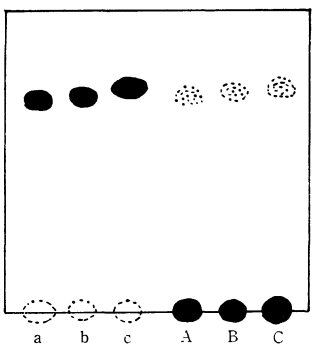

Fig. 1. A paper chromatogram of alkyl dihydrogen phosphate and the reaction products.
a: Ethyl dihydrogen phosphate
b: *n*-Propyl dihydrogen phosphate
c: *n*-Butyl dihydrogen phosphate
A: Reaction product (Ethyl)
B: Reaction product (*n*-Propyl)
C: Reaction product (*n*-Butyl)

Table II. The R_f value of the free acid and the reaction products

	Free acid	Reaction product
Ethyl	0.73	Retained strongly
n-Propyl	0.74	Retained strongly
n-Butyl	0.76	Retained strongly

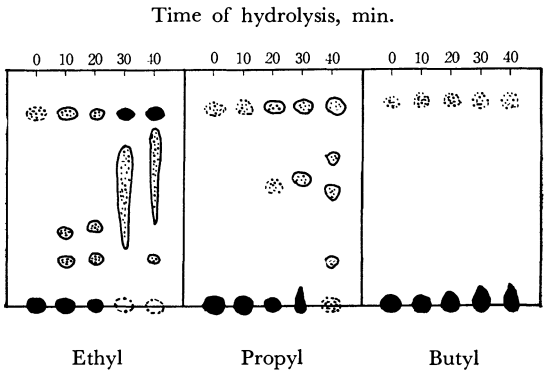

Fig. 2. The formation of hydrolysis products at pH 2.5 and 60°C.

As is shown in Fig. 2, the AAPP possesses a considerable stability upon hydrolytic degradation in an acidic solution.

The X-Ray Diffraction Pattern of AAPP and Its By-product.—The X-ray diffraction pattern of AAPP is illustrated in Fig. 3.

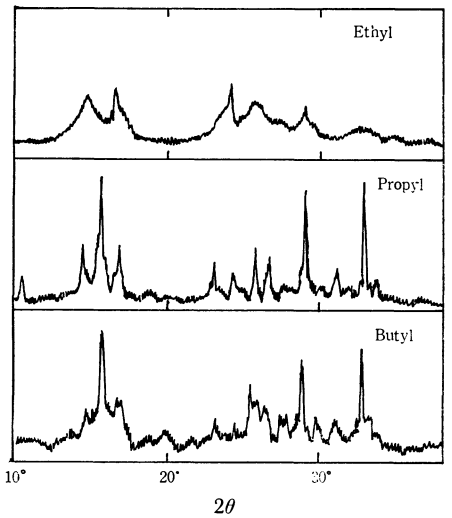

Fig. 3. The X-ray diffraction pattern of the reaction products.

As is apparent from the diffraction patterns, AAPP is always a crystalline substance. As the number of carbon atoms in the alkyl group increases, however, the crystallinity of the AAPP tends to increase. The crystallinity of the AAPP obtained from mono-ethyl dihydrogen phosphate is fairly poor in comparison with that obtained from propyl and butyl compounds. The poor crystallinity of the ethyl compound may be thought of as being caused by the hygroscopicity of the product.

Table III shows the spacing of the main interference with AAPP; it is always almost the same

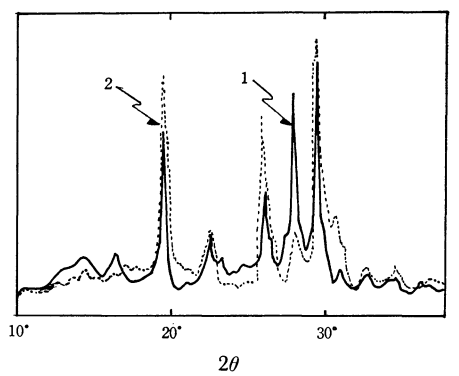

Fig. 4. The X-ray diffraction pattern of an insoluble substance and cyanuric acid.
1: Insoluble substance
2: Cyanuric acid (Reagent)

TABLE III. X-RAY DIFFRACTOMETRIC ANALYSIS OF THE REACTION PRODUCTS

Sample	Main interference															
	A		B		C		D		E		F		G		H	
	d Å	I/I_1	*d* Å	I/I_1	*d* Å	I/I_1	*d* Å	I/I_1	*d* Å	I/I_1	*d* Å	I/I_1	*d* Å	I/I_1	*d* Å	I/I_1
Ethyl	5.99	0.92	—	—	5.31	1.00	3.74	0.84	3.45	0.77	—	—	3.06	0.77	2.71	0.54
n-Propyl	6.03	0.44	5.64	1.00	5.31	0.48	3.80	0.40	3.45	0.44	3.35	0.40	3.06	0.84	2.71	0.84
n-Butyl	6.06	0.56	5.64	1.00	5.34	0.67	3.80	0.50	3.47	0.61	3.38	0.56	3.08	0.83	2.72	1.00

TABLE IV. DATE OBTAINED BY THE X-RAY DIFFRACTOMETRY OF AN INSOLUBLE SUBSTANCE AND CYANURIC ACID

Sample	Main interference											
	A		B		C		D		E		F	
	d Å	I/I_1	*d* Å	I/I_1	*d* Å	I/I_1	*d* Å	I/I_1	*d* Å	I/I_1	*d* Å	I/I_1
Cyanuric acid	4.53	1.00	3.99	0.19	3.39	0.61	3.01	1.00	2.24	0.27	2.17	0.25
Insol. substance	4.51	0.73	3.99	0.37	3.40	0.53	3.02	1.00	2.24	0.21	2.16	0.21

interferecne, regardless of the alkyl type. Therefore, the products can reasonably be regarded as phosphates with similar crystalline structures.

A water insoluble by-product was recrystallized in hot water (85—90°C) and then dried. The recrystallized substance was identified by the X-ray diffractometry as cyanuric acid, which was formed by the thermal decomposition of urea. The X-ray diffraction pattern and the spacing of the main interference of an insoluble substance and a pure reagent of cyanuric acid are shown in Fig. 4 and Table IV respectively.

As can be seen, the pattern and the main interference of the insoluble substance agree well with those of pure cyanuric acid.

The Infrared Absorption Spectra of AAPP. —In this work the infrared spectra of samples were examined as powder in the 4000—700 cm^{-1} range. These spectra have been investigated with a view to assigning characteristic frequencies to molecular groupings and to generally correlating the absorption with the molecular structure.

AAPP was mixed with potassium bromide and pressed into a disk; then the infrared spectra were measured and further compared with Nujol mulls. Figure 5 shows some typical spectra of these products; a potassium bromide tablet technique was employed for the measurements.

As can be seen from Fig. 5, a considerable variation was observed throughout the spectra. Some salts, e. g., *n*-propyl and *n*-butyl compounds, particularly afford broad and poorly resolved peaks.

The characteristic absorption bands of P–O–P, P–O–C (where C is aliphatic carbon) and the NH_4^+ ion were found in each spectrum in the ranges ~890 (P–O–P stretching), 760—740 (harmonics of P–O–P bending), 1010 (P–O–C stretching), 1390—1410 (NH_4^+, N–H stretching) cm^{-1}.

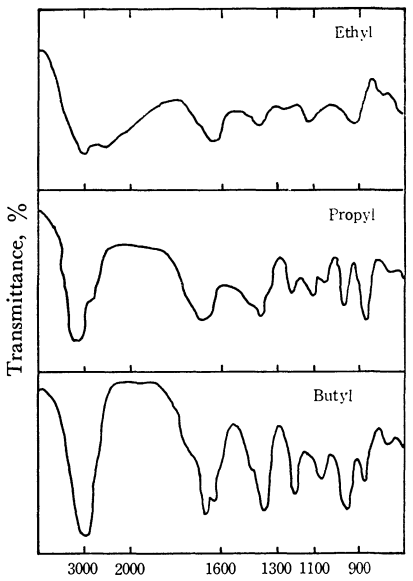

Fig. 5. The infrared absorption spectra of the reaction products.

This evidence strongly supports the view that AAPP is poly-condensed phosphate containing alkyl and ammonium radicals in the molecule.

The Mechanism of the Reaction.—A useful method for the preparation of condensed phosphate containing nitrogen has recently been developed by the present authors,[1] in this method a phosphoric acid or alkali metal dihydrogen phosphate is thermally treated with urea.

Similar condensation reactions have also been observed in the interaction of alkyl dihydrogen phosphate with urea. As has been stated above, the preparation of AAPP through the thermal reaction of alkyl dihydrogen phosphate with urea

is accompanied by the following chemical reactions; alkyl dihydrogen phosphate and urea are subjected to the thermal reaction with greater ease; carbon dioxide gas and a stimulative gas (which is considered to be isocyanic acid) are generated, small amounts of ammonia gas and cyanuric acid as trimer of isocyanic acid are formed in the final stage of the reaction. On the basis of these observations as well as of chromatographic, infrared and X-ray diffractometric measurements, the mechanism given below seems reasonable for the reaction of alkyl dihydrogen phosphate and urea.

Assumption for the Mechanism of the Reaction.—First of all, urea is decomposed into ammonia and carbon dioxide with water.

$$(NH_2)_2CO + H_2O \rightarrow 2NH_3 + CO_2 \qquad (1)$$

The water is thought to come from the hydroxyl radical of two moles of dihydrogen orthophosphates.

A small part of the urea can also be decomposed into cyanuric acid and ammonia in the following way when cyanuric acid is formed as a by-product of the reaction:

$$3(NH_2)_2CO \rightarrow (HNCO)_3 + 3NH_3 \qquad (2)$$

Thus, the formation of AAPP may be illustrated by the following equation:

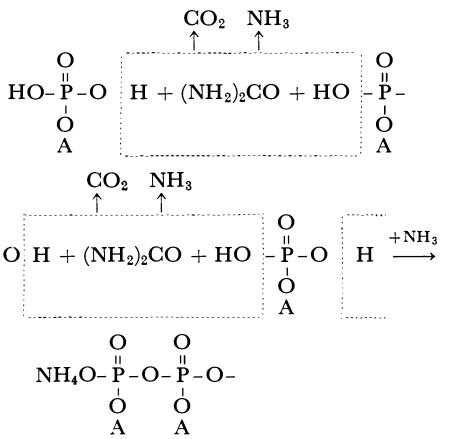

(3)

As has been recognized by Hochwalt and his co-workers[6] in the thermal decomposition of alkyl hydrogen phosphate, the alkyl group in phosphate may also be decomposed partially into free acid and olefine by heating. The ammonia produced by the reactions 1, 2, and 3 can subsequently be neutralized with the hydroxyl radical of the poly-condensed phosphate according to the following equation:

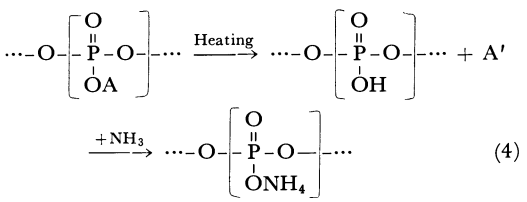

(4)

Where $A = C_nH_{2n+1}$, $A' = C_nH_{2n}$, etc.

Therefore, the alkyl group of this compound may partially be replaced by the ammonium group in a random way.

Summary

When alkyl dihydrogen phosphate and urea are mixed and subjected to thermal reaction at 120—200°C, the thermal decomposition of urea, the condensation of alkyl dihydrogen phosphate, and a partial neutralization of the acid with ammonia have been brought about, this yielding alkyl ammonium polyphosphate (AAPP).

Observations with infrared spectroscopy, paper chromatography and chemical analysis have disclosed that the reaction products are long-chain phosphates containing alkyl and ammonium group in a skeleton P–O–P.

The average chain length, *n*, of AAPP is estimated by calculation to be more than 20.

No substantial difference in crystalline form has been found among the various AAPPs' tested.

The products are more or less hygroscopic, although the hygroscopicity of AAPP decreases with an increase in the number of carbon atoms in the alkyl group.

It has also been found that AAPP is reasonably stable upon the hydrolytic degradation of the P–O–P linkage in an acidic, hot aqueous solution.

6) C. A. Hochwalt, J. M. Lum and J. E. Malowan, *Ind. Eng. Chem.*, **34**, 19 (1942).

BULLETIN OF THE CHEMICAL SOCIETY OF JAPAN VOL. 39 2400—2405 (1966)

A Spectrophotometric Determination of Iron(III) with ω-Aminoacetophenone-*N*, *N*-diacetic Acid Oxime*

By Takeshi ANDO** and Keihei UENO

Department of Organic Synthesis, Faculty of Engineering, Kyushu University, Hakozaki, Fukuoka

(Received September 10, 1965)

The oximes of aminoacetone-*N*, *N*-diacetic acid, ω-aminoacetophenone-*N*, *N*-diacetic acid, *p*-bromo-ω-aminoacetophenone-*N*, *N*-diacetic acid and 2-glycylthiophene-*N*, *N*-diacetic acid have been synthesized as the colorimetric reagents for iron(III). The most favourable result was obtained with the oxime of ω-aminoacetophenone-*N*, *N*-diacetic acid, which forms a stable orange red chelate with iron(III), showing an absorption maximum at 420 mμ. With the use of this reagent, 0—25 p. p. m. of iron(III) can be determined at pH 5.5. It should be noticed that this reagent is almost specific for iron(III); serious interferences were only observed for copper(II), vanadate, fluoride and phosphate ions.

During the course of our investigation of the synthesis of keto derivatives of methyliminodiacetic acid,[1] the color reactions of these ligands with various metal ions have been studied with a hope of finding new colorimetric reagents of analytical importance. In these studies, it has been found that 1-amino-propan-2-one-*N*, *N*-diacetic acid or aminoacetone-*N*, *N*-diacetic acid (I) (AADA) gave a red coloration with iron(III) in the presence of hydroxylamine hydrochloride and hydrogen peroxide; the photometric determination of iron (III) based on this color reaction has been reported.[2] The results of the detailed investigation of the mechanism of the color reaction with AADA proved that the chromogenic substance was an oxime of AADA(AADA-OX), which reacted with iron(III) to form a red chelate. This finding, together with the fact that the molar absorptivity of iron chelate of AADA-OX is not large enough (1.6×10^3), stimulated us to investigate new colorimetric reagents of the related structure.

The compounds investigated in this study are ω-aminoacetophenone-*N*, *N*-diacetic acid oxime (II) (AAPDA-OX), *p*-bromo-ω-aminoacetophenone-*N*, *N*-diacetic acid oxime (III) (Br-AAPDA-OX), and 2-glycylthiophene-*N*, *N*-diacetic acid oxime (IV) (GTDA-OX).

The comparative study of these compounds showed that AAPDA-OX and Br-AAPDA-OX

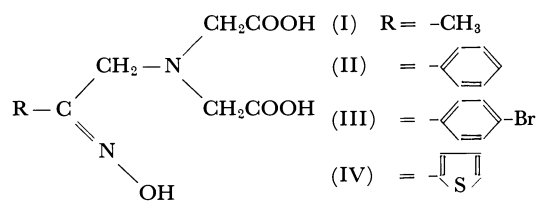

gave the most intense coloration with iron(III) with an absorption maximum in the 410—420 mμ region and that these compounds could be used as a specific colorimetric reagent for iron(III). However, AAPDA-OX may be more suitable for practical purposes because this compound can be synthesized more easily than Br-AAPDA-OX.

This paper will report on the results of an investigation of the synthesis and the use of AAPDA-OX as a colorimetric reagent for iron(III). The molar absorptivity of Fe-AAPDA-OX chelate is 2.0×10^3. This is smaller than that of Fe-1, 10-phenanthroline (1.1×10^4); however, AAPDA-OX is almost specific for iron(III). Of the common ions investigated, serious interferences were observed for only copper(II), vanadate, fluoride and phosphate ions. The results suggest that AAPDA-OX can be used as a specific iron reagent in the practical determination of iron at a relatively higher concentration level in the presence of a large amount of foreign ions. The results also indicate that a new type of colorimetric reagent for iron(III) can be developed using AAPDA-OX as a mother compound.

Experimental

The Syntheses of Reagents.—Oximes of the Keto-derivatives of iminodiacetic acid were synthesized by the condensation of the corresponding acid and the free hydroxylamine. As an example, the synthesis of AAPDA-OX(II) be described.

* Contribution No. 87 from the Department of Organic Synthesis, Faculty of Engineering, Kyushu University.

** Present address; Chemical Laboratory, Department of General Education, Kyushu University, Ootsubomachi, Fukuoka.

1) a) T. Ando, This Bulletin **36**, 1593 (1963); b) T. Ando and K. Ueno, *Inorg. Chem.*, **4**, 375 (1965).

2) H. Takama, T. Ando and K. Ueno, *Japan Analyst*, **13**, 345 (1964).

Anhydrous sodium carbonate (1.05 g.) was added slowly to a suspension of 5 g. of ω-aminoacetophenone-*N*, *N*-diacetic acid[1b] in 15 ml. of water; this made a clear solution of the monosodium salt of the acid. To this solution was added 14 ml. of an aqueous ethanol (1 : 3 by volume) solution of free hydroxylamine prepared from 1.50 g. of hydroxylamine hydrochloride; the mixture was then heated on a water bath at 70—80°C, with occasional shaking. After the mixture had stood overnight at room temperature, the pale yellow solution was concentrated under reduced pressure almost to dryness, while the bath temperature was kept below 60°C. To the residue, 250 ml. of ethanol was added, and the solution was kept in a refrigerator overnight. The resulting monosodium salt of the oxime was filtered off, and washed with ethanol and then with ether. Yield: 7 g. The pure monosodium salt of AAPDA-OX was obtained by repeated recrystallizations from 90% ethanol. The pure oxime was obtained as colorless needles which decomposed at 129—130°C (they colored at 122°C). This material has two moles of the water of crystallization; one mole of which was lost when it was heating at 40°C over phosphorus pentoxide in vacuo, while the remaining water was removed only by heating, the material at 70°C. However, reliable analytical data corresponding to the anhydrous material could not be obtained since it was very hygroscopic.

The structure for oxime was also supported by the infrared spectra, in which a carbonyl band at 1690 cm^{-1} characteristic of the starting material disappeared in the oxime derivatives.

The physical properties and the results of analyses of the oximes are summarized in Table I. The monosodium salts of these oximes are very soluble in water and soluble in hot methanol and ethanol, but insoluble in ether, benzene, dioxane and petroleum ether. All attempts to obtain the free acid form of oximes were unsuccessful, since the oximes were easily hydrolyzed in a low pH region.

pH Titration Study.—An automatic recording titrator, Metrohm Potentiograph E 336, was employed for the pH titration study. The titration was conducted in an atmosphere of nitrogen at room temperature. A 100-ml. portion of a 1×10^{-3} M solution of monosodium salt of AAPDA-OX was titrated with a 0.1 N sodium hydroxide solution in the absence and in the presence of equimolar amounts of metal ions.

Absorption Spectral Study.—*Reagents.*—AAPDA-OX solution. A 0.001 M solution was prepared by dissolving a monosodium salt of oxime.

A 0.01 M standard iron(III) solution was prepared from ferric nitrate. This solution was standardized by EDTA titration.

The buffer solutions were acetates of standard compositions.

All the other reagents were of analytical grade unless otherwise specified.

Apparatus.—A Hitachi Model EPS-2 recording spectrophotometer was used for the measurements of the absorption spectra, while a Hitachi Model FPW-4 filter photometer was used for the photometric measurements. A Hitachi-Horiba Model P glass electrode pH meter was used for the pH measurements.

Standard procedure for the measurements of the absorption spectra: To a solution containing 312 μg. of iron(III), 5 ml. of a buffer solution (pH 5.5) and 5 ml. of a 0.001 M oxime solution were added; the mixture was then diluted to 25 ml. After 30 min., an absorption spectrum of the resulting solution was measured against water, using standard 1-cm, cells. The results are shown in Fig. 1. For the absorbance measurements, a similar procedure was followed, using a photometer equipped with a filter with a maximum transmittance at 420 mμ.

Results and Discussion

Absorption Spectra.—The absorption spectra of the iron(III) chelates of oximes and of the reagent blank are shown in Fig. 1. The reagent blank consists of iron and the buffer solution.

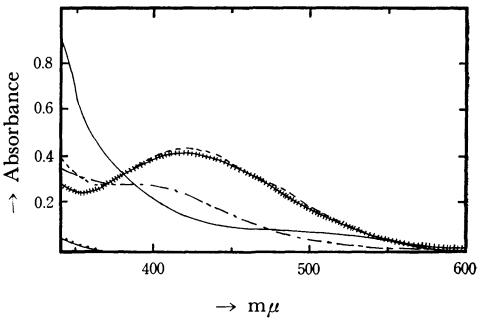

Fig. 1. Absorption spectra of oximes (12.5 p.p.m. of Fe).

- – – AADA-OX Na
- ||||||| AAPDA-OX Na
- – – – *p*-Br-AAPDA-OX Na
- —— GTDA-OX Na
- ▲▲▲ Blank···Fe(III)-Acetate Buffer

None of free oxime reagents showed any absorption in the visible region. The iron(III) chelate of GTDA-OX gave no absorption maximum in this region. On the contrary, the iron(III) chelates of AAPDA-OX and Br-AAPDA-OX gave a maximum at around 420 mμ. The iron(III) chelate of AADA-OX gave a shoulder at around 390 mμ, and the absorption spectra is identical with that of the aminoacetone-*N*, *N*-diacetic acid—hydroxylamine hydrochloride — hydrogen peroxide—iron(III) system, which was reported on previously.[2] Therefore, the colored complex due to iron(III) was proved to be the iron(III) chelate of AADA-OX.

The molar absorptivity of the iron chelates of AAPDA-OX and Br-AAPDA-OX were calculated as 2.0×10^3 and 2.1×10^3 respectively. These values are not so high as 1, 10-phenanthroline, but these oximes are still effective as the colorimetric reagents for iron(III). However, the synthesis of AAPDA-OX is much easier than that of Br-AAPDA-OX. After considering these results, AAPDA-OX was chosen as a colorimetric reagent for iron(III) in this study.

Structures of the Ligand and the Iron Chelate.—As has been described in the Experimental part, the results of elementary analyses

agree fairly well with the proposed formula of the oximes. The infrared spectra of oximes, observed as Nujol mull on the solid sample as well as on the deuterium oxide solution, indicated the disappearance of the carbonyl band of the starting materials. These results all support the oxime structure.

In order to get semi-quantitative information on the interaction of various metal ions with oximes, a pH titration study was carried out on AAPDA-OX in the absence and in the presence of various metal ions. The titration curves are reproduced in Fig. 2. As is clear from the figure, a fairly strong interaction between iron(III) and AAPDA-OX can be seen in the acid region.

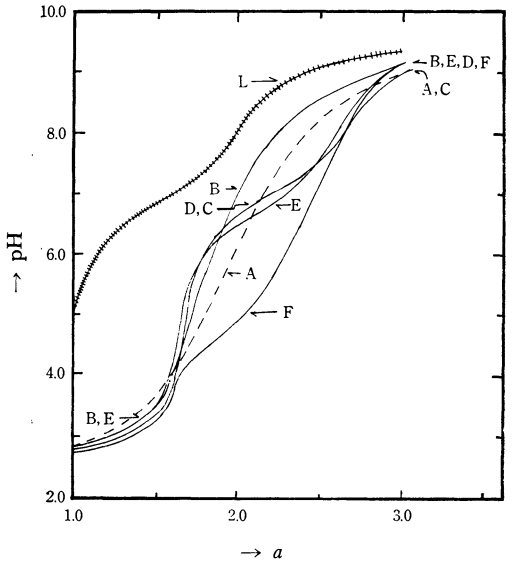

Fig. 2. Titration curves of monosodium AAPDA-OX in the abssence and presence of equivalent amount of various ions.
L, ligand; A, Fe(III); B, Cd(II); C, Zn(II); D, Ni(II); E, Co(II); F, Cu(II). *a* denotes moles of base (0.1 N NaOH) added per mole of ligand. Concentration of ligand and metal ions···about 1×10^{-3} M.

To determine the combining ratio of iron to a ligand, the continuous variation study was carried out on the Fe-AAPDA-OX system at pH 5.5. As is shown in Fig. 3, the results clearly indicate the formation of the chelate in only a 1 : 1 metal ligand ratio. Since iron(III) has a coordination number of 6, the iron(III) chelate of AAPDA-OX may possibly have a structure such as is shown in Fig. 4. Since there still remains a problem of the geometric arragement of the imino hydroxyl group (syn and anti), more experimental data is needed to settle this problem.

Conditions for the Photometric Determination of Iron(III).—In order to find the optimum conditions for the photometric determination of

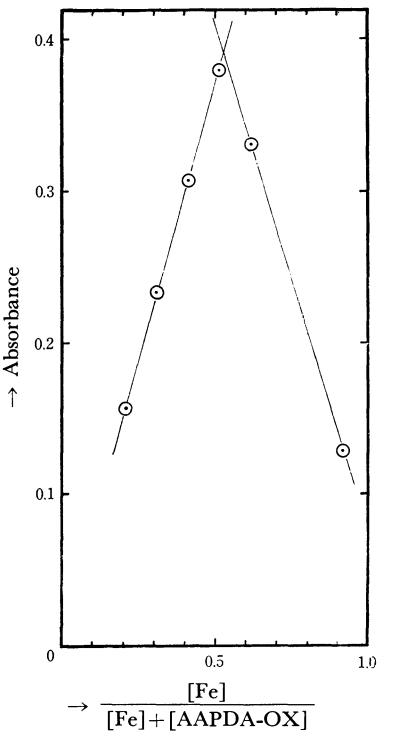

Fig. 3. Continuous variation study on AAPDA-OX-iron(III) system. [Fe(III)]+[AAPDA-OX] =0.01 M. pH=5.5. wavelength=420 mμ.

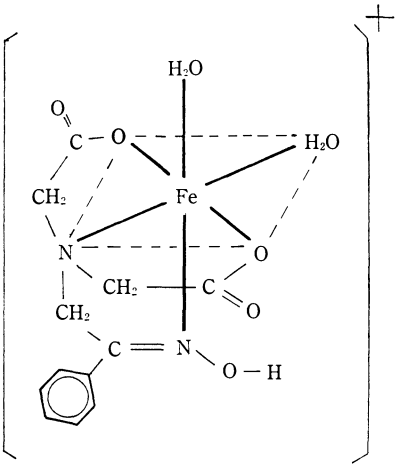

Fig. 4. Possible structure of the colored complex.

iron(III) with AAPDA-OX, various factors influencing the coloration, such as the pH, the amount of reagent, and the standing time, have been investigated.

The Effect of the pH.—The variations in the absorbance of the iron(III) chelate of AAPDA-OX at 420 mμ with a change in pH are shown in Fig. 5. The standard procedure for the measurement of absorption spectra was followed, with acetate

Table I. Monosodium salts of oximes

	Oximes	Recrystallized from	M.p. (with decomposition), °C	Water of crystallization	Elementary analyses[a] Calculated, % C H N	Found, % C H N
I	AADA-OX	85% ethanol	154—155	1 mole	for $C_7H_{11}O_5N_2Na\cdot H_2O$ 34.43 5.36 11.47	34.08 5.37 11.47
II	AAPDA-OX	90% ethanol	129—130	2 moles	for $C_{12}H_{13}O_5N_2Na\cdot 2H_2O$ 44.44 5.28 8.65	44.70 5.18 8.95
III	Br-AAPDA-OX	90% ethanol	134—135	2 moles	for $C_{12}H_{12}O_5N_2BrNa\cdot 2H_2O$ 35.75 4.00 6.95	36.01 3.95 7.24
IV	GTDA-OX	95% ethanol	above 170 (gradually decomposed)	2 moles	for $C_{10}H_{11}O_5N_2SNa\cdot 2H_2O$ 36.36 4.54 8.48	36.23 4.55 8.24

a) Elementary analyses were carried out at the Elementary Analysis Center of Kyushu University.

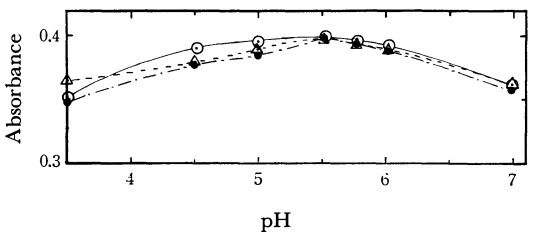

Fig. 5. Effect of pH on absorbance (12.5 p.p.m. of Fe).

●———● standing time 15 minutes
△- - - -△ standing time 1 hour
⊙———⊙ standing time 20 hours

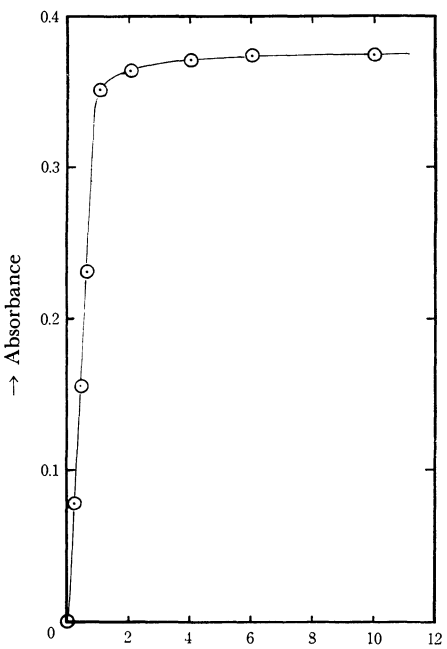

Fig. 6. Effect of the amount of reagent on the color developement (11.0 p.p.m of Fe).

buffers of different pH values, and their absorbances were measured after various standing times. It may be seen from this figure that the absorbance changes very slightly over the pH range from 4.0 to 7.0. Especially, in the pH range from 5.0 to 6.0, the absorbance is almost constant within the limits of experimental error. Therefore, the acetate buffer solution of pH 5.5 was chosen in this experiment. The amount of buffer solution had not much influence on the absorbance, since the acetato-iron(III) complex has no significant absorption at 420 mμ under these conditions.

The Amount of AAPDA-OX.—The effect of the amount of the reagent on the color development was studied. As is shown in Fig. 6, when more than four times as much reagent as iron was employed,

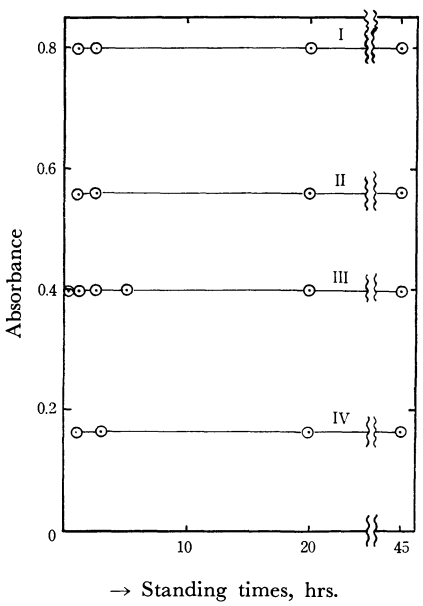

Fig. 7. Effect of the standing time for the color development.
I, Fe=25.0 p.p.m.; II, Fe=17.5 p.p.m.; III, Fe=12.5 p.p.m.; IV, Fe=7.0 p.p.m.

the absorbance became almost constant. Accordingly, 5 ml. of a 1×10^{-1} M solution of AAPDA-OX was added to a sample solution containing 50 to 625 μg. of iron(III).

The Stability of the Color.—The color developed by the standard procedure was found to be very stable over many hours, as is shown in Fig. 7. It was not neccessary to wait for the full color development, as the color reached its maximum immediately after the reagents were mixed. However, the absorbance was measured after 0.5—1.0 hr. in this experiment.

Calibration Curve.—To the series of sample solutions containing 60—600 μg. of iron(III), the standard procedure described in the experimental part was applied, and the absorbances of the resulting color at 420 mμ were plotted against their concentrations. As is shown in Fig. 8, the system follows Beer's law in the concentration range from 0 to 25 p. p. m. of iron(III).

The Effects of Diverse Ions.—The effects of diverse ions were investigated on the solutions containing 312 μg. of iron(III) and various amounts of individual diverse ions. The cations, except for manganese and chromium, were added as the nitrate, but manganese and chromium were added as sulfate and chloride respectively. The data in Table II show the tolerance limits of each ion.

As the table shows, cadmium, manganese(II), lead and ammonium do not interfere, even if they are present at a concentration level hundreds of

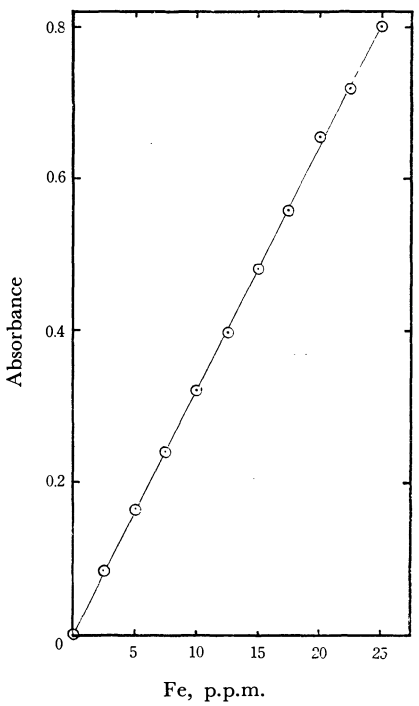

Fig. 8. Calibration curve for the determination of iron(III) with AAPDA-OX.

Table II. Effects of diverse ions for the determination of 312 μg. of iron(III)

Ions	Ions added μg.	Found Fe μg.	Relative error, %
Al(III)	3000	300	−3.85
	1500	305	−2.24
	750	310	−0.64
Cd(II)	24000	298	−4.49
	12000	315	+0.95
	6000	310	−0.64
Co(II)	600	320	+2.56
	300	318	+1.92
Cr(III)	525	318	+1.92
	263	310	−0.64
Cu(II)	625	345	+10.58
	63	318	+1.92
Mn(II)	44000	312	0.00
	22000	312	0.00
	8800	315	+0.95
Ni(II)	29500	300	−3.85
	5900	315	+0.95
	2950	310	−0.64
Pb(II)	41400	290	−7.05
	20700	315	+0.95
	10350	310	−0.64
Zn(II)	3250	295	−5.45
	1950	311	−0.32
	1300	312	0.00
NH_4^+	90000	318	+1.92
	45000	312	0.00
MoO_4^{2-}	80000	320	+2.56
	40000	315	+0.95
	8000	305	−2.24
WO_4^{2-}	4955	283	−9.29
	3300	308	−1.28
	1650	305	−2.24
VO_4^{3-}	990	360	+15.38
Cl^-	355000	320	+2.56
	177500	318	+1.92
SO_4^{2-}	480000	318	+1.92
	240000	315	+0.95
CH_3COO^-	295000	310	−0.64
	147000	315	+0.95
PO_4^{3-}	48000	103	−66.99
	950	305	−2.24
F^-	2000	278	−10.90
	200	298	−4.49

times that of iron. Nickel, aluminum, and zinc do not interfere up to concentrations of several tens times of the amount of iron. The negative errors observed in the presence of a large amount of these interfering ions may be due to the consumption of the reagent by the formation of stable but colorless complexes with these cation; the error may be lessened by the use of a fairly large amount of the reagent. Cobalt(II) and chromium(III) show a positive error if they are present in an amount more than twice that of iron(III). Copper(II) seriously interferes, giving a positive error. The cations which give a positive error are apt

to form stable and colored complexes, and so they should be masked or separated by appropriate methods. The anions, such as chloride, sulfate and acetate, do not interfere, even if they are present at concentration levels several thousands of times that of iron. Hundreds times of the level of molybdate and tens times of the level of tungstate do not interfere either; however, as was expected for iron(III), fluoride and phosphate seriously interfere with the determination by the formation of stable fluoro- and phosphato-complexes respectively.

It is clear from these results that AAPDA-OX is almost specific for iron, and that this reagent can be used as a colorimetric reagent for iron(III) in the presence of fairly large amounts of various ins.

It is interesting to note that the degrees of interference by these cations are parallel with the degrees of chelate formation, as estimated from the titration curves in Fig. 2. The extent of the pH drop is largest for copper, intermediate for cobalt and nickel, and smallest for cadmium and zinc. Thus, the interference with the cations is caused not only by the formation of colored complexes with the reagent, but also by the formation of stable chelates even if they are colorless.

A Comparison with Other Methods. — Of the various colorimetric reagents for iron, 2, 2'-bipyridine, 1, 10-phenanthroline and 5, 8-diphenyl-1, 10-phenanthroline have been known as the most favourable reagents because of their sensitivity.[3] They form strongly-colored complexes of the hexacovalent type and chelates (FeA_3^{2+}) with iron(II) in weakly acidic, neutral, or weakly alkaline media. The complexes are fairly stable, and the reagents are highly selective for iron. However, nickel, cobalt and copper are known to form colored complexes with these reagents, giving erroneous results. The limiting amounts of the interfering ions for various reagents are compared in Table III.

As has described above, the molar absorptivity of Fe-(AAPDA-OX) is about one fifth that of Fe-(phenanthroline)$_3$. Therefore, AAPDA-OX can not compete with the phenanthroline reagents in it's sensitivity; however, as is shown in Table III, AAPDA-OX is more specific than the phenanthroline reagents for iron. As has been discussed in the previous section, by the use of this reagent iron(III) can be determined in the presence of a fairly large amount of cations, especially in the presence of nickel. It should also be noticed that AAPDA-OX reacts with iron(III) ion immediately, resulting in a maximum coloration, whereas it is necessary to wait for a while to reach a maximum coloration with phenanthroline reagents, because that color reaction involves the reduction of iron(III) to iron(II).

Table III. Limiting amounts of interfering ions for various reagents

Ion	Reagents: AAPDA-OX (for 12.5 p.p.m. of Fe(III)) p.p.m.	1, 10-Phenanthroline[4] (for 2 p.p.m. of Fe(III) p.p.m.	2, 2'-Bipyridine[5] for 5 p.p.m. of Fe(III) p.p.m.
Al(III)	50	0	—
Cd(II)	600	50	5
Co(II)	20	10	2
Cr(III)	20	0	1.5
Cu(II)	2	10	5
Mn(II)	2000	500	5
Ni(II)	250	2	2.5
Pb(II)	800	500	—
Zn(II)	80	10	2.5
NH_4^+	3600	500	—
MoO_4^{2-}	200	∞	—
WO_4^{2-}	150	5	3.5
VO_4^{3-}	0	0	—
Cl^-	7100	500	precipitated
SO_4^{2-}	1900	500	—
CH_3COO^-	12000	500	—
PO_4^{3-}	30	20	—
F^-	0	500	—

The result of this investigation also indicates that a new type of colorimetric reagents for iron could be developed by starting from AADA-OX or AAPDA-OX as a mother compound.

The authors wish to thank Mrs. Hiroko Yamaguchi for her laboratory assistance in the analytical work. They are also grateful for the Ministry of Education of the Japanese Government for its financial assistance.

3) E. B. Sandell, "Colorimetric Determination of Traces of Metals," 3rd Ed., Interscience Publishers, New York (1959), p. 537.

4) W. B. Fortune and M. G. Mellon, *Ind. Eng. Chem., Anal. Ed.*, **10**, 60 (1938).

5) M. L. Moss and M. Mellon, ibid., **14**, 862 (1942).

BULLETIN OF THE CHEMICAL SOCIETY OF JAPAN VOL. 39 2406—2410 (1966)

A Study of the Hydration of Calcium Orthoplumbate. VII. The Mechanism of the Formation of Hydrate

By Masumi Koishi

Department of Applied Chemistry, Faculty of Science, Tokyo College of Science, Kagurazaka, Shinjuku-ku, Tokyo

(Received November 15, 1965)

The hydration processes of calcium orthoplumbate are studied by means of a twin-type conduction calorimeter. The curves of the differential electromotive force vs. the hydration time have two characteristic maxima, corresponding to two exothermic processes: the first one is due to the immersion and dissolution of calcium orthoplumbate, while the second one is caused by the formation of crystalline hydrates. The heat liberated by the first process is about 1.14 cal./g. Ca_2PbO_4, while that liberated by the second process is about 52.22 cal./g. Ca_2PbO_4. The reaction in the second process proceeds by the 2/3 order; this may be explained by assuming that the rate of the reaction is determined by the surface area of the calcium orthoplumbate being hydrated.

Many investigations of the reactions of calcium orthoplumbate with water have been reported[1] but most of the investigations have been those of reactions above 100°C; few experiments[2] have been carried out concerning hydration below 100°C.

In previous papers[2] we reported the compositions of completely hydrated products of calcium orthoplumbate and the process of hydrating them at various temperatures below 100°C; we made our study by the use of X-ray diffraction analysis, thermobalance analysis, chemical analysis, and electron microscopy. In this paper, the hydration of calcium orthoplumbate will be examined by a twin-type conduction microcalorimeter in order to obtain the heats of hydration and, therefrom, some information on the mechanism of the hydration process.

Experimental

Material.—*Calcium Orthoplumbate.* — Ca_2PbO_4 (or $2CaO \cdot PbO_2$) was prepared by heating an equimolar mixture of lead oxide and calcium carbonate in air at 700°C for 8 hr. The product was identified by X-ray diffraction and chemical analysis. The composition found was PbO_2: 66.71%, CaO: 32.00%, and free calcium as $Ca(OH)_2$: 1.47%. The specific gravity was 5.7. The specific surface area determined by the BET method with an nitrogen adsorption of 3.01 m^2/g. Four chemical reagents, lead oxide, lead peroxide, calcium hydroxide, and calcium carbonate, were employed as reference samples for the analysis of X-ray diffraction patterns, using CuK_α radiation.

Apparatus and Procedure

Apparatus for Hydration Reaction.—*Calorimeter.*—The twin-type conduction calorimeter employed in this work was a commercial model, CM-502, of Ôyodenki Kenkyujo.[3] While this calorimeter is based on the principle which Tian & Calvet first developed, a brief description of the apparatus will be appropriate here. The apparatus is shown in Fig. 1. The main part of the apparatus consists of two pairs of similar calorimeters, each having a 70 ml. reaction cell, a stirrer,

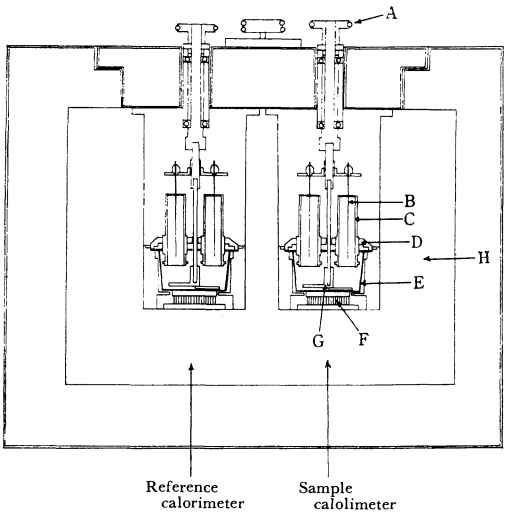

Fig. 1. Principal diagrams of twin-type conduction calorimeter.
A, Pulley; B, Needle; C, Sample-holding tube; D, Lid; E, Reaction cell; F, Thermoelement; G, Stirrer; H, Aluminum block (standard bed)

1) J. W. Mellor, "Comprehensive Treatise of Theoretical and Inorganic Chemistry," Vol. 7, Longmans, Green and Co., London (1931), Term of the Plumbate.

2) M. Koishi and K. Meguro, *J. Chem. Soc. Japan, Ind. Chem. Sect. (Kogyo Kagaku Zasshi)*, **67**, 2001, 2005 (1964); M. Koishi and K. Meguro, *J. Japan Soc. Colour Material (Shikizai Kyokaishi)*, **39**, 20 (1966).

3) K. Hagiwara, *An Explanatory Note of the CM-502-type Conduction Calorimeter* (Ôyodenki Kenkyujo) (1963); K. Amaya, *Bussei*, **4**, 588 (1963) (in Japanese).

two sample-holding tubes, breakers, a calibrated electric heater, and a thermoelement. The two calorimeters are surrounded by an aluminum block. All the tubes are sealed with rubber membrane and are supported by a lid attached to a main rod from the top plate of the aluminum block. The needles for breaking the rubber film in order to drop the sample into water are connected to the stirrer. The needles slip down with the rotation of the stirrer and so break the rubber membrane. The temperature difference between the two calorimeters produced by the immersion of sample into water is detected by a thermoelement. The electromotive force of the thermoelement of this apparatus is 6.5 mV./deg., and the optimum sensitivity is about 5×10^{-4}°C under the present operating conditions.

Procedure.—After the bottom of all the tubes have been sealed with rubber membrane, about 1.0—14.0 g. of calcium orthoplumbate is weighed into one of the sample-holding tubes of the sample calorimeter. This tube and another empty one* of the sample calorimeter are set on a lid. Another pair of empty tubes are placed on a lid in the reference calorimeter to serve as compensators. Equal volumes of distilled water (20 ml.) are then introduced both into the sample cell and into the reference cell. After the two calorimeters have been set in position, they are kept for about 5 hr. at the desired temperature in order to attain an equilibrium. Then, the sample is dropped into water and the heat liberated in the calorimeter is recorded as the differential electromotive force. After the hydration reactions of calcium orthoplumbate have been completed in the calorimeter, a known amount of electrical energy is supplied to one of the calorimeters to calibrate for the heat liberated. One example of the recorded thermograms is shown in Fig. 2. The amount of heat (Q_1 cal.) liberated by the reaction is calculated by the following equation:

$$Q_1 = \frac{S_1}{S_2} \times Q_2$$

where S_1 denotes the area under the curve of the diagram, corresponding to the liberated heat Q_1, and where, similarly, Q_2 and S_2 denote the heat supplied as electrical energy and the corresponding area respectively.

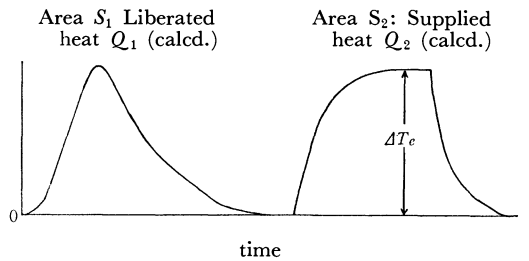

Fig 2. Standard diagram of record.

* The empty tube is for use in the case of a bulky sample.

The Determination of the Apparatus Constant of the Calorimeter.—The calorimeter of this experiment is schematically shown by the block diagram in Fig. 3. The heat liberated in the reaction cell, E, is conducted away in two ways; one is the direct escape from E to H (aluminum block), and the other is that through F (the thermoelement). If the heat is assumed to escape exclusively through the thermoelement, F, both the generation and the absorption of the heats by the sample per unit time (dQ/dt) are given by the following equation:

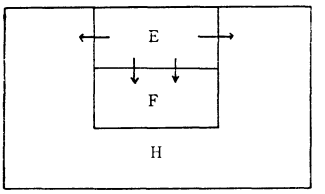

E: Reaction cell
F: Thermoelement
H: Aluminum block

Fig. 3. Block diagram of calorimeter.

$$dQ/dt = \sigma\cdot\Delta T + H\cdot d(\Delta T)/dt \quad (1)$$

where Q denotes the heat liberated in the sample calorimeter, σ is the effective thermal transmissive coefficient of the thermoelement, F (cal./deg. sec.), and ΔT is the temperature difference between the reaction cell and the cell of the reference calorimeter. The constant H stands for the effective heat capacity of E.

The ΔT recording for the electrical energy in Fig. 2 tends to level off, and in this region Eq. 1 reduces to:

$$\sigma = W/\Delta T_e \quad (2)$$

where W denotes the supplied electrical energy (watt), and ΔT_e is the temperature difference from the base line at the stationary state, because $d(\Delta T)/dt=0$ at the stationary state. H is calculated by:

$$d\ln(\Delta T) = -\frac{\sigma}{H}dt \quad (3)$$

from the ΔT recording curve after the supply of electrical energy is stopped.

The values of σ and H obtained here are 4.72×10^{-2} cal./deg. sec. and 25.30 cal./deg. Using these values, Eq. 1 may be rewritten as:

$$dQ/dt = 4.72\times10^{-2}\times\Delta T+25.30\times d(\Delta T)/dt \quad (4)$$

Results and Discussion

The Heat of the Hydration of Anhydrous Calcium Orthoplumbate.—The determination of

Table I. The values of the heat liberated during the hydration

Ca_2PbO_4/H_2O (molar ratio)	Duration of experiment, hr	Total heat liberated, cal.	Heat liberated, cal./g.		
			First process	Second process	Total
1/30	18	636.28	1.47	53.10	54.57
1/70	18	268.50	1.20	52.50	53.70
1/200	18	90.70	1.03	50.80	51.83
1/300	18	62.06	1.13	52.10	53.23
1/400	18	46.80	0.88	52.61	53.49

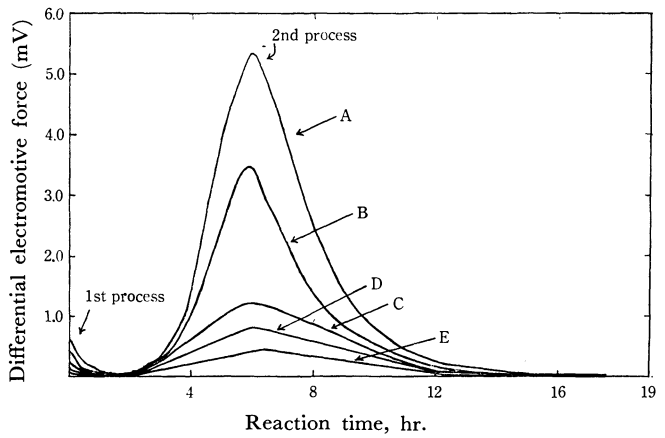

Fig. 4. Recorded curves at the hydration of calcium orthoplumbate.

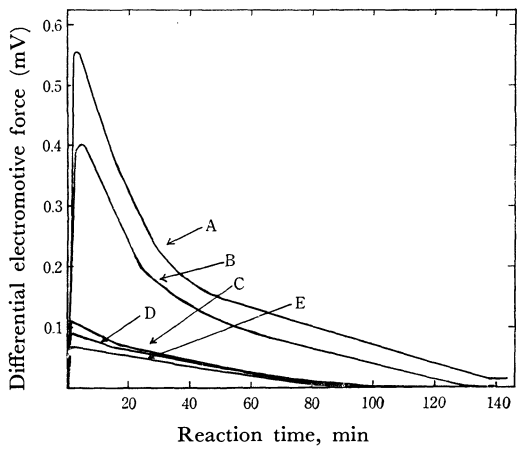

Fig. 5. Recorded curves in the first process at the hydration of calcium orthoplumbate.

the heat liberated in the process of hydrating calcium orthoplumbate is carried out at 20°C. In the hydration of calcium orthoplumbate, the recorded curves which have two maxima corresponding to to the first and the second exothermic processes of hydration are shown in Figs. 4 and 5.

Table I lists the heats of hydration in each process separately. The values of the total heat evolved in the two processes are proportional to the weight of the calcium orthoplumbate specimens; it was about 53.36 cal./g. This proportionality can be explained on the assumption that only a part of the water reacted with calcium orthoplumbate, while the rest of the water did not take part in the hydration reaction.

The X-ray diffraction of the solid, which was filtered off after the first process, did not show the presence of the hydrate of calcium orthoplumbate, as Fig. 6 shows. This suggests that the first process is the immersion and dissolution of calcium orthoplumbate, and that it does not involve the hydration process.

Zettlemoyer[4] observed that the heat of immersion of a solid in various butyl derivatives forms a nearly linear plot against the dipole moment of the functional group in the wetting liquid, and that the slope of the line can be used as a measure of the polarity of the solid. By Zettlemoyer's treatment, the polarity of calcium orthoplumbate can be shown to be as small as that of Teflon and Graphon. In fact, the heats of immersion of calcium orthoplumbate in *n*-butyl alcohol* and *n*-butyric acid* are less than 0.035 cal./g. (1.16×10^{-6} cal./cm^2), as is shown in Fig. 7. Considering the small amount of the heat of immersion, the heat evolved in the first process is mainly due to the heat of dissolution of calcium orthoplumbate into water. The heat of dissolution calculated by neglecting the heat of immersion is about 1.14 cal./g. Ca_2PbO_4.

4) A. C. Zettlemoyer, J. J. Chessick and C. H. Hollabaugh, *J. Phys. Chem.*, **62**, 489 (1958).

* Reagents: commercial extra pure.

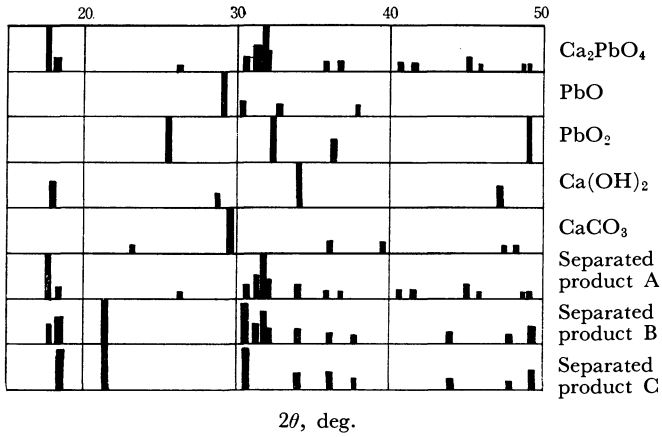

Fig. 6. X-ray diffraction patterns of anhydrous and hydrated calcium orthoplumbate, and reference samples.
Separated product A: after the first process
Separated product B: intermediate one during the second process
Separated product C: after the second process

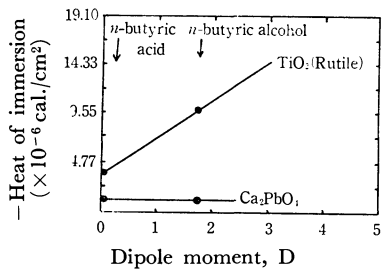

Fig. 7. Heat of immersion versus dipole moment relation for calcium orthoplumbate and titanium dioxide (rutile).

Analysis of the Second Process. — After the immersion and dissolution of calcium orthoplumbate have been completed, the second process (the hydration process) is followed by the X-ray diffraction of the solid, as is shown in Fig. 6. The growth of the peaks of the hydrate with the lapse of the hydration time is evident in this figure. Assuming that water rapidly reaches the surface of calcium orthoplumbate through its hydrated layer, and that the rate of the second process is proportional to the surface area of calcium orthoplumbate as a spherical particle, the following relation holds:

$$dx/dt = k \cdot n \cdot s \tag{5}$$

where x is the amount of hydration at t min. per gram of calcium orthoplumbate; s, the area of the calcium orthoplumbate surface at t min., and n, the number of particles per gram of calcium orthoplumbate.

If the reaction proceeds uniformly on the spherical particles with the diameter a, including the hydrated layer with thickness of $\Delta/2$, as is shown in Fig. 8, s is given by:

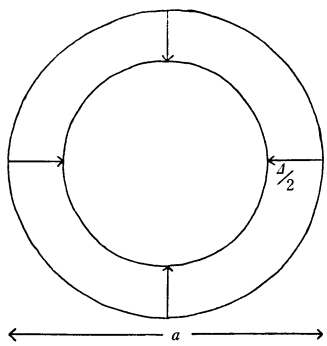

Fig. 8. Simplified model for hydration of calcium orthoplumbate with water.

$$s = 4\pi(a-\Delta)^2/4 = \pi(a-\Delta)^2 \tag{6}$$

When the reaction is completed, $t \to \infty$ and $x \to x_\infty$; then we have:

$$\frac{4/3 \cdot \pi(a/2)^3 \cdot n}{4/3 \cdot \pi\{(a-\Delta)/2\}^3 \cdot n} = \frac{a^3}{(a-\Delta)^3} = \frac{x_\infty}{x_\infty - x} \tag{7}$$

Taking account of Eq. 7, s is given by:

$$s = \pi \cdot a^2 \cdot \{(x_\infty - x)/x\}^{2/3} \tag{8}$$

The n value is expressed in terms of density, ρ, as:

$$n = \frac{1}{4/3 \cdot \pi(a/2)^3 \cdot \rho} = \frac{6}{\pi \cdot a^3 \cdot \rho} \tag{9}$$

From Eqs. 5, 8, and 9, we obtain:

$$dx/dt = (6k/a\rho) \cdot \{(x_\infty - x)/x_\infty\}^{2/3} \tag{10}$$

The integration of Eq. 10 gives:

$$-3\{(x_\infty - x)/x_\infty\}^{1/3} = (6k/a\rho x_\infty) \cdot t \tag{11}$$

Thus, the value of $(x_\infty - x)^{1/3}$ may be expected to be proportional to t.

In the present experiment the value of x was not measured directly, but it can reasonably be assumed that the value of x is porportional to the value of Q, and that the value can be calculated from the following equation:

$$Q = 4.72\times10^{-2}\times\Delta T\cdot t + 25.30\times\Delta T$$

which can be derived by integration of Eq. 1.* Thus, the term $(x_\infty - x)^{1/3}$ may be replaced by

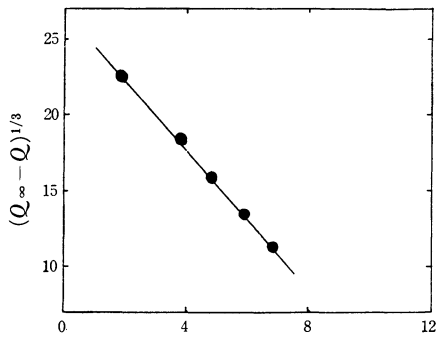

Fig. 9-(a)

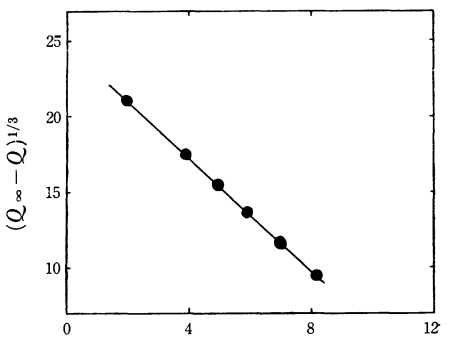

Fig. 9-(b)

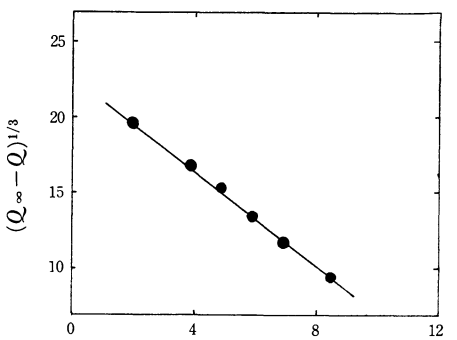

Fig. 9-(c)

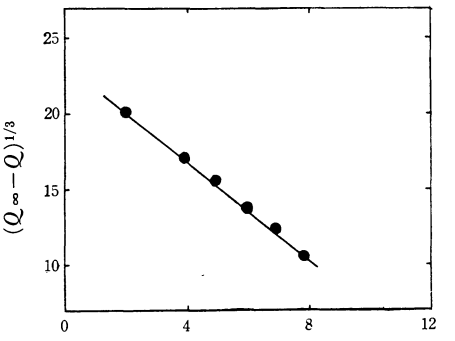

Fig. 9-(d)

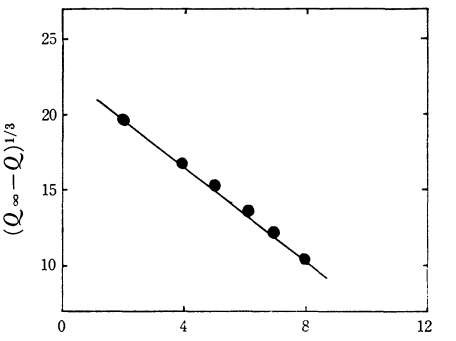

Fig. 9—(e)

Figs. 9-(a)—(e). The relation between the reaction time and $(Q_\infty - Q)^{1/3}$. Molar ratio of Ca_2PbO_4/H_2O are kept (a)=1/30, (b)=1/70, (c)=1/200, (d)=1/300 and (e)=1/400.

$(Q_\infty - Q)^{1/3}$ without any serious error. Figure 9-(a)—(e) show the $(Q_\infty - Q)^{1/3}$-t plot. The linear relation in Figs. 9-(a)—(e) indicates the general correctness of the assumption that the second process proceeds through the hydrated layer as a 2/3 order reaction.

The author wishes to express his gratitude to Professor Tsunetaka Sasaki of Tokyo Metropolitan University for his continuous encouragement and the inspection of this paper. The author also wishes to express his gratitude to Professor Kenjiro Meguro of Tokyo College of Science for his helpful discussions throughout this work, and to thank Kiyoichi Hagiwara and Shogo Enomoto for their help during the course of these experiment.

* The effective heat capacity, H, in Eq. 1 depends, in principle, on the amount of the specimen employed. However, all the ΔT-vs.-time calibration curves coincide for different fillings of the specimen within the precision of the present experimental set-up.

BULLETIN OF THE CHEMICAL SOCIETY OF JAPAN VOL. 39 2411—2414 (1966)

The Chemical Equilibrium of the $2H_2S+SO_2=3S+2H_2O$ Reaction in Solfataras of the Nasudake Volcano

By Yoshihiko MIZUTANI and Tsutomu SUGIURA

Institute of Earth Sciences, Faculty of Science, Nagoya University, Chikusa-ku, Nagoya

(Received February 7, 1966)

The stability of native sulfur in solfataras depends upon the temperature, the pressure, and the chemical composition of the solfataric gases with which native sulfur is in equilibrium. The equilibrium constant of the $2H_2S+SO_2=3S_{(s,l)}+2H_2O$ reaction may be expressed as:

$$K = \frac{X^2_{H_2O}}{X^2_{H_2S} X_{SO_2} P},$$

where X is the mole fraction of the gaseous components in the system and where P is the total pressure on the system. By the use of this relationship, the equilibrium temperature of natural solfataric gases with respect to the reaction may be estimated, provided the theoretical value of K, the chemical composition, and the pressure of natural solfataric gases are known. The attainment of chemical equilibrium of the reaction in solfataric gases of the Nasudake Volcano has been examined by comparing the estimated equilibrium temperature with the observed outlet temperature of the solfataras. The results indicate that the native sulfur occurring in the solfataras is approximately in equilibrium with the solfataric gases. On this basis, an attempt has also been made to explain the behavior of hydrogen sulfide and sulfur dioxide in solfataric gases.

Many investigators have discussed the chemistry of volcanic gases in terms of thermodynamics. Ellis[1] made comprehensive thermodynamic calculations on the variation in the chemical composition of volcanic gases with the temperature and with the pressure. Krauskopf[2] also made thermodynamic calculations on the feasibility of the vapor transportation of heavy metals in magmatic vapor. Recently, Matsuo[3] presented similar calculations with relevance to the possibility of a heterogeneous reaction in magma effecting the creating of volcanic gases.

On the other hand, the thermodynamics were applied to interpreting the results from the analyses of natural volcanic gases by Oana[4] and by Matsuo[5]. Their studies showed that, in high-temperature volcanic gases, the chemical equilibrium is seemingly established, at least with respect to the $3H_2+SO_2=H_2S+2H_2O$ and $CO+H_2O=CO_2+H_2$ reactions.

In the present paper, the authors will attempt to extend the application of thermodynamics to the heterogeneous reaction, $2H_2S+SO_2=3S_{(s,l)}+2H_2O$, in natural solfataras. The authors wish to examine the attainment of chemical equilibrium in solfataric gases during its ascent toward the surface. In addition, it is important to consider the effect of the chemical equilibrium of the reaction upon the hydrogen sulfide and sulfur dioxide portions of solfataric gases.

Results and Discussion

The Character of Solfataric Gases of the Nasudake Volcano.—Mizutani, Sugiura and Oana[6] analyzed solfataric gases of the Nasudake Volcano, Tochigi, Japan, and found some correlation between the temperature of the solfataras and the behavior of the major chemical components of the gases. For example, there is a notable increase in the amounts of hydrogen sulfide and sulfur dioxide in the temperature range between 100 and 200°C when the amount of the sulfur compounds in the gases is plotted against the outlet temperature of the solfataras. This finding led the present authors to conclude that the major part of the sulfur compounds in the gases at temperatures between 100 and 200°C was contributed secondarily by subterranean native sulfur accumulated through previous solfataric activities of this volcano. There is also a trend toward an increase in the ratio of hydrogen sulfide to sulfur dioxide in the gases with a lowering of the temperature.

In this solfataric area, native sulfur is mined by introducing solfataric gases into artificial gas channels, where native sulfur is then deposited as the

1) A. J. Ellis, *Am. J. Sci.*, **255**, 416 (1957).
2) K. B. Krauskopf, *Econ. Geol.*, **52**, 786 (1957).
3) S. Matsuo, *J. Earth Sci. Nagoya Univ.*, **8**, 222 (1960).
4) S. Oana and K. Takahashi, *Geol. Survey Japan, Report*, **170**, 115 (1957).
5) S. Matsuo, *J. Earth Sci. Nagoya Univ.*, **9**, 80 (1961).
6) Y. Mizutani, T. Sugiura and S. Oana, Read at the Meeting of the Volcanological Society of Japan, October 1961.

temperature falls. Small pools of liquid sulfur are usually found at the openings of gas channels.

The Chemical Equilibrium of the $2H_2S+SO_2=3S+2H_2O$ Reaction.—In solfataras, native sulfur usually occurs in three different forms: rhombic, monoclinic, and liquid, depending on the temperature. Therefore, the following three reactions must be considered:

$$2H_2S + SO_2 = 2H_2O + 3S_{(rh.)}, \quad \text{for } T<95.6°C \quad (1)$$

$$2H_2S + SO_2 = 2H_2O + 3S_{(mono.)}, \quad \text{for } T=95.6—119°C \quad (2)$$

$$2H_2S + SO_2 = 2H_2O + 3S_{(s,l)}, \quad \text{for } T>119°C \quad (3)$$

The appearance or disappearance of native sulfur in solfataras may be controlled by the temperature, the total pressure, and the chemical composition of the gases in equilibrium with the native sulfur. The equilibrium constants of these reactions may be expressed as:

$$K = \frac{X^2_{H_2O}}{X^2_{H_2S}X_{SO_2}P} \quad (4)$$

where K is the equilibrium constant, X is the mole fraction of the gaseous components in the system, and P is the total pressure on the system.

The theoretical equilibrium constant for these reactions may be calculated from the free-energy change for these reactions by using the $\ln K=-\Delta F/RT$ relation, where ΔF is the free-energy change, R is the gas law constant, and T is the absolute temperature of the system. The values of the free-energy change for these reactions may be obtained from the thermodynamic data given by Kubaschewski and Evans[7] and Rossini et al.[8] The temperature functions of the equilibrium constant obtained are:

for Reaction 1:

$$\log K_1 = -11.43+0.333\log T+1.53\times10^{-3}T + 7720\,T^{-1}+1.73\times10^4\,T^{-2} \quad (5)$$

for Reaction 2:

$$\log K_2 = -11.35+0.302\log T+1.76\times10^{-3}T + 7690\,T^{-1}+1.73\times10^4\,T^{-2} \quad (6)$$

and for Reaction 3:

$$\log K_3 = -18.90+3.09\log T+1.28\times10^{-3}T + 7900\,T^{-1}+1.73\times10^4\,T^{-2} \quad (7)$$

The relation between the equilibrium constant and the temperature obtained from these equations is shown in Fig. 1.

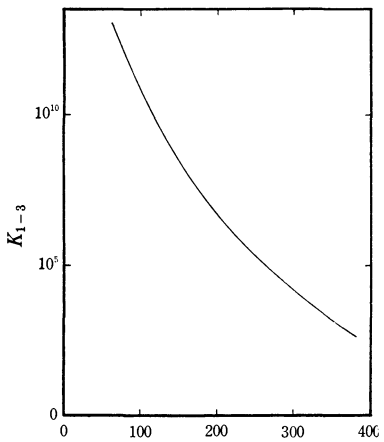

Fig. 1. Relation between equilibrium constant and temperature with respect to reaction $2H_2S+SO_2=3S_{(s,l)}+2H_2O$.

By the use of these relations, the equilibrium temperature of natural solfataric gases with respect to the above reactions may be estimated from the observed value of K. For solfataric gases of the Nasudake Volcano the observed value of $X^2_{H_2O}/X^2_{H_2S}X_{SO_2}$ may be obtained from the analytical data of the gases given by Mizutani et al.[9] Some examples of the data are given in Table I. The observed values of $X^2_{H_2O}/X^2_{H_2S}X_{SO_2}$ thus obtained are given in Table II. The equilibrium temperature of the solfataric gases may be estimated from these values, provided the total pressure on the system is known. The total pressure of the gases is assumed to be 1 atm. for the first approximation, because the gases are emitted from openings of gas channels with a rather low static pressure (close to 1 atm.).[10] The equilibrium temperatures thus estimated are given in Table II.

By comparing the estimated equilibrium temperatures with the observed outlet temperatures, the degree of the attainment of the chemical equilibrium of the reaction at the outlet of the solfataras may be examined. As is shown in Table II, the equilibrium temperatures obtained for the solfataras with native sulfur deposits are almost in agreement with the observed temperatures, although the former are always slightly higher than the latter. This implies that the native sulfur deposits occurring in solfataras are approximately in equilibrium with the solfataric gases from which the native sulfur deposit is formed, and possibly that, in the solfataric gases, the sulfur vapor is also in equilibrium with the water vapor, hydrogen sulfide and sulfur dioxide, through the reaction:

7) O. Kubaschewski and E. I. Evans, "Metallurgical Thermochemistry," John Wiley, New York (1956).
8) F. D. Rossini et al., "Selected Values of Chemical Thermodynamic Properties," Natl. Bur. Standards (1952), p. 500.
9) Y. Mizutani et al., Unpublished Data.
10) S. Sakuma, *Bull. Volcanol. Soc. Japan, 2nd Ser.*, *1*, 1 (1957).

TABLE I. CHEMICAL COMPOSITION OF SOLFATARIC GASES OF VOLCANO NASUDAKE

Solfatara	M-2c	OE-1	O-1	U-1
Date	1961	1962	1961	1961
Temp., °C	410	190	181	132
H_2O, l./1000 l.	993.6	991.7	982.6	991.4
CO_2, l./1000 l.	2.0	1.24	1.3	1.4
H_2S, l./1000 l.	3.08	4.23	13.7	4.10
SO_2, l./1000 l.	0.71	2.41	1.64	2.12
HCl, l./1000 l.	0.250	0.214	0.51	0.91
HF, l./1000 l.	0.041	0.056	0.14	0.01
O_2, l./1000 l.	0.000	0.000	0.000	0.000
H_2, ml./1000 l.	310	100	57	<10
N_2, ml./1000 l.	21	36	40	<86
Ar, ml./1000 l.	0.19	0.39	0.24	—
CH_4, ml./1000 l.	0.96	2.1	2.6	< 3
CO, ml./1000 l.	0.07	0.39	—	—

TABLE II

Solfatara	Sampling date	Native sulfur in gas channel	Mole fractions* $\times 10^3$			H_2S/SO_2	$\frac{X^2_{H_2O}}{X^2_{H_2S}X_{SO_2}}$	Equilibrium temp. °C	Observed outlet temp. °C	Difference Eq. T.− outlet T.
			X_{H_2O}	X_{H_2S}	X_{SO_2}					
T-1	1961	+	995.4	4.2	0.49	8.6	$10^{8.06}$	161	118	+43
T-1	1962	+	997.1	2.3	0.62	3.7	$10^{8.48}$	151	119	+32
T-1	1963	+	996.3	3.6	0.11	33	$10^{8.84}$	142	120	+22
S-1	1961	+	996.6	3.2	0.16	20	$10^{8.78}$	143	120	+23
S-1	1962	+	996.7	2.6	0.72	3.6	$10^{8.31}$	154	129	+25
U-1	1961	+	993.8	4.2	2.1	2.0	$10^{7.43}$	179	132	+47
U-1	1963	+	992.7	4.8	2.5	1.9	$10^{7.23}$	185	140	+45
O-2c	1963	+	992.0	4.6	3.4	1.4	$10^{7.14}$	187	160	+27
O-1	1961	−?	984.6	13.7	1.6	8.6	$10^{6.51}$	207	181	+26
OE-1	1962	−?	993.3	4.2	2.4	1.8	$10^{7.37}$	181	190	−9
O-2	1961	−?	987.6	11.1	1.3	8.5	$10^{6.79}$	199	195	+4
M-2a	1960	−	993.7	5.9	0.36	16	$10^{7.90}$	165	195	−30
O-2b	1963	−	992.9	3.9	3.1	1.3	$10^{7.33}$	181	217	−36
O-2	1963	−	993.2	4.0	2.8	1.4	$10^{7.34}$	181	230	−49
M-2a	1961	−	997.3	5.9	0.36	2.6	$10^{8.58}$	146	261	−115

* $X_{H_2O}+X_{H_2S}+X_{SO_2}=1$

$$3/n\,S_{n(gas)} + 2H_2O = 2H_2S + SO_2 \qquad (8)$$

The Behavior of Hydrogen Sulfide and Sulfur Dioxide in Solfataric Gases.—The foregoing finding facilitates the understanding of the behavior of sulfur compounds in solfataric gases. If it is assumed that ascending volcanic water vapor comes into contact with subterranean native sulfur deposits for a sufficient time to react with them, the following reactions may be expected between water vapor and native sulfur:

$$3S_{(s,l)} + 2H_2O = 2H_2S + SO_2 \qquad (9)$$

$$H_2S = H_2 + S_{(s,l)} \qquad (10)$$

Then, on the assumption that the chemical equilibrium is established in this system, the hydrogen sulfide, sulfur dioxide, and hydrogen contents of the gas phase at a given P, T condition may be estimated by solving the following simultaneous equations:

$$K_4 = \frac{X^2_{H_2O}}{X^2_{H_2S}X_{SO_2}P} \qquad (11)$$

$$K_5 = \frac{X_{H_2}}{X_{H_2S}} \qquad (12)$$

$$\frac{2(X_{H_2S}+X_{H_2}+X_{H_2O})}{2X_{SO_2}+X_{H_2O}} = 2 = \text{Ratio of hydrogen to oxygen atoms} \qquad (13)$$

$$X_{H_2O} + X_{H_2S} + X_{SO2} + X_{H_2} = 1 \qquad (14)$$

where K_4 and K_5 are the equilibrium constants of reactions 9 and 10 respectively, P is the total pressure on the system, and X is the mole fraction of the gaseous components in the system. For the value of K_4, Eqs. 5, 6 and 7 are used again, and the value of K_5 is calculated from the standard thermodynamic properties of the chemical components in the way described above. The equation of K_5 obtained is:

$$\log K_5 = -9.475 + 2.470 \log T + 0.343 \times 10^{-3} T - 770\, T^{-1} + 1.313 \times 10^{3}\, T^{-2} \quad (15)$$

The equilibrium amounts of hydrogen sulfide, sulfur dioxide, and hydrogen in the gas phase, as calculated from the simultaneous equations, are illustrated graphically in Fig. 2.

The equilibrium figure obtained shows that the H_2S/SO_2 ratio of the gas phase is always approximately 2.0, while the hydrgoen sulfide, sulfur dioxide, and hydrogen contents in the gas phase vary with the change in the P, T condition, because the hydrogen content is always so small as to be negligible as compared with the hydrogen sulfide and sulfur dioxide contents.

In the Nasudake Volcano, some solfataric gases of the low-temperature type show a H_2S/SO_2 ratio close to 2 and a paucity of hydrogen (in

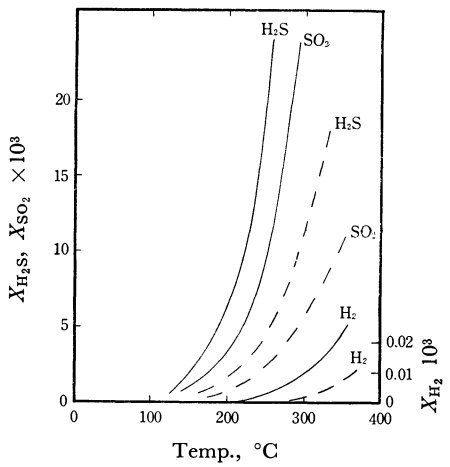

Fig. 2. Equilibrium amounts of H_2S, SO_2 and H_2 for system $S_{(liquid)}$-$H_2O_{(vapor)}$.
Solid line: $P_{H_2O}+P_{H_2S}+P_{SO_2}+P_{H_2}=1$ atm.
Broken line: $P_{H_2O}+P_{H_2S}+P_{SO_2}+P_{H_2}=100$ atm.

Table I, OE-1 and U-1). This probably implies that the major part of the sulfur compounds in the gases is derived from native sulfur deposits through the above reactions. The addition of sulfur compounds of this sort may also occur in low-temperature solfataras other than OE-1 and U-1. The situation must, however, be somewhat different from that considered for OE-1 and U-1, because the H_2S/SO_2, ratio of the gases from those solfataras is far different from 2. The gases coming from such solfataras may be considered to be products of reactions between native sulfur deposits and volcanic gases containing

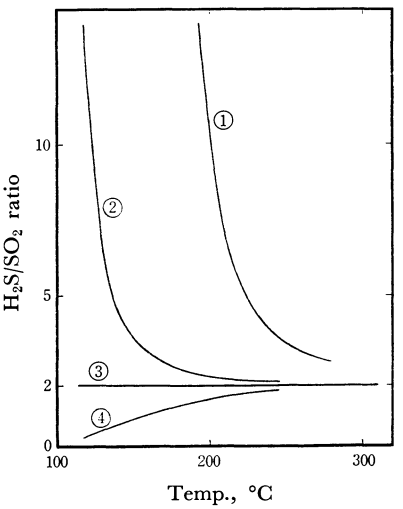

Fig. 3. Equilibrium ratio of H_2S to SO_2 for system S - H_2O - extra H_2S, SO_2 or H_2.
P=1 atm.
①: H/O=2.020 (H_2O : extra H_2S or H_2=990 : 10)
②: H/O=2.002 (H_2O : extra H_2S or H_2=999 : 1)
③: H/O=2.000
④: H/O=1.996 (H_2O : extra SO_2=999 : 1)

appreciable amounts of hydrogen sulfide, sulfur dioxide, and hydrogen. When such reactions proceed and reach an equilibrium in the gases, the equilibrium ratio, H_2S/SO_2, should deviate from 2 because the mass balance, the H/O atomic ratio in the system, is different from 2; Fig. 3 shows the effect of adding extra chemical components to the water vapor in the S-H_2O system. In other words, the equilibrium amounts of hydrogen sulfide and sulfur dioxide in the final products of the reactions at a given P, T condition are varied by the change in the amounts of such extra chemical components as hydrogen sulfide, sulfur dioxide, and hydrogen in the gases.

The natural situation in most low-temperature solfataras may be more complicated than this simple model indicates, but the general features of the variation in hydrogen sulfide and sulfur dioxide contents in the gases ought to be accounted for by this model if the above reactions reach equilibrium in the solfataras.

The authors wish to express their deep appreciation to Professor Shinya Oana of Nagoya University and Dr. Sadao Matsuo of Tokyo Kyoiku University for their helpful suggestions and for their encouragement throughout this work.

BULLETIN OF THE CHEMICAL SOCIETY OF JAPNA VOL. 39 2415—2417 (1966)

Preparation of *cis*- and *trans*-Dichlorobis(ethylenediamine)-Iridium(III) Chlorides

By Sigeo KIDA

Department of Chemistry, Wakayama University, Masago-cho, Wakayama

(Received March 30, 1966)

Potassium tetrachloro(ethylenediamine)iridate(III) and *cis*-dichlorobis(ethylenediamine) iridium(III) chloride were obtained by the reaction of iridium(III) chloride and ethylenediamine in a weakly acid aqueous solution. The condition for the formation of each compound depends on the mole ratio of iridium to ethylenediamine and pH of the solution. Trans-dichlorobis(ethylenediamine)iridium(III) chloride was prepared from potassium tetrachloro(ethylenediamine)iridate-(III) and ethylenediamine.

The geometrical configurations of the two isomers were determined by infrared spectra, and checked by ultraviolet spectra.

In the study of electronic spectra of d^6 complexes, it was desired to discuss the spectra of a series of complexes, *cis*- and *trans*-$[M\ Cl_2en_2]^{n+}$ (M= Co(III),[1] Rh(III),[2] Ir(III) and Pt(IV),[3] where preparation of all compounds, except iridium(III) complexes, have been reported. Therefore, it has been attempted to prepare *cis*- and *trans*- dichlorobis(ethylenediamine)iridium(III) complexes.

Anderson and Basolo[2] have prepared *cis*- and *trans*-dichlorobis(ethylenediamine)rhodium(III) complexes from an aqueous solution of rhodium(III) chloride, ethylenediaminedihydrochloride and potassium hydroxide (with the mole ratio of 1 : 2 : 4). However, iridium(III) analogues have not been obtained by the similar methods so far attempted, because iridium (III) chloride readily hydrolyzes in an alkaline or even neutral solution to form amorphous precipitate, and therefore, boiling this mixture with ethylenediamine leads to formation of tris(ethylenediamine)iridium(III) complex irrespective of the ratio of ethylenediamine to iridium.

In the present study, iridium(III) chloride was tried to react with ethylenediamine in a weakly acid medium, with various ratios of ethylenediamine to iridium. In this way, potassium tetrachloro-(ethylenediamine)iridate(III), $K[IrCl_4en]$, was obtained, and then *cis*-dichlorobis(ethylenediamine) iridium(III) chloride, *cis*-$[IrCl_2en_2]Cl$. The trans isomer was prepared from $K[IrCl_4en]$ and ethylenediamine.

Experimental

Preparation of a Solution of Iridium(III) Chloride from Iridium Metal.—Five grams of iridium powder was heated at 300—400°C with 15 g. of sodium hydroxide and 10 g. of sodium peroxide in a nickel crucible for one hour, ($Ir+3\ Na_2O_2 \rightarrow IrO_3+3\ Na_2O$). The resulting black mixture was dissolved in 150 ml. of water forming a colloidal solution. This was neutralized with hydrochloric acid, and added another 20 ml. of concentrated hydrochloric acid. When this solution was boiled for 30 min., iridium(VI) oxide was reduced to iridium(IV) chloride evolving chlorine gas to form dark brown solution, ($IrO_3+6\ HCl \rightarrow IrCl_4+Cl_2+3\ H_2O$). Iridium(IV) chloride was further reduced to iridium(III) chloride by adding hydrogen sulfide, ($6\ IrCl_4+H_2S+2\ H_2O \rightarrow 6\ IrCl_3+SO_2+6\ HCl$). The red-brown solution thus prepared contained iridium-(III) chloride and much excess of sodium chloride and hydrochloric acid.

***cis* - Dichlorobis (ethylenediamine) iridium (III) Chloride.**—The iridium(III) chloride solution, prepared by the method described above, was neutralized with potassium hydroxide and adjusted at pH 3 with acetic acid. This solution, containing 533 mg. of iridium, was diluted with water to 300 ml., and boiled in a 500 ml. round-bottom flask. To the boiling solution 25 ml. of 2% aqueous ethylenediamine(Ir/en=1/3) was slowly added. It was boiled for 3 hr., being frequently supplied with water to keep the volume constant. Then, this solution was evaporated to form crystals of sodium chloride and potassium chloride, cooled, and filtered. This procedure was repeated twice until the solution was concentrated to 15 ml. After one night yellow prisms were formed in the solution. These crystals were separated by filtration, washed with ethanol, and recrystallized from 6 N hydrochloric acid solution; yield, 276 mg.. The well-formed bright light-yellow prisms were obtained. This compound is fairly soluble in water, (soluble more than 1.1 g. in 100 ml. of water at 10°C).

Found: C, 11.42; H, 4.26; N, 12.93. Calcd. for $[IrCl_2en_2]Cl$: C, 11.47; H, 3.85; N, 13.38%.

Potassium Tetrachloro(ethylenediamine)Iridate (III).—The iridium(III) chloride solution prepared by the method described before, was neutralized with

1) "Inorganic Syntheses," Vol. 2, McGraw-Hill, New York (1946), p. 222.

2) S. Anderson and F. Basolo, *J. Am. Chem. Soc.*, **82**, 4423 (1960).

3) F. Basolo, J. C. Bailar Jr. and B. R. Tarr, ibid., **72**, 2433 (1950).

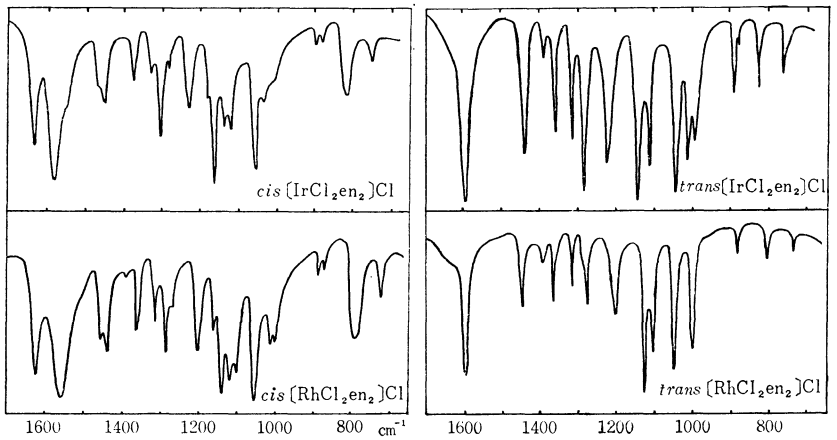

Fig. 1. Infrared spectra of *cis*- and *trans*- $[IrCl_2en_2]Cl$, with comparison of the Rh(III) analogues whose geometrical configurations were already known.

potassium hydroxide, and was again acidified by adding 1.2 g. of acetic acid. The solution containing 1 g. of iridium was diluted to 200 ml. with water, and boiled. To the boiling solution, 0.6 g. of ethylenediamine in 30 ml. of water was slowly added (Ir/en=1/2). The solution was boiled for 3 hr., being kept the volume constant by frequent addition of water, and then evaporated to about 60 ml. When cooled, the solution was quickly filtered to separate off the resulting crystals of sodium chloride and potassium chloride. The filtrate was strongly acidified with conc. hydrochloric acid, and again evaporated to 30 ml., cooled, and quickly filtered. After standing one night at room temperature, the filtrate yielded orange-red crystals, which were separated by filtration, washed with water and ethanol. Upon further evaporation of the filtrate, more crystals may be obtained. All these crystals were recrystallized from 6 N hydrochloric acid; yield, 768 mg.. The orange-red crystals thus obtained contain 2 molecules of water for one atom of iridium, and readily lose crystal water when heated at 100°C. This compound is sparingly soluble in cold water and fairly soluble in hot water.

Found: C, 5.57; H, 2.17; N, 6.25. Calcd. for $K[IrCl_4en]$: C; 5.55; H, 1.86; N, 6.47%.

***trans*-Dichlorobis(ethylenediamine)Iridium(III) Chloride.**—One half gram of $K[IrCl_4en]\cdot 2H_2O$, was dissolved in 30 ml. of hot water. Three milliliters of 1% aqueous ethylenediamine was slowly added to this solution which was stirred and heated on a steam bath. After the addition of ethylenediamine, the solution was kept at 95—100°C for one hour, and its color gradually changed from red to orange. Then another 3 ml. of 1% aqueous ethylenediamine was slowly added to the hot solution, and the solution was heated at 95—100°C for one hour as before. Throughout the above processes, the volume of the solution had been kept at 30 ml. by frequent supply of water. The solution was evaporated on a steambath to a small volume—ca. 3 ml., and left at room temperature for one night. The resulting orange-red crystals, the unreacted starting material, was filtered off. The filtrate was acidified with conc. hydrochloric acid, and concentrated to a very small volume—less than 1 ml. Upon ice cooling, light yellow flakes were formed in the solution. These crystals were filtered, and recrystallized with 6 N hydrochloric acid; yield, 96 mg. This compound is very soluble in water, (much more soluble than the cis isomer), and fairly soluble in 99% ethanol.

Found: C, 11.27; H, 4.33; N, 13.02. Calcd. for $[IrCl_2en_2]Cl$: C, 11.47; H, 3.85; N, 13.38.

Discussion

The *cis*- and *trans*-isomers were identified by infrared spectra. Morris and Busch[4] pointed out that in diacidobis(ethylenediamine)cobalt(III) complexes trans isomer has one strong absorption near 1600 cm^{-1}, while the corresponding band of a *cis* isomer always splits into two bands. Examining the spectra, which are shown in Fig. 1, one could easily determine the geometrical configuration of the two isomers which has been obtained in this study.

The UV spectrum of aqueous solution of each new compound was measured, and the first spin-allowed bands of the cobalt(III), rhodium(III) and iridium(III) complexes were listed in Table I. It is seen in Table I that the first spin-allowed

Table I. Absorption maxima of the first spin-allowed bands of dichlorobis(ethylenediamine) complexes of Co(III), Rh(III) and Ir(III)

M	Co(III)*		Rh(III)		Ir(III)	
	$\bar{\nu}$(kK.)	log ε	$\bar{\nu}$(kK.)	log ε	$\bar{\nu}$(kK.)	log ε
cis-$[MCl_2en]^+$	18.64	1.95	28.5	2.27	34.2	2.15
trans-$[MCl_2en]^+$	16.12	1.61	24.4	1.92	28.9	1.66

* M. Linhard and M. Weigel, *Z. anorg. u. allgem. Chem.*, **271**, 101 (1952).

4) M. L. Morris and D. H. Busch, *J. Am. Chem. Soc.*, **82**, 1521 (1960).

band of *cis*-isomer is located in the shorter wavelength region and has higher intensity than that of the trans isomer in the case of the iridium(III) complexes, as in the cases of the cobalt(III) and the rhodium(III) complexes whose geometrical configurations were already determined. This fact implies that the investigation of ultraviolet spectra supports the conclusion on the geometrical configuration deduced from IR spectra. The detailed discussion of electronic spectra will be reported separately.

The author wishes to express his thanks to Mr. Tsuyoshi Yamoto for his help in the experiments. This research has been financially supported in part by a grant of the Ministry of Education, to which author's thanks are due.

BULLETIN OF THE CHEMICAL SOCIETY OF JAPAN VOL. 39 2417—2424 (1966)

Metal Complexes of Amino Acids. III.[1] The Circular Dichroism of Cobalt(III) Ammine and Ethylenediamine Complexes with L-Amino Acids

By Takaji YASUI, Jinsai HIDAKA and Yoichi SHIMURA

Department of Chemistry, Faculty of Science, Osaka University, Toyonaka, Osaka

(Received May 19, 1966)

In order to study the vicinal effect of the L-amino acid coordinated in a complex on the central metal ion, a number of cobalt(III) L-amino acid complexes of three types were prepared, i. e., $[Co(NH_3)_5(L\text{-amH})]X_3$, $[Co(L\text{-am})(NH_3)_4]SO_4$, and *trans*-$[Co\ en_2(L\text{-amH})_2]X_3$, where L-amH denotes an L-amino acid, and where X is Cl, Br, or I. The circular dichroism (CD) and the rotatory dispersion (RD) spectra of their aqueous solutions were measured in the wavelength range from 650 to 300 mμ. In the region of the first absorption band, both the $[Co(NH_3)_5(L\text{-amH})]^{3+}$ and the *trans*-$[Co\ en_2(L\text{-amH})_2]^{3+}$ ions show one or two CD bands to be expected in complexes of the C_{4v} symmetry with a structure of the $[Co\ N_5O]$-type and of the D_{4h} symmetry with a structure of the *trans*-$[Co\ N_4O_2]$-type respectively. The positions of the CD bands observed in the *trans* complexes coincide well with the maxima of the split components, Ia and Ib, of the first absorption band. The CD spectra of different $[Co(L\text{-am})(NH_3)_4]^{2+}$ ions, in which L-am is a bidentate ligand, show a variety of behavior; they are discussed from a stereochemical point of view. An intense CD band of the $[Co(L\text{-prol})(NH_3)_4]^{2+}$ ion at about 510 mμ can be attributed to the vicinal effect of an asymmetric nitrogen atom of the coordinated L-prolinate ion. For the *trans*-$[Co\ en_2(L\text{-amH})_2]X_3$ complexes, the rotatory parameters and rotatory strengths were calculated by means of analyses of the experimental CD and RD curves.

Circular dichroism (CD) spectra have been proved to give useful information on the splittings of d→d absorption bands of metal complexes with a rather low symmetry. On the other hand, such splittings are not always observed in ordinary absorption curves.

It is well known that a metal complex containing an optically-active ligand (for example, optically-active amino acid,[2-7] tartaric acid, [8,9] or propylenediamine),[10] shows some weak CD bands in the region of its d→d absorption band as a result of the vicinal effect of the optically-active center in the ligand on the central metal ion. Of these ligands, the optically-active amino acids* behave in

1) Part II of this series: T. Yasui and Y. Shimura, This Bulletin, **39**, 604 (1966).
2) Y. Shimura, ibid., **31**, 315 (1958).
3) C. T. Liu and B. E. Douglas, *Inorg. Chem.*, **3**, 1356 (1964).
4) J. H. Dunlop and R. D. Gillard, *J. Chem. Soc.*, **1964**, 2822.
5) J. Fujita, T. Yasui and Y. Shimura, This Bulletin, **38**, 654 (1965).
6) T. Yasui, J. Hidaka and Y. Shimura, *J. Am. Chem. Soc.*, **87**, 2762 (1965).
7) T. Yasui, This Bulletin, **38**, 1746 (1965).
8) D. C. Bhatnagar and S. Kirshner, *Inorg. Chem.*, **3**, 1256 (1964).
9) K. M. Jones and E. Larsen, *Acta Chem. Scand.*, **19**, 1210 (1965).
10) J.-P. Mathieu, *Ann. Phys.*, **19**, 335 (1944).

* The following abbreviations will be used: L-alaH=$CH_3CH(NH_3^+)COO^-$; L-ala=$CH_3CH(NH_2)COO^-$; L-serH=$CH_2(OH)CH(NH_3^+)COO^-$; L-ser=$CH_2(OH)CH(NH_2)COO^-$; L-valH=$(CH_3)_2CHCH(NH_3^+)COO^-$; L-val=$(CH_3)_2CHCH(NH_2)COO^-$; L-thrH=$CH_3CH(OH)CH(NH_3^+)COO^-$; L-thr=$CH_3CH(OH)CH(NH_2)COO^-$; L-leuH=$(CH_3)_2CHCH_2CH(NH_3^+)COO^-$; L-leu=$(CH_3)_2CHCH_2CH(NH_2)COO^-$; L-isoleu=$CH_3CH_2CH(CH_3)CH(NH_2)COO^-$; L-phalaH=$CH_2(C_6H_5)CH(NH_3^+)COO^-$; L-phala=$CH_2(C_6H_5)CH(NH_2)COO^-$; L-prolH=$NH_2^+CH_2CH_2CH_2CHCOO^-$; L-prol=$NHCH_2CH_2CH_2CHCOO^-$.

an especially interesting way in that they can be coordinated both as unidentate and as bidentate ligands.

In a previous paper,[5] pentammine and tetrammine cobalt(III) complexes containing optically-active amino acids were reported, and it was suggested that the magnitude of the anomalous rotatory dispersion (RD) in the region of the first absorption band depends mainly on the conformational mobility of the optically-active ligand coordinated. In the present paper, the CD spectra of cobalt(III) ammine and ethylenediamine complexes which contain various L-amino acids will be described. The relationship among the ordinary absorption spectra and CD and some RD spectra will be considered precisely on the basis of the vicinal effect. Previously, several workers[2,11-14] made analyses of RD curves, but it was quite difficult to establish the individual inversive dispersions by the RD curve analyses alone. It was, therefore, been desirable to study in more detail the relation among the CD, the RD, and the ordinary absorption curves. In relation to this point, the present paper will discuss some typical d→d absorption bands of the cobalt(III) complexes of a new type, *trans*-[Co en_2(L-amH)$_2$]X_3.

Experimental

Preparation.—By evaporating a mixed aqueous solution of $[Co(OH_2)(NH_3)_5](ClO_4)_3$[15] and an excess of L-amino acid below 60°C, the $[Co(NH_3)_5$(L-amH)$]X_3$ complex was obtained in a good yield. In this condition, the L-amino acid coordinates to cobalt(III) as a unidentate ligand[5] by an oxygen atom of the carboxyl group. At temperatures higher than 60°C, it was difficult to obtain the desired complexes because of the decomposition of $[Co(OH_2)(NH_3)_5]^{3+}$. The complexes with L-valine, L-leucine and L-threonine were readily soluble in methanol and were insoluble in ethanol.

The $[Co(am)(NH_3)_4]SO_4$ complexes have already been reported on by one of the present authors,[2,16] who prepared the complexes from [Co Cl$(OH_2)(NH_3)_4$]-SO_4 and glycine, DL-alanine or L-leucine in ammoniacal alkaline solutions. In the present work, however, all of the $[Co$(L-am$)(NH_3)_4]SO_4$ complexes were obtained from the reaction of $[Co(OH_2)(NH_3)_5](ClO_4)_3$ with L-amino acid in the presence of activated charcoal. This method was proved to be superior to that described previously in respect to the yield and the diminution of the by-product. The *trans*-[Co en_2(L-amH)$_2$]X_3 complex was prepared by the evaporation almost to dryness of an aqueous solution containing $[Co(OH_2)_2$-$en_2](ClO_4)_3$[17] and an excess of L-amino acid at a temperature higher than 70°C. The *trans* complexes are very soluble in water. At temperatures lower than 70°C, $[Co(OH_2)en_2$(L-amH)$]X_3$ is produced mainly.

The preparation of *trans*-$[Co(NH_3)_4$(L-amH)$_2]X_3$ was attempted by similar ways, but all such attempts were unsuccessful.

$[Co(NH_3)_5$(L-valH)$]Cl_3$.—An aqueous solution containing 5 g. of $[Co(OH_2)(NH_3)_5](ClO_4)_3$[15] and 3 g. of L-valine in 30 ml. of warm water was gradually evaporated almost to dryness on a water bath at about 55°C. To the resulting material there was added a solution containing 5 g. of potassium chloride in a small amount of water, and then 50 ml. of methanol was added. After the potassium perchlorate which settled had been removed, a large amount of an ethanol-ether mixture (2 : 1) was added, drop by drop, to the filtrate. The pinkish powder obtained was washed with ethanol and then with ether. The crude complex was recrystallized from 95% methanol by adding ethanol. The pinkish-orange complex obtained was then dried in a vacuum desiccator.

Found: C, 16.28; H, 7.19; N, 22.16. Calcd. for $CoC_5H_{26}N_6O_2Cl_3$: C, 16.33; H, 7.14; N, 22.86%.

$[Co(NH_3)_5$(L-leuH$)]Cl_3$ and $[Co(NH_3)_5$(L-thrH$)]$-Cl_3.—These complexes were prepared by the method described above for the L-valine complex.

Found: C, 18.29; H, 7.23; N, 22.21. Calcd. for $CoC_6H_{28}N_6O_2Cl_3$: C, 18.88; H, 7.41; N, 22.02%.

Found: C, 13.45; H, 6.68; N, 22.67. Calcd. for $CoC_4H_{24}N_6O_3Cl_3$: C, 13.00; H, 6.56; N, 22.74%.

$[Co(NH_3)_5$(L-serH$)]Cl_3$.—The crude complex was obtained by the same way as was used for the L-valine complex; it was recrystallized from a small amount of water by adding methanol.

Found: C, 9.98; H, 6.25; N, 23.56. Calcd. for $CoC_3H_{22}N_6O_3Cl_3$: C, 10.13; H, 6.25; N, 23.64%.

$[Co(NH_3)_5$(L-prolH$)]I_3\cdot 3H_2O$.—This was isolated by adding potassium iodide to a reaction mixture prepared by the method mentioned above.

Found: C, 9.00; H, 4.56; N, 11.88; H_2O, 8.04. Calcd. for $CoC_5H_{24}N_6O_2I_3\cdot 3H_2O$: C, 8.65; H, 4.37; N, 12.11; H_2O, 7.79%.

$[Co$(L-val$)(NH_3)_4]SO_4\cdot H_2O$.—To an aqueous solution containing 5 g. of $[Co(OH_2)(NH_3)_5](ClO_4)_3$ and 1.5 g. of L-valine in 50 ml. of warm water, about 0.2 g. of activated charcoal was added. The mixture was evaporated on a water bath at 80°C to a volume of about 12 ml. After the resultant solution had been cooled to room temperature, a solution of 2.5 g. of potassium sulfate in 10 ml. of water was added to it. The solution was filtered, and then about 50 ml. of methanol was added, drop by drop, to the filtrate. The crude compound formed was collected, and washed with methanol and then with ether. The pinkish-orange crystals were separated into flakes by adding a small amount of methanol to an aqueous solution of the product.

Found: C, 16.81; H, 6.63; N, 19.20; H_2O, 4.93. Calcd. for $CoC_5H_{22}N_5O_6S\cdot H_2O$: C, 16.81; H, 6.78; N, 19.60; H_2O, 5.04%.

$[Co$(L-ser$)(NH_3)_4]SO_4$, $[Co$(L-leu$)(NH_3)_4]SO_4$ and $[Co$(L-prol$)(NH_3)_4]SO_4\cdot 3H_2O$.—These complexes were

11) M. Kobayashi, *J. Chem. Soc. Japan, Pure Chem. Sect. (Nippon Kagaku Zasshi)*, **64**, 648 (1934).
12) J.-P. Mathieu, *Bull. soc. chim.*, **(5)3**, 476 (1936); ibid., **(5)6**, 873 (1937); *J. chim. phys.*, **33**, 78 (1936).
13) J. Hidaka, Y. Shimura and R. Tsuchida, This Bulletin, **33**, 847 (1960).
14) J. G. Brushmiller, E. L. Amma and B. E. Douglas, *J. Am. Chem. Soc.*, **84**, 3227 (1962).
15) O. Hassel and G. B. Naess, *Z. anorg. Chem.*, **174**, 24 (1928).
16) Y. Shimura, This Bulletin, **31**, 173 (1958).
17) M. Linhard and G. Stirn, *Z. anorg. Chem.*, **268**, 105 (1952).

obtained in orange crystals by methods similar to that used for the L-valine complex above.

Found: C, 11.21; H, 5.66; N, 21.29. Calcd. for $CoC_3H_{18}N_5O_7S$: C, 11.00; H, 5.56; N, 21.40%.

Found: C, 20.37; H, 6.75; N, 19.58. Calcd. for $CoC_6H_{24}N_5O_6S$: C, 20.39; H, 6.86; N, 19.82%.

Found: C, 15.38; H, 6.89; N, 17.46; H_2O: 13.20. Calcd. for $CoC_5H_{20}N_5O_6S\cdot 3H_2O$: C, 15.34; H, 6.71; N, 17.90; H_2O, 13.81%.

$[Co(L\text{-isoleu})(NH_3)_4]SO_4\cdot H_2O$, $[Co(L\text{-thr})(NH_3)_4]SO_4$ and $[Co(L\text{-phala})(NH_3)_4]SO_4\cdot H_2O$.—These complexes were separated by recrystallizing from warm water the crude products which were obtained by procedures similar to that used for the L-valine complex. These complexes were sparingly soluble in water.

Found: C, 18.98; H, 7.07; N, 19.02; H_2O, 4.40. Calcd. for $CoC_6H_{24}N_5O_6S\cdot H_2O$: C, 19.04; H, 7.07; N, 18.86; H_2O, 4.85%.

Found: C, 14.10; H, 5.99; N, 20.56. Calcd. for $CoC_4H_{20}N_5O_7S$: C, 14.08; H, 5.92; N, 20.53%.

Found: C, 26.69; H, 5.99; N, 17.57; H_2O, 4.42. Calcd. for $CoC_9H_{22}N_5O_6S\cdot H_2O$: C, 26.86; H, 5.98; N, 17.28; H_2O, 4.45%.

***trans*-$[Co\ en_2(L\text{-alaH})_2]Cl_3$.**—To an aqueous solution containing 5 g. of $[Co(OH_2)_2en_2](ClO_4)_3$[17] in 50 ml. of water, 2.2 g. of L-alanine was added. The mixture was then evaporated almost to dryness on a water bath at about 80°C. After cooling, the crude product obtained was dissolved in 80 ml. of water. To the solution was added 3.5 g. of potassium chloride, and then 10 ml. of methanol. The potassium perchlorate which was deposited was removed from the violetish-red solution by filtration. A few drops of concentrated hydrochloric acid and a small amount of ethanol were added to the filtrate, and the solution was kept in a refrigerator for several hours. The violetish-red crystals obtained were then washed with a water-ethanol mixture (1 : 1), with ethanol, and then with ether. This complex was recrystallized from water by adding a small amount of ethanol.

Found: C, 25.92; H, 6.66; 18.33. Calcd. for $CoC_{10}H_{30}N_6O_4Cl_3$: C, 25.90; H, 6.53; N, 18.13%.

***trans*-$[Co\ en_2(L\text{-serH})_2]Cl_3$, *trans*-$[Co\ en_2(L\text{-thrH})_2]Cl_3\cdot 2H_2O$, and *trans*-$[Co\ en_2(L\text{-prolH})_2]Br_3$.**—These complexes were prepared by procedures similar to that described above for the L-alanine complex.

Found: C, 24.39; H, 6.22; N, 17.40. Calcd. for $CoC_{10}H_{30}N_6O_6Cl_3$: C, 24.25; H, 6.11; N, 16.96%.

Found: C, 25.98; H, 7.00; N, 15.04; H_2O, 6.19. Calcd. for $CoC_{12}H_{34}N_6O_6Cl_3\cdot 2H_2O$: C, 25.73; H, 6.86; N, 15.01; H_2O, 6.43%.

Found: C, 25.96; H, 5.37; N, 13.11. Calcd. for $CoC_{14}H_{34}N_6O_4Br_3$: C, 26.30; H, 5.37; N, 13.15%.

***trans*-$[Co\ en_2(L\text{-leuH})_2]Br_3\cdot 2.5H_2O$.** — The violet needle crystals were separated by adding a large amount of acetone to a solution which was obtained by a method similar to that used for the L-alanine complex.

Found: C, 26.92; H, 6.54; N, 11.35; H_2O, 5.99. Calcd. for $CoC_{16}H_{44}N_6O_4Br_3\cdot 2.5H_2O$: C, 26.38; H, 6.51; N, 11.54; H_2O, 6.19%.

Measurements.—The visible and ultraviolet absorption spectra were measured by using a Beckman DU spectrophotometer. The CD curves were obtained by a Model ORD/UV-5 spectrophotometer of Japan Spectroscopic Co., and by a Shimadzu QR-50 spectrophotometer with a CD attachment, while the RD curves were recorded with an ORD/UV-5 spectrophotometer. The concentrations of complexes were 1/20 or 1/30 mole/l. for $[Co(NH_3)_5(L\text{-amH})]X_3$, 1/30 mole/l. for $[Co(L\text{-am})(NH_3)_4]X_2$, and 1/20 or 1/30 mole/l. for *trans*-$[Co\ en_2(L\text{-amH})_2]X_3$. All the measurements were made in aqueous solutions and at room temperature.

Results and Discussion

Circular Dichroism.—The CD and absorption data of $[Co(NH_3)_5(L\text{-amH})]^{3+}$ ions are summarized in Table I, while representative curves are shown, with their RD curves, in Fig. 1. The absorption curve is one typical of a $[Co\ N_5O]$-type complex; this indicates that the L-amino acid is coordinated to the cobalt(III) ion as a unidentate ligand.

Recently, Larsen and Olsen[18] have reported on the $[Co(NH_3)_5(OCOR^*)]^{2+}$ and *trans*-$[Co(NH_3)_4(OCOR^*)_2]^+$ of an optically-active carboxylic acid anion, $OCOR^{*-}$. According to their CD measurements, no CD band was found in the region of the first absorption band. All of the present complexes with L-amino acid as a unidentate ligand, however, exhibit CD bands in the corresponding region. These facts suggest that the

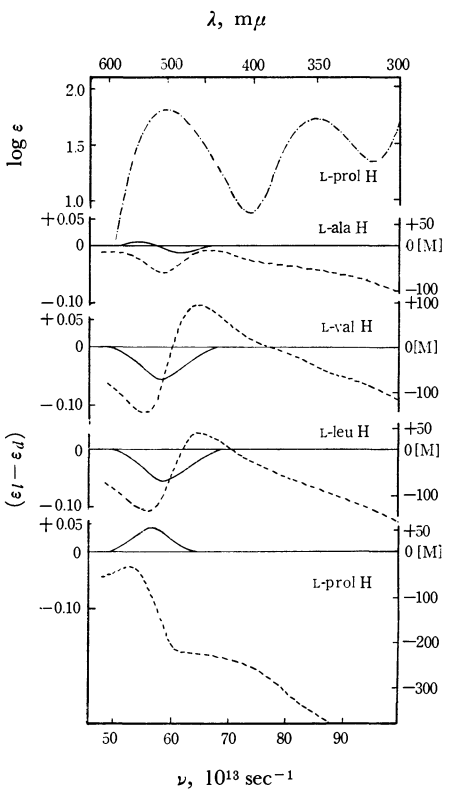

Fig. 1. Absorption (—·—), CD (——) and RD (- - -) curves of $[Co(NH_3)_5(L\text{-amH})]^{3+}$ ions.

18) E. Larsen and I. Olsen, *Acta Chem. Scand.*, **18**, 1025 (1964).

TABLE I. THE CD AND ABSORPTION DATA OF $[Co(NH_3)_5(L\text{-amH})]^{3+}$, $[Co(L\text{-am})(NH_3)_4]^{2+}$ AND *trans*-$[Co\ en_2(L\text{-amH})_2]^{3+}$ IONS IN AQUEOUS SOLUTIONS

Complex ion	I Band				II Band			
	λ_{ext}^{CD} mμ	$(\varepsilon_l-\varepsilon_d)$	λ_{max}^{AB} mμ	(log ε)	λ_{ext}^{CD} mμ	$(\varepsilon_l-\varepsilon_d)$	λ_{max}^{AB} mμ	(log ε)
$[Co(NH_3)_5(L\text{-alaH})]^{3+}$	543	$(+0.00_5)$	500	(1.83)	—	—	350	(1.73)
	484	(-0.01_5)						
$[Co(NH_3)_5(L\text{-serH})]^{3+}$	505	(-0.05_5)	500	(1.83)	—	—	350	(1.73)
$[Co(NH_3)_5(L\text{-valH})]^{3+}$	505	(−0.05)	500	(1.81)	—	—	350	(1.71)
$[Co(NH_3)_5(L\text{-thrH})]^{3+}$	508	(−0.10)	500	(1.82)	—	—	350	(1.72)
$[Co(NH_3)_5(L\text{-leuH})]^{3+}$	505	(−0.05)	500	(1.82)	—	—	350	(1.73)
$[Co(NH_3)_5(L\text{-phalaH})]^{3+}$	505	(-0.08_5)	500	(1.82)	—	—	348	(1.72)
$[Co(NH_3)_5(L\text{-prolH})]^{3+}$	525	(+0.04)	500	(1.85)	—	—	348	(1.93)
$[Co(L\text{-ala})(NH_3)_4]^{2+}$	547	(-0.02_5)	493	(1.89)	351	(−0.02)	348	(1.95)
	512	(+0.07)						
	495	(−0.22)						
$[Co(L\text{-leu})(NH_3)_4]^{2+}$	544	(−0.05)	492	(1.90)	350	(−0.06)	349	(1.97)
	505	(+0.04)						
	458	(−0.30)						
$[Co(L\text{-phala})(NH_3)_4]^{2+}$	546	(−0.06)	495	(1.91)	353	(−0.06)	348	(1.99)
	508	(+0.02)						
	458	(−0.34)						
$[Co(L\text{-prol})(NH_3)_4]^{2+}$	556	(−0.07)	495	(1.89)	342	(−0.05)	348	(2.00)
	508	(+0.42)						
	450	(−0.21)						
$[Co(L\text{-val})(NH_3)_4]^{2+}$	540	(−0.16)	495	(1.91)	353	(−0.07)	349	(1.97)
	462	(−0.34)						
$[Co(L\text{-isoleu})(NH_3)_4]^{2+}$	540	(-0.12_5)	493	(1.90)	355	(-0.06_5)	348	(1.96)
	460	(−0.32)						
$[Co(L\text{-ser})(NH_3)_4]^{2+}$	476	(−0.32)	492	(1.88)	355	(-0.02_5)	347	(1.95)
$[Co(L\text{-thr})(NH_3)_4]^{2+}$	469	(−0.30)	492	(1.90)	355	(−0.04)	348	(1.97)
trans-$[Co\ en_2(L\text{-alaH})_2]^{3+}$	550	(−0.14)	542	(1.72)	346	$(+0.03_8)$	355	(1.80)
	445	(-0.05_2)	446	(1.46)				
trans-$[Co\ en_2(L\text{-serH})_2]^{3+}$	548	(-0.28_6)	542	(1.72)	350	$(+0.03_8)$	355	(1.79)
	445	(-0.01_5)*	446	(1.46)				
trans-$[Co\ en_2(L\text{-leuH})_2]^{3+}$	552	(−0.33)	542	(1.74)	349	$(+0.05_5)$	355	(1.82)
	445	(-0.04_2)*	445	(1.46)				
trans-$[Co\ en_2(L\text{-thrH})_2]^{3+}$	550	(−0.34)	544	(1.74)	350	(+0.03)	355	(1.81)
	440	$(+0.01_1)$*	446	(1.47)				
trans-$[Co\ en_2(L\text{-prolH})_2]^{3+}$	540	(−0.03)	544	(1.74)	345	(+0.02)	355	(1.80)
	445	(−0.04)	443	(1.45)				

* These values were estimated from the curve analysis.

vicinal effect of the asymmetric carbon atom on the cobalt(III) ion may be more effective in the amino acid complexes than in the carboxylic acid complexes. The $[Co(NH_3)_5(L\text{-amH})]^{3+}$ ion belongs approximately to the C_{4v} symmetry, so two absorption components, $^1A_1 \rightarrow {}^1A_2$ and $^1A_1 \rightarrow {}^1E_a$, may be expected in the first absorption band region.[19] As may be seen in Fig. 1 and Table I, the L-alanine complex shows two weak CD bands, with signs opposite to each other. It is reasonable to assign these two CD bands to the transitions of $^1A_1 \rightarrow {}^1A_2$ and $^1A_1 \rightarrow {}^1E_a$.

The other L-amino acid complexes show only a negative CD band at about 505 mμ. It may be assumed that each single CD peak of these complexes is a residual one resulting from an overlap or a cancellation of the two CD components. On the other hand, a positive CD peak was observed for the L-proline complex at 525 mμ. The difference in sign between the L-proline complex and the other L-amino acid complexes may be explained from the occlusion of the asymmetric carbon atom of L-proline in a sieged pyrrolidine ring.

The CD and absorption data of the complex ions containing L-amino acid as a bidentate ligand are also summarized in Table I. Some CD and RD curves of these complex ions are shown in

19) H. Yamatera, This Bulletin, **31**, 95 (1958).

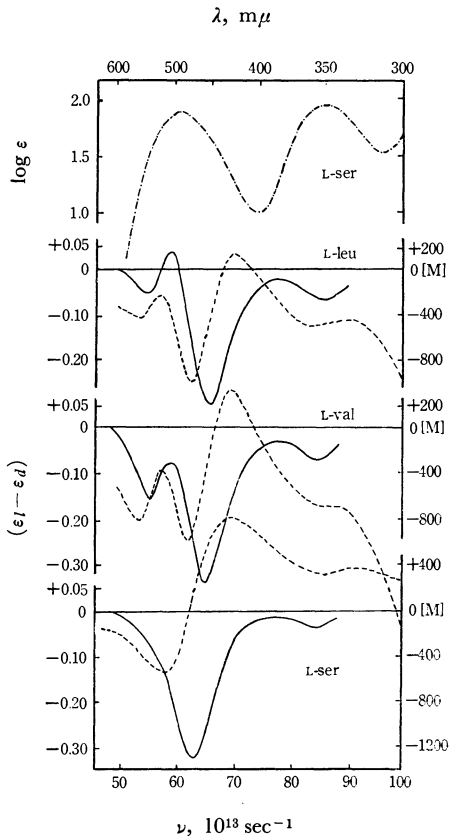

Fig. 2. Absorption (—·—), CD (——) and RD (- - -) curves of $[Co(L\text{-am})(NH_3)_4]^{2+}$ ions.

Fig. 2. The first absorption band does not show any indication of a split on the ordinary absorption curve. Now, the true symmetry of $[Co(L\text{-am})(NH_3)_4]^{2+}$ is C_1, so a T_{1g} level under an O_h symmetry should split into three ^1A levels, and three $^1A \rightarrow {}^1A$ transitions, which are magnetic-dipole allowed, should be observed in the first absorption band region. As may be seen in Fig. 2, the CD curve of the L-leucinato complex shows three components, at 544, 505 and 458 mμ, in this region. This fact suggests that the first absorption band of a complex of this type can actually split into three components.

Experimentally the L-amino-acidato-tetrammine complexes are divided into the following three groups, according to the behavoir of the CD curves in the region of the first absorption band:

(1) L-am=L-ala, L-leu and L-phala. The complexes of this group exhibit three CD bands in the first absorption band region; their signs are (−), (+) and (−) (from longer to shorter wavelengths).

(2) L-am=L-val and L-isoleu. These complexes exhibit two CD bands, of a negative sign, in the first absorption band region.

(3) L-am=L-ser and L-thr. These complexes exhibit only one CD band, of a negative sign, in the first absorption band region.

The differences among these groups are less explicit in their RD curves than in their CD curves.

Stereochemically, the differences among these complexes are concentrated in the three substituents, $R_{(1)}$, $R_{(2)}$ and $R_{(3)}$, on the β-carbon atom of the amino acid ligands; in the group 1, $R_{(1)}=R_{(2)}=H$ and $R_{(3)}=H$, $CH(CH_3)_2$ or C_6H_5; in group 2, $R_{(1)}=H$, $R_{(2)}=CH_3$ and $R_{(3)}=CH_3$ or C_2H_5; in group 3, $R_{(1)}=H$, $R_{(2)}=OH$ and $R_{(3)}=H$ or CH_3. By the construction of molecular models, it is shown that some intramolecular interactions exist between a coordinated ammonia molecule and the substituents on the β-carbon atom (Fig. 3).

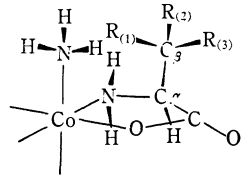

L-leu: $R_{(1)}=H$, $R_{(2)}=H$, $R_{(3)}=CH(CH_3)_2$
L-val: $R_{(1)}=H$, $R_{(2)}=CH_3$, $R_{(3)}=CH_3$
L-ser: $R_{(1)}=H$, $R_{(2)}=OH$, $R_{(3)}=H$

Fig. 3. The interaction between a coordinated ammonia molecule and substituted groups at the β-carbon atom of the chelated amino acid in $[Co(L\text{-am})(NH_3)_4]^{2+}$ ions.

Of course, internal rotations occur around the C_α—C_β axis, and it will be pointed out that, for example, the internal rotations are more hindered in the L-valinato complex ($R_{(1)}=H$, $R_{(2)}=R_{(3)}=CH_3$) than in the L-alaninato complex ($R_{(1)}=R_{(2)}=R_{(3)}=H$). In the group 3 complexes, the intramolecular interactions of another kind may also be possible, namely, a hydrogen bond between the coordinated ammonia and the $R_{(2)}=OH$ substituent on the β-carbon atom:

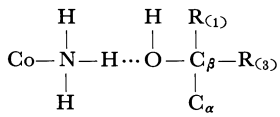

It is difficult, however, at present to relate the behavior of CD curves to the stereochemical differences considered above.

On the whole, the CD curve of $[Co(L\text{-prol})(NH_3)_4]^{2+}$ shows a behavior similar to that of the L-leucinato complex, but the positive CD component at about 508 mμ is more intense than that of the other complexes (Fig. 4 and Table I). As was pointed out in previous papers,[6,7] the asymmetric nitrogen atom of the bidentatically-coordinated L-prolinate has a forced configuration antipodal to that of the similarly-coordinated D-prolinate. In the present complex, one of the reasons why the CD band at 508 mμ predominates is the vicinal effect of such a nitrogen atom of the L-prolinate.

TABLE II. THE ROTATORY PARAMETERS AND ROTATORY CD

L-amH	K	λ_K^{CD} mμ	$(\varepsilon_l-\varepsilon_d)_{ext}$	Δ_K^{CD} (red) mμ	Δ_K^{CD} (blue) mμ	R_K^{CD} {×10^{42}(c.g.s.)}
L-alanine	Ia	550	−0.140	46.7	46.3	−48.1
	Ib	445	−0.052	45.0	46.0	−21.6
	II	346	+0.033	31.8	30.2	+12.0
L-serine	Ia	548	−0.286	50.7	50.5	−107
	Ib	445	−0.015	38.3	39.5	−5.32
	II	350	+0.033	27.3	28.0	+10.6
L-leucine	Ia	552	−0.330	49.0	49.0	−119
	Ib	445	−0.042	33.0	39.0	−13.8
	II	349	+0.055	26.0	25.0	+16.3
L-threonine	Ia	550	−0.340	49.5	51.8	−127
	Ib	440	+0.011	30.0	29.0	+2.99
	II	350	+0.030	30.5	29.2	+10.4

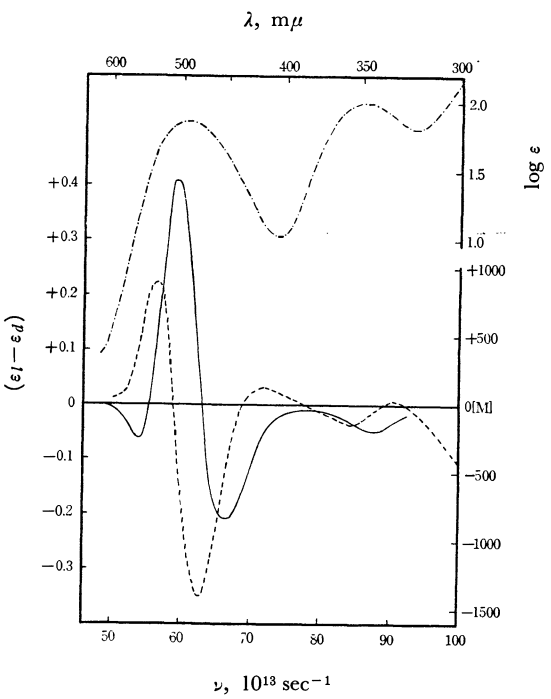

Fig. 4. Absorption (—·—), CD (——) and RD (- - -) curves of $[Co(L\text{-prol})(NH_3)_4]^{2+}$ ion.

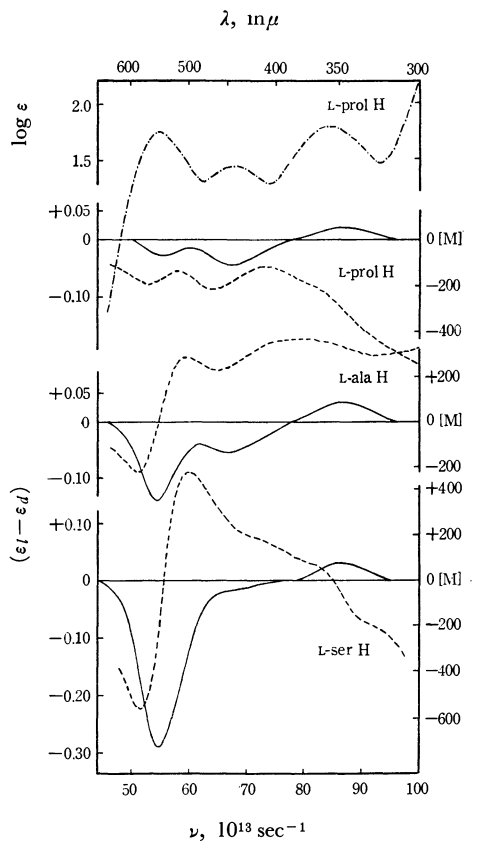

Fig. 5. Absorption (—·—), CD (——) and RD (- - -) curves of *trans*-$[Co\,en_2(L\text{-amH})_2]^{3+}$ ions.

Single negative CD bands are commonly observed in the second absorption band region of the $[Co(L\text{-am})(NH_3)_4]^{2+}$ complexes. They are all almost the same in magnitude and are located in the region from 342 to 355 mμ; these CD bands will be useful in the determination of the configurations of amino acids.

The CD and absorption data of *trans*-$[Co\,en_2(L\text{-amH})_2]^{3+}$ ions are listed in Table I, while their CD and RD curves are shown in Figs. 5 and 6. Their absorption spectra coincide well with those of *trans*-$[Co(OCOR)_2en_2]^+$ and of *trans*-$[Co(OCOR)_2(NH_3)_4]^+$.[20] It is well known that the first absorption band of the *trans*-$[Co\,N_4O_2]$-type complex with the D_{4h} symmetry splits into two components, Ia ($^1A_{1g} \rightarrow {}^1E_g$) and Ib ($^1A_{1g} \rightarrow {}^1A_{2g}$),[20,21] which are magnetic-dipole allowed.

20) M. Linhard and M. Weigel, *Z. anorg. Chem.*, **264**, 321 (1951).
21) K. Kuroda and P. S. Gentile, This Bulletin, **38**, 1368 (1965); ibid., **38**, 2159 (1965).

STRENGTHS FOR THE *trans*-[Co en$_2$(L-amH)$_2$]$^{3+}$ COMPLEX ION

RD								
λ_K^{RD} mμ	$[M]_{ext}$ (red)	$[M]_{ext}$ (blue)	Δ_K^{RD} (red) mμ	Δ_K^{RD} (blue) mμ	R_K^{RD} {$\times 10^{42}$(c.g.s.)}	R_K^{RD}/R_K^{CD}	$[M]=\frac{k}{\lambda^2-\lambda_0^2}$ $\lambda_0(\mu)$	k
547	−245	+280	40.0	48.0	−46.1	0.96	0.216	+16.2
440	−85	+95	42.0	39.0	−18.1	0.84		
341	+61	−61	29.0	29.0	+11.3	0.94		
543	−530	+555	43.0	47.0	−98.2	0.92	0.265	−9.1
442	−34	+32	34.5	32.0	−5.42	1.02		
346	+56	−56	30.0	30.0	+10.7	1.00		
550	−615	+635	45.0	46.2	−113	0.95	0.246	+7.5
443	−89	−76	32.8	33.3	−13.4	0.97		
351	+93	+91	24.2	25.0	+14.1	0.87		
551	−609	+650	45.0	49.0	−117	0.92	0.245	−29.0
448	+22	−20	30.0	26.0	+2.87	0.96		
353	+66	−64	25.5	22.0	+9.55	0.92		

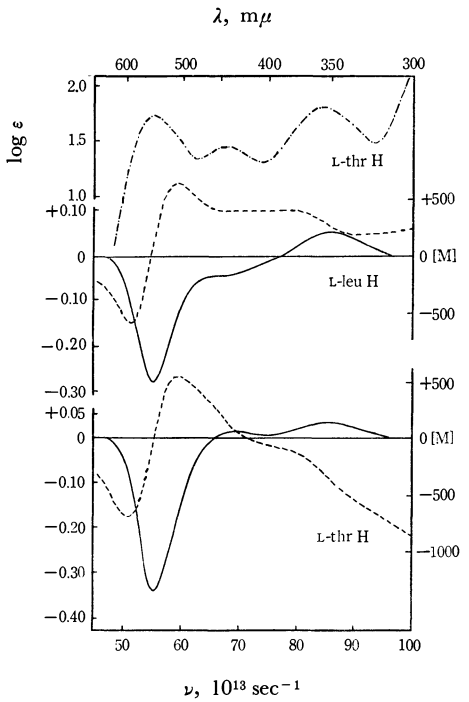

Fig. 6. Absorption (—·—) CD (——) and RD (- - -) curves of *trans*-[Co en$_2$(L-amH)$_2$]$^{3+}$ ions.

The absorption and the CD spectra of *trans*-[Co-en$_2$(L-amH)$_2$]$^{3+}$ exhibit the two first band components; their extremum positions are consistent with each other (Table I).

In the region of the second absorption band, the CD bands of the *trans*-[Co en$_2$(L-amH)$_2$]$^{3+}$-type complexes are situated in a narrow range from 350 to 345 mμ. It is interesting that all of these CD bands have a positive sign, in contrast to those of the [Co(L-am)(NH$_3$)$_4$]$^{2+}$-complex ions.

Rotatory Strength.—In general, it is quite difficult to analyze the observed CD and RD curves into individual component curves, since the first or the second absorption bands are contributed by two or three absorption components which are located very close to each other. When the absorption band splits largely, however, the analysis can be made easily and precisely. In the case of the first absorption band of *trans*-[Co en$_2$(L-amH)$_2$]$^{3+}$, this condition is quite well satisfied, as may be seen in Figs. 5 and 6. The rotatory parameters and rotatory strengths of the individual absorption components were calculated by curve analyses from the observed CD and RD curves of *trans*-[Co en$_2$(L-amH)$_2$]$^{3+}$; the results are summarized in Table II.

The RD curves were analyzed using Moscowitz's Eq. 1:[22]

$$[M_K(\lambda)] = \frac{2[\theta^\circ_K]}{\sqrt{\pi}}\left[\exp\left(-\frac{\lambda-\lambda_K^{CD}}{\Delta_K^{CD}}\right)^2 \times \int_0^{\lambda-\lambda_K^{CD}/\Delta_K^{CD}} e^{x^2}dx - \frac{\Delta_K^{CD}}{2(\lambda+\lambda_K^{CD})}\right] \quad (1)$$

where $[\theta^\circ_K] \simeq 3300(\varepsilon_l-\varepsilon_d)_{ext}$ is the extremum value of the CD band for the Kth transition, λ_K^{CD} is the wavelength of the CD band extremum, and Δ_K^{CD} is the $1/e$-halfwidth of the CD band.

The curve analyses were made by the following steps. In the first, the CD bands which were assumed to be Gaussian on the wavelength scale of the abscissa were separated from the observed CD curve by using the equation:

$$(\varepsilon_l-\varepsilon_d) = (\varepsilon_l-\varepsilon_d)_{ext} \exp\{-(\lambda-\lambda_K^{CD})^2/(\Delta_K^{CD})^2\} \quad (2)$$

Each inversive RD curve was calculated by substituting the parameters estimated from the Gaussian CD band into Eq. 1, and then the resultant individual RD curves were subtracted from the observed RD curve. From the residual curve, the constants in Drude's equation (λ_0 and k) were

22) A. Moscowitz, "Optical Rotatory Dispersion" (C. Djerassi, ed.), McGraw-Hill, New York (1960), p. 150.

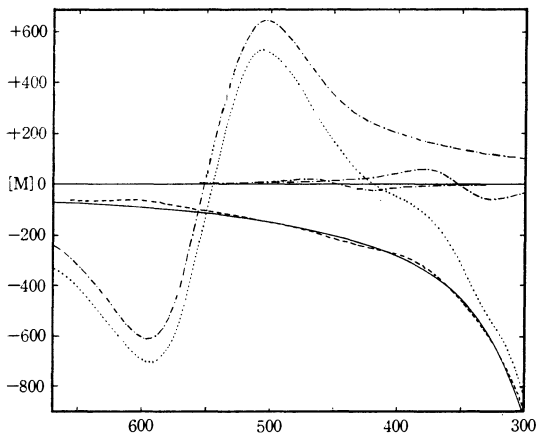

Fig. 7. The analyses of RD curves of *trans*-[Co en$_2$(L-thrH)$_2$]$^{3+}$ ion; (·····) observed RD curve, (—·—) individual RD curves of each absorption components, (- - -) observed curve minus the sum of individual RD curves and (——) Drude's curve.

estimated by the method of Lowry[23] (Table II).

In the second step, independent of the CD data mentioned above, the individual RD curve of each absorption component was again determined by subtracting Drude's curve from the observed RD curve, and by analyzing the residual curve into several individual RD curves. These treatments were made separately both on the longer and on the shorter wavelength sides of the inversive center, λ_K^{RD}. The individual RD components obtained for *trans*-[Co en$_2$(L-thrH)$_2$]$^{3+}$ are shown in Fig. 7 as an example.

It is possible to estimate the rotatory strengths from the data of the CD bands in the first step, and also from the RD data in the second step.

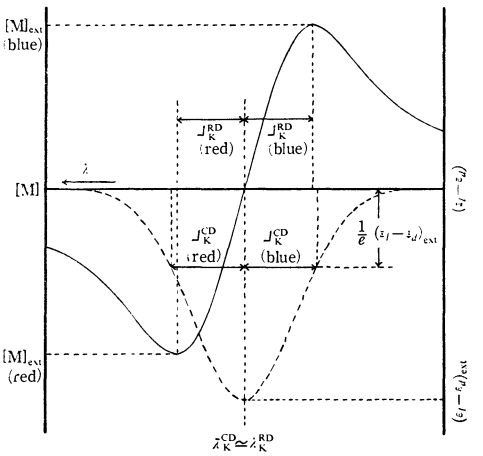

Fig. 8. Parameters for the isolated CD and RD curves.

The rotatory strength from the CD data, R_K^{CD}, is given by:

$$R_K^{CD}\simeq 2.03\times 10^{-39}(\varepsilon_l-\varepsilon_d)_{ext}\{\Delta_K^{CD}(\text{red})+\Delta_K^{CD}(\text{blue})\}/(\lambda_K^{CD}) \quad (3)$$

while the rotatory strength from the RD data, R_K^{RD}, is given by:

$$R_K^{RD}\simeq 5.46\times 10^{-43}\{[M]_{ext}(\text{red})-[M]_{ext}(\text{blue})\}\times\{\Delta_K^{RD}(\text{red})+\Delta_K^{RD}(\text{blue})\}/(\lambda_K^{RD}) \quad (4)$$

The parameters which appear in Eqs. 3 and 4 are defined as in Fig. 8, and a relation, $\Delta_K^{RD}\simeq 0.9233\times\Delta_K^{CD}$, exists[24] for the ideal case in which Moscowitz's Eq. 1 holds perfectly.

As may be seen in Table II, the experimental values of R_K^{CD} are approximately equal to those of R_K^{RD}; furthermore, the positions of λ_K^{RD} coincide well with those of λ_K^{CD} within the range of ± 5 mμ. These facts prove the adequacy of the equations used and of the curve analyses.

23) T. M. Lowry, "Optical Rotatory Power," Longmans, Green and Co., London (1935), p. 419.

24) F. Woldbye, *Tech. Inorg. Chem.*, **4**, 249 (1965).

BULLETIN OF THE CHEMICAL SOCIETY OF JAPAN VOL. 39 2425—2429 (1966)

The Oligomerization of Isoprene by Cobalt or Iron Complex Catalysts

By Akira MISONO, Yasuzo UCHIDA, Masanobu HIDAI and Yoshiro OHSAWA

Department of Industrial Chemistry, Faculty of Engineering, The University of Tokyo, Hongo, Tokyo

(Received November 26, 1965)

The reaction of isoprene by the catalyst systems composed of cobalt(III) or iron(III) acetylacetonate, an electron donor, and triethylaluminum was studied. It was found that isoprene is selectively dimerized to form a mixture of 1, 5- and 2, 5-dimethyl-1, 5-cyclooctadiene by the catalyst prepared by the reaction of iron(III) acetylacetonate, 2, 2'-dipyridyl, and triethylaluminum. The intermediate complex of the reaction was then examined by studying the effects of the molar ratio of the catalyst components on the reaction or by the measurement of the electronic absorption spectra of the reaction solution. The reaction of butadiene with the catalyst systems described above was also carried out and compared with that of isoprene.

Several complex catalyst systems for the selective dimerization or trimerization of butadiene have been reported, most of them composed of first-row transition metal complexes and organometallic compounds. On the other hand, only a few complex catalyst systems for the dimerization or trimerization of isoprene[1] have been found, although various cyclic dimers of isoprene have been obtained by thermal or photosensitized reaction. It has now been found that isoprene is selectively dimerized to form a mixture of 1, 5- and 2, 5-dimethyl-1, 5-cyclooctadiene by the catalyst combining iron(III) acetylacetonate, triethylaluminum, and a proper bidentate electron donor such as 2, 2'-dipyridyl or *o*-phenanthroline. This paper will be concerned with the reaction of isoprene by the catalyst systems composed of cobalt(III) or iron(III) acetylacetonate, an electron donor, and triethylalumium, in particular, by the above-mentioned catalyst system. Moreover, the intermediate complex of the reaction will be discussed by studying the effects of the molar ratio of the catalyst components on the reaction and by analyzing the electronic absorption spectra of the reaction solution.

Experimental

Reagents. — Isoprene and 2, 3-dimethylbutadiene were dried over anhydrous calcium sulfate and distilled under an atmosphere of nitrogen.

Triethylaluminum (Ethyl Corp., U. S. A.) was used without further purification.

The electron donors were those of commercial reagents or were prepared by the usual methods.

Benzene was purified by conventional procedures.

Procedure.—Experiments were carried out in a 30-ml. glass tube, a 200-ml. glass autoclave, or a 100-ml. stainless autoclave. Benzene, isoprene and triethylaluminum were added in a dry nitrogen atmosphere.

In a typical reaction, 20 ml. of benzene, 10 ml. of isoprene, and 0.33 g. of triethylaluminum were added, in this order, to an autoclave which had been charged with 0.353 g. of iron(III) acetylacetonate and 0.156 g. of 2, 2'-dipyridyl. The autoclave was then heated at 90°C and stirred for 1 hr.

After the reaction, the solution was washed with dilute hydrochloric acid and with water, and dried over anhydrous sodium sulfate. Then the solution was fractionated by distillation. The dimers were isolated by fractional distillation at a reflux ratio of at least 1 : 6 in a rectifying column, or by preparative gas chromatography. For the analysis of the products, gas chromatography was also used.

Analysis.—*Gas Chromatography.*—The dimers of isoprene were analyzed by using a copper tube (3 m. long and 4 mm. in diameter) packed with polydiethylene glycol succinate on Diasolid (Nihon Kuromato, Ltd.). The conditions were as follows; column temperature, 110°C; flash evaporator temperature, 220°C; carrier gas (helium) speed, 30 ml./min. The isomers of dimethyl-1, 5-cyclooctadiene were detected by using a 3 m. β, β'-oxydipropionitrile column (column temperature, 124°C; flash evaporator temperature, 220°C; carrier gas speed, 30 ml./min.).

Infrared Spectra.—The infrared spectra of the products were taken with a Nihon-bunko double-beam spectrometer, Model 401-G.

Electronic Spectra.—The electronic spectra of the reaction solution were recorded by using 0.1 mm.-path-length spacer cells on a Hitachi spectrometer Model EPS.

NMR Spectra.—The spectra were recorded on a Nihon Denshi apparatus JEOL Model 3H-60.

Results and Discussion

Structural Assignments of Products.—The products formed by the reaction of isoprene with a catalyst combining cobalt or iron acetylacetonate, an electron donor, and triethylaluminum are given in Table I. The product with a relative retention time below 3.7 based on benzene was supposed to be a dimer of isoprene.

1) L. I. Zaharkin, *Doklady Akad. Nauk, SSSR,* **131**, 1069 (1960); G. Wilke, *Angew. Chem.*, **75**, 10 (1963); L. I. Zaharkin, *Izv. Akad. Nauk, SSSR,* **1964**, 168.

TABLE I. REACTION PRODUCTS OF ISOPRENE BY IRON OR COBALT COMPLEX CATALYSTS

Catalyst	Products							
	1.6	2.3	2.7	3.0	3.7	6.0	6.3*	Polymer
Fe-Al		t	t	t	t			m
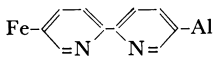	s	s			l			
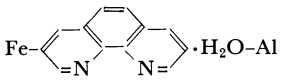	t	s	t		m			
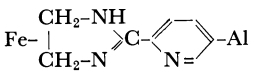		t	t	t	s			m
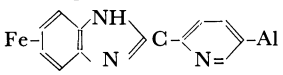								l
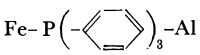					t			
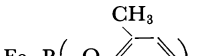								l
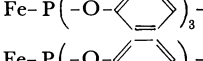								l
Co-Al	t	s			s	t	s	l
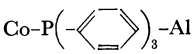		t			t			
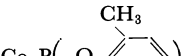		t			t			

Abbreviations:

Fe: iron(III) acetylacetonate, Co: cobalt(III) acetylacetonate, Al: triethylaluminum

The yields of the products were indicated by the symbols l (above 50%), m (10—50%), s (1—10%), and t (below 1%).

* Relative retention time of product based on benzene

Reaction conditions:

Al/Fe: 3; Donor/Metal acetylacetonate: 1 (mole ratio); React. temp.: 90°C; React. time: 1 hr.

The analytical gas chromatography of reaction products formed by the catalyst prepared by the reaction of iron(III) acetylacetonate, 2, 2'-dipyridyl, and triethylaluminum showed three peaks, of which the relative retention times were 1.6, 2.3, and 3.7 respectively. Here, at present, these will be designated as A, B, and C respectively, in which C was the main product, the yields of A and B being low. The main product, C, was isolated by fractional distillation. The analytical results of C were as follows, where the values in parentheses are the theoretical values calculated for $C_{10}H_{16}$;

Molecular weight	138 (136)
Elementary analysis	C: 87.70%, H: 11.82% (C: 88.17%, H: 11.84%)
Refractive index	n_D^{20}: 1.4881
Boiling point	80°C/23 mmHg
Iodine value	350

The results of molecular weight determination, elementary analysis, and iodine value indicated that C had the formula of $C_{10}H_{16}$, with two double bonds; hence, it was considered a cyclodimer. Twelve cyclodimers of isoprene of $C_{10}H_{16}$ can be formulated; their structures may be grouped as six cyclobutenes, four cyclohexenes, and two cyclooctadienes. All of cyclobutenes and cyclohexenes contain one terminal vinyl or methylene group at least. The infrared spectrum of C (shown in Fig. 1), however, showed no bands characteristic of the group. Therefore, C was supposed to be 1, 5-dimethyl-1, 5-cyclooctadiene (I), or 2, 5-dimethyl-1, 5-cyclooctadiene (II), or a mixture of them. The infrared spectrum, the boiling point, and the refractive index of C were essentially identical with those of a mixture of I and II given

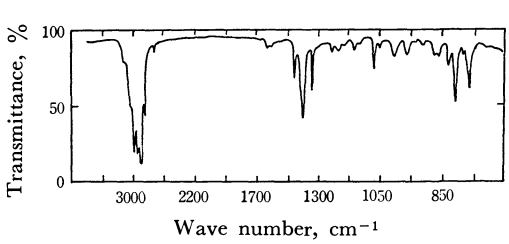

Fig. 1. Infrared spectrum of the fraction of b. p. 80°C/23 mmHg.

by Binder.[2] Furthermore, on the basis of the relative intensities of the bands in the infrared specturm at 1070 and 1093 cm^{-1} which have been considered to be characteristic of I and II respectively,[3] it was concluded that C was a mixture of I and II, and that II was the main constituent. These two isomers, I and II, were also detected by gas chromatography by using a β, β'-oxydipropionitrile column; here the ratio of II to I was determined to be about 4. On the other hand, the NMR spectrum of C (shown in Fig. 2) showed three resonances, at 8.3, 7.8, and 4.8 τ, which were assigned, respectively, to six

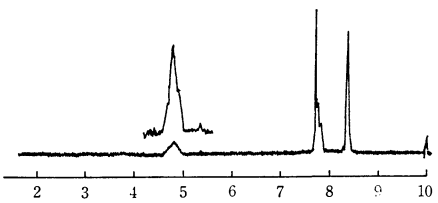

Fig. 2. NMR spectrum of the fraction of b. p. 80°C/23 mmHg.

methyl protons next to a double bond, eight methylene protons next to a double bond, and two ethylenic protons.

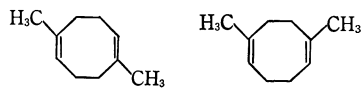

(I) (II)

The boiling points of A and B were so near that their separation was difficult. As they were also formed in the case of thermal reaction, however, they were considered to be thermal dimers. The fraction with a b. p. of 75—77°C/23 mmHg was about 70% B and 30% C. By the infrared spectrum of the fraction, B was identified as 1-methyl-4-isopropenyl-1-cyclohexene or/and 2-methyl-4-isopropenyl-1-cyclohexene. The fraction with a b. p. of 69—71°C/23 mmHg was about 50% A and 50% B. The infrared spectrum of the fraction indicated that A was 1, 4-dimethyl-4-vinyl-1-cyclohexene or/and 2, 4-dimethyl-4-vinyl-1-cyclohexene.

The Effects of Electron Donors.—Table II shows the effects of electron donors upon the reaction of isoprene with the catalyst prepared by the reaction of iron(III) acetylacetonate and triethylaluminum. Isoprene did not react to the catalyst composed of iron(III) acetylacetonate, triphenylphosphine, and triethylaluminum, although the linear dimers are formed in the case of butadiene.[4] When triphenylphosphite or tri(*o*-tolyl)phosphite was added as a catalyst component, polymers were formed. The addition of a bidentate ligand such as 2, 2'-dipyridyl or *o*-phenanthroline gave the cyclodimers selectively, while the addition of a bidentate ligand such as 2(2'-pyridyl)imidazoline or 2(2'-pyridyl)benzimidazole led to the formation of polymers. These facts indicate that the reaction of isoprene by the catalyst composed of iron(III) acetylacetonate, an electron donor and triethylaluminum was greatly affected by the nature of the electron donor as a catalyst component.

TABLE II. EFFECTS OF ELECTRON DONORS UPON THE REACTION OF ISOPRENE BY THE CATALYST COMPOSED OF IRON(III) ACETYLACETONATE AND TRIETHYLALUMINUM

Donor	Conv. %	Yield of dimers, %	
none	30	t	
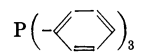	9		
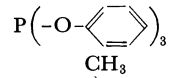	74	t	polymer
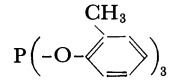	54	t	polymer
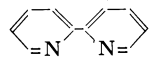	100	92	
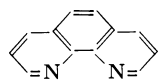	67	36	
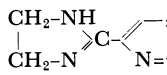	50	5	polymer
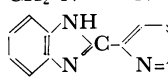	100		polymer

Reaction conditions:
Al/Fe: 3; C_5H_8/Fe: 100; Donor/Fe: 1;
React. temp.: 90°C; React. time: 1 hr.

The Reaction of Isoprene by the Catalyst Composed of Iron(III) Acetylacetonate, 2, 2'-Dipyridyl and Triethylaluminum.—*The Effects of the Molar Ratio of the Catalyst Components.*—The effects of the molar ratio of 2, 2'-dipyridyl to iron-(III) acetylacetonate on the reaction are shown in Fig. 3. The most active catalyst system for the cyclic dimerization was formed when one mole of 2, 2'-dipyridyl was added to one mole of iron(III) acetylacetonate. When more than one mole of 2, 2'-dipyridyl was added to one mole of iron(III) acetylacetonate, both the conversion of isoprene and the yield of the cyclic dimers decreased. The same phenomena had been observed in the cyclic dimerization of butadiene with the same catalyst system.[4] On the other hand, 2, 3-dimethyl-1, 3-butadiene did not react with the same catalyst.

2) J. L. Binder, K. C. Eberly and G. E. P. Smith, *J. Polymer Sci.*, **38**, 229 (1959).
3) G. S. Hammond, *J. Org. Chem.*, **28**, 3302 (1963).
4) M. Hidai, K. Tamai, Y. Uchida and A. Misono, This Bulletin, to be published.

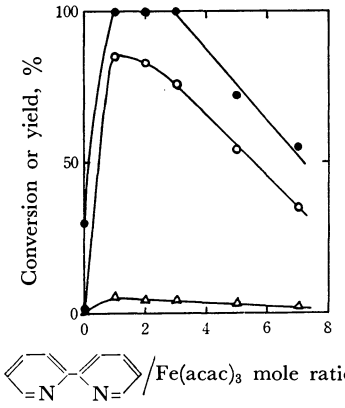

Fig. 3. Effect of molar ratio of 2, 2'-dipyridyl to iron(III) acetylacetonate.
●: Conversion of isoprene, %
○: Yield of 1,5(2,5)-dimethyl-1,5-cyclooctadiene, %
△: Yield of 1(2)-methyl-4-isopropenyl-1-cyclohexene, %
Reaction conditions:
$AlEt_3/Fe(acac)_3$: 3; $C_5H_8/Fe(acac)_3$: 100;
Reactn. time: 1 hr.; Reactn. temp.: 90°C

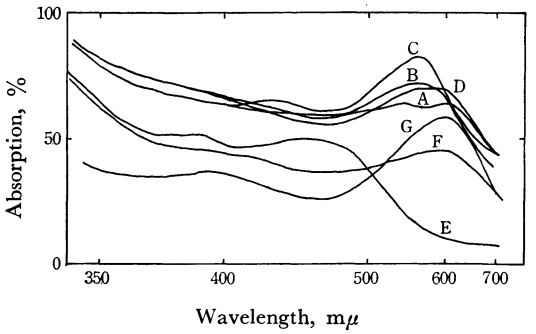

Fig. 4. Electronic absorption spectra of reaction solutions.
Molar ratios are as follows;
A: Fe : Dip : Al : Bz = 1 : 1 : 3 : 10^3
B: Fe : Dip : Al : IP : Bz = 1 : 1 : 3 : 70 : 10^3
C: Fe : Dip : Al : BD : Bz = 1 : 1 : 3 : 10^2 : 10^3
D: Fe : Dip : Al : DMBD : Bz = 1 : 1 : 3 : 70 : 10^3
E: Fe : Dip : Al : IP : Bz = 1 : 1 : 8 : 70 : 10^3
F: Fe : Dip : Al : IP : Bz = 1 : 8 : 3 : 70 : 10^3
G: Benzene solution of $Fe(dip)_2Et_2$[5] prepared by the reaction of $Fe(acac)_3$, 2, 2'-dipyridyl, and $AlEt_2(OEt)$ in ether
where
Fe: $Fe(acac)_3$, Dip: 2,2'-dipyridyl, Al: $AlEt_3$, Bz: benzene, IP: isoprene, BD: butadiene, DMBD: 2,3-dimethylbutadiene.

Figure 4 shows the electronic absorption spectra of the solution prepared by the reaction of iron(III) acetylacetonate, 2, 2'-dipyridyl, triethylaluminum and a diene monomer in various ratios at room temperature. The solution obtained by the reaction of iron(III) acetylacetonate, 2, 2'-dipyridyl, and triethylaluminum (molar ratio; 1 : 1 : 3) showed a maximum absorption peak at about 600 mμ and a dark blue color. This absorption peak, which was considered to be due to the charge transfer between the iron atom and 2, 2'-dipyridyl, shifted to about 550 mμ and the solution became purple when butadiene or isoprene was present. However, the shift was not observed when an excess of 2, 2'-dipyridyl was added.

These facts indicate that a dark blue complex is formed by the reaction of iron(III) acetylacetonate, 2, 2'-dipyridyl, and triethylaluminum, and that this blue complex is changed into a purple complex by the addition of butadiene or isoprene, in which the diene monomers besides 2, 2'-dipyridyl are coordinated to a low valent iron atom. When an excess of 2, 2'-dipyridyl is present, the ligands occupy all, or at least the greater part, of the coordinating sites of the low valent iron atom and, therefore, prevent the approach of the diene monomer. Thus, when an excess of 2, 2'-dipyridyl was present, the reaction of isoprene was depressed. On the other hand, the fact that the solution obtained by the reaction of iron(III) acetylacetonate, 2, 2'-dipyridyl, and triethylaluminum (molar ratio: 1 : 1 : 3) in the presence of 2, 3-dimethyl-1, 3-butadiene was dark blue indicates that the monomer is not coordinated to the low valent iron atom.

Figure 5 shows the effects of the molar ratio of triethylaluminum to iron(III) acetylacetonate on the reaction. When the molar ratio of triethylaluminum to iron(III) acetylacetonate was below 3, the reaction solution was purple and the cyclic

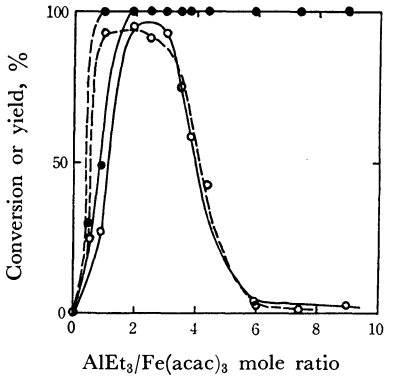

Fig. 5. Effect of molar ratio of triethylaluminum to iron(III) acetylacetonate.
●: Conversion of isoprene, %
○: Yield of cyclic dimers, %
——: Reactn. temp., 40°C
----: Reactn. temp., 50°C
Reaction conditions:
=N N= /$Fe(acac)_3$: 1; $C_5H_8/Fe(acac)_3$: 100;
Reactn. time: 1 hr.

5) A. Yamamoto, K. Morifuji, S. Ikeda, T. Saito, Y. Uchida and A. Misono, *J. Am. Chem. Soc.*, **87**, 4652 (1965).

Table III. Effects of mixing order of catalyst components

Mixing order	Reactn. temp. °C	Reactn. time min.	Conv. %	Yield of cyclic dimers, %
Fe-Dip-Bz-IP-Al	50	60	100	96
Fe-Dip-Bz-Al-IP	50	60	92	88
Fe-Dip-Bz-BD-Al	50	240	73	45
Fe-Dip-Bz-Al-BD	50	300	30	25

Reaction conditions:
Fe/Al: 3; Dip/Fe: 1; IP/Fe: 100; BD/Fe: 200 (mole ratio)

dimers of isoprene were formed selectively. However, when the molar ratio was above 6, the reaction solution turned reddish brown, as is shown in Fig. 4, and only polymers were formed.

The Effect of the Mixing Order of the Catalyst Components. — In the dimerization of butadiene with a cobalt complex catalyst or in the trimerization of butadiene with an iron complex catalyst, it has been reported that the order of mixing the catalyst components and butadiene had a great effect on the reaction.[6] The effects of the mixing order of the catalyst components on the formation of the cyclic dimers of isoprene or butadiene by the catalyst composed of iron(III) acetylacetonate, 2, 2'-dipyridyl, and triethylaluminum are shown in Table III. Evidently the rate of the formation of the cyclic dimers was greater when iron(III) acetylacetonate, 2, 2'-dipyridyl, isoprene or butadiene, and triethylaluminum were mixed in this order than when triethylaluminum was allowed to react with iron(III) acetylacetonate and 2, 2'-dipyridyl in the absence of isoprene or butadiene. These results indicate that when iron(III) acetylacetonate and 2, 2'-dipyridyl are reacted with triethylaluminum in the presence of the diene monomer, a purple complex, which is supposed to be an intermediate complex for the cyclic dimerization, is easily formed, while when iron(III) acetylacetonate, 2, 2'-dipyridyl, triethylaluminum, and the diene monomer are mixed in this order, the dark blue complex first formed by the reaction of iron(III) acetylacetonate, 2, 2'-dipyridyl and triethylaluminum does not easily react with the diene monomer to form the purple complex.

A Comparison of Isoprene and Butadiene.— It has been reported that butadiene is dimerized to form the linear dimers by the cobalt complex catalyst prepared by the reaction of cobalt(III) acetylacetonate and triethylaluminum or by the iron complex catalyst prepared by the reaction of iron(III) acetylacetonate, triphenylphosphine, and triethylaluminum.[4,6] However, in these catalyst systems, the reactivity of isoprene was not so great as butadiene and linear dimers were not formed. On the other hand, when the catalyst composed of iron(III) acetylacetonate, 2, 2'-dipyridyl, and triethylaluminum was used, with which butadiene is dimerized to form the cyclic dimers, isoprene reacted more easily than butadiene and the cyclic dimers were similarly formed. These facts indicate that the coordination state of a diene monomer to a low valent cobalt or iron tom in the case of the formation of linear dimers is different from that in the case of the formation of cyclic dimers, and that isoprene is not likely to have a coordination state giving linear dimers.

6) T. Saito, T. Ohno, Y. Uchida and A. Misono, *J. Chem. Soc. Japan, Ind. Chem. Sect. (Kogyo Kagaku Zasshi)*, **66**, 1099 (1963); M. Hidai, Y. Uchida and A. Misono, This Bulletin, **38**, 1243 (1965).

BULLETIN OF THE CHEMICAL SOCIETY OF JAPAN VOL. 39 2430—2433 (1966)

Studies of the Organic Reaction of Metal Carbonyl. X.* The Oxo Reaction of Ethyl Acrylate—The Effects of the Reaction Conditions on the Distribution of the Products

By Yoshinobu TAKEGAMI, Chikao YOKOKAWA and Yoshihisa WATANABE

Department of Fuel Chemistry, Faculty of Engineering, Kyoto University, Sakyo-ku, Kyoto

(Received November 26, 1965)

The ratio between the α- and β-carbethoxypropionaldehyde formed in the oxo reaction of ethyl acrylate is affected by various reaction conditions; the proportion of β-carbethoxypropionaldehyde increases with an increase in the reaction temperature, but decreases with an increase in the partial pressure of carbon monoxide or hydrogen. These effects can be explained on the basis of the reaction mechanism between cobalt hydrocarbonyl and ethyl acrylate (Y. Takegami et al., This Bulletin, **37**, 1190 (1964)): in the first step of the reaction, ethyl acrylate reacts with cobalt hydrocarbonyl to give, selectively, α-carbethoxypropionylcobalt carbonyl (I), and then I isomerizes to β-carbethoxypropionylcobalt carbonyl (II). Accordingly, the rates of two competitive reactions, the isomerization of I to II and the reduction of I to the corresponding aldehyde, may be the factors determining the distribution of the oxo reaction products. Under the oxo reaction conditions, the isomerization of I to II seems to occur more easily at a relatively high temperature and to be prohibited by a high pressure of carbon monoxide. On the other hand, a relatively high pressure of hydrogen seems to be favorable to the reduction of I to the aldehyde.

Previous work[1] in this laboratory has demonstrated that the reaction of ethyl acrylate with cobalt hydrocarbonyl gives two isomeric acylcobalt carbonyls (α- and β-carbethoxypropionylcobalt carbonyl); that is, in the first step of the reaction, the α-carbon atom of the ethyl acrylate is selectively carbonylated to give α-carbethoxypropionylcobalt carbonyl, and then this isomerizies to the acylcobalt carbonyl with a straight chain structure. This fact strongly indicates that, in the reaction between cobalt hydrocarbonyl and olefin, the rates of the addition of cobalt hydrocarbonyl to an olefinic bond and the isomerization of acylcobalt carbonyls are the factors determining the distribution of the products. It is reasonable to consider that, under the oxo conditions, such an isomerization of acylcobalt carbonyls occurs, having a great effect on the distribution of the products. In the oxo reaction of 1-olefins, the effect of the reaction conditions on the distribution of the products has been studied in detail by several workers.[2] However, no attention has been paid to the effect of the isomerization of acylcobalt carbonyls.

The aim of the present investigation is to study whether the isomerization of alkyl and acylcobalt carbonyls does indeed occur in the oxo reaction of ethyl acrylate, by examining in detail the effects of various reaction conditions.

Experimental

Reaction Procedures.—An autoclave (300 ml.), made of 18-8 nickel-chrom-iron steel and equipped with a magnetic stirrer, was used. Eighty milliliters of toluene, 10 ml. of a dicobalt octacarbonyl solution in toluene (containing 0.22 to 0.24 g. of cobalt as calculated from the carbonyl content), and 20 ml. of ethyl acrylate were placed into the autoclave. After the air in the autoclave had been replaced with hydrogen, hydrogen and carbon monoxide were introduced at certain pressures. The autoclave was then kept at a certain temperature until the guage pressure ceased to decline.

Analysis of the Products.—The products were identified by mixed gas chromatography with authentic samples. A column (3 m. long and 3 mm. in diameter), filled with dilauryl phthalate on cerite, was used. The column temperature was 110 to 125°C, and the rate of flow of the carrier gas (hydrogen) was 50 to 100 ml. per min.

The infrared absorption spectrum of the toluene solution was recorded by the use of a Shimadzu Model IR-27 spectrophotometer.

Materials.—Dicobalt octacarbonyl solution in toluene was prepared according to the method described in a

* Presented at the 18th Annual Meeting of the Chemical Society of Japan, Osaka, April, 1965. Part IX: Y. Takegami, Y. Watanabe, H. Masada and C. Yokokawa, This Bulletin, **39**, 1499 (1966).

1) Y. Takegami, C. Yokokawa, Y. Watanabe, H. Masada and Y. Okuda, This Bulletin, **37**, 1190 (1964).

2) V. L. Hughes and I. Kirshenbaun, *Ind. & Eng. Chem.*, **49**, 1999 (1957); *Petroleum Refiner*, **37**, 209 (1958); P. Pino, F. Piacenti and P. P. Neggiani, *Chem. & Ind.*, **1961**, 1400.

previous paper.[3] Ethyl acrylate, toluene and other materials were commercial products which had been proved by gas chromatography to be sufficiently pure. As authentic samples, the following commercial chemicals were used: α- and β-carbethoxypropionaldehyde and β-carbethoxypropyl alcohol.

Results and Discussion

The effects of the reaction conditions (the temperature, the partial pressures of hydrogen and carbon monoxide, and the solvents) on the ratio of the products were examined; the results are summarized in Tables I and II. Under the conditions used, 80 to 90% of ethyl acrylate was converted to α- and β-carbethoxypropionaldehyde. In Tables I and II, the values of the reaction times during which a pressure drop was observed, relative of that of Exp. 12, are shown as a measure of the relative reaction rate.

The Effect of the Reaction Temperature.— The relation between the reaction temperature and the percentage of α-carbethoxypropionaldehyde, and that between the reaction temperature and the relative rate, are illustrated in Figs. 1 and 2.

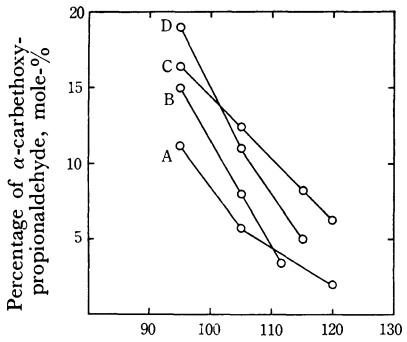

Fig. 1. The percentage of α-carbethoxypropionaldehyde vs. the reaction temperature.
A: H_2 80 atm., CO 40 atm.
B: H_2 80 atm., CO 80 atm.
C: H_2 80 atm., CO 120 atm.
D: H_2 120 atm., CO 80 atm.

As Fig. 1 shows, the percentage of the branched aldehyde decreased almost proportionally with an increase in the reaction temperature, when the initial pressures of hydrogen and carbon monoxide were fixed. With simple 1-olefins, the yield of branched aldehyde increases with an increase in the reaction temperature.[2] In this point, the behavior of ethyl acrylate is different from that of the simple 1-olefins in the oxo reaction. This contrast may be attributed to an ester group of ethyl acrylate. On the other hand, in the reaction of ethyl acrylate with cobalt hydrocarbonyl, a relatively high reaction tmperature is favorable to the formation of a product with a straight chain structure.[1] Therefore, the reaction temperature in the oxo reaction of ethyl acrylate has an effect on the distribution of the products similar to that in the reaction of cobalt hydrocarbonyl. This fact seems to support the consideration[4] that a cobalt catalyst in the oxo reaction acts as cobalt hydrocarbonyl. It may reasonably be considered that the oxo reaction of ethyl acrylate follows this reaction scheme, similar to that of the reaction of cobalt hydrocarbonyl[1]:

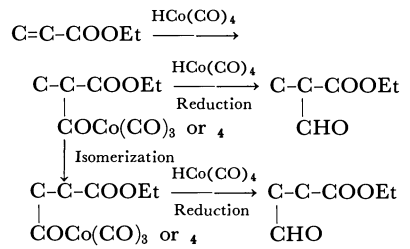

In the light of the reaction scheme, the distribution of the two aldehydes seems to be controlled by the isomerization and reduction of α-carbethoxypropionylcobalt carbonyl, which is obtained by the reaction of ethyl acrylate with cobalt hydrocarbonyl. It has been shown[1] that the isomerization of this acylcobalt carbonyl occurs easily at a relatively low temperature (-10 to 25°C). In the oxo reaction, a higher temperature seems to be more favorable to this isomerization, from α-carbethoxypropionylcobalt carbonyl to β-carbethoxypropionylcobalt carbonyl, then causing the percentage of β-carbethoxy propionaldehyde to increase.

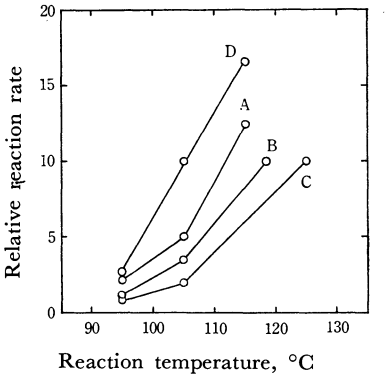

Fig. 2. The relative reaction rate vs. the reaction temperature.
A: H_2 80 atm., CO 40 atm.
B: H_2 80 atm., CO 80 atm.
C: H_2 80 atm., CO 120 atm.
D: H_2 120 atm., CO 80 atm.

3) C. Yokokawa, Y. Watanabe and Y. Takegami, This Bulletin, **37**, 677 (1964).

4) L. Kirch and M. Orchin, *J. Am. Chem. Soc.*, **80**, 4428 (1958); **81**, 3597 (1959); R. F. Heck and D. S. Breslow, ibid., **83**, 4023 (1961).

TABLE I. THE OXO REACTION OF ETHYL ACRYLATE

Exp. No.	Reaction conditions: Temp. °C	Partial pressure,*1 atm. H_2	Partial pressure,*1 atm. CO	Time*2 min.	Conversion of ethyl acrylate %	Relative reaction rate*4	Products,*3 mole- %: *n*-Aldehyde	*iso*-Aldehyde	*n*-Alcohol
1	100—110	80	80	50	93	3.4	92	8.0	—
2	120—133	40	120	60	92	3.4	96	2.5	1.5
3	100—110	40	80	75	93	1.7	95.8	4.2	—
4	100—110	120	80	40	93	10	88.8	11.2	—
5	100—110	25	80	70	90	1.3	95.3	4.7	—
6	100—110	160	80	35	93	10	83.3	14.7	2.0
7	100—110	80	120	70	95	2	87.5	12.5	—
8	100—110	80	40	45	94	5	94.4	5.6	—
9	90—100	80	80	85	93	0.8	85	15	—
10	90—100	40	80	140	85	0.5	94	6.0	—
11	90—100	120	80	60	95	2.5	80	18.5	1.5
12	90—100	80	120	75	91	1	83.6	16.4	—
13	90—100	80	40	45	90	2.3	88.7	11.3	—
14	100—125	80	80	35	95	6	92.2	3.3	4.5
15	110—135	40	80	40	90	5	96	3.0	1.0
16	110—120	120	80	25	89	16	91.5	5.0	3.5
17	110—120	80	40	30	83	12	94.5	5.0	0.5
18	110—120	80	120	30	93	12	92	2.0	0
19	110—125	80	120	30	91	—	92	6.3	1.7
20	110—125	80	40	30	80	—	98	2.0	—
21	110—125	80	80	30	80	—	93.5	5.5	—

*1 Initial pressure.
*2 From the time when the reaction temperature reached to the certain one to that when pressure drop ceased.
*3 *n*-Aldehyde: β-carbethoxypropionaldehyde, *iso*-aldehyde: α-carbethoxypropionaldehyde, and *n*-alcohol: β-carbethoxy-*n*-propyl alcohol.
*4 The values of the reaction time, during which pressure drop was observed, relative to that of Exp. 12.

TABLE II. THE OXO REACTION OF ETHYL ACRYLATE—THE EFFECTS OF A MIXED SOLVENT

Exp. No.	Reaction conditions*1: Temp. °C	Partial pressure, atm. H_2	Partial pressure, atm. CO	Time min.	Relative reaction rate	Products,*2 mole- %: *n*-Aldehyde	*n*-Alcohol	Diethyl succinate	*iso*-Aldehyde	*iso*-Alcohol	*iso*-Aldehyde + *iso*-alcohol
22	100—103	80	80	35	5	24.6	4.6	57.5	11.0	2.3	13.3
23	100—110	80	80	35	6	34.2	3.6	53.1	7.3	1.8	9.1
24	95—100	40	80	65	1.3	46.5	2.1	42.9	6.4	2.1	8.5

*1 Solvent: toluene - ethyl alcohol (60 : 25 in volume). In every case, about 95% of ethyl acrylate.
*2 Cf. Table I. *iso*-Alcohol: α-carbethoxy-*n*-propyl alcohol.

As Fig. 2 shows, the reaction rate increased with an increase in the reaction temperature.

The Effect of the Partial Pressure of Carbon Monoxide.—The relation between the initial pressures of carbon monoxide and the percentage of β-carbethoxypropionaldehyde is illustrated in Fig. 3.

The percentage of α-carbethoxypropionaldehyde increased with an increase in the initial pressure of carbon monoxide when the other reaction conditions were fixed (Fig. 3). Previous work[1,5] in this laboratory has demonstrated that the isomerization of the acylcobalt carbonyls (butyryl- and β-carbethoxypropionylcobalt carbonyl, etc.) generally occurs more rapidly under nitrogen than under carbon monoxide. Under oxo conditions, the isomerization of β-carbethoxypropionylcobalt carbonyl seems to be difficult at relatively high pressures of carbon monoxide; then the percentage of α-carbethoxypropionaldehyde increases with an increase in the carbon monoxide pressure. This fact supports the reaction scheme mentioned above.

5) Y. Takegami, C. Yokokawa, Y. Watanabe, H. Masada and Y. Okuda, This Bulletin, **37**, 181 (1964); ibid., **38**, 787 (1965); ibid., **39**, 1495 (1966).

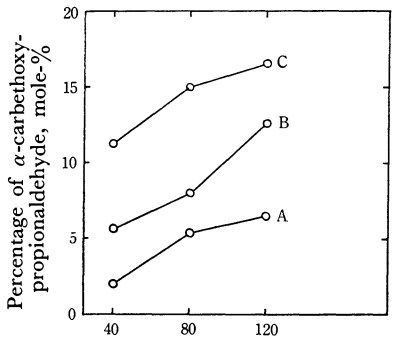

Fig. 3. The percentage of α-carbethoxypropionaldehyde vs. the initial pressure of carbon monoxide.

A: H_2 80 atm., Temp. 120°C
B: H_2 80 atm., Temp. 105°C
C: H_2 80 atm., Temp. 95°C

The relative reaction rate decreases with an increase in the initial pressure of carbon monoxide (cf. Exps. 1, 7 and 8).

The Effect of the Partial Pressure of Hydrogen.—The relation between the initial pressure of hydrogen and the percentage of α-carbethoxypropionaldehyde is shown in Fig. 4.

As Fig. 4 shows, the percentage of α-carbethoxypropionaldehyde increases almost proportionally with an increase in the partial pressure of hydrogen; when the initial pressure of carbon monoxide and the reaction temperature were fixed at 80 atm. and 100—110°C respectively, and when the initial pressures of hydrogen were 40, 80, 120 and 160 atm., the percentages of the aldehyde were 4.0, 8.0, 11.2 and 14.7 mole-% respectively.

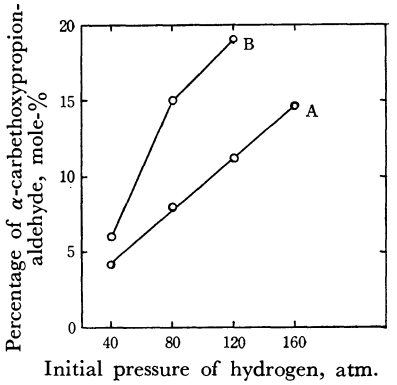

Fig. 4. The percentage of α-carbethoxypropionaldehyde vs. the initial pressure of hydrogen.

A: CO 80 atm., Temp. 105°C
B: CO 80 atm., Temp. 95°C

The relative reaction rate also increases with an increase in the partial pressure of hydrogen (cf. Exps. 1, 3, 4, and 5). The rate of the oxo reaction of simple 1-olefins may be represented as follows:[6]

$$\text{rate} = \frac{k_1 P_{H_2}}{k_2 P_{CO} + k_3 P_{H_2}}$$

k: constant
P: partical pressure

This equation seems to be applicable to the case of ethyl acrylate.

From the standpoint of the reaction scheme, higher pressures of hydrogen are considered to be more favorable to the reduction of α-carbethoxypropionylcobalt carbonyl to the corresponding aldehyde rather than to its isomerization; hence, the formation of α-carbethoxypropionaldehyde seems to be relatively promoted. From this consideration, it may be suggested that the proportion of α-carbethoxypropionaldehyde increases with an increase in the reaction rate when the partial pressure of carbon monoxide and the reaction temperature are fixed. With simple 1-olefins, the oxo reaction rate is remarkably affected by the concentration of the catalyst and solvent.*[1,2] Thus, with ethyl acrylate also the distribution of the products may be affected by solvents.

The Effect of the Solvent.—The effect of a mixed solvent, toluene - ethyl alcohol (60 : 25 in volume), on the reaction rate and the distribution of the products was also examined (Table II).

As the reaction products, the two aldehydes, two alcohols (α- and β-carbethoxy-*n*-propyl alcohol) and diethyl succinate were obtained. The diethyl succinate appeared to be formed by the reaction of β-carbethoxypropionylcobalt carbonyl with ethyl alcohol.

By comparing the results of Exps. 1 and 10 with those of Exps. 23 and 24 respectively, the reaction rate in the mixed solvent was found to be about two times as large as that in pure toluene when the other conditions were fixed; moreover, the percentage of the branched-chain products in the mixed solvent was evidently larger, supporting the assumption that the proportion of the branched-chain products increases with an increase in the reaction rate if the partial pressure of carbon monoxide and the reaction temperature are the same.

* For example, the oxo reaction rate of acrylonitrile in ethyl alcohol is about five times as large as that in benzene.[7]

6) G. Natta, R. Ercoli, S. Castellano and F. H. Barbieri, *J. Am. Chem. Soc.*, **76**, 4049 (1954); R. A. Martin, *Chem. & Ind.*, **1954**, 1536; H. W. Sternberg, R. Markby and I. Wender, *J. Am. Chem. Soc.*, **79**, 6116 (1957).

7) J. Kato, H. Wakamatsu, Y. Iwanaga and T. Yoshida, *J. Chem. Soc. Japan, Ind. Chem. Sect. (Kagyo Kagaku Zasshi)*, **64**, 2139 (1961).

BULLETIN OF THE CHEMICAL SOCIETY OF JAPAN VOL. 39 2434—2437 (1966)

The Isocyanurates. III. The Formation of Tributyl Isocyanurates from Butyl Bromides in the Presence of 1-Butanol

By Atsuo NAGASAWA, Hisao KITANO and Kenichi FUKUI

Department of Hydrocarbon Chemistry, Faculty of Engineering, Kyoto University, Sakyo-ku, Kyoto

(Received December 20, 1965)

The reaction of *n*-butyl or *s*-butyl bromide with potassium cyanate in dimethylformamide was carried out at 100°C for 3 hr. to give tri-*n*-butyl or tri-*s*-butyl isocyanurate. In this process, the presence of unpolymerized *n*-butyl or *s*-butyl isocyanate in the reaction mixture was detected by treating the mixture with benzylamine, thus forming 1-*n*-butyl- or 1-*s*-butyl-3-benzyl urea. The presence of 1-butanol in the reaction system resulted in an increase in the yield of the corresponding isocyanurates. This tendency was remarkable when *s*-butyl bromide was used as a starting material. The addition of *n*-butyl *N*-*n*-butyl- or *n*-butyl *N*-*s*-butylcarbamate to the reaction system strongly accelerated the formation of isocyanurates. The acceleration due to the addition of 1-butanol described above was, therefore, attributed to the effect of carbamates formed in the reaction system. An attempt to trimerize *n*-butyl or *s*-butyl isocyanate in the presence of carbamates and dimethylthylformamide, or in the presence of carbamates and potassium cyanate, resulted in failure. Therefore, carbamates acted as strong accelerators for the trimerization of butyl isocyanates, in cooperation with basic alkali metal salts, such as potassium cyanate, in dimethylformamide.

Previous papers[1] have described how trialkyl or trialkenyl isocyanurates were prepared by the reaction of alkyl or alkenyl halides with alkali cyanates in an aprotic solvent, such as dimethylformamide or dimethylsulfoxide. In this process, the formation of 1, 3-dialkyl urea was often observed when the reaction mixture was poured into water immediately after the desired reaction time. This fact supported indirectly the idea that the reaction between alkyl halides and alkali cyanates generated alkyl isocyanates at the first step,[2] and that those were subsequently polymerized to trialkyl isocyanurates by the catalysis of alkaline compounds (e. g., alkali cyanate)[3] present in the reaction mixture. Therefore, the presence of the unpolymerized alkyl isocyanate in the reaction mixture caused a depression in the yield of trialkyl isocyanurate.

In order to promote the trimerization of isocyanates, an isocyanate-polymerizing catalyst,[4] such as potassium carbonate, sodium benzoate, pyridine or triethylamine, was added to the reaction system. However, all such attempts resulted in failure in the reaction system containing alkyl halides.

On the other hand, some compounds bearing a hydroxyl or an imino group were found to be effective in the trimerization of an initially-formed alkyl isocyanate, even in the presence of alkyl halides.

In the present work, the effects of the addition of 1-butanol, *n*-butyl *N*-*n*-butyl- or *n*-butyl *N*-*s*-butylcarbamate on the reaction of *n*-butyl or *s*-butyl bromide with potassium cyanate in dimethylformamide were studied. The reaction mixture was treated by the following two methods: (I) the reaction mixture was allowed to stand for 24 hr. and then distilled to obtained isocyanurates, and (II) the reaction mixture was quenched at the end of the reaction period and mixed with benzylamine, thus converting the remaining isocyanate into 1-butyl-3-benzyl urea.

A previous paper[1] described how the reaction 1 between *n*-butyl bromide and potassium cyanate, together with water, afforded 1, 3-di-*n*-butyl urea in an 80 to 87% yield (based on the water added) and how the yield of tri-*n*-butyl isocyanurate decreased with the amount of the water added. In this reaction, the decomposition of potassium cyanate proceeded easily in the presence of more than 0.6 mol. of water per mole of the cyanate.

$$n\text{-}C_4H_9Br + KNCO + H_2O \xrightarrow{DMF} (n\text{-}C_4H_9NH)_2CO + (n\text{-}C_4H_9NCO)_3 \quad (1)$$

In the reaction 2 of *n*-butyl bromide with potassium cyanate in the presence of 1-butanol, the use of an equimolar amount of butanol to butyl bromide resulted in the yield of *n*-butyl *N*-*n*-butylcarbamate being limited to 47%, while that of tri-*n*-butyl

1) K. Fukui and H. Kitano, Japanese Pat. 282402 (1961); K. Fukui, F. Tanimoto and H. Kitano, This Bulletin, **33**, 1586 (1965).
2) K. Fukui and H. Kitano, Japanese Pat. 282468 (1961).
3) T. Yamabe, A. Nagasawa, H. Kitano and K. Fukui, *J. Chem. Soc., Japan, Ind. Chem. Sect. (Kogyo Kagaku Zasshi)*, **66**, 821 (1963).
4) A. W. Hofmann, *Ber.*, **18**, 764 (1885); W. J. Balon, U. S. Pat. 2353518 (1958); A. W. Hofmann, *Jahresber. Fortschritte Chem.*, **1862**, 335.

TABLE I. THE REACTION OF *n*-BUTYL OR *s*-BUTYL BROMIDE AND POTASSIUM CYANATE WITH OR WITHOUT 1-BUTANOL

Reactant (mole)	Method* employed	Yield of the product, %		
		$C_4H_9NHCONHCH_2C_6H_5$	$(C_4H_9NCO)_3$	$C_4H_9NHCO_2C_4H_9$-*n*
n-C_4H_9Br (0.2) KNCO (0.3)	I	0	83	—
	II	51	27	—
n-C_4H_9Br (0.4) KNCO (0.6) *n*-C_4H_9OH (0.4)	I	0	36	47
	II	0	35	47
s-C_4H_9Br (0.2) KNCO (0.3)	I	0	73	—
	II	40	31	—
s-C_4H_9Br (0.6) KNCO (0.9) *n*-C_4H_9OH (0.6)	I	0	63	12
	II	0	62	11

* Method I: Distillation of the reaction mixture;
Method II: The addition of benzylamine to the reaction mixture.

isocyanurate reached 36%, much higher than in the case of the addition of water (13%). Moreover, when *s*-butyl bromide was used in place of *n*-butyl bromide, this trend became remarkable and a 63% yield of tri-*s*-butyl isocyanurate was obtained (Eq. 3):

$$n\text{-}C_4H_9Br + KNCO + n\text{-}C_4H_9OH \xrightarrow{DMF} n\text{-}C_4H_9NHCO_2C_4H_9\text{-}n + (n\text{-}C_4H_9NCO)_3 \quad (2)$$

$$s\text{-}C_4H_9Br + KNCO + n\text{-}C_4H_9OH \xrightarrow{DMF} s\text{-}C_4H_9NHCO_2C_4H_9\text{-}n + (s\text{-}C_4H_9NCO)_3 + CH_3CH{=}CHCH_3 \quad (3)$$

The two methods, I and II, were adopted for the reaction with and without the use of 1-butanol. Table I indicates the results.

The clear difference between the results from I and II observed in the absence of 1-butanol implies that considerable amounts of isocyanates remained unpolymerized for several hours in the reaction mixture (Eq. 4), while, in the presence of 1-butanol, I and II were not appreciably different, indicating the absence of free isocyanates in the reaction mixture.

$$C_4H_9Br + KNCO \xrightarrow[\text{Method I}]{} (C_4H_9NCO)_3$$
$$C_4H_9Br + KNCO \xrightarrow[\text{Method II}]{C_6H_5CH_2NH_2} C_4H_9NHCONHCH_2C_6H_5 + (C_4H_9NCO)_3 \quad (4)$$

Table I also apparently illustrates that the addition of 1-butanol to the reaction system 4 served to increase the yield of tributyl isocyanurates.

On the basis of our observations that the addition of water to the reaction system 4 did not increase the yield of the isocyanurate,[1] we assumed that the trimerization of butyl isocyanates was accelerated neither by water, nor by urea, nor by 1-butanol, but by *n*-butyl *N*-butylcarbamates derived from the reaction with 1-butanol. In this regard, it may be recollected that Kogon[5] carried out the trimerization of phenyl isocyanate in the presence of ethyl carbanilate and *N*-methyl morpholine.

The effect of the addition of half a more of *n*-butyl *N*-*n*-butyl- or *n*-butyl *N*-*s*-butylcarbamate per mole of *n*-butyl or *s*-butyl bromide on the reaction of butyl bromides with potassium cyanate in dimethylformamide was examined in order to confirm that *N*-monosubstituted carbamates may be expected to promote the trimerization of aliphatic isocyanates. In this reaction 5, the yields of tributyl isocyanurates were about 80% and there was no butyl isocyanate remaining in the reaction mixture which was detectable by the benzylamine method II described above.

$$C_4H_9Br + KNCO \xrightarrow[C_4H_9NHCO_2C_4H_9]{DMF} (C_4H_9NCO)_3 \quad (5)$$

Furthermore, the trimerization 6 of *n*-butyl or *s*-butyl isocyanate with a *n*-butyl *N*-*n*-butylcarbamate-dimethylformamide mixture led to the recovery of the isocyanates in about a 90% yield, while the reaction 7 of the isocyanates in the presence of potassium cyanate and the carbamate in toluene resulted in the recovery of the isocyanates in almost a quantitative yield:

$$C_4H_9NCO \xrightarrow[n\text{-}C_4H_9NHCO_2C_4H_9\text{-}n,\ DMF]{} (C_4H_9NCO)_3 \quad (6)$$

$$C_4H_9NCO \xrightarrow[n\text{-}C_4H_9NHCO_2C_4H_9\text{-}n,\ KNCO]{} (C_4H_9NCO)_3 \quad (7)$$

The trimerization 8 of the isocyanates with the carbamate and potassium cyanate in dimethylformamide gave isocyanurates in twice the yield of the reaction 8 in the absence of the carbamate:

$$C_4H_9NCO \xrightarrow[n\text{-}C_4H_9NHCO_2C_4H_9\text{-}n,\ KNCO,\ DMF]{} (C_4H_9NCO)_3 \quad (8)$$

Consequently, it was concluded that *n*-butyl *N*-butyl-carbamates exhibited a strong accelerating ability in the trimerization of butyl isocyanates

5) I. C. Kogon, *J. Am. Chem. Soc.*, **78**, 4911 (1956).

in cooperation with basic alkali metal salts, such as potassium cyanate, in dimethylformamide, in spite of the presence of butyl bromides, which reduced the isocyanate-trimerizing property of some basic compounds described in the preliminary experiment; this information will be useful for the syntheses of isosyanurates from aliphatic halides and alkali cyanates.

Experimental

Materials.—*n*-Butyl and *s*-butyl bromides were prepared from the corresponding alcohols by the usual methods.[6,7] We described the purity of potassium cyanate[5] and dimethylformamide in a previous paper[1]. *n*-Butyl and *s*-butyl isocyanates were prepared by the phosgenation[9] of anhydrous *n*-butyl or *s*-butylamine hydrochloride in tetralin and were purified by treating them with calcium oxide and molecular sieves, followed by fractional distillation. The specimens used had the following physical properties: *n*-butyl; b. p. 115°C, n_D^{20} 1.4058 (Ref.[10] b. p. 113—116°C, n_D^{20} 1.4060) and *s*-butyl; b. p. 102°C, n_D^{20} 1.3995 (Ref.[10] b. p. 99—101°C, n_D^{20} 1.3989). *n*-Butyl *N*-*n*-butylcarbamate (b. p. 102°C/4 mmHg, n_D^{20} 1.4359) and *n*-butyl *N*-*s*-butylcarbamate (b. p. 91—92°C/4 mmHg, n_D^{15} 1.4429) were prepared by the reaction of an excess of pure *n*-butanol with butyl isocyanates (the specimens described above) and were purified by distillation under reduced pressure. These carbamates were identified with the authentic samples prepared by Curry's method.[11]

The Reaction of *n*-Butyl or *s*-Butyl Bromide with Potassium Cyanate.—*(A) Method I (The Distillation of the Reaction Mixture).*—In a three-necked flask fitted with a reflux condenser, a thermometer, and a mercury-sealed mechanical stirrer, there was placed a mixture of 27.4 g. (0.2 mole) of *n*-butyl or *s*-butyl bromide, 24.3 g. (0.3 mole) of potassium cyanate, and 100 g. (1.4 mole) of dimethylformamide. The mixture was well stirred and then kept at 100±1°C for 3 hr. After the reaction mixture had then been allowed to stand for 24 hr. at room temperature, it was filtered to removed inorganic salts. The filtrate was distilled under reduced pressure to give dimethylformamide and tri-*n*-butyl isocyanurate (b. p. 160—162°C/4 mmHg, n_D^{20} 1.4720[10]) or tri-*s*-butyl isocyanurate (b. p. 138—140°C/4 mmHg, n_D^{15} 1.4600[10]). The yields of the isocyanurates are shown in Table I.

(B) Method II (The Addition of Benzylamine to the Reaction Mixture).—The reaction of *n*-butyl bromide with potassium cyanate was carried out as in the case of Method I. After 3 hr., the reaction mixture was quickly quenched with ice water; the inorganic precipitates were filtered off, and the filtrate was at once mixed with 26.8 g. (0.25 mole) of benzylamine. The resulting mixture was allowed to stand for 24 hr. at room temperature and then poured into cold water to afford a white crystalline mass. The mass was collected by filtration, washed with water and *n*-butyl ether, and recrystallized from a methyl ethyl ketone-ligroin mixture (1 : 1) to give 1-*n*-butyl-3-benzyl urea, m. p. 101°C.

Found: N, 13.5%. Calcd. for $C_{12}H_{18}ON_2$: N, 13.6%.

The filtrate was poured into a saturated sodium chloride solution and extracted with benzene. The extract was dried over anhydrous magnesium sulfate overnight and distilled under reduced pressure to give tri-*n*-butyl isocyanurate.

When *s*-butyl bromide instead of *n*-butyl bromide was used in this experiment, 1-*s*-butyl-3-benzyl urea, m. p. 102.5°C, tri-*s*-butyl isocyanurate and butene-2 were obtained.

Found: N, 13.4% Calcd. for $C_{12}H_{18}ON_2$: N, 13.6%.

These results are summarized in Table I.

The Reaction of *n*-Butyl Bromide with Potassium Cyanate in the Presence of 1-Butanol.—A mixture of 54.8 g. (0.4 mole) of *n*-butyl bromide, 48.6 g. (0.6 mole) of potassium cyanate, 200 g. (2.8 mole) of dimethylformamide and 29.6 g. (0.4 mole) of 1-butanol was kept at 100±1°C for 3 hr. with stirring. The reaction mixture was then treated by the two methods, I and II, to give *n*-butyl *N*-*n*-butylcarbamate (b. p. 97—98°C/3 mmHg, n_D^{20} 1.4726) and tri-*n*-butyl isocyanurate (b. p. 158—160°C/3 mmHg). The results are shown in Table I. The yields of the above products which depend upon the amount of 1-butanol added are listed in Table II.

Table II. The reaction of *n*-butyl bromide with potassium cyanate in the presence of 1-butanol

n-C_4H_9OH / n-C_4H_9Br mole/mole	Yield (A) of n-$C_4H_9NHCO_2$-C_4H_9-n %	Yield (B) of $(n$-$C_4H_9NCO)_3$ %	Total yield (A+B) %
0.5	35	47	82
1.0	47	36	83
1.5	56	28	84
2.0	61	22	83
4.0	83	—	83

The Reaction of *s*-Butyl Bromide with Potassium Cyanate in the Pressence of 1-Butanol.—In both methods, I and II, the top of the reflux condenser was connected with a trap chilled by a dry ice-methanol bath. A mixture of 83.2 g. (0.6 mole) of *s*-butyl bromide, 72.9 g. (0.9 mole) of potassium cyanate, 300 g. (4.2 mole) of dimethylformamide, and 42.6 g. (0.6 mole) of 1-butanol was maintained at 100±1°C for 5 hr. with stirring. The reaction mixture, when then treated by the above methods, yielded *n*-butyl *N*-*s*-butylcarbamate (b. p. 90—91°C/4 mmHg, n_D^{15} 1.4428) and tri-*s*-butyl isocyanurate (b. p. 137—139°C/4 mmHg). The results are shown in Table I, while the effects of the amount of 1-butanol added on the yields of the carbamate and the isocyanurate are summarized in Table III. In this table, the yield of butene-2 was determined from the bromine number of the distillate in the trap.

6) O. Kamm and C. S. Marvel, "Org. Syntheses," Coll. Vol. I, 28 (1956).
7) C. R. Noller and R. Dinsmore, ibid., Coll. Vol. II, 359 (1948).
8) A. Scattergood, "Inorg. Syntheses," **2**, 87 (1953).
9) M. W. Farlow, "Org. Syntheses," **31**, 62 (1951).
10) R. J. Slocombe, E. E. Hardy, J. H. Saunders and R. L. Jenkins, *J. Am. Chem. Soc.*, **72**, 1888 (1950).
11) H. H. Curry and J. P. Mason, *J. Am. Chem. Soc.*, **73**, 5043 (1951).

Table III. The reaction of *s*-butyl bromide with potassium cyanate in the presence of 1-butanol

n-C_4H_9OH / s-C_4H_9Br mole/mole	Yield (A) of s-$C_4H_9NHCO_2C_4H_9$-s %	Yield (B) of $(s$-$C_4H_9NCO)_3$ %	Yield (C) of $CH_3CH{=}CHCH_3$ %	Total yield (A+B+C) %
0.5	30	42	6	78
1.0	11	62	4	77
1.5	15	58	3	76
2.0	16	57	1	74
4.0	17	54	0.5	72

The Reaction of *n*-Butyl or *s*-Butyl Bromide with Potassium Cyanate in the Presence of *n*-Butyl *N*-Butylcarbamates.—A mixture of 27.4 g. (0.2 mole) of *n*-butyl or *s*-butyl bromide, 24.3 g. (0.3 mole) of potassium cyanate, 100 g. (1.4 mole) of dimethylformamide, and 17.3 g. (0.1 mole) of *n*-butyl *N*-*n*-butyl or *n*-butyl *N*-*s*-butylcarbamate specimens, was heated at 100±1°C for 3 hr. The reaction mixture was then treated by Methods I and II to give tri-*n*-butyl and tri-*s*-butyl isocaynurate respectively. The yields of the isocyanurates by the two methods, are shown in Table IV. The carbamate added was recovered in a quantitative yield.

Table IV. The reaction of *n*-butyl or *s*-butyl bromide with potassium cyanate in the presence of *n*-butyl *N*-butylcarbamates

Reactant	Carbamate	Method*	Yield of isocyanurate, %
n-C_4H_9Br	n-$C_4H_9NHCO_2C_4H_9$-n	I	83
		II	81
s-C_4H_9Br	s-$C_4H_9NHCO_2C_4H_9$-s	I	73
		II	72

* Method I: Distillation of the reaction mixture; Method II: The addition of benzylamine to the reaction mixture.

Attempted Trimerizations of *n*-Butyl and *s*-Butyl Isocyanates.—After a mixture listed in Table V was heated at 100±1°C for 3 hr. while being stirred, the resultant mixture was quenched with ice water and 5 ml. of the mixture was pipetted out. The sample was then mixed with 20 ml. of a 0.5 N di-*n*-butylamine-dioxane solution and allowed to stand for 2 hr. at room temperature. The residual isocyanate content in the sample was determined by titrating the excess of di-*n*-butylamine with a 0.1 N hydrochloric acid - ethanol solution, using bromocresol purple as the indicator.[3] The results are shown in Table V.

Table V. The attempted trimerization of *n*-butyl and *s*-butyl isocyanates

Components of the reaction mixture*	Recovered C_4H_9NCO %
n-C_4H_9NCO, $CH_3C_6H_5$	99.5
n-C_4H_9NCO, n-$C_4H_9NHCO_2C_4H_9$-n, KCNO, $CH_3C_6H_5$	99.4
n-C_4H_9NCO, $HCON(CH_3)_2$	90.9
n-C_4H_9NCO, n-$C_4H_9NHCO_2C_4H_9$-n, $HCON(CH_3)_2$	91.0
n-C_4H_9NCO, KCNO, $HCON(CH_3)_2$	83.5
n-C_4H_9NCO, n-$C_4H_9NHCO_2C_4H_9$-n, $HCON(CH_3)_2$, KCNO	65.4
s-C_4H_9NCO, $CH_3C_6H_5$	99.4
s-C_4H_9NCO, n-$C_4H_9NHCO_2C_4H_9$-n, $CH_3C_6H_5$, KCNO	99.6
s-C_4H_9NCO, $HCON(CH_3)_2$	89.2
s-C_4H_9NCO, n-$C_4H_9NHCO_2C_4H_9$-n, $HCON(CH_3)_2$	89.4
s-C_4H_9NCO, KCNO, $HCON(CH_3)_2$	81.5
s-C_4H_9NCO, n-$C_4H_9NHCO_2C_4H_9$-n, $HCON(CH_3)_2$, KCNO	61.6

* C_4H_9NCO: 0.01 mole, n-$C_4H_9NHCO_2C_4H_9$-n: 0.005 mole, KCNO: 2.5×10^{-5} mole, $CH_3C_6H_5$: 10 ml., $HCON(CH_3)_2$: 10 ml.

With regard to Table V, toluene was used as a diluent of the isocyanates in order to obtain accurate results from the analysis of the reaction mixture in the absence of dimethylformamide, because toluene itself did not influence the polymerization of the isocyanates.

BULLETIN OF THE CHEMICAL SOCIETY OF JAPAN VOL. 39 2438—2441 (1966)

The Photochemical Sulfoxidation of Alkylbenzenes[1]

By Yoshiro OGATA, Yasuji IZAWA, Takao TSUDA and Katsuhiko TAKAGI

Department of Applied Chemistry, Faculty of Engineering, Nagoya University, Chikusa-ku, Nagoya

(Received February 3, 1966)

The photochemical sulfoxidation of alkylbenzenes with sulfur dioxide and oxygen in acetic anhydride to give the corresponding sulfonic acids has been studied. The sulfoxidation of the higher alkylbenzenes, such as that with a side-chain of trimerized propylene (ABTP) with a total average mol. wt. of 253 and that with a linear side-chain (ABL) with an average mol. wt. of 254, and also that of ethylbenzene give, by homolytic reaction, the corresponding sulfonic acids substituted at their side-chains. In contrast, the sulfonation of *m*-xylene occurs at the benzene ring by ionic reaction, while toluene gives a very poor yield of sulfonic acid. The surface activities of the resulting sodium alkylbenzenesulfonate with their sulfonate group at the side-chain were comparable to the corresponding ring-substituted sulfonates.

The present authors have previously postulated, for the photochemical sulfoxidation of *n*-hexane, a mechanism involving the simultaneous steps of a radical chain reaction and a molecular mechanism; the primary process seems to involve two processes, i. e., energy transfer and hydrogen abstraction with excited sulfur dioxide,[2] the ratio of reactivities of C–H bonds (primary : secondary : tertiary) being 1 : 0.8—1.3 : 3.2—6.2.[3]

It is well-known that the sulfonation of alkylbenzenes with sulfur trioxide occurs via an electrophilic attack on the benzene ring. However, little is known about the photochemical sulfoxidation of alkylbenzenes, though perhaps they are attacked at the side-chain via a radical mechanism. At the same time, the ionic sulfonation with sulfur trioxide is conceivable because of the possible photooxidation of sulfur dioxide to sulfur trioxide.[4]

The present paper will deal with the results obtained in a study of the photochemical sulfoxidation of various alkylbenzenes, such as toluene, ethylbenzene, *m*-xylene, alkylbenzene with a side-chain of trimerized propylene (ABTP) and alkylbenzene with a linear side-chain (ABL).

Experimental

Materials.—ABTP was purified by the fractionation of commercial material, b. p. 80°C/3 mmHg, n_D^{25} 1.4887, average mol. wt., 253, with an alkyl chain of 12—13 carbon atoms. ABL was of a commercial grade, prepared by the Friedel-Crafts reaction of chlorinated paraffin with benzene, b. p. 309—325°C, average mol. wt., 254, with an alkyl chain of 11—16 carbon atoms. The mol. wt. was determined cryoscopically in a benzene solution. Toluene, b. p. 109—110°C, ethylbenzene, b. p. 135—136°C; n_D^{18} 1.4971, and *m*-xylene, b. p. 138—138.5°C, were purified by the fractionation of commercial materials of an extra pure grade. Acetic anhydride, carbon tetrachloride, sulfur dioxide, oxygen, sodium *o*-toluenesulfonate and sodium *p*-toluenesulfonate were commercial materials and were used without further purification.

Sodium toluene-ω-sulfonate was prepared by the same procedure as was used by Johnson and Ambler.[5] Sodium *m*-xylene-ω-sulfonate was prepared by the reaction[5] of ω-bromo-*m*-xylene,[6] b. p. 117—120°C/60 mmHg, with anhydrous sodium sulfite. Sodium *p*-ethylbenzenesulfonate was prepared by the reaction of ethylbenzene with concentrated sulfuric acid at 136°C; the m. p. of its sulfonamide was 106—108°C (lit.[7] m. p. 109°C). Sodium 2, 4-dimethylbenzene-1-sulfonate was prepared by the reaction of *m*-xylene with concentrated sulfuric acid at 100—110°C; the m. p. of its acid was 58—59°C (lit. m. p. 59.8°C[8] and 63—64°C).[9] The sodium sulfonates with a ring-sulfonate group were prepared by the sulfonation of the corresponding ABTP and ABL with concentrated sulfuric acid.

The ultraviolet spectra were measured by a Shimadzu automatic recording spectrophotometer (Type SV-50A), and the infrared spectra, by a Perkin-Elmer grating infrared spectrophotometer (Type 337).

The Photochemical Sulfoxidation of Ethylbenzene.—Ethylbenzene (1.6 g., 0.015 mole), acetic anhydride (0.1 ml.), and carbon tetrachloride (150 ml.) were placed in a quartz reaction vessel. Sulfur dioxide (9 l./hr.) and oxygen (4.5 l./hr.) were introduced simultaneously into the ethylbenzene solution (0.01 mol./l.) at 17—22°C under the irradiation of ultraviolet light (Toshiba HSL-100 UV) for 12 hr. After the irradiation had ended, the resulting sulfonic acid was extracted with hot water (ca. 60 ml.). The extract was then neutralized with sodium carbonate and

1) Contribution No. 85. Presented in part at the 4th Symposium on Oil Chemistry, Tokyo, October, 1965.

2) Y. Ogata, Y. Izawa and T. Tsuda, *Tetrahedron*, **21**, 1349 (1965).

3) Y. Ogata, Y. Izawa and T. Tsuda, This Bulletin, **38**, 1984 (1965).

4) A. Coehn, *Z. Elektrochem.*, **13**, 545 (1907).

5) T. B. Johnson and J. A. Ambler, *J. Am. Chem. Soc.*, **36**, 381 (1914).

6) E. F. G. Atkinson, *J. Chem. Soc.*, **91**, 1696 (1907).

evaporated to dryness on a water bath, and the residue was further dried under a vacuum. The residue was then extracted with ethanol to give sodium ethylbenzenesulfonate as a light yellow solid (0.06 g.; 2.2%).

The Photochemical Sulfoxidation of Toluene.—Toluene (21.8 g., 0.24 mol.) and acetic anhydride (1.3 ml.) were placed in a quartz vessel. Sulfur dioxide (2 l./hr.) and oxygen (0.7 l./hr.) were then introduced simultaneously into the solution at 18—20°C under the irradiation of ultraviolet light for 12 hr. After the irradiation had ended, a work-up similar to the sulfoxidation of ethylbenzene gave a trace of a product; its infrared spectrum showed absorptions at 1135, 1015 and 650 cm^{-1} due to characteristic absorption bands of sulfonate.

The Photochemical Sulfoxidation of Alkylbenzenes.—A solution of ABTP (10 g., 0.04 mol.) and acetic anhydride (0.3 ml.) in carbon tetrachloride (100 ml.), after being dried with Drierite, was placed in a quartz vessel. Sulfur dioxide (7 l./hr.) and oxygen (3.5 l./hr.) were introduced simultaneously into the solution at 17—20°C under the irradiation of ultraviolet light (Toshiba H-400PUV) for 12 hr. After the irradiation had ended, water (ca. 1 ml.) was added to the reaction mixture and it was stirred at 40—50°C for 1 hr. in order to complete the decomposition of the acetyl phenylalkanesulfonyl peroxide. The resulting sulfonic acid was extracted with hot water (ca. 60 ml.), and isopropanol (ca. 60 ml.) was added to the extract. The solution was then neutralized with sodium carbonate, and further sodium carbonate added to the solution until the separated aqueous layer was saturated at 40°C. The separated isopropanol layer was dried with anhydrous sodium sulfate and evaporated to dryness on a water bath, and the residue was further dried under a vacuum. The yield of sodium sulfonate was about 0.4 g. (3%). The crude sulfonate was extracted with ethanol to give sodium sulfonate of ABTP (0.16 g.).

The sulfoxidation of ABL was carried out similarly. The yield was 2.9%.

The Photochemical Sulfoxidation of *m*-Xylene.—*m*-Xylene (21.5 g., 0.2 mol.), acetic anhydride (1.3 ml.) and carbon tetrachloride (75 ml.) were placed in a quartz vessel. Sulfur dioxide (7.0 l./hr.) and oxygen (3.5 l./hr.) were introduced simulatneously into the solution at room temperature under the irradiation of ultraviolet light for 9 hr. After the irradiation had ended, a work-up similar to that used for ethylbenzene gave the sodium sulfonate (yield 1.0%).

Results and Discussion

The photochemical sulfoxidation of various alkylbenzenes gave the corresponding sulfonic acids in yields lower than those for *n*-hexane and *n*-decane[2] (see Table I). The lowering of the yields may be due to an inner-filter effect of alkylbenzenes as a substrate, although the λ_{max} value of sulfur dioxide (290 mμ) is longer than those of the substrates. Table II summarizes the ultraviolet and the infrared spectral data on the sodium sulfonates obtained from the sulfoxidized ethylbenzene, ABTP, with an average mol. wt. of 253 (with a side-chain consisting of 12—13 carbon atoms), and ABL, with an average mol. wt. of 254 (with a side-chain of 11—16 carbon atoms). The sulfonate from ethylbenzene showed a λ_{max} value at 256 mμ in water and characteristic infrared absorption bands at 1168 and 1048 cm^{-1} (assigned to the S–O stretching vibrations), at 650 cm^{-1} (assigned to the C–S stretching vibration) and at 734 and 696 cm^{-1} (assigned to the out-of-plane C–H deformation vibrations of five adjacent hydrogen atoms in the benzene ring). Similarly, the sodium sulfonate from ABTP showed a λ_{max} value at 250 mμ in dilute aqueous ethanol and characteristic infrared absorption bands at 1180 and 1045 cm^{-1} (assigned to the S=O stretching vibrations), at 648 cm^{-1} (assigned to the C–S stretching vibration) and at 758 and 695 $cm.^{-1}$ (assigned to the out-of-plane C–H deformation of five adjacent hydrogen atoms in the benzene ring). The sodium sulfonate from ABL showed a λ_{max} value at 258 mμ in ethanol and similar characteristic infrared absorption bands.

As Table III shows, however, the absorption peaks of all authentic alkylbenzenesulfonates with a sulfonate group at the benzene ring are observed above 260 mμ, while those with a sulfonate group at the side-chain shift to below 258 mμ.

On the other hand, the photochemical sulfoxidation of *m*-xylene was found to give a product with a sulfonate group in the benzene ring, i. e., 2, 4-dimethylbenzene-1-sulfonate, which was identified by ultraviolet and infrared spectroscopy (Tables II and III). Although the sulfoxidation of toluene gave a trace of a product which showed the infrared characteristic absorption bands associated with the sulfonate group, attempts to detect the position of the sulfonate group were unsuccessful.

On the basis of these facts, the sulfoxidation of the alkylbenzenes with secondary and/or tertiary hydrogen atoms in the side-chain, such as ethylbenzene, ABTP and ABL, may be described as follows:

$$SO_2 \xrightarrow{h\nu} SO_2^* \longrightarrow SO_2^{**} \quad (1)[10]$$

(Singlet state) (Triplet state)

$$Ph(CH_2)_nCH_3 + SO_2^{**} \longrightarrow PhCH(CH_2)_{n-1}CH_3 + \cdot H + SO_2 \quad (2)$$

$$PhCH(CH_2)_{n-1}CH_3 + SO_2 \longrightarrow PhCHSO_2(CH_2)_{n-1}CH_3 \xrightarrow{O_2} \cdots \quad (3)$$

In contrast, *m*-xylene gave ring-substituted products via an ionic mechanism with sulfur trioxide as an attacking species, since another probable

7) L. Sempotowski, *Ber.*, **22**, 2663 (1889).
8) J. M. Craft, ibid., **34**, 1352 (1901).
9) F. A. H. Schreinemakers, *Rec, trav. chim.*, **16**, 420 (1898).
10) R. B. Cundall and T. F. Palmer, *Trans. Faraday Soc.*, **56**, 1211 (1960).

TABLE I. PHOTOCHEMICAL SULFOXIDATION OF ALKYLBENZENES

Alkylbenzene (mol.)		Ac_2O ml.	Solvent (ml.)	Irrad. time hr.	Yield[a] %
Toluene	(0.24)	1.3	None	12	Trace
			CCl_4 (75)	4	Trace
Ethylbenzene	(0.015)	0.1	CCl_4 (150)	12	2.2
ABTP	(0.04)	0.3	CCl_4 (100)	12	3.0
ABL	(0.04)	0.3	CCl_4 (100)	12	2.9
m-Xylene	(0.2)	1.3	CCl_4 (75)	9	1.0

a) The yield of the sodium sulfonate based on the used alkylbenzenes.

TABLE II. UV AND IR SPECTRAL DATA OF THE RESULTING SULFONATES IN THE SULFOXIDATION

Sodium sulfonate	UV λ_{max} (mμ)	IR (KBr disk) Out-of-plane C-H deformation of adjacent hydrogen in benzene ring (cm^{-1})				
		1-H	2-H	3-H	4-H	5-H
Toluene	—	—	—	—	—	—
Ethylbenzene	256[a]	None	None	None	None	734, 696
ABTP	250[b]	None	None	None	None	758, 695
ABL	258[c]	None	None	None	None	751, 699
2,4-Dimethyl-benzene-1-	275.7[d]	874 (?)	832	None	None	None

a) In water.
b) In aqueous ethanol.
c) In ethanol.
d) In methanol.

TABLE III. UV AND IR SPECTRAL DATA OF THE AUTHENTIC SAMPLES

Sodium sulfonate	UV λ_{max} (mμ)	IR (KBr disk) Out-of-plane C-H deformation of adjacent hydrogen in benzene ring (cm^{-1})				
		1-H	2-H	3-H	4-H	5-H
o-Toluene	267[a]	None	None	None	753	None
p-Toluene	261[a]	None	815	None	None	None
ω-Toluene	258[a]	None	None	None	None	731, 693
p-Ethylbenzene	261[a] 262[b]	None	831	None	None	None
o- or *p*-ABTP	261[c]	None	830	None	758	None
p-ABL	268[b]	None	828	None	None	None
2,4-Dimethylbenzene-1-	275.7[d]	874	836	None	None	None
m-Xylene-*ω*-	273.2[d]	892	None	771	None	None

a) In water.
b) In ethanol.
c) In aqueous ethanol.
d) In methanol.

mechanism involving the excitation of a C-T complex between *m*-xylene and sulfur dioxide is unlikely because the complex has not been detected in carbon tetrachloride by ultraviolet spectroscopy. The sulfoxidation of toluene occurred only with difficulty. These facts can be explained by an equilibrium (Eq. 3′) where the benzyl radical is more stabilized than the *ω*-toluenesulfonyl radical.[11]

$$PhCH_2\cdot + SO_2 \rightleftarrows PhCH_2\dot{S}O_2 \qquad (3')$$

Consequently, *m*-xylene is probably sulfonated with the sulfur trioxide obtained from the photooxidation[4] of sulfur dioxide by the reactions of Eqs. 4 and 5:

$$SO_2 + O_2 \xrightarrow{h\nu} SO_3 \qquad (4)$$

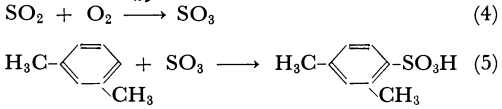

(5)

The very poor yield of the toluenesulfonate may be due to the fact that *m*-xylene is attacked by electrophilic sulfur trioxide more rapidly than toluene.

11) M. S. Kharasch and A. T. Reed, *J. Am. Chem. Soc.*, **61**, 3089 (1939).

A similar example of radical and ionic substitutions under irradiation has been reported in photochemical thiocyanation,[12] i. e., the reaction with thiocyanogen chloride in acetic acid occurs completely at the side-chain of ethylbenzene, but only partially at the ring of *m*-xylene, and entirely at the ring of mesitylene.

Table IV. The surface and the water-kerosene interfacial tensions of the aqueous solutions of sodium sulfonates of ABTP and ABL at 20°C

Position of substituted sulfonate group		Surface tension[a] dyne/cm.		Interfacial tension[b] dyne/cm.	
		0.1 g.%	0.05 g.%	0.1 g.%	0.05 g.%
ABTP	Side-chain	45.9	49.3	11.5	15.1
	Benzene	29.8	33.5	2.7	—
ABL	Side-chain	40.6	43.2	2.3	5.2
	Benzene	35.0	37.1	0.7	3.3

a) By Du Nouy tensiometer. The surface tension of distilled water is 68.7 dyne/cm. at 20°C.

b) By Du Nouy tensiometer. The interfacial tension between distilled water and kerosene is 35.8 dyne/cm. at 20°C.

12) R. G. R. Bacon and R. G. Guy, *J. Chem. Soc.*, **1961**, 2428.

m-Xylyl chloride and an aromatic carboxylic acid of an unknown structure were detected by gas chromatography and infrared spectroscopy respectively as minor side-reaction products in the photosulfoxidation of *m*-xylene. The latter showed the characteristic infrared peaks of aromatic carboxylic acid at 1720, 1690 and 1277 cm^{-1}. *m*-Xylyl chloride appears to be obtained by the chlorine-atom abstraction of the *m*-xylyl radical from the solvent, carbon tetrachloride,[13] while the carboxylic acid seems to be formed by the photooxidation of *m*-xylene.

The side-chain sulfonation of ABTP and ABL is a novel reaction. The surface and the water-kerosene interfacial tensions of the aqueous solutions of sodium sulfonates of ABTP and ABL are tabulated in Table IV, together with those of the ring-sulfonated ones. The results show that the side-chain-sulfonated ABTP and ABL are also good surfactants.

The authors wish to thank the Seitetsu Chemical Co., and the Nissan Chemical Co. for their gifts of materials.

13) C. Walling and M. J. Gibian, *J. Am. Chem. Soc.*, **86**, 3902 (1964).

BULLETIN OF THE CHEMICAL SOCIETY OF JAPAN VOL. 39 2441—2443 (1966)

The Reaction of Optically Active Silver β-Phenylisobutyrate with Halogen

By Shigeru OAE, Teruya KASHIWAGI and Seizi KOZUKA

Department of Applied Chemistry, Faculty of Engineering, Osaka City University, Sumiyoshi-ku, Osaka

(Received February 4, 1966)

The Hunsdiecker reaction of optically active silver β-phenylisobutyrate with bromine was carried out, and racemic β-phenylisopropyl bromide and optically atcive 3-methyl-7-bromohydrocoumarin were obtained as the major products. Meanwhile, the Simonini reaction was also performed with the same optically active acid and iodine; 1-phenyl-2-propyl β-phenylisobutyrate was obtained as the product here. Upon the hydrolysis of the ester, the resulting alcohol, β-phenylisopropyl alcohol, was found to be racemic. From these observations, the mechanisms involving the formation of the incipient free radical during the reactions were suggested for both the reactions.

There are two different pathways for the reaction between silver carboxylate and halogen, depending mainly upon the molarity of halogen used. One is known as the Hunsdiecker reaction[1]; it gives an alkyl halide, carbon dioxide and silver halide, when a silver carboxylate is treated with a one mole equivalent of halogen, usually bromine; the other pathway, known as the Simonini reaction,[1] gives an ester, carbon dioxide and silver halide, using two moles of halogen and generally employing iodine.

As for the Hunsdiecker reaction, a few stereochemical studies have been carried out using various optically active silver carboxylates. Bell and

1) a) R. G. Johnson and R. K. Ingham, *Chem. Revs.*, **56**, 219 (1956). b) C. V. Wilson, *Org. Reactions*, **9**, 332 (1957).

Smyth[2] reported that the Hunsdiecker reaction of optically active silver benzylethylacetates gave an almost completely inactive 2-bromo-1-phenylbutane. A similar racemization was reported by Arnold and Morgan[3] and also by Heintzeler[4]; they favored a radical process for this reaction. Meanwhile, there has been a report by Arcus, Campbell and Kenyon[5] that the Hunsdiecker reaction of silver (+)-α-phenylpropionate gave (+)-α-phenylethyl bromide to the extent of a 43.1% inversion of the configuration. On the other hand, no stereochemical study has been reported of the Simonini reaction.

During our recent studies of the thermal decompositions of diacyl peroxides,[6] we have had occasion to synthesize a few optically active carboxylic acids; thus we have extended the mechanistic investigation into the nature of these two reactions using an optically active silver carboxylate, namely silver β-phenylisobutyrate, in the hope of accumulating additional supporting evidence for the free radical nature of these reactions.

Results and Discussion

The Hunsdiecker Reaction.—A mixture of optically active silver β-phenylisobutyrate and bromine (in a one-to-one molar ratio) was refluxed in carbon tetrachloride for about 11 hr. The products obtained were practically racemized β-phenylisopropyl bromide, carbon dioxide, an optically active lactone (identified as 3-methyl-7-bromohydrocoumarin), silver bromide, and optically active β-phenylisobutyric acid. The yields and optical rotations of these products will be shown in the Experimental section.

The expected product of the Hunsdiecker reaction, β-phenylisopropyl bromide (obtained in about an 18% yield) was almost completely racemized within the range of experimental error. This result agreed well with the previous results reported[2-4] for similar reactions using other optically active carboxylic acids. The present stereochemical outcome can serve to support the free radical mechanism suggested for the formation of the bromide, as has been suggested by previous workers.[2-4,7]

β-Phenylisobutyric acid could be a reaction product, formed via the acyl hypobromite; however, the stereochemical outcome (retention) does not indicate whether β-phenylisobutyric acid is the recovered material or the reaction product.

It is interesting to note here that the formation of a substantial amount of 3-methyl-7-bromohydrocoumarin was obtained in this reaction. Although the formation of lactone in the Hunsdiecker reaction has rarely been reported, it may not be particularly unusual when the Hunsdiecker reaction is applied to a carboxylic acid that bears a phenyl group at the β-position. In fact, Pandit and Dirk[8a] reported that 4-phenylcoumarin and 4-phenylhydrocoumarin were obtained in 43 and 25% yields respectively in the reaction of silver salt of 3, 3-diphenylpropionic acid with bromine, while similar formations of lactones were reported by Berr[1a] and Wilt[8b]. The structure of the lactone, 3-methyl-7-bromohydrocoumarin, was confirmed from the information on infrared spectra, and NMR spectra and from an elemental analysis.

The Simonini Reaction.—The reaction of iodine in ether or a carbon tetrachloride solution with optically active silver β-phenylisobutyrate at a boiling temperature yields optically active 1-phenyl-2-propyl β-phenylisobutyrate, carbon dioxide, silver iodide, and optically active β-phenylisobutyric acid. In this case, however, no detectable amount of the lacton was formed. The ester obtained was then subjected to alkaline hydrolysis in order to examine the stereochemical change in the alcohol moiety. The results will be shown in the Experimental section.

The β-phenylisopropyl alcohol thus obtained from the hydrolysis of the ester was completely racemized, indicating that the ester was formed via a symmetrical intermediate, probably the 1-phenyl-2-propyl radical, at the initial stage of the formation of 1-phenyl-2-propyl iodide; this iodide eventurally would react with the silver salt to form the ester in the following stage of the ionic process.[9]

Experimental

(+)- and (−)-Silver β-Phenylisobutyrate.—Optically active β-phenylisobutyric acid was prepared following DeTar's method.[10] The optically active acid ($[\alpha]_D^{17}$ +21.7, *c* 0.0559 and $[\alpha]_D^{15}$ −9.8, *c* 0.0254) was neutralized with aqueous potassium hydroxide, and the hot solution was treated with a one-equivalent amount of aqueous silver nitrate. The preciptated silver salt was washed with water and acetone, and then dried on phosphorous pentoxide in vacuo.

2) F. Bell and I. F. B. Smyth, *J. Chem. Soc.*, **1949**, 2372.
3) R. T. Arnold and P. Morgan, *J. Am. Chem. Soc.*, **70**, 4248 (1948).
4) M. Heintzeler, *Ann.*, **569**, 102 (1950).
5) C. L. Arcus, A. Campbell and J. Kenyon, *J. Chem. Soc.*, **1949**, 1510.
6) S. Oae, T. Kashiwagi and S. Kozuka, *Chem. & Ind.*, **1965**, 1694.
7) a) C. C. Price, "Mechanisms of the Reaction of Carbon-Carbon Double Bonds," Interscience, Publishers, New York (1946), p. 55. b) W. T. Smith, Jr., and R. L. Hull, *J. Am. Chem. Soc.*, **72**, 3309 (1950).
8) a) U. K. Pandit and I. P. Dirk, *Tetrahedron Letters*, No. 14, 891 (1963). b) J. W. Wilt and J. A. Lundquist, *J. Org. Chem.*, **29**, 921 (1964).
9) a) J. D. Roberts and H. E. Simmons, Jr., *J. Am. Chem. Soc.*, **73**, 5487 (1951). b) R. N. Haszeldine and A. G. Sharpe, *J. Chem. Soc.*, **1952**, 993. c) H. Wielland and F. G. Fischer, *Ann.*, **446**, 49 (1926).
10) D. F. DeTar and C. Weis, *J. Am. Chem. Soc.*, **79**, 3045 (1957).

The Hunsdiecker Reaction.—Silver salt (6 g.) was suspended with stirring in boiling dry carbon tetrachloride (54 ml.), to which bromine (3.6 g.) was then added. The solution was heated under refluxing for about 8 hr., allowed to stand overnight, and then refluxed with stirring for 3 hr. During this period, the evolution of a detectable amount of carbon dioxide was noticed by passing the gas through a saturated barium hydroxide solution. The reaction mixture was filtered. The filtrate was washed with 30 ml. of 10% sodium bicarbonate and then with water, and then the aqueous layer was extracted with carbon tetrachloride. The carbon tetrachloride layers were then combined and dried over sodium sulfate. There were thus obtained 0.8 g. of β-phenylisopropyl bromide (b. p. 90°C/10 mmHg) and 150 mg. of 3-methyl-7-bromohydrocoumarin (b. p. 126—130°C/1 mmHg; m. p. 127—128°C) by fractional distillation, and 0.75 g. of the tarry residue was left. β-Phenylisopropyl bromide, which was identified by comparing its infrared spectrum with that of an authentic sample, was practically all racemized; $[\alpha]_D^{20}$ +1.3, *c* 0.0365 (using (−)-silver salt), +0.88, *c* 0.0756 (using (+)-silver salt). 3-Methyl-7-bromohydrocoumarin was in the form of colorless crystalline plates, m. p. 127—128°C (from ethyl alcohol), Found: C, 50.22; H, 4.11. Calcd. for $C_{10}H_9O_2Br$: C, 49.82; H, 3.76; spectral peaks appeared at: IR: 1760 cm^{-1} and 1715 cm^{-1}; UV: λ_{max}^{EtOH} 275, 283, 321 mμ; λ_{min}^{EtOH} 298 mμ; 60 MC. NMR (Deuterochloroform): a doublet at 1.36 τ, a multiplet at 2.87 τ, and a multiplet at 7.12 τ. The peak areas are in the ratio of 1 : 1 : 1. The position of bromine on the benzene ring was assigned from the NMR spectra, thus, 5-H; multiplet at 6.88 τ, 6-H; doublet at 7.43 τ, 8-H; singlet at 7.29 τ, (intensities 1 : 1 : 1). $[\alpha]_D^{22}$ +12.0, *c* 0.029 (using (+)-silver salt). Meanwhile, 1 g. of optically active β-phenylisobutyric acid ($[\alpha]_D^{20}$ +21.2, *c* 0.0636 (using (+)-silver salt), −9.8 (using (−)-silver salt), b. p. 122°C/2 mmHg) was obtained by acidifying the water layer with concentrated sulfuric acid.

The Simonini Reaction.—Optically active silver β-phenylisobutyrate (8 g.) was suspended in dry ether (50 ml.), into which was then stirred iodine (3.7 g). in dry ether (17 ml.). The solution immediately turned light yellow. It was then refluxed for 3 hr. under a nitrogen stream. The carbon dioxide (about 0.18 g.) evolved was trapped through an aqueous barium hydroxide solution. The silver iodide was separated from the reaction mixture by filtration; the filtrate was washed initially with a 5% aqueous potassium hydroxide solution, then with aqueous sodium thiosulfate, and finally with water, and then dried over sodium sulfate. Only 2.3 g. of optically active 1-phenyl-2-propyl β-phenylisobutyrate ($[\alpha]_D^{15}$ +30.8, *c* 0.0635 (using (+)-silver salt), −12.9, *c* 0.0416 (using (−)-silver salt), b. p. 145°C/1 mmHg) was obtained from the ether layer. One gram of optically active β-phenylisobutyric acid ($[\alpha]_D^{13}$ +21.7, *c* 0.0584 (using (+)-silver salt), −9.8 (using (−)-silver salt)) was obtained from the water layer.

By using carbon tetrachloride instead of ether as a solvent, a similar result was also obtained.

The hydrolysis of the optically active ester (1.3 g.) was performed by allowing it to dissolve in a mixture of potassium hydroxide (0.5 g.), water (0.2 g.), and methyl alcohol (12 ml.) at room temperature for 3 hr. Optically inactive β-phenylisopropyl alcohol (b. p. 74—76°C/3 mmHg, $[\alpha]_D^{15}$ +0.5, *c* 0.054 (using the (+)-ester), +0.7, *c* 0.0353 (using the (−)-ester)) and optically active β-phenylisobutyric acid ($[\alpha]_D^{13}$ +21.7, *c* 0.0431 (using the (+)-ester), −9.8, *c* 0.0254 (using the (−)-ester)) were obtained. In a separate experiment, it was confirmed that there was no change in optical rotation for this and a similar alcohol under the same conditions as in the hydrolysis.

The optical rotations of all the above samples were measured in absolute ethyl alcohol.

The authors wish to thank Dr. Tetsushi Yamashita, Department of Chemistry, Faculty of Science, Osaka City University, for his help in the use of the polarimeter, and Dr. Yutaka Asahi, Laboratory of Takeda Chem. Ind., Ltd., for his collaboration in the NMR study.

BULLETIN OF THE CHEMICAL SOCIETY OF JAPAN VOL. 39 2444—2449 (1966)

Heptafulvenes. V. Some Substitution Reactions of 2, 3-Dimethoxy-8, 8-dicyanoheptafulvenes

By Yoshio KITAHARA,*1 Kozo DOI*2 and Tadahiro KATO*1

Chemical Research Institute of Non-Aqueous Solutions, Tohoku University, Katahira-cho, Sendai

(Received February 19, 1966)

Methoxyl groups of alkyl-2, 3-dimethoxy-8, 8-dicyanoheptafulvenes were easily replaced by various kinds of nucleophilic reagents to give the corresponding substituted-8, 8-dicyanoheptafulvenes. There exists a difference in reactivity between the two methoxyl groups located at the 2 and 3 positions of 8, 8-dicyanoheptafulvenes. The isopropyl group at the 4 position of 2, 3-dimethoxy-8, 8-dicyanoheptafulvene hindered some substitution reactions of the methoxyl group at the 3 position.

The previous paper[1] reported the formation of 2, 3-dimethoxy-8, 8-dicyanoheptafulvene and its alkyl derivatives. Since isopropyl-2, 3-dimethoxy-8, 8-dicyanoheptafulvene (I) possesses the large dipole moment of 8.85 Debye units, there may be considered to be a large contribution of the ionic structure (II).[2a] The π-electron density at each atom in the heptafulvene derivative has also been calculated by Katagiri[2b] (Fig 1).

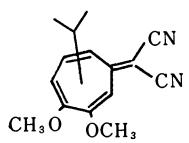

(I)

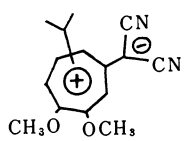

(II)

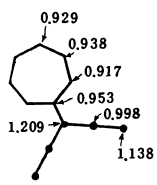

Fig. 1. π-Electron density at each atom in 8,8-divinyl heptafulvene (by Katagiri).

On the basis of these data, the methoxyl groups at the 2 and 3 positions of I may be expected to undergo various kinds of nucleophilic substitution reactions, and it is reasonable to expect that there is a difference between the reactivities of the methoxyl groups at the 2 and 3 positions and that the group at the 3 position might be more reactive if other factors are not considered.

When 5-isopropyl-2, 3-dimethoxy-8, 8-dicyanoheptafulvene (III) is allowed to react with such amines as ammonia, methylamine and dimethylamine, the disubstituted products, V, VI and VII, respectively, are formed.

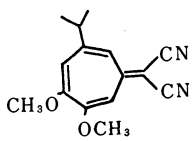

(III)

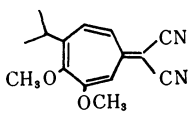

(IV)

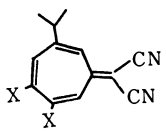

(V) X=NH_2
(VI) X=$NHCH_3$
(VII) X=$N(CH_3)_2$

V reacts with acids or acid chlorides to give as products VIII, IX, X and XI, all of which have an imidazole nucleus. The possibility of these condensation products being 1, 3-diazaazulene derivatives (structure b) was eliminated by an examination of their infrared and ultraviolet absorption spectra. The infrared spectra of these compounds show conjugated nitriles at 2175 and 2195 cm^{-1}, and their ultraviolet spectra are completely different from that of 1, 3-diazaazulene.[3] III reacts with guanidine to give the corresponding condensation product. From its molecular formula and its spectral data, it was concluded

*1 Present address: Department of Chemistry, Tohoku University, Katahira-cho, Sendai.

*2 Present address: Hirosaki University, Bunkyo-machi, Hirosaki.

1) Y. Kitahara, K. Doi and T. Kato, This Bulletin, **37**, 1747, 1750 (1964).

2a) S. Katagiri, K. Doi, Y. Kitahara and H. Azumi, ibid., to be published. T. Nozoe and K. Takase, "Dai Yuki Kagaku" (Comprehensive Organic Chemistry), **13**, Asakura-shoten, Tokyo (1960), p. 531.

2b) By private communication, Katagiri calculated the π-electron density at each atom of the hypothetical 8, 8-divinyl heptafulvene.

3) I. Murata, This Bulletin, **33**, 56 (1960).

that the product has the heptafulvene structure (XIIa or XIIb).

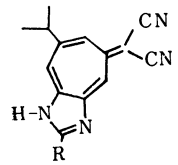

(a)

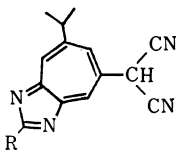

(b)

(VIII) R=H
(IX) R=CH_3
(X) R=Ph
(XI) R=*p*-NO_2·Ph

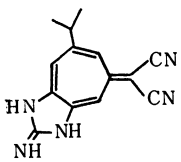

(XIIa)

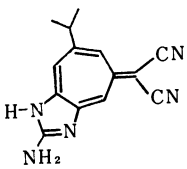

(XIIb)

4-Isopropyl-2, 3-dimethoxy-8, 8-dicyanoheptafulvene (IV) gave a yellow crystalline substance (XIII) and a white crystalline substance (XIV) in almost equal amounts upon reaction with liquid ammonia. The composition of both XIII and XIV satisfies $C_{13}H_{14}N_4$, but their ultraviolet absorption spectra are quite different. The spectrum of XIII is similar to that of 8, 8-dicyanoheptafulvene, but the spectrum of XIV, which shows no absorption in the longer wave region and which is similar to that of dicyanostyrene, suggests that XIV does not possess a heptafulvene structure. XIV seems to be a six-membered ring compound formed by rearrangement reaction* during the formation of XIII.

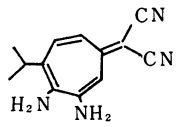

(XIII)

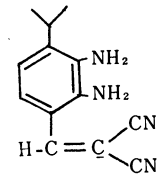

(XIV)

III readily undergoes substitution reactions with sodium ethoxide or sodium ethyl mercaptide, affording a disubstituted product, XV or XVI respectively. In the case of IV, however, the reaction with sodium ethyl mercaptide affords not a disubstituted product but monosubstituted product (XVII); this is due to the steric hindrance of the isopropyl group to the attack of the anionoid reagent.

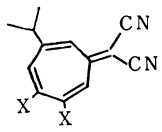

(XV) X=OC_2H
(XVI) X=SC_2H_5

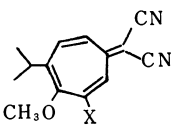

(XVII) X=SC_2H_5

IV reacts with hydrazine to afford a monohydrazino compound (XVIIIa or XVIIIb). The XVIIIa structure is more likely for the compound since the steric hindrance of the isopropyl group would be expected to prevent the 3-methoxyl group from substituting.

The reaction of III with sodium hydrogen sulfide gives a monosubstituted product whose composition corresponds to XIX. XIX is acidic, and the mercapto group is readily methylated by diazomethane to yield XX. By the reaction with ethylenediamine or with hydrazine, III does not afford a disubstituted product, but gives a monosubstituted product, XXI or XXII. For each of these monosubstituted products, there are two possible structures, a and b.

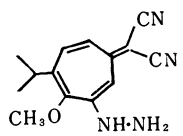

(XVIIIa)

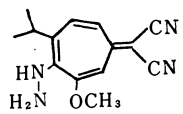

(XVIIIb)

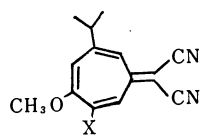

(a)

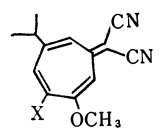

(b)

(XIX) X=SH
(XX) X=SCH_3
(XXI) X=NH·$(CH_2)_2$·NH_2
(XXII) X=NH·NH_2

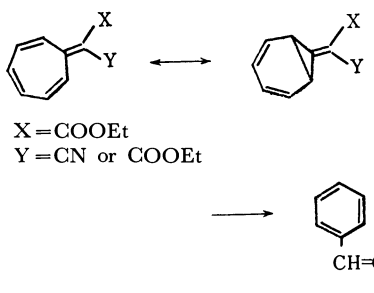

X=COOEt
Y=CN or COOEt

* However, the chemical proof of the structure of XIV will be the subject of further investigation. It is known that 8, 8-disubstituted heptafulvenes undergo a base-catalyzed rearrangement to styrene derivatives; for example, Kitahara and Doi[4] found that 8-cyano-8-ethoxycarbonylheptafulvene and 8, 8-diethoxycarbonylheptafulvene are unstable in alkali and that they easily rearrange to styrene derivatives in the presence of sodium methoxide.

4) Heptafulvenes III, ibid., **37**, 1754 (1964).

It is not apparent that the methoxyl group at the 2 position of III is more reactive than that of the 3 position. Because III lacks the steric interference from an adjacent isopropyl group, unlike IV, the two possible structures, a and b, must be considered as equally likely. However, the ultraviolet and infrared absorption spectra support a.[5]

On the basis of these results, it may be concluded that there is a difference between the reactivities of the methoxyl groups at the 2 and 3 positions, and that the one at the 2 position undergoes nucleophilic substitution reactions more easily.

The above conclusion is not in accord with the results calculated by Katagiri. This inconsistency is considered to arise from the interaction between the adjacent two methoxyl groups, and from complication factors, such as the π-p conjugation between the lone paired electrons of the oxygen atom of the methoxyl and the electrons in the ring, which cause discrepancies in the simple calculation.

The hydrazino group of XVIII can be removed by treatment with cupric sulfate - acetic acid to give XXIII, which reacts readily with certain amines to produce the corresponding aminoheptafulvenes, XXIV, XXV or XXVI. However, XXIII does not react with dimethylamine, apparently because of the steric hindrance of the isopropyl group adjacent to the methoxyl group.

The methoxyl group of XXIII is readily hydrolyzed with alkali to yield the corresponding hydroxy compound, which is considered to have the XXVIIa structure rather than the tautomeric keto form, XXVIIb, on the basis of the following facts: (i) the ultraviolet absorption spectrum of the hydroxy compound is similar to that of heptafulvene, (ii) the infrared absorption spectrum of the compound indicates the presence of a conjugated nitrile, and (iii) the compound gives an acetate (XXVIII).

When treated with cupric sulfate - acetic or hydrochloric acid, XXIV affords 3-isopropyl-8, 8-dicyanoheptafulvene (XXIX) or 3-chloro-4-isopropyl-8, 8-dicyanoheptafulvene (XXX) respectively.

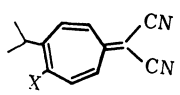

(XXIII) X=OCH_3 (XXVIIa) X=OH
(XXIV) X=$NH \cdot NH_2$ (XXVIII) X=OAc
(XXV) X=NH_2 (XXIX) X=H
(XXVI) X=$NHCH_3$ (XXX) X=Cl

XXII yields XXXI by the analogous dehydrazination reaction. The methoxyl group of XXXI

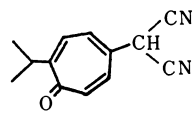

(XXVIIb)

is readily replaced by amino groups to produce the aminoheptafulvenes, XXXII, XXXIII or XXXIV. Because of the absence of the steric interference of the isopropyl group, XXXI gives XXXV by reaction with dimethylamine.

The dehydrazination of XXXII gives 2-isopropyl-8, 8-dicyanoheptafulvene XXXVI. XXXII readily condenses with tropone to yield the corresponding condensation products, XXXVII.

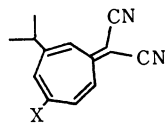

(XXXI) X=OCH_3 (XXXIV) X=$NHCH_3$
(XXXII) X=$NH \cdot NH_2$ (XXXV) X=$N(CH_3)_2$
(XXXIII) X=NH_2 (XXXVI) X=H

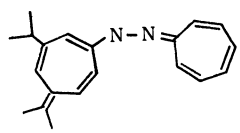

(XXXVII)

Experimental

The Reaction of 5-Isopropyl-2, 3-dimethoxy-8, 8-dicyanoheptafulvene (III) with Amines.—*Liquid Ammonia.*—A mixture of 1.5 g. of III and 30 ml. of liquid ammonia was allowed to stand at room temperature for 2 days. The evaporation of the resulting red solution left a yellow crystalline residue which was then dissolved in ethanol and chromatographed over alumina. The recrystallization of the eluted crystals from methanol gave orange needles of V, m. p. >260°C.

Found: C, 68.98; H, 5.92; N, 24.56. Calcd. for $C_{13}H_{14}N_4$: C, 69.00; H, 6.24; N, 24.76%.

UV λ_{max}^{MeOH} mμ (log ε): 245 (4.11), 335 (4.45), 405 (4.45).

Liquid Methylamine.—By a procedure similar to that described above, 500 mg. of III and 30 ml. of liquid methylamine afforded 430 mg. of orange scales (VI) after recrystallization from ethanol, m. p. 260—261°C (decomp.).

Found: C, 71.08; H, 6.54; N, 21.53. Calcd. for $C_{15}H_{18}N_4$: C, 70.83; H, 7.13; N, 22.03%.

UV λ_{max}^{MeOH} mμ (log ε): 258 (4.14), 330 (4.36), 425 (4.42).

Liquid Dimethylamine.—A mixture of 700 mg. of III and 50 ml. of liquid dimethylamine, after recrystallization from ethanol, yielded 500 mg. of VII as red prisms, m. p. 184—185°C.

Found: C, 72.14; H, 7.38; N, 19.44. Calcd. for $C_{17}H_{22}N_4$: C, 72.30; H, 7.85; N, 19.84%.

5) Heptafulvenes VII, to be published.

UV λ_{max}^{MeOH} mμ (log ε): 285 (4.01), 340 (4.17), 455 (4.24).

The Reaction of 2, 3-Diamino-5-isopropyl-8, 8-dicyanoheptafulvene V with Acids or Acid Derivatives.—*With Formic Acid.*—A mixture of 5 ml. of 80% formic acid and 400 mg. of V was refluxed for 30 min. After the excess formic acid had been removed under reduced pressure, the resulting red crystalline material was recrystallized from methanol to yield 180 mg. of red scales (VIII), m. p. >280°C.

Found: C, 71.19; H, 4.74; N, 23.80. Calcd. for $C_{14}H_{12}N_4$: C, 71.16; H, 5.12; N, 23.72%.

UV λ_{max}^{MeOH} mμ (log ε): 245 (4.20), 290 (4.00), 410 (4.52).

With Acetic Anhydride.—A mixture of 300 mg. of V and 20 ml. of acetic anhydride was refluxed for one hr., after which the acetic anhydride was distilled off under reduced pressure. The addition of water to the residue precipitated red crystals (200 mg.) which, after filtration, were taken up in ethanol and passed through an alumina column. The recrystallization of the eluted material from ethanol gave red scales (IX), m. p. >300°C.

Found: C, 71.68; H, 5.11; N, 21.95. Calcd. for $C_{15}H_{14}N_4$: C, 71.97; H, 5.64; N, 22.39%.

UV λ_{max}^{MeOH} mμ (log ε): 250 (4.27), 295 (4.17), 415 (4.54).

With Benzoyl Chloride.—A solution of 400 mg. of V in 10 ml. of anhydrous pyridine was mixed with 1.5 mol. equivalents of benzoyl chloride and allowed to stand at room temperature overnight. After the pyridine had been distilled off, the residue was refluxed in 20 ml. of methanol for one hr. and then allowed to cool. The red crystalline deposit (300 mg.), after recrystallization from an ethyl acetate-methanol (1 : 1) mixture, afforded reddish violet scales (X), m. p. >300°C.

Found: C, 76.93; H, 4.71; N, 17.53. Calcd. for $C_{20}H_{16}N_4$: C, 76.90; H, 5.16; N, 17.94%.

UV λ_{max}^{MeOH} mμ (log ε): 240 (4.30), 265 (4.24), 330 (4.50), 410 (4.57).

With p-Nitrobenzoyl Chloride.—The reaction between V and *p*-nitrobenzoyl chloride was carried out in a manner similar to that described above. The crude crystals obtained from the reaction of 220 mg. of V and 200 mg. of *p*-nitrobenzoyl chloride in 10 ml. of pyridine were recrystallized from acetone to afford blackish-violet scales (XI), m. p.—300°C.

Found: C, 67.42; H, 4.21; N, 19.57. Calcd. for $C_{20}H_{15}N_5O_2$: C, 67.22; H, 4.23; N, 19.60%.

UV λ_{max}^{MeOH} mμ (log ε): 260 (4.31), 337 (4.57), 413 (4.62).

The Reaction of III with Guanidine.—III (500 mg.) was added to a solution of 200 mg. of guanidine hydrochloride in ethanolic sodium ethoxide (prepared from 50 mg. of sodium and 20 ml. of absolute ethanol), and the mixture was refluxed for 5 hr. The removal of the ethanol afforded a red oil which was then chromatographed over alumina. Ethyl acetate was used as the solvent; 100 mg. of the crystals were obtained from early fractions which, after recrystallization from ethyl acetate, afforded XV as orange plates, m. p. 143—144°C.

Found: C, 71.75; H, 6.86; N, 9.27. Calcd. for $C_{17}H_{20}N_2O_2$: C, 71.80; H, 7.09; N, 9.85%.

UV λ_{max}^{MeOH} mμ (log ε): 245 (4.29), 275 (4.16), 295 (4.17), 408 (4.45).

Then (1 : 1 ethyl acetate-methanol) crystals (210 mg.) were obtained; on recrystallization from ethanol, they gave XII as red needles, m. p. >290°C.

UV λ_{max}^{MeOH} mμ (log ε): 255 (4.13), 310 (4.23), 330 (4.28), 410 (4.54).

Picrate: m. p. 262—263°C (decomp.) Found: C, 49.95; H, 3.47; N, 23.02. Calcd. for $C_{14}H_{13}N_5 \cdot C_6H_3N_3O_7$: C, 50.00; H, 3.35; N, 23.32%.

The Reaction of III with Sodium Ethyl Mercaptide.—A mixture of 250 mg. of III and 20 ml. of ethyl mercaptan containing 50 mg. of sodium was refluxed for 8 hr., and then most of the mercaptan was distilled off. The residue was diluted with 50 ml. of water, and extracted with ethyl acetate. The ethyl acetate extract was washed with water, dried over magnesium sulfate, and evaporated to yield 150 mg. of red crystals which, after recrystallization from ethanol, gave red scales of XVI, m. p. 106—107°C.

Found: C, 64.17; H, 6.34; N, 8.50. Calcd. for $C_{17}H_{20}N_2S_2$: C, 64.54; H, 6.37; N, 8.86%.

UV λ_{max}^{MeOH} mμ (log ε): 295 (sh.), 345 (4.27), 438 (4.45).

The Reaction of III and Sodium Hydrogen Sulfide.—A sodium ethoxide solution (prepared from 5 ml. of absolute ethanol and 70 mg. of sodium) was saturated with hydrogen sulfide, and then 200 mg. of III was added. After the mixture had been heated for several minutes, the ethanol was removed and the residue was diluted with dilute sulfuric acid to afford 200 mg. of yellow crystals (XIX), m. p. 219—220°C (decomp.). When XIX was heated in ethanol, it changed into an insoluble blackish-red material which could not be purified.

A suspension of 200 mg. of the crude XIX in ethanol was treated with an excess of diazomethane. After the solvent had been removed, the residue was dissolved in benzene and passed through an alumina column. The evaporation of the solvent afforded red needles (XX), m. p. 174—175°C.

Found: C, 66.13; H, 6.14; N, 9.97. Calcd. for $C_{15}H_{16}N_2OS$: C, 66.16; H, 5.92; N, 10.29%.

UV λ_{max}^{MeOH} mμ (log ε): 260 (4.15), 330 (4.04), 415 (4.47).

The Reaction of III with Ethylenediamine.—To a solution of 50 ml. of absolute ethanol containing 90 mg. of sodium, 260 mg. of ethylenediamine hydrochloride and 510 mg. of III were added, the mixture was then refluxed for one hr. The removal of the ethanol afforded a red oil which, after being chromatographed over alumina using ethanol, yielded 300 mg. of crystals. Recrystallization from ethanol gave orange plates (XXI), m. p. 248—250°C (decomp.).

Found: C, 67.77; H, 6.77; N, 19.37. Calcd. for $C_{16}H_{20}N_4O$: C, 67.58; H, 7.09; N, 19.71%.

UV λ_{max}^{MeOH} mμ (log ε): 250 (4.17), 350 (4.55), 410 (4.37).

The Reaction of III with Hydrazine.—A large excess of 80% hydrazine was added to a suspension of 400 mg. of III in 40 ml. of ethanol at 50°C. The mixture was heated for 5 min., and then diluted with 200 ml. of water to give 260 mg. of crystals. Recrystallization from an ethanol-ethyl acetate mixture afforded orange scales (XXII), m. p. 204—205°C (decomp.).

Found: C, 65.72; H, 5.93; N, 21.84. Calcd. for $C_{14}H_{16}N_4O$: C, 65.60; H, 6.29; N, 21.86%.

UV λ_{max}^{MeOH} mμ (log μ): 240 (4.24), 325 (4.33), 405 (4.44).

The Reaction of 4-Isopropyl-2, 3-dimethoxy- 8, 8-dicyanoheptafulvene (IV) with Liquid Ammonia.—A mixture of 450 mg. of IV and 40 ml. of liquid ammonia was allowed to stand overnight at room temperature, and then the ammonia was distilled off. The residue was treated with methanol. The methanol-insoluble yellow crystalline material (150 mg.) was dissolved in ethanol and chromatographed over alumina to afford yellow crystals (XIII), m. p. >260°C.

Found: C, 68.93; H, 6.23; N, 24.95. Calcd. for $C_{13}H_{14}N_4$: C, 69.00; H, 6.24; N, 24.76%.

UV λ_{max}^{MeOH} mμ (log ε): 225 (4.25), 245 (4.01), 330 (4.38), 410 (4.47).

From the methanol-soluble part, 150 mg. of white needles (XIV), m. p. >270°C, were obtained.

Found: C, 68.43; H, 6.01; N, 24.42. Calcd. for $C_{13}H_{14}N_4$: C, 69.00; H, 6.24; N, 24.76%.

UV λ_{max}^{MeOH} mμ (log ε): 225 (4.26), 300 (4.36).

The Reaction of IV with sodium Ethyl Mercaptide.—To 30 ml. of ethyl mercaptan containing 80 mg. of sodium, 500 mg. of IV were added, and then the mixture was refluxed for 8 hr. After the ethyl mercaptan had been removed, the residue was treated with water and extracted with ethyl acetate. The ethyl acetate extract was washed with dilute sulfuric acid and then with water. Drying over magnesium sulfate and the removal of the solvent afforded 500 mg. of a red oil, which was then taken up in benzene and chromatographed on alumina. Red plates (XVII), m. p. 131—132°C, were obtained after recrystallization from ethanol.

Found: C, 66.82; H, 6.06; N, 9.63. Calcd. for $C_{16}H_{18}N_2OS$: C, 67.11; H, 6.34; N, 9.78%.

UV λ_{max}^{MeOH} mμ (log ε): 225 (3.87), 335 (4.26), 442 (4.42).

The Reaction of IV with Hydrazine.—By the procedure described for the formation of XXII from III, 200 mg. of red needles (XVIII), m. p. 208—209°C, were obtained from 300 mg. of IV.

Found: C, 65.98; H, 6.06; N, 21.99. Calcd. for $C_{14}H_{16}N_4O$: C, 65.60; H, 6.29; N, 21.86%.

UV λ_{max}^{MeOH} mμ (log μ): 243 (4.09), 315 (4.24), 405 (4.42).

The Dehydrazination of 2-Hydrazino-5-isopropyl-3-methoxy-8, 8-dicyanoheptafulvene (XXII).—Into a boiling suspension of 200 mg. of XXII in a mixed solvent of 5 ml. of acetic acid and 5 ml. of water, 10 ml. of a 10% aqueous cupric sulfate solution was stirred, drop by drop. The boiling was continued for 20 min., after which time gas evolution ceased. The reaction mixture was allowed to come to room temperature, and then diluted with water and extracted with ethyl acetate. The ethyl acetate extract was washed with a dilute aqueous sodium hydroxide solution and then with water, dried over magnesium sulfate, and evaporated. The brown crystalline residue was dissolved in ethyl acetate and passed through an alumina column. The crystals (100 mg.) so obtained were recrystallized from ethanol to give orange needles (XXXI), m. p. 175.5—177.5°C.

Found: C, 74.09; H, 5.85; N, 12.51. Calcd. for $C_{14}H_{14}N_2O$: C, 74.31; H, 6.24; N, 12.38%.

UV λ_{max}^{MeOH} mμ (log ε): 238 (4.29), 280 (3.85), 418 (4.48).

The Dehydrazination of XVIII.—The procedure was the same as that described for the dehydrazination of XXII. Red prisms (XXIII), m. p. 141—142°C, after recrystallization from ethanol, were obtained from XVIII.

Fonnd: C, 74.36; H, 6.12; N, 12.54. Calcd. for $C_{14}H_{14}N_2O$: C, 74.31; H, 6.24; N, 12.38%.

UV λ_{max}^{MeOH} mμ (log ε): 238 (4.03), 250 (4.04), 428 (4.50).

Depending on the experimental conditions, orange needles, m. p. 255°C (decomp.), could be obtained in addition to XXIII.

Found: C, 64.36; H, 5.74; N, 18.63. Calcd. for $C_{16}H_{18}N_4O_2$: C, 64.41; H, 6.08; N, 18.78%.

UV λ_{max}^{MeOH} mμ (log ε): 240 (4.09), 307 (4.29), 410 (4.58).

IR: 3250 (NH), 1660, 1626, 1285 cm^{-1}.

From the results of microanalysis and a study of its infrared spectrum, the above compound was deduced to be 2-acetylhydrazino-4-isopropyl-3-methoxy-8, 8-dicyanoheptafulvene.

The Reaction of XXIII with Hydrazine.—To a solution of 100 mg. of XXIII in 2 ml. of ethanol there was added 27 mg. of a 80% hydrazine hydrate aqueous solution. The concentration of this solution afforded 50 mg. of red crystals which were recrystallized from ethanol to give red prisms (XXIV), m. p. 187—188°C (decomp.).

Found: C, 68.92; H, 5.81; N, 25.13. Calcd. for $C_{13}H_{14}N_4$: C, 69.00; H, 6.24; N, 24.76%.

UV λ_{max}^{MeOH} mμ (log ε): 250 (4.12), 330 (3.89), 465 (4.56).

The Reaction of XXIII with Ammonia.—A mixture of 50 mg. of XXIII and 10 ml. of methanolic ammonia was allowed to stand overnight at room temperature; then the solvent was removed. The resulting crystalline material was recrystallized from ethanol to give orange prisms (XXV), m. p. 234—235°C (decomp.).

Found: C, 73.90; H, 5.67; N, 20.27. Calcd. for $C_{13}H_{13}N_3$: C, 73.90; H, 6.20; N, 19.89%.

UV λ_{max}^{MeOH} mμ (log ε): 250 (4.17), 308 (3.88), 465 (4.59).

The Reaction of XXIII with Methylamine.—To a solution of 50 mg. of XXIII in 4 ml. of ethanol, 1 ml. of a 40% aqueous methylamine solution was added; the mixture was then refluxed for 5 min. On cooling to room temperature, 50 mg. of orange needles (XXVI), m. p. 256—257°C (decomp.), were obtained.

Found: C, 75.05; H, 6.26; N, 18.64. Calcd. for $C_{14}H_{15}N_3$: C, 74.64; H, 6.71; N, 18.65%.

UV λ_{max}^{MeOH} mμ (log ε): 220 (4.31), 255 (4.10), 325 (3.85), 465 (4.57).

The Reaction of XXIII with Dimethylamine.—To a solution of 50 mg. of XXIII in 6 ml. of ethanol, 1 ml. of a 33% aqueous dimethylamine solution was added. The concentration of this mixture afforded 20 mg. of orange needles, m. p. 255—256°C (decomp.), which were identified as XXVI by microanalysis and by a study of their infrared spectrum. XXVI seems to be formed by the reaction of XXIII with the methylamine contained in the dimethylamine.

3-Hydroxy-4-isopropyl-8, 8-dicyanoheptafulvene (XXVII).—A mixture of 200 mg. of XXIII, 20 ml. of water, and 2 N sodium hydroxide was heated. The acidification of the resulting red solution with sulfuric acid precipitated crystals which were recrystallized from benzene-methanol to afford orange prisms (XXVII), m. p. 226—227°C (decomp.).

Found: C, 73.36; H, 5.23; N, 13.40. Calcd. for $C_{13}H_{12}N_2O$: C, 73.56; H, 5.70; N, 13.20%.

UV λ_{max}^{MeOH} mμ (log ε): 243 (4.19), 295 (3.64), 440 (4.60).

The Acetylation of XXVII.—After a mixture of 150 mg. of XXVII and 2 ml. of acetic anhydride has been refluxed for 1 hr., the solvent was distilled off. The recrystallization of the residue from methanol afforded 80 mg. of orange scales (XXVIII) m. p. 137—138°C.

Found: C, 71.07; H, 5.24; N, 11.28. Calcd. for $C_{15}H_{14}N_2O_2$: C, 70.85; H, 5.55; N, 11.02%.

UV λ_{max}^{MeOH} mμ (log ε): 235 (4.10), 257 (4.11), 397 (4.43).

3-Chloro-4-isopropyl-8, 8-dicyanoheptafulvene (XXX).—Into a boiling solution of 2 g. of cupric sulfate in 4 ml. of water, a solution of 100 mg. of XXIV in 6 ml. of concentrated hydrochloric acid was stirred, drop by drop. The heating was continued until the evolution of nitrogen gas ceased. After it had then been allowed to cool to room temperature, the mixture was diluted with water and extracted with ethyl acetate. The extract was washed with water and dried over magnesium sulfate, and the solvent was distilled off. The red, oily residue, after being chromatographed over alumina using a mixed solvent of benzene and ethyl acetate (5 : 1), afforded 20 mg. of orange needles (XXX), m. p. 143—144°C.

Found: C, 68.08; H, 4.59; N, 12.20. Calcd. for $C_{13}H_{12}N_2Cl$: C, 67.69; H, 4.81; N, 12.15%.

UV λ_{max}^{MeOH} mμ (log ε): 240 (4.07), 257 (4.09), 397 (4.40).

3-Isopropyl-8, 8-dicyanoheptafulvene (XXIV).—Into a boiling solution of 5 g. of cupric sulfate in 10 ml. of water and 5 ml. of acetic acid, 180 mg. of XXIV were stirred and then the mixture was heated for 10 min. After being allowed to cool to room temperature, the reaction mixture was extracted with ethyl acetate. The extract was washed with dilute sodium hydroxide and then with water, and dried. The removal of the solvent afforded orange crystals which, after being chromatographed over alumina using a benzene-ethyl acetate (10 : 1) mixture, gave 50 mg. of crystals. Recrystallization from ethanol-cyclohexane gave red needles (XXIX), m. p. 120—121°C.

Found: C, 79.49; H, 5.83; N, 14.33. Calcd. for $C_{13}H_{12}N_2$: C, 79.56; H, 6.16; N, 14.28%.

UV λ_{max}^{MeOH} mμ (log ε): 232 (4.06), 255 (4.10), 397 (4.42).

3-Hydrazino-5-isopropyl-8, 8-dicyanoheptafulvene (XXXII).—By the procedure described for the formation of XXIV from XXIII, 200 mg. (after recrystallization from ethanol) of red prisms (XXXII), m. p. 218—219°C (decomp.), were obtained from 300 mg. of XXXI.

Found: C, 69.12; H, 5.73; N, 24.65. Calcd. for $C_{13}H_{14}N_4$: C, 69.00; H, 6.24; N, 24.76%.

UV λ_{max}^{MeOH} mμ (log ε): 244 (4.20), 330 (3.93), 465 (4.50).

The Condensation Reaction of XXXII with Tropone.—To a solution of 50 mg. of XXXII in 10 ml. of methanol, 4 drops of tropone were added; this mixture was then refluxed for 1.5 hr. After the methanol had been removed, 30 mg. of crystals were obtained. Recrystallization from ethanol gave reddish-violet scales (XXXVII), m. p. 227°C (decomp.).

Found: C, 76.38; H, 5.74; N, 17.47. Calcd. for $C_{20}H_{18}N_4$: C, 76.40; H, 5.77; N, 17.82%.

UV λ_{max}^{MeOH} mμ (log μ): 515 (4.64).

The Reaction of XXXI with Ammonia.—According to the procedure described for the formation of XXV from XXIII, 100 mg. of red prisms (XXXIII), m. p. 260—261°C (decomp.), were obtained from 150 mg. of XXXI.

Found: C, 73.80; H, 5.85; N, 19.91. Calcd. for $C_{13}H_{13}N_3$: C, 73.90; H, 6.20; N, 19.89%.

UV λ_{max}^{MeOH} mμ (log. ε): 242 (4.19), 315 (3.81), 455 (4.48).

The Reaction of XXXI with Methylamine.—When treated by the procedure used for the conversion of XXIII into XXVI, 100 mg. of XXXI afforded 90 mg. of orange needles (XXXIV), m. p. 247—248°C (decomp.).

Found: C, 74.96; H, 6.29; N, 19.27. Calcd. for $C_{14}H_{13}N_3$: C, 75.31; H, 5.87; N, 18.82%.

UV λ_{max}^{MeOH} mμ (log ε): 245 (4.32), 300 (sh.) 320 (3.93), 355 (3.93), 463 (4.53).

The Reaction of XXXI with Dimethylamine.—To a solution of 100 mg. of XXXI in 2 ml. of ethanol, 3 ml. of 33% aqueous dimethylamine was added, then the mixture was refluxed for 1 hr. The concentration of the reaction mixture afforded 40 mg. of red prisms (XXXV) after recrystallization from ethanol.

Found: C, 75.48; H, 6.72; N, 18.00. Calcd. for $C_{15}H_{17}N_3$: C, 75.28; H, 7.16; N, 17.56%.

UV λ_{max}^{MeOH} mμ (log μ): 250 (4.19), 333 (3.90), 465 (4.53).

2-Isopropyl-8, 8-dicyanoheptafulvene (XXXVI).—The procedure was the same as that described for the dehydrazination of XXIV. From 100 mg. of XXXII, 40 mg. of red needles (XXXVI), m. p. 111°C, were obtained.

The authors gratefully acknowledge the award of Maintenance Grants from Sankyo Co. Thanks are also due to Miss Yoko Endo and Miss Yukiko Endo for their elemental analyses.

BULLETIN OF THE CHEMICAL SOCIETY OF JAPAN VOL. 39 2450—2453 (1966)

Heptafulvenes. VI. The Structure of 2, 3-Diamino-8, 8-dicyanoheptafulvene Hydrochloride

By Tadahiro KATO*

Chemical Research Institute of Non-Aqueous Solutions, Tohoku University, Katahira-cho, Sendai

(Received February 11, 1966)

2, 3-Diamino- and 2, 3-bismethylamino-8, 8-dicyanoheptafulvenes gave the corresponding crystalline salts of hydrochloride. From the infrared and ultraviolet spectra, it was concluded that these hydrochlorides are the derivatives of the hydrochloride of 2-aminotropoimine.

In a previous paper,[1] it has been reported that 5 - isopropyl - 2, 3 - dimethoxy - 8, 8 - dicyanoheptafulvene (I) yielded the corresponding diamino compounds II, III and IV respectively, by the reactions with the amines RR'NH (R, R'=H and/or CH_3). It is possible that, besides the heptafulvene structure (A), II and III take a tautomeric 2-aminotropoimine structure, such as B or C.

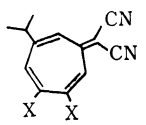

(I) X=OCH_3 (II) X=NH_2
(III) X=$NHCH_3$ (IV) X=$N(CH_3)_2$

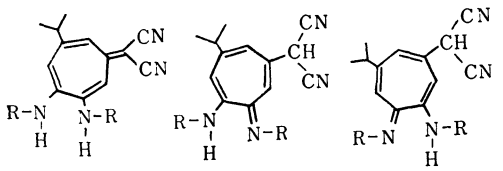

(A) (B) (C)

R=H, CH_3

Recently Brasen and his coworkers[2,3] have reported that the product obtained by the reaction of 4-bromo-1-(*p*-tolylamino)-7-(*p*-tolylimino)-1, 3, 5-cycloheptatriene (V) with malononitrile is not 2-aminotropoimine (VIa), but 3, 4-bis-(*p*-tolylamino)-8, 8-dicyanoheptafulvene (VIb).

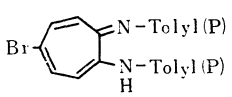

V

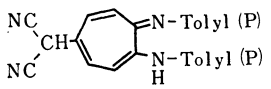

VIa

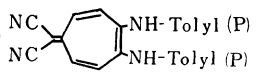

VIb

The infrared absorption spectra of II, III and IV display absorptions at 2200—2190 cm^{-1} due to the presence of conjugated cyano groups; and four strong absorption bands of two primary amino groups in II, while two strong bands assigned to two secondary amino groups in III are observed in the 3500—3100 cm^{-1} region (Table I).

TABLE I. INFRARED SPECTRA OF 2,3-DIAMINO-8,8-DICYANOHEPTAFULVENES AND THEIR HYDROCHLORIDES

Compound	IR spectra, cm^{-1}		
	NH region	CN region	
II	3490, 3420, 3310, 3254	2170 (S) 2195 (S)	1693, 1643, 1610
III	3380, 3200	2170 (S) 2195 (S)	1625
IV	—	2175 (S) 2195 (S)	1605
VII	3140 3300	2270 (W)	1690, 1645
VIII	3300, 3160	2265 (W)	1695, 1625
X	3430, 3300, 3170	—	1705, 1695, 1645
XI	3440, 3320 3160	—	1735, 1695, 1638

The shapes of the ultraviolet absorption spectra of II and III are similar to that of I in methanol.

It can be concluded from these spectral data that II and III possess a heptafulvene structure, both in solution and in the solid state. This conclusion is in good agreement with the results obtained by Brasen and Benson.

* Present address: Department of Chemistry, Tohoku University, Katahira-cho, Sendai.

1) Y. Kitahara, K. Doi and T. Kato, This Bulletin, **39**, 2444 (1966).

2) W. R. Brasen, H. E. Holmquist and R. E. Benson, *J. Am. Chem. Soc.*, **83**, 3125 (1961).

3) W. R. Brasen and R. E. Benson, ibid., **83**, 3135 (1961).

On the other hand, it has become clear that there is a large contribution of an ionic structure, quite similar to that of azulene,[4] to 8, 8-dicyanoheptafulvenes.[5]

Azulene is reported to exist as a tropylium cation in a strongly acidic medium[6,7] and the cation has been isolated as a stable crystalline salt.[8]

It may therefore, be anticipated that heptafulvenes can also exist as cations of the tropylium type in a strongly acidic medium, the cations being stabilized by amino groups at the 2 and 3 positions.

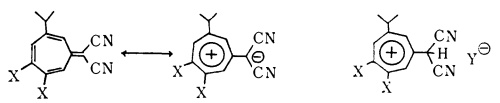

X=OCH_3
=NRR′ (R′=H, CH_3)

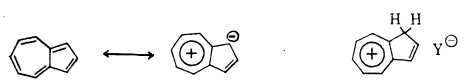

The addition of concentrated hydrochloric acid to compound II at room temperature gives a solution; after several minutes, pale yellow crystals (VII) begin to separate out. The composition of this compound corresponds to $C_{13}H_{14}N_4 \cdot HCl \cdot H_2O$, i. e., an addition product of II with one mole each of hydrochloric acid and water. Compound III also affords a yellow crystalline addition product (VIII), with one mole each of hydrochloric acid and water, i. e., $C_{15}H_{18}N_4 \cdot HCl \cdot H_2O$. Compounds VII and VIII are pale in color compared with the original compounds, II and III, suggesting that they have a different chromophore from those of II and III.

Meanwhile, when compound II or III is treated with hydrochloric acid, two ways of protonation are possible; either the protonation occurs at a nitrogen atom, forming D or E, or the dicyanomethylene groups is protonated, forming a tropylium cation (F), which is similar to the 2-aminotropoimine protonated at the imine nitrogen.

The infrared spectra of VII and VIII show a weak absorption band at 2260—2270 cm^{-1} due to a cyano group which is no longer conjugated. The ultraviolet absorption spectra of these compounds in methanol are similar to that of heptafulvene itself. In 6 N hydrochloric acid, however, they display quite different absorption maxima from those of II or III. Therefore, it can be concluded that VII and VIII have a structure similar to the hydrochloride of 2-aminotropoimine (F).

IV dissolves in 6 N hydrochloric acid, but attempts to isolate a crystalline salt analogous to VII or VIII were unsuccessful. When IV is heated in the same acid, two dimethylamino groups of IV are hydrolyzed, affording 2, 3-dihydroxy - 5 - isopropyl- 8, 8 - dicyanoheptafulvene (IX). Accordingly, the following deduction might be made; owing to the steric interference of the four methyl groups of the two adjacent dimethylamino groups, it becomes impossible for IV to form the structure corresponding to F, in which the lone paired electrons of the nitrogens and the π-electrons of the ring overlap. In a hydrochloric acid solution, IV exists as D or E, i. e., the hydrochloride of a tertiary amine maintaining the heptafulvene structure, which is hydrolyzed to IX. The above deduction is also supported by a similarity between the ultraviolet absorption spectra of IV in 6 N hydrochloric acid and in methanol.

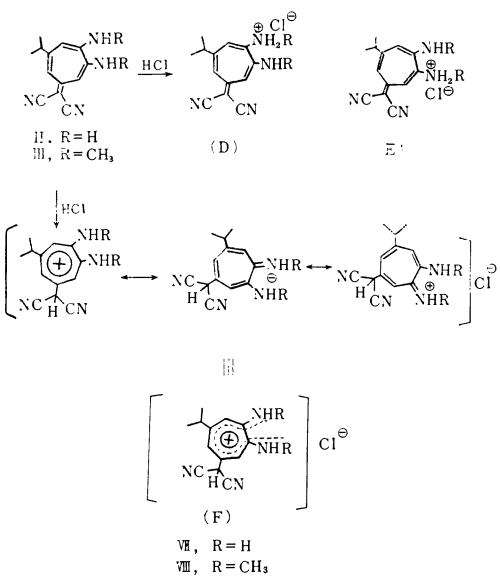

When VII is heated in concentrated hydrochloric acid, a white crystalline compound (X), $C_{12}H_{16}O_2N_2 \cdot HCl$, is obtained, while when it is heated in methanolic hydrochloric acid, VII affords a pale yellow crystalline compound (XI), $C_{13}H_{18}O_2N_2 \cdot HCl$. X and XI are also obtained directly from II by heating it in hydrochloric acid and hydrochloric acid - methanol respectively.

In the infrared spectra of X and XI, no bands to be assigned to cyano groups are present; instead of them, bands at 1705 and 1735 cm^{-1} due to carboxyl and ester groups appear in the spectra of X and

4) A. G. Anderson, Jr., and B. M. Steckler, ibid., **81**, 4941 (1959).
5) S. Katagiri, K. Doi, Y. Kitahara and H. Azumi, This Bulletin, to be published.
6) Pl. A. Plattner, E. Heilbronner and S. Weker, *Helv. Chim. Acta*, **35**, 1036 (1952).
7) L. H. Chopard-dit-Jean and E. Heilbronner, ibid., **35**, 2170 (1952).
8) K. Hafner, *Ann.*, **625**, 108 (1959); **650**, 35 (1961).

XI respectively. The ultraviolet absorption spectra of these compounds are quite similar to that of VII in 6 N hydrochloric acid; this suggests that VII, X and XI possess the same chromophore (Fig. 1). Accordingly, it can be concluded that X and XI are both hydrochlorides of 2-aminotropoimine derivatives.

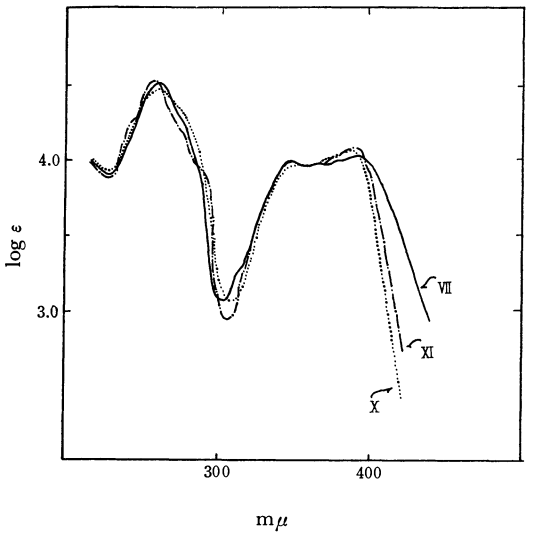

Fig. 1. Ultraviolet spectra of VII in 6 N HCl, X, XI in MeOH.

The infrared absorption spectra of these hydrochlorides, VII, X and XI are similar to each other through the whole spectral region; furthermore, they are very similar to that of the hydrochloride of 2, 5-diaminotropoimine[9] (XII) (Table II). It might, therefore, be assumed that the hydrochlorides of these compounds have similar structures.

TABLE II. IR SPECTRA OF SOME DERIVATIVES OF 2-AMINOTROPOIMINE HYDROCHLORIDES

Compound	IR spectra, cm^{-1}							
VII	1590	1524	1473	1385	1365	1290	1190	1040
VIII	1590	1535	1473	1375	1350	1273	1195	1015
X	1590	1525	1472	1385	1357	1280	1196	1040
XI	1590	1522	1472	1384	1367	1300	1195	1015
XII	1590	1525	1482	1390	1350	1276	1207	1000
XIV	1595		1485	1375	1360	1295	1200	1030

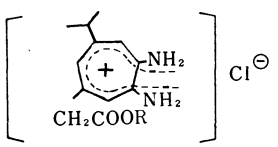

(X) R=H
(XI) R=CH_3

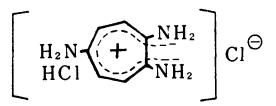

(XII)

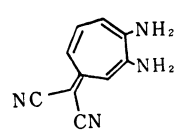

(XIII)

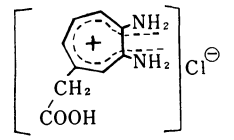

(XIV)

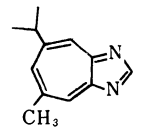

(XV)

Similarly, on being heated in hydrochloric acid, 2, 3-diamino-8, 8-dicyanoheptafulvene (XIII) yields XIV, whose ultraviolet and infrared absorption spectra are quite similar to those of X.

When X is heated in 80% formic acid, it gives a 1, 3-diazaazulene derivative (XV).[10,11]

Experimental

2, 3-Diamino-5-isopropyl-8, 8-dicyanoheptafulvene Hydrochloride (VII).—one hundred milligrams of II were dissolved in 1 ml. of 12 N hydrochloric acid; to this solution, active charcoal* was added, and then the charcoal was filtered off. The filtrate, on standing at room temperature, deposited to give pale yellow needles, which were filtered off and washed with water to give 80 mg. of VII, m. p. 216°C (decomp.).

Found: C, 55.60; H, 5.78. Calcd. for $C_{13}H_{14}N_4 \cdot HCl \cdot H_2O$: C, 55.60; H, 6.11%.

UV λ_{max}^{MeOH} mμ (log ε): 260(4.37), 338(4.30), 408 (4.30).

$\lambda_{max}^{6\,N\,HCl}$ mμ (log ε): 263(4.51), 350(3.99), 395(4.0).

5-Isopropyl-2, 3-bis(methylamino)-8, 8-dicyanoheptafulvene Hydrochloride (VIII).—A mixture of 120 mg. of III and 1 ml. of 12 N hydrochloric acid was heated on a water bath for a short time. The mixture then turned orange. The addition of 3 ml. of water to the solution afforded 120 mg. of yellow crystals (VIII); m. p. 211—212°C (decomp.).

Found: C, 58.17; H, 6.43; N, 17.80. Calcd. for $C_{15}H_{18}N_4 \cdot HCl \cdot H_2O$: C, 58.33; H, 6.88; N, 18.11%.

UV λ_{max}^{MeOH} mμ (log ε): 243 (4.26), 338 (4.32), 430 (4.48).

9) T. Nozoe, M. Sato and T. Matsuda, *Sci. Repts. Tohoku Univ., First Ser.*, **37**, 407 (1953).
10) I. Murata, This Bulletin, **33**, 56 (1960).
11) T. Nozoe, T. Mukai and I. Murata, *J. Am. Chem. Soc.*, **76**, 3352 (1954).

* Active charcoal was found to be very effective for the purification of the hydrochlorides of 2, 3-diamino-8, 8-dicyanoheptafulvene derivatives.

$\lambda_{max}^{6\,N\ HCl}$ mμ (log ε): 280 (4.63), 358 (4.14), 420 (4.13).

When an ethanol solution of VIII was chromatographed on alumina, using ethanol as the eluting solvent, it yielded yellow crystals, m. p. 255°C (decomp.), which were identified as III by a mixed melting point determination and by a study of the infrared absorption spectrum.

The Reaction of 2, 3-Bis(dimethylamino)-5-isopropyl-8, 8-dicyanoheptafulvene (IV) with Hydrochloric Acid.—The addition of 3 ml. of 6 N hydrochloric acid to a solution of 100 mg. of IV in 3 ml. of ethanol yielded a deep red solution. To this solution a small amount of active charcoal was added, after which the mixture was heated for 30 min. in a water bath. The charcoal was then filtered off, and most of the enthanol of the filtrate was distilled off, affording a crystalline compound (50 mg.), m. p. 234°C (decomp.). An ethanol solution of this compound was treated with diazomethane in ether to yield a yellowish-orange crystalline compound, m. p. 177—178°C, which was proved to be 5-isopropyl-2, 3-dimethoxy-8, 8-dicyanoheptafulvene by a mixed melting point determination with an authentic sample and by a study of its infrared absorption spectrum.

The Reaction of 2, 3-Diamino-5-isopropyl-8, 8-dicyanoheptafulvene (II) with Methanolic Hydrochloric Acid.—a) A mixture of II (100 mg.) and 1 ml. of a 12 N hydrochloric acid-methanol (1 : 1) solution was heated on a water bath for 30 min., and then treated with active charcoal. After the charcoal had then been filtered off, the filtrate was allowed to cool to room temperature; it then gave 80 mg. of yellow prisms (XI), m. p. 221°C (decomp.), after recrystallization from a 12 N hydrochloric acid - methanol (1 : 1) mixture.

Found: C, 57.49; H, 7.09; N, 10.51. Calcd. for $C_{13}H_{18}N_2O_2 \cdot HCl$: C, 57.64; H, 7.07; N, 10.35%.

UV λ_{max}^{MeOH} mμ (log ε): 260 (4.53), 348 (3.99), 390 (4.07).

b) A mixture of II (150 mg.) and 12 N hydrochloric acid (3 ml.) was heated for 20 min., treated with active charcoal, and then filtered. After the filtrate had then been cooled, orange crystals were obtained (100 mg.), those were recrystallized from 12 N hydrochloric acid, affording needles (X), m. p. 275°C (decomp.).

Found: C, 56.31; H, 6.13; N, 10.93; Cl, 14.17. Calcd. for $C_{12}H_{16}N_2O_2 \cdot HCl$: C, 56.30; H, 6.68; N, 10.90; Cl, 13.81%.

UV λ_{max}^{MeOH} mμ (log ε): 260 (4.48), 348 (3.97), 390 (4.00).

2-Amino-4-carboxymethyltropoimine Hydrochloride (XIV).—A mixture of 120 mg. of XIII and 12 N hydrochloric acid (3 ml.) was heated for 5 min. It turned orange. After the heating had been continued at 90°C for 30 min., the solution was treated with active charcoal and the charcoal was filtered off. On cooling, white needles (XIV) (80 mg.), m. p. 270°C (decomp.), were obtained.

Found: C, 50.29; H, 4.86; N, 12.84; Cl, 16.75. Calcd. for $C_9H_{10}N_2O_2 \cdot HCl$: C, 50.35; H, 5.16; N, 13.06; Cl, 16.51%.

UV λ_{max}^{MeOH} mμ (log ε): 257 (4.40), 348 (4.00), 395 (4.04).

7-Isopropyl-5-methyl-1, 3-diazaazulene (XV).—A mixture of 220 mg. of X and 5 ml. of 80% formic acid was refluxed for one hr. The solvent was then distilled under reduced pressure, giving a red oil (XV) (100 mg.), which was then purified by chromatoraphy on alumina, using methanol as the elution solvent.

UV λ_{max}^{MeOH} mμ (log ε): 225 (4.10); 257 (4.18), 370 (3.61), 358 (3.86). Picrate: m. p. 195°C (decomp.).

Found: C, 52.15; H, 4.00; N, 16.95. Calcd. for $C_{18}H_{17}N_5O_7$: C, 52.05; H, 4.13; N, 16.84%.

The author wishes to express his gratitude to Professor Yoshio Kitahara of this Institute for his kind guidance and encouragement throughout this study. The author is also indebted to Professor Kozo Doi of Hirosaki University for his interest and valuable advice concerning this work, and to the Misses Yoko Endo and Yukiko Endo for their microanalyses.

BULLETIN OF THE CHEMICAL SOCIETY OF JAPAN VOL. 39 2454—2458 (1966)

Intramolecular Hydrogen Bonds. VIII.[1] Isomeric Hydroxycyclohexylcarbinols and Bis-hydroxymethyl-cyclohexanes

By Nobuo Mori and Yojiro Tsuzuki

Department of Chemistry, Tokyo College of Science, Kagurazaka, Shinjuku-ku, Tokyo

(Received February 21, 1966)

The preferential direction of intramolecular hydrogen bonding in isomeric hydroxycyclohexylcarbinols in dilute carbon tetrachloride solutions has been investigated by infrared spectroscopy. The 1-hydroxy isomer contains a tertiary hydroxyl group predominantly bonded to the oxygen atom of a primary hydroxyl, while the *cis*- and *trans*-2-hydroxy isomers contain a primary hydroxyl group mainly bonded to the oxygen atom of a secondary hydroxyl; the other isomers are internally unbonded. On the other hand, bis-hydroxymethyl-cyclohexanes other than the 1, 1- and 1, 2-isomers are unbonded. These findings can be explained in terms of the acidity of the hydroxyl groups and the steric effect on the orientation of the groups.

The direction and extent of intramolecular hydrogen bonding is particularly sensitive to changes in molecular structure and conformation. In intramolecularly hydrogen-bonded diol systems, the direction of the bonding of one hydroxyl group to another depends on the acidity and/or the basicity of the groups as well as on the steric environment around them; the steric requirement for the orientation of the groups often appears to be more influential than their acidity. For example, when the diols are those which contain a tertiary and a primary hydroxyl group in the 1, 2-position, the steric crowding about the tertiary hydroxyl group causes its hydrogen atom to be directed towards the primary hydroxyl group, resulting in hydrogen-bond formation with the oxygen atom of the latter,[2] although the former group is more basic or proton-accepting than the latter.[3] In *cis*-cyclohexane-1, 2-diols the so-called 1, 3-diaxial steric interaction being exercised on an axial hydroxyl group causes its hydrogen atom to be directed out of the cyclohexane ring; then the hydrogen atom is bonded with the oxygen atom of an equatorial hydroxyl.[2]

In the present investigation, such a preferential direction of hydrogen bonding has been investigated in hydroxycyclohexylcarbinols by means of infrared spectroscopy. Further, this investigation has dealt with the intramolecular hydrogen bonding in bis-hydroxymethyl-cyclohexanes.

Experimental

Samples.—Hydroxycyclohexylcarbinols were prepared in the usual manner by reducing the corresponding hydroxycyclohexane-carboxylates[4] with lithium aluminum hydride in ether. Bis-hydroxymethyl-cyclohexanes were similarly synthesized from the diethyl esters of cyclohexane-dicarboxylic acids.[5,6] They were purified through recrystallizations or redistillations; their physical constants closely agreed with those reported in the literature (see Table I).

Infrared Measurements.—The hydroxyl stretching region was measured by a method previously described,[4] using lithium fluoride optics with carbon tetrachloride solutions in concentrations of 0.004 mol./l. or less at ca. 25°C. Such a concentration was sufficiently low to avoid any intermolecular hydrogen bonding.

Results and Discussion

The data of the observed apparent hydroxyl bands are summarized in Table I, together with the physical constants of the samples.

In cyclohexane systems, characteristic unbonded hydroxyl frequencies[3,13,14] are 3635—3640 cm^{-1} for primary hydroxyl groups, 3627—3632 cm^{-1} and 3623—3630 cm^{-1} for axial and equatorial secondary hydroxyl respectively, and 3613—3619 cm^{-1} for tertiary hydroxyl; each frequency is that of the apparent band peak, which is practically assigned to the hydroxyl group in the sterically-most-preferable one of the three orientations around the C–O axis.[15] In practice for the exact assignment of an apparent free hydroxyl band one should also take account of an additional weaker absorption due to the hydroxyl group in the

1) Part VII: N. Mori, Y. Tanaka and Y. Tsuzuki, This Bulletin, **39**, 1490 (1966).
2) L. P. Kuhn, *J. Am. Chem. Soc.*, **80**, 5950 (1958).
3) L. P. Kuhn, ibid., **74**, 2492 (1952).
4) N. Mori, S. Omura, N. Kobayashi and Y. Tsuzuki, This Bulletin, **38**, 2149 (1965).
5) G. H. Haggis and L. N. Owen, *J. Chem. Soc.*, **1953**, 399.
6) G. H. Haggis and L. N. Owen, ibid., **1953**, 404.
13) A. R. H. Cole, G. T. A. Müller, D. W. Thornton and R. L. S. Willix, *J. Chem. Soc.*, **1959**, 1218.
14) A. R. H. Cole, P. R. Jefferies and G. T. A. Müller, ibid., **1959**, 1222.
15) M. Oki and H. Iwamura, This Bulletin, **32**, 950 (1959).

TABLE I. SUMMARY OF THE COMPOUNDS AND THEIR INFRARED DATA

No.		B. p. °C/mmHg (M. p. °C)	n_D	ν_{OH} cm^{-1}	log I_0/I	$\Delta\nu_{1/2}$ cm^{-1}
I	1-OH	(76.5[7])		3638 3586	0.22 0.29	} 90
II	*cis*-2-OH	125—126/7[8] (49—51)		3642 (sh.) 3628 3538	 0.74 0.57	} 35 58
III	*trans*-2-OH	125—126/7[8]	1.4835(25°C)	3638 (sh.) 3623 3535	 0.81 0.96	} 44 60
IV	*cis*-3-OH	132/9[9]	1.4890(23°C)	3637 3622	0.64 0.75	} 36
V	*trans*-3-OH	134—136/6[9,10]	1.4874(25°C)	3638 3628	0.58 0.72	} 40
VI	1-CH_2OH[11]			3640 3550		
VII	*cis*-2-CH_2OH[3,12]			3633 3496		
VIII	*trans*-2-CH_2OH[3,12]			3631 3479		
IX	*cis*-3-CH_2OH	(59[5])		3640	1.68	24
X	*cis*-4-CH_2OH	154/9[6]	1.4868(20°C)	3635	1.03	30
XI	*trans*-4-CH_2OH	(66—66.5[6])		3637	1.17	28

other less-preferable orientations; this absorption appears generally as a broadening of the band, centered at a frequency lower by 10—15 cm^{-1} than the apparent peak frequency.[15] In fact, 1, 3- and 1, 4-bis-hydroxymethyl-cyclohexanes (IX—XI), which are internally unbonded, show only one sharp band, at ca. 3637 cm^{-1} somewhat broadened on the lower frequency side. 3-Hydroxycyclohexylcarbinols (IV and V) which are also internally unbonded show two band-peaks at ca. 3637 and 3625 cm^{-1}; the higher intensity of the lower frequency-free secondary hydroxyl band (see the table) may be attributed to such an absorption of the free primary hydroxyl group overlapped with the band. However, when the free secondary hydroxyl band is much stronger than the free primary hydroxyl, as is observed in the spectra (cf. Fig. 2) of 2-hydroxycyclohexylcarbinols (II and III), such an absorption of the primary hydroxyl group, overlapped with the stronger band, is practically negligible, especially for the purpose of confirming the preferential direction of hydrogen bonding.

In this paper, the term "free hydroxyl group" includes both the hydroxyls which contain an unbonded hydrogen atom (i. e., those not participating in any hydrogen bond) and the hydroxyls whose oxygen atom is bonded to the hydrogen atom of another hydroxyl, since the bonding of the oxygen atom of a free hydroxyl group to the hydrogen atom of another hydroxyl has, in general, little effect upon the frequency of the free hydroxyl.[2,3]

1-Hydroxycyclohexylcarbinol (I).—The resolution of the observed spectrum is far from complete, in spite of the relatively wide spacing of 52 cm^{-1} between the band-peaks (3638 and 3586 cm^{-1}), so its graphical separation has been examined by a method previously described.[1,4] This method, shown in Fig. 1, assumes, for convenience, that the individual band-components are symmetric; after subtracting two strong, substantially symmetric bands from the spectrum, a weak broad band remains with a peak frequency

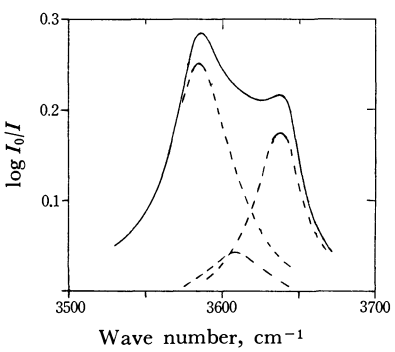

Fig. 1. Infrared spectrum of 1-hydroxycyclohexylcarbinol (I):
Apparent: ——; Separated: ----

7) M. Mousseron, *Compt. rend.*, **224**, 1230 (1947).
8) H. B. Henbest and B. B. Millward, *J. Chem. Soc.*, **1960**, 3575.
9) D. S. Noyce and D. B. Denney, *J. Am. Chem. Soc.*, **74**, 5912 (1952).
10) H. L. Goering and C. Serres, ibid., **74**, 5908 (1952).
11) P. von R. Schleyer, ibid., **83**, 1368 (1961).
12) L. P. Kuhn, P. von R. Schleyer, W. F. Baitinger and L. Eberson, ibid., **86**, 650 (1964).

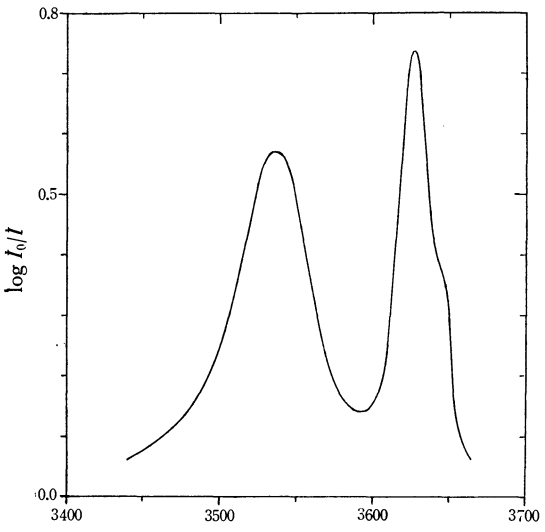

Fig. 2. Infrared spectrum of *cis*-2-hydroxycyclohexylcarbinol (II).

of 3615 cm^{-1}. The resulting band absorbances (and half-band widths in cm^{-1}) are 0.17 (38) for the 3638 band, 0.04 (30) for the 3615 band, and 0.25 (36) for the 3586 band. The separated weak band seems to be due to an additional absorption, (which will be assigned later), rather than to the intrinsic unsymmetry of the strong bands.

This carbinol may take the four interconvertible, internally bonded chair-forms Ia—Id, in which all the valence bonds of any two adjacent atoms are fully staggered:

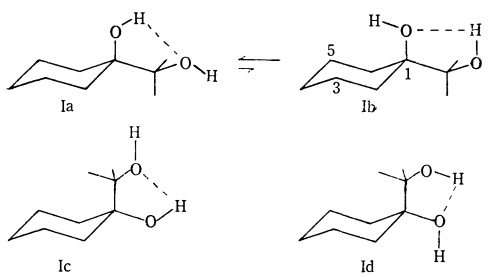

In assigning the bands to the hydroxyl groups in these forms, one must first take the thermodynamical stability and the population of these forms into account. The difference in free energy between equatorial and axial hydroxyl groups lies in a range of −0.4 to −0.9 kcal./mol.[16]; for the hydroxymethyl group the difference is unknown, but it is expected to be nearly equal to the −1.5 to −1.9 kcal./mole given for the methyl.[16] Since the difference of −1 kcal./mole (the difference between the two averaged values) at 25°C corresponds to an equilibrium constant of ca. 5.3, as calculated using the van't Hoff isotherm, the carbinol may exist predominantly in a chair form containing the hydroxyl group in the axial position. The preference of the axial hydroxyl-containing form holds even when the hydrogen bonding is present, since no large entropy and enthalpy effect may be expected on the equilibrium between the bonded forms. Of the axial hydroxyl-containing forms, Ia and Ib, the preferable one may be Ia, in which the tertiary hydroxyl group is bonded to the oxygen atom of the primary hydroxyl, in spite of the former being more basic or proton-accepting than the latter. The reason is that the axial hydrogens on C_3 and C_5 in Ib may sterically repel the hydrogen of the tertiary hydroxyl group, causing it to be directed out of the cyclohexane ring and then towards the primary hydroxyl, as in Ia. The repulsion can then be removed by going to Ia. This expectation agrees well with the infrared data; the strong bands at 3638 and 3586 cm^{-1} are predominantly due to the free primary hydroxyl group and the bonded axial tertiary hydroxyl group respectively in Ia. The latter frequency agrees well with the 3586 cm^{-1} of the bonded tertiary hydroxyl group in 1, 1-diethylethyleneglycol.[2] On the other hand, the free tertiary hydroxyl group and the bonded primary hydroxyl group in Ib may together principally contribute to the weak band at 3615 cm^{-1}; this is supported by the fact that the frequency agrees with that of ordinary free tertiary hydroxyl groups and with the 3612 cm^{-1} of the bonded primary hydroxyl groups in ethyleneglycols.[2,3]

Further, the separation by 29 cm^{-1} between the free and the bonded tertiary hydroxyl band agrees with the 32 cm^{-1} of ethyleneglycol and 1, 1-diethylethyleneglycol,[2] but it is lower than either the 50 cm^{-1} of 1, 1,-diisopropylethyleneglycol[2] or the ca. 80 cm^{-1} of 1, 1-di-*t*-butylethyleneglycol.[2] Such a lowering in frequency resulting from the 1, 1-disubstitution may chiefly be attributed to the so-called Thorpe-Ingold effect,[17] which results in the decrease in valence angle between the other two bonds of C_1; therefore, the above fact suggests that the cyclohexane ring does not suffer from such an effect, and that, at the same time, the steric repulsion between the hydroxyl group on C_1 and the axial hydrogens on C_3 and C_5 is not so high as to change the valence angle of C_1 to any significant extent.

2-Hydroxycyclohexylcarbinols (II and III).— As Fig. 2 shows, the spectra are of a completely-resolved doublet with peak-frequencies of 3625 and 3536 cm^{-1}; the higher frequency band has a weak shoulder, centered at ca. 3640 cm^{-1}. An

16) E. L. Eliel, "Stereochemistry of Carbon Compounds," McGraw-Hill Book Co., New York, N. Y. (1962), p. 236.

17) R. M. Beesley, C. K. Ingold and J. F. Thorpe, *J. Chem. Soc.*, **107**, 1030 (1915); C. K. Ingold, ibid., **119**, 305 (1921); see also Refs. 3 and 12.

examination of the rough graphical separation shows that the absorbance of the shoulder separated from the spectrum is about 0.19 for II and 0.17 for III.

For *cis*-carbinol II, the axial hydroxyl-containing forms, IIa and IIb, may similarly be preferable to the equatorial hydroxyl-containing forms. The steric environment around the hydroxyl groups included in the hydrogen bond may be essentially the same in both IIa and IIb, so the difference in acidity between the hydroxyl groups may be considered to be a major factor in deciding the direction of hydrogen bonding; therefore, IIa, in which the less basic primary hydroxyl group is bonded to the oxygen atom of the more basic secondary hydroxyl, should be more favorable than IIb. Accordingly, the strong band at 3628 cm^{-1} may primarily be assigned to the free secondary axial hydroxyl group in IIa, while the weak absorption at 3642 cm^{-1} may primarily be assigned to the free primary hydroxyl in IIb. The strong band at 3538 cm^{-1} is mainly due to the bonded primary hydroxyl group in IIa, together with a minor proportion of the bonded secondary hydroxyl in IIb.

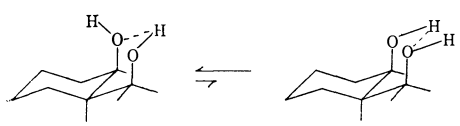

IIa IIb

As for *trans*-carbinol III, only the diequatorial forms, IIIa and IIIb, are possible for hydrogen bonding for the following reasons: (1) any diaxial form should be unfavorable for hydrogen bonding in view of the distance between the hydroxyl groups, and in view of the fact that any such form includes 1, 3-diaxial interactions between the axial hydrogens and the groups, while (2) the diequatorial forms include only the so-called skew interaction between the groups, an interaction which is much lower in energy than the 1, 3-diaxial interaction, and they acquire in addition the stabilization resulting from the hydrogen bond. In IIIa and IIIb, the nature of the hydroxyl groups may similarly be a major factor in controlling the equilibrium between the forms. Accordingly, the strong bands at 3623 and 3535 cm^{-1} may mostly be due to the free secondary hydroxyl group and the bonded primary hydroxyl group in IIIa, while the weak shoulder at 3638 cm^{-1} may be due to the free primary hydroxyl in IIIb.

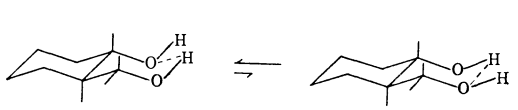

IIIa IIIb

As has been mentioned above, the expected preferential direction of hydrogen bonding of the primary hydroxyl group toward the oxygen atom of the secondary hydroxyl agrees very well with the infrared data. In this connection, there has been an interesting report[18] on the direction of hydrogen bonding in some triterpenoid 3, 24-diols. Urs-12-ene-3β, 24-diol (A) has the primary hydroxyl group bonded to the oxygen atom of the equatorial secondary hydroxyl, the 3α-isomer with the diaxial structure (B) contains no hydrogen bonding, and methyl hederagenin with the diequatorial structure prefers form C to D. It is surprising that the hyderogen bonding in methyl hederagenin is opposite in preferential direction to those in carbinols II and III, the reason for this is not clear at the present time.

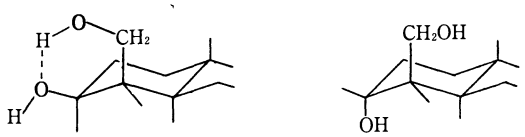

A B

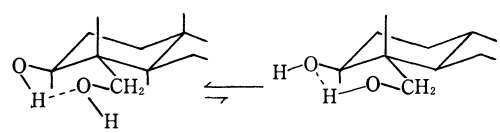

C D

3-Hydroxycyclohexylcarbinols (IV and V).— These are internally unbonded. The diaxially fixed structure of *cis*-3-hydroxycyclohexylcarbinol is known[19] to show a bonded hydroxyl band at 3460 cm^{-1}; this fact is not necessarily inconsistent with the absence of bonding in *cis*-carbinol IV for the following reason: the stabilization due to hydrogen bonding in the diaxial conformation can not be sufficient to overcome the instabilization due to the steric repulsion between the diaxial atoms and groups, in view of the fact that the difference in free energy between the diequatorial and the unbonded diaxial conformation is expected to be of the relatively high value of ca. −2.4 kcal./mol.[20] (corresponding to an equilibrium constant of 56), while the ordinary OH–O type intramolecular hydrogen bonding to form a seven-membered ring results in a large decrease in entropy of −10

18) A. R. H. Cole and G. T. A. Müller, *J. Chem. Soc.*, **1959**, 1224.
19) J. Tadanier, *J. Org. Chem.*, **28**, 1744 (1963).
20) Approximated by adding the corresponding values for a hydroxyl and a hydroxymethyl group, since such summations have been verified to be approximately correct in some cases.[21,22]
21) S. J. Angyal and D. J. McHugh, *Chem. & Ind.*, **1956**, 1147.
22) N. L. Allinger and M. A. Miller, *J. Am. Chem. Soc.*, **83**, 2145 (1961); E. L. Eliel and H. Haubenstock, *J. Org. Chem.*, **26**, 3503 (1961).

e. u., with an enthalpy of 2.7 kcal./mol.[23] In other words, the bonded diaxial form, if any, exists in a population so low as to make it impossible to observe its spectral band. In fact, intramolecular hydrogen bonding is present when the difference in free energy is relatively low, e. g., such as the −1.9 kcal./mol.[21] for *cis*-cyclohexane-1, 3-diol, which is known to be hydrogen-bonded.[3]

Bis-hydroxymethyl-cyclohexanes (VI—XI). —The 1, 3- and 1, 4-isomers are internally unbonded, while the 1, 1- and 1, 2-isomers are bonded. The absence of bonding in the *cis*-1, 3-isomer IX can be explained by essentially the same reason as that mentioned in the case of *cis*-3-hydroxycyclohexylcarbinol IV; in this case, however, the difference in free energy between the diequatorial and the diaxial form should be much higher. In the case of the *cis*-1, 4-isomer X, on the other hand the most important factor may be that this compound can not take the boat or twist conformation required for ordinary hydrogen bondings between 1- and 4-*cis* groups.[24]

The authors are thankful to Mr. Teruo Kajiura and Mr. Tadao Tamura of the Government Chemical Industrial Research Institute of Tokyo for the infrared measurements.

23) L. P. Kuhn and R. A. Wires, *J. Am. Chem. Soc.*, **86**, 2161 (1964).

24) R. D. Stolow, P. M. McDonagh and M. M. Bonaventure, ibid., **86**, 2165 (1964), and references cited therein.

BULLETIN OF THE CHEMICAL SOCIETY OF JAPAN VOL. 39 2458—2463 (1966)

Copolymerization of Vinyl Chloride and Ethylene Initiated by Trialkylboron-Peroxide Catalyst Systems

By Akira MISONO and Yasuzo UCHIDA

Department of Industrial Chemistry, Faculty of Engineering, The University of Tokyo, Hongo, Tokyo

and Kunikazu YAMADA

Central Research Laboratory, Sekisui Chemical Co., Shimamoto-cho, Mishima-gun, Osaka

(Received February 21, 1966)

Low-pressure copolymerization was carried out in a water-methanol mixture(1 : 1 by weight) at 0°C. It was found that, when hydroperoxides were used as cocatalysts, triethylboron and tri-*n*-butylboron were active as catalysts, while triphenylboron was inactive. As cocatalysts, hydroperoxides were more active than disubstituted peroxides. The highest catalytic activity was observed when the cocatalyst/catalyst molar ratio was 0.4. The initiating radical has been suggested to be the hydroxy radical, and the initiating mechanism has been discussed briefly. The yield and the reduced specific viscosity of the copolymer decrease rapidly with an increase in the ethylene content of the monomer mixture. The monomer reactivity ratios were: r_1(vinyl chloride)=4.16 and r_2(ethylene)=0.05. This indicates that the copolymerization reaction proceeds via a normal radical mechanism. The resulting copolymer shows characteristic absorption peaks at 750 cm^{-1} in the infrared spectrum and at 8.37 τ in the NMR spectrum.

Since Furukawa et al.[1] and Ashikari[2] found that alkyl derivatives of boron acted as powerful radical initiators for vinyl polymerization, many studies have been reported on the polymerization and copolymerization of various vinyl monomers. The copolymerization of vinyl chloride and ethylene at a high pressure has been studied in some detail by Burkhalt et al.[3] and Erussalimsky et al.[4] However, no details have been reported on the radical copolymerization of these monomers at a low pressure.

In the course of their studies of the copolymerization of vinyl chloride and ethylene, the present authors found that trialkylboron and hydroperoxides provided excellent catalyst systems which copolymerize these monomers to high-molecular-weight copolymers with a high ethylene content, even at low temperatures. In order to study this subject further, the authors carried out some experiments; they thus obtained the interesting results to be reported here.

1) J. Furukawa, T. Tsuruta and S. Inoue, *J. Polymer Sci.*, **26**, 234 (1957).
2) N. Ashikari, ibid., **28**, 250, 641 (1958).
3) R. D. Burkhalt and N. L. Zutty, ibid., **A1**, 1137 (1963).
4) B. Erussalimsky, F. Suntoff and N. Tumarkin, *Makromol. Chem.*, **66**, 205 (1963).

Experimental

Materials.—Vinyl chloride supplied by the Chisso Co. was used without further purification; no impurity was detected in it by gas chromatography. Ethylene supplied by the Nihon Petroleum Co. was used without further purification; no impurity was detected in it by gas chromatography. Triethylboron was prepared from ethylmagnesium bromide and boron trifluoride according to the method of Brown[5] (b. p. 92—112°C). Tri-*n*-butylboron was prepared from *n*-butylmagnesium bromide and boron trifluoride according to the method of Johnsen et al.[6] (b. p. 116°C/21 mmHg). Triphenylboron was prepared from phenylmagnesium bromide and boron trifluoride according to the method of Krause et al.[7] The reaction mixture containing triphenylboron was extracted with benzene several times; then the benzene extract was concentrated and distilled (b.p. 154°C/3 mmHg). The peroxides were used without further purification, while methanol was purified by distillation. Ion-exchanged water was boiled prior to use.

Polymerization.—The reaction vessel was a stainless steel autoclave with a 300 ml. capacity and equipped with an electro-magnetic stirring device. Trialkylboron and peroxide were separately sealed into a glass ampule with a 1 ml. capacity attached to the stirring rod of the autoclave. A measured quantity of the reaction medium, a water-methanol mixture (1 : 1 by weight), was introduced into the autoclave, and the inner air was evacuated by a vaccum pump after the autoclave had been cooled to −30°C. Then a measured quantity of vinyl chloride was introduced into the autoclave from a glass pressure tube. When the temperature of the autoclave reached 0°C, ethylene was introduced from a storage tank and the reaction was started by breaking glass ampules containing catalytic components by means of ethylene pressure. Afterward, the reaction temperature was kept within 0±3°C. After a given time, the reaction was stopped by expelling the residual monomers as soon as possible. The resulting copolymer was filtered, washed repeatedly with water and methanol, and dried in vacuo at 50°C. The crude copolymer thus obtained was then precipitated by adding a tetrahydrofuran solution of the copolymer to methanol, filtered, dried in vacuo at 50°C, and subjected to the following analyses.

Analyses of the Copolymer.—The reduced specific viscosity of the copolymer was measured using 5 g./l. cyclohexanone solution at 30°C. The composition of the copolymer was calculated from the results of the elemental analyses of C, H and Cl. The infrared spectrum of the copolymer was masured with a Hitachi double-beam spectrometer, model EPI-S2 (potassium bromide disk). The NMR spectrum of the copolymer was measured with a Nihon Denshi high-resolution NMR spectrometer, model C-60, in a 10% solution of monochlorobenzene at 60°C, using tetramethylsilane as the internal standard.

Results and Discussion

The Effect of the Catalytic Composition.—Henceforth, alkylboron will be called the catalyst, and the other component, the cocatalyst, according to custom. In many studies using alkylboron as the catalyst, oxygen is used as the cocatalyst. However, considering the difficulty of accurately measuring of the oxygen amount, the authors decided to use organic or inorganic peroxides instead of oxygen.

The results of copolymerization with catalytic systems consisting of various catalysts and cocatalysts are summarized in Table I. It may clearly be seen that if either the catalyst or the cocatalyst is absent, copolymerization does not occur. When trialkylboron is used as the catalyst, the cocatalytic activities decrease in the following order:

t-butyl hydroperoxide ≫ cumene hydroperoxide > benzoyl peroxide > hydrogen peroxide, α, α'-azobisisobutyronitrile, di-*t*-butyl peroxide.

Hydroperoxides are more active than disubstituted peroxides when they are combined with trialkylboron. On the other hand, when *t*-butyl hydroperoxide is used as the cocatalyst, the activities of the catalyst are in the following order:

tri-*n*-butylboron ≈ triethylboron ≫ triphenylboron.

On the basis of the above results, the catalyst system consisting of tri-*n*-butylboron or triethylboron and *t*-butyl hydroperoxide was used in every copolymerization experiment to be reported on in this paper unless otherwise mentioned.

Figure 1 shows the influence of the cocatalyst/catalyst molar ratio on the yield and the reduced specific viscosity of the copolymer. The catalytic activity changes remarkably with the ratio, being highest at the ratio of 0.4. The ethylene content of the copolymer also becomes highest at the same ratio. These results are in agreement with those

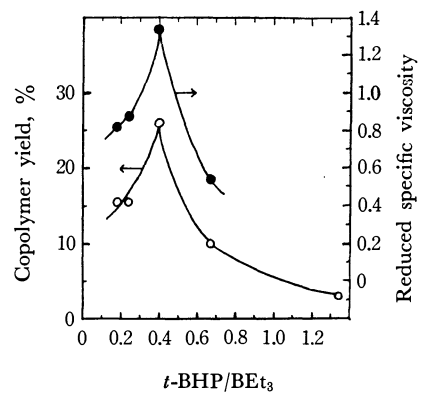

Fig. 1. Effect of *t*-BHP/BEt_3 molar ratio on yield and reduced specific viscosity of copolymer.
experimental condition; vinyl chloride: 25.0 g., ethylene 14.8 l., *t*-BHP: 0.77 mmol., water: 93 g., methanol: 93 g., polyvinyl alcohol: 0.25 g., temperature: 0°C, time: 5 hr.

5) H. C. Brown, *J. Am. Chem. Soc.*, **67**, 374 (1945).
6) J. R. Rohnson, H. R. Snyder and M. G. van Campen, ibid., **60**, 115 (1938).
7) E. Krause and R. Nitshe, *Ber.*, **55**, 1261 (1922).

Table I. Copolymerization results with various catalyst systems

Catalyst	Amount mmol.	Cocatalyst	Amount mmol.	Conversion %	η_{sp}/C	VCl content mol.%
BEt_3	3.30	—	—	trace	—	—
BEt_3	—	*t*-BHP	0.85	0	—	—
BEt_3	1.92	*t*-BHP	0.77	28.6	1.026	80.58
BEt_3	1.90	CHP	1.26	9.82	0.786	82.82
BEt_3	1.87	BPO	1.25	5.31	0.406	93.81
BEt_3	1.83	H_2O_2	1.22	4.98	0.965	86.08
BEt_3	1.88	*t*-BPB	1.24	4.55	0.568	90.93
BEt_3	1.88	AIBN	1.25	4.11	0.366	94.93
BEt_3	1.92	di-*t*-BPO	1.28	4.12	0.496	91.07
BBu_3	2.13	*t*-BHP	0.85	30.1	1.076	84.55
BPh_3	1.90	*t*-BHP	0.76	0	—	—

Polymerization condition: vinyl chloride, 25.0 g. (0.40 mol.); ethylene, 14.8 l. (at 30°C, 0.60 mol.); polyvinyl alcohol, 0.25 g.; water, 93 g.; methanol, 93 g.; temperature, 0°C; time, 5 hr.
Abbreviations: BEt_3, triethylboron; BBu_3, tri-*n*-butylboron; BPh_3, triphenylboron; *t*-BHP, *t*-butyl hydroperoxide; CHP, cumene hydroperoxide; BPO, benzoyl peroxide; *t*-BPB, *t*-butyl perbenzoate; AIBN, α,α-azobisisobutyronitrile; di-*t*-BPO, di-*t*-butyl peroxide

found in vinyl chloride[8] and vinyl acetate[9] polymerizations carried out in the presence of the trialkylboron-oxygen catalyst system, in which the highest catalytic activity has been observed at the point where trialkylboron exists in about a three fold excess over oxygen.

Furukawa et al.[10] have supposed that the initiating mechanism of an organometallic compound-peroxide catalyst system in vinyl chloride polymerization would be as follows:

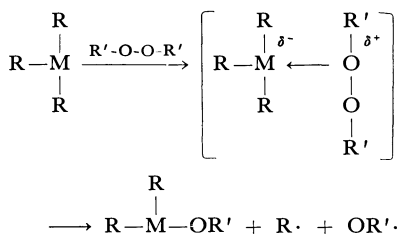

where the metal may be either aluminum or boron. They have supposed that the resulting radicals might be able to initiate the vinyl polymerization, but no experimental support has been given.

The present authors could isolate a low-molecular-weight copolymer on solution polymerization in *n*-hexane using the triethylboron-cumene hydroperoxide catalyst system. The infrared spectrum of the resulting copolymer is shown in Fig. 2. Before the treatment with benzoyl chloride, the copolymer shows a stretching vibration of the hydroxy group at 3430 cm^{-1}, this vibration disappears when the copolymer is treated with benzoyl chloride, and a new stretching vibration absorption of the carbonyl group appears at 1700 cm^{-1}. The rest of the spectrum is the same as that of the high-molecular-weight copolymer to be shown later.

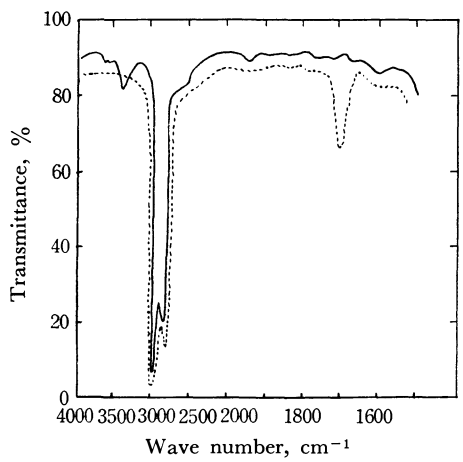

Fig. 2. Infrared spectra of low molecular weight copolymer.
Full line; untreated copolymer
Dotted line; after benzoylation

Hansen et al.,[11] after studying the reaction of triethylboron and oxygen in *n*-hexane, have suggested that an ethyl radical was formed during the reductive decomposition of a peroxide of triethylboron with an excess of triethylboron. In another report,[12] they have shown, from the results of kinetic studies of the polymerization of methylmethacrylate by the triethylboron-oxygen catalyst system, that the highest rate of polymerization was

8) G. Borsini and M. Cippolla, *J. Polymer Sci.*, **B2**, 291 (1964).
9) F. Ide and Y. Takayama, *J. Soc. Chem. Japan, Ind. Chem. Sect. (Kyogyo Kagaku Zasshi)*, **63**, 529 (1960).
10) J. Furukawa, T. Tsuruta and S. Shiotani, *J. Polymer Sci.*, **40**, 237 (1959).
11) R. L. Hansen and R. R. Hamann, *J. Phys. Chem.*, **67**, 2868 (1963).
12) R. L. Hansen, *J. Polymer Sci.*, **A2**, 4215 (1964).

obtained when the triethylboron concentration was twice the oxygen concentration. Also, Bawn et al.[13] and Welch[14] have reported similar findings concerning the initiation mechanism of the trialkylboron-oxygen catalyst system.

From the results of the present authors and those of the other authors cited above, it seems better to consider, also in the case of the trialkylboron-peroxide systems, the initiating radical as arising from such a mechanism in which the 1 : 1 complex of trialkylboron and peroxide is reduced by another molecule of trialkylboron rather than from Furukawa's mechanism. One probable mechanism may be as follows:

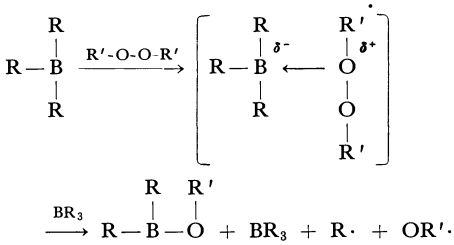

Hydroperoxides might be able to coordinate to the boron atom of trialkylboron with less steric hindrance and might, hence, show a greater catalytic activity.

The Effects of the Monomer Composition. —The effects of the monomer composition on the yield and the reduced specific viscosity of the copolymer are shown in Fig 3. As the ethylene content in the monomer mixture increase, both the yield and the viscosity of the copolymer decrease rapidly, ethylene does not polymerize under the present experimetnal conditions.

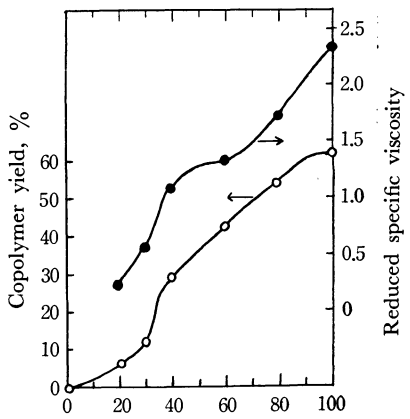

Fig. 3. Effect of monomer composition on yield and reduced specific viscosity of copolymer.
Experimental condition; vinyl chloride+ethylene: 1.0 mol., BBu_3: 2.18 mmol., *t*-BHP/BBu_3: 0.40, water: 93 g., methanol: 93 g., polyvinyl alcohol: 0.25 g., temperature: 0°C, time: 5 hr.

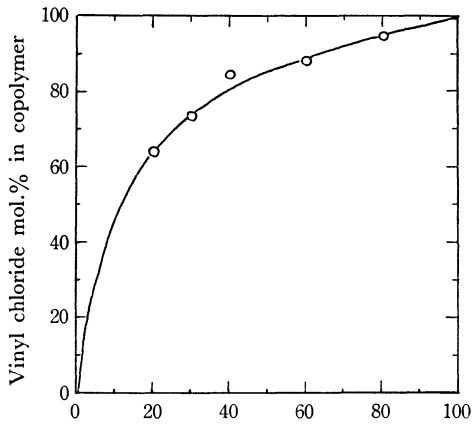

Fig. 4. Effect of monomer composition on copolymer composition.
Experimental condition; vinyl chloride+ethylene; 1 mol., BBu_3: 2.18 mmol., *t*-BHP/BBu: 0.40, water: 93 g., methanol: 93 g., polyvinyl alcohol: 0.25 g., temperature: 0°C, time: 5 hr.

The copolymer composition curve is shown in Fig. 4. The monomer reactivity ratios determined from the Finemann-Ross plot are r_1(vinyl chloride)=4.16 and r_2(ethylene)=0.05. These values almost equal those obtained by the authors using the *t*-butyl hydroperoxide - ascorbic acid catalyst system[15] (r_1=4.70, r_2=0.08). This indicates that the copolymerization reaction proceeds via a normal radical mechanism. The monomer reactivity ratios obtained by the authors are slightly different from those of Burkhalt et al.[1] (r_1=3.60, r_2=0.24) and Erussalimsky et al.[2] (r_1=1.85, r_2=0.20), which have been obtained from high-pressure copolymerization studies.

The Infrared and NMR Spectra of the Copolymer.—The infrared spectra of the copolymers containing 64.08 and 84.55 mol.% of vinyl chloride respectively are shown in Fig. 5. Most of the spectra show features intermediate between those of polyvinyl chloride and those of polyethylene, but a characteristic absorption absent in both homopolymers is observed at 750 cm^{-1}, the intensity of which absorption increases with an increase in the ethylne content of the copolymer.

Sheppard et al.[16] have studied the infrared spectra of polymethylene halides and found that the methylene rocking vibration absorption, which appeared at 720 cm^{-1} in polymethylene, shifted to a higher region, between 770 cm^{-1} and 790 cm^{-1}, in the case of trimethylene or pentamethylene

13) C. E. H. Bawn, D. Margerison and N. M. Richardson, *Proc. Chem. Soc.*, **1959**, 397.
14) F. J. Welch, *J. Polymer Sci.*, **61**, 243 (1962).
15) A. Misono et al., unpublished data.
16) J. K. Brown and N. Sheppard, *Trans. Faraday Soc.*, **231(A)**, 555 (1952).

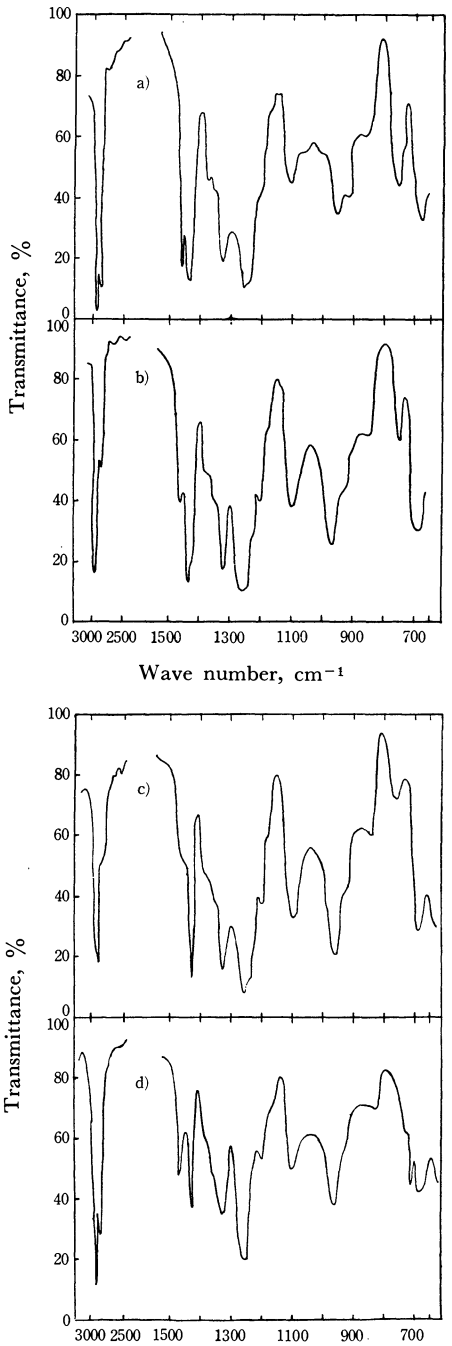

Fig. 5. Infrared spectra of copolymers and mixture of homopolymers.
a) Copolymer containing 64.08 mol.% of vinyl chloride
b) Copolymer containing 84.55 mol.% of vinyl chloride
c) Copolymer containing 94.69 mol.% of vinyl chloride
d) Mixture of polyvinyl chloride and poly ethylene (80: 20 molar ratio)

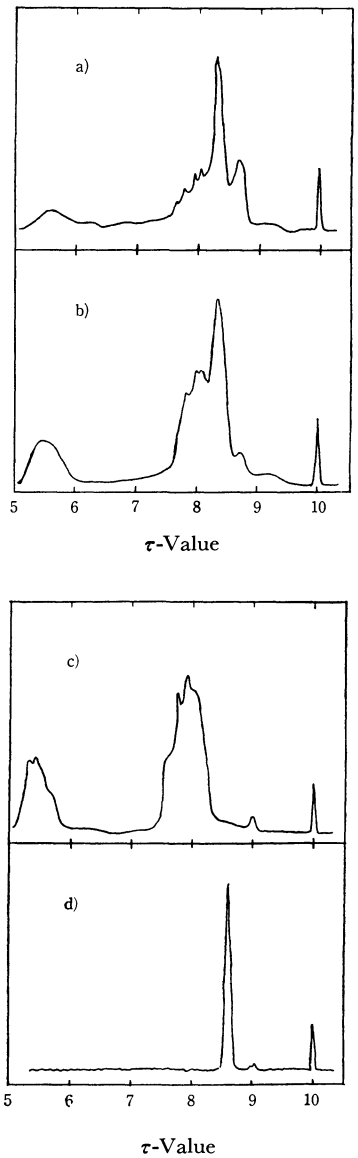

Fig. 6. NMR spectra of copolymers and homopolymers.
a) Copolymer containing 64.08 mol.% of vinyl chloride
b) Copolymer containing 84.55 mol.% of vinyl chloride
c) Polyvinyl chloride d) Polyethylene

chloride. From these observations, it seems reasonable to assign the absorption at 750 cm^{-1} observed in the copolymer to the following structure in the copolymer chain:

$$-CHCl-CH_2-CH_2-CH_2-CHCl$$

The NMR spectra of the copolymers containing 64.08 and 84.55 mol.% of vinyl chloride are shown in Fig. 6. The characteristic absorption is observed at 8.32 τ, whereas absorptions at 7.78

τ, 7.96 τ and 5.46 τ are also observed in polyvinyl chloride. Johnsen has made assignments of these absorptions in polyvinyl chloride.[17] An absorption at 8.68 τ is observed also in polyethylene. The characteristic absorption at 8.32 τ may be assigned to the following structure in the copolymer chain:

$$-CHCl-CH_2-CH_2-$$

Summary

The copolymerization of vinyl chloride and ethylene has been carried out by the use of various trialkylbron-peroxide catalyst systems. A catalyst system consisting of triethylboron or tri-*n*-butylboron and *t*-butyl hydroperoxide showed the best activity. As for the molar ratio of the two catalyst components, the highest catalytic activity was observed when the *t*-butyl hydroperoxide/triethylboron molar ratio was 0.4. The initiating radical was supposed to be a hydroxy radical from the results of a study of the infrared spectra of a low-molecular-weight copolymer. The initiating radical might arise from the reductive degradation of a 1 : 1 complex of trialkylboron and peroxide with excess of trialkylboron. The yield and the reduced specific viscosity of the copolymer changed greatly with the composition of the monomer mixture; the richer the vinyl chloride content in the monomer mixture, the higher the yield and viscosity. The monomer reactivity ratios were determined to be r_1(vinyl chloride) : 4.16 and r_2-(ethylene) : 0.05. The infrared spectrum of the copolymer showed a characteristic absorption at 750 cm^{-1}, and also in the NMR spectrum at 8.32 τ. These characteristic absorptions might be assigned to a boundary structure in the copolymer chain as follows:

$$-CHCl-CH_2-CH_2-CH_2-$$

17) U. Johnsen, *J. Polymer Sci.*, **54**, S6 (1961).

BULLETIN OF THE CHEMICAL SOCIETY OF JAPAN VOL. 39 2463—2466 (1966)

The Direct Introduction of an Ethoxycarbonyl Group by the Photolysis of Some Substituted Formates in Solution

By Yasuo SHIGEMITSU, Tamotsu TOMINAGA, Takashi SHIMODAIRA,* Yoshinobu ODAIRA and Shigeru TSUTSUMI

Department of Chemical Technology, Faculty of Engineering, Osaka University, Miyakojima-ku, Osaka

(Received February 22, 1966)

The direct introduction of an ethoxycarbonyl group by the photolysis of various substituted formates ($RCO_2C_2H_5$) was carried out. Both ethyl cyanoformate and ethyl chloroformate effectively underwent ethoxycarbonylation by a hydrogen-donating solvent such as cyclohexane, with the yields of 19% and 15%, respectively. On the other hand, the photolysis of ethyl acetate, diethyl carbonate, and ethyl carbamate gives mainly carbinols and carbon monoxide instead of ethyl carboxylate. On the basis of these results, the effects of the substituent in the formate on the ethoxycarbonylation were considered. First, the electronic effect of the substituent R has an influence on the position of the bond fission of the formate. Cyano and chloro groups, which are the electron-withdrawing substituents, weaken the R-carbon bond in the formates. Second, the ability of the hydrogen abstraction of the radical R produced by the photolysis of the formate is very important in the ethoxycarbonylation. Thus, it is clear that there is a relationship between the electron affinity of the radical R and the yield of the ethyl carboxylate.

Since the chloroformylation of cyclohexane by the photolysis of oxalyl chloride was investigated by Kharasch,[1] photochemical studies of the direct introduction of important functional groups, e. g., the nitroso,[2] cyano,[3] carbamoyl[4] and ethyl oxalyl groups,[5] have been extensively carried out. Little attention, however, has been paid to direct alkoxycarbonylation, though this is very valuable

* Present address: Mizonokuchi Research Laboratory, Mitsubishi Petrochemical Company, Ltd., Kawasaki.

1) M. S. Kharasch and H. C. Brown, *J. Am. Chem. Soc.*, **64**, 329 (1942).

2) M. A. Naylor and A. W. Anderson, *J. Org. Chem.*, **18**, 115 (1953).

3) E. Müller, *Chem. Ber.*, **96**, 670, 2319 (1963).

4) DovElad, *Tetrahedron Letters*, No. **2**, 77 (1963).

5) Y. Odaira, T. Tominaga, T. Sugihara and S. Tsutsumi, ibid., No. **36**, 2527 (1964).

TABLE I. ETHOXYCARBONYLATION WITH THE PHOTOLYSIS OF FORMATE (RCO_2Et)

R	Electron affinity of R, kcal./mol.	Solvent	Carboxylate, %[a]	Other liquid products,[b] %[a]
Cl	87		15	-Cl (5)
CN	64		19	-$COCO_2Et$ (3)
CN	64	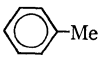	37	
H	—		4	-CH(OH)Me(I) (3), -CH_2OH(II) (3), EtOH(III) (7), -OEt(IV) (2)
Me	26		Trace	I (9), II (6), III (8) IV (3), MeCHO (9)
EtO	34		Trace	I (0.5), II (0.1)
EtO	34		Trace	-CH(OH)Me(V) (18)
NH_2	28		None	V (Trace)

a) Basis on consumed formate.
b) The dimer of the solvent is excluded from this Table. See experimental for the amounts of the dimer.

in organic synthesis. In our preliminary report,[6] the possibility of the direct introduction of an ethoxycarbonyl group into cyclohexane by means of the photolysis of ethyl cyanoformate was verified. In this paper, we wish to report on ethoxycarbonylation by the photolysis of various substituted formates, focusing attention on the effect of the substituent in the formate on the ethoxycarbonylation.

Results and Discussion

Although the photochemical reactions of alkyl esters (e. g., RCO_2R') are very complicated, it is generally considered that the following four primary steps proceed through the excitation of the molecule by the $n\rightarrow\pi^*$ transition of the carbonyl group in the esters:

$$R\text{-}\overset{\overset{O}{\|}}{C}\text{-}OR' \xrightarrow[n\rightarrow\pi^*]{h\nu} \left[R\text{-}\overset{\overset{O}{\|}}{C}\text{-}OR'\right]^* \quad [I]$$

$$[I] \longrightarrow R\cdot + \cdot\overset{\overset{O}{\|}}{C}\text{-}OR' \quad (1)$$

$$[I] \longrightarrow R\text{-}\overset{\overset{O}{\|}}{C}\cdot + \cdot OR' \quad (2)$$

$$[I] \longrightarrow RH + CO_2 + \text{Olefin} \quad (3)$$

$$[I] \longrightarrow R\cdot + CO + \cdot OR' \quad (4)$$

Of the above four steps, step 1, leading to the formation of an alkoxycarbonyl radical, will be most important for the alkoxycarbonylation. It is, however, well known that the alkoxycarbonyl radical produced in step 1 is so unstable that it decomposes exothermically to carbon dioxide and a free alkyl radical with an activation energy of only about 1—2 kcal./mol.[7]:

$$\cdot\overset{\overset{O}{\|}}{C}\text{-}OR' \longrightarrow CO_2 + \cdot R' \quad (5)$$

The results of ethoxycarbonylations by the photolysis of various formates in hydrogen-donating solvents are summarized in Table I. In spite of the above disadvantage, the data shown in Table I indicate that both ethyl cyanoformate and ethyl chloroformate, among others, effectively underwent ethoxycarbonylation by hydrogen-donating solvents. However, contrary to expectation, carbinols and carbon monoxide, not ethyl carboxylate, were mainly obtained in the photolysis of ethyl acetate, diethyl carbonate and ethyl carbamate. From these results, it is found that the R substituent in the formate influences the nature of the product of the photolysis of the formate. Therefore, it seems

6) T. Tominaga, Y. Odaira and S. Tsutsumi, This Bulletin, **37**, 596 (1964).
7) P. Gray and J. C. J. Thynne, *Nature*, **191**, 1357 (1961).

to be more reasonable to assume that the substituent in the formate plays a very important role in the photolytic behavior of the formate; the following two effects of the substituent may then be considered.

First, the electronic effect of the substituent has a considerable influence on the position of the bond fission of the formate. From the fact that the photolysis of ethyl cyanoformate and ethyl chloroformate affords ethyl carboxylate exclusively, it seems that the electron-withdrawing substituents weaken the R-carbon bond in the formates, thus causing this bond to break easily upon photolysis. Consequently, step 1 proceeds predominantly to produce the ethoxycarbonyl radical. The fact that carbon monoxide and carbinols are the major products in the photolyses of the other formates in Table I means that the electron-releasing substituents, e. g., methyl, ethoxy and amino groups, probably make the R-carbon bond fission conversely difficult. Consequently, the photolysis of the formates must proceed through step 2 to produce an acyl radical and an alkoxy radical. The acyl radical may decompose immediately to carbon monoxide and an alkyl radical. There is also a possibility that carbon monoxide may be produced directly by the photolysis of the formates through step 4.

Second, the ethoxycarbonylation is influenced by the ability of the R radical produced by step 1 to produce hydrogen abstraction. As is well-known, the chloro atom and the cyano radical, which have large electron affinities, effectively abstract the hydrogen of the solvent. On the other hand, the hydrogen-abstraction ability of methyl, alkoxy and amino radicals, which have small electron affinities, is not so powerful as that of the above radicals, even if these radicals are generated through step 1. In the case of the photolysis of diethyl carbonate in cyclohexane, the ethyl cyclohexanecarboxylate obtained was only small amount; carbon dioxide was the major product in the gaseous products. Therefore, the ethoxycarbonyl radical decomposes to carbon dioxide and the ethyl radical, as is shown in step 5.

Interestingly, ethyl cyano- and ethyl chloroformate react in a little different manner, as indicated by the composition of their products. Ethylene was a major gaseous product of the photolysis of ethyl cyanoformate. On the contrary, ethyl chloroformate afforded mainly ethane. In addition, the obtainable dimer of the solvent was very little in the photolysis of the former as compared with that of the latter. These results suggest that the transition state of the hydrogen abstraction is different in the cases of the two formate. Presumably, the ethoxycarbonylation with ethyl cyanoformate proceeds through a somewhat four-centered mechanism, or the intramolecular hydrogen abstraction of the formate leads to hydrogen cyanide, carbon dioxide and ethylene through a six-membered transition state, as is shown hereunder:

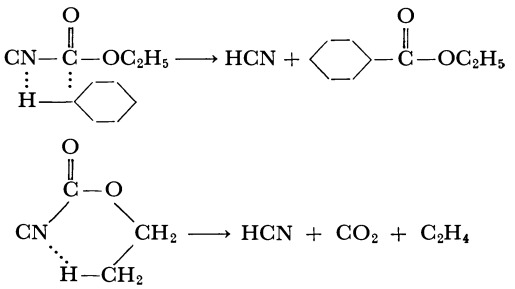

On the other hand, ethyl chloroformate may dissociate to a chloro atom and an ethoxycarbonyl radical. Then, the chloro atom generated would abstract the hydrogen of the solvent, thus producing a free solvent radical. This solvent radical may combine with the ethoxycarbonyl radical, or it may dimerize by itself.

Furthermore, in order to examine the effect of the substituent R', the phenoxycarbonylation of cyclohexane by means of the photolysis of phenyl chloroformate was also attempted. In this reaction, phenol was obtained as the major product, together with a small amount of phenyl cyclohexanecarboxylate. This result leads us to assume that a phenoxycarbonyl radical generated through step 1 may be easily decomposed to carbon monoxide and a phenoxy radical because of its large resonance stabilization.

Further studies of ethoxycarbonylation by means of ethyl cyanoformate will be presented elsewhere.

Experimental[8]

Materials.—Ethyl cyanoformate was prepared in a 54% yield from ethyl chloroformate and sodium cyanide according to the procedure of Sheppard,[9] b. p. 116—118°C, n_D^{20} 1.3812: phenyl chloroformate was synthesized in a 54% yield by the method of Raiford and Inman from phenol and phosgene in the presence of dimethylaniline,[10] b. p. 84—87°C/23—24 mmHg, $n_D^{29.5}$ 1.5067, the other formates and solvents were commercial-grade chemicals; they were purified by the usual methods and distilled before use.

The Photolysis of Ethyl Chloroformate.—A mixture of ethyl chloroformate (38 g., 0.35 mol.) and cyclohexane (147 g., 1.75 mol.) was irradiated with a 350 W. high-pressure mercury arc lamp for 25 hr. under nitrogen at room temperature. During the irradiation, the continuous evolution of gas was observed and 450 ml. gas was collected. Hydrogen chloride was identified qualitatively as the precipitate of silver chloride. The other gaseous products were analyzed by gas chromatography using a 2.5-m. active carbon column. The main gaseous products were carbon dioxide, ethane, and carbon monoxide, plus small amounts of methane

8) Melting points are uncorrected.
9) W. A. Sheppard, *J. Org. Chem.*, **27**, 3756 (1962).
10) L. C. Raiford and G. O. Inman, *J. Am. Chem. Soc.*, **56**, 1586 (1934).

and ethylene. The liquid products were fractionally distilled and analyzed by gas chromatography using a 2.5-m. Si DC-550 column and an Apiezone N column. The conversion percentage of ethyl chloroformate was about 6%. The high-boiling products (1.7 g.) were ethyl cyclohexanecarboxylate (15%, based on the ethyl chloroformate consumed), cyclohexyl chloride (4.5%), and bicyclohexyl, plus small amounts of methyl cyclohexylcarbinol, diethyl oxalate, and ethyl cyclohexane.

The Photolysis of Ethyl Cyanoformate.—The irradiation of a solution of ethyl cyanoformate (39.6 g., 0.4 mol.) in cyclohexane (168 g., 2.0 ml.) was carried out under the same conditions as above for 50 hr. The gas evolved amounted to about 300 ml., consisting of carbon dioxide, carbon monoxide, ethylene, and small amounts of methane. Hydrogen cyanide was determined qualitatively as silver cyanide. The conversion percentage of ethyl cyanoformate was about 33%. The main liquid products were ethyl cyclohexanecarboxylate (3.9 g, 19%) and ethyl cyclohexaneglyoxylate (0.7 g., 3%). The above α-ketoester was isolated by preparative gas chromatography using a 3-m. Si DC-550 column. 2,4-Dinitrophenylhydrozone was recrystallized from ethyl alcohol to yield yellow needles, m. p. 158—160°C. A mixed-melting-point determination with an authentic sample of ethyl cyclohexaneglyoxylate 2, 4-dinitrophenylhydrazone showed no depression. Small amounts of ethyl alcohol, cyclohexyl cyanide, propionitrile, and bicyclohexyl were identified by gas chromatography. The photolysis of ethyl cyanoformate in toluene was also carried out using a 1-KW. high-pressure mercury arc lamp for 40 hr. The ultimate yield of ethyl phenylacetate was about 37%. The photolysis of ethyl cyanoformate at the wave length of 3660 Å did not occur to any appreciable extent. The effective wave length in the photolysis of the formates seemed to be shorter than 3660 Å.

The Photolysis of Ethyl Formate.—A mixture of ethyl formate (148 g., 2.0 mol.) and cyclohexane (420 g., 5.0 mol.) was irradiated with a 350-W. high-pressure mercury arc lamp for 68 hr. About 2800 ml. of gas was evolved, consisting largely of carbon monoxide. The other gaseous products were carbon dioxide and ethane, plus small amounts of methane and ethylene. The conversion of ethyl formate was about 32%. The main liquid products were bicyclohexyl (4.8 g.), ethyl cyclohexanecarboxylate (3.8 g., 3.8%), methyl cyclohexylcarbinol (3.2 g.), cyclohexylcarbinol (2.2 g.), ethyl alcohol (2.2 g.), and acetone (2.2 g.). Small amounts of acetaldehyde, diethyl oxalate, and ethoxycyclohexane were also obtained.

The Photolysis of Ethyl Acetate.—A mixture of ethyl acetate (105.6 g., 1.2 mol.) and cyclohexane (252 g., 3.0 mol.) was irradiated for 50 hr. The conversion of ethyl acetate was about 37%. The gaseous products (2500 ml.) were carbon monoxide, ethylene, carbon dioxide, methane, and ethane. The liquid products were methyl cyclohexylcarbinol (5.5 g.), cyclohexylcarbinol (4.6 g.), bicyclohexyl (16 g.), ethoxycyclohexane (1.6 g.), ethyl alcohol (1.6 g.), and acetaldehyde (1.7 g.). Ethyl cyclohexanecarboxylate, however, was present in only a very small amount.

The Photolysis of Diethyl Carbonate.—A mixture of diethyl carbonate (59 g., 0.5 mol.) and cyclohexane (336 g., 4.0 mol.) was irradiated for 30 hr. The conversion rate of diethyl carbonate was about 21%. The gaseous products (300 ml.) were carbon dioxide, carbon monoxide, ethane, ethylene, methane, *n*-butane, and hydrogen. Almost the only liquid product was a polymeric substance (5.8 g.). Small amounts of bicyclohexyl (0.8 g.) and methyl cyclohexylcarbinol (0.1 g.) were also obtained. Ethyl cyclohexanecarboxylate, cyclohexylcarbinol, and ethyl alcohol were present only in trace amounts.

The photolysis of diethyl carbonate in tetrahydrofuran was also carried out. A mixture of diethyl carbonate (47.2 g., 0.4 mol.) and tetrahydrofuran (144 g., 2.0 mol.) was irradiated for 75 hr. under the same conditions. The gaseous products (1100 ml.) were almost the same as those of the above case, except that carbon monoxide instead of carbon dioxide was the main product. The main liquid products obtained were methyl-2-tetrahydrofurylcarbinol (1.7 g.) and 2, 2′-ditetrahydrofuryl (2.8 g.). Small amounts of ethyl 2-tetrahydrofurancarboxylate and 2-tetrahydrofurylcarbinol were also obtained.

The Photolysis of Ethyl Carbamate.—A mixture of ethyl carbamate (44.5 g., 0.5 mol.) and tetrahydrofuran (144 g., 2.0 mol.) was irradiated for 110 hr. The total volume of gas evolved was about 850 ml. The main gaseous product was carbon monoxide. Carbon dioxide, ethane, ethylene, methane, and hydrogen were also identified. After the tetrahydrofuran had been removed, the residue was cooled overnight and then filtered. Hydrochloric acid (1.5 N) was added to the filtrate, and the solution was extracted with ether. The ethereal solution was washed by 5% aqueous sodium bicarbonate and water successively, and dried over sodium sulfate. After the ether had been removed, the residue was fractionally distilled under reduced pressure. 2, 2′-Ditetrahydrofuryl (0.5 g.) and small amounts of methyl-2-tetrahydrofurylcarbinol were obtained. However, ethyl 2-tetrahydrofurancarboxylate was not obtained.

The Photolysis of Phenyl Chloroformate.—A mixture of phenyl chloroformate (109.6 g., 0.7 mol.) and cyclohexane (343 g., 4.2 mol.) was irradiated with a 1-KW. high-pressure mercury arc lamp for 7.2 hr. The gaseous products were hydrogen chloride and carbon monoxide. The conversion of phenyl chloroformate was about 27%. The main liquid product was phenol (12.6 g.). Phenyl cyclohexanecarboxylate was obtained only in trace amounts.

We are indebted to Mr. Koichi Matsumoto and Mr. Takeshi Fujimoto for their excellent assistance.

BULLETIN OF THE CHEMICAL SOCIETY OF JAPAN VOL. 39 2467—2470 (1966)

Hydrogenation and Hydrogenolysis. IX.[1] The Hydrogenation of Benzyl Alcohol with Platinum Metal Catalysts

By Shigeo NISHIMURA and Michiko HAMA

Department of Industrial Chemistry, Tokyo University of Agriculture and Technology, Koganei, Tokyo

(Received February 28, 1966)

The rate of the hydrogenation of benzyl alcohol with a rhodium catalyst decreases markedly in the course of the reaction, accompanied by the formation of an increasing amount of cyclohexanecarboxaldehyde with the conversion of the alcohol. The decrease in the rate is only slight with a platinum catalyst, however, and the formation of the aldehyde is much less than with the rhodium catalyst. It has been shown that cyclohexanecarboxaldehyde is an effective catalyst poison in the hydrogenation of benzyl alcohol, but that cyclohexylcarbinol is not. 1-Cyclohexenylcarbinol, an intermediate of the hydrogenation, isomerizes to cyclohexanecarboxaldehyde during the hydrogenation on rhodium and 7 : 3 rhodium-platinum catalysts to a greater extent than on the platinum catalyst. Cyclohexanecarboxaldehyde is hydrogenated only very slowly, but the rate with the platinum catalyst is about four times greater than that with the rhodium catalyst. These results may account for the different behaviors of the rhodium or 7 : 3 rhodium-platinum catalyst and the platinum catalyst observed in the hydrogenation of benzyl alcohol.

It has been reported in a previous paper that the hydrogenation of benzyl alcohol to cyclohexylcarbinol is not successful with a rhodium-platinum catalyst because of a marked decrease in the rate in the course of the reaction,[2] although benzyl ethers, benzyl acetate and α-substituted benzyl alcohols are easily hydrogenated to give good yields of the corresponding saturated compounds with the same catalyst.[2-4] Such a phenomenon was also observed in the hydrogenation with a supported rhodium catalyst.[5] Benzyl alcohol may be hydrogenated to cyclohexylcarbinol in a good yield, either with an Adams platinum catalyst in alcohols containing a small amount of acetic acid[6,7] or, better, with a ruthenium catalyst in the presence of water.[1] The present study was undertaken to elucidate the cause of the deactivation of rhodium and rhodium-platinum catalysts observed in the hydrogenation of benzyl alcohol.

Experimental

Materials.—Benzyl alcohol of the G. R. grade was used after a fresh and careful distillation under reduced pressure. Cyclohexylcarbinol was prepared by the hydrogenation of benzyl alcohol with ruthenium hydroxide catalyst[8] in the presence of water, a typical run being shown in the following: 43 g. of benzyl alcohol was hydrogenated with the addition of 10 ml. of water at 90°C under 80—100 kg./cm^2 of hydrogen pressure, using 0.1 g. of the catalyst. The hydrogen uptake was complete in 3.5 hr. The distillation of the product after extraction with ether gave 37 g. of cyclohexylcarbinol, b. p. 91.5°C/22—23 mmHg (81% yield). Cyclohexanecarboxaldehyde was prepared by the oxidation of cyclohexylcarbinol with chromium trioxide in acetic acid and purified via the sodium hydrogen sulfite adduct.[9] 1-Cyclohexenylcarbinol was prepared by the reduction of methyl 1-cyclohexenecarboxylate[10] with lithium aluminum hydride.[11] The purity of the compounds prepared was well confirmed by means of gas chromatography.

Catalysts.—The oxide catalysts of platinum and 7 : 3 rhodium-platinum were prepared by the Adams method.[12,13] The rhodium hydroxide catalyst was prepared by adding a slight excess of a lithium hydroxide solution to a hot aqueous solution of rhodium chloride, followed by a thorough washing with hot, distilled water.

Hydrogenation. — All the hydrogenations were carried out at 25°C under the atmospheric pressure of hydrogen, using isopropyl alcohol as the solvent. Benzyl alcohol (0.5 g.) and additives were added, together with the solvent, after the metal oxide had been reduced to the metal with hydrogen in the solvent containing a small amount of acetic acid (0.02 ml.), the total amount of the solvent used being 10 ml. Rhodium

1) Part VIII: Y. Takagi, T. Naito and S. Nishimura, This Bulletin, **37**, 585 (1964).
2) S. Nishimura, ibid., **34**, 32 (1961).
3) S. Nishimura, ibid., **33**, 566 (1960).
4) S. Nishimura and H. Taguchi, ibid., **36**, 318 (1963).
5) J. H. Stocker, *J. Org. Chem.*, **27**, 2288 (1962).
6) S. Nishimura, This Bulletin, **32**, 1155 (1959).
7) Y. Ichinohe and H. Itō, ibid., **37**, 887 (1964).
8) Y. Takagi, T. Naito and S. Nishimura, ibid., **38**, 2119 (1965).
9) N. Zelinsky and J. Gutt, *Ber.*, **40**, 3050 (1907).
10) W. J. Bailey and R. A. Baylouny, *J. Am. Chem. Soc.*, **81**, 2126 (1959).
11) B. Lythgoe, S. Trippett and J. C. Watkins, *J. Chem. Soc.*, **1956**, 4060.
12) R. Adams, V. Voorhees and R. L. Shriner, "Organic Syntheses," Coll. Vol. I, 2nd Ed., 463 (1941).
13) S. Nishimura, This Bulletin, **34**, 1544 (1961).

hydroxide was reduced to metal in isopropyl alcohol without the addition of acetic acid, since the presence of the acid greatly retarded the reduction of the hydroxide and since the hydrogenation of benzyl alcohol with this catalyst occurred without the addition of acetic acid.[14] Hydrogenation products were analyzed directly by gas chromatography using a column containing PEG-6000.

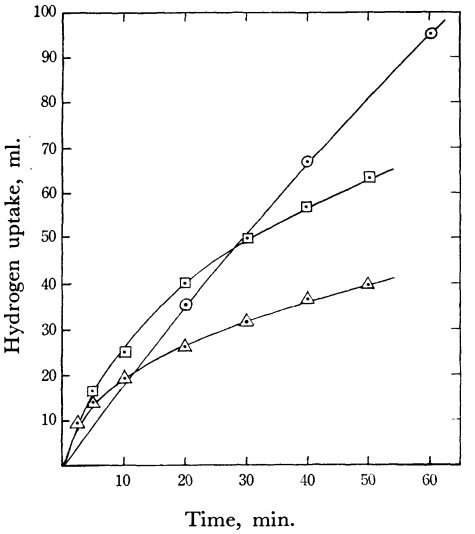

Fig. 1. Hydrogenation of benzyl alcohol.
- ⊡ Hydrogen uptake with rhodium catalyst
- ◬ Hydrogen uptake with 7: 3 rhodium-platinum catalyst
- ⊙ Hydrogen uptake with platinum catalyst

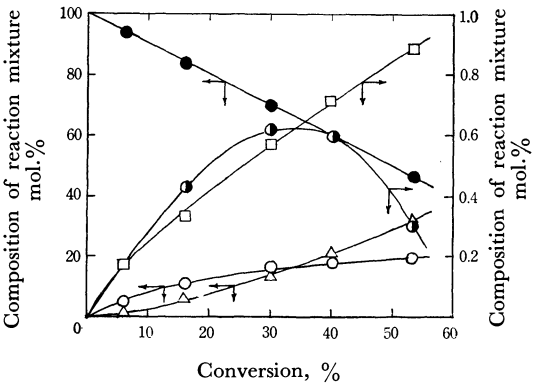

Fig. 2. Products of the hydrogenation of benzyl alcohol with rhodium catalyst.
- □ Cyclohexanecarboxaldehyde
- ○ Cyclohexylcarbinol
- ◑ 1-Cyclohexenylcarbinol
- △ Toluene
- ● Benzyl alcohol

14) The rhodium hydroxide catalyst used in this study probably contains a much smaller amount of alkaline substances than the oxide catalysts of the Adams type (cf. Ref. 8).

Results and Discussion

The hydrogen uptake in the hydrogenation of benzyl alcohol with rhodium, 7 : 3 rhodium-platinum and platinum catalysts is shown in Fig. 1. It may be seen that the rate of the hydrogenation decreases markedly in the course of a reaction with the rhodium and 7 : 3 rhodium-platinum

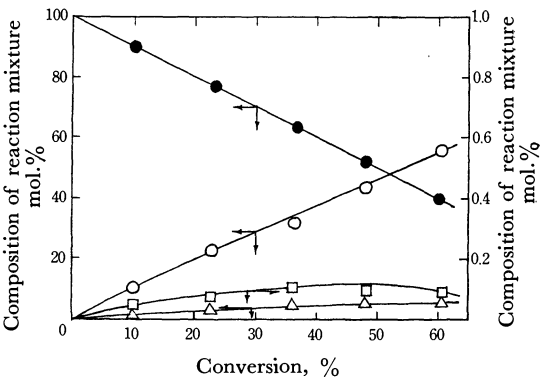

Fig. 3. Products of the hydrogenation of benzyl alcohol with platinum catalyst.
- □ Cyclohexanecarboxaldehyde
- ○ Cyclohexylcarbinol
- △ Toluene
- ● Benzyl alcohol

catalysts. The decrease in the rate is only slight with the platinum catalyst, however. Figures 2 and 3 show the changes in the amounts of the products formed in the course of the hydrogenation with the rhodium catalyst and with the platinum catalyst respectively. The most pronounced difference in the products seems to be that, with the rhodium catalyst, the formation of cyclohexanecarboxaldehyde is much greater than with the platinum catalyst and that it increases with conversion, whereas with the platinum catalyst the aldehyde is formed in an amount only 0.1% of the reaction mixture, even at the maximum, and then decreases gradually after about a 40% conversion. 1-Cyclohexenylcarbinol was also detected in the course of the rhodium-catalyzed hydrogenation, but it decreased rapidly after about 40% conversion.

Since it may be supposed from the above results that the cyclohexanecarboxaldehyde formed during the hydrogenation may be a catalyst poison, the effect of the addition of the aldehyde was then studied and compared with the effect of added cyclohexylcarbinol (Fig. 4). It may be seen that the hydrogenation of benzyl alcohol is markedly inhibited by the addition of cyclohexanecarboxaldehyde, while the addition of cyclohexylcarbinol has little effect on the rate of the hydrogenation. The effect of the addition of 1-cyclohexenylcarbinol

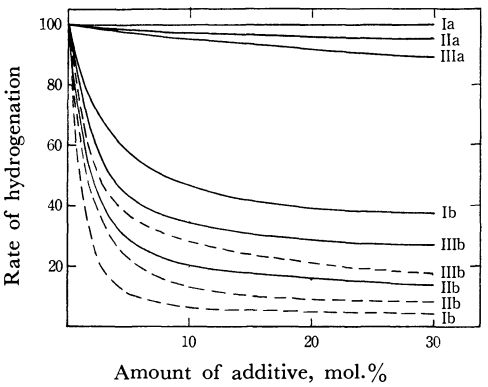

Fig. 4. The effects of added cyclohexylcarbinol and of cyclohexanecarboxaldehyde in the hydrogenation of benzyl alcohol.
I: Rhodium II: 7:3 Rhodium-platinum
III: Platinum a: Cyclohexylcarbinol
b: Cyclohexanecarboxaldehyde
——: Added in mixture with benzyl alcohol
- - -: Added before the addition of benzyl alcohol

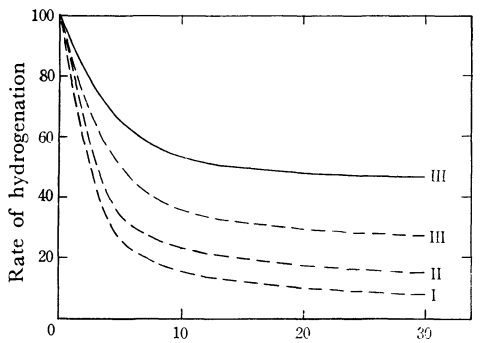

Fig. 5. The effect of the addition of 1-cyclohexenylcarbinol on the rate of the hydrogenation of benzyl alcohol.
I: Rhodium II: 7:3 Rhodium-platinum
III: Platinum
——: Added in mixture with benzyl alcohol
- - -: Added before the addition of benzyl alcohol

was also studied (Fig. 5), since the unsaturated alcohol is produced as an intermediate of the hydrogenation and is probably the precursor of the aldehyde formed in the hydrogenation.

It may be seen from Fig. 5 that the addition of 1-cyclohexenylcarbinol also inhibits the hydrogenation, although to a somewhat lesser extent than in the case of cyclohexanecarboxaldehyde. It may also be seen that the decrease in the rate is more pronounced in the hydrogenation with the rhodium catalyst than with the platinum catalyst. It should be noted that the hydrogenation is more retarded when the compounds are added before the addition of benzyl alcohol than when they are previously admixed with benzyl alcohol, as is shown in Figs. 4 and 5. Table I shows the products of the hydrogenation of 1-cyclohexenylcarbinol with rhodium, 7 : 3 rhodium-platinum and platinum catalysts. The hydrogenations with rhodium and and 7 : 3 rhodium-platinum catalysts are accompanied by the formation of cyclohexanecarboxaldehyde (about 18%). Such an isomerization occurs to a much lesser extent with the platinum catalyst (about 5%).[15] Thus, the action of cyclohexenylcarbinol as a catalyst poison probably results from the formation of the aldehyde by isomerization during the hydrogenation. The hydrogenation of the aldehyde was found to occur only very slowly, especially with the rhodium catalyst (hydrogen uptake: 3 ml./hr., 50 mg. catalyst). With the platinum catalyst the aldehyde is hydrogenated at a rate about four times greater than with the rhodium catalyst.

Table I. Products of the hydrogenation of 1-cyclohexenylcarbinol

Catalyst	Product, %		
	Cyclohexylcarbinol	Cyclohexanecarboxaldehyde	Hydrocarbons
Platinum[a]	94.8	5.2	Trace
7:3 Rhodium-Platinum	75.0	18.1	6.9
Rhodium	75.9	17.8	6.3

a) Products obtained in 84% hydrogenation.

From the results described above, it is very probable that the deactivation observed in the hydrogenation of benzyl alcohol with rhodium and rhodium-platinum catalysts is caused by the cyclohexanecarboxaldehyde formed by the isomerization of 1-cyclohexenylcarbinol, which is expected to be produced in a considerable amount as an intermediate of the hydrogenation, although the amount of it detected in the course of the hydrogenation was rather small.[16] The hydrogenation with the platinum catalyst is only slightly poisoned, because the isomerization of 1-cyclohexenylcarbinol occurs to a much lesser extent and the aldehyde formed by the isomerization is hydrogenated much faster than with the rhodium catalyst. It is known that ruthenium catalysts hydrogenate aliphatic aldehydes to alcohols with ease;[17,18]

15) The hydrogenation with the palladium hydroxide catalyst was accompanied by an extensive hydrogenolysis, affording 74% of methylcyclohexane along with 20.5% of cyclohexylcarbinol, 1.6% of cyclohexanecarboxaldehyde, and other products.

16) Cf. S. Siegel, G. V. Smith, B. Dmuchovsky, D. Dubbell and W. Halpern, *J. Am. Chem. Soc.*, **84**, 3136 (1962).

17) G. Gilman and G. Cohn, "Advances in Catalysis," Vol. IX, Academic Press, New York (1957), p. 733.

18) Y. Takagi, *Sci. Papers Inst. Phys. Chem. Research (Tokyo)*, **57**, 105 (1963).

this may account for the rapid hydrogenation of benzyl alcohol with these catalysts. The formation of cyclohexanecarboxaldehyde is not possible, at least in the absence of water, in the hydrogenation of benzyl ethers and esters, which are both hydrogenated easily with rhodium and rhodium-platinum catalysts. α-Substituted benzyl alcohols, which are also hydrogenated rapidly with rhodium and rhodium-platinum catalysts,[2-5] may give saturated ketones in the course of the hydrogenation, but it is probable that the adsorption of ketones on catalyst metals will not be so strong as that of aldehydes[19] and that the hydrogenation of ketones may occur more rapidly than in the case of aldehydes.[2,20]

It is an interesting fact that the ratio of the toluene to the cyclohexylcarbinol formed in the hydrogenation of benzyl alcohol increases with conversion with the rhodium catalyst, while it is nearly unchanged during the hydrogenation with the platinum catalyst (see Figs. 2 and 3). This suggests that the hydrogenation of the benzene nucleus is more inhibited by the presence of cyclohexanecarboxaldehyde than is the hydrogenolysis of the hydroxyl group. This is further supported by the observation that the hydrogenolysis of benzyl alcohol with a palladium catalyst is not inhibited at all by the addition of the aldehyde.

The authors are indebted to the Mitsubishi Chemical Industries Co., Ltd., for its financial support.

19) The hydrogenation of benzyl alcohol with the rhodium catalyst was not retarded at all, even by the addition of 30 mole% of acetone (unpublished).

20) E. Beitner, E. Roginsky and P. N. Rylander, *J. Org. Chem.*, **24**, 1955 (1959).

BULLETIN OF THE CHEMICAL SOCIETY OF JAPAN VOL. 39 2470—2473 (1966)

Altenin. II. The Structure of Altenin

By Noboru SUGIYAMA, Choji KASHIMA, Yoshitaka HOSOI and Tsuneo IKEDA

Department of Chemistry, Tokyo Kyoiku University, Otsuka, Tokyo

and Ryotaro MOHRI

The Liberal Arts Department, Tottori University, Tachikawa-cho, Tottori

(Received March 15, 1966)

Altenin, a metabolite of *Alternaria Kikuchiana* Tanaka, produces the black spot disease on the leaves and fruits of the pear. The optimum conditions for a 200-l. tank culture of this fungus will be described. Altenin has been tentatively deduced as being an ethyl ester of a C_7-carboxylic acid. Of the four expected tautomeric structures, the probability of a furanose ring structure will be demonstrated. There is only one asymmetric center in altenin, at the position α to the ethoxycarbonyl group; this belongs to the L-lactic acid configuration.

It has been demonstrated that one of the metabolites of the fungus *Alternaria Kikuchiana* Tanaka produces the black spot disease on pear leaves and fruit.[1] This substance has been isolated from the culture filtrate and designated "Altenin."[2,3] Altenin is a faint yellow liquid. The spectral and chemical data of altenin allows one to tentatively deduce it as an ethyl α-hydroxy carboxylate with a methyl reductone residue.

Results and Discussion

Altenin gives only one spot on a silica-gel thin-layer chromatogram with a benzene-acetone (1 : 1 v/v) mixture; its R_f value is 0.76, while that of methyl red, a pilot dye, is 0.37.

The molecular peak in the mass spectrum of altenin appears at *m/e* 218; altenin does not contain sulfur and halogen, as can be seen from the fact that the isotope peak, *m/e* 220 (M+2), is very weak compared with the molecular peak. From the molecular weight, 218, and the results of elementary analysis, the molecular formula of altenin may be determined to $C_9H_{14}O_6$. It is apparent that altenin does not contain an aromatic ring.

In an infrared absorption spectrum, an OH absorption at 3400 cm^{-1} and a C=O absorption at

1) I. Hiroe, S. Nishimura and W. Sato, *Transaction of the Tottori Society of Agriculture Science (Tottori Nogeikagaku Kaishi)*, **11**, 291 (1958).

2) N. Sugiyama, C. Kashima, M. Yamamoto and R. Mohri, This Bulletin, **38**, 2028 (1965).

3) N. Sugiyama, C. Kashima, M. Yamamoto, T. Sugaya and R. Mohri, ibid., **39**, 1573 (1966).

1730 cm^{-1} are observed. However there is no absorption band in the region between 1700 and 1600 cm^{-1}. This suggests that altenin has neither carboxyl group nor an olefinic double bond.

The nuclear magnetic resonance spectrum of altenin is given in Table I. The quartet at 4.83 τ is assigned to a methine proton, which is deshielded by an electron withdrawing group and which is coupled to a methyl group at 8.48 τ. The quartet at 5.80 τ is assigned to an ester methylene proton, which is coupled with a methyl group at 8.71 τ. Therefore, the presence of an ethoxycarbonyl group in altenin may be concluded. Similar to the methine proton of ethyl α-hydroxy levulinate[4] at 5.90 τ, the methine proton of altenin at 5.83 τ is deshielded by the oxygen atom. The doublet of 8.54 τ is coupled with the 5.83 τ methine proton. The broad band between 6.9 and 8.0 τ disappears upon deuterium exchange; it shows the presence of two hydroxyl protons. The nuclear magnetic resonance spectrum lacks signals due to a methyl group attached to a quaternary carbon or acetyl group.

The ultraviolet absorption spectrum shows an absorption maximum at 275 mμ (ε 228) in ethanol; it also shows a small shift to a shorter wavelength in acidic ethanol. The optical rotatory dispersion spectrum of altenin is shown in Fig. 3, the specific rotation at 589 mμ being $-5.1°$.

Altenin behaves as a reducing agent in reaction with Tillman's reagent,[5] manganese dioxide[6]

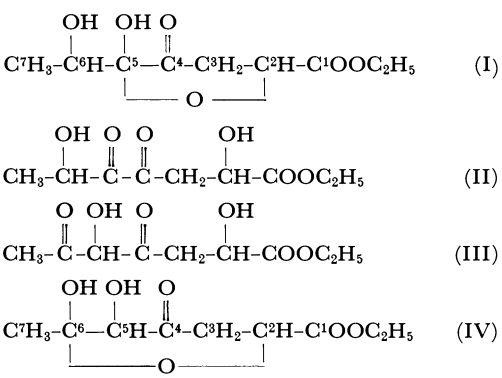

Fig. 1. Structure of altenin.

and Tollens' reagent. The red violet color of Tillman's reagent in acetic acid is decolorized; manganese dioxide is reduced, and silver nitrate is reduced to silver metal in an alkaline solution. These color reactions are characteristic of reductones, acyloins, and ascorbic acid. These properties suggest structures I to IV (Fig. 1) as conceivable for altenin.

4) A. Rossi and A. Lauchenauer, *Helv. Chim. Acta*, **30**, 1501 (1947).
5) F. Cramer and W. Krum, *Chem. Ber.*, **86**, 1586 (1953).
6) F. Feigl and H. T. Cardoso, *Rev. Brasil. Biol.*, **2**, 117 (1942).

The mass specturm of altenin is shown in Fig. 2. The base peak, *m/e* 45, might represents CH_3–CH–OH and C_2H_5–O groups. The peaks at *m/e* 45, 73 and 145 (M-73) suggest the presence of an ethoxycarbonyl group. The peaks at *m/e* 102 and 115 are obtained from the cleavage of the molecule into two parts; that at 102 might also be due to an O–CH–$COOC_2H_5$ fragment. The peak at *m/e* 85 can be accounted for by CH–$COOC_2H_5$ minus one proton, and that at 89 can be accounted for by CH_3–CH(–OH)–C(–O)$_2$ or CH_3–C(–O)$_2$–CH–OH; these high intensive peaks can not be expected from structures II and III. The structures I and IV, in which the lactol ring is present, thus seem to be more reasonable than structures II and III.

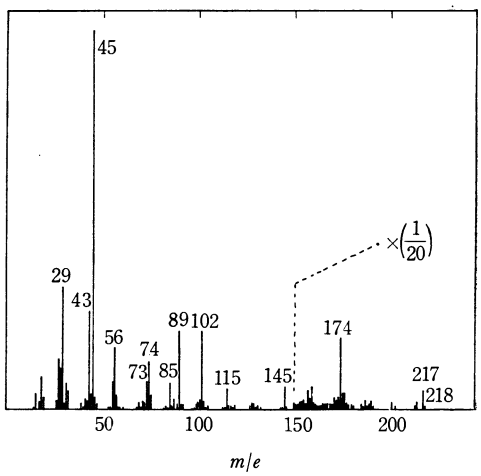

Fig. 2. Mass spectrum of altenin.

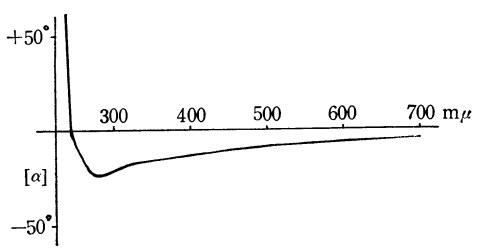

Fig. 3. ORD spectrum of altenin.

The hydroxyl group at C-6 is indicated by the splitting of the methine signal at 4.83 τ to a quartet. However a hydroxyl group of reductones can be rearranged through the endiol tautomer. The presence of an α-hydroxy carbonyl (–CO–CH–OH) group in strucutres II and III, its absence in the structure I, and the absence of the methine proton at C-6 in IV suggest the preference of I to II, III and IV.

Ethyl α-hydroxy levulinate has a structure similar to II and III, and it cannot cyclize to lactol linkage. However, the doublet of methylene

protons of altenin at 8.54 τ is more shielded than the β-methylene protons of ethyl α-hydroxy levulinate at 6.97 τ. In general, the α-methylene protons of aliphatic ketones and cyclohexanones are deshielded but the deshielding effect of the carbonyl group in cyclopentanone is weak[7] and the β-methylene protons of tetrahydrofurane is not influenced by the oxygen atom.[7] Therefore, the methylene protons of C-3 of I may be expected to be at a high field.

The peak intensity of altenin at 7.98 τ is about one half that of a proton; it is probably to be assigned to the methyl group at C-7 of III and IV. The signal of acetyl protons of diacetyl carbinol appears as a singlet at 7.80 τ. Since the peak ratio at 8.48 and 7.98 τ (2.5 : 0.5) is nearly proportional to the ratio of tautomers (I and II): (II and IV), the tautomers I and II may be thought to comprise 85 per cent, while III and IV comprise 15 per cent.

These four tautomeric structures are also found in osones. Petuely[8] reported that D-glucosone preferred the lactol ring form to the open-chain form. Bayne[9] obtained the triisopropylidene glucosone, and demonstrated the presence of a furanose ring. Therefore, it seems most probable for altenin to have the structure I, which has a furanose ring.

Since the carbon at C-6 is enolizable to its endiol tautomer, the only asymmetric center in altenin is the carbon C-2. The specific rotation of altenin is similar to that of α-hydroxy heptanoic acid $[\alpha]_D$ $-4.4°$, which has L-lactic acid configuration.

The substance of structure I or its tautomers was synthesized by the condensation of 3-acetoxy acetylacetone and ethyl glyoxylate with potassium amide; it was thus demonstrated that it showed the same phytopathogenic activity and R_f value as altenin. The details of this will be reported in the near future.

Experimental

The Cultivation of the Fungus Alternaria Kikuchiana Tanaka.—The culture broth (3 l.) of *Alternaria Kikuchiana* Tanaka (No. 5), which was cultured on an ager (0.1%) slant, was transferred into a 200 l. fermenter tank charged with 120 l. of a medium containing sucrose (4.0%), monobasic potassium phosphate (1.1%), dibasic ammonium phosphate (0.2%), potassium chloride (0.05%) and magnesium sulfate (0.05%); it was then cultivated at 30°C for 8 days under aeration (20 l./min.) with stirring. On the second or third day, the fermenter was filled with foam. An antifoam agent (silicon oil) was added on the third day. The activity test with pear leaves showed the highest value on the ninth day; this cultivation was 1.22 times as active as that of the stationary cultivation using the Czapek-Dox medium.

Material.—From the culture filtrate of this fungus, altenin was isolated by a previously-reported method.[3] Altenin is a yellow liquid, which is unstable above 60°C. The R_f value of altenin on silica-gel thin-layer chromatography with a benzene-acetone (1 : 1 v/v) mixture was 0.76, while that of methyl red, a pilot dye, was 0.37. The R_f value on paper (Toyo paper No. 53) chromatography with water saturated with benzene was 0.87.

Found*1: C, 50.95; H, 7.56. Calcd. for $C_9H_{14}O_6$: C, 49.54; H, 6.47.

Mass Spectrum.*2—The mass spectrum of altenin was measured by a Hitachi RMU-6D mass spectrometer; it vaporized at 80°C, and ionized at 70 V., and its ions accelarated at 1800 V. The molecular peak was observed at *m/e* 218, and the base peak, at *m/e* 45.

Infrared and Ultraviolet Absorption Spectra.—In the infrared absorption spectrum (liquid film), absorptions were observed at 3440, 2980, 1740, 1450, 1380, 1270, 1200, 1130, 1100, 1050, 1020, 940, 860 and 760 cm^{-1}. The ultraviolet absorption spectrum showed an absorption maximum at 276 mμ (ε 228) in ethanol and at 273 and 370 mμ in acidic ethanol.

Nuclear Maguetic Resonance Spectrum.*3—An Hitachi H-60 high resolution nuclear magnetic resonance spectrometer was used; the solvent was a mixture of carbon tetrachloride and deuterochloroform for altenin, and only deuterochloroform for ethyl α-hydroxy levulinate. For the deuterium exchange of the hydroxyl proton, deuterium oxide was added to the altenin solution. TMS was used as the inner

Table I. Nuclear megnetic resonance spectrum of altenin

τ, p. p. m.	Intensity	Coupling	J, c. p. s.
4.83	1H	quartet	7.0
5.80	2H	quartet	7.0
5.83	1H	triplet	
6.9—8.0	2H	multiplet	
7.98	0.5H	singlet	
8.46	2.5H	doublet	7.0
8.54	2H	doublet	7.0
8.71	3H	triplet	7.0

Table II. Nuclear magnetic resonance spectrum of ethyl α-hydroxy levulinate

τ, p. p. m.	Intensity	Coupling	J, c. p. s.
5.78	2H	quartet	7.0
5.90	1H	triplet	8.0
6.97	2H	doublet	8.0
7.80	3H	singlet	
8.72	3H	triplet	7.0

7) H. Primas, K. Frei and Hs. H. Gunthard, *Helv. Chim. Acta*, **41**, 35 (1958).
8) F. Petuely, *Montash. Chem.*, **83**, 765 (1952).
9) S. Bayne, G. A. Collie and J. A. Fewster, *J. Chem. Soc.*, **1952**, 2766.

*1 Elementary analyses were made by Mr. Kyusaburo Furuhashi of Department of Chemistry, Tokyo Kyoiku University.
*2 The mass spectra were measured by courtesy of Dr. Hiroshi Satoh of Hitachi Co. Ltd.
*3 The NMR spectra were measured by courtesy of Dr. Kisaburo Yamazaki and Dr. Takamichi Ichimura of Yamanouchi Pharmaceutical Co. Ltd.

standard. The τ value, intensity, coupling type and coupling constant are listed in Tables I and II.

Optical Rotatory Dispersion Spectrum.[*4]—The optical rotatory dispersion spectrum of altenin, which was recorded on a ORD/UV-5 spectrometer made by the Japan Spectroscopic Co., Ltd., in methanol at 28°C, is shown in Fig. 3. Altenin showed a levo specific rotation at 589 mμ and an inversion from levo to dextro specific rotation at 245 mμ.

The Color Reactions.—*With Tillman's Reagent.*—The silica-gel thin layer chromatogram of altenin was obtained by spraying it with Tillman's reagent dissolved in acetic acid. After a few minutes' warming, the color of the thin layer became pink, while the altenin spot remained colorless.

With Manganese Dioxide.—Manganese dioxide was prepared on the filter paper using aqueous potassium permanganate. A drop of an altenin solution was put on a test paper, and after a few minutes the paper was immersed in an aqueous benzidine hydrochloride solution. The paper color became blue, while the altenin spot remained colorless. In this test, ascorbic acid exhibits a strongly positive, while acetoin exhibits only a weak positive, reaction.

With Silver Nitrate.—The paper strip on which altenin had been developed by water saturated with benzene was immersed in a silver nitrate acetone solution, then in an alcoholic sodium hydroxide solution and finally in an aqueous sodium thiosulfate solution. The spot of altenin was blackened by the reduction of silver ions to metal.

The authors wish to express their hearty thanks to Professor Tatsukichi Kobayashi and Dr. Isei Nakamura, Department of Agriculture, Tokyo Kyoiku University, for their kind advice on the cultivation of the fungi and for their generous permission for us to use the 200 l. fermenter at that university. This work was supported by a grant from the Matsunaga Science Foundation.

[*4] ORD spectra were recorded by courtesy of Dr. Takuzo Nishimura of Sankyo Co., Ltd.

BULLETIN OF THE CHEMICAL SOCIETY OF JAPAN VOL. 39 2473—2476 (1966)

Studies of Unnatural Amino Acids and Their Peptides. II. The Syntheses of DL-β-(4-Thiazolyl)-α-alanine and Its Peptides*1

By Hiroshi WATANABE, Shigeru KUWATA, Tatsuo SAKATA*2 and Keizo MATSUMURA*3

Laboratory of Chemistry, Faculty of Science, Kōnan University, Okamoto, Higashinada, Kobe

(Received March 15, 1966)

DL-β-(4-Thiazolyl)-α-alanine has been synthesized in a good yield by the condensation of 4-thiazolylmethyl chloride and diethyl acetamidomalonate, and by the subsequent hydrolysis of the product. The *N*-carbobenzoxy derivative of this amino acid could be prepared easily and transformed to its *p*-nitrophenyl ester and *t*-butoxycarbonylhydrazide, but it was found difficult to obtain the methyl ester or the benzyl ester directly from this amino acid. Carbobenzoxy-DL-β-(4-thiazolyl)-α-alanyl-glycine benzyl ester has been synthesized by several coupling methods: its yield decreased in the following order: *p*-nitrophenyl ester > dicyclohexylcarbodiimide (glycine ester was used as a free base) > azide > dicyclohexylcarbodiimide (glycine ester *p*-toluenesulfonate was used without triethylamine) > dicyclohexylcarbodiimide (glycine ester *p*-toluenesulfonate was used with triethylamine) > mixed anhydride. The alkaline hydrolysis of the protected dipeptide ester afforded the *N*-protected peptide in a good yield. Decarbobenzoxylation did not proceed smoothly by catalytic hydrogenation, in which hydrogen was absorbed slowly and incompletely, while it proceeded normally with hydrobromic acid in acetic acid.

As one of a series of studies of unnatural amino acids and their peptides,[1] the syntheses of DL-β-(4-thiazolyl)-α-alanine and its peptides will be reported in this paper. This amino acid has already been synthesized in several ways.[2,3] First, the authors prepared this compound by

*1 This work was presented at the 18th Annual Meeting of the Chemical Society of Japan, April, 1965.

*2 Present address: Sakata Seiryu Kogyo Co., 132 Tsukuda-cho, 5 chome, Nishiyodagawa-ku, Osaka.

*3 Present address: Nippon Zoki Pharmaceutical Co., Ltd., 18 Hirano, Nishiwaki-cho, Higashisumiyoshi-ku, Osaka.

1) Part I: This Bulletin, **38**, 1461 (1965).

2) R. G. Jones, E. C. Kornfeld and K. C. McLaughlin, *J. Am. Chem. Soc.*, **72**, 4526 (1950).

3) W. T. Caldwell and S. M. Fox, ibid., **73**, 2935 (1951).

reproducing the method of Caldwell and Fox[3] (illustrated in Scheme 1), but they found the results unsatisfactory in some step. When 2 mol. of sodium ethyl acetamidomalonate were allowed to react with one mole of thiazolylmethyl chloride hydrochloride, according to the method of the literature,[3] the condensation product was somewhat difficult to separate from the unreacted acetamidomalonate present in a large excess, and the hydrolysate of the product was contaminated with glycine, as was confirmed by paper chromatography. Hence, we modified the method so as to use the thiazolylmethyl chloride as a free base and the equimolar sodium ethyl acetamidomalonate, as in the report of Jones et al.[2] In this way we succeeded not only in avoiding the

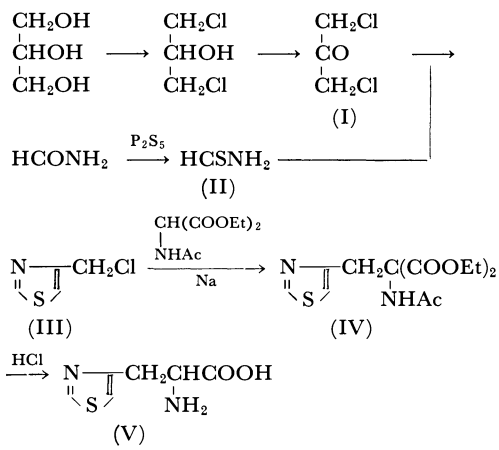

Scheme 1. The synthetic route of DL-β-(4-thiazolyl)-α-alanine.

contamination with acetamidomalonate, but also in raising the yield of the condensation product up to 58% of the theoretical amount in a large-scale reaction. The hydrolysis of the condensation product proceeded smoothly when it was boiled with 6 N hydrochloric acid for 8 hr., and the amino acid was obtained as hydrochloride in an almost quantitative yield.

In the case of an unnatural amino acid containing a heterocyclic ring, the methods generally used for the peptide synthesis are not always suitable because they may be accompanied by undesirable side reactions resulting from the heterocyclic ring. For instance, as has already been reported,[1] in order to remove the formyl group from formylfurylalanine the oxidative cleavage method can not be used because of the simultaneous destruction of the furan ring. Thus, the validity of some typical methods of peptide synthesis was examined for this amino acid.

The carbobenzoxy derivative of this amino acid was prepared by a usual method without any difficulty, while the attempts to esterify this amino acid with methyl alcohol and hydrogen chloride, or with benzyl alcohol and *p*-toluenesulfonic acid in the presence of benzene, resulted in failure.

The coupling reaction of carbobenzoxythiazolylalanine with another amino acid was demonstrated using glycine benzyl ester as an amine component. Though the alkyl ester of thiazolylalanine could not be obtained, carbobenzoxythiazolylalanine *p*-nitrophenyl ester could be prepared by condensing the protected amino acid with *p*-nitrophenol by dicyclohexylcarbodiimide. In the same way, the *t*-butoxycarbonylhydrazide of the carbobenzoxylated amino acid could be obtained by condensing both the components by the dicyclohexylcarbodiimide method, and this compound was used as an intermediate for the azide method. The results of some coupling reactions are summarized in Table I. The yield decreased in connection with the coupling methods in the following order: *p*-nitrophenyl ester > dicyclohexylcarbodiimide (glycine ester was used as a free base) > azide > dicyclohexylcarbodiimide (glycine ester *p*-toluenesulfonate was used without triethylamine) > dicyclohexylcarbodiimide (glycine ester *p*-toluenesulfonate was used with triethylamine) > mixed anhydride. It is noteworthy that, in the condensation of carbobenzoxythiazolylalanine with glycine benzyl ester *p*-toluenesulfonate with dicyclohexylcarbodiimide, a somewhat higher yield was obtained in the absence of triethylamine than in its presence.

The alkaline hydrolysis of the protected peptide ester proceeded smoothly, and carbobenzoxythiazolylalanylglycine was obtained in an excellent yield after the neutralization of the reaction mixture with the equivalent hydrochloric acid.

One of the most important problems is that of estimating the validity of the hydrogenolytic decarbobenzoxylation method of these amino acid derivatives, because they contain a sulfur atom as a constituent. Therefore, precise studies were made by using a quantitative hydrogenation apparatus. Carbobenzoxythiazolylalanine was hydrogenated in the apparatus, using palladium as a catalyst in the presence of sodium hydroxide to remove the carbon dioxide which was evolved during the reduction; the absorption-rate of hydrogen was then compared with that of carbobenzoxyphenylalanine. Though the reduction of carbobenzoxyphenylalanine proceeded smoothly and finished in a short time, that of carbobenzoxythiazolylalanine proceeded very slowly and was still incomplete even after 2 hr. On the basis of these results, we have reached the conclusion that the hydrogenolytic removal of the protecting group is unfavorable in these amino acid derivatives. It was shown, on the other hand, that the carbobenzoxy group was easily split off with hydrogen bromide in acetic acid, and a free peptide, which was proved chromatographically pure, was obtained

by the subsequenttreatment of the reaction product with an ion exchange resin.

Experimental

α, γ-Dichloroacetone (I).—α, γ-Dichlorohydrin was prepared from glycerol by passing hydrogen chloride through it at 100—110°C,[4] then it was oxidized to I with sodium dichromate, according to the method of Conant and Quayle.[4] B. p. 170—175°C.

Thioformamide (II).—This was prepared according to the method of Schmitz,[5] by the action of phosphorus pentasulfide on formamide in tetrahydrofuran; the oily, crude product was used for the next reaction without purification.

(4-Thiazolyl)-methyl Chloride Hydrochloride (III).—This was prepared according to the method of Caldwell and Fox[3] by condensing I and II in acetone. When the resulting crude material (65% yield) was sublimed at 130—140°C under reduced pressure, the pure substance was obtained as pale yellow needles melting at 167—168°C (85—90% yield).

Diethyl (4-Thiazolyl)-methyl Acetamidomalonate (IV).—(4-Thiazolyl)-methyl chloride, which was obtained as a viscous oil by treating III with alkali, was condensed with acetamidomalonate in ethanol, using sodium as the condensing agent, at 40°C for 5 days. The yield was 58%; m. p. 104—105°C (lit.[3] m. p. 104—105°C).

DL-β-(4-Thiazolyl)-α-alanine (V).—IV was hydrolyzed by refluxing it with 6 N hydrochloric acid for 8 hr.; V-hydrochloride was thus obtained in a 93% yield. The free amino acid was obtained in a 87% yield by treating the hydrochloride with ion exchange resin (Amberlite CG-120). M. p. 226—229°C (decomp.) (darkened from ca. 200°C) (lit.[2] m. p. 227—230°C). R_f=0.40 (circular paper chromatography; solvent, *n*-butanol : acetic acid : water=5 : 4 : 1).

***N*-Carbobenzoxy-DL-β-(4-thiazolyl)-α-alanine (VI).**—Carbobenzoxy chloride (28.2 g.) was added, drop by drop, to a solution of V (24 g.) in a sodium hydroxide solution (sodium hydroxide 6 g.; water 150 cc.) with stirring under ice-cooling. The solution was kept alkaline by adding a sodium hydroxide solution. After the addition of carbobenzoxy chloride, stirring was continued for 1 hr. The clear reaction mixture was then extracted with ether, and the pH of the aqueous layer was adjusted to 4 with hydrochloric acid. The white crystals which formed were collected and washed thoroughly with water. The yield was 40 g. (94%); m. p. 122—124°C. For analysis it was recrystallized from dichloromethane; m. p. 130—131°C.

Found: C, 55.05; H, 4.71; N, 9.35. Calcd. for $C_{14}H_{14}O_4N_2S$: C, 54.89; H, 4.61; N, 9.15%.

***N*-Carbobenzoxy-DL-β-(4-thiazolyl)-α-alanine *p*-Nitrophenyl Ester (VII).**—Dicyclohexylcarbodiimide (1 g.) was added to the solution of VI (1.5 g.) and *p*-nitrophenol (0.7 g.) in dichloromethane (40 cc.); the mixture was then stirred for 3 hr. and allowed to stand overnight at room temperature. The dicyclohexylurea was filtered off, and the filtrate was washed with a cold potassium carbonate solution and water until the aqueous phase became colorless. The organic layer was dried with sodium sulfate and concentrated under reduced pressure. The residual solid was recrystallized from ethanol. The yield was 0.77 g. (37%); m. p. 101—103°C.

Found: C, 56.27; H, 3.99; N, 9.28. Calcd. for $C_{20}H_{17}O_6N_3S$: C, 56.20; H, 4.01; N, 9.83%.

***N*-Carbobenzoxy-DL-β-(4-thiazolyl)-α-alanine *t*-Butoxycarbonylhydrazide (VIII).** — Dicyclohexylcarbodiimide (2.1 g.) dissolved in dichloromethane (5 cc.) was added to a solution of VI (3.0 g.) and *t*-butoxycarbonylhydrazine (1.4 g.) in dichloromethane (ca. 50 cc.) under ice-cooling. When the reaction mixture was stirred for 1 hr., voluminous crystals were separated (probably due to the crystallization of *t*-butoxycarbonylhydrazine). By adding more dichloromethane (10 cc.) and methanol (26 cc.), almost all the crystals were dissolved; then the mixture was allowed to stand overnight at room temperature. Acetic acid (2 cc.) was added, and the mixture was stirred for 1 hr. The dicyclohexylurea was then filtered off, and the filtrate was concentrated to dryness. The resulting solid mass was recrystallized from methanol. The yield was 2.43 g. (59%). To remove the trace of dicyclohexylurea, the crystals were dissolved in a small volume of hot ethanol, and then water was added into this solution. The dicyclohexylurea which separated was filtered off, and then the filtrate was allowed to stand overnight at room temperature. The crystals obtained in this way melted sharply at 158.5—160°C, and their analytical data agreed well with the theoretical values.

Found: C, 54.25; H, 6.13; N, 13.17. Calcd. for $C_{19}H_{24}O_5N_4S$: C, 54.27; H, 5.75; N, 13.33%.

***N*-Carbobenzoxy-DL-β-(4-thiazolyl)-α-alanylglycine Benzyl Ester (IX).**—*The Azide Method.*—VIII (1.8 g.) was added to methanolic hydrogen chloride (50 cc.); then, after the evolution of carbon dioxide had ceased, the clear solution was evaporated under reduced pressure. The resulting, strongly hygroscopic solid was dissolved in 1 N hydrochloric acid (4.3 cc.), and ethyl acetate (20 cc.) was added. A solution of sodium nitrite (0.3 g.) in water (2 cc.) was added at −10°C and, then, 2 min. later, 50% potassium carbonate (10 cc.) was added at the same temperature. Then the organic layer was separated, and the aqueous layer was extracted with ethyl acetate (20 cc.). The combined organic layer was dried with sodium sulfate. On the other hand, glycine benzyl ester *p*-toluenesulfonate (2 g.) was dissolved in a small volume of water, made alkaline by the addition of 50% potassium carbonate, and extracted with ethyl acetate 3 times (total volume: 40 cc.). After dried with sodium sulfate, the ester solution was combined with the azide solution and kept in a refrigerator for 2 days. After filtered and washed successively with water, a 0.5% sodium bicarbonate solution, and water, the ethyl acetate solution was dried with sodium sulfate. The solid mass (1.3 g.), obtained by evaporating off the solvent, melted at 110—112°C. After recrystallization from ethanol, it melted at 114—115°C (1.13 g., 58%).

Found: C, 61.24; H, 5.24; N, 8.89. Calcd. for $C_{23}H_{23}O_5N_3S$: C, 60.91; H, 5.11; N, 9.27%.

The p-Nitrophenyl Ester Method.—To a solution of VII

4) J. B. Conant and O. R. Quayle, "Organic Syntheses," Coll. Vol. I, 292, 211 (1948).

5) Wm. R. Schmitz, U. S. Pat. 2682558; *Chem. Abstr.*, **49**, 9029e (1955).

TABLE I. RESULTS OF THE COUPLING REACTIONS OF CARBOBENZOXYTHIAZOLYLALANINE AND GLYCINE BENZYL ESTER

Coupling method	Z-Thia-OH g.	H-Gly-OBz·TosOH g.	Et_3N cc.	Form of amine component	Product g.	Yield, %	M. p., °C
Azide	1.8[a]	2	—	Free base	1.13	58	114—115
p-Nitrophenyl ester	0.57[b]	0.5	0.3	Salt+Et_3N	0.45	74	111.5—113
Mixed anhydride	4.2	5.3	2.2	Salt+Et_3N	2.2	35	114—114.5 (sintered at 112)
DCC	1.5	1.8	—	Free base	1.58	71	113—114 (sintered at 112)
DCC	2.9	3.5	1.6	Salt+Et_3N	1.55	36	106—111.5
DCC	1.5	1.8	—	Salt	0.91	41	111—114 (sintered at 108)

a=Z-Thia-NHNHBOC; b=Z-Thia-ONP

Z: $C_6H_5CH_2OCO$–, -Thia-: 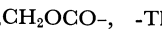 , Bz: $-CH_2C_6H_5$, Tos: $CH_3C_6H_4SO_2$–,

DCC: Dicyclohexylcarbodiimide, BOC: $(CH_3)_3COCO$–, ONP: $-OC_6H_4NO_2$

(0.57 g.) in dichloromethane (40 cc.), there was added glycine benzyl ester *p*-toluenesulfonate (0.5 g.) and triethylamine (0.3 cc.); then the mixture was allowed to stand at room temperature overnight. After washed thoroughly with 5% hydrochloric acid, 0.5% sodium bicarbonate, and water, the solution was dried with sodium sulfate and evaporated under reduced pressure, leaving a viscous, pale yellow oil. By cooling the ethyl acetate solution of the oil, white needle crystals were obtained.

The Mixed Anhydride Method.—To a solution of VI (4.2 g.) and triethylamine (2 cc.) in dichloromethane (60 cc.), ethyl chloroformate (1.37 cc.) was added, drop by drop, at −30°C with stirring. The mixture was then kept at −15—−10°C for 5 min. To the somewhat reddish-brown solution thus obtained, a mixture of glycine benzyl ester *p*-toluenesulfonate (5.3 g.) and triethylamine (2.2 cc.) in dichloromethane (20 cc.) was added with stirring, then allowed to stand overnight at room temperature. The dichloromethane solution was washed successively with water, 5% hydrochloric acid, 0.5% sodium bicarbonate, and water, and dired with sodium sulfate. After the solvent had been evaporated off, a yellowish-brown semi-solid (5.1 g.) was obtained. Recrystallization from ethyl acetate afforded needle crystals.

The Dicyclohexylcarbodiimide Method. — To a solution of VI (1.5 g.) in dichloromethane (30 cc.) there was added a dichloromethane solution of glycine benzyl ester (prepared from 1.8 g. of glycine benzyl ester *p*-toluenesulfonate by neutralizing with potassium carbonate and extracting with dichlorometane). After dicyclohexylcarbodiimide (1.2 g.) in dichloromethane (3 cc.) had been added, the reaction mixture was stirred for 3 hr. at room temperature and then allowed to stand overnight at this temperature. After dicyclohexylurea had been filtered off, the solution was washed successively with 5% hydrochloric acid, 0.5% sodium bicarbonate, and water, and dried with sodium sulfate. After the solvent had been evaporated off, the pale yellow, syrupy residue was crystallized from ethyl acetate (the yield was 1.58 g. (71%)). Instead of free glycine benzyl ester, a mixture of glycine benzyl ester *p*-toluenesulfonate and the equimolar triethylamine, in one case, and glycine benzyl ester *p*-toluenesulfonate alone, in the other case, were used.

All of these results are summarized in Table I, together with those of the other coupling methods.

***N*-Carbobenzoxy-DL-thiazolylalanyl-glycine (X).**—To a methanolic solution (400 cc.) of IX (3.3 g.), 1 N sodium hydroxide (10 cc.) was added; the solution was then allowed to stand at 25°C for 1 hr. with occasinal shaking. About a half of the solvent was then distilled off under reduced pressure, and water was added. After filtration, the solution was neutralized with 1 N hydrochloric acid (10 cc.). The resulting white precipitates were collected, washed thoroughly with water, and air-dried. The yield was 2.3 g. (87%); m. p. 179—181°C (from ethanol).

Found: C, 52.63; H, 4.97; N, 11.40. Calcd. for $C_{16}H_{17}O_5N_3S$: C, 52.88; H, 4.72; N, 11.56%.

The Hydrogenation of Carbobenzoxy-DL-phenylalanine and Carbobenzoxy-DL-thiazolylalanine.—A solution of carbobenzoxy-DL-phenylalanine (0.5 g., 1.67 mmol.) in aqueous methanol (methanol, 25 cc.; water, 10 cc.) and 1 N sodium hydroxide (4 cc.) was placed in a hydrogenation flask containing a palladium catalyst (0.1 g.) in water (20 cc.) which had previously been equilibrated with hydrogen. After the air in the apparatus had been completely replaced with hydrogen, stirring was started; the decreasing volume of the hydrogen was measured against the time. The same experiment was then carried out with carbobenzoxy-DL-thiazolylalanine (0.5 g., 1.63 mmol). In the latter case only about one-third of the theoretical amount of hydrogen was absorbed, even after 2 hr., while in the former case the hydrogenation was complete after 15 min.

DL-Thiazolylalanyl-glycine (XI).—To a 25% solution of hydrogen bromide in acetic acid (3 cc.), X (0.5 g.) was added. After the evolution of carbon dioxide had ceased, water was added and the mixture was extracted with ether. The aqueous layer was then decolorized, the pH was adjusted to ca. 6 with aqueous ammonia, and the solution was allowed to pass through an Amberlite CG-120 (H^+ form) column. After the column had been thoroughly washed with water, the absorbed free peptide was eluted with aqueous ammonia. The eluate was then decolorized, concentrated to a small volume under reduced pressure, and finally lyophilized. The yield was 0.31 g. (92% calculated as hemihydrate); m. p. 158—160°C (sintered at 154°C). Paper chromatography gave only one spot: R_f=0.34.

Found: C, 39.93; H, 5.37; N, 16.84. Calcd. for $C_8H_{11}O_3N_3S\cdot{}^1/_2H_2O$: C, 40.33; H, 5.08; N, 17.64.

BULLETIN OF THE CHEMICAL SOCIETY OF JAPAN VOL. 39 2477—2479 (1966)

Studies of Acenaphthene Derivatives. XII.[1] On the Red Substance Obtained from Acenaphthenequinone and Ammonia

By Otohiko TSUGE and Masashi TASHIRO

The Research Institute of Science and Industry, Kyushu University, Hakozaki, Fukuoka

(Received March 17, 1966)

In order to elucidate the chemical structure of red crystals (A) obtained from the reaction of acenaphthenequinone (I) with ammonia, the reaction of I with ammonia, formamide or benzylamine was reinvestigated. It has been made clear again that the compound A is not acenaphthazine (II) but acenaphtho[1, 2-b]isoimidazole-2-spiro-2'-acenaphthenone (III), and that Schönberg's assumption of the structure of the compound A is incorrect. That reaction of I with benzylamine afforded II as yellow needles in a good yield. Also, it has been found that the reaction product (B) of I with formamide is a mixture of almost equal amounts of II and III.

The previous work[2] of this series has shown that the chemical structure of the red compound A, the reaction product of acenaphthenequinone (I) with ammonia, is neither acenaphthenequinonimide anhydride ($C_{24}H_{12}ON_2$)[3] nor acenaphthazine (II),[4] but acenaphtho[1, 2-b]isoimidazole-2-spiro-2'-acenaphthenone (III).

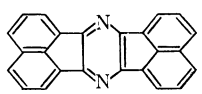

II

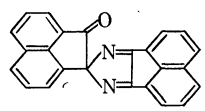

III

Recently, Schönberg and Singer[5] obtained a red substance identical with the compound A by the reaction of I with formamide in the presence of acetic acid;[6] they objected to our proposed structure III for the compound A as a misconception resulting from the treatment of an impure substance. On the basis of its analyses, a study of its infrared spectrum,[7] and its being similar to phenanthrazine, they concluded that the compound A is acenaphthazine (II), whose structure was early suggested by Schönberg and Nedzati.[4]

In the preceding paper,[1] however, it has been shown that II is formed as yellow needles in the reaction of I with primary aliphatic amines, such as methyl-, ethyl- and benzylamine, and the reaction course of the formation of II was also suggested.

Consequently, we are compelled to reexamine our assignment of III for the compound A to see whether it is attributable to the results of the treatment of an impure substance, and to see whether II is the main product in the reaction of I with ammonia or formamide.

In the reaction of I with ammonium carbonate in acetic acid, red crystals (A) are formed.[2] The crude product just after the reaction and the product purified by means of recrystallization from pyridine or by means of sublimation over iron powder are in agreement with the formula $C_{24}H_{12}ON_2$ (III), but not with Schönberg's formula $C_{24}H_{12}N_2$ (II), and the infrared spectrum of the crude product, which showed the absorption band at 1704 cm^{-1} assigned to the carbonyl group, was also almost the same as that of the purified

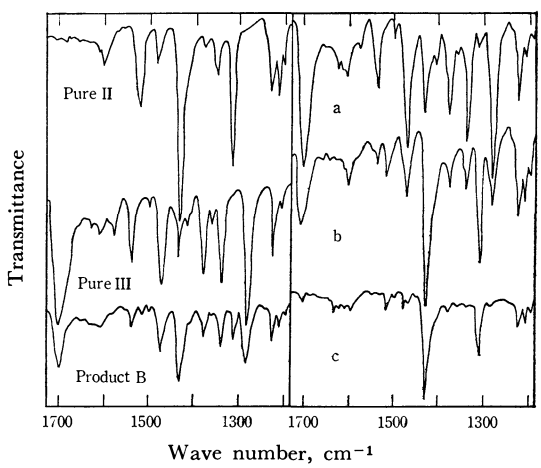

Fig. 1. Infrared spectra of the crude and purified II and III in KBr disk.

a: II obtained from the reaction of I with formamide

b, c: Substance purified three or five times by sublimation respectively

1) Part XI: O. Tsuge and M. Tashiro, This Bulletin, **38**, 399 (1965).
2) O. Tsuge and M. Tashiro, ibid., **36**, 970 (1963).
3) C. Graebe and E. Gfeller, *Ann.*, **276**, 1 (1893).
4) A. Schönberg and F. Nedzati, *Ber.*, **54**, 238 (1921).
5) A. Schönberg and E. Singer, *Chem. Ber.*, **98**, 3436 (1965).
6) It has been reported that the crude product was contaminated by an oxygen-containing substance.[5]
7) Although it was shown that its infrared spectrum did not exhibit any carbonyl bond, its spectrum was not given.

product. These observations indicate that our substance is a pure and single compound.

The reaction of I with an excess amount of benzylamine afforded II, benzal benzylamine and *N*-benzylnaphthalimide. Unlike III, II is yellow needles, and it is more easily purified by sublimation than III. As benzal benzylamine is the condensation product of benzaldehyde[8] and benzylamine, it is resonable to conclude that the reaction proceeds through the previously-proposed course.[1]

As Chart 1 shows, *N*-benzylacenaphthenequinonimine (IV) rearranges to the Schiff base (V), which in turn hydrolyzes to yield benzaldehyde and 1, 2-aminoacenaphthenole (VI). The self-condensation of VI leads to the formation of dihydroacenaphthazine (VII), which easily dehydrogenates to II. On the other hand, benzaldehyde reacts with benzylamine to form benzal benzylamine.

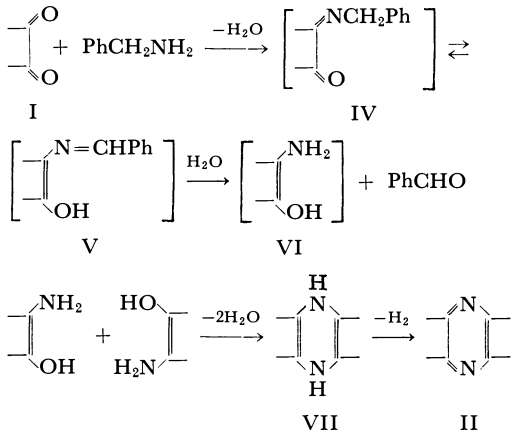

$$PhCHO + PHCH_2NH_2 \longrightarrow PhCH{=}NCH_2Ph$$

Chart 1

The infrared and ultraviolet spectra of II and III are given in Figs. 1 and 2 respectively. The infrared spectrum of III exhibited the sharp band at 1704 cm^{-1} ascribed to the carbonyl group. In view of its elemental analyses and the results of oxidation[2] as well as its infrared spectrum, the compound A may be said to be in accord with the structure of III.

The infrared spectrum of the crude product (B) just after the reaction of I with formamide is also shown in Fig. 1. On the basis of its infrared spectrum, which revealed all the distinctive bands of II and III (as are shown in Fig. 1) and of the ultraviolet spectra (cf. Fig. 2), it may be supposed that the product B is a mixture of II and III.

If the product B was extracted with chloroform and if the chloroform-extract was then recrystallized from pyridine, a red substance whose infrared

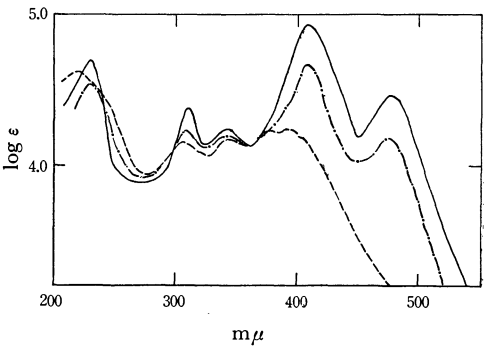

Fig. 2. Ultraviolet spectra of II, III and product B in concentrated sulfuric acid.
—— II
---- III
—·— Product B

spectrum was superimposed on that of III was obtained. On the other hand, the more repeatedly the purification of the product B was done by sublimation, the weaker the strength of the band at 1704 cm^{-1} ascribed to the carbonyl group became; finally yellow needles, m. p. 438°C, the infrared spectrum of which was the same as that of II, were obtained.

The infrared spectra of the product B as purified by recrystallization and by sublimation are also shown in Fig. 1.

The quantitative estimation of II and III in the product B was established by using the ratio method,[9] which was carried out by the measurement of the absorbances, a_1 and a_2, for the bands at 1320 and 1704 cm^{-1}, respectively. Thus, samples of a mixture consisting of specified amounts of II and III were prepared, and the absorbances, a_1 and a_2 were measured according to the baseline

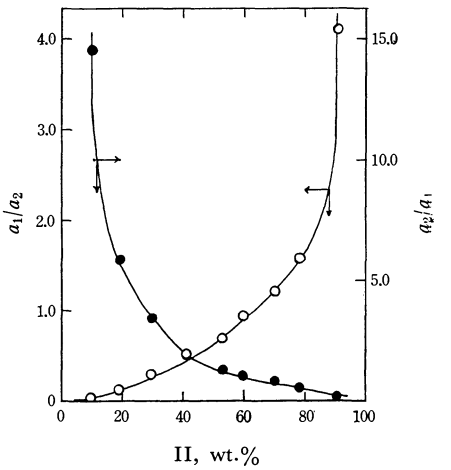

Fig. 3. Calibration curves.

8) Benzaldehyde was isolated and identified as 2, 4-dinitrophenylhydrazone.[1]

9) S. Takagi, "Experiment and Calculation of Quantitative Analyses" (in Japanese), Vol. III, Kyoritsu, Tokyo (1961), p. 91.

method. The calibration curves plotting the relationship between a_1/a_2 or a_2/a_1 and the concentration (wt. %) of II are shown in Fig. 3.

According to the calibration curves thus obtained, it was found that the product B consisted of II (45%) and III (55%). In the reaction of I with formamide known as the Leukart reaction, I reacts with the ammonia which is formed in the reaction process to give III, besides the usual reaction.

Experimental

The Reaction of I with Ammonium Carbonate in Glacial Acetic Acid.—As has been described previously,[2] a mixture of I (1.0 g.) and ammonium carbonate (13.0 g.) in glacial acetic acid (30 ml.) was refluxed for 1 hr. to afford red crystals (0.38 g.). These crude red crystals were washed with hot acetic acid and with acetone, and then dried in vacuo.

Some of the crystals were recrystallized from pyridine, and another part was purified by sublimation over iron powder. The infrared spectrum of the crude product was almost the same as that of the purified product. The elemental analytical data of the red crystals are given in Table I.

Table I. Elemental analytical data of red crystals

Sample	Found, %		
	C	H	N
Crude	83.97	3.33	8.39
	83.81	3.39	8.35
Recrystallized from pyridine	83.97	3.36	8.36
	83.78	3.28	8.40
Sublimated	84.07	3.18	8.47

Calcd. for $C_{24}H_{12}N_2$ (II): C, 87.79; H, 3.68; N, 8.53%.
Calcd. for $C_{24}H_{12}ON_2$ (III): C, 83.71; H, 3.51; N, 8.14%.

The Reaction of I with Benzylamine.—A mixture of I (16 g.) and benzylamine (25 g.) was heated at 80°C for 1 hr. During this time the mixture turned brown. After it had cooled, the mixture was washed with benzene (250 ml.); 6.1 g. of brown crystals were left (m. p. over 400°C). Recrystallization from nitrobenzene or sublimation over iron powder afforded acenaphthazine (II) as yellow needles, m. p. 438°C (decomp.).

Found: C, 87.79; H, 3.65; N, 8.75. Calcd. for $C_{24}H_{12}N_2$: C, 87.79; H, 3.68; N, 8.53%.

After the benzene washings had been dried over sodium sulfate and the benzene had then been removed, distillation in vacuo gave 8.6 g. of a colorless oil (138°C/3 mmHg) and a residue. The distillate was proved, by a study of its infrared spectrum, to be identical with the benzal benzylamine which was prepared from benzaldehyde and benzylamine. On the other hand, the residue was washed with a small amount of hot isopropyl alcohol; this left pale yellow crystals which, on recrystallization from isopropyl alcohol, afforded 3.0 g. of *N*-benzylnaphthalimide as pale yellow needles, m. p. 195—195.5°C.[1]

The Reaction of I with Formamide.—A mixture of I (2.5 g.), formamide (40 ml.), and glacial acetic acid (1 ml.) was heated at 170—180°C for 20 min. The same treatment as has been previously used[2] gave 1.5 g. of red crystals, which were found to be a mixture of II (45%) and III (55%) by the spectroscopic determination. The crude product (300 mg.) was extracted with chloroform (300 ml.), leaving insoluble red crystals which consisted of II (55%) and III (45%). The chloroform extract was concentrated in vacuo to afford red crystals (100 mg.) which were a mixture of II (40%) and III (60%). The fractional recrystallization of the crystals from pyridine gave almost pure III as red needles; their infrared spectrum is also given in Fig. 1.

The chloroform-insoluble crystals were purified by sublimation over iron powder. The more repeatedly sublimation was done, the greater was the relative amount of II in the crystals (Table II).

Table II. Variation in the relative amounts of II and III with sublimation

Number of times	Composition (wt. %)		Number of times	Composition (wt. %)	
	II	III		II	III
1	64	36	4	85	15
2	70	30	5*	~100	
3*	83	17			

* Infrared spectra are given in Fig. 1.

Schönberg et al.[5] may have failed to recognize that II is red crystals, because II as red crystals appears to be contaminated with a trace amount of III.

Also, the reaction in the absence of acetic acid gave red crystals which consisted of II (55%) and III (45%).

The Spectroscopic Determination of II and III in Compound B.—The infrared absorption measurements were made with a Koken IR-S double-beam spectrophotometer equipped with a sodium chloride prism.

Potassium chloride disks containing II and III, in which the weight percentages of III were 10.0, 21.7, 30.0, 39.8, 47.9, 59.7, 70.1, 80.7 and 90.2% respectively, were prepared. The absorbances, a_1 and a_2, for the bands at 1320 and 1704 cm^{-1} respectively were measured by the baseline method.

The calibration curves obtained by the ratio method are shown in Fig. 3.

The authors are indebted to the staff of the Analytical Service Centre of this university and Mr. Eiji Shiozaki of this laboratory for their microanalyses.

BULLETIN OF THE CHEMICAL SOCIETY OF JAPAN VOL. 39 2480—2485 (1966)

Kinetic Studies of the Solution Polymerization of Trioxane Catalyzed by $BF_3 \cdot O(C_2H_5)_2$. VI. The Catalytic Mechanism of Boron Trifluoride Coordination Complexes in Ethylene Dichloride

By Tetsuro MIKI, Toshinobu HIGASHIMURA and Seizo OKAMURA

Department of Polymer Chemistry, Faculty of Engineering, Kyoto University, Sakyo-ku, Kyoto

(Received March 18, 1966)

The initiation mechanism in the cationic polymerization of trioxane by the BF_3 coordination complex catalyst was studied in ethylene dichloride at 30°C. The coordination complexes of BF_3 with diethyl ether (Et_2O), ethyl alcohol (EtOH) and acetic acid (AcOH) were used as catalysts. Under similar conditions, the rates of polymerization decreased in the order: $BF_3 \cdot EtOH > BF_3 \cdot AcOH > BF_3 \cdot Et_2O$, whereas the molecular weights of the polymers decreased in the order: $BF_3 \cdot Et_2O > BF_3 \cdot EtOH \simeq BF_3 \cdot AcOH$. The molecular weight of the polymer formed was unaffected by the addition of the same compound as the donor molecule in the BF_3 coordination complex. However, on the addition of EtOH to the polymerization system catalyzed by $BF_3 \cdot Et_2O$, the rate of polymerization increased and the molecular weight of the polymer decreased. On the other hand, the addition of Et_2O to the system catalyzed by $BF_3 \cdot EtOH$ decreased the rate of polymerization and increased the molecular weight of the polymer formed. The order of catalytic reactivity and the effect of the additive support the idea that the initiation reaction is not an interaction of the BF_3 molecule with trioxane but an addition of the cation produced from the BF_3 coordination complex to the trioxane molecule.

It has been reported that the polymerization of trioxane catalyzed by boron trifluoride (BF_3) is initiated by a direct interaction of BF_3 with trioxane without a cocatalyst such as water, and that it proceeds through a zwitter-ion or by a free-ion mechanism,[1] as is shown in Eq. 1. According to this scheme, the true initiating species of

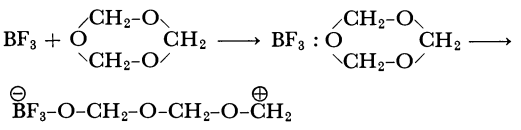

$$\rightleftarrows BF_3\text{-}O\text{-}CH_2\text{-}O\text{-}CH_2\text{-}O^{\oplus}{=}CH_2 \qquad (1)$$

trioxane polymerization catalyzed by BF_3 coordination complexes may be the BF_3 derived from the BF_3 coordination complex molecule, rather than the actual BF_3 coordination complex molecule itself. On the other hand, as reported in a previous paper,[2] it has been found that water is necessary as a cocatalyst to initiate the polymerization by $BF_3 \cdot O(C_2H_5)_2$ in *n*-hexane. This fact suggests that an initiation mechanism through the formation of a BF_3-trioxane coordination complex does not apply in *n*-hexane.

In this paper, the catalytic mechanism involving BF_3 coordination complexes in the solution polymerization of trioxane will be discussed. In addition, the effect of some additives on the polymerization has been investigated in order to clarify the initiation mechanism. As a result, it is concluded that the BF_3 coordination complex itself participates in the initiation of trioxane polymerization; that is, trioxane is attacked by a cationic species produced directly by the ionization of the BF_3 coordination complex.

Experimental

The procedures of the polymerization, the measurement of the viscosity number, and the method of purifying trioxane, ethylene dichloride and $BF_3 \cdot O(C_2H_5)_2$ were the same as those described in previous papers.[2,3] The coordination complexes of BF_3 with two molecules of ethyl alcohol and acetic acid were purified by distilling, in a vacuum, commercial materials (b. p., $BF_3(C_2H_5OH)_2$: 77.5—78°C/11—12 mmHg, $BF_3(CH_3CO_2H)_2$: 78—79°C/18—22 mmHg). The density of these catalysts was measured approximately by the usual piconometer technique at 20°C; $BF_3(C_2H_5OH)_2$: 1.18_1 (lit.,[4] 1.164, $BF_3 \cdot C_2H_5OH$; 1.272), $BF_3(CH_3CO_2H)_2$: 1.37_6 (lit.,[4] 1.342, $BF_3 \cdot CH_3CO_2H$; 1.496). Although precise measurement was very difficult due to the hygroscopic character of these compounds, these values show that these catalysts can approximately be treated

1) V. Jaacks and W. Kern, *J. Polymer Sci.*, **48**, 391 (1962).
2) T. Higashimura, T. Miki and S. Okamura, This Bulletin, **38**, 2067 (1965).
3) T. Higashimura, T. Miki and S. Okamura, ibid., **39**, 25 (1966).
4) N. N. Greenwood, *Quant. Rev.*, **8**, 1 (1954); G. A. Olah, D. R. Martin and J. M. Canon, "Friedel-Crafts and Related Reactions," Vol. I, Ed by G. A. Olah, Interscience Publishers, John Wiley & Sons, Inc., New York (1963), Chap. 4, 6, 8.

as the coordination complexes of BF_3 with two donor molecules.

Results

The Effect of the Nature of the Donor Molecule in the BF_3 Coordination Complex Catalyst on the Polymerization Reaction.— Ethyl ether (Et_2O), ethyl alcohol (EtOH) and acetic acid (AcOH) were selected as donor molecules, and the coordination complexes of BF_3 with these compounds were used as catalysts. It was found by preliminary experiments that, in the case of the $BF_3(EtOH)_2$ and $BF_3(AcOH)_2$ catalysts, the order of reaction with respect to the catalyst was smaller than one, and that the molecular weights of the polymers formed decreased with an increase in the catalyst concentration, as was shown in the case of the $BF_3 \cdot Et_2O$ catalyst.[2,3]

Figure 1 shows the effect of the donor molecule

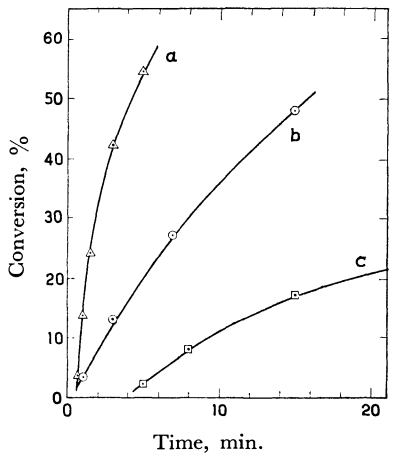

Fig. 1. Effect of the kind of the donor molecule in the BF_3 coordination complex catalyst on the rate of polymerization in ethylene dichloride at 30°C.
($[M]_0$; 3.3 mole/l., $[H_2O]$; 2—3 mmole/l., Catalyst (mmole/l.); a(△): $BF_3(EtOH)_2$ (10.0), b(○): $BF_3(AcOH)_2$ (9.8) and c(□): $BF_3 \cdot Et_2O$ (10.0))

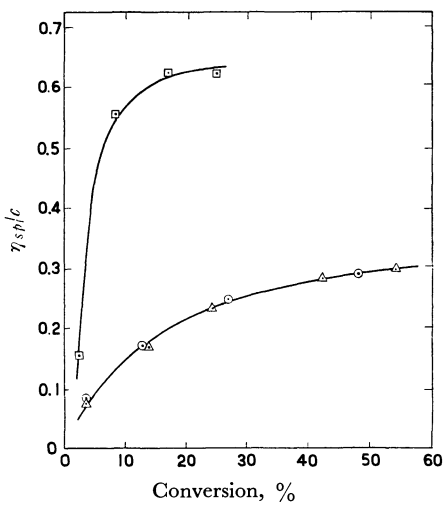

Fig. 2. Effect of the kind of the donor molecule in the BF_3 coordination complex catalyst on the molecular weight of the polymer formed in ethylene dichloride at 30°C.
($[M]_0$; 3.3 mole/l., $[H_2O]$; 2—3 mmole/l., Catalyst (mmole/l.); a(△): $BF_3(EtOH)_2$ (10.0), b(○): $BF_3(AcOH)_2$ (9.8) and c(□): $BF_3 \cdot Et_2O$ (10.0))

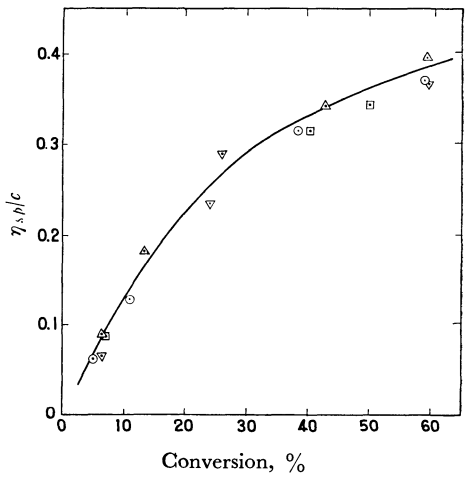

Fig. 3. Effect of the concentration of added EtOH on the molecular weight of the polymer formed by $BF_3(EtOH)_2$ in ethylene dichloride at 30°C.
($[M]_0$; 3.3 mole/l., $[H_2O]$; 3 mmole/l., $[BF_3(EtOH)_2]$; 10.0 mmole/l., [EtOH]; (△): 0, (○): 2.2, (▽): 4.4 and (□): 8.8 mmole/l.)

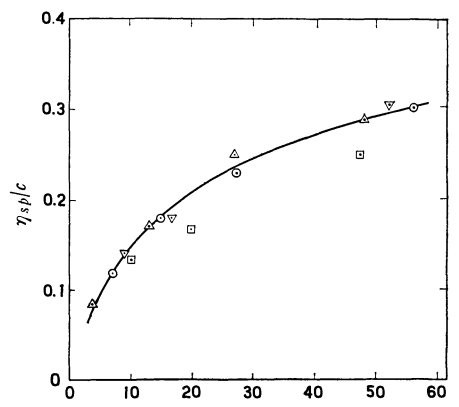

Fig. 4. Effect of the concentration of added AcOH on the molecular weight of the polymer formed by $BF_3(AcOH)_2$ in ethylene dichloride at 30°C.
($[M]_0$; 3.3 mole/l., $[H_2O]$; 3 mmole/l., $[BF_3(AcOH)_2]$; 9.8 mmole/l., [AcOH]; (△): 0, (○): 2.5, (▽): 4.9 and (□): 9.9 mmole/l.)

on the polymerization rate, while Fig. 2 shows its effect on the molecular weight of the polymer formed under similar conditions. In all cases, the molecular weights of the polymer formed increased with an increase in the polymer yield. This fact may be explained in terms of a larger initiation rate than the propagation rate and no termination reaction, as has been shown in a previous paper[3] and in another report.[5]

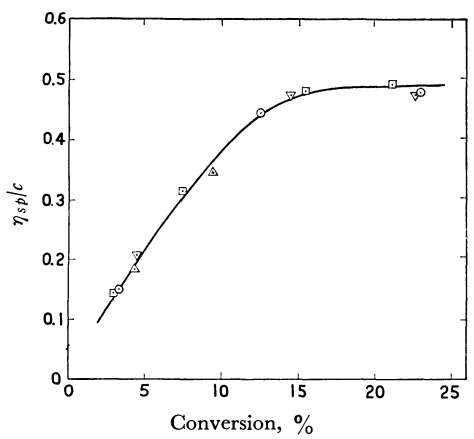

Fig. 5. Effect of the concentration of added Et_2O on the molecular weight of the polymer formed by $BF_3 \cdot Et_2O$ in ethylene dichloride at 30°C. ($[M]_0$; 3.3 mole/l., $[H_2O]$; 7 mmole/l., $[BF_3 \cdot Et_2O]$; 10 mmole/l., $[Et_2O]$; (○): 0, (△): 1.9, (□): 5.0 and (▽): 10 mmole/l.)

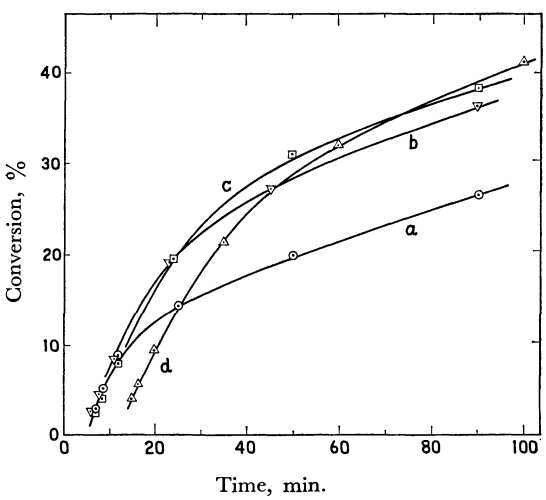

Fig. 6. Effect of the concentration of added EtOH on the rate of polymerization catalyzed by $BF_3 \cdot Et_2O$ in ethylene dichloride at 30°C. ($[M]_0$; 3.3 mole/l., $[H_2O]$; 2 mmole/l., $[BF_3 \cdot Et_2O]$; 10.0 mmole/l., [EtOH]; a(○): 0, b(▽): 2.5, c(□): 4.9 and d(△): 9.9 mmole/l.)

5) T. Kagiya, M. Hatta and K. Fukui, *Chem. High Polymers, Japan*, **20**, 730, 737 (1963).

As is clear from Fig. 1, the polymerization rates decrease in the order:

$$BF_3(EtOH)_2 > BF_3(AcOH)_2 > BF_3 \cdot Et_2O.$$

As may be seen in Fig. 2, the molecular weights of the polymers obtained at a fixed polymer yield decrease in the order:

$$BF_3 \cdot Et_2O > BF_3(EtOH)_2 \simeq BF_3(AcOH)_2.$$

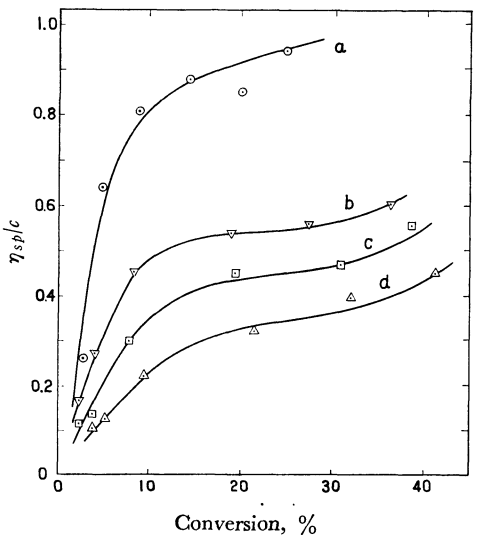

Fig. 7. Effect of the concentration of added EtOH on the molecular weight of the polymer formed by $BF_3 \cdot Et_2O$ in ethylene dichloride at 30°C.
($[M]_0$; 3.3 mole/l., $[H_2O]$; 2 mmole/l., $[BF_3 \cdot Et_2O]$; 10.0 mmole/l., [EtOH]; a(○): 0, b(▽): 2.5, c(□): 4.9 and d(△): 9.9 mole/l.)

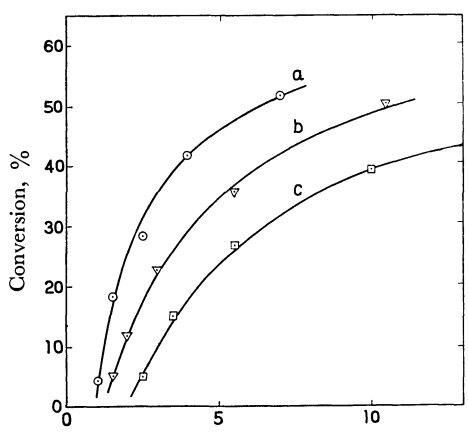

Fig. 8. Effect of the concentration of added Et_2O on the rate of polymerization catalyzed by $BF_3(EtOH)_2$ in ethylene dichloride at 30°C. ($[M]_0$; 3.3 mole/l., $[H_2O]$; 1.8 mmole/l., $BF_3(EtOH)_2$; 7.3 mmole/l., $[Et_2O]$; a(○): 0, b(▽): 2.0, and c(□): 5.0 mmole/l.)

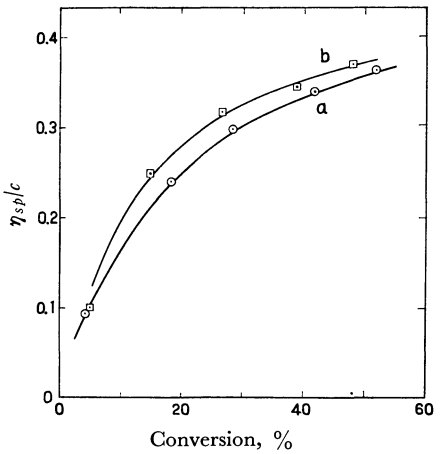

Fig. 9. Effect of the concentration of added Et_2O on the molecular weight of the polymer formed by $BF_3(EtOH)_2$ in ethylene dichloride at 30°C.
([M]$_0$; 3.3 mole/l., [H_2O]; 1.8 mmole/l., [$BF_3(EtOH)_2$]; 7.3 mmole/l., [Et_2O]; a(○): 0 and b(□): 5.0 mmole/l.)

The Effect of Additives on the Polymerization.—Figures 3, 4, and 5 show the effect of the additive (X), when this is the same as the donor molecule in the BF_3·X coordination complex, on the molecular weight of the polymer formed by BF_3·X. The X is EtOH in Fig. 3, AcOH in Fig. 4, and Et_2O in Fig. 5.

Figure 6 shows the effect of added EtOH on the rate of polymerization catalyzed by BF_3·Et_2O, while Fig. 7 shows its effect on the molecular weight of the polymer formed by BF_3·Et_2O.

Figure 8 shows the effect of added Et_2O on the rate of polymerization catalyzed by $BF_3(EtOH)_2$, while Fig. 9 shows its effect on the molecular weight of the polymer formed in the reaction.

Discussion

In vinyl polymerization catalyzed by Lewis acids, there are many cases in which a cocatalyst is necessary.[6] In the trioxane polymerization catalyzed by BF_3, however, no necessity for a cocatalyst has been suggested.[1] In this case, the boron trifluoride - trioxane coordination complex should be formed if the polymerization is to occur according to Eq. 1. Then the ring of this complex opens and the polymerization proceeds either through a free-ion or zwitter-ion mechanism.

According to this suggestion, the following mechanisms may be proposed for the trioxane polymerization catalyzed by BF_3 coordination complexes, where X is a donor molecule:

$$BF_3{\cdot}X \rightleftharpoons BF_3 + X \qquad (2)$$

$$BF_3 + \text{O}\bigcirc \longrightarrow BF_3{\cdot}\text{O}\bigcirc \qquad (2')$$

or

$$BF_3{\cdot}X + \text{O}\bigcirc \rightleftharpoons BF_3{\cdot}\text{O}\bigcirc + X \qquad (3)$$

In either case, the rate of polymerization will be controlled by the concentration of the BF_3-trioxane coordination complex formed. Consequently, the variation in the concentration of this complex with the character of the donor molecule will now be discussed.

According to Eqs. 2 and 3, it may be considered that the BF_3-trioxane coordination complex is more easily produced when the strength of the BF_3-donor bond is weaker. The BF_3-donor bond energy is considered to be larger when the ionization potential of the donor molecule is small.[7] The ionization potential decreases in the order[8]:

$$AcOH > EtOH > Et_2O.$$

Therefore, the BF_3-donor bond energy will decrease in the order:

$$BF_3 \cdot Et_2O > BF_3(EtOH)_2 > BF_3(AcOH)_2.$$

The BF_3-donor bond energy of the 1 : 2 complexes used in this paper is considered to be in the same order as that of the corresponding 1 : 1 complexes, since the 1 : 2 complexes are formed by an additional donor-acceptor interaction of the second molecule, not with BF_3, but with the proton of the donor molecule in the corresponding 1 : 1 complex.[4] Therefore, it might be expected that the rates of polymerization catalyzed by these complexes decrease in the order:

$$BF_3(AcOH)_2 > BF_3(EtOH)_2 > BF_3 \cdot Et_2O.$$

This order, however, does not agree with the experimental results.

According to Eq. 2 or 3 the structure of the growing chain end is considered to be always the same, independent of the kind of donor molecule in the BF_3 coordination complex. As the rate of polymerization catalyzed by $BF_3(EtOH)_2$ is, as Fig. 1 shows, larger than that catalyzed by $BF_3(AcOH)_2$, the concentration of the BF_3-trioxane coordination complex formed by the $BF_3(EtOH)_2$ catalyst is considered to be larger than that formed by the $BF_3(AcOH)_2$ catalyst. Therefore, the molecular weight of the polymer formed by the former ought to be smaller than that formed by

6) A. G. Evans, D. Holden, P. H. Plesch, M. Polanyi, H. A. Skinner and M. A. Weinberger, *Nature*, **158**, 94 (1946); and their studies of this series. "The Chemistry of Cationic Polymerizations," Ed. by P. H. Plesch, Pergamon Press, London (1963).

7) H. A. Skinner "Cationic Polymerization and Related Complexes", Ed. by P. H. Plesch, W. Heffer & Sons Ltd., Cambridge (1953), p. 28.

8) J. D. Morrison and A. J. C. Nicholson, *J. Chem. Phys.*, **20**, 1021 (1952).

the latter, at the same polymer yield. This speculation does not agree with the experimental result, either.

However, for the purposes of the above speculation, it is necessary to assume that the free AcOH or EtOH resulting from the exchange reaction does not act as a transfer agent. In fact, as is shown in Figs. 3 and 4, AcOH and EtOH do not act as transfer agents to any significant degree when these additives are employed at lower concentrations than that of the corresponding catalyst.

In view of the above-mentioned facts, the mechanism of the initiation reaction for trioxane polymerization according to Eqs. 2 and 3 must be rejected. Indeed, the exchange reaction according to Eqs. 2 and 3 might occur to produce the BF_3-trioxane coordination complex, but this complex does not seem to play an essential part in the polymerization reaction.

Another mechanism for the initiation reaction of trioxane polymerization must also be taken into account. The vinyl polymerization catalyzed by $BF_3 \cdot X$ coordination complexes is considered to be initiated by the attack of the alkyl cation, resulting from an ionization of the $BF_3 \cdot X$ coordination complex, on the monomer, and to proceed through an ion-pair mechanism, as is shown in Eq. 4:[9]

$$BF_3 \cdot X \rightleftarrows BF_3Y\ominus R\oplus$$

$$BF_3Y\ominus R\oplus + M \longrightarrow R\text{-}M\oplus \cdots BF_3Y\ominus \qquad (4)$$

$R\oplus$: a proton or alkyl cation

We believe that this idea may also be adopted in the trioxane polymerization on the grounds of the following considerations.

The rate of polymerization catalyzed by $BF_3(EtOH)_2$ is, as Fig. 1 shows, larger than that catalyzed by $BF_3(AcOH)_2$. However, the molecular weights of the polymers obtained at the same polymer yield in both systems are nearly equal. The latter fact means that the numbers of the polymer molecules produced in both polymerization systems under similar conditions are equal; that is, the concentrations of the initiating species, or of the growing chains, are equal in both systems. This speculation is supported by the fact that the addition of a small amount of an additive (X) to the $BF_3 \cdot X_2$ catalyst does not affect the molecular weight of the resultant polymer. As the initiating species is a proton solvated by the corresponding donor molecule in both cases, the difference in the polymerization rate between both catalysts can probably be ascribed to that of the rate of propagation reaction. This implies that there is a difference in the structure of the growing chain end or in the gegen ion between the two polymerization systems, as is suggested in the usual vinyl polymerization. Therefore, it may be concluded that, in the trioxane polymerization, the $BF_3 \cdot X$ coordination complex is partially ionized in a polar solvent, and that the resulting cation attacks the monomer.

The rate of polymerization catalyzed by $BF_3(EtOH)_2$ is, as is shown in Fig. 1, much larger than catalyzed by $BF_3 \cdot Et_2O$. The initiating species is considered to be a proton solvated by ethyl alcohol (or an ethoxonium ion) in the $BF_3(EtOH)_2$ catalyst, and an ethyl cation in $BF_3 \cdot Et_2O$, while the gegen ion is considered to be the same in both catalysts according to Eq. 4. This supposition has been confirmed in the polymerization of styrene catalyzed by these similar catalysts.[10] Therefore, the differences between the two catalysts in the rate of polymerization and in the molecular weight of the polymers may be due to the initiation step. As the degree of ionic dissociation of molten $BF_3(EtOH)_2$ is about sixty times larger than that of molten $BF_3 \cdot Et_2O$,[11] it may be anticipated that the former will also be ionized more easily than the latter in ethylene dichloride. Therefore, the larger rate of polymerization and the lower molecular weight of the polymer in $BF_3(EtOH)_2$ than in $BF_3 \cdot Et_2O$ are probably caused by the higher concentration of the initiating species in $BF_3(EtOH)_2$ than in $BF_3 \cdot Et_2O$. Also, the difference in the rate of polymerization between the two catalysts may be partly ascribed to a difference in the reactivity of the initiating species; that is, to the difference in reactivity between a proton (solvated by ethyl alcohol) and an ethyl cation.

Thus, the mechanism for the function of the BF_3 coordination complex according to Eq. 4 can explain the experimental results. As has been shown in a previous paper,[2] $BF_3 \cdot Et_2O$ cannot initiate the polymerization of trioxane without a cocatalyst such as water in a non-polar solvent. It may probably be concluded that, on the basis of such a mechanism, the polymerization of trioxane catalyzed by BF_3 does not occur without a cocatalyst.

In the trioxane polymerization catalyzed by $BF_3 \cdot Et_2O$, the polymer yield in a given period of time increased upon the addition of a small amount of water in ethylene dichloride.[2] In this work the effect of EtOH on the trioxane polymerization catalyzed by $BF_3 \cdot Et_2O$ was also studied. As is clear from Figs. 6 and 7, the addition of EtOH increases the polymer yield in a given period of time and decreases the molecular weight of the polymer formed. This result indicates that, besides the occurrence of the usual transfer reaction of a growing chain to EtOH, it can be supposed that the exchange reaction, as is shown in Eq. 5,

9) e. g., J. P. Kennedy, *J. Polymer Sci.*, **38**, 263 (1959).

10) S. Aoki and M. Imoto, *Makromol. Chem.*, **65**, 243 (1963).

11) N. N. Greenwood and R. L. Martin, *J. Chem. Soc.*, **1953**, 1427 (1953).

takes place upon the addition of $BF_3 \cdot Et_2O$ to a monomer solution containing a small amount of EtOH. Such an exchange reaction with respect to BF_3 has been observed by NMR spectroscopy.[12]

$$BF_3 \cdot Et_2O + EtOH \rightleftarrows BF_3 \cdot EtOH(\text{or } BF_3(EtOH)_2) + Et_2O \quad (5)$$

The increase in the polymerization rate upon the addition of a small amount of EtOH is probably due to the simultaneous occurrence of the polymerization catalyzed by $BF_3(EtOH)_2$, which has a much larger ability to produce the initiating species than does $BF_3 \cdot Et_2O$.

According to this speculation, the addition of Et_2O to the polymerization system catalyzed by $BF_3(EtOH)_2$ ought to lead to the following reaction (Eq. 6); the polymerization may then proceed through two kinds of catalyst.

$$BF_3(EtOH)_2 + Et_2O \rightleftarrows BF_3 \cdot Et_2O + 2EtOH \quad (6)$$

As the concentration of $BF_3(EtOH)_2$ decreases upon the equilibrium of Eq. 6, and as the $BF_3 \cdot Et_2O$ catalyst has only a small tendency to form the initiating species, the total concentration of the initiating species will decrease in comparison with the case without the additive. Consequently, the rate of polymerization will decrease and the molecular weight of the polymer will increase, since the molecular weight of the formed polymer increases with the decrease in the catalyst concentration, as has been reported in a previous paper.[3] The experimental results support this speculation, as is shown in Figs. 8 and 9. That is, the rate of polymerization decreases and the molecular weight of the polymer increases upon the addition of Et_2O to the trioxane-$BF_3(EtOH)_2$ system. The increase in the molecular weight was not caused by an experimental error in the viscosity measurement. In fact, the molecular weight of the polymer was decreased by the addition of AcOH instead of Et_2O under the same conditions.[13]

If the additive acts only as a transfer agent, it should only decrease the molecular weight of the polymer formed. However, in the present paper, the additive caused an increase in the polymerization rate or in the molecular weight of the polymer formed, depending on the particular system examined. These facts mean that the additive participates in the initiation of the polymerization reaction. Therefore, it may concluded that the polymerization reaction of trioxane occurs according to Eq. 4, not according to Eqs. 2 and 3.

12) R. A. Craig and R. E. Richards, *Trans. Faraday Soc.*, **59**, 1962 (1963); A. C. Rutenberg, A. A. Palko and J. S. Drury, *J. Am. Chem. Soc.*, **85**, 2702 (1963).

13) T. Miki, T. Higashimura and S. Okamura, unpublished data.

BULLETIN OF THE CHEMICAL SOCIETY OF JAPAN VOL. 39 2485—2489 (1966)

The Reaction of *N*-Acylurethans with Phenyl Glycidyl Ether Accompanying Acyl Migration

By Yoshio IWAKURA, Shin-ichi IZAWA and Fusakazu HAYANO

Department of Synthetic Chemistry, Faculty of Engineering, The University of Tokyo, Hongo, Tokyo

(Received March 19, 1966)

N-Acylethylurethans reacted with phenyl glycidyl ether to produce 3-acyl-5-phenoxymethyl-2-oxazolidones, 5-phenoxymethyl-2-oxazolidone and *N*-(2-acyloxy-3-phenoxypropyl)ethylurethans. The reaction mechanism involving acyl migration was discussed.

In an earlier paper[1] it has been shown that the addition condensation reaction between *N*-arylurethan and phenyl glycidyl ether occurs to form 2-oxazolidone in the presence of tertiary amines as catalysts:

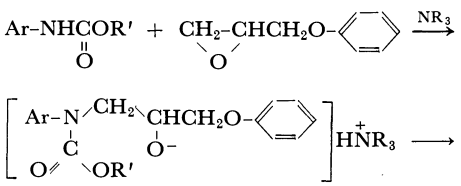

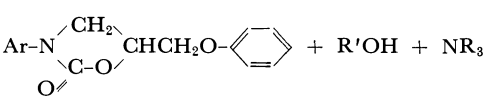

However, *N*-alkylurethans do not react with phenyl glycidyl ether. Further investigation of the reaction between *N*-(*p*-substituted phenyl)-urethans and phenyl glycidyl ether showed that electron-withdrawing substituents facilitated the reaction.

1) Y. Iwakura and S. Izawa, *J. Org. Chem.*, **29**, 379 (1964).

N-Acylurethans have been chosen in this study because of the electron-withdrawing ability of the acyl group. It is expected that 3-acyl-5-phenoxymethyl-2-oxazolidone will be obtained according to the following equation:

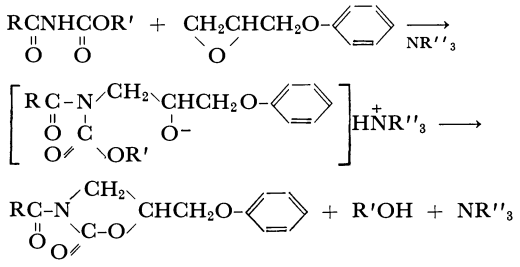

Results

The reaction of *N*-acylethylurethan with phenyl glycidyl ether was more complicated than had been expected. When this reaction was carried out at 70°C for 3—8 hr. in an organic solvent such as toluene or dimethylacetamide, using triethylenediamine as the catalyst, the products were 3-acyl-5-phenoxymethyl-2-oxazolidone and also 5-phenoxymethyl-2-oxazolidone. Moreover, *N*-(2-acyloxy-3-phenoxypropyl)ethylurethan, formed as the result of the N→O migration of the acyl group, was obtained. The reaction conditions and product ratios are listed in Table I.

The 3-acyl-5-phenoxymethyl-2-oxazolidones obtained by this reaction were identical with the authentic samples synthesized from acyl chlorides and 5-phenoxymethyl-2-oxazolidone. 5-Phenoxymethyl-2-oxazolidone was synthesized from 2-hydroxy-3-phenoxypropylamine and diethylcarbonate according to Homeyer's method:[2]

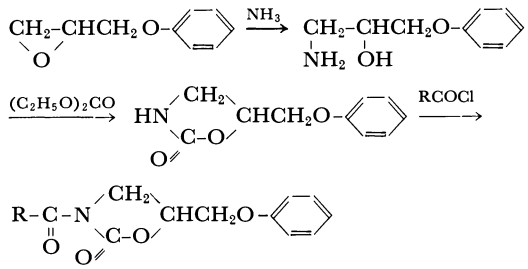

The infrared spectra of 3-acyl-5-phenoxymethyl-2-oxazolidones showed two strong absorptions, at 1700 cm^{-1} and 1760 cm^{-1} which were assignable to the carbonyl groups in cyclic urethan and in the acyl substituent respectively. In the infrared spectrum of 5-phenoxymethyl-2-oxazolidone, the carbonyl absorption appeared at 1740 cm^{-1} and the NH-stretching at 3340 cm^{-1}, but no amide band at 1530 cm^{-1} (NH-deformation) was observed. Physical and analytical data on 3-acyl-5-phenoxymethyl-2-oxazolidones are listed in Table II.

N-(2-Acyloxy-3-phenoxypropyl)ethylurethans were characterized by elementary analysis, infrared spectra, and by a study of the saponification equivalent. These data are listed in Table III.

Discussion

The most likely reaction mechanism for the simultaneous formation of 3-acyl-5-phenoxymethyl-2-oxazolidone (IV) and *N*-(2-acyloxy-3-phenoxypropyl)ethylurethan (V) is the one which involves the common intermediate (III) formed by

Table I. Reaction of *N*-acylethylurethans with phenyl glycidyl ether

Expt.[a]	Moles of starting material	Solvent,	ml.	Reaction time hr.	Cat.,[b] g.	Recovery %	Yield, %		
							Acyl-oxazolidone	*N*-Unsubst.-oxazolidone	Acyloxy-urethan
A-1	0.04	Toluene	10	3	0.1	46	16	0	26
A-2	0.04	Toluene	10	3	0.2	24	44	5	12
A-3	0.04	Toluene	10	3	0.3	18	46	18	0
A-4	0.04	Toluene	10	8	0.2	23	47	16	0
A-5	0.04	DMAc	10	3	0.05	13	37	0	28
A-6	0.04	DMAc	10	3	0.1	5	42	7	20
A-7	0.04	DMAc	10	3	0.2	0	35	35	0
A-8	0.04	DMAc	10	8	0.2	0	46	45	0
P-1	0.08	Toluene	12	3	0.2	27	18	0	45
P-2	0.08	Toluene	12	8	0.2	19	19	0	41
P-3	0.04	DMAc	10	8	0.2	0	25	32	21
n-B-1	0.08	Toluene	15	8	0.2	26	18	0	43
n-B-2	0.04	DMAc	10	8	0.2	14	16	17	31
i-B-1	0.053	Toluene	10	8	0.2	7	24	2	47

a) Letters stand for *N*-substituent: A=acetyl, P=propionyl, B=butyryl.
b) Triethylenediamine.

2) A. H. Homeyer, U. S. Pat. 2399118 (April 23, 1946).

TABLE II. PROPERTIES OF 3-ACYL-5-PHENOXYMETHYL-2-OXAZOLIDONES

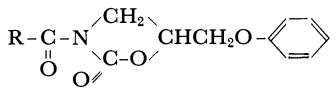

R	M. p., °C	Formula	Anal., % Calcd. / Found			$\nu_{C=O}$, cm^{-1}	
			C	H	N		
CH_3	114.5—115.5	$C_{12}H_{13}NO_4$	61.27 61.22	5.57 5.50	5.96 5.89	1700	1760
C_2H_5	122—124	$C_{13}H_{15}NO_4$	62.64 62.35	6.07 5.90	5.62 5.73	1710	1760
$CH_3(CH_2)_2$	77— 78	$C_{14}H_{17}NO_4$	63.86 63.57	6.51 6.47	5.32 5.07	1700	1760
$(CH_3)_2CH$	99—101	$C_{14}H_{17}NO_4$	63.86 64.16	6.51 6.56	5.32 5.30	1690	1780

TABLE III. PROPERTIES OF *N*-(2-ACYLOXY-3-PHENOXYPROPYL)ETHYLURETHANS

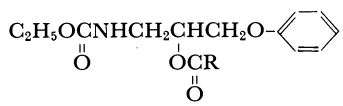

R	B. p., °C/mmHg	Formula	Mol. wt.	Saponification equivalent	Anal., % Calcd. / Found			$\nu_{C=O}$, cm^{-1}	
					C	H	N		
CH_3	147—148/0.03	$C_{14}H_{19}NO_5$	281	281	59.77 59.88	6.81 6.57	4.98 4.97	1730	1700
C_2H_5	150—153/0.05	$C_{15}H_{21}NO_5$	295	293	61.00 60.93	7.17 7.21	4.74 4.75	1720 (broad)	
$CH_3(CH_2)_2$	165—168/0.15	$C_{16}H_{23}NO_5$	309	311	62.12 62.30	7.49 7.41	4.53 4.51	1730	1700
$(CH_3)_2CH$	150—153/0.04	$C_{16}H_{23}NO_5$	309	307	62.12 62.79	7.49 7.30	4.53 4.30	1730	1700

the addition reaction of *N*-acylurethan (I) to phenyl glycidyl ether (II), as is depicted in Chart 1. The alkoxide anion in III can attack the carbonyl carbon either in the amide or urethan group intramolecularly. If the anion attacks the urethan carbonyl to cleave the acyl-oxygen linkage, IV and the ethoxide ion will be formed, while the attack on the amide carbonyl, followed by acyl-nitrogen cleavage, will result in the formation of V. The 5-phenoxymethyl-2-oxazolidone (VII) is considered to have resulted either from IV or V by the reaction of the ethoxide anion formed from III in the course of the formation of IV. The presence of ethanol and ethyl acetate was detected by the gas chromatographic analysis of the reaction mixture of I and II. As the ethoxide anion may possibly abstract the proton from $\overset{+}{H}N\leftarrow$ to form ethanol, it cannot be expected that all of the ethoxide anions will effect the conversion of IV or V to VII.

When 3-acetyl-5-phenoxymethyl-2-oxazolidone (IVa) was treated with ethanol and sodium ethoxide in toluene, VII was obtained. On the contrary, no reaction occurred when IVa was treated with ethanol in the presence of triethylenediamine instead of sodium ethoxide. VII was also obtained by the hydrolysis of V with alcoholic sodium hydroxide. However, no change in the infrared spectrum of the solution of V in toluene was recognized after it had been heated for 8 hr. in the presence of triethylenediamine. The formation of VII, rather than of *N*-(2-hydroxy-3-phenoxypropyl)ethylurethan, from V by hydrolysis is explained by the reaction scheme as being through the intermediate VI, just as that of IV from I and II proceeds through III.

The phenomenon of acyl migration in 2-aminoethanol derivatives and in similar compounds is well known, and reaction mechanisms have been proposed by many authors.[3-6] According to these authors, acyl migrations are reversible and the N→O migration proceeds in acidic media, whereas the O→N migration proceeds in basic media. In addition, when the amino group is acylated after the N→O migration has taken place, no more reverse migration of acyl group (O→N) proceeds, even when it is treated with alkali.

3) L. H. Welsh, *J. Am. Chem. Soc.*, **69**, 128 (1947).
4) A. P. Phillips and R. Baltzly, ibid., **69**, 200 (1947).
5) L. H. Welsh, ibid., **71**, 3500 (1949).
6) G. E. McCasland, ibid., **73**, 2295 (1951).

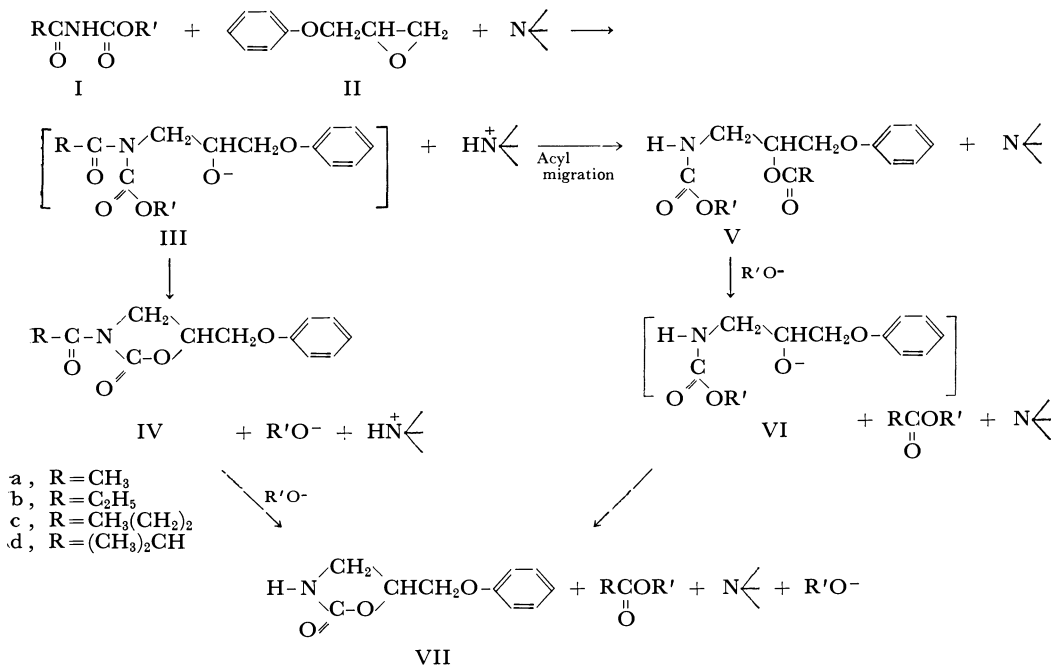

Chart 1

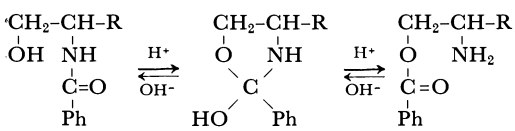

In the reaction of I with II, the N→O migration proceeded in basic media. The reverse migration of the acyl group, from V to III, was excluded, because prolonged reactions did not result in a decrease in V nor in an increase in IV, as is shown in Experiments P-1 and P-2. The change in the yield of V in Experiments A-3 and A-5 is the result of the formation of VII from V. The fact that the infrared spectrum of the solution of V in toluene did not change after it had been heated for 8 hr. also indicates that no migration from V to III proceeds. These experimental results may be explained by the difference in basicity between nitrogen and oxygen atoms.

In the reaction of epoxides with nucleophiles, the latter may attack either of the two epoxide-ring carbon atoms, leading to $-CH_2-O$ or $>CH-O$ fission. These two routes are usually referred to as "normal" and "abnormal" ring-opening respectively. In the reaction of I with II, normal opening was shown by NMR spectral study to occur. As Table IV shows, the methin protons of IV and VII give a signal at a field lower than that of 4-isopropyl-2-oxazolidone prepared from 2-hydroxy-1-isopropylethylamine and phosgene by 1.3 p. p. m. A similar observation about the effect of the neighboring atom on the chemical shift has been shown in the spectra of the $O-CH_3$ proton and the $N-CH_3$ proton, and it has been indicated that the $O-CH_3$ proton gives a signal at a field lower than that of the $N-CH_3$ proton by about 1 p. p. m., presumably because of the inductive effect of the neighboring oxygen atom.[7] The NMR spectra of IVa and VII were completely identical with those of 3-acetyl-5-phenoxymethyl-2-oxazolidone and 5-phenoxymethyl-2-oxazolidone prepared by Homeyer's method. Since the opening of the epoxide ring by ammonia is considered to be normal, the oxazolidones prepared by Homeyer's method are 5-substituted ones.

TABLE IV. NMR SPECTRAL DATA FOR METHIN PROTONS IN OXAZOLIDONE RINGS

2-Oxazolidones	δ, p. p. m.
3-Acetyl-5-phenoxymethyl	4.90
5-Phenoxymethyl	4.90
3-Phenyl-5-phenoxymethyl[a]	4.90
4-*i*-Propyl[b]	3.62

a) Prepared from *N*-phenylethylurethan and phenyl glycidyl ether.
b) Prepared from 2-hydroxy-1-isopropylethylamine.

Experimental

***N*-Acylurethans.**—*N*-Acylethylurethans were prepared from acyl chlorides and ethyl carbamate as has

7) N. S. Bhacca and D. H. Williams, "Application of N. M. R. Spectra in Organic Chemistry," Holden-Day Co., London (1964), p. 39.

been described in the literature.[8] Their melting points and nitrogen analysis data were:

N-Acetyl, m. p. 77.5—78.5°C.

Found: N, 10.80. Calcd. for $C_5H_9NO_3$: N, 10.68%.

N-Propionyl, m. p. 78—81°C.

Found: N, 9.59. Calcd. for $C_6H_{11}NO_3$: N, 9.65%.

N-*n*-Butyryl, m. p. 63—65°C.

Found: N, 8.85. Calcd. for $C_7H_{13}NO_3$: N, 8.80%.

N-*i*-Butyryl, m. p. 100—101°C.

Found: N, 8.67. Calcd. for $C_7H_{13}NO_3$: N, 8.80%.

The Reaction of *N*-Acylethylurethan and Phenyl Glycidyl Ether.—A typical procedure (A-2) was as follows. A mixture of 5.24 g. (0.04 mol.) of *N*-acetylethylurethan and 6.00 g. (0.04 mol.) of phenyl glycidyl ether in 10 ml. of toluene was heated to 70°C, and then 0.2 g. of triethylenediamine was added to the mixture. The mixture was refluxed at 70°C for 3 hr. under reduced pressure. After the solvent had been removed in a vacuum, the reaction mixture was distilled at 0.4 mmHg. *N*-Acetylethylurethan was recovered by sublimation at first, and then phenyl glycidyl ether was distilled at 71—74°C. A fraction boiling at 160—190°C at 0.1 mmHg was collected (5.88 g.). This was a pale yellow, viscous liquid consisting of a mixture of 3-acetyl-5-phenoxymethyl-2-oxazolidone, 5-phenoxymethyl-2-oxazolidone and *N*-(2-acetoxy-3-phenoxypropyl)ethylurethan; it crystallized partially after it had stood overnight. It was treated with 30 ml. of cold ether and filtered to remove liquid *N*-(2-acetoxy-3-phenoxypropyl)ethylurethan. The crystalline part weighed 4.24 g. A portion of 2.00 g. of the crystals was treated with 200 ml. of boiling cyclohexane and filtered in hot to extract 3-acetyl-5-phenoxymethyl-2-oxazolidone. The remaining crystals were treated by the same method four times using each 200 ml. of cyclohexane. Finally, 0.15 g. of 5-phenoxymethyl-2-oxazolidone was obtained as an insoluble material which was proved to be free from 3-acetyl-5-phenoxymethyl-2-oxazolidone on the basis of infrared spectral analysis. It was further purified by recrystallization from 1500 ml. of cyclohexane; m. p. 121—122°C.

Found: C, 62.43; H, 5.52; N, 7.40. Calcd. for $C_{10}H_{11}NO_3$: C, 62.16; H, 5.74; N, 7.25%.

Five filtrates obtained from the above treatments were combined and evaporated. The residue (1.75 g.) was recrystallized from a mixture of 500 ml. of ether and 10 ml. of acetone to give 3-acetyl-5-phenoxymethyl-2-oxazolidone, m. p. 114.5—115.5°C.

Found: C, 61.22; H, 5.50; N, 5.89. Calcd. for $C_{12}H_{13}NO_4$: C, 61.27; H, 5.57; N, 5.96%.

A liquid portion of the *N*-(2-acetoxy-3-phenoxypropyl)ethylurethan obtained at the beginning of this fractionation procedure was evaporated to give 1.29 g. of *N*-(2-acetoxy-3-phenoxypropyl)ethylurethan. Distillation gave a pure product, b. p. 147—148°C at 0.03 mmHg.

Found: C, 59.88; H, 6.57; N, 4.97. Calcd. for $C_{14}H_{19}NO_5$: C, 59.77; H, 6.81; N, 4.98%.

The yields of 3-acetyl-5-phenoxymethyl-2-oxazolidone, 5-phenoxymethyl-2-oxazolidone, and *N*-(2-acetoxy-3-phenoxypropyl)ethylurethan were 4.16 g. (44%), 0.35 g. (5%), and 1.37 g. (12%) respectively, on the basis of the above-mentioned fraction collected at 160—190°C at 0.1 mmHg.

The Saponification Equivalent of *N*-(2-Actloxy-3-phenoxypropyl)ethylurethan.—A typical procedure was as follows. Into a 100-ml. Erlenmeyer flask, 0.7465 g. of *N*-(2-acetoxy-3-phenoxypropyl)ethylurethan was taken. Fifteen milliliters of a 0.5 N alcoholic sodium hydroxide solution was then added to the flask. The solution was allowed to stand at room temperature for 1.5 hr., and then it was warmed at 40°C for 5 min. The excess alkali was titrated by means of 0.2 N hydrochloric acid. The saponification equivalent was found from the amount of alkali consumed to be 281 (calcd. 281).

The hydrolyzed mixture was evaporated under reduced pressure, and then the residue was recrystallized from ether to give white crystalline 5-phenoxymethyl-2-oxazolidone.

The Hydrolysis of 3-Acetyl-5-phenoxymethyl-2-oxazolidone.—A solution of 0.820 g. of 3-acetyl-5-phenoxymethyl-2-oxazolidone in 20 ml. of 0.5 N alcoholic sodium hydroxide was allowed to stand for 8 hr. at room temperature. The mixture was then evaporated under reduced pressure, and the residual solid was washed with 1 ml. of water to give 0.376 g. (56%) of 5-phenoxymethyl-2-oxazolidone.

The Acylation of 5-Phenoxymethyl-2-oxazolidone.—A typical procedure was as follows. A mixture of 1.93 g. (0.01 mol.) of 5-phenoxymethyl-2-oxazolidone and 1.1 g. (0.011 mol.) of triethylamine in 50 ml. of benzene was heated to 80°C. Into the mixture, a solution of 1.10 g. (0.01 mol.) of propionyl chloride in 20 ml. of benzene was added, drop by drop, over a 10-min. period. As the reaction proceeded, triethylamine hydrochloride precipitated. The mixture was refluxed for 2 hr. and filtered in hot to remove triethylamine hydrochloride. The filtrate was evaporated under reduced pressure, and the residual white solid was washed with 5 ml. of water to remove the triethylamine hydrochloride completely. The crude product weighed 2.67 g. (100%). It was distilled at 0.04 mmHg, and the fraction boiling at 162—165°C was collected to give 1.95 g. (74%) of 3-propionyl-5-phenoxymethyl-2-oxazolidone. After the recrystallization from diethyl ether had been repeated, pure 3-propionyl-5-phenoxymethyl-2-oxazolidone was obtained; m. p. 122—124°C.

Found: C, 62.95; H, 5.66; N, 5.67. Calcd. for $C_{13}H_{15}NO_4$: C, 62.64; H, 6.07; N, 5.62%.

8) D. Ben-Ishai and E. Katchalski, *J. Org. Chem.*, **16**, 1025 (1951).

BULLETIN OF THE CHEMICAL SOCIETY OF JAPAN VOL. 39 2490—2494 (1966)

2-Oxazolidones from Glycidyl Ether Reactions with Acid Amides

By Yoshio IWAKURA and Shin-ichi IZAWA

Department of Synthetic Chemistry, Faculty of Engineering, The University of Tokyo, Hongo, Tokyo

(Received March 19, 1966)

The reaction between acid amides and aryl glycidyl ethers was carried out using tertiary amine as the catalyst. 2-Oxazolidone derivatives were obtained by the reaction of trichloroacetanilide or trifluoroacetanilide with aryl glycidyl ether. Acyl migration occurred in the reaction of acetanilide with phenyl glycidyl ether.

In a previous paper[1] we reported that 2-oxazolidone ring formation occurred in the reaction between epoxides and urethans. The reaction has been shown to proceed through a nucleophilic attack of the imide group of urethans on an epoxy ring, followed by an intramolecular exchange of alcohols with a carbon-oxygen bond scission in urethan linkage. Keeping in mind that the epoxides can react with the imide groups of urethans under the catalysis of tertiary amines, and that acid amides and urethans have the same imide groups, the reactivity of the epoxy ring with acid amide will be studied here.

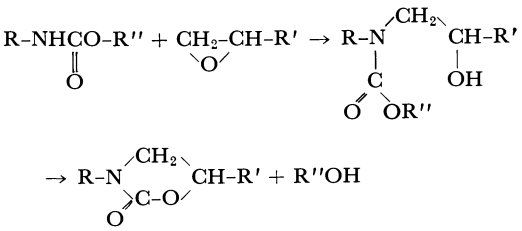

A mixture of equimolar acetanilide and phenyl glycidyl ether, with a small amount of triethylamine as a catalyst, was heated at 100°C for 5 hr. The infrared spectra of the reaction mixture showed an

TABLE I

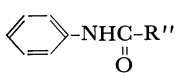

R''	M. p.,	(Lit.)	Anal. of N, % Calcd.	Found	Results of the reaction with phenyl glycidyl ether at 100°C for 2 hr.
CH_3-	113—114	(114)	10.37	10.31	Gave V, VII[a]
	131—132	(134)	8.26	8.41	Gave V, VII
Cl-	116—117	(117)	6.86	7.01	Gave V, VII
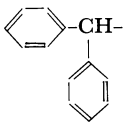	91—93	(94)	5.87	5.98	Gave V, VII and a little amounut of IV
$ClCH_2$-	163.5—164	(164)	7.11	7.07	Side reaction[b]
Cl_2CH-	208—209	(204)	11.57	11.39	Side reaction[c]
Cl_3C-	193—194	(194)	6.05	6.29	Gave IV in good yield[d]
O_2N-	179—180	(180)	4.88	4.78	Side reaction[c]
O_2N- -CH_2-	205—206		10.93	10.68	Side reaction[c]
F_3C-	88—89	(91)	7.41	7.27	Gave IV in good yield[d]
HCF_2CF_2-	66—68	(69)	6.33	6.45	Side reaction[c]
NC-CH_2-	194—195	(198)	17.49	17.53	Side reaction[c]

a) Identified by preparing acetates (VIa and VIIIa).
b) *N, N'*-diphenyldiketopiperazine was obtained in good yield.
c) It was difficult to estimate the structure of products from the infrared spectra of reaction mixture.
d) 3-Phenyl-5-phenoxymethyl-2-oxazolidone was obtained quantitatively.

1) Y. Iwakura and S. Izawa, *J. Org. Chem.*, **29**, 379 (1964).

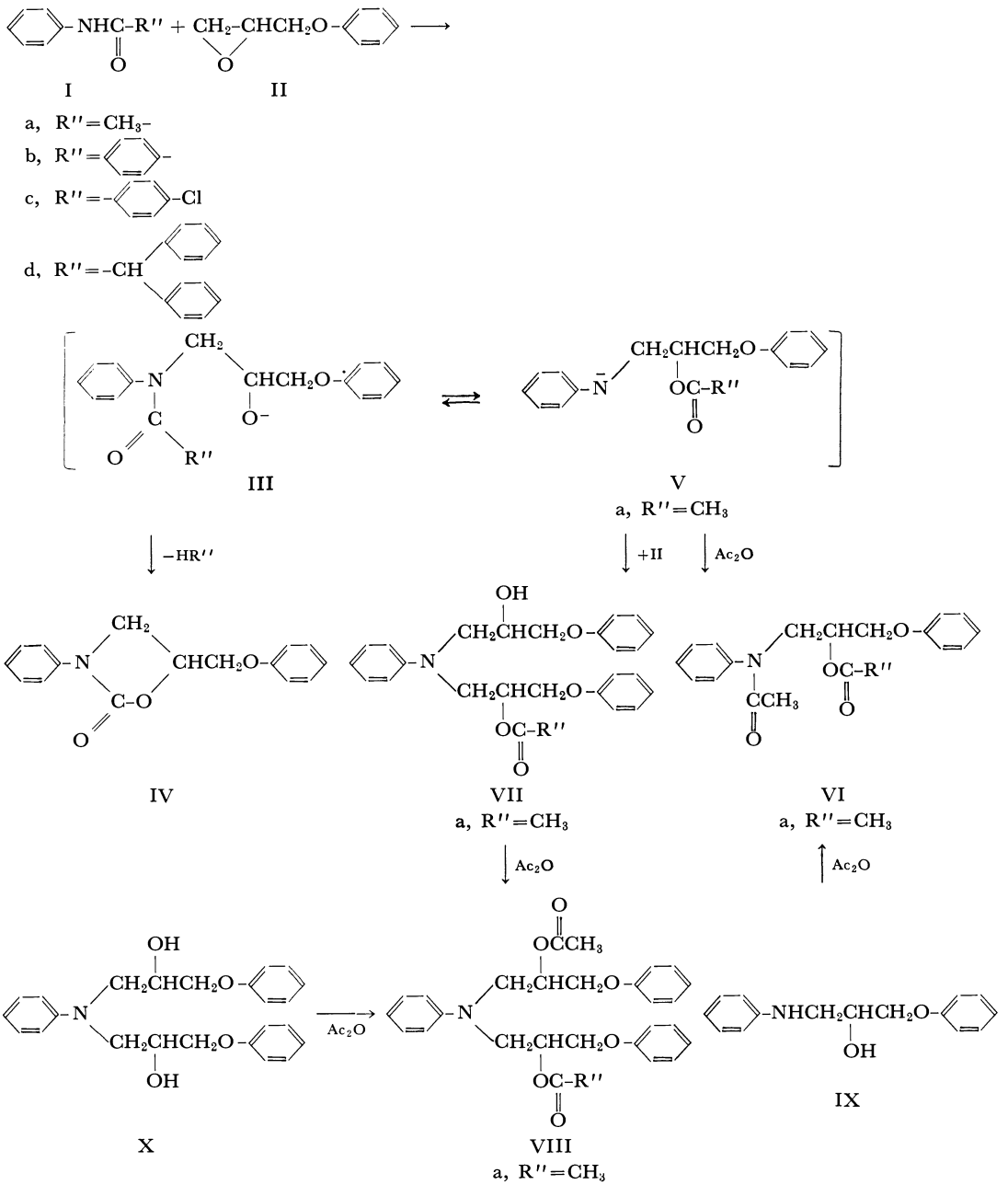

Chart 1

appearance of a new strong absorption at 1735 cm^{-1} and a decrease in the intensity of the amide band of the starting material. The acetylation of the products without separation gave VIa and VIIIa, as Chart 1 shows. The structure of VIa and VIIIa were confirmed to be diacetates of *N*-(3-phenoxy-2-hydroxypropyl)aniline (IX) and *N*, *N*-bis(3-phenoxy-2-hydroxypropyl)aniline (X) respectively, by comparing the melting point and the infrared spectra with the authentic samples prepared via the acetylation of IX and X according to Kier and Penland's method.[2]

These results suggested that the nucleophilic attack of the imide group of acid amide on the epoxy ring occurred easily as had been expected, but that the intramolecular acyl migration reaction proceeded exclusively in the intermediate, III, to give esteramine (Va), since carbon-carbon bond scission was difficult. Further reaction of

2) L. B. Kier and R. B. Penland, ibid., **25**, 1865 (1960).

TABLE II

$$R\text{-}NHC\text{-}R''$$
$$\|$$
$$O$$

R	R''	M.p., °C	Formula	Anal., % Calcd. / Found C	H	N	Products of the reaction with phenyl glycidyl ether at 130°C for 2 hr.
	Cl_3C-	91—93	$C_8H_6Cl_3NO$	40.28 40.58	2.54 2.58	5.87 5.98	2-Oxazolidone[a]
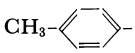	Cl_3C-	110.5—111.5	$C_9H_8Cl_3NO$	42.80 42.89	3.19 3.22	5.55 5.66	2-Oxazolidone
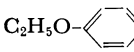	Cl_3C-	124—126	$C_{10}H_{10}Cl_3NO_2$	42.50 42.69	3.57 3.71	4.96 5.20	2-Oxazolidone
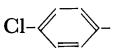	Cl_3C-	124.5—125.5	$C_8H_5Cl_4NO$	35.20 35.33	1.85 1.81	5.13 5.25	2-Oxazolidone
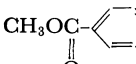	Cl_3C-	115—118	$C_{10}H_8Cl_3NO_3$	40.50 40.46	2.72 2.84	4.72 4.58	2-Oxazolidone[b]
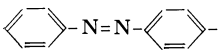	Cl_3C-	143—145	$C_{14}H_{10}Cl_3N_3O$	49.08 49.27	2.94 2.96	12.27 12.55	2-Oxazolidone[c]
	F_3C-	88—89	$C_8H_6F_3NO$	50.80 50.88	3.20 3.31	7.41 7.27	2-Oxazolidone
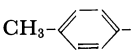	F_3C-	109—111	$C_9H_8F_3NO$	53.20 53.37	3.97 3.94	6.89 7.08	2-Oxazolidone
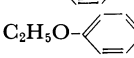	F_3C-	139—140	$C_{10}H_{10}F_3NO_2$	51.50 51.22	4.32 4.40	6.01 5.93	2-Oxazolidone
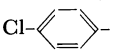	F_3C-	122—123	$C_8H_5ClF_3NO$	42.97 43.05	2.25 2.35	6.27 6.59	2-Oxazolidone
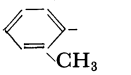	F_3C-	79—80	$C_9H_8F_3NO$	53.20 53.30	3.97 3.92	6.89 6.90	No reaction[d]

a) 2-Oxazolidones were identified by comparing melting point and infrared spectra with authentic samples.

b) 3-(*p*-Methoxycarbonylphenyl)-5-phenoxymethyl-2-oxazolidone was recrystallized from ethanol, m. p. 195—197°C. Found: C, 65.94; H, 5.23; N, 4.17. Calcd. for $C_{18}H_{17}NO_5$: C, 66.05; H, 5.24; N, 4.28%.

c) 3-(*p*-Phenylazophenyl)-5-phenoxymethyl-2-oxazolidone was recrystallized from ethanol, m. p. 184—186°C. Found: C, 70.69; H, 5.16; N, 11.32. Calcd. for $C_{22}H_{19}N_3O_3$: C, 70.76; H. 5.13; N, 11.25%.

d) The acid amide employed was recovered quantitatively.

TABLE III

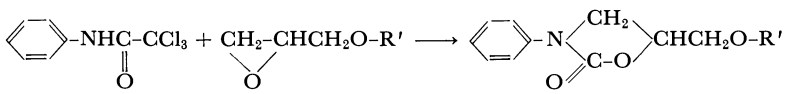

R'	Reaction temp. °C	Reaction time hr.	Yield, %	M. p., °C	Formula	Anal., % Calcd. / Found C	H	N
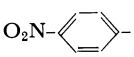	90	5	70	198—199	$C_{16}H_{14}N_2O_5$	61.14 61.16	4.49 4.61	8.91 8.97
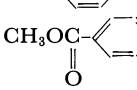	95	4	78	144—146	$C_{18}H_{17}NO_5$	66.05 65.83	5.24 5.31	4.28 4.34
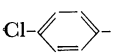	95	5	75	192—194	$C_{16}H_{14}ClNO_3$	63.25 63.46	4.64 4.83	4.61 4.63
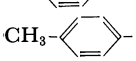	90	6	85	197—198	$C_{17}H_{17}NO_3$	72.06 72.26	6.05 6.28	4.94 4.96
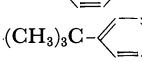	90	6	80	138—140	$C_{20}H_{23}NO_3$	73.82 73.52	7.12 7.10	4.30 4.24
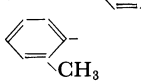	90	6	73	91—94	$C_{17}H_{17}NO_3$	72.06 72.35	6.05 6.10	4.94 5.11
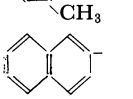	90	6	88	206—208	$C_{20}H_{17}NO_3$	75.25 75.37	5.37 5.37	4.39 4.47

Va with phenyl glycidyl ether occurred, yielding VIIa because the reactivity of the imino group of Va was higher than that of Ia.

In order to investigate the possibility of carbon-carbon bond scission in the reaction intermediate, III, an electron-withdrawing group was introduced into the acid component of acid amides. The acid amides prepared and the results of the reaction between these compounds and phenyl glycidyl ether are listed in Table I. The fact that only trifluoro- and trichloroacetanilides gave the 2-oxazolidone derivatives (IV) shows that a moderately strong electron-withdrawing ability is necessary to break the carbon-carbon bond in the intermediate, III.

The infrared spectra of the reaction mixture between phenyl glycidyl ether and *p*-nitrobenzanilide, *p*-nitrophenylacetanilide, dichloroacetanilide, 1, 1, 2, 2-tetrafluoropropionanilide, and cyanoacetanilide showed that some side reactions occurred, but they were not studied further.

N-Aryl-trichloroacetamides and *N*-aryl-trifluoroacetamides were prepared by the condensation of the corresponding amines and trichloro- or trifluoroacetyl chlorides. The reaction between these amides and phenyl glycidyl ether gave 3-aryl-5-phenoxymethyl-2-oxazolidones in good yields, as had been expected. The results are listed in Table II.

Trichloroacetanilide and aryl glycidyl ethers also produced 3-phenyl-5-aryloxymethyl-2-oxazolidones, as Table III shows.

Experimental

Glycidyl Ethers.—These were prepared by the condensation of the corresponding phenols and epichlorohydrin, as has been described in our previous paper.[1] A typical preparation will be described below.

***p*-Chlorophenyl Glycidyl Ether.**—To a mixture of 128.5 g. (1.0 mol.) of *p*-chlorophenol and 370 g. (4 mol.) of epichlorohydrin was added 54 g. (1.0 mol.) of sodium methylate in 400 ml. of methanol drop by drop with stirring during 1-hr. period at room temperature; the mixture was then stirred for an additional 1 hr. After the epichlorohydrin had been removed, the residue was distilled under reduced pressure to give 144 g. (78%) of *p*-chlorophenyl glycidyl ether, b. p. 115—116°C/2 mmHg; n_D^{25} 1.5419.

Acid Amides.—These were prepared by the condensation reaction of the corresponding amines with acid chlorides. Examples will be shown below.

***α*-Chloroacetanilide.**—To a solution of 22.6 g. (0.2 mol.) of monochloroacetyl chloride in 100 ml. of benzene was added 18.6 g. (0.2 mol.) of aniline and 20.2 g. (0.2 mol.) of triethylamine in 200 ml. of benzene with stirring at 10—20°C; the mixture was then allowed to stand for 3 hr. After the triethylamine hydrochloride had been filtered out and the benzene removed, the resulting crystalline solid was recrystallized from water to give 21.7 g. (64%) of α-chloroacetanilide, m. p. 163.5—164°C.

***α, α, α*-Trifluoroacetanilide.**—To a solution of 9.3 g. (0.1 mol.) of aniline and 10.1 g. (0.1 mol.) of triethylamine in 100 ml. of acetone was added 13.3 g. (0.1 mol.) of trifluoroacetyl chloride in 60 ml. of acetone with stirring at −10°C. The mixture was then allowed to stand for 1 hr. at room temperature. After the triethylamine hydrochloride had been filtered out and the acetone had been removed, the resulting crystalline solid was recrystallized from *n*-hexane to give 40.7 g. (72%) of α, α, α-trifluoro-*p*-ethoxyacetanilide, m. p. 139—140°C.

The Reaction between Acid Amides and Glycidyl Ethers.—A mixture of equimolar amounts of acid amide and glycidyl ether, with triethylenediamine as a catalyst, was heated at 100°C for 2 hr. An example will be shown below.

The Reaction of Phenyl Glycidyl Ether with Acetanilide.—A mixture of 13.5 g. (0.1 mol.) of acetanilide and 15.0 g. (0.1 mol.) of phenyl glycidyl ether was heated at 100°C in order to dissolve both ingredients, and then 0.1 g. of triethylenediamine was added. The mixture was heated at 100°C for 2 hr. After cooling, the reaction mixture was poured into a solution of 100 g. of acetic anhydride in 80 g. of pyridine and allowed to stand overnight at room temperature. Pyridine and acetic anhydride were removed by distillation under reduced pressure, and the residue was recrystallized from ethyl acetate to give 9.5 g. of *N*, *N*-bis(3-phenoxy-2-hydroxypropyl)aniline diacetate (VIIIa). After the ethyl acetate had been evaporated from the filtrate, the residue was recrystallized from ethanol to give 9.8 g. *N*-(3-phenoxy-2-hydroxypropyl)aniline diacetate (VIa). Acetanilide (4.1 g.) was recovered from the filtrate. The structures of VIa and VIIIa were confirmed by a mixed-melting-point determination and by comparing the infrared spectra with those of authentic samples.

The Preparation of Authentic Samples (VIa and VIIIa).—*N-(3-Phenoxy-2-hydroxypropyl)aniline Diacetate (VIa).*—To 9.5 g. (0.1 mol.) of redistilled aniline, which was maintained at 120°C, 4.5 g. (0.03 mol.) of phenyl glycidyl ether was added over 1-hr. period. The mixture was then heated for an additional 15 min. and distilled at 10 mmHg to recover the unreacted aniline. The pressure was then reduced further, and 6.5 g. of a viscous oil, b. p. 180—185°C (0.1 mmHg), was distilled. After the oil had been dissolved in a toluene - petroleum ether mixture, upon cooling 5.9 g. (80.9%) of *N*-(3-phenoxy-2-hydroxypropyl)aniline (IX) crystallized, m. p. 60—62°C (lit, 61—63°C). A mixture of IX (5.0 g.), pyridine (30 g.), and acetic anhydride (40 g.) was allowed to stand for 1 day at room temperature. Pyridine and acetic anhydride were removed by distillation under reduced pressure, and the residue was recrystallized several times from ethanol to give 4.8 g. (71.4%) of VIa, m. p. 96—97°C.

Found: C, 69.82; H, 6.43; N, 4.26. Calcd. for $C_{19}H_{21}NO_4$: C, 69.71; H, 6.47; N, 4.28%.

N, N-Bis(3-phenoxy-2-hydroxypropyl)aniline Diacetate (VIIIa).—To a boiling solution of 6.5 g. (0.02 mol.) of IX in 30 ml. of benzene was added drop by drop with stirring 4.5 g. (0.03 mol.) of phenyl glycidyl ether in 50 ml. of benzene. The mixture was then heated under reflux for an additional hour. After the benzene had been removed, the residue, without purification, was dissolved in pyridine - acetic anhydride mixture; the solution was then allowed to stand for 1 day. The

pyridine and acetic anhydride were removed by distillation under reduced pressure, and the residue was recrystallized several times from ethyl acetate to give 5.7 g. (59.7%) of VIIIa, m. p. 171—172°C.

Found: C, 70.29; H, 6.55; N, 3.00. Calcd. for $C_{28}H_{31}NO_6$: C, 70.42; H, 6.54; N, 2.93%.

3-Aryl-5-aryloxymethyl-2-oxazolidones.—The results of the reaction between acid amides and glycidyl ethers are listed in Tables II and III. Experimental examples will be given below.

A. The Reaction of α, α, α-Trichloroacetanilide with Phenyl Glycidyl Ether.—A mixture of 7.2 g. (0.03 mol.) of α, α, α-trichloroacetanilide, 4.5 g. (0.03 mol.) of phenyl glycidyl ether, and 0.1 g. of triethylenediamine was heated at 100°C for 2 hr. After cooling, the adduct was recrystallized from acetone to give 6.5 g. (80%) of 3-phenyl-5-phenoxymethyl-2-oxazolidone, m. p. 138—139°C. A mixed-melting-point determination with an authentic sample showed no depression.

B. The Reaction of α, α, α-Trifluoro-*p*-methylacetanilide with Phenyl Glycidyl Ether.—A mixture of 6.1 g. (0.03 mol.) of α, α, α-trifluoro-*p*-methylacetanilide, 4.5 g. (0.03 mol.) of phenyl glycidyl ether, and 0.1 g. of triethyl benzylammonium bromide was heated at 110°C for 2 hr. After cooling, the adduct was recrystallized from acetone to give 7.4 g. (87%) of 3-*p*-tolyl-5-phenoxymethyl-2-oxazolidone, m. p. 149—151°C. A mixed-melting-point determination with an authentic sample showed no depression.

C. The Reaction of α, α, α-Trichloroacetanilide with *p*-Methoxycarbonylphenyl Glycidyl Ether.—A mixture of 11.9 g. (0.05 mol.) of α, α, α-trichloroacetanilide, 10.4 g. (0.05 mol.) of *p*-methoxycarbonylphenyl glycidyl ether, and 0.2 g. of triethyl benzylammonium bromide was heated at 95°C for 4 hr. After cooling, the adduct was recrystallized from ethanol to give 12.8 g. (78%) of 3-phenyl-5-(*p*-methoxycarbonylphenoxymethyl)-2-oxazolidone, m. p. 144—146°C.

Found: C, 65.83; H, 5.31; N, 4.34. Calcd. for $C_{18}H_{17}NO_5$: C, 66.05; H, 5.24; N, 4.28%.

BULLETIN OF THE CHEMICAL SOCIETY OF JAPAN VOL. 39 2494—2499 (1966)

Copolymerizations of 1-Phthalimido-1, 3-butadiene and 1-Succinimido-1, 3-butadiene[1]

By Kenichi MURATA and Akira TERADA[2]

Government Industrial Research Institute, Osaka; Ikeda, Osaka

(Received March 24, 1966)

1-Phthalimido-1, 3-butadiene (1-PB) and 1-succinimido-1, 3-butadiene (1-SB) were copolymerized readily with acrylonitrile, methyl methacrylate and styrene, but somewhat less readily with vinyl acetate. The monomer reactivity ratios for the system with styrene were calculated by the Fineman-Ross method and found to be r_1(1-PB)=1.48, r_2(St)=0.32 for the 1-phthalimido-1, 3-butadiene-styrene system, and r_1(1-SB)=1.62, r_2(St)=0.28 for the 1-succinimido-1, 3-butadiene - styrene system. The Q, e-values for these systems were successively evaluated and obtained as Q(1-PB)=1.57, e(1-PB)=+0.06, Q(1-SB)=1.76 and e(1-SB)=+0.09, when Q(St)=1.0 and e(St)=−0.8. Likewise, such values for *N*-vinyl phthalimide (VPI) and *N*-vinyl succinimide (VSI) were investigated in order to compare them with the values obtained above for the imidobutadienes; they were shown to be r_1(VPI)=0.09 and r_2(St)=6.3 for the *N*-vinyl phthalimide - styrene system, and r_1(VSI)=0.07 and r_2(St)=9.6 for the *N*-vinyl succinimide - styrene system. Subsequently, the following Q and e values were determined: Q(VPI)=0.09, e(VPI)=−0.13, Q(VSI)=0.06, and e(VSI)=−0.17.

As part of the investigation of aminobutadienes and related compounds, experiments have presented some results of the syntheses of several imidobutadiene monomers,[3-6] and of attempts to improve the dyeability of polypropylene fiber[7] and to make high-equivalent anion exchange resins.[8] Since it became desirable to determine some of the reactivity parameters of the imidobutadienes toward polymerization and copolymerization, a previous paper has dealt with the polymerization and copolymerization of 2-phthalimido-1, 3-butadiene and the determination of the Q, e-parameters.[9]

1) Paper VII on Aminobutadienes: Abstracts of the 17th Annual Meeting of the Chemical Society of Japan, Tokyo, April, 1964.

2) Present address: Department of Industrial Chemistry, Kyushu Institute of Technology, Tobata-ku, Kitakyushu.

3) A. Terada, *J. Chem. Soc. Japan, Pure Chem. Sect. (Nippon Kagaku Zasshi)*, **81**, 1773 (1960).

4) A. Terada and S. Takahashi, ibid., **83**, 485 (1962).

5) A. Terada and K. Murata, ibid., **83**, 490 (1962).

6) A. Terada and K. Murata, Abstracts of the Meeting on Olefin Chemistry of the Society of Organic Synthetic Chemistry, Japan, Tokyo, November, 1964.

7) A. Terada, Abstracts of the Ōita Meeting of the Chemical Society of Japan, Ōita, December, 1965.

8) A. Terada and K. Murata, Japanese Pat. 468683 (1966).

9) K. Murata and A. Terada, Paper VI on Aminobutadienes, *J. Polymer Sci.*, **A**, Nov., (1966), in press.

Likewise, data presented in one of the previous reports[10] have demonstrated that 1-phthalimido- and 1-succinimido-1, 3-butadienes easily polymerize, using a free radical source, to give high polymers, and that the polymerizations take place smoothly even by a cationic process. The purpose of the present investigation is to extend these data to copolymerization systems with various vinyl monomers, and to supply some of the basic data for the above-mentioned utilizations. The copolymerizations of each of these imidobutadiene monomers with acrylonitrile (AN), methyl methacrylate (MMA), styrene (St) and vinyl acetate (VAc), and, in addition, the copolymerizations of *N*-vinyl phthalimide and *N*-vinyl succinimide with such vinyl monomers will also be described. The monomer reactivity ratios for the copolymerization systems of these imidobutadienes and of vinyl imides with styrene will be determined, and the evaluation of the *Q*, *e*-parameters will also be attempted according to the Alfrey-Price scheme.[11]

Experimental

Materials.—1-Phthalimido-1, 3-butadiene (1-PB) and 1-succinimido-1, 3-butadiene (1-SB) were prepared as previously reported,[5] and obtained as yellow needles with a m. p. of 114.5—116°C, and as white crystals with a m. p. of 75—76°C respectively. *N*-Vinyl phthalimide (VPI) was prepared via the pyrolysis of the *N*-β-acetoxyethylphthalimide obtained after the condensation of monoethanolamine with phthalic acid and following acetylation; it was obtained as pale yellow needles (from methanol), 85—86°C (lit., 86,[12,13] 85.5—86°C[14,15]). *N*-Vinyl succinimide (VSI) was prepared by a similar manner, using succinic acid and monoethanolamine as the starting meterials; it was obtained as white crystals, m. p. 48—48.5°C (lit., m. p. 48,[16] 48.5,[17] 48—49°C)[18]. The other vinyl monomers, acrylonitrile (b. p. 76—77°C), methyl methacrylate (b. p. 44.5—46°C/118 mmHg), styrene (b. p. 46.5—47°C/24 mmHg) and vinyl acetate (b. p. 71—71.5°C), were obtained commercially as reagent grade materials, just prior to use they were purified to the above state according to the usual manner.[19] Benzoyl peroxide (analytical-grade reagent) was purified by repeated precipitations into methanol from a chloroform solution and then dried under a vacuum, m. p. 104°C. Purified dimethylformamide was prepared by repeated fractional distillations through a 30 cm. fractionating-distillation column after dehydration over anhydrous sodium sulfate; the middle fraction was used as a solvent for the polymerization, b. p. 65—66°C/40 mmHg.

Polymerization Procedure.—This was carried out as usual.[9,10]

Results and Discussion

The Copolymerization of 1-Phthalimido-1, 3-butadiene.—Table I shows the results of the radical copolymerization of this monomer with various comonomers in the bulk state or in solution. The infrared spectra of the resulting copolymers are illustrated in Fig. 1.[20] In each of the spectra, there is a strong absorption band, showing a *trans* di-substituted ethylenic bond internal in the polymer chain, as has been shown previously in the case of the homopolymer.[10] This obviously indicates

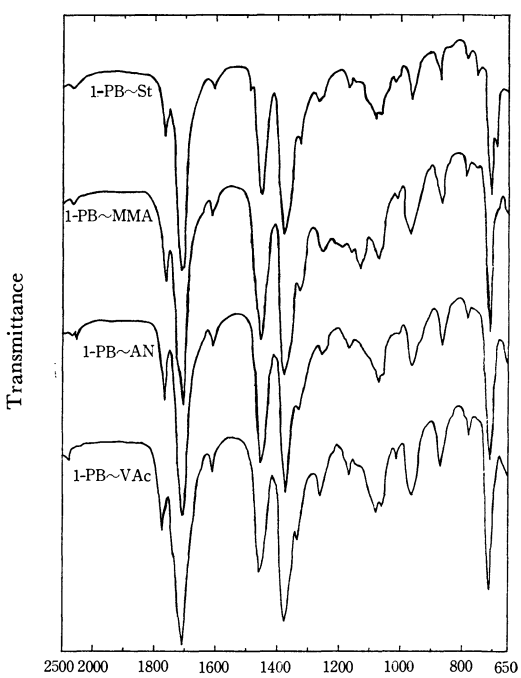

Fig. 1. Infrared spectra of copolymers of 1-phthalimido-1, 3-butadiene with various vinyl monomers.

10) A. Terada and K. Murata, Paper V on Aminobutadienes: Abstracts of the Tokuyama Meeting of the Chemical Society of Japan, Tokuyama, May, 1961.
11) T. Alfrey and C. C. Price, *J. Polymer Sci.*, **2**, 101 (1947).
12) M. Bachstez, *Chem. Ber.*, **46**, 3087 (1913).
13) U. S. Pat. 2276840.
14) T. Yoshida and H. Hirakawa, *J. Chem. Soc. Japan, Ind. Chem. Sect. (Kogyo Kagaku Zassi)*, **55**, 83 (1952).
15) S. Akiyoshi, K. Yanagi and T. Matsuda, ibid., **59**, 658 (1956).
16) U. S. Pat. 2231905.
17) A. F. Nikolaev and S. N. Ushakov, *Izvest. Akad. Nouk. S. S. S. R., Otdel. Khim. Nauk.*, **1957**, 1235; *Chem. Abstr.*, **52**, 6283 (1958).
18) J. Furukawa, A. Ōnishi and T. Tsuruta, *J. Chem. Soc. Japan, Ind. Chem. Sect. (Kogyo Kagaku Zassi)*, **60**, 350 (1957).
19) The Society of Polymer Science, Japan, "Synthetic Methods of Monomers," in "Lectures on High Polymer Experiments (Kobunshi Zikken Koza)," Vol. 9, Ed. by S. Kambara, Kyoritsu Publ. Co., Tokyo (1957).
20) Taken in Nujol Paste by a Hitachi Infrared Spectrophotometer, Model EPI-2.

TABLE I. THE COPOLYMERIZATIONS OF 1-PHTHALIMIDO-1, 3-BUTADIENE (M_1) WITH VARIOUS VINYL MONOMERS (M_2) IN THE PRESENCE OF 1.0 mole-% OF BENZOYL PEROXIDE AT 60°C

M_1	M_2		DMF[a]	Time	Yield	N[b]	m_1	m_2[c]
10^{-4}mole			ml.	hr.	wt.-%	wt.-%	mole-%	
10	St	90	—	24	40.8	2.19 2.08	18.6	81.4[d]
10	MMA	90	—	20	83	1.34 1.38	19.3	80.7[d]
10	AN	90	—	20	90	—	—	—
10	VAc	90	—	24	8.5	5.71 5.76	65.8	34.2
15	St	35	1.50	20	16.2	4.96	55.6	44.4
15	MMA	35	2.00	20	19.3	5.00	55.2	44.8
15	AN	35	2.00	20	26.9	8.88	72.4	27.6
15	VAc	35	1.50	24	13.0	6.45	82.7	17.3

a) Dimethylformamide.
b) Determined by the Micro-Dumas method.
c) Calculated by means of the nitrogen content.
d) Calculated by means of the average value of the nitrogen content.

that the monomer arrangement in the copolymerization is mainly of the 1, 4-type, also. The absorption peaks at 1710 and 1770 cm^{-1} in these spectra are assigned to the phthalimido-carbonyl; another striking band, at 710 cm^{-1}, is that of the *o*-di-substituted benzene of phthalimido. 1-Phthalimido-1, 3-butadiene easily copolymerizes with these monomers, whereas vinyl acetate enters into the copolymer somewhat less readily.

In an attempt to determine the relative reactivity ratios for the 1-phthalimido-1, 3-butadiene - styrene system, the copolymerization in a dimethylformamide solution was carried out at 60°C; the monomer ratio in the initial charge was varied, while benzoyl peroxide was used as the free radical source at a concentration of 2.0 mol.-% in each case (Table II).

TABLE II. THE COPOLYMERIZATION OF 1-PHTHALIMIDO-1, 3-BUTADIENE (M_1) AND STYRENE (M_2) AT 60°C

M_1	M_2	DMF	Time	Yield	N, %	m_1[a]	m_2[a]
10^{-4}mole		ml.	hr.	wt.-%	wt.-%	mole-%	
10	90	0.30	6.0	11.4	2.30 2.41	20.9	79.1
10	45	1.00	5.0	8.0	3.85 3.78	38.1	61.9
10	30	1.00	6.0	8.3	4.37 4.25	45.4	54.6
20	30	1.50	6.0	9.1	4.86 5.14	56.2	43.8
15	10	1.00	5.0	8.1	5.84 5.98	73.3	26.7

a) Calculated by means of the average value of the nitrogen content.

The M_1 and M_2 in Table II represent the molar concentrations of 1-phthalimido-1, 3-butadiene and styrene respectively at the initial feeding, while m_1 and m_2 are the molar fractions of them in the resulting copolymers as determined by the Micro-Dumas method. According to the Fineman-Ross plot,[21] we obtain:

$$r_1(\text{1-PB}) = 1.48$$

$$r_2(\text{St}) = 0.32$$

The copolymer composition curve for this system, calculated from these r_1 and r_2 values, is shown in

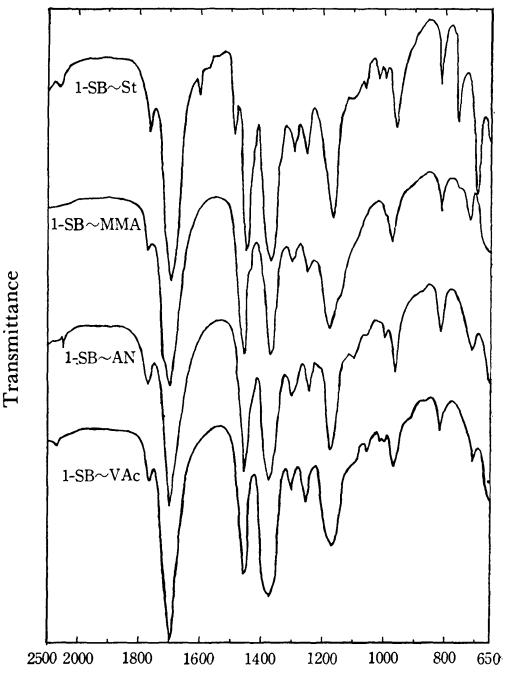

Fig. 2. Infrared spectra of copolymers of 1-succinimido-1, 3-butadiene with various vinyl monomers.

21) M. Fineman and S. D. Ross, *J. Polymer Sci.*, **5**, 269 (1950).

Table III. The copolymerizations of 1-succinimido-1, 3-butadiene (M_1) with various vinyl monomers (M_2) in the presence of 1.0 mole-% of benzoyl peroxide at 60°C

M_1	M_2		DMF	Time	Yield	N	m_1	m_2
10^{-4}mole			ml.	hr.	wt.-%	wt.-%	mole-%	
15	St	35	0.50	20	31.6	{4.98 {4.88	43.7	56.3
30	MMA	70	1.00	20	25.9	5.87	53.4	46.6
30	AN	70	1.00	20	53.5	12.28	62.2	37.8
15	VAc	35	0.50	20	11.8	{7.78 {7.74	74.6	25.4
8	VAc	61	—	24	3.5	8.22	81.8	18.2

Fig. 3; it gives the best fit to the experimental data.

The Copolymerization of 1-Succinimido-1, 3-butadiene.—The results of the radical copolymerizations with various vinyl monomers are presented in Table III, while the infrared spectra of the resulting copolymers are illustrated in Fig. 2.

The strong absorption bands at 1700 and 1770 cm^{-1}, assignable to succinimido-carbonyl, are found in all of the polymer spectra; this fact and the data in Table III clearly show that this monomer could copolymerize preferentially with all of such comonomers as well as in the above case of 1-phthalimido-1, 3-butadiene. However, only vinyl acetate was less reactive to enter into the copolymer.

Table IV. The copolymerization of 1-succinimido-1, 3-butadiene (M_1) and styrene (M_2) in the presence of 1.0 mole-% of benzoyl peroxide at 60°C

M_1	M_2	DMF	Time	Yield	N	m_1	m_2
10^{-4}mole		ml.	hr.	wt.-%	wt.-%	mole-%	
10	90	0.50	3.0	6.8	{2.85 {2.89	23.6	76.4
15	35	0.50	3.0	5.3	{5.64 {5.57	51.4	48.6
22.5	27.5	0.50	2.5	4.2	{6.69 {6.53	63.3	36.7
20	20	0.50	2.5	5.4	{6.81 {7.05	67.2	32.8
30	20	0.50	2.0	4.1	{7.36 {7.59	74.2	25.8

By the usual treatment, we obtain Table IV and;

$$r_1(\text{1-SB}) = 1.62$$

$$r_2(\text{St}) = 0.28$$

The copolymer composition curve calculated for this system agrees exactly with the experimental results (Fig. 4).

The Copolymerizations of *N*-Vinyl Phthalimide and *N*-Vinyl Succinimide.—Tables V and VI show the results of the copolymerizations of *N*-vinyl phthalimide and of *N*-vinyl succinimide respectively with styrene. Similar calculations of the monomer reactivity ratios give the following values:

$$r_1(\text{VPI}) = 0.09^{22)}$$

Table V. The copolymerization of *N*-vinyl phthalimide (M_1) and styrene (M_2) in the presence of 1.0 mole-% of benzoyl peroxide at 60°C

M_1	M_2	DMF	Time	Yield	N	m_1	m_2
10^{-4}mole		ml.	hr.	wt.-%	wt.-%	mole-%	
10	90	0.50	2.5	6.9	0	0	100
15	35	0.50	2.0	2.4	0.81	6.3	93.7
20	20	0.50	2.5	3.2	1.57	12.7	87.3
35	15	1.00	5.0	5.6	3.08	27.0	73.0
40	10	1.00	5.0	3.3	3.60	32.6	67.4

Table VI. The copolymerization of *N*-vinyl succinimide (M_1) and styrene (M_2) in the presence of 1.0 mole-% of benzoyl peroxide at 60°C

M_1	M_2	DMF	Time	Yield	N	m_1	m_2
10^{-4}mole		ml.	hr.	wt.-%	wt.-%	mole-%	
10	40	0.50	4.0	10.4	0.42	3.1	96.9
15	35	0.50	4.0	9.0	{0.58 {0.61	4.5	95.5
20	30	0.50	4.0	8.6	0.77	5.8	94.2
25	25	0.50	4.0	7.6	{1.21 {1.23	9.2	90.8
30	20	0.50	4.0	6.9	1.73	13.2	86.8
35	15	0.50	4.0	5.8	{2.36 {2.40	18.4	81.6
40	10	0.70	4.0	4.8	3.48	27.3	72.7

$$r_2(\text{St}) = 6.3$$

and;

$$r_1(\text{VSI}) = 0.07^{24)}$$

$$r_2(\text{St}) = 9.6$$

22) Recently, Nikolaev et al.[23] have dealt with the copolymerization system of vinyl phthalimide with styrene; their results are $r_1(\text{VPI})=0.075\pm0.03$ and $r_2(\text{St})=8.3\pm0.3$. These results are very close to the results obtained here.

23) A. F. Nikolaev and M. N. Tereshchenko, *Vysokomolekul Siedin*, **6**, 379 (1964); *Chem. Abstr.*, **61**, 5771 (1964).

24) Furukawa et al.[25] and, independently, Hopff and Schlumbon[26] have also investigated this copolymerization system, *N*-vinyl succinimide and styrene, and their results were $r_1=0.09$ and $r_2=7.0$, and $r_1=0.07$ and $r_2=10.5$ respectively.

25) J. Furukawa, T. Tsuruta, H. Fukatani and N. Yamamoto, *J. Chem. Soc. Japan, Ind. Chem. Sect. (Kogyo Kagaku Zassi)*, **60**, 1085 (1957).

26) H. Hopff and P. Schlumbon, *Makromol. Chem.*, **43**, 173 (1961).

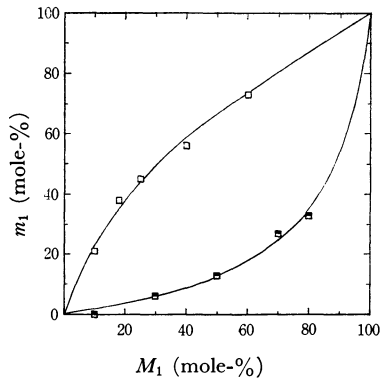

Fig. 3. Copolymerization curves. The solid lines were calculated for the monomer reactivity ratios of each copolymerization system.

□: 1-PB～St
■: VPI～St

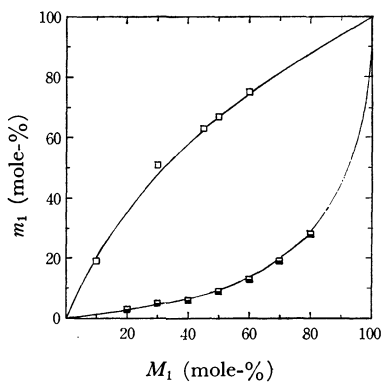

Fig. 4. Copolymerization curves. The solid lines were calculated for the monomer reactivity ratios of each copolymerization system.

□: 1-SB～St
■: VSI～St

TABLE VII. Q, e-PARAMETERS AND ULTRAVIOLET ABSORPTION MAXIMA OF IMIDO-MONOMERS

Monomer	Q	e	UV, mμ λ_{max}	UV, mμ ε_{max}
1-Phthalimido-1, 3-butadiene	1.57	+0.06	278.5	35400[8]
1-Succinimido-1, 3-butadiene	1.76	+0.09	248	26000[5]
2-Phthalimido-1, 3-butadiene	5.0	−0.05[9]	219	55000[4]
2-Succinimido-1, 3-butadiene	—	—	219.5	18500[4]
1, 3-Butadiene	1.33	−0.8[27]	217	21000
N-Vinyl phthalimide	0.09	−0.13	234.5	26200[8]
	0.41	−1.63[29]		
	0.21	−1.14[28]		
N-Vinyl succinimide	0.06	−0.17	212	17900[5]
	0.10	−0.12[25]		
	0.15	−0.27		
	0.15	−0.25[26]		
	0.13	−0.23[34]		
Ethylene	0.03	−0.43[32]	175	10000
N-Vinyl pyrrolidone	0.087	−1.22[31]	235	14700
N-Vinyl ethylurea	0.14	−1.6[33]		
N-Vinyl ethylcarbamate	0.12	−1.9[33]		
N-Vinyloxazolidone	0.07	−0.8[33]		

27) T. Alfrey, J. J. Bohrer and H. Mark, "Copolymerization," Interscience Publishers, New York (1952), p. 91.

28) Nikolaev et al. have obtained the Q and e-values of *N*-vinyl phthalimide as Q=0.41 and e=−1.63 from the copolymerization with vinyl acetate,[29] they also obtained them as Q=0.21 and e=−1.14 from the system with styrene.[28] While there are large differnces between these values and the values we present here, the discrepancy can be explained as follows: In general, when the Q and e values are calculated, two values for the e are usually given. Nikolaev et al. have chosen the more negative e value of the two in each case; however, we have taken the less negative e value (−0.05) between −0.8+0.75 and −0.8−0.75, with regard to the values for *N*-vinyl acetamide (e=−1.39 and −1.44)[30] and for *N*-vinyl pyrrolidone (e=−1.22)[31] and also to those of such other related *N*-vinyl compounds as *N*-vinyl succinimide reported on hitherto.

29) A. F. Nikolaev, S. N. Ushakov, L. P. Vishnevetskaya, N. A. Voronova and E. I. Rodina, *Vysokomolekul Soedin*, **4**, 1053 (1962); *Chem. Abstr.*, **59**, 10243 (1963).

30) Yu-Wu Hsu, S. S. Skorokhodov and A. A. Vansheidt, ibid., **6**, 1291 (1964); *Chem. Abstr.*, **61**, 14790 (1964).

31) J. F. Bork and L. E. Coleman, *J. Polymer Sci.*, **43**, 413 (1960).

32) R. D. Burkhart and N. L. Zutty, ibid., **A1**, 1137 (1963).

33) From the report by R. Hart and D. Timmerman, *Makromol. Chem.*, **31**, 223 (1959).

34) L. J. Young, *J. Polymer Sci.*, **54**, 411 (1961).

The *Q*, *e*-Parameters.—The calculated copolymer composition curves of these imido-monomers are figured as in Fig. 3 and in Fig. 4 respectively from the above-obtained monomer reactivity ratios.

From these curves the following considerations are possible. These two imidobutadienes preferentially enter into the copolymers, while the two vinyl imides do so less readily. The curves of the two imidobutadienes are so similar that they are virtually superimposable; those of the vinyl imides are very similar to each other also. Therefore, it may be concluded that the natures and the effects of these two imido groups on the monomer reactivity are very similar and that, therefore, the reactivity differences between the imidobutadienes and vinyl imides on copolymerization are due to the differences between butadienyl and vinyl.

To investigate the structural features of these imido-monomers, the Q and e-parameters were evaluated from the above-indicated monomer reactivity ratios according to the Alfrey-Price scheme,[11] using the values of $Q=1.0$ and $e=-0.8$ for styrene. The calculated Q and e-values, and those of the other monomers of related type which have appeared in the literature, are shown in Table VII, along with their ultraviolet spectral data for the sake of comparison. The respective pairs of the Q and e-parameters of 1-phthalimido- and 1-succinimido-1, 3-butadienes, and of *N*-vinyl phthalimide and *N*-vinyl succinimide are very similar to each other. This fact indicates that the effects of the two substituents on the radical copolymerizations of such monomers closely resemble each other, as has already been established.

The Q values of 1-phthalimido- and 1-succinimido-1, 3-butadienes are much larger than those of *N*-vinyl phthalimide and *N*-vinyl succinimide. This means that, by the substituting butadienyl group for vinyl, the conjugated systems in the former two are more extended and more resonance-stabilized than in the latter two. A clear proof for this is the conclusion to be drawn from their ultraviolet spectroscopic data (Table VII), in which such imidobutadienes exhibit a more bathochromic displacement of their K bands and a much greater increase in intensity than do *N*-vinyl imides.[3,5] Similar relationships also hold in comparison with the Q value of 1, 3-butadiene.[27] Those of 1-imido-1, 3-butadienes indicate somewhat larger values; this means a similar extension of the butadienyl conjugation to the imido-nitrogen.

When the e value of 1, 3-butadiene (-0.8) is compared, those of such 1-imido-1, 3-butadienes exhibit a decrease and become near to zero. This fact may be explained by the M-effect of carbonyls in both the imido rings serving, in the opposite direction, to reduce the electron-donating power of the imido-nitrogen extending over the butadiene chain, because there is a so-called Branch-Calvin cross conjugation in these structures. Similar relationships and explanations should also hold between ethylene and *N*-vinyl imides. The e values for *N*-vinyl pyrrolidone and other *N*-vinyl acylamide are remarkably more negative than that of *N*-vinyl succinimide (Table VII); this fact may give support to our theory here.

The authors wish to thank Professor Shizunobu Hashimoto of Doshisha University for his helpful suggestions in this work and Mrs. Masako Hayashi for her elemental analyses.

BULLETIN OF THE CHEMICAL SOCIETY OF JAPAN VOL. 39 2500—2502 (1966)

The Solvent Effect on the Rates of Autoxidation of *o*-Cresol[1]

By Yoshiro OGATA and Takashi MORIMOTO

Department of Applied Chemistry, Faculty of Engineering, Nagoya University, Chikusa-ku, Nagoya

(Received March 25, 1966)

The effects of alcohols, carbonyl compounds and dimethyl sulfoxide on the pyridine-cuprous chloride-catalyzed autoxidation of *o*-cresol in benzene have been studied kinetically by estimating the consumption of oxygen. The rate is first-order in the concentration of *o*-cresol and one-half order in the partial pressure of oxygen at constant concentrations of pyridine and cuprous chloride in a solvent of methanol-benzene (20 : 80 in vol.). The reaction in a benzene solution is retarded by the addition of below 0.1 vol.% methanol or ethanol; having passed through a minimum at ca. 0.1 vol.%, it is accelerated by the addition of alcohol more than 0.1 vol.%. The reaction in a benzene solution is retarded by the addition of carbonyl compounds. A probable mechanism which explains these solvent effects is discussed.

In our previous report[2] it has been suggested that the pathway for the pyridine - cuprous chloride-catalyzed autoxidation of *o*-cresol in a benzene solution involves the reaction of *o*-cresol anion and an autoxidized pyridine - copper complex. The similar autoxidation of 2, 6 - dimethylphenol catalyzed by the pyridine - cuprous salt complex is sometimes carried out in a mixed solvent, e. g., benzene - isopropanol or toluene - isopropanol.[3] However, the autoxidation of aniline by the same catalyst is retarded on addition of methanol.[4]

The present study was undertaken to clarify the kinetic solvent effect on the pyridine-cuprous chloride-catalyzed autoxidation of *o*-cresol.

Results and Discussion

The rates were measured in the presence of anhydrous magnesium sulfate to eliminate the water which is formed as a product and which inhibits the reaction.

The rate of absorption of oxygen at constant concentrations of pyridine and cuprous chloride in methanol-benzene (20 : 80 in vol.) is expressed as:

$$-\frac{dp}{dt} = k[\mathrm{CrlH}]\,p^{1/2} \qquad (1)$$

Here, [CrlH] is the concentration of *o*-cresol and p is the partial pressure of oxygen. This rate law agrees with that in pure benzene as previously reported; therefore, the oxidation in benzene containing 20 vol.% methanol may also involve the same mechanism.

Table I. The 1.5th- and second-order rate constants for the autoxidation of *o*-cresol at constant concentration of catalyst, pyridine (0.2467 M) and cuprous chloride (5.05×10^{-3} M), in methanol-benzene (20 : 80) at 35°C

o-Cresol M	O_2 press. p, mmHg	1.5th-order const $mmHg^{1/2}\,M^{-1}\,min^{-1}$	Second-order const. $M^{-1}\,min^{-1}$
0.1889	100	4.63	5.50
0.1889	200	4.57	3.45
0.1889	400	4.58	2.29
0.0994	200	5.15	3.50

$$o\text{-}CH_3C_6H_4OH + C_5H_5N \overset{\text{fast}}{\rightleftharpoons} o\text{-}CH_3C_6H_4O^- + C_5H_5\overset{+}{N}H \qquad (2)$$

$$m\,C_5H_5N + n\,Cu^+ \overset{\text{fast}}{\rightleftharpoons} (C_5H_5N)_m(Cu^+)_n \qquad (3)$$

$$2(C_5H_5N)_m(Cu^+)_n + O_2 \overset{\text{fast}}{\rightleftharpoons} [(C_5H_5N)_m(Cu^+)_n]_2O_2 \qquad (4)$$

$$[(C_5H_5N)_m(Cu^+)_n]_2O_2 \overset{\text{fast}}{\rightleftharpoons} 2(C_5H_5N)_m(Cu^+)_nO\cdot \qquad (5)$$

$$(C_5H_5N)_m(Cu^+)_nO\cdot + o\text{-}CH_3C_6H_4O^- \overset{\text{slow}}{\longrightarrow} o\text{-}CH_3C_6H_4O\cdot + \text{etc.} \qquad (6)$$

Figure 1 illustrates the effect of the addition of alcohols, carbonyl compounds and dimethyl sulfoxide on the pyridine-cuprous chloride-catalyzed autoxidation of *o*-cresol in benzene. As shown in the figure, the rate constant decreased on addition of below 0.1 vol.% methanol, but with above 0.1 vol.% methanol the constant increased with increasing concentration of methanol, approaching a constant value at more than 20 vol.% methanol. The ratio of the rate constant in 20 vol.% methanol

1) Contribution No. 87.
2) Y. Ogata and T. Morimoto, *Tetrahedron*, **21**, 2791 (1965).
3) *Chem. Eng. News*, **42**, Dec. 7, 1964, p. 57.
4) K. Kinoshita, This Bulletin, **32**, 777 (1959).

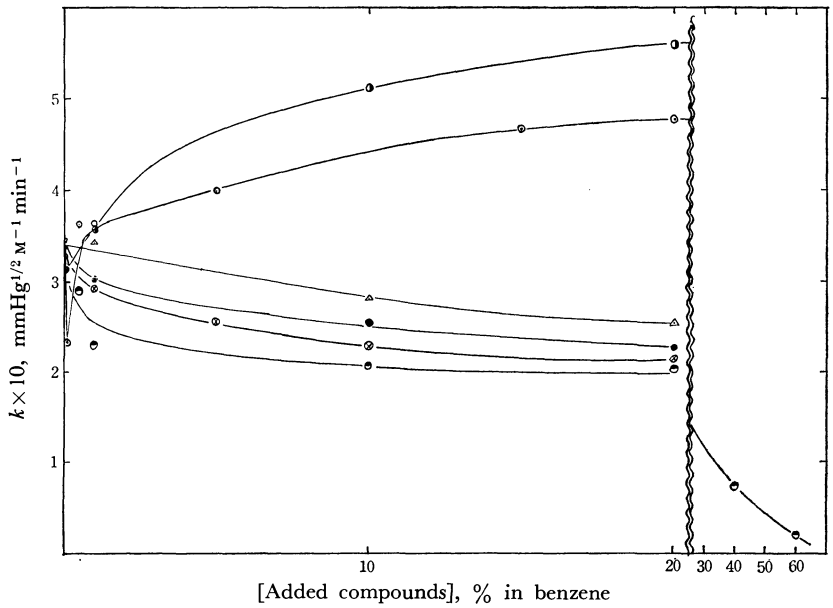

Fig. 1. The solvent effect on the rate constant for the autoxidation of *o*-cresol in benzene at 35°C or at constant oxygen pressure (p=200 mmHg) and at constant concentration of catalyst: [CuCl]=5.05×10^{-5} M and [pyridine]=0.2469 M. Initial concn. of *o*-cresol: 0.1918 M. ⊙, Methanol; ◑, Ethanol; △, Methyl ethyl ketone; ●, Dimethylformamide; ⊗, Ethyl acetate; ◓, Dimethyl sulfoxide.

to that in pure benzene was about 1.3. These phenomena are not due to the formation of formaldehyde from methanol, since no absorption of oxygen was observed in the absence of *o*-cresol and no formaldehyde was detected in the effluent gas.

In contrast, the rate constant gradually decreased with increasing concentration of carbonyl compounds or dimethyl sulfoxide. For example, in 60 vol.% dimethyl sulfoxide in benzene, the rate was too low to measure.

This retardation with carbonyl or sulfoxide compounds may be due to the deactivation of the catalyst, (i) by the substitution of a carbonyl or sulfoxide compound for pyridine molecule:

$$Py_mCu^+{}_n + (\rangle C{=}O) \rightleftarrows Py_{m-1}(\rangle C{=}O)Cu^+{}_n + Py \quad (7)$$

or (ii) by the steric inhibition of the approach of molecular oxygen to the active site of catalyst by a coordinated carbonyl or sulfoxide compound:

$$Py_mCu^+{}_n + (\rangle C{=}O) \rightleftarrows Py_mCu^+{}_n(\rangle C{=}O) \quad (8)$$

Although the rate increased with an increase in the dielectric constant[2,5] by the addition of chlorobenzene (ε=5.62[6]), the reaction was retarded by the addition of dimethylformamide (ε=37.6[7]) or dimethyl sulfoxide (ε=46[8]) to the solvent. These results suggest that the catalyst is deactivated by the coordination of the oxygen atom in these compounds.

On the other hand, methanol may act as an acid, as shown in the following equilibrium:

$$C_5H_5N + CH_3OH \rightleftarrows C_5H_5\overset{+}{N}H + CH_3O^- \quad (9)$$

$$\text{or } C_5H_5N^+\cdots H\cdots\overset{-}{O}CH_3$$

It is expected that methoxide anion, like carbonyl compounds, will coordinate with the catalyst to retard or inhibit the reaction. In fact, the pyridine solution containing *o*-cresol and cuprous chloride absorbs oxygen (1.38×10^{-4} mole after 180 min. at 13.9 mmHg), but no absorption was observed on addition of 10 vol.% methanol to the solvent. At a lower concentration of pyridine (below 1 M) in a benzene solution, the reaction may be retarded by a small amount of methanol, probably because the methoxide ion formed acts much like carbonyl compounds, while the reaction is accelerated by the addition of more than 0.1 vol.% methanol, as is obvious in Fig. 1. It is difficult to explain this acceleration at present, but it is probable that an increase in the dielectric constant and solvation power by the addition of methanol results in an increase in the concentration of the more

5) G. F. Endres, A. S. Hay and J. W. Eustance, *J. Org. Chem.*, **28**, 1300 (1963).
6) J. A. Riddick and E. E. Toops, Jr., "Organic Solvents," in "Technique of Organic Chemistry," Vol. VII, Ed. by A. Weissberger, Interscience, New York (1955), p. 190.
7) J. Parker, *Quart. Revs.*, **16**, 163 (1962).
8) T. J. Wallace, H. Pobiner, F. A. Baron and A. Schriesheim, *J. Org. Chem.*, **30**, 3147 (1965).

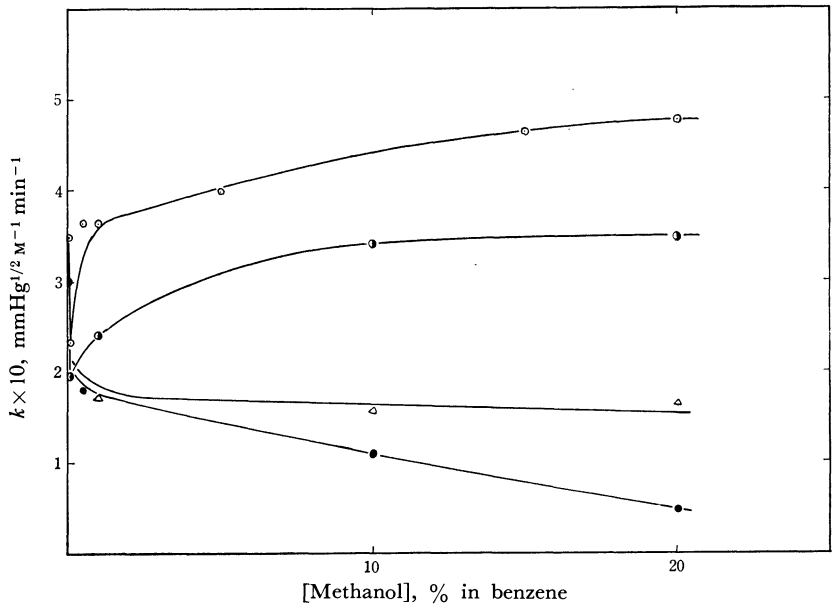

Fig. 2. The effects of concentrations of methanol and pyridene on the rate constant for the autoxidation of *o*-cresol in benzene at 35°C at constant concentration of CuCl (5.05×10^{-5} M) and *o*-cresol (0.1918 M) and constant oxygen pressure (200 mmHg).
⊙, [pyridene]=0.247 M; ◑, 0.99 M; △, 2.48 M; ●, 4.99 M.

reactive *o*-cresol anion and that this effect surpasses the deactivation of the catalyst by methanol.

At higher concentrations of pyridine (over 2 M), the oxidation was always inhibited or retarded by the addition of methanol in any concentration. The effect of the methanol concentration on the rate constant at various pyridine concentrations is illustrated in Fig. 2. Apparently, at higher concentrations of pyridine (e. g., over 2 M), the rate constant decreases with increasing concentration of methanol. On the other hand, at lower concentrations of pyridine (below 1 M), the rate constant sharply decreases and then increases with increasing concentration of methanol. These facts seem to support the above assumption that the deactivation with methanol is not caused by methanol itself, but by methoxide ions, which can only be produced by the presence of pyridine.

A similar effect is expected for the autoxidation of 2, 6-dimethylphenol by the same catalyst. In fact, the acceleration was appreciable by the addition of 20 vol% ethanol or isopropanol to a benzene solution at 0—35°C at initial concentrations of 0.1979 M 2, 6-dimethylphenol, 0.2461 M pyridine, and 5.05×10^{-3} M cuprous chloride. However, the reaction in both pure benzene and the mixed solvent was too rapid for the rate constants to be compared (80% conversion after 20 min. at 35°C in pure benzene).

Experimental

Materials.—*o*-Cresol, cuprous chloride, pyridine, and benzene were purified as reported previously.[2] Methanol (b. p. 64.1—64.5°C), ethanol (b. p. 78.1—78.2°C), methyl ethyl ketone (b. p. 78.8—79.1°C) and ethyl acetate (b. p. 77.0—77.2°C) were purified by rectification. Dimethylformamide (b. p. 56.5—56.7°C/27 mmHg) and dimethyl sulfoxide (b. p. 85—87°C/25 mmHg) were distilled in a vacuum after having been dried over anhydrous potassium carbonate. 2, 6-Dimethylphenol was recrystallized from *n*-hexane (m. p. 44.0—44.5°C).

Rate Measurements.—The same apparatus and procedure[2] were used for the rate measurements.

The Detection of Formaldehyde.—Oxygen gas, after having been passed through the reaction solution, was bubbled into an aqueous solution of sodium sulfate containing thymolphthalein as an indicator. No color was observed. This proved the absence of formaldehyde.

The authors wish to thank Mr. Kazuo Matsuyama for his helpful assistance in performing these experiments.

BULLETIN OF THE CHEMICAL SOCIETY OF JAPAN VOL. 39 2503—2508 (1966)

The Synthesis of an Etiojervane Analog of Progesterone[1]

By Tadashi MASAMUNE, Kazuhiko ORITO and Akio MURAI

Department of Chemistry, Faculty of Science, Hokkaido University, Sapporo

(Received March 25, 1966)

N-Acetyl-22, 27-iminojerva-5, 12-diene-3β, 23α-diol-11-one, prepared from jervine by Masamune et al. (*J. Org. Chem.*, **29**, 2282 (1964)), was submitted to a Birch reduction and then to a modified Wolff-Kishner reduction to yield 22, 27-iminojerv-5-ene-3β, 23α-diol. The compound was then degraded, according to the procedure by Johnson et al. (*Tetrahedron Letters*, **1963**, 545), to a methyl ketone, which was then further oxidized by the Oppenauer method to give 17α-ethyletiojerv-4-ene-3, 20-dione.

In the past decade considerable attention has been paid to the modification of the basic steroid skeleton of hormones in search of analogs with enhanced or more specific physiological properties. In view of the natural occurrence[2] of the C-nor-D-homosteroid ring system, the synthesis of hormone analogs seemed to be a particularly attractive subject. Etiojervane[3] analogs of testosterone, epiandrosterone and so on have recently been prepared, using the available hecogenin and/or jervine as the starting materials.[4-6] In the present paper we will describe the synthesis of C-nor-D-homoprogesterone.

Jervine (I), one of the most readily-available veratrum alkaloids, was selected as the starting material for our investigation. Two processes for the degradation of I to nitrogen-free compounds have been reported in the literature. One, which was developed by Fried et al.[7] and improved by Okuda et al.[8] and by us,[9] involves the fragmentation of I, by treatment with Lewis acids, to 17-ethyletiojerva-5, 12, 17(20)-terien-3β-ol-11-one (II).

It was deemed efficient to utilize the ethylidene moiety of II to prepare an acetyl side chain of progesterone, and it was attempted to reduce the 12, 13-double bond selectively. The double bond could not be hydrogenated catalytically, however, without a concomitant reduction of the 17, 20-double bond. The Birch reduction of II gave rise to a mixture containing a considerable amount of the starting material (II), from which only a compound, $C_{21}H_{30}O_2$, m. p. 236—237°C, showing a peak at 1730 cm^{-1}, could be isolated in a very low yield. Next, the selective reduction of the 12, 13-double bond in the glycol[10] (III) prepared from II was reexamined under various conditions, as a glycol system would be converted into an acetyl group by the Serini reaction.[11] However, neither the Birch reduction nor the catalytic hydrogenation of III was shown to be of any value in the proposed synthesis.[10] The treatment of the glycol acetate (IIIa) with alkali yielded a multicomponent mixture, from which only etiojerv-5-ene-3, 11, 17-trione 3-ketal[4] (IV), formed by fission of the 17, 20-bond, was isolated, in a moderate yield, by chromatography.

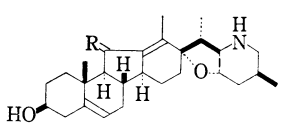

I: R=O
VI: R=H_2

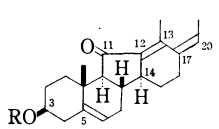

II

1) Part VI of "C-Nor-D-homosteroids and Related Alkaloids"; Part V: T. Masamune, I. Yamazaki and M. Takasugi, This Bulletin, **39**, 1090 (1966).

2) Most of the veratrum alkaloids and the fritillaria alkaloids possess this modified skeleton; C. R. Narayanan, "Progress in the Chemistry of Organic Natural Products," Vol. XX, Springer-Verlag, Wien (1962), p. 298; H, G. Boit, "Ergebnisse der Alkaloid-Chemie bis 1960," Akademie-Verlag, Berlin (1961), p. 758.

3) The designations "etiojervane and jervane" will be used to describe 17aβ-methyl-C-nor-D-homo-18-nor-5α, 13α-androstane and the corresponding cholestane analog respectively; cf. Ref. 4, 5 and 7.

4) S. M. Kupchan and S. D. Levine, *J. Am. Chem. Soc.*, **86**, 701 (1964).

5) W. F. Johns and I. Laos, *J. Org. Chem.*, **30**, 4220 (1965) and the references cited there.

6) H. Mitsuhashi and N. Kawahara, *Tetrahedron*, **21**, 1215 (1965), and the references cited there.

7) J. Fried and A. Klingsberg, *J. Am. Chem. Soc.*, **75**, 4929 (1953).

8) S. Okuda, K. Tsuda and H. Kataoka, *Chem. & Ind.*, **1961**, 512.

9) Footnote 8 of Ref. 4.

10) S. M. Kupchan, T. Masamune and G. W. A. Milne, *J. Org. Chem.*, **29**, 755 (1964).

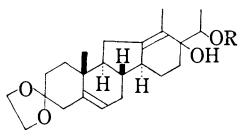

III: R=H
IIIa: R=Ac

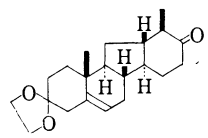

IV

The other degradation process was developed by Johnson et al.;[12] it requires the presence of hydroxyl and secondary amino group in the nitrogen ring as in that of veratramine (V). However, V would not be an appropriate starting material, in view of the yield in isolation from natural plants or in chemical preparations.[13,14] On the other hand, in order to obtain intermediates suitable for degradation from the readily-available alkaloids, jervine (I) or 11-deoxojervine[14] (VI), it was necessary to cleave the ether linkage in those compounds. A reexamination of the references revealed that the fission of the ether linkage took place in several ways.[13-17] The following two reactions appeared to be effective, considering the yields and stabilities of the products; the Birch reduction of I to 8, 9-dihydroisojervine[17] (VII), and the catalytic hydrogenation of VI over platinum in acetic acid to 11-deoxo-5, 6, 8, 9-tetrahydroisojervine[18] (VIII).

The degradation of VIII was first undertaken, as VIII possessed no oxygen function on C-11 and appeared to be suitable for the present plan. VIII was converted to a *N*-chloro derivative with *N*-chlorosuccinimide, which gave, when treated with sodium methoxide and then hydrolyzed with acid, an aldehyde (IX) in an over-all yield of 89%. The aldehyde was further degraded, with *n*-butyl nitrite and sodium *n*-butoxide in *n*-butanol, to an oxime, which was extracted with 2 N aqueous sodium hydroxide solution and then purified by acetylation with acetic anhydride and pyridine. The acetate, m. p. 139—140°C, obtained in a 35% yield from IX, exhibited, in agreement with the assigned structure of X, strong peaks at 1788 (*N*-acetoxyl) and 1737 cm^{-1} (3-acetoxyl) in the infrared spectrum and five sharp singlets at τ 7.38, 7.71, 7.99, 8.31 and 9.39 in the NMR spectrum. The singlets were attributed to the 21-methyl, *N*-acetoxyl, 3-acetoxyl, 18-methyl and 19-methyl groups respectively. However, an attempted hydrolysis of the oxime to a ketone was unsuccessful; the treatment of the crude oxime with hydrochloric acid in refluxing ethanol gave a compound with a m. p. of 157°C, in a 40% yield; this compound showed no strong absorption in the carbonyl region of the infrared spectrum. It might probably be an isooxazoline derivative. Next, the oxime acetate (X) was heated in glacial acetic acid on a water bath; it yielded a crystalline material, which showed two superimposable spots on thin layer-chromatograms and which resisted further purification. Furthermore, the elemental analysis showed that it contained almost the same percentage of nitrogen as the original acetate, indicating no fission of the C–N bond.

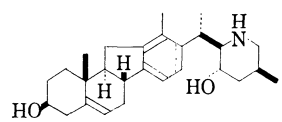

V

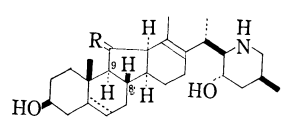

VII: R=O, Δ^5
VIII: R=H_2, 5αH

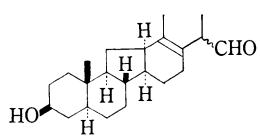

IX

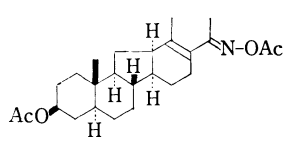

X

The preparation of 8, 9-dihydroisojervine (VII) by the Birch reduction[17] of I was improved by replacing the dioxane used previously as a solvent by tetrahydrofuran. The acetylation of VII, followed by hydrolysis and isomerization with alkali, proceeded smoothly, and afforded an α, β-unsaturated ketone (XI) in a good yield.[17] The next step in the synthesis required the reduction

11) L. F. Fieser and M. Fieser, "Steroids," Reinhold Publ. Corp., New York, N. Y. (1959), p. 628.
12) R. W. Franck and W. S. Johnson, *Tetrahedron Letters*, **1963**, 545.
13) T. Masamune, Y. Mori, M. Takasugi and A. Murai, ibid., **1964**, 913.
14) T. Masamune, Y. Mori, M. Takasugi, A. Murai, S. Ohuchi, N. Sato and N. Katsui, This Bulletin, **38**, 1374 (1965).
15) a) O. Wintersteiner and M. Moore, *J. Am. Chem. Soc.*, **75**, 4938 (1953); O. Wintersteiner and M. Moore and B. M. Iselin, ibid., **76**, 5609 (1954); B. M. Iselin and O. Wintersteiner, ibid., **76**, 5619 (1954); O. Wintersteiner and M. Moore, *J. Org. Chem.*, **29**, 262 (1964). b) O. Wintersteiner and M. Moore, *Tetrahedron*, **21**, 779 (1965).
16) W. G. Dauben, W. W. Epstein, M. Tanabe and B. Weinstein, *J. Org. Chem.*, **28**, 293 (1963).
17) T. Masamune, M. Takasugi, M. Gohda, H. Suzuki, S. Kawahara and T. Irie, ibid., **29**, 2282 (1964).
18) T. Masamune, M. Takasugi and Y. Mori, *Tetrahedron Letters*, **1965**, 489. It was suggested in the reference that a double bond would exist at C-13-C-17. This disposition was confirmed by the transformation of VIII to 11-deoxo-5, 6-dihydrojervine. It will be discussed later (T. Masamune and A. Murai, unpublished results).

of the 12, 13-double bond. Wintersteiner and Moore[15b] observed that the double bond in a 5, 6-dihydro derivative (XII) of XI could be hydrogenated over platinum in acetic acid. However, the product (XIII) was unstable to alkali and readily isomerized.[19] Furthermore, it was supposed that the hydrogenation of the 12, 13-double bond in XI under the aforementioned conditions would accompany the reduction of the 5, 6-double bond. Thus, XI was treated with lithium in liquid ammonia. It produced the corresponding 12, 13-dihydro derivative (XIV), m. p. 148—149°C. The assigned structure was confirmed by a stong absorption at 1737 cm^{-1} in the infrared spectrum and by a broad peak (1H) at τ 4.63 in NMR spectrum. The over-all yield from I to XIV was 40% (4 steps). With the purpose of confirming the stereochemistry, XIV was hydrogenated over platinum in acetic acid. The product, obtained in a good yield, was found to be identical with 22, 27-iminojervane-3β-23α-diol-11-one *N*-acetate (XV), the configuration of which had been established by Wintersteiner and Moore.[19] Thus, both the hydrogens on C-12 and C-13 in XIV were proved to have an α-configuration.

In order to prepare a progesterone analog, the reduction of the 11-carbonyl to methylene group was necessary. A modification of the Huang-Minlon procedure for the Wolff-Kishner reduction of XIV resulted in the removal of the oxygen on C-11, with the concomitant hydrolysis of the *N*-acetyl group; 22, 27-iminojerv-5-ene-3β, 23α-diol (XVI), m. p. 221—223°C, was isolated in a 60% yield after purification. Since XIV was recovered unchanged by reflux with alkali in a mixture of dimethylsulfoxide and diethylene glycol, no epimerization is considered to take place at the carbons adjacent to C-11 during the reduction. A comparison of the NMR spectrum of the triacetate (XVIa), m. p. 155—156°C, with that of XIV supports this conclusion; in the former, the signal due to the 19-methyl protons appeared at τ 9.03, while the corresponding signal of the latter appeared at τ 8.98. The magnitude of the downfield shift caused by the 11-carbonyl function was almost equal to the deshielding effect (0.07 p.p.m.) of a 11-ketonic group found in the study of the NMR spectra of a series of 22, 27-imino-17, 23-oxidojervane derivatives[20]; it was remarkably different from the corresponding effects in compounds possessing a B/C *cis*-fused linkage.[21]

The next step of the synthesis was the degradation of XVI; this was carried out in the way described above to yield an oxime (XVII), m. p. 192—193°C, in a 60% yield from XVI (4 steps). No trouble was encountered in the hydrolysis of XVII; treatment with a mixture of pyruvic acid and acetic acid gave a crude methyl ketone (XVIII) which, in turn, was submitted to the Oppenauer oxidation. Chromatographic purification yielded 17α-ethyletiojerv-4-ene-3, 20-dione (XIX), m. p. 168—169°C, in a 21% yield from XVII (2 steps). In accord with the assigned structure, this C-nor-D-homoprogesterone had prominent peaks at 1715 (20-carbonyl), 1663 (3-carbonyl) and 1616 cm^{-1} (conjugated double bond) in the infrared spectrum, and an absorption maximum at 237 mμ (ε 20200) in the ultraviolet spectrum. It also exhibited two singlets, at τ 8.87 and 7.86 (each 3H, the 19- and 21-methyl groups respectively) and one doublet (3H, J=6 c. p. s., the 18-methyl group) in the NMR spectrum. The acetyl side chain was assigned the α-configuration for the following reasons. The side chain at C-17 of XVI had the β-configuration and was *cis*-oriented relative to the methyl group at C-13. If the acetyl group in XIX had the same (β) configuration, treatment with alkali would cause epimerization at C-17. However, XIX was recovered unchanged after attempts to effect the epimerization by heating XIX under reflux in a 5% methanolic potassium hydroxide solution for 2 hr. This fact indicates that both the methyl at C-13 and the acetyl function at C-17 possess the equatorial conformation and are *trans* to each other. Hence, the acetyl group must have the

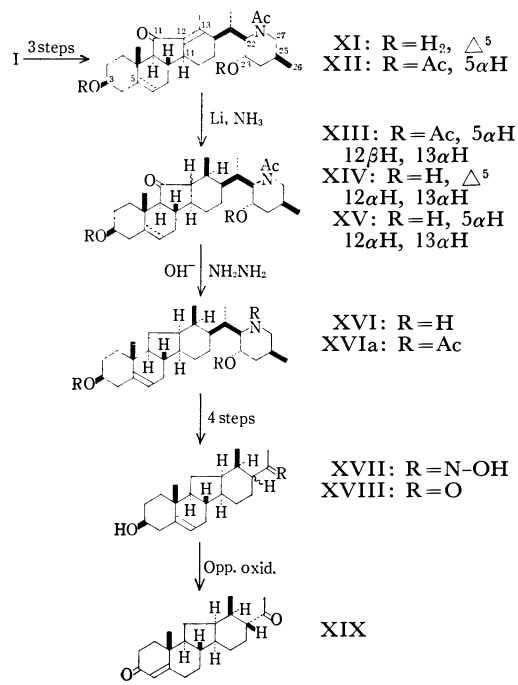

19) O. Wintersteiner and M. Moore, *Tetrahedron*, **20**, 1947 (1964).
20) T. Masamune, N. Sato, K. Kobayashi, I. Yamazaki and Y. Mori, ibid., in press. The deshielding effects of the 3β-acetoxyl and 3β-hydroxyl groups are 0.03 and 0.02 p. p. m. respectively.
21) J. P. Kitney, A. By, T. Inaba and S. Y. Leong, *Tetrahedron Letters*, **1965**, 2911; D. M. Bailey, D. P. G. Hamon and W. S. Johnson, ibid., **1963**, 555.

α-configuration, and the epimerization must have taken place during the hydrolysis or the Oppenauer oxidation.

Experimental

The melting points are uncorrected. The optical rotations and the ultraviolet spectra were measured in 95% methanol and 99% ethanol, and the infrared spectra, in Nujol, unless otherwise stated. The NMR spectra were taken in deuterochloroform at 60 Mc., using tetramethylsilane as an internal standard.

The Alkali Treatment of 17-Ethyletiojerva-5, 12-diene-17, 20-diol-3-one 20-Acetate 3-Ethylene Ketal[10] (IIIa).—To dioxane (5 ml.) containing IIIa (0.2 g.), a 1N aqueous sodium hydroxide solution (5 ml.) was added, and then the whole solution was refluxed for 40 min. After the solvent had been removed, the residue was treated with water and three 10 ml. portions of chloroform. The chloroform solution gave, after it had been washed with water, dried with anhydrous sodium sulfate and evaporated to dryness, an oily substance (0.22 g.) which was then chromatographed on alumina (2.0 g.). Fractions eluted with petroleum ether and a mixture of petroleum ether and benzene (1 : 1) crystallized and amounted to 0.15 g. Repeated recrystallizations from *n*-hexane afforded etiojerv-5-ene-3, 11, 17-trione 3-ethylene ketal (IV, 0.05 g.), m. p. 156—157.5°C, which was identical with a sample prepared according to the literature.[4] IR (chloroform): ν_{max} 1738, 1714, 1104 and 1083 cm^{-1}.

Found: C, 73.32; H, 8.30. Calcd. for $C_{21}H_{28}O_4$: C, 73.22; H, 8.19%.

11-Deoxo-5, 6, 8, 9-tetrahydroisojervine (VIII) and the 3, 23, *N*-Triacetyl Derivative. — When 11-deoxojervine[14] (VI; 7.01 g.) was hydrogenated in the presence of pre-reduced Adams' platinum (2.23 g.) at room temperature in acetic acid (140 ml.), 832 ml. of hydrogen (2.05 mol.) was absorbed after 29 hr. After the catalyst and the solvent had then been removed, the residue was treated with water (40 ml.), 6N aqueous ammonia (30 ml.) and chloroform (50 ml.); the chloroform-addition compounds of VIII remained suspended between the aqueous and the chloroform layers. The chloroform compound (7.23 g.), after being collected by filtration, washed with water, and dried, was recrystallized from acetone to yield VIII (4.96 g.), m. p. 143—146°C. Recrystallization from acetone gave an analytical sample (3.64 g.), m. p. 156—157°C; $[\alpha]_D^{20}$ −59.4°; IR; ν_{max} 3300, 1032 and 878 cm^{-1}.

Found: C, 78.31; H, 10.83; N, 3.33. Calcd. for $C_{27}H_{45}O_2N$: C, 78.02; H, 10.91; N, 3.37%.

Compound VIII (3.37 g.) was acetylated with acetic anhydride (30 ml.) and pyridine (40 ml.) on a steam bath for 2 hr. The residue, obtained after the solvents had been removed by azeotropization with benzene, was crystallized from aqueous methanol; it had a m. p. of 153.5—155°C. Recrystallization from the same solvent afforded a pure sample (3.45 g.) of the triacetyl derivative, m. p. 157—159°C; IR: ν_{max} 1738, 1634 and 1238 cm^{-1}; NMR: a broad multiplet which consisted of three peaks centered at τ 4.93, 5.17 and 5.33 (3H, protons on C-3, C-22 and C-23),[22] a singlet at τ 8.34 3H, 18-methyl protons) and a singlet at τ 9.28 (3H, 19-methyl protons).

Found: C, 73.22; H, 9.40; N, 2.55. Calcd. for $C_{33}H_{51}O_5N$: C, 73.16; H, 9.49; N, 2.59%.

17-Ethyl-20-formyletiojerv-13(17)-en-3β-ol (IX).—A suspended mixture of *N*-chlorosuccinimide (0.50 g.) in ether containing 11-deoxo-5, 6, 8, 9-tetrahydroisojervine (VIII; 1.45 g.) was stirred at room temperature for 1.5 hr. The ether layer was then washed with three 25 ml. portions of water, dried and evaporated to yield a mixture of crystals (1.39 g.). This mixture was used for the next step without further purification, as it colored at room temperature. It was dissolved in methanol (60 ml.); then to the solution there was added a methanol solution containing sodium methoxide (prepared from 0.7 g. of sodium and 30 ml. of methanol) under cooling and in a stream of nitrogen. The solution was allowed to stand at room temperature for 3 hr. and then evaporated below 33°C. The residue was stirred vigorously with 1N hydrochloric acid (120 ml.) at room temperature for 1 or 2 days, until the resinous materials were changed to amorphous powder. The powder (IX) was collected by filtration, washed repeatedly with water, and found to amount to 1.02 g.; UV: only end absorption, ε 1890 at 220 mμ; IR (chloroform); ν_{max} 3575, 3400, 2705 and 1719 cm^{-1}; NMR: a broad peak centered at τ 0.47 (aldehyde proton), a singlet at τ 8.31 (3H, 18-methyl protons), a doublet centered at τ 8.87 (3H, J=7 c. p. s., 21-methyl protons) and a singlet at τ 9.27 (3H, 19-methyl protons).

Found: C, 79.80; H, 10.29. Calcd. for $C_{22}H_{34}O_2$: C, 79.95; H, 10.37%.

17-Ethyl-20-oximinoetiojerv-13(17)-en-3β-ol and the Diacetyl Derivative (X).—To a cooled *n*-butanol solution (2 ml.) containing the aldehyde IX (0.20 g.) and freshly-prepared *n*-butyl nitrite (0.20 g.), was added a 1N sodium *n*-butoxide solution in *n*-butanol (2 ml.), and the whole solution was then kept in a refrigerator for 12 hr. After an excess of dry ice and a small volume of water had been added, the solution was evaporated below 43°C under reduced pressure, and the residue was extracted with chloroform. The chloroform solution was shaken with a 2N aqueous sodium hydroxide solution, which was then neutralized carefully with 2N hydrochloric acid and extracted with chloroform. The chloroform solution gave, after the solvent had been removed, an oxime (0.09 g.) which showed one spot on thin-layer chromatograms but which resisted crystallization; UV: λ_{max} 413 (1760) and 246 mμ (ε 5550); IR (chloroform): ν_{max} 3580, 3290, 1663 and 1602 cm^{-1}.

Found: C, 76.34; H, 10.19; N, 4.02. Calcd. for $C_{21}H_{33}O_2N$; C, 76.09; H, 10.03; N, 4.23%.

The afore-mentioned oxime (0.26 g.) was acetylated with acetic anhydride (1.5 ml.) and pyridine (3 ml.) at room temperature for 14 hr. A crude diacetate, obtained on the removal of the solvents by azeotropization with benzene, crystallized on trituration with isopropyl ether; it was collected by filtration. On recrystallization from acetone-isopropyl ether, the diacetyl derivative (X; 0.22 g.) had a m. p. of 139—140°C; UV: λ_{max} 350 (4660) and 251 mμ (ε 13250); IR: ν_{max} 1788, 1737, 1671 and 1581 cm^{-1}.

Found: C, 72.31; H, 9.05; N, 3.19. Calcd. for $C_{25}H_{37}O_4N$: C, 72.25; H, 8.98; N, 3.37%.

22, 27-Iminojerva-5, 12-diene-3β, 23α-diol-11-one

22) Footnote 33a of Ref. 17.

***N*-Acetate (XI).**—The Birch reduction of jervine (I) to 8, 9-dihydroisojervine (VII) was carried out according to a procedure reported previously,[17] except that tetrahydrofuran was used as the solvent instead of dioxane; because of the high melting point, the latter was frozen in liquid ammonia, including its starting material, and the yield was sometimes decreased. From 4.0 g. of jervine dissolved in tetrahydrofuran (100 ml.), a crude 8, 9-dihydroisojervine (3.21 g.), m. p. 158—160°C, was obtained. Recrystallization from a mixture of acetone and methanol (9 : 1) afforded the pure sample of VII (3.01 g.), m. p. 161—163°C.

The acetylation of VII proceeded much as has been described in the literature;[17] 5.0 g. of 8, 9-dihydroisojervine was converted to 5.81 g. of the triacetyl derivative, m. p. 163—164°; $[\alpha]_D^{29}$ +95.0°; NMR: a broad peak centered at τ 4.62 (1H, proton on C-6), a broad multiplet which consisted of three peaks centered at τ 4.98, 5.18 and 5.37 (3H, protons on C-3, C-22 and C-23), singlet at τ 8.15 (3H, 18-methyl protons), a doublet centered at τ 8.92 (6H, J=6 c. p. s., 21- and 26-methyl protons), a singlet at τ 9.03 (3H, 19-methyl protons).

Found: C, 71.49; H, 8.34; N, 2.26. Calcd. for $C_{33}H_{47}O_6N$: C, 71.58; H, 8.56; N, 2.53.

A solution of the triacetyl derivative (4.14 g.) in methanol (160 ml.) containing 5% potassium hydroxide was refluxed for 40 min. in a stream of nitrogen. The solution was then evaporated, diluted with water (100 ml.), stirred at room temperature overnight, and filtrered. The precipitates thus collected crystallized, after being dried, on trituration with acetone; then those had a m. p. of 214—217°C. Recrystallization from a mixture of ethanol and acetone (2 : 3) afforded XI (3.17 g.), m. p. 218—219°; $[\alpha]_D^{29}$ −93.0°; UV: λ_{max} 254 mμ (ε 19000); IR: ν_{max} 1701, 1614 and 1055 cm^{-1}; NMR: a broad peak centered at τ 4.63 (1H, proton on C-6), a singlet at τ 7.92 (18-methyl protons), two doublets centered at τ 8.73 and 9.15 (each 3H, J=7 and 6 c. p. s., 21- and 26-methyl protons or vice versa) and a singlet at τ 8.98 (3H, 19-methyl protons).

Found: C, 74.26; H, 9.13; N, 2.93. Calcd. for $C_{29}H_{43}O_4N$: C, 74.16; N, 9.23; N, 2.98.

22, 27-Iminojerv-5-ene-3β, 23α-diol-11-one *N*-Acetate (XIV).—To liquid ammonia (350 ml.) cooled with a dry ice - acetone mixture and containing lithium (604 mg.), 22, 27-iminojerv-5, 12-dien-3β, 23α-diol-11-one *N*-acetate (XI, 4.0 g.) was added over a 5-min. period; the whole mixture was then stirred for another 15 min. The blue color of the mixture disappeared on the addition of ammonium chloride (12 g.), and then the ammonia was removed. The residue was extracted with four 40-ml. portions of chloroform, and the chloroform solution was evaporated to dryness after it had been washed with water and dried with anhydrous sodium sulfate. The residue (3.18 g.) crystallized on trituration with acetone; then it was recrystallized from a mixture of acetone and ethanol (3 : 2) to yield XIV (3.04 g.), m. p. 248—249°; $[\alpha]_D^{29}$ −85°; IR: ν_{max} 3425, 1737, 1600 and 1065 cm^{-1}.

Found: C, 73.72; H, 9.59; N, 4.31. Calcd. for $C_{29}H_{45}O_4N$: C, 73.84; H, 9.62; N, 4.23.

The Hydrogenation of 22, 27-Iminojerv-5-ene-3β, 23α-diol-11-one *N*-Acetate (XIV).—Compound XIV (0.10 g.) was hydrogenated in the presence of pre-reduced Adams' platinum (62 mg.) at room temperature in acetic acid (12 ml.); 7 ml. of hydrogen was absorbed in 20 min. After the catalyst and the solvent had been removed, the residue was treated with three 30-ml. portions of chloroform and a 5% aqueous sodium carbonate solution (5 ml.). The chloroform solution was washed with water, dried, and then evaporated to dryness. The residue (97 mg.) was crystallized from acetone, and then recrystallized from 90% aqueous ethanol. The product (92 mg.), m. p. 271—274°C, was identified as a known compound, 22, 27-iminojervane 3β, 23α-diol-11-one *N*-acetate[19] (XV), by a mixed-melting-point determination and by a comparison of the infrared and NMR spectra with those of XV.

The Alkali Treatment of 22, 27-Iminojerv-5-ene-3β, 23α-diol-11-one *N*-Acetate (XIV).—Compound XV (0.1 g.) was suspended in a mixture of diethylene glycol (50 ml.), water (0.5 ml.), and dimethylsulfoxide (10 ml.) containing potassium hydroxide (1.0 g.). The mixture was refluxed at 205°C for 2 hr. in a stream of nitrogen when it was homogenous. To the cooled solution, water (35 ml.) was added, and then the whole mixture was stirred for a while and filtered. The precipitates (62 mg.) thus collected were treated with 1 N hydrochloric acid (7 ml.) and chloroform (45 ml.). The chloroform solution gave a crystalline compound, which had a m. p. of 247—248.5°C and which amounted to 45 mg. after recrystallization from a mixture of acetone and ethanol (3 : 2). It was proved identical with the starting material (XIV) by a comparison of the infrared spectra and by thin-layer chromatography on silica gel (methanol-benzene, 4 : 1). On the other hand, the acidic layer was made alkaline and extracted with chloroform. From the chloroform solution, nothing remained after the solvent had been removed.

22, 27-Iminojerv-5-ene-3β, 23α-diol (XVI) and the 3, 23, *N*-Triacetyl Derivative (XVIa).—To freshly-distilled diethylene glycol (130 ml.), sodium (3.0 g.) was added; the mixture was then heated for a while and cooled. To this solution anhydrous hydrazine[23] (18 ml.) was added, and the mixture was refluxed for 30 min. and cooled. After the addition of 22, 27-iminojerv-5-ene-3β, 23α-diol-11-one *N*-acetate (XIV, 2.0 g.), the entire mixture was heated at 180°C for 48 hr., heated further to 210°C to remove the excess hydrazine, and again refluxed for another 24 hr. To the cooled solution, water (200 ml.) was added, and the mixture was stirred at room temperature overnight. The precipitates thus formed were collected by filtration and dried to yield a crude deoxo derivative (XVI; 1.52 g.). Repeated recrystallizations, each fraction being checked by paper chromatography,[24] afforded a pure sample (1.05 g.) of XVI, m. p. 221—223°C; IR: no absorption near 1700 cm^{-1}.

Found: C, 78.20; H, 10.81; N, 3.08. Calcd. for $C_{27}H_{45}O_2N$: C, 78.02; H, 10.91; N, 3.37.

Compound XVI (0.15 g.) was acetylated with acetic anhydride (1 ml.) and pyridine (2.5 ml.) at room temperature overnight. The solution was poured into ice water (200 ml.), stirred for 4 hr., and then filtered. The crude triacetate (XVIa; 198 mg.), m. p. 153—155°C, obtained after the washing and drying of the

23) L. I. Smith and K. L. Howard, *Org. Synth.*, **24**, 53 (1944).

24) Footnote 40 of Ref. 17.

precipitates, was recrystallized from aqueous methanol to yield pure sample of 22, 27-iminojerv-5-ene-3β, 23α-diol 3, 23, *N*-triacetate, m. p. 155—156°C; $[\alpha]_D^{20}$ −75.0°; IR: ν_{max} 1742, 1732, 1641, 1244, and 1025 cm^{-1}.

Found: C, 73.18; H, 9.66; N, 2.50. Calcd. for $C_{33}H_{51}O_5N$: C, 73.16; H, 9.49; N, 2.59.

17-Ethyl-20-formyletiojerv-5-en-3β-ol.—Into methanol containing 22, 27-iminomerv-5-ene-3β, 23α-diol (XVI; 1.0 g.) *N*-chlorosuccinimide (385 mg.) was stirred below 30°C, and then the entire mixture was stirred for another 2.5 hr. The solution was concentrated to 50 ml. below 30°C under reduced pressure. Into the solution, cooled with an ice bath, there was stirred in a stream of nitrogen sodium (2.3 g.) dissolved in absolute methanol (50 ml.). The whole solution was allowed to stand at 0°C for 2.5 hr. and then evaporated below 35°C under diminished pressure. The residual oil was mixed with water (50 ml.), and then with 2 N hydrochloric acid (50 ml.). The heterogeneous mixture was vigorously stirred at room temperature overnight and then filtered. The precipitates (835 mg.) had a m. p. of 160—165°C after being washed with water and dried. Two recrystallizations from a mixture of acetone and methanol (4 : 1) yielded 17-ethyl-20-formyletiojerv-5-en-3β-ol (720 mg.), m. p. 173—180°C; IR: ν_{max} 3495, 2735 and 1715 cm^{-1}; NMR: a broad peak centered at τ 4.67 (1H, olefinic proton on C-6), a doublet centered at τ 9.02 (3H, J=7 c. p. s., 21-methyl protons) and a singlet at τ 9.01 (3H, 19-methyl protons).

Found: C, 79.85; H, 10.19. Calcd. for $C_{22}H_{34}O_2$: C, 79.95; H, 10.39%.

17-Ethyl-20-oximinoetiojerv-5-en-3β-ol (XVII).—To absolute methanol (2.1 ml.) containing *n*-butyl nitrite (0.3 ml.) and the afore-mentioned aldehyde (0.10 g.), there was added, under cooling with ice and in a stream of nitrogen, sodium (96 mg.) dissolved in absolute methanol (2.1 ml.); the whole mixture was then allowed to stand in a refrigerator for 22 hr. The solution was made acidic to pH 4 with concentrated hydrochloric acid and evaporated to dryness. The residue was treated with water and five 20-ml. portions of warm chloroform; the chloroform solution was then shaken with a saturated aqueous sodium chloride solution, dried and evaporated. The residual oil crystallized on trituration with acetone; it had a m. p. of 180—184°C. The collected crystals (65 mg.) were twice recrystallized from a mixture of acetone and methanol (4 : 1) to yield the oxime (XVII; 52 mg.), m. p. 192—193°; $[\alpha]_D^{20}$ −27°; IR: ν_{max} 3340, 1680 and 1060 cm^{-1}.

Found: C, 76.19; H, 10.04; N, 3.86. Calcd. for $C_{21}H_{33}O_2N$: C, 76.09; H, 10.03; N, 4.23%.

17-Ethyletiojerv-5-en-3β-ol-20-one (XVIII) and 17-Ethyletiojerv-4-ene-3, 20-dione (XIX).—17-Ethyl-20-oximinoetiojerv-5-en-3β-ol (XVII; 0.41 g.) was suspended in a mixture of pyruvic acid (1.8 ml.), water (18 ml.) and acetic acid (18 ml.), and then refluxed for 3 hr. under a stream of nitrogen. The mixture became homogeneous on being heated. The cooled solution was diluted with water (40 ml.) and made strongly alkaline with a concentrated aqueous sodium hydroxide solution. After ethanol (30 ml.) had been added, the solution was treated with five 30-ml. portions of ether. The ether solution gave, after being washed with water and dried, an oil (221 mg.) which was crystallized from isopropyl ether to yield the crude methyl ketone (XVIII; 209 mg.), m. p. 96—103°C. This ketone was used for the next step without further purification.

The afore-mentioned methyl ketone (XVIII; 150 mg.) was dissolved in a mixture of toluene (100 ml.) and cyclohexanone (5 ml.); 3 ml. of the toluene was then distilled off in order to remove the water from the system. Aluminum isopropoxide (500 mg.) was added, and the reaction mixture was refluxed for 5 hr. under stirring and then cooled. It was distilled with steam for 5 hr. to remove the organic solvents. The residual mixture was extracted with four 30-ml. portions of ether; the ether layer, after being washed with water and dried, was evaporated to dryness. The residue (158 mg.) was purified by thin-layer chromatography on silica gel (ether-acetone, 3 : 2). The extraction of the main spot with chloroform and the subsequent evaporation of the solvent afforded the crude 17α-ethyletiojerv-4-ene-3, 20-dione (XIX), which was recrystallized from a mixture of acetone-methanol (7 : 3) to yield a pure sample (60 mg.), m. p. 168—169°C; $[\alpha]_D^{20}$ +129°.

Found: C, 80.20; H, 9.52. Calcd. for $C_{21}H_{30}O_2$: C, 80.21; H, 9.62%.

The authors wish to express their thanks to Professor Toshi Irie for his encouragment, and also to Professor Shigenobu Okuda, the University of Tokyo, and to Dr. Issei Iwai, Sankyo Co., Ltd., for providing them with crude jervine. They are also indebted to Dr. Toshio Sato and to Mr. Shigezo Shimokawa for the measurement of the NMR spectra.

BULLETIN OF THE CHEMICAL SOCIETY OF JAPAN VOL. 39 2509—2512 (1966)

Sesquiterpenes from *Dictyopteris Divaricata*. II.[1] Dictyopterol and Dictyopterone

By Etsuro KUROSAWA, Motowo IZAWA, Koji YAMAMOTO,* Tadashi MASAMUNE and Toshi IRIE

Department of Chemistry, Faculty of Science, Hokkaido University, Sapporo

(Received March 28, 1966)

The structures of new sesquiterpenes, dictyopterol and dictyopterone, isolated from the essential oil of a brown algae, *Dictyopteris divaricata* Okamura ("Yezoyahazu"), have been shown to be selinen-1β-ol and selinen-1-one, respectively, on the basis of chemical and spectral data. Dictyopterol is an inseparable mixture of α- and β-isomers.

During the course of a search on the sesquiterpenes from the essential oil of *Dictyopteris divaricata* Okamura, a sesquiterpene alcohol has been isolated.[2] The present paper is concerned with the structural elucidation of the alcohol and also of a new ketone isolated during the studies. On the basis of the experimental evidence described below, the alcohol, designated dictyopterol (I), and the ketone, dictyopterone (II), are shown to be selinen-1β-ol and selinen-1-one, respectively.

Dictyopterol (I), $C_{15}H_{24}O$, $[\alpha]_D^{22}$ $-30.8°$, was obtained in ca. 0.12% yield from the neutral fraction of the essential oil of the seaweed. The infrared spectrum indicated the presence of a secondary hydroxyl group at ν 3400 and 1038 cm^{-1} and terminal methylene groups at ν 1642 and 888 cm^{-1}. The NMR spectra measured at 60 and 100 Mc. showed a signal due to an olefinic methyl group at τ 8.25 and two sharp peaks at τ 9.31 and 9.23. The latter peaks altogether involved three protons and the ratio of the intensity of the respective peaks was about 3 : 2. A broad signal due to an olefinic proton, centered at τ 4.7, appeared besides two peaks due to the terminal methylene protons at τ 5.47 and 5.29. However, the intensity of the absorption at lowest field was equivalent to only about 0.4 proton. Similar signals were observed in the NMR spectrum of dictyopterol acetate (III), obtained by acetylation of I with acetic anhydride in pyridine. These NMR spectral data suggested that the alcohol was probably a mixture (about 2 : 3) of structural isomers caused by the different disposition of a double bond, i. e., α- (Ia) and β-dictyopterol (Ib); the peaks in the high field were attributable to a tertiary methyl group. This inference was supported by hydrogenation and the oxidation experiments. The catalytic hydrogenation of dictyopterol acetate (III) over Adams' catalyst in acetic acid followed by hydrolysis gave quantitatively tetrahydrodictyopterol (IV), $C_{15}H_{28}O$, which was shown to be a single compound in all respects. This saturated alcohol should be bicyclic and showed in its NMR spectrum the presence of a secondary methyl group at τ 9.21, a tertiary methyl group at τ 9.17, and an isopropyl group at τ 9.12. Selenium dehydrogenation of III gave eudalene (V), suggesting that IV possessed a selinane skeleton, a view that was confirmed later.

Oxidation of I with chromium trioxide in pyridine afforded a mixture of two isomeric ketones, $C_{15}H_{22}O$, which were separated by chromatography. One of these ketones was identical with dictyopterone (II), isolated from the essential oil, and the other was an α, β-unsaturated ketone (VI), λ 227 mμ

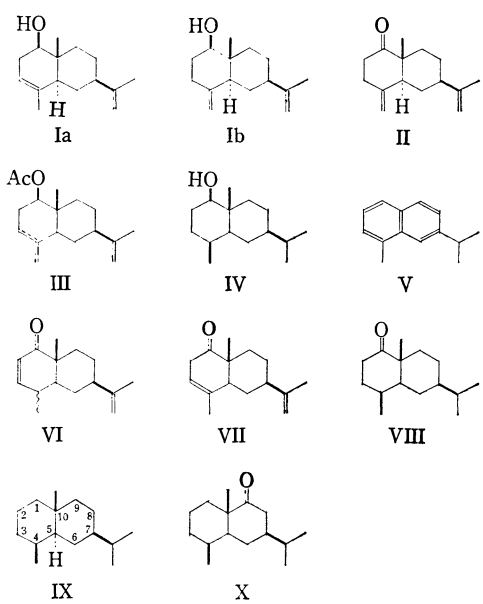

1) Part V of "Constituents from Marine Plants"; Part IV, T. Irie, M. Suzuki, E. Kurosawa and T. Masamune, *Tetrahedron Letters*, **1966**, 1837.

* Present address: Research Laboratory, Mitsubishi Rayon Co., Ootake, Hiroshima.

2) T. Irie, K. Yamamoto and T. Masamune, This Bulletin, **37**, 1053 (1964).

(log ε 4), ν 1680 cm^{-1}. Since only a small amount of the latter was available, no chemical investigation could be carried out. However, neither α- nor β-dictyopterol was characterized as an allylic alcohol. Hence, this α, β-unsaturated ketone was probably formed by migration of a double bond from a β, γ-position, i. e., VII.

Dictyopterone (II), $C_{15}H_{22}O$, $[\alpha]_D^{21}$ −12.5°, was newly isolated from the neutral fraction of the essential oil beside I and was also obtained by the oxidation of I as mentioned above. The infrared spectrum showed the presence of a six-membered ring carbonyl (ν 1710 cm^{-1}) and terminal methylene group (ν 1640, 890 cm^{-1}). The NMR spectrum indicated the presence of two terminal methylene groups at τ 5.34 and 5.07 (total 4H), a methyl group on an olefinic carbon at τ 8.28, and a tertiary methyl group at τ 9.05. This unsaturated ketone II was stable toward alkali, indicating that the double bond is not located at a β, γ-position relative to the carbonyl group. When II was reduced with lithium aluminum hydride in tetrahydrofuran, a corresponding alcohol was obtained, the NMR spectrum of which showed a sharp singlet at τ 9.31 (3H), a doublet (J=2 c. p. s.) at τ 8.25 (3H), and broad peaks at τ 5.47 and 5.29 (total 4H). It was found that this alcohol was identical with one of the components of I, i. e., β-dictyopterol (Ib), by comparisons of the infrared and NMR spectra of this alcohol and I.

Catalytic hydrogenation of II yielded tetrahydrodictyopterone (VIII), $C_{15}H_{26}O$, which was also obtained by the chromium trioxide oxidation of IV; VIII displayed positive Zimmermann test. Treatment of VIII with heavy water in the presence of sodium deuteroxide in dioxane afforded a dideuterio derivative (mass spectrum: *m/e* 224). The ketone therefore has $-CH_2-CO-\dot{C}(\dot{C})-C$ grouping.

The Wolff-Kishner reduction of VIII gave (+)-selinane (IX); this transformation has now established the carbon skeleton as well as the stereochemistry of the tertiary methyl and the isopropyl group in VIII, and tetrahydrodictyopterone should therefore be selinan-1-one (VIII). The alternative structure X (selinan-9-one) is ruled out because the α, β-unsaturated ketone VI was formed by the oxidation of I and because tetrahydrodictyopterone showed the infrared spectrum different from that of dihydrocanarone[3] (X). Optical rotatory dispersion curves of II and VIII showed small positive and samll negative Cotton effects, respectively. Furthermore, the mass spectra of both VIII and its dideuterio derivative showed a remarkable peak at *m/e* 178 which was formulated as follows, supporting the structure of VIII.

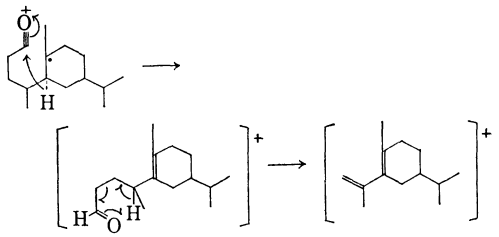

m/e 178

Finally, the conformation of the hydroxyl group in I is equatorially disposed and, therefore, β-oriented because tetrahydrodictyopterol acetate showed in its NMR spectrum a broad multiplet (half-band width ca. 16 c. p. s.) at τ 5.6 attributable to an axial hydrogen on a carbon bearing the acetoxyl group.

All the facts discussed above show that Ia, Ib, and II are the most favorable structures for α- and β-dictyopterols and dictyopterone, respectively.

These 1-oxygenated selinenes may be considered to be formed biogenetically as a result of *trans*-anti-parallel oxidative cyclization of a germacrane-type intermediate XI.[4]

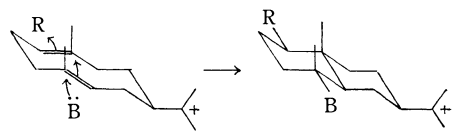

XI

Experimental

The melting points are uncorrected. The ultraviolet and infrared spectra were measured using a Hitachi spectrophotometer and a Nippon Bunko 402-G or IR-S spectrophotometer, respectively. The NMR measurements were performed in carbon tetrachloride with a Nippon Denshi 60-Mc. spectrophotometer using tetramethylsilane as an internal reference unless otherwise stated. The ORD and mass spectra were measured with a Nippon Bunko ORD/UV-5 and a Hitachi RMU-6 mass spectrometer, respectively.

The Isolation of Dictyopterol (I) and Dictyopterone (II).—a) The neutral fraction[2] of the essential oil from *D. divaricata* was submitted to distillation in vacuo; after removal of fractions up to b. p. 106.5°C/4 mmHg, the residual oil (14 g.) was chromatographed on silica gel containing 20% Celite. The benzene eluate was rechromatographed over neutral alumina, and a mixture of dictyopterol and δ-cadinol was obtained. Repeated chromatography afforded dictyopterol free from δ-cadinol, but a better result was obtained by

3) V. K. Hinge, A. D. Wagh, S. K. Paknikar and S. C. Bhattacharyya, *Tetrahedron*, **21**, 3197 (1965); cf. A. D. Wagh, S. K. Paknikar and S. C. Bhattacharyya, *J. Org. Chem.*, **29**, 2479 (1964).

4) Cf. J. B. Hendrickson, *Tetrahedron*, **7**, 82 (1959).

the following treatment. A mixture of dictyopterol and δ-cadinol was treated with acetic anhydride and pyridine, and the crude product was taken up in *n*-hexane and chromatographed over neutral alumina. Elution with *n*-hexane - benzene (3 : 1) yielded dictyopterol acetate (III) (488 mg.) as pure (T.L.C.), colorless oil, $[\alpha]_D^{19}$ −15.5° (*c* 2.0, EtOH); ν_{max}^{film} 3080, 1742, 1642, 1240, 1026, 890 cm^{-1}; NMR: τ 9.25, 9.17 (total 3H, two singlets), 8.29 (more than 3H, doublet, J= 2 c. p. s.), 8.02 (3H, singlet), 5.5 (1H, multiplet), 5.34, 5.28 (total more than 3H, broad multiplets), and 4.8 (ca. 0.4H, broad multiplet).

Found: C, 78.02; H, 10.02. Calcd. for $C_{17}H_{26}O_2$: C, 77.82; H, 9.99%.

The above acetate III (278 mg.) dissolved in a mixture of methanol (50 ml.) and ether (5 ml.) was added to 5% aqueous potassium hydroxide (10 ml.), and the solution was kept aside at room temperature for 2 days. After addition of water and removal of the organic solvent in vacuo, the residue was extracted with ether. The ether extracts were washed, dried and evaporated, giving an oily product which was chromatographed on neutral alumina. Elution with benzene - ethyl acetate (5 : 1) afforded pure (T. L. C.) I as a colorless oil, $[\alpha]_D^{22}$ −30.8° (*c* 2.08, CCl_4); ν_{max}^{film} 3400, 3080, 1642, 1038, 888 cm^{-1}; NMR: τ 9.31, 9.23 (total 3H, two singlets), 8.25 (more than 3H, doublet, J=2 c. p. s.), 6.6 (1H, broad multiplet), 5.47, 5.29 (total more than 3H, broad multiplets), and 4.7 (ca. 0.4H, broad multiplet). Mass spectrum: *m/e* (rel. abund.) 220 (100), 205 (81), 202 (84), 161 (91), 159 (84), 133 (83), 93 (82), 81 (71).

Found: C, 81.47; H, 10.65. Calcd. for $C_{15}H_{24}O$: C, 81.76; H, 10.98%.

The *n*-hexane - benzene (3 : 1) eluate in the chromatography of the residual oil described above, was rechromatographed over neutral alumina, and dictyopterone (II) was obtained (161 mg.), $[\alpha]_D^{21}$ −12.5° (*c* 2.16, CCl_4); ν_{max}^{film} 3080, 1710, 1640, 890 cm^{-1}; NMR: τ 9.05 (3H, singlet), 8.26 (3H, doublet, J=2 c. p. s.), 5.30, 5.07 (total 4H, broad multiplets).

Found: C, 82.73; H, 10.02. Calcd. for $C_{15}H_{22}O$: C, 82.51; H, 10.16%.

b) The neutral fraction (25 g.) of the essential oil was chromatographed on neutral alumina and eluted successively with *n*-hexane, benzene, ether, and ethyl acetate. The product (ca. 7 g.) obtained from the eluates with ether and ethyl acetate was distilled with steam. The distillate was extracted with ether and dried. After removal of the solvent, the residual oil was chromatographed on silica gel. Each eluate was treated as described above, yielding I and II.

The Hydrogenation of Dictyopterol Acetate (III).—Dictyopterol acetate (III) (208 mg.) in glacial acetic acid (15 ml.) was hydrogenated over Adams' catalyst (15 mg.) at room temperature until gas absorption ceased (2 mol. of hydrogen was absorbed after 2 hr.). The catalyst was removed by filtration and the solvent was evaporated under reduced pressure. The residual oil was chromatographed on alumina. The fraction eluted with *n*-hexane - benzene (3 : 1) afforded pure (T. L. C.) tetrahydrodictyopterol acetate (196 mg.). ν_{max}^{film} 1742, 1240, 1024 cm^{-1}; NMR: τ 9.12 (9H, doublet, J=6 c. p. s.), 9.08 (3H, singlet), 8.05 (3H, singlet), 5.6 (1H, broad multiplet).

Found: C, 76.95; H, 11.25. Calcd. for $C_{17}H_{30}O_2$: C, 76.64; H, 11.35%.

Tetrahydrodictyopterol (IV).—To a solution of the afore-mentioned tetrahydro-acetate (190 mg.) in a mixture of methanol (20 ml.) and ether (5 ml.) was added 5% aqueous potassium hydroxide (3 ml.), and the mixture was allowed to stand at room temperature for 2 days. After addition of water to the reaction mixture, the organic solvent was removed in vacuo and the residue was extracted with ether. The ether solution was washed with 0.5 N hydrochloric acid, 2% sodium bicarbonate solution, and then with water, successively. Removal of the solvent afforded an oily material, which was chromatographed on alumina. The fraction eluted with benzene - ethyl acetate (5:1) gave pure (T. L. C.) tetrahydrodictyopterol (IV) (136 mg.). ν_{max}^{film} 3400, 1020 cm^{-1}. NMR: τ 9.21 (3H, doublet, J=6 c. p. s.), 9.17 (3H, singlet), 9.12 (6H, doublet, J=6 c. p. s.), 6.9 (1H, broad multiplet).

Selenium Dehydrogenation of Dictyopterol Acetate (III).—A mixture of III (80 mg.) and selenium (85 mg.) was heated in a sealed tube at 282—294°C for 6 hr. The reaction mixture was extracted with ether and the ether extracts were dried. After removal of the solvent, the residue was chromatographed on alumina thin layer using *n*-hexane. The fraction of R_f=1 33 mg.) was identified as eudalene (V), λ_{max}^{EtOH} mμ (ε): 228 (36.700), 282 (3200), 320 (383). ν_{max}^{film} 1630, 1600, 1510, 1380, 1360, 1300, 1170, 1150, 1080, 1042, 878, 830, 750 cm^{-1}.

Picrate: m. p. 87—89°C, yellow needles (from ethanol).

The Oxidation of Dictyopterol (I).—A solution of I (109 mg.) in dry pyridine (5 ml.) was added to a complex of chromium trioxide (300 mg.) and pyridine (3 ml.) and the mixture was set aside at room temperature overnight. The reaction mixture was distilled with steam and the distillate was extracted with ether. The ether extracts were washed with 0.5 N hydrochloric acid, 0.5 N sodium hydroxide solution, then with water and dried. After removal of the solvent in vacuo, the residual oil was chromatographed on alumina. The fraction eluted with *n*-hexane - benzene (3 : 1) afforded pure (T. L. C.) oily product (61 mg.), which was identified as dictyopterone (II) in all respects.

The fraction eluted with benzene gave an α, β-unsaturated ketone (14 mg.). λ_{inf}^{EtOH} 227 mμ (log ε 4). ν_{max}^{film} 1680 cm^{-1}.

The Alkaline Treatment of Dictyopterone (II).—A mixture of II (12 mg.) and 5% methanolic potassium hydroxide was refluxed for 1 hr. After addition of water and removal of the methanol in vacuo, an oily product was extracted with ether and the ether extracts were washed with water and dried. On removal of the solvent, the starting material II was recovered unchanged.

The Reduction of Dictyopterone (II) with Lithium Aluminum Hydride.—To a suspension of lithium aluminum hydride (25 mg.) in dry tetrahydrofuran (10 ml.), a solution of II (59 mg.) in the same solvent (5 ml.) was added and then the mixture was refluxed for 2 hr. After being cooled, the mixture was decomposed by the addition of water and acidified with dilute sulfuric acid. The solution was extracted with ether and the ethereal layer was washed with 2% sodium

bicarbonate solution and then with water and dried. After removal of the solvent, the residual oily product was chromatographed on alumina. The product eluted with benzene - ethyl acetate (5 : 1) was identified as β-dictyopterol (Ib) by a comparison of the infrared and NMR spectra. ν_{max}^{film} 3400, 3080, 1642, 1038, 888 cm^{-1}. NMR: τ 9.31 (3H, singlet), 8.25 (3H, doublet, J=2 c. p. s.), 6.6 (1H, broad quartet), 5.47 and 5.29 (total 4H, broad multiplets).

Tetrahydrodictyopterone (VIII).—Dictyopterone (29 mg.) in glacial acetic acid (6 ml.) was hydrogenated over Adams' catalyst (3 mg.) at room temperature. After 2 hr. the catalyst was removed and the acetic acid solution was neutralized with 5% aqueous potassium hydroxide. The neutral solution was extracted with ether and the ethereal layer was washed with water and dried. Removal of the solvent afforded an oily product, which was chromatographed on alumina. The fraction eluted with benzene gave oily saturated ketone VIII (22 mg.). $[\alpha]_D^{22}$ −41.6° (c 1.01, MeOH). The ultraviolet spectrum showed only an end absorption. ν_{max}^{film} 1705, 1390, 1372, 1285, 1140, 1077, 1010, 916 cm^{-1}. NMR: τ 9.12 (6H, doublet, J=6 c. p. s.), 8.92 (3H, singlet), 8.92 (3H, doublet, J=7 c. p. s.). Mass spectrum: m/e (rel. abund.) 222 (92), 220 (92), 178 (98), 135 (79), 109 (74), 81 (81), 43 (100).

The Oxidation of Tetrahydrodictyopterol (IV).—The oxidation of IV (110 mg.) with chromium trioxide was carried out as described in the case of I, yielding a crude oily product which was chromatographed over alumina. The fraction eluted with n-hexane - benzene (3 : 1) was identified as tetrahydrodictyopterone (VIII) obtained by the catalytic hydrogenation of II.

The Wolff-Kishner Reduction of Tetrahydrodictyopterone (VIII).—To a solution of sodium (250 mg.) in diethylene glycol (7 ml.), VIII (45 mg.) in the same solvent (3 ml.) and 100% hydrazine hydrate (1.3 ml.) were added, and the mixture was heated at 180—185°C for 20 hr. After addition of water, the mixture was extracted with ether. The ether extracts were washed with water, dried and the ether was removed in vacuo. The oily product thus obtained was chromatographed on alumina. The fraction eluted with n-hexane afforded a colorless oil, $[\alpha]_D^{22}$ +15°, which was identified as (+)-selinane (IX) by a comparison of its infrared spectrum with that appeared in the literature.[5]

Deuterium Exchange Experiment of Tetrahydrodictyopterone (VIII).—Deuterium exchange was effected by heating VIII (32 mg.) in N sodium deuteroxide solution (0.5 ml.) and dry dioxane (1.5 ml.) at 100°C for 10 min. After cooling, the solvent was distilled off under diminished pressure. To the product was added a mixture of heavy water (0.7 ml.) and dry dioxane (1.5 ml.), and the mixture was heated and most of the solvent was then evaporated in vacuo. This procedure was repeated two times, and finally the residue was extracted with dry ether. Removal of the ether yielded tetrahydrodictyopterone-d_2 (24 mg.) as a colorless oil. Mass spectrum: m/e (rel. abund.) 224 (100), 222 (92), 178 (98), 163 (81), 135 (72), 109 (65), 81(64), 43(62).

The authors wish to express their thanks to Professor Koshiro Miyahara for measurements of mass spectra and to Mr. Seiichiro Ohnishi of Toyo Rayon Co. and Mr. Shigezo Shimokawa for measurements of NMR spectra. They are also indebted to Miss Akiko Maeda for her elemental analyses.

5) J. Pliva, M. Herac, V. Herout and F. Šorm, "Die Terpene. Sammlung der Spektren und Physikalischen Konstanten," Teil I. Akademie-Verlag, Berlin (1960).

BULLETIN OF THE CHEMICAL SOCIETY OF JAPAN VOL. 39 2512—2516 (1966)

The Chemistry of Polyazanes. VI. The Oxidation of ω, ω'-Dibenzoylcarbohydrazide

By Hiroshi MINATO, Ryuki HISADA* and Mitsugu TANAKA*

Department of Chemistry, International Christian University, Mitaka, Tokyo

(Received April 7, 1966)

ω, ω'-Dibenzoylcarbohydrazide (DBC) was oxidized with sodium hypochlorite in an aqueous ethanolic solution at $-70°C$. At first the solution had a deep red color, but it gradually faded away. The products of the reaction isolated were benzoic acid, ethyl benzoate, carbon dioxide, 2-phenyl-1, 3, 4-oxadiazol-5-one, and N, N'-dibenzoylhydrazine. Then, DBC was oxidized with hypochlorous acid, the products of this reaction were not very different from those obtained with sodium hypochlorite. A plausible mechanism was presented, which assumed the formation of bis(benzoylimino)urea, which was then decomposed heterolytically by the nucleophilic attack of ethanol and water molecules.

Compounds containing a chain of several nitrogen atoms have been investigated in our laboratories

* The American Chemical Society-Petroleum Research Fund Scholar.

in the last few years.[1-5] In relation to these compounds, our attention has been drawn to a compound in which a chain of four nitrogen atoms is intercepted by a carbonyl group, namely, bis-(benzoylimino)urea (BIU). In BIU, two benzoyl radicals are connected with –N=N–C(=O)–N=N–, which may change spontaneously into gaseous nitrogen molecules and a carbon monoxide molecule. If BIU is prepared and if it then decomposes at very low temperatures into two benzoyl radicals, two nitrogen molecules and one carbon monoxide molecule, BIU might be used as an initiator of polymerization at very low temperatures.

Stollé and Krauch[6] observed that the oxidation of ω, ω'-dibenzoylcarbohydrazide (DBC) with an aqueous sodium hypochlorite solution gave a yellow-red color, and that the color immediately disappeared with evolution of gas. They did not, however, elucidate the structure and the nature of the compound possessing the yellow-red color.

The oxidation of DBC with an aqueous sodium hypochlorite solution and with a hypochlorous acid solution has now been investigated in detail and will be described in this paper.

Experimental

ω, ω'-Dibenzoylcarbohydrazide (DBC).—DBC was prepared according to the method of Stollé and Krauch.[6] Seventy grams of carbohydrazide (0.716 mol.) was dissolved in 750 ml. of a 1.6 N sodium hydroxide solution. To this solution, 202 g. of benzoyl chloride (1.423 mol.) was stirred, drop by drop, with cooling. After the mixture had been allowed to stand for 12 hr., the precipitates were filtered off, and washed with water and ether. The yield of crude DBC was 200 g. (0.672 mol.). It was recrystallized from ethanol. M. p. 204.5°C (lit.: 205°C).

The Oxidation of DBC with a Sodium Hypochlorite Solution.—First, a blank test was run in order to check whether ethanol, used as an antifreeze solvent, is oxidized with sodium hypochlorite. One milliliter of a 6.965% aqueous sodium hypochlorite solution and 3.0 ml. of water were mixed at 0°C. To this solution 25.0 ml. of ethanol was added, and the mixture was immediately cooled to −70°C. Then 1.5 g. of potassium iodide, 3 ml. of glacial acetic acid, and 15 ml. of ethanol were added. After it had been warmed to room temperature, the solution was titrated with a 0.1037 N sodium thiosulfate solution. The titer was 9.70 ml. In the absence of ethanol, the titer was 9.75 ml.

Run 1.—Fifteen milliliters of a 6.965% aqueous sodium hypochlorite solution (13.41 mmol.) and 45 ml. of water were mixed at 0°C. Three-hundred-seventy-five milliliters of cooled ethanol was added to this solution, and this mixture was immediately cooled to −70°C. Then this cooled mixture was added to a solution of 2.091 g. of DBC (6.67 mmol.) in 300 ml. of ethanol which had been cooled to −70°C. The mixed solution had a deep red color at −70°C. After about 3 min., the color turned orange and gradually faded away. The solution was stirred for about 2 more hr. at −70°C, and then warmed to room temperature.

After it had been allowed to stand for a day, the mixture was distilled by the use of a 30-cm. Vigreux column. The ethanol was then distilled off, and a small amount of a brown residue remained. Sixty milliliters of ether was added to this residue, and the ethereal solution was dried with anhydrous sodium sulfate. After the evaporation of ether under reduced pressure, reddish-brown solids, weighing 1.40 g., remained. This solid material was divided into a petroleum ether-soluble fraction and a petroleum ether-insoluble fraction. The infrared spectrum of the petroleum ether-soluble fraction indicated the presence of benzoic acid and ethyl benzoate. It was found, by the use of the absorption of benzoic acid at 1415 cm^{-1} and that of ethyl benzoate at 1110 cm^{-1}, that 0.689 g. of benzoic acid (5.65 mmol.) and 0.164 g. of ethyl benzoate (1.09 mmol.) were present in this fraction.

The petroleum ether-insoluble fraction consisted of crystals weighing 0.261 g. and melting at 135°C. After they had been recrystallized three times from water, the crystals melted at 138—139°C. The crystals were identified as 2-phenyl-1, 3, 4-oxadiazol-5-one from the infrared spectrum and from the melting point of the mixture with an authentic sample (m. p. 139°C).[7]

Run 2.—Run 2 was different from Run 1 with respect to the work-up; after the reaction was over, the solution was acidified and the amount of carbon dioxide was analyzed.

Twenty milliliters of a 0.765 M aqueous sodium hypochlorite solution (15.30 mmol.) and 40 ml. of water were mixed at 0°C. Three-hundred-seventy-five milliliters of cooled ethanol was then added to this solution, and the mixture was immediately cooled to −70°C. Then this cooled mixture was added to a solution of 2.270 g. of DBC (7.61 mmol.) in 300 ml. of ethanol which had been cooled to −70°C in a one-liter, four-necked flask equipped with a mercury-sealed stirrer and with an outlet leading to an apparatus for the measurement of carbon dioxide. The mixed solution had a deep red color at −70°C. After about two minutes, however, the color turned orange. The mixed solution was stirred for two hours at −70°C. Then it was warmed to room temperature, and 13.81 ml. of 1.108 M hydrochloric acid (15.30 mmol.) was added. In order to determine the amount of carbon dioxide present, the solution was swept by a stream of a CO_2-free air, which was then led to a tube containing soda-lime. The increase in the weight of the soda-lime tube

1) H. Minato and M. Oku, This Bulletin, **38**, 1529 (1965).
2) H. Minato and T. Fujisawa, ibid., **39**, 1054 (1966).
3) H. Minato, M. Oku and S. Chan, ibid., **39**, 1049 (1966).
4) H. Minato, M. Ibata and H. Iwai, *J. Chem. Soc. Japan, Ind. Chem. Sect. (Kogyo Kagaku Zasshi)*, **69**, 184 (1966).
5) H. Minato, H. Tateno and H. Yokokawa, This Bulletin, in press.
6) R. Stollé and K. Krauch, *Ber.*, **47**, 727 (1914).
7) A. Dornow and K. Bruncken, ibid., **82**, 121 (1949).

was 0.1575 g. after the carbon dioxide had been completely absorbed. The pH of the mixed solution was 3.0.

After it had then been allowed to stand for a day, the solution was distilled by the use of water bath kept at 85°C. When about 10 ml. of the residual liquid was present in the flask, the distillation was stopped. Then the distillate was carefully redistilled unitl about 100 ml. remained in the flask, and the residual liquid was gas-chromatographed by the use of a Shimadzu GC-2B gas chromatograph; the presence of ethyl benzoate was detected and 2.33 mmol. of ethyl benzoate was found by the use of diphenyl ether as the internal standard.

To the 10-ml. residue of the first distillation, 300 ml. of ether was added. White precipitates were filtered off and found to be sodium chloride. When the ethereal solution was distilled, the residue was a mixture of white precipitates and a brown pasty oil. The white solids were filtered off, washed, and recrystallized from ethanol; m. p. 235—240°C. The infrared spectrum was exactly the same as that of authentic *N*, *N'*-dibenzoylhydrazine (m. p. 234—238°C).[8]

When the filtrate and washings were evaporated, a brown, pasty residue weighing 2.052 g. was obtained. This was found to be a mixture of benzoic acid and ethyl benzoate by a study of its infrared spectrum. 5.39 mmol. of benzoic acid and 2.22 mmol. of ethyl benzoate were found to be present.

Carbon monoxide was found to be absent among the reaction products in a separate experiment using iodine pentoxide and potasssium iodide.

The Oxidation of DBC with Hypochlorous Acid.—First, a blank test was run in order to check whether or not ethanol was oxidized with hypochlorous acid. 2.003 g. of a 0.732 M aqueous hypochlorus acid solution was cooled to 0°C. To this solution 50 ml. of ethanol and 6 ml. of water were added, and the mixed solution was immediately cooled to −70°C. Then 2 g. of potassium iodide, 3 ml. of glacial acetic acid, and 30 ml. of ethanol were added to the solution. After it had been warmed to room temperature, the solution was titrated with a 0.1037 N sodium thiosulfate solution. The titer was 27.65 ml., which corresponded to a 0.728 M hypochlorous acid solution. This test showed that only 0.55% of the hypochlorous acid initially present was consumed by the reaction with ethanol.

21.60 ml. of a 0.640 M aqueous hypochlorous acid solution (13.82 mmol.) and 38.4 ml. of water were mixed at 0°C. After 375 ml. of cooled ethanol had then been added to this solution, the mixture was immediately cooled to −70°C. Then this cooled mixture was added to a solution of 2.052 g. of DBC (6.88 mmol.) in 300 ml. of ethanol which had been cooled to −70°C in a one-liter, four-necked flask equipped with a mercury-sealed stirrer and with an outlet leading to an apparatus for the determination of carbon dioxide. The mixture did not acquire a deep red color, but only a light yellow color. After it had been kept at −70°C for two hours, it was warmed to room temperature. The increase in the weight of the soda-lime tube was 0.1530 g., corresponding to the evolution of 3.47 mmol. of carbon dioxide. After it had then been allowed to stand at room temperature for a day, the mixed solution was distilled. 6.18 mmol. of ethyl benzoate was found to be present in the distillate by the use of a Shimadzu GC-2B gas chromatograph. The residue was washed with petroleum ether, and the white solids (m. p. 127°C) were found, by a study of the infrared spectrum, to be *N*-benzoyl-*N'*-ethoxycarbonylhydrazine (m. p. 127°C). The petroleum ether-washings were evaporated to yield an oil weighing 0.6154 g. Its infrared spectrum showed that it contained 0.671 mmol. of benzoic acid and 2.04 mmol. of ethyl benzoate.

The Oxidation of DBC with Sodium Hypochlorite and the Reduction of the Oxidation Product with Hydrogen Sulfide.—Ten milliliters of a 0.433 M aqueous sodium hypochlorite solution (4.33 mmol.) and 7.5 ml. of water were mixed at 0°C. One hundred milliliters of cooled ethanol was added to this solution, and this mixture was immediately cooled to −70°C. Then this cooled mixture was added to a solution of 0.642 g. of DBC (2.15 mmol.) in 90 ml. of ethanol which had been cooled to −70°C. When the mixed solution possessed a deep red color, 4.5 ml. of a 1.0 M hydrochloric acid solution was added, after which hydrogen sulfide was passed into this mixed solution for five minutes. Then it was warmed to room temperature.

After the mixture had been allowed to stand at room temperature for a day, it was distilled. Most of the liquid was distilled at about 79°C, but a yellowish residue remained. It was shaken with 20 ml. of water, and the precipitates were filtered; this treatment was repeated four times. Then the precipitates were shaken with 20 ml. of ether, and the solids were filtered; this procedure was repeated four times. The white solids obtained weighed 0.115 g. (0.385 mmol.), and melted at 199—203°C. The infrared spectrum was exactly the same as the infrared spectrum of the authentic DBC. After the ethereal washings had been evaporated, a yellowish-brown residue, weighing 0.309 g., remained. The infrared spectrum showed that the residue contained 0.034 mmol. of benzoic acid and 0.306 mmol. of ethyl benzoate.

Results and Discussion

ω, *ω'*-Dibenzoylcarbohydrazide (DBC) was oxidized with sodium hypochlorite at −70°C in a mixture of water and ethanol; the latter was used as the anti-freeze. When DBC and the

TABLE I. PRODUCTS OF OXIDATION OF DBC

Product (mol./mol. DBC)	Oxidant: NaOCl Run 1	NaOCl Run 2	HOCl
Benzoic acid	0.847	0.708	0.098
Ethyl benzoate	0.163	0.598	1.195
2-Phenyl-1, 3, 4-oxadiazol-5-one	0.241	—	—
N, *N'*-Dibenzoylhydrazine	—	0.075	—
N-Benzoyl-*N'*-ethoxycarbonylhydrazine	—	—	0.194
Carbon dioxide	(not determined)	0.468	0.505
% C_6H_5 accounted for	62.6	72.8	74.4
% CO accounted for	49.7	64.1	72.9

8) H. H. Hatt, "Organic Syntheses," Coll. Vol. II., 208 (1943).

oxidant were mixed, the mixed solution had a deep red color, but this gradually faded away. The results of an analysis of the products of the reaction are shown in Table I.

The products of the decomposition of bis-(benzoylimino)urea (BIU), which was supposed to be the oxidation product of DBC, indicate that BIU did not decompose homolytically with the production of free radicals. The products of the reaction are best described by the nucleophilic attack of ethanol or water molecules or ethoxide or hydroxide ions upon benzoyl carbon atoms of BIU, as is shown in Fig. 1. When sodium hypochlorite was used as the oxidizing agent, the medium was alkaline, the ethoxide ions and hydroxide ions present may be supposed to be far more nucleophilic than the ethanol and water molecules.

If DBC was oxidized in a non-alkaline condition, BIU formed might decompose homolytically to yield free radicals. In order to check this possibility, DBC was oxidized with hypochlorous acid. The products of the decomposition of BIU in an acid medium, shown in Table I, indicate that the BIU formed was attacked by ethanol and water molecules and decomposed heterolytically rather than homolytically. The products of decomposition were not very different from those formed in an alkaline condition. 0.24 mol. of 2-phenyl-1, 3, 4-oxadiazol-5-one was produced from one mole of BIU in Run 1 with sodium hypochlorite. In the case of Run 2, hydrochloric acid was added to the reaction mixture after the reaction had been completed; this acidification must have decomposed 2-phenyl-1, 3, 4-oxadiazol-5-one. When hypochlorous acid was used as the oxidant, none of this heterocyclic compound was detected.

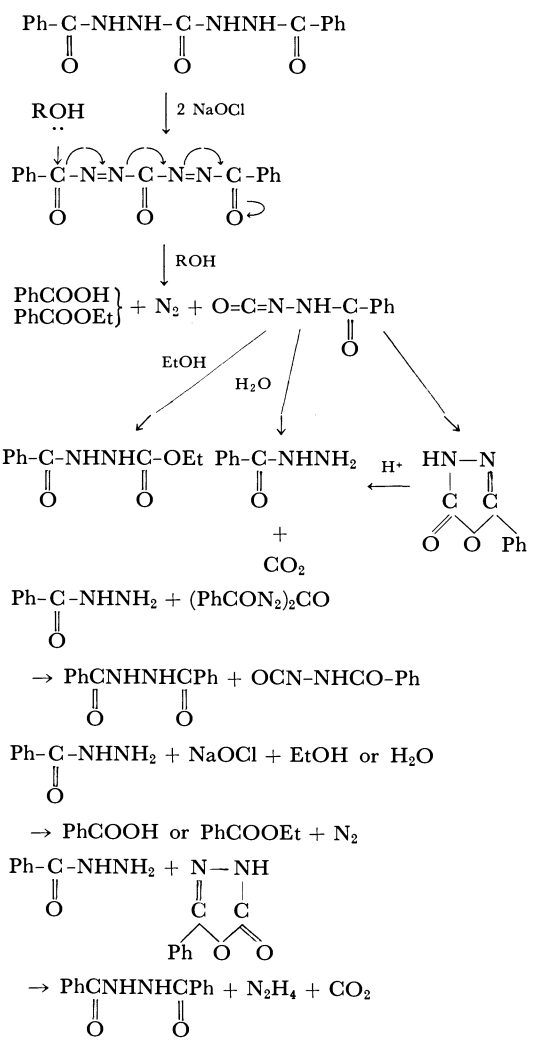

Fig. 1. Plausible scheme of decomposition of BIU.

The behavior of the deep red substance can best be explained by assuming that bis(benzoylimino)-urea is produced by the oxidation of DBC. However, in order to confirm this, the deep red substance was reduced by hydrogen sulfide. Stollé oxidized *N, N'*-diacetylhydrazine and obtained diacetyldiimide, which was a deep red and unstable oil. He then reduced it with hydrogen sulfide and thus obtained *N, N'*-diacetylhydrazine again.

Soon after the DBC solution and sodium hypochlorite solution had been mixed and the deep red color produced, hydrogen sulfide gas was introduced in order to reduce the deep red substance. After the work-up, about 18% of the amount of DBC originally present was isolated. All the data, including those of this reduction experiment, can best be explained by assuming that the deep red substance produced by the oxidation of DBC is bis(benzoylimino)urea.

The nucleophilic attack of ethoxide and hydroxide ions upon BIU under alkaline conditions seems reasonable, but the equally fast attack of ethanol and water molecules on BIU under acid conditions seems somewhat surprising. Probably the azo double bonds are protonated, and this protonation induces the nucleophilic attack of ethanol and water molecules.

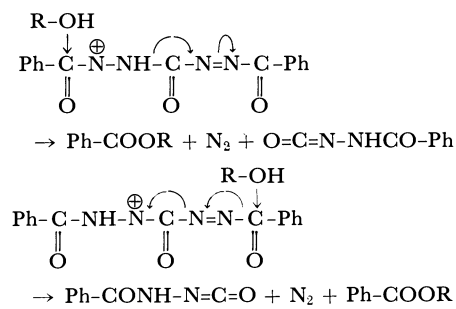

When DBC was oxidized under acid conditions, no deep red color was observed, even at the instant

of mixing the reactants. This fact is reasonable, since the protonated BIU is not likely to have a deep color.

The structures of benzoylphenyldiimide,[9] bis-(phenylimino)urea,[10] and dibenzoyldiimide[11] are somewhat related to the structure of BIU, and it is interesting to note their behavior in hydroxylic solvents:

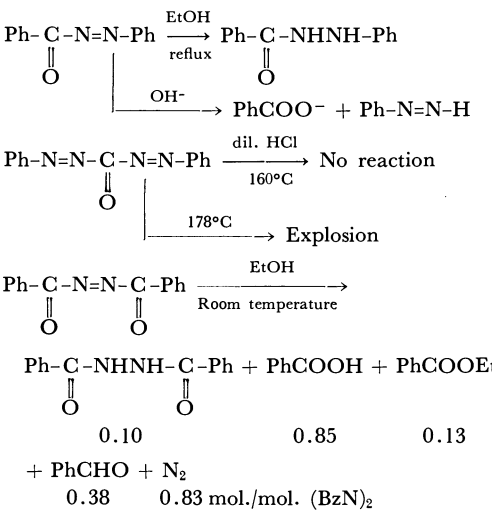

The decomposition of dibenzoyldiimide is especially interesting. Leffler and Bond[11] determined the rates of its decomposition and found that $k_1 = 7.33 \times 10^{-6}$ sec^{-1} in benzene at 100°C (initial concentration $(C_0) = 0.03$ M); $k_1 = 137 \times 10^{-6}$ sec^{-1} in benzyl alcohol at 61.9°C ($C_0 = 0.0051$ M); $k_1 = 75.6 \times 10^{-6}$ sec^{-1} ($C_0 = 0.008$ M), and $k_1 = 124 \times 10^{-6}$ sec^{-1} ($C_0 = 0.0135$ M) in ethanol at 19.69°C.

Although both the products and the kinetics of the decomposition seem to suggest that the decomposition of the diimide in ethanol at 20°C is an ionic reaction initiated by the nucleophilic attack of ethanol on the benzoyl carbon, Leffler and Bond favored a free radical mechanism. Since they found acrylonitrile to polymerize in a benzene solution at 75°C, they thought the decomposition of the diimide in benzene at 75°C was likely to involve some homolytic decomposition. They argued that ethyl benzoate could be formed from the radical-ethanol complexes by the loss of hydrogen to another radical or to a molecule of dibenzoyldiimide, and that the second oxygen needed for the conversion of benzoyl radical to benzoic acid probably came from the solvent ethanol. These arguments seem unsatisfactory. They did not explain the formation of *N, N'*-dibenzoylhydrazine, either.

On the basis of the findings of the decomposition of bis(benzoylimino)urea, an ionic mechanism seems to be a better mechanism for the decomposition of dibenzoyldiimide, at least in ethanol near room temperature. The following reaction scheme seems to explain the reaction products:

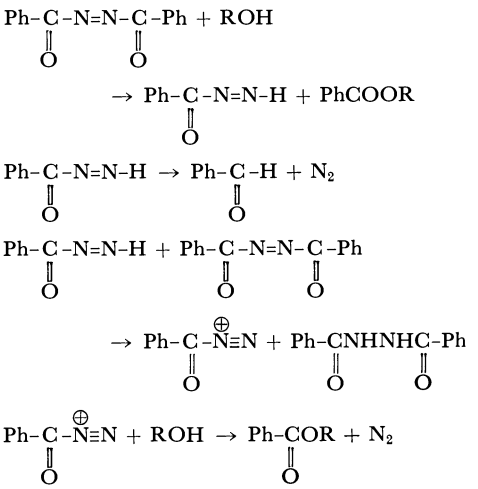

Grateful acknowledgment is made to the donors of The Petroleum Research Fund, administered by the American Chemical Society, for their support of this research.

9) G. Ponzio and G. Charrier, *Gazz. Chem. Ital.*, **39**, I, 598 (1909); S. G. Cohen and J. Nicholson, *J. Org. Chem.*, **30**, 1162 (1965).
10) E. Bamberger, *Ber.*, **44**, 3745 (1911).
11) J. E. Leffler and W. B. Bond, *J. Am. Chem. Soc.*, **78**, 336 (1956).

BULLETIN OF THE CHEMICAL SOCIETY OF JAPAN VOL. 39 2517—2520 (1966)

The Reaction of Halogenated Biacetyl Monoximes with Esters of Amino Acids

By Masatoshi SUGIYAMA, Mitsuo MASAKI and Masaki OHTA

Laboratory of Organic Chemistry, Tokyo Institute of Technology, Ookayama, Tokyo

(Received April 7, 1966)

1-Chloro-2-oximino-3-butanone (I) was prepared by the nitrosation of chloroethyl methyl ketone with an alkyl nitrite. I was treated with the L-leucine ethyl ester (II) to give 2-(2-oximino-3-oxobutylamino)-4-methylvalerate (III) and 2-[*N*, *N*-bis(2-oximino-3-oxobutyl)amino]-4-methylvalerate (IV). In a similar manner, 1-bromo-3-oximino-2-butanone (V) was treated with II to give 2-(3-oximino-2-oxobutylamino)-4-methylvalerate (VI). The reaction of the carbonyl group of III and VI with hydroxylamine and hydrazine was also studied. The treatment of VI with ammonia gave 6-(2-oximinoethyl)-3-isobutyl-2-hydroxypyrazine. Reactions of I and V with other esters of amino acids were also carried out.

It has been shown in our laboratory[1] that the reaction of α-haloximes with amino acid derivatives gives *N*-(2-oximinoalkyl)amino acid derivatives in good yields and that it is useful for synthesizing 2-hydroxypyrazines. In the present research this reaction was further studied by using monohalogenated biacetyl monoximes, in which a reactive carbonyl group is present besides a halogen atom.

Recently, Ogloblin has prepared 1-chloro-2-oximino-3-butanone (I) by treating methyl vinyl ketone with nitrosyl chloride and showed that the reaction of I with hydroxylamine hydrochloride or phenylhydrazine yielded the corresponding carbonyl derivatives, while I reacted with diethylamine to give 1-diethylamino-2, 3-butanedione-2-oxime.[2] However, it has not yet been clarified in the reaction of I with primary amines whether the carbonyl group is condensed or the chlorine atom is displaced.

1-Chloro-2-oximino-3-butanone (I) was prepared by a more convenient method than Ogloblin's: the chloroethyl methyl ketone obtained from acetyl chloride and ethylene[3] was treated with an alkyl nitrite to give I in a good yield.

When I was treated with two mole equivalents of the L-leucine ethyl ester (IIa) in an ethereal solution, one mole equivalent of hydrochloride of IIa separated immediately, and ethyl 2-(2-oximino-3-oxobutylamino)-4-methylvalerate (IIIa) was obtained in a 44% yield, while there was also a 38% yield of ethyl 2-[*N*, *N*-bis(2-oximino-3-oxobutyl)amino]-4-methylvalerate (IVa). Both products were characterized by hydrolysis with 2 N sodium hydroxide to the corresponding acids (VIIa and VIIIa). The infrared spectrum of IIIa showed strong absorption bands at 1730 ($COOC_2H_5$) and 1685 cm^{-1} (C=O conjugated with C=N). The acid (VIIa) was treated with hydroxylamine in an alkaline solution to give 2-(2, 3-dioximinobutylamino)-4-methylvaleric acid (IXa). When I was treated with the DL-phenylalanine ethyl ester (IIb) in the same manner as in the case of IIa, ethyl 2-(2-oximino-3-oxobutylamino)-3-phenylpropionate (IIIb) was obtained.

From the above facts, it became clear that, in the reaction of I with esters of amino acids, condensation with the carbonyl group did not occur, but the chlorine atom was exclusively displaced. The reaction of 1-bromo-3-oximino-2-butanone (V)[4] with the ester of amino acids was then attempted, though the reactions of α-halo ketones with primary amines have been known to be generally very complex.[5] There has been no report about the reaction of V except with thioformamide or thiobenzamide.[6]

When V was treated with piperidine in an ethereal solution, 1-piperidino-3-oximino-2-butanone was obtained in a good yield. The treatment of V with the L-leucine ethyl ester (IIa) in an ethereal solution gave the expected ethyl 2-(3-oximino-2-oxobutylamino)-4-methylvalerate (VIa) in a 46% yield. In the same manner, V reacted with other esters of amino acids to yield *N*-(3-oximino-2-oxobutyl)amino acid esters (VI) (Fig. 1). VI was characterized by a study of its infrared spectrum, in which strong absorption bands at 1720

1) M. Masaki and M. Ohta, This Bulletin, **36**, 922, 1177 (1963).
2) K. A. Ogloblin and A. A. Potekhin, *Zh. Obshch. Khim.*, **34**, 2688 (1964); *Chem. Abstr.*, **61**, 14519 (1964).
3) F. Sondheimer and R. B. Woodward, *J. Am. Chem. Soc.*, **75**, 5438 (1953).
4) M. P. Doerner, U. S. Pat. 2821555 (1958); *Chem. Abstr.*, **52**, 9198 (1958).
5) C. L. Stevens, P. Blumbergs and M. Munk, *J. Org. Chem.*, **28**, 331 (1963).
6) H. Erlenmeyer and H. Ueberwasser, *Helv. Chim. Acta*, **23**, 197 (1940); A. Silberg and A. Benkeo, *Chem. Ber.*, **97**, 1915 (1964).

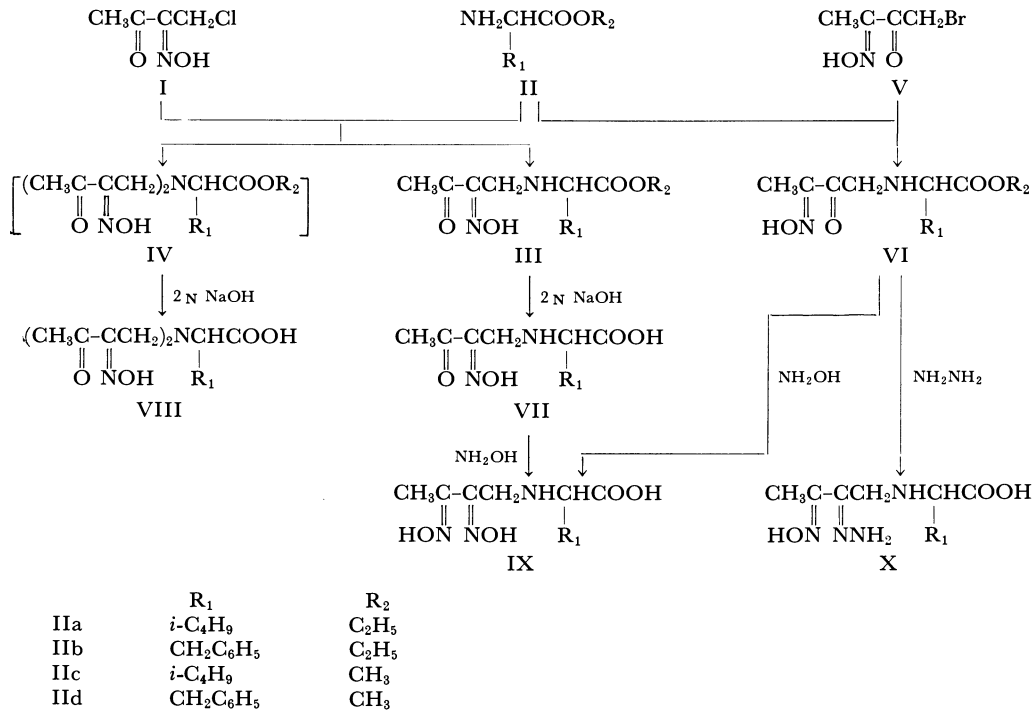

	R_1	R_2
IIa	i-C_4H_9	C_2H_5
IIb	$CH_2C_6H_5$	C_2H_5
IIc	i-C_4H_9	CH_3
IId	$CH_2C_6H_5$	CH_3

Fig. 1.

$(COOR_2)$ and 1685 cm^{-1} (C=O) appeared, as well as by the reactions described below. VIa was converted to IXa by treatment with hydroxylamine, followed by the hydrolysis of the oily product in an aqueous alkali; VId gave 2-(2-hydrazono-3-oximinobutylamino)-3-phenylpropionic acid (Xd) when treated with hydrazine hydrate and then subjected to hydrolysis.

When VIa was treated with ammonia in methanol, 6-(2-oximinoethyl)-3-isobutyl-2-hydroxypyrazine was obtained in a poor yield.

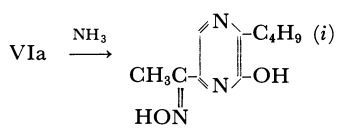

Experimental

1-Chloro-2-oximino-3-butanone (I). — 4-Chloro-2-butanone was prepared from acetyl chloride and ethylene according to Sondheimer's method.[3] Into a solution of 4-chloro-2-butanone (64 g.) in absolute ether (300 ml.), hydrogen chloride was introduced at the rate of 3—5 bubbles a second. The gaseous ethyl nitrite (1.5 mole equivalent) [prepared from sodium nitrite (55.2 g.), ethanol (36.8 g.), and sulfuric acid (39.2 g.)] was introduced with vigorous stirring into the solution at 30—35°C during a six-hour period. After all the ethyl nitrite had passed in, the stirring and the addition of hydrogen chloride were continued for an additional thirty minutes. The ethereal solution was then treated with activated charcoal and concentrated under reduced pressure to give a brown crystalline product, which was washed with carbon tetrachloride to yield I (43 g., 53%). The product was sufficiently pure for further experiments. A part of the product was recrystallized twice from benzene into the form of colorless plates, m. p. 92—93°C (lit.[2] 89—90°C).

The Reaction of I with L-Leucine Ethyl Ester (IIa).—To a solution of the L-leucine ethyl ester (IIa, 7 g.) in absolute ether (30 ml.), I (3 g.) was added with ice-cooling. Hydrochloride of the ester (IIa) separated immediately. The mixture was then allowed to stand at room temperature overnight. The hydrochloride (4.3 g.) was filtered off and washed with ether. The combined ethereal solution was extracted with 130 ml. (50+50+30 ml.) of 1 N hydrochloric acid. The aqueous extract was neutralized with sodium carbonate until pH 3, thus separating a small quantity of an oil, which was removed by extracting with ether. The aqueous layer was further neutralized with sodium carbonate to pH 6 to give ethyl 2-(2-oximino-3-oxobutylamino)-4-methylvalerate (IIIa; 2.5 g.; 44%, calculated on I). Two recrystallizations from n-hexane gave colorless needles, m. p. 96.5—97.5°C.

Found: C, 55.98; H, 8.82; N, 11.00. Calcd. for $C_{12}H_{22}N_2O_4$: C, 55.79; H, 8.58; N, 10.85%.

The combined ethereal layer and extract were dried over anhydrous sodium sulfate and concentrated to give an oily product (1.9 g.), which was then dissolved in 2 N sodium hydroxide (20 ml.) and allowed to stand at room temperature overnight. After being diluted with water (40 ml.) and treated with activated charcoal, the solution was neutralized with 4 N acetic acid to give 2-[N, N-bis(2-oximino-3-oxobutyl)amino]-4-methylvaleric acid (VIIIa; 1.4 g.; 38%, calculated on I), which was then recrystallized twice from 50% aqueous

dimethylformamide into the form of colorless prisms, m. p. 171—172°C.

Found: C, 50.66; H, 6.97; N, 12.66. Calcd. for $C_{14}H_{23}N_3O_6$: C, 51.05; H, 7.04; N, 12.76%.

2-(2-Oximino-3-oxobutylamino)-4-methylvaleric Acid (VIIa).—In 2 N sodium hydroxide (10 ml.) IIIa (0.46 g.) was dissolved; the resultant solution was allowed to stand at room temperature overnight. The solution was treated with activated charcoal, and then neutralized with 4 N acetic acid to afford a product (0.35 g., 85%) which was then recrystallized from dimethylformamide into the form of colorless prisms, m. p. 230°C (decomp.).

Found: C, 52.43; H, 7.91. Calcd. for $C_{10}H_{18}N_2O_4$: C, 52.16; H, 7.88%.

Ethyl 2-(2-Oximino-3-oxobutylamino)-3-phenylpropionate (IIIb).—To a solution of the DL-phenylalanine ethyl ester (IIb, 12.6 g.) in absolute ether (150 ml.), I (4.2 g.) was added with ice-cooling; the mixture was then allowed to stand at room temperature overnight. After the precipitate (6.8 g.) had been removed from the mixture, the filtrate was allowed to stand in a refrigerator to separate crystals gradually. After three hours the crystals (3.1 g.) were collected, and the filtrate was washed with water and extracted with 1 N hydrochloric acid. The acidic extract was treated with activated charcoal and neutralized with sodium carbonate until pH 6 to give the product (1.9 g.). The total yield was 5 g. (55%). An analytical sample was obtained, by recrystallization from ethyl acetate, as colorless needles, m. p. 119—120°C.

Found: C, 61.87; H, 7.03; N, 9.69. Calcd. for $C_{15}H_{20}N_2O_4$: C, 61.63; H, 6.90; N, 9.58.%

2-(2, 3-Dioximinobutylamino)-4-methylvaleric Acid (IXa).—To a solution of VIIa (1.9 g.) in 1 N sodium hydroxide (30 ml.) hydroxylamine hydrochloride (0.8 g.) was added. After the resultant solution had been allowed to stand at room temperature for two days, it was treated with activated charcoal and acidified with 20% aqueous acetic acid to give IXa (1.9 g., 94%), which was then recrystallized from dimethyl formamide into the form of colorless prisms, m. p. 257—258°C.

Found: N, 17.04. Calcd. for $C_{10}H_{19}N_3O_4$: N, 17.13%.

1-Bromo-3-oximino-2-butanone (V).—This compound was prepared from bromobiacetyl and hydroxylamine according to Doerner's method.[4] Colorless plates; m. p. 85—86°C (lit.[4] 86—87°C).

1-Piperidino-3-oximino-2-butanone.—To a solution of piperidine (1.7 g.) in absolute ether (70 ml.) V (1.8 g.) was added, after which the mixture was allowed to stand at room temperature for three hours. The precipitate was then collected by filtration and washed with water in order to remove the hydrobromide of piperidine, thus obtaining a product (1.1 g.). The above ethereal filtrate was washed with water, dried over anhydrous sodium sulfate, and concentrated under reduced pressure to give a crystalline product (0.4 g.). The total yield was 1.5 g. (82%). Recrystallization from ethyl acetate gave colorless needles, m. p. 135°C (decomp.).

Found: N, 15.28. Calcd. for $C_9H_{16}N_2O_2$: N, 15.21%.

Ethyl 2-(3-Oximino-2-oxobutylamino)-4-methylvalerate (VIa).—The following experiment was typical of the procedures used for the reaction of V with amino acid esters (II).

To a solution of the L-leucine ethyl ester (IIa, 12.7 g., 0.08 mole) in absolute ether (150 ml.), V (7.2 g., 0.04 mole) was added, the mixture was then allowed to stand at room temperature overnight. The precipitate was collected by filtration and washed with water, and the collected crystals were treated with water, in order to remove the hydrobromide; this yielded the product (1.3 g.). After being washed with water and dried over anhydrous sodium sulfate, the combined ethereal filtrate and washing were concentrated under reduced pressure. The crystalline residue was dissolved in carbon tetrachloride in order to filter it, thus giving VIa (3.4 g.). The total yield was 4.7 g. (46%); an analytical sample was obtained, by recrystallization from carbon tetrachloride, as colorless needles, m. p. 124.5—125.5°C (decomp.).

Found: C, 55.85; H, 8.34; N, 11.07. Calcd. for $C_{12}H_{22}N_2O_4$: C, 55.79; H, 8.58; N, 10.85%.

Ethyl 2-(3-Oximino-2-oxobutylamino)-3-phenylpropionate (VIb).—This ester was obtained from V (3.9 g.) and the DL-phenylalanine ethyl ester (IIb, 8.4 g.) in a 51% yield. Recrystallization from ethanol gave colorless needles, m. p. 121—122°C (decomp.).

Found: C, 61.58; H, 6.96; N, 9.63. Calcd. for $C_{15}H_{20}N_2O_4$: C, 61.63; H, 6.90; N, 9.58%.

Methly 2-(3-Oximino-2-oxobutylamino)-4-methylvalerate (VIc). — This ester was obtained from V (14.4 g.) and the L-leucine methyl ester (IIc, 23 g.) in a 40% yield. Recrystallization from methanol gave colorless needles, m. p. 149°C (decomp.).

Found: C, 54.09; H, 8.40; N, 11.62. Calcd. for $C_{11}H_{20}N_2O_4$: C, 54.08; H, 8.25; N, 11.47%.

Methyl 2-(3-Oximino-2-oxobutylamino)-3-phenylpropionate (VId).—This ester was obtained from V (7.2 g.) and the DL-phenylalanine methyl ester (IId, 14.3 g.) in a 40% yield. Recrystallization from ethanol gave colorless needles, m. p. 138—139°C (decomp.).

Found: C, 60.61; H, 6.82; N, 9.90. Calcd. for $C_{14}H_{18}N_2O_4$: C, 60.42; H, 6.52; N, 10.07%.

The Reaction of VIc with Hydroxylamine.—To a solution of hydroxylamine [from hydroxylamine hydrochloride (0.43 g.) and sodium (0.15 g.) in methanol (20 ml.)], VIc (1.5 g.) was added; the suspension was warmed at 60—64°C for four hours and then allowed to stand at room temperature overnight. The resultant solution was evaporated under reduced pressure, and the residue was dissolved in ethyl acetate (10 ml.) and filtered. After the ethyl acetate had been removed under reduced pressure, the resultant brown oil was dissolved in 2 N sodium hydroxide (10 ml.) and allowed to stand at room temperature overnight. The alkaline solution was treated with activated charcoal and neutralized until pH 6 with 4 N acetic acid, thus obtaining crystals (0.55 g., 36%); these crystals were recrystallized from dimethylformamide into colorless prisms, m. p. 239.5°C (decomp.). The identity of this product with the IXa prepared from VIIa was confirmed by a mixed-melting-point determination and by a comparison of their infrared spectra.

2-(2-Hydrazono-3-oximinobutylamino)-3-phenylpropionic Acid (Xd).—To a suspension of VId (1 g.) in methanol (20 ml.) hydrazine hydrate (0.4 g.) was added, after which the suspension was refluxed for four hours. The resultant solution was concentrated

under reduced pressure, and the residual brown oil was dissolved in 2 N sodium hydroxide (10 ml.). After being allowed to stand at room temperature overnight, the solution was neutralized until pH 6 with 4 N acetic acid, thus giving yellowish crystals (0.4 g., 40%) which were recrystallized from dimethylformamide into the form of yellow prisms, m. p. 168—169°C (decomp.).

Found: N, 19.99. Calcd. for $C_{13}H_{18}N_4O_3$: N, 20.13%.

6-(2-Oximinoethyl)-3-isobutyl-2-hydroxypyrazine.—A suspension of VIa (4.8 g.) in methanol (100 ml.) was saturated with ammonia with ice-cooling and then allowed to stand at room temperature for two days. The resultant red solution was concentrated under reduced pressure to afford a red residue, which was dissolved in water (100 ml.) and extracted with ether. The ethereal extract was dried over anhydrous sodium sulfate, and then concentrated under reduced pressure to give a mixture of a yellow oil and crystals. The mixture was dissolved in ethyl acetate (2 ml.) for filtration, and the crystals (0.2 g., 5%) were recrystallized twice from ethyl acetate to give colorless needles, m. p. 200.5—201.5°C (decomp.).

λ_{max}^{EtOH} 245 mμ (ε=11100), 330 (10200), and 340 (10100, sh.).

Found: C, 57.63; H, 7.26; N, 20.29. Calcd. for $C_{10}H_{15}N_3O_2$: C, 57.40; H, 7.23; N, 20.08%.

BULLETIN OF THE CHEMICAL SOCIETY OF JAPAN VOL. 39 2520—2522 (1966)

Styrene Derivatives. IX. 2-Benzyl-2-phenyl-3-aminomethyl-trimethylene Oxides and Related Compounds[1]

By Akira TERADA

Department of Industrial Chemistry, Kyushu Institute of Technology, Tobata-ku, Kitakyushu

(Received April 14, 1966)

3-Chloromethyl-4-chloro-1, 2-diphenylbutan-2-ol was obtained by a Grignard reaction of 2-benzoyl-1, 3-dichloropropane using benzyl chloride, which was turned into 2-benzyl-2-phenyl-3-chloromethyl-trimethylene oxide by the alkali dehydrochlorination. Heating this oxide with an excess of piperidine at 170°C for 22 hr. gave 2-benzyl-2-phenyl-3-piperidinomethyl-trimethylene oxide and a small amount of 1, 2-diphenyl-3-piperidinomethyl-2, 4-butanediol. The same procedures with morpholine gave 2-benzyl-2-phenyl-3-morpholinomethyl-trimethylene oxide; with ethanolic dimethyl amine, however, afforded only 1, 2-diphenyl-3-dimethylamino-methyl-2, 4-butanediol.

During the synthetic studies of styrene derivatives which have been developed in our former laboratory,[2] 2-benzoyl-1, 3-dichloropropane (I) was previously prepared from acetophenone via the 5-benzoyl-1, 3-dioxane obtained by the acidic-aldol condensation of acetophenone with formaldehyde.[3] The present paper will deal with the syntheses of 2-benzyl-2-phenyl-3-aminomethyl-trimethylene oxides and the hydrated aminodiol compounds, using this 2-benzoyl-1, 3-dichloropropane as a synthetic intermediate. We expect to be able thus to determine the physiological activities of these amino compounds and the availabilities in the field of synthetic drugs, and also some information about the reaction course.

The reaction of I with a Grignard solution prepared from benzyl chloride easily gave 3-chloromethyl-4-chloro-1, 2-diphenylbutan-2-ol (II). The dehydrochlorination of II with an excess of ethanolic potassium hydroxide under reflux preferentially afforded III as the product. The compound III did not decolorize permanganate, and its infrared spectrum shows a strong band at 966 cm^{-1} assignable to trimethylene oxide[4] and has neither the characteristic peak of hydroxyl nor of the vinylidene group. Therefore, the structure of III must be 2-benzyl-2-phenyl-3-chloromethyl-trimethylene oxide.

It was found that the remaining chlorine atom in the compound III was too stable to react with either such an alkali as above or the amines used in this report under such mild conditions as below 100°C, but when it was heated at 160—170°C over 20 hr. it could be substituted with such amines to give the attempted amino compounds, besides 1, 2-diphenyl-3-aminomethyl-2, 4-butanediols. The VI amines were also confirmed to be trimethylene oxide compounds; their infrared spectra clearly indicate the characteristic band of the trimethylene oxide ring in the region near 980 cm^{-1}.

1) Styrene Derivatives, Paper VIII: A. Terada, *J. Chem. Soc. Japan, Pure Chem. Sect. (Nippon Kagaku Zasshi)*, **81**, 1465 (1960).

2) Government Industrial Research Institute, Osaka, Oyodo-ku, Osaka.

3) A. Terada, *J. Chem. Soc. Japan, Pure Chem. Sect. (Nippon Kagaku Zasshi)*, **81**, 612 (1960).

4) G. M. Barrow and S. Searles, *J. Am. Chem. Soc.*, **75**, 1175 (1953).

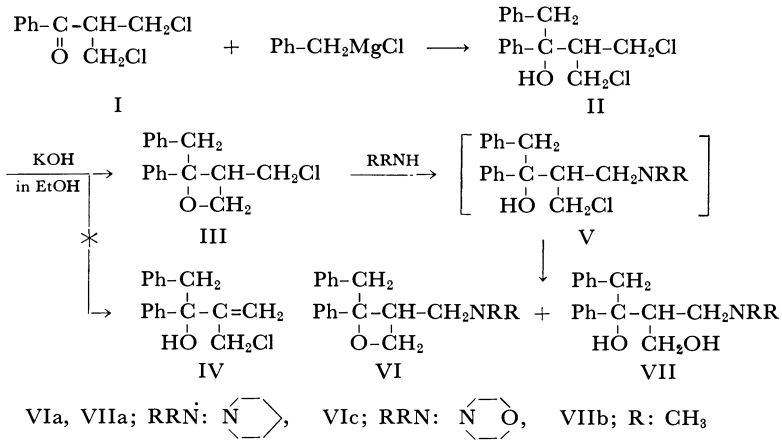

Fig. 1

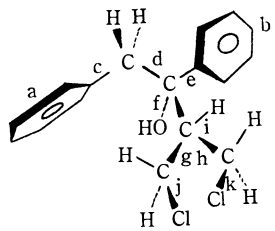

Fig. 2

The conformation of II may be sketched stereochemically as in Fig. 2 using a Stuart-type molecular model in which the ring a is nearly horizontal and the ring b almost vertical. The observation of the model also strongly suggests that the free rotations about the bonds of c, d, e, f, g and h are virtually impossible, and that in view of their preferred conformations, both the chlorine atoms may jut together to this side. The repulsion between two chlorine atoms should, therefore, be so large that it is obvious that one of the chlorines is excessively reactive. However, both the chlorine atoms can not be placed in the *trans* conformation to the *i*-hydrogen, because there are serious restrictions of free rotation about the bonds g and h as has been mentioned above. The chlorine atom will preferentially react with the hydroxyl group of the back side, and the system will proceed to a ring closure to give the trimethylene oxide (III) by an S_N2 reaction rather than to a formation of the vinylidene compound (IV) by a *trans* E2 reaction.

It is believed that the bimolecular substitution of the remaining chlorine atom in the compound III with amine will be hindered greatly by the crowded back and that, therefore, it will be less reactive. We, therefore, assume that the compound III reacts with such amines to form an intermediate V, aminated chlorohydrin, which is a normal addition product of trimethyleneoxide ring opening effected exclusively by steric reasons, and that it immediately turns into the principal product, VI, as is shown in Fig. 1. Support for this conclusion can be obtained by the following fact. Searles and Gregory have reported that, while trimethylene oxide reacts with amines less readily at moderate temperatures, when the temperature rises to 150°C it undergoes ring opening to give the corresponding aminopropanols in good yields.[5]

Experimental

3-Chloromethyl-4-chloro-1, 2-diphenylbutan-2-ol (II).—An ethereal solution of benzyl magnesium chloride was prepared in the usual manner with 50 ml. of anhydrous ether, 6.1 g. of magnesium foils, and 28.2 g. (0.22 mol.) of benzyl chloride in 50 ml. of anhydrous ether. A solution of 43.4 g. (0.2 mol.) of 2-benzoyl-1, 3-dichloropropane[3] in 85 ml. of anhydrous ether was added, drop by drop, into the Grignard reagent under vigorous stirring and ice cooling over a period of 25 min. The reaction mixture became cloudy in the early stages of the reaction, and then it became clear. After it had settled overnight at room temperature, the mixture was treated with ice water, made acidic with hydrochloric acid, and taken up in benzene. The benzene solution was washed with water, a saturated sodium bicarbonate solution, and water again, and then dried over anhydrous sodium sulfate. Upon the removal of the solvent under reduced pressure and cooling, 29.8 g. (48.2%) of crude crystals were yielded. Recrystallization from benzene-petroleum benzine gave an analytical sample of II melting at 76—77.5°C.

Found: C, 65.89; H, 6.03. Calcd. for $C_{17}H_{18}Cl_2O$: C, 66.03; H, 5.87%.

ν_{max}^{Nujol} 3704 (OH); 3035, 1603, 1504 (phenyl); 1344, 1151 (tertiary alcohol); 761, 746, 692 cm^{-1} (monosubstituted benzene).[6]

2-Benzyl-2-phenyl-3-chloromethyltrimethylene Oxide (III).—A sample of 15.2 g. (0.05 mol.) of II

5) S. Searles and V. P. Gregory, *J. Am. Chem. Soc.*, **76**, 2789 (1954).

6) The infrared spectra were taken on a Perkin-Elmer spectrophotometer, Model 21 (NaCl).

was refluxed with 2.8 g. (0.05 mol.) of potassium hydroxide in 10 ml. of ethanol. The reaction was exothermic, and potassium chloride crystals were precipitated immediately. After another hour's refluxing, the reaction mixture was poured into water and taken up in benzene. The benzene layer was washed with water until the washings were neutral, and then dried over anhydrous sodium sulfate. The remaining oil, upon the removal of the solvent, was induced to crystallize by trituration with petroleum benzine under cooling. The isolated crude crystals (5.33 g.; 39%) were recrystallized from petroleum benzine to give an analytical sample of III, white crystals, m. p. 83.5—84.5°C.

The use of a two-molar equivalent of potassium hydroxide against III gave a yield nearly twice as good.

Found: C, 74.71; H, 6.44; Cl, 12.92. Calcd. for $C_{17}H_{17}ClO$: C, 74.85; H, 6.28; Cl, 13.00%.

ν_{max}^{Nujol} 3021, 1600, 1495 (phenyl); 1155, 1145, 1029, 774, 750, 711, 702 (mono-substituted benzene); 966 cm^{-1} (trimethylene oxide).[4]

The Reaction of III with Piperidine.—A mixture of 2.20 g. (8.07 mmol.) of III and 5.50 g. of piperidine (b. p. 106°C) in a sealed tube was heated at 170°C for 22 hr. The contents were then evaporated under reduced pressure, and the remaining oil, after being alkalized with a dilute sodium hydroxide solution, was repeatedly extracted with benzene. The benzene solution was washed with water and dried over anhydrous sodium sulfate. After the removal of the solvent, the oily product was combined with 1.5 ml. of concentrated hydrochloric acid to give a white precipitate of the hydrochloride. Crystallization from water yielded 1.65 g. (55.8%) of crystals, m. p. 197—198°C. An analytical sample was obtained from another recrystallization, m. p. 200—201°C, 2-benzyl-2-phenyl-3-piperidinomethyl-trimethylene oxide hydrochloride · a half hydrate (VIa·HCl·1/2 H_2O).

Found: C, 72.01; H, 8.10; N, 4.13; H_2O, 3.10. Calcd. for $C_{22}H_{27}NO\cdot HCl\cdot 1/2H_2O$: C, 72.01; H, 7.97; N, 3.82; H_2O, 2.45%.

ν_{max}^{Nujol} 3635, 3289, 1621 (H_2O); 2710—2410 (tertiary amine hydrochloride); 979 (trimethylene oxide); 767, 754, 699, 695 cm^{-1} (mono-substituted benzene).

The anhydrous hydrochloride was obtained by drying it at 100°C under a vacuum until a constant weight was obtained, but the melting point remained unchanged. The infrared spectrum of the dried hydrochloride showed no absorption bands characteristic of the water of crystallization in the region of 3635, 3289 and 1621 cm^{-1}.

Free Amine (VIa).—This was obtained as usual, m. p. 49.5—50.5°C. It may be hydrated, because the following infrared spectral data show a weak absorption peak of the hydroxyl group. When the mother liquor, from which VIa·HCl had been effectively removed, was concentrated, a small amount of white crystals remained. Recrystallization from water gave an analytical sample of 1, 2-diphenyl-3-piperidinomethyl-2, 4-butanediol hydrochloride (VIIa·HCl), m. p. 219—220°C.

Found: C, 70.28; H, 8.20; N, 3.92. Calcd. for $C_{22}H_{29}NO_2\cdot HCl$: C, 70.29; H, 8.04; N, 3.73%.

ν_{max}^{Nujol} 3413, 3215 (OH); 2732—2410 (tertiary amine hydrochloride); 3030, 1605, 1502 (phenyl); 1136 (C–O, tertiary alcohol); 1064 (C–O, primary alcohol); 771, 755, 702, 698 cm^{-1} (mono-substituted benzene).

The Reaction of III with Dimethyl Amine in Ethanol.—A sample of 1.37 g. (5 mmol.) of III was dissolved in 7.0 g. of 33% ethanolic dimethyl amine and heated in a sealed tube at 170°C for 33 hr. After working-up as usual, the oily product was repeatedly extracted with dilute hydrochloric acid under heating. The combined extract was concentrated under diminished pressure, and the remaining crystals were washed with acetone to give 0.77 g. (45.9%) of 1, 2-diphenyl-3-dimethylaminomethyl-2, 4-butanediol hydrochloride (VIIb·HCl) as white crystals, m. p. 213—214°C.

Found: C, 66.74, 66.90; H, 7.98, 7.97; N, 4.14, 4.03. Calcd. for $C_{19}H_{25}NO_2\cdot HCl\cdot 1/3H_2O$: C, 66.74; H, 7.27; N, 4.10%.

ν_{max}^{Nujol} 3279 (OH); 3049, 1603, 1493 (phenyl); 2801 (N-CH_3); 1377 (methyl); 1060 (C–O, primary alcohol); 765, 744, 703, 699 cm^{-1} (mono-substituted benzene).

Free Amine (VIIb).—This was obtained as usual, m. p. 135—136°C (from benzene).

Found: C, 75.96; H, 8.38. Calcd. for $C_{19}H_{25}NO_2$: C, 76.22; H, 8.42%.

ν_{max}^{Nujol} 3378 (OH); 3012, 1600, 1493 (phenyl); 2793 (N-CH_3); 1376 (methyl); 1059 (C–O, primary alcohol); 768, 747, 699, 696 cm^{-1} (mono-substituted benzene).

The Reaction of III with Morpholine.—A mixture of 2.725 g. (10 mmol.) of III and 8.70 g. (100 mmol.) of morpholine (b. p. 128°C) was heated in a sealed glass tube at 170°C for 28 hr. After working-up as usual and the subsequent hydrochlorination of the product, crystallization from *n*-butanol gave 1.58 g. (47.2%) of 2-benzyl-2-phenyl-3-morpholinomethyl-trimethylene oxide hydrochloride (VIc·HCl), m. p. 197.5—202°C. Recrystallization from water raised the melting point to 203—204.5°C, white crystals.

Found: C, 69.94; H, 7.57; N, 3.99. Calcd. for $C_{21}H_{25}NO_2\cdot HCl$: C, 70.08; H, 7.03; N, 3.89%.

ν_{max}^{KBr} 3360, 2710, 2690, 2480 (tertiary amine hydrochloride); 1960, 1895, 1815, 1758, 780, 764, 748, 700 (mono-substituted benzene); 1600, 1580, 1490 (phenyl); 980 cm^{-1} (trimethylene oxide).

Free Amine (VIc).—This was obtained by the same procedure in a 48.2% yield, and also from the alkali treatment of the above hydrochloride, white needles (VIc·1/3H_2O), m. p. 67—68°C (from petroleum benzine).

Found: N, 4.37; H_2O, 1.87. Calcd. for $C_{21}H_{25}NO_2\cdot 1/3H_2O$: N, 4.25; H_2O, 1.82%.

ν_{max}^{KBr} 3470, 1631 (water of crystallization); 3080, 3040, 1610, 1500 (phenyl); 1958, 1885, 1818, 1760, 773, 756, 705 (mono-substituted benzene); 980 cm^{-1} (trimethylene oxide).

The anhydrous VIc was obtained as usual; it showed no absorption bands of the infrared spectrum characteristic of the water of crystallization at such regions as 3470 and 1631 in the above hydrated sample.

The author wishes to thank Professor Ichiro Hirao for his excellent support to this work and Mr. Takahisa Masuda for his experimental assistance.

BULLETIN OF THE CHEMICAL SOCIETY OF JAPAN VOL. 39 2523—2526 (1966)

The Analysis of Activators in Several Phosphors

By Yoshihide KOTERA, Tadao SEKINE and Masao TAKAHASHI

Government Chemical Industrial Research Institute, Tokyo, Shibuya-ku, Tokyo

(Received December 24, 1965)

The activators in the zinc sulfide phosphors were analyzed by colorimetry. The reagents were *p*-dimethylaminobenzylidene-rhodanine for the determination of silver in zinc sulfide and sodium dithiocarbamate, and zinc dibenzyldithiocarbamate for copper. The analytical procedures were discussed, and the range of the activator content to which these procedures are applicable was clarified. The methods were then used to determine the activator contents in the phosphors in the form of powder and single crystals; the results obtained make it clear that the activators are dissipated during the firing process in the preparation of phosphors and that copper is incorporated during the single-crystal preparation.

It is well known that the quantity of activators in the phosphors is one of the most important factors in determining their characteristics. The quantity of activators has been analyzed by several researchers, while, because of a variety of combinations between the host lattice materials and activators, it is necessary to extend the analytical method to all phosphors. We have reported on the application of polarography to the analysis of activators in calcium silicate phosphors,[1] and Rathje[2] has published a paper on the analysis of silver in zinc sulfide phosphors by flame-photometry.

The aim of the present research is to establish the methods of analyzing silver and copper in zinc sulfide phosphors. The method consists of the preparation of a sample solution and the determination of activators by colorimetry; the results obtained make it clear that the activators are dissipated during the firing process in the preparation of phosphor and that copper is incorporated during the single-crystal preparation.

The Analysis of Silver in the Zinc Sulfide Phosphors Activated by Silver by Colorimetry.—*a) Principle.*—It is well known that the colorimetric analysis of silver is carried out by using dithizone or rhodanine derivatives. The absorption curve of silver rhodanine has a peak at ca. 470 mμ, as is shown in Fig. 1; the figure was obtained by using an interference filter and a photocell. This absorption is affected by the presence of oxidizing agent, including chloride ions, therefore, the agents should be completely removed from the sample solution.

b) Experimental.—Reagents and Materials: All reagents were of the reagent grade. Zinc sulfide phosphors were prepared by the usual procedure in our laboratory. The amounts of silver added to zinc sulfide before firing ranged from 10^{-3} to 10^{-5} mole per mole of zinc sulfide. *p*-Dimethylaminobenzylidene-rhodanine was dissolved in methanol.

Apparatus: Tokyo Koden Co.'s Photoelectric Colorimeter 7A.

Sample Preparation: Weigh 0.5—1.0 g. of the sample of phosphor, add ca. 10 ml. of a concentrated hydrogen peroxide solution and heat in a evaporating dish with watch-glass cover until the mixture has completely dried. Repeat the evaporation after adding ca. 5 ml. of concentrated nitric acid, then dissolve the residue with ca. 1 ml. of concentrated nitric acid. After cooling, add water to make the whole volume to 100 ml. Take 10 ml. of this solution out with a pipette, add 0.2 ml. of a 0.05% rhodanine solution, and agitate carefully. After 10 min., measure the absorption at 470 mμ by means of an interference filter.

Standard Preparation: The standards used to obtain the analytical absorption curve were made by dissolving in 0.1 N nitric acid various amounts of silver nitrate crystals dried previously at 110°C. Standards in the range from 0.1 to 4 p. p. m. of silver in 0.1 N nitric acid were prepared and treated in the same manner as the samples.

Absorption Curve: The absorption curve was obtained for the solution which contains 1 p. p. m. of silver and 0.2 ml. of *p*-dimethylaminobenzylidene-rhodanine in 10 ml. by means of interference filter, and is shown in Fig. 1. From the figure it is convenient to use the interference filter at 470mμ.

Color Stability: The stability of the colored solution is shown in Fig. 2, which shows that the analysis is most accurately carried out when the solution is held constant for 5 min., after the addition of rhodanine and for not longer than 15 min. When the colored solution is held for one day, there is a colored precipitate.

The Effect of the Silver Concentration on the Absorbance: The absorbance of the colored solution was obtained

1) Y. Kotera, M. Yonemura and T. Sekine, This Bulletin, **28**, 132 (1955).
2) A. O. Rathje, *Anal. Chem.*, **27**, 1583 (1955).

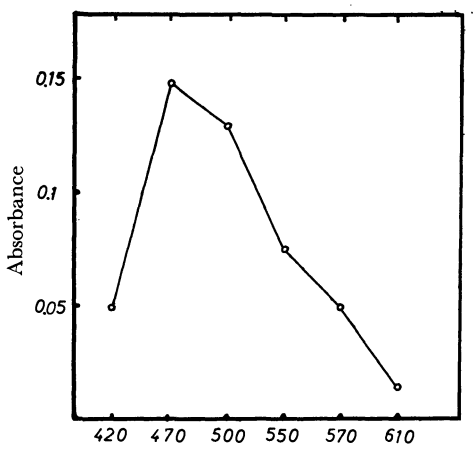

Fig. 1. Absorption curve of Ag-rhodanine.

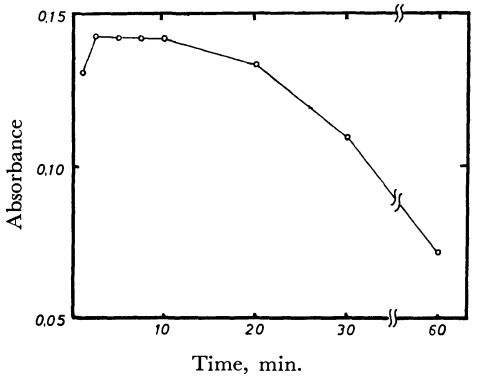

Fig. 2. Effects of standing time on the absorbance.

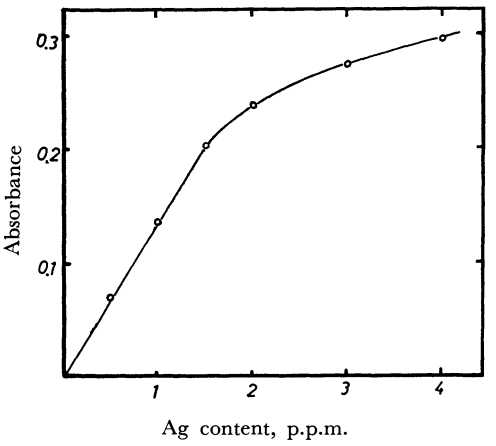

Fig. 3. Effects of silver concentrations on the absorbance.

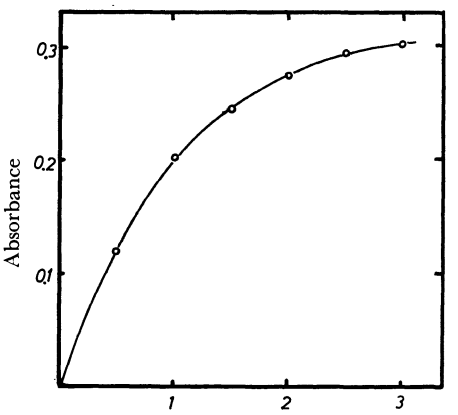

Fig. 4. Calibration curve.
Wavelength 470 mμ

in the 0.1 to 4 p.p.m. range of silver; it is shown in Fig. 3. From the figure it is possible to determine silver in the range from 0.1 to 1 p. p. m.

The Effect of the Presence of Zinc Sulfate on the Absorbance: When a sample of phosphor is treated as described above, the solution contains a certain amount of zinc sulfate prepared by the hydrogen peroxide oxidation of sulfide. It is, therefore, necessary to test the effect of zinc sulfate upon the absorbance. Various amounts of silver were added to the precipitated zinc sulfide; after they had been dried at 110°C, these samples were treated as had been the sample phosphors. The absorbance of the colored solution is shown in Fig. 4 as the function of the amount of silver. A comparison of Fig. 4 with Fig. 3 will show the effect of zinc sulfate; the colored solution was more stable in this case than without sulfate. The determination of the silver amount in sample phosphors was carried out by the use of the curve in Fig. 4.

c) Results and Discussion.—Zinc sulfide phosphors, which had been prepared by adding various amounts of silver before firing and by subsequent firing at 110°C for 2 hr., were analyzed; the results are shown in Table I. The same samples were washed after firing either by distilled water or by a potassium cyanide solution (5%), and the results for both samples were tabulated. As expected, a part of the silver dissipates during firing, while a part of the residual silver does not diffuse in the crystal lattice of zinc sulfide phosphors, but changes to silver sulfide, adhering on their crystal surface; the amount is estimated to be the difference in the results for the two washing agents. As for the analytical procedure, it was difficult to dissolve zinc sulfide phosphors without separating sulfur or its compound. This difficulty was overcome by the use of an oxidizing agent, for example, hydrogen peroxide, in our procedure; the residual oxidizing agent should be removed completely before the addition of rhodanine.

The Analysis of Copper in the Zinc Sulfide Phosphors Activated by Copper by Sodium Dithiocarbamate. — *a) Principle.* — The

TABLE I. ANALYTICAL RESULTS OF SILVER IN SILVER-ACTIVATED ZINC SULFIDE PHOSPHORS

Sample: Amount of silver added to zinc sulfide before firing (g. a./mol.)	Silver content determined, wt.%: treatment after firing: H_2O	KCN soln.
10^{-3}	0.058	0.030
6×10^{-4}	0.033	0.019
3×10^{-4}	0.014	0.016
10^{-4}	0.0051	0.0091
6×10^{-5}	0.0007	0.0017
3×10^{-5}	0.0019	—
10^{-5}	0	0

analysis of a trace of copper has been widely carried out colorimetrically. Dithiocarbamate compounds, dithizone, 1-10 phenanthroline derivatives, cuprizon, etc. are commonly used as the coloring agents. Dithiocarbamate compounds were selected for this research.

b) Experimental.—Reagents and Materials: $CuSO_4\cdot 5H_2O$ was used; it had been prepared in the Osaka Industrial Research Institute for analytical use. The other reagents were of the reagent grade. The zinc sulfide precipitated was given by the Dai Nippon Toryo Co., while the zinc sulfide phosphors and their single crystals were prepared in our laboratory.

Apparatus: This was the same as in the case of silver determination.

Sample Preparation: Weigh ca. 0.1 g. of a sample of phosphor, and then dissolve it in concentrated hydrochloric acid. Add to this solution 10 ml. of a 10% EDTA-2Na aq. solution, 2 drops of a 0.1% Crezol Red solution, and 5 ml. of a 1 N ammonium citrate solution; then add concentrated aqueous ammonia until the color of the indicator changes. Make the total volume to 50 ml. and transfer to a separating funnel. Add 5 ml. of a 0.1% sodium diethyldithiocarbamate solution and 10 ml. of chloroform, and agitate vigorously for ca. 2 min. Take out the colored layer of chloroform in a 25-ml. measuring flask, add 10 ml. of chloroform to the residual aqueous part, and agitate for 1 min. Take out the chloroform layer in the same measuring flask, and make the total volume to 25 ml. by adding ca. 5 ml. of chloroform. Transfer the solution into the colorimeter cell and measure the absorbance by means of a 420 mμ filter.

Standard Preparation: Dissolve the precipitated zinc sulfide in hydrochloric acid, add the standard solution of copper to this solution, treat it in the manner described above, and obtain the relationship between the amount of copper and the absorbance. The results obtained, shown in Fig. 5, indicate that the determination of copper between 0.5 and 1 p. p. m. is possible by this procedure.

c) Results and Discussion.—Single crystals of zinc sulfide prepared by the vapor-transport method were analyzed. The results, shown in Table II, show that copper is easily introduced during the single crystals preparation; work is now in progress in our laboratory attempting to reduce the copper content in the single crystals. Hydrogen chloride, bromine, and iodine are used in the vapor-transport method; they are tabulated in Table II. The difference in copper content among the three samples might be explained by the volatility difference in the materials used in the crystal preparation.

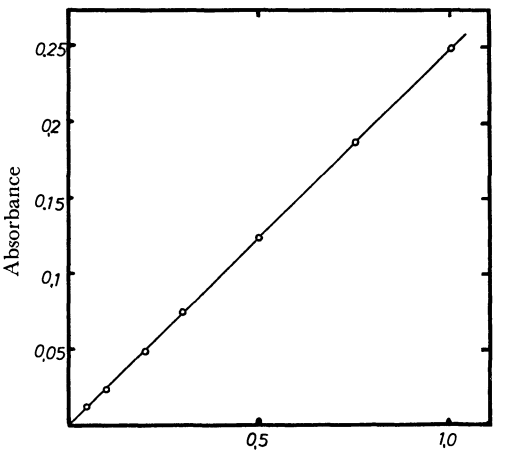

Fig. 5. Calibration curve (relation between the amount of copper and the absorbance).

TABLE II. ANALYTICAL RESULTS OF IMPURITY COPPER IN ZINC SULFIDE SINGLE CRYSTALS PREPARED BY THE VAPOR-TRANSPORT METHOD

Sample	Copper content determined wt.%
ZnS-HCl	0.017
ZnS-Br_2	0.007
ZnS-I_2	0.011

The Analysis of Copper by Zinc Dibenzyldithiocarbamate.—*a) Experimental.—Sample Preparation:* Weigh 0.5 to 1.0 g. of a sample of phosphor, and dissolve it in concentrated hydrochloric acid. After boiling this solution to remove the hydrogen sulfide, add concentrated hydrochloric acid or distilled water to make the whole volume to 100 ml. of a 1 N hydrochloric acid solution, and then transfer it into a separating funnel. Add to this exactly 10 ml. of a 0.01% zinc dibenzyldithiocarbamate solution in carbon tetrachloride, and agitate the mixture vigorously for ca. 1 min. Transfer the yellow-colored layer of carbon tetrachloride into the colorimeter cell, and measure the absorbance at 420 mμ.

The standard preparation and the other procedures are almost the same as in the case of sodium dithiocarbamate. The relation between the

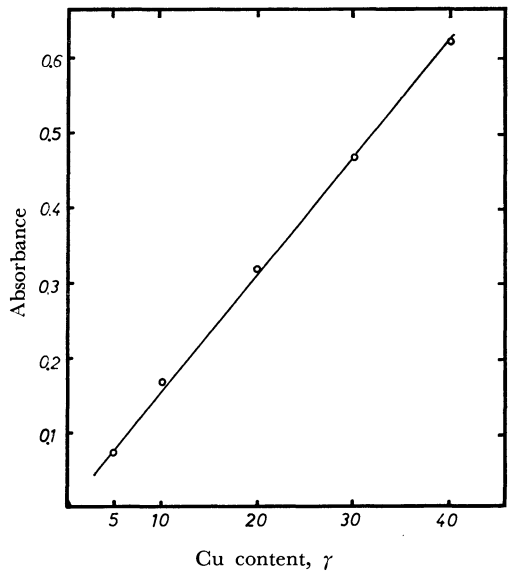

Fig. 6. Calibration curve (relation between the amount of copper and the absorbance).

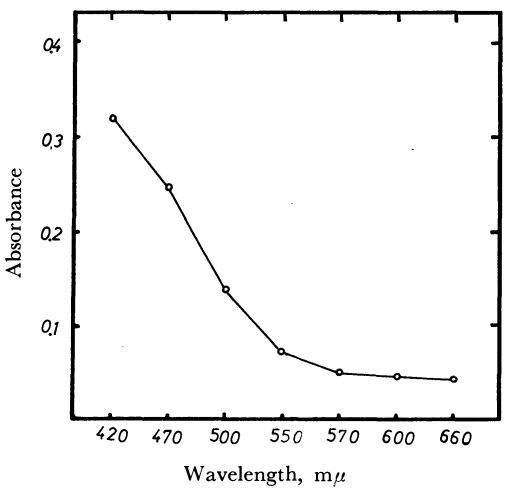

Fig. 7. Absorption curve of Cu-dithiocarbamate.

amount of copper and the absorbance, shown in Fig. 6, indicates the possibility of determining copper in the range from 5 to 40 p. p. m.

The absorption curve of the copper dithiocarbamate solution measured as a function of the wavelength is shown in Fig. 7, while the stability of the colored solution is shown in Fig. 8.

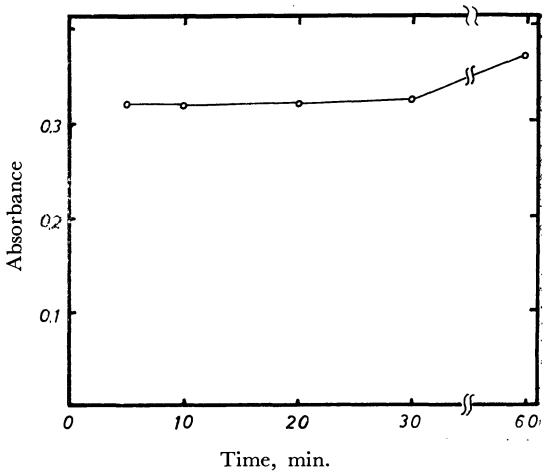

Fig. 8. Effects of standing time on the absorbance.

c) Results and Discussion.—Zinc sulfide phosphors activated by copper were prepared, and the copper content was determined by the procedure described above. The results obtained, shown in Table III, indicate that copper does not dissipate so much in the case of zinc sulfide phosphors, whose copper content is low, as does silver in zinc sulfide.

TABLE III. ANALYTICAL RESULTS OF COPPER IN COPPER ACTIVATED ZINC SULFIDE PHOSPHORS

Sample Amount of copper added to zinc sulfide before firing, g. a/mol.	Copper content determined, wt.%
10^{-4}	0.0067
10^{-5}	0.00077

It may be concluded that the analysis of copper in zinc sulfide phosphors is accurately carried out by the use of sodium diethylthiocarbamate for copper contents ranging from 0.5 to 1 p. p. m. and by the use of zinc dibenzyldithiocarbamate in the range from 5 to 40 p. p. m.

We thank Dai-Nippon-Toryo Co. for offering precipitated zinc sulfide.

BULLETIN OF THE CHEMICAL SOCIETY OF JAPAN VOL. 39 2527—2531 (1966)

The Catalytic Hydrogenation of Aniline in Fluidized Beds[1)]

By Etsuro ECHIGOYA, Hiroshi HAGIWARA* and Akio SAKURAI

Research Laboratory of Resources Utilization, Tokyo Institute of Technology, Ookayama, Meguro-ku, Tokyo

(Received January 11, 1966)

The hydrogenation of aniline in fluidized beds was studied. As a result of the experiments, the following conclusions were obtained: 1) The reaction rate of the catalytic hydrogenation of aniline in the temperature range between 150°C and 180°C was approximately first-order with respect to hydrogen. In the case of a large molar ratio of hydrogen to aniline, however, the reaction rate became zeroth-order with respect to aniline. 2) A good agreement was obtained between the conversion by the fluidized-bed experiment and the values calculated on the model of the contact-time distribution for low degrees of conversion. For high degrees of conversion, the deviation of the values calculated using this model from the experimental value was found to be about 10%. It was suggested that this model can well be applied to predicting the conversion for zeroth-order reaction within the limits of uncertainty given above.

Studies of the catalytic hydrogenation of aniline have previously been reported by the present authors. In this paper, the study of the hydrogenation of aniline in fluidized beds will be reported. The fluidization technique has been widely used in the chemical industry. The quantitative design of a fluidized bed reactor is, however, complicated by the gas by-passing the reaction zone via bubbles and channelling, with the result that the conversions obtained in fluidized beds are often lower than those in fixed bed at the same space velocity. Consequently, many modified reactor models have been proposed to represent the behavior of the gas flows in the fluidized bed. The experimental results of fluidized-bed runs will be analyzed in this paper in terms of the contact-time distribution model reported before.[2)]

Experimental

The Preparation of Catalysts.—*20% Cobalt-alumina.*—Powdered alumina was added to a solution of cobalt nitrate. The slurry was stirred for some time, and to it was then slowly added at 20°C a quantity of dissolved ammonium carbonate in a slight excess. The mixture was then heated and kept at 60—70°C for 5 hr. After being filtered and washed, the precipitate was dried at 100°C and calcined at 500°C for 2 hr. At this reaction temperature, the catalyst powder could be fluidized satisfactorily.[3)]

Rate Constant Measurements.—The reaction rate constant was measured by a flow-type fixed bed in a Pyrex reactor (1.8 cm. ID and 80 cm. long). The reactor was immersed in a fluidized thermal bath in order to maintain the desired reaction temperature. The temperature was controlled automatically within a range of 1.0—1.5°C. About 5—10 g. of a cobalt-alumina catalyst was placed on a porous glass disk, and a thin glass thermowell was inserted from the top of the reactor. The heat of the reaction for this process was about 40 kcal./mol. Then, under the experimental conditions, a temperature gradient in the longitudinal direction of the catalyst bed was obtained. The mean temperature was estimated from the temperature distribution curves. The activity of the catalyst became almost constant after 2 hr.; the variation in the catalyst activity with reaction time was almost negligible for 30 hr. No effects of the different particle size of the catalyst on the reaction rate was observed. After the steady state of the catalyst's activity was reached, the reaction rate was estimated by the integral method.

Fluidized-bed Equipment.—The equipment used for the fluidization experiments consisted of a glass tube 90 cm. long and 5 cm. ID. Its lower part had a porous glass plate and was connected to a conical section for preheating. The temperature of the reactor was controlled by an external electric furnace. The equipment was surrounded with heating wires and was insulated with asbestos. The temperatures within the bed were measured by chromel-alumel thermocouples in glass wells located at the axis and on the inside of the reactor wall. The temperature distribution of the bed was occasionally checked by moving the thermocouples vertically throughout the bed. The observed difference in temperature between top and bottom was not more than 1 to 1.5°C.

The Measurement of the Contact-time Distribution Functions.—A method described before[2)] was used in the investigation of the contact-time distribution function in the fluidized bed. Propane was used as the adsorbent, and argon, as an inert gas.

Gas Analysis.—Samples were analyzed by gas chromatography. Separations were made by a 3 m. coulmn of polyethyleneglycol 20000 on polytetrafluoroethylene, with hydrogen as the carrier gas. The temperature of the column was 180°C.

---

* Present address: Yoshitomi Pharmaceutical Ind. Ltd., Yoshitomi, Fukuoka.

1) E. Echigoya, H. Hagiwara and A. Sakurai; presented at the 31th Annual Meeting of Chemical Engineering in Japan, Tokyo, April, 1966.

2) M. Iwasaki, I. Furuoya, H. Sueyoshi, T. Shirasaki and E. Echigoya, *Chem. Eng. (Kagaku Kogaku)*, **29**, 892 (1965).

3) E. Echigoya, H. Hagiwara and A. Sakurai, This Bulletin, in press.

Catalyst.—The cobalt catalyst used in the kinetic studies in both fixed and fluidized beds was the 150—200 Tyler mesh fraction of the catalyst. The bulk density of the catalyst containing 20 wt.% cobalt was 0.998—1.02 g./cc.; it was reduced for 2 hr. at 450°C.

Velocity at the Minimum Fluidization.—The minimum fluidization velocity, (U_{mf}) [cm./sec.] was taken as the value at which the pressure drop across the reactor vs. hydrogen flow curve showed a discontinuity. In cases where no sharp discontinuity occurred, the intersection of the two parts of the curve was selected as the value defining U_{mf}. The average value of U_{mf} over the experimental range used 160 to 200°C was 2 cm./sec.

Experimental Results and Discussion

Kinetic Data.—The rate equation for a catalytic reaction in a flow system may be written as:

$$W/F = y_0 \int_0^x dx/r \qquad (1)$$

where W: the catalyst weight [g.]
F: the total molar feed of the reaction mixture [mol./hr.]
y_0: the mole fraction of aniline in the reaction mixture
x: the conversion
r: the reaction rate [mol./g. cat. hr.]

The hydrogenation of aniline followed approximately a first order reaction kinetics with respect to hydrogen in the 150°C—180°C temperature range, for which the equation is:

$$r = k_c C_{H_2} = k\,(m-3x)/(1+m-3x) \qquad (2)$$

where k_c: the specific reaction rate
C_{H_2}: the concentration of hydrogen
k: $=k_c(\pi/RT)$ [mol./g. cat. hr.], π: the total pressure [atm.]
m: the molar ratio of hydrogen to aniline
R: the gas constant
T: the reaction temperature [°K]
x: the conversion

When Eq. 2 is substituted into Eq. 1 and integrated by assuming an idealized piston flow, the following equation is obtained:

$$1/k(m+1)\int_0^x (1+m-3x)dx/(m-3x) = W/F$$

$$f(m,\ x) = (1/m+1)x + \{1/(3(m+1))\}\ln[1/\{1-(3/m)x\}] = k(W/F) \qquad (3)$$

The value of the rate equation found was as follows (Fig. 2):

Temp., °C		
160	1.35×10^{-3}	(mol./g. hr.)
170	1.9×10^{-3}	
180	2.4×10^{-3}	
190	2.75×10^{-3}	

The temperature dependence of the rate constants was evaluated from the Arrehenius plot over the temperature range from 150 to 180°C. An overall activation energy (E) of 12 kcal./mol. was calculated from the slope of the plot, log k vs. $1/T$. The kinetic data could be written also in the following simple form in the case of a large value of m.[4]

$$k(W/F) = f(m,\ x) = Mx \qquad (M = 1/m) \qquad (4)$$

The above equation shows that the reaction rate is zero order with respect to aniline.

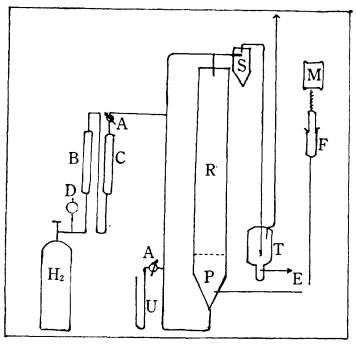

Fig. 1. Arrangement of experimental equipment.

A	flow control valve	M	feed motor
B	oxygen eliminator	P	preheater
C	flow meter	R	reactor unit
D	pressure gauge	S	cyclone
E	analysis unit	U	mercury manometer
F	aniline feed syringe	T	trap

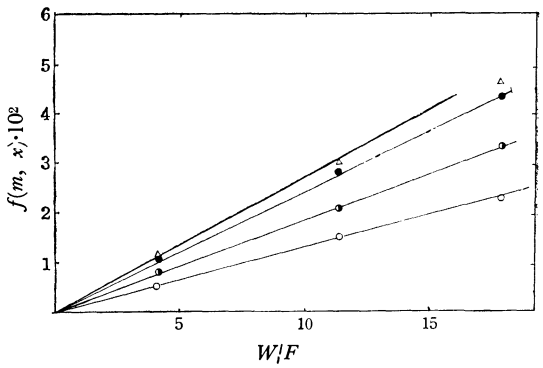

Fig. 2. Kinetics of hydrogenation of aniline with a fixed bed.
○ 160°C, ◑ 170°C, ● 180°C

Fluidized-bed Runs.—Fluidized-bed runs were made in a 2-inch-ID reactor over the temperature range between 150°C and 230°C. The results of a fluidized-bed run are shown in Table I, while a typical run is demonstrated in Fig. 3. The conversion data for the fluidized-bed were plotted as a function of the dimensionless number $k/(W/F)$. The dashed line represents the conversion in a fixed bed. All the data fall below the dashed line. An apparent rate constant, k', may be estimated from Eq. 5 for fluidized beds, but it depends on the catalyst activity, the gas-solid contact behavior,

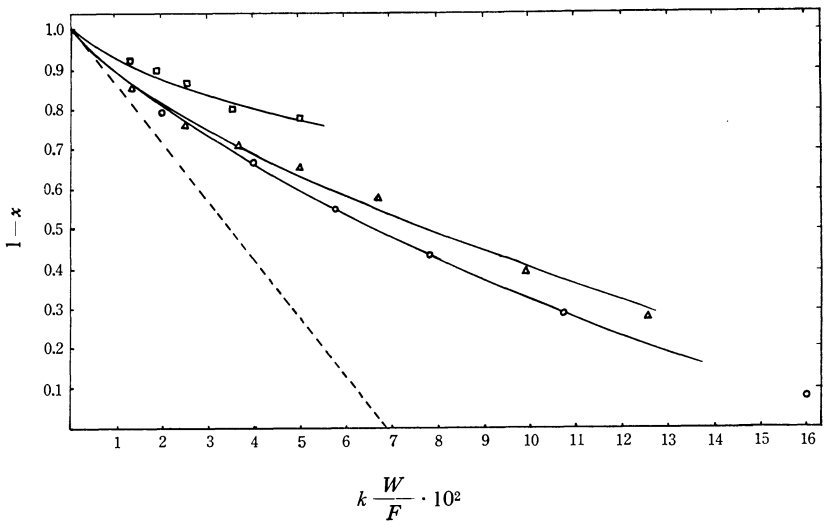

Fig. 3. The experimental data for fluidized bed (Reac. temp. 180°C).
U: ○ 3.34, △ 5.34, □ 10.69 cm./sec.

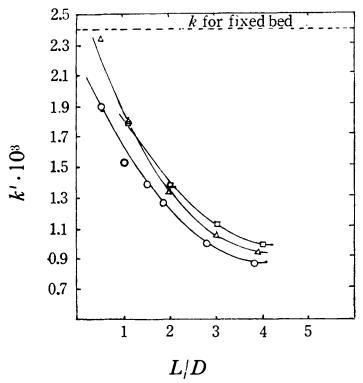

Fig. 4. Apparent rate constant as a function of L/D ratio and gas velocity for a fluidized bed.
k': rate constant (fluidized bed)
k: rate constant (fixed bed)
U: ○ 3.34, △ 5.34, □ 10.69 cm./sec.

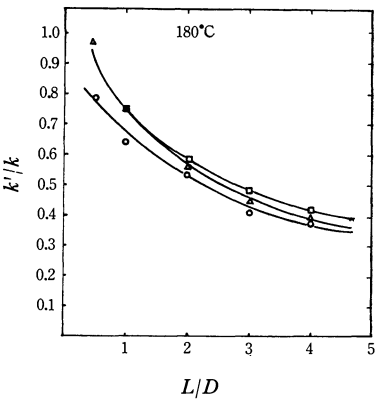

Fig. 4′ k'/k as a function of L/D ratio and gas velocity for the fluidized bed.
k': rate constant (fluidized bed)
k: rate constant (fixed bed)
U: ○ 3.34, △ 5.34, □ 10.69 cm./sec.

and the temperature.

$$k' = (F/W)Mx \tag{5}$$

When the catalyst activity and the temperature are held constant, k'/k is a measure of the efficiency of the fluidized bed as a device for the gas-solid contact. The fixed bed value is also shown in Fig. 4 for the sake of comparison. The value of k' appears to decrease rapidly with an increase in the bed height and to decrease slightly with a decrease in the gas velocity. At a lower temperature (for example, 160°C), the effects of these parameters on k' were not very large.

The Application of the Contact-time Distribution Model.—Fluidized beds have been characterized by the distribution of residence time. The use of a residence-time distribution $E(\varphi)$ is, however, restricted to homogeneous reactions of the first-order. It seems desirable, therefore, to define a contact-time or reaction-time W/F in connection with heterogeneous reactions. For the zeroth-order reaction, the mean fraction of reactant remaining at the exit of the bed is given below in terms of the contact time:[4]

$$1-x = \int_0^{\theta_{11m}} (1-K\theta)C(\theta)\mathrm{d}\theta \tag{6}$$

where $K=(k/M)(W/F)$, $\theta_{11m}=(W/F)_{11m}/(W/F)$; W/F: the mean contact time [hr. g./mol.]; $(W/F)_{11m}$: the contact time when x attains to

4) E. Echigoya, K. Toyoda and K. Morikawa, presented at the 30th Annual Meeting of Chemical Engineering in Japan, Osaka, April, 1965.

TABLE I. EXPERIMENTAL RESULTS IN THE FLUIDIZED BED

	W/F [g. hr./mol.]	U cm./sec.	Conversion % Reaction temp. 160°C	170°C	180°C	190°C	200°C	210°C	220
49 g.	8.3	3.34	15.5	20.0	23.6	24.5	23.0	22.5	18
	5.2	5.34	8.7	12.4	17.9	17.5	15.6	16.2	15
	2.6	10.69	5.1	5.7	7.8	8.2	8.2	8.0	
98 g.	16.6	3.34	27.5	34.0	37.5	38.4	374	33.0	27
	10.4	5.34	17.8	23.6	23.1	23.0	26.5	23.2	20
	5.1	10.69	8.9	12.4	14.6	15.0	13.8	11.7	7
145 g.	24.6	3.34	34.8	45.1	51.7	51.0	48	40.5	32
	15.4	5.34	23.1	30.4	34.7	35.7	35.0	31.4	25
	7.6	10.69	11.4	15.2	17.7	18.4	17.5	13.0	7
194 g.	32.9	3.34	40.0	54.5	63	62.5	57	47.7	36
	20.6	5.34	27.2	36.0	42	42.1	40.3	37.1	34
	10.1	10.69	13.6	17.0	21.5	22.4	20.4	17.2	11
266 g.	45.2	3.34	42.5	57.4	68	66.5	61.0	52.2	38
	28.3	5.34	32.3	40.8	46.5	46.0	42.5	39.5	35
	13.9	10.69	16.5	21.1	24.6	25.5	24.0	21.6	17
395 g.	67.1	3.34	67	82.3	90	85.1	75.0	66.4	49
	42.0	5.34	44	53.8	60.0	57.5	50.4	43.1	34
	20.6	10.69	22.6	27.4	31	30.6	28.2	24.6	19
496 g.	53.0	5.34	54.0	65.2	71	67.3		51.5	

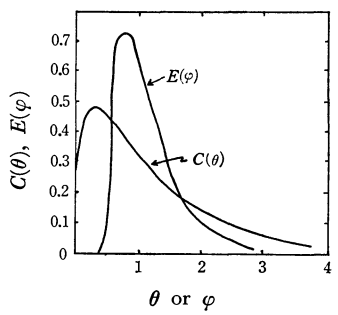

$L/D=3$, $U=3.5$ cm./sec.

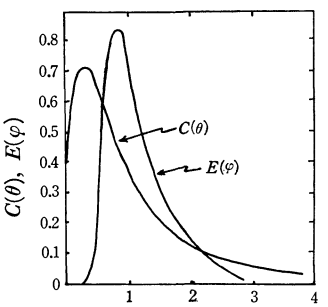

$L/T=5$, $U=5.5$ cm./sec.

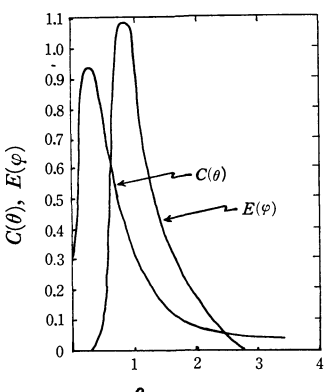

$L/D=3$, $U=10.5$ cm./sec.

Fig. 5. Contact time distribution $C(\theta)$ and sidence time distribution $E(\varphi)$.

1 [hr. g./mol.] $C(\theta)$: contact time distribution function (see lit. 2) [mol./hr. g.]. This equation was normalized with respect to W/F, the average contact time. $C(\theta)$ could be estimated by the input (pulse) response technique. Some examples of the curves of $C(\theta)$ are shown in Fig. 5. The distribution of residence time for an inert gas (obtained by an input-response technique) is superimposed on the contact-time distribution plots in Fig. 5. The conversion curve calculated by Eq. 6 is compared with the experimental values in Fig. 6. From the comparison, a good agreement between the calculated conversion on the model and the experimentally-determined conversion was obtained for low degrees of conversion. However, for high degrees of conversion, the calculated value was a little low compared with that of the experimental conversion. From these data, it may be concluded that the $C(\theta)$ curve can give enough information for predicting the conversion in the zeroth-order reaction.

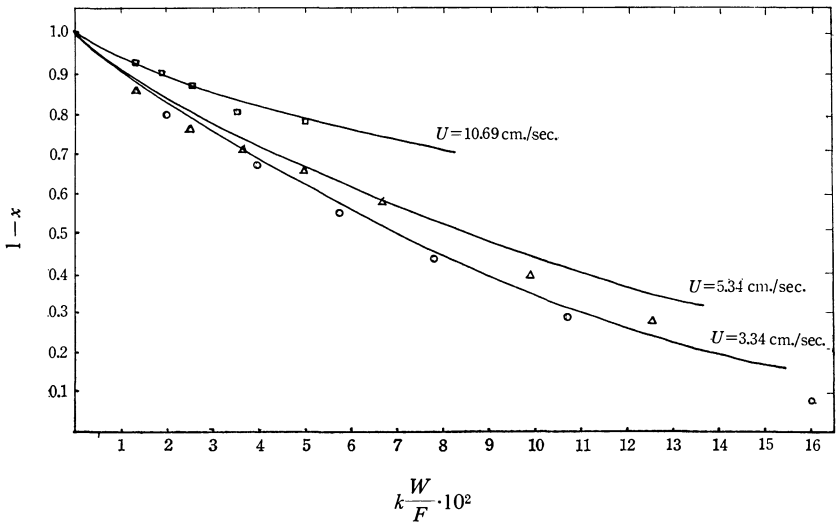

Fig. 6. The calculated values from the contact time distribution (180°C) model (full lines).
○, △, □……experimental points

Summary

1) The catalytic hydrogenation of aniline to cyclohexylamine over a cobalt alumina catalyst was carried out in the fluidized bed under the following conditions; the temperature range: 160—220°C, W/F: [g. hr./mol.] 2.6—67.

2) The reaction rate was found to be of the zeroth-order with respect to aniline in the case of a large molar ratio of hydrogen to aniline, using the fixed bed.

3) It was found that the contact-time distribution model could be usefully applied to predicting the conversion for the zeroth-order reaction in the fluidized bed within limits of 10%.

The authors wish to thank Professor Kiyoshi Morikawa for his useful discussion and constant guidance.

NOTES

A Chemical Examination of *Euphorbia hirta Linn.*

By D. R. GUPTA and S. K. GARG

Department of Chemistry, University of Roorkee, Roorkee, India

(Received September 1, 1965)

Euphorbia hirta Linn. (Fam: Euphorbiaceae; Hindi, Dudhi) is a small herb which grows throughout the hotter parts of India. This plant has been medicinally used in the teratment of bowel complaints, coughs, dysentery, colic pains, bronchial affections, and asthma.[1] Some varieties of *Euphorbia hirta,* viz., procumbens, pedilantus calcaratus and pedilantus tehuacanus, have been chemically examined by earlier workers.[2] We have now undertaken a systematic chemical examination of *Euphorbia hirta Linn.,* which has not yet been worked up. In a previous communication,[3] the free organic acids of the stems and leaves of this plant were reported. The present work will concern the chemical examination of the petroleum ether and ethanol extracts of the stems and the ethanol extract of the flowers of *Euphorbia hitra Linn.*

Experimental

Air-dried, powdered stems (2 kg.) were successively soxhletted with petroleum ether (b. p. 60—80°C) and ethanol for 30 hr.

The Examination of the Petroleum Ether Extract of the Stems.—The petroleum ether extract was concentrated and left in a refrigerator overnight; the white solid (7.2 g.) which thereupon separated, was filtered and dissolved in petroleum ether, and then chromatographed over Brockmann alumina (64×4 cm.) using petroleum ether, benzene, chloroform and their mixtures as eluants, as is shown in Table I. Eluants were collected in fractions of 30—40 ml. each and evaporated to dryness.

Fractions 1—14 gave a waxy material which, on repeated crystallisation from ethanol, afforded silky needles (1.2 g.), m. p. 84°C.

Found: C, 82.14; H, 14.12. Calcd. for $C_{30}H_{62}O$: C, 82.19; H, 14.15%.

The compound was soluble in benzene, chloroform, ethyl ether and petroleum ether, but was insoluble in water. It was identified as myricyl alcohol by a mixed m. p. determination with an authentic sample and by the preparation of its acetyl derivative,[4] m. p. 71.5°C, and a chloro derivative,[4] m. p. 64°C.

Found: Cl, 7.50. Calcd. for $C_{31}H_{63}Cl$: Cl, 7.54%.

TABLE I

Fraction No.	Eluant	Residue left on the evaporation of the solvents
1—14	Petroleum ether (b. p. 60—80°C)	Waxy material
15—24	Petroleum ether+Benzene (5: 1 v/v)	Colourless solid
25—32	Petroleum ether+Benzene (3: 2 v/v)	Colourless solid
33—40	Petroleum ether+Benzene (1: 1 v/v)	Nil
41—49	Benzene	Short needles
50—58	Benzene+Chloroform (3: 2 v/v)	Shining flakes
59—66	Benzene+Chloroform (1: 1 v/v)	Shining flakes
67—72	Chloroform	Nil

Fractions 15—32 gave a colourless solid which, when crystallised from a methanol-chloroform mixture, afforded needle-shaped crystals (1.1 g.), m. p. 281°C.

Found: C, 84.46; H, 11.71. Calcd. for $C_{30}H_{50}O$: C, 84.51; H, 11.74%.

This product gave colour reactions characteristic of triterpenes, including Noller's test. A sequence of colour (yellow→orange→red→purple) was developed when the compound was treated with thionyl chloride in the presence of tin. The compound was identified as taraxerol by a mixed m. p. determination and by the preparation of its acetate,[5] m. p. 304°C, and a benzoate,[5] m. p. 292°C.

Fractions 41—49, on crystallisation from benzene, gave colourless needles (2.4 g.), m. p. 260—261°C.

Found: C, 84.44; H, 11.82. Calcd. for $C_{30}H_{50}O$: C, 84.51; H, 11.74%.

The compound, which gave no colour reaction in Salkowski or Liebermann-Burchard reaction or with tetranitromethane reagent was identified as friedelin

1) R. N. Chopra, S. L. Nayar and I. C. Chopra, "Glossary of Indian Medicinal Plants," C. S. I. R., New Delhi, India (1956), p. 113.

2) H. Estrada, *Bol. Inst. Quim. Univ. Nacl. Auton. Mex.,* **11**, 15 (1959).

3) D. R. Gupta and S. K. Garg, *Indian J. Appl. Chem.,* **28**, 113 (1965).

4) M. C. Sheth and C. M. Desai, Science and Culture, **20**, 243 (1954).

5) S. Burrows and J. C. E. Simpson, *J. Chem. Soc.,* **1938**, 2042.

by a mixed m. p. determination and by preparing its derivatives, i. e., friedelinol,[6] m. p. 299°C; oxime acetate,[7] m. p. 239°C, and friedelin-2, 4-dinitrophenyl hydrazone,[7] m. p. 297—298°C.

Fractions 50—66 gave shining flakes which, on repeated crystallisation from a methanol - ethyl acetate mixture, yielded coloruless flakes (1.4 g.), m. p. 136—137°C.

Found: C, 84.15; H, 12.16. Calcd. for $C_{29}H_{50}O$: C, 84.05; H, 12.08%.

The compound was fairly soluble in benzene, methanol ethanol, and was readily soluble in chloroform, ethyl ether and ethyl acetate. The compound gave a positive Salkowskii-Hesse reaction and developed a green colour in the Liebermann-Burchard reaction. It formed an acetate,[8] m. p. 126°C; a benzoate,[8] m. p. 144°C, and a digitonide,[9] m. p. 230°C. The compound was identified as β-sitosterol by a mixed m. p. determination and by the formation of a mixed chromatogram of the compound with an authentic sample of β-sitosterol.

The Examination of the Ethanol Extract of the Stems.—The ethanol extract was concentrated under reduced pressure and then kept overnight in a refrigerator; it thereupon left a greenish, waxy material (4.1 g.), which was then dissolved in petroleum ether and then chromatographed over Brockmann alumina (32×2 cm.) using petroleum ether, benzene, chloroform and their mixtures as eluants, as is shown in Table II. Eluants were collected in fractions of 30—40 ml. each and evaporated to dryness.

Table II

Fraction No.	Eluant	Residue left on the evaporation of the solvents
1—10	Petroleum ether (b. p. 60—80°C)	Way material
11—17	Petroleum ether+Benzene (3: 2 v/v)	White solid
18—25	Petroleum ether+Benzene (1: 1 v/v)	White solid
26—30	Benzene	Nil
31—35	Benzene+Chloroform (3: 2 v/v)	Nil
36—40	Benzene+Chloroform (1: 1 v/v)	Nil
41—44	Chloroform	Nil

Fractions 1—10 gave a waxy material which, on repeated crystallisation from a mixture of methanol-acetone-benzene (1 : 1 : 1 v/v), gave a colourless solid (2.2 g.), m. p. 68°C.

Found: C, 85.44; H, 14.71. Calcd. for $C_{31}H_{64}$: C, 85.32; H, 14.67%.

Its infrared absorption spectrum did not indicate the presence of any functional groups. It did not absorb bromine and, on oxidation with air in the presence of potassium permanganate and boric acid at 200°C, gave an alcohol,[10] m. p. 58°C. The compound was identified as hentriacontane.[11]

Fractions 11—25 gave a white solid which, on crystallisation from a chloroform-methanol mixture, afforded colourless needles (1.3 g.), m. p. 199°C.

Found: C, 84.46; H, 11.78. Calcd. for $C_{30}H_{50}O$: C, 84.51; H, 11.74%.

The substance gave a positive Liebermann-Burchard reaction for a triterpene. It formed an acetate,[12] m. p. 237°C, which produced a yellow colouration with tetranitromethane; a benzoate,[12] m. p. 232°C, and a *p*-nitrobenzoate,[12] m. p. 258°C. The compound was identified as β-amyrin by a mixed m. p. determination with an authentic sample.

The Examination of the Flowers of *Euphorbia hirta Linn.*—Fresh flowers of *Euphorbia hirta Linn.* (2 kg.) were soxhletted with ethanol for 30 hr. Ethanol was distilled off from the extract under reduced pressure, and the sticky mass left was taken up in water (100 ml.). The aqueous solution was extracted with petroleum ether to remove the fatty material and chlorophyll, and then extracted with ethyl ether in a liquid-liquid extractor. The ether was removed, and the residue left was taken up in methanol and filtered. Distilling off the methanol afforded a yellow solid which, on crystallisation from pyridine, gave yellow needles (4.2 g), m. p. 360°C.

Found: C, 55.64; H, 2.02. Calcd. for $C_{14}H_6O_8$: C, 55.62; H, 1.98%.

The compound gave a green colour with ferric chloride, dissolved in aqueous sodium hydroxide with a bright yellow colour, and gave a positive Griessmeyer reaction. The compound was identified as ellagic acid by a mixed m. p. determination with an authentic sample and by the preparation of its tetraacetate,[13] m. p. 342—343°C, and an ellagorubin,[14] m. p. 218—219°C. It was further confirmed by paper chromatography,[15] using Whatman filter paper No. 1, and an aqueous solution of 60% formamide buffered at pH 3.5 with formic acid as the developer. The chromatogram was exposed to ammonia vapours in order to locate ellagic acid as yellow spot. The co-chromatography of the compound with an authentic sample of ellagic acid gave a single yellow spot with a R_f value of 0.58.

Summary

Petroleum ether and ethanol extracts of the stems of *Euphorbia hirta Linn.* were submitted to chromatography over Brockmann alumina using petroleum ether, benzene, chloroform and their mixtures as eluants, myricyl alcohol, taraxerol, friedelin, β-sitosterol, hentriacontane and β-amyrin were isolated, while the ethanol extract of the flowers

6) S. Rangaswami and K. Sambamurthy, *Proc. Indian Acad. Sci.*, **54A**, 99 (1961).
7) N. L. Drake and S. A. Shrader, *J. Am. Chem. Soc.*, **57**, 1854 (1935).
8) A. Chatterjee and S. K. Roy, *J. Indian Chem. Soc.*, **36**, 268 (1959).
9) A. Sinha, *Indian J. Appl. Chem.*, **23**, 40 (1960).
10) H. Nobori and A. Yoneshiro, *J. Soc. Chem. Ind. Japan*, **48**, 79 (1945).
11) I. M. Heilbron, R. F. Phipers and H. R. Wright, *J. Chem. Soc.*, **1934**, 1573.
12) L. C. King, C. D. Ball, B. Riegel, C. E. Schweitzer, P. G. Smith and E. W. Meyer, *J. Am. Chem. Soc.*, **65**, 1168 (1943).
13) R. C. Sharma, A. Zaman and A. R. Kidwai, *Indian J. Chem.*, **2**, 254 (1964).
14) L. Jurd, *J. Am. Chem. Soc.*, **79**, 6043 (1957).
15) A. Singh and V. N. Sharma, *Indian J. Chem.*, **2**, 253 (1964).

of *Euphorbia hirta Linn.* gave only ellagic acid. The above compounds were characterized by their physical and chemical properties and by the preparation of their derivatives.

It is interesting to observe that *Euphorbia hirta Linn.* contains myricyl alcohol, taraxerol and ellagic acid, besides friedelin, β-amyrin, hentriacontane and β-sitosterol already reported[2] in some varieties of *Euphorbia hirta.*

The authors are thankful to Dr. A. R. Kidwai, Aligarh, for supplying authentic samples of ellagic acid and taraxerol; to Dr. W. U. Malik, Professor of Chemistry, University of Roorkee, Roorkee, for providing laboratory facilities, and to C. S. I. R., New Delhi, for a Junior Research Fellowship to one of the authors (S. K. G.).

Ethylene Polymerization by Bisarenechrome π-Complex Compounds

By Yoshio TAZIMA and Sadao YUGUCHI

Central Research Lab. Toyo Rayon Co., Ltd., Otsu, Shiga

(Received November 9, 1965)

Ethylene polymerization by a binary catalyst system composed of bisarenechrome π-complex cations and an organoaluminum compound was investigated. The bisarenechrome π-complex compounds used were bisbiphenylchrome iodide, chromate, dichromate, thiocyanate, tetrathiocyano diammono chromate, etc. Instead of biphenyl, such other benzene derivatives as benzene, toluene, and mesitylene were also used as ligands.

As an organoaluminum compound, $Al(i\text{-}Bu)_3$ was the most suitable; the other organoaluminum compounds, such as $AlEt_3$ and $AlEt_2Cl$, showed less catalytic activity.

Figure 1 shows the relation of the polymerization temperature and the weights of the solid polymer formed during the initial 10 min. with the binary system of the bisbiphenylchrome compound (abbreviated as $(C_6H_5C_6H_5)_2CrX^-$) and 4 mmol. of $Al(i\text{-}Bu)_3$. As a solvent toluene was used, and the ethylene pressure was 40 kg./cm^2.

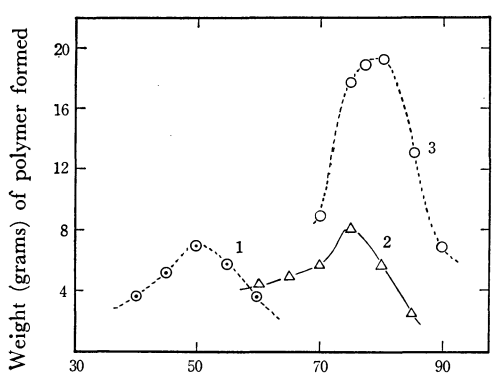

Fig. 1. 1 $(C_6H_5C_6H_5)_2Cr(NH_3)_2Cr(SCN)_4$ $\sim$ $Al(i\text{-}Bu)_3$
2 $[(C_6H_5C_6H_5)_2Cr]_2CrO_4$ $\sim$ $Al(i\text{-}Bu)_3$
3 $[(C_6H_5C_6H_5)_2Cr]_2Cr_2O_7$ $\sim$ $Al(i\text{-}Bu)_3$

Bisbiphenylchrome dichromate showed a maximum activity at 80°C; bisbiphenylchrome chromate, at 75°C, and bisbiphenylchrome tetrathiocyano diammono chromate, at 50°C. The order of the catalytic activity of bisbiphenylchrome compounds as a component of the binary system with $Al(i\text{-}Bu)_3$ is as follows:

$$[(C_6H_5C_6H_5)_2Cr]_2Cr_2O_7 > [(C_6H_5C_6H_5)_2Cr]_2CrO_4 > [(C_6H_5C_6H_5)_2Cr][(NH_3)_2Cr(SCN)_4] > (C_6H_5C_6H_5)_2CrI$$

The same tendencies were observed for other ligands, such as benzene, toluene and mesitylene.

The orders of catalytic activities of bisarenechrome π-complex compounds with the same anion species are as follows:

$$X^- : I^-$$
$$(C_6H_6)_2CrI > (C_6H_5CH_3)_2CrI > [C_6H_3(CH_3)_3]_2CrI > (C_6H_5C_6H_5)_2CrI$$

$$X^- : [(NH_3)_2Cr(SCN)_4]^-$$
$$(C_6H_5C_6H_5)_2Cr[NH_3)_2Cr(SCN)_4] > [C_6H_3(CH_3)_3]_2Cr[(NH_3)_2Cr(SCN)_4] > (C_6H_5CH_3)_2Cr[(NH_3)_2Cr(SCN)_4] > (C_6H_5)_2Cr[(NH_3)_2Cr(SCN)_4]$$

It should especially be noted that bisbiphenylchrome chromate or bisbiphenylchrome dichromate alone has the catalytic activity for ethylene polymerization without the presence of an organoaluminum compound. Table I shows the results obtained at different temperatures by using bisbiphenylchrome chromate or bisbiphenylchrome dichromate. Bisbiphenylchrome chromate showed increased activity above 75°C, and bisbiphenylchrome dichromate, above 80°C. The temperature (75°C or 85°C) accorded with the temperature of the maximum catalytic activity of each binary

system with $Al(i\text{-}Bu)_3$. Bisbiphenylchrome dichromate or bisbiphenylchrome chromate was inferrior to bisbenzene chrome dichromate or bisbenzenechrome chromate in catalytic activity.

Table I. Ethylene polymerization with $[(\phi_2)_2Cr]_2CrO_4$ or $[(\phi_2)_2Cr]_2Cr_2O_7$
Polymerization hour: 1 hr.

Catalyst		Temp. °C	Polymer formed, g.
$[(\phi_2)_2Cr]_2CrO_4$	0.05 g.	60	0.15
$[(\phi_2)_2Cr]_2CrO_4$	0.05 g.	75	0.45
$[(\phi_2)_2Cr]_2CrO_4$	0.05 g.	85	0.50
$[(\phi_2)_2Cr]_2CrO_4$	0.05 g.	100	0.50
$[(\phi_2)_2Cr]_2Cr_2O_7$	0.05 g.	60	0.13
$[(\phi_2)_2Cr]_2Cr_2O_7$	0.05 g.	75	0.45
$[(\phi_2)_2Cr]_2Cr_2O_7$	0.05 g.	85	0.75
$[(\phi_2)_2Cr]_2Cr_2O_7$	0.05 g.	100	0.70

Table II. Ethylene polymerization with oxidized product of bisbiphenylchrom

Polymerization temp., °C	Polymer formed, g.
75	0.55
100	0.75
150	0.60

Bisbiphenylchrome $(C_6H_5C_6H_5)_2Cr(O)$ (chrome is zero valency) showed catalytic activity for ethylene polymerization after it had been oxidized and activated by heating it above 75°C.

The results of some experiments obtained by the oxidized product of bisbiphenylchrome are shown in Table II. One procedure was as follows:

After the oxidation of $(C_6H_5C_6H_5)_2Cr$ (0.2 g.) dissolved in toluene (50 ml.) with oxygen (3 kg./cm^2) at 30°C for 1 hr. in an autoclave (100 ml.), oxygen was removed by stirring it at 75°C for 30 min. under a nitrogen atmosphere. Then ethylene was introduced up to a pressure of 40 kg./cm^2. Above 75°C, the oxidized product showed some catalytic activity, but the activity was lower than that of bisbenzene-chrome. Bisarenechromium compounds were prepared[1,2] by reducing chromium(III) chloride with benzene derivatives (benzene, toluene, mesitylene, and biphenyl) in the presence of aluminum and aluminum chloride in a sealed tube at 150°C, and by then decomposing the reduction products with methanol and water, followed by a treatment of the decomposed products with potassium salts. Bisbiphenylchromium was prepared by reducing the preceding product with $Na_2S_2O_3$.

1) E. O. Fischer and W. Hafner, *Z. Naturforsch.*, **10b**, 655 (1955).
2) E. O. Fischer and W. Hafner, *Z. anorg. allgem. Chem.*, **286**, 14b (1956).

The Preparation and Some Properties of *N*-Monomethylated L-Amino Acids

By Mitsuo EBATA, Yasuo TAKAHASHI and Hideo OTSUKA

Shionogi Research Laboratory, Shionogi & Co., Ltd., Fukushima-ku, Osaka

(Received January 10, 1966)

N^{α}-Monomethylated amino acids which can be grouped as the unusual amino acids have been found in natural products. Most of them are present in a series of antibiotics which have been discovered and elucidated during the last several years. They are *N*-methyl-L-isoleucine, *N*-methyl-L-valine (Enniatins);[1,2] sarcosine, *N*-methyl-L-alanine, *N*-methyl-L-valine, *N*-methyl-L-isoleucine (Actinomycins);[3] *N*-methyl-L-phenylglycine (L-α-phenylsarcosine), *N*, β-dimethyl-L-leucine (Etamycin);[4] *N*, *N'*-dimethyl-L-cystine, *N*-methyl-L-valine, *N*-methyl-L-alloisoleucine, *N*, γ-dimethyl-L-alloisoleucine (Quinoxaline antibiotics);[5-7] *N*-methyl-L-phenylalanine (Staphylomycin)[8] and *N*-methyl-L-leucine (Sporidesmolides).[9] Two of the *N*-methylamino acids, *N*-methyl-D-tyrosine (D-surinamine) and *N*-methyl-L-tryptophan (L-abrin),

1) Pl. A. Plattner and U. Nager, *Helv. Chim. Acta*, **31**, 665, 2192 (1948).
2) M. M. Shemyakin, Yu, A. Ovchinnikov, A. A. Kiryushkin and V. I. Ivanov, *Tetrahedron Letters*, **7**, 301 (1962).
3) H. Brockmann, *Angew. Chem.*, **72**, 939 (1960); *Ann. N. Y. Acad. Sci.*, **89**, 323 (1960).
4) J. C. Sheehan, H. G. Zachan and W. B. Lawson, *J. Am. Chem. Soc.*, **80**, 3349 (1959).
5) H. Otsuka and J. Shoji, *J. Antibiotics (Tokyo)*, **A16**, 52 (1963).
6) H. Otsuka and J. Shoji, ibid., **A18**, 134 (1965).
7) J. Shoji, K. Tori and H. Otsuka, *J. Org. Chem.*, **30**, 2772 (1965).
8) H. Vanderhaeghe and G. Permentier, *J. Am. Chem. Soc.*, **82**, 4414 (1960).
9) D. W. Russell, *Biochim. Biophys. Acta*, **45**, 411 (1960).

TABLE I. SOME PROPERTIES OF

N-Methylamino acid	Formula	Yield* %	M. p. °C
N-Methyl-L-alanine	$C_4H_9O_2N$	19	260—263
N^{α}-Methyl-L-arginine	$C_7H_{16}O_2N_4$	26	260
N-Methyl-L-aspartic acid	$C_5H_9O_4N \cdot {}^1/_2H_2O$	28	168
N-Methyl-L-cysteic acid	$C_4H_9O_5NS$	24	219—220
N, *N'*-Dimethyl-L-crystine	$C_8H_{16}O_4N_2S_2 \cdot 1/2H_2O$	34	206—208 dec.
N-Methyl-L-glutamic acid	$C_6H_{11}O_4N \cdot {}^3/_4H_2O$	3	131
N-Methyl-glycine(sarcosine)	$C_3H_7O_2N$	—	215 dec.
N-Methyl-L-isoleucine	$C_7H_{15}O_2N$	31	240
N-Methyl-L-leucine	$C_7H_{15}O_2N$	42	220 sub.
N^{α}-Methyl-L-lysine(hydrochloride)	$C_7H_{16}O_2N_2 \cdot HCl$	38	234—235
N-Methyl-L-phenylalanine	$C_{10}H_{13}O_2N$	14	233—237 dec.
N-Methyl-L-serine	$C_4H_9O_3N$	27	194
N-Methyl-L-threonine	$C_5H_{11}O_3N$	14	240
N-Methyl-L-tyrosine(L-surinamine)	$C_{10}H_{13}O_3N \cdot {}^1/_8H_2O$	34	149
N-Methyl-L-valine	$C_6H_{13}O_2N$	36	300

* Yield was calculated from each parent amino acid.
** As *N*-methylamino acid/parent amino acid. Solvent, BuOH : AcOH : H_2O=4 : 1 : 2; temperature,
*** Color yield ratio=Ninhydrin color yield of *N*-methylamino acid/ninhydrin color yield of original
I Estimated from the analytical chart of the automatic amino acid analyzer. The reaction was
II Measured by the method of Moore and Stein.[23] The conditions of the reaction was as described
a In 6 N HCl, acetic acid (1 : 1) b In 5 N HCl

were found in cabbage tree bark[10] and in *Abrus precatorius*[11-13] respectively. It, therefore, can not be doubted that *N*-methylamino acids play a very important role as constituents of peptide or depsipeptide antibiotics.

For the synthesis of the *N*-methylamino acids, however, there is still no simple and generally applicable method except for the method of Quitt et al.,[14] in which the temporary benzylation and the reductive methylation are involved. They have demonstrated that this method is an excellent one by preparing *N*-methylated L-alanine, L-valine, L-leucine, L-phenylalanine, L-serine, L-lysine and L-arginine. However, it has been considered that the kind of *N*-methylamino acids prepared was not sufficient to claim that this is a generally-applicable method.

In the present work the authors have shown that this method is, certainly, a generally-applicable simple method for the preparation of the most *N*-methylamino acids; they have shown this by preparing *N*-monomethyl derivatives of aspartic acid, glutamic acid, isoleucine, threonine and tyrosine, together with the amino acids described above. However, a few exceptions or limitations have been found; namely, the *N*-methylations of histidine and of tryptophan were not achieved. The final products obtained gave large values of negative optical rotations in both cases, while the values of the elemental analyses agreed very nearly with those of the respective expected methylated products. The structures of the products were still obscure, since these compounds have not yet been investigated in detail. *N*-Benzyl-*N*-methyl-L-methionine was prepared in this work in a 54% yield from L-methionine. However, the debenzylation of the compound was not carried out, even in the presence of large amounts of a palladium-barium sulfate catalyst. The treatment of the compound with sodium in liquid ammonia also failed to remove the benzyl group. *N*-Benzyl-L-glutamic acid was prepared with only a 7.4% yield. This indicates that the γ-carboxyl group of glutamic acid exerts a steric hindrance when the Schiff base of glutamic acid with benzaldehyde is formed. For the synthesis of *N*, *N'*-dimethyl-L-cystine, L-thiazolidine-4-carboxylic acid was more useful as the starting material.[15] *N*-Methyl-L-cysteic acid was obtained by the oxidation of *N*, *N'*-dimethyl-L-cystine with performic acid.

The optical rotations of *N*-methylamino acids have already been described in the literature, although the reported values do not always agree. We measured the rotations in 6 N hydrochloric acid unless we otherwise state. The results obtained are listed in Table I. Among the *N*-methylamino acids prepared, we have found that arginine,

10) E. Winterstein, *Z. Physiol. Chem.*, **105**, 20 (1919).
11) T. Hoshino, *Ann.*, **520**, 31 (1935).
12) W. M. Cahill and R. W. Jackson, *J. Biol. Chem.*, **126**, 29 (1938).
13) T. Yoshida and S. Fukuyama, *J. Biochem. (Tokyo)*, **34**, 429 (1941); **36**, 249 (1944).
14) P. Quitt, J. Hellerback and K. Vogler, *Helv. Chim. Acta*, **46**, 327 (1963).
15) S. Ranter and H. T. Clarke, *J. Am. Chem. Soc.*, **59**, 200 (1937).

N-METHYL-L-AMINO ACIDS

$[\alpha]_D^{24-25}$ $c=1-2$	$[M]_D^{N\text{-Methyl amino acid}}$ minus $[M]_D^{\text{Amino acid}}$	Taste	R_f-value ratio**	Color yield ratio with ninhydrin at 570 mμ***	
				I	II
+10.4	−1.0	Slightly sweet	1.1	0.081	0.458
+34.2	+16.1	Slightly sweet	1.8	0.189	0.599
+25.3	+13.3	Sour	1.4	0.039	0.355
+ 6.7	—	—	—	0.083	0.745
+98.8	+723[b]	Tasteless	1.5	0.125	—
+30.6	+6.5	Sour	1.2	0.066	0.344
—	—	Sweet	1.1	0.190	0.473
+46.1	+14.0	Tasteless	1.1	0.014	0.599
+30.0	+26.9	Tasteless	1.1	0.064	0.894
+28.5	+29.8	Faintly sweet	1.2	0.877	1.078
+26.6	+38.9	Tasteless	1.1	0.203	—
+ 9.8	−4.2	Tasteless	1.1	0.045	0.638
−15.9	−3.3	Sweet	1.5	0.065	0.721
+29.3[a]	+58.6[a]	Tasteless	1.2	0.186	—
+29.3	+10.3	Tasteless	1.1	0.023	0.433

22°C; paper, Toyo Roshi No. 51 filter paper; ascending-frame technique was used.
amino acid.
carried out at 100°C for 15 min. at pH 4.9. The ratio, sample solution : ninhydrin solution was 1 : 0.5.
above except ninhydrin concentrations. The ratio, sample solution: ninhydrin solution was 1 : 2.

isoleucine, serine and tyrosine gave somewhat higher values than those of the literature (*N*-methyl-L-arginine, +32.9;[14] *N*-methyl-L-isoleucine, +44.8;[1] *N*-methyl-L-serine, +8.0;[14] and *N*-methyl-L-tyrosine, +19.8[16]). The optical rotations of several *N*-methylamino acids were the same or somewhat lower than those reported by Quitt et al.; nevertheless, they were still higher than those of the derivatives prepared by the classical method (*N*-methyl derivatives of alanine, aspartic acid, lysine, phenylalanine and valine).[16,17] This is one evidence that the method of Quitt et al. is a generally-applicable, simple method for the preparation of *N*-methylamino acids.

The rotational shifts of amino acids induced by *N*-methylation were also observed; they also are listed in the table. In the fact that the values for the latter compounds are invariably more positive than for those for the former, there seems to be a striking rule, as has been pointed out by Izumiya and his associates.[18] However, three exceptions to this rule appeared to occur in the cases of L-alanine, L-serine and L-threonine. We must, therefore, recall the correlation between optically-active amino acid and glycyl-amino acid. In this case, no correlation can be drawn with the introduction of a glycyl residue at the *N*-acyl position.[19-21]

The R_f-values determined upon the one-dimensional paper chromatography of *N*-methylamino acids are listed in Table I as ratios to those of the parent amino acids. The R_f-values of *N*-methylamino acids are usually higher than those of the parent amino acids. Thin-layer chromatography on silica gle G with the same solvent gave almost the same R_f-value as each of the original parent amino acids.

The tastes of *N*-methylamino acids were tested in comparison with those of the L- and D-series of amino acids. The results obtained are shown in Table I. (Of course, the properties are not nowadays important in identifying the individual amino acids.) As far as the tastes of these *N*-methylamino acids were tested, they reproduced the characteristics of the parent L-amino acid series.[22]

The effect of *N*-methylamino acids on the growth of *Escherichia coli* K 12 and *Bacillus subtilis* PCI 219 strains was investigated using the paper-disk method. None of the 14 *N*-methylamino acids tested inhibited the growth of the both microorganisms in a nutrient medium until the concentrations became 0.05 per cent (500 μg./ml.).

It is well known that ninhydrin can react not

16) E. Fischer and W. Lopschitz, *Ber.*, **48**, 377 (1915).
17) Keller-Schierlein, M. L. Michailovic and V. Prelog, *Helv. Chim. Acta*, **42**, 305 (1959).
18) N. Izumiya, A. Nagamatsu and S. Ota, *Kyushu Mem. Med. Sci.*, **4**, 1 (1953).
19) R. Mozingo, D. E. Wolf, S. A. Harris and K. Folkers, *J. Am. Chem. Soc.*, **65**, 1013 (1943).
20) P. Karrer, *Helv. Chim. Acta*, **6**, 957 (1923).
21) P. Karrer and A. Schlosser, ibid., **6**, 411 (1923).
22) A. Meister, "Biochemistry of the Amino Acids," Academic Press, New York (1957), p. 76.

only with α-amino acids, but also with *N*-monoalkylated α-amino acids at neutral pH values.[23,24] In the present work, the color yields with ninhydrin of *N*-methylamino acids were compared with those of the original amino acids by an automatic amino-acid analyzer (Hitachi KLA type 2) and by the method of Stein and Moore.[23] The results obtained are listed in Table I. Although the *N*-methylamino acids generally react with ninhydrin quantitatively, at least 20—30 min. are necessary for their complete reaction at 100°C. The color yields were considerably lower than those of the original amino acids under the conditions used, as is shown in the table. This indicates that the heating was not enough to produce the maximum reaction between ninhydrin and *N*-methylamino acids. In the ninhydrin reaction with *N*-methylamino acids, it was considered that demethylation might occur before color developing, since the absorption spectra of the ninhydrin color reaction of amino acid and *N*-methylamino acid gave the same type of curves.

The conversion of an L-amino acid to the corresponding *N*-methylamino acid is accompanied by some shift in the infrared absorption spectrum when these spectra are measured under the same conditions. Comparisons were performed in each case of amino acid esters and *N*-methylamino acid esters in the same solvent. In this work two main shifts of the absorption band were found, from 6.13 μ to 6.36 μ and from 6.58 μ to 6.80 μ, corresponding to the change from the $-NH_2^+ \cdot Cl^-$ to the $-NH^+-CH_3 \cdot Cl^-$ group.

Grateful acknowledgement is hope by made to Dr. Kaoru Kuriyama and his staff for their optical rotation measurements, to Dr. Satoshi Mizukami and his staff for their microanalyses, and to Miss Shizuko Kitamura for her technical assistance.

23) S. Moore and W. H. Stein, *J. Biol. Chem.*, **176**, 367 (1948).
24) C. E. Dalgleish, A. W. Johnson, A. R. Todd and L. C. Vinning, *J. Chem. Soc.*, **1950**, 2946.

On 2-Cyanotropone Derivatives

By Toyonobu Asao and Masao Kobayashi*[1]

Department of Chemistry, Faculty of Science, Tohoku University, Katahira-cho, Sendai

(Received November 24, 1965)

It is known[1] that nucleophilic reagents generally attack at the 7-position of 2-halotropones to give so-called abnormal substitution products. However, it has been reported[2] that the attack of the sulfides on 2-holotropones occurs exclusively at the 2-position (normal substitution).

The present authors have investigated the reaction[3] of 2-bromotropones with cuprous cyanide to see whether the reaction is normal or abnormal. In addition, some reactions of 3-cyanotropolone will be reported in this paper.

The two hydrazinotropones,[4] 2-hydrazino-6-isopropyl- and 2-hydrazino-4-isopropyltropones (I and II), derived from the methyl ethers of hinokitiol were decomposed with cupric sulfate in hydrobromic acid to give isomeric 2-bromotropone derivatives, III and IV respectively. The treatment of III and IV with an excess of cuprous cyanide gave a good yield of two cyanoisopropyltropones (V and VI), which, on being heated with 75% sulfuric acid, were hydrolyzed to the carboxyisopropyltropones, VII and VIII respectively. From the evidence which follows, it is apparent that the formation of the cyanotropones from the bromotropones proceeds by normal substitution; accordingly, V and VII are 2-cyano- and 2-carboxy-6-isopropyltropones respectively, while VI and VIII are 2-cyano- and 2-carboxy-4-isopropyltropones respectively.

In general, yields of the abnormal substitution products of 6-substituted 2-halotropones are very low as a result of the steric interference of the substituents; mainly rearrangement products are obtained, whereas the conversion of III into V results in a good yield. The infrared spectra of V and VII appeared at 810 and 792 cm^{-1} respectively, similar to the out-of-plane deformation band of 2, 6-disubstituted tropones.[5] On the other hand, the out-of-plane deformation bands of

*1 Present address: Mitsubishi Rayon Co., Ltd., Otake, Hiroshima.

1) Cf. T. Nozoe et al., "Dai Yuki Kagaku (Comprehensive Organic Chemistry)," Vol. XIII, Asakura Shoten, Tokyo (1960), Chapter 7.

2) K. Matsui, This Bulletin, **33**, 1448 (1960).

3) T. Nozoe, S. Seto and S. Matsumura, *Proc. Japan Acad.*, **28**, 483 (1952).

4) S. Seto, *Sci. Repts. Tohoku Univ.*, **I**, **36**, 126 (1952).

5) 2, 4-Disubstituted tropones show characteristic absorptions in the 810—840 cm^{-1} range, while 2, 6-disubstituted tropones show theirs in the 770—800 cm^{-1} range (T. Nozoe, K. Takase and M. Yasunami, to be published).

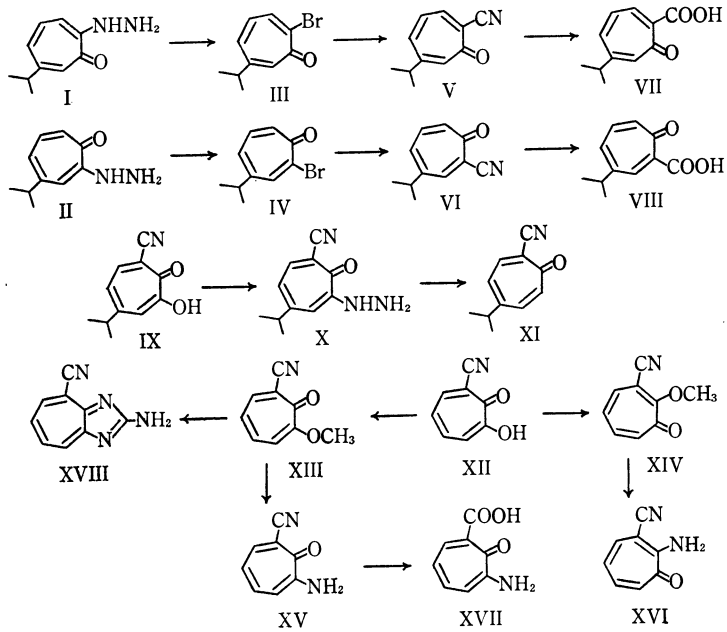

VI (at 830 cm^{-1}) and of VIII (at 843 cm^{-1}) were similar to those of 2, 4-disubstituted tropones.[5]

The above conclusions were confirmed by the following reactions. 7-Cyano-2-hydrazino-4-isopropyltropone (X), obtained by the reaction[6] of 3-cyano-6-isopropyltropolone (IX) with hydrazine, was decomposed with cupric sulfate in acetic acid to yield 2-cyano-5-isopropyltropone (XI). The compound XI is clearly different from VI; the infrared of XI shows a band at 860 cm^{-1}, which is a reasonable value[7] for the out-of-plane deformation band of 2, 5-disubstituted tropones. The ultraviolet spectra of three isopropyl-2-cyanotropones are shown in Fig. 1.

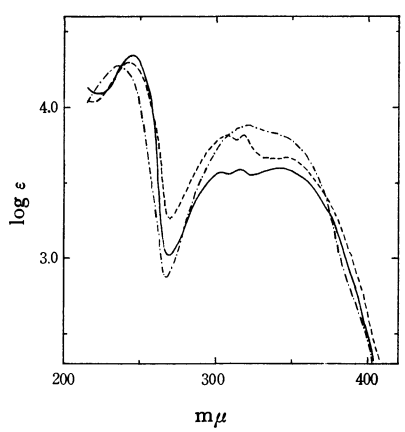

Fig. 1. U. V. absorption spectra of isopropyl derivatives of 2-cyanotropone in methanol.
—— (V) ---- (VI) —·—· (XI)

The two methyl ethers (XIII and XIV)[6] which were obtained from 3-cyanotropolone (XII), when allowed to react with liquid ammonia, afforded 7-cyano- and 3-cyano-2-aminotropone (XV and XVI) respectively, and the hydrolysis of XV afforded 2-amino-7-carboxytropone (XVII).

It is known that the reaction of XIII and ethyl cyanoacetate gives a complex mixture,[8] while the reaction[9] with guanidine affords 2-amino-4-cyano-1, 3-diazaazulene (XVIII) in a good yield.

Experimental*2

2-Bromo-6-isopropyltropone (III).—To a gently boiling solution of cupric sulfate (37 g.) in water (37 ml.), a solution of 2-hydrazino-6-isopropyltropone (I) (3.7 g.) in 48% hydrobromic acid (30 ml.) was added; the mixture was then heated at around 100°C for 3 min. After it had cooled, water (50 ml.) was added, and the solution was extracted with chloroform. The extract was dried over sodium sulfate, chromatographed on an alumina column, and eluted with chloroform. From the first effluent, pale yellow crystals (3 g.) were obtained. Recrystallization from petroleum ether gave III as colorless needles, m. p. 56—57°C.

Found: C, 53.05; H, 4.75. Calcd. for $C_{10}H_{11}$·OBr: C, 52.88; H, 4.83%.

λ_{max}^{MeOH} mμ (log ε): 237^{sh} (4.28), 247 (4.31), 320 (3.83).

6) T. Nozoe, Y. Kitahara, K. Takase and I. Murata, This Bulletin, **37**, 1292 (1964).

7) Y. Kitahara, *Sci. Repts. Tohoku Univ.*, **I**, **39**, 275 (1956); Y. Ikegami, *Kagakuno-Ryoiki, Extra* **38**, 79 (1959).

8) Cf. T. Nozoe et al., "Dai Yuki Kagaku (Comprehensive Organic Chemistry)," Vol. XIII, Asakura Shoten, Tokyo (1960), p. 377.

9) T. Nozoe, T. Mukai, K. Takase, I. Murata and K. Matsumoto, *Proc. Japan Acad.*, **29**, 452 (1953).

*2 All melting points are uncorrected.

2-Bromo-4-isopropyltropone (IV).[*3] — According to the procedure discribed above, 2-bromo-4-isopropyltropone (500 mg.) was obtained as a pale yellow oil from 600 mg. of 2-hydrazino-4-isopropyltropone (II).

Found: C, 52.44; H, 4.93. Calcd. for $C_{10}H_{11}OBr$: C, 52.88; H, 4.83%.

λ_{max}^{MeOH} mμ (log ε): 225[sh] (3.99), 248 (4.17), 323 (3.80).

2-Cyano-6-isopropyltropone (V).—A mixture of III (390 mg.) and cuprous cyanide (800 mg.) was heated at 125°C for 2 hr. while being occasionally stirred. The resulting black solid was extracted with chloroform. The evaporation of the solvent gave dark brown crystals, which were then dissolved in benzene and chromatographed on an alumina column to give 240 mg. of yellow crystals. Recrystallization from methanol gave V as pale yellow plates, m. p. 98—99.5°C.

Found: N, 7.71. Calcd. for $C_{11}H_{11}ON$: N, 8.09%.

λ_{max}^{MeOH} mμ (log ε): 246 (4.35), 303 (3.58), 315 (3.59), 343 (3.60).

IR (Nujol): 2225 cm^{-1} (C≡N).

2-Cyano-4-isopropyltropone (VI).—A mixture of IV (160 mg.) and cuprous cyanide (350 mg.) was heated at 125°C for 2 hr. while being occasionally stirred. The resulting solid was extracted with chloroform; a reddish oil was obtained by the evaporation of the solvent. Distillation gave 100 mg. of VI as a pale yellow oil, b. p. about 125°C/0.5 mmHg.

Found: N, 8.27. Calcd. for $C_{11}H_{11}ON$: N, 8.09%.

λ_{max}^{MeOH} mμ (log ε): 245 (4.31), 305 (3.82), 318 (3.82), 340 (3.67).

IR (Liquid): 2222 cm^{-1} (C≡N).

2-Carboxy-6-isopropyltropone (VII).—A solution of V (150 mg.) in 75% sulfuric acid (1 ml.) was heated at 150—155°C for 30 min., and then poured onto ice thus affording crystals. Recrystallization from benzene-cyclohexane gave 77 mg. of VII as pale yellow needles, m. p. 76—77°C.

Found: C, 69.02; H, 6.20. Calcd. for $C_{11}H_{12}O_3$: C, 68.73; H, 6.29%.

λ_{max}^{MeOH} mμ (log ε): 240 (4.34), 304[sh] (3.74), 316 (3.77).

2-Carboxy-4-isopropyltropone (VIII).—After it had been heated at 155°C for 20 min., a solution of 80 mg. of VI in 75% sulfuric acid (0.5 ml.) was poured onto ice to give crystals. Recrystallization from benzene-cyclohexane gave VIII as pale yellow needles, m. p. 120—121°C.

Found: C, 68.93; H, 6.21. Calcd. for $C_{11}H_{12}O_3$: C, 68.73; H, 6.29%.

λ_{max}^{MeOH} mμ (log ε): 238 (4.27), 319 (3.90).

2-Cyano-7-hydrazino-5-isopropyltropone (X).—A solution of 3-cyano-6-isopropyltropolone (IX) (200 mg.) and 80% hydrazine hydrate (100 mg.) in ethanol (1.5 ml.) was refluxed for 15 min. After the solvent had then been evaporated, the residue was dissolved in ethanol and passed through an alumina column to yield 30 mg. of yellow crystals. Recrystallization from ethanol gave X as orange yellow prisms, m. p. 147—148°C.

Found: C, 64.90; H, 6.12; N, 20.50. Calcd. for $C_{11}H_{13}ON_3$: C, 65.00; H, 6.45; N, 20.68%.

[*3] This experiment was carried out by Dr. Masafumi Yasunami.

2-Cyano-5-isopropyltropone (XI).—To a heated solution of X (130 mg.) in a mixture of acetic acid (3 ml.) and water (3 ml.), a solution of cupric sulfate (0.6 g.) in water (6 ml.) was added. The mixture was then heated for 15 min., water (15 ml.) was added, and the solution was extracted with chloroform. After the solution had been dried over sodium sulfate, the solvent was removed to leave a reddish oil which was distilled under reduced pressure to give XI as a pale yellow oil (30 mg.).

Found: N, 7.95. Calcd. for $C_{11}H_{11}ON$: N, 8.09%.

λ_{max}^{MeOH} mμ (log ε): 237 (4.28), 321 (3.89), 340[sh] (3.83).

IR (Liquid): 2233 cm^{-1} (C≡N).

2-Amino-7-cyanotropone (XV).—A solution of XIII (700 mg.) in liquid ammonia (7 ml.) in sealed tube was allowed to stand at room temperature overnight. The excess ammonia was then removed, and the residue was recrystallized from methanol to give XV as yellow crystals (400 mg.), m. p. 207.5—209°C.

Found: C, 65.19; H, 4.58; N, 18.71. Calcd. for $C_8H_6ON_2$: C, 65.75; H, 4.18; N, 19.17%.

λ_{max}^{MeOH} mμ (log ε): 220 (4.07), 250 (4.34), 273 (4.13), 283[sh] (4.01), 349(3.99), 424 (4.31).

Acetate.—Yellow plates (from ethanol); m. p. 238.5—239°C.

Found: C, 63.66; H, 4.00; N, 14.89. Calcd. for $C_{10}H_8O_2N_2$: C, 63.82; H, 4.29; N, 14.89%.

2-Amino-3-cyanotropone (XVI).—By the procedure described above, XVI was obtained from 3-cyano-2-methoxytropone (XVI) as yellow crystals, m. p. 138—140°C.

Found: C, 65.61; H, 4.05; N, 18.93. Calcd. for $C_8H_6ON_2$: C, 65.75; H, 4.18; N, 19.17%.

λ_{max}^{MeOH} mμ (log ε): 225[sh] (4.12), 248 (4.30), 270 (4.04), 345 (4.01), 406 (4.06).

2-Amino-7-carboxytropone (XVII).—A solution of XV (400 mg.) in 75% sulfuric acid (2.8 ml.) was heated at 160°C for 45 min. and then poured onto ice to yield a brown solid. Recrystallization from methanol afforded XVII as yellow crystals (150 mg.), m. p. 264°C (decomp.).

Found: C, 57.78; H, 4.19; N, 8.27. Calcd. for $C_8H_7O_3N$: C, 58.18; H, 4.28; N, 8.48%.

λ_{max}^{MeOH} mμ (log ε): 249 (4.25), 272 (4.00), 344 (3.88), 418 (4.19).

Acetate.—Yellow needles (from ethanol); m. p. 218—219°C (decomp.).

Found: C, 58.29; H, 4.21; N, 6.71. Calcd. for $C_{10}H_9O_4N$: C, 57.97; H, 4.38; N, 6.76%.

Methyl Ester.—The methylation of XVII with diazomethane gave yellow needles, m. p. 145—146.5°C.

Found: C, 60.60; H, 5.05; N, 7.82. Calcd. for $C_9H_9O_3N$: C, 60.33; H, 5.06; N, 7.82%.

λ_{max}^{MeOH} mμ (log ε): 240[sh] (4.34), 245 (4.36), 265 4.01), 274[sh] (3.93), 344 (3.99), 409 (4.11).

2-Amino-4-cyano-1, 3-diazaazulene (XVIII). — A solution of 2-methoxy-7-cyanotropone (XIII) (100 mg.), guanidine hydrochloride (71 mg.), and sodium methoxide (15.7 mg.) in absolute ethanol (1.5 ml.) was refluxed for 1 hr. The brown precipitate (60 mg.) was washed with water and recrystallized from *n*-butanol, affording XVIII as reddish-orange plates, m. p. 305°C (decomp.).

Found: C, 63.54; H, 3.41; N, 32.65. Calcd. for $C_9H_6N_4$: C, 63.52; H, 3.55; N, 32.93%.

λ_{max}^{MeOH} $m\mu$ (log ε): 263 (4.46), 302 (3.93), 364 (4.11), 428 (3.89).

The authors wish to express their gratitude to Professor Tetsuo Nozoe for his kind and unfailing guidance throughout this work.

A Structural Study of Complex Chromic-Ferrocyanide and -Ferricyanide by Means of Ultrasonic Waves

By Wahid U. MALIK and Jahan SINGH*

Chemical Laboratories, University of Roorkee, Roorkee, India

(Received January 11, 1966)

Sette[1] has discussed and reviewed the use of ultrasonic velocities in the determination of molecular structures and the structure of liquids. Work on complex barium-citrate has been carried out by Prakash and Pandey,[2] and by Subrahmanyam.[3] These methods have, however, not been extensively employed to determine the composition and structure of coordination compounds. This is especially true for metal ferrocyanogen complexes, where, except for some preliminary studies on potassium ferrocyanide, nothing worth mentioning has so far been done. Investigations in this direction were, therefore, considered desirable.

The ultrasonic method cannot be applied to all the known metal ferro-cyanogen complexes, since most of them exist as insoluble compounds. Recently Malik,[4,5] during the course of his investigations into these compounds, came across a number of new ferrocyanogen complexes, like that of chromium, molybdenum, etc., which could exist in a soluble state. It was thought that some of these could be put to ultrasonic analysis and so ascertain their composition. In this communication the preliminary results on sono-metric study of chromic ferro- and ferricyanides have been reported.

Experimental

Standard solutions of chromium(III) chloride and potassium ferrocyanide and potassium ferricyanide were prepared by dissolving A. R. grade reagents in doubly-distilled water. A series of mixtures were then prepared according to Job's method[6] of continuous variation. These mixtures were allowed to stand for some time to attain equilibrium and to complete the reaction (as determined by the change in colour from light yellow to orange-red and by shifts in the absorption maximum). The velocity in each mixture was determined by the optical diffraction[7,8] method. An X-cut quartz crystal was suspended in a rectangular glass vessel containing the experimental mixture in such a manner that the crystal hung parallel to one side of the vessel. This crystal was then connected to a Hartley oscillator to produce ultrasonic waves. The stationary waves were formed in a liquid to give regions of compression and rarefraction, which act like a diffraction grating. The readings of the direct slit and diffraction orders were taken on the scale of the telescope. The velocity was calculated by the formula:

$$V=\frac{n\cdot f\cdot \lambda\cdot D}{x} \qquad (1)$$

where f = the frequency of the Hartley oscillator for the impedance matching of crystal
n = the number of the diffraction order
λ = the wavelength of the source of light
D = the distance between the optical centre of the objective of the telescope and the scale
x = the distance between the nth order and the direct image of the slit.

The apparatus used was made by the Andhra Scientific Co., India. For this apparatus $D=100$ cm., and the least count of the scale is 0.01 cm. In our observations, $f=3$ mc./s., $\lambda=5893$ A. U. and $n=1$ (1st order). By putting these values into Eq. 1, we get:

$$V=\frac{176.79}{x} \text{ m./sec.} \qquad (2)$$

From Eq. 2 the velocity was calculated for different mixtures. These results are shown in Tables I and II.

Results and Discussion

From the graphs for Job's method it was found that the ultrasonic velocity gradually decreases, reaches a minimum, and then increases again. In graph No. 1 the minimum occurs at the point of 0.5 ratio $Cr^{3+}/(Cr^{3+}+Fe(CN)_6^{4-})$ at a composition

* Present address: Department of Physics, Regional Engineering, College Kurukshetra, India.

1) D. Setter, *Ric. Sci.*, **20**, 102 (1950).
2) S. Prakash and J. D. Pandey, *J. Phy. Chem.*, **68**, 3078 (1964).
3) S. V. Subrahmanyam and P. J. Reddy, *J. Phys. Soc. Japan*, **17**, 1061 (1962).
4) W. U. Malik, *J. Sci. Ind. Res.*, **20B**, 213 (1961).
5) W. U. Malik, *J. Ind. Chem. Soc.*, **38**, 293 (1961).
6) P. Job, *Ann. Chim.*, **9**, 113 (1928).
7) P. Debye and F. W. Sears, *Proc. Natl. Acad. Sci. U. S. A.*, **18**, 410 (1932).
8) E. C. Richardson, "Ultrasonic Physics," 2nd Ed., Elsevier Co., N. Y. (1962).

of 1 : 1. This indicates the maximum complex formation at that point. In graph 2 the minimum occurs at the point of 0.6 ratio $Cr^{3+}/(Cr^{3+}+Fe(CN)_6^{3-})$ at a composition of 3 : 2.

Had there been no interaction between the two solutions, the curve would be linear. When the complex formation is at a maximum, the ultrasonic velocity is at a minimum.

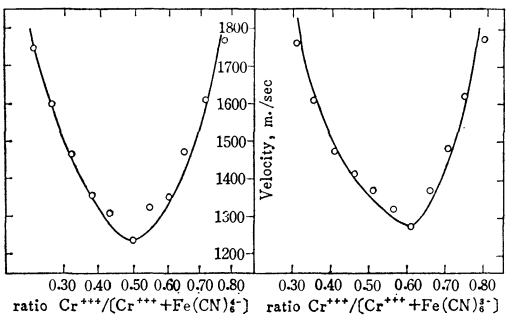

Fig. 1 Fig. 2

Graphs showing the variation of ultrasonic velocities of chromic ferrocyanide (Fig. 1) and chromic ferricyanide (Fig. 2) with different ratio of chromic (Cr^{3+}) to the complex ($Cr^{3+} + Fe(CN)_6^{4-}$ and $Cr^{3+} + Fe(CN)_6^{3-}$).

By a comparison of graphs 1 and 2, it may be seen that the velocity is more in the case of chromic-ferricyanide than in that of chromic-ferrocyanide. This difference may be attributed to the difference in the degree of hydration of chromic ferro- and ferricyanide particles, since both these compounds give colloidal precipitates. A confirmation of these results is found in the work of Malik[9] on the composition (using spectrophotometric and amperometric methods) and colloidal behaviour (sol-gel transformation) of chromic-ferro- and ferricyanides.

Tables I and II show the ultrasonic velocities of chromic-ferrocyanide and chromic-ferricyanide complexes respectively.

Table I

0.1 M $CrCl_3$ + 0.1 M $K_4Fe(CN)_6$
Total volume = 100 cc.

Sample No.	Vol. of $CrCl_3$ cc.	Vol. of $K_4Fe(CN)_6$ cc.	Ratio	x cm.	V m./s.
1	25	75	0.25	0.10	1767.9
2	30	70	0.30	0.11	1607.2
3	35	65	0.35	0.12	1473.3
4	40	60	0.40	0.13	1359.9
5	45	55	0.45	0.135	1309.6
6	50	50	0.50	0.14	1262.8
7	55	45	0.55	0.132	1339.3
8	60	40	0.60	0.13	1359.9
9	65	35	0.65	0.12	1473.3
10	70	30	0.70	0.11	1607.2
11	75	25	0.75	0.10	1767.9

Table II

0.1 M $CrCl_3$ + 0.1 M $K_3Fe(CN)_6$
Total volume = 100 cc.

Sample No.	Vol. of $CrCl_3$ cc.	Vol. of $K_3Fe(CN)_6$ cc.	Ratio	x cm.	V m./sec.
1	25	75	0.25	0.09	1964.3
2	30	70	0.30	0.10	1767.9
3	35	65	0.35	0.11	1607.2
4	40	60	0.40	0.12	1473.3
5	45	55	0.45	0.125	1414.3
6	50	50	0.50	0.13	1359.9
7	55	45	0.55	0.135	1309.5
8	60	40	0.60	0.14	1262.8
9	65	35	0.65	0.13	1359.9
10	70	30	0.70	0.12	1473.3
11	75	25	0.75	0.11	1607.2
12	80	20	0.80	0.10	1767.9

Thanks are due to the Head of the Physics Department, University of Roorkee, for allowing us to carry out some of this study in his laboratory.

9) W. U. Malik, D. Sc. Thesis, Aligarh University, India (1960).

Studies of *C*-Substituted Tartaric Acid. III. The Preparation of Isomeric 1, 2-Dihydroxycyclohexane-1, 2-dicarboxylic Acids and the Optical Resolution of the Racemate

By Susumu TATSUMI, Masami IMAIDA and Yoshiharu IZUMI

Division of Organic Chemistry, Institute for Protein Research, Osaka University, Kita-ku, Osaka

(Received January 28, 1966)

1, 2-Dihydroxycyclohexane-1, 2-dicarboxylic acid is a kind of *C, C'*-dialkyltartaric acid. This hydroxy acid contains two asymmetric centers; hence, it exists in two optically inactive modifications. One is a racemic form which may be resolved into optically active forms, while the other is a meso form. The optically active and inactive forms, therefore, are interesting substances from the stereochemical point of view in relation to tartaric acid. Moreover, in a previous paper[1] from our laboratory, it was reported that a Raney nickel catalyst treated with an aqueous solution of this optically active hydroxy acid exhibits an asymmetric hydrogenation activity in the hydrogenation of methyl acetoacetate to methyl 3-hydroxybutyrate. However, there have been no reports on the preparation of the two optically inactive or active forms of this hydroxy acid.

In the present work, 1, 2-dihydroxycyclohexane-1, 2-dicarboxylic acid was prepared from 1, 2-cyclohexanedione and was then separated into the meso (I) and racemic (II) forms on the basis of the different solubilities of their calcium salts in water. The purity of each salt was checked by a study of the infrared spectrum.[2] Subsequently, the optical resolution of II was performed in an aqueous solution with brucine. The optical rotation values of the optically active isomers were as follows: (+)-isomer, $[\alpha]_D^{20}$ +31.0° (*c* 2, water); (−)-isomer, $[\alpha]_D^{20}$ −30.5° (*c* 2, water).

Experimental*

The Preparation of 1, 2-Dihydroxycyclohexane-1, 2-dicarboxylic Acid.—One hundred and twenty-nine grams of sodium cyanide was dissolved in 250 ml. of cold water in a 2 l. three-necked flask fitted with a stirrer and a dropping funnel. Into the cold solution, a 220 ml. portion of concentrated hydrochloric acid was added, drop by drop, with the temperature of the solution maintained below 20°C under a hood. After the addition of hydrochloric acid was complete, 3.6 g. of potassium carbonate was added, and then 115 g. of 1,2-cyclohexanedione[3] was added, drop by drop. The reaction mixture was stirred for 3 hr. at room temperature and then allowed to stand overnight. To the mixture, a 600 ml. portion of concentrated hydrochloric acid was added, after which the solution was kept for an hour at room temperature. Inorganic salts were removed by filtration, and the filtrate was refluxed for 5 hr. The hydrolyzed solution was decolorized with charcoal and then evaporated to dryness under reduced pressure. The residue was extracted with four 100 ml. portions of ethanol, and the white residue was discarded. The alcohol extracts were combined and evaporated to a syrup. This was dissolved in 3 l. of ethanol and esterified by blowing dry hydrogen chloride gas into the solution. The alcohol was distilled off in vacuo, and the diethyl ester of the acid was collected at 116—119°C/2 mmHg. Yield, 84 g.

Eighty-four grams of the ester were refluxed with 150 ml. of 12% hydrochloric acid for 5 hr. The hydrolyzate was then concentrated to a syrup under reduced pressure. This was taken up in 100 ml. of water and concentrated again. To remove free hydrochloric acid, water was added and the evaporation was repeated. The resulting viscous syrup was dissolved in 80 ml. of hot ethyl acetate, and then a 20 ml. portion of petroleum ether was added to the solution. After the mixture had stood overnight in a refrigerator, white crystals were collected by suction. Yield, 50 g.

Found: C, 47.31; H, 5.85. Calcd. for $C_8H_{12}O_6$: C, 47.06; H, 5.92%.

Separation into the Meso (I) and Racemic (II) Forms.—*The Preparation of Calcium Salts of I and II.*—Fifty grams of isomeric acids and 36 g. of calcium chloride dihydrate were dissolved in 2.8 l. of water. The resulting solution was adjusted to pH 5 with 10% sodium hydroxide, and then left to stand overnight at room temperature. The calcium salt which precipitated was collected by suction. In order to purify the salt, it was decomposed with hydrochloric acid and then neutralized with a sodium hydroxide solution. The decomposition and neutralization were repeated alternately three times, with the purity of the salt being checked on the basis of its infrared spectrum.[2] In this way, 18 g. of the pure calcium salt of I was obtained.

Found: C, 37.00; H, 4.70. Calcd. for $C_8H_{10}O_6Ca \cdot H_2O$: C, 36.91; H, 4.65%.

The mother liquor of the calcium salt of I was concentrated to dryness under reduced pressure. Four recrystallizations of the residue from boiling water gave 19 g. of the pure salt of II.

Found: C, 39.57; H, 4.20. Calcd. for $C_8H_{10}O_6Ca$: C, 39.66; H, 4.16%.

The Preparation of I and II.—Thirty grams of the

1) Y. Izumi, S. Tatsumi and M. Imaida, This Bulletin, **39**, 1087 (1966).
2) S. Tatsumi, ibid., **39**, 2202 (1966).
* All melting points are uncorrected.
3) R. S. Schreiber, "Organic Syntheses," Vol. 32, 35 (1951).

calcium salt of I was dissolved in 120 ml. of 2 N hydrochloric acid, and then the resulting solution was evaporated to dryness under reduced pressure. The residue was extracted with four 50 ml. portions of acetone, and the white residue was discarded. The acetone extracts were combined and evaporated to dryness in vacuo, yielding 23 g. of crude I. Recrystallization from ethyl acetate - petroleum ether (4 : 1) gave 20 g. of pure I. M. p. 154°C.

Found: C, 47.14; H, 5.96. Calcd. for $C_8H_{12}O_6$: C, 47.06; H, 5.92%.

Thirty grams of the calcium salt of II was treated as has been described above. 18.5 g. of pure II was thus obtained. M. p. 180°C.

Found: C, 46.72; H, 5.97. Calcd. for $C_8H_{12}O_6$: C, 47.06; H, 5.92%.

The Optical Resolution of II.—Twenty grams of II and 39 g. of brucine were dissolved in 600 ml. of boiling water, and the resulting solution was allowed to stand overnight in an ice box. The crystals of the brucine salt which precipitated were collected by suction; six recrystallizations of this salt from ten parts of boiling water gave 16 g. of the pure brucine salt of II. This salt was suspended in 150 ml. of water and decomposed with 35 ml. of N sodium hydroxide. The precipitated brucine was removed by filtration, and the alkaline filtrate was washed with 20 ml. of chloroform, neutralized with concentrated hydrochloric acid, and then evaporated to a syrup. To this a small amount of water was added, and the resulting solution was decolorized with charcoal and evaporated to dryness. The residue was extracted several times with 10 ml. volumes of acetone. The acetone extracts were combined and again evaporated to a syrup. The syrupy product was dried over sulfuric acid in a vacuum desiccator. In this way, 4.4 g. of (+) II was obtained. Recrystallization from ethyl acetate - petroleum ether (3 : 1) gave 3.8 g. of optically pure (+)-II. $[\alpha]_D^{20}$ +31.0° (*c* 2, water).

Found: C, 47.11; H, 5.81. Calcd. for $C_8H_{12}O_6$: C, 47.06; H, 5.92%.

The mother liquor of the brucine salt of (+)-II was concentrated to dryness under reduced pressure. The brucine salt of (−)-II was collected and treated as has been described above. 2.0 g. of optically pure (−)-II were thus obtained. $[\alpha]_D^{20}$ −30.5° (*c* 2, water).

Found: C, 47.14; H, 5.94%.

This research was made possible by the support of the Ajinomoto Co., Inc., Tokyo. The authors wish also to express their deep thanks to Miss Kiku Koike of this Institute for carrying out the elemental analyses.

A Redox Titration of Vanadium(IV), Hypochlorite, Hypobromite and a Mixture of Vanadium(IV) and Vanadium(V)

By J. P. TANDON and K. L. CHAWLA

Department of Chemistry, University of Rajasthan, Jaipur, India

(Received February 2, 1966)

Vanadium(IV) in an alkaline solution can be rapidly and quantitatively oxidised to vanadium(V) in an inert atmosphere by the use of a hypochlorite or hypobromite solution. This forms the basis of the methods of the determination of vanadium(IV), hypochlorite and hypobromite to be described in the present paper.

To an alkaline solution of vanadium(IV) sulphate, a known excess of a standardised hypohalite solution is added. After destroying the excess with a known amount of arsenic(III) oxide solution, the excess of arsenic(III) is finally determined by titration with a hypohalite solution, using methyl red as the indicator. For determining the amount of hypohalite, its known volume is added to an excess of a vanadium(IV) solution in the presence of alkali; then the vanadium(V) so formed is titrated with iron(II) sulphate, using *N*-phenylanthranilic acid as the indicator. These methods have the advantage that the reactions are rapid at room temperature, and the excess of the oxidising solution in the determination of vanadium(IV) is easily and completely removed. However, all the titrations must be carried out in an atmosphere of purified nitrogen, since the auto-oxidation of vanadium(IV) is serious in an alkaline medium. A method for the determination of vanadium(IV) and vanadium(V) mixtures is also suggested.

Experimental and Results

Reagents.—All the chemicals used were products of the British Drug House (B. D. H.), Analar (A. R.) or of the E. Merck Company.

The Vanadium(IV) Sulphate Solution.—Prepare an approximately 0.05 M solution containing 0.05 M sulphuric acid and standardise against permanganate at about 80°C.

The Hypochlorite and Hypobromite Solutions.—Prepare approximately 0.05 M solutions as described by Erdey and Vigh[1] and standardise iodometrically.

The Arsenic(III) Oxide Solution.—Prepare a 0.25 M solution.

1) L. Erdey and K. Vigh, *Talanta*, **10**, 439 (1963).

The Procedure for the Determination of Vanadium(IV) with Hypochlorite of Hypobromite.—Place 5 to 10 ml. of a vanadium(IV) sulphate solution in a titration vessel, bubble nitrogen in for about 10 min., and add 5 to 10 ml. of 4 M sodium hydroxide and 5 to 10 ml. of the previously-standardised hypochlorite or hypobromite solution. When the solution becomes almost colourless (after 2—3 min.), add 5 to 10 ml. of a 0.05 M arsenic(III) oxide solution. Add 10 ml. of 6 M hydrochloric acid and 1—2 drops of methyl red indicator, and titrate the excess of arsenic(III) with the hypochlorite or hypobromite solution. A few results are recorded in Table I.

Table I. Determination of vanadium(IV) (V^{IV}—V^{V} change)

Amount of vanadium(IV), mmol.		
Taken	Found	% Error
0.5070	0.5039	−0.61
0.5070	0.5077	+0.14
0.5320	0.5350	+0.56
0.5750	0.5740	−0.17

The Procedure for the Determination of Hypochlorite or Hypobromite.—Place about 10 ml. of a vanadium(IV) sulphate solution in a titration vessel, bubble nitrogen in for about 10 min., and add about 5 ml. of 4 M sodium hydroxide and 2 to 5 ml. of the hypochlorite or hypobromite solution. After 2 to 3 min., add 30 ml. of 6 M sulphuric acid and titrate the vanadium(V) with iron(II) sulphate, using *N*-phenylanthranilic acid as the visual indicator. A few results are given in Table II.

The Procedure for the Determination of Vanadium(IV) and Vanadium(V) in a Mixture.—For the determination of vanadium(IV) in the mixture, follow the procedure described earlier. In another aliquot, acidify the mixture with 6 M sulphuric acid to make the overall acidity about 3 M, and then titrate the vanadium(V) with iron(II) sulphate. A few results are given in Table III.

Table II. Determination of hypochlorite and hypobromite

Oxidising agent		Found by procedure described mmol.	Found iodometrically mmol.	% Error
Hypochlorite	(i)	0.2522	0.2520	+0.08
	(ii)	0.2515	0.2520	−0.12
	(iii)	0.2044	0.2038	+0.24
Hypobromite	(i)	0.0566	0.0567	+0.17
	(ii)	0.1690	0.1688	+0.11
	(iii)	0.1917	0.1910	+0.37

Tables I to III show that, in the concentration ranges from 0.2780 to 0.5750 mmol. of vanadium(IV) and 0.0567 to 0.2522 mmol. of hypohalites, the accuracy of the present method is ±0.6% and ±0.4% respectively. The variation co-efficient is ±0.15%.

The Effects of Foreign Substances.—The determination of vanadium(IV) is subject to interference by even a small amount of ammonia, urea, sulphide, thiosulphate, tetrathionate and hydrogen peroxide, whereas in the determination of hypochlorite and hypobromite, cerium(IV), chromium(VI), vanadium(V), etc., which are reduced by iron(II), interfere.

The authors wish to thank Professor R. C. Mehrotra for his keen interest in the work and for providing the facilities, and to the Council of Scientific and Industrial Research, New Delhi, for the award of a Junior Research Fellowship to K. L. C.

Table III. Determination of mixtures of vanadium(IV) and vanadium(V)

Amount of vanadium(IV) mmol.		Amount of vanadium(V) mmol.		% Error	
Taken	Found	Taken	Found	V(IV)	V(V)
0.2780	0.2778 (i)	0.7190	0.7190	−0.07	0.00
0.2780	0.2778 (ii)	0.5752	0.5763	−0.07	+0.19
0.2875	0.2865 (iii)	0.2738	0.2738	−0.35	0.00
0.2875	0.2865 (iv)	0.1369	0.1369	−0.35	0.00
0.5750	0.5783 (v)	0.1369	0.1369	+0.57	0.00

The Oxidation of Terpene Compounds with *t*-Butyl Chromate. IX.[1] The Oxidation of (+)-*p*-Menth-1-ene

By Takayuki SUGA, Masako SUGIMOTO, the late Kôzô FUJITA and Tamon MATSUURA

Department of Chemistry, Faculty of Science, Hiroshima University, Hiroshima

(Received February 14, 1966)

The oxidation of *p*-menth-1-ene with *t*-butyl chromate in carbon tetrachloride has been reported by Dupont et al.[2] to afford carvotanacetone, piperitone, and possibly 2-methyl-5-isopropyl-1, 4-hydroquinone. On the other hand, Fujita et al.,[3] in a previous paper of this series, have reported that *t*-butyl chromate oxidation of *p*-menth-1-ene in benzene yielded only carvotanacetone. We have now re-examined this oxidation in order to check the point of the oxidative attack.

The oxidation was conducted in accordance with the technique presented in a previous report of ours[3]; it has been confirmed to yield (±)-carvotanacetone (a 25% yield based on the sample taken), (+)-piperitone (26%), and traces of carvacrol, thymol and (+)-phellandric acid, by a combination of fractional distillation, column chromatography, gas chromatography, and a study of the absorption spectra and the functional derivatives. Not even a trace of the hydroquinone, which has been found by Dupont et al.,[2] could be detected.

The present results indicate that *t*-butyl chromate oxidizes equally each of two active methylenes (C-3 and C-6) of *p*-menth-1-ene to a ketone group; this differs from Fujita's results[3] on the oxidation of this hydrocarbon. The presence of phellandric acid suggests that an active methyl group at C-1 was, to a small extent, oxidized to a carboxyl, possibly via an aldehydic group. It was, moreover, noteworthy that optically inactive carvotanacetone resulted from the oxidation of an active methylene adjacent to the C*-atom in the $-C^*(R)=CH-$ system, while piperitone formed by the oxidation of the methylene in the $-C(R)=CH-CH_2-$ grouping partially retained its optical activity. The same phenomenon has also been observed in the *t*-butyl chromate oxidation of (+)-limonene[4] and (+)-*p*-menth-3-ene[5]; the cause of such phenomena is not yet completely clear.

Experimental

Oxidation. — (+)-*p*-Menth-1-ene (b. p. 85°C/40 mmHg, n_D^{25} 1.4531, d_4^{25} 0.8205, $[\alpha]_D^{27}$ 96.6°) was synthesized from (+)-limonene (b. p. 85°C/40 mmHg, $[\alpha]_D^{14}$ 121.9°) by catalytic partial hydrogenation according to the method of Ref. 5 cited in Ref. 3. A benzene solution of *t*-butyl chromate was prepared from 108.6 g. of chromium trioxide, 241.6 g. of *t*-butyl alcohol, and 550 ml. of benzene following the method reported.[1,3] Then, each of this oxidant solution and (+)-*p*-menth-1-ene (50.0 g.) was simultaneously dropped into a flask over a 6 hr. period at 50°C under agitation in an atmosphere of carbon dioxide. After the mixture had been stirred for 24 hr., glacial acetic acid (70 g.) and acetic anhydride (110 g.) was added to the mixture; it was then stirred further at the same temperature for 6 hr. The treatment of the mixture according to the usual method[1,3] gave 51.0 g. of a reaction mixture, which was then fractionated into three fractions and a residue (7.6 g.) by distillation. The residue seemed to be a chromium-containing polymerized substance.

The Identification of the Oxidation Products.— 1) The first fraction (9.0 g.; b. p. 71—84°C/40 mmHg) was the unchanged hydrocarbon, judging from its gas chromatogram and infrared spectrum.

2) The second fraction (25.9 g.; b. p. 88—112°C/10 mmHg) was found to consist of equal amounts of two components by a study of its chromatostrip and by gas chromatographic analyses. This fraction was chromatographed on a silica gel column with a mixture of ethyl acetate and *n*-hexane. The first elute (b. p. 75°C/4 mmHg, n_D^{25} 1.4740, d_4^{25} 0.9382, $[\alpha]_D^{25}$ 0° (*c* 9.5, ethanol); λ_{max}^{hexane} 231 and 312 mμ (ε 12200 and 57); $\nu_{max}^{liq.}$ 1668 (C=O), 1438 ($-CH_2CO-$), 903 (>C=CH–) cm^{-1}; NMR (CCl_4, p.p.m. from internal tetramethylsilane) 0.81_s (3H), 0.96_s (3H), 1.68_s (3H), 6.60_{br} (1H)) gave (±)-carvotanacetone 2, 4-dinitrophenylhydrazone (m.p. and mixed m.p. 192—193°C and semicarbazone (m. p. and mixed m. p. 177—178°C).

The second elute showed the following physical properties: b. p. 78°C/3 mmHg, n_D^{25} 1.4745, d_4^{25} 0.9293; $[\alpha]_D^{11}$ +11.32° (*c* 6.5, ethanol), lit.,[6] $[\alpha]_D^{20}$ +49.8°; λ_{max}^{hexane} 225 and 332 mμ (ε 15000 and 32), lit.,[7] λ_{max}^{hexane} 225 and 333 mμ (ε 17800 and 35); $\nu_{max}^{liq.}$ 1666 (C=O), 1437 ($-CH_2CO-$), 871 (>C=CH–) cm^{-1}; NMR (CCl_4, p. p. m. from internal tetramethylsilane) 0.78_d (J=6 c. p. s., 3H), 0.88_d (J=6 c. p. s., 3H), 1.87_s (3H), 5.68_s(1H); it was confirmed to be (+)-piperitone by

1) Paper VIII of this series: T. Matsuura and T. Suga, *J. Org. Chem.*, **30**, 518 (1965).
2) G. Dupont, R. Dulou and O. Mondou, *Bull. soc. chim. France*, **1953**, 60.
3) K. Fujita and T. Matsuura, *J. Sci. Hiroshima Univ., Ser. A*, **18**, 455 (1955).
4) K. Fujita, ibid., **24**, 691 (1960).
5) K. Fujita, This Bulletin, **34**, 968 (1961).
6) J. Read and H. G. Smith, *J. Chem. Soc.*, **1923**, 2267.
7) R. G. Cooke and A. K. Macbeth, ibid., **1938**, 1408.

preparing the 2, 4-dinitrophenylhydrazone (m. p. 117—118°C; lit.,[8] 117-—118°C) and the semicarbazone (m. p. 229—230°C; lit.,[9] 226—227°C).

3) The third fraction (3.5 g.; b. p. 112—152°C/10 mmHg) was diluted with petroleum ether and shaken with a 5% sodium hydroxide solution. The extraction of the alkaline solution with ether gave a phenolic substance (λ_{max}^{hexane} 276 and 282 mμ (ε 2000 and 2000); $\nu_{max}^{liq.}$ 3361, 1425, 1229 (OH), 3019, 1621, 1590 (aromatic), 1386, 1370 (isopropyl) cm^{-1}). It was shown, by gas chromatography using a 3 m.-column of 5.6% SE-30 on siliconized Gaschrom P at 150°C, to consist of carvacrol (t_R 6.6 min.) and thymol (t_R 6.9 min.).

4) A crystalline mass (0.25 g.) deposited from the viscid oil which was obtained as a holdup in the distilling apparatus. The recrystallization of the mass from dilute ethanol gave white needles showing a m. p. of 148—149°C ($[\alpha]_D^{25}$ +90.4° (*c* 1.4, methanol), λ_{max}^{hexane} 220 mμ (ε 11000), and *m/e* 168 (M^+), 125 (M-43), 123 (M-45) and 70 (base peak) in the mass spectrum). The needles were confirmed to be (+)-phellandric acid by a comparison of their infrared spectrum in a carbon disulfide solution with that of (−)-phellandric acid (m. p. 146—147°C, $[\alpha]_D^{25}$ 109.0° (*c* 2.5, ethanol); λ_{max}^{hexane} 220 mμ (ε 10800)), which was prepared from (−)-perillaldehyde in our laboratory.

8) G. Dupont, R. Dulou and P. Crabbe, *Bull. soc. chim. France*, **1955**, 621.

9) J. C. Bardham, N. C. De and B. B. Datta, *J. Chem. Soc.*, **1951**, 3195.

Zero-order Catalysis at Low Catalyst Concentrations

By R. L. Failes and V. R. Stimson

University of New England, Armidale, N. S. W., Australia

(Received February 16, 1966)

Several cases of gas-phase catalysis by hydrogen halides (HX) have been noted where the rate is zero-order in the catalyst; in particular, the hydrogen bromide-catalysed decomposition of tertiary butyl ethyl ether to produce isobutane,[1] and the hydrogen chloride-catalysed decomposition of acetaldehyde[2] have been noted. The kinetic forms assigned to these decompositions are $^{1}c\mu X_{1,0}$ or $^{1}cXXM_{1,0}$, and $^{2}cXXM_{3/2,0}$ at high pressures of hydrogen bromide and hydrogen chloride respectively. (The superscripts 1 and 2 refer to the order of initiation; c indicates a catalysed chain; μ, X and M indicate the entities involved in the termination, and the subscripts give the order of the reaction in the substrate and in the catalyst respectively[3]). The experimental results in the first case are somewhat obscured by another reaction, but in the second case the variation of the rate with the catalyst concentration at low pressures is clear: with an increasing pressure of hydrogen chloride, the reaction velocity increases above that of the uncatalysed reaction in a non-linear manner, attaining a constant value for catalyst pressures above 20—150 mmHg, depending on the temperature. Consideration of this case affords an answer to the interesting question of what happens in a catalysed reaction of the zero order in a catalyst when the catalyst concentration is decreased.

For the mechanism:

$$M + M \rightarrow R_1 + M_1 + M \quad (1)$$

$$R_1 + HX \rightarrow P_1 + X \quad (2)$$

$$X + M \rightarrow HX + R_2 \quad (3)$$

$$R_2 \rightarrow P_2 + R_1 \quad (4)$$

$$X + X + M \rightarrow X_2 + M \quad (5a)$$

$$X + R_1 + M \rightarrow R_1X + M \quad (5b)$$

$$R_1 + R_1 + M \rightarrow R_1R_1 + M \quad (5c)$$

where M=acetaldehyde, $R_1=\dot{C}H_3$, and $X=\dot{C}l$,

$$[R_1]/[X]=k_3[M]/k_2[HX]$$

in the steady state.

From the individual rate parameters listed in Table I

$$[\dot{C}H_3]/[\dot{C}l] \fallingdotseq 5\times[CH_3CHO]/[HCl] \text{ at } 700°K.$$

Even allowing for a considerable error in the rate

Table I.

Reaction	E kcal. mol^{-1}	log A sec^{-1} cc. mol^{-1} or sec^{-1}	Ref.
2	2.1	11.7	4, 2
2	4.5	12.2	5, 2
3	5.0	13.3	6, 2
4	16.0	11.5 (Estimated)	7

1) V. R. Stimson and E. J. Watson, *Austral. J. Shem.*, **19**, 75 (1966).
2) N. Imai, T. Fujii and O. Toyama, This Bulletin, **38**, 410 (1965).
3) R. L. Failes and V. R. Stimson, *Austral. J. Chem.*, **17**, 851 (1964).
4) R. J. Cvetanovic and E. W. R. Steacie, *Can. J. Chem.*, **31**, 158 (1953).
5) H. O. Pritchard, J. B. Pyke and A. F. Trotman-Dickenson, *J. Am. Chem. Soc.*, **77**, 2629 (1955).
6) W. A. Alexander and H. J. Schumacher, *Z. physik. Chem.*, **B44**, 57 (1939).
7) F. B. Marcotte and W. A. Noyes, *J. Am. Chem. Soc.*, **74**, 783 (1952).

constants, it is clear that the termination 5a is not likely to persist at low pressures of hydrogen chloride, and that the alternatives, 5b and/or 5c will predominate. These are also likely to be in their termolecular range and to lead to the $^{2}c\beta XM_{1,1/2}$ and $^{2}c\beta\beta M_{1/2,1}$ rate forms respectively. As $[R_1]/[R_2] \doteqdot 60$, for $[HX] = 10^{-6}$ mol. cc^{-1}, termination involving R_2 need not be considered.

The experimental results[2] at low hydrogen chloride pressures indicate that the rate is less than first-order in the catalyst, but it is not apparent whether or not a change of order in the substrate has taken place. If two termination steps occur simultaneously, the order will not be clearly integral or half-integral.

In principle, as the concentration of the catalyst is decreased the uncatalysed reaction must at some point become predominant. Where this takes place depends on the competition between Steps 2 and 6:

$$R_1 + M \rightarrow P_1 + R_2 \qquad (6)$$

Lower pressures of HX favour Step 6. However, in the case of acetaldehyde and hydrogen chloride, the uncatalysed mechanism is evidently slower than the catalysed mechanism down to very small pressures of hydrogen chloride.

The Photolysis of Propylene at 1849Å

By Shigeyoshi ARAI, Shoji SHIDA and Takeo NISHIKAWA

Laboratory of Physical Chemistry, Tokyo Institute of Technology, Ookayama, Meguro-ku, Tokyo

(Received March 7, 1966)

A number of studies have been made on the mercury-photosensitized reaction of olefins, but only a few on the direct photolysis.[1-4] In a previous paper[3] we reported a study on the photolysis of butene-1 by the light of 1849 Å, and compared the results with those which had been obtained in the mercury-photosensitized reaction.

The present note concerns a similar study on the photolysis of propylene at 1849 Å. As for the mercury-photosensitized reaction of propylene, it has been known that the primary step is the formation of an excited molecule, which either decomposes or collisionally deactivates,[5] and that the splitting of the C–H bond is the predominant process.[5-8]

The purest propylene commercially available (99.9%) was used after distillation; gas chromatographic analysis did not show any impurity. The absence of mercury vapor in the reacting system was confirmed experimentally.[3] The light source and the method of product analysis are similar to those in the previous work.[3] Dimethylsulfolane and squalane columns were used in gas chromatography. Some experiments were also made on the mercury-photosensitized reaction.

On irradiation the amounts of most products linearly increase initially, but gradually curve off after a few minutes. The latter fact may be ascribed to the decrease in the transparency of the quartz window due to the possible deposit of polymers. The light intensity has no appreciable effect on the relative yields of products. The rates of formation of all the products measured are practically independent of the propylene pressure over the 10—70 mmHg range, although slight, linear increases with the pressure were detected. This pressure dependence is quite different from that observed in the mercury-photosensitized reaction.

TABLE I. RELATIVE YIELDS OF THE PRODUCTS IN THE PHOTOLYSIS OF PROPYLENE AT 1849Å NORMALIZED TO $C_2H_6=1.00$

Time of irradiation, 1 min.
Pressure of propylene, 20 mmHg
Room temperature

Product	Relative yield
Hydrogen	0.76
Methane	0.67
Acetylene	1.00
Ethylene	0.93
Ethane	0.58
Propane	1.00
Allene	0.20
Methylacetylene	0.40
n-Butane	~0
i-Butane	0.74
Butene-1	1.3
2-Methylpentane	0.73
4-Methylpentene-1	1.8
2,3-Dimethylbutane	~0
n-Hexane	~0

1) M. C. Sauer and L. M. Dorfman, *J. Chem. Phys.*, **35**, 497 (1961).
2) H. Okabe and J. R. McNesby, ibid., **36**, 601 (1962).
3) N. Harumiya, S. Shida and S. Arai, This Bulletin, **38**, 142 (1965).
4) H. Okabe, H. D. Beckey and W. Groth, private communication.
5) A. B. Callear and R. J. Cvetanovic, *J. Chem. Phys.*, **24**, 873 (1950).
6) F. P. Lossing, D. G. H. Marsden and J. B. Farmer, *Can. J. Chem.*, **34**, 701 (1956).
7) M. Avrahmi and P. Kebarle, *J. Phys. Chem.*, **67**, 354 (1963).
8) C. A. Heller and A. S. Gordon, *J. Chem. Phys.*, **42**, 1262 (1965).

where all the products showed marked maxima in the pressure region of 10—30 mmHg. This indicates that the life-time before the decomposition of the excited state is very short, less than 10^{-9} sec. This behavior is similar to that found in the photolysis of butene-1. Table I shows the relative yields of products, normalized to $C_2H_6=1.00$.

For simplicity the following three primary processes are assumed, although others could occur.

$$C_3H_6+h\nu \rightarrow H+C_3H_5(\text{allyl}) \quad (1)$$

$$C_3H_6+h\nu \rightarrow CH_3+C_2H_3(\text{vinyl}) \quad (2)$$

$$C_3H_6+h\nu \rightarrow CH_2+C_2H_4 \quad (3)$$

The first two have generally been used for the mercury-photosensitized reaction,[5-8] and the last one has recently been found by Okabe et al. by the field ion mass spectrometer in the photolysis at 1849 Å. All the products found can be qualitatively explained with these primary processes and the subsequent radical reactions. It is to be noted, however, that butene-1 may be formed by the following two reactions.

$$CH_3 + C_3H_5 \rightarrow C_4H_8 \quad (4)$$

$$CH_2 + C_3H_6 \rightarrow C_4H_8 \quad (5)$$

The yield of C–C bond split, 2 and 3, producing methyl and methylene may be given by $CH_4+2C_2H_6+i\text{-}C_4H_{10}+C_4H_8=3.15$. On the other hand, the yield of C–H bond split, 1, producing allyl radicals may be give by the summed yield, 4-methylpentene-1 + allene + methylacetylene + xC_4H_8 = 2.40 + xC_4H_8, where x means the unknown fraction of butene-1 formed by 4.

Apart from the details of the formation of each products, it may be seen from Table I that the C–C bond split occurs to a comparable extent as the C–H bond split. This conclusion is in contrast with the results in the mercury-photosensitized reaction. Further, the result that the C–C bond split is more favored in the direct photolysis at 1849 Å than in the sensitized reaction is in accord with that obtained in the photolysis of butene-1 in the previous work.[3]

The Potassium Fluoride-catalyzed Reaction. IV. The Michael Addition of Nitroalkanes to α, β-Unsaturated Compounds

By Satoshi KAMBE

Oyama College of Technology, Oyama Tochigi

and Heinosuke YASUDA*

The Institute of Physical and Chemical Research, Bunkyo-ku, Tokyo

(Received March 28, 1966)

Wakamatsu and Shimo[1] recently reported liquid ammonia-catalyzed Michael additions of nitroalkanes to acrylonitrile and other acceptors, but such a catalyst has not generally been utilized in synthesis. In connection with previously-reported additions[2-4] of reactive methylene compounds to α, β-unsaturated compounds, using potassium fluoride as the catalyst, the present study deals with the additions of nitroalkanes to such Michael acceptors as acrylonitrile, methyl acrylate, methyl methacrylate, methyl crotonate, dimethyl fumarate and methyl cinnamate.

The addition of nitromethane to acrylonitrile in 95% ethanol containing potssium fluoride at the refluxing temperature of the solution gave crystalline tris(β-cyanoethyl)nitromethane (I) after one hour, even when a 1 : 1 molar proportion of the reactants was used. When dioxane-water (9 : 1) was employed as the solvent, the addition product I was obtained in a very low yield (0.2%); on the other hand, the starting materials were recovered unreacted in the case of a dioxane (anhydrous) solution under the same conditions. Adamcik et al.[5] have already observed that no cyanoethylation occurs in such nonhydroxylic solvents as dioxane and tetrahydrofuran.

In the cyanoethylation of nitromethane, it is noted that the yield of I is dependent upon the concentration of potassium fluoride used. The use of 0.01 mole of the fluoride per mole of nitromethane yielded 11% of I, but 0.1 mole of the catalyst gave a 63% yield. Furthermore, the nature of the solvent has a remarkable effect on the rate of the reaction and on the product yield. The yield increased with the solvating ability of the solvent in the following order;

$(CH_3)_3COH < (CH_3)_2CHOH <$
50% aqueous $C_2H_5OH \approx$ 95% C_2H_5OH

* Present address: Laboratory of Chemistry, Faculty of Education, Utsunomiya University, Utsunomiya.

1) S. Wakamatsu and K. Shimo, *J. Org. Chem.*, **27**, 1609 (1962).

2) H. Yasuda, H. Midorikawa and S. Aoyama, *Sci. Papers, Inst. Phys. Chem. Res., Tokyo*, **53**, 19 (1959).

3) S. Kambe, H. Yasuda and H. Midorikawa, ibid., **58**, 118 (1964).

4) S. Kambe and H. Yasuda, ibid., **58**, 148 (1964).

5) J. A. Adamcik and E. J. Miklasiewicz, *J. Org. Chem.*, **28**, 336 (1963).

TABLE I. NITRO COMPOUNDS OBTAINED FROM NITROALKANES

Compound	R_1	R_2	R_3	R_4	R_5	B. p. °C/mmHg	Lit. °C/mmHg	Reac. time hr.	Yield %
I	$(CH_2)_2CN$	$(CH_2)_2CN$	H	H	CN	a)		2	63
II	CH_3	H	H	H	CN	106—107/2	107—110/2[b]	2	67
III	C_2H_5	H	H	H	CN	112—113/2	110/1[c]	2	52
IV	CH_3	CH_3	H	H	CN	108—109/2	105—107/1[c]	2	53
V	H	H	H	H	$COOCH_3$	79— 80/1	82— 83/3[c]	5	34
IV	H	$(CH_2)_2COOCH_3$	H	H	$COOCH_3$	141—143/1		5	48
VII	CH_3	H	H	H	$COOCH_3$	89— 90/2	88— 89/2[c]	5	31
VIII	CH_3	$(CH_2)_2COOCH_3$	H	H	$COOCH_3$	154—155/2		5	40
IX	C_2H_5	H	H	H	$COOCH_3$	97— 98/2	97/2[c]	5	24
X	C_2H_5	$(CH_2)_2COOCH_3$	H	H	$COOCH_3$	164—165/2		5	53
XI	CH_3	CH_3	H	H	$COOCH_3$	77— 78/1	77—78.5/1.3[c]	5	80
XII	H	H	H	CH_3	$COOCH_3$	76— 77/2	82— 83/3[c]	10	29
XIII	CH_3	H	H	CH_3	$COOCH_3$	88— 89/2	88— 89/2[c]	10	31
XIV	C_2H_5	H	H	CH_3	$COOCH_3$	94— 95/4	90— 93/4[c]	10	34
XV	CH_3	CH_3	H	CH_3	$COOCH_3$	75— 76/2	72/1.3[d]	10	27
XVI	H	H	CH_3	H	$COOCH_3$	77— 79/1		20	24
XVII	CH_3	H	CH_3	H	$COOCH_3$	98— 99/2		20	6
XVIII	C_2H_5	H	CH_3	H	$COOCH_3$	92— 93/1		20	5
XIX	CH_3	CH_3	CH_3	H	$COOCH_3$	91— 92/1		20	4
XX	CH_3	CH_3	$COOCH_3$	H	$COOCH_3$	116—118/1	118—120/1[d]	7	54

a) M. p. 114—115°C. Lit., m. p. 114°C. H. A. Bruson and T. W. Riener, *J. Am. Chem. Soc.*, **65**, 25 (1943).
b) G. D. Buckley, T. J. Elliott, F. G. Hunt and A. Lowe, *J. Chem. Soc.*, **1947**, 1505.
c) N. J. Leonard and G. L. Shoemaker, *J. Am. Chem. Soc.*, **71**, 1760 (1949).
d) M. C. Kloetzel, *J. Am. Chem. Soc.*, **70**, 3571 (1948 .

In general, all primary and secondary alcohols react easily with acrylonitrile in the presence of alkaline catalysts to form the corresponding alkoxypropionitriles, but a negligible amount of ethoxypropionitrile is obtained, even in the presence of ethanol, when potassium fluoride is used.

Acrylonitrile also reacted with other nitroalkanes within two hours (see Table I). Prolonged heating (for more than two hours) did not increase the yield. No bis- or tris-cyanoethylated products were obtained in these reactions even in the presence of an excess of acrylonitrile.

Methyl acrylate readily condensed with nitroalkanes within five hours at about 80°C under the catalytic influence of potassium fluoride. The variation in adducts obtained may be attributed to the difference in the number of replaceable hydrogen atoms of the acidic nitro compounds. 2-Nitropropane, thus, gave only a 1 : 1-addition product, whereas the other nitroalkanes examined yielded 1 : 1- and 1 : 2-adducts in each case (see Table I).

In the addition of nitroalkanes to methyl methacrylate, methyl crotonate and methyl cinnamate in the presence of potassium fluoride, the yield decreased in the following order;

$CH_2=C(CH_3)COOCH_3 > CH_3CH=CHCOOCH_3 > C_6H_5CH=CHOOCH_3$

Methyl 2-methyl-4-nitrobutanoate (XII), for example, was obtained when methyl methacrylate was allowed to react with nitromethane at about 80°C for less than ten hours. Methyl crotonate gave the corresponding adduct XVI with nitromethane, but the relative yield was much lower than those obtained from the methacrylate, even after treatment had been continued for twenty hours. Methyl cinnamate, however, gave no evidence of reaction with the nitroalkanes examined, even after they had been refluxed for thirty hours, and it was recovered quantitatively.

This phenomenon[6] has also been observed in other Michael additions. This suggests that the substitution of the methyl or phenyl group at the β-position of the acceptor would offer a larger steric hindrance to nitroalkane addition than the substitution of the methyl group at the α-position.

The extension of these studies to dimethyl fumarate had disclosed an advantage of employing potassium fluoride as a catalyst; i. e., the fumarate yielded dimethyl 3-methyl-3-nitro-1, 2-butanedicarboxylate (XX) from 2-nitropropane, but the addition products from the other nitroalkanes examined could not be purified by means of distillation.

The results obtained are shown in Table I, along with the infrared data.

6) R. Connor and Wm. R. McClellan, ibid., **3**, 570 (1939).

AND α,β-UNSATURATED MATERIALS

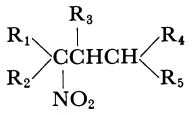

Forumula	C, % Calcd.	C, % Found	H, % Calcd.	H, % Found	N, % Calcd.	N, % Found	C≡N str. cm^{-1}	C=O str. (ester) cm^{-1}	NO_2 str. asym. cm^{-1}	NO_2 str. sym. cm^{-1}
							2250m		1542 s	1340m
							2240m		1540 s	1350m
							2250m		1550 s	1345m
							2240m		1540 s	1345m
$C_5H_9O_4N$	40.81	41.02	6.12	6.02	9.52	9.48		1730 s	1550 s	1345m
$C_9H_{15}O_6N$	46.35	46.35	6.43	6.26	6.00	5.89		1730 s	1545 s	1350sh
								1730 s	1543 s	1360m
$C_{10}H_{17}O_6N$	48.58	48.72	6.88	6.64	5.66	5.58		1730 s	1538 s	1360m
								1738 s	1550 s	1350m
$C_{11}H_{19}O_6N$	50.57	50.86	7.27	6.98	5.36	5.27		1730 s	1540 s	1320m
								1735 s	1538 s	1350m
								1725 s	1550 s	1340sh
								1730 s	1545 s	1358m
								1730 s	1550 s	1340m
								1738 s	1540 s	1348m
$C_6H_{11}O_4N$	51.89	51.29	5.94	5.90	7.56	7.67		1730 s	1550 s	1350sh
$C_7H_{13}O_4N$	47.99	48.01	7.48	7.66	8.00	7.80		1733 s	1548 s	1360m
$C_8H_{15}O_4N$	50.78	51.09	7.99	7.52	7.40	7.27		1730 s	1550 s	1360sh
$C_8H_{15}O_4N$	50.78	49.78	7.99	7.56	7.40	7.40		1735 s	1540 s	1350m
								1730 s	1542 s	1343m

e) U. S. Pat. 2361259 (1944); *Chem. Abstr.*, **39**, 2079 (1945).
Abbriviation; s, strong. m, medium, sh, shoulder. str., stretching. asym., asymmetric. sym., symmetric. The infrared data were obtained by Shimazu IR-27C infrared spectrophotometer. Compound I was measured in KBr disk, and all other compounds were measured in liquid film.

Experimental*

The Addition of Nitroalkanes to Acrylonitrile. —A mixture of an appropriate nitroalkane (0.1 mole) and acrylonitrile (0.1 mole, 5.3 g.) in ethanol (50 ml.) containing potassium fluoride (0.01 mole, 0.58 g.) was heated to reflux on a water bath for a suitable number of hours (cf, Table I). After the catalyst had been removed by filtration, the reaction mixture was poured into water (20 ml.). The resulting oily matter was extracted with ether, and the ethereal extract was dried over anhydrous calcium chloride. After the solvent had then been removed, the residual oil was distilled fractionally under diminished pressure. The results obtained are summarized in Table I. In the case of nitromethane, the only product obtained was that of the tris-cyanoethylation; no mono- or bis-cyanoethylated product was detected.

The Addition of Nitroalkanes to α,β-Unsaturated Esters. — The procedure used was essentially the same as that described above. The yields are also listed in Table I.

The authors wish to express their gratitude to Dr. Hiroshi Midorikawa of the Institute of Physical and Chemical Research for his continued encouragement. We also wish to thank Miss Toshiko Takizawa for her able assistance.

* All boiling and melting points are uncorrected.

The 1 : 1 Complex Formation of Triaryl Isocyanurates with Organic Solvents

By Yoshio IWAKURA, Keikichi UNO and Norio KOBAYASHI

Department of Synthetic Chemistry, Faculty of Engineering, University of Tokyo, Bunkyo-ku, Tokyo

(Received March 18, 1966)

During the course of an investigation of isocyanate polymerization, it has been found that triaryl isocyanurates tend to form 1 : 1 complexes with various organic solvents.

Table I. Analytical data of complexes
$(R\text{-}NCO)_3\text{-}X$

R	X	Composition	Analysis, % Calcd. C	H	N	Found C	H	N
Phenyl	DMF	$C_{24}H_{22}N_4O_4$	66.96	5.15	13.02	66.99	5.17	12.95
p-Tolyl	DMF	$C_{27}H_{28}N_4O_4$	68.62	5.97	11.86	68.85	5.93	11.93
p-Tolyl	Benzene	$C_{30}H_{27}N_3O_3$	75.45	5.70	8.80	75.67	5.53	8.82
p-Tolyl	Acetone	$C_{27}H_{27}N_3O_4$	70.88	5.95	9.19	70.86	5.93	9.48
p-Methoxyphenyl	DMF	$C_{27}H_{28}N_4O_7$	62.30	5.42	10.76	61.55	5.20	10.70
p-Methoxyphenyl	Benzene	$C_{30}H_{27}N_3O_6$	68.56	5.18	8.00	68.55	5.30	7.90
p-Methoxyphenyl	Acetone	$C_{27}H_{27}N_3O_7$	64.15	5.38	8.71	64.04	5.34	8.60
p-Chlorophenyl	DMF	$C_{24}H_{19}N_4O_4Cl_3$	54.00	3.59	10.50	54.40	3.87	10.59
p-Chlorophenyl	Acetone	$C_{24}H_{18}N_3O_4Cl_3$*	55.56	3.50	8.10	55.37	3.53	7.94

* Cl: Calcd., 20.50%. Found, 20.67%.

Table II. C=O Band frequencies of 1 : 1 complexes (Nujol mull)

R	X	cm^{-1}
Phenyl	—	1710
Phenyl	DMF	1700, 1670
p-Tolyl	—	1765, 1715, 1690
p-Tolyl	DMF	1700, 1675
p-Tolyl	Benzene	1700
p-Tolyl	Acetone	1700
p-Methoxyphenyl	—	1765, 1715, 1690
p-Methoxyphenyl	DMF	1700, 1680
p-Methoxyphenyl	Benzene	1700
p-Methoxyphenyl	Acetone	1700
p-Chlorophenyl	—	1770, 1715, 1690
p-Chlorophenyl	DMF	1700, 1670
p-Chlorophenyl	Acetone	1700

Triaryl isocyanurates have previously been reported by Tsuzuki and his co-workers[1] to form 1 : 1 complexes with alkylene carbonates, such as ethylene carbonate, propylene carbonate, and chloroethylene carbonate. This paper will discuss the formation of 1 : 1 complexes of triphenyl, tri-*p*-tolyl, tri-*p*-methoxyphenyl, and tri-*p*-chlorophenyl isocyanurates with *N, N*-dimethylformamide (DMF), benzene, and acetone.

When triaryl isocyanurates were boiled in such a solvent for about 2 hr., complexes were formed and isolated as colorless crystals on cooling or by the removal of the solvent. They were characterized by elemental analyses (Table I) and by infrared spectra analyses. The infrared absorption spectra of complexes contain almost all the principal bands of both components, but the relative intensity and the frequency of the C=O stretching absorption bands varied remarkably. The C=O bands of triaryl isocyanurates and complexes are summarized in Table II.

Methanol and ether did not form complexes with triaryl isocyanurates, and attempts to prepare such complexes as triphenyl isocyanurate-benzophenone and tri-*p*-tolyl isocyanurate-pyridine were unsuccessful.

The complex was stable for a long period at room temperature under reduced pressure, but it decomposed to the original two components on being heated above 100°C in vacuo. When the complexes of triphenyl isocyanurate-DMF and tri-*p*-methoxyphenyl isocyanurate-benzene were submitted to thermogravinometric analysis, there was observed a weight loss corresponding to the amount of the solvent in the complex in the temperature range from 70 to 150°C. The complexes show the melting points of the original triaryl isocyanurates because of the liberation of the solvents by the heating.

Experimental

Triaryl Isocyanurates.—Triphenyl isocyanurate (m. p. 280°C), tri-*p*-tolyl isocyanurate (m. p. 264°C), tri-*p*-methoxyphenyl isocyanurate (m. p. 260°C), and tri-*p*-chlorophenyl isocyanurate (m. p. 318°C) were prepared by the method given in the literature.[2]

1 : 1 Complexes of Triaryl Isocyanurates with Solvents.—The data of the elemental analysis and the characteristic infrared absorption bands are listed in Table I and Table II respectively. They were prepared by the same procedure. A typical synthesis is described below.

The Synthesis of the Triphenyl Isocyanurate-DMF Complex.—Triphenyl isocyanurate (0.5 g.) was treated with boiling DMF (15 ml.) for 2 hr. After the reaction mixture had cooled, the DMF was removed by distillation under reduced pressure. The colorless crystals which were then precipitated were washed with ether. Yield, 83%.

1) R. Tsuzuki, K. Ichikawa and M. Kase, *J. Org. Chem.*, **25**, 1009 (1960).

2) J. Idris Jones and N. G. Savill, *J. Chem. Soc.*, **1957**, 4392.

Studies on Amino-hexoses. X. A Synthesis of *p*-Acetaminophenyl *N*-Acetyl-β-muramide

By Satoko ISEMURA and Yoshio MATSUSHIMA

Department of Chemistry, Osaka University, College of Science, Toyonaka

(Received April 2, 1966)

Lysozyme, the enzyme which exerts a bacteriolytic influence, has been found to split the bacterial cell-wall mucopeptides at the site of the glycosidic bond of the *N*-acetyl muramic acid component.[1] However, the substrate specificity of the enzyme is not very clear because of the complexity of the chemical structure of the mucopeptides. Lysozyme is also known to split the glycosidic bonds of chitin[2] and glycol chitin[3], both of which have no *N*-acetyl muramic acid as a component. The present work has been undertaken as a part of the project for the elucidation of the substrate specificity of lysozyme. The course of the synthesis of the model substrate (Fig. 1) followed basically the method reported by one of the present authors.[4] *p*-Nitrophenyl *N*-acetyl-β-D-glucosaminide (I)[5] was reduced to the *p*-aminophenyl compound (II), which was converted to the *p*-acetaminophenyl compound (IV) by acetylation and *O*-deacetylation. The benzylidene derivative of IV was condensed with L-α-chloropropionic acid, and the product, after mild acid hydrolysis, was the desired *p*-acetaminophenyl *N*-acetyl-β-muramide. The methyl ester was obtained by methylation with diazomethane. Egg-white lysozyme revealed no activity on either of these model substrates.

Experimental

p-Aminophenyl 2-Acetamido-2-deoxy-β-D-glucopyranoside (II).—I (4.4 g.) and 32 g. of ferrous sulfate hydrate ($FeSO_4 \cdot 7H_2O$) were suspended in 600 ml. of water, and then 2 ml. of 2 N hydrochloric acid was added. The suspension was stirred and heated to 60°C. Eight milliliters of concentrated ammonium hydroxide (ca. 28%) was added in one portion, and then three 3 ml. portions of ammonium hydroxide were added at two-minute intervals. After the mixture had been stirred for fifteen minutes, the precipitates were removed by filtration and the filtrates were concentrated in vacuo. The concentrate was extracted with methanol, evaporated, and desalted by passing it through a column of Dowex-1 (OH^- form). The eluate was concentrated in vacuo, and the residue was recrystallized from ethanol, giving 2.7 g. (67%) of colorless crystals which melted at 225—228°C (uncorr.). $[\alpha]_D^{16}$ +7.6° (*c* 0.92, water).

Found: C, 53.87; H, 6.80; N, 8.80. Calcd. for $C_{14}H_{20}O_6N_2$: C, 53.84; H, 6.45; N, 8.97%.

p-Acetaminophenyl 2-Acetamido-3,4,6-tri-*O*-acetyl-2-deoxy-β-D-glucopyranoside (III).—II (5.8 g.) was dissolved in a mixture of 60 ml. of acetic anhydride and 60 ml. of pyridine. The temperature of the reaction mixture was raised to 50°C in ten minutes, and then the mixture was poured into ice water. The crystalline product was collected by filtration and was recrystallized from ethanol. The colorless crystals thus obtained weighed 5.6 g. (63%) and melted at 245°C (uncorr.). $[\alpha]_D^{16}$ −40.3° (*c* 0.92, pyridine).

Found: C, 55.04; H, 5.83; N, 5.79. Calcd. for $C_{22}H_{28}O_{10}N_2$: C, 54.99; H, 5.87; N, 5.83%.

p-Acetaminophenyl 2-Acetamido-2-deoxy-β-D-glucopyranoside (IV).—III (3 g.) was dissolved in 75 ml. of absolute methanol. After the addition of 3 ml. of 1 N sodium methoxide, the solution was shaken for several minutes. A de-*O*-acetylated product separated and was collected and recrystallized from methanol, giving 1.5 g. (68%) of colorless crystals which melted at 236—237°C (uncorr.). $[\alpha]_D^{16}$ +6.1° (*c* 1.02, water).

Found: C, 54.01; H, 6.13; N, 7.79. Calcd. for $C_{16}H_{22}O_7N_2$: C, 54.23; H, 6.26; N, 7.91%.

p-Acetaminophenyl 2-Acetamido-4,6-*O*-benzylidene-2-deoxy-β-D-glucopyranoside (V).—IV (3.2 g.), 40 ml. of freshly-distilled benzaldehyde and 3.2 g. of anhydrous zinc chloride were shaken together in a closed bottle for 24 hr. The reaction mixture was then poured into ice water, and the insoluble material was separated from the water layer by decantation. The product gave, after it had been washed with petroleum ether and recrystallized from ethanol, 2.8 g. (70%) of colorless crystals which melted at 258—262°C (uncorr.). $[\alpha]_D^{16}$ −10° (*c* 1.83, dimethylformamide).

Found: C, 62.01; H, 6.08; N, 6.26. Calcd. for $C_{23}H_{26}O_7N_2$: C, 62.43; H, 5.92; N, 6.33%.

p-Acetaminophenyl 2-Acetamido-4,6-*O*-benzylidene-3-*O*-(D-1'-carboxyethyl)-2-deoxy-β-D-glucopyranoside (VI).—V (2.7 g.) was dissolved in 105 ml. of freshly-distilled dimethylformamide, and the mixture was heated to 30°C. Sodium hydride (0.7 g., suspended in mineral oil at ca. a 50% concentration) was added, and the mixture was stirred for one hour. After the reaction temperature had been raised to 40°C, 3.8 g. of L-α-chloropropionic acid was added, and then 2.8 g. more of sodium hydride was added after 30 min. Stirring was continued overnight without applying any exteranl heating. Water was added in order to decompose the excess sodium hydride, and the mixture was concentrated in vacuo. The concentrate was dissolved in water, and the solution, after it had been washed with chloroform, was made acidic (pH

1) M. R. J. Salton and J. M. Ghuysen, *Biochim. Biophys. Acta*, **36**, 552 (1959); **45**, 355 (1960).
2) L. R. Berger and R. S. Weiser, ibid., **26**, 517 (1957).
3) K. Hamaguchi and M. Funatsu, *J. Biochem.*, **46**, 1695 (1959).
4) Y. Matsushima and J. T. Park, *J. Org. Chem.*, **27**, 3581 (1962).
5) *Biochemical Preparations*, **10**, 118 (1963).

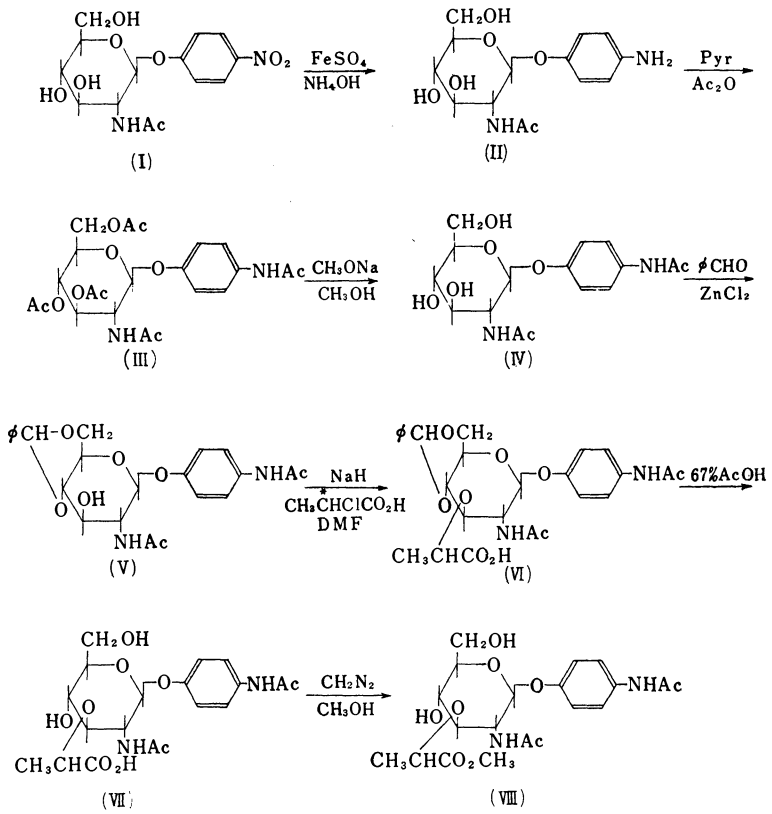

Fig. 1. The reaction sequence of the synthesis.

2.8) by adding hydrochloric acid while the mixture was kept at the temperature of ice water. The precipitates were collected and recrystallized from ethanol, giving 1.4 g. (43%) of colorless crystals which melted at 248—250°C (uncorr.). $[\alpha]_D^{16}$ +15.4° (*c* 0.72, dimethylformamide).

Found: C, 58.73; H, 6.30; N, 5.05. Calcd. for $C_{26}H_{30}O_9N_2 \cdot H_2O$: C, 58.64; H, 6.06; N, 5.26%.

The hydrochloric acid hydrolysis of VI gave a product which showed a spot identical to that of muramic acid on a paper chromatogram with the solvent system of phenol-water (75 : 25). VI showed an absorption band at 1740 cm^{-1} in the infrared spectrum, a band due to carboxyl carbonyl.

***p*-Acetaminophenyl 2-Acetamido-3-*O*-(D-1'-carboxyethyl)-2-deoxy-β-D-glucopyranoside (VII).**—In the 67% acetic acid, VI was boiled for ten minutes. After the solution had then been evaporated in vacuo, there remained a syrup which failed to crystallized.

***p*-Acetaminophenyl 2-Acetamido-3-*O*-(methyl-D-1'-ethylcarboxylate)-2-deoxy-β-D-glucopyranoside (VIII).**—An ethereal solution of diazomethane was dropped into the methanol solution of VII until a persistent yellow color remained. After evaporation in vacuo, the residual syrup was dissolved in a small amount of methanol; the mixture was then allowed to stand at −20°C. The crystals thus obtained were recrystallized from methanol, giving a specimen which melted at 210—213°C (uncorr.). $[\alpha]_D^{16}$ +17° (*c* 0.94, methanol).

Found: C, 54.03; H, 6.54; N, 5.93. Calcd. for $C_{20}H_{28}O_9N_2$: C, 54.54; H, 6.41; N, 6.36%.

This investigation was supported by U. S. Public Health Service Grant No. AI-04586-04.

On the Relative Rate of Energy Transfer from the Excited Argon Atom

By Masaru NISHIKAWA and Niro MATSUURA

Department of Pure and Apllied Sciences, College of General Education, University of Tokyo, Komaba, Meguro-ku, Tokyo

(Received April 15, 1966)

A reduction in the spark-breakdown potential[1] and the starting potential for the glow discharge in neon by small traces of argon[2] has long been recognized; it is often called the Penning effect. A similar effect of a contaminant gas in reducing W-values upon the ionization of rare gases under irradiation has been interpreted as resulting from energy transfer from the excited species of the latter, leading to the subsequent ionization of the former.[3] The effect has been employed in a sensitive detector for gas chromatography. Recently, Collinson et al. studied the effect in the argon butane system from the viewpoint of radiation chemistry in an electric field,[4] in which it was necessary for them to evaluate the relative rate constant for energy transfer, $k_8/(k_{2a}+k_{2b})$, as in their terminology;

$$Ar^*+B \rightarrow Ar+B^++e^- \quad (2a)$$

$$Ar^*+B \rightarrow Ar+(\text{uncharged species}) \quad (2b)$$

$$Ar^*+Ar \text{ (or wall)} \rightarrow Ar+Ar \text{ (or wall)} \quad (8)$$

They estimated the value from the known relative rate,[3] 4000, for the ionization of argon in trace amounts by metastable neon atoms to the de-excitation of the latter by ground-state neon atoms, together with the correction for the difference in cross-sectional areas for the various species. Thus, $k_8/(k_{2a}+k_{2b}) = (1/4000) \times (\sigma_{Ar}^2/\sigma_{Ne}\cdot\sigma_B)$, which, when suitable figures are supplied, yields 6000 as the value.

The objective of the present note is to show that the rate can be obtained also from their own data on ion current measurements.

In their system primary electrons produced by the action of radiation are accelerated to an energy capable of exciting argon to metastable states;

$$e^- \rightarrow e_{en}^- \quad (5)$$

$$e_{en}^- + Ar \rightarrow Ar^* + e^- \quad (6)$$

Let a "primary" electron - accelerated in the field between each collision - produce α metastable atoms per cm. of its path in field direction. Of the α metastable atoms,[5] a fraction proportional to $k_{2a}[B]/\{(k_{2a}+k_{2b})[B]+k_8[A]\}$ enters into Reaction 2a. Thus the increase in the number of electrons along the length, dx, is $N_x\cdot\alpha\cdot dx\cdot k_{2a}[B]/\{(k_{2a}+k_{2b})[B]+k_8[A]\}$ per N_x electrons. By intergrating from $x=0$ to $x=d$;

$$N/N_0 = i/i_0 = \exp(\alpha\cdot d\cdot k_{2a}[B]/\{(k_{2a}+k_{2b})[B] + k_8[A]\})$$

where N_0 is the number of electrons per sec., and i_0, the current produced initially by irradiation. This is essentially the equation for Townsend discharge,[6] as Collinson et al. noted, although they used a different (but equivalent) expression. If the equation applies to the present case, the plot of $1/\ln(i/i_0)$ vs. [A]/[B] should give straight lines, whose slope-to-intercept ratio should then yield the desired relative rate. The data of i/i_0 read from their Fig. 3, at least the initial portion of the curves where [B] is sufficiently small,[7] are shown to lie on straight lines in Fig. 1. The relative rate

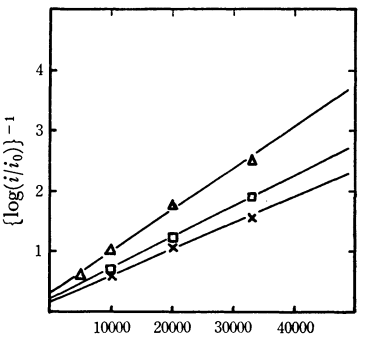

Fig. 1. Plot of $\{\log(i/i_0)\}^{-1}$ vs. [A]/[B]
Field strength; △, 3900 V./cm., □, 4800 V./cm., ×, 5700 V./cm.
(Read from Fig. 3 of Ref. 4.)

thus obtained is approximately 4500, this is in agreement with Collinson's estimation for any one of straight lines, and so seems to indicate the validity of the treatment. The value is of the same order as that of 2270 obtained recently by Lipsky when

1) F. M. Penning, *Naturwissenschaften*, **15**, 818 (1927).
2) F. M. Penning and C. C. J. Addink, *Physica*, **1**, 1007 (1934).
3) W. P. Jesse and J. Sadauski, *Phys. Rev.*, **100**, 1755 (1955).
4) E. Collinson, J. F. Todd and F. Wilkinson, *Discussions Faraday Soc.*, **36**, 83 (1963).
5) This statement only applies to the case where [B] is sufficiently low compared with [A]. At higher [B], e^- collides with B suppressing electron-multiplication sequence.
6) A. von Engel, "Ionized Gases," 2nd Ed., Chapter 7, Oxford University Press, London (1965).
7) See Ref. 5.

no electron multiplication occurs.[8] The agreement can be said to be fair if a large difference in the experimental conditions and the lack of exact data are taken into consideration. The larger value estimated in this paper may be due to the drastic change in conditions where electron multiplication predominates, and/or to the larger ion current measured by Collinson et al., which, as is pointed out by Lipsky, might be caused by the higher drift velocity of electrons in the presence of polyatomic contaminant than in that of pure argon. Corrections for the latter effect are expected to alter the value to bring it closer to Lipsky's value.

A similar study is now in progress with the Ar-NH_3 system, partly in connection with the sensitized production of hydrazine; the results will be published elsewhere.

8) M. M. Shahin and S. R. Lipsky, *J. Chem. Phys.*, **41**, 2021 (1964).

The Stereochemistry of Sulfoxide in the Base-Catalyzed Hydrogen-Isotopic Exchange of Aryl-Methyl Sulfoxide[1]

By Yong-He KHIM, Waichiro TAGAKI, Masahiro KISE, Naomichi FURUKAWA and Shigeru OAE

Department of Applied Chemistry, Faculty of Engineering, Osaka City University

(Received April 23, 1966)

Because of the possible 3d orbital resonance of the following type:

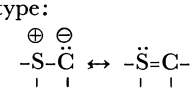

the base-catalyzed hydrogen-isotopic exchange of the methyl or methylene group attached to a trivalent or tetravalent sulfur group has been known to take place very readily,[2] and the stereochemistry of both the sulfone and the sulfoxide stabilized carbanions have been pretty well worked out.[3,4]

When the incipient carbanion is presumed to be stabilized by a trivalent sulfur group, such as sulfinyl or sulfonio, an interesting problem is raised regarding the stereochemistry at the sulfur atom attached to the carbanion if one uses an optically-active sulfur group. A study of this kind would be quite significant, since it would answer the hitherto often-argued question of whether or not the π-bond between the sulfur atom and the carbon atom is of the 2p-3p overlapping type, with the promotion of the unshared outer valence electrons on the sulfur atom to a d-orbital, or if the π-bond is of the 2p-3d overlapping type.[5] That is, if the π-bond is of the 2p-3p overlapping type, the carbanion formation will result in the racemization of the trivalent sulfur group, while the retention of the configuration of the sulfur group will be observed if the carbanion is stabilized by a 2p-3d overlapping-type conjugation. Recently Cram et al. have observed a complete retention of the configuration of the sulfoxide group in the base-catalyzed racemization of optically-active 2-octyl phenyl sulfoxide, that has two asymmetric centers.[3c] We have chosen a simpler system, but with only one asymmetric center, namely, (+)-*p*-toly methyl sulfoxide, we have found that the base-catalyzed hydrogen isotopic exchange does not accompany the racemization of the sulfoxide group.

An optically-active *p*-tolyl methyl sulfoxide was prepared from the reaction of optically-active (−)-menthyl (−)-*p*-toluenesulfinate with methylmagnesium iodide[6] and was then subjected to base-catalyzed hydrogen isotopic exchange in various solvents in order to examine the possible racemization, along with the H–D exchange on the methyl group attached to the sulfoxide.

The solvents used were ethanol-d_1, *t*-butanol-d_1, and dimethyl sulfoxide. Ethanol-d_1 and *t*-butanol-d_1 were prepared from the reaction of deuterium oxide with sodium ethoxide and potassium *t*-butoxide respectively.[7]

1) Paper XII on Sulfoxides. XI; S. Oae, K. Kikukawa, N. Kunieda and W. Tagaki, This Bulletin, **39**, 614 (1966).

2) a) J. Hochberg and K. F. Bonhoeffer, *Z. Physik. Chem.*, **184A**, 419 (1939); b) W. E. V. Doering and L. K. Levy, *J. Am. Chem. Soc.*, **77**, 509 (1955).

3) a) D. J. Cram, W. D. Nielsen and B. Rickborn, ibid., **82**, 6415 (1960); b) D. J. Cram, D. A. Scott and W. D. Nielsen, ibid., **83**, 3696 (1961); c) D. J. Cram and A. S. Wingrone, ibid., **85**, 1096, 1101 (1963).

4) a) S. Oae and C. C. Price, ibid., **80**, 3425, 4938 (1958); b) S. Oae, W. Tagaki and A. Ohno, ibid., **83**, 5036 (1961); c) S. Oae, "3d Orbital Resonance Involving the Sulfur Atom in Organic Sulfides," in "Org. Sulfur Compounds," Vol. IV, Ed. by N. Kharasch, Pergamon Press (in press).

5) G. Suld and C. C. Price, *J. Am. Chem. Soc.*, **83**, 1770 (1961).

6) K. Mislow, M. Green, P. Laur, J. T. Melillo, T. Simmons and A. L. Ternay, Jr., ibid., **87**, 1958 (1965).

7) S. Oae, W. Tagaki and A. Ohno, *Tetrahedron*, **20**, 423 (1964).

TABLE I. THE BASE-CATALYZED HYDROGEN-DEUTERIUM EXCHANGE AND RACEMIZATION REACTION OF *p*-TOLYL METHYL SULFOXIDE

Sulfoxide	Solvent	Base	Molar ratio[a]	Temp. °C	Time hr.	H-D[b] Exchange %	$[\alpha]_D$
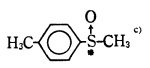	C_2H_5OD[d]	C_2H_5ONa	(1 : 5 : 0.5)	30—35	15	60	+152°
	C_2H_5OD[d]	C_2H_5ONa	(1 : 10 : 0.5)	105—110	15	66	+148.7°
	$(CH_3)_3COD$[e]	$(CH_3)_3COK$	(1 : 10 : 0.5)	105—110	15	20	+149°
	$(CH_3)_2SO$	$(CH_3)_3COK$	(1 : 15 : 2)	105—110	15	—	+148.2°
	$(CH_3)_2SO$	$(CH_3)_3COK$	(1 : 20 : 5)	130—135	20	not recovered[f]	

a) The molar ratio is starting sulfoxide : solvent : base.
b) The deuterium contents were analyzed by means of infrared and nuclear magnetic resonance spectroscopy.
c) $[\alpha]_D^{25}$ +152.3° (*c* 2.68, ethanol).
d) Deuterium content: 70%.
e) Deuterium content: 60%.
f) The starting sulfoxide seems to be decomposed.

The sulfoxide was recovered quantitatively, and from its melting point, ultraviolet absorption, infrared and nuclear magnetic resonance spectroscopic analyses it was found to be identical with the starting sulfoxide, except that the sulfoxide recovered was found to have incorporated a considerable amount of deuterium at the methyl group. However, the sulfoxide was found to have retained its configuration completely. The experimental conditions and the results are shown in Table I.

Although a substantial hydrogen isotopic exchange was observed to occur at the *p*-methyl group at a high temperature and with a prolonged heating, only a very small amount of hydrogen isotopic exchange at the para methyl group was observed when the reaction was performed under the relatively mild conditions in which a substantial amount of hydrogen isotopic exchange was found to take place at the other methyl group.

Moreover, the configuration around the sulfur atom of the trivalent sulfur group is retained regardless of any change in the solvent used.

These observations appear to suggest strongly that the carbanion attached to a trivalent sulfur group such as sulfoxide is stabilized by the resonance involving the 2p-orbital of carbon and the 3d-orbital of sulfur.

Experimental

(−)-Menthyl (−)-*p*-Toluenesulfinate.—The sulfinate was prepared, according to the method reported by Mislow et al.,[6] from 18.8 g. of (−)-menthol and 21 g. of *p*-toluenesulfinyl chloride[8] to give 8 g. of (−)-menthyl (−)-*p*-toluenesulfinate. (60%) M. p. 105—106°C; $[\alpha]_D^{20}$ −201° (*c* 2.0, acetone).

(+)-*p*-Tolyl Methyl Sulfoxide.[6]—To a solution of (−)-menthyl (−)-*p*-toluenesulfinate (6.2 g.) in anhydrous ether (50 ml.), an ether solution of methyl magnesium iodide (prepared from 5.36 g. of methyl iodide and 1.02 g. of magnesium was added drop by drop at room temp. After it had been stirred for an hour, the reaction mixture was quenched with aqueous ammonium chloride. The ether layer was separated, washed with water, and then dried over mangesium sulfate. After the ether had been removed, the residue was cooled in an ice bath, then the precipitate was filtered to give crude (+)-*p*-tolyl methyl sulfoxide, which was recrystallized from *n*-hexane. (3.0 g., 92%) M. p. 75—76°C; $[\alpha]_D^{25}$ +152.3° (*c* 2.0, ethanol). Lit.[6] m. p. 73—74°C; $[\alpha]_D^{25}$ +145.5° (*c* 2.0, acetone).

The Base-catalyzed Hydrogen-deuterium Exchange and Racemization Reaction of (+)-*p*-Tolyl Methyl Sulfoxide.—The H–D exchange and racemization reaction of the sulfoxide was performed using both C_2H_5OD and *t*-BuOD as solvents. The bases used were sodium ethoxide and potassium *t*-butoxide. Ethanol-*O*-*d* and *t*-butanol-*O*-*d* were prepared from the corresponding alkoxides with deuterium oxide.[7] The deuterium contents were determined by means of infrared and NMR studies. The D content was about 70%. A typical run was as follows: optically active (+)-*p*-tolyl methyl sulfoxide (0.3 g.) and sodium ethoxide (0.052 g.) were dissolved in ethanol-*O*-*d* (0.46 g.) and sealed in a glass ampoule. The ampoule was then heated in an oil bath at 105—110°C. After it had been heated for 15 hr., the reaction mixture was evaporated and the sulfoxide was recovered by extracting it with ether. (0.2 g., m. p. 75—76°C from *n*-hexane.) The optical activity of the recovered sulfoxide was checked by using a polarimeter and found to be $[\alpha]_D^{25}$ +148.7° (*c* 2.68, ethanol). The deuterium content of the methyl group attached to the sulfoxide was determined by NMR spectra.

Found: 60—66% (τ=7.27 singlet.).

When DMSO was used as a solvent, the racemization reaction of the sulfoxide was carried out with only one base, namely, potassium-*t*-butoxide.

The authors are grateful to Professor Toshiro Miwa for his collaboration in the NMR study.

8) "Organic Syntheses," Coll. Vol. 4, 937 (1963).

SHORT COMMUNICATIONS

Ethylenediamine Conjugates of Bis-*O*-carboxymethylsalicylaldehyde-alkylenediimine-copper*

By Tsuguo TANAKA, Shigeharu KONO,** Keiko MIYAHARA and Kazuko KATSUKI

Department of Science and Technology, Saga University, Honjo, Saga

(Received June 23, 1966)

The isolation and the structures of the penta-coordinate addition compounds of bis-salicylaldehyde - ethylenediimine - copper with acids and phenols have previously been reported.[1] Therefore, it now seems of interest to synthesize some side-chain acid bis-salicylaldehyde-ethylenediimine-copper substances and examine their chemical behavior.

Yellow - green bis - *O* - carboxymethylsalicylaldehyde - ethylenediimine-copper (I, $n = 2$) - $2H_2O$, (Found: C, 49.80; H, 4.83; N, 5.71; Cu 13.36. Calcd. for $C_{20}H_{18}N_2O_6Cu$-$2H_2O$: C, 49.84; H, 4.60; N, 5.68; Cu, 13.19%.) was synthesized through copper salt of *O*-carboxymethylsalicylaldehyde. Found: C, 47.13; H, 4.13, Cu, 13.86. Calcd. for $C_{18}H_{14}O_8Cu$-$2H_2O$: C, 47.20; H, 3.69; Cu, 13.88%.

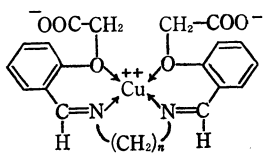

(I, *n*)

The 1660 cm^{-1} peak in its infrared spectra as well as the 830 mμ absorption maximum in its visible spectra support a partially-polarized[2] ionic structure.[3]

Ethylenediamine conjugate (II, $n=2$) was obtained by the reaction of (I, $n=2$) with two moles of ethylenediamine in an alcoholic solution.

The analytical results (Found: C, 46.72; H, 6.49; N, 13.95; Cu, 10.34. Calcd. for $C_{24}H_{36}N_6O_7Cu$-$3H_2O$: C, 45.16; H, 6.63; N, 13.17; Cu, 9.96%.) and the titration curve (Fig. 1) substantiate the formula, [(I, $n=2$)-$2C_2H_4(NH_2)_2$-$H]^+(OH)^-$-$3H_2O$, of the ethylenediamine conjugate (II, $n=2$). The 1578 cm^{-1} peak of the prefectly-ionized carboxylate ion[4] in the infrared spectra and the 570 mμ absorption maximum in the visible region, unlike those of the chelate (I, $n=2$), reveal the structural difference between (I, $n=2$) and (II, $n=2$). By dehydration (II, $n=2$) changes, by way of a blue modification (weight decrease; Found: 8.35%. Calcd. for $3H_2O$: 8.47%), into a green compound (weight decrease: Found; 11.1%; Calcd. for $4H_2O$: 11.3%), which, in dry air or in an oxygen atmosphere, changes into a gray modification (III, $n=2$) (weight increase: 2.56—2.96% and, slowly, 3.6—4.0%).

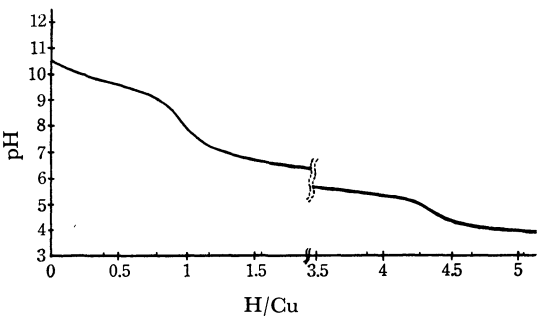

Fig. 1. Titration of (II, $n=2$), 186.67 mg. in 50 ml. H_2O, titrated with 1.0 N HCl ($f=1.135$).

Several bis-*O*-carboxymethylsalicylaldehyde-alkylenediimine-copper (II, $n=2$—6)-$2H_2O$ substances and their ethylenediamine conjugates (II, $n=2$—6) are given in Table I.

Table I. Bis-*O*-carboxymethylsalicylaldehyde-ethylenediimine-copper (I, *n*)-$2H_2O$ and their ethylenediamine conjugate (II, *n*)

$n=$	(I, *n*) Color	(II, *n*) Color
2	yellow-green	purple
3	green	purple
4	green-blue	purple
6	pale-blue	purple

* Part VIII of "Some Addition Compounds of Salicylaldehyde-ethylenediimine - copper." Partly reported in the Proceedings of the IX I. C. C. C., St. Moritz, 1966.

** Eisai Pharmaceutical Company.

1) T. Tanaka, *J. Chem. Soc. Japan, Pure Chem. Sect.* (*Nippon Kagaku Zasshi*), **83**, 1179 (1962).

2) A. Rosenberg, *Acta Chim. Scand.*, **10**, 840 (1956).

3) H. Ozima, *J. Chem. Soc. Japan, Pure Chem. Sect.* (*Nippon Kagaku Zasshi*), **86**, 718 (1965).

4) T. Tanaka, ibid., **81**, 1013 (1960); K. Nakamoto, Y. Morino, and A. E. Martell, *J. Am. Chem. Soc.*, **83**, 4528 (1961).

The Micro Determination of Palladium with *p*-Ethoxy-chrysoidine

By J. P. TANDON and S. S. GOYAL

Department of Chemistry, University of Rajasthan, Jaipur, India

(Received August 2, 1966)

The use of a number of chromogenic reagents in the determination of platinum metals has been reported. For instance, Grigore Popa and his co-workers[1] described the spectrophotometric determination of palladium with chrysoidine within the range from 1 to 15 μg. palladium/ml. In the present investigations, the use of *p*-ethoxy-chrysoidine, which contains the chromogenic group ($-OC_2H_5$), in the spectrophotometric determination of palladium will be described; it will be shown to be more sensitive than chrysoidine.

The absorption spectra of the dye and palladium complex are shown in Fig. 1. The maximum difference in absorbance (Δ-absorbance) between the dye and the palladium complex is found at 465 mμ at pH 2.2. The complex is formed by adding 0.5 ml. of a 0.002 M palladium solution to a mixture of 10 ml. of a sodium acetate - hydrochloric acid buffer solution (pH 2.2) and 1.0 ml. of a 0.002 M dye solution in a 50-ml. volumetric flask. The solution is then diluted to the mark with double-distilled water and mixed thoroughly. A dye blank is also prepared under similar conditions. The Δ-absorbance between the dye blank and the palladium complex is at its maximum in the 2.0—2.4 pH range. The colour under these conditions develops instantaneously and is stable for at least one hour. There is no variation in the Δ-absorbance over the temperature range of 15—45°C. The presence of excess palladium, however, helps in the coagulation of the complex.

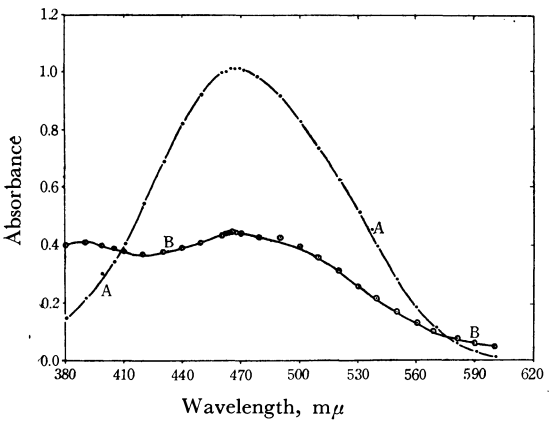

Fig. 1. Absorption spectra. pH 2.2
A: Reagent (4×10^{-5} M), against water
B: Reagent (4×10^{-5} M) + Pd (2×10^{-5} M), against water

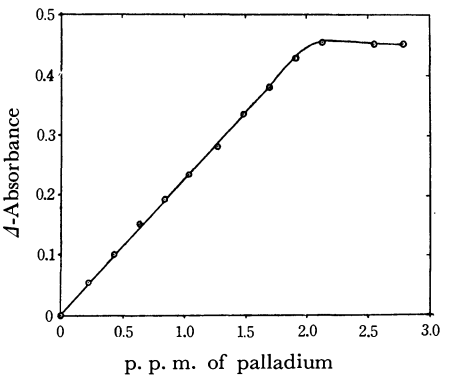

Fig. 2. Beer's law curve. pH 2.2

Beer's law holds over the 0—1.9 p. p. m. palladium/ml. range at 465 mμ (Fig. 2); the molar absorptivity is 2.5×10^4, and the sensitivity is 0.004 μg. palladium/cm^2, corresponding to $\log I_0/I = 0.001$.

Composition studies by Vosburgh and Cooper's method[2] and by the slope-ratio method[3] indicate the formation of only one compound, with a ratio of palladium to dye of 1 : 2.

Further, more detailed studies are now in progress.

1) G. Popa, V. Croitoru and D. Costache, *Studia Univ. Babes-Bolyai, Ser. Chem.*, **8**(1), 195 (1963).

2) W. C. Vosburgh and G. R. Cooper, *J. Am. Chem. Soc.*, **63**, 437 (1941).

3) A. E. Harvey and D. L. Manning, ibid., **72**, 4448 (1950).

The Hydrogen Isotope Effects Arising from the Reaction of Hydrated Electrons

By Shin-ichi OHNO

Japan Atomic Energy Research Institute, Tokai-mura, Ibaraki

(Received August 23, 1966)

The measurement of hydrogen isotope effects has been applied to the elucidation of the reactions occurring during the radiolysis of water.[1-3] The question still remains unclear, however, because of the complicated set of reaction processes involved. This communication will present the isotope effect in the formation of H atoms arising from the reaction between e^-_{aq} and proton donors.

In a H_2O-D_2O mixture containing 1 M methanol, the photochemically-produced electron from 10^{-3} M $K_4[Fe(CN)_6]$[4] reacts with the added solute, SH:

$$e^-_{aq} + SH \rightarrow \begin{matrix} H + S^- \\ \searrow \\ D + S^- \end{matrix} \qquad (1)$$

The hydrogen atoms thus produced, H and D, react with CH_3OH to yield H_2 and HD respectively, the observed value of (H_2/HD) giving directly the hydrogen atom ratio, $(H/D)_a$, arising from Reaction 1. The separation factors defined by $S=(H/D)_a/(H/D)_{solvent}$ are given in Table I. The value for the hydrogen ion (H_2SO_4) confirms the values previously arrived at using radiation chemical data.[2,3] The hydrogen ion exists as H_3O^+, HD_2O^+, H_2DO^+ and D_3O^+; the estimated fraction of each species can be obtained from the literature.[5]

Table I. Isotope separation factors for the hydrogen atom formation from some solutes

[SH]	pH	S
0.01—1.2 N H_2SO_4	—	3.5±0.2
0.01—0.2 M KH_2PO_4	—	7.7
0.5—1 M NH_4Cl	—	11.0
0.1—0.8 M HCN, KCN	7.4—9.0	1.8
0.1—0.36 M H_3BO_3, $Na_2B_4O_7$	7.2—7.5	10.4

On the assumption that each species has an equal probability of reaction with e^-_{aq}, one can compute the relative rate of bond breaking, (k_H/k_D), where:

$$e^-_{aq} + HD_2O^+ \begin{matrix} \xrightarrow{k_H} H + D_2O \\ \xrightarrow[k_D]{} D + HDO \end{matrix}$$

An Arrhenius plot of $\log(k_H/k_D)$ vs. $1/T$ (the data of Table II) gave a value of 1340±20 cal. mol^{-1} for the difference in the activation energy of O–H and O–D bond fission in the hydronium ion. This value is close to the value (~1200 cal. mol^{-1}) which the infrared evidence gives[6] for the difference in zero-point energy between O–H and O–D bonds in the hydronium ion. One may further predict that the activation energy for the reaction of e^-_{aq} with D_3O^+ is about 4.5 kcal. mol^{-1}, since the pulse radiolysis study[7] has shown that the activation energy for the reaction, $e^-_{aq}+H_3O^+$, equals 3.2 kcal. mol^{-1}.

Table II. The effect of temperature on the isotope effect in the case of hydrogen ion

Temp., °C	2.0	10.4	21.6	30.2	40.8
S	4.35	4.16	3.80	3.64	3.61
k_H/k_D	5.40	5.07	4.36	4.09	4.03

1) J. H. Baxendale and G. Hughes, *Z. Phys. Chem.*, **14**, 306 (1958).
2) C. Lifshitz, *Can. J. Chem.*, **41**, 2175 (1963).
3) M. Anbar and D. Meyerstein, *J. Phys. Chem.*, **69**, 698 (1965).
4) S. Ohno and G. Tsuchihashi, This Bulletin, **38**, 1052 (1965).
5) C. G. Swain and R. F .W. Bader, *Tetrahedron*, **10**, 200 (1960).
6) J. Jortner and G. Stein, *Intern. J. Appl. Radiation Isotopes*, **7**, 198 (1960).
7) J. K. Thomas, S. Gordon and E. J. Hart, *J. Phys. Chem.*, **68**, 1524 (1964).

Preparation of a Novel Schiff Base Complex of Lanthanum(III)

By Toshiyuki Isobe,† Sigeo Kida†† and Seizo Misumi†

† *Department of Chemistry, Faculty of Science, Kyushu University, Fukuoka*

†† *Department of Chemistry, Wakayama University, Wakayama*

(Received August 30, 1966)

A Schiff base,

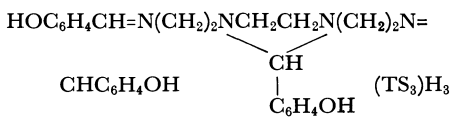

from triethylenetetramine and salicylaldehyde was reported as a multidentate ligand by Mukkerjee.[1] Sarma et al.[2,3] have found that when the base, $(TS_3)H_3$, reacts with such metal ions as cobalt(III), iron(III), manganese(III), gallium(III), aluminum(III), cobalt(II), nickel(II) and copper(II), one molecule of salicylaldehyde is hydrolyzed and a metal complex of a sexadentate ligand, HOC_6H_4-$CH{=}N(CH_2)_2NH(CH_2)_2NH(CH_2)_2N{=}CHC_6H_4$-OH $(TS_2)H_2$, is formed. No metal complexes of TS_3 have ever been obtained as pure crystals, in spite of the elaborated investigations.

In this paper we report the preparation of a metal complex of $(TS_3)^{3-}$ using lanthanum(III) ion as a central metal.

White crystals, which were prepared from lanthanum(III) perchlorate and $(TS_3)H_3$ in methanol, were found by the elementary analysis to have the formula of $La(TS_3)$ (Found: C, 54.23; H, 4.63; N, 9.50; La, 23.2. Calcd. for $LaC_{27}H_{27}N_4O_3$: C, 54.55; H, 4.58; N, 9.42; La, 23.3%). The infrared spectrum supported our present conclusion, since no N–H, O–H and ClO_4^- bands were observed in 3500—3000 and 1100 cm^{-1} region. Although this ligand has seven coordination atoms, it is sterically impossible for this ligand to form a heptadentate chelate with one metal ion. The molecular weight determination by the use of the "Vapor Pressure Osmometer" has shown that this compound is dimeric, and the structure as shown in Fig. 1 is assumed as the most probable one.

It appears that the formation of TS_3 complex is due to the fact that the coordination number and coordination place are not so rigid in lanthanide(III) ions as in other metal ions, since metal-ligand linkage of the lanthanum(III) complex is mainly ionic and the ionic radius of lanthanum(III) ion is relatively large.

The preparation of similar complexes of a series of lanthanide ions is in progress. The results will be reported shortly with the more detailed discussion on the structures of this type of compounds.

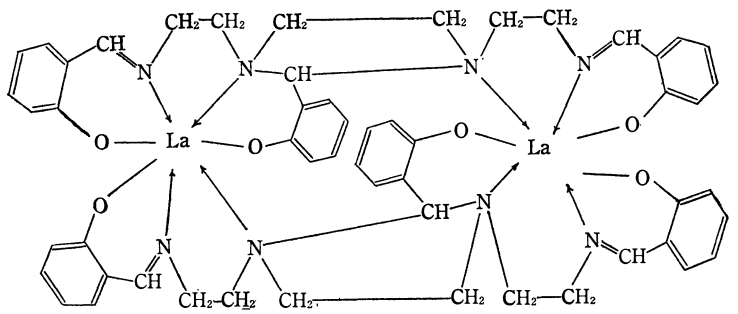

Fig. 1

1) A. K. Mukherjee, *Science and Culture*, **19**, 107 (1953).

2) B. D. Sarma and J. C. Bailar, Jr., *J. Am. Chem. Soc.*, **77**, 5476 (1955).

3) B. D. Sarma, K. R. Lay, R. E. Sievers and J. C. Bailar, Jr., ibid., **86**, 14 (1964).

Solvent Effects on Charge-transfer Spectra with Implications for the Electron-transfer Reaction in the Excited State

By Noboru MATAGA, Tadashi OKADA and Noriyuki YAMAMOTO

Department of Chemistry, Faculty of Engineering Science, Osaka University, Toyonaka, Osaka

(Received September 2, 1966)

The solvent effects on charge-transfer (CT) spectra are very interesting and important in relation to the electronic structures of and electronic processes in the CT complexes. However, there are only a few clear-cut experimental results concerning this problem. The findings of Czekalla and Meyer[1] on the tetrachlorophthalic anhydride-hexamethylbenzene complex seem to be very important in establishing the mechanism of CT interaction. However, their experimental findings appear to be somewhat complicated by the fluorescence spectra arising from some unknown impurities in the polar solvents.

We have found another very clear-cut example of a very large solvent dependence of the CT fluorescence spectrum at room temperature. It is the pyrene - *N*, *N*-dimethylaniline 1 : 1 complex, which is formed only in the excited electronic state.[2] We have made detailed studies of the electronic structure of the complex, of the complex formation, and of the decomposition processes, by measuring the fluorescence quantum yields and the fluorescence rise and decay curves.

The wave numbers of the band maxima of the CT fluorescence are shown in the table, where ε is the static dielectric constant and n_D is the refractive index of the solvent for the sodium D line. In contrast to the case of the CT absorption spectra,[3] where the values of $\tilde{\nu}_m$ depend on the optical dielectric constant, the $\tilde{\nu}_m$ values in the present case are primarily connected with the static dielectric constant of the solvent. This result is a direct consequence of the very polar structure of this complex in the excited state. The lifetime of the fluorescent state of this complex is very long (ca. 150 ns in *n*-hexane and toluene solutions), according to our measurements. Therefore, the equilibrium state with respect to the solute-solvent interactions may be reached completely during the lifetime of the excited state.

Accordingly, we may be able to apply the ordinary theories of the solvent effect to the present system. The dipole moment of this complex in the excited state has been estimated to be ca. 10 *D* in such slightly or moderately polar solvents as benzene, toluene, and monochlorobenzene. However, in more polar solvents, such as dichloroethane and pyridine, we have observed considerable deviations from the simplified theories; this indicates a large increase in the dipole moment of the complex due to the interactions between the solute and surrounding polar solvent molecules. Moreover, in the even more polar solvent, benzonitrile, the fluorescence yield is very small and the $\tilde{\nu}_m$ value is a little larger than those in the case of pyridine and dichloroethane solutions.

It seems that these findings for the benzonitrile solution can be interpreted as follows. Because the distance between the pairs in the complex may be considerably large as a result of the strong solvation by the polar solvent molecules, the delocalization interaction between them may be rather small, leading to the smaller red shift of the fluorescence. Furthermore, the rather strong fluorescence quenching in benzonitrile may cause a considerable shortening of the excited-state lifetime. Accordingly, the equilibrium state of the solute-solvent interactions might not be established during the lifetime of the fluorescent state.

These results indicate the importance of the higher-order effects of solute-solvent interactions in the case of CT complexes, effects which finally induce electron transfer and complete ionic dissociation, leading to complete fluorescence quenching in such strongly polar solvents as acetonitrile and alcohols.[2]

TABLE I. WAVE NUMBERS OF THE FLUORESCENCE BAND MAXIMA

Solvent	n_D	ε	$\tilde{\nu}$ (10^4 cm^{-1})
n-Hexane	1.37486	1.89	2.30
p-Xylene	1.49581	2.270	2.17
Benzene	1.5011	2.284	2.15
Toluene	1.49413	2.379	2.14
Monochlorobenzene	1.52481	5.621	2.09
Dichloroethane	1.44795	10.360	2.00
Pyridine	1.5067	12.30	1.93
Benzonitrile	1.5272	25.20	$\gtrsim$2.00

1) J. Czekalla and K.-O. Meyer, *Z. Phys. Chem., N. F.*, **27**, 185 (1961).
2) N. Mataga, T. Okada and K. Ezumi, *Mol. Phys.*, **10**, 203 (1966); International Conf. on Luminescence, Budapest, 1966.
3) H. M. Rosenberg and D. Hale, *J. Phys. Chem.*, **69**, 2490 (1965).

The Luminescence of the Heteropolar Excimer in the Cyclohexane Matrix

By Noboru MATAGA, Tadashi OKADA and Hiroo OOHARI

Department of Chemistry, Faculty of Engineering Science, Osaka University, Toyonaka Osaka

(Received September 2, 1966)

It has been established now that many aromatic hydrocarbons, such as pyrene, perylene, anthracene, chrysene, phenanthrene, and triphenylene, form stable complexes with such aromatic amines as *N*, *N*-dimethylaniline (DMA), *N*, *N*-dimethyltoluidines (DMT's), and *N*, *N*-dimethylnaphthylamines (DMNA's) only in the excited state.[1] The most important contribution to the intermolecular forces in these complexes seems to be charge transfer from the amine to the excited aromatic hydrocarbon.

Because the complexes are formed only in the excited state, it may be convenient to call the complex the "heteropolar excimer" in contrast to a "homopolar excimer" such as the pyrene excimer, in order to distinguish it from the ordinary CT complex which exists in the ground state as well as in the excited state.

In order to study the electronic processes in the heteropolar excimer at low temperatures, we have measured the fluorescence emission and excitation spectra, and also the fluorescence rise and decay curves. From the results of these measurements, we have confirmed that the heteropolar excimer can be produced easily in the rigid cyclohexane matrix at low temperatures. For example, in the pyrene (10^{-5} mol./l.)-DMA(10^{-2} mol./l.) system, only the long-wavelength and structureless fluorescence band, which seems to be ascribed to the heteropolar excimer, can be observed from 300°K to 77°K. However, when the temperature is lowered, the fluorescence band maximum shifts to red at first, and then makes a blue shift to approximately the same position as it has at 300°K, as one can see in the following:

T (°K)	300	273	240	230—210	190—100
λ_{max}(mμ)	440	450	465	480	440

The relative fluorescence yield and the fluorescence decay time change in a similar way; i. e., they both have minima at ca. 220°K. These facts seem to indicate that some state of the heteropolar excimer which differs from that in the solution at room temperature may be forced to arise in the cyclohexane matrix. However, when the DMA concentration is small (10^{-4} mol./l.), the fluorescence of the complex can be observed only at the wavelength region of 440—450 mμ. Therefore, one of the possible mechanisms for the appearance of the longer-wavelength fluorescence might be the formation of a more highly aggregated state than the 1 : 1 complex. In the above-described systems, no time delay of the heteropolar excimer fluorescence from the exciting light pulse (with a half-value-width of ca. 10 ns) was detected, in contrast to the fact that we have observed a time delay of ca. 100 ns in a liquid paraffin solution at room temperature. This fact may suggest that the stable complex is already formed in the ground state. However, the shape of the fluorescence excitation spectra at various temperatures is practically the same as that of the solution at room temperature, where the complex is not formed in the ground state. Accordingly, although the charge transfer interaction in the ground state is very weak, there may be donor-acceptor pairs with such a small distance between them that they can form the heteropolar excimer immediately after excitation.

When aniline, naphthylamines, *N*-methylaniline, and *N*, *N*-dimethylbenzylamine are used as electron donors in a solution at room temperature, contrary to the case where DMA, DMT's, and DMNA's are used as electron donors, we cannot observe any heteropolar excimer fluorescence, but only a quenching of the aromatic hydrocarbon fluorescence. Although the mechanism of this quenching is not very clear at the present stage of the investigation, it seems quite plausible that a charge transfer interaction in the encounter complex, followed by some very efficient, radiationless transition, plays an important role in these cases. Accordingly, if we can stabilize the complex in a rigid matrix at low temperature in order to decrease the probability of the radiationless transition, it might be possible to observe the heteropolar excimer fluorescence even in these cases.

Actually, we have observed the fluorescence spectra of heteropolar excimers of pyrene complexed with *N*, *N*-dimethylbenzylamine, aniline, and *N*-methylaniline at ca. 450—470 mμ in the cyclohexane matrix at low temperatures. However, in the case of these complexes, the fluorescence yield is much smaller than in the case of complexes of pyrene with DMA and DMT's. That is, even at low temperatures in the rigid matrix, the radiationless process is quite predominant in the former complexes compared with that in the latter ones.

More detailed studies, including studies of other heteropolar excimers, will be published in the near future.

1) N. Mataga, K. Ezumi and T. Okada, *Mol. Phys.*, **10**, 201 (1966); N. Mataga, T. Okada and K. Ezumi, ibid., **10**, 203 (1966); International Conf. on Luminescence, Budapest, 1966; N. Mataga and K. Ezumi, **This Bulletin, to be published.**

The Crystal Structure of Carbazole

By Masayasu KURAHASHI, Makoto FUKUYO and Akira SHIMADA

Department of Chemistry, Faculty of Science, Osaka City University, Sumiyoshi-ku, Osaka

and Akio FURUSAKI and Isamu NITTA

Faculty of Science, Kwansei Gakuin University, Nishinomiya

(Received September 24, 1966)

The analysis has been performed to make clear whether hydrogen bonds N–H···N are formed in carbazole crystal and whether the molecule is planar. Single crystals in colorless plates were obtained by keeping the melted substance slightly below its melting point, 237°C. The crystals are orthorhombic with four molecules in a unit cell of dimensions $a=7.76$, $b=19.15$ and $c=5.74$ Å. The density measured by floatation in sulfuric acid was 1.29 g./cm^3 and the calculated value is 1.31 g./cm^3. The space group was found to be $Pn2_1a$ or $Pnma$. Since Wilson statistics showed the existence of a center of symmetry, it was decided that the corresponding space group was the latter.

Using the multiple-film technique, intensity data were obtained from zeroth-layer Weissenberg photographs around the main axes a, b and c, taken with filtered Cu$K\alpha$ radiation. The intensities of reflexions were estimated visually with a calibrated scale.

The approximate co-ordinates of nitrogen and carbon atoms were obtained by the trial method considering packing. The structure thus obtained was refined initially by electron density projections on (001) and (100) and finally by the least-squares method.

The discrepancy index R calculated with the final least-squares co-ordinates is respectively 0.14 for $hk0$, 0.15 for $0kl$ and 0.14 for $h0l$ if non-observed reflexions were omitted. The final electron density projection along the c-axis and the crystal structure projected on (010) are shown in Fig. 1 and Fig. 2 respectively.

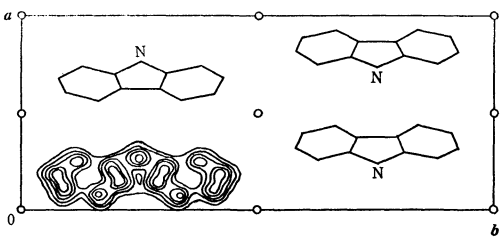

Fig. 1. Crystal structure projected on (001).

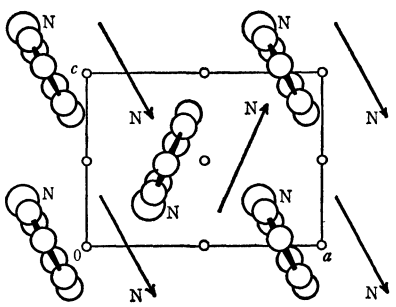

Fig. 2. Crystal structure projected on (010).

Carbazole molecule is planar, and a crystallographic mirror plane normal to the b-axis passes through the N atom and is perpendicular to the molecular plane. The N···N distance is 3.89 Å, and this shows that the hydrogen bond is not formed in the crystal as expected by Aihara[1] (1953) from the measurement of the vapor pressure.

Fluorene[2] crystal takes the same space group as carbazole and resembles closely to that of carbazole in both cell dimensions and atomic parameters. A full paper will be published in the near future.

1) A. Aihara, *J. Chem. Soc. Japan, Pure Chem. Sect. (Nippon Kagaku Zassi)*, **76**, 492 (1955).
2) D. M. Burns and J. Iball, *Proc. Roy. Soc.*, **A227**, 200 (1955).

BULLETIN OF THE CHEMICAL SOCIETY OF JAPAN VOL. 39 2565—2571 (1966)

Vibrational Spectra and Structure of Substituted Unsaturated Carbonyl Compounds. VI. β-Halogeno- and β-Halogenodeuteriovinyl Ketones

By Janusz DABROWSKI and Krystyna KAMIEŃSKA-TRELA

Institute of Organic Chemistry, Polish Academy of Sciences, Warsaw, Poland

(Received March 17, 1966)

The infrared spectra of several chloro-, bromo- and iodovinyl ketones and their partly deuterated derivatives were investigated in the liquid state and in solutions. A Raman spectrum of one of these substances was also obtained. It has been shown that, unlike enamino- and hydroxyvinyl ketones, the title compounds exhibit fairly characteristic absorption bands due to carbonyl and skeletal vibrations. The splittings observed in the double bond stretching region are accounted for by rotational isomerism. Several assignments of the group frequencies are proposed.

It has been shown that β-amino[1-3] and β-hydroxy substituted α, β-unsaturated ketones[4] are characterized by partial equalization of the double and single bonds causing strong coupling of the C=O and C=C stretching vibrations and very large frequency shifts. On the other hand the carbonyl and vinyl bands of the unsubstituted vinyl ketones are less shifted,[5,6] the corresponding vibrations being practically localized. It is therefore, interesting to investigate unsaturated ketones with substitutents of various types in the β position and compare their spectral characteristics with those obtained in the two extreme cases mentioned.

In the present work halogens were the substituents in the β position. In order to obtain as far as possible detailed assignments, all substituents were systematically varied (R–CO–CR′=CR′–X; R= CH_3, C_2H_5, *n*-C_3H_7, *i*-C_3H_7 or *t*-C_4H_9; R′=H or D; X=Cl, Br or I) The $\nu_{C=O}$ and $\nu_{C=C}$ vibrations were found to be practically localized and characteristic. Moreover, a number of vibrations in the fingerprint region are also fairly characteristic as could be established by comparison of the spectra of related compounds; this is particularly distinct in the case of β-chloro, bromo and iodo derivatives of ethyl vinyl ketone (compounds IV, VI and VII, Fig. 1) where large parts of the spectra are almost true copies of each other.

Of particular interest are the band splittings observed within the 1500—1700 cm^{-1} region which have been shown in this study to be caused by rotational isomerism.

Recently a number of β-chlorovinyl ketones were spectroscopically investigated by Benson and Pohland[7]; as already pointed out[8] the resolving power of the apparatus used by these authors must have been insufficient and the significant fact of splitting of the absorption bands was overlooked.

A number of infrared and Raman bands of the parent homologue, i. e. methyl-β-chlorovinyl ketone and three of its deuterated derivatives have been assigned in the previous paper of this series.[8]

Experimental

All substances studied in the present work were prepared according to conventional methods. These are listed in Table I. The syntheses of new compounds are described below.

Alkyl-β-chloro-α, β - dideuteriovinyl ketones were synthesized from deuterioacetylene and acyl chlorides similarly as the nondeuteriated chlorovinyl ketones described previously[9] and purified by threefold distillation:

Ethyl-β-chloro-α, β-dideuteriovinyl ketone (V), b. p. 50—51°C/18mmHg, n_D^{25} 1.4586, yield 68.1%;

n-Propyl-β-chloro-α, β-dideuteriovinyl ketone (IX), b. p. 100°C/60 mmHg, n_D^{25} 1.4609, yield 32.0%

Isopropyl-β-chloro-α, β-dideuteriovinyl ketone (XI), b. p. 75—76°C/43 mmHg, n_D^{25} 1.4582, yield 65.0%.

Spectral purity of the deuteriated species was established by the fact that the bands at 3050—3100 cm^{-1} due to C–H vinyl stretch were absent from all spectra of deuteriovinyl compounds while new bands

1) K. Kotera, *Yakugaku Zasshi*, **80**, 1275 (1960).
2) J. Dabrowski, *Spectrochim. Acta*, **19**, 4751 (1963).
3) J. Dabrowski and K. Kamienska-Trela, ibid., **22**, 211 (1966).
4) R. Mecke and E. Funck, *Z. Elektrochem.*, **60**, 1124 (1956).
5) K. Noack and R. N. Jones, *Can. J. Chem.*, **39**, 2201, 2225 (1961).
6) J. Kossanyi, *Bull. Soc. Chim.*, **1965**, 704.
7) W. R. Benson and A. E. Pohland, *J. Org. Chem.*, **29**, 385 (1964).
8) J. Dabrowski and J. Terpiński, ibid., **31**, 2159 (1966).
9) A. N. Nesmeyanov, N. K. Kochetkov and M. I. Rybinskaya, *Izv. Akad. Nauk SSSR, Otd. Khim. Nauk*, **1950**, 350.

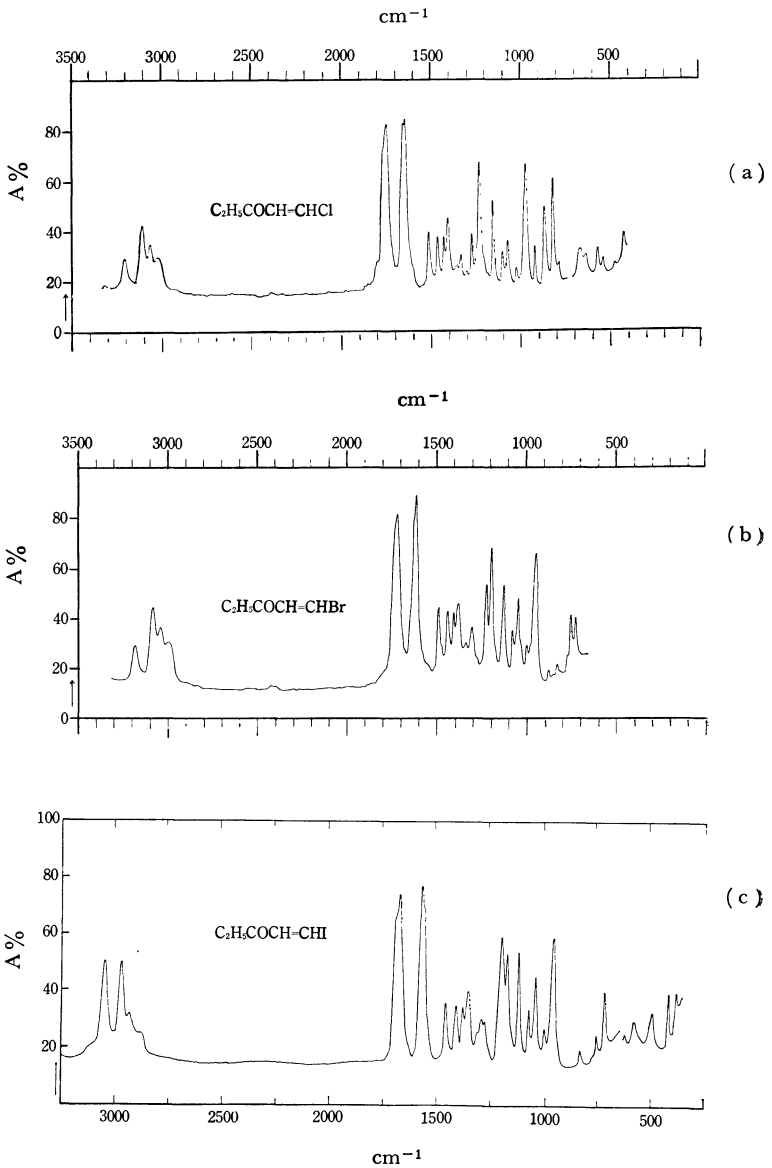

Fig. 1. (a) Infrared spectrum of 1-chloropenten-1-one-3 (IV); neat, liquid film.
(b) Infrared spectrum of 1-bromopenten-1-one-3 (VI); neat, liquid film.
(c) Infrared spectrum of 1-iodopenten-1-one-3 (VII); neat substance; 3250—650 cm^{-1}: melted, film, 650—400 cm^{-1}: crystalline, film.

due to corresponding C–D vibrations arose at 2260—2300 cm^{-1}.

Ethyl-β-bromovinyl ketone (VI) was prepared according to the method described by Niemirowski and co-workers[10] from 4.3 g. (0.0525 mole) of pentyn-1-one-3 and 14 g. of 41% HBr (0.071 mole, water solution). Yield 5.3 g. (62% theor.). Colourless liquid with b. p. 68°C/16 mmHg, n_D^{25} 1.4961.

Found: C, 37.05; H, 4.44; Br, 48.19. Calcd.: C, 36.84; H, 4.33; Br, 49.03%.

Ethyl-β-iodovinyl ketone (VII) was obtained from 5 g. (0.04 mole), ethyl-β-chlorovinyl ketone and 10 g. (0.067 mole) of sodium iodide in acetone solution in the same manner as described by Kochetkov[11] for other homologues. Yield 8.4 g. (60% theor.); white leaflets with m. p. 32—33°C (from pentane).

Found: I, 60.15%. Calcd.: I, 60.42%.

The solvents were purified by the methods used previously.[2] Measurements were carried out using a Hilger H-800 double-beam spectrometer with sodium chloride and potassium bromide optics. Melted substances were investigated in an electrically heated cell and low-melting, crystalline samples in the low-temperature cell described previously.[2] The spectra

10) W. D. Niemirowski, L. F. Czelpanova and A. A. Pietrov, *Zh. Obshch. Khim.*, **31**, 2552 (1961).

11) N. K. Kochetkov, *Dokl. Akad. Nauk SSSR*, **82**, 593 (1952).

TABLE I. WAVE NUMBERS (cm^{-1}) OF THE ABSORPTION BANDS OF β-HALOGENOVINYL KETONES IN THE DOUBLE BOND STRETCHING REGION

Substance and reference to synthesis	Solvent	M mole/l.	Cell thickness mm.	Absorption band A C=O *s-cis*	B C=O *s-trans*	C C=C *s-trans*	D C=C *s-cis*
1	2	3	4	5	6	7	8
$CH_3COCH=CHCl$[9] (I)	—	—	film	1691	1677	1585**	
				1631?			
	C_2Cl_4	0.38	0.06	1697	1686	1583	
$CH_3COCH=CHBr$[10] (II)	—	—	film	1690 sh	1679	1584**	
	C_6H_{12}	0.07	0.28	1707 sh	1691	1586	1581 sh
	CH_3OH	0.63	0.04		1678	1580	
$CH_3COCH=CHI$[11] (III)	—[b]		film	1750	1658	1610	1570
				1687			1541
	—[c]		film		1675[a]	1569[a]	
	C_6H_{14}	0.05	0.27	1706	1691	1570	1559 sh
	CH_3OH	0.6	0.04		1671	1566	
$C_2H_5COCH=CHCl$[9] (IV)	—	—	film	1697 sh	1680	1594	1584
	C_6H_{12}	0.09	0.28	1703	1690	1604	1583
	CH_3CN	0.30	0.09	1701	1682	1594	1583
	CH_3OH	0.86	0.04	1704 sh	1679	1593	1585
$C_2H_5COCD=CDCl$ (V)	—	—	film	1691	1681	1564**	
	C_6H_{14}	0.25	0.09	1702	1695	1567	1537?
	CH_3CN	0.24	0.09	1691	1681	1564	
	CH_3OH	1.6	0.02		1680	1562	
$C_2H_5COCH=CHBr$ (VI)	—	—	film	1693 sh	1681	1592 sh	1581
	C_6H_{12}	0.06	0.28	1707	1694	1592 sh	1581
	CH_3OH	0.64	0.04	1685	1679 sh	1592 sh	1582
$C_2H_5COCH=CHI$ (VII)	—[b]		film	1686	1656	1576	1564 sh
					1627		
	—[c]		film	1691 sh	1681	1575	1562
	C_6H_{12}	0.05	0.28	1704	1691	1576	
	CH_3OH	0.63	0.04		1678	1575	1566 sh
n-$C_3H_7COCH=CHCl$[9]	—	—	film	1689 sh	1679	1587**	
(VIII)	C_6H_{12}	0.07	0.22	1699	1688	1587	
	CH_3OH	0.07	0.04		1673	1586	
n-$C_3H_7COCD=CDCl$ (IX)	—				1683	1563	
	C_2Cl_4	0.13	0.22		1690	1563	
i-$C_3H_7COCH=CHCl$[13] (X)	—		film	1695	1679	1591**	
	C_2Cl_4	0.24	0.06	1699	1684	1590	
	CH_3CN	0.32	0.06	1694	1677	1589	
	CH_3OH	1.10	0.02	1691	1679	1588	
i-$C_3H_7COCD=CDCl$ (XI)	—		film	1690	1683 sh	1560**	
	C_2Cl_4	0.23	0.06	1692	1678 sh	1558	1543 sh
	CH_3OH	0.46	0.02		1676	1557	
$(CH_3)_3CCOCH=CHCl$[14]	—		film	1695		1595	1580 sh*
(XII)	C_2Cl_4	0.07	0.18	1696		1595	1580*
	CH_3OH	0.70	0.04	1690		1592	1579*

* With respect of this band in XII see discussion on p. 2569.
** Overlapping bands of both *s-trans* and *s-cis* forms.
a) Asymetrically broadened, b) Crystalline film, c) Melted film

13) N. K. Kochetkov, *Dokl. Akad. Nauk SSSR*, **84**, 289 (1952).

14) N. K. Kochetkov, I. Ambrush, I. I. Ambrush and E. S. Severin, *Zh. Obsch. Khim.*, **28**, 3024 (1958).

Table II. Wave numbers (cm^{-1}) of the absorption bands of β-halogenovinyl ketones below 1500 cm^{-1}

Compound	Assignment								
	CH_3 asym	CH_2 scissor.	CH_3 sym	H/C=C/H in-plane	H/C=C/H out-of-plane	D/C=C/D in-plane	D/C=C/D out-of-plane	C-Cl stretch *s-trans*	C-Cl stretch *s-cis*
$CH_3COCH=CHBr$ (II)	1424m		1365 s	1291m	946 s				
$CH_3COCH=CHI$ (III) liquid	1418m		1361 s	1286m	948 s				
$CH_3COCH=CHI$ (III) crystalline	1420m		1363w	a)	958 s				
$C_2H_5COCH=CHCl$ (IV) IR spectrum	1459m	1412m	1378m	1288w	944 s			846 s	800 s
$C_2H_5COCH=CHCl$ (IV) Raman spectrum	1458m	1410m	1378vw	1290vs	b)			840m	800m
$C_2H_5COCD=CDCl$ (V)	1460m	1411m	1379m			952m	701 s	794vs	769vs
$C_2H_5COCH=CHBr$ (VI)	1460m	1411m	1379m	1283m	946 s				
$C_2H_5COCH=CHI$ (VII) liquid	1453m	1408m	1376m	1287w	948vs				
$C_2H_5COCH=CHI$ (VII) crystalline	1454m	1410m	1377m	1286w	961vs				
n-$C_3H_7COCH=CHCl$ (VIII)	1458m	1458m 1406m	1371m	1292m	943 s			853m	829m
n-$C_3H_7COCD=CDCl$ (IX)	1467m	1467m 1414m	1378m			960m	701 s	774 s	761 s
i-$C_3H_7COCH=CHCl$ (X)	1470 s		1388 s 1370m	1292m	943vs			846 s	779vs
i-$C_3H_7COCD=CDCl$ (XI)	1467 s		1387m 1370w			953m	698 s	793 s	759vs
$(CH_3)_3CCOCH=CHCl$ (XII)	1466m 1478 s		1397m 1370m	1308m	940 s				837 s

a) Absent from the spectrum of crystalline film. b) Very weak or absent from Raman spectrum.

were calibrated with polystyrene and indene.[12] The frequencies are accurate to within ±1—2 cm^{-1}.

Results and Discussion

Tables I and II contain spectral data of all compounds examined; in addition representative spectra are depicted in the figures.

The spectra of the great majority of the compounds examined exihibit more peaks in the 1500—1750 cm^{-1} region than expected for molecules containing one C=O and one C=C bond; where only two peaks occur, at least additional shoulders can be observed. The occurrence of these additional absorption bands and/or shoulders cannot be explained by association effects since their intensities are practically independent of concentration. For instance, the relative intensity of the four absorption bands between 1500 and 1700 cm^{-1} in the spectrum of ethyl chlorovinyl ketone remains practically unchanged when the initial 2.4×10^{-1} M solution is diluted to 3.4×10^{-2} M concentration. Besides, the intensity of the band occurring at the lowest of these frequencies increases in hexane solution as compared with pure liquid, while exactly an opposite effect would be expected if association played any role here. *Cis-trans* isomerism can also be excluded in this discussion since β-chlorovinyl ketones were shown by NMR spectra to consist in at least 95% of the trans form[7] and the additional infrared bands are too strong to be caused by small admixtures of other molecules. Moreover substances I, IV and XII were proved by gas-liquid chromatography to be homogeneous in about 99%.

In the previous paper of this series it has been shown that methyl-β-chlorovinyl ketone[8] exists in two rotational forms. No doubt, this is also true for the β-halogenovinyl ketones studied in this work. The present results concerning spectra of several differently substituted homologues of the parent methyl-β-chlorovinyl ketones provide strong support for this concept although neither simplification of the spectra upon crystallization (compounds I, IVand V) nor any marked temperature dependence of the intensity of the absorption bands could be observed in the majority of cases (see, however, discussion on iodo ketones, III and IV, p. 2570). The two rotational forms are

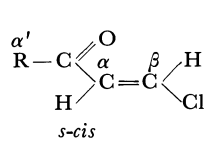

s-cis

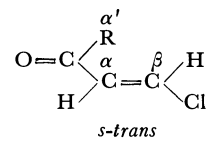

s-trans

12) R. N. Jones and A. Nadeu, *Spectrochim. Acta*, **20**, 1175 (1964).

most likely the *s-cis* and *s-trans* ones, the latter being more stabilized by resonance.

According to the data of Jones and Noack[5] and to the Stuart-Briegleb atomic models the *s-cis* form is free of strain while the *s-trans* one is sterically hindered. Therefore, the C=O group in the latter conformation is probably forced out of the plane of the C=C bond, especially in the higher homologues. However, the true gauche form is not likely to exist as its formation would mean a considerable loss of resonance energy; hence, with increasing size of the α'-substituent, the equilibrium between the *quasi-s-trans* form* and the plane, strain-free *s-cis* one will tend to shift towards the latter. This tendency is clearly illustrated by the spectra of five ketones (I, IV, VIII, X and XII) bearing different alkyls in α' position (Fig. 2). In all but one (XII) of these spectra the carbonyl band is distinctly split; the peak occurring at lower frequency (B) weakens with increasing volume of the α' substituent (in XII only an inflection is observable) thus permitting its assignment to the sterically hindered *s-trans* form; consequently band A can be attributed to the *s-cis* form. The remaining chloro ketones investigated here (II, III, V—VII, IX, XI) fit well in this scheme (see discussion below). With the olefinic C=C stretching vibrations the situation is somewhat more complex. In the majority of cases splitting of the $\nu_{C=C}$ band could not be observed; it is likely that the bands of the two conformers coincide in the spectra. The same was noted for unsubstituted α,β-unsaturated ketones.[6] *t*-Butyl-β-chlorovinyl ketone exhibits two intense bands at frequencies consistent with the $\nu_{C=C}$ vibration, but these do not seem to correspond to different conformational forms, since the lack of a distinct second $\nu_{C=O}$ band suggests rather a mono-component system. Besides, the whole spectrum is much simpler than those of the other compounds investigated. Therefore, the splitting in this particular case is probably due to other factors, possibly to Fermi resonance. Only one of the compounds investigated here: 1-chloropenten-1-one-3 (IV, Fig. 3) shows in the double-bond spectral region four intense bands (A, B, C, D), two of which (C, D) can be attributed to the $\nu_{C=C}$ vibrations in the two rotational isomers. The assignments follow from the intensity changes of these bands in solvents of various polarity: in neat liquid and in solution in acetonitrile, bands B and C increase markedly in intensity as compared with the solution in hexane; this simultaneous change means that band C is due to the $\nu_{C=C}$ vibration of the *s-trans* form, since band B was assigned in the above discussion of Fig. 2 to this form. Band D corresponds therefore to $\nu_{C=C}$ of the *s-cis* form.

The authors are aware of the dangers of interpretation based solely on intensity changes in solvents. Nevertheless, the range of these changes exceeds here so much the values expected for the pure solvent effect on band intensity that the interpretation postulating the equilibrium shift *s-cis*$\rightleftarrows$*s-trans* seems to be justified, provided Fermi

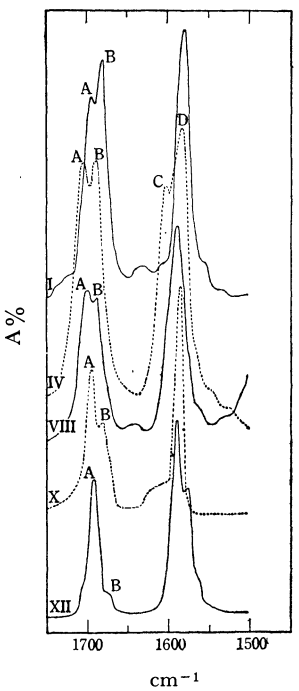

Fig. 2. Infrared spectra of β-chlorovinyl ketones in nonpolar solvents.
I: methyl-, IV: ethyl-, VIII: *n*-propyl-, X: isopropyl-, XII: *t*-butyl-β-chlorovinyl ketones.
Solvent concentrations and cell thicknesses are given in Table I.

* Called further *s-trans*.

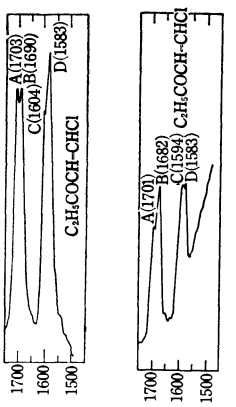

Fig. 3. Infrared spectrum of 1-chloropenten-1-one-3 (IV).
(a) C_6H_{12} solution (b) CH_3CN solution
Concentrations and cell thicknesses are given in Table I.

resonance is not involved.

The assignments derived here are in agreement with those obtained for unsubstituted α,β-unsaturated ketones.[5,6] In particular, the regularity, consisting in wider frequency separation between the C=O and C=C stretching bands in the case of the *s-cis* isomer, can now be extended on corresponding β-chloro substituted ketones. For *s-cis* 1-chloropenten-1-one-3 $\nu_{C=O}-\nu_{C=C}=120$ cm^{-1} and for *s-trans* $\Delta\nu=86$ cm^{-1}, both values being considerably greater in comparison with those for ketones lacking polar substituents as well as with those containing the dialkylamino group in the β position, where the corresponding differences can be evaluated at about 90 cm^{-1} for the *s-cis* and 70 cm^{-1} or less for *s-trans* form. The fact, that in chloro ketones the differences $\nu_{C=O}-\nu_{C=C}$ are greater than in unsubstituted ketones, while in enamino ketones[3] they are equal or smaller, can be readily understood since a halogen is known to lower the $\nu_{C=C}$ frequency and to enhance the $\nu_{C=O}$ one, whereas an amino substituent lowers both of them, $\nu_{C=O}$ being usually somewhat more shifted.

Furthermore, the assignments presented above can be reconciled with the Raman intensities of 1-chloropenten-1-one-3 (IV, Fig. 4) on the basis of the idea of the in-phase and out-of-phase stretching vibrations of the two double bonds in the system O=C–C=C. In the Raman spectrum bands B and D are very intense while A and C occur in hexane solution as inflections only being undetectable in neat liquid. According to Sobolev and Alexanyan,[15] (see also discussion in[8]) (1) the intense Raman bands of α,β-unsaturated ketones are due to the in-phase vibration both in the *s-trans* and in the *s-cis* form, the bands due to corresponding out-of-phase vibrations being much weaker and (2) the in-phase and out-of-phase vibrations have a reverse order of frequencies in these two rotational isomers, i. e. $\nu_{sym}>\nu_{as}$ in the *s-trans* form, and $\nu_{sym}<\nu_{as}$ in the *s-cis* one. Our results fit in very well in this scheme: the intense Raman band B assigned to the $\nu_{C=O}$ vibration of the *s-trans* form has its counterpart in the weak inflection C due to the $\nu_{C=C}$ mode of the same form (i. e. $\nu_{sym}\approx\nu_{C=O}$ and $\nu_{as}\approx\nu_{C=C}$); correspondingly, inflection A and band D can be ascribed to the C=O and C=C stretch respectively in the *s-cis* form (i. e. $\nu_{as}\approx\nu_{C=O}$ and $\nu_{sym}\approx\nu_{C=C}$).

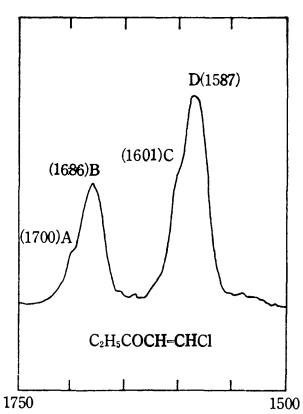

Fig. 4. Raman spectrum of 1-chloropenten-1-one-3; 50% by weight solution in hexane.

In addition to the five β-chlorovinyl ketones discussed above seven other β-halogenovinyl ketones (II, III, V—VII, IX and XI) were examined in order to investigate the influence of bromine, iodine and deuterium substituents on the position of the $\nu_{C=O}$ and $\nu_{C=C}$ bands. It is obvious that all these compounds exist likewise in two rotational forms, since (1) their liquid-state and solution spectra contain additional bands and/or shoulders in the 1700—1500 cm^{-1} region and (2) the spectra of solid methyl- and ethyl-β-iodovinyl ketones (III and VII) are markedly simplified between 650 and 1500 cm^{-1} as compared with the liquids: the bands 1286, 1237, 1150 and 864 cm^{-1} disappear from the spectrum of solid III and band 1273 cm^{-1} from that of solid VII. The fact that crystallization causes simultaneous complication in the 1700—1500 cm^{-1} region (Fig. 5), instead of the expected simplification, can be explained by assuming splittings by crystal field. In other respects the assignments of the $\nu_{C=O}$ and $\nu_{C=C}$ bands coincide with those for chloro ketones (Table I).

The solvent sensitivity of the $\nu_{C=O}$ and $\nu_{C=C}$ bands of halogenovinyl ketones differs strongly from that of aminovinyl ketones.[3] While the $\nu_{C=O}$ bands of both rotational isomers are clearly solvent-sensitive (Table I), the $\nu_{C=C}$ bands are in most cases constant within the limits of experimental error, showing that—contrary to what was observed for aminovinyl ketones—mechanical coupling between the two modes is much weaker than in amino ketones. This conclusion agrees with the calculations made by Sadlej and Sadlej[16] who showed the bond orders of the single and double bonds of the system O=C–C=C to be largely equalized in enamino ketones and but slightly changed (as compared with normal values) in halogenovinyl ketones. It should be noted that the $\nu_{C=O}$ frequencies of β-halogenovinyl ketones coincide almost exactly with those of unsubstituted vinyl ketones.[6] This indicates that the mesomeric effect of halogens counterbalances the inductive effect.

A general tendency, already noticed for enamino ketones, is the lowering of the $\nu_{C=C}$ frequency by 24—31 cm^{-1} upon vinyl deuteration (Table I).

15) E. V. Sobolev and V. T. Aleksanyan, *Izv. Akad. Nauk SSSR, Otd. Khim. Nauk*, **1965**, 1336.

16) A. Sadlej and M. Sadlej, *Bull. Acad. Polon. Sci., Sér. Sci Chim.*, **13**, 625 (1965).

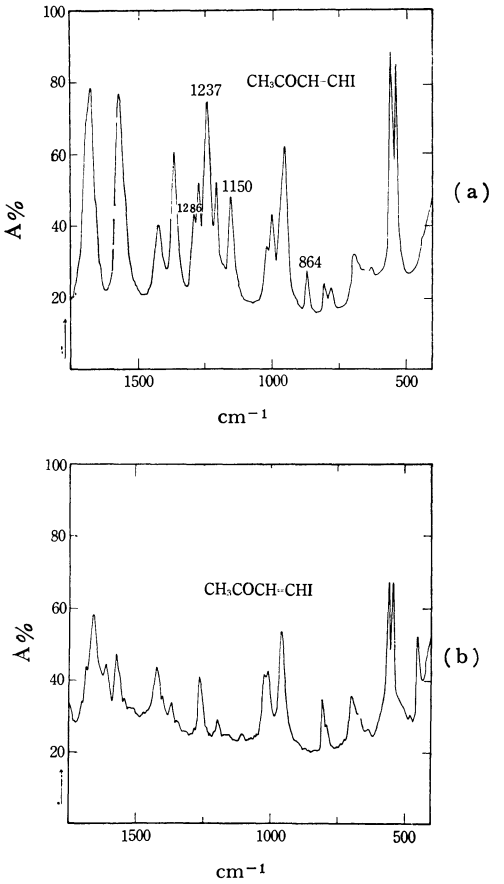

Fig. 5. Infrared spectrum of 1-iodobuten-1-one-3. (a) liquid film, (b) crystalline film

However, the $\nu_{C=O}$ frequency is insensitive to deuteration in chloro ketones, whereas in enamino ketones the reverse is true. This demonstrates once more that mechanical coupling between $\nu_{C=C}$ and $\nu_{C=O}$ in halogenovinyl ketones is not very strong.

The spectral region below 1500 cm^{-1} cannot be fully interpreted because of the occurrence of many noncharacteristic vibrations. Yet, there are some regularities which permit to draw definite conclusions in regard to several important absorptions or, at least, to suggest tentative assignments.

First of all, the CH_2 scissoring and both the doubly degenerate and symmetrical bending modes of the CH_3 group can rather easily be recognized; the data given in Table II show that there is no marked difference with respect to aliphatic saturated ketones.[17] There are, however, in several spectra absorption bands of medium intensity between 1300 and 1358 cm^{-1}, the origin of which cannot be estimated with certainty at the time being.

The C–H vinyl bending modes were assigned on the basis of deuteration studies. The in-plane bending vibration gives rise to a band within the range 1283—1298 cm^{-1}, the only strong deviation taking place in the case of compound XII (1308 cm^{-1}). These bands shift upon deuteration to 952—960 cm^{-1}. The C–H out-of-plane vibration occurs at 940—944 cm^{-1} for chloro ketones (IV, VIII, X and XII), at 946 for bromo ketones and at 948 for iodo ketones; the band of the C–D out-of-plane vibrations of chloro ketones V, IX and XI occurs at 698—701 cm^{-1}. All isotopic shifts are of the expected magnitude ($\nu_H/\nu_D \approx 1.35$).

The assignments of the ν_{C-Cl} frequencies follow from the intensity changes in various solvents. In the previous paper[8] it was noticed, that in hexane solution the lower of the two ν_{C-Cl} bands occurring at about 800—830 cm^{-1} grows up; the same effect was now confirmed in the case of compound IV. On the basis of the interpretation of the intensity changes in the 1700—1500 cm^{-1} region (p. 2569) this frequency can be ascribed to the *s-cis* form. The ν_{C-Cl} frequency of the *s*-trans form of the non-deuteriated ketones falls in most cases to the narrow range 846—853 cm^{-1} (Raman band in IV at 840 cm^{-1}) while those of the *s-cis* form are more variable. In IV the *s-cis* ν_{C-Cl} band occurs at 800 cm^{-1} both in Raman and infrared spectra, in VIII at 829 cm^{-1}. In X first band occurs at 846 cm^{-1} and there is no other strong band in this region except that at 779 cm^{-1}. Since the band splittings in the double-bond stretching region point to rotational isomerism, the latter band can be assumed to correspond to the second conformer. For XII the situation seems to be different: the first band lies at 837 cm^{-1} and the next one at a much lower value 753 cm^{-1}; according to what was already said in the discussion on the 1700—1500 cm^{-1} region (p. 2569) it may be concluded that substance XII containing the voluminous *t*-butyl radical exists practically in one conformational form, viz. *s-cis* with a ν_{C-Cl} frequency of 837 cm^{-1}.

In vinyl deuterated compounds V, IX and XI the ν_{C-Cl} bands are displaced to lower frequencies by 20—79 cm^{-1}. Although, on the basis of the intensity data, we believe our assignments of the ν_{C-Cl} bands to be correct, we admit freely that they are not as unambiguous as was case with methyl-β-chlorovinyl ketone[8] for which no other strong bands occurred in the whole spectral region theoretically possible for the C–Cl stretching vibrations.

The ν_{C-Br} and ν_{C-I} frequencies cannot unambiguously be assigned on the basis of data now available. Assignments for other frequencies within the region 400—1500 cm^{-1} will be given in the coming paper of this series.

The spectra discussed in the present paper will be submitted to the DMS catalogue.

17) A. R. Katritzky and S. Øksne, *Spectrochim. Acta*, **17**, 1286 (1961).

BULLETIN OF THE CHEMICAL SOCIETY OF JAPAN VOL. 39 2572—2576 (1966)

Determination of Angular Orientation of Rigid Group in Molecular Crystal: Vector-set Seeking Method

Yukiteru KATSUBE

Himeji Institute of Technology, Himeji

and Yoshio SASADA and Masao KAKUDO

Institute for Protein Research, Osaka University, Kita-ku, Osaka

(Received March 23, 1966)

In order to determine the angular orientation of the rigid atomic group, such as benzene ring, in a molecular crystal, a new method for interpreting a distribution of peaks near the origin of two-dimensional Patterson function has been described in this paper. Similar methods for solving the Patterson function by the aid of the rigid groups have been proposed by several authors, but the present method, vector-set seeking method, differs from them in the procedure to find a satisfactory fit of a vector-set of the rigid group on the Patterson function and in a criterion for a correct choice of the angular orientation. Satisfactory results for the known structures of salicylamide and α-pyridone and the unknown structure of *m*-hydroxybenzamide were quickly obtained by the application of this method.

In the early stage of crystal structure analysis, the orientation of a rigid atomic group in the unit cell provides useful information of the interpretation of the Patterson function. The optical transform method has been used for this purpose.[1] It has been realized that the interpretation of the Patterson peaks near the origin is also effective in some cases.[2] Recently, several systematic procedures for solving the Patterson function with the aid of the rigid group of known spatial atomic arrangement have been proposed and applied successfully to the practical crystal structure determinations.[3,4] However, a large scale computer would be required and even on such computer it might take rather long computational time.

We have developed on the same line somewhat different procedure, the vector-set seeking method, which is convenient to deal with two-dimensional Patterson function and could be done on the smaller computer. It was proved that this method worked well for some practical structure determinations. The present paper includes the procedure of the vector-set seeking method and its application.

Description of the Method

The angular orientation of the rigid group in a molecule is defined by θ, φ and ψ, which are the angles of the rotations with respect to the three mutually orthogonal reference axes, X, Y and Z respectively. In the application of the vector-set seeking method for the projection of the Patterson function, this expression of the rotation is more convenient than that by Eulerian angles.

The procedure of this method is as follows. A plausible model of the rigid group defined by the orthogonal coordinate system is first rotated about two axes, X and Y, and then finally about the third axis, Z. The model after such three independent rotations is projected along the axis of the final rotation, Z. The vector-set consisting of interatomic vectors in the projected model is superposed on the projected Patterson function, so that two systems coincide in the origin and the axis of projection. The relation of the crystallographic axes with the reference axes is indicated in the figure for each example. The summation of the values of the Patterson function at the ends of the vectors is carried out over all the vector-set. If necessary, the Patterson function may be modified by some function of the distance from the origin.

The sum obtained by this procedure would give a degree of the fitness between the vector-set having a given angular orientation and the Patterson function; we shall call it 'fit-factor'. In the practical applications, the fit-factor is computed at every point (θ, φ, ψ), with suitable intervals of the three angular coordinates. It is natural to assume that the angular coordinates which give the largest value, the best fitting, within a reasonable range of the rotation correspond to the correct orientation of the rigid group in the crystal.

1) C. A. Taylor and H. Lipson, "Optical Transforms," Bell and Son, London (1965).
2) W. Cochran, *Acta Cryst.*, **4**, 376 (1951).
3) P. Tollin and W. Cochran, ibid., **17**, 1322 (1964).
4) C. E. Nordman and K. Nakatsu, *J. Am. Chem. Soc.*, **85**, 353 (1963).

Application

This method was tested with the known structures of salicylamide[5] and α-pyridone[6], and with the unknown structure of *m*-hydroxybenzamide.[7] In these examples, the whole molecules were taken as the rigid group. The Patterson function computed for the grid points at suitable intervals was stored in the computer. The value of the function at the end of the vector was obtained by means of the interpolation by a second order equation.[8] In the case of the non-interpolation, the value on the nearest grid point from the end of the vector was taken. The angles, θ, φ and ψ, were stepwisely changed with intervals of 15° in the first stage, and of 5° to 10° in the search in the neighborhood of the maxima.

Salicylamide.—(a=12.92, b=4.98, c=21.04 Å, β=91.8°, $I2_1/a$). The Patterson function projected on (010) was computed for the grid points at intervals of $a/64$ and $c/128$. A planar molecular model of salicylamide was set up with generally accepted bond lengths and angles. Only the Patterson function within 5.3 Å from the origin was stored in the computer, because all the intramolecular vectors of the model will be within this region. The value of the origin of the Patterson function was taken as zero. Both the seekings with the interpolation and with the non-interpolation were carried out. The difference between the results of these two seekings was very small, and the angular orientation of the molecule in the projection was uniquely determined. Figure 1 shows a part of the result. The highest peak appeared at θ=40°, φ=20° and ψ=−20°. In

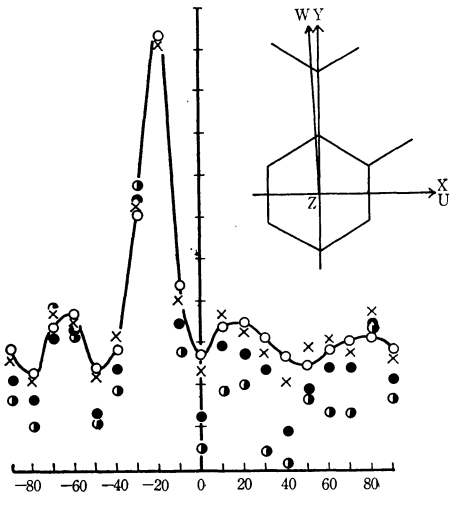

Fig. 1 (a)

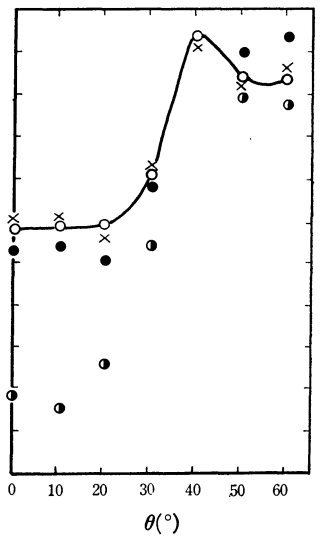

Fig. 1 (b)

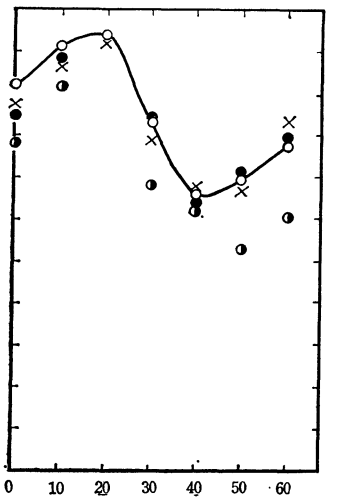

Fig. 1 (c)

Fig. 1. Variation of 'fit-factor,' in salicylamide,
(a) by the rotation of ψ at θ=40° and φ=20°,
(b) by that of θ at φ=20° and ψ=−20° and
(c) by that of φ at θ=40° and ψ=−20°.
○ interpolated, with equi-weighted vector-set.
× non-interpolated, with equi-weighted vector-set.
● non-interpolated, with weighted vector-set.
◑ non-interpolated, with weighted vector-set and Patterson function modified by distance from origin.
The values plotted by the other symbols than × were given by subtracting a constant from the fit-factors which were standardized so as to give the same value at the best fitting.

5) Y. Sasada, T. Takano and M. Kakudo, This Bulletin, **37**, 940 (1964).
6) B. R. Penford, *Acta Cryst.*, **6**, 591 (1953).
7) Y. Katsube, Y. Sasada and M. Kakudo, This Bulletin, **39**, 6107 (1966).
8) J. Ladell and J. L. Katz, *Acta Cryst.*, **7**, 460 (1954).

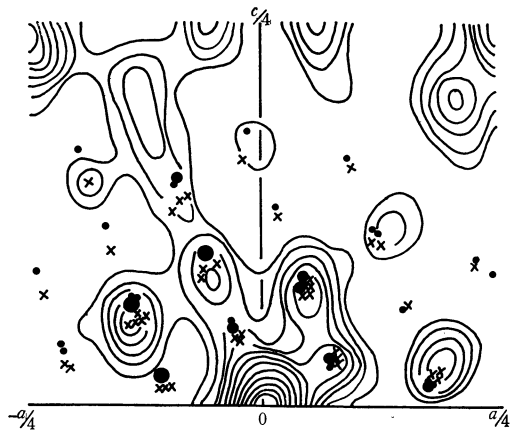

Fig. 2. Patterson projection of salicylamide and vector-set at the best fitting.
● model structure, × true structure

Fig. 2, the projected vector-set with this angula orientation of the model structure and that of th true structure are superposed on the Patterso projection. As seen from Fig. 2, the projecte vector-set obtained by this method is in good agreement with that of the correct structure already known, within the limits of error to be expected.

α-Pyridone.—($a=13.63$, $b=5.89$, $c=5.67$ Å, $P2_12_12_1$) The Patterson function projected on (001) was computed for the grid points at intervals of $a/60$ and $b/30$. In the seeking with the interpolation, there appeared some broad peaks with the shoulders, and it was unable to determine uniquely the angular orientation. However, it was not so difficult to find out the most probable angular orientation to be $\theta=-15°$, $\varphi=65°$ and $\psi=-45°$,

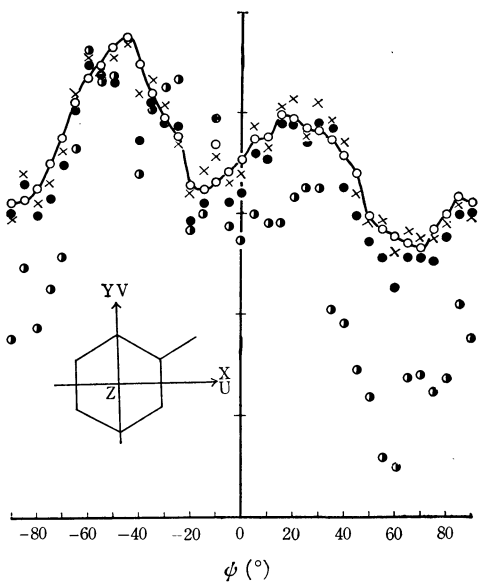

Fig. 3 (a)

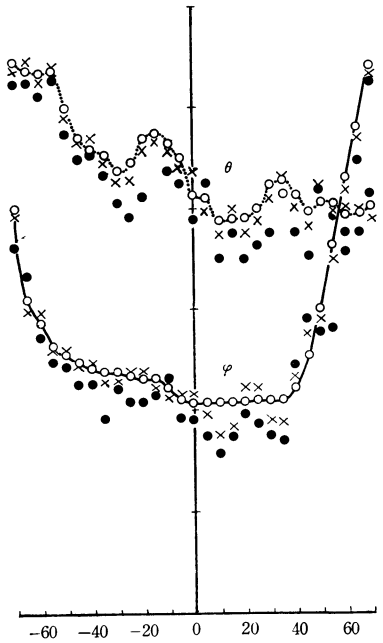

Fig. 3 (b)

Fig. 3. Variation of 'fit-factor,' in α-pyridone,
(a) by the rotation of ψ at $\theta=-15°$ and $\varphi=65°$,
(b) by that of θ at $\varphi=65°$ and $\psi=-45°$ (dotted curve) and by that of φ at $\theta=-15°$ and $\psi=-45°$ (full curve).

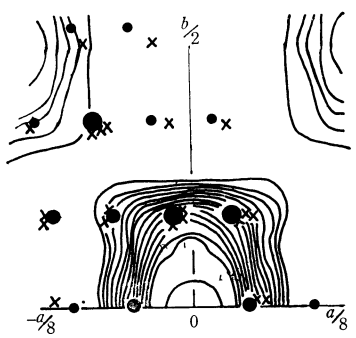

Fig. 4. Patterson projection of α-pyridone and vector-set at the best fitting.

through the inspection of the Patterson function superposed on the possible vector-sets given by the seeking within a limit of rotations due to the unit cell dimensions. This was in good agreement with the orientation of the true structure in the projection. The result of seeking in every five degree of the rotation is shown in Fig. 3, and the vector-set of the model with the orientation corresponding to these angles and that of the true structure superposed on the Patterson projection is also shown in Fig. 4.

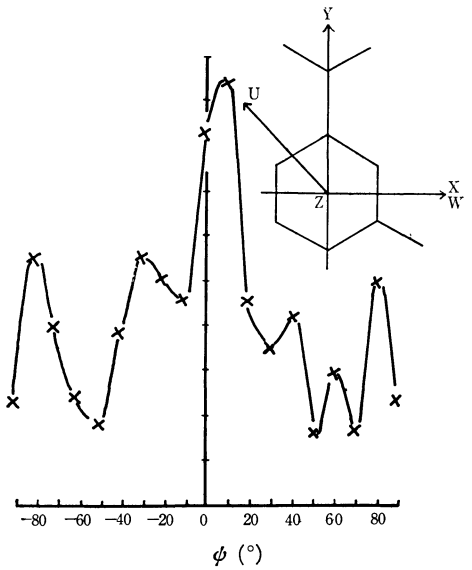

Fig. 5. Variation of 'fit-factor,' in *m*-hydroxybenzamide, by the rotation of ϕ at $\theta=0°$ and $\varphi=45°$.

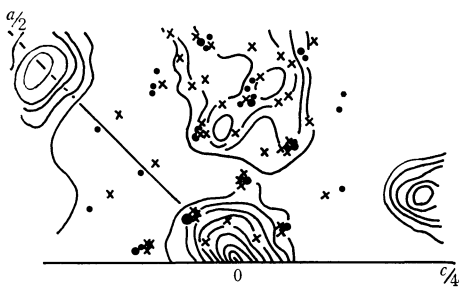

Fig. 6. Patterson projection of *m*-hydroxybenzamide and vector-set at the best fitting.

***m*-Hydroxybenzamide.** — ($a=11.59$, $b=5.03$, $c=15.53$ Å, $\beta=136.1°$, $P2_1/c$). The Patterson function projected on (010) was computed for the grid points at intervals of $a/64$ and $c/64$. In the seeking with the non-interpolation, the angular orientation of the benzene ring in the projection was determined with the planar molecular model consisting of the atoms of equal weight. A complete analysis of the crystal structure has been carried out with the knowledge on the angular orientation of the benzene ring obtained by this method. The result of the seeking is shown in Fig. 5, and the vector-set of the model with the orientation at the best fitting and that of the true structure is also shown in Fig. 6.

Discussion

In the crystals mentioned above, it was possible to find the orientation of the molecule in the projection by the application of this method. Since the maxima corresponding to the best fittings in the crystals of salicylamide and of *m*-hydroxybenzamide were sharp, the angular orientations of these molecules were quickly determined.

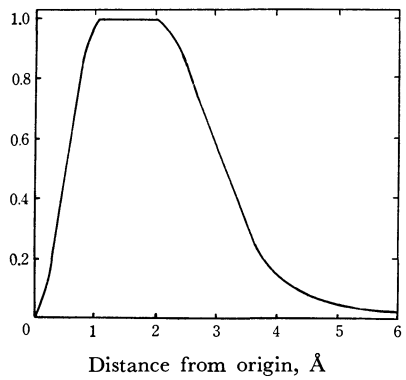

Fig. 7. Modification function against Patterson function to avoid the disturbance from the neighboring molecules.

When a part of the molecule, say the benzene ring, was taken as a rigid group, the peak in the fit-factor distribution became broader and lower. Although it was difficult, in general, to assign the orientation of the group, this method still worked well in some cases.

The fit-factor, especially in the seeking with the non-interpolation, was greatly affected by the rotation about the axis of the projection. Therefore, it may lead to a false orientation unless the rotation about this axis is carried out at relatively close intervals; the interval of the rotation angle should be decided by a correlation between the longest vector in the set and the size of the mesh of the Patterson function calculated. When there is the ambiguity in the estimation of the best fitting, as seen in the case of α-pyridone, the angular orientation may be estimated by the search of the largest fit-factor within the allowable angular region of the rotation; the dimension of the axis of the projection limits correlatively the ranges of θ and φ. However, in such a case, it may be difficult to find out the correct orientation by only the application of this method.

In the crystal of the molecule composed of the atoms of approximately equal weight, as seen from the present examples, it may be not necessary to use the weighted vector-set.

It is not always the case, even in that of the rigid molecule, that the angular coordinates for the best fitting give the correct angular orientation, because of the difference in geometries between the model used and the true molecule. In the crystal of *m*-hydroxybenzamide, in spite of the twist between a carboxyamide group and benzene ring, the angular coordinates obtained from the best fitting was very close to those of the benzene

ring in the true structure. The difference between their geometries was suggested by the disagreement between the vector-set of the model structure and that of the true structure, as shown in Fig. 6. It seems that the small difference between their geometries does not give rise to a serious problem for the determination of the approximate angular orientation of the molecule.

Different orientations due to the symmetry of the projected Patterson function may also influence the correct choice of the angular orientation. In the case of α-pyridone, two vector-sets related by the symmetry may overlap to some extent, and the Patterson peaks may not appear exactly in the positions corresponding to the points of the vector-sets; in fact, the peaks near the origin were mostly unresolved. It seems that the difficulty in the determination of the angular orientation of the α-pyridone molecule arose from this fact.

The intermolecular vectors may disturb the determination of the angular orientation. In order to minimize such obstruction, the values of the Patterson function were modified by a function of the distance from the origin, because the probability that the Patterson function at a point is due to only the intramolecular interactions decreases with increasing distance from the origin. In the present work, the modification as shown in Fig. 7 was used; the modification of this type also corresponded to the removal of the origin peak in the Patterson function. But the removal of the effects from the intermolecular vector and the origin peak was not greatly going to help the search of the best fitting; the latter resulted in the low background in the fit-factor distribution.

The vector-set seeking method was also applied to the crystal of salicylamide with the Patterson function sharpened by the factors of $\{3.5\exp 2\sin^2\theta/\lambda^2)\}$. This brought almost a similar result to the seeking with the unsharpened Patterson function. However, this helped the identification of the angular coordinates for the best fitting, because the maximum peak became sharper than that with the unsharpened Patterson function.

In the present work, a program was written in the machine language of NEAC 2230 computer. The computing time for the seeking with the interpolation is about 3.5 sec. per evaluation of a fit-factor' for a given angular orientation of the model containing ten atoms, while that for the non-interpolation is about 2.5 sec.

BULLETIN OF THE CHEMICAL SOCIETY OF JAPAN VOL. 39 2576—2583 (1966)

The Crystal Structure of *m*-Hydroxybenzamide

By Yukiteru KATSUBE

Himeji Institute of Technology, Himeji

and Yoshio SASADA and Masao KAKUDO

Institute for Protein Research, Osaka University, Kita-ku, Osaka

(Received March 23, 1966)

Crystals of *m*-hydroxybenzamide are monoclinic with four molecules in a unit cell of dimensions $a=11.59$, $b=5.03$, $c=15.53$ Å, $\beta=136.1°$, space group $P2_1/c$. An approximate angular orientation of the molecule in the cell was quickly obtained by an application of the vector-set seeking method. The location of the molecule was then determined with the help of the orientation. The positional and anisotropic thermal parameters of the carbon, nitrogen and oxygen atoms were refined by means of the least-squares method with three-dimensional intensity data. The final R factor was 0.138. The carboxyamide group and benzene ring twist to each other about the C–C bond by an angle of 24.4°. The interatomic distances and bond angles are close to those expected. The molecules are linked by three types of hydrogen bonds to form the infinite double-layered sheets perpendicular to the c axis, and the crystal structure shows somewhat different features from those of the related compounds.

In the serial studies of the crystal structures of some aromatic carboxyamides, it has been found that there are several types of molecular arrangement connected by hydrogen bonds.[1-4] Although

1) Y. Takaki, Y. Sasada and T. Watanabe, *Acta Cryst.*, **13**, 693 (1960).
2) C. Tamura, H. Kuwano and Y. Sasada, ibid., **14**, 693 (1961).
3) S. Orii, T. Nakamura, Y. Takaki, Y. Sasada and M. Kakudo, This Bulletin, **36**, 788 (1963).
4) Y. Sasada, T. Takano and M. Kakudo, ibid., **37**, 940 (1964).

the complete interpretation of these crystal structures in terms of interatomic interaction is impossible at the present stage, it will be of some significance to determine the crystal structures of carboxyamides with various substitutes.

In the previous paper, the authors have reported the structure of salicylamide (*o*-hydroxybenzamide).[4] In this compound, the hydroxy group in the ortho position to the carboxyamide group plays some role in the molecular association by hydrogen bonding, and in consequence the crystal structure shows somewhat different features from those already reported.

It might be interesting to compare the molecular linkage and molecular dimensions of *m*-hydroxybenzamide with those of salicylamide. The present paper will describ the threedimensional X-ray analysis of *m*-hydroxybenzamide.

Experimental and Crystal Data

Crystals were obtained from an alcohol-water solution as colorless hexagonal plates.

The unit cell dimensions were determined from oscillation and Weissenberg photographs about the b and c axes. The crystal and physical data found are as follows:

m-Hydroxybenzamide: $C_7H_7NO_2$, Molecular weight: 137.14.

Monoclinic: $a=11.59\pm0.03$, $b=5.03\pm0.03$, $c=15.53\pm0.03$ Å, $\beta=136.1\pm0.5°$.

Absent spectra: $(h0l)$ when l is odd, $(0k0)$ when k is odd.

Space group: $P2_1/c$.

Density (by flotation): 1.449 g.cm^{-3}.

Density (calculated): 1.451 g.cm^{-3}.

Four molecules per unit cell.

Volume of the unit cell: 627.78 Å^3.

Linear absorption coefficient for Cu$K\alpha$ radiation: $\mu=10.44$ cm^{-1}.

Total number of electron per unit cell: $F(000)=288$.

Equi-inclination Weissenberg photographs for 0—3 layers around the b axis were taken with filtered Cu$K\alpha$ radiation. In order to determine the approximate interlayer scales, Weissenberg photograph of $(hk0)$ zone was also taken. Intensities of the reflections were estimated visually against a calibrated intensity scale prepared using the same crystal. The multiple-film technique was used to correlate strong and weak reflections, ranging in relative intensities from 12000 to 1. The number of independent reflections observed was 706, representing about 70% of the total accessible reflections in the recorded layers. Corrections for Lorentz and polarization factors were applied in the usual way. The crystal used were square in cross section with rectangular dimensions 0.10×0.05 cm. Therefore, absorption and secondary extinction effect might be negligible, and corrections for them were omitted. The observed structure factors were first set onto an absolute scale by Wilson's method,[5] and the scale factors were further improved during the later stage of the refinement.

Structure Determination

Orientation of the Molecule.—In order to determine the orientation of the molecule, the vector-set seeking method described in the previous paper[6] was applied; the vector set of the planar molecular model was superposed on the Patterson projection on (010) and the best fitting between them was searched by varying stepwisely the angular orientation of the molecule. The maximum of the degree of fitting was found at $\theta=0°$, $\varphi=45°$ and $\psi=10°$, while there were some other high peaks in the fitting at the different rotations. It is naturally expected that the orientation of the molecule is given by the angles corresponding to the best fitting if the carboxyamide group is coplanar with the benzene ring. However, the coplanarity of the molecule may not necessarily be fulfilled in the present compound. Therefore, the orientation corresponding to the second highest peak was also saved for the subsequent refinement.

Location of the Molecule in the Unit Cell.—It was expected from the normal van der Waals radii that the atoms would be located only outside the circles centered at the symmetry elements of the unit cell, as shown in Fig. 1. The initial x and z coordinates of the atoms in the molecule for the possible orientations were assigned easily in a rather limited allowable region. They were adjusted by trial with the aid of the structure factor maps for some strong reflections. The discrepancy factor, $R=\sum||F_o|-|F_c||/\sum|F_o|$, was about 0.6 for both orientations at this stage.

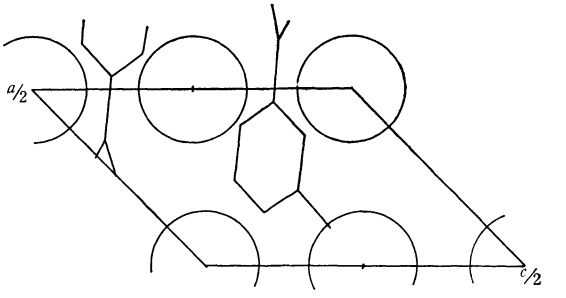

Fig. 1. Forbidden regions for the location of the molecule. The final position of the molecule is indicated.

5) A. J. C. Wilson, *Nature*, **150**, 152 (1942).
6) Y. Katsube, Y. Sasada and M. Kakudo, This Bulletin, **39**, 6108 (1966).

TABLE I. THE FINAL ATOMIC COORDINATES AND TEMPERATURE FACTORS

Atom	x/a	y/b	z/c	$B_{ij}\times10^5$					
				B_{11}	B_{22}	B_{33}	B_{12}	B_{13}	B_{23}
C(1)	0.3662	0.2182	0.3524	738	2198	466	357	826	67
C(2)	0.1971	0.2519	0.2572	663	1671	493	−233	818	−115
C(3)	0.1292	0.4526	0.1706	731	1787	618	86	990	94
C(4)	0.2324	0.6251	0.1813	931	2873	529	1094	925	780
C(5)	0.4037	0.5984	0.2782	943	1836	722	439	1417	963
C(6)	0.4700	0.3985	0.3630	825	328	496	−68	1042	61
C(7)	0.6541	0.3551	0.4710	968	−28	679	178	1389	84
N	0.7492	0.5606	0.5089	916	402	634	−274	1005	−151
O(1)	0.7059	0.1305	0.5196	666	1426	626	438	889	433
O(2)	0.0940	0.0890	0.2466	627	2961	651	−476	889	309

	Attached to	x/a	y/b	z/c	B (Å^2)
H(1)	C(1)	0.4174	0.0472	0.4247	0.67
H(2)	O(2)	0.1334	−0.0943	0.2984	2.24
H(3)	C(3)	0.0003	0.4422	0.0890	3.45
H(4)	C(4)	0.1817	0.8009	0.1096	2.34
H(5)	C(5)	0.4749	0.7453	0.2688	5.44
H(6)	N	0.7033	0.7765	0.4826	5.62
H(7)	N	0.8769	0.5639	0.5939	1.90

In the Fourier projection for the model corresponding to the maximum peak in the vector-set seeking, all the atoms except those in the carboxy-amide group were resolved. On the other hand, the Fourier projection for another orientation did not look encouraging to continue the refinement, because there appeared the regions of low electron density around the positions of the assumed atoms and areas of high density where no atom was placed.

The x and z coordinates in the former model were further refined by successive five Fourier syntheses. The R factor reduced to 0.27. Because of the overlapping of the atoms in the carboxy-amide group, their coordinates were improved by the trial method, until the R factor dropped to 0.22.

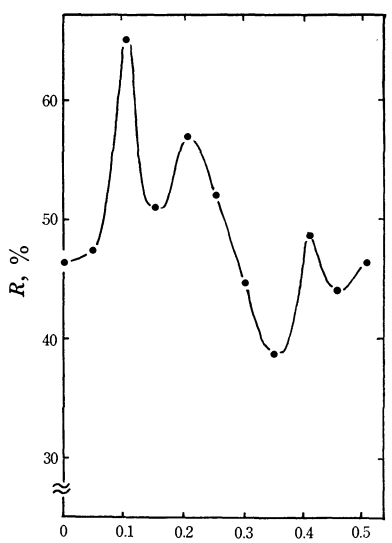

Fig. 2. Minimum residual calculation.

Determination of y Coordinates.—The y coordinates of the atoms were obtained by the one-dimensional minimum residual method.[7] The molecular model constructed from the fixed x and z coordinates was translated successively along the b axis; fifteen ($hk0$) reflections were included in the computation. It gave uniquely the y coordinates, as seen from Fig. 2, where the abscissa shows the coordinates of the reference atom C(7). Successive two Fourier refinements for ($hk0$) reduced the R factor to 0.30.

Three-dimensional Refinement.—Three positional parameters and one isotropic temperature factor for each atom were refined by least-squares method where off-diagonal matrix elements were neglected. The scale factors for the various layer lines were adjusted after every cycle. In the computation, 827 reflections in the four layers about the b axis, some of which were unobserved, were included. Five cycles of the refinement reduced the R factor to 0.23. At this stage, a three-dimensional (F_o-F_c) synthesis was made, but it did not show the positions of hydrogen atoms. Therefore, four hydrogen atoms were placed on the benzene ring plane and at a distance of 1.0 Å outward from the carbon atoms, and the hydrogen atoms of the hydroxy and the amino

7) A. K. Bhuiya and E. Stanley, *Acta Cryst.*, **17**, 746 (1964).

TABLE II. OBSERVED AND CALCULATED STRUCTURE FACTORS

F_o	F_c
H = 0	
28.5	-27.9
53.0	57.0
23.3	22.5
25.6	25.2
13.0	-10.1
8.2	8.5
H = 1	
23.4	-23.8
26.0	-29.9
29.8	28.5
16.1	-14.1
3.6	-2.3
11.6	12.5
2.9	3.0
H = 2	
47.7	-51.0
65.0	-67.3
6.0	-7.1
14.6	-15.4
3.7	-5.5
5.9	-4.5
H = 3	
2.2	-1.4
51.0	50.3
6.6	-5.1
0	1.5
4.4	-3.7
H = 4	
9.8	-9.3
21.0	21.1
5.1	4.6
6.3	6.8
6.6	5.6
H = 5	
13.8	-13.4
8.4	-8.8
0	1.6
0	-1.5
1.4	0.1
H = 6	
12.8	-11.9
8.6	8.7
18.0	-16.3
H = 7	
8.1	-6.8
14.1	13.5
4.8	-5.4
H =8	
10.1	8.5
0	-0.7
4.5	-3.5
H = 9	
4.6	4.4
1.4	-3.2
H = 1	
35.7	-38.3
0	0.3
23.9	-23.6
4.1	-4.8
17.9	-18.2
15.3	16.1
11.5	-13.3
H = 2	
4.3	2.9
97.6	-100.9
40.4	-43.5
3.3	3.9
10.0	-11.0
15.9	-15.3
10.6	9.3
H = 3	
44.7	41.6
52.4	56.7
38.7	37.8
17.5	16.2
13.0	13.7
2.2	3.0
9.8	10.7
8.4	-7.9
H = 4	
47.3	45.5
1.7	-1.5
29.9	27.4
10.5	-10.0
35.8	31.6
14.8	-13.5
3.6	2.9
6.0	5.7
H = 5	
32.6	-26.9
34.8	-33.3
32.3	-29.5
35.7	-34.0
19.8	-14.0
11.2	-11.0
0	-0.6
4.4	-4.7
H = 6	
17.0	15.8
9.9	-6.7
17.2	15.3
7.3	6.7
4.5	4.1
6.2	5.7
7.9	-5.6
2.0	-2.1
H = 7	
9.8	7.8
10.4	11.4
22.1	20.6
21.0	-18.8
31.4	31.0
0	0
9.7	9.4
1.4	-0.1
2.5	3.0
H = 8	
1.4	-0.9
15.9	-14.9
6.3	-7.1
8.5	-8.0
7.1	-8.6
10.4	-9.8
5.3	-5.3
1.9	1.7
1.4	0.6
H = 9	
6.8	-6.6
2.6	-1.1
21.3	20.9
5.9	-5.9
7.2	-7.9
22.6	20.4
4.8	-4.6
5.9	-6.1
0	0.6
H = 10	
0	0.2
5.7	7.0
25.7	-24.0
27.3	29.6
9.3	-8.2
6.7	7.1
2.6	-2.0
4.9	5.8
H = 11	
4.3	-4.6
1.8	1.3
12.0	-11.9
11.5	12.0
29.8	-31.5
2.1	2.7
3.3	-4.4
2.2	-1.0
10.7	-14.3
H = 12	
10.6	10.7
3.4	-4.8
0	-0.8
18.8	19.6
3.0	-3.4
0	0.2
5.4	5.6
1.6	1.9
H = 13	
1.7	2.9
2.8	2.8
3.9	4.5
0	0
7.6	8.0
4.6	7.0
0	-1.2
H = 14	
5.0	-7.8
3.8	-8.9
9.7	-10.3
K = 1	
H = 0	
29.6	32.1
20.9	20.7
8.3	-8.3
1.2	-1.7
11.0	-11.4
0	0.8
8.9	8.5
12.6	14.5
0	0.1
9.2	-9.0
H = 1	
11.8	11.0
18.0	16.4
4.6	6.2
23.3	-21.9
21.4	19.5
2.9	3.3
18.5	-18.6
9	5.8	-6.8
10	8.0	8.0
H = 2		
0	29.5	-31.6
1	8.9	-9.5
2	2.9	2.5
3	3.3	3.8
4	23.8	-21.9
5	8.3	-9.6
6	4.5	3.6
7	13.5	16.0
H = 3		
0	20.0	-19.4
1	8.9	-9.7
2	4.9	4.3
3	3.8	3.0
4	6.0	6.1
5	0	-2.1
6	6.8	-8.1
H = 4		
0	11.3	12.6
1	13.9	-14.4
2	10.0	11.8
3	0	1.8
4	0	-1.2
5	6.8	-5.6
6	2.8	3.2
7	6.2	6.4
H = 5		
0	0	1.3
1	7.4	7.8
2	4.5	-4.7
3	8.3	8.5
4	6.8	-5.7
5	4.6	4.8
H = 6		
0	4.5	-5.4
1	4.7	-3.5
2	0	0.6
3	6.7	-8.2
H = 7		
0	0	0.9
1	4.8	-6.7
2	0	-1.0
3	4.2	-4.6
H = 8		
0	6.6	9.8
1	6.2	7.5
H = 9		
0	3.0	-2.6
1	5.8	7.1
H = 10		
0	4.6	5.7
H = 1		
-2	60.0	57.5
-3	31.6	32.0
-4	4.9	4.2
-5	17.6	16.4
-6	2.1	3.0
-7	11.2	-10.9
-8	0	-1.9
-9	13.6	12.1
-10	11.7	11.6
-11	4.8	4.7
-12	8.6	-9.2
-13	0	-0.1
-14	6.2	-2.7
H = 2		
-1	18.8	17.1
-2	14.0	12.0
-3	73.1	-76.3
-4	65.4	-74.9
-5	24.4	23.8
-6	28.9	27.5
-7	35.1	-32.1
-8	17.2	-16.6
-9	0	-0.1
-10	2.3	-3.4
-11	6.8	-8.4
-12	0	-2.3
-13	7.8	-6.7
-14	7.7	8.1
-15	2.9	-1.4
H = 3		
-1	0	-1.1
-2	4.7	3.6
-3	26.8	-21.0
-4	23.8	21.8
-5	32.3	32.9
-6	14.3	-12.2
-7	17.0	-16.8
-8	8.9	-8.1
-9	6.9	-4.8
-10	11.6	11.0
-11	0	0.2
-12	0	-1.7
-13	3.9	4.4
-14	0	1.6
-15	9.0	-8.6
H = 4		
-1	35.3	35.7
-2	23.8	19.7
-3	14.4	-15.2
-4	39.5	36.2
-5	17.1	15.0
-6	2.9	2.3
-7	31.4	29.3
-8	27.4	25.7
-9	14.5	15.6
-10	0	1.5
-11	7.8	7.1
-12	0	-0.3
-13	8.4	9.0
-14	0	0
H = 5		
-1	0	2.0
-2	26.1	-23.7
-3	0	0.6
-4	15.5	-15.9
-5	27.4	20.6
-6	3.1	-3.4
-7	10.0	-10.1
-8	26.3	-23.4
-9	5.6	-5.7
-10	4.1	-5.0
-11	7.6	-8.3
-12	0	0.5
-13	4.8	3.4
-14	6.7	-5.7
-15	6.3	-7.2
-16	0	1.2
H = 6		
-1	4.2	-2.9
-2	8.4	-7.7
-3	0	3.9
-4	13.2	-11.9
-5	41.9	-37.2
-6	0	-2.1
-7	3.6	3.9
-8	14.0	-12.4
-9	17.0	-17.4
-10	7.3	-7.7
-11	7.6	-6.9
-12	0	2.2
-13	14.4	-15.7
-14	4.5	-4.4
-15	0	0
-16	0	0.4
-17	3.3	-3.8
-18	2.4	3.8
H = 7		
-1	9.4	-9.6
-2	23.1	24.9
-3	6.1	-4.5
-4	4.1	2.7
-5	6.2	-5.9
-6	17.8	16.7
-7	13.7	13.6
-8	24.5	23.4
-9	10.1	-7.0
-10	12.8	13.0
-11	10.9	11.7
-12	8.0	7.1
-13	8.3	9.4
-14	6.8	6.5
-15	8.1	8.7
-16	0	0
-17	0	-2.2
-18	0	1.2
H = 8		
-1	0	-0.6
-2	10.6	-13.2
-3	26.9	30.0
-4	4.6	5.8
-5	9.0	-12.1
-6	7.6	-7.3
-7	16.3	17.1
-8	4.3	5.0
-9	11.6	10.7
-10	11.8	-12.6
-11	4.6	5.1
-12	0	-1.0
-13	0	-1.1
-14	4.8	5.4
-15	4.7	5.5
-16	4.4	-5.6
-17	3.0	3.3
-18	0	-0.3
H = 9		
-1	4.4	-5.8
-2	6.6	-9.7
-3	8.7	9.0
-4	8.4	9.3
-5	0	-0.7
-6	23.3	-27.2
-7	0	2.4
-8	4.6	-5.3
-9	6.5	-7.8
-10	10.5	-12.3
-11	0	0.2
-12	0	-0.4
-13	9.7	-13.5
-14	19.3	-20.1
K = 2		
H = 0		
5.1	6.4
45.1	45.2
3.5	4.9
3.5	-3.1
6.0	6.9
17.6	17.6
0	-1.1
12.2	11.9
6.1	6.0
7.5	9.5
H = 1	
14.9	15.4
27.4	-27.8
12.1	-12.5
17.7	-15.8
8.1	8.8
18.8	-18.9
8.7	9.0
4.6	-4.9
3.9	-3.7
12.0	-13.0
0	0
5.2	-6.2
H = 2	
9.2	10.1
1.6	2.2
15.2	-17.5
4.1	4.4
3.2	2.9
25.3	-23.6
15.4	-15.5
4.8	5.0
7.0	-7.4
3.6	-4.7
H = 3	
12.4	-10.9
19.1	16.6
9.5	-8.8
6.3	6.9
11.0	13.2
31.4	30.7
8.8	-9.1
7.0	7.5
0	-1.7
H = 4	
0	0.9
5.0	5.3
11.5	11.7
11.3	-11.4
3.9	-5.8
0	0
4.5	7.8
3.3	-4.8
H = 5	
12.5	-14.7
24.5	-25.5
17.8	18.0
4.8	-4.6
5.5	-6.8
2.5	-3.1
0	0
9.8	-13.0
H = 6	
11.5	-12.6
29.0	26.8
0	-1.3
0	0.1
4.8	-5.8
4.1	5.2
2.5	3.5
H = 7	
8.4	9.9
5.4	6.0
2	-0.9
2.2	3.1
H = 8	
6.3	6.8
4.0	-4.5
2	-1.5
8.1	-9.5
H = 1	
13.2	-13.5
5.6	5.6
12.5	-12.7
18.9	-18.1
8.1	-8.8
4.1	2.8
15.0	-13.4
0	0.9
9.0	9.8
4.8	-5.7
5.4	-7.8
H = 2	
4.9	-7.9
20.8	-19.6
0	-0.5
10.1	-6.8
26.3	27.9
3.2	-3.7
15.6	15.4
0	-0.1
5.1	6.7
6.7	-8.5
10.1	12.4
0	0.5
4.2	5.9
H = 3	
35.1	36.6
0	1.1
4.8	5.6
10.9	11.0
6.8	7.5
22.3	-22.9
10.8	-10.5
13.8	14.0
0	-1.5
0	0.6
0	-1.5
4.0	3.8
7.3	-8.3
H = 4	
11.7	-13.5
24.8	25.6
6.0	-7.2
6.4	-6.8
21.5	-24.2
11.7	11.9
27.5	27.3
8.8	8.9
29.1	-29.5
2.7	-2.7
0	-1.0
4.8	-4.5
0	1.6
5.8	6.2
3.1	-4.2
H = 5	
13.8	-16.6
4.8	3.3
13.3	12.9
4.8	5.7
26.8	-27.3
10.0	9.2
2.0	2.9
20.9	-21.6
3.3	5.1
13.4	12.3
9.6	12.5
3.9	-4.9
0	-1.0
0	0.5
5.8	8.0
3.4	-5.5
H = 6	
3.6	-4.2
2.4	3.0
22.2	22.6
14.2	-16.1
9.8	-7.8
6.4	-5.9
13.5	14.7
10.9	-13.8
2.4	4.0
5.7	8.8

TABLE II. (continued)

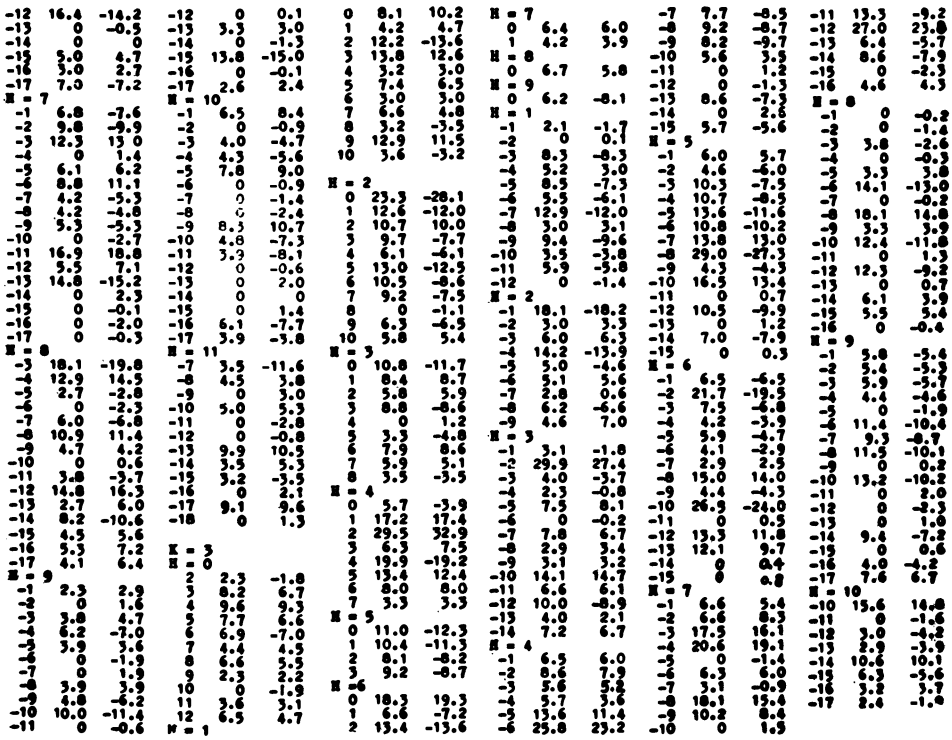

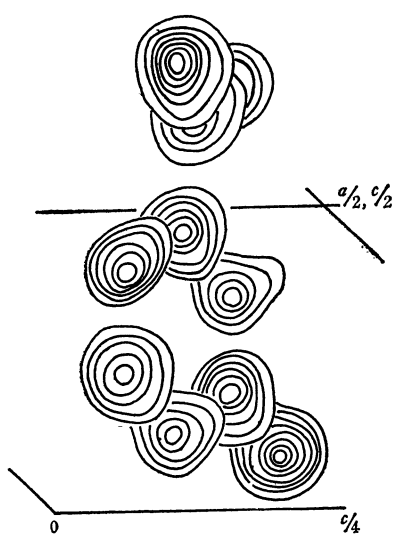

Fig. 3. The final electron density distribution. Composite diagram of sections parallel to the (010). Contours are at intervals of 1.0 eÅ^{-3}, the lowest one being 2.0 eÅ^{-3}.

groups were located at the positions expected from the hydrogen bonding. Further refinement of the structure was made by least-squares with a block-diagonal matrix approximation; anisotropic temperature factors in the form of

$$\exp\{-(B_{11}h^2+B_{22}k^2+B_{33}l^2+B_{12}hk+B_{13}hl+B_{23}kl)\}$$

were assigned for the non-hydrogen atoms. Three cycles of the block-diagonal least-squares refinement yielded the R factor of 0.138 for all the independent reflections. If the unobserved reflections were omitted, the R factor became 0.118. Atomic scattering factors for the carbon, nitrogen and oxygen were taken from Berghuis, Haanapple, Potters, Loopstra, MacGillavry and Veenendaal,[8] and those for the hydrogen from McWeeny.[9] The final atomic coordinates and anisotropic temperature factors are given in Table I. Observed and calculated structure factors are listed in Table II. The final three-dimensional electron density distribution viewed down the b axis is shown in Fig. 3.

All numerical computations except for the final refinement were done on NEAC 2230 and NEAC 2206 computers with programs written by the authors. The least-squares method with block-diagonal approximation was made on an IBM 7090 with program written by T. Ashida.

8) J. Berghuis, Ij. M. Haanappel, M. Potters, B. O. Loopstra, C. H. MacGillavry and A. L. Veenendaal, ibid., **8**, 478 (1955).
9) R. McWeeny, ibid., **4**, 513 (1951).

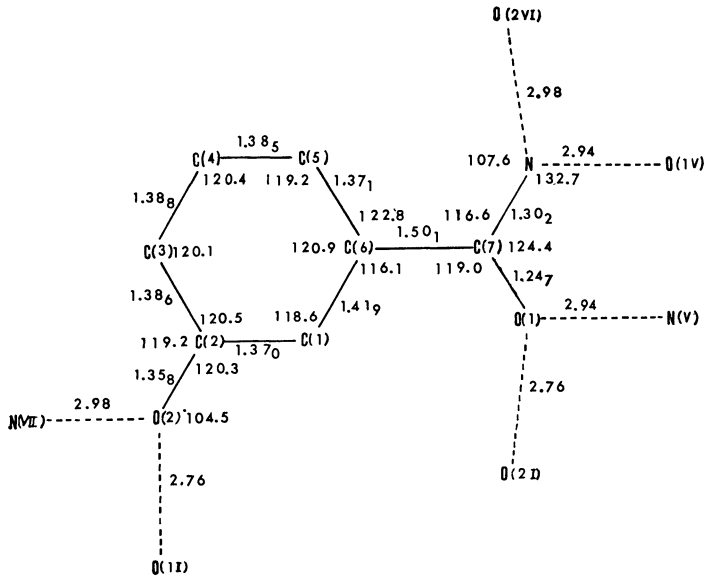

Fig. 4. Bond lengths (Å) and bond angles (°).

Description of the Structure and Discussion

Molecular Structure.—Bond lengths and bond angles found in the *m*-hydroxybenzamide molecule are shown in Fig. 4. The average standard deviations of the atomic coordinates are 0.014, 0.011 and 0.008 Å for carbon, nitrogen and oxygen atoms respectively. Therefore, the estimated standard deviations of the bond lengths are 0.020 Å in C–C, 0.018 Å in C–N and 0.016 Å in C–O. Although small fluctuations among the C–C bond lengths in the benzene ring are probably significant, detailed discussion about this will not be given because of low degree of accuracy. The average C–C bond length, 1.39 Å, and average C–C–C bond angle, 120.0°, in the benzene ring are in good agreement with the standard values. The dimensions of the carboxyamide group in the *m*-hydroxybenzamide, C–N=1.30_2 Å and C–O=1.24_7 Å, are close to those found in the related crystals: C–N=1.31_2 Å and C–O=1.24_4 Å in α-pyrazinamide,[1] C–N=1.29 Å and C–O=1.25 Å in *m*-methylbenzamide,[3] C–N=1.30_9 Å and C–O=1.22_2 Å in salicylamide,[4] C–N=1.34 Å and C–O=1.22 Å in nicotinamide,[10] C–N=1.31 Å, and C–O=1.24 Å in benzamide.[11] The bond length between the ring carbon and hydroxy oxygen atoms is 1.35_8 Å, which does not differ significantly from the values found in the salicylamide, 1.36_1 Å, salicylic acid, 1.358 Å,[12] and α-resorcinol, 1.36 Å.[13]

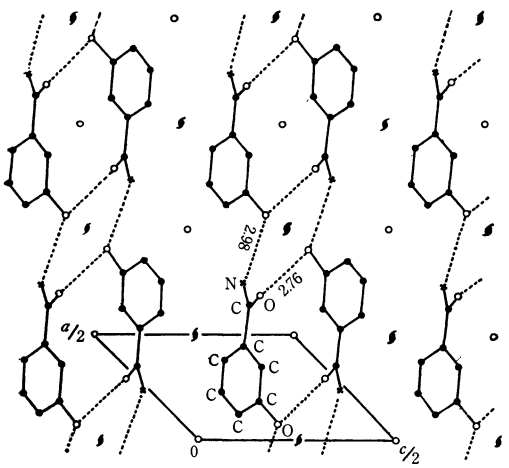

Fig. 5. Arrangement of the molecules viewed down the b axis.

The plane of the benzene ring (including C(7) and O(2)) can be represented by the equation:

$$y' = -0.0368x' - 1.2750z' + 4.3267$$

where $x' = x\sin\beta$, $y' = y$ and $z' = z + x\cos\beta$. The coefficients of the equation were determined by the least-squares method. The perpendicular displacements of the atoms from the mean plane are shown in Table III. The six carbon atoms in the benzene ring are coplanar within an experimental error. On the other hand, the carboxyamide group and the benzene ring twist to each

10) W. B. Wright and G. S. D. King, ibid., **7**, 285 (1954).
11) B. R. Penfold and J. C. B. White, ibid., **12**, 130 (1959).
12) M. Sundarlingam and L. H. Jensen, ibid., **18**, 1053 (1965).
13) J. M. Robertson, *Proc. Roy. Soc.*, **A157**, 79 (1936).

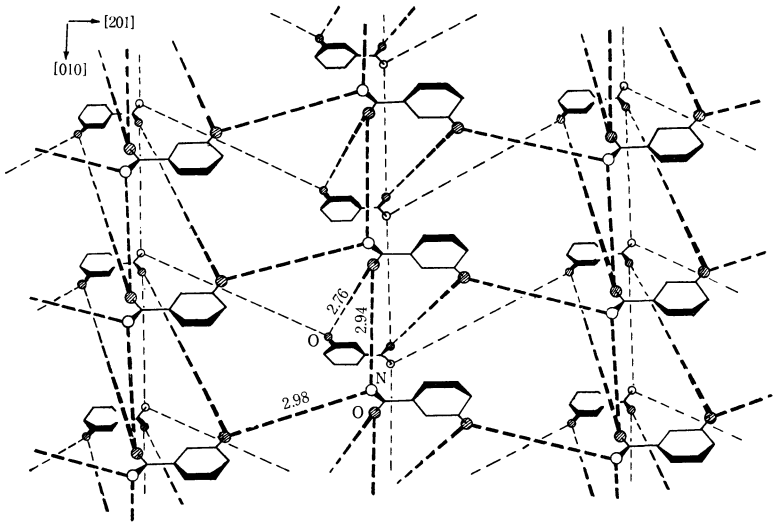

Fig. 6. A schematical drawing of the double-layered sheet formed by hydrogen bonds.

TABLE III. PERPENDICULAR DISPLACEMENTS OF ATOMS FROM THE MEAN PLANE OF THE BENZENE RING

Atom	Displacement Å
C(1)	0.025
C(2)	0.005
C(3)	0.006
C(4)	−0.001
C(5)	−0.007
C(6)	0.000
C(7)	−0.009
O(2)	−0.019

other around the C(6)–C(7) bond, and the angle between the planes of the benzene ring and the carboxyamide group is 24.4°. In many related crystals, the plane of the carboxyamide group makes an angle of about 25° with that of the benzene ring. This twist has been interpreted as the effect of steric hindrance between the hydrogen atom in the amino group and that in the ortho position of the ring.

Crystal Structure.—The crystal structure projected down the b axis is illustrated in Fig. 5, and the intermolecular distances less than 4.0 Å are listed in Table IV. There are three types of hydrogen bonds. The reference molecule at (x, y, z) is connected by the first set of OH···O (amide) of length 2.76 Å with the molecule at $(1-x, -y, 1-z)$, to form a molecular pair across the center of symmetry. The pairs are piled up infinitely along the b axis by the second set of NH···O (amide) of length 2.94 Å. The third hydrogen bonds, NH···O (hydroxy), of length 2.98 Å join the neighboring piles which are related to each other by the screw axis. Thus all the hydrogen atoms capable of participating the hydrogen bonding have been utilized and the endless double-layered sheets perpendicular to the c axis are formed as seen from Fig. 5. Figure 6 shows a schematical drawing of this double-layered sheet. This type of the molecular linkage by the hydrogen bonds has been first found in the present crystal.

TABLE IV. INTERMOLECULAR DISTANCES

From atom at x, y, z	To atom	In molecule	Distance(Å)
C(1)	C(1)	I	3.87
C(1)	C(6)	II	3.84
C(1)	C(7)	II	3.62
C(2)	C(7)	II	3.77
C(4)	C(7)	IV	3.62
C(5)	C(7)	IV	3.65
C(5)	C(6)	IV	3.72
C(5)	C(5)	IV	3.85
C(6)	C(6)	II	3.92
C(4)	N	IV	3.82
C(1)	O(1)	I	3.18
C(2)	O(1)	I	3.37
C(3)	O(2)	III	3.69
C(5)	O(1)	IV	3.82
C(7)	O(2)	VI	3.60
O(2)	N	II	3.30
O(2)	O(2)	III	3.38
	Hydrogen bond		
N	O(1)	V	2.94
N	O(2)	VI	2.98
O(2)	O(1)	I	2.76

Molecule I at $1-x, -y, 1-z$
II $1-x, 1-y, 1-z$
III $-x, {}^1/_2+y, {}^1/_2-z$
IV $1-x, {}^1/_2+y, {}^1/_2-z$
V $x, 1+y, z$
VI $1+x, {}^1/_2-y, {}^1/_2+z$

The intermolecular distances except the hydrogen bonds require no special comment, all corresponding to the van der Waals interaction. The molecular arrangement described here can reasonably explain the presence of cleavage parallel to the $(10\bar{4})$ plane.

The authors wish to express their thanks to Dr. Tamaichi Ashida for permitting the use of the programs of the least-squares with block-diagonal approximation. They are also indebted to Japan IBM Co., Ltd. which offerred machine time of an IBM 7090 under the University Contribution System.

BULLETIN OF THE CHEMICAL SOCIETY OF JAPAN VOL. 39 2583—2588 (1966)

The Radiolysis of Crystalline Oxalato Metal Complexes. The Effects of Coordinating Metal Ions on the Radiolysis of Oxalate

By Akira SUGIMORI*

Japan Atomic Energy Research Institute, Tokai-mura, Naka-gun, Ibaraki

(Received April 14, 1966)

Coordinated oxalates in metal complexes are more reactive under γ-irradiation than are ionic oxalates. This suggests that the covalency between the metal ion and the ligand in oxalato metal complexes promotes the reactivity of the ligand. The reaction of the ligand is also affected by the central metal ions. In $K_3[Co(C_2O_4)_3]\cdot 3H_2O$ and $K_3[Fe(C_2O_4)_3]\cdot 3H_2O$, the coupled reduction of central metal ions with the oxidative decomposition of the ligand to carbon dioxide occurs at relatively high G values. In $K_3[Cr(C_2O_4)_3]\cdot 3H_2O$, the redox reaction of the central metal ion is small and the ligand decomposes into carbon dioxide and carbon monoxide. In $K_3[Al(C_2O_4)_3]\cdot 3H_2O$, the formation of glyoxal and formic acid instead of carbon monoxide is significant.

It is well-known that the reactions of the ligand molecule in coordination compounds are affected by the central metal ions. As for the photochemistry of metal complexes, the photochemical reactions of oxalato metal complexes have been studied extensively.[1,2] It has been concluded that the photo-induced electron transfer from the ligand to such central metal ions as iron(III), cobalt(III) and manganese(III) results in the high quantum yield of the decomposition of the ligand molecule.

Our study aims at the elucidation of the effects of central metal ions on the radiolytic decomposition of the ligand molecule (in this case, oxalate) by comparing the results of radiolysis with those of photolysis.

Several papers have dealt with the radiation-induced reactions of metal complexes in aqueous solutions.[3-6] The radiation-induced reaction of an aqueous system is, however, not suitable for comparison with the photo-induced reaction, because the radiation-induced reaction is initiated by the reactive intermediates produced by the radiolysis of water, while the photochemical reaction is initiated by the direct excitation of the solute. On the other hand, the direct excitation of the complexes by an ionizing radiation can be expected in the radiolysis of crystalline complexes. Therefore, the radiolysis of crystalline oxalato metal complexes was studied in order to elucidate the effects of metal ions in the excitation of the complexes by ionizing radiations. A preliminary report has already been published.[7] Moreover, recently, a study of the radiolysis of several oxalatocobalt(III)-complex salts was reported by Sano, Matsubara and Saito.[8]

Results and Discussion

The Reactivities of Ionic Oxalate in Salts and Coordinated Oxalate in Metal Complexes. —The radiation-chemical reactivities of ionic

* Present address: Department of Chemistry, Faculty of Science and Technology, Sophia University, 7-Kioicho, Chiyoda-ku, Tokyo.

1) C. A. Parker and C. G. Hatchard, *Proc. Roy. Soc.*, **A235**, 518 (1956); *J. Phys. Chem.*, **63**, 22 (1959).

2) G. B. Porter, J. G. W. Doering and S. Karanka, *J. Am. Chem. Soc.*, **84**, 4028 (1962).

3) E. A. Hausman and T. W. Davis, ibid., **76**, 5341 (1954).

4) J. W. Swinnerton, *Dissertation Abstr.*, **20**, 527 (1959).

5) A. Sugimori and G. Tsuchihashi, This Bulletin, **34**, 713 (1960).

6) N. Matsuura, N. Shinohara and M. Takizawa, *J. Chem. Soc. Japan, Pure Chem. Sect. (Nippon Kagaku Zasshi)*, **86**, 590 (1965).

7) A. Sugimori and G. Tsuchihashi, This Bulletin, **34**, 449 (1961).

8) H. Sano, N. Matsubara and N. Saito, ibid., **38**, 333 (1965).

oxalate and of coordinated oxalate were compared. In order to avoid the additional effects caused by the reduction or oxidation reactions of central metal ions in metal complexes, the radiolysis of potassium trioxalatoaluminate(III), the central ion of which is resistant to reduction and oxidation, was compared with that of oxalate salts.

Table I lists the G values for the decomposition

TABLE I. THE DECREASE IN THE REDUCING POWER OF THE OXALATE SALTS AND THE OXALATO METAL COMPLEX BY γ-IRRADIATION

Compound	Dose rate eV./g.hr.	Dose eV./g.	G(−Reducing power)
$H_2C_2O_4\cdot 2H_2O$			10.1*
$H_2C_2O_4$	2.6×10^{19}	8.2×10^{21}	8.0
$K_3[Al(C_2O_4)_3]\cdot 3H_2O$			9.9*
$Na_2C_2O_4\cdot H_2O$	1.4×10^{19}	2.8×10^{21}	0.4
	2.5×10^{19}	7.9×10^{21}	0.03
$K_2C_2O_4\cdot H_2O$	4.5×10^{19}	9.6×10^{21}	0.8
	4.5×10^{19}	1.2×10^{22}	0.8
$NaHC_2O_4\cdot H_2O$	2.4×10^{19}	8.5×10^{21}	1.5
$FeC_2O_4\cdot 2H_2O$	8.8×10^{19}	8.1×10^{21}	0.1

* Is obtained from the yield-dose curve.

(the number of molecules decomposed per 100 eV. of the absorbed energy of radiation) of ionic and coordinated oxalates, values which were determined by titration with potassium permanganate.

Ionic oxalates in sodium oxalate, potassium oxalate, and iron(II) oxalate showed lower G values for decomposition than the coordinated oxalate in potassium trioxalatoaluminate(III). The G value of the aluminum complex was similar to that of oxalic acid (hydrous and anhydrous). Sodium hydrogen oxalate showed an intermediate G value. These results suggest that the covalency between oxygen and metal/or hydrogen is important for the reactivity of oxalates against ionizing radiation.

Crystal water has a slight effect on the radiolysis of oxalate. Hydrated oxalic acid and hydrated iron(II) oxalate have reactivities similar to those of anhydrous oxalic acid and anhydrous sodium oxalate respectively.

The Radiolysis of Trioxalato Metal Complexes.—*General Features.*—In addition to the effect of the covalency described above, the oxidation and reduction of the central metal ions affect the reaction mechanism of the ligand. Before discussing this problem, however, the general features of the radiolysis of trioxalato metal complexes should be described. Gamma-irradiation brings about the decomposition of the ligand and a change in the oxidation state of metal ions, and gives gaseous, liquid and solid products. Among the reaction products, gaseous products show an interesting feature. Gamma-irradiation gave two kinds of gaseous products: the gas evolved by irradiation, and the gas evolved by dissolving the irradiated complex in water. In some cases, the content of the gas evolved from the γ-ray irradiated complex was different from that of the gas evolved by dissolving the irradiated complex in water. The most remarkable example is the case of potassium trioxalatochromate(III). When it was irradiated at a total dose of 2.3×10^{22} eV./g., it gave a gaseous product at a G value of 1.8; this product consisted of 58% carbon dioxide, 37% carbon monoxide, and 5% hydrogen. The G value of the gas evolved by treating the irradiated complex with water was 0.5; this gas consisted solely of carbon dioxide. This fact suggests that the gas evolved by dissolving the irradiated complex is not the gas occluded in the irradiated complex crystals. The existence of a precursor for carbon dioxide may be expected. An infrared spectroscopic study of irradiated potassium trioxalatochromate(III) suggested that carbon dioxide was trapped in the form of hydrogen carbonate ions.[9]

The quantities of the evolved gas and the decomposed oxalato metal complexes are plotted against the absorbed radiation dose in Figs. 1, 2 and 3.

As is shown in the figures, the quantities of the evolved gas and the decomposed complexes are proportional to the absorbed dose.

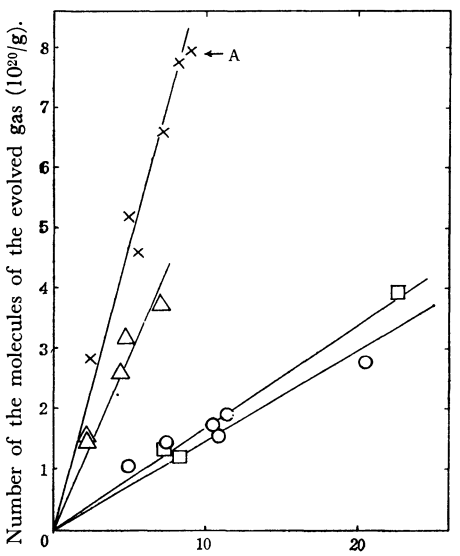

Fig. 1. Relations between the number of the molecules of the evolved gas and the absorbed radiation dose.
—○— $K_3[Al(C_2O_4)_3]\cdot 3H_2O$
—□— $K_3[Cr(C_2O_4)_3]\cdot 3H_2O$
—△— $K_3[Fe(C_2O_4)_3]\cdot 3H_2O$
—×— $K_3[Co(C_2O_4)_3]\cdot 3H_2O$
A Irradiated at −50°C

9) A. Sugimori, To be published.

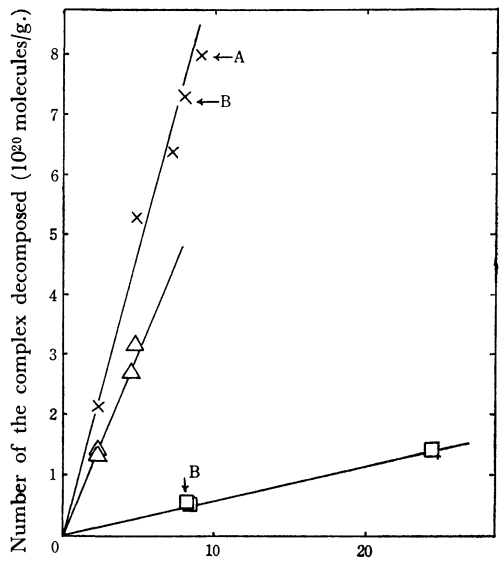

Fig. 2. Relations between the number of the complex decomposed and the absorbed radiation dose.
—□— $K_3[Cr(C_2O_4)_3]\cdot 3H_2O$
—△— $K_3[Fe(C_2O_4)_3]\cdot 3H_2O$
—×— $K_3[Co(C_2O_4)_3]\cdot 3H_2O$
A Irradiated at −50°C
B Irradiated in the air

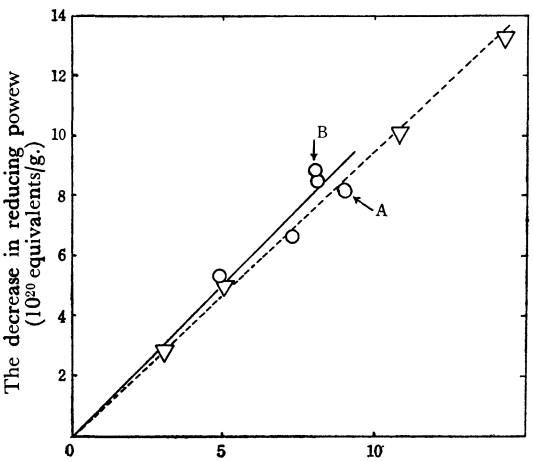

Fig. 3. Relations between the decrease in reducing power and the absorbed radiation dose.
—○— $K_3[Al(C_2O_4)_3]\cdot 3H_2O$
—▽— $H_2C_2O_4\cdot 2H_2O$
A Irradiated at −50°C
B Irradiated in the air

The existence of air and the change in the irradiation temperature from room temperature to −50°C slightly affect the decomposition of the complex (Figs. 1, 2 and 3).

Effects of Central Metal Ions on the Decomposition of the Ligand.—The decomposition of the ligand depends on the nature of the central metal ions.

i) $K_3[Fe(C_2O_4)_3]\cdot 3H_2O$ and
$K_3[Co(C_2O_4)_3]\cdot 3H_2O$.

The results of the radiolysis of potassium trioxalatoferrate(III) and potassium trioxalatocobaltate-(III) are summarized in Table II.

Table II. The radiolysis of potassium trioxalatoferrate(III) and potassium trioxalatocobaltate(III)

	$K_3[Fe(C_2O_4)_3]\cdot 3H_2O$		
	Dose (eV./g.)	*G* value	Composition of the gas (%)
Evolved gas		6.8*	
	7.1×10^{21}	6.3	H_2 0, CO 0, CO_2 100
The gas evolved by dissolving the irradiated complex	7.1×10^{21}	1.5	H_2 0, CO 0, CO_2 100
Fe(II)		7.2*	
The decrease of the complex		6.1*	
	$K_3[Co(C_2O_4)_3]\cdot 3H_2O$		
	Dose (eV./g.)	*G* value	Composition of the gas (%)
Evolved gas		11.1*	
	5.4×10^{21}	8.6	H_2 0, CO 0, CO_2 100
The gas evolved by dissolving the irradiated complex	5.4×10^{21}	1.3	H_2 0, CO 0, CO_2 100
The decrease of the complex		10.3*	

* Is obtained from the yield-dose curve.

The features of the radiolysis of these complexes are:

1) The *G* values of the gaseous products and the decomposed complexes were greater than those of the other complexes.

2) The gaseous product consisted entirely of carbon dioxide.

3) In the case of potassium trioxalatoferrate-(III), iron(II) was produced at a *G* value similar to those of the total gaseous product and the decomposed complex.

The radiation-induced reaction of potassium trioxalatoferrate(III) is very simple. The main reaction of the ligand is the decomposition to carbon dioxide; side reactions to give carbon monoxide and hydrogen are negligible. The coupled reduction of the central metal ion with the oxidative decomposition of coordinated oxalate takes place

solely. This reaction is the same as that of the photolysis of the complex. Excited states which are the same as that in photolysis may be produced selectively and effectively by γ-irradiation. The reaction mechanism proposed for the photolysis[1] may be applied to the radiation-induced reaction:

$$[Fe^{III}(C_2O_4)_3]^{3-} \xrightarrow{\gamma\text{-rays}} [Fe^{III}(C_2O_4)_3]^{3-*} \quad (1)$$
(excited state)

$$[Fe^{III}(C_2O_4)_3]^{3-*} \rightarrow \left[\begin{array}{l} O \\ \| \\ O \end{array}\!\!>\!C\!-\!C\!<\!\!\begin{array}{l} O \\ \| \\ O \end{array}\!\!>\!Fe^{II}(C_2O_4)_2\right]^{3-} \quad (2)$$

$$\left[\begin{array}{l} O \\ \| \\ O \end{array}\!\!>\!C\!-\!C\!<\!\!\begin{array}{l} O \\ \| \\ O \end{array}\!\!>\!Fe^{II}(C_2O_4)_2\right]^{3-} \rightarrow$$

$$C_2O_4^- + [Fe^{II}(C_2O_4)_2]^{2-} \quad (3)$$

$$C_2O^-_4 + [Fe^{III}(C_2O_4)_3]^{3-} \rightarrow$$

$$2CO_2 + [Fe^{II}(C_2O_4)_3]^{4-} \quad (4)$$

Similar reactions would take place in the radiolysis of potassium trioxalatocobaltate(III). In this case, the structure of the cobalt(II) complex has been studied by the infrared spectroscopic method.[9] The cobalt(II) produced by γ-irradiation preferentially forms four coordinate dioxalato complexes. This means that the reduction of the central metal ion is followed by the elimination of one oxalate ion and a reorganization in the coordination sphere.

ii) $K_3[Cr(C_2O_4)_3]\cdot 3H_2O$.

1) The formation of carbon monoxide and hydrogen was remarkable.

2) The G value for the decomposition of the complex was small.

3) The content of the evolved gas was different from that of the gas obtained by dissolving the irradiated complex in water.

The radiolysis of potassium trioxalatochromate(III) is very different from those of potassium trioxalatoferrate(III) and potassium trioxalatocobaltate(III). The reduction of chromium(III) to chromium(II) was not observed. On the other hand, the oxidation of the central metal ion was observed, although the yield was very small. The G value of chromium(VI) was found to be 0.003—0.004. The lack of a conjugation of reactions between the ligand and the central metal ion in potassium trioxalatochromate(III) would result in a lower reactivity toward γ-irradiation.

TABLE III. THE RADIOLYSIS OF POTASSIUM TRIOXALATOCHROMATE(III)

	Dose (eV./g.)	G value	Composition of the gas (%)	
Evolved gas		1.8*		
	2.3×10^{22}	1.8	H_2	5
			CO	37
			CO_2	58
	8.0×10^{21}	—	H_2	2
			CO	36
			CO_2	62
The gas evolved by dissolving the irradiated complex	2.3×10^{22}	0.5	H_2	0
			CO	0
			CO_2	100
The decrease of the complex		0.6*		

* Is obtained from the yield-dose curve.

The lower reactivity of the complex has also been observed in the photolysis of the complex.[2] Trioxalatocobaltate(III) and trioxalatoferrate(III) are easily decomposed by ultraviolet irradiation, but trioxalatochromate(III) is very resistant to ultraviolet light. This fact also suggests that, in the radiation-induced reaction, the same excited molecules as in the photochemical reaction are preferentially produced.

iii) $K_3[Al(C_2O_4)_3]\cdot 3H_2O$

TABLE IV. THE RADIOLYSIS OF POTASSIUM TRIOXALATOALUMINATE(III)

	Dose (eV./g.)	G value	Composition of the gas (%)	
Evolved gas		1.5*		
	1.0×10^{22}	1.7	H_2	2
			CO	5
			CO_2	93
The gas evolved by dissolving the irradiated complex	1.0×10^{22}	2.9	H_2	0
			CO	0
			CO_2	100
Decrease in the reducing power		9.9*		

* Is obtained from the yield-dose curve.

The reaction of the complex is similar to that of potassium trioxalatochromate(III). However, some quantitative differences were observed:

1) The carbon dioxide content in the evolved gas was larger than that of the chromium complex.

2) The contribution of the gas obtained by dissolving the irradiated complex to the total gaseous product is larger than that in the case of the chromium complex.

In this case, the yield of carbon dioxide, the oxidized product, was much superior to the yield of carbon monoxide, the reduced product, if the large contribution of the gas evolved by dissolving the irradiated complex in water was taken into account. Since the oxidation and the reduction of aluminum(III) are difficult, the reduction products of oxalate ions may be expected. The formation of aldehyde and formic acid was observed. The infrared spectra of the aldehyde 2, 4-dinitrophenylhydrazone suggest that the aldehyde consists mainly of glyoxal: G=0.2 was given for the aldehydic product. A volatile acidic substance, presumably formic acid, and with a G value of 0.4, was formed.

A similar reaction occurs in the radiolysis of oxalic acid. The formation of glyoxal and formic acid was also observed.

Since the decomposition of oxalate occurred in a small yield in the case of ionic oxalate, it is evident that the coordination bond between aluminum-(III) and oxalate plays an important role in the radiation-induced reaction of the coordinated oxalate ion.

Experimental

Materials.—Commercially-available oxalic acid, sodium oxalate, potassium oxalate (guaranteed-grade reagent of the Kanto chemical Co.) and iron(II) oxalate (extra pure-grade reagent of the Kanto Chemical Co.) were used without any further purification. Sodium hydrogen oxalate was prepared by mixing the solutions of oxalic acid and sodium oxalate in an equal molar ratio. Potassium trioxalatoaluminate(III), potassium trioxalatochromate(III), potassium trioxalatoferrate(III) and potassium trioxalatocobaltate(III) were prepared according to the method described in "Inorganic Synthesis."[10]

Gamma-Ray Irradiation.—The irradiation cell was a cylindrical tube with a break-off seal. About one gram of the crystalline oxalato metal complexes or oxalate salts was put in the cell, and the cell was sealed off in a vacuum. The cell was covered with black paper to protect the contents from the light when the sample was sensitive to light.

Cobalt-60 γ-ray sources of 10000 and 16000 curies were used. The dose rate was measured by Fricke dosimetry, which was modified for the measurements of larger doses by using acidic solutions of ferrous sulfate saturated with nitrogen gas. The dose was calculated assuming that $G(Fe^{3+})=8.2$.

The correction of the absorbed radiation energy arising from the difference in the electron densities of the dosimeter and samples was also applied.

Irradiation at low temperatures was carried out by using a thermostat placed in the irradiation facility.

Analysis of the Products.—*i) Gaseous products.*—The vessel containing the irradiated complex was connected to the vacuum system, the volume of which had been measured. Then the break-off seal was cut off. The total volume of the gaseous products was calculated from the pressure increase in the vacuum system. The composition of the gas was determined by means of mass spectrometric analysis.

ii) The Gas Evolved by Dissolving the γ-Ray Irradiated Complex.—The vessels containing the irradiated complex and water were arranged in a vacuum line, as is shown in Fig. 4. The water in B was degassed by boiling the contents several times in a vacuum. Then the whole system except for B was evacuated thoroughly. After evacuation, the vacuum system was isolated from the pump. Then the water in B was introduced into A, and the irradiated complex in A was dissolved. After the whole sample had been dissolved in water, the vessel, A, was cooled with dry ice. Then the

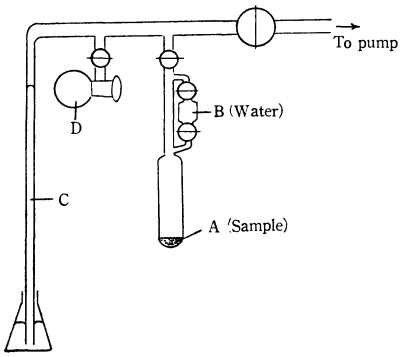

Fig. 4. Vacuum system for the analysis of the gas evolved by dissolving the irradiated complex in water.
A Irradiated sample, B Water,
C Mercury manometer, D Gas sampler for mass spectrometric analysis.

volume and the composition of the gas were determined in the same way as in *i*).

iii) Reducing Power.—After irradiation, the whole contents of the irradiation vessel were transfered into a measuring flask and dissolved in water. The solution was then titrated with potassium permanganate in acidic media. The comparison of the reducing power before and after γ-irradiation gave the decomposition of oxalate ions. This analysis was, however, applied only to oxalic acid, oxalte salts and potassium trioxalatoaluminate(III).

iv) Carbonyl Compound.—The determination of the carbonyl compounds produced in the irradiated oxalic acid and potassium trioxalatoaluminate(III) was

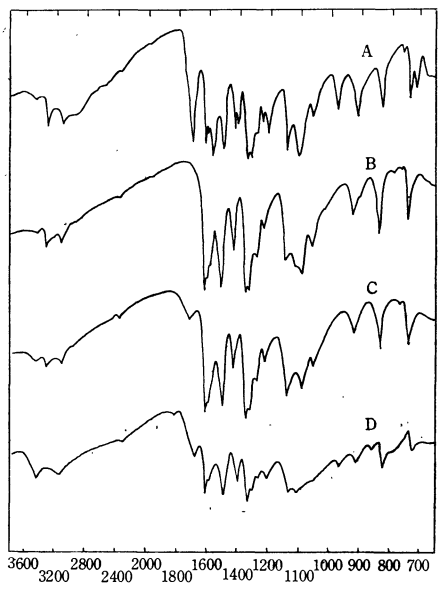

Fig. 5. Infrared spectra of the 2,4-dinitrophenylhydrazones of glyoxylic acid (A), glyoxal (B), and radiolytically-produced aldehydes from $H_2C_2O_4\cdot 2H_2O$ (C) and $K_3[Al(C_2O_4)_3]\cdot 3H_2O$ (D).

10) J. C. Bailar, Jr., and E. M. Jones, "Inorganic Synthesis," Vol. 1, Mcgraw-Hill, New York (1939), p. 35.

carried out by precipitating them with 2, 4-dinitrophenylhydrazine. The melting point of the 2, 4-dinitrophenylhydrazone was 280°C in the radiolytic product of oxalic acid, and 240°C in the radiolytic product of potassium trioxalatoaluminate(III). Since the melting point of glyoxal 2, 4-dinitrophenylhydrazone is 328°C, the carbonyl compound obtained in radiolysis is not considered to be pure glyoxal. However, the 2, 4-dinitrophenylhydrazone was turned purple by the action of alkali, which is specific for bis-2, 4-dinitrophenylhydrazone of $-\overset{O}{\overset{\|}{C}}-\overset{O}{\overset{\|}{C}}-$. The infrared spectra of the 2, 4-dinitrophenylhydrazone of the radiolytically-produced aldehyde, together with those of glyoxal and glyoxylic acid, are shown in Fig. 5. Since the infrared spectra of the 2, 4-dinitrophenylhydazone of the radiolytically-produced aldehyde, especially in oxalic acid, were very similar to those of glyoxal, the main component of the radiolytically produced aldehyde may be assumed to be glyoxal. However, a small peak at $\sim 1700\ cm^{-1}$ which can not be explained by glyoxal is to be ascribed to an impurity, presumably glyoxylic acid.

v) Volatile Acidic Substance.—The solution of the γ-ray irradiated sample was acidified with sulfuric acid. The solution was steam-distilled, and the distillate was titrated with a sodium hydroxide solution.

vi) Iron(II).—Iron(II), which was produced in the radiolysis of potassium trioxalatoferrate(III), was determined to be a bipyridyl complex.

vii) Residual Metal Complex.—The irradiated oxalato metal complex was dissolved in water, and the residual oxalato metal complex was determined by the spectrophotometric method. For the determination of potassium trioxalatochromate(III), the absorption bands at 420 and 570 mμ were used. For potassium trioxalatocobaltate(III), the bands at 420 and 605 mμ were used. For the determination of potassium trioxalatoferrate-(III), the shoulder at 263 mμ was used.

The author is very grateful to Professor Kenjiro Kimura for his kind guidance and encouragement throughout this work. The author is also very grateful to Drs. Akibumi Danno, Gen-ichi Tsuchihashi, and Shin-ichi Ohno for their helpful discussions.

BULLETIN OF THE CHEMICAL SOCIETY OF JAPAN VOL. 39 2588—2597 (1966)

The Quenching Action of Benzoic Acid and Methylbenzoate on the Fluorescence of Naphthalene Derivatives. III. The Solvent Effect on the Quenching of the Fluorescence of Dimethylnaphthylamine by Methylbenzoate

By Takuji MIWA and Masao KOIZUMI

Department of Chemistry, Faculty of Science, Tohoku University, Katahira-cho, Sendai

(Received April 15, 1966)

The fluorescence and absorption spectra and the quenching of the fluorescence of *N*, *N*-dimethyl-2-naphthylamine by methylbenzoate have been measured in cyclohexane, benzene, *p*-dioxane, isopropyl ether, ethyl ether, ethyl acetate, tetrahydrofuran, acetone and *N*, *N*-dimethylformamide (in the order of DK values). The fluorescence and the absorption spectra show a red-shift with the polarity of the solvent. By the method of Lippert and Mataga, the dipole moment of the excited fluorescer molecule has been estimated to be 4.1D. In nonpolar and weakly polar solvents, the methyl benzoate-added systems give fluorescence spectra with a swell or a shoulder on the long wavelength side, but this does not occur in *N*, *N*-dimethylformamide. When methyl benzoate is used as the solvent, two peaks of fluorescence are observed. The new emission has been interpreted as a charge-transfer emission, and the temperature-dependence of the fluorescence spectra has led to the conclusion that an encounter of fluorescent and quencher molecules is prerequisite for the appearance of CT emission. The quenching efficiencies in different solvents have been dealt with in reference to that in *N*, *N*-dimethylformamide, since the quenching in this solvent has been found to be almost encounter-controlled. A general correlation has been found between the quenching efficiency and the polarity of the solvent. The quenching mechanism and also the appearance of the CT emission have been discussed.

In previous papers,[1] the quenching action of benzoic acid and its ester on the fluorescence of some naphthalene derivatives was discussed from the viewpoint of a charge transfer (CT) mechanism. Most of the results were favorable to this

1) T. Miwa and M. Koizumi, This Bulletin, **38**, 529 (1965).

viewpoint, but there was no conclusive evidence. The purpose of the present paper is to give further evidence for the CT mechanism of the quenching action of methyl benzoate (MB) on *N*, *N*-dimethyl-2-naphthylamine (DMNA) by studying the solvent effect on the fluorescence spectra and on the quenching action.

Weller was the first to offer confirmative evidence for the CT mechanism of quenching. Leonhard and Weller,[2] for instance, studied the quenching action of aniline, *N*, *N*-dimethylaniline, etc., on the fluorescence of perylene and found that the efficiency of quenching depends largely on the polarity of the solvent; for example, it is large in acetonitrile, but quite small in benzene. They also found that a new emission due to a CT complex between fluorescer and quencher is observable only in nonpolar solvents. Further, by means of a flash technique, they succeeded in detecting the radical anion of perylene in polar solvents, whereas only the enhancement of the T–T absorption was observed in nonpolar solvents. Mataga et al.[3] extended such studies using similar systems. These works led us to expect analogous phenomena in the system of DMNA and MB; we have found that this is really true. Besides, we have ascertained the dipole moment of the excited DMNA by employing the method of Mataga and Lippert.[4]

Experimental

Material.—Acetone of Wako Junyaku, G. R. grade, was stored over potassium permangnate for 3 days, boiled for 2 hr., and then, after distillation, dried over potassium carbonate and finally fractionated. The middle half (b. p. 56.5°C) was used. Ethyl acetate was kept over anhydrous potassium carbonate and then fractionated carefully. Ethyl ether and isopropyl ether of Kanto Kagaku, G. R. grade, were treated with a 10% solution of sodium carbonate for 24 hr. and then dehydrated with anhydrous calcium chloride and finally with sodium. The ethers were repeatedly decanted, and fresh sodium was added until no hydrogen evolved. They were then distilled slowly over sodium. Tetrahydrofuran of Kanto Kagaku, G. R. grade, was repeatedly treated with fresh sodium and decanted until the evolution of hydrogen stopped. It was then distilled over sodium. Methyl benzoate, E. P. grade, was washed with a concentrated aqueous solution of potassium carbonate and dried over anhydrous pottassium carbonate and then over anhydrous mangesium sulfate. After being distilled under reduced pressure, it was passed through 1-meter silica gel column and then distilled in vacuo. The sample thus purified showed no impurity luminescence when the excitation wavelength is longer than 320 mμ. *p*-dioxane, benzene and cyclohexane were purified in the same way as in a previous paper.[1]

Procedure.—The absorption spectra were measured with a Hitachi ESP III recording spectrophotometer. The fluorescence and action spectra were measured with an Aminco-Bowman spectrofluorimeter. The samples were usually not degassed. The temperature was maintained at 25°C. Some measurements were made at low temperatures down to the liquid nitrogen temperature. The concentration of *N*, *N*-dimethyl-2-naphthylamine was always 10^{-4} M. The excitation wavelength was usually 350 mμ. In dealing with the intensity data, the peak intensities were used without any correction for the spectral sensitivity of the instrument. The solvent effect on the optical density at the exciting wavelength, which was usually very small, was taken into account.

Results

The Solvent Effects on the Absorption and Fluorescence Spectra of DMNA in the Absence and in the Presence of MB.—The absorption spectra show a red shift and become broader as the polarity of the solvent increases. The addition of MB has a similar effect, the magnitude of which decreases with the increase in the polarity of the solvent.

In Table I some of the data on the absorption spectra are tabulated. Most of them will be used in the discussion below.

The solvent effects and the effect of the addition of MB on the fluorescence spectra of DMNA are

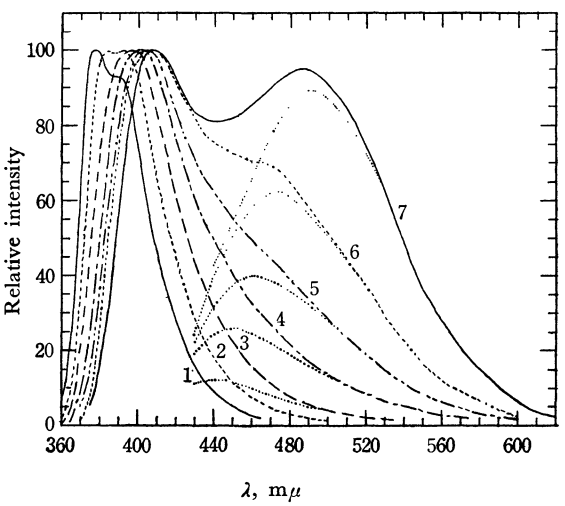

Fig. 1. Fluorescence spectra of DMNA-MB in cyclohexane.
MB: 1) 0, 2) 0.198, 3) 0.793, 4) 2.38, 5) 3.97, 6) 5.55, 7) 7.93 M (no cyclohexane)
dotted line, emission of the longer wavelength component (see text)

2) H. Leonhardt and A. Weller, *Z. physik. Chem., N. F.*, **29**, 277 (1961); *Ber. Bunsges. phys. Chem.*, **61**, 791 (1963).

3) N. Mataga, K. Ezumi and G. Takahashi, Symposium on Photochemistry, Tokyo (1964); N. Mataga and K. Ezumi, Symposium on Molecular Structure, Nagoya (1965); N. Mataga and M. Okada, ibid.

4) N. Mataga, Y. Kaifu and M. Koizumi, This Bulletin, **29**, 465 (1956); E. Lippert, *Z. Elektrochem.*, **61**, 962 (1957).

Table I. Absorption spectra data for DMNA in the absence and in the presence of MB

	Solvent	In the Absence of MB: [DMNA] M	λ_{max} of the first abs. band mμ	λ_{max} of the second abs. band mμ	*op.d.* at 350 mμ (d)	Oscillator strength for the first abs. band (f_i)	$\frac{(f/n_D)_i}{(f/n_D)_9}$	In the presence of MB: λ_{max} of the first abs. band [MB]: 0.801	[MB]: 1.60	[MB]: 2.40
1)	Cyclohexane	1.00×10^{-4}	351.5	287.0, 297.6	0.287	0.039	0.84	352.5	352.5	353.5
2)	Benzene	1.00×10^{-4}	356.6	290.6, 300.6	0.294	0.050	1.03	356.5	356.5	357.5
3)	*p*-Dioxane	1.12×10^{-4}	355	289.0, 299.1	0.319	0.047	1.03	355	355	356
4)	Isopropyl ether	1.00×10^{-4}	352	287.4, 297.2	0.284	0.045	1.03	352	353	354
5)	Ethyl ether	1.00×10^{-4}	352	287.3, 297.3	0.294	0.046	1.06	352	353	
6)	Ethyl acetate	1.00×10^{-4}	354	288.0, 297.9	0.288	0.047	1.06	354	354	354.5
7)	Tetrahydrofuran	1.00×10^{-4}	354.5	289.0, 298.8	0.292	0.053	1.16	355	355	355.5
8)	Acetone	1.00×10^{-4}	355	—	0.280	0.049	1.13	355	355	355
9)	*N*, *N*-Dimethylformamide	1.00×10^{-4}	357	290.0, 299.5	0.287	0.046	1.00	357	357.5	358
10)	Methyl benzoate	1.00×10^{-4}	358	—	0.281	0.054	1.13	—	—	—

Table II. Some characteristics of the emission spectra for the DMNA-MB system

	Solvent	In the absence of MB: [DMNA] M×10⁴	λ_{max} of the fluorescence spectra mμ	F_{0i}/F_{09}	$\alpha_i \equiv \left(\frac{F_{0i}}{F_{09}}\right)\left(\frac{d_9}{d_i}\right)$	In the presence of MB: [MB] : 0.801 M λ_{max} of the s. flu.	λ_{max} of the l. flu.	[MB] : 2.40 M λ_{max} of the s. flu.	λ_{max} of the l. flu.
1)	Cyclohexane	1.00	379	0.720	0.720	396		401	450±2
2)	Benzene	1.00	395	0.865	0.844	398		403	470±4
3)	*p*-Dioxane	1.12	400	1.24	1.12	404		406	478±5
4)	Isopropyl ether	1.00	390	0.467	0.472	398		404	467±3
5)	Ethyl ether	1.00	393	0.671	0.655	401			467±3*
6)	Ethyl acetate	1.00	402	0.654	0.652	404		407	480±7
7)	Tetrahydrofuran	1.00	403	0.819	0.805	405		406	485±5
8)	Acetone	1.00	409	0.645	0.661	410		411	505±10
9)	*N*, *N*-Dimethylformamide	1.00	412	1.00	1.00	413		413	
10)	Methyl benzoate	1.00	406,490	0.00260	0.00266				

*[MB], 1.60 M

Table III. The data for the calculation of the dipole moment of excited DMNA

	Solvent	$\tilde{\nu}_{a\,max}$ cm^{-1}	$\tilde{\nu}_{f\,max}$ cm^{-1}	$\tilde{\nu}_{a\,max}-\tilde{\nu}_{f\,max}$ cm^{-1}	ε at 25°C	n_D at 25°C	μ (D)	η (cpoise) at 25°C
1)	Cyclohexane	28450	26390 (27700)*	2060	2.020	1.4274	0	0.898
2)	Benzene	28050	25320	2730	2.273	1.4980	0	0.6028
3)	*p*-Dioxane	28170	25000	3170	2.280	1.42025	0.45	1.16
4)	Isopropyl ether	28410	25640	2770	3.88	1.36618	1.22	0.379
5)	Ethyl ether	28410	25450	2960	4.335 (20°C)	1.35272 (20°C)	1.15	0.233
6)	Ethyl acetate	28250	24880	3370	6.02	1.36979	1.81	0.421
7)	Tetrahydrofuran	28210	24810	3400	7.39	1.40355	1.68	0.51 (20°C)
8)	Acetone	28170	24450	3720	20.70	1.35609	2.72	0.305
9)	*N*, *N*-Dimethylformamide	28010	24270	3740	36.71	1.4269	3.86	0.908
10)	Methyl benzoate	27930	24630	3300	6.548	1.4961	1.86	1.846

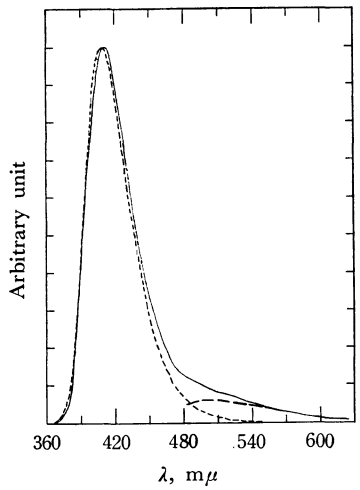

Fig. 2. Fluorescence spectra of DMNA-MB in acetone.

---- DMNA (1×10^{-4} M) in acetone
—— DMNA (1×10^{-4} M) + MB (2.40 M) in acetone
—— Emission of the longer wavelength component

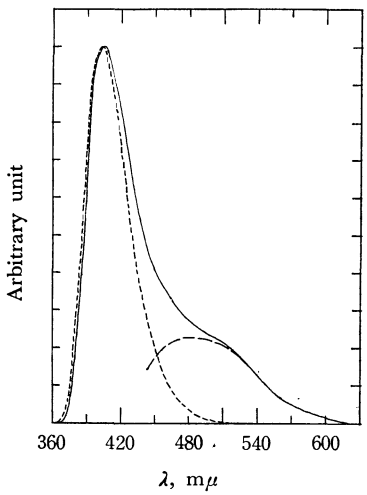

Fig. 3. Fluorescence spectra of DMNA-MB in ethyl acetate.

---- DMNA (1×10^{-4} M) in ethyl acetate
—— DMNA (1×10^{-4} M) + MB (2.40 M) in ethyl acetate
—— Emission of the longer wavelength component

similar to those on the absorption spectra, but more pronounced. As for the latter effect, it is remarkable in cyclohexane, but very small in dimethylformamide. A notable finding is that the tail in the long-wavelength side grows gradually with the addition of MB, and in most solvents a shoulder and, in favorable cases, a new peak comes to be

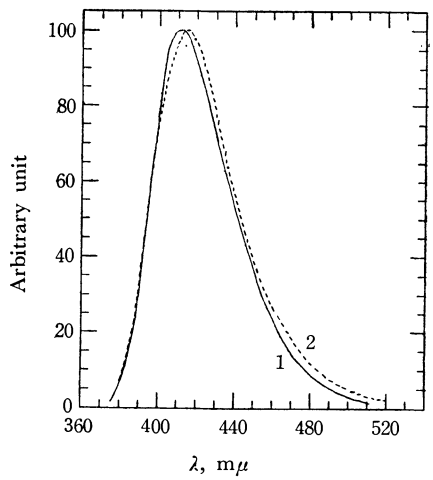

Fig. 4. Fluorescence spectra of DMNA-MB in dimethylformamide.

1) DMNA (1×10^{-4} M) in dimethylformamide
2) DMNA (1×10^{-4} M) + MB (2.40 M) in dimethylformamide

observed. This phenomenon is observed easily in less polar solvents. In *N*, *N*-dimethylformamide, which is the most polar solvent in the present experiment, the above change is very weak. When 10^{-4} M DMNA is dissolved in pure MB, there exist two emission bands, with peaks at 406 mμ and 490 mμ. These two peaks are about the same height, but the integrated intensity for the latter is much larger because of its broad shape. The real difference is probably still larger in view of the spectral sensitivity of the photometer. Some typical examples of the fluorescence spectra are shown in Fig. 1—4, where the peak height of the short-wavelength emission is normalized to unity. The real intensity decreases with the increase in the MB concentration. It may be seen that the solvent effect on the new emission is much larger.

To make sure that this new emission is not due to any impurity which might be present in MB, the excitation spectra were taken on various systems and at various wavelengths of emission spectra. The results confirmed that the new band originates from the light absorption of DMNA, since the excitation spectra agreed quite well with the absorption spectra of DMNA. In Table II some characteristic data on the emission spectra are tabulated. The relative intensities of fluorescence with reference to *N*, *N*-dimethylformamide as the solvent, (F_{0i}/F_{09}), and the relative quantum efficiencies, $(F_{0i}/F_{09})\times(d_9/d_i)_{350}$, where d_i is the optical density in solvent i at 350 mμ (the suffix, 0, indicates the non-existence of MB), are listed since they will be useful for the later discussion. The peak position of the longer-wavelength emission was evaluated by subtracting the shorter-wavelength emission from the total. Since this procedure involves some

arbitrariness, however, the data given are not very reliable.

The Dipole Moment of the Excited DMNA.—Since the absorption and emission spectra in various solvents have been measured, the dipole moment of the excited DMNA molecule can be evaluated by means of the following formula:[4]

$$hc(\tilde{\nu}_a-\tilde{\nu}_f) = \frac{(\mu_e-\mu_g)^2}{a^3}\left[\frac{2(\varepsilon-1)}{2\varepsilon+1}-\frac{2(n_D^2-1)}{2n_D^2+1}\right] + \text{const.} + \text{small terms} \quad (1)$$

The data necessary for the calculation are given in Table III.

The dipole moments and the viscosities of the solvents are listed so that they can be used in the later discussion. ε and n are the values at 25°C. The plot $\tilde{\nu}_a-\tilde{\nu}_f$ vs. $\{2(\varepsilon-1)/2(\varepsilon+1)-2(n_D^2-1)/(2n_D^2+1)\}$ is given in Fig. 5. Assuming a (the cavity radius in Onsager's theory) in Eq. 1 as ~3 Å, the value of $\mu_e-\mu_g$ was found to be 4.1D (Debye). This is reasonable in view of the values of 4.5D, 4.4D, and 3.5D reported for *N*, *N*-dimethyl-1-naphthylamine, 1-naphthylamine, and 2-naphthylamine by Mataga et al.[4] Thus it was confirmed that the excited state of DMNA is highly polar.

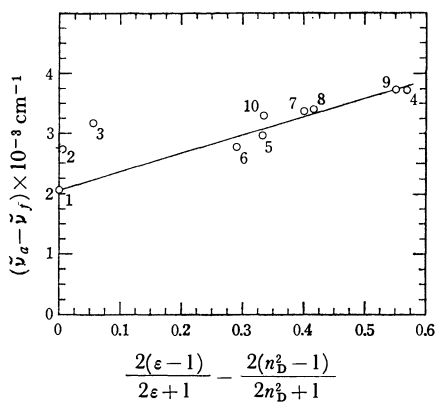

Fig. 5. Evaluation of the dipole moment of the excited DMNA.
Solvent: 1) cyclohexane, 2) benzene, 3) *p*-dioxane, 4) acetone, 5) ethyl ether, 6) isopropyl ether 7) ethyl acetate, 8) tetrahydrofuran, 9) *N*, *N*-dimethylformamide, 10) methyl benzoate

Intensity Relations on the Fluorescence of DMNA.—In all the solvents, the fluorescence intensities of DMNA decrease upon the addition of MB. In Figs. 6, 7, and 8, the values of $(F_{0i}d_i/F_id_{0i})-1$ are plotted against the MB concentrations. Since all the plots deviate more or less from the Stern-Volmer relation with the increase in the concentration of the quencher, the quenching constants, K_A, in terms of this equation were evaluated from the slopes of the curves at the point of origin. They are given in Table IV, along with the values obtained from the $(F_{0i}d_i/F_id_{0i})-1$ values at 0.160 and 0.801 M concentrations of MB (K_B and K_C). The moderate agreement of the K_A, K_B and K_C values assures the reliability of the data.

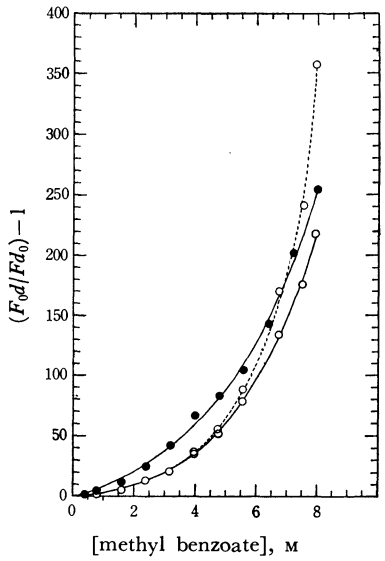

Fig. 6. $(F_{0i}/F_i)(d_i/d_{0i})-1$ vs. [MB] plot for
—○— , benzene solution;
—●— , cyclohexane solution (corrected for impurity luminescence in MB);
--○-- , cyclohexane solution (uncorrected).
(corrected values only are given in Figs. 7 and 8).

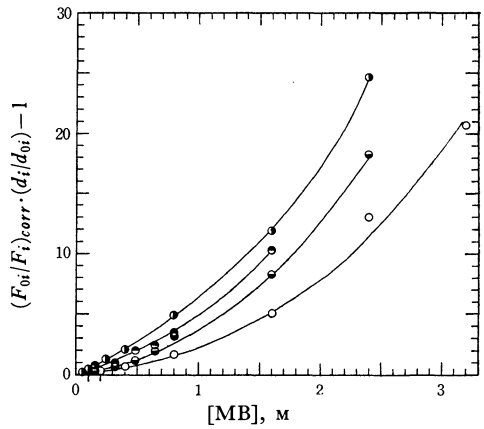

Fig. 7. $(F_{0i}/F_i)(d_i/d_{0i})-1$ vs. [MB] plot for
◑ benzene solution;
◓ ethyl ether solution;
◒ isopropyl ether solution;
○ cyclohexane solution;

When the concentrations of MB are 1.60, 2.40, and 3.20 M, a new emission band of the longer wavelength becomes notable in most cases. As a

TABLE IV. INTENSITY RELATION OF THE FLUORESCENCE

	Solvent	K_A	K_B	K_C	[MB] : 0.801 M			[MB] : 1.60 M		
					$\left(\frac{F_{0i}}{F_i}\right)\left(\frac{d_i}{d_{0i}}\right)-1$	$\frac{F_i}{F_{i500}}$	$\frac{F_0\left(\frac{d_i}{d_{0i}}\right)-F_i}{F_{i500}}$	$\left(\frac{F_{0i}}{F_i}\right)\left(\frac{d_i}{d_{0i}}\right)-1$	$\frac{F_i}{F_{i500}}$	$\frac{F_0\left(\frac{d_i}{d_{i0}}\right)-F_i}{F_{i500}}$
1)	Cyclohexane	1.7	1.6	2.1	1.70	24.4	41.6	5.10	13.3	68.0
2)	Benzene	5.2	5.1	6.1	4.85	17.5	85.0	11.9	8.80	105
3)	*p*-Dioxane	11	9.7	12	10.0	13.6	135	28.3	6.18	170
4)	Isopropyl ether	2.2	1.9	4.0	3.21	17.6	56.4	8.33	8.09	67.4
5)	Ethyl ether	3.9	4.8	4.4	3.47	14.4	49.9	10.3	7.41	75.5
6)	Ethyl acetate	24	23	28	22.1	12.9	285	45.7	6.61	302
7)	Tetrahydrofuran	25	25	29	23.2	10.8	253	52.8	6.84	366
8)	Acetone	64	59	65	52.5	26.0	1365	114	12.5	1419
9)	*N*, *N*-Dimethylformamide	72	69	93	74.1	25.6	1984	179	21.2	3779

TABLE V.

	Solvent	$Z_i=\frac{8RT}{3000\,\varepsilon_i}$	$K_{cal}=Z_i\tau_0$	$\beta_i=d_i\frac{Z_i}{Z_9}$	$\frac{K_{Ai}}{K_{A9}}$	$\gamma_{Ai}=\frac{K_{Ai}}{K_{A9}\beta_i}$	$\frac{K_{Ci}}{K_{C9}}$	$\gamma_{Ci}=\frac{K_{Ci}}{K_{C9}\beta_i}$
1)	Cyclohexane	7.36×10^9	74	0.728	0.024	0.033	0.023	0.032
2)	Benzene	10.96×10^9	110	1.27	0.072	0.057	0.066	0.052
3)	*p*-Dioxane	5.70×10^9	57	0.874	0.15	0.17	0.13	0.15
4)	Isopropyl ether	17.43×10^9	174	1.13	0.031	0.027	0.043	0.038
5)	Ethyl ether	28.35×10^9	284	2.55	0.054	0.021	0.047	0.018
6)	Ethyl acetate	15.69×10^9	157	1.41	0.33	0.23	0.30	0.21
7)	Tetrahydrofuran	12.74×10^9	127	1.41	0.35	0.25	0.31	0.22
8)	Acetone	21.66×10^9	217	1.97	0.89	0.45	0.70	0.36
9)	*N*, *N*-Dimethylformamide	7.28×10^9	73	1.00	1.00	1.00	1.00	1.00

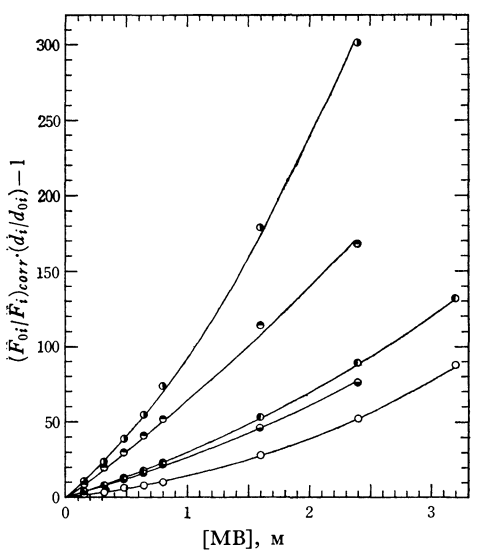

Fig. 8. $(F_{0i}/F_i)(d_i/d_{0i})-1$ vs. [MB] plot for
◑ *N*, *N*-dimethylformamide solution;
◓ acetone solution;
◐ tetrahydrofuran solution;
◒ ethyl acetate solution;
○ *p*-dioxane solution.
[DMNA], 1.12×10^{-4} M for *p*-dioxane
1.00×10^{-4} M for all the other solvents

measure of the intensities of this emission, $\{(F_{0i}d_i/d_{0i})-F_i\}/F_{i500}$ (F_{i500} is the fluorescence intensity at 500 mμ) and F_i/F_{i500} are listed in Table IV; for the sake of comparison, $(F_{0i}d_i/F_id_{0i})-1$ for the intrinsic emission of DMNA is also listed. The intensity at 500 mμ was used because the intensity at the peak is difficult to evaluate on account of the superposition of the two emission bands. It should be noted that the values of F_{i500} used as the measures of the new emission become more and more overestimated as the solvent polarity increases, because the solvent effect on this new emission is quite large. Thus, the data are only approximate in nature. However, a general tendency is observed for $\{(F_{0i}d_i/d_{0i})-F_i\}/F_{i500}$ to increase as the quenching constant K increases, whereas F_i/F_{i500} decreases at first, shows a minimum, and then increases again. Such tendencies may clearly be seen from Figs. 9 and 10 where $(F_0d_i/d_{0i}-F_i)/F_{i500}$ and F_{i500}/F_i are plotted, respectively against the concentration of MB. Moreover, Fig. 9 shows that the former quantity increases with the concentration of MB, while a comparison of Fig. 9 with Figs. 6, 7 and 8 indicates that the concentration effect on it is far less than on F_i. Figure 10 shows, on the other hand, that F_{i500}/F_i increases remarkably with the concentration of MB in most cases.

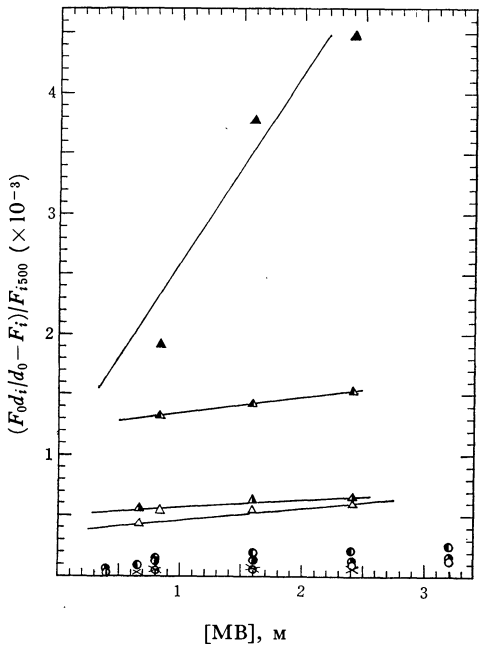

Fig. 9. $(F_0d_i/d_{0i}-F_i)/F_{i500}$ vs. [MB] plot for
○ cyclohexane, ◑ benzene, ◐ dioxane,
× isopropyl ether, △ ethyl acetate,
◭ tetrahydrofuran, ◭ acetone,
▲ *N N*-dimethylformamide.

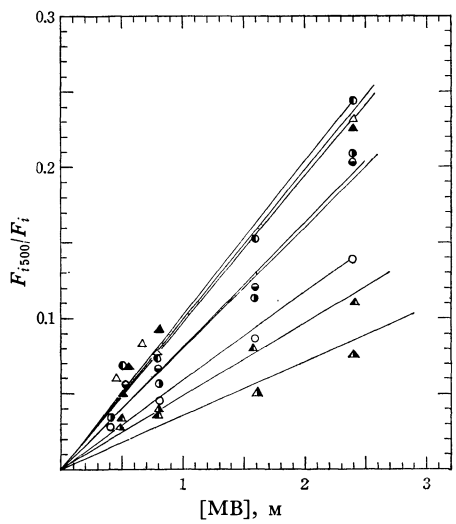

Fig. 10. F_{i500}/F_i vs. [MB] plot for
○ cyclohexane, ◑ benzene, ◐ dioxane,
◒ isopropyl ether, △ ethyl acetate,
▲ tetrahydrofuran, ◭ acetone,
◭ *N*, *N*-dimethylformamide.

The Effect of Temperature on the Fluorescence Spectra.—To make clear the nature of quenching as well as the origin of a new emission, the spectra were measured at different temperatures down to −182°C. The fluorescence spectra of DMNA 10^{-4} M in cyclohexane at this temperature is extremely sharp in comparison with those at room temperature. When 6.41 M of MB was added to the above solution, the intensity of the fluorescence at room temperature decreases remarkably and the spectra consist of the two emission bands with peaks at 406 and 486 mμ. At −182°C the

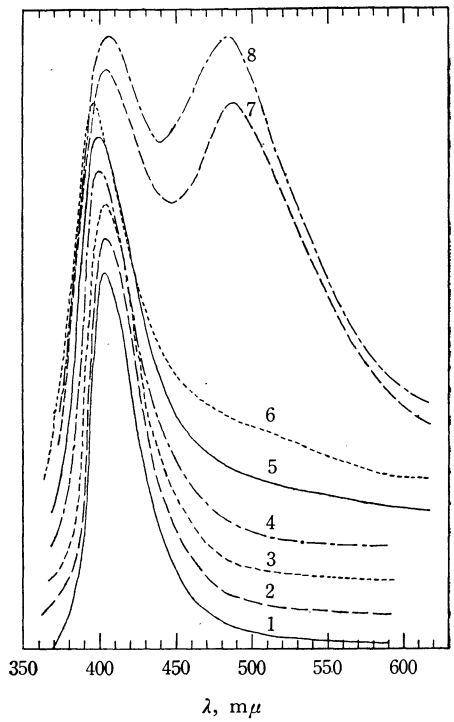

Fig. 11. Temperature dependence of the fluorescence spectra of DMNA-MB in cyclohexane.
[DMNA] : 1.00×10^{-4} M, [MB] : 6.41 M
temperature (°C): 1) −182, 2) −158, 3) −138, 4) −94, 5) −50, 6) −43, 7) −38, 8) −31
Intensity ratio of the normal fluorescence of DMNA : 8) 1, 7) 1.1, 6) 12, 5) 23, 4) 61, 3) 52, 2) 49, 1) 63

emission consists of a single sharp band of a high intensity with a peak at 404 mμ. The shapes of the fluorescence spectra at different temperatures from −182°C up to −31°C are shown in Fig. 11. From the figure it may be seen that, at −31°C and at −38°C, there are two emission bands similar to those at room temperature. Although only one band occurs below −43°C, the tail in the longer wavelength gradually rises with the rise of temperature; the intensity decreases to some extent at −50°C. The intensities at −38°C and at −31°C are quite small.

It should be noted that the above change proceeds as the sample melts. Thus the crystal begins to soften in appearance near −50°C, and around −43°C it partly begins to melt. At −38°C more than two-thirds of the crystals melts, until the melting ends at −31°C. The above observation leads

to the conclusion that the quenching of the fluorescence is dynamic and, further, that a new emission arises from the encounter of an excited fluorescer molecule with a quencher molecule.

All the facts observed strongly support the view that the new emission is due to an excited CT complex. Hereafter, it will be designated as a CT emission.

Discussion

Since the quenching in the present investigation is dynamic in nature, the discussion can be made on the basis of a Stern-Volmer eq. of the following type:

$$\Phi_0/\Phi = F_0/F = 1 + \gamma Z\tau_0[\mathrm{Q}] = 1 + \frac{\gamma Z}{k_f}\Phi_0[\mathrm{Q}] \tag{2}$$

where Φ and Φ_0 are the quantum yields of fluorescence in the presence and in the absence of the quencher. The experimentally-determined quenching constant, K_A, is:

$$K_A = \frac{\gamma Z}{k_f}\Phi_0 \tag{3}$$

where Z is the bimolecular rate constant for an encounter process and γ, the quenching efficiency for each encounter. Further, τ_0 and Φ_0 are written as follows:

$$\tau_0 = \frac{1}{k_f + k_d + k_{q02}[\mathrm{O_2}]} \tag{4}$$

$$\Phi_0 = \frac{k_f}{k_f + k_d + k_{q02}[\mathrm{O_2}]} \tag{5}$$

where k_f, k_d and k_{q0_2} are, respectively, the rate constants for emission, monomolecular deactivation, and bimolecular deactivation due to oxygen.

Now the Z value for each solvent can be estimated from the Stokes-Einstein formula, $8\boldsymbol{R}T/3000\eta$; the values are listed in Table V. $\tau_0 Z$ gives the quenching constant provided γ is unity. The values of $\tau_0 Z$ obtained by putting $\tau_0 = 10^{-8}$ sec. (estimated from the oscillator strength) are also given in the table (K_{cal}). A comparison of K_{cal} with K_A in Table IV will show that, in the case of *N*, *N*-dimethylformamide, they agree quite well. Of course, this is rather fortuitous, but there is no doubt that the quenching in this case is almost entirely diffusion-controlled. In all the other solvents, K_A is much less than K_{cal}. Therefore, it is appropriate to discuss the relative quenching efficiency with reference to $(Z\Phi_0/k_f)_9$ (9 is the numbering index for *N*, *N*-dimethylformamide). The relative quenching constant for solvent i is, then,

$$K_{Ai}/K_{A9} = (\gamma Z\Phi_0)_i/(Z\Phi_0)_9 = \frac{\gamma_i Z_i}{Z_9}\alpha_i = \gamma_i\beta_i \qquad \beta_i = \frac{Z_i}{Z_9}\alpha_i \tag{6}$$

by assuming that $k_{f9} = k_{fi}$. This is approximately correct since the values of $(f/n_D)_i/(f/n_D)_9$ given in Table I are unity within +10% (except cyclohexane). The values for $\alpha_i = \Phi_{0i}/\Phi_{09}$ are given in Table II. The quenching efficiency for solvent i can, thus, be calculated from:

$$\gamma_i = \frac{K_{Ai}}{K_{A9}\beta_i}$$

The values of β_i, K_{Ai}/K_{A9} and γ_{Ai} are tabulated in Table V. The analogous quantities on the basis of K_C are also given to make sure that the values of γ_{Ci} thus obtained are quite reliable for comparing the quenching efficiency. Figure 12

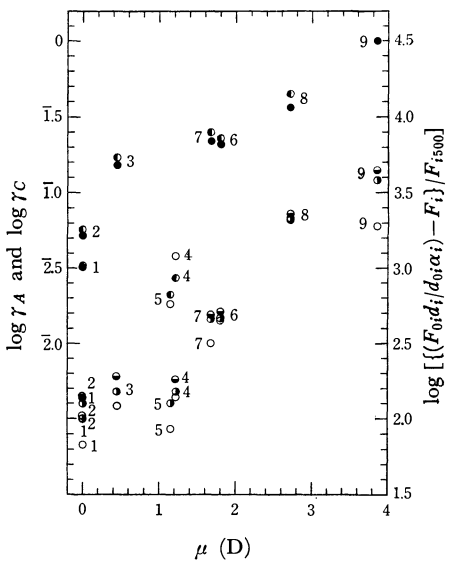

Fig. 12. $\log\gamma$ and $\log[\{(F_{0i}d_i/d_{0i}\alpha_i)-F_i\}/F_{i500}]$ vs. μ.
● $\log\gamma_{Ci}$
◐ $\log\gamma_{Ai}$
○ $\log[\{(F_{0i}d_i/d_{0i}\alpha_i)-F_i\}/F_{i500}]$ [MB] : 0.81 M
◑ $\log[\{(F_{0i}d_i/d_{0i}\alpha_i)-F_i\}/F_{i500}]$ [MB] : 1.60 M
◒ $\log[\{(F_{0i}d_i/d_{0i}\alpha_i)-F_i\}/F_{i500}]$ [MB] : 2.40 M
1 cyclohexane, 2 benzene, 3 *p*-dioxane, 4 isopropyl ether, 5 ethyl ether, 6, ethyl acetate, 7 tetrahydrofuran, 8 acetone, 9 dimethylformamide

shows the plot of γ_i and $\{(F_{0i}d_i/d_{0i}\alpha_i)-F_i\}/F_{i500}$ against the dipole moments (μ) of the solvent molecules. Broadly speaking, there is a correlation between them except for some irregularity in the solvents with a low polarity. In Figs. 13 and 14, $(F_{0i}d_i/d_{0i}-F_i)/F_{i500}$ and F_i/F_{i500} are plotted against K_C. These two figures suggest that solvents can be classified into two groups, one with a low polarity from cyclohexane to ether type compounds (1 to 5), and the other with a higher polarity from ethyl acetate to *N*, *N*-dimethylformamide (from 6 to 9). Hereafter these two groups will be denoted as group 1 and group 2.

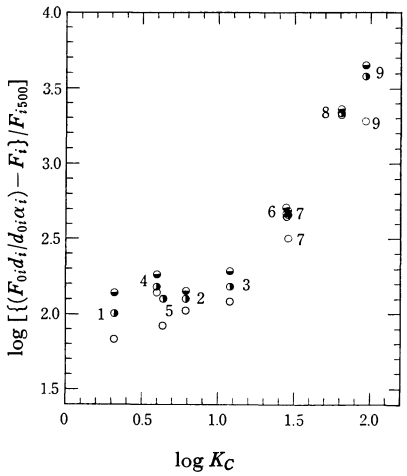

Fig. 13. $\log[\{(F_{0i}d_i/d_{0i}\alpha_i)-F_i\}/F_{i500}]$ vs. $\log K_C$.
● [MB] : 0.801 M, ○ [MB] : 1.60 M,
◑ [MB] : 2.40 M
1 cyclohexane, 2 benzene, 3 *p*-dioxane, 4 isopropyl ether, 5 ethyl ether, 6 ethyl acetate, 7 tetrahydrofuran, 8 acetone, 9 dimethylformamide.

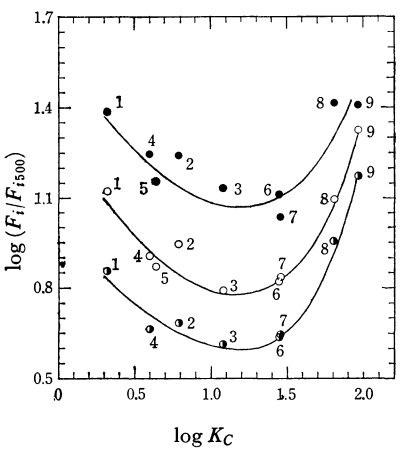

Fig. 14. $\log F_i/F_{i500}$ vs. $\log K_C$ plot.
● [MB] : 0.801 M, ○ [MB] : 1.60 M,
◑ [MB] : 2.40 M
1 cyclohexane, 2 benzene, 3 *p*-dioxane, 4 isopropyl ether, 5 ethyl ether, 6 ethyl acetate, 7 tetrahydrofuran, 8 acetone, 9 dimethylformamide

These two types of behaviour, as well as the results in Fig. 12, can well be comprehended on the basis of Weller's scheme for quenching. According to it, the quenching in nonpolar solvents is related to the formation of the CT complex, whereas the quenching in polar solvents occurs through the formation of radical ions. Plausible schemes for the two types of solvents are as follows:[5]

5) Cf. Ref. 3.

A) In nonpolar solvents

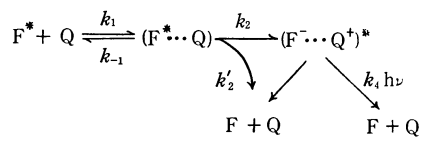

and

B) in highly polar solvents

$$F^* + Q \underset{k_{-1}}{\overset{k_1}{\rightleftarrows}} (F^*\cdots Q) \underset{k_3}{\rightarrow} F^- + Q^+$$

Thus, in nonpolar solvents an encounter complex $(F^*\cdots Q)$ which has, more or less, a CT character, has two alternative paths, denoted by k_{-1} and k_2 or k_2'; their magnitudes depend upon the solvent, but usually $k_{-1}>k_2, k_2'$. $(F^-\cdots Q^+)^*$, which is reached by the k_2 path, is a stable CT complex capable of emission; its emissivity depends on the environment. k_2', which was included for the sake of generality, denotes another process of deactivation which occurs during the course of CT complex formation. On the other hand, an encounter complex in the highly-polar solvents, being quite a different type from that in nonpolar solvents, proceeds mainly along k_3 instead of k_2 and forms free ionic species. In the solvents with medium polarity, the k_2 and k_3 processes may compete with each other.

If one assumes, as is plausible, that the quenching efficiency in scheme A is far less than in scheme B, then the general tendency seen in Fig. 12 may be easily interpreted. Further, it is natural to consider that the A scheme prevails for group 1, whereas scheme B becomes gradually predominant for group 2. The analysis on the basis of the above scheme, however, requires much more data than those obtained above.

Below we will give only the plausible interpretation of the results shown in Figs. 9, 10, 13 and 14 by introducing a CT emission probability, ϕ_{CT}, which gives a ratio between the CT emission and the effective collisional quenching. Assuming Stern-Volmer's equation, the following relations can easily be derived:

$$F_{500} = \frac{Z\gamma[Q]\phi_{CT}}{k_f + k_d + k_{q0}[O_2] + Z\gamma[Q]} \tag{6}$$

$$\frac{F_{500}}{F} = \frac{Z\gamma[Q]\phi_{CT}}{k_f} \tag{7}$$

$$\frac{F_0 - F}{F_{500}} = \frac{k_f\tau_0}{\phi_{CT}} \tag{8}$$

From Eq. 8, F_0-F/F_{500} or, more rigorously, $(F_0d_i/d_{0i}-F_i)/F_{i500}$ should depend merely on ϕ_{CT}. The slight dependence of ϕ_{CT} on [MB], as seen in Fig. 9, may perhaps be due to the quenching of the CT complex by MB. Alternatively, it may be due to the inadequeacy of the Stern-Volmer relation. Putting approximately $k_f\tau_0 \approx$

1, the solvents belonging to group 1 have ϕ_{CT} values ranging from 0.5×10^{-2} to 2×10^{-2}, whereas the solvents in group 2 have ϕ_{CT} values of $<0.5\times10^{-2}$. As may be seen from Fig. 13, ϕ_{CT} generally decreases with K_C; in group 1 it decreases very little, while in group 2 it decreases to a large extent.

The results in Fig. 14 and 10 can now be interpreted by means of Eq. 7. Thus in group 1, $Z\gamma$ increases while ϕ_{CT} decreases with the polarity, but since the former effect outweighs the latter, F_i/F_{500} decreases, as may be seen in Fig. 14. In group 2, on the other hand, the effect of the decrease in ϕ_{CT} predominates, since the increase of $Z\gamma$ is not so great (the maximum value of γ is 1); as a result, F_i/F_{500} again increases. The rather good linearity holding for the plots in Fig. 10 (as compared with Figs. 6, 7 and 8) may perhaps be due to the ϕ_{CT} factor, which decreases with the concentration of MB.

Thus, all the results can be interpreted if one assumes that, in group 1, $Z\gamma$ increases whereas ϕ_{CT} decreases a little with the polarity, and that in group 2 $Z\gamma$ increases and ϕ_{CT} decreases remarkably. These assumptions are quite natural in view of schemes A and B. It is not possible, however, to decide quantitatively how the contributions of schemes A and B depend upon the solvent polarity, and nor to decide how each elementary reaction in scheme A is influenced by the solvent polarity.

In summary, it may be said that in group 2 the formation of radical ions becomes easier with the solvent polarity, and that this is the main cause of the high quenching efficiency and the low CT emission. Although in group 1, the CT emission seems to become more easily observable with the polarity of the solvent, this is most probably due to the increase in γZ; the probability of the CT emission itself seems to decrease a little with the solvent polarity. The latter remark, however, must be further scrutinized in view of the irregular behavior to be seen in Fig. 12. The influence of the solvent polarity upon the emissivity of CT complex awaits further study.

BULLETIN OF THE CHEMICAL SOCIETY OF JAPAN VOL. 39 2597—2602 (1966)

Studies of the Quenching of the Fluorescence of Acridine Orange from the Standpoint of Charge-Transfer

By Tomoko KOMIYAMA, Takuji MIWA and Masao KOIZUMI

Department of Chemistry, Faculty of Science, Tohoku University, Katahira-cho, Sendai

(Received April 15, 1966)

The quenching action of *N*, *N*-dimethylaniline, nitrobenzene, *s*-trinitrobenzene and tetracyanoethylene on the fluorescence of acridine orange (AO) has been studied using ethanol and dioxane as solvents. In these solvents AO exists as cations or neutral molecules. In the former solvent, the quenching actions of the above substances on these two species have been investigated separately. The quenching constants, *K*'s (in reference to the Stern-Volmer equation) of the above substances (in the above sequence) in ethanol are (34—35), (19.6), (53.6) and (~90) for cations and (8.4), (72.8), (—), and (—) for neutral molecules (in 1./mol.). Thus, when quenchers are electron acceptors, *K* increases with the accepting power: nitrobenzene<*s*-trinitrobenzene<tetracyanoethylene. Further, acceptors are more efficient quenchers on neutral molecules than on cations (nitrobenzene), whereas the reverse is true for donors (*N*, *N*-dimethylaniline). In dioxane the quenching constants are generally somewhat smaller than in ethanol, but a basic similarity has been confirmed. All the results support the view that the present quenching phenomena are closely related to a charge-transfer process.

An electron transfer mechanism for the quenching of fluorescence has been postulated for a long time, but it was only in 1961 that the first evidence for it was presented by Weller.[1]

According to this mechanism, it is expected that a fluorescer with an electron-donating (accepting) power is quenched by an electron-accepting (donating) substance, and that the quenching constant runs parallel with the electron-accepting (donating) power of a quencher. This paper will deal, from such a viewpoint, with the quenching action of a few substances on the fluorescence of acridine orange, which may act as an electron donor or acceptor as the case may be. Besides, acridine orange exists as cations (acid) or neutral

1) H. Leonhardt and A. Weller, *Z. physik. Chem., N. F.*, **29**, 277 (1961); *Ber. Bunsges. Phys. Chem.*, **61**, 791 (1963).

molecules (base) according to the experimental conditions (see below); it is, therefore, interesting to compare the quenching efficiency of each substance on these two species.

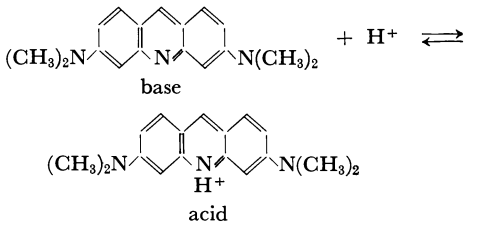

Experimental

Materials.—Acridine Orange: a double salt of Tokyo Kasei, G. R. grade, was purified by precipitating the free base from a dilute sodium hydroxide solution, dissolving the precipitate in chloroform (G. R.), and chromatographing it on activated silica-alumina treated with hydrochloric acid. The main band was collected, dissolved in chloroform-methanol, concentrated, and then cooled to −20°C. The precipitate thus obtained was filtered and dried in air and finally in vacuo for several hours at 70°C.[2] M. p. 181°C.

N, N-Dimethylaniline of a G. R. grade of Tokyo Kasei was dried over potassium carbonate, distilled under reduced pressure in a nitrogen atmosphere, and finally submitted to vacuum distillation. The sample was stored in a sealed ampoule.

Triethylamine of a G. R. grade of Tokyo Kasei was dreid over sodium, distilled under reduced pressure in a nitrogen atmosphere, and then stored in a sealed ampoule.

Nitrobenzene, G. R. grade of Tokyo Kasei, was dried with phophorus pentoxide and distilled under reduced pressure. [5.7°C]. *s*-Trinitrobenzene, G. R. grade of Tokyo Kasei, was recrystallized from water two times. After being dried, it was further recrystallized from carbon tetrachloride two times.

Tetracyanoethylene, G. R. grade of Tokyo Kasei, was purified by sublimation three times. The solution soon got a tint of reddish violet, perhaps from an impurity.

Trichloroacetic acid of Kanto Kagaku, G. R. grade, was purified by recrystallization from benzene three times.

Ethanol of Wako Junyaku, G. R. grade, was fractionally distilled. B. p. 78°C.

Dioxane, G. R. grade of Wako Junyaku, was boiled under reflux for a few days over sodium and then distilled twice. B. p. 101°C.

Benzene of Wako Junyaku, G. R. grade, was dried over sodium and then distilled. B. p. 80.1°C.

Methanol of Wako Junyaku, G. R. grade, was fractionally distilled. B. p. 64.5°C.

Procedures.—The fluorescence intensities, fluorescence spectra and action spectra were measured by an Aminco-Bowman spectrofluorimeter. Correction for sensitivity dependence on the wavelength was not made on the fluorescence spectra. The absorption spectra were measured with a Hitachi EPS III autorecording spectrometer.

Results and Discussion

The Absorption and Fluorescence Spectra of Acridine Orange.—According to Zanker,[2] association becomes apparent above 10^{-5} M of acridine orange in an aqueous solution; Mataga reported similar association phenomena in pyridine, acrylonitrile and ethanol.[3] The recent results of Olszowski and Ruziewicz,[4] however, are quite different from Mataga's results. They assigned the two bands with peaks at ~20000 cm^{-1} and ~23400 cm^{-1} which appear separately or simultaneously in various solvents to cations (acid) and neutral molecules (base) respectively. This assignment was confirmed by the present investigation. As is shown in Fig. 1, acridine orange 7.35×10^{-5} M in ethanol gives a single peak at 495 mμ,

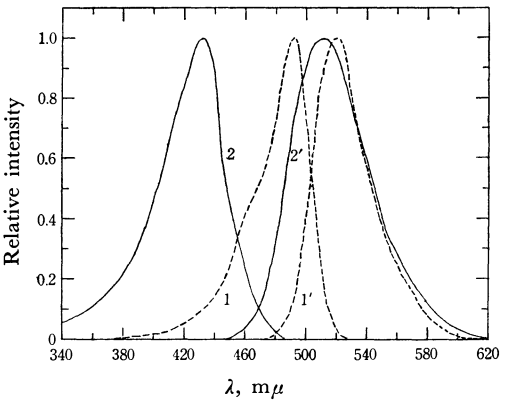

Fig. 1. Fluorescence and absorption spectra of acridine orange (7.35×10^{-6} M) in ethanol.

1 Absorption spectra
1′ Fluorescence spectra
} (in ethanol)

2 Absorption spectra
2′ Fluorescence spectra
} (in alkaline ethanol)

with a shoulder[5] near 460 mμ while the fluorescence spectrum obtained by 490 mμ excitation has a single peak at 522 mμ. When ethanol which has been made alkaline by adding a few pieces of sodium hydroxide is used as a solvent, the absorption peak is at 433 mμ with $\varepsilon_{max}=$ 24900 and the fluorescence spectrum obtained by 430 mμ excitation has a peak at 510 mμ. Figure 2 shows the change in the absorption spectra when trichloroacetic acid or triethylamine is added to a 1.96×10^{-5} M solution of acridine orange in

2) V. Zanker, *Z. physik. Chem.*, **199**, 225 (1952); **200**, 250 (1952).

3) N. Mataga, This Bulletin, **30**, 375 (1957).

4) A. Olszowski and Z. Ruziewicz, ibid., **37**, 1883 (1964).

5) Although the above shoulder seems to suggest the existence of a dimer, Zanker made it clear that there is no sign of association in a dilute ethanol solution. Cf. V. Zanker, Dissertation, T. H. Munchen (1948).

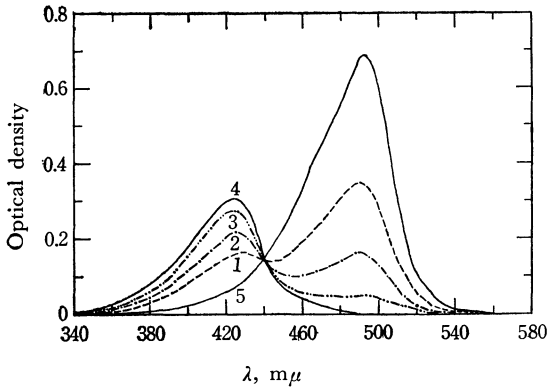

Fig. 2. Absorption spectra of acridine orange (1.96×10^{-5} M) in dioxane.

1) Without addition of a third component
2) With 2.8×10^{-5} M triethylamine
3) With 2.8×10^{-4} M triethylamine
4) With 7.11×10^{-4} M triethylamine
5) With 4.14×10^{-5} M trichloroacetic acid

dioxane. When more than 7.1×10^{-3} M of triethylamine is added, only the peak at 426 mμ due to neutral species becomes notable, whereas upon the addition of trichloroacetic acid of 4.14×10^{-5} M, only the peak of the cation at 492 mμ survives. There is an isosbestic point at 442 mμ. Thus, it is in complete accord with the general behavior of the acid-base system. The molar absorbances for cationic and neutral species were estimated to be 4.29×10^{4} and 1.55×10^{4}, respectively. Figure 3 shows a similar change in the fluorescence spectra obtained by the excitation at the isosbestic point. The neutral and cationic species have fluorescence peaks at, respectively, 500 and 530 mμ. From the intensity ratio when excited by the light of the isosbestic point, the ratio of the apparent fluorescence quantum yields of the two species was decided to be neutral: cation=1 : 2.5. Using the data taken from these two figures, the fraction of the cation, x_C can be calculated from the following equations:

$$x_C = \frac{[\text{cation}]}{[\text{total AO}]} = \frac{D_i - D_{iB}}{D_{iC} - D_{iB}} \quad (1)$$

$$x_C = \frac{F_i - 0.4F_{iB}}{F_{iC} - 0.4F_{iB}} \quad (2)$$

where D_i, is the optical density of the solution in question, where D_{iC} and D_{iB} are, respectively, the optical densities of the cation and the base when they exist in a pure form and at the same concentration (all at a certain wavelength, i), where F_i is the fluorescence intensity of the solution in question, and where F_{iB} and F_{iC} are the relative intensities when the intensity for each species at the peak of the fluorescence spectra is taken as unity. It should be added that Eq. 2 is derived on the assumption that there is no shift of equilibrium during the lifetime. Figure 4, which shows the relation between the two sets of x_C-values obtained from Eqs. 1 and 2, verifies that no essential shift occurs during the lifetime of the excited state.

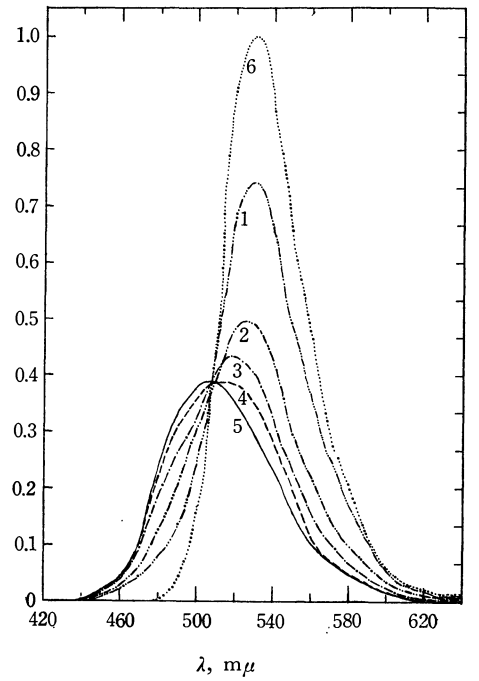

Fig. 3. Fluorescence spectra of acridine orange (1.96×10^{-5} M) in dioxane.

1) Without a third component
With triethylamine of
2) 2.8×10^{-5} M
3) 5.6×10^{-5} M
4) 2.8×10^{-4} M
5) 8.4×10^{-4} M
6) With trichloroacetic acid of 4.14×10^{-5} M

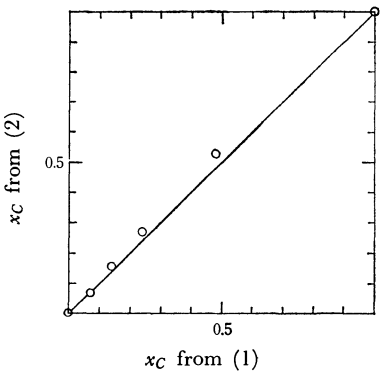

Fig. 4.

The Quenching Action of the Added Substances in Ethanol. — This was examined separately on cations and on neutral molecules. The quenching constants on cations were obtained

by measuring the relative height of the fluorescence spectra at 522 mμ upon excitation at 490 mμ. The quenching constants for neutral molecules were similarly determined by measuring the fluorescence intensity in an alkaline ethanol solution at 510 mμ, with the exciting wavelength at 430 mμ. In all cases it was confirmed that the addition of a quencher does not appreciably affect the absorption spectra of acridine orange. *N*, *N*-Dimethylaniline gives a weak absorption, extending from 380 to 450 mμ, when the concentration is large. This is due to its interaction with the dissolved oxygen,[6] but the excitation in this wavelength region does not give any sign of emission. The absorption spectra of nitrobenzene extend to around 450 mμ; this was taken into account in the measurement in the alkaline solution. *s*-Trinitrobenzene and tetracyanoethylene, both of which are strong electron acceptors, also do not affect the absorption nor the fluorescence spectra of acridine orange. This rules out any specific interaction between fluorescer and quencher. A small band of trinitrobenzene in the 450—600 mμ region is also not affected by the addition of acridine orange. The same holds for the other bands. The absorption spectra of tetracyanoethylene in ethanol is also not essentially affected by the addition of acridine orange. However, trinitrobenzene in the alkaline solution reacts chemically, and the solution becomes red in color. The addition of tetracyanoethylene to the alkaline solution of acridine orange, on the other hand, causes the fluorescence spectra to change into cationic-type spectra. Since tetracyanoethylene is a strong π-acid, some kind of ion-pair may be formed. At any rate, the above situations prevent the determination of the quenching constants of trinitrobenzene and tetracyanoethylene in an alkaline solution.

The results are given in Table I, while some examples of the Stern-Volmer plot are given in Fig. 5.

The results given in Table I can be well comprehended on the basis of a charge-transfer mechanism of quenching. Thus, the order of quenching efficiency on cations, — nitrobenzene < trinitrobenzene < tetracyanoethylene—agrees with that of the electron-accepting power of these substances. Further, *N*, *N*-dimethylaniline, which is considered to act as an electron donor, is a more efficient quencher on cations than on neutral molecules, whereas the reverse is true for nitrobenzene.

The Quenching Action of the Added Substances in Dioxane.—The quenching phenomena were studied with a solution containing both cation and neutral species of acridine orange; suitable

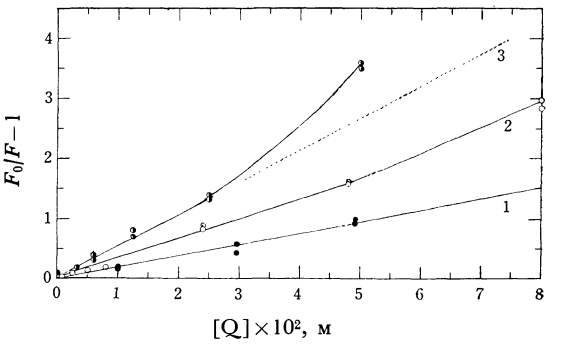

Fig. 5-a. $F_0/F-1$ vs. concentration of quenchers
quencher: 1) Nitrobenzene
2) *N*, *N*-Dimethylaniline
3) *s*-Trinitrobenzene

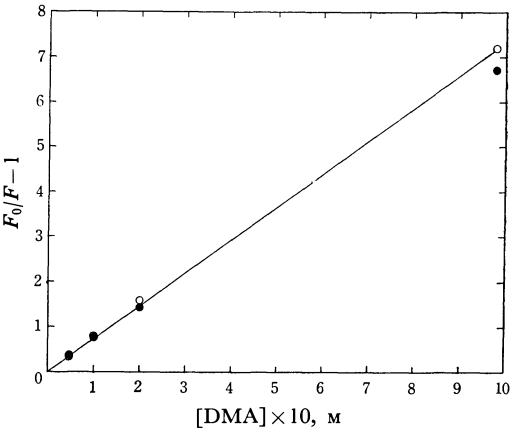

Fig. 5-b. $F_0/F-1$ vs. concentration of nitrobenzene in alkaline ethanol (EtOH+NaOH).
Concentration of AO, 7.35×10^{-6} M
Excitation wavelength—open circle: 440 mμ;
filled circle: 420 mμ

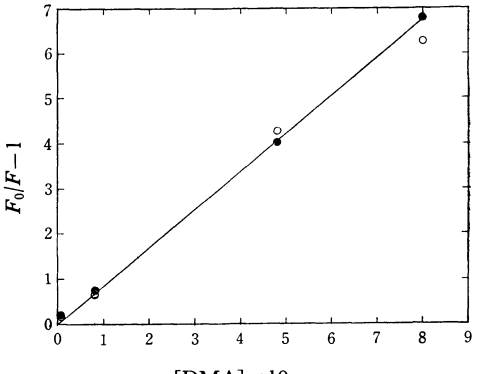

Fig. 5-c. $F_0/F-1$ vs. concentration of *N*, *N*-dimethylaniline in alkaline ethanol (EtOH+NaOH).
Concentration of AO, 4.90×10^{-6} M
Excitation wavelength—open circle, 450 mμ;
filled circle, 430 mμ

6) D. F. Evans, *J. Chem. Soc.*, **1953**, 345; **1957**, 1351, 3885; **1959**, 2753; *Proc. Roy. Soc.*, **A255**, 55 (1960).

Table I. Quenching constants of some substances on the fluorescence of AO in ethanol

Quencher	Concn. of AO M	Concn. range of quencher, M	Quenching for cation	Const. K^*(l. mol^{-1}) for neutral species
N,*N*-Dimethylaniline	4.90×10^{-5}	2.4×10^{-3}—4.8×10^{-2}	34.5	
	4.90×10^{-6}	8.0×10^{-3}—8.0×10^{-1}		8.4
Nitrobenzene	7.35×10^{-6}	4.9×10^{-3}—9.8×10^{-2}	19.6	
	7.35×10^{-6}	4.9×10^{-3}—9.8×10^{-2}		73
s-Trinitrobenzene	7.35×10^{-6}	3.1×10^{-3}—5.0×10^{-2}	53.6	
Tetracyanoethylene	7.35×10^{-6}	5.6×10^{-3}	(90)	

* $K=(F_0/F-1)/[Q]$
F_0 and F are respectively the fluorescence intensities in the absence and in the presence of a quencher.

exciting wavelengths were chosen and the fluorescence intensities at different wavelengths were compared. The data were analyzed on the basic assumption that no essential shift of equilibrium occurs during the lifetime of the excited state. When the wavelength of the exciting light, i, is not the one at the isosbestic point, F_j, the fluorescence intensity at the j wavelength is approximately given by:

$$F_j = x_C F_{Cj}\frac{\varepsilon_C}{\varepsilon_0} + \frac{1}{2.5}(1-x_C)F_{Bj}\frac{\varepsilon_B}{\varepsilon_0} \qquad (3)$$

where ε_C, ε_B and ε_0 are, respectively, the molar absorbance of cation and base at the i wavelength and that at the isosbestic point. From this equation it was confirmed that, except in very extreme cases, the fluorescence behavior of cation and base can be studied separately by choosing the exciting lights at 490 and 430 mμ respectively and by measuring the intensity at 530 and 490 mμ respectively. In some cases the change in the fluorescence spectra and in the action spectra caused by the addition of a quencher were made use of in getting semi-quantitative information on quenching.

***N*, *N*-Dimethylaniline.**—Figure 6 gives the Stern-Volmer plot for cation and neutral species. The quenching constant for neutral species was determined by the use of a solution containing 2.80×10^{-4} M of triethylamine. The results are, for cation, $K=20$ l./mol. and for base, $K=0$ l./mol.

Nitrobenzene.—With the increase in the concentration of nitrobenzene, the superposition of the absorption of nitrobenzene becomes notable in the shorter wavelength region. The fluorecscence spectra observed when the excitation wavelength is 490 mμ, as well as the action spectra obtained at 530 mμ of the fluorescence spectra, are not essentially affected by the addition of nitrobenzene.

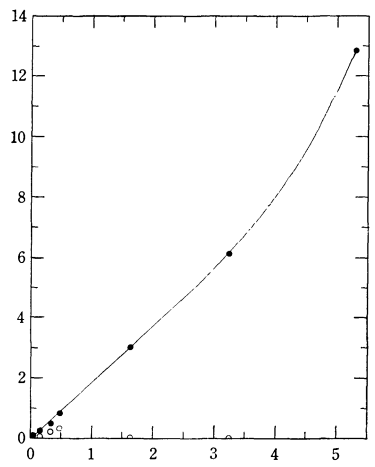

Fig. 6. $F_0/F-1$ vs. concentration of *N*,*N*-dimethylaniline in dioxane.
Concentration of acridine orange 1.96×10^{-5} M
Excitation wavelength—filled circle: 490 mμ;
open circle, 430 mμ
Fluorescence wavelength—filled circle, 530 mμ;
open circle 500 mμ

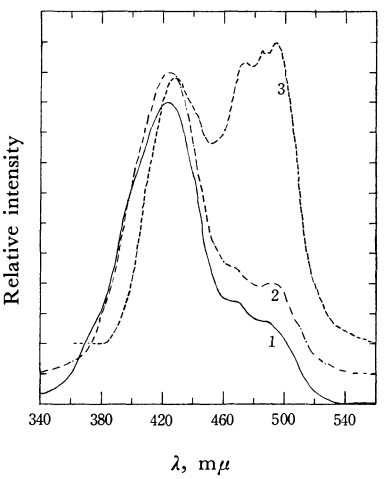

Fig. 7. The effect of the addition of nitrobenzene on the fluorescence excitation spectra of AO (1.95×10^{-5} M) in dioxane.
Concentration of nitrobenzene: (1) 0 M, (2) 9.8×10^{-2} M, (3) 9.8×10^{-1} M
Fluorescence wavelength, 500 mμ
Some structures near 500 mμ of curve 3 are due to the characteristics of the Xe - arc lamp emission.

This implies that the fluorescence of the cation is not quenched very much by nitrobenzene. On the other hand, the action spectra taken at 500 mμ of the fluorescence spectra, as Fig. 7 shows, depend on the concentration of nitrobenzene to a great extent. Thus, there is scarcely any doubt that nitrobenzene quenches neutral molecules more efficiently than cations. The quenching constants evaluated from the intensities at 530 and 490 mμ with the exciting lights at 495 and 430 mμ respectively, are ~10 and ~30 l./mol.

Trinitrobenzene.—As in ethanol, a weak absorption from 550 to 600 mμ is not due to the interaction of trinitrobenzene and acridine orange, but to trinitrobenzene itself. The measurement of the fluorescence intensities at 530 and 490 mμ, with the exciting lights at 490 and 430 mμ respectively, gives, as the quenching constants for cations and neutral species respectively, ~55 and ~70 l./mol. The fluorescence spectra taken with exciting lights of shorter wavelengths and the action spectra taken at 490 and 510 mμ of fluorescence spectra also indicated that the neutral species is more quenched than the cation.

Tetracyanoethylene.—With the addition of tetracyanoethylene, the absorption spectra change into cationic-type spectra, just as in ethanol. The fluorescence spectra also become cationic-type spectra; however, their peaks shift slightly toward blue. The quenching constant of tetracyanoethylene on the ion-pair is ~70 l./mol. from the Stern-Volmer plot. The appoximate quenching constants in the dioxane solution are summarized in Table II.

TABLE II. APPROXIMATE QUENCHING CONSTANTS OF SOME SUBSTANCES ON THE FLUORESCENCE OF AO IN DIOXANE

Quencher	K for cation l. mol^{-1}	K for base l. mol^{-1}
N,*N*-Dimethylaniline	~20	~ 0
Nitrobenzene	~10	~30
s-Trinitrobenzene	~55	~70
Tetracyanoethylene	70	

Relations similar to those in ethanol are apparent in this case. All the quenching constants in dioxane are somewhat smaller than in ethanol. This is consistent with the results reported by Miwa and Koizumi.[7]

Conclusion

All the results obtained in the present experiment strongly support a charge-transfer mechanism of quenching. Besides, it has been confirmed that the acid-base equilibrium does not shift essentially during the lifetime of the excited state.

7) T. Miwa and M. Koizumi, This Bulletin, **39**, 2588 (1966).

BULLETIN OF THE CHEMICAL SOCIETY OF JAPAN VOL. 39 2603—2608 (1966)

The Photo-ionization of Molecules in Solutions. III. Photo-ionization and Recombination Processes of *N*, *N*, *N'*, *N'*-Tetramethyl-*p*-phenylenediamine in Various Organic Solvent

By Naoto YAMAMOTO, Yoshihiro NAKATO and Hiroshi TSUBOMURA

Department of Chemistry, Faculty of Engineering Science, Osaka University, Toyonaka, Osaka

(Received April 21, 1966)

Flash photolysis studies of *N*,*N*,*N'*,*N'*-tetramethyl-*p*-phenylenediamine (TMPD) were made in various solvents at room temperature. The transient absorption spectrum of the cation, $TMPD^+$, was observed in polar solvents. The transient was also observed in a viscous, non-polar solvent. It has a spectrum different from that of $TMPD^+$. Its absorbance is proportional to the flash-light intensity, and it decays exponentially, with $\tau_e=82$ μ sec. This absorption is attributed to the triplet-triplet transition of TMPD. With aerated solutions, no transient spectrum was observed. The fluorescence and the phosphorescence of TMPD caused by direct excitation were investigated, together with those induced by the recombination of electrons and $TMPD^+$ in non-polar matrices stimulated either thermally or by infrared light. The absorption spectra of TMPD in a non-polar matrix at a low temperature were investigated by means of the cross-illumination method, and the time dependence of the absorption was followed. The ionization and the recombination processes were then discussed by the use of these results.

It was found by Lewis and Lipkin[1] that *N*, *N*, *N'*, *N'*-tetramethyl-*p*-phenylenediamine (TMPD) in a rigid matrix at the temperature of liquid air forms the $TMPD^+$ cation by ultraviolet irradiation. The electronic and vibronic properties of the excited states of TMPD and $TMPD^+$ were investigated using the technique of photoselection in a rigid medium at a low temperature.[2] Recently, the existence of an electron ejected into a medium by photo-ionization has been argued by an ESR study.[3] Albrecht and his collaborators have studied the photoionization process of TMPD[4-6] and the recombination process of the ionized species[5-8] in a nonpolar matrix at a low temperature. From these results, they concluded that a two-step mechanism involving the triplet state is responsible for the photo-ionization of benzene derivatives in rigid glasses.[4] Porter et al. sugested the same mechanism for the photo-ionization of aromatic hydrocarbons.[9] Claridge and Willard have found that photoejected electrons from TMPD in matrices containing alkyl halides cause the decomposition of alkyl halides, leading to the appearance of ESR signals of alkyl radicals.[10] Van Voorst and Hoijtink have recently found that solvated electrons are formed by the photo-ejection of electrons from aromatic negative ions in 2-methyl-tetrahydrofuran matrices.[11] Hamill and his co-workers have also been studying similar electron-ejection and capture processes by using radiolysis techniques.[12]

We ourselves have previously studied the photo-excitation and photo-ionization of TMPD and the recombination of the ionized species in a variety of media at various temperatures.[13,14] The work on the room-temperature photolysis has been mainly done by the flash-photolysis technique.

Experimental

Commercially-available TMPD dihydrochloride was neutralized in an aqueous solution with ammonia.

1) G. N. Lewis and D. Lipkin, *J. Am. Chem. Soc.*, **64**, 2801 (1942).
2) A. C. Albrecht, ibid., **77**, 4454 (1955); **82**, 3813 (1960).
3) E. Dolan, *J. Chem. Phys.*, **37**, 2508 (1962).
4) K. D. Cadogan and A. C. Albrecht, ibid., **43**, 2550 (1965).
5) G. E. Johnson, W. M. McClain and A. C. Albrecht ibid., **43**, 2911 (1965).
6) G. E. Johnson and A. C. Albrecht, International Conference on Photosensitization in Solids, I. I. T., Chicago, 1964.
7) E. Dolan and A. C. Albrecht, *J. Chem. Phys.*, **37**, 1149 (1962); **38**, 567 (1963).
8) W. M. McClain and A. C. Albrecht, ibid., **43**, 465 (1965).
9) W. A. Gibbons, G. Porter and M. I. Savadatti, *Nature*, **206**, 1355 (1965).
10) R. F. C. Claridge and J. E. Willard, *J. Am. Chem. Soc.*, **87**, 4992 (1965).
11) J. D. W. van Voorst and G. J. Hoijtink, *J. Chem. Phys.*, **42**, 3995 (1965).
12) M. Kondo, M. R. Ronayne, J. P. Guarino and W. H. Hamill, *J. Am. Chem. Soc.*, **86**, 1297 (1964).
13) H. Tsubomura, N. Yamamoto, K. Kimura, T. Sato, H. Yamada, M. Kato, G. Yamaguchi and Y. Nakato, This Bulletin, **38**, 2021 (1965).
14) H. Tsubomura, N. Yamamoto and Y. Nakato, to be published.

The TMPD thus formed was extracted with ether, dried, and sublimed twice in a vacuum.

The solvent used in this experiment were MP (1 part methylcyclohexane, 1 part isopentane), EPA (5 parts ether, 5 parts isopentane, 2 parts ethanol), pyridine, *n*-heptane, ethanol, acetonitrile, liquid paraffin, and cyclohexanol. The ether was purified by distillation. The methylcyclohexane and isopentane were purified by passing them through activated silica gel. The ethanol was purified by drying it over magnesium ribbon and by distilling it in a 120 cm. column. The acetonitrile was refluxed over phosphorus pentoxide, distilled over anhydrous potassium carbonate to remove the phosphorus pentoxide, and finally fractionally distilled in the same column. The *n*-heptane was fractionally distilled. The EP-grade cyclohexanol, liquid paraffin and pyridine were used without further purification.

In the case of polar solvents, TMPD was dissolved in the solvent after it had been degassed by the freezed-pump-thaw technique. In the case of non-polar solvents, the solution was prepared by the conventional method, and then degassed by the same technique.

Flash-photolysis measurements at room temperature were made by the use of a glass cell with quartz windows (200 mm. long, 16 mm. in diameter). Two photolysis flash lamps, one placed at each side of the cell, were connected in series to a condenser a 5-μF capacity working up to 15 kV. Each lamp was made of a quartz glass tube, 20 cm. long and 1.0 cm. in diameter, with tungsten-electrodes at both ends. Those tubes were filled with argon up to a pressure of about 100 mmHg. A small quartz spectro-flash lamp, with a capillary middle portion, was connected to a 2.5 μF condenser working up to 7.5 kV. The lamps were fired by powerful trigger pulses. The time interval between the photolysis-flash and the spectro-flash can be controlled in the range from 1 μsec. to 1 sec. through a delay circuit. The electric power supply and the trigger pulse generator of this instrument were provided by the Nakano Electric Co. The duration times of both the photolysis-flash and the spectro-flash were found to be less than 3 μsec. The transient absorption spectra were obtained photographically with Fuji Neopan SSS film (ASA 200) by the use of a plane-grating spectrograph 1 m. in focal length (Shimadzu GE-100). The decay-curve measurements of the transient absorption were performed by recording the cathode currents of a photomultiplier (EMI 9552B) with a synchroscope or a recorder.

For the measurements of emission spectra at a low temperature, a degassed TMPD matrix contained in a cylindrical cell 10 mm. in diameter was put into a quartz Dewar. For the measurement of the usual fluorescence and phosphorescence spectra of TMPD, the sample was illuminated by focusing light from a 250-W. high-pressure mercury lamp (Ushio HMB-250D) through a filter (Toshiba UV-D2; transparent from 320 to 390 mμ). The emission of the sample was focused on the slit of a 50-cm. grating spectrograph (Nalumi RM 23), the emission spectra were then photographed. The emission spectrum induced by the infrared illumination of the ultraviolet-irradiated TMPD in the MP matrix was obtained by repeating the following procedures about eighty times: (1) ultraviolet irradiation for 30 sec., followed by (2) a 60-sec. dark period, then (3) infrared illumination and the photographing of the induced emission for 30 sec. The infrared light used was obtained from the mercury lamp through a filter (Toshiba VR-69) transparent from 690 mμ to 3 μ. For the measurement of the thermoluminescence spectrum, the sample was drawn out from the Dewar after irradiation by ultraviolet light at the temperature of liquid nitrogen; it was then held in front of the spectrograph until it melted. The decay of the emission spectra was measured in a MP matrix at 77°K by recording the cathode currents of a photomultiplier (RCA 1P28), placed near the sample, by means of a synchroscope through a cathode-follower circuit.

Results

The Flash Photolysis of TMPD.—The flash photolysis of about 5×10^{-4} mol./l. solutions of TMPD in some deoxygenated solvents at room temperature resulted in the appearance of transient absorption spectra, while in some other no new spectrum was obtained at all. These results are tabulated in Table I. The spectra obtained in ethanol, acetonitrile, and cyclohexanol agree with that of $TMPD^+$ formed by chemical oxidation. The spectrum obtained in liquid paraffin does not exactly agree with that of $TMPD^+$, though they have features similar to some extent, as Fig. 1 shows. Decay curves of the transient absorption spectra in a liquid paraffin solution and an ethanol solution are shown in Figs. 2 and 3 respectively. In the liquid paraffin solution, the decay is of the first order and the life-time is 82 μsec. In ethanol and in acetonitrile, the decay is, rather, of the second order and the life-time is very long. The characteristic violet color of $TMPD^+$ remains visible for more than a day. When these solutions were aerated, no transient absorption spectrum was observed by a flash illumination,

TABLE I. APPEARANCE OF TRANSIENT ABSORPTION BY FLASH ILLUMINATION AT ROOM TEMPERATURE

Solvent	Dielectric constant	Temp., °C	Viscosity (centipoise)	Temp., °C	Appearance
Ethanol	24.30	25	1.20	20	Yes (long life)
Acetonitrile	37.5	—	0.345	25	Yes (long life)
Cyclohexanol	15.0	25	68	20	Yes (weak)
Amyl alcohol	ca. 15	20	4.65	30	No
Pyridine	12.3	25	0.974	20	No
Heptane	ca. 1.8	20	0.409	20	No
Ether	4.2	27	0.24	20	No
Liq. paraffin	ca. 1.8	—	ca. 500	—	Yes ($82\frac{1}{2}\mu$sec.)

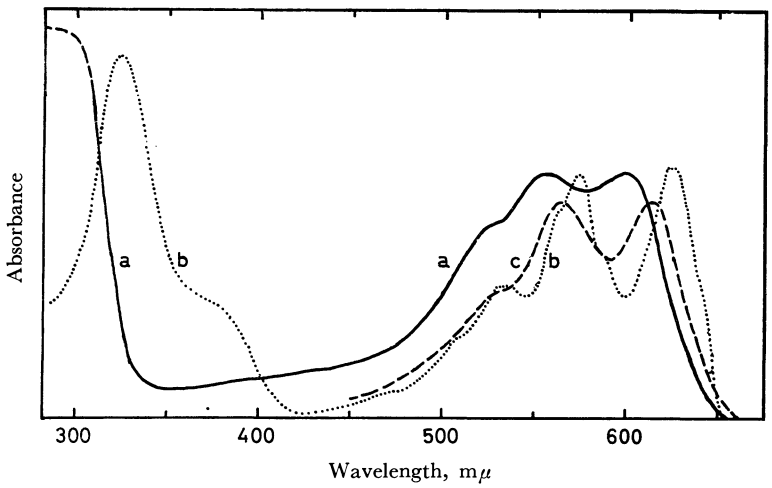

Fig. 1. a) Transient absorption spectrum formed by the flash photolysis of TMPD in liquid paraffin at room temperature.
b) Absorption spectrum formed by the ultraviolet illumination of TMPD in ethanol at 77°K.
c) Absorption spectrum of Wurster's blue perchlorate in ethanol at room temperature.

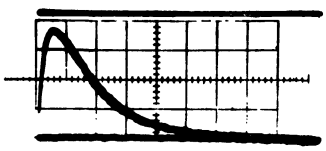

Fig. 2. A decay curve of a transient absorption at 560 mμ formed by flash photolysis of liquid paraffin of TMPD at room temperature. The upper and lower lines indicate 100% and 0% absorption, respectively. The time scale is 50 μsec. per main division.

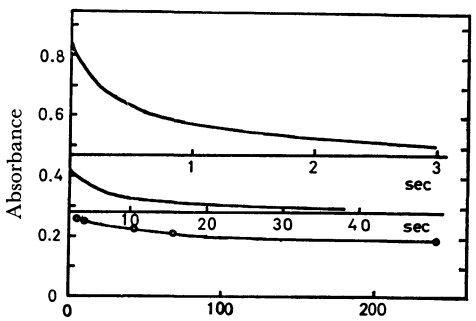

Fig. 3. Decay of the transient absorption (λ= 610 mμ) in ethanol at room temperature produced by the flash photolysis of TMPD.

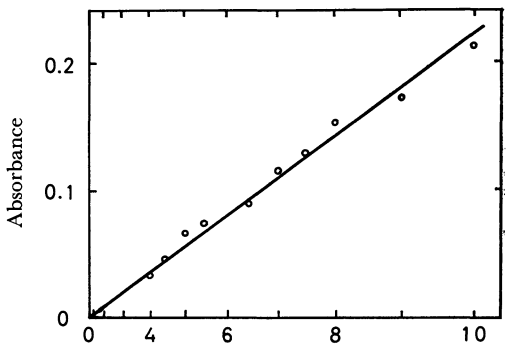

Fig. 4. Dependence of the transient absorption (λ=560 mμ) in liquid paraffin solution of TMPD on the flash light intensity. It is assumed that the flash light intensity is proportional to the square of charging-up-voltage of a 5 μF condenser.

except in the acetonitrile solution.

The correlation between the transient absorption and the intensity of flash light was studied for 10^{-5} mol./l. liquid paraffin solutions of TMPD. Since the intensity curves of the flash light with respect to time do not change with the charging-up-voltages of the condenser, it may be assumed that the light intensity at any moment is proportional to the square of the voltage. The intensity of the transient absorption was found to be proportional to V^2, as Fig. 4 shows.

Luminescence at a Low Temperature.— The UV-irradiated TMPD in non-polar (MP or liquid paraffin) matrices at 77°K shows an afterglow stimulated by infrared light or by warming up the matrix, as has been reported by Albrecht and his co-workers.[7,8] The spectra obtained photographically by the method described earlier in this paper are shown in Fig. 5 by curves b and c. The normal fluorescence (F, λ=375 mμ) and phosphorescence (P, λ=470 mμ) spectra of TMPD are

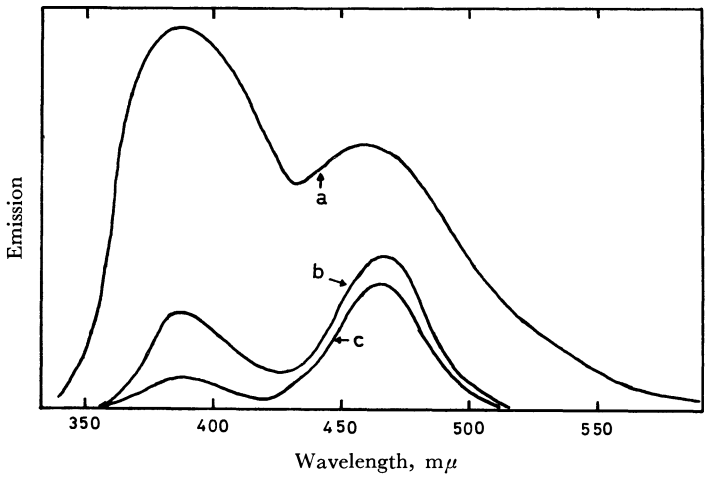

Fig. 5. Emission spectra in MP matrix at 77°K.
a) Emission spectrum of TMPD excited by ultraviolet (mainly 313 mμ). Two peakes at 376 mμ and 470 mμ are the fluorescence and the phosphorescence of TMPD, respectively.
b) Induced emission spectrum obtained by infrared illumination after ultraviolet irradiation.
c) Thermoluminescence spectrum obtained by elevating temperature.

also shown in Fig. 5a. The results of these emission spectra indicate that the induced emission consists of the fluorescence and the phosphorescence of TMPD respectively. The P/F ratios of the induced emission are larger than that of the normal emission of TMPD. In the case of the liquid paraffin matrix, the emission induced by infrared illumination was observed visually at temperatures ranging from 77°K to 120°K. Emission was found to continue until the temperature of the solution became about −30°C. However, no induced emission was observed in the case of polar matrices (ethanol or EPA) by any method. The time dependence of the IR-induced emission in the MP matrix at 77°K was also measured and found to agree with that reported by Albrecht et al.[8]

Absorption Spectra at Low Temperature. —In order to get more information on the nature of the transient absorption obtained by the flash photolysis of TMPD in a viscous solvent at room temperature, the abosprption spectra of about 10^{-5} mol./l. TMPD in a MP matrix at 77°K were measured photographically by means of the cross-illumination method. The 250-W. high-pressure mercury lamp, equipped with a Toshiba UV-D2 filter, was used as the exciting light source. As the spectral light source, a 500-W. Xenon lamp was used. The spectra were photographed by the use of a Nalumi RM 23 spectrograph. In Fig. 6, curve a shows the absorption spectrum taken by an exposure which began 5 sec. after the ultraviolet light came on and continued for 5 sec. Curve b shows the spectrum taken just before the ultraviolet light went off. Curve c shows the spectrum taken by the recording spectrophotometer many minutes after the ultraviolet light went off.

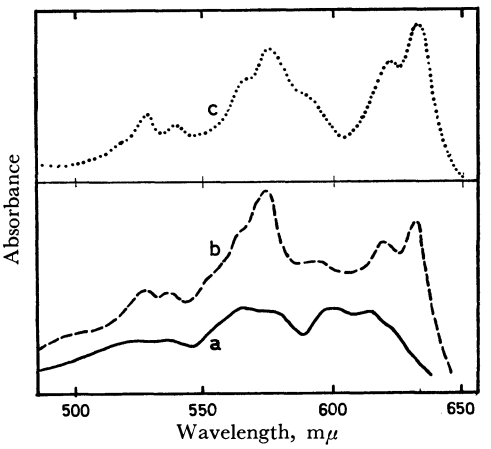

Fig. 6. Absorption spectra of MP matrix of TMPD obtained photographically by means of the cross illumination method at 77°K.
a) The absorption spectrum taken at 5 sec. after the UV light was on.
b) The sample was irradiated by UV light for 5 min. The absorption spectrum taken just before the UV light was off.
c) The absorption spectrum taken at many minutes after the UV light was off.

Discussion

We may conclude from the following reasons that the transient absorption spectrum obtained by the flash photolysis of TMPD in liquid paraffin (Fig. 1, curve a) is the T-T′ absorption of TMPD:

1) The spectral feature is different from that of $TMPD^+$ (Fig. 1).

2) Its absorption intensity is proportional to

the intensity of the photolysis flash light, while it would be proportional to its square if the two-step photo-ionization mechanism proposed by Albrecht et al. was correct.

3) Its absorbance is larger than that of $TMPD^+$ formed by a single-flash photolysis with the same flash apparatus of a degassed ethanol solution, while the quantum yield of $TMPD^+$ formation in a non-polar matrix at 77°K is much less than that in a polar matrix at 77°K.[15] On the other hand, if it is the T-T' absorption, the larger intensity in liquid paraffin can reasonably be attributed to its larger viscosity which stabilizes the triplet state.

4) The decay of the transient absorption in a liquid paraffin solution is exponential. This means a first-order decay process; therefore, it does not correspond to a recombination process between a cation and a free electron. The life-time (82 μsec.) is in the range of those of the triplet states of aromatic hydrocarbons.[16]

The transient absorption spectra obtained in polar solvents at room temperature are identical to that of $TMPD^+$, and the decay curve is nearly a hyperbola. For polar solvents, therefore, photo-ionization is easily produced by flash illumination at room temperature and the ionized species has a remarkably long life-time (one or two days).

For solvents with low dielectric constants and low viscosities, no transient absorption is observed at room temperature. In this case, the first excited triplet state of TMPD is supposed to have a life-time so short that it is impossible to detect it. Also, TMPD is not photo-ionized in such solvents.

When these solutions are aerated, no transient absorption is observed, except for the acetonitrile solution. In a liquid paraffin solution at room temperature, the fluorescence of TMPD is not quenched by the existence of O_2.[15] When ethanol or acetonitrile solution is aerated after the transient absorption is formed by the flash, no oxygen effect on the absorption is observed. It is also well known that an excited triplet state of aromatic hydrocarbon is quenched by O_2.[16] Our results concerning the O_2 effect are consistent with the two-step mechanism of the photo-ionization which occurs via the triplet state of TMPD.

It was pointed out by Albrecht and McClain,[8] on the basis of their photo-electric measurements, that the P/F ratio of the phosphorescence and fluorescence intensity in the induced emission is different from that in the normal TMPD emission. They, therefore, suggested that a direct transfer from the recombining electron to the triplet state occurs to some extent, for if the transfer occurs only to the singlet state, the P/F ratio should be the same as that for the normal emission of TMPD. Our results, shown in Fig. 5, curve b, is in agreement with their results, showing that the P/F ratio is much larger in the infrared-stimulated emission. The P/F ratio in the thermoluminescence, as shown by Fig. 5, curve c, is still larger, indicating that the probability of the transfer to the triplet state is larger in this case.

In polar media, no emission is observed either by infrared ($\lambda > 690$ mμ) or by elevating the temperature. This suggests that the potential trough for the electrons is so deep that the energy of infrared light is not sufficient to release it. At an elevated temperature, the electron recombination will lead to the ground state of TMPD. Ultraviolet-irradiated TMPD in an EPA matrix shows an ESR spectrum composed of ill-resolved quintets, which might correspond to a radical $CH_3\dot{C}HOH$,[17] whereas in the MP matrix a strong sharp peak is obtained at the free-spin g value. The results in EPA seem to indicate that most of the ejected electrons react with the solvent, possibly causing $CH_3\dot{C}HOH$ or $C_2H_5O^-$. However, to solve the question of whether the model of electrons-deeply-trapped-in-the-solvent does or does not apply in this case, we need more experimental knowledge on these matters.

The change in the absorption spectrum with time as measured by the cross-illumination method at a low temperature (Fig. 6) clearly indicates that two species are present. One corresponds to Curve a, which coincides well with the T-T' absorption spectrum obtained by the flash illumination of the liquid paraffin solution at room temperature (Fig. 1a), although the vibrational structure is more evident in this case, probably because of the low temperature. Curves b and c are almost identical; they evidently represent the spectrum for $TMPD^+$. The change in these spectra with time is more clearly seen by Fig. 7. When the ultraviolet lamp is on, the T-T' absorption rapidly increases within a few seconds, that is to say, it

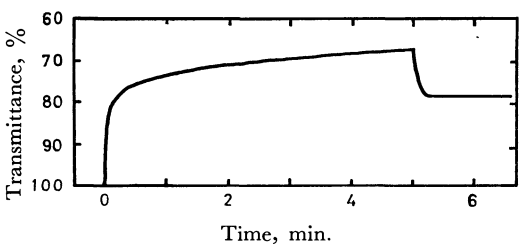

Fig. 7. Time dependence of the absorption (λ= 575 mμ), which consists of the transient and the stable components, in MP matrix of TMPD at 77°K by cross illumination method. At time, t=0, ultraviolet light is on. At t=5 min., light off.

15) Unpublished results in our laboratry.
16) G. Porter and M. W. Windsor, *Discussions Faraday Soc.*, **17**, 178 (1954).
17) Unpublished results from our laboratry. The details will be reported in the near future.

is of the same order as the life-time, τ_e, of the triplet state. (The life-time, τ_e, of the triplet state of TMPD has been determined by us, from the decay of its phosphorescence, to be 2.12 sec.) Then the absorption increases almost linearly with time. During this period, it may be supposed that the T-T' absorbance keeps a constant value and that the absorbance due to $TMPD^+$ steadily increases. When the ultraviolet lamp is off, the component of the absorbance arising from the T-T' transition decays again within a few seconds, and the total absorbance drops to a constant value due to $TMPD^+$. These results, together with the flash-photolysis results with a liquid paraffin solution, clearly demonstrate that there are two bands due to different species in the same wavelength region. Their spectra have also been unambiguously determined.

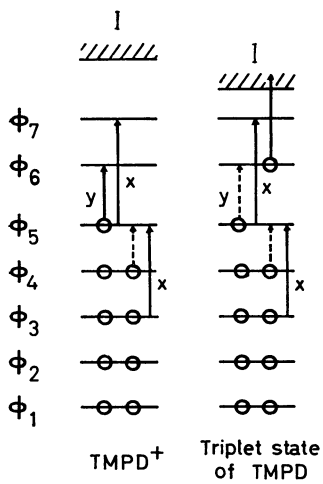

Fig. 8. Scheme of the molecular orbitals and the electron configurations of $TMPD^+$ and the triplet state of TMPD.

It is of theoretical interest to compare the two spectra and to interpret them on the basis of the molecular orbital theory. Figure 8 shows schematically the molecular orbitals (MO's) and the electron configurations of $TMPD^+$ and the triplet state of TMPD. It was determined by Albrecht that the visible spectrum of $TMPD^+$ is X-polarized, that the near ultraviolet hump (λ=370 mμ) is Y-polarized, and that the ultraviolet peak (λ=320 mμ) is X-polarized. According to calculations made by Kimura and Mataga,[18] these bands correspond mainly to the one-electron excitations, $\phi_3 \rightarrow \phi_5$, $\phi_5 \rightarrow \phi_6$, and $\phi_5 \rightarrow \phi_7$. The $\phi_4 \rightarrow \phi_5$ excitation should be in the infrared region, it may not appear because it is a forbidden transition.

If one assume that the MO's and the orbital energies of the triplet states are analogous to those for $TMPD^+$, the visible T-T' band is clearly due to the $\phi_3 \rightarrow \phi_5$ excitation. The $\phi_5 \rightarrow \phi_6$ excitation in this case must inevitably lead to a singlet state, therefore, it is a forbidden transition. The absorption band corresponding to this transition must, therefore, be very weak. This explains very well the lack of a near ultraviolet hump for the spectra of the triplet state of TMPD. The ultraviolet absorption might then correspond to the $\phi_5 \rightarrow \phi_7$ excitation. In this case, however, the ionization threshold will be considerably lower than that for TMPD. It is, therefore, doubtful whether the ultraviolet absorption is due to $\phi_5 \rightarrow \phi_7$ excitation or to the transition leading to ionization ($\phi_6 \rightarrow$ I).

If we tentatively assume that the latter is the case, the wavelength at which the ultraviolet absorption starts (ca. 340 mμ) would correspond to the vertical ionization potential for the triplet-state TMPD in an MP matrix, leading to 3.6 eV., a bit larger than the value proposed by Cadogan and Albrecht (3.2 eV.). By the addition of the excitation energy from the ground to the triplet state of TMPD (3.0 eV.), the ionization potential is found to be 6.6 eV.

The authors are grateful to Professors A. C. Albrecht and J. E. Willard for showing us parts of their papers prior to publication.

18) K. Kimura and N. Mataga, to be published in the near future.

BULLETIN OF THE CHEMICAL SOCIETY OF JAPAN VOL. 39 2609—2612 (1966)

Kinetic Studies of Ammonia Oxidation in Shock Waves. III. The Radiation of Excited OH Radicals

By Tetsu TAKEYAMA and Hajime MIYAMA

Basic Research Laboratories, Toyo Rayon Company, Ltd., Tebiro, Kamakura, Kanagawa

(Received April 22, 1966)

Mixtures of ammonia and oxygen in argon were heated by reflected shock waves to temperatures between 1600 and 2100°K, and the ultraviolet radiation from $OH(^2\sum^+)$ was observed by means of monochromator and a photomultiplier. The radiation profiles showed two types of radiation: a strong spike which appeared after an induction period, and a weak and constant-level emission, which followed the spike and persisted for up to 500 μsec. The former emission was observed also in the oxidation of hydrogen, methane, and acetylene, but the latter emission was observed only in the oxidation of methane and acetylene. The temperature coefficients of the intensities of the latter emission divided by the sum of spectral emissivities were found, for the oxidation of ammonia, not large enough to be explained by the thermal excitation of the ground-state $OH(^2\pi)$ to the $^2\sum^+$ state. Possible reaction processes for this chemiluminescence were proposed to explain the experimental results.

OH radicals in the ground state, $^2\pi$, have been found, by absorption spectrophotometry, to persist more than one millisecond in oxidation reactions of hydrogen,[1] methane,[2] acetylene,[3] and ammonia[4] in shock waves. On the contrary, excited OH radicals, $^2\sum^+$, were observed in the detonation of hydrocarbons to last for a very short period, showing spike in their time history of radiation.[5] Also, the chemiluminescence of excited OH in hydrogen-oxygen reactions was studied in detail recently.[6]

In the course of the study of the ammonia oxidation, we have measured the change with time in concentrations of excited OH radicals and other intermediate species simultaneously.[4] We have thereby found the interesting fact that the spike of OH radiation is followed by a weak radiation which persists at an essentially constant level from 100 to 500 μsec. This prompted us to clarify whether the radiation is chemiluminescent or thermal in nature, and to see whether or not the same type of radiation is observed in the oxidation of other fuels.

Experimental

The experimental apparatus and procedure have been described in detail previously.[3,4,7] In brief, the ultraviolet radiation of OH has been observed through a quartz window, mounted 5.5 mm. from the end wall of the shock tube, by a Shimadzu QR-500 monochromator and a Hamamatsu-TV R106 photomultiplier. The monochromator has been set at 3067 Å, and its slit width, at 0.15 mm., allowing a band pass of 6 Å. The incident shock speed has been measured by two platinum-thin-film thermometers, stationed 139.0 mm. apart, and an electronic counter. After each run, the debris of the Lumirror (polyester film) diaphragm was taken out of the shock tube, and the quartz window was cleaned. Gas mixtures were prepared manometrically in an all-glass apparatus, and stirred magnetically for at least an hour before being used in the experiment.

Calculation

That the radiation of OH observed in the oxidation of ammonia is chemiluminescent in nature has been determined in the following manner.

The basic phenomenological law for the emission of radiation at wave-number ω from uniformly-distributed radiators is[8]:

$$R_\omega = R_\omega^0[1-\exp(-P_\omega X)], \quad (1)$$

where R_ω is the total spectral radiancy; R_ω^0, the black body radiancy; P_ω, the spectral absorption coefficient, and X, the optical density. The term in brackets is referred to as the spectral emissivity, α_ω. Thus, the spectral intensity, I_ω, measured in the experiment by a monochromator and a photo-

1) H. Miyama and T. Takeyama, *J. Chem. Phys.*, **41**, 2287 (1964).
2) H. Miyama and T. Takeyama, This Bulletin, **38**, 37 (1965).
3) T. Takeyama and H. Miyama, ibid., **38**, 936 (1965).
4) T. Takeyama and H. Miyama, *J. Chem. Phys.*, **42**, 3737 (1965); This Bulletin, **38**, 1670 (1965).
5) G. J. Minkoff, A. J. Everett and H. P. Broida, Fifth Symposium (International) on Combustion, Reinhold Publishing Corporation, New York (1955), p. 799.
6) E. F. Belles and M. R. Lauver, *J. Chem. Phys.*, **40**, 415 (1964).
7) T. Takeyama and H. Miyama, This Bulletin, in press.
8) S. S. Penner, "Quantitative Molecular Spectroscopy and Gas Emissivities," Addison-Wesley Publishing Company, Inc., Mass. (1959).

multiplier may be represented by:

$$I_\omega = AR^0_\omega \alpha_\omega, \tag{2}$$

where A is a constant determined by the selected conditions of the optical system and the measuring instruments. By applying Wien's radiation law, $R^0_\omega = B\exp(-\boldsymbol{h}c\omega/\boldsymbol{k}T)$, to Eq. 2, the following relation can be obtained:

$$I_\omega/\alpha_\omega = C(\omega)\exp\left(-\frac{\boldsymbol{h}c\omega}{\boldsymbol{k}T}\right), \tag{3}$$

where C is a coefficient which is variable with the wave number but which is independent of the temperature, and where $\boldsymbol{h}$, c, and $\boldsymbol{k}$ are Planck's constant, the light velocity, and Boltzmann's constant respectively. Therefore, for the thermal radiation, a plot of $\log(I_\omega/\alpha_\omega)$ vs. $1/T$ would give a straight line, the slope of which corresponds to $-\boldsymbol{h}c\omega/\boldsymbol{k}$.

In the actual measurement, the monochromator allows a band pass of several angstrom, and, hence, a certain number of spectral lines reach the photomultiplier. Accordingly, the observed intensity, I, is a sum of the intensity of each line; namely:

$$I = \sum_i I_i \tag{4}$$

On the assumption that, for a narrow range of wave numbers, the right hand side of Eq. 3 may be represented approximately by the value for the average wave number, ω_{av}, the following relation can be obtained from Eqs. 3 and 4:

$$\frac{I}{\sum_i \alpha_i} = C(\omega_{av})\exp\left(-\frac{\boldsymbol{h}c\omega_{av}}{\boldsymbol{k}T}\right) \tag{5}$$

Thus, the plot of $\log(I/\sum_i \alpha_i)$ vs. $1/T$ gives a check on whether the radiation is thermal or chemiluminesent.

As we measure the spectral-line emission, the radiancy for the isolated spectral line, R_L, must be used rather than R_ω, which refers to the radiancy at wave number ω, in the calculation of emissivities by means of Eq. 5. Taking into account the natural-line-, the collision-, and the Doppler-broadening effects, the following relation is valid[8]:

$$\frac{R_L(\ln 2)^{1/2}}{2R^0{}_\omega b_D} = \frac{1}{2}\int_{-\infty}^{\infty}[1-\exp(-P_{|\xi|}X)]\,d\xi,$$

where;

$$P_{|\xi|} = P'\left(\frac{a}{\pi}\right)\int_{-\infty}^{\infty}\frac{\exp(-y^2)}{a^2+(\xi-y)^2}\,dy, \tag{7}$$

$$P' = \frac{S}{\omega_0}\left(\frac{mc^2}{2\pi\boldsymbol{k}T}\right)^{1/2} = \frac{S}{b_D}\left(\frac{\ln 2}{\pi}\right)^{1/2}, \tag{8}$$

$$a = \frac{(b_N+b_C)}{b_D}(\ln 2)^{1/2}, \tag{9}$$

$$\xi = \frac{\omega-\omega_0}{\omega_0}\left(\frac{mc^2}{2\boldsymbol{k}T}\right)^{1/2} = \frac{\omega-\omega_0}{b_D}(\ln 2)^{1/2} \tag{10}$$

and where b_N, b_C, and b_D refer to the natural line-, the collision-, and the Doppler-broadening respectively; where S refers to the integrated absorption, a, to the line-shape parameter, and ω_0, to the wave number at the line center and where m is the mass of electrons. All these quantities can be estimated from the experimental conditions; accordingly, P can be numerically calculated by using one of several approximate expressions of Eq. 7.[7,8]

However, the results of the computations of these approximate formulae have been conveniently summarized[9] in the "curves of growth," where the dimensionless parameter, $R_L(\ln 2)^{1/2}/2b_D R^0_{\omega_0}$, is plotted against $\log(10.6P'X)$ for various values of the line-shape parameter, a. Therefore, the emissivity for each spectral line, R_L/R^0_ω, can be estimated from the curves of growth.

Results and Discussion

Figure 1 shows profiles of the ultraviolet radiation of OH radicals due to the $^2\Sigma^+ \rightarrow {}^2\Pi$ transition, and of the ultraviolet absorption of ammonia at 2245 Å,[7]

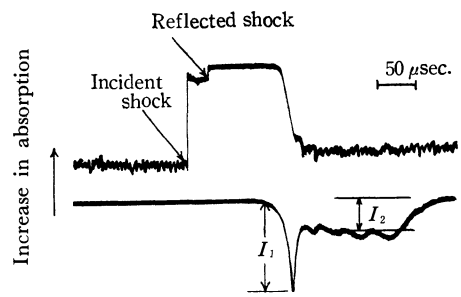

Fig. 1. Typical, oscillogram; upper trace shows NH_3 absorption measured at 2245 Å and lower trace OH emission at 3067 Å. Composition of gas mixture, Ar 90% - NH_3 6% - O_2 4%; initial pressure, 60.1 mmHg; incident shock velocity, 985.8 m/sec.; reflected shock temperature, 1930°K; equilibrium pressure, 4.74 atm.

which have been obtained by shock-heating mixtures of ammonia and oxygen diluted in argon to 1930°K. These profiles are essentially the same for all the experiments: the intensity of OH emission rises steeply, after an induction period, to a sharp maximum; there follows an approximately exponential decay to 1/4—1/8 the level of the maximum, and then the intensity remains at this level for a period varying from 100 μsec. for the strong shock (T_5=1980°K) to 500 μsec. for the weak (T_5=1650°K), until finally it falls to zero emission.

We were more interested in the weak emission, I_2, than in the strong emission, I_1, because, so far as we know, no paper has yet been published on

9) A. C. G. Mitchell and M. W. Zemansky, "Resonance Radiation and Excited Atoms," Cambridge at University Press, Cambridge (1961), p. 132.

TABLE I. VALUES OF SPECTRAL EMISSIVITIES ESTIMATED FROM CURVES OF GROWTH
(Mixture, Ar 90% - NH_3 6% - O_2 4%; initial pressure, 55.0 mmHg; incident shock speed, 999.6 m./sec.; equilibrium temperature, 2785°K; equilibrium pressure, 4.550 atm.; a,[a] 0.735; b_D,[b] 0.1494 cm^{-1})

Line	ω, cm^{-1}	J''[c]	S_J[d]	log $(10.6P'X)$[e]	$\frac{R_L(\ln 2)^{1/2}}{2b_DR_\omega^0}$	α_i[f]
R_1^7	32626	$7^1/_2$	26.9	1.59	1.97	0.707
R_1^{11}	625	$11^1/_2$	43.7	1.62	2.07	0.743
R_1^6	618	$6^1/_2$	22.7	1.57	1.93	0.693
R_1^{12}	616	$12^1/_2$	47.8	1.63	2.09	0.750
R_1^5	607	$5^1/_2$	18.4	1.55	1.86	0.668
R_1^{13}	603	$13^1/_2$	51.9	1.63	2.09	0.750
R_1^4	593	$4^1/_2$	14.2	1.52	1.80	0.646
R_2^{10}	589	$9^1/_2$	37.0	1.63	2.09	0.750
R_2^9	587	$8^1/_2$	32.9	1.63	2.09	0.750
R_1^{14}	586	$14^1/_2$	56.0	1.63	2.09	0.750
R_2^{11}	586	$10^1/_2$	41.0	1.63	2.09	0.750
R_2^8	582	$7^1/_2$	28.8	1.62	2.07	0.743
R_2^{12}	579	$11^1/_2$	45.1	1.64	2.14	0.768
R_1^3	578	$3^1/_2$	10.1	1.46	1.64	0.589
R_2^7	573	$6^1/_2$	24.8	1.61	2.07	0.743
R_2^{13}	567	$12^1/_2$	49.1	1.64	2.14	0.768
R_1^{15}	565	$15^1/_2$	57.2	1.62	2.07	0.743
R_1^2	560	$2^1/_2$	6.1	1.37	1.40	0.502
R_2^6	559	$5^1/_2$	20.7	1.60	2.00	0.718

a) Calculated from the empirical formula[10]: $a=450p/T$, where p is in atm., and T in degrees Kelvin.
b) Calculated from the equation[8]: $b_D=(2\boldsymbol{k}T\boldsymbol{N}\ln 2/Mc^2)^{1/2}\omega_0$, where $\boldsymbol{k}$, $\boldsymbol{N}$, M and c refer to Boltzmann's constant, Avogadro's number, molecular weight of OH, and velocity of light respectively; the averaged value of 32590 cm^{-1} was used as ω_0.
c) Total angular momentum of lower state.
d) Line strength of Ref. 11, Table IV.
e) Calculated from the relation[12]: $10.6P'X=23.1S_J/(2J''+1)$.
f) Calculated from the relation $\alpha_i=\frac{R_L}{R_\omega^0}$.

this emission. Thus, we tried to identify the nature of I_2 by the method described above; measurements were mainly made of two mixture (Ar 90% - NH_3 6% - O_2 4% and Ar 90% - NH_3 4% - O_2 6%) which had been investigated previously.[4]

Since the slit width of the monochromator allowed a band pass from 3064 to 3070 Å, nineteen spectral lines of R_1 and R_2 branches of (0, 0) band in the $^2\Sigma^+\rightarrow{}^2\Pi$ transition were regarded as contributing to the intensity of emission; the satellite branches, R_{21} and S_{21}, were neglected because of their weakness compared with R_1 and R_2. The values of emissivities calculated for one set of experimental condition are presented in Table I. The equilibrium temperature and pressure[13] have been used in the calculation, since the majority of the ammonia (more than 95%) has reacted before I_2 appears, as is shown in Fig. 1; accordingly, the reaction system can be considered to be close to the equilibrium condition.

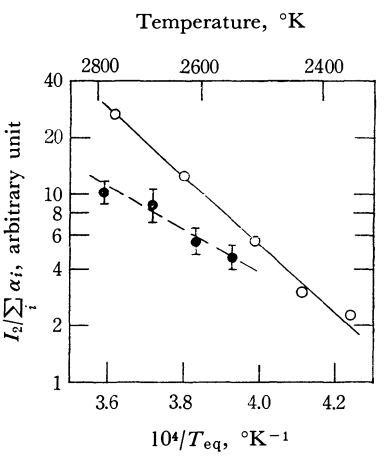

Fig. 2. Plot of log (I_2/α_i) against reciprocal temperature. Open circles represent data obtained for mixture of 90%Ar, 4%NH_3, and 6%O_2, and solid circles for mixture of 90%Ar, 6%NH_3, and 4%O_2.

10) W. E. Kaskan, *J. Chem. Phys.*, **31**, 944 (1959).
11) G. H. Dieke and H. M. Crosswhite, "The Ultraviolet Bands of OH," Bumblebee Rept. No. 86, The Johns Hopkins University, 1948.
12) T. Carrington, *J. Chem. Phys.*, **31**, 1243 (1959).
13) We are greatly indebted to Prof. W. C. Gardiner, Jr. of University of Texas for the equilibrium-state calculation.

The temperature dependence of the intensity of emission is shown in Fig. 2 as a plot of $\log(I_2/\sum_i \alpha_i)$ vs. $1/T$; the temperature coefficients are 56 and 82 kcal./mol., less than the quantity needed for the thermal excitation of OH ($^2\Pi$).

The dependence of the intensity of I_2 upon the equilibrium concentration of OH, H, O_2 and H_2 was studied by using several mixtures presented in Table I of the previous paper[7] (Part II of this series).

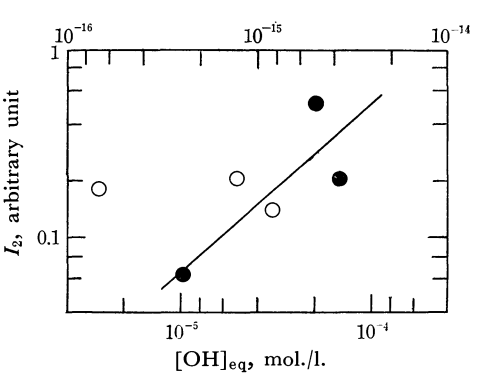

Fig. 3. Intensity of OH emission against equilibrium concentration of OH (open circles) and against the products of equilibrium concentration of H, O_2 and H_2 (solid circles). Slope of the solid line is about 0.9 by inspection.

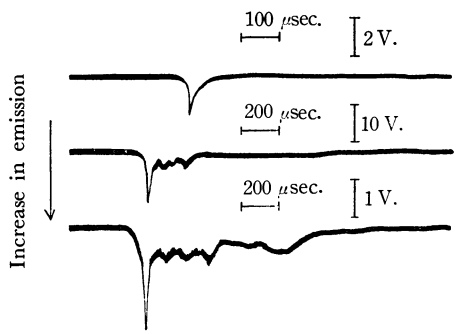

Fig. 4. Profiles of OH emission observed in oxidations of other fuels.
Top trace: Ar 90% - H_2 6.67% - O_2 3.33%; initial pressure, p_1, 100.3 mmHg; incident shock velocity, w_1, 722.3 m./sec.; reflected shock temperature, T_5, 1150°K; reflected shock pressure, p_5, 2.60 atm.
Middle trace: Ar 90% - C_2H_2 4% - O_2 6%; p_1, 100.3 mmHg; w_1, 716.0 m./sec.; T_5, 1135°K; p_5, 2.82 atm.
Bottom trace: Ar 90% - CH_4 3% - O_2 7%; p_1, 79.9 mmHg; w_1, 903.6 m./sec.; T_5, 1690°K; p_5, 4.30 atm.

It was found that the intensity of I_2 is independent of the equilibrium OH concentration $[OH]_{eq}$ over the concentration range from 3.2×10^{-5} to 3.2×10^{-6} mol./l., but that it is approximately proportional to $[H]_{eq}[H_2]_{eq}[O_2]_{eq}$ when $[OH]_{eq}$ is kept almost constant, as is shown in Fig. 3.

For purposes of comparison, measurements were made of the OH emission in reactions of hydrogen, methane, and acetylene with oxygen. The profiles obtained are shown in Fig. 4. Although the profiles for the oxidation of methane and acetylene are similar to those for ammonia oxidation, that for the oxidation of hydrogen is very different from the others; no weak emission following a spike can be observed.

The temperature coefficients of the intensity of OH emission, I_2, obtained in Fig. 2 for both mixtures are definitely less than that required for the termal excitation:

$$OH(^2\Pi) + M \rightarrow OH(^2\Sigma^+) + M \quad -93.5\,\text{kcal./mol.} \qquad (I)$$

indicating that the excited OH radicals are produced by chemical reaction processes. This is supported also by the fact that the intensity of I_2 is independent of the ground-state OH concentration.

The proportionality of I_2 to $[H]_{eq}[H_2]_{eq}[O_2]_{eq}$ seems to suggest that the following excitation mechanism is valied:

$$H + O_2 + H_2 \rightarrow OH^* + H_2O \qquad (II)$$

This mechanism has been proposed by Belles and Lauver[6] for the OH* chemiluminescence observed during the induction period of the hydrogen-oxygen reaction. The absence of I_2 in the hydrogen-oxygen reaction, as is shown in Fig. 4, suggests that most of the hydrogen has been used up before the appearance of I_2 emission. On the contrary, considerable amounts of hydrogen are produced near the end of the ammonia oxygen reaction (order of 10^{-4} mol./l., according to equilibrium calculation); therefore, Reaction II can be considered to be operating during the period when I_2 is observed. A similar explanation may serve for the acetylene-oxygen and methane-oxygen reactions. However, Reaction II is not the only possibility. Further studies will be required to elucidate a detailed mechanism for this chemiluminescence.

The authors wish to express their thanks to Dr. W. C. Gardiner, Jr., and Dr. Soji Tsuchiya for their helpful discussions and criticisms, and to Messrs. Kazutoshi Sugiyama and Akio Sawa for their assistance in the experiment.

BULLETIN OF THE CHEMICAL SOCIETY OF JAPAN VOL. 39 2613—2615 (1966)

A Comparison of the Radiation-Induced Reaction with Photochemical and Thermal Reactions. I. The Radiation-Induced Isomerization of *o*-Nitrobenzaldehyde in the Solid State

By Akira SUGIMORI, Kōichi NAKATA and Hachiro HIRAI

Department of Chemistry, Faculty of Science and Technology, Sophia University, Chiyoda-ku, Tokyo

(Received May 2, 1966)

The radiation-induced reaction of *o*-nitrobenzaldehyde in the solid state was investigated. Isomerization to *o*-nitrosobenzoic acid preferentially took place. This suggests that the γ-ray irradiation produces effectively the excited *o*-nitrobenzaldehyde which is identical with that produced by ultraviolet irradiation.

The radiation-induced reaction has often been compared with the photochemical reaction using rather simple compounds.[1-5] However, only a few studies have been carried out with complex compounds.

The photochemical reaction of *o*-nitrobenzaldehyde was studied by Ciamician and Silber,[6] and by Leighton and Lucy.[7] These studies showed that the following isomerization proceeds intramolecularly both in solid state and in a solution, with no side reaction.

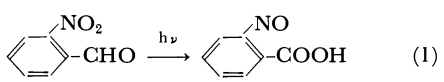

(1)

This system is considered to be suitable for the comparison of radiation-induced reaction with the photochemical reaction from the following reasons. First, little kinetical consideration is needed for the interpretation of the reaction because of the intramolecular rearrangement. Secondly, the photochemical reaction of *o*-nitrobenzaldehyde has already been elucidated, not only with a solution but also with the solid state. Direct excitation by ionizing radiation can not be expected with a solution.

Results and Discussion

The results of the analysis of the gaseous products from the γ-ray-irradiated solid *o*-nitrobenzaldehyde are listed in Table I.

Table I. Gaseous products from the γ-ray irradiated *o*-nitrobenzaldehyde

i) Condition of irradiation
Dose Rate : 3.3×10^{19} eV./g.hr.
Total Dose : 2.0×10^{22} eV./g.

ii) G(total gaseous products)$=0.2$

Component	
CO_2	82%
CO	16%
H_2	2%
NO_2, NO, N_2O	—

No oxides of nitrogen (N_2O, NO and NO_2) were observed to be formed. The evolved gas consisted of carbon dioxide, carbon monoxide, and a small amount of hydrogen. However, the yields of the gaseous products were small and the G value for the total gaseous products was found to be 0.2.

In contrast with the small G value of the radiolytic decomposition, the radiation-induced isomerization of *o*-nitrobenzaldehyde to *o*-nitrosobenzoic acid proceeds in a highly efficient manner. The results of the analyses of the γ-ray-irradiated *o*-nitrobenzaldehyde are shown in Table II.

Table II. The analysis of the γ-ray irradiated *o*-nitrobenzaldehyde

Run	1	2	3
Absorbed radiation dose (eV./g.)	5.0×10^{21}	2.1×10^{22}	2.4×10^{22}
Purity of the sample (%)	97.7	97.7	97.7
Formed *o*-nitroso-benzoic acid (%)	6.6	34.1	37.6
Unreacted *o*-nitro-benzaldehyde (%)	91.0	62.3	56.8
Side reaction (%)	0.1	1.3	3.3

1) G. J. Mains and A. S. Newton, *J. Phys. Chem.*, **65**, 212 (1961).
2) H. A. Dewhurst, ibid., **63**, 813 (1959).
3) R. B. Cundall and P. A. Griffith, *Discussions Faraday Soc.*, **36**, 111 (1963).
4) M. Katayama, J. C. Whitmer and C. N. Trumbore, *J. Am. Chem. Soc.*, **84**, 4025 (1962).
5) A. Scala and P. Ausloos, *J. Phys. Chem.*, **70**, 260 (1966).
6) G. Ciamician and P. Silber, *Ber.*, **34**, 2040 (1901).
7) P. A. Leighton and F. A. Lucy, *J. Chem. Phys.*, **2**, 760 (1934).

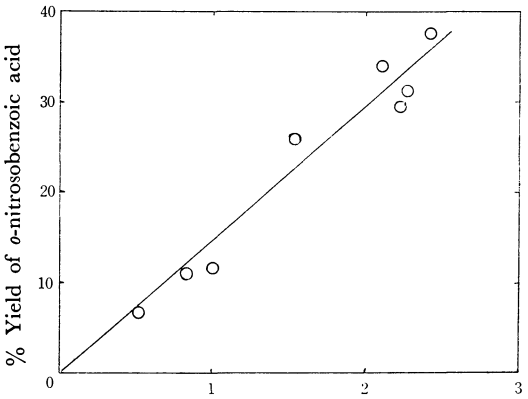

Absorbed radiation dose ($\times 10^{22}$ eV./g.)

Fig. 1. Relation between the yield of *o*-nitrosobenzoic acid and the absorbed radiation dose.

The formation of *o*-nitosobenzoic acid is plotted against the absorbed radiation dose in Fig. 1.

As is shown in Table II, the formation of *o*-nitrosobenzoic acid can explain more than 90% of the reaction of *o*-nitrobenzaldehyde. At a rather high dose of irradiation, where 35.4% of the original *o*-nitrobenzaldehyde was consumed (Run 2 in Table II), the side reaction was only 3.8% of the isomerization.

A linear relationship was observed between the yield of *o*-nitrosobenzoic acid and the absorbed radiation dose in the range where the conversion was below 40%. The *G* value for the *o*-nitrosobenzoic acid formed is found from Fig. 1 to be 5.8.

Since the *G* value of the main reaction is 5.8, the *G* value of the side reaction can be estimated as 0.2—0.5. Most of the side reaction may be explained by the reaction that gives rise to the formation of gaseous products, because the *G* value for the gaseous products is nearly equal to the *G* value for the side reaction. Judging from the composition of the gaseous products, the side reactions may be:

(2)

(3)

The reactions to give oxides of nitrogen and hydrogen are negligible.

Since carbon dioxide is considered to come from the secondary decomposition of the initially-produced *o*-nitrosobenzoic acid, the only side reaction at the initial stage is the decarbonylation reaction (reaction 3). Reaction 3 plays a minor part in the side reactions (it comprises 1/6 of the total side reactions), so the side reactions at the initial stage may be smaller than as evaluated above.

These facts indicate that the γ-ray irradiation gives rise preferentially to the isomerization of *o*-nitrobenzaldehyde to *o*-nitrosobenzoic acid.

It can be said that the identity of the reaction in such a special case as the isomerization of *o*-nitrobenzaldehyde to *o*-nitrosobenzoic acid indicates the identity of the reaction mechanism and the identity of the excited molecules included in the reaction. In the radiation-induced reaction of *o*-nitrobenzaldehyde, the same excitation as that in photochemical reaction is preferentially produced. Analogous results have been obtained in the radiolysis of oxalato metal complexes.[8] These compounds have an efficient reaction path for the absorption of light (the supply of relatively low energy), and the radiation-induced reaction occurs selectively and with a high effciency through this reaction path.

As to the yields of the isomerization by light and by ionizing radiation, the following explanation may hold.

Leighton and Lucy showed that the quantum yield of the isomerization is 0.5 for ultraviolet light of 3660 Å (3.4 eV.), 3130 Å (4.0 eV.), and 2537 Å (4.4 eV.).[7] Therefore, the supply of at least about 7 eV. of light energy is necessary for each *o*-nitrosobenzoic acid molecule. On the other hand, the *G* value of the isomerization in γ-ray irradiation was 5.8. This means that 17 eV. of radiation energy is required for the production of each *o*-nitrosobenzoic acid molecule. This suggests that most of the radiation energy absorbed was lost in the form of heat without bringing the molecules of *o*-nitrobenzaldehyde to excitation.

Experimental

Materials.—Commercially-available *o*-nitrobenzaldehyde (guaranteed reagent-grade; Tokyo Kasei Co.) was used without further purification. The purity of the sample, which was determined by the gravimetric analysis to be 2, 4-dinitrophenylhydrazone, was 97.7%. *o*-Nitrosobenzoic acid was produced by the ultraviolet irradiation of *o*-nitrobenzaldehyde in a benzene solution.[6]

Gamma-Irradiation.—One to two grams of *o*-nitrobenzaldehyde were sealed in a tube with a break-off seal in a vacuum. The samples were irradiated by Co-60 γ-rays in the irradiation facility, equipped with a Co-60 source of 16000 curies, at the Japan Atomic Energy Research Institute.

Gaseous Products.—The break-off seal of the tube containing the γ-ray-irradiated *o*-nitrobenzaldehyde was cut in the vacuum system, the volume of which had been measured in advance. The pressure increase in the vacuum system permitted us to determine the quantity of gas evolved. Some of the gaseous products were analyzed by the mass spectrometric method. A CEC Model 103C mass spectrometer was used. The quantity of CO_2 was estimated from the peak at $m/e=44$. The ratio of CO to CO_2 was evaluated from the peaks.

8) A. Sugimori, This Bulletin, **38**, 2583 (1966).

at $m/e=12$ and 44. The hydrogen content was estimated from the peak at $m/e=2$. The lack of the peak at $m/e=30$ indicates the absence of N_2O, NO and NO_2.[9]

The Determination of *O*-Nitrosobenzoic Acid.—Gamma ray-irradiated *o*-nitrobenzaldehyde was treated three times with each 5-ml. portion of benzene, and the benzene-insoluble substance was collected on a sintered glass filter. It was dried at 80°C and weighed. The substance was identified as *o*-nitrosobenzoic acid from its infrared spectra (Fig. 2).

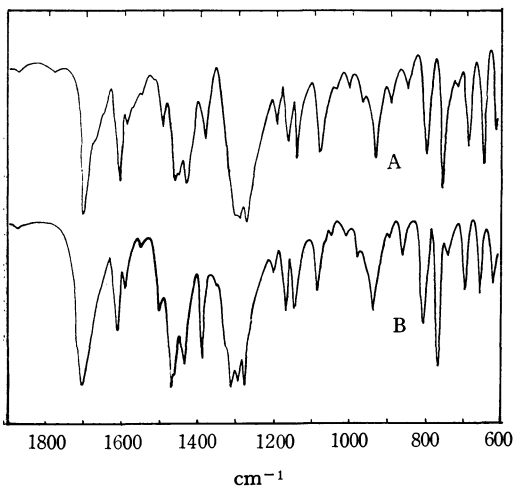

Fig. 2. Infrared spectra of *o*-nitrosobenzoic acid (A) and the benzene-insoluble substance from γ-irradiated *o*-nitrobenzaldehyde (8.0×10^{21} eV./g.) (B). Nujol mull method.

The Determination of the Residual *O*-Nitrobenzaldehyde.—Benzene-soluble portions of the γ-ray-irradiated *o*-nitrobenzaldehyde were collected. The solvent was evaporated by leaving the solution to stand at room temperature for several days in the dark in order to protect it from photo-isomerization. Figure 3 shows the infrared spectra of the benzene-soluble substance from the *o*-nitrobenzaldehyde irradiated at 8.1×10^{21} eV./g. of the absorbed radiation dose (10.7% of conversion).

All of the bands except that at 1785 cm^{-1} can be accounted for by *o*-nitrobenzaldehyde.

All the infrared spectra of γ-ray-irradiated *o*-nitrobenzaldehyde (Fig. 4) can be explained by the superposition of those of *o*-nitrobenzaldehyde and *o*-nitrosobenzoic acid, except for the weak band at 1785 cm^{-1}, which probably came from side reaction.

The quantitative analysis of *o*-nitrobenzaldehyde was carried out by gravimetric analysis in the form of 2, 4-dinitrophenylhydrazone. The residue, after the evaporation of benzene, was dissolved in ethanol and treated with an acidic solution of 2, 4-dinitrophenylhydrazine.

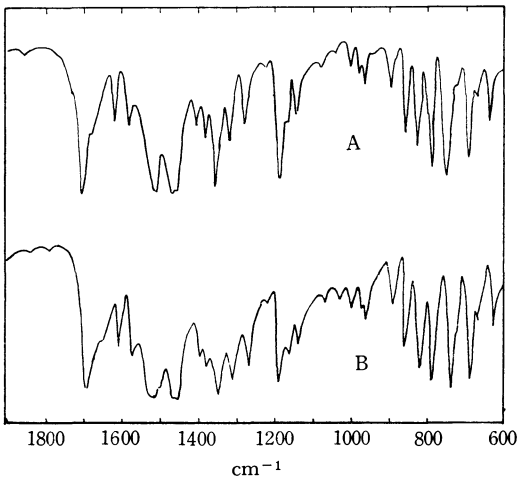

Fig. 3. Infrared spectra of *o*-nitrobenzaldehyde (A) and the benzene-soluble substance from γ-irradiated *o*-nitrobenzaldehyde (8.1×10^{21} eV./g.) (B). Nujol mull method.

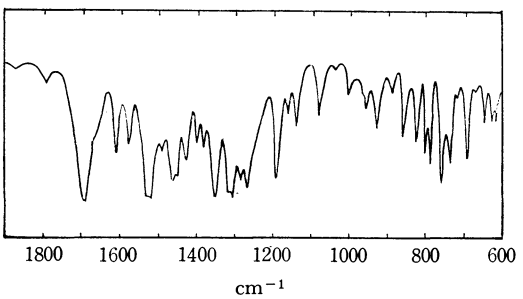

Fig. 4. Infrared spectra of γ-irradiated *o*-nitrobenzaldehyde (2.1×10^{22} eV./g.). Nujol mull method.

The 2, 4-dinitrophenylhydrazone thus formed was then collected on a sintered glass filter and weighed.

Annealing.—It was shown that the prolonged standing of the irradiated sample caused a secondary reaction of the initial product. A sample which had been stored for 8 months after a 1.5×10^{22} eV./g. irradiation showed a higher yield of the side reaction (31% against the isomerization), while the samples which were analyzed soon after irradiation gave side reactions of below 10% as is shown in Table II. The infrared absorption at 1785 cm^{-1} cited above is due to this side reaction.

The authors wish to thank Professor Yoshiyuki Urushibara, Dr. Shin-ichi Ohno and Dr. Akio Hosaka for their helpful discussions. Thanks are also due to Dr. Akibumi Danno and the members of the Cobalt-60 Irradiation Facility of Japan Atomic Energy Research Institute for γ-irradiation and Mr. Hitoshi Hashimoto for mass spectrometric analysis.

9) "Catalog of Mass Spectral Data," American Petroleum Institute Res. Project No. 44, Serial No. 96, 1218 and 95.

BULLETIN OF THE CHEMICAL SOCIETY OF JAPAN VOL. 39 2616—2624 (1966)

Unit Cell Metastable-form Constants of Various Phthalocyanines

By Michio Ashida,* Natsu Uyeda and Eiji Suito

Institute for Chemical Research, Kyoto University, Takatsuki, Osaka

(Received May 2, 1966)

Thin films of phthalocyanine compounds formed on cleaved surfaces of muscovite by the vacuum-condensation method showed well-defined single-directional orientation when their substrates were preheated at 300°C for one hour and then kept at 150°C. Their electron diffraction patterns were fiber diagrams, the fiber period of which coincided with the unit-cell length of the b-axis of the individual compounds. When the substrates were preheated at 400°C for one hour and then kept at 150°C, the films formed on the muscovite surface were composed of discrete crystals with a different orientation. Electron-diffraction patterns from the films revealed that the b-axis of the crystal was inclined to the substrate surface. The cross-grating patterns of the (*h*0*l*) plane were obtained when the inclination of the films was properly adjusted to the incident beam. The unit-cell constants of platinum-phthalocyanine vacuum-condensed on muscovite were revealed to be as follows with the monoclinic space group $C2/c$: $a=23.18$ Å, $b=3.818$ Å, $c=23.84$ Å, and $\beta=91.9°$. Films of Cu-, Co-, Fe-, Ni- and metal-free phthalocyanines exhibited an orientation similar to that of the platinum derivative. High-resolution electron-diffraction patterns revealed that all the compounds assumed a conspicuous isomorphism with one another and occurred in the metastable forms of their dimorphs.

The polymorphism of some phthalocyanine derivatives was very briefly described by German investigators[1] for the first time. Later, Hamm and van Norman[2] examined the microcrystals of copper-phthalocyanine by electron microscopy and identified the dimorphs with two different characteristic electron-diffraction patterns. Susich[3] found the polymorphs of metal-free phthalocyanine by X-ray diffraction. Wiswall[4] also referred to polymorphic pairs of copper-, nickel- and zinc-phthalocyanines. Ebert and Gottlieb[5] reported the differences in infrared absorption spectra and X-ray diffraction diagrams due to the dimorphs with respect to copper-, metal-free, cobalt-, nickel- and zinc-phthalocyanines. Furthermore, Karasek and Decius[6] observed polymorphic crystalline states of metal-free phthalocyanine by depositing a film of the material directly onto a highly-polished and relatively cool rock salt at a pressure of 10^{-5} mmHg.

Robertson[7,8] and Robertson and Woodward[9,10] extensively investigated the crystal structures of the stable forms of phthalocyanine and its metal derivatives by X-ray diffraction using single crystals which had been prepared by sublimation under a low pressure of carbon dioxide. On the other hand, the metastable forms of several phthalocyanine derivatives have been reported by many investigators, as has been mentioned above, but there is very little information available on the crystal data. The only report on the crystal data of the metastable forms was that on copper-phthalocyanine, determined by means of X-ray powder diffraction by Robinson and Klein.[11] Since the metastable form was obtained only as a fine powder, with a small tendency to form single crystals which were large enough, the accurate determination of the crystal data for the metastable form involves many difficulties when the ordinary method is used.

In a previous paper,[12] the present authors reported that films of phthalocyanine compounds vacuum-condensed on a cleaved face of muscovite epitaxialy grew when the substrate was maintained at a temperature of 150°C to 170°C. Since the films thus prepared was composed of crystals which assumed a well-defined orientation, an electron diffraction pattern obtained from the film showed a fiber or a single crystal diagram, from which the crystal axes and the cell dimensions might be

* Present address: Department of Industrial Chemistry, Faculty of Engineering, Kobe University, Nada-ku, Kobe.

1) P. B. Report, 700336, p. 7945.
2) F. A. Hamm and E. van Norman, *J. Appl. Phys.*, **19**, 1097 (1948).
3) G. Susich, *Anal. Chem.*, **22**, 426 (1950).
4) R. H. Wiswall, Jr., U. S. Pat. 2486351.
5) A. A. Ebert, Jr., and H. B. Gottlieb, *J. Am. Chem. Soc.*, **74**, 2806 (1952).
6) F. W. Karasek and J. C. Decius, ibid., **74**, 4716 (1952).
7) J. M. Robertson, *J. Chem. Soc.*, **1935**, 615.
8) J. M. Robertson, ibid., **1936**, 1195.
9) J. M. Robertson and I. Woodward, ibid., **1937**, 219.
10) J. M. Robertson and I. Woodward, ibid., **1940**, 36.
11) M. T. Robinson and G. E. Klein, *J. Am. Chem. Soc.*, **74**, 6294 (1952).
12) E. Suito, N. Uyeda and M. Ashida, *Nature*, **194**, 273 (1962).

determined with ease even though each crystal was very small. The present authors[13] also studied the orientation overgorwth of platinum-, copper- and zinc-phthalocyanines vacuum-condensed on muscovite by electron diffraction; they thus found that all three compounds showed a conspicuous isomorphism with one another and that copper- and zinc-phthalocyanines occurred in the metastable forms of their dimorphs. As for the metastable form of copper-phthalocyanine, the analysis of the electron diffraction pattern of the film revealed that the crystal data reported by Robinson and Klein[11] failed reasonably to explain the results on the film and that another, more appropriate crystal structure should be proposed instead. Honigmann et al.[14] studied the metastable form of copper-phthalocyanine and its chloroderivatives by X-ray diffraction and supported the present authors' proposition that the metastable form of copper-phthalocyanine was isomorphous with platinum-phthalocyanine.

When the depositing conditions were modified, another, different orientation occurred with the same metastable phase. These condensation methods were also extended to derivatives other than platinum-, copper- and zinc-phthalocyanines, which had previously been reported on. Using films which assumed two different kinds of orientation, the crystal data of the individual materials were estimated directly from the electron-diffraction pattern. In the present paper, the crystal data will be determined for the metastable forms of platinum-, copper-, cobalt-, iron-, nickel- and metal-free phthalocyanines with regard to the vacuum-condensed films by means of high-resolution electron diffraction.

Experimental

Materials.—Platinum-, copper- and metal-free phthalocyanines were supplied by the Sumitomo Kagaku Co. Cobalt-phthalocyanine was synthesized from phthalonitrile and anhydrous cobalt chloride, while iron-phthalocyanine was synthesized from phthalonitrile and anhydrous ferric chloride, by the method established by Barrett et al.[15] All of these materials were purified by repeated sublimation in a low-pressure stream of carbon dioxide at a temperature above 500°C. The products were obtained as small needle-like crystals, which were established as assuming the stable forms reported by Robertson.

The Preparation of Vacuum-condensed Films.—A 2×2 cm^2 cleaved sheet of muscovite was placed in a Pyrex glass tube, and then this tube was inserted in an electric furnace, as Fig. 1 shows. The purified material was sublimated from a conical-type heater of tungsten wire. The heater was placed in the part

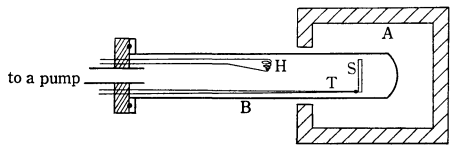

Fig. 1. Schematic diagram of appratus.
A: electric furnace, B: Pyrex glass tube
S: substrate mica sheet, T: thermocouple
H: tungsten heater (evaporation source)

of the tube protruding from the furnace because of the necessity of keeping the material from sublimation during the preliminary thermal treatment of muscovite. About 2 mg. of the material was condensed vertically onto a cleaved face of muscovite in a vacuum of 5×10^{-5} mmHg. The thickness of the films was estimated to be in a range from 500 Å to 900 Å. The rate of deposition was 20—30 Å/min. The specimen for an electron microscopy was prepared by the wet-stripping method after it had been reinforced by evaporated carbon film. Thalium chloride evaporated on phthalocyanine films was used as the standard specimen for the high-resolution diffraction work.

The Determination of Densities.—As the quantity of the material deposited on muscovite was too small for the density to be measured, powderly crystals of the metastable form prepared by the acid-paste method[16] were used in place of the sublimated films. The densities of the materials were determined by a 5% methyl alcohol displacement in a 25 ml. pycnometer.

Results

a) Platinum-phthalocyanine.—When muscovite was preheated at 300°C for one hour and held at 150°C, the film condensed on it was composed of laminar crystal strips which parallelly grew in a definite direction, as is shown in Fig. 2(a). An electron-diffraction pattern from the film shows the fiber structure shown in Fig. 2(b). The fiber axis coincides with the longitudinal direction of the crystals, and the fiber period is 3.81 Å.

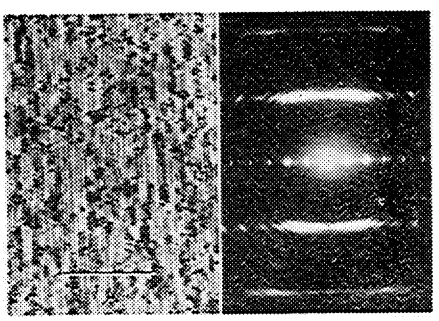

(a) (b)

Fig. 2. Electron micrograph (a) and electron diffraction pattern (b) of Pt-phthalocyanine film vacuum-condensed on muscovite which is preheated at 300°C and kept at 150°C.

13) N. Uyeda, M. Ashida and E. Suito, *J. Appl. Phys.*, **36**, 1453 (1965).
14) B. Honigmann, H. Lenne and R. Schrödel, *Z. Krist.*, **122**, 185 (1965).
15) P. A. Barrett, C. E. Dent and R. P. Linstead, *J. Chem. Soc.*, **1936**, 1719.
16) E. Suito and N. Uyeda, *Kolloid-Z.*, **193**, 97 (1963).

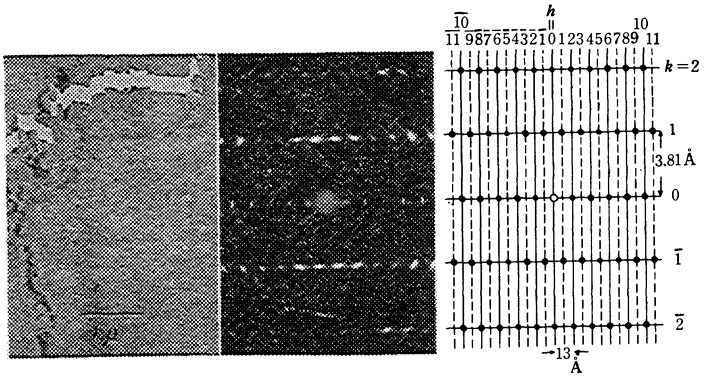

(a) (b)

Fig. 3. Electron micrograph (a) and electron diffraction pattern (b) of single crystal film of Pt-phthalocyanine and its schematic diagram (c).

On the equator, two sets of reflection spots simultaneously appeared, corresponding to an interplanar spacing of 13.1 Å and 11.9Å. As has been reported previously[13] the appearance of the two sets of equatorial reflection spots indicates that the film consists of at least two kinds of crystal strips with different lattice orientations. The crystal structure of platinum-phthalocyanine determined by Robertson has the following unit-cell dimensions with the monoclinic space group $P2_1/a$: $a=23.9$ Å, $b=3.81$ Å, $b=16.9$ Å, and $\beta=129.6°$. Since the fiber period obtained from the diffraction pattern showed a good coincidence with the unit lentgth of the b-axis, the b-axis of the crystal strips turned out to be parallel to the longitudinal direction. As for the two characteristic reflections on the equator, the spacings of 13.1 Å and 11.9 Å corresponded to the (001) and ($20\bar{1}$) planes respectively, planes which are almost perpendicular to each other and which share the b-axis as the zone axis. However, a closer observation of the electron diffraction pattern revealed that it was necessary to reconsider the designation of the crystal axes. A perfect single crystal was obtained in the part of the film prepared as above. Figs. 3(a) and (b) show respectively, an electron micrograph and electron diffraction pattern from the film. In Fig. 3(b), the maximum lattice period along the meridian is 3.81 Å, which is the same value as that of the fiber diagram. On the other hand, the period of 13.1 Å in the equatorial direction corresponded to 001 and its higher-order reflections, according to Robertson's assignment. This means that the diagram shows the reciprocal lattice plane with the index of $0kl$. However, when the reflection spots appearing on the lines of $k=1$ and 3 are taken into account, it is obvious that the period along the equator should take twice as long as that given by Robertson by adding the periods displayed to the broken lines in Fig. 3(c). If the equator is identified as the a* axis of the reciprocal lattice, then all the reflection spots in Fig. 3(b) may be indexed as in Fig. 3(c). The possible reflection is as follows: h is even in ($h00$), k is even in ($0k0$), and $k+k$ is even in ($hk0$).

When a muscovite substrate was preheated at 400°C for one hour and kept at 170°C, the film condensed on it was composed of discrete crystallites, as Fig. 4(a) shows. The electron-diffraction pattern in Fig. 4(b) is apparently a superposition of two identical diagrams, both composed of layered zones of reflection spots. The appearance of these layered zones in the individual diagrams is to be ascirbed to the position of the main-zone axes of the sublimated crystal, which tilts against the substrate face and consequently against the electron beam. The orientation will be described in detail in another report. However, it must be noted here that the crystallites are divided into

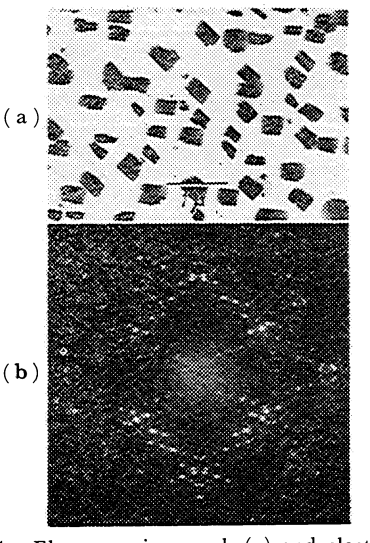

Fig. 4. Electron micrograph (a) and electron diffraction pattern (b) of Pt-phthalocyanine film vacuum-condensed on muscovite which is preheated at 400°C and kept at 170°C.

two groups, which can be defined by a plane of symmetry, normal with regard to the total film plane, as far as the lattice orientation is concerned. The b-axis stands somewhat obliquely to the film plane. Therefore, when the film is tilted against the incident electron beam so that the b-axis of the crystal becomes parallel to the beam, the intensity distribution of the reflection spots is symmetrized with respect to the point of origin, as is shown in Fig. 5. As the incident beam is

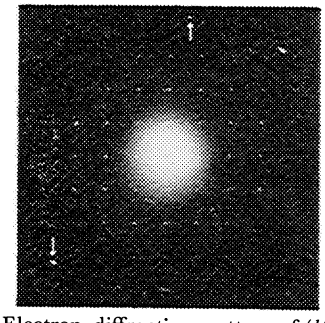

Fig. 5. Electron diffraction pattern of ($h0l$) plane of Pt-phthalocyanine obtained by tilting the film shown in Fig. 4.

parallel to the b-axis of the crystal, the diagram shows the reciprocal lattice points with the $h0l$ indices. Since the b-axis of the crystals taking another orientation does not become parallel to the incident beam, and since the unit length of the b* reciprocal axis is considerably longer than those of the a* and c* axes, the reflection from these crystals of another group gave rise to only a few extra spots, indicated with arrows in the figure. The cross-grating pattern consisted of two arrays of reflection spots, with periods of 13.1 Å and 11.9 Å, which cross each other at an angle of 88.1°. Since the interplanar spacings agreed with those obtained from the fiber diagram, both crystals were assigned the same structure. When the a* axis of the reciprocal lattice was associated with the period of 13.1 Å described above, the c* axis was to be ascribed to the other period, 11.9 Å. The unit lengths of a- and c-axes and the axial angle, β, were directly obtained from the pattern. The possible reflection was as follows: both h and l are even in ($h0l$). Although these possible reflections in ($h00$), ($0k0$), ($hk0$) and ($h0l$) appear in both space groups, C_s^4–C_c and C_{2h}^6–$C2/c$, it is well known that platinum-phthalocyanine is a planar molecule which has a center of symmetry. On the basis of these results, the unit cell constants were determined to be as given in Table I (1). As has been mentioned above, the new designation of the crystal axes was given by the substitution of (200) and (002) respectively for the (001) and ($20\bar{1}$) planes assigned by Robertson.

On the basis of such a transformation of the

Table I. Unit cell constants of Pt-phthalocyanine

	(1)	(2)	Cf. Robertson's data
a	26.18 Å	26.2 Å	23.9 Å
b	3.818 Å	3.81 Å	3.81 Å
c	23.84 Å	23.9 Å	16.9 Å
β	91.9°	95.1°	129.6°
Space group	$C_{2h}^6=C2/c$	$C_{2h}^6=C2/c$	$C_{2h}^5=P2_1/a$
Mols. per cell	4	4	2
d(calcd.)	1.96	1.97	1.97
d(found)	1.94	1.98	1.98

(1): Obtained from the crystal vacuum-condensed on muscovite,
(2): Correction of Robertson's data.

Table II. Interplanar spacings of Pt-phthalocyanine vacuum-condensed on muscovite

d(Å) (1)	I/I_0	(hkl)	d(Å) (2)	d(Å) (3)
13.12	vs.	200	13.09	13.1
11.99	s.	002	11.92	11.9
9.14	w.	$20\bar{2}$	8.965	9.19
8.43	w.	202	8.668	8.49
6.56	s.	400	5.545	6.56
5.96	s.	004	5.960	5.95
5.61	m.	$20\bar{4}$	5.495	5.60
4.62	w.	$40\bar{4}$	4.483	4.60
4.37	w.	600	4.363	4.37
4.19	vw.	$60\bar{2}$	4.143	4.21
4.01	vw.	602	4.054	4.00
3.78	m.	110	3.778	3.78
3.62	m.	$11\bar{2}$	3.607	3.61
3.41	m.	$11\bar{3}$	3.419	3.41
3.28	vw.	800	3.272	3.28
3.21	vw.	$31\bar{3}$	3.218	3.22
3.03	m.	$31\bar{4}$	3.035	3.03
2.99	vw.	314	2.999	2.99
2.95	m.	115	2.954	2.95
2.86	vw.	513	2.857	2.86
2.61	vw.	$71\bar{2}$, 316	2.609	2.61
2.52	vw.	117	2.524	2.52
2.46	w.	317	2.457	2.46
2.33	w.	$71\bar{5}$	2.353	2.33
2.17	vw.	119	2.164	2.17
2.11	vw.	$31\bar{9}$	2.126	2.11
1.99	w.	519	1.990	1.99
1.91	w.	020	1.909	1.91
1.85	vw.	023	1.86	1.86
1.76	w.	225	1.76	1.76
1.70	w.	226	1.70	1.70
1.65	vw.	426	1.65	1.65

(1): Observed values from the film vacuum-condensed on muscovite.
(2): Calculated values from the crystal data (1) in Table I.
(3): Calculated values from the crystal data (2) in Table II

crystal axes, the original crystal data reported by Robertson should be corrected as in Table I (2). When the values in the column (1) are compared with those in the column (2), the coincidence is fairly good except for the value of the axial angle, β. The interplanar spacings evaluated from the fiber diagram are given in Table II (1). Tables II (2) and (3) show the interplanar spacings calculated from the cell constants given in Tables I (1) and (2) respectively. In Table II, the values in the column (2) agreed with those in the column (1) except for sevsral spacings, which had the index of $(h0l)$. These discrepancies were apparently caused by the difference in the axial angle, β, which will be discussed in a latter section.

b) Copper-phthalocyanine.—In the case of copper-phthalocyanine, films showed a fiber structure similar to that of platinum-phthalocyanine when the substrate muscovite was preheated at 300°C for one hour and held at 150°C during the vacuum-deposition. Figures 6(a) and (b) show the electron micrograph and electron-diffraction pattern of the film respectively. The fiber period was 3.79 Å, and the two sets of equatorial reflections had periods of 13.0 Å and 11.9 Å in Fig. 6(b). Since these values were quite similar to those of the platinum derivative, the crystal of vacuum-condensed copper-phthalocyanine film was ac-accounted for in terms of the isomorph with the platinum derivative. Consequently, it seems reasonable to assign the fiber period and the two long periods on the equator for the principal axial lengths of copper-phthalocyanine in the same way as for the platinum derivative.

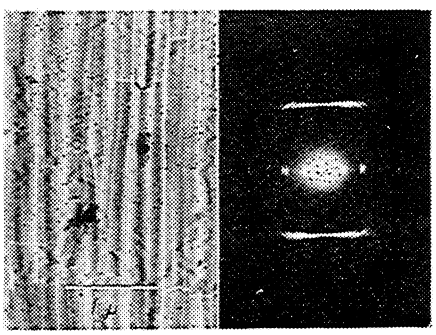

(a) (b)

Fig. 6. Electron micrograph (a) and electron diffraction pattern (b) of Cu-phthalocyanine film vacuum-condensed on muscovite which is preheated at 300°C and kept at 150°C.

Films sublimated onto muscovite which had been preheated at 400°C for one hour and held at 150°C were composed of many small crystals, as Fig. 7(a) shows. The electron-diffraction pattern from the film revealed that the b-axis of the crystals stood obliquely on the substrate face in a way similar to that of the platinum derivative. When

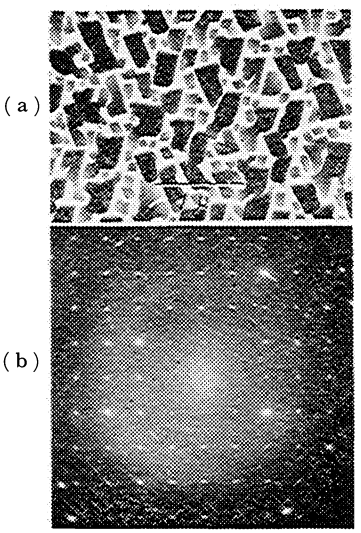

(a)

(b)

Fig. 7. Electron micrograph (a) of Cu-phthalocyanine film vacuum-condensed on muscovite which is preheated at 400°C and kept at 150°C and electron diffraction pattern (b) of $(h0l)$ plane of Cu-phthalocyanine obtained by tilting the film (a).

the film was tilted against the incident beam so that the b-axis of the crystals became parallel to it, the electron diffraction pattern gave the cross-grating pattern of the $(h0l)$ plane shown in Fig. 7(b). In the cross-grating pattern, the interplanar spacings with the periods of 12.9 Å and 11.9 Å, which cross each other at the angle of 89.6°, agreed with those of the two sets of reflections on the equator in the fiber diagram. Since the crystal was found to be the isomorph of the platinum derivative, the reflection spots should be indexed in the same way. Conseuqenctly, the cell constants of the copper-phthalocyanine vacuum-condensed on muscovite were determined to be as given in Table III (1). The interplanar spacings in Table IV (I) were obtained from the fiber diagram, while those in Table IV (2) were calculated from the cell constants given in Table III (1). The values in two series showed good

Table III. Unit ceel constants of metastable form of Cu-phthalocyanine

	(1)	(2)
	$a=25.92$ Å	$a=25.92$ Å
	$b=3.790$ Å	$b=3.790$ Å
	$c=23.92$ Å	$c=24.10$ Å
	$\beta=90.4°$	$\beta=90.4°$
Space group	$C^6_{2h}=C2/c$	$C^6_{2h}=C2/c$
Mols. per cell	4	4
d(calcd.)	1.62	1.605
d(found)		1.62

(1): Film vacuum-condensed on muscovite.
(2): Powder prepared by acid paste method.

agreement. It was found that the crystal vacuum-condensed onto muscovite was the same metastable form as that prepared by the acid-paste method.[16] The interplanar spacings in Table IV (3) were obtained from the latter crystal by X-ray diffractometry. As each value in this column agrees well with those in the columns (1) and (2), each spacing may reasonably be indexed as in the column (3). Reversely, on the basis of the index, the cell constants were calculated from the values in Table IV(3) to be as given in Table III(2). They showed good agreement with those obtained from the vacuum-condensed film.

c) Other Phthalocyanines. — Vacuum-condensed films of iron-, cobalt-, metal-free and nickel-phthalocyanines also assumed the single directional orientation similar to that of the platinum derivative, as Figs. 8(a), (b), (c) and (d) respectively show. Figures 9(a), (b), (c) and (d) are, respectively, the electron diffraction patterns from these films. The fiber periods of these diagrams were in the range from 3.5 to 3.8 Å, and two sets of reflection spots appeared on the equator at definite intervals for each set. The findings suggest

Table IV. Interplanar spacings of Cu-phthalocyanine vacuum-condensed on muscovite and prepared by acid paste method (in Å)

d(1)	I/I_0	d(2)	(hkl)	d(3)	I/I_0	d(4)
13.01	vs.	12.96	200	12.96	vs.	12.96
11.90	s.	11.96	002	12.05	vs.	12.05
			202	8.817	m.	8.816
6.48	s.	6.480	400			
5.99	m.	5.980	004			
5.64	w.	5.678	402	5.671	w.	5.681
			$20\bar{4}$	5.479	w.	5.478
4.32	m.	4.320	600			
			602	4.068	w.	4.067
4.01	w.	3.989	006			
3.77	w.	3.750	110			
3.68	m.	3.705	$11\bar{1}$	3.704	m.	3.70
3.59	m.	3.579	$11\bar{2}$	3.560	m.	3.580
3.40	m.	3.395	$11\bar{3}$			
3.33	m.	3.336	312	3.338	m.	3.338
3.22	m.	3.186	313	3.233	m.	3.233
2.97	m.	2.967	512			
2.93	w.	2.950	115			
2.85	w.	2.853	513			
2.59	w.	2.589	712			
2.52	w.	2.525	117			
2.41	w.	2.423	317			
1.89	w.	1.895	020			

(1): Observed values from the film vacuum-condensed on muscovite
(2): Calculated values from the crystal data (1) in Table III
(3): Observed values from powder prepared by acid paste method
(4): Calculated values from the crystal data (2) in Table III

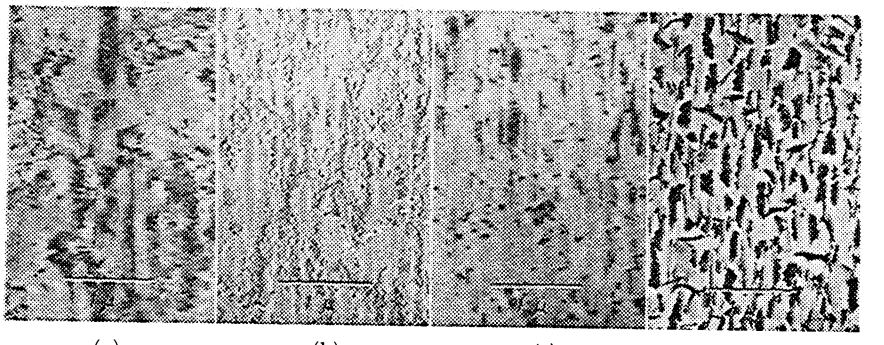

(a) (b) (c) (d)

Fig. 8. Electron micrographs of (a) Fe-, (b) Co, (c) metal-free and (d) Ni-phthaloyanine films vacuum-condensed on muscovite which is preheated at 300°C and kept at 150°C

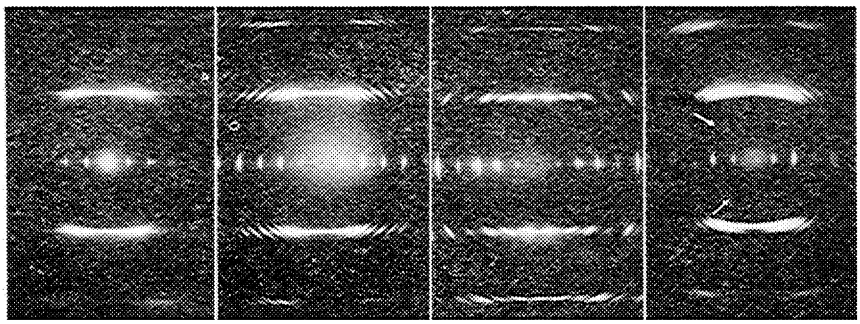

(a) (b) (c) (d)

Fig. 9. Electron diffraction patterns of (a) Fe-, (b) Co-, (c) metal-free and (d) Ni-phthalocyanine films vacuum-condensed on muscovite which is preheated at 300°C and kept at 150°C.

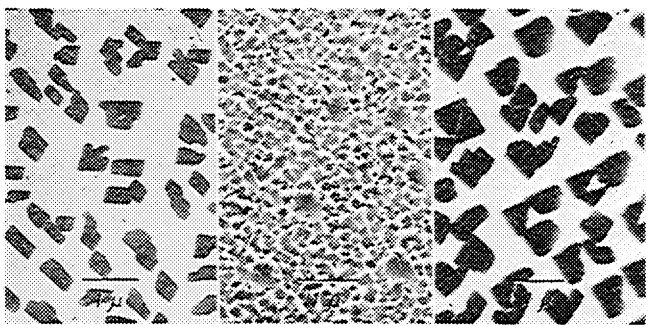

(a) (b) (c)

Fig. 10. Electron micrographs of (a) Fe-, (b) Co- and (c) metal-free phthalocyanine films vacuum-condensed on muscovite which is preheated at 400°C and kept at 150°C.

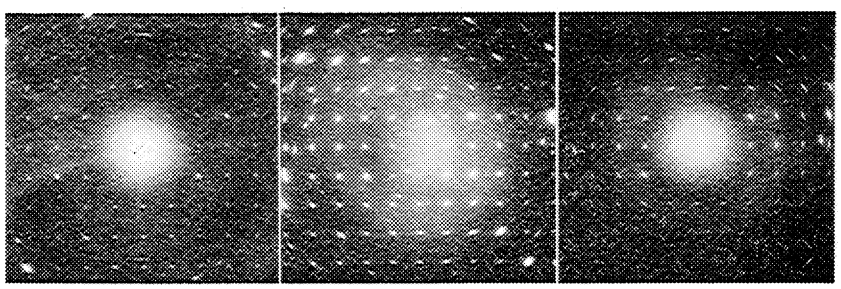

(a) (b) (c)

Fig. 11. Electron diffraction patterns of ($h0l$) plane of (a) Fe-, (b) Co- and (c) metal-free phthalocyanines obtained by tilting the films shown in Fig. 10, respectively.

not only that all four compounds occur in the metastable forms of their dimorphs, but also that they are conspicuously isomorphic with the platinum derivative. Table V shows the interplanar spacings evaluated from these fiber diagrams.

When the substrate muscovite was preheated at 400°C for one hour and then maintained at a temperature of 150°C to 200°C for the deposition, the films of iron-, cobalt- and metal-free phthalocyanines were composed of small crystals, the b-axis of which stood obliquely on the substrate face, as Figs. 10(a), (b) and (c), respectively, show. The cross-grating patterns of their ($h0l$) planes were obtained from the films exhibited in Figs. 11(a), (b) and (c) when these films were tilted against the incident beam in a way similar to that used with the platinum derivative. The unit lengths of the b-axes of these phthalocyanines were obtained from the fiber diagrams, while the unit lengths of the a- and c-axes and the axial angle, β, were determined from the cross-grating patterns. The unit cell constants were determined to be as given in Table VI for the metastable forms of these phthalocyanines; in the table the unit cell constants of platinum- and copper-phthalocyanines are again reproduced for the sake of reference. When the

TABLE V. INTERPLANAR SPACINGS OF Fe-, Co-, Ni- AND METAL-FREE PHTHALOCYANINES VACUUM-CONDENSED ON MUSCOVITE

	Fe-Pc			Co-Pc			H_2-Pc			Ni-Pc		
(*hkl*)	*d*(o)*	*I*	*d*(c)**	*d*(o)	*I*	*d*(c)	*d*(o)	*I*	*d*(c)	*d*(o)	*I*	*d*(c)
200	13.1	vs.	12.95	12.9	vs.	12.94	13.1	s.	13.07	13.06	s.	13.07
002	12.5	vs.	12.05	12.6	vs.	12.04	11.9	vs.	11.98	12.12	vs.	12.13
202										8.54	w.	8.544
400	6.55	s.	6.535	6.47	s.	6.470	6.56	s.	6.535	6.56	m.	6.535
004	6.05	s.	5.990	6.27	s.	6.020	5.96	vs.	5.990	6.06	s.	6.065
$20\bar{4}$										5.68	m.	5.688
204										5.34	w.	5.334
600	4.34	m.	4.360	4.32	m.	4.311	4.35	m.	4.360	4.36	m.	4.357
006	4.13	vw.	3.993	4.18	w.	4.013	3.97	w.	3.993	4.05	m.	4.043
110	3.72	m.	3.726	3.72	m.	3.711	3.77	m.	3.774	3.77	m.	3.751
$11\bar{1}$				3.66	w.	3.668	3.73	w.	3.730	3.68	m.	3.713
$11\bar{2}$	3.58	m.	3.560	3.56	w.	3.547	3.61	s.	3.603	3.56	w.	3.571
310	3.49	s.	3.451	3.43	m.	3.439						
311	3.43	vw.	3.416									
$11\bar{3}$	3.39	vw.	3.380	3.36	vw.	3.369	3.42	s.	3.416			
800	3.25	vw.	3.267	3.25	vw.	3.235	3.25	vw.	3.267	3.24	s.	3.267
313	3.17	w.	3.171	3.15	w.	3.160	3.20	m.	3.210	3.19	s.	3.173
510	3.07	w.	3.046	3.05	w.	3.038				3.05	vw.	3.068
$11\bar{5}$	2.95	vw.	2.949	2.96	vw.	2.948	2.97	m.	2.967			
513	2.89	m.	2.848	2.88	w.	2.842	2.84	w.	2.864	2.82	w.	2.823
$71\bar{2}$	2.63	w.	2.578	2.58	vw.	2.573	2.59	w.	2.612			
117	2.51	vw.	2.529	2.49	vw.	2.500						
317				2.45	w.	2.433				2.43	vw.	2.417
$71\bar{5}$				2.33	vw.	2.313						
518				2.14	vw.	2.136	2.17	w.	2.173			
519				1.99	vw.	2.005						
020	1.88	w.	1.883	1.87	w.	1.875	1.91	w.	1.907			
023	1.84	w.	1.833	1.82	vw.	1.826	1.84	w.	1.855			

* *d*(o): observed value ** *d*(c): calculated value

TABLE VI. UNIT CELL CONSTANTS OF VARIOUS PHTHALOCYANINES VACUUM-CONDENSED ON MUSCOVITE

	Pt-Pc	Cu-Pc	Fe-Pc	Co-Pc	Ni-Pc	H_2-Pc
a	26.18 Å	25.92 Å	25.90 Å	25.88 Å	26.15 Å	26.14 Å
b	3.818 Å	3.790 Å	3.765 Å	3.750 Å	3.790 Å	3.814 Å
c	23.84 Å	23.92 Å	24.10 Å	24.08 Å	24.26 Å	23.97 Å
β	91.9°	90.4°	90.0°	90.2°	94.8°	91.1°
Space group	*C*2/*c*	*C*2/*c*	*C*2/*c*	*C*2/*c*	*C*2/*c*	*C*2/*c*
d(calcd.)	1.96	1.62	1.59	1.61	1.57	1.42
d(found)	1.94	1.62		1.65	1.62	1.44

fiber diagram was compared with the cross-grating pattern, the interplanar spacings which are associated with two sets of reflections on the equator were found to be 13.1 Å and 12.5 Å for the iron derivative, and 12.9 Å and 12.5 Å for the cobalt derivative, while the periods corresponding with these reflections in the cross-grating patterns were 12.9 Å and 12.05 Å for the former and 12.94 Å and 12.04 Å for the latter. In the cases of iron- and cobalt-phthalocyanines, therefore, the interplanar spacings calculated from the unit cell constants given in Table VI showed a discrepancy of about 4% from those obtained with the fiber diagrams. No serious difference was observed in metal-free phthalocyanine.

In the case of nickel-phthalocyanine, extra spots always appeared between the equator and the first-layer line in the fiber diagram, as is shown with arrows in Fig 9(d). The film was composed of laminar crystal strips, giving rise to a raft structure as a whole, and beard-like crystals appearing among the raft structure, as Fig. 8(d) shows. The reflections from the former crystals produced the fiber pattern, while those from the latter crystals appeared as extra spots. As for the nickel derivative, no films which showed another orientation

were obtained. In the fiber diagram, the maximum lattice period along the meridian was 3.79 Å and the interplanar spacings were 13.07 Å and 12.13 Å, these spacings are associated with two sets of reflections on the equator. Since these values were very similar to those of other phthalocyanines, the interplanar spacings obtained from the fiber diagram were indexed as in Table V. The unit-cell constants of nickel-phthalocyanine given in Table VI were then calculated from the interplanar spacings thus indexed.

Discussion

Robertson[7] and Linstead and Robertson[17] reported that metal-free, beryllium-, manganese-, iron-, cobalt-, nickel- and copper-phthalocyanines were isomorphic and that the unit lengths of their b-axis fell in the range from 4.71 Å to 4.84 Å, and that only the platinum-phthalocyanine had the unit length of the b-axis of 3.81 Å and was not isomorphic with the others. As is well known, however, their investigations were restricted to the stable forms of these compounds; no account was taken of the metastable form. Honigmann et al.[14] suggested that the individual unit cells of phthalocyanine compounds should contain four molecules and that, considering its isomorphic behavior with other phthalocyanine derivatives, the space group of platinum-phthalocyanine was transformed into $B2_1/a$. However, the space group assigned by them was based on the molecular orientation reported by Robertson and Woodward.[10] Recently, Brown[18] proposed that the space group of platinum-phthalocyanine should be corrected by means of a new interpretation that $C2/c$ of the monoclinic system is more plausible, since it is twice as large as that reported by Robertson. His proposition coincides well with the crystal data reported in the present paper. Consequently, it may be concluded that the unit cell constants of platinum-phthalocyanine should be transformed to those give in Table I(2). In Table II, the values in the column (1) agreed well with those in (2). On the other hand, there were small discrepancies between the values in (3) and those in (1) and (2) as a result of the difference in the axial angle, β. The result shows that the laminar crystals which assume the single directional orientation have the same structure as that investigated by Robertson, while the crystals which have the b-axis standing obliquely on the substrate face are distorted from the original structure, possibly because of the bond forces between the deposited crystal and the substrate muscovite.

As for the metastable form of copper-phthalocyanine prepared by the acid-paste method, Robinson and Klein reported the crystal to be $P4/m$ of the tetragonal system with the following unit cell constants: $a=17.376$ Å and $b=12.790$ Å.[11] This crystal, however, unfortunately cannot explain the present results which are directly obtained by electron diffraction. It should be reasonable to take the lattice spacing of 3.79 Å into consideration in determining the basic configuration of the unit cell, not only because the fiber diagram of the diffraction requires them, but also because this spacing is nearest the case of platinum-phthalocyanine and some other condensed polycyclic aromatic compounds.[19] The cell constants represented in this paper were confirmed with the results obtained by X-ray diffraction.

In the cases of iron- and cobalt-phthalocyanines, the unit length of the c-axis showed a discrepancy of less than 4% between the value obtained from the fiber diagram and that obtained from the cross-grating pattern. This discrepancy may be caused by the lattice distortion of the deposited crystal, which is accompanied by a slight change in the molecular arrangement in the crystal due to the lattice orientation relative to the substrate muscovite. Consequently, except for copper- and platinum-phthalocyanines, which were confirmed with a crystal prepared by another method, the crystal data obtained from the vacuum-condensed films may be expected to show some deviation. In spite of such possible deviations, however, it is believed that these crystal data are very useful for the study of the metastable form of phthalocyanine compounds because the metastable form of phthalocyanine compounds have not yet been obtained in the large, single-crystalline state from which the crystal data were determined by X-ray diffraction.

The authors would like to express their sincere thanks to Dr. C. J. Brown, University College, London, for his kind information about the crystal data of platinum- and copper-phthalocyanines.

17) R. P. Linstead and J. M. Robertson, *J. Chem. Soc.*, **1936**, 1736.
18) C. J. Brown, Private communication (1966).
19) H. Akamatu and K. Nagamatsu, *J. Colloid Sci.*, **2**, 593 (1947).

BULLETIN OF THE CHEMICAL SOCIETY OF JAPAN VOL. 39 2625—2631 (1966)

The Orientation Overgrowth of Metal-phthalocyanines on the Surface of Single Crystals. I. Vacuum-condensed Films on Muscovite

By Michio ASHIDA*

Institute for Chemical Research, Kyoto University, Takatsuki, Osaka

(Received May 2, 1966)

When substrate muscovite is preliminarily heated at 300°C for one hour and then kept at 150°C to 200°C during deposition in vacuo, Cu-phthalocyanine films condensed on it show parallel b-axis orientations, including single- and triple-directional orientations. The b-axis of the crystal runs parallel to the substrate face. On the other hand, when the substrate is preliminarily heated at 400°C and then kept at 150°C, films vacuum-condensed on it occur in a standing b-axis orientation. The high-resolution electron-diffraction pattern of the film reveals that the a-, b- and c-axes of the crystal are inclined to the normal of the substrate face at angles of about 75°, 32° and 118° respectively. An electron micrograph of the film shows that as discrete crystals grow they orient themselves in either of two different directions. The crystal which assumes the standing b-axis orientation has its $(31\bar{3})$ plane almost parallel to the substrate face. Pt-phthalocyanine film also assumes the standing b-axis orientation, in which the a-, b- and c-axes of the crystal are inclined to the normal of the substrate face at angles of about 74°, 35° and 120° respectively. It turns out that the molecular plane comes in contact with the muscovite surface in the case of the standing b-axis orientation. A plausible explanation of the origin of these orientations is presented in terms of the dehyroxylation of the surface mica layer caused by the thermal treatment.

The epitaxial growth of thin crystalline film has been investigated by many workers; they have mostly been interested in metals or inorganic compounds. As for the organic compounds, Willems[1] and Kleber and Meyer[2] observed the orientation overgrowth of some compounds by light microscopy. However, the method based on light microscopy was limited to cases where the overgrown crystals have a well-defined morphology. Moreover, the lack of exact information on the crystal structures of most of those compounds made it impossible to discuss in detail the orientation of the crystals relative to the substrate in terms of a difinite lattice structure. In a previous paper,[3] it was reported that the condensed polycyclic aromatic compounds, which are frequently referred to as the organic semiconductors, show an epitaxial growth when those materials are condensed onto a cleaved face of muscovite crystal. Furthermore, it was observed by electron microscopy and electron diffraction that platinum-, copper- and zinc-phthalocyanines vacuum-condensed on muscovite assumed the single- and triple-directional orientations.[4] It turned out in previous investgations that the b-axes of crystals always ran parallel to the substrate surface.

When substrate muscovite was treated at a higher temperature in advance of the deposition of these materials, films of many phthalocyanine compounds showed quite a different orientation. Using these oriented films, the crystal data were determined for the metastable forms of several phthalocyanine derivatives by the high-resolution electron-diffraction method.[5]

In this work, the effect of the thermal treatment of muscovite will be studied concerning the orientation overgrowth of copper-phthalocyanine. The orientation of the evaporated film of phthalocyanine will also be examined in relation to the substrate by electron microscopy as well as by electron diffraction.

Experimental

The metal-phthalocyanines used in this work was purified by repeated sublimation in a stream of carbon dioxide at low pressure and at a temperature above 500°C. A freshly-cleaved thin film of muscovite about 20 mm. square was placed in a Pyrex glass tube situated in an electric furnace. The substrate was heated at an appropriate temperature in a vacuum of about 5×10^{-5} mmHg. The purified material was then vacuum-sublimated onto muscovite following the

* Present address: Department of Industrial Chemistry, Faculty of Engineering, Kobe University, Nada-ku, Kobe.

1) J. Willems, *Z. Elektochem.*, **56**, 345 (1952).

2) W. Kleber and K. Meyer, *Z. anorg. u. allgem. Chem.*, **296**, 164 (1958).

3) E. Suito, N. Uyeda and M. Ashida, *Nature*, **194**, 273 (1962).

4) N. Uyeda, M. Ashida and E. Suito, *J. Appl. Phys.*, **36**, 1453 (1965).

5) M. Ashida, N. Uyeda and E. Suito, This Bulletin, **39**, 2616 (1966).

same procedure as that described in the previous work.[5] The crystallographic principal axes of muscovite were determined in its basal plane by polarizing microscopy. The specimen used for electron microscopy was prepared by the wet-stripping method.

Results

Three Types of Orientation.—Films vacuum-condensed onto muscovite showed various orientations according to the evaporating conditions. Generally speaking, the typical orientations may be classified into the following three groups.

A. Parallel b-Axis Orientations. — A-1. The Single-directional Orientation.—When substrate muscovite was preheated at 300°C for one hour and then kept at a temperature between 150°C and 170°C, the film condensed showed a well-defined single-directional orientation, whose electron micrograph and electron diffraction pattern are shown in Figs. 1(a) and (b) respectively. As has been

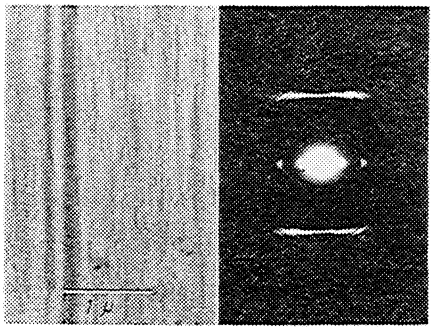

(a) (b)

Fig. 1. Electron micrograph (a) and electron diffraction pattern (b) of copper-phthalocyanine film which assumed the single-directional orientation.

described in a previous paper,[4] films were composed of laminar crystal strips; it was revealed by the analysis of the fiber diagram obtained from the film that at least two kinds of lattice orientations may be assumed to show a longitudinal direction in individual strips which always run parallel to their b-axes. As for the relative orientation of the evaporated film to the substrate, the b-axis of the former was parallel to either of the two directions, which made $\pm 60°$ with the b-axis of the muscovite crystal.[6]

A-2. The Triple-directional Orientation. — The triple-directional orientation was observed when films were prepared at the substrate temperature of 200°C without any preliminary thermal treatment. The electron micrograph shown in Fig. 2(a) exhibits that the film was built up of triangular labyrinthine networks of slender crystal strips.

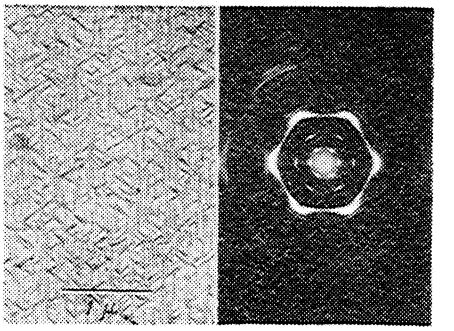

(a) (b)

Fig. 2. Electron micrograph (a) and electron diffraction pattern (b) of copper-phthalocyanine film which assumed the triple-directional orientation.

Corresponding to such a configuration of the film, the diffraction pattern also had a hexagonal appearance, as Fig. 2(b) shows. The pattern is a superposition of three identical fiber diagrams, each of which is essentially the same as that of the single-directional orientation.

B. The Standing b-Axis Orientation.—When the substrate muscovite was heated in advance at 400°C for one hour and then kept at 150°C, the film was composed of small, flaky crystals which grew by orienting themselves along either of the two different directions designated as AA′ and BB′ in Fig. 3(a). These wedge-like crystals were separated from one another, making the total film discrete, unlike the above two cases. The electron diffraction pattern in Fig. 3(b) is apparently

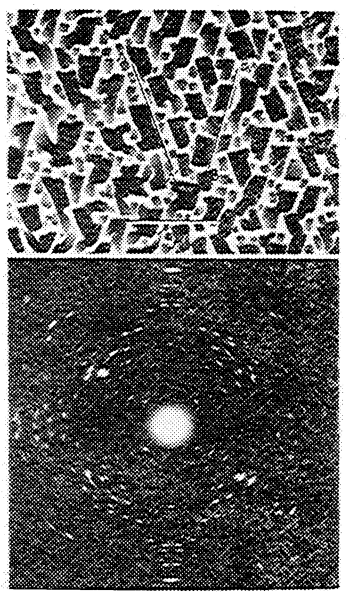

(a)

(b)

Fig. 3. Electron micrograph (a) and electron diffraction pattern (b) of copper-phthalocyanine film which assumed the standing b-axis orientation.

6) E. Suito, N. Uyeda, M. Ashida and K. Yamamoto, *Proc. Japan Acad.*, **42**, 54 (1966).

a superposition of two identical diagrams, both composed of layered zones of reflection spots. Naturally, the angle defined by those two sets of parallel layered lines is identical with that defined by the two directions AA′ and BB′. The appearance of these layered zones in the individual diagrams should be ascribed to the position of the main zone axes of the evaporated crystal, which are tilted against the substrate face and, consequently, against the electron beam. This orientation will be described in a later section.

The Relation between the Evaporating Conditions and the Orientation Overgrowth of Copper-phthalocyanine.—As has been described above, three groups of orientations of copper-phthalocyanine vacuum-condensed on muscovite take parallel b-axis orientations, which includes single- and triple-directional orientations, and the standing b-axis orientation. The appearance of these different orientations depends on the evaporating conditions, one of which is expected to be the thermal treatment of muscovite. In an effort to determine the effect of thermal treatment, the change in the orientation was also studied with various combinations of the time and the temperature of preheating; the effect of the temperature at which the material was finally deposited was also studied.

Generally, the film formed on substrate muscovite at room temperature was composed of granular crystals with a random orientation. An epitaxial growth of phthalocyanine occurred when the temperature of substrate was not lower than about 100°C. As the substrate temperature was increased, the deposited crystal grew larger and assumed a better orientation until around 200°C, above which point the orientation became worse again. When the substrate was kept at temperatures above 200°C, a film was built up of long, flaky crystals, which occurred in the stable form and which grew in a random direction, without any relative orientation to the substrate structure.

The effect of the preliminary thermal treatment of muscovite on orientation overgrowth is summarized in Fig. 4. In this case, the substrate temperature was kept at 150°C during sublimation for all the experiments. Since the single- and triple-directional orientations both take the b-axis of crystals parallel to the muscovite surface and occasionally mix with one another, the temperature range for the appearance of these orientations can not be defined by sharp critical points. When the temperature of the thermal treatment was under 350°C, the deposited crystals always assumed the parallel b-axis orientation, in which the single-directional orientation occurred only in a considerably limited range of temperature, as follows: the substrate muscovite was treated in advance at 300°C for one hour, and the substrate temperature during sublimation was kept in the range from

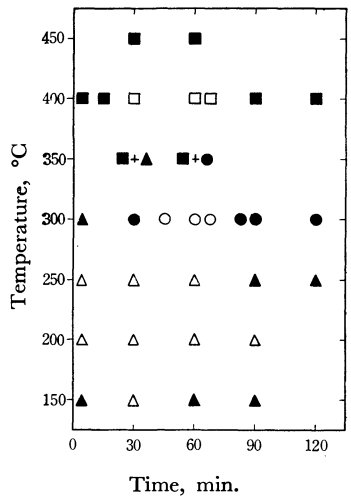

Fig. 4. The effect of preliminarily thermal treatment of muscovite on orientation overgrowth of Cu-phthalocyanine. The substrate temperature is kept at 150°C during sublimation.
□: Standing b-axis orientation
■: Nearly standing b-axis orientation
○: Single-directional orientation
●: Nearly single-directional orientation
△: Triple-directional orientation
▲: Nearly triple-directional orientation

150°C to 170°C. The triple-directional orientation appeared under all conditions, except for the range of temperature mentioned above. On the other hand, when the thermal treatment was carried out above 350°C, the deposited crystals assumed the standing b-axis orientation. Therefore, the orientation overgrowth on muscovite was found to change its state from one to the other when the temperature of the preliminary thermal treatment was around 350°C. Moreover, when the substrate muscovite was exposed to water vapor after a thermal treatment at 400°C and then treated under 300°C in vacuo, the film condensed on it again showed a triple-directional orientation. Consequently, the alternation of orientation seems to depend on the variation in the surface structure of muscovite, which is not necessarily accompanied by the decomposition of the crystal lattice of the substrate but which occurs reversibly in regard to the temperature range mentioned above.

The Determination of the Standing b-Axis Orientation.—Each elementary cross-grating pattern in Fig. 3(b) consists of three parallel zones. On the basis of the unit-cell constants of the metastable form,[5] the reflection spots were indexed as in Fig. 5. The zone which includes the point of origin appears as the intersection of the reciprocal lattice points as well as their elongated intensity regions, which have the index of $k=0$ with the Ewald sphere. The other zones, which do not

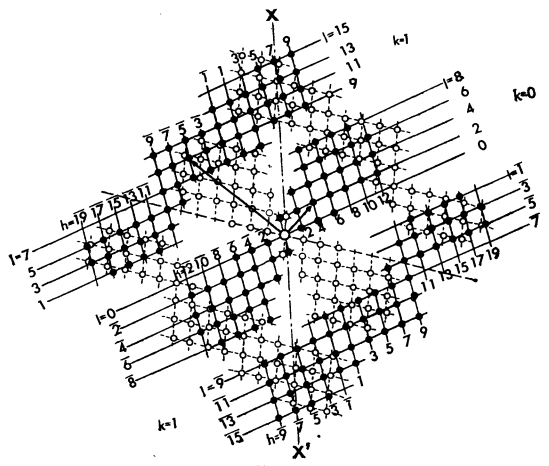

Fig. 5. The interpretation of the diffraction pattern shown in Fig. 3(b). A cross-section of the reciprocal lattice points of the crystal with the Ewald sphere. The reciprocal lattice points 402 and $\bar{5}19$ lie directly on the Ewald sphere.

include the point of origin, correspond to the reciprocal lattice planes of $k=\pm 1$. When the interplanar spacings obtained from the diffraction spots were compared with those calculated from the cell constants, the reciprocal lattice points, 402 and $\bar{5}19$, were found to lie directly on the Ewald sphere. Consequently, the a-, b- and c-axes of the crystal are inclined to the normal of the substrate surface at angles of about 75°, 32° and 118° respectively. On the other hand, the normal of the $(31\bar{3})$ plane is inclined to the a-, b- and c-axes at angles of about 69°, 33° and 113° respectively. When two sets of angles were compared, the crystal which assumed the standing b-axis orientation has its $(31\bar{3})$ plane almost parallel to the substrate face. The reflection diagram in Fig. 5 implies the plane of C_{2v} symmetry, XX', which was found to make an angle of 60° with the

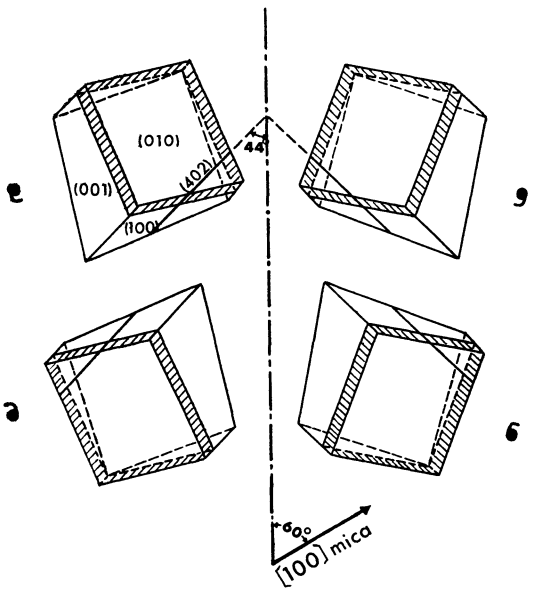

Fig. 6. Schematic diagram of the projection of crystals which assumed the standing b-axis orientation on the muscovite surface. The hatched zone shows unit cell dimensions. The (402) plane is perpendicular to the muscovite surface.

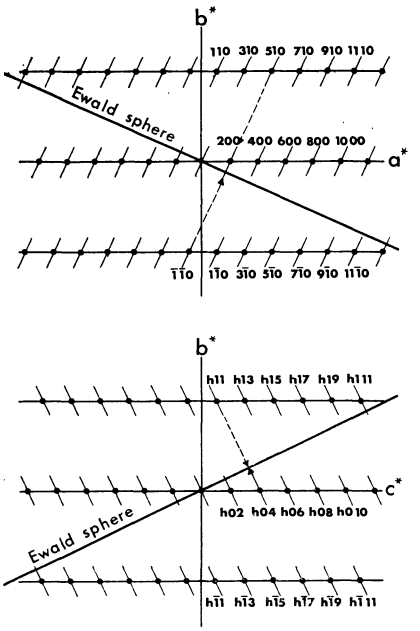

Fig. 7. Schematic diagrams of the elongation in the intensity region of the reciprocal lattice points. A: cross-section with 001 layer, B: cross-section with 100 layer.

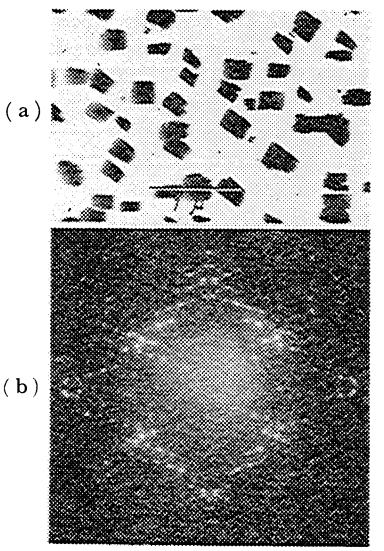

Fig. 8. Electron micrograph (a) and electron diffraction pattern (b) of platinum-phthalocyanine film which assumed the standing b-axis orientation.

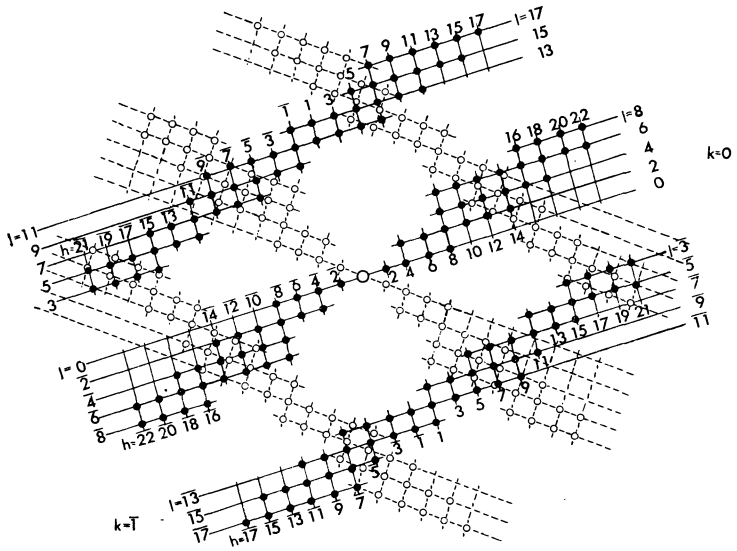

Fig. 9. The interpretation of the diffraction pattern shown in Fig. 8(b).

a-axis of muscovite. The projection of the crystals onto the muscovite face is shown schematically in Fig. 6, where the individual unit cells are designated with hatched zones. The orientation of these four crystals can be defined by two kinds of symmetries, one of which is a plane of mirror symmetry which makes an angle of 60° with the a-axis of muscovite and stands perpendicular to its surface, while the other is an axis of the two-fold symmetry. The projection of the b-axis of the evaporated crystals to the surface makes an angle of about 44° with the plane of symmetry. The top face of the crystal corresponds to the (010) plane, and the side faces, to the (100) and (001) planes.

In the diffraction pattern, the reflections which have the same value of h or l but which differ in the index k, did not appear on the same line. This was probably caused by the elongation in the intensity region in a somewhat unusual direction. Since the external form of the crystal is wedge-shaped, the thickness of the crystal measured normal to the $(31\bar{3})$ plane, which is almost parallel to the substrate face, may be very thin in the vicinity of the edge. Consequently, it may be supposed that the intensity regions of the reciprocal lattice points are elongated along the normal to the $(31\bar{3})$ plane and are crossed by the Ewald sphere, which is parallel to the basal plane of the crystal, as Fig. 7 shows. According to the figure, it is clear that the points with the indices of $51l$ fall on the same line as those with the indices of $\bar{1}\bar{1}l$; it is clear also that the line includes the points with the indices of $20l$. Similarly, the points with the $h$ll indices fall on the same line as those with the h04 indices.

The standing b-axis orientation was also observed in other phthalocyanine compounds. Platinum-phthalocyanine, for example, assumed a similar orientation, as Figs. 8(a) and (b) show. The cross-grating pattern is interpreted as is shown in Fig. 9 by the method described above. In the case of platinum-phthalocyanine, it turned out that two reciprocal lattice points, 402 and $\bar{3}19$, lie directly on the Ewald sphere, and that the a-, b- and c-axes of the crystal which assumed the standing b-axis orientation made angles of about 74°, 35° and 120° respectively with the normal of the substrate face. The projection of the b-axis of the crystal onto the substrate face made an angle of about 44° with the plane of symmetry.

Discussion

Vacuum-condensed films of copper-phthalocyanine occur in the metastable form of its dimorphs and were found to be isomorphic with platinum-phthalocyanine.[4] Such isomorphic behavior of the phthalocyanine derivatives has also been found in the case of stable crystals of beryllium-, iron- cobalt-, nickel-, copper- and metal-free phthalocyanines.[7,8]

According to Robertson,[7] the molecular plane has the same inclination of 45.8° to the b-axis in the cases of nickel- and metal-free phthalocyanines of the stable form. Therefore, the molecule in the metastable form of copper-phthalocyanine is expected to be inclined to the b-axis at an angle similar to that of the platinum derivative, which has a conspicuous isomorphic structure, although

7) J. M. Robertson, *J. Chem. Soc.*, **1935**, 615.
8) R. P. Linstead and J. M. Robertson, ibid., **1935**, 1736.

no exact information has been obtained as far as copper-phthalocyanine is concerned. However, the relative orientation of platinum-phthalocyanine to the substrate may reasonably be interpreted on the basis of this isomorphism.

The crystal structure of the platinum derivative has the following unit cell dimensions with the monoclinic space group $C2/c$: $a=26.18$ Å, $b=3.818$ Å, $c=23.84$ Å, and $\beta=91.9°$.[5] The molecules of platinum-phthalocyanine appear to be strictly planar and stack themselves so that they are closely packed in a column, facing each other, parallel, and inclined alternatively along the c-axis. The central platinum atom lies at the center of a square-bonded configuration with four nitrogen atoms, and four other nitrogen atoms make a bridge between the isoindole rings. The molecular axes, L and M, are defined through the center of the molecule and the latter nitrogen atoms (see Fig. 11). When a projection is taken normal to the molecular plane, the corresponding atoms in parallel molecules along the b-axis shift along the molecular axis, M, one from another. The angles between the molecular axes and the crystal axes are given in Table I. The normal direction of the $(21\bar{4})$ plane, which is approximately parallel to

Table I. Orientation of platinum-phthalocyanine molecule in the crystal

	Angles between molecular axes and crystal axes			Angles between crystal axes and the normal to the $(21\bar{4})$ plane
	L.	M.	N.*	
b-Axis	85.7°	63.9°	26.5°	31.0°
c-Axis**	71.4	32.9	116.1	123.0

* Molecular axis N is the normal to the molecular plane.

** The c-axis is transformed from the a-axis assigned by Robertson.

the substrate face, makes such angles with the crystal axes as are given in the last column of Table I. Because the discrepancy between the angles in the third column (N) and those in the last one was quite small, it is evident that the molecular plane is parallel to the surface of muscovite in this case. On the other hand, each molecule in the crystal with the parallel b-axis orientation stands on a carbon atom in one of the outer benzene rings.[4] Consequently, when the crystal assumes the parallel or the standing b-axis orientation, the planar molecules in the individual crystals are located on the substrate face, as is shown schematically in Fig. 10. On the basis of this experimental finding, there may considered to be an atomic matching between the deposited and the substrate crystals at the interface.

When it is tentatively assumed that the hexagonal network of potassium ions on the cleavage face is perfect and that a nitrogen atom on the molecular axis M (e. g., m), defined as the point of origin,

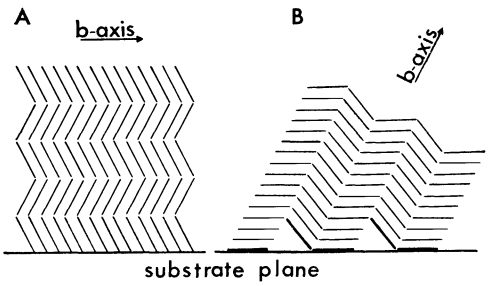

Fig. 10. Schematic diagrams of orientation of platinum-phthalocyanine molecules in the crystal. A: the crystal with the parallel b-axis orientation, B: the crystal with the standing b-axis orientation.

is located on a potassium ion (e. g., K_1), one nitrogen atom on the molecular axis (e. g., p) is in contact with a potassium ion (e. g., K_2), and a nitrogen atom bonded to the central platinum atom (e. g., a) also comes into contact with a potassium ion (e. g., K_3) as is shown schematically in Fig. 11. The projections of the a-, b- and c-axes of the crystal onto the molecular plane are exhibited with a_p, b_p and c_p directively. In this case, the neighboring molecules are distributed on the substrate face as is shown in the figure. The closest molecule along the a-axis is located at the nearest site of potassium ions (e. g., K_4, K_5, K_6 and K_7) with four nitrogen atoms on the molecular axes (e. g., m′, n′, p′ and q′). Similarly, the next parallel molecule in the direction of the c-axis is located at the nearest site of potassium ions (e. g., K_8, K_9 and K_{10}) with three nitrogen atoms (e. g., n″, q″ and c″). If molecules are located on the surface of muscovite in such a manner, the direction of b_p, which is the projection of the b-axis of the crystal onto the substrate face, makes an angle of about 44° with the direction, K, which makes an angle of 60° with the a-axis of muscovite (a_M). The angle of 44° coincides with that between the plane of symmetry of the two different crystal orientations and the projection of the b-axis on the substrate face, which was formerly determined from the electron diffraction pattern. By a comparison of these two results, it may be confirmed that the orientation of the M axis and, consequently, all the molecules have an orientation such as is shown in Fig. 11. Because the phthalocyanine crystal has a symmetry of two-fold screw rotation and the molecule along the b-axis shifts in with the direction of +M or −M, the orientation of the deposited crystals has a symmtery of C_{2v}.

Although the top layer of muscovite apparently has a hexagonal symmetry, the orientation overgrowth of phthalocyanine compounds appeared only in a mirror symmetry. The plane of symmetry made ±60° with the a-axis of muscovite. As has been described in a previous paper,[4] the

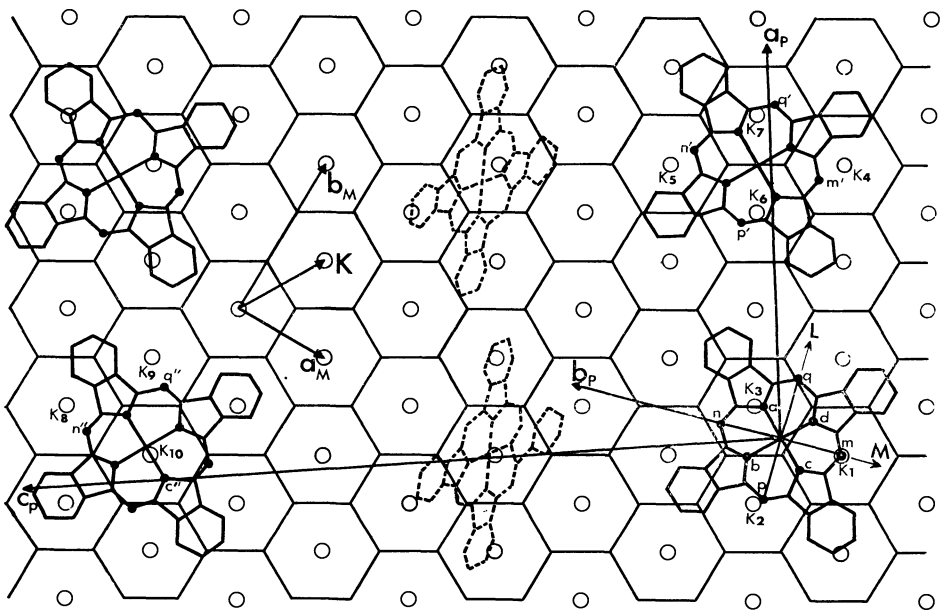

Fig. 11. Schematic diagram of the relative orientation of platinum-phthalocyanine to muscovite face when the crystal assumes the standing b-axis orientation. The directions a_M and b_M are the (100) and (010) directions of muscovite, respectively. Phthalocyanine molecules shown with dotted line are not contacted to the muscovite surface.

intersection of the plane of symmetry with the muscovite face coincides with the direction of the staggering in the top mica layer at the surface. It should be noted that the muscovite structure with a monoclinic symmetry, instead of a hexagonal one, gives rise to a latent influence upon nucleation and to a further growth of deposited films of phthalocyanine compounds, not only in the case of the parallel b-axis orientation, but also in the case of the standing b-axis orientation.

The orientation of the deposited crystal films varied from the parallel b-axis to the standing b-axis as a function of the thermal treatment of muscovite; there was quite a sharp critical transition point. The dehydroxylation of muscovite gradually begins at a temperature about 400°C in vacuo without a general destruction of the crystal lattice.[9] It is known that the phthalocyanine molecule, which has many aromatic rings, shows a strong repulsive force against water. Therefore, it is reasonable to postulate that the deposited molecules of phthalocyanine stand on the substrate muscovite so that the molecular planes separate from its surface as much as possible as a result of the repulsive force between the molecule and water included in muscovite. The resulting film shows a parallel b-axis orientation, whereas when the substrate muscovite was treated at 400°C, the planar molecule lies parallel to the substrate face because of the diminution of the repulsive force by the dehydroxylation of muscovite. The crystals thus nucleated by deposited molecules grow in the direction of the b-axis, which inclines obliquely to the substrate face, and the resulting film becomes discrete in the case of the standing b-axis orientation.

In the case of the metastable crystal of the copper-phthalocyanine film, which assumed the standing b-axis orientation, each crystal axis was observed to incline to the substrate face at an angle similar to that of platinum-phthalocyanine. Therefore, it seems that the molecular plane of copper-phthalocyanine inclines to the crystal axes at approximately the same angles as those of platinum-phthalocyanine. Consequently, it can reasonably be explained that the planar molecule of copper-phthalocyanine comes into parallel contact with the substrate face in a manner similar to that of the platinum derivative.

The author is very grateful to Professor Eiji Suito of the Institute for Chemical Research, Kyoto University, for his interst and support; he wishes also to thank Dr. Natsu Uyeda of the same Institute for his many helpful discussions and suggestions during this work. He is indebted to Professor Wasaburo Jono and Professor Teizo Watanabe of Kobe University for thier encouragement in this work.

9) M. Ashida, T. Watanabe and W. Jono, This Bulletin, **39**, 2047 (1966).

BULLETIN OF THE CHEMICAL SOCIETY OF JAPAN VOL. 39 2632—2638 (1966)

The Orientation Overgrowth of Metal-phthalocyanines on the Surface of Single Crystals. II. Vacuum-condensed Films of Copper-phthalocyanine on Alkali Halides

By Michio ASHIDA*

Institute for Chemical Research, Kyoto University, Takatsuki, Osaka

(Received May 2, 1966)

Cleaved faces of KCl, KBr and NaCl crystals were used as substrates. When copper-phthalocyanine is vacuum-condensed onto either KCl or KBr, the films on it take a standing b-axis orientation, which shows a C_{4v} symmetry. The major planes of symmetry coincide with those of KCl and KBr. The crystals on KBr show an azimuthal angular shift of about $+12°$ or $-12°$ in respect to the major symmetry axes, [010] and [100], of the substrate crystal. When the films have the standing b-axis orientation, the planar molecule in the crystal comes into parallel contact with the cleavage face of the substrate. It may be presumed that the bridge nitrogen atoms in a phthalocyanine molecule are placed on the potassium ions in the (001) planes of KCl and KBr. The films on KCl and KBr are composed of finely-divided rectangular crystals and dendrites; the former are concentrated at steps on the cleavage face to produce a decorative pattern, while the latter appear on the smooth surface. The formation in various types of crystals are interpreted in terms of the rate of nucleation and growth. The films vacuum-condensed onto NaCl are composed of laminar crystals which have a random orientation.

In previous papers,[1,2] the orientation overgrowth of phthalocyanine compounds was investigated on a cleavage face of muscovite. Films vacuum-condensed onto muscovite occurred in two different types of orientations, which were called the parallel b-axis orientation and the standing b-axis orientation. This difference appeared mostly to depend upon the condition of the thermal treatment of muscovite. With regards to the orientation of the phthalocyanine crystal relative to substrate muscovite, it was suggested that planar molecules in the crystal came into contact with the cleavage face of muscovite, and that bridge nitrogen atoms in a phthalocyanine molecule were connected with the surface potassium ions in the (001) plane of muscovite when the film took the standing b-axis orientation.

In an effort to elucidate the effect of potassium ions in a substrate on the orientation overgrowth of phthalocyanine, the vacuum-condensed film was studied on the cleavage faces of alkali halides. Karasek and Decius[3] reported that vacuum-sublimated films of metal-free phthalocyanine on rock salt appeared in either of its dimorphs, depending upon the substrate temperature. By X-ray diffractometry, they also found that the crystals were of the metastable form if the substrate temperature was lower than 200°C. However, they did not refer to the orientation of the deposited films relative to the substrate.

For the present paper, vacuum-condensed films of copper-phthalocyanine on cleavage faces of alkali halides were observed by electron microscopy. The appearance of various crystals in their growth process was then interpreted on the basis of the topography of the substrate surface. The orientation of the film was determined by electron diffraction. The orientation of the deposited crystal relative to the substrate alkali halides will be discussed on the basis of the molecular arrangement in the crystal.

Experimental

Powdery commercial copper-phthalocyanine was purified by repeated sublimation in a low-pressure stream of carbon dioxide at a temperature above 500°C. The purified material was sublimated from a tungsten basket onto the cleavage faces of alkali halides in a vacuum evaporator. The single crystals of alkali halides used in this work were potassium chloride, potassium bromide and sodium chloride. The crystals were cleaved in air and immediately placed in a Pyrex glass tube, as has been mentioned in a previous paper.[2] The specimens used for electron microscopy were prepared by the wet-stripping method.

Results

The Morphology of the Vacuum-condensed Crystals.—*(a) Crystals on the Cleavage Face of Potassium Chloride.* — When copper-phthalocyanine

* Present address: Depertment of Industrial Chemistry, Faculty of Engineering, Kobe University, Nada-ku, Kobe.

1) N. Uyeda, M. Ashida and E. Suito, *J. Appl. Phys.*, **36**, 1453 (1965).
2) M. Ashida, This Bulletin, **39**, 2625 (1966).
3) F. W. Karasek and J. C. Decius, *J. Am. Chem. Soc.*, **74**, 4716 (1952).

was vacuum-condensed onto a cleavage face of potassium chloride at 150°C, various crystal shapes were observed in the growth process of the deposit. At the early stage of condensation, the film was composed of three types of crystals, with different shapes, as is shown in Fig. 1. Very fine

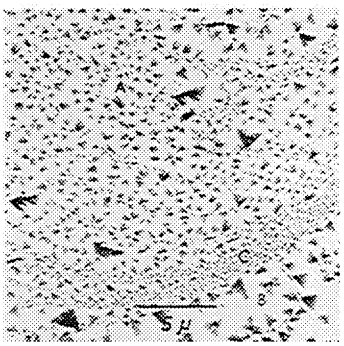

Fig. 1. Electron micrograph of Cu-phthalocyanine vacuum-condensed onto a cleavage face of KCl at the early stage of sublimation.

crystals like A, the size of which was about 100 Å, were observed all over the substrate face. In the part B, large dendrites appeared, while relatively small rectangular crystals came together in the part C. The curved pattern was formed by the latter crystals in the part B. As the film thickness was increased, the dendrites grew larger until the ends of their branches reached the curved zone, as is shown in Fig. 2(a), while small crystals condensed on the curved zone came into contact

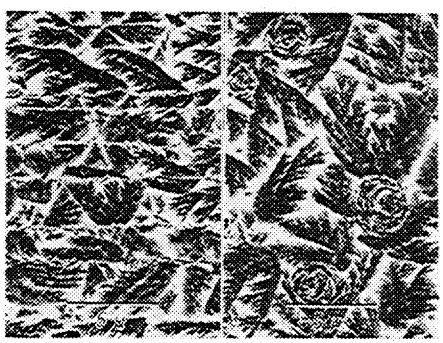

(a) (b)

Fig. 2. Electron micrographs of Cu-phthalocyanine films vacuum-condensed onto cleavage faces of KCl.

with each other without showing any tremendous growth. These curved lines formed by the crystallites may be attributed to the decorative effect similar to that pointed out by Basset and Pashley[4] for the metallic deposit on alkali halides and other inorganic crystals. It is well known that the

4) G. A. Basset and D. W. Pashley, *Phil. Mag.*, **3**, 1042 (1958).

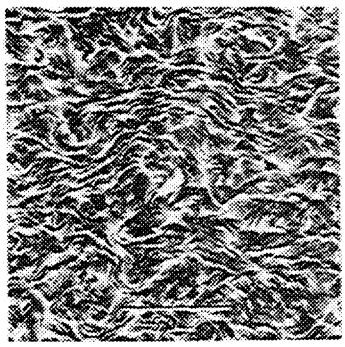

Fig. 3. Electron micrograph of Cu-phthalocyanine films vacuum-condensed onto a cleavage face of KCl when the rate of sublimation is increased.

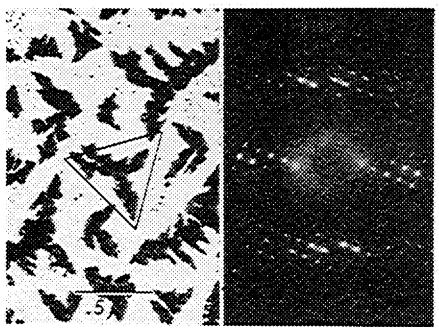

(a) (b)

Fig. 4. Electron micrograph (a) and selected area diffraction pattern (b) of Cu-phthalocyanine vacuum-condensed onto a cleavage face of KCl at the substrate temperature of 200°C.

decoration pattern shows the topography of the cleavage face. Sometimes, small crystals were observed to lie on concentric circles in the early stages. These crystals were aggregated in the circles to form a cabbage-like shape, shown in Fig. 2(b), when the amounts of the condensed crystals were increased. When the rate of deposition was increased, the film was composed of small crystals which were connected to form a wave-like pattern, as is shown in Fig. 3. When the substrate temperature was higher than 200°C, the film was composed of only discrete crystals with a dendrite structure, as Fig. 4(a) shows. Figure 4(b) shows a selected area-diffraction pattern from the triangular dendtrite shown in Fig. 4(a); this pattern revealed that the dendrite was a well-defined single crystal. Although the deposited crystal occurred in various types depending on either the condensation conditions or the topography of the cleavage face, all the crystals were found to have the same crystal habit on a close observation of electron micrographs as well as of electron-diffraction patterns. It is obvious that the dendrites shown in Figs. 1 and 4 are formed from rectangular crystals which were aggregated to one another with a definite orientation. The cabbage-like

features in Fig. 2(b) are apparently composed of a number of small rectangular crystals assembled on the concentric circles. In the process of crystal growth, the difference in the way of the secondary aggregation of these elementary rectangular crystals gave rise to various shapes.

(b) Crystals on the Cleavage Face of Potassium Bromide.—When the cleavage face of potassium bromide was used as the substrate, the film vacuum-condensed on it was composed of small rectangular crystals and dendrites, as Fig. 5 shows, which were

Fig. 5. Electron micrograph of Cu-phthalocyanine vacuum-condensed onto a cleavage face of KBr.

similar to those formed on potassium chloride. The small crystals arranged in a row were distributed all over the surface, as were the dendrites.

(c) Crystals on the Cleavage Face of Sodium Chloride.—In contrast to the film formed on either potassium chloride or potassium bromide, the film on sodium chloride was composed of crystals with entirely different features, as Fig. 6(a) shows.

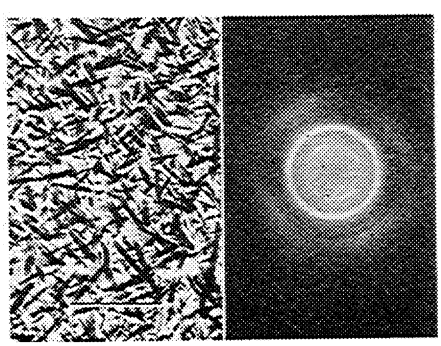

(a) (b)

Fig. 6. Electron micrograph (a) and diffraction pattern (b) of Cu-phthalocyanine vacuum-condensed onto a cleavage face of NaCl.

The laminar crystals grew in random directions, and the size of the crystals was apparently not uniform. No evident orientation was observed in the electron diffraction pattern, as may be seen in Fig. 6(b).

The Determination of the Crystal Orientation.—*(a) The Orientation of the Crystal Deposited*

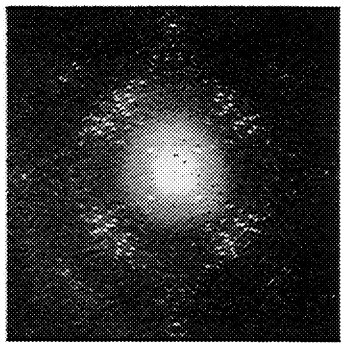

Fig. 7. High resolution electron diffraction pattern of Cu-phthalocyanine film vacuum-condensed onto a cleavage face of KCl. Crystals assume the standing b-axis orientation.

on Potassium Chloride.—Although the films condensed onto the cleavage face of potassium chloride were composed of crystals with various shapes, as has been described above, the electron diffraction patterns from those films, all gave the same pattern, as is shown in Fig. 7, this revealed that all the crystals assumed the same lattice orientation. The diffraction pattern consisted of four sets of identical cross-grating patterns, each of which was essentially the same as the single crystal pattern shown in Fig. 4(b). Therefore, it turned out that the film included eight groups of crystals, in each of which the orientation was the same. The total diffraction pattern is schematically reproduced in Fig. 8, in which the white circles represent the basic single crystal pattern associated with the two groups of the crystals which have a C_2 symmetry. Although the total pattern appeared to be complicated, it can be configurated

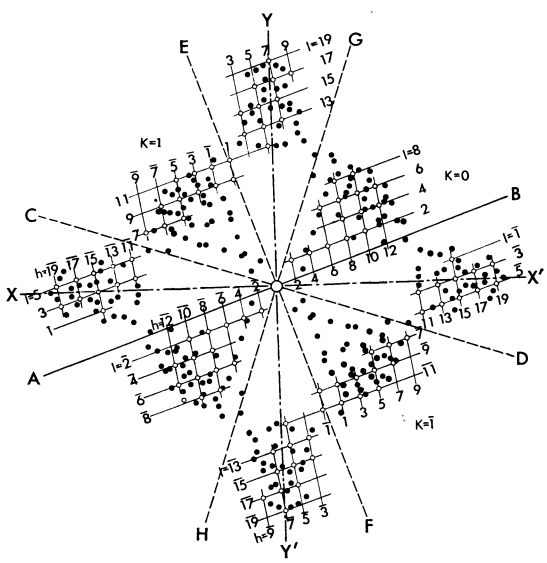

Fig. 8. The interpretation of the diffraction pattern shown in Fig. 7. White circles are the representation of the basic single crystal pattern.

by the systematic superposition of this elementary pattern, which is essentially the same as that shown in Fig. 4(b), with the major axes of C_{4v} symmetry, XX' and YY', which further coincide with the [100] and [010] directions of potassium chloride respectively.

Another result derived from the analysis of this elementary pattern is that the individual crystals have the $(31\bar{3})$ plane as the basal one facing parallel to the substrate crystal. As the AB line appears as the projection of the c* reciprocal axis in the elementary pattern, so other lines, CD, EF and GH, are similar projections of c* axes associated with individual crystal groups. The angle between the projection of each c* reciprocal axis and the nearest major axis of symmetry was found to be almost 20°.

(b) The Orientation of the Crystal Deposited on Potassium Bromide.—The films condensed onto potassium bromide were composed of crystals similar to those on potassium chloride, excepting that the high-resolution electron-diffraction pattern from the film revealed a somewhat different orientation of the deposited crystals. Figure 9 shows the

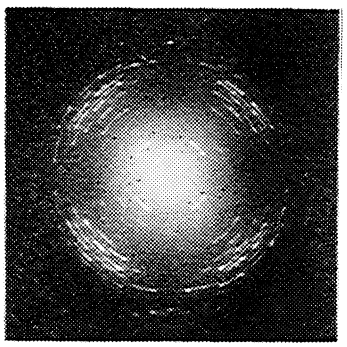

Fig. 9. High resolution electron diffraction pattern of Cu-phthalocyanine film vacuum-condensed onto a cleavage face of KBr.

electron-diffraction pattern obtained from the film. Also, in this case the crystals turned out to assume the standing b-axis orientation, in which the $(31\bar{3})$ plane of the crystal lies parallel to the cleavage face of potassium bromide. The pattern indicated that the orientation of crystals has a C_{4v} symmetry, the major axes of which again coincide with the [010] and [100] directions of potassium bromide. Therefore, the crystals may be classified into eight orientation groups, defined by two planes of symmetry which finally coincide with the (100) and (010) planes of potassium bromide; these planes are designated by XX' and YY'. The arc spots revealed that crystallites included in the individual groups were oriented with an azimuthal angular shift of about 12°. Thus, the projection of the reciprocal c* axis on the basal plane falls into an angular range defined,

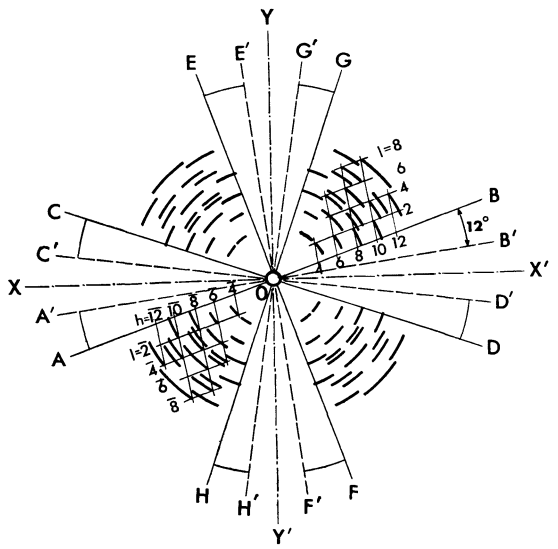

Fig. 10. The interpretation of the diffraction pattern shown in Fig. 9.

for instance, by AB and A'B' for one group of crystallites. Since the pattern has the C_{4v} symmetry, the angular ranges of the projection of the c* axis are defined by sets of CD:C'D', EF:E'F' and GH:G'H' for the other groups, as is shown in Fig. 10. Even in this case, each crystallite condensed onto potassium bromide again occurred in the standing b-axis orientation, which made the $(31\bar{3})$ plane parallel to the substrate surface.

Discussion

As has been described in the previous paper,[1] vacuum-condensed films of copper-phthalocyanine occur in the metastable form, the crystal structure of which is isomorphic with that of the platinum derivative. The a-, b- and c-axes of the copper-phthalocyanine crystal in the standing b-axis orientation are inclined to the normal of the substrate surface at angles of about 75°, 32° and 118° respectively. In the case of the platinum-phthalocyanine crystal with the standing b-axis orientation on muscovite, the main axes are inclined to the normal of the substrate face at angles similar to those of the copper derivative, and the molecular plane faces the substrate face.[2] Therefore, it seems that the molecular plane of copper-phthalocyanine in the alternative lattice rows in the basal face comes into parallel contact with the substrate face. The metastable form of copper-phthalocyanine has the following unit cell dimensions with a monoclinic space group $C2/c$: $a=25.82$ Å, $b=3.79$ Å, $c=23.72$ Å and $\beta=90.4°$.[5] As the

5) M. Ashida, N. Uyeda and E. Suito, This Bulletin, **39**, 2616 (1966).

axial angle, β, is nearly equal to a right angle, the a* and c* axes of the reciprocal lattice are approximated by the directions along the a- and c-axes of the real crystal respectively. Consequently, the projection of the reciprocal c* axis on the basal plane shown in Figs. 8 and 10 may be considered the projection of the c-axis on the substrate face.

The cleavage face of the potassium chloride crystal is the (001) plane, in which K^+ ions and Cl^- ions are alternatively located in the [100] and [010] directions at the distance of 3.14 Å, as is shown in Fig. 11. A phthalocyanine molecule

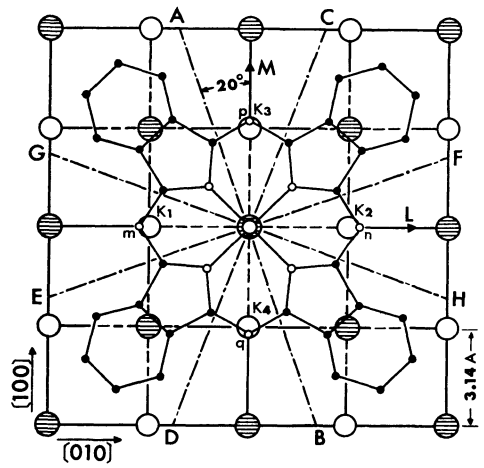

Fig. 11. The lattice structure of the cleavage face of KCl and the orientation relative to the deposited molecule of Cu-phthalocyanine.

is usually represented by a set of two molecular axes, L and M, which are defined through the center of the molecule through the bridge nitrogen atoms, as Fig. 11 shows. A projection of the c-axis of the crystal on a molecular plane makes an angle of about 20° with the M molecular axis, and the b-axis of the crystal is projected on a molecular plane in the direction of the M molecular axis.

According to Kobayashi,[6] the electrons in the phthalocyanine molecule are distributed on the bridge nitrogen atoms at the highest density; this causes an electrophilic effect to occur at these nitrogen atoms.[7] As the potassium ion has an electron-attractive force, the bridge nitrogen atoms of phthalocyanine possibly tend to come closer to the potassium ion. In the case of crystals deposited on potassium halides, it seems reasonable to consider that the bridge nitrogen atoms of the molecule which parallelly faces the (001) plane of the substrate crystal come into contact with the potassium ions on the cleavage plane. When it is tentatively assumed that four nitrogen atoms on the L and M molecular axes (e. g., m, n, p and q) are located on potassium ions (e. g., K_1, K_2, K_3 and K_4), the projection of the c-axis of the crystal on the substrate plane makes an angle of either $+20°$ or $-20°$ with the [100] direction of potassium chloride, as is shown by the line AB or CD; these lines give rise to two crystals with a plane of mirror symmetry, as is shown in Figs. 12 A and B. It should be noted that this angle coincides with that between the projection of the reciprocal c* axis of the phthalocyanine crystal and the [100] direction of potassium chloride as revealed by the electron-diffraction pattern. In addition to this choice of the c-axis, the above molecule parallel along the b-axis shifts in either the +M or −M direction depending upon the staggering of the overlapping molecule; this results in two different crystals by the axis of two-fold symmetry, as is shown in Figs. 12 A and C. The

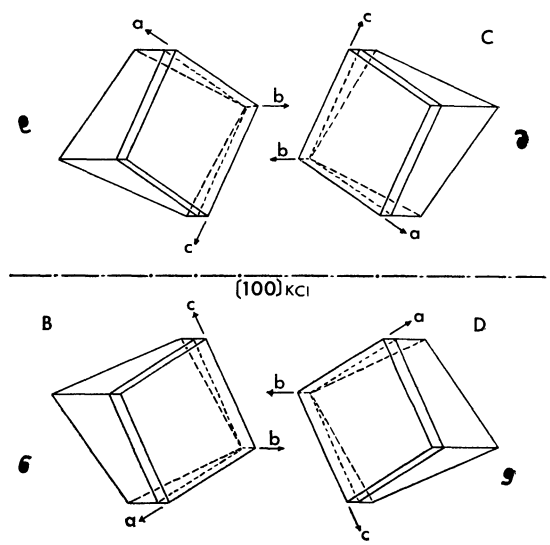

Fig. 12. Schematic diagram of the projection of crystals on the cleavage face of KCl.

M molecular axis can also lie parallel to the [010] direction of potassium chloride; that is, the staggering of the overlapping molecule may happen in four other ways in the [010] direction, thus forming a final crystal which has a projection of the c-axis like either EF or GH. Thus, the total film configuration involves a C_{4v} symmetry as far as the orientation of the individual crystallites is concerned.

Even though the same standing b-axis orientation appeared on potassium chloride, the crystal deposited onto potassium bromide showed an apparent azimuthal angular shift in the plane of the film. A cleavage face of potassium bromide is the (001) plane, in which K^+ ions and Br^- ions are located in the [100] and [010] directions at a

6) H. Kobayashi, *J. Chem. Soc. Japan, Pure Chem. Sect. (Nippon Kagaku Zasshi)*, **82**, 272 (1961).
7) C. J. Pedersen, *J. Org. Chem.*, **22**, 127 (1957).

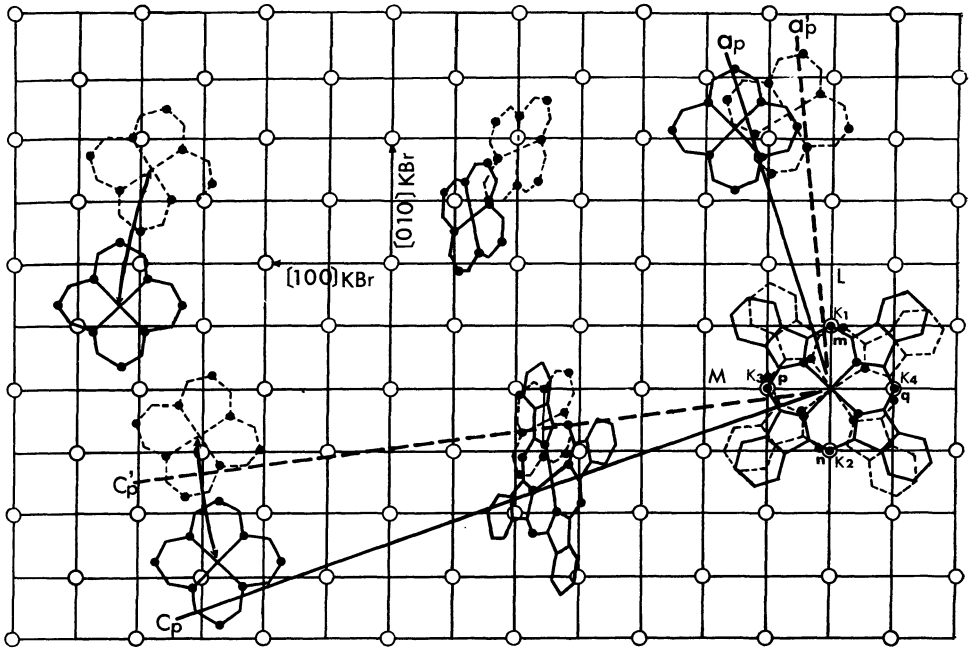

Fig. 13. The lattice structure of the cleavage face of KBr and the orientation relative to the deposited molecule of Cu-phthalocyanine.

distance of 3.29 Å, as is shown in Fig. 13. As has been described above, if four nitrogen atoms on the L and M molecular axes (e. g., m, n, p and q) of phthalocyanine, defined as the point of origin, are located on potassium ions (e. g., K_1, K_2, K_3 and K_4), the nitrogen atoms in the neighboring molecules are projected on the substrate face as is shown schematically in the figure. In this case, the projection of the c-axis, C_p, makes an angle of 20° with the [100] direction of potassium bromide. This angle coincides with that between the projection of the reciprocal c* axis of the phthalocyanine crystal, AB, and the [100] direction of potassium bromide as is revealed by the electron diffraction in Fig. 9. Since the orientation of the deposited crystals is distributed in an angular range of about 12° in azimuth, the projection of the c-axis lies between C_p and C_p'; that is, the molecules in the crystal may be rotated on the substrate face as is shown by the dotted line. The above characteristic orientation may plausibly be ascribed to the difference in misfitting between the deposit and the substrate crystal. The interaction betweeen the molecule and the substrate will also vary depending upon the differences in the negative ions.

The deposited crystals of phthalocyanine appeared in a C_{4v} symmetric orientation on the (001) planes of potassium chloride and potassium bromide. The planes of mirror symmetry corresponded to the (100) and (010) planes of potassium halides. On the contrary, phthalocyanine crystals deposited onto the (001) plane of muscovite, which apparently has a hexangonal symmetry, showed only a C_{2v} symmetry,[1,2] this symmetry was considered to be due to the influence of the staggering in the mica layer under the cleavage face. This suggestion was supported by the present finding that the orientation of the phthalocyanine crystal had the same symmetry as that of the substrate face in the case of alkali halide, which has no such staggering as muscovite.

The crystal growth of evaporated films consists of two factors, the rates of nucleation and its growth. A variation in the crystal shape is caused by the contribution of the two factors. When phthalocyanine is deposited onto a cleavage face of potassium chloride, the preferential nucleation occurs at steps on the substrate face. Fast nucleation causes a number of fine crystals at the steps. On the contrary, the deposited molecule can relatively freely move over the smooth parts of the surface; thus it collides with other deposited molecules to form a large aggregate, and the nuclei grow to a large dendrite on these parts. As the rate of sublimation is increased, the deposited molecules have more chance to collide, thus leading to the nucleation predominate in number. Therefore, fine crystals appeared all over the surface with uniform dimensions and formed a continuous film with a wave-like pattern, as is shown in Fig. 4. In contrast to the crystals deposited onto potassium chloride, the film formed on muscovite was composed of small rectangular crystals; dendrites

were not observed even when the film had the same standing b-axis orientation.[2] Since a cleavage face of muscovite is considered to be fairly smooth in an atomic scale over a limited area, this appearence is probably due to the difference in nucleation velocity. It seems that the molecules deposited onto muscovite have a lower mobility than those on potassium chloride, and that the difference in mobility depends upon the bonding force of the interface between deposit and the substrate.

Recently, Ino et al.[8] investigated the epitaxial growth of metal on a surface of sodium chloride which has been cleaved either in an ultrahigh vacuum of 10^{-7} to 10^{-9} mmHg or in a rather poor vacuum of 10^{-4} to 10^{-5} mmHg; they concluded that some gas molecule adsorbed on the sodium chloride surface is necessary for the epitaxial growth of a single crystal of f. c. c. metal. Furthermore, Mattews and Grünbaum[9] established that moist air modified the (001) plane of sodium chloride in such a way that f. c. c. metals tend to grow epitaxially upon it. In the present experimental results, the film condensed on sodium chloride has a random orientation. Phthalocyanine as well as condensed polycyclic aromatic compounds repulse water rather strongly. Since adsorbed water molecules could not be removed from the cleavage face of sodium chloride under the present experimental conditions, it is reasonable to postulate that the orientation overgrowth of copper-phthalocyanine on sodium chloride is disturbed by the adsorbed water molecules. This assumption was further confirmed by the use of sodium chloride cleaved in vacuo. In this case, the deposited crystals were found to have the standing b-axis orientation. The results will appear in detail in a future report.

The author is very grateful to Professor Eiji Suito of the Institute for Chemical Research, Kyoto University, for his interest and support; he wishes also to thank Dr. Natsu Uyeda of the same Institute for his many helpful discussions and suggestions during this work. Moreover, he is indebted to Professor Wasaburo Jono and Professor Teizo Watanabe of Kobe University for their encouragement in this work.

8) S. Ino, D. Watanabe and S. Ogawa, *J. Phys. Soc. Japan*, **19**, 881 (1964).
9) J. W. Matthews and E. Grünbaum, *Appl. Phys. Letters*, **5**, 106 (1964).

BULLETIN OF THE CHEMICAL SOCIETY OF JAPAN VOL. 39 2638—2642 (1966)

The Mechanism of the Catalytic Hydrogenation of Propene on Nickel, Palladium, and Platinum (The Application of Microwave Spectroscopy to Isotopic Analysis)[1]

By Kozo Hirota and Yoshie Hironaka[2]

Faculty of Science, Osaka University, Toyonaka, Osaka

(Received May 6, 1966)

The catalytic hydrogenation of propene with deuterium gas and its isotopic exchange reaction with deuterium oxide have been carried out at room temperature, and the remaining propene has been subjected to microwave spectroscopic analysis so as to determine the isotopic isomer-distribution of propene-d_1 and -d_2. From the results, the following conclusions have been drawn: (1) the rate-determining step in the hydrogenation on platinum as well as nickel and palladium catalysts is the addition of hydrogen to the half-hydrogenated species; (2) the kinds of chemisorbed species and their distribution prior to the rate-determining step are not always the same, but depend on the metals, and (3) the life-time of the chemisorbed propene is shorter than the successive time interval of its exchange process on nickel, but this is not the case on platinum nor, probably, on palladium.

In previous reports,[3,4] the chemisorbed states of propene on nickel and palladium catalysts were investigated on the basis of the subspecies-distributions[5] of propene-d_1 in the products of the exchange and hydrogenation reaction with deuterium gas and deuterium oxide:

1) Presented at the 19th annual meeting of the Chemical Society of Japan, April 1, 1966.

2) Present address: Research Institute of Science and Industry, Osaka University.

3) J. Hirota and Y. Hironaka, *J. Catalysis*, **4**, 602 (1965); K. Hirota, Y. Hironaka and E. Hirota, *Tetrahedron Letters*, **1964**, 1645.

4) Y. Hironaka and K. Hirota, This Bulletin, **38**, 1558 (1965).

5) Subspecies may be called "isotopic isomers."

$$C_3H_6 + nD_2 \rightarrow C_3H_{8-y}D_y, \text{ and } C_3H_{6-x}D_x, \quad (1a)$$

$$C_3H_6 + nD_2O \rightarrow C_3H_{6-x}D_x. \quad (1b)$$

It has been proposed that the main chemisorbed states of propene are the associative-type I on nickel and the π-allyl-type II on palladium. In addition, both reactions were found to occur with the half-hydrogenated state, C_3H_7, as an intermediate.

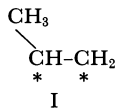

I

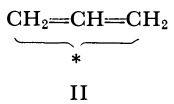

II

Since these findings are very important to a discussion of the mechanism of catalytic hydrogenation, a similar investigation was made of platinum, using the mass spectrometric and microwave-spectroscopic methods in the analysis, as adopted in previous reports. The object of the present paper is not only to report the new knowledge obtained and to discuss it from the standpoint of the mechanism of catalytic hydrogenation in general, but also to report the superiority of microwave spectroscopy for isotopic analysis.

Experimental

The platinum catalyst was prepared from chloroplatinum acid by reduction with formaldehyde.

The other materials and procedures were the same as those in the cases of nickel and palladium.[3,4] The subspecies distribution of propene-d_2 in the product was determined, as was that of propene-d_1, by applying the microwave spectroscopic method to the samples, without any separating procedure.

The reaction times in both reactions were selected in such a way that the parameter, $\phi=\frac{1}{6}\sum_x xd_x$, an indication of the exchange degree, took a value similar to that of nickel and palladium (about 10%). (Cf. Table I (A))

Results

Table I (B) shows the isotopic distribution of the deuteropropenes remaining after the reactions. Deuteropropenes with higher x values can be observed, because d_5 and d_6 were negligibly small in the cases of most nickel and palladium catalysts.

The distribution of deuterium in the propene-D_2 system was slightly wider than that in the propene-D_2O system when Ni and Pd were used as catalysts, but, according to the present research, the deuterium-distribution of the proepene-D_2O system is, on the contrary, wider than that of the propene-D_2 system.

In the subspecies distrubtion of propene-d_1, shown in Table II, the characteristic differences of the three catalysts are obvious. There is a tendency for the methylene group to be most exchangeable on platinum, though only the methine group was easily exchanged in the case of nickel; there is also a difference in the case of palladium, by which all the three groups were exchanged with nearly equal probabilities. However, it is

Table I. Experimental conditions and deuterium-distribution of reaction products

(A) Experimental condition

No.	Catalyst	g.	Sample (mole$\times 10^{-3}$)				Reaction	
			C_3H_6	D_2O	D_2	C_3H_6/D_2	Temp.	Time
5505	Pt-black	0.50	2.18	—	1.09	2.0	20°C	20 min.
41017	Pt-black	0.30	2.18	9.9	—	—	25°C	100 hr.

(B) Distribution of deuterium in remaining propene (%)

No.	d_0	d_1	d_2	d_3	d_4	d_5	d_6	$\phi=\frac{1}{6}\sum xd_x$
5505	60.6	21.9	9.5	4.7	2.6	0.7	—	11.5
41017	53.5	26.9	8.9	4.9	2.7	1.9	1.1	14.7

Table II. Distribution of subspecies (%) of propene-d_1*

No. of run subspecies	5505 Pt, D_2O	41017 Pt, D_2O	3513** Ni, D_2O	3515** Pd, D_2O
CH_2D-CH=CH_2	21.1±1.7	19.5±2.1	22.5±2.7	59.2±2.2
	(7.0)	(6.5)	(7.5)	(19.7)
t-CH_3-CH=CHD	39.1±3.3	47.4±4.8	9.5±2.1	13.1±1.3
c-CH_3-CH=CHD	13.1±2.5	5.8±1.4	9.9±2.2	13.7±1.5
CH_3-CD=CH_2	26.7±3.6	27.3±4.5	58.1±5.1	14.1±1.3

* Trans- and cis-form denotes the position of deuterium against the CH_3 group.

** These two runs, reported already, were shown for the sake of comparison.

Table III The subspecies distribution of propene-d_2 in the products of the metal/D_2O systems

Subspecies		Ni		Pd		Pt	
		Obs.	(Calcd.)	Obs.	(Calcd.)	Obs.	(Calcd.)
CHD_2-CH=CH_2	3,3-d_2	10.0	(11.3)	25.4	(43.6)	25.5	(6.4)
CH_2D-CD=CH_2	2,3-d_2	38.7	(39.6)	19.0	(14.8)	12.1	(24.3)
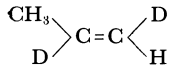	*trans*-1,2-d_2	15.8	(17.1)	5.4	(3.5)	8.7	(4.0)
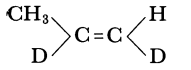	*cis*-1,2-d_2	17.1	(17.1)	5.6	(3.5)	18.4	(32.4)
CH_3-CH=CD_2	1,1-d_2	4.9	(2.8)	7.5	(3.4)	15.8	(6.8)
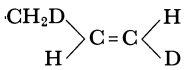	*trans*-1,3-d_2	6.9	(6.8)	18.7	(15.6)	15.9	(23.1)
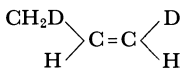	*cis*-1,3-d_2	7.1	(6.8)	18.4	(15.6)	3.7	(2.8)

important in the case of platinum that the exchange degree of $CH_3CH{=}CHD$ is not the same as between its cis- and trans-forms, irrespective of which is used, deuterium gas (No. 5505) or deuterium oxide (No. 41017). Considering this, the same tendency may exist in the case of the Pd/D_2O system,[3] though it is at present difficult to derive such a conclusion because the difference lies within the limits of experimental error.

The above findings can also be confirmed qualitatively by the clear difference in the infrared spectra of the products obtained by the use of the the three catalysts.

In Table III, the subspecies distribution of propene-d_2 is shown in addition to the data on Ni and Pd, which have already been mentioned.[3] The discrepancies among the distributions of the three catalysts and the calculated values shown in brackets will be discussed below.

Discussion

The Half-hydrogenated State. — In view of the similarity between the two reactions, 1a and 1b, in the substancies distribution of C_3H_6-d_1 (Table II), it can be said that the catalytic hydrogenation proceeds on platinum via the half-hydrogenated state, C_3H_7, in the same scheme as on nickel and palladium, making the step A rate-determining at room temperature. In other words, the exchange reaction occurs by the back ward process of the step B

$$\underset{*}{C_3H_6} \underset{-H}{\overset{H}{\rightleftarrows}} \underset{*}{C_3H_7} \xrightarrow{H} C_3H_8 \qquad (2)$$

(B) (A)

$$\underset{* \ *}{C_3H_6} + D \rightarrow \underset{*}{C_3H_6D} \rightarrow \underset{* \ *}{C_3H_5D} + H \qquad (3)$$

because the coincidence of No. 5505 and No. 41017 in the subspecies distribution of propene-d_1 is too close for the other reaction schemes to be possible.

However, in deriving this conclusion, it must be remembered that the water molecule is, as usual, assumed to exist dissociatively on the metal surface.

$$H_2O \longrightarrow \underset{*}{HO} + \underset{*}{H} \qquad (4)$$

Though the non-dissociative adsorption of water molecule is also possible on some parts of metal surfaces,[6] the state seems to be indifferent to the present exchange reaction in view of the above results.

Such being the situation, the scheme of Eq. 3 may be justified, and the so-called Rideal mechanism, Eq. 5, seems to be implausible; i. e., the possibility that the half-hydrogenated state is formed only by the reaction of the hydrogen molecule and chemisorbed propene in one step[7] is of less importance.

$$\underset{* \ *}{C_3H_6} + H_2 \longrightarrow \underset{*}{C_3H_7} + \underset{*}{H} \qquad (5)$$

However, the scheme of the exchange reaction, Eq. 1b, proposed on nickel may not necessarily be derived. The scheme of the reaction may be different on palladium and on other metals. The chemisorbed states[8] of propene are not always the same; rather, they may differ according to the metals as well as according to the reaction conditions. These points will be investigated below.

The Distribution of the d_1 Subspecies.— The characteristic features of the activity of platinum, clarified by the subspecies distribution of propene-d_1, suggest that some new chemisorbed species is produced from propene on platinum simultaneously with the associative state which is

6) G. C. Bond, "Catalysis by Metals," Academic Press, New York (1962), p. 219.

7) G. H. Twigg, *Discussions Faraday Soc.*, **8**, 152 (1950).

8) Besides, there is a possibility that the associative state, $\underset{* \ *}{C_3H_6}$, is π-bonded rather than σ-bonded to the surface on some metals.

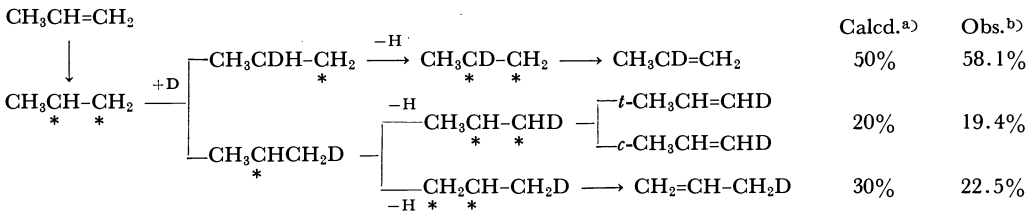

	Calcd.[a]	Obs.[b]
$CH_3CD=CH_2$	50%	58.1%
t-$CH_3CH=CHD$ + c-$CH_3CH=CHD$	20%	19.4%
$CH_2=CH-CH_2D$	30%	22.5%

Fig. 1. Scheme of the associative mechanism of the exchange reaction.

a) Percentage of the products on the right side are calculated by neglecting the isotopic effect during hydrogenation and dehydrogenation.

b) The result of Ni/D_2O system (No. 3513) is shown for the sake of the comparison.

predominant on nickel. In explanation of this, the existence of a dissociative state may be suggested; such a state would especially explain the predominance of the trans-form over the cis-form of CH_3–CH=CHD in the product. Such a suggestion is not new, because the state has already been mentioned on platinum by Farkas[9] and has been proposed by Burwell,[10] who expressed the states as follows:

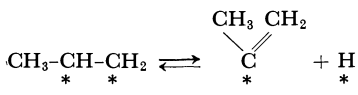

(IIIa) (6a)

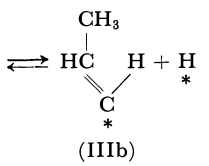

(IIIb) (6b)

Both dissociative states, IIIa and IIIb, are convenient in explaining the broad distribution of deuterated propenes. Of the two dissociative states, however, the state IIIb, CH_3–CH=$\overset{*}{C}$H, would be more abundant, because less CH_3CDCH_2 is produced than the sum of *trans-* and *cis*-CH_3-CHCHD. The chemisorbed species may lie on the metal plane perpendicularly because of the steric hindrance of the methyl group. Therefore, the exchange occurs as follows:

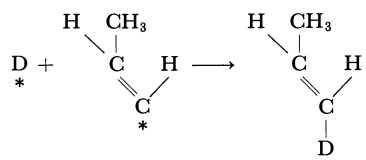

(7)

On the other hand, an alternative explanation on the basis of the associative chemisorbed state is possible; i. e., because of the presence of the methyl group, the propene may not be chemisorbed parallel to the metal plane, but may take an inclined state. However, the production of the trans-form from such a state is hard to explain without introducing another assumption into the exchange process.

Parallel with the dissociative process, the exchange reaction on platinum may be realized by the associative process proposed for on nickel; it is shown diagramatically in Fig. 1. According to this scheme, the production of 3-d_1, 2-d_1 and, t- and c-1-d_1 can be explained quantitatively, because the isotopic effect can be neglected, and the subspecies distribution of propene-d_1 can be given by Eq. 8 on the assumption that the addition of D to $CH_3\overset{*}{C}H-\overset{*}{C}H_2$ occurs at an equal rate:

$$3\text{-}d_1 : 2\text{-}d_1 : (t+c)\text{-}1\text{-}d_1 = 3 : 5 : 2 \qquad (8)$$

The application of Eq. 8 to the data of nickel gives a semi-quantitative coincidence between theory and experiment. However, the Pt/D_2O system (No. 41017) gives a different result. By assuming the associative mechanism on platinum, the amounts of c-1-d_1 and t-1-d_1 are made equal to be 5.8% and the percentages of other subspecies are calculated (cf. Table IV). It is evident from the table that, except for t-1-d_1, the amounts agree well with the calculated values.

Table IV. The isotopic distribution of the propene-d_1 produced on platinum catalysts (%)
(Run: No. 41017)

	c-1-d_1	t-1-d_1	3-d_1	2-d_1
Obs.	5.8	47.8	19.5	27.3
Calcd.	(5.8)	(5.8)	19.4	29.0

This indicates that the difference between 47.8 and 5.8% (i. e., 42.0%) in t-1-d_1 results from the occurrence of the dissociative mechanism, while the residual 5.8% results from that of the associative mechanism.

Finally, it must be mentioned that, by the associative mechanism, the d_1-distribution of Pd/D_2O cannot be explained at all. Judging from the above reasoning, the dissociative mechanism may possibly play some role in the exchange reaction in the case of palladium as well as in those of platinum.

9) A. Farkas and L. Farkas, *J. Am. Chem. Soc.*, **60**, 22 (1938).

10) R. L. Burwell, Jr., *Chem. Revs.*, **57**, 895 (1957).

Distribution of Propene-d_2.—In Table III, the calculated subspecies distribution of propene-d_2 is shown in parentheses. Those values have been obtained on the assumption that the second exchange occurs independently and in the same way as that of the first. In the case of nickel, the values coincide well, indicating that the second exchange occurs independently of the first exchange. This finding, already reported by Morino and Hirota,[11] can be explained by the fact that the desorption of the propene-d_1 produced occurs at a faster rate than the second exchange process at the same chemisorbed state. However, since no such tendency is indicated in the case of platinum, the chemisorbed state on this metal may have a life-time sufficient to allow both processes to have some correlation. Of course, it cannot be said, from the results shown in Table III alone, that the lifetime of chemisorbed propene on platinum is longer than that on nickel.

As for palladium, an intermediate property of nickel and platinum is suggested in the present distribution, as it is in the propene-d_1 distrubtion. Such a result may be brought about from the adsorbed state on palladium, which is of the π-allyl type, as has been suggested in a previous paper.

11) Y. Morino and E. Hirota, *J. Chem. Soc. Japan, Pure Chem. Sect. (Nippon Kagaku Zasshi)*, **85**, 535 (1964).

Conclusion

As far as the reaction conditions in the present paper are concerned, the following conclusions are obtained: (i) the rate-determining step in the catalytic hydrogenation on nickel, palladium and platinum is the addition of hydrogen to the half-hydrogenated species, C_3H_7; (ii) the kinds of chemisorbed species and their distribution prior to the rate-determining step, however, vary with the metal, and (iii) the life-time of the chemisorbed propene is shorter than the successive interval of its exchange process so far as nickel is concerned, while this may not be true in the case of platinum and probably in that of palladium as well.

It must be mentioned, however, that further investigations are now going on in order to investigate if the above conculsions, especially Eq. 2, are applicable to these metals irrespectively of their methods of preparation and the presence of carriers.

We wish to express our sincere thanks to Professor Yonezo Morino and Dr. Eizi Hirota, the University of Tokyo, for their discussions and help in performing the present research.

BULLETIN OF THE CHEMICAL SOCIETY OF JAPAN VOL. 39 2643—2645 (1966)

Studies of the Aqueous Solution of a Surface Active Substance by Means of an Ultrasonic Interferometer. III. Determinations of Ionic and Nonionic Hydrations of Sodium Alkyl Sulfate

By Koji SHIGEHARA*

Department of Chemistry, Faculty of Science, Tokyo Metropolitan University, Setagaya-ku, Tokyo

(Received May 13, 1966)

The amounts of water of ionic and nonionic hydration were calculated for sodium alkyl sulfate in the state of molecular dispersion from the data obtained by the author and under the assumptions usually adopted: (a) the solution, as a whole, consists of several volume elements of different compressibilities; (b) the ionic radical together with its hydration water is incompressible; (c) the compressibility of the water of nonionic hydration for the CH_2 group of the hydrocarbon chain is the same as that of ordinary ice; (d) the compressibility and the molar volume of the CH_2 radical in the state of molecular dispersion are the same as those in the micellar state. The water of hydration was calculated to be 2.1 mole per mole of the CH_2 radical, and 4.9 mole per mole of the ionic radical, the latter value being the same as that of the solute in the micellar state previously reported. The molar volume of the water of nonionic hydration is found to be slightly less than that of free water, in accordance with the prediction of others. The dehydration of sodium alkyl sulfate caused by the addition of inorganic electrolyte has also been observed.

In previous papers,[1,2] it has been shown that differential ultrasonic interferometry is one of the most useful methods for the study of aqueous solutions of surface active substances. The sound velocity measurement by this method, together with the density measurement, makes possible the calculation of the compressibility and the critical micelle concentrations (CMC) of aqueous solutions of several alkyl sulfates with or without the addition of inorganic electrolytes, and from these data the compressibility, the molar volume and the hydration number of ionic micelle were determined. It has been inferred therefrom that the hydrocarbon interior of the ionic micelle is liquid-like rather than solid-like; the nonionic hydration of CH_2-chain is also one of the most important factors responsible for the dissolution of the surface active substance, and the builder action of the inorganic electrolyte is due not only to the decrease in the mutual repulsion of the ionized head group of the surface active substance caused by the gegenion attachment to this group, but also to the decrease in the amount of nonionic hydration of the CH_2-chain of the surface active substance. However, no quantitative discussion of the nature and the amount of the nonionic hydration of the CH_2-chain of a surface active substance has yet been reported. The present paper will give an estimation of the nonionic hydration of the CH_2-chain of the surfactant molecule.

Calculation

A solution (total volume, V; compressibility, β) is assumed to consist of several volume elements, v_1, v_2,$\cdots$, of different compressibilities, β_1, β_2,$\cdots$, in such a manner as:[1]

$$V = v_1 + v_2 + \cdots \quad (1)$$

$$V\beta = v_1\beta_1 + v_2\beta_2 + \cdots \quad (2)$$

Then, for a solution of an alkyl sulfate below CMC, we have:

$$V = V_1(n_1 - nn_x - nn_yN) + V_2nn_yN + V_3nN + V_4n \quad (3)$$

$$V\beta = V\beta_1 + V_2nn_yN(\beta_2 - \beta_1) + V_3nN(\beta_3 - \beta_1) + V_4n(\beta_4 - \beta_1) \quad (4)$$

where n_1 and n denote the mole numbers of the solvent and the solute in the solution of the volume (V) respectively; n_x, the mole number of the water of ionic hydration per mole of the SO_4Na radical; n_y, the mole number of the water of nonionic hydration per mole of the CH_2 radical of the alkyl chain; N, the number of carbon atoms in a solute molecule; V_1 and V_2, the molar volume of free water and the water of nonionic hydration respectively; V_3, the molar volume of the CH_2 radical of the solute molecule; V_4, the molar volume of the SO_4Na radical together with its n_x moles of

* Present address: Ocean Research Institute, The University of Tokyo, Nakano-ku, Tokyo.

1) T. Sasaki and K. Shigehara, IVth International Congress of Surface Activity, B/IV. 13, Brussels, Belgium (1964); K. Shigehara, This Bulletin, **38**, 1700 (1965).

2) K. Shigehara, This Bulletin, **39**, 2332 (1966).

hydration water; and β, β_1, β_2, β_3 and β_4, the compressibility of the solution as a whole and of the parts which have the molar volumes of V_1, V_2, V_3 and V_4 in the solution respectively. Thus, the terms of the right hand side of Eq. 3 indicate the volumes of free water, the water of hydration of the hydrocarbon chain, the hydrocarbon chain, and the hydrated ionic head respectively in that order. From Eqs. 3 and 4, we obtain:

$$\overline{V} = (-n_y V_1 + n_y V_2 + V_3)N + V_4 - n_x V_1 \quad (5)$$

$$d\beta/dC = [V_2(\beta_2 - \beta_1) + V_3(\beta_3 - \beta_1)]N + V_4(\beta_4 - \beta_1) \quad (6)$$

where $\overline{V}$ denotes the partial molar volume of alkyl sulfate, and C, the molarity of the solute ($C=n/V$).

It is assumed that such ionic radicals as HSO_4^- and $-SO_4^-$ (alkyl sulfate), and its hydration water, are incompressible, as has been accepted by many authors,[3] that V_3 and β_3 are equal to the molar volume (V_m) of CH_2 in the micelle and the compressibility (β_m) of the hydrocarbon parts in the micelle respectively, and that β_2 is equal to the compressibility (β_{ice}) of ordinary ice, as was accepted by Sasaki and Yasunaga[4] and by Shiio et al.[5] The last assumption is also in accordance with the view that the water molecule is oriented towards the CH_2 radical and that they form an ice-like structure by means of H-bonds between them, thus producing a microscopic "iceberg" around dissolved molecules of hydrocarbon.[6,7] The following equations can then be obtained for the solution of alkyl sulfates below CMC:

$$\overline{V} = (-n_y V_1 + n_y V_2 + V_m)N + V_4 - n_x V_1 \quad (7)$$

$$d\beta/dC = [V_2(\beta_{ice} - \beta_1) + V_m(\beta_m - \beta_1)]N - V_4\beta_1 \quad (8)$$

where the values of β_1, β_{ice}, β_m, V_1 and V_m are 44.082,[1] 11.1,[8] 70.1[1] (all in 10^{-12} cm^2/dyn.), 18.094[9] and 17.1[1] (both in cc./mol.) respectively.

In his previous papers,[1] the author has reported empirical equations* corresponding to those of Eqs. 7 and 8:

$$\overline{V} = 15.9N + 46 \quad (9)$$

$$d\beta/dC = -0.776\times10^{-12}\times N - 5.94\times10^{-12} \quad (10)$$

where $\overline{V}$ and $d\beta/dC$ are expressed in cc./mol. and (cm^2/dyn.)/(mol./l.) respectively.

By comparing Eq. 7 with Eq. 9, and Eq. 8 with Eq. 10, with due consideration of the difference in units, the n_x, n_y, V_2 and V_4 values are calculated to be as shown in Table I.

TABLE I

Radical	Amount of hydration water of (mol./mol.)	Molar volume of hydrated (cc./mol.)	Molar volume of hydration water of (cc./mol.)
SO_4Na	4.9	135	—
CH_2	2.1	—	17.5

The mole number of the water of ionic hydration per mole of the SO_4Na radical, $n_x=4.9$, and the molar volume of the hydrated SO_4Na radical, $V_4=135$ (cc./mol.), are consistent with those of the solute in the micellar state, determined independently in previous papers.[1] The mole number of the water of nonionic hydration per mole of the CH_2 radical, $n_y=2.1$, agrees with Butler's assumption,[6] which he adopted to calculate the heat of hydration of a homologous series of alcohols. There he considered that two hydrogen atoms of the CH_2 radical give rise to two H-bonds around it. The molar volume of the water of nonionic hydration, $V_2=17.5$ cc./mol., is slightly less than that of free water. This fact agrees with those reported by other authors.[7] All these facts lead us to the conclusion that the assumptions used in the calculation are permissible.

In a preceding paper,[2] the present author has reported that the $\overline{V}$ value of alkyl sulfate is not affected by the addition of inorganic electrolyte, that $d\beta/dC$ below CMC increases with the concentration of the added electrolyte, and that the extrapolated value of $d\beta/dC$ to $N=0$ shows the same value independently of the presence of the added electrolyte (Fig. 1). From these results and from Eqs. 7 and 8, the n_x, n_y, V_2 and V_4 values in the presence of inorganic electrolytes are obtained by a calculation similar to that mentioned above. It was confirmed that the values of n_x, V_2 and V_4 thus obtained were not affected by the addition of inorganic electrolytes. On the other hand, as is shown in Fig. 2, the mole number of the water of nonionic hydration per mole of the CH_2 radical, n_y, decreases with the increase in the concentration of inorganic electrolytes until it reaches a minimum value which is about 80% of the n_y value in the absence of electrolytes. This

* The measurements at 30°C.

9) "International Critical Tables," Vol. III, McGraw-Hill Book Co., New York (1928), p. 26.

3) A. Passynski, *Acta Physicochimica USSR*, **8**, 385 (1938); Y. Wada, S. Shimobo, M. Oda and J. Nagumo, *Applied Phys. (Oyo Buturi)*, **17**, 257 (1948); T. Yasunaga and T. Sasaki, *J. Chem. Soc. Japan, Pure Chem. Sect. (Nippon Kagaku Zassi)*, **72**, 87, 89 and 366 (1951); T. Sasaki and T. Yasunaga, This Bulletin, **28**, 269 (1955); K. Tamura and T. Sasaki, ibid., **36**, 975 (1963).

4) T. Sasaki and T. Yasunaga, This Bulletin, **26**, 175 (1953).

5) H. Shiio, T. Ogawa and H. Yoshihashi, *J. Am. Chem. Soc.*, **77**, 4980 (1955).

6) J. A. V. Butler, *Trans. Faraday Soc.*, **33**, 229 (1937).

7) H. S. Frank and M. W. Evans, *J. Chem. Phys.*, **13**, 507 (1945); W. F. Claussen and M. F. Polglase, *J. Am. Chem. Soc.*, **74**, 4817 (1952); F. Franks and D. J. G. Ives, *J. Chem. Soc.*, **1960**, 741; J. T. Davies and E. K. Rideal, "Interfacial Phenomena," Academic Press, New York and London (1961), pp. 18 and 163.

8) F. Joha and P. Scherrer, *Helv. Phys. Acta*, **25**, 35 (1952).

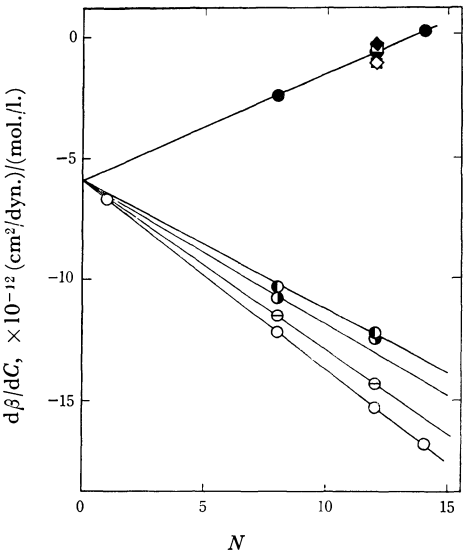

Fig. 1. $d\beta/dC$ vs. N.

Below CMC:
○ Without electrolyte
⊖ 0.05 N NaCl
◑ 0.1 N NaCl
◐ 0.5 N NaCl

Above CMC:
● Without electrolyte
■ 0.05 N NaCl
◇ 0.1 N NaCl
□ 0.5 N NaCl
◆ 1 N NaCl

confirms the view inferred in the former report[2] that the addition of inorganic electrolytes not only serves to increase the gegenion attachment, as is generally believed, but may also remove water of hydration from the hydrophobic chain of surface active substances. Both of these factors may be considered to decrease the CMC of the surface active substance.

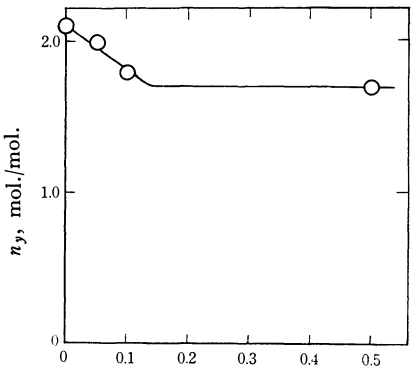

Fig. 2. n_y vs. concentration of NaCl.

The author wishes to express his deep gratitude to Professor Tsunetaka Sasaki of our University for his kind direction and valuable criticism. The cost of this research has been defrayed by a grant of the Ministry of Education given to Professor Sasaki.

BULLETIN OF THE CHEMICAL SOCIETY OF JAPAN VOL. 39 2645—2647 (1966)

The Physical Properties and Crystal Structure of 2-Bromo-1, 1, 1-trichloro-2-methylpropane

By Tsutomu KOIDE, Tsutomu ODA, Osamu WASHIO* and Kazuo FUJITA**

Laboratory of Chemistry, Osaka University of Liberal Arts and Education, Tennoji, Osaka

(Received May 16, 1966)

2-Bromo-1, 1, 1-trichloro-2-methylpropane gives a plastic crystal, named by Timmermans (*J. Chim. Phys.*, **35**, 331 (1938)), which is optically isotropic and which has a density of 1.97 g./cc. at 25°C. The X-ray data can be interpreted with a body-centered cubic lattice, with 7.42 Å for the unit cell length containing two molecules. The symmetry interpretation gives a crystal structure of a disordered orientation of molecules. It was found, by means of optical measurements and differential thermal analysis, that there is a phase transition at about −62°C, below which the crystal is in a lower symmetry.

In our previous papers,[1-5] several hexasubstituted ethane derivatives expressed by the formula

* Present adrress, Gojo High School, Gojo, Nara.
** Died, Oct. 1960.

1) T. Oda and T. Koide, This Bulletin, **29**, 208 (1956).
2) T. Koide, T. Oda and I. Nitta, ibid., **29**, 738 (1956).
3) T. Koide, T. Oda and I. Nitta, ibid., **30**, 119 (1957).
4) T. Koide, S. Takeuchi, T. Oda, Y. Yamada and I. Taguchi, ibid., **30**, 683 (1957).
5) T. Koide, Y. Kato and T. Oda, ibid., **33**, 1572 (1960).

$X_{3-n}(CH_3)_nC\text{-}C(CH_3)_mX_{3-m}$ were studied from the point of view of crystal chemistry. It was observed that all the investigated substances undergo a phase transition in the solid state and that their high temperature modifications belong to the cubic structure, in which the molecular arrangement is in a disordered state.

It seems that it would be interest to see what effect may occur in the molecular behavior in the crystal, when substitution is extended to three species of atoms and groups such as chlorine, bromine and methyl groups, since they have nearly equal van der Waals radii.[6] In the present paper, the authors have studied 2-bromo-1, 1, 1-trichloro-2-methylpropane by means of X-ray diffraction, differential thermal analyses and optical measurements.

Experimental and Results

Material.—2-Bromo-1, 1, 1-trichloro-2-methylpropane was prepared by the bromination of chloreton with phosphorus pentabromide, following the method of Willgrerodt and Dürr.[7] The material obtained was purified by fractional melting and further by recrystallization three times from ether. The final purification was effected by fractional sublimation in a high vacuum (about 10^{-5} mmHg). The crystal shows plasticity and high volatility, its fumes irritating the eyes and nose.

Physical Properties.—The melting point was to be 160°C, and it sublimes at almost the same temperature. The density was found to be 1.97 g./cc. at 25°C by the flotation method using an aqueous solution of zinc chloride.

Optical Observation.— Under a polarized microscope, the optical properties of the crystal were observed at room and at lower temperatures. The cryostat used for the low-temperature measurements is described in Ref. 5. In the temperature range between room temperature and about −60°C, the crystal was found to be optically isotropic, indicating that the crystal is cubic. At about −60°C, it was suddenly transformed into a birefrigent polycrystal.

X-Ray Study.—A single crystal was sealed in a thin-walled Pyrex glass capillary tube. Within the capillary tube, a Pyrex glass rod almost filling the space was inserted to prevent the loss of crystal by sublimation.

Using Cu$K\alpha$ radiation ($\lambda=1.54$ Å) filtered through a nickel foil and adjusting [110] as the axis of rotation, we prepared a series of 30° oscillation photographs, covering a range of about 90°.

Laue photographs were also taken with X-rays parallel to [100], [110] and [111]. They show that the point-group symmetry of the crystal is T_d-$\bar{4}3m$ or O-43 or O_h-$m3m$. All the spectra appearing in oscillation photographs were extinguished except those of $h+k+l=2n$, they can be indexed with a body-centered cubic lattice with a unit cell of the side of $a=7.42$ Å.

The density indicates that two molecules are present in the unit cell, giving the calculated density to be 1.59 g./cc.

Differential Thermal Analysis (D. T. A.).—The apparatus and procedure of D. T. A. have been described elsewhere.[2] The investigated temperature range was from about −80°C to the melting point, 160°C. Two thermal anomalies were observed. One of them occurs at about −62°C on cooling, and at −35°C on heating. It is in accordance with the anomlies observed by a polarized microscope. Another anomaly was found at 160°C, corresponding to the melting point.

Discussion

The unit cell length of the cubic crystal of 2-bromo-1, 1, 1-trichloro-2-methylpropane, 7.42 Å, is comparable with the value of 7.43 Å given for hexachloroethane and that of 7.46 Å given for 1, 1, 1, 2-tetrachloro-2-methylpropane, even though the substance under investigation contains a bromine atom which has a larger van der Waals radius, 1.9 Å, than that of the chlorine atom, 1.8 Å.[6]

Since the unit cell contains two molecules, it is reasonable to place the centers of the mass of molecules at the lattice points, 0, 0, 0 and 1/2, 1/2, 1/2. The proper symmetry of these points is T_d-$\bar{4}3m$ or O-43, or O_h-$m3m$, so that the molecular symmetry in the crystal should have one of these cubic point groups. On the other hand, if we consider that the free molecule has the skew configulation (Fig. 1), the highest symmetry that the molecule

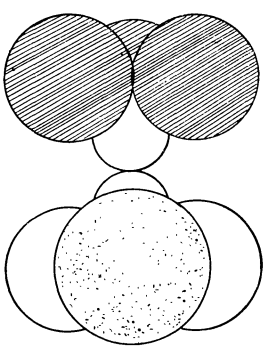

Fig. 1. The assumed skew configuration for the free molecule of 2-bromo-1, 1, 1-trichloro-2-methylpropane, $Br(CH_3)_2C\text{-}CCl_3$. The small circles represent carbon atoms, the larger circles the methyl groups, the dotted circle the bromine atom and the hatched one the chlorine atoms.

6) L. Pauling, "The Nature of the Chemical Bond," 3rd Ed., Cronell Univ. Press, Ithaca, New York (1960), p. 260.

7) C. Willgrerodt and F. Dürr, *J. prakt. Chem.*, **2**, 39, 284 (1889).

could have is C_s-m. In order for such a molecule of low symmetry to aquire an apparent high symmetry, it is necessary to take into consideration some statistical arrangements of molecules, as we have done in the cases of several other plastic crystals.[1-5,8]

Such a statistically-disordered molecular arrangement may disappear at lower temperatures. Thus the phase transition occuring at about $-62°C$ is perhaps the extreme temperature, below which the arrangement of the molecule is in an ordered state. The optical observation indicates that the crystal below the transition point possesses a lower crystal symmetry.

The authors wish to express their hearty thanks to Professor Isamu Nitta and Professor Tokunosuke Watanabé for their interest during this study.

8) C. D. West, *Z. Krist.*, **88**, 195 (1934).

BULLETIN OF THE CHEMICAL SOCIETY OF JAPAN VOL. 39 2647—2652 (1966)

Szilard-Chalmers Reaction of Anionic Cobalt Complex Ions on Ion-Exchange Resins*[1]

By Tatsuo MATSUURA

Institute for Atomic Energy, Rikkyo University, Sajima, Yokosuka

and Tetsuo HASHIMOTO*[2]

Faculty of Science, Kanazawa University, Kanazawa

(Received November 15, 1965)

The recoiling behavior of $[Co(C_2O_4)_3]^{3-}$, $[Co(NO_2)_6]^{3-}$ and $[Co(CN)_6]^{3-}$ ions on in anion-exchanger was studied both by the dynamic and the static methods under various conditions. As the stability of the complex decreases, the separable yield increased as a general trend, and the effectiveness of the dynamic method in obtaining higher yield than the static method was clearly demonstrated. On the other hand, specific activity increased with increasing stability of the complex, i. e., with decreasing G values. The increase of pH generally decreased the separable yield and increased the specific activity. The effects of mesh size of resin and preirradiation by gamma rays were also studied. Since the observed tendency that the separable yield decreased with increasing stability constant of the complex ion seems to be a general one, a theoretical interpretation for this relationship was attempted.

Extensive studies have been made of the recoil chemistry of cobalt complexes, possibly because of the availability of stable complexes of this element and of the ease in activating the element and in measuring its activity. One of the authors has recently introduced a "dynamic method" using a complex-loaded ion-exchanger, as a new technique for elucidating the recoil process as well as for enriching radioisotopes; and this method has an advantage in obtaining a yield higher than the usual static method in the cases of $[Co(NH_3)_6]^{3+}$, $[Co\,en_3]^{3+}$,[1] and $[Cr(C_2O_4)_3]^{3-}$ ions.[2]

In this paper, a few anionic cobalt complex ions, $[Co(C_2O_4)_3]^{3-}$,[3] $[Co(NO_2)]^{3-}$,[4] and $[Co(CN)_6]^{3-}$,[5] were chosen as the target resin form, and the yield and specific activity of the separable fraction were estimated both by the dynamic and the static methods. Since it is already known that there are many factors affecting these quantities, this study was also performed under various experimental conditions: different irradiation positions in a reactor,[1,6] different pH of the eluent,[2,7] differing mesh size of resin,[8] and pre-irradiation by gamma rays.[6,9] The G values of the complexes adsorbed on the resin by gamma rays were also

*1 Presented in part at the 9th Symposium on Radiochemistry, Hiroshima, October, 1965.

*2 Present address: Research Reactor Institute, Kyoto University, Kumatori-cho, Osaka.

1) T. Matsuura, *J. Inorg. Nucl. Chem.*, **27**, 2669 (1965).

2) T. Matsuura, Y. Sensui and T. Sasaki, *Radiochimica Acta*, **4**, 85 (1965).

3) a) D. C. Hoffman and D. S. Martin, Jr., *J. Phys. Chem.*, **56**, 1097 (1952).
b) N. Saito, H. Sano and N. Matsubara, The 7th Symposium on Radiochemistry, Sendai, 1963.

4) T. Costea and I. Dema, *J. Inorg. Nucl. Chem.*, **24**, 1021 (1962).

5) H. Rauscher and G. Harbottle, ibid., **4**, 155 (1957).

6) T. Matsuura, ibid., **28**, 313 (1966).

7) Y. Sensui and T. Matsuura, This Bulletin, **38**, 1171 (1965).

8) T. Matsuura and T. Sasaki, *Radiochimica Acta*, **5**, 212 (1966).

9) T. Matsuura, *J. Inorg. Nucl. Chem.*, **28**, 2093 (1966).

determined in this work in order to determine the interrelation of this value with the stability of complex and specific activity.[10]

Since the dependence of the yield on the nature of the complexes i. e. on their relative stability is one of the main concerns of this paper, and since the tendency that the higher the stability the lower the separable yield is what we have already observed with the two cationic cobalt complexes, $[Co(NH_3)_6]^{3+}$ and $[Co\,en_3]^{3+}$,[1,6] a theoretical consideration was attempted also in this paper as a first approach to a more rigorous treatment.

Experimental

Preparation of the Samples.—The complex salt, $K_3[Co(C_2O_4)_3]$, $Na_3[Co(NO_2)_6]$ and $K_3[Co(CN)_6]$, were prepared by the method described in "Inorganic Syntheses," and were purified by repeated crystallization. Ion exchange resin, Dowex 1X8, was sieved in the dry condition and beads of 120—150 and 40—50 mesh size were chosen as the sample resins.

After the resin was well-conditioned, it was converted into these complex ion forms by treating with an excess amount of about 0.1 N solution of the complex salts, and washed thoroughly with water. The resin was then treated with nitric acid solutions of known pH, which were to be used for elution of the separable species. The complex ion form of the resin was prepared as late as possible prior to the irradiation.

Irradiation and Separation.—In static irradiation experiments, about 2 ml. of the sample resin was taken into a polyethylene vial with about 0.5 ml. of the digesting liquid mentioned above and irradiated batchwise in the rotary specimen rack* and in the thermal column (with lead shield)* of the Rikkyo University TRIGA reactor. After being irradiated for 20 min. and 2 hr. in the respective irradiation positions, each sample was transferred into a glass column with a filter on which about 1 ml. of acetate-ion form resin was bedded, and then nitric acid of a definite pH was passed through the resin as an eluent of the enriched cobalt species at a flow rate of about 2—4 ml./min. The effluent was sampled in seven 25 ml. portions with a fraction collector.

In experiments by the dynamic method, the simultaneous separation of the recoiling species during irradiation was carried out in the thermal column or in the central thimble* as reported previously.[1,2] The volumes of the complex-ion form of resin irradiated were 10 ml. and 2 ml. for the respective irradiation positions, while the volume of the bed resin was fixed at 1 ml. throughout the experiment. The irradiations were done for two hours during the reactor operation and for an additional one and half hours after the shutdown of the reactor, and the elution was continued at a constant flow rate of 4 ml./min.[8] The effluent was collected with a fraction collector as in the static method.

It should be reported that in the case of the oxalatocomplex (green colored), a pink colored anionic species with relatively high specific activity was observed in the bed resin as an intermediate between the parent species and the completely aquated one. The species is considered to be $[Co(C_2O_4)_2]^{2-}$,[11] and it was eluted by 0.02 N nitric acid. Likewise, with the nitrocomplex (yellowish brown), a yellow colored anionic species with a relatively low specific activity appeared in the bed, and it was eluted in later portions of effluents when nitric acid of more than 0.01 N was used as an eluent. This species has not yet been identified.

Measurements.—The activity of the aliquots of effluent and of the resin was determined with a well type NaI(Tl) scintillation detector connected to a single channel analyzer. The measurements of specific activities for static runs were made for the most enriched, first two or three fractions of the eluents. Activation analysis using ^{60m}Co measured with a multichannel analyzer, or colorimetry by the nitroso-R salt method was employed in the determination of the non-active cobalt in the eluents.[1,6]

Determination of the *G* Values.—The G values of decomposition of the complex ion adsorbed on the ion-exchange resin were measured as follows. After 1 ml. of the sample resin which had been digested in a small amount of water or nitric acid of pH 2.0 was irradiated with gamma rays of a cobalt 60 source for 2—24 hr. at a dose rate of $(2—5)\times10^5$ r./hr., the decomposed cobalt species were eluted with about 100 ml. of nitric acid of pH 2.0 and their amount was determined as before. The calculation is based on the assumption that 1 r. of gamma rays deposits 6.08×10^{13} eV./(g. water) multiplied by the density of resin, i. e., 7.30×10^{13} eV./(ml. resin).[10]

Results and Discussion

Separable Yield.—The results obtained are shown in Tables I—IV, from which the following conclusions can be drawn.

The dynamic method was found to give higher separable yield than the static method as a general trend, especially in cases of $[Co(C_2O_4)_3]^{3-}$ and $[Co(NO_2)_6]^{3-}$ ions (except the case of the former complex ion irradiated in the central thimble as stated below) and under the condition of low pH of the eluent. As was observed already in the $[Cr(C_2O_4)_3]^{3-}$ study,[2,7] the separable yield, irrespective of whether dynamic or static method was used, increased with decreasing pH of the eluent. As to the effects of irradiation position, exact conclusions cannot be drawn because the irradiation and storage times were different for the static irradiations in the two different positions.

The order of increasing separable yield with the three complexes in the same pH region is $[Co(C_2O_4)_3]^{3-} < [Co(NO_2)_6]^{3-} < [Co(CN)_6]^{4-}$, i. e., it is approximately in the order of decreasing stability of the complex ion. Since this dependence of the separable yield on the stability of the complex ion

10) T. Matsuura, *Intern. J. Appl. Radiation and Isotopes*, submitted for publication.

* The thermal neutron flux (Φ_{th}, n/cm² sec.) and the exposure rate (D r_0/hr.) at these irradiation positions are: $\Phi_{th}=5\times10^{11}$, $D=1.4\times10^6$ for r. s. r., $\Phi_{th}=3\times10^{10}$, $D=7\times10^3$ for t. c., and $\Phi_{th}=4\times10^{12}$, $D=5\times10^7$ for c. t.

11) Gmelins Handbuch der Anorg. Chemie, Co[A], p. 355 (1932).

Table I. Separable yield and specific activity of enriched fraction for various pH of eluent and irradiation conditions

(The values of specific activity are shown in the square brackets.)

Resin*1 form	pH of eluent	Yield (%) and specific activity (μc./mg.) Static method in r. s. r. (irradiated for 20 min.)	Static method in t. c. (irradiated for 2 hr.)	Dynamic method in t. c. (irradiated for 2 hr.)
$[Co(C_2O_4)_3]^{3-}$	6*2	70.7 [1.5]	50.4 [0.3]	86.6 [1.4]
	6*2 (40—50 mesh)	43.4 [1.0]	36.0 [0.2]	55.0 [0.5]
	4.0	76.7 [1.8]	51.5 [0.4]	74.6 [1.5]
$[Co(NO_2)_6]^{3-}$	6*2	7.9, 7.6 [0.5]	7.3 [0.1]	3.8 [0.5]
	3.0	8.5 [0.8]	10.3 [0.1]	13.9 [0.4]
	2.5	16.9 [0.7]	10.7 [0.1]	47.7 [0.2]
	2.0	52.1 [0.6]	49.9 [0.1]	97.7, 90.2 [0.2]
	2.0 (40—50 mesh)	34.5 [0.8]	34.4 [0.1]	61.0 [0.1]
$[Co(CN)_6]^{3-}$	6*2	0.8 [—]	3.1 [—]	5.2 [—]
	3.0	6.1, 5.2 [400]	6.8 [200]	5.9 [120]
	2.0	7.4, 7.0 [150]	7.7 [100]	8.6 [50]
	2.0 (40—50 mesh)	6.5, 5.9 [100]	9.6 [20]	9.9 [20]
	1.0	11.0 [70]	10.4 [20]	16.5 [0.2]
	0*3	46.8 [0.2]	46.9 [0.05]	89.9 [0.01]

*1 The mesh size of resin is 120—150 mesh except as otherwise noted.
*2 Pure H_2O
*3 1 N HNO_3

Table II. Separable yield and specific activity of enriched fraction irradiated by the dynamic method in the central thimble

(The mesh size of resin is 120—150 mesh; the irradiation time is 2 hr., except as otherwise noted.)

Resin form	pH of eluent	Yield %	Specific activity μc./mg.
$[Co(C_2O_4)_3]^{3-}$	6*1	17.0	1.4
	6*1,*2	7.1	1.4
	6*1,*2,*3	8.0	1.2
$[Co(NO_2)_6]^{3-}$	2.0	98.3	2.0
$[Co(CN)_6]^{3-}$	2.0	16.3	80

*1 See Table I.
*2 Flow rate is 2 ml./min.
*3 Irradiated for 40 min.

Table III. Effect of pre-irradiation by gamma ray

(Total gamma exposure is $(4.4—4.8)\times10^6$ r.; irradiations were done in the thermal column for 2 hr.)

Resin form	pH of eluent	Yield %	Specific activity μc./mg.
$[Co(C_2O_4)_3]^{3-}$	6*	13.6	0.04
$[Co(NO_2)_6]^{3-}$	2.0	39.4	0.1
$[Co(CN)_6]^{3-}$	2.0	6.4	5

* See Table I.

is the same as was already observed with $[Co(NH_3)_6]^{3+}$ and $[Co\,en_3]^{3+}$ under a variety of experimental conditions[1,6] and since it seems to be a general tendency, a theoretical interpretation is presented in a later section.

Table IV. Approximate G values of the complex ions

(Total gamma exposure is $(1—5)\times10^6$ r. The eluent is nitric acid of pH 2.)

Resin form	Digesting liquid	G Value
$[Co(C_2O_4)_3]^{3-}$	H_2O	10.0
$[Co(NO_2)_6]^{3-}$	H_2O	>15
	HNO_3(pH 2)	>31
$[Co(CN)_6]^{3-}$	H_2O	0.004
	HNO_3(pH 2)	0.016

As were observed with $[Cr(C_2O_4)_3]^{3-}$,[7] and $[Co(NH_3)_6]^{3+}$,[1], an increase of the mesh size of the resin decreased the yield for the cases of $[Co(C_2O_4)_3]^{3-}$ and $[Co(NO_2)_6]^{3-}$ ions. It is inferred that in these cases the rate of recombination is comparable with the rate of diffusion of the separable species in the resin phase.

Pre-irradiation by gamma rays brought about only a small decrease in yield in the $[Co(CN)_6]^{3-}$ case, although it was found that this treatment caused very large decreases in yield of the $[Co(NH_3)_6]^{3+}$ and $[Co\,en_3]^{3+}$ cases.[6,9]

Specific Activity.—Table I shows that the specific activity is almost unchanged whether the dynamic or static method is employed. This was anticipated from the previous work.[1,2,6,7] It can be seen from the data that the values for the dynamic method in the thermal column and of the static method in the rotary specimen rack are almost equal, but those of the static method in the

thermal column are a little smaller than the above two methods. This is probably due to the difference of standing time after irradiation. The tendency of the specific activity to decrease with decreasing pH of the eluent is the same as was observed in the case of $[Cr(C_2O_4)_3]^{3-}$.[2,7]

While the separably yield decreased with increasing stability of the complex ion, the specific activity increased with the stability.[6] As can be seen from Table IV, this order is the same as the decrease in G values.[10] Although the value of the specific activity of about 400 μc./mg. in the case of cyano-complex was the largest one yet obtained in this laboratory for the cobalt compound,[1,6] it is smaller than those reported in the solid state irradiation of this complex salt.[5]

Anomalous Results for the Trioxalato Ion Case in Irradiation at High Exposure Rate.—Table II shows that the separable yield in the case of the $[Co(C_2O_4)_3]^{3-}$ ion form which had been dynamically irradiated in the central thimble was considerably lower than those of other irradiation conditions, with an anomalous elution diagram as shown in Fig. 1. Since this unexpected decrease of yield is the first case encountered in experiments by the dynamic method, it seems worthwhile to consider this in detail.

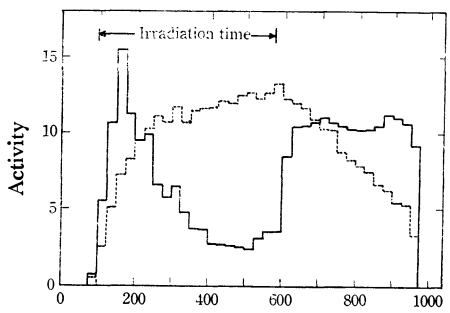

Fig. 1. Elution diagram of $[Co(C_2O_4)_3]^{3-}$ ion form.
—— Irradiated in the central thimble (pH 6, 120—150 mesh).
—— Irradiated in the the thermal column (pH 6, 40—50 mesh).
* Unit of ordinate: 10^4 c.p.m./5 ml. for solid line. 10^3 c.p.m./5 ml. for broken line.

As this anomaly occurred only in the case of $[Co(C_2O_4)_3]^{3-}$ ion irradiated in the central thimble, it can be inferred that the radiation decomposition products of this complex at the high exposure rate may play some role, and that they are probably the same species which are formed by the following photochemical decomposition of this complex ion:[12]

$$\begin{cases} 2[Co(C_2O_4)_3]^{3-} \xrightarrow{h\nu} 2Co(C_2O_4) + 3C_2O_4^{2-} + 2CO_2 \\ C_2O_4^{2-} + H_2O \xrightarrow{h\nu} HCO_2^- + CO_2 + OH^- \end{cases}$$

During irradiation, these fragments and the carbonate ion therefrom may combine with the primary elutable species such as $Co^*(C_2O_4)$ and Co^{*2+} ion into the non-elutable anionic species, such as $[Co^*(C_2O_4)(CO_3)]^{2-}$, $[Co^*(CO_3)_2]^{2-}$, $[Co^*(C_2O_4)(HCO_3)]^-$, etc. These complexes are supposed to be unstable from the analogy of the tricarbonate complex ion in aqueous solution[13] and to exist only in high concentration of the carbonate, which is the situation in the high exposure rate. Following the supposed decrease of carbonate centration after the shutdown of the reactor, these temporary complexes will immediately dissociate into the original elutable species.

Theoretical Discussion of the Dependence of Yield on the Stability of Complexes.—Although the increase of the separable yield with decreasing stability of the complex ion seems to be a general trend, this view has not been reported before. The authors believe this is because too many parameters, especially in batch irradiation experiments, have vitiated a knowledge of the true initial yield.[14] In fact, in this laboratory it has also been observed that the yield of $[Co\ en_3]^{3+}$ on the resin, for example, varied widely from more than ninety percent to as small as a few percent, depending on the irradiation conditions;[6] nevertheless, the yield was always lower than that of $[Co(NH_3)_6]^{3+}$ for all irradiation conditions. However, the fact that the dynamic method which has been developed gave large yield values even under the most disadvantageous conditions for the batch results[1,6] suggests that this method can generally provide nearly the highest, so to speak, initial separably yield,[8] except with the anomalous case mentioned above. The term initial or inherent yield is used to describe the radiochemical yield of the chemical entities into which the energetic recoiling atoms become finally incorporated immediately after they are thermalized through the epithermal reaction in that chemical environment.[7]

Thus, accepting the observed tendency to be generally true, the following theoretical interpretation for the dependence of the inherent separable

12) a) T. B. Copestake and N. Uri, *Proc. Roy. Soc.*, **A228**, 252 (1955).
b) I. G. Murgulescu and T. Oncescu, *Z. Physik. Chem.*, **214**, 238 (1962).
c) G. B. Porter, J. G. Doering and S. Karanka, *J. Am. Chem. Soc.*, **84**, 4027 (1962).
d) Gmelins Handbuch der Anorg. Chemie, Co [A], p. 424 (1932).
e) W. W. Wendlandt and E. L. Simmons, *J. Inorg. Nucl. Chem.*, **27**, 2317 (1965).

13) M. Mori, M. Shibata and E. Kyuno, This Bulletin, **29**, 883 (1956).
14) S. R. Veljković and G. Harbottle, *J. Inorg. Nucl. Chem.*, **24**, 1517 (1962).

yield on the stability of the complex ion has been made as a first approach to a more rigorous treatment. For the sake of simplicity, the following assumptions were made.

1) The chemical forms of the parent complex ion and the separable species are $[CoL_6]^{3-}$ and $[Co(H_2O_6)]^{2+}$, respectively, and the formation of the intermediate complex is negligible.

2) The energy state of the parent and the separable species is regarded to be schematically as shown in Fig. 2. Here, ΔF_0 and F_a are the standard free energy change and the activation energy of the following reaction, respectively:

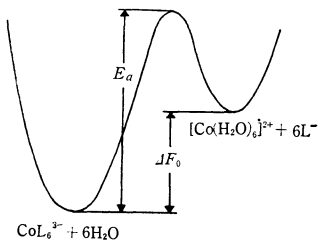

Fig. 2. Assumed energy state of the radioactive cobalt species after thermalization.

$$[CoL_6]^{3-} + 6H_2O + e^- = [Co(H_2O)_6]^{2+} + 6L^- \quad (1)$$

3) Because the central atom or whole molecule of the complex ion upon neutron-capturing becomes very much excited by recoiling compared with the activation energy, the final products which are formed after their thermalization are immediately distributed irrespective of the excited state in such a proportion that reaction 1 is in equilibrium at room temperature.

4) The complexing ability of the free ligand is assumed to be constant irrespective of pH, and, the effects of the concentration of the coexisting solute, of the complexing constant of the solute and of its acid dissociation constant on the equilibrium of Eq. 1 are negligible.

Reaction 1 can be divided into the following two processes:

$$[CoL_6]^{3-} + 6H_2O = [Co(H_2O)_6]^{3+} + 6L^- \quad (2)$$

$$[Co(H_2O)_6]^{3+} + e^- = [Co(H_2O)_6]^{2+} \quad (3)$$

The standard free energy change for each reaction is correlated with the stability constant of the complex ion (K) and the reduction potential of cobaltic ion (E_{red}) as follows:

$$\Delta F_s = -\boldsymbol{R}T \ln (1/K) \quad (4)$$

$$\Delta F_{red} = -FE_{red} \quad (5)$$

where $\boldsymbol{R}$, T and F are the gas constant, absolute temperature, and the Faraday constant, respectively. The overall standard free energy change for reaction 1 is

$$\Delta F_0 = \Delta F_s + \Delta F_{red} = \boldsymbol{R}T \ln K - FE_{red} \quad (6)$$

By using assumption 3, the distribution of the species involved in the reaction 1 can be expressed by

$$(N_a)(N_1)^6/(N_c)(N_w)^6 = [(Z_a)(Z_l)^i/(Z_c)(Z_w)^6] = \exp(-\Delta F_0/\boldsymbol{R}T) \quad (7)$$

where N_a, N_l, N_c and N_w are the number of molecules involved in the reaction 1 for $[Co(H_2O)_6]^{2+}$, L^-, $[CoL_6]^{3-}$ and H_2O, respetively, and Z_a, Z_l, Z_c and Z_w are the partition functions of these species. Assuming $N_l/N_a = N_w/N_c$ for every six-coordinated complex, Eq. 7 is expressed by

$$(N_a/N_c)^7 = [\exp(-\Delta F_0/\boldsymbol{R}T)] \quad (8)$$

On the other hand, the initial separable yield (Y) obtained by the experiment can be represented by

$$Y = N_a/(N_a + N_c) \quad (9)$$

Combining Eqs. 8 and 9

$$Y = 1/[\exp(\Delta F_0/7\boldsymbol{R}T) + 1] \quad (10)$$

Inserting the Eq. 6 into 10

$$Y = 1/[K^{1/7} \exp(-FE_{red}/7\boldsymbol{R}T) + 1] \quad (11)$$

$$(1/Y - 1) = K^{1/7} \exp(-FE_{red}/7\boldsymbol{R}T)$$

$$\ln(1/Y - 1) = (1/7) \ln K - (FE_{red}/7\boldsymbol{R}T) \quad (12)$$

Converting into common logarithms,

$$\log(1/Y - 1) = (1/7) \log K - 0.4343(FE_{red}/7\boldsymbol{R}T) \quad (13)$$

Equation 13 shows that $\log(1/Y - 1)$ should increase linearly with an increase in $\log K$ of the complex ion and should have a slope of (1/7) and an ordinate constant of $-0.4343\ FE_{red}/7\boldsymbol{R}T$ ($= -4.45$)[15] respectively.

The experimental values at pH 2 for these complexes obtained by the dynamic method are plotted against $\log K$[12a,15,16] in Fig. 3. Although the $[Co(C_2O_4)_3]^{3-}$ ion cannot be rigorously treated in this way, it is shown as a reference value. (The value at pH 6 was used for this case, because the yield at pH 2 was found to be almost the same as that at pH 6 by a preliminary experiment.)

The values for the cationic cobalt complexes, $[Co(NH_3)_3]^{3+}$ and $[Co\,en_3]^{3+}$, are not shown in this figure, because there are no values for the experimental conditions corresponding to the anionic complexes. However, since the initial yields for these cases should be very small in spite of the large $\log K$ values,[6] it is evident that they deviate much from this theoretical curve. It can be inferred that this discrepancy might be due to

15) W. M. Latimer, "Oxidation Potentials" Second Edition, Prentice-Hall, Inc. (1959), p. 214.

16) J. Bjerrum, G. Schwarzenbach and L. G. Sillén, "Stability Constants," Part II, Inorganic Ligands, The Chemical Society, London (1958), p. 34.

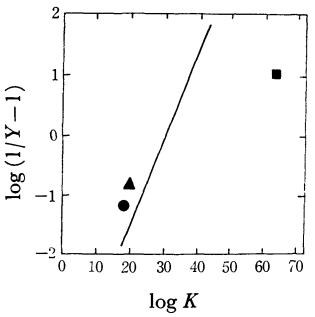

Fig. 3. Dependence of the initial separable yield (Y) on the stability constant of the complex (K).
▲ —— $[Co(C_2O_4)_3]^{3-}$ ion form.
● —— $[Co(NO_2)_6]^{3-}$ ion form.
■ —— $[Co(CN)_6]^{3-}$ ion form.
(The line is the theoretical slope.)

the differing behavior of the intermediate complexes; while the intermediate ammine complexes are labile and elutable as bivalent cations and thus usually can be classified as the separable species,[6] the anionic intermediates may be considerably stable and resistant to aquation or elution and thus the separable yield will be considerably low.

At any rate, the present theory agrees with the experimental data only qualitatively. However, if the main reasoning is correct, the authors believe this theory can further be refined by introducing additional parameters, such as the pH value, acid dissociation constant of the ligand, the concentration of the coexisting solute, and its complexing and acid dissociation constants, and by considering the existence and the behavior of the intermediates mentioned above.

The authors wish to thank IAEA, which supported this work through the research contract (No. 221/RB). They also wish to thank Professor Masanobu Sakanoue of Kanazawa University for his kind encouragment on this work.

BULLETIN OF THE CHEMICAL SOCIETY OF JAPAN VOL. 39 2652—2655 (1966)

On the Preparation of Cadmium Sulfoselenide by the Wet Processes

By Koshiro HASHIMOTO,* Goro YAMAGUCHI** and Yoshitomo TODA*

* *Department of Industrial Chemistry, Chiba Institute of Technology, Yatsu, Narashino-shi, Chiba*
** *Department of Industrial Chemistry, The University of Tokyo, Hongo, Tokyo*

(Received December 1, 1965)

The super-homogeneous coprecipitation method, in which the binary solution reactants made to mix and react in a moment, thus reducing a super-homogeneous precipitate, has been used recently in the preparation of catalysts. The coloring temperature of the cadmium sulfoselenide red pigment can be lowered to 350°C by this method, while, when the usual wet method is used, the temperature is between 450 and 650°C. This is because a very homogenous solid solution can be formed by the super-homogeneous coprecipitation method. This method is also effective in making an anionic solid solution of A(X, Y) with different anions of X and Y. Spectral reflectance measurements and X-ray analysis in the present work have shown that the coloring temperature has been considerably lowered and the transformation of the β-Cd(Se, S) into the α form has been accelerated by the method.

Cadmium red is a substantial inorganic pigment with a clear tone; it is used in ceramics, glasses, enamels, and resins. This pigment has been considered to be a cadmium sulfoselenide which was a continuous solid solution of cadmium sulfide and cadmium selenide. However, the relation between the compositions and the color has hardly been discussed at all.[1-3] There are various combination of starting materials and processes used in the preparation of cadmium sulfoselenide. The processes are classified into wet and dry methods. In the wet method, the pigment is obtained by sintering the coprecipitate, which has been prepared by treating an aqueous solution of sodium sulfoselenide an aqueous solution of cadmium sulfide; the coloring temperature has been reported to be between 470 and 640°C by Stuckert,[4] between 450 and 650°C by Yamanouchi,[1] between 550 and 650°C by Eroles and Friedberg.[5] In this case, the binary solution is made to mix and react

1) S. Yamanouchi, *J. Ceram. Assoc. Japan (Yogyo Kyokai Shi)*, **60**, 676 (1952).
2) Milligna, *J. Phys. Chem.*, **38**, 797 (1934).
3) H. Kohl, *Ber. Deut. Keram. Ges.*, **4**, 181 (1935).
4) L. Stuckert, *Glashutte*, **64**, 364 (1934).
5) A. J. Eroles and A. L. Friedberg, *J. Am. Ceram. Soc.*, **48**, 223 (1965).

in a moment, and then a super-homogeneous coprecipitate can be obtained. This is the super-homogeneous coprecipitation method which has been used recently in the preparation of catalysts.[6-8]

The authors will report in this paper the results of an examination of the thermal transformation of the coprecipitate (the β-Cd(Se, S) into the α form) by spectral reflectance measurements and by X-ray diffraction analysis.[2,9]

Experimental

The Preparation of Solutions.—Table I shows the effect of selenium upon the color. The poorer the selenium content, the more yellowish the color; the richer, the darker.[1] The lattice dimensions, a_0 and c_0 increase with a rise in the cadmium selenide content. Since the linearity between the lattice dimension and the content is almost complete, the concentration of cadmium sulfide or cadmium selenide in a pigment can be exactly determined by means of the X-ray diffraction patterns.[5,10] E-3 is the best color tone among them; the procedure for obtaining it is follows (the chemicals used in this experiment are commercially-available chemically-pure reagents). A cadmium salt solution (sp. gr. 1.4) is made by dissolving 98.42 g. of cadmium sulfate ($CdSO_4 \cdot 8/3H_2O$) in 102 cc. of distilled water. A sodium sulfoselenide solution is made by dissolving 85.7 g. of sodium sulfide ($Na_2S \cdot 9H_2O$) into 200 cc. of water, and by then dissolving 11.05 g. of metallic selenium into it with heating; the solution is used after filtration (sp. gr. 1.13). When cadmium sulfide is made, of course, metallic selenium is not added. In order to carry out a sudden and homogeneous reaction in a mixer, an intermediate aqueous solution such as a sodium sulfate solution (sp. gr. 1.21) is required.

The Preparation of Coprecipitates.—a) The usual method consists of adding a sodium sulfate solution to a cadmium sulfate solution and by then pouring a sulfoselenide solution into it, then obtaining a coprecipitate by stirring, as usual. The reason why a sodium sulfate solution is added is to set up the same conditions as in the following new method. The precipitate is filtered, washed by warm water, and dried at 100°C.

b) In the new method, at first, the double amount of a cadmium sulfate solution mentioned above is put into a 1.8 l. mixer, and then a sodium sulfate solution is slowly added along the wall of the container by means of a separating funnel. The two aqueous solutions easily separate into two layers as a result of the difference in specific gravity. A sodium sulfoselenide solution added by the same method makes the triple layers. The state is shown in Fig. 1. When switched on, the solution suddenly becomes homogeneous, and a precipitate is formed uniformly every part of the solution.

The samples obtained by the a) method (the usual method) are said to form the A-system, and those by the b) method (the new method), the B-system. In order to establish the characteristics of the new coprecipitative method, the authors also made CdS precipitates

Table I. Effect of selenium upon color

Chemical analysis, color measurement and X-ray analysis.

These specimens sintered at 550°C are complete solid solution by X-ray diffraction patterns.

Reactants—$CdSO_4 \cdot 8/3H_2O$ is 40% aq. sol., $Na_2S \cdot 9H_2O$ is 30% aq. sol. and Se is metallic selenium

Chemical analysis of pigments—Cd: EDTA, S: converted to SO_4 and estimated as Ba_2SO_4, Se: reducted to metallic selenium.

Color measurement—Y: Lightness, P_e: Excitation purity, λ_d: Dominant wavelength.

Sample	Reactants			Chemical analysis				
	$CdSO_4$	Na_2S	Se	Cd	S	Se	SO_4	Total
	g.			%				
E-1	98.4	89.4	4.7	71.56	17.27	7.83	3.40	100.07
E-2	98.4	87.5	7.8	69.98	15.64	10.80	2.70	99.12
E-3	98.4	85.7	11.0	66.83	13.70	14.39	2.50	97.42
E-4	98.4	82.9	15.8	65.09	12.23	20.81	0.64	98.77

Composition		Color measurement			Lattice parameter (Hexagonal)	
CdSe	CdS	Y	P_e	λ_d	a_0	c_0
mol. %		%	%	mμ	Å	
15.5	84.5	31.9	72.0	594.8	4.16	6.77
22.0	78.0	25.6	68.7	606.5	4.17	6.78
30.7	69.3	15.6	52.9	611.2	4.18	6.80
44.7	55.3	11.2	35.9	619.2	4.19	6.81

6) T. Shirasaki, *Catalyzer (Shokubai)*, **6**, 37 (1964).
7) M. Okada, *Report of the Chiba Institute of Technology*, **5**, 18 (1964).
8) L. Gordon, "Precipitation from a Homogeneous Solution," John Wiley & Sons, London (1959).
9) F. Ulrich and W. Zachariasen, *Z. Krist.*, **62**, 260 (1925).
10) K. Hashimoto, *Report of the Chiba Institute of Technology*, **2**, 43 (1962).

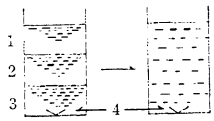

Fig. 1. The illustration of reactor (mixer) for B-system.
1: Sodium sulfoselenide aq. sol. (sp. gr. 1.13) or sodium sulfide aq. sol.
2: Intermediate aq. sol., sodium sulfate aq. sol. (sp. gr. 1.21)
3: Cadmium sulfate aq. sol. (sp. gr. 1.4)
4: Rotor

by these two methods.

Sintering.—A dried precipitate (25 g.) is powdered in an agate motor; then it is put into a vitreous quartz Tamman tube (35 mm. in internal diameter) supplied with nitrogen gas (1 l./min.) and heated in the vertical electric furnace, taking care that every part of the sample is equal in temperature. Each sample is heated quickly, kept at the given temperature (350, 400, 450, 500 or 550°C) for 30 min., and then cooled in air. Again it is powdered in the agate motor.

Measuring Apparatus.—The Shimadzu Hardy-type photoelectric colorimeter is used for the spectral reflectance measurements. Color measurements are carried out by determining x, y, and z by the 30-division method, and Y, P_e and λ_d, according to the indications of the C. I. E. method.

The Shimadzu X-ray apparatus is used; the characteristic X-ray is Cu$K\alpha$=1.539 Å. MgO is used as the internal standard.

Results and Discussion

The Preparation of Samples.—Precipitates obtained from liquid-liquid reactions are not always homogeneous microscopically in their compositions. This fact has been reported in the field of gravimetric analysis, and attempts have recently been made to get homogeneous precipitates. In the formation of a solid solution of the A(X, Y) type, the diffusion velocities of X and Y across the boundary membranes are different, and so it is impossible that compositions of every particle of precipitate are A(X, Y) exactly. Furthermore the phenomenon of the crystallization of precipitates is not chemical equilibrium but chemical kinetics. The initial precipitate may differ from the following precipitate in composition. By the use of the method in mixing two solutions uniformly during the induction period in the formation of nuclei, a precipitate of the same composition and size may be formed from a supersaturated solution. This is especially very effective in a supersaturated solution of slightly soluble salt, for its induction period is momentary. Thus, the precipitate obtained by the new method (the B-system) may be thought to be highly homogeneous compared with the precipitate formed by the usual coprecipitation method (the A-system). The differences between these two systems will be discussed below.

The Results of Color Measurement.—The spectral reflectance curves of the precipitates of cadmium sulfoselenide sintered at the given temperatures are shown in Fig. 2 and Table II. The precipitates of both the A-system and the B-system are amorphous and hardly change at all up to 300°C. The B-system begins to show a reddish tone at 350°C, but the A-system does so at 400°C. Therefore, the B-system is more reddish than the A-system at the same temperature. This may be ascertained from the dominant wavelength. At 500°C the A-system develops the same color as that of B-system sintered at 450°C. This difference is also found in the results of X-ray diffraction analysis.

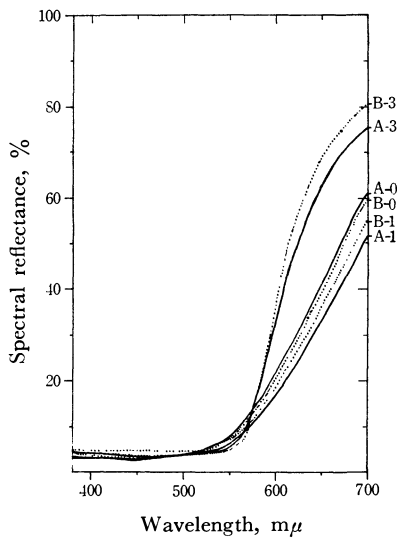

Fig. 2. The spectral reflectance curves of A- and B-system coprecipitates sintered at 350 and 450°C and without heat-treatment.

TABLE II. CHANGE OF COLOR THROUGH SINTERING
A: A-system (usual method)
B: B-system (new method)

Sample	Sintering temp. °C	Lightness %	Excitation purity %	Dominant wavelength mμ
A-0		13.0	65.9	596.2
A-1	350	10.6	57.7	598.3
A-2	400	12.9	60.2	603.0
A-3	450	15.6	68.2	605.7
A-4	500	15.7	65.0	607.0
A-5	550	16.2	65.0	609.0
B-0		12.4	60.0	596.0
B-1	350	11.6	51.7	601.9
B-2	400	12.5	58.2	606.1
B-3	450	16.0	65.2	607.3
B-4	500	16.0	62.3	608.0
B-5	550	16.5	60.1	608.0

X-Ray Diffraction Patterns.—The X-ray diffraction patterns of α-CdS obtained from cadmium sulfide precipitates of A- and B-systems sintered at 450°C; a typical one is shown in Fig. 3. These patterns show the conversion of the amorphous precipitate of cadmium sulfide into α-CdS (the wurtzite structure) by heating, because the broad peak splits into three characteristic peaks, which correspond to (100), (002) and (101) in the wurtzite structure. The thermal transformation of Cd(Se, S) can be studied qualitatively from these peaks, as is shown in Fig. 4. Up to about 300°C no change can be found in these patterns, but at 350°C the spilt peaks in the B-system become observable. This fact shows that the crystallization process corresponds exactly to the coloring process. At 450°C both are transformed into the substance of the wurtzite structure. The A-system develops a color as if it contained a smaller amount of selenium. From this fact, the A-system precipitate may be more inhomogeneous than the B-system and part of the selenium may be lost by the difference between the diffusion velocity of the solid and the missing velocity of the vapor at a low temperature. The diffusion velocity may be faster than the missing velocity of vapor above 500°C; in this case selenium can form a solid solution with CdS. There is no difference in the transformation temperature between the A- and the B-systems in the case of a cadmium sulfide precipitate consisting of only A(X). From this fact, the transition may have no close relation to the defect in the crystalline structure or the particle size of the precipitate, but rather a close relation to the homogeneity of the precipitate. Such a process would be effective in the precipitation of uniform solid solution. It may be possible to contain traces of impurities uniformly in the precipitate.

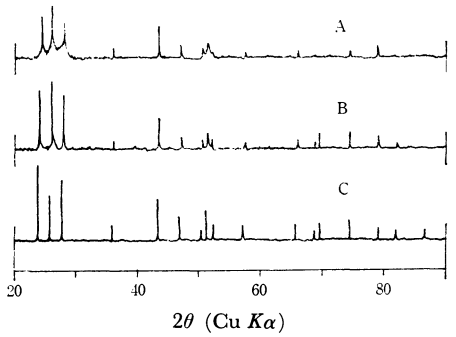

Fig. 3. The X-ray diffraction patterns of α-CdS.
A: A-system sintered at 450°C
B: B-system sintered at 450°C
C: Typical one from β-CdS sintered in H_2S gas at 900°C

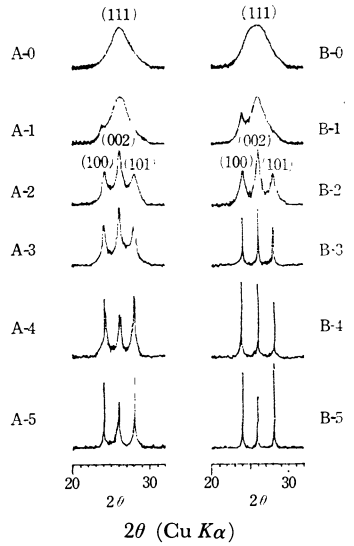

Fig. 4. The thermal transformation of A- and B-system Cd (Se, S) coprecipitates on the X-ray diffraction patterns.
A-0 and B-0: Starting precipitate
A-1 and B-1: Sintered at 350°C
A-3 and B-3: Sintered at 450°C

Conclusions

1) The optimum temperature of the cadmium sulfoselenide red pigment can be lowered by utilizing the super-homogeneous coprecipitation method.

2) The super-homogeneous coprecipitation method is an important way to obtain the precipitate of a uniform constitution of A(X, Y)-type solid solutions.

3) When selenium is partially substituted for sulfur, the transition to the wurtzite structure occurs at a lower temperature.

4) A precipitate of cadmium sulfoselenide showing the amorphous X-ray diffraction patterns can be transformed, even at 350°C.

BULLETIN OF THE CHEMICAL SOCIETY OF JAPAN VOL. 39 2656—2665 (1966)

The Catalytic Hydrolysis of Oligophosphates by Ethylenediamine-Copper(II) and Poly-L-lysine-Copper(II) Complexes

By Yoshiki MORIGUCHI

Department of Chemistry, Faculty of Science, Hiroshima University, Higashisenda-machi, Hiroshima

(Received December 29, 1965)

The hydrolysis of some oligophosphates (tetra-, penta- and hexaphosphates) has been studied at 45°C in the absence and in the presence of a metal complex, and the relation between the nature of the complex catalyst and the composition of the degradation products has been investigated on oligophosphates as substrates, especially on pentaphosphate. In the presence of the Cu(II)-en (1 : 1) complex, the intermediate chain of pentaphosphate is attacked to produce trimeta- and pyrophosphates as the main products; the hydrolytic reaction is apparently of a first-order kinetics which depends on the concentration of the catalyst. The Cu(II) - Poly-Lys complex shows a strong catalytic activity and attacks pentaphosphate exclusively, thus producing orthophosphate as the main product. The optimum conditions for the catalytic effect on the hydrolysis of pentaphosphate are as follows: 1) the ratio of the NH_2 repeat unit of Poly-Lys to a mole of pentaphosphate ($[-NH_2]_i/[P_5]_i$) is about 1.6 at pH 8, the concentration of Cu(II) being constant; 2) the molar ratio of Cu(II) to the NH_2 repeat unit of Poly-Lys ($[Cu]_i/[-NH_2]_i$) is 1.0: 3) the activity reaches a maximum at about pH 10. Attempts have been made to explain these results on the basis of the structure of the Cu(II) - Poly-Lys complex.

The catalytic action of various metal chelates on the hydrolysis of Sarine and DFP (diisopropyl phosphofluoridate) has been studied by Martell and his co-workers.[1-3] The catalytic hydrolysis of polyphosphates by metal ions and chelates has also been studied by several workers.[4-6] In view of the fact that metal ions play a significant role in the catalytic action of the natural enzyme, metal complexes are some of the most interesting catalysts. Previous investigations of the metal complex catalysts have almost exclusively been kinetic studies; little attention has been paid to such peculiarities in the catalytic action as the action of the natural enzyme.[7,8] The present work was undertaken to investigate the relation between the nature of the metal complex catalyst and the kind of degradation products of the substrate as described in a previous report.[9] Polyphosphates with the 4—6 degree of polymerization, i. e., oligophosphates, were used as substrates for the purpose described above.

The ethylenediamine-copper(II) (Cu(II)-en) and poly-L-lysine - copper(II) (Cu(II) - Poly-Lys) complexes were used as catalysts. Though both of the ligands are similar in N-coordination to copper, Poly-Lys is a polypeptide and may be expected to have some catalytic effect on the ability to form higher-order structures (e.g. the α-helix configuration).

Experimental

Reagents.—Oligophosphates were prepared by the same method as has been reported previously.[10] Trimetaphosphate was prepared by the pyrolysis of sodium dihydrogenphosphate containing ^{32}P.[11] Ethylenediamine and cupric nitrate, $Cu(NO_3)_2 \cdot 3H_2O$, were both of the G. R. grade and were used without further purification. The concentrations of cupric ion and ethylenediamine were standardized by means of chelatometric[12] and potentiometric titrations respectively. Poly-L-lysine was of the pure hydrobromide form with a molecular weight of 85000.

* Present address: Department of Organic Synthesis, Faculty of Engineering, Kyushu University, Hakozaki, Fukuoka.

1) R. C. Courtney, R. L. Gustafson, S. J. Westerback, Hyytiainen, S. C. Charberek, Jr., and A. E. Martell, *J. Am. Chem. Soc.*, **79**, 3030 (1957).
2) R. L. Gustafson and A. E. Martell, ibid., **84**, 2309 (1962).
3) R. L. Gustafson, G. S. Charberek, Jr., and A. E. Martell, ibid., **85**, 598 (1963).
4) R. Hofstetter and A. E. Martell, ibid., **81**, 4461 (1959).
5) J. M. Rainey, *J. Inorg. & Nucl. Chem.*, **26**, 1415 (1964).
6) W. Wieker and E. Thilo, *Z. anorg. Chem.*, **306**, 48 (1960).
7) W. L. Koltun, R. N. Dexter, R. E. Clark and F. R. N. Gurd, *J. Am. Chem. Soc.*, **80**, 4188 (1958).
8) J. P. Collman and D. A. Buckingham, ibid., **85**, 3039 (1963).
9) Y. Moriguchi and M. Miura, This Bulletin, **38**, 678 (1965).
10) M. Miura and Y. Moriguchi, ibid., **37**, 1522 (1964).
11) Van Wazer, "Phosphorus and Its Compounds," Vol. I, Interscience Publisher, New York (1958), p. 618.
12) K. Ueno, "Chelatometric Titration (Kireto Tekitei Hō)," Nankodo, Tokyo (1964), p. 148; V. Suk, M. Malat and A. Jenickova, *Collection Czechslov. Chem. Commun.*, **20**, 158 (1955).

Procedure.—The pH of the sample solution, which was made up of an oligophosphate and a catalyst, was adjusted by adding nitric acid or tetramethylammonium hydroixde. The ionic strength of the solution was maintained at 0.1 by adding tetramethylammonium nitrate. The pH of the solution was readjusted within ±0.5 pH unit at regular intervals. The solution (2.5—3.0 ml.) was kept at 45°C in a small test tube coated by silicone and was shaken vigorously at intervals. A part of the solution (0.05—0.1 ml.) was taken out at regular intervals, and the degradation products were identified and quantitatively determined by ion-exchange chromatography. Each degradation product was separated in response to the degree of polymerization by ion-exchange chromatography using ^{32}P as a tracer.[9,13] Its quantity, which was recorded on a chart by a linear count-rate meter, was determined by measuring the area of the separated peak on the chart by means of a planimeter. The H-form of Dowex 1 X4 (100—200 mesh) was used as the ion-exchange resin. The eluent used in the ion-exchange chromatography was an aqueous solution of sodium chloride, the concentration of which was continuously changed from 0.22 M to 0.6 M during elution. The pH of the eluent was adjusted to 9.2 by an ammonia-ammonium chloride buffer.

As a precipitate was formed in the oligophosphate-Poly-Lys system, it was separated by means of a centrifuge. A part of the supernatant solution was used for ion-exchange chromatography, and another part was used for the estimation of the ratio of the ^{32}P in the supernatant solution to that in the precipitate.

Results and Discussion

The experimental conditions and the results of hydrolytic degradation are summarized in Table I. A part of these results are quoted from Otani's data[13] for reference. As may be seen in Table I, the degradation ratio increases with the increase in the the chain length of oligophosphate and with the decrease in the pH of the sample solution. Cupric ion or its complexes show a catalytic action on the hydrolysis; this action is especially remarkable in the presence of the Cu(II)-Poly-Lys complex.

The Degradation in the Absence of Metal Ions and Complexes.—The hydrolytic degradations of tetra- and hexaphosphates at pH 8 and those of pentaphosphate at pH 4 and 8 are shown in Fig. 1 as a function of the reaction time. The ordinate of the figure, "Number of phosphorus atoms (%)," is expressed by the percentages of the total ^{32}P contained in the substrate and the degradation products. Each value of the degradation products is shown by the vertical distance between neighboring curves. These results, which are represented in Fig. 2a, can be expressed by the following equation:

$$k_1 t = 2.303 \log (100/P_n) \quad (1)$$

where P_n is the percentage of oligophosphate with the n degree of polymerization at the reaction time, t, and k_1, the first-order rate constant.

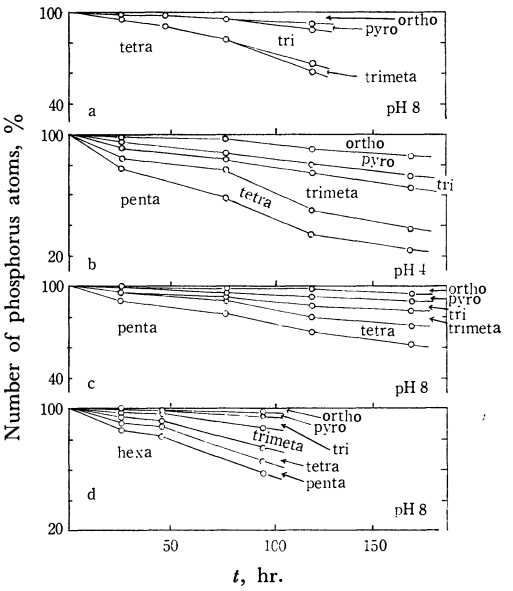

Fig. 1. The relation between the composition of degradation products and the reaction time in the absence of metal ion and complex. Initial concentration of oligophosphates, $[P_n]_i$; a: $[P_4]_i = 6.85 \times 10^{-3}$ M, b, c: $[P_5]_i = 4.07 \times 10^{-3}$ M, d: $[P_6]_i = 1.07 \times 10^{-2}$ M.

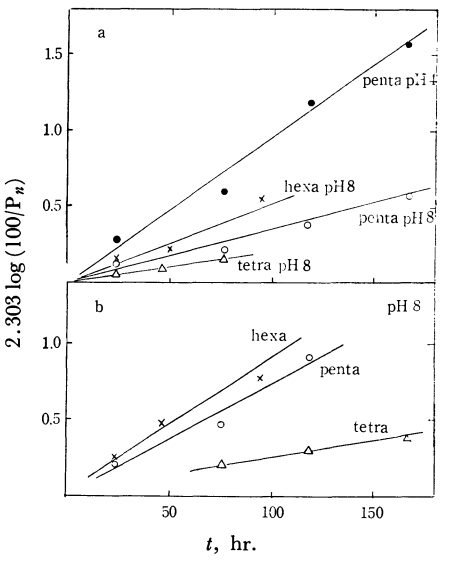

Fig. 2. The validity of the first-order kinetics (Eq. 1) in the hydrolytic gradation of oligophosphates.
a: no catalyst (cf. Fig. 1),
b: in the presence of Cu(II) (cf. Fig. 5)

13) S. Otani, M. Miura and T. Doi, *J. Chem. Soc. Japan, Ind. Chem. Sect. (Kogyo Kagaku Zasshi)*, **66**, 593 (1963).

It has been found from several studies[13,14] that the hydrolysis of oligophosphates is of the first-order at low concentrations of substrate. This may also be confirmed as in Fig. 2a.

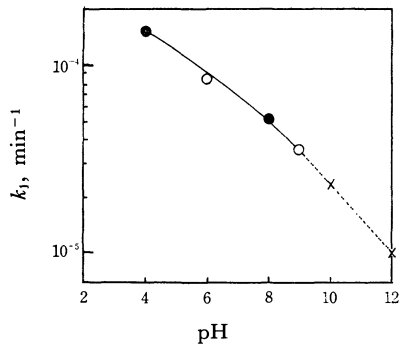

Fig. 3. The relation between the first-order rate constant in the hydrolysis of pentaphosphate and the pH in the absence of Cu(II) and complex.
●: Values obtained by the author (cf. Figs. 1b and 1c).
○: Values obtained by Otani et al.[13]
×: Extrapolated values.

The pH dependence of the first-order rate constant in the hydrolysis of pentaphosphate is shown in Fig. 3. Several stuides have been done on the pH-effect on the hydrolysis of polyphosphates,[6,13,15,16]; it can be concluded from these results that the hydrolysis rate increases with the decrease in pH because the hydrogen ion behaves as a catalyst, and that the terminal chain of polyphosphates is mainly attacked in the higher pH region, whereas the intermediate chain is also attacked in the lower pH region. These conclusions have been confirmed in the present study as may be seen in Figs. 1b, 1c and 3 and Table I; that is, the hydrolysis rate is greater at pH 4 than at pH 8, and the type of degradation is the terminal (a) and intermediate (b) chain attacks at pH 4, while it is the terminal chain attack (a) at pH 8.

$$\text{pentaphosphate} \rightarrow \text{tetra-} + \text{ortho-} \qquad \text{(a)}$$

$$\text{pentaphosphate} \rightarrow \text{trimeta-} + \text{pyro-} \qquad \text{(b)}$$

The dependence of the rate constants at pH 4 and 8 on the degree of the polymerization of oligophosphates is shown in Fig. 4. A part of the data are quoted from Otani's paper.[13] A similar study has been done at 60°C by Wieker.[17] The relation between the rate constant and the degree of polymerization can be expressed by Eq. 2, when the polyphosphate chain is attacked at random and the attack depends only on the statistical factor with relation to the degree of polymerization:

$$k_{P_n} = (n-1)k_{P_2} \qquad n > 2 \rightarrow n \geqq 2 \qquad (2)$$

where k_{P_n} is the rate constant of polyphosphate

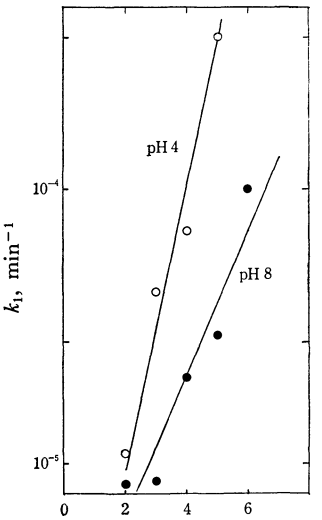

Fig. 4. The relation between the first-order rate constant and the degree of polymerization of oligophosphates.

with the degree of polymerization, n, and k_{P_2}, the rate constant of pyrophosphate. Though the rate constant in Fig. 4 increases linearly with the degree of polymerization, neither of the two straight lines agrees with Eq. 2. This may indicate that the hydrolytic degradation of oligophosphates depends on the electrostatic effect caused by the charge on the polyphosphate chain.

The Formation of Trimetaphosphate.— As may be seen in Figs. 1a, 1c and 1d, the formation of trimetaphosphate increases with the degree of polymerization when the pH is kept constant. The formation of trimetaphosphate from tetraphosphate has recently been reported by Otani et al. of our laboratory.[13] In view of the fact that crystalline Kurrol's salt, which is a kind of polyphosphate, has a spiral structure with four tetrahedra, $-PO_3-$, per pitch,[18] trimetaphosphate may be formed from the polyphosphate chain by such a mechanism as that the polyphosphate chain is constricted to form some spiral structure like Kurrol's salt, with trimetaphosphate then being formed from such a part, as is shown in Fig. 17.[19]

14) J. P. Crowther and A. E. R. Westman, *Can. J. Chem.*, **32**, 42 (1954).
15) E. Thilo and W. Wieker, *Z. anorg. u. allgem. Chem.*, **291**, 164 (1957).
16) J. P. Crowther and A. E. R. Westman, *Can. J. Chem.*, **34**, 969 (1956).
17) W. Wieker, *Z. Elektrochem.*, **64**, 1047 (1960).
18) K. H. Jost and E. Thilo, *Cristallographia*, **6**, 828 (1961).
19) E. Thilo, "Advances in Inorganic and Radio Chemistry," Vol. IV, Academic Press Inc., New York (1962).

It may, therefore, be concluded that the probability of spiral formation to give trimetaphosphate increases with the increase in the degree of polymerization, and that even the tetraphosphate with four tetrahedra will probably form trimetaphosphate.

The Degradation in the Presence of Copper(II).—The results of hydrolytic degradation are shown in Fig. 5, where the molar ratio of cupric ions to oligophosphate is 1.0. The pH of the solution was kept at 4 or 8 for pentaphosphate and at 8 for tetra- and hexaphosphates. It has been reported[4-6] that the transition metals and a large quantity of alkali metals have a catalytic effect on the hydrolysis of polyphosphates. A comparison of Figs. 5a, 5c and 5d with Figs. 1a, 1c and 1d will indicate that the cupric ion acts as a weak catalyst that it seems to accelerate the formation of trimetaphosphate by the intermediate chain attack. The acceleration of the formation of ortho- and trimetaphosphates in the presence of alkali metals and alkaline earth metals has also been reported in the hydrolysis of polyphosphates with a high degree of polymerization by Wieker et al.[6] The results in Fig. 2b indicate that the hydrolytic reaction is of the first-order in the presence of cupric ions in not too high a concentration.

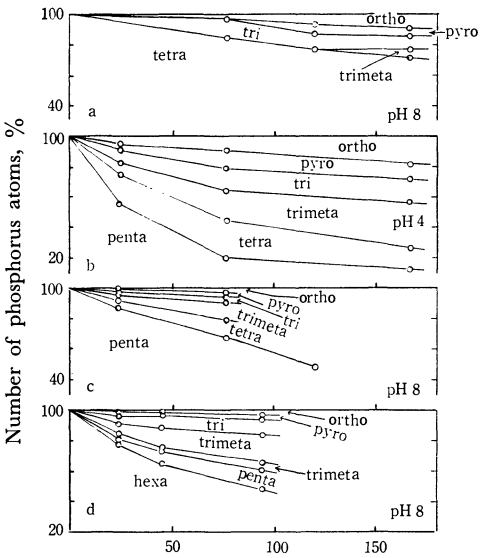

Fig. 5. The relation between the composition of degradation products and reaction time in the presence of Cu(II). Initial concentrations of oligophosphates, $[P_n]_i$, and Cu(II), $[Cu]_i$; a: $[P_4]_i=6.60\times10^{-3}$ M, $[Cu]_i=6.60\times10^{-3}$ M, b, c: $[P_5]_i=4.40\times10^{-3}$ M, $[Cu]_i=4.40\times10^{-3}$ M, d: $[P_6]_i=1.03\times10^{-2}$ M, $[Cu]_i=1.03\times10^{-2}$ M.

The Degradation in the Presence of the Cu(II)-en Complex.—The relation between the composition of degradation products and the reaction time for pentaphosphate at pH 4 and 8 are shown in Figs. 6b and 6c, and those for tetra- and hexaphosphates at pH 8, in Figs. 6a and 6d. The molar ratio of cupric ions and that of ethylenediamine to oligophosphate were 1.0 in each experiment. As may be seen in these figures, the Cu(II)-en complex has a considerable catalytic effect on the hydrolysis of oligophosphates at pH 8; the main products are pyro- and trimetaphosphates for the pentaphosphate substrate and tri- and trimetaphosphates for the hexaphosphate substrate. These results suggest that the Cu(II)-en complex catalyst attacks exclusively the intermediate chain of oligophosphates, thus forming trimetaphosphate.

As may be seen in Figs. 5b and 6b at pH 4, the hydrolysis rate (cf. Table I) and the composition of degradation products when both ethylenediamine and cupric ions are present are similar to those when cupric ions alone are present. These results indicate that in both cases the same catalyst species acts in the hydrolysis of pentaphosphate. The species seems to be hydrated cupric ions

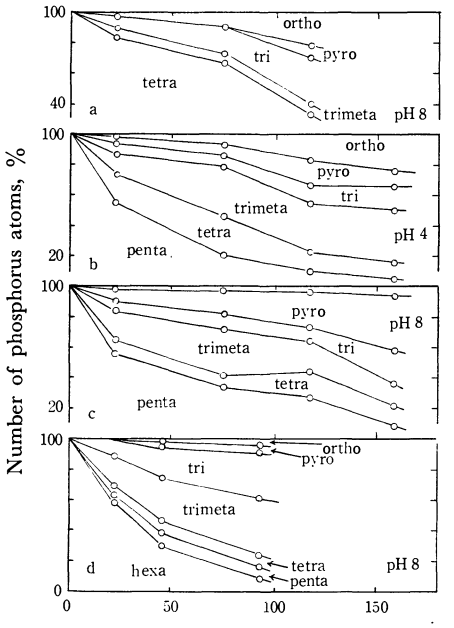

Fig. 6. The relation between the composition of degradation products and the reaction time in the coexistence of Cu(II) and ethylenediamine. Initial concentrations of oligophosphates, $[P_n]_i$, Cu(II), $[Cu]_i$ and ethylenediamine, $[en]_i$; a: $[P_4]_i=6.20\times10^{-3}$ M, $[Cu]_i=6.20\times10^{-3}$ M, $[en]_i=6.20\times10^{-3}$ M, b, c: $[P_5]_i=4.07\times10^{-3}$ M, $[Cu]_i=4.07\times10^{-3}$ M, d: $[P_6]_i=1.06\times10^{-2}$ M, $[Cu]_i=1.06\times10^{-2}$ M, $[en]_i=1.06\times10^{-2}$ M.

Table I. Hydrolysis of oligophosphates and trimetaphosphate at 45°C, ionic strength 0.1 ($(CH_3)_4NNO_3$)

Oligophosphate P_n	Degree of polymerization	pH	Condition of degradation: Metal M	Ligand*1 L	Molar ratio: M/P_n	Molar ratio: L/P_n	$-NH_2/P$*2	Degradation ratio (%)*3	Catalytic activity ratio*4	$k_1\times10^5$ (min^{-1})*5
Pyrophosphate P_2	2	4	—	—	0	0	0	0		1.3±0.2
		8	—	—	0	0	0	0		0.3
		8	Cu(II)	en	0.4	0.4	2/5	6.0		3.7±1.0
		8	Cu(II)	Poly-Lys	0.4	2.0×10^{-3}	2/5	2.1		
Tri- P_3	3	4	—	—	0	0	0	8.3		6.6†
		8	—	—	0	0	0	0.5	1.0	0.4
		8	Cu(II)	en	0.6	0.6	2/5	2.0	4.0	4.5±1.2
		8	Cu(II)	Poly-Lys	0.6	4.2×10^{-3}	2/5	7.1		
Tetra- P_4	4	8	—	—	0	0	0	4.4	1.0	3.8±0.4
		8	Cu(II)	—	1.0	0	0	$(16.5)_{70}$		4.0±0.4
		8	Cu(II)	en	1.0	1.0	2/4	15.5	3.5	13±2.0
Penta- P_5	5	4	—	—	0	0	0	23.6	1.0	15±0.1
		4	Cu(II)	—	1.0	0	0	43.7	1.9	39±7.0
		4	Cu(II)	en	1.0	1.0	2/5	44.5	1.9	43±2.0
		4	Cu(II)	Poly-Lys	0.71	3.6×10^{-3}	2/7	46.3	2.0	
		8	—	—	0	0	0	10.5	1.0	5.2±0.1
		8	Cu(II)	—	1.0	0	0	13.3	1.3	11±1.0
		8	Cu(II)	en	1.0	1.0	2/5	43.8	4.2	23±3.0
		8	Cu(II)	Poly-Lys	0.71	3.6×10^{-3}	2/7	60.3	5.8	
		8	Cu(II)	Poly-Lys	1.0	5.0×10^{-3}	2/5	77.9	7.4	
		10	Cu(II)	—	1.0	0	0	14.4		19±7.0
Hexa- P_6	6	8	—	—	0	0	0	15.5	1.0	10±4.0
		8	Cu(II)	—	1.0	0	0	24.1	1.6	17±2.0
		8	Cu(II)	en	1.0	1.0	2/6	42.0	2.7	42±2.0
Trimeta- P_3	3	8	—	—	0	0	0	$(1.6)_{70}$		
		8	Cu(II)	Poly-Lys	0.43	3.0×10^{-3}	2/7	21.4		
		8	Cu(II)	Poly-Lys	0.6	4.2×10^{-3}	2/5	32.6		

*1 en: ethylenediamine $NH_2CH_2CH_2NH_2$; Poly-Lys: poly-Lysine $-[-CHCONH-]-_n$ M. W. 85000
$(CH_2)_4NH_3Br$

*2 Number of repeat unit of Poly-Lys (side chain amino group $-NH_2$) or that of amino group of en per phosphorus atom of oligophosphate.

*3 Percentage of substrate degradated at the reaction time 22 hr. except ( )$_{70}$ which is the one at 70 hr.

*4 Ratio of the degradation ratio in the presence of catalyst to that in the absence of catalyst at the same pH.

*5 First-order rate constants (hydrolysis rate) estimated from Eq. 1. (†: quoted from Otani's data[13]).

(aquo-complex), since little Cu(II)-en 1 : 1 chelate exists at pH 4. On the other hand, the form of the Cu(II)-en complex, which predominantly has a catalytic effect at pH 8, seems to be monohydroxo, Cu en(OH)(H_2O), or dihydroxo, Cu en-$(OH)_2$, chelate.[2]

The degradation ratio at the reaction time of 70 hr. and the apparent rate constant are plotted against the concentration of Cu(II)-en in Fig. 7. The initial concentration of pentaphosphate and the molar ratio of copper(II) to ethylendiamine were kept constant. The degradation ratio and the apparent first-order rate constant, k_{obs}, estimated by using Eq. 5, increase linearly with the concentration of catalyst. The simplest kinetics which is applicable to the results seems to be represented by Eqs. 3—6:

$$\text{pentaphosphate} \xrightarrow{{}^1k_1} \text{degradation products} \quad (3)$$

$$\text{pentaphosphate} + \text{catalyst} \xrightarrow{{}^2k_1} \text{degradation products} + \text{catalyst} \quad (4)$$

$$k_{obs}t = 2.303 \log (100/P_5) \quad (5)$$

$$k_{obs} = {}^1k_1 + {}^2k_1C \quad (6)$$

where k_{obs} is the apparent first-order rate constant (observed value) and C, the concentration of the metal complex catalyst. The value extrapolated to the zero concentration of the catalyst, ${}^1k_1$, does not agree with the value observed in the absence of the Cu(II)-en complex, k_{obs}. This may show that the catalytic effect of hydrogen ions and that of the Cu(II)-en complex on the hydrolysis of pentaphosphate are not always independent, but correlate with each other.

The dependence of the composition of degradation products at half-life on the catalyst concentration is shown in Fig. 8. The molar ratio of copper(II) to ethylenediamine in each experiment was kept

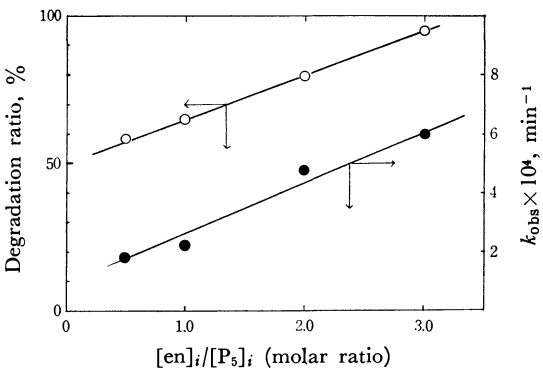

Fig. 7. The dependence of degradation ratio (%) at the reaction time 70 hr. and the apparent first-order rate constant (Eq. 5) on the Cu(II)-en catalyst concentration at pH 8.
Initial concentration of pentaphosphate, [P$_5$]$_i$: [P$_5$]$_i$: 4.07×10^{-3} M, molar ratio of Cu(II) to ethylenediamine: 1.0.

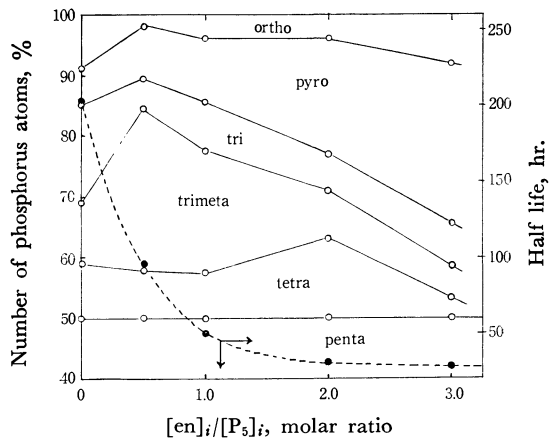

Fig. 8. The dependence of the composition of degradation products at half left on the Cu(II)-en catalyst concentration (life ordinate scale) and the dependence of the half life in the hydrolytic degradation of pentaphosphate on the Cu(II)-en catalyst concentration (right ordinate scale) at pH 8 (cf. Fig. 7).

constant at 1.0. The formation of pyrophosphate increases with the concentration of Cu(II)-en, as may be seen in Fig. 8. From the fact that the pyrophosphate and the triphosphate are hardly degraded in the presence of the Cu(II)-en complex (cf. Table I), it seems reasonable to conclude that the reaction shown in Eq. 7 becomes predominant with an increase in the concentration of the Cu(II)-en complex.

$$\text{pentaphosphate} \longrightarrow 2\ \text{pyro-} + \text{ortho-} \quad (7)$$

The Degradation in the Presence of the Cu(II)-Poly-Lys Complex.—The catalytic effect of the Cu(II)-Poly-Lys complex on the hydrolysis of oligophosphates was studied by using pentaphosphate; the results are shown in Figs. 9—16. Figures 9—11 show the dependence of the ^{32}P

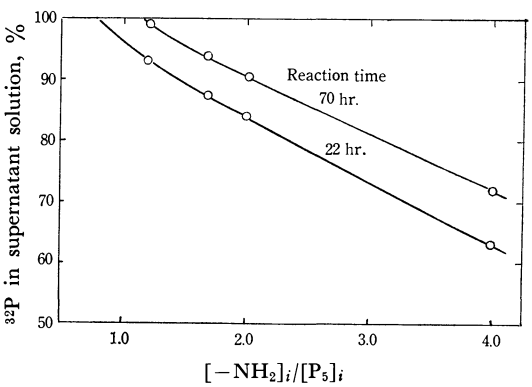

Fig. 9. The dependence of ^{32}P percentage in the supernatant solution of pentaphosphate-Poly-Lys-Cu(II) system on the Poly-Lys concentration (repeat unit molar concentration, [$-NH_2$]) at pH 8.

TABLE II. HYDROLYTIC DEGRADATION OF PENTAPHOSPHATE IN THE PRESENCE OR IN THE ABSENCE OF PRECIPITATE AT 45°C, pH 8

No.	^{32}P (%) In the supernatant solution						In the precipitate	Total
	Ortho-	Pyro-	Tri-	Tetra-	Penta-	Trimeta-	As penta	
1	13.9	10.0	6.0	20.6	30.1	9.6	9.6	100
2	3.0	7.5	6.1	9.1	39.2	7.5	27.6	100

No. 1 Degradation was carried out in the presence of precipitate at 45°C for 22 hr.
No. 2 After degradation for 5 hr. at 45°C in the presence of precipitate, the supernatant solution separated from the precipitate was kept at 45°C for 17 hr.
$[P_5]_i$, $[-NH_2]_i/[P_5]_i$ and $[Cu]_i/[-NH_2]_i$ were 1.63×10^{-3} M, 1.43 and 0.5, respectively, in both cases.

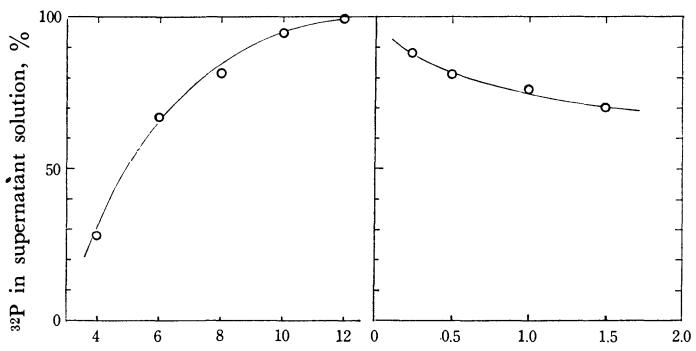

Fig. 10. Fig. 11.

Fig. 10. The pH dependence of ^{32}P percentage in the supernatant solution of pentaphosphate - Poly-Lys - Cu(II) system.
$[Cu]_i/[-NH_2]_i$ and $[-NH_2]_i/[P_5]_i$: kept constant, 0.5 and 1.43, respectively.

Fig. 11. The dependence of ^{32}P percentage in the supernatant solution of pentaphosphate - Poly-Lys - Cu(II) system on the number of Cu(II) per repeat unit of Poly-Lys at pH 8.
$[-NH_2]_i/[P_5]_i$: kept constant, 1.43.

percentage in the supernatant solution on the concentrations of Poly-Lys, hydrogen ions and cupric ions respectively. These experiments were carried out at 45°C for 22 hr.; all the ^{32}P in the precipitate was assumed to be of the pentaphosphate form in estimating the degradation ratio.** Figure 12 shows the relation between the composition of the degradation products and the reaction time. The molar ratios of cupric ions to pentaphosphate are 0.71 and 1.0 in Figs. 12a and 12b respectively. The repeat unit of Poly-Lys per pentaphosphate is 1.43 in Fig. 12a and 2.0 in Fig. 12. The pH dependence of the hydrolysis of pentaphosphate in the presence of the Cu(II) - Poly-Lys complex is shown in Fig. 13, where all the experimental conditions except the pH value are the same as those in the case of Fig. 12a. Figure 14 shows the dependence of the degradation ratio on the concentration of the Cu(II)-Poly-Lys complex, the ratio of cupric ions to the repeat unit of Poly-Lys being kept constant at 1 : 2. Figure 15 shows the relation between the concentration of cupric ions and the degradation ratio, where the ratio of the repeat unit of Poly-Lys to pentaphosphate is kept constant at 1.43. Figure 16, obtained from the experiments in Fig. 14, shows the relation between the composition of the degradation products and the concentration of the Cu(II)-Poly-Lys complex. All of the initial concentrations of pentaphosphate in Figs. 9—15 are kept constant at 1.60×10^{-3} M.

Although the catalytic action of various amino-acids and synthetic polypeptides has been studied in the hydrolysis of DFP[3,20] and *p*-nitrophenyl-acetate[21,22] as substrates, the peculiar action of

** It could not be determined in this case whether or not all ^{32}P in the precipitate remained in the pentaphosphate form; therefore, in practice, it seems probable that the degradation ratio of pentaphosphate is somewhat greater than the value obtained in the present paper.

20) T. Wagner-Jauregg, B. E. Hackley, Jr., T. A. Lies, O. O. Owens and R. Proper, *J. Am. Chem. Soc.*, **77**, 922 (1955).
21) S. Saito, This Bulletin, **38**, 4 (1965).
22) J. Noguchi and T. Saito, "Polyamino Acids, Polypeptides and Proteins," Ed. by M. A. Stahmann, Univ. of Wisconsin Press, Madison (1962), p. 313.

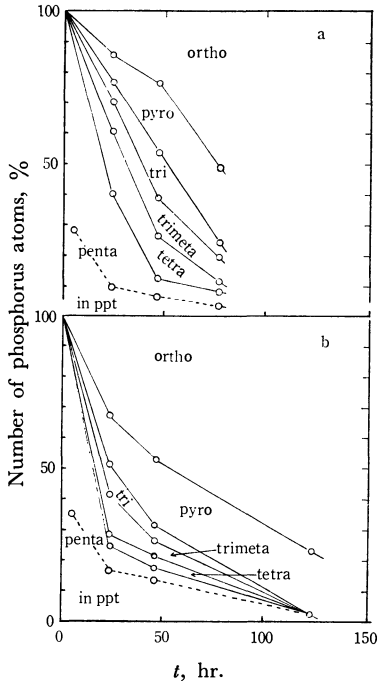

Fig. 12. The relation between the composition of degradation products and the reaction time in the coexistence of Cu(II) and Poly-Lys at pH 8.
Broken line: ^{32}P as pentaphosphate form in the precipitate (%).

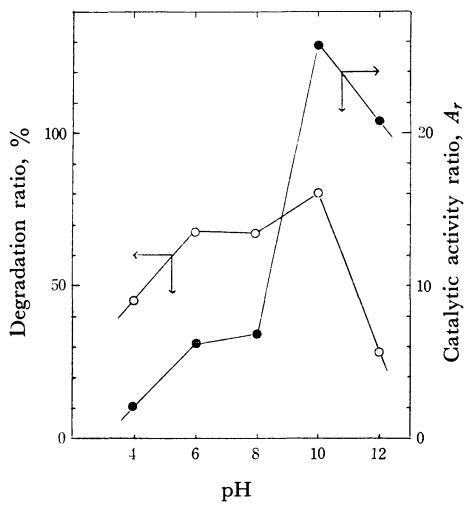

Fig. 13. Effect of pH on the hydrolysis of pentaphosphate in the coexistence of Cu(II) and Poly-Lys. Reaction time: 22 hr.
Left ordinate scale: degradation ratio (%)
Right ordinate scale: catalytic activity ratio, A_r, defined by

$$A_r = D_r/D_{r_0}$$

D_r: Degradation ratio (%) in the coexistence of Cu(II) and Poly-Lys.
D_{r_0}: Degradation ratio (%) in the absence of Cu(II) and Poly-Lys (cf. Fig. 3).

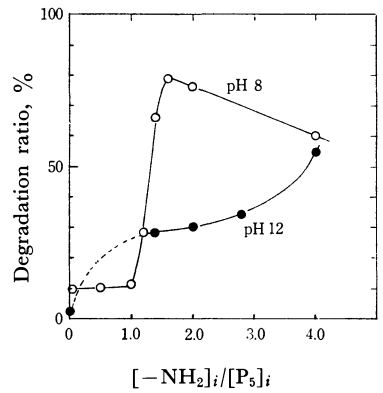

Fig. 14. The dependence of degradation ratio of pentaphosphate on the concentration of Cu(II)-Poly-Lys. Reaction time: 22 hr.

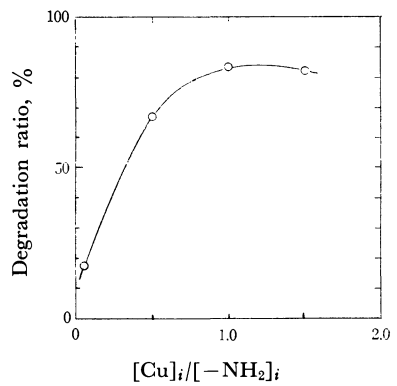

Fig. 15. The relation between the concentration of Cu(II) and the degradation ratio of pentaphosphate in the coexistence of Cu(II) and Poly-Lys at pH 8. Reaction time: 22 hr.

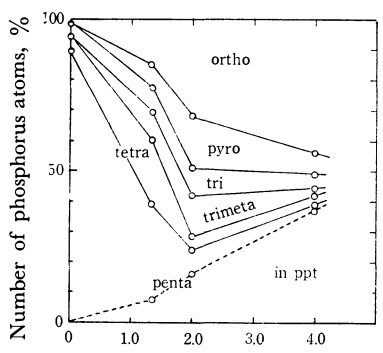

Fig. 16. The relation between the composition of degradation products and the number of Poly-Lys repeat unit per pentaphosphate in the coexistence of Cu(II) and Poly-Lys at pH 8 (cf. Fig. 14). Reaction time: 22 hr.
Broken line: ^{32}P as pentaphosphate form in the precipitate (%).

the catalyst on the substrate has not been investigated, probably because the substrates are too simple. As may be seen in Table I and Figs. 6 and 12, the catalytic action of the Cu(II) - Poly-Lys complex is very remarkable and differs from that of the Cu(II)-en complex in the main product of the hydrolytic degradation. The main product in the former case is orthophosphate, while those in the latter are pyro- and trimetaphosphates. Though ethylenediamine and Poly-Lys are both N-coordination ligands to copper(II), the catalytic effects in the hydrolysis of pentaphosphate differ from each other in the main products. This is probably due to the specific structure of Poly-Lys and to the remarkable catalytic action to be decribed below.

Orthophosphate may be formed from pentaphosphate by the following reactions:

pentaphosphate ⟶ tetra- + ortho-

tetra- ⟶ tri- + ortho-

tri- ⟶ pyro- + ortho- (8)

pentaphosphate ⟶ tri- + pyro-

tri- ⟶ pyro- + ortho- (9a)

pentaphosphate ⟶ trimeta- + pyro-

trimeta- ⟶ pyro- + ortho- (9b)

As may be seen in Figs. 12a, 12b and Table I, pyrophosphate does not degrade at all practically and the degradation ratios of tri- and trimetaphosphates are much less than that of pentaphosphate. From these facts in the presence of the Cu(II) - Poly-Lys complex, it seems reasonable to assume that the predominant reaction in bringing about the remarkable formation of orthophosphate in the initial stage of the reaction is not the intermediate chain attack represented by Eq. 9a or 9b, but the terminal chain attack, Eq. 8.

The composition of the precipitate which is formed by the interaction between a part of pentaphosphate and the Cu(II) - Poly-Lys catalyst can not be determined in the present work. Although the precipitate may also contain the degradation products from the reaction (8), (9a) or (9b), it is probable that most of the oligophosphates in the precipitate are pentaphosphate because the ^{32}P contained in the precipitate decreases with an increase in the reaction time (cf. broken lines in Figs. 13a and 12b) and in the degradation products in the supernatant solution. From the facts that there is remarkable difference between the degradations in the presence and in the absence of the precipitate and that the degradation ratio decreases upon the separation of the precipitate (Table II) it is found in the initial stage of the reaction that a great portion of the Cu(II) - Poly-Lys catalyst exists in the precipitate with a part of pentaphosphate and that the catalyst is liberated with the degradation of pentaphosphate from the precipitate to a bulk solution. The formation of precipitates by the interaction between polyphosphate and Poly-Lys depends on the pH, the concentration of Poly-Lys and that of cupric ions (Figs. 9—11), and the interaction seems to be considerably electrostatic in character.[23]

As may be seen in Figs. 13—15, there are three optimum conditions for the catalytic effect of the Cu(II) - Poly-Lys complex: 1) the remarkable catalytic effect appears only when the molar ratio of Poly-Lys to pentaphosphate, $[-NH_2]_t/[P_5]_t$, reaches a value which is larger than about 1.2 and attains a maximum at about 1.6; 2) the catalytic activity increases with the molar ratio of copper(II) to the NH_2 repeat unit of Poly-Lys, $[Cu]_t/[-NH_2]_t$, and attains a maximum at 1.0, and 3) the catalytic activity reaches a maximum at about pH 10. These results lead us to the following conclusions: 1) when the concentration of Poly-Lys is much lower than that of pentaphosphate, hardly any catalytic activity appears because the cupric ions which play an important role in the catalytic effect are masked by the complexation with pentaphosphate; 2) although copper(II) complexes with various compositions and structures may exist in the pentaphosphate - Poly-Lys - Cu(II) system, some of these species have the most remarkable catalytic activity; that is, the Cu(II)-Poly-Lys complex with 2 : 1 composition ratio of the side chain amino group to copper(II) or the hydroxo-complex with a 1 : 1 composition ratio acts on pentaphosphate and forms a mixed chelate such as that shown in Fig. 18a or 18b, so that the pentaphosphate is liable to suffer decomposition by the Cu(II) - Poly-Lys chelate[4], and 3) in view of the fact that the configuration of Poly-Lys becomes α-helix in the pH region above 10.5,[24] the results shown in Fig. 13 may indicate that there is some relation between the α-helix configuration of Poly-Lys and its catalytic activity.

It may be assumed from the variation in the color of the precipitate of the pentaphosphate-Poly-Lys - Cu(II) system that the complex species at pH 8—10 is different from that at 12. The

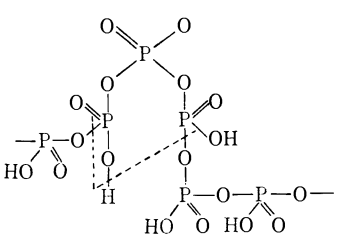

Fig. 17.

23) G. Felsenfeld and S. Huang, *Biochim. et Biophysica Acta*, **34**, 234 (1959).
24) P. Doty, K. Imahori and E. Klemperer, *Pro. Nat. Acad. Sci.*, **44**, 424 (1958).

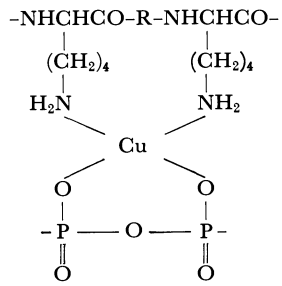

Fig. 18a.

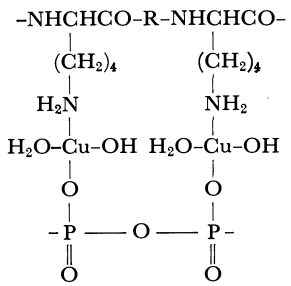

Fig. 18b.

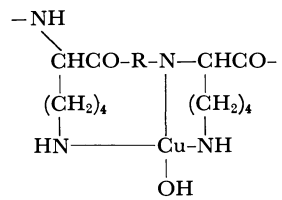

Fig. 18c.

R: -(-NHCHCO-)-$_n$
|
$(CH_2)_4NH_2$

copper(II) atom in the light blue-green complex at pH 8—10 may be coordinated with one or two nitrogen atoms of the amino group of Poly-Lys (e. g. Fig. 18a or 18b), while that in the red-purple complex at pH 12 may be coordinated with the nitrogen atom of the peptide bond, –CONH–, in the main chain of Poly-Lys as well as the nitrogen atom of the side chain (e. g. Fig. 18c). As may be seen in Figs. 13 and 14, the former complex is catalytically more active than the latter because the active sites of copper(II) for pentaphosphate are occupied by nitrogen atoms of Poly-Lys. The color of the latter complex may be due to the biuret reaction from the interaction between cupric ions and polypeptides at high pH values. The chelate shown in Fig. 18a, 18b or 18c is an example of the conceivable structures; the structure with relation to the α-helix configuration can not be discussed in detail in this report for lack of data of the optical rotatory dispersion.

The oligophosphate - Poly-Lys - Cu(II) system is not suitable for the kinetic investigation because the precipitate is formed in this system. Kinetic studies of the oligophosphate - Poly-α, L-glutamate - magnesium(II) and -copper(II) systems are in progress.

The author whishes to express his sincere gratitude to Professor Masaji Miura for his kind guidance and constant encouragement throughout this work. He also wishes to thank Professor Keihei Ueno of Kyushu University for his understanding of this work, Dr. Kiwamu Yamaoka of the National Institutes of Health (U. S. A.) for supplying the Poly-L-lysine and Miss Fumiko Sakiue for her technical assistance.

BULLETIN OF THE CHEMICAL SOCIETY OF JAPAN VOL. 39 2666—2668 (1966)

Studies of Some Telluro-Vanadomolybdates

By Sarju PRASAD and K. C. PATHAK

Chemical Laboratories, Banaras Hindu University, Varanasi-5, India

(Received January 11, 1966)

Ammonium telluro-vanadomolybdate, $6(NH_4)_2O \cdot TeO_3 \cdot 3V_2O_5 \cdot 4MoO_3 \cdot 15H_2O$, has been synthesized, its properties studied, and its composition determined by analytical methods. Copper, silver, calcium, strontium, barium and lead salts have then been prepared from the ammonium salt. D. T. A. of ammonium and strontium salts have been carried out to investigate the thermal changes. The infrared spectra of the ammonium salt and its dehydrated product have been recorded, and the characteristic frequencies assigned.

A large number of condensation products of molybdenum and vanadium have been reported.[1] Gibbs[2] prepared two heterotriammonium phosphovanadomolybdates, $8(NH_4)_2O \cdot P_2O_5 \cdot 8V_2O_5 \cdot 14MoO_3 + 50H_2O$ and $7(NH_4)_2O \cdot 2P_2O_5 \cdot V_2O_5 \cdot 48MoO_3 + 30H_2O$, by boiling ammonium phosphomolybdate with an ammonium vanadate solution. Later Blum[3] confirmed Gibbs by showing the possibility of the condensation of vanadium, molybdenum and phosphorus and by isolating $5(NH_4)_2O \cdot P_2O_5 \cdot 11V_2O_5 \cdot 11MoO_3 \cdot 50H_2O$.

Telluric acid has been condensed to form heteropoly salts with molybdic acid,[4-6] and a series of vanadotellurites have been reported by Jena.[7]

The formation of heteropoly salts of tellurium with molybdic acid[8] and vanadium pentoxide[9] to form various salts has been studied in this laboratory. A heterotritellurovanadotungstate series[10] has also been investigated. This work is now extended to a study of the heterotrisalt formation of tellurium, vanadium and molybdenum. This paper will report the preparation of ammonium telluro-vanadomolybdate and its salts with copper, silver, calcium, strontium, barium and lead. The differential thermal analysis technique has been applied to a study of the thermal changes in the case of ammonium and strontium salts and the infrared spectra of the ammonium salt and its dehydrated product (the compound heated above 300°C) recorded in the KBr phase.

Experimental and Results

Ammonium Telluro-vanadomolybdate. — A mixture of telluric acid and 18.72 g. of ammonium metavanadate was refluxed in an ammoniacal medium for four hours. Twenty-six grams of molybdic acid dissolved in a sufficient quantity of aqueous ammonium was then added to the above solution, and the mixture was refluxed for another 8 hr. The solution was then evaporated to a small bulk and kept in a refrigerator for crystallization. The crystalline ammonium telluro-vanadomolybdate which was obtained was recrystallized and analyzed. Found: $(NH_4)_2O$, 15.98; TeO_3, 9.63; V_2O_5, 28.45; MoO_3, 31.08; H_2O, 14.86. Calcd. for $6(NH_4)_2O \cdot TeO_3 \cdot 3V_2O_5 \cdot 4MoO_3 \cdot 15H_2O$: $(NH_4)_2O$, 16.61; TeO_3, 9.346; V_2O_5, 29.06; MoO_3, 30.65; H_2O, 14.37%.

A yellow crystalline substance highly soluble in water, the compound is decomposed by acids and alkalies.

Copper Salt.—A greenish-yellow compound was precipitated when a dilute solution of copper sulfate was added to the ammonium salt solution. Found: CuO, 24.82; TeO_3, 9.53; V_2O_5, 28.62; MoO_3, 31.08; H_2O, 5.95. Calcd. for $6CuO \cdot TeO_3 \cdot 3V_2O_5 \cdot 4MoO_3 \cdot 6H_2O$: CuO, 25.36,; TeO_3, 9.33; V_2O_5, 29.01; MoO_3, 30.60; H_2O, 5.738%.

Silver Salt.—This is an orange yellow compound obtained by adding a dilute silver nitrate solution to the ammonium salt solution. The salt is blackened when exposed to light. Found: Ag_2O, 49.08; TeO_3, 6.62; V_2O_5, 18.92; MoO_3, 21.48; H_2O, 3.90. Calcd. for $6Ag_2O \cdot TeO_3 \cdot 3V_2O_5 \cdot 4MoO_3 \cdot 5H_2O$: Ag_2O, 50.02; TeO_3, 6.32; V_2O_5, 19.65; MoO_3, 20.72; H_2O, 3.239%.

Calcium Salt.—When a dilute solution of calcium acetate is added to the ammonium salt solution, a yellow compound is separated. It is

1) "Gmelins Handbuch der Anorganischen Chemie," 8 Auflage System-Nummer **53**, Verlag Chemie, Berlin (1935), p. 376.
2) W. Gibbs, *Am. Chem. J.*, **5**, 391 (1883).
3) W. Blum, *J. Am. Chem. Soc.*, **30**, 1858 (1908).
4) A. Miolati, *Z. Physik. Chem.*, **70**, 330 (1910).
5) V. W. Meloche and W. Woodstock *J. Am. Chem. Soc.*, **51**, 171 (1929).
6) S. R. Wood and A. Carlson, ibid., **61**, 1810 (1939).
7) C. Jena, "Uber Verbindungen Welche Vanadisaure und Tellurigesaure enthalten Giessen," (1907) (J. W. Mellor, "A Comprehensive Treatise on Theoretical and Inorganic Chemistry," Vol. 11, Longman Green & Co. (1931), p. 81).
8) S. Prasad and K. C. Pathak, *J. Indian Chem. Soc.*, **42**, 373 (1965).
9) S. Prasad and K. C. Pathak, to be published.
10) S. Prasad and K. C. Pathak, to be published.

decomposed by acids. Found: CaO, 18.48; TeO_3, 9.64; V_2O_5, 31.08; MoO_3, 32.96; H_2O, 7.84. Calcd. for $6CaO \cdot TeO_3 \cdot 3V_2O_5 \cdot 4MoO_3 \cdot 8H_2O$: CaO, 18.93; TeO_3, 9.88; V_2O_5, 30.73; MoO_3, 32.41; H_2O, 8.104%.

Strontium Salt.—This a yellow compound obtained by adding a dilute solution of strontium acetate to the ammonium salt solution. The compound was filtered after some time and analyzed. Found: SrO, 30.86; TeO_3, 8.28; V_2O_5, 26.22; MoO_3, 28.86; H_2O, 5.78. Calcd. for $6SrO \cdot TeO_3 \cdot 3V_2O_5 \cdot 4MoO_3 \cdot 7H_2O$: SrO, 30.40; TeO_3, 8.586; V_2O_5, 26.70; MoO_3, 28.16; H_2O, 6.162%.

Barium Salt.—When a dilute solution of barium chloride was added to the ammonium salt solution, a yellow compound began to separate. It was kept for few hours to settle, and then filtered, dried and analyzed. The compound is decomposed by acids. Found: BaO, 38.34; TeO_3, 7.12; V_2O_5, 23.53; MoO_3, 24.62; H_2O, 6.39. Calcd. for $6BaO \cdot TeO_3 \cdot 3V_2O_5 \cdot 4MoO_3 \cdot 8H_2O$: BaO, 38.95; TeO_3, 7.437; V_2O_5, 23.13; MoO_3, 24.39; H_2O, 6.099%.

Lead Salt.—A heavy yellow precipitate was obtained by adding a solution of lead nitrate to the ammonium salt solution. Found: PbO, 50.02; TeO_3, 6.12; V_2O_5, 19.48; MoO_3, 21.47; H_2O, 2.91. Calcd. for $6PbO \cdot TeO_3 \cdot 3V_2O_5 \cdot 4MoO_3 \cdot 5H_2O$: PbO, 49.12; TeO_3, 6.442; V_2O_5, 20.03; MoO_3, 21.13; H_2O, 3.301%.

Estimations. — Tellurium was estimated as metallic tellurium[11]; ammonia, as has been described earlier[8]; molybdenum, by precipitating it as molybdenum sulfide and igniting to molybdenum(VI) oxide, and vanadium, by titrating it against a standard potassium permanganate solution at 70°C in a dilute sulfuric acid medium. The other metals were estimated by standard methods. The water content was determined by difference as not all the water molecules were removed at 120°C.

The differential thermal analysis of ammonium and strontium salt was carried out by the method described in an earlier communication.[9] The infrared spectra of the ammonium salt and its dehydrated product (the compound heated at 300°C) was recorded between 2 and 15 μ on a Perkin-Elmer infracord in a potassium bromide medium by the disc-technique method.

Discussion

The composition of ammonium telluro-vanadomolybdate has been determined by analytical methods. Its anionic nature has been confirmed by passing a freshly-prepared solution of the ammonium salt through a cation exchange resin (Amberlite IR 120); in this case the tellurium, vanadium and molybdenum contents of the solution remained unchanged. In precipitated copper, silver, calcium, strontium, barium and lead salts, the anion has the same composition in all cases.

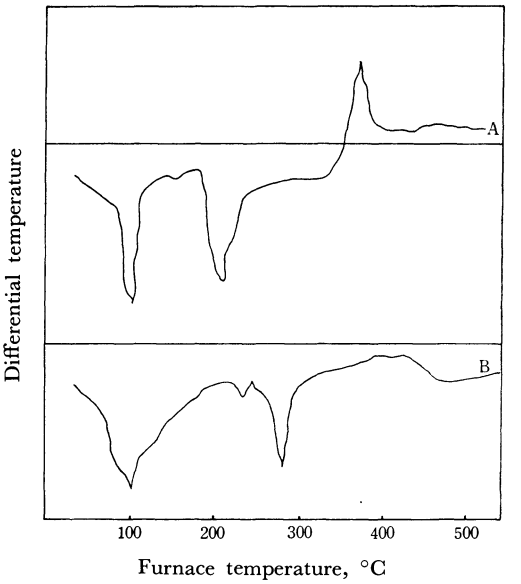

Fig. 1. Differential thermal analysis curves.
A. Ammonium telluro-vanadomolybdate
B. Strontium telluro-vanadomolybdate

The D. T. A. curve of the ammonium salt reveals two endotherms, at about 105 and 210°C, and a characteristic exotherm at about 370°C. The two endothermic peaks correspond to the dehydration of the compound; 6 water molecules are removed at 105°C, and the rest at about 210°C. The characteristic exothermic peak at 370°C is due either to the oxidation or to the decomposition of ammonia at the surface of molybdenum(VI) oxide or vanadium(V) oxide serving as a catalyst. The characteristic exotherm around this temperature has been observed while studying the D. T. A. of ammonium molybdate[12] and ammonium vanadate.[13] The oxidation of ammonia in the last stage of decomposition may be suggested as a possible source of exothermic heat.

In the case of strontium salt the water molecules are removed in two different temperature ranges, first at 105°C and the others at about 280°C, resulting in two endothermic peaks.

In the infrared spectrum of ammonium telluro-vanadomolybodate a broad band is observed in the region of 3400 cm^{-1} which is due to the intermixing of the N–H vibration of ammonium ions with the O–H stretching vibration of water. A sharp peak at 1650 cm^{-1} is observed; it represents

11) V. Lenher and A. W. Homberger, *J. Am. Chem. Soc.*, **30**, 387 (1908).

12) E. Ma, This Bulletin, **37**, 171 (1964).

13) M. Taniguchi and T. R. Ingraham, *Can. J. Chem.*, **1964**, 2467.

the bending mode of the O–H vibrations of water. The spectrum of the above salt was recorded after heating it to 300°C; it was thus observed that the above bands are eliminated and that the overall spectrum is considerably altered. A strong peak at 1400 cm^{-1} is due to the hydrogen bonding of the constitutional water molecules held in the interstices of the crystal lattice; this has also been confirmed by the D. T. A. curve. These water molecules are firmly bound, but they are released at quite a higher temperature, one which may be sufficient to break the bonds.

The broad band in the 840—900 cm^{-1} region indicates the predominant character of V–O valence vibrations in conjunction with Mo–O vibrations; this character has been confirmed by a study of the spectrum of the heated salt, in which the complexity arising from the different bond has vanished and two distinct peaks at 910 and 980 cm^{-1} are observed.

The sincere thanks of the authors are due to the authorities of the Banaras Hindu University for providing facilities. One of the authors (K. C. P.) is also thankful to the Council of Scientific and Industrial Research, New Delhi, for a Fellowship. We are also thankful to Professor C. N. R. Rao, I. I. T., Kanpur, for infrared spectra.

BULLETIN OF THE CHEMICAL SOCIETY OF JAPAN VOL. 39 2668—2671 (1966)

Stability Constants of Uranyl Chelates with Nuclear-Substituted Salicylic Acids

By J. Mohan Rao and U. V. Seshaiah

Department of Chemistry, Osmania University, Hyderabad (Dn), India

(Received January 25, 1966)

The formation of an orange-red coloured water soluble chelate between uranyl ion and *p*-aminosalicylic acid with maximum absorption at 460 mμ is reported. The colour of the complex is fairly stable and attains maximum intensity at a pH 4.5. The composition of the complex has been evaluated by Job's and mole ratio methods employing absorbance data and has been found to be 1 : 1 with respect to metal and ligand. The stability constants of the uranyl chelates of certain nuclear substituted salicylic acids, such as, 3-nitrosalicylic, 5-sulphosalicylic, β-resorcylic and *p*-aminosalicylic acids have been determined and the validity of the linear relationship between ligand basicity and the metal chelate stability studied. Based on pH and adsorption studies, tentative structures for the above uranyl chelates have also been proposed.

The complex formation of substituted salicylic acids, such as amino-, alkyl-, chloro-, and nitrosalicylic acids, has been studied in detail with ferric and aluminium ions. It was observed by Foye et al.[1] that the sequence of stabilities with both the metals was parallel to the ionisation constants of the ligands. However, no such studies of the stability constants of uranyl chelates with nuclear-substituted salicylic acids have been carried out.

Baiulescu[2] has introduced a new method for the colorimetric determination of *p*-aminosalicylic acid based on the facts that the above ligand develops a characteristic orange-red colour with uranyl ions and that the complex obeys Beer's law. However, no details regarding the stoichiometry and stability constant have been reported. Recently, Rajam and Martell[3] have studied the formation of a 1 : 1 uranyl-5-sulphosalicylate employing the pH-titration technique; they reported its stability constant ($\log K$) to be 10.62. The formation of a red water-soluble chelate between uranyl ions and β-resorcylic acid[4] with a metal-ligand ratio of 1 : 1, which is also confirmed by the present authors, has been studied by spectrophotometric methods, but no data regarding the stability constant have been presented. While studying the chelate formation of 3-nitrosalicylic acid with ferric ions, the present authors have observed spectrophotometrically and potentiometrically that 3-nitrosalicylic acid forms a 1 : 1 chelate with uranyl ions.[5]

The present communication will describe the

1) O. F. William and J. G. Turcotte, *J. Pharma. Sci.*, **51**, 329 (1962).

2) Gh. Baiulescu, *Acad. rep. popular Romine, Studii Cercetari Chim.*, **6**, 433 (1958); *Chem. Abstr.*, 12931d, (1959).

3) K. S. Rajam and A. E. Martell, *J. Inorg. Nucl. Chem.*, **26**, 789 (1964).

4) M. N. Desai and B. M. Desai, *Curr. Sci.*, **34**, No. 8, 244 (1965).

5) J. M. Rao and U. V. Seshayya, unpublished work.

studies in the complex formation of uranyl ions with *p*-aminosalicylic acid in some detail, as well as the evaluation and comparison of the stability constants of uranyl *p*-aminosalicylate, β-resorcylate and 3-nitrosalicylate chelates. Spectrophotometric, pH and ion exchange methods were employed in the studies of the above systems. pH titrations of the uranyl ion-5-sulphosalicylic and salicylic acids with the metal-ligand ratio of 1 : 1 were also carried out, and the stability constants were evaluated for purposes of comparison.

Experimental

A standard solution of uranyl nitrate was prepared from a B. D. H. Analar sample by direct weighing; the uranium content was gravimetrically confirmed as uranium oxide. For spectrophotometric studies, an uranyl perchlorate solution was prepared by dissolving the uranium hydroxide, precipitated from a known volume of a standard uranyl nitrate solution, in dilute perchloric acid. Fresh solutions of ligands, *p*-aminosalicylic (PAS), β-resorcylic (RA), 3-nitrosalicylic (NSA), 5-sulphosalicylic (5-SSA), and salicylic (SA) acids were prepared by direct weighing and were standardised potentiometrically and titrimetrically.

All the spectrophotometric measurements were carried out by means of a UNICAM SP 600 spectrophotometer. pH titrations were carried out with the help of a Ludwig pH meter, type-12.

Results and Discussion

The development of an orange-red colour when sodium *p*-aminosalicylate was mixed with uranyl ions is almost instantaneous and is pH-dependent. The absorbance of the mixture containing uranyl perchlorate and *p*-aminosalicylic acid in the ratio of 1 : 3 attains a maximum intensity at pH=4.5.

The Composition of the Complex.—The method of Voshburg and Cooper[6] was employed to determine the nature of the complex formed in the solution. All the mixtures, containing metal-ligand in ratios of 1 : 1, 1 : 2, and 1 : 3, showed a maximum absorption at 460 mμ; this isoabsorptive point suggests the formation of only one complex in solution. Job's continuous variation[7] and mole ratio methods[8] were employed to establish the stoichiometry of the complex.

In Job's continuous variation method, equimolecular aqueous solutions (1×10^{-3} M) of the metal and ligand were mixed in complementary quantities and the absorption was measured at 460 mμ and at pH=4.5. The Job curve (Fig. 1, curve A) obtained by plotting the optical densities against the composition of the coloured solutions has shown a peak at the mole fraction of 0.5 of the metal to the ligand, indicating the formation of 1 : 1 complex.

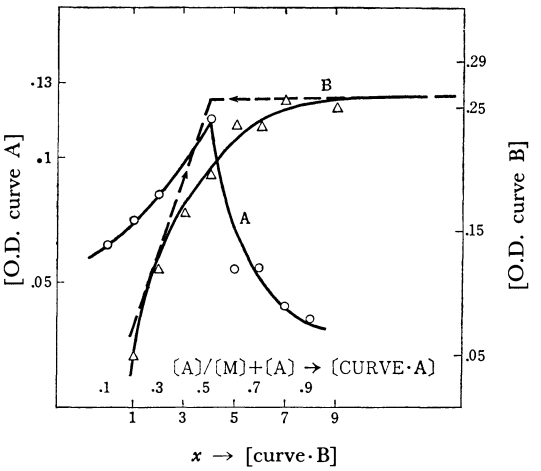

Fig. 1. Composition of the complex by Job's method and mole ratio methods.
A, [A]/([M]+[A])=mole fraction; B, x=ml. of 5×10^{-3} M ligand added to 4 ml. of 5×10^{-3} M uranyl solution. Total volume=20 ml. pH=4.5; λ=460 mμ

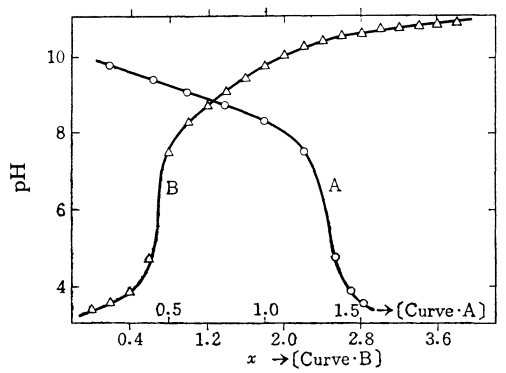

Fig. 2. Curve A, Formation of β-resorcylic acid.
$\bar{n}$=Average number of protons held per mole of anion residue; ($x=\bar{n}$)
Curve B, Potentiometric titration of resorcylic acid in 0.10 M KNO_3 at 28°C with 0.05 M NaOH. ($x=a$, equivalents of base added.)

In the mole ratio method too, the plot of the optical densities against the amount of ligand added to the metal shows a clear break at one equivalent of the ligand, confirming the 1 : 1 ratio of the metal to the ligand in the complex.

The Interaction of Uranyl Ions with Nuclear-Substituted Salicylic Acids.—Potentiometric titrations for the 1 : 1 ratio of uranyl ions to various ligands were performed at the same ligand concentration. The results of the experimental measurements are presented in Fig. 3, curves A, B, C, D, and E. The titration curves indicate qualitatively the relative magnitudes of the stabilities of

6) W. C. Voshburg, and C. R. Cooper, *J. Am. Chem. Soc.*, **63**, 437 (1941).
7) P. Job, *Ann. Chim.*, **11**, 97 (1936).
8) A. E. Harvey, and D. L. Manning *J. Am. Chem. Soc.*, **72**, 4488 (1950).

the uranyl chelates. Precipitations were found at the end of the titrations; they were probably caused by disproportionation to the metal hydroxide or by the hydrolysis of the 1 : 1 chelate.

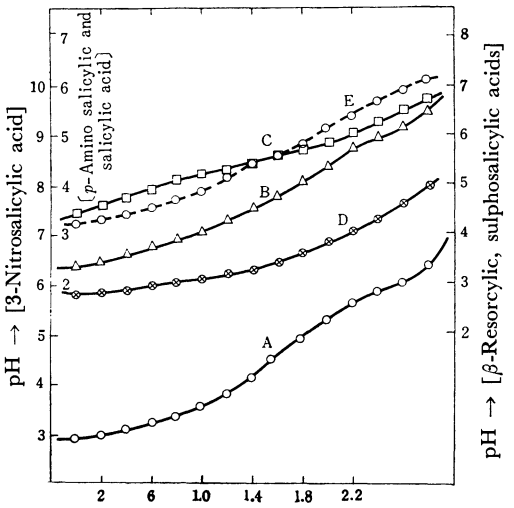

Fig. 3. Potentiometric titration of uranyl chelates of substituted salicylic acids in 0.10 M KNO_3 at 28°C with molar ratio 1:1 of ligand to uranyl ions.
A, 3-nitrosalicylic acid; B, resorcylic acid; C, *p*-aminosalicylic acid; D, 5-sulphosalicylic acid; and E, salicylic acid.

Acid Dissociation Constants of β-Resorcylic Acid.—The step-by-step ionisation of β-resorcylic acid with its step constants can be expressed as follows:

$$H_3A \rightleftharpoons H_2A^- + H^+; \quad k_1 = \frac{(H_2A^-)(H\cdot)}{(H_3A)}$$

$$H_2A^- \rightleftarrows HA^{2-} + H^+; \quad k_2 = \frac{(HA^{-2})(H\cdot)}{(H_2A^-)}$$

$$HA^{2-} \rightleftarrows A^{3-} + H^+; \quad k_3 = \frac{(A^{3-})(H\cdot)}{(HA^{2-})}$$

where the parentheses indicate the concentrations of the respective ions.

The values of k_1 and k_2, the first and the second acid dissociation constants, of the β-resorcylic acid (H_3A) were determined by titrating the free acid in the presence of mineral acid (HNO_3) with standard, carbon dioxide-free sodium hydroxide (Fig. 2B). Various values of $\bar{n}$, the average number of protons held per anion residue, calculated from the following equations[9] have been plotted against the pH (Fig. 2A):

$$\bar{n} = \frac{(H_2A^-) + 2(H_3A)}{C_A}; \quad (H_2A^-) = aC_A + (H\cdot)$$

and $(H_3A) = C_A - (H_2A^-)$ in low-buffer regions and $(H_2A^-) = (a-1)C_A - (OH^-)$; $(HA^{2-}) = C_A - (H_2A^-)$ in higher buffer regions.

where a = equivalents of base added, and
C_A = total anion concentration.

The third dissociation constant, k_3, has been evaluated from the potentiometric data, using the algebraic method of Schwarzenbach et al.[10]:

$$(HA^{2-}) = (a-2)C_A - (OH^-);$$

$$(A^{3-}) = C_A - (HA^{2-}); \quad k_3 = \frac{(A^{3-})(H\cdot)}{(HA^{2-})}$$

The present value of $k_1 = 2.2 \times 10^{-4}$ slightly differs from the reported value of 4.73×10^{-4} [11] obtained conductometrically. The values of k_2 and k_3 have been worked out to be 4.5×10^{-10} and 1.16×10^{-11} respectively. The literature, however, does not reveal any values for these two constants for purposes of comparison.

The Stability Constants of the Chelates.—The equilibrium involved in the metal chelate formation of a 1 : 1 system (metal-ligand) may be expressed as:

$$UO_2^{2+} + A^{2-} \rightleftarrows UO_2A; \quad K = \frac{(UO_2A)}{(UO_2^{2+})(A^{2-})}$$

where K is the stability constant of the chelate. The stability constants of the complexes have been evaluated employing Bjerrum's method as modified by Chaberek and Martell.[12] In the case of a 1 : 1 complex, the various factors involved in the K of the chelate are obtained by using the following equations:

$$(A^{2-}) = \frac{(2-a)C_A - (H\cdot) + (OH^-)}{\frac{2(H\cdot)^2}{k_1k_2} + \frac{(H\cdot)}{k_2}}$$

$$K = \frac{C_A - x(A^{2-})}{(A^{2-})[C_M + x(A^{2-}) - C_A]}$$

where

$$x = \frac{(H\cdot)^2}{k_2k_1} + \frac{(H\cdot)}{k_2} + 1$$

where k_1 and k_2 are the suitable acid dissociation constants of the ligands, and where C_M = the total metal ion concentration.

The values of the stability constants of the uranyl chelates (Table I) indicate a gradual increase in the stability of the chelates as the basic nature of the donor group of the ligand increases. The stabilities of the uranyl chelates were found to increase in the sequence; 3-nitrosalicylic < 5-sulphosalicylic < β-resorcylic < salicylic < *p*-aminosalicylic acids. Moreover, as was predicted by the thermodynamically-derived equation of Ernst and

9) S. Chaberek, Jr., and A. E. Martell, ibid., **74**, 5052 (1952).

10) G. Schwarzenbach, E. Kampitsch and R. R. Steiner, *Helv. Chem. Acta*, **28**, 837 (1945).

11) J. E. F. Dippy, *J. Chem. Soc.*, **1959**, 1717.

12) S. Chaberek, Jr., and A. E. Martell, *J. Am. Chem. Soc.*, **74**, 5052 (1952).

Table I. Stability constants of uranyl chelates of salicylic acids

Temperature = 28±0.1°C
Ionic strength (μ) = 0.10 M (KNO_3)

Sl. No.	Ligand	pk_1	pk_2	pk_1k_2	log K
1*	3NSA	1.90	10.33	12.23	8.57
2*	5SSA	2.50	11.75	14.25	10.70
3	RA	3.65	10.94	14.61	11.98
4*	SA	2.98	13.59	16.57	13.12
5*	PAS	4.08	13.75	17.82	14.41

* The values of the acid dissociation constants have been abstracted from earlier works.

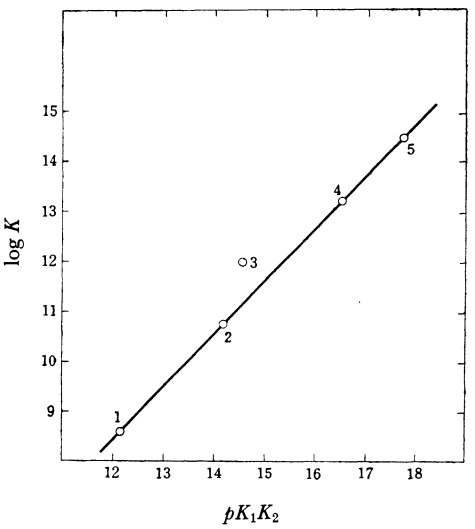

Fig. 4. Linear relationship of log K vs. $p(K_1K_2)$.
(1) 3-nitrosalicylic acid (2) sulphosalicylic acid (3) β-resorcylic acid (4) salicylic acid (5) p-aminosalicylic acid.

Menashi,[13] and as has been proposed by many workers,[14-16] the plot of $\log_{10}K$ against $p(k_1k_2)$ yields a straight line, as is shown in Fig. 4, for the complexes of the uranyl ions with both salicylic and substituted salicylic acids.

Under the experimental conditions, it seems that all the above ligands react with uranyl ions in 1 : 1 ligand-metal ratio, liberating two protons; the adjacent carboxylic and the phenolic groups seem to be responsible for the binding of the metal atom in the complexes. The structure with the reactive moiety may be tentatively represented as:

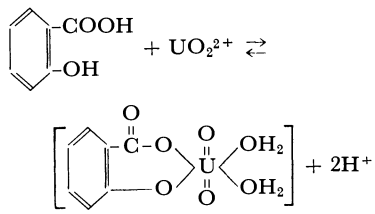

Similar structures have been assigned to the ferric complexes of p-aminosalicylate,[17] 5-sulphosalicylate,[18] β-resorcylate[19] and o-cresotate[20] by earlier workers. Further, the non-ionic nature of all the chelates, uranyl-3-nitrosalicylic, β-resorcylic and p-aminosalicylic acids was confirmed by their non-adsorption on both cation exchange resin, Rexyn 102(H), and anion exchange resin, Rexyn AG-7(Cl-SO_4).

Summary

1) The composition of the uranyl p-aminosalicylic acid chelate was found by spectrophotometric methods to be 1 : 1 with respect to the metal-ligand ratio.

2) The stability constants of uranyl-salicylate and substituted salicylate chelates were determined, and the validity of the linear relationship between the ligand basicity and the metal chelate stability was studied.

3) The second and third acid dissociation constants of β-resorcylic acid were determined from potentiometric data.

4) The stabilities of uranyl chelates were found to increase in the sequence:

3-nitrosalicylic acid < 5-sulphosalicylic < β-resorcylic < salicylic < p-aminosalicylic acids.

5) Substituents were found to play an important role in this case.

The authors are grateful to Professor N. V. Subba Rao for his keen interest in their investigations.

13) Z. L. Ernst and J. Menashi, *Trans. Faraday Soc.*, **59**, 2838 (1963).
14) M. Calvin and K. W. Wilson, *J. Am. Chem. Soc.*, **67**, 2003 (1945).
15) D. D. Perrin, *J. Chem. Soc.*, **1958**, 3125
16) S. P. Datta, R. Leberman and B. R. Rabin, *Trans. Faraday Soc.*, **55**, 1982, 2141 (1959).
17) R. C. Das and S. C. Aditya, *J. Indian Chem. Soc.*, **37**, 557 (1960).
18) R. T. Foley and R. C. Anderson, *J. Am. Chem. Soc.*, **70**, 1195 (1948).
19) M. L. N. Reddy and U. V. Seshayya, *J. Indian Chem. Soc.*, **41**, 289 (1964).
20) K. G. Divekar, *J. Sci. Ind. Res.*, **21B**, 309 (1962).

BULLETIN OF THE CHEMICAL SOCIETY OF JAPAN VOL. 39 2672—2677 (1966)

Electrode Processes Followed by Chemical Reactions Involving Electroactive Species. II. A Study on the Substitution Reaction Involving Chromium(II)

By Kazuko OGINO (née EBATA) and Nobuyuki TANAKA

Department of Chemistry, Faculty of Science, Tohoku University, Katahira-cho, Sendai

(Received March 30, 1966)

The one-electron reduction wave of hexamminechromium(III) ions at the dropping mercury electrode splits into two steps by the presence of manganese(II) and ethylenediaminetetraacetatomanganate(II) (MnY^{2-}; Y^{4-} represents a quadrivalent ethylenediaminetetraacetate anion) ions. The limiting current of the first step was considered to depend on the rate of the formation of CrY^{2-} by the substitution reaction of MnY^{2-} and chromium(II) ions which were produced at the electrode by the reduction of the chromium(III) complex ions. From the change in the limiting current of the first step by the change of the concentrations of Mn^{2+}, MnY^{2-} and H^+, the rate constants of the complex-forming reaction

$$Cr^{2+} + HY^{3-} \underset{k_{1b}}{\overset{k_{1f}}{\rightleftharpoons}} CrY^{2-} + H^+$$

were obtained to be $k_{1f}=8\times10^7$ l.mol^{-1}sec^{-1}, $k_{1b}=4\times10^4$ l.mol^{-1}sec^{-1} (ionic strength 1.0, 25°C).

In the previous papers[1,2] the mechanisms of the electrode reaction of hexamminechromium(III) in the presence of ethylenediaminetetraacetate (EDTA) was reported. The one-electron reduction wave of hexamminechromium(III) is affected by the presence of ethylenediaminetetraacetatomanganate(II) ions. The mechanism of this phenomenon is considered to be one similar to that observed in the presence of EDTA; chromium(II) ions produced at the electrode by the reduction of the chromium(III) complex react with manganese(II)-EDTA to form chromium(II)-EDTA complexes, which are oxidized at the electrode as long as the potential is sufficiently positive, resulting in a decrease of the net cathodic current. The reactions can be expressed as*

$$Cr(NH_3)_6^{3+} + e \rightarrow Cr^{2+} + 6NH_3 \quad (1a)$$

$$Cr^{2+} + MnY^{2-} \rightleftharpoons CrY^{2-} + Mn^{2+} \quad (1b)$$

$$CrY^{2-} \rightleftharpoons CrY^{-} + e \quad (1c)$$

where Y^{4-} represents a quadrivalent EDTA anion.

The determination of rate constants by means of the analysis of the limiting kinetic current due to the following chemical reaction seems to be convenient for reactions involving unstable substances, though it has been applied to the actual reaction only in a few cases involving organic substances.[3-5] Equations giving the relation between the current at a constant potential and the rate constants of the following chemical reaction were given by Alberts and Shain.[4] In this paper, these equations are applied to the determination of the rate constants of Reaction 1b, a substitution reaction of chromium(II) and manganese(II)-EDTA complex ions.

Experimental

Hexamminechromium(III) chloride was prepared according to the method of Mori.[6] The solution of manganese(II) chloride was standardized amperometrically against the solution of disodium ethylenediaminetetraacetate, which in turn was standardized against a standard copper(II) nitrate solution.

Solutions containing manganese(II) and manganese(II)-EDTA complex ions were obtained by adding appropriate amounts of the manganese(II) chloride and the ethylenediaminetetraacetate solutions before each measurement. The pH of the solution was adjusted with acetate buffer solution and the ionic strength was adjusted to be 1.0 with sodium chloride. Gelatin was added as a maximum suppressor by 0.005 %.

1) N. Tanaka and K. Ebata, *J. Electroanal. Chem.*, **8**, 120 (1964).

2) K. Ebata, *Sci. Repts. Tohoku Univ. Ser. I*, **47**, 191 (1964).

* It was shown previously[1] that the aquation of hexamminechromium(II) ions is more rapid than the direct substitution with EDTA. Since the reaction of chromium(II) with manganese(II)-EDTA is much slower than that with EDTA, it may be considered that the reaction of chromium(II) with manganese(II)-EDTA takes place via an aquo complex.

3) I. Tachi and M. Senda, "Advances in Polarography," Vol. 2, Ed. by I. S. Longmuir, Pergamon Press, London (1960), p. 454.

4) G. S. Alberts and I. Shain, *Anal. Chem.*, **35**, 1859 (1963).

5) R. S. Nicholson, J. M. Wilson and M. L. Olmstead, ibid., **38**, 542 (1966).

6) M. Mori, *J. Chem. Soc. Japan, Pure Chem. Sect. (Nippon Kagaku Zassi)*, **74**, 253 (1953).

The current-time curves during the life of a mercury drop were recorded using a Rikadenki ERJ1 recorder with an RLDC-201 preamplifier. In the following sections of this paper, the word "current", denoted by i, means the instantaneous current observed 4 seconds after the beginning of the mercury drop growth, unless otherwise stated. The dropping mercury electrode used had an m value of 1.42 mg./sec. and a drop time, t_d, 5.54 sec. in a deaerated 0.1 M sodium perchlorate solution at −0.5 V. vs. SCE and 60 cm. mercury height. A saturated calomel electrode (SCE) with a large surface area served as an anode. All measurements were carried out at 25°C.

Results

When manganese(II) and manganese(II)-EDTA complex ions are present in the solution in a large excess over chromium(III) complex ions, Eqs. 1a to 1c can be symbolyzed as

$$A_1 + n_1e \rightarrow A_2 \quad (2a)$$

$$A_2 \underset{l_b}{\overset{l_f}{\rightleftharpoons}} A_3 \quad (2b)$$

$$A_3 + n_2e \rightleftharpoons A_4 \quad (2c)$$

where A_1, A_2, A_3 and A_4 correspond to $Cr(NH_3)_6^{3+}$, Cr^{2+}, CrY^{2-} and CrY^- in Eqs. 1a to 1c respectively, and l_f and l_b are the forward and the backward first-order rate constant of Reaction 2b. Symbols n_1 and n_2 represent numbers of electrons involved in electrochemical reactions; positive and negative values of n's correspond to the reduction and the oxidation process respectively. In the system given by Eqs. 2a to 2c, the case $n_1n_2<0$ is physically impossible if A_1 is a substitution-labile complex. For Reactions 1a to 1c, where A_1 is a substitution-inert complex ion, the value of n_1 is 1 and that of n_2 is −1.

Substances A_1, A_2 and A_3 in Eqs. 2a to 2c obey the following equations when the mass transfer process is controlled by the linear diffusion.

$$\frac{\partial[A_1]}{\partial t} = D_1\frac{\partial^2[A_1]}{\partial x^2} \quad (3a)$$

$$\frac{\partial[A_2]}{\partial t} = D_2\frac{\partial^2[A_2]}{\partial x^2} - l_f[A_2] + l_b[A_3] \quad (3b)$$

$$\frac{\partial[A_3]}{\partial t} = D_3\frac{\partial^2[A_3]}{\partial x^2} + l_f[A_2] - l_b[A_3] \quad (3c)$$

where $[A_j]$ and D_j are the concentration and the diffusion coefficient of species A_j, respectively. The initial and the boundary conditions are

$$t = 0,\ x>0:\ [A_1]=[A_1]_0,\ [A_2] = [A_3] = 0 \quad (4)$$

$$t>0,\ x = 0:\ [A_1] = [A_3] = 0 \quad (5a)$$

$$D_2\frac{\partial[A_2]}{\partial x} = -D_1\frac{\partial[A_1]}{\partial x} \quad (5b)$$

$$t>0,\ x\rightarrow\infty:\ [A_1]=[A_1]_0,\ [A_2] = [A_3] = 0 \quad (6)$$

where $[A_1]_0$ is the concentration of A_1 in the bulk of the solution. The boundary condition 5a expresses that, in the potential region in question, the rates of electrochemical reactions 2a and 2c are much greater than the rate of diffusion.

The solution to the equations was given by Alberts and Shain[4] under the assumption that $D_2=D_3$. The kinetic part of the current, i_k, is given by one of Eqs. 8, 12 and 13, according to the magnitude of the equilibrium constant of Reaction 2b*:

$$K = \frac{l_f}{l_b} = \frac{[A_3]_e}{[A_2]_e} \quad (7)$$

where $[A_j]_e$ is the concentration of A_j at equilibrium.

(a) For $K > 1$:

$$i_k = i_d\frac{n_2}{n_1}\frac{K}{K-1}\left\{1 - \exp(-lt) - 2\theta\exp(-K^2\theta^2)\int_\theta^{K\theta}\exp(\lambda^2)d\lambda\right\} \quad (8)$$

where

$$l = l_f + l_b \quad (9)$$

$$\theta = \sqrt{\frac{lt}{K^2-1}} \quad (10)$$

and i_d is the diffusion current observed in the absence of Reaction 2b:

$$i_d = n_1Fq[A_1]_0\sqrt{\frac{D_1}{\pi t}} \quad (11)$$

where q is the area of the electrode surface.

(b) For $K = 1$:

$$i_k = i_d\frac{n_2}{n_1}\left[1 - \frac{1}{lt}\left\{1 - \exp(-lt)\right\}\right] \quad (12)$$

(c) For $K < 1$:

$$i_k = i_d\frac{n_2}{n_1}\frac{K}{1-K}\left[\theta\sqrt{\pi}\exp(K^2\theta'^2)\times\left\{\mathrm{erf}(\theta') - \mathrm{erf}(K\theta')\right\} - \left\{1 - \exp(-lt)\right\}\right] \quad (13)$$

where

$$\theta' = \sqrt{\frac{lt}{1-K^2}} \quad (14)$$

$$\mathrm{erf}(\lambda) = \frac{2}{\sqrt{\pi}}\int_0^\lambda \exp(-y^2)dy \quad (15)$$

When $K^2\ll1$ is satisfied, θ' can be simplified as

$$\theta' = \sqrt{lt} \quad (16)$$

Thus, when the value of K is known, rate constants l_f and l_b can be computed from the value of i_k/i_d which is obtained experimentally.

The addition of manganese(II) chloride to the solution of hexamminechromium(III) caused a

* More simplified solutions of Eqs. 3a to 3c, obtained at several limited conditions, are given in Ref. 2.

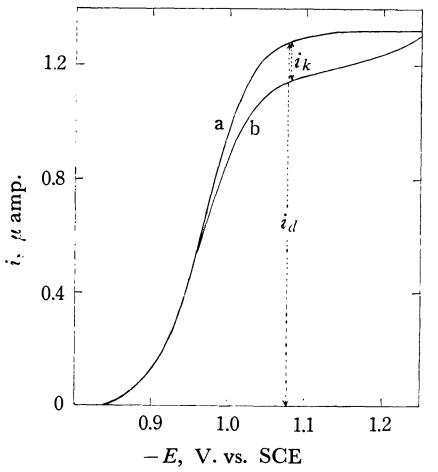

Fig. 1. Current-potential curves of 0.4 mM $Cr(NH_3)_6^{3+}$ in the presence of 0.089 M Mn^{2+} (curve a) and 0.074 M $Mn^{2+}+0.0039_8$ M MnY^{2-} (curve b) in solutions of ionic strength 1.0 (NaCl) and pH 4.94 containing 0.1 M acetate buffer and 0.005% gelation.

small positive shift (2—3 mV. by 0.1 M $MnCl_2$) in the half-wave potential of hexamminechromium-(III) without changing the shape of the wave. When both manganese(II) and manganese(II)-EDTA complex ions were present, the wave showed a decrease in the current in the potential region more positive than about -1.25 V. as shown in Fig. 1, where the diffusion current observed in the absence of manganese(II)-EDTA is denoted by i_d, and the decrease in current by the addition of manganese(II)-EDTA, by i_k. The value of i_k was found to be proportional to the concentration of hexamminechromium(III) chloride. Table I gives the relation between the mercury height and i_k observed just before the mercury drop detaches the capillary. That i_k is independent of the mercury height indicates a kinetic nature of i_k. The value of i_k/i_d was dependent on the pH

Table I. Values of i_k (at $t=t_d$)* at -1.06 V.vs. SCE at various heights of mercury reservoir**

Mercury height*** cm.	i_k (at $t=t_d$) μ amp.
68.5	0.168
58.5	0.173
48.5	0.163
38.5	0.173

* i_k observed just before the mercury drop detaches the capillary.

** Measurements were made in the solution of ionic strength 1.0 (NaCl), pH 4.94 containing 0.40 mM $Cr(NH_3)_6^{3+}$, 0.0079_6 M MnY^{2-}, 0.089_2 M Mn^{2+}, 0.005% gelatin and 0.1 M acetate buffer.

*** Corrected for the back pressure.

and concentrations of manganese(II) and manganese(II) - EDTA complex ions.

As manganese(II) and manganese(II)-EDTA complex ions are present in a large excess under the experimental condition, the apparent equilibrium constant of Reaction 1b is given as

$$K = \frac{l_f}{l_b} = \frac{[CrY^{2-}]_e}{[Cr^{2+}]_e} = \frac{K_{CrY}}{K_{MnY}} \frac{[MnY^{2-}]}{[Mn^{2+}]} \quad (17)$$

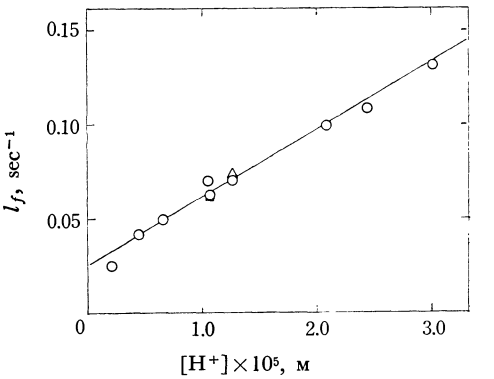

Fig. 2. Values of l_f as a function of the hydrogen ion concentration* in solutions of ionic strength 1.0 (NaCl) containing 0.4 mM $Cr(NH_3)_6^{3+}$, 0.1 M acetate buffer, 0.005% gelatin, a M Mn^{2+} and b M MnY^{2-}.

	○	△	□
a	0.089_3	0.179	0.044_6
b	0.0079_5	0.0159	0.0039_8

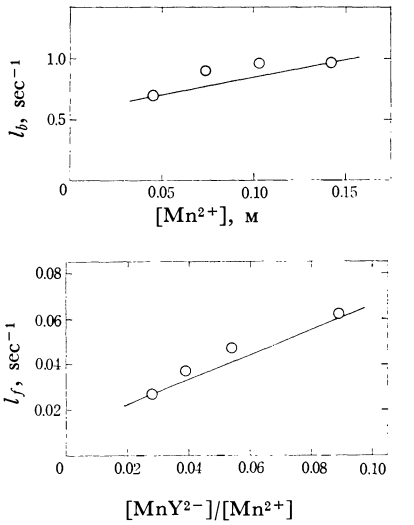

Fig. 3. Variation of l_f and l_b with the change of $[Mn^{2+}]$ in solutions of ionic strength 1.0 (NaCl), pH 4.94 containing 0.4 mM $Cr(NH_3)_6^{3+}$, 0.0039_8 M MnY^{2-}, 0.1 M acetate buffer and 0.005% gelatin.

* The hydrogen ion concentration was assumed to be equal to antilog(-pH).

where K_{CrY} and K_{MnY} are the stability constants of CrY^{2-} and MnY^{2-} respectively. The values of the stability constants at ionic strength 0.1 at 20°C were reported to be $10^{13.61}$ for CrY^{2-} [7] and $10^{13.58}$ for MnY^{2-} [8], respectively. When it is assumed that the ratio K_{CrY}/K_{MnY} does not vary considerably with changes of ionic strength from 0.1 to 1.0 and of temperature from 20°C to 25°C, Eq. 17 becomes

$$K = 1.07[MnY^{2-}]/[Mn^{2+}] \quad (18)$$

As the ratio $[MnY^{2-}]/[Mn^{2+}]$ was less than 0.1 under the experimental condition, Eqs. 13 and 16 were employed for the calculation of the rate constants of Reaction 1b.* Rate constants l_f and l_b obtained at various pH's and concentrations of manganese(II) and manganese(II)-EDTA complex ions are plotted in Figs. 2 and 3.

Discussion

The following reaction paths can be assumed for Reaction 1b:

$$(I)\quad MnY^{2-} + jH^+ \rightleftharpoons Mn^{2+} + H_jY^{(j-4)+} \text{ (fast)} \quad (19a)$$

$$(j = 0, 1, 2, \cdots)$$

$$Cr^{2+} + H_jY^{(j-4)+} \underset{k_{Ijb}}{\overset{k_{Ijf}}{\rightleftharpoons}} CrY^{2-} + jH^+ \text{ (slow)} \quad (19b)$$

$$(II)\quad MnY^{2-} + jH^+ \rightleftharpoons MnH_jY^{(j-2)+} \text{ (fast)} \quad (20a)$$

$$Cr^{2+} + MnH_jY^{(j-2)+} \underset{k_{IIjb}}{\overset{k_{IIjf}}{\rightleftharpoons}} CrH_jY^{(j-2)+} + Mn^{2+} \text{ (slow)} \quad (20b)$$

$$CrH_jY^{(j-2)+} \rightleftharpoons CrY^{2-} + jH^+ \text{ (fast)} \quad (20c)$$

In Path I, Reaction 19a, the dissociation reaction of manganese(II)-EDTA, was assumed to be in equilibrium for the following reason. If Reaction 19a is rate-determining in Path I, it is expected that the rate of chromium(II)-EDTA formation, and hence i_k, is governed by the rate of Reaction 19a and is independent of the concentration of hexamminechromium(III). This is against the experimental result which showed a proportionality between i_k and the chromium(III) concentration.

When Reaction 1b proceeds via Paths I and II, the first-order rate constants of Reaction 1b with respect to Cr^{2+} and CrY^{2-} are given by

$$l_f = \frac{1}{K_{MnY}} \frac{[MnY^{2-}]}{[Mn^{2+}]} \sum_{j=0} \{k_{Ijf}[H^+]^j (\prod_{\nu=0}^{j} K_\nu)\} + [MnY^{2-}] \sum_{j=0} (k_{IIjf} K_{MnH_jY}[H^+]^j) \quad (22)$$

$$l_b = \sum_{j=0} (k_{Ijb}[H^+]^j) + [Mn^{2+}] \sum_{j=0} (k_{IIjb} K_{CrH_jY}[H^+]^j) \quad (23)$$

where K_{MnH_jY} and K_{CrH_jY} are the stability constants of protonated complexes, e. g.,

$$K_{MnH_jY} = \frac{[MnH_jY^{(j-2)+}]}{[MnY^{2-}][H^+]^j} \quad (24)$$

It is defined that K_{MnH_jY} and K_{CrH_jY} are equal to 1 for $j=0$. For $j=1$, the following values were reported at ionic strength 0.1 at 20°C: $K_{MnHY}=10^{3.1}$;[8] $K_{CrHY}=10^{3.00}$.[7] The symbol K_ν in Eq. 22 denotes a reciprocal of the acid dissociation constant of $H_\nu Y^{(\nu-4)+}$, and is defined to be equal to 1 for $\nu=0$; for $\nu=1, 2, 3$ and 4, the values of K_ν were reported to be $10^{10.26}$, $10^{6.16}$, $10^{2.67}$ and $10^{1.99}$ respectively at ionic strength 0.1 at 20°C.[9]

That l_f and hence l_b change linearly with the change in hydrogen ion concentration as shown in Fig. 2 indicates that j in Eqs. 22 and 23 takes only the values 0 and 1.

The first terms of Eqs. 22 and 23 correspond to rate constants for Path I and the second terms to those for Path II. Equations 22 and 23 indicate that if Path II is the predominant path of Reaction 1b, l_f should be constant as long as $[MnY^{2-}]$ is kept constant, and that l_b should be proportional to $[Mn^{2+}]$. They also indicate that, when Path I is predominant, l_b should be independent of concentrations of both manganese(II) and manganese(II)-EDTA complex ions, and l_f should be independent of $[Mn^{2+}]$ and $[MnY^{2-}]$ as long as the ratio $[MnY^{2-}]/[Mn^{2+}]$ is constant. The values of l_f and l_b obtained at different concentrations of manganese(II) and manganese(II)-EDTA complex ions with the same ratio of $[MnY^{2-}]/[Mn^{2+}]$ are given in Fig. 2, where all the values lie near a single straight line. Figure 3 shows that l_f is not constant by the change of $[MnY^{2-}]/[Mn^{2+}]$, but that it varies almost proportionally with the change of $[MnY^{2-}]/[Mn^{2+}]$, when $[MnY^{2-}]$ is kept constant. It is also shown that l_b is not proportional to $[Mn^{2+}]$. It may be concluded from these that the predominant path of Reaction 1b under conditions where the ratio $[MnY^{2-}]/[Mn^{2+}]$ is considerably large and pH is low is

$$MnY^{2-} + H^+ \rightleftharpoons Mn^{2+} + HY^{3-} \text{ (fast)} \quad (25a)$$

$$Cr^{2+} + HY^{3-} \underset{k_{1b}}{\overset{k_{1f}}{\rightleftharpoons}} CrY^{2-} + H^+ \text{ (slow)} \quad (25b)$$

The rate constants of Reaction 25b are obtained

7) R. L. Pecsok, L. D. Shields and W. P. Schaefer, *Inorg. Chem.*, **3**, 114 (1964).
8) G. Schwarzenbach and E. Freitag, *Helv. Chim. Acta*, **34**, 1503 (1951).
* The effect of mercury drop growth was neglected.
9) G. Schwarzenbach and H. Ackermann, *Helv. Chim. Acta*, **30**, 1798 (1947).

Table II. Rate constants of reaction 26 (25°C)

M^{2+}	Ionic strength	k_{1f} l. mol^{-1} sec^{-1}	k_{1b} l. mol^{-1} sec^{-1}	Method	Investigators
Cr^{2+}	1.0	8×10^{7}	4×10^{4}	Polarographic kinetic current	The present authors
Co^{2+}	0.2	8×10^{6}	3×10	Polarographic diffusion current	Tanaka and Ogino[10]
Ni^{2+}	0.2	1.1×10^{4}	(5×10^{-5})	Polarographic diffusion current	Tanaka and Sakuma[11]
	1.25		8.0×10^{-4}	Spectrophotometry	Margerum and Bydalek[12]
Cu^{2+}	0.2	3×10^{9}	(9.5)	Polarographic diffusion current	Tanaka and Kato[13]
Zn^{2+}	0.2	$>10^{8}$		Polarographic diffusion current	Tanaka and Ogino[14]
	0.5	1.6×10^{9}	7×10^{2}	Polarographic kinetic current	Fujisawa and Tanaka[16]
Cd^{2+}	0.1	8.5×10^{8}	(4.0×10^{2})	Polarographic half-wave potential	Koryta and Zábransky[15]
	0.5	(2.3×10^{9})	1.1×10^{3}	Polarographic kinetic current	Fujisawa and Tanaka[16]
Pb^{2+}	0.2	1.1×10^{10}	(2.2×10^{2})	Polarographic diffusion current	Tanaka and Ogino[17]

Values in parentheses are those calculated from values of k_{1f} or k_{1b} and the equilibrium constant of Reaction 26[18] by the present authors.

from the plots in Figs. 2 and 3, and are given in Table II. Rate constants of other paths are not determined because of the rather large error.

The rate constants of Reaction 25b obtained here are compared with those of reactions similar to Reaction 25b involving other bivalent metal ions.

$$M^{2+} + HY^{3-} \underset{k_{1b}}{\overset{k_{1f}}{\rightleftharpoons}} MY^{2-} + H^{+} \qquad (26)$$

The values of k_{1f} and k_{1b} for several metal ions are also given in Table II. The dissociation rate constant k_{1b} for chromium(II) is larger than any of those for other metal ions given in the table.

It was reported by Eigen[19,20] that the rate-determining step of the complex-forming reaction of many metal ions is the substitution of a water molecule from the coordination sphere of the metal ions.

$$M(H_2O)_x\cdots L \overset{k_{H_2O}}{\rightleftharpoons} ML\cdot(H_2O)_{x-1}\cdots H_2O \qquad (27)$$

The values of k_{H_2O} for many bivalent metal ions are given in references 19 and 20. Reaction 26 can be considered to proceed in several consecutive steps

$$\begin{aligned} M(H_2O)_x{}^{2+} + HY^{3-} &\overset{K_{ass.}}{\rightleftharpoons} M(H_2O)_x{}^{2+}\cdots HY^{3-} \\ &\overset{k_{H_2O}}{\rightleftharpoons} M(HY)(H_2O)_{x-1}{}^{-}\cdots H_2O \\ &\rightleftharpoons \cdots \rightleftharpoons MY(H_2O)_y{}^{2-} + (x-y)H_2O + H^{+} \end{aligned} \qquad (28)$$

The first step, an outer-sphere association, and the steps following the substitution of a water molecule are more rapid than the substitution step, and hence the overall rate constant, k_{1f}, can be written as

$$k_{1f} = K_{ass.}k_{H_2O} \qquad (29)$$

The outer-sphere association constant, $K_{ass.}$, is not considered to vary considerably with different metal ions of the same charge according to the theory of the ion association by Bjerrum,[21] and therefore, a parallelism is expected to exist between values of k_{1f} and k_{H_2O}. Actually the order of Ni(II) $<$ Co(II) $<$ Cd(II) $<$ Cu(II) $<$ Pb(II) and that of Co(II) $<$ Zn(II) for k_{1f} are the same as those for k_{H_2O} reported by Eigen. These orders can be

10) N. Tanaka and H. Ogino, The 15 th Annual Symposium on Coordination Chemistry, Kanazawa, October 1965.
11) N. Tanaka and Y. Sakuma, This Bulletin, **32**, 578 (1959).
12) D. W. Margerum and T. J. Bydalek, *Inorg. Chem.*, **2**, 683 (1963).
13) N. Tanaka and K. Kato, This Bulletin, **32**, 1376 (1959).
14) N. Tanaka and H. Ogino, unpublished.
15) J. Koryta and Z. Zábranský, *Collection Czech. Chem. Commun.*, **25**, 3153 (1960).
16) T. Fujisawa and N. Tanaka, *J. Chem. Soc. Japan, Pure Chem. Sect.* (*Nippon Kagaku Zasshi*), **87**, 965 (1966).
17) N. Tanaka and H. Ogino, This Bulletin, **36**, 175 (1963).
18) L. G. Sillén and A. E. Martell, "Stability Constants of Metal Ion Complexes," Chemical Society, London (1964).
19) M. Eigen, "Advances in the Chemistry of Coordination Compounds" Ed. by S. Kirschner, Macmillan, New York (1961), p. 371.
20) M. Eigen, *Pure Appl. Chem.*, **6**, 97 (1963).
21) H. S. Harned and B. B. Owen, "The Physical Chemistry of Electrolytic Solutions," Reinhold Publishing, New York (1950), p. 42.

understood when the crystal field activation energies for the dissociation mechanism and the Jahn-Teller effect are considered.[20] Though the k_{H_2O} value for chromium(II) has not been reported, it is expected that k_{H_2O} for chromium(II) which has four d electrons is larger than those for nickel(II) and cobalt(II) from the view points of the crystal field activation energies and of the Jahn-Teller effect. Thus, it may be considered to be valid that the value of k_{1f} for chromium(II) obtained in this study is larger than those for cobalt(II) and nickel(II).

BULLETIN OF THE CHEMICAL SOCIETY OF JAPAN VOL. 39 2677—2680 (1966)

Polarographic and Potentiometric Studies of Indium(III)- and Europium(III)-Iminodiacetate Complexes

By Seizo MISUMI and Makoto AIHARA

Department of Chemistry, Faculty of Science, Kyushu University, Hakozaki, Fukuoka

(Received March 31, 1966)

The successive chelate formation constants for In(III)- and Eu(III)-IDA complexes were obtained by potentiometric titration and calculation by Bjerrum's method. The values of $\log K_1$ and $\log K_2$ for the In(III)-IDA complex are 9.54 and 8.87, and those for the Eu(III)-IDA complex are 6.22 and 4.72, respectively. The electrode reactions of these complexes were studied polarographically and found to be irreversible and diffusion-controlled. The ionic states of these complexes before reduction in the vicinity of the electrode surface were estimated to be $[InY_2(OH)]^{2-}$ or InY_2^- and $Eu(H_2O)_x^{3+}$. The rate constant, $(k_f^\circ)_B$, of the electron transfer for the Eu(III)-IDA complex was calculated to be 1.3×10^{-20} cm.sec^{-1}.

The polarography of complexes of some metal ions (e. g., zinc(II) and cadmium(II)[1]) with iminodiacetic acid (IDA) and the chelate formation constants of IDA complexes of rare earths[2] and some other metal ions[3] obtained by potentiometric titration have been investigated by serveral workers. In this paper, polarographic studies of indium(III)- and europium(III)-IDA complexes, of their electrode reaction, the rate constant, and the ionic state in the vicinity of electrode surface, are presented. The chelate formation constants for these complexes have also been determined by using Bjerrum's method.

Experimental

Reagents.—Stock solutions of indium(III) and europium(III) were prepared by dissolving metal perchlorates (more than 99.9% pure in distilled water; they were standardized volumetrically. The concentration of each stock solution was 0.01 M. Reagent-grade IDA (made by Wako Pure Chemical Industries) was used without any further purification.

A stock solution of monopotassium iminodiacetate (IDA-1K salt) was prepared by neutralizing IDA with a potassium hydroxide solution, and the concentration of IDA was adjusted to 0.5 M. A borate buffer (H_3BO_3-KCl-KOH) was used to adjust the pH of the solution. The ionic strength (μ) was adjusted with potassium chloride. A carbonate-free potassium hydroxide solution was prepared by the ion-exchange method.[4] All the other chemicals used were of an analytical reagent grade.

Apparatus.—A Yanagimoto PA-102 pen-recording polarograph was used to record the current-voltage curves. An H-type cell connected with a saturated calomel electrode (SCE) was used. The capillary used had a flowing weight, m, of mercury of 1.474 mg. sec^{-1} and a drop time, t_d, of 4.97 sec. drop^{-1} at the applied potential of -1.1 V. vs. SCE in an air-free 0.05 M IDA solution at a corrected height ($h_{corr.}$) of the mercury column of 68.41 cm. The measurement of the pH was made with a Hitachi pH meter, EHM-1 type. A titration apparatus consisting of a Horiba pH meter, P type, a titration vessel, and a thermostat was used. The titration vessel was a 150 ml. beaker fitted with a rubber stopper with holes for electrodes, a microburet, a thermometer, a gas inlet and outlet tubes; it was enveloped with a water jacket to maintain the solution at 25.0 ± 0.1°C during the measurements.

Procedure. — *Potentiometric Titration.*—Solutions of 1 : 1, 1 : 2, 1 : 3 and 1 : 5 ratios of metal ion to IDA were used. A sample solution was made up to 50 ml. or 100 ml., where the ionic strength was kept at 0.3 by the addition of potassium chloride. Purified nitrogen

1) K. W. Bernaver, D. Walz and S. Fallab, *Helv. Chim. Acta*, **41**, 2094 (1958).
2) L. C. Thompson, *Inorg. Chem.*, **1**, 490 (1962).
3) S. Chaberek, Jr., and A. E. Martel, *J. Am. Chem. Soc.*, **74**, 5052 (1952).
4) A. Albert and E. P. Serjeant, "Ionization Constants of Acids and Bases," Methuen and Co., Ltd., London (1962).

gas was passed through the solution; the solution was meanwhile being stirred in order to remove any carbon dioxde from the solution. Then the solution was titrated with 0.1 N potassium hydroxide, and the pH was measured. All experiments were carried out at a constant temperature of 25.0±0.1°C.

Polarography.—To a solution indium(III) or europium-(III) containing an appropriate quantity of IDA, a borate buffer solution was added in order to adjust the pH to the required value. Potassium chloride was also added to keep an ionic strength of 0.3. The solution was prepared at 25.0±0.1°C, and purified nitrogen gas was passed through the solution for about 30 min. in order to remove any dissolved oxygen before a polarogram was recorded.

Results and Discussion

Potentiometric Titration.—The acid dissociation constant and the chelate formation constant were determined by the method outlined by Chabereck and Martel.[3]

The Dissociation Constant of IDA. — The dissociation constant of IDA was calculated by a direct algebraic method, using a titration curve. The values obtained were $pk_1=3.01$ and $pk_1=9.60$* at 25.0±0.1°C and $\mu=0.3$(KCl).

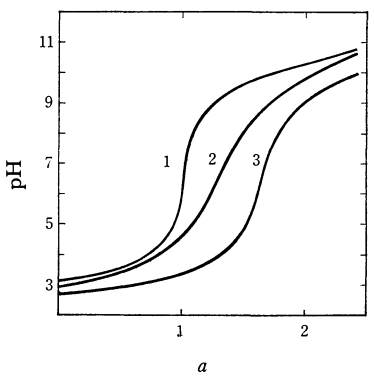

Fig. 1. Titration curves.
1) IDA, 2) $[Eu^{3+}]/[IDA]=1/3$,
3) $[In^{3+}]/[IDA]=1/5$
a=moles of base added per mole of acid.

The Chelate Formation Constant. — The chelate formation constant was calculated by using Bjerrum's method. In a solution with a 1 : 1 ratio of metal(III) to IDA, a hydrolytic buffer region appeared. However, from the solution with a 1 : 5 ratio of indium(III) to IDA or a 1 : 3 ratio of europium(III) to IDA, it disappeared, as Fig. 1 shows. The formation functions for In(III)- and Eu(III)-IDA complexes, plotted in Fig. 2, give a clear indication of the formation of

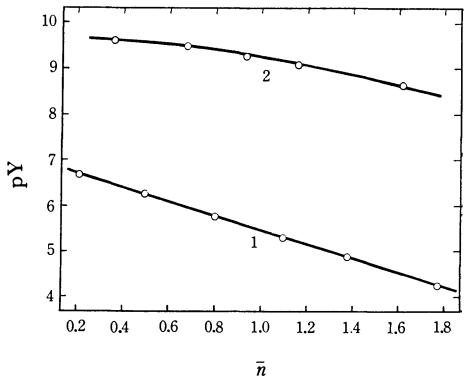

Fig. 2. Formation functions.
1) Eu(III)-IDA complex, 2) In(III)-IDA complex. $\bar{n}$=average number of donor groups bound per metal ion present. pY=negative logarithm of anion concentration, Y^{2-}.

the 1 : 1 and 1 : 2 complexes. The values of the successive chelate formation constants obtained are as follows:

	$\log K_1$	$\log K_2$
In^{3+}	9.54	8.78
Eu^{3+}**	6.22	4.72

Polarography.—Typical polarograms of In(III)- and Eu(III)-IDA complexes in borate buffer solutions are shown in Fig. 3.

Each complex ion shows a single reduction wave. The half-wave potentials for In(III)- and Eu(III)-IDA complexes shifted to the more negative side than that of the reduction wave of the corresponding metal aquo ion.

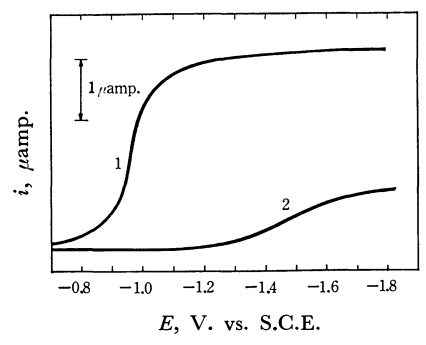

Fig. 3. Current-voltage curves of indium(III) and europium(III) in 0.05 M IDA solution.
1) $[In^{3+}]=0.5$ mM, pH=9.2; 2) $[Eu^{3+}]=0.5$ mM, pH=11.0

The Dependence of the Limiting Current on the Pressure of the Dropping Mercury Electrode.—The relation between limiting currents and various heights of the mercury column is shown in Table I.

* L. C. Thompson reported that $pk_1=2.58$ and $pk_2=9.33$ at 25°C and that $\mu=0.1$ (Ref. 2).

** L. C. Thompson: $\log K_1=6.73$ and $\log K_2=5.38$ (Ref. 2).

Table I. Dependence of limiting current on the height of mercury column

a) In(III)-IDA complex

$h_{corr.}$, cm.	i_l, μamp.	$i_l/\sqrt{h_{corr.}}$
53.41	2.828	0.395
63.41	3.144	0.395
73.41	3.372	0.394

0.5 mM In^{3+} in 0.05 M IDA medium, pH=9.2

b) Eu(III)-IDA complex

$h_{corr.}$, cm.	i_l, μamp.	$i_l/\sqrt{h_{corr.}}$
58.20	0.578	0.0757
63.21	0.604	0.0759
68.21	0.626	0.0758

0.5 mM Eu^{3+} in 0.05M IDA medium, pH=11.4

The values of $i_l/\sqrt{h_{corr.}}$ were found to be 0.395 ±0.001 μamp. $cm^{-1/2}$ for the In(III)-IDA complex and 0.0758±0.0001 μamp. $cm^{-1/2}$ for the Eu(III)-IDA complex. These results obviously indicate that the limiting currents for both In(III)- and Eu(III)-IDA complexes are diffusion-controlled.

Reversibility.—The reversibility of the electrode reaction for the In(III)- or the Eu(III)-IDA complex was verified by plotting log $i/(i_d-i)$ vs. E. As is shown in Table II, the mean values of the reciprocal slope for the In(III)-IDA complex and that for the Eu(III)-IDA complex were found to be 0.041 V. and 0.079 V. respectively. The mean values of αn were, therefore, 1.4 and 0.75 respectively, where α is the transfer coefficient and n, the number of electrons associated with the electrode reaction. Consequently, the electrode reactions for In(III)- and Eu(III)-IDA complexes were irreversible; three electrons change in the former, while one electron changes in the latter.

The Effects of the pH on Reduction Waves.—Polarograms were recorded with 0.5 mM Eu(III) or In(III) in 0.05 M IDA solutions at various pH's. The results are shown in Table II. The half-wave potential for the In(III)-IDA complex shifted to the more negative side as the pH increased from 9.2 to 10.6, whereas the half-wave potential for the Eu(III)-IDA complex was independent of the pH in the pH range from 9.2 to 12.0. The values of $d(-E_{1/2})_c/d\log C_{OH^-}$ calculated from the experimental data are as follows:

$$d(-E_{1/2})_c/d \log C_{OH^-} = 0.054$$

for the In(III)-IDA complex

$$d(-E_{1/2})_c/d \log C_{OH^-} = 0$$

for the En(III)-IDA complex

where $(E_{1/2})_c$ is the half-wave potential of complex ions and C_{OH^-} the concentration of hydroxyl ions.

The diffusion current for the In(III)-IDA complex decreased with an increase in the pH. It was supposed that the decrease in the diffusion current was caused by the precipitation of basic substances on the electrode. The diffusion current for the Eu(III)-IDA complex, on the other hand, was almost the same in the pH range from 10.0 to 12.0.

Table II. Effects of pH on reduction wave

a) In(III)-IDA complex

pH	$(E_{1/2})_c$ V. vs. SCE	i_d μamp.	Reciprocal slope mV.	αn
9.2	−0.977	3.244	39	1.5
9.5	−0.997	3.188	42	1.4
9.8	−1.020	3.032	42	1.4
10.2	−1.035	2.716	42	1.4
10.6	−1.057	1.744	42	1.4
		mean value	41	1.4

0.5 mM In^{3+} in 0.05 M IDA medium μ=0.3

b) Eu(III)-IDA complex

pH	$(E_{1/2})_c$ V. vs. SCE	i_d μamp.	Reciprocal slope mV.	αn
9.2	−1.427	0.552	74	0.80
9.8	−1.425	0.576	70	0.84
10.0	−1.425	0.620	82	0.72
11.0	−1.424	0.614	84	0.70
12.0	−1.426	0.616	83	0.71
		mean value	79	0.75

0.5 mM Eu^{3+} in 0.05 M IDA medium μ=0.3

The Effects of the Concentration of IDA on the Reduction Wave.—Polarograms were recorded in the range of the concentration of IDA from 5 mM to 50 mM at pH 9.2 for the In(III)-IDA complex and from 30 mM to 60 mM at pH 11.4 for the Eu(III)-IDA complex. The results are shown in Table III.

Table III. Effects of concentration of IDA on reduction wave

a) In(III)-IDA complex

Concn. of IDA mM	$(E_{1/2})_c$ V. vs. SCE	i_d μamp.	Reciprocal slope mV.	αn
5	−0.983	2.960	41	1.4
10	−0.987	3.188	42	1.4
25	−0.981	3.208	42	1.4
50	−0.980	3.224	40	1.5
		mean value	41	1.4

In^{3+}: 0.5 mM, pH=9.2 μ=0.3

b) Eu(III)-IDA complex

Concn. of IDA mM	$(E_{1/2})_c$ V. vs. SCE	i_d μamp.	Reciprocal slope mV.	αn
30	−1.378	0.630	77	0.77
40	−1.393	0.628	75	0.79
50	−1.411	0.604	76	0.78
60	−1.422	0.630	79	0.75
		mean value	77	0.77

Eu^{3+}: 0.5 mM, pH=11.4. μ=0.3.

The half-wave potentials for the In(III)-IDA complex were independent of the IDA concentration, but that for the Eu(III)-IDA complex shifted to the more negative side with an increase in the IDA concentration. Thus:

$$d(-E_{1/2})_c/d\log C_{IDA}=0 \text{ for the In(III)-IDA complex at pH 9.2}$$

and:

$$d(-E_{1/2})_c/d\log C_{IDA}=0.150 \text{ for the Eu(III)-IDA complex at pH 11.4,}$$

where C_{IDA} was the concentration of the complexing agent, IDA. The diffusion current for the In(III)-IDA complex increased with increasing IDA concentrations, while that for the Eu(III)-IDA complex was almost constant.

The Electrode Process and the Species of Complex in the Vicinity of the Electrode Surface. — If an irreversible electrode process for the metal M(III) complex takes place according to the following scheme:

$$MX_p^{3-pb} \rightleftarrows MX_q^{3-qb} + (p-q)X^{b-}$$
$$MX_q^{3-qb} + ne \rightarrow MX_q^{(3-qb-n)} \qquad (1)$$

where p is the maximum number of ligands (X^{b-}) attached to a metal ion in the bulk solution; q, the number of ligands attached to a metal ion in the vicinity of the electrode surface, and n, the number of electrons associated with the electrode reaction, an equation derived by Matsuda and Ayabe[5] for the current-voltage curve due to an irreversible electrode reaction of a complex ion is applicable. Therefore, as the electrode reaction of In(III)- or Eu(III)-IDA complex is irreversible and diffusion-controlled, the half-wave potential, $(E_{1/2})_c$, is given by Eq. 2[5]:

$$(E_{1/2})_c=2.3\frac{RT}{\alpha nF}[\log(k_f^0)_B f_{MX_p}/\sqrt{D_{MX_p}} + 0.5\log t_d - 0.053 - (p-q)\log(f_x D_x)] \qquad (2)$$

where $(k_f^0)_B$ is the forward reduction rate constant of the electron transfer process at the potential of the normal hydrogen potential; D_{MX_p}, the diffusion coefficient of the complex metal ion, MX_p^{3-pb}; t_d, the drop time; C_x, the concentration of the complexing agent, and f_{MX_p} and f_x, the activity coefficients of the complex metal ion and the complexing agent respectively. From Eq. 2, a plot of $-(E_{1/2})_c$ vs. $\log(f_x C_x)$ should produce a straight line with a slope equal to $(p-q)\ 2.3\ RT/\alpha n F$; the value of the tangent for $-(E_{1/2})_c$ vs. $\log f_x C_x$ is given by:

$$d(-E_{1/2})_c/d\log f_x C_x=(p-q)\ 0.0591/\alpha n$$

As the electrode reaction for the In(III)-IDA complex is an irreversible three-electron change ($n=3$) and is independent of the IDA concentration between 5 mM to 50 mM, the value of $(p-q)$ for OH in the case of the In(III)-IDA complex was calculated to be about 1, by using the observed value, 1.4, of αn in the pH range from 9.2 to 10.6. On the assumption that $p=2$ or $p=1$ for OH, for example, the $[InY_2(OH)]^{2-}$ or InY_2^- species would participate in the electron transfer process, where H_2Y indicates IDA. On the other hand, as the electrode reaction for the Eu(III)-IDA complex is irreversible, of a one-electron change ($n=1$), and independent of pH values from 9.2 to 12.0, the value of $(p-q)$ for IDA was calculated to be about 2, by using the observed value, 0.77, of αn in the range of the IDA concentration from 30 mM to 60 mM. Therefore, if it is assumed that $p=2$ for IDA, for example, the $Eu(H_2O)_x^{3+}$ species would participate in the electron transfer process, the transfer coefficient, α, being equal to 0.77.

The value of the forward rate constant, $(k_f^0)_B$, of the electron transfer process for the Eu(III)-IDA complex was calculated for the IDA concentration of 0.05 M with the value of the half-wave potential of -1.178 V. vs. NHE; a diffusion coefficient of the Eu(III)-IDA complex, D_{MX_p}, of 1.16×10^{-6} cm^2 sec^{-1}, and a drop time of 3.91 sec., provided that $f_{MX_p}=f_x=1$. The value obtained was:

$$\log(k_f^0)_B=-19.9 \quad (k_f^0 \text{ cm. sec}^{-1})$$

In conclusion, the above results indicate that the species which participate directly in the electron transfer process are mainly $[InY_2(OH)]^{2-}$ or InY_2^- and $Eu(H_2O)_x^{3+}$.

The authors wish to thank the Ministry of Education for the financial support granted this research.

5) H. Matsuda and Y. Ayabe, *Z. Elektrochem.*, **63**, 1164 (1959).

BULLETIN OF THE CHEMICAL SOCIETY OF JAPAN VOL. 39 2681—2684 (1966)

Studies of Scandium in Various Solutions. III. The Solvent Extraction and Complex Formation of Scandium(III) with Acetylacetone and Thenoyltrifluoroacetone

By Tatsuya SEKINE, Akira KOIZUMI and Mitsuo SAKAIRI

Department of Chemistry, Tokyo College of Science, Kagurazaka, Shinjuku-ku, Tokyo

(Received April 13, 1966)

The distribution of scandium(III) at a tracer concentration was determined between chloroform with acetylacetone or thenoyltrifluoroacetone and 0.1 M aqueous perchlorate solutions at 25°C. The change in the distribution ratio of the metal ion with the change in the chelating acid concentration or with the change in the hydrogen-ion concentration was explained in terms of the extraction of the tris chelate complexes into the organic phase and the formation of the primary complexes in the aqueous phases. The equilibrium constants in these systems were determined graphically, by a curve-fitting method to be as follows:

$$K_{ex}=[ScA_3]_{org}[H^+]^3/[Sc^{3+}][HA]^3_{org}$$

$$K_1=[ScA^{2+}]/[Sc^{3+}][A^-]$$

HA	Acetylacetone	Thenoyltrifluoroacetone
$\log K_{ex}$	−6.35	−1.30
$\log K_1$	8.3	7.1

Acetylacetone (AA) and thenoyltrifluoroacetone (TTA) in various organic solvents have been used for the extraction of scandium(III) in aqueous solutions.[1-5]

For the present paper, the authors studied the distribution of trace amounts of scandium(III) between chloroform solutions of AA or TTA and aqueous solutions of 0.1 M (Na, H)ClO_4 at 25°C; they also determined the extraction constants and the stability constants of scandium(III) aqueous complexes with these β-diketones.

Statistical Treatment

The distribution equilibrium of scandium(III) in an aqueous phase into an immiscible organic phase with an organophilic chelating acid, HA, may be described as follows:

$$Sc^{3+} + 3HA(org) \rightleftarrows ScA_3(org) + 3H^+ \quad (1)$$

$$K_{ex} = [ScA_3]_{org}[H^+]^3/[Sc^{3+}][HA]^3_{org} \quad (2)$$

In the equations, the subscript *"org"* denotes a species in the organic phase, while the absence of a subscript denotes a species in the aqueous phase.

The concentration of scandium in the two phases may be determined radiometrically, and the net distribution ratio may be defined as:

$$D = [Sc(III)]_{org,total}/[Sc(III)]_{total} \quad (3)$$

When it is assumed that (i) scandium(III) exists in the aqueous phase only as Sc^{3+} or as the chelate complexes, ScA^{2+}, ScA_2^+,⋯, and that (ii) scandium(III) exists in the organic phase only as the neutral tris chelate complex, ScA_3, the net distribution ratio in Eq. 3 may be described as:

$$D = [ScA_3]_{org}/([Sc^{3+}]+[ScA^{2+}]+[ScA_2^+]+\cdots) \quad (4)$$

The statistical treatment of the distribution ratios may then be carried out by applying the law of mass action.[6]

The complex formation equilibria in the aqueous phase may be described as:

$$Sc^{3+} + nA^- \rightleftarrows ScA_n^{3-n} \quad (5)$$

$$\beta_n = [ScA_n^{3-n}]/[Sc^{3+}][A^-]^n \quad (6)$$

By introducing Eqs. 2 and 6 into Eq. 4, the following equation is obtained:

$$D[H^+]^3[HA]^{-3}_{org} = K_{ex}/(1+\beta_1[A^-]+\beta_2[A^-]^2+\cdots) \quad (7)$$

The chelating acid is distributed between the two phases as:

$$HA \rightleftarrows HA(org) \quad (8)$$

$$K_D = [HA]_{org}/[HA] \quad (9)$$

1) J. Starý and E. Hladký, *Anal. Chim. Acta*, **28**, 227 (1963).
2) A. M. Poskanzer and B. M. Foreman, *J. Inorg. Nucl. Chem.*, **16**, 323 (1961).
3) E. Sheperd and W. W. Meinke, *U. S. Atomic Energy Comm. Report, AECU*-3879.
4) T. C. Rains, H. P. House and O. Menis, *Anal. Chim. Acta*, **22**, 315 (1960).
5) T. Sekine, *Proceedings 7th International Conference on Coordination Chemistry*, **7J4**, Stockholm (1962).
6) J. Rydberg, *Acta Chem. Scand.*, **4**, 1503 (1950).

The chelating acid may dissociate in the aqueous phase as:

$$HA \rightleftarrows H^+ + A^- \quad (10)$$

$$K_a = [H^+][A^-]/[HA] \quad (11)$$

When a certain volume of an organic phase with the chelating acid at an initial concentration, $[HA]_{org,initial}$ is equilibrated with an aqueous phase of the same volume, the following equation holds:

$$[HA]_{org,initial} = [HA]_{org} + [HA] + [A^-] \quad (12)$$

From Eqs. 9, 11 and 12, the following equations can be introduced:

$$[A^-] = [HA]_{org,initial}/(1+K_a^{-1}[H^+] + K_D K_a^{-1}[H^+]) \quad (13)$$

$$[HA]_{org} = [HA]_{org,initial}/(1+K_D^{-1} + K_D^{-1}K_a[H^+]^{-1}) \quad (14)$$

Thus, the values $[A^-]$ and $[HA]_{org}$ at the equilibrium can be calculated from the initial concentration of the chelating acid in the organic phase, the hydrogen ion concentration, and the two equilibrium constants, K_D and K_a. The extraction constant and the stability constants of the scandium complexes may then be determined by introducing these values into Eq. 7.

Experimental

Reagents.—Scandium-46 was obtained from the New England Nuclear Co., U. S. A., as a hydrochloric acid solution. This was diluted with 0.1 M perchloric acid and used as the stock solution. All of the reagents were of a reagent grade. Acetylacetone and thenoyltrifluoroacetone were obtained from Dojindo & Co., Ltd. The sodium perchlorate was recrystallized two times from water. The chloroform was washed three times with water. The other reagents were used without further purification.

Procedures.—All of the procedures were carried out in a thermostatted room at 25±0.5°C. Stoppered glass tubes (volume: 20 ml.) were employed to equilibrate the two phases. The tracer solution, a buffer solution, a 0.1 M sodium perchlorate solution, and finally a chloroform solution of acetylacetone or thenoyltrifluoroacetone were placed in the tubes. Sulfanilate or pyridine (the initial concentration was 0.01 M) was used as the buffer. In some experiments, the scandium tracer in the aqueous phase was first extracted with the chelating acid into the organic phase and the scandium in the organic phase was back-extracted into fresh aqueous solutions. The initial volume of the two phases was always 5.0 ml., and the initial concentration of scandium in either the aqueous or the organic phase was 6×10^{-5} M.

The two phases in the tubes were agitated by a mechanical rotator for more than one hour and centrifuged at 2000 r. p. m. for three minutes. A 2-ml. portion was then pipetted from both the phases and transferred into small test tubes. The γ-radioactivity of the solutions was measured with a well-type (NaI) scintillation counter. A small portion was also taken from the aqueous phase, and the hydrogen ion concentration was measured potentiometrically, using 0.010 M perchloric acid +0.09 M sodium perchlorate as the standard of $-\log [H^+]=2.000$.

Results

Figures 1 and 2 give the distribution ratio of scandium(III) in the acetylacetone (AA) systems or the thenoyltrifluoroacetone (TTA) systems at various hydrogen ion concentrations. Figure 1 shows the log$D$ vs. $-\log [H^+]$ plot when the initial concentration of the chelating acids in the organic phase is 0.100 M while Fig. 2 gives the log$D$ $[H^+]^3$ vs. log $[HA]_{org}$ plot when the initial concentration of the chelating acid is different. In Fig. 1, the open circles give the data obtained when the tracer was initially added to the organic phase. The straight line of slope three in the figures are the calculated distribution curves obtained from the extraction constants, K_{ex}, in Table II.

The K_D and K_a values for AA and TTA which appear in the literature were introduced into Eqs. 13 and 14. The equations thus obtained are given in Table I.

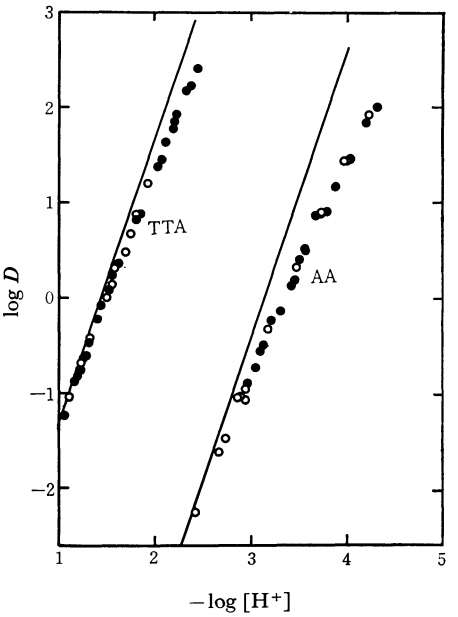

Fig. 1. Distribution of Sc(III) between chloroform with 0.1 M (initial concentration) chelating acid and 0.1 M (Na, H)ClO_4 at 25°C as a function of $-\log [H^+]$.
Open circles; extraction of Sc(III) in the aqueous phase into the organic phase.
Closed circles; back-extraction of Sc(III) in the organic phase into the aqueous phase.
The straight line for the TTA plot is $\log D = -3\log [H^+] - 4.32$ and that for the AA plot is $\log D = -3\log [H^+] - 9.44$.

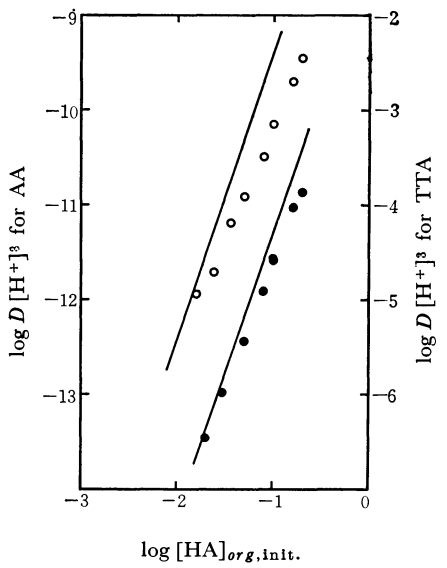

Fig. 2. Distribution of Sc(III) between chloroform with chelating acid and 0.1 M (Na, H)ClO_4 as a function of the initial chelating acid concentration in the organic phase.
Open circles; acetylacetone (AA)
Closed circles; thenoyltrifluoroacetone (TTA)

TABLE I. CONCENTRATION OF CHELATING ACIDS IN THE TWO PHASES AT 25°C

Organic phase; chloroform
Aqueous phase; 0.1 M (H, Na)ClO_4

(A) HA=Acetylacetone

$\log K_D = 1.37$[6] $\log K_a = -8.82$[6]

$[A^-] = [HA]_{org,initial}/(1+1.56\times10^{10}[H^+])$

$[HA]_{org} = [HA]_{org,initial}/(1.04+6.79\times10^{-11}[H^+]^{-1})$

(B) HA=Thenoyltrifluoroacetone

$\log K_D = 1.84$[5] $\log K_a = -6.23$[7]

$[A^-] = [HA]_{org,initial}/(1+1.18\times10^{8}[H^+])$

$[HA]_{org} = [HA]_{org,initial}/(1.01+8.51\times10^{-9}[H^+]^{-1})$

TABLE II. EQUILIBRIUM CONSTANTS FOR THE EXTRACTION AND THE COMPLEX FORMATION OF SCANDIUM(III) AT 25°C

Organic phase; chloroform
Aqueous phase; 0.1 M (H, Na)ClO_4
$K_{ex} = [ScA_3]_{org}[H^+]^3/[Sc^{3+}][HA]^3_{org}$
$K_1 = [ScA^{2+}]/[Sc^{3+}][A^-]$

HA	Acetylacetone	Thenoyltrifluoroacetone
$\log K_{ex}$	−6.35	−1.30
$\log K_1$	8.3_2	7.1_4

7) J. C. Reid and M. Calvin, *J. Am. Chem. Soc.*, **72**, 2948 (1950).

Figures 3 and 4 give $\log D\,[H^+]^3[HA]^{-3}_{org}$ vs. log[A⁻] plot calculated from the data in Figs. 1 and 2 and Table I.

From Eq. 7, the following equation is obtained:

$$\log D[H^+]^3[HA]^{-3}_{org} = \log K_{ex} - \log(1+\beta_1[A^-] + \beta_2[A^-]^2+\cdots) \quad (15)$$

Equation 15 shows that the $\log D\,[H^+]^3[HA]^{-3}_{org}$ vs. log[A⁻] plot will be found to fit one of the family of standard curves[8-10]:

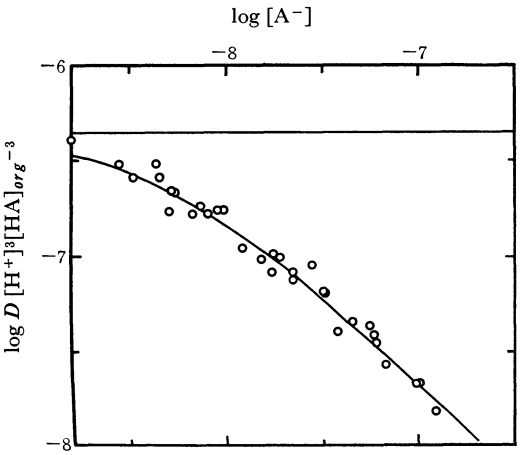

Fig. 3. Change in the extraction constant of Sc(III) with AA as a function of the concentration of the dissociated chelating acid in the aqueous phase.
The solid curve shows $\log D\,[H^+]^3[HA]^{-3}_{org}$ vs. $-\log(1+2.0\times10^8[A^-])$.

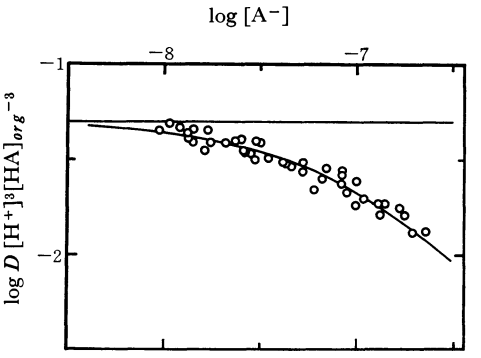

Fig. 4. Change in the extraction constant of Sc(III) with TTA as a function of the concentration of the dissociated chelating acid in the aqueous phase.
The solid curve shows $\log D\,[H^+]^3[HA]^{-3}_{org}$ vs. $-\log(1+1.3\times10^7[A^-])$.

8) L. G. Sillén, *Acta Chem. Scand.*, **10**, 186 (1956).
9) F. J. G. Rossotti and H. Rossotti, "The Determination of Stability Constants in Solution," McGraw-Hill Book Co., Inc., New York (1961).
10) T. Sekine and Y. Hasegawa, This Bulletin, **39**, 240 (1966).

$$\left.\begin{aligned} X &= \log v \\ Y &= -\log(1+\sum_{n=1}^{n} p_n v^n) \end{aligned}\right\} \quad (16)$$

After several trials, it was found that both of the plots in Figs. 3 and 4 fit the standard curve $X=\log v$; $Y=\log(1+v)$. The best-fit constants obtained from the curve-fitting are listed in Table II. The solid curves in Figs. 3 and 4 show the statistical curves calculated from these constants.

Discussion

In the present study, the aqueous phase was always 0.1 M (Na, H)ClO_4, and the hydrogen ion concentration was larger than 10^{-4} M. Therefore, the hydrolysis of Sc^{3+} in the aqueous phase may not be very much, because the hydrolysis constant of scandium in 0.1 M ($NaClO_4$) at 25°C was reported to be $[ScOH^{2+}][H^+][Sc^{3+}]=10^{-4.74}$.[11] The formation of polynuclear complexes may be negligible because the total concentration of scandium in the aqueous phase is less than 6×10^{-5} M; thus, Assumption i described in the previous section, may be valid in the present systems. The scandium complexes in the organic phase may be in the ScA_3 form in both the AA and TTA systems, because no remarkable deviation of the plot in Figs. 2 to 4 is observed even when the organic concentration of the chelating acid is larger or smaller than 0.1 M (cf. Ref. 5). Thus, it may be concluded that Assumption ii is also valid in the present systems. The distribution ratios obtained both by the extraction from the aqueous phase and by the back-extraction from the organic phase agree within the range of experimental error; this may indicate that the distribution equilibrium of scandium is established under the present experimental conditions.

The plots in Figs. 3 and 4 scatter somewhat from the fitted curve given by a solid curve, and as a result the limit of the error of the constants will be rather large. Therefore, the $\log K_{ex}$ are given to three figures, while the $\log\beta_1$ are given to only two figures.

Starý[12] listed the extraction constants of scandium(III) into benzene with AA ($\log K_{ex}=-5.83$) and TTA ($\log K_{ex}=-0.77$).

Wakahayashi, Oki, Omori and Suzuki[13] studied the distribution of scandium(III) chelate into various solvents. They reported that the net distribution ratio of scandium(III) between chloroform and 0.1 M (Na, H)ClO_4 was $\log D=0.41$ for the AA chelate and $\log D=-0.54$ for the TTA chelate when $-\log[A^-]=7.80$. Their figure for the TTA chelate seems to agree with the present results, but their value for the AA chelate seems to be a little higher. They did not give any constants for the complex formation in the aqueous phase.

Izatt and his co-workers[14] gave the stability constants for the AA complexes of scandium(III) at zero ionic strength and at 30°C as $\log K_1=8.0$ and $\log K_2=7.2$ ($\log\beta_2=15.2$). The $\log K_1$ in their work is of the same order as that in the present work, but the formation of a secondary complex of the $\log\beta_2$ around 15 can not be concluded from the present results (cf. Fig. 3).

No stability constant for scandium TTA complexes seems to have been reported.

Part of this work was carried out at the Laboratory of Nuclear Chemistry, the Institute of Physical and Chemical Research, Tokyo. The authors are very grateful to Professor Nobufusa Saito, the head of that Laboratory. The authors are also very grateful to Mr. Ichiro Kobayashi and Mr. Ichiro Sakamoto of the present laboratory for their experimental aid.

11) M. Kilpatrick and L. Pokras, *J. Electrochem. Soc.*, **101**, 39 (1954).

12) J. Starý, "The Solvent Extraction of Metal Chelates," Pergamon Press Ltd., Oxford (1964), p. 42.

13) T. Wakahayashi, S. Oki, T. Omori and N. Suzuki, *J. Inorg. Nucl. Chem.*, **26**, 2265 (1964).

14) R. M. Izatt, W. C. Fernerius, C. G. Haas, Jr., and B. P. Block, *J. Phys. Chem.*, **59** 170 (1955).

BULLETIN OF THE CHEMICAL SOCIETY OF JAPAN VOL. 39 2685—2690 (1966)

The Radioactivation Analysis of Semiconductor Graphite for Nitrogen by the $^{14}N(p, \alpha)^{11}C$ Reaction

By Tadashi NOZAKI

Institute of Physical and Chemical Research, Yamato-machi, Saitama

and Takayasu OKUO and Hiroyuki AKUTSU,

University of Electrocommunication, Chôfu, Tokyo

and Michiaki FURUKAWA

Faculty of Science, The University of Tokyo, Hongo Tokyo

(Received April 14, 1966)

The excitation curve for the $^{14}N(p, \alpha)^{11}C$ reaction was measured up to a proton energy of 15 MeV.; the reaction was found to have a fairly high cross section for a sensitive determination of nitrogen by radioactivation. A convenient technique was developed for the rapid quantitative conversion of the irradiated graphite into carbonate within a closed system. This technique makes possible the determination of a trace (down to several p.p.b.) of nitrogen in pyrolytic graphite. Discussions of the possible interference (i. e., that of boron by the $^{11}B(p, n)^{11}C$ reaction) will also be given. The nitrogen content of the pyrolytic graphite sample was found to vary markedly according to the starting material and to the preparation conditions.

The development of reliable methods for determining an ultra-trace quantity of nitrogen has been required because of its ultimate importance in the physicochemical study of hyper-pure substances, especially of semiconductor materials. Previously, we reported, in a short communication,[1] that radioactivation analysis by means of the $^{14}N(p, \alpha)^{11}C$ reaction is useful for determining a trace quantity of nitrogen in pyrolytic graphite for semiconductors. In this paper, the excitation curve for the $^{14}N(p, \alpha)^{11}C$ reaction, a detailed description of the chemical process, and some results of the determination will be given, along with a discussion of the possible interferences.

Pyrolytic graphite is prepared by the thermal decomposition of an organic vapor, the carbon from the organic substance depositing onto a heated substrate to give gradually a crystalline, lustrous plate with profitable semiconductor characteristics. The pyrolytic graphite prepared from pyridine was found to have fascinating semiconductor properties.[2] The presence of a trace quantity of nitrogen is considered to give it these properties.

As is shown in Table I, all previously-reported methods are unsatisfactory for determining a trace of nitrogen in graphite; they are either inapplicable to the matrix or are of insufficient sensitivity. Further, since nitrogen is abundant in air, the sample surface, the analytical reagents and apparatus are always contaminated with it. The present method is of a very high sensitivity (a few p.p.b. of nitrogen) and is free from the contamination effect. Further, because of its extreme thermal stability, pyrolytic graphite is a suitable matrix to be analyzed by charged-particle activation; a sample with less thermal stability is apt to melt or decompose during the irradiation.

A chemical process involving a rapid quantitative decomposition of the irradiated graphite is necessary, as will be explained later. Since pyrolytic graphite is quite resistant to chemical attack, some ingenuity is required for the decomposition. The technique described in this paper is not only suitable for the present purpose, but is useful also for the rapid quantitative decomposition of many kinds of substances within a closed system.

The Excitation Curve for the $^{14}N(p, \alpha)^{11}C$ Reaction, and a Discussion of Possible Interferences

The excitation curve for the $^{14}N(p, \alpha)^{11}C$ reaction up to 15 MeV. was measured by the stacked-foil method; the results are given in Fig. 1. Because of the possible error involved in the proton-beam monitoring and in the absolute activity measurements, the absolute value of the cross section is less certain than the shape of the excitation curve, although the uncertainty must be within 20%. The mean recoil range of the ^{11}C produced by 14.2 MeV. protons was also measured by inserting a recoil catcher in the stack; it was found to be 0.36 mg./cm^2.

The irradiation of carbon itself with 15 MeV.

1) T. Nozaki and K. Yazawa, This Bulletin, **37**, 1891 (1964).

2) K. Takeya, Y. Yazawa, N. Okuyama and H. Akutsu, *Phys. Rev. Letters*, **15**, 111 (1965).

Table I. Analytical methods for trace nitrogen

Method	Detection limit*	Application to graphite	Removal of surface contamination	Interference etc.
Vacuum fusion	~1 p. p. m.	×	×	
Kjeldahl	>1 p. p. m.	×	×	Contamination from reagents
Emission spectroscopy	~10 p. p. m.	○	△	Contamination by residual air
Mass spectroscopy	~10 p. p. b.	△	×	Contamination by residual air
Radio-activation analysis $^{14}N(n, 2n)^{13}N$	a few p. p. m.	○	○	Difficulty in the chemical separation of nitrogen
Radio-activation analysis $^{14}N(\gamma, n)^{13}N$	a few p. p. m.	○	○	Difficulty in the chemical separation of nitrogen
Radio-activation analysis $^{14}N(p, \alpha)^{11}C$	several p. p. b.	○	○	$^{11}B(p, n)^{11}C$

○: Suitable, △: Difficult, ×: Impracticable
* For a convenient matrix.

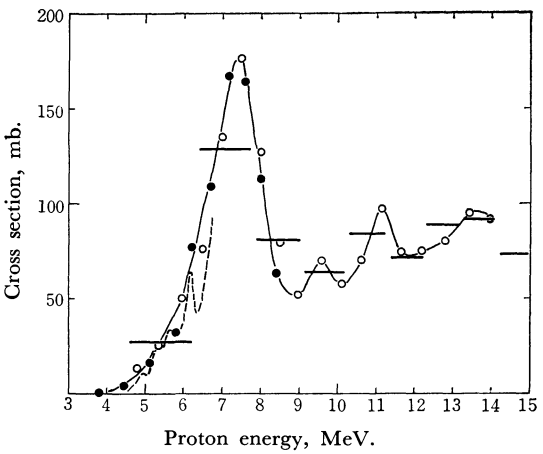

Fig. 1. The excitation curve for the $^{14}N(p, \alpha)^{11}C$ reaction.
Full line: Our result (—: nylon; ○, ●: aluminum nitride)
Broken line: Blaser's result[13]

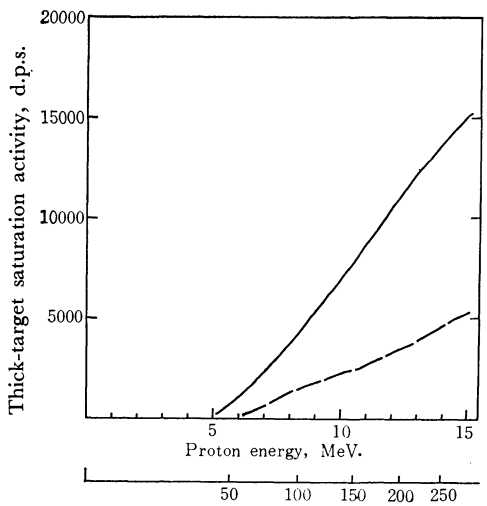

Fig. 2. The thick-target saturation activity of ^{11}C. (see text)
—— $^{11}B(p, n)^{11}C$
—— $^{14}N(p, \alpha)^{11}C$

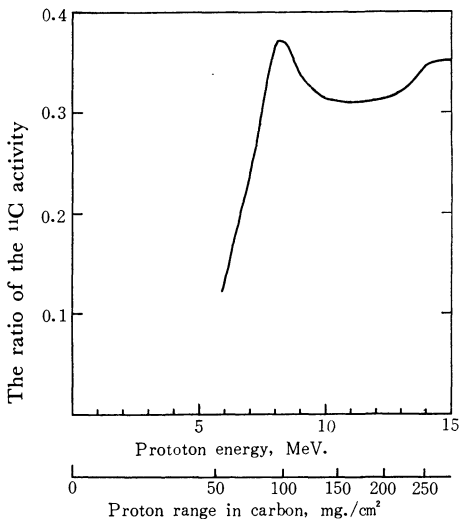

Fig. 3. The ratio of the ^{11}C activity formed from nitrogen to that from boron. (see text)

protons gives no ^{11}C, since the threshold for the $^{12}C(p, pn)^{11}C$ reaction is 20.2 MeV. There is, however, another reaction, namely, $^{11}B(p, n)^{11}C$, which gives ^{11}C on the proton irradiation.[3] Figure 2 shows the thick-target saturation activity of ^{11}C produced by irradiating carbon containing 1 p.p.m. (by weight) of nitrogen or of boron (natural isotopic composition) with a 1 μamp. proton beam. Figure 3 shows the ratio of the ^{11}C activity formed from nitrogen to that formed from boron, when a thick matrix containing equal amounts (weight fraction) of the two elements is irradiated with protons. The thick-target yield varies with the nature (the stopping power) of the matrix, but the ratio is almost independent of it.

As is evident from Fig. 2 and Fig. 3, in the presence of boron nitrogen cannot be determined by proton activation in a single irradiation. Alternately, two irradiations at different proton energies, followed by the solution of the pair of simultaneous equations thus obtained, do not seem to

3) M. Furukawa, Y. Ishizaki, Y. Nakano, T. Nozaki, Y. Saji and S. Tanaka, *J. Phys. Soc. Japan*, **15**, 2167 (1960).

give accurate results. By radioactivation analysis using the $^{10}B(d, n)^{11}C$ reaction, an ultra-trace quantity of boron can be determined in the presence of nitrogen. However, this method is not suitable for the graphite matrix because of the simultaneous formation of a very high activity of ^{13}N due to the $^{12}C(d, n)^{13}N$ reaction.

Fortunately, however, the determination of a trace of boron in graphite has been well studied because of its importance in nuclear engineering. Both direct spectrography[4] and spectrography or spectrophotometry after ashing the sample in the presence of calcium oxide or lanthanum oxide[5,6] are useful. In the latter process, the methods developed for determining an ultra-trace quantity of boron in transistor-grade silicon[7] or in germanium are also applicable with slight modifications. Hence, it appears preferable to determine boron by one of the above method prior to the proton activation.

It was certain, however, that most of our present samples contained much less boron than nitrogen, because they were prepared from pyridine. Hence, without the prior determination of boron, their nitrogen content could be determined reliably.

The Elimination of the Surface Contamination

Surface contamination is easily eliminated by removing a surface layer of a suitable, uniform thickness after the irradiation. The layer thickness depends on the recoil range of the radio-nuclide and on the roughness of the initial surface. It has been shown previously that a surface layer of about 5 times the thickness corresponding to the recoil range should be removed.[8] Hence, for the present case, a surface layer about 1.8 mg./cm^2 thick should be removed. However, since the uniform removal of such a thin surface is difficult and since the initial surface roughness is not precisely known, it is considered preferable to grind off a surface layer of a greater thickness (5 to 10 mg./cm^2).

Chemical Process

The nuclide ^{11}C has a 20.4 min. half-life and emits positrons but no γ-rays. The proton irradiation of carbon gives a high activity of ^{13}N by the $^{13}C(p, n)^{13}N$ reaction,[9] the abundance of ^{13}C being 1.1%. ^{13}N also emits positrons and has a 10.0 min. half-life. Many kinds of impurities also give positron emitters on proton irradiation. Therefore, a trance of nitrogen in graphite cannot be determined by nondestructive γ-ray spectrometry; a chemical purification of the ^{11}C involving a rapid decomposition of the sample is required. In the purification, the matrix graphite itself is the carrier of ^{11}C.

After the irradiation with charged particles, the radionuclide formed is not distributed uniformly in the sample, and the radiation effect might have changed the chemical reactivity of the irradiated portion. Therefore, a quantitative treatment of the pyrolytic graphite involving its oxidation under drastic conditions is required until a homogeneous phase containing all of the carbon is obtained.

Wet oxidation in a mixture of sulfuric and condensed polyphosphoric acid provided a useful method of decomposing the sample. Kiba and his associates[10] describe the stoichiometrical oxidation of charcoals and naturally-occurring graphite with potassium iodate in condensed polyphosphoric acid. For the present purpose, the technique they described should, however, be slightly modified, because pyrolytic graphite is more resistive to oxidation than charcoals and graphites of other sources, and because a larger quantity (up to 1 g.) of the sample should be oxidized. The following modifications proved to be convenient: (1) a mixture of sulfuric and condensed polyphosphoric acid was used as the oxidation medium[11]; (2) a small quantity of perchloric acid was added near the end of the oxidation; and (3) the reaction temperature was raised slowly but continuously in the course of the reaction. Without these modifications, the oxidation was often incomplete with the formation of the so-called graphitic acid, which was still less oxidizable than the graphite itself. The fine pulverization of the sample with the aid of added alumina or silica[10] was of ultimate importance for the smooth oxidation. The perchloric acid, oxidizing the deep-colored molecular iodine formed in the reaction, was effective also in facilitating the observation of the reaction from outside.

The equipment shown in Fig. 4 was devised for oxidizing the graphite and absorbing quantitatively the carbon dioxide formed to yield a homogeneous phase. The oxidation and the absorption were carried out in a closed system. The absorbed carbon dioxide was further purified, because it probably contained such radiochemical impurities as were distilled from an oxidizing medium.

4) E. g. F. W. J. Garton, *Spectrochem. Acta*, **9**, 297 (1957).
5) E. g. T. Nakajima, M. Takahashi and M. Morishita, *J. Atom. Energy Soc. Japan*, **3**, 104 (1961).
6) E. g. T. Takeuchi, M. Suzuki and Y. Miwa, *J. Chem. Soc. Japan, Ind. Chem. Sect. (Kogyo Kagaku Zasshi)*, **64**, 1367 (1961).
7) E. g. G. H. Morrison and R. L. Rupp, *Anal. Chem.*, **29**, 892 (1957).
8) K. Saito, T. Nozaki, M. Furukawa, S. Tanaka and H. Cheng, *Intern. J. Appl. Radiation Isotopes*, **14**, 358 (1963).
9) A. B. Whitehead, *Can. J. Phys.*, **36**, 1283 (1958).
10) T. Kiba, S. Ohashi, T. Takagi and Y. Hirose, *Japan Analyst*, **2**, 446 (1953).
11) M. Ura, *J. Chem. Soc. Japan, Pure Chem. Sect. (Nippon Kagaku Zasshi)*, **78**, 316 (1957).

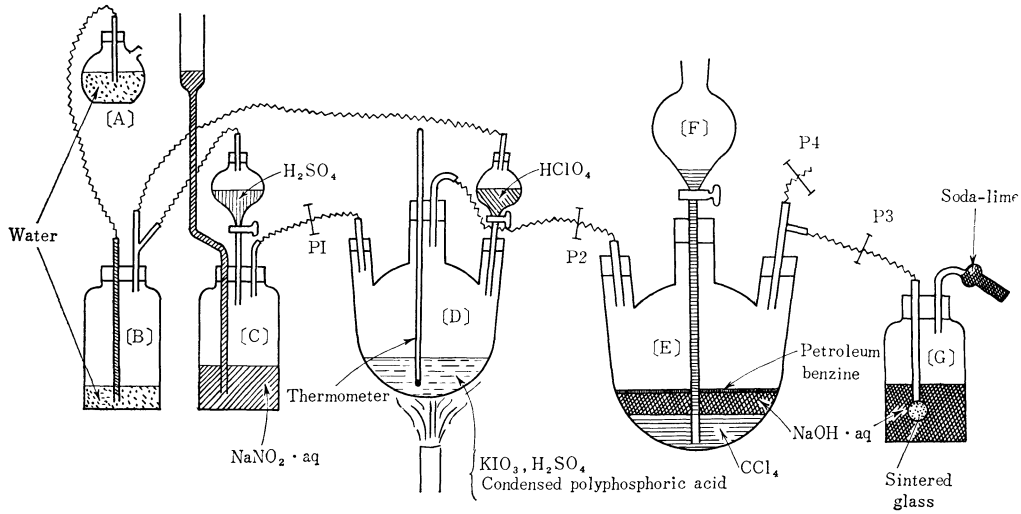

Fig. 4. Equipment for the chemical process.
P: Pinch-cock; ~~ : Rubber tube

It was then converted into barium carbonate for activity and recovery measurements. The details concerning the operation of the equipment are given in the Experimental Section.

It took 40 to 50 min. for the barium carbonate to be obtained after the irradiation. Its radiochemical purity was so high that a satisfactory decay curve was obtained by measuring the annihilation radiation with a simple scintillation counter.

The Calculation of the Nitrogen Content

For a sample of a given nitrogen content (e. g., 1 p. p. m.), the absolute ^{11}C-activity induced in it can be calculated by the use of the integral excitation curve (Fig. 2) when the sample thickness, the initial proton energy, the proton-beam current, and the irradiation duration are known. Also, the absolute ^{11}C-activity contained in the analyzed sample (at the end of the irradiation) can be calculated by the use of the measured activity and recovery and of the counting efficiency. The above two calculations were made for each sample, and its nitrogen content was obtained from the resultant values.

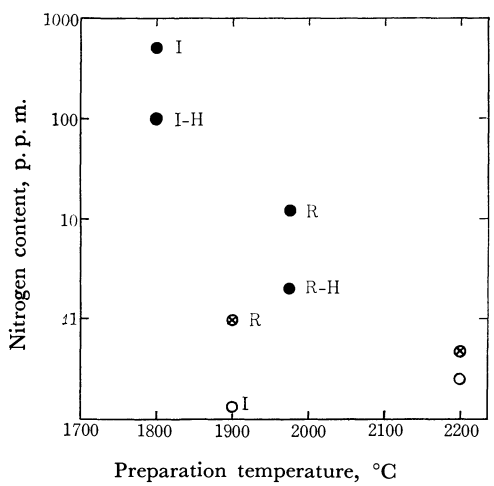

Fig. 5. Nitrogen content of the pyrolytic graphite.
●: Prepared from pyridine ; ○: Prepared from propane; ⊗: Prepared from propane in nitrogen atmosphere.
I : By induction heating ; R : By resistance heating ; −H: Heat-treated.

The Results of the Analysis

Some of the analytical results are given in Fig. 5. Figure 6 shows the decrease in nitrogen content on heat treatment, in which samples prepared from pyridine at 2150°C were kept at 2300°C in a nitrogen atmosphere (ca. 10 cmHg). Although the interference of boron should be taken into account for the sample with a low nitrogen content, the following facts can be derived unambiguously:

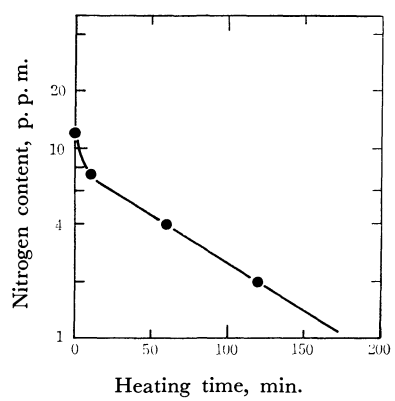

Fig. 6. Escape of the nitrogen on heat treatment.

(1) the sample from pyridine contains much more nitrogen than that from propane; (2) the presence of nitrogen gas in the preparation of pyrolytic graphite from propane does not make the nitrogen concentration in the product markedly higher; (3) the nitrogen concentration in the sample from pyridine depends on the temperature of the preparation—the higher the temperature, the lower the content; and (4) when the sample from pyridine is heated, the nitrogen content decreases.

Experimental

The Measurement of the Excitation Curve.—Nylon films of a known thickness (ca. 20 mg./cm^2) with thin aluminum foils (also of a known thickness) on both sides of each film were stacked. The stack was bombarded with a proton beam (15 MeV., 0.1 μamp.) from the cyclotron of the Institute for Nuclear Study, The University of Tokyo, for 1 min., the integrated beam current being read by an integrator. Each of the nylon films with the aluminum foils was sandwiched between bronze plates (ca. 3 mm. thick) for counting. The annihilation radiation from each sandwich was measured by a scintillation counter with a single channel analyzer, whose counting efficiency was calibrated with a standard ^{22}Na source. By following the decay, the sample activity was found to consist only of ^{11}C and ^{13}N. Thus, after the analysis of decay curve, the cross section of the ^{14}N(p, α)^{11}C reaction was calculated for each of the films.

The energy loss[12] (in MeV.·cm^2/g.) of charged particles in a compound is regarded as the sum of that in each element making up the compound in proportion to its weight fraction (the additivity rule). However, when the proton energy at each of the nylon films was calculated by the use of the additivity rule, an unreasonable result was obtained: the reaction appeared to have a considerably large cross section for proton energies below its threshold. There are two possible explanations of this result: (1) an incorrectness in the additivity rule for compounds consisting of light elements, especially for those containing hydrogen, or (2) a change in the thickness of the films in the course of the irradiation. No apparent thickness change, however, was observed in the irradiated part of the film. Hence, the value given by the additivity rule was slightly modified and used for the present calculations.

A more reliable experiment was undertaken by the use of a stack consisting of aluminum nitride films and aluminum foils. Fine powder of aluminum nitride was suspended in acetone, and allowed to deposit onto an aluminum foil of a known thickness to form a uniform film with the aid of a small, known quantity of polyvinyl acetate as a binder. The thickness of film was determined from its weight and area. Two stacks were bombarded with proton beams of different initial energies. The excitation curves obtained by the use of the stack material and of the additivity rule for the proton energy loss are of a reasonable form, agreeing with Blaser's result in the low-energy region.[13]

12) R. M. Sternheimer, *Phys. Rev.*, **115**, 137 (1959).

The Preparation of the Pyrolytic Graphite.—In a stream of propane or pyridine vapor (4 to 7 mmHg), a substrate plate was heated (1800 to 2200°C) by direct current (resistance heating) or by induction. The pyrolytic graphite grew at a rate of 50 to 300 μ/hr. The sample preparation from propane was also carried out in the presence of nitrogen (6 to 10 mmHg).

Irradiation, and the Removal of the Surface Contamination.—A rectangular window (10 mm.× 20 mm.) was cut in a metal plate thick enough to stop the protons. A graphite plate (0.4 to 2.0 mm. thick) slightly larger than the window was placed between a water-cooled target holder and the window of the metal plate, well in contact with both. It was then irradiated with a deflected proton beam (14 MeV., 10 μamp., 10 min.), the beam current being recorded. Since a part of the beam impinged on the metal plate at the edges of the window, the activity induced in it was measured and compared with that obtained on irradiating the metal plate without a window under the same conditions. Thus, the beam flux received by the sample itself was determined.

The sample surface was removed as uniformly as possible by grinding on a flat plate with the aid of fine alundum powder (both sides for a thin sample, one side for a thick sample). The thickness of the surface layer removed was determined by measuring the surface area and the loss of weight. The sample was then pulverized in a tall iron mortar in the presence of alumina powder (ca. 1 g.).

The Chemical Process.—In Fig. 4, A and B were for supplying a suitable pressure, while C was for generating nitrous fumes (gas formed on treating sodium nitrite with sulfuric acid).

Condensed polyphosphoric acid convenient for the present purpose was prepared by heating orthophosphoric acid up to 300°C during 40 min. and keeping it at 300°C for 20 min. The condensed polyphosphoric acid (50 ml.), sulfuric acid (35 ml.) and potassium iodate (25 g.) were added into D (500-ml. three-necked flask), and the mixture was heated gently. Into E (1-l. three-necked flask) were added carbon tetrachloride (300 ml.), carbonate-free sodium hydroxide solution (1.5 N, 200 ml.), and petroleum benzine (a few milliliters) to form three layers. When the temperature of the mixture in D reached 160°C, the air in D and E was replaced by nitrous fumes streaming from P1 to P4. After P1 and P4 had been closed, the stopper of the central neck of D was momentarily opened, and the pulverized sample was quantitatively added through the neck. Gentle heating was continued.

When oxidation began, a part of the carbon tetrachloride was pushed into F. Then E was shaken from outside to remove the petroleum benzine layer by being absorbed in the carbon tetrachloride beneath the sodium hydroxide solution. When the evolution of carbon dioxide became feeble even at 230°C, perchloric acid (60%; less than a few milliliters) was carefully dripped into D. A gentle shaking of D and E was necessary throughout to cause the oxidation process to proceed smoothly. When all of the sample had been oxidized, P1 was opened and the carbon dioxide remaining in D was carried into E with nitrous fumes.

13) J. P. Blaser, P. Marmier and M. Sempert, *Helv. Phys. Acta*, **25**, 442 (1952).

Without A and B, neither the sulfuric acid not the perchloric acid could be added smoothly. Without the replacement of air by nitrous fumes, the air expelled most of the sodium hydroxide solution into F before the carbon dioxide came into E. The nitrous fumes also served as a hold-back carrier for ^{13}N. Without the benzine layer, nitrous fumes were freely absorbed by the sodium hydroxide before the commencement of oxidation, and air entered E from F. The determination of the carbonate in E proved that the quantitative conversion of the graphite sample into the carbonate had taken place.

Hydrazine hydrate (60%; 20 ml.) and hydrochloric acid (2 N; 200 ml.) were successively added to E from F, with P3 open and P2 closed. The carbon dioxide thus evolved was caught by carbonate-free sodium hydroxide solution (1.5 N; 100 ml.) in G. The heat of neutralization evolved in E effectively caused the carbon dioxide to be forced into G, the vapor of benzine and carbon tetrachloride filling the vacancy in E. The solution in G was added to a hot solution of barium chloride (0.5 N, an amount equivalent to the sample carbon), and the barium carbonate was filtered off with suction and washed with hot water. The recovery of the sample carbon was determined gravimetrically after the activity measurement.

The Activity Measurement.—The annihilation radiation of ^{11}C in the barium carbonate was measured by a calibrated scintillation counter with a single channel analyzer. The decay of the barium carbonate activity was followed to ascertain the radiochemical purity. Also, the γ-ray spectra of some of the barium carbonate samples were measured by a multi-channel analyzer to ascertain the absence of γ-rays other than the annihilation radiation.

The authors wish to express their gratitude to Professor Ken-ichi Takeya and Dr. Kazuhiko Yazawa of the University of Electrocommunication for their kind encouragement. They are also indebted to members of the Semiconductor Research Group of the same university for their aid in the analytical practice, and to the cyclotron crew of the Institute for Nuclear Study, The University of Tokyo, for help in the cyclotron irradiation.

BULLETIN OF THE CHEMICAL SOCIETY OF JAPAN VOL. 39 2690—2695 (1966)

A Geochemical Study of Iodine in Volcanic Gases

By Fumihiro HONDA, Yoshihiko MIZUTANI, Tsutomu SUGIURA and Shinya OANA

Institute of Earth Science, Faculty of Science, Nagoya University, Chikusa-ku, Nagoya

(Received May 20, 1966)

Volcanic gases from several active volcanoes in Japan have been analyzed for iodine and chlorine: Showashinzan (I=0.025—0.20 mg.I/kg.H_2O, Cl=238—1830 mg.Cl/kg.H_2O), Iwatesan (I=0.053—0.19, Cl=2720—3360), Issaikyoyama (I=0.030—0.087, Cl=104—213), Nasudake (I=0.16—3.9, Cl=188—9460), Yakedake (I=0.58—0.93, Cl=1250—1730), Kuju-Ioyama (I=0.13—1.3, Cl=266—8000), Kirishima-Ioyama (I=0.036—0.84, Cl=200—4200), and Miharayama (I=0.45—1.5, Cl=1640—2180). Each volcano has a characteristic I/Cl ratio. Analyses have also been made of hot-spring waters from the environs of Nasudake, Kuju-Ioyama, and Kirishima-Ioyama. It is indicated that the hot-spring waters are similar in I/Cl ratio to the volcanic gases from the same area.

In a previous paper,[1] the abundance and the behavior of halogens in the volcanic gases were investigated. As to the iodine, however, some uncertainties remained because of the paucity of analytical data. For this paper, the iodine and chlorine contents of volcanic gases from eight active volcanoes in Japan (Showashinzan, Iwatesan, Issaikyoyama, Nasudake, Yakedake, Kuju-Ioyama, Kirishima-Ioyama, and Miharayama) have been investigated.

The iodine and chlorine contents of some hot-spring waters around Nasudake, Kuju-Ioyama, and Kirishima-Ioyama have also been investigated in order to examine the similarity in I/Cl ratio between hot-spring waters and volcanic gases from the same area.

Experimental

The Sampling of Volcanic Gases.—Through a glass tubing inserted into the fumarole, volcanic gases were introduced into a cold trap, in which the water vapor in the gases was condensed; the halogens were completely dissolved in the condensed water.[1] The solution was then subjected to the following analyses.

The Determination of Iodine and Chlorine.—The methods for the determination of these elements are:

1) T. Sugiura, Y. Mizutani and S. Oana, *J. Earth Sci., Nagoya Univ.*, **11**, 272 (1963).

TABLE I. IODINE AND CHLORINE CONTENTS OF VOLCANIC GASES

Showashinzan Fumarole	Temp., °C	Cl mg./kg.H_2O	I mg./kg.H_2O	I/Cl×10^4
A-1, 1958	759	856	0.097	1.1
A-1, 1960	722	926	0.064	0.69
A-6a, 1959	700	1040	0.10	1.0
A-6a, 1960	695	1040	0.13	1.2
A-1, 1962	662	1760	0.20	1.1
C-2, 1959	645	970	0.11	1.2
A-1, 1963	635	1830	0.12	0.66
C-2, 1960	605	1310	0.11	0.87
C-2, 1962	538	625	0.083	1.3
A-4a, 1958	470	1090	0.12	1.1
B-4a, 1959	464	250	0.040	1.6
A-4a, 1959	460	1130	0.13	1.2
B-5, 1960	446	538	0.061	1.2
C-4, 1959	430	1310	0.16	1.2
B-3, 1961	375	318	0.043	1.3
B-6, 1960	347	547	0.066	1.2
B-1a, 1959	328	285	0.033	1.2
B-4b, 1959	300	290	0.040	1.6
B-1b, 1960	260	264	0.025	0.92
C-3, 1958	222	328	0.052	1.6
B-6, 1961	200	1220	0.15	1.2
C-3, 1959	194	234	0.033	1.4
C-3, 1960	187	242	0.063	2.9
Iwatesan Sampling date	Temp., °C	Cl mg./kg.H_2O	I mg./kg.H_2O	I/Cl×10^4
Oct. 13, 1964	206	2720	0.16	0.59
Oct. 13, 1964	206	3100	0.053	0.17
Oct. 13, 1964	206	3360	0.19	0.57
Issaikyoyama Sampling date	Temp., °C	Cl mg./kg.H_2O	I mg./kg.H_2O	I/Cl×10^4
Jan. 11, 1956	213	213	0.087	4.1
Oct. 10, 1958	141	104	0.030	2.9
Nasudake Fumarole	Temp., °C	Cl mg./kg.H_2O	I mg./kg.H_2O	I/Cl×10^4
M-1, 1960	489	429	0.56	13
M-1, 1959	480	600	0.71	12
M-2c, 1961	410	510	0.53	11
M-1, 1963	396	360	0.31	8.6
M-1, 1965	370	191	0.21	11
M-2b, 1960	352	480	0.57	12
M-4a, 1965	340	188	0.19	10
M-4b, 1965	261	460	0.29	6.3
O-1b, 1965	228	710	0.63	8.9
M-2a, 1960	195	9460	3.7	3.9
O-2a, 1965	165	196	0.20	10
U N-1, 1965	158	4280	1.5	3.5
U-1, 1961	132	1810	0.49	2.7
O-2b, 1965	125	188	0.16	8.5
O-1, 1959	119	3180	3.9	12
O E-1, 1965	119	410	0.40	9.8
M-3, 1960	97	8700	0.67	0.77
Yakedake Fumarole	Temp., °C	Cl mg./kg.H_2O	I mg./kg.H_2O	I/Cl×10^4
Y-2, 1965	163	1730	0.58	3.4
Y-6, 1965	168	1250	0.93	7.4

TABIE I. (Continued)

Kuju-Ioyama Fumarole	Temp., °C	Cl mg./kg.H_2O	I mg./kg.H_2O	I/Cl×10^4
KH-1, 1960	508	1340	1.3	9.7
KH-1d, 1964	360	8000	1.1	1.4
KH-3a, 1964	350	6580	0.89	1.5
KX-2a, 1964	180	5700	0.67	1.2
KO-3, 1964	160	7160	0.91	1.3
KO-1, 1964	155	5000	0.58	1.2
KX-3, 1964	150	6480	1.2	1.9
KX-1b, 1964	140	7440	1.3	1.7
KX-2b, 1964	120	5160	0.60	1.2
KH-1g, 1964	96	266	0.13	5.0
Kirishima-Ioyama Fumarole	**Temp., °C**	**Cl mg./kg.H_2O**	**I mg./kg.H_2O**	**I/Cl×10^4**
EE-1, 1965	220	2160	0.61	2.9
ES-3, 1965	202	1920	0.55	2.8
ES-4, 1965	201	1680	0.52	3.1
ES-1, 1965	187	2020	0.80	3.9
EE-2, 1965	178	350	0.12	3.4
EE-3, 1965	132	200	0.036	1.8
EW-1, 1965	128	4000	0.14	0.35
EE-4, 1965	121	4200	0.84	2.0
Miharayama* Sampling date	**Temp., °C**	**Cl mg./kg.H_2O**	**I mg./kg.H_2O**	**I/Cl×10^4**
May 2, 1959	388	1640	0.45	2.2
May 12, 1959		1840	1.3	7.1
May 26, 1959		2180	1.5	6.9
May 27, 1959	392	1920	1.5	7.8

* These samples were given by K. Noguchi at Tokyo Metropolitan University.

Cl Mercuric thiocyanate[2]

I The catalytic oxidation of $FeSCN^{2+}$ [3]

Most of the samples contained an appreciable amount of sulfide which interferes with both chlorine and iodine analyses. Accordingly, samples were heated with sodium carbonate and hydrogen peroxide in order to oxidize the sulfide to sulfate.[2] The solution was then subjected to the above-mentioned analyses.

Continuous Observation of the Iodine and Chlorine Contents of Volcanic Gases.—Continuous observations over a short period (3—5 hr.) were made in order to examine the constancy in iodine and chlorine contents of volcanic gases from several fumaroles of Showashinzan and Nasudake. Samples were collected from a fumarole at about 20-min. intervals. In each sampling time, each about 15 min. long, about 100 ml. of condensed water was collected.

Results

The analytical results are listed in Tables I to III, while the sampling sites of the volcanic gases and hot-spring waters are shown geographically in Fig. 1.

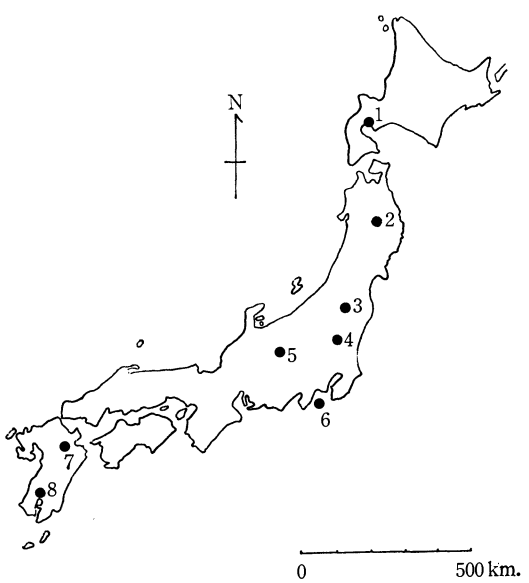

Fig. 1. Sampling site of volcanic gases and hot spring waters.

1. Showashinzan
2. Iwatesan
3. Issaikyoyama
4. Nasudake
5. Yakedake
6. Miharayama
7. Kuju-Ioyama
8. Kirishima-Ioyama

2) S. Utsumi, *J. Chem. Soc. Japan, Pure Chem. Sect. (Nippon Kagaku Zasshi)*, **81**, 401 (1960).

3) S. Utsumi, M. Shiota, N. Yonehara and I. Iwasaki, ibid., **85**, 32 (1964).

TABLE II. IODINE AND CHLORINE CONTENTS OF HOT-SPRING WATERS IN THE ENVIRONS OF NASUDAKE

Locality	Temp., °C	Cl mg./l.	I mg./l.	I/Cl×10⁴
Oana	84	80	0.037	4.6
Yumoto-shika-yu	73	124	0.0080	0.65
Yumoto-gyonin-yu	60	104	0.0035	0.34
Benten-yu	52	48	0.010	2.1
Benten-yu	49	23	0.095	41
Benten-yu	45	22	0.010	4.5
Iimori	41	129	0.057	4.4
Takao-onsen	39	97	0.039	4.0
Kakko-onsen	37	107	0.015	1.2
Hot spring pool	28	53	0.0050	0.95

IODINE AND CHLORINE CONTENTS OF HOT-SPRING WATERS IN THE ENVIRONS OF KUJU-IOYAMA

Locality	Temp., °C	Cl mg./l.	I mg./l.	I/Cl×10⁴
Odake-onsen	92	1430	0.23	1.6
Suji-yu	60	286	0.050	1.7
Kora-yu	56	30	0.0036	1.2
Hizen-yu	55	263	0.035	1.3
Senshaku-yu	44	218	0.033	1.5
Hokkein-onsen	44	107	0.011	1.0
Ukenokuchi-onsen	41	224	0.013	0.51
Kan-no-jigoku		25	0.0026	1.0
Hossho-onsen		75	0.042	5.6

IODINE AND CHLORINE CONTENTS OF HOT-SPRING WATERS IN THE ENVIRONS OF KIRISHIMA-IOYAMA

Locality	Temp., °C	Cl mg./l.	I mg./l.	I/Cl×10⁴
Maruo bore	94	242	0.069	2.9
Ebino bore	93	4	0.000	< 1
Iodani-tessen	71	65	0.0078	1.1
Iodani-myobansen	66	63	0.0098	1.6
Ebino	56	152	0.010	0.66

Discussion and Conclusion

The following facts may be seen in Tables I to III:

1) The I/Cl ratio (in weight) of volcanic gases ranges from 10^{-3} to 10^{-5}. Most of the samples, however, have values from 10^{-3} to 10^{-4}. This value agrees with that given in the previous paper[1].

2) The I/Cl ratio of volcanic gases differs in different volcanoes, while the gases show a comparatively constant Br/Cl ratio.[1] The average I/Cl ratios are: Showashinzan (1.2×10^{-4}), Iwatesan (0.44×10^{-4}), Issaikyoyama (3.5×10^{-4}), Nasudake (temp. >300°C: 10.7×10^{-4}; temp.< 300°C: 6.7×10^{-4}), Yakedake (5.4×10^{-4}), Kuju-Ioyama (1.4×10^{-4}—two values were excluded from the average), Kirishima-Ioyama (temp.> 200°C: 3.0×10^{-4}; temp. <200°C: 2.3×10^{-4}), and Miharayama (6.0×10^{-4}).

3) The I/Cl value of volcanic hot-spring waters nearly agrees with that of the volcanic gases to which the hot-spring waters are believed to be related genetically.

4) The constancy in the I/Cl value is fairly good at each fumarole over a period of 2 to 3 hr. The results of continuous observations at the A-1 fumarole of Showashinzan show that the gases have a constant I/Cl value, while the iodine and chlorine contents vary widely. At Nasudake, it is observed that each of the fumaroles shows a constant I/Cl value with respect to the time change, though their values differ considerably from one fumarole to the other (Tables I and III).

The Behavior of Iodine in Volcanic Gases.— The gases of Kuju-Ioyama show a constant I/Cl value, though they show no clear relationship between the halogen content and the gas temperature. The gases of Showashinzan show a linear relationship between the iodine content and the gas temperature, as Fig. 2 shows. In addition, the gases have a conspicuously constant I/Cl ratio over a wide range of gas temperatures (187—759°C). This implies that the cause of the variation in iodine content is probably the same as that of the variation in chlorine.

It has already been reported by Mizutani[4] that the chlorine content of Showashinzan gases decreases linearly with a lowering of the temperature, and that the dilution effect of mixing water vapor into original gases is responsible for the variation in the chemical composition of the gases during

4) Y. Mizutani *J. Earth Sci., Nagoya Univ.*, **10**, 125 (1962).

TABLE III. CONTINUOUS OBSERVATION OF IODINE AND CHLORINE CONTENTS OF VOLCANIC GASES

Nasudake
M-1, 1965 Temp. 370°C

Sampling time	Cl mg./kg.H_2O	I mg./kg.H_2O	I/Cl×10^4
2 : 15—2 : 25	195	0.24	12
2 : 30—2 : 40	188	0.20	11
2 : 45—2 : 55	198	0.21	11
3 : 00—3 : 10	185	0.20	11
3 : 15—3 : 25	195	0.20	10
3 : 30—3 : 40	195	0.22	11
3 : 45—3 : 55	188	0.22	12
4 : 00—4 : 10	190	0.20	11
4 : 15—4 : 25	195	0.23	12
4 : 30—4 : 40	185	0.21	11

Nasudake
M-4a, 1965 Temp. 340°C

Sampling time	Cl mg./kg.H_2O	I mg./kg.H_2O	I/Cl×10^4
9 : 20— 9 : 38	185	0.21	11
9 : 40— 9 : 53	180	0.19	11
9 : 55—10 : 08	188	0.15	8.0
10 : 10—10 : 23	180	0.16	8.9
10 : 25—10 : 39	193	0.15	7.8
10 : 41—10 : 54	205	0.25	12
10 : 57—11 : 12	188	0.20	11
11 : 14—11 : 30	185	0.20	11
11 : 34—11 : 50	188	0.21	11
11 : 53—12 : 08	190	0.22	12

Nasudake
M-4b, 1965 Temp. 261°C

Sampling time	Cl mg./kg.H_2O	I mg./kg.H_2O	I/Cl×10^4
9 : 20— 9 : 38	443	0.26	5.9
9 : 40— 9 : 53	458	0.38	8.3
9 : 55—10 : 08	458	0.24	5.2
10 : 10—10 : 23	465	0.24	5.2
10 : 25—10 : 39	470	0.23	4.9
10 : 41—10 : 54	448	0.30	6.7
10 : 57—11 : 12	463	0.32	6.9
11 : 14—11 : 30	468	0.34	7.3
11 : 34—11 : 50	463	0.26	5.6
11 : 53—12 : 08	465	0.33	7.1

Nasudake
O-2a, 1965 Temp. 165°C

Sampling time	Cl mg./kg.H_2O	I mg./kg.H_2O	I/Cl×10^4
11 : 13—11 : 26	195	0.22	11
11 : 30—11 : 47	200	0.21	11
11 : 51—12 : 04	198	0.20	10
12 : 07—12 : 22	198	0.20	10
12 : 26—12 : 44	202	0.20	10
13 : 24—13 : 37	193	0.19	10
13 : 41—13 : 54	195	0.20	10
13 : 58—14 : 13	195	0.19	10
14 : 16—14 : 29	193	0.18	9.3
14 : 32—14 : 48	190	0.19	10

Nasudake
O-2b, 1965 Temp. 125°C

Sampling time	Cl mg./kg.H_2O	I mg./kg.H_2O	I/Cl×10^4
11 : 13—11 : 26	180	0.16	8.9
11 : 30—11 : 47	200	0.15	7.5
11 : 51—12 : 04	193	0.20	10
12 : 07—12 : 22	185	0.13	7.0
12 : 26—12 : 44	203	0.16	7.9
13 : 24—13 : 37	135	0.14	10
13 : 41—13 : 54	210	0.16	7.6
13 : 58—14 : 13	173	0.14	8.1
14 : 16—14 : 29	213	0.19	8.9
14 : 32—14 : 08	190	0.16	8.4

Showashinzan
A-1, 1961 Temp. 703°C

Sampling time	Cl mg./kg.H_2O	I mg./kg.H_2O	I/Cl×10^4
15 : 00—15 : 10	1130	0.060	0.53
15 : 20—15 : 30	940	0.063	0.67
15 : 40—15 : 50	1250	0.075	0.60
16 : 00—16 : 10	1480	0.096	0.65
16 : 20—16: 30	1200	0.068	0.57
16 : 40—16 : 50	1340	0.083	0.62
17 : 00—17 : 10	1290	0.091	0.71
17 : 20—17 : 30	1190	0.086	0.72
17 : 40—17 : 50	1400	0.087	0.62
18 : 00—18 : 10	950	0.060	0.63

B-5, 1960 Temp. 446°C

Sampling time	Cl mg./kg.H_2O	I mg./kg.H_2O	I/Cl×10^4
9 : 00	535	0.056	1.0
10 : 00	545	0.066	1.2
11 : 00	528	0.065	1.2
12 : 00	532	0.056	1.1
13 : 00	540	0.061	1.1
14 : 00	530	0.061	1.1

their effusion process. On the contrary, in the gases of Nasudake and Kirishima-Ioyama, iodine behaves differently from chlorine. In the cases of Nasudake, the I/Cl ratio of the gases varies widely with the gas temperature, as Fig. 3 shows. Gases with temperatures above 300°C show values of $(10—13)\times10^{-4}$, while gases with temperatures between 100°C and 300°C have values of $(0.8—12)\times10^{-4}$.

The gases of Kirishima-Ioyama are similar in this respect to those of Nasudake. The I/Cl value given for the gases with temperatures above 200°C shows $(2.8—3.1)\times10^{-4}$, while for the gases with temperatures below 200°C the value is $(0.35—3.9)\times10^{-4}$. The change in I/Cl ratio implies that the deposition and/or the addition of iodine and chlorine occurs in the gases as the temperature falls. Some evidence for the addition of some chemical components, including chlorine, to volcanic gases were suggested in the investigations

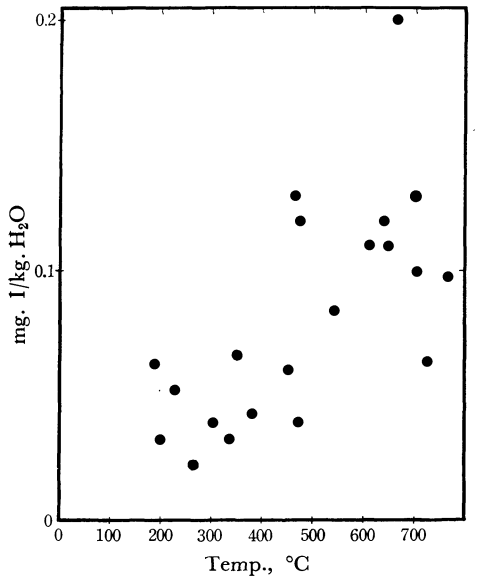

Fig. 2. Corelation between gas temperature and the iodine content of the gases of Showashinzan.

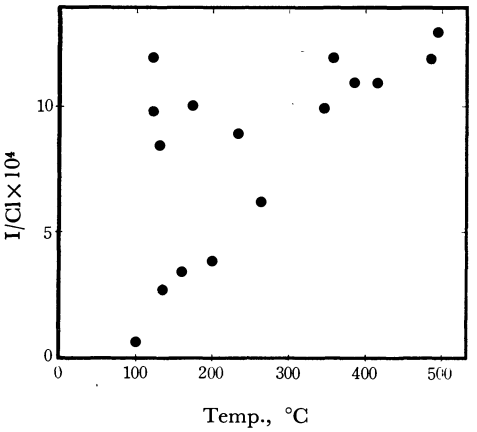

Fig. 3. Corelation between gas temperature and the I/Cl ratio of the gases of Nasudake.

by Mizutani et al.[5] and Suzuoki[6] of the chemical nature of the gases of Nasudake.

Both of these studies agree that the increase in chlorine in the gases is possibly caused by the contribution of the chlorine compounds which have accumulated in the subsurface during past effusion processes. Yoshida et al.[7] studied the halogen compounds sublimed from powdered volcanic rocks on heating; they showed that iodine behaves differently from chlorine during the volatilization and sublimation processes. Actually, volcanic sublimates, particularly alkali and ammonium chlorides, have lower I/Cl values (10^{-5}—10^{-6}),[7-9] than volcanic gases. If an appreciable quantity of halogens is supplied from such a deposit to the volcanic gases, the I/Cl value of the gases may be decreased, while the halogen content of the gases increases. It seems reasonable to explain the difference in I/Cl ratio with the decrease in the temperature as being caused by the increasing contribution of halogens from a secondary source, such as volcanic sublimates, though a problem remains as to the process of the discharge of halogens in deposits.

The authors express their gratitude to Dr. Nobuyuki Nakai for his helpful discussions.

5) Y. Mizutani, T. Sugiura and S. Oana, Read the abstract at the Meeting of the Volcanological Society of Japan, Oct., 1961.
6) T. Suzuoki, This Bulletin, **38**, 1946 (1965).
7) M. Yoshida, I. Makino, N. Yonehara and I. Iwasaki, This Bulletin, **38**, 1436 (1965).
8) Y. Mizutani, *J. Earth Sci., Nagoya Univ.*, **10**, 149 (1962).
9) K. Noguchi, T. Goto, S. Ueno and M. Ichikuni, *Bull. Volcanol. Soc. Japan (Kazan), 2nd Series*, **5**, 163 (1961).

BULLETIN OF THE CHEMICAL SOCIETY OF JAPAN VOL. 39 2696—2702 (1966)

The Effects of the Temperature on the γ-Radiation-Induced Polymerization of Ethylene*

By Sueo MACHI, Miyuki HAGIWARA, Masao GOTODA and Tsutomu KAGIYA

Japan Atomic Energy Research Institute, Takasaki Radiation Chemistry Research Establishment, Takasaki, Gunma

(Received January 18, 1966)

The gamma-radiation-induced polymerization of ethylene was carried out/over the wide range of temperature from 30 to 200°C at pressure ranging from 100 to 400 kg./cm^2 and at dose rates from 2×10^3 to 4×10^5 rad./hr. It was shown that the rate of polymerization is rapidly accelerated at 30°C, that the degree of acceleration decreases with an increase in the reaction temperature, and that above 100°C the rate is independent of the time. It was correspondingly shown that the molecular weight of the polymer increases with the reaction time, at 30°C, that its increment for a unit of time decreases with an increase in the temperature, and that the molecular weight is independent of the time above 100°C. By means of a kinetical discussion it was concluded that the rate of the termination reaction, which is almost eliminated at 30°C, increases with the temperature and attains a value comparable to that of initiation above 100°C. The dose rate exponents of the polymerization rate and molecular weight were shown to vary with the reaction temperature. Namely, the exponents were evaluated as 0.9 and 0 at 30°C, 0.8 and −0.1 at 100°C, and 0.7 and −0.2 at 140 and 200°C, for the polymerization rate and the molecular weight respectively. It was assumed from these high exponents that the termination may occur above 100°C in a first-order reaction to a considerable extent. Under a constant pressure, the polymer yield was shown to decrease with the temperature from 30 to 60—80°C, and then to increase at high temperatures from 80 to 200°C. On the other hand, the molecular weight of the polymer simply decreases with the temperature from 30 to 200°C. The chain transfer reaction is considered to be almost negligible at 30—70°C. The number of polymer chains for a constant reaction time and monomer concentration is independent of the temperature from 30 to 70°C, while it increases with the temperature from 70 to 200°C. The effects of pressure on the polymer yield and molecular weight were also investigated at 140°C.

In previous papers[1,2] the γ-radiation-induced bulk polymerization of ethylene at normal temperatures was characterized by a steady increase in the polymerization rate and in the molecular weight of polymer with the reaction time. From the kinetic study,[2] the existence of a long-lived radical has been suggested; this has been confirmed by the results of the experiments of the two-stage irradiation method.[3] On the other hand, it was recently shown that the phenomena of the rate acceleration and the increase in the molecular weight with the time vanish, and that the molecular weight is considerably lowered at high reaction temperatures, as has previously been reported briefly.[4] This paper attempts to elucidate the specific influences of the reaction temperature on the γ-radiation-induced polymerization of ethylene in bulk.

Experimental

The reaction vessel, the irradiation facilities, and the experimental procedures are the same as have been reported in a previous paper.[2] The ethylene used was commercially available and 99.9% pure (free of CO and H_2S), containing 21 p. p. m. of acetylene and 0.3 p. p. m. of oxygen. Polymerizations were carried out to low conversion in order to maintain the pressure essentially constant, and the temperature was constant within ±1°C for the duration of the experiment.

Results and Discussion

The Effect of the Temperature on Chain Termination.—A marked acceleration in rate and an increase in the number-average molecular weight with the reaction time have been reported in the γ-radiation-induced polymerization of ethylene at normal temperatures.[1,2] On the other hand, in the polymerization at high temperatures (above 100°C), no increase in the polymerization rate and molecular weight were observed, as has already been reported briefly.[4]

---

* Presented at the 18th Annual Meeting of the Chemical Society of Japan, Osaka, April, 1965.

1) S. Machi, M. Hagiwara, M. Gotoda and T. Kagiya, *J. Polymer Sci.*, **B2**, 765 (1964).
2) S. Machi, M. Hagiwara, M. Gotoda and T. Kagiya, This Bulletin, **39**, 675 (1966).
3) S. Machi, M. Hagiwara, M. Gotoda and T. Kagiya, *J. Polymer Sci.*, **A3**, 2931 (1965).
4) S. Machi, M. Hagiwara, M. Gotoda and T. Kagiya, ibid., **A3**, 3029 (1965).

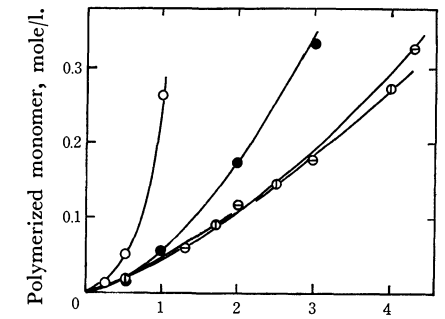

Fig. 1a.

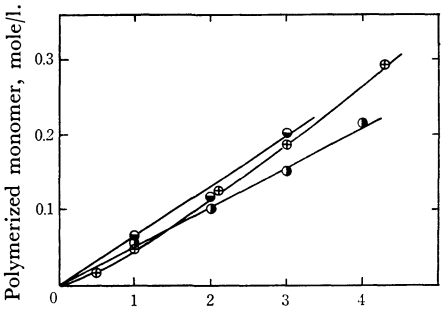

Fig. 1b.

Fig. 1. The amount of polymerized monomer vs. reaction time at various reaction temperatures. (Reaction pressure, 400 kg./cm²; dose rate, 2.5×10^4 rad./hr.; reaction temperature, 30 (○), 58 (●), 62 (⊖), 70 (⊕), 86 (⊕), 100 (◑), 140°C (◒))

The results of the experiments which were carried out at various reaction temperatures from 30 to 200°C, at a dose rate of 2.5×10^4 rad./hr. and at a pressure of 400 kg./cm², are summarized in Table I. Figures 1a and 1b show the relation between the amount of the polymerized monomer (i. e., the polymer yield) and the reaction time. They show that the amount of the polymerized monomer increases rapidly with the time at lower temperatures and less rapidly at higher temperatures. In order to show the time dependency of the amount of the polymerized monomer, it is plotted on a logarithmic scale in Fig. 2. The slopes of the line are the time exponents of the polymer yield, which are listed in Table II. It is found that the time exponent at 30°C is 2.1 and that it decreases with the increase in the temperature to unity at temperatures of 100°C and above. In other words, the rate of polymerization increases almost proportionally with the time at 30°C, the increase in the rate for unit time becomes less with an increase in the temperature, and finally the rate becomes independent of the time. Namely, the rate acceleration is observed at 30 to 86°C, its degree decreases with the temperature, and it is not observed at 100 and 140°C.

Table I. Effects of reaction temperature on polymer yield and molecular weight

Reaction temp. °C	Reaction time hr.	Polymer yield g.	Molecular weight $\bar{M}_n \times 10^{-4}$
30	0.26	0.03	7.0
	0.53	0.14	14.7
	1.0	0.74	26.6
58	0.50	0.05	6.5
	1.0	0.16	11.5
	2.0	0.49	17.5
	3.0	0.93	23.0
62	0.50	0.05	4.7
	1.3	0.17	7.6
	2.0	0.33	9.9
	3.0	0.50	11.3
	4.3	0.91	14.0
70	0.50	0.06	4.3
	1.7	0.25	6.0
	2.5	0.41	7.4
	4.0	0.76	9.0
86	0.50	0.05	2.4
	1.0	0.14	3.1
	2.1	0.35	3.5
	3.0	0.52	3.6
	4.3	0.82	3.8
100	1.0	0.16	1.8
	2.0	0.28	1.9
	3.0	0.43	2.0
	4.0	0.60	2.1
120	2.0	0.34	1.9
140	1.0	0.18	1.3
	2.0	0.33	1.2
	3.0	0.58	1.2
160	2.0	0.42	0.99
180	2.0	0.54	0.83
200	2.0	0.70	0.64

Reaction pressure, 400±5 kg./cm²; dose rate, 2.5×10^4 rad./hr.; volume of reaction vessel, 100 ml.

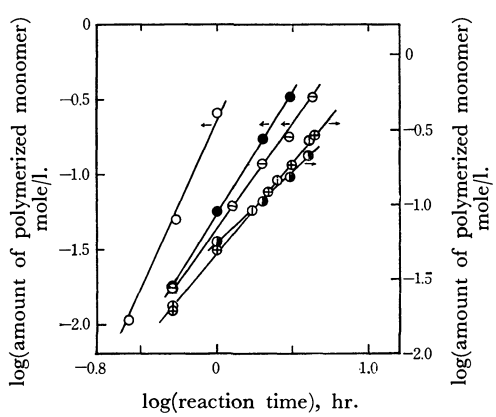

Fig. 2. Relation between the amount of polymerized monomer and reaction time shown in logarithmic scale at various temperatures. (Notes and reaction conditions are the same as shown in Fig. 1.)

Table II. Time exponent of polymer yield at various reaction temperatures

Reaction temp. °C	Time exponent of polymer yield
30	2.1
58	1.7
62	1.4
70	1.2
86	1.2
100	1.0

Reaction pressure, 400±5 kg./cm²; dose rate, 2.5 ×10⁴ rad./hr.

The effect of the reaction temperature on the increase in the molecular weight with the reaction time is shown in Fig. 3. The molecular weight of polymer formed at 30°C is shown to be proportional to the time. This feature, together with the rate acceleration, have been explained[2] on the assumption that the termination and transfer do not take place to any appreciable extent. It has been also suggested that the life of the polymer radical is long and that the accumulation of polymer radicals causes the rate acceleration. In the polymerization from 58 to 86°C, it is observed that the molecular weight increases with the time and that the increment for the unit of time decreases with a rise in the temperature. This corresponds to the above fact, i. e., the degree of rate acceleration decreases with temperature. These corresponding facts may indicate that the rate of chain termination increases with rise in the temperature, the average life-time of the polymer radical, therefore, becomes shorter, and the extent of radical accumulation decreases.

Above 100°C the polymerization rate and molecular weight are shown to remain constant, independently of the reaction time, in Figs. 1b and 3. This suggests that the rate of the termination becomes comparable to that of the initiation. The life of the radical is not long, but normal, and the stationary state is realized.

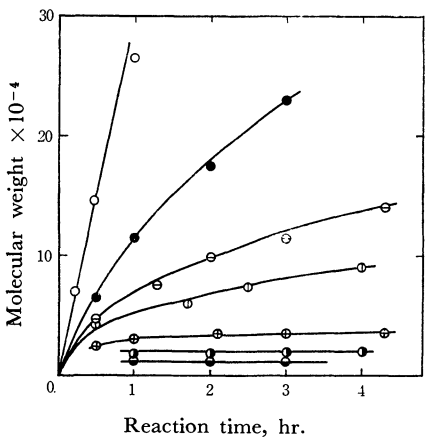

Fig. 3. Molecular weight vs. reaction time at various temperatures. (Notes and reaction conditions are the same as shown in Fig. 1.)

The Order of the Termination Reaction.— In order to elucidate the termination reaction, the dependence of the polymerization rate and the molecular weight on the irradiation dose rate was investigated at various temperatures from 30 to 200°C, the results are summarized in Table III. The rate and the molecular weight are plotted on logarithmic scales against the dose in Figs. 4 and

Table III. Effects of dose rate on polymer yield and molecular weight at various temperatures

Reaction temp. °C	Dose rate rad./hr. ×10⁻⁴	Reaction time hr.	Polymer yield g.	Molecular weight $\bar{M}_n$ ×10⁻⁴
30	39	0.33	0.73	7.8
	15	0.50	0.63	9.7
	6.3	0.55	0.38	13.2
	0.73	2.0	0.70	42.5
100	39	0.50	0.61	1.2
	15	1.0	0.56	1.2
	6.3	2.0	0.54	1.4
	1.0	5.0	0.37	2.0
	0.50	6.0	0.26	2.2
140	15	1.0	0.56	0.9
	6.3	2.0	0.65	1.0
	1.0	4.1	0.35	1.3
	0.50	5.0	0.27	1.4
	0.19	6.6	0.19	1.9
200	39	0.50	1.15	0.45
	15	1.0	0.90	0.46
	6.3	1.0	0.65	0.47
	1.0	4.0	0.59	0.64
	0.50	6.0	0.62	0.70

Reaction pressure, 400±5 kg./cm²; volume of reaction vessel, 100 ml. Data for dose rate of 2.5 ×10⁴ rad./hr. are listed in Table I.

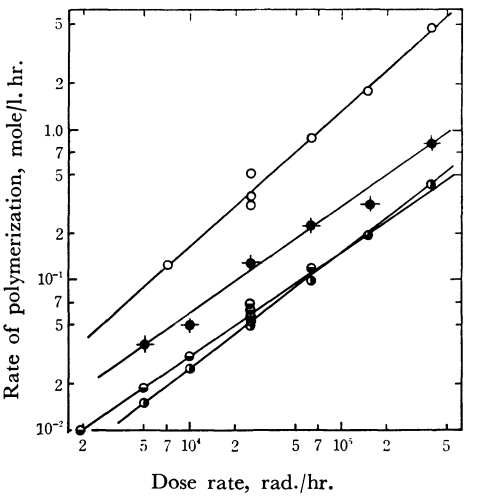

Fig. 4. Effect of dose rate on the rate of polymerization at various temperatures.
(Reaction pressure, 400 kg./cm²; reaction temperature, 30 (○), 100 (◑), 140 (◒), 200°C (◆))

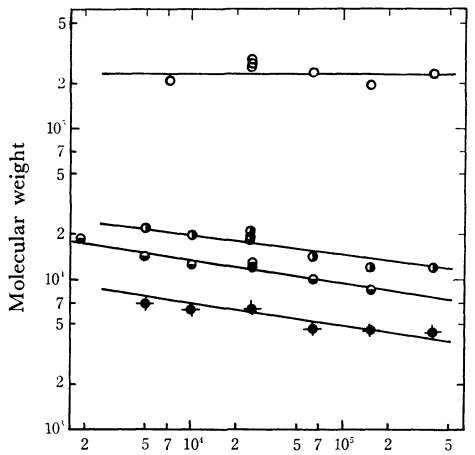

Fig. 5. Effect of dose rate on the molecular weight at various temperatures.
(Notes and reaction conditions are the same as shown in Fig. 4.)

5 respectively. Here, since the rate and the molecular weight increase with the time at 30°C, the data in these figures have been normalized to a fixed reaction time of one hour. The dose rate exponents of the rate and the molecular weight evaluated from the slope of these lines are shown in Table IV. The dose rate exponents for both the rate and the molecular weight are shown to decrease with a rise in the temperature from 30 to 140°C; they remain constant at temperatures from 140 to 200°C.

TABLE IV. DOSE RATE EXPONENTS OF POLYMERIZATION RATE AND MOLECULAR WEIGHT AT VARIOUS TEMPERATURES

Reaction temp., °C	Dose rate exponent of rate	Dose rate exponent of molecular weight
30	0.9	0.0
100	0.8	−0.1
140	0.7	−0.2
200	0.7	−0.2

Reaction conditions are the same as shown in Table III.

It has already been shown in a previous paper[2] that the exponents at 30°C of 0.9 (approximately unity) for the rate and 0 for the molecular weight coincide with the reaction scheme at normal temperatures; i. e., we may assume no termination reaction. The exponents for the polymerization above 100°C (i. e., 0.8 and 0.7 for the rate, and −0.1 and −0.2 for the molecular weight) are higher than the common exponents of 0.5 and −0.5 for the rate and molecular weight in the case of second-order termination with respect to the polymer radical. These high exponents may indicate that first-order termination with respect to the polymer radical is predominant. The first-order termination is assumed to be brought about by a reaction between the polymer radical and the radical of a low molecular weight which has little effect on the molecular weight of high polymers.

The fact that these exponents decrease with a rise in the temperature indicates that the contribution of the second-order termination, i. e., the mutual termination of the polymer radicals, increases with the temperature from 100 to 200°C.

The Evaluation of the Rate of Termination.—The rates of termination at various temperatures from 58 to 76°C are evaluated by means of the analysis[5] of the data on the polymer yield on the basis of the following elementary reactions, which have been proposed[2] for the γ-radiation-induced polymerization of ethylene in bulk:

1. Initiation

$$M \xrightarrow{k_i} R_1 \qquad R_i = k_i \rho_M I \qquad (1)$$

2. Ethylene excitation and dimerization

$$M \rightleftarrows M^*$$
$$M + M \overset{K_e}{\rightleftarrows} M_2^* \qquad f_{M_2^*} = K_e f_M^2 \qquad (2)$$

3. Propagation

$$R_1\cdot + M_2^* \xrightarrow{k_p} R_3\cdot$$
$$\cdots\cdots \qquad R_p = k_p[R\cdot] f_{M_2^*} \qquad (3)$$
$$R_{n-2}\cdot + M_2^* \xrightarrow{k_p} R_n\cdot$$

4. Termination

$$R_n\cdot + Z \xrightarrow{k_{t1}} P_n \qquad R_t = k_{t_1}[R\cdot][Z] +$$
$$R_m\cdot + R_n\cdot \xrightarrow{k_{t2}} P_{m+n} \qquad k_{t_2}[R\cdot]^2 \qquad (4)$$

5. Transfer

$$R_n\cdot + Y \xrightarrow{k_{tr}} P_n + Y\cdot$$
$$R_{tr} = k_{tr}[R\cdot][Y] \qquad (5)$$

where M represents the ethylene monomer; $R_n\cdot$, an active polymer chain composed of n monomers; $[R\cdot]$ total concentration of all active polymer chains irrespective of size; M*, the excited monomer; M_2^* the excited dimer; Y the substance with which the activity of the radical is transferred; Z, the substance by which the radical is deactivated; P_n, the dead polymer composed of n monomers; R_i, R_p, R_{tr}, and R_t, the rates of initiation, propagation, transfer, and termination; k_i, k_p, k_{tr}, and k_t, the rate constants of these reactions; ρ_M the density of ethylene; I, the dose rate; f_M, the fugacity of ethylene; $f_{M_2^*}$, the fugacity of the excited dimer, and K_e the equilibrium constant of the 2nd step.

5) T. Kagiya, M. Izu, S. Machi and K. Fukui, paper presented at the 14th Polymer Symposium, Kyoto, October, 1965.

The rate of polymerization, R, is written:

$$R = k_p K_e [\mathrm{R}\cdot] f_M^2 \quad (6)$$

where R represents the overall polymerization rate. [R·] is given in the non-stationary state;

$$[\mathrm{R}\cdot] = \int R_i dt - \int R_t dt \quad (7)$$

Since no second-order termination in the polymer radical takes place below 100°C, Eq. 7 is:

$$[\mathrm{R}\cdot] = \int k_i \rho_M I dt - \int k_{t_1} [\mathrm{R}\cdot][\mathrm{Z}] dt \quad (8)$$

Here, [R·] on the right side being replaced by Eq. 6,

$$[\mathrm{R}\cdot] = k_i \rho_M I t - (k_{t_1}[\mathrm{Z}]/k_p K_e f_M^2) \cdot \int R dt \quad (9)$$

where $\int R dt$ corresponds to the amount of the polymerized monomer, M_p. By substituting [R·] in Eq. 6 with Eq. 9, R is written:

$$R = k_i k_p K_e \rho_M f_M^2 I t - k_{t_1}[\mathrm{Z}] M_p \quad (10)$$

By integrating Eq. 10 with time,

$$\int R dt = M_p = (1/2) \cdot k_t k_p K_e \rho_M f_M^2 I t^2 - k_{t_1}[\mathrm{Z}] \int M_p dt \quad (11)$$

$$M_p / \int M_p dt = (1/2) \cdot k_i k_p K_e \rho_M f_M^2 I t^2 / \int M_p dt - k_{t_1}[\mathrm{Z}] \quad (12)$$

According to Eq. 12, $(M_p/\int M_p dt)$ is plotted in Fig. 6 against $(t^2/\int M_p dt)$, where $\int M_p dt$ is calculated from Fig. 1 by a graphical method. The values of $k_{t_1}[\mathrm{Z}]$, i. e., the rate of termination, are determined from the intercept on the axis of

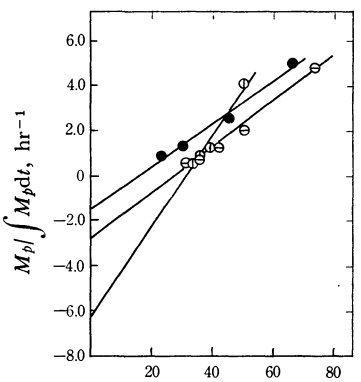

Fig. 6. $M_p/\int M_p dt$ vs. $t^2/\int M_p dt$.
(Notes and reaction conditions are the same as shown in Fig. 1.)

TABLE V. RATE OF CHAIN TERMINATION AT VARIOUS TEMPERATURES

Reaction temp. °C	Rate of termination $k_{t_1}[\mathrm{Z}]$ hr^{-1}
58	1.5
62	2.8
70	6.1

Reaction pressure, 400±5 kg./cm²; dose rate, 2.5 ×10⁴ rad./hr.

$M_p/\int M_p dt$; they are summarized in Table V. The rate of termination is shown to increase with the reaction temperature.

The Effects of the Temperature on the Polymer Yield and the Molecular Weight.— As is shown in Figs. 1 and 3, the effects of the temperature on the polymer yield and molecular weight are complicated because of their time dependency. Figure 7 shows how the polymer

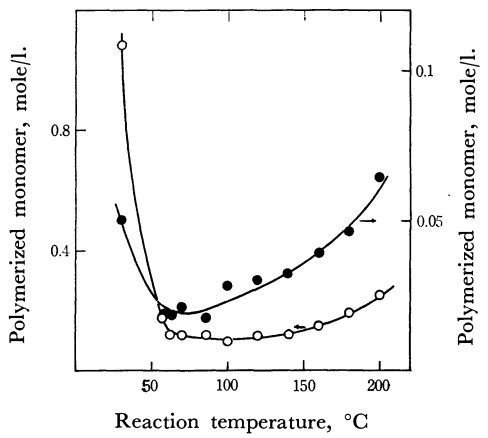

Fig. 7. Effect of reaction temperature on the amount of polymerized monomer.
(Reaction pressure, 400 kg./cm²; dose rate, 2.5 ×10⁴ rad./hr.; reaction time, 0.5 (●), 2.0 hr. (○). Data at 100, 200°C for 0.5 hr., and 62, 70°C for 2.0 hr. are calculated from those at other reaction time.)

yield at the reaction times of 0.5 and 2.0 hr. varies with reaction temperature. It is shown that the polymer yield decreases rapidly with the temperature from 30 to 60°C, remains almost constant from 60 to 80—100°C, and increases in the higher temperature region (to 200°C). Figure 8 indicates that the molecular weight of the polymer formed at 0.5 and 2.0 hr. under the constant pressure of 400 kg./cm² simply decreases with a rise in the reaction temperature, and that it is very sensitive to the temperature from 30 to 100°C. The effect is shown to become larger as the polymerization proceeds.

The Effects of the Temperature on Chain Initiation and Transfer.—The number-average

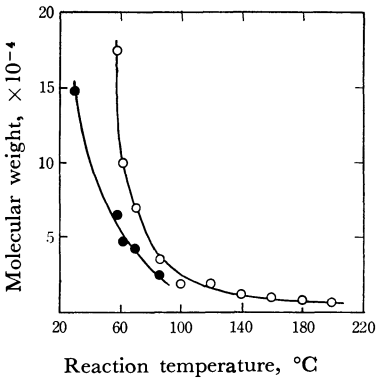

Fig. 8. Effect of reaction temperature on the molecular weight.
(Notes and reaction conditions are the same as shown in Fig. 7. Data at 62, 70°C. for 2.0 hr. are calculated from those at other reaction time.)

degree of polymerization at a given reaction time is written for the polymerization in the non-stationary state, assuming no termination by the recombination of polymer radicals, which is almost realized below 100°C:

$$1/\overline{DP}_n = \int R_i dt / \int R_p dt + \int R_{tr} dt / \int R_p dt \quad (13)$$

where $\overline{DP}_n$ represents the number-average degree of polymerization. From the above reaction scheme, Eq. 13 is, then,

$$1/\overline{DP}_n = k_t \rho_M I(t/M_p) + (k_{tr}/k_p)[Y]/K_e f_M^2 \quad (14)$$

According to Eq. 14, $1/\overline{DP}_n$ is plotted in Fig. 9 against t/M_p to give an almost linear relation. The fact that the lines in Fig. 9 pass through the point of origin indicates that the transfer reaction does not take place at temperatures from 30 to 70°C.

The relation between the number of moles of polymer chains (N_p) for a unit of ethylene concentration and the reaction time is shown in Fig. 10, where N_p is evaluated as the ratio of the amount of the polymerized monomer to the number-

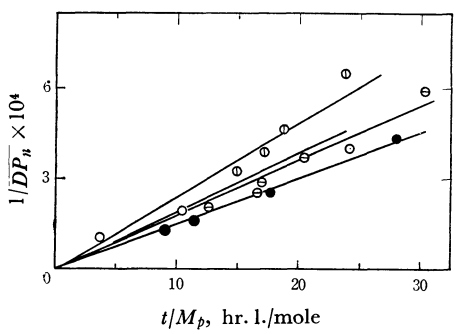

Fig. 9. $1/\overline{DP}_n$ vs. t/M_p.
(Notes and reaction conditions are the same as shown in Fig. 1.)

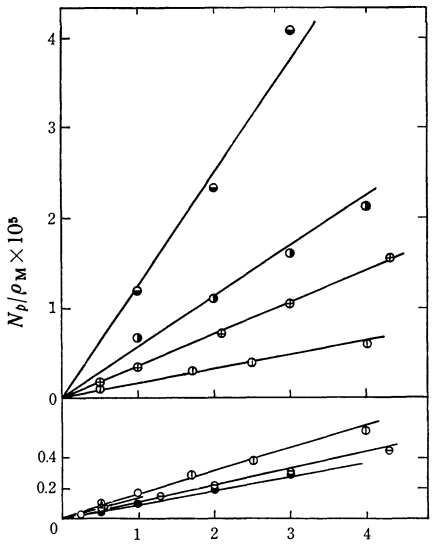

Fig. 10. Number of moles of polymer chains per unit ethylene concentration vs. reaction time at various temperatures.
(Notes and reaction conditions are the same as shown in Fig. 1.)

average molecular wight of the polymer, i. e., $M_p/\overline{M}_n$. It is observed that N_p/ρ_M (i. e., the number of moles of polymer chains formed divided by the concentration of ethylene) increases almost proportionally with the time at the respective temperatures because of successive initiation by continuous radiation. The number of moles of polymer chains formed per unit of reaction time (i. e., N_p/t, the rate of the increase in number of polymer chains) is shown in Table VI and Fig. 11 for various reaction temperatures. It is shown

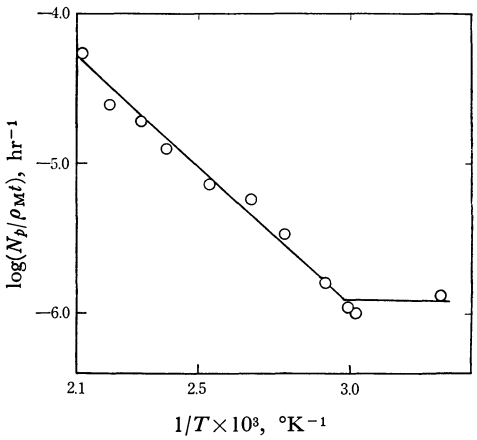

Fig. 11. Effect of temperature on the rate of increasing in the number of polymer chains.
(Reaction pressure, 400 kg./cm^2; dose rate, 2.5×10^4 rad./hr.)

TABLE VI. EFFECT OF REACTION TEMPERATURE ON THE RATE OF INCREASING IN THE NUMBER OF MOLES OF POLYMER CHAINS

Reaction temp. °C	$N_p/\rho_M t$ hr^{-1} $\times 10^5$
30	0.13
58	0.10
62	0.11
70	0.16
86	0.33
100	0.57
120	0.71
140	1.23
160	1.92
180	3.10
200	5.55

Reaction pressure, 400±5 kg./cm^2; dose rate, 2.5 $\times 10^4$ rad./hr.

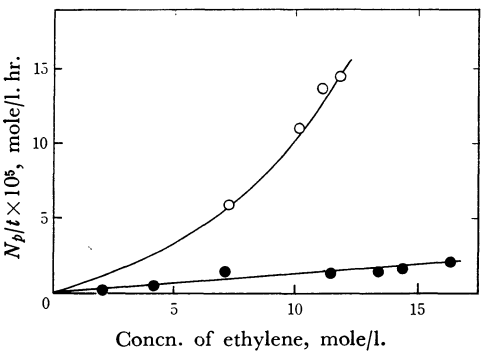

Fig. 12. N_p/t vs. concentration of ethylene. (Reaction temperature, 30 (●), 140°C (○); dose rate, 2.5×10^4 rad./hr.)

that N_p/t is almost independent of the temperature from 30 to 70°C, where the chain transfer does not take place. The rate of initiation is, therefore, known to be independent from the temperature of this range. On the other hand, the higher temperature range, N_p/t is shown to increase with the temperature and an apparent activation energy of about 8 kcal./mole was observed. It is also noted that the polymer yield increases with the temperature over the same range (shown in Fig. 7). Since no evidence for the absence of chain transfer is given in this temperature range, the activation energy may be ascribed not only to the initiation reaction but also to the transfer reaction.

TABLE VII. EFFECTS OF REACTION PRESSURE ON POLYMER YIELD AND MOLECULAR WEIGHT AT 140°C

Ethylene Pres. kg./cm^2	Ethylene Fugacity kg./cm^2	Ethylene Concn. mol./l.	Reaction time hr.	Polymer yield g.	Molecular weight $\bar{M}_n$ $\times 10^{-4}$
100	80	3.4	46.1	0.25	—
200	144	7.3	6.0	0.23	0.66
300	200	10.1	2.0	0.22	0.99
350	228	11.1	2.0	0.33	1.2
400	261	11.8	listed in Table I		

Dose rate, 2.5×10^4 rad./hr.; volume of reaction vessel, 100 ml.

The Effect of the Pressure on the Polymer Yield and the Molecular Weight at 140°C.— The results of experiments where ethylene pressure varies from 100 to 400 kg./cm^2 are summarized in Table VII. It is shown that the amount of polymerized monomers and the molecular weight per unit of reaction time increase with the ethylene pressure. The number of moles of polymer chains per unit of time is plotted in Fig. 12 against the concentration of ethylene for the polymerization at 140 and 30°C. The direct proportionality which was previously reported[6] is observed at 30°C. On the other hand, at 140°C with the same concentration of ethylene, N_p is greater than 30°C and is not proportional to the concentration of ethylene. This difference between 30 and 140°C may indicate that additional processes related to ethylene occur at 140°C to increase the number of polymer chains. They may be the additional initiation and/or the transfer with the monomer.

6) S. Machi, M. Hagiwara, M. Gotoda and T. Kagiya, *J. Polymer Sci., A-1*, **4**, 1517 (1966).

BULLETIN OF THE CHEMICAL SOCIETY OF JAPAN VOL. 39 2703—2706 (1966)

Syntheses of Isomeric Methylpseudoionones and Isomeric Pseudoionones by Means of the Wittig Reaction

By Kazuhiro SASAKI

Ichikawa Works, Kobayashi Perfumery Co., Ltd., Ichikawa, Chiba

(Received February 18, 1966)

Four isomeric methylpseudoionones and two isomeric pseudoionones were separately synthesized by the Wittig reaction of citral a or citral b with the corresponding phosphonates. Two isomeric pseudoionones were also synthesized by the Wittig reaction of citral a or citral b with 2-oxopropylidenetriphenylphosphorane. The configurations and the conformations of the dienone systems in four methylpseudoionones and two pseudoionones were discussed on the basis of the infrared and ultraviolet absorption data.

Since butanone has an active methyl and an active methylene group, the condensation of citral (I) with butanone results in the formation of two pairs of methylpseudoionones, i. e., *n*-methylpseudoionones (II) and isomethylpseudoionones (III). The four isomers have been isolated as their semicarbazones or phenylsemicarbazones.[1,2] The direct synthesis of each isomer, however, has never been reported.

Recently, II, III, and pseudoionone (IV) were synthesized by the reaction of citral (an isomeric mixture) with the corresponding 2-oxoalkylidenetriphenylphosphoranes,[3] but the configurations and the conformations of the dienone systems were not described.

In the present experiment, the syntheses of each isomeric methylpseudoionone and pseudoionone were attempted by the use of the corresponding phosphonates, according to the modified Wittig reaction.[4] The phosphonates employed in the present investigation were prepared by the Michaelis-Arbuzov reaction.[5]

Diethyl 2-oxopropylphosphonate (V) was treated successively with sodium amide and with a 96 : 4 mixture of citral a (Ia) and citral b (Ib) (Ia-rich I) to afford a 95 : 5 isomeric mixture of *trans*-3, *trans*-5-pseudoionone (IVa) and its 5-*cis* isomer (IVb). The treatment of V with a 2 : 98 mixture of Ia and Ib (Ib-rich I) in the same way gave a 2 : 98 mixture of isomers, IVa and IVb. These products were confirmed by gas chromatographic identification with authentic samples obtained by the aldol condensation of Ia-rich I or Ib-rich I with acetone, by a study of the infrared spectra*1 of the products (Table I)*2, and by elementary analyses of the semicarbazones.*3 IVa and IVb were also prepared by the reaction of 2-oxopropylidenetriphenylphosphorane (VI) with Ia-rich I or Ib-rich I for the sake of comparison. The results (Table II) show that the phosphonate method gave better yields than the phosphorane method, and that the reaction proceeded substantially stereospecifically (only *trans* isomers were produced).

Table I. Some characteristic absorption bands in the infrared spectra of the modified Wittig reaction products (liquid film)

	ν(C=O) cm^{-1}	ν(C=C) cm^{-1}	δ(C-H) cm^{-1}
IVa	1668 vs, 1688 vs*	1633 vs, 1590 vs	975 s
IVb	1668 vs, 1687 vs*	1631 vs, 1588 vs	973 s
IIa	1667 vs, 1688 vs*	1631 vs, 1593 vs	977 s
IIb	1667 vs, 1687 vs*	1630 vs, 1593 vs	973 s
IIIa	1662 vs	1632 vs, 1596 m	
IIIb	1662 vs	1630 vs, 1592 m	

* Splitting carbonyl bands.

Each isomeric mixture rich in *trans*-4,*trans*-6-*n*-methylpseudoionone (IIa), its 6-*cis* isomer (IIb), *trans*-3, *trans*-5-isomethylpseudoionone (IIIa), or its

1) H. Barbier, Y. R. Naves and P. Ardizio, *Bull. soc. chim. France*, **1951**, 254.
2) Y. R. Naves, H. Barbier and P. Ardizio, ibid., **1951**, 639.
3) K. Fujiwara, H. Takahashi and M. Ohta, This Bulletin, **35**, 2042 (1962).
4) Cf. W. S. Wadsworth and W. D. Emmons, *J. Am. Chem. Soc.*, **83**, 1733 (1961).
5) G. M. Kosolapoff, "Organophosphorus Compounds," 1st Ed., J. Wiley & Sons Inc., New York, N. Y. (1950), Chap. 7.
6) H. Köster, *Chem. Ber.*, **80**, 248 (1947).

*1 The infrared spectra were measured through the courtesy of Dr. Yoshitaka Matsuoka and Mr. Kenya Sakaguchi of the Eisai Research Laboratories.

*2 The infrared and ultraviolet absorption spectra of the products (as mixtures) were measured without further purification.

*3 This conclusion might be supported by the following reports: Surber and his co-workers observed that the preparation of the α, β-*cis* form of methyl ketones unsaturated in the α, β- and γ, δ-positions with respect to the carbonyl group proves practically impossible (W. Surber, V. Theus, L. Colombi and H. Schinz, *Helv. Chim. Acta*, **39**, 1299 (1956)). Naves and his co-workers reported that the most probable configuration for III and IV is *trans*-3, *trans*-5 or *trans*-3, *cis*-5, while that for II is *trans*-4, *trans*-6 or *trans*-4, *cis*-6 (Ref. 2).

Table II. Pseudoionones obtained by means of the Wittig reactions

Reagent		Reaction conditions	B. p. of product °C/mmHg	Yield, %	Composition of product*4 (IVa : IVb)	d_4^{20}	n_D^{20}	Semicarbazone $C_{14}H_{23}N_3O$*5 M. p.*6 °C	Anal. Calcd., %	Found, %
Ia-rich I	VI	4 hr. at 100—110°C	95—100/0.5	26	95 : 5					
Ib-rich I	VI	4 hr. at 100—110°C	95—96/0.8	19	7 : 93					
Ib-rich I	VI	4 hr. at 100—110°C 1/2 hr. at 142°C	98—100/0.9	37	11 : 89					
Ia-rich I	V	See Experimental	100—105/0.6	49	95 : 5	0.9073	1.4891	139.5—141	C : 67.43	67.25
									H : 9.30	9.38
									N : 16.85	17.03
Ib-rich I	V	See Experimental	92—98/0.8	48	2 : 98	0.9086	1.4862	139—140	C : 67.43	67.08
									H : 9.30	9.33
									N : 16.85	17.05

Table IV. Methylpseudoionones prepared by means of the modified Wittig reaction

Reagent		B. p. of product °C/mmHg	Yield, %	Composition of product*4 IIa	IIb	IIIa	IIIb	d_4^{20}	n_D^{20}	Crystalline derivatives*5,*7 M. p. °C	Anal. Semicarbazone $C_{15}H_{25}N_3O$ Calcd., %	Found, %	4-Phenylsemicarbazone $C_{21}H_{29}N_3O$ Calcd., %	Found, %
Ia-rich I	VII	111—114/0.55	75	93.1	5.2	0.8	0.8	0.8959	1.5264	153—154			C : 74.30	74.39
													H : 8.61	8.75
													N : 12.38	12.46
Ib-rich I	VII	107—111/0.75	67	2.8	95.5		1.7	0.9015	1.5227	138.5—140			C : 74.30	74·15
													H : 8.61	8.66
													N : 12.38	12.60
Ia-rich I	VIII	94—98/0.2	63	1.4		94.1	4.5	0.9117	1.5299	184—186	C : 68.40	68.15		
											H : 9.57	9.78		
											N : 15.96	16.20		
Ib-rich I	VIII	88—92/0.07	62		3.0	3.2	93.8	0.9110	1.5250	169—171	C : 68.40	68.68		
											H : 9.57	9.59		
											N : 15.96	16.21		

5-*cis* isomer (IIIb) was prepared by the reaction of Ia-rich I or Ib-rich I with diethyl 2-oxobutylphosphonate (VII) or diethyl 1-methyl-2-oxopropylphosphonate (VIII). All these products were identified by a comparison of their retention times with those of authentic samples rich in II and rich in III, which were prepared in the manner described by Köster.[6] The identifications were supported by the infrared*1 and ultraviolet absorption spectra of the products (Tables I and III)*2

Table III. UV absorption data (in EtOH)

	λ_{max} (mμ)	ε_{max}
IIa	293	24500
	(292)[7]	(22500)[7]
IIb	293.5	23100
IIIa	294	24500
	(293.5)[7]	(25000)[7]
IIIb	295	23500
IV	(291)[8]	(21000)[8]

and by elementary analyses of the carbonyl derivatives*3. The results are summarized in Table IV.

$(EtO)_2P(O)CHCOCH_2R + NaNH_2 \rightarrow$
$\quad\quad\quad

IIIb). Many authors have reported such a carbonyl splitting in the infrared spectra of *trans*-3-penten-2-one and its 5-alkyl homologs; they have ascribed the effect to an equilibrium between the *s-cis* and *s-trans* conformations.[12-15] On the other hand, it has been reported that no such carbonyl splitting is observed in the infrared spectra of 3-methyl-*trans*-3-penten-2-one and its 3-ethyl homolog, which have the same partial enone structure as that of isomethylpseudoionones (IIIa, IIIb); it has also been reported that the spectral properties of 3-methyl-*trans*-3-penten-2-one and its 3-ethyl homolog are very close to those of the ketones with a fixed *s-trans* conformation.[14] Although no definite evidence can be offered except the infrared spectral data, the conjugated enone systems of *n*-methylpseudoionones (IIa, IIb) and pseudoionones (IVa, IVb) seem to exist in an equilibrium between *s-cis* and *s-trans* conformations, while the systems of isomethylpseudoionones (IIIa, IIIb) may exist predominantly or exclusively in the *s-trans* conformation.

The infrared spectra of *n*-methylpseudoionones (IIa, IIb), isomethylpseudoionones (IIIa, IIIb), and pseudoionones (IVa, IVb) showed two absorption bands due to C=C stretching vibrations at 1630—1633 and 1588—1596 cm^{-1}. The intensities of both bands in the spectra of *n*-methylpseudoionones (IIa, IIb) and pseudoionones (IVa, IVb) were nearly equal, while the intensity of the band at 1592 or 1596 cm^{-1} in the spectra of isomethylpseudoionones (IIIa, IIIb) was weakened. This weakened intensity could be ascribed to an effect of the C-3 methyl group, which should polarize the C-3 double bond in the direction opposite to the effect of the carbonyl group.[14]

Experimental

Materials.—Citrals (Ia-rich I and Ib-rich I) were isolated from commercial lemongrass oil by the procedure described in a previous paper.[16] Ia-rich I: b. p. 66—68°C /0.7 mmHg, Ia : Ib=96 : 4. Ib-rich I: b. p. 61—63°C 10.7 mmHg, Ia : Ib=2 : 98. 2-Oxopropylidenetriphenylphosphorane (VI) was obtained by the reaction of chloroacetone and triphenylphosphine, followed by the treatment of the resultant 2-oxopropylidenetriphenylphosphonium chloride with 10% sodium carbonate.[17] Diethyl 2-oxopropylphosphonate (V) was prepared from triethyl phosphite and bromoacetone. B. p. 75—78°C/0.3 mmHg; yield 53%; $\nu_{C=O}$ 1714, $\nu_{P=O}$ 1259, ν_{P-O} 1165, ν_{C-O} 1025 cm^{-1}. Diethyl 2-oxobutylphosphonate (VII) was prepared from triethyl phosphite and bromomethyl ethyl ketone. B. p. 91—95°C/0.7 mmHg; yield 65%; $\nu_{C=O}$ 1713, $\nu_{P=O}$ 1256, ν_{P-O} 1167, ν_{C-O} 1026 cm^{-1}. Diethyl 1-methyl-2-oxopropylphosphonate (VIII) was prepared from triethyl phosphite and 1-bromoethyl methyl ketone. B. p. 70—73°C/0.25 mmHg; yield 11%; $\nu_{C=O}$ 1716, $\nu_{P=O}$ 1253, ν_{P-O} 1167, ν_{C-O} 1027 cm^{-1}.

The Reaction of a 96 : 4 Citral Mixture (Ia-rich I) or a 2 : 98 Citral Mixture (Ib-rich I) with 2-Oxopropylidenetriphenylphosphorane (VI).—A solution of 3.04 g. (0.02 mole) of Ia-rich I and 6.37 g. (0.0 2mole) of VI in 70 ml. of *n*-butyl ether was heated while being stirred on an oil bath. When the reaction has been completed the solvent was evaporated, a small amount of cold ether was added to the residue, and the crystallized triphenylphosphine oxide was filtered off and washed with ether. The combined filtrate and washings were then dried over anhydrous sodium sulfate. After the solvent had been removed, the residue was distilled off under reduced pressure to give 1.0 g. of a 95 : 5 mixture of IVa and IVb. The same procedure with Ib-rich I gave 0.8 g. of a 7 : 93 mixture of IVa and IVb. In the reaction with Ib-rich I, the prolongation of the reaction time by one half-hour at a refluxing temperature resulted in the formation of 1.4 g. of a 11 : 89 mixture of IVa and IVb.

The Modified Wittig Reaction with the Phosphonates.—To a suspension of 1.95 g. (0.05 mole) of sodium amide in 30 ml. of dry tetrahydrofuran (THF), there was added a solution of 9.71 g. (0.05 mole) of V in 20 ml. of dry THF with stirring and cooling. After the addition was complete, the temperature of the reaction mixture was gradually raised to −3—−1°C, after which the reaction was continued at that temperature until the evolution of ammonia had ceased. The reaction mixture was then again cooled below −10°C, and a solution of 7.61 g. (0.05 mole) of Ia-rich I or Ib-rich I in 20 ml. of dry THF was added. The reaction mixture was gradually warmed to room temperature and allowed to stand overnight. The solvent being evaporated under reduced pressure, the residue was poured into a large excess of water and extracted with ether. The ethereal extract was washed with water and dried over anhydrous sodium sulfate. After the solvent had been removed, the oily residue was distilled under reduced pressure to afford 4.7 g. of a 95 : 5 mixture, or 4.6 g. of a 2 : 98 mixture, of IVa and IVb.

The products rich in IIa, rich in IIb, rich in IIIa, and rich in IIIb, were prepared in a similar manner.

The author wishes to express his deep gratitude to Professor Masaki Ohta and Assistant Professor Rokuro Sudo of the Tokyo Institute of Technology and to Dr. Kazuyoshi Fujiwara of Tamura Veterinary Chemicals, Ltd., for their constant interest and encouragement. Thanks are also due to Mr. Kenjiro Kobayashi, President of Kobaysahi Perfumery Co., Ltd., and Mr. Mitsuhiro Takahashi, Director of the same company, for their permission to publish this work.

12) Cf. I. Bell, E. R. H. Jones and M. C. Whiting, ibid., **1958**, 1313.
13) Cf. R. D. Campbell and N. H. Cromwell, *J. Am. Chem. Soc.*, **79**, 3456 (1959).
14) R. Meck and K. Noack, *Chem. Ber.*, **93**, 210 (1960).
15) K. Noack and R. N. Jones, *Can. J. Chem.*, **39**, 2225 (1961).
16) K. Sasaki, *J. Chem. Soc. Japan, Pure Chem. Sect. (Nippon Kagaku Zasshi)*, **87**, 763 (1966).
17) F. Ramirez and S. Dershowitz, *J. Org. Chem.*, **22**, 41 (1957).

BULLETIN OF THE CHEMICAL SOCIETY OF JAPAN VOL. 39 2707—2713 (1966)

Studies of Poly-β-benzyl-L-aspartate Helix. I. The Synthesis and Rotatory Dispersion of Copolymers of β-*p*-Methyl, Chloro, Cyano, or Nitrobenzyl-L-aspartate with β-Benzyl-L-aspartate

By Masahisa HASHIMOTO and Jiro ARITOMI

Research Laboratory, Dainippon Pharmaceutical Co., Ltd., Ebie, Fukushima-ku, Osaka

(Received February 19, 1966)

β-*p*-Methyl, chloro, cyano and nitrobenzyl-L-aspartates were synthesized, and the respective homopolymers and copolymers of these β-(*p*-substituted benzyl)-L-aspartates with β-benzyl-L-aspartate were prepared. The introduction of a methyl, chloro, or cyano group into the para position of the aromatic ring in the side chain of poly-β-benzyl-L-aspartate (PBLA) also causes a reversal from the left- to the right-handed in the helical sense of the polypeptide in a chloroform solution, as in the case of the nitro group. The residue of the copolymers where the transition takes place contained: nitro, 20—30; cyano, 40—50; chloro, ca. 50; and methyl group, ca. 70 mol.-%. These values may indicate the relative stabilities between the PBLA helix and poly-β-(*p*-substituted benzyl)-L-aspartate helices. These series of copolymers had no absorption band in the longer wavelength region except for a nitrobenzyl series, which had an absorption band at around 330 mμ. The absence of an absorption band resulted in a normal b_0 value. The results suggest that the factors which determine the helical sense of the PBLA helix are not very simple and that the left-handed helix of PBLA is much less stable.

It has been shown that poly-β-benzyl-L-aspartate (PBLA) forms the left-handed α-helix in a chloroform solution.[1,2] Recently Goodman and his co-workers have reported that the introduction of a nitro group in the para position of the aromatic ring in the side chain of poly-β-benzyl-L-aspartate causes a reversal from the left- to the right-handed in the helical sense of the polypeptide in a chloroform solution.[3,4] It has also been suggested that the right-handed helix is stabilized by the nitro-aromatic groups in the side chain, which form an electronically-coupled side chain helix rigidly arrayed about the main chain helix.

These findings stimulated our interest in studying the helical sense of poly-β-benzyl-L-aspartate homologues which have other side chains. In this paper, we shall describe the synthesis of poly-β-(*p*-methylbenzyl)-L-aspartate (PMeBLA), poly-β-(*p*-chlorobenzyl)-L-aspartate (PClBLA), poly-β-(*p*-cyanobenzyl)-L-aspartate (PCNBLA), and also poly-β-(*p*-nitrobenzyl)-L-aspartate (PNBLA), together with the copolymers derived from these β-(*p*-substituted benzyl)-L-aspartates and β-benzyl-L-aspartate. It will be described as well how optical rotatory dispersion data show that the introduction of a methyl, chloro, or cyano group in the aromatic side chain also causes a reversal in helical sense of the polypeptide in a chloroform solution, as in the case of a nitro group.

Results and Discussion

Syntheses.—β-Benzyl-L-aspartate (BLA) has been prepared by the partial hydrolysis of α, β-dibenzyl-*N*-carbobenzoxy-L-aspartate[5] and by selective β-esterification using concentrated hydrochloric acid[6] or aqueous sulfuric acid[7]. Goodman et al.[4] have prepared β-*p*-nitrobenzyl-L-aspartate by the nitration of β-benzyl-L-aspartate with nitronium fluoroborate.

In the present study, β-(*p*-substituted benzyl)-L-aspartates were prepared by the direct β-esterification of L-aspartic acid with *p*-substituted benzyl alcohol. β-*p*-Methylbenzyl-L-aspartate (MeBLA) was obtained in only a trace amount by using concentrated hydrochloric acid, but it was prepared in a 10% yield by using *p*-toluenesulfonic acid as the catalyst. β-*p*-Chlorobenzyl-L-aspartate (ClBLA) and β-*p*-cyanobenzyl-L-aspartate (CNBLA) were obtained in better yields by using *p*-toluenesulfonic acid than by using concentrated hydrochloric acid as the catalyst. The esterification of L-aspartic

1) R. H. Karlson, K. S. Norland, G. D. Fasman and E. R. Blout, *J. Am. Chem. Soc.*, **82**, 2268 (1960).
2) E. M. Bradbury, A. R. Downie, A. Elliott and W. E. Hanby, *Proc. Roy. Soc. (London)*, **A259**, 110 (1960).
3) M. Goodman, C. M. Deber and A. M. Felix, *J. Am. Chem. Soc.*, **84**, 3773 (1962).
4) M. Goodman, A. M. Felix, C. M. Deber, A. R. Brause and G. Schwartz, *Biopolymers*, **1**, 371 (1963).
5) A. Berger and E. Katchalski, *J. Am. Chem. Soc.*, **73**, 4084 (1951).
6) N. Izumiya, Z. Uchio and T. Yamashita, *J. Chem. Soc. Japan, Pure Chem. Sect. (Nippon Kagaku Zassi)*, **79**, 420 (1958).
7) T. Hayakawa, J. Noguchi, H. Nishi, S. Ikeda, T. Yamashita and T. Isemura, ibid., **82**, 601 (1961).

acid with *p*-nitrobenzyl alcohol, using *p*-toluenesulfonic acid as the catalyst, afforded a mixture of β-*p*-nitrobenzyl and α-*p*-nitrobenzyl-L-aspartates, with the former predominant. However, hydrochloric acid also gave a mixture, with the former predominant. It was more favorable to obtain the β-isomer of *p*-nitrobenzyl-L-aspartate by the reaction using concentrated hydrochloric acid than to use *p*-toluenesulfonic acid, since the repeated recrystallizations needed to separate the β-isomer lowered the yield.

In order to confirm that these synthesized esters were β-esters and L-isomers, these esters were treated with aqueous ammonia to convert them to asparagine, which was identified as L-asparagine monohydrate. The *N*-carboxyanhydrides (NCA) of these esters were prepared by a method similar to that of Karlson et al.[1] (method B). The polymerizations of NCA's were carried out in glass ampules, in which the air was replaced with dry nitrogen, using triethylamine[8] as an initiator ($A/I=100$).

Optical Rotatory Dispersion in a Chloroform Solution.—*1) The Poly-β-(p-methylbenzyl)-L-aspartate and Copolymers of β-p-Methylbenzyl-L-aspartate with β-Benzyl-L-aspartate.*—The values of b_0 derived from the Moffitt equation[9] have been empirically correlated with the sense of helix; the b_0 values of −630 obtained for poly-γ-benzyl-L-glutamate have been associated with the right-handed helix, and that of +600 for poly-β-benzyl-L-aspartate have been correlated with the left-handed one.[10]

The optical rotatory measurement of PMeBLA in a chloroform solution gave b_0 values ($\lambda_0=212$ mμ) of −680, which seem to indicate that PMeBLA exists in a right-handed helix. However, Fasman[11] pointed out that the sign is not always an indication of the helical sense. If PMeBLA exists in a right-handed helix, the copolymer of β-*p*-methylbenzyl-L-aspartate with β-benzyl-L-aspartate, which have been demonstrated to exist in a left-handed helix in a chloroform solution,[1,2] must exhibit a drastic change in b_0 values when the copolymer composition varies. Truly, b_0 values displayed a sharp change when they were plotted against copolymer composition (Fig. 1a). The values of λ_c and $[\alpha]_{546}$ also showed drastic changes (Table I). PMeBLA showed values of 256 for λ_c which are empirically correlated with a right-handed helix.[12] These typical drastic and abrupt changes in b_0, λ_c, and $[\alpha]_{546}$ indicate that a transition from the left-handed helix of PBLA to the right-handed helix of PMeBLA occurs at ca. a 70 mol.-% methyl residue content.

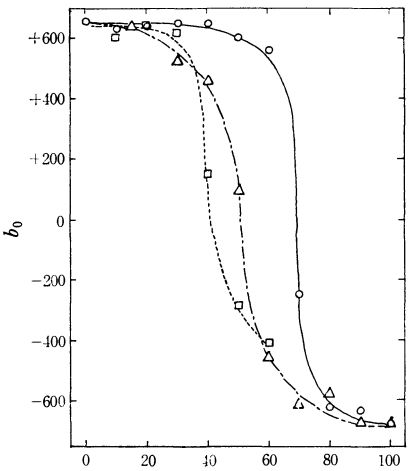

Fig. 1. Values of b_0 against copolymer composition; a) ○—○, copolymers of BLA and MeBLA, b) △-·-△, copolymers of BLA and ClBLA, c) □---□, copolymers of BLA and CNBLA.

TABLE I. COPOLYMERS OF β-*p*-METHYLBENZYL-L-ASPARTATE WITH β-BENZYL-L-ASPARTATE

Polymer No.	Mol-% of methylbenzyl residues*1	b_0*2	λ_c*2	$[\alpha]_{546}$*2	η_{sp}/C*3
C0014	0	+659	152	−178	0.38
C3011	9.9	+631	154	−178	0.34
C3021	19.8	+645	139	−175	0.41
C3031	29.9	+651	146	−172	0.29
C3041	39.9	+653	142	−166	0.30
C3051	49.9	+602	148	−159	0.36
C3061	59.9	+564	148	−158	0.27
C3071	70.0	−248	230	−128	0.17
C3081	80.0	−623	254	−114	0.25
C3091	90.1	−631	257	−110	0.20
C3101	100.0	−680	256	−120	0.31

*1 Mol.-% of residues in polymerization mixture of NCA's.
*2 At 30.0±0.5°C.
*3 $C=0.5\%$, dichloroacetic acid.

2) The Poly-β-(p-chlorobenzyl)-L-aspartate and Copolymers of β-p-Chlorobenzyl-L-aspartate with β-Benzyl-L-aspartate.—Drastic changes in b_0, λ_c, and $[\alpha]_{546}$ similar to those shown above were observed for this series of copolymers (Fig. 1b, Table II). These results reveal that a reversal in the helical sense from the left-handed helix of PBLA to the right-handed helix of PClBLA takes place at a nearly equimolar composition of these residues.

3) The Copolymers of β-Cyanobenzyl-L-aspartate with β-Benzyl-L-aspartate.—Data are shown in Fig. 1c and Table III. Unfortunately, copolymers with cyano-residue contents greater than 60 mol.-%

8) E. R. Blout and R. H. Karlson, *J. Am. Chem. Soc.*, **78**, 941 (1956).
9) W. Moffitt, *J. Chem. Phys.*, **25**, 467 (1956).
10) E. R. Blout and R. H. Karlson, *J. Am. Chem. Soc.*, **80**, 1259 (1958).
11) G. D. Fasman, *Nature*, **193**, 681 (1962).
12) J. A. Schellman and C. G. Schellman, *J. Polymer Sci.*, **49**, 129 (1961).

Table II. Copolymers of β-*p*-chlorobenzyl-L-aspartate with β-benzyl-L-aspartate

Polymer No.	Mol.% of chlorobenzyl residues*1	b_0*2	λ_c*2	$[\alpha]_{546}$*2	η_{sp}/C*3
C1021	15.1	+644	149	−168	0.40
C1031	30.0	+522	156	−146	0.33
C1041	40.0	+458	164	−139	0.41
C1051	49.9	− 93	218	−115	0.39
C1061	60.0	−454	254	−105	0.32
C1071	70.1	−612	263	−99	0.26
C1081	79.9	−578	265	−92	0.30
C1091	90.0	−677	267	−97	0.23
C1101	100.0	−686	269	−94	0.21

*1 Mol.% of residues in polymerization mixture of NCA's.
*2 At 27.5±0.5°C.
*3 C=0.5%, dichloroacetic acid.

Table III. Copolymers of β-*p*-cyanobenzyl-L-aspartate with β-benzyl-L-aspartate

Polymer No.	Mol.% of cyanobenzyl residues*1	b_0*2	λ_c*2	$[\alpha]_{546}$*2	η_{sp}/C*3
C4011	10.0	+613	138	−165	0.73
C4021	20.0	+615	142	−174	0.69
C4031	30.0	+626	147	−167	0.69
C4041	39.9	+156	193	−135	0.64
C4051	50.0	−280	234	−98.6	0.54
C4061	60.0	−401	259	−83.5	0.30

*1 Mol.% of residues in polymerization mixture of NCA's.
*2 At 30.0±0.5°C.
*3 C=0.5%, dichloroacetic acid.

were insoluble in chloroform. In this series a transition from the left-handed to the right-handed helix occurs at a 40—50 mol.-% cyano-residue content.

4) The Copolymers of β-Nitrobenzyl-L-aspartate with β-Benzyl-L-aspartate.—Goodman et al.[4] have reported that a transition from the left-handed helical sense of PBLA to the right-handed helical sense of PNBLA occurs at a 26—32 mol.-% nitro-residue content, and that copolymers with more than a 32% nitro-residue content have large negative b_0 values. In our series a transition takes place at a 20—30 mol.-% nitro residue, Moffitt's plots for copolymers containing 30 and 40 mol.-% nitro residues are non-linear, and those with nitro-residue contents greater than 40 mol.-% are insoluble in chloroform (Table IV).

Table IV. Copolymers of β-*p*-nitrobenzyl-L-aspartate with β-benzyl-L-aspartate

Polymer No.	Mol.% of nitrobenzyl residues*1	b_0*2	$[\alpha]_{546}$*2	η_{sp}/C*3
C2011	10.2	+613	−168	0.31
C2021	20.1	−7.6	−155	0.24
C2031	30.2	N. L.	−157	0.31
C2041	40.0	N. L.	−157	0.24
C2101	100.0	—	—	0.13

*1 Mol.% of residues in polymerization mixture of NCA's.
*2 At 27.5±0.5°C, N. L.; Moffitt's plot was non linear, —; insoluble in chloroform.
*3 C=0.5%, dichloroacetic acid.

In the present study, as has been described above, the optical rotatory dispersion studies with series of copolymers of β-benzyl-L-aspartate and *p*-substituted esters are carried out. The introduction not only of a nitro group but also of a methyl, chloro, or cyano group in the para position of the aromatic ring in the side chain of poly-β-benzyl-L-aspartate causes a reversal from the left- to the right-handed in the helical sense of the polypeptide in chloroform.

Goodman and his co-workers[4] have proposed an explanation based on competitive hydrogen bonding between the carbonyls of the side-chain esters and the main-chain amides. They have suggested that if PBLA were in a right-handed helical conformation, normal intramolecular hydrogen bonding could be disrupted through the interaction of main-chain NH groups with suitably-placed side-chain ester groups. The stabilization of the right-handed conformation in the poly-β-*p*-nitrobenzyl-L-aspartate helix has been explained by assuming that nitroaromatic groups form an electronically-coupled side-chain helix; they have also suggested that when the nitro group is not present, certain $\pi-\pi^*$ transitions are absent, or that there is insufficient π-electron cloud density to allow side chains to overlap.

In our studies, PMeBLA, PClBLA, and PCNBLA have neither an asymmetric absorption band in the long wavelength region nor the enhanced b_0 values which have been reported on PNBLA.[4] Ultraviolet absorption spectra[13] show that these three have small molar extinction coefficients compared with that of PNBLA. Especially, PMeBLA and PClBLA have molar extinction coefficients associated with the aromatic groups which do not differ much from that of PBLA. Nevertheless, these polymers are in right-handed helices. It is remarkable that the helical sense is reversed even by a methyl group which is weakly electron-releasing in contrast with the strongly electron-withdrawing nitro group. Therefore, it is unlikely that stabilization forces of an electronically-coupled aromatic group in the side chain are the primary forces which bring about a reversal

13) Molar extinction coefficients are as follows: PBLA, $\lambda_{max}^{CHCl_3}$ 259 mμ (ε, 210); PMeBLA, $\lambda_{max}^{CHCl_3}$ 265 mμ (ε, 281); PClBLA, $\lambda_{max}^{CHCl_3}$ 268 mμ (ε, 254); PCNBLA, λ_{max}^{DMF} 274 mμ (ε, 825); PNBLA, λ_{max}^{DMF} 275 mμ (ε, 7770).

into a right-handed helix, just as Goodman et al. have proposed for PNBLA. The helix reversals found in the present study also can not be interpreted by the dipole properties of the *p*-substituted benzene rings, since the effects of the introduction of a methyl group on the dipole properties of the aromatic ring should be opposite to those of the other three groups. (The dipole moments of mono-substituted benzenes, Ph-X, are as follows[14]: CH_3, $-0.4(\times 10^{-18})$; Cl, 1.58; C≡N, 4.0; NO_2, 3.98, where the dipole moment of $\overrightarrow{Ph-X}$ is taken to be positive.)

However, in the series of nitro, cyano, chloro, and methyl groups, the transitions occur at 20—30, 40—50, ca. 50, and ca. 70 mol.-%. These values may indicate relative stabilities between PBLA helix and poly-β-(*p*-substituted benzyl)-L-aspartate helices. From these values, it is evident that the helix of PNBLA is the most stable and that that of PMeBLA is the most unstable among the homopolypeptides in the present study. However, the stabilities relative to the PBLA helix differ much less between PCNBLA and PClBLA, while the difference is significant between PMeBLA and PClBLA. These results can be interpreted neither by the electronic nor by the dipole properties of *p*-substituted benzene rings.

These results suggest that the factors which determine the helical sense of PBLA helix are not simple, and that the left-handed helix of PBLA is far less stable.

Experimental

Samples and Apparatus.—The optical rotatory dispersion was measured with a Rudolph photoelectric polarimeter, model 200-S, using a mercury lamp as the light source. Measurements were made at five wavelengths from 5780 to 3650 Å; the concentration was 0.5% w/v, and the path length was 2 dm. The chloroform used was refluxed over and distilled from phosphorus pentoxide.

The mole-per-cent residue content for each of the copolymers is given in a molar ratio in the polymerization mixture of NCA's.[15] The measurements of viscosity were made on solutions in dichloroacetic acid at a concentration of 0.5% w/v using an Ostwald viscometer (35°C) for a qualitative comparison of the relative molecular weights of the various preparations.

Preparation.[16]—*β-Benzyl-L-aspartate.*—The preparation was carried out according to the procedure of Hayakawa, Noguchi, et al.[7] A 32% yield of white powder was obtained; m. p. 221°C (decomp.) $[\alpha]_D^{24}$ +24.4 (*c* 1, 0.1 N HCl).

β-p-Methylbenzyl-L-aspartate. — A mixture of well-pulverized L-aspartic acid (10.0 g.), *p*-toluenesulfonic acid (14.4 g.), and *p*-methylbenzyl alcohol (9.2 g.), which had been prepared by the reduction of *p*-methylbenzaldehyde with sodium borohydride in a methanol solution, was heated at 80°C for 2 hr. with stirring; during the reaction water was removed three or four times under reduced pressure from a reaction vessel. After water (150 ml.) had been added to the reaction mixture and it had been washed with ether (150 ml.), the aqueous layer was neutralized by adding sodium bicarbonate; after the mixture had then stood in a cold place, the precipitate was filtered and recrystallized from water (300 ml.). After decoloring with Norit, β-*p*-methylbenzyl-L-aspartate was obtained (1.70 g. (9.5%)) as white leaflets; m. p. 225—226°C (decomp.) $[\alpha]_D^{25}$ +14.3 (*c* 1, glacial acetic acid).

Found: C, 60.46; H, 6.44; N, 6.02. Calcd. for $C_{12}H_{15}O_4N$: C, 60.75; H, 6.37; N, 5.90%.

β-p-Chlorobenzyl-L-aspartate.—A mixture of L-aspartic acid (1.2 g.), *p*-toluenesulfonic acid (1.5 g.), and *p*-chlorobenzyl alcohol (2.5 g.), which had been prepared by the hydrolysis of *p*-chlorobenzyl chloride in an aqueous sodium carbonate solution, was treated according to the same procedure as was used for β-*p*-methylbenzyl-L-aspartate; recrystallization from boiling water furnished 1.3 g. (58.5%) of the product as white leaflets, m. p. 208°C (decomp.), $[\alpha]_D^{23}$ +25.6 (c 1, glacial acetic acid).

Found: C, 51.35; H, 4.58; N, 5.32; Cl, 13.94. Calcd. for $C_{11}H_{12}O_4NCl$: C, 51.27; H, 4.69; N, 5.44; Cl, 13.76%.

A similar procedure but using concentrated hydrochloric acid instead of *p*-toluenesulfonic acid afforded the product in about a 15% yield.

β-p-Cyanobenzyl-L-aspartate. — The procedure was exactly the same as was used for β-*p*-methylbenzyl-L-aspartate (yield 10—15%); m. p. 187—188°C (decomp.), $[\alpha]_D^{25.5}$ +11.2 (*c* 1, glacial acetic acid).

Found: C, 57.88; H, 5.04; N, 11.60. Calcd. for $C_{12}H_{12}O_4N_2$: C, 58.06; H, 4.87; N. 11.29%.

p-Cyanobenzyl alcohol was prepared by the chlorination of *p*-methylbenzonitrile, followed by hydrolysis with aqueous·potassium carbonate.[17]

β-p-Nitrobenzyl-L-aspartate. — a) A mixture of *p*-nitrobenzyl alcohol (15 g.) and L-aspartic acid (7 g.) was stirred for 0.5 hr., with the temperature kept at 110°C; concentrated hydrochloric acid (3 ml.) was added. After the mixture had been stirred for 2 hr., concentrated hydrochloric acid (1 ml.) was added; then the mixture was stirred for another hour. During the reaction water was removed from the reaction vessel two or three times under reduced pressure. The reaction mixture was then diluted with water, neutralized with sodium bicarbonate, and filtered. Treatment with Norit and recrystallization from water afforded pale yellow crystals whose infrared spectra have two

14) C. P. Smyth, "Dielectric Behavior and Structure," McGraw-Hill, New York (1955), p. 253.

15) For almost these copolymers prepared, the results of their elementary analyses agreed, within ±0.35%, with the values calculated from the molar ratios of the NCA's in the polymerizations. The chloro-residue contents of the copolymers of ClBLA with BLA were determined by the ultraviolet spectra (utilizing the aromatic absorption bands) and by the infrared spectra (utilizing the out-of-plane deformation bands of the aromatic rings). These results agree, within 2 mol.%, with the mixing molar ratios of the NCA's in the polymerizations. For all the copolymers, their molar ratios may, therefore, not differ much from those of the NCA's in the polymerization mixtures.

16) All melting points are uncorrected.

17) J. N. Ashley, H. J. Barber, A. J. Ewins, G. Newberg and A. D. H. Self, *J. Chem. Soc.*, **1942**, 103.

ester-carbonyl stretching absorptions (1740 cm^{-1} and 1720 cm^{-1}). Repeated recrystallizations from hot water gave leaflets (2.7 g.); m. p. 190.5—191°C (decomp.), $[\alpha]_D^{19.5}$ +16.7 (*c* 2, glacial acetic acid), which have a single ester-carbonyl stretching absorption at 1720 cm^{-1} in the infrared spectrum; this was proved to be the β-ester by the conversion to L-asparagine to be described below.

Found: C, 49.17; H, 4.70; N, 10.31. Calcd. for $C_{11}H_{12}O_6N_2$: C, 49.26; H, 4.51; N, 10.44%.

On the other hand, the concentration of the mother liquor gave crystals which have an ester-carbonyl stretching absorption at 1740 cm^{-1}, with a weak shoulder at 1720 cm^{-1}. Repeated recrystallizations afforded α-*p*-nitrobenzyl-L-aspartate (m. p. 180—181.5°C (decomp.), ester νC=O 1740 cm^{-1}). The specimen was converted to L-isoasparagine monohydrate, which was identified by a comparison of its infrared spectrum with that of an authentic sample.[18]

b) The same procedure utilizing *p*-toluenesulfonic acid as was used for β-*p*-methylbenzyl-L-aspartate afforded a mixture which contained more α-esters than was obtained by the procedure of (a).

Conversions of p-Substituted Benzyl-L-aspartates to L-Asparagine.—To establish that these *p*-substituted benzyl-L-aspartates are β-esters and that no racemization takes place during the preparation of the products, these esters were converted as follows. β-*p*-Methylbenzyl-L-aspartate (0.517 g.) was treated with 28% aqueous ammonia at 100°C for 25 hr. in the sealed glass ampule. The solution was then heated to remove the ammonia and washed with ether, the aqueous layer was concentrated, and the residue was recrystallized from aqueous alcohol to give crystals (0.264 g.); m.p. 230°C (decomp.), $[\alpha]_D^{24.5}$ +31.0 (*c* 1, 6 N HCl); reported for L-asparagine monohydrate[2] $[\alpha]_D^{20}$ +31.2.

Found: C, 32.07; H, 7.00; N, 18.35. Calcd. for $C_4H_8N_2O_3 \cdot H_2O$: C, 32.00; H, 6.70; N, 18.66%.

Exactly the same treatments of β-(*p*-chloro, *p*-cyano and *p*-nitro)-benzyl-L-aspartates (0.49, 0.53, and 0.53 g.) as for β-*p*-methylbenzyl-L-aspartate were carried out to afford 0.18, 0.23 and 0.26 g. of L-asparagine monohydrate; their specific rotations were as follows: $[\alpha]_D^{24.5}$ +29.6, +33.7 and +30.7 (*c* 1, 6 N HCl) respectively.

β-Benzyl-L-aspartate-N-carboxyanhydride. — The procedure of Karlson et al.[1] (method B) utilizing the reaction of phosgene with β-benzyl-L-aspartate suspended in anhydrous dioxane[19] at 40°C and the recrystallization of the anhydride from ethyl acetate-*n*-hexane furnished the product as needles.

β-p-Methylbenzyl-L-aspartate-N-carboxyanhydride.—The same procedure as that described above for β-*p*-methylbenzyl-L-aspartate (10.0 g.) afforded the product (7.0 g.) as leaflets, m. p. 129—131°C, $[\alpha]_D^{27}$ −30.6 (*c* 2.6, ethyl acetate).

Found: C, 59.22; H, 5.09; N, 5.45. Calcd. for $C_{13}H_{13}NO_5$: C, 59.31; H, 4.98; N, 5.32%.

β-p-Chlorobenzyl-L-aspartate-N-carboxyanhydride.—The same procedure as has been described above for β-*p*-chlorobenzyl-L-aspartate (15.0 g.) gave the product (5.8 g.) as leaflets, m. p. 162°C (decomp.), $[\alpha]_D^{24}$ −30.1 (*c* 1.5, ethyl acetate).

Found: C, 50.81; H, 3.65; N, 4.74; Cl, 21.86. Calcd. for $C_{12}H_{10}O_5NCl$: C, 50.81; H, 3.55; N, 4.94; Cl, 12.50%.

β-p-Cyanobenzyl-L-aspartate-N-carboxyanhydride.—The same procedure as has been described above for β-*p*-cyanobenzyl-L-aspartate (8.0 g.) and the recrystallization of the anhydride from dioxane-*n*-hexane furnished the product (6.5 g.) as leaflets, m. p. 153—154°C (decomp.), $[\alpha]_D^{27}$ −53.6 (*c* 2.4, dioxane).

Found: C, 57.06; H, 3.95; N, 10.12. Calcd. for $C_{13}H_{10}O_5N_5$: C, 56.94; H, 3.68; N, 10.22%.

β-p-Nitrobenzyl-L-aspartate-N-carboxyanhydride.—M. p. 174—176°C (decomp.), $[\alpha]_D^{25}$ −48.5 (*c* 1.5, dioxane). (Found: C, 48.91; H, 3.67; N, 9.22%.)

Poly-β-benzyl-L-aspartate and Poly-β-p-methyl chloro, cyano or nitrobenzyl-L-aspartate.—A typical polymerization was carreid out as follows: to 7 ml. of dioxane[17] containing 0.4 ml. of a solution of 100 mg. of triethylamine in 10 ml. of dioxane, 1.0 g. of β-benzyl-L-aspartate-*N*-carboxyanhydride was added; A/I=100. The clear solution in a glass ampule[20] (dried for 7 hr. at 140°C) was sealed under an atmosphere of dry

Table V

Polymer No.	MeBLA-NCA mg.	BLA-NCA mg.	Methylbenzyl content mol.%	Triethylamine* mg.	A/I**	Yield %
C3011	104	896	9.9	4.0	100	76
C3021	207	793	19.8	4.0	100	83
C3031	310	687	29.9	4.0	100	84
C3041	411	586	39.9	4.0	100	87
C3051	513	488	49.9	4.0	100	86
C3061	611	387	59.9	3.9	100	84
C3071	711	289	70.0	3.9	100	86
C3081	808	191	80.0	3.9	100	83
C3091	903	94	90.1	3.8	100	84
C3101	1000	0	100.0	3.8	100	85

* A solution of 0.10 g. in 10 ml. dioxane; the triethylamine was purified by refluxing over and distilling from sodium metal.

** Molar ratio of the total anhydride to initiator.

18) J. Kovacs, H. N. Kovacs and R. Ballina, *J. Am. Chem. Soc.*, **85**, 1839 (1963).

19) L. F. Fieser, "Experiments in Organic Chemistry," 2nd Ed., Heath, Boston, Mass. (1941), p. 361.

20) Sealed glass ampules were used for the polymerization to prevent the moisture.

TABLE VI

Polymer No.	ClBLA-NCA mg.	BLA-NCA mg.	Chlorobenzyl content mol.%	Triethylamine* mg.	A/I**	Yield %
C1015	152	750	15.1	3.6	100	73
C1031	295	606	30.0	3.5	100	60
C1041	389	513	40.0	3.5	100	73
C1051	479	423	49.9	3.4	100	67
C1061	568	332	60.0	3.4	100	77
C1071	652	244	70.1	3.3	100	78
C1081	737	163	79.9	3.3	100	75
C1091	821	80	90.0	3.2	100	76
C1101	1470	0	100.0	5.3	100	81

* A solution of 0.10 g. in 10 ml. dioxane; the triethylamine was purified by refluxing over and distilling from sodium metal.
** Molar ratio of the total anhydride to initiator.

TABLE VII

Polymer No.	CNBLA-NCA mg.	BLA-NCA mg.	Cyanobenzyl content mol.%	Triethylamine* mg.	A/I**	Yield %
C4011	109	889	10.0	4.0	100	81
C4021	216	785	20.0	4.0	100	84
C4031	321	680	30.0	3.9	100	82
C4041	423	578	39.9	3.9	100	82
C4051	524	477	50.0	3.9	100	84
C4061	623	377	60.0	3.8	100	86
C4075	720	200	76.6	3.8	100	26
C4081	816	185	80.0	3.8	100	27
C4091	909	93	89.9	3.7	100	19
C4101	1050	0	100.0	3.7	100	46

* A solution of 0.10 g. in 10 ml. dioxane; the triethylamine was purified by refluxing over and distilling from sodium metal.
** Molar ratio of the total anhydride to initiator.

TABLE VIII

Polymer No.	NBLA-NCA mg.	BLA-NCA mg.	Nitrobenzyl content mol.%	Triethylamine* mg.	A/I**	Yield %
C2011	119	884	10.2	4.0	100	74
C2021	230	772	20.1	3.9	100	52
C2031	340	666	30.2	3.8	100	76
C2041	440	560	40.0	3.8	100	71
C2101	1070	0	100.0	3.7	100	34

* A solution of 0.10 g. in 10 ml. dioxane; the triethylamine was purified by refluxing over and distilling from sodium metal.
** Molar ratio of the total anhydride to initiator.

nitrogen and allowed to stand for 3.5 days at 30°C. The solution was poured into 80 ml. of diethyl ether in order to precipitate the polymer, which was washed with ether and reprecipitated from a chloroform solution with ether and dried at 60°C in vacuo.

These β-*p*-methyl, chloro, cyano, and nitrobenzyl-L-aspartate-*N*-carboxyanhydrides were polymerized according to the same procedure as was used for β-benzyl-L-aspartate. The quantities used and the yields obtained for these polymers are summarized in Tables V—VIII. Poly-β-*p*-cyano and nitro benzyl-L-aspartates were reprecipitated from a dimethylformamide solution with ether.

PMeBLA; Found: C, 65.63; H, 6.11; N, 6.58. Calcd. for $C_{12}H_{13}O_3N$: C, 65.74; H, 5.98; N, 6.39%. PClBLA; Found: C, 55.08; H, 4.44; N, 5.77; X, 11.99. Calcd. for $C_{11}H_{10}C_3NCl$: C, 55.13; H, 4.21; N, 5.84; X, 14.79%. PCNBLA; Found: C, 62.73; H, 4.49; N, 11.99. Calcd. for $C_{12}H_{10}N_2O_3$: C, 62.20; H, 4.38; N, 12.17%. PNBLA; Found: C, 52.39; H, 4.26; N, 11.05. Calcd. for $C_{11}H_{10}O_5N_2$: C, 52.80; H, 4.03; N, 11.20%.

Copolymers of β-p-Methylbenzyl-L-aspartate with β-Benzyl-L-aspartate.—Tabel V summarizes the quantities used

and the yields obtained for these copolymers. A typical polymerization was as follows: 0.513 g. of β-*p*-methylbenzyl-L-aspartate-*N*-carboxyanhydride and 0.488 g. of β-benzyl-L-aspartate-*N*-carboxyanhydride (1 : 1 molar ratio) were dissolved in 7.0 ml. of dioxane. To a total of 14.3% w/v NCA's in a dioxane solution, 0.40 ml. of a solution of 100 mg. of triethylamine in 10 ml. of dioxane was added ($A/I=100$). The mixed solution in a glass ampule was sealed under an atmosphere of dry nitrogen and allowed to stand for 3.5 days at 30°C. The workup was the same as for poly-β-benzyl-L-aspartate described above.

Copolymers of β-p-Chlorobenzyl-L-aspartate with β-Benzyl-L-aspartate.—Table VI summarizes the yields obtained for these copolymers. Polymerizations were carried out in a manner similar to that employed for the copolymers of MeBLA with BLA. The NCA's were in a 5% w/v solution, and polymerizations were allowed to proceed for 7.5 days.

Copolymers of β-p-Cyanobenzyl-L-aspartate with β-Benzyl-L-aspartate.—Table VII summarizes the quantities used and the yields obtained for these copolymers. Polymerizations were carried out according to the procedure used for the copolymers of MeBLA with BLA. The NCA's were in a 10% solution for C4011—C4051 and in a 5% solution for C4061—C4091, and polymerizations were allowed to proceed for 5 days. The copolymers were dissolved in chloroform for C4011—C4061 and in dimethylformamide for C4075—C4091, and they were precipitated with ether.

Copolymers of β-p-Nitrobenzyl-L-aspartate with β-Benzyl-L-aspartate.—Table VIII summarizes the quantities used and the yields obtained for these polymers. Polymerizations were carried out according to the procedure used for the copolymers of MeBLA with BLA. The solutions of NCA's were 5% except C2101 (3%), and polymerizations were allowed to stand for 5 days.

The authors wish to express their gratitude to Professor Takehiko Shimanouchi and Professor Kazutomo Imahori, The University of Tokyo, for their encouragement throughout this work. They are indebted to Professor Tatsuo Miyazawa and Dr. Kozo Hamaguchi of Institute for Protein Research, Osaka University for the use of Rudolph photoelectric polarimeter. They are also grateful to Dr. Shinsuke Ose, Dr. Hideji Takamatsu and Dr. Kiyoshi Nakamura of this laboratory for their encouragement and valuable discussions and also greatly indebted to Mr. Satoshi Arakawa for his kind help in the course of their experiments.

BULLETIN OF THE CHEMICAL SOCIETY OF JAPAN VOL. 39 2713—2720 (1966)

Studies of Poly-β-benzyl-L-aspartate Helix. II. The Circular Dichroism and Optical Rotatory Dispersion of Copolymers of β-*p*-Methyl, Chloro, or Cyanobenzyl-L-aspartate with β-Benzyl-L-aspartate

By Masahisa HASHIMOTO

Research Laboratory, Dainippon Pharmaceutical Co., Ltd., Ebie, Fukushima-ku, Osaka

(Received February 19, 1966)

The observation of the circular dichroism (240—290 mμ) due to the aromatic side chain indicates that, in a chloroform solution, even the side-chain aromatic rings of the copolyaspartate chain in the right-handed helix are in a regular arrangement to form an outer helix. On the contrary, for the copolyaspartate chain in the left-handed helix, the aromatic rings are much less regular. The ORD measurements indicate that, in a dimethylformamide solution, the poly-β-benzyl-L-aspartate chain is essentially in a random coil form, whereas the para-substituted derivatives are essentially in a right-handed helix. Accordingly, for each series of copolymers, the transition from a random coil form to a right-handed helix is observed as the molar content of the para-substituent is increased. The copolypeptide chain of β-benzyl-L-aspartate and β-(*p*-methylbenzyl)-L-aspartate (molar ratio, 1 : 1) takes either the left-handed helix in a chloroform solution or the right-handed helix in a dimethylformamide solution. Accordingly, for this copolypeptide, the transition from the left to right-handed conformation is observed at the mixing volume ratio, 90 : 10, of the chloroform-dimethylformamide solution.

Goodman et al.[1] have reported that the left-handed helix of poly-β-benzyl-L-aspartate (PBLA) is reversed to the right-handed sense by the introduction of the nitro group in the para-position of the side-chain aromatic ring. They have proposed that this right-handed conformation is stabilized by an electronically-coupled nitroaromatic side-chain helix rigidly arrayed about the main chain helix. In the previous paper,[2] the present author and Aritomi have revealed that the helix reversal

1) M. Goodman, A. M. Felix, C. M. Deber, A. R. Brause and G. Schwartz, *Biopolymers*, **1**, 371 (1963).

2) Part I of this series: M. Hashimoto and J. Aritomi, This Bulletin, **39**, 2707 (1966).

is also brought about by the introduction of the methyl, chloro, or cyano groups at the para-position of the benzyl group. This is quite clear since, for each series of the copolymers of β-benzyl-L-aspartate (BLA) with β-(*p*-methyl, chloro, or cyanobenzyl)-L-aspartate (MeBLA, ClBLA, or CNBLA), a sharp change in b_0 values[3] has been observed with the variation in the molar contents of the para-substituent.

In this paper, the author will present; (1) the results of the optical rotatory dispersion (ORD) and circular dichroism (CD) measurements of the above copolymers in a chloroform solution, in the absorption region (around 240—290 mμ) of the side-chain aromatic rings, and (2) the results of the ORD measurements of the copolymers in a dimethylformamide solution in the visible and near-ultraviolet regions. The evidence obtained to establish the conformations of the side-chain aromatic rings of the copolymers in a chloroform solution will be presented, and the conformations of the copolymer chains in dimethylformamide will be discussed.

Experimental

The samples of the copolymers used in the present study are the same as those used in the previous report[2] except for PClBLA (C1102), which was synthesized in a similar way but by adopting anhydride to the initiator ratio, 50.

Chloroform obtained from E. Merck AG was treated with molecular sieves (4A, Tomoe Kogyo Co., Tokyo) to remove a small amount of ethanol. The dimethylformamide (DMF) used was purified by distillation, and the dichloroacetic acid (DCA) was purified by vacuum distillation.

Ultraviolet ORD and CD measurements were carried out through the courtesy of Professor Kazutomo Imahori of College of General Education, The University of Tokyo, on a JASCO, model ORD/UV5, optical rotatory dispersion recorder with a CD attachment equipped with a xenon light source at 30°C. The CD measurements were made at the minimum scanning speed (10 mμ/10 min.). Fused-quartz cells 10 mm. and 1 mm. long were used. Identical cells and solutions were used in both ORD and CD measurements; the solutions were prepared to be around 2 in optical density. ORD and CD data are expressed in terms of $[m']$ and θ respectively, and their units are both deg.cm²/decimole. The refractive index was estimated from the Sellmeir equation, using the indices of chloroform observed at 434 and 589 mμ.

The ultraviolet absorption measurements were carried on a Hitachi EPS-2U spectrophotometer.

Optical rotatory dispersion measurements in the near-ultraviolet and visible regions were carried through the courtesy of Professor Tatsuo Miyazawa and Dr. Kozo Hamaguchi of the Institute for Protein Research, Osaka University, on a Rudolph, model 200-S, photoelectric polarimeter using a mercury lamp as the light source. The values of b_0 and λ_c were calculated from measurements at five wavelengths, from 5780 to 3650 Å; the concentration was 0.5% w/v, and the path length was 2 dm. In the Moffitt plot, the dispersion of the refractive index is neglected, using the values at the sodium D line.

Results and Discussion

Ultraviolet Rotatory Dispersions and Circular Dichroisms of Copolymers of β-Benzyl-L-aspartate with β-*p*-Methyl, Chloro, and Cyanobenzyl-L-aspartate in a Chloroform Solution.—*a) Copolymers of BLA with CNBLA.*— The copolymer of BLA with CNBLA containing 60 mol.-% cyano residues had b_0 values of −401 in a chloroform solution.[2] The ORD curve (Fig. 1a) of the cpolymer showed a negative plain

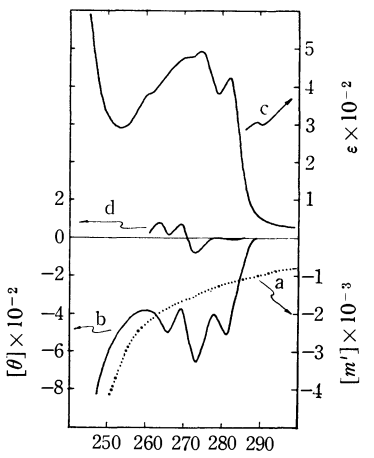

Fig. 1. Curves of ORD (a), CD (b), and UV (c) in chloroform, and CD (d) in chloroform containing 10%v/v dichloroacetic acid for the copolymer of BLA with CNBLA containing 60 mole per cent cyano residues.

curve, and no definite Cotton effect was found in the region from 260 to 290 mμ. However, the CD measurements for this copolymer gave, in this region, a distinct negative CD peak involving fine vibrational structures. This dichroism is evidently associated with the side-chain aromatic rings of the copolymer. This negative ellipticity decreased remarkably in a chloroform solution containing 10% dichloroacetic acid (Fig. 1d). Therefore, it is clear that the CD of this copolymer in a chloroform solution is not essentially due to an optically active chromophore, which still gives rise to CD in a random coil form. (For poly-L-tyrosine, it has been reported that one of the CD bands, observed at 245 mμ in a helical conformation, persists in a random conformation.[4]) Accordingly,

3) W. Moffitt, *J. Chem. Phys.*, **25**, 467 (1956); W. Moffitt and J. T. Yang, *Proc. Natl. Acad. Sci. U. S.* **42**, 596 (1956).

4) G. D. Fasman, E. Bodenheimer and C. Lindblow, *Biochemistry*, **3**, 1665 (1964); S. Beychok and G. D. Fasman, ibid., **3**, 1675 (1964).

the results may be attributed to the fact the negative CD curve involving fine vibrational structures evidently arises from a regular arrangement of the side-chain aromatic rings of this copolymer in a helical conformation. The increasing negative ellipticity with the decrease in the wavelength below 250 mμ observed for the copolymer may suggest that the copolymer has a negative ellipticity for the n-π^* transition near 220 mμ, which is associated with a right-handed α-helix.[5] The above results are consistent with the negative b_0 values (−401).[2]

The ORD and CD curves of the copolymer of BLA with CNBLA containing 30 mol.-% cyano residues are shown in Figs. 2a and 2b respectively. In the region from 250 mμ to 280 mμ, a very weak positive ellipticity was found. The increasing positive ellipticity with a decrease in the wavelength below 250 mμ suggests that this copolymer exists in a left-handed α-helix which is opposite in the helical sense to that of the copolymer containing 60 mol.-% cyano residues. This result is also consistent with the positive b_0 values (+626) observed for this copolymer.[2]

The CD curve of poly-β-benzyl-L-aspartate (PBLA) shows a small ellipticity involving fine structures (Fig. 3b). The magnitude of this ellipticity is rather small; however, the results were reproducible. The peaks in CD curves either in Figs. 2b or 3b do not correspond to those in UV spectra; however, these two CD curves are fairly similar to each other, both in their shape and in the position of the peaks. A comparison of the magnitude of their ellipticity may be meaningless because of the weakness in their ellipticity. However, the fact that the absolute magnitude of the ellipticity of PBLA associated with the aromatic

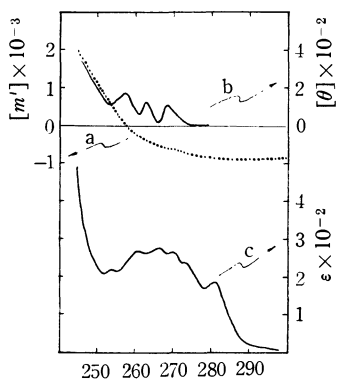

Fig. 2. Curves of ORD (a), CD (b), and UV (c) in chloroform for the copolymer of BLA with CNBLA containing 30 mole per cent cyano residues.

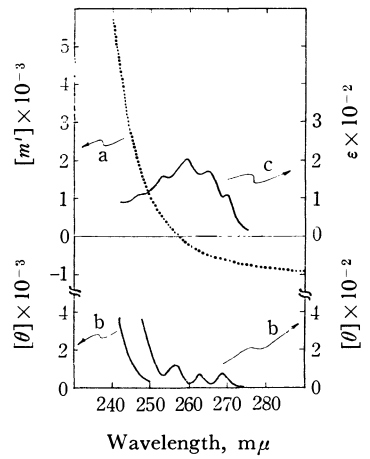

Fig. 3. Curves of ORD (a), CD (b), and UV (c) for PBLA in chloroform solution.

group is smaller than that of the copolymer in Fig. 1b may indicate that the side-chain aromatic rings of PBLA are packed with much less regularity. The same conclusion can be obtained for the side-chain of the copolyaspartate containing 30 mol.-% cyanobenzyl residues, since the magnitude of the CD peak is far less than that of the copolymer in Fig. 1b.

The CD curve of poly-γ-benzyl-L-glutamate (PBLG) may be seen in Fig. 4a. This polypeptide showed no significant ellipticity in the region of the absorption of the aromatic group. This finding indicates that the aromatic rings in PBLG are not in a regular orientation in a chloroform solution, although in oriented solid film Tsuboi has elucidated, from his infrared studies, that the aromatic rings of this polypeptide are held in a regular orientation.[6]

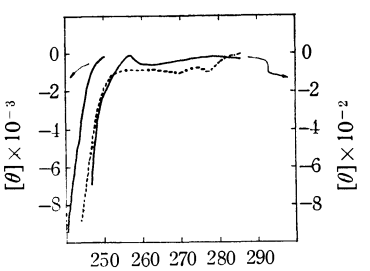

Fig. 4. CD of PBLG (a), ——, and the copolymer of BLA with ClBLA containing 50 mole per cent chloro residues (b), ·····, in chloroform.

b) Copolymers of BLA with MeBLA.—The UV, ORD, and CD curves of copolymers of BLA with MeBLA containing 80 and 60 mol.-% methyl residues in a chloroform solution are shown in Figs.

5) G. Holzwarth, W. B. Gratzer and P. Doty, *J. Am. Chem. Soc.*, **84**, 3194 (1962).

6) M. Tsuboi, *J. Poly. Sci.*, **59**, 139 (1962).

5 and 6 respectively, while the results concerning a homopolymer, poly-β-(*p*-methylbenzyl)-L-aspartate (PMeBLA), are shown in Fig. 7. The ellipticity observed for PMeBLA is to some extent larger than that of the copolymer containing 80 mol.-% methyl residues. The negative CD curves observed for these polypeptides are different in magnitude and in the wavelength of their maximum ellipticity. However, the wavelengths of the CD peaks of these polypeptides are in good agreement with the wavelengths of their UV absorption peaks. These results may indicate that both the methylbenzyl and benzyl groups are regularly arranged

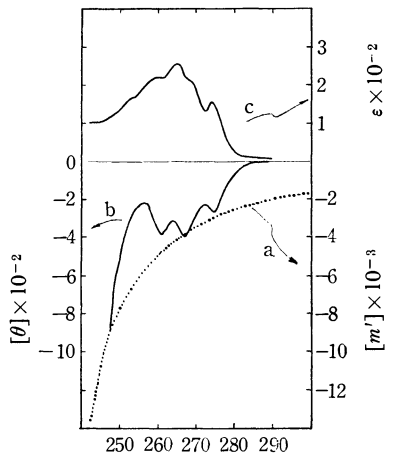

Fig. 5. Curves of ORD (a), CD (b), and UV (c) in chloroform for the copolymer of BLA with MeBLA containing 80 mole per cent methyl residues.

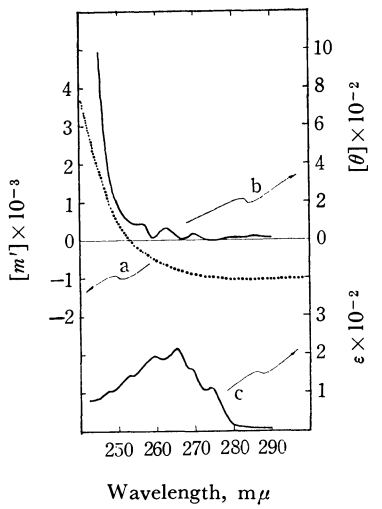

Fig. 6. Curves of ORD (a), CD (b), and UV (c) in chloroform for the copolymer of BLA with MeBLA containing 60 mole per cent methyl residues.

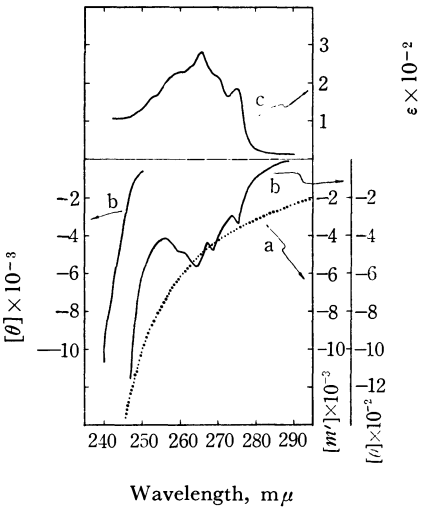

Fig. 7. Curves of ORD (a), CD (b), and UV (c) in chloroform for PMeBLA.

and contribute to the ellipticity. On the contrary, for the copolymer containing 60 mol.-% methyl residues the CD curve (Fig. 6b) is almost the same as that of PBLA (Fig. 3b). This result indicates that this copolymer exists in a left-handed helix and that the methylbenzyl group does not contribute to the ellipticity. Therefore, the side-chain aromatic rings of this copolymer may be said to be much less regularly packed as in PBLA.

c) Copolymers of BLA with ClBLA.—The UV, ORD, and CD curves in a chloroform solution of a copolymer of BLA with ClBLA containing 60 and 40 mol.-% chloro residues are shown in Figs. 8 and 9 respectively, while the results concerning a homopolymer, poly-β-(*p*-chlorobenzyl)-L-aspartate (PClBLA), are shown in Fig. 10. The

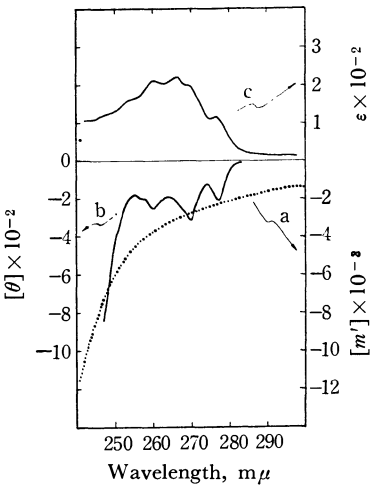

Fig. 8. Curves of ORD (a), CD (b), and UV (c) in chloroform for the copolymer of BLA with ClBLA containing 60 mole per cent chloro residues.

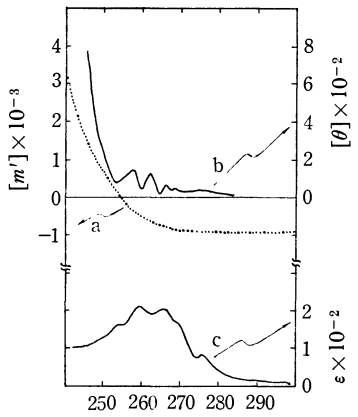

Fig. 9. Curves of ORD (a), CD (b), and UV (c) in chloroform for the copolymer of BLA with ClBLA containing 40 mole per cent chloro residues.

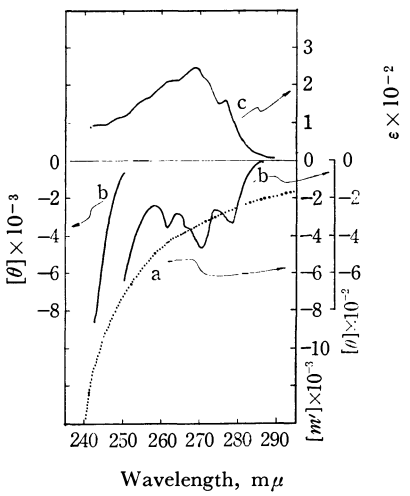

Fig. 10. Curves of ORD (a), CD (b), and UV (c) in chloroform for PClBLA.

results may be interpreted similarly as in case of the BLA-MeBLA series described above. A copolymer of BLA with ClBLA containing 50 mol.-% chloro residues gave no significant CD curve in the region of the side-chain aromatic group (Fig. 4b). Judging from the b_0 value, −93, in a chloroform solution,[2] the copolymer exists essentially in a random coil. As is evident from Figs. 7b and 8b, the ellipticity associated with the aromatic rings is comparatively large in magnitude if the backbone is folded in the right-handed helix, while the left-handed helix exhibits a negligible amount of ellipticity for the side-chain chromophore. Thus, if equal amounts of the left- and right-handed helices exist, the CD value due to the right-handed helix would exceed that of the left-handed one, and the resulting CD curve should be one similar in shape to, and a half the magnitude of, that of the right-handed helix (Fig. 10). However, since no significant peak was detected in the CD curve of the copoly-(BLA-ClBLA) (50 : 50), as may be seen in Fig. 4b, the assumption of the mixture of the left- and right-handed helices for this copolymer should be discarded; rather, the copolymer has been proved to exist in a random coil. The amount and the sense of the helical conformation judging from CD measurements of PClBLA and three copolymers (chlororesidue contents; 40, 50, and 60 mol.-%) are consistent with those obtained from b_0 analysis.[2]

A pronounced increase in negative ellipticity and negative ORD with a decrease in the wavelength below 250 mμ was observed for both PMeBLA and PClBLA. This result indicates that both PMeBLA and PClBLA have a negative ellipticity for the n-π^* transition near 220 mμ; it leads to the conclusion that both polypeptides exist in the right-handed helix, although the ultraviolet absorption of chloroform prevents the direct measurement of the n-π^* transition around 220 mμ. On the other hand, a positive ellipticity and a positive ORD curve were observed for PBLA, which exists in the left-handed α-helix. In each series of copolymers, the transition from the left- to the right-handed helix, depicted by the change in the signs of ellipticity and optical rotation parameter, takes place in a narrow range of composition.

The ellipticities observed for PMeBLA and PClBLA at 250 mμ, are about twice as large as that observed for PBLG, although this comparison is only qualitative because their ellipticity steeply changes around 250 mμ. The ellipticity around 240 mμ observed for PMeBLA and PClBLA in chloroform is also about twice as large as that for poly-γ-methyl-L-glutamate, as estimated from the results of Holtzwarth et al.[7] The ORD curve of PBLA in chloroform in the present study is in accordance with that in methylene dichloride reported by Blout.[8] However, for PClBLA and PMeBLA the observed optical rotations at 250 mμ are about twice and one-and-a-half times as large, respectively, as that for poly-α, L-glutamic acid in a water solution (pH, 4.3; the helical form), as estimated from the results of Blout et al.[9] The above comparison indicates that, for PClBLA and PMeBLA, the CD and ORD around 240 mμ are both larger in magnitude than the ordinary polypeptides in the right-handed α-helix. These results may be due to the contributions to CD and ORD of the aromatic absorption band around

7) G. Holzwarth and P. Doty, *J. Am. Chem. Soc.*, **87**, 218 (1965).
8) E. R. Blout, *Biopolymers*, **Symp. No. 1**, 397 (1964).
9) E. R. Blout, I. Schmier and N. S. Simmons, *J. Am. Chem. Soc.*, **80**, 1259 (1958).

220 mμ[10] and/or of the ester-carbonyl absorption around 220—230 mμ resulting from the regular arrangement of the side-chain group. However, qualitatively the above results do not change the conclusion obtained as to the helical sense of the polypeptides.

In the present study, the negative CD bands were found in the 250—290 mμ region, whereas no definite Cotton effect was observed in this region, for the polypeptide chains forming the right-handed helix. The Kronig-Kramers transform relating ellipticity to rotation has been shown to lead to the following relation when the circular dichroism is in a Gaussian form:[11]

$$[\theta^\circ] = \pm 0.82 \frac{n_\lambda^2 + 2}{3} ([m'_{max}] - [m'_{min}])$$

where $[\theta^\circ]$ is the maximum ellipticity of the band, and $[m']$ is the reduced mean residue rotation. This relation suggests that Cotton effects should be observed in the 250—290 mμ region for the present, right-handed polypeptides. (Even when the CD curve deviates from a Gaussian curve, the relation should hold qualitatively.) Furthermore, essentially the same selection rules hold on ORD and CD even in the case of a vibration-coupled optically active chromophore.[12] The largest observed ellipticity associated with the aromatic chromophore in the present study is −650 (Fig. 1b). The value of $(n_\lambda^2+2)/3$ in the above formula is about 0.7 in the region from 260 mμ to 290 mμ; thus, the value of the $0.82(n_\lambda^2+2)/3$ term, is about 1.2. Therefore, if this maximum ellipticity (−650) is completely due to a band, the above relation leads to an estimation that a trough, about 280 in magnitude, should appear in the ORD curve. However, as is evident from Fig. 1b, the three peaks of CD lie close together. In addition, the contribution of the large ellipticity (ca. -1.5×10^4) of the n-π^* transition around 220 mμ to this region cannot be excluded completely. Therefore, if one assumes that the net maximum ellipticity for the band is about a half of the observed value after the correction of the contributions from the other bands, this ellipticity may, practically speaking, not be so large as to give rise to a definite Cotton effect. This situation is less profound in the other polypeptides in the present study.

The results of the ORD and CD measurements described above indicate qualitatively but strongly that a reversal in the helical sense really takes place in each series of copolymers, and that PClBLA and PMeBLA in a chloroform solution exist in the right-handed α-helix. The results also lead to the conclusion that, in the right-handed helix, the side-chain aromatic rings of the copolyaspartate chain are arranged regularly to form an outer helix, whereas in the left-handed helix the aromatic rings are much less regular.

From the results in the present study, it can not be determined whether or not an outer helix formed by the side-chain aromatic rings contributes to the stability of the right-handed helix of the main chain.

The Optical Rotatory Dispersion in Dimethylformamide.—In a chloroform solution PBLA is known to exist in a left-handed α-helix,[13,14] whereas in a dimethylformamide (DMF) solution PBLA has been estimated to be essentially in a random conformation from the studies of the copolymers of BLA and *p*-nitrobenzyl-L-aspartate.[1]

The results of the ORD measurements in the present study of homopolymers and copolymers of BLA with CNBLA, ClBLA, or MeBLA are listed in Tables I—III respectively.

In the series of copolymers of BLA and CNBLA, the specific rotations at 546 mμ are ca. −100 for the copolymers containing cyanoresidues of more than 30 mol.-% (C4101—C4041); the value sharply decreases to ca. −40 with a decrease in the cyanoresidue content, as Table I shows. (PBLA itself and the copolymers up to a 30 mol.-% cyanoresidue content were less soluble in DMF, and 0.25% solutions were used for the measurements instead of a 0.5% solution.) The results indicate that there is a transition.

A similar change are found in the b_0 value, just as in case of specific rotation. The b_0 values of

TABLE I. COPOLYMERS OF β-*p*-CYANOBENZYL-L-ASPARTATE WITH β-BENZYL-L-ASPARTATE IN DMF*

Polymer No.	Mol.-% of cyanobenzyl residues	b_0	$[\alpha]_{546}$	λ_c
C0014	0	−315	−40	283
C4011	10.0	−307	−26	292
C4021	20.0	−276	−58	252
C4031	30.0	−422	−97	249
C4041	39.9	−533	−107	251
C4051	50.0	−568	−115	247
C4061	60.0	−548	−110	249
C4071	76.6	−580	−109	248
C4081	80.0	−490	−99	249
C4091	89.9	−496	−100	250
C4101	100	−483	−105	251

* At 30°C; the concentration was 0.5% w/v for C4041-C4101, and 0.25% w/v for the others.

10) L. C. Jones, Jr., and L. W. Taylor, *Anal. Chem.*, **27**, 235 (1955).
11) J. A. Schellman and C. Schellman, "The Proteins," II, Ed. by H. Neurath, Academic Press, New York (1964), p. 84; A. Moscowitz, "Optical Rotatory Dispersion," Ed. by C. Djerassi, McGraw-Hill, New York (1960), p. 150.
12) W. Moffitt and A. Moscowitz, *J. Chem. Phys.*, **30**, 648 (1959).
13) R. H. Karlson, K. S. Norland, G. D. Fasman and E. R. Blout, *J. Am. Chem. Soc.*, **82**, 2268 (1960).
14) E. M. Bradbury, A. R. Downie, A. Elliott and W. E. Hanby, *Proc. Roy. Soc.*, **A259**, 110 (1960).

−480——580 for the copolymers (C4101—C4041) become sharply less (ca. −300) for the rest of the copolymers (C4021—C0014). As has been reported in the previous paper,[2] the b_0 value of PBLA in a chloroform solution was +659 (left-handed helix), whereas the value of PClBLA or PMeBLA was −680 (right-handed helix). Karlson et al. have shown that the b_0 value of ca. −250 is attributable to the residual contribution for PBLA in a random chain.[13] If this residual contribution exists in the left- and right-handed helical conformations of poly-L-aspartate esters, the b_0 values should differ not only in sign but also in magnitude according to the sense of the helix. The small difference in b_0 value between the above-mentioned left- and right-handed poly-L-aspartate esters leads to the conclusion that the residual contribution to the b_0 value is small for these polypeptides in a helical solvent like chloroform. Therefore, the b_0 value of ca. −660 can possibly be expected for poly-L-aspartate esters in a DMF solution if they exist in the right-handed helix.

On the other hand, the b_0 values of PBLA were observed to be −315 and −280 in DMF and DCA solutions respectively. The similarity in the b_0 values of the two solvents suggests that PBLA exists essentially in a random coil in a DMF solution because DCA has been revealed as a random coil solvent for PBLA by Karlson et al.[13] This fact seems to be an exception for PBLA, because DMF is usually considered to be a helix-promoting solvent.

As for λ_c values observed for this series of copolymers in a DMF solution, no sharp change in λ_c was found as the molar content of the cyano residue varied. λ_c values of 251 and 285 were observed for PCNBLA and PBLA respectively, both in a DMF solution. These values are ordinally correlated with the right-handed helix,[15] since the constant, λ_c, usually has a value of 210 or less for the random-coil form (for poly-γ-benzyl-L-glutamate[16] and poly-γ-methyl-L-glutamate[17] in a DCA solution, 180 and 187 were reported as the respective λ_c values). The plot for λ_c of PBLA in a DCA solution was nonlinear, but it could roughly be estimated to be 280—310. Considering that both values of b_0 and λ_c obtained for PBLA in a DMF solution coincide with those for a DCA solution, it may be deduced that these unusually high values should be correlated with a random coil form. Another example of anomaly is found for poly-L-tyrosine (λ_c=330) in its coiled form.[18] Thus, both λ_c and b_0 strongly suggest that PBLA exists in a random form in a DMF solution.

On the other hand, the b_0 values of −580——480 observed for the copolymers of BLA and CNBLA containing cyano residues more than 30 mol.-% in a DMF solution are somewhat smaller than the value for PClBLA or PMeBLA in a chloroform solution, but considerably larger than the value for PBLA in a DMF solution. The evidence that some copolymer in a DMF solution is in a right-handed helix may be derived from the fact that a sharp change in b_0 value from ca. −600 to ca. +600 was found for a copoly-L-aspartate ester (BLA-MeBLA 1 : 1) in chloroform-DMF solutions, as will be described later. Consequently, the b_0 values of −580——480 indicate that the copolymers are mainly in a right-handed helix, and possibly partially in a random coil form also. The nonlinear change in b_0 and $[\alpha]_{546}$ values (Table I) observed for a series of copolymers of BLA and CNBLA in DMF solution reflect a transition from a right-handed helix to a random-coil form, a transition which occurs as the molar content of the cyano residue is decreased. There is a possibility that the transition also affects the solubilities of the copolymers in DMF.

The results of the ORD measurements of the copolymers of BLA with ClBLA and with MeBLA are shown in Tables II and III. For these series the results are essentially the same as with a series of copolymers of BLA and CNBLA; PClBLA and PMeBLA themselves exist mainly in a right-handed helix, and in the case of copolymers with BLA transitions, from a right-handed helix to a random-coil form, were found at 15—30 and 30—40 mol.-% of chloro and methyl residue contents respectively.

The above finding that poly-β-(*p*-substituted benzyl)-L-aspartates exist in a right-handed helix in a DMF solution was confirmed by another piece of evidence that PClBLA showed a helix-to-coil transition in a DMF-DCA solvent system (as is shown in Fig. 11). When DCA was added to the PClBLA solution in DMF up to a 24% v/v of DCA,

Table II. Copolymers of β-*p*-chlorobenzyl-L-aspartate with β-benzyl-L-aspartate in DMF*

Polymer No.	Mol.-% of chlorobenzyl residues	b_0	$[\alpha]_{546}$	λ_c
C1021	15.1	−299	−60	258
C1031	30.0	−489	−91	259
C1041	40.0	−553	−103	258
C1051	49.9	−534	−103	258
C1061	60.0	−572	−111	257
C1071	70.1	−569	−117	258
C1081	79.9	−562	−122	257
C1091	90.0	−609	−122	260
C1101	100	−554	−110	253

* At 27.5°C; the concentration was 0.5% w/v except C1021 (0.25% w/v).

15) Ref. 11 (The Proteins), p. 78.
16) J. T. Yang and P. Doty, *J. Am. Chem. Soc.*, **79**, 761 (1957).
17) M. Goodman, E. E. Schmitt, I. Listowsky, F. Boardman, I. G. Rosen and M. A. Stake, "Polyamino Acids, Polypeptides and Proteins," The University of Wisconsin Press, Wisconsin (1962), p. 195.
18) J. D. Coombes, E. Katchalski and P. Doty, *Nature*, **185**, 534 (1960).

TABLE III. COPOLYMERS OF β-*p*-METHYLBENZYL-L-ASPARTATE WITH β-BENZYL-L-ASPARTATE IN DMF*

Polymer No.	Mol.-% of methylbenzyl residues	b_0	$[\alpha]_{546}$	λ_c
C3011**	9.9	—	—	—
C3021	19.8	−266	−53	253
C3031	29.9	−298	−80	241
C3041	39.9	−496	−110	251
C3051	49.9	−532	−105	250
C3061	59.9	−525	−111	248
C3071	70.0	−576	−120	250
C3081	80.0	−614	−123	250
C3091	90.1	−544	−118	251
C3101	100	−491	−111	251

* At 30°C; the concentration was 0.5% w/v for C3051-C3101, and 0.25% w/v for the others.
** Not observed because of its poor solubility in DMF.

the solution became turbid; the further addition of DCA caused the precipitation of PClBLA. The same phenomenon occurred in the reversed procedure when DMF was added to a PClBLA solution in DCA up to a 70% v/v of DMF. The small magnitude of the observed optical rotation of PClBLA in DMF or DCA solutions resulted in the somewhat scattered b_0 plot of Fig. 11. However, the nonlinear change in the b_0 value in Fig. 11 evidently indicates that a helix-to-coil transition takes place as the DCA content in DMF increases.

Finally, a clear-cut transition from the left- to the right-handed helix should be mentioned for a copoly-BLA: MeBLA (molar ratio, 1 : 1). This

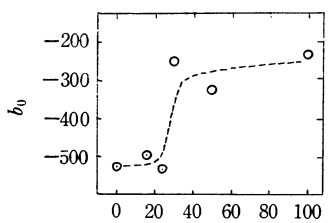

Fig. 11. b_0 Values of PClBLA versus solvent composition (DMF-DCA).

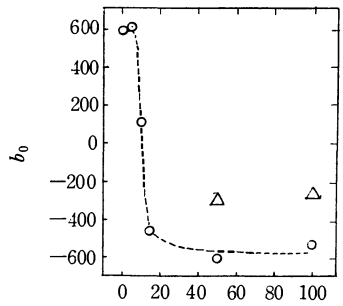

Fig. 12. b_0 Values of the copolymer of BLA with MeBLA containing 50 mole per cent methyl residues versus solvent composition (○ chloroform-DMF; △ DMF-DCA).

copolypeptide chain takes either the left-handed helix in a chloroform solution or the right-handed helix in a DMF solution (b_0 value; +602 in $CHCl_3$, −532 in DMF). For this copolymer in chloroform-DMF solutions, the observed b_0 values as a function of the solvent composition are illustrated in Fig. 12. The sharp change in b_0 value from ca. +600 to ca. −600 obviously indicates that the transition from the left- to right-handed helix occurs at the mixing volume ratio, 90 : 10, of the chloroform-DMF solution. Therefore, it may also be expected that a transition from the right-handed helix conformation to a random-coil form can be observed in the DMF-DCA solvent system. Such experiments were, indeed, attempted, but unfortunately the transition was not observed because of the precipitation of the copolymer when DCA was added in about a 10% v/v ratio to its DMF solution.

The author wishes to express his gratitude to Professor Takehiko Shimanouchi, The University of Tokyo, for his encouragement. He is also indebted to Professor Kazutomo Imahori and Dr. Masaru Shiraki, The University of Tokyo, for their useful discussions. Moreover, he is grateful to Dr. Shinsuke Ose, Dr. Hideji Takamatsu, and Dr. Kiyoshi Nakamura of this laboratory for their encouragement and valuable discussions, and also to Mr. Satoshi Arakawa for his kind help in the experiments.

BULLETIN OF THE CHEMICAL SOCIETY OF JAPAN VOL. 39 2721—2723 (1966)

A New Method for the Phosphorylation of Alcohols by Means of Bromine and Dibenzylhydrogen Phosphite

By Teruaki MUKAIYAMA, Hajime KOUDA and Kyoko KODERA

Laboratory of Organic Chemistry, Tokyo Institute of Technology, Ookayama, Meguro-ku, Tokyo

(Received March 12, 1966)

Various alkyldihydrogen phosphates were obtained in good yields by reacting alcohols, dibenzylhydrogen phosphite, and bromine in the presence of triethylamine, followed by catalytic hydrogenation. When benzyl alcohol and diethyl phosphite were used in the above reaction, only the oxidation of the latter took place, giving diethylhydrogen phosphate in an excellent yield. These results suggest that the above phosphorylation of alcohol proceeds through a quaternary phosphonium salt, i. e., dibenzyloxyalkyloxyhydroxy phosphonium bromide, which is then converted into an alkylbenzylhydrogen phosphate. The effect of tertiary amines on this type of phosphorylation was also examined.

The reactions of various phosphorous compounds with monobromocyanoacetamide and benzylalcohol, and the phosphorylation of alcohols and phenols by means of dibenzyl phosphite (or phosphorous acid) and monobromocyanoacetamide, have been studied in detail.[1-5]

This paper will describe an improved synthesis of monoesters of phosphoric acid, a method in which bromine in the presence of triethylamine is employed as an oxidizing reagent in place of the monobromocyanoacetamide mentioned in the above experiments. In this phosphorylation, it was found that bromine was a more reactive and effective oxidizing reagent than monobromocyanoacetamide, which was prepared from bromine and cyanoacetamide. When bromine was added to a mixture of ethanol, dibenzyl phosphite, and triethylamine in benzene under ice cooling, triethylamine hydrobromide was immediately separated. After the triethylamine hydrobromide (98%) and benzene had been removed and the benzylbromide had been fractionated (97%), the residue, benzylethylhydrogen phosphate, was hydrogenated without further purification.

Thus ethyldihydrogen phosphate was obtained in a 81% yield as its anilinium salt.

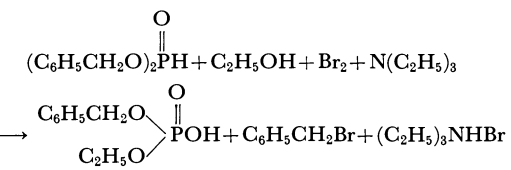

1) T. Hata and T. Mukaiyama, This Bulletin, **35**, 1106 (1962).
2) T. Hata and T. Mukaiyama, ibid., **37**, 103 (1964).
3) T. Mukaiyama, O. Mitsunobu and T. Obata, *J. Org. Chem.*, **30**, 101 (1965).
4) O. Mitsunobu, T. Obata and T. Mukaiyama, ibid., **30**, 1071 (1965).
5) T. Obata and T. Mukaiyama, This Bulletin, in press.

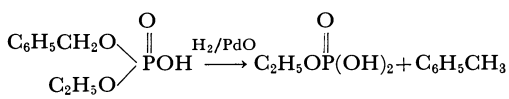

In a similar fashion, *n*-propyl, isopropyl, *n*-butyl or bornyldihydrogen phosphate was obtained as the anilinium salt in a 98, 78, 82, or 30% yield respectively. Bromine is more reactive than monobromocyanoacetamide, and the phosphorylation of alcohols takes place rapidly at a lower temperature, resulting in the formation of the desired phosphates in good yields without the use of excess alcohols.

It has been reported that the phosphorylation of phenol by the use of dibenzylphosphate and monobromocyanoacetamide gave a 79% yield of phenyldihydrogen phosphate as the anilinium salt. In the present experiment, however, the phosphorylation of phenol failed, and only bromophenols were obtained. Apparently, the isolation of phosphorous acid (as anilinium salt) in a 72% yield, after catalytic hydrogenation, indicates that dibenzyl phosphite did not participate in this reaction and that the preferential bromination of phenol occurred.

There are two possible pathways for the formation of monoalkyl phosphate by this procedure: (A) Initially a quaternary phosphonium salt (I) is formod. The intermediate (I) is then converted into another quaternary phosphonium salt (II), which is in turn decomposed to alkylbenzyl phosphate and benzyl bromide. (B) Initially the $(C_6H_5CH_2O)_2(HO)PBr_2$ compound is formed. This compound is then converted to benzylbromophosphonate, $(C_6H_5CH_2O)(HO)\overset{\overset{O}{\|}}{P}Br$, by the elimination of benzyl bromide. The bromophosphonate thus formed reacts with an alcohol in the presence of triethylamine to yield the corresponding alkylbenzyl phosphate.

TABLE I. THE PHOSPHORYLATION OF ALCOHOLS BY MEANS OF DIBENZYL PHOSPHITE AND BROMINE IN THE PRESENCE OF TRIETHYLAMINE

Alcohol	Product: Phosphate (anilinium salt) $ROP(=O)(OH)O^-$ R	Yield %	M. p. °C	Analyses, % Calcd. C	Calcd. H	Calcd. N	Found C	Found H	Found N	R_f [1]
C_2H_5OH	C_2H_5	81	157—158	43.83	6.39	6.56	42.62	7.32	6.48	0.37
n-C_3H_7OH	*n*-C_3H_7	98	152—153	46.35	6.87	6.01	45.58	7.05	6.01	0.43
i-C_3H_7OH	*i*-C_3H_7	78	165—166	46.35	6.87	6.01	46.07	6.78	6.05	0.41
n-C_4H_9OH	*n*-C_4H_9	82	140—142	48.44	7.48	5.69	48.58	7.29	5.67	0.53
$C_{10}H_{17}OH$ (borneol)	$C_{10}H_{17}$	30	195—196	58.89	7.62	4.29	58.91	7.93	4.39	0.63

1) solvent system ; *n*-propanol - concentrated ammonium hydroxide - water, 6 : 3 : 1.

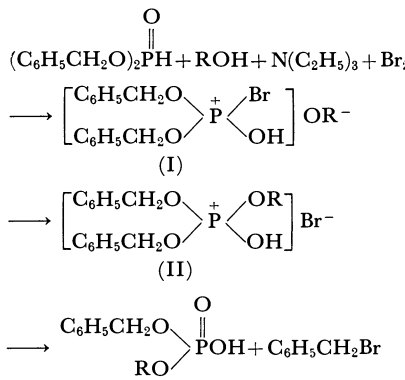

In order to differentiate the two alternatives, A and B, the reaction was tried using diethyl phosphite, benzyl alcohol, and bromine in the presence of triethylamine. In this case, since the ethyl group is not so easily eliminated as the benzyl group or hydrogen, it can be expected that diethyl phosphate will be formed according to the mechanism A, while diethylbenzyl phosphate will be formed according to the mechanism B. When the reaction was carried out at 0°C diethyl phosphate (68%), benzyl bromide (86%), and triethylamine hydrobromide (90%) were obtained. Therefore, it can be concluded that the key intermediate of the above-mentioned phosphorylation is the quaternary phosphonium salt (II), rather than benzylbromophosphonate.

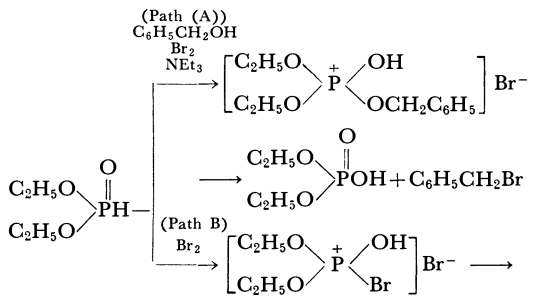

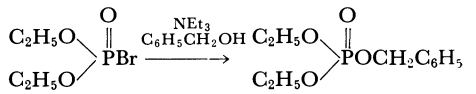

In order to examine the effect of tertiary amines on this type of phosphorylation, the reaction of diethyl phosphite, bromine, and benzyl alcohol in the presence of triethylenediamine, *N*-methylmorpholine, pyridine, or hexamethylenetetramine was attempted under identical conditions (see Table II). The results show that the yield of diethyl phosphate is influenced by the basicity of amine, increasing with an increase in the basicity.

Concerning the phosphorylation of alcohol with phosphorous compounds and halogen, it has been reported by Kirby[6] that 4-hydroxy but-2-enyl phosphate was obtained in a 86.5% yield by treating butene-1, 4-diol with iodine, and phosphorous acid in the presence of triethylamine. In the present experiment, however, it was found that the reaction of iodine, dibenzyl phosphite,

TABLE II. THE REACTION OF DIETHYL PHOSPHITE WITH BROMINE AND BENZYL ALCOHOL IN THE PRESENCE OF VARIOUS TERTIARY AMINES

Tertiary amines	Diethyl phosphite yield, %	Benzyl bromide yield, %	Tertiary amines hydrobromide yield, %
Triethylamine	68	86	90
Triethylenediamine	60	74	98[1]
N-Methylmorpholine	36	74	66
Pyridine	50	65	34
Hexamethylenetetramine	68	49	—[2]

1) The yield of the salt is shown as triethylenediamine dihydrobromide.
2) Pure hexamethylenetetramine monohydrobromide could not be isolated because of the contamination of *N*-benzylhexamethylenetetraminium bromide.

6) A. J. Kirby, *Chem. & Ind. (London)*, **1963**, 1877.

and alcohols in the presence of triethylamine resulted in the formation of a large quantity of unidentified red tarry products.

Experimental

Reagents.—The solvents, alcohols, and amines were purified and dried by ordinary procedures. Diethyl phosphite[7] and dibenzyl phosphite[8] were prepared according to the procedures described in the literature.

The Phosphorylation of Alcohols by Means of Bromine and Dibenzyl Phosphite in the Presence of Triethylamine.—A solution of bromine (1.60 g.; 0.01 mole) in 10 ml. of benzene was vigorously stirred, drop by drop, into a solution of dibenzyl phosphite (2.70 g.; 0.01 mole), ethanol (0.50 g.; 0.01 mole), and triethylamine (1.01 g.; 0.01 mole) in 10 ml. of benzene under ice cooling. After stirring had been continued for 1 hr., the solution was heated at 40—50°C for an additional hour. The solution was then allowed to stand overnight and filtered to remove triethylamine hydrobromide (1.77 g.; 98%; m. p. 246—247°C). From the filtrate, benzene and benzyl bromide (1.68 g.; 97%; b. p. 75—82°C/23 mmHg) were fractionated, and the residue was dissolved in 50 ml. of 99% ethanol. The solution was then hydrogenated over palladium oxide (100 mg.) at room temperature under atomospheric pressure. After the absorption of quantitative amount of hydrogen, the catalyst was removed by filtration and the solution was concentrated to about 10 ml. under reduced pressure. Aniline (1.9 g.) was then added, giving anilinium ethyldihydrogen phosphate (1.76 g.; 81%; m. p. 155—157°C). The anilinium salt was purified by chromatography (cellose-*n*-butanol - water) and recrystallized from acetonitrile-water, m. p. 157—158°C. A mixed-melting-point determination with an authentic sample was not depressed.

Found: C, 42.23; H, 7.83; N, 6.48. Calcd. for $C_8H_{14}NO_4P$: C, 43.84; H, 6.39; N, 6.56%.

Ethyl phosphate itself was also identified with an authentic specimen by paper chromatography (R_f 0.37) *n*-propyl, isopropyl, *n*-butyl, and bornyldihydrogen phosphates were obtained as their anilinium salts by the phosphorylation of *n*-propanol, isopropanol, *n*-butanol and borneol respectively (see Table I).

The Reaction of Diethyl Phosphite with Benzyl-Alcohol and Bromine in the Presence of Triethylamine.—A solution of bromine (1.60 g.; 0.01 mole) in 10 ml. of benzene was vigorously stirred, drop by drop, into a solution of diethyl phosphite (1.38 g.; 0.01 mole), benzyl alcohol (1.10 g.; 0.01 mole), and triethylamine (1.01 g.; 0.01 mole) in 10 ml. of benzene under ice cooling. The mixture was then allowed to stand overnight and filtered to remove triethylamine hydrobromide (1.63 g.; 90%). From the filtrate, benzyl bromide (1.48 g.; 86%; b. p. 75—85°C/23 mmHg) and diethyl phosphate (1.05 g.; 68%; b. p. 114—117°C/0.02 mmHg) were obtained by fractionation. Diethyl phosphate was identified with an authentic sample by paper chromatography (R_f 0.70; solvent system, *n*-propanol - concentrated ammonium hydroxide - water 6 : 3 : 1).

The Reaction of Diethyl Phosphite with Bromine and Benzyl Alcohol in the Presence of Various Tertiary Amines.—A solution of bromine (1.60 g., 0.01 mole) in 10 ml. of benzene was vigorously stirred, drop by drop, into a solution of diethyl phosphite (1.38 g.; 0.01 mole), benzyl alcohol (1.10 g.; 0.01 mole) and triethylenediamine (0.60 g.; 0.005 mole) under ice cooling. The mixture was then allowed to stand overnight and filtered to remove triethylenediamine dihydrobromide (1.24 g.; 98% d. p. 347—348°C). From the filtrate, benzyl bromide (1.29 g.; 74% b. p. 70—84°C/6 mmHg) and diethyl phosphate (0.92 g.; 60%; b. p. 118—121°C/0.03 mmHg) were obtained by fractionation.

Similarly, diethyl phosphate was obtained in yields ranging from 68% to 36% by treating alcohol with diethyl phosphite and benzyl alcohol and bromine in the presence of various amines, such as pyridine, *N*-methylmorpholine and hexamethylenetetramine. The results are listed in Table II.

The Reaction of Phenols and Dibenzyl Phosphite with Bromine in the Presence of Triethylamine.—A solution of bromine (1.60 g.; 0.01 mole) in 10ml. of benzene was vigorously stirred, drop by drop, into a solution of dibenzyl phosphite (2.70 g.; 0.01 mole), phenol (0.95 g.; 0.01 mole) and triethylamine (1.01 g.; 0.01 mole) in 10 ml. of benzene under ice cooling. The mixture was allowed to stand overnight and then filtered to remove triethylamine hydrobromide (1.73 g.; 95%). From the filtrate, *o*-bromophenol (34%; it was identified by gas chromatography) was removed by distillation under reduced pressure. The residue was dissolved in 30 ml. of 99% alcohol and hydrogenated over palladium oxide (100 mg.) at room temperature under atmospheric pressure. After the absorption of hydrogen had ceased, the catalyst was removed by filtration and the solvent was removed under reduced pressure. The residue was dissolved in 10 ml. of 95% alcohol, and aniline (1.9 g.) was added to the solution. The anilinium salt of phosphorous acid (1.25 g.; 71.5%; m. p. 170—173°C) was obtained; recrystallization from acetonitrile-water raised the melting point to 173—175°C. It was identified by paper chromatography (R_f 0.31; an authentic sample, R_f 0.30; solvent system, *n*-propanol - concentrated ammonium hydroxide - water, 6 : 3 : 1).

Found: C, 41.21; H, 6.26; N, 8.32. Calcd. for $C_6H_{10}NO_3P$: C, 41.14; H, 5.71; N, 8.32%.

Similarly, phosphorous acid (m. p. 172—173°C) resulted as anilinium salt in the case of the reaction of *p*-nitrophenol, and no depression was observed in a mixed-melting-point determination with an authentic sample.

The authors wish to express their hearty thanks to Dr. Oyo Mitsunobu and Mr. Teisuke Obata for their kind help during the course of this experiment, and to Miss Keiko Nakamura for her microanalysis.

7) H. McCombie, B. C. Saunders and G. J. Stacey, *J. Chem. Soc.*, **1945**, 380.
8) F. R. Atherton, H. T. Openshaw and A. R. Todd, ibid., **1945**, 382.

BULLETIN OF THE CHEMICAL SOCIETY OF JAPAN VOL. 39 2724—2728 (1966)

The Chemistry of Polyazanes. V. The Mechanism of the Oxidation of Benzalphenylhydrazone

By Hiroshi MINATO, Hiroo TATENO* and Hiroshi YOKOKAWA*

Department of Chemistry, International Christian University, Mitaka, Tokyo

(Received March 18, 1966)

Benzalphenylhydrazone was oxidized with amyl nitrite and with sodium hypoiodite, and the products of the oxidation were analyzed. The products identified were dibenzaldiphenyltetrazone, α-benzilosazone and unoxidized benzalphenylhydrazone. The mechanism of the oxidation was discussed.

The oxidation of benzalphenylhydrazone (I) was investigated by several chemists many years ago, but the mechanisms proposed were not convincing, nor were the products of the oxidation quantitatively studied.

Minunni[1] oxidized the benzalphenylhydrazone with mercuric oxide, and obtained the compound II, dibenzaldiphenyltetrazone.

$$\underset{\text{(I)}}{C_6H_5CH{=}NNHC_6H_5} \xrightarrow[\text{or AmONO or NaOI}]{\text{HgO}}$$

(m. p. 158°C)

$$\underset{\text{(II)}}{\begin{matrix}C_6H_5CH{=}NNC_6H_5\\ |\\ C_6H_5CH{=}NNC_6H_5\end{matrix}} \quad \text{and/or} \quad \underset{\text{(III)}}{\begin{matrix}C_6H_5C{=}NNHC_6H_5\\ |\\ C_6H_5N{-}N{=}CHC_6H_5\end{matrix}}$$

(m. p. 186°C) (m. p. 202°C)

$$\text{and/or} \quad \underset{\text{(IV}_\alpha\text{)}}{\begin{matrix}C_6H_5C{=}NNHC_6H_5\\ |\\ C_6H_5C{=}NNHC_6H_5\end{matrix}}$$

(m. p. 208°C)

Pechmann[2] oxidized the benzalphenylhydrazone with amyl nitrite and also obtained compound II.

Ingle and Mann[3] repeated Pechmann's experiment and obtained a compound melting at 202°C as well as the compound II melting at 186°C. Ingle and Mann assigned the structure III to this new compound. Then Ingle and Mann, using sodium hypoiodite as a new oxidizing agent, obtained a compound melting at 208°C as well as the compound II. They assigned the structure IV, benzilosazone, to this compound. However, the benzilosazone formed by mixing benzil and phenylhydrazine melts at 225°C. Therefore, they named the oxidation product (m. p. 208°C) as α-benzilosazone, and called the osazone (m. p. 225°C) formed from benzil and phenylhydrazone β-benzilosazone.

$$C_6H_5CH{=}NNHC_6H_5 \xrightarrow{\text{NaOI}} \text{(II)}$$

$$+ \quad \underset{\text{(IV}_\alpha\text{) m. p. 208°C}}{\begin{matrix}C_6H_5{-}C{=}N\diagdown NHC_6H_5\\ |\\ C_6H_5{-}C{=}N\diagup NHC_6H_5\end{matrix}}$$

$$\begin{matrix}C_6H_5{-}C{=}O\\ |\\ C_6H_5{-}C{=}O\end{matrix} + 2C_6H_5N_2H_3 \rightarrow$$

$$\underset{\text{(IV}_\beta\text{) (m. p. 225°C)}}{\begin{matrix}C_6H_5{-}C{=}N\diagup NHC_6H_5\\ |\\ C_6H_5{-}C{=}N\diagdown NHC_6H_5\end{matrix}}$$

However, they did not mention anything about the reason why IV_α, not IV_β, was produced by the oxidation of benzalphenylhydrazone.

This investigation was undertaken in order to find out: 1) the products of the oxidation of benzalphenylhydrazone by amyl nitrite and sodium hypoiodite; 2) whether or not compound III was present in the oxidized mixture, and 3) a plausible mechanism for the oxidation of benzalphenylhydrazone.

Experimental

Benzalphenylhydrazone (I).—By mixing phenylhydrazine and benzaldehyde in ethanol, yellow crystals of benzalphenylhydrazone were produced. After the recrystallization from ethanol, they melted at 155—156°C. (Literature: 156°C).

β-Benzilosazone (IV_β). — A hot ethanol solution containing 4.5 g. of phenylhydrazine hydrochloride (0.032 mol.) and 11.3 g. of sodium acetate (0.1486 mol.) was added to an ethanol solution containing 3 g. of benzil (0.0142 mol.). Bright yellow crystals were recrystallized from a 2 : 1 mixture of benzene and ethanol. M. p. 224—225°C (Literature: 225°C).

The Oxidation of Benzalphenylhydrazone (I) by Amyl Nitrite.—Five grams of benzalphenylhydrazone (I) (0.0255 mol.) was dissolved in 100 ml. of ether, and 6.0 ml. (0.0403 mol.) of amyl nitrite was

* American Chemical Society-Petroleum Research Fund Scholar.

1) G. Minunni, *Gazz.*, **22**, 228 (1892).

2) H. von Pechmann, *Ber.*, **26**, 1045 (1893).

3) H. Ingle and H. H. Mann, *J. Chem. Soc.*, **67**, 607 (1895).

added to this solution. The mixture was heated on a water-bath at 40—50°C for 6 hr. This solution was orange yellow at first, but on further heating it became darker, and yellow crystals precipitated. Brown nitrogen dioxide gas evolved for several hours.

The mixture was cooled, and the yellow crystals were filtered and washed with ethanol and ether; yield, 0.5690 g.; m. p. 184—186°C. This was identified as dibenzaldiphenyltetrazone (II) from its melting point and its infrared spectrum. The filtrate was evaporated to dryness to yield 5.114 g. of a yellowish-red residue. This residue was divided by repeated recrystallization from ether and ethanol into three fractions. The first fraction, weighing 0.0212 g., was identified as the benzalphenylhydrazone (I) by a study of its melting point and its infrared spectrum. The second fraction, weighing 3.990 g., was identified as α-benzilosazone, (IV_α) from a study of its melting point and its infrared spectrum. The third fraction, weighing 1.003 g., was an oily substance which was not identified.

The Oxidation of Benzalphenylhydrazone (I) by Iodine and Sodium Ethoxide.—Ten grams of benzalphenylhydrazone (I) (0.0510 mol.) in 200 ml. of ether were added to a solution of 1.59 g. of sodium (0.0650 mol.) in 20 ml. of ethanol. Then an ethereal solution of 6.57 g. (0.0510 mol.) of iodine was gradually stirred into this mixture over a 1.5 hr. period at room temperature. Then the solution was shaken with 50 ml. of a saturated solution of sodium sulfite in order to remove the last trace of iodine. Upon the evaporation of the ether, 10.773 g. of a brownish-red, somewhat resinous residue was obtained. This residue was divided into four fractions by repeated recrystallizations from ethanol, ethyl acetate, and/or benzene. The first three fractions were identified, by a study of infrared spectra and their melting points, as 0.296 g. of dibenzaldiphenyltetrazone (II) (0.71 mmol.), 4.943 g. of α-benzilosazone (IV_α) (12.67 mmol.), and 1.256 g. of benzalphenylhydrazone (I) (6.41 mmol.). It was not possible to identify the fourth fraction, which was viscous and resin-like.

An Attempt to Oxidize α-Methylphenylhydrazone of Benzaldehyde.—A solution of 1.008 g. of the α-methylphenylhydrazone of benzaldehyde (0.0048 mol.) in 12 ml. of diethyl ether and a solution of 0.15 g. of sodium (0.0066 mol.) in 2 ml. of ethanol was mixed; a solution of 1.67 g. of iodine (0.0066 mol.) in 10 ml. of ether was then stirred, drop by drop, into this mixture. The solution thus prepared was treated in a manner similar to that described above for the oxidation of benzalphenylhydrazone. The white crystals obtained was recrystallized from ethanol; yield, 0.892 g. The melting point (105—107°C) and the infrared spectrum of these crystals were identical with those of an authentic sample of the α-methylphenylhydrazone of benzaldehyde.

An Attempt to Reduce β-Benzilosazone.—To a mixture of 3.7 g. of β-benzilosazone (0.0095 mol.), 90 ml. of ethanol and 20 ml. of benzene, 82 g. of a 3% sodium amalgam (0.0107 mol.) was added, at one time, at 90°C, and in a carbon dioxide atmosphere; the mixture was then stirred for 9 hr. at 90°C. The yellow color of β-benzilosazone disappeared within 2 hr. of the stirring. After 9 hr., the reaction mixture became white and highly viscous. It was neutralized with a 10% hydrochloric acid solution to pH 7.2. The mercury was removed, and the solution was made strongly acid by the addition of concentrated hydrochloric acid. When the solution was concentrated by the evaporation of the solvents, a pale green solution was obtained. When diethyl ether was added to this solution, white crystals obtained; yield, 0.43 g.; m. p. 242—244°C. From the mother liquor, 0.30 g. of white crystals were obtained; m. p. 183—184°C. When the filtrate was further evaporated, a dark brown solution of a high viscosity remained.

Results and Discussion

The products of the oxidation of benzalphenylhydrazone (I) with amyl nitrite are summarized in Table I. Pechmann[2] oxidized benzalphenylhydrazone with amyl nitrite; he identified only the dibenzaldiphenyltetrazone (II), which was very little soluble in ethanol and was easily isolated. When Ingle and Mann[3] repeated Pechmann's experiment, they found a compound melting at 202°C as well as the tetrazone (II). They assigned the structure III to this compound, but the assignment was made without any convincing evidence. Our experiment did not indicate the presence of the compound III. Since our experiment did not account for 100% of the starting material, the production of the compound III was not completely excluded. However, our data seem to imply that the compound melting at 202°C was most likely an impure form of α-benzilosazone, which melted at 208°C.

Table I. Products of oxidation of benzalphenylhydrazone with amyl nitrite*

Product	g.	mmol.	mol./mol. I
$C_6H_5CH{=}NNHC_6H_5$	0.0212	0.108	0.004
$C_6H_5CH{=}N{-}N{-}C_6H_5$ | $C_6H_5CH{=}N{-}N{-}C_6H_5$	0.569	1.46	0.057
$C_6H_5C{=}N{-}NHC_6H_5$ | $C_6H_5C{=}N{-}NHC_6H_5$	3.990	10.2	0.400
	% Accounted for		92.8% of I

* Five grams of benzalphenylhydrazone (25.5 mmol.) was mixed with 40.3 mmol. of amyl nitrite in ethanol.

The products of the oxidation of benzalphenylhydrazone with sodium hypoiodite are summarized in Table II. Ingle and Mann[3] did the same oxidation; they reported the formation of II and IV_α, but did not give any quantitative data. A comparison of Tables I and II reveals that, in the case of the oxidation with sodium hypoiodite, the smaller percent of the starting material was accounted for and about 13% of I remained unoxidized, even though a stoichiometric amount of the oxidant was present. The residue, which was unidentifiable, was resinous. These facts seem to indicate that a part of the sodium hypoiodite

TABLE II. PRODUCTS OF OXIDATION OF BENZALPHENYLHYDRAZONE WITH IODINE AND SODIUM ETHOXIDE*

Product	g.	mmol.	mol./mol. I
$C_6H_5CH{=}NNHC_6H_5$	1.256	6.41	0.126
$C_6H_5CH{=}N{-}NC_6H_5$ | $C_6H_5CH{=}N{-}NC_6H_5$	0.296	0.710	0.014
$C_6H_5C{=}NNHC_6H_5$ | $C_6H_5C{=}NNHC_6H_5$	4.943	12.67	0.249
	% Accounted for		65.2% of I

* Ten grams of benzalphenylhydrazone (51.0 mmol.) in ether was mixed with an ethanolic solution of 1.59 g. of sodium (65.0 mmol.) and with an ethereal solution of 6.57 g. (51.0 mmol.) of iodine.

was used to oxidize some of the oxidation products to resinous substances. α-Benzilosazone possesses oxidizable hydrogens; a plausible scheme of this oxidation may be shown as follows:

$$\begin{array}{l} C_6H_5{-}C{=}N{-}NHC_6H_5 \\ \quad | \\ C_6H_5{-}C{=}N{-}NHC_6H_5 \\ \quad (IV_\alpha) \end{array} \xrightarrow{NaOI} \begin{array}{l} C_6H_5{-}C{=}N{-}N{-}C_6H_5 \\ \quad | \quad\quad | \\ C_6H_5{-}C{=}N{-}N{-}C_6H_5 \end{array}$$

$$+ \begin{array}{l} C_6H_5{-}C{=}N{-}NHC_6H_5 \\ \quad | \\ C_6H_5{-}C{=}N{-}N{-}C_6H_5 \\ \quad | \\ C_6H_5{-}C{=}N{-}N{-}C_6H_5 \\ \quad | \end{array} + \text{others}$$

As to the mechanism of the oxidation of benzalphenylhydrazone, neither Pechmann nor Ingle and Mann proposed anything. Minunni[1] proposed the following mechanism.

By the abstraction of a hydrogen atom attached to nitrogen, a radical, $C_6H_5CH{=}\dot{N}\dot{N}C_6H_5$ (A), is formed. This free radical, with a divalent nitrogen-atom, is unstable and rearranges to $C_6H_5\dot{C}{=}NNHC_6H_5$ (B) with a trivalent carbon atom.

$$\underset{(I)}{C_6H_5CH{=}NNHC_6H_5} \rightarrow \underset{(A)}{C_6H_5CH{=}\dot{N}\dot{N}C_6H_5} \rightarrow \underset{(B)}{C_6H_5\dot{C}{=}NNHC_6H_5}$$

The combination of A-A results in the tetrazone (II), while that of B-B results in the osazone (IV).

The mechanism proposed by Minunni seems to be unacceptable for two reasons. First, the radical B appears to be a more stable radical than the radical B. In the radical A, the odd electron is in resonance with the p-electrons of C=N and two benzene rings; hence, this radical is a rather well-stabilized radical. The radical B, on the other hand, is not so stable, since the odd electron is in resonance with the p-electrons of only one benzene ring. Therefore, it is unlikely that the radical A rearranges to the less stable radical B. Second, the combination of two B radicals should produce the thermodynamically more stable osazone, the β-form, not the α-form. In order, for the radical B to be stabilized, the p-orbital with the odd electron must be parallel with the p-orbitals of the benzene ring. When this rotation occurs, the radical becomes symmetrical, and the combination of B-B should yield the more stable β-osazone. For these two reasons, Minunni's mechanism seems to be unacceptable.

Sidgwick[4] explained this reaction by assuming the initial formation of two radicals; the radical A formed by the hydrogen-abstraction from the α-nitrogen of I, and the radical B formed by the hydrogen-abstraction from the α-carbon of I:

$$\underset{(A)}{C_6H_5CH{=}N{-}\dot{N}{-}C_6H_5} \leftarrow \underset{(I)}{C_6H_5CH{=}N{-}NHC_6H_5} \rightarrow \underset{(B)}{C_6H_5\dot{C}{=}NNHC_6H_5}$$

The combination of A-A will form II, while that of B-B will form IV. However, Sidgwick's explanation does not solve any of the difficulties mentioned above in connection with Minunni's mechanism. Since the radical A appears to be much more stable than the radical b, the hydrogen abstraction most likely will take place on the α-nitrogen, not on the α-carbon. The combination of two B radicals should yield the β-benzilosazone, but the osazone isolated by the experiment was the α-form.

We wish to propose and describe a plausible mechanism for the oxidation of benzalphenylhydrazone.

The abstraction of hydrogen takes place on the α-nitrogen atom of I and yields the radical A, which is stabilized by the resonance expressed by the limiting forms, A and C.

$$C_6H_5CH{=}NNHC_6H_5 \rightarrow [\underset{(A)}{C_6H_5CH{=}N{-}\dot{N}{-}C_6H_5} \leftrightarrow \underset{(C)}{C_6H_5\dot{C}H{-}N{=}N{-}C_6H_5}]$$

The combination of A-A results in the formation of II. The combination of C-C will yield the compound IV', which is then expected to tautomerize to IV_α:

$$(C) + (C) \rightarrow \underset{(IV')}{\begin{array}{l} C_6H_5CH{-}N{=}N{-}C_6H_5 \\ \quad | \\ C_6H_5CH{-}N{=}N{-}C_6H_5 \end{array}} \rightarrow \underset{(IV_\alpha)}{\begin{array}{l} C_6H_5{-}C{=}N\diagdown NHC_6H_5 \\ \quad | \\ C_6H_5{-}C{=}N\diagup NHC_6H_5 \end{array}}$$

The combination of A-A is a combination of electronegative nitrogen atoms, which must be less favorable than the combination of C-C. In the actual experiments, the benzilosazone (IV) was

4) N. V. Sidgwick, "Organic Chemistry of Nitrogen," Clarendon Press, Oxford (1937), p. 464.

found in a much greater quantity than the tetrazone (II).

In order to defend this mechanism, the following three conditions must be satisfied:

(1) The trivalent carbon radical B, $C_6H_5\dot{C}=NNHC_6H_5$, is not formed from the oxidation of I.

(2) The azo form IV′ should tautomerize to the hydrazone form IV under the experimental conditions.

(3) The tautomerism should yield the α-osazone, which is less stable than the β-osazone.

In an attempt to establish that the hydrogen atom of the α-carbon is not abstracted, the α-methylphenylhydrazone of benzaldehyde was prepared and was subjected to oxidation with sodium hypoiodite. After crystallization and washing, 90% of the α-methylphenylhydrazone was isolated as crystals; this fact indicates that the hydrogen atom on the α-carbon atom of the benzalphenylhydrazone will not be abstracted either.

The problem of the tautomerism from the azo form IV′ to the hydrazone form IV is rather complex. In 1961, Zollinger[5] wrote that "it has always been found that the hydrazone is the more stable species. Since the rate of rearrangement of the azo into the hydrazone form is in general very low, azo compounds can readily be isolated in spite of this. The reaction is favored by solvents able to provide protons and is catalyzed by acids and bases, but no exact investigations have yet been undertaken."

Brough et al.[6] prepared 1′-(*p*-chlorophenyl)-benzeneazomethane by the oxidation of the corresponding hydrazo-compound; they found that it was fairly stable at 0°C, but isomerized to the hydrazone in methanol at room temperature.

$$p\text{-Cl-}C_6H_4\text{-}CH_2\text{-N=N-}C_6H_5 \xrightarrow{CH_3OH} p\text{-Cl-}C_6H_5\text{-CH=N-NH-}C_6H_5$$

However, 1′,1′-diphenylbenzeneazomethane, C_6H_5-N=N-$CH(C_6H_5)_2$, is rather stable and melts at 73—75°C. Perhaps the compound IV′ resembles 1′-(*p*-chlorophenyl)-benzeneazomethane rather than 1′, 1′-diphenylbenzeneazomethane, and perhaps the compound IV′ easily isomerizes to IV_α.

In order to ascertain what actually happens, an attempt was made to reduce IV_β so as to prepare IV′. When the β-benzilosazone IV_β was subjected to reduction with an excess amount of sodium amalgam or lithium aluminum hydride in an inert atmosphere, a mixture of several compounds always resulted, and it was not possible to prepare the compound IV′. Although the attempt to ascertain the easy isomerism from IV′ to IV_α failed, it seems likely that the isomerization proceeds under experimental conditions which are either basic (sodium hypoiodite) or acidic (amyl nitrite).

Now the problem of the tautomerism to the α-osazone, not to the β-osazone, should be dealt with. When the azo form IV′ tautomerizes to the osazone, two types of transition state seem possible, as is illustrated in Fig. 1. The IV′ form may tautomerize to IV either by way of the transition state of a four-membered ring, as is shown in Fig. 1 (a), or by way of the transition state of a five-membered ring, as is shown in Fig. 1(b). The transition state of Fig. 1(b) seems more favorable than that of Fig. 1(a), since the nitrogen atom and the hydrogen atom are more closely situated in Fig. 1(b) than in Fig. 1(a). If the compound IV′ tautomerizes to IV by way of the five-membered transition state, the osazone formed must be the α-osazone. When a compound like 1′, 1′-diphenylbenzeneazomethane is to tautomerize to a hydrazone, it must go through a four-membered transition state. It is highly likely that the rate of the tautomerization of IV′ to IV_α is much faster than that of 1′, 1′-diphenylbenzeneazomethane.

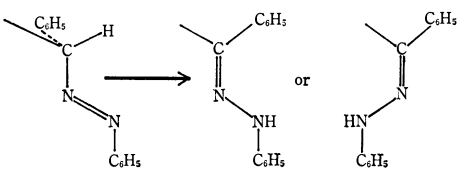

Fig. 1(a)

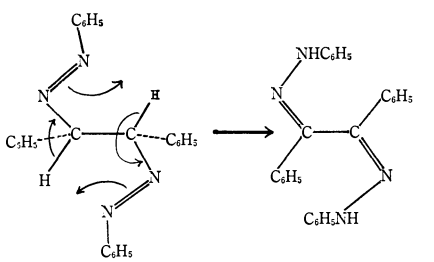

Fig. 1(b)

Thus, the mechanism proposed above as plausible seems to account for the available experimental data fairly well.

When Milligan and Minor[7] oxidized benzalphenylhydrazone with ammoniacal silver nitrate in dimethylformamide, they isolated two products, one melting at 201°C, and the other, at 187°C. They assigned the structure III to the former and the IV′ structure to the latter. Their assignment is surprising, especially in view of the existing experimental data.

5) H. Zollinger, "Azo and Diazo Chemistry," Interscience Publishers, New York (1961), p. 327.

6) J. N. Brough, B. Lytge and P. Waterhouse, *J. Chem. Soc.*, **1954**, 4069.

7) T. W. Milligan and B. C. Minor, *J. Org. Chem.*, **27**, 4663 (1962).

The compound melting at 186°C was obtained from the oxidation of benzalphenylhydrazone with mercuric oxide,[1] amyl nitrite,[2,3] or sodium hypoiodite.[3] Minunni,[1] Pechmann,[2] and Ingle and Mann[3] assigned the structure II to this compound. Both Pechmann[2] and Ingle and Mann[3] reduced the compound melting at 186°C and obtained benzalphenylhydrazone, I. This fact is consistent with the structure II, but not with the structure IV', which was suggested by Milligan and Minor.

The compound melting at 186°C is "very insoluble in almost all solvents, and dissolves but sparingly in hot benzene and chloroform."[3] This solubility characteristic seems to go better with the structure II than with the structure IV'. Such azo compounds as $C_5H_5N{=}NCH(C_6H_5)_2$ and $(C_6H_5)_2CHN{=}NCH(C_6H_5)_2$ very readily dissolve in benzene and chloroform, and even in ligroin. It seems unlikely that the compound possessing the structure IV' is very insoluble in almost all solvents.

The only data which seems to favor the structure IV' is its NMR spectrum, which shows the aromatic multiplet at −436 c. p. s. and another signal at −343 c. p. s. (4.28 τ), the latter "corresponding in position and intensity to that expected for two protons on benzylic carbon atoms substituted by azo-unsaturation."[7] However, the compound melting at 186°C was only sparingly soluble in hot chloroform, and the NMR spectrum measured in deuteriochloroform may not be too reliable. It was not possible to prepare a 0.001 M solution of the compound in chloroform due to its small solubility. The reduction with phenylhydrazine and the solubility of the compound melting at 186°C seem to be more persuasive than the NMR spectrum.

The compound melting at 208°C was converted to β-benzilosazone (IV_β) (m. p. 225°C) by heating it with phenylhydrazine, or by heating it with ethyl succinate.[3] The compound yielded benzil and triphenylosotriazole, 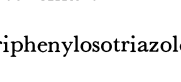 , upon reaction with sulfuric acid and water. β-Benzilsazone yielded only benzil and no triphenylosotriazole upon reaction with sulfuric acid and water. On the basis of these findings, Ingle and Mann[3] assigned the structure IV_α to the compound melting at 208°C. Its infrared spectrum was very much similar to, but not superimposable upon, that of β-benzilosazone.

The compound melting at 202°C was assigned the structure III by Ingle and Mann[3] and by Milligan and Minor[7], but without any convincing evibence. Its ultraviolet spectrum ($\lambda_{max}^{CHCl_3}$ 298, 335 mμ: ε, 19400, 37000) and infrared spectrum (NH at 3330 cm^{-1} and ArC=N– at 1590, 1543, 1485 cm^{-1})[7] were very similar to those of α-benzilosazone melting at 208°C ($\lambda_{max}^{CHCl_3}$ 295 (18300), 340 mμ (33200); 3330, 1590, 1543, 1485 cm^{-1}). It seems that the compound melting at 202°C may be the impure α-benzilosazone (m. p. 208°C).

Grateful acknowledgment is made to the donors of The Petroleum Research Fund, administered by the American Chemical Society, for support of this research.

BULLETIN OF THE CHEMICAL SOCIETY OF JAPAN VOL. 39 2728—2733 (1966)

Syntheses of L-Sorbosylthymines and Related Compounds[1)]

By Kanji TOKUYAMA and Mitsuru KATSUHARA

Shionogi Research Laboratory, Shionogi & Co., Ltd., Fukushima-ku, Osaka

(Received July 11, 1966)

1, 3, 4, 5-Tetra-*O*-acetylsorbopyranosylureas were prepared from sorbopyranosyl chloride via 1, 3, 4, 5-tetra-*O*-acetylsorbopyranosylisocyanates. 1-Ureido- and 6-ureidosorbofuranoses were obtained from the corresponding aminosorboses. The transformations of the ureas thus obtained into *N*-(sorbose)thymines were achieved, although with difficulty, by the direct condensation of halogeno- or tosylsorboses with metal salts of thymine.

A variety of nucleosides have received considerable interest in connection with their potential biochemical activities. However, synthetic studies have dealt almost exclusively with the preparation of aldose derivatives, such as ribosylpyrimidines or glucosylpurines. This paper will discuss the introduction of the thymine group into sorboses at the C-1, C-2, and C-6 positions through urea derivatives.

1) Sorboses. Part VIII. For Part VII, see K. Tokuyama, M. Kiyokawa and M. Katsuhara, *J. Org. Chem.*, **30**, 4057 (1965).

Mercuric salts of thymine or theophylline in inert solvents are generally employed for nucleoside synthesis.[2-5] The condensation of the salts with 1, 3, 4, 5-tetra-*O*-acetyl-α-L-sorbopyranosyl chloride (I)[6] in xylene did not give any of the expected nucleoside; instead, a colorless sirup with no chlorine and nitrogen was obtained. It showed a positive resorcin test (Seliwanoff test),[7] a strong band due to an enol acetate, a weak band due to a double bond in the infrared, and an ultraviolet maximum at 210 mμ. These facts suggested that the structure of the product was 2-deoxy-1, 3, 4, 5-tetra-*O*-acetyl-L-sorbopyranos-2, 3-ene (II) or -1, 2-ene. The NMR spectrum, showing a singlet (two protons) at τ 5.24 due to the $-CH_2-$ at the C-1 position and no signals at a lower field, was consistent with the structure of II. The condensation reaction in such a polar solvent as *N*, *N*-dimethylformamide (DMF) or nitromethane in the presence of mercuric cyanide[8,9] gave the same results. The formation of II was observed even in the absence of the salt to a small extent. Therefore, this type of reaction was thought to be not suitable for sorbose nucleoside synthesis.

Another promising route to sorbosylthymine utilizes urea derivatives[10-14] (for the scheme, see Charts 1 and 2). Thus I was treated with silver isocyanate in anhydrous toluene under heating. The sirup produced showed a strong band at 2245 cm^{-1} characteristic of the N=C=O stretching vibration.[15] Thin-layer chromatography revealed that the sirup was a mixture of the major α, β-anomers (III and IV) and the minor II.

The ammonolysis of the sirup mixture of the III and IV isocyanates was performed by adding methanolic ammonia at 0°C; the subsequent fractional recrystallization furnished *N*-(1, 3, 4, 5-tetra-*O*-acetyl-α-L-sorbopyranosyl)urea (V) and the β-anomer of V (VI). The ureas, V and VI, gave satisfactory analyses and revealed absorptions at 1659 and 1530 cm^{-1} characteristic of the -CO-NH- group. From the optical rotations, V was determined to have the α-configuration, and VI, the β-configuration.

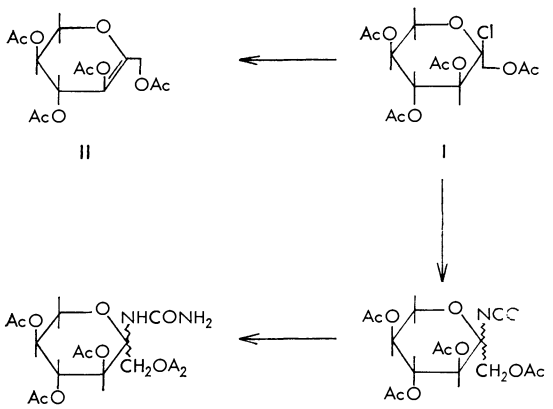

Chart 1

The α-urea V was condensed with 2-methyl-3-methoxyacryloyl chloride (XI) in pyridine.[12,16] After the reaction product had been purified by silica gel-column chromatography, 1-(1, 3, 4, 5-tetra-*O*-acetyl-α-L-sorbopyranosyl)-3-(2-methyl-3-methoxyacryloyl)urea (VII) was obtained as a colorless powder. This showed an ultraviolet absorption at 255 mμ. The ring closure and simultaneous deacetylation of this compound by

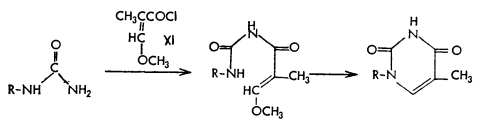

V ($R=R_1$) VII ($R=R_1$) VIII ($R=R_1'$)
VI ($R=R_2$) IX ($R=R_2$) X ($R=R_2'$)
XXIII ($R=R_3$) XXV ($R=R_3$) XXVII ($R=R_3$)
XXIV ($R=R_4$) XXVI ($R=R_4$) XXVIII ($R=R_4$)

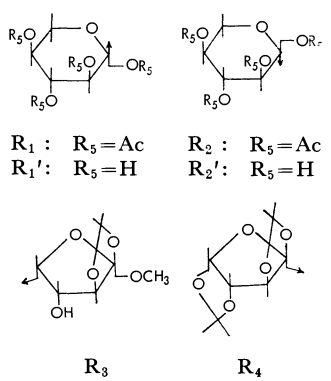

Chart 2

2) N. Yung and J. J. Fox, *Methods Carbohydrate Chem.*, **2**, 108 (1963).
3) E. Fischer and B. Helferich, *Ber.*, **47**, 210 (1914).
4) J. Daroll and B. A. Lowky, *J. Am. Chem. Soc.*, **73**, 1650 (1951).
5) H. M. Kissman, C. Pidacks and B. R. Baker, ibid., **77**, 18 (1955).
6) H. H. Schlubach and G. Graefe, *Ann.*, **532**, 211 (1937).
7) A. Atake and N. Seno, "Jikken Kagaku Koza," Bd. 23, Ed. by Chem. Soc. of Japan, Publisher, Maruzen, Tokyo (1957), p. 374.
8) B. Coxon and H. G. Fletcher, *J. Am. Chem. Soc.*, **85**, 2637 (1963).
9) N. Yamaoka, K. Aso and K. Matsuda, *J. Org. Chem.*, **30**, 149 (1965).
10) M. N. Schrool, *Rec. Trav. Chim.*, **22**, 1 (1903).
11) A. Hynd, *Biochem. J.*, **20**, 195 (1926).
12) B. Helferich and W. Kosche, *Ber.*, **59**, 69 (1926).
13) T. Naito and T. Kawakami, *Chem. Pharm. Bull.*, **10**, 627 (1962).
14) T. Ukita, R. Hamada and M. Yoshida, ibid., **12**, 454 (1964).
15) H. Hoyer, *Chem. Ber.*, **89**, 2677 (1962).
16) T. Naito and M. Sano, *Chem. Pharm. Bull.*, **9**, 709 (1961).

treament with monomethylamine, followed by the purification of the reaction product by cellulose column chromatography, afforded a brown sirup (VIII). The sirup VIII showed analytical data corresponding to those of L-sorbosylthymine, a positive resorcin test, and the ultraviolet maximum at 303 mμ characteristic of thymine. Similarly, β-L-sorbopyranosylthymine (X), λ_{max}^{UV} 285 mμ, was prepared from the β-urea VI via 1-(1, 3, 4, 5-tetra-*O*-acetyl-β-L-sorbopyranosyl)-3-(2-methyl-3-methoxyacryloyl)urea (IX). The sorbopyranosylthymines thus obtained, VIII and X, were unstable; e. g., they released the thymine moiety upon mild acetylation.

The introduction of thymine into the C-1 and C-6 positions of L-sorbose was also studied. Previously we observed that the condensation of 1-*O*-tosyl-2, 3 : 4, 6-di-*O*-isopropylidene-α-L-sorbofuranose (XII) with 2-thiouracil in DMF gave *S*-substituted (XIII) and *O*, *S*-disubstituted thiouracil (XIV).[1] The analogous condensation of XII with the sodium salt of thymine was attempted. However, the product formed was 1-deoxy-1-dimethylamino-2, 3 : 4, 6-di-*O*-isopropylidene-α-L-sorbofuranose (XV), which was identified by comparison with an authentic sample prepared by the reaction of XII with dimethylamine. The formation of XV in this reaction is interesting, but we have no reasonable explanation for this finding at the present time. On the other hand, the treatment of XII with the sodium salt of theophylline in DMF gave the expected compound (XVI), which showed a band characteristic of theophylline in the infrared spectrum. Therefore, the introduction of the thymine group into the C-1 and C-6 positions of sorbose was carried out through ureidosorbose in a way similar to that used with VIII and X.

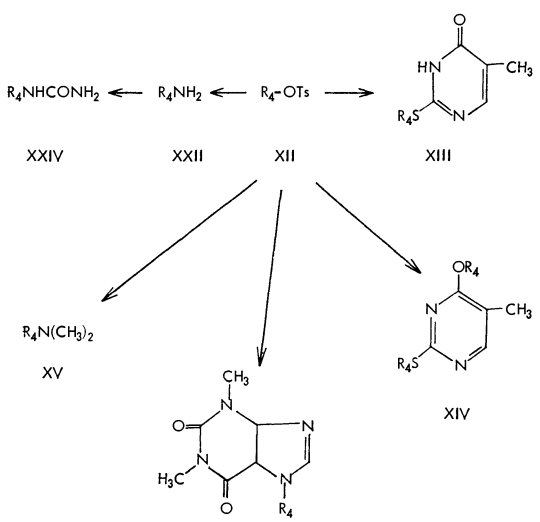

Chart 3

2, 3 : 4, 6-Di-*O*-isopropylidene-α-L-sorbofuranose (XVII)[17] was converted into 1-*O*-methyl-2, 3 : 4, 6-di-*O*-isopropylidene-α-L-sorbofuranose (XVIII) with methyl iodide in the presence of sodium ethoxide in liquid ammonia. In the methylation of XVII, methyl iodide and sodium alkoxide in liquid ammonia were more satisfactorilly used than dimethylsulfate in an alkaline medium[18] or methyl iodide and potassium in liquid ammonia and an inert solvent.[19] The partial deacetonation of XVIII gave a monoacetonated compound (XIX), which was then converted into 6-tosylate (XX) on tosylation under cooling. The heating of XX with liquid ammonia led to 1-*O*-methyl-6-deoxy-6-amino-2, 3-*O*-isopropylidene-α-L-sorbofuranose (XXI).

When XXI (or the 1-deoxy-1-amino-2, 3 : 4, 6-di-*O*-isopropylidene-α-L-sorbofuranose (XXII) previously reported[20]) in dilute alcohol was treated with potassium cyanate in the presence of one equivalent of acetic acid, the crystalline urea derivative XXIII (or XXIV), was obtained. This product XXIII (or XXIV) was then condensed with XI by a procedure similar to that used for V (see Chart 2); this produced an unstable intermediate XXV (or XXVI) which showed an ultraviolet absorption at 250 mμ. Without purification, XXV (or XXVI) was immediately treated with aqueous ammonia. There was thus isolated by thin-layer chromatography the desired thymine derivative XXVII (or XXVIII). The product XXVII (or XXVIII) gave analytical data corresponding to the structure and showed a positive resorcin test and the ultraviolet absorption at 270 mμ characteristic of thymine.

The thymine derivatives of L-sorbose obtained above, VIII, X, XXVII and XXVIII, were found to be unstable, and they were slowly converted into sorbose or aminosorboses at room temperature. The conversion was found to be more rapid in an aqueous solution.

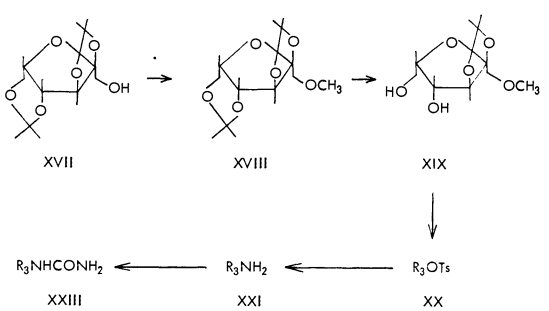

Chart 4

17) T. Reichstein, *Helv. Chim. Acta*, **17**, 311 (1934).
18) E. L. Hirst and E. Percival, *Methods Carbohydrate Chem.*, **2**, 145 (1963).
19) R. S. Tipson, ibid., **2**, 150 (1963).
20) K. Tokuyama, This Bulletin, **37**, 1133 (1964).

Experimental[21]

1, 3, 4, 5-Tetra-*O*-acetyl-*α*-L-sorbopyranosyl Chloride (I).—A mixture of 1, 3, 4, 5-tetra-*O*-acetyl-*α*-L-sorbopyranose (6 g.)[6,22] and aluminum chloride (15.5 g.) in chloroform (90 ml.) was stirred at room temperature for 1 hr. The precipitates were removed by filtration and washed with ether (400 ml.), and the washings were combined with the filtrate. The combined solution was then washed with cold water, cold aqueous sodium bicarbonate, and cold water successively. The dried solution was evaporated under reduced pressure to leave a yellow sirup which was purified by silica gel-column chromatography with benzene and ether (9 : 1 v/v). The recrystallization of the thus-purified sirup from ether and petroleum ether gave needles (1.8 g.); m. p. 62—64°C, $[\alpha]_D^{25}$ −83.2 (*c* 1.027, chloroform).[6]

Found: C, 45.85; H, 5.22; Cl, 9.67. Calcd. for $C_{14}H_{19}O_9Cl$: C, 45.92; H, 5.32; Cl, 9.23%.

The Reaction of Mercuric Salt of Thymine with I.—To a suspension of mercuric salt of thymine (2.1 g.)[2] in dry xylene (150 ml.), there was added a dry xylene solution (25 ml.) of I (1.8 g.). Traces of water were removed by azeotropic distillation with xylene (50 ml.). After it had been refluxed for 1.5 hr., the solution was concentrated to a sirup which showed, on thin-layer chromatography, no spot with a positive resorcin test and ultraviolet absroption. The purification of the sirup on an alumina column (neutral) (25 g.) with benzene gave a colorless sirup (II) (220 mg.); $[\alpha]_D^{22}$ +217.6 (*c* 1.032, chloroform).

Found: C, 51.06; H, 5.81. Calcd. for $C_{14}H_{18}O_9$: C, 50.91; H, 5.49%.

1, 3, 4, 5-Tetra-*O*-acetyl-L-sorbopyranosyl Isocyanate (III and IV).—A solution of I (0.6 g.) in anhydrous toluene (6 ml.) was added to a suspension of silver isocyanate (0.45 g.)[23] in anhydrous xylene (10 ml.), and the mixture was heated at 100—110°C for 2.5 hr. under stirring. After it had been cooled, the precipitates (silver chloride and unreacted silver isocyanate) formed were removed by filtration and washed with toluene, and the washings were combined with the filtrate. The combined solution was then concentrated to about 1—2 ml. under reduced pressure, and to the residue there was added 10—20 ml. of petroleum ether (20 ml.). The upper organic layer was separated by decantation from a small amount of the yellow sirup precipitated. A yellow sirup (0.54 g.) was obtained on the removal of the solvent. IR cm^{-1} $\nu_{N=C=O}$ 2245 (liquid film). The thin-layer chromatogram (silica gel) showed two major spots (III and IV) and one minor spot (II).

***N*-(1, 3, 4, 5-Tetra-*O*-acetyl-L-sorbopyranosyl)urea (V and VI).**—Silver chloride was removed by filtration from a reaction mixture of I (9.4 g.) and silver isocyanate (7.2 g.) by a similar procedure to those used above for III and IV. When ammonia was bubbled into the filtrate under stirring at 0°C, crystals appeared immediately. After 5 min., the crystals (5.98 g.) were filtered, washed with ether, and dissolved in chloroform and methanol (20 : 1 v/v); petroleum ether was then added to the solution until crystals appeared again. The recrystallization of the resultant crystals from methanol gave colorless needles (VI) (1.53 g.); m. p. 194—195°C, $[\alpha]_D^{24.5}$ +65.1 (*c* 1.049, methanol).

Found: C, 46.05; H, 5.85; N, 7.40. Calcd. for $C_{15}H_{22}N_2O_{10}$: C, 46.15; H, 5.68; N, 7.18%.

From the mother liquor (chloroform-methanol-petroleum ether), the *α*-anomer (V) (1.49 g.) was obtained; this was recrystallized from methanol, m. p. 217—219°C, $[\alpha]_D^{23.5}$ −34.4 (*c* 0.973, chloroform).

Found: C, 46.35; H, 5.79; N, 7.34. Calcd. for $C_{15}H_{22}N_2O_{10}$: C, 46.15; H, 5.68; N, 7.18%.

1-(1, 3, 4, 5-Tetra-*O*-acetyl-*α*-L-sorbopyranosyl)-3-(2-methyl-3-methoxyacryloyl)urea (VII). — To a suspension of V (2.0 g.) in chloroform (20 ml.), XI (1.5 g.)[24] and pyridine (0.8 ml.) were added. The mixture was stirred for 2 days at room temperature. After the precipitates had been removed by filtration, the solvent was removed under reduced pressure and the residue was dissolved in chloroform (20 ml.), and washed with 5% sodium bisulfite, 5% sodium bicarbonate, and water successively. The dried solution was then evaporated under reduced pressure to leave a yellow sirup. This sirup was washed with petroleum ether. A plae yellow powder (2.05 g.) was thus obtained. λ_{max}^{UV} 255 mμ (ethanol).

Found: C, 49.39; H, 5.85; N, 5.66. Calcd. for $C_{20}H_{28}N_2O_{12}$: C, 49.18; H, 5.78; N, 5.74%.

***N*-(*α*-L-Sorbopyranosyl)thymine (VIII).** — To a solution of VII (2 g.) in hot ethanol (10 ml.), 40% aqueous monomethylamine (12 ml.) was added in several portions within 4 hr. at 80—85°C. The mixture was concentrated under reduced pressure, and the residue was washed with chloroform, dissolved in ethanol (8 ml.), and subjected to column chromatography on cellulose (2.4×52 cm.). The column was eluted with *n*-butanol-ethanol-water (4-1-5, v/v), and 5 ml. portion of each of the effluents was taken. The fractions (tubes Nos. 43—47) which showed ultraviolet absorption were combined, and the solvent was evaporated to give a hygroscopic brown sirup (40 mg.). $[\alpha]_D^{23}$ −25.1 (*c* 0.987, water), λ_{max}^{UV} 303 mμ (water).

Found: C, 42.70; H, 6.42; N, 9.09. Calcd. for $C_{11}H_{16}N_2O_7 \cdot H_2O$: C, 42.99; H, 6.23; N, 9.12%.

1-(1, 3, 4, 5-Tetra-*O*-acetyl-*β*-L-sorbopyranosyl)-3-(2-methyl-3-methoxyacryloyl)urea (IX). — A suspension of VI (1.3 g.) in chloroform (12 ml.) was mixed with XI (1.0 g.) and pyridine (0.6 ml.), and then treated by a procedure similar to that used for VII. A pale yellow powder (1.33 g.) was obtained; λ_{max}^{UV} 255 mμ (ethanol).

Found: C, 49.13; H, 5.98; N, 5.42. Calcd. for $C_{20}H_{28}N_2O_{12}$: C, 49.18; H, 5.78; N, 5.74%.

***N*-(*β*-L-Sorbopyranosyl)thymine (X).**—IX (1.33 g.) was treated by a procedure similar to that used for VIII. Crude X was then purified from this by cellulose-column chromatography using *n*-butanol-ethanol-water in a way similar to that described above. The fractions (tubes Nos. 45—46) that showed ultraviolet absorption were combined and concentrated to dryness

21) Melting points were determined on a Kofler block. The NMR spectra were measured on a Varian A-60 spectrometer at 60 Mc. in deuteriochloroform at room temperature, using tetramethylsilane as an internal standard.

22) Y. Khouvine and M. G. Arragon, *Bull. soc. chim. France*, **1938**, 1404.

23) G. Dean, *J. Chem. Soc.*, **1904**, 1371.

24) G. Shaw and R. N. Warrener, ibid., **1958**, 153.

under reduced pressure. A brown sirup (0.05 g.) was thus obtained. $[\alpha]_D^{24}$ −9.6 (*c* 0.660, water), λ_{max}^{UV} 285 mμ (water).

Found: C, 41.57; H, 6.28; N, 8.15. Calcd. for $C_{11}H_{16}N_2O_7 \cdot 2H_2O$: C, 40.74; H, 6.22; N, 8.64%.

1-Deoxy-1-ureido-2, 3 : 4, 6-di-*O*-isopropylidene-α-L-sorbofuranose (XXIV).—To a hot solution of XXII (3.8 g.) in ethanol (20 ml.) there was added a solution of potassium cyanate (1.6 g.) in water (20 ml.) and then glacial acetic acid (1.1 ml.). After it had been heated on a boiling water bath for 25 min., the solution was concentrated under reduced pressure. The recrystallization of the residual sirup from methanol and *n*-hexane gave colorless needles (2.4 g.); m. p. 180°C (decomp.), $[\alpha]_D^{28}$ −29.7 (*c* 1.060, chloroform).

Found: C, 51.20; H, 7.52; N, 9.51. Calcd. for $C_{13}H_{22}H_2O_6$: C, 51.64; H, 7.34; N, 9.27%.

***N*-(1-Deoxy-2, 3 : 4, 6-di-*O*-isopropylidene-α-L-sorbofuranose-1)thymine (XXVIII).**—The treatment of XXIV (1.51 g.) in chloroform (15 ml.) and pyridine (0.5 ml.) with XI (1.0 g.) in a way similar to that used for VIII gave an intermediate (XXVI) [1.67 g., λ_{max}^{UV} 250 mμ (ethanol)] as a yellow sirup. To a solution of XXVI (1.47 g.) in hot ethanol (4 ml.), aqueous ammonia was then added in several portions within 6 hr. at 80—90°C. After the solvent had been removed, a yellow powder was obtained; this was purified into a colorless powder by alumina thin-layer chromatography with chloroform and acetone (1 : 1, v/v). $[\alpha]_D^{24}$ −8.5 (*c* 1.017, chloroform), λ_{max}^{UV} 270 mμ (water).

Found: C, 55.52; H, 6.81; N, 7.51. Calcd. for $C_{17}H_{24}O_7N_2$: C, 55.43; H, 6.56; N, 7.61%.

1-*O*-Methyl-2, 3 : 4, 6-di-*O*-isopropylidene-α-L-sorbofuranose (XVIII).—Small pieces of sodium (12.8 g.) were slowly added to a solution of XVII (135 g.) in liquid ammonia (300 ml.) at about −40°C. To the solution, ethanol (about 40 ml.) was added to discharge the blue color of sodium, and then methyl iodide (77 g.) was then added over a 1 hr. period. After 2 hrs.' stirring, the ammonia was allowed to evaporate, and the solution was extracted with benzene. The benzene solution was washed with water and dried, and the solvent was removed. The distillation of the residual sirupy crystals gave XVIII (165 g.); b. p. 111°C/2 mmHg; m. p. 53°C, $[\alpha]_D^{23}$ −11.1 (*c* 1.075, acetone).

Found: C, 57.09; H, 7.67. Calcd. for $C_{13}H_{22}O_6$: C, 56.95; H, 8.03%.

1-*O*-Methyl-2, 3-*O*-isopropylidene-α-L-sorbofuranose (XIX).—A solution of XVIII (41.8 g.) in 60% acetic acid (100 ml.) was warmed at 80°C for 1 hr. The reaction mixture was then cooled, made alkaline with sodium hydroxide, and extracted with chloroform. After the solvent had been removed, the residue was distilled to give a colorless sirup (25.35 g.); b. p. 140°C/2 mmHg, $[\alpha]_D^{23}$ +33.3 (*c* 1.191, chloroform).

Found: C, 51.58; H, 7.83. Calcd. for $C_{10}H_{18}O_6$: C, 51.28; H, 7.69%.

1-*O*-Methyl-6-*O*-tosyl-2, 3-*O*-isopropylidene-α-L-sorbofuranose (XX).—Into a solution of XIX (5.4 g.) in pyridine (15 ml.), tosyl chloride (3.76 g.) was stirred in small portions under cooling. After having been stirred at 0—−5°C for 7 hr., the reaction mixture was poured into a saturated sodium carbonate solution (100 ml.) and extracted with chloroform, which had previously been washed with water and dried; the solvent was then evaporated under reduced pressure. The recrystallization of the residue from benzene and *n*-hexane gave colorless needles; m. p. 37°C, $[\alpha]_D^{23}$ +21.4 (*c* 1.129, chloroform).

Found: C, 52.21; H, 5.73; S, 8.61. Calcd. for $C_{17}H_{24}O_8S$: C, 52.58; H, 6.19; S, 8.24%.

1-*O*-Methyl-6-deoxy-6-amino-2, 3-*O*-isopropylidene-α-L-sorbofuranose (XXI).—A solution of XX (150 g.) and liquid ammonia (150 ml.) in an autoclave was heated on a boiling-water bath for 20 hr. After the liquid ammonia had been removed, the residue was extracted with chloroform and the solvent removed. The distillation of the residue gave a colorless sirup (32 g.); b. p. 125°C/3 mmHg, m.p. 55°C, $[\alpha]_D^{24.5}$ +8.3 (*c* 1.074, methanol).

Found: C, 51.46; H, 8.32; N, 5.82; CH_3O, 13.11. Calcd. for $C_{10}H_{19}NO_5$: C, 51.50; H, 8.15; N, 6.01; CH_3O, 13.30%.

1-*O*-Methyl-6-deoxy-6-ureido-2, 3 : 4, 6-di-*O*-isopropylidene-α-L-sorbofuranose (XXIII).—To a hot solution of XXI (1.8 g.) in ethanol (7 ml.), there was added a solution of potassium cyanate (0.8 g.) in water (7 ml.), and then glacial acetic acid (0.6 ml.). After being heated on a boiling water bath for 3 hr., the solution was concentrated and extracted with ethyl acetate, and the solvent was removed. The recrystallization of the residue from ethanol and *n*-hexane gave colorless rods; m. p. 184°C (decomp.), $[\alpha]_D^{25}$ −22.4 (*c* 1.006, ethanol).

Found: C, 47.58; H, 7.29; N, 9.89. Calcd. for $C_{11}H_{20}O_6$: C, 47.83; H, 7.25; N, 10.14%.

***N*-(6-Deoxy-1-*O*-methyl-2, 3-*O*-isopropylidene-α-L-sorbofuranose-6)thymine (XXVII).**—The treatment of XXIII (0.95 g.) in chloroform (10 ml.) and pyridine (0.6 ml.) with XI (0.6 g.) in a way similar to that used for VII gave an intermediate (XXV) [1.1 g., λ_{max}^{UV} 250 mμ (ethanol)]. The compound XXV thus obtained was treated by the procedure used for XXVIII. The crude product was purified by silica-gel thin layer chromatography. XXVII (0.049 g.) was obtained as a colorless sirup; $[\alpha]_D^{25}$ −34.9 (*c* 0.988, ethanol), λ_{max}^{UV} 270 mμ (water).

Found: C, 49.71; H, 6.66; N, 7.56. Calcd. for $C_{15}H_{22}N_2O_7 \cdot H_2O$: C, 49.99; H, 6.71; N, 7.77%.

7-(1-Deoxy-2, 3 : 4, 6-di-*O*-isopropylidene-α-L-sorbofuranose-1)theophylline (XVI).—Theophylline (1.8 g.) was dissolved in hot water (ca. 100 ml.) containing potassium carbonate (0.7 g.), and the water was removed under reduced pressure. The residue was well dried in a desiccator. The potassium salt of theophylline thus obtained was added to DMF (40 ml.) containing XII (3 g.). The solution was refluxed for 10 hr. After it had cooled, the solution was filtered, the filtrate was evaporated to dryness under reduced pressure, and the residue was extracted with chloroform. The solvent was removed, and the residue was recrystallized from ether to give colorless needles of XVI (0.62 g.); m. p. 181—183°C; $[\alpha]_D^{24}$ −2.7 (*c* 1.033, chloroform).

Found: C, 54.01; H, 6.35; N, 13.39. Calcd. for $C_{19}H_{26}N_4O_7$: C, 54.02; H, 6.20; N, 13.26%.

1-Deoxy-1-dimethylamino-2, 3 : 4, 6-di-*O*-isopropylidene-α-L-sorbofuranose (XV).—A mixture of XII (5 g.), 40% aqueous dimethylamine (25 ml.), and methanol (25 ml.) in an autoclave was heated on

a boiling water bath for 30 hr. After cooling, the solution was evaporated and extracted with chloroform, which had previously been washed with water and dried, and then evaporated. The distillation of the residue gave a colorless sirup (2.4 g.); b. p. 105—107°C/5 mmHg, $[\alpha]_D^{24}$ −1.5 (*c* 1.105, chloroform).

Found: C, 58.38; H, 8.89; N, 4.89. Calcd. for $C_{14}H_{25}NO_5$: C, 58.51; H, 8.77; N, 4.87%.

A mixture of the potassium salt of thymine (1 g.) and XII (3 g.) in DMF (50 ml.) was refluxed for 20 hr. After it had cooled, the solution was filtered, and the filtrate was evaporated under reduced pressure. The distillation of the residue gave XV (0.8 g.).

The authors wish to express their deep gratitude to Dr. Ken'ichi Takeda, Director of this Laboratory, for his encouragement.

BULLETIN OF THE CHEMICAL SOCIETY OF JAPAN VOL. 39 2733—2735 (1966)

Organic Sulfur Compounds. XIII. The Reactions of *p*-Toluenesulfinyl Chloride with Azides

By Michio KOBAYASHI* and (in part) Asami YAMAMOTO

Department of Chemistry, Yokohama City University, Kanazawa-ku, Yokohama

(Received April 18, 1966)

Attempts to prepare a sulfinyl azide resulted in the formation of the sulfonyl azide, disulfide, and thiolsulfonate; of these products, the first two were considered to be disproportionation products of the intermediate, sulfinyl azide. The reaction of a sulfinic acid with hydrazoic acid gave a sulfonamide. No rearrangement similar to the Curtius or the Schmidt reaction was observed.

Recently a photochemical rearrangement of a sulfonyl azide has been reported,[1] although this class of compounds has been established as giving no intramolecularly rearranged products on thermal decomposition.[2-5] No sulfinyl azide (I) has, to the authors' knowledge, yet been prepared. Since the analogous carboxylic azides are known to decompose thermally to give nitrogen and the rearranged product, isocyanate (reaction 1), it seemed of interest to study the reactions which could proceed through the intermediate formation of a sulfinyl azide. If a sulfinyl azide was actually produced and then lost its nitrogen to generate a sulfinyl nitrene (II), an intramolecular rearrangement to a *N*-sulfinylamine (III) would be expected.

$$\underset{\underset{\|}{O}}{RC}\text{-}N_3 \rightarrow RN{=}C{=}O + N_2 \qquad (1)$$

$$\underset{\underset{O}{\downarrow}}{RS}\text{-}N_3 \rightarrow \underset{\underset{O}{\downarrow}}{R\text{-}S}\text{-}\underset{|}{N}\text{-} + N_2 \qquad (2)$$

(I) (II)

$$II \rightarrow R\text{-}N{=}S{=}O \qquad (3)$$

(III)

In this paper, the results of attempts to synthesize sulfinyl azides by several alternative routes will be described.

When sodium azide was treated with *p*-toluenesulfinyl chloride in benzene, only a small amount of nitrogen was evolved. After the reaction was quenched by water a considerable amount of *p*-toluenesulfinic acid was recovered, whereas there was no indication of the presence of *p*-toluidine, which should be formed by the hydrolysis of the expected product of the rearrangement, *N*-sulfinyl-*p*-toluidine. When methylene chloride was used as the solvent, the reaction was again sluggish, and the volume of the nitrogen evolved was only one-tenth of the calculated amount. Among the reaction products, 15 mol.% of *p*-toluenesulfonyl azide was detected by infrared spectroscopy.

On the other hand, the reaction in acetonitrile was rather rapid. After the reaction mixture had been let stand for 4 days at room temperature, the mixture was diluted with water and extracted with methylene chloride; the formation of a substantial amount of *p*-toluenesulfonyl azide was again observed, while there was no trace of sulfinyl-*p*-toluidine or *p*-toluidine in the products.

The reaction between silver azide and *p*-toluenesulfinyl chloride in benzene was also very slow and stopped halfway.

Sodium azide and silver azide are almost insoluble in the above solvents. This was considered to be the main reason for the slow rate of reaction.

* To whom inquiries should be addressed: Department of Chemistry, Faculty of Science, Tokyo Metropolitan University, Setagaya-ku, Tokyo.

1) W. Lwowski and E. Scheiffele, *J. Am. Chem. Soc.*, **87**, 4359 (1965).
2) O. C. Dermer and M. T. Edmison, ibid., **77**, 70 (1955).
3) J. F. Heacock and M. T. Edmison, ibid., **82**, 3460 (1960).
4) G. Smolinsky and B. I. Feuer, ibid., **86**, 3085 (1964).
5) J. E. Franz, C. Osuch and M. W. Dietrich, *J. Org. Chem.*, **29**, 2922 (1964).

Indeed, when a solution of *p*-toluenesulfinyl chloride in *N*, *N*-dimethylformamide was slowly added to a solution of sodium azide in the same solvent, which could dissolve some sodium azide upon being warmed, the evolution of nitrogen started immediately and reached a total of 78 mol.%. From the reaction mixture, 40 mol.% of *p*-toluenesulfonyl azide and small amounts of *p*, *p*-ditolyl disulfide, *p*-toluenesulfonamide, and sodium *p*-toluenesulfonate were isolated. Again in this case, *p*-toluidine or *N*-sulfinyl-*p*-toluidine was not detected among the products.

Reactive *N*-sulfinylamines, such as sulfinyl sulfonamide, have been reported to react with dimethylformamide to give azomethine derivatives[6]; the reaction of *N*, *N*-diphenylformamide with sulfinyl sulfonamide has been also described.[7] Therefore, it is possible that the reaction of sodium azide with *p*-toluenesulfinyl chloride in dimethylformamide gave a sulfinylamine, which reacted further with the solvent to form a condensed product instead of *p*-toluidine. However, no reaction was observed between *N*-sulfinylaniline and dimethylformamide when these reactants were heated on a water bath for several hours. This suggests that if a *N*-sulfinylamine (III) was formed by the intramolecular rearrangement of a sulfinyl nitrene (II), the former would be stable under the reaction conditions and could, therefore, be isolated.

The material balance in the reaction of sodium azide with *p*-toluenesulfinyl chloride in dimethylformamide was far from satisfactory. Most probably, some reaction product other than the sulfinylamine reacted with the solvent to give volatile compounds, which could escape notice during the treatment of the reaction mixture.

Finally, the reaction of *p*-toluenesulfinyl chloride with a solution of tetra-*n*-butylammonium azide in benzene was examined. The reaction proceeded very rapidly at room temperature, accompanied by the evolution of about 75 mol.% of nitrogen. Among the products, *p*-toluenesulfonyl azide (38%), *p*-tolyl *p*-toluenethiolsulfonate (13%), and *p*, *p*-ditolyl disulfide were detected. A close examination of every fraction of the reaction mixture confirmed the absence of *N*-sulfinyl-*p*-toluidine and its hydrolyzed product.

Consequently, the reaction of *p*-toluenesulfinyl chloride with azide ions may be concluded to result not in the formation of the expected rearrangement product of the sulfinyl nitrene II, but in the formation of several other possible products; their formation can best be explained by assuming the disproportionation of the possible intermediate, a sulfinyl azide I, as is shown below:

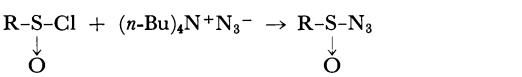

(4)

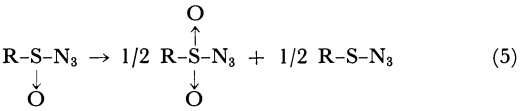

(5)

(IV)

(6)

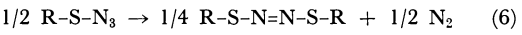

(7)

Although the existence of sulfenyl azides has not been established, Kharasch[8] has described how the reaction of sulfenyl chlorides with sodium azide gives the disulfide as the only isolatable product, probably via the reactions 6 and 7.

Although the mechanism of the formation of the thiolsulfonate is uncertain at present, the following reaction sequence may be tentatively presumed to be applicable:

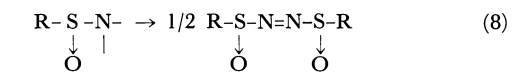

(8)

(III) (V)

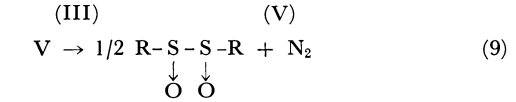

(9)

(VI)

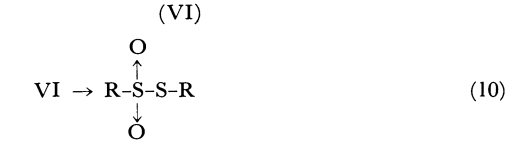

(10)

The reaction of *p*-toluenesulfinic acid with hydrogen azide in a benzene-water mixture was also attempted in order to find out whether any reaction similar to the Schmidt reaction of carboxylic acids occurs. The only product identified was *p*-toluenesulfonamide, and no toluidine salt was detected, showing the absence of the molecular rearrangement in this reaction also. The formation of sulfonamide could be attributed to the following reaction mechanism:

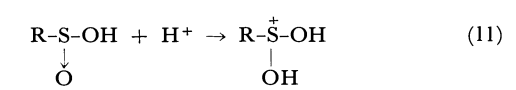

(11)

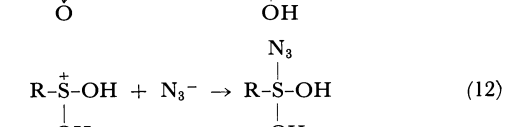

(12)

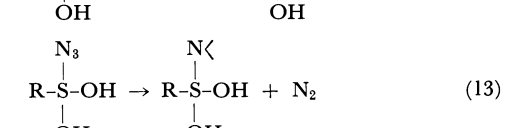

(13)

(VII)

6) G. Kresze and R. Albrecht, *Angew. Chem.*, **74**, 781 (1962); R. Albrecht, G. Kresze and B. Mlakar, *Chem. Ber.*, **97**, 483 (1964).
7) G. Tosolini, *Chem. Ber.*, **94**, 2731 (1961).
8) N. Kharasch, "Organic Sulfur Compounds," Vol. 1, Pergamon Press, New York (1961), p. 377.

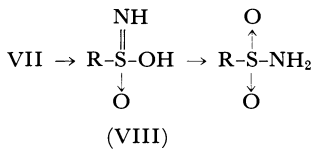

(VIII)

Although the proposed intermediate, the hydroxysulfoximine VIII, is not known, the related sulfoximine IX has been shown to be formed by the reaction of a sulfoxide with hydrazoic acid,[9] probably according to the following reaction mechanism:

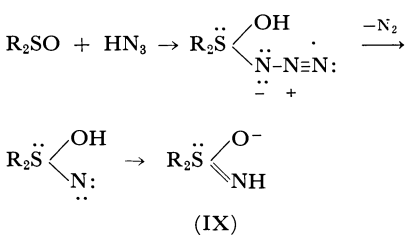

(IX)

Experimental

Materials.—Tetra-*n*-butylammonium azide was prepared by distilling an aqueous hydrogen azide solution, collecting the distillate directly in a solution of tetra-*n*-butylammonium hydroxide in water, and evaporating the resulting salt solution to complete dryness under reduced pressure.[10]

The Reaction of *p*-Toluenesulfinic Acid with Hydrazoic Acid.—To a cooled mixture of 1 g. of sodium azide, 1 ml. of water, and 6 ml. of benzene, 0.7 g. of concentrated sulfuric acid was added. A solution of 1.5 g. of *p*-toluenesulfinic acid in benzene was added to the above solution under cooling. After one night, the benzene layer was separated and evaporated to leave 0.5 g. of *p*-toluenesulfonamide. The aqueous layer was made alkaline and extracted with ether in order to check for the presence of *p*-toluidine, but no residue remained after the evaporation of the solvent.

The Reaction of Sodium Azide with *p*-Toluenesulfinyl Chloride in Dimethylformamide.—When 1.5 g. of sodium azide was warmed with 200 ml. of dimethylformamide which had been dehydrated by calcium hydride and rectified, most of the salt dissolved. When a solution of 4.0 g. of sulfinyl chloride (23 mmol.) in 15 ml. of the same solvent was then added to the above azide solution at room temperature, the reaction started immediately, accompanied by a rapid evolution of gas; the total volume of gas was 450 ml. (18 mmol.) The solvent was removed from the reaction mixture under reduced pressure, and the residue was treated with methylene chloride. From the insoluble part, 0.59 g. (15 mol.%) of *p*-toluenesulfonamide and some sodium *p*-toluenesulfonate were isolated. The part soluble in methylene chloride was fractionated by column chromatography over alumina to obtain 0.16 g. of *p, p*-ditolyl disulfide (2.8 mol.%) and 1.8 g. of *p*-toluenesulfonyl azide (39 mol.%).

The Reaction of Tetra-*n*-butylammonium Azide with *p*-Toluenesulfinyl Chloride.—To a warm solution of 4.1 g. of the azide (14.4 mmol.) in 100 ml. of dry benzene, there was added, drop by drop, 2.5 g. of sulfinyl chloride (13.9 mmol.) in 30 ml. of benzene; a vigorous evolution of gas was observed, the volume totalling 245 ml. (75 mol.%). After one night, the reaction mixture was shaken with water, the benzene layer was dried, and subjected directly to infrared measurement; it was estimated that 1.04 g. of *p*-toluenesulfonyl azide (76% of the theoretical yield based on the reactions 4 and 5) and 0.52 g. of *p*-tolyl *p*-toluenethiolsulfonate (13 mol.%) were formed. The elution chromatography of the solute of the above solution with petroleum ether gave 0.43 g. of pure *p, p*-ditolyl disulfide (identified by its m. p. and infrared spectrum) (48% of the theoretical yield based on the reactions 5—7); its presence in the original benzene solution could not be detected by infrared spectroscopy because of the coincidence of the key bands of the disulfide with those of the other major products. The aqueous extract of the reaction mixture was evaporated to dryness under reduced pressure to give 4.0 g. of tetra-*n*-butylammonium chloride (14 mmol.); no *p*-toluenesulfonic acid nor amine compound was detected in this residue by means either of infrared spectroscopy or of such other characteristic reactions as the formation of *S*-benzylthiuronium sulfonate.

9) F. Misani, T. W. Fair and L. Reiner, *J. Am. Chem. Soc.*, **73**, 459 (1951); H. R. Bentley and J. K. Whitehead, *J. Chem. Soc.*, **1950**, 2081; **1952**, 1572.

10) E. D. Hughes, C. K. Ingold, S. F. Mok, S. Patai and Y. Pocker, *J. Chem. Soc.*, **1957**, 1228.

BULLETIN OF THE CHEMICAL SOCIETY OF JAPAN VOL. 39 2736—2738 (1966)

Organic Sulfur Compounds. XIV. The Reactions of Sulfinic Esters and Related Compounds with Hydrazine

By Michio KOBAYASHI* and Asami YAMAMOTO

Department of Chemistry, Yokohama City University, Kanazawa-ku, Yokohama

(Received April 18, 1966)

Anhydrous hydrazine reacted with sulfinic esters under mild reaction conditions to give disulfides, which were in turn, upon prolonged heating, reduced by hydrazine to mercaptans. Aromatic thiolsulfonates and sulfonyl chlorides were also reduced by hydrazine, whereas aromatic sulfoxides and sulfinic acids were not reduced under comparable reaction conditions. A mixture of hydrazine with a sulfinic ester or another of the reducible sulfur compounds described above can hydrogenate carbon-carbon double bonds and triple bonds. A mechanism involving the intermediate formation of diimide is proposed.

The reactions of hydrazine hydrate with ethyl benzenesulfinate and methyl β-naphthalenesulfinate have been described by Curtius,[1] and the formation of nitrogen and disulfides has been observed. Although these reactions have been claimed to be expressed by the following equation, no details of the material balance have been given and no reaction mechanism has yet been discussed.

$$4\,\mathrm{R\text{-}\overset{\overset{\mathrm{O}}{\downarrow}}{S}\text{-}OR'} + 3\,N_2H_4\cdot H_2O \rightarrow 2\,(\mathrm{RS\text{-}})_2 + 4\,\mathrm{R'OH} + 7\,H_2O + 3\,N_2 \quad (1)$$

In an attempt to prepare the hitherto-unknown sulfinyl hydrazides, the reactions of anhydrous hydrazine with alkyl sulfinates and sulfinyl chlorides have been studied by the present authors. Ethyl *p*-toluenesulfinate and hydrazine reacted very slowly at room temperature, but vigorously at 60—80°C to form about one mole of gaseous product and *p*,*p*-ditolyl disulfide in an almost theoretical yield. Ethyl *p*-bromobenzenesulfinate reacted similarly to give 1.5 mole of gas and di-*p*-bromophenyl disulfide in a quantitative yield. Ethyl benzenesulfinate gave 1.25 mole of gas and diphenyl disulfide in good yields. The amounts of the gaseous product were always more than the calculated figures based on the equation 1.

Upon prologned heating, the reaction proceeded further to give the thiophenols. For instance, *p*-bromobenzenesulfinic ester gave *p*-bromothiophenol in a good yield.

The reaction between *p*-toluenesulfinyl chloride (I) and hydrazine was very vigorous, even at −60°C; di-*p*-tolyl disulfide was the major product. This reaction could be expressed by the following formula:

$$4\,\mathrm{CH_3C_6H_4\text{-}\overset{\overset{\mathrm{O}}{\downarrow}}{S}\text{-}Cl} + 7\,N_2H_4 \rightarrow 2\,(\mathrm{CH_3C_6H_4S\text{-}})_2 + 3N_2 + 4\,N_2H_5Cl + 4\,H_2O \quad (2)$$

(I)

In all the reactions described above, the formation of the desired sulfinyl hydrazide was not observed; this suggests the low stability of this class of compounds.

The reactions of several other organic sulfur compounds with anhydrous hydrazine were also examined. *p*-Toluenesulfinic acid did not react with hydrazine, and the acid was recovered unchanged upon the acidification of the reaction mixture. Diphenyl sulfoxide was also unreactive towards hydrazine.

p-Tolyl *p*-toluenethiolsulfonate (II) reacted very rapidly with hydrazine, in either the presence or absence of the solvent, to form a considerable quantity of gas, as well as di-*p*-tolyl disulfide and *p*-toluenesulfinic acid in good yields. When the reaction was carried out in ethanol for several hours at the boiling point, *p*-thiocresol and sulfinic acid were the products.

Many studies of the reactions between thiolsulfonates and anionoid reagents have been published.[2] For instance, with cyanide anions or hydroxide anions:

$$\mathrm{RSO_2SR'} + CN^- \rightarrow \mathrm{RSO_2^-} + \mathrm{R'SCN} \quad (3)$$

$$\mathrm{RSO_2SR'} + OH^- \rightarrow \mathrm{RSO_2^-} + \mathrm{R'SOH} \quad (4)$$

with thiolate anions[3]:

$$\mathrm{RSO_2SR'} + \mathrm{R''SH} \rightarrow \mathrm{RSO_2H} + \mathrm{R'SSR''} \quad (5)$$

with amines[4]:

$$\mathrm{RSO_2SR'} + \mathrm{R''NH_2} \rightarrow \mathrm{RSO_2H} + \mathrm{R'SNHR''} \quad (6)$$

* To whom inquiries should be addressed: Department of Chemistry, Faculty of Science, Tokyo Metropolitan University, Setagaya-ku, Tokyo.

1) T. Curtius and F. Lorenzen, *J. pr. Chem.*, [2] **58**, 160 (1898).

2) N. Kharasch, *Chem. Revs.*, **59**, 583 (1959).

3) T. F. Parsons, J. D. Buckman, D. E. Pearson and L. Field, *J. Org. Chem.*, **30**, 1923 (1965).

4) B. G. Boldyrev and S. A. Kolensnikova, *Zh. obshch. khim.*, **35**, 198 (1965).

In all these reactions, the anionoid reagents attacked the thiolsulfonate on the sulfide sulfur. By analogy, the hydrazine molecule may be expected to react with the thiolsulfonate according to the following formula to give the sulfenyl hydrazide in the first stage:

$$RSO_2SR' + N_2H_4 \rightarrow RSO_2H + R'SNHNH_2 \quad (7)$$

The overall reaction may then be expressed by the following equation:

$$RSO_2SR' + 1/4\ N_2H_4 \rightarrow RSO_2H + R'SSR' + 1/4\ N_2 \quad (8)$$

As has been described above, the volume of the gaseous products in the reactions of hydrazine with sulfinate esters exceeded the volume of nitrogen calculated on the basis of the reaction 1. This suggests the formation of some hydrogen molecule according to the reaction shown below:

$$2\ R\text{-}\underset{\underset{O}{\downarrow}}{S}\text{-}OR' + 3\ N_2H_4 \rightarrow (RS\text{-})_2 + 3\ N_2 + 3H_2 + 2\ R'OH + 2\ H_2O \quad (9)$$

This idea has led us to examine the reaction of sulfinate esters, or other reducible organic sulfur compounds, with hydrazine in the presence of cyclohexene. If the hydrogen in the reaction 9 is formed in a reactive state, cyclohexene would be reduced to cyclohexane. Actually, when a mixture of cyclohexene (60 mmole), hydrazine (30 mmole), and methyl *p*-toluenesulfinate (12 mmole) in ethanol was warmed, 9 mole% per ester of cyclohexane was formed. In the presence of a large excess of hydrazine, the formation of 1.5 mole of cyclohexane, 0.9 mole of di-*p*-tolyl disulfide, and 1.2 mole of gas was observed. These results may be expressed by the following formula:

$$R\text{-}\underset{\underset{O}{\downarrow}}{S}\text{-}OCH_3 + 3/2\ N_2H_4 + 3/2\ C_6H_{10} \rightarrow 3/2\ C_6H_{12} + (RS\text{-})_2 + 3/2\ N_2 + CH_3OH + H_2O \quad (10)$$

The reaction between di-*p*-tolyl disulfide, cyclohexene, and an excess of hydrazine also gave cyclohexane (75—87 mole% per mole disulfide). Cyclohexene was reduced by a mixture of *p*-tolyl *p*-toluenethiolsulfonate and hydrazine to give cyclohexane in a 50 mole% yield per thiolsulfonate and *p*-toluenesulfinic acid in a 83% yield. This reaction may be represented by the equation below:

$$2\ RSO_2SR + N_2H_4 + C_6H_{10} \rightarrow (RS\text{-})_2 + 2\ RSO_2H + N_2 + C_6H_{12} \quad (11)$$

A mixture of *p*-toluenesulonyl chloride and hydrazine reduced cyclohexene to give 1.3 mole of cyclohexane per mole of sulfonyl chloride; *p*-toluenesulfinic acid was another major product.

Acetylenic triple bonds can be hydrogenated, too. When a solution of tolan (3.3 mmole), ethyl *p*-toluenesulfinate (2.60 mmole), and a large excess of hydrazine in ethanol was refluxed for 5 hr., the formation of bibenzyl (65 mole%) and *trans*-stilbene (19 mole%) was observed.

As the common reactive hydrogenator in the above reductions, diimide (III) is considered the most plausible. In the reaction with sulfinate esters and sulfinyl chlorides, a sulfinyl hydrazide (IV) could be formed as an intermediate; this could in turn decompose to give the sulfenic acid and diimide:

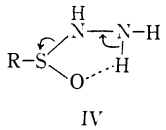

$$\longrightarrow RSOH + HN{=}NH \quad (12)$$

IV III

In the next step, the sulfenic acid could be reduced with excess hydrazine, not with diimide, to give the disulfide.

In the case of thiolsulfonates, the sulfenyl hydrazide formed in the reaction 7 would decompose to the sulfide and diimide:

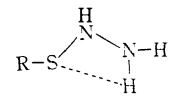

$$\longrightarrow RSH + HN{=}NH \quad (13)$$

The disulfide could also give the sulfenyl hydrazide according to the reaction shown below:

$$RSSR + N_2H_4 \rightarrow RSH + RSNHNH_2 \quad (14)$$

By assuming the reactions 12—14, the amount of cyclohexane formed may be seen to correspond well with the calculated yield of diimide in these reactions. It has also been confirmed that no reduction of cyclohexene is observed, even upon prolonged boiling, with hydrazine in ethanol except when a sulfur compound is added.

Recently there have been many investigations on the reduction with diimide.[5-15] Diimide has

5) a) E. J. Corey, W. L. Mock and D. J. Pasto, *Tetrahedron Letters*, **1961**, 347. b) E. J. Corey, D. J. Pasto and W. L. Mock, *J. Am. Chem. Soc.*, **83**, 2957 (1961).

6) a) S. Huenig, H. R. Mueller and W. Thier, *Tetrahedron Letters*, **1961**, 353. b) S. Huenig and H. R. Mueller, *Angew. Chem.*, **74**, 215 (1962).

7) E. J. Corey and W. L. Mock, *J. Am. Chem. Soc.*, **84**, 685 (1962).

8) R. Appel and W. Buechner, *Angew. Chem.*, **73**, 807 (1961); *Ann.*, **654**, 1 (1962).

9) J. K. Stille and T. Anyos, *J. Org. Chem.*, **27**, 3352 (1962).

10) E. E. van Tamelen, R. S. Dewey and R. J. Timmons, *J. Am. Chem. Soc.*, **83**, 3725 (1961).

11) R. S. Dewey and E. E. van Tamelen, ibid., **83**, 3729 (1961).

12) E. E. van Tamelen, R. S. Dewey, M. F. Lease and W. H. Pirkel, ibid., **83**, 4302 (1961).

13) E. E. van Tamelen and R. J. Timmons, ibid., **84**, 1067 (1962).

14) R. Buyle, A. V. Overstraeten and F. Eloy, *Chem. Ind.*, **1964**, 839.

15) E. W. Garbisch, Jr., S. M. Schildcrout, D. B. Patterson and C. M. Sprecher, *J. Am. Chem. Soc.*, **87**, 2932 (1965).

been produced by several methods, including the oxidation of hydrazine, the decomposition of hydroxylamine-*O*-sulfonic acid, and the decomposition of azodicarboxylate, but the methods particularly related to the present investigation are the decomposition of the sulfonylhydrazine[6a,11,15] and the alkaline decomposition of chloroacetylhydrazide.[14] The reaction of the sulfonylhydrazine in the presence of a base to give diimide and a sulfinic acid is especially reminiscent of the reactions investigated in this paper:

$$RSO_2NHNH_2 \rightarrow RSO_2H + NH{=}NH \qquad (15)$$

Most probably, in the reaction of sulfonyl chlorides with hydrazine described above, this sulfonylhydrazine is formed in the first stage of the reaction.

The steric course of the hydrogenation by diimide has been shown to be *cis*.[5b,6a,7] In the reduction of tolan with ethyl sulfinate and hydrazine described above, the formation of *trans*-stilbene, not the expected *cis*-stilbene, was observed. Considering that thiophenol is a powerful catalyst for the *cis-trans* isomerization of doulbe bonds, the above result may be explained in terms of the isomerization of the primary product, *cis*-stilbene, to the *trans* isomeride in the presence of *p*-thiocresol, formed as another main product.

In the literature, the reduction efficiency of sulfonylhydrazines has been reported to be rather poor; for instance, the amount of the alkene reduced was 0.2—0.3 mole per mole of sulfonylhydrazine.[15] On the contrary, the efficiency of the sulfinate esters or other sulfur compounds described in this paper in the reduction of cyclohexene is very good. This may be attributable to the presence of a large excess of hydrazine, in which the rate of the decay of diimide to nitrogen and hydrogen or to nitrogen and hydrazine[14] could be retarded.

Experimental

Materials.—Anhydrous hydrazine was prepared by boiling hydrazine hydrate with sodium hydroxide and barium oxide successively.

The Reaction between Ethyl *p*-Bromobenzenesulfinate and Hydrazine.—When 1.0 g. of the ester and 0.7 ml. of hydrazine were mixed at room temperature, the reaction proceeded very slowly at first, but after some time the exothermal reaction, accompanied by the evolution of gas, was started; the total gas volume was 150 ml. (1.6 mole). Upon the dilution of the reaction mixture with water, di-*p*-bromophenyl disulfide was obtained in a nearly quantitative yield.

The Reaction of *p*-Toluenesulfinyl Chloride with Hydrazine.—To a mixture of 4 g. of hydrazine and 1 ml. of anhydrous pyridine, cooled in a dry ice-acetone bath, 7 g. of sulfinyl chloride was added slowly; a very vigorous reaction, accompanied by the evolution of gas, occurred to give a solid mass, from which 2.5 g. of di-*p*-tolyl disulfide and 1 g. of *p*-toluenesulfinic acid were then isolated.

The Reaction of *p*-Tolyl *p*-Toluenethiolsulfonate with Hydrazine.—When 0.7 ml. of hydrazine was added, drop by drop, to 2 g. of the thiolsulfonate, a vigorous reaction started, and about 20 mole% of gas was evolved. After an hour, the mixture was diluted with water to leave 1 g. of di-*p*-tolyl disulfide.

The Reduction of Cyclohexene with Methyl *p*-Toluenesulfinate and Hydrazine.—A mixture of 2.0 g. of the methyl ester, 5.0 g. of cyclohexene, and 1.0 g. of hydrazine in 40 ml. of anhydrous methanol was warmed on a water bath for one hour. The reaction mixture was then diluted with water, and the organic layer was separated, dried, and analyzed by gas liquid chromatography (a 1 m. tricresyl phosphate column at 82°C), and found to contain 1.83% of cyclohexane. A similar reaction of 5.0 g. of ethyl *p*-toluenesulfinate, 5.0 g. of cyclohexene, and 5.0 g. of hydrazine in 40 ml. of ethanol at 70—80°C gave 750 ml. of gas in 8 hr. Analysis by gas chromatography revealed the formation of 1.48 mole of cyclohexane per mole of the sulfinate ester. The extraction of the water layer with methylene chloride gave 3.0 g. of di-*p*-tolyl disulfide.

The Reduction with Di-*p*-tolyl Disulfide.—A mixture of 3.0 g. of the disulfide, 5.0 g. of hydrazine, and 5.0 g. of cyclohexene in 40 ml. of ethanol was warmed at 65°C for 11 hr.; 180 ml. of gas was thus evolved. By treatment similar to that of the above reaction, the formation of 75 mole% cyclohexane (based on the disulfide) was indicated.

The Reduction of Tolan.—A solution of 585 mg. of tolan, 2 g. of hydrazine, and 480 mg. of ethyl *p*-toluenesulfinate in 15 ml. of absolute ethanol was refluxed for 5 hr. The reaction mixture was then diluted with water, extracted with *n*-hexane, and fractionated by elution chromatography over alumina with petroleum ether. Bibenzyl, di-*p*-tolyl disulfide, and *trans*-stilbene were eluted in this order. Since the separation of bibenzyl from the disulfide was incomplete, the yield of these compounds was estimated by infrared spectroscopy and found to be 401 mg. of bibenzyl and 127 mg. of the disulfide, whereas the yield of *trans*-stilbene was 113 mg. No *cis*-stilbene was detected.

BULLETIN OF THE CHEMICAL SOCIETY OF JAPAN VOL. 39 2739—2744 (1966)

The Ionic Telomerization of Conjugated Diene Compounds. I. The Cationic Telomerization of Butadiene with Its Hydrochlorides at Low Temperatures

By Teruzo ASAHARA and Hideo KISE

Institute of Industrial Science, The University of Tokyo, Azabu-Shinryudocho, Minato-ku, Tokyo

(Received May 7, 1966)

The telomerization of butadiene with its hydrochlorides (1-chlorobutene-2 and 3-chlorobutene-1) at low temperatures in the presence of cationic catalysts was investigated. The aim of the present investigation is to explore methods to control the molecular weight of the products with various reaction conditions, and to determine the properties and structure of the telomers obtained. The activity of several cationic catalysts at −50——40°C, and the effects of the conversion and the ratio of chlorobutene to butadiene (RCl/Bu) on the yield and average molecular weights of the telomers were investigated. The products were divided into simple adducts and higher telomers by vacuum distillation. The fraction of the 1 : 1 adduct contained three isomers, one of which was 1-chlorooctadiene-2, 6. The structure and properties of the higher telomers were investigated by the aid of the infrared spectra, the average molecular weight, the iodine value, and elementary analysis. On the basis of the results, the reaction mechanism was discussed.

There is information in the literature about the cationic telomerizations of conjugated dinene compounds with compounds of the allyl halide type. For example, the reactions of isoprene and butadiene with their hydrochlorides in the presence of stannic chloride were investigated by Leets[1] and Petrov[2]; the adducts of a 1 : 1 ratio were thus isolated by vacuum distillation. It was found that the relative amounts of the simple addition products and higher telomers depend primarily on the degree of conversion of the reaction. It was also shown that the addition of allyl and alkyl halides to butadiene and isoprene goes in accordance with Markovnikov's rule and occurs at both the 1, 4 and 1, 2 positions. However, the higher telomers are very complex and have not previously been investigated, and knowledge about the reaction mechanism is lacking.

This paper will be concerned, in particular, with the comparison of the activity of several cationic catalysts in the telomerization of butadiene with its hydrochlorides at low temperatures, and with the effect of the initial ratio of the chlorobutene to butadiene on the degree of conversion of the reaction and on the average molecular weight of the resultant telomers. The structure of telomers will also be discussed.

Experimental

The Synthesis of Chlorobutene.—1-Chlorobutene-2 and 3-chlorobutene-1, which were used as telogens, were prepared according to the method described by Dolnick.[3] The two isomers were separated by the fractional distillation of the obtained products, which consisted of about 65% 1-chlorobutene-2 (b. p. 83—85°C), 32% 3-chlorobutene-1 (b. p. 63—66°C), and a trace of a third product with a lower boiling point. The total yield of chlorobutenes was about 85%. In the present experiments 1-chlorobutene-2 was used as a telogen.

Telomerization.—Butadiene was dried before use by passing it through a column of anhydrous calcium chloride and sodium hydroxide. The purity was found to be above 99.3%. Ethyl bromide was purified by washing it several times with chilled concentrated sulfuric acid and water, drying it on calcium chloride, and distilling it.

A 500-ml. round-bottomed glass flask, equipped with a sealed stirrer, a thermometer, a condenser, and an inlet for gas, was cooled in a dry ice-aceton bath under a nitrogen stream; then it was charged with known amounts of the telogen, butadiene, and ethyl bromide. After the temperature of the solution had reached −50——55°C, the catalyst, contained in a part of the ethyl bromide, was slowly added. The reaction is exothermic, and the temperature of the solution rises as the reaction proceeds. The rate of the addition of the catalyst solution was adjusted to keep the temperature of the solution under −35°C. After the telomerization, a small amount of pyridine was added to stop the reaction, and then *n*-hexane was added. The precipitated pyridine/catalyst complex was separated, and the solution was washed with a 5% sodium carbonate solution, a 5% hydrochloric acid solution, and then water, and dried on anhydrous calcium chloride. The solvent and the unreacted chlorobutene and butadiene were distilled off under a vacuum by a water jet pump, and the residue was subjected to vacuum distillation.

1) K. V. Leets, *Zh. Obshch. Khim.*, **28**, 1823 (1957).
2) A. A. Petrov, X. B. Valiyan, L. I. Vunina-Kriborukoba and T. B. Yakobleba, ibid., **29**, 1576 (1959).
3) U. S. Pat. 2573695 (1951).

Analysis.—*Molecular Weight.*—The molecular weight of the products was measured in a toluene solution with a Mechrolab vapor-pressure osmometer, model 301A, at 37°C. Squalane was used as the standard material.

Infrared Spectra.—The spectra of the telomers were taken with a Hitachi-Perkin-Elmer double-beam grating spectrophotometer, model 125. The evaluation of the absorption intensity was made by the ordinary base-line method.

Gas Chromatography.—The adducts with a 1 : 1 ratio of butadiene to chlorobutene were analyzed by a Hitachi-Perkin-Elmer F6 gas chromatograph with a flame ionization detector. The separation column was a stainless steel tube packed with Diasolid S (Nihon Chromato Kogyo, Ltd.); the liquid phase was silicon grease (10%).

The Amount of Unsaturation.—The degree of the unsaturation of telomers was determined by the Wijs method in a carbon tetrachloride solution.

Results and Discussion

1) The Activity of Catalysts. — Several cationic catalysts were used in the telomerization of butadiene with 1-chlorobutene-2. The findings on their catalytic activities are shown in Table I. Zinc chloride is partially insoluble in the reaction solution. Table I shows that, under the present reaction conditions, aluminum chloride and ferric chloride have considerable catalytic ability, but the other catalysts investigated gave only a small amount of a product. Stannic chloride in dichloromethane was used as a catalyst at 15—20°C by Petrov[2]; it gave an appreciable amount of the 1 : 1 adduct and higher telomers. However, in the present experiment at low temperatures, stannic chloride in ethyl bromide gives only a very small amount of telomers with higher molecular weights, and scarcely any of the 1 : 1 adduct. All the products are yellow-brownish viscous liquids and contain little of the simple adduct, except for the ferric chloride being used as the catalyst.

Table I. Telomerization of butadiene with 1-chlorobutene-2 by cationic catalysts

Catalyst	C/Bu mole	EtBr/Bu vol.	Time min.	Yield %	Av. mol. wt.
$AlCl_3$	0.010	1.5	240	50.4	457
$FeCl_3$	0.015	2.2	240	65.8	527
$SnCl_4$	0.020	1.5	420	2.6	394
$ZnCl_2$	0.029	1.5	1380	1.2	—
BF_3Et_2O	0.058	2.6	240	0.3	—
BF_3Et_2O*	0.106	1.8	240	3.0	1235

RCl/Bu, 1.0 (molar ratio);* RCl/Bu, 0.5 (molar ratio)

On the basis of these results, aluminum chloride and ferric chloride were employed in the following experiments.

2) Conversion and Molecular Weight.—The yield and the molecular weight of the products are plotted against the reaction time in Fig. 1. The reaction nears completion during a short period; therefore, the reaction must be stopped in the early stages if we are obtain lower telomers by the control of the conversion. Under these conditions, the average molecular weight of the telomer is limited to less than about 530; other conditions must be used to obtain the higher telomers.

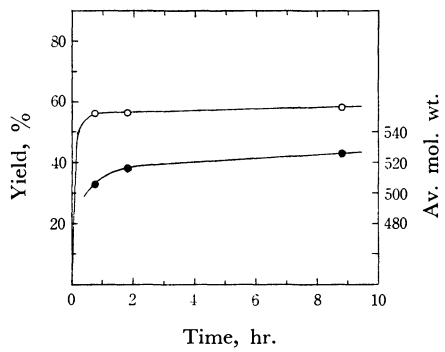

Fig. 1. Changes in yield and average molecular weight of telomer with reaction time.
RCl/Bu=1.0 (molar ratio); $AlCl_3$/Bu=0.01 (molar ratio); EtBr/Bu=1.5 (volume ratio)
○: Yield ●: Average molecular weight

3) Telomerization with Two Chlorobutene Isomers and the Polymerization of Chlorobutene.—As has previously been mentioned, two isomeric chlorobutenes are obtained by the addition of hydrogen chloride to butadiene. When it is used as a telogen under the same reaction conditions, 1-chlorobutene-2 gives a little higher yield and average molecular weight of telomers (Table II, Nos. 1 and 2). However, the analysis by gas chromatography shows that the 1 : 1 adducts of butadiene and each of these two chlorobutenes are composed of nearly the same proportions of isomers, and that the higher telomers from each of these two chlorobutenes have nearly the same infrared spectra. These results indicate that the carbonium cation shown below is formed by the interaction between chlorobutene and the catalyst in the initiation process:

$$CH_3-\overset{+}{C}H\cdots CH\cdots CH_2$$

The difference in the yield of telomers may be attributable to the difference in the rate of the initiation reaction.

Experiment No. 3 in Table II shows that the polymerization of 1-chlorobutene-2 by the action of aluminum chloride affords polymers with a low unsaturation. A small amount of dimer was isolated by distillation (21% of total product; b. p. 60—72°C/1 mmHg).

Found: C, 52.81; H, 7.64; Cl, 39.10. Calcd. for $(C_4H_7Cl)_2$: C, 53.05; H, 7.80; Cl, 39.15%.

No condensation product was found. Therefore, in the system which contains both butadiene and chlorobutene, the polymerization of chlorobutene and the grafting of a growing carbonium ion onto the preformed telomers are also plausible (see section 8).

TABLE II. TELOMERIZATION OF BUTADIENE WITH TWO CHLOROBUTENE ISOMERS AND POLYMERIZATION OF CHLOROBUTENE

Expt. No.	Telogen	Yield, % Soluble	Yield, % Insoluble	Av. mole wt.	Iodine value
1	1-Cl-But-2	50.4	—	457	201
2	3-Cl-But-1	37.7	—	419	216
3	1-Cl-But-2	60.3	—	466	25
4	—	0.5	38.0	—	—

No. 1—3: $AlCl_3$/RCl, 0.01 (molar ratio); RCl/Bu, 1.0 (molar ratio); EtBr/Bu, 1.5 (vol. ratio); Reaction time, 240 min.
No. 3: Reaction in the absence of butadiene.
No. 4: Polymerization of butadiene. $AlCl_3$/Bu, 0.02 (molar ratio); EtBr/Bu, 1.5 (vol. ratio); Reaction time, 100 min.

4) The Effect of the RCl/Bu Ratio.—As Figs. 2 and 3 show, the yield and the average molecular weight of telomers depend on the initial ratio of chlorobutene to butadiene. When aluminum chloride was used as a catalyst, the maximum yield of telomers is obtained at RCl/Bu=0.7. In the region where RCl/Bu is lower than 0.7, the insoluble product is obtained; it increases in amount with the decrease in the RCl/Bu ratio. Moreover, almost all the product obtained from the polymerization of butadiene in the absence of chlorobutene is insoluble in ordinary organic and inorganic solvents (Table II, No. 4). These products are probably caused by branching. As

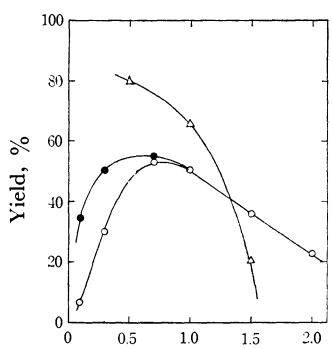

Fig. 2. Effect of the ratio of chlorobutene to butadiene on the yield of telomer.
Reaction time: 4 hr.
○: Catalyst: $AlCl_3$; $AlCl_3$/Bu=0.01 (molar ratio); ●: Insoluble telomor; △: Catalyst: $FeCl_3$; $FeCl_3$/Bu=0.015 (molar ratio)

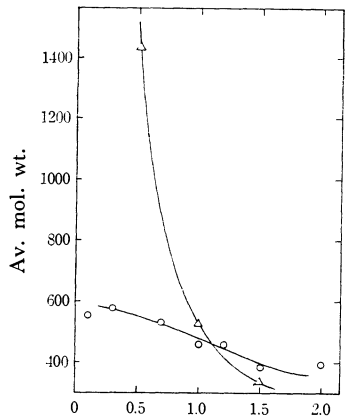

Fig. 3. Effect of the ratio of chlorobutene to butadiene on the average molecular weight of telomer.
Reaction time: 4 hr.
○: Catalyst: $AlCl_3$; $AlCl_3$/Bu=0.01 (molar ratio)
△: Catalyst: $FeCl_3$; $FeCl_3$/Bu=0.015 (molar ratio)

will subsequently be described, the total unsaturation of higher telomers is always low, and it is obviously due to the reactivity of the telomers preformed in side reactions. Grafting and cyclization are suggested, at least as contributory factors.

On the other hand, with ferric chloride as a catalyst, the yield of telomers increases monotonously with the decrease in the RCl/Bu ratio; in the low region of this ratio, the product is a very adhesive semisolid, only a small part of which is insoluble.

The increase in the RCl/Bu ratio causes a decrease in the average molecular weight of products when both aluminum chloride and ferric chloride are used as the catalyst. However, the decrease in the average molecular weight is larger when ferric chloride is used than when aluminum chloride is used.

On the basis of these results, it may be concluded that ferric chloride is the most convenient of the catalysts investigated for controlling the molecular weight of telomers in the telomerization of butadiene with 1-chlorobutene-2.

5) Lower Telomers.—The telomerization of butadiene with 1-chlorobutene-2 was carried out to various extents of the reaction. The increasing degree of reaction is accompanied by an increasing total yield of telomers and by a decrease in the yield of lower adducts (Table III). This agrees with the finding of Leets[1] that, in the telomerization of isoprene with prenyl chloride in dichloromethane in the presence of stannic chloride, the yield of monoterpene chloride increases in the early stages of the reaction, but then decreases

in the later stages; the increase in the yield of polyterpene chloride follows the opposite pattern. This may be due to the consumption of the preformed 1 : 1 adduct by some side reactions or by its addition to butadiene as a telogen, producing higher adducts.

TABLE III. CONVERSION AND LOWER TELOMERS

RCl/Bu mole	EtBr/Bu vol.	Time min.	Conversion %	Lower adducts in telomer, %
1.0	2.20	240	65.8	13.9
1.2	2.22	90	15.9	51.7
1.2	2.23	130	53.9	27.5
1.2	2.23	180	54.4	25.7
1.5	2.30	240	20.5	43.3

Telogen, 1-chlorobutene-2; Catalyst, $FeCl_3$

The fraction with a b. p. of 50—65°C/10 mmHg (I) was again divided into two fractions: 50—58°C/10 mmHg (II) and 58—65°C/10 mmHg (III).

II: Found: C, 64.99; H, 8.81; Cl, 23.43.
III: Found: C, 64.10; H, 8.73; Cl, 24.51.
Calcd. for $H(C_4H_6)_2Cl$: C, 66.43; H, 9.06; Cl, 24.51%.

The gas chromatogram of II has two main peaks, which overlap one another, whereas that of III consists of only one peak. The III content in the fraction I is about 61%. The infrared spectrum of the fraction II (Fig. 4, curve 4) exhibits the characteristic stretching (1645 cm^{-1}) and deformation (910 cm^{-1}) bands of a vinyl group, together with the stretching (1665 cm^{-1}) and deformation (965 cm^{-1}) bands of the -CH=CH- grouping. The spectrum of the fraction III (Fig. 4, curve 3) has only the bands of -CH=CH- (965 and 1665 cm^{-1}). The cationic addition of chlorobutene to butadiene is known to abide by Markovnikov's rule; therefore, the structures of the 1 : 1 adducts may be shown as follows:

CH_3-CH=CH-CH_2-CH_2-CH=CH-CH_2Cl (A)

CH_3-CH=CH-CH_2-CH_2-$CHCl$-CH=CH_2 (B)

CH_2=CH-CH(-CH_3)-CH_2-CH=CH-CH_2Cl (C)

CH_2=CH-CH(-CH_3)-CH_2-$CHCl$-CH=CH_2 (D)

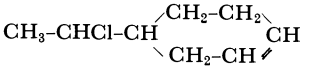

(E)

From the results mentioned above, the fraction III is determined to be A. The fraction II is considered, from the infrared spectrum, probably to be a mixture of B and C. The iodine values of II and III are 325 and 315 respectively, values which correspond to 92.8 and 90.0% of the theoretical value based on the assumption that two C–C double bonds are present in each molecule. Consequently, the amount of cyclic product (E) must be small.

6) The Infrared Spectra of Higher Telomers.—The infrared spectra of higher telomers, obtained from telomerizations under various conditions, were taken and the amounts of *trans*-1, 4, *cis*-1, 4 and 1, 2 linkages were determined by the method described by Richardson[4] and by Golub[5]. The *trans*-1, 4 linkage predominates, accounting for 80—85% of the total observed unsaturation. The contents of 1, 2 and *cis*-1, 4 linkages are determined to be 9—15% and 2—10% respectively. The structures of telomers vary with the RCl/Bu ratio, the conversion, the structure of chlorobutenes, and the catalysts, but the differences are small and no definite trend can be discerned.

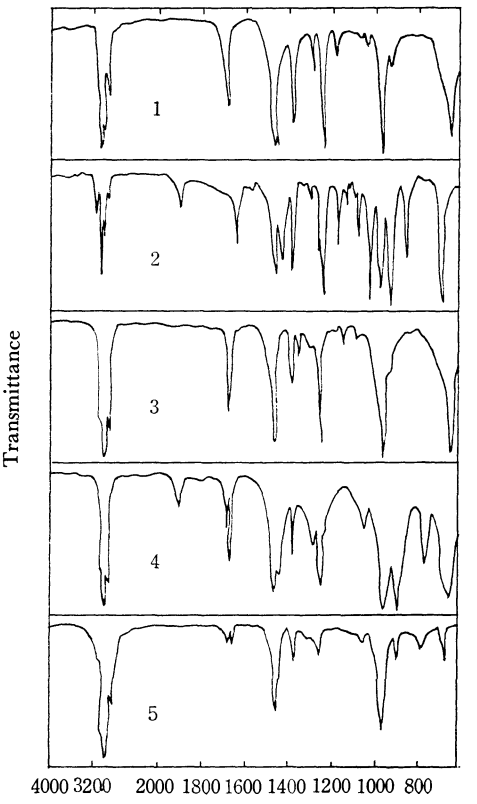

Fig. 4. Infrared spectra of telogens and telomers.
1: 1-Chlorobutene-2 2: 3-Chlorobutene-1
3: Fraction III 4: Fraction II
5: Higher telomer

7) The Unsaturation of Telomers.—The amount of the unsaturation of higher telomers was determined by the Wijs method in a carbon tetrachloride solution. According to Kemp,[6] the iodine value of polybutadiene depends on the

4) W. S. Richardson, *J. Polymer Sci.*, **13**, 229 (1954).
5) M. A. Golub, ibid., **25**, 373 (1957).
6) A. R. Kemp and H. Peters, *Ind. Eng. Chem., Anal. Ed.*, **15**, 453 (1943).

Table IV. Amount of unsaturation in telomers

Expt. No.	RCl/Bu mole	Catalyst	Conversion %	Av. mol. wt.	Iodine value	Unsaturation %
1	0.3	$AlCl_3$	50.6	577	251	57.2
2	0.7	$AlCl_3$	55.2	530	201	45.9
3	1.0	$AlCl_3$	50.4	457	201	46.5
4	1.0	$AlCl_3$	12.8	346	222	52.7
5	1.5	$AlCl_3$	36.0	384	195	45.7
6	2.0	$AlCl_3$	22.7	396	179	42.0
7	0.5	$FeCl_3$	79.8	1436*	147	32.1
8	1.0	$FeCl_3$	65.8	527	194	44.3
9	1.5	$FeCl_3$	20.5	340	253	60.4
10	0.5	BF_3Et_2O	4.1	1235*	289	63.0

* Eighty cubic centimeters of carbon tetrachloride were used becauce of the low solubility of the telomers in carbon tetrachloride - acetic acid solution.

Table V. Structural factors of telomers

Expt.* No.	α	β	Av. No. a	Av. No. b	Av. No. c	% a	% b	% c
1	4.97	1.85	7.34	0.85	2.63	67.8	7.9	24.3
2	3.05	2.60	5.33	1.60	2.14	58.8	17.6	23.6
3	2.65	2.52	4.16	1.52	1.54	57.6	21.1	21.3
5	2.46	2.23	3.26	1.23	1.32	56.1	21.2	22.7
7	2.91	7.43	14.19	6.43	6.88	51.6	23.4	25.0
8	2.22	3.44	4.20	2.44	1.18	53.7	31.2	15.1
9	2.77	1.79	3.17	0.79	0.78	66.9	16.7	16.4

* Numbers are in common with Table IV.

reaction time and on the amount of excess iodine chloride. Therefore, the effects of the amount of iodine chloride and the reaction time on the iodine value of the telomer with a molecular weight of about 550 were studied; it was concluded that, in the presence of about a 60% excess of idoine chloride, the addition of iodine chloride to the C–C double bond in telomers nears completion after 3 hr. The results are shown in Table IV. The theoretical unsaturation is always low, and it may be taken as evidence of the occurrence of some side reactions. As will be shown below, various side reactions may possibly occur, particularly grafting and cyclization which involve the loss of unsaturation.

When aluminum chloride is used as a catalyst, the theoretical unsaturation of telomers decreases somewhat with the increase in the RCl/Bu ratio. However, in case of ferric chloride, an appreciable increase in the theoretical unsaturation is observed.

The amount of the residual unsaturation also depends on the conversion. It increases with the decrease in the conversion. This is considered to be due to the predominance of the side reactions as a result of the decrease in the butadiene concentration and the increase in the telomer concentration at the later stage of the reaction.

8) The Mechanism of the Reaction.—The reaction mechanism of the cationic telomerization of butadiene with chlorobutene is known to be as follows:

Initiation:

$$\left.\begin{matrix}CH_3\text{-}CH{=}CH\text{-}CH_2Cl\\ CH_3\text{-}CHCl\text{-}CH{=}CH_2\end{matrix}\right\} + AlCl_3 \longrightarrow$$

$$CH_3\text{-}\overset{+}{C}H\text{---}CH\text{---}CH_2 + AlCl_4^- \qquad (1)$$

Propagation:

$$CH_3\text{-}\overset{+}{C}H\text{---}CH\text{---}CH_2 + (n-1)CH_2{=}CH\text{-}CH{=}CH_2$$

$$\longrightarrow H(C_4H_6)_{n-1}CH_2\text{-}\overset{+}{C}H\text{---}CH\text{---}CH_2 \qquad (2)$$

Transfer reaction:

$$H(C_4H_6)_{n-1}CH_2\text{-}\overset{+}{C}H\text{---}CH\text{---}CH_2 + CH_3\text{-}CH{=}CH\text{-}CH_2Cl \longrightarrow$$

$$H(C_4H_6)_nCl + CH_3\text{-}\overset{+}{C}H\text{---}CH\text{---}CH_2 \qquad (3)$$

Termination:

$$H(C_4H_6)_{n-1}CH_2\text{-}\overset{+}{C}H\text{---}CH\text{---}CH_2 + AlCl_4^-$$

$$\longrightarrow H(C_4H_6)Cl + AlCl_3 \qquad (4)$$

The finding that the proportion of the 1, 4-1, 4 adduct in the mixture of the 1 : 1 adduct is about 61% suggests that the probability of finding the positive charge on the terminal carbon atom of a growing carbonium ion is about 78%. This is

compatible with the value in the butadiene polymerization.[7]

Several side reactions are also possible; they are shown as follows:

Grafting:

$$-CH_2-CH=CH-CH_2- + -CH_2^+ \longrightarrow -CH_2-\overset{+}{C}H-\underset{CH_2-}{CH}-CH_2- \quad (5)$$

Hydride-ion transfer from the telomer:

$$\begin{matrix}-CH-CH_2-\\ |\\ CH=CH_2\end{matrix} + -CH_2^+ \longrightarrow \begin{matrix}\overset{+}{C}-CH_2-\\ |\\ CH=CH_2\end{matrix} + -CH_3 \quad (6)$$

Proton transfer to the telomer:

$$-CH_2-CH=CH-CH_2- + -CH_2-CH=CH-CH_2^+ \longrightarrow -CH_2-\overset{+}{C}H-CH_2-CH_2- + -CH=CH-CH=CH_2 \quad (7)$$

Intramolecular tranfser reactions:

$$\begin{matrix}CH_2-CH\\ /\quad \|\\ -CH_2-CH\ \overset{+}{C}H_2-CH\\ \quad |\\ CH_2=CH\end{matrix} \longrightarrow \begin{matrix}-CH_2-\overset{+}{C}-CH_2-CH=CH-CH_3\\ \quad\quad |\\ \quad CH_2=CH\end{matrix} \quad (8)$$

$$\begin{matrix}\quad\quad CH_2-CH_2\\ -CH=CH\ \diagup \quad\quad \diagdown\\ \quad\quad \overset{+}{C}H_2-CH \quad\quad CH\\ \quad\quad\quad\quad\quad\quad \diagdown\quad /\\ \quad\quad\quad\quad\quad\quad CH_2-CH\end{matrix} \longrightarrow \begin{matrix}\quad\quad\quad\quad CH_2-CH_2\\ \quad\quad\quad\quad\quad\quad\quad\quad \diagdown\\ -\overset{+}{C}H-CH\quad\quad\quad\quad CH\\ \quad\quad\quad\quad\quad\quad\quad\quad /\\ \quad\quad\quad\quad\quad\quad CH_2-CH\end{matrix} \quad (9)$$

Reactions 5 and 9 cause a decrease in the average iodine value of telomer mixtutes. Reactions 5, 6 and 7 give telomers with more than one chlorine atom, but reactions 6 and 7 have no effect on the average chlorine contents in the telomer mixtures.

The telomers which are formed by reactions 1—4 can be represented by the general formula, $H(C_4H_6)_nCl$. However, the low amount of unsaturation, the formation of insoluble telomers, and the high chlorine contents in higher telomers suggest the presence of side reactions. Thus, telomers represented by the general formula $[H(C_4H_6)_\alpha Cl]_\beta$ are obtained. The values of α and β were calculated from the results of the elementary analysis and the average molecular weights (Table V).

If a telomer is formed by a times of propagation (Eq. 2), b times of grafting (Eq. 5), and c times of cyclization (Eq. 9), and if the reaction is initiated exclusively by Eq. 1, the following relations must hold:

$$\begin{aligned}\alpha\beta &= a + b + 1\\ \beta &= b + 1\\ F &= a - c + 1\end{aligned} \quad \text{(i)}$$

where F represents the average number of the residual C–C double bonds in a telomer and can be obtained from the iodine value determination. Equation i can then be rewritten as follows:

$$\begin{aligned}a &= \beta(\alpha - 1)\\ b &= \beta - 1\\ c &= \beta(\alpha - 1) + 1 - F\end{aligned} \quad \text{(ii)}$$

The calculated values of a, b and c are given in Table V. When aluminum chloride is used as the catalyst, the increase in the RCl/Bu ratio causes an increase in the proportion of grafting, with a decrease in the contribution of propagation. On the other hand, when ferric chloride is used as the catalyst, the proportion of propagation increases with the RCl/Bu ratio. The cyclization occurs almost independently of the RCl/Bu ratio. The high occurrence of cylization in Exp. 7 may be related to a very high conversion of the reaction.

Knowledge about reactions 6, 7 and 8 is lacking; there is no direct evidence for any of these reactions.

7) P. H. Plesch ed., "The Chemistry of Cationci Polymerization," Pergamon Press Ltd., London (1963), p. 356.

BULLETIN OF THE CHEMICAL SOCIETY OF JAPAN VOL. 39 2745—2749 (1966)

The Reactions of 1-Chloro-2-oximino-3-butanone

By Mitsuo MASAKI, Masatoshi SUGIYAMA, Suehiro TAYAMA, and Masaki OHTA

Laboratory of Organic Chemistry, Tokyo Institute of Technology, Ookayama, Meguro-ku, Tokyo

(Received May 9, 1966)

The reaction of 1-chloro-2-oximino-3-butanone (I) with thiourea at 50—60°C gave *S*-(2-oximino-3-oxobutyl)thioformamidine hydrochloride (II), which upon being heated in an aqueous solution, then gave 2-amino-4-(1-oximinoethyl)thiazole (III). The treatment of I with aminoacetonitrile gave a mixture of *N*-(2-oximino-3-oxobutyl)aminoacetonitrile (IV) and *N*, *N*-bis(2-oximino-3-oxobutyl)aminoacetonitrile (V), which were confirmed as the corresponding amidoxime and benzoyl or *p*-nitrobenzoyl derivatives respectively. The reaction of I or 3-chloro-2-oximinopropiophenone with barium thiocyanate gave the corresponding acyclic thiocyanates (VI), while the reaction of *anti*-bromoacetophenone oxime with barium thiocyanate yielded 2-amino-4-phenylthiazole-3-oxide. That the cyclization reaction between the oximino and the cyano groups of V or VI did not occur seemed to favor the *syn*-chloromethyl conformation of the oximino group in I, a mechanism for which is hereby proposed.

The reaction of halogenated biacetyl monooximes has received only scant attention, but they seem to be useful for some synthetic reactions because they have three functional groups. The reaction of 1-bromo-3-oximino-2-butanone with thioformamide or thiobenzamide has been known to give the corresponding thiazole derivatives.[1] Recently, Ogloblin and Potekhin reported the preparation of 1-chloro-2-oximino-3-butanone (I) and its reactions with hydroxylamine hydrochloride, phenylhydrazine, or diethylamine to give the corresponding carbonyl derivatives or substituted product.[2]

We have shown in a previous paper that the reaction of I with amino acid esters, as an example of primary amines, gave products formed not by the condensation of the carbonyl group, but by the displacement of chlorine in I.[3] In the present experiment, the reactions of I with thiourea, aminoacetonitrile, and barium thiocyanate were examined.

The reaction of I with thiourea in ethanol at 50—60°C gave *S*-(2-oximino-3-oxobutyl)thioformamidine hydrochloride (II), which was characterized by elementary analysis and by a study of the infrared spectrum of the free base. When II was boiled in an aqueous solution and then neutralized with ammonia, a crystalline product, m. p. 206—207°C, was obtained. The elementary analysis of the product indicated that the empirical formula, $C_5H_7N_3OS$, held, a formula compatible with the cyclic structure, 2-amino-4-(1-oximinoethyl)thiazole (III) or 2-imino-4-methyl-5-oximino-5, 6-dihydro-2*H*-1, 3-thiazine (IV).

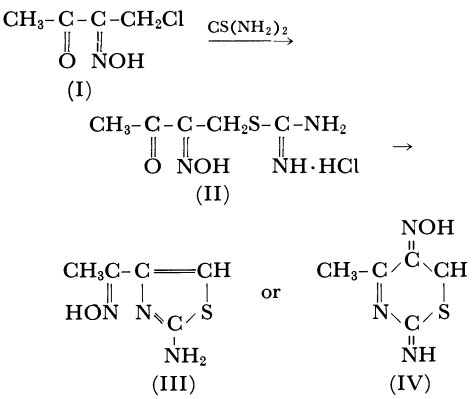

Garreau reported the treatment of 1-chloro-2, 3-butanedione with thiourea to give a substance, m. p. 230°C, the structure of which he claimed to be 4-acetyl-2-aminothiazole (V), though the possibility of the thiazine structure (VI) could not be excluded.[4]

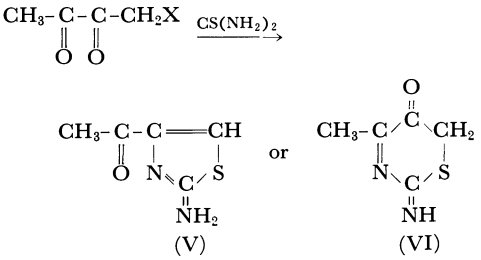

X=Cl or Br

1) M. Erlenmeyer and H. Ueberwasser, *Helv. Chim. Acta*, **23**, 197 (1940); A. Silberg and A. Benkoe, *Chem. Ber.*, **97**, 1915 (1964).

2) K. A. Ogloblin and A. A. Potekhin, *J. Gen. Chem. USSR*, **34**, 2710 (1964).

3) M. Sugiyama, M. Masaki and M. Ohta, This Bulletin, submitted for publication.

4) Y. Garreau, *Chem. Zentr.*, **1947**, 731; *Chem. Abstr.*, **51**, 12148 (1957).

The substance, m. p. 230°C, prepared from 1-bromo-2, 3-butanedione and thiourea was treated with hydroxylamine to give the corresponding oxime, which was confirmed to be identical with the substance, m. p. 206—207°C obtained above. The identical product was also obtained directly by the reaction of 1-bromo-3-oximino-2-butanone with thiourea.

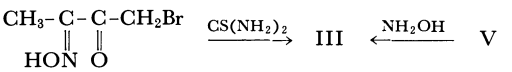

On the basis of these results, as well as infrared and ultraviolet spectral data, the substance with a m. p. of 206—207°C was concluded to be 2-amino-4-(1-oximinoethyl)thiazole (III); accordingly, the substance with a m. p. of 230°C, obtained from 1-bromo-2, 3-butanedione and thiourea, must be 4-acetyl-2-aminothiazole (V).

The infrared spectrum of III showed two absorption bands, at 3380 and 3305 cm^{-1}, which could be ascribed to asymmetric and symmetric NH_2-stretching vibrations, as the relationship of the wave numbers of the two bands accorded well with the equation of Bellamy-Williams.[5] The presence of the primary amine corresponded only with the III structure.

The ultraviolet spectrum of III showed two absorption maxima, at 224.5 and 270 mμ; this also supported the thiazole structure, since unsubstituted thiazole has an absorption maximum at 235 mμ[6] and the maximum bands of 2-amino-4-phenylthiazole were observed at 230.5 and 285 mμ.

A probable pathway for the formation of III from II would be the initial cyclization of II to give V and hydroxylamine, which then reacts to give III. A similar ring-closure by the loss of hydroxylamine was also observed in the reaction of bromoacetophenone oxime with thiourea; when bromoacetophenone oxime and thiourea were heated in an ethanolic solution for twenty minutes, 2-amino-4-phenylthiazole was obtained in a quantitative yield.

When I was treated with two equivalents of aminoacetonitrile in ethyl acetate at room temperature, an oily product was obtained with a quantitative amount of aminoacetonitrile hydrochloride. The oily product was soluble in water, and its purification was difficult. The treatment of the crude product with hydroxylamine afforded 2-(2-oximino-3-oxobutylamino)acetoamidoxime (VII), while treatment with benzoyl chloride gave *N*, *N*-bis(2-benzoyloximino-3-oxobutyl)amino acetonitrile (VIII). Thus, the oily product is probably a mixture of *N*-(2-oximino-3-oxobutyl)-aminoacetonitrile (IX) and *N*, *N*-bis(2-oximino-3-oxobutyl)aminoacetonitrile (X). Reaction with *p*-nitrobenzoyl chloride gave the corresponding di-*p*-nitrobenzoyl derivatives (XI, XII), from the yields of which the oily product appeared to include nearly equivalent amounts of IX and X (Scheme 1).

Sharp et al. described the reaction of α-oximino-

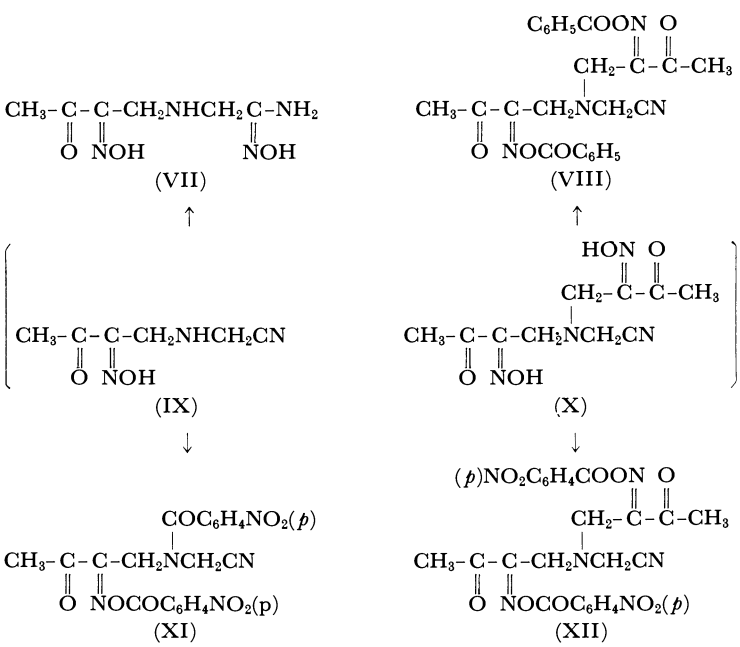

Scheme 1

5) L. J. Bellamy, "The Infra-red Spectra of Complex Molecules," 2nd, Methuen, London; John Wiley, New York (1958), p. 250.

6) A. R. Katritzky, "Physical Methods in Heterocyclic Chemistry," Vol. II, Academic Press, New York and London (1963), p. 59.

carbonyl compounds with α-aminonitrile to give 2-aminopyrazine-1-oxides.[7] The analogous ring closure between oximino and cyano groups of IX was attempted by treatment in the presence of acids or by the conversion of the nitrile into the iminoether, but the corresponding cyclic compound was not isolated.

The reaction of 1-chloro-2-oximino-1-phenylpropane with barium thiocyanate has been reported to give 2-amino-4-methyl-5-phenylthiazole-3-oxide.[8] When 3-chloro-2-oximinopropiophenone (XIII, R=C_6H_5) was treated with barium thiocyanate, it gave not the corresponding cyclic compound (XV), but 2-oximino-3-oxo-3-phenylpropyl thiocyanate (XIV, R=C_6H_5), which was characterized by elementary analysis and by the presence of absorption bands near 2130 cm^{-1} (-SCN) in the infrared spectrum as well as by the negative ferric chloride reaction. The treatment of I with barium thiocyanate gave an oily product, which also had absorption bands near 2130 cm^{-1} in the infrared spectrum and did not show a color reaction with ferric chloride.

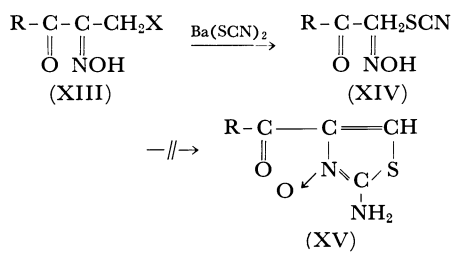

(XIII) (XIV) (XV)

R=C_6H_5, CH_3

Although, in the case of the synthesis of aminopyrazine oxide[7] or aminothiazole oxide[8], neither the configuration of the oximes nor the mechanism of the cyclization reactions has been discussed, the pathways of those cyclization reactions probably involve an attack by the nitrogen of the oximino group on the carbon of the cyano group (see XVII). Therefore, if the hydroxyl group in the oxime of I has an *anti*-configuration to the chloromethyl group (I-a), IX or XIV may be expected to undergo ring closure readily, while if both groups are situated in the *syn*-configuration (I-b), the cyclization reaction of IX or XIV would not easily take place.

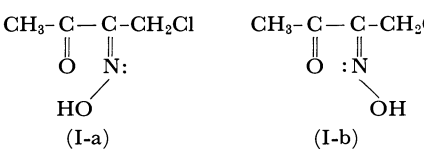

(I-a) (I-b)

When *anti*-bromoacetophenone oxime (XVI) was treated with barium thiocyanate, the cyclization reaction occurred expectedly, and 2-amino-4-phenylthizaole-3-oxide (XVIII), which shows a positive ferric chloride reaction, was obtained.

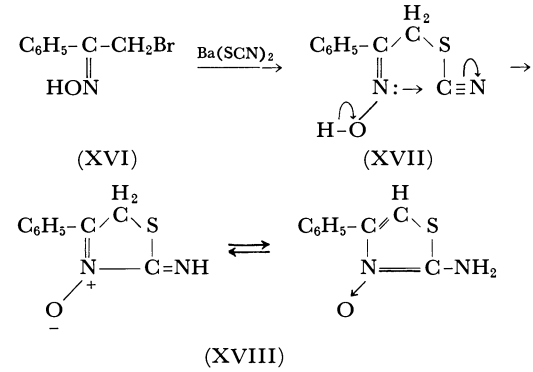

(XVI) (XVII)

(XVIII)

Thus, the fact that the cyclization reaction of IX or XIV did not occur may be ascribed to the *syn*-chloromethyl configuration (I-b) of the oxime in I.[9]

Experimental

***S*-(2-Oximino-3-oxobutyl)thioformamidine (The Free Base of II).**—A mixture of thiourea (1.5 g.) and I (2.7 g.) in ethanol (40 ml.) was heated at 50—60°C for 2 hr. and then left standing at room temperature overnight. The solution was evaporated under reduced pressure to give an oily residue, which was the hydrochloride (II). The oily residue (II) was dissolved in water (40 ml.) and treated with activated charcoal. A half of the solution was neutralized with sodium bicarbonate (1.7 g.) to separate yellow crystals (2.7 g.). (The remaining half of the solution was used for the cyclization reaction in the next section.) The product (1 g.) was dissolved in 0.5 N hydrochloric acid (15 ml.), treated with activated charcoal, and then reprecipitated by neutralizing it with a clear aqueous solution of sodium bicarbonate (0.6 g. in 9 ml. of water). After it had been washed twice with water and twice with ethanol, it was analyzed. Fine yellow crystals; m. p. 128—130°C (decomp.). IR: ν_{max}^{KBr} 3300 (-NH-), 3000—2200 (broad band), and 1650 cm^{-1} (-C=O).

Found: C, 34.91; H, 5.05; N, 24.12. Calcd. for $C_5H_9N_3O_2S$: C, 34.28; H, 5.18; N, 23.99%.

2-Amino-4-(1-oximinoethyl)thiazole (III).—*a) From II.*—The remaining half of the solution of II described above was heated on a boiling water bath for 3 hr. After it had then cooled to room temperature, the solution was neutralized with an aqueous ammonia to separate almost colorless crystals, which were recrystallized twice from water by using activated charcoal. Colorless needles; m. p. 205—206°C. The product showed no depression in mixing tests with the specimen obtained by either the b) or the c) method. UV: λ_{max}^{EtOH} 224.5 mμ (ε=15700) and 270 (sh., 7700). IR:

7) W. Sharp and F. S. Spring, *J. Chem. Soc.*, **1951**, 932; J. J. Gallagher, G. T. Newbold, W. Sharp and F. S. Spring, ibid., **1952**, 4870.

8) A. Dornow, H. H. Marquardt and H. Paucksch, *Chem. Ber.*, **97**, 2165 (1964).

9) The *syn*-chloromethyl conformation of I might be supported by the fact that the melting point of 1-diethylamino-2, 3-butanedione-2-oxime[2] derived from I is essentially identical with that of authentic *syn*-1-diethylamino-2, 3-butanedione-2-oxime.[10]

10) G. B. Bachman and D. E. Welton, *J. Org. Chem.*, **12**, 221 (1947).

ν_{max}^{KBr} 3380 (*asym*-NH_2), 3305 (*sym*-NH_2), and 1650 cm^{-1} (-C=O).

Found: C, 38.86; H, 4.55; N, 26.93. Calcd. for $C_5H_7N_3OS$: C, 38.22; H, 4.49; N, 26.74%.

b) From 4-Acetyl-2-aminothiazole.—When thiourea (1.9 g.) was added to a solution of 1-bromo-2, 3-butanedione (4.2 g.) in ethanol (20 ml.), the mixture became a clear solution with an exothermic reaction; then colorless crystals soon separated. The resultant mixture was heated under reflux for 30 min. The crystals were collected and recrystallized from water to yield 4-acetyl-2-aminothiazole hydrobromide as colorless needles; m. p. 248—250°C (decomp.). (Found: N, 12.24%). The treatment of the hydrobromide with aqueous sodium bicarbonate gave the free base with a m. p. of 229—231°C (decomp.) (lit.[4] 230°C). A solution of the free base (0.95 g.), hydroxylamine hydrochloride (0.5 g.), and potassium hydroxide (0.4 g.) in methanol (50 ml.) was heated under reflux for 4 hr., after which the solvent was removed under reduced pressure; the residual solid was recrystallized twice from water and once from *n*-butanol to give 0.5 g. of colorless needles; m. p. 207—208°C.

c) From 1-Bromo-3-oximino-2-butanone. — Thiourea (0.76 g.) was added to a solution of 1-bromo-3-oximino-2-butanone (1.8 g.) in ethanol (15 ml.). The mixture soon became a clear solution with exothermic reaction. The solution was heated under reflux for 30 min. and then cooled to room temperature to give a crystalline product. An aqueous solution of the product was treated with sodium bicarbonate to give colorless crystals (0.5 g.), which were recrystallized from the solvent described in a) and b) to give colorless needles; m. p. 206—207°C.

The Reaction of Phenacylbromide Oxime with Thiourea.—A mixture of phenacylbromide oxime (2.0 g.) and thiourea (0.75 g.) in ethanol (20 ml.) was heated on a boiling water bath for 20 min. and then allowed to stand at room temperature for 1 hr. After the solution had been concentrated under reduced pressure, the residue was treated with water. The crystals were washed successively with an aqueous solution of sodium bicarbonate and with water. Yield, 1.6 g. Recrystallization from ethanol gave colorless needles; m. p. 150—151°C (lit.[11] 151—152°C). UV: λ_{max}^{EtOH} 230.5 mμ (ε=22300) and 285 (7400).

The Reaction of I with Aminoacetonitrile.—To a solution of aminoacetonitrile (4.5 g., 0.08 mole) in ethyl acetate (70 ml.), I (5.4 g., 0.04 mole) was added. The solution was then allowed to stand at room temperature overnight. After the hydrochloride of aminoacetonitrile (3.7 g.; 94.6%) had been filtered off, the filtrate was evaporated under reduced pressure to give an oily product which was readily soluble in water and alcohol, but not in ether or benzene. In order to remove the impurities, the oily product dissolved in ethyl acetate was chromatographed on alumina. After elution with ethyl acetate, the elute was evaporated to give a reddish oil, "oily product A," which was used for the following reactions.

2-(2-Oximino-3-oxobutylamino)acetoamidoxime Hydrochloride (VII).—A solution of the oily product A (2 g.) and hydroxylamine (1 g.) in methanol (25 ml.) was allowed to stand at room temperature for two days. The solution was then evaporated under reduced pressure to give an oily product. A solution of the product in ethanol (20 ml.) was treated with dry hydrogen chloride and allowed to stand in a refrigerator overnight. The solvent was evaporated under reduced pressure, and the residual product was treated with activated charcoal in ethanol. Yield, 1.34 g. Recrystallization from ethanol-ether gave white crystals; m. p. 140°C (decomp). IR: ν_{max}^{KBr} 2900—2500 (broad band) and 1690 cm^{-1} (-C=O).

Found: C, 31.87; H, 5.65; N, 25.08. Calcd. for $C_6H_{13}N_4O_3Cl$: C, 32.04; H, 5.79; N, 24.92%.

***N, N*-Bis(2-benzoyloximino-3-oxobutyl)aminoacetonitrile (VIII).**—A solution of benzoyl chloride (4 g.) in ethyl acetate was slowly stirred at −10—−5°C into a solution of the oily product A (4.4 g.) and pyridine (2.25 g.) in ethyl acetate (100 ml.). After the addition was complete, stirring was continued at that temperature two more hours. The solution was then washed with water, an aqueous solution of sodium bicarbonate, and again with water, dried over anhydrous sodium sulfate, and then evaporated under reduced pressure. The oily product was treated with isopropyl alcohol (20 ml.) to give a crystalline product (1 g.). Several recrystallizations from isopropyl alcohol gave *N, N*-bis(2-benzoyloximino-3-oxobutyl)aminoacetonitrile.

Colorless needles; m. p. 140—141°C. IR: ν_{max}^{KBr} 1765 (-C=O), 1708 (-C=O), and 1230 cm^{-1} (-COO-).

Found: C, 62.28; H, 5.00; N, 12.29. Calcd. for $C_{24}H_{22}N_4O_6$: C, 62.33; H, 4.80; N, 12.12%.

The *p*-Nitrobenzoylation of the Product Derived from I and Aminoacetonitrile.—A solution of *p*-nitrobenzoyl chloride (7.4 g., 0.04 mole) in ethyl acetate (40 ml.) was stirred, drop by drop, at −10—−5°C into a solution of the oily product A, prepared from I (2.7 g., 0.02 mole), aminoacetonitrile (2.2 g., 0.04 mole), and pyridine (3.2 g.) in ethyl acetate (40 ml.). After the stirring had been continued at that temperature for 8 hr., the mixture was washed with water; thereby a crystalline product (1.5 g.) was separated. The recrystallization of the crystalline product from acetonitrile gave *N*-*p*-nitrobenzoyl-*N*-(2-*p*-nitrobenzoyloximino-3-oxobutyl)aminoacetonitrile (X) as fine yellowish needles; m. p. 187°C (decomp.). IR: ν_{max}^{KBr} 1770 (-COO-), 1710 (-C=O), 1655 (-CONH-), 1530 ($-NO_2$), 1350 ($-NO_2$), and 1230 cm^{-1} (-COO-).

Found: C, 53.03; H, 3.49; N, 5.65. Calcd. for $C_{20}H_{15}N_5O_8$: C, 52.98; H, 3.34; N, 15.45%.

The organic layer in the above reaction was dried over anhydrous sodium sulfate and evaporated under reduced pressure. The residual product was then treated with activated charcoal in chloroform. After the chloroform had been evaporated under reduced pressure, the oily residue was crystallized by teatment with isopropyl alcohol. The crystalline product (1.5 g.) was repeatedly recrystallized from a mixture of acetonitrile and ethanol (7 : 3) to give *N, N*-bis(2-*p*-nitrobenzoyloximino-3-oxobutyl)aminoacetonitrile (XII) as yellowish needles; m. p. 162—163°C. IR: ν_{max}^{KBr} 1765 (-COO-), 1710 (-C=O), 1530 ($-NO_2$), 1350 ($-NO_2$), and 1230 cm^{-1} (-COO-).

Found: C, 52.50; H, 3.80; N, 15.49. Calcd. for $C_{24}H_{20}N_6O_{10}$: C, 52.17; H, 3.65; N, 15.21%.

3-Chloro-2-oximinopropiophenone (XIII).— The

11) R. M. Dodson and L. C. King, *J. Am. Chem. Soc.*, **67**, 2242 (1945).

procedure for the preparation of 3-chloropropiophenone was modified from the method of Matsumoto and Hata.[12] The main modification was that chloroform was used as the solvent instead of tetrachloroethane. In this case, 3-chloropropiophenone was directly obtained without the isolation of phenyl vinyl ketone.

Benzoyl chloride (422 g.; 3 mole) was added, with stirring and ice-cooling, to a mixture of aluminum chloride (414 g.; 3.1 mole) and absolute chloroform (1000 ml.). Ethylene was then introduced into the stirred mixture at such a rate that all was absorbed, the internal temperature being kept between 10—15°C for 40 hr. The reaction mixture was poured into a mixture of hydrochloric acid (426 ml.) and ice (2.3 kg.). The organic layer was washed successively with dilute hydrochloric acid, an aqueous solution of sodium carbonate, and water, and dried over anhydrous sodium sulfate. After the chloroform had been evaporated under reduced pressure, the residual crystalline product was washed with petroleum ether and treated with activated charcoal in benzene or ether to give 3-chloropropiophenone (213 g.). On the concentration of the washings of petroleum ether, an additional product (72 g.) was obtained. The total yield was 285 g. (56.4%); m. p. 46—47°C (lit. 53—55°C[12]).

The nitrosation of 3-chloropropiophenone was carried out in a manner similar to that in the case of 1-chloro-3-butanone.[3] Colorless prisms with a m. p. of 111—112°C was obtained in a 83% yield (lit. 113—114°C[12]; 110—110.5°C[2]).

The Reaction of 3-Chloro-2-oximinopropiophenone with Barium Thiocyanate.—A solution of barium thiocyanate (3 g.) in ethanol (15 ml.) was gradually added to a solution of 3-chloro-2-oximinopropiophenone (4 g.) in ethanol (20 ml.), and then the mixture was refluxed for 1 hr. The precipitate was filtered off, and the filtrate was evaporated under reduced pressure to give an brown residue, which was treated with activated charcoal in benzene (20 ml.). After the benzene had been evaporated under reduced pressure, the residual red oil (4.5 g.) was allowed to stand at room temperature to crystallize. The crystalline product was purified by passing the methanolic solution through an alumina column. Recrystallization from benzene gave 2-oximino-3-oxo-3-phenylpropyl thiocyanate (XIV, $R=C_6H_5$) as colorless needles; m. p. 91—93°C. The product showed no color reaction with ferric chloride. IR: ν_{max}^{KBr} 2150 (-SCN) and 1670 cm^{-1} (-C=O).

Found: N, 12.79. Calcd. for $C_{10}H_8N_2O_2S$: N, 12.72%.

5-Phenyl-2-aminothiazole-1-oxide (XVIII). — A solution of barium thiocyanate (1.5 g.) in ethanol (15 ml.) was added, drop by drop, to a solution of *anti*-2-bromoacetophenone oxime[13] (XVI, 2 g.) in ethanol (20 ml.), and the mixture was warmed at 35°C for 1 hr. After the precipitated barium chloride was filtered off, the solution was concentrated under reduced pressure to give an oily product. The oily product was purified by means of unactivated-alumina column chromatography to yield a caramel (1.5 g.), which showed a blue color with ferric chloride and which had no infrared absorption in the region of the -SCN group. The picrate of XVIII was obtained by refluxing a solution of the caramel (0.5 g.) and picric acid (0.5 g.) in ethanol (40 ml.) for 1 hr., followed by the evaporation of the ethanol. Recrystallization from ethanol gave yellow plates; m. p. 171—172°C.

Found: C, 43.01; H, 2.82; N, 16.67. Calcd. for $C_{15}H_{11}N_5O_8S$: C, 42.76; H, 2.63; N, 16.63%.

12) T. Matsumoto and K. Hata, ibid., **79**, 5506 (1957).

13) H. Korton and R. Scholl, *Ber.*, **34**, 1907 (1901).

BULLETIN OF THE CHEMICAL SOCIETY OF JAPAN VOL. 39 2750—2755 (1966)

Studies of the Hydrocracking of Lignin. I. The Hydrocracking of Desulfonated Sulfite Waste Lignin

By Motoyoshi OSHIMA, Kan KASHIMA, Teruo KUBO
Haruro TABATA and Hiroshi WATANABE

The Noguchi Institute, Kaga, Itabashi-ku, Tokyo

(Received November 15, 1965)

The raw material for the hydrocracking was prepared by treating alcohol fermented sulfite waste liquor with lime, desulfonating the thus-prepared slurry by heating, and deashing the precipitate with sulfur dioxide. The hydrocracking was run with a high-boiling fraction of lignin-hydrogenated oil as the solvent (pasting oil) and with Fe-promotor-sulfur as the catalyst. The yield of monophenols was 24% (based on klason lignin) with a 100% recovery of the pasting oil under reaction conditions of a temperature of 430°C, an initial hydrogen pressure of 130 kg./cm^2, and a catalyst dosage of 3% (based on the lignin). The higher reaction pressure resulted in a slight increase in the yield of monophenols. The formation of non-volatile pitch decreased with the increase in the initial pressure up to 130 kg./cm^2 but a further increase of the pressure exerted no effect. The higher reaction temperature gave more hydrogen absorption and a higher yield of monophenols, and less pitch formation and pasting oil recovery. However, it is essential to select reaction conditions where the highest yield of monophenols is obtained with a 100% recovery of the pasting oil.

Numerous studies of the hydrogenation of lignin have been reported since 1931.[1] Particularly from the end of the 1930's through the 1940's, Harris and Adkins,[2] Hachihama and Jodai,[3] and Lautsch[4] conducted energetic research, mainly for academic purposes. Although few studies were conducted with commercial applications in mind, the yield of phenols, the possible major commercial products, was low, and no particular consideration was paid to the recovery of the solvent, which was the most critical factor in considering the economic feasibility of the process.

Recently, Sakakibara et al.[5] hydrogenated wood-hydrolysis lignin (concentrated sulfuric acid process) with cyclohexanol as the solvent and with a CuCrO type catalyst, the yield of the acidic fraction was 38.9%.

Giesen[6] claimed in his patent that a 55% yield (lignin base) of the 150—325°C (6 mmHg) fraction could be obtained by hydrogenating wood-hydrolysis lignin (Scholler process) using xylenols as the solvent, of which a 100% recovery was claimed. The studies of lignin hydrogenation with phenol, cyclohexanol, tetralin, crude petroleum oil and other materials as the solvents have been reported by one of the present authors.[7] The solvent recovery was very low in the above work, and the low solvent recovery made the process economically unattractive.

In lignin hydrocarcking processes, it is usual to use a solvent in an amount from 1 to 3 times as great as that of lignin. Excellent solvents for the lignin hydrocracking process, such as phenols, sometimes react with lignin in the course of hydrocracking; this makes the analysis and evaluation of the process very complicated.

For the purpose of eliminating the above-mentioned complications and disadvantages, the present authors utilized as a solvent the high-boiling-point fraction of the lignin-hydrogenated product; a 100% recovery of the solvent was successfully achieved by the so-called pre-stabilization of the high-boiling-point fraction. The process proposed here is the one where monophenols are obtained from lignin. The effects of various reaction conditions were fully studied.

Although the present authors[8] have reported a fairly high liquefaction yield (yield of liquid material) and a high yield of monophenols, further detailed experimental work has proved that the

1) A. Lindbalt, *Ing. Vetenskaps Akad.*, No. 107, p. 7 (1931).
2) E. E. Harris, J. D'Ianni and H. Adkins, *J. Am. Chem. Soc.*, **60**, 1467 (1938).
3) Y. Hachihama and M. Jodai, *J. Soc. Chem. Ind. (Kōgyō Kwagaku Zassi)*, **43**, 280 (1940); ibid., **44**, 773 (1941).
4) W. Lautsch and G. Piazolo, *Ber.*, **70**, 486 (1943).
5) K. Takubo, A. Sakakibara and T. Araki, FAO Technical Panel on Wood Chemistry, Tokyo (Japan) 10—15, 10, (1960).
6) G. Giesen, U. S. Pat. 2870133 (1959).
7) K. Kashima and T. Osada, *J. Chem. Soc. Japan, Ind. Chem. Sect. (Kogyo Kagaku Zasshi)*, **64**, 916 (1961).
8) K. Kashima, *Annual Report of the Noguchi Inst.*, **9**, 23 (1960); ibid., **11**, 327 (1962); M. Oshima and K. Kashima, FAO Technical Panel on Wood Chemistry, Tokyo (Japan) 10—15, 10 (1960). M. Oshima, Panel Discussion, Lignin Symposium held in Chicago in 1961.

previously-published data should be rechecked because of the complicated effect of the solvent and the poor analytical techniques previously utilized. The work reported on here is the reinvestigation of the previous work and, hence, the conclusion of our work.

Experimental

The Preparation of Lignin (Desulfonated SWL).—Alcohol-fermented softwood sulfite waste liquor (solid content, 12%) (15 kg.) and calcium hydroxide (0.25 kg.) were mixed and agitated for 30 min. at 70°C, the precipitate thus formed was collected by a centrifugal seperater, 0.05 kg. of calcium hydroxide was added to the filtrate, it was heated for 30 min. at 70°C, and the precipitate was collected. The combined filter cake weighed roughly 3 kg. (containing approx. 50% water). The alcohol-fermented sulfite waste liquor (1.5 kg.) was mixed with the filter cake and heated for 1 hr. at 195°C. The precipitated desulfonated lignin (with 20—30% ash) was filtered, suspended in water, and acidified with SO_2 gas. The deashed lignin was filtered, washed, and dried. The lignin thus prepared will hereafter be referred to as desufonated SWL for the sake of simplicity. The lignin was analyzed and found to be as follows: lingin (klason lignin), 92.2%; ash, 4.7%; total sulfur; 2.4%. The moisture content ranged from 3 to 6%. The lignin sample used in this study was manufactured by the above-mentioned authors' process and supplied by the Crown Zellerbach Corporation, U. S. A.

The Preparation of the Catalyst.[9]—Reduced iron, copper powder, tin powder and sulfur (in an atomic ratio of Fe : Cu : Sn : S=10 : 1 : 1 : 12) were charged into a porcelain ball mill with three times as much water as the combined weight of the above ingredients and crushed and mixed for about one day. After the catalyst had settled, the water layer was discarded and the catalyst was stored wet. (The catalyst should always be wet in order to prevent the loss of its activity). The well-settled catalyst slurry contained approx. 50% water.

The catalyst will be referred to as the standard catalyst hereafter.

Pasting Oil (Solvent).—Pasting oil was the stabilized highboiling-point fraction (b. p.>247°C) of the hydrocracking product of lignin. The pasting-oil fraction was collected from several runs of a bench-scale pilot-plant unit. The authors named this fraction "green pasting oil."

When the green pasting oil was used as the solvent, an excessive degradation took place in it, thus a 100% recovery of the oil was very difficult, and the reproducibility of the data was very poor. The green pasting oil was pretreated as follows to make a so-called stabilized pasting oil. The green pasting oil was hydrogenated with the standard catalyst at a specified temperature. A fraction boiling above 247°C was recovered; this fraction, desulfonated SWL, and the standard catalyst were then mixed and hydrogenated again under same conditions. The fraction of the product boiling above 247°C was the pre-stabilized (or simply stabilized) pasting oil at the specified temperature. Unlike the green pasting oil, the stabilized pasting oil could be recycled with fairly reproducible results without excessive degradation.

Reaction Procedure.—Specified amounts of desulfonated SWL, stabilized pasting oil, a catalyst, and, for better agitation, a rod 13 mm. in diameter and 460 mm. long were charged into an autoclave (2.8 l.; externally-heated rotating type). Hydrogen was then charged in up to the specified pressure, the autoclave was rotated (23 r. p. m.) and heated to the specified temperature within 3 hr.,*1 kept at that temperature for 2 hr., and then left to cool while the autoclave was rotated and the final pressure was recorded.

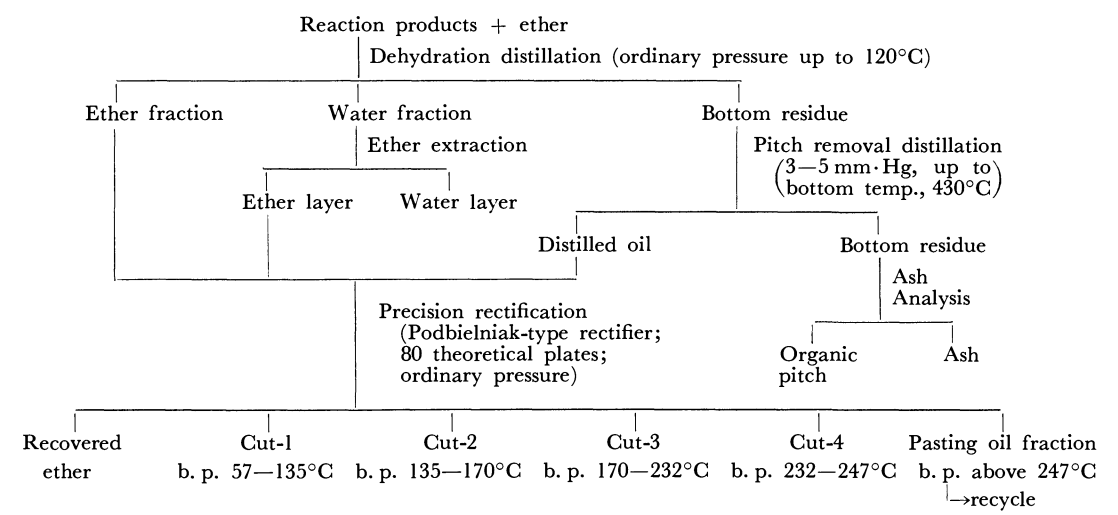

Fig. 1. The fractionation of the reaction products.

9) M. Oshima, Y. Maeda and K. Kashima, Can. Pat. 700210; U. S. Pat. 3223698; M. Oshima and K. Kashima, Japanese Pat. 405634 (1963).

*1 A faster heating-up time results in a poorer reproducibility of the results. Hence, no isothermal condition was obtained in the reaction. Therefore, the reaction temperatures and pressures are not exact in a strict sense.

After the gas had been purged, the autoclave was opened and the contents were washed out with ethyl ether.

The Fractionation and Analysis of the Reaction Products.—Cut-2 through cut-4 (Fig. 1) were analyzed by gas chromatography for the monophenol content. The apparent yield of monophenols was a little higher than the actual yield since some neutrals were contained in the phenol fractions of the gas chromatogram. For the sake of brevity, the monophenol yields in this paper are the figures calculated from the chromatogram without any alkaline extraction (see "Neutrals in Monophenols Fraction"). The weights of individual phenols were assumed to be proportional to the areas occupied on the chromatogram. This assumption had been verified in the authors' laboratory. For cut-2, containing large amounts of low-boiling materials, the inner standard method, with *p*-cresol as the standard, was used. The gas chromatograph was operated as follows: Stationary phase, dilaurylphthalate; column, 5 m. long, 0.6 cm. in diameter; temp., 170°C; carrier gas, H_2, 180 cc./min. An example of the gas chromatograms is shown in Fig. 2.

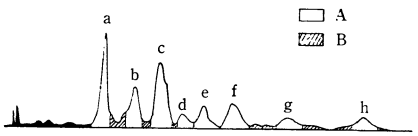

Fig. 2. Analysis of monophenols in the gas chromatogram of cut-3.
a phenol, b *o*-cresol, c *m*- and *p*-cresole
d 2-ethylphenol, e 2, 4-xylenol, f 3- and 4-ethylphenols g 2-(*n*-propyl)phenol, h 4-(*n*-propyl)phenol
A identified phenols, B unidentified phenols
Monophenols = A + B

The Analysis of Neutrals in the Monophenol Fraction.—The different fractions of cut-3 were combined, and then 50 g. of this mixture was treated as is shown in Fig. 3.

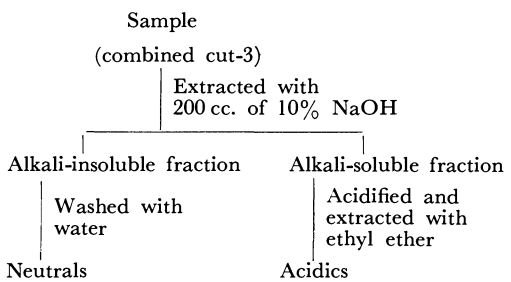

Fig. 3. The analysis of neutrals.

The neutral fraction thus obtained was gas chromatographed, and the relative areas on the chromatogram were subtracted from the areas of monophenols on the chromatogram (Fig. 2.) Thus the true amounts of the individual monophenols were obtained.

Definition of Terms.—Intitial pressure (I. press.): Gauge pressure of hydrogen gas charged into the autoclave at room temperature (kg./cm²). Maximum pressure (Max. press.): Maximum gauge pressure (kg./cm²) (it does not necessarily appear at the reaction temperature). Amount of catalyst (A. C.): (catalyst charged (dry basis))/(klason lignin charged) × 100(%). Pasting oil recovery (P. O. R.): (fraction boiling above 247°C recovered)/(oil boiling above 247°C charged) × 100(%).

Monophenols yield (M. P. Y.): (amount of monophenols analyzed by chromatogram)*2/(klason lignin charged) × 100(%). Liquefaction yield (L. Y.): (Total oil boiling above 57°C recovered-Pasting oil charged)/(klason lignin charged) × 100(%). Pitch yield (P. Y.): (organic pitch)/(klason lignin charged) × 100(%). Hydrogen absorption index (H. A. I.): this is not an accurate measure of the hydrogen absorption. See "Effect of Hydrogen Pressure." (Initial pressure − final pressure)/(klason lignin charged) × 100(%) (kg./cm²/100 g. room temp.).

Results and Discussions

The experimental results are tabulated in Table I.

The Effect of the Amount of Catalyst.—Figure 4 shows that a catalyst amount of 3% based on lignin is sufficient for the reaction.

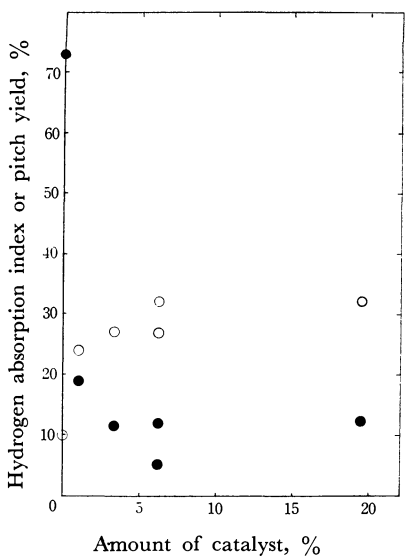

Fig. 4. Effects of amount of catalyst on hydrogen absorption index (○) and pitch yield (●).

The Monophenol Yield.—From the commercial point of view, the most valuable products from the lignin hydrocracking are monophenols; a 100% recovery of pasing oil should also be secured. Under too mild conditions, the pasing oil recovery exceeds 100%. By running with more severe reaction conditions, one can make the recovery of pasting oil lower and the yield of monophenols higher. As the reaction conditions giving a 100%

*2 For the details, see "Fractionation and Analysis of the Reaction Products" and "Neutrals in the Monophenols Fraction".

Table I. Experimental results

Run No.	Reaction temp. °C	I. press. kg./cm²	Max. press. kg./cm²	A. C. %	P.O.R.	M.P.Y. %	L.Y. %	P.Y. %	H.A.I.	Amount of charge*
37—45	365	98	200	6.2	114	13.9	45.8	26.1	19	B
37—38	400	100	220	6.2	114	17.6	45.8	10.2	25	B
36—55	405	94	226	5.9	101.5	24.7	37.9	14.7	26	A
37—51	405	132	280	6.9	109	20.9	48.6	9.1	28	B′
37—18	405	161	341	6.2	112	19.6	51.6	9.5	29	B
36—52	415	92	219	5.9	102	24.8	41.2	11.2	31	A
36—35	420	87	221	6.0	103.5	24.6	43.2	10.3	19	A
36—44	420	95	232	5.9	103	23.2	39.6	14.3	29	A
37—15	420	95	192	6.2	106	21.8	40.5	13.0	25	B
37—14	420	132	280	6.2	108.5	21.3	46.8	11.6	27	B
37—17	420	160	338	6.2	107	20.2	51.5	8.8	29	B
36—48	425	89	234	5.9	99	23.2	33.2	22.0	24	A
36—38	425	90	215	6.0	98.5	27.7	32.1	12.2	33	A
36—53	425	92	218	5.9	99	27.7	39.3	9.8	32	A
36—54	425	92	213	5.9	100	26.5	36.2	14.1	33	A
36—56	425	95	229	5.9	101.5	23.6	36.8	10.9	28	A
37—46	430	50	140	6.2	78	22.0	−8.6	47.0	12	B
36—41	430	89	216	6.0	104	22.4	39.6	17.9	25	B
37—49	430	100	220	6.2	103.5	23.0	34.5	11.0	34	B
37—20	430	133	280	6.2	104.5	26.1	46.5	8.6	34	B
37—23	430	160	357	6.2	103.5	—	45.4	6.1	40	B′
37—28	435	100	251	6.2	107	21.6	44.2	16.6	25	B
37—34	435	100	221	6.2	97	28.9	35.2	11.0	26	B
37—30	435	101	240	6.9	106.5	24.6	46.5	11.7	30	B′
37—40	435	120	333	0	62	—	−41	73	9.7	B
37—44	435	125	270	19.5	105	26.3	48.8	12.4	32	B
37—47	435	128	290	1.0	97.5	24.4	29.4	19.0	24	B
37—19	435	130	280	6.2	105	21.6	47.2	12.2	27	B
37—25	440	130	286	3.3	102	26.4	41.0	11.5	27	B
37—29	440	130	287	6.2	100	29.2	41.4	5.2	32	B′
37—21	440	165	345	6.2	93.5	38.9	41.2	5.6	35	B
37—22	440	165	351	6.2	107	—	48.4	8.6	32	B
37—26	440	180	400	6.2	98	29.8	48.3	6.2	29	B
37—35	445	160	360	6.2	94	33.7	35.8	5.0	32	B
37—41	445	160	355	6.2	105.5	26.7	50.7	7.0	32	B

* The followings were charged into the autoclave.

Symbol	Desulfonated SWL g.	Stabilized pasting oil g.
A	190	450
B	240	370
B′	170	262

recovery of pasting oil must be used commercially, the yield of monophenols under those conditions is very important in considering the commercialization of the process.

Monophenol yields from several runs under identical reaction conditions, such as the reaction temperature and pressures, were compared, but no definite conclusion could be drawn because of the scattered data. However, very remarkable correlations between the monophenol yield and the pasting oil recovery were observed when the initial pressures were nearly equal. This is illustrated by Fig. 5, where monophenol yield are plotted for all the runs with catalyst amounts of between 3 and 7%, and at various temperatures. From the figure we can see that the monophenol yield at initial pressures from 90 to 100 kg./cm² is 26—27%, while at more than 130 kg./cm² it is 29—30%, when pasting oil is fully recovered. No effect of the blending ratio of lignin to pasting oil on the monophenol yield was observed.

The Effect of the Hydrogen Pressure.— As is shown in Fig. 6, generally speaking, the hydrogen absorption index tends to increase and the

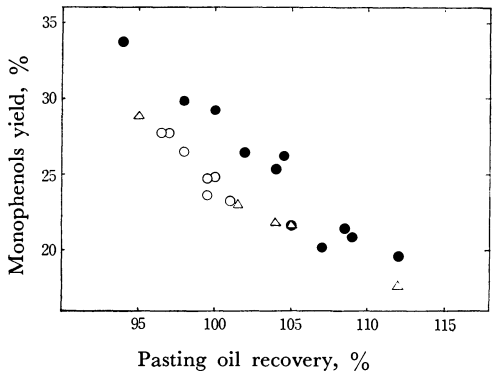

Fig. 5. Relation between pasting oil recovery and monophenols yield at initial pressures: of 90—100 kg./cm² (○, △), or above 130 kg./cm² (●),
○: 190 g. desulfonated SWL & 450 g. pasting oil were charged
●, △: 240 g. desulfonated SWL & 370 g. pasting oil were charged

pitch yield, to decrease with an increase in the initial hydrogen pressure up to approximately 130 kg./cm², but any further increase exerts no effect on the pitch yield.

Monophenol yields at 100% recovery of pasting oil tend to increase with the hydrogen initial pressure (Fig. 5).

The Effect of the Reaction Temperature.—The hydrogen absorption index, the pitch yield, the monophenol yield, and the pasting oil recovery as plotted against the reaction temperatures give a series of fairly scattered points on the graphs. As an example, relations between the reaction temperatures and the monophenol yield are shown in Fig. 7.

The statistical analysis of the data gave the results tabulated in Table II.

Table II shows that there are definite correlations between the temperature and the four variables with a 99% confidence level. That is to say,

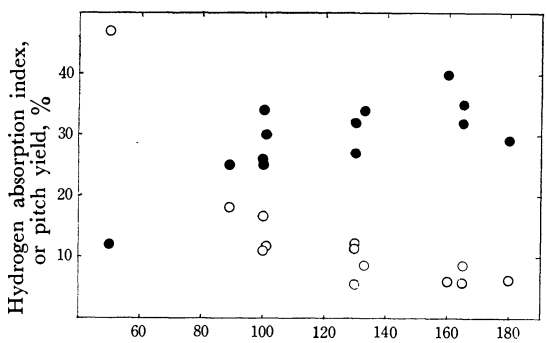

Fig. 6. Plots of initial hydrogen pressure versus hydrogen absorption index (●) and pitch yield (○).
Reaction temp. : 430—440°C

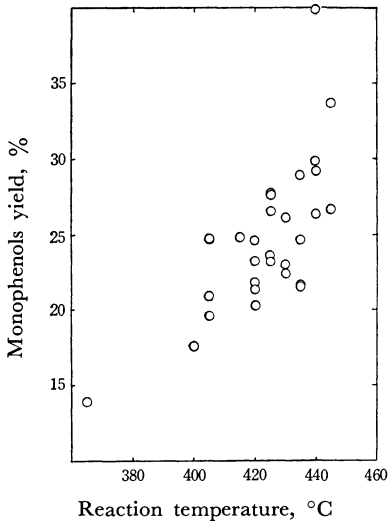

Fig. 7. Relation between reaction temperature and monophenols yield.

Table II. Relations between reaction temperatures and various yields

(Reaction conditions : initial pressure, above 87 kg./cm², catalyst, 3—8% lignin)

	H.A.I.	P.Y.	P.O.R.	M.P.Y.
Number of runs	31	31	31	29
First-order regression	162	210	226	342
Residual	448	443	531	317
Variance ratio	10.4**	13.7**	12.3**	29.2**

$F^1_{29}(0.01)=7.60$ $F^1_{27}(0.01)=7.63$

Table III. The neutrals content in the individual monophenols

	A	B
Phenol	11.4	3.3
o-Cresol	7.9	32.6
m, *p*-Cresols	19.8	6.8
2-Ethylphenol	2.2	19.0
2, 4-Xylenol	7.7	26.8
3 and 4-Ethylphenols	15.0	10.5
2-(*n*-Propyl)phenol	2.0	19.0
4-(*n*-Propyl)phenol	7.9	1.8
Unidentified phenols	16.2	41.4
Total monophenols	90.1	18.2
Unidentified compounds	9.9	94.0
Grand total	100.0	25.6

A : Analysis by the procedure described in "Fractionation and Analysis of the Reaction Products" (% based on cut-3).
B : Neutrals in individual peaks of the gas chromatogram (% of the individual peaks).

higher reaction temperatures give a higher hydrogen absorption index and monophenol yield and a lower pitch yield and pasting oil recovery.

Neutrals in the Monophenol Fraction.— Neutrals in the monophenol fraction as defined in "Fractionation and Analysis of the Reaction Products" were quantitatively analyzed according to the procedures described in "Analysis of Neutrals in the Monophenol Fraction."

The neutrals content in the individual peaks of Fig. 2 are found to be as in Table III.

Table III shows that in the so-called monophenol, the yields shown in the figures and tables contain about 18% neutrals on the average. No complete analysis of the neutrals in monophenols fractions of individual runs has yet been made, however, and so the monophenol yield as defined by "Fractionation and Analysis of the Reaction Products" was used throughout this paper.

The authors would like to express their appreciation to the Noguchi Institute for the permission to publish this study, and to the Crown Zellerbach Corporation, U. S. A., for their cooperation.

BULLETIN OF THE CHEMICAL SOCIETY OF JAPAN VOL. 39 2755—2759 (1966)

Studies of the Hydrocracking of Lignin. II. The Components of Lignin Hydrocracking Products

By Motoyoshi OSHIMA, Kan KASHIMA, Teruo KUBO
Haruro TABATA and Hiroshi WATANABE

The Noguchi Institute, Kaga, Itabashi-ku, Tokyo

(Received November 15, 1965)

The components of the hydrocracking products of alcohol-fermented softwood sulfite waste lignin were identified by rectification, gas chromatography, and IR spectrophotometry. In the acidic fraction (b. p. 170—232°C) phenol, *o*-cresol, 2,6-xylenol, *m*-cresol, *p*-cresol, 2-ethylphenol, 2, 4-xylenol, 2, 5-xylenol, 4-ethylphenol, 3-ethylphenol, 3, 5-xylenol, 2-(*n*-propyl)phenol, 3, 4-xylenol, 4-(*n*-propyl)phenol and 3-(*n*-propyl)phenol were identified. In the neutral fraction (b. p. 170—232°C) naphthalene, 2-methylnaphthalene, and tetralin were identified. In the fraction (b. p. 135—170°C) ethylbenzene, *m*-xylene, *p*-xylene, *o*-xylene, and *n*-propylbenzene were found. In the fraction boiling between 57 and 135°C toluene was identified.

The preceding paper reported on our study of the reaction conditions of the hydrocracking process. In the analysis of monophenols in that paper, the component contents were determined merely by the retention time and the percentages of the areas of peaks in the gas chromatogram.

In this paper, a detailed investigation of the components of the products of the runs conducted with the refined lignin (desulfonated SWL) as the raw material and pre-stabilized pasting oil as the solvent will be reported. Precise rectification, alkaline extraction, gas chromatography, and infrared spectrophotometry techniques resulted in the identification of eleven acidic components and four neutral components, besides the compounds previously reported by some of the present authors. *p*-Cresol, *o*-cresol, 4-ethylphenol and 4-(*n*-propyl)-phenol had been reported to be obtained from the products of lignin hydrocracking with phenol solvent,[1] and *m*-xylene, *p*-xylene, *o*-xylene and ethylbenzene were obtained from the runs with a tetralin solvent.[2]

Experimental Procedures

Cuts-1—4 of all the runs reported in the previous paper[3] were collected and combined. Cut-1, an alkali-unextracted portion of cut-2, and alkali-extracted and unextracted portions of cut-3 were gas chromatographed; the peaks to be identified were numbered for the sake of convenience.

Cut-2 and cut-3 were rectified and separated into fractions with narrow boiling-point ranges. From each fraction, after the contaminating component had been removed by alkali extraction if necessary, the component to be identified was collected from the effluent of the gas chromatograph. (No rectification of cut-1 was conducted. Cut-1 was directly gas chromatographed, and the components desired were collected.)

The components were identified from their boiling points, retention times in the gas chromatogram,

1) K. Kashima, H. Tabata and H. Watanabe, *J. Chem. Soc. Japan, Ind. Chem. Sect. (Kogyo Kagaku Zasshi)*, **64**, 919 (1961).

2) K. Kashima and T. Osada, ibid., **64**, 916 (1961).

3) M. Oshima, K. Kashima, T. Kubo, H. Tabata and H. Watanabe, This Bulletin, **39**, 2750 (1966).

Table I. Operating conditions of the gas chromatograph

Procedure	1	2	3
Purpose	Identification	Identification	Collection of components
Stationary phase	DLP*	CE**	CE
Column; Inside dia.	6 mm.	10 mm.	10 mm.
Length	5 m.	5 m.	7.5 m.
Carrier gas	H_2	H_2	H_2
Flow rate of gas	180 cc./min.	300 cc./min.	300 cc./min.
Quantity of sample	0.01 cc.	0.01 cc.	0.5—1.0 cc.

* Dilaurylphthalate
** Celanese ester No. 9 manufactured by the Celanese Corporation.

and infrared spectra. The alkali-extraction procedure has been explained in a previous paper.[3]

Analysis and Collection by Gas Chromatograph.—A model GC-1B gas chromatograph manufactured by Shimadzu Seisaku-sho was used under the operating conditions as shown in Table I.

Infrared Analysis.—When the authentic material was available, the infrared spectrum of the authentic material was compared with that of the sample obtained from lignin. Infrared charts (IRDC Card)*1 were used instead of the standard spectrum when no standard sample was available.

Results and Discussions

Combined Cut-3.—A precision rectification was made with a 1 kg. sample of the combined cuts-3+4 (cut-3; 750 g., cut-4; 250 g.) as prepared by the procedure mentioned before. The fractions collected are shown in Table II.

Acidic Fraction.—The acidic fraction of combined cut-3 was gas chromatographed as shown in Fig. 1.

Individual peaks on the gas chromatogram were named PA-1 through PA-11; their relative retention times (RRT), like that of phenol as the standard, are listed in Table III.

The relative retention times of the standard phenolic reagents are shown in Table IV.

The fractions shown in Table II were extracted with alkali if necessary and gas chromatographed. From the effluent of the chromatograph, portions corresponding to the peaks to be identified were collected by cold trapping and were subjected to infrared analysis. Although some peaks were easily identified by simply comparing the infrared spectra of the components with those of the standards, while others were mixtures; some more comments will be given below.

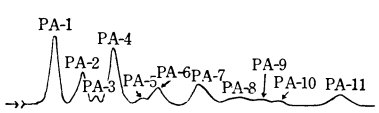

Fig. 1. Gas chromatogram of acidic fraction of cut-3.
Column, CE; Column temp., 170°C

Table II. Rectification of cut-3+4*

Fraction No.	B. p., °C	Amount, g.
1	175—177.4	23.1
2	179.5	26.3
3	181.5	47.0
4	186.0	11.5
5	190.0	10.8
6	191.6	29.0
7	195.5	7.0
8	199.0	31.5
9	200.0	44.0
10	201.0	90.7
11	201.6	25.7
12	204.8	10.9
13	207.6	5.6
14	212.0	55.9
15	213.8	4.5
16	216.0	38.8
17	217.2	43.0
18	220.0	40.1
19	221.4	8.8
20	223.0	10.3
21	224.0	9.3
22	224.8	12.0
23	225.8	16.8
24	226.2	7.3
25	227.8	11.3
26	228.2	5.4
27	229.4	6.8
28	231.0	13.2
29	232.2	35.6
30	233.4	47.8
31	235.0	30.0
Still residue		193.0

* Podbilniak type rectifier with 80 theoretical plates was used at a reflux ratio of 30 : 1—40 : 1.

PA-4.—From the acidic fraction of fr-10, a portion corresponding to PA-4 was gas chromatographically collected. Figure 2(a) is the infrared spectrum of PA-4.

*1 Published by the Infrared Data Committee of Japan.

Table III. Relative retention times of individual peaks

Stationary phase	CE	DLP
PA—1	1.0	1.0
2	1.3	1.3
3	1.4	—
4	1.6	1.6
5	1.9	1.9
6	2.0	2.0
7	2.4	2.4
8	2.8—2.9	2.8, 2.9
9	3.0	3.0
10	3.2	3.2
11	3.8	3.8

Table IV. Relative retention times of some standard materials

Stationary phase	CE	DLP
Phenol	1.00	1.00
o-Cresol	1.3	1.3
2,6-Xylenol	1.4	1.5
p-Cresol	1.6	1.6
m-Cresol	1.6	1.7
2-Ethylphenol	1.9	1.9
2,4-Xylenol	2.0	2.0
2,5-Xylenol	2.0	2.0
4-Ethylphenol	2.4	2.4
3-Ethylphenol	2.4	2.4
3,5-Xylenol	2.4	2.8
2-(*n*-Propyl)phenol	2.7	2.8
3,4-Xylenol	2.8	2.9
4-(*n*-Propyl)phenol	3.8	3.8

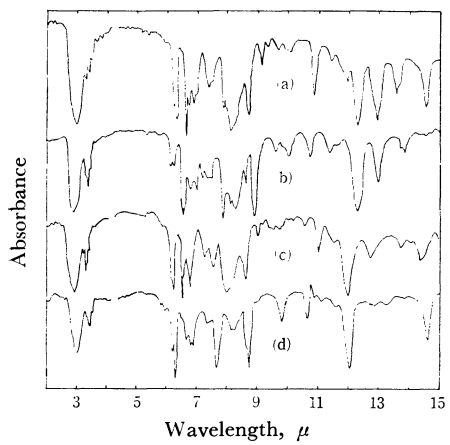

Fig. 2. IR spectra of PA-4 (a), PA-6 (b), PA-7 collected from fr-18 (c) and PA-7 collected from fr-19 (d). (Liquid film method)

The absorptions of PA-4 at 10.8 μ, 11.4 μ and 14.5 μ belong to *m*-cresol, and those at 11.9 μ and 12.3 μ, to *p*-cresol.

PA-6.—The infrared spectrum of PA-6, collected as before from the acidic fraction of fr-10, is shown in Fig. 2(b). Figure 2(b) shows that PA-6 was composed mainly of 2, 4-xylenol (7.9 μ and 13.0 μ). Weak absorptions of 2, 5-xylenol (10.0 μ, 10.7 μ and 13.8 μ) were also detected.

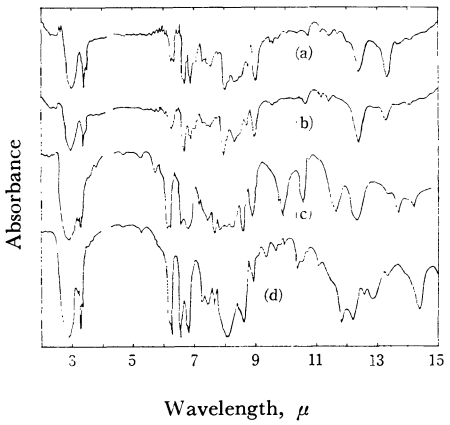

Fig. 3. IR spectra of PA-8 collected from fr-18 (a), from fr-19 (b) and from fr-23 (c), and PA-11 (d). (Liquid film method)

PA-7.—The infrared spectra of two PA-7 fractions collected from acidic fractions of fr-18, and fr-19 respectively, are shown in Figs. 2(c) and 2(d).

In the spectrum of PA-7 collected from fr-18, absorptions of 4-ethylphenol (12.1 μ) and those of 3-ethylphenol (11.0 μ, 12.8 μ and 14.4 μ) are observed. The PA-7 collected from fr-19 gave an infrared spectrum almost identical to that of 3, 5-xylenol.

PA-8.—Three PA-8 fractions were collected from fr-18, fr-19 and fr-23 separately.

As is shown in Figs. 3(a) and 3(b), the infrared

Table V. Identified components in acidic fraction of combined cut-3

Gas chromatographic Peak No.	Identified component
PA-1	Phenol
PA-2	*o*-Cresol
PA-3	2,6-Xylenol*
PA-4	*m*- and *p*-Cresols
PA-5	2-Ethylphenol
PA-6	2,4- and 2,5-Xylenols
PA-7	3-, and 4-Ethylphenols, 3,5-xylenol
PA-8	2-(*n*-Propyl)phenol, 3,4-xylenol and at least one unidentified compound
PA-9	Unidentified
PA-10	Unidentified
PA-11	4-(*n*-Propyl)phenol, 3-(*n*-propyl)phenol

* No IR spectrum was obtained because gas chromatographic collection of the peak was difficult.
The component was identified from RRT and boiling point.

spectra of two PA-8 fractions resemble that of 2-(*n*-propyl)phenol very closely (12.3 μ, 13.3 μ and others), except that the absorption at 12.3 μ is stronger than that of the standard sample, indicating the presence of some unknown meterials in PA-8. The infrared spectrum of PA-8 (Fig. 3(c)) collected from fr-23 is identical with that of 3, 4-xylenol.

PA-11.—Figure 3(d) shows the infrared spectrum of PA-11, collected from the acidic fraction of fr-29.

Absorption of 4-(*n*-propyl)phenol (12.2 μ and 12.6 μ) and those of 3-(*n*-propyl)phenol (11.1 μ, 11.8 μ, 12.9 μ and 14.4 μ) are observed in the spectrum of PA-11.

The above results are summarized in Table V.

Neutral Fraction.—Figure 4 is a gas chromatogram of the alkali-insoluble portion of the combined cut-3. The major peaks in Fig. 4 were named PN-1 through PN-5.

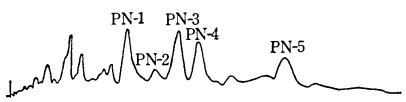

Retention time

Fig. 4. Gas chromatoram of neutral fraction of cut-3. Column, CE; Column temp., 170°C

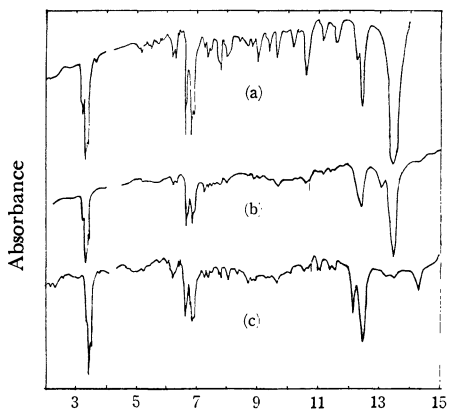

Wavelength, μ

Fig. 5. IR spectra of PN-1 (a), PN-2 (b) and PN-5. (Liquid film method)

PN-1.—The infrared spectrum of PN-1 collected from the neutral fraction of fr-10 is shown in Fig. 5(a) and is identical with that of tetralin.

PN-2.—The infrared spectrum of PN-2 collected from the neutral fraction of fr-10 is shown in Fig. 5(b); it indicates that PN-2 is 1, 2-dialkylbenzene. From its boiling point (approx. 200°C), PN-2 was estimated to be 2-methylbutylbenzene.

PN-3.—The alkaline extraction of fr-14 gave a white crystalline precipitate as an alkali-insoluble fraction. The melting point of the crystals was 79.5°C. Its gas chromatographic retention time, infrared spectrum, and mixed melting point showed that the compound was naphthalene.

PN-5.—PN-5 was collected from the neutral fraction of fr-29; it was found, from Fig. 5(c), to be composed mainly of 2-methylnaphthalene.

Table VI. Identified components in the neutral fraction of combined cut-3

Gas chromatographic peak No.	Identified component
PN-1	Tetralin
PN-2	2-Methylbuthylbenzene
PN-3	Naphthalene
PN-5	2-Methylnaphthalene

The results are summarized in Table VI.

Combined Cut-2.—Table VII shows the results of the rectification of the combined cut-2. The gas chromatogram of the neutral fraction of the combined cut-2, with the peak numbers of p-1 through p-19, is shown in Fig. 6.

From the neutral portions*2 of several fractions,

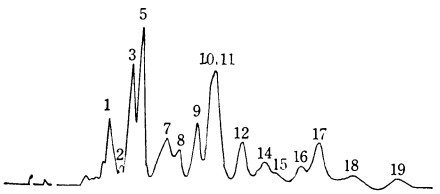

Retention time

Fig. 6. Gas chromatogram of neutral fraction of cut-2.
Column, CE; Column temp., 130°C

Table VII. Rectification of combined cut-2

Fraction No.	B.p., °C	Amount, g.
1	108.4—124.6	15.0
2	128.6	8.8
3	131.6	12.5
4	133.3	5.6
5	134.3	12.0
6	139.8	10.7
7	144.0	14.7
8	148.4	10.1
9	153.0	13.5
10	155.0	10.8
11	159.0	12.4
12	161.2	8.2
13	162.6	18.1
14	167.4	18.1
15	169.6	12.0
16	173.2	11.1
17	175.0	7.6

*2 A small amount of phenol was present in the fractions because of the incomplete rectification.

Table VIII. Identified components in the combined cut-2

Gas chromatographic peak No.	Identified component
p-3	Toluene
p-9	Ethylbenzene
p-10	*m*-, and *p*-Xylenes
p-12	*o*-Xylene
p-16	*n*-Propylbenzene

the main components were gas chromatographically-collected*3 and the infrared spectra of the components were measured. The infrared spectra thus obtained were compared with those of standard samples, and the compounds listed in Table VIII were identified.

Further, the types of components were estimated by infrared analysis to be as follows; peak Nos. 5, 6, 7, 8, 11 and 18 were aliphatic hydrocarbons, while peak Nos. 14, 17 and 19 were aromatic hydrocarbons.

The combined cut-2 was thus found to be mainly composed of hydrocarbons.

Combined Cut-1.—A gas chromatogram of the combined cut-1, with the peak numbers p-1 through p-6, is shown in Fig. 7. The retention times (RT) of the peaks, and those of standard samples which were suspected to be components of cut-1, are shown in Tables IX and X respectively.

Table IX. Retention times of components of combined cut-1

Peak No.	RT, min.
1	3.2
2	3.5
3	8.0
4	13.0
5	16.0
6	18.6

*3 The gas chromatograph column temperature was changed from 100°C to 150°C depending on the vapor pressures of the fraction to be collected.

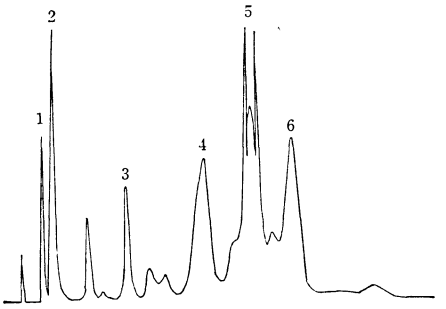

Fig. 7. Gas chromatogram of cut-1.
Column, DLP; Column temp., 100°C

Table X. Retention times of some standard

Sample	RT, min.
Acetone	3.2
n-Heptane	6.5
Cyclohexane	6.0
Methanol	2.3
Ethanol	2.9
n-Butanol	9.9
Methyl ethyl ketone	5.5
Toluene	16
Benzene	7.7

Among the peaks of cut-1, only p-1 and p-5 have identical retention times with those of the standard samples, i. e., acetone and toluene respectively. Acetone is used as a solvent in the treatment of lignin reaction products; hence, no conclusion can be drawn as to whether a part of the acetone originates from lignin or not.

Although many gas chromatographic peaks in the combined cuts-1 remain unidentified, it was concluded that substantial amounts of *n*-heptane, cyclohexane, ethanol, *n*-butanol, methyl ethyl ketone and benzene were not present in cut-1.

The authors would like to express their appreciation to the Noguchi Institute for the permission to publish this study.

BULLETIN OF THE CHEMICAL SOCIETY OF JAPAN VOL. 39 2760—2763 (1966)

Studies of the Hydrocracking of Lignin. III. The Hydrocracking of Various Types of Lignin

By Motoyoshi OSHIMA, Kan KASHIMA, Hiroshi WATANABE
Haruo TABATA and Teruo KUBO

The Noguchi Institute, Kaga, Itabashi-ku, Tokyo

(Received November 15, 1965)

Three types of raw material for lignin hydrocracking were prepared and their reactivities were compared in relation to the refined lignin reported in the authors' previous paper (*Bull. Chem. Soc. Japan*, **39**, 2750 (1966)). The raw materials were prepared; 1) by autoclaving the alcohol-fermented sulfite waste liquor (heat-precipitated lignin); 2) by drying the liquor (dried SWL), and 3) by concentrating the liquor (concentrated SWL). Although these three types of lignin are less costly to prepare, they showed poor reactivities in the hydrocracking process. Heat-precipitated lignin gave a 16—20% monophenol yield [Analyzed by rectification and gas chromatography (no alkaline extraction was conducted).] at a 100% recovery level of pasting oil. No definite monophenol yield figures could be concluded in the runs with dried or concentrated SWL because of the scattered data. The poor reproducibility of data in the cases of these two types of lignin is discussed.

In the previous paper, the hydrocracking of the refined lignin (desulfonated SWL) was reported on in detail.[1] Although the yield of monophenols was high, the cost of the lignin was too high for the commercial success of the process.

In the present paper, several types of lignin which are less costly to prepare were investigated. The lignins studied here are; a lignin solid prepared by simply autoclaving the fermented sulfite waste liquor—heat-precipitated lignin, a lignin solid prepared by drying the same waste liquor—dried SWL, and a thick lignin paste containing a 50% solid from the same origin—concentrated SWL.

Experimental Procedures

Heat-precipitated Lignin. — Ten killograms of alcohol-fermented sulfite waste liquor (softwood) was heated to 210°C over a 3 hr. period, kept at that temperature for 1 hr., and then cooled overnight. The lignin solid precipitated was filtered, washed, and dried.

The analysis showed the solid contained lignin (Klason lignin) (83.5%) and inorganic ash (13.3%) (on a dry basis).

Dried SWL.—Alcohol-fermented sulfite waste liquor was concentrated to a 50% solid content and oven-dried at 110°C. This was prepared and supplied by the Crown Zellerbach Corporation, U. S. A. The content of the solid on the dry basis was; lignin (analyzed by the β-naphthylamine method) (56.8%) and inorganic ash (13.9%).

Concentrated SWL.—This was also supplied by the Crown Zellerbach Corporation, U. S. A. The content was: water (48.7%), lignin (analyzed by the β-naphthylamine method) (28.9%), and inorganic ash (7.2%).

The Preparation of the Catalyst.—The standard catalyst used in our previous paper[1] was used here; it consisted of reduced iron, copper powder, tin powder, and sulfur in an atomic ratio of 10 : 1 : 1 : 12.

The reaction procedures, the separation and the analysis of the reaction products have been described in the previous paper[1] and the terms have been defined there.

Results and Discussions

Tables I, II and III show the results of the runs with heat-precipitated lignin, dried SWL, and con-concentrated SWL as the raw materials respectively.

Monophenol Yield.—In considering the commercial feasibility of the process, the yield of monophenols at a 100% recovery of pasting oil is very important, as has been described in the previous paper.[1]

Figures 1 and 2 show the relations between the monophenol yield and the pasting-oil recovery in the runs with heat-precipitated lignin, dried SWL, and concentrated SWL respectively. The data points in Figs. 1 and 2 are distributed over a considerably wide range as compared with the case of refined lignin in the previous paper. The reason for the scattered data will be discussed later.

Table IV, correlation analysis, shows that, although the first-order regression may be concluded for the runs with heat-precipitated lignin with more than a 99% confidence level, no correlation can be assumed for the runs with dried SWL or concentrated SWL.

In the runs with heat-precipitated lignin as the raw material, the monophenol yield at 100% pasting

1) M. Oshima, K. Kashima, T. Kubo, H. Tabata and H. Watanabe, This Bulletin **39**, 2750 (1966).

Table I. Heat-precipitated lignin
(Initial hydrogen pressure; 170 kg./cm²)

Run No.	A. C.*1 %	Reaction temp., °C	P. O. R.*2 %	M. P. Y.*3 %	P. Y.*4 %	Lignin/P. O.†
68	10	370	113	8.7	25.8	0.4
75	8	370	103	5.7	26.9	0.5
56	5	400	105	11.6	14.6	0.7
60	5	400	106	14.3	21.1	0.5
69	7	440	104	15.5	12.2	0.7
96	6	440	100	17.7	16.9	0.6
97	6	440	98.8	17.9	11.5	0.6
101	5	440	103	18.3	14.2	0.6
102	5	440	103	17.0	12.0	0.6
109	6	440	97.8	16.1	27.3	0.6
112	6	440	92.3	28.4	9.7	0.6
113	6	440	102	22.1	13.0	0.6
116	6	440	97.4	18.5	14.8	0.6
120	5.5	440	103	18.2	11.0	0.6
127	5.5	440	95.0	26.2	12.1	0.6
128	5.5	440	95.5	20.0	16.6	0.6
130	5.5	440	103	16.4	15.5	0.6
137	5.6	440	99.8	19.2	11.0	0.6
146	5.6	440	102	15.8	20.0	0.6
149	5.6	440	100	16.1	9.5	0.6
131	6	470	82.3	33.0	6.2	0.6
138	6	470	82.7	26.0	9.6	0.6

*1 Amount of catalyst on the basis of klason lignin
*2 Pasting oil recovery
*3 Monophenols yield
*4 Pitch yield
† Klason lignin/pasting oil

Table II. Dried SWL

Run No.	A. C.* %	Reaction temp., °C	P. O. R. %	M. P. Y. %	P. Y. %	Lignin/P. O.
55	7	370	93.4	10.8	60.4	0.36
59	8	370	88.7	11.7	70.9	0.36
63	7	370	95.0	13.1	47.6	0.40
54	7	400	89.6	21.0	50.8	0.38
58	7	400	94.3	14.5	54.7	0.43
62	7	400	95.5	11.0	51.4	0.46
124	6	400	90.3	16.7	42.7	0.42
148	6	400	98.7	19.1	43.7	0.42
57	7	440	85.5	29.2	31.0	0.38
61	7	440	91.1	28.8	26.7	0.38

* On the basis of lignin as determined by β-naphthylamine method.

Table III. Concentrated SWL

Run No.	A. C.* %	Reaction temp., °C	P. O. R. %	M. P. Y. %	P. Y. %	Lignin/P. O.
143	6.9	370	125	9.4	42.2	0.96
121	6.9	400	127	12.4	27.1	0.96
126	6.9	400	115	16.7	14.4	0.96
132	6.9	400	105	11.7	38.6	0.96
139	6.9	400	119	14.1	18.3	0.96
141	6.9	400	114	10.1	28.8	0.96
145	6.8	400	119	11.9	34.2	0.96
133	6.9	440	113	15.4	16.6	0.96
136	6.9	440	103	15.3	27.6	0.96

* On the basis of lignin as determined by β-naphthylamine method.

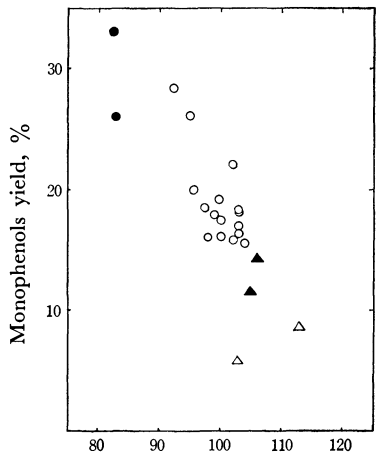

Fig. 1. Relation between monophenols yield and pasting oil recovery.
Reaction temperature: △ 370°C, ▲ 400°C
○ 440°C, ● 470°C

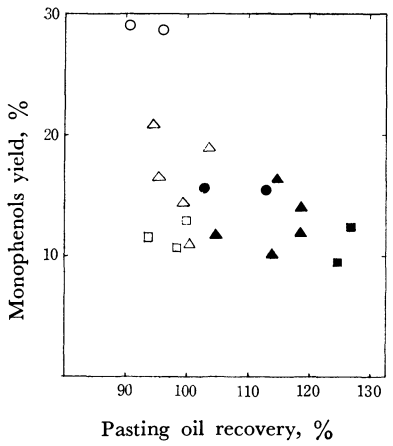

Fig. 2. Relation between monophenols yield and pasting oil recovery.

Reaction temp.	Raw material: Concentrated SWL	Raw material: Dried SWL
370°C	■	□
400°C	▲	△
440°C	●	○

Table IV. Correlation analysis:
Pasting oil recovery and monophenol yield

	Heat-precipitated lignin	Dried SWL	Concentrated SWL
No. of runs	22	10	9
First-order regression	635.4	99	6.8
Residual	306.6	420.3	43.8
F	41.5**	1.88	1.11

oil revovery level was 16—20%. In the case of dried SWL or concentrated SWL, no definite conclusions have been drawn as to the monophenol yield.

The Effect of the Reaction Temperature.—From Fig. 1, a general trend may be observed for higher reaction temperatures to result in higher monophenol yields and lower pasting oil recoveries in the case of heat-precipitated lignin. The same trend, though not so clear, may also be observed in the cases of dried and concentrated SWL. These results show that an excessive degradation of both lignin and pasting oil, even though stabilized, takes place at higher temperatures.

The relations between the pitch yield and the reaction temperature are analyzed in Table V.

Table V. Correlation analysis:
Pitch yield and reaction temperature

	Heat-precipitated lignin	Dried SWL	Concentrated SWL
No. of runs	22	10	9
First-order regression	365.2	1023	246.4
Residual	353	515.6	514.2
F	20.6**	15.9**	3.36

Higher reaction temperatures give lower pitch yields in the cases of heat-precipitated lignin and dried SWL. No clear correlation was obtained in the case of concentrated SWL because of highly-scattered data.

The Reactivities of Various Types of Lignin.—The monophenol yields from the runs of the refined lignin are much higher than those from the runs of the three types of lignin in this study.

A very marked difference in pasting-oil recovery was observed between the runs with dried SWL and concentrated SWL. In the case of dried SWL, it was extremely difficult to get a pasting-oil recovery of more than 100%. On the contrary, in the case of concentrated SWL, it was hard to obtain a pasting-oil recovery of less than 100%.

Such a difference between concentrated SWL and dried SWL was unexpected since these two types of lignin are very close in their structures and impurities. As reasons for the difference, the following three can be postulated: (1) In the drying operation, the condensation of the lignin structure took place. (2) Excess water in concentrated SWL exerted some unknown effects on the reaction. (3) In the runs with concentrated SWL, the ratio of pasting oil to lignin was kept low because of the limitation of reaction pressure. With dried SWL, the ratio was more than 2, but in the case of concentrated SWL, it was around 1. The solvent-lignin ratio might have had some effects. The true reason is yet to be determined.

Pitch yields in the runs with the three types of lignin were much higher than the 5—10% pitch yields in the runs with the refined lignin reported previously.

The effect of the reaction temperature is very significant in the cases of heat-precipitated lignin and dried SWL, but it was less in the runs with concentrated SWL. This may clearly be seen from Figs. 1 and 2 and Table V.

The Effects of Other Reaction Conditions.—No significant effects of the hydrogen initial pressure (30—170 kg./cm^2), the amount of catalyst (3—30% of the lignin), and the rate of revolution of the autoclave (23—80 r.p.m.) were observed. In order to improve the dispersion of the catalyst, attempts were made to prepare catalysts by ball-milling the ingredients in acetone or pasting oil instead of water, but no significant effect was observed.

The Reproducibility of the Data.—A poor reproducibility of data was encountered in the study of the three types of lignin in this paper as compared with the case of the refined lignin. This made the interpretation of data quite difficult. Various efforts to eliminate the poor reproducibility were all fruitless. Impurities present in the three types of lignin might have exerted some serious effects.

Especially in cases of dried SWL and concentrated SWL, the problem was critical. By closely observing the course of the reaction conducted in a vertical mechnaically-agitated autoclave, we found the following evidence to show that the mixture of lignin and pasting oil first changed to a soft pitch-like solid mass before it was degraded by hydrocracking:

(1) When the temperature of the autoclave reached 200°C, a rubbing sound was heard from the autoclave. (2) An exothermic reaction was observed around 200°C. (3) If the autoclave was opened as soon as the reaction temperature reached 200°C, it was found that the autoclave contained a soft pitchy solid.

In the cases of heat-precipitated lignin and refined lignin, both of which had been prepared by heat precipitation processes, the above phenomena were not observed. In the cases of dried and concentrated SWL, the possible poor dispersion of the solid and the non-uniformity of the temperature in the reaction mass might have resulted in the poor reproducibility of the data and the low yield.

The authors would like to express their appreciation to the Noguchi Institute for the permission to publish this study.

BULLETIN OF THE CHEMICAL SOCIETY OF JAPAN VOL. 39 2763—2767 (1966)

Studies of the Hydrocracking of Lignin. IV. The Evaluation of the Catalysts

By Motoyoshi OSHIMA, Kan KASHIMA, Haruro TABATA
Hiroshi WATAMABE and Teruo KUBO

The Noguchi Institute, Kaga, Itabashi-ku, Tokyo

(Received November 15, 1965)

In order to find a more active catalyst than the standard catalyst (*Bull. Chem. Soc. Japan*, **39**, 2750) (1966)), some seventeen materials were tested in the hydrocracking reaction of lignin. Although no catalyst was found that would alter the economic picture of the process, several interesting pieces of information were obtained. Selenium and zinc iodide gave a very high hydrogen absorption, indicating their activities as the catalyst. The reaction mechanism with these catalysts, seemed, however, very different from that with the standard catalyst. They resulted in high neutral yields and poor phenol yields. Cobalt octacarbonl, cobalt sulfide, ammonium molybdate, Raney iron, iron pentacarbonyl, nickel oxalate, and Ni-S showed fair activities. A closer evaluation of some of the above catalysts revealed that the standard catalyst was, at least at present, the most preferable catalyst.

The standard catalyst discussed in previous papers,[1-3] consisted of iron, copper, tin and sulfur in an atomic ratio of 10 : 1 : 1 : 12. The catalyst was discovered by improving the Fe-S*-type catalyst, which was originally employed in the study of coal hydrogenation.[4]

* The expression, for example, Ni-S, shows that the catalyst was produced by the wet-ball milling of Ni and S powders.

1) M. Oshima, K. Kashima, T. Kubo, H. Tabata and H. Watanabe, This Bulletin, **39**, 2750 (1966).

2) M. Oshima, K. Kashima, T. Kubo, H. Tabata and H. Watanabe, ibid., **39**, 2756 (1966).

3) M. Oshima, K. Kashima, H. Watanabe, H. Tabata and T. Kubo, ibid., **39**, 2760 (1966).

4) E. Munekata, Japanese Pat. 152898 (1942).

Sulfur has been known to show a slight activity in the hydrocracking reaction. In this study, selenium and tellurium, belonging to the same group as sulfur in the periodical table, were examined as catalysts of the reaction.

Halogenated metals, such as ferric chloride, or stannous iodide, had been used in the hydrogenation of coal. This type of compound was suspected to be also active in the lignin hydrogenation. Zinc iodide was tested as an example of this type of catalyst.

Compounds of nickel, cobalt, or molybdenum have long been known as catalysts for various types of hydrogenation reactions. Studied in this paper were: nickel compounds such as Ni–S* and nickel oxalate, cobalt compounds such as cobalt sulfide and cobalt octacarbonyl, a molybdenum compound (ammonium molybdate), iron compounds such as iron pentacarbonyl, and Raney iron.

Experimental Procedures

Raw Material Lignin. — Three types of lignin, refined lignin (desulfonated SWL), heat-precipitated lignin, and dried SWL, were used in the present study. For a detailed explanation of the preparative procedures and an analysis see our previous papers.[1,3]

The Preparation of Catalysts. — Selenium and tellurium were commercial reagent of the metallic grade. Ammonium molybdate ($(NH_4)_6Mo_7O_{24}\cdot 4H_2O$), zinc iodide, nickel oxalate, zinc oxide, and cobalt sulfide were also commercial reagents (Extra Pure grade). Ni-S was prepared by milling a mixture of nickel and sulfur in an 1:1 atomic ratio in aqueous media using a porcelain ball mill. Iron aluminum alloy (Fe 44.36%, Al 50.2%) was treated with a caustic solution by the usual procedure to prepare Raney iron. The catalyst was stored in dry ethanol.

Cobalt octacarbonyl ($Co_2(CO)_8$) was prepared as follows. Cobaltous carbonate ($CoCO_3$) (13.7 g.) and petroleum ether (150 ml.) were charged into a stainless steel autoclave, pressurized to 250 kg./cm^2 with 1 : 1 mixture of hydrogen and carbon monoxide gas, and heated for 3 hr. at 150—160°C. The product was then filtered, and the filtrate cooled. The crystallized cobalt octacarbonyl was filtered and dried under a dry carbon monoxide atomosphere.

In order to prepare iron pentacarbonyl, pyrite cynder was reduced in a hydrogen stream for 5—6 hr. at 630—730°C; 80 g. of it was then charged in a 500 ml. stainless steel autoclave and pressurized to 170 kg./cm^2 with carbon monoxide gas and kept at 190—200°C for 3 hr. The autoclave was cooled, the remaining gas was purged, and the autoclave was pressurized again to 170 kg./cm^2 with fresh carbon monoxide gas and heated at 190—200°C for 3 hr. The iron pentacarbonyl ($Fe(CO)_5$) thus formed was separated from unreacted iron powder by filtration.

The standard catalyst was a ball-milled mixture of iron, copper, tin and sulfur with an atomic ratio of 10 : 1 : 1 : 12. The details of the preparative procedures have been given in a previous paper.[1]

Reaction Conditions.—The reaction conditions are tabulated in Table I.

Conditions A, C and D, where a xylenol mixture was used as the solvent, were for the preliminary evaluation of the catalyst, while B and E were the regular reaction procedures. The types of lignin used were the ones which were of particular interest at the time when the study was made, hence, there is no special meaning in the selection of lignin.

The activity of the catalysts were tested and compared with the standard catalyst under these conditions. First catalysts were evaluated preliminarily under the conditions A, C and D, only those with promising activities were subjected to full evaluation under the B and E conditions.

The reaction condition B is identical with the one used in Part III.[3] A lower reaction temperature was used in D and E in order to observed the activity at a lower temperature.

A commerially-available industrial-grade xylenol-mixture was distilled to remove a low-boiling fraction (b. p. below 205°C); the residue was then used as the solvent.

The stabilized pasting oil was prepared by a usual procedure fully described in a previous paper.[1]

The Separation and Analysis of the Product.—For A, C and D, the procedure described in Fig. 1 was used.

With the runs under B and E reaction conditions the analytical procedures were the same as in the previous paper.[1]

Definitions of Terms.—The terms used in this paper are as have been described in the previous paper[1] except for the following. In the preliminary runs;

Table I. A list of the reaction conditions

Reaction conditions	A	B	C	D	E
Autoclave	300 ml. Shaking	3 l. Rotating	3 l. Rotating	3 l. Rotating and agitating	3 l. Agitating
Solvent	Xylenols	Stabilized pasting oil	Xylenols	Xylenols	Stabilized pasting oil
Raw material	Refined lignin	Heat-precipitated lignin	Refined lignin	Dried SWL	Dried SWL
Reaction temp., °C	400	400	400	360	360
Reaction time, hr.	2	2	2	2	2
Initial pressure, kg./cm^2	130	170	130	130	130
Raw-material charged, g.	17	230	170	250	250
Solvent charged, g.	30	400	300	350	350

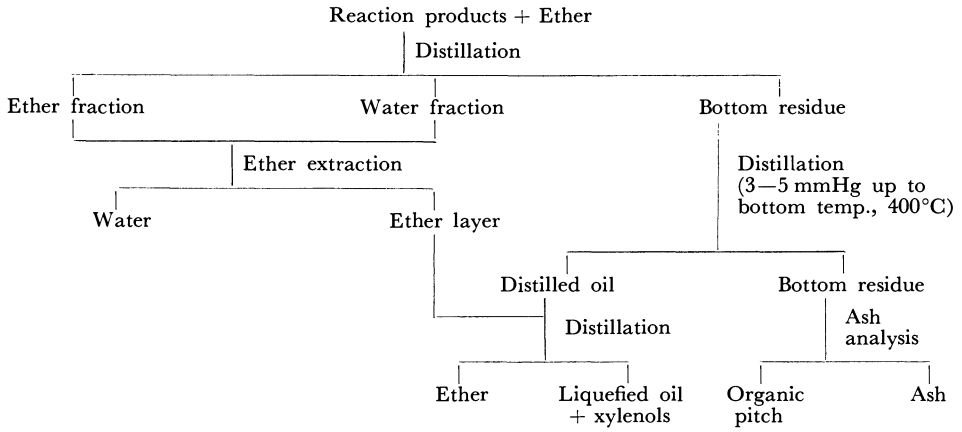

Fig. 1. The separation and analysis of the products of preliminary runs (Conditions A, C and D).

Liquefaction yield (L. Y.)=(distillable oil recovered-xylenol charged)/(lignin charged)×100%. In all the runs; Pressure difference (ΔP)=(Initial hydrogen pressure at room temp.—Final pressure at room temp.) (kg./cm^2)

Table II. Preliminary runs (Condition A)

Run No.	Catalyst	A. C.*1	L. Y.	P. Y.*2	Δp
2—18	Standard	10.4	41.0	19.5	21
2—22	Standard	11.1	27.2	30.1	18
2—30	Se	20.8	35.1	22.8	40
2—32	Se	2.08	22.2	41.2	41
2—37	Se	6.95	10.4	22.9	17

*1 Amount of catalyst
*2 Pitch yield

Results and Discussion

Selenium,[5] Tellurium and Zinc Iodide.—Table II shows the results of the preliminary runs with selenium metal as the catalyst under the condition A. A high hydrogen absorption of 21% (lignin charged) was observed when selenium was used. This cannot be explained by the consumption of hydrogen by selenium to form hydrogen selenide. As compared with the runs with a 10% standard catalyst, the run with 2% selenium gave more organic pitch, but the runs with selenium more than 7% the quantity of lignin gave an almost comparable pitch yield.

Selenium, suspected to be a peculiar catalyst in the preliminary runs, was fully evaluated under the B reaction condition, which is identical with that of Table I of Part III of a previous report.[3] As is shown in Table III, a remarkably high hydrogen absorption was observed, as had been expected. The neutral materials in the cut-3 fraction comprized, however, as much as 73% of the total.

The gasification was almost twice as much as the run with the standard catalysts and amounts of neutral materials and low boilers were high. Thus, the reaction mechanism seemed to be different from that with the standard catalyst. From a commercial point of view, the selenium catalyst was concluded to be less desirable than the standard catalyst. Tellurium was examined under the C reaction condition (Table IV). Tellurium showed a hydrogen absorption almost comparable to that of the standard catalyst, but the amount of organic pitch residue was exceptionally large. Tellurium was thus rejected.

Zinc iodide also gave a very high final-initial pressure difference. The product oil, however, was dark brown, tarry material and gave much non-distillable pitch (Table IV). The reaction mechanism seems to be different from the standard catalyst. A combination of zinc iodide and sulfur gave less pressure difference and a higher pitch yield than did zinc iodide without sulfur.

Other Miscellaneous Catalysts.—Although a vertical, mechanically-agitated autoclave and a horizontal, rotating autoclave were used (Table

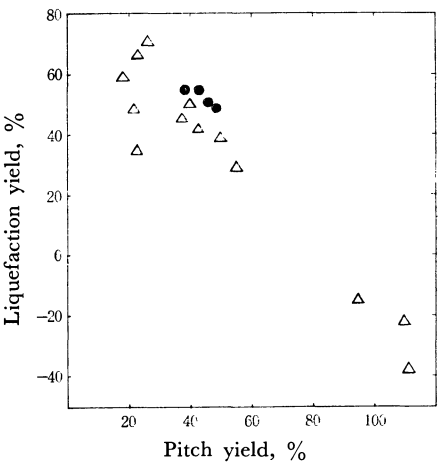

Fig. 2. Liquefaction yield against pitch yield.
● Standard catalyst

5) M. Oshima, K. Kashima, H. Tabata, T. Kubo and H. Watanabe, Japanese Pat, 460177 (1965).

Table III. Evaluation of selenium catalyst (Condition B)

Run No.	Catalyst	A. C.	P. O. R.*1	M. P. Y.*2	L. Y.	P. Y.	G & L*3
37—115	Se	21.6	96.8	5.79	32.6	16.1	52.1

*1 Pasting oil recovery *2 Monophenols yield *3 Gasification and loss

Table IV. Preliminary runs (Condition C)

Run No.	Catalyst	A. C.	ΔP	L. Y.	P. Y.
2—44	Standard	10.9	32	59.2	18.7
2—47	Standard	10.7	29	44.7	18.1
2—51	Te	18.1	31	44.2	29.7
2—52	ZnI_2	10.1	42	—	35.3
2—54	ZnI_2+S	14.6	27	19.7	50.1

Table V. Preliminary runs (Conditions D)

Run No.	Catalyst	A. C.	L. Y.	P. Y.	ΔP	Autoclave*
3— 50	Standard	30W	51.1	45.6	37	R
3— 51	Standard	30W	49.3	48.4	39	R
3— 63	Standard	30W	55.3	38.5	42	A
3— 65	Standard	30W	55.0	43.4	38	A
3— 52	None	None	−21.6	110.0	3	R
3— 59	S	15	−15.1	94.8	9	R
3— 69	ZnO	30	38.8	50.0	30	R
3— 76	ZnO	30	29.1	43.9	30	A
3— 67	Ni-S	30W	45.3	37.5	42	A
3— 68	$NiC_2O_4 \cdot 2H_2O$	20	50.3	40.3	37	A
3— 74	Zn-S	30W	−38.1	111.3	1	A
3— 88	$(NH_4)_6Mo_7O_{24} \cdot 4H_2O$	30	34.8	22.4	61	A
3—100	$(NH_4)_6Mo_7O_{24} \cdot 4H_2O$	30	48.7	21.9	60	A
3— 7	$Co_2(CO)_8$	30	59.0	18.0	50	A
3— 21	CoS	30W	66.0	22.8	51	A
3— 75	Raney Fe	20W	41.8	42.5	29	A
4— 10	$Fe(CO)_5$	20	70.6	26.2	38	A

* R: Rotating autoclave, A: Agitating autoclave, W: Weight of catalyst in a wet state

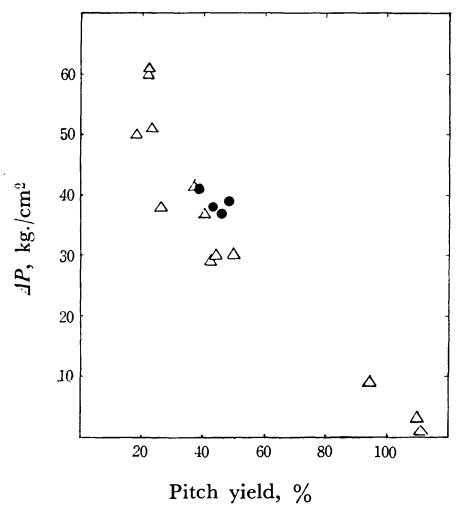

Fig. 3. Pressure difference between final-initial pressure against pitch yield.
● Standard catalyst

V), no difference was observed. These data gave the relation between the pitch yield and the liquefaction yield, and that between the pitch yield and the final-initial pressure difference, shown in Figs. 2 and 3 respectively.

Ni-S and nickel oxalate behaved almost identically as the standard catalyst. Raney iron was almost comparable to the above three. Cobalt sulfide and cobalt octacarbonyl showed a large final-initial pressure difference and a very low pitch yield. The two catalysts seemed to be better than the standard catalyst as far as the preliminary examination was concerned. Ammonium molybdate and iron pentacarbonyl showed a pressure difference comparable to that of the standard catalyst. They also showed a low pitch yield and a high liquefaction yield.

Zinc oxide unexpectedly showed a fair activity, though it was a little inferior to the standard catalyst. On the other hand, Zn-S showed no activity. Elemental sulfur showed very little activity.

Table VI. Evaluation of ammonium molybdate and iron pentacarbonyl (Condition E)

Run No.	Catalyst	A. C.	L. Y.	P. Y.	ΔP	M. P. Y.	P. O. R.
3—99	Standard	30	34.8	46.1	36	11.2	100.9
3—11	Standard	30	34.8	48.3	31	11.8	101.1
3—19	Standard	30	39.7	52.6	35	7.9	103.8
3—16	$(NH_4)_6Mo_7O_{24}\cdot 4H_2O$	30	47.4	32.3	57	9.9	106.5
3—17	$(NH_4)_6Mo_7O_{24}\cdot 4H_2O$	30	47.2	36.8	57	14.6	102.8
3—18	$(NH_4)_6Mo_7O_{24}\cdot 4H_2O$	30	51.2	37.2	54	8.6	108.2
3—20	$(NH_4)_6Mo_7O_{24}\cdot 4H_2O$	30	64.9	27.5	62	17.8	103.2
3—22	$Fe(CO)_5$	20	47.8	44.6	29	10.9	104.4
3—23	$Fe(CO)_5$	15	43.9	38.8	39	10.3	106.8
3—24	$Fe(CO)_5$	20	35.9	46.2	38	9.3	102.9
3—25	$Fe(CO)_5$	15	15.6	51.7	25	7.0	97.4

Ammonium Molybdate and Iron Pentacarbonyl. — In the preliminary examination described in the previous section, cobalt sulfide, cobalt octacarbonyl, ammonium molybdate, and iron pentacarbonyl seemed to be a little more active than the standard catalyst. The former two are expensive and so are not attractive for the commercial process. The latter two, ammonium molybdate and iron pentacarbonyl, were studied in detail under the E reaction condition (Table VI).

Statistical analysis showed that no difference in pitch yield, pressure difference, and monophenol yield could be deduced between the standard catalyst and the iron pentacarbonyl catalyst. In the case of ammonium molybdate, a higher pressure difference and a lower pitch yield than in the case of the above two catalysts can be concluded with more than a 99% confidence level. However, as far as the monophenol yield and the pasting oil recovery are concerned, no clear differences could be concluded to exist among the three catalysts studied.

From the commercial point of view, the monophenol yield at a 100% recovery of pasting oil is a critical factor. From this point of view, three catalysts showed almost identical activities. Considering the cost of preparation, the standard catalyst is, at least at present, the most desirable catalyst for the hydrocracking of lignin.

The authors would like to express their appreciation to the Noguchi Institute for the permission to publish this study.

NOTES

The Synthesis of 3-*t*-Butyl-6-methyl-2-benzofurylacetic Acid

By the late D. S. DEORHA and Padma GUPTA

Chemistry Department, University of Rajasthan, Jaipur, India

(Received September 14, 1965)

Arylacetic acid is made from an aromatic aldehyde by the hydrolysis of derived azlactone to pyruvic acid and by subsequent oxidation. During the investigation it has been observed that the azlactones of a few 2-formylbenzofurans offer resistance to hydrolysis, which therefore sometimes results only in tars. Moreover, the derived pyruvic acids are so sensitive to oxidation by alkaline hydrogen peroxide that the reaction is hard to control and sometimes furnishes sticky intractable gums. The reaction explored by Jennings[1] for the conversion of *m*-nitrobenzaldehyde to *m*-nitrophenylacetic acid has been successfully used by Dean and coworkers[2]; it has now been extended to the preparation of 3-*t*-butyl-6-methyl-2-benzofurylacetic acid from 2-formyl-3-*t*-butylbenzofuran.

For this purpose 2-hydroxy-4-methylphenyl *t*-butyl ketone (I, R=H), and 5-methyl-2-pivaloylphenoxyacetic acid (I, R=CH_2COOH) have been prepared and converted into 3-*t*-butyl-6-methylbenzofuran (II, R=H), which, when dimethylformamide and phosphorus oxychloride[3] are employed, yields 2-formyl-3-*t*-butyl-6-methylbenzofuran (II, R=CHO) in a good yield. The orientation of the formyl group in it has been confirmed by its oxidation to the carboxylic acid (II, R=COOH), which is identical with that formed by the cyclisation of the phenoxyester (I, R=$CH_2COOC_2H_5$) and by subsequent hydrolysis (II, R=$COOC_2H_5$). Thus, 4-[(3′-*t*-butyl-6′-methyl-2′-benzofuryl)methylene]-2-phenyloxazolin-5-one (III), obtained from 2-formyl-3-*t*-butyl-6-methylbenzofuran (II, R=CHO) by heating it with hippuric acid and sodium acetate in acetic anhydride, reacts with hydrazine hydrate to yield α-benzamido-β-(3-*t*-butyl-6-methyl-2-benzofuryl)acrylohydrazide (IV, R=$NHNH_2$). The latter, with nitrous acid, forms α-benzamido-β-(3-*t*-butyl-6-methyl-2-benzofuryl) acryloazide (IV, R=N_3). Upon being refluxed in dry benzene this azide furnishes 4-[(3′-*t*-butyl-6′-methyl-2′-benzofuryl)methyl]-6-phenyl-2*H*-1, 3, 5-oxadiazin-2-one (V), which, with hydrochloric acid, yields 3-*t*-butyl-6-methyl-2-benzofurylacetic acid (II, R=CH_2COOH).

Though more steps are involved in this method, it gives purer products and all the reactions proceed quite smoothly.

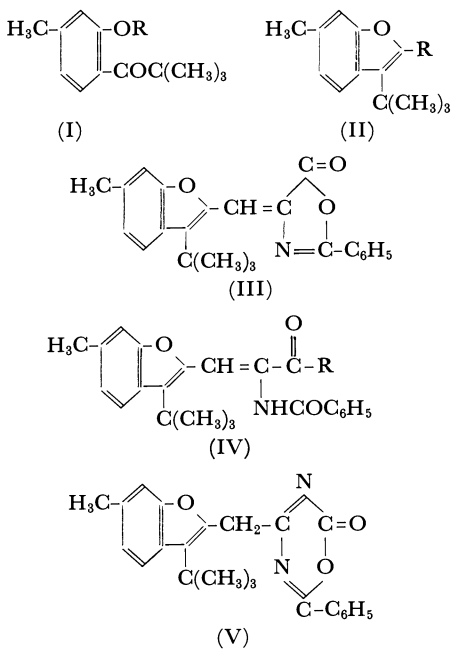

Experimental

2-Hydroxy-4-methylphenyl *t*-Butyl Ketone.—Pivalyl chloride (13.0 g.) was added gradually to a solution of *m*-cresol (10.8 g.) in dry ether (50 ml.) containing dry pyridine (9 ml.), the temperature maintained below 10°C. After it had been kept for 18 hr. at room temperature, the mixture was treated with water and then extracted with ether. The ether extract was thoroughly washed with aqueous sodium bicarbonate and then with water. The evaporation of the ether left an oil which, on distillation (b. p. 130°C/20 mmHg), furnished 3-methylphenyl pivalate[4] (17 g.) as a colorless oil.

1) K. F. Jennings, *J. Chem. Soc.*, **1957**, 1512.
2) F. M. Dean, D. S. Deorha, J. C. Knight and T. Francis, ibid., **1961**, 327.
3) M. Bisagni, Ng. Ph. Buu Hoi and R. Royer, ibid., **1955**, 3688.
4) R. Batzly, W. S. Ide and A. P. Phillips, *J. Am. Chem. Soc.*, **77**, 2522 (1955).

To the above ester (5 g.) finely-powdered anhydrous aluminum chloride (5 g.) was added in small quantities at room temperature. The reaction commenced immediately. After the addition, the mixture was heated at 70°C for 12 hr. The complex was decomposed with ice and 10 ml. of concentrated hydrochloric acid. The product, which was isolated with ether in the usual way, was distilled, whereby hydroxy ketone (2 g.) was obtained as a viscous liquid, b. p. 150°C/0.3 mmHg.

Found: C, 74.82; H, 8.46. Calcd. for $C_{12}H_{16}O_2$: C, 75.00; H, 8.33%.

With hydroxylamine the ketone formed an oxime which separated from benzene as colorless crystals, m. p. 164°C.

Found: N, 6.88. Calcd. for $C_{12}H_{17}NO_2$: N, 6.76%.

Ethyl 5-Methyl-2-pivaloylphenoxyacetate. — A mixture of 2-hydroxy-4-methylphenyl *t*-butyl ketone (15.5 g.), anhydrous potassium carbonate (40 g.), ethyl chloroacetate (10.2 g.), potassium iodide (0.1 g.), and dry acetone (150 ml.) was refluxed on a water bath for 18 hr. and then filtered. The residue was washed with hot acetone, and the combined acetone filtrates were distilled. The residue was crystallized from ethanol as colorless plates (21 g., 91%), m. p. 63°C.

Found: C, 69.25; H, 8.10. Calcd. for $C_{16}H_{22}O_4$: C, 69.03; H, 7.97%.

Its 2, 4-dinitrophenylhydrazone separated from ethanol in the form of yellow needles, m. p. 152°C.

Found: N, 12.00. Calcd. for $C_{22}H_{26}N_4O_7$: N, 12.22%.

5-Methyl-2-pivaloylphenoxyacetic Acid. — The foregoing ester (10 g.) was heated with sodium hydroxide (5%, 100 ml.) and ethanol (15 ml.) until it dissolved (2 hr.). The acidification of the cooled and diluted solution furnished the *phenoxyacetic* acid, which crystallized from ethanol as needles (8 g., 90%), m. p. 143°C.

Found: C, 67.34; H, 7.40. Calcd. for $C_{14}H_{18}O_4$: C, 67.17, H, 7.25%.

Its 2, 4-dinitrophenylhydrazone was crystallized from ethanol in the form of orange plates, m. p. 230°C.

Found: N, 13.28. Calcd. for $C_{20}H_{22}N_4O_7$: N, 13.02%.

3-*t*-Butyl-6-methylbenzofuran.—The above phenoxyacetic acid (14.0 g.) was mixed with anhydrous sodium acetate (25 g.) and acetic anhydride (50 ml.), kept at 160°C (oil bath) for 3 hr., and then poured into cold water (200 ml.). After 24 hr. the product was extracted with ether in the usual way. The removal of the ether left an oil which was distilled under reduced pressure as a colorless liquid (7.5 g., 73%, b. p. 100°C/5 mmHg).

Found: C, 83.14; H, 8.70. Calcd. for $C_{13}H_{16}O$: C, 82.93; H, 8.57%.

2-Formyl-3-*t*-butyl-6-methylbenzofuran.—a) An ice-cold mixture of *N*, *N*-dimethylformamide (3.5 ml.) and freshly-distilled phosphorus oxychloride (3.5 ml.) was added to a solution of 3-*t*-butyl-6-methylbenzofuran (1.0 g.) in *N*, *N*-dimethylformamide (3.5 ml.). The mixture was then heated on a water bath for 4 hr., cooled, diluted with water, and neutralized with sodium bicarbonate. After 2 hr., the product was extracted with ether in the usual way, and recovered by the evaporation of the solvent. The residue was crystallized from ethanol, furnishing the 2-formylbenzofuran (1.0 g., 89%) in the form of colorless needles, m. p. 60°C.

Found: C, 77.90; H, 7.30. Calcd. for $C_{14}H_{16}O_2$: C, 77.71; H, 7.45%.

b) A solution of 3-*t*-butyl-6-methylbenzofuran (1.0 g.) in ether (10 ml.) containing hydrogen cyanide (0.7 ml.) and aluminum chloride (1.0 g.) was saturated at 0°C with hydrogen chloride, kept for 24 hr., and then evaporated in a current of air. The hydrolysis of the residue with 40 ml. of water at 0°C, and then on a boiling water bath for 1 hr., gave a low-melting solid. The product was isolated by ether in the usual way. The removal of the ether left a residue which, on crystallization from ethanol, furnished 2-formyl-3-*t*-butyl-6-methylbenzofuran (0.35 g., 30%) in the form of colorless needles, m. p. and mixed m. p. with the above sample under a), 60°C.

The 2, 4-dinitrophenylhydrazone separated from ethanol in the form of red crystals, m. p. 261°C.

Found: N, 14.40. Calcd. for $C_{20}H_{20}N_4O_5$: N, 14.14%.

4-[(3'-*t*-Butyl-6'-methyl-2'-benzofuryl)methylene]-2-phenyloxazolin-5-one.— A mixture of the above-mentioned formylbenzofuran (4.65 g.), benzoylglycine (7 g.), anhydrous sodium acetate (4.0 g.), and acetic anhydride (25 ml.) was heated on a water bath for 2 hr., cooled, diluted with ethanol (100 ml.), and kept overnight. The crystalline solid was then filtered and crystallized from ethanol as orange yellow needles (7.7 g., 72%), m. p. 195°C.

Found: N, 4.15. Calcd. for $C_{23}H_{21}NO_3$: N, 3.09%.

α-Benzamido-β-(3-*t*-butyl-6-methyl-2-benzofuryl) Acrylohydrazide. — To a suspension of the finely-powdered oxazolone (5.0 g.) in ethanol (150 ml.), 99% hydrazine hydrate (0.7 g.) was added. This mixture was vigorously stirred until the color had been discharged. The solid was then collected and crystallized from ethanol to furnish acrylohydrazide (5.4 g., 89%) in the form of light yellow needles, m. p. 187°C.

Found: N, 10.59. Calcd. for $C_{23}H_{25}N_3O_3$: N, 10.74%.

4-[3'-*t*-Butyl-6'-methyl-2'-benzofuryl)methyl]-6-phenyl-2*H*-1, 3, 5-oxadiazin-2-one.—An ice-cold solution of sodium nitrite (0.3 g.) in a minimum amount of water was added slowly to a solution of the α-benzamido-β-(3-*t*-butyl-6-methyl-2-benzofuryl) acrylohydrazide (1 g.) in glacial acetic acid (25 ml.), the temperature being kept below 10°C. After 30 min., the yellow crystalline precipitate was filtered, washed with water, and dried in air.

The crude azide (1 g.) (decomp. 136°C) was then extracted from a soxhlet thimble with benzene (50 ml.); when concentrated and cooled, the benzene extracts deposited a product which, on recrystallization from benzene, gave the oxidiazine (0.7 g., 85%) in the form of orange-yellow needles, m. p. 214°C.

Found: N, 7.20. Calcd. for $C_{23}H_{22}N_2O_3$: N, 7.48%.

3-*t*-Butyl-6-methyl-2-benzofurylpyruvic Acid. — A mixture of 4-[(3'-*t*-butyl-6'-methyl-2'-benzofuryl)-methylene]-2-phenyloxazolin-5-one (1.0 g.) and potassium hydroxide (20%, 20 ml.) was boiled under reflux until the oxazolone dissolved completely. The condenser was then removed, and the hydrolysis was completed by gentle boiling until ammonia could no longer be detected in the issuing vapors. During the latter part of the reaction, the volume of the solution was kept at 20ml. by the occassional addition of water.

The solution was then diluted with water (50 ml.) and filtered. The cold filtrate was acidified with concentrated hydrochloric acid, and then warmed on a steam bath to 60°C. In this form, the pyruvic acid separated in a granular form and was easily filtered. The benzoic acid formed in the reaction remained in solution. The pyruvic acid crystallized from benzene as colorless plates (0.25 g., 24%), m. p. 206°C.

Found: C, 70.20; H, 6.40. Calcd. for $C_{16}H_{18}O_4$: C, 70.01; H, 6.61%.

3-*t*-Butyl-6-methyl-2-benzofurylacetic Acid.—a) A suspension of the above-mentioned oxadiazine (3.74 g.) in acetic acid (40 ml.) and 5 N hydrochloric acid (5 ml.) was refluxed until its dissolution was complete and the color of the solution had been completely discharged, whereafter dilution with water precipitated the 2-benzofurylacetic and benzoic acids. The latter was leached out with water at 60°C, leaving the crude 2-benzofurylacetic acid, which was then crystallized from aqueous ethanol (1 : 1) in colorless plates (2.0 g., 85%), m. p. 130°C.

Found: C, 73.00; H, 7.95. Calcd. for $C_{15}H_{18}O_3$: C, 73.13; H, 7.83%.

b) A solution of the crude pyruvic acid (1.0 g.) in aqueous potassium hydroxide (5 ml., 10%) at 0°C was mixed with hydrogen peroxide (20 ml., 100 vol.), warmed until effervescence began, cooled to 0°C, diluted with ice water, and finally acidified with concentrated hydrochloric acid. The 3-*t*-butyl-6-methyl-2-benzofurylacetic acid thus precipitated crystallized from aqueous ethanol (1 : 1) as colorless plates (0.31 g., 35%), m. p. and mixed m. p. with the sample under a), 130°C.

Its methyl ester, prepared by diazomethane, crystallized from benzene in the form of colorless needles, m. p. 52°C.

Found: C, 73.96; H, 7.60. Calcd. for $C_{16}H_{20}O_3$: C, 73.79; H, 7.74%.

3-*t*-Butyl-6-methyl-2-benzofurylcarboxylic Acid.—a) Ethyl 5-methyl-2-pivaloylphenoxyacetate (1.08 g.) was dissolved in ethanol (10 ml.), and a solution of sodium ethoxide (0.2 g. of sodium in 10 ml. of dry ethanol) was added. The solution was heated on a water bath for 15 min. and then diluted with water (20 ml.). The clear solution was acidified with 5 N hydrochloric acid. The product was crystallized from ethanol in the form of colorless prisms (0.4 g., 40%), m. p. 234°C.

Found: C, 73.19; H, 7.18. Calcd. for $C_{14}H_{16}O_3$: C, 73.00; H, 7.00%.

b) 2-Formyl-3-*t*-butyl-6-methylbenzofuran (1.0 g.) was dissolved in purified acetone (50 ml.), and a solution of potassium permanganate (0.6 g.) in water (20 ml.) was added. The solution slowly deposited manganese dioxide; after 18 hr., this was removed by means of sulfur dioxide. The solution was then diluted with water, and the solid that separated was collected, dissolved in ether, and extracted with a sodium bicarbonate solution. The extract was acidified with 5 N hydrochloric acid to give the acid (0.5 g., 46%), which was crystallized from ethanol, m. p. and mixed m. p. with the above sample under a), 234°C.

The thanks of the authors are due to Professor R. C. Mehrotra, Head of the Chemistry Department, University of Rajasthan, Jaipur, for providing facilities, and to the Council of Scientific and Industrial Research, New Delhi, for awarding a fellowship to P. G.

Vibrational Analysis of Substituted and Perturbed Molecules. Direct Determination of Force Constants from the Coriolis Interaction

By C. David Bass* and Jack S. Margolis**

North American Aviation Science Center, Thousand Oaks, California

(Received September 22, 1965)

Molecular spectroscopists generally acknowledge the importance of obtaining the molecular force constants since there is much potential information contained in them if they can be determined accurately enough. For example, these force constants may be related to the chemical bonding and the electronic structure; they are useful to the spectroscopist for predicting the molecular frequencies beyond the range of his instruments and in interpreting the combination and overtone bands he observes. Also, determining accurate values of the anharmonic forces goes hand in hand with determing the harmonic forces. The analysis required to obtain molecular force constants using the $\boldsymbol{F}$-$\boldsymbol{G}$ matrix techniques rapidly becomes very complex as the molecular size increases and must proceed in a backward manner.

A great deal of the computational difficulties of the $\boldsymbol{F}$-$\boldsymbol{G}$ matrix procedure has been obviated by means of the molecular Green's function.[1)]

* Present Address: TRW Systems, Inc. One Spare Park, Redondo Beach, California.

** Present Address: Jet Propulsion Laboratory 480 Oak Grove Drive, Pasadena, Califonia.

1) a) R. E. DeWames and T. Wolfram, *J. Chem. Phys.*, **40**, 853 (1964); b) C. D. Bass, L. Lynds, T. Wolfram and R. E. DeWames, ibid., **40**, 3611 (1964); c) T. Wolfram, C. D. Bass, R. E. DeWames and L. Lynds, This Bulletin, **39**, 201 (1966); d) L. Lynds, T. Wolfram and C. D. Bass, *J. Chem. Phys.*, **43**, 3775 (1965).

For XY_3 planar molecules, the Green's function method allows direct computation of the mixing parameter connecting two modes of the same symmetry type using only the observed frequencies as input data. The force constants can then be calculated directly from the mixing parameter. It is not necessary to make mathematical approximations in order to solve the equations and so computational errors are negligible. However, the number of molecular frequencies available to the computation are usually not more than just sufficient to determine the force constants, and since the off-diagonal components[2] of the force constant matrix are very sensitive to small variations of the frequencies there will remain large uncertainties in the values of these numbers. It is important to find measurable quantities which determine the force in a less sensitive way. One such quantity is the Coriolis coefficient. Mills,[3] Meal and Polo,[4] Kristiansen and Cyvin,[5] Boyd and Longuet-Higgins[6] have shown how to relate the Coriolis coefficient to force constants.

Calculations

The Coriolis coefficient, ζ_r, can be measured directly from the splitting of the degenerate frequencies of a molecular vibration. Following the procedure of Boyd and Lonquet-Higgins[6] we denote the two real normal coordinates of a degenerate vibration P_r, Q_r; these are written in a basis of mass adjusted cartesian coordinate u_k, v_k, w_k:

$$u_k=\sqrt{m_k}x_k;\quad v_k=\sqrt{m_k}y_k;\quad w_k=\sqrt{m_k}z_k.$$
$$P_r=\sum_j \alpha_{rj}S_j;\quad Q_r=\sum_j \alpha_{rj}S_j. \tag{1}$$

As an example of this we apply the method to the calculations of the mixing parameter for a molecule of type XY_3-planar. The normal coordinates for this molecule have been tabulated in Ref. 1b.

This leads to the following expression for the Coriolis coefficient ζ_3:

$$\zeta_3=\sum_k \begin{vmatrix} \frac{\partial P_r}{\partial u_k} & \frac{\partial P_r}{\partial v_k} \\ \frac{\partial Q_r}{\partial u_k} & \frac{\partial Q_r}{\partial v_k} \end{vmatrix}$$
$$=\frac{1}{A^2d_1{}^2d_2{}^2}[3r^2(a^2d_1{}^2-2ad_1+1)-d_2{}^2(2ad_1+3r^2)]. \tag{2}$$

This may be rewritten as an equation with a as the unknown:

$$d_1{}^2(3r^2-d_2{}^2\zeta_3)a^2-4d_1{}^3a-d_1{}^2(3r^2+d_2{}^2\zeta_3)=0. \tag{3}$$

As a specific illustration we shall consider the case of BF_3. From the potential constants $F_{33}=6.303\times10^5$, $F_{34}/d=-0.259\times10^5$, and $F_{44}/d^2=0.528\times10^5$ (all force constants are millidynes/Angstrom), Meal and Polo[4] calculated $\zeta_3=0.83$ for BF_3. Substitution of this value for ζ_3 into Eq. 3 gives a value -1.2761 for a, which compares with $a=-1.2765$ calculated from Eq. 12, Ref. 1b. The force field, calculated from the equations in 1c is: $F_{33}=6.310\times10^5$, $F_{34}/d=-0.3198\times10^5$, $F_{44}/d^2=0.528\times10^5$. The frequencies used to obtain the latter results appear in a publication of Ladd et al.[7] Aside from F_{34}/d, which is the potential constant most sensitive to observed frequencies, the results are in substantial agreement.

However, a different set of data, (Ref. 5) results in a quite different force field, as calculated by the Wilson method: $F_{33}=7.4068\times10^5$, $F_{34}/d=-0.6398\times10^5$, $F_{44}/d^2=0.50013\times10^5$. The value of ζ_3 calculated in Ref. 5 is 0.717. Abramowitz has recently measured ζ_3 and found a value 0.70.[8] Equation 2 gives $a=-1.0385$ for $\zeta_3=0.70$, and, using the frequencies of Ref. 5 with the equations of 1c: $F_{33}=7.5807\times10^5$, $F_{34}/d=0.7934\times10^5$, $F_{44}/d^2=0.5060\times10^5$. Equation 12, Ib gives $a=-1.1261$. There is substantial agreement within this last set of data, the largest discerpancy again appearing in F_{34}/d.

The new result of Abramowitz indicates that the BF_3 vibrational data of Kristiansen and Cyvin[5] is more reliable that other reported data. Utilizing the simple formalism of this paper, and our previous results (1a—1b) we have performed the calculations with much less effort than earlier investigators.

2) We are speaking of off-diagonal in the sense of a matrix constructed in a basis of internal coordinates. However, the Green's function analysis is most conveniently carried out in a basis of external cartesian coordinates which form an ortho-normal set. The advantage is that we deal with unitary matrices.

3) I. M. Mills, *J. Mol. Spectroscopy*, **5**, 334 (1960).

4) J. H. Meal and S. R. Polo, *J. Chem. Phys.*, **24**, 1126 (1956).

5) L. Kristiansen and S. J. Cyvin, *J. Mol. Spect.*, **11**, 185 (1963).

6) D. J. R. Boyd and H. C. Longuet-Higgins, *Proc. Royal Soc.*, **A213**, 55 (1952).

7) J. A. Ladd, W. J. Orville-Thomas and B. C. Cox, *Spectrochimica Acta*, **19**, 1911 (1963).

8) S. Abramowitz, Private Communication, *J. Chem. Phys.*, **43**, 4213 (1965).

o-Methyl Proton Chemical Shifts in Sterically-much-hindered Aromatic Ketones

By Kazuhiro MARUYAMA

Department of Chemistry, Faculty of Science, Kyoto University, Sakyo-ku, Kyoto

(Received February 16, 1966)

Proton chemical shifts of α-hydrogen atom in the aromatic side chain have theoretically been explained by the ring current model. Furthermore, it is known experimentally that *o*-carboxy, *o*-carbonyl, and *o*-nitro substituents cause a paramagnetic shift (i. e., a shift to a lower τ-value) of about 0.2—0.3 p. p. m. to the α-hydrogen atom of the methyl group on the aromatic ring.[1] The present author has found that *o*-methyl protons of sterically-much-hindered ketones, alkyl-substituted benzophenone derivatives and alkyl-substituted pivalophenone derivatives show, rather, a shift to a higher τ-value of about 0.2—0.3 p. p. m. The results are shown in Table I. NMR spectra for all compounds were obtained in a carbon tetrachloride solution using tetramethylsilane as the inner reference. Carbon tetrachloride solutions with concentrations from five to ten percent were used for all the measurements because there was no appreciable difference in chemical shifts within this concentration for these compounds. The values of the chemical shifts were corrected by the side-band method. A 60 Mc. 3H-60 spectrometer, manufactured by the Japan Electron Optics Laboratory, was used in these measurements.

Synthetic method and their physical constants of the compounds from No. 22 to No. 27 have been reported in this Bulletin.[2]

As one can easily see in Table I, methyl protons of the 2, 6-position and of the 2, 6, 2′, 6′-position of alkylated benzophenone derivatives (No. 14—No. 21) appear at a considerably higher field side than do methyl protons of sterically-less-hindered benzophenone derivatives (No. 7—No. 13). In methylated pivalophenone derivatives, again, methyl protons of the 2-position and of the 2, 6-position appear at a higher field side. Because the paramagnetic shielding effect of the *o*-carboxy, *o*-carbonyl, and *o*-nitro groups on the methyl group will be most effective if the benzene ring and these substituents have coplanarity, the observed effects (i. e., the shift to a higher field side) in sterically-much-hindered ketones might be due to the loss of coplanarity among two benzene rings, the carbonyl group, and methyl groups.* Methyl-proton chemical shifts of 2, 6, 2′-trimethylbenzophenone (No. 15) are likely to be typical and to show these circumstances most clearly: 2, 6-CH_3, $\delta(10-\tau)$: 2.04, 2′-CH_3, δ : 2.64. That is to say, 2, 6-CH_3 protons appear at a higher field side than do 2-CH_3 of 2-methylbenzophenone, and 2′-CH_3 appears at a far lower field side than that. Considering the molecular model, the two benzene rings in 2, 6, 2′-trimethylbenzophenone are exactly perpendicular to each other at the most strain-free average molecular state, and the 2′-methyl group may take the position which is affected most effectively by the magnetic deshielding effect of the carbonyl group (see Fig. 1). On

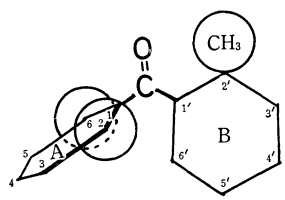

Fig. 1. Configuration of 2, 6, 2′-trimethylbenzophenone.

the other hand, 2- and 6-methyl groups must be under the influence of the magnetic shielding effect of the carbonyl group because the plane of the carbonyl double bond and the plane of the disubstituted benzene ring are perpendicular; then the signal moves upfield. Although two benzene rings in 2, 6, 2′, 6′-tetramethylbenzophenone are also able to be perpendicular to each other with a slight sterical repulsion of a methyl group (i. e., 6′-CH_3 on ring B) and a benzene ring (i. e., ring A), this state could not be the most strain-free molecular state. Two benzene rings and the carbonyl group should take a twisted position to each other in the more strain-free state, and then the four methyl groups may be non-equivalent in this state. Two of the four methyl groups can be near the other benzene ring, and the other two methyl groups near the

1) J. C. P. Schwarz, "Physical Method in Organic Chemistry," Oliver and Boyd, London (1964), p, 175.
2) H. Suzuki, H. Wada, K. Maruyama and R. Goto, This Bulletin, **39**, 1201 (1966).

* The experimental results of UV measurements made on an extensive series of methyl-substituted benzophenones by Rekker and Nauta indicate a loss of coplanarity between two benzene rings attributed to the steric effects of *o*- and *o*′-substituted methyl groups. R. F. Rekker and W. T. Nauta, *Rec. Trav. Chim.*, **73**, 969 (1954); **77**, 714 (1958); **80**, 747 (1961); **80**, 764 (1961).

TABLE I. PROTON CHEMICAL SHIFTS OF METHYL GROUP OF ALKYLATED BENZOPHENONES AND OF ALKYLATED PIVALOPHENONES AT 23°C

No.	Compound	CH_3	Proton chemical shifts $\delta(10-\tau)$	Others
1	Toluene	2.32		
2	*o*-Xylene	2.23		
3	*o*-Nitrotoluene	2.45		
4	*o*-Carboxytoluene	2.62		
5	*m*-Carboxytoluene	2.37		
6	*p*-Carboxytoluene	2.37		
	Benzophenone derivatives			
7	2-Methyl-	2.23		
8	3-Methyl-	2.22		
9	4-Methyl-	2.21		
10	2, 2'-Dimethyl-	2.35		
11	2, 4'-Dimethyl-	2.21	(2-CH_3), 2.33 (4'-CH_3)	
12	2-Methyl-4'-*t*-butyl-	2.23		1.22 (*t*-Bu)
13	4, 4'-Dimethyl-	2.33		
14	2, 4, 6-Trimethyl-	1.98	(2, 6-CH_3), 2.23 (4-CH_3)	
15	2, 6, 2'-Trimethyl-	2.04	(2, 6-CH_3), 2.64 (2'-CH_3)	
16	2, 6-Dimethyl-4-*t*-butyl-	2.06		1.32 (*t*-Bu)
17	2, 6-Dimethyl-4-*t*-butyl-4'-nitro-	2.00		1.30 (*t*-Bu)
18	2, 6-Dimethyl-4-*t*-butyl-4'-chloro-	2.05		1.32 (*t*-Bu)
19	2, 6, 2', 6'-Tetramethyl-	2.04		
20	2, 6, 2', 6'-Tetramethyl-4, 4'-di-*t*-butyl-	2.06		1.26 (*t*-Bu)
21	2, 4, 6, 2', 4', 6'-Hexamethyl-	1.98	(2, 6, 2', 6'-CH_3), 2.17 (4, 4'-CH_3)	
	Pivalophenone derivatives			
22	2, 4-Dimethyl-	2.07	(2-CH_3), 2.22 (4-CH_3)	1.14 (*t*-Bu)
23	2, 3, 4-Trimethyl-	1.99	(2-CH_3), 2.07 (3-CH_3), 2.18 (4-CH_3)	1.14 (*t*-Bu)
24	2, 4, 5-Trimethyl-	2.07	(2-CH_3), 2.15 (4, 5-CH_3)	1.14 (*t*-Bu)
25	2, 4, 6-Trimethyl-	2.06	(2, 6-CH_3), 2.18 (4-CH_3)	1.14 (*t*-Bu)
26	2, 3, 4, 5-Tetramethyl-	2.01	(2-CH_3), 2.14 (3, 5-CH_3), 2.21 (4-CH_3)	1.14 (*t*-Bu)
27	2, 3, 5, 6-Tetramethyl-	1.98	(2, 6-CH_3), 2.16 (3, 5-CH_3)	1.14 (*t*-Bu)

carbonyl. However, this state is interconvertible with a rotation of C_1—C—$C_{1'}$ bondings without

any appreciable sterical repulsion through the molecular state in which two benzene rings are perpendicular to each other. Thus, four methyl groups are supposed to become equivalent to the average molecular state. Recently, Mislow and co-workers[3] have observed the methyl proton chemical shifts of *o*, *o'*-bridged biphenyl derivatives and found that the signal moved upfield with an increase in the angle of torsion between the two benzene rings; they ascribed this effect to the magnetic shielding effect of the other benzene ring on which the methyl was not attached. Therefore, a part of the shielding effect might also be ascribed to that of the benzene ring in 2, 6, 2', 6'-tetramethylbenzophenone. Thus, four methyl groups may be supposed to be under the magnetic shielding effect of both the carbonyl group and the benzene ring, although it is not clear which is the more important of the said shielding effects.

A similar explanation may be applied to all the compounds examined here which show a shift to the upfield side of the methyl proton signal.

3) K. Mislow, M. A. W. Glass, H. B. Hopps, E. Simon and G. H. Wahl, Jr., *J. Am. Chem. Soc.*, **86**, 1710 (1964).

Extended Hückel Calculations Including the Outer Orbitals: Ethylene, Methyl Chloride and Related Compounds

By Hiroshi KATO, Hideyuki KONISHI and Teijiro YONEZAWA

Faculty of Engineering, Kyoto University, Sakyo-ku, Kyoto

(Received March 7, 1966)

LCAO calculations including the outer atomic orbitals (AO) have been carried out for small molecules by several authors.[1,2] In this note, the extended Hückel method proposed by Hoffmann[3] is modified so that the molecular orbitals (MO) are constructed not only by the valence AO's but also by the outer AO's. The calculations are made for planar ethylene, twisted ethylene, methyl chloride, and the transient species, $(Cl\cdots CH_3\cdots Cl)^-$, appearing in S_N2-type reactions. The calculations are carried out by several methods. The following AO's are included in each method:

A: valence AO's

B: valence AO's + $3s_C$, $3p_C$ AO's,

C: valence AO's + $3s_C$, $3p_C$ AO's + $2s_H$, $2p_H$ AO's,

D: valence AO's + $3s_C$, $3p_C$ AO's + $3d_C$, $3d_{Cl}$ AO's,

where $3s_C$ and $3p_C$ refer to the 3s and 3p AO's of the carbon atom and so on.

The adopted values of the Coulomb integrals of the outer AO's are as follows: −3.75 eV. for the carbon 3s AO; −2.35 eV. for the carbon 3p AO's;[4] −3.40 eV. for the hydrogen 2s, 2p AO's, and −1.47 eV. and −1.60 eV. for the carbon and chlorine 3d AO's respectively.[5] The orbital exponents of these AO's, derived from the rule in Ref. 2, which are necessary in calculating the overlap integrals, are 0.500 for the hydrogen AO's, 0.483 for the carbon AO's, and 2.0333 for the chlorine AO's. The geometries of the treated compounds have already been given in our previous paper,[6,7] where the adopted configurations for the transient species, $(Cl\cdots CH_3\cdots Cl)^-$, were denoted by the notations b-IV and b-VI.[7]*

The calculated values of the total electronic energy, the highest occupied (HO), the lowest vacant (LV), and the next LV orbital energies of the normal and twisted ethylene molecules are listed in Table I (a), along with the methods adopted. The same quantities calculated for the methyl chloride and the transient species are given in Table I (b). Remarkable effects of the inclusions of the outer AO's are seen on the lowerings of the vacant MO energies. For normal ethylene, the first $\pi-\sigma^*$ transition energies are

Table I. The calculated total energies, E, the HO, LV and the next LV orbital energies (in eV.)

(a)	C_2H_4	E	HO	LV	Next LV
Normal	A	−210.83	−13.24	−8.25	+8.14
	B	−212.47	−13.24	−8.46	−5.17
	C	−215.75	−13.24	−8.80	−5.87
Twisted	A	−207.33	−10.39	+11.02	+12.94
	B	−208.99	−10.41	−5.17	−3.61
	C	−214.19	−10.75	−5.71	−5.04

(b) CH_3Cl and the species b-IV, b-VI

	Method	E	HO	LV
CH_3Cl	A	−249.79	−13.80	+1.09
	B	−250.20	−13.80	−4.43
	D	−250.47	−13.81	−4.96
b-IV	A	−388.77	−13.76	−3.77
	B	−389.43	−13.79	−5.51
	D	−389.82	−13.82	−6.05
b-VI	A	−386.01	−12.61	−3.52
	B	−386.83	−12.68	−5.45
	D	−387.43	−12.78	−5.89

Table II. The atomic orbital bond populations, $N(r-s)$, of the C-Cl bonds in the b-VI compounds

Method	s/r	$N(r-s)$			
		$2s_C$*	$2p\sigma_C$	$3s_C$	$3p\sigma_C$
B	$3s_{Cl}$*	−0.042	0.053	0.035	−0.022
	$3p\sigma_{Cl}$	−0.043	0.189	0.0	0.003
D	$3s_{Cl}$	−0.031	0.056	0.028	−0.022
	$3p\sigma_{Cl}$	−0.040	0.191	0.0	0.002

* The notation $2s_C$ denotes the carbon 2s AO, and $3s_{Cl}$ is the chlorine 3s AO and so on.

1) E. g., J. Jacobs, *Proc. Phys. Soc.*, **A68**, 72 (1955).
2) H. Lefebvre-Brion and C. M. Moser, *J. Mol. Spectro.*, **13**, 418 (1964).
3) R. Hoffmann, *J. Chem. Phys.*, **39**, 1397 (1963).
4) H. Hosoya, Summary of the 18th Annual Meeting of the Chem. Soc. of Japan (1965), p. 480.
5) C. E. Moore, "Atomic Energy Levels," Natl. Bureau of Standards, Washington (1949).
6) T. Yonezawa, H. Konishi, H. Kato, K. Morokuma and K. Fukui, *J. Chem. Soc. Japan, Ind. Chem. Sect. (Kogyo Kagaku Zasshi)*, **69**, 869 (1966).
7) H. Kato, K. Morokuma, T. Yonezawa and K. Fukui, This Bulletin, **38**, 1749 (1965).

* The configurations of these compounds are as follows: for the b-IV compounds, the C–Cl$^-$ distance is 2.4 Å; for the C–Cl, 1.95 Å and the Cl–C–H angle is 100°, and for the b-VI symmetrical configuration, the C···Cl is 2.05 Å, and the Cl–C–H angle, 90°.

21.4 eV. by Method A, and 7.4 eV. by Method C. As to the total energies, the lowerings in the twisted ethylene are larger than those in normal ethylene.

The same tendencies are found in the methyl chloride and its anions. Namely, the differences between the HO and LV orbital energies of methyl chloride are 15 eV. by Method A and 9 eV. Method D, whereas the corresponding observed value is about 8 eV.[7] The largest lowering of the total energy of the compounds in Table I (b) is found in the species with a symmetrical configuration, b-VI. Further, by population analysis of the above compounds it is shown that the carbon 3s AO participates in the C—Cl bondings while the 3pσ AO does not, as Table II shows. In other words, it may be suggested that the hybrids formed by the carbon 2pσ and 3s AO's take part mainly in the C—Cl bonding at the transition state of S_N2-type reactions. The contributions of the 3d AO's to the ground state of chlorinated compounds are found to be negligibly small.

Accordingly, it may be concluded that the inclusion of the outer AO's improves especially the excited states of the normal molecules and the ground states of the unstable compounds or of those containing atoms with unusual valencies. Hence, the improvement made in Methods B, C and D may be useful in discussing the σ-σ^* transition and the ^{13}C–H coupling constants in NMR of various compounds. Full details of these results will be published in the near furture.

The authors wish to thank Professor Saburo Nagakura and Dr. Haruo Hosoya for their kind advice.

The Reaction of Cuprous Ethanethiolate with 1, 2-Dibromoethylene

By Masuo MURAKAMI and Kozo TAKAHASHI

Central Research Laboratory, Yamanouchi Pharmaceutical Co., Ltd., Itabashi-ku, Tokyo

(Received March 28, 1966)

In 1959, Adams and Ferretti[1] reported that *S*-ethyl hydrogen thiocarbonate was formed by the oxidation of ethyl ethynyl sulfide, which had been obtained from the reaction between 1, 2-dibromoethylene and cuprous ethanethiolate, with hydrogen peroxide. It is generally accepted that the thiocarbonic acid and their primary esters are exceedingly unstable in the free state, but their derivatives, such as salts, neutral esters and amides, are sufficiently stable.

Since the observation of Adams and Ferretti about the stability of *S*-ethyl hydrogen thiocarbonate seems unusual, we have repeated their experiments; we have found that the reaction between 1, 2-dibromoethylene and cuprous ethanethiolate does not lead to ethyl ethynyl sulfide, but to 1, 2-bis-ethylthioethylene, which is subsequently converted to the corresponding sulfone by oxidation.

The reaction of cuprous ethanethiolate with commercial 1, 2-dibromoethylene*1 was carried out according to the reported procedure.[1] The product **I**, b. p. 104—108°C at 18 mmHg, was isolated in a 49% yield, while a large amount of tarry material remained:

$$Br\text{-}CH{=}CH\text{-}Br + CuSC_2H_5 \longrightarrow C_2H_5S\text{-}CH{=}CH\text{-}SC_2H_5 \quad (I)$$

The infrared spectrum of I was similar to that of Adams and Ferretti's product (b. p. 61°C at 1 mmHg), which they assumed to be ethyl ethynyl sulfide. It showed a strong band at 1260 cm^{-1}, but not those absorptions at 3300 cm^{-1} and 2100—2140 cm^{-1} which are characteristic of monosubstituted acetylenes. The results of elementary analysis (Found: C, 48.37; H, 8.06; S, 43.35), Calcd. for $C_6H_{12}S_2$: C, 48.63; H, 8.16; S. 43.25%. gas chromatography*2 and NMR spectrum (3.90 τ(s), 3.93 τ(s), 7.29 τ(q), 7.33 τ(q), 8.70 τ(t), 8.72 τ(t)) indicated that I was a mixture of about equal amounts of two stereoisomeric 1, 2-bis-ethylthioethylenes. When I was oxidized with hydrogen peroxide in acetic acid as reported before, two isomeric products were isolated; they were then purified by recrystallization from ethanol. The first product **II**, m. p. 145—146°C, is less soluble than the second product **III**, m. p. 90—91°C, which is easily soluble in water. The yields were 35% and 41% respectively. The analysis leads to identical empirical formulas ($C_2H_6O_2S$) for both products; the would-be *S*-ethyl hydrogen thiocarbonate, m. p. 145—146°C, prepared by

1) R. Adams and A. Ferretti, *J. Am. Chem. Soc.*, **81**, 4927 (1959).

*1 Infrared spectrum and NMR spectrum showed that the material is a mixture of about equal amount of cis and trans form.

*2 Gas chromatography on Silicon DC 550 column (1 m.) with hydrogen as carrier gas at 100°C showed two peaks with about equal peak-height.

Adams and Ferretti[1] also gives the same formula. These facts demonstrate that II is apparently identical with the Adams and Ferretti's product. Both of the isomers thus obtained are neutral substances, and they show two strong bands, at 1310 cm^{-1} and 1120 cm^{-1}, in the infrared spectrum, which can be assigned to the stretching vibration of a sulfone group.

When both isomers are hydrogenated over palladium-carbon, one mole of hydrogen was absorbed easily, yielding a theoretical amount of 1, 2-bis-ethylsulfonylethane, m. p. 137—139°C, which does not depress the melting point of the authentic sample.[2]

$\longrightarrow C_2H_5SO_2CH{=}CHSO_2C_2H_5 \longrightarrow$

(II): trans $C_2H_5SO_2CH_2CH_2SO_2C_2H_5$

(III): cis

2) Beckman, *J. Prakt. Chem.*, **17**, 469 (1878).

From these results, we may conclude that II and III are geometrical isomers[3] of 1, 2-bis-ethylsulfonylethylene.

Boonstra and Rinzema[4] reported that ethyl ethynyl sulfide[5] shows characteristic bands at 3330 cm^{-1} and 2040 cm^{-1} in the infrared spectrum. From these findings, it is evident that the Adams and Ferretti's products are 1, 2-bis-ethylthioethylene and *trans*-1, 2-bis-ethylsulfonylethylene, but not ethyl ethynyl sulfide and *S*-ethyl hydrogen thiocarbonate. It is also shown that the reaction of 1,2-dibromoethylene with cuprous ethanethiolate proceeds in the same way as that with cuprous thiophenolate.[1]

3) M. F. Shostakovskii, E. N. Prilezhaeva, L. V. Tsymbal and L. G. Stolyarova, *Zh. Obshch. Khim.*, **30**, 3143 (1960).

4) H. J. Bonstra and L. C. Rinzema, *Rec. Trav. Chim.*, **79**, 962 (1960).

5) J. F. Arens and T. Doornbos, ibid., **75**, 481 (1956) and other papers of J. F. Arens et al.

Complex Formation of Indium(III) with Oxalate Ion in 1M Sodium Perchlorate Media

By Yuko HASEGAWA and Tatsuya SEKINE

Department of Chemistry, Tokyo College of Science, Kagurazaka, Shinjuku-ku, Tokyo

(Received April 13, 1966)

Much work has been devoted to the complex formation of indium(III) in aqueous solutions with various ligands.[1] It has been shown that indium(III) is a good acceptor of various ligands, forming stable complexes in aqueous solutions.

The complex formation of some trivalent metal ions with oxalate ion has also been studied, and it has been reported[2] that lanthanum(III), europium(III), luthetium(III) and americium(III) form oxalate complexes, $MC_2O_4^+$, $M(C_2O_4)_2^-$ and $M(C_2O_4)_3^{3-}$, in 1 M sodium perchlorate media.

For the complex formation of indium(III), Lacroix reported[3] that a tripositive indium ion combines with two oxalate ions. Moreover, White, Tang and Li[4] reported that indium(III) forms a complex species, $InHC_2O_4^{2+}$. However, no quantitative data on the successive formation of indium(III) complexes seem to have been published.

For the present paper, the authors studied the complex formation of indium(III) with oxalate ions in 1 M $Na(ClO_4)$ at 25°C. A liquid-liquid distribution method was employed in conjunction with an indium-114 m tracer in order to keep the metal ion concentration very low and to avoid the formation of indium oxalate precipitates. The complex formation was determined from the decrease in the metal extraction with thenoyltrifluoroacetone. The stability constants were determined graphically by a curve-fitting method.

Experimental

Most of the reagents and procedures were the same as those described previously[5,6] except the following.

Tracer and Reagents.—Indium-114 (half-life; 50.0 days) was prepared by the irradiation of five-nine indium metal with thermal neutrons in the JRR-2 reactor of the Japan Atomic Energy Institute. The irradiated sample was dissolved in aqua regia and evaporated to dryness. The residue was dissolved in perchloric acid and used as the stock tracer solution. The chloroform was washed three times with water.

Procedures.—In the present study, sulfanilic acid-sulfanilate was used to buffer the aqueous phase between pH 3.0 to 3.4, and a chloroform solution of 0.01 M

1) L. G. Sillen and A. E. Martell, "Stability Constants," Spec. Pub. **17**, the Chemical Society, London (1964).
2) T. Sekine, *Acta Chem. Scand.*, **19**, 1476 (1965).
3) S. Lacroix, *Ann. Chim.*, **4**, 5 (1949).
4) J. M. White P. Tang and N. C. Li, *J. Inorg. Nucl.*, **14**, 255 (1960).
5) T. Sekine and Y. Hasegawa, This Bulletin, **39**, 240 (1966).
6) T. Sekine, M. Sakairi and Y. Hasegawa, This ibid., **39**, 2141 (1966).

thenoyltrifluoroacetone (TTA) was used as the organic phase. The initial concentration of indium(III) in the aqueous phase was always less than 3×10^{-7} M.

Results and Discussion

The dissociated oxalate ion concentration in the solutions at different hydrogen ion concentrations was calculated from the total oxalate concentration, using the acid dissociation constant. The details of the statistical treatment have been given in previous papers[2,5,6]; only the final equations will be given in Table I.

Table I. Abrribations and equations

D: Net distribution ratio

$$D=\frac{\gamma\text{-radioactivity per ml. org. phase}}{\gamma\text{-radioactivity per ml. aq. phase}} \quad (1)$$

D_0: Distribution ratio in the absence of ligands

$$D_0=[InA_3]_{org}/[In^{3+}]_{aq} \quad (2)$$

K_{ex_0}: Extraction constants

$$K_{ex_0}=D_0[H^+]^3[HA]_{org}^{-3} \quad (3)$$

$=10^{-3.83}$ (determined from the data in Fig. 1)

β_n: The stability constant for the "nth" complex

$$\beta_n=[InL_n^{3-2n}]/[In^{3+}][L^{2-}]^n \quad (4)$$

$$\log(1+\sum\beta_n[L^{2-}]^n)^{-1} = \log D[H^+]^3[HA]_{org}^{-3}/K_{ex_0} \quad (5)$$

Figure 1 gives the $\log D$ vs. $-\log[H^+]$ plot when the aqueous phase contains no oxalate. The plot in the figure falls on the straight line of slope 3 (cf. Eq. 3).

The stability constants of the oxalate complexes may be calculated by Eq. 5, and the stability constants may be determined by a "curve-fitting" method.[5,6]

The stability constants for the complex $InC_2O_4^+$ and $In(C_2O_4)_2^-$ species were determined by the curve-fitting method as $\log\beta_1=5.30$ and $\log\beta_2=10.52$. Figure 2 gives the $\log D[H^+]^3[HA]_{org}^{-3}/K_{ex_0}$ vs. $\log[C_2O_4^{2-}]$ plot, together with the curve calculated from the stability constants obtained by the curve-fitting method.

Under the present experimental conditions, the hydrolysis of indium(III) may be neglected (for the calculation of the stability constants) because the hydrolysis constants have been given as $10^{-4.4}=[InOH^{2+}][H^+]/[In^{3+}]$ and $10^{-3.9}=[In(OH)^{2+}][H^+]/[InOH^+]$.[7]

It seems that the experimental data can be explained by assuming only the primary and the secondary complexes within the present oxalate concentration range. No stability constants of indium(III) oxalate complexes have been reported which can be directly compared with the present

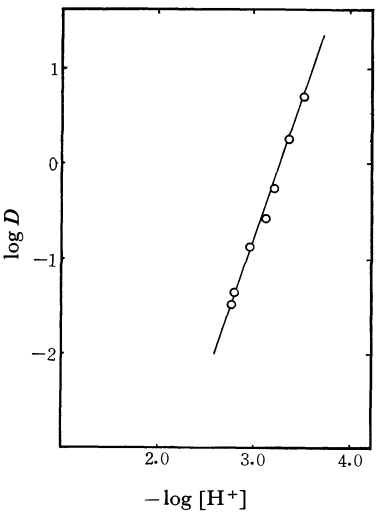

Fig. 1. Distribution ratio of indium(III) as a function of hydrogen ion concentration at 25°C when oxalate ion is absent in the aqueous phase.
Organic phase: 0.01 M TTA in chloroform
Aqueous phase: 1.0 M $NaClO_4$

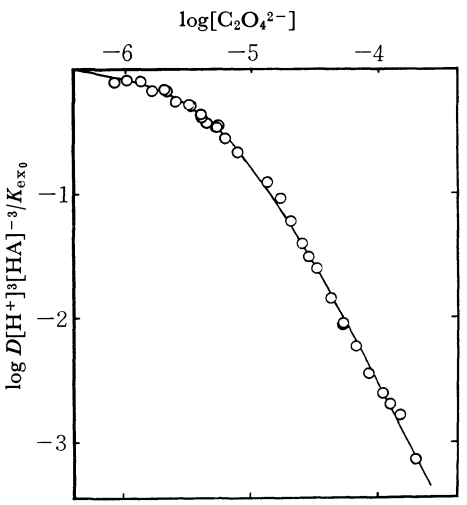

Fig. 2. Variation of $D[H^+]^3[HA]_{org}^{-3}$ of indium(III) as a function of the concentration of oxalate ion at 25°C.
Organic phase: 0.01 M TTA in chloroform
Aqueous phase: 1.0 M $Na(ClO_4)$
The solid curve shows $\log D[H^+]^3[HA]_{org}^{-3}K_{ex_0}^{-1} = -\log(1+2.0\times10^5[C_2O_4^{2-}]+3.3\times10^{10}\times[C_2O_4^{2-}]^2)$

results, nor have such constants been reported for the oxalate complexes of aluminum(III), gallium(III) or thallium(III) under similar experimental conditions except for those by Dutt and Sur[8] in 1 M potassium nitrate at 32°C. It may be

7) G. Biederman, *Arkiv Kemi*, **9**, 277 (1956); *Rec. Trav. Chim.*, **75**, 716 (1956).

8) N. K. Dutt and B. Sur, *Z. anorg. Chem.*, **293**, 195 (1957).

seen in their results that the K_2 of the aluminum(III) oxalate complex ($\log K_2 = 5.45$) is of the same order as that of the indium(III) complex in the present study ($\log K_2 = 5.22$).

The stability constants for the primary and the secondary oxalate complexes of lanthanum(III), europium(III), luthetium(III) and americium(III)[2] under the same experimental conditions are a little smaller than those of indium(III); the tertiary complex, such as was always found for these trivalent ions, was not found for indium(III).

Part of the present work was carried out at the Laboratory of Nuclear Chemistry, the Institute of Physical and Chemical Research, Tokyo. The authors are very grateful to Professor Nobufusa Saito, the head of the laboratory. The authors are also grateful to Dr. Tadashi Nozaki and Dr. Mariko Inarida for their experimental aid.

A Powerful New Aldol Condensation Agent, Ba_3N_4[1]

By Yoshiyuki OKAMOTO and J. C. GOSWAMI

Research Division, School of Engineering and Science, New York University, University Heights, New York

(Received April 26, 1966)

The thermal decomposition of many inorganic azides, especially those of heavy metals, proceeds explosively and results in the formation of the corresponding metal and nitrogen.[2] However, we have found that barium azide, $Ba(N_3)_2$, decomposes smoothly in organic solvents such as decalin or tetralin at the temperature of their respective boiling points to yield nitrogen and a fine black powder, barium pernitride, Ba_3N_4.[3,4]

Barium pernitride obtained was found to be exceedingly reactive with water and air. We now wish to report that this compound is also a highly active catalyst for an aldol condensation. Indeed, barium pernitride exhibits much greater reactivity than that of aluminum tri-*t*-butyl alcoholate, known as a powerful catalytic agent for this reaction.[5]

The typical results are described as follows. Barium azide (10 g.) and decalin or tetralin (50 ml.) were placed in a 100 ml. pyrex three-neck flask equipped with a Liebig reflux condenser. The air in the apparatus was replaced with dry nitrogen. The flask was heated slowly in an oil bath. The decomposition reaction started within 20 min. and after the solvents reached the boiling point, the mixture was refluxed for 30—40 min. to complete the reaction.

Upon cooling the system, the solvent was replaced with 50 ml. dried ether under a stream of dry nitrogen. Dried acetone (25 g.) was added dropwise into the suspension of Ba_3N_4 in ether with stirring at -15 to -20°C during 30 min. Mesityl oxide (14.2 g., b. p. 133°C/757 mmHg, 2, 4-dinitrophenylhydrazone m. p. 204°C) and diacetone alcohol (5.8 g., b. p. 160°C/757 mmHg, 2, 4-dinitrophenyl hydrazone m. p. 202°C) were obtained as the main products. When an excess of Ba_3N_4 was used, the dehydrate, mesityl oxide, was the only product formed (according to Eq. 1).

Ba_3N_4 (prepared from 12.2 g. $Ba(N_3)_2$) suspended in 60 ml. ether was reacted with 32 g. acetophenone at 30°C for 1 hr. Dypnone (25 g., b. p. 133°C/0.5 mmHg, 2, 4-dinitrophenylhydrazone m. p. 167°C, authentic compound m. p. 167°C[5]) was obtained.

$$R\text{-}\overset{\overset{O}{\|}}{C}\text{-}CH_3 + Ba_3N_4 \xrightarrow{\text{ether}} R\text{-}\overset{\overset{O}{\|}}{C}\text{-}\overset{\overset{H}{|}}{C}=\overset{\overset{CH_3}{|}}{C}\text{-}R + N_2 + NH_3 + Ba(OH)_2 \quad (1)$$

where $R=CH_3$ or C_6H_5.

1) Decomposition of Azides. II. Part I: Y. Okamoto and J. C. Goswami, *Inorg. Chem.*, **5**, 1281 (1966).

2) For general discussion and references: a) F. P. Bowden and A. D. Yoffe, "Fast Reactions in Solids," Academic Press, Inc., New York, N. Y. (1958); b) P. Gray, *Quart. Revl (London)*, **1963**, 441.

3) Y. Okamoto and J. C. Goswami, *Inorg. Chem.*, **5**, 1281 (1966).

4) A possible constitution of Ba_3N_4 is the barium tetrazane salt, $3Ba^{+2}$ $(-\overset{|}{N}-\overset{|}{N}-\overset{|}{N}-\overset{|}{N}-)^{6-}$. Further investigation of the structure is being studied currently.

5) W. Wayne and H. Adkins, *Org. Syn.*, **21**, 39 (1941).

Two Crystal Forms and the Fluorescence Spectra of 9, 10-Dichloroanthracene

By Harumitsu KUWANO and Michio KONDO

Central Research Laboratories, Sankyo Co., Ltd., Shinagawa-ku, Tokyo

(Received May 2, 1966)

It has been pointed out by Stevens[1] that the fluorescence spectra of aromatic hydrocarbons in the solid state have a close relationship to their crystal structures. According to him, aromatic hydrocarbons of type A show slightly red-shifted emission spectra, preserving molecular vibrational structures, whereas crystals of type B exhibit broad, structureless emission bands at considerably longer wavelengths than the corresponding molecular fluorescence in solutions.

Bock et al.[2] reported the fluorescence spectrum of 9, 10-dichloroanthracene (DClA) at various temperatures. They reported that, at room temperature, the spectrum exhibits a broad band with something of a structure and with peaks at about 470 and 490 mμ. On the other hand, Stevens and Dickinson[3] reported a single green-fluorescence band, with a peak about 540 mμ, for sublimed DClA. This fact has stimulated us to verify the existence of the two crystal forms of DClA.

Results and Discussion

Materials.—DClA was purified by column chromatography through alumina and recrystallized from benzene. Crystal-form α was obtained as long, yellow plates from benzene, alcohol or carbon tetrachloride. Form β was obtained as greenish-yellow plates on sublimation or by heating the α-form crystal above 180°C.

Lattice Constants and Crystal Structures.—The lattice constants of the α and β forms of DClA were determined by the usual X-ray technique. The crystal data for the α and β forms are summarized in Table I, together with the values reported by Trotter.[4]

The lattice constants of the α form agree excellently with those reported by Trotter. This leads to the conclusion that the α form is identical with that analyzed by Trotter.[5] According to his result, molecules are stacked along the a-axis, with their molecular planes nearly perpendicular to the a-axis. Adjacent molecules in the stacked column are separated by about 3.5 Å. In the projection along the a-axis, the long axes of two adjacent molecules are seen to be at an angle of about 60° to each other.

A crystal structure analysis of the β form is now in progress. Preliminary results reveal that the molecular stacking along the a-axis resembles the 9, 10-dibromoanthracene crystal, the structure of which has been analyzed by Trotter.[6] Namely, as can be seen from the value of the a-axis, the molecular planes are nearly parallel to the bc plane and the molecules in a stacking column are completely superposable on the bc plane when they are projected along the a-axis. In this regard, the β form is in sharp contrast to the α form, although both α and β forms belong to the type B.

Fluorescence Spectra. — The fluorescence spectra were recorded with a Shimadzu model SV-50 AL spectrophotometer equipped with an accessory for measuring the emission spectra of solid samples.

The fluorescence spectra measured on polycrystalline powders of the α and β forms of DClA at room temperature are shown in Fig. 1, together with that measured in a cyclohexane solution.

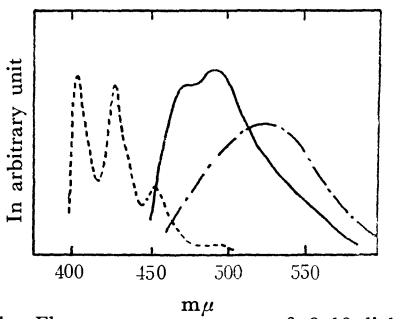

Fig. 1. Fluorescence spectrum of 9, 10-dichloroanthracene.
----: in cyclohexane ——: α form
— — —: β form

Emission bands in the crystalline state are at longer wavelengths than that in the solution. The α form exhibits a broad spectrum with peaks at about 470 and 490 mμ, whereas the β form shows a broad structureless band, with a peak at about

1) B. Stevens, *Spectrochim. Acta*, **18**, 439 (1962).
2) E. Bock, J. Ferguson and W. G. Schneider, *Can. J. Chem.*, **36**, 507 (1958).
3) B. Stevens and T. Dickinson, *Spectrochim. Acta*, **19**, 1865 (1963).
4) J. Trotter, *Acta Cryst.*, **11**, 564 (1958).
5) J. Trotter, ibid., **12**, 54 (1959).
6) J. Trotter, ibid., **11**, 803 (1958).

Table I. Crystal data of two crystal forms of 9,10-dichloroanthracene

	α Form		β Form
	Present work	Trotter	
a	7.04 Å	7.04 Å	3.87 Å
b	17.95 Å	17.93 Å	8.58 Å
c	8.60 Å	8.63 Å	16.98 Å
α	90°	90°	106°31′
β	103°06′	102°56′	94°56′
γ	90°	90°	95°04′
Space group	$P2_1/a$	$P2_1/a$	$P\bar{1}$ or $P1$
V	1059 Å^3	1062.3 Å^3	535 Å^3
Z	4	4	2
$d_{calcd.}$	1.549 g. cm^{-3}	1.545* g. cm^{-3}	1.535 g. cm^{-3}
$d_{obsd.}$	1.549 g. cm^{-3}	1.525 g. cm^{-3}	1.532 g. cm^{-3}

* A value recalculated from their lattice constants.

525 mμ.* The spectrum reported by Bock et al. resembles the present one on the α form, but the emission band reported by Stevens and Dickinson is located at a slightly longer wavelength than that of the β form reported herein.

As has been mentioned, the α and β forms of DClA both belong to the type B. These closely-stacked structures with interplanar distances of about 3.5 Å seem to be favorable for the formation of excimers. The broad structureless emission of the β form is separated from the 0–0 band of the emission spectrum in a cyclohexane solution by about 5800 cm^{-1}. For aromatic hydrocarbons in solutions, it has been pointed out that the excimer fluorescence spectra are located at positions lower than the 0–0 bands of monomer emissions by about 6000 cm^{-1}.[7] Furthermore, pyrene, a typical crystal with a dimer structure, shows a structureless emission band quite similar to the excimer fluorescence observed in solutions of moderately-high concentrations (10^{-2} mol./l.) as regards its shape and its position.[1] Therefore, the fluorescence spectrum of the β form can be regarded as being due to the excimer state.

On the other hand, it is not easy to explain the structure of the emission band of the α form. This band has a frequency lower than that of the 0–0 band of the monomer emission by about 3600 cm^{-1}. This band may be explained by; (a)"a weak excimer state" or (b) "a unimolecular degradation of an excited state strongly perturbed in crystals." Recently, it has been reported[8] that anthracene in cyclohexane at a low temperature (20°K) shows an excimer fluorescence with some structure located at a position lower than the 0–0 band of monomer emission by only about 2000 cm^{-1}. This fact seems to suggest the superiority of the explanation (a) over (b), but the possibility of (b) cannot be ruled out. Therefore, a more satisfactory explanation should be obtained from studies of the temperature dependence of the fluorescence spectra of the α and β forms of DClA.

Many theortical papers[9] have appeared on the excimer configuration, but no definite conclusion has yet been obtained. The present results will at least throw some light on this problem.

* The excitation spectra of the α and β forms were only a little different. This means that the absorption spectra of the α and β forms are essentially indentical.

7) J. B. Birks, M. D. Lumb and I. H. Munro, *Proc. Roy. Soc.*, **A280**, 289 (1964).

8) J. Ferguson, *J. Chem. Phys.*, **43**, 306 (1965).

9) T. Azumi and S. P. McGlynn, ibid., **42**, 1675 (1965), and references cited therein.

A Correlation of Catalytic Activity for the Oxidation of Carbon Monoxide and the Adsorption of Carbon Dioxide on Nickel Oxide

By Junko KONDO, Toshio UCHIJIMA and Yukio YONEDA

Department of Synthetic Chemistry, Faculty of Engineering, The University of Tokyo, Hongo, Tokyo

(Received May 10, 1966)

Various kinds of physical or chemical properties of oxides have previously been discussed, e. g., semiconductivity,[1] the decomposition pressure of oxides,[2] reducibility,[3] the heat of the formation of oxides,[4] and the rate of isotopic exchange reaction in molecular oxygen,[5] in attempts to find a parameter which is capable of accounting for the oxidation activity of nickel oxide catalysts.

It is generally accepted that carbon dioxide is adsorbed on the oxygen atom of the nickel oxide surface in the form of the "CO_3-complex," the existence of which was ascertained by both infrared spectroscopic[6] and micro-calorimetric[7] studies. The nature of the surface oxygen would be made clear by the measurement of the interaction between carbon dioxide and the catalyst surface. The adsorption of carbon dioxide will be examined in this study by means of the gas chromatographic technique for the purpose of obtaining the parameter for the catalytic activity of the oxidation of carbon monoxide.

The apparatus was a conventional assembly used for gas chromatography, modified by an additional small reactor. The oxidation of carbon monoxide with oxygen, diluted with helium as a carrier gas, was performed on grayish-green nickel oxide, which had been prepared by calcining basic nickel carbonate in air at 700°C for 8 hr. Molecular Sieve 5A was packed in the analytical column.

In order to observe the behavior of the adsorbed carbon dioxide, a gas sample (0.1 ml.) of carbon dioxide, mixed with a small amount of argon, was injected at the top of the nickel oxide catalyst column and the values of the retention times of carbon dioxide and argon were measured. The true retention volume of carbon dioxide was calculated from the flow rate and the retention time of argon.

The extent of the oxidation of carbon monoxide by gaseous oxygen on nickel oxide was determined first, and then that by nickel oxide itself, that is, reduction rate of nickel oxide by carbon monoxide. The rate constant of the oxidation of carbon monoxide by gaseous oxygen, k_o, was obtained by injecting the stoichiometric reaction mixture of carbon monoxide (0.5 ml.), oxygen (0.25 ml.) and helium (0.25 ml.) as a pulse. The reduction rate constant of nickel oxide by carbon monoxide, k_r, was derived in the same way using a mixture of carbon monoxide (0.5 ml.) and helium (0.5 ml.). The conversion of carbon monoxide to carbon dioxide both by gaseous oxygen, x_o, and by nickel oxide, x_r, was obtained from the decrease in the gas chromatographic peak height of carbon monoxide. The reaction kinetics being assumed to be first order with respect to the total pressure, the rate constants, k_o and k_r, were calculated as

$$k_o = F/W\,[\ln\,(1-x_o)^{-1}] \qquad (1)$$

and

$$k_r = F/W\,[\ln\,(1-x_r)^{-1}] \qquad (2)$$

respectively, where F (ml./min.) is the flow rate of the carrier gas and W (g.) is the weight of the catalyst.

The relationship between x_r and the retention volume of carbon dioxide, $V(CO_2)$, is shown in Table I. Both the true retention volume and the reduction rate constant are large under oxidized conditions and small under reduced conditions.

Table I. Relationship between retention volume of CO_2 on nickel oxide column and amount of reduction of nickel oxide by CO

Amount of catalyst, 4 g. Temperature, 140°C

Pretreatment	$V(CO_2)$, ml.	x_r, %
Oxidation	14.9	31
Reduction	8.0	16
Reoxidation	10.8	26

As to the retention volume, this may coincide with the schematic model of the adsorption of carbon dioxide on the surface oxygen proposed by Stone.[7]

Correlation of the oxidation rate of carbon monoxide or the reduction rate of nickel oxide

1) G. Parravano and M. Boudart, *Advances in Catalysis*, **7**, 47 (1955).
2) G. Rienacker and G. Schneeberg, *Z. anorg. u. allgem. Chem.*, **282**, 222 (1955).
3) W. H. M. Sachtler and N. H. De Boer, "Proceedings of the Third International Congress on Catalysis," North-Holland Publishing Company, Amterdam (1965), p. 252.
4) Y. Morooka and A. Ozaki, *J. Catalysis*, **5**, 116 (1966).
5) G. K. Boreskov, *Advances in Catalysis*, **15**, 285 (1965).
6) R. P. Eischens and W. A. Pliskin, ibid., **9**, 662 (1957); **10**, 1 (1958).
7) F. S. Stone, ibid., **13**, 1 (1962).
8) D. Chee and Y. Yoneda, to be published.

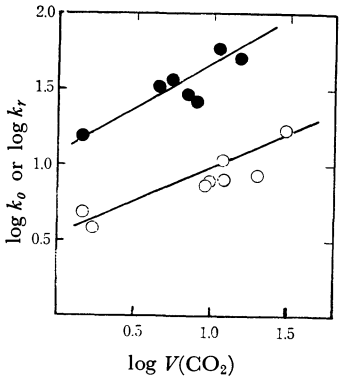

Fig. 1. Correlation between reaction rate constants and retention volume of CO_2 on nickel oxide at 120°C.

● Oxidation rate constant of carbon monoxide, k_o, in Eq. 1.
○ Reduction rate constant of nickel oxide, k_r, in Eq. 2.

with the retention volume of carbon dioxide over a nickel oxide catalyst is plotted in Fig. 1 for various conditions, such as oxidized or reduced, and fresh or poisoned. The oxidation rate of carbon monoxide by oxygen gas on nickel oxide is parallel to the reduction rate of nickel oxide by carbon monoxide. This correlation may reflect the fact that the more reactive surface oxygen for carbon monoxide the catalyst has, the more active is the catalyst for the catalytic oxidation of carbon monoxide.

By means of surface potential measurements, Chee and Yoneda[8] revealed recently that the surface state of nickel oxide during the oxidation of carbon monoxide is the oxidized one, irrespective of pretreatment and that the rate-determining step of this reaction is the process of the reaction between gaseous carbon monoxide and adsorbed oxygen.

A parallel correlation between the two kinds of rate constants and the retention volume of carbon dioxide seems to be reasonable, since the same surface oxygen may interact with carbon dioxide in both cases, and it may determine the catalytic activity as well.

On the basis of the above results and discussion, it may be concluded that the surface oxygen on which carbon dioxide is adsorbed can control the oxidation rate of carbon monoxide, and that the ability of carbon dioxide adsorption on nickel oxide is an important parameter for the catalytic activity of the oxidation of carbon monoxide. The value of the retention volume of carbon dioxide is the product of the number of adsorption sites and the equilibrium constant of the adsorption. In order to clarify the nature of the active center for the oxidation reaction of carbon monoxide on nickel oxide, it will be necessary to distinguish the amount of the adsorption of carbon dioxide from the adsorption strength. This problem will be dealt in another paper.

The authors wish to thank Dr. Yasukazu Saito and Dr. Dong Hyeon Chee for their many helpful discussions and suggestions during this work.

An Interpretation of Observed Long-range Couplings

By Kensuke TAKAHASHI*

The Chemical Research Institute of Non-Aqueous Solutions, Tohoku University, Katahira-cho, Sendai

(Received June 4, 1966)

Long-range spin-spin interactions between protons separated more than three bonds in saturated and unsaturated compounds have recently become the subject of a number of reports.[1] With respect to this problem, the importance of the straight zig-zag path (the M- or W-rule) in saturated systems has been pointed out by Rassat et al.[2] A similar case holds with some aromatics.[3] In this note, we should like to point out the additivity of the coupling constants with respect to the paths across which the long-range couplings take place. Such an empirical rule has not yet been pointed out in the previous reports. It seems to fit especially the large long-range couplings observed. The decrease in the coupling constant with the increase in the number of the bonds between nuclei was pointed out by Aihara.[4] Therefore, when the

* Present address: Department of Industrial Chemistry, Nagoya Institute of Technology, Gokiso-cho, Showa-ku, Nagoya.

1) S. Sternhell, *Rev. Pure and Appl. Chem.*, **14**, 15 (1964); many references are cited therin.

2) A. Rassat, C. W. Jefford, J. M. Lehn and B. Waegell, *Tetrahedron Letters*, **1964**, 233.

3) a) K. Takahashi, T. Kanda, F. Shoji and Y. Matsuki, This Bulletin, **38**, 508 (1965); b) M. M-Smith, S. T. Reid and S. Sternhell, *Tetrahedron Letters*, **1965**, 2393.

4) E. Aihara, *J. Chem. Phys.*, **26**, 1347 (1957).

TABLE I. SOME EXAMPLES SHOWING THE ADDITIVE CONTRIBUTION OF THE EFFECTIVE COUPLING PATHS BETWEEN TWO PROTONS

No.	Compound	No. of bonds	No. of paths	Observed coupling constant, c.p.s.	Ref.
1	2-Endo, 3-endocamphane-2,3-diol	4	1	1.4, 1.0	a
2	Exo-3-substituted norcamphors	4	1	3—4	b
3	Bicylo(2,2,1)-heptanes	4	1	1	b
4	*cis*-1,3-Dihalogenocyclohexanes	4	1	1.9	c
5	Bicyclo(2,1,1)-hexanes	4	2	7	b
6	Tricyclo(1,1,1,0)-pentane	4	3	14	d
7	1,3-Dioxanes	5	2	0.9	e
8	Thianaphthenes	6	1	0.6	f
9	Indoles	6	1	0.4	g
10	Thienopyrroles	6	2	1.3	h
11	Thienothiophene	6	2	1.55	i

a) F. A. L. Anet, *Can. J. Chem.*, **39**, 789 (1961); b) J. Meinwald and Y. C. Meinwald, *J. Am. Chem. Soc.*, **85**, 2514 (1963); c) H. M. vanDort and Th. J. Sekuur, *Tetrahedron Letters*, **1963**, 1301; d) S. Masamune, *J. Am. Chem. Soc.*, **86**, 735 (1964); e) Ref. 6; f) Ref. 3; g) Ref. 3b; h) R. J. Tuite, A. D. Josey, H. R. Snyder, *J. Am. Chem. Soc.*, **82**, 4360 (1960); i) B. Gestblom, R. A. Hoffman and S. Rodamar, *Acta Chem. Scand.*, **18**, 1222 (1964).

magnitudes of the coupling constants are first compared, the number of the bonds between nuclei must be taken into consideration. The notation of J^n_{ij} will be used here; n denotes the number of bonds between two nuclei, i and j, in series. The magnitude of the J^4 value between two protons is too small to be observed in usual saturated compounds, but it sometimes amounts to about 2 c. p. s. with one straight zig-zag path, as is shown by the examples of Nos. 1, 2, 3 and 4 in Table I. A theoretical approach to this problem was formulated by Barfield.[5] On the other hand, in bicyclo(2, 1, 1)hexanes (No. 5 in Table I), J^4 amounts to about 7 c. p. s., and, in this case, the number of paths connecting two protons is two; therefore, the magnitude of coupling may be expected to be approximately twice as much as is the case with only one path. No. 6 in Table I shows an abnormally large long-range coupling of 14 c. p. s.; this magnitude of coupling is considered to be about three times the magnitude of the examples with only one path. Recently, the J^5 value between protons has been observed with some 1, 3-dioxanes;[6] in this case the paths are also considered to be two. J^6 values between protons have been observed with some aromatics.[2] As can be seen from a comparison between the values of Nos. 10 and 11 and Nos. 8 and 9 in Table I, the cases with two paths show values of the coupling constants about twice as large as those in which only one path is effective. From the above-mentioned data, it may be concluded that the additive contribution of the effective coupling paths holds, to a good approximation, in the long-range couplings observed.

5) M. Barfield, ibid., **41**, 3825 (1964).

6) K. C. Ramey and J. Messick, *Tetrahedron Letters*, **1965**, 4423; J. Delmau and J. Duplan, ibid., **1966**, 559.

SHORT COMMUNICATIONS

The Crystal Structure of Meso-pentane-2, 4-diol Borate

By Shunsuke KURIBAYASHI

Government Industrial Research Institute, Osaka, Midorigaoka, Ikeda

(Received August 19, 1966)

In the course of a structural investigation of the model substances of polyvinyl alcohol, we have analyzed the crystal structure of meso-pentane-2, 4-diol borate.[1] This compound crystallizes in a monoclinic form, with unit cell dimensions of $a=15.36$ Å, $b=13.39$ Å, $c=7.60$ Å, and $\beta=113.0°$ The systematic absences of the reflections show that the space group is $C2/c$ or Cc. As the statistical test of the intensity distributions suggests that there exists a center of symmetry in the crystal, it was decided that the space group was $C2/c$. As this compound is very hygroscopic and is easily dissolved in nearly all kinds of solvents, it was very difficult to determine the density of the crystal. However, from the fact that the crystal is a little heavier than water, it is reasonable to consider that there are 8 molecule in the unit cell.

Multiple film equi-inclination Weissenberg photographs about the c axis were taken with CuK_α radiation for layers from 0 up to 6, while the intensities were estimated visually against a standard scale.

The structure was analyzed mainly by the Patterson projection along the c axis. The positional and thermal parameters of each atom so obtained were then refined by the least-square method. The reliability index, R, for (hkl) reflections at this stage of analysis is 18%, omitting the unobserved reflections. The final electron density projection along the c axis is shown in Fig. 1.

Surrounding the center of symmetry, two molecules are hydrogen-bonded, as is shown in Fig. 2, the distance of the hydrogen bond being about 2.8 Å. The boron atom is surrounded by three oxygen atoms, which form an almost equilateral triangle about the boron; these four atoms are nearly coplanar. The two CH groups and the two oxygen atoms are almost on one plane; all the carbon atoms also form a plane. These three planes, namely, the plane containing all the carbon atoms, that containing two CH groups and two oxygen atoms, and that containing the BO_3 group, intersect to form a chair-like structure. The details of the structure analysis will be reported in the near future.

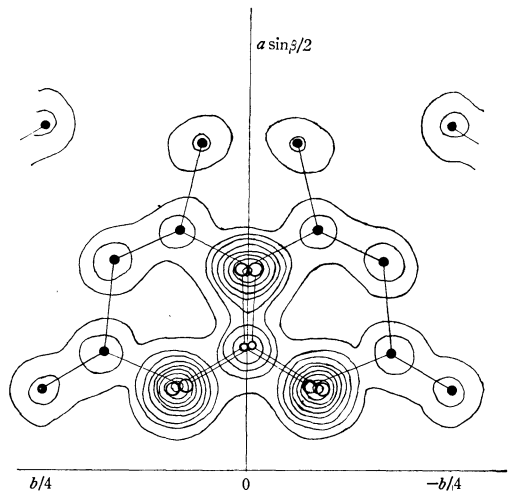

Fig. 1. The final electron density projection on the (001). Contours are in arbitrary unit. Black circles indicate carbon atoms, small open circles indicate boron atoms, and large open circles indicate oxygen atoms.

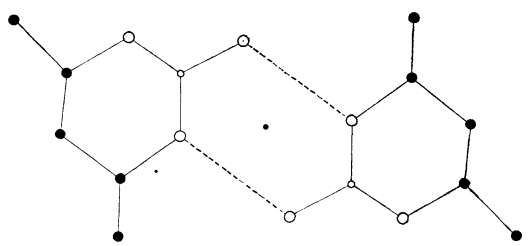

Fig. 2. Two hydrogen bonded molecules. The broken lines indicate the hydrogen bonds, small black circle indicates the center of symmetry. Other circles are as in Fig. 1.

1) E. Nagai, S. Kuribayashi, M. Shiraki and M. Ukita, *J. Polymer Sci.*, **35**, 295 (1959).

A Retentive S_Ni Hydrolysis in Aqueous Acrylonitrile and the Polymerization of Acrylonitrile Initiated by the S_Ni Hydrolysis Intermediate

By Kunio Okamoto, Kôichi Komatsu and Haruo Shingu

Department of Hydrocarbon Chemistry, Faculty of Engineering, Kyoto University, Sakyo-ku, Kyoto

(Received July 13, 1966)

As a result of continuation of our search[1] for the solvent systems in which the S_Ni solvolysis of simple alkyl derivatives involves retention of configuration, we found the water-acrylonitrile system being added to the examples of such retentive solvents. We also found that the acrylonitrile, used as the solvolytic solvent, concomitantly polymerizes, most probably being initiated by the S_Ni ion-pair intermediate.

The hydrolysis of α-phenylethyl chloride (2.61 g., α_D[2] +31.00°) was conducted in 97 wt.% aqueous acrylonitrile (90 cc.) in the presence of added triethylamine (0.201 M) at 90—91°C for 50 hr. Polyacrylonitrile[3] (16.1 wt.% of the starting nitrile), resulted in during the course of the reaction, was separated after treatment of the reaction mixture with ether and water; the ethereal solution was worked up in the usual way and then distilled in vacuo. The fraction A (0.842 g., b. p. 42—58°C/2.5 mmHg; the mixture of styrene, α-phenylethyl alcohol and unchanged α-phenylethyl chloride) and the succeeding fraction B (0.157 g., bath temp. 30—40°C/0.15 mmHg; almost pure α-phenylethyl alcohol) were respectively acetylated with acetic anhydride in pyridine to give α-phenylethyl acetates[4] with α_D +2.01° and α_D +2.02°. The content of the unchanged chloride (0.440 g.) in the fraction A was estimated from the chloride ion analysis of the water washings of the acetylation products; styrene (0.113 g.) was recovered from the acetylation products as a component eluted by *n*-hexane in the elution chromatography over basic alumina; α-phenylethyl acetate was eluted by benzene. The rotation of the unchanged chloride (α_D +0.264°) was calculated on the basis of the rotations of the fraction A and the α-phenylethyl alcohol,[5] contained in the fraction A. From the titrimetric chloride ion analysis of the washings of the reaction mixture the completion of the hydrolysis was estimated to be 58.1%.

These results indicate that 6.31%[6] of the optical activity of the starting chloride was retained in the acetate derived from α-phenylethyl alcohol, and that the acetate possesses the same configuration as that of the chloride. In other words, the hydrolysis to 58.1% completion gave α-phenylethyl alcohol with 6.31% of retention of the configuration, since the acetylation process gives no change to the optical purity and the configuration of the alcohol.[7] Although the titrimetric first-order rate constant for this hydrolysis showed appreciable decreasing tendency, the S_Ni-character of this hybrolysis seems to be undoubtful on the basis of the predominant racemization of the product (93.7%) and of the unchanged chloride (99.1%). The specific solvation of the acrylonitrile molecule to the S_Ni ion-pair intermediate would be responsible for this unusual steric course of the hydrolysis.

The rate of the concomitant polymerization of acrylonitrile, estimated from wt.% yield of polyacrylonitrile at intervals, was as high as about eight fold of the rate in the absence of α-phenylethyl chloride; this rate increased with the increasing initial concentration of α-phenylethyl chloride and decreased with the decreasing water content in aqueous acrylonitriles. The added triethylammonium chloride and styrene, in the absence of the chloride, were found to have no appreciable accelerating action on this polymerization. From these findings, we conclude that this polymerization is most probably initiated by the S_Ni ion-pair intermediate produced from α-phenylethyl chloride and that the specific solvation above mentioned may also be responsible for this initiation.

1) a) K. Okamoto, K. Takeuchi and H. Shingu, This Bulletin, **35**, 521 (1962); b) K. Okamoto, H. Yamada, I. Nitta and H. Shingu, ibid., **39**, 299 (1966); c) K. Okamoto, M. Hayashi and H. Shingu, ibid., **39**, 408 (1966).

2) α_D signifies the rotation, neat, l dm., at 20—22°C.

3) The almost identical infrared spectrum with the authentic polyacrylonitrile. The inherent viscosity, 0.525 (DMF, 0.5%).

4) n_D^{25} 1.4931 and 1.4915, respectively. The acetate, the alcohol and styrene were identified by their infrared spectra.

5) The rotation of this alcohol, α_D +0.690°, estimated from that observed for the corresponding acetate. The maximum rotation of R-(+)-α-phenylethyl acetate, α_D 129° (lit. α_D^{28} 117°, H. R. Snyder and J. H. Brewster, *J. Am. Chem. Soc.*, **71**, 291, 4165 (1949)), determined from the results of the preliminary acetylation of the optically active α-phenyl ethyl alcohol. The maximum rotation of R-(+)-α-phenylethyl alcohol, α_D 44.2° (cf. Ref. 1b or 1c).

6) Calculated from the mean value of the rotations of the acetates obtained from the fraction A and B. The maximum rotation of R-(+)-α-phenylethyl chloride was taken as 125° (cf. Ref. 1b or 1c).

7) The second run (71% completion) afforded α-phenylethyl alcohol with 4.7% of retention of the configuration.

Circular Dichroism of Lanthanide(III) Complexes

By Sigeo KIDA

Department of Chemistry, Wakayama University, Masago-cho, Wakayama

and Toshiyuki ISOBE and Seizo MISUMI

Department of Chemistry, Faculty of Science, Kyushu University, Fukuoka

(Received September 24, 1966)

There have been reported a number of studies on the circular dichroism (CD) of metal complexes with optically active ligands. However, these studies have been limited to the absorption bands due to the d-d transitions; no studies of the Cotton effect associated with the absorption due to the f-f transitions have ever been reported, except for magnetic optical rotation studies.[1] Katzin and Barnett[2] have suggested the appearance of the Cotton effect of the tartarato complexes of some lanthanide(III) ions in an alkaline aqueous solution, but they have not yet shown any experimental data. In this paper we will report the results of the CD measurements of some lanthanide (III) complexes with optically active ligands.

The measurements have been carried out on aqueous alkaline solutions of tartarato-, lactato-, alaninato-, serinato- and valinato complexes of neodymium(III) and propylen ediamine tetraacetato complexes of praseodymium(III), neodymium-(III) samarium(III), dysprosium(III) and erbium-(III). The circular dichroism was clearly observed in the region of each absorption band (one of which is shown in Fig. 1), even though the intensity is very weak compared with that of a d-complex. This is to be expected from the fact that the f-electrons in lanthanide(III) complexes are better shielded than d-electrons in ordinary transition metal complexes. In some cases the results were rather ambiguous because of too weak intensities.

As may be seen in Fig. 1, a few CD components

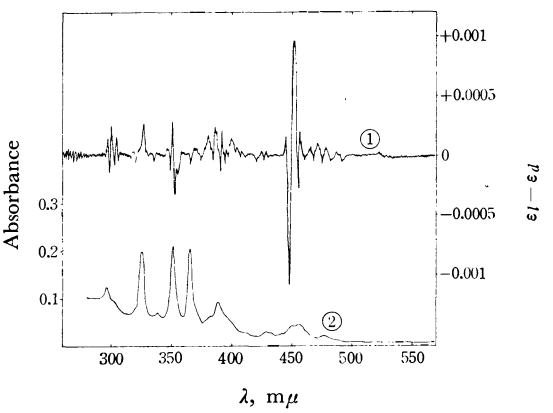

Fig. 1. CD and absorption spectra of levo-propylenediamine tetra acetato complex of dysprosium(III) in aqueous solution (0.1 F, pH= 10.63), 1 cm. cell. 25°C.
(1) CD spectrum (2) Absorption spectrum

are observed for each absorption band; these components may be attributable to the ligand-field splitting. It is interesting that the absorption bands due to f-f transitions can be resolved into so minute peaks by CD measurements.

A more detailed discussion will be reported later.

1) For instance, Y. R. Shen, *Phys. Rev.*, **133** (2A), 511 (1964).
2) L. I. Katzin and M. L. Barnett, *J. Phys. Chem.*, **68**, 3779 (1964).

Nuclear Magnetic Resonance Spectra of Organophosphorus Compounds. I. Long-range Coupling between Phosphorus and Proton through Four Bonds

By Kensuke TAKAHASHI,* Taro YAMASAKI and Goh MIYAZIMA

The Chemical Research Institute of Non-Aqueous Solutions, Tohoku University, Katahira-cho, Sendai
The Research Institute of Mineral Dressing and Metallurgy, Tohoku University, Naga-machi, Sendai
Naka Works, Hitachi, Ltd., Ichige-cho 882, *Katsuta, Ibaragi*

(Received September 28, 1966)

In this communication, we will compare the results of the coupling constants observed in some organophosphorus compounds of the type of $(EtO)_nPCl_{3-n}$ with those of $(EtO)_nPXCl_{3-n}$ (X=O or S, and n=3, 2 or 1). Some data were given in Table I and a typical proton spectrum of $EtOPOCl_2$ was shown in Fig. 1. The doubling

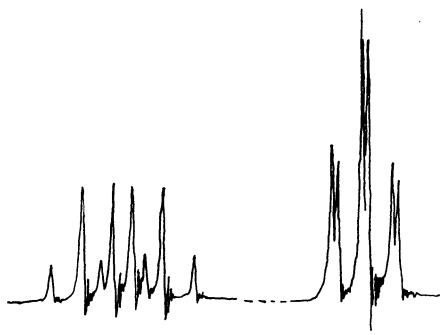

Fig. 1. The proton magnetic resonance spectrum of $EtOPOCl_2$ at 60Mc p. s. Applied magnetic field increases from left to right.

of the usual 3—4 pattern of the ethyl group is clearly observed in Fig. 1. This is ascribed to the coupling between phosphorus and protons in methyl and methylene groups. As has been shown in Table I, the long-range coupling between phosphorus and proton through four bonds was observed in six pentavalent compounds but unresolved one in three trivalent compounds. The magnitude of the long-range coupling, $^4J_{PH}$, seems to increase in the order of P, PS and PO, while that of the $^3J_{PH}$ increases in the order of P, PO and PS; the effect of the substitution of oxygen by sulfur in the $^4J_{PH}$ is opposite to that in the $^3J_{PH}$. The substitution of an ethoxy group by chlorine causes the increase of the coupling constants both between phosphorus and methyl protons and between phosphorus and methylene protons. This kind of effect caused by some electronegative groups has been discussed by Hendrickson et al.,[1] but the long-range coupling between phosphorus and proton through four bonds has not yet been reported except some acetylenic compounds.[2] The coupling constants between protons in these compounds are almost constant. Another point of interest is that we can determine the relative sign of the coupling constants in this system using the double resonance technique. Preliminary results show $^3J_{PH}$ and $^4J_{PH}$ in $EtOPOCl_2$ (No. 4 in Table I) have the same relative sign. This was determined by partial irradiation of the methylene protons. Spectra were examined on the liquid containing a small amount of TMS as an internal reference. The proton and phosphorus resonances were observed at 60 and 24.288 Mc. p. s. respectively, using a Hitachi H-60 type spectrometer system.

TABLE I. NMR DATA OF SOME ORGANOPHOSPHORUS COMPOUNDS

No.	Compound	Coupling constant, c.p.s.			Chemical shift, p.p.m.*	
		$^3J_{PH}$**	$^4J_{PH}$	$^3J_{HH}$	δ_{CH_3}	δ_{CH_2}
1	$EtOPCl_2$	$8._5$	<0.5	7	1.35	4.27
2	$(EtO)_2PCl$	8	<0.5	7	1.29	4.05_5
3	$(EtO)_3P$	8	<0.5	7	1.21	3.81
4	$EtOPOCl_2$	$11._5$	1.2	7	1.44	4.42_5
5	$(EtO)_2POCl$	10	1.0	7	1.36_5	4.25_5
6	$(EtO)_3PO$	$8._5$	0.7	7	1.28_5	4.04
7	$EtOPSCl_2$	13	1.0	7	1.46	4.43
8	$(EtO)_2PSCl$	11	0.8_5	7	1.37	4.26_5
9	$(EtO)_3PS$	10	0.7	7	1.27_5	4.06

* Referred to TMS
** The notation $^nJ_{ij}$ denotes the coupling constant between nuclei i and j through n bonds.

* Present address: Department of Industrial Chemistry, Nagoya Institute of Technology, Gokiso-cho, Showa-ku, Nagoya.

1) J. B. Hendrickson, M. L. Maddox, J. J. Sims and H. D. Kaesz, *Tetrahedron*, **20**, 449 (1964).
2) C. Charrier, M.-P. Simmonnin, W. Chodkiewicz and P. Cadiot *Compt. rend*, **258**, 1537 (1964).

The π-Type Conjugation in the Cyclopropylmethyl Cation

By Teijiro YONEZAWA, Hiroshi NAKATSUJI and Hiroshi KATO

Faculty of Engineering, Kyoto University, Sakyo-ku, Kyoto

(Received October 5, 1966)

The high conjugative ability of the cyclopropyl group with an adjacent π orbital has been established experimentally[1] and theoretically.[2-4] For the cyclopropyl derivatives, Walsh predicted that this conjugation would be most effective when these compounds were in a "bisected" conformation (I in Fig. 1). Recently his prediction has been confirmed by Pittman and Olah through their NMR measurements.[1]

In the present paper, we will treat quantitatively the electronic structures of the two conformers, "bisected" (I) and "non-bisected" (II) (see Fig. 1), of the cyclopropylmethyl cation with our newly-developed semi-empirical ASMO-SCF method.[5] The geometry chosen for the cyclopropyl group is the same as that in cyclopropane, while the C_1–C_5 bond distance (in Fig. 1) is assumed to be 1.50 Å.

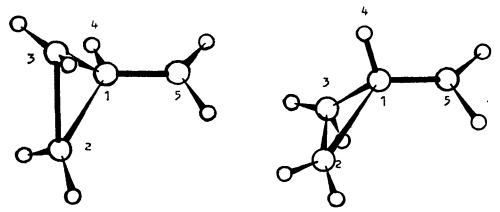

Fig. 1. The configurations of "bisected" (I) and "non-bisected" (II) conformers. In the I form, the atoms H_4, C_1 and the terminal CH_2 group are on the same plane, and in the II form the C_1–H_4 bond is perpendicular to the plane of the terminal CH_2 group.

TABLE I. THE ATOM AND AO BOND POPULATIONS IN CYCLOPROPYL GROUP

Compound	C_1–C_2	p_1–p_2	C_1–H_4	$p_{\sigma 1}$–h
Bisected (I)	0.585	0.309	0.847	0.523
Non-bisected (II)	0.650	0.378	0.785	0.464
Cyclopropane	0.651	0.367	0.839	0.539

The calculated total energies show that the I form is more stable than the II form by 0.813 eV. The π atomic orbital (AO) population of the C_5 atom is 0.443 in I and 0.280 in II. As to the atom bond population between the C_1 and C_5 atoms, the values are 1.015 in I and 0.924 in II, while the π AO bond populations are 0.203 in I and 0.113 in II; other π AO bond values obtained by the same method include 0.425 in ethylene, 0.114 in the ethyl cation, and -0.022 in ethane. Accordingly, it may be concluded that the π-conjugation in the I form is quite strong and that it contributes greatly to the stabilization of the I form.

The atom bond populations of C_1–C_2 and C_1–H_4 are collected in Table I, together with the corresponding values in cyclopropane. The table implies that the values of C_1–C_2 in the II form and of C_1–H_4 in the I form do not suffer much change, compared with the values in the cyclopropane, while remarkable changes do occur in C_1–C_2 in I and in C_1–H_4 in II. Further, in Table I, the sum of the AO bond populations between the three p AO's belonging to the C_1 and C_2 atoms, denoted by p_1–p_2 in Table I, and the value between the $p\sigma$ AO of the C_1 atom and the 1s AO of the H_4 atom ($p_{\sigma 1}$–h) are also indicated. Hence, the following conclusion may be drawn; the large changes in the atom bond population of C_1–C_2 in I and of C_1–H_4 in II are mainly caused by the changes in p_1–p_2 in I and in $p_{\sigma 1}$–h in II. As may be seen in Fig. 1, the p AO of the C_1 atom conjugating with the vacant π AO of the C_5 atom also participates in the C–C bonding in the I form and in the C–H bonding in the II form. Accordingly, the above-mentioned changes are largely due to the interactions between the p AO of the C_1 atom and the vacant π AO.

From the above discussions, it is clear that the stabilization in the I form arises mainly from π-type interaction between the vacant π AO of the sp^2 carbon and the π-like AO's in the ring carbons.

The transition energies for the first excitation may be evaluated as 6.60 eV. and 5.04 eV., and the oscillator strengths as 0.054 and 0.015, for I and II respectively. These transitions may be attributed to the intramolecular charge transfer from the cyclopropane ring to the vacant π AO of the sp^2 carbon.

1) C. U. Pittman, Jr., and G. A. Olah, *J. Am. Chem. Soc.*, **87**, 5123 (1965).
2) A. D. Walsh, *Trans. Faraday Soc.*, **45**, 179 (1949).
3) C. A. Coulson and W. E. Moffitt, *Phil. Mag.*, **40**, 1, (1949).
4) R. Hoffmann, *J. Chem. Phys.*, **40**, 2840 (1964); *Tetrahedron Letters*, **43**, 3819 (1965).
5) T. Yonezawa, K. Yamaguchi and H. Kato, This Bulletin, to be published; Abstract of the Symposium on Molecular Structure, Osaka (1966), p. 49.

* In Ref. 1 it is stated that the energy difference between these two conformers might be larger than 8—10 kcal./mol.